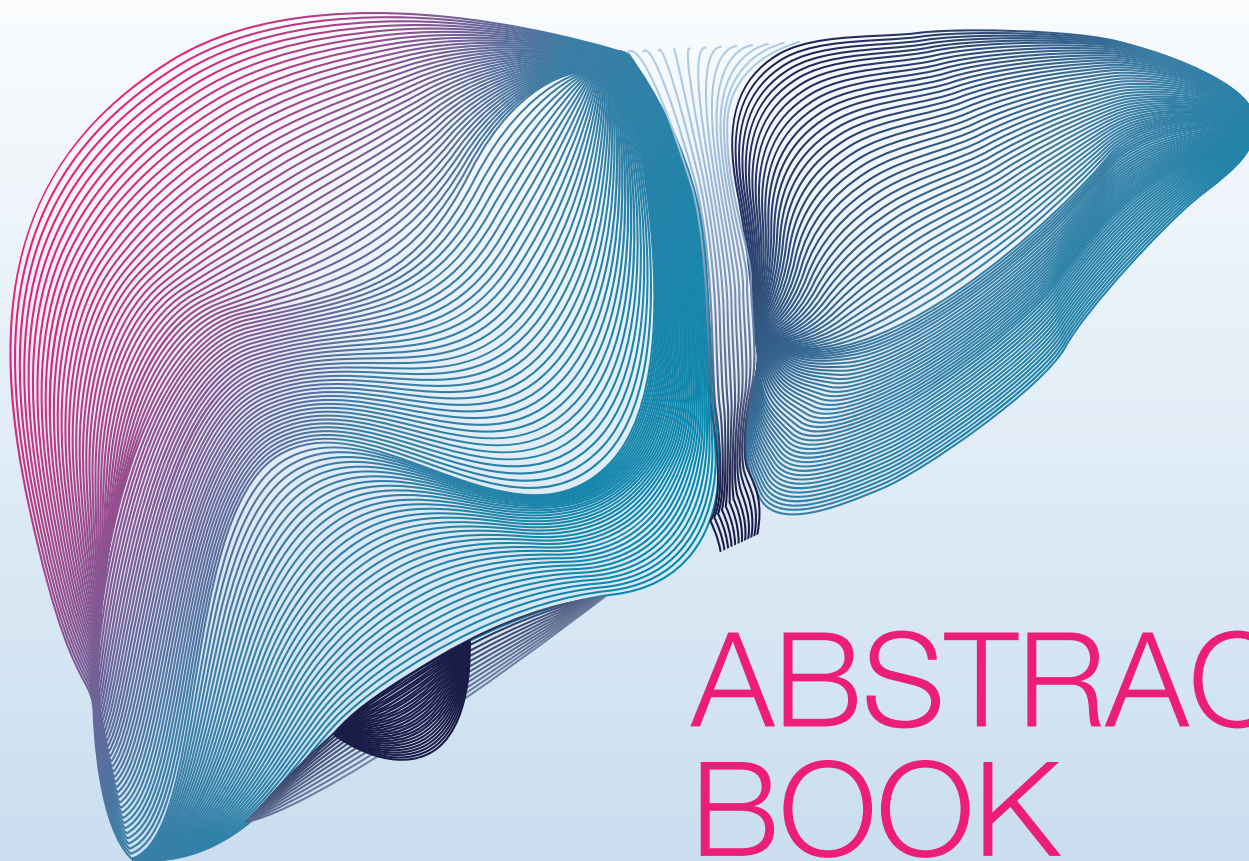


JOURNAL OF HEPATOLOGY

The Home of Liver Research

 **EASL** CONGRESS
Vienna, Austria
21–24 June 2023



ABSTRACT BOOK

JOURNAL OF HEPATOLOGY

The Home of Liver Research

EDITOR IN CHIEF

Paolo Angeli, Italy

DEPUTY EDITOR

Patrizia Burra, Italy

CO-EDITORS

Vlad Ratziu, France | Bruno Sangro, Spain |
Frank Tacke, Germany | Stefan Zeuzem, Germany

ASSOCIATE EDITORS

Alcohol and Drug-Related Liver Diseases

Einar S. Björnsson, Iceland
Alexandre Louvet, France

Cholestasis and Autoimmune Diseases

Tom H. Karlsen, Norway
Verena Keitel, Germany
Ulrich Beuers, Netherlands

Complications of Cirrhosis and Liver Failure

Paolo Caraceni, Italy
Javier Fernández, Spain
Constantine Karvellas, Canada
Wim Laleman, Belgium

Disease Burden and Public Health

Gregory Dore, Australia

Genetics

Carmen Berasain, Spain

Gut-Liver Axis

Bernd Schnabl, USA
Jonel Trebicka, Germany

Hepatic and Biliary Cancer

Jesper Andersen, Denmark
John Bridgewater, UK
Stephen L. Chan, Hong Kong
Tim Greten, USA

Tom Lüdde, Germany

Jean-Charles Nault, France
Maria Reig, Spain
Lorenza Rimassa, Italy

Imaging and Non-Invasive Tests

Annalisa Berzigotti, Switzerland
Maxime Ronot, France

Immunology

Barbara Rehermann, USA

Liver Fibrosis

Massimo Pinzani, UK

Liver Surgery and Transplantation

Pierre-Alain Clavien, Switzerland
Julie K. Heimbach, USA
Francesco P. Russo, Italy

NAFLD

Quentin Anstee, UK
Elisabetta Bugianesi, Italy
Jacob George, Australia
Wajahat Mehal, USA

Pathology

Christine Sempoux, Switzerland

Statistics, A.I. and Modelling Outcomes

Fabrice Carrat, France
Sylvie Chevret, France
Julian Varguese, Germany
Terry CF Yip, Hong Kong

Vascular Liver Diseases

Jordi Gracia-Sancho, Spain

Viral Hepatitis

Thomas Baumert, France
Maria Buti, Spain
Markus Cornberg, Germany
Edward J. Gane, New Zealand
Man-Fung Yuen, Hong Kong

Consultants

Julius Chapiro, USA
Peter Jepsen, Denmark

SPECIAL SECTION EDITORS

Reviews

Michael Trauner, Austria

Snapshot

Sara Montagnese, Italy
Alexander Ploss, USA

Website/Social Media

Jesus Bañales, Spain

What is your diagnosis?

Xavier Forns, Spain

EDITORIAL BOARD

Alcohol and Drug-Related Liver Diseases

Raul Andrade, Spain
Michael R. Lucey, USA
Philippe Mathurin, France
Laura E. Nagy, USA
Georges-Philippe Pageaux, France
Mark R. Thursz, UK

Basic Science

Javier Cubero, Spain
José Fernandez-Checa, Spain
Chandrashekar Gandhi, USA
Mathias Heikenwälder, Germany
Irene Ng, China
Cecilia Rodrigues, Portugal
Detlef Schuppan, Germany

Cholestatic and Autoimmune Diseases

Martti Färkkilä, Finland
Michael Heneghan, UK
Gideon Hirschfield, Canada
Pietro Invernizzi, Italy
Ansgar Lohse, Germany
Xiong Ma, China
Aldo J. Montano-Loza, Canada
Atsushi Tanaka, Japan

Complications of Cirrhosis and Liver Failure

Juan G. Abraldes, Canada
Banwari Agarwal, UK
Jasmohan S. Bajaj, USA
William Bernal, UK
Andrés Cárdenas, Spain
Claire Francoz, France
Guadalupe Garcia-Tsao, USA
Pere Ginés, Spain
Thierry Gustot, Belgium
Mattias Mandorfer, Austria
Sebastian Marciano, Argentina
Salvatore Piano, Italy
Shiv K. Sarin, India

Puneeta Tandon, Canada

Reiner Wiest, Switzerland

Epidemiology/Public Health

Jeffrey Lazarus, Spain
Uwe Siebert, Austria

Genetics

Frank Lammert, Germany
Stefano Romeo, Sweden

Gut-Liver Axis

Sofia Forslund, Germany
Aleksander Krag, Denmark

Hepatic and Biliary Cancer

Ann-Lii Cheng, Taiwan
Laura Dawson, Canada
Peter R. Galle, Germany
Chiun Hsu, Taiwan
Katie Kelley, USA
Josep Llovet, USA
Tim Meyer, UK
Pierre Nahon, France
Hayato Nakagawa, Japan
Jinsil Seong, Republic of Korea
Beicheng Sun, China
Juan Valle, UK

Immunology

Mala Maini, UK
Elsa Solà, Spain

Liver Fibrosis

Scott Friedman, USA
Tatiana Kisseleva, USA
Isabelle Leclercq, Belgium
Robert E. Schwartz, USA
Thierry Tordjmann, France
Holger Willenbring, USA

Liver Surgery and Transplantation

Martina Gambato, Italy
Giacomo Germani, Italy
Vincenzo Mazzaferro, Italy

Rajender K. Reddy, USA

Alberto Sánchez-Fueyo, UK
Gonzalo Sapichin, Canada
Christian Toso, Switzerland

NAFLD

Leon Adams, Australia
Guruprasad Aithal, UK
Helena Cortez-Pinto, Portugal
Henning Grønbaek, Denmark
Rohit Loomba, USA
Giulio Marchesini, Italy
Philip N. Newsome, UK
Elizabeth E. Powell, Australia
Manuel Romero-Gómez, Spain
Arun Sanyal, USA
Jörn Schattenberg, Germany
Giovanni Targher, Italy
Luca Valenti, Italy
Grace Wong, Hong Kong
Vincent Wong, Hong Kong
Shira Zelber-Sagi, Israel

Non-invasive Diagnoses and Imaging

Jérôme Boursier, France
Laurent Castera, France
Thierry de Baere, France
Richard (Dick) L. Ehman, USA
Salvatore Petta, Italy
Jordi Rimola, Spain
Riad Salem, USA

Pathology

Karoline Lackner, Austria
Valerie Paradis, France
Peter Schirmacher, Germany
Dina Tiniakos, UK
Achim Weber, Switzerland

Pediatrics

Emmanuel Jacquemin, France
Pietro Vajro, Italy

Statistics, A.I. and Modeling Outcomes

Calogero Camma, Italy
Jeremie Guedj, France

Vascular Liver Diseases

Yasuko Iwakiri, USA
Vincenzo La Mura, Italy
Pierre-Emmanuel Rautou, France

Viral Hepatitis

Alessio Aghemo, Italy
Sandra Ciesek, Germany
James Fung, Hong Kong
Jason Grebely, Australia
Ira Jacobson, USA
Patrick Kennedy, UK
Pietro Lampertico, Italy
Darius Moradpour, Switzerland
Jean-Michel Pawlotsky, France
Thomas Pietschmann, Germany
Charles Rice, USA
Jian Sun, China
Robert Thimme, Germany
Stephan Urban, Germany
Heiner Wedemeyer, Germany
Fabien Zoulim, France

EDITORS EMERITUS

Dame Sheila Sherlock†, Founding Editor, UK (1985-1989)
Jean-Pierre Benhamou†, France (1990-1994)
Gustav Paumgartner, Germany (1995-1999)
Juan Rodés†, Spain (2000-2004)
Massimo Colombo, Italy (2005-2009)
Didier Samuel, France (2010-2014)
Rajiv Jalan, UK (2015-2019)

EDITORIAL OFFICE

Manager

Joël Walicki

Coordinators

Jiyeong Adams
Duncan Anderson

Assistant

Kristina Jajcevic
Graphic Arts Project Manager
Pablo Echeverria

EASL GOVERNING BOARD

SECRETARY GENERAL

Thomas Berg, Germany

VICE SECRETARY

Aleksander Krag, Denmark

TREASURER

Francesco Negro, Switzerland

SCIENTIFIC COMMITTEE

Tobias Böttler, Germany
Virginia Hernández-Gea, Spain

Anna Lleo, Italy

Jean-Charles Nault, France

Bogdan Procopet, Romania

Debbie Shawcross, UK

Eric Trepo, France

Saskia van Mil, Netherlands

EDUCATIONAL COUNCILLORS

Ulrich Beuers, Netherlands
Sven Francque, Belgium (elect)

EU POLICY COUNCILLOR

Maria Buti, Spain

EXTERNAL AFFAIRS COUNCILLOR

Francesco Paolo Russo

INTERNAL AFFAIRS COUNCILLOR

Ahmed Elsharkawy

EASL Office

Journal of Hepatology Editorial Office
7 rue Daubin
1203 Geneva, Switzerland
Tel.: +41 (0) 22 807 0363
E-mail: jhepatology@easloffice.eu

Application for EASL Membership can be done at <https://easl.eu/community/join-the-community/>

© 2023 European Association for the Study of the Liver. Published by Elsevier B.V. All rights reserved.

This journal and the individual contributions contained in it are protected under copyright, and the following terms and conditions apply to their use in addition to the terms of any Creative Commons or other user license that has been applied by the publisher and the European Association for the Study of the Liver to an individual article:

Photocopying: Single photocopies of single articles may be made for personal use as allowed by national copyright laws. Permission is not required for photocopying of articles published under the CC BY license nor for photocopying for non-commercial purposes in accordance with any other user license applied by the publisher and the European Association for the Study of the Liver. Permission of the publisher and the European Association for the Study of the Liver and payment of a fee is required for all other photocopying, including multiple or systematic copying, copying for advertising or promotional purposes, resale, and all forms of document delivery. Special rates are available for educational institutions that wish to make photocopies for non-profit educational classroom use.

Derivative Works: Users may reproduce tables of contents or prepare lists of articles including abstracts for internal circulation within their institutions or companies. Other than for articles published under the CC BY license, permission of the publisher and the European Association for the Study of the Liver is required for resale or distribution outside the subscribing institution or company. For any subscribed articles or articles published under a CC BY-NC-ND license, permission of the publisher and the European Association for the Study of the Liver is required for all other derivative works, including compilations and translations.

Storage or Usage: Except as outlined above or as set out in the relevant user license, no part of this publication may be reproduced, stored in a retrieval system or transmitted in any form or by any means, electronic, mechanical, photocopying, recording or otherwise, without prior written permission of the publisher and the European Association for the Study of the Liver.

Permissions: For information on how to seek permission visit www.elsevier.com/permissions.

Author rights: Author(s) may have additional rights in their articles as set out in their agreement with the publisher and the European Association for the Study of the Liver (more information at <http://www.elsevier.com/authorsrights>).

Notice: Practitioners and researchers must always rely on their own experience and knowledge in evaluating and using any information, methods, compounds or experiments described herein. Because of rapid advances in the medical sciences, in particular, independent verification of diagnoses and drug dosages should be made. To the fullest extent of the law, no responsibility is assumed by the publisher or the European Association for the Study of the Liver for any injury and/or damage to persons or property as a matter of products liability, negligence or otherwise, or from any use or operation of any methods, products, instructions or ideas contained in the material herein.

Although all advertising material is expected to conform to ethical (medical) standards, inclusion in this publication does not constitute a guarantee or endorsement of the quality or value of such product or of the claims made of it by its manufacturer.

Publication information: *Journal of Hepatology* (ISSN 0168-8278). For 2023, volumes 78 and 79 are scheduled for publication. Subscription prices are available upon request from the Publisher or from the Elsevier Customer Service Department nearest you or from this journal's website (<http://www.elsevier.com/locate/jhep>). Further information is available on this journal and other Elsevier products through Elsevier's website: (<http://www.elsevier.com>). Subscriptions are accepted on a prepaid basis only and are entered on a calendar year basis. Issues are sent by standard mail (surface within Europe, air delivery outside Europe). Priority rates are available upon request. Claims for missing issues should be made within six months of the date of dispatch.

Orders, claims, and journal enquiries: Please visit our Support Hub page <https://service.elsevier.com> for assistance.

Advertising information: Advertising orders and enquiries can be sent to: **USA, Canada and South America:** Elsevier Inc., 360 Park Avenue, Suite 800, New York, NY 10169-0901, USA; phone: (+1) (212) 989 5800. **Europe and ROW:** Robert Bayliss, Pharma Solutions, Elsevier Ltd., 125 London Wall, London EC2Y 5AS, UK; phone: (+44) 207 424 4454; e-mail: r.bayliss@elsevier.com.

Author enquiries: Visit the Elsevier Support Center (<https://service.elsevier.com/app/home/supporthub/publishing>) to find the answers you need. Here you will find everything from Frequently Asked Questions to ways to get in touch.

You can also check the status of your submitted article via https://service.elsevier.com/app/answers/detail/a_id/29155/ or find out when your accepted article will be published via https://service.elsevier.com/app/answers/detail/a_id/5981/.

Funding body agreements and policies: Elsevier has established agreements and developed policies to allow authors whose articles appear in journals published by Elsevier, to comply with potential manuscript archiving requirements as specified as conditions of their grant awards. To learn more about existing agreements and policies please visit <http://www.elsevier.com/fundingbodies>.

Special regulations for authors: Upon acceptance of an article by the journal, the author(s) will be asked to transfer copyright of the article to EASL. Transfer will ensure the widest possible dissemination of information.

USA mailing notice: *Journal of Hepatology* (ISSN 0168-8278, USPS 11087) is published monthly by Elsevier B.V. Radarweg 29, 1043 NX Amsterdam, the Netherlands. Airfreight and mailing in the USA by agent named World Container Inc, 150-15, 183rd Street, Jamaica, NY 11413, USA. Periodicals postage paid at Brooklyn, NY 11256.

POSTMASTER: Send address changes to *Journal of Hepatology*, Air Business Ltd, c/o World Container INC 150-15, 183rd St, Jamaica, NY 11413, USA.

Subscription records are maintained at Elsevier B.V. Radarweg 29, 1043 NX Amsterdam, the Netherlands.

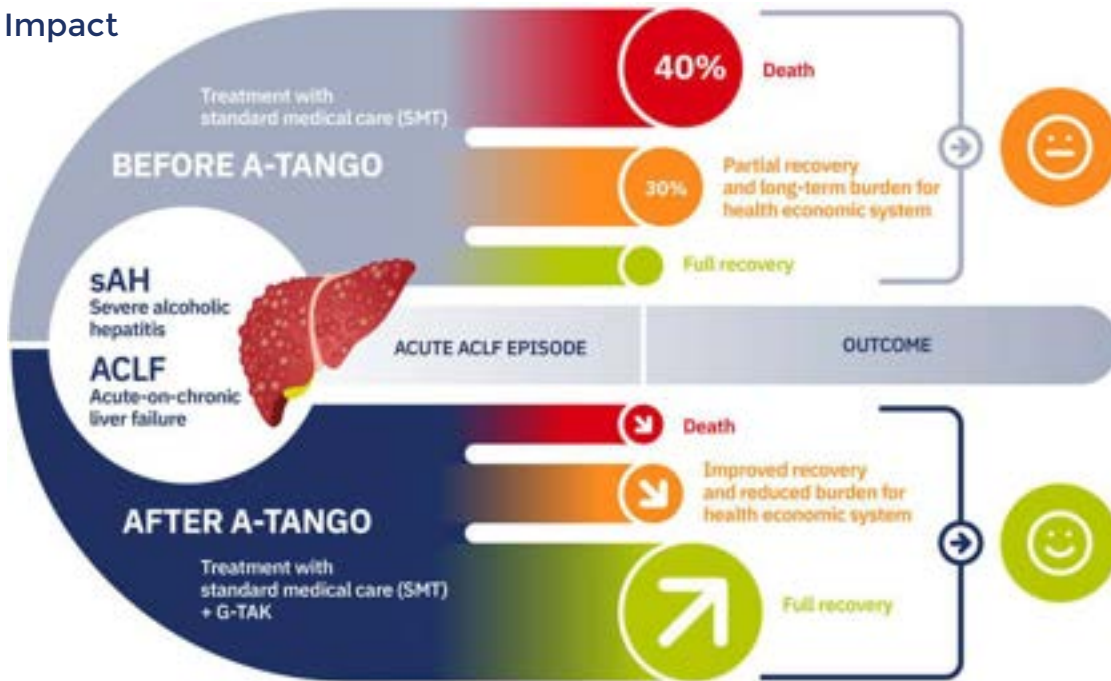
Air Business Ltd is acting as our mailing agent.

© The paper used in this publication meets the requirements of ANSI/NISO Z39.48-1992 (Permanence of Paper).

Printed by Henry Ling Ltd., Dorchester, UK

The A-TANGO project - featuring G-TAK, a novel combinatorial therapy for acute-on-chronic liver failure (ACLF)

Expected Impact



- More than 10 million people suffer from decompensated cirrhosis worldwide.
- Effective treatment of ACLF is an urgent and unmet need.
- A-TANGO performs Phase II clinical studies of G-TAK, a novel and innovative therapeutic strategy that aims to reduce inflammation and improve hepatocyte proliferation.
- A-TANGO also strives to identify reliable biomarkers for better patient stratification and increased survival.

14 partners, one goal:
Helping cirrhosis patients
in Europe!



www.a-tango.eu
info@atango.eu

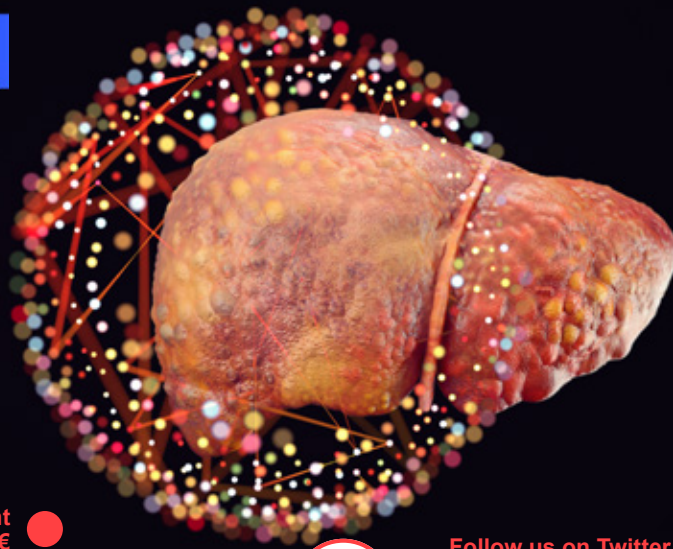


project duration	grant amount	8 countries	kick-off
5.0 years	6.0 million €	14 institutions	1st March 2021




This project has received funding from the European Union's Horizon 2020 research and innovation programme under grant agreement No 945096.



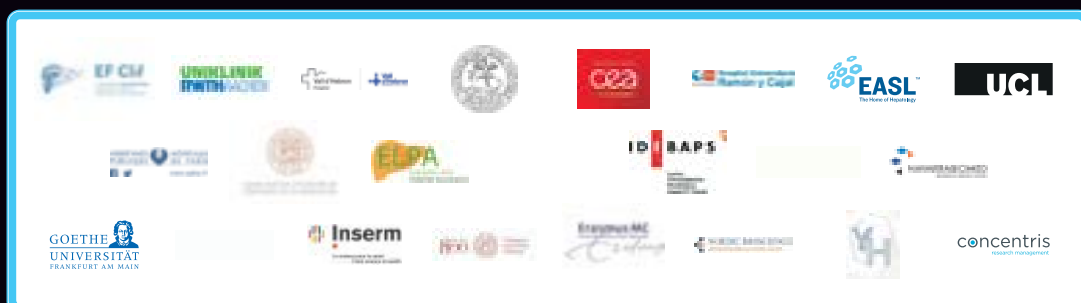


www.decision-for-liver.eu



 [decision-project](#)

- ① Pathophysiologic elucidation of acute decompensated cirrhosis at the systems level (genetics, epigenetics, transcriptomics, metabolomics, lipidomics, miR, and analysis of extracellular vesicles)
- ② Integration of existing clinical data and new multi-omics data from 2,200 patients with more than 8,600 measurements
- ③ Development of new combinatorial therapies
- ④ Optimization of therapies using existing and new animal models
- ⑤ Development of novel and robust tests for prediction of outcome following traditional treatment versus response to new therapies
- ⑥ Phase II clinical trials to test new combination therapies
- ⑦ Creation of new guidelines for outcome prediction and personalized treatment of acute decompensated cirrhosis to prevent ACLF to death



Liver Matters

Voices and views from our community



- + **ALEH: The Latin American perspective on fighting liver disease**
- + **Across generations and fields: EASL members tell their stories**
- + **Introducing the new EASL Scientific Committee**
- + **and much more...**

READ THE
BLOG



easl.eu/easl-blog

JOURNAL OF HEPATOLOGY

VOLUME **78**, SUPPLEMENT **1**, PAGES **S1–S1314**

Abstract Book of EASL Congress 2023
21–24 June 2023, Vienna, Austria

Publication of this Abstract supplement was supported by the European Association for the Study of the Liver (EASL)

ELSEVIER

Open-access eLearning anytime, anywhere



8,700+ resources available
38 CME-accredited courses

- 19 CPG slide decks
- 5,500 ePosters
- 24,200 registered users
- 2,800 webcasts



JOURNAL OF HEPATOLOGY

VOLUME 78, SUPPLEMENT 1, PAGES S1–S1314

CONTENTS

Oral Presentations	S1
General session I	S1
General session II	S7
Late-breaker Orals	S10
Nurses & AHPs Forum	S15
Alcohol-related liver disease and drug-induced liver injury	S18
Cirrhosis Experimental	S20
Gut microbiome/organ crosstalk	S24
Liver tumours – Basic	S27
NAFLD: Diagnostics and non-invasive assessment	S30
Viral hepatitis B/D - New treatments	S34
Cirrhosis and its complications: Clinical	S37
Experimental liver fibrosis	S41
(1) Immune-mediated and cholestatic liver diseases	S44
Liver transplantation and hepatobiliary surgery	S47
Liver tumours – Therapy	S50
NAFLD: Therapy	S53
Viral hepatitis B/D - Current treatments	S55
(2) Immune-mediated and cholestatic diseases	S59
Liver immunology	S62
Liver tumours - Clinical except therapy	S65
NAFLD: Clinical aspects	S69
Public health - viral hepatitis	S72
Senescence, circadian rhythm and sexual dimorphism	S75
Cirrhosis and its complications: Portal Hypertension	S78
Liver failure and regeneration	S82
NAFLD: Experimental	S85
Public Health - Except viral hepatitis	S88

Rare liver diseases	S90
Viral hepatitis C	S95
Poster Presentations	S100
Late-breaker Posters	S100
Acute liver failure and drug induced liver injury	S126
Alcohol-related liver disease	S145
Cirrhosis and its complications ACLF and Critical illness	S182
Cirrhosis and its complications Experimental and pathophysiology	S205
Cirrhosis and its complications Other clinical complications except ACLF	S233
Cirrhosis and its complications Portal Hypertension	S279
Fibrosis Stellate cell biology	S321
Gut microbiota and liver disease Liver-organ crosstalk	S342
Hepatocyte biology	S358
Immune-mediated and cholestatic disease Clinical aspects	S366
Immune-mediated and cholestatic Experimental and pathophysiology	S409
Liver development and regeneration	S433
Liver immunology	S442
Liver transplantation and hepatobiliary surgery	S454
Liver tumours Clinical aspects except therapy	S489
Liver tumours Experimental and pathophysiology	S524
Liver tumours Therapy	S571
NAFLD Clinical aspects except therapy	S600
NAFLD Diagnostics and non-invasive assessment	S647
NAFLD Experimental and pathophysiology	S730
NAFLD Therapy	S806
Non-invasive assessment of liver disease except NAFLD	S831
Nurses and Allied Health Professionals	S845
Public Health Except viral hepatitis	S854
Public Health Viral hepatitis	S872
Rare liver diseases (including paediatric and genetic)	S936
Viral Hepatitis Experimental and pathophysiology	S1013
Viral hepatitis AE Clinical aspects	S1052
Viral hepatitis B and D Clinical aspects	S1054
Viral Hepatitis B and D Current therapies	S1130
Viral Hepatitis B and D New therapies, unapproved therapies or strategies	S1147

Viral Hepatitis C Clinical aspects including follow up after SVR	S1172
Viral hepatitis C Therapy and resistance	S1204
Author Index	S1213
Disclosures: no commercial relationships	S1306
Disclosures: commercial relationships	S1310
Reviewers list	S1314

Registration of Clinical Trials

The *Journal of Hepatology* endorses the policy of the WHO and the International Committee of Medical Journal Editors (ICMJE) on the registration of clinical trials. Therefore, any trial that starts recruiting on or after July 1, 2005 should be registered in a publicly owned, publicly accessible registry and should satisfy a minimal standard dataset. Trials that started recruiting before that date will be considered for publication if registered before September 13, 2005.

More detailed information regarding clinical trials and registration can be found in *New Engl J Med* 2004; 351:1250–1251 and *New Engl J Med* 2005; 352:2437–2438.

Available online at www.sciencedirect.com

 **ScienceDirect**
for online access via your library



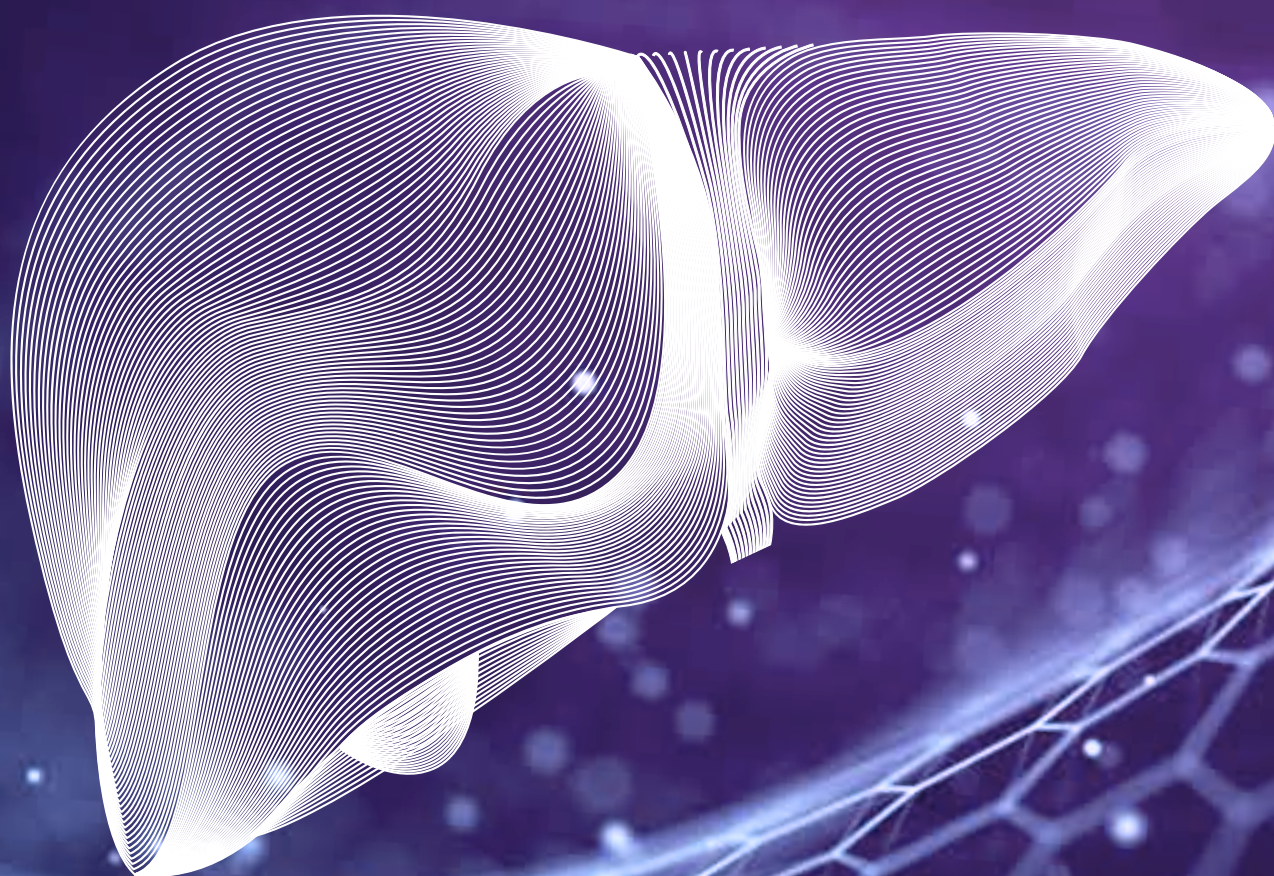
EASL

Milan, Italy
5–8 June

CONGRESS
2024

The International Liver Congress™

Save the date



easlcongress.eu

#EASLCongress

FUTURE EVENTS

2023–2024

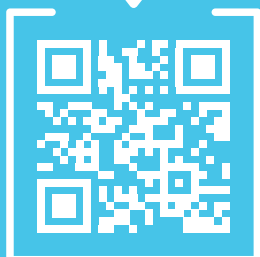
2023

21–23	September	EASL NAFLD Summit	Prague, Czechia
-------	-----------	-------------------	-----------------

2024

22–24	February	EASL Liver Cancer Summit	Rotterdam, The Netherlands
5–8	June	EASL Congress 2024	Milan, Italy
TBC	September	EASL NAFLD Summit 2024	TBC
TBC	TBC	AASLD-EASL Endpoints	USA

SEE OUR
CALENDAR





EASLTM

The Home of
Hepatology

THE LANCET



Ursula von der Leyen
President of the European Commission

The EASL–*Lancet* Liver Commission

The EASL–*Lancet* Liver Commission
has published a landmark report on
liver diseases in Europe.

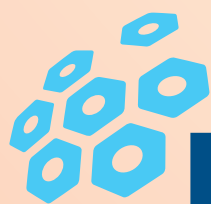
DOWNLOAD
THE REPORT



CHECK OUT
THE WEBSITE



Let's unite Hepatology



EASL™ The Home of
Hepatology

JOIN OUR
COMMUNITY



Patient & Advocate Forum: **Making the patient voice heard**

WATCH
ON DEMAND





EASL QUIZ

- + Testing your guidelines knowledge **since June 2020**
- + Sharpening your skills

TEST YOUR
KNOWLEDGE



Earn up to two badges
with gamification on
EASL Campus



EASL JOURNAL CLUB

SCAN FOR
MORE INFO



- + Hear directly from authors and experts in the field
- + Get answers to your questions
- + Take part every month



Your weekly hepatology broadcast news
Every Wednesday at 18:00 CET

Topics:

- + JHEP Live**
- + YIs Choice**
- + Nurses & AHPs Focus**
- + and more...**

WATCH
ON DEMAND





Understanding Gene ENvironment Interaction in ALcohol-related hepatocellular carcinoma

A project that will use AI models to integrate genetic and non-genetic information, including digital imaging, to develop novel cost-effective strategies towards prevention and early-stage detection of ALD-HCC

AIM:

- To portray genetic and environmental determinants promoting ALD-HCC;
- To evaluate how they interact at cellular level in human samples and preclinical models to get novel insights into liver carcinogenesis and identify chemopreventive targets; and
- To assess how they modulate the risk of ALD-HCC in several retrospective and prospective cohorts of patients included in HCC surveillance programs.



The GENIAL Project is funded by the European Union within the Horizon Europe programme under grant agreement No 101096312.

JOURNAL OF HEPATOLOGY

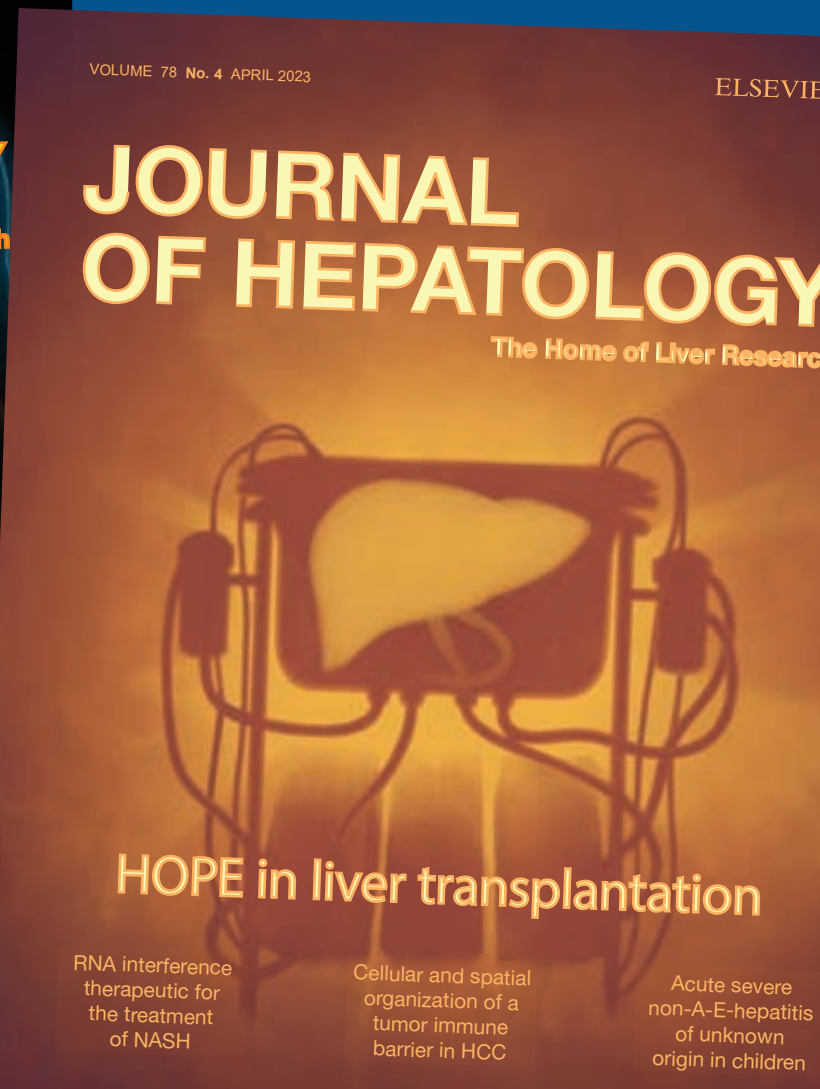
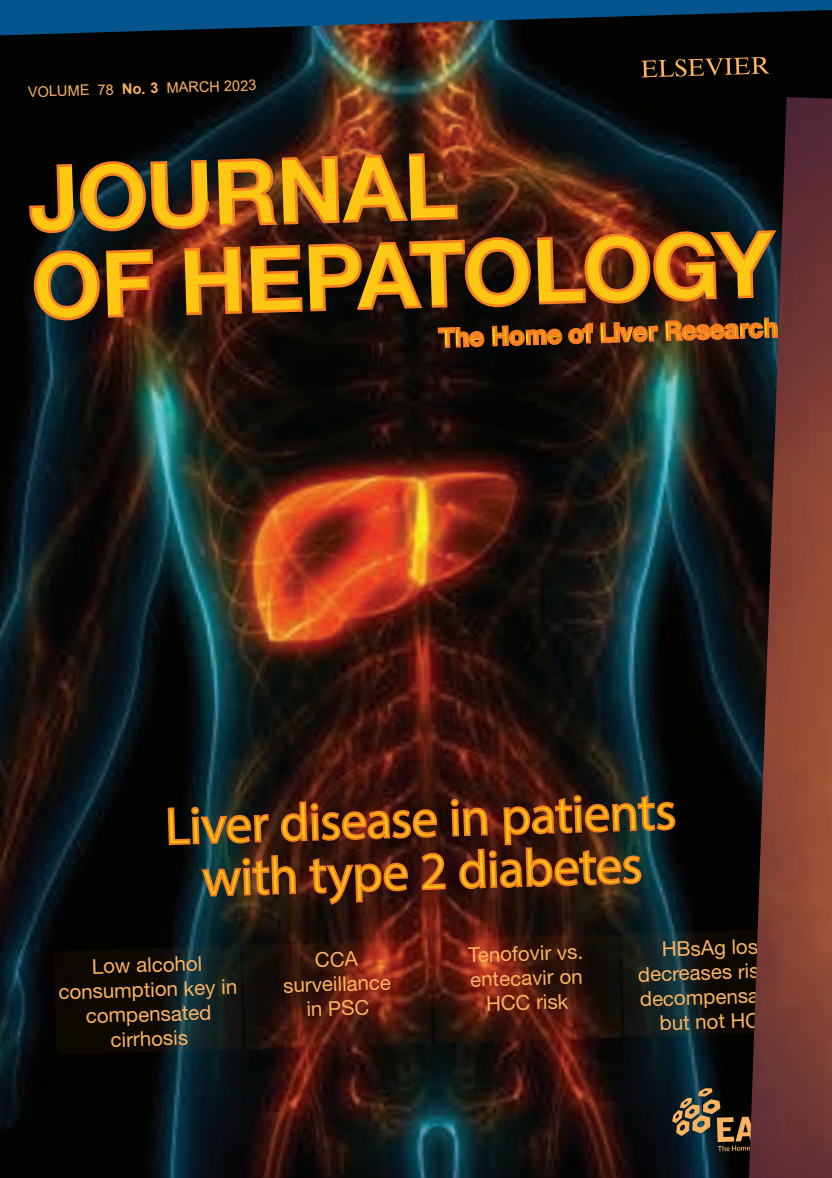
The Home of Liver Research



- + Premium hepatology journal
- + International Editorial team led by Prof. Paolo Angeli
- + 2021 Impact Factor: 30.083

**Submit your
article now**

SCAN FOR
MORE INFO



JHEP|Reports

Innovation in Hepatology



EASL's first open-access journal

+ **Discoverability**

Indexed by PubMed Central,
Clarivate, and Scopus

+ **Speed**

Time to first decision: 3.6 weeks
Acceptance to online publication: 2.2 weeks

+ **Excellence**

High-quality peer review guaranteed by an
international Editorial team led by Prof. Jessica Zucman-Rossi

**Submit your
article now**

SCAN FOR
MORE INFO





Liver Interinvestigation: Testing Marker Utility in Steatohepatitis

- 54 partners
- 14 countries for clinical recruitment
- True public-private co-funding model

The overarching aim of LITMUS is to develop, robustly validate and advance towards regulatory qualification biomarkers that diagnose, risk stratify and/or monitor NAFLD/NASH progression and fibrosis stage.

litmus-project.eu
imi.europa.eu



The LITMUS project has received funding from the Innovative Medicines Initiative 2 Joint Undertaking under grant agreement No. 777377. This Joint Undertaking receives support from the European Union's Horizon 2020 research and innovation programme and EFPIA.

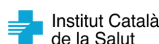
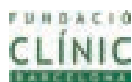
LIVER SCREEN

Screening for liver fibrosis population-based study across European Countries

**A project that will change the paradigm
of diagnosis of chronic liver diseases**

AIM:

**To assess the prevalence of liver fibrosis in the general population
using Transient Elastography, with the objective of establishing
criteria for screening for liver fibrosis in the population.**



MICROBiome-based biomarkers to PREDICT decompensation of liver cirrhosis and treatment response



Project duration
6 1/4 years

Start
01 January 2019

Follow-us on Twitter and LinkedIn:

 @MicrobPredict

 MICROB-PREDICT

Grant amount
15 million €

10 Countries
22 Partners

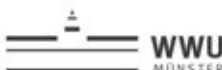
www.microb-predict.eu



will investigate

the human microbiome to identify predictors and mechanisms associated with the development of decompensation of cirrhosis and progression to **acute-on-chronic liver failure (ACLF) and death.**

- New microbiome-based tests for better stratification of cirrhosis patients
- Personalized prediction and prevention of decompensation and ACLF
- Clinical trial to predict response to treatment
- Modern, effective nanobiosensors as clinical tools with improved specificity
- More personalized treatment
- Increased survival times
- Decreased costs for the health systems



This project has received funding from the European Union's Horizon 2020 research and innovation programme under grant agreement No 825694.



EASLTM

Nurses & AHPs

On the frontline of hepatology

SCAN FOR
MORE INFO



- + Nurses & AHPs Task Force
- + Nurses & AHPs webinars
- + Nurses & AHPs Forum
- + Rising Star Award
- + Abstracts & Bursaries at events



EASLTM

Young Investigators

The future of hepatology



SCAN FOR
MORE INFO



- + YIs Task Force
- + YIs webinars
- + EASL Schools & Masterclasses
- + Fellowships & Mentorships
- + EASL Emerging Leader Award
- + Abstracts & Bursaries at events
- + YIs newsletter

THURSDAY 22 JUNE

General session I

GS-001

Primary results from MAESTRO-NASH a pivotal phase 3 52-week serial liver biopsy study in 966 patients with NASH and fibrosis

Stephen Harrison¹, Pierre Bedossa², Cynthia Guy³, Jörn Schattenberg^{4,5,6}, Rohit Loomba⁷, Rebecca Taub⁸, Dominic Labriola⁸, Sam Moussa⁹, Guy Neff¹⁰, Arun Sanyal¹¹, Mazen Nouredin¹², Meena Bansal¹³, Naim Alkhouri¹⁴, Vlad Ratzu¹⁵.
¹Pinnacle Research, United States; ²LiverPat, France; ³Duke University, United States; ⁴Mainz University, Germany; ⁵Metabolic Liver Research Program, I. Department of Medicine, University Medical Center Mainz, Mainz, Germany; ⁶Department of Internal Medicine I, University Medical Center of the Johannes Gutenberg-University, Mainz, Germany, Germany; ⁷UCSD, United States; ⁸Madrigal Pharmaceuticals, United States; ⁹Adobe Research, United States; ¹⁰Covenant Research, United States; ¹¹VCU, United States; ¹²CSHS, United States; ¹³Mount Sinai, United States; ¹⁴AZ Liver, United States; ¹⁵Inserm, France
 Email: rebeccataub@yahoo.com

Background and aims: MAESTRO-NASH (NCT03900429) is an ongoing 54-month, Phase 3, registrational double blind, placebo-controlled NASH clinical trial to study the effect of once daily 80 mg or 100 mg resmetirom as compared with placebo in patients with NASH and liver fibrosis. Eligibility required: presence of ≥ 3 metabolic risk factors, FibroScan VCTE ≥ 8.5 kPa, baseline MRI-PDFF $\geq 8\%$ and biopsy-proven NASH with fibrosis stage 1B, 2, or 3 and NAFLD activity score (NAS) ≥ 4 with at least 1 in each NAS component. An analysis of the Week 52 primary end points of MAESTRO-NASH were conducted and presented here. Week 52 dual primary end points included resolution of NASH (ballooning 0, inflammation 0, 1 with at least a 2-pt reduction in NAS) with no worsening of fibrosis OR ≥ 1 stage reduction in fibrosis with no worsening of NAS. The key secondary end point was % reduction in LDL-C at Week 24.

Method: 966 patients were enrolled at ~200 global sites. Liver biopsies were read by two central pathologists using glass slides (primary analysis) with results combined using a statistical algorithm to generate a single treatment effect; if readers disagreed on the response for either primary end point, a supportive consensus read using digitized images was conducted. The mITT population excluded 11 patients with liver biopsies after Week 60 due to COVID site issues.

Results: Baseline characteristics included age 57 (11) (mean (SD)), female 56%, white 90%, BMI 36 (7), type 2 diabetes 67%, hypertension 78%, dyslipidemia 71%, FibroScan VCTE 13 kPa (7), CAP 348 (38), MRI-PDFF 18 (7)% fat fraction, baseline liver biopsy NAS ≥ 5 84%, baseline fibrosis stage: F3-62%, F2-33%, F1B-5%. Both primary histologic end points and the key secondary end point (LDL cholesterol lowering) were met at both doses (table); consensus review confirmed results. Similar results for both end points were obtained by both central pathologists, and results were independent of diabetes status or

baseline fibrosis stage. Multiple other liver biopsy end points were met including NASH resolution and fibrosis reduction (combined) and a 2-stage reduction in fibrosis. Biomarker end points including reduction in ALT, AST and GGT, ELF, MRI-PDFF, CAP and FibroScan VCTE were met. Resmetirom appeared generally safe and well-tolerated with similar numbers of SAEs across groups and an increase in the incidence of diarrhea and nausea in resmetirom treatment groups only at the beginning of therapy.

Figure.

End points	Resmetirom 80 mg (n = 316)	p value	Resmetirom 100 mg (n = 321)	p value	Placebo (n = 318)
Primary End points (Dual)					
NASH resolution (ballooning 0, inflammation 0, 1) with ≥ 2 -point reduction in NAS and no worsening of fibrosis	26%	<0.0001	30%	<0.0001	10%
≥ 1 -stage improvement in fibrosis with no worsening of NAS	24%	0.0002	26%	<0.0001	14%
Key Secondary End point					
LDL-C lowering (24 weeks)	(24 -12%)	<0.0001	-16%	<0.0001	1%

Conclusion: NASH resolution and fibrosis reduction end points on liver biopsy were achieved at both resmetirom doses in a large Phase 3 pivotal clinical trial. Resmetirom appeared safe and was generally well-tolerated. These data support the potential for resmetirom treatment to provide benefit to patients with NASH and liver fibrosis.

GS-002-YI

Myeloid IL-8 enrichment associates with immunotherapy resistance in advanced hepatocellular carcinoma

Tsz Tung Kwong¹, Zhewen Xiong², Yiling Zhang², Patrick Pak-Chun Wong², Jingying Zhou², Alfred Sze-Lok Cheng², Stephen Chan¹.
¹The Chinese University of Hong Kong, Department of Clinical Oncology, Hong Kong; ²The Chinese University of Hong Kong, School of Biomedical Sciences, Hong Kong
 Email: tsztungkwong@cuhk.edu.hk

Background and aims: Despite the therapeutic options with immunotherapy have been emerging in advanced hepatocellular carcinoma (HCC), durable response is confined to a small fraction of patients. Thereby, ineffectiveness of immune checkpoint blockade (ICB) and resistance acquisition caused by the immunosuppressive drivers including inflammatory cytokines and myeloid cells within the liver tumor microenvironment (TME) had to be tackled urgently. In this study, we analyzed the immune contexture of advanced HCC patients before and after pembrolizumab treatment to investigate the role of myeloid IL-8 in ICB-resistance mechanism and aim to intervene the IL-8 pathway through inhibition of its receptor by a clinical in-use CXCR2 antagonist.



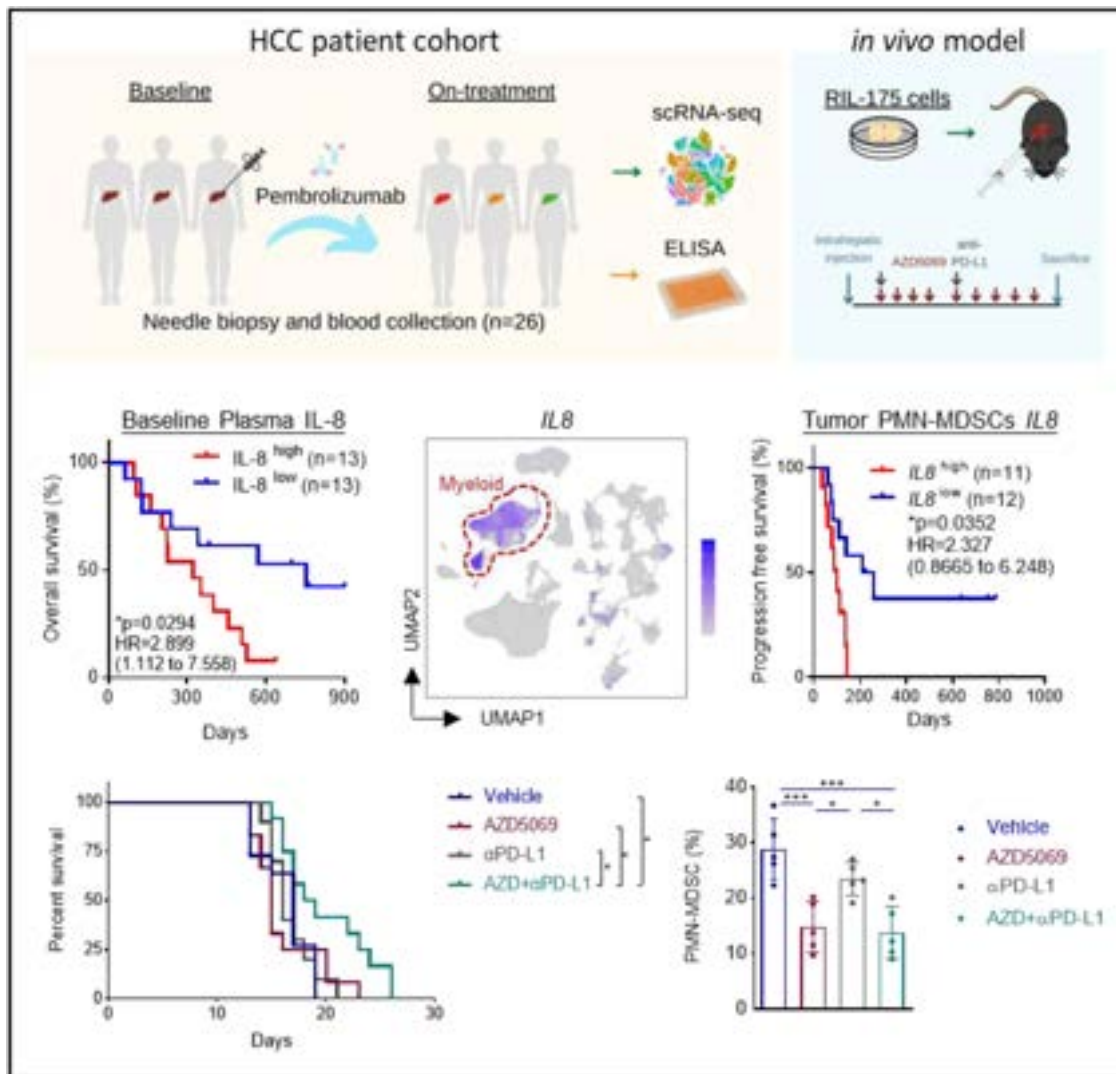


Figure: (abstract: 002).

Method: Patients with advanced HCC (n = 26) were enrolled prior to pembrolizumab therapy with their baseline and on-treatment biopsies collected to perform single cell RNA transcriptomic analysis. Simultaneously, circulating IL-8 level was quantified in the paired peripheral blood samples. Therapeutic efficacy of CXCR2 pathway inhibition by AZD5069 in potentiating ICB response was evaluated in our ICB-resistant orthotopic mouse model which is generated by serial *in vivo* passaging of anti-PD-L1 residual tumor. Profiling of immune landscape in the TME were assessed by high-parameter flow cytometry.

Results: In our advanced HCC cohort with anti-PD-1 treatment, patients with higher baseline plasma IL-8 had worse overall survival compared to those with lower IL-8 level (hazard ratio (HR), 2.899, 95% confidence interval (CI), 1.112–7.558; p=0.0294). Single cell RNA sequencing further revealed that IL-8 was originated from myeloid cell cluster in tissue biopsies. In particular, the upregulated expression of *IL8* on polymorphonuclear myeloid-derived suppressor cells (PMN-MDSCs) were strongly linked with poorer progressive free survival (HR, 2.327; 95% CI, 0.867–6.248; p = 0.0352). Inhibition of the IL-8 receptor with a CXCR2 antagonist (AZD5069) improved the survival benefit of anti-PD-L1 treatment in our ICB-resistant orthotopic pre-clinical HCC model. Mechanistically, the suppression of CXCR2 signaling hindered the MDSC recruitment to tumor site, in

turn reverted the immunosuppression in the TME which favors ICB treatment.

Conclusion: We demonstrated the importance of myeloid IL-8/CXCR2 pathway in ICB-resistance from our advanced HCC cohort which paved way for IL-8 to become a novel prognostic target for immunotherapy. Blocking CXCR2 could reduce MDSC trafficking and overcome ICB-resistance in our pre-clinical HCC model, suggesting a promising combination regimen in future development. This work is supported by the Collaborative Research Fund C4045-18W.

GS-003

Rivaroxaban improves survival and decompensation in cirrhotic patients with moderate liver dysfunction. Double-blind, placebo-controlled trial

Angela Puente Sanchez¹, Fanny Turon^{2,3}, Javier Martinez^{3,4}, Jose Ignacio Fortea¹, Manuel Hernandez-Guerra⁵, Edilmar Alvarado-Tapias^{3,6}, Monica Pons⁷, Marta Magaz^{2,3}, Elba Llop⁸, Carmen Álvarez-Navascués⁹, José Castellote Alonso¹⁰, Marina Berenguer¹¹, Helena Masnou^{3,12}, Rafael Bañares^{3,13}, Marta Casado¹⁴, Javier Ampuero¹⁵, Georgina Casanovas¹⁶, Carlos Redondo¹, Patricia Huelin¹, Luis Téllez^{3,4}, Dalia Morales Arraez⁵, Manuel Rodríguez⁹, Victoria Aguilera¹¹, Anna Baiges^{2,3}, Virginia Hernandez-Gea^{2,3}, Christie Perelló⁶,

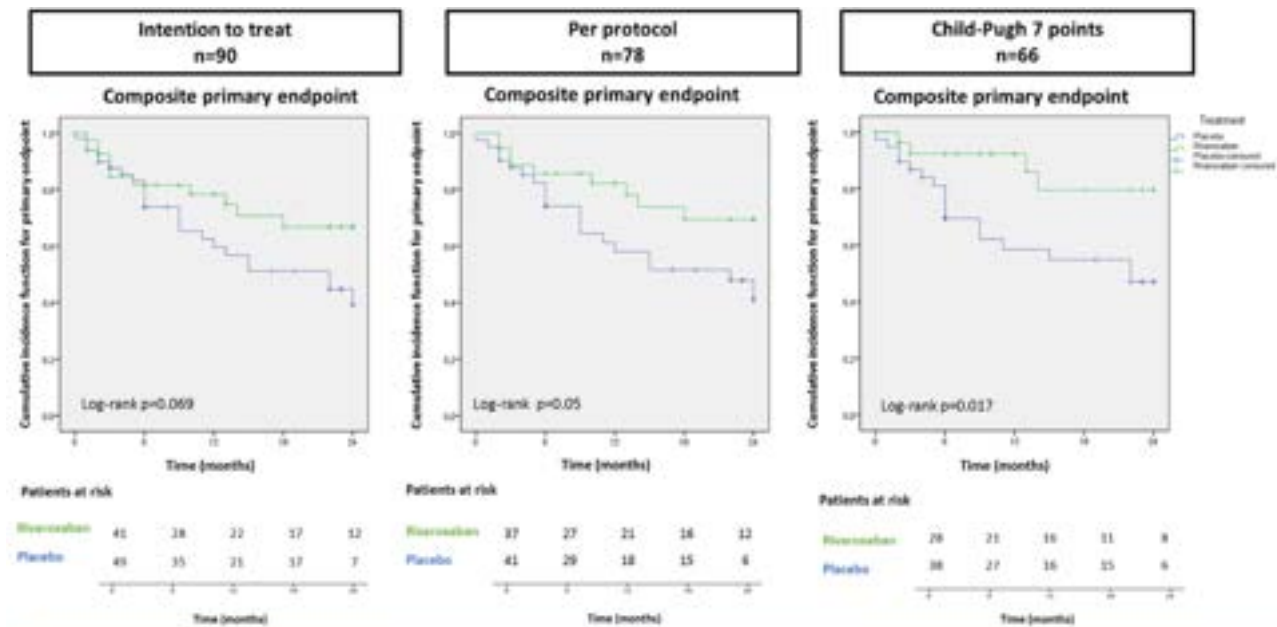


Figure: (abstract: 003).

José Luis Calleja Panero⁸, Joan Genesca⁷, Cándid Villanueva^{3,6}, Carlos González-Alayón⁵, Agustín Albillos^{3,4}, Javier Crespo¹, Juan Carlos García Pagan^{2,3}. ¹Marqués de Valdecilla University Hospital. IDIVAL, Liver Unit. Gastroenterology department, Santander, Spain; ²Hospital Clínic, Barcelona Hepatic Hemodynamic Laboratory, Liver Unit. Institut de Investigacions Biomèdiques August Pi i Sunyer (IDIBAPS), University of Barcelona. Health Care Provider of the European Reference Network on Rare Liver Disorders (ERN-Liver), Barcelona, Spain; ³Centro de Investigación Biomédica en Red de Enfermedades Hepáticas y Digestivas (CIBEREHD), Spain; ⁴Ramón y Cajal University Hospital- IRYCIS (Madrid). University of Alcalá, Gastroenterology and Hepatology department, Madrid, Spain; ⁵Canarias University Hospital, Gastroenterology and Hepatology department, Tenerife, Spain; ⁶Hospital de la Santa Creu i Sant Pau. Biomedical Research Institute Sant Pau (IIB Sant Pau). 08025 Barcelona. Universitat Autònoma de Barcelona, Bleeding Unit. Gastroenterology and hepatology department, Barcelona, Spain; ⁷Vall d'Hebron University Hospital, Vall d'Hebron Research Institute (VHIR), Vall d'Hebron Barcelona Hospital Campus, Autonomous University of Barcelona, Liver Unit, Barcelona, Spain; ⁸Puerta De Hierro University Hospital, Gastroenterology and Hepatology department, Madrid, Spain; ⁹Hospital Central de Asturias, Gastroenterology department, Oviedo, Spain; ¹⁰Bellvitge Hospital, Gastroenterology department, Barcelona, Spain; ¹¹La Fe University Hospital, Hepatology and Liver Transplantation Unit, Valencia, Spain; ¹²Germans Trias i Pujol Hospital, Liver Unit. Instituto de Investigación Germans Trias i Pujol (IGTP), Badalona, Spain; ¹³Gregorio Marañón University Hospital, Gastroenterology department, Madrid, Spain; ¹⁴Torrecañadas Hospital, Gastroenterology department, Almería, Spain; ¹⁵Virgen del Rocío University Hospital, Gastroenterology department, Sevilla, Spain; ¹⁶Hospital Clínic, Medical Statistics Core Facility, Institut D'Investigacions Biomèdiques August Pi i Sunyer (IDIBAPS), Barcelona, Spain
Email: angelapuente@hotmail.com

Background and aims: Observational studies and a non-double-blind non-placebo randomized study suggested that anticoagulation decreases the probability of developing portal hypertension (PHT) complications and improves survival in cirrhotic patients. However, anticoagulation is not routinely used in these patients showing that stronger evidence is required. Our study aimed to evaluate the efficacy/safety of the direct anticoagulant Rivaroxaban (Rban) in patients with cirrhosis.

Method: Randomized, double-blind, placebo-controlled multicenter trial (EudraCT: 2014-005523-27) in cirrhotic patients with PHT and moderate liver dysfunction (Child-Pugh:7–10) of Rban 10 mg/24 hours vs. placebo for 24 months. Primary composite end point: development of a PHT complication (grade>II ascites, grade>II encephalopathy, or PHT related bleeding) or death/transplantation whatever occurred first. An intention-to-treat (mITT) and per-protocol (PP) analysis was performed.

Results: 90 patients were included (Age: 58.1 ± 7.6 years; 82.2% male; Child-Pugh: 7.4 ± 0.8 ; MELD: 12.4 ± 2.5 ; 86.7% alcoholic cirrhosis), median follow-up: 10.1 (0.4–24) months. 49 received placebo (P) and 41 Rban. In the mITT analysis, 34 patients developed the primary end point, 23 (46.9%) in the P vs 11 (26.8%) in the Rban group, with an actuarial cumulative probability of primary end point at 1 and 2 years of 40.1% and 60.9% in P vs 21.6 and 33.2% in Rban (Log-rank; $p = 0.069$). This difference reached statistical significance (HR = 0.466 [95% CI 0.222–0.980] $p = 0.044$) when adjusted by Child-Pugh. This beneficial effect of Rban was especially relevant in the subgroup of Child-Pugh B7 ($n = 66$) (HR: 0.292 [95% CI 0.098–0.870] $p = 0.017$). The main benefit relies in the prevention of ascites (Log-rank; $p = 0.056$). Twelve patients had a protocol deviation due to therapeutic non-compliance. In the PP analysis (41 P and 37 Rban), the main event was reached in 19 P (38.7%) vs. 9 (21.9%) in the Rban group (Log-rank; $p = 0.05$). Figure.

Thirty-one non-PHT bleeding events were registered in twenty four patients (26.6%) [placebo ($n = 10$) vs Rban ($n = 22$), OR 3.34 (95% CI 1.36–7.74) $p = 0.008$]. However, no differences were observed in major bleeding events: P ($n = 2$) vs Rban ($n = 6$): OR 4.02. (95% CI 0.767–21.167, $p = \text{NS}$). One death associated with major bleeding (hemoperitoneum) was recorded in the P group.

Conclusion: In cirrhotic patients with moderate liver dysfunction, rivaroxaban improves PHT complication-free survival without significantly increasing major bleeding events.

ORAL PRESENTATIONS

CS-004-YI

Vulnerable offspring: a nationwide Danish cohort study of adverse health outcomes in offspring of parents with alcohol-related liver disease compared to controls

Peter Jepsen¹, Joe West^{2,3}, Frederik Kraglund¹, Colin Crooks², Anna Emilie Kann⁴, Joanne Morling², Gro Askgaard¹. ¹Aarhus Universitetshospital, Aarhus, Denmark; ²University of Nottingham, United Kingdom; ³Nottingham University Hospitals NHS Trust and the University of Nottingham, NIHR Nottingham Biomedical Research Centre (BRC), United Kingdom; ⁴Zealand University Hospital, Køge, Denmark
Email: gask@dadlnet.dk

Background and aims: Offspring of parents with alcohol-related liver disease (ALD) likely grow up in families with significant exposure and access to alcohol and may themselves be vulnerable to adverse health outcomes. We compared the risk of adverse health outcomes in such offspring to that of controls.

Method: We used nationwide healthcare registries to identify offspring of parents diagnosed with ALD (ICD-10: K70.x) in Denmark 1996–2018 and age- and gender-matched controls (20:1). We compared the incidence rates of: diagnosis of ALD, any alcohol-related hospital contacts, emergency room visits for fractures or injury, hospital contacts for intentional or accidental poisoning, and

Figure 1. Incidence rate ratios of alcohol-related outcomes in offspring of individuals with ALD (n = 60,708) compared to age- and sex matched controls (n = 1,213,380), overall and stratified by gender and ALD parent's educational level. Outcomes are: Alcohol-related liver disease (black), any alcohol-related hospital contact (red), fracture or injury (green), intentional or accidental poisoning (blue) and death (purple).

The figure shows that the risk of alcohol-related hospital contacts is higher in offspring of individuals with ALD of primary [incidence rate ratio, 2.63 (95%CI: 2.58-2.68)] than of higher educational level [incidence rate ratio, 1.60 (95%CI: 2.58-2.68)] compared to controls.

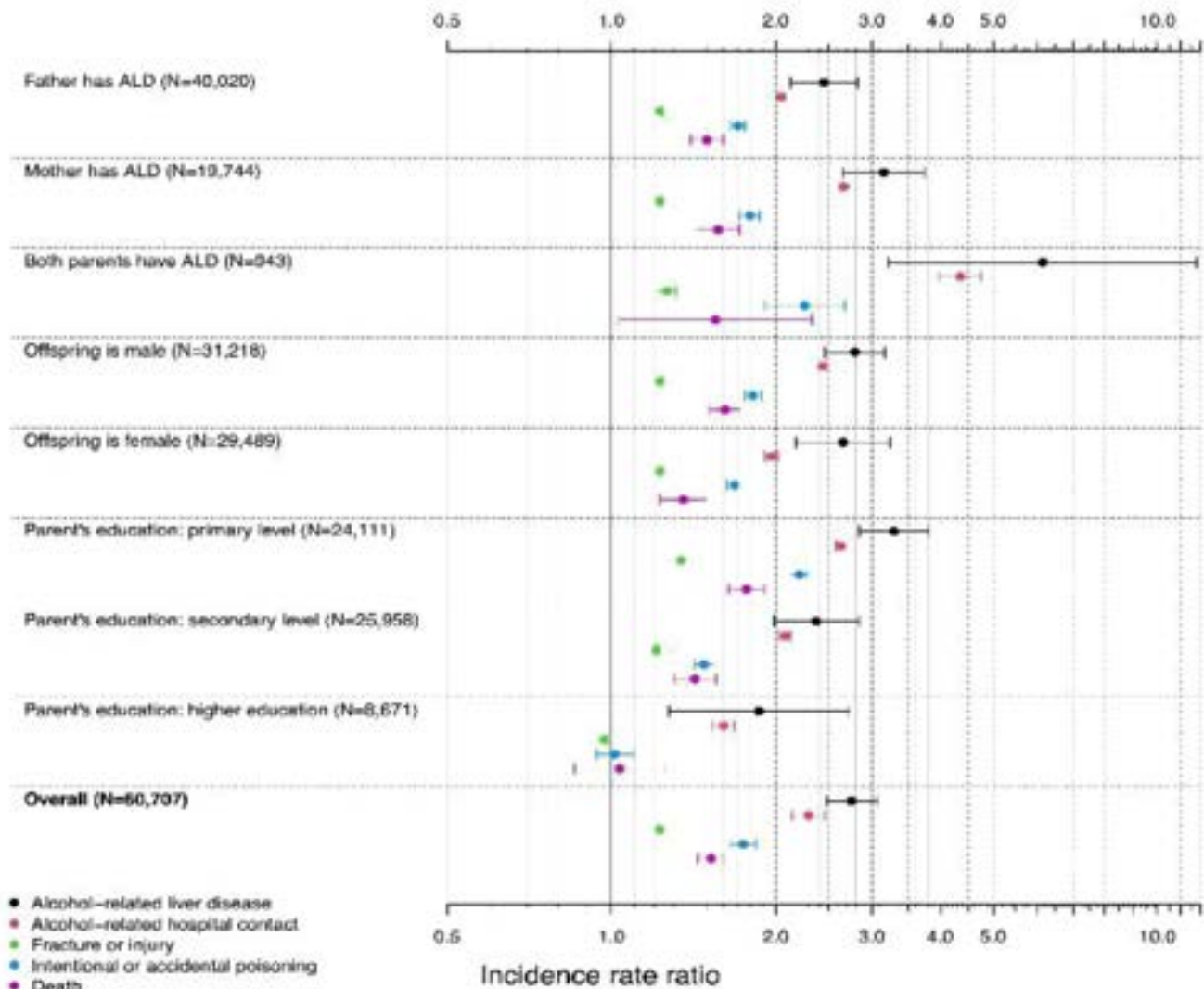


Figure: (abstract: 004).

all-cause death in offspring of parents with ALD with that of the matched controls, overall and within subgroups. We used a self-controlled case series design to examine whether hospitalization for poisoning was more likely to occur during the first year after the parent's ALD diagnosis vs. at any other time among offspring aged 13–25 years.

Results: There were 60,708 offspring of parents with ALD and 1,213,380 matched controls. Offspring had a median age of 31 years (IQR 23–39) when their parent was diagnosed with ALD; 51% were male. Offspring had a higher incidence rate of ALD, any alcohol-related hospital contacts, fractures or injury, poisoning, and all-cause death compared to controls (Figure 1). Offspring whose ALD parent had only primary education experienced higher risks compared to controls, than offspring whose parents had a higher education [incidence rate ratios (IRR) for an alcohol-related hospital contact compared to controls were 2.63 (95%CI: 2.58–2.68) vs 1.60 (95%CI: 1.53–1.68) respectively]. Offspring aged 13–25 years were most likely to have their first admission for poisoning in the first year after their parent's ALD diagnosis than at any other time (IRR = 1.25, 95% CI: 1.01–1.55), suggesting that the event of the parent's diagnosis of ALD might cause the offspring to self-harm.

Conclusion: Offspring of parents with ALD have a higher risk of adverse health outcomes; only the minority with well-educated parents are partially protected from those consequences. The first year after a parent's ALD diagnosis is a particularly vulnerable time for the offspring of a young age with respect to hospitalization with poisoning.

GS-005

Selective activation of the IL-2 pathway in CD8⁺ T cells drives antiviral activity to Hepatitis B Virus (HBV)

Francesco Andreata¹, Kelly Moynihan², Pietro Di Lucia¹, Danielle Peppas², Irene Ni², Henri Nguyen², Chiara Perucchini¹, Mike Chin², Elisa Bono¹, Leonardo Giustini¹, Paul Bessette², Andy Yeung², Craig Gibbs², Ivana Djuretic², Matteo Iannacone¹. ¹San Raffaele Scientific Institute, Division of Immunology, Transplantation and Infectious Diseases, Milan, Italy; ²Asher Biotherapeutics, San Francisco, United States
Email: iannacone.matteo@hsr.it

Background and aims: CD8⁺ T cells are critical for mediating anti-viral activity against Hepatitis B virus (HBV); however, CD8⁺ T cell

responses against HBV antigens may be deficient in chronically infected HBV patients.^{1–3} In murine HBV models that recapitulate key features of HBV-induced CD8⁺ T cell dysfunction, IL-2-based therapy (but not PD-1 checkpoint blockade) successfully rescued CD8⁺ T cell function and anti-viral immunity⁴, suggesting that the IL-2 pathway may be a promising approach to reinvigorate CD8⁺ T cell immunity. Unfortunately, IL-2-based therapeutics are limited by pleiotropy, as IL-2 receptors are expressed broadly on many cell types, including regulatory T cells (Tregs) and natural killer (NK) cells, which may oppose anti-viral responses or contribute to toxicity, respectively. We developed a cis-targeted IL-2 fusion protein called AB359 that selectively acts on CD8⁺ T cells in order to evaluate its potential for the treatment of chronic HBV.

Method: AB359 was generated by fusing an attenuated IL-2 mutein to an anti-CD8 antibody, and activity was characterized on human cells. Cynomolgus monkeys were dosed with AB359 and peripheral blood pharmacodynamics were assessed by flow cytometry. AB359's murine surrogate, muAB359, was tested in a murine HBV model⁵.

Results: In a murine HBV model⁵, muAB359 significantly increased the number of HBV-reactive CD8⁺ T cells in the liver without substantial changes to NK and Treg numbers. The expanded HBV-specific CD8⁺ T cells following muAB359 treatment showed enhanced expression of IFN γ and granzyme B relative to controls. Therapy with muAB359 resulted in strong anti-HBV activity: a single dose of muAB359 demonstrated over 100-fold reduction in serum HBV core DNA and a 79% decrease in serum Hepatitis B surface antigen (HBsAg) levels. In contrast, an untargeted not- α IL-2 (CTRL-IL2) demonstrated preferential expansion of IL-2R β ^{high} NK cells, modest CD8⁺ T cell expansion, and minimal changes to IFN γ and granzyme B expression by HBV-reactive CD8⁺ T cells following therapy. As a result, less robust viral control was observed with CTRL-IL2; a 9.5-fold reduction in HBV core DNA and a 37% decrease in HBsAg were observed. In cynomolgus monkeys, AB359 induced the selective expansion of peripheral blood CD8⁺ T cells by approximately 20-fold without substantial changes to NK and Treg numbers.

Conclusion: Selectively providing an IL-2 signal to CD8⁺ T cells via cis-targeting shows considerable anti-viral activity in a preclinical model of HBV, with superior performance to an untargeted IL-2. These data support the development of AB359 as a therapy for the treatment of chronic HBV.

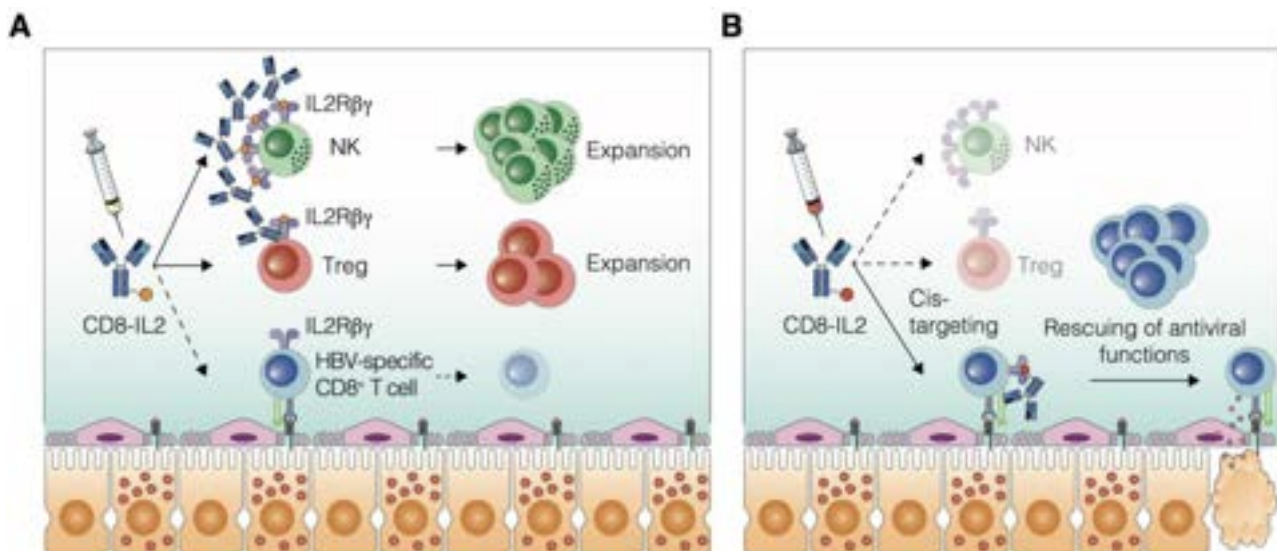


Figure: (abstract: 005): "Cis-targeting of IL-2 to CD8⁺ T cells avoids the pleiotropy associated with untargeted IL-2 therapy and drives potent anti-HBV immunity"

ORAL PRESENTATIONS

CS-006

Randomised controlled trial of ceftriaxone versus no antibiotic to prevent infection in patients with Child-Pugh A cirrhosis with acute variceal bleeding

Anany Gupta^{1,1}, Samagra Agarwal¹, Sanchit Sharma², Deepak Gunjan³, Srikanth Gopi³, Jamshed Nayer⁴, Anoop Saraya¹. ¹All India Institute Of Medical Sciences, Department of Gastroenterology and HNU, New Delhi, India; ²Liver Unit, Queen Elizabeth Hospital, Birmingham, United Kingdom, Liver Unit, Birmingham, United Kingdom; ³All India Institute Of Medical Sciences, Department of Gastroenterology and HNU, New Delhi, India; ⁴All India Institute Of Medical Sciences, Department of emergency medicine, New Delhi, India
Email: ansaraya@yahoo.com

Background and aims: Administering antibiotics reduce the risk of bacterial infections and improve survival in advanced

decompensated cirrhosis presenting with acute variceal bleeding. However, their role in patients with Child-Pugh A cirrhosis with variceal bleed is not clearly defined. We studied the impact of antibiotic prophylaxis on outcomes in patients with Child-A cirrhosis.

Method: We conducted a single centre open label randomised controlled trial with a non-inferiority study design. Eligible patients of Child-A cirrhosis with suspected variceal bleeding were randomly assigned at presentation to receive either 5-day course of intravenous Ceftriaxone (active control) or no antibiotic (test regimen). Patients were otherwise managed as per Baveno-VI recommendations for variceal bleeding. The primary outcome was incidence of infection at day-5 in both arms. Secondary outcomes were incidence of early rebleeding and mortality at day-5, new onset decompensation at 6 weeks and 6-week mortality in both arms.

Results: One hundred eighty patients of Child-A cirrhosis with variceal bleeding (Mean age 45.1±13.1 years, 76.9%males) of

	Overall N=180	Ceftriaxone N=90	No antibiotic N=90	P value
Age [mean (SD)](years)	45.06 (13.06)	44.23 (12.49)	45.92 (13.63)	0.399
Female (%)	40 (23.3)	19 (22.1)	21 (24.4)	0.857
Co-morbidity				
Diabetes Mellitus (%)	54 (32.5)	23 (28.4)	31 (36.5)	0.345
Hypertension	25 (15.1)	10 (12.3)	15 (17.6)	0.461
Heart disease (%)	4 (2.4)	4 (4.9)	0 (0.0)	0.117
ETIOLOGY (%)				0.206
Viral	23 (13.9)	7 (8.6)	16 (18.8)	
Alcohol	80 (43.4)	44 (49.4)	36 (37.6)	
NAFLD	36 (21.7)	17 (21.0)	19 (22.4)	
Viral+NAFLD	2 (1.2)	2 (2.5)	0 (0.0)	
Alcohol+NAFLD	2 (1.2)	0 (0.0)	2 (2.4)	
INDEX PRESENTATION (%)				0.621
Ascites	59 (35.5)	26 (32.1)	33 (38.8)	
Bleed	104 (62.7)	53 (65.4)	51 (60.0)	
BASELINE Grade-1 ASCITES DURING THIS EPISODE OF BLEED	22 (13.3)	11 (13.6)	11 (12.9)	1
Hemoglobin (g/dl) [mean (SD)]	8.19 (1.98)	7.91 (1.93)	8.46 (2.00)	0.074
TLC/mm3 [mean (SD)]	6.72 (2.30)	6.84 (2.42)	6.61 (2.18)	0.53
Platelet X1000/mm3 [mean (SD)]	120.73 (30.33)	124.50 (27.64)	117.05 (32.65)	0.11
Urea (mg/dl) [mean (SD)]	37.38 (10.99)	36.86 (10.55)	37.89 (11.43)	0.548
Creatinine (mg/dl) [mean (SD)]	0.80 (0.16)	0.81 (0.17)	0.80 (0.15)	0.499
Bilirubin (mg/dl) mean (SD)]	2.14 (3.15)	2.17 (3.45)	2.11 (2.86)	0.902
Albumin(g/dl) [mean (SD)]	3.84 (0.25)	3.83 (0.24)	3.84 (0.27)	0.796
INR (mean (SD))	1.32 (0.77)	1.35 (1.10)	1.29 (0.15)	0.613
CRP DAY 1 /mg/dl [mean (SD)]	14.11 (28.45)	29.60 (42.19)	2.50 (3.55)	0.243
Procalcitonin (mg/dl) DAY 1 (mean (SD))	1.05 (2.08)	2.38 (2.88)	0.04 (0.04)	0.153
Endoscopy				0.094
Esophageal variceal bleed	157 (87.3)	79 (87.8)	78 (86.7)	
Gastric variceal bleed	23 (12.7)	11 (12.2)	12 (13.3)	
Active bleeding	16 (9.6)	12 (14.8)	4 (4.7)	
DAY 5 OUTCOMES				
Infection	16 (9.6)	10 (12.3)	6 (7.1)	0.373
Site of infection				
Spontaneous bacterial peritonitis	10 (6.0)	7 (8.6)	3 (3.5)	0.29
Urinary tract infection*	7 (4.2)	4 (4.9)	3 (3.5)	0.948
Lower respiratory tract infection *	2 (1.2)	2 (2.5)	0 (0.0)	0.456
Bacteremia	4 (2.4)	3	1	0.561
Multi-drug resistant organisms	2 (1.2)	2 (2.5)	0	0.456
Multiple site infection	2 (1.2)	2 (2.5)	0	0.456
Jaundice	2 (1.2)	2 (2.5)	0 (0.0)	0.456
HE	14 (8.5)	8 (9.9)	6 (7.1)	0.726
Rebleed	4 (2.4)	4 (4.9)	0 (0.0)	0.117
Mortality	2 (1.2)	2 (2.5)	0	0.456
6 WEEKS OUTCOME				
Infection	2 (1.4)	2 (3.1)	0 (0.0)	0.426
Jaundice	1 (0.7)	1 (1.5)	0 (0.0)	0.954
Rebleeding	11 (8.0)	7 (10.8)	4 (5.5)	0.406
Ascites				0.754
Grade 1 ascites	3 (2.2)	2 (3.1)	1 (1.4)	
Grade 2 ascites	5 (3.6)	2 (3.1)	3 (4.1)	
6-week Mortality	3 (1.6)	2 (2.5)	1 (1.4)	0.93

*. Lower respiratory tract infection and urinary tract infection developed in addition to SBP in patients

Figure: (abstract: 006).

predominant non-viral aetiology (alcohol 43.4%; NAFLD 21.7%) were randomised. Baseline characteristics including MELD score were comparable between two arms. The incidence of 5-day infection in Ceftriaxone arm and no antibiotic arm was 7% (95%CI: 2.8–15.1%) and 12% (6.02–20.8%) respectively ($p=0.397$; non-inferiority margin met). Spontaneous bacterial peritonitis following early decompensation was the most common site of infection in both groups (10/16; 66.7%). The incidence of rebleeding at day-5 (4.9 vs 0; $p=0.117$), in hospital mortality (2.5% vs 0%; $p=0.456$), new onset decompensation at 6-weeks (16.0% vs 11.8%; $p=0.566$) and 6-week mortality (2.5% vs 1.4%; $p=0.93$) were comparable across both the arms although non-inferiority could not be established.

Conclusion: Among patients with Child-A cirrhosis with acute variceal bleeding, the incidence of post-bleed infections and other outcomes in those receiving no antibiotics was comparable to those receiving ceftriaxone (CTRI/2021/06/033939).

FRIDAY 23 JUNE

General session II

GS-007

Faecal microbiota transplant restores gut barrier function and augments ammonia metabolism in patients with advanced cirrhosis: a randomised single-blind placebo-controlled trial

Lindsey A Edwards¹, Charlotte Woodhouse^{1,2}, Sunjae Lee³, Benjamin H. Mullish⁴, Theo Portlock⁵, Lilianeleny Meoli¹, Victoria Kronsten^{1,2}, Julian Marchesi⁴, Ane Zamalloa², Thomas Tranah^{1,2}, Vishal Patel^{1,2,6}, Saeed Shoaie^{5,7}, Simon Goldenberg⁸, Debbie L. Shawcross^{1,2}. ¹King's College London, Institute of Liver Sciences, School of Immunology and Microbial Sciences, Faculty of Life Sciences and Medicine, London, United Kingdom; ²King's College Hospital NHS Foundation Trust, Institute of Liver Studies, London, United Kingdom; ³Gwangju Institute of Science and Technology, School of Life Sciences, Gwangju, Korea, Dem. People's Rep. of; ⁴Imperial College London, Division of Integrative Systems Medicine and Digestive Disease, Department of Surgery and Cancer, Faculty of Medicine, London, United Kingdom; ⁵King's College London, Centre for Host-Microbiome Interactions, Dental Institute, London, United Kingdom; ⁶The Roger Williams Institute of Hepatology London (Foundation for Liver Research), London, United Kingdom; ⁷Science for Life Laboratory, KTH-Royal Institute of Technology, Stockholm, Sweden; ⁸Guy's and St Thomas' Hospitals NHS Trust, Centre for Clinical Infection and Diagnostics Research, London, United Kingdom
Email: lindsey.edwards@kcl.ac.uk

Background and aims: Patients with cirrhosis have reduced gut bacterial diversity, and a gut microbiome over-represented by pathobionts. This, coupled with gut barrier damage and bacterial translocation, increases susceptibility to infection and death. Bacterial translocation is a significant driver of cirrhosis-associated immune dysfunction which increases the susceptibility to developing infection. Faecal microbiota transplant [FMT] has been shown to restore gut diversity and improve hepatic encephalopathy (HE) in 10 patients with cirrhosis. We hypothesised that modifying the gut microbiota with FMT may alter intestinal barrier function, mucosal immunity and microbial ammonia metabolism in patients with cirrhosis.

Method: We performed a placebo-controlled randomised single-blinded feasibility trial of FMT transplanted in 32 patients with advanced cirrhosis (MELD score 10–16) [NCT02862249]. 50 grams of liquid frozen FMT versus placebo [allocated in a 3:1 ratio] was administered into the jejunum via endoscopy. To assess efficacy in

modulating the patient's own microbiome and inflammatory status: blood and stool were collected at baseline and day 7, 30 and 90 post-FMT/placebo. Cytokine production, markers of barrier integrity (electrochemiluminescence/ELISA), global metabolite profile (¹H-NMR) and faecal proteomics (LC-MS/MS) were assessed.

Results: Deep metagenomic sequencing confirmed FMT increased recipient species richness with significant donor engraftment. FMT significantly reduced stool carriage of *E. faecalis* and other pathobionts. FMT reduced biomarkers of inflammation and increased markers associated with gut barrier repair. FMT led to a reduction at 30-days in plasma ammonia ($p=0.0006$). Faecal ammonia was higher in the FMT group versus placebo at days 30 ($p=0.011$) and 90 ($p=0.025$). Faecal proteomics quantified 301 proteins, 154 proteins found were of human origin and 147 were of bacterial origin. Many of these proteins were found to be both human and microbial enzymes. In converse to the enzymes found reduced in blood, increases in the abundance of microbial enzymes involved in denitrification and ammonification were observed in the stool [enzyme EC.4.3.1.1 (aspartate ammonia-lyase), with 17 high-confidence peptides, was enhanced in patients administered FMT versus placebo ($p=0.031$)]. Enzymes required for nitrogen assimilation and excretion via the urea cycle were enhanced, with enhanced secretion of urinary hippurate ($p=0.0299$) at day 30 in FMT versus placebo.

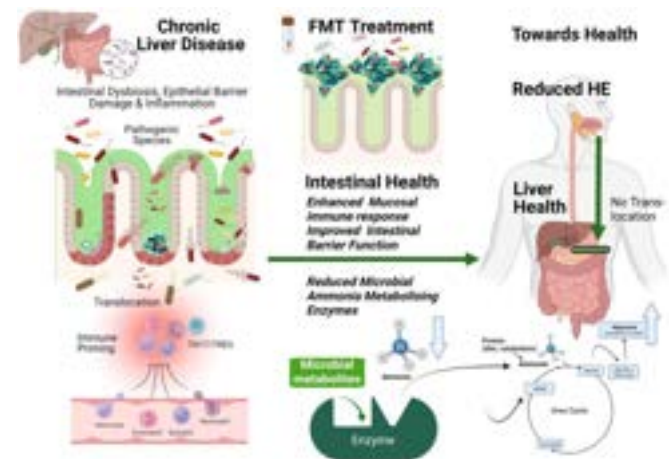


Figure:

Conclusion: These data support FMT as playing an important role in enteric pathogen reduction, altering the gut-microbiota to promote inflammatory restoration of the gut barrier. FMT reduced microbial-associated ammonia production in the blood and upregulated ammonia excretion in stool and augmenting the anaerobic metabolism of L-aspartate providing proof of concept that FMT augments ammonia metabolism, central in the pathogenesis of HE.

GS-008-YI

Naltrexone is safe and effective in achieving abstinence and reducing alcohol craving in cirrhotic patients: a double blind randomized placebo controlled trial

Manasa Alla¹, S Muralikrishna Shashtry¹, Mohit Varshney¹, Vinod Arora¹, Shiv Kumar Sarin¹. ¹Institute of Liver and Biliary Sciences, New Delhi, India
Email: shivsarin@gmail.com

Background and aims: Continued alcohol use is the single important driver of long term outcomes in alcohol associated liver diseases. But there are no FDA approved drugs for alcohol use disorder (AUD) that have been approved in patients with liver cirrhosis. Considering the importance of maintaining abstinence and the positive effect on survival in patients with alcohol liver disease, this study assumes importance in establishing safety and efficacy of naltrexone in patients with alcohol related liver disease.

ORAL PRESENTATIONS

Method: This is a single centre double blind placebo controlled randomized trial conducted in ILBS hospital (April 2020–July 2022) in patients with compensated cirrhosis with AUD. 147 patients were screened and 100 consecutive patients with compensated cirrhosis fulfilling the DSM -5 criteria for AUD as per inclusion and exclusion criteria of the study were enrolled and randomized between Naltrexone or placebo, given for 12 weeks. The primary objective was proportion of patients achieving and maintaining alcohol abstinence at 12 weeks and secondary objectives were proportion of patients maintaining abstinence at 6 months and 12 months, adverse effects, lapses and relapses at 3, 6 and 12 months. Behavioural therapy and counselling was offered to both the groups.

Results: Baseline demographics, clinical characteristics, AUDIT and ODDS scores were comparable between the groups. Significantly higher number of patients i.e., 32/50 (64%) achieved abstinence with Naltrexone compared to placebo at 12 weeks {11/50 (22%)}, $P < 0.001$. Similarly maintenance of abstinence after 6 months of follow-up was higher with Naltrexone {22% vs. 8%, $P = 0.09$ }. Number of lapses at 12 weeks {14/50 (28%) vs. 27/50 (54%), $P = 0.01$ } were significantly lower in Naltrexone group. Relapses were higher with the placebo {14/50 (28%) vs. 6/50 (12%), $P = 0.07$ }. Mean craving scores were significantly lower with Naltrexone by 12 weeks- ODDS-O score (6.63 ± 1.16 vs 9.29 ± 1.78 , $P < 0.01$) and ODDS-C score (6.35 ± 1.23 vs 9.02 ± 1.86 , $P < 0.01$). Significant difference in visual analog scale for craving was also noted between the groups in comparison of means values (4.27 ± 1.301 vs 6.51 ± 1.27 , $P < 0.01$). Adverse events were comparable in both the groups and none required discontinuation of drug. Mild abdominal discomfort was the most common adverse effect noted in 5/50 (10%) patients in Naltrexone group vs. 3/50 (6%) in placebo, $P = 0.71$. 2/50 (4%) patients in naltrexone group developed jaundice with bilirubin values >3 mg/dl, likely due to continued alcohol consumption and as a part of disease progression.

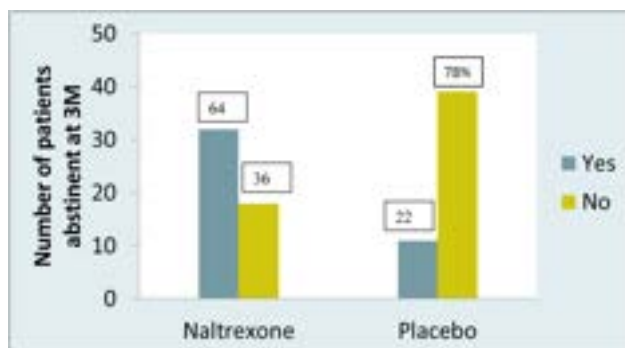


Figure:

Conclusion: Naltrexone can be safely administered for AUD in patients with compensated cirrhosis and is effective in achieving abstinence and as well as decreasing the craving scores at 3 months.

GS-009

Endoscopy sleeve gastropasty is an effective treatment in steatohepatitis patients: a prospective, multicenter, randomized trial

Javier Abad Guerra¹, Elba Llop¹, María Teresa Arias Loste², Diego Burgos Santamaria³, José Luis Martínez Porras¹, Javier Graus³, Paula Iruzubieta², Belén Ruiz Antoran¹, Manuel Romero Gomez⁴, Agustin Albillos³, Javier Crespo², José Luis Calleja Panero¹. ¹Puerta de Hierro Hospital, Spain; ²Marques de Valdecilla Hospital, Spain; ³Ramon y Cajal Hospital, Spain; ⁴Virgen del Rocio Hospital, Spain
Email: javiabad83@gmail.com

Background and aims: Non-alcoholic steatohepatitis (NASH) affect over 5% of the population, and patients are at risk of progressing to cirrhosis. Life-style intervention with diet and exercise achieving a weight loss $>10\%$ promotes NASH resolution, but this goal is only

achieved by $<25\%$ of the patients. Endoscopic sleeve gastropasty (ESG) with Overstitch[®] system has recently emerged as a safe and effective option to promote weight loss in patients with obesity. We report the results of a multicenter, randomized, controlled and double-blind study to evaluate the efficacy and safety of ESG in NASH patients.

Method: 40 patients were 1:1 randomized to ESG with OverStitch[®] (Apollo Endosurgery) plus lifestyle modification vs. endoscopic simulated intervention (ESI) with upper endoscopy plus lifestyle modification. Inclusion criteria included biopsy proven NASH with NAS ≥ 3 and fibrosis stage from F1 to F3. 18 patients from the ESG group and 19 from the ESI group completed follow-up. (72 weeks). We evaluated changes from baseline to end of follow-up in body weight, liver function tests, liver stiffness by Fibroscan[®] and liver histology.

Results: (mean \pm SD) Both groups had similar clinical characteristics at baseline. 55% of the patients were men, with a median age of 56.5 years (23–69). The mean BMI was 37.85. Half of patients had type 2 diabetes. Total body weight loss (TBWL) was $9.47\% (\pm 9.38)$ in ESG group vs $3.91\% (\pm 5.43)$ in ESI group ($p < 0.05$). Only patients in the ESG group achieved more than 15% of their body weight (22.2%). Liver stiffness decreased $5.63 (\pm 7.17)$ KPa in ESG group vs $0.2 (\pm 5.38)$ KPa in ESI group ($p < 0.05$). Steatosis was significantly reduced in ESG group (-0.94 ± 0.87) vs ESI group (-0.26 ± 0.99). NAS score, but not fibrosis stage, was reduced in patients achieving weight loss $>10\%$ (-4 ± 0.94 vs. -0.81 ± 1.62 , $p < 0.01$). Only 2 patients of the ESG group had adverse events that required admission (perigastric hematoma and perigastric collection), that resolved conservatively in 72 hours.

Table 1:

WEIGHT CHANGES (n)	ESI (19)	ESG (18)	p
N° patients weight lost% (SD)	11 (57.9)	17 (94.4)	0.010
TBWL% (SD)	-3.91 (5.43)	-9.47 (9.38)	0.025
LIVER STIFFNESS CHANGES (n)	ESI (18)	ESG (16)	p
LS KPa (SD)	-0.2 (5.38)	-5.63 (7.17)	0.017
HISTOLOGICAL CHANGES (n)	ESI (19)	ESG (18)	p
NAS score (SD)	-1.47 (2.01)	-1.89 (2.11)	0.544
Steatosis (SD)	-0.26 (0.99)	-0.94 (0.87)	0.033
Lobulillar inflammation (SD)	-0.53 (0.84)	-0.44 (0.86)	0.771
Ballooning (SD)	-0.68 (0.75)	-0.50 (0.86)	0.490
HISTOLOGICAL BY WEIGHT CHANGES (n)	No weight loss (9)	Weight loss (28)	p
NAS score (SD)	-0.22 (1.48)	-2.14 (2)	0.012
HISTOLOGICAL BY WEIGHT CHANGES (n)	Weight loss $<10\%$ (27)	Weight loss $>10\%$ (10)	p
NAS score (SD)	-0.81 (1.62)	-4 (0.94)	<0.001
Steatosis (SD)	-0.22 (0.75)	-1.60 (0.84)	<0.001
Lobulillar inflammation (SD)	-0.26 (0.86)	-1.10 (0.32)	0.005
Ballooning (SD)	-0.33 (0.68)	-1.30 (0.67)	<0.001
Fibrosis (SD)	-0.48 (1.22)	-0.30 (0.95)	0.674

Conclusion: ESG is an effective and safe method to promote weight reduction associated with significant improvement in liver stiffness and histological parameters in patients with NASH and obesity that achieve a significant weight loss. ESG could be an option in the management of obese patients with NASH failing to lose weight by life-style intervention.

CS-010

An integrative multi-omic approach defines therapeutic pathways associated with altered cell state and chromatin organisation in human liver fibrosis

Elliot Jokl¹, Aoiheann Mullan¹, Varinder Athwal¹, Kara Simpson¹, Nigel Hammond², Sokratia Georgaka², Syed Murtuza-Baker², Oliver Street², Neil Hanley¹, Karen Piper Hanley¹. ¹The University of Manchester, Division of Diabetes, Endocrinology and Gastroenterology, Manchester, United Kingdom; ²The University of Manchester, United Kingdom
Email: karen.piperhanley@manchester.ac.uk

Background and aims: Liver fibrosis is characterised by the deposition of pathological extracellular matrix from myofibroblasts, leading to progressive scarring and loss of organ function. As a progressive step in most chronic liver diseases, fibrosis is almost always diagnosed too late with limited treatment options. There is a massive unmet clinical need to halt tissue damaging fibrosis. In this study we have utilised a multi-omic integrative approach to define a novel targetable pathway driving profibrotic myofibroblasts.

Method: In human liver cirrhosis, we carried out single cell RNA and Assay for Transposase-Accessible Chromatin (ATAC) sequencing to deconvolute our multi-cell spatial transcriptomic (ST) using the Visium platform. Molecular mechanisms were validated in vitro and in vivo through genetic manipulation of the actin cytoskeleton and modelling in fibrosis.

Results: Through an integrative approach using RNA, ATAC and ST sequencing we defined molecular signatures associated with human liver myofibroblasts. Computational approaches identified altered cell state driven by nuclear lamina proteins in scar associated myofibroblasts (Figure). In cell biology, the nuclear lamina provides nuclear elasticity and chromatin organisation. Through in vitro and in vivo interrogation, we investigated how physical tension from increasing scar alters spatial organisation of the genome and transcription in liver fibrosis. We uncovered that when myofibroblasts encounter a stiffer environment (e.g. due to fibrosis) the nuclear response is to soften. Significantly, this is in parallel to a radical shift in cytoskeletal cell shape and pro-fibrotic gene expression. Through uncoupling the actin cytoskeleton by *Pak1*-loss (P21-activated kinase 1 associated with actomyosin signalling) we highlight a functional mechanoreponse of myofibroblasts driven by nuclear deformation and H3K9me3-mediated chromatin remodelling. These findings are consistent with a profound switch in profibrotic gene expression and one that further permits their migratory, contractile phenotype. By integrating chromatin accessibility profiles (ATAC and RNA sequencing) we provide insight into the transcription network and open chromatin landscape underlying the switch in profibrotic myofibroblast states, emphasizing mechanoadaptive pathways linked to PAK1 as key drivers. In addition, we demonstrated increased chromatin accessibility parallels loss of heterochromatin H3K9me3 marks in profibrotic myofibroblasts. The correlation with enhanced nuclear adaptation, measured by atomic force microscopy (AFM), and pro-fibrotic gene expression as myofibroblasts switch to an activated pro-fibrotic phenotype supports the idea that H3K9me3 compacts chromatin structure and restricts gene expression programmes.



Figure: Spatial transcriptomics and data integration of human cirrhotic liver. Human cirrhotic liver. Sections were stained for HandE for visual landmarks and localisation of Visium spots defined by spatially-significant gene clusters. Gene expression of lamin A (LMNA) located in the tissue section representing scar associated myofibroblast spatial clusters.

Conclusion: This study provides insight into the chromatin landscape and nuclear mechanics driving pro-fibrotic myofibroblasts and highlights actomyosin-dependent mechanisms linked to chromatin state as urgently needed therapeutic targets in liver disease.

CS-011

IMbrave050: Efficacy, safety and patient-reported outcomes (PROs) for adjuvant atezolizumab (atezo) + bevacizumab (bev) vs active surveillance in hepatocellular carcinoma (HCC) patients at high risk of disease recurrence after resection or ablation

Ahmed Kaseb¹, Minshan Chen², Pierce Chow³, Masatoshi Kudo⁴, Han Chu Lee⁵, Adam Yopp⁶, Lars Becker⁷, Sairy Hernandez⁸, Bruno Kovic⁹, Qinsu Lian⁸, Ning Ma⁸, Chun Wu¹⁰, Shukui Qin¹¹, Ann-Lii Cheng¹². ¹MD Anderson Cancer Center, Houston, TX, United States; ²Sun Yat-sen University Cancer Center, Guangdong Province, China, China; ³National Cancer Centre Singapore, Singapore and Duke-NUS Medical School Singapore, Singapore, Singapore; ⁴Kindai University, Osaka, Japan, Japan; ⁵Asan Medical Center, University of Ulsan College of Medicine, Seoul, Republic of Korea, Korea, Dem. People's Rep. of; ⁶UT Southwestern Medical Center, Dallas, TX, United States; ⁷F Hoffmann-La Roche, Basel, Switzerland, Switzerland; ⁸Genentech, Inc., South San Francisco, CA, United States; ⁹Hoffmann-La Roche Limited, Mississauga, ON, Canada, Canada; ¹⁰Roche (China) Holding Ltd., Shanghai, China, China; ¹¹Jinling Hospital of Nanjing University of Chinese Medicine, Nanjing, China, China; ¹²National Taiwan University Cancer Center and National Taiwan University Hospital, Taipei, Taiwan
Email: akaseb@mdanderson.org

Background and aims: In IMbrave050, adjuvant atezo + bev demonstrated a statistically significant and clinically meaningful improvement in recurrence-free survival (RFS) vs active surveillance in patients (pts) at high risk of HCC recurrence following resection or ablation with curative intent. Further, the safety of atezo + bev was generally manageable. Here, we additionally report PRO data from IMbrave050.

Method: IMbrave050 (NCT04102098) enrolled pts HCC pts at high risk of recurrence following resection or ablation. Pts were randomized to Arm A (atezo + bev) or Arm B (active surveillance). Pts in Arm A received atezo 1200 mg + bev 15 mg/kg IV q3w for a period of one year (17 cycles). Pts in Arm B underwent active surveillance for one year and were eligible to crossover to atezo + bev following independent review facility (IRF) confirmation of recurrence. The primary end point was IRF-assessed RFS. Pre-specified exploratory analyses included change from baseline in global health status (GHS)/quality of life (QoL), physical functioning, role functioning, emotional functioning, and social functioning. Clinically meaningful deterioration was defined as a ≥ 10 -point decrease. Pts completed the IL42-EORTC QLQ-C30 (reduced) questionnaire at baseline and then at every odd treatment/surveillance visit through Cycle 17.

Results: The ITT population included 334 pts in both Arms A and B. With a median follow-up time of 17.4 mo (clinical cutoff date: 21 Oct 2022), IRF-RFS HR was 0.72 (95% CI: 0.56, 0.93; $p = 0.0120$). In the safety population, Grade 3 or 4 adverse events occurred in 41% of 332 Arm A pts and 13% of 330 Arm B pts. In ITT pts, IL42 completion rates remained $\geq 93\%$ in both arms from baseline through treatment/surveillance Cycle 17. Mean scores at baseline in both arms were high and similar, as measured by the GHS/QoL and physical, role, emotional and social functioning scales. Mean changes from baseline were not considerable through Cycle 17 and were similar between arms as evidenced by overlapping 95% CIs. Pts' GHS/QoL and functioning was maintained through Cycle 17, with no clinically meaningful deterioration observed at any time.

Conclusion: Statistically significant and clinically meaningful improvement in RFS was seen in pts receiving atezo + bev vs active surveillance. Atezo + bev safety was generally manageable, and consistent with the established safety profiles of each therapeutic agent and with the underlying disease. PRO outcome analyses

ORAL PRESENTATIONS

revealed similar overall health-related QoL (HRQoL) and functioning between atezo + bev and active surveillance, and that treating high-risk pts with HCC with adjuvant atezo + bev following procedures with curative intent did not result in a clinically meaningful deterioration in HRQoL or function.

© 2023 American Society of Clinical Oncology, Inc. Reused with permission. This abstract was presented at the 2023 ASCO Annual Meeting. All rights reserved.

GS-012

Week 48 results of the phase 3 D-LIVR study, a randomized double-blind, placebo-controlled trial evaluating the safety and efficacy of Lonafarnib-boosted with Ritonavir with or without Peginterferon Alfa in patients with chronic hepatitis delta

Ohad Etzion¹, Saeed Sadiq Hamid², Tarik Asselah³, George Sebastian Gherlan⁴, Adela Turcanu⁵, Tsarynna Petrivna⁶, Lisa Weissfeld⁷, Ingrid Choong⁸, Colin Hislop⁸, David Apelian⁸, Maria Buti⁹, Liana Gheorghe¹⁰, Elena Laura Iliescu¹⁰, Natalia Voronkova¹¹, Natalia Barsukova, Soo Aleman¹², Jordan J. Feld¹³, Nancy S Reau¹⁴, Maurizia Brunetto¹⁵, Pietro Lampertico¹⁶, Theo Heller¹⁷, Chris Koh¹⁷, Cihan Yurdaydin¹⁸, Jeffrey Glenn¹⁹, ¹Soroka University Medical Center, Israel; ²Ag Khan University, Pakistan; ³University of Paris, France; ⁴Fundatia "Dr. Victor Babes", Romania; ⁵ISMP Spitalul Clinic Republican "Timofei Mosneaga", Moldova; ⁶Medical Center "OK!Clinic" of international Institut of Clinical Research LLC, Ukraine; ⁷Statistics Collaborative, Inc, United States; ⁸Eiger BioPharmaceuticals, Inc, United States; ⁹Hospital Universitari Vall d'Hebron, Spain; ¹⁰Institutul Clinic Fundeni, Romania; ¹¹H-Clinic, LLC, Russian Federation; ¹²Karolinska Universitetssjukhuset Huddinge, Sweden; ¹³University Health Network, Canada; ¹⁴Rush University Medical Center, United States; ¹⁵Azienda Ospedaliero Universitaria Pisana (Presidio di Cisanello), Italy; ¹⁶University of Milan/ Fondazione IRCCS CA' Granda Ospedale Maggiore Policlinico, Italy; ¹⁷National Institute of Diabetes and Digestive and Kidney Diseases, United States; ¹⁸Koc University Hospital, Turkey; ¹⁹Stanford University School of Medicine, United States
Email: ohadet34@yahoo.com

Background and aims: Chronic hepatitis delta (CHD) is the most severe form of human viral hepatitis for which there is no FDA approved therapy. Lonafarnib (LNF) is a farnesyl transferase inhibitor that interferes with HDV virion assembly through inhibition of the interaction of the large delta antigen with hepatitis B surface antigen. The purpose of this study is to evaluate the safety and efficacy of LNF boosted with ritonavir (RTV) ± peginterferon alfa-2a (Alfa) for the treatment of CHD.

Method: D-LIVR (NCT03719313) is a randomized, double-blind, placebo-controlled, parallel-group clinical trial. Adults with CHD and compensated liver disease were enrolled and randomized (7:5:2:2) to receive LNF 50 mg BID + RTV 100 mg BID (oral), LNF 50 mg BID + RTV 100 mg BID + Alfa 180 mcg QW (combo), Alfa 180 mcg QW (Alfa), or placebo for 48 weeks, followed by 24 weeks post-treatment. All patients were on background entecavir or tenofovir throughout the study. Paired liver biopsies were obtained at baseline (BL) and Week 48. The primary end point was a composite response of HDV RNA decline ≥ 2 log IU/ml and ALT normalization in the LNF arms compared to placebo at Week 48. Key secondary end points included the components of the primary end point and the rate of patients achieving >2 point improvement in histology activity index score without worsening of fibrosis (histology end point) at Week 48 compared to BL.

Results: A total of 407 patients (mean age 42.7 years, 69% male, 73% white) were enrolled, of whom 405 were randomized to the oral (n = 178), combo (n = 125), Alfa (n = 52) and placebo arms (n = 52). At BL, mean ALT, total bilirubin, albumin, platelets and HDV RNA levels were comparable across the four arms. 27% of patients had evidence of cirrhosis per investigator assessment. At Week 48, by intention to treat analysis, composite response rate was 10.1% (oral), 19.2%

(combo), 9.6% (Alfa) and 1.9% (placebo). Composite response rates for both LNF-based arms were statistically significant vs placebo arm (p = 0.0044, oral; p < 0.001, combo). HDV RNA decline of ≥ 2 log IU/ml was observed in 14.6% (p = 0.0026, oral) and 32% (p < 0.001, combo), vs 3.8% (placebo). ALT normalization was achieved in 24.7% (p = 0.003, oral) and 34.4% (p < 0.001, combo), vs 7.7% in placebo. Of the 229 evaluable paired liver biopsies, statistically significant improvement in the histology end point was seen between the combo (35/66, 53%, p = 0.0139) and placebo arms (8/30, 27%), but not between the oral or Alfa and the placebo arms. Overall, both LNF-based regimens were well-tolerated, with comparable rates of treatment discontinuations across all arms.

Table:

Endpoint	Oral (n=178)	Combo (n=125)	Alfa (n=52)	Placebo (n=52)
Primary Endpoint ¹	10.1% p=0.0044 ²	19.2% p<0.0001 ¹	9.6%	1.9%
≥ 2 Log Decline in HDV RNA	14.6% p=0.0026 ²	32% p<0.0001 ¹	36.5%	3.8%
ALT Normalization	24.7% p=0.003 ²	34.4% p<0.0001 ¹	11.5%	7.7%
	Oral (n=177)	Combo (n=124)	Alfa (n=51)	Placebo (n=51)
Histology Endpoint ¹	33% (35) p=0.61 ²	53% (35) p=0.0139 ²	38% (10) p=0.46 ²	27% (8)

¹ ≥ 2 log decline in HDV RNA + ALT normalization

² Compared to placebo

³ >2 point improvement in histology activity index score without worsening of fibrosis

Conclusion: The Phase 3 D-LIVR trial achieved the primary efficacy end point for both LNF-based regimens compared to placebo with oral arm matching and combo arm doubling the Alfa response rate. Encouragingly, statistically significant histologic improvement was observed in the combo arm. Week 72 results of this trial are awaited.

Late-breaker Orals

SATURDAY 24 JUNE

LBO-01

Simvastatin plus Rifaximin to prevent ACLF in patients with decompensated cirrhosis. A randomised, double-blind, placebo-controlled, phase-3 trial: the liverhope efficacy trial

Elisa Pose¹, César Jiménez², Giacomo Zaccherini³, Daniela Campion⁴, Salvatore Piano⁵, Frank Erhard Uschner⁶, Koos de Wit⁷, Olivier Roux⁸, Kohilan Gananandan⁹, Wim Laleman¹⁰, Cristina Solé¹¹, Sonia Alonso¹², Berta Cuyas¹³, Xavier Ariza¹⁴, Adria Juanola¹, Ann T Ma¹⁵, Laura Napoleone¹, Jordi Gratacos¹, Marta Tonon¹⁶, Enrico Pompili^{17,18}, Jordi Sánchez-Delgado¹⁹, Marta Carol¹, Martina Perez¹, Núria Fabrellas²⁰, Judit Pich¹, Claudia Martell¹, Georgina Casanovas¹, Gemma Domenech¹, Ferran Torres¹, Víctor Manuel, Vargas Blasco², Paolo Caraceni¹⁷, Carlo Alessandria⁴, Paolo Angeli¹⁶, Jonel Trebicka²¹, Ulrich Beuers²², Claire Francoz⁸, Raj Mookerjee⁹, Rafael Bañares²³, German Soriano¹³, Ruben Hernaez²⁴, Andrew S. Allegretti²⁵, Manuel Morales-Ruiz¹, Miquel Serra²⁶, Hugh Watson²⁷, Juan G Abraldes²⁸, Patrick S. Kamath²⁹, Pere Ginès¹. ¹Hospital Clínic de Barcelona, Barcelona, Spain; ²Vall d'Hebron University Hospital, Barcelona, Spain; ³University of Bologna, Italy; ⁴Azienda Ospedaliero-Universitaria Città della Salute e della Scienza di Torino, Torino, Italy; ⁵Padova University Hospital, Padova, Italy; ⁶Goethe-Uni Frankfurt (Campus Riedberg), Frankfurt am Main, Germany; ⁷Amsterdam UMC, locatie AMC, Amsterdam, Netherlands; ⁸Hospital Beaujon AP-HP, Clichy, France; ⁹UCL

Institute for Liver, United Kingdom; ¹⁰UZ Leuven, Leuven, Belgium; ¹¹Parc Taulí, Sabadell, Spain; ¹²Gregorio Marañón General University Hospital, Madrid, Spain; ¹³Recinte Modernista de Sant Pau, Barcelona, Spain; ¹⁴Hospital de Sant Joan Despí Moisès Broggi, Sant Joan Despí, Spain; ¹⁵University Health Network, Toronto, Canada; ¹⁶University of Padova, Padova, Italy; ¹⁷Alma Mater Studiorum-Università di Bologna, Bologna, Italy; ¹⁸Hospital Clínic de Barcelona, Liver Unit, Barcelona, Spain; ¹⁹Hospital Parc Taulí de Sabadell, Sabadell, Spain; ²⁰Universitat de Barcelona, Barcelona, Spain; ²¹Universität Münster-Fürstenberghaus, Münster, Germany; ²²University of Amsterdam, Amsterdam, Netherlands; ²³Hospital Gregorio Marañón Pharmacy, Madrid, Spain; ²⁴Baylor College of Medicine, Houston, United States; ²⁵Massachusetts General Hospital, Boston, United States; ²⁶University of Zurich, Zürich, Switzerland; ²⁷Evotec (France) SAS-Campus Curie, Toulouse, France; ²⁸University of Alberta, Edmonton, Canada; ²⁹Mayo Clinic, Rochester, United States
Email: EPOSE@clinic.cat

Abstract LBO-01 is under embargo until Saturday 24 June 2023, 11:00.

This abstract will be made publicly available on the congress website at 11:00 (CEST) on the day of its presentation at the congress. Industry must not issue press releases – even under embargo – covering the data contained in abstracts selected to be highlighted during official EASL Press Office activities or in official EASL Press Office materials until the individual embargo for each data set lifts. Media must not issue coverage of the data contained in abstracts selected to be highlighted during official EASL Press Office activities or in official EASL Press Office materials until the individual embargo for each data set lifts.

Journalists, industry, investigators and/or study sponsors must abide by the embargo times set by EASL. Violation of the embargo will be taken seriously. Individuals and/or sponsors who violate EASL's embargo policy may face sanctions relating to current and future abstract submissions, presentations and visibility at EASL Congresses. The EASL Governing Board is at liberty to ban attendance and/or retract data.

Copyright for abstracts (both oral and poster) on the website and as made available during The International Liver Congress™ 2023 resides with the respective authors. No reproduction, re-use or transcription for any commercial purpose or use of the content is permitted without the written permission of the authors. Permission for re-use must be obtained directly from the authors.

LBO-02

Safety and efficacy of VIR-2218 with or without pegylated interferon alfa in virally-suppressed participants with chronic hepatitis B virus infection: post-treatment follow-up

Man-Fung Yuen¹, Young-Suk Lim², Ki Tae yoon^{3,4}, Tien Huey Lim⁵, Jeong Heo⁶, Pisit Tangkijvanich⁷, Won Young Tak⁸, Vaidehi Thanawala⁹, Daniel Cloutier⁹, Shenghua Mao⁹, Andre Arizpe⁹, Andrea Cathcart⁹, Sneha V. Gupta⁹, Carey Hwang⁹, Edward J. Gane¹⁰. ¹Department of Medicine, Queen Mary Hospital, School of Clinical Medicine; State Key Laboratory of Liver Research, The University of Hong Kong, Hong Kong, China; ²Department of Gastroenterology, Liver Center, Asan Medical Center, University of Ulsan College of Medicine, Seoul, Korea, Rep. of South; ³Liver Center, Pusan National University Yangsan Hospital, Yangsan, Korea, Rep. of South; ⁴Division of Gastroenterology and Hepatology, Department of Internal Medicine, Pusan National University College of Medicine, Yangsan, Korea, Rep. of South; ⁵Department of Gastroenterology and Hepatology, Middlemore Hospital, Auckland, New Zealand; ⁶Department of Internal Medicine, College of Medicine, Pusan National University and Biomedical Research Institute, Pusan National University Hospital, Busan, Korea, Rep. of South; ⁷Faculty of Medicine, Chulalongkorn University, Bangkok, Thailand; ⁸Division of Gastroenterology and Hepatology, Department of Internal Medicine, Kyungpook National University Hospital, School of Medicine Kyungpook National University, Daegu, Korea, Rep. of South; ⁹VIR Biotechnology Inc., San Francisco, United States; ¹⁰Department of Medical and Health Sciences, University of Auckland, Auckland, New Zealand
Email: mfyuen@hku.hk

Abstract LBO-02 is under embargo until Saturday 24 June 2023, 11:00.

This abstract will be made publicly available on the congress website at 11:00 (CEST) on the day of its presentation at the congress. Industry must not issue press releases – even under embargo – covering the data contained in abstracts selected to be highlighted during official EASL Press Office activities or in official EASL Press Office materials until the individual embargo for each data set lifts. Media must not issue coverage of the data contained in abstracts selected to be highlighted during official EASL Press Office activities or in official EASL Press Office materials until the individual embargo for each data set lifts.

Journalists, industry, investigators and/or study sponsors must abide by the embargo times set by EASL. Violation of the embargo will be

ORAL PRESENTATIONS

taken seriously. Individuals and/or sponsors who violate EASL's embargo policy may face sanctions relating to current and future abstract submissions, presentations and visibility at EASL Congresses. The EASL Governing Board is at liberty to ban attendance and/or retract data.

Copyright for abstracts (both oral and poster) on the website and as made available during The International Liver Congress™ 2023 resides with the respective authors. No reproduction, re-use or transcription for any commercial purpose or use of the content is permitted without the written permission of the authors. Permission for re-use must be obtained directly from the authors.

LBO-03

A phase 3, randomized, double-blind, placebo-controlled study evaluating the efficacy and safety of cilofexor in patients with non-cirrhotic primary sclerosing cholangitis (PRIMIS)

Michael Trauner¹, Cynthia Levy^{2,3}, Atsushi Tanaka⁴, Zachary Goodman⁵, Douglas Thorburn⁶, Deepak Joshi⁷, Kimmo Salminen⁸, Kidist Yimam⁹, Hiroyuki Isayama¹⁰, Aldo J Montano-Loza¹¹, Mark Danta^{12,13}, Holger Hinrichsen¹⁴, Pietro Invernizzi^{15,16}, Xiangyu Liu¹⁷, Xiaomin Lu¹⁷, Muhsen Alani¹⁷, William Barchuk¹⁷, Timothy R. Watkins¹⁷, Mark Genovese¹⁷, Christopher Bowlus¹⁸. ¹Medical University of Vienna, Division of Gastroenterology and Hepatology, Department of Medicine III, Vienna, Austria; ²University of Miami Miller School of Medicine, Division of Digestive Health and Liver Diseases, Miami, United States; ³University of Miami Miller School of Medicine, Schiff Center for Liver Diseases, Miami, United States; ⁴Teikyo University School of Medicine, Department of Medicine, Tokyo, Japan; ⁵Inova Fairfax Hospital, Center for Liver Diseases, Falls Church, United States; ⁶Royal Free Hospital, The Sheila Sherlock Liver Centre and UCL Institute of Liver and Digestive Health, London, United Kingdom; ⁷King's College Hospital, Institute of Liver Studies, London, United Kingdom; ⁸Turku University Hospital, Division

of Gastroenterology, Department of Medicine, Turku, Finland; ⁹California Pacific Medical Center, Department of Hepatology and Liver Transplantation, San Francisco, United States; ¹⁰Juntendo University, Department of Gastroenterology, Graduate School of Medicine, Tokyo, Japan; ¹¹University of Alberta, Division of Gastroenterology and Liver Unit, Edmonton, Canada; ¹²UNSW, School of Clinical Medicine, Faculty of Medicine, Sydney, Australia; ¹³St Vincent's Hospital, Department of Gastroenterology, Sydney, Australia; ¹⁴Gastroenterologisch-Hepatologisches MVZ Kiel GmbH, Kiel, Germany; ¹⁵Fondazione IRCCS San Gerardo dei Tintori, Gastroenterology Unit, Monza, Italy; ¹⁶University of Milano-Bicocca, Department of Medicine and Surgery, Monza, Italy; ¹⁷Gilead Sciences, Inc, Foster City, United States; ¹⁸University of California Davis School of Medicine, Division of Gastroenterology and Hepatology, Sacramento, United States
Email: michael.trauner@meduniwien.ac.at

Abstract LBO-03 is under embargo until Saturday 24 June 2023, 11:00. This abstract will be made publicly available on the congress website at 11:00 (CEST) on the day of its presentation at the congress. Industry must not issue press releases – even under embargo – covering the data contained in abstracts selected to be highlighted during official EASL Press Office activities or in official EASL Press Office materials until the individual embargo for each data set lifts. Media must not issue coverage of the data contained in abstracts selected to be highlighted during official EASL Press Office activities or in official EASL Press Office materials until the individual embargo for each data set lifts.

Journalists, industry, investigators and/or study sponsors must abide by the embargo times set by EASL. Violation of the embargo will be taken seriously. Individuals and/or sponsors who violate EASL's embargo policy may face sanctions relating to current and future abstract submissions, presentations and visibility at EASL Congresses. The EASL Governing Board is at liberty to ban attendance and/or retract data.

Copyright for abstracts (both oral and poster) on the website and as made available during The International Liver Congress™ 2023 resides with the respective authors. No reproduction, re-use or transcription for any commercial purpose or use of the content is permitted without the written permission of the authors. Permission for re-use must be obtained directly from the authors.

LBO-04

Deep learning predicts sensitivity to atezolizumab-bevacizumab from digital slides of hepatocellular carcinoma

Qinghe Zeng^{1,2}, Christophe Klein², Stefano Caruso³, Pascale Maille⁴, Daniela Allende⁵, Beatriz Minguez⁶, Massimo Iavarone⁷, Massih Ningarhari⁸, Andrea Casadei Gardini⁹, Federica Pedica¹⁰, Margherita Rimini¹¹, Riccardo perbellini¹², Camille Boulagnon-Rombi¹³, Alexandra Heurgue-berlot¹⁴, Marco Maggioni¹⁵, Mohd. Rela¹⁶, Mukul Vij¹⁷, Sylvain Baulande¹⁸, Patricia Legoix¹⁹, Sonia Lameiras¹⁹, Ismail Labga²⁰, Christine Sempoux²⁰, Antonia Digkilia²¹, Narmin Ghaffari-Laleh²², Jakob Nikolas Kather²³, Omar El Nahhas²⁴, Pooja Navale²⁵, Callie Torres²⁵, Tung-Hung Su²⁶, Rondell Graham²⁷, María Salcedo²⁸, María Bermúdez²⁹, Nguyen H. Tran³⁰, Jean-Michel Pawlotsky³¹, Gontran Verset³², Eric Trépo³³, Maria Varela³⁴, Andrés Castano-García³⁴, Dominique Wendum³⁵, Giuliana Amaddeo³⁶, Helene Regnault³⁷, Marie Lequoy³⁵, Alba Díaz³⁸, María Reig³⁹, Pompilia Radu⁴⁰, Jean-François Dufour⁴¹, Stephen Chan⁴², Purva Gopal⁴³, Léa Bruges⁸, Viviane Gnemmi⁴⁴, Jean Charles Nault⁴⁵, Hyungjin Rhee⁴⁶, Young Nyun Park⁴⁷, Mercedes Iñarrairaegui⁴⁸, Josep Maria Argemi⁴⁹, Bruno Sangro⁵⁰, Antonio D'Alessio⁵¹, Bernhard Scheiner⁵², David J. Pinato⁵³, Matthias Pinter⁵², Valérie Paradis⁵⁴, Aurélie Beaufrière⁵⁵, Simon Peter⁵⁶, Lorenza Rimassa⁵⁷, Luca Di Tommaso⁵⁸, Arndt Vogel⁵⁹, Sophie Michalak⁶⁰, Jerome Boursier⁶⁰, Nicolas Loménie⁶¹, Marianne Zioli⁶², Julien Calderaro³⁶. ¹Laboratoire d'Informatique Paris Descartes (LIPADE), Université Paris Cité, France; ²Centre d'Histologie, d'Imagerie et de Cytométrie (CHIC), Centre de Recherche des Cordeliers; ³Inserm UMR 1662, France; ⁴Université Paris Est Créteil, INSERM, IMRB, F-94010 Créteil, France; ⁵Cleveland Clinic, United States; ⁶Liver Unit, Hospital Vall d'Hebron, Barcelona, Catalonia, Spain; ⁷Fondazione IRCCS Cà Granda Ospedale Maggiore Policlinico, University of Milan, Italy; ⁸Centre Hospitalier Universitaire de Lille, Hôpital Huriez, Maladies de l'Appareil Digestif, Lille, France; ⁹Department of Oncology, Vita-Salute San Raffaele University, IRCCS San Raffaele Scientific Institute Hospital, Milan, Italy; ¹⁰IRCCS San Raffaele Hospital, Italy; ¹¹IRCCS San Raffaele Scientific Institute Hospital, Department of Oncology, Vita-Salute San Raffaele University, Milan, Italy; ¹²Division of Gastroenterology and Hepatology, Fondazione IRCCS Cà Granda Ospedale Maggiore Policlinico, Milan, Italy; ¹³Reims University Hospital, Department of Pathology, Reims, France; ¹⁴Reims University Hospital, Department of Hepatology, Reims, France; ¹⁵Department of Pathology, Fondazione IRCCS Cà Granda Ospedale Maggiore Policlinico, Italy; ¹⁶The Institute of Liver Disease and Transplantation, Dr. Rela Institute and Medical Centre, Bharath Institute of Higher Education and Research, Chennai, India; ¹⁷Dr Rela Institute and Medical Centre, Bharath Institute of Higher Education and Research, Chennai, India; ¹⁸Institut Curie Research Center, France; ¹⁹Institut Curie Genomics of Excellence (ICGex) NGS Platform, Institut Curie, Paris, France; ²⁰University Hospital of Lausanne (CHUV), Switzerland; ²¹Department of Oncology, Centre Hospitalier Universitaire

Vaudois, 1011 Lausanne, Switzerland; ²²Department of Medicine III, University Hospital RWTH Aachen, RWTH Aachen university, Aachen, Germany; ²³TU Dresden, Germany; ²⁴Else Kroener Fresenius Center for Digital Health, Medical Faculty Carl Gustav Carus, Technical University Dresden, Dresden, Germany; ²⁵Department of Pathology and Immunology, Washington University in St. Louis, St. Louis, MO, 63110, USA; ²⁶Division of Gastroenterology and Hepatology, Department of Internal Medicine, National Taiwan University Hospital, Taipei, Taiwan; ²⁷Mayo Clinic, United States; ²⁸Pathology Department, Hospital Universitario Vall d'Hebron, Vall d'Hebron Barcelona Hospital Campus, Spain; ²⁹Liver Cancer Research Group, Liver Diseases, Vall d'Hebron Institut de Recerca (VHIR), Vall d'Hebron Barcelona Hospital Campus, 08035 Barcelona, Spain; ³⁰Oncology Mayo clinic, United States; ³¹Hôpitaux Universitaires Henri Mondor, France; ³²Department of Gastroenterology, Hepatopancreatology and Digestive Oncology, Hôpital Erasme, Belgium; ³³Laboratory of Experimental Gastroenterology, Université Libre de Bruxelles, Brussels, Belgium; ³⁴Liver Unit, Division of Gastroenterology and Hepatology, Hospital Universitario Central de Asturias, Oviedo, Spain; ³⁵Hôpital Saint-Antoine, France; ³⁶Centre hospitalier universitaire Henri-Mondor, France; ³⁷Assistance Publique-Hôpitaux de Paris, Henri Mondor University Hospital, Department of Hepatology, Paris, France; ³⁸Barcelona Clinic Liver Cancer (BCLC) Group, Department of Pathology, Hospital Clínic de Barcelona, Universitat de Barcelona, Barcelona, Spain; ³⁹Barcelona Clinic Liver Cancer (BCLC), Liver Unit, Hospital Clinic of Barcelona, IDIBAPS, CIBEREHD, Universidad de Barcelona, Barcelona, Spain; ⁴⁰Department of Visceral Surgery and Medicine, Inselspital, Bern University Hospital, University of Bern, Switzerland; ⁴¹Swiss NASH Fondation, Switzerland; ⁴²Department of Clinical Oncology and State Key Laboratory of Translational Oncology, Sir YK Pao Centre for Cancer, The Chinese University of Hong Kong, Hong Kong SAR, People's Republic of China; ⁴³The University of Texas Southwestern Medical Center, United States; ⁴⁴Service d'Anatomie Pathologique, Centre de Biologie Pathologique, CHU Lille, 59037 Lille, France; ⁴⁵Inserm, France; ⁴⁶Department of Radiology, Research Institute of Radiological Science, Center for Clinical Imaging Data Science, Severance Hospital, Yonsei University College of Medicine, Seoul, Korea, Rep. of South; ⁴⁷Yonsei University College of Medicine, Korea, Rep. of South; ⁴⁸Liver Unit, Clínica Universidad de Navarra, Av. Pio XII, 36, 31008, Pamplona, Spain; ⁴⁹University of Navarra, Spain; ⁵⁰Clínica Universitaria. Universidad de Navarra, Spain; ⁵¹Department of Surgery and Cancer, Imperial College London, Hammersmith Hospital, London, UK; ⁵²Division of Gastroenterology and Hepatology, Department of Internal Medicine III, Medical University of Vienna, Vienna, Austria; ⁵³Department of Surgery and Cancer, Imperial College London, Hammersmith Hospital, Du Cane Road, W120HS, United Kingdom; ⁵⁴APHP, France; ⁵⁵Centre de recherche sur l'inflammation, INSERM1149, Université Paris Cité, Paris, France; ⁵⁶Department of Gastroenterology, Hepatology and Endocrinology, Hannover Medical School, Hannover, Germany; ⁵⁷Department of Biomedical Sciences, Humanitas University, Via Rita Levi Montalcini 4, Pieve Emanuele, Milan 20072, Italy; ⁵⁸Pathology Unit, IRCCS Humanitas Research Hospital, Via Manzoni 56, Rozzano, MI, Italy; ⁵⁹Department of Gastroenterology, Hepatology and Endocrinology, Hannover Medical School, Germany; ⁶⁰Angers University Hospital, France; ⁶¹Laboratoire d'Informatique Paris Descartes (LIPADE), Université Paris Cité, Paris, France; ⁶²Hôpital Jean-Verdier, France

Email: julienalderaro@gmail.com

Background and aims: Atezolizumab-bevacizumab combination therapy is the standard of care for advanced hepatocellular carcinoma (HCC). Objective responses are however observed only in a minority of patients and the development of predictive biomarkers is critical to improve patient stratification and outcomes. The ABRs gene signature has been previously developed to this aim¹, however, molecular profiling techniques remain very challenging to

ORAL PRESENTATIONS

implement into clinical practice as they require expertise in molecular biology and bioinformatics. Our goal was to develop a regression based deep-learning model to estimate the ABRs expression value directly from HCC histological digital slides, and determine if this model could predict progression-free survival (PFS) in treated patients.

Method: We trained our model (ABRS-P) using the public TCGA dataset (n = 336). Image features extracted from whole-slide images were fed along with ABRs gene signature expression as the label, into a model fit for gene expression prediction/regression analysis. The model was externally validated on two independent datasets: a resection series (n = 225, Henri Mondor University Hospital) and a biopsy series (n = 157, Henri Mondor and Avicenne University Hospitals), which differed significantly from the discovery dataset in gene profiling technology (3' RNA sequencing) and slide staining and encoding formats. The predictive value was then tested on an multicentric series of 122 biopsy samples from patients treated by atezolizumab-bevacizumab. A control series of patients (n = 44) treated by other systemic therapies was also investigated. Finally, to obtain insights into the biological features of areas that significantly impact ABRs-P predictions, we performed spatial transcriptomics on HCC samples and matched prediction heatmaps with *in situ* gene expression profiles.

Results: Using cross-validation, the mean Pearson correlation coefficient (r) of ABRs-P was 0.62 (0.46-0.72), with a median p value of 9.37E-09. The ABRs-P generalised well on the resection external validation series with a r = 0.60, p = 1.81E-23. A small drop in performance (r = 0.53) was observed in the biopsy validation set, but the correlation was still highly significant (p = 1.52E-12). Patients with ABRs-P High tumors showed prolonged PFS (p = 0.014) after initiation of atezolizumab-bevacizumab treatment. No impact of the ABRs-P prediction was observed on PFS in patients treated with other systemic therapies. Spatial transcriptomics showed significantly higher ABRs gene expression, along with upregulation of various other immune effectors, in tumor areas with high ABRs-P predicted values.

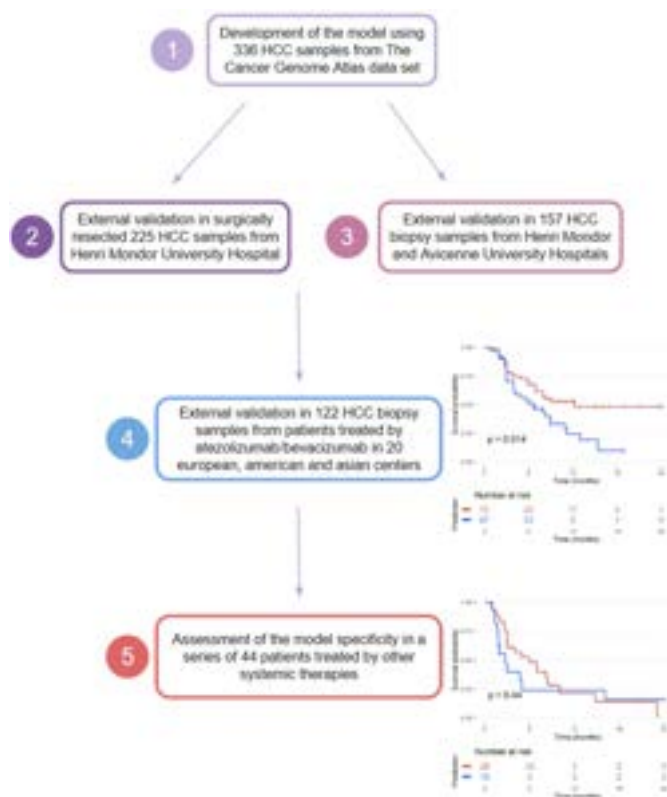


Figure:

Conclusion: Our study demonstrates that AI applied on HCC digital slides is able to predict PFS in patients treated by atezolizumab-bevacizumab. These approaches pave the way for the development of inexpensive and fast biomarkers of sensitivity to targeted therapies that could be easily implemented in clinical practice. Finally, we also show that the combination of AI prediction heat maps with spatial transcriptomics provides insights on the molecular features associated with areas with high predictive value. This could be applied to other cancers or diseases and improve our understanding of the biological mechanisms that drive outcomes or responses to treatments.

LBO-05

Pegozafermin for the treatment of non-alcoholic steatohepatitis patients with F2/F3 fibrosis: a multi-center, randomized, double-blind, placebo-controlled Phase 2b trial (ENLIVEN)

Rohit Loomba¹, Arun Sanyal², Kris Kowdley³, Deepak Bhatt⁴, Naim Alkhouri⁵, Juan P Frias⁶, Pierre Bedossa⁷, Stephen Harrison⁸, Don Lazas⁹, Robert Barish¹⁰, Millie Gottwald¹¹, Shibao Feng¹¹, Germaine D. Agollah¹¹, Cynthia (Cindy) Hartsfield¹¹, Hank Mansbach¹¹, Maya Margalit¹², Manal Abdelmalek¹³. ¹University of California San Diego, NAFLD Research Center, Division of Gastroenterology and Hepatology, Department of Medicine, San Diego, United States; ²Virginia Commonwealth University, Division of Gastroenterology, Hepatology, and Nutrition, Richmond, United States; ³Liver Institute Northwest, Seattle, United States; ⁴Icahn School of Medicine at Mount Sinai Health System, Dr. Valentin Fuster Professor of Cardiovascular Medicine, New York, United States; ⁵Arizona Liver Health, Phoenix, United States; ⁶Velocity Clinical Research, Los Angeles, United States; ⁷Liverpat, Paris, France; ⁸Pinnacle Clinical Research, San Antonio, United States; ⁹ObjectiveHealth, Nashville, United States; ¹⁰Ocala GI Research, Ocala, United States; ¹¹89bio, San Francisco, United States; ¹²89bio, Rehovot, Israel; ¹³Mayo Clinic, Division of Hepatobiliary Disease, Rochester, United States
Email: cindy.hartsfield@89bio.com

Abstract LBO-05 is under embargo until Friday 23 June 2023, 08:30.

This abstract will be made publicly available on the congress website at 08:30 (CEST) on the day of its presentation at the congress. Industry must not issue press releases – even under embargo – covering the data contained in abstracts selected to be highlighted during official EASL Press Office activities or in official EASL Press Office materials until the individual embargo for each data set lifts. Media must not issue coverage of the data contained in abstracts selected to be highlighted during official EASL Press Office activities or in official EASL Press Office materials until the individual embargo for each data set lifts.

Journalists, industry, investigators and/or study sponsors must abide by the embargo times set by EASL. Violation of the embargo will be taken seriously. Individuals and/or sponsors who violate EASL's embargo policy may face sanctions relating to current and future abstract submissions, presentations and visibility at EASL Congresses. The EASL Governing Board is at liberty to ban attendance and/or retract data.

Copyright for abstracts (both oral and poster) on the website and as made available during The International Liver Congress™ 2023 resides with the respective authors. No reproduction, re-use or transcription for any commercial purpose or use of the content is permitted without the written permission of the authors. Permission for re-use must be obtained directly from the authors.

taken seriously. Individuals and/or sponsors who violate EASL's embargo policy may face sanctions relating to current and future abstract submissions, presentations and visibility at EASL Congresses. The EASL Governing Board is at liberty to ban attendance and/or retract data.

Copyright for abstracts (both oral and poster) on the website and as made available during The International Liver Congress™ 2023 resides with the respective authors. No reproduction, re-use or transcription for any commercial purpose or use of the content is permitted without the written permission of the authors. Permission for re-use must be obtained directly from the authors.

LBO-06

Mycophenolate mofetil is superior to azathioprine for the induction of remission in treatment-naïve autoimmune hepatitis [CAMARO trial]

Romée Snijders^{1,2}, Anna Stoelinga³, Tom Gevers^{2,4,5}, Simon Pape^{1,2}, Maaïke Biewenga³, Maarten Tushuizen³, Robert Verdonk⁶, Henk-Marijn De Jonge⁷, Jan Maarten Vrolijk⁸, Sjoerd Bakker⁹, Thomas Vanwolleghem^{2,10}, Ynto de Boer^{2,11}, Martine Baven-Pronk¹², Ulrich Beuers^{2,11}, Adriaan Van der Meer¹³, Nicole van Gerven¹⁴, Marijn Sijtsma¹⁵, Bart Verwer¹⁶, Manon van IJzendoorn¹⁷, Manon van Herwaarden¹⁸, Floris van den Brand¹⁹, Kerim Sebib Korkmaz²⁰, Aad van den Berg²¹, Maureen Guichelaar²², Amar Levens³, Bart Van Hoek³, Joost P.H. Drenth^{1,2}. ¹Radboud University Medical Center; ²European Reference Network on Hepatological Diseases (ERN RARE-LIVER), Germany; ³Leiden University Medical Center, Netherlands; ⁴Maastricht University, Netherlands; ⁵Maastricht University Medical Center, Netherlands; ⁶St. Antonius Hospital, Netherlands; ⁷Jeroen Bosch Hospital, Netherlands; ⁸Rijnstate Hospital, Netherlands; ⁹Elisabeth-Tweesteden Hospital, Netherlands; ¹⁰Antwerp University Hospital, Belgium; ¹¹Amsterdam University Medical Centers, Netherlands; ¹²Groene Hart Hospital, Netherlands; ¹³Erasmus University Medical Center, Netherlands; ¹⁴Rode Kruis Hospital, Netherlands; ¹⁵St. Jansdal Hospital, Netherlands; ¹⁶Spaarne Gasthuis, Netherlands; ¹⁷Hospital Bernhoven, Netherlands; ¹⁸Deventer Hospital, Netherlands; ¹⁹OLVG Oost, Netherlands; ²⁰IJsselland Hospital, Netherlands; ²¹University Medical Center Groningen, Netherlands; ²²Medisch Spectrum Twente, Netherlands
Email: Romee.Snijders@radboudumc.nl

Abstract LBO-06 is under embargo until Saturday 24 June 2023, 11:00. This abstract will be made publicly available on the congress website at 11:00 (CEST) on the day of its presentation at the congress. Industry must not issue press releases – even under embargo – covering the data contained in abstracts selected to be highlighted during official EASL Press Office activities or in official EASL Press Office materials until the individual embargo for each data set lifts. Media must not issue coverage of the data contained in abstracts selected to be highlighted during official EASL Press Office activities or in official EASL Press Office materials until the individual embargo for each data set lifts. Journalists, industry, investigators and/or study sponsors must abide by the embargo times set by EASL. Violation of the embargo will be

WEDNESDAY 21 JUNE

Nurses & AHPs Forum

OS-001

Refractory ascites in cirrhosis is associated with a major psychological burden in patients with cirrhosis and caregivers

Ana Belen Rubio Garcia^{1,2}, Rebeca Moreira³, Marta Carol^{2,3}, Martina Perez^{2,3}, Marta Cervera^{2,3}, Ruth Nadal³, Jordi Gratacos³, Anita Arslanow³, Adria Juanola³, Anna Soria³, Elisa Pose³, Isabel Graupera³, Pere Ginès^{2,3}, Núria Fabrellas⁴. ¹Hospital Clinic of

ORAL PRESENTATIONS

Barcelona, Hepatology, Spain, ²Faculty of Medicine and Health Sciences, Spain, ³Hospital Clinic of Barcelona, Spain, ⁴Faculty of Medicine and Health Sciences, University of Barcelona, Spain
Email: anabrubio96@gmail.com

Background and aims: Refractory ascites is common in patients with cirrhosis and represents a major challenge for nurses caring for patients with liver diseases. The management of refractory ascites has been investigated extensively. However, there is very little information on the psychological impact of this condition in patients and the burden for their caregivers. The aim of this study was to investigate the psychological burden of refractory ascites in patients and effects on caregivers.

Method: Qualitative phenomenological study, the study population included outpatients with cirrhosis and refractory ascites. Sociodemographic and clinical data was collected from all patients. Psychological experiences were collected through semi-structured individual interviews to patients and caregivers. The analysis of the interviews was carried out by transcription and subsequent reading and re-reading of the description of the interpretative experiences. Subsequently, the content was analyzed to code the obtained information and grouped into categories. The sample was determined by data saturation. In patients, overall quality of life (QoL) was assessed by the short form survey 36 (SF-36) and liver specific QoL by the Chronic Liver Disease Questionnaire (CLDQ). Caregivers were asked to complete the SF-36 as well as the Zarit Burden Interview to measure caregiving burden.

Results: A total of 26 patients were included in the study (13 patients and 13 main caregivers). The mean age of the patients was 65 years. Nine patients (69%) were male and the main etiologic factor was alcohol consumption. Patients had a marked impairment in QoL in both physical and mental components. Main clinical symptoms were related to loss of appetite and weight loss, exhaustion, and insomnia. Patients reported a marked psychological impact mainly due to their decreased ability to move and reduced social activity ("I am very tired, I am always very tired"). Patients frequently reported mood swings ("I can open the window and disappear and that's it...") and symptoms of depression, yet some patients also expressed feelings of acceptance and resilience. The psychological impact was also very high in caregivers who had a major burden, as assessed by a median Zarit score of 57 (SD \pm 12).

Conclusion: Refractory ascites has a profound psychological impact on patients and their informal caregivers. This psychological impact should be evaluated and treated to help improve patients and caregivers wellbeing.

OS-002

Pharmacist led telemonitoring and titration of carvedilol for ambulatory patients with compensated cirrhosis and clinically significant portal hypertension

Sheridan Rodda^{1,2}, Chloe McAinch^{1,2}, Aparna Morgan^{2,3}, Eliza Flanagan^{2,3,4}, Edward Saxby^{2,3}, Jo Hunter^{1,2}, Sue Kirsal^{1,2}, Sally Bell^{3,4}, Suong Le^{2,3,5}. ¹Monash Health, Pharmacy Department, Melbourne, Australia; ²Monash University, Monash Digital Therapeutics and Innovation Laboratory, Melbourne, Australia; ³Monash Health, Department of Gastroenterology and Hepatology, Melbourne, Australia; ⁴Monash University, Department of Medicine, Melbourne, Australia; ⁵Monash University, School of Clinical Sciences, Melbourne, Australia
Email: roths2@hotmail.com

Background and aims: Carvedilol is frequently under-prescribed and under-dosed in patients with compensated cirrhosis and clinically significant portal hypertension (CSPH), despite significant mortality benefits. We aimed to investigate the feasibility, safety, and patient acceptability of a novel pharmacist led telemonitoring and titration service for achieving guideline directed carvedilol therapy (GDCT).

Method: We conducted a mixed methods study to prospectively evaluate the Optimising One Medication for Patients with Cirrhosis

(OOMPa-C) clinic. A new model of care and GDCT titration protocol was developed by Pharmacy, Hospital in the Home and the Department of Gastroenterology and Hepatology at Monash Health Australia. During April to December 2022, 22 ambulatory adult patients with compensated cirrhosis and CSPH were trained to self-record daily blood pressure (BP) using a Bluetooth machine paired to a smartphone application. Pharmacists reviewed the results on a web-based platform and conducted twice weekly video consultations with patients. Doses were titrated per GDCT up to 12.5 mg daily as tolerated. Semi-structured interviews were conducted by the OOMPa-C pharmacist at the final consult.

Results: Of 22 participants, 20 (91%) were successfully titrated over a median of 14 days (interquartile range (IQR):12.5–17) with a median of 4 (IQR:3–5) pharmacist consults. Overall 18 (82%) participants took 12.5 mg per day at completion and 20 (91%) adhered to monitoring on at least 90% of enrolled days. One participant (4.5%) experienced respiratory adverse effects requiring treatment cessation. The figure summarises the themes identified from the 21 participants that completed interviews. The BP machine and app were reported as easy to use. Convenience was the most cited benefit; saving time, money and effort by receiving care in the privacy and comfort of home. Participants were happy to use the service again and recommend it to others. Clinical safety and data security were not a concern.

Table:

Theme	Barriers	Facilitators
Perceived ease of use	Issues with app, phone, BP machine Work routines Illness Telehealth application	Regular routines Alerts/reminders Family/carers Use of familiar video call method Flexible review times Accessibility of pharmacist via phone
Perceived usefulness	Little perceptible benefit (preventive medication)	More information and visibility for BP and pulse Respectful communication More education on carvedilol
Intention to use the service	Medication adverse effects	Referring doctor Altruism (research setting) Perceived trustworthiness of staff
Perceptions of technology	Low self-esteem Apprehension	Family/carers

Conclusion: A virtual carvedilol dose titration service (telemonitoring combined with pharmacist telehealth reviews) achieved GDCT and was feasible, safe and acceptable to patients with compensated cirrhosis and CSPH.

OS-003

Feasibility of a home-based, virtually-delivered, group exercise intervention in older patients with liver cancer (TELEX-Liver Cancer)

Kate Hallsworth^{1,2}, Sam Orange^{1,3}, Misti McCain^{1,3}, Roisin Fallen-bailey¹, Helen Louise Reeves^{1,2,3}. ¹Faculty of Medical Sciences, Newcastle University, Newcastle upon Tyne, United Kingdom; ²The Liver Unit, Newcastle upon Tyne Hospitals NHS Foundation Trust, Newcastle upon Tyne, United Kingdom; ³Northern Institute for Cancer Research, Newcastle University, Newcastle upon Tyne, United Kingdom
Email: kate.hallsworth@ncl.ac.uk

Background and aims: Hepatocellular carcinoma (HCC) is often diagnosed at an intermediate/advanced stage; less than a third of patients are offered potentially curative treatments. For many,

maintaining quality-of-life (QoL) and independence throughout cancer treatment (s) and beyond is a core objective of clinical care. Strong evidence supports supervised exercise as an effective way to improve QoL in older adults with cancer and age-related comorbidities. Multiple barriers to the implementation of system-wide exercise programmes exist on both an organisational and individual patient level.

The aim of the study was to investigate whether it is feasible and safe to deliver supervised group exercise via videoconferencing to patients with HCC in their own home.

Method: TELEX-Liver Cancer was a non-randomised feasibility study for patients with HCC aged ≥ 60 years. Primary outcomes focussed on recruitment, retention, exercise adherence, and safety. Patients were asked to attend exercise classes, twice-weekly for ~45 minutes via online videoconferencing for 10 weeks in their own home. Each class included both aerobic and resistance training. Physical function was assessed pre-/post-intervention and patient-reported outcomes were collected via postal questionnaire.

Results: From November 2021 to September 2022, 45 patients were invited to participate and 19 provided consent (recruitment rate 42%). Participants had a mean age of 74 years, were on average 22 months post-diagnosis and 11 months post-treatment. Participants completed 76% of planned exercise sessions. 15/19 (79%) patients completed assessments of physical function and 14/19 (74%) patients returned study questionnaires. Hand grip strength ($p = 0.002$), Liver Frailty Index ($p < 0.001$) and 5-times chair stand ability ($p = 0.002$) significantly improved from pre- to post-intervention. No adverse events occurred during exercise sessions.

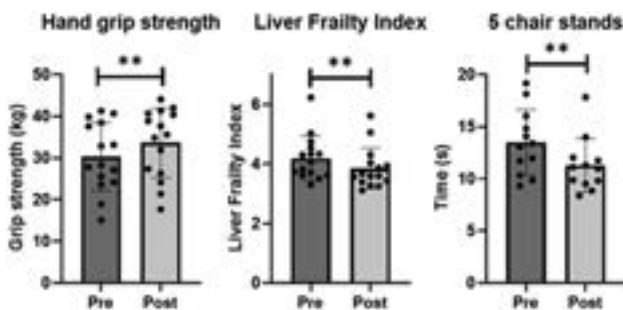


Figure:

Conclusion: It is feasible and safe to deliver supervised group exercise via videoconferencing to patients with HCC in their own home. Patients also benefited from improvements in physical functional. These findings will inform the design of a future, adequately-powered randomised controlled trial to evaluate the efficacy of the intervention.

OS-004-YI

Community dispensed hepatitis C virus treatment for 'hard to reach' opiate substitution treatment service users in Dublin: an intervention to address HCV infection eradication

Gillian Farrell¹, Kieran Harkin², Miriam Coghlan¹, Nessa Quinn¹, Colm Bergin¹. ¹St. James's Hospital, GUIDe Clinic, Dublin, Ireland;

²Merchants Quay Ireland, Ireland

Email: gilfarrell@stjames.ie

Background and aims: The GUIDe Clinic is Ireland's largest hospital-based infectious diseases' clinic. We run a very successful HCV treatment clinic; however, a number of our target patient group were regularly failing to attend clinic appointments, of which a disproportionate number were homeless. With the ambition of becoming 'HCV Free by 2023' we developed an alternative 'linkage to treatment' pathway. In September 2020 we established a partnership with Merchants Quay Ireland (MQI)-a not for profit organisation that provides services for people who are homeless and those with

addiction issues. The aim of the programme was to link otherwise 'hard to reach' populations to HCV DAA curative treatment.

Method: GUIDe Nurse and MQI General Practitioner (GP) set up and ran a fortnightly HCV clinic for patients who attended the opiate substitution treatment (OST) clinic based in MQI. This service offered a 'one-stop-shop' service where patients with HCV were assessed, educated, baseline bloods collected, fibroscan performed, drug-drug-interaction (DDI) checked and registered for treatment all within one clinical visit-as they attended for their OST review. DAAs were prescribed within this clinic and patients received their DAAs from the community pharmacy. Data was retrospectively collected using Electronic Patient Record (EPR) and Excel spreadsheet.

Results: 283 patients were registered to GP in MQI for OST (Opiate Substitution Treatment), of whom 239 (84%) had blood borne viral (BBV) screening. 89 (37%) of these patients were HCV Ag or PCR positive and were referred for DAA workup.

Of this patient group (N = 89),

- 40 were linked to our community dispensed DAA treatment
- 21 were linked to DAA treatment elsewhere (e.g. hospital based clinic, drug treatment centre or prison HCV treatment programme)
- 14 disengaged from MQI service
- 11 subsequently tested HCV RNA negative
- 3 died.

40 patients were treated in our programme and eligible for inclusion for analysis. All were HIV negative, fibroscan score < 12 KPa.

- 40 patients (7 (17.5%) female, 33 (88.5%) male) received 42 courses of DAA treatment.
- 6 patients received > 1 DAA course, having been previously treated elsewhere, or else requiring re-treatment.
- Regimens Prescribed: SOF/VLP (Epclusa) 26; G/P (Maviret) 14, SOF/VLP/VOX (Vosevi) 1, SOF/GP 1.

DAA Treatment Outcome Data (N = 42):

On Treatment Analysis:

24 (57%) SVR12 achieved

10 (24%) Failed to attend for SVR bloods: either lost to follow-up (LTFU) or declining bloods

3 (7%) treatment failure (2 successfully re-treated, 1 early discontinuation and now LTFU)

4 (10%) Re-infection (1 patient successfully re-treated, 1 linked to re-treatment elsewhere, 1 in prison and listed for DAA re-treatment with Prison in-reach service, 1 still actively trying to link with re-treatment 1 (2%) RIP

Conclusion: This model of care and treatment delivery programme has proved to be very successful to date, with many patients that failed to be treated in standard clinics, now successfully treated and cured. Many other patients were successfully linked to alternative treatment programmes. Although absolute numbers are small the high re-infection rate is concerning, and highlights the need for ongoing BBV molecular screening and rapid access to re-treatments in this high risk population group. The next challenge is to offer HCV screening and treatment to persons sleeping rough or living in unstable accommodation in a community based setting to optimise patient engagement and compliance and outcomes.

THURSDAY 22 JUNE

Alcohol-related liver disease and drug-induced liver injury

OS-005-YI

Clinical course of biopsy-controlled alcohol-related liver disease

Stine Johansen^{1,2}, Mads Israelsen¹, Nikolaj Torp^{1,2}, Katrine Thorhauge^{1,2}, Johanne Kragh Hansen^{1,2}, Katrine Prier Lindvig^{1,2}, Peter Andersen¹, Emil Deleuran Hansen^{1,2}, Camilla Dalby Hansen^{1,2}, Ida Ziegler Spedtsberg^{1,2}, Ida Villesen^{1,2}, Katrine Bech¹, Sönke Detlefsen^{2,3}, Helene Bæk Juel⁴, Ditlev Rasmussen¹, Torben Hansen⁴, Aleksander Krag^{1,2}, Maja Thiele^{1,2}. ¹Odense University Hospital, Fibrosis, fatty liver and steatohepatitis research center Odense (FLASH), Denmark; ²University of Southern Denmark, Department of Clinical Research, Faculty of Health Sciences, Denmark; ³Odense University Hospital, Department of Pathology, Denmark; ⁴University of Copenhagen, Novo Nordisk Foundation Center for Basic Metabolic Research, Denmark
Email: stine.johansen@rsyd.dk

Background and aims: Alcohol-related liver disease (ArLD) is associated with high morbidity and mortality but there is a lack of good prospective studies characterising the natural history of ArLD in more detail than epidemiological studies. We aimed to investigate the clinical course of biopsy-controlled ArLD according to baseline fibrosis stage including the risk of progression to decompensation and death.

Method: We prospectively followed a cohort of patients with a history of excessive alcohol intake (≥ 36 g/day for men and ≥ 24 g/day for women) and no prior decompensation. At baseline, we performed liver biopsies, genotyping of four single nucleotide polymorphisms in PNPLA3, MBOAT7, TM6SF2, HSD17B13, and clinical investigations. During follow-up, we manually reviewed patients' medical health records for all hospital contacts, new diagnoses/complications, reports of alcohol intake and all-cause mortality. First and further decompensation were defined according to the Baveno VII recommendations.

Results: We followed a total of 459 ArLD patients for a median of 5.9 years (IQR 4.5–7.8). Mean age at baseline was 57 ± 10 years, 76% male, fibrosis stage F0-1/F2/F3-4 = 57%/23%/20%. Patients reported a median of 15.5 years of excessive drinking. During follow-up, 67 patients decompensated of whom 46 developed at least one further decompensation, and 101 patients died (figure). All-cause mortality increased with higher fibrosis stage from 1.4 deaths per 100 person-years for stage F0-1, to 5.0 deaths per 100 person-years for stage F2, and 9.3 deaths per 100 person-years for stage F3-4. The cause of death was hepatic in 38%, non-hepatic in 43% and unknown in 20% of cases. The most frequent type of first decompensation was ascites (60%) followed by hepatic encephalopathy (25%) and variceal bleeding (15%). The incidence of decompensations during follow-up increased with baseline fibrosis stage: 5 out of 260 = 1.9% for stage F0-1, 17 out of 107 = 15.9% for stage F2, and 45 out of 91 = 49.5% for stage F3-4. Baseline fibrosis stage (hazard ratio, HR = 3.11; 95%CI 1.54–6.30) and excessive drinking during follow-up (HR = 4.80; 95%CI 3.28–7.02) were independent predictors of a first decompensation. PNPLA3 and TM6SF2 were predictors of decompensation in univariable regression but did not exhibit independent prognostic information.

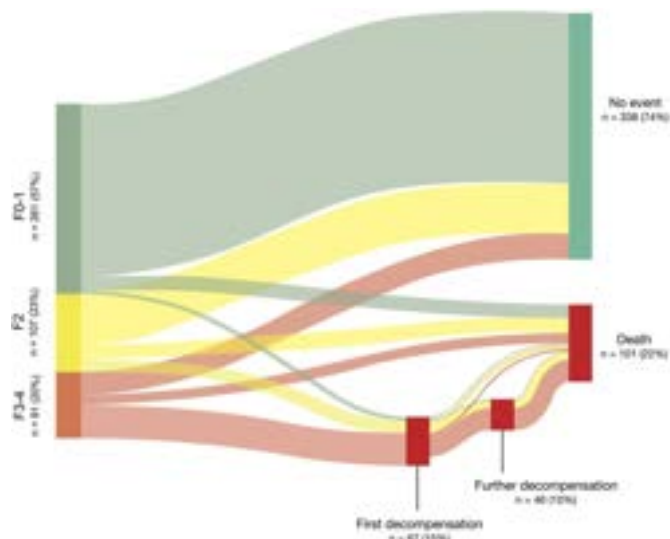


Figure:

Hepatocellular carcinoma occurred in 14 patients (3%) after a median of 3 years (IQR 1.3–6.4) with eight of the cases detected prior to first decompensation.

Conclusion: In this prospective cohort with 5.9 years of follow-up, patients with alcohol-related liver disease experienced a high 5-year risk of decompensation and death, even in patients with only moderate fibrosis (F2) at baseline. Continuous excessive drinking predicted decompensation independent of fibrosis stage.

OS-006-YI

Plasma multi-omics outlines association of urobilinogen with corticosteroid non-response, inflammation, intestinal permeability and outcome in severe alcoholic hepatitis

Jaswinder Maras¹, Manisha Yadav¹, Babu Mathew¹, Sadam H Bhat¹, Neha Sharma¹, Gaurav Tripathi¹, Nupur Sharma¹, Vasundhara Bindal¹, Sushmita Pandey¹, Jitendra Kumar¹, Pushpa Yadav¹, Ravinder Singh¹, Mojahidul Islam¹, Ashima Bhaskar², Ved Dwivedi², Nirupma Trehanpati¹, Shvetank Sharma¹, Shiv Kumar Sarin³.

¹Institute of Liver and Biliary Sciences, Molecular and Cellular Medicine, New Delhi, India; ²International Centre For Genetic Engineering And Biotechnology, New Delhi, India; ³Institute of Liver and Biliary Sciences, Hepatology, New Delhi, India

Email: jassi2param@gmail.com

Background and aims: Severe alcoholic hepatitis (SAH) has a high mortality and corticosteroid therapy is effective in 60% patients. Reliable indicators of response to therapy and mortality in SAH are needed.

Method: Altogether 223 SAH patients, 70 in derivative [50 responders (R) and 20 non-responders (NR)] and 153 in validation cohort [136 R, 17 NR] were included. Plasma metabolic and meta-proteomic phenotype was studied using UHPLC-HRMS and validated using Machine-Learning (ML). Temporal metabolic changes were assessed using Weighted Metabolome Correlation Network Analysis (WMCNA). Functional properties (inflammatory nature, effect on membrane integrity, effect on glucocorticoid receptor expression and downstream signaling) of nonresponse indicator were assessed in vitro on primary healthy neutrophils and primary mice enterocytes.

Results: Baseline plasma metabolomics discriminated NR ($p < 0.05$) with significant increase in urobilinogen (3.6-fold), cholesterol sulfate (6.9-fold), Adenosine monophosphate (4.7-fold) levels. Baseline plasma meta-proteome showed increase in alpha, beta diversity and clusters of orthologous groups of protein functions; biosynthesis of secondary metabolites, and others as a characteristic feature of NR ($p < 0.05$). Temporal change in the metabolite expression post- corticosteroid therapy was higher in responders ($p < 0.05$) whereas NR remained metabolically inactive. Plasma

urobilinogen predicted non-response [AUC = 0.94] with a hazard-ratio of 1.5 (1.2–1.6) and cut-off >0.07 mg/ml segregated non-survivors ($p < 0.01$, log-rank) and showed >98% accuracy using ML. Plasma urobilinogen expression correlated with circulating bacterial peptide known for converting bilirubin to urobilinogen ($r^2 > 0.7$; $p < 0.05$). A significant increase in neutrophil activation marker (CXCR1, NGAL), oxidative stress (NOXO1, NOXA1, NOX1, and NOX4), and pro-inflammatory cytokine genes (IL15, IL7, TNF α , IL6, IL8, and IL11) was observed post-treatment of primary healthy neutrophils with urobilinogen. Additionally, urobilinogen promoted corticosteroid resistance by enhancing the expression of GR β , trans-repression genes under GR α (inflammatory genes- NFkB, MAPK-MAP, IRF) and downregulating the expression of GR α , and transactivation (anti-inflammatory genes- NFkB-IkB) genes. Urobilinogen also dysregulated intestinal membrane junction proteins (gap junction protein 1, occludin and desmoglein) which promoted leaky gut.

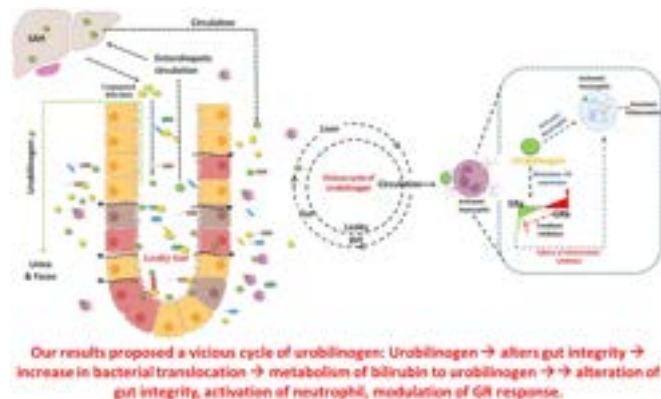


Figure:

Conclusion: Plasma metabolome/meta-proteome can stratify pre-therapy steroid response. Increase in plasma Urobilinogen modulates gut integrity and increases bacterial translocation. Increase in circulatory bacteria increases metabolism of circulatory bilirubin to urobilinogen. This vicious cycle of increase in urobilinogen again modulate gut integrity, increases activation of neutrophil and modulate glucocorticoid receptor activity thereby contributing to Non-response.

OS-007

Prior drug allergies are associated with worse outcome in patients with idiosyncratic drug-induced liver injury: an analysis from the Spanish DILI registry

Pablo Solis-Munoz^{1,2}, Inmaculada Medina-Cáliz¹, Rocío Romero Flores¹, Miguel Zoubek¹, Judith Sanabria-Cabrera¹, M Robles-Díaz^{1,3}, Miren García Cortes^{1,3}, Aida Ortega-Alonso^{1,3}, Jose Pinazo Bandera^{1,3}, MR Cabello¹, Raul J. Andrade^{1,3}, Maria Isabel Lucena^{1,3}, Hao Niu^{1,3}, Ismael Alvarez-Alvarez^{1,3}. ¹UGC de Aparato Digestivo, Servicio de Farmacología Clínica, Instituto de Investigación Biomédica de Málaga y Plataforma en Nanomedicina-IBIMA Plataforma BIONAND, Hospital Universitario Virgen de la Victoria, Universidad de Málaga, Málaga, Spain; ²Unidad de Investigación, Hospital Universitario Santa Cristina, Instituto de Investigación Sanitaria La Princesa, Madrid, Spain; ³Centro de Investigación Biomédica en Red, Enfermedades Hepáticas y Digestivas (CIBERehd), Madrid, Spain
Email: andrade@uma.es

Background and aims: Drug allergies encompass a plethora of hypersensitivity reactions with heterogeneous mechanisms. Whether the presence of prior drug allergies (PDA) is related with the outcome in patients that develop idiosyncratic drug-induced liver injury (DILI) remains uncertain. We aimed to determine the differences in clinical phenotype and outcomes of DILI patients according to the presence or absence of PDA.

Method: The demographics, clinical, biochemical and outcome information of patients included in the Spanish DILI Registry was analyzed, and the previous history of PDA was carefully examined. Cases of non-drug allergies, other types of adverse drug reactions, or insufficiently documented allergies were not considered PDA. Drugs were classified according to the Anatomical Therapeutic Chemical (ATC) Classification System. Differences between groups were tested with the Mann-Whitney U test, or the chi-square test or Fisher's exact test, as appropriate.

Results: Of 913 cases with a first episode of DILI, 62 (6.8%) patients presented with well-documented PDA (6.8%). Patients with PDA exhibited an older age (60 vs. 54 years, respectively; $p = 0.011$). Although hepatocellular injury predominated in both groups, compared to patients with no history of drug allergies, cases with PDA showed significantly lower median values of alkaline phosphatase (1.6 vs. $1.4 \times \text{ULN}$; $p = 0.027$) and platelet count (226 vs. $189 \times 10^3/\text{ml}$; $p = 0.011$), while aspartate aminotransferase (AST) showed a trend towards increased levels in patients with PDA (6.2 vs. $8.7 \times \text{ULN}$; $p = 0.049$). Fatal outcome was more common in patients with PDA (15% vs. 3.1%; $p < 0.001$). Indeed, seven cases (11%) developed a liver-related death compared to 1.6% who did not suffer from drug allergy ($p < 0.001$). Fatal cases with PDA were predominantly women (78% vs. 55% in non-fatal cases; $p = 0.282$), and all of them presented with hepatocellular injury, jaundice, and required hospitalization. Moreover, fatal cases with PDA had increased total bilirubin levels (14 vs. $4.1 \times \text{ULN}$ in non-fatal cases; $p < 0.001$), but lower platelet count (189 vs. $226 \times 10^3/\text{ml}$ in non-fatal cases; $p = 0.013$). The most common pharmacological groups implicated in PDA were anti-infectives (53%), central nervous system agents and musculoskeletal system drugs (14% each). The most frequent drugs implicated in PDA were penicillin (31%), acetylsalicylic acid and codeine (4% each). In 16 patients with PDA (26%), the drugs that caused the allergy and the DILI belonged to the same ATC group, and in five cases (8.1%), they belonged to the same drug class.

Conclusion: Our findings support the hypothesis that a previous history of an immunoallergic reaction related to drugs is associated with a worse outcome in patients with DILI. Patients with PDA presenting with hepatocellular damage, jaundice and lower platelet count were more likely to develop a fatal outcome.

OS-008-YI

Tumor necrosis factor-inducible gene 6 protein suppresses release of cluster of differentiation 44 intracellular domain, and attenuates alcohol-induced liver damages and activation of hepatic stellate cells

Jinsol Han¹, Chanbin Lee^{1,2}, Youngmi Jung^{1,3}. ¹Pusan National University, Department of Integrated Biological Science, Pusan, Korea, Rep. of South; ²Pusan National University, Institute of Systems Biology, Pusan, Korea, Rep. of South; ³Pusan National University, Department of Biological Sciences, Pusan, Korea, Rep. of South
Email: y.jung@pusan.ac.kr

Background and aims: Alcohol-related liver disease (ALD) is global prevalent chronic liver disease caused by excessive and/or habitual alcohol consumption. However, the effective and practical treatment against ALD has not been developed. Previously, we have demonstrated that tumor necrosis factor-inducible gene 6 protein (TSG-6), one of cytokines released from mesenchymal stem cells, reduces liver fibrosis and induces successful liver repair in mice with chronically damaged liver. TSG-6 was also shown to attenuate activation of hepatic stellate cells (HSCs), a main player in liver fibrosis, by interacting with cluster of differentiation 44 (CD44). CD44 is cleaved and releases its intracellular domain (ICD) fragment, which translocates into the nucleus and turn on fibrotic genes, contributing to liver fibrosis. However, it remains unclear whether and how TSG-6 has protective function in ALD. Hence, we investigated therapeutic effect of TSG-6 and its underlying mechanism in mice with ALD.

ORAL PRESENTATIONS

Method: 7-week-old male C57BL/6 mice were fed isocaloric pair diet (the CON group) or 5% (v/v) ethanol-containing Lieber-DeCarli liquid diet (EtOH group) for 12 weeks. At 9 weeks after the liquid diet, 50 ng of TSG-6 (EtOH + TSG-6) or saline (EtOH + Veh) as vehicle was intraperitoneally injected every other day along with feeding liquid diet for 3 additional weeks. These experimental mice were sacrificed 12 weeks after the diet feeding to collect blood and liver samples. Human primary HSCs at 70% confluence were serum starved overnight and cultured in medium containing 2% FBS with 20 ng/ml of TSG-6 or saline for 6 hr, 12 hr and 24 hr.

Results: Chronic alcohol feeding increased liver weight/body weight (LW/BW) ratio and caused severe liver damage including fat accumulation, hepatocyte death, inflammation and fibrosis. However, the EtOH + TSG-6 group had significantly lower LW/BW ratio and less alcohol-induced liver damage than the EtOH + Veh group had. Moreover, TSG-6 treatment remarkably reduced liver fibrosis in EtOH treated mice. The both levels of full-length CD44 and ICD significantly increased in the EtOH + Veh group compared with the EtOH + TSG-6 group. The nuclear translocation of CD44/ICD was also significantly reduced in TSG-6-treated alcohol-fed mice. Immunostaining for CD44 showed that CD44-positive HSCs-looking cells were more apparent in the EtOH + Veh group than the TSG-6 treated group. In addition, TSG-6 treatment significantly alleviated expression of CD44/ICD and suppressed its nuclear accumulation in human primary HSCs, leading to HSC inactivation.

Conclusion: These findings demonstrate that TSG-6 attenuates alcohol-induced liver damage and fibrosis, by blocking cleavage of CD44 to CD44/ICD, and suggest that TSG-6 has therapeutic potential for ALD with fibrosis.

OS-009

Efficacy of N-acetylcysteine to prevent anti-tuberculosis drug-induced liver injury: a randomized controlled trial

Supot Nimanong¹, Kittichai Samaithongcharoen¹, Watcharasak Chotiyaputta¹, Suppareak Disayabutr², Phunchai Charatcharoenwitthaya¹, Siwaporn Chainuvati¹, Tawesak Tanwandee¹. ¹Division of Gastroenterology, Department of Medicine, Siriraj Hospital, Mahidol University, Bangkok, Thailand; ²Division of Respiratory Disease and Tuberculosis, Department of Medicine, Siriraj Hospital, Mahidol University, Bangkok, Thailand
Email: supotgi@gmail.com

Background and aims: Hepatitis is a common complication of anti-tuberculosis therapy, especially from isoniazid. Slow acetylator status in the N-acetyltransferase 2 (NAT2) genotype is a significant risk factor of anti-tuberculosis drug-induced liver injury (AT-DILI). There is scanty data of N-acetylcysteine (NAC) to prevent AT-DILI. This study was aimed to explore the efficacy of NAC to prevent clinically significant AT-DILI.

Method: We conducted a randomized, open-labeled, controlled trial in patients with newly diagnosed tuberculosis (TB) who received standard anti-TB regimen. Patients with HIV infection or chronic liver disease were excluded. The enrolled patients were randomized to using NAC 1,200 mg/day for 2 months (NAC group) or anti-TB drugs alone (control group). Acetylator status of NAT2 was determined and liver function tests were assessed at baseline, 2 weeks, 2 and 6 months. Clinically significant hepatitis was defined as elevated aspartate aminotransferase (AST) or alanine aminotransferase (ALT) more than 5 times of baseline levels.

Results: Among 82 enrolled patients, the mean age was 54 years, 53.7% were male, 30% were NAT2 slow acetylator, mean AST was 25 IU/ml, mean ALT was 22 IU/ml which were not significantly different between NAC (n = 40) and control group (n = 42). The prevalence of clinically significant hepatitis was 19.5%. All events occurred within 2 months and 50% occurred within 2 weeks. The number of patients in NAC group who had clinically significant hepatitis were 5% and 15% at 2 weeks and 2 months respectively, compared with 14.3% and 23.8% in control group, which were not significantly different. Among NAT2

slow acetylator patients (n = 24), there was no hepatitis in NAC group, whereas 50% of control group had hepatitis at 2 months, which was significantly different (p = 0.02). No adverse effect of NAC was observed. Multivariate analysis revealed NAT2 slow acetylator was the only predictor of AT-DILI (hazard ratio 3.60 [1.07–12.15]; p = 0.039).

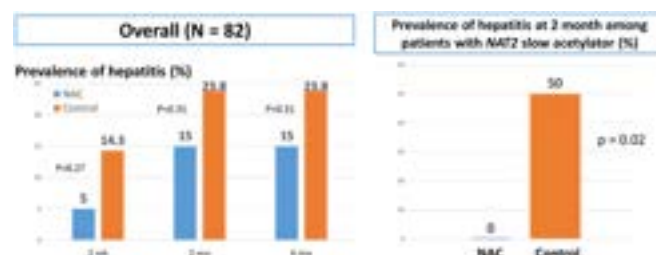


Figure:

Conclusion: Hepatitis is a common complication within 2 months of anti-TB therapy. NAC is safe and can prevent AT-DILI in patients with NAT2 slow acetylator.

Cirrhosis Experimental

OS-010-YI

Dysregulation of the FXR-FGF19 pathway indicates impaired gut-liver axis signalling in patients with cirrhosis

Benedikt Simbrunner¹, Benedikt Hofer¹, Philipp Schwabl¹, Kerstin Zinöber¹, Oleksandr Petrenko¹, Claudia Fuchs¹, Georg Semmler¹, Rodrig Marculescu², Mattias Mandorfer¹, Christian Datz³, Michael Trauner¹, Thomas Reiberger¹. ¹Division of Gastroenterology and Hepatology, Department of Medicine III, Medical University of Vienna, Vienna, Austria, Austria; ²Department of Laboratory Medicine, Medical University of Vienna, Austria, Austria; ³Department of Internal Medicine, General Hospital Oberndorf, Teaching Hospital of the Paracelsus Medical University Salzburg, Salzburg, Austria, Austria
Email: thomas.reiberger@meduniwien.ac.at

Background and aims: Experimental studies demonstrated impaired Farnesoid X receptor (FXR)-fibroblast growth factor 19 (FGF19) signalling in liver disease. This study aimed to characterize the FXR-FGF19 pathway along the gut-liver axis in patients with cirrhosis and investigate associations with disease severity.

Method: Patients with cirrhosis undergoing hepatic venous pressure gradient measurement with or without transjugular liver biopsy (n = 107, n = 53 liver biopsy; n = 5 control livers without background disease) or colonoscopy with ileum biopsy (n = 37; n = 6 liver-healthy controls) were included. Expression of genes reflecting hepatic and intestinal FXR activation and intestinal barrier integrity was assessed by qPCR. Bile acid (BA) and FGF19 levels in the systemic circulation were measured.

Results: Systemic BA correlated with FGF19 levels (r = 0.461; p < 0.001) and were significantly higher in patients with decompensated vs. compensated cirrhosis. Hepatic SHP expression was significantly lower in patients with cirrhosis than in controls (p < 0.001), reflecting reduced hepatic FXR activation. FGF19 (r = 0.512, p < 0.001) and BA (r = -0.487, p < 0.001) levels in the systemic circulation correlated negatively with CYP7A1 expression in the liver, but not with hepatic SHP or CYP8B1, indicating dysfunctional FXR-dependent BA feedback signalling in the liver. Furthermore, decreased expression of FXR, SHP and FGF19 was observed in the ileum of patients with cirrhosis. Surprisingly, intestinal FGF19 gene expression was not linked to systemic FGF19 levels. The expression of intestinal barrier proteins

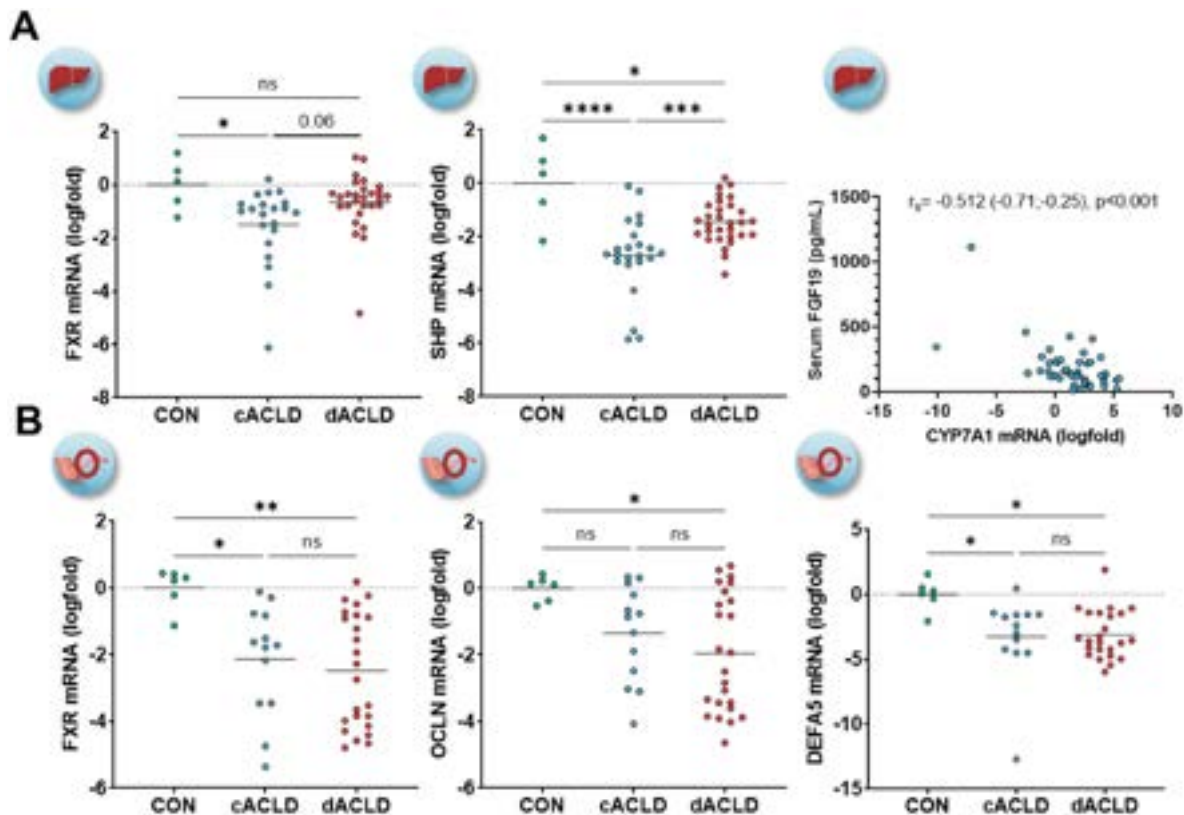


Figure: (abstract: OS-010-YI).

zonula occludens-1, occludin, and alpha-5-defensin correlated with SHP and decreased in patients with decompensated cirrhosis as compared to controls.

Conclusion: FXR signalling is dysregulated at key intersections of the gut-liver axis in patients with cirrhosis. Decreased FXR activation in the ileum was associated with reduced expression of intestinal barrier proteins in patients with cirrhosis. These translational data are highly relevant for ongoing efforts investigating whether targeting the FXR-FGF19 pathway in the gut-liver axis may ameliorate bacterial translocation in cirrhosis.

OS-011-YI

Restoration of epithelial and vascular intestinal barriers and splanchnic macrophage function mediates the halting of bacterial translocation by propranolol in cirrhotic rats with ascites

Elisa Castillo^{1,2}, Lorena Paule^{1,2}, Leticia Munoz^{1,2}, Manuel Ponce-Alonso^{3,4}, Rosa del Campo^{3,4}, Oscar Pastor⁴, Miguel A Ortega^{1,5}, Melchor Álvarez-Mon^{1,2,6}, Agustín Albillos^{1,2,4}.

¹Universidad de Alcalá: Facultad de Medicina y Ciencias de la Salud, Alcalá de Henares, Spain; ²CIBERehd-Liver and Digestive Diseases Networking Biomedical Research Centre, Spain; ³CIBERinfec- Center for Biomedical Research Network of Infectious Diseases, Spain; ⁴Hospital Universitario Ramón y Cajal IRYCIS, Madrid, Spain; ⁵CIBER-Center for Biomedical Research Network, Spain; ⁶Hospital Universitario Príncipe de Asturias, Alcalá de Henares, Spain

Email: elisa.castillo@uah.es

Background and aims: It has been hypothesized, but not proven, that restoration of the intestinal barrier damaged in cirrhosis could mediate the non-hemodynamic effects of propranolol (Prop). Prop

has also been suggested to be associated with improved survival in acute-on-chronic liver failure (ACLF). We aimed to i) study the effects of Prop on the epithelial and vascular intestinal barriers, microbiota, and immune system of cirrhotic rats with ascites, and ii) explore whether any effect is also present in cirrhotic rats with ACLF.

Method: Cirrhosis was induced in Wistar rats by CCl₄ gavage or bile duct ligation (BDL). Prop (Prop) (30 mg/kg/d, p.o.) or vehicle (Veh) was administered for 2 weeks from ascites development (Cirrhosis group, n = 40). ACLF was induced by LPS (6 microg/kg, i.p., 7 and 3 days before sacrifice) in rats already on Prop or Veh (ACLF group, n = 37). In the ileum, we evaluated the epithelial and vascular intestinal barriers, the microbiota adhering to the mucosa, bacterial translocation (BT), and peritoneal macrophage activation and function.

Results: Prop normalized the ileal microbiota of CCl₄-cirrhotic rats by reducing the elevated proportions of Gammaproteobacteria, Verrucomicrobium, and Bacteroidota. BT was reduced 2.5-fold by Prop (Table). Compared to Veh, Prop increased ileal mucus thickness and ZO-1 and occludin expression and reduced the expression of TNF-alpha, IFN-gamma, and IL-23. Prop improved the ileal vascular barrier, as shown by reductions in the PV1/CD34 ratio and liver detection of dextran in an intestinal loop assay. Prop exerted similar effects in BDL cirrhotic rats. In peritoneal macrophages, Prop ameliorated the increased RT1B expression (mean ± SD: from 33.8% ± 5.4% to 18.5% ± 3.2%, p < 0.01) and TNF-alpha production (from 24.4% ± 6.9% to 5.8% ± 2.7%, p < 0.01) and restored the phagocytosis (from 8.3% ± 2.4% to 29.9% ± 5.3%, p < 0.01). BT (89% vs. 91%), ileal mucous thickness (9.5 ± 3.4 vs. 10.1 ± 4.6 μm), ZO-1 expression (0.09 vs. 0.11 R.E.), and PV1/CD34 (0.83 ± 0.13 vs. 0.75 ± 0.17) were similar in ACLF rats on Prop or Veh.

Table:

	Controls n = 5	CCl ₄ cirrhosis	
		Vehicle n = 7	Propranolol n = 6
Small intestine (ileum)			
Mucus thickness (microm)	87 ± 6	13 ± 7 [*]	40 ± 15 [†]
ZO-1 (R.E.)	1	0.15 [*]	0.65 [†]
Occludin (R.E.)	1	0.22 [*]	0.59 [†]
TNF-α (R.E.)	1	121.6 [*]	73.8 [†]
IFN-γ (R.E.)	1	3.6 [*]	1.9 [†]
IL-23 (R.E.)	1	2.2 [*]	1.6 [†]
PV1/CD34	0.04 ± 0.03	0.81 ± 0.11 [*]	0.52 ± 0.09 [†]
4KDa-dextran in liver	0	11 ± 3 [*]	3 ± 1 [†]
Bacterial translocation			
Mesenteric lymph nodes (%)	0	86 [*]	33 [†]
Ascites (%)	0	57 [*]	0 [†]

*p < 0.001 vs. healthy controls;

†p < 0.05 vs. vehicle; R.E., relative expression.

Conclusion: Prop halts gut and hepatic BT in cirrhotic rats with ascites, but not in those with ACLF. Prop mediates these effects by restoring the integrity of the epithelial and vascular intestinal barriers and the activity of the splanchnic innate immune system.

OS-012-YI

Novel insights on liver endothelial mechanobiology in cirrhosis: role of calcium integrin-binding protein 1

Cong Wang¹, Sonia Selicean¹, Eric Felli¹, Yeldos Nulan¹, Sergi Guixé-Muntet², Juanjo Lozano², Jaime Bosch¹, Annalisa Berzigotti¹, Jordi Gracia-Sancho^{1,2}. ¹University of Berne and Inselspital, Department of Visceral Surgery and Medicine, Berne, Switzerland; ²IDIBAPS-Hospital Clinic Barcelona-CIBEREHD, Liver Vascular Biology, Barcelona, Spain
Email: jgracia@reccerca.clinic.cat

Background and aims: Liver microcirculatory malfunction is a key event in liver cirrhosis and portal hypertension, being liver sinusoidal endothelial cells (LSECs) central players in this pathological situation. We previously delineated how increased liver stiffness *per se* dysregulates sinusoidal cells phenotype by altering cells nuclear morphology. Reversing this mechanism may open novel therapeutic approaches based on targeting stiffness-modulated molecular factors (SMMFs). A possible SMMFs is calcium and integrin-binding protein-1 (CIB1), a small, ubiquitously expressed protein involved in many processes, and dysregulated in liver cancer and fibrosis. This study aimed at investigating the mechanotransduction mechanisms promoting endothelial dedifferentiation in cirrhosis, with a particular focus on CIB1 mechanobiology.

Method: Primary LSECs were cultured 48 h on tunable stiffness polyacrylamide gels (healthy, soft stiffness: 0.5 kPa vs. pathologic: 30 kPa). RNAseq was performed and dysregulated pathways were determined by Ingenuity Pathway Analysis. CIB1 expression and cellular localization was measured in healthy and cirrhotic human and rat liver tissues and cells. The effects of depleting CIB1 using siRNA were investigated in endothelial cells cultured at pathologic stiffness.

Results: Pathologic stiffness (30 kPa) induced significant changes in LSECs transcriptome as demonstrated by the dysregulation of 224 genes in comparison to soft substrate (p < 0.05; FC 1.5). Top dysregulated pathways were related to CIB1 functions, involving

integrin, sirtuin, hepatic fibrosis, actin cytoskeleton and mTOR signaling. Immunofluorescence on healthy LSECs and HUVECs cultured at 0.5 and 30 kPa confirmed that CIB1 significantly translocates to the cytoplasm on a stiff substrate (+46.7% and +93.3% respectively), which was prevented using nuclear mechanotransduction inhibitors (cytochalasin D plus nocodazol). Importantly, overexpression and translocation of CIB1 were confirmed in human cirrhotic liver (+20%) and primary cirrhotic LSEC (+40.8%). Cirrhotic rat LSECs showed significant re-translocation into the nucleus when cultured on healthy-like substrate (-231.6%) (all p < 0.05). Finally, CIB1 knock-down reversed LSECs nuclear morphology to a healthy spherical shape on 30 kPa, which was associated with improved LSECs phenotype as demonstrated by the amelioration of pathways related to LSECs dysfunction such as inflammation, DNA damage and repair, nitric oxide signal transduction, ROS scavenging activity, as well as a reduced nuclear membrane trafficking.

Conclusion: We demonstrate that CIB1 is a key regulator of LSECs mechanotransduction and dysfunction in liver cirrhosis. The reversibility of the effects of CIB1 makes it, or its downstream molecular pathways, potential novel therapeutic targets for chronic liver disease and portal hypertension.

OS-013

ETS2 alleviates HMGB1 and LPS triggered excessive inflammation in acute-on-chronic liver failure

Lulu He¹, Xi Liang², Jiaojiao Xin¹, Dongyan Shi¹, Jinjin Luo¹, Jiaqi Li¹, Jing Jiang¹, Jun Li¹. ¹The First Affiliated Hospital, Zhejiang University School of Medicine, State Key Laboratory for Diagnosis and Treatment of Infectious Diseases, Collaborative Innovation Center for Diagnosis and Treatment of Infectious Diseases, Hangzhou, China; ²Taizhou Central Hospital (Taizhou University Hospital), Precision Medicine Center, Taizhou, China
Email: lijun2009@zju.edu.cn

Background and aims: Hepatitis B virus-related acute-on-chronic liver failure (HBV-ACLF) is characterized by rapid deterioration of liver function with pre-existing chronic liver diseases (CLDs), and shows high short-term mortality. This study aims to identify potential biomarkers in ACLF pathogenesis and clarify the potential mechanisms.

Method: Peripheral blood mononuclear cells from patients with HBV-ACLF (n = 50), patients with chronic liver disease (n = 19) and healthy subjects (n = 14) were subjected to transcriptome analysis. The potential biomarkers ETS2 were subsequently validated in vivo and in vitro with myeloid-specific ETS2 deficiency mice and ETS2 deficient macrophages.

Results: Transcriptome analysis identified ETS2 as the top differentially expressed genes. ETS2 expression levels were significantly higher in ACLF patients than patients with chronic liver disease and normal controls (all p < 0.001). High accuracy of ETS2 for ACLF short-term mortality (28-/90-day) prediction were observed (AuROC value: 0.9083/0.7725) (all p < 0.001). The activation of innate immune and the suppression of adaptive immune were observed in ACLF patients with high ETS2 expression. In vivo studies showed that myeloid-specific ETS2 deficiency aggravates the impairment of liver function, promotes the induction of pro-inflammatory cytokines and hepatocyte apoptosis. Ablation of ETS2 in macrophages increased the levels of high-mobility group box 1 (HMGB1) and LPS-induced IL-6 and IL-1β significantly (p < 0.05), and nuclear factor-κB inhibitor abolished the suppressive effect of ETS2.

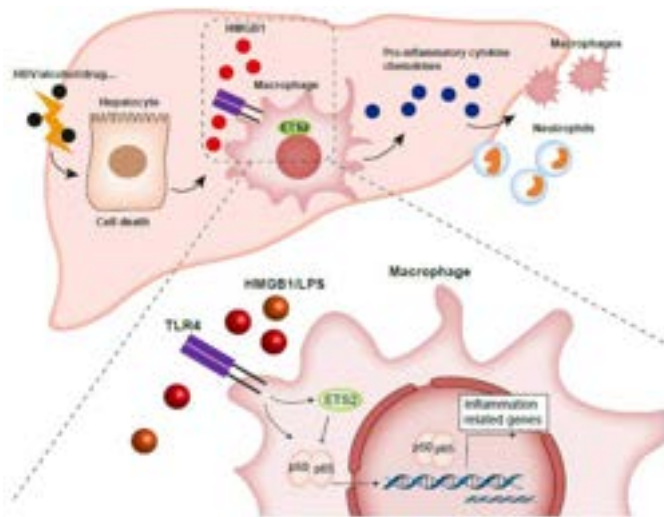


Figure:

Conclusion: Our study describes the role of ETS2 as a prognostic biomarker of ACLF patients. ETS2 protect mice from liver failure via alleviation of HMGB1-lipopolysaccharide-triggered inflammation response in macrophages, and serve as a potential therapeutic target for ACLF.

OS-014-YI

Longitudinal change in the plasma metabolite indicates therapeutic plasma exchange in acute-on chronic liver failure patients should be done every 12 hours

Jaswinder Maras¹, Gaurav Tripathi¹, Vasundhara Bindal¹, Babu Mathew¹, Manisha Yadav¹, Nupur Sharma¹, Sadam H Bhat¹, Neha Sharma¹, Sushmita Pandey¹, Abhishak Gupta¹, Meenu Bajpai², Shiv Kumar Sarin³, Rakhi Maiwall³. ¹Institute of Liver and Biliary Sciences, Department of molecular and cellular medicines, New Delhi, India; ²Institute of Liver and Biliary Sciences, Department of Transfusion Medicine, Institute of Liver and Biliary Sciences, New Delhi, India; ³Institute of Liver and Biliary Sciences, Department of hepatology, New Delhi, India
Email: jassi2param@gmail.com

Background and aims: Therapeutic plasma exchange (TPE) has shown some benefits in ACLF patients as it reduces inflammatory cytokines, albumin/water-bound toxins and improves the survival of ACLF patients. Analogous changes in the plasma metabolic landscape post-TPE in ACLF patients are unknown and could predict non-survival or TPE requirements.

Method: In this study, TPE was performed on ACLF patients (N = 42), and plasma samples of patients were collected at pre-therapy (baseline), mid-therapy, post-therapy, and at 6hrs and 12hrs post-therapy, respectively. A total of 250 plasma samples were subjected to untargeted metabolomics using HRMS. Temporal change in the plasma metabolic profile of non-survivors was compared to survivors

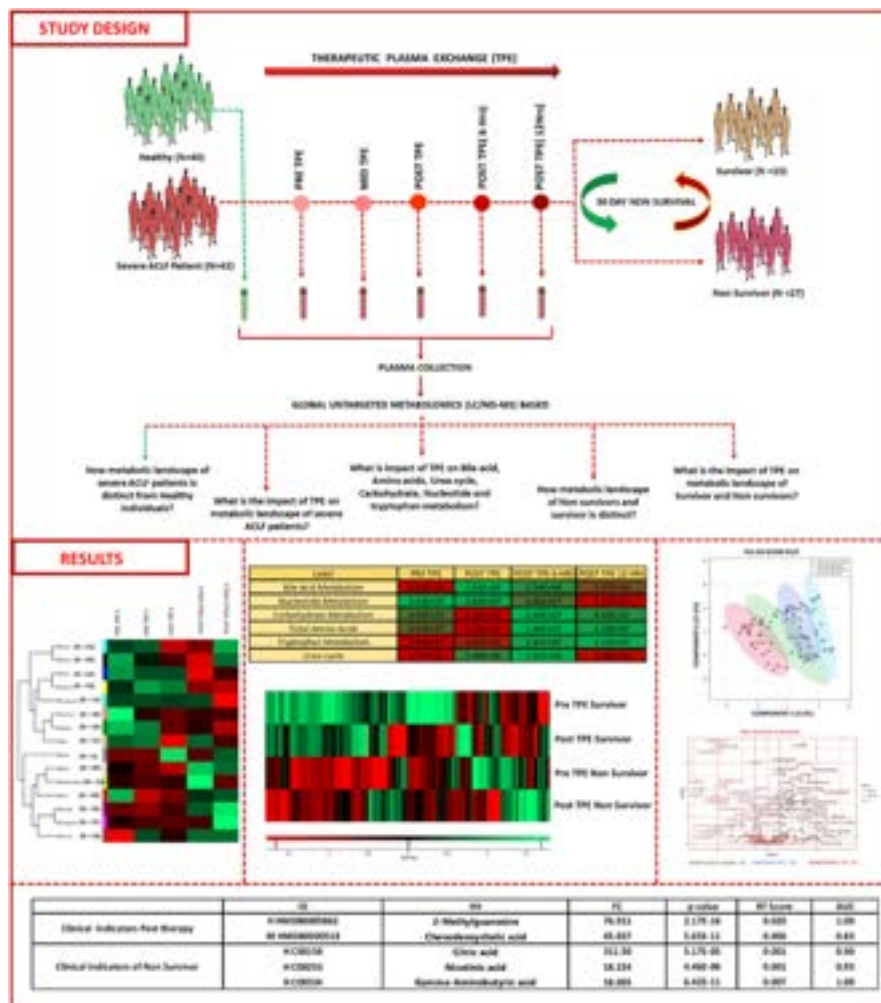


Figure: (abstract: OS-014-YI).

(30 days) using weighted metabolome correlation network analysis (WMCNA). Non-survivor-specific metabolites were identified (baseline) and subjected to clinical correlation and outcome prediction.

Results: Plasma metabolomics identified 620 features. ACLF patients, as compared to healthy, showed 142 metabolites (Up-77; Down-65 (FC >1.5, $p < 0.05$)). Partial Least Square-Discriminant Analysis (PLS-DA) analysis and hierarchical clustering segregated ACLF patients. ACLF patients showed dysregulated energy, nucleotide, amino acid metabolism, and others. Analysis of Post TPE compared to pre-TPE showed 130 metabolites (Up-63; Down-67 (FC >1.5, $p < 0.05$)) differentially expressed. PLS-DA and hierarchical clustering showed clear distinction in the post-therapy metabolic landscape of ACLF patients. TPE specifically remodelled Tryptophan, Carbohydrate, Urea, and bile acid metabolism. Post-therapy levels of chenodeoxycholic acid and others (FC >76, AUC >0.9, $p < 0.05$) were responsible for the segregation of post-therapy metabolotype. WMCNA and pathway enrichment analysis revealed a temporal post-TPE decrease in the urea cycle, bile acids, and tryptophan metabolism, whereas amino acids and carbohydrate metabolism-linked metabolites were increased. Interestingly the metabolic profile of ACLF showed a reversal of metabolotype in 6 hrs which got prominent by 12 hrs suggesting an urgent need for another TPE. The plasma of non-survivors was highly enriched for DAMPS/PAMPS compared to survivors. Further, single TPE very effectively clears the plasma of survivors but was found ineffective for non-survivors. Non-survivors showed a significant increase in Citric acid, Nicotinic acid, and others (FC >10, AUC >0.99, $p < 0.05$), which directly correlated with the severity and clinical factors (MELD, SOFA, and others, $R^2 > 0.7$, $p < 0.05$) and can be used as a putative indicator for non-survival or requirement of TPE.

Conclusion: Temporal change in the metabolic phenotype of ACLF patients is predictive of TPE response, and an increase in plasma level of Citric acid, Nicotinic acid, and others by 12 hrs post TPE warrants an urgent need for another TPE in ACLF patients.

Gut microbiome/organ crosstalk

OS-015

Unexpected function of the cell cycle kinase Cyclin E/CDK2 for control of intestinal barrier: implications for gut-liver communication, liver fibrosis and liver cancer

Anna Verwaayen¹, Julia Hennings¹, Christian Penner¹, Adrien Guillot², Tobias Otto¹, Nicole Treichel³, Thomas Clave³, Christian Trautwein¹, Yulia Nevzorova⁴, Christian Liedtke¹. ¹University Hospital RWTH Aachen, Department of Medicine III, Germany; ²Charité Universitätsmedizin Berlin, Department of Hepatology and Gastroenterology, Germany; ³Institute of Medical Microbiology, Functional Microbiome Research Group, University Hospital RWTH Aachen, Germany; ⁴Department of Immunology, Ophthalmology and ENT, Complutense University School of Medicine, Madrid, Spain, Spain
Email: cliedtke@ukaachen.de

Background and aims: E-type Cyclins (i.e. CCNE1, CCNE2) and their associated Cyclin-dependent kinase 2 (CDK2) control the transition from quiescence to the S-phase of the cell cycle. In addition, recent data point to several non-canonical functions of E-cyclins. In previous work, we demonstrated that constitutive deletion of the Cyclin E1 gene (*Ccne1*) in mice protected from liver fibrosis and hepatocellular carcinoma (HCC), while the underlying mechanisms are incompletely understood. In the present study, we tested the hypothesis that *Ccne1* expression contributes to liver fibrosis and hepatocarcinogenesis through modulation of the gut-liver axis and activation of Hepatic Stellate Cells (HSCs).

Method: We generated mice deficient for the whole Cyclin E/CDK2 complex in intestinal epithelial cells (i.e. *Ccne1*, *Ccne2*, and *Cdk2*, referred to as TKO mice). TKO mice at the age of twelve weeks were analysed for intestinal proliferation, gut barrier function, microbiota profiles and liver phenotypes. We also generated mice with deletion of *Ccne1* in Lecithin retinol acyltransferase (*Lrat*)-expressing cells (*Ccne1^{DHSC}*) targeting HSCs. *Ccne1^{DHSC}* mice were either subjected to the Carbon tetrachloride/Diethylnitrosamine (DEN/CCl₄) model to induce liver fibrosis and HCC, or fed with the Lieber-DeCarli alcohol liquid diet to challenge the intestinal barrier. Identification of *Lrat*-expressing cells in the gut was performed using *Lrat-cre* reporter mice and multiplex immunostaining.

Results: Unexpectedly, TKO mice were characterized by enhanced gut barrier and up-regulation of Tight junction protein 1 (*Tjp1*), which was associated with reduced gene expression of Toll-like receptor 4 (*Tlr4*) in the liver. Additionally, TKO mice showed changes in microbial composition. *Ccne1^{DHSC}* mice had significantly reduced liver fibrosis and HCC burden after DEN/CCl₄ treatment, which was related to impaired HSC activation and reduced hepatic *Tlr4* signaling. Importantly, *Lrat-cre* driven gene deletion did not only target HSCs, but also intestinal myofibroblasts and subpopulations of epithelial cells in the gut. Accordingly, *Ccne1^{DHSC}* mice had reduced intestinal permeability and improved liver injury after chronic ethanol feeding.

Conclusion: Cyclin E1 is an important driver of liver fibrosis and HCC. These functions are mediated at least in part through HSC activation. We provide unexpected evidence that the Cyclin E/CDK2 complex is involved in the control of intestinal permeability. Thus, reduced liver fibrosis and HCC as found in *Ccne1^{-/-}* or *Ccne1^{DHSC}* mice might be supported by enhanced intestinal barrier and modulation of the gut-liver crosstalk.

OS-016

Association of gut microbiome with prospective risk of hepatocellular carcinoma in chronic hepatitis B patients: a prospective nested case-control study

Zhixian Lan¹, Qiuhong You¹, Kaifeng Wang¹, Rui Deng¹, Rong Fan¹, Xieer Liang¹, Dekai Zheng¹, Jinlin Hou¹, Jian Sun¹. ¹State Key Laboratory of Organ Failure Research, Guangdong Provincial Key Laboratory of Viral Hepatitis Research, Department of Infectious Diseases, Nanfang Hospital, Southern Medical University, China
Email: doctorsunjian@qq.com

Background and aims: Case-control studies showed a possible relationship between gut microbiome and hepatocellular carcinoma (HCC), but longitudinal study was lacking. Here, we aimed to prospectively investigate the association of gut microbiome with subsequent risk of HCC in chronic hepatitis B (CHB) patient.

Method: SEARCH-B Study (NCT02167503) was conducted to evaluate the effect of anti-viral treatment on long-term outcome on patients with CHB, which have included 3798 patients so far. Fecal samples have been collected when patients were enrolled in this cohort. A total of 70 incident HCC cases were ascertained after a median follow-up of 2.9 years. Using a prospective nested case-control design, 70 incident HCC cases and 280 controls were selected at a ratio of 1:4 by propensity score matching. 16S rRNA gene sequencing was performed to characterize the composition of gut microbiota. Cox proportional hazards models were used for the association of different taxonomies as well as KEGG pathways with overall HCC risk adjusted for age, gender, albumin, platelet and body mass index (BMI). Spearman correlation analysis was performed on different taxonomies and KEGG pathways to assess their correlations. The significant threshold is $p < 0.05$.

Results: At the order level, we found that *Gemellales* was associated with an increased risk of HCC with an HR (95% CI) of 1.22 (1.05–1.42). At the family level, a higher risk of HCC was also linked to greater richness of *Gemellaceae* and *Peptostreptococcaceae* with HR (95% CI) of 1.19 (1.02–1.37) and 1.18 (1.03–1.35) respectively. At the genus level, *Blautia* was significantly associated with higher risk of HCC (HR (95%

CI): 1.27 (1.03–1.57)). However, genus *Roseburia* and *Ralstonia* were significantly linked to a decreased incidence of HCC with HR (95% CI) of 0.61 (0.38–0.99) and 0 (0.00–0.64) respectively. The analysis of microbial functional characteristics showed that secondary bile acid biosynthesis pathway was related with a higher risk of developing HCC (HR (95% CI): 1.32 (1.04–1.67)). Furthermore, risky order *Gemellales*, family *Gemellaceae*, family *Peptostreptococcaceae* and genus *Blautia* were positively correlated with the risky secondary bile acid biosynthesis pathway, with which protective genus *Roseburia* were negatively correlated.

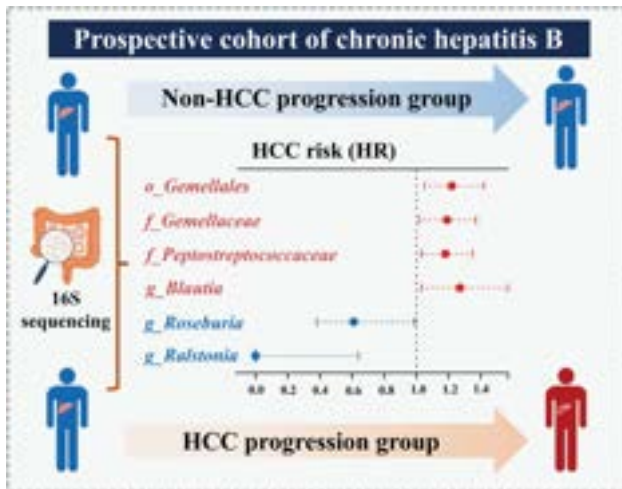


Figure:

Conclusion: This study demonstrated that several gut bacterial taxa were prospectively associated with HCC risk in our CHB cohort, which indicated that gut microbiome may play a significant role in the etiology of HCC in CHB patients, but more experiments are needed to clarify the causal relationships.

OS-017-YI

Serum villin-1 level-a tell-tale sign of gut barrier failure in patients with cirrhosis and acute decompensation

David Tornai¹, Boglárka Balogh¹, Aniko Csillag¹, Budai András², András Kiss², Péter Antal-Szalmás³, Gábor Méhes⁴, Lukács Baráth⁴, Tamas Tornai⁵, Istvan Tornai¹, Zsuzsanna Vitális¹, Nóra Sipeki^{1,6}, Patricia Kovats¹, Jonel Trebicka^{7,8}, Maria Papp¹. ¹University of Debrecen, Division of Gastroenterology, Department of Internal Medicine, Faculty of Medicine, Debrecen, Hungary; ²Semmelweis University, Department of Pathology, Forensic and Insurance Medicine, Faculty of Medicine, Budapest, Hungary; ³University of Debrecen, Department of Laboratory Medicine, Faculty of Medicine, Debrecen, Hungary; ⁴University of Debrecen, Department of Pathology, Faculty of Medicine, Debrecen, Hungary; ⁵Semmelweis University, Institute of Pancreatic Diseases, Budapest, Hungary; ⁶Faculty of Medicine, University of Debrecen, Division of Gastroenterology, Department of Internal Medicine, Debrecen, Hungary; ⁷University of Münster, Department of Internal Medicine B, Münster, Germany; ⁸European Foundation for Study of Chronic Liver Failure, EF-CLIF, Barcelona, Spain
Email: papp.maria@med.unideb.hu

Background and aims: Dysfunctional and leaky gut barrier are characteristics of cirrhosis and associated with disease progression and mortality. Utility of biomarkers, indicating the presence and extent of intestinal barrier dysfunction, remains a controversial issue in the prognosis and risk stratification of decompensated cirrhosis. Villin-1 (VIL1) is an actin-bundling protein, present in the intestinal, renal and biliary brush border. VIL1 is downregulated in response to chronic injury and diverse cellular stressors, including the microbiome, while during acute stress it is redistributed from the brush border to the basolateral membrane, which facilitates its release into

the blood. We investigated clinical significance of serum VIL1 levels in patients with cirrhosis and acute decompensation (AD).

Method: Patients (n = 86) and healthy controls (HC; n = 50) from the MICROB-PREDICT cohort were tested for serum VIL1 by ELISA. Four patient severity sub-groups were defined according to the PREDICT study (stable AD (SDC), unstable AD (UDC), pre-ACLF and ACLF [acute-on-chronic liver failure]). VIL1 immunohistochemistry (IHC) evaluation of duodenum biopsy was performed in a sub-cohort of the patients (n = 13) and controls (n = 11).

Results: Serum VIL1 levels were decreased in SDC patients (median [IQR]: 6.5 [4.9–10.4] vs 12 [8.4–14.9] ng/ml, p < 0.001) compared to controls and increased in more severe disease. This difference was confirmed in duodenum tissue by IHC. Significantly higher serum VIL1 levels were detected in pre-ACLF patients compared to those who did not develop ACLF (10.7 [7.8–22.9] vs 6.9 [5.0–10.5] ng/ml, p = 0.004), while in ACLF survivors decreased VIL1 levels were observed on day-7 compared to day-0 (9.8 [7.3–14.6] vs 12.7 [9.7–18.1] ng/ml, p = 0.010). High serum VIL1 levels (≥16.17 ng/ml) predicted 90-day mortality (AUROC:0.73, 95%CI: 0.563–0.888, p = 0.013) and in combination with high (≥50) CLIF-C AD score the prediction accuracy was excellent (both is high: 75%; all other together: 8% mortality, LogRank p < 0.001). High serum VIL1 level was able to predict mortality both in the presence (20% vs 62% LogRank p = 0.030) and absence (14% vs 40% LogRank p = 0.008) of renal failure.

Conclusion: Besides the six organ failures included in CLIF-SOFA, patients with cirrhosis and AD may also develop intestinal failure, as an additional organ failure. Serum VIL1 level could reliably indicate this organ failure and made the mortality risk stratification performed by CLIF-C OF score more accurate.

The MICROB-PREDICT project has received funding from the European Union's Horizon 2020 research and innovation programme under grant agreement No 825694. This abstract reflects only the author's view, and the European Commission is not responsible for any use that may be made of the information it contains.

OS-018-YI

Offspring of obese mothers have a higher risk for hepatocellular carcinoma through the transmission of an altered gut microbiome

Beat Moeckli^{1,2}, Vaihere Delaune¹, Benoit Gilbert³, Andrea Peloso¹, Graziano Oldani¹, Sofia El Hajji², Florence Slits², Quentin Gex², Stéphanie Lacotte², Christian Toso^{1,2}. ¹Geneva University Hospitals, Department of Surgery, Geneva, Switzerland; ²University of Geneva, Transplantation and hepatology laboratory, Genève, Switzerland; ³University of Geneva, Department of rheumatology, Genève, Switzerland
Email: beat.moeckli@gmail.com

Background and aims: The obesity pandemic leads to rising number of obese women of reproductive age. Emerging evidence suggests that maternal obesity has a negative impact on the long-term health of offspring. Additionally, obesity is an independent risk factor for malignancies and particularly hepatocellular carcinoma (HCC). The aim of our study is to investigate the impact of maternal obesity on the risk for HCC in the offspring and identify potential mechanisms of transmission.

Method: Female mice were fed either a high fat (HFD) or a normal diet (ND) before mating. Offspring received ND throughout life. In the offspring we studied the gut microbiome, liver histology, inflammatory patterns and tumor load in a diethylnitrosamine induced HCC mouse model. To normalize the gut microbiome, we co-housed offspring of HFD and ND mothers after weaning. The composition of the gut microbiota was assessed through 16S rRNA sequencing.

Results: Maternal obesity induced a distinguishable shift in the microbial composition towards decreased microbial diversity (2.56 vs. 2.92, p = 0.0089), increased proportions of Firmicutes and decreased abundance of Bacteroidota. Only at 40 weeks female HFD offspring developed steatosis (9.43 vs 3.09%, p = 0.0023) and a higher

ORAL PRESENTATIONS

number of inflammatory infiltrates (4.8 vs 1.0, $p = 0.018$) compared to ND offspring. Additionally inflammatory markers such as *TLR4*, *MHCII*, *iNOS* and *CXCL16* were overexpressed in offspring of obese mothers. A higher proportion of female HFD offspring developed liver tumors after DEN induction (79.8 vs 37.5%, $p = 0.0084$) with a higher total tumor volume at 36 weeks (234 vs $3 \mu\text{m}^3$, $p = 0.0041$). Co-housing offspring of obese and lean mothers corrected the gut microbiome composition and co-housing normalized the tumor number and volume to the level of ND offspring. Abundance of Erysipelotrichaceae was positively ($R = 0.46$, $p = 0.003$) and Lachnospiraceae negatively ($R = -0.35$, $p = 0.029$) correlated with tumor load.

Conclusion: Maternal obesity increases the susceptibility for chronic liver disease and HCC in the offspring. The transmission of an altered gut microbiome appears to play an important role in this increased risk profile.

OS-019

Lactobacillus protects against leaky gut, future decompensation, and hepatic encephalopathy in patients with cirrhosis

Patricia Bloom¹, Vincent B. Young¹, Anna Lok¹. ¹University of Michigan, United States

Email: pbbloom@med.umich.edu

Background and aims: Several complications of cirrhosis result from the translocation of bacteria or their products across a leaky gut; however, little is known about how mucosal bacteria (lining the intestinal epithelia) influence intestinal permeability and clinical cirrhosis outcomes. We aimed to assess if mucosal bacteria associate with intestinal permeability and predict future hospitalization for hepatic decompensation.

Method: We obtained duodenum, ileum, and colon tissue biopsies from patients with cirrhosis. Patients were excluded if they recently used non-rifaximin antibiotics or immunosuppression. Composition of the mucosal microbiota was determined via 16S rRNA gene

sequencing and epithelial permeability assessed by measuring transepithelial electrical resistance (TEER). Patients were followed until they met the primary outcome of hospitalization for cirrhosis decompensation or were censored at last visit, liver transplantation, or death. Associations between microbiota relative abundance and clinical outcomes were assessed in a beta binomial model with a false discovery rate of 0.05.

Results: We studied 58 patients with cirrhosis and obtained biopsies from 49 duodenums, 16 ileums, and 20 colons. Patients had median MELD 8 (IQR 7, 10), 62% were male, 16 (28%) had a history of hepatic encephalopathy (HE) and 28 (49%) had a history of ascites. In follow-up of median 192 days (IQR 79, 548), 14 were hospitalized for cirrhosis decompensation after median 90 days (IQR 50, 173), 7 of which were due to overt HE (2 of these patients had prior HE, 5 did not).

Including all gut segments, a beta binomial model found 37 mucosal bacteria were associated with future hospitalization for decompensation (5 positively associated, 32 protective) and 28 were associated with future overt HE episodes (5 positively associated, 23 protective). Of the taxa identified in these models, a *Lactobacillus* was significantly correlated with higher TEER (less leaky gut; $r^2 = 0.23$, $p = 0.05$), and protective of future overt HE and hospitalization for decompensation (Figure).

Sensitivity analyses were performed on duodenal samples only, the gut segment with the largest number of samples. A beta binomial model found 17 mucosal bacteria were associated with hospitalization for decompensation and 15 with future overt HE. Duodenal *Lactobacillus* was protective of future overt HE and decompensation.

Conclusion: Certain mucosal bacteria are associated with future cirrhosis decompensation hospitalizations and overt HE. *Lactobacillus*, a known probiotic, was associated with intact epithelial permeability and protected against HE and cirrhosis decompensation. Targeting mucosal microbiota and intestinal permeability may prevent HE and hospitalization among patients with cirrhosis.

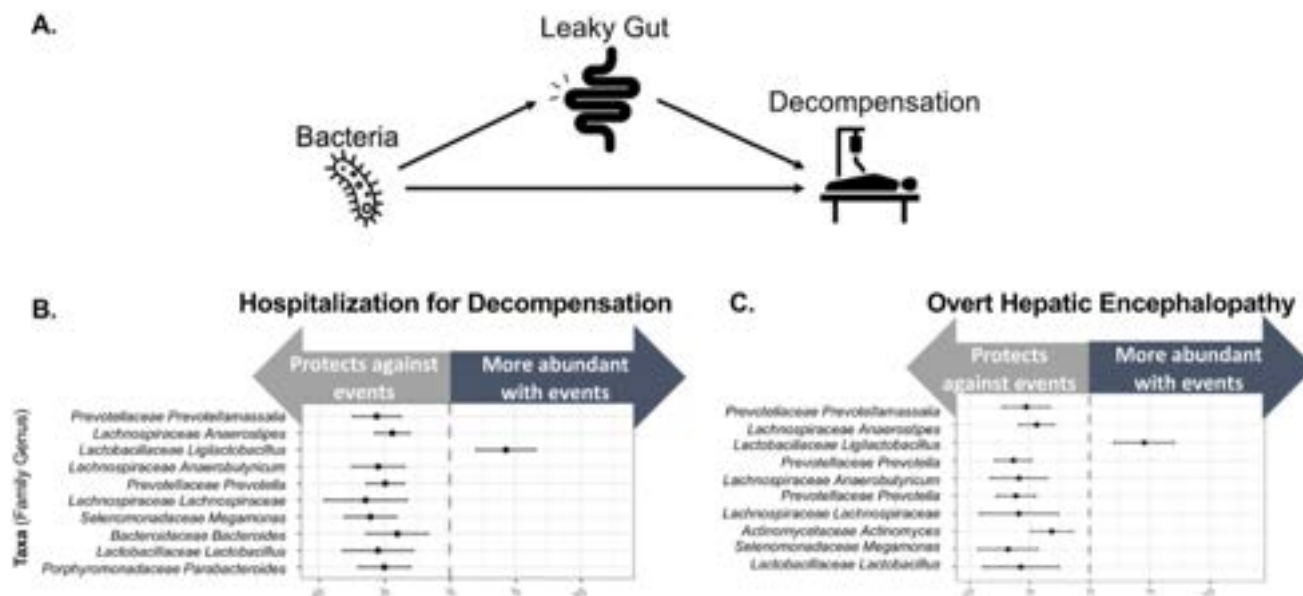


Figure: (abstract: OS-019): (A) Proposed causative pathway to cirrhosis decompensation; (B) Top 10 taxa that predicted hospitalization for decompensation; (C) Top 10 taxa that predicted overt hepatic encephalopathy

Liver tumours – Basic

OS-020-Y1

Multiplatform single cell spatial dissection of the invasive front of hepatocellular carcinoma (HCC) reveals molecular insights into tumor progression

Josephine Zhang¹, Nia Adeniji², Akanksha Suresh³, Lea Lemaitre¹, Vivek Charu⁴, Brendan Visser⁵, C. Andrew Bonham⁶, Renumathy Dhanasekaran¹. ¹Stanford University School of Medicine, Medicine- Division of Gastroenterology and Hepatology, Stanford, United States; ²UCSF School of Medicine, Medicine, San Francisco, United States; ³The Johns Hopkins University School of Medicine, Medicine, Baltimore, United States; ⁴Stanford University School of Medicine, Pathology, Stanford, United States; ⁵Stanford University School of

Medicine, Surgery- General Surgery, Stanford, United States; ⁶Stanford University School of Medicine, Surgery- Multi-Organ Transplantation, Stanford, United States
Email: dhanaser@stanford.edu

Background and aims: Cells at the invasive edge of a tumor evade immune surveillance and drive tumor progression. However, characterization of HCC cells along the tumor edge has remained elusive. Here, we used three powerful spatial technologies to perform multiregional profiling of primary HCC lesions and identify how heterogenous tumor evolution from the central core to the invasive edge drives disease progression.

Method: We prospectively obtained 30 tissue samples from HCC tumor specimens of 7 patients undergoing surgical resection, under appropriate IRB approval. We generated a tissue microarray of these samples to analyze 48,458 cells from three distinct regions: tumor core (7 samples, 15,668 cells), invasive edge (14 samples, 23,234 cells), and uninvolved liver (10 samples, 9,556 cells). We used CODEX, a 42-plex immunofluorescent imaging approach, to identify cell

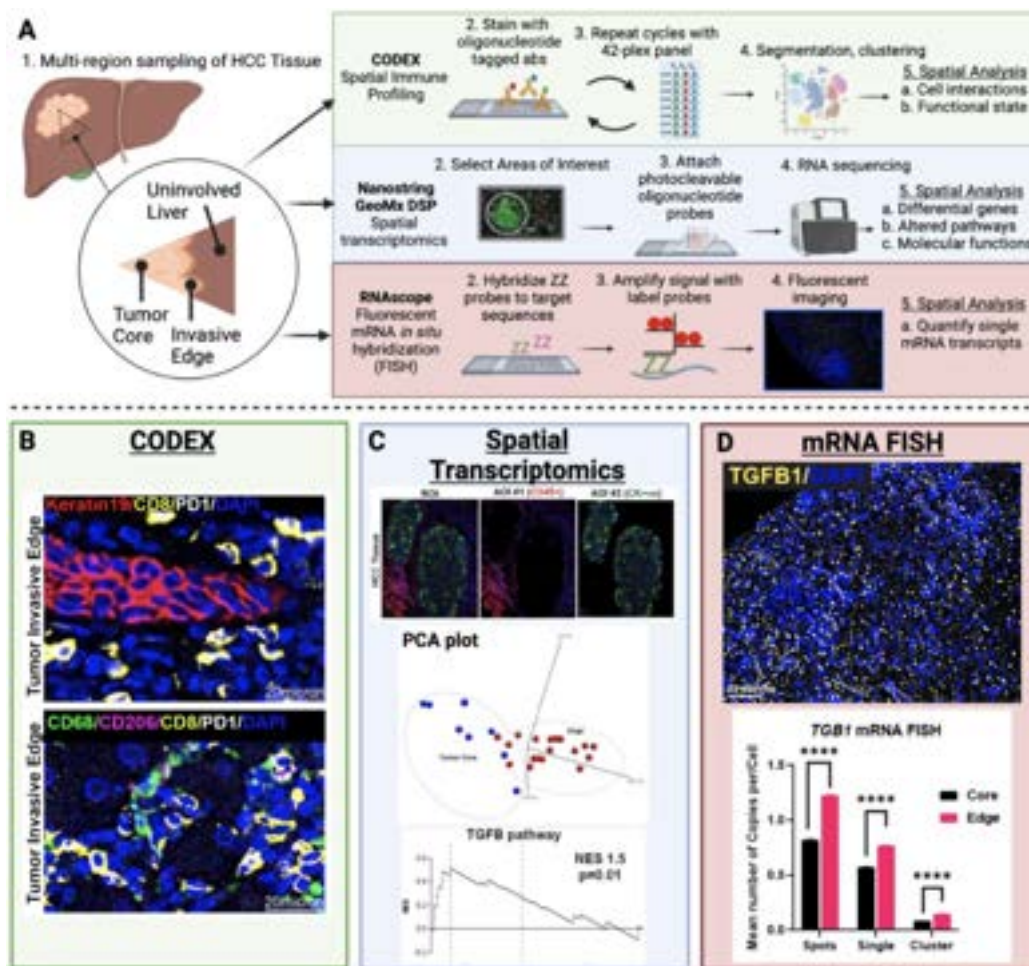


Figure 1. A) Study design: Multi-region sampling of HCC tissue followed by single cell spatial analysis. We use three powerful technologies : CODEX, a 42-plex immunofluorescent imaging approach, Nanostring GeoMx, a spatial transcriptomic platform, and RNAscope, an mRNA FISH assay. B) CODEX reveals enrichment of CK 19+ cancer stem-like cells at the invasive edge and their interaction with exhausted CD8+ T cells. C) Spatial transcriptomics determines gene expression in the CK tumor compartment and CK-/CD45+ TME. PCA plot indicates separate clusters between tumor core and invasive edge. The TGFβ pathway is the most upregulated pathway along the edge. D) mRNA FISH validates TGFβ upregulation, showing that TGFβ1 transcripts are more abundant at the invasive edge than in the tumor core.

Figure: (abstract: OS-020-Y1).

populations and interactions. A spatial transcriptomic platform, Nanostring GeoMx, determined gene expression and molecular pathway involvement of 1,812 genes in regions of interest classified into tumor (CK+) and microenvironment (TME) (CK-/CD45+). We used fluorescent RNA *in situ* hybridization (mRNA FISH) to validate gene expression at the single-cell level (Fig. 1A).

Results: We identified 20 unique tumor, immune, and stromal cell types in our samples with CODEX. The invasive edge had a higher proportion of endothelial cells ($p=0.003$), CD4+ T cells ($p=0.01$), exhausted CD8+ T cells ($p=0.04$), and fibroblasts ($p=0.04$) than the uninvolved liver. Moreover, the edge had a higher proportion of CK19+ cancer stem-like cells ($p=0.03$) than the tumor core. The CK19+ cancer stem-like cells interacted with exhausted CD8+ T cells ($p=0.01$), CD4+ T cells ($p=0.02$), and fibroblasts ($p=0.04$) more frequently at the invasive edge than at the core (Fig. 1B). We also observed more frequent interactions between CD206+ and PDL1+ M2-like macrophages and CD8+ T cells ($p=0.02$). Spatially resolved transcriptomics identified 141 genes that were differentially expressed in the CK+ tumor compartment of invasive edge vs the core, including upregulation of several genes which promote pro-tumoral inflammation (*SERPINE1*, *IL6ST*, *CD81*, *NCOR1*, *PSEN1*). The TME of the invasive edge vs the core showed differential expression of 38 genes including upregulation of immune modulating genes (*CD164*, *ST6GAL1*, *ITCH*) (Fig. 1C). Enrichment analysis revealed that TGF-beta pathway was the top upregulated pathway in the invasive edge (NES 1.46, $p=0.01$). Through mRNA FISH, we validated that *TGFB1* mRNA transcripts, both as single copies and clusters per cell, were indeed more abundant in the invasive edge than the core (47% of cells in the edge vs. 36% in the core ($p < 2.810^{-16}$)) (Fig. 1D).

Conclusion: We integrate multiplatform single cell spatial data from multi-region sampling of HCC and demonstrate dramatic remodeling of the immune microenvironment along the invasive edge of the tumor. Compared to the core, the invasive edge of the tumor is enriched in aggressive CK19+ cancer stem-like cells and exhausted CD8+ T cells which interact with each other and with M2-like macrophages. Further, we determine and validate TGF-beta pathway activation as the master regulator of cancer stemness and anti-tumor immunity along the invasive edge. Collectively, our spatial analysis provides mechanistic insights into how molecular events along the edge fuel tumor progression and identifies molecular targets for therapy.

OS-021-YI

Myeloid-derived cells suppress CD8+ T cells by arginase-1 through interaction with stellate cells in the microenvironment of hepatocellular carcinoma

Sung Eun Choi¹, Jong-Min Jeong¹, Kyurae Kim¹, Won-il Jeong^{1,2}. ¹Korea Advanced Institute of Science and Technology (KAIST), Graduate School of Medical Science and Engineering (GSMSE), Daejeon, Korea, Rep. of South; ²Center for the Hepatic Glutamate and Its Function, KAIST, Daejeon, Korea, Rep. of South
Email: wijeong@kaist.ac.kr

Background and aims: Hepatocellular carcinoma (HCC) is one of the leading causes of deaths worldwide and its occurrence relies heavily on the onset of liver cirrhosis. Various hepatic and immune cells, namely hepatic stellate cells and macrophages, are reported to be activated near the tumour area during HCC development, and yet their mechanisms of migration or intercellular interaction have not been fully elucidated. Here, we aim to investigate the mechanism regulating the migration of pro-tumorigenic immature macrophages and their interaction with activated HSCs (aHSCs) in the HCC microenvironment.

Method: 2-week-old male mice were intraperitoneally injected with 20 mg/kg diethylnitrosamine (DEN) for HCC induction and bred for 40 weeks for tumour formation. eGFP+, CX₃CR1GFP/GFP, or Arg1-YFP Ly6C+ bone marrow (BM) cells were adoptively transferred to observe the migration of immature macrophages and their interaction with

aHSCs via arginase-1 (Arg1) expression. Mice with myeloid-specific depletion of Arg1 (LyzM^{ΔArg1}) were utilised to observe the changes in CD8+ T cell proliferation and HCC progression. *In vitro* co-culture system was adopted to further confirm the findings *in vivo*.

Results: The frequency of CD14⁺CD11b⁺HLA-DR⁻ and CD11b⁺Ly6G⁻Ly6C^{high} macrophages was elevated in blood and liver tissues of clinical and DEN-induced HCC, respectively, whereas the frequency of hepatic CD8+ T cells was decreased compared to healthy controls. From the adoptive transfer of eGFP+ BM cells, we found that CD11b⁺Ly6G⁻Ly6C^{high} macrophages were located particularly near the aHSCs in the peritumour area, expressing high level of CX₃CR1, Arg1, and iNOS. In CX₃CR1-depleted HCC-bearing mice, the expression of Arg1, iNOS and IL-10 was reduced in hepatic immune cells along with markedly reduced interaction of Ly6C+ cells with CX₃CL1+ aHSCs. Ly6C+ BM cells co-cultured with aHSCs revealed that immature Ly6C+ BM cells highly expressed Arg1 while the expression of genes related to retinoid metabolism (*Raldh1*, *RARα/β*, *RXRα/β*) was elevated in aHSCs, indicating that Arg1 expression in immature macrophages may have been induced by retinoids produced from aHSCs. In fact, co-incubation of CD8+ T cells with Ly6C+ BM cells pre-co-cultured with aHSCs exhibited suppressed proliferation of CD8+ T cells, supporting the acceleration of HCC. These findings *in vitro* were further confirmed by reduced hepatic tumorigenesis in LyzM^{ΔArg1} mice compared to controls.

Conclusion: We showed that CX₃CR1-expressing CD11b⁺Ly6G⁻Ly6C^{high} cells migrate and interact with aHSCs in the peritumour region. Retinoids produced from the aHSCs induce Arg1 expression in the migrated immature macrophages, subsequently depriving CD8+ T cells of arginine to be used for proliferation and promoting the progression of HCC. By proposing the abovementioned mechanism, we suggest CX₃CR1 and Arg1 as potential therapeutic targets of HCC.

OS-022

In vivo cancer-associated fibroblast specific gene silencing for anti-stromal therapy in primary liver cancer using novel siRNA loaded polypeptide nanoparticles

Paul Schneider¹, Leon Capelo², Heyang Zhang², Matthias Barz², Barbara Schoers³, Oezlem Akilli-Oeztuerk³, Mustafa Diken³, Karina Benderski⁴, Alexandros Marios Sofias⁴, Twan Lammers⁴, Markus Möhler⁵, Peter Galle⁵, Matthias Bros⁶, Leonard Kaps⁵.
¹University medicine at the Johannes Gutenberg University in Mainz, 1st Medical Unit, Mainz, Germany; ²Leiden Academic Center for Drug Research, Netherlands; ³TRON-Translational Oncology, Germany; ⁴Institute for Experimental Molecular Imaging, RWTH University Hospital Aachen, Department of Nanomedicine and Theranostics, Germany; ⁵University Medical Center Mainz, First Department of Medicine, Germany; ⁶University Medical Center Mainz, Department of Dermatology, Germany
Email: leonardkaps@googlegmail.com

Background and aims: Cancer associated fibroblasts (CAF) support tumor growth and metastasis in the tumor microenvironment (TME) and are therefore promising target cells for anti-stromal therapy in solid tumors [Kaps, Schuppan; Cells 2020]. We have designed a novel polypeptide nanoparticle (NP) with improved endosomal escape for small interfering RNA (siRNA) delivery into stroma cells of hepatocellular carcinoma (HCC) [Birke et al., Prog. Polym. Sci. 2018]. NPs loaded with CAF targeting siRNA were tested in a murine model of primary liver cancer.

Method: In vitro screening for CAF relevant target genes revealed that the CAF derived microfibrillar-associated protein 5 (MFAP-5) was highly upregulated in fibroblasts (3T3 fibroblasts and MHSC-SV40 hepatic stellate cells) when co-cultured with HCC cells (Dt81Hepa1-6). NPs have been designed utilizing the triblock copolymer polysarcosine-b-poly(-benzyl glutamic acid)-b-polylysine, which enables co-loading of siRNA and desloratidin, an antihistamine that triggers endosomal release of siRNA after cell

uptake. NPs loaded with Cy-5.5 labeled control siRNA were efficiently taken up by fibroblasts and induced a robust knockdown (<50%) at low siRNA concentrations (≤ 5 nM) in these cell lines as assessed by FACS and qPCR analysis, respectively. For the HCC model, B6 mice were intrasplenically injected with 500,000 HCC cells to develop macroscopic tumor lesions exclusively in their livers after 28 days. In vivo studies using NPs loaded with Cy5.5 labeled control siRNA were performed in healthy and HCC mice. After intravenous injection, NPs distributed preferentially to the liver (>80%), while biodistribution did not differ between healthy versus tumor mice. Ex vivo FACS analysis of digested livers confirmed a cellular uptake of NPs in CAF (FAP+) >macrophages (CD45+, F4/80+, CD11b+) >dendritic cells (CD45+, F4/80+, CD11c+). For in vivo anti-stromal therapy, tumor mice (n = 5) received three intravenous injections of NPs loaded with anti-MFAP-5 siRNA (corresponding to 0.5 or 1 mg/kg siRNA) in week four, while controls received equal concentrations of NPs loaded with non-targeting scrambled siRNA (scsiRNA).

Results: Liver weights of mice treated with anti-MFAP-5 siRNA were significantly ($*p < 0.05$) lower compared to mice treated with encapsulated scsiRNA, indicating less hepatic tumor burden. Efficient in vivo knockdown of MFAP-5 was confirmed on RNA and protein level by qPCR and FACS analysis, respectively, while controls had similar MFAP-5 levels like healthy mice. The treatment was well tolerated by the mice and serum parameters for liver- and nephrotoxicity were in the normal range. Histological analysis of liver sections revealed that markers of tumor vascularization (e.g. CD34, CD105) were downregulated by the siRNA treatment in the TME, suggesting that the knockdown of MFAP-5 may inhibit angiogenesis.

Conclusion: Liver targeting NPs loaded with siRNA induced a gene specific knockdown of CAF derived MFAP-5 and demonstrated a convincing antitumor effect by interference with angiogenesis in the TME of HCC.

OS-023-YI

Remodeling of myeloid cells during hepatocellular carcinoma driven by beta-catenin activation

Camille Joubel^{1,2}, Lucie Poupel¹, Julie Sanceau¹, Sabine Colnot¹, Angélique Gougelet¹. ¹INSERM UMRS 1138 Cordeliers Research Center, Team "Oncogenic functions of beta-catenin in the liver", Paris, France; ²Université Paris Cité, Doctoral School 561 HOB, Paris, France
Email: camille.joubel@inserm.fr

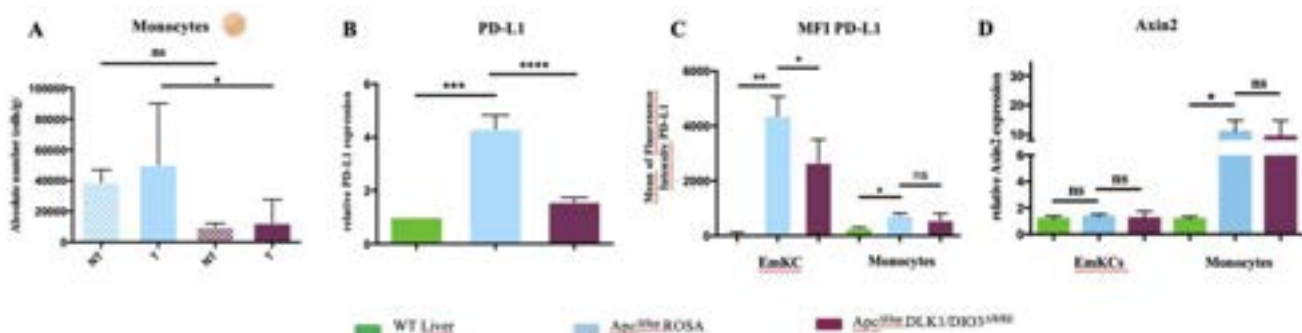
Background and aims: Hepatocellular Carcinoma (HCC) is the paradigm of inflammation-associated tumors and is one of the

deadliest cancers in the world. Recently, immunotherapies (IT) give promising results in almost 30% of HCC, while mutations in beta-catenin signaling detected in 30% of HCCs appear to be associated with resistance to IT. In the liver, coexist resident Kupffer cells (emKCs), able to self-renew, and inflammatory monocyte-derived macrophages (moKCs) recruited and differentiated from circulating monocytes upon liver injuries. Our work aims at exploring how an oncogenic beta-catenin signal in hepatocytes gives rise to a switch from protective emKCs to inflammatory moKCs permissive to HCC and how it affects response to IT.

Method: We have created relevant murine models, targeted *Apc* or *Ctnnb1*, that closely recapitulate human HCC features and enables kinetic studies from early pre-neoplastic states to advanced tumors (Loesch et al, JHep, 2022; Gougelet et al. Gastroenterology, 2019). Non-parenchymal cells (NPCs) are freshly isolated together with pre-neoplastic hepatocytes by liver perfusion or from murine tumors. They are either analyzed by flow cytometry or cultured, alone or with hepatocytes, for further analyses. In parallel, cell supernatants were collected to study exosome content after their purification by ultracentrifugation.

Results: Tumorigenesis driven by beta-catenin is associated with a strong infiltration of monocytes and a gradual replacement of emKCs by moKCs in both tumors and adjacent non-tumor tissues. We showed that beta-catenin activation in pre-neoplastic hepatocytes leads to an activation of this pathway at distance in emKCs and monocytes. More strikingly, the expression of the immune checkpoint inhibitor PD-L1 on both cells is induced in both preneoplastic livers and tumors. We additionally highlighted that non-coding RNAs (ncRNAs) produced from the *DLK1/Dio3* locus, a positive target of the beta-catenin that we recently found to be involved in liver tumorigenesis, are encapsulated into exosomes and oversecreted by preneoplastic hepatocytes and NPCs activated for the beta-catenin pathway. The impairment of the *DLK1/Dio3* locus by CRISPR/Cas9 significantly impaired the proportions of monocytes in tumors and non-tumors tissues as well as PD-L1 expression.

Conclusion: During early steps of liver tumorigenesis, pre-neoplastic hepatocytes with beta-catenin overactivation educate surrounding myeloid cells through their subsequent activation for beta-catenin signaling and the downstream induction of ncRNAs produced from the *DLK1/Dio3* locus in favor of HCC progression. These ncRNAs seems to participate to myeloid cell education, in part through exosomal transfer communication and PD-L1 dysregulation. We are now exploring their potential implication in the resistance to IT of this group of HCC.



The impairment of the *DLK1/Dio3* locus (*DLK1/DIO3^{ΔWRE}*) in *Apc^{ΔHep}* livers limits the recruitment of monocytes in tumors and non-tumor tissues (A). It also decreases the induction of Cd274 (PD-L1), seen in RT-qPCR in *Apc^{ΔHep}* tumors (B). PD-L1 expression was mainly detected by cytometry on monocytes and emKCs (C). The activation of beta-catenin signaling in *Apc^{ΔHep}* hepatocytes induces Axin2 expression in monocytes (D).

Figure: (abstract: OS-023-YI): Beta-catenin overactivated hepatocytes reprogram myeloid cells during HCC progression.

OS-024-YI

Scavenger receptor MARCO is associated with an immunosuppressive microenvironment and tumor progression in intrahepatic cholangiocarcinoma

Aloña Agirre Lizaso¹, Maider Huici Izaguirre¹, Colm O'Rourke², Ekaterina Zhuravleva², Ana Korosec^{3,4}, Mikel Azkargorta^{5,6}, Felix Elortza^{5,6}, Sumera I. Ilyas⁷, Gregory Gores⁷, Jesper Andersen², Gernot Schabba^{3,4}, Luis Bujanda^{1,5}, Pedro Miguel Rodríguez^{1,5,8}, Omar Sharif^{3,4}, Jesus Maria Banales^{1,5,8,9}, María Jesús Perugorria^{1,5,10}.

¹Department of Liver and Gastrointestinal Diseases, Biodonostia Health Research Institute-Donostia University Hospital - University of the Basque Country (UPV/EHU), San Sebastian, Spain; ²Biotech Research and Innovation Centre (BRIC), Department of Health and Medical Sciences, University of Copenhagen, Copenhagen, Denmark; ³Institute for Vascular Biology, Centre for Physiology and Pharmacology, Medical University Vienna, Vienna, Austria; ⁴Christian Doppler Laboratory for Arginine Metabolism in Rheumatoid Arthritis and Multiple Sclerosis, Vienna, Austria; ⁵CIBERehd, Instituto de Salud Carlos III (ISCIII), Madrid, Spain; ⁶Proteomics Platform, CIC bioGUNE, ProteoRed-ISCIII, Bizkaia Science and Technology Park, Derio, Spain; ⁷Division of Gastroenterology and Hepatology, Mayo Clinic, Rochester, United States; ⁸IKERBASQUE, Basque Foundation for Science, Bilbao, Spain; ⁹Department of Biochemistry and Genetics, School of Sciences, University of Navarra, Pamplona, Spain; ¹⁰Department of Medicine, Faculty of Medicine and Nursing, University of the Basque Country (UPV/EHU), Leioa, Spain
Email: matxus.perugorria@biodonostia.org

Background and aims: Cholangiocarcinoma (CCA) comprises a heterogeneous group of malignant tumours with dismal prognosis. During the last years, different studies have highlighted the key role of the immune system in the development of intrahepatic CCA (iCCA) and several combinational therapies targeting the tumour micro-environment (TME) have shown promising results for anti-cancer therapy. In this regard, the macrophage receptor with collagenous structure (MARCO) is a class A scavenger receptor found on particular subsets of macrophages that has been described to play a determining role in macrophage polarization and consequently in adaptive immune responses in many solid tumours. However, its role in iCCA is still unknown. This study aims to unravel the role of MARCO in iCCA development and progression.

Method: The cell-type specific MARCO expression was examined in iCCA human tumours by using publicly available single-cell RNA sequencing data from different studies and MARCO-expressing tumour-associated macrophages (TAMs) were phenotypically characterized. MARCO mRNA expression was analyzed in human control and iCCA liver tissue samples and associated to different immune cell types and immune-functionality scores employing state-of-the-art technologies as ConsensusTME, Tumour Immune Dysfunction and Exclusion (TIDE) tool and Tumour Immunophenotype Profiling (TIP). To study the role of MARCO in murine cholangiocarcinogenesis, wild type (WT) and *Marco*^{-/-} mice were subjected to 3 different iCCA murine models and flow cytometry analysis of the TME was carried out to characterize different lymphocytic and myeloid populations.

Results: Single-cell RNA sequencing data indicate that MARCO is expressed in a specific subtype of TAMs in patients with iCCA. Besides, high MARCO expression levels in the liver samples of patients with iCCA are linked with worse clinical outcome. In line with this, MARCO expression in human iCCA tumours is associated to cell types involved in tumour progression such as M2 macrophages, and related with T cell dysfunction. Regarding the potential role of MARCO in murine models of iCCA, *Marco*^{-/-} mice show a trend to be protected from iCCA development, the mechanisms behind this effect being likely associated to a reduction of the innate immune cells such as CD9⁺Ly6C⁺F4/80⁺ resident macrophages and type-2 innate lymphoid cells (ILC2). Noteworthy, in a context of a syngeneic orthotopic experimental model, *Marco*^{-/-} mice exhibit a reduced presence of immune checkpoint molecules in innate and adaptive immune cells, including a lower percentage of PD-L1⁺Ly6C⁺F4/80⁺ resident

macrophages and, PD-1⁺ and CTLA-4⁺ cytotoxic CD8⁺ T cells in comparison to WT mice. In addition, MARCO deficiency significantly improves the overall survival of mice subjected to the orthotopic injection of syngeneic CCA cells into the liver. This was associated with a reduction of the tumour metastasis in the lungs.

Conclusion: High MARCO expression is associated to a worse outcome in patients with iCCA and is associated to an immunosuppressive TME. Importantly, *Marco*^{-/-} mice display a reduced presence of immunosuppressive cell populations and present an increased overall survival. Therefore, MARCO arises as a novel therapeutic target for iCCA.

NAFLD: Diagnostics and non-invasive assessment

OS-025

A clinical care pathway to detect advanced liver disease in patients with type 2 diabetes through automated fibrosis score calculation and electronic reminder messages: a randomised controlled trial

Xinrong Zhang¹, Terry Cheuk-Fung Yip¹, Grace Lai-Hung Wong¹, Wei-Xuan Leow², Yan Liang¹, Lee-Ling Lim³, Guanlin Li¹, Luqman Ibrahim³, Huapeng Lin¹, Che To Lai¹, Henry LY Chan¹, Alice Pik-Shan Kong¹, Wah-Kheong Chan², Vincent Wai-Sun Wong¹.
¹The Chinese University of Hong Kong, Department of Medicine and Therapeutics, Hong Kong; ²University of Malaya, Gastroenterology and Hepatology Unit, Malaysia; ³University of Malaya, Endocrinology Unit, Malaysia
Email: wongv@cuhk.edu.hk

Background and aims: The majority of patients with non-alcoholic fatty liver disease (NAFLD) are seen at primary care and non-hepatology settings. Although several studies have demonstrated the successful implementation of clinical care pathways with the involvement of highly motivated clinicians, the findings may not be generalised. We aimed to test the hypothesis that automated fibrosis score calculation and electronic reminder messages could increase the detection of advanced liver disease in patients with type 2 diabetes.

Method: In this pragmatic, single-blind, randomised controlled trial at 5 general medical or diabetes clinics in Hong Kong and Malaysia, we randomly assigned patients in a 1:1 ratio to the intervention group with Fibrosis-4 index and aspartate aminotransferase-to-platelet ratio index automatically calculated based on routine blood tests followed by electronic reminder messages to alert clinicians of abnormal results, or the control group with usual care. The primary outcome was the proportion of patients with increased fibrosis scores who received appropriate care (referred for hepatology care or specific fibrosis assessment) within 1 year. This trial is registered with ClinicalTrials.gov, number NCT04241575.

Results: Between May 19, 2020, and Oct 14, 2021, 1379 patients were screened, of whom 533 and 528 were assigned to the intervention and control groups, respectively. A total of 55 out of 165 (33.3%) patients with increased fibrosis scores in the intervention group received appropriate care, compared with 4 of 131 (3.1%) patients in the control group ($p < 0.001$) (Table). Overall, 11 of 533 (2.1%) patients in the intervention group and 1 of 528 (0.2%) patients in the control group were confirmed to have advanced liver disease (liver stiffness ≥ 10 kPa and/or cirrhotic complications) ($p = 0.006$). Among patients attending hepatology care, 33 had NAFLD, and 22 had no liver disease identified.

	Intervention group	Control group	p value
Primary outcome			
Proportion of patients with high fibrosis scores who were referred for hepatology care or further fibrosis assessment	55/145 (33.3)	4/131 (3.1)	<0.001
Secondary outcomes			
Proportion of patients in the entire cohort who were referred for hepatology care or further fibrosis assessment	57/533 (10.7)	6/526 (1.1)	<0.001
Proportion of patients with low fibrosis scores who were referred for hepatology care	1/368 (0.3)	2/397 (0.5)	>0.999
Proportion of patients confirmed to have advanced liver disease*	11/533 (2.1)	1/526 (0.2)	0.006

Figure:

Conclusion: Automated fibrosis score calculation and electronic reminders can increase identification of advanced liver disease in patients with type 2 diabetes at non-hepatology settings. However, over half of patients with increased fibrosis scores did not receive appropriate care, and a minority of referred patients actually had advanced liver disease. The findings of this trial serve as the basis to further refine the clinical care pathway.

OS-026

Performance of the AGA clinical care pathway in identifying patients with at-risk non-alcoholic steatohepatitis: combined data from multiple therapeutic clinical trials including more than 5,000 patients (in collaboration with NAIL-NIT consortium)

Naim Alkhouri¹, Julie Dubourg², Stephen Harrison³, Michael Charlton⁴, Vlad Ratziu⁵, Jörn Schattenberg⁶, Sophie Jeannin Megnier², Mazen Nouredin⁷. ¹Arizona Liver Health, Chandler, United States; ²Summit Clinical Research, San Antonio, United States; ³University of Oxford, United Kingdom; ⁴UChicago Medicine, Chicago, United States; ⁵Institute for Cardiometabolism and Nutrition, France; ⁶University medicine at the Johannes Gutenberg University in Mainz, Mainz, Germany; ⁷Houston Methodist Hospital, Houston, United States
Email: jdubourg@summitclinicalresearch.com

Background and aims: The American Gastroenterological Association (AGA) has released guidelines in 2021 to identify non-alcoholic steatohepatitis (NASH) patients with at least stage 2 fibrosis (at-risk NASH) that will benefit from referral to hepatology and potential use of pharmacologic agents. We aimed to assess the utility of the recommended score-based parts of these algorithms (FIB-4 and Vibration Controlled Transient Elastography (VCTE)) in the setting of non-cirrhotic NASH clinical trials in the United States.

Method: We combined screening data from 6 ongoing non-cirrhotic NASH phase 2 trials (>5,000 patients). We assessed the proportion of NASH patients with at least stage 2 fibrosis for each risk-category based on FIB-4 and liver stiffness measurement (LSM) by VCTE. We also assessed the proportion of at-risk NASH with a non-alcoholic fatty liver disease activity score (NAS) of at least 4 and excluding fibrosis 4.

Results: 2,119 patients with histology results were included for final analysis, with 2,119 (100%) of those having FIB-4 data and with 1,105 (52%) of those having LSM data. The table shows the proportion of patients in each risk-category meeting AGA target population as well as the classic non-cirrhotic NASH trial population. 1,254 patients with FIB-4 <1.3 would not have been referred to hepatology clinic but 430 (30%) of those had at-risk NASH on liver biopsy (missed cases). 388 patients with FIB-4 >1.3 had LSM on VCTE of <8 kPa but 16 (76%) of those had at-risk NASH on biopsy. In patients with FIB-4 >2.67, 65% had at-risk NASH on biopsy and in those with LSM of 8–12 kPa and >12 kPa, 67% and 65% had at risk NASH, respectively.

AGA Guidelines			Clinical trial Target
AGA Guidelines Criteria		N of patients with data	N of NASH patients with at least fibrosis stage 2
Low risk Group FIB-4 <1.3		1,254	430 (34%)
Intermediate Risk Group FIB-4 > 1.3 to 2.67	LSM <8 kPa	21	16 (76%)
	LSM 8 to 12 kPa	212	142 (67%)
	LSM >12 kPa	255	201 (79%)
High risk group FIB-4 ≥ 2.67		80	63 (79%)
			380 (30%)

Figure:

Conclusion: Using the AGA clinical care pathway in the setting of clinical trial may lead to missing patients with biopsy-proven at-risk NASH. In patients considered high-risk based on the pathway, two thirds have at-risk NASH and will potentially benefit from clinical trial and future pharmacologic treatments.

OS-027

Performance of vibration controlled transient elastography and related scores to identify at-risk non-alcoholic steatohepatitis patients: combined data from multiple trials including more than 5,000 patients (in collaboration with NAIL-NIT consortium)

Mazen Nouredin¹, Julie Dubourg², Stephen Harrison³, Sophie Jeannin Megnier², Vlad Ratziu⁴, Michael Charlton⁵, Naim Alkhouri⁶, Jörn Schattenberg⁷. ¹Houston Methodist Hospital, Houston, United States; ²Summit Clinical Research, San Antonio, United States; ³University of Oxford, United Kingdom; ⁴Institute for Cardiometabolism and Nutrition, France; ⁵UChicago Medicine, Chicago, United States; ⁶Arizona Liver Health, Chandler, United States; ⁷University medicine at the Johannes Gutenberg University in Mainz, Mainz, Germany
Email: jdubourg@summitclinicalresearch.com

Background and aims: Non-alcoholic steatohepatitis (NASH) with Fibrosis (F) F2-F3 patients is the target population for phase 2b/3 NASH clinical trials. High screening failure (SF) rate on biopsy has slowed down enrollment and drug development. Subsequently non-invasive tests (NITs) have been developed to reduce SF rate on biopsy. We aim to assess composite scores related to vibration-controlled transient elastography (VCTE), namely FAST and Agile 3+ and compare them to traditional VCTE cut offs to identify NASH patients with F2 and F3 in clinical trial settings.

Method: We combined screening data from 6 ongoing biopsy-proven therapeutic NASH trials (>5,000 patients). Liver histology data were read centrally. We assessed the diagnostic accuracy of FAST and liver stiffness measurements (LSM) on VCTE, using published cut-offs (0.5 for FAST and 8.2 kPa for LSM) to identify NASH patients with F2-F3. We also assessed the diagnostic accuracy of Agile 3+ and LSM on VCTE, using published cut-offs (0.6 for Agile 3+ and 9.7 kPa for LSM) to identify NASH patients with F3. Patients with F4 were excluded. We calculated the following diagnostic performance indices: sensitivity (Se), specificity (Sp), negative predictive value (NPV), positive predictive value (PPV), positive likelihood ratio (LR+), negative likelihood ratio (LR-) and the correct classification (CC).

Results: 1,048 patients with liver histology and NIT data were included, with a fibrosis prevalence of: 92 (9%) for F0, 231 (22%) for F1, 290 (28%) for F2, and 435 (42%) for F3. The average age was 54.7 years, 644 (61%) were females and 439 (42%) were Hispanics. The Se, Sp, NPV, PPV and CC are shown in the table. Overall, FAST had better Sp, NPV, PPV, LR+ and CC than the traditional LSM value of 8.2 kPa for patients with NASH F2-F3. Agile 3+ had better Sp, PPV, LR+, LR- and CC than the traditional LSM value of 9.7 kPa for patients with NASH F3.

NASH F2-F3								
NIT	Published Cut-offs	Se	Sp	NPV	PPV	Correct Classification	LR+	LR-
FAST	0.5	76.7	51.7	58.2	71.7	0.67	1.59	0.45
LSM	8.2	94.4	8.4	48.6	62.2	0.61	1.03	0.66
NASH F3								
Agile 3+	0.6	67.6	62.0	76.2	51.6	0.64	1.78	0.52
LSM	9.7	82.9	35.7	77.7	43.5	0.53	1.29	0.48

Figure:

Conclusion: In a pooled data analysis from a large cohort of NASH patients enrolled in Phase 2 clinical trials we showed that FAST and Agile 3+ are better screening tests than liver stiffness alone for patients with NASH F2-F3 and, NASH F3, respectively. We recommend using these scores as screening criteria in phase 2b/3 NASH trials.

OS-028

Prediction of outcomes in patients with non-alcoholic fatty liver disease by initial measurements and subsequent changes in magnetic resonance elastography

Takashi Kobayashi¹, Michihiro Iwaki¹, Asako Nogami¹, Masato Yoneda¹, Satoru Saito¹, Atsushi Nakajima¹. ¹Yokohama city university graduate school of medicine, Department of gastroenterology and hepatology, Japan
Email: yoneda@yokohama-cu.ac.jp

Background and aims: Liver fibrosis is strongly correlated with prognosis in non-alcoholic fatty liver disease (NAFLD). We investigated whether liver stiffness measured (LSM) by magnetic resonance elastography (MRE) and its changes can predict clinical outcomes in patients with NAFLD.

Method: A retrospective analysis of 405 NAFLD patients who had undergone at least two magnetic resonance elastography (MRE) was conducted. The patients were divided into five groups corresponding to fibrosis stages 0–4 based on their initial LSM. Additionally, based on the difference between two LSMs (Δ LSM), the patients were classified as progressors (Δ LSM $\geq +19\%$) and non-progressors (Δ LSM $< +19\%$). Cumulative outcomes were calculated using Kaplan-Meier analysis and compared by log-rank test.

Results: The mean duration from the initial MRE to the end of follow-up was 72.64 ± 25.80 months. In the interval between serial MREs (mean: 23.51 ± 0.47 months), 52 (12.8%) were progressors and 353 (87.2%) were non-progressors. According to the groups based on initial LSM, there were significant differences in the cumulative incidence of decompensated cirrhosis ($p < 0.001$), hepatocellular carcinoma (HCC) ($p < 0.001$), liver-related events ($p < 0.001$), extrahepatic malignancies ($p = 0.049$) and overall mortality ($p < 0.001$), but no significant differences in cardiovascular disease ($p = 0.203$). Hazard ratios (HRs) for progressors to non-progressors were

significantly higher for decompensated cirrhosis (HR = 12.08, $p = 0.009$), HCC (HR = 25.02, $p = 0.008$), and liver-related events (HR = 12.79, $p = 0.012$), but not for extrahepatic malignancies (HR = 2.66, $p = 0.179$), cardiovascular disease (HR = 5.396, $p = 0.317$), or overall mortality (HR = 1.207, $p = 0.821$) (Figure A–F). Among patients with no clinical evidence of cirrhosis ($n = 385$), the HR of cirrhosis development for progressors versus non-progressors was 60.15 ($p < 0.001$), which was significant. Even within the subgroup with low initial LSM ($n = 296$), corresponding to fibrosis stages 0–2, which has been considered a good prognosis, the HR for progressors versus non-progressors was significantly high for liver-related events (HR = 77.45, $p = 0.009$) and overall clinical events (HR = 10.32, $p = 0.012$).

Conclusion: In addition to initial LSM, Δ LSM can predict liver-related events in patients with NAFLD, even for low initial LSM. Their integrated evaluation can provide more detailed risk stratification and sort out high-risk patients with NAFLD from those previously considered low-risk.

OS-029

Analytical and clinical validation of AIM-NASH: a digital pathology tool for artificial intelligence-based measurement of non-alcoholic steatohepatitis histology

Stephen Harrison¹, Hanna Pulaski², Marlena Vitali², Laryssa Manigat², Stephanie Kaufman², Hypatia Hou², Susan Madasu², Sara Hoffman², Adam Stanford-Moore², Robert Egger², Janani Iyer², Jonathan Glickman², Murray Resnick², Neel Patel², Cristin Taylor², Shraddha Mehta², Robert Myers³, Chuhan Chung⁴, Scott Patterson⁵, Anne-Sophie Seifling⁶, Anne Minnich⁷, Vipul Baxi⁷, Mani Subramanian³, Arun Sanyal⁸, Quentin Anstee⁹, Rohit Loomba¹⁰, Vlad Ratzu¹¹, Katy Wack². ¹Pinnacle Clinical Research, United States; ²PathAI, United States; ³OrsoBio, Inc, United States; ⁴Imiphar, Inc, United States; ⁵Gilead Sciences, Inc., United States; ⁶Novo Nordisk, Denmark; ⁷Bristol Myers Squibb, United States; ⁸Virginia Commonwealth University, United States; ⁹Newcastle University, United Kingdom; ¹⁰UCSD School of Medicine, United States; ¹¹Sorbonne Université, France

Email: stephenharrison87@gmail.com

Background and aims: The gold standard for participant enrollment and end point assessment in NASH clinical trials is manual histologic

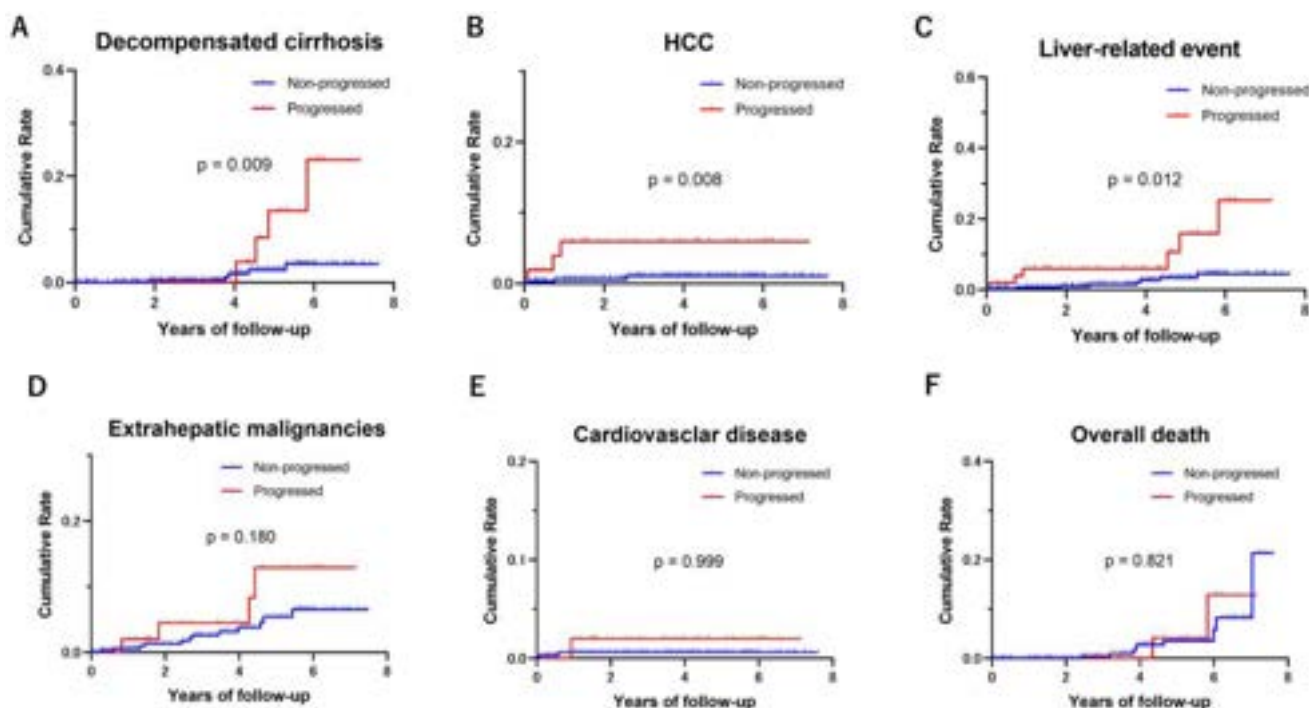


Figure: (abstract: OS-028).

assessment of a liver biopsy. The NASH CRN scoring system has suboptimal reproducibility, even amongst expert hepatopathologists (HPs). High variability limits assessment of change over time and therapeutic response. Here, we describe the validation of AIM-NASH (AI-based Measurement of NASH Histology) (PathAI, v1.1.0), an AI-powered, assistive digital pathology tool that detects and scores the key histologic features of NASH (steatosis (ST), lobular inflammation (LI), hepatocellular ballooning (HB), and fibrosis). Analytical Validation (AV), Overlay Validation (OV) and Clinical Validation (CV) studies were conducted to determine the accuracy and precision of AIM-NASH as an aid to HPs in NASH scoring.

Method: Ground Truth: (GT) NASH CRN scores for AV/CV were determined via consensus by a panel of 3 experts. AV: The AIM-NASH algorithm alone was evaluated for non-inferior accuracy to HPs manual reads (MRs) (Figure 1). Algorithm repeatability (at one site) and reproducibility (at 3 sites) with Leica AT2 scanners was evaluated against a target agreement of >85%. OV: Assessed the accuracy of AI-

derived heatmap overlays, per visual feature, with target true positive and false positive success (TPS/FPS) rates of ≥85%. CV: HPs' AI-assisted performance was assessed for non-inferior accuracy to MRs within a NASH clinical trial workflow, totaling 1501 anonymized biopsies from 3 trials.

Results: AV: [Accuracy] AIM-NASH was superior to MRs for HB (weighted kappa (κ_w) difference 0.17; $p < 0.0001$) and non-inferior (margin of 0.1) for ST, LI, and fibrosis (κ_w) differences 0.05, 0.01, and 0.02; all $p < 0.02$. [Repeatability] Mean intra-scanner overall percent agreement (OPA) rates for ST, LI, HB, and fibrosis were 0.93, 0.96, 0.96, and 0.93 (all $p < 0.0001$). [Reproducibility]: Mean inter-site OPAs between scans for ST, LI, HB, and fibrosis were 0.86, 0.85, 0.91, and 0.87 ($p = 0.002-0.53$). OV: All overlays met TPS/FPS criteria of ≥85%. CV: AI-assisted reads were superior to MRs for LI and HB (κ_w improvements 0.12 and 0.15; both $p < 0.0001$) and non-inferior for ST and fibrosis (κ_w differences 0.003 and -0.009). The AI-assist workflow also showed superior accuracy over MRs when evaluating for NASH

Table 1: Agreement of AIM-NASH-assisted reads and GT versus MR and GT in CV with literature comparison

Clinical Validation feature	n	Weighted kappa, (95% CI)	Difference, (95% CI)	P-value for non-inferiority	P-value for superiority	Average manual Inter-reader Weighted Kappa from literature ¹
Steatosis: AI-assist	1467	0.677, (0.652, 0.703)	0.003, (-0.028, 0.037)	<0.001	0.3365	0.609
Steatosis: MR	1481	0.674, (0.651, 0.695)				
LI: AI-assist	1465	0.419, (0.361, 0.46)	0.123, (0.069, 0.173)	<0.0001	<0.0001	0.328
LI: MR	1478	0.297, (0.264, 0.328)				
HB: AI-assist	1465	0.563, (0.519, 0.601)	0.150, (0.108, 0.195)	<0.0001	<0.0001	0.517
HB: MR	1476	0.414, (0.385, 0.441)				
Fibrosis: AI-assist	1429	0.653, (0.627, 0.676)	-0.009, (-0.042, 0.022)	<0.0001	0.7445	0.484
Fibrosis: MR	1453	0.663, (0.642, 0.683)				
NASH Assessment*: AI-assist	1463	0.632 (0.593, 0.67)	0.12 (0.064, 0.166)			0.399***
NASH Assessment*: MR	1474	0.512 (0.477, 0.547)				
NASH Resolution: AI-assist	1463	0.532 (0.47, 0.542)	0.162 (0.093, 0.205)			Not reported
NASH Resolution: MR	1474	0.370 (0.324, 0.413)				

Reference: 1. Davison BA, Harrison SA, Cotter G, Alkhouri N, Sanyal A, Edwards C, et al. Suboptimal reliability of liver biopsy evaluation has implications for randomized clinical trials. *J Hepatol.* 2020;73(6).

*NASH Assessment defined as NAS ≥4 and each H&E component ≥1

**NASH Resolution defined as ballooning=0, inflammation of 0 or 1, and any steatosis

***Unweighted kappa, all others reported are weighted.

Table: (abstract: OS-029).

resolution (HB=0, LI=0, 1) with a κ_w difference 0.16 ($p < 0.01$) (Table 1).

Conclusion: AIM-NASH is highly repeatable and reproducible, with accuracy ranging from comparable to superior relative to HPs. AIM-NASH-assisted HPs are superior to unaided HPs in assessing NASH resolution, HB, and LI. These results are notable given high HP disagreement in HB and LI evaluation. The data suggest AIM-NASH may reduce the impact of rater variability on NASH clinical trial end points and subsequently allow for a more consistent and reliable assessment of therapeutics being developed in the field.

Viral hepatitis B/D - New treatments

OS-030

Treatment with siRNA JNJ-73763989 plus nucleos (t)ide analogue (NA) decreases HBsAg and HDV RNA levels in patients with chronic hepatitis D (CHD): part 1 of the REEF-D study

Heiner Wedemeyer¹, Edward J. Gane², Kosh Agarwal³, Fehmi Tabak⁴, Xavier Forns⁵, Ulus Akarca⁶, Morozov Viacheslav⁷, Soo Aleman⁸, Maria Buti⁹, ŞGurdal Yilmaz¹⁰, Pietro Lampertico^{11,12}, Julia Niewczas¹³, John Jerzowski¹⁴, Thomas Kakuda¹⁵, Isabelle Benoot¹⁶, Nonko Pehlivanov¹⁷, Oliver Lenz¹⁶, Michael Biermer¹⁶. ¹Dept. of Gastroenterology, Hepatology and Endocrinology, Hannover Medical School, Hannover, Germany; ²New Zealand Liver Transplant Unit, University of Auckland, Auckland, New Zealand; ³Institute of Liver Studies, King's College Hospital, London, United Kingdom; ⁴Istanbul University, Istanbul, Turkey; ⁵Liver Unit, Hospital Clinic Barcelona, IDIBAPS, University of Barcelona, Barcelona, Spain; ⁶Division of Gastroenterology, Department of Internal Medicine, University of Ege School of Medicine, Izmir, Turkey; ⁷Medical Company Hepatolog, Samara, Russian Federation; ⁸Department of Infectious Diseases, Karolinska University Hospital/Karolinska Institutet, Stockholm, Sweden; ⁹Hospital General Universitari Val de Hebron and CIBER-EHD del Instituto Carlos III, Barcelona, Spain; ¹⁰Trabzon Karadeniz Technical University Farabi Hospital, Trabzon, Turkey; ¹¹Foundation IRCCS Ca' Granda Ospedale Maggiore Policlinico, Division of Gastroenterology and Hepatology, Milan, Italy; ¹²CRC "A. M. and A. Migliavacca" Center for Liver Disease, Department of Pathophysiology and Transplantation, University of Milan, Milan, Italy; ¹³Janssen-Cilag, Solna, Sweden; ¹⁴Janssen Research and Development, LLC, Titusville, United States; ¹⁵Janssen Research and Development, LLC, Brisbane, United States; ¹⁶Janssen Pharmaceutica NV, Beerse, Belgium; ¹⁷Janssen Research and Development, LLC, Raritan, United States
Email: wedemeyer.heiner@mh-hannover.de

Background and aims: Hepatitis D virus (HDV) requires hepatitis B surface antigen (HBsAg) to form infectious viral particles. The siRNA JNJ-73763989 (JNJ-3989) has been shown to profoundly reduce HBsAg in chronic hepatitis B patients. In the REEF-D study, the antiviral effect of JNJ-3989 was evaluated for the first time in patients with CHD to investigate whether reduction of HBsAg would lead to reduction of HDV replication, resulting in a therapeutic benefit of JNJ-3989 for patients with CHD.

Method: REEF-D, a 2-part, phase 2, multicenter, randomized, double-blind, placebo-controlled study, included adults with CHD, including compensated cirrhosis. Patients were randomized 4:1 to receive JNJ-3989 (100 mg subcutaneously every 4 weeks) + NA for 144 weeks (active arm) or placebo + NA for 52 weeks followed by JNJ-3989 + NA for 96 weeks (deferred treatment arm) with 48 weeks of off-treatment follow-up. Changes in serum viral markers (HBsAg and HDV RNA) and safety (alanine aminotransferase [ALT] levels) were assessed. The primary composite end point was the proportion of patients with HDV RNA decline from baseline of $\geq 2 \log_{10}$ IU/ml (or undetectable) and normal ALT at Week 48. Antiviral activity in Part 1

was used to expand the study (Part 2). Data from Part 1, Week 48 interim analysis are reported here.

Results: Of 22 patients enrolled in REEF-D Part 1, 17 and 5 were randomized to the active and deferred treatment arms, respectively. Treatment with JNJ-3989 led to robust reductions in HBsAg, and subsequently, HDV RNA. Twelve of 17 (70.6%) patients in the active arm had treatment-emergent ALT elevations ($\geq 3 \times$ upper limit of normal [ULN] and $\geq 2 \times$ nadir) between Weeks 8 and 20, which were associated with HDV RNA rebound, limited transient HBV DNA increase in most patients, but no clear impact on HBsAg decline, and resulted in early treatment discontinuation in 8 patients. Grade 3/4 ALT elevations were observed, with no cases of decompensation. In general, ALT levels returned to baseline values after treatment discontinuation in those patients. Among the 9 JNJ-3989-treated patients still on-treatment at Week 48, mean (standard error [SE]) HBsAg change from baseline was -1.75 (0.29) \log_{10} IU/ml in the active arm vs -0.07 (0.04) \log_{10} IU/ml for the 5 patients in the deferred treatment arm. Mean (SE) change from baseline in HDV RNA was -1.52 (0.38) \log_{10} IU/ml and -0.23 (0.15) \log_{10} IU/ml in the active and deferred treatment arms, respectively. Four of 17 (23.5%) patients in the active arm achieved the primary composite end point vs none from the deferred treatment arm. Among the 5 patients without ALT elevations, 4 (80.0%) achieved the primary composite end point, 2 (40.0%) of whom had HDV RNA <lower limit of quantification of the assay. Aside from ALT elevations, safety outcomes were unremarkable. Predefined antiviral criteria to initiate Part 2 of the study were met and the observation of ALT flares predominantly in patients with high HBsAg and HDV RNA levels at baseline led to exclusion of patients with cirrhosis or HBsAg $>10,000$ IU/ml and HDV RNA $>100,000$ IU/ml.

Conclusion: This is the first proof-of-concept study showing that an HBsAg-targeting agent leads to simultaneous reduction of HBsAg and HDV RNA in patients with CHD. Clinically relevant ALT elevations were frequent and associated with increases in HDV RNA and led to treatment discontinuation. However, patients without ALT elevations generally had a continuous reduction of HDV RNA, 4/5 of whom met the primary efficacy end point.

OS-031

Safety and antiviral activity of short-duration combinations of the investigational small interfering ribonucleic acid VIR-2218 with the neutralizing, vaccinal monoclonal antibody VIR-3434: post-treatment follow-up from the Phase 2 MARCH trial

Edward J. Gane¹, Alina Jucov^{2,3}, Marta Dobryanska^{4,5}, Ki Tae Yoon⁶, Tien Huey Lim⁷, Andre Arizpe⁸, Daniel Cloutier⁸, Michael Chattergoon⁸, Shenghua Mao⁸, Sneha V. Gupta⁸, Gregory Camus⁸, Carey Hwang⁸, Young-Suk Lim⁹. ¹Faculty of Medicine, University of Auckland, Auckland, New Zealand; ²Arensia Exploratory Medicine GmbH, Düsseldorf, Germany; ³Nicolae Testemițanu State University of Medicine and Pharmacy, Chișinău, Moldova; ⁴Medical Center of Limited Liability Company "Harmoniia krasny," Kyiv, Ukraine; ⁵Arensia Exploratory Medicine, Kyiv, Ukraine; ⁶Pusan National University Yangsan Hospital, Pusan National University College of Medicine, Yangsan, Korea, Rep. of South; ⁷Department of Gastroenterology, Middlemore Hospital, Auckland, New Zealand; ⁸Vir Biotechnology, Inc., San Francisco, United States; ⁹Asan Medical Center, University of Ulsan College of Medicine, Seoul, Korea, Rep. of South
Email: edgane@adhb.govt.nz

Background and aims: There is an unmet need for a finite, curative, and well-tolerated treatment regimen for chronic hepatitis B virus (HBV) infection. VIR-2218 is an investigational small interfering ribonucleic acid (siRNA) targeting the HBx region of HBV genome, and VIR-3434 is an investigational fragment crystallizable (Fc)-engineered human monoclonal antibody targeting the conserved antigenic loop of HBsAg. This phase 2 open-label trial (MARCH) evaluated the safety, tolerability, and antiviral activity of short-duration combination regimens of VIR-2218 and VIR-3434 for the

treatment of chronic HBV infection. Here, we report data through 24-week post-treatment follow-up from the first cohorts of the MARCH study.

Method: This open-label study included adults with chronic HBV infection who received continuous nucleos(t)ide reverse transcriptase inhibitor therapy for ≥ 2 months. Cohorts 2 and 3 were restricted to participants with HBsAg $< 3,000$ IU/ml at screening. Participants in Cohort 1 received VIR-2218 200 mg on day 1 and on weeks 4, 8, 12, 16, and 20, plus 5 weekly (QW) doses of VIR-3434 75 mg between weeks 16 and 20. Participants in Cohorts 2 and 3 received 3 doses of VIR-2218 200 mg on day 1 and weeks 4 and 8, plus 12 QW doses of VIR-3434 18 mg (Cohort 2) or 75 mg (Cohort 3) from day 1 through week 11. The primary end points were the proportion of participants with treatment-emergent adverse events (TEAEs), serious adverse events (SAEs), and HBsAg loss at EOT and at 24 weeks post-EOT.

Results: A total of 40 participants were enrolled across Cohorts 1 ($n = 17$), 2 ($n = 4$), and 3 ($n = 19$). Mean HBsAg change from baseline over time by cohort is presented in the Figure. HBsAg gradually rebounded after EOT but remained $> 1 \log_{10}$ IU/ml below baseline on average in all cohorts at time of last available follow-up (24 weeks post-EOT for Cohort 1 and 28 weeks post-EOT for Cohorts 2 and 3). No participants achieved HBsAg loss or functional cure. TEAEs were observed in 50% (20/40) of participants overall. All TEAEs were mild or moderate except for one Grade 3 TEAE of creatine kinase elevation observed in Cohort 3. No TEAEs led to treatment discontinuation.

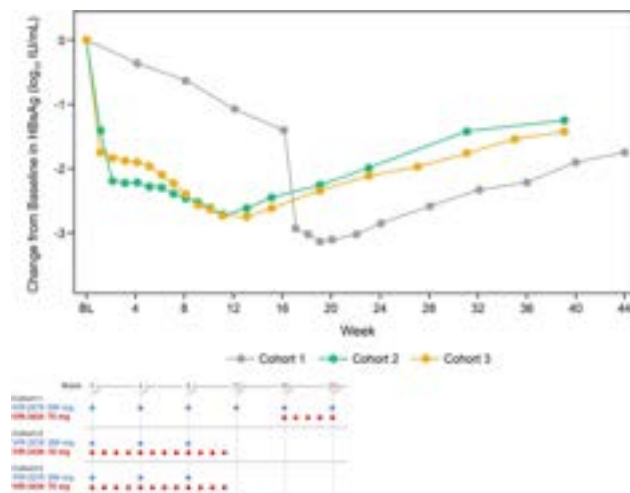


Figure: Mean HBsAg Change from Baseline by Cohort (\log_{10} IU/ml)

Conclusion: By 24 weeks post-EOT, HBsAg levels rebounded in all treatment groups but remained $> 1 \log_{10}$ IU/ml below baseline on average. Combination therapy with VIR-2218 and VIR-3434 was generally well tolerated with no safety signals observed to date. Regimens evaluating 24 or 48 weeks of VIR-2218 and VIR-3434, with and without PEG-IFN α , are ongoing.

OS-032

A PKA-associated liver-tissue rheostat curbs T cell receptor signalling and effector function of virus-specific CD8 T cells in chronic viral hepatitis

Miriam Bosch¹, Nina Kallin¹, Donakonda Sainitin¹, Hannah Wintersteller¹, Anna Fürst¹, Jitao David Zhang², Carlos Ramirez³, Carl Herrmann³, Maïke Hofmann⁴, Robert Thimme⁴, Ulrike Protzer⁵, Jan Boettcher¹, Dirk Wohlheuer¹, Souphalone Luangsang², Percy A. Knolle¹. ¹Institute of Molecular Immunology, School of Medicine, Technical University of Munich (TUM), Munich, Germany; ²Roche Pharmaceutical Research and Early Development, Switzerland; ³Health Data Science Unit, Medical Faculty Heidelberg and BioQuant, Germany; ⁴Klinik für Innere Medizin II,

University Hospital Freiburg, Germany; ⁵Institute of Virology, Technical University of Munich, Germany
Email: miriam.bosch@tum.de

Background and aims: Antigen-specific CD8 T cell immunity is crucial for clearance of viral liver infections such as Hepatitis B virus (HBV) infection. During persistent HBV infection, however, a functional CD8 T cell response is missing and to date cannot be induced by immune therapies. We aimed at determining the mechanisms determining the functional inhibition of CD8 T cells during persistent viral infection of the liver.

Method: We used a preclinical model system with adenoviral gene transfer of the HBV genome or ovalbumin to investigate virus-specific immunity during persistent or acute-resolving viral liver infection. Antigen-specific CD8 T cells from liver and spleen were analyzed by flow cytometry, RNAseq and tissue sections by confocal microscopy. HBV-specific CD8 T cells from patients with chronic HBV infection were compared to the results from preclinical models.

Results: Hepatic CXCR6⁺CD69⁺ virus-specific CD8 T cells during persistent viral liver infection had a liver-resident phenotype in transcriptome and flow cytometry analysis. However, T cells did not respond to cognate stimulation with cytokine production and cytotoxicity. Transcriptional network analysis of dysfunctional compared to cytotoxic CXCR6⁺CD8T cells revealed elevated cAMP signaling indicated by increased Crem (cAMP responsive element modulator) activity as single differentiating transcription factor in persistent infection. We did not observe a rescue of anti-viral T cell immunity in mice lacking the inhibitory Crem isoform ICER in T cells, and therefore searched for post-translational mechanisms influencing T cell immunity. Strikingly, PKA phosphorylation at S114 was elevated in dysfunctional CXCR6⁺CD8T cells confirming increased cAMP signaling. Pharmacologically induced cAMP signaling caused loss of functionality in previously highly cytotoxic CXCR6⁺CD8T cells isolated after resolved infection. Importantly, increased cAMP signaling curbed T cell receptor signaling shown by reduced phosphorylation of Lck, Akt and Erk rendering virus-specific CXCR6⁺CD8T cells unable to respond to cognate stimulation. Confocal microscopy revealed increased contact between prostanoid-producing liver sinusoidal endothelial cells (LSECs) and dysfunctional CXCR6⁺CD8T cells recognizing peptide presented on infected hepatocytes, and coculture with LSECs led to increased cAMP-signaling in T cells pointing at spatially regulated cAMP signaling in persistent viral infection.

Conclusion: We identify a liver-tissue rheostat enforced by LSECs increasing cAMP-signaling in virus-specific CXCR6⁺CD8T cells during persistent hepatotropic infection that renders T cells non-responsive to stimulation through TCR signaling. Our results further identify molecular markers for identification of T cells influenced by the liver tissue rheostat and allow to explore novel targeted immune therapies to reconstitute virus-specific immunity in chronic hepatitis B.

OS-033

Novel, high accuracy prediction models of hepatocellular carcinoma based on longitudinal data and cell-free DNA signatures

Rong Fan¹, Lei Chen², Hao Yang³, Siru Zhao¹, Zhengmao Li³, Yunsong Qian⁴, Hong Ma⁵, Jingfeng Liu⁶, Junqi Niu⁷, Chuanxin Wang⁸, Jian Bai³, Jianping Xie⁹, Xiaotang Fan¹⁰, Qing Xie¹¹, Chunying Wang¹², Song Yang¹³, Honglian Bai¹⁴, Xiaoguang Dou¹⁵, Lin Wu³, Guoqing Jiang¹⁶, Qi Xia¹⁷, Dan Zheng¹⁸, Huiying Rao¹⁹, Jie Xia²⁰, Jia Shang²¹, Pujun Gao²², Dong-Ying Xie²³, Yanlong Yu²⁴, Yongfeng Yang²⁵, Hongbo Gao²⁶, Yali Liu²⁷, Aimin Sun²⁸, Yongfang Jiang²⁹, Yan-Yan Yu³⁰, Jian Sun¹, Hong-Yang Wang², Jinlin Hou¹. ¹Guangdong Provincial Key Laboratory of Viral Hepatitis Research, Guangdong Provincial Clinical Research Center For Viral Hepatitis, Department of Infectious Diseases, Nanfang Hospital, Southern Medical University, Guangzhou, China; ²Department of Hepatobiliary Medicine, Shanghai Eastern Hepatobiliary Surgery

ORAL PRESENTATIONS

Hospital, Shanghai, China; ³Berry Oncology Corporation, Beijing, China; ⁴Hepatology Department, Ningbo Hwamei Hospital, University of Chinese Academy of Sciences, Ningbo, China; ⁵Liver Research Center, Beijing Friendship Hospital, Capital Medical University, Beijing, China; ⁶The United Innovation of Mengchao Hepatobiliary Technology Key Laboratory of Fujian Province, Mengchao Hepatobiliary Hospital of Fujian Medical University, Clinical Oncology School of Fujian Medical University, Fujian Cancer Hospital, Fuzhou, China; ⁷Hepatology Unit, No. 1 Hospital affiliated to Jilin University, Changchun, China; ⁸Department of Clinical Laboratory, The Second Hospital, Cheeloo College of Medicine, Shandong University, Jinan, China; ⁹Department of Infectious Diseases, Xiangya Hospital, Central South University, Changsha, China; ¹⁰Department of Hepatology, First Affiliated Hospital of Xinjiang Medical University, Urumqi, China; ¹¹Department of Infectious Diseases, Ruijin Hospital, Shanghai Jiao Tong University School of Medicine, Shanghai, China; ¹²Xuzhou Infectious Diseases Hospital, Xuzhou, China; ¹³Beijing Ditan Hospital, Capital Medical University, Beijing, China; ¹⁴The Department of Infectious Disease, The First People's Hospital of Foshan, Foshan, China; ¹⁵Department of Infectious Diseases, Shengjing Hospital of China Medical University, Shenyang, China; ¹⁶Department of Hepatobiliary Surgery, Clinical Medical College, Yangzhou University, Yangzhou, China; ¹⁷Department of Infectious Diseases, Zhejiang University 1st Affiliated Hospital, Hangzhou, China; ¹⁸Department of Gastroenterology, The Central Hospital of Wuhan, Tongji Medical College, Huazhong University of Science and Technology, Wuhan, China; ¹⁹Peking University Hepatology Institute, Peking University People's Hospital, Beijing, China; ²⁰Department of Infectious Diseases, Southwest Hospital, Third Military Medical University (Army Medical University), Chongqing, China; ²¹Henan Provincial People's Hospital, Zhengzhou, China; ²²The First Hospital of Jilin University, Jilin, China; ²³Department of Infectious Diseases, Sun Yat-Sen University 3rd Affiliated Hospital, Guangzhou, China; ²⁴Chifeng Clinical Medical School of Inner Mongolia Medical University, Chifeng, China; ²⁵The Second Hospital of Nanjing, Nanjing, China; ²⁶8th People's Hospital, Guangzhou, China; ²⁷Beijing Youan Hospital, Capital Medical University, Beijing, China; ²⁸Henan Institute of Medical and Pharmaceutical Sciences, Zhengzhou University, Zhengzhou, China; ²⁹Liver Disease Research Center, the Second Xiangya Hospital, Central South University, Changsha, China; ³⁰Department of Infectious Diseases, First Hospital of Peking University, Beijing, China Email: jlhoumu@163.com

Background and aims: Current hepatocellular carcinoma (HCC) risk scores do not reflect changes in the risk assessment of HCC resulting from liver disease progression/regression over time. Moreover, majority of HCC risk scores perform unsatisfactorily among cirrhotic patients. Therefore, we aimed to develop and validate novel prediction models by using multivariate longitudinal data with or without incorporating cell-free DNA (cfDNA) signatures.

Method: A total of 13,728 patients from 2 nationwide multicentre prospective cohorts (Search-B CHB cohort and PreCar cirrhotic cohort) were enrolled in the study. aMAP HCC risk score [J Hepatol, 2020], calculated by age, sex, platelets, albumin and total bilirubin, was evaluated for each patient using baseline data. Low-pass whole genome sequencing was used to derive multi-modal cfDNA fragmentomics features for PreCar cirrhotic patients. Longitudinal Discriminant Analysis algorithm was used to estimate the risk of HCC development.

Results: We developed and externally validated two novel HCC prediction models with greater accuracy called aMAP-2 and aMAP-2 Plus scores. The aMAP-2 score, calculated with longitudinal data of aMAP score, AFP and ALT during up to 8-year follow-up, performed superbly in the Search-B training (N = 3,706; AUC: 0.84) and external validation (N = 5,796; AUC: 0.85) CHB cohorts, and performed moderately in PreCar cirrhotic cohort (N = 4226; AUC: 0.73). In Search-B training cohort, aMAP-2 score could clearly divide patients into low-risk (3191, 86.1%), and high-risk (514, 13.9%), with 5-year cumulative incidences of 1.4% and 15.7% ($p < 0.0001$), respectively. The significant difference of future HCC incidence between aMAP-2 score identified low- and high-risk groups were also demonstrated in Search-B validation and PreCar cohorts. The aMAP-2 Plus score, developed by incorporating cfDNA signatures (Nucleosome, Fragment and Motif scores) based on aMAP-2 score, could further optimize the performance in predicting HCC development, especially for cirrhotic patients (AUC: 0.86–0.89). These two HCC prediction models both exhibited broadly better performance than the other existing HCC risk scores. Moreover, the aMAP-2 Plus score also played a potential role in very-early diagnosis of HCC, by alarming HCC occurrence 3.5 months earlier, on average. More importantly, among the PreCar cirrhotic patients, the application of stepwise approach (aMAP → aMAP-2 → aMAP-2 Plus) could identify 90.9% and 9.0% of

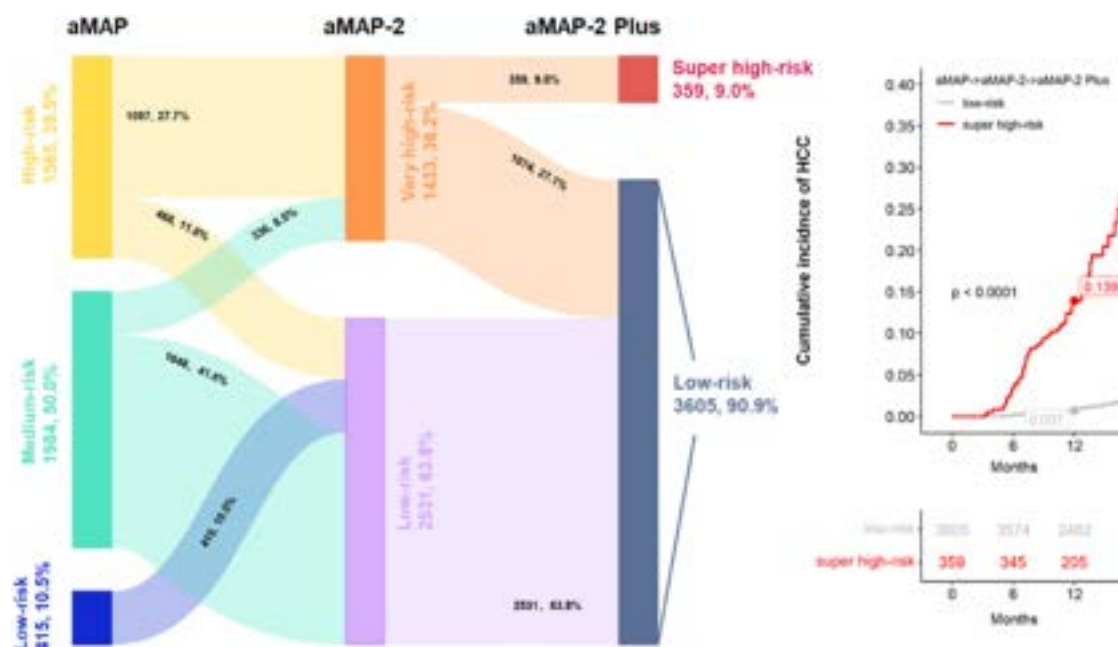


Figure: (abstract: OS-033).

cirrhotic patients with annual HCC incidence of 0.7% and 13.9%, respectively ($p < 0.0001$, Figure).

Conclusion: aMAP-2 and aMAP-2 Plus scores represent more accurate models in predicting HCC for patients with or without cirrhosis. The stepwise application of aMAP scores (aMAP → aMAP-2 → aMAP-2 Plus) provides an improved enrichment strategy of super high-risk HCC patients, which could effectively guide nationwide individualized HCC surveillance.

OS-034

A gene editing approach for chronic hepatitis B: elimination of hepatitis B virus in vivo by targeting cccDNA and integrated viral genomes with a sequence-specific ARCUS nuclease

Cassandra Gorsuch¹, Paige Nemec¹, Mei Yu², Simin Xu², Dong Han², Jeff Smith¹, Janel Lape¹, Nicholas Van Buuren², Ricardo Ramirez², Robert Muench², Meghan Holdorf², Becket Feierbach², Greg Falls¹, Jason Holt², Wendy Shoop¹, Emma Sevigny¹, Forrest Karriker¹, Robert Brown¹, Amod Joshi¹, Tyler Goodwin¹, Ying Tam³, Paulo Lin³, Sean Semple³, Neil Leatherbury¹, William E. Delaney², Derek Jantz¹, Emily Harrison¹, Amy Rhoden Smith¹. ¹Precision BioSciences, United States; ²Gilead Sciences, United States; ³Acuitas Therapeutics, Canada
Email: cassie.gorsuch@precisionbiosciences.com

Background and aims: ARCUS nucleases can be engineered to recognize conserved DNA sequences in the Hepatitis B virus (HBV) genome and provide a strategy for chronic hepatitis B (CHB) treatment. Persistence of CHB is attributed to maintenance of the intrahepatic pool of viral covalently closed circular DNA (cccDNA) and expression of immunosuppressive Hepatitis B surface antigen (HBsAg) from integrated HBV. Current therapies have no direct impact on cccDNA or expression of HBsAg from integrated virus. ARCUS nucleases expressed in hepatocytes can cut both cccDNA and integrated viral genomes leading to removal of cccDNA and inhibition of viral gene expression. We describe a potential curative approach for CHB using a highly specific engineered ARCUS nuclease (ARCUS-POL) targeting the HBV genome.

Method: Through iterative rounds of protein engineering, ARCUS-POL nucleases were optimized to exhibit high levels of on-target editing with minimal off-target activity. Efficacy and specificity were then tested *in vitro* in primary human hepatocytes (PHHs) infected with HBV and a HepG2 cell line with an integrated partial HBV genome. To evaluate ARCUS-POL *in vivo*, novel episomal adeno-associated virus (AAV) mouse and non-human primate (NHP) models were developed containing a portion of the HBV genome serving as a surrogate for cccDNA. Clinically relevant delivery was achieved through systemic administration of lipid nanoparticles (LNPs) containing ARCUS-POL mRNA.

Results: ARCUS-POL mRNA was transfected into HBV-infected PHHs, resulting in >75% reductions of both cccDNA and HBsAg. Importantly, ARCUS-POL produced no detectable translocations in PHHs using hybrid capture followed by long-read sequencing. After transient delivery of ARCUS-POL into cells containing integrated HBV DNA, >80% on-target editing was achieved with subsequent HBsAg reductions. In both mouse and NHP AAV models, a significant decrease in total AAV copy number and high on-target indel frequency was observed after LNP delivery of ARCUS-POL mRNA. In the case of the mouse model, which supports HBsAg expression, circulating surface antigen was durably reduced by 96%.

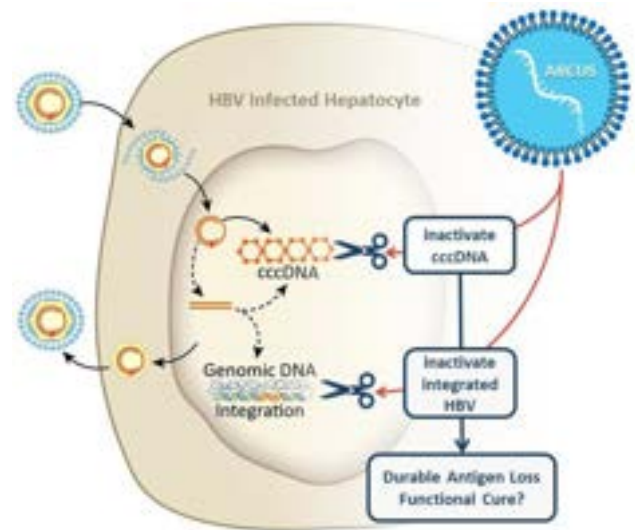


Figure:

Conclusion: ARCUS-POL nucleases were able to eliminate cccDNA and reduce HBsAg expression from integrated HBV without inducing translocations. Together, these data support a potential gene editing approach and cure for CHB.

FRIDAY 23 JUNE

Cirrhosis and its complications: Clinical

OS-035-YI

Development and validation of the AMMON-OHE model to risk stratify cirrhotic outpatients for occurrence of overt hepatic encephalopathy

María Pilar Ballester^{1,2}, Thomas Tranah³, Lorenz Balcar⁴, Alessandra Fiorillo², Javier Ampuero⁵, Annarein Kerbert^{6,7}, Karen Louise Thomsen^{6,7}, Desamparados Escudero-García¹, Mattias Mandorfer⁴, Thomas Reiberger⁴, Debbie L. Shawcross³, Manuel Romero Gomez⁵, Carmina Montoliu², Juan Antonio Carbonell-Asins², Rajiv Jalan⁷. ¹Hospital Clínico Universitario de Valencia, Digestive Disease, Spain; ²INCLIVA Biomedical Research Institute, Spain; ³King's College London, Institute for Liver Studies, United Kingdom; ⁴Medical University of Vienna, Vienna Hepatic Hemodynamic Laboratory, Austria; ⁵Virgen del Rocio University Hospital, Digestive Disease Department, Spain; ⁶Aarhus University Hospital, Denmark; ⁷University College London, Liver Failure Group, United Kingdom
Email: mapibafe@gmail.com

Background and aims: Neuropsychological and psychophysical tests are recommended for the risk assessment for overt hepatic encephalopathy (OHE), but their accuracy is limited. Hyperammonaemia is central in the pathogenesis of OHE, but its predictive utility is unknown. This study aimed to determine the role of neuropsychological or psychophysical tests and ammonia and to develop the AMMON-OHE model for risk stratification regarding subsequent OHE development in outpatients with liver cirrhosis.

Method: This observational, prospective study included 426 outpatients without previous OHE from 3 liver units followed for a median of 2.5 years. Psychometric hepatic encephalopathy score (PHES) <−4 or critical flicker frequency (CFF) <39 was considered abnormal. Ammonia was normalized to upper limit of normal (AMM-

ORAL PRESENTATIONS

ULN) at the respective reference laboratory. Multivariable frailty competing risk analyses and fast unified random forest were performed to predict future OHE and to develop the AMMON-OHE model. External validation of the model was carried out using 267 and 381 patients from two independent liver units.

Results: Significant differences were found in time-to-OHE (log-rank $p < 0.001$) according to PHES and CFF tests and ammonia, with the highest risk in patients with abnormal PHES plus high AMM-ULN (HR: 4.4; 95% CI: 2.4–8.1, $p < 0.001$ compared with normal PHES and AMM-ULN) (Figure 1). On multivariable analysis, AMM-ULN but not PHES or CFF was an independent predictor for development of OHE (HR: 1.4; 95% CI: 1.1–1.9; $p = 0.015$). The AMMON-OHE model included sex, diabetes, albumin, creatinine and AMM-ULN, and showed a C-index of 0.844 and 0.728 in the two validation cohorts, respectively.

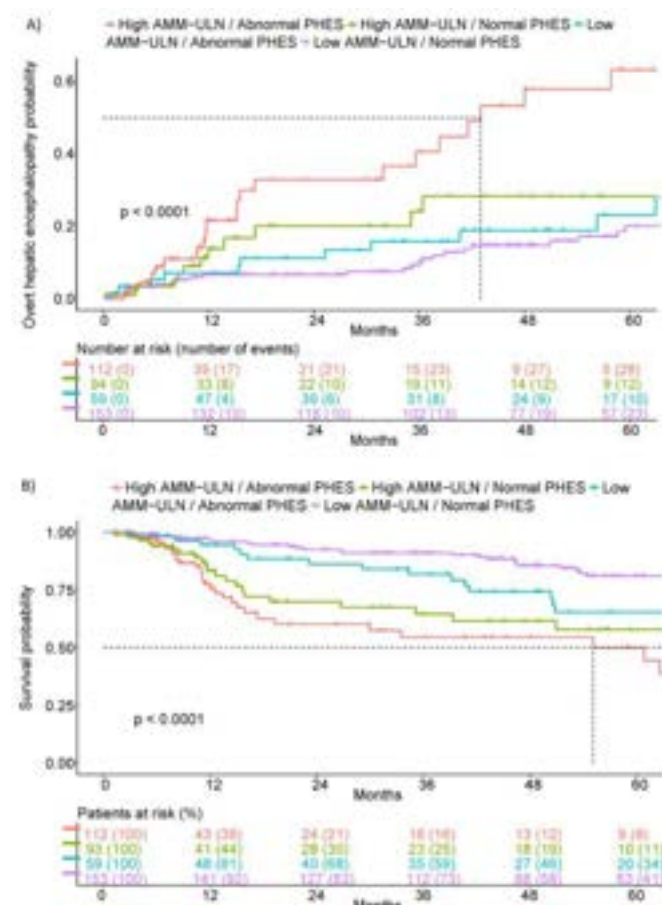


Figure:

Conclusion: This study developed and validated the AMMON-OHE model, comprising readily available clinical and biochemical variables that can be used to identify outpatients with cirrhosis at highest risk for developing a first episode of OHE.

OS-036

Efficacy and safety of lusutrombopag in a real-world Italian series of cirrhotic patients with severe thrombocytopenia undergoing invasive procedures: the Reality study

Paolo Gallo¹, Antonio De Vincentis¹, Valeria Pace Palitti², Maurizio Russello³, Anthony Vignone^{4,5,6}, Domenico Alvaro⁴, Raffaella Tortora⁶, Marco Biolato⁷, Maurizio Pompili⁷, Vincenza Calvaruso⁸, Marzia Veneziano⁸, Valerio Rosato⁹, Ernesto Claar⁹, Rosanna Villani¹⁰, Antonio Izzi¹¹, Raffaele Cozzolongo¹², Marco Distefano¹³, Vincenzo Messina¹⁴, Enrico Ragone¹⁵, Rodolfo Sacco¹⁰, Pierluigi Cacciatore², Alessandra Moretti¹⁶, Francesca Terracciani¹, Antonio Picardi¹,

Umberto Vespasiani Gentilucci¹. ¹Fondazione Policlinico Campus Biomedico Rome, Italy; ²ASL Pescara, Italy; ³Arnas Garibaldi Catania, Italy; ⁴Sapienza University of Rome, Italy; ⁵Policlinico Umberto I, Rome, Italy; ⁶SAORN Cardarelli, Naples, Italy; ⁷Fondazione Policlinico Universitario Gemelli Rome, Italy; ⁸University of Palermo, Italy; ⁹Betania Hospital Naples, Italy; ¹⁰University of Foggia, Italy; ¹¹D. Cotugno Hospital Naples, Italy; ¹²"S de Bellis" Research Hospital, Castellana Grotte (Bari), Italy; ¹³Umberto I Hospital Siracusa, Italy; ¹⁴S. Anna and S. Sebastiano Hospital Caserta, Italy; ¹⁵Monaldi Hospital Naples, Italy; ¹⁶San Filippo Neri Hospital Rome, Italy
Email: paolo.gallo@policlinicocampus.it

Background and aims: Severe thrombocytopenia (platelet count less than 50,000/ μ L) complicates the management of patients with chronic liver disease by increasing the risk of bleeding for invasive procedures and sometimes delaying lifesaving treatments. In the last years, thrombopoietin (TPO) receptor agonists such as lusutrombopag have been developed in order to avoid platelet transfusion and associated concerns. Real-world data on the efficacy and safety of the drug are limited to sparse reports or administrative databases. We aimed to evaluate the first post-marketing European cohort of cirrhotic patients treated with lusutrombopag in order to verify efficacy and safety of the drug in a real-world setting.

Method: In the REAL-world Lusutrombopag treatment in Italy (REALITY) study, we collected data of consecutive cirrhotic patients receiving lusutrombopag before invasive procedures between March 2021 and November 2022 from 15 Italian hepatologic centers, mostly belonging to the "Club Epatologi Ospedalieri" (CLEO). Efficacy, i.e., the capability of lusutrombopag to raise platelet count to $\geq 50,000/\mu$ L and avoid transfusions, as well as treatment-related adverse events, were captured and analyzed.

Results: Fifty patients were enrolled (median age 66 years, female 30%, Child-Pugh A/B/C 67/27/6%). Ten patients (20%) had a previous medical history of portal vein thrombosis. Chronic viral hepatitis was the most common cause of liver disease (42%), followed by the non-alcoholic fatty liver disease (28%). Interventional radiology (44%) and endoscopic (32%) were the most common procedures involved: thermal ablation (14%) and transarterial chemoembolization (14%) of liver cancer, liver biopsy (15%), endoscopic band ligation (18%), other endoscopic operative procedures (14%). Lusutrombopag induced a significant increase in platelet count [from 36,500 (33,000–43,000)/ μ L] to 61,500 (52,000–80,750), $p < 0.01$]. The efficacy of lusutrombopag was 78%, while 11 patients (22%) did not reach the platelet threshold of 50,000/ μ L and required platelet transfusions before the invasive procedure. Notably, the efficacy of lusutrombopag was significantly lower in the 9 patients with a baseline platelet count $\leq 30,000/\mu$ L compared to the 41 patients with a baseline count $> 30,000/\mu$ L (4% Vs 85%, respectively, $p < 0.01$). There were no hemorrhagic events in this series. *De novo* portal vein thrombosis was observed in 2 patients.

Conclusion: In this first real-world European series of cirrhotic patients with severe thrombocytopenia treated with lusutrombopag before invasive procedures, the drug confirmed efficacy and safety profiles in line with those observed in registrative trials. According to our results, patients with baseline platelets $\leq 30,000/\mu$ L are unlikely to respond to the drug.

OS-037

Pregnancy outcomes in women with liver cirrhosis: a prospective UK obstetric surveillance system national cohort study

Melanie Nana¹, Agata Majewska¹, Mussarat Rahim², Victoria Geenes¹, Paul Seed¹, Caroline Ovadia¹, Marian Knight³, Michael Heneghan², Catherine Williamson¹. ¹King's College London, Women's Health, London, United Kingdom; ²Institute of Hepatology, King's College London, United Kingdom; ³National Perinatal Epidemiology Unit, United Kingdom
Email: melanie.nana@kcl.ac.uk

Background and aims: The number of women entering pregnancy with cirrhosis is increasing, yet there is a paucity of data to inform

evidence-based management and counselling of these patients. In the first prospective study of cirrhosis in pregnancy we aimed to determine its national incidence and management, and to describe maternal and fetal outcomes in this group.

Method: A prospective, national cohort study was performed using the UK Obstetric Surveillance System between 2017 and 2020. Rates of adverse perinatal outcomes were compared with published rates of adverse perinatal outcomes in uncomplicated pregnancies or at population level using logistic regression, and prediction of adverse pregnancy outcomes by ALBI score was determined by calculating the area under the receiver operating characteristic curve (AUROC) (Stata 17.0 and GraphPad Prism v9).

Results: In total, 52 eligible cases were reported (denominators were determined by available data for specific adverse outcomes. The causes of cirrhosis are illustrated in Figure 1.

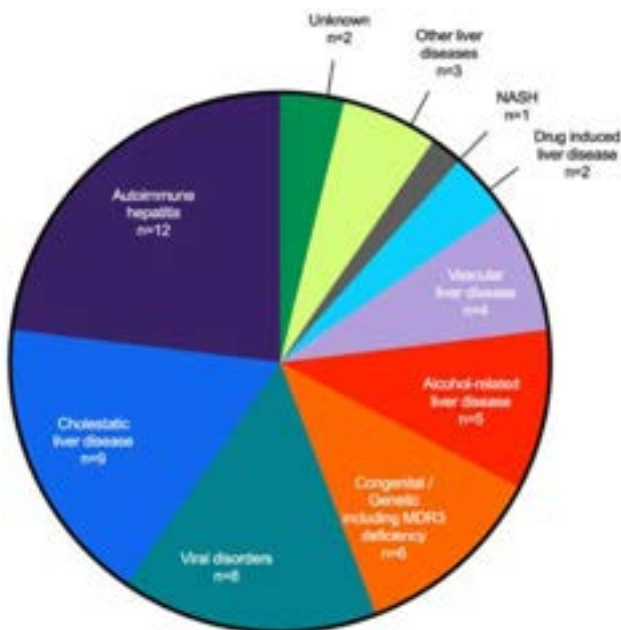


Figure: Underlying causes of cirrhosis. Abbreviations: NASH-non-alcoholic steatohepatitis; MDR3-multidrug resistance protein 3.

Only 17/42 (40.5%) of women received pre-pregnancy counselling. In total, 49/52 (94.2%) conceived spontaneously; three miscarried. Maternal decompensation occurred in seven women, defined by jaundice (n = 2), ascites (n = 3) and encephalopathy (n = 1). The worst ALBI score in pregnancy predicted maternal decompensation AUROC 0.80 (p = 0.03). During the pregnancy 26/49 (53.0%) had an endoscopy, of which 34.6% had uncomplicated variceal banding. Untreated varices were associated with increased rates of variceal bleed (p = 0.01). In total, 9/52 (17.3%) women developed cholestasis. Four women required intensive care unit (ICU) admission, none required liver transplant, and none died. There were 42 live births: 51.2% were preterm, 44.2% had low-birth-weight; there was one stillbirth; and two neonatal deaths (both a consequence of extreme prematurity). The worst ALBI score in pregnancy predicted pre-term birth AUROC 0.74 (p = 0.03). When compared to a healthy reference population, cirrhotic women were at increased risk of cholestasis in pregnancy (OR 29.4, 95% CI 13.8–61.6, p < 0.001), ICU admission (OR 42.5, 95% CI 15.2–118.8, p < 0.001), pre-term birth (OR 13.2, 95% CI 7.12–24.4, p < 0.001), low-birth-weight (OR 12.0, 95% CI 6.5–22.0, p < 0.001), neonatal intensive care unit admission (OR 4.4, 95% CI 2.4–8.2, p < 0.001) and neonatal death (OR 31.795 CI 7.6–131.4, p < 0.001).

Conclusion: High numbers of women with cirrhosis in pregnancy conceive spontaneously. Pre-pregnancy counselling is paramount to ensuring that women are optimised for pregnancy, including having screening and appropriate management of varices and being counselled regarding the increased rates of maternal and neonatal complications. The ALBI score predicts maternal decompensation and pre-term birth.

OS-038

Substitution of even one non-vegetarian meal with plant-based alternatives associate with lower ammoniogenesis in patients with cirrhosis who follow a western diet: a randomized clinical trial

Andrew Fagan¹, Bryan Badal¹, Victoria Tate¹, Travis Mousel¹, Mary Leslie Gallagher¹, Puneet Puri¹, Michael Fuchs¹, Brian Davis¹, Jennifer Miller¹, Jasmohan S Bajaj¹. ¹Virginia Commonwealth University and Richmond VAMC, United States

Email: jasmohan.bajaj@vcuhealth.org

Background and aims: Dietary preferences (Vegetarian, vegan, meat) could differentially influence ammoniogenesis in cirrhosis and hepatic encephalopathy (HE). Most Western populations follow meat-based diets but the impact of intermittent diet substitution on ammoniogenesis is unclear. Aim: Determine impact of substituting one meal with equicaloric and protein containing vegan, vegetarian or meat on ammonia levels in outpatients with cirrhosis on a Western non-vegetarian diet.

Method: Outpatients with cirrhosis with/without prior HE (on stable lactulose/rifaximin) on a stable Western meat-based diet were enrolled. We excluded those with MELD>23, unclear cirrhosis diagnosis, BMI (<18.5 or >40), prior TIPS, recent antibiotic/probiotic use, HE treatment<2 months, or valproate/steroid use.

Subjects were randomized 1:1:1 into the 3 meals which had equivalent protein (20 gm) and calories. Meals were freshly prepared by our dietician. These consisted of a burger (meat substitute patty for vegan, bean-burger for vegetarian and pork/beef patty for meat) with bun and low-salt potato chips and water. Baseline dietary history, cirrhosis details, MELD-Na were collected, after overnight fasting, all patients ate the entire meal under observation. They remained fasting for the remaining 3 hours, where they were kept under observation. Venous ammonia levels were drawn at baseline and hourly for 3 hours post-meal (Fig 1A). Baseline characteristics and changes in ammonia levels were compared within and between groups.

Results: We enrolled 30 men; ten each were randomized per meal group. All subjects finished the meals and none developed HE symptoms or confusion during the observation period. There were no baseline differences in age, MELD-Na, prior HE, lactulose, rifaximin, PPI and ascites (Fig 1B) between the groups.

Ammonia levels: At baseline, no significant differences in ammonia levels were observed (Figure 1B). However, the ammonia levels over time increased significantly from baseline (p = 0.007) only in the meat-based group but not the vegan (p = 0.45) or vegetarian (p = 0.84) group. As shown in figure 1C, serum ammonia levels between groups were significantly higher in the meat group compared to the other 2 groups at hours 1, 2 and 3 post-meal. There were no differences between the ammonia level changes at any timepoint between the vegan and vegetarian groups.

Conclusion: Substitution of even one meat-based meal with vegan or vegetarian alternatives has the potential to reduce ammoniogenesis in outpatients with cirrhosis regardless of prior HE. Intermittent plant-based options for protein could be considered in patients with cirrhosis who usually follow a Western diet.



Figure: (abstract: OS-038).

OS-039-YI

Head-to-head comparison of the prognostic performance of the hepatic venous pressure gradient and non-invasive tests in compensated advanced chronic liver disease

Matthias Jachs¹, Lukas Hartl¹, Benedikt Simbrunner¹, Georg Semmler¹, Lorenz Balcar¹, Benedikt Hofer¹, Michael Schwarz¹, David JM Bauer¹, Albert Stättermayer¹, Matthias Pinter¹, Michael Trauner¹, Thomas Reiberger¹, Mattias Mandorfer¹. ¹Medical University of Vienna, Austria

Email: mattias.mandorfer@meduniwien.ac.at

Background and aims: Models based on platelet count (PLT) and liver stiffness measurement (LSM; ANTICIPATE) or von Willebrand factor antigen (VWF) to PLT ratio (VITRO) are applied to estimate the probability of/rule in- or rule-out clinically significant portal hypertension (CSPH), and thus, stratify risk and guide NSBB therapy in patients with compensated advanced chronic liver disease (cACLD). However, head-to-head comparisons of their prognostic utility for first hepatic decompensation and comparisons with the minimally invasive hepatic venous pressure gradient (HVPG) are lacking.

Method: Patients with cACLD, defined by LSM ≥ 10 kPa, who underwent same-day assessment of HVPG, LSM, and VITRO between 2007 and 2022 were included. Patients' individual ANTICIPATE-derived probability for CSPH was calculated based on PLT and LSM according to the published formula. Long-term follow-up data on first hepatic decompensation was recorded. Time-dependent AUROC analyses and competing risk regressions were performed.

Results: We included 445 cACLD patients: median age: 54.1 years; 66.7% male; etiology: 51.7% viral, 20.8% ALD, 18.9% NAFLD/cryptogenic, while 8.8% other. The median HVPG was 12 (IQR: 8–17) mmHg with a CSPH prevalence of 61.5%. The median PLT, VWF, and VITRO levels were 109 (80–156) G/L, 243 (188–306) %, and 2.24 (1.29–3.52), respectively. The median estimated probability of CSPH based on the ANTICIPATE model was 80.0 (47.0–94.2) %. The cumulative incidences of first hepatic decompensation were 4.4%, 7.6%, and 13.3% at 1, 2, and 3 years of follow-up. HVPG, VITRO, and CSPH-probability according to ANTICIPATE conferred similar time-dependent prognostic value in

AUROC analyses (Figure; panel A), with VITRO showing the numerically highest values over time. In competing risk analyses adjusted for model for end-stage liver disease (MELD) score and serum albumin levels, HVPG (adjusted subdistribution hazard ratio [aSHR]: 1.092 [95%CI:1.048–1.140] per mmHg; $p < 0.001$), VITRO (aSHR: 1.138 [1.066–1.210] per unit; $p < 0.001$), and ANTICIPATE-CSPH probability (aSHR: 1.022 [1.010–1.034] per %; $p < 0.001$) all predicted first decompensation during follow-up. When stratifying the cohort by previously proposed decision rules (HVPG ≥ 10 mmHg vs. < 10 mmHg, VITRO ≥ 2.5 vs. < 2.5 , and ANTICIPATE-CSPH probability $\geq 60\%$ vs. $< 60\%$), all biomarkers accurately discriminated between patients at negligible risk and those at substantial risk of hepatic decompensation, as shown in the Figure (panels B–D).

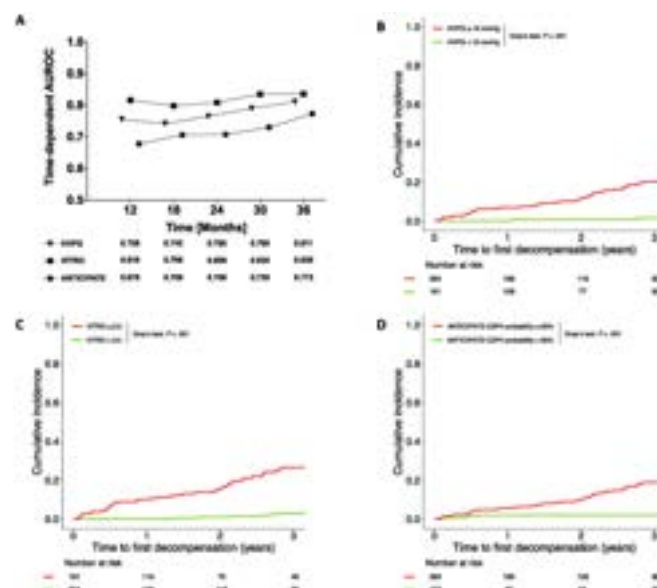


Figure:

Conclusion: Non-invasive CSPH surrogates, i.e., the ANTICIPATE-CSPH probability, and even more, VITRO, have a high prognostic performance that is similar to minimally invasive HVPG-measurement. Thus, they provide clinically meaningful information and accurately identify candidates for medical therapies to prevent first hepatic decompensation.

Experimental liver fibrosis

OS-041-YI

X-box binding protein 1 (XBP1) in hepatic stellate cells (HSC) mitigates liver fibrosis

Hanghang Wu¹, Hui Ye^{1,2}, Juan Francisco Vilchez-Gómez¹, Marcos Fernandez Fondevila^{3,4}, Aveline Filliol⁵, Robert F. Schwabe⁵, Javier Vaquero^{6,7,8}, Rafael Bañares^{6,7,8}, Ruben Nogueiras^{3,4,9}, Eduardo Martínez-Naves¹, Scott Friedman¹⁰, Yulia Nevzorova^{1,7,8}, Francisco Javier Cubero^{1,7,8}. ¹Complutense University of Madrid, Spain; ²ZhongDa Hospital Southeast University, China; ³University of Santiago de Compostela-Instituto de Investigación Sanitaria, Spain; ⁴CIBER Fisiopatología de la Obesidad y Nutrición (CIBEROBN), Instituto de Salud Carlos III, Spain; ⁵Columbia University, United States; ⁶Hospital General Universitario Gregorio Marañón, Spain; ⁷Instituto de Investigación Sanitaria Gregorio Marañón (IISGM), Spain; ⁸Centro de Investigación Biomédica en Red de Enfermedades Hepáticas y Digestivas (CIBEREHD), Spain; ⁹Galician Agency of Innovation (GAIN), Xunta de Galicia, Santiago de Compostela, Spain; ¹⁰Icahn School of Medicine at Mount Sinai, United States
Email: hangwu@ucm.es

Background and aims: Hepatic fibrosis is a pathogenic condition triggered by persistent inflammation, in which hepatic stellate cells (HSC) are the main cell type responsible for the overexpression of extracellular matrix (ECM) proteins. Recently, it was reported that myeloid-specific XBP1 deficiency or pharmacological inhibition of XBP1 protected the liver against fibrosis. In this study, we aimed to investigate the role of XBP1 in HSCs.

Method: Mice harboring a conditional floxed allele of *Xbp1* (*Xbp1^{flf}*), were crossed with *Lrat-Cre* mice to obtain a HSC-specific knockout of *Xbp1* (*Xbp1^{ΔHSC}*). Overnight-fasted 8–12 week-old male *Xbp1^{flf}* and *Xbp1^{ΔHSC}* mice were either fed a MCD diet, challenged with carbon tetrachloride (CCl₄) [0,6 ml/kg] or corn oil for 4 weeks, or given a Western diet (WD) in combination with CCl₄ [0,2 ml/kg] for 12 weeks- the FAT-NASH model. Upon sacrifice, qRT-PCR, Western blot, and IF analysis, were performed. In addition, functional experiments were carried out in primary isolated XBP1-deficient HSC and in LX2 cells treated with TGFβ (0–24 h) or vehicle. Finally, scRNA-seq of HSC from fibrotic mouse liver induced by 19 injections of CCl₄ and HSCs from normal and cirrhotic human livers was used.

Results: Interestingly, *Xbp1^{ΔHSC}* mice exhibited significantly increased lipid accumulation (Oil Red O) and steatosis as well as cell death (TUNEL, CC3) and compensatory proliferation (Ki-67), compared with *Xbp1^{flf}* knockout mice, after 4 weeks of MCD diet. Moreover, one month of CCl₄ challenge triggered elevated serum markers of liver damage (ALT, AST) in *Xbp1^{ΔHSC}*. These changes were accompanied with aggravated periportal fibrosis (HandE, Sirius red), a robust overexpression of αSMA expression- a marker of HSC activation-, and other ECM components (Vimentin, Desmin), and the production of proinflammatory proteins (*Tnfα*, *IL-6*, *Tgfβ*). Finally, the FAT-NASH preclinical model exacerbated liver injury, periportal fibrosis and inflammation in *Xbp1^{ΔHSC}* compared with *Xbp1^{flf}* mice. Additionally, LX2 cells challenged with TGFβ exhibited increased

markers of the IRE1-XBP1. Finally, enrichment of XBP1 in HSCs was found in fibrotic murine and cirrhotic human livers.

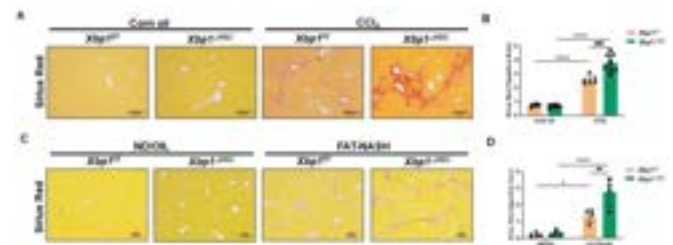


Figure:

Conclusion: Our data highlighted a novel function of *Xbp1* specifically in HSCs in NAFLD/NASH models by mitigating NAFLD/NASH-induced injury. Thus ER stress modulation specifically in HSC could potentially be used clinically to satisfy the current lack of effective treatments against hepatic fibrosis.

OS-042-YI

Novel insights on the contribution of collagen degradative macrophages to liver fibrosis resolution

Maria Fernandez-Fernandez^{1,2}, Paloma Ruiz-Blazquez^{1,2}, Valeria Pistorio^{1,3,4}, Celia Martinez-Sanchez^{2,5}, Michele Costanzo⁴, Paula Iruzueta⁶, Susana Núñez², Ekaterina Zhuravleva⁷, Jesper Andersen⁷, Margherita Ruoppolo⁴, Javier Crespo⁶, M. Carmen Garcia-Ruiz^{1,2,5,8}, Mar Coll^{2,5,9}, Luigi Pavone⁴, José Fernandez-Checa^{1,2,5,8}, Anna Moles^{1,2,5}. ¹Instituto de Investigaciones Biomédicas de Barcelona (IIBB-CSIC), Spain; ²Centro de Investigación Biomédica en Red de Enfermedades Hepáticas y Digestivas (CIBEREHD), Spain; ³Sorbonne Université, Inserm, Centre de Recherche Saint-Antoine (CRSA), Spain; ⁴University of Naples Federico II, Spain; ⁵Institut d'Investigacions Biomèdiques August Pi i Sunyer (IDIBAPS), Spain; ⁶Department of Gastroenterology and Hepatology, Marqués de Valdecilla University Hospital, Research Institute Marqués de Valdecilla (IDIVAL), Spain; ⁷Biotech Research and Innovation Centre (BRIC), Department of Health and Medical Sciences, University of Copenhagen, Spain; ⁸USC Research Center for ALPD, United States; ⁹Medicine Department, Faculty of Medicine, University of Barcelona, Spain
Email: anna.moles.fernandez@gmail.com

Background and aims: Liver fibrosis is caused by an excessive accumulation of extracellular matrix (ECM) proteins. Macrophages are important effectors for ECM remodelling through recycling of the ECM within acidic compartments and can contribute to liver fibrosis resolution. Proteases, such as cathepsins, are essential for lysosomal proteolytic activity; however, their contribution to ECM remodelling within the macrophages is unknown. Thus, the aim of this study was to investigate the proteolytic and degradative signalling pathways associated to macrophages during liver fibrosis.

Method: A novel macrophage-cathepsin D KO mouse strain (CtsD^{ΔMyel}) was generated by breeding *LysMCre* (macrophages) with *CtsD*-floxed mice. Fibrosis was established by chronic CCl₄ administration and bile duct ligation in CtsD^{flf} or CtsD^{ΔMyel} mice and determined by hydroxyproline, Sirius Red, α-SMA, Col1A1 and TGF-β RT-PCR. Proteomic profile was determined by LC-MS/MS in fibrotic livers. Reversion was assessed 72 h post-challenge in a 4-week CCl₄ model. Collagen degradation in liver was determined by R-CHP staining. Macrophage polarization and proteolytic secretome was assessed by RT-PCR and protease array, respectively. Collagen degradation and endocytosis was determined by FACS in Kupffer cells (KC). Single-cell RNA sequencing analysis was performed using GSE136103 dataset.

Results: ScRNAseq analysis and CtsD IHP demonstrated high expression of CtsD in liver macrophages from cirrhotic patients. Next, CtsD^{ΔMyel} mouse was validated by FACS and WB in KC and dual IHP (F4/80-CtsD) in liver. CtsD deletion in macrophages enhanced liver fibrosis with enriched matrisome proteomic signatures in chronic CCl₄ and BDL models. Analysis of KC isolated from 72h-CCl₄-treated livers demonstrated significantly lower expression of markers associated with resolutive macrophages (CD206, TREM-2 and TGF-β) and defective proteolytic secretome profile in CtsD^{ΔMyel} KC. In addition, CtsD^{ΔMyel} KC displayed defective proteolytic processing of collagen I without impairment of the Endo180 receptor-mediated endocytosis demonstrated by FACS. Analysis of CtsD macrophage subclusters in control and cirrhotic human livers, confirmed cirrhotic CtsD-expressing subclusters were differentially enriched in ECM degradation and organization signalling pathways. In addition, it revealed a decrease in the number of CtsD-expressing macrophage subclusters in cirrhotic livers, which could contribute to inadequate ECM recycling, perpetuating fibrosis and hampering resolution. Indeed, CtsD^{ΔMyel} mouse was unable to remodel collagen in vivo when subjected to a fibrosis reversion model determined by both percentage of HP and fluorescent intensity of collagen hybridizing peptide (CHP) binding to liver tissue.

Conclusion: CtsD is essential in regulating the collagenolytic activity of macrophages during liver fibrosis and is part of a novel and currently unknown degradome landscape of restorative macrophages.

OS-043

Atypical Chemokine receptors regulate the induction of 'disease-associated' LSEC by modulating Endothelial-to-Mesenchymal transition (EndMT) during liver fibrosis

Christina Gkantzikoudi¹, Antal Rot¹, William Alazawi¹, Neil Dufton¹.

¹Queen Mary University of London, United Kingdom

Email: n.dufton@qmul.ac.uk

Background and aims: Single cell RNA sequencing of cirrhosis patients (Ramachandran et al., 2019) and murine models of fibrosis (Su et al., 2020 and Ruan et al., 2021) have revealed the induction of 'disease-associated' Liver Sinusoidal Endothelial Cells (LSEC) correlate with liver fibrosis. Meta-analysis of these datasets shows that loss of endothelial identity and acquisition of mesenchymal characteristics, a process termed endothelial-to-mesenchymal transition (EndMT), are a common trait of 'disease-associated' LSEC. Our research was the first study to establish EndMT correlates with progressive fibrosis in murine models and human end-stage liver

disease (Dufton et al., 2017). We aim to determine the contribution of EndMT to 'disease-associated' LSEC during fibrogenesis. Secondly, we noted that LSEC undergo a switch in expression of Atypical Chemokine Receptors (ACKRs), from ACKR4 in healthy liver to ACKR1 during injury. Our study assessed the role of ACKRs in the regulation of EndMT during liver injury using ACKR1 and ACKR4-deficient mice.

Method: Carbon tetrachloride (CCl₄) was administered for 2, 4 and 8 weeks in ACKR4^{egfp-KO} and ACKR1^{KO} mice. To characterise LSEC subtypes we assessed 12 phenotypic markers by spectral flow cytometry. LSEC were gated using live cells, singlets and CD31⁺ CD45⁻ populations and analyzed by tSNE using the co-expression of LSEC markers with mesenchymal markers (e.g. Thy-1, TAGLN, and PDGFRα) to identify EndMT following CCl₄. Histograms show the expression of individual markers within each cluster corresponding to their colour. Localisation of LSEC subtypes were confirmed by immunofluorescent microscopy (IF).

Results: Healthy LSEC were distributed in four clusters 1: Lyve1^{hi} EMCN^{hi}, 2: CD31^{hi} Thbd^{hi}, 3: CD31^{lo} EMCN^{lo} and 4: CD31^{lo} ICAM1^{lo} (Fig. 1A). 8-weeks CCl₄ significantly reduced the number and composition of LSEC in clusters 1–4 and gave rise to three unique populations of EndMT cells 5: Thy-1^{hi} PDGFRα^{hi} CD34^{neg} 6: TAGLN^{hi} CD34^{med} and 7: Thy-1^{hi} PDGFRα^{mid} CD34^{hi} (Fig. 1B). IF revealed these EndMT populations predominantly arise in peri-central LSEC.

ACKR4^{egfp-KO} reporter mice revealed ACKR4 expression in peri-central LSEC in healthy tissue. ACKR4 gene expression was significantly downregulated in WT following CCl₄. Conversely, ACKR1 expression was absent in healthy LSEC but markedly upregulated in peri-central regions following CCl₄. CCl₄ treated ACKR1-deficient mice maintained their vascular architecture with reduced collagen deposition and reduced number of cells undergoing EndMT compared to WT. ACKR4-deficient mice displayed augmented fibrogenesis at all time points characterized by increased collagen-deposition, significant disruption of EC identity and increased EndMT.

Conclusion: We observed three distinct 'disease-associated' LSEC subtypes arose with characterised features of EndMT. These clusters may represent different stages of EndMT that occur with LSEC transitioning from Cluster 3, to acquire mesenchymal traits in Cluster 6 before reaching complete EndMT (Cluster 5 and 7). ACKR1^{KO} mice were protected from both EndMT and fibrogenesis while ACKR4^{egfp-KO} mice displayed an opposite phenotype suggesting regulation of ACKRs during liver injury is a crucial determinant of vascular health and liver fibrosis.

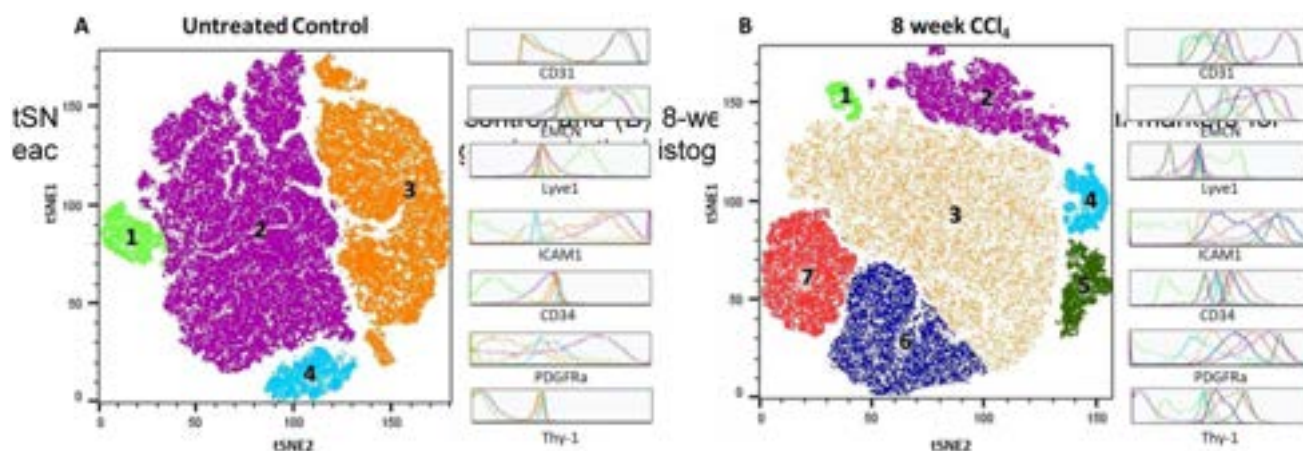


Figure: (abstract: OS-043): tSNEs plots display LSEC from (A) control and (B) 8-week CCl₄ WT mice with individual markers for each cluster shown by corresponding colour in the histograms.

OS-044-YI

Single-cell multiomics defines candidate transcription factors regulating pathogenic macrophage differentiation in murine liver fibrosis

Eleni Papachristoforou¹, Elena Sutherland¹, Neil Henderson¹,
Prakash Ramachandran¹. ¹University of Edinburgh, Centre for
Inflammation Research, United Kingdom
Email: eleni.papachristoforou@ed.ac.uk

Background and aims: Hepatic macrophages are key regulators of fibrosis progression and regression. Recent work using single-cell RNA-sequencing (scRNAseq) has identified a subpopulation of TREM2+CD9+ scar-associated monocyte-derived macrophages (SAMac) which expand in fibrotic human and murine liver tissue and regulate fibrosis. However, whilst the transcriptome of this macrophage population has now been well defined, the key transcriptional regulators of SAMac differentiation and phenotype remain unknown. To address this, we aimed to apply scRNAseq and single-cell ATAC-seq (scATACseq) in a murine model of liver fibrosis, to study transcription factor (TF) enrichment in monocyte and macrophage subpopulations at single-cell resolution.

Method: Liver injury was induced in C57BL/6J mice by carbon tetrachloride (CCl₄) twice weekly for 4 weeks. Age matched uninjured mice were controls. scRNAseq and scATACseq was performed on FACS-purified immune cells from blood and liver tissue of CCl₄ injury (n = 6 scRNAseq; n = 4 scATACseq) and controls (n = 6 scRNAseq; n = 4 scATACseq) using the 10X Genomics Chromium platform. Computational analysis was performed in R.

Results: Unsupervised clustering of scRNAseq data enabled atlasing of populations of immune cells. Mononuclear phagocytes (MP) were

reclustered, identifying 17 distinct subpopulations (Fig) including Trem2+Cd9+Gpnmb+ macrophages which expanded in fibrotic liver tissue and were transcriptionally similar to the corollary SAMac population in human fibrotic livers. Trajectory inference performed using Sevelo, demonstrated that murine SAMac derived from the recruitment and differentiation of circulating Ly-6C^{hi} monocytes. Having defined macrophage heterogeneity and differentiation kinetics using the scRNAseq data, scATACseq cell type clusters were then annotated by employing Seurat label transfer methodology (Fig). Differential TF motif enrichment was assessed in annotated scATACseq MP subpopulations using SIGNAC (Fig). We identified enrichment for previously described TFs such as the *Cebp* family in Ly-6C^{hi} blood monocytes, *Nr4a1* in Ly-6C^{lo} monocytes, *Runx1* in dendritic cells and *Nr1h3* (*Lxra*) in resident Kupffer cells. Focussing on SAMac, this population was enriched for AP-1 family members, *Nfe2*, *Batf*, *Smad2/3* as well as the transcriptional repressor *Bach2* and the antioxidant regulator *Nfe2l2*. Hence, the differentiation of monocytes into SAMac results in a distinct motif profile, suggesting that complex signals within the fibrotic niche are crucial to determining SAMac phenotype.

Conclusion: Single-cell multiomics identifies novel candidate transcriptional regulators of SAMac differentiation and expansion in the fibrotic liver. These data provide a framework for future functional studies aiming to selectively target and modulate SAMac transcription as an antifibrotic strategy for liver disease.

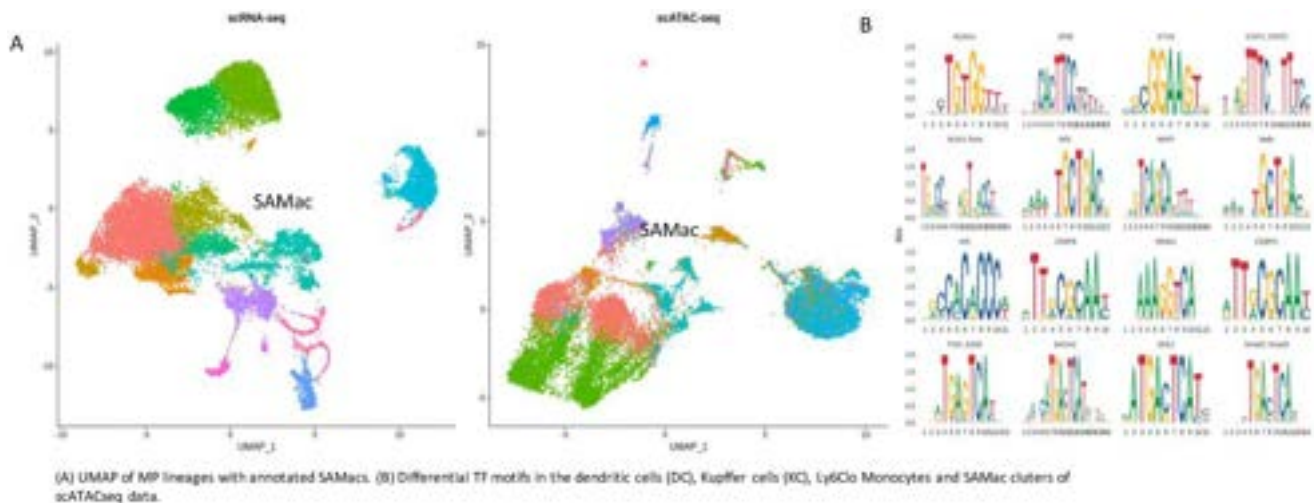


Figure: (abstract: OS-044-YI).

(1) Immune-mediated and cholestatic liver diseases

OS-045

Long-term real-world experience with obeticholic acid in primary biliary cholangitis: the Italian recapitulate study

Francesca Terracciani¹, Antonio De Vincentis¹, Daphne D'Amato², Anna Morgando², Ester Vanni², Mauro Viganò³, Domenico Alvaro⁴, Rosanna Venere⁴, Ana Lleo⁵, Francesca Colapietro⁵, Elisabetta Degasperi⁶, Raffaella Viganò⁷, Edoardo Giovanni Giannini⁸, Sara Labanca⁸, Valentina Feletti⁹, Alessandro Mussetto⁹, Raffaele Cozzolongo¹⁰, Francesco Losito¹⁰, Maurizio Pompili¹¹, Francesca Ponziani¹¹, Grazia Niro¹², Rosa Cotugno¹², Pietro Pozzoni¹³, Luchino Chessa¹⁴, Giuseppe Cuccorese¹⁵, Valeria Pace Palitti¹⁶, Maurizio Russello¹⁷, Maria Rita Cannavò¹⁷, Evelise Frazzetto¹⁸, Gaetano Bertino¹⁸, Marco Marzoni¹⁹, Natalia Terreni²⁰, Teresa Zolfino²¹, Carlo Saitta²², Adriano Pellicelli²³, Barbara Coco²⁴, Maurizia Brunetto²⁴, Nora Cazzagon²⁵, Annarosa Floreani²⁵, Luigi Muratori²⁶, Floriano Rosina²⁷, Marco Distefano²⁸, Gaetano Scifo²⁸, Leonardo Baiocchi²⁹, Giuseppe Grassi^{29,30}, Rodolfo Sacco³¹, Antonio Izzi³², Saveria Lory Croce³³, Cecilia Fiorini³⁴, Fabio Marra³⁴, Loredana Simone³⁵, Olivia Morelli³⁶, Ludovico Abenavoli³⁷, Fabrizio Pizzolante³⁸, Nicoletta De Matthaeis³⁸, Miki Scaravaglio³⁹, Giancarlo Gimignani⁴⁰, Valentina Boano⁴¹, Giulia Francesca⁴², Massimo Marignani⁴³, Silvia Fanella⁴³, Marco Giaccetto⁴⁴, Antonino Castellaneta⁴⁵, Guido Poggi⁴⁶, Valerio Buzzanca⁴⁹, Paolo Scivetti⁴⁷, Annalisa Tortora¹¹, Silvia Casella⁴⁸, Valentina Bellia⁴⁹, Barbara Omazzi⁵⁰, Giuliano Alagna⁵¹, Chiara Ricci⁵², Paolo Poisa⁵², Pietro Invernizzi³⁹, Cristina Rigamonti⁴², Vincenza Calvaruso⁴⁴, Marco Carbone³⁹, Umberto Vespasiani Gentilucci¹. ¹University Campus Bio-Medico of Rome, Internal Medicine and Hepatology, Italy; ²Città della salute e della scienza, Turin, Italy, Gastroenterology Unit, Italy; ³San Giuseppe Hospital, Milan, Italy, Italy; ⁴University La Sapienza, Rome, Italy, Department of Translational and Precision Medicine, Italy; ⁵Humanitas Clinical and Research Center IRCCS, Humanitas University, Milan, Italy, Italy; ⁶Foundation IRCCS Ca' Granda Ospedale Maggiore Policlinico, Italy; ⁷Niguarda Hospital, Milan, Italy, Italy; ⁸University of Genoa, IRCCS Ospedale Policlinico San Martino, Italy; ⁹Santa Maria Delle Croci Hospital, Ravenna, Italy, Italy; ¹⁰National Institute of Gastroenterology "S de Bellis" Research Hospital, Castellana Grotte (Bari), Italy, Italy; ¹¹Policlinico Gemelli, Sapienza University, Rome, Italy, Italy; ¹²Fondazione Casa Sollievo Della Sofferenza IRCCS, San Giovanni Rotondo, Foggia, Italy, Italy; ¹³Alessandro Manzoni Hospital, Lecco, Italy, Italy; ¹⁴University Hospital of Cagliari, Italy; ¹⁵Ospedale "R.Dimiccoli", Barletta, Italy; ¹⁶Santo Spirito Hospital, Pescara, Italy, Italy; ¹⁷Arnas Garibaldi, Catania, Italy, Italy; ¹⁸University Hospital Policlinico Vittorio Emanuele, Catania, Italy, Italy; ¹⁹Università Politecnica delle Marche, Ancona, Italy, Italy; ²⁰Valduce Hospital, Como, Italy, Italy; ²¹Brotzu Hospital, Cagliari, Italy, Italy; ²²University Hospital of Messina "Policlinico G. Martino", Messina, Italy, Italy; ²³San Camillo Hospital, Rome, Italy, Italy; ²⁴University Hospital of Pisa, Italy; ²⁵Padua University Hospital, Padua, Italy, Italy; ²⁶Università di Bologna, Policlinico di Sant'Orsola, Italy; ²⁷Medical Team Torino, Torino, Italy, Italy; ²⁸Umberto I Hospital, Syracuse, Italy, Italy; ²⁹Tor Vergata University Hospital, Rome, Italy; ³⁰Policlinico di torvergata, Epatologia, Italy; ³¹Ospedali Riuniti, Foggia, Italy, Italy; ³²Cotugno Hospital, Napoli, Italy, Italy; ³³Clinica Patologie Fegato, Azienda Sanitaria Universitaria Integrata Di Trieste, Italy; ³⁴University of Florence, Florence, Department of Experimental and Clinical Medicine, Italy; ³⁵Azienda Ospedaliero-Universitaria Di Ferrara, Ferrara, Italy, Italy; ³⁶Università Degli Studi Di Perugia, Italy, Italy;

³⁷University "Magna Graecia" of Catanzaro, Italy, Italy; ³⁸Fondazione Policlinico Universitario A. Gemelli IRCCS, Università Cattolica Del Sacro Cuore, Rome, Italy, Italy; ³⁹University of Milano-Bicocca, European Reference Network on Hepatological Diseases (ERN RARE-LIVER), San Gerardo Hospital, Monza, Italy, Italy; ⁴⁰San Paolo Hospital, Civitavecchia; Padre Pio Hospital Bracciano, Italy; ⁴¹Cardinal Massaia Hospital, Asti, Italy, Italy; ⁴²Azienda Ospedaliero-Universitaria Maggiore della Carità, Novara, Italy, Italy; ⁴³School of Medicine and Psychology University "Sapienza", Azienda Ospedaliera S. Andrea, Rome, Italy; ⁴⁴University of Palermo, Palermo, Italy, Italy; ⁴⁵Policlinico di Bari Hospital, Bari, Italy, Italy; ⁴⁶Istituto Di Cura Città Di Pavia, Pavia, Italy, Italy; ⁴⁷Azienda Sanitaria Locale Di Biella, Biella, Italy, Italy; ⁴⁸Spedali Civili Gardone Val Trompia, Brescia, Italy, Italy; ⁴⁹Valtellina e Alto Lario Hospital, Sondrio, Italy, Italy; ⁵⁰Guido Salvini Hospital, Rho, Italy, Italy; ⁵¹Ospedale SS. Annunziata Sassari, Italy; ⁵²Spedali Civili, Brescia, Italy, Italy
Email: f.terracciani@unicampus.it

Background and aims: Primary biliary cholangitis (PBC) is a chronic inflammatory and autoimmune cholestatic liver disease, which, if left untreated, can lead to cirrhosis and the need for liver transplantation. A variable percentage of patients (25–40%) are non-responder to first-line therapy with ursodeoxycholic acid (UDCA). In 2016, obeticholic acid (OCA) has been approved for patients non-responder or intolerant to UDCA. A number of studies have already reported post-marketing experiences with OCA; however, they are limited by small sample sizes and short follow-up. Aim of the RECAPITULATE study is to provide long-term results concerning real-world treatment with OCA in a large Italian cohort of PBC patients.

Method: Centres belonging to the "Italian PBC registry," the PBC task force of "Club Epatologi Ospedalieri" (CLEO) and "Associazione Italiana Gastroenterologi Ospedalieri" (AIGO), the "Sicilian PBC Network" and the "PBC Project Piemonte-Liguria-Valle D'Aosta" participated to data collection. Data from all patients followed at those centres receiving at least one dose of OCA, and with a follow-up of at least 6 months, were captured. Cumulative incidences of OCA response and discontinuation were evaluated through Aalen-Johansen (taking into account the competing risk of discontinuation) and Kaplan-Meier estimators, respectively.

Results: Data on 441 PBC patients (median age 58 years, women 88%, median time on OCA therapy 24 months), enrolled from 50 Italian centres, were analyzed. 153 patients (34%) were cirrhotics and 59 (13%) were PBC/autoimmune hepatitis (AIH) overlap. Observed response probabilities according to POISE criteria at 12/24/36 months were 37.5/43.5/47.2%, respectively. OCA was discontinued in 86 patients (19%). Discontinuation probabilities at 12/24/36 months were 12.8/17.7/22.9%, respectively. Leading causes of discontinuation were pruritus (41 patients, 48%), and hepatic events (19 patients, 21%). Cirrhotics showed lower response probabilities (25.9/27.7/34.8% at 12/24/36 months; $p < 0.01$ Vs non-cirrhotics), and higher discontinuation probabilities (19.9/27.6/34.6% at 12/24/36 months; $p < 0.01$ Vs non-cirrhotics). Response and discontinuation probabilities in PBC/AIH overlap were not significantly different to those observed in "pure PBC" ($p = 0.20$). Liver stiffness measurements (LSM) by vibration-controlled-transient-elastography (VCTE) were available for 309/114/69 patients at 0/12/24 months. LSMs were not different at 12 months compared with baseline either in Poise non-responders or responders. Conversely, at 24 months, LSMs were significantly reduced with respect to baseline in Poise responders [7.5 (5.4–9.5) Vs 7.9 (6.1–11.3), $p = 0.01$], but not in non-responders ($p = 0.96$).

Conclusion: Results from the Italian RECAPITULATE study confirm in a real-world setting the long-term efficacy and safety of second-line PBC treatment with OCA. These first data concerning LSM variation over time under OCA treatment suggest a reduction only in Poise responders, but need to be verified in a larger sample size.

OS-046

Results from a planned interim analysis of a randomized, double-blind, active-controlled trial evaluating the effects of obeticholic acid and bezafibrate on serum biomarkers in primary biliary cholangitis

Vaclav Hejda¹, Alexandre Louvet², Antonio Civitarese³, Lynda Szczech³, Heng Zou³, Frederik Nevens⁴. ¹University Hospital in Pilsen, Pilsen, Czech Republic; ²University Hospital of Lille, Lille, France; ³Intercept Pharmaceuticals Inc, Morristown, United States; ⁴University Hospital KU Leuven, Belgium
Email: antonio.civitarese@interceptpharma.com

Background and aims: Bezafibrate (BZF), a pan-agonist of the peroxisome proliferator-activated receptors, benefits patients with primary biliary cholangitis (PBC) who have an inadequate response to ursodeoxycholic acid (UDCA). Obeticholic acid (OCA), a potent farnesoid X receptor agonist, was approved as second-line treatment for PBC in 2016. This planned interim analysis of an ongoing phase 2, randomized, active-controlled trial assessed whether a combination of OCA and BZF may improve serum biomarkers for PBC more than BZF monotherapy, while also monitoring the safety and tolerability of the novel combination.

Method: While continuing their UDCA treatment (if any), subjects with PBC were randomized 1:1:1 to receive 12 weeks of once daily oral BZF 200 mg + placebo (B200), BZF 400 mg + placebo (B400), BZF 200 mg + OCA 5 mg titrated to 10 mg at week 4 (OCA/B200), or BZF 400 mg + OCA 5 mg titrated to 10 mg at week 4 (OCA/B400). End points included comparisons of serum biomarker levels of PBC-induced liver damage: alkaline phosphatase (ALP), alanine transaminase (ALT), aspartate aminotransferase (AST), gamma-glutamyl transferase (GGT), and total bilirubin (TB). Safety was assessed by monitoring of adverse events (AEs) and laboratory values.

Results: This planned interim analysis from the first 45 of the anticipated 72 subjects focused on short-term changes in biochemical indicators of improved outcomes in PBC. Relative to baseline values, only subjects receiving OCA/B400 showed a highly significant reduction in ALP to within normal range (60% of subjects) at week 4, which continued to improve through week 12 (**Figure**). Subjects receiving OCA/B400 also exhibited the greatest reductions in biomarkers and normalized levels of total bilirubin (100%), ALT (100%), and GGT (70%) by week 12. Two events of pruritus (20%) were reported in B200, 3 (25%) in B400, 2 (17%) in OCA/B200, and none in OCA/B400. Five of 23 (22%) subjects who received OCA discontinued the study: 2 withdrew consent (one in each combination group), 2 experienced treatment-emergent AEs (TEAEs; OCA/B400), and 1 violated the inclusion/exclusion criteria (OCA/B200). Four subjects experienced severe or serious TEAEs deemed non-drug related (atrial fibrillation [2 events], breast cancer, and pleural mesothelioma malignant). No deaths occurred in this study.

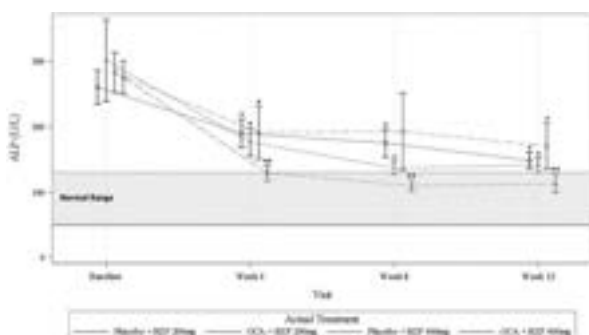


Figure: Effect of BZF (200 or 400 mg) and placebo or BZF (200 or 400 mg) and OCA (5–10 mg) on ALP levels in subjects with PBC. All treatment groups showed reductions from baseline in ALP, but only the highest dose combination (BZF 400 mg + OCA 5–10 mg) reduced the mean ALP levels to within normal range. Data are shown as mean values \pm standard error of the mean. * $p < 0.05$, ** $p < 0.0001$.

Conclusion: The results of this planned interim analysis suggest that short-term combination of BZF and OCA was well tolerated and has therapeutic potential in the reduction of biomarkers of PBC-related liver damage.

OS-047-YI

Results of the prospective multicentre European R-LIVER registry reveal the unmet clinical needs of autoimmune hepatitis

Ida Schregel¹, Maria Papp², Nóra Sipeki², Patricia Kovats^{2,3}, Richard Taubert⁴, Bastian Engel⁴, Alejandro Campos-Murguía⁴, George Dalekos⁵, Nikolaos Gatselis⁵, Kalliopi Zachou⁵, Piotr Milkiewicz^{6,7}, Maciej K. Janik⁶, Joanna Raszeja-Wyszomirska⁶, Henriette Ytting⁸, Felix Braun¹, Christian Casar¹, Ansgar W. Lohse¹, Christoph Schramm^{1,9,10}. ¹University Medical Centre Hamburg-Eppendorf, I. Department of Medicine, Hamburg, Germany; ²Faculty of Medicine, University of Debrecen, Division of Gastroenterology, Department of Internal Medicine, Debrecen, Hungary; ³Faculty of Medicine, University of Debrecen, Kálmán Laki Doctoral School, Debrecen, Hungary; ⁴Hannover Medical School, Hannover, Germany; ⁵General University Hospital of Larissa, Department of Medicine and Research Laboratory of Internal Medicine, National Expertise Center of Greece in Autoimmune Liver Diseases, Larissa, Greece; ⁶Medical University of Warsaw, Department of Hepatology, Transplantology and Internal Medicine, Warsaw, Poland; ⁷Pomeranian Medical University, Translational Medicine Group, Szczecin, Poland; ⁸Hvidovre University Hospital of Copenhagen, Copenhagen, Denmark; ⁹University Medical Centre Hamburg-Eppendorf, Martin Zeitz Center for Rare Diseases, Hamburg, Germany; ¹⁰University Medical Centre Hamburg-Eppendorf, Hamburg Center for Translational Immunology (HCTI), Hamburg, Germany
Email: i.schregel@uke.de

Background and aims: Prospective multicentre data on the treatment and outcome of adult autoimmune hepatitis (AIH) patients is lacking. The European Reference Network for Hepatological Diseases (ERN RARE-LIVER) launched the prospective, quality-controlled R-LIVER registry on rare liver diseases including data from newly diagnosed patients with autoimmune liver diseases. The aim of this study was to assess presentation, treatment heterogeneity and outcome under real-world conditions to describe the landscape of AIH in Europe.

Method: Data was collected prospectively between 01/2015 and 10/2022 at time of diagnosis of AIH, and after 6- and 12-months follow-up. Patients with concomitant liver diseases other than fatty liver disease at diagnosis were excluded. Treatment response was defined as normalization of ALT since in our cohort, correlation of ALT with histological activity could not be improved by the addition of serum IgG levels.

Results: 227 patients from six centres were included in the final analysis (81.5% female) with a median age at diagnosis of 55 years. Liver biopsy was performed in 96%, of whom 81.3% presented with a moderate to severe mHAI and 25.4% with severe Fibrosis (F3/F4). 24/227 patients presented with acute-severe AIH (including three patients receiving liver transplantation who were further excluded). After six months ALT was below ULN in 58% (130/224) and after 12 months, in 69.2% (155/224) of patients. In 36.6% steroids were withdrawn within the first year resulting in a steroid-free response in 29.4% (66/224) of patients.

In multivariate analysis corrected for centre site, older age at diagnosis (OR = 1.03 [95%CI 1.01–1.05]; $p = 0.007$), severe fibrosis (OR 0.38 [95% 0.16–0.89]; $p = 0.026$) and change of treatment between baseline and six-months follow-up (OR 0.40 [95% CI 0.2–0.86]; $p = 0.018$) were associated with treatment response at 12 month-follow-up.

Change of treatment, mostly due to intolerance, occurred in 30.4% within the first six months and in another 13.4% in the following six months. Of those who had a treatment change within the first six months, in only 57.4% ALT was below ULN at 12 months-follow-up.

ORAL PRESENTATIONS

After 12 months, 62.9% were still on first-line therapy (azathioprine and/or steroids). Overall, 16 different treatment regimens were administered within the first year of follow-up.

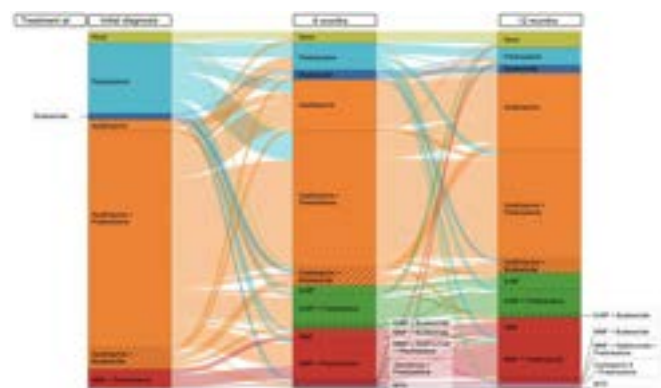


Figure 5: Sankey diagram showing treatment regimens and flows between treatment regimens at diagnosis, at 6 months and at 12 months ($n = 224$; 3 patients excluded due to liver transplantation). Steroids: Prednisolone (light blue), budesonide (striped). Immunosuppressive Treatment: Azathioprine (orange), MMF (red), 6-MP (green), tacrolimus (purple), cyclosporine A (pink), MTX (brown).

Conclusion: The results from this European multicentre prospective registry demonstrate a high rate of drug intolerance within the first six months of AIH therapy leading to change of treatment regime in 30.4%. The landscape of AIH-treatment is heterogeneous even in expert centres throughout Europe with nearly one third of patients not reaching normalization of serum ALT levels until 12 months-follow-up and less than one third of patients with steroid-free treatment response. Those high rates of failure highlight the unmet needs in the care of people suffering from AIH.

OS-048-YI

Risk of cancer and subsequent mortality in primary biliary cholangitis: a population-based cohort study of 3,052 patients

Axel Wester¹, Johanna Schönau², Jörn Schattenberg³, Hannes Hagström¹. ¹Karolinska Institutet, Department of Medicine Huddinge, Sweden; ²University Medical Center of the Johannes Gutenberg-University, Germany; ³Metabolic Liver Research Program, University Medical Center of the Johannes Gutenberg-University Mainz, Germany
Email: axel.wester@ki.se

Background and aims: Primary biliary cholangitis (PBC) is a rare cholestatic liver disease. Incident cancer is a concern. Previous studies have described an increase in hepatocellular carcinoma (HCC), but the risk of non-hepatic cancer and the cancer risk across subgroups is largely unknown.

Method: We used the Swedish National Patient Register to identify all patients who were newly diagnosed with PBC between 2002 and 2019. Patients were matched for age, sex, and municipality with up to ten reference individuals from the general population. Incident cancer was recorded from the National Cancer Register. Cox regression was used to investigate the rates of cancer and post-cancer mortality, adjusted for potential confounders. The cumulative incidence of cancer was calculated while accounting for the competing risk of death.

Results: We identified 3,052 patients with PBC and 26,792 reference individuals and followed them for a median of 5.5 and 7.0 years, respectively. The median age was 64 years and 85% were women. At ten years of follow-up, the cumulative incidence of any cancer in patients with PBC was 14.3% (95% confidence interval [CI] 12.8–15.9),

compared to 11.8% (95% CI 11.3–12.2) in the reference population (adjusted hazard ratio [aHR] 1.4, 95% CI 1.2–1.5). Although the rate of HCC was particularly high (aHR 30.9; 95% CI 14.8–64.6), PBC was also associated with non-HCC cancer (aHR 1.2, 95% CI 1.1–1.4), including gastrointestinal (aHR 1.5, 95% CI 1.1–1.9), lung (aHR 1.5, 95% CI 1.1–2.2) and lymphoma (aHR 2.9, 95% CI 1.9–4.6). The cancer rates were similarly increased across age and sex subgroups, but more prominently increased in patients with cirrhosis (aHR 2.1; 95% CI 1.4–3.0). Following a diagnosis of cancer, patients with PBC had higher one-year mortality rates compared to reference individuals (aHR 1.4, 95% CI 1.1–1.8), which was mainly driven by HCC (non-HCC related mortality: aHR 1.2, 95% CI 0.9–1.6).

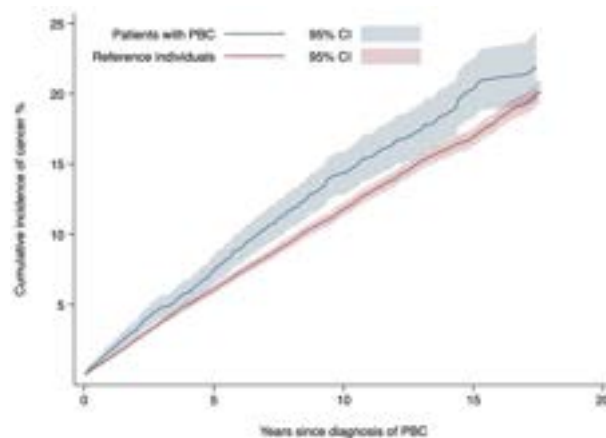


Figure:

Conclusion: Patients with PBC have a significantly higher risk of cancer compared to the general population. PBC was associated with both HCC and non-hepatic cancers as well as higher mortality following a diagnosis of cancer.

OS-049-YI

Lack of biochemical response after diagnosis is associated with cirrhosis development during follow-up in autoimmune hepatitis

Charlotte Slooter¹, Patrick Maisonneuve², Francesca Colapietro³, Floris van den Brand¹, Marco Lenzi⁴, Paolo Muratori⁴, Nanda Kerker⁵, George Dalekos⁶, Kalliopi Zachou⁶, Maria Isabel Lucena⁷, Mercedes Robles-Díaz⁷, Daniel E. Di Zeo-Sánchez⁷, Raul J. Andrade⁷, Aldo Montano-Loza⁸, Ellina Lytvyak⁸, Gerd Bouma¹, Rodrigo Liberal⁹, Ana Lleó³, Ynto de Boer¹. ¹Amsterdam University Medical Center, Netherlands; ²European Institute of Oncology, Italy; ³Humanitas University, Italy; ⁴University of Bologna, Italy; ⁵Golisano Children's Hospital, University of Rochester Medical Center, United States; ⁶University Hospital of Larissa, Greece; ⁷Virgen de Victoria University Hospital, University of Málaga, Spain; ⁸University of Alberta Hospital, Edmonton, Canada; ⁹Centro Hospitalar Sao Joao, Porto, Portugal
Email: y.deboer1@amsterdamumc.nl

Background and aims: The aim of treatment in autoimmune hepatitis (AIH) is the achievement of complete biochemical response defined as normalization of aminotransferases and immunoglobulin G (IgG) in order to prevent further progression of the disease and the development of cirrhosis. Studies with enough power that assess prognostic factors are scarce. The aim of this study is to identify prognostic factors in the world's largest AIH cohort from the International Autoimmune hepatitis (AIH) Group retrospective registry (IAIHG-RR).

Method: This retrospective, observational, multicentre study included all patients with a clinical diagnosis of AIH and available follow-up data from the IAIHG-RR. Logistic regression and Cox regression were used to identify independent risk factors for lack of biochemical response and development of cirrhosis. Analysis of cirrhosis development was restricted to the four centres that reported date of cirrhosis development.

Results: This analysis included 1700 patients with a median follow-up of 10 (range 0–49) years. In those with available data on response, no normalization of aminotransferases and IgG within 6 months after treatment initiation was observed in 418 (32%) and 153 (22%) patients, respectively. Overall, 224 (32%) patients did not achieve complete biochemical response and 114 (37%) developed cirrhosis after a median of 8 (range 0–33) years. Predictors of lack of biochemical response were cirrhosis at diagnosis (HR 2.6 95% CI 1.7–4.0), anti-smooth muscle antigen (SMA) (HR 0.5 95% CI 0.3–0.7), and the laboratory values alkaline phosphatase (ALP) (HR 1.0 95% CI 1.0–1.0) and IgG (HR 1.1 95% CI 1.0–1.1) at first evaluation. Predictors of cirrhosis development included variant syndromes with primary biliary cholangitis (PBC) (HR 2.0 95% CI 1.0–4.0) and primary sclerosing cholangitis (PSC) (HR 6.7 95% CI 2.6–17.6) as well as lack of biochemical response (HR 4.2 95% CI 2.1–8.2).

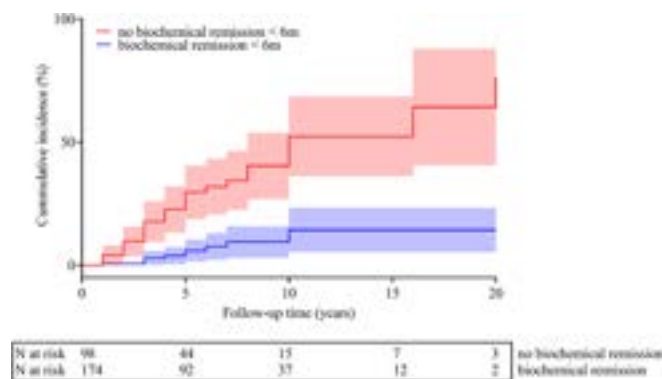


Figure: Cumulative incidence of cirrhosis development according to response to treatment in patient with AIH ($p < 0.001$ log-rank).

Conclusion: Cirrhosis at diagnosis, SMA, ALP and IgG were associated with lack of biochemical response. Predictors of cirrhosis development after diagnosis were lack of biochemical response and the presence of variant syndromes. This finding supports IAIHG statement that treatment of AIH should aim at complete biochemical response within 6 months, as defined by normalization of both liver enzymes and IgG. Close follow-up and more aggressive treatment of these patients may be warranted.

Liver transplantation and hepatobiliary surgery

OS-050-YI

APRI+ALBI score is superior to Indocyanine Green (ICG) clearance and LiMax test in the prediction of posthepatectomy liver failure—an international multicenter study of 14581 patients

Jonas Santol^{1,2}, Sarang Kim¹, Hubert Hackl³, Lindsey Gregory⁴, Ruth Baumgartner⁵, Anastasia Lemekhova⁶, Emrullah Birgin⁷, Severin Gloor⁸, Eva Braunwarth⁹, Markus Ammann¹⁰, Johannes Starlinger¹¹, David Pereyra¹², Daphni Ammon¹², Marijana Ninkovic⁹, Anna Kern¹², Felix Huber¹², Jeremias Weninger¹², Yawen Dong¹, Cornelius Thiels⁴, Susanne Warner⁴, Rory L. Smoot⁴, Mark Truty⁴, Michael Kendrick⁴, David M. Nagorney⁴, Sean Cleary⁴, Katrin Hoffmann⁶, Stefan Gilg¹³, Alice Assinger², Thomas Grünberger¹, Patrick Starlinger⁴. ¹HPB Center, Vienna Health Network, Clinic Favoriten, Department of Surgery, Wien, Austria; ²Center for Physiology and Pharmacology, Medical University of Vienna, Institute of Vascular Biology and Thrombosis Research, Vienna, Austria; ³Biocenter, Medical University of Innsbruck, Division of Bioinformatics, Austria; ⁴Mayo Clinic, Department of Surgery, Division of Hepatobiliary and Pancreatic Surgery, Rochester, United States; ⁵Karolinska University Hospital, Department of Oncology, Sweden; ⁶Heidelberg University Hospital, Department of General, Visceral, and Transplantation Surgery, Germany; ⁷University Medicine Mannheim, Medical Faculty Mannheim, Heidelberg University, Department of Surgery, Germany; ⁸Inselspital, Bern University Hospital, University of Bern, Department of Visceral Surgery and Medicine, Switzerland; ⁹Medical University of Innsbruck, Department of Visceral, Transplantation and Thoracic Surgery, Austria; ¹⁰State Hospital Wiener Neustadt, Department of Surgery, Austria; ¹¹37binary UG, Berlin, Germany; ¹²Medical University of Vienna, Department of General Surgery, Division of Visceral Surgery, Austria; ¹³Karolinska University Hospital, Department of HPB surgery, Sweden
Email: tellsantol@gmail.com

Background and aims: APRI+ALBI, a score calculated using only aspartate aminotransferase, platelet count, albumin and bilirubin, and dynamic liver function tests like ICG clearance and LiMax have been evaluated for their predictive potential for posthepatectomy liver failure (PHLF). The aim of this study was to compare the predictive potential of these parameters for PHLF grade B + C and validate our findings using an international multicenter cohort and a logistic regression-based prediction model.

Method: 622 patients undergoing major and minor liver resection with preoperative ICG clearance measurement and 192 patients undergoing hepatic surgery, with preoperative LiMax test assessment were included from a prospectively maintained database. PHLF grade B + C was defined according to the ISGLS criteria. To form a validation cohort 1906 patients with available preoperative APRI+ALBI score from 8 different international institutions were included. Finally, 12056 patients from the NSQIP database, who underwent hepatic surgery and where a preoperative APRI+ALBI score could be calculated, were included to generate a logistic regression-based prediction model along with generalized additive models to capture non-linearities.

Results: Predictive potential of the APRI+ALBI score for PHLF grade B + C was superior to ICG clearance and LiMax, when comparing areas under the curve (AUC) (ICG cohort: APRI+ALBI AUC = 0.785, ICG-R15 AUC = 0.643, ICG-PDR AUC = 0.643; LiMax cohort: APRI+ALBI AUC = 0.868, LiMax AUC = 0.536). We then defined two cutoffs for APRI+ALBI. A low-risk cutoff of ≥ -2.43 , to assess which patients could safely be resected (negative predictive value (NPV) = 98%, $p < 0.001$) and a high-risk cut-off of ≥ -0.86 , to identify which patients were most likely to develop PHLF B + C (positive predictive value (PPV) = 56%, $p < 0.001$). Both cutoffs proved independent of other parameters and confounders in two multivariable models (low-risk multivariable

ORAL PRESENTATIONS

model: low-risk cutoff, $p < 0.001$, odds ratio (OR), 5.751, 95% confidence interval (CI), 2.193–15.082; high-risk multivariable model: high-risk cutoff, $p < 0.001$, OR, 20.534, CI, 4.946–85.252. The cutoffs showed similar results in the validation cohort (≥ -2.43 NPV = 93%, $p < 0.001$; ≥ -0.86 PPV = 29%, $p < 0.001$; ≥ -0.98 PPV = 33%, $p < 0.001$). To evaluate dynamic risk increase more precisely, in a next step, we developed a logistic regression based dynamic risk assessment model (Fig. 1). We were able to demonstrate and validate that with a rising APRI+ALBI score a concomitant exponential increase in risk can be observed.

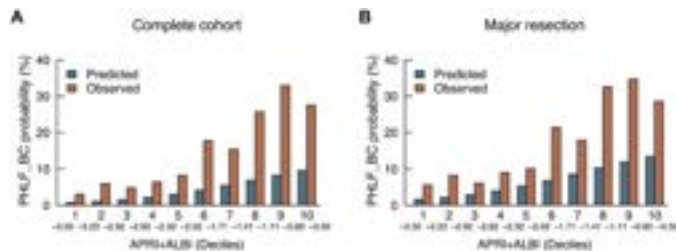


Figure 1: Logistic regression based dynamic risk assessment model, calculated for the whole cohort (A) and for major resections only (B).

Conclusion: APRI+ALBI can be calculated using only routine preoperative laboratory parameters. We can demonstrate that APRI+ALBI is superior to ICG clearance and LiMAX testing, as two frequently used dynamic liver function tests, in the prediction of PHLF grade B + C. Using high- and low-risk cutoffs, we were able to assess which patients could safely undergo surgery and which patients had the highest postoperative risk to develop PHLF B + C. We were able to validate our findings, using an international multicenter validation cohort. Importantly, we could ultimately develop and validate a dynamic risk assessment model for clinically significant PHLF based on simple APRI/ALBI scoring to increase predictive accuracy for the individual patient.

OS-051-YI

MicroRNA based prediction of posthepatectomy liver failure and mortality outperforms established markers of preoperative risk assessment

Anna Kern¹, David Pereyra², Hubert Hackl³, Susanna Skalicky⁴, Jonas Santol^{5,6}, Jeremias Weninger², Sarah Brunner², Valerie Laferl², Yannick Herrmann², Thomas Grünberger⁵, Matthias Hackl⁴, Alice Assinger⁶, Patrick Starlinger⁷. ¹General Hospital of Vienna, Department of General Surgery, Division of Visceral Surgery, Medical University of Vienna, Vienna, Austria; ²General Hospital of Vienna, Department of General Surgery, Division of Visceral Surgery, Medical University of Vienna, Austria; ³Medical University of Innsbruck, Division of Bioinformatics, Austria; ⁴TamiRNA GmbH, Austria; ⁵Clinic Favoriten, Department of Surgery, HPB Center, Vienna Health Network, Austria; ⁶Institute of Vascular Biology and Thrombosis Research, Center for Physiology and Pharmacology, Medical University of Vienna, Austria; ⁷Mayo Clinic, Rochester, Department of Surgery, Division of Hepatobiliary and Pancreatic Surgery, Rochester, United States
Email: tellkern@gmail.com

Background and aims: Posthepatectomy liver failure (PHLF) continues to be the most significant factor determining outcomes after hepatic resection, accounting for nearly half of postoperative mortality. In this study, we evaluated if the simple assessment of circulating microRNAs (miRs) can predict PHLF, and could outperform other liver function tests, such as indocyanine green (ICG) clearance, hepatic venous pressure gradient (HVPG) and liver maximum capacity (LiMAX) test.

Method: A total of 329 patients, all undergoing liver resection in 3 different hospitals in Vienna, Austria, were included and postoperative outcome was assessed. Our previously described miR-Score

(HepatomiR) was assessed preoperatively, as well as other well established predictors of PHLF.

Results: HepatomiR was superior to all other analyzed liver function tests in the prediction of PHLF and PHLF grades B and C (PHLF: HepatomiR: area under the curve (AUC) = 0.770, Fig. 1A) (PHLF: plasma disappearance rate (PDR): AUC = 0.569; retention rate at 15 minutes (R15): AUC = 0.618; HVPG: AUC = 0.530; LiMAX: AUC = 0.540, Fig. 1B) (PHLF B+C: HepatomiR: AUC = 0.755, Fig. 1C) (PHLF B+C: PDR: AUC = 0.634; R15: AUC = 0.653; HVPG: AUC = 0.530; LiMAX: AUC = 0.593). Also, strong predictive potential for PHLF was observed when analyzing HepatomiR in the respective tumor subgroups (colorectal cancer liver metastases (mCRC): AUC = 0.799; hepatocellular carcinoma (HCC): AUC = 0.723; cholangiocellular carcinoma (CCA): AUC = 0.701; other: AUC = 0.949, Fig. 1D). We could validate the previously published low-risk cut-off $P > 0.59$ (negative predictive value = 91.5%) and high-risk cut-off $P > 0.68$ (positive predictive value = 77%) for PHLF and document a close association with postoperative overall survival. Economic analyses demonstrated a significant reduction of health care costs utilizing improved patient risk-stratification.

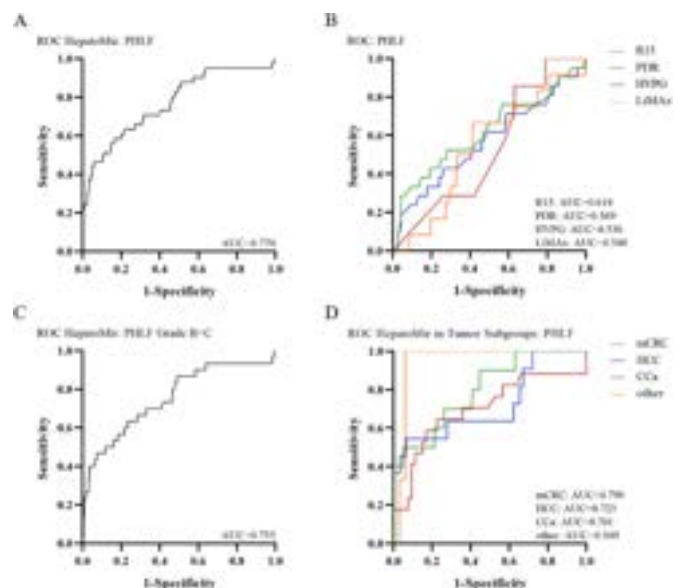


Figure:

Conclusion: The simple assessment of 3 circulating miRs outperforms several liver function tests utilized in daily clinical practice in the prediction of PHLF. Moreover, HepatomiR allowed identification of patients that died rapidly after hepatic resection, which might be better served with alternative treatments. Economic assessment let us to demonstrate, that optimized preoperative risk-assessment lead to a significant reduction of health care costs.

OS-052

Prehabilitation intervention to maximize early recovery (PRIMER) in liver transplantation: a randomized, controlled trial

Marina Serper¹, Lauren Jones¹, Thomas Clement¹, Kristen Dwinells², Derek Zaleski², Peter Reese¹. ¹University of Pennsylvania, United States; ²Hospital of the University of Pennsylvania, United States
Email: marinas2@pennmedicine.upenn.edu

Background and aims: Frailty and impaired functional status are associated with adverse outcomes on the liver transplant (LT) waitlist and after transplantation. Prehabilitation prior to LT has rarely been tested. We conducted a two-arm patient randomized trial to evaluate the efficacy of a behavioral intervention to promote exercise and physical activity prior to LT.

Method: This was a 12-week, prospective study comparing enhanced usual care to a home-based, remote monitoring behavioral intervention. A total of 30 patients were randomized 2:1 to intervention (n-

20) vs. control (n = 10). The intervention arm included financial incentives and text-based reminders that were linked to personal fitness trackers (Nokia Go) to gradually increase daily steps by 15% in 2-week intervals (6 in total). Weekly check-ins with study staff were incentivized to promote adherence and assess barriers to physical activity. Both arms received personalized dietary and physical activity recommendations based on a nutrition assessment, short physical performance battery (SPPB), and frailty. The primary outcomes were feasibility and acceptability. Secondary outcomes included mean end-of-study (week 11–12) step counts, SPPB, grip strength, and body composition (PhA). We fit regression models for secondary outcomes with arm as the exposure adjusting for baseline performance using robust standard errors.

Results: Mean age was 61, 47% were female, median MELD-Na was 13. One third were frail or pre-frail by the liver frailty index (LFI), 40% had impaired mobility by SPPB, nearly 40% had sarcopenia by bioimpedance PhA, 23% had prior falls, and 53% had diabetes. Study retention was 27/30 (90%; 2 unenrolled from intervention, 1 lost to follow-up in control arm). Self-reported adherence to exercise during weekly check-ins was about 50%; most common barriers were fatigue, weather, liver-related symptoms. Figure 1 shows mean step counts by arm (Panel A) and % adherence to daily step targets (Panel B) by each 2-week interval. Mean baseline daily steps counts were: overall: M 2186 SD (1166); control: M 2632 SD (1599); intervention: M 1924 SD:758). End of study step counts were nearly 1000 steps higher for intervention vs. control: $\beta = 997$, 95% CI 147–1847; $p = 0.023$). On average, the intervention group achieved daily step targets 51% of the time.

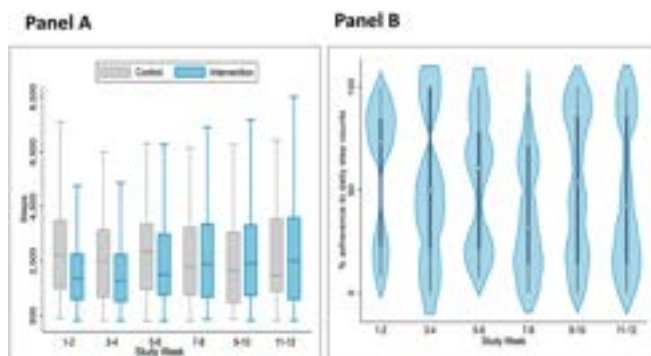


Figure 1: Panel A. Steps counts by arm during each 2-week interval; Panel B. Percent adherence to step count goals during each 2-week interval in the intervention arm.

Conclusion: A home-based intervention with financial incentives and text-based nudges increased walking by one third over baseline in LT candidates with functional impairment and malnutrition. Adherence to physical activity was three-fold higher than reported in recent studies. Home-based prehabilitation is feasible and hold promise for larger trials.

OS-053-YI

Type of calcineurin inhibitor versus long-term outcome following liver transplantation for primary biliary cholangitis-an ELTR study

Maria van Hooff¹, Rozanne de Veer¹, Vincent Karam², René Adam², Wojciech Polak³, Hasina Pashtoun¹, Sarwa Darwish Murad¹, Christophe Corpechot⁴, Darius F. Mirza⁵, Michael Heneghan⁶, Peter Lodge⁷, Gabriel Oniscu⁸, Douglas Thorburn⁹, Michael Allison¹⁰, Herold Metselaar¹, Caroline den Hoed¹, Adriaan Van der Meer¹.

¹Erasmus MC Transplant Institute, University Medical Center Rotterdam, Department of Gastroenterology and Hepatology, Netherlands; ²Hôpital Paul Brousse, Université Paris-Saclay Villejuif, European Liver Transplant Registry, Department of Hepatobiliary and Pancreatic Surgery and Liver Transplantation AP-HP, France; ³Erasmus MC Transplant Institute, University Medical Center Rotterdam, Department of Surgery, Division

of HPB and Transplant Surgery, Netherlands; ⁴Saint-Antoine Hospital, Assistance Publique-Hôpitaux de Paris; Inserm UMR_S938, Saint-Antoine Research Center, Sorbonne University, Paris, Reference Center for Inflammatory Biliary Diseases and Autoimmune Hepatitis, European Reference Network on Hepatological Diseases (ERN Rare-Liver), France; ⁵Queen Elizabeth Hospital, Birmingham, Department of HPB Surgery, Liver Unit, United Kingdom; ⁶King's College Hospital, London, Institute of Liver Studies, United Kingdom; ⁷The Leeds Teaching Hospitals NHS Trust, United Kingdom; ⁸Edinburgh Transplant Centre, Royal Infirmary of Edinburgh, United Kingdom; ⁹Royal Free Hospital, London, Department of Hepatology and Liver Transplantation, United Kingdom; ¹⁰Cambridge University Hospitals NHS Foundation Trust, Cambridge NIHR Biomedical Research Centre, Cambridge, Liver Unit, United Kingdom
Email: m.vanhooff@erasmusmc.nl

Background and aims: Tacrolimus is the preferred calcineurin inhibitor (CNI) following liver transplantation (LT). As compared to cyclosporine, however, tacrolimus has been linked to a more frequent recurrence of Primary Biliary Cholangitis (PBC), which was recently shown to negatively impact graft and patient survival. Therefore, the aim of this study was to assess the relation between the type of CNI and long-term graft and patient survival following LT for PBC.

Method: Cox proportional hazard analyses were used to assess the association between the type of CNI and graft or recipient survival among adult patients with PBC in the European Liver Transplant Registry (ELTR) who received a DBD graft between 1990 and 2021. Graft failure was defined as re-transplantation irrespective of the cause, as ELTR contained no data on recurrence PBC. Patients were not included in case of concomitant liver disease or in case they did not reach one year of follow-up with a functioning graft. The type of CNI was based on the registered maintenance immunosuppressive regimen, or in case this was not available, on the initial regimen.

Results: In total, the ELTR included 5306 PBC patients who received a DBD LT between 1990 and 2021. Overall, these patients were followed for a median of 8.3 years (IQR 2.0–15.9), during which 2213 patients lost their graft and/or died. The 5-year cumulative graft and recipient survival rates were 77.7% (95%CI 76.5–78.9) and 82.0% (95%CI 80.8–83.2), respectively. Of the 5306 patients, 443 (8.3%) patients did not (yet) reach one year of follow-up and 797 (15.0%) lost their graft or died during the first year. Among the remaining 4066 patients, there was no information concerning immunosuppressive drugs in 891 (21.9%) patients. The study population for the primary aim thus included 3175 PBC patients; 2764 (87.1%) females, median age at LT of 55.4 years (IQR 48.8–61.4), and a median year of LT of 2001 (IQR 1996–2009). Tacrolimus was used in 2056 (64.8%) patients and cyclosporine in 819 (25.8%), while 283 (8.9%) did not use any CNI and 17 (<0.01%) used both. Among patients using a single CNI, tacrolimus was not associated with higher risk of graft loss (HR 0.95, 95%CI 0.83–1.08, $p = 0.397$) or death (HR 0.91, 95%CI 0.80–1.04, $p = 0.150$). Adjusting for age, gender, year of LT, ischemia time and donor age did not change the association between the type of CNI and graft loss (aHR 0.97, 95%CI 0.82–1.15, $p = 0.751$) or death (aHR 0.96, 95%CI 0.81–1.14, $p = 0.636$). Findings were consistent in clinically relevant subgroups (e.g. based on age and time of LT) and sensitivity analyses including events in the first year post-LT (range of aHR for type of CNI was 0.83–1.22, $p > 0.100$ for all).

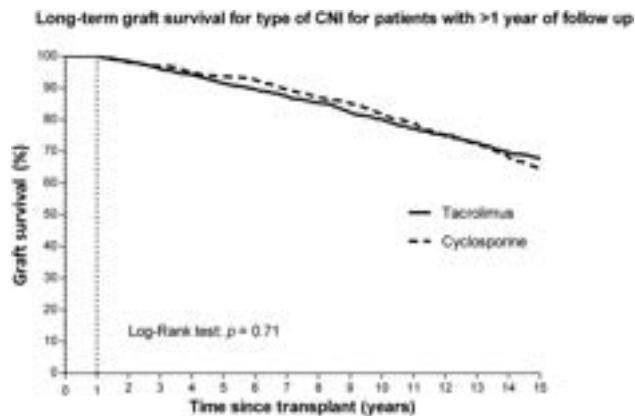


Figure:

Conclusion: Among adult PBC patients transplanted with DBD liver grafts, the type of CNI was not associated with long-term graft survival or recipient survival. These results justify the continued use of tacrolimus after DBD LT in the patients with PBC.

Liver tumours – Therapy

OS-055

Characterization and burden of non-hepatocellular carcinoma focal lesions detected during surveillance of patients with cirrhosis

Pierre Nahon¹, Layese Richard², Nathalie Ganne-Carrié¹, Cagnot Carole³, Etienne Audureau², Pierre-André Natella¹. ¹APHP Avicenne, France; ²APHP Henri Mondor, France; ³ANRS, France
Email: pierre.nahon@aphp.fr

Background and aims: Hepatocellular carcinoma (HCC) surveillance is challenged by the detection of hepatic focal lesions (HFL) of other types. The aim was to describe the incidence, characteristics and outcomes of non-HCC HFL detected in patients with cirrhosis.

Method: We analyzed data obtained from medical files of French patients with cirrhosis included in protocolized multicentre HCC surveillance programs (prospective ANRS CirVir and CIRRAL cohorts,

HCC 2000 trial). Incidences of HFL, applied recall procedures, diagnoses and outcomes were analyzed.

Results: 3295 patients were studied. After a median follow-up of 59.8 months, 1024 (31.1%) patients developed at least one HFL (5-yr incidence: 33.3%). Following recall procedures 391 (38.2%) were considered as HCCs (5-yr incidence: 12.1%, Fig1A). The 633 (61.8%) remaining lesions corresponded to non-HCC HFL (5-yr incidence: 21.1%). These lesions were more frequently detected in younger patients with non-viral cirrhosis, with less severe liver disease and better screening compliance. Rates of uninodular lesions were similar in both groups (66.2% vs 65.7%), as was the examination that enabled detection (ultrasound 62.6% vs 59.7%). 283 (72.6%) HCC patients were classified as BCLC 0 or A. The diagnostic procedures performed for non-HCC HFL were available in 389 patients [median additional cross-sectional examination 1 (min: 0, max: 6), 0.7 exams per year (IQR : 0–1.4)]. Sixty-three/389 (16.1%) non-HCC HFL were not subsequently confirmed by recall procedures. One hundred and four/389 (26.7%) non-HCC HFL remained undetermined. A diagnosis of benign liver tumour was assessed for 206/389 (52.9%) HFL (cyst = 41, angioma = 38, vascular fistula = 37, regeneration nodule = 33, dysplastic nodule = 15, perfusion defect = 15, pseudo-lesion = 4, others = 23). Sixteen/389 (4.1%) malignant tumours (cholangiocarcinoma = 15, metastases = 1) were diagnosed. Overall survival of patients with non-malignant HFL was similar to that of patients who never developed HFL during follow-up (5-year survival 92% vs 88%, $P=0.07$, Fig1B). Extra-hepatic mortality was the first cause of death in these 2 groups (60.3% and 63.7%).

Conclusion: The incidence of non-HCC HFL reaches 20% at 5 years and corresponds to two-thirds of lesions detected in patients enrolled in screening programs. This burden must be taken into account in cost-effectiveness analyses of future surveillance programs using more sensitive imaging techniques such as abbreviated MRI.

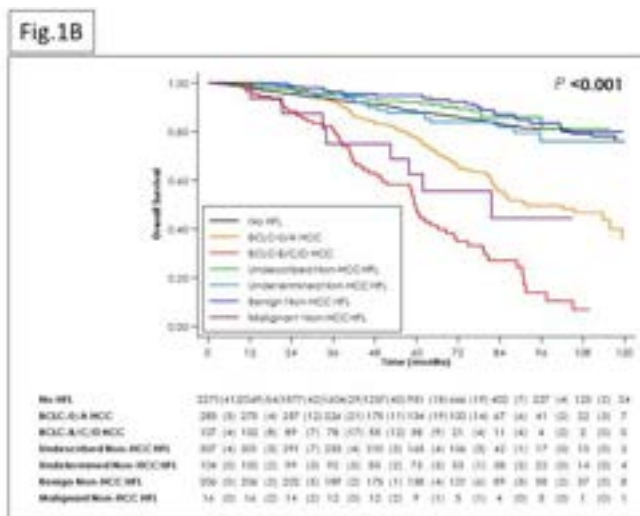
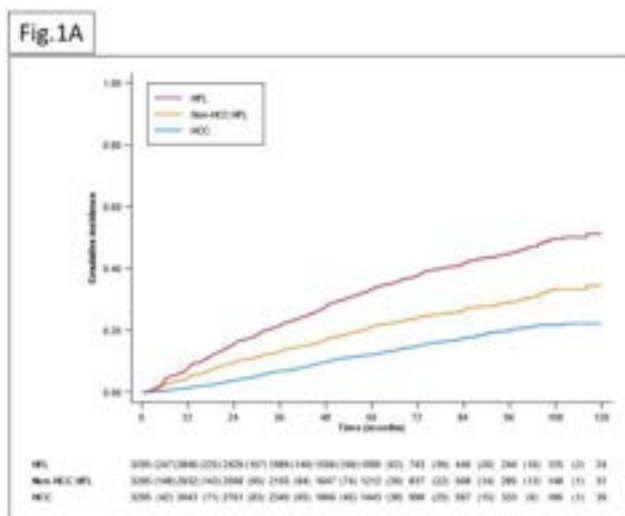


Figure: (abstract: OS-055).

OS-057

Risk of bleeding and thromboembolic events with atezolizumab/bevacizumab or lenvatinib in patients with hepatocellular carcinoma: a multicenter, retrospective study

Najib Ben Khaled¹, Marie Möller², Leonie Jochheim³, Catherine Leyh³, Ursula Ehmer⁴, Katrin Böttcher⁴, Hans Benno Leicht², Monika Rau², Friedrich Sinner⁵, Marino Venerito⁵, Simon Johannes Gairing⁶, Friedrich Foerster⁶, Enrico de Toni¹, Andreas Geier², Florian P Reiter².

¹Department of Medicine II, University Hospital, LMU Munich, Munich, Germany; ²Division of Hepatology, Department of Medicine II, University Hospital Würzburg, Würzburg, Germany; ³Department of Gastroenterology and Hepatology, University Hospital Essen, University of Duisburg-Essen, Essen, Germany; ⁴Internal Medicine II, Klinikum rechts der Isar, TU Munich, Munich, Germany; ⁵Department of Gastroenterology, Hepatology and Infectious Diseases, Otto-von-Guericke University Hospital Magdeburg, Magdeburg, Germany; ⁶Department of Medicine I, University Medical Center of the Johannes-Gutenberg University Mainz, Germany

Email: najib.benkhaled@med.uni-muenchen.de

Background and aims: The combination of atezolizumab and bevacizumab demonstrated superiority over the tyrosine kinase inhibitor (TKI) sorafenib in patients with advanced hepatocellular carcinoma (HCC). VEGF-inhibition with bevacizumab or TKI is associated with the risk of bleeding and thromboembolic events, which is of particular concern in HCC patients. In the pivotal IMBrave150 trial, there was a numerically higher rate of bleeding and arterial thromboembolic events with atezolizumab/bevacizumab compared to sorafenib. The current first-line alternative to a treatment with atezolizumab/bevacizumab is lenvatinib, which demonstrated longer progression free survival and higher objective response rates compared to sorafenib. However, data comparing the safety of atezolizumab/bevacizumab and lenvatinib are lacking. In this study, we evaluated the risk of bleeding and thromboembolic events with atezolizumab/bevacizumab versus lenvatinib in a large, multi-centric real-world population.

Method: Data from HCC cohorts of six tertiary centers in Germany were used for analysis. In total n=262 patients treated with atezolizumab/bevacizumab (treated between Jun. 2019 and Oct. 2022) and n = 136 patients treated with lenvatinib (treated between Sept. 2018 and Jun. 2022) were evaluated. Occurrence of bleeding or thromboembolic events within 3 months after initiation of therapy was assessed. For statistical analysis, normality of the data was assessed by Shapiro-Wilk test, followed by Student's t test or Mann Whitney test. Fisher's exact test was applied for contingency tables.

Results: Both groups were balanced with respect to demographics, presence of liver cirrhosis and variceal status (see figure). Median length of therapy was not different between groups (atezolizumab/bevacizumab 105 vs. lenvatinib 108 days, p = 0.96). Surrogate markers of portal hypertension such as platelet count (atezolizumab/bevacizumab 195.7 ± 107.9 vs. lenvatinib 187.7 ± 99.8 × 10⁹/L; p = 0.75) or spleen size (atezolizumab/bevacizumab 12.5 ± 2.6 vs. lenvatinib 12.6 ± 2.7 cm; p = 0.99) showed no differences between groups.

Bleeding episodes were described in 46 of 262 (17.6%) patients receiving atezolizumab/bevacizumab compared to 16 of 136 (11.8%) patients receiving lenvatinib (p = 0.15, Odds Ratio 1.60, 95% CI 0.86–2.95). Variceal hemorrhage occurred in 8 of 262 (3.0%) patients treated with atezolizumab/bevacizumab versus 5 of 136 (3.6%) patients treated with lenvatinib (p = 0.77, Odds Ratio 0.83, 95% CI 0.26–2.28). Thromboembolic events were reported in 20 of 260 (7.6%) patients in the atezolizumab/bevacizumab cohort compared to 5 of 136 (3.6%) patients in the lenvatinib cohort (p = 0.19, Odds Ratio 2.1, 95% CI 0.81–5.23).

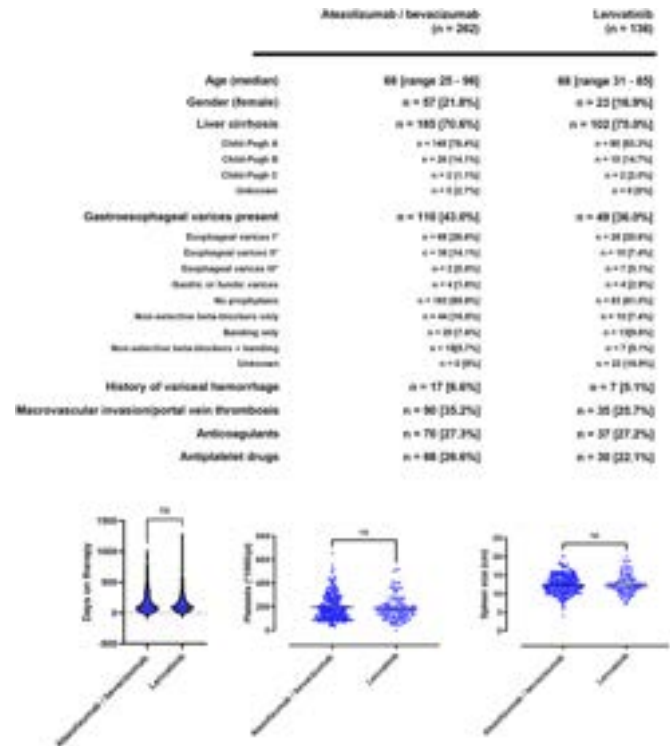


Figure:

Conclusion: Rates of bleeding and thromboembolic events did not differ significantly between atezolizumab/bevacizumab and lenvatinib and may not be helpful in choosing between the two treatments. Future prospective studies are needed to confirm our results.

OS-058

Multimodal integrative genomics and pathology analyses in neoadjuvant nivolumab treatment for borderline resectable HCC

Tan-to Cheung¹, Daniel Ho¹, Shirley Lyu¹, Qingyang Zhang¹, Yu Tsui¹, Tiffany Yu¹, Karen Sze¹, Joyce Lee¹, Vince Lau¹, Yin-Lun Chu², Simon Tsang², Wong She¹, Roland Leung², Thomas Yau¹, Irene Oi-Lin Ng¹. ¹The University of Hong Kong, Hong Kong; ²Queen Mary Hospital, Hong Kong
Email: iolng@hku.hk

Background and aims: Immunotherapy has resulted in pathologic responses in hepatocellular carcinoma (HCC) but the benefits and molecular mechanisms of neoadjuvant immune checkpoint blockade are largely unknown. In this study, we evaluated the efficacy and safety of pre-operative nivolumab (anti-PD1) in patients with borderline resectable HCC and investigated the molecular determinants for predicting treatment response.

Method: A single-arm study was designed to assess the clinical benefit of Neoadjuvant treatment with nivolumab in patients with untreated, borderline resectable HCC. Between July 2020 and November 2021, 20 treatment-naïve HCC patients with intermediate and locally advanced tumors received preoperative nivolumab at 3 mg/kg for 3 cycles prior to surgical resection. Pathological examination of pre- and post-operative tumour specimens, RNA-sequencing to devise the cellular and molecular profiles of patients' HCC tumours, and plasma cell-free DNA and copy number variation (CNV) to derive a non-invasive biomarker anti-PD1 response score were used.

ORAL PRESENTATIONS

Results: Of the 20 patients, 19 underwent surgical resection on-trial. The majority (90%) of patients had locally advanced stage and 10% had intermediate stage per Hong Kong Liver Cancer (HKLC) staging classification. 70% of the patients were HBV carriers and the remaining 5 had chronic alcohol consumption. Seven (36.8%) of the 19 patients had major pathologic tumor necrosis ($\geq 60\%$) in the post-nivolumab resection specimens, with 3 having almost complete ($>90\%$) tumor necrosis. The tumor necrosis was hemorrhagic and often accompanied with increased or dense immune cell infiltrate at the border of the tumors. None of the patients developed major adverse reactions contradicting hepatectomy. RNA-sequencing analysis on both pre-nivolumab tumor biopsies and post-nivolumab resected specimens revealed a change in the immune cellular landscape. In the cases with major pathologic necrosis, the proportion of CD8T cells in the HCC tissues predominantly increased after treatment. Immunohistochemistry for CD8 and CD4 T cells showed result consistent with those of the cellular deconvolution. With subsequent gene set enrichment analysis, we detected an overall upregulation of immune response, particularly lymphocyte activation and differentiation, consistent with our findings in the cellular landscape. Moreover, to investigate non-invasive biomarker for nivolumab response, we evaluated, on plasma cell-free DNA of the patients, the copy number variation (CNV) using target-panel sequencing and derived a CNV-based anti-PD1 score. The score correlated with the extent of tumor necrosis, and was validated in a Korean patient cohort with anti-PD1 treatment.

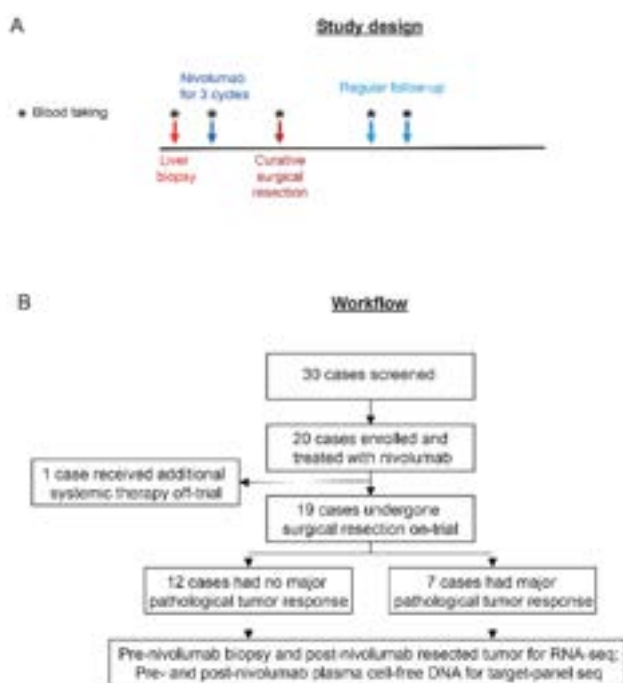


Figure:

Conclusion: Our study demonstrates that neoadjuvant nivolumab is safe and has promising clinical activity in borderline resectable HCC patients. We also identify potentially useful non-invasive biomarker predicting anti-PD1 responsiveness. Significant immune cell-related tumor necrosis observed in the post-nivolumab hepatectomy specimens signifies that successful restoration of cytotoxic immunity is the key determinant for immune checkpoint blockade response.

OS-059-YI

Predicting response to atezolizumab plus bevacizumab in advanced hepatocellular carcinoma using single-cell RNA-sequencing-derived gene signatures

Sarah Cappuyns^{1,2,3,4,5}, Marta Piqué-Gili^{1,2}, Roger Esteban-Fabré^{1,2}, Gino Philips^{4,5}, Roser Pinyol², Vincent Vandecaveye^{6,7}, Jordi Abril-Fornaguera^{1,2}, Philipp Haber^{1,8}, Chris Verslype³, Eric Van Cutsem³, Diether Lambrechts^{4,5}, Augusto Villanueva¹, Jeroen Dekervel³, Josep Llovet^{1,2,9}. ¹Tisch Cancer Institute, Icahn School of Medicine at Mount Sinai, Mount Sinai Liver Cancer Program, Division of Liver Diseases, NY, United States; ²Institut d'Investigacions Biomèdiques August Pi i Sunyer (IDIBAPS), Liver Cancer Translational Research Laboratory, Spain; ³UZ/KU Leuven, Digestive Oncology, Department of Gastroenterology, Belgium; ⁴Katholieke Universiteit Leuven, Laboratory for Translational Genetics, Department of Human Genetics, Leuven, Belgium; ⁵Vlaams Instituut voor Biotechnologie, Center for Cancer Biology, Leuven, Belgium; ⁶UZ Leuven, Radiology Department, Belgium; ⁷Katholieke Universiteit Leuven, Laboratory of Translational MRI, Department of Imaging and Pathology, Belgium; ⁸Charité Universitätsmedizin Berlin, Germany; ⁹Institució Catalana de Recerca i Estudis Avançats, Spain
Email: sarahcappuyns@hotmail.com

Background and aims: Single-cell transcriptomic profiling (scRNAseq) is a powerful explorative technique that has helped in the characterisation of tumour immune cell infiltration and how it relates to treatment response in advanced HCC (aHCC). Here, we aimed to 1) derive gene expression signatures that recapitulate distinct single-cell derived immune cell types that can be applied to bulk RNAseq data and to 2) evaluate whether these signatures are associated with clinical response in aHCC treated with atezolizumab plus bevacizumab (atezo + bev), current standard of care.

Method: Using scRNAseq data from 31 aHCC tumour biopsies (91,169 single cells), we defined gene signatures for 35 cell phenotypes using a customized bio-informatics pipeline based on differential gene expression analysis. Signatures were validated in an independent, publicly available scRNAseq dataset of 22 HCC patients (Ma *et al.* JHep 2021). To evaluate the power of single-cell derived signatures to capture the presence of specific intra-tumoural cell types in bulk transcriptomic data, we analysed three cohorts comprising a total of 547 HCC tumour samples: 1) 399 early HCCs, 2) 83 anti-PD1-treated aHCCs and 3) 65 aHCCs treated with atezo + bev in frontline. We performed a) single-sample Gene Set Enrichment Analysis (ssGSEA) and b) Nearest Template Prediction (NTP) analysis, and ssGSEA-derived scores and class prediction results were correlated with both known HCC immune subclasses and objective response to therapy (mRECIST).

Results: We successfully generated highly specific gene signatures for 21 out of 35 single-cell derived cell types. As expected, signature enrichment analysis using the bulk transcriptome of 399 early HCCs revealed that the 'immune-active' and 'exhausted' HCC subclasses (Sia *et al.* Gastroenterology 2017) were enriched in both T-cell and myeloid signals. In contrast, the inflamed profile of the 'immune-like' subclass (Montironi *et al.* Gut 2022) was mostly driven by myeloid populations, in particular PDL1⁺ CXCL10⁺ macrophages, previously associated with response to immunotherapy at the single-cell level (Cappuyns *et al.* ILC 2022). In aHCC, 12% of tumours (n = 17/148) were enriched in PDL1⁺ CXCL10⁺ macrophages in bulk RNAseq (using the NTP-method). Importantly, their presence was associated with response to both anti-PD1 (n = 4/12 responders vs. 0/16 non-responders; p = 0.02) and atezo + bev (n = 6/18 responders vs. 1/39 non-responders; p = 0.003), thus identifying responders with a specificity of 100% and 97.5% and a positive predictive value of 100% and 86.6%, respectively.

Conclusion: Using scRNAseq data from immunotherapy-treated aHCC patients, we generated gene signatures representative of 21 distinct cell phenotypes. The presence of PDL1⁺ CXCL10⁺

macrophages was associated with response to atezo + bev, confirming their essential role in facilitating the efficacy of immunotherapy in aHCC.

NAFLD: Therapy

OS-060

A Phase 2a, randomized, active-comparator-controlled, open-label study to evaluate the efficacy and safety of efinopegdutide in individuals with non-alcoholic fatty liver disease

Manuel Romero Gomez¹, Eric Lawitz², R. Ravi Shankar³, Eirum Chaudhri³, Jie Liu³, Raymond Lam³, Keith Kaufman³, Samuel Engel³. ¹University of Seville/Virgen del Rocio University Hospital, Institute of Biomedicine of Seville (HUVR/CSIC/US)/Digestive Diseases Unit and CIBERehd, Seville, Spain; ²University of Texas Health Science Center at San Antonio-UT Health San Antonio, Texas Liver Institute, San Antonio, United States; ³Merck and Co Inc, MRL, Rahway, United States

Email: mromerogomez@us.es

Background and aims: Currently, there are no approved therapies for non-alcoholic steatohepatitis (NASH). This study was conducted to assess the effects of the GLP-1/glucagon receptor co-agonist efinopegdutide (EFI), relative to the selective GLP-1 receptor agonist semaglutide (SEMA), on liver fat content (LFC) in patients with non-alcoholic fatty liver disease (NAFLD), and to inform on the role of EFI as a therapy for NASH.

Method: This was a Phase 2a, randomized, active-comparator-controlled, parallel-group, open-label study in subjects with NAFLD (18–70 years, BMI 25–50 kg/m², stable body weight, without type 2 diabetes mellitus (T2DM), or with T2DM with an A1C ≤8.5% controlled by diet ± stable dose of metformin). During a 4-week screening period, an MRI-PDFF was performed to determine LFC. Participants with an LFC of ≥10% were randomized in a 1:1 ratio to open-label SC EFI 10 mg Q1W or SC SEMA 1.0 mg Q1W for 24 weeks, stratified according to concurrent diagnosis of T2DM. Both drugs were titrated to the target dose over an 8-week time period. The primary efficacy end point was the least squares (LS) mean relative reduction from baseline in LFC (%) after 24 weeks of treatment.

Results: Among 145 randomized subjects (EFI n = 72, SEMA n = 73), 55.2% were male, 35.2% were Hispanic and 33.1% had T2DM. At baseline, the mean BMI was 34.3 kg/m² and the mean LFC was 20.3%. The LS mean relative reduction from baseline in LFC at Week 24 was significantly ($p < 0.001$) greater with EFI (72.7% [95% CI: 66.8, 78.7]) than with SEMA (42.3% [95% CI: 36.5, 48.1]) (figure). Median relative reductions from baseline in LFC at Week 24 were 83.8% with EFI and 44.4% with SEMA. Greater proportions of participants had relative reductions from baseline at Week 24 in LFC of ≥30%, ≥50% and ≥70% with EFI (81.9%, 77.8%, and 70.8%, respectively) compared with SEMA (67.1%, 43.8%, and 12.3%, respectively) (figure). A greater proportion of participants achieved normal LFC (<5%) at Week 24 with EFI (66.7%) compared with SEMA (17.8%). Both treatment groups had an LS mean relative reduction from baseline in body weight at Week 24 ($p = 0.085$ for EFI 8.5% vs SEMA 7.1%). The relative reductions from baseline in LFC at Week 24 by weight loss category (≤5%, >5% to ≤10%, and >10% reduction in body weight from baseline) were greater in the EFI group (52.4%, 76.6%, and 86.2%, respectively) than in the SEMA group (13.4%, 39.6%, and 64.2%, respectively). There were no meaningful differences between the two treatment groups in the incidence of overall, serious, or drug-related adverse events, including adverse events that led to discontinuation.

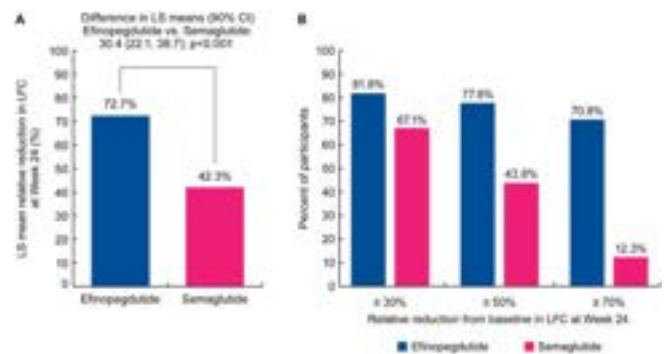


Figure: (A) LS mean relative reduction from baseline in LFC at Week 24 and (B) proportions of participants with relative reductions from baseline in LFC at Week 24 of ≥30%, ≥50% and ≥70%

Conclusion: In this study in patients with NAFLD, treatment with EFI 10 mg weekly led to a significantly greater reduction in LFC than SEMA 1 mg weekly. EFI may offer an effective treatment option for patients with NASH.

OS-061

Multicenter, randomized, double-blind, placebo-controlled trial of Fatty Acid Synthase (FASN) inhibitor, denifanstat, versus placebo in the treatment of biopsy-proven NASH: A 26-week interim analysis of the FASCINATE-2 Phase 2B trial

Marie O'Farrell¹, Katharine Grimmer¹, Alithea Zetter¹, Wen-Wei Tsai¹, George Kemble¹, Rohit Loomba², Eduardo Bruno Martins¹, Stephen Harrison³. ¹Sagimet Biosciences, San Mateo, United States; ²University of California, San Diego, Dept of Medicine, NAFLD Research Center, La Jolla, United States; ³Pinnacle Clinical Research, San Antonio, United States

Email: marie.ofarrell@sagimet.com

Background and aims: Denifanstat (DEN) is a first-in-class FASN inhibitor. In the completed FASCINATE-1 study, patients with NAFLD treated with denifanstat for 12 weeks showed significant reductions of liver fat, ALT, low density lipoprotein cholesterol (LDL) and N-terminal type III collagen propeptide (PRO-C3). DEN exhibited a well-tolerated safety profile. The FASCINATE-2 (NCT04906421) study, is a Ph2b, placebo-controlled, double-blind study of DEN compared to placebo in 168 biopsy-confirmed NASH patients. The primary end points will evaluate safety and histological impact of a 50 mg daily oral dose of DEN compared to placebo after 52 weeks. A planned interim analysis (IA) at Week 26 of treatment was performed using non-invasive assessments including de novo lipogenesis assessment, MRI-PDFF and ALT.

Method: Adults ≥18 years were enrolled in this study with a screening biopsy confirming F2-F3 fibrosis and a NAFLD activity score (NAS) ≥4 with a score of at least 1 in each of the following parameters: steatosis, balloon degeneration and lobular inflammation. In the IA, the first 52 patients on study for 26 weeks with a baseline MRI-PDFF of ≥8% liver fat were evaluated. 30 of these patients received 50 mg of DEN and 22 received placebo; 65% were diabetic; mean ALT 62.7 U/L; mean liver fat by MRI-PDFF 19.3%; and 54% had F3 fibrosis.

Results: DEN inhibited FASN activity as demonstrated by reduction of plasma levels of the saturated fatty acid triglyceride tripalmitin (−42.0% vs +21.5%, $p < 0.002$). FASN inhibition resulted in a relative reduction of liver fat from baseline in DEN-treated patients compared to placebo (−34.1% vs −1.5%, $p < 0.002$). Importantly, 67% of DEN-treated patients reduced their liver fat by ≥30% (67% vs 18%, $p < 0.002$) and approximately half of these responders decreased liver fat by ≥50%. ALT also dropped significantly in the DEN-treated group (−16.5 U/L vs −4.0 U/L, $p < 0.05$). Recent studies show an MRI-PDFF reduction of ≥30% combined with an ALT reduction of ≥17 U/L highly correlate with histological improvement. The proportion of DEN patients achieving this combined metric was significantly improved (37% vs 9%, $p < 0.05$). Fibrosis markers declined from baseline with DEN

ORAL PRESENTATIONS

treatment; enhanced liver fibrosis (ELF) score (-0.34 vs -0.02 , $p < 0.05$) and PRO-C3 (-4.4 ng/ml vs -0.28 ng/ml, $p < 0.05$). Consistent with Ph2a results, LDL was significantly decreased by DEN (-12.4 mg/dL vs 0.0 mg/dL, $p < 0.05$) while FGF-21 increased ($+0.21$ vs -0.04 ng/ml, $p < 0.05$), indicating improved metabolism. There were no treatment-related serious adverse events, and the majority of adverse events were mild to moderate in nature (Grade 1 and 2).

Conclusion: Denifanstat showed a strong improvement of key non-invasive disease markers in NASH patients after 26 weeks of treatment. These data suggest that denifanstat will have a positive impact on histological end points in FASCINATE-2.

OS-062

Phase 1 study of the RNA interference therapeutic ALN-HSD in healthy adults and patients with non-alcoholic steatohepatitis

Arun Sanyal¹, Jörg Tübel², Prajakta Badri³, Sarah Bond³, Nune Makarova³, Weizhi Zhao³, Satyajit Karnik⁴, Farshad Kajbaf³, Benjamin Olenchock⁴, Joshua Friedman³, John Gansner³. ¹Virginia Commonwealth University, Division of Gastroenterology, Hepatology and Nutrition, Richmond, VA, United States; ²Richmond Pharmacology and St. George's University of London, London, United Kingdom; ³Alnylam Pharmaceuticals, Cambridge, MA, United States; ⁴Regeneron Pharmaceuticals, Tarrytown, NY, United States
Email: jgansner@alnylam.com

Background and aims: Non-alcoholic steatohepatitis (NASH) is a prevalent chronic liver disease that can lead to progressive fibrosis, cirrhosis, and hepatocellular carcinoma. Genome-wide association studies have identified loss-of-function variants in the hydroxysteroid 17-beta dehydrogenase 13 (HSD17B13) gene that are associated with a reduced risk of chronic liver disease and progression from steatosis to steatohepatitis. ALN-HSD is an investigational, subcutaneously administered, N-acetylgalactosamine (GalNAc)-conjugated small interfering RNA (siRNA) targeting liver-expressed HSD17B13 mRNA, in development for the treatment of NASH. Here, we present interim results of the Phase 1 study of ALN-HSD.

Method: ALN-HSD-001 (NCT04565717) is a two-part, randomized, double-blind, placebo-controlled, multi-center, single-ascending dose and multiple-dose study designed to evaluate the safety, tolerability, pharmacokinetic (PK), and pharmacodynamic (PD) effects of ALN-HSD in healthy adults (Part A) and adult patients with NASH (Part B). The primary end point is frequency of adverse events (AEs). Secondary end points include characterization of ALN-HSD plasma and urine PK and change from baseline of liver HSD17B13 mRNA.

Results: In Part A, which is complete, 58 healthy adults were randomized 3:1 to receive a single dose of study drug (ALN-HSD or placebo) in ascending dose groups from 25 to 800 mg. The only AE occurring in at least 10% of subjects treated with ALN-HSD was injection site reaction ($n=5/44$; 11%), all mild in severity and transient. One serious AE (SAE) of tonsillitis was reported and deemed unrelated to study drug. Consistent with other GalNAc-conjugated siRNAs, plasma concentrations of ALN-HSD declined rapidly by 24 hours post-dose. ALN-HSD showed a slightly more than dose proportional increase in exposures across doses. Across doses, ALN-HSD showed 17–37% excretion in urine. In Part B, which is ongoing, 46 patients with NASH were randomized 4:1 to receive ALN-HSD (25, 200, or 400 mg) or placebo on Day 1 and Day 85 (12 weeks apart). Liver biopsies were performed at baseline and either Day 169 or Day 337. At data cut-off, 45 patients received at least one dose of study drug. The only AE occurring in at least 10% of all patients was upper respiratory tract infection (13.3%), all deemed unrelated to study drug. Two SAEs, appendicitis and skin laceration, were also deemed unrelated to study drug. There was no evidence of drug-induced liver injury. In the cohorts with Day 169 liver PD data, ALN-HSD was associated with dose-dependent reduction of HSD17B13 mRNA. ALN-HSD was also associated with numerically lower liver enzymes and biopsy-derived non-alcoholic fatty liver disease activity score over six months relative to placebo.

Dose (mg)	N	Change from baseline of liver HSD17B13 mRNA at Day 169 (%)	
		Mean (SD)	Median [Range]
Placebo	5	4.6 (10.7)	4.7 [-11.7, 18.1]
25	6	-38.7 (24.7)	-39.8 [-67.2, -4.5]
200	6	-68.7 (8.6)	-71.5 [-79.3, -55.8]
400	7	-73.2 (9.7)	-78.3 [-80.9, -53.7]

Figure:

Conclusion: ALN-HSD has exhibited an encouraging safety and tolerability profile to date, with robust reduction in liver HSD17B13 mRNA expression. A Phase 2 study has been initiated to further investigate ALN-HSD in patients with NASH (NCT05519475).

Co-funded by Alnylam Pharmaceuticals and Regeneron Pharmaceuticals, Inc.

OS-063

Pemvidutide, a glp-1/glucagon dual receptor agonist, significantly reduces liver fat, fibro-inflammation, and body weight in patients with non-alcoholic fatty liver disease: a 24-week multicenter, randomized, double-blind, placebo-controlled trial

Stephen Harrison¹, Shaheen Tomah², John Suschak², Scot Roberts², Jay Yang², Liang He², Bertrand Georges², Lakisha Rodwell-Green², Randy Brown², M. Scott Harris², Sarah Browne². ¹Pinnacle Research, San Antonio, United States; ²Altimmune, Inc, Gaithersburg, United States
Email: stephenharrison87@gmail.com

Background and aims: Pemvidutide is a long-acting, balanced GLP-1/glucagon (GCG) dual receptor (R) agonist under development for the treatment of NASH and obesity. The balanced 1:1 potency ratio combines the reduced caloric intake effects of GLP-1R agonism with the increased energy expenditure and lipometabolic effects of CGCR agonism. This study assessed the efficacy, safety, and tolerability of pemvidutide on liver fat content (LFC), body weight and non-invasive markers of fibro-inflammation in patients with NAFLD over 24 weeks of treatment.

Method: Subjects were randomized 1:1:1:1 to receive 1.2 mg, 1.8 mg, and 2.4 mg pemvidutide, or placebo weekly for 12 weeks with an optional 12-week extension for a total of 24 weeks of treatment. There was no dose titration at 1.2 mg or 1.8 mg; a brief 4-week titration was used at 2.4 mg. The primary efficacy end point was the reduction in LFC from baseline after 12 and 24 weeks of treatment. Key secondary end points included: reductions in serum alanine aminotransferase (ALT), corrected T1 (cT1) and percent (%) body weight loss from baseline after 12 and 24 weeks of treatment.

Results: 94 subjects were randomized and dosed, and 66 subjects participated in the 12-week extension study. Mean baseline body mass index (BMI), LFC by MRI-PDFF, cT1, and ALT were approximately 36 kg/m², 22%, 920 ms and 37 IU/L, respectively. Twenty-seven (29%) participants had type 2 diabetes (T2D), and 71 (75.5%) were of Hispanic ethnicity. The primary end point was met in all pemvidutide treatment groups at both 12 and 24 weeks (Table 1). Significant reductions in absolute and relative LFC were noted at both time-points, with a mean relative LFC reduction of 76.4% at the 2.4 mg dose at 24 weeks, with 100% of subjects achieving $\geq 30\%$ reduction in LFC and approximately 50% achieving normalization, defined as LFC $\leq 5\%$. cT1 decreased significantly from baseline, with 84.6% of subjects across all pemvidutide treatment groups achieving a reduction of ≥ 80 ms in cT1 at week 24 compared to 0% of subjects receiving placebo. Serum ALT levels decreased significantly in a dose-dependent manner, particularly in subjects with baseline ALT ≥ 30 IU/L, with all pemvidutide treatment groups achieving mean reductions ≥ 17 IU/L. Weight loss of 7.2% and 5.3% were achieved in patients without and with T2D at the 1.8 mg dose at 24 weeks. Pemvidutide was well-tolerated, with no serious or severe AEs related to study drug, and low rates of AEs leading to study discontinuation.

Table:

	Week 12				Week 24			
	placebo	pemvi 1.2 mg	pemvi 1.8 mg	pemvi 2.4 mg	placebo	pemvi 1.2 mg	pemvi 1.8 mg	pemvi 2.4 mg
Change in LFC								
Absolute reduction (%)	0.2	8.9	14.7	11.3	1.6	11.2	17.0	15.6
Relative reduction (%)	4.4	46.6	68.5	57.1	14.0	56.3	75.2	76.4
30% reduction (%)	4.2	65.0	94.4	85.0	5.6	76.9	92.3	100
50% reduction (%)	0.0	40.0	72.2	70.0	0.0	61.5	84.6	72.7
Normalization ($\leq 5\%$)	0.0	20.0	55.6	50.0	0.0	30.8	53.8	45.5
Change in ALT								
All subjects (IU/L)	-6.2	-11.2	-13.8	-13.6	-2.2	-13.3	-13.7	-15.2
Baseline ALT ≥ 30 (IU/L)	-12.6	-17.8	-20.8	-27.0	-3.1	-17.0	-17.7	-20.6
Change in cT1								
Proportion of subjects with 80 ms reduction in cT1 (%)	0.0	87.5	83.3	85.7	0.0	85.7	75.0	100.0
Weight loss								
Without diabetes (%)	0.2	3.4	4.9	3.5	1.2	5.2	7.2	5.8
With diabetes (%)	0.5	3.3	3.8	4.4	3.4	4.3	5.3	3.5

Conclusion: Pemvidutide led to rapid and potent reductions in LFC, serum ALT, cT1, and body weight, and was well-tolerated without the use of dose titration. These findings support a high likelihood of histopathologic improvement in NASH patients in a forthcoming paired liver biopsy study.

OS-064-YI

Calorie restriction by time restricted intermittent fasting is better than standard calorie restriction in improving the metabolic profile and hepatic fibrosis in patients with non-alcoholic fatty liver disease

Deepankshi Aggarwal¹, Ajay Kumar Duseja², Arka De², Sanjay Bhadada³, Naveen Kalra⁴, Nancy Sahni⁵. ¹Post Graduate Institute of Medical Education and Research, Internal Medicine, Chandigarh, India; ²Post Graduate Institute of Medical Education and Research, Hepatology, Chandigarh, India; ³Post Graduate Institute of Medical Education and Research, Endocrinology, Chandigarh, India; ⁴Post Graduate Institute of Medical Education and Research, Radiodiagnosis and Imaging, Chandigarh, India; ⁵Post Graduate Institute of Medical Education and Research, Dietetics, Chandigarh, India
Email: ajayduseja@yahoo.co.in

Background and aims: Lifestyle interventions including diet modification and exercise causing weight-loss are recommended as first line treatment for patients with non-alcoholic fatty liver disease (NAFLD)/non-alcoholic steatohepatitis (NASH) with overweight/obesity. Even though found to be beneficial in weight reduction, efficacy of intermittent fasting (IF) in improving liver disease in patients with NAFLD is still evolving. Aim of the present study was to compare the effectiveness of calorie restriction by intermittent fasting (IF) with standard of care calorie-restriction (SOC) in improving hepatic steatosis, inflammation and fibrosis in patients with NAFLD.

Method: In this open label randomized study, 68 overweight/obese patients [as per Asia-Pacific cut offs-body mass index (BMI) ≥ 23 Kg/m²] with NAFLD were randomised to IF and SOC groups. After calculating daily calorie requirement (30–35 kcal/Kg/day), patients in both groups were advised 30% calorie restriction either by IF or SOC. IF regimen was 16:8-IF [time restricted feeding (TRF)], [meals for 8-hours followed by fasting of 16-hours daily]. Changes in anthropometry, components of metabolic syndrome, hepatic steatosis [ultrasound and controlled attenuation parameter (CAP)], hepatic inflammation [liver enzymes and FibroScan-AST (FAST) score] and hepatic fibrosis [APRI, FIB-4, NFS, liver stiffness measurement (LSM) on Fibroscan], were assessed at 6 months with intra-group and inter-group analysis.

Results: Of 68, 6 patients in each group were lost to follow-up; remaining 56 (M: F 1:1) patients (28 in each group, comparable mean age and BMI) were analyzed. Patients in both groups had significant

reduction in waist circumference, weight and BMI from baseline [4.3%, 5.88% and 6.1% reduction in IF ($p < 0.001$) versus 2.7%, 4.71% and 4.6% reduction in SOC group ($p < 0.001$)] with no difference between the groups. There was significant reduction in mean blood pressure, fasting blood glucose, total cholesterol, low-density lipoprotein levels in IF group in comparison to baseline ($p < 0.001$) and in comparison to SOC group ($p = 0.012$). There was significant improvement in hepatic steatosis in both the groups [mean CAP reduction in IF group 316 ± 43.78 to 287.7 ± 46.4 dB/m ($p < 0.001$); SOC group 323.1 ± 40.34 to 300.89 ± 45.7 dB/m ($p < 0.001$)] with no difference between the groups. In those with elevated ALT, there was significant reduction in mean ALT in both IF group [(from 74.1 ± 49 to 38.2 ± 26.4 U/ml ($p < 0.001$)] and SOC group [54.39 ± 36.7 to 37.9 ± 27.3 U/ml ($p < 0.006$)] with no difference between the groups. Similarly, significant reduction in mean FAST score was observed in both IF [from 0.38 ± 0.23 to 0.21 ± 0.18 ($p < 0.001$)] and in SOC group [from 0.32 ± 0.18 to 0.21 ± 0.19 ($p < 0.001$)] with no difference between the groups. IF group showed significant reduction in mean LSM on Fibroscan in comparison to baseline [6.42 ± 2.28 to 5.89 ± 2.12 kPa ($p < 0.016$)] whereas there was no significant reduction in LSM in SOC group. The proportion of patients having $>20\%$ reduction in LSM were also significantly higher in IF [21.4% ($n = 6$)] compared to SOC group [3.5% ($n = 1$)] ($p < 0.04$). The mean reduction in APRI, FIB-4 and NFS was not significant in either group.

Conclusion: Calorie restriction by time restricted intermittent fasting is better than standard calorie restriction in improving the metabolic profile and hepatic fibrosis; both IF and SOC are equally effective in causing weight reduction and improving hepatic steatosis and inflammation in NAFLD.

Viral hepatitis B/D - Current treatments

OS-065-YI

Predictors of severe flares after nucleos (t)ide analogue cessation- results of a global cohort study (RETRACT-B study)

Edo Dongelmans¹, Grishma Hirode^{2,3,4}, Bettina Hansen^{2,5,6}, Chien-Hung Chen⁷, Tung-Hung Su⁸, Wai-Kay Seto⁹, Arno Furquim d'Almeida¹⁰, Stijn Van Hees¹⁰, Margarita Papatheodoridi¹¹, Sabela Lens¹², Grace Wong¹³, Sylvia Brakenhoff¹, Rong-Nan Chien¹⁴, Jordan J. Feld^{2,3,4}, Henry Ly Chan¹⁵, Xavier Forns¹², George Papatheodoridis¹¹, Thomas Vanwolleghem¹⁰, Man-Fung Yuen⁹, Yao-Chun (Holden) Hsu¹⁶, Jia-Horng Kao⁸, Markus Cornberg¹⁷, Milan Sonneveld¹, Rachel Wen-Juei Jeng¹⁴, Harry LA Janssen^{1,2}. ¹Erasmus MC, Department of Gastroenterology and Hepatology, Rotterdam, Netherlands; ²Toronto General Hospital, Toronto Centre for Liver Disease, Canada; ³The Toronto Viral Hepatitis Care Network (VIRCAN), Canada; ⁴University of Toronto, Institute of Medical Science, Canada; ⁵Erasmus MC, Department of Epidemiology, Biostatistics, Netherlands; ⁶University of Toronto, Institute of Health Policy, Management and Evaluation, Canada; ⁷Kaohsiung Chang Gung Memorial Hospital, Division of Hepatogastroenterology, Department of Internal Medicine, Taiwan; ⁸National Taiwan University Hospital, Division of Gastroenterology and Hepatology, Department of Internal Medicine, Taiwan; ⁹The University of Hong Kong, Department of Medicine and State Key Laboratory of Liver Research, Hong Kong; ¹⁰Antwerp University Hospital, Department of Gastroenterology and Hepatology, Belgium; ¹¹Medical School of National and Kapodistrian University of Athens, Department of Gastroenterology, Greece; ¹²University of Barcelona, Liver Unit, Hospital Clínic de Barcelona, IDIBAPS and CIBEREHD, Spain; ¹³The Chinese University of Hong Kong, Medical Data Analytics Centre (MDAC), China; ¹⁴Chang Gung Memorial Hospital Linkou Medical Center, Chang Gung University, Department of Gastroenterology and Hepatology, Taiwan; ¹⁵The Chinese University of

ORAL PRESENTATIONS

Hong Kong, Faculty of Medicine, China; ¹⁶E-Da Hospital/I-Shou University, Division of Gastroenterology and Hepatology, Taiwan; ¹⁷Hannover Medical School, Germany; Centre for Individualized Infection Medicine (CiiM), Department of Gastroenterology, Hepatology and Endocrinology, Germany
Email: e.dongelmans@erasmusmc.nl

Background and aims: Flares after nucleos (t)ide analogue (NA) cessation are common and potentially harmful. Predictors of severe withdrawal flares are required for risk stratification and to guide off-treatment follow-up.

Method: This is a retrospective, international, multicenter cohort study including patients with chronic hepatitis B (CHB) who were virally suppressed and hepatitis B e antigen (HBeAg) negative at the time of NA cessation. Flares after NA withdrawal were defined as mild, moderate or severe based on a ALT level of 5-, 10- or 20 times or more the upper limit of normal (ULN). Multivariable cox regression analyses (adjusted for age, sex, previous interferon and NA therapy, type of NA, HBsAg- and ALT levels at withdrawal, cirrhosis and HBeAg status at start of treatment) were performed censoring at re-treatment and loss-to-follow-up. A sub-group analysis was performed to investigate the association between HBV DNA levels at 12 weeks after withdrawal and subsequent flare risk, excluding patients with a flare before or at 12 weeks.

Results: Among 1557 included patients, 356 (22.9%) developed a mild flare during follow-up of which 70% occurred within the first year after withdrawal and with a 5-year cumulative incidence of 31.9%. One-year cumulative incidences for ALT flares $\geq 5\times$, $\geq 10\times$, $\geq 20\times$ ULN were 18.6%, 10.0% and 3.4%, respectively (see figure). Fifteen (4.2%) patients decompensated after a mild flare of which 9 subsequently developed a severe flare resulting in 1 death.

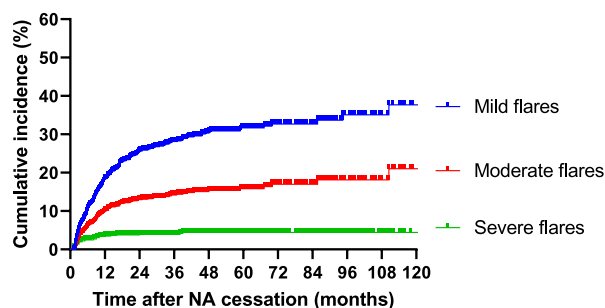


Figure:

Multivariable analyses showed that older age (aHR 1.02, 95%CI 1.01–1.03), male sex (aHR 1.49 95%CI 1.11–1.99), higher HBsAg levels at NA withdrawal (100–1,000 IU/ml; aHR 2.15, 95%CI 1.47–3.16, >1,000 IU/ml; aHR 2.79, 95% CI 1.85–4.22) and Tenofovir (TDF) vs. Entecavir therapy (aHR 2.23, 95%CI 1.76–2.83) were predictive for any flare ($\geq 5\times$ ULN). TDF therapy (aHR 2.50, 95%CI 1.78–3.49), previous NA-therapy (aHR 1.53, 95%CI 1.04–2.25) and a HBsAg level >1,000 IU/ml at withdrawal (aHR 2.41, 95%CI 1.38–4.19) were predictive for moderate flares. Only TDF therapy was associated with an increased risk of severe flares (aHR 4.06, 1.92–8.58).

When focusing on available HBV DNA data from 12 weeks after NA-cessation (n = 685), only levels between 2,000–10,000 IU/ml (aHR 2.15, 95%CI 1.00–4.61) and >10,000 IU/ml (aHR 4.63, 95%CI 2.42–8.86) were associated with an increased risk of mild flares (HBV-DNA <100 IU/ml as reference).

Conclusion: Flares are common after NA withdrawal and were predominantly observed in the first year after NA cessation and could result in liver decompensation or death. Older age, male sex, increased HBsAg levels at end of treatment and TDF therapy before drug withdrawal were associated with a higher risk of flares. HBV DNA kinetics after stopping NA may be used to stratify the risk of flares, with an increased risk observed among patients with an HBV DNA level >2,000 and >10,000 IU/ml 12 weeks after NA withdrawal.

OS-066

HDV-RNA decline less than 1 log after 6 months of BLV 2 mg monotherapy could define poor-response and lead to therapeutic decision. Data from real-life cohort

Victor de Lédighen¹, Edouard Bardou-Jacquet², Sophie Metivier^{3,3}, Nathalie Ganne-Carrié⁴, Veronique Loustaud-Ratti⁵, Marie-Noëlle Hilleret⁶, Laurent Alric³, Anne Minello Franza⁷, Tarik Asselah⁴, Dominique Roulot⁴, Isabelle Fouchard Hubert⁸, Stanislas Pol⁴, Bruno Roche⁴, Valérie Canva⁹, Xavier Causse¹⁰, Anne Gervais⁴, Frederic Heluwaert¹¹, Jérôme Dumortier¹², Karine Lacombe⁴, Caroline Lascoux-Combe⁴, Louis d'Alterroche¹³, Patrick Mialhes¹⁴, Leon Muti¹⁵, Isabelle Ollivier-Hourmand¹⁶, Christiane Stern⁴, Isabelle Rosa¹⁷, Fabien Zoulim¹⁸, Juliette Foucher¹.
¹CHU Bordeaux, France; ²CHU rennes, France; ³CHU Toulouse, France; ⁴APHP, France; ⁵CHU Limoges, France; ⁶CHU Grenoble, France; ⁷CHU Dijon, France; ⁸CHU Angers, France; ⁹CHU Lille, France; ¹⁰CH Orléans, France; ¹¹CH Annecy, France; ¹²CHU Lyon, France; ¹³CHU Tours, France; ¹⁴CH Bourg en Bresse, France; ¹⁵CHU Clermont-Ferrand, France; ¹⁶CHU Caen, France; ¹⁷CHI Créteil, France; ¹⁸INSERM, France
Email: victor.deledighen@chu-bordeaux.fr

Background and aims: Bulevirtide (BLV) is a lipopeptide inhibiting the HBV/HDV entry into the hepatocytes. Significant HDV-RNA decline was observed in HBV/HDV patients who received 48 weeks of BLV in monotherapy or in combination with PEG-interferon α 2a (PEG-IFN α). The aim of this analysis was to evaluate the efficacy of BLV 2 mg daily with or without PEG-IFN α 2a in HDV patients with poor early virologic response in the French BLV early access program.

Method: 118 HDV patients (male 67.8%, mean age 42 years, cirrhosis 52%, median HDV-RNA 6.52 log₁₀ IU/ml) with chronic HDV infection, with compensated cirrhosis/severe fibrosis or moderate fibrosis with elevated ALT levels were included in this analysis. Patients received at least 6 months of BLV 2 mg QD SC alone or in combination with PEG-IFN α once weekly according to physician's choice. Poor response was defined as HDV-RNA decline lower than 1 or 2 log₁₀ IU/ml at M3 or M6. The evaluation at M12 and M18 was performed only in patients who continued treatment during 12 and 18 months respectively.

Results: From baseline, median HDV RNA (log₁₀ IU/ml) and median ALT levels (IU/L) declined overtime: M3 –1.33 and –27, M6 –3.48 and –29, and M12 –3.83 and –33, respectively. Algorithm of virologic response in BLV monotherapy is proposed in Figure. In the BLV group (N = 59), among the 23 patients with HDV-RNA decline <1 log at M3, 8/21 (38%), 2/21 (9.5%), and 11/21 (52.4%) had HDV-RNA decline <1 log, between 1 and 2 log, and >2log at M6, respectively. In the 10 patients who had HDV-RNA <1 log at M6, HDV-RNA decline <1 log, between 1 and 2 log, and >2log at M18 was observed in 6 (60%), 4 (40%), and 0% of patients, respectively. In these patients, ALT <1.5 at M18 was observed in 2/6 (33.3%), 3/4 (75%), and 0% of patients, respectively. In the BLV + PEG-IFN group, at M3, only 4/58 (7%) of patients had HDV-RNA decline <1 log, and 10/58 (17%) had HDV-RNA decline between 1 and 2 log. Among the 6 patients with HDV RNA decline <2 log at M6, 3/5 (60%) had decline <2 log at M18.

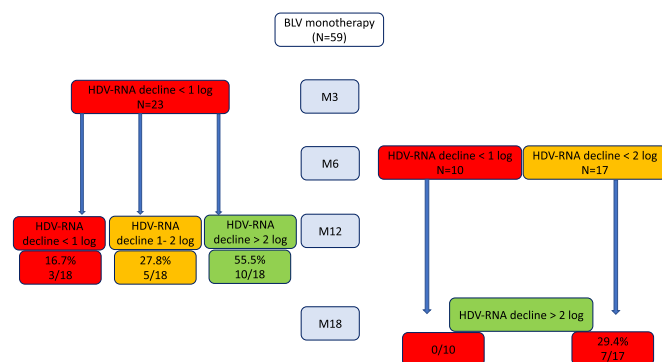


Figure: Algorithm of virologic response in BLV monotherapy

Conclusion: For the first time, in patients receiving BLV monotherapy 2 mg daily, we could define a subgroup of poor-responders with low probability to improve virological response overtime. The data of this real-life cohort suggest that BLV monotherapy should be stopped and another strategy offered in patients with HDV-RNA decline <1 log at M6. This strategy needs to be evaluated in future studies.

OS-067

Long-term efficacy of tenofovir alafenamide in HBeAg-positive and -negative chronic hepatitis B patients treated for up to 8 years in 2 phase 3 studies

Maria Buti^{1,2}, Kosh Agarwal³, Henry Ly Chan⁴, Wai-Kay Seto⁵, Young-Suk Lim⁶, Maurizia Brunetto⁷, Wan-Long Chuang⁸, Harry Janssen^{9,10}, Scott Fung¹¹, Namiki Izumi¹², Maciej Jablowski¹³, Frida Abramov¹⁴, Hongyuan Wang¹⁴, Leland Yee¹⁴, Roberto Mateo¹⁴, John F. Flaherty¹⁴, Calvin Pan¹⁵, Shalimar¹⁶, Patrick Marcellin¹⁷, Edward J. Gane¹⁸. ¹Hospital Universitario Vall d'Hebron, Barcelona, Spain; ²CIBEREHD del Instituto Carlos III, Madrid, Spain; ³King's College Hospital NHS Foundation Trust, Institute of Liver Studies, London, United Kingdom; ⁴Chinese University of Hong Kong, HMA office, 9/F Union Hospital, Tai Wai, Hong Kong; ⁵The University of Hong Kong, Department of Medicine and School of Clinical Medicine, Pok Fu Lam, Hong Kong; ⁶University of Ulsan College of Medicine, Asan Medical Center, Seoul, Korea, Rep. of South; ⁷Azienda Ospedaliero-Universitaria Pisana, Pisa, Italy; ⁸Kaohsiung Medical University Hospital, Kaohsiung City, Taiwan; ⁹University Health Network, Toronto Centre for Liver Disease, Toronto, Canada; ¹⁰Erasmus University Medical Center, Rotterdam, Netherlands; ¹¹University of Toronto, Department of Medicine, Toronto, Canada; ¹²Japanese Red Cross Musashino Hospital, Department of Gastroenterology and Hepatology, Tokyo, Japan; ¹³Medical University of Lodz, Łódź, Poland; ¹⁴Gilead Sciences, Inc., Foster City, United States; ¹⁵New York University Grossman School of Medicine, NYU Langone Health, New York, United States; ¹⁶All India Institute Of Medical Sciences, New Delhi, India; ¹⁷Hôpital Beaujon, Hepatology department, Clichy, France; ¹⁸Auckland Clinical Studies, Symonds St, Auckland, New Zealand Email: frida.abramov@gilead.com

Background and aims: In 2 similarly designed double-blind (DB), randomized (2:1), Phase 3 studies (Study 108 in HBeAg-negative patients [N=425] and Study 110 in HBeAg-positive patients [N=873]), tenofovir alafenamide (TAF) demonstrated noninferior efficacy relative to tenofovir disoproxil fumarate (TDF) in the blinded assessments. After completing up to 3 years (yr) of DB treatment, all patients were eligible to receive open-label (OL) TAF through week 384 (yr 8). Here we present the final 8-yr results.

Method: Efficacy was assessed for each study by missing equals excluded (M=E) approach of the full analysis set and included serial assessments for viral suppression (HBV DNA <29 IU/ml), ALT normalization by 2018 AASLD criteria, serologic responses, and fibrosis change by serum FibroTest. Resistance analyses, including deep sequencing of HBV pol/RT (at baseline and annually), for those with virologic breakthrough/blip, persistent viremia, or treatment discontinuation with viremia were performed, as was phenotyping of qualifying samples.

Results: Of 1298 randomized and treated patients, 1157 (89%; 775 TAF; 382 TDF) entered the OL phase, including 180 and 202 TDF-treated patients who began OL TAF at week 96 (TDF-OL TAF 6 yr) or week 144 (TDF-OL TAF 5 yr) based on timing of a protocol amendment. Overall, 974 (75%) participants completed OL study treatment. The most common reasons for discontinuation were withdrawal of consent, loss to follow-up, or investigator discretion. Similar high rates of virologic suppression and ALT normalization were achieved and maintained over 8 yr in all treatment groups (Table). Sequence/phenotyping analysis through 6 yr showed no resistance to TAF; resistance analyses at yr 8 are ongoing.

Table.: Results at Yr 8^a.

n/N (%)	TAF 8 yr	TDF-TAF 6 yr	TDF-TAF 5 yr
Study 108			
HBV DNA < 29 IU/ml	201/208 (97)	43/44 (98)	57/58 (98)
Normalized ALT ^b	147/189 (78)	30/41 (73)	44/57 (77)
HBsAg loss/	8/199 (4)	0/41	1/58 (2)
Seroconversion	6/199 (3)	0	0
Mean (SD) log ₁₀ IU/ml	-0.62 (0.924)	-0.50 (0.526)	-0.61 (0.758)
change in HBsAg			
Mean change in	-0.05 (0.142)	-0.04 (0.174)	0.00 (0.158)
FibroTest score (SD)			
Study 110			
HBV DNA < 29 IU/ml	370/392 (94)	74/81 (91)	108/112 (96)
Normalized ALT ^b	295/380 (78)	55/79 (70)	83/103 (81)
HBsAg loss/	171/373 (46)	32/73 (44)	50/108 (46)
Seroconversion	114/373 (31)	20/73 (27)	36/108 (33)
HBsAg loss/	9/384 (2)	4/76 (5)	3/109 (3)
Seroconversion	6/384 (2)	4/76 (5)	3/109 (3)
Mean (SD) log ₁₀ IU/ml	-0.89 (1.211)	-1.09 (1.424)	-1.09 (1.268)
change in HBsAg			
Mean change in	-0.05 (0.155)	-0.04 (0.158)	-0.01 (0.142)
FibroTest score (SD)			

^aFull analysis set by missing = excluded analysis. ^bPopulation included only patients with ALT above ULN at baseline.

Conclusion: After 8 yr of treatment with TAF or up to 6 yr after switch from TDF, virologic suppression rates remained high across all groups; up to 33% achieved HBeAg/HBeAb seroconversion, while HBsAg loss was low (≤5%).

OS-068

Efficacy and safety at 96 weeks of bulevirtide 2 mg or 10 mg monotherapy for chronic hepatitis D: results from an interim analysis of a phase 3 randomized study

Heiner Wedemeyer¹, Soo Aleman², Maurizia Brunetto^{3,4}, Antje Blank⁵, Pietro Andreone⁶, Pavel Bogomolov⁷, Vladimir Chulanov⁸, Nina Mamonova⁸, Natalia Geyvandova⁸, Morozov Viacheslav⁹, Olga Sagalova¹⁰, Tatyana Stepanova¹¹, Dmitry Manuilov¹², Renee-Claude Mercier¹², Qi An¹², John F. Flaherty¹², Anu Osinusi¹², Audrey Lau¹², Julian Schulze zur Wiesch¹³, Markus Cornberg¹⁴, Stefan Zeuzem^{15,16}, Pietro Lampertico^{17,18}. ¹Medizinische Hochschule Hannover, Klinik für Gastroenterologie, Hepatologie und Endokrinologie, Hannover, Germany; ²Karolinska University Hospital/Karolinska Institute, Department of Infectious Diseases, Stockholm, Sweden; ³Azienda Ospedaliero-Universitaria Pisana, Italy; ⁴University of Pisa, Department of Clinical and Experimental Medicine, Pisa, Italy; ⁵Heidelberg University Hospital, Clinical Pharmacology and Pharmacoepidemiology, Heidelberg, Germany; ⁶University of Modena and Reggio Emilia, Baggiovara Hospital, Internal Medicine, Modena, Italy; ⁷Moscow Regional Research Clinical Institute after M.F. Vladimirov, Moscow, Russian Federation; ⁸FSBI National Research Medical Center for Phthiopolmonology and Infectious Diseases of the Ministry of Health of the Russian Federation, Russian Federation; ⁹LLC Medical Company "Hepatolog," Samara, Russian Federation; ¹⁰Federal state-funded institution of higher education "Southern Ural State Medical University of Ministry of Health of the Russian Federation", Chelyabinsk, Russian Federation; ¹¹Limited liability company "Clinic of Modern Medicine," Moscow, Russian Federation; ¹²Gilead Sciences, Inc., Foster City, United States; ¹³Universitätsklinikum Hamburg-Eppendorf, Medizinische Klinik Studienambulanz Hepatologie, Hamburg, Germany; ¹⁴Medizinische Hochschule Hannover, Klinik für Gastroenterologie, Hepatologie und Endokrinologie, Hannover, Germany; ¹⁵University Hospital Frankfurt, Frankfurt am Main, Germany; ¹⁶University Hospital Frankfurt, Department of Medicine, Frankfurt am Main, Germany; ¹⁷Foundation

ORAL PRESENTATIONS

IRCCS Ca' Granda Ospedale Maggiore Policlinico, Division of Gastroenterology and Hepatology, Milan, Italy; ¹⁸University of Milan, CRC "A. M. and A. Migliavacca" Center for Liver Disease, Milan, Italy
Email: wedemeyer.heiner@mh-hannover.de

Background and aims: Bulevirtide (BLV) is a first-in-class, entry inhibitor for chronic hepatitis D (CHD) which was conditionally approved in the EU in July 2020. Results from the Week 48 primary end point analysis for MYR301 (NCT03852719), a phase 3 randomized study, showed monotherapy with BLV at 2 mg/d or 10 mg/d given subcutaneously was superior to no active anti-HDV treatment based on the combined viral and biochemical response. Efficacy was similar at the 2 dose levels and BLV was generally safe and well tolerated. Here, we present findings from the predefined week 96 interim analysis of this ongoing study.

Method: 150 patients with CHD were randomized (1:1:1) and stratified based on the presence/absence of compensated cirrhosis as follows: Arm A: no active anti-HDV treatment for 48 weeks followed by BLV 10 mg/d for 96 weeks (n = 51), and Arms B or C: immediate treatment with BLV at 2 mg/d (n = 49) or 10 mg/d (n = 50), respectively, each for 144 weeks, with follow-up of 96 weeks after end of treatment (i.e. up to Week 240). The combined response was defined as undetectable HDV RNA or decrease by $\geq 2 \log_{10}$ IU/ml from baseline and ALT normalization; other end points included viral response (undetectable HDV RNA or decrease by $\geq 2 \log_{10}$ IU/ml from baseline), ALT normalization, \log_{10} change in HDV RNA and change in liver stiffness (LS) by transient elastography (TE).

Results: Baseline characteristics were similar between groups and included: mean (SD) age 41.8 (8.4) years, 57% males, 83% White, 47% with compensated cirrhosis, mean (SD) HDV RNA 5.05 (1.34) \log_{10} IU/ml, mean (SD) ALT 110.9 (69.0) U/L, mean (SD) LS of 15 (8.9) kPa; and

61% were on concomitant nucleos(t)ide analogues therapy. Of 150 patients, 143 (95%) completed 96 weeks of treatment. Week 96 efficacy responses were improved vs. Week 48 (Table). At Week 96, similar combined responses were seen in arms B and C. Viral and biochemical responses were also similar among arms B and C. BLV was safe and well tolerated; there were no drug discontinuations, serious AE (SAE) or deaths attributed to BLV. Increases in bile acids without a correlation to pruritus or other symptoms were noted with BLV treatment. Injection site reactions occurred in a higher proportion receiving 10 mg/d dosing.

Conclusion: BLV continues to be safe and well tolerated as monotherapy for CHD through Week 96. Virological and biochemical responses increased with longer term therapy.

OS-069

Prophylaxis of HBV-recurrence after liver transplantation in patients with HCC: risk of HCC recurrence from a large, multicentre retrospective study from Italy

Patrizia Burra¹, Sara Battistella¹, Francesco Paolo Russo¹, Laura Turco², Chiara Manuli³, Alberto Calleri³, Luisa Pasulo⁴, Valerio Giannelli⁵, Clara DiBenedetto⁶, Laura Mameli⁷, Alberto Ferrarese⁸, Simona Marengo⁹, Flaminia Ferri¹⁰, Ilaria Lenci¹¹, Domenico Forastiere¹², Silvia Schiavone², Vittoria Vero², Luca Vizioli², Agnese Carroli¹, Gabriella Frassanito¹³, Giulia Scandali¹⁴, Marco Biolato¹⁵, Ezio Fornasiere¹⁶, Francesca Ponziani¹⁵, Gianluca Svegliati-Baroni¹⁴, Edoardo Giovanni Giannini⁹, Pierluigi Toniutto¹⁶, Alfonso Galeota Lanza¹⁷, Maria Grazia Rendina¹², Maria Francesca Donato⁶, Stefano Fagioli⁴, Nicola De Maria¹³, Maria Cristina Morelli², Silvia Martini³, Silvia Trapani¹⁸, Paolo Antonio Grossi¹⁹, Alessio Aghemo^{20,21}, Alberto Zanetto¹.

¹Gastroenterology and Multivisceral Transplant Unit, Padova University Hospital, Department of Surgery, Oncology and Gastroenterology, Italy;

²Internal Medicine Unit for the Treatment of Severe Organ Failure, IRCCS Azienda Ospedaliero-Universitaria di Bologna, Italy; ³Division of Gastroenterology, Molinette Hospital, Città della Salute e della Scienza,

Efficacy and safety results for BLV at Weeks 48 and 96

	Arm A Delayed Treatment/BLV 10mg (N = 51)		Arm B BLV 2 mg (N = 49)		Arm C BLV 10 mg (N = 50)	
	Week 48	Week 96 (48 week BLV 10 mg)	Week 48	Week 96	Week 48	Week 96
Combined Response:						
Responder n (%)	1 (2)	20 (39)	22 (45)	27 (55)	24 (48)	28 (56)
95% CI (%)	(0, 10)	(26, 54)	(31, 60)	(40, 69)	(34, 63)	(41, 72)
Viral Response:						
Responder n (%)	2 (4)	46 (90)	36 (73)	37 (76)	38 (76)	41 (82)
95% CI (%)	(0, 13)	(79, 97)	(59, 85)	(61, 87)	(62, 87)	(69, 91)
Undetectable HDV RNA:						
Responder n (%)	0	12 (24)	6 (12)	10 (20)	10 (20)	18 (36)
95% CI (%)	(0, 7)	(13, 38)	(5, 25)	(10, 34)	(10, 34)	(23, 51)
ALT normalization:						
Responder n (%)	6 (12)	22 (43)	25 (51)	31 (63)	28 (56)	32 (64)
95% CI (%)	(4, 24)	(29, 58)	(36, 66)	(48, 77)	(41, 70)	(49, 77)
Change from BL in HDV RNA levels (\log_{10} IU/mL):						
least square means (95% CI)	0.0 (-0.4, 0.3)	-3.6 (-4.0, -3.3)	-2.6 (-3.0, -2.3)	-3.2 (-3.6, -2.8)	-3.0 (-3.4, -2.7)	-3.6 (-4, -3.2)
Change from BL in HBsAg levels (\log_{10} IU/mL):						
least square means (95% CI)	0.0 (-0.1, 0.1)	-0.2 (-0.3, 0.0)	0.1 (-0.0, 0.2)	-0.2 (-0.4, -0.1)	0.1 (0.0, 0.2)	-0.1 (-0.3, 0.0)
Change from BL in liver stiffness (kPa):						
least square means (95% CI)	0.3 (-0.8, 2.6)	-3.0 (-4.6, -1.5)	-3.1 (-4.7, -1.5)	-4.0 (-5.6, -2.5)	-3.2 (-4.9, -1.5)	-4.7 (-6.3, -3.2)
Adverse Events at Week 96						
Number (%) of patients with:						
Any AE	39 (77)	47 (96)	41 (84)	47 (96)	44 (88)	48 (96)
Any Grade ≥ 3 AE	4 (8)	7 (14)	5 (10)	9 (18)	4 (8)	8 (16)
Any AE related to BLV	0	22 (43)	24 (49)	25 (51)	36 (72)	36 (72)
Any SAE	1 (2)	3 (6) [†]	2 (4)	2 (4)	1 (2)	4 (8)

BL, baseline; CI, confidence interval.

Undetectable HDV RNA defined as below lower limit of quantification (target not detected). ALT normalization defined as: ≤ 31 U/L for females and ≤ 41 U/L for males (Russian sites); or ≤ 34 U/L for females and ≤ 49 U/L for males (all other sites). Confidence intervals were calculated using Clopper-Pearson (exact) for proportions.

[†]Includes 1 death due to plasma cell myeloma not related to study treatment.

Figure: (abstract: OS-068).

Turin, Italy; ⁴Gastroenterology, Hepatology and Liver Transplantation Unit, ASST Papa Giovanni XXIII, Bergamo, Italy; ⁵Liver Unit, Azienda Ospedaliera San Camillo Forlanini, Rome, Department of Liver Transplant, Italy; ⁶Fondazione IRCCS Ca' Granda Ospedale Maggiore Policlinico, Division of Gastroenterology and Hepatology, Milan, Italy; ⁷Liver and Pancreas Transplant Center, Azienda Ospedaliera Brotzu, Cagliari, Italy; ⁸Gastroenterology, Azienda Universitaria Integrata Verona, Verona, Italy; ⁹Gastroenterology Unit, Department of Internal Medicine, University of Genoa, IRCCS Ospedale Policlinico San Martino, Genoa, Italy; ¹⁰Department of Translational and Precision Medicine, Sapienza University of Rome, Rome, Italy; ¹¹Hepatology Unit, Tor Vergata University, Rome, Italy; ¹²U.O.C. Gastroenterologia Universitaria, Azienda Ospedaliero-Universitaria-Policlinico di Bari, Bari, Italy; ¹³Gastroenterology-OHBP Surgery and Liver Transplant, AOU Policlinico di Modena, Modena, Italy; ¹⁴Liver Injury and Transplant Unit, Polytechnic University of Marche, Ancona, Italy; ¹⁵Department of Medical and Surgical Sciences, CEMAD, Fondazione Policlinico Universitario Agostino Gemelli IRCCS, Rome, Italy; ¹⁶Hepatology and Liver Transplantation Unit, Azienda Sanitaria Universitaria Integrata, Udine, Italy; ¹⁷Hepatology Unit, Cardarelli Hospital, Naples, Italy; ¹⁸Italian National Transplant Center, National Institute of Health, Rome, Italy; ¹⁹Department of Medicine and Surgery, University of Insubria-ASST Sette Laghi, Varese, Italy; ²⁰Division of Internal Medicine and Hepatology, Department of Gastroenterology, IRCCS Humanitas Research Hospital, Rozzano, Italy; ²¹Department of Biomedical Sciences, Humanitas University, Pieve Emanuele, Italy
Email: burra@unipd.it

Background and aims: Discontinuation of hepatitis B (HBV) immune globulin (HBIG) after liver transplantation (LT) for HBV-related cirrhosis with and without hepatocellular carcinoma (HCC) represents a challenging option. The adherence to this option in real-life practice is unknown. In a contemporary cohort of patients transplanted for HBV, with and without HCC, we aimed to: 1) assess the rate of HBV recurrence (HBV-R); 2) evaluate risk factors for HBV-R; 3) evaluate the association between HBV-R and HCC recurrence (HCC-R) and patient survival.

Method: This is a multicentric, retrospective study designed by the "Permanent Transplant Commission" of the Italian Association for the Study of the Liver; 20 LT Italian centres were invited to participate and 17 were finally included. All recipients who underwent LT for HBV-related liver disease were considered for inclusion. Exclusion criteria were: LT prior to January 1, 2010; age < 18 years old; combined transplantation; HIV coinfection; duration of follow-up after LT < 12 months. HBV-R was defined by positivity of HBV-DNA and/or HBsAg. Uni and multivariate linear regression analysis were used to identify predictors of HBV/HCC-R.

Results: 1115 patients were included (77% male; median age 57 years old). Indications for LT were HCC (51%), decompensated cirrhosis (41.2%), acute on chronic liver failure (ACLF) (3.4%), and acute liver failure (ALF) (4.2%). Median MELD at LT was 15 (10-21). Data regarding HBV prophylaxis were available in 984 (88%) of patients. Among them, life-long HBIG+nucl(t)oside analogues (NA) were used in 94.4%; withdrawal HBIG+life-long NA in 2.8%; HBIG alone in 0.5%; NA alone in 2.3%. Overall rate of HBV-R was 2.2% (median time after LT: 7 months [2-15]). Patients who received life-long HBIG+NA had lower rates of HBV-R than those in whom HBIG were withdrawn and those who received NA alone (1.4% vs. 10.7% vs. 13.6%; respectively, $p < 0.001$). HBV-R was associated with a lower survival after LT ($p = 0.008$). No association was found between HBV-R and MELD, HBV-DNA positivity or title >2000 UI/L at time of LT, HCC, use of anti-HBc donor. In patients transplanted for HCC ($n = 535$), the rate of HBV-R was 2.8% and of HCC-R was 10.3% (median time from LT: 17 months). Rate of HBV-R was higher in patients with vs. without HCC-R (14.6% vs. 1.2%; $p < 0.001$). Vascular invasion, TNM, AFP, and HBV-R were associated with HCC-R. Multivariate analysis showed that HBV-R was the only parameter independently associated with HCC-R (HR: 20;

CI95% 5-86; $p < 0.001$). HCC-R was associated with a significantly reduced survival after LT (5-year survival 36% vs. 94%; $p < 0.001$).

Conclusion: Life-long HBIG+NA is the most commonly used scheme for HBV-R prophylaxis after LT in Italy, leading to a low risk of HBV-recurrence. In LT recipients, HBV recurrence is associated with an increased risk of death. In patients transplanted for HCC, HBV-R is independently associated with HCC recurrence. Therefore, discontinuation of HBIG in these patients should be considered only in the setting of clinical trials.

(2) Immune-mediated and cholestatic diseases

OS-070

Development and validation of a score predicting response to obeticholic acid in primary biliary cholangitis: the OCA response score (ORS)

Antonio De Vincentis¹, Francesca Terracciani², Daphne D'Amato³, Pietro Invernizzi⁴, Anna Morgando³, Rinaldo Pellicano³, Ester Vanni³, Mauro Viganò⁴, Domenico Alvaro⁵, Rosanna Venere⁵, Ana Lleo⁴, Francesca Colapietro⁴, Elisabetta Degasperis⁴, Raffaella Viganò⁴, Edoardo Giovanni Giannini⁶, Sara Labanca⁶, Valentina Feletti⁵, Alessandro Mussetto⁵, Raffaele Cozzolongo⁵, Francesco Losito⁵, Maurizio Pompili⁵, Francesca Ponziani⁵, Grazia Niro⁵, Rosa Cotugno⁵, Pietro Pozzoni⁷, Luchino Chessa⁷, Giuseppe Cuccorese⁷, Valeria Pace Palitti⁷, Maurizio Russello⁷, Maria Rita Cannavò⁷, Evelise Frazzetto⁷, Gaetano Bertino⁷, Marco Marzoni⁷, Natalia Terreni⁷, Teresa Zolfino⁷, Carlo Saitta⁷, Adriano Pellicelli⁵, Barbara Coco⁷, Maurizio Brunetto⁷, Nora Cazzagon⁷, Annarosa Floreani⁷, Luigi Muratori⁷, Floriano Rosina⁷, Marco Distefano⁷, Gaetano Scifo⁷, Leonardo Baiocchi⁷, Giuseppe Grassi⁷, Rodolfo Sacco⁷, Antonio Izzi⁷, Saveria Lory Croce⁷, Cecilia Fiorini⁷, Fabio Marra⁷, Loredana Simone⁷, Olivia Morelli⁷, Ludovico Abenavoli⁷, Fabrizio Pizzolante⁷, Nicoletta De Matthaeis⁷, Miki Scaravaglio⁷, Giancarlo Gimignani⁷, Valentina Boano⁷, Giulia Francesca⁷, Massimo Marignani⁷, Silvia Fanella⁷, Marco Giaccetto⁷, Antonino Castellaneta^{7,8}, Guido Poggi⁷, Valerio Buzzanca⁷, Paolo Scivetti⁹, Annalisa Tortora⁷, Silvia Casella⁷, Valentina Bellia⁷, Barbara Omazzi⁷, Giuliano Alagna⁷, Chiara Ricci⁷, Paolo Poisa⁷, Cristina Rigamonti¹⁰, Vincenza Calvaruso⁷, Umberto Vespasiani Gentilucci⁷, Marco Carbone⁷. ¹University Campus Biomedico of Rome, Rome, Italy; ²campus, Italy; ³Torino, Italy; ⁴Milano, Italy; ⁵Roma, Italy; ⁶genova, Italy; ⁷A, Italy; ⁸Policlinico di Bari, Gastroenterologia, Bari, Italy; ⁹Ospedale degli infermi Biella, Medicina Interna, Ponderano (BI), Italy; ¹⁰Università degli Studi del Piemonte Orientale, Department of Translational Medicine, Novara, Italy
Email: a.devincentis@policlinicocampus.it

Background and aims: Obeticholic acid (OCA) is the only approved second-line treatment for patients with primary biliary cholangitis (PBC), and has been shown to provide an effective biochemical response in around ~40% of patients, according to POISE criteria. We aimed to derive and validate a predictive score (OCA response score, ORS) for predicting response to OCA at 12 and 24 months.

Method: We exploited data from the Italian recapitulate database including centers from the Italian PBC Registry, the Sicilian PBC Network, the PBC Project Piemonte-Liguria-Valle D'Aosta and CLEO/AIGO PBC study group. Multivariable Cox's regressions with backward selection method were applied to obtain parsimonious predictive models, including pre-treatment variables and/or the change of ALP/ULN and total bilirubin after 6 months' therapy. Biochemical response was evaluated according to the POISE (alkaline phosphatase (ALP)/upper limit of normal (ULN) <1.67 with a reduction of at least 15%, and a normal bilirubin) and ALP/ULN <1.67 criteria. Discrimination and calibration were evaluated by c-

statistics and comparing observed and predicted probabilities, and internally validated with bootstrap resampling procedure.

Results: We selected 441 subjects (median age 58, women 88%, cirrhosis 34%, median follow-up 24 months) with at least 6 months' observation after of OCA prescription. The observed response rates were 38%, 47% for POISE and 58%, 67% for ALP/ULN <1.67 criteria at 12 and 24 months. A score including age, pre-treatment pruritus, cirrhosis, ALP/ULN, GGT/ULN and bilirubin (ORS), and one that includes also the relative change of ALP/ULN and total bilirubin after 6 months (ORS+), showed good discrimination for response by POISE (c-statistics = 0.76 and 0.84, for ORS and ORS+, respectively) and by ALP/ULN <1.67 (c-statistics = 0.78 and 0.89, for ORS and ORS+, respectively). Bootstrap validation evidenced modest overfitting (slopes > 0.90) and consistent discrimination. The score also disclosed a good calibration (mean absolute errors < 0.04 for prediction of POISE and ALP/ULN <1.67 response at 24 months according to ORS and ORS+).

Conclusion: We derived and internally validated the ORS, that accurately predicts OCA response at 12 and 24 months. This could enhance allocation of second-line therapies in PBC with a personalised medicine approach. The present performances will need validation in external cohorts.

OS-071-YI

Laminin 511-E8 is an autoantigen in IgG4-related cholangitis patients that protects cholangiocytes against T lymphocyte-induced epithelial barrier dysfunction

David Trampert¹, Remco Kersten¹, Aldo Jongejan², Dagmar Tolenaars¹, Stan van de Graaf¹, Ulrich Beuers¹. ¹Tytgat Institute for Liver and Intestinal Research, Amsterdam Gastroenterology Endocrinology Metabolism (AGEM), Amsterdam University Medical Centers, Department of Gastroenterology and Hepatology, Netherlands; ²Amsterdam University Medical Centers, Department of Clinical Epidemiology, Biostatistics and Bioinformatics, Netherlands
Email: u.h.beuers@amsterdamumc.nl

Background and aims: IgG4-related disease is a systemic, lymphocyte driven, fibroinflammatory disorder. The most common organ manifestations are autoimmune pancreatitis (AIP) and IgG4-related cholangitis (IRC). Laminin 511-E8 is an extracellular matrix protein and autoantibodies against laminin 511-E8 have been described in

AIP. We have previously demonstrated that laminin 511-E8 protects human cholangiocytes against toxic bile acids (J Hepatol. 2022; 77 (S1): 603). Additionally, laminin 511-E8 appears to aid in establishing barrier function and lymphocyte recruitment. Here, we aimed to investigate whether IRC patients have autoantibodies against laminin 511-E8 and via which mechanisms laminin 511-E8 could further contribute to cholangiocyte health.

Method: Anti-laminin 511-E8 autoantibody positivity in patient sera was assessed by ELISA and compared to healthy control and primary sclerosing cholangitis (PSC) sera. *In vitro*, human H69 cholangiocytes were treated with recombinant laminin 511-E8, after which RNA sequencing was performed. For permeability assays, Transwell inserts were coated with recombinant laminin 511-E8 alongside BSA control coating, after which H69 cholangiocytes were seeded onto the inserts. In addition, T lymphocytes were activated *in vitro* and then added to the basolateral compartment of the co-culture system to better mimic the phenotype of IRC. The effect of laminin 511-E8 coating was studied by subjecting confluent H69 monolayers to 4kD FITC-dextran permeability assays.

Results: Seven out of 52 patients (13.5%) with IRC had autoantibodies against laminin 511-E8 confirming that laminin 511-E8 is an autoantigen in patients with IRC. In contrast, no PSC patients and one healthy control had autoantibodies against laminin 511-E8. RNA sequencing of H69 cholangiocytes treated with recombinant laminin 511-E8 compared to controls showed differential expression of genes involved in cell barrier function and inflammation. Permeability assays revealed that laminin 511-E8 reduced leakage of FITC-dextran past the H69 monolayer. When Transwell inserts were coated with recombinant laminin 511-E8 in the co-culture setup, H69 cholangiocytes were protected from T lymphocyte-induced epithelial barrier dysfunction.

Conclusion: In this study we establish that laminin 511-E8 is an autoantigen in a subset of IRC patients. RNA sequencing and FITC-dextran permeability assays indicate that laminin 511-E8 enhances barrier function and protects cholangiocytes against T lymphocyte-induced epithelial barrier dysfunction. In addition to the previously reported effects of laminin 511-E8 protecting cholangiocytes against toxic bile acids, we speculate that autoantibodies against laminin 511-E8 may contribute to the pathogenesis of IRC by impairing cholangiocyte barrier function with increased inflammatory bile duct damage.

FITC-dextran permeability in human H69 cholangiocytes co-cultured with and without stim. T cells

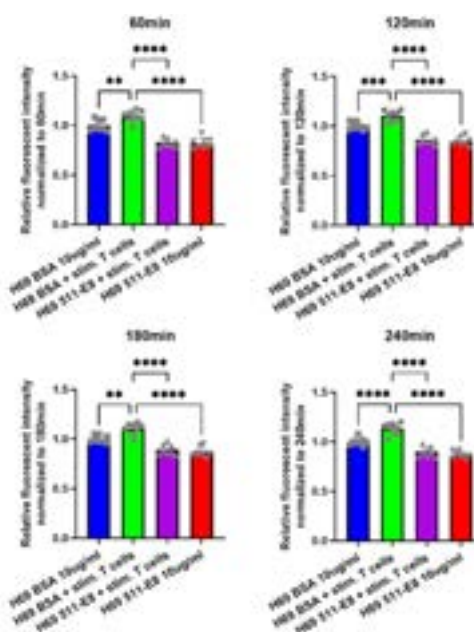
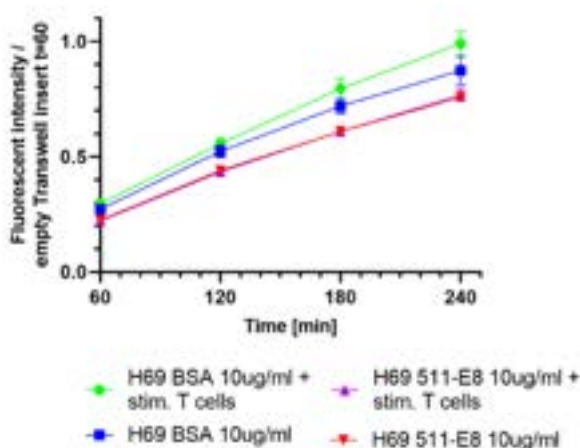


Figure: (abstract: OS-071-YI).

OS-072

Maralixibat leads to significant reductions in bilirubin for patients with progressive familial intrahepatic cholestasis: data from MARCH-PFIC

Lorenzo D'Antiga¹, Alexander Miethke², Douglas Mogul³, Tiago Nunes³, Will Garner³, Pamela Vig³, Richard Thompson⁴.

¹Hospital Papa Giovanni XXIII, Paediatric Hepatology, Gastroenterology and Transplantation, Bergamo, Italy; ²Cincinnati Children's Hospital Medical Center, Cincinnati, Ohio, United States; ³Mirum Pharmaceuticals, Inc., Foster City, California, United States; ⁴King's College London, Institute of Liver Studies, London, United Kingdom
Email: ldantiga@asst-pg23.it

Background and aims: Progressive Familial Intrahepatic Cholestasis (PFIC) refers to inherited disorders of abnormal bile formation causing pruritus, chronic liver disease, and increased serum bile acid (sBA) levels. Evidence exists that elevated serum bilirubin levels portend poor outcomes in PFIC. Ileal bile acid transporter inhibitors (IBATi) interrupt enterohepatic circulation of bile acids. We evaluated the pre-specified secondary end point of the impact of maralixibat (MRX) on bilirubin and a post-hoc analysis of bilirubin normalization in the MARCH-PFIC study.

Method: MARCH-PFIC enrolled patients with a genetic diagnosis of PFIC, pruritus, and elevated sBA. Patients were randomized to MRX 570 µg/kg BID or placebo (PBO) for 26 weeks. Changes were determined as the difference between MRX and PBO groups for Change from Baseline (CFB) to the average of the final 3 measurements (Weeks 18, 22 and 26) using a mixed-effects model with recurrent measurements. Total/direct bilirubin (TB/DB) categories were defined as normal ($\leq 1.2/0.3$ mg/dL) or abnormal ($> 1.2/0.3$ mg/dL).

Results: Analysis included 64 patients from the All-PFIC cohort (13 FIC1, 31 nt-BSEP, 9 MDR3, 7 TJP2, and 4 MYO5B); patients were randomized to MRX (n = 33) or PBO (n = 31). Baseline median (Q1, Q3) TB in the MRX and PBO groups were 2.8 (1.4, 5.5) and 2.6 (0.8, 5.5) mg/dL, and DB were 2.1 (0.9, 4.0) mg/dL and 1.9 (0.5, 4.3) mg/dL, respectively. The study achieved significant CFB between MRX vs PBO for TB (-1.1 vs +0.9 mg/dL; group difference: 2.0; p = 0.047) and DB (-0.8 vs +0.8 mg/dL; group difference: 1.5; p = 0.048). Among individuals with abnormal Baseline bilirubin (total: n = 46; direct: n = 56), there was a significant CFB between MRX vs PBO groups for DB (-0.8 vs +1.0 mg/dL; group difference: -1.8; p = 0.042). For the post-hoc analysis assessing bilirubin normalization, pre and post bilirubin values were available for 60 individuals (32 MRX; 28 PBO). For the MRX group, TB normalized in 40% (10/25) of patients with abnormal Baseline values, and no patient went from normal to abnormal TB (0/7). For the PBO group, TB never normalized in those with abnormal Baseline values (0/18) and instead became abnormal for 30% (3/10) of patients. For DB, the MRX group also showed greater frequency of normalization vs PBO (34% vs 7%). Among all individuals that normalized TB, sBA was reduced by 94.9% (95% CI: 68.5%, 98.9%), whereas for those individuals that did not normalize TB, sBA only decreased by 13.3% (95% CI: 1.4, 34.0); p < 0.0001. For treatment-emergent adverse-event reporting, bilirubin increases were observed less frequently in MRX vs PBO (14.9% vs 19.6%).

Conclusion: MRX is the only IBAT inhibitor to demonstrate significant decreases in TB/DB compared to PBO in children with PFIC and across PFIC types. 40% of MRX patients with abnormal Baseline bilirubin achieved normalization vs none in the PBO group, suggesting that MRX may yield clinically meaningful improvements in liver health in patients with PFIC.

OS-073

Prognostic significance of liver stiffness progression in primary biliary cholangitis

Laurent Lam¹, Fabrice Carrat¹, Pierre-Antoine Soret², Sara Lemoine², Bettina Hansen^{3,4}, Gideon Hirschfield⁴, Aliya Gulamhusein⁴, Aldo J Montano-Loza⁵, Ellina Lytvayak⁵, Albert Pares⁶, Olivas Ignasi⁶, John Eaton⁷, Karim Osman⁷, Christoph Schramm⁸, Marcial Sebode⁸,

Ansgar W. Lohse⁸, George Dalekos⁹, Nikolaos Gatselis⁹, Frederik Nevens¹⁰, Nora Cazzagon¹¹, Alessandra Zago¹¹, Francesco Paolo Russo¹¹, Nadir Abbas¹², Palak Trivedi¹², Douglas Thorburn¹³, Francesca Saffioti¹³, Laszlo Barkai¹³, Davide Roccarina¹³, Vincenza Calvaruso¹⁴, Anna Fichera¹⁴, Adele Delamarre¹⁵, Natalia Sobenko¹⁶, Maria Alejandra Gracia Villamil¹⁶, Medina-Morales Esli¹⁷, Alan Bonder¹⁷, Vilas Patwardhan¹⁷, Cristina Rigamonti¹⁸, Marco Carbone¹⁹, Pietro Invernizzi¹⁹, Laura Cristofori¹⁹, Adriaan Van der Meer²⁰, Rozanne de Veer²⁰, Ehud Zigmund²¹, Yehezkel Eyal²¹, Andreas E Kremer²², Ansgar Deibel²², Tony Bruns²³, Karsten Große²³, Aaron Wetten²⁴, Jessica Dyson²⁴, David Jones²⁴, Jérôme Dumortier²⁵, Georges-Philippe Pageaux²⁶, Victor de Lédinghen¹⁵, Olivier Chazouillères², Christophe Corpechot².
¹Sorbonne Université, INSERM, Institut Pierre Louis d'Epidémiologie et de Santé Publique (IPLESP), Paris, France; ²Saint-Antoine Hospital, Assistance Publique-Hôpitaux de Paris, Sorbonne University, Reference Center for Inflammatory Biliary Diseases and Autoimmune Hepatitis, Paris, France; ³Erasmus MC, Department of Epidemiology and Biostatistics, Rotterdam, Netherlands; ⁴University of Toronto, Toronto Centre for Liver Disease, Toronto, Canada; ⁵University of Alberta, Division of Gastroenterology and Liver Unit, Edmonton, Canada; ⁶University of Barcelona, Hospital Clínic, Liver Unit, Barcelona, Spain; ⁷Mayo Clinic, Division of Gastroenterology and Hepatology, Rochester, United States; ⁸University Medical Center Hamburg-Eppendorf, Department of Medicine I and Martin Zeitz Center for Rare Diseases, Hamburg, Germany; ⁹General University Hospital of Larissa, Department of Medicine and Research Laboratory of Internal Medicine, Larissa, Greece; ¹⁰University Hospitals KU, Division of Hepatology and Liver Transplantation, Leuven, Belgium; ¹¹University of Padova, Department of Surgery, Oncology and Gastroenterology, Padova, Italy; ¹²University Hospitals Birmingham, Liver Unit, Birmingham, United Kingdom; ¹³Royal Free Hospital, University College London Institute for Liver and Digestive Health, London, United Kingdom; ¹⁴University of Palermo, Section of Gastroenterology and Hepatology, Palermo, Italy; ¹⁵University Hospitals of Bordeaux, Department of Hepatology, Pessac, France; ¹⁶Italian Hospital of Buenos Aires, Department of Hepatology and Liver Transplantation, Buenos Aires, Argentina; ¹⁷Beth Israel Deaconess Medical Center, Boston, Department of Medicine, Division of Gastroenterology, Boston, United States; ¹⁸Università del Piemonte Orientale, Department of Internal Medicine, Novara, Italy; ¹⁹University of Milano-Bicocca, Center for Autoimmune Liver Diseases, Monza, Italy; ²⁰Erasmus University Medical Center, Department of Gastroenterology and Hepatology, Rotterdam, Netherlands; ²¹Tel Aviv Sourasky Medical Center, Research Center for Digestive Tract and Liver Diseases, Tel Aviv, Israel; ²²University Hospital Zürich, Department of Gastroenterology and Hepatology, Zurich, Switzerland; ²³University Hospital RWTH Aachen, Department of Medicine III, Aachen, Germany; ²⁴Newcastle upon Tyne Hospitals NHS Foundation Trust and Newcastle University, Department of Hepatology and Liver Transplantation, Newcastle, United Kingdom; ²⁵Edouard Herriot Hospital, Hospices Civils de Lyon, Department of Gastroenterology and Hepatology, Lyon, France; ²⁶University Hospital of Montpellier, Department of Hepatology and Liver Transplantation, Montpellier, France
Email: christophe.corpechot@aphp.fr

Background and aims: The prognostic value of point measurement of liver stiffness (LSM) by vibration-controlled transient elastography (VCTE) in patients with primary biliary cholangitis (PBC) has been established. However, the association between LSM progression over time and the occurrence of adverse clinical events in these patients is poorly known. Our aim was to evaluate the risk of adverse clinical events associated with longitudinal changes of LSM in a large cohort of PBC patients.

Method: A large retrospective cohort study (24 centres, 13 countries) of patients with PBC, followed-up using VCTE (Fibroscan) over the past 15 years whilst on ursodeoxycholic acid (UDCA) therapy, was performed. Patients with follow-up ≤ 12 months, those diagnosed

ORAL PRESENTATIONS

with autoimmune hepatitis overlap syndrome, and those exposed to second-line therapies (i.e., fibrates, obeticholic acid, corticosteroids) at any time were excluded. Unreliable LSM values, defined by an interquartile/median ratio >30%, were excluded from the analysis. Advanced PBC was defined by LSM ≥ 10 kPa. Biochemical response to UDCA was defined by the Paris-2 criteria. The primary composite end point was time to adverse clinical events, defined as death, liver transplantation, or liver-related complications. Joint models for longitudinal and time-to-event data, adjusted for age and sex, were used to assess the association between changes in LSM and clinical outcomes.

Results: A total of 4408 LSMs performed in 2244 patients (female 90.8%; mean age 58.4 years; advanced disease 25.4%; mean prior treatment with UDCA 5.9 years) were analyzed. A total of 217 adverse clinical events occurred during 10122.3 patient-years (incidence, 21.4 per 1000 patient-years). Any increase in LSM was associated with an increased risk of poor clinical outcomes (Figure), with an overall hazard ratio per 10% increase in LSM/year of 1.47 (95% CI 1.40–1.55, $p < 0.001$). This association was consistent regardless of age (≤ 45 years; > 45 years) and LSM (< 8 kPa; > 8 kPa and ≤ 15 kPa; ≥ 15 kPa) risk groups at baseline. Conversely, LSM progression was significantly higher in patients who met the primary end point than in those who did not ($p < 0.05$). No association was found between LSM progression and baseline values of LSM, except in the youngest patients (≤ 45 years; $p < 0.05$) and those who did not have an adequate response to UDCA ($p < 0.01$).

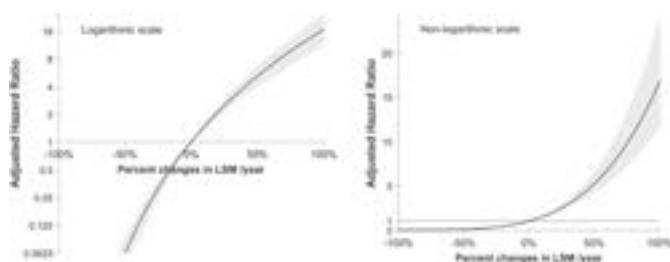


Figure: Adjusted risk of adverse clinical events associated with LSM progression over time.

Conclusion: In patients with PBC treated with UDCA, progression of LSM over time is associated with poorer clinical outcomes regardless of age and LSM values at baseline. LSM values on UDCA are associated with LSM progression in the youngest patients and those with inadequate biochemical response to UDCA.

OS-074-YI

A3907, a systemic ASBT inhibitor, improves cholestasis in mice by inhibiting multi-organ bile acid transport and shows translational relevance to human

Francisco J. Caballero^{1,2}, Pedro Miguel Rodrigues^{2,3,4}, Aloña Agirre Lizaso², Paula Olaizola², Laura Izquierdo-Sánchez², María Jesús Perugorria^{1,2,3}, Luis Bujanda^{1,2,3}, Bo Angelin⁵, Sara Straniero⁵, Anna Wallebäck⁶, Ingemar Starke⁶, Per-Göran Gillberg⁶, Ellen Strängberg⁶, Fredrik Wangsell⁶, Jan Mattsson⁶, Henrik B. Hansen⁷, Erik Lindström⁶, Peter Akerblad⁶, Jesus Maria Banales^{2,3,4,8}. ¹University of the Basque Country, Department of Medicine, Faculty of Medicine and Nursing, Spain; ²Biodonostia Health Research Institute, Liver and Gastrointestinal Diseases, Spain; ³National Institute for the Study of Liver and Gastrointestinal Diseases (CIBERehd, "Instituto de Salud Carlos III"), Spain; ⁴Ikerbasque, Basque Foundation for Science, Spain; ⁵Karolinska Institutet at Karolinska University Hospital Huddinge, CardioMetabolic Unit, Department of Medicine and Clinical Department of Endocrinology, Sweden; ⁶Albireo AB, Göteborg, Sweden; ⁷Gubra, Denmark; ⁸University of Navarra, Department of Biochemistry and Genetics, Spain
Email: jesus.banales@biodonostia.org

Background and aims: Cholestasis is characterized by impaired bile flow leading to intrahepatic accumulation of bile constituents, including bile acids (BAs). Sustained cholestasis can progress to advanced stages of liver disease, increasing the risk of hepatobiliary malignancies and liver failure. The apical sodium-dependent BA transporter (ASBT) is pivotal for BA reabsorption in the ileum, bile ducts and kidneys, contributing to BA overload during cholestasis by preventing BA excretion. Our aim was to explore the therapeutic and translational potential of a novel oral systemic ASBT inhibitor (A3907) for the treatment of cholestasis.

Method: The pharmacological profile of A3907, its therapeutic potential in experimental models of cholestasis, and its translational potential in healthy human subjects was investigated.

Results: A3907 was a potent and selective inhibitor of both mouse and human ASBT displaying significant systemic biodistribution in healthy rodents. Daily oral administration of A3907 for 7 days promoted fecal BA excretion in healthy mice without affecting urine BA levels. A3907 was evaluated in two animal models of cholestasis, *Mdr2*^{-/-} and BDL mice. Daily oral administration of A3907 resulted in high systemic exposure in both models. In the *Mdr2*^{-/-} mice, 4-week oral treatment with A3907 significantly reduced liver-to-body and spleen-to-body weight ratios, serum bile acids, plasma markers of liver injury, and liver markers of inflammation, fibrosis, and ductular reaction. Interestingly, A3907 prevented apoptosis in cultured cholangiocytes exposed to high concentrations of GCDCA (1 mM), also indicating a direct cholangioprotective effect. In the BDL mice, oral A3907 administration for 11 days enhanced renal BA clearance resulting in substantial reduction of serum and biliary BA levels. As a result, the pronounced body weight loss observed in BDL mice was prevented by A3907 administration. Furthermore, A3907 treatment led to marked reduction in serum transaminases (AST and ALT), bilirubin, and urea, and liver histopathological analysis revealed reduced inflammatory cell infiltration and fewer necrotic areas in the treated animals. Finally, the translational potential of A3907 into clinical practice was investigated in a placebo-controlled Phase 1 study, showing that A3907 was well-tolerated in human subjects at pharmacologically active doses.

Conclusion: A3907 is the first oral systemic ASBT inhibitor that acts at the level of the intestine, liver and kidney and robustly attenuates cholestatic liver damage in experimental models. A3907 was well-tolerated in human subjects at doses reaching systemic exposures comparable to those required for therapeutic effects in animal models of cholestasis. Collectively these results highlight the promising translational potential of A3907 for the treatment of cholestatic diseases.

Liver immunology

OS-075

Single-cell atlas of liver myeloid cells with cure of chronic viral hepatitis

Ang Cui^{1,2}, Bo Li^{1,2}, Michael Wallace³, Anna Gonye³, Christopher Oetheimer³, Hailey Patel³, Pierre Tonnerre³, Jacinta Holmes³, David Lieb¹, Brianna Yao¹, Aileen Ma¹, Kela Roberts¹, Marcos Damasio³, Jonathan Chen^{1,3}, Daphnee Pious³, Charles Carlton-Smith³, Joelle Brown³, Ravi Mylvaganam³, Jeremy Fung³, Moshe Sade-Feldman^{1,3}, Jasneet Aneja³, Jenna Gustafson³, Eliana Epstein³, Shadi Salloum³, Cynthia Brisac³, Ashraf Thabet³, Arthur Kim³, Georg Lauer³, Nir Hacohen^{1,3}, Raymond Chung³, Nadia Alatrakchi³. ¹Broad Institute of MIT and Harvard, United States; ²Harvard University, United States; ³Massachusetts General Hospital and Harvard Medical School, United States
Email: angcui@broadinstitute.org

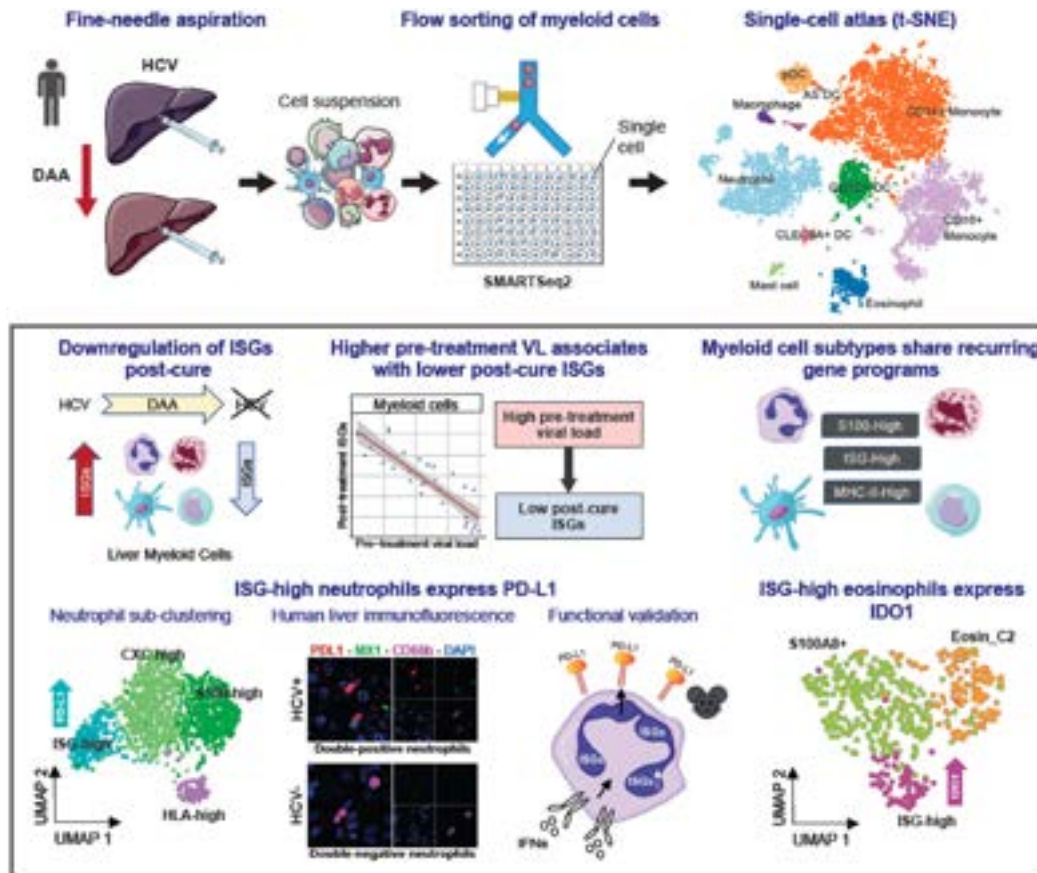


Figure: (abstract: OS-075-Y1).

Background and aims: Direct-acting antivirals (DAAs) are now able to cure nearly all patients infected with the hepatitis C virus (HCV), representing the only definitive cure of a human chronic viral infection to date. DAAs provide a valuable opportunity to study immune pathways in the reversal of chronic immune failures in humans.

Method: To leverage this opportunity, we used plate-based single-cell RNA-seq (scRNA-seq) to deeply profile myeloid cells from liver fine needle aspirates (FNAs) in HCV patients before and after DAA treatment. We comprehensively characterized liver neutrophils, eosinophils, mast cells, conventional dendritic cells (cDCs), plasmacytoid dendritic cells (pDCs), classical monocytes, non-classical monocytes, and macrophages, and defined fine-grained subpopulations of several cell types.

Results: We discovered cell-type-specific changes post-cure, including an increase in *MCM7+STMN1+* proliferating CD1C+ cDCs, which may support restoration from chronic exhaustion. We observed an expected downregulation of interferon stimulated genes (ISGs) post-cure as well as an unexpected inverse relationship between pre-treatment viral load and post-cure ISG expression in each cell type, revealing a link between viral loads and sustained modifications of the host's immune system. We found an upregulation of PD-L1/L2 expression in ISG-high neutrophils and IDO1 expression in eosinophils, pinpointing cell subpopulations crucial for immune regulation. We identified three recurring gene programs shared by multiple cell types, distilling core functions of the myeloid compartment.

Conclusion: This comprehensive scRNA-seq atlas of human liver myeloid cells in response to a cure of chronic viral infections reveals principles of liver immunity and provides immunotherapeutic insights.

OS-076

Liver-on-chip platform for studying recruitment and differentiation of circulating monocytes

Aleksandra Aizenshtadt¹, Mathias Busek^{1,2}, Inger Øynebråten^{1,3}, Shadab Abadpour^{1,4}, Anna Katharina Frank^{1,5,6,7}, Alexey Golovin¹, Justyna Stokowiec¹, Alexandre Corthay^{1,3}, Espen Melum^{1,4,5,6,7}, Stefan Krauss^{1,2}, ¹University of Oslo, Hybrid Technology Hub, Institute of Basic Medical Science, Oslo, Norway; ²Oslo University Hospital, Department of Immunology and Transfusion Medicine, Oslo, Norway; ³Oslo University Hospital, Department of Pathology, Oslo, Norway; ⁴Oslo University Hospital, Department of Transplant Medicine and Institute for Surgical Research, Oslo, Norway; ⁵Oslo University Hospital, Norwegian PSC Research Center, Department of Transplantation Medicine, Division of Surgery, Inflammatory Diseases and Transplantation, Oslo, Norway; ⁶Oslo University Hospital, Research Institute of Internal Medicine, Division of Surgery, Inflammatory Diseases and Transplantation, Oslo, Norway; ⁷University of Oslo, Institute of Clinical Medicine, Faculty of Medicine, Oslo, Norway
Email: aleksandra.aizenshtadt@medisin.uio.no

Background and aims: Recent studies based on single-cell and spatial (proteo)genomics uncovered a significant diversity of immune cells in the liver, reflecting metabolic zonation, and might be altered during diseases. For instance, circulating monocytes can be recruited to damaged liver tissue and change fate depending on signals from the microenvironment. An expanded population of recruited macrophages is believed to affect the progression of liver diseases. The exact mechanisms and functions of recruited macrophages are not fully understood, partially due to the absence of relevant human *in vitro* models. The aim of this study was to establish an *in vitro* system for functional studies of circulating immune cells in

ORAL PRESENTATIONS

the context of their recruitment and interactions with healthy and diseased 3D liver tissue representations with metabolic zonation.

Method: We developed medium compositions for generating and maintaining human pluripotent stem cells-derived periportal (zone 1) and pericentral (zone 3)-like liver organoids (HLO). The zone-specific phenotype of the HLOs was demonstrated by immunofluorescence, gene expression analysis, proteomics. Functional assays included drug metabolism, production of albumin, urea, glutamine and accumulation of glycogen. Using a recently developed pump-less recirculation Organ-on-a-Chip (rOoC) platform, healthy and diseased zoned HLOs were co-cultured with human primary CD14⁺ monocytes, isolated from peripheral blood mononuclear cells (PBMC). Confocal imaging, flow cytometry and multiplex assay of cytokines were employed for the analysis of interaction between HLOs and monocytes.

Results: We present a novel *in vitro* model for studying interactions between circulating human immune cells and liver tissue representations with metabolic zonal identity (Fig. a) in a rOoC platform (Fig. b). In this setting, HLOs could be cultured for at least 2 weeks while retaining viability and functionality. Moreover, disease phenotype (hepatic steatosis or drug-induced liver injury, DILI) can be induced in HLOs in a rOoC platform in response to free fatty acids or acetaminophen (APAP) (Fig. c), respectively. Monocytes could be circulated in the rOoC platform without trapping, activation or decrease in viability. The functional interactions between zoned HLOs and circulating monocytes were analyzed in control and disease-mimicking conditions. We observed an increased migration of monocytes toward APAP-treated HLOs compared to untreated HLOs (Fig. c). The multiplex analysis of cytokines and *in situ* immunophenotyping enabled a thorough characterization of deployment and disease-dependent alterations of monocytes and liver cells “on chip”.

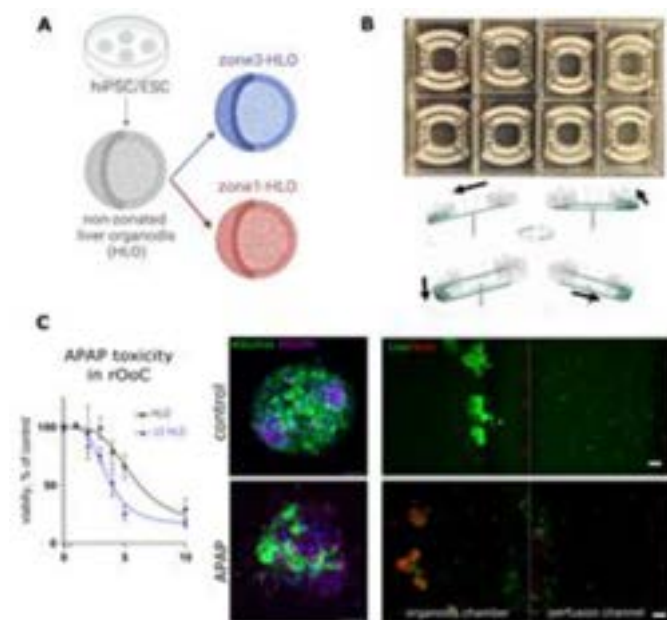


Figure: The Liver-on-chip platform. A) Scheme of generation of zoned HLO. B) rOoC chips in the culture 8-wells format, and scheme of rOoC perfusion. C) Example of disease model in rOoC-APAP-induced liver injury. “On chip” confocal imaging showing expression of albumin (green) and PDGFR (magenta) in control and APAP-treated HLO. Live/dead staining was used for the visualization of monocytes (green dots) migration toward APAP-treated organoids.

Conclusion: In this proof-of-concept study, we developed a novel platform for modelling the interactions between zoned liver 3D representations and circulating immune cells “on chip.” The platform provides an improved tool for a scalable and personalized evaluation of human liver responses to drug interventions and disease modelling.

OS-077

Liver immunity index: circulating HBV-specific CXCR6⁺ CD8T cells mirror intrahepatic anti-viral T cell immunity and predict immune control in models of chronic hepatitis B

Hannah Wintersteller¹, Miriam Bosch¹, Donakonda Sainitin¹, Anna Kosinska^{2,3}, Edanur Ates-Öz^{2,3}, Christine Wurmser⁴, Dietmar Zehn⁴, Ulrike Protzer^{2,3}, Dirk Wohlleber¹, Percy A. Knolle^{1,3}.

¹Institute of Molecular Immunology, Technical University of Munich, Germany;

²Institute of Virology, Technical University of Munich, Germany;

³German Center for Infection Research, Munich, Germany;

⁴Division of Animal Physiology and Immunology, School of Life Sciences Weihenstephan, Freising, Germany

Email: percy.knolle@tum.de

Background and aims: Persistent hepatic viral infections, such as chronic hepatitis B, are characterized by a scarcity and dysfunction of virus-specific CD8T cells detected in the liver and the circulation. Immunotherapies, such as therapeutic vaccination, thus aim to reinvigorate and expand virus-specific CD8T cell immunity to control viral infection in the liver. Since liver biopsies are difficult to obtain, we sought to identify markers on circulating antigen-specific CD8 T-cells that reflect the immune response at the site of infection in the liver and could be used for immune monitoring of immune therapies.

Method: We used pre-clinical models of adenoviral hepatocyte-specific delivery of nominal antigens and HBV genomes to study the dynamics of virus-specific T cell responses by flow cytometry and single-cell RNA sequencing (scRNAseq).

Results: After adenoviral transduction of hepatocytes, we detected generation of CXCR6⁺ virus-specific CD8T cells with a liver-resident phenotype that were absent from the spleen. During an acute infection, CXCR6⁺ CD8T cells were potent effector cells, expressing high levels of Granzyme B and TNF/IFN γ after *ex vivo* stimulation. CXCR6⁺ CD8T cells in a persistent infection of the liver were rendered dysfunctional. Strikingly, during clearance of hepatic infection, high numbers of circulating CXCR6⁺ CD8T cells were detected in peripheral blood, whose phenotype and functionality were identical to their counterparts in the liver, and most importantly predicted outcome. Notably, CXCR6⁺ CD8T cells developed solely when recognizing their antigen in the liver and not after systemic DNA vaccination in the absence of infection, which led to formation of circulating CX₃CR1⁺ effector T cells. scRNAseq analysis of sorted, virus-specific CD8T cells confirmed co-clustering of CD8T cells from the liver and blood but not spleen.

Conclusion: Our results reporting the occurrence of HBV-specific CXCR6⁺CD8T cells in the circulation, that have previously seen their antigen in the liver, provide the basis for using CXCR6 as a predictive marker for intrahepatic immune responses during monitoring of immune therapies, such as therapeutic vaccination, in patients with chronic hepatitis B.

OS-079-YI

2D-interactome of the tumor immune-microenvironment reveals immunosuppressive T cells in primary sclerosing cholangitis-associated cholangiocarcinoma

Jenny Krause¹, Christian Casar², Sonja Haenzelmann^{3,4,5}, Fabian Hausmann^{3,4}, Robin Khatri^{3,4}, Camilla Engblom⁶, Srustidhar Das^{7,8}, Dominik Kyllies⁵, Tobias Poch¹, Dorothee Schwinge¹, Franziska Muscate^{1,9}, Filippo Cortesi^{1,9}, Asmus Heumann⁹, Tarik Ghabban⁹, Lutz Fischer¹⁰, Till Clauditz¹¹, Christian F. Krebs^{5,12}, Victor Puelles⁵, Eduardo Villablanca^{7,8}, Samuel Huber^{1,12}, Stefan Bonn^{3,4,12}, Christoph Schramm^{1,12}, Nicola Gagliani^{1,9,12}.

¹University Medical Center Hamburg-Eppendorf, I. Department of Medicine, Hamburg, Germany; ²University Medical Center Hamburg-Eppendorf, Bioinformatics Core, Hamburg, Germany; ³University Medical Center Hamburg-Eppendorf, Institute of Medical Systems Biology, Hamburg, Germany; ⁴University Medical Center Hamburg-Eppendorf, Center for Biomedical AI, Hamburg, Germany; ⁵University Medical Center Hamburg-Eppendorf, III. Department of Medicine, Hamburg, Germany; ⁶Karolinska Institute, Department of Cell and Molecular Biology, Stockholm, Sweden; ⁷Karolinska Institute and University Hospital, Division of Immunology and Allergy, Department of Medicine Solna, Stockholm, Sweden; ⁸Center of Molecular Medicine, Stockholm, Sweden; ⁹University Medical Center Hamburg-Eppendorf, Department of General, Visceral and Thoracic Surgery, Hamburg, Germany; ¹⁰University Medical Center Hamburg-Eppendorf, Department for Visceral Transplant Surgery, Hamburg, Germany; ¹¹University Medical Center Hamburg-Eppendorf, Department of Pathology, Hamburg, Germany; ¹²University Medical Center Hamburg-Eppendorf, Hamburg Center for Translational Immunology, Hamburg, Germany

Email: je.krause@uke.de

Background and aims: Primary Sclerosing Cholangitis (PSC) is the greatest risk factor for Cholangiocarcinoma (CCA), its most feared complication (1, 2). Curative therapeutic options are limited, and its pathogenesis is still only partially understood. Altered T cell function has recently been described in patients with PSC, characterized by a pro-inflammatory CD4⁺ T_{EM} phenotype dominated by IL-17 producing cells (T_H17) (3–5). In CCA, highly activated immunosuppressive regulatory Foxp3⁺ T cells (Foxp3⁺ T_{REG}) have been linked to unfavourable outcome (6). The tumor immune-microenvironment (TIME) of PSC-associated CCA (PCS-CCA) has never been thoroughly characterized, thus whether T_H17 or Foxp3⁺ T_{REG} contribute to TIME of PSC-associated CCA remains unknown.

Method: To understand the composition and function of the TIME in PSC-CCA, we applied state-of-the-art single-cell multi-omics, as well as spatial transcriptomics (ST). By using a combination of novel analyses such as interactome and spot deconvolution, we overcame the limitation of 1-dimensional biased morphological experiments, revealing the cellular neighborhood composition and the comprehensive 2D interactome of PSC-CCA TIME.

Results: We provide the first comprehensive characterization of the TIME in PSC-CCA. We developed a new method to elucidate the 2D-immune-interactome based on single-cell multi-omics, and thereby identified immunosuppressive T cell interaction within the PSC-CCA TIME. Trajectory analyses and scTCR-Seq suggests plasticity of CD4⁺ T_{EM} with a T_H17 polarization-state towards Foxp3⁺ T_{REG} in PSC-CCA. ST spot deconvolution revealed the neighborhood composition of Foxp3⁺ T_{REG} within the tumor, showing proximity to CCA cells and cancer associated fibroblasts. Finally, we found *TGFB1*, a cytokine known to promote the conversion of CD4⁺ T cells to Treg, gene expression increased in tumors when compared to the adjacent liver.

Conclusion: We here generated the first comprehensive multi-omics dataset on the complex TIME of PSC-CCA proposing potential therapeutic targets. By revealing the 2D-immune-interactome, we identified location and cellular network of Foxp3⁺ T_{REG} and suggested them as a potent mediator of tumor maintenance. We further suggest TGFB1 from the tumor microenvironment to be the potential

cytokine able to polarize CD4⁺ T_{EM} in the liver toward immunosuppressive regulatory T cells in PSC-CCA, and thus impair antitumorigenic function of cytotoxic CD8⁺ T cells.

References

1. Aune D, et al. Primary sclerosing cholangitis and the risk of cancer, cardiovascular disease, and all-cause mortality: a systematic review and meta-analysis of cohort studies. *Sci Rep* 2021;11:10646.
2. Karlsen et al. Primary sclerosing cholangitis-a comprehensive review. *J Hepatol* 2017;67:1298–1323.
3. Katt J, et al. Increased T helper type 17 response to pathogen stimulation in patients with primary sclerosing cholangitis. *Hepatology* 2013;58:1084–1093.
4. Sebode M, Peiseler M, et al. Reduced FOXP3 (+) regulatory T cells in patients with primary sclerosing cholangitis are associated with IL2RA gene polymorphisms. *J Hepatol* 2014;60:1010–1016.
5. Schwinge D, et al. Dysfunction of hepatic regulatory T cells in experimental sclerosing cholangitis is related to IL-12 signaling. *J Hepatol* 2017;66:798–805.
6. Alvisi G, et al. Multimodal single-cell profiling of intrahepatic cholangiocarcinoma defines hyperactivated Tregs as a potential therapeutic target. *J Hepatol* 2022.

Liver tumours - Clinical except therapy

OS-080-YI

Platelet, elastography, age, sex and etiology for hepatocellular carcinoma surveillance in patients with advanced chronic liver disease: Please algorithm

Wenji Gu¹, Victor de Lédighen², Christophe Aubé³, Aleksander Krag⁴, Christian Strassburg⁵, Laurent Castera⁶, Jérôme Dumortier⁷, Mireen Friedrich-Rust⁸, Stanislas Pol⁹, Ivica Grgurevic¹⁰, Yasmin Zeleke⁸, Michael Praktiknjo¹, Sven Francque¹¹, Halima Gottfriedová¹², Thomas Vanwolleghem¹¹, Ioan Sporea¹³, Ida Tješić-Drinković¹⁰, Chang Johannes⁵, Sanda Mustapic¹⁰, Philipp Schindler¹, Florian Rennebaum¹, Maria Kjærgaard⁴, Olivier Guillaud⁷, Cristina Margini¹⁴, Christophe Cassinotto¹⁵, Jan Best¹⁶, Ali Canbay¹⁶, Pierre-Emmanuel Rautou⁶, Maxime Ronot⁶, Filipe Andrade⁶, David Jm Bauer^{17,17}, Benedikt Simbrunner¹⁷, Georg Semmler¹⁷, Thomas Reiberger¹⁷, Jerome Boursier³, Ditlev Nytoft Rasmussen⁴, Valérie Vilgrain⁶, Aymeric Guibal⁷, Stefan Zeuzem⁸, Camille Vassord⁹, Luisa Vonghia¹¹, Renata Senkerikova¹², Alina Popescu¹³, Annalisa Berzigotti¹⁴, Wenping Wang¹⁸, Wim Laleman¹⁹, Maja Thiele⁴, Christian Jansen⁵, Jonel Trebicka¹. ¹University Hospital Muenster, Germany; ²Bordeaux University Hospital, France; ³Angers University Hospital, France; ⁴Odense University Hospital, Denmark; ⁵Bonn University Hospital, Germany; ⁶Paris Beaujon University Hospital, France; ⁷Lyon Edouard Herriot University Hospital, France; ⁸Frankfurt University Hospital, Germany; ⁹Paris Cochin University Hospital, France; ¹⁰Dubrava University Hospital, Croatia; ¹¹Antwerp University Hospital, Belgium; ¹²Institute for Clinical and Experimental Medicine, Prague, Czech Republic; ¹³“Victor Babes” University of Medicine and Pharmacy, Romania; ¹⁴Bern University Hospital, Switzerland; ¹⁵University hospital of Montpellier, France; ¹⁶University Hospital Knappschaftskrankenhaus, Germany; ¹⁷Medical University of Vienna, Austria; ¹⁸Zhongshan University Hospital of Fudan University, China; ¹⁹University Hospitals Leuven, Belgium

Email: jonel.trebicka@ukmuenster.de

Abstract OS-080-YI is under embargo until Friday 23 June 2023, 17:15. This abstract will be made publicly available on the congress website at 17:15 (CEST) on the day of its presentation at the congress. Industry must not issue press releases – even under embargo – covering the data contained in abstracts selected to be highlighted during official EASL Press Office activities or in official EASL Press Office materials until the individual embargo for each data set lifts.

ORAL PRESENTATIONS

Media must not issue coverage of the data contained in abstracts selected to be highlighted during official EASL Press Office activities or in official EASL Press Office materials until the individual embargo for each data set lifts.

Journalists, industry, investigators and/or study sponsors must abide by the embargo times set by EASL. Violation of the embargo will be taken seriously. Individuals and/or sponsors who violate EASL's embargo policy may face sanctions relating to current and future abstract submissions, presentations and visibility at EASL Congresses. The EASL Governing Board is at liberty to ban attendance and/or retract data.

Copyright for abstracts (both oral and poster) on the website and as made available during The International Liver Congress™ 2023 resides with the respective authors. No reproduction, re-use or transcription for any commercial purpose or use of the content is permitted without the written permission of the authors. Permission for re-use must be obtained directly from the authors.

OS-081

Epidemiology and characteristics of hepatocellular carcinoma in France: results of the first 2000 patients in real-life situations from the French prospective chief cohort

Eric Nguyen Khac¹, Philippe Merle², Ben Khadhra Hajer³, Giuliana Amaddeo⁴, Thomas Decaens⁵, Thomas Uguen⁶, Jean-Frédéric Blanc⁷, Nathalie Ganne-Carrié⁸, Mohamed Bouattour⁹, Stéphane Cattani¹⁰, Christine Silvain¹¹, Ghassan Riachi¹², Jean Marie Peron¹³, Rodolphe Anty¹⁴, Jean-Pierre Bronowicki¹⁵, Aurore Baron¹⁶, Georges-Philippe Pageaux¹⁷, Veronique Loustaud-Ratti¹⁸, Frédéric Oberti¹⁹, Manon Allaire²⁰, Sylvain Manfredi²¹, Yasmina Ben Merabet²², Isabelle Ollivier-Hourmand²³, Marie Lequoy²⁴, Jean Baptiste Nousbaum²⁵, Moana Gelu-Simeon²⁶, Lucien Grados³, Pierre Nahon⁸, Charlotte Costentin⁵, Gerard Ducournau³, Olivier Ganry³. ¹Amiens University Hospital, Hepato-Gastroenterology and Oncology digestive, Amiens, France; ²CHU Lyon, France; ³CHU Amiens, France; ⁴CHU Henry Mondor Créteil, France; ⁵CHU Grenoble, France; ⁶CHU Rennes, France; ⁷CHU Bordeaux, France; ⁸CHU Avicennes Bobigny, France; ⁹CHU Beaujon Clichy, France; ¹⁰CHU Lille, France; ¹¹CHU Poitiers, France; ¹²CHU Rouen, France; ¹³CHU Toulouse, France; ¹⁴CHU Nice, France; ¹⁵CHU Nancy, France; ¹⁶CH Sud Francilien, France; ¹⁷CHU Montpellier, France; ¹⁸CHU Limoges, France; ¹⁹CHU Angers, France; ²⁰CHU GH Pitié Salpêtrière, France; ²¹CHU Dijon, France; ²²CHU Paul Brousse Villejuif, France; ²³CHU Caen, France; ²⁴CHU Saint Antoine Paris, France; ²⁵CHU Brest, France; ²⁶CHU Guadeloupe, France
Email: nguyen-khac.eric@chu-amiens.fr

Background and aims: Hepatocellular carcinoma (HCC) is the first cause of primary liver cancer, constantly increasing, and the 3rd cause of cancer death worldwide. The objective of the study is to describe the epidemiology and management of HCC in France.

Method: CHIEF is a prospective and nationwide observational cohort initiated in September 2019, with the aim to include all patients with HCC in a real-life situation. The clinical, biological, radiological and therapeutic characteristics of the patients were collected with a follow-up for 5 years for each patient.

Results: 2043 patients were included from September 2019 to September 2021 in 31 centers. The analysis involved 1640 patients, with 68 years of median age, 86% of men, BMI at 26.8 kg/m². HCC was diagnosed by a screening program in 35.2% of cases, associated with better survival (84.7% at 1 year $p < 0.0001$) compared to those diagnoses during a complication. A diagnostic by liver biopsy was performed in 46.3% of cases. Cirrhosis was present in 70.8% of cases, with median MELD 9 IQR [7;11], Child-Pugh A in 77.8%, median ALBI score at -2.4 [-2.7; -1.9] (ALBI 1: 36.3%, ALBI 3: 7%), esophageal varices of grade ≥ 2 in 28.4%. The etiologies were at least alcohol in 58.5% of cases, metabolic syndrome in 39%, and viral infection in 23.3% (16.4% HCV). HCC was diagnosed within the Milan criteria in 32.9%, with a median AFP level of 39 ng/ml IQR [7-562], a portal thrombosis in 5.9% and a metastatic condition in 10.7% of cases. The distribution of BCLC stages 0, A, B, C and D was 6.1%, 29.8%, 28.8%, 32.1% and 3.2% respectively. The median follow-up of new cases was 17.8 months 95% CI [17.3;18.5], IQR [13.7;23.3], with 29.1% of death. The survivals at 6 months, 1 year and 18 months were 84.9% 95%CI [82.8;87], 76.7% [74.2;79.2] and 69.3% [66.4; 72.3]. Median overall survival was not reached. First-line therapeutic access was 40.5% for curative treatments, 36.2% for locoregional procedures, 19.2% for systemic treatments and 4% palliative. The 1-year survival rates for BCLC stages 0, A, B, C and D were 95.6%, 89.7%, 81.7%, 54.9% and 40% (log rank test $p < 0.0001$). BCLC 0, A and B median survivals were not reached. They were 14.6 months and 6.1 months for BCLC stages C and D. The 1-year survival rates for curative, locoregional and systemic treatments were 92.9% 82.2% and 57.8% ($p < 0.0001$). Among the systemic treatments, the atezolizumab-bevacizumab combination was used as much as first-line TKIs (18.8% for each treatment), with a median survival of 17.05 months versus 9 months for TKIs ($p < 0.0001$).

Conclusion: The first analysis of the CHIEF cohort provides epidemiological data and recent therapeutic results in real life. In this cohort, the overall survival at 1 year, the survivals observed for the treatments applied, and the access to curative treatments seem interesting. First-line immunotherapy shows comparable survival in real life as in trials.

OS-082

Glycemic control as a modifiable and independent risk factor for the development of liver, biliary tract and pancreatic cancer: a territory-wide study of 273,421 patients with diabetes mellitus

Xianhua Mao¹, Ka Shing Cheung^{1,2}, Jing Tong Tan¹, Lung-Yi Mak¹,
Chi Ho Lee¹, CL Chiang³, Ho Ming Cheng¹, Rex Wan-Hin Hui¹,
Man-Fung Yuen¹, Wai Keung Leung¹, Wai-Kay Seto^{1,2}. ¹The University
of Hong Kong, Medicine, Hong Kong; ²The University of Hong Kong-
Shenzhen Hospital, Medicine, China; ³The University of Hong Kong,
Clinical Oncology, Hong Kong
Email: wkseto@hku.hk

Background and aims: Diabetes mellitus (DM) is an established risk factor for liver, biliary and pancreatic cancer, but the impact of glycemic control on the development of these cancers in patients with DM has not been well-investigated.

Method: We identified adults (age ≥ 18 years) newly diagnosed with DM between 2000 and 2015 via a territory-wide electronic healthcare registry in Hong Kong. DM was identified by (i) the American Diabetes Association criteria with two abnormal test results of hemoglobin A1c (HbA1c) $\geq 6.5\%$ or fasting plasma glucose ≥ 7 mmol/L, (ii) use of antidiabetic medications, or (iii) international classification of diseases (ICD-9) coding. An initial lead-in period of three years from the date of DM diagnosis was used to minimize reverse causality, with optimal glycemic control defined as mean HbA1c $< 7\%$ from at least two values within the lead-in period. Average successive variabilities of HbA1c were calculated to assess the variability. Outcomes of interest were incident liver, biliary (gall-bladder and extrahepatic biliary tract), and pancreatic cancer development. A multivariable Cox regression model was used to calculate the adjusted hazard ratio (aHR) of cancer development with glycemic control. Additional sensitivity analyses (Table 1) were applied to assess robustness of results.

Results: Among 421,818 screened individuals, 273,421 patients with DM (mean age 61.5 ± 11.7 years, 52.6% male) were included. The median follow-up duration was 6.7 (4.4–10.1) years, with the occurrence of 2,018, 517, and 721 liver, biliary and pancreatic

cancers respectively. When compared with a mean HbA1c $\geq 7\%$, a level $<7\%$ was independently associated with a lower risk of liver cancer (aHR: 0.74; 95% CI: 0.67–0.81), biliary tract cancer (0.67; 0.56–0.80), and pancreatic cancer (0.83; 0.71–0.97). The associations remained significant after 1:2 propensity score matching (HR 0.68–0.80), inverse probability of treatment weighting (HR 0.71–0.85), and via other sensitivity analyses (Table 1). A lower risk of liver cancer was observed regardless of presence or absence of obesity (aHR 0.69–0.78); aspirin intake (aHR 0.71–0.75); or viral hepatitis (aHR 0.68, 0.59–0.79; and aHR 0.78, 0.69–0.88 respectively). Significant associations were also demonstrated in biliary tract cancer regardless of smoking, hypertension, and hyperlipidemia (aHR 0.46–0.74). For pancreatic cancer, the association was significant in non-smokers, normotensive and non-dyslipidemia individuals (aHR 0.80–0.82), but became insignificant when these metabolic risk factors were present.

Conclusion: Optimal glycemic control with mean HbA1c <7% was independently associated with a lower risk of cancers of the liver, biliary tract, and pancreas among patients with DM. Glycemic control is a modifiable risk factor which can influence oncoprotective strategies for hepatobiliary and pancreatic cancers.

OS-083-YI

Natural history and management of recurrent hepatocellular carcinoma after liver transplantation: a multicenter nationwide study

Massih Ningarhari¹, Camille Henry¹, Emmanuel Boleslawski¹,
Camille Besch², François Faitot², Eric Assenat³, Astrid Herrero³,
Jose Ursic-Bedoya³, Fabien Robin⁴, Thomas Uguen⁴, Teresa Antonini⁵,
Domitille Erard⁵, Sylvie Radenne⁵, Bleuenn Brusset⁶,
Thomas Deacons⁶, Manon Allaire⁷, Filomena Conti⁷, Hélène Barraud⁸,
Laure Elkrief⁸, Ephrem Salame⁸, Olivier Boillot⁹, Jérôme Dumortier⁹
Line Carolle Ntandja Wandji¹, Alexandre Louvet¹, Philippe Mathurin¹,
Sebastien Dharancy¹, Guillaume Lassailly¹. ¹CHU Lille, France; ²CHU
Strasbourg, France; ³CHU Montpellier, France; ⁴CHU Rennes, France;
⁵HCL Lyon, Croix-Rousse, France; ⁶CHU Grenoble, France; ⁷APHP, Pitié-
Salpêtrière, France; ⁸CHU Tours, France; ⁹HCL Lyon, Edouard-Herriot,
France

Email: massih.ningarhari@chu-lille.fr

Background and aims: Liver transplantation (LT) is the best curative treatment for hepatocellular carcinoma (HCC). Recurrence of HCC (rHCC) still occurs in approximately 15% of patients at 5 years after LT despite stringent selection criteria, and significantly impairs post-

Table 1. Effect of Optimal Glycemic Control on Risk of Liver, Biliary Tract, and Pancreatic Cancers.

	HRs of cancers (95%CI)		
	Liver	Biliary tract	Pancreas
Main analyses			
Age-adjusted HR	0.85 (0.78-0.93)	0.81 (0.74-0.89)	0.74 (0.67-0.81)
Model 2*	0.80 (0.67-0.95)	0.69 (0.57-0.83)	0.67 (0.56-0.80)
Model 3†	0.87 (0.75-1.01)	0.83 (0.71-0.97)	0.83 (0.71-0.97)
Sensitivity analyses			
PS matching	0.73 (0.66-0.81)	0.68 (0.56-0.83)	0.80 (0.68-0.95)
IPTW	0.80 (0.73-0.88)	0.71 (0.59-0.85)	0.85 (0.73-0.99)
Mean A1c <6.5% vs. ≥6.5%	0.69 (0.62-0.77)	0.53 (0.42-0.67)	0.75 (0.62-0.90)
Based on at least three A1c values during lead-in period	0.77 (0.69-0.85)	0.66 (0.53-0.82)	0.86 (0.72-1.02)
A1c ASV <25% quartile vs. ≥25%	0.74 (0.66-0.83)	0.86 (0.70-1.06)	0.76 (0.63-0.91)

*A multivariable Cox proportional-hazards regression model accounted for the following covariates: baseline characteristics (age, sex, BMI, duration of diabetes, smoking, alcohol abuse, hyperlipidemia, hypertension) and medication use during follow-up (statins, aspirin, NSAID, metformin, sulfonylureas, insulin, SGLT-2i, DPP-4i, GLP-1a).

†Model 3 included model 2 covariates and further adjusted for chronic hepatitis B and C infection, cirrhosis, and liver compensation in liver cancer; gallstone, cholangitis, calculus of bile duct, and cholecystitis in biliary tract cancer; acute and chronic pancreatitis in pancreatic cancer.

ASV, average successive variability; BMI, body mass index; CI, confidence interval; DPP-4i, dipeptidyl peptidase-4 inhibitors; GLP-1a, glucagon-like peptide-1 agonists; HR, hazard ratio; IPTW, inverse probability of treatment weighting; NSAID, non-steroidal anti-inflammatory drug; PS, propensity score; SGLT-2i, sodium-glucose cotransporter-2 inhibitors.

Figure: (abstract: OS-082).

ORAL PRESENTATIONS

transplant survival. More data on the natural history, clinical presentation, efficacy and safety of treatments are needed to optimize the management of rHCC in the specific context of transplanted patients.

Method: Observational, retrospective study in 9 French transplantation centers, including all patients with rHCC after LT between 01/01/2008 and 31/12/2020. Patients' characteristics at LT and at recurrence were collected. We evaluated factors associated with overall survival (OS) from the date of recurrence, treatment in terms of efficacy and safety, and the impact of immunosuppressive (IS) drug management.

Results: Two-hundred-and-fifty-five patients were included (median age 63 years, HCC/alcohol 55%). The median time between LT and recurrence was 23 months (IQR 11.8–45.4) and was predominantly only extrahepatic (60%), with bone lesions in 35% of cases. AFP at recurrence was only weakly correlated to last AFP before LT (Spearman $r = 0.36$). Recurrence was very early (<6 months) in 12% of cases and very late (>5 years) in 18% of cases. Early and late recurrences were similar in terms of anatomical sites. Size of the main nodule on the explant pathology ($p = 0.01$) and the last AFP before LT ($p = 0.01$) were associated with earlier recurrence.

Median OS was 18.2 months (95%CI: 15.1–21.7) from the date of recurrence. Overall 5-year post-LT survival was 45% (95%CI: 39–52), 31% of patients ($n = 78$) received a curative treatment (surgery or percutaneous destruction) at the first recurrence, with a subsequent 5-year recurrence-free survival of recurrence of 19% (95% CI: 11–34). When considering systemic treatments, sorafenib was the most commonly used TKI ($n = 131$, 86%), while the use of the atezolizumab and bevacizumab was limited ($n = 6$). 10-year OS post-LT was 46% (95% CI: 34–62) for patients who were amenable to curative treatment at recurrence 6% (95% CI: 0.3–12) for non-curative treatment. In multivariate analysis, non-curative treatment (HR 2.76, $p < 0.001$), recurrence later than 2 years after LT (HR 0.15, $p = 0.001$), WHO PS 1 (HR 1.69, $p = 0.01$) or >1 (HR 8.1, $p < 0.001$), AFP level at recurrence >100 ng/ml (HR 1.83, $p = 0.03$) and concomitant intra- and extra-hepatic recurrence (HR 1.54, $p = 0.04$) were associated with OS after HCC recurrence. Change of listing criteria for HCC in France in 2013 (Milan criteria versus AFP model) did not impact on rHCC prognosis.

Forty-nine percent of patients experienced grade 3/4 toxicity, and treatment discontinuation was required in 38%. There was no significant association between mTOR inhibitors, calcineurin inhibitors or mycophenolate mofetil management with survival or safety profile of systemic treatments.

Conclusion: Recurrence HCC after LT is a predominantly extrahepatic disease, and 20% of recurrences occur more than 5 years after LT. OS could be improved by aggressive management in selected patients, resulting in those patients in 46% survival 10 years after LT. Timing of recurrence after LT has a major prognostic impact. TKIs have a manageable toxicity profile, no impact of IS drugs on the prognosis of the disease or on the tolerance of systemic treatments.

OS-084-YI

Weakly supervised intrahepatic tumour classification from routine tumour biopsy: a proof of concept

Paul Emile Zafar^{1,2}, Aurélie Beaufrère^{1,3}, Nora Ouzir², Miguel Albuquerque¹, Jules Grégory⁴, Kévin Mondet¹, Jean Christophe Pesquet², Valérie Paradis¹. ¹APHP Hôpital Beaujon, Pathology FHU MOSAIC, Clichy, France; ²CentraleSupélec, France; ³Curie, U900 CBIO Team, France; ⁴APHP Hôpital Beaujon, Radiology FHU MOSAIC, France

Email: aurelie.beaufriere@aphp.fr

Background and aims: Primary liver malignancies define a wide spectrum of tumours, including hepatocellular carcinoma (HCC), intrahepatic cholangiocarcinoma (iCCA) and combined hepatocarcinoma (CHCC-CCA) recognised by the presence of HCC and iCCA features. Due to CHCC-CCA's heterogeneity, diagnosis using conventional histology with Hematein Eosin Safran (HES) staining is challenging, especially on biopsy samples. This study aims to automatically classify primary liver malignancies on biopsy samples using a weakly supervised learning method based on deep convolutional neural networks (CNN).

Method: We constituted 119 biopsies of primary liver malignancies (Beaujon Hospital, Clichy, France) divided into training and validation sets of 90 and 29 samples, respectively. Two liver pathologist experts examined each sample's whole slide HES image (WSI). After annotating the tumour/non-tumour areas, tiles of 125 μm^2 (256 pixels) were extracted from the WSIs and used to train a ResNet18

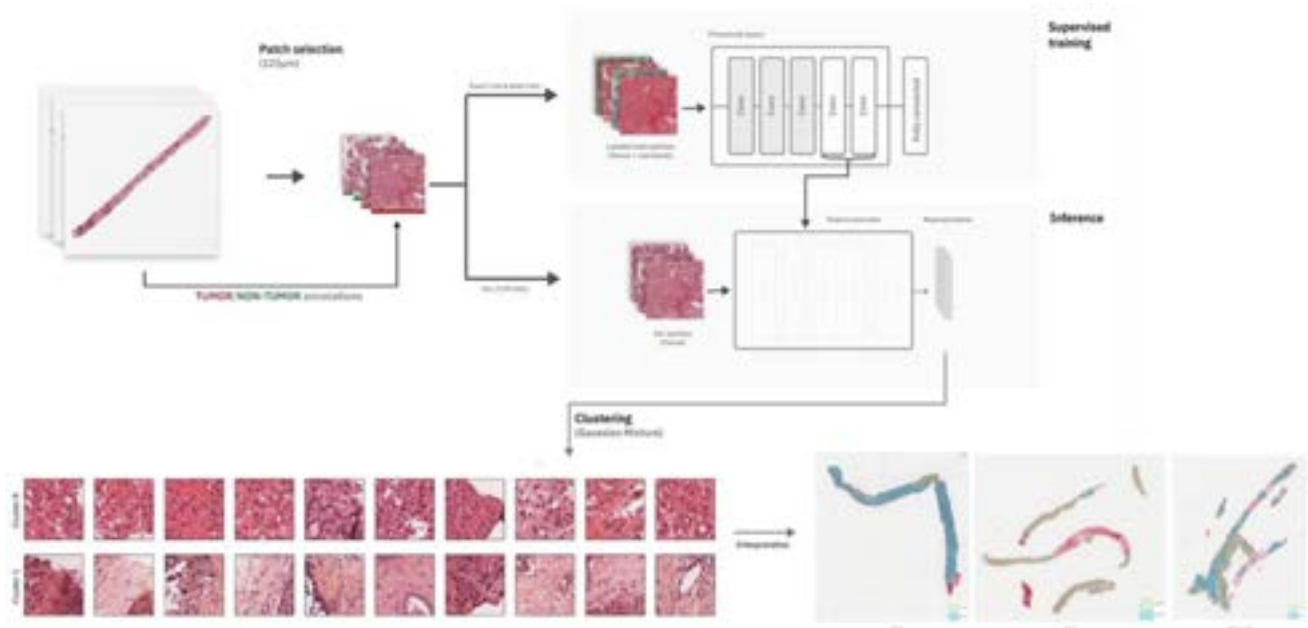


Figure: (abstract: OS-084-YI).

CNN. The tumour/non-tumour annotations of the WSIs served as (weak) labels during training (Figure), while the network's last convolutional layer was used to extract new tumour tile features. Without knowledge of the precise labels of the malignancies, we then applied an unsupervised clustering algorithm to the newly extracted features and explored the results using different numbers of clusters. **Results:** First, pathological reviewing classified the training and validation sets into HCC (n = 33 and n = 11), iCCA (n = 28 and n = 9), and cHCC-CCA (n = 29 and n = 9), respectively. We then analysed the results of the proposed weakly supervised method using 2 to 8 clusters. No specific cluster associated with cHCC-CCA was identified. In the case of 2 clusters, cluster 0 contained mainly HCC histological features (76% of the tiles) while cluster 1 contained mainly iCCA features (92% of the tiles) (Figure). This two-clusters model was assessed on the validation set by quantifying the proportion of clusters 0 (representative of HCC) and 1 (representative of iCCA). For HCC and iCCA, the diagnostic agreement between the pathological diagnosis and the model predictions (major contingent) was 100% for HCC (11/11 cases) and 78% for iCCA (7/9 cases). For cHCC-CCA, we observed a highly variable proportion of each cluster type (cluster 0: 5–90%; cluster 1: 9–94%). The diagnostic agreement of the major contingent in pathology predicted by the model was 89% (8/9 cases). **Conclusion:** This study shows that a weakly supervised learning method applied to primary liver malignancy biopsy can identify specific morphological features of HCC and iCCA. While no specific features of cHCC-CCA were recognized, assessing the proportion of HCC and iCCA tiles within a slide could improve the identification of cHCC-CCA in biopsies.

NAFLD: Clinical aspects

OS-085

Use of antidiabetic and lipid-lowering medications associated with lower scores of liver fibrosis biomarkers in non-alcoholic steatohepatitis (NASH) patients

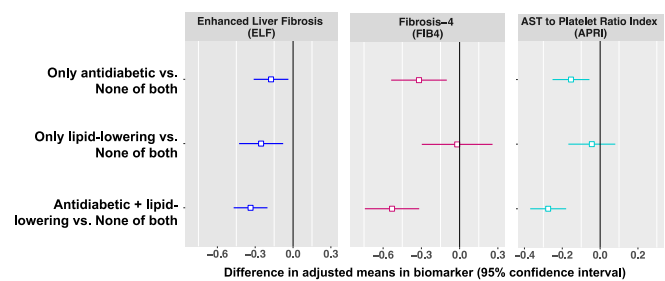
Jun Wang¹, Dora Ding¹, Xiaorong Shao¹, Lily Ma¹, Jun Xu¹, Jason Melehan¹, Lisa Boyette¹, Timothy R. Watkins¹, Catherine Jia¹, Vlad Malkov¹, Andrew Billin¹, Shahed Iqbal¹. ¹Gilead Sciences, Inc., United States
Email: jun.wang37@gilead.com

Background and aims: The effects of antidiabetic or lipid-lowering drug use on liver fibrosis biomarkers in NASH patients are not well documented. We investigated the associations between use of antidiabetic or lipid-lowering drugs and blood liver fibrosis biomarkers. Additionally, we assessed if the associations vary by patient's genetic predisposition to NASH.

Method: We conducted a cross-sectional analysis of baseline data from two completed phase III trials of NASH patients with bridging fibrosis (NCT03053050, N = 785) or compensated cirrhosis (NCT03053063, N = 864). Use of antidiabetic (metformin, GLP-1RA, Pioglitazone, SGLT2 inhibitors and DPP4 inhibitors) and lipid-lowering (statins and fibrates) drugs were obtained from trial baseline data. Among patients who provided blood samples for sequencing (N = 1077), a polygenic risk score (PRS) for NASH was derived for those of European ancestry (N = 742) using 6 variants from prior genome-wide association or exome sequencing studies: *PNPLA3*, *TM6SF2*, *HSD17B13*, *GCKR*, *MBOAT7* and *LEPR*. Outcomes included composite scores measured at baseline: Fibrosis 4 (FIB-4), AST to platelet ratio index (APRI) and Enhanced Liver Fibrosis (ELF). Linear regression models were used, adjusting for age, sex, race, BMI, HbA1C and triglyceride.

Results: Study participants (N = 1649) were predominantly ≥50 years old (82%), female (59%) and White (75%). About 61% (N = 1008) of

patients used any antidiabetic drugs, most of whom used Metformin alone or in combination (901/1008, 89%). Among patients who used lipid-lowering drugs (N = 750), the majority used statins (657/750, 88%). Overall, use of any antidiabetic or any lipid-lowering drugs was inversely associated with all biomarkers and the associations were stronger among those using both types of drugs (Figure). Compared to patients who used neither drug, patients using both drugs had an average 0.34 (95% Confidence Interval [CI] = -0.47, -0.20) lower ELF, 0.53 (95%CI = -0.74, -0.32) lower FIB-4 and 0.27 (95%CI = -0.37, -0.18) lower APRI scores. Among patients of genetically inferred European ancestry (N = 742), the associations were stronger in those with high PRS (>median PRS; N = 364) than those with low PRS (≤median PRS; N = 378) for FIB-4 (interaction p = 0.01) or APRI (interaction p = 0.004). Use of both drugs was significantly associated with an average 0.50 lower FIB-4 (95%CI = -0.92, -0.07) in patients with high PRS while no such association in patients with low PRS. Similar patterns were seen for APRI. However, there was no statistically significant interaction for ELF.



None of both (none of any antidiabetic and any lipid-lowering drugs): N = 460; only antidiabetic drug: N = 420; only lipid-lowering drug: N = 168; any antidiabetic + any lipid-lowering drugs: N = 561.

Figure:

Conclusion: Use of antidiabetic and lipid-lowering drugs was inversely associated with biomarkers of liver fibrosis. Among patients of European ancestry, stronger associations were observed in those at high genetic risk of NASH development and progression. Prospective studies may provide further insights into potential benefits of these drugs.

OS-086

Stratification of liver fat content in non-alcoholic steatohepatitis patients with significant liver fibrosis using the MEFIB-Index and MRI-PDFF and its association with hepatocellular carcinoma, decompensation, and mortality

Sung Won Lee^{1,2}, Daniel Huang^{1,3}, Veeral Ajmera¹, Monica Tincopa¹, Jaclyn Bergstrom¹, Nabil Nouredin¹, Maral Amangurbanova¹, Harris Siddiqi¹, Egbert Madamba¹, Abdul Majzoub⁴, Tarek Nayfeh⁴, Nobuharu Tamaki⁵, Namiki Izumi⁵, Atsushi Nakajima⁶, Ramazan Idilman⁷, Mesut Gumusoy⁷, Digdem Kuru Öz⁸, Ayse Erden⁸, Mazen Nouredin⁹, Rohit Loomba¹. ¹University of California at San Diego, NAFLD Research Center, Division of Gastroenterology, San Diego, United States; ²College of Medicine, The Catholic University of Korea, Division of Gastroenterology and Hepatology, Seoul, Korea, Rep. of South; ³National University of Singapore, Department of Medicine, Yong Loo Lin School of Medicine, Singapore; ⁴Mayo Clinic, Evidence-Based Practice Center, United States; ⁵Musashino Red Cross Hospital, Department of Gastroenterology and Hepatology, Japan; ⁶Yokohama City University, Department of Gastroenterology and Hepatology, Japan; ⁷Ankara University School of Medicine, Department of Gastroenterology, Turkey; ⁸Ankara University School of Medicine, Department of Radiology, Turkey; ⁹Houston Liver institute, United States
Email: roloomba@health.ucsd.edu

Background and aims: Progression of liver fibrosis in non-alcoholic steatohepatitis (NASH) patients often result in a decrease in hepatic fat to <5%. However, there are limited data on the differences in prognosis according to the liver fat content and fibrosis in NASH patients. Therefore, we aimed to compare the prognosis of patients

ORAL PRESENTATIONS

stratified by liver fat content and fibrosis using the MEFIB-Index (magnetic resonance elastography [MRE] ≥ 3.3 Kpa + FIB-4 ≥ 1.6) and magnetic resonance imaging-derived proton density fat fraction (MRI-PDFF).

Method: A total of 456 patients from three countries with both MRE and MRI-PDFF at baseline were enrolled, and 294 patients with longitudinal follow-up were retrospectively analyzed. MEFIB-negative, MEFIB-positive + MRI-PDFF ≥ 5 , and MEFIB-positive + MRI-PDFF < 5 were defined as having no significant liver fibrosis, significant liver fibrosis with higher liver fat content (higher liver fat content group), and significant liver fibrosis with lower liver fat content (lower liver fat content group), respectively. Cox proportional hazards model was used to assess the factors associated with the composite primary outcome of hepatocellular carcinoma (HCC), decompensation, and mortality.

Results: In this meta-analysis of individual participants (IPDMA), the lower liver fat content group consisted of patients with older age, and higher proportion of diabetes and hypertension. Also, compared to the higher liver fat content group, the lower liver fat content group had lower alanine aminotransferase, albumin, platelet counts, and prolonged prothrombin time. The rates of decompensation, HCC, and death were highest in the lower liver fat content group with 1%, 1%, 2% occurrence in the no significant liver fibrosis group; 22%, 13%, 13% in the higher liver fat content group; 32%, 14%, 14% in the lower liver fat content group, respectively. In multivariate analysis, lower liver fat content in patients with significant liver fibrosis was associated [HR = 74.6 (95%CI: 7.2–768.4, $p = 0.0003$)] with the composite outcome of HCC, decompensation, and mortality.

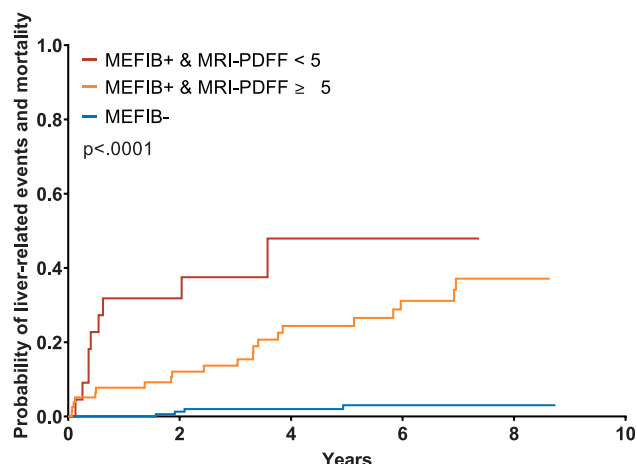


Figure: Cumulative incidence of primary outcome (decompensation, HCC, or death) stratified by MEFIB and MRI-PDFF

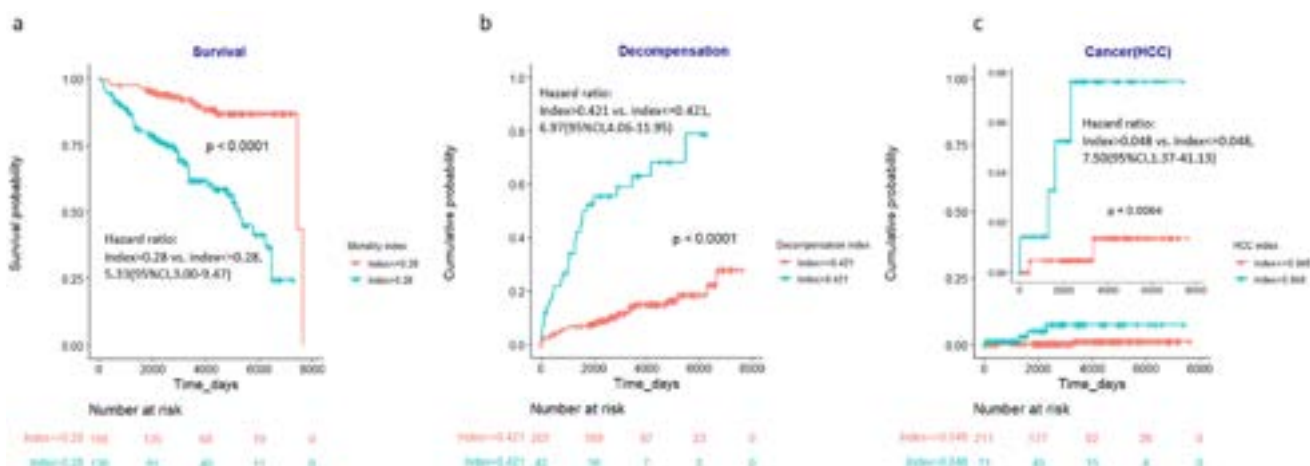


Figure: (abstract: OS-087).

Conclusion: The combination of MEFIB-Index and MRI-PDFF is a useful tool to stratify prognosis according to liver fat content and fibrosis in NASH patients. Lower liver fat content in NASH patients with significant fibrosis is associated with an increase in HCC, hepatic decompensation, and mortality.

OS-087

Digital pathology using stain-free imaging indices allows direct prediction of all-cause mortality, hepatic decompensation and hepatocellular carcinoma development in patients with non-alcoholic fatty liver disease

Timothy Kendall¹, Dean Tai², Gideon Ho², Yayun Ren², Elaine Chng², Jonathan Fallowfield¹. ¹University of Edinburgh, United Kingdom; ²HistoIndex Pte Ltd, Singapore
Email: tim.kendall@ed.ac.uk

Background and aims: Digital quantification of scarring from either stained liver sections or stain-free imaging reduces observer-related variability in the histological assessment of non-alcoholic fatty liver disease (NAFLD). To date, computational methods have mainly provided ordinal scores analogous to those provided by a pathologist as disease outcomes are strongly correlated with stage. Direct prediction of outcomes from tissue, without using fibrosis stage as a surrogate, has not been possible due to the absence of suitable event-rich cohort data. Using SteatoSITE (<https://steatosite.com/>), a resource containing integrated clinical and pathological data, we undertook stain-free imaging to generate tools predictive of patient outcomes using architectural features unapparent to human observers.

Method: Unstained sections from a training set of 294 biopsies were imaged using second harmonic generation/two-photon excitation fluorescence microscopy. Using sequential feature selection, 10, 10 and 5 parameters were chosen out of 184 fibrosis parameters and a linear regression method was used to construct individual indices for risk of all-cause mortality, hepatic decompensation and hepatocellular carcinoma (HCC), respectively. Time-to-event analysis was performed using the Kaplan-Meier method, with death as a competing risk for decompensation and HCC, and distributions compared using the log-rank test (Fig. 1). A Cox proportional hazards model was used to estimate hazard ratios (HRs). The predictive power of the risk indices was compared with the assigned NASH-CRN fibrosis stage (F0/1/2 v F3/4) and the stain-free imaging derived qFibrosis stage (qF0/1/2 v qF3/4).

Results: The newly defined "Mortality Index" had greater predictive power for all-cause mortality (index > 0.28 vs. ≤ 0.28 , HR 5.33, 95% confidence intervals (CI) 3.00–9.47, $p = 0.000$) than either NASH-CRN or qFibrosis stage. The "Decompensation Index" had greater predictive power for decompensation events (index > 0.421 vs. ≤ 0.421 , HR 6.97, 95% CI 4.05–11.9, $p < 0.0001$).

0.421, HR 6.97, 95% CI 4.06–11.95, $p = 0.000$) than either NASH-CRN stage or qFibrosis stage. Finally, the “HCC Index” had greater predictive power for HCC development (index >0.048 vs. ≤ 0.048 , HR 7.50, 95% CI 1.37–41.13, $p = 0.020$) than either NASH-CRN stage or qFibrosis stage.

Conclusion: Using liver biopsy material with linked long-term clinical outcome data, we developed tools that directly predict hard end points in patients with NAFLD and do not rely on ordinal fibrosis scores as a surrogate. These tools have greater predictive value than pathologist-assigned NASH-CRN fibrosis stage or computationally-assigned qFibrosis stage. These indices will be validated in an additional NAFLD cohort but may provide direct tissue-to-outcome predictions that aid clinical decision-making, offer more nuanced participant stratification and meaningful end points in clinical trials.

OS-088

Effect of semaglutide 2.4 mg on alanine aminotransferase in adolescents with obesity: a post-hoc analysis of the STEP TEENS trial

Daniel Weghuber¹, Inge Gies², Lise Lotte Gluud³, Aske Thorn Iversen⁴, Maximilian Jara⁵, Signe Schmidt⁶, Rasmus Sørrig⁵, Martin Wabitsch⁷, Mazen Nouredin^{8,9}. ¹Department of Pediatrics, Paracelsus Medical University, Salzburg, Austria; ²Department of Pediatrics, Division of Pediatric Endocrinology, Universitair Ziekenhuis Brussel, Brussels, Belgium; ³Gastro Unit, Copenhagen University Hospital Hvidovre and Department of Clinical Medicine, University of Copenhagen, Copenhagen, Denmark; ⁴Biostatistics, Novo Nordisk A/S, Søborg, Denmark; ⁵Global Medical Affairs, Novo Nordisk A/S, Søborg, Denmark; ⁶Medical and Science, Novo Nordisk A/S, Søborg, Denmark; ⁷Division of Pediatric Endocrinology and Diabetes, Department of Pediatrics and Adolescent Medicine, Ulm University Medical Center, University of Ulm, Ulm, Germany; ⁸Sherrie and Alan Conover Center for Liver Disease and Transplantation, Houston Methodist Hospital, Houston, TX, United States; ⁹Houston Research Institute, Houston, TX, United States
Email: NouredinMD@houstonresearchinstitute.com

Background and aims: Increased body mass index (BMI) is associated with a greater incidence of non-alcoholic fatty liver disease (NAFLD) and its advanced forms, such as steatohepatitis. Weight loss can improve hepatic parameters, such as alanine aminotransferase (ALT) levels, in patients with NAFLD/steatohepatitis. Change in ALT levels is associated with histological response in patients with steatohepatitis. The phase 3, double-blind, placebo-controlled, STEP TEENS trial (NCT04102189) demonstrated the efficacy and safety of semaglutide 2.4 mg once weekly for weight management among adolescents with obesity. This post hoc analysis of the STEP TEENS trial examined the change in ALT levels and presumed NAFLD in adolescents treated with semaglutide 2.4 mg vs placebo.

Method: Adolescents (aged 12 to <18 years) with obesity (BMI $\geq 95^{\text{th}}$ percentile), or overweight (BMI $\geq 85^{\text{th}}$ percentile) with ≥ 1 weight-related comorbidity, were randomised 2:1 after a 12-week lifestyle intervention run-in phase (consisting of diet and physical activity counselling) to receive semaglutide 2.4 mg once weekly (or maximum tolerated dose) or placebo for 68 weeks, plus lifestyle intervention. Change in ALT from baseline to week 68 was a prespecified secondary end point, assessed using a mixed model for repeated measurements using data from the on-treatment period for the trial product estimand (assessed the treatment effect if all participants remained on treatment without using rescue interventions).

Results: Overall, 201 participants were randomised. Mean parameters at baseline were: age 15.4 years, body weight 107.5 kg and

BMI 37.0 kg/m². Participants were 62% female, 38% had elevated ALT (>25.8 U/L in males, >22.1 U/L in females) and 34% were presumed to have NAFLD (defined as BMI $\geq 85^{\text{th}}$ percentile, fatty liver index ≥ 60 [a surrogate index of fatty liver based on BMI, waist circumference, triglycerides and gamma-glutamyl transferase] and elevated ALT). The geometric mean ALT level at baseline was 23 U/L vs 20 U/L in the semaglutide vs placebo groups, respectively. The change from baseline in ALT with semaglutide was significantly greater vs placebo (-18.1% vs -1.1% ; estimated treatment difference [95% confidence interval] -23.7% [points -28.8 , -3.6]; $p = 0.015$). At week 68, mean ALT levels decreased from baseline levels in participants treated with semaglutide who achieved a weight loss of $\geq 10\%$, but not in those with $<10\%$ weight loss (Table). Estimated ALT changes in participants with presumed NAFLD were -15.5% vs 10.6% with semaglutide vs placebo, respectively (estimated treatment difference -23.7%) (Table). Of participants with elevated baseline ALT levels, 53.8% vs 33.3% had normal levels at week 68 with semaglutide vs placebo, respectively. Participants reporting hepatic-related adverse events (mostly non-serious) were higher in the semaglutide 2.4 mg group (7.5%) than with placebo (1.5%). The imbalance was mainly driven by events reported at the day of randomisation (without exposure to semaglutide) and events in subjects with pre-existing hepatic disorders.

Table Change in ALT parameters

Endpoints	Semaglutide 2.4 mg	Placebo		
Participants with elevated ALT ^a				
Geometric mean ALT level at week 0, U/L (CV)	n = 56 42 (51.2)	n = 20 40 (51.1)		
Mean change from baseline at week 68, %	-20.1	0.50		
Treatment difference, %-points (95% CI)	-20.5 (-38.5, 2.8)			
Participants with presumed NAFLD ^b				
Geometric mean ALT level at week 0, U/L (CV)	n = 50 43 (51.4)	n = 18 39 (48.7)		
Mean change from baseline at week 68, %	-15.5	10.6		
Treatment difference, %-points (95% CI)	-23.7 (-41.7, 0)			
ALT ratio to baseline at week 68 by % body weight loss, geometric mean (CV)				
< 10% weight loss ^c	n = 39 1.00 (56.6)	n = 44 1.04 (43.2)		
≥ 10% weight loss	n = 72 0.67 (65.3)	n = 5 0.99 (36.5)		
≥ 20% weight loss	n = 44 0.62 (67.1)	n = 2 1.22 (57.7)		
ALT levels by % body weight loss, geometric mean, U/L (CV)				
Weight loss at week 68	Semaglutide		Placebo	
	Baseline	Week 68	Baseline	Week 68
< 10% weight loss ^c	n = 53 24.4 (72.8)	n = 39 27.4 (72.6)	n = 62 19.9 (72.1)	n = 44 21.0 (58.4)
≥ 10% weight loss	n = 81 22.6 (68.3)	n = 72 15.9 (49.9)	n = 5 15.0 (49.5)	n = 5 14.8 (27.2)

Observed data from on-treatment analysis.

^aElevated ALT was defined as levels > 25.8 U/L in males and > 22.1 U/L in females.¹

^bPresumed NAFLD was defined as BMI $\geq 85^{\text{th}}$ percentile, FLI (a surrogate index of fatty liver based on BMI, waist circumference, triglycerides and gamma-glutamyl transferase) ≥ 60 and elevated ALT.^{1,2}

^cIncludes participants who gained weight.

ALT, alanine aminotransferase; BMI, body mass index; CI, confidence interval; CV, coefficient of variation in %; FLI, fatty liver index; n, number of participants with an observation at the visit; NAFLD, non-alcoholic fatty liver disease.

1. Schwimmer JB, et al. *Gastroenterology* 2010;138:1357–64;

2. Arshad T, et al. *Hepatol Commun* 2021;5:1676–88.

Figure:

Conclusion: In the STEP TEENS trial, treatment with semaglutide 2.4 mg once weekly for 68 weeks was associated with a significant reduction in ALT vs placebo in adolescents with obesity.

OS-089

Non-alcoholic steatohepatitis disease progression in participants from the United States TARGET-NASH real world longitudinal observational study

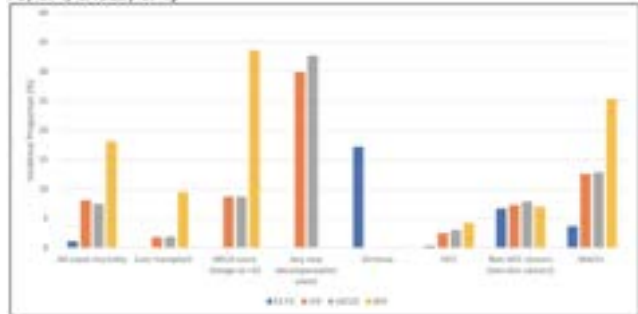
Claudio Sartini¹, Bryan Rudolph¹, Mandy Fraessdorf², Heather Morris³, Derek Gazis³, Andrea Mospan³, Michael Fried³, Michael Roden⁴, Brent Tetri⁵, Kenneth Cusi⁶, Philip N Newsome^{7,7}.
¹Boehringer Ingelheim, United States; ²Boehringer Ingelheim, Germany; ³Target RWE, United States; ⁴German Diabetes Center, Germany; ⁵St. Louis University, United States; ⁶University of Florida, United States; ⁷University of Birmingham, United Kingdom
 Email: hnmorris@targetrwe.com

Background and aims: Estimating progression rate is essential for understanding the comprehensive burden of disease and informing future clinical trial designs. The aim of this study was to describe demographic and clinical characteristics in a large multi-centre cohort of NASH participants followed in routine clinical practice and determine the occurrence of health outcomes.

Method: Adults from the US TARGET-NASH longitudinal observational study were followed from August 2016-October 2021. Participants had a biopsy or clinical NASH diagnosis with significant fibrosis (stage F2/3/4). Demographic and clinical characteristics were analyzed in 4 groups: non-cirrhotic NASH F2-F3, compensated cirrhosis (cF4), compensated advanced chronic liver disease (cACLD-no signs of decompensation and ≥ 1 of the following: FibroScan liver stiffness ≥ 15 kPa, NASH F3/F4 on biopsy, gastric/esophageal varices on endoscopy, or cirrhosis and findings of portal hypertension noted on imaging) and decompensated cirrhosis (dF4). Progression outcomes included all-cause mortality, progression from non-cirrhosis to cirrhosis, compensated to decompensated cirrhosis, and liver-related and cardiovascular events. Incidence rates and incidence proportion for all outcomes were estimated in each group.

Results: Of the 1,852 participants, median age was 59 years, BMI was 34.1 kg/m², mostly female (59%), and non-Hispanic white (77%). 699 (38%) were classified as F2-F3, 1153 (62%) as F4 (795 cF4, 358 dF4). Among the 1,494 (81%) with no signs of decompensation, 428 (29%) were defined as cACLD. Participants with F4 (vs F2-F3) were 6 years older, had a higher prevalence of diabetes ($p = 0.02$), and similar BMI; lower ALT, higher GGT, higher glucose levels, and higher FIB-4 score ($p < 0.001$). The cACLD group was older with a higher FIB-4 (compared to non-cACLD and F2-F3). Over an average follow-up (FU) time of about 4 years, the incidence rate per 1000 person-years (py) for all-cause mortality was 42 per 1000 py in dF4, 18 per 1000 py in cACLD, 19 per 1000 py in cF4, and 3 per 1000 py in F2-F3. In the F2-F3 group, 120 (17%) progressed to cirrhosis (49 per 1000 py, average FU time 3.5 years); in the cF4 group, 238 (30%) progressed to decompensation (89 per 1000 py, average FU time 3.4 years). For completeness, the incidence proportion for all outcomes is summarized in Figure 1.

Incidence proportion for disease progression outcomes¹ by NASH groups (F2-F3, cF4, cACLD, dF4)



¹ HCC= Hepatocellular carcinoma; MELD= model for end-stage liver disease; PACE+ = events or procedures indicative of all-cause death, non-fatal PE, non-fatal stroke, coronary revascularization or unstable angina

² MELD outcome was only assessed in cirrhotic patients with a MELD ≤ 12 prior to index

Figure:

Conclusion: This is a large US multi-center study using real-world data to examine NASH disease progression longitudinally. Although rates of progression to cirrhosis were similar compared to previous studies, substantially lower mortality incidence rates were found for participants in dF3/4 subgroups. The real world evidence from our study inform the natural history of NASH and can provide additional rationale and justification in clinical trials design, including enrollment criteria, duration of the trials, and the choice of end points.

Public health - viral hepatitis

OS-090-YI

Estimating the residual risk of hepatitis B mother-to-child transmission in The Gambia, 30 years after HBV vaccine implementation

Gibriel Ndow¹, Rohey Bangura¹, Erwan Vo Quang¹, Fatoumatta Touray¹, Abdoullie Jatta¹, Jainaba Barry¹, Sulayman Bah¹, Fatou Bintou Nyassi¹, Queen Bola-Lawal¹, Alhagie Touray¹, Sainabou Drammeh¹, Hawa Cham¹, Gavin Cloherty², Gora Lo³, Coumba Toure-Kane³, Lamin Bojang^{1,4}, Yusuke Shimakawa⁵, Umberto D'Alessandro⁴, Maud Lemoine⁶. ¹MRC Unit The Gambia at LSHTM, Hepatitis Group, Disease Control and Elimination Theme, Fajara, Gambia; ²Abbott Labs, United States; ³IRESEF, Senegal; ⁴MRC Unit The Gambia at LSHTM, Fajara, Gambia; ⁵Institut Pasteur, Paris, France; ⁶Imperial College London, Metabolism, Digestion and Reproduction, London, United Kingdom

Email: gndow@mrc.gm

Abstract OS-090-YI is under embargo until Friday 23 June 2023, 17:15. This abstract will be made publicly available on the congress website at 17:15 (CEST) on the day of its presentation at the congress. Industry must not issue press releases – even under embargo – covering the data contained in abstracts selected to be highlighted during official EASL Press Office activities or in official EASL Press Office materials until the individual embargo for each data set lifts. Media must not issue coverage of the data contained in abstracts selected to be highlighted during official EASL Press Office activities or in official EASL Press Office materials until the individual embargo for each data set lifts.

Journalists, industry, investigators and/or study sponsors must abide by the embargo times set by EASL. Violation of the embargo will be taken seriously. Individuals and/or sponsors who violate EASL's embargo policy may face sanctions relating to current and future abstract submissions, presentations and visibility at EASL Congresses. The EASL Governing Board is at liberty to ban attendance and/or retract data.

Copyright for abstracts (both oral and poster) on the website and as made available during The International Liver Congress™ 2023 resides with the respective authors. No reproduction, re-use or transcription for any commercial purpose or use of the content is permitted without the written permission of the authors. Permission for re-use must be obtained directly from the authors.

OS-091

Finding undiagnosed hepatitis C cases: using machine learning to identify clinical attributes and social determinants of health to improve the screening-to-diagnosis ratio and improve efficiency and linkage to care

Linda Chen^{1,2,3}, John Wolf¹, Bruce Kreter¹, Pranava Goundan⁴, Qin Ye⁴, Ravi Ippili⁴, Abhinav Bansal⁴, Shubhankar Thakar⁴. ¹Gilead Sciences, United States; ²Gilead Sciences, Medical Affairs, Foster City, United States; ³Gilead Sciences, Medical Affairs, Foster City, United States; ⁴ZS Associates, United States
Email: linda.chen24@gilead.com

Abstract OS-091 is under embargo until Friday 23 June 2023, 17:15.

This abstract will be made publicly available on the congress website at 17:15 (CEST) on the day of its presentation at the congress. Industry must not issue press releases – even under embargo – covering the data contained in abstracts selected to be highlighted during official EASL Press Office activities or in official EASL Press Office materials until the individual embargo for each data set lifts. Media must not issue coverage of the data contained in abstracts selected to be highlighted during official EASL Press Office activities or in official EASL Press Office materials until the individual embargo for each data set lifts.

Journalists, industry, investigators and/or study sponsors must abide by the embargo times set by EASL. Violation of the embargo will be taken seriously. Individuals and/or sponsors who violate EASL's embargo policy may face sanctions relating to current and future abstract submissions, presentations and visibility at EASL Congresses. The EASL Governing Board is at liberty to ban attendance and/or retract data.

Copyright for abstracts (both oral and poster) on the website and as made available during The International Liver Congress™ 2023 resides with the respective authors. No reproduction, re-use or transcription for any commercial purpose or use of the content is permitted without the written permission of the authors. Permission for re-use must be obtained directly from the authors.

OS-092-YI

Development of a behaviour-based score predicting hepatocellular carcinoma among patients with chronic hepatitis B virus infection in France (ANRS CO22 HEPATHER)

Clémence Ramier¹, Camelia Protopopescu¹, Massimo Levvero^{2,3,4}, Vincent Di Beo¹, Lucia Parlati⁵, Fabienne Marcellin¹, Celine Dorival⁶, Marta Lotto¹, Fabrice Carrat^{6,7}, Marc Bourliere^{1,8}, Maria Patrizia Carrieri¹. ¹Aix Marseille Univ, INSERM, IRD, SESSTIM, Sciences Économiques and Sociales de la Santé and Traitement de l'Information Médicale, ISSPAM, Marseille, France; ²INSERM U1052, CNRS UMR-5286, Cancer Research Center of Lyon (CRCL), Lyon, France; ³University of Lyon, Université Claude-Bernard (UCBL), Lyon, France; ⁴Hospices Civils de Lyon (HCL), Lyon, France; ⁵Université de Paris Cité; INSERM U1016; AP-HP, Hôpital Cochin, Département d'Hépatologie/Addictologie, Paris, France; ⁶Institut National de la Santé et de la Recherche Médicale (INSERM), Institut Pierre Louis d'Epidémiologie et de Santé Publique, Sorbonne Université, Paris, France; ⁷Hôpital Saint-Antoine, Unité de Santé Publique, Assistance Publique-Hôpitaux de Paris (AP-HP), Paris, France; ⁸Hôpital Saint Joseph, Département d'hépatologie et gastroentérologie, Marseille, France
Email: clemence.ramier@inserm.fr

Background and aims: Hepatocellular carcinoma (HCC) is the third cancer-related cause of death worldwide and 90% of cases are attributable to either unhealthy alcohol use or viral hepatitis. People infected with hepatitis B virus (HBV) have an increased risk of developing HCC. To date, predictive scores of HCC are mainly based on clinical data and do not include behaviours. We aimed to develop an easy-to-use score based on both behaviours and routine medical data predicting HCC in chronic HBV patients.

Method: The study population included chronic HBV patients with no history of HCC enrolled between 2012 and 2018 in the French ANRS CO22 HEPATHER cohort. The study population was randomly split into a training set (70%) and a testing set (30%). A Cox proportional hazards model for time to HCC was estimated on the training set. Variables with a p value <0.20 in univariable analyses were included in the multivariable analysis, then a backward selection procedure based on an alpha error <0.05 was used. Points were assigned to each variable in the final multivariable model by dividing its coefficient by the coefficient associated with a 10-year

ORAL PRESENTATIONS

increase in age, then rounded. A prediction score for HCC was calculated as the sum of three points. The optimal cut-off predicting the risk of HCC was computed using Youden index on 1000 bootstrap samples. The score's predictive performance was rated on the testing set and compared to other published scores using the area under the receiver operating characteristic curve (AUROC).

Results: The study population (N = 4,370) was 63% male, 65% were aged <50 years and 3.6% were infected with hepatitis Delta virus (HDV). During the 8-year follow-up (25,900 person-years), 55 patients (1.3%) developed a HCC. In the multivariable model, age, unhealthy alcohol use (>2 and >3 standard units/day for women and men, respectively), tobacco smoking, HDV infection, low platelet count and receiving HBV treatment were associated with increased HCC risk. The ADAPTT score (Age, Delta, Alcohol, Platelet, Tobacco, Treatment) (Table 1) ranged from 0 to 16, a score ≥6 indicating a high risk of HCC. Comparisons with existing scores suggested higher performance for ADAPTT score (AUROC = 0.848) than for PAGE-B (AUROC = 0.783), REAL-B (AUROC = 0.787) and THRI (AUROC = 0.776) scores.

AUROC	ADAPTT score
	0.848
Age: 50–59 years	+1
Age: 60–69 years	+2
Age ≥70 years	+3
HDV infection	+3
Past or current unhealthy alcohol use	+2
Platelet count <200 × 10 ⁹ /L	+2
Tobacco smoking ≥20 pack-years	+2
Receiving HBV treatment	+4

Conclusion: Based on easy-to-collect behavioural data and routine medical data, the ADAPTT score shows higher performance than existing scores for predicting HCC in patients with chronic HBV infection. Though further validation on other datasets is needed, this score, implementable in all settings, including primary care and decentralized areas, can facilitate follow-up of at-risk patients.

OS-093-YI

Chronic hepatitis B virus infection and risk of stroke types: a prospective cohort study of 0.5 million Chinese adults

Elizabeth Hamilton¹, Ling Yang^{1,2}, Iona Millwood^{1,2}, Zhengming Chen^{1,2}, ¹Clinical Trial Service Unit and Epidemiological Studies Unit (CTSU), Nuffield Department of Population Health, Oxford, United Kingdom; ²Medical Research Council Population Health Research Unit (MRC PHRU), Nuffield Department of Population Health, Oxford, United Kingdom

Email: elizabeth.hamilton@univ.ox.ac.uk

Background and aims: Stroke is a leading cause of mortality and permanent disability in China, with large and unexplained geographic variations in rates of different stroke types. Chronic hepatitis B virus (HBV) infection is prevalent among adult Chinese and may play a role in stroke aetiology.

Method: The prospective China Kadoorie Biobank included >0.5 million adults aged 30–79 years who were recruited from ten (five urban and five rural) geographically diverse areas of China during 2004–2008, with measurement of hepatitis B surface antigen (HBsAg) positivity at baseline. During 11-years of follow-up, a total of 59,117 incident stroke cases were recorded (>90% confirmed by neuroimaging), including 11,318 intracerebral haemorrhage (ICH), 49,971 ischaemic stroke (IS), and 995 subarachnoid haemorrhage (SAH) and 3,036 other/unspecified stroke. Cox regression models were used to estimate adjusted hazard ratios (HRs) for risks of stroke types associated with HBsAg positivity. In a subset of 17,833

participants, levels of liver enzymes and lipids were measured and compared between HBsAg positive and negative individuals.

Results: Overall, 3.0% (men: 3.4%; women: 2.8%) of participants were positive for HBsAg at baseline. HBsAg-positivity was associated with an increased risk of ICH (adjusted HR = 1.29, 95% CI 1.16–1.44), similarly for fatal (n = 5,982; 1.36, 1.16–1.59) and non-fatal (n = 5,336; 1.23, 1.06–1.44) ICH. There were no significant associations of HBsAg positivity with risks of IS (0.97, 0.92–1.03), SAH (0.87, 0.57–1.33), or other/unspecified stroke types (1.12, 0.89–1.42). Individuals who were HBsAg-positive, compared to those who were HBsAg-negative, had significantly lower levels of TC (4.41 vs 4.61 mmol/L), LDL-C (2.19 vs 2.32 mmol/L), TG (1.42 vs 1.61 mmol/L) and albumin (41.4 vs 42.1 g/L), and higher levels of ALT (28.0 vs 21.7 u/L) and AST (33.2 vs 28.2 u/L). The association of HBsAg with ICH was attenuated with adjustment for liver enzymes in the subset (from 1.28, 1.01–1.62 to 1.22, 0.95–1.56).

Figure: Number of events and adjusted HRs for risks of different stroke types associated with HBsAg positivity among 500,991 participants.

Stroke types	Number of events		Risk of stroke ^a	
	HBsAg negative	HBsAg positive	HR (95% CI)	P value
Intracerebral haemorrhage	10,992	326	1.29 (1.16–1.44)	6.3 × 10 ⁻⁶
Ischaemic stroke	48,817	1,154	0.97 (0.91–1.03)	0.29
Subarachnoid haemorrhage	973	22	0.87 (0.57–1.33)	0.53
Other or unspecified stroke	2,964	72	1.12 (0.89–1.42)	0.34
Total stroke	57,691	1,426	1.02 (0.97–1.07)	0.52

^aStratified by (5-year categories), sex, study site (10 sites) and adjusted for education (3 levels), smoking, alcohol, physical activity, regular fruit, meat or dairy intake, BMI, systolic blood pressure, prevalent diabetes and cancer. Abbreviations: HBsAg, hepatitis B surface antigen; ICD-10, International Statistical Classification of Diseases and Related Health Problems 10th Revision.

Conclusion: Among Chinese adults, chronic HBV infection is associated with a significantly high risk of ICH, but not other types of stroke and the association with ICH may be mediated through multiple mechanisms, including liver dysfunction and lipid metabolism.

OS-094

The first mass reactive vaccination campaign against hepatitis E in Bentiu, South Sudan: feasibility, vaccination coverage and two-dose vaccine effectiveness

Robin Nesbitt¹, Vincent Kinya Asilaza², Priscilla Gitahi², Patrick Nkemenang², Melat Haile³, Jetske Duncker³, Etienne Gignoux³, Manuel Albela³, Primitivo Gakima³, Joseph Wamala⁴, Zelig Antier², Kediende Chong⁵, Monica Rull³, Andrew Azman^{3,6}, Iza Ciglemecki³, John Rumunu⁵. ¹Epicentre, Paris, France; ²Médecins sans Frontières, South Sudan; ³Doctors Without Borders, Genève, Switzerland; ⁴World Health Organisation, South Sudan; ⁵Ministry of Health, South Sudan; ⁶Johns Hopkins University, Baltimore, United States

Email: robin.nesbitt@epicentre.msf.org

Abstract OS-094 is under embargo until Friday 23 June 2023, 17:15.

This abstract will be made publicly available on the congress website at 17:15 (CEST) on the day of its presentation at the congress.

Industry must not issue press releases – even under embargo – covering the data contained in abstracts selected to be highlighted during official EASL Press Office activities or in official EASL Press Office materials until the individual embargo for each data set lifts. Media must not issue coverage of the data contained in abstracts selected to be highlighted during official EASL Press Office activities

or in official EASL Press Office materials until the individual embargo for each data set lifts.

Journalists, industry, investigators and/or study sponsors must abide by the embargo times set by EASL. Violation of the embargo will be taken seriously. Individuals and/or sponsors who violate EASL's embargo policy may face sanctions relating to current and future abstract submissions, presentations and visibility at EASL Congresses. The EASL Governing Board is at liberty to ban attendance and/or retract data.

Copyright for abstracts (both oral and poster) on the website and as made available during The International Liver Congress™ 2023 resides with the respective authors. No reproduction, re-use or transcription for any commercial purpose or use of the content is permitted without the written permission of the authors. Permission for re-use must be obtained directly from the authors.

Senescence, circadian rhythm and sexual dimorphism

OS-095-YI

Hepatocyte senescence is linked with extrahepatic organ injury, failure of regeneration and mortality in patients with acute indeterminate hepatitis

Mohsin Hassan¹, Su Lin², Pavitra Kumar¹, Fausto Andreola², Adrien Guillot¹, Andrew Hall², Frank Tacke¹, Alberto Quaglia², Thomas Bird³, Rajiv Jalan², Cornelius Engelmann^{1,2,4}. ¹Charité Campus Virchow Clinic, Department of Hepatology and Gastroenterology, Berlin, Germany; ²University College London; ³Institute for Liver and Digestive Health, University College London, London, United Kingdom; ⁴University of Edinburgh, Beatson Institute, Glasgow, United Kingdom; ⁴Berlin Institute of Health, Berlin, Germany
Email: cornelius.engelmann@charite.de

Abstract OS-095-YI is under embargo until Friday 23 June 2023, 17:15. This abstract will be made publicly available on the congress website at 17:15 (CEST) on the day of its presentation at the congress. Industry must not issue press releases – even under embargo – covering the data contained in abstracts selected to be highlighted during official EASL Press Office activities or in official EASL Press Office materials until the individual embargo for each data set lifts. Media must not issue coverage of the data contained in abstracts selected to be highlighted during official EASL Press Office activities or in official EASL Press Office materials until the individual embargo for each data set lifts.

Journalists, industry, investigators and/or study sponsors must abide by the embargo times set by EASL. Violation of the embargo will be taken seriously. Individuals and/or sponsors who violate EASL's embargo policy may face sanctions relating to current and future abstract submissions, presentations and visibility at EASL Congresses. The EASL Governing Board is at liberty to ban attendance and/or retract data.

Copyright for abstracts (both oral and poster) on the website and as made available during The International Liver Congress™ 2023 resides with the respective authors. No reproduction, re-use or transcription for any commercial purpose or use of the content is permitted without the written permission of the authors. Permission for re-use must be obtained directly from the authors.

OS-096-YI

DNA damage induced-senescence shifts the cellular bioenergetics capacity from glycolysis to oxidative phosphorylation in mouse hepatocytes

Pavitra Kumar¹, Mohsin Hassan¹, Frank Tacke¹, Cornelius Engelmann^{1,2,3}. ¹Charité Universitätsmedizin Berlin, Department of Hepatology and Gastroenterology, Berlin, Germany; ²Berlin Institute of Health (BIH), Berlin, Germany; ³University College London, Institute for Liver and Digestive Health, London, United Kingdom
Email: cornelius.engelmann@charite.de

Background and aims: Cellular senescence is a state in which cells become resistant to growth-promoting stimuli and apoptosis, resulting in permanent cessation of cellular proliferation. This leads to a prolonged 'zombie-like' state, which can have detrimental effects on tissues relying on their regenerative capacity for homeostasis, such as the liver. Cells undergo a drastic metabolic shift as they adapt to senescent phenotype, potentially affecting the function of the liver. Therefore, in the present study, we aim to characterize, specifically, the link between DNA-damage-induced senescence and metabolic capacity in primary hepatocytes and hepatocyte-derived liver organoids.

Method: Primary hepatocytes, isolated by collagenase-perfused mouse liver (C57B6/J; 18–23 weeks), were cultured overnight in William's E-medium (+2% FBS, L-glutamine, and hepatocyte growth supplements). Hepatocyte-derived organoids were developed in a 3D matrix for two weeks. Cells or organoids were treated with the DNA

damage inducers, cisplatin (DNA cross-linker and alkylating agent), BIBR-1532 (telomerase inhibitor), and 5-azacytidine (DNA-methyl transferase inhibitor) for 24 hours. Senescence was assessed by SA- β galactosidase activity, immunofluorescence, and immunoblotting (p53, p21, and γ H2Ax), and senescence-associated secretory phenotype (SASP) candidates. Cellular bioenergetics was measured by XFe Seahorse analyser (substrates: 10 mM glucose, 2 mM pyruvate, and 1 mM glutamine).

Results: Dosages and time of treatment were optimized on the primary hepatocytes (five dosages and four-time points, 12 hours, 24 hours, 48 hours, and 72 hours). The results showed that cisplatin, 5-azacytidine, and BIBR-1532 increased phosphorylation of histone (γ H2Ax), a DNA damage marker, by 10-fold ($p < 0.001$), 5-fold ($p < 0.001$), and 10-fold ($p < 0.001$), respectively. Additionally, cisplatin, 5-azacytidine, and BIBR1532 increased SA β -galactosidase activity by 15-fold ($p < 0.001$), 6-fold ($p < 0.001$), and 11-fold ($p < 0.001$), respectively (Fig. 1A). Arrested proliferation is an important feature of senescence cells and the primary hepatocytes have limited proliferation in 2D culture. To overcome this limitation, we validated the results in hepatocyte-derived organoids. Coincided with DNA damage, cisplatin, 5-azacytidine, and BIBR1532 stabilized p53, increased p21 levels, and SASP (CCL2, CXCL2, IL6, IL10, TNF α , and MMP13) among which BIBR-1532 being the most potent to increase p21 and cisplatin is the most potent to stabilize p53 and increase SASP production. DNA damage-associated senescence reduced the basal glycolysis and oxidative phosphorylation. However, in contrast to the studies in immortalized cell lines, DNA damage inducers extended the bioenergetics capacity towards oxidative phosphorylation from glycolysis significantly. Hydroxy urea (a negative control for oxidative phosphorylation) inhibited oxidative phosphorylation and hence it extended the cellular respiration capacity towards glycolysis along with the increased senescent phenotype (Fig. 1B).

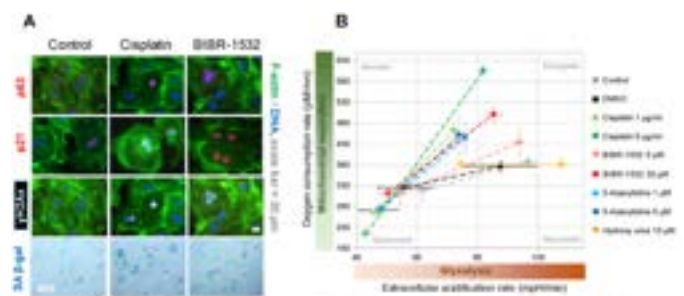


Figure 1. Effect of DNA damage on cellular bioenergetics and senescence markers on mouse hepatocytes treated for 24 hours **A)** senescence markers **B)** cell energy phenotype measured by XFe Seahorse analyser

Figure:

Conclusion: Cisplatin (DNA cross-linker), BIBR-1532 (telomerase inhibitor), and 5-azacytidine (DNA-methyl transferase inhibitor) induce senescence phenotype in mouse primary hepatocytes. DNA damage-induced senescence shifts the cellular bioenergetics capacity from glycolysis to oxidative phosphorylation, which may affect the hepatocytes' response to toxins and inflammation.

OS-097

CLOCK Δ 19 circadian disruption primes myofibroblasts for accelerated activation and fibrotic progression

Elliot Jokl¹, Jessica Llewelyn², Kara Simpson¹, Oluwatobi Adegboye¹, James Pritchett³, Leo Zeef¹, Qing-Jun Meng¹, Karen Piper Hanley¹. ¹University of Manchester, United Kingdom; ²Perelman School of Medicine at the University of Pennsylvania, Philadelphia, United States; ³Manchester Metropolitan University, United Kingdom
Email: elliot.jokl@manchester.ac.uk

Background and aims: Non-Alcoholic Fatty Liver Disease (NAFLD) is an increasing health burden with an estimated incidence of around 25%. Progressive disease is associated with fibrosis, characterised by

deposition of extracellular matrix (ECM) proteins by hepatic stellate cells (HSCs). Circadian rhythm governs many aspects of liver physiology and its disruption exacerbates chronic disease. However, the impact of disrupted circadian rhythm in pro-fibrotic HSCs remains to be investigated. In this study we investigate whether genetic disruption of circadian homeostasis predisposes HSCs to instigate fibrotic changes in the liver.

Method: Circadian rhythm was disrupted *in vitro* and *in vivo* using CLOCK mutant mice (CLOCK $\Delta 19$). HSC characteristics were investigated by western blot and genomic analysis. *In vivo* CLOCK $\Delta 19$ livers were assessed at basal state and during CCl₄ induced fibrosis. HSC CLOCK $\Delta 19$ genomic data was integrated with ATAC-seq from WT HSCs to generate a putative CLOCK regulome.

Results: Livers from CLOCK $\Delta 19$ mutant mice showed a higher baseline collagen (COL1) deposition and significantly worse fibrotic injury after CCl₄-induced fibrosis. Mutant livers had significantly increased scar formation (~40%), accumulation of myofibroblasts (~50%) and increased serum liver enzymes compared to control animals. HSCs isolated from PER2:LUC mice (displaying critical circadian rhythm measured by luciferase activity of the Per2 gene) were shown to display an intrinsic circadian rhythm. To investigate the role of circadian rhythm in HSCs further, genomic analysis demonstrated quiescent HSCs from CLOCK $\Delta 19$ mice had higher expression of RhoGDI pathway components, a suppression of genes associated with lipid metabolism, and had accelerated *in vitro* activation of pro-fibrotic genes on plastic. Through data integration,

we discovered chromatin regions (through ATAC-seq peaks) containing CLOCK binding motifs were differentially accessible during HSC activation. Our data suggested CLOCK may act in qHSCs to suppress profibrotic genes involved in focal adhesions and promote the expression of genes involved in lipid metabolism associated with quiescence.

Conclusion: Taken together, our data suggests disrupted circadian rhythm primes HSCs to a profibrotic state associated with dysregulated metabolic and mechanotransduction genes. This promotes an enhanced response to fibrotic-insult, driving more rapid progression of disease. Genes involved in the CLOCK regulome that underlie the HSC primed state include several secreted ECM candidates as urgently needed biomarkers of disease progression in NAFLD.

OS-098

Perturbation of rhythmicity of the circadian clock-oscillator in hepatic stellate cells is associated with liver fibrosis

Emilie Crouchet¹, Mayssa Dachraoui¹, Frank Jühling¹, Marine Oudot¹, Clara Ponsolles¹, Laura Heydmann¹, Cloé Gadenne¹, Julien Moehlin¹, Natascha Roehlen¹, Romain Martin¹, Nicolas Brignon¹, Laurent Mailly¹, Yuji Teraoka², Hiroshi Aikata², Michio Imamura², Hiromi Abe-Chayama², Kazuaki Chayama², Fabio Del Zompo¹, Antonio Saviano¹, Sarah Durand¹, Catherine Schuster¹, Patrick Pessaux¹, Joachim Lupberger¹, Atish Mukherji¹, Thomas Baumert¹. ¹Université de Strasbourg, Inserm, Institut de

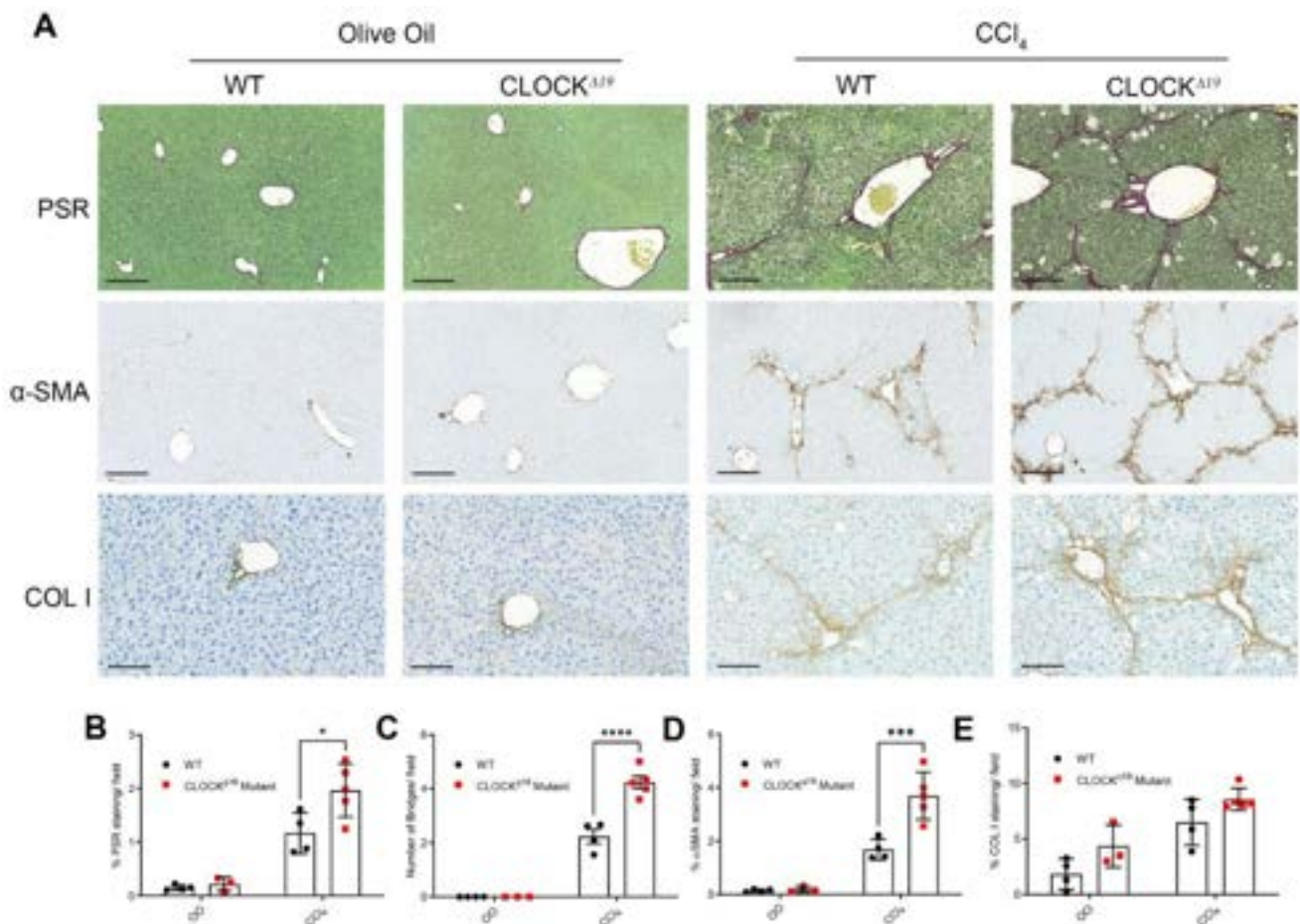


Figure: (abstract: OS-097): CLOCK $\Delta 19$ mice show an enhanced fibrotic response to CCl₄. (A) Staining for fibrillar collagen (PSR) and IHC of α -SMA and COL1 in olive oil- and CCl₄-treated mice shows enhanced fibrosis in the CLOCK $\Delta 19$ mutant. (B-E) Quantification of IHC showing significantly elevated (B) PSR staining, (C) bridging fibrosis and (D) α -sma expression in CCl₄ treated mice. (E) COL1 shows a non-significant trend towards higher levels in the CLOCK $\Delta 19$ mice (two way ANOVA, * = $p < 0.05$, *** = $p < 0.001$, **** = $p < 0.0001$, $n = 3-5$). Error bars represent the mean \pm SD

ORAL PRESENTATIONS

Recherche sur les Maladies Virales et Hépatiques Inserm, UMR_S1110, France; ²Institute of Biomedical and Health Sciences, Hiroshima University, Japan
Email: thomas.baumert@unistra.fr

Abstract OS-098 is under embargo until Friday 23 June 2023, 17:15.

This abstract will be made publicly available on the congress website at 17:15 (CEST) on the day of its presentation at the congress.

Industry must not issue press releases – even under embargo – covering the data contained in abstracts selected to be highlighted during official EASL Press Office activities or in official EASL Press Office materials until the individual embargo for each data set lifts. Media must not issue coverage of the data contained in abstracts selected to be highlighted during official EASL Press Office activities or in official EASL Press Office materials until the individual embargo for each data set lifts.

Journalists, industry, investigators and/or study sponsors must abide by the embargo times set by EASL. Violation of the embargo will be taken seriously. Individuals and/or sponsors who violate EASL's embargo policy may face sanctions relating to current and future abstract submissions, presentations and visibility at EASL Congresses. The EASL Governing Board is at liberty to ban attendance and/or retract data.

Copyright for abstracts (both oral and poster) on the website and as made available during The International Liver Congress™ 2023 resides with the respective authors. No reproduction, re-use or transcription for any commercial purpose or use of the content is permitted without the written permission of the authors. Permission for re-use must be obtained directly from the authors.

OS-099

Gender differences in repair mechanisms of chronic cholangiopathies with progressive fibrosis

Massimiliano Cadamuro^{1,2}, Labjona Haxhiaj³, Chiara Montanaro³, Erica Villa⁴, Annarosa Floreani⁵, Nora Cazzagon⁵, Giovannella Baggio³, Mario Strazzabosco⁶, Paolo Simioni^{1,2,7}, Luca Fabris^{1,6,8}. ¹Padua University-Hospital, General Internal Medicine Unit, Italy; ²University of Padua, Department of Medicine (DIMED), Italy; ³University of Padua, Italy; ⁴University of Modena and Reggio Emilia, Gastroenterology, Italy; ⁵University of Padua, DISCOG, Italy; ⁶Yale University, Digestive Disease Section, Liver Center, United States; ⁷University of Padua, Thrombotic and Haemorrhagic Disease Unit and Haemophilia Center, Department of Medicine (DIMED), Italy; ⁸University of Padua, Department of Molecular Medicine (DMM), Italy
Email: massimiliano.cadamuro@unipd.it

Background and aims: In chronic liver disease pathophysiology, gender dimorphism is much less characterized compared with degenerative disorders affecting other organs. Repair mechanisms are instrumental to direct fibrogenesis and progression of chronic inflammatory conditions. Therefore, we investigated the gender-specific differences in tissue repair culminating in liver fibrogenesis and sustained by activation of hepatic progenitor cells (HPC) and ductular ductular reaction (DR) in two models of diseases of the

biliary epithelium (cholangiopathies) featuring progressive fibrosis. We considered the Pkhd1^{del4/del4} and the Mdr2^{-/-} mouse models, orthologous of the human congenital hepatic fibrosis/Caroli's disease (CHF/CD) and primary sclerosing cholangitis (PSC), respectively, and in sections of human PSC and CHF/CD.

Method: Serial sections of liver tissue specimens of PSC (n = 9 M/n = 5 F) and CHF/CD (n = 3 M/n = 1 F), along with Pkhd1^{del4/del4} (n = 11 M/n = 23 F), and Mdr2^{-/-} mice (n = 5 M/n = 3 F), were stained with Sirius Red (histological staining) and with immunohistochemistry for myofibroblasts (α -SMA), macrophages (CD68, human samples only), and RDC/DR (K19). Extent of DR, fibrosis, inflammation and number of HPC were evaluated with computer-assisted morphometry.

Results: In both mouse models and human diseases, fibrosis resulted higher in M compared with F, without significant differences in myofibroblast accumulation and HPC activation. In both Mdr2^{-/-} mice and PSC patients, extension of DR was more prominent in M than F, whereas in Pkhd1^{del4/del4} mice, dysgenetic biliary lesions were greater in F than in M. In addition, in PSC samples, the number of CD68+ macrophages was higher in M as respect to F. Similar trends were also found in human CHF/CD samples.

Conclusion: This study shows gender-specific differences in tissue repair mechanisms of the biliary epithelium in both mouse models and human samples of PSC and CHF/CD. In particular, we found more severe fibrogenesis associated with more intense inflammatory infiltrate dominated by macrophages in males compared to females, thereby providing mechanistic evidence of the more severe clinical course of chronic liver diseases affecting men as reported in viral and metabolic etiologies.

SATURDAY 24 JUNE

Cirrhosis and its complications: Portal Hypertension

OS-100-YI

Hemodynamic response determines further decompensation and survival in patients with decompensated cirrhosis

Claudia Pujol^{1,2}, Marta García Guix^{1,2}, Anna Brujats^{1,2}, Edilmar Alvarado-Tapias^{1,2,3}, Anna Huerta^{1,2}, Berta Cuyas^{1,2}, Maria Poca^{1,2,3}, Xavier Torras^{1,2}, Àngels Escorsell^{1,2,3}, Cándid Villanueva^{1,2,3}. ¹Hospital Santa Creu i Sant Pau, Department of Gastroenterology, Barcelona, Spain; ²Institut de Recerca Sant Pau-Universitat Autònoma de Barcelona, Barcelona, Spain; ³Centro de Investigación Biomédica en Red de Enfermedades Hepáticas y Digestivas (CIBERehd), Instituto de Salud Carlos III, Madrid, Spain
Email: cpujolc@santpau.cat

Background and aims: Different stages can be identified in decompensated cirrhosis, such as bleeding alone or with other concomitant decompensation, and ascites without bleeding. The development of further decompensation determines prognosis in each of these stages. This study investigates the influence of hemodynamic response to β -blockers on the risk of further decompensation and survival in each substage of decompensated cirrhosis.

Method: Patients admitted due to variceal bleeding (VB) were consecutively included, differentiating those who only had VB (VBAlone) from those with concomitant ascites (As) (with or without encephalopathy) (VBPlus). Patients with ascites and varices without previous bleeding (AsAlone) referred during the study period for primary prophylaxis, were also investigated. An

hemodynamic study was performed before starting therapy with β -blockers and was repeated after 1–2 months to assess the response. The risk of outcomes was estimated in a competing risks (CR) framework considering death and liver transplant as competing events.

Results: 476 patients with decompensated cirrhosis were included, 103 with VBA alone, 186 with VBPlus and, 187 with AsAlone. During a mean follow-up of 32 months (IQR 12–58), the risk of death and of further decompensation, were higher in AsAlone group than in VBA alone group and higher in VBPlus than in the other two groups. Survival probability was significantly worse in patients with further decompensation than in those without, in each of the 3 substages ($<70\%$ at 3rd-year), and was lower in patients with VBPlus (37% at 3rd-year) than in the other groups. Among patients without further decompensation, survival probability was similar in the 3 substages ($\geq 83\%$ at 3rd-year). HVPG-decrease was an independent predictor of further decompensation and death. An HVPG-decrease $\geq 10\%$ from baseline (defining HDK-response) was achieved in 43% of patients. Overall, patients with HDK-response vs those without, had lower risk of further decompensation (sHR = 0.31, 95%CI = 0.24–0.39), and lower risk of death (sHR = 0.23, 95%CI = 0.17–0.32). Similar results favoring HDK-responders were observed in each substage separately.

Conclusion: At each decompensation of cirrhosis (bleeding, ascites or both), the risk of death is higher in patients developing further decompensation. With each decompensation, those patients achieving an HVPG-decrease $\geq 10\%$ have lower risk of further decompensation and better survival. Our results suggest that therapies effectively decreasing HVPG (such TIPS) may be valuable in decompensated patients without HDK-response to β -blockers.

OS-101-YI

Comparison of 1-day vs 3-days intravenous terlipressin in cirrhotic patients with acute variceal bleeding: open-label randomized control trial

Manas Vaishnav¹, Sagnik Biswas¹, Shekhar Swaroop¹, Arnav Aggarwal¹, Abhinav Anand¹, Piyush Pathak¹, Shalimar¹. ¹All India Institute of Medical Sciences, New Delhi, India
Email: drshalimar@yahoo.com

Background and aims: In patients with acute variceal bleeding (AVB), the optimal duration of vasoconstrictor therapy after endoscopic therapy with band ligation is unclear. Expert guidelines recommend vasoconstrictor therapy for 1-day to 5-days. We aimed to compare the efficacy of 1-day terlipressin therapy vs 3-days of terlipressin in cirrhosis patients with AVB post-endoscopic intervention. We also measured HVPG on day 1 and day 3 in both groups. The

primary objective was to compare the rebleeding rates at 5-days between the two groups. The secondary objectives were to compare rebleeding and mortality at 6 weeks. We also assessed the change in HVPG between days 1 and 3 (HVPG response rate).

Method: In this open-label, randomized controlled trial, cirrhosis patients with AVB were randomized to receive either 1-day or 3-days of terlipressin therapy post-endoscopic intervention. Rebleeding and mortality were noted on day 5 and after 6 weeks. HVPG measurements were done after the first endoscopy and after 72 hours.

Results: Of the 149 patients randomized, 74 were randomized to the 1-day and 75 to 3-day group. There were no differences in baseline clinical as well as laboratory parameters between the 2 groups. Failure to control bleeding at 24 hours in the 1-day and 3-days [0 vs 2 (2.7%), $p = 0.497$], 5-days rebleeding rate [3 (4.1%) vs 4 (5.3%), $p = 1.000$], and 5-day mortality [1 (1.4%) vs 1 (1.3%), $p = 1.000$] were similar. At 6 weeks, rebleeding [9 (12.2%) vs 10 (13.3%), $p = 0.830$] and mortality [5 (6.8%) vs 4 (5.3%), $p = 0.745$] were similar (Figure 1a and b). HVPG response (defined as $\geq 10\%$ reduction from baseline) was similar in both groups. Patients who received 3-days of terlipressin therapy experienced more adverse effects as compared to 1-day therapy [42 (45%) vs 28 (37.8%), $p = 0.026$].

Conclusion: As compared to 3 days therapy, 1 day of terlipressin was associated with similar rebleeding rates at 5-days and 6 weeks, 42-days mortality, and HVPG response rate at day 3. One-day terlipressin therapy is associated with fewer adverse effects than 3-days therapy.

OS-102

The new diagnostic criteria of portopulmonary hypertension identify a group of patients with cirrhosis at high risk of death

Luis Téllez^{1,2,3,4}, Antonio Guerrero¹, Jesus Donate¹, Miguel Ángel Rodríguez-Gandía^{1,2,3}, Susana del Prado⁵, Andrés Tenes⁶, Rosa Martín-Mateos^{1,2,3}, Rosario González Alonso^{1,2,3}, Javier Martínez^{1,2,3,4}, Miguel García González^{1,2,3}, Rubén Sánchez-Aldehuelo^{1,2}, Diego Burgos Santamaria^{1,2,3}, Beatriz Mateos Muños^{1,2,3}, María Torres Guerrero^{1,6}, Jose Luis Lledo Navarro^{1,2,3}, Agustín Albillos^{1,2,3,4}. ¹Hospital Universitario Ramón y Cajal, Gastroenterology and Hepatology, Madrid, Spain; ²Instituto Ramón y Cajal de Investigación Sanitaria-IRYCIS, Madrid, Spain; ³Universidad de Alcalá: Facultad de Medicina y Ciencias de la Salud, Alcalá de Henares, Spain; ⁴CIBER-Center for Biomedical Research Network, Madrid, Spain; ⁵Hospital Universitario Ramón y Cajal, Cardiology, Madrid, Spain; ⁶Hospital Universitario Ramón y Cajal, Respiratory Diseases, Madrid, Spain
Email: luistevilla@gmail.com

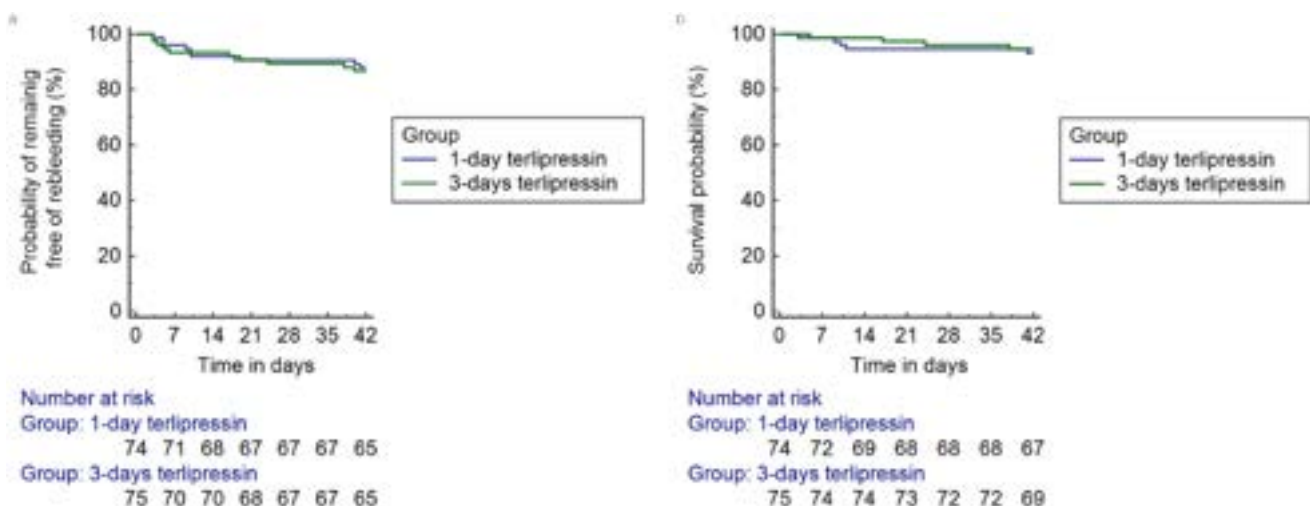


Figure: (abstract: OS-101-YI): (a) Cumulative probability of remaining free of bleeding at 6 weeks (log rank $p = 0.820$) (b) Cumulative probability of survival at 6 weeks (log rank $p = 0.691$)

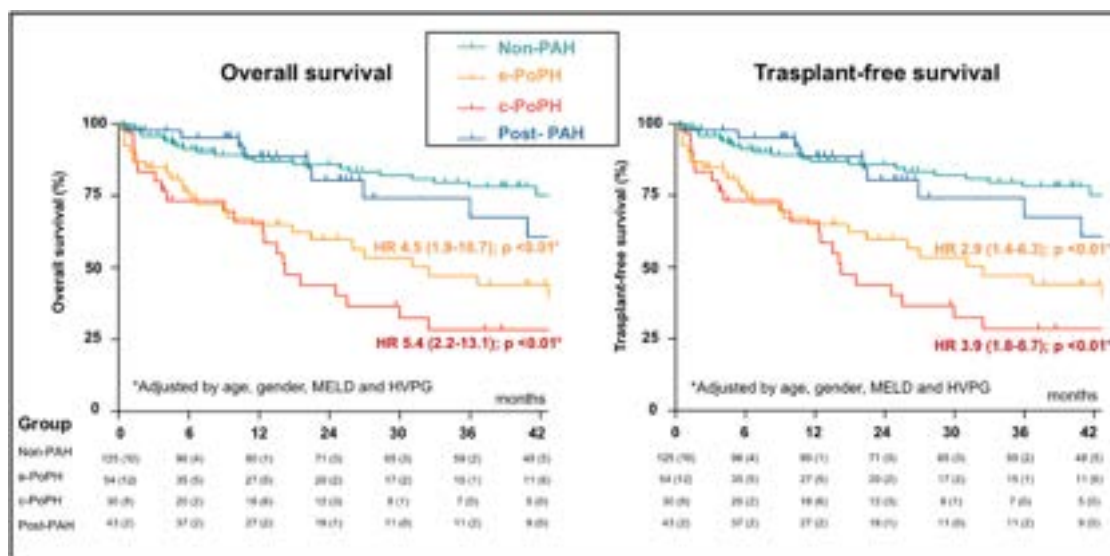


Figure: (abstract: OS-102).

Background and aims: The new diagnostic criteria of pulmonary arterial hypertension (PAH) use lower cut-offs for mean pulmonary arterial pressure (mPAP) (before: 25; now: 20 mmHg) and pulmonary vascular resistance (PVR) (before: 3; now: 2 Woods Units (WU)) to define portopulmonary hypertension (PoPH). Using these criteria, we can identify a group of patients with early precapillary PAH (e-PoPH: mPAP 20–25 mmHg and PVR ≥ 2 WU), whose prognostic significance in cirrhosis has not been studied. The primary aim was to analyze the impact on the prognosis of the new PAH criteria in patients with cirrhosis and portal hypertension; the secondary objective was to identify non-invasive predictors of PoPH according to new criteria.

Method: Observational study including prospectively all consecutive patients with cirrhosis and HVPG >5 mmHg evaluated by hepatic and right heart catheterization between 2015 and 2022. The patients were classified as Non-PAH (mPAP <20 mmHg); e-PoPH (mPAP = 20–25 mmHg and RVP ≥ 2 WU); classic PoPH or c-PoPH (mPAP ≥ 25 mmHg and RVP ≥ 3 WU); postcapillary PAH or post-PAH (mPAP ≥ 20 mmHg and pulmonary artery wedged pressure ≥ 15 mmHg). The variables associated with a worse prognosis (death or transplantation) were analyzed using Cox regression, and the predictors of HAPoP using binary logistic regression.

Results: (mean, SD). 258 patients were followed-up for 104 (28) months (72.5% male; age 58.6 (9.1) years). Non-PAH: 48.4%; e-PoPH: 20.9%; c-PoPH: 11.6%; post-PAH: 16.7%. Poorer liver function (MELD), higher portal hypertension (HPVG), and the presence of PAH were independently associated with worse overall survival and transplant-free survival ($p < 0.01$).

The prognosis of patients with PoPH, whether early (HR 4.5 (1.9–10.7)) or classic (HR 5.4 (2.2–13.1)), was worse ($p < 0.01$) than that of those without PAH or with post-PAH (overall-survival and transplant-free survival) (Figure). Those with PoPH (early or classic) had higher ($p < 0.05$) levels of C-reactive protein, brain natriuretic peptide (BNP), and uric acid and lower levels of albumin than those without PAH. The variables independently associated with PoPH were the existence of a portosystemic shunt (OR 6.8 (2.0–22.8)) and BNP >80 pg/ml (OR 13.1 (2.7–65.0)). Tricuspid regurgitation velocity (AUC 0.82 (0.7–0.9), $p < 0.01$) and right atrial area (AUC 0.86 (0.8–0.9), $p < 0.01$) were the echocardiographic parameters that best discriminated the presence of PoPH.

Conclusion: The new diagnostic criteria of PAH identify a group of patients with cirrhosis and early PoPH at high risk of death. We have identified clinical and analytical variables that allow us to suspect the existence of PoPH according to new criteria.

OS-103-YI

Outcomes of a therapeutic stepwise approach involving low-dose systemic thrombolysis for managing acute portomesenteric thrombosis

Ahmed Hashim¹, Aashish Pandya¹, Naz Kanani Alviri¹, Hannah Old¹, Jonathan King¹, Louise China¹, Dominic Yu¹, David Patch¹. ¹Institute for Liver and Digestive Health, Royal Free Hospital, London, United Kingdom
Email: ahmed.hashim@nhs.net

Background and aims: Acute non-malignant portomesenteric thrombosis (PMT) is challenging to manage and can often result in bowel infarction leading to high morbidity and mortality. We report a large series of patients presenting with this condition who received our novel step-wise therapeutic protocol, aiming to describe the rates of recanalization, symptom control and complications. Our protocol published originally in 2019–adopts a step-ladder approach involving the infusion of systemic low-dose tissue plasminogen activator (L-tPa) for 72 hours initially and up to a maximum of 7 days. Depending on the clinical and radiological response, the treatment is escalated to Catheter-Directed Thrombolysis (CDT) followed by Transjugular Intrahepatic Portosystemic Shunt (TIPS) when indicated.

Method: We conducted a retrospective analysis of clinical records of patients with acute PMT who undertook the stepwise regimen above at Royal Free Hospital between December 2019 and August 2022.

Results: The total number of patients included was 42 patients; 25 (60%) were males. The mean age was 46 (SD = 13). Hereditary thrombophilia was identified in 17 (40%) patients and acquired prothrombotic conditions were observed in 15 (36%) cases (2 had a recent COVID-19 infection and 3 received the ChAdOx1 vaccine). Three patients had underlying chronic liver disease. All patients had thrombosis of the superior mesenteric vein (SMV) on cross-sectional imaging. Main portal vein thrombosis (PVT) was found in 38 (90%) patients whereas thrombosis of all three-vessel (PVT + SMV + splenic vein) was present in 25 (60%). All patients had persistent abdominal pain despite standard anticoagulation prior to the initiation of L-tPa. The median time to initiation of L-tPa ($n = 39$) was 12 (IQR = 12) days of symptoms and the mean duration of L-tPa infusion was 95 (SD = 48) hours. CDT was undertaken in 21 (50%) patients, of whom, two-thirds (15/21) had the local therapy delivered through EKOS™ endovascular system. TIPS was inserted in 18 patients (43%) and remained patent at discharge in 16/18 (89%). A degree of recanalization was observed in 33 (79%). Around half of the patients ($n = 20$) did not require intensive or high-dependency care admission. The

majority 31 (80%) received warfarin as long-term anticoagulation (5 were maintained on Apixaban). At a median follow-up of 10 (IQR = 12) months, complete symptom resolution was achieved in 26/37 (70%). Recanalization was maintained in 26/40 (65%) and TIPSS remained patent in 14/18 (78%). Nine patients required bowel resection within a median duration of 11 (IQR = 10.5) days from presentation. The mean length of small bowel resected was 67 cm (SD = 50). One patient was discharged with a stoma and needed parenteral nutrition and another suffered an intracranial haemorrhage. Minor bleeding occurred in 10 patients. One death was recorded (due to bowel ischemia).

Conclusion: Our stepwise protocol achieved good recanalization and patency rates, and sustained symptom control was observed in the majority of patients. While some patients inevitably required surgical intervention, bowel continuity was eventually achieved in almost all cases.

OS-104

Long-term outcome following liver transplantation for patients with acute on chronic liver failure grade 3 (ACLF-3): a retrospective matched-controlled study

Florent Artru^{1,2}, Sophie-Caroline Sacleux³, José Ursic Bedoya⁴, Clementine Levy², Marion Khaldi², Charles Le Goffic², Eric Levesque³, Sébastien Dharancy², Emmanuel Boleslawski², Gilles Lebuffe², Philippe Ichai³, Audrey Coilly³, Eleonora De Martin³, Eric Vibert³, Samir Jaber⁴, Astrid Herrero⁴, Magdalena Meszaros⁴, Clement Monet⁴, Didier Samuel³, Philippe Mathurin², Georges-Philippe Pageaux⁴, Faouzi Saliba³, Alexandre Louvet². ¹King's College Hospital, United Kingdom; ²CHU Lille, France; ³Hopital Paul Brousse, France; ⁴CHU Montpellier, France
Email: florent.artru@kcl.ac.uk

Background and aims: Utility, a major principle for allocation in the context of scarce medical resources, is questioned in patients with

acute-on chronic liver failure (ACLF) grade 3 who undergo liver transplantation (LT). Indeed, while the evidence is growing regarding an acceptable 1-year survival after LT, very scarce data reports long-term patients and graft survivals that are the final aim of LT. We aimed to explore long-term outcomes of patients included the 3 center retrospective French experience published in 2017.

Method: All patients with ACLF grade 3 (n = 73) as well as their matched controlled (on sex and age) with ACLF 2 (n = 145), 1 (n = 119) and no ACLF (n = 292) that have participated in the princeps study published in J Hepatol were included. We explored 5- and 10-year patient and graft survivals, causes of death and their predictive factors.

Results: Patients with ACLF grade 3 were male in 70% with a median age of 57 years old. Alcohol was the main cause of cirrhosis (53%) and septic shock (49%) the main primary reason for admission in intensive care unit. At time of LT, MELD score was 40 and CLIF-C ACLF 67. Median follow-up was 9 years. In patients with ACLF 3, 2, 1 and no ACLF, 5- and 10-year patient survivals were respectively 73% vs. 71% vs. 76% vs. 79% (p = 0.3) and 57% vs. 58% vs. 59% vs. 65% (p = 0.3). In cox-regression analysis ACLF grade was not associated with 5- (RR 1.1, 95%CI: 0.95–1.29, p = 0.16) and 10-year survival (RR 1.1 95%CI: 0.97–1.22, p = 0.11). 5- and 10-year graft survivals were respectively 67% vs. 68% vs. 74% vs. 73% (p = 0.4) and 50% vs. 53% vs. 58% vs. 60% (p = 0.3). At 10 years in ACLF 3 patients, 30 died and 5 were retransplanted. The leading causes of death were infections (33%), and cardiovascular events (23%) and reasons for retransplantation were chronic rejection (60%) and biliary complications (40%). Multivariable analyses identified Charlson comorbidity index (CCI) (RR 1.59, 95%CI: 1.12–2.26, p = 0.009 and RR 1.37, 95%CI: 1.05–1.78, p = 0.019) at LT and the number of RBC packs transfused (RR 1.18, 95%CI: 1.10–1.34, p = 0.0001 and RR 1.17, 95%CI: 1.07–1.27, p = 0.0003) as independently associated with 5- and 10-year patients' survival while age, etiology of cirrhosis, MELD score, sarcopenia, donor-risk index were not.

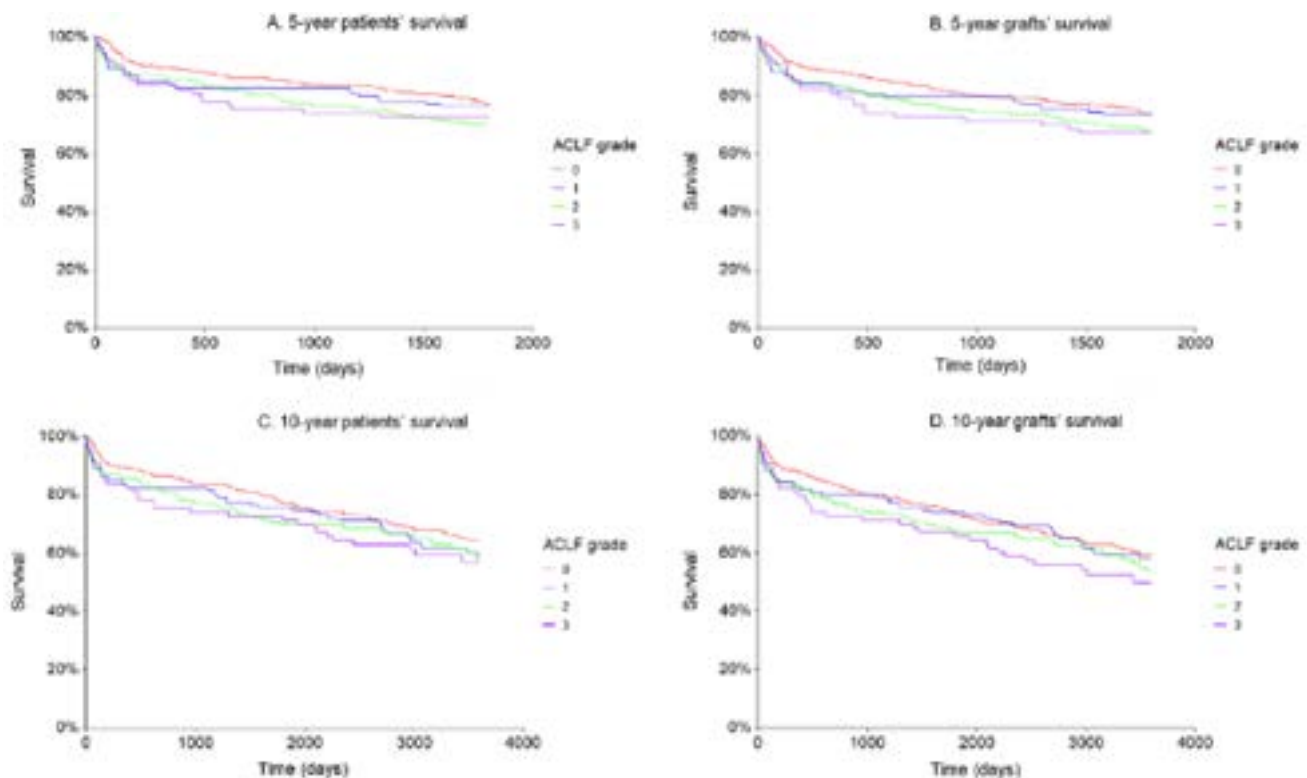


Figure: (abstract: OS-104): 5-year patients (A) and graft (B) survival, and 10-year patients (C) and graft (D) survivals in patients with ACLF 3 (n = 73) and their matched controls with ACLF 2 (n = 145), 1 (n = 119) and no ACLF (n = 292).

Conclusion: 5- and 10-year patients and graft survivals in ACLF 3 patients were not significantly different from their matched controls with lower ACLF grade or absence of ACLF. 5-year patients' survival is higher than that of the 50%–70% threshold defining the utility of liver graft. To further improve outcomes efforts should focus on candidates' selection (CCI associated with long-term survival) and prevention of infection and cardiovascular events standing as the main causes of death.

Liver failure and regeneration

OS-105

Hepatic nerve endings are rewired by cholestatic injury to connect inflamed lymphatics to sites of ductular remodelling

Luke Noon^{1,2,3}, Anne-Laure Cattin², Jemima Burden², Luigi Aloia², Giulia Casal², Marina Berenguer⁴, Judith Pérez⁴, Alison Lloyd². ¹CIPF Centro de Investigación Príncipe Felipe, Valencia, Spain; ²MRC Laboratory for Molecular Cell Biology, United Kingdom; ³CIBER-Center for Biomedical Research Network, Madrid, Spain; ⁴La Fe University and Polytechnic Hospital, Valencia, Spain
Email: lnoon@cipf.es

Background and aims: Hepatic nerves regulate blood flow, metabolism and regeneration, yet we have almost no understanding of the structure, function, or cell-specificity of nerve endings in liver. In this study we set out to map the “connectome” of peripheral nerves in murine liver, taking a cross-scale approach to visualize, quantify and reconstruct nerve terminals using correlative light and electron microscopy (CLEM) and 3D-electron microscopy (EM).

Method: Plp-EGFP transgenic mice were used to identify hepatic nerves in portal tracts by EGFP fluorescence and hone in on the ultrastructural features of the neural niche by CLEM. Array tomography-based scanning EM (SEM) was then used to scale-up sampling around nerves and compare “healthy” adult liver to that of “injured” mice fed 0.1% 3,5-diethoxycarbonyl-1,4-dihydrocollidine (DDC). The resulting volume (v)EM image database was annotated, segmented and 3D-rendered using the Webknossos open source platform.

Results: We identified 187 individual axonal contacts in “healthy” liver (n=3) and 208 in “injured” liver (n=3) from a total tissue volume of 165835 μm^3 . Our survey of hepatic nerve endings revealed Schwann cells in portal tracts support a wider network of “naked” axons protruding into the surrounding stroma, making multitude contacts with fibroblasts (21.9% of total), macrophages (6.4%), and the basal lamina of blood vessels (36.9%) and bile ducts (2.7%). Axons also formed prominent varicosity-like contacts abutting hepatocytes of the limiting plate (31.6%). Remarkably, we observed a close physical association between hepatic nerves and lymphatic vessels, that was confirmed in human liver. Nerve terminals contacting lymphatics in healthy liver were rare (0.53%), but their density increased dramatically with injury (8.79-fold) indicating axonal remodelling. Axon tracing also revealed individual nerve fibres connected inflamed lymphatics with hepatocytes of the canals of Hering-the epithelial interface where ductular remodelling occurs upon DDC injury. Moreover, synapse-like structures penetrating the basal lamina of ductular progenitors could be traced back to axons protruding from nearby lymphatic tissue (see figure). Together, our results demonstrate hepatocytes and cholangiocytes of the Canals of Hering are connected in series by nerves emanating from lymphatic tissue.

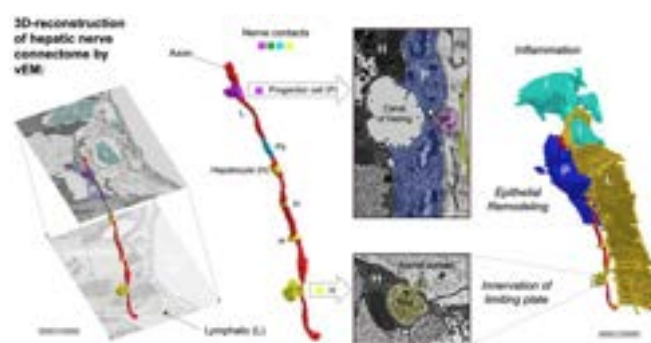


Figure:

Conclusion: We showcase a new workflow that enables quantitative mapping and visualization of peripheral nerve connectomes in liver at the ultrastructural level, revealing multiple novel features of hepatic nerve endings. Our analysis uncovers local circuitry connecting regenerative epithelial surfaces in series with nearby lymphatic tissue, raising the extraordinary possibility that the detection/response to injury is coordinated between inflamed lymphatic tissue and progenitor cells by hepatic nerves.

OS-106-YI

The silencing of Sox9 impairs ductular reaction expansion while enhancing the differentiation of DR cells into hepatocytes

Arthur de Schaetzen¹, Maxime De Rudder¹, Isabelle Leclercq¹. ¹Institut de recherche expérimentale et clinique, Pôle d'hépatogastro-entérologie, Woluwe Saint Lambert, Belgium
Email: arthur.deschaetzen@uclouvain.be

Background and aims: After acute damage or liver resection the liver regenerates and each cell compartment proliferates to repopulate the cells that were lost. In chronic liver disease, hepatocytes are found in a state of replicative senescence and are no longer able to duplicate. In such a setting, cholangiocytes proliferate and invade the parenchyma, in a phenomenon called the ductular reaction (DR). Cells of the ductular reaction have the ability to differentiate in hepatocytes, offering an alternative path for regeneration. Observations in animal models show nevertheless that DR cells generate only a modest fraction of hepatocytes. Hence strategies to enhance DR-derived regeneration are needed to significantly support liver function in chronic diseases.

Sox9 is a transcription factor that determines the biliary fate of the bipotential precursor to cholangiocytes and hepatocytes during embryogenesis. Sox9 ectopic expression is proposed to direct liver epithelial cells towards the biliary lineage. Here we hypothesize that the silencing of Sox9 in cells of the ductular reaction will ease their shift towards the hepatocyte lineage, thereby enhancing their contribution to liver regeneration.

Method: We used $\text{Opn}^{\text{CreERT2}} : \text{Rosa26R}^{\text{YFP}} : \text{Sox9}^{\text{floxed}}$ transgenic mice in which the injection of Tamoxifen drives the constitutive expression of YFP and the silencing of Sox9 in cholangiocytes alone. Any cell expressing YFP is a cholangiocyte or its progeny. $\text{Sox9}^{\text{Chol}} \text{KO}$ and controls with intact Sox9 expression received carbon tetrachloride (CCl_4) for 6 weeks to cause chronic hepatocellular damage. In a separate experiment, we first treated mice with CCl_4 to induce DR and then operate Sox9 silencing in cholangiocytes, followed by a 2 weeks recovery period before harvest.

Results: In response to tamoxifen injection, we observed expression of YFP in 71% ($\pm 1.9\%$) of cholangiocytes together with deletion of Sox9 in 100% of them in $\text{Sox9}^{\text{Chol}} \text{KO}$ mice. In controls mice 82% ($\pm 3.5\%$) of cholangiocytes expressed YFP and all of them expressed Sox9. After 6 weeks of CCl_4 , the magnitude of the ductular reaction, as measured by the area of Ck19^+ cells, was significantly lower in $\text{Sox9}^{\text{Chol}} \text{KO}$ than in controls. Patches of $\text{YFP}^+/\text{HNF4}\alpha^+$ hepatocytes generated from the DR were present in all animals, but similar in density in $\text{Sox9}^{\text{Chol}} \text{KO}$ and in controls, this regardless whether the

ductular reaction was weak (Sox9^{Chol} KO) or vigorous (controls), supporting that Sox9 deletion favors differentiation of DR cells. To further support this, we silenced Sox9 after the induction of the DR in chronic hepatocellular injury, and examined livers after a 2 weeks recovery period. We confirmed that tamoxifen injection effectively induced YFP expression and silenced Sox9 in 68% and 100% of DR cells respectively in Sox9^{Chol} KO and in 83% and 0% of DR cells in controls. The number of YFP⁺ hepatocytes was significantly increased in Sox9^{Chol} KO compared to controls (figure).

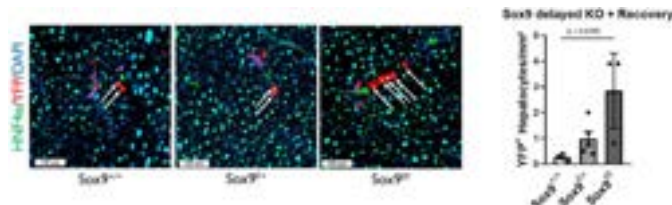


Figure: Livers with homozygous deletion of Sox9 (Sox9^{Chol} KO) and with heterozygous deletion of Sox9 (Sox9^{+/+}) are compared with livers with wild type Sox9 alleles (Sox9^{+/+}). Statistical analysis: one-way anova

Conclusion: We generated a model for inducible and cholangiocyte-specific YFP expression along with Sox9 silencing: the Opn^{iCreERT2} : Rosa26R^{YFP} : Sox9^{flxed} mice. With this model, we showed that the silencing of Sox9 impairs the expansion of DR cells. Furthermore, the silencing of Sox9 in DR cells enhances their hepatocytic differentiation.

OS-107-YI

Bio-molecular map of albumin identifies signatures of severity and early mortality in acute liver failure

Neha Sharma¹, Jaswinder Maras¹, Sushmita Pandey¹, Manisha Yadav¹, Babu Mathew¹, Vasundhara Bindal¹, Nupur Sharma¹, Gaurav Tripathi¹,

Sadam H Bhat¹, Rakhi Maiwall², Shvetank Sharma¹, Shiv Kumar Sarin².
¹Institute of Liver and Biliary Sciences, Molecular and Cellular Medicine, New Delhi, India; ²Institute of Liver and Biliary Sciences, Hepatology, New Delhi, India
Email: jassi2param@gmail.com

Background and aims: Acute liver failure (ALF) has high mortality and corresponds to changes in plasma albumin levels and functions. Whether the bio-molecular analysis of albumin could identify signatures of the severity of the hepatic injury and early mortality in ALF is unknown.

Method: A total of 225 subjects (200 ALF and 25 healthy controls) were enrolled in the study protocol. Albumin was purified and analysed in the training cohort (ALF Non-Survivors; n=32, ALF-survivors; n=8 and Healthy Controls; n=5) for modification, functionality, and bounded multi-omics signatures (Proteins, Lipids, Metabolites, and bacterial peptides) followed by validation in a test cohort of 160 ALF patients using machine learning (ML) approach.

Results: Albumin oxidative state, plasma oxidation, and glycosylation were higher in ALF, specifically in ALF-non-survivors (p<0.05). Purified albumin from non-survivors showed significant multi-omics alterations as indicated by multivariate Partial least squares-discriminant analysis (PLS-DA) and alpha/beta-diversity indices (p<0.05). Albumin bio-molecular profile of non-survivors showed a significant (p<0.05) increase in bound biomolecules linked to inflammation, Advance Glycation End-products (AGE) signaling, amino-acid (arginine, proline) metabolism, bile acids, mitochondria breakdown (carnitines and beta-oxidation) and bacterial peptides of phylum Proteobacteria, Firmicutes, Verrucomicrobia, and others. Increased bacterial taxa (Listeria, Clostridium, and others) functionality correlated with serum Triglyceride; TG (4:0/12:0/12:0), Phosphatidylserine; PS (39:0) and metabolites (Porphobilinogen, Nicotinic Acid, and others) in non-survivors (R²>0.7, p<0.05). Multiomics signature-based probability of detection (POD) for non-

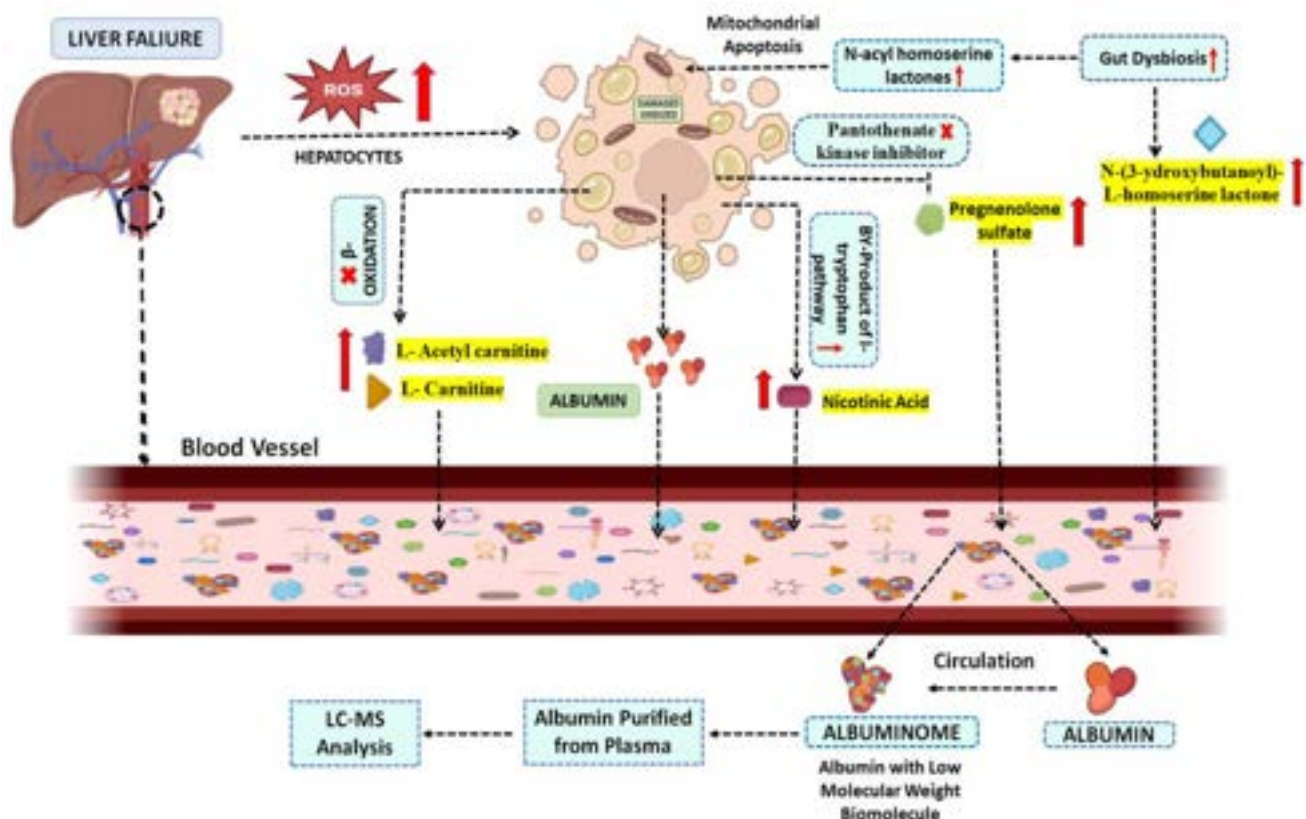


Figure: (abstract: OS-107-YI): Albumin-bounded Biomolecule shows ongoing mitochondrial failure and hyperinflammation state in ALF Patients

ORAL PRESENTATIONS

survival in ALF was >90% and correlated with albumin functionality and clinical parameters ($R^2 > 0.85$). POD metabolites showed diagnostic efficiency of 98% (AUC = 0.98 [0.95–1.0]) for early mortality prediction in ALF ($p < 0.05$). Specific increase in binding of L-acetylcarnitine, L-carnitine, N-(3-hydroxybutanoyl)-L-homoserine lactone (linked to mitochondrial failure), nicotinic acid (a by-product of tryptophan metabolism) and pregnenolone lactone (a pantothenate kinase inhibitor) to albumin were seen in non-survivors. It was validated using five machine learning algorithms in test cohort 1 (plasma and paired one drop blood) and showed >98% accuracy for early mortality prediction.

Conclusion: Albumin bio-molecular composition is hyperoxidized and deranged in ALF patients. Novel albuminome signatures can segregate ALF patients who are likely to have early mortality or require emergency liver transplantation.

OS-108-YI

Investigating the PD-1/PD-L pathway and macrophage responses in acute-on-chronic liver failure

Dimitrios Patseas¹, Eoin Mitchell¹, Emilio Flint², Tong Liu¹, Sujit Mukherjee¹, Lucia Possamai¹, Mark J W McPhail³, Christine Bernsmeier², Evangelos Triantafyllou¹. ¹Imperial College London, Department of Metabolism, Digestion and Reproduction, London, United Kingdom; ²University of Basel, Department of Biomedicine, Basel, Switzerland; ³King's College London, Department of Inflammation Biology, London, United Kingdom
Email: e.triantafyllou@imperial.ac.uk

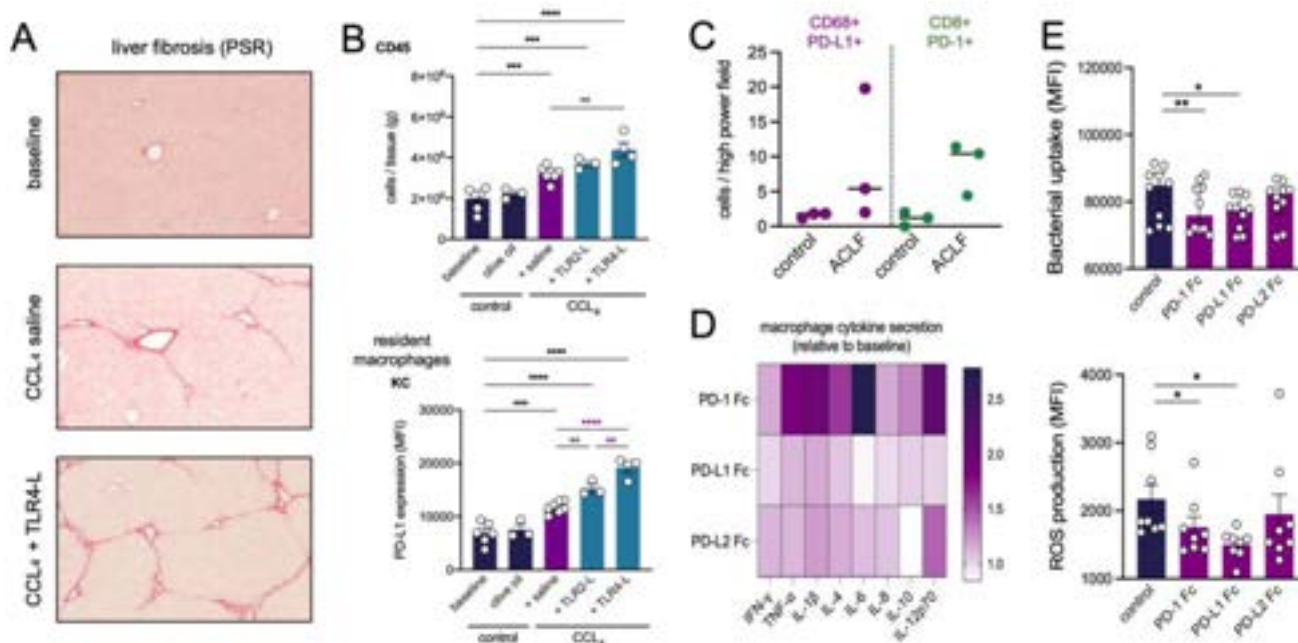
Background and aims: Macrophage dysfunction and bacterial infections are common in acute-on-chronic liver failure (ACLF) and contribute to mortality. PD-1/PD-L related adaptive immune dysfunction has been documented in alcoholic hepatitis, HBV/HCV infection, and anti-PD-1 (L1) therapy is approved for HCC. We also found that PD-1/PD-L axis impaired macrophage antimicrobial responses in murine acute liver injury. However which inflammatory cues trigger this axis' upregulation, and how it modulates

macrophage function, remain unknown. We explored this using human tissue samples, cell culture, and in vivo models.

Method: WT male mice were intraperitoneally (i.p.) treated with CCl₄ (0.4 ml/kg), twice-weekly for 6 weeks, and then were i.p. dosed with saline, TLR2-L (Pam3CSK4; 20 ug) or TLR4-L (LPS; 100 ug) ligand for 24 h before culling. FFPE murine liver tissue was histologically examined, and phenotyping of myeloid cells was performed by flow cytometry. Liver tissue sections of ACLF patients and pathological controls were imaged using multiplex immunofluorescent (mIF) staining. Effects of TLR-ligand (TLR-L) 24 h treatment on human monocyte-derived macrophage (MoMF) PD-L1 were assessed by flow cytometry. In additional experiments, MoMF were primed for 24 h with TLR4-L (100 ng/ml; LPS) and then treated for 24 h with Ig control, PD-1, PD-L1 or PD-L2 Fc proteins (5 ug/ml) to activate the PD-1/PD-L axis. Macrophage *E. coli* pHrodo uptake, ROS production, and cytokine secretion levels were assessed by flow cytometry and Meso Scale Discovery kit.

Results: We found that TLR4-L, TLR5-L and TLR9-L (but not TLR2, TLR3, or TLR7-L) agonism upregulated PD-L1 expression on human MoMF [TLR4: 38,054 vs TLR5: 43,120 vs TLR9: 32,806 vs CTRL: 9,048; (MFI), all $p < 0.05$]. Also, our in vivo analyses revealed that TLR4-L (LPS) treated CCl₄ mice were characterized by increased liver inflammation and Kupffer cell (Fig. A–B) or MoMF (not shown) PD-L1 levels, in comparison with TLR2-L and saline treated CCl₄ mice (Fig. A–B). Human liver tissue mIF showed that ACLF patients had higher numbers of CD68+ PD-L1+ macrophages and CD8+ PD-1+ cells (Fig. C). We found that PD-1 axis' agonism on human LPS-primed MoMF with PD-1 or PD-L1 proteins (but not PD-L2) resulted in altered pro-inflammatory cytokine secretion (Fig. D) and reduced bacterial uptake and ROS production (Fig. E).

Conclusion: Our findings show that macrophage PD-L1 is differentially induced by microbial toxins (TLR-L) such as LPS, both in vitro and in experimental liver fibrosis and ACLF. Mechanistically, we found that PD-1 axis' activation on LPS-primed macrophages causes negative "back-signaling" by reducing their bactericidal functions.



(A–B) MOUSE MODELS OF FIBROSIS & ACLF. AFTER 6-WEEK I.P. CCl₄ (0.4 U/L) TREATMENT, WT MICE RECEIVED I.P. SALINE OR TLR2-L OR TLR4-L 24h BEFORE CULL. (A) REPRESENTATIVE HISTOLOGICAL STAINS. (B) NUMBER OF CD45+ LIVER CELLS & KUPFFER CELL PD-L1 EXPRESSION. (C) DATA SHOW CD68+ PD-L1+ AND CD8+ PD-1+ CELLS IN HUMAN ACLF & CONTROLS. (D–E) KC MONOCYTE-DERIVED MACROPHAGES (7 DAYS) WERE TREATED FOR 24h WITH RECOMBINANT Ig Fc CONTROL OR PD-1 Fc OR PD-L1 Fc OR PD-L2 Fc PROTEIN (5 UG/ML) TO ACTIVATE THE PD-1 PATHWAY. CELL BACTERIA PHAGOCYTOSIS (PHRODO) AND REACTIVE OXYGEN SPECIES (ROS) PRODUCTION WERE MEASURED BY FLOW CYTOMETRY. CYTOKINE SECRETION WAS MEASURED BY MSD KIT.

Figure: (abstract: OS-108)

Future work will evaluate PD- (L)1 and/or TLR-directed immunomodulatory therapeutic approaches for improving hepatic macrophage antimicrobial responses in ACLF.

OS-109-YI

Neutrophils promote chronic liver injury resolution

Silvia Ariño¹, Laura Sererols-Viñas¹, Beatriz Aguilar-Bravo¹, Raquel A Martínez-García de la Torre¹, Iván Ballesteros², Andrea Rubio-Ponce², Daniela Cerezo-Wallis³, Alex Guillaumon¹, Juanjo Lozano⁴, Andrés Hidalgo^{2,3}, Pau Sancho-Bru^{1,4}. ¹*Institut d'Investigacions Biomèdiques August Pi Sunyer (IDIBAPS), Spain;* ²*National Center for Cardiovascular Research Carlos III, Spain;* ³*Yale University School of Medicine, United States;* ⁴*Centro de Investigación Biomédica en Red de enfermedades hepáticas y digestivas (CIBERehd), Spain*
Email: sarinom@recerca.clinic.cat

Background and aims: Advanced chronic liver injury is characterized by the loss of hepatocyte function, fibrosis accumulation, ductular reaction expansion and neutrophil recruitment. Previous results from our group have shown that neutrophils participate in chronic liver injury progression. However, neutrophils' contribution to chronic liver damage repair remains elusive. Therefore, the aim of the present study is to investigate the role of neutrophils in chronic liver injury resolution and regeneration.

Method: Injury regression was evaluated by immunohistochemistry and serum transaminase levels in a mouse model treated for 3 weeks with DDC diet which was followed by resolution periods of 1, 3 or 5 days of standard diet administration. To investigate neutrophils' role, neutrophils were depleted using a transgenic mouse in which the diphtheria toxin receptor is expressed under the neutrophil specific promoter Mrp8. Depletion impact was evaluated during 5 days of regression by immunohistochemistry and gene expression. Finally, we performed bulk-sequencing analysis of isolated neutrophils from healthy liver, injured liver after 3 weeks of DDC and injury resolution after 3 days of regression.

Results: We observed an imminent decrease of transaminase levels after 24 hours of DDC diet withdrawal. At histological level, hepatocyte proliferative peak was achieved at 3 days of resolution. However, a significant decrease of neutrophils and ductular reaction and fibrosis regression were not observed until day 5 of resolution. The specific depletion of neutrophils during a 5-days resolution period showed a reduced ductular reaction and fibrosis regression. Moreover, there was a lower number of proliferative hepatocytes in the neutropenic model, suggesting the participation of neutrophils in hepatocyte regeneration in the context of injury resolution. Finally, neutrophil sequencing analysis showed that liver neutrophils from injury resolution recover the expression of pathways related to interferon type I, apoptosis and autophagy, which were lost in DDC liver-injured neutrophils. Moreover, liver neutrophils from injury resolution were enriched in pathways related to LPS-response, cell migration and mitogenic factors (IL6 and TNFα) secretion when compared to healthy and DDC liver neutrophils.

Conclusion: Our study shows the participation of neutrophils in chronic liver injury resolution. Moreover, our data indicate that neutrophils are a plastic cell population and suggest their capacity to acquire a pro-resolutive phenotype and to promote liver regeneration.

NAFLD: Experimental

OS-110

Spatial proteotranscriptomics identifies macrophage heterogeneity in patients with at-risk non-alcoholic steatohepatitis

Dina Tiniakos^{1,2}, Asier Antoranz-Martinez³, Trieu My Van⁴, Daniel Newhouse⁴, James Clark¹, Ann K Daly¹, Tania Roskams³, Quentin Anstee^{1,5}, Olivier Govaere^{1,3}. ¹*Newcastle University, Translational and Clinical Research Institute, Faculty of Medical Sciences, United Kingdom;* ²*National and Kapodistrian University of Athens, Dept of Pathology, Aretaieio Hospital, Greece;* ³*KU Leuven and University Hospitals Leuven, Department of Imaging and Pathology, Translational Cell and Tissue Research, Belgium;* ⁴*NanoString Technologies, United States;* ⁵*Newcastle upon Tyne Hospitals NHS Trust, Newcastle NIHR Biomedical Research Centre, United Kingdom*
Email: olivier.govaere@kuleuven.be

Background and aims: Patients with "at-risk" NASH (NAS $\geq 4 + F \geq 2$) are a key recruitment group for drug trials as they are more likely to progress to cirrhosis. Besides lobular inflammation and hepatocellular ballooning at an advanced fibrosis stage, the biopsies of these patients often exhibit lipogranuloma and monocyte-derived macrophages infiltration in the portal tract. The dynamics between the response of Kupffer cells to parenchymal damage and the influx of circulating immune cells, are still poorly understood. In this study, we aimed to resolve the spatial heterogeneity of the macrophage population in at-risk NASH and their relationship to histopathological features.

Method: GeoMx Human Whole Transcriptome Atlas profiling was performed on 8 biopsies from patients with NASH fibrosis stage 3. Regions of interest were selected based on (1) the presence of portal inflammatory infiltration, (2) steatosis with lobular inflammation and/or lipogranulomas, and (3) parenchyma without steatosis. Fluorescent CD68, CD45 and pan-keratin markers were used to segment the different macrophage, immune cell and epithelial cell populations from each region. A total of 80 segments were processed for high throughput RNA sequencing. The clinical relevance of the identified differentially expressed genes were explored in extant bulk RNA sequencing data from 206 NAFLD patients. Key targets were validated on protein level using the Multiple Iterative Labelling by Antibody Neodeposition method. All samples were scored by an expert liver pathologist according to the semi-quantitative NASH-CRN Scoring System.

Results: Comparison of parenchymal steatohepatitis-associated (SH-) macrophages with portal (PT-) macrophages and Kupffer cells from parenchyma without steatosis identified 352 and 218 differentially expressed genes respectively. PT-macrophages displayed a typical immature/monocyte phenotype, lacking the expression of scavenger receptors (*MSR1*, *CD36*, *CD163*), and expressing lymphocyte-regulatory genes (*CCL19*, *CCL21*, *CD48*, *IL7R*, *CCL5*). Compared to Kupffer cells in areas without steatosis, SH-macrophages showed features of both monocytes (high expression of *LSP1*, glycoprotein NMB and lysozyme) and mature macrophages (high *MSR1* expression). In addition, SH-macrophages displayed an increase in metabolic- and phagocytosis-related genes. Exploring the clinical relevance of key markers in bulk RNASeq data showed that *CCL19* expression was linearly correlated with the fibrosis stage, lobular inflammation and hepatocyte ballooning scores, but not with the steatosis grade. In contrast, *GNMB* and lysozyme mRNA expression reflected predominantly NASH activity, as it was significantly associated with steatosis, lobular inflammation and hepatocyte ballooning scores, but not with fibrosis. At the protein level, *GNMB*-positive macrophages were observed in steatotic areas with active inflammation and lipogranulomas.

ORAL PRESENTATIONS

Conclusion: This study identified a steatohepatitis-associated macrophage subpopulation in patients with at-risk NASH, with unique characteristics compared to portal macrophages and Kupffer cells from non-steatotic liver parenchyma highlighting macrophage heterogeneity. Furthermore, we showed the clinical relevance of steatohepatitis-associated macrophages in the grading and staging of the NAFLD spectrum.

OS-111

Intestinal Angptl4 perturbs gut barrier function in NAFLD

Damien Chua¹, Hong Sheng Cheng¹, Nguan Soon Tan^{1,2}. ¹Lee Kong Chian School of Medicine, Singapore, Singapore; ²Nanyang Technological University, Singapore, School of Biological Sciences, Singapore
Email: NSTAN@ntu.edu.sg

Background and aims: The disruption of the gut-liver axis, which involves a complex interplay of intestinal and hepatic processes, contributes to the onset and progression of liver diseases. The gut barrier functions are compromised in NAFLD patients, which increases the exposure of the liver to pathogen-mediated microbial patterns and microbial-derived metabolites. The identification of the elements of the gut-liver axis primarily damaged in NAFLD offers possibilities for intervention. Early studies have implicated angiotensin-like 4 protein (Angptl4) as a potential link between gut microbiota and adiposity. However, the role of intestinal Angptl4 in the gut-liver axis is poorly understood. Here, we examined the role of intestinal Angptl4 as a prime pathological player of gut-liver axis in NAFLD.

Method: We developed a human-relevant diet-induced NAFLD mouse model based on thermoneutral housing, LIDPAD (Liver Disease Progression Aggravation Diet) and a control diet of defined ingredients. Intestinal epithelium-specific Angptl4 deleted (Angptl4^{int/-}) mice were fed NASH-inducing LIDPAD and control diet. Liver histology and CellROX were performed to assess the liver damage and oxidative stress. RNA-seq of liver and intestinal epithelium and gene ontology analyses were performed. Liver histology and CellROX were performed to assess the liver damage and oxidative stress. Gut permeability was assessed using a FITC-dextran permeability assay and qPCR of tight junction proteins. Whole-mount immunofluorescence imaging was performed to reveal alteration in the spatial distribution of the intestinal structure and vasculature.

Results: Angptl4^{int/int} mice developed hepatic steatosis at 1–4 weeks of LIDPAD that progressed to NASH by 8–12 weeks. Fibrosis was prevalent in 90% of LIDPAD-fed Angptl4^{int/int} mice from 12 weeks onwards. Hepatic transcriptomic and gene ontology analyses to identify early events that underpin NAFLD onset revealed acute-phase response and hepatic response to LPS between weeks 1–4. Functional hepatic analysis revealed increased hepatocyte oxidative stress and lipid peroxidation in the liver as early as 2 weeks after diet feeding, before the presentation of NASH. Consistently, Angptl4^{int/-} mice had reduced gut permeability and hepatic oxidative stress damages compared with Angptl4^{int/int} mice. Furthermore, LIDPAD-fed Angptl4^{int/int} mice gained more body weight with larger liver and epididymal adipose tissue than Angptl4^{int/-} mice.

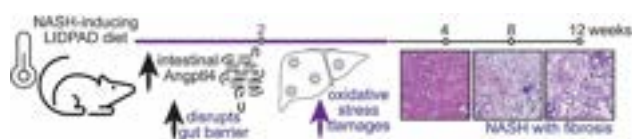


Figure:

Conclusion: Our observations suggest an integral role for intestinal Angptl4 in regulating gut barrier functions associated with early diet-induced liver injury and adiposity associated with diet-induced NAFLD.

OS-112

The transcriptional function of TCF7L2 is spatially restricted in liver and regulates zoned metabolic pathways that contribute to NAFLD

Irisilla Ayala¹, Skanda Hebbale¹, Christopher Shannon², Ivan Valdez³, Luis Cruz-Moreno¹, Terry Bakewell¹, Marcel Fourcaudot¹, Sami Heikkinen⁴, Luke Norton¹. ¹University of Texas Health San Antonio (UTHSA), United States; ²University College Dublin, Ireland; ³University of Texas Southwestern Medical Center (UTSW), United States; ⁴University of Eastern Finland, Finland
Email: nortonl@uthscsa.edu

Background and aims: The prevalence of non-alcoholic fatty liver disease (NAFLD) is 40–80% in people with Type 2 Diabetes (T2D). Single nucleotide polymorphisms in the transcription factor 7-like 2 (TCF7L2) gene are significantly associated with T2D, but the metabolic function of TCF7L2 remains to be fully elucidated. TCF7L2 is a transcriptional effector of the WNT/beta-catenin signaling pathway, and we previously demonstrated that it regulates key zonally expressed metabolic genes in hepatocytes. Here we investigated the spatial transcriptional role of TCF7L2 in mouse liver using multimodal single nuclei genomics, and determined the impact of TCF7L2 transcriptional inactivation on zoned metabolic pathways and the development of severe NAFLD.

Method: Using single nuclei RNA-Seq and ATAC-Seq, we examined the spatial expression and DNA binding activity of TCF7L2 across the mouse liver lobule. We visualized TCF7L2 transcriptional activity in liver using TCF/Wnt signaling reporter mice, which express eGFP downstream of the conserved TCF/LEF DNA binding site. The transcriptional activity of TCF7L2 was ablated in liver by breeding mice with a floxed Tcf7l2 exon 11, which encodes part of the DNA binding domain (DBD), to albumin-Cre mice to create liver specific TCF7L2 mutant mice (Hep-TCF7L2^{DBD}). The impact of TCF7L2 inactivation on the development of fibrosis in NAFLD was investigated in Hep-TCF7L2^{DBD} mice fed a choline-deficient amino acid-defined high fat (CDAHFD) diet for 8-weeks. In liver samples harvested from these mice, we examined the disruption to zoned metabolic pathways including cholesterol, bile and glutamine/glutamate metabolism.

Results: Our multimodal single nuclei methodology reliably isolated distinct hepatocyte populations in mouse liver. We found that the expression of Tcf7l2 mRNA was ubiquitous across the liver lobule, but that the presence of the consensus TCF/LEF DNA binding motif in ATAC peaks was significantly enriched in zone 3 pericentral hepatocytes. Consistent with this, immunofluorescence analysis of TCF/Wnt reporter mice revealed GFP staining that was highly restricted to zone 3 hepatocytes. In Hep-TCF7L2^{DBD} mice, the expression of zone 3 marker genes was abolished, and was associated with disruptions to cholesterol and bile acid metabolism, and glutamine/glutamate homeostasis. Following the CDAHFD, Hep-TCF7L2^{DBD} mice developed more severe fibrosis, and expressed elevated levels of genes involved in fibrogenesis, collagen synthesis and TGF-beta signaling.

Conclusion: Our findings suggest that under normal conditions, TCF7L2 activity is spatially regulated in mouse liver, and that its transcriptional activity is required for pericentral hepatocyte function. We also demonstrate that disrupted pericentral zonation may contribute to the development of severe NAFLD by interfering with several zoned metabolic pathways.

OS-113

Macrophage-derived osteopontin protects from non-alcoholic steatohepatitis

Hui Han¹, Xiaodong Ge¹, Sukanta Das¹, Romain Desert¹, Zhuolun Song¹, Dipti Athavale¹, Wei Chen¹, Sai Komakula¹, Daniel Lantvit¹, Grace Guzman¹, Natalia Nieto¹. ¹University of Illinois at Chicago, Pathology, Chicago, United States
Email: nnieto@uic.edu

Background and aims: Osteopontin (OPN, encoded by the *SPP1* gene) is an immunomodulatory protein involved in chronic liver disease. The expression of OPN in macrophages (MFs) from healthy liver is relatively low; however, it markedly increases in non-alcoholic steatohepatitis (NASH). Our aim was to determine whether MF-derived OPN is protective or pathogenic in NASH.

Method: *Spp1* knock-in and knock-out mice in myeloid cells (*Spp1*^{KI Mye} and *Spp1*^{ΔMye}) and liver MFs (*Spp1*^{KI MF}) were generated. Mice were fed a NASH-inducing or an isocaloric control diet for 6 months. Livers were pathologically evaluated by HandE staining and immunohistochemistry. RNA-seq, lipidomics and metabolomics analyses were done in total liver. MFs were isolated and RNA-seq was performed. Fatty acid metabolism was analyzed with the Seahorse. The crosstalk between MFs and hepatocytes (HEPs) was studied using a co-culture system.

Results: Both genders of *Spp1*^{KI Mye} mice were fully protected from NASH. The NASH activity score, liver triglycerides (TGs) and cholesterol were significantly decreased in *Spp1*^{KI Mye} compared to control and *Spp1*^{ΔMye} mice. The latter presented the worst phenotype. *Spp1*^{KI MF} recapitulated the protection achieved in *Spp1*^{KI Mye} mice. Metabolomics and lipidomics analyses revealed that livers from *Spp1*^{KI Mye} mice showed less saturated fatty acid-containing TGs, which correlated with up-regulation of urea cycle metabolites. Gene expression enrichment analysis revealed that mitochondrial arginase-2 (*Arg2*) but not cytosolic arginase-1 (*Arg1*), was up-regulated mainly in HEPs from *Spp1*^{KI Mye} mice. The increase in ARG2 was associated with higher NAD⁺/NADH ratio and ATP levels in total liver. HEPs from *Spp1*^{KI Mye} showed higher mitochondrial respiration and fatty acid oxidation (FAO), which were reduced by ablation of *Arg2* in HEPs. Transcriptomics and gene network analyses revealed that Oncostatin-M (OSM) was induced in *Spp1*^{KI Mye} MFs regardless of diet. Treatment of HEPs with OSM induced *Arg2* and FAO while they were blocked by co-treatment with a STAT3 inhibitor.

Conclusion: MF-derived OPN protects from diet-induced NASH in mice. The ARG2-mediated increase in mitochondrial respiration and FAO is responsible for the protective effect. OSM induced in MFs from *Spp1*^{KI Mye} mice up-regulates ARG2 in HEPs through STAT3. Future work will focus on delineating how OPN induces OSM in MFs.

OS-114-YI

Dissecting NAFLD pathomechanisms using primary mouse liver and blood cells in a microfluidic perfusable compartmentalized liver-on-a-chip model

Hanyang Liu¹, Marlene Kohlhepp¹, Guo Yin¹, Jana Hundertmark¹, Felix Heymann¹, Kehinde Aina², Alexander Mosig², Frank Tacke¹, Adrien Guillot¹. ¹Charité Universitätsmedizin Berlin, Department of

Hepatology and Gastroenterology, Berlin, Germany; ²University Hospital Jena, Center for Sepsis Control and Care and Institute of Biochemistry II, Jena, Germany

Email: hanyang.liu@charite.de

Background and aims: Non-alcoholic fatty liver disease (NAFLD) is a chronic liver condition defined by lipid accumulation in liver parenchymal cells (steatosis) associated with varying degrees of lipotoxicity, hepatocellular injury, inflammation and fibrosis. The liver sinusoids are lined by liver sinusoidal endothelial cells (LSECs) and represent the interface between circulating blood and liver resident macrophages (Kupffer cells, KCs) on one hand, liver epithelial cells (mainly hepatocytes) and hepatic stellate cells (HSCs) on the other hand. Thus, the liver sinusoid microenvironment includes all cellular players involved in NAFLD pathogenesis. Current in-vivo mouse NAFLD models present ethical challenges, and traditional in-vitro approaches cannot recapitulate the complex cellular interplay and the involvement of circulating cells. In this project, we aim at establishing and testing a primary cell biochip-based liver sinusoid model for the study of NAFLD driving mechanisms.

Method: Our liver-on-chip model consists of two distinct seeding chambers separated by a porous membrane. A microfluidic system can differentially perfuse both chambers. Primary mouse hepatocytes, HSCs, KCs and LSECs are isolated from fresh liver tissues, while peripheral blood mononuclear cells (PBMCs) were isolated from the vena cava of the same animal. Free fatty acids (palmitic and oleic acids) were used to induce hepatic steatosis. Lipid deposition, cellular lipotoxicity and inflammation were evaluated by lipid droplet and live/dead immunostaining, or immune cell tracking and flow cytometry. NAFLD-relevant markers were measured by qRT-PCR. The pan-PPAR agonist lanifibranor was used to test the relevance of our model for therapeutic agent testing. Acetaminophen (paracetamol) was used as a model of acute drug-induced injury.

Results: Five cell types were successfully isolated from mouse livers, and seeded in the biochip system, followed by PBMC perfusion for 48 hours. We found that FFA stimulation resulted in hepatocellular lipid deposition, cell injury and immune cell mobilization, as well as the induction of NAFLD-associated inflammatory cytokines. Lanifibranor treatment attenuated the FFA-induced observations. Similarly, acetaminophen induced acute hepatocyte injury and immune cell activation.

Conclusion: Our data demonstrate the relevance of the liver-on-chip model to study NAFLD and acute liver injury, suggesting that it is an innovative tool for functional and molecular studies.

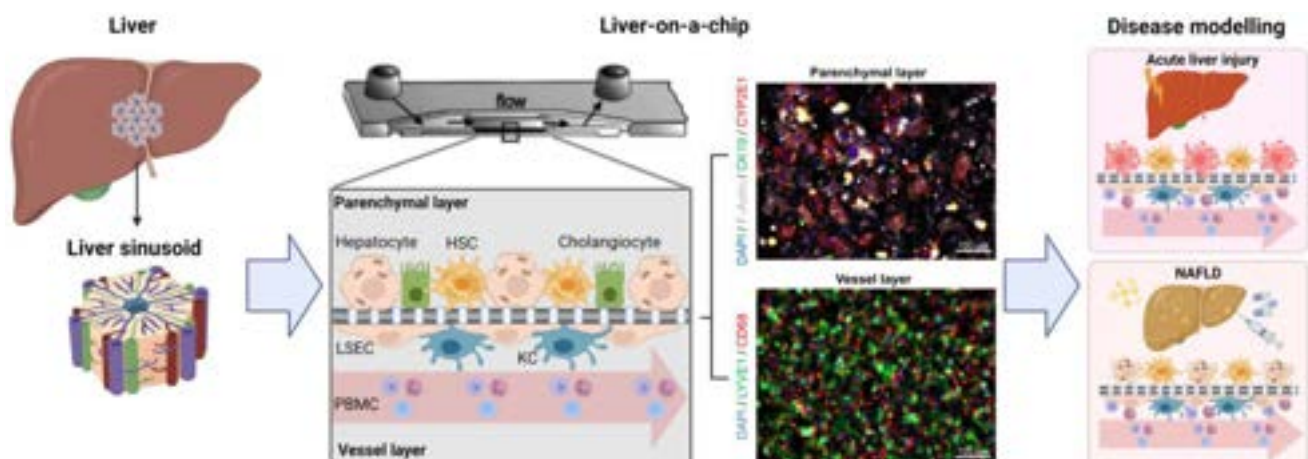


Figure: (abstract: OS-114-YI)

Public Health - Except viral hepatitis

OS-115-YI

Who is safe from chronic liver disease? A population-based approach for early detection in the US

Nakia Chung¹, Ajitha Mannalithara¹, Vivek Charu¹, W. Ray Kim¹.

¹Stanford University School of Medicine, Stanford, United States

Email: wrkim@stanford.edu

Abstract OS-115-YI is under embargo until Saturday 24 June 2023, 14:00. This abstract will be made publicly available on the congress website at 14:00 (CEST) on the day of its presentation at the congress. Industry must not issue press releases – even under embargo – covering the data contained in abstracts selected to be highlighted during official EASL Press Office activities or in official EASL Press Office materials until the individual embargo for each data set lifts. Media must not issue coverage of the data contained in abstracts selected to be highlighted during official EASL Press Office activities or in official EASL Press Office materials until the individual embargo for each data set lifts.

Journalists, industry, investigators and/or study sponsors must abide by the embargo times set by EASL. Violation of the embargo will be taken seriously. Individuals and/or sponsors who violate EASL's embargo policy may face sanctions relating to current and future abstract submissions, presentations and visibility at EASL Congresses. The EASL Governing Board is at liberty to ban attendance and/or retract data.

Copyright for abstracts (both oral and poster) on the website and as made available during The International Liver Congress™ 2023 resides with the respective authors. No reproduction, re-use or transcription for any commercial purpose or use of the content is permitted without the written permission of the authors. Permission for re-use must be obtained directly from the authors.

OS-116-YI

Increased risk of hepatocellular carcinoma among first-degree relatives of patients with biopsy-proven NAFLD – a multigenerational nationwide cohort study

Fahim Ebrahimi^{1,2}, Tracey Simon³, Hannes Hagström⁴, Jiangwei Sun¹, David Bergman¹, Bjorn Roelstraete¹, Jonas Ludvigsson^{1,5,6}. ¹Karolinska Institutet, Department of Medical Epidemiology and Biostatistics (MEB), Stockholm, Sweden; ²Clarunis-University Center for Gastrointestinal and Liver Diseases Basel, Gastroenterology and Hepatology, Basel, Switzerland; ³Harvard Medical School, Gastroenterology and Hepatology, Boston, United States; ⁴Karolinska University Hospital, Division of Hepatology, Stockholm, Sweden; ⁵Örebro University Hospital, Department of Pediatrics, Örebro, Sweden; ⁶Columbia University, Department of Medicine, New York, United States

Email: f.ebrahimi@outlook.com

Background and aims: Non-alcoholic fatty liver disease (NAFLD) is the fastest growing cause of hepatocellular carcinoma (HCC). First-degree relatives (FDR) of patients with NAFLD are at substantially increased risk to develop NAFLD themselves, however little is known about their risk for HCC.

Method: We conducted a nationwide, population-based cohort study including all Swedish adults with biopsy-proven NAFLD in Sweden 1966–2017 (n = 11,924), who were matched to ≤5 population controls (n = 56,634) by age, sex, calendar year and county of residence. Leveraging the Swedish Total Population Register, we identified all first-degree relatives (fathers, mothers, siblings, offspring) (n = 48,032) and spouses (n = 9,406) of patients with NAFLD and of controls (n = 248,463; and n = 47,718 respectively). All first-degree relatives and spouses were followed from the time of NAFLD diagnosis or matching in their relative or from 18 years of age, whichever occurred last. We used Cox proportional hazards model to calculate multivariable adjusted HRs (aHRs) and 95% confidence intervals (CIs) for the risk of incident HCC.

Results: Over a median of 17.2 years, 86 (0.22%) NAFLD FDRs were diagnosed with incident HCC, compared to 285 (0.14%) control FDRs, yielding a significantly increased relative risk (13.0 vs. 8.4/100,000 PY; difference = 4.6/100,000 PY; aHR = 1.74, 95% CI = 1.32 to 2.28). The excess risk for HCC did not differ across generations: parents (36.9/100,000 PY, aHR = 2.01, 95% CI = 1.24 to 3.26), siblings (15.9/100,000 PY, aHR = 1.73, 95% CI = 1.04 to 2.88), offspring (5.3/100,000 PY, aHR = 1.46, 95% CI = 0.84 to 2.56). The risk was highest among FDRs of NAFLD patients with histological confirmation of fibrosis or cirrhosis (aHR = 2.77, 95% CI = 1.50 to 5.14) when compared to FDR of those with simple steatosis or NASH without fibrosis (aHR = 1.56, 95% CI = 1.15 to 2.12). There was no difference in HCC risk between NAFLD spouses and control spouses (17.9 vs. 14.4/100,000 PY, aHR = 1.30, 95% CI = 0.80 to 2.12).

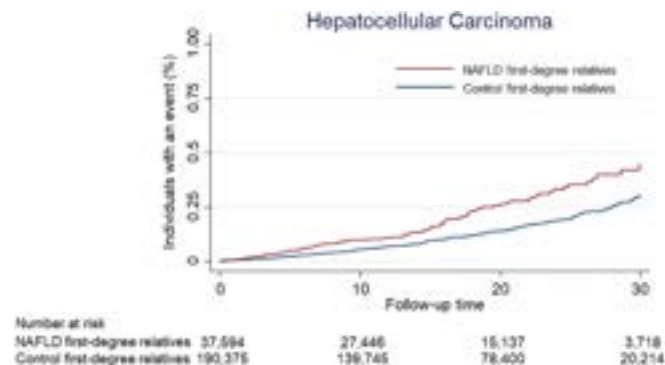


Figure:

Conclusion: First-degree relatives of patients with NAFLD, but not patient spouses were at increased risk of HCC, indicating that shared biological or early environmental factors might contribute to these elevated risks. Screening for risk factors of HCC-such as underlying NAFLD-might be considered in first-degree relatives of patients with NAFLD, especially when the patient already has signs of fibrosis or cirrhosis.

OS-117

Socioeconomic disparities and primary liver cancer incidence between 2006 and 2016: analyze by subtypes, a French population-based study

Nga Nguyen¹, Bertille Comoz¹, Joséphine Bryere², Anne-Marie Bouvier³, Jean Baptiste Nousbaum⁴, Guy Launoy², Veronique Bouvier², Isabelle Ollivier-Hourmand¹. ¹CHU de Caen, Calvados, Caen, France; ²Centre Francois Baclesse, Calvados, Caen, France; ³INSERM UMR 1231, France; ⁴CHU de Brest, France
Email: bertille.comoz@hotmail.fr

Background and aims: Hepatocellular carcinoma (HCC) and intrahepatic cholangiocarcinoma (iCCA) are the two most frequent histological subtypes of primary liver cancer (PLC). Despite different risk factors, these two types of cancer are often pooled in most epidemiological studies, as they are coded in databases under the common code C22 according to the ICD-O-3 classification. The aim of this study was to measure the association of socio-economic disparities on the incidence of these two subtypes of PLC.

Method: Data provided from FRANCIM the French cancer registry network, which covers 20% of the French territory, between 2006 and 2016. HCC was defined by topographic code C22.0 and morphological codes 8000, 8001 and 8170-8175. iCCA was defined by topographic code C22.1 and morphological codes 8000, 8001, 8050, 8140-8141, 8160-8161, 8260, 8440, 8480-8500 and 8570-8572. Each patient's address was geolocalized and assigned to an IRIS, the smallest geographic unit in France. The socio-economic environment was assessed by the European deprivation index (EDI). The EDI based on the 2011 national census was used for each IRIS. Crude and standardized Incidence rates with 95% confidence intervals (CI) were estimated as the number of newly diagnosed cancer cases per 100,000 inhabitants. These were given for each IRIS, sex and age group using a 15-year increment: 15-29, 30-44, 45-59, 60-74, 75 and over. Incidence rates by national quintiles were calculated, with quintile 1 (Q1) characterizing the most affluent areas and quintile 5 (Q5) characterizing the most deprived areas. A Poisson regression by subtypes was performed to model the impact of deprivation on the incidence of HCC and iCCA separately, using the continuous EDI.

Results: Between 2006 and 2016, the study population included 22 249 cases of PLC: 17 732 men and 4 517 women, over the period. HCC accounts for 79.64% of PLC with a male/female ratio of 5.6 and a mean age at diagnosis of 69 years. iCCA accounts for 16.97% of PLC with a male/female ratio of 1.44 and a mean age at diagnosis of 71 years. The overall age- and sex-standardised incidence rates were 11.46 per 100 000 person-years for HCC and 2.39 per 100 000 person-years for iCCA.

There was an over incidence rate of HCC in quintiles 2, 3, 4, and 5 compared to quintile 1: Q1 10.28 [9.9-10.66] per 100 000 person-year, Q2 11.43 [10.48-12.47] ($p < 0.0001$), Q3 11.81 [10.82-12.89] ($p < 0.0001$), Q4 12.26 [11.25-13.37] ($p < 0.001$), Q5 11.53 [10.57-12.57] ($p < 0.0001$). By contrast there was no difference for iCCA: Q1 2.25 [2.08-2.43] per 100 000 person-year, Q2 2.37 [1.96-2.85] ($p 0.3614$), Q3 2.44 [2.02-2.95] ($p 0.1422$), Q4 2.50 [2.07-3.00] ($p 0.06$), Q5 2.40 [1.99-2.89] ($p 0.2506$).

Using Poisson regression and analysis of the $\beta 1$ coefficient, a significant association was found between the deprivation and the risk of HCC (positive and significant $\beta 1$ coefficients) for both men and women. By contrast, there was no significant association between environment and the risk of iCCA (Table 1).

Table 1. Socioeconomic disparities in liver cancer incidences in French registries between 2006 and 2016 by subtypes.

	Estimated EDI coefficient, $\beta 1$	CI [95%]	P-value	Exp ($\beta 1$)
PLC				
Total	0.0112	[0.0079-0.0144]	<.0001	1.01
Men	0.0053	[0.0016-0.0090]	0.0054	1.01
Women	0.0133	[0.0062-0.0204]	0.0002	1.01
HCC				
Total	0.0121	[0.0085-0.0157]	<.0001	1.01
Men	0.0064	[0.0024-0.0104]	0.0018	1.01
Women	0.0150	[0.0062-0.0239]	0.0009	1.02
iCCA				
Total	0.0015	[-0.0072-0.0102]	0.7407	
Men	0.0054	[-0.0067-0.0175]	0.3823	
Women	-0.0031	[-0.0161-0.0099]	0.6392	

If the $\beta 1$ coefficient is significantly different from the 0 value and positive, there is an increase in cancer risk for the most deprived areas. If $\beta 1$ is significant and negative, the risk of cancer is higher for the deprived areas.

Conclusion: This population-based study showed that HCC account for the vast majority of PLC. Its incidence is lower in most affluent areas, and the risk of HCC is related to socioeconomic disparities, contrary to the risk of iCCA. This reinforces the need to study separately, HCC and iCCA, and to adjust public health measures to each subtype of PLC.

Key words: Epidemiology, cancer registries, socioeconomic inequalities, deprivation index, hepatocellular carcinoma, intrahepatic cholangiocarcinoma.

OS-118

Metabolic dysfunction associated fibrosis-5 (MAF-5) score to identify at-risk liver fibrosis and to predict prognosis in a population-based setting

Laurens van Kleef¹, Sven Francque², Jhon Prieto-Ortiz³, Milan Sonneveld¹, Carlos B Sanchez Luque³, Robin G Prieto-Ortiz³, Wilhelmus Kwanten², Luisa Vonghia², An Verrijken², Christophe De Block², Zouhir Gadi², Harry La Janssen¹, Robert De Knecht¹, Willem Pieter Brouwer¹. ¹Erasmus MC University Medical Centre Rotterdam, Gastroenterology and Hepatology, Netherlands; ²UZA, Gastroenterology and Hepatology, Belgium; ³Center for Liver and Digestive Diseases (CEHYD), Bogota, Colombia
Email: w.p.brouwer@erasmusmc.nl

Background and aims: There is an unmet need for non-invasive tools to improve case-finding and aid primary care professionals in referring patients at high risk of advanced liver disease.

Method: A metabolic dysfunction associated fibrosis (MAF-5) score was developed: an age-independent anthropometric-based non-invasive test, using the NHANES 2017-2020 as training set. Individuals with metabolic dysfunction were selected with complete data on potential score components ($n = 6,333$). Fibrosis was defined as liver stiffness (LSM) ≥ 8.0 kPa. Diagnostic accuracy was evaluated in the entire group and clinically relevant subgroups and compared to the FIB-4, NFS and SAFE. The score was externally validated with LSM ≥ 8.0 kPa in an elderly population with metabolic dysfunction (Rotterdam study, $N = 2,699$), with shear-wave elastography (SWE ≥ 9.3 kPa) and biopsy-proven NAFLD according to METAVIR (Bogota cohort, $N = 231$) and with biopsy-proven NAFLD according to NASH-CRN (Antwerp cohort, $N = 562$). Finally the score was tested for prognostic performance against all-cause mortality in participants from the NHANES III with metabolic dysfunction ($N = 9,679$).

Results: The MAF-5 score comprised waist circumference, BMI, diabetes, AST and platelets. With this score, 60.3% was predicted at low risk (MAF-5 < 0), 14.6% at intermediate risk (MAF-5 0-1) and 25.1% at high risk (MAF-5 > 1) of liver fibrosis. The observed fibrosis prevalence in these groups were 3.6%, 9.3% and 29.1%, respectively. The AUC of the MAF-5 (0.81) was significantly higher than the FIB-4 (0.60), NFS (0.70) and SAFE (0.73). The MAF-5 showed similar performance in detecting LSM ≥ 8 kPa in an elderly population, as

ORAL PRESENTATIONS

well as for SWE ≥ 9.3 kPa. MAF-5 was significantly associated with the presence of liver fibrosis according to both NASH-CRN (median MAF-5 for stages F0F1/F2/F3/F4: 0.8/2.3/3.4/4.2, $p < 0.001$) and METAVIR (median MAF-5 0.66/1.12/2.57/3.5, $p < 0.001$). Finally, MAF-5 score > 1 was associated with increased risk of all-cause mortality in both unadjusted and adjusted models (HR 1.65, 95% 1.51–1.79).

Conclusion: The MAF-5 score is an inexpensive tool to identify individuals with metabolic dysfunction at high risk of liver fibrosis and all-cause mortality in a primary care setting, using only easily obtainable variables. Given the MAF-5 outcompetes other first-line non-invasive tests, it can prevent unnecessary referrals and avoid extra diagnostic expenses.

OS-119-YI

Machine learning models are superior to FIB-4 as a first line stratification tool for liver disease in the community

Huw Purrsell^{1,2}, Mohamed Mostafa³, Lucy Bennett⁴, Richard Hammersley³, Oliver Street², The ID LIVER Consortium², Karen Piper Hanley², Joanne Morling⁴, Manish Patel³, Neil Hanley^{1,2}, Neil Guha⁴, Varinder Athwal^{1,2}. ¹Manchester University NHS Foundation Trust, Manchester, United Kingdom; ²University of Manchester, Faculty of Biology, Medicine and Health, Manchester, United Kingdom; ³Jiva.AI, Cardiff, United Kingdom; ⁴Nottingham University Hospitals NHS Foundation Trust and the University of Nottingham, NIHR Nottingham Biomedical Research Centre, United Kingdom
Email: Huw.Purrsell@mft.nhs.uk

Abstract OS-119-YI is under embargo until Saturday 24 June 2023,

14:00. This abstract will be made publicly available on the congress website at 14:00 (CEST) on the day of its presentation at the congress. Industry must not issue press releases – even under embargo – covering the data contained in abstracts selected to be highlighted during official EASL Press Office activities or in official EASL Press Office materials until the individual embargo for each data set lifts. Media must not issue coverage of the data contained in abstracts selected to be highlighted during official EASL Press Office activities or in official EASL Press Office materials until the individual embargo for each data set lifts.

Journalists, industry, investigators and/or study sponsors must abide by the embargo times set by EASL. Violation of the embargo will be taken seriously. Individuals and/or sponsors who violate EASL's embargo policy may face sanctions relating to current and future abstract submissions, presentations and visibility at EASL Congresses. The EASL Governing Board is at liberty to ban attendance and/or retract data.

Copyright for abstracts (both oral and poster) on the website and as made available during The International Liver Congress™ 2023 resides with the respective authors. No reproduction, re-use or transcription for any commercial purpose or use of the content is permitted without the written permission of the authors. Permission for re-use must be obtained directly from the authors.

Rare liver diseases

OS-120

Fazirsiran reduces liver Z-alpha-1 antitrypsin synthesis, decreases globule burden and improves histological measures of liver disease in adults with alpha-1 antitrypsin deficiency: a randomized placebo-controlled phase 2 study

Virginia Clark^{1,2}, Charlton Strange³, Pavel Strnad⁴, Antonio Sanchez⁵, Paul Yien Kwo⁶, Vítor Magno Pereira⁷, Bart Van Hoek⁸, Igor Barjaktarevic⁹, Angelo Guido Corsico¹⁰, Monica Pons¹¹, Monica Goldklang¹², Meagan Gray¹³, Brooks Kuhn¹⁴, Hugo Vargas¹⁵, John M. Vierling¹⁶, Raj Vuppalaanchi¹⁷, Mark Brantly¹, Naomi Kappe⁸, Ting Chang¹⁸, Thomas Schluep¹⁸, Min Yi¹⁸, James Hamilton¹⁸, Javier San Martin¹⁸, Rohit Loomba¹⁹. ¹University of Florida, Gainesville, FL, USA, United States; ²University of Florida, Gainesville, United States; ³Medical University of South Carolina, Charleston, SC, USA, United States; ⁴University Hospital Aachen, Aachen, Germany, United States; ⁵University of Iowa, Iowa City, IA, USA, United States; ⁶Stanford University, Stanford, CA, USA, United States; ⁷Funchal Central Hospital, Funchal, Madeira, Portugal, United States; ⁸Leiden University Medical Center, Leiden, Netherlands, Netherlands; ⁹University of California Los Angeles, CA, USA, United States; ¹⁰Foundation IRCCS San Matteo Hospital and Pavia University, Pavia, Italy, Italy; ¹¹Vall d'Hebron University Hospital, Barcelona, Spain, United States; ¹²Columbia University Medical Center, New York, USA, United States; ¹³University of Alabama at Birmingham, Birmingham, AL, USA, United States; ¹⁴UC Davis Medical Center, Sacramento, CA, USA, United States; ¹⁵Mayo Clinic in Arizona, Phoenix, AZ, USA, United States; ¹⁶Baylor College of Medicine, Houston, TX, USA, United States; ¹⁷Indiana University School of Medicine, IN, USA, United States; ¹⁸Arrowhead Pharmaceuticals, Pasadena, CA, USA, United States; ¹⁹UC San Diego Medical Center, San Diego, CA, USA, United States
Email: virginia.clark@medicine.ufl.edu

Background and aims: Alpha-1 antitrypsin (AAT) deficiency, caused by homozygous protease inhibitor ZZ (PiZZ) mutations, results in production of mutant Z-proteins (Z-AAT) that aggregate in hepatocytes, leading to progressive liver dysfunction and fibrosis. Fazirsiran, an investigational RNA interference therapeutic, degrades liver Z-AAT messenger RNA to reduce Z-AAT synthesis. This study evaluated safety, pharmacodynamic and histologic effects of fazirsiran in adults with PiZZ AAT deficiency.

Method: This ongoing, placebo (PBO)-controlled, phase 2 study (NCT03945292) randomized participants (PTP) to subcutaneous PBO or fazirsiran 25/100/200 mg doses. The primary end point was change from baseline (BL) in serum Z-AAT concentration at week (wk) 16. PTP with biopsy-proven liver fibrosis underwent liver biopsy at BL and received treatment on day 1, wk 4, and then every 12 wks, and underwent a second liver biopsy at or after wk 48. PTP without liver fibrosis received 2 treatment doses on day 1 and wk 4. Three blinded central pathologists scored and adjudicated histological parameters, including hepatic globule burden (periodic acid-Schiff-diastase [PAS+D] staining (score 0–9), portal inflammation (score 0–3), and fibrosis score (F0–F4 METAVIR staging). Change from BL in serum and total liver Z-AAT concentrations were measured using liquid chromatography-tandem mass spectrometry.

Results: Forty PTP were enrolled (PBO [n = 14]; fazirsiran 25 mg [n = 9], 100 mg [n = 8], 200 mg [n = 9]). Fazirsiran reduced serum Z-AAT levels in a dose-dependent manner at wk 16 compared with PBO ($p < 0.001$), with mean relative reductions of 92% in the 200 mg group. Sustained reductions in serum Z-AAT up to wk 52 were observed with fazirsiran treatment. At post-BL liver biopsy, median reduction in liver Z-AAT was 94% with fazirsiran, compared with a median increase of 26% with PBO. Concomitant reduction from BL in hepatic PAS+D globule burden was observed with fazirsiran (mean [standard deviation (SD)] score of 5.9 [2.24] at BL and 2.3 [2.24] at post-BL visit), compared with no change with PBO (mean [SD] score of 6.9 [1.76] at BL and 6.6 [2.13] at post-BL visit). In PTP with BL score >0 , portal inflammation improved in 5/12 PTP in the fazirsiran group vs. 0/8 PTP in the PBO group. In PTP with adjudicated liver fibrosis $>F0$ at BL, ≥ 1 -point improvement in METAVIR score occurred in 7/14 PTP in the fazirsiran group vs. 3/8 PTP in the PBO group. Fazirsiran was well tolerated without any adverse events leading to study/drug discontinuation and no treatment-associated decline in pulmonary function.

Conclusion: Fazirsiran reduced serum and liver concentrations of Z-AAT and hepatic PAS+D globule burden in all treated PTPs compared with PBO, leading to improved liver portal inflammation. These results support further development of fazirsiran in larger phase 3 studies.

Funded by Arrowhead. Editorial support provided by Oxford PharmaGenesis, funded by Takeda Development Center Americas, Inc.

OS-121-YI

Performance of spleen stiffness measurement by vibration-controlled transient elastography to rule out high-risk varices in patients with porto-sinusoidal vascular disorder

Lucile Moga^{1,2}, Valérie Paradis^{2,3}, Koushik Gudavalli⁴, Joel Silva^{5,6}, Antonio Colecchia^{7,8}, Federico Ravaioli^{9,10}, Oana Nicoara-Farcu^{11,12}, Giulia Tosetti¹³, Annalisa Berzigotti¹⁴, Bogdan Procopet¹¹, Macarena Simón-Talero¹⁵, Laura Turco¹⁶, Francisco Capinha¹⁷, Laure Elkrief¹⁸, Jose Alberto Ferrusquia Acosta¹⁹, Odile Gorla²⁰, Lorenz Balcar²¹, Lannes Adrien^{22,23}, Vincent Mallet²⁴, Armelle Poujol-Robert²⁵, Dominique Thabut^{26,27}, Pauline Housset-Debry²⁸, Yu Jun Wong²⁹, Thomas Reiberger²¹, Teresa Monllor-Nunell¹⁹, Giovanni Vitale¹⁶, Carlos Noronha Ferreira¹⁷, Judit Vidal-González¹⁵, Andreea Fodor¹¹, Antonina Antonenko¹⁴, Riccardo Caccia¹³, Fanny Turon¹², Elton Dajti⁹, Filippo Schepis⁷, Federica Indulti⁷, Guilherme Macedo^{5,6}, Sai Prasanth Rampally⁴, Audrey Payancé^{1,2}, Castera Laurent^{2,30}, Arun Valsan⁴, Aurélie Plessier¹, Pierre-Emmanuel Rautou^{1,2}. ¹Hôpital Beaujon-

Assistance Publique-Hôpitaux de Paris, Hepatology-Centre de Référence des Maladies Vasculaires du Foie, Clichy, France; ²Inserm, Centre de recherche sur l'inflammation-UMR 1149, Paris, France; ³Hôpital Beaujon-Assistance Publique-Hôpitaux de Paris, Département d'Anatomie Pathologique, Clichy, France; ⁴Amrita Institute of Medical Sciences, Hepatology and Transplantation Unit, Department of Gastroenterology, Kochi, India; ⁵Centro Hospitalar e Universitário de São João, Gastroenterology Department, Porto, Portugal; ⁶Faculdade de Medicina da Universidade do Porto, Porto, Portugal; ⁷University Hospital of Modena, Gastroenterology Unit, Department of Medical Specialties, Modena, Italy; ⁸University of Modena and Reggio Emilia, Modena, Italy; ⁹University Hospital of Bologna, Department of Medical and Surgical Sciences, Bologna, Italy; ¹⁰University of Bologna, Bologna, Italy; ¹¹University of Medicine and Pharmacy "Iuliu Hatieganu," 3rd Medical Clinic and Regional Institute of Gastroenterology and Hepatology "Prof. Dr. Octavian Fodor," Hepatology Department, Cluj-Napoca, Romania; ¹²Hospital Clinic, Hepatic Hemodynamic Department, Liver Unit, Barcelona, Spain; ¹³Foundation IRCCS Ca' Granda Ospedale Maggiore Policlinico, Division of Gastroenterology and Hepatology, Milano, Italy; ¹⁴Inseppital, Universitätsklinik für Viszerale Chirurgie und Medizin, Bern, Switzerland; ¹⁵Hospital Vall d'Hebron, Liver Unit, Department of Internal Medicine, Barcelona, Spain; ¹⁶IRCCS Azienda Ospedaliero-Universitaria di Bologna, Internal Medicine Unit for the Treatment of Severe Organ Failure, Bologna, Italy; ¹⁷Centro Hospitalar Universitário Lisboa Norte, Serviço de Gastrenterologia e Hepatologia, Lisboa, Portugal; ¹⁸CHRU de Tours-Hôpital Trousseau, Service d'Hépatogastro-Entérologie, Tours, France; ¹⁹Hospital Universitari Parc Taulí, Liver Unit, Sabadell, Spain; ²⁰Hôpital Charles Nicolle-CHU de Rouen, Service d'Hépatogastroentérologie et Oncologie digestive, Rouen, France; ²¹Medical University of Vienna, Department of Medicine III-Division of Gastroenterology and Hepatology, Vienna, Austria; ²²CHU Angers, Hépatogastro-entérologie et oncologie digestive, Angers, France; ²³CHU Angers, Maine et Loire, ANGERS, France; ²⁴Hôpital Cochin-Assistance Publique-Hôpitaux de Paris, Gastro-entérologie et hépatologie, Paris, France; ²⁵Hôpital Saint-Antoine-Assistance Publique-Hôpitaux de Paris, Hépatologie, Paris, France; ²⁶Hôpital Pitié Salpêtrière-Assistance Publique-Hôpitaux de Paris, Hépatogastroentérologie Department, Liver Intensive Care Unit, Paris, France; ²⁷Inserm, Centre de recherche Saint-Antoine-UMR-S 938, Paris, France; ²⁸Hôpital Pontchaillou-CHU de Rennes, Centre hépatogastro-digestif-Maladies du foie, Rennes, France; ²⁹Changi General Hospital, Department of Gastroenterology and Hepatology, Singapore, Singapore; ³⁰Hôpital Beaujon-Assistance Publique-Hôpitaux de Paris, Hépatologie, Clichy, France
Email: lucile.moga@gmail.com

Background and aims: Spleen stiffness is associated with the severity of portal hypertension in patients with cirrhosis. Baveno VII consensus suggests that screening endoscopy can be safely avoided in patients with cirrhosis and a spleen stiffness measurement (SSM) by vibration-controlled transient elastography (VCTE) ≤ 40 kPa as they have a low probability of high-risk varices (HRV). In porto-sinusoidal vascular disorder (PSVD), endoscopic screening for varices is recommended in all patients. Whether SSM could also avoid endoscopies in patients with PSVD is currently unknown. This study aimed to evaluate the performance of SSM by VCTE to rule out high-risk varices (i.e. large varices, or red spot signs, or previous variceal band ligation) in patients with PSVD.

Method: All the patients with PSVD, according to Baveno VII definition, and at least one sign of portal hypertension, who underwent a liver biopsy between 2012 and 2022 at our center, and SSM by VCTE using FibroScan[®] performed within two years before or after an endoscopy, have been included. Patients with cavernoma or complete portal vein thrombosis at the time of liver biopsy, prior TIPS, or tense ascites at the time of SSM by TE, have not been included. Performance of SSM by VCTE was externally validated in a cohort of PSVD patients from 21 VALDIG centers, using the same inclusion and non-inclusion criteria.

ORAL PRESENTATIONS

Results: 154 patients were included in the derivation cohort: 56% men, median age 53, 75% with ≥ 1 condition known to be associated with PSVD. Median INR was 1.08 (IQR 0.99–1.24), median serum bilirubin 14 $\mu\text{mol/L}$ (IQR 9–22), and median serum creatinine 70 $\mu\text{mol/L}$ (IQR 61–86). A history of variceal bleeding was present in 16% of the patients, and 46% had HRV. Median SSM was 46.8 kPa (IQR 30.0–70.3). By univariate analysis, platelet count, serum bilirubin, serum albumin, spleen size, portosystemic collaterals, partial occlusion of portal venous axis, LSPS, and SSM by VCTE were associated with HRV status. By multivariate logistic regression analysis, only serum bilirubin ($p=0.003$) and SSM by VCTE ($p<0.0001$) remained associated with HRV. SSM by VCTE ≤ 40 kPa had a sensitivity of 87% to rule out HRV. This cutoff would avoid 45% of screening endoscopies, but with 13% of HRV missed, and a negative predictive value (NPV) of 87%. SSM by VCTE ≤ 40 kPa combined with serum bilirubin $<17 \mu\text{mol/L}$ had a sensitivity of 96% to rule out HRV, and could avoid 34% of screening endoscopies, with 4% of HRV missed, and a NPV of 94%. In the validation cohort including 207 patients with similar characteristics, the combination of SSM and serum bilirubin could avoid 17% of screening endoscopies, with 4.7% of HRV missed, and a NPV of 86% (Fig.). Sensitivity analyses restricted to patients with an interval between SSM and endoscopy <6 months, or to patients without a history of bleeding, gave even better results. We tested SSM ≤ 40 kPa combined with platelet count $\geq 150\text{G/L}$, and observed that HRV missed rate was $>5\%$.

Conclusion: This study gathering a total of 361 patients with PSVD showed that SSM by VCTE ≤ 40 kPa combined with serum bilirubin $<17 \mu\text{mol/L}$ identifies patients with PSVD with very low risk ($<5\%$) of HRV, in whom screening endoscopy can be avoided.

OS-122

Final results from a phase 1/2, 48-month, open-label extension study of givosiran in patients with acute intermittent porphyria

Eliane Sardh¹, Manisha Balwani², David Rees³, Karl Anderson⁴, Gang Jia⁵, Marianne T Sweetser⁵, Bruce Wang⁶. ¹Karolinska University

Hospital, Karolinska Institutet, Stockholm, Sweden; ²Icahn School of Medicine, Department of Genetics and Genomic Sciences, New York, United States; ³King's College Hospital, United Kingdom; ⁴University of Texas Medical Branch, United States; ⁵Alnylam Pharmaceuticals, United States; ⁶University of California San Francisco, Department of Medicine and UCSF Liver Center, San Francisco, United States
Email: eliane.sardh@ki.se

Background and aims: Acute hepatic porphyrias (AHPs) are rare genetic disorders that can lead to accumulation of the neurotoxic intermediates 5-aminolevulinic acid (ALA) and porphobilinogen (PBG). The clinical presentation of AHPs, including the most common AHP, acute intermittent porphyria (AIP), is characterized by acute neurovisceral attacks, chronic symptoms, and long-term complications. Givosiran is an RNA interference therapeutic for AHP. In a phase 1 study in AIP (NCT02452372), once-monthly givosiran treatment led to sustained reductions in ALA and PBG levels and a lower annualized rate of porphyria attacks and hemin use versus placebo. We report final results from a phase 1/2 open-label extension study (NCT02949830) of the safety and efficacy of up to 48 months of givosiran treatment.

Method: Patient eligibility criteria for this multicenter study were AIP diagnosis, completion of the phase 1 trial, and absence of a prophylactic hemin regimen. Patients received givosiran 2.5 mg/kg once monthly, 5.0 mg/kg once monthly, or 5.0 mg/kg once every 3 months; eventually, all patients transitioned to 2.5 mg/kg once monthly.

Results: Of 16 patients enrolled, 14 completed the study. Mean (SD) age was 37.4 (12.0) years. Most patients were White (81%) and female (88%). Fourteen patients (88%) reported at least 1 adverse event (AE) related to study drug. The most common treatment-related AEs were injection-site erythema ($N=6$; 38%) and injection-site pruritus ($N=4$; 25%); most were mild or moderate in severity, and none led to treatment discontinuation. One (6%) patient experienced a serious treatment-related AE of anaphylaxis, leading to study withdrawal. Two patients experienced AEs of elevated alanine aminotransferase, and 1 experienced elevated blood homocysteine. Long-term treatment with givosiran 2.5 mg/kg once monthly led to a sustained

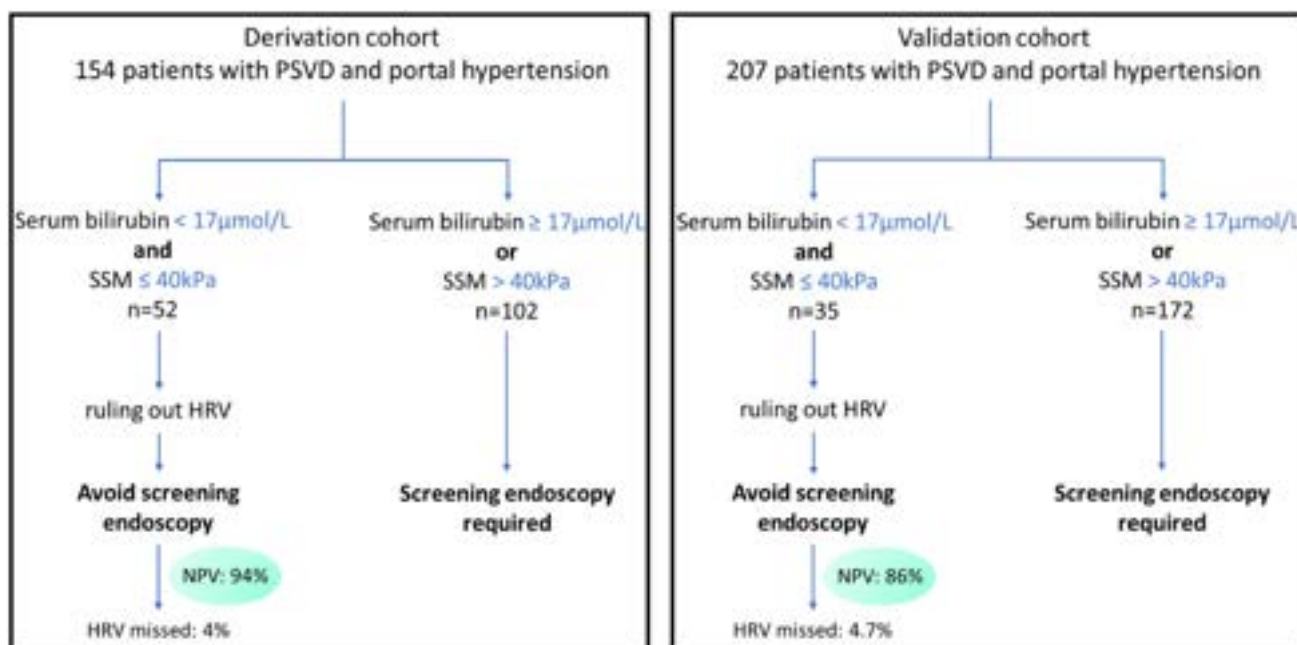


Figure 1. Performance of spleen stiffness measurement by vibration-controlled transient elastography combined with serum bilirubin to rule out high-risk varices in patients with porto-sinusoidal vascular disorder

Figure: (abstract: OS-121-YI)

reduction in composite porphyria attacks, with a mean annualized attack rate of 0.4 (98% reduction), as well as a decrease in the mean rate of hemin use, from 33.1 doses/year during run-in to 0.9 dose/year (97% reduction) during this study. Sustained reductions in ALA and PBG levels were also observed. Exploratory assessments showed that quality-of-life scores improved over time.

Conclusion: This longest follow-up (up to 48 months) of patients receiving monthly givosiran treatment demonstrated acceptable safety, durable clinical response, and improvements in quality-of-life scores.

OS-123-YI

Porto sinusoidal vascular liver disorder: natural history and long-term outcome

Marta Magaz¹, Heloïse Giudicelli-Lett², Juan Abalde³, Oana Nicoara-Farcu⁴, Neil Rajoriya⁵, Ashish Goel⁵, Karlén Raymenants⁶, Sophie Hilaire², Luis Téllez⁷, Laure Elkrief⁸, Lara Orts⁹, Akash Shukla¹⁰, Hélène Larrue¹¹, Helena Degroote¹², Victoria Aguilera Sancho¹³, Elba Llop¹⁴, Laura Turco¹⁵, Stefania Gioia¹⁶, Giulia Tosetti¹⁷, Niccolò Bitto¹⁷, Chiara Becchetti¹⁸, Edilmar Alvarado-Tapias¹⁹, Cristina Roig¹⁹, Raquel Diaz²⁰, Michael Praktikjnjo²¹, Anna-Lena Konicek²¹, Guillem Soy⁹, Pol Olivas¹⁹, Jose Ignacio Fortea²², Helena Masnou²³, Angela Puente²², Alba Ardevol²³, Mari Carmen Alvarez-Navascues²⁴, Marta Romero-Gutiérrez²⁵, Bernhard Scheiner²⁶, Georg Semmler²⁶, Mattias Mandorfer²⁶, Filipe de Sousa Damião²⁷, Anna Baiges¹, Fanny Turon¹, Macarena Simón-Talero²⁸, Carlos González-Alayón²⁹, Alba Díaz³⁰, Maria Ángeles García-Criado³¹, Andrea de Gottardi³², Joan Genesca²⁸, Olivier Roux², Carlos Noronha Ferreira²⁷, Thomas Reiberger²⁶, Manuel Rodríguez²⁴, Rosa M Morillas²³, Sarah Shalaby¹, Javier Crespo²², Jonel Trebicka²¹, Rafael Bañares²⁰, Cándid Villanueva¹⁹, Annalisa Berzigotti¹⁸, Massimo Primignani³³, Vincenzo La Mura¹⁷, Oliviero Riggio¹⁶, Filippo Schepis³⁴, Federica Indulti³⁴, Bogdan Procopet⁴, Xavier Verhelst¹², José Luis Calleja Panero¹⁴, Christophe Bureau¹¹, Filipe Gaio Castro Nery³⁵, Agustin Albillos⁷, Frederik Nevens⁶, Virginia Hernandez-Gea¹, Dhiraj Tripathi⁵, Pierre-Emmanuel Rautou², Juan Carlos Garcia Pagan¹. ¹Hepatic hemodynamic lab, Barcelona, IDIBAPS, CIBEREHD, ERN-Liver., Spain; ²Service d'Hépatologie, Centre de Référence des Maladies Vasculaires du Foie, DHU Unity, Pôle des Maladies de l'Appareil Digestif, Hôpital Beaujon, AP-HP, Clichy, France., France; ³Liver Unit, Division of Gastroenterology, University of Alberta, Edmonton, AB, Canada., Canada; ⁴Regional Institute of Gastroenterology and Hepatology "Octavian Fodor", Hepatology Department and "Iuliu Hatieganu" University of Medicine and Pharmacy; 3rd Medical Clinic, Cluj-Napoca, Romania., Romania; ⁵The Liver Unit, University Hospital Birmingham NHS Foundation Trust, Birmingham, UK, United Kingdom; ⁶Department of Gastroenterology and Hepatology, University Hospital KU Leuven, Leuven, Belgium., Belgium; ⁷Department of Gastroenterology and Hepatology, Hospital Universitario Ramón y Cajal, IRYCIS, CIBEREhd, Universidad de Alcalá, Madrid, Spain., Spain; ⁸Service d'Hépatogastroentérologie, CHU de Tours, France. Université de Paris, Centre de recherche sur l'inflammation, Inserm, U1149, CNRS, ERL8252, F-75018 Paris, France., France; ⁹Hospital Clinic, Spain; ¹⁰Seth GS Medical College and KEM Hospital, Sion, Mumbai, India., India; ¹¹Department of Hepatology, Rangueil Hospital, CHU Toulouse, University Paul Sabatier of Toulouse, France., France; ¹²Department of Gastroenterology and Hepatology, Ghent University Hospital, Ghent, Belgium., Spain; ¹³Liver Transplantation and Hepatology Unit, Hospital Universitari i Politècnic La Fe, Valencia, Spain. CIBEREhd (Centro de Investigación Biomédica en Red en Enfermedades Hepáticas y Digestivas, Valencia Spain), Instituto de Salud Carlos III., Spain; ¹⁴Liver Unit, Hospital U, Puerta de Hierro. Universidad Autónoma de Madrid, CIBEREhd, Madrid, Spain., Spain; ¹⁵Department of Gastroenterology and Hepatology, University of Modena and Reggio Emilia and Azienda Ospedaliero-Universitaria di Modena, Italy., Italy; ¹⁶Department of Gastroenterology and Hepatology,

Centre for the Diagnosis and Treatment of Portal Hypertension, "Sapienza" University of Rome, Rome, Italy., Italy; ¹⁷Foundation IRCCS Ca' Granda Ospedale Maggiore Policlinico, Division of Gastroenterology and Hepatology, CRC "A.M. and A. Migliaivacca" Center for Liver Disease, Milan, Italy., Italy; ¹⁸University Clinic for Visceral Surgery and Medicine, Inselspital, Bern University Hospital, University of Bern, Bern, Switzerland., Switzerland; ¹⁹Liver Unit, Department of Gastroenterology Hospital Sant Pau, Barcelona, Autonomous University, Barcelona, Spain. Centro de Investigación Biomédica en Red de Enfermedades Hepáticas y Digestivas (CIBEREhd), Barcelona, Spain, Spain; ²⁰Department of Gastroenterology and Hepatology, University Gregorio Marañón Hospital, IISGM, CIBEREhd, Barcelona, Spain., Spain; ²¹Department of Internal Medicine I, University Hospital Bonn, Bonn, Germany., Germany; ²²Liver Unit, Digestive Disease Department, Marqués de Valdecilla University Hospital, Santander, Cantabria University, Spain., Spain; ²³Liver Unit, University Hospital Germans Trias i Pujol, Badalona, Spain. Centre for Biomedical Research in Liver and Digestive Diseases Network (CIBEREhd), Spain; ²⁴Liver Unit, Department of Gastroenterology and Hepatology, Hospital Universitario Central de Asturias, University of Oviedo, Oviedo, Spain., Spain; ²⁵Liver Unit, Department of Gastroenterology, Hospital Virgen de la Salud, Toledo, Spain., Spain; ²⁶Vienna Hepatic Hemodynamic Lab, Medical University of Vienna, Vienna, Austria., Austria; ²⁷Department of Gastroenterology and Hepatology, Hospital de Santa Maria-Centro Hospitalar Universitário Lisboa Norte, Lisbon, Portugal., Portugal; ²⁸Liver Unit, Department of Internal Medicine, Hospital Universitari Vall d'Hebron, Vall d'Hebron Research Institute (VHIR), Vall d'Hebron Barcelona Hospital Campus, CIBEREhd, Universitat Autònoma de Barcelona, Barcelona, Spain., Spain; ²⁹Liver Unit, Department of Gastroenterology and Hepatology, Hospital Universitario de Canarias. Tenerife, Spain., Spain; ³⁰Department of Histopathology, Hospital Clínic, Institut de Investigacions Biomèdiques August Pi i Sunyer (IDIBAPS), University of Barcelona, Barcelona., Spain; ³¹Department of Radiology, Hospital Clínic, University of Barcelona, Barcelona., Spain; ³²Servizio di Gastroenterologia e Epatologia, Ente Ospedaliero Cantonale, Università della Svizzera Italiana, Lugano, Switzerland., Switzerland; ³³Foundation IRCCS Ca' Granda Ospedale Maggiore Policlinico, Division of Gastroenterology and Hepatology, CRC "A.M. and A. Migliaivacca" Center for Liver Disease, Milan, Italy., Spain; ³⁴Department of Gastroenterology and Hepatology, University of Modena and Reggio Emilia and Azienda Ospedaliero-Universitaria di Modena, Italy., Italy; ³⁵Liver Unit, Centro Hospitalar do Porto, Hospital Sto Antonio, Porto, Portugal., Portugal Email: martamagazm@gmail.com

Background and aims: The natural history and prognostic factors in portosinusoidal vascular disorder (PSVD) are not well understood. Aim: to describe the natural history of and prognostic factors in PSVD patients with portal hypertension (PH).

Method: Retrospective multicentric study of patients with PSVD and PH prospectively registered in 28 European centres. PSVD patients without an associated condition, or with an associated condition that usually impacts on life expectancy (e.g. autoimmune hypothyroidism), or with a controlled associated condition were classified as having "no or mild associated conditions." The remaining PSVD patients with an active associated condition known to potentially negatively impact life expectancy, (e.g. severe lupus with kidney involvement), were classified as having a "severe associated condition." Cox analysis was performed to identify variables with an independent predictive value for transplant-free survival.

Results: A total of 587 patients (38% women) were identified. At PSVD diagnosis, median age was 47 (33;59) years; 377 (64%) were asymptomatic. 210 patients had a PH complication as first manifestation: 87 (41%) variceal bleeding, 92 (43.8%) ascites, 25 (12%) variceal bleeding plus ascites, 11 (5%) hepatic encephalopathy (HE; 4 of them together with variceal bleeding and in 7 coexistent with ascites) and 13 (6%) dyspnea (seven of them coexisting with ascites). Median Child-Pugh at diagnosis was 5 (5;6), MELD 8 (7;11), total serum bilirubin 1 (0.6;1.4) mg/dL, INR 1.1 (1;1.2). Associated conditions

ORAL PRESENTATIONS

included: autoimmune (23%), hematologic (9%), HIV (9%), azathioprine (8%), oxaliplatin (7%), prothrombotic (8%), hereditary (4%), others (1%), while 32% had no other conditions (idiopathic). In 157 patients, the associated persistent condition was considered severe. Median follow-up was 68 [1–469] months. Fifty (9%) patients were transplanted and 109 (19%) died (59 non-liver related death). Transplant-free survival was 97%, 93%, 83%, and 72% at 1, 2, 5, and 10 years, respectively. We developed a predictive model based on multivariable Cox regression analyses for transplant free survival including age, ascites, serum bilirubin, creatinine and albumin at diagnosis, and the severity of the associated underlying condition that showed good discrimination and calibration (bootstrapped c-statistic: 0.82, Integrated calibration index at 3 and 6 years: 0.008 and 0.011) (nomogram). An accurate HVPG was available in 327 patients (without vein-vein communications). The median value was 7 mmHg (4;11). In this subgroup of patients, HVPG improved the predictive value of the model.

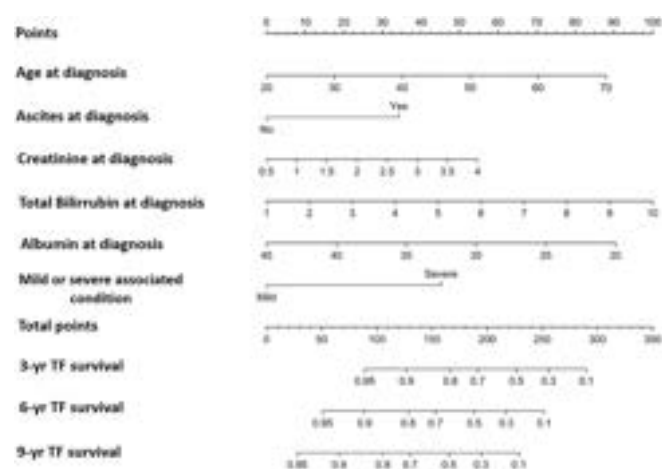


Figure:

Conclusion: Prognosis of patients with PSVD and PH is strongly determined by the presence of associated diseases. If diagnosis is made at the time of preserved liver function, long-term prognosis is good reinforcing the need of early diagnosis and management in centers of expertise.

OS-124-YI

Diagnosis by liver stiffness measurement of sinusoidal obstruction syndrome/veno-occlusive disease after hematopoietic stem cell transplantation: results from the Italian multicentric prospective study (ELASTOVOD)

Federico Ravaoli^{1,2,3}, Antonio Colecchia², Francesco Barbato¹, Jacopo Peccatori⁴, Anna Grassi⁵, Barbara Sarina⁶, Maurizio Pompili⁷, Simona Sica⁷, Franco Locatelli⁸, Simone Cesaro⁹, Chiara Nozzoli¹⁰, Anna Paola Iori¹¹, Lucia Prezioso¹², Stella Santarone¹³, Franca Fagioli¹⁴, Attilio Olivieri¹⁵, Ester Vanni¹⁶, Giorgia Specchia¹⁷, Edoardo Benedetti¹⁸, Francesco Zallio¹⁹, Fabrizio Pane²⁰, Francesca Carobolante²¹, Maria Cristina Menconi²², Fabio Benedetti²³, Francesca Patriarca²⁴, Michele Malagola²⁵, Riccardo Varaldo²⁶, Francesco Onida²⁷, Vincenzo Pavone²⁸, Amanda Vestito¹, Luigi Colecchia¹, Elton Dajti¹, Luigina Vanessa Alemanni¹, Giovanni Marasco¹, Fabio Ciceri⁴, Arcangelo Prete¹, Andrea Pession¹, Davide Festi¹, Francesca Bonifazi¹.
¹IRCCS Azienda Ospedaliero-Universitaria di Bologna, Bologna Italy, Italy; ²Gastroenterology Unit, Department of Medical Specialties (CHIMOMO), University of Modena and Reggio Emilia, Italy, Italy; ³Alma Mater Studiorum-Università di Bologna, Department of Medical and Surgical Sciences, Bologna, Italy; ⁴Unit of Hematology and Bone Marrow Transplantation, Division of Regenerative Medicine, Stem Cells and Gene Therapy, IRCCS San Raffaele Scientific Institute, Milan, Italy, Italy; ⁵ASST

Papa Giovanni XXIII, Bergamo, Italy, Italy; ⁶Bone Marrow Unit, Humanitas Cancer Center, Rozzano, Milan, Italy, Italy; ⁷Department of Hematology Catholic University of Sacred Heart, Rome, Italy, Italy; ⁸Department of Hematology/Oncology, IRCCS Ospedale Pediatrico Bambino Gesù, Rome, Italy; ⁹Department of Gynecology/Obstetrics and Pediatrics, Sapienza University, Rome, Italy, Italy; ¹⁰Oncematologia Pediatrica, Azienda Ospedaliera Universitaria Integrata, Verona, Italy, Italy; ¹¹Department of Cellular Therapies and Transfusion Medicine, Careggi University Hospital, Florence, Italy, Italy; ¹²Department of Translational and Precision Medicine, Division of Allogeneic Transplantation, "Sapienza" University of Rome, Rome, Italy, Italy; ¹³Hematology and BMT Unit, Azienda Ospedaliero-Universitaria di Parma and Department of Medicine and Surgery, University of Parma, Italy, Italy; ¹⁴Department of Hematology, Transfusion Medicine and Biotechnologies, Ospedale Civile, Pescara, Italy, Italy; ¹⁵Pediatric Onco-Hematology, Città della Salute e della Scienza di Torino, Turin, Italy, Italy; ¹⁶Clinica di Ematologia Azienda Ospedaliero-Universitaria, Ospedali Riuniti di Ancona, Ancona, Italy, Italy; ¹⁷Gastroenterology Unit, Città della salute e della scienza, Turin, Italy, Italy; ¹⁸Department of Emergency and Organ Transplantation (D.E.T.O.), Hematology Section, University of Bari, Italy, Italy; ¹⁹Hematology Unit, Department of Oncology, University of Pisa, Italy, Italy; ²⁰Hematology Department, SS Antonio and Biagio and C. Arrigo Hospital, Alessandria Italy, Italy; ²¹UOC di Ematologia e Trapianti di Midollo, Azienda Ospedaliera Universitaria Federico II di Napoli, Napoli, Italy; ²²Dipartimento di Medicina clinica e Chirurgia, Università di Napoli Federico II, Napoli, Italy, Italy; ²³UOC Ematologia, Ospedale dell'Angelo, Venezia, Mestre, Italy, Italy; ²⁴Pediatric Oncohematology Unit, Azienda Ospedaliera Universitaria Pisana, Pisa, Italy, Italy; ²⁵Department of Clinical and Experimental Medicine, Hematology and Bone Marrow Transplant Unit, University of Verona, Verona, Italy, Italy; ²⁶Clinica Ematologica, Azienda sanitaria Universitaria Integrata, DAME, Università di Udine, Udine, Italy, Italy; ²⁷Unit of Blood Diseases and Stem Cell Transplantation, ASST-Spedali Civili di Brescia, Department of Clinical and Experimental Sciences, University of Brescia, Brescia, Italy, Italy; ²⁸IRCCS Policlinico San Martino IST, Genova, Italy, Italy; ²⁹Hematology and Bone Marrow Transplantation Center, Fondazione IRCCS Ospedale Maggiore Policlinico/University of Milan, Milan, Italy, Italy; ³⁰A.O. C. Panico, U.O.C. Ematologia e Trapianto, Tricase, Italy, Italy
 Email: f.ravaoli@unibo.it

Background and aims: Sinusoidal obstruction syndrome (SOS), also known as veno-occlusive-disease (VOD), remains a serious complication for patients undergoing hematopoietic stem cell transplantation (HSCT). Improving diagnosis with non-invasive methods needs to be urgently investigated. Consequently, we aimed to evaluate the diagnostic role of the measurement of liver stiffness (LSM), assessed with different ultrasound elastography techniques, for diagnosing SOS.

Method: This interventional prospective multicenter clinical trial, from April 2018 to December 2021, consecutively and prospectively examined 1089 patients from 25 Italian centres undergoing HSCT. Sixty-nine (6.3%) patients were excluded for inadequate data quality; among the remaining 1020 patients, 80 did not perform at least one LSM assessment after HSCT and were consequently excluded. Patients were followed according to the protocol by a dense clinical, laboratory, and imaging program during hospitalization for HSCT and until the diagnosis of SOS, death, or +100-day follow-up. LSM was performed before the HSCT (T0), on days +9/10 (T1), +15/17 (T2), and +22/24 (T3) after the. The diagnosis of SOS was performed clinically by each participating centre. The primary end point of the study was the diagnostic role for SOS by LSM assessed by different elastographic methods (ClinicalTrials.gov-number-NCT03426358)

Results: Among the 941 patients, 774 were adults, and 167 were children. Characteristics of the populations enrolled were reported in Table. Sixty per cent of patients were male with a mean age of 43.7 (SD 20.25) at the time of HSCT; the main HSCT indication was AML (40.3%), ALL (16.9%), NHL (7.1%), and myelofibrosis (6.6%). Most HSCTs

were allogeneic (95%) from peripheral blood stem cell sources (79.2%) and myeloablative intensity conditioning (63.3%). The +100-days overall survival was 96.5% [95%CI 90.2–100] in the whole population and 75.0% [95%CI 53.3–100] in the SOS group (78.6% [95%CI 39.2–100] in mild and moderate and 50.0% [95%CI 18.4–100] in very severe). LSM was measured in kilopascals (kPa) in 90.9% and meter-second (m/sec) in 9.1% of cases and evaluated by transient elastography (FibroScan, Echosens, Paris), 2D shear wave elastography (2D-SWE), and point shear wave elastography (p-SWE) in 76%, 12.9%, and 11.1%, respectively. Median LSM values prior-HSCT (T0) were 4.9 kPa [IQR 3.9–6.13] and 1.18 m/sec [IQR 1.01–1.4] with no significant difference (p value 0.350) according to SOS occurrence both by kPa (4.9vs5.0) and by m/sec (1.19vs1.02). LSM time point by time point (Fig1A), LSM values increased significantly in patients who developed SOS and differed between SOS severity grades (Fig1B). LSM values on the day of clinical diagnosis were significantly ($p < 0.0001$) associated both with SOS (OR 1.424 [95%CI 1.308–1.549]) and showed good diagnostic performance with a c-statistic of 0.975 [95%CI 0.948–1.000]. Comparable results were observed when LSM was evaluated in adults and paediatrics cohorts and by m/sec. Combination of the rule-in (25 kPa) and rule-out (6 kPa) cut-offs with deltaLSM (2x) in a stepwise algorithm achieved high values of PPV (84.2–98) and NPV (95–99) in all cohorts.

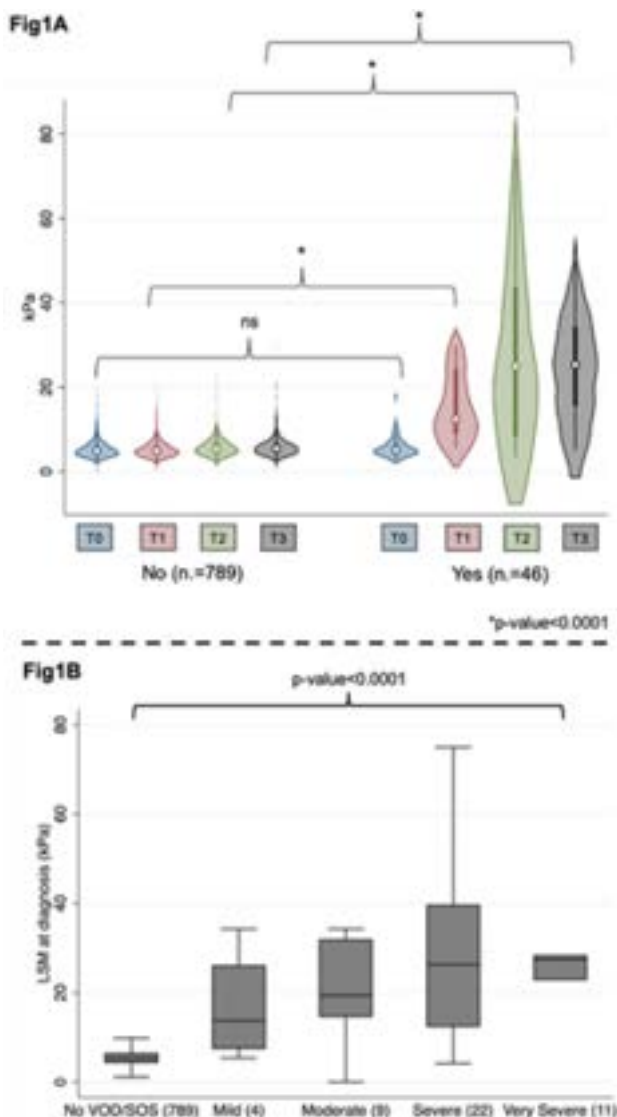


Figure 1:

Conclusion: LSM, regardless of the elastography modality, has proven to be an accurate diagnostic tool for SOS. This non-invasive method can support the multidisciplinary team formed by hepatologists and haematologists and allows for diagnosing SOS/VOD.

Viral hepatitis C

OS-125

Outcomes of early vs late treatment initiation in solid organ transplantation from HCV NAT+ donors to HCV-uninfected recipients: results from the HCV-TARGET study

Wesam Aleyadeh¹, Elizabeth Verna², Hany Elbeshbeshy³, Mark S Sulkowski⁴, Coleman I. Smith⁵, Jama Darling⁶, Richard Sterling⁷, Andrew Muir⁸, Lucy Akushevich⁶, Danie La¹, Michael W. Fried⁶, Jordan J. Feld¹. ¹Toronto General Hospital, Toronto Center for Liver Disease, Toronto, Canada; ²Columbia University Irving Medical Center, New York, United States; ³Saint Louis University School of Medicine, St. Louis, United States; ⁴The Johns Hopkins University School of Medicine, Baltimore, United States; ⁵MedStar Georgetown University Hospital, Washington, United States; ⁶University of North Carolina at Chapel Hill, Chapel Hill, United States; ⁷VCU Health System Authority, Richmond, United States; ⁸Duke University Medical Center, Durham, United States
Email: jordan.feld@uhn.ca

Background and aims: In North America (NA), the ongoing opioid overdose crisis has led to increasing organ transplantation from hepatitis C (HCV)-infected donors to HCV-uninfected recipients (D+/R-). While early treatment is recommended in societal guidelines, the optimal timing of antiviral therapy remains unclear. We compared the safety and efficacy of early vs late HCV treatment initiation in D+/R- non-liver solid organ recipients.

Method: Enrolled patients were treated with direct-acting antiviral (DAA) regimens per local standard of care at 10 NA sites. We compared efficacy and safety of HCV treatment between those who started before/within 7 days of transplant (Early) and those treated >7 days post-transplant (Late). The primary end point is sustained virological response (SVR12), defined as HCV RNA negativity 12 weeks post-treatment completion.

Results: 56 participants received Early treatment which included glecaprevir/pibrentasvir ± ezetimibe (GLE/PIB ± E) (n = 48) and sofosbuvir/velpatasvir (SOF/VEL) (n = 8). Treatment was initiated immediately before transplantation in GLE/PIB ± E, and by median day 5 and 4 in GLE/PIB and SOF/VEL, respectively. 102 participants received Late treatment which included SOF/VEL (n = 45), GLE/PIB (n = 49) and other regimens (n = 6). Two patients in the Late group did not start DAA treatment. Late treatment was initiated a median of 31 (range 8–114) days post-transplant. Median total treatment days was 8 (range 7–93) in Early vs 85 (range 51–111) in Late ($p < 0.0001$). There were 79 kidney, 50 lung, 23 heart, and 6 mixed transplants with similar distribution between groups. The proportion who achieved SVR12 was 92.9% (95% CI: 82.7–98.0) in the Early and 91.0% (95%CI: 83.6–95.8) in the Late groups, respectively. No participant in Early treatment group experienced non-response or relapse. In the Late group, 2 patients did not respond to treatment and 3 had post-treatment relapse. Of those with available virologic outcomes (n = 148) 100% (95% CI: 93.2–100.0) in Early and 94.8% (95%CI: 88.3–98.3) in Late groups achieved SVR12, respectively. Acute cellular rejection occurred in 11 (19.6%) recipients in the Early and 25 (25.0%) in the Late group, with 7 (12.5%) and 5 (4.9%) cases of biopsy-proven rejection requiring treatment. There were 11 patient deaths; all unrelated to HCV or HCV therapy: 8 in the Early group (1 during treatment), and 4 in the Late group (1 pre- and 3-post-treatment). HCV treatment was well tolerated in both groups.

	ET	LT	All		ET	LT	All
	N=56 (%)	N=100 (%)	N=158 (%)		N=56 (%)	N=100 (%)	N=158 (%)
Male Sex	40 (71.4%)	62 (62.0%)	102 (65.4%)	Organ transplanted			
Age, yrs (mean, min-max)	57 (26-76)	61 (20-80)	59 (20-80)	Heart	7 (12.5%)	16 (16.0%)	23 (14.6%)
Race				Heart And Lung	0 (0.0%)	1 (1.0%)	1 (0.6%)
Caucasian	35 (62.5%)	66 (66.0%)	101 (64.7%)	Kidney	32 (57.1%)	47 (47.0%)	79 (50.0%)
Black or African American	11 (19.6%)	27 (27.0%)	38 (24.4%)	Kidney And Heart	0 (0.0%)	2 (2.0%)	2 (1.3%)
Asian or Other	10 (17.9%)	7 (7.0%)	17 (10.9%)	Kidney And Pancreas	3 (5.4%)	0 (0.0%)	3 (1.9%)
HCV Genotypes				Lung	14 (25.0%)	34 (34.0%)	48 (30.8%)
1	13 (23.2%)	64 (64.0%)	77 (49.4%)	ALT (IU/L) Median (min-max)	20 (6-86)	19 (5-99)	20 (5-99)
2	5 (8.9%)	8 (8.0%)	13 (8.3%)	AST (IU/L) Median (min-max)	20 (8-88)	21 (8-76)	20 (8-88)
3	10 (17.9%)	18 (18.0%)	28 (17.9%)	T. Bilirubin (mg/dL) Median (min-max)	0.5 (0.2-1.9)	0.5 (0.2-5.3)	0.5 (0.2-5.3)
Not reported	28 (50.0%)	10 (10.0%)	38 (24.4%)	Achieved SVR (those with virological outcomes)	100 (93.2-100.0)	94.8 (88.3-98.3)	96.2 (92.3-98.9)
HIV Positive	1 (1.8%)	0 (0.0%)	1 (0.6%)	Complications			
Treatment Regimens				Fibrosing Cholestatic Hepatitis	0 (0%)	1 (1%)	1 (0.6%)
SOF/VEL	8 (14.3%)	44 (44.0%)	52 (32.9%)	Glomerulonephritis	3 (5.3%)	2 (2%)	5 (3.2%)
SOF/VEL+ Ribavirin	0 (0.0%)	1 (1.0%)	1 (0.6%)	Renal failure acute	6 (10.7%)	34 (34%)	40 (25.6%)
GLE/PIB + Ezetimibe	32 (57.1%)	0 (0.0%)	32 (20.3%)	Renal failure acute attributed to HCV therapy	5 (8.9%)	5 (5%)	10 (6.4%)
GLE/PIB	16 (28.6%)	49 (49.0%)	65 (41.1%)	Acute graft rejection	11 (19.6%)	25 (25%)	36 (23.1%)
GLE/PIB SOF/LDV	0 (0.0%)	1 (1.0%)	1 (0.6%)	Acute graft rejection biopsy-proven acute rejection requiring treatment	7 (12.5%)	5 (5%)	12 (7.7%)
SOF/LDV	0 (0.0%)	3 (3.0%)	3 (1.9%)	SOF/VEL – sofosbuvir/velpatasvir; GLE/PIB – glecaprevir pibrentasvir; SOF/LDV – sofosbuvir/ledipasvir; EBR/GZR – elbasvir/grazoprevir; ET – Early Treatment; LT – Late Treatment			
EBR/GZR	0 (0.0%)	2 (2.0%)	2 (1.3%)				

Figure: (abstract: OS-125) Recipient characteristics and outcomes

Conclusion: Solid non-liver organ transplantation in D+/R- recipients was safe with excellent graft and patient survival. Early treatment led to a non-significant lower rate of virological failure despite shorter duration treatment with numerically fewer episodes of acute rejection than with delayed therapy, supporting guideline recommendations for prompt treatment initiation.

OS-126

Unusual HCV subtypes and retreatment outcomes in a cohort of European DAA-experienced patients

Julia Dietz¹, Christiana Graf¹, Christoph P. Berg², Kerstin Port³, Katja Deterding³, Peter Buggisch⁴, Johannes Vermehren¹, Georg Dultz¹, Kai-Henrik Peiffer¹, Andreas Geier⁵, Tony Bruns⁶, Christophe Moreno⁷, Janina Trauth⁸, Thomas Discher⁸, Thomas Berg⁹, Andreas E. Kremer¹⁰, Beat Müllhaupt¹⁰, Stefan Zeuzem¹, Christoph Sarrazin^{1,11}. ¹Department of Internal Medicine I, Goethe University Hospital, Frankfurt, Germany jVermehren@gmx.de ²Department of Gastroenterology, Hepatology, and Infectiology, University Hospital Tübingen, Tübingen, Germany (christoph.berg@med.uni-tuebingen.de) ³Department of Gastroenterology, Hepatology and Endocrinology, Medizinische Hochschule Hannover, Hannover (Port. Kerstin@mh-hannover.de, deterding.katja@mh-hannover.de) ⁴Institute for Interdisciplinary Medicine IFI, Hamburg (buggisch@ifi-medizin.de) ⁵Division of Hepatology, Department of Medicine II, University Hospital Würzburg, Würzburg (Geier_A2@ukw.de) ⁶Department of Medicine III, University Hospital Aachen, Aachen, Germany (tbruns@ukaachen.de) ⁷Department of Gastroenterology, Hepatopancreatology and Digestive Oncology, CUB Hôpital Erasme, Université Libre de Bruxelles, Brussels, Belgium (Christophe.Moreno@erasme.ulb.ac.be) ⁸Department of Medicine II, Justus Liebig University Gießen (Thomas.Discher@innere.med.uni-giessen.de, Janina.Trauth@innere.med.uni-giessen.de) ⁹Section of Hepatology, Department of Gastroenterology and Rheumatology, University Hospital Leipzig, Leipzig, Germany (Thomas.Berg@medizin.uni-leipzig.de) ¹⁰Swiss Hepato-Pancreato-Biliary Center and Department of Gastroenterology and Hepatology, University Hospital Zürich, Zürich, Switzerland (andreas.kremer@usz.ch, beat.muellhaupt@usz.ch) ¹¹St. Josefs-Hospital, Wiesbaden, Germany Email: julia.dietz@em.uni-frankfurt.de

Background and aims: The global HCV elimination targets could be achieved with highly effective direct acting antivirals (DAAs) for treatment of hepatitis C virus (HCV) infection. However, studies showed that unusual HCV genotypes (GT) that are uncommon in industrialised countries are associated with lower SVR (sustained virologic response) rates and second generation DAAs are not available in all countries. This study aimed to describe the prevalence of unusual GT and resistance-associated substitutions (RASs) among European DAA-failure patients.

Method: We have identified 1314 patients who had failed IFN-free DAA treatment in the European Resistance database between 2014 and 2022. NS3, NS5A and NS5B were amplified and population sequenced and RASs that had >2-fold increased DAA susceptibility were analysed. All HCV geno- and subtypes were re-evaluated sequence-based.

Results: Overall, 4% (58/1314) of DAA-failure patients were infected with an unusual subtype. We found different frequencies of unusual GT among DAA treatment failures, namely 46% (27/58) GT4 (4b, 4c 4f, 4n, 4o, 4r, 4v), 24% (14/58) (3b, 3g, 3h, 3i, 3k; 24%), 12% (7/58) GT6 (6e, 6f, 6n, 6r), 10% (6/58) GT1 (1c, 1e, 1i) and 4% (2/58) each of GT2k and GT5a. The majority of patients with unusual GT (79%, 46/58) had failed to first-generation DAAs (LDV/SOF, DCV/SOF, 2D/3D, SOF/RBV, GZR/EBR) and only 21% (12/58) had failed to second-generation DAAs such as VEL/SOF or G/P. Characteristic NS5A RASs at positions 28, 30 and 31 were detected particularly in GT3 (86%, 12/14) and in GT4 (96%, 23/24) after DAA failure, whereas RASs were less frequent in the other GTs. Y93H was rarely detected overall. 76% (44/58) of patients had started retreatment, most with VOX/VEL/SOF (n = 29) and overall 95% (39/41) with completed follow-up after end of retreatment) achieved SVR across all regimens. Two patients with cirrhosis had virological treatment failure. One patient with GT4r had failed to respond to VEL/SOF/RBV and another with GT3b had failed to VOX/VEL/SOF.

Conclusion: We found unusual HCV GT in 4% of DAA failure patients, mainly after failure to first generation DAA regimens. Retreatment with second generation DAAs was effective with 95% SVR. The lack of global availability of second generation DAAs could lead to the global HCV elimination targets not being met.

OS-127-YI

The risks of first hepatic decompensation and HCC remain constant during long-term follow-up and can be stratified by a one-time assessment after HCV-cure

Georg Semmler^{1,2}, Sonia Alonso Lopez^{3,4,5}, Monica Pons⁶, Sabela Lens⁷, Elton Dajti⁸, Marie Griemsmann⁹, Alberto Zanetto¹⁰, Lukas Burghart¹¹, Stephanie Hametner-Schreil¹², Lukas Hartl^{1,2}, Adriana Ahumada³, Sergio Rodriguez-Tajes⁷, Paola Zanaga¹⁰, Michael Schwarz^{1,2,11}, Clara Uson³, Mathias Jachs^{1,2}, Anna Pocurull⁷, Maria Luisa Manzano Alonso¹³, Dominik Ecker¹², Daniel Riado¹⁴, Beatriz Mateos Muñoz¹⁵, Michael Gschwantler¹¹, Francesco Paolo Russo¹⁰, Francesco Azzaroli⁸, Benjamin Maasoumy⁹, Thomas Reiberger^{1,2}, Xavier Forns⁷, Joan Genesca^{6,16}, Rafael Bañares^{3,4,5}, Mattias Mandorfer^{1,2}. ¹Medical University of Vienna, Division of Gastroenterology and Hepatology, Department of Internal Medicine III, Vienna, Austria; ²Medical University of Vienna, Vienna Hepatic Hemodynamic Lab, Division of Gastroenterology and Hepatology, Department of Internal Medicine III, Vienna, Austria; ³Hospital General Universitario Gregorio Marañón, Liver Unit, Madrid, Spain; ⁴Instituto De Investigación Sanitaria Gregorio Marañón (IISGM), Madrid, Spain; ⁵Universidad Complutense de Madrid, Madrid, Spain; ⁶Vall d'Hebron University Hospital, Vall d'Hebron Institut of Research (VHIR), Vall d'Hebron Barcelona Hospital Campus, Universitat Autònoma de Barcelona, Liver Unit, Barcelona, Spain; ⁷Hospital Clínic, Universitat de Barcelona, Liver Unit, Barcelona, Spain; ⁸University of Bologna, Department of Medical and Surgical Sciences (DIMEC), Bologna, Italy; ⁹Hannover Medical School, Department of Gastroenterology, Hepatology and Endocrinology, Hannover, Germany; ¹⁰Padua University Hospital, Gastroenterology and Multivisceral Transplant Unit, Department of Surgery, Oncology, and Gastroenterology, Padua, Italy; ¹¹Klinik Ottakring, Department of Internal Medicine IV, Vienna, Austria; ¹²Ordensklinikum Linz Barmherzige Schwestern, Department of Internal Medicine IV, Linz, Austria; ¹³Hospital Universitario 12 De Octubre, Liver Unit, Madrid, Spain; ¹⁴Hospital Universitario Fundación Alcorcón, Liver Unit, Madrid, Spain; ¹⁵Hospital Universitario Ramón y Cajal, Liver Unit, Madrid, Spain; ¹⁶Centro de Investigación Biomédica En Red de Enfermedades Hepáticas y Digestivas (CIBERehd), Instituto de Salud Carlos III, Madrid, Spain
Email: mattias.mandorfer@meduniwien.ac.at

Background and aims: The number of individuals who will be treated for and cured from HCV infection world-wide is expected to exceed 1 million per year for the next decade. In those with compensated advanced chronic liver disease (cACLD), the risks of *de-novo* hepatocellular carcinoma (HCC) and hepatic decompensation are decreased but not completely abolished by HCV-cure. Thus, risk stratification is key to decrease resource utilization by individualizing post-treatment management. We evaluated whether the incidences of HCC and hepatic decompensation decrease with time after HCV-cure and whether the discriminatory ability of a one-time post-treatment assessment is maintained during long-term follow-up.

Method: We retrospectively analyzed cACLD patients with paired liver stiffness measurement (LSM) and platelet count (PLT) before and after HCV-cure by interferon-free therapies from 7 European regions. Cumulative incidence curves were used to estimate the incidence of hepatic decompensation/HCC over time in the overall group and throughout previously defined risk strata (i.e., Baveno VII criteria for clinically significant portal hypertension after HCV-cure and Semmler et al. J Hepatol 2022 for HCC).

Results: 2347 patients (mean age 60 ± 12 years, 60% male, 21% obese, 21% diabetes) with a median LSM of 16.3 kPa (IQR: 12.1–24.5, 25% ≥25 kPa) before HCV-cure were followed for a median of 6.0 years after treatment. Interestingly, the incidence of first hepatic decompensation was strictly linear with 65 patients (2.8%) developing hepatic decompensation before eventually being diagnosed with HCC (incidence rate 0.57/100 patient years, incidence at 6 years: 3.1%, Figure-panel A). Similarly, incidence of HCC was also linear with 184

patients (7.8%) developing HCC (incidence rate 1.60/100 patient years, incidence at 6 years: 8.3%). Stratifying the risks for hepatic decompensation according to Baveno VII (Figure-panel B) and for HCC according to Semmler et al (algorithm based on age, LSM, albumin and alcohol consumption, Figure-panel C) after HCV-cure identified subgroups with a distinct prognosis during long-term follow-up, even after limiting prediction to events occurring >3 years after HCV-cure.

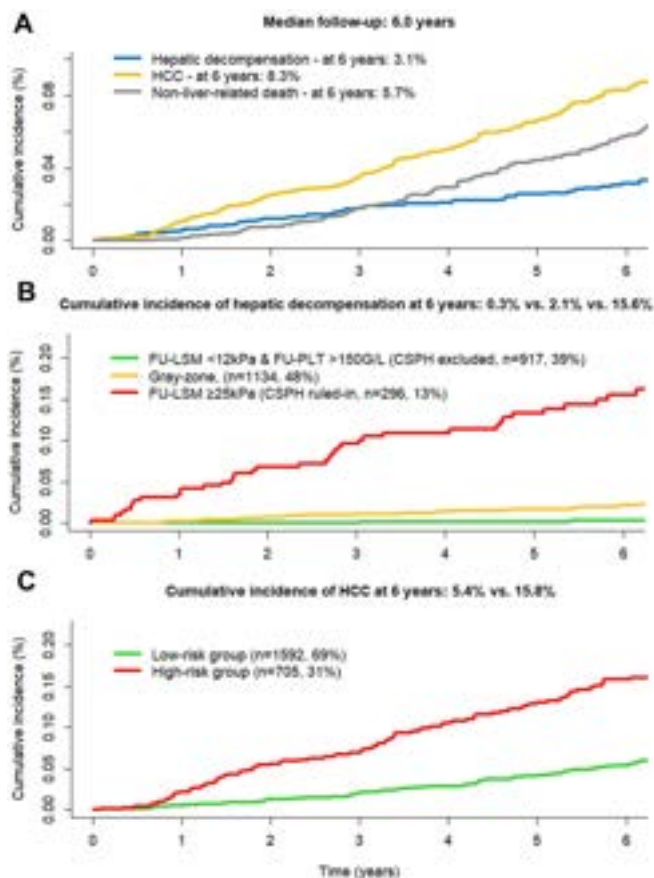


Figure:

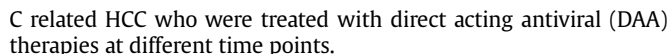
Conclusion: In patients with cACLD, the risks of hepatic decompensation, and more importantly, HCC remain constant after HCV-cure, even in the long-term (>3 years). A one-time post-treatment risk stratification based on non-invasive criteria confers important prognostic information that is maintained during long-time follow-up, as the hazards over time remain proportional.

OS-128

Achieving a hepatitis C cure in those with hepatocellular carcinoma is associated with an improvement in overall survival: real world data

Maria Guerra Veloz¹, Sital Shah¹, James Lok¹, Riham Soliman¹, Almuthana Mohamed¹, Mary D Cannon¹, Paul Ross², Ivana Carey¹, Kosh Agarwal¹. ¹King's College Hospital, Institute of Liver Studies, London, United Kingdom; ²Guy's and St Thomas' NHS Foundation Trust, Oncology, London, United Kingdom
Email: maria.guerraveloz@nhs.net

Background and aims: Achieving sustained virological response (SVR) has proved to improve clinical outcomes/survival rates in patients with chronic hepatitis C and HCC. However, the optimal time frame for delivering antiviral therapy in those with active infection remains unclear. The aim of this study was to provide real-world data on virological response and overall survival in patients with hepatitis



Method: This retrospective cohort study included hepatitis C virus (HCV) positive patients who were diagnosed with HCC and managed at King's College Hospital between January 2015 and 2020. Follow-up data was collected until death, liver transplantation or April 2022, whichever came first. Patients with historical or active HCC were included and information about tumour stage and treatments modality were collected. The latter was defined as curative (ablation, resection or liver transplantation) or non-curative (TACE, SIRT, SBRT or systemic therapy). The primary outcome was to compare the SVRs in both HCC groups, and the secondary outcome was to measure the overall survival.

Results: Of the 98 patients included, 82.7% (81) had active HCC at the time of DAA therapy and 17.3% (11) had a historical HCC. The majority (84.7%) were cirrhotic with compensated liver disease and 52% received curative HCC therapy. The overall SVR rate was 81.6%, but decreased to 75.7% in patients with active HCC. In the multivariate analysis, the presence of active HCC at the time of HCV therapy (HR, 5.46; 95% CI, 1.25–23.82, $p = 0.024$) and the number of HCC nodules (2.19 CI 95% 1.08–4.41, $p = 0.029$) were the only factors associated with not achieving SVR. Failure to achieve SVR (HR, 9.9; 95% CI, 2.16–46.01, $p = 0.003$), the presence of more advanced chronic liver disease (i.e. Child Pugh B/C HR 3.7; 95% CI 1.46–9.58) and administration of non-curative treatments (HR 3.2; 95% CI 1.19–8.44) were associated with mortality. The overall survival was higher in those who achieved SVR (130 m 95% CI 85–174) and this was consistently irrespective of treatment timing (historical HCC 119 m, 95% CI 102–135; active HCC 78 m, 95% CI 67–88), tumor stage (BCLC A 104 m, 95% CI 93–116; BCLC B/C 60 m, 95% CI 63–85) and treatment intent (curative 117 m (95% CI 107–128) and non-curative 75 m (95% CI 59–91) (log-rank test $p = 0.003$).

Conclusion: Treating Hepatitis C in patients with HCC is feasible with acceptable SVR rates.

Failure to achieve SVR is one of the main factors associated with mortality. Overall survival was higher in those who achieved SVR and this was independent of tumor stage or treatment modality.

OS-129-YI

Real-world effectiveness of voxilaprevir/velpatasvir/sofosbuvir in hepatitis C patients with prior failure to DAA treatment

Christiana Graf^{¶1}, Elisabetta Degasperi², Roberta D'Ambrosio²,
Jordi Llaneras³, Johannes Vermehren¹, Georg Dultz¹, Nils Wetzstein⁴,
Eva Herrmann⁵, Stefan Zeuzem¹, Maria Buti³, Pietro Lampertico²,
Julia Dietz¹, Christoph Sarrazin^{1,6}. ¹University Hospital Frankfurt,
Department of Internal Medicine I, Frankfurt, Germany; ²Foundation
IRCCS Ca' Granda Ospedale Maggiore Policlinico, Division of
Gastroenterology and Hepatology, Milan, Italy; ³Hospital Universitari
Vall d'Hebron, Department of Medicine of the UAB (Universitat
Autònoma de Barcelona), Barcelona, Spain; ⁴University Hospital
Frankfurt, Department of Internal Medicine, Infectious Diseases,
Frankfurt, Germany; ⁵Goethe University Frankfurt, Institute of
Biostatistics and Mathematical Modeling, Frankfurt, Germany;
⁶St. Josefs-Hospital, Medizinische Klinik II, Wiesbaden, Germany
Email: christiana.graf@kgu.de

Abstract OS-129-YI is under embargo until Saturday 24 June 2023, 14:00. This abstract will be made publicly available on the congress website at 14:00 (CEST) on the day of its presentation at the congress. Industry must not issue press releases – even under embargo – covering the data contained in abstracts selected to be highlighted during official EASL Press Office activities or in official EASL Press Office materials until the individual embargo for each data set lifts. Media must not issue coverage of the data contained in abstracts selected to be highlighted during official EASL Press Office activities or in official EASL Press Office materials until the individual embargo for each data set lifts.

Journalists, industry, investigators and/or study sponsors must abide by the embargo times set by EASL. Violation of the embargo will be taken seriously. Individuals and/or sponsors who violate EASL's embargo policy may face sanctions relating to current and future abstract submissions, presentations and visibility at EASL Congresses. The EASL Governing Board is at liberty to ban attendance and/or retract data.

Copyright for abstracts (both oral and poster) on the website and as made available during The International Liver Congress™ 2023

resides with the respective authors. No reproduction, re-use or transcription for any commercial purpose or use of the content is permitted without the written permission of the authors. Permission for re-use must be obtained directly from the authors.

Late-breaker Posters

WEDNESDAY 21 TO SATURDAY 24 JUNE

LBP-01

HCV and HBV prevalence and associated risk factors among people who inject drugs in Kenya

Matthew Akiyama¹, Lindsey Riback¹, Mercy Nyakowa², Chenshu Zhang¹, Sarah Masyuko², Rose Wafula², Nazila Ganatra².

¹Albert Einstein College of Medicine/Montefiore Medical Center, Medicine, Bronx, United States; ²Kenya Ministry of Health, Kenya
Email: makiyama@montefiore.org

Background and aims: Injection drug use is an important risk factor for viral hepatitis in sub-Saharan Africa, but factors associated with seropositivity are poorly understood. Understanding the prevalence and transmission risk factors is critical to reducing prevalence and incidence among people who inject drugs (PWID). We assessed factors associated with hepatitis C antibody (anti-HCV) and hepatitis B (HBV) positivity among PWID in Kenya.

Method: We are recruiting 3,500 PWID from needle and syringe programs sites in Kenya. Participants are recruited using respondent driven sampling, complete biobehavioral surveys and receive HCV, HBV, and HIV testing. We conducted this analysis using chi-square tests for categorical values and t-tests for continuous variables.

Results: Among the 1526 participants enrolled, participants are mainly male (89.9%) and 34.4 years old (SD=±8.6) on average. Roughly one-fifth, 314 (20.6%) are anti-HCV positive; regional prevalence is highest in the Coast (175/589, 29.7%), followed by Nairobi (137/589, 23.3%), and Western Region (2/348, 0.6%). HBV surface antigen (HBsAg) follows a similar gradation to HCV moving inland. Overall HBsAg prevalence is 1.4%; 13/589 (2.2%), 6/589 (1.0%) and 2/348 (0.6%), respectively. HBV-positive participants were significantly more likely to be female (23.8% vs 9.9%, $p=0.036$), which was not the case for HCV (12.7% vs 9.4%, $p=0.09$). However, both HCV-positive and HBV-positive PWID were more likely to have a main sexual partner who injects (30.4% vs 19.9%, $p=0.023$) and (55.6% vs 21.5%, $p=0.028$), respectively. HCV-positive PWID were more likely to have used supplies previously used by others at their last injection; needle (17.8% vs 7.8%, $p<0.001$) and cookers (23.3% vs 9.0%, $p<0.001$) when compared to their HCV-negative counterparts. Similar supply sharing patterns were identified for HBV status, HBV-positive PWID were more likely to share needles (23.8% vs 9.7%, $p=0.031$) and cookers (28.6% vs 11.7%, $p=0.018$). HCV-positivity was also associated with a history of incarceration (52.9% vs 43.9%, $p=0.004$), more years injecting (9.7 vs 5.4, $p<0.001$), and exchanging sex to be injected in the last 30 days (0.25% vs. 1.61%, $p=0.011$).

Conclusion: Rising anti-HCV prevalence in Kenya (20.6% vs 13.0% in our previous survey) could be attributable to high engagement in risk behaviours such as shared injection equipment, suggesting a need to expand harm reduction interventions and include targeted approaches among PWID with sexual partners who also inject. Due to differing risk factors for HCV and HBV, once size fits all intervention may not be optimal. While preliminary, we anticipate these data will

inform policy makers and programs on identifying viral hepatitis elimination and prevention strategies among PWID. Next steps include performing next generation HCV sequencing and phylogenetic analysis to characterize transmission networks and determine factors associated with transmission and cluster membership. We anticipate the latter will be leveraged for targeted elimination strategies to reduce viral hepatitis among PWID with potential for generalizability to other resource limited settings.

LBP-02

Using FIB-4's parameters an explainable black-box machine learning model outperforms FIB-4 index on the diagnosis of advanced fibrosis of non alcohol related fatty liver disease patients in three cohorts from China, Malaysia and India

Athanasios Angelakis^{1,2,3}, Tianlu Chen^{4,5}. ¹Amsterdam Public Health Research Institute, Netherlands; ²University of Amsterdam, Netherlands;

³Amsterdam University Medical Centers, Netherlands; ⁴Shanghai Jiao Tong University, China; ⁵Sixth People's Hospital, China

Email: a.angelakis@amsterdamumc.nl

Background and aims: Non-alcoholic fatty liver disease (NAFLD) affects over 25% of the general population. FIB-4 index for liver fibrosis is an important non-invasive test which can be used to distinguish advanced fibrosis (F012 vs. F34 in metavir score). Our aim is to tune an explainable machine learning model using as features FIB-4's variables which outperforms FIB-4 on the diagnosis of early/advanced fibrosis of patients with NAFLD.

Method: We use three cohorts from China (train), Malaysia (test1) and India (test2) consisting of 540 (early/advanced fibrosis) 391/149, 147 (116/31) and 97 (65/32) patients with liver biopsy validated hepatic fibrosis. The features of the datasets are: age, sex, alanine transaminase (ALT), aspartate transaminase (AST), platelet (PLT), the ratio AST/PLT and the FIB-4 score. For training the machine learning model on the train dataset and we test it on the test1 and on the test2. For tuning we use 10-fold cross validation (10CV) in order to gain more confidence in our machine learning model regarding its robustness. Even though the number of data instances of our train set is relatively low, we use categorical gradient boosted trees (catboost) which has shown great performance on similar size tabular datasets; it hardly overfits and it is robust. We use feature engineering in order to add more dimensions to our features' space taking powers of products of the initial features. Tuned catboost's parameters' values are: iterations: 111, learning_rate: 0.12 and depth: 16; all other parameters have default values. From explainable artificial intelligence we use shapley values in order to understand the weight of features regarding the predictability of catboost.

Results: We compare our catboost's performance with the FIB-4 score. Catboost on the training set using 10CV, on the test1 and one the test2 achieved the following performance: 10CV: Spec: 0.9301 ± 0.0616 CI95[0.8235, 1.000], Sens: 0.5546 ± 0.1005 CI95[0.3226, 0.75], AUC: 0.7950 ± 0.0649 CI95[0.6809, 0.8902], test1: Spec: 0.9545, Sens: 0.4576, AUC: 0.7976, test2: Spec: 0.7759, Sens: 0.4872, AUC: 0.643. The performance of the FIB-4 using 1.3 as cutoff value was the following on the training set 10CV: Spec: 0.8500 ± 0.0744 CI95 [0.7436, 0.9667], Sens: 0.4893 ± 0.0855 CI95[0.3750, 0.6667], AUC: 0.6997 ± 0.0692 CI95[0.5691, 0.7871], test1: Spec: 0.9109, Sens: 0.4783, AUC: 0.7514, test2: Spec: 0.7414, Sens: 0.4359, AUC: 0.5964.



Using our method we observe a relative big improvement of the AUC on the train, test1 and test2 datasets regarding the performance of FIB-4, namely: 13.41%, 6.15% and 7.81%. Using shapley values we observe that the ten most important features regarding the predictability of catboost are: PLT^{*11} , PLT^{*8} , ALT^{*11} , PLT^{*9} , ALT^{*10} , $FIB4^{*3}$, Age^{*11} , $FIB4^{*2}$, $FIB4^{*7}$, $FIB4^{*5}$. None of this belongs to the initial features.

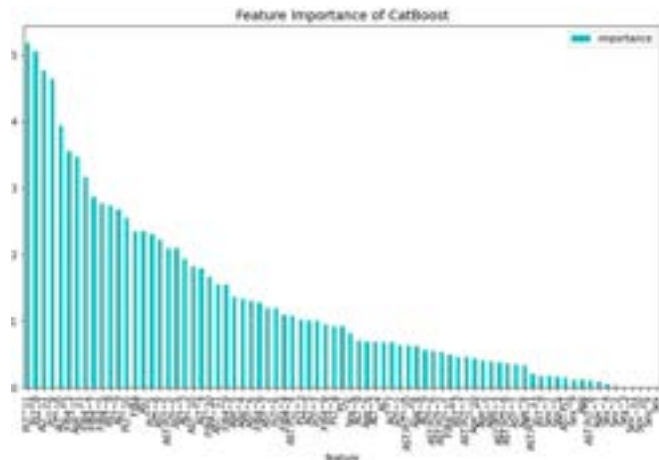


Figure:

Conclusion: Using data science approach, catboost, feature engineering and as features sex and FIB-4's variables, we achieve better performance and more robust solution, than the FIB-4. Using explainable artificial intelligence we identify the importance of powers of the variables of FIB-4 which could lead to an improved version of FIB-4. In addition, we think we should start considering that the classification of NAFLD patients to early versus advanced fibrosis is not a problem which could be approached by linear cut-off values only. It is a more complicated problem and data science using explainable artificial intelligence could help.

LBP-03

Safety and efficacy of continuous infusion terlipressin (BIV201) in patients with decompensated cirrhosis and refractory ascites: a phase 2, randomized, controlled, open-label study

Jasmohan Bajaj¹, Ethan Weinberg², K. Rajender Reddy², Andrew Keaveny³, Michael Porayko⁴, David Koch⁵, Paul Thuluvath⁶, Douglas Simonetto⁷, Paolo Angeli⁸, Sujit Janardhan⁹, Eric Orman¹⁰, Sammy Saab¹¹, Jeffrey Zhang¹², Susan Clausen¹³, Joseph Palumbo¹³, Penelope Markham¹³. ¹Richmond VA Medical Center, United States; ²University of Pennsylvania, United States; ³Mayo Clinic, Jacksonville, FL, United States; ⁴Vanderbilt University, United States; ⁵Medical University of South Carolina, United States; ⁶Mercy Medical Center, United States; ⁷Mayo Clinic, Rochester, United States; ⁸University of Padova, Italy; ⁹Rush University, United States; ¹⁰Indiana University, United States; ¹¹David Geffen School of Medicine, University of California, Los Angeles, United States; ¹²Princeton Pharmatech, United States; ¹³BioVie Inc., United States

Email: jasmohan.bajaj@va.gov

Background and aims: Patients with cirrhosis and refractory ascites have a poor quality of life. The standard of care (SOC), which includes regular large-volume therapeutic paracentesis (TP), provides only temporary relief and is associated with significant medical complications. Terlipressin, an analog of vasopressin, improves renal perfusion and excretion. BIV201 (terlipressin administered as a continuous infusion by a small ambulatory pump) is being evaluated for reduction of ascites accumulation and related complications in a prospective, phase 2b, open-label, randomized trial.

Method: Fifteen, out of a total of 30, adult patients with diuretic-resistant ascites due to decompensated cirrhosis and 3 to 9 TPs within

the previous 60 days were enrolled, monitored for 14-28 days, and randomized 2:1 to receive either continuous infusion of BIV201 (3 mg/day; dose-adjusted to 2-4 mg/day) for two 28-day cycles plus SOC, separated by an up to 56-day washout period, or SOC alone, respectively, for a total of 180 days, followed by a 180-day, long-term follow-up phase. Here we report interim data analysis for safety, change in ascites accumulation (total ascites volume removed by TP), and related parameters.

Results: Mean age of the 15 enrolled patients was 61.3 years, mean MELD-Na was 15.4, and the mean CTP score was 8.7. 10 patients were randomized to receive BIV201 plus SOC and 5 patients received SOC alone. Five (50%) patients in the BIV201 group completed both 28-day infusion cycles; 5 patients discontinued during or at the end of treatment cycle 1. One patient in the SOC-only group withdrew consent at randomization. Patients who completed both treatment cycles of BIV201 plus SOC (n = 5) experienced mean reductions of 43% (p = 0.063) in ascites accumulation and 47% (p = 0.021) in the mean number of monthly TPs, during the 3 months of treatment, compared with 3 months prior to treatment, vs respective mean reductions of 13% (p = 0.561) and 21% (p = 0.263) in the SOC-only group. In these patients, after 28 days of treatment, BIV201 treatment was associated with significant improvements in ascites-related symptoms scores (p = 0.006), pharmacodynamic measures related to ascites pathophysiology (reduction in serum creatinine [p = 0.019] and plasma renin activity [p = 0.048]), and health-related quality of life measured by the Chronic Liver Disease Questionnaire (p = 0.002), mainly driven by improvements in the abdominal domain. Treatment was generally well tolerated with 1 treatment-related serious adverse event (hyponatremia), which resolved upon treatment withdrawal.

Conclusion: These data indicate that treatment with BIV201 plus SOC may significantly reduce ascites accumulation and its associated symptoms compared with SOC alone. If confirmed in future studies, the current safety profile of BIV201 may support its use for outpatient administration in the treatment of refractory ascites.

LBP-04

Long-term trends of circulating hepatitis B virus RNA and hepatitis B core-related antigen levels in persons with HIV and functional hepatitis B cure during tenofovir therapy

Lorin Bègre^{1,2}, Anders Boyd³, Marie-Laure Plissonnier⁴, Barbara Testoni⁴, Franziska Suter-Riniker⁵, Charles Bèguelin¹, Jürgen Rockstroh⁶, Huldrych Günthard^{7,8}, Alexandra Calmy⁹, Matthias Cavassini¹⁰, Hans Hirsch¹¹, Massimo Levrero^{4,12}, Gilles Wandeler¹, Fabien Zoulim^{4,12}, Andri Rauch¹. ¹Department of Infectious Diseases, Inselspital, Bern University Hospital, University of Bern, Bern, Switzerland; ²Graduate School for Health Sciences, University of Bern, Bern, Switzerland; ³Department of Infectious Diseases, Research and Prevention, Public Health Service of Amsterdam, and stichting hiv monitoring, Amsterdam, Netherlands; ⁴UMR Inserm U1052-CNRS 5286, Cancer Research Center of Lyon (CRCL), Lyon, France; ⁵Institute for Infectious Diseases, University of Bern, Bern, Switzerland; ⁶HIV-Clinic, Department of Medicine I, University Hospital Bonn, Bonn, Germany; ⁷Department of Infectious Diseases, University Hospital Zurich, Zurich, Switzerland; ⁸Institute of Medical Virology, University of Zurich, Zurich, Switzerland; ⁹Division of Infectious Diseases, University Hospital Geneva, University of Geneva, Geneva, Switzerland; ¹⁰Division of Infectious Diseases, Lausanne University Hospital, University of Lausanne, Lausanne, Switzerland; ¹¹Division of Infectious Diseases and Hospital Epidemiology, University Hospital Basel, University of Basel, Basel, Switzerland; ¹²Hepatology Department, Hospices Civils de Lyon and University of Claude Bernard Lyon 1 (UCLB1), Lyon, France

Email: lorinaaron.begre@insel.ch

Background and aims: Hepatitis B core-related antigen (HBcrAg) and circulating hepatitis B virus (HBV) RNA correlate with intrahepatic covalently closed circular DNA (cccDNA) levels and cccDNA transcriptional activity. Both markers may help improve the understanding of the determinants of functional HBV cure during antiviral

POSTER PRESENTATIONS

therapy. We aimed to compare long-term trends of HBcrAg and circulating HBV RNA levels in persons with HIV and HBV treated with tenofovir disoproxil fumarate or tenofovir alafenamide in the Swiss HIV Cohort Study.

Method: We included 29 participants experiencing functional HBV cure during tenofovir-containing antiretroviral therapy (ART) and 29 participants without functional HBV cure matched 1:1 based on age, sex, prior treatment with lamivudine and CD4+ T-cell count. We defined functional HBV cure as a quantitative hepatitis B surface antigen (qHBsAg) level <0.05 IU/ml. We measured qHBsAg, HBV DNA, HBcrAg and HBV RNA every six months during the first two years after the initiation of tenofovir and annually thereafter. We assessed the cumulative proportion of participants with undetectable HBV DNA, HBV RNA and HBcrAg levels using Kaplan-Meier estimators in participants with detectable levels at tenofovir start, and compared participants with and without functional HBV cure using Fisher's exact and log-rank tests.

Results: Median follow-up time was 12 years (interquartile range [IQR] 8-14), with functional HBV cure occurring after a median of 4 years (IQR 1-8). Prior to starting tenofovir, 48/58 (83%) participants received lamivudine for a median duration of 6 years (IQR 4-8). At tenofovir start, 15/58 (26%) had HBV DNA levels <20 IU/ml, 7/49 (14%) had HBcrAg levels $\leq 3 \log_{10}$ U/ml and 17/49 (35%) had HBV RNA levels <10 copies/ml without significant differences between participants with and without functional HBV cure. All participants with functional HBV cure and 28/29 (97%) without cure achieved HBV DNA <20 IU/ml on tenofovir ($p=1.00$). Among participants with functional HBV cure, 23/29 (79%) ever achieved HBcrAg $\leq 3 \log_{10}$ U/ml and all achieved HBV RNA <10 copies/ml before or at the time of the first qHBsAg <0.05 IU/ml. In comparison, 23/29 (79%) participants without cure achieved HBV RNA <10 copies/ml ($p=0.02$) and 14/29 (48%) achieved HBcrAg $\leq 3 \log_{10}$ U/ml ($p=0.03$). The cumulative proportions of participants with HBV DNA <20 IU/ml, HBcrAg levels

$\leq 3 \log_{10}$ U/ml and HBV RNA <10 copies/ml in persons with and without functional HBV cure are depicted in the Figure.

Conclusion: HBV RNA levels decreased to undetectable levels in all persons with HIV and functional HBV cure, whereas a fifth of the persons without cure had detectable HBV RNA levels on long-term tenofovir-containing ART despite HBV DNA suppression. HBcrAg levels decreased during tenofovir therapy, but remained detectable in approximately 20% of persons with and 50% of persons without functional HBV cure.

LBP-05

Dramatic reductions in hepatic steatosis accompanied by improved HbA1c following a 4-week treatment of obese/diabetic/NAFLD patients with DD01, a novel long-acting GLP-1/glucagon receptor agonist

Adam Bell¹, Dennis To¹, Subbu Karanth¹, Svetlana Sosnovtseva¹, Yen-Huei Lin¹, Jaehee Shin². ¹DandD Pharmatech, Neuraly, Inc, Gaithersburg, United States; ²DandD Pharmatech, Seongnam-si, Korea, Rep. of South

Email: acbell@neuralymed.com

Background and aims: DD01 is a novel, long-acting dual agonist of the GLP-1 and glucagon receptors. In rodent and non-human primate models, DD01 improved glycemic control, reduced hepatic steatosis, and resulted in weight loss. In rodents the effect on liver fat was more significant than achieved with a comparable dose of semaglutide, consistent with the expected effect of increased hepatic lipolysis achieved through activation of the glucagon receptor. Based on these pharmacologic effects, DD01 was evaluated for safety and its effect on diabetes, obesity, and NAFLD in humans.

Method: A Phase 1 study was conducted in subjects with overweight/obese subjects with type 2 diabetes and NAFLD. Doses from 1-80 mg were evaluated in both single-ascending and multiple-ascending (4 once-weekly doses) cohorts of 8. Safety, tolerability, and PK were assessed for all dose groups. Fasting and post-prandial glucose,

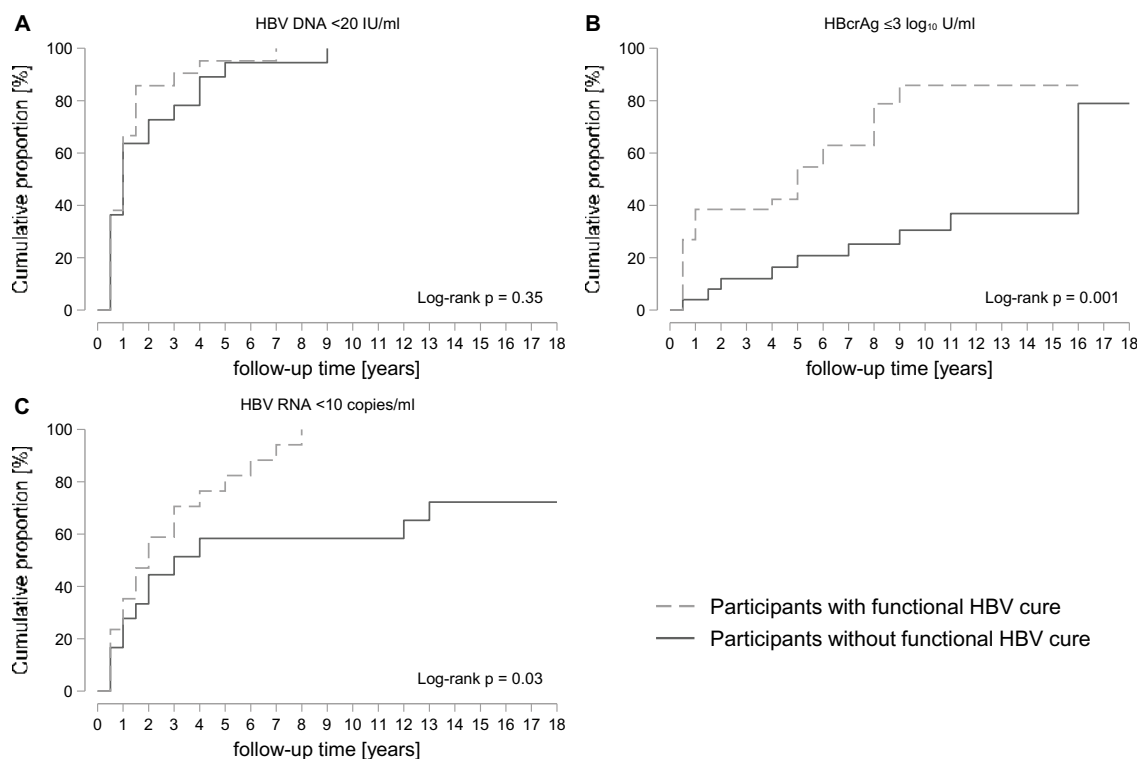


Figure: (abstract: LBP-04): Kaplan Meier curves for cumulative proportions with HBV DNA <20 IU/ml (A), HBcrAg $\leq 3 \log_{10}$ U/ml (B) and circulating HBV RNA <10 copies/ml (C) after starting tenofovir-containing antiretroviral therapy, stratified on participants with and without functional HBV cure on tenofovir.

insulin, and glucagon were measured periodically during the dosing period and during a mixed-meal tolerance tests conducted at baseline and after the last dose was administered for each cohort. Liver fat was measured by MRI-PDFF on Day -1 and Day 36. HbA1c and body weight were assessed pre-dose and at the end of 4 weeks dosing.

Results: DD01 treatment resulted in rapid, clinically significant reductions in hepatic steatosis. Reductions in HbA1c were observed at lower and overlapping doses and this was accompanied by reductions in caloric intake and weight loss. DD01 was generally safe and well tolerated. Adverse events were as expected for a GLP-1R agonist and primarily GI-related. DD01 has a half-life of 7-8 days. Following only 4 once-weekly treatments with DD01, up to 100% of patients achieved $\geq 30\%$ reduction in liver fat as assessed by MRI-PDFF. In the high dose group, all subjects achieved at least a 40% reduction in liver fat with a mean reduction of 52% whereas the change from baseline liver fat in the placebo group was only 2.8%. Substantial reductions in liver fat were observed at doses with minimal effect on body weight underscoring the importance of direct lipogenic action achieved through the glucagon receptor in the liver. Meaningful and rapid improvements in steatosis were observed at well-tolerated doses that did not cause significant weight loss, potentially uncoupling the need for weight loss to precede or coincide with significant improvements in liver health. Over the 4-week treatment period, improved HbA1c, decreased meal-related glucose, and mild weight loss accompanied dose-dependent reductions in hepatic steatosis. DD01 is a dual-pathway GLP-1R agonist augmenting the benefits of the incretin pathway through activation of the glucagon pathway.

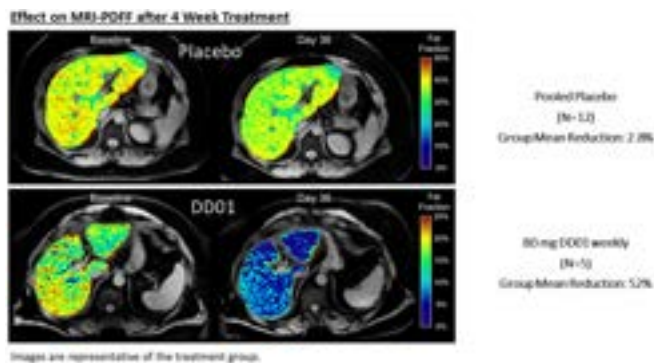


Figure:

Conclusion: DD01 acts through the GLP-1 receptor and glucagon receptor pathways to improve glucose control and rapidly reduce hepatic steatosis. Weight loss is observed at higher doses and it appears that rapid resolution of hepatic steatosis can be achieved independent of weight loss. The combined effects of DD01 may be useful in the treatment of NASH and NAFLD both with and without co-occurring diabetes.

LBP-06

Preventing liver disease with policy measures to tackle alcohol consumption and obesity: a microsimulation study

Lise Retat¹, Laura Webber¹, Peter Jepsen², Helena Cortez-Pinto³, Markiyan Mitchyn⁴, Jeffrey Lazarus⁵, Alexander Martin¹, Francesco Negro⁶, Pierre Nahon⁷, John Guzek⁴, Nick Sheron^{8,9}, Joshua Card-Gower¹, Shira Zelber-Sagi⁹, Hannah Graff⁴, Maria Buti¹⁰.
¹HealthLumen Ltd, London, United Kingdom, United Kingdom;
²Department of Hepatology and Gastroenterology, Aarhus University Hospital, Aarhus, Denmark, Denmark; ³Clínica Universitária de Gastroenterologia, Centro de Nutrição e Metabolismo, Faculdade de Medicina, Universidade de Lisboa, Portugal, Portugal; ⁴HealthLumen Ltd, London, United Kingdom, United Kingdom; ⁵Barcelona Institute for Global Health (ISGlobal), Hospital Clinic, University of Barcelona, Barcelona, Spain, Spain; ⁶Division of Gastroenterology and Hepatology,

University Hospitals, Geneva, Switzerland, Switzerland; ⁷AP-HP, Hôpitaux Universitaires Paris Seine Saint-Denis, Liver Unit, Bobigny; Université Sorbonne Paris Nord, France; ⁸The Foundation for Liver Research, The Institute of Hepatology, London, United Kingdom; ⁹School of Public Health, University of Haifa, Haifa, Israel, Israel; ¹⁰Liver Unit, Hospital Universitario Vall d'Hebron, and CIBEREHD del Instituto de Salud Carlos III, Barcelona, Spain
 Email: lise.retat@healthlumen.com

Background and aims: Chronic liver disease (CLD) causes 1.8% of all deaths in Europe. Without policies to mitigate harmful alcohol consumption and obesity, that proportion will continue to increase. This study aims to estimate the impact of policy interventions targeting alcohol and obesity on the incidence of CLD and primary liver cancer in France, the Netherlands, and Romania.

Method: A validated and peer-reviewed microsimulation model was employed using data from online public databases and published literature. Static and dynamic trends in alcohol consumption and body mass index (BMI) respectively were projected from 2022 to 2030. We modeled the incidence of CLD and liver cancer under three policy scenarios versus an inaction scenario. The policies were 1€ minimum unit pricing (MUP) on alcohol; a combination of 0.7€ MUP and a sugar sweetened beverage (SSB) tax; and a combination of 0.7€ MUP, SSB tax, and a volumetric tax on alcohol.

Results: All policies had an important impact ranging from a 2% to 7% reduction in annual incidence of chronic liver disease and liver cancer by 2030. The 1€ MUP policy had the largest predicted impact: In the three countries combined, that policy would result in 11,550 fewer cases of CLD and 7,921 fewer cases of liver cancer by 2030. Policy interventions combining a €0.7 MUP, an SSB tax, and a volumetric tax on alcohol would prevent nearly as many cases: 7,317 cases of CLD and 5,390 cases of liver cancer by 2030 compared with the inaction scenario.

Conclusion: In conclusion, we can reduce the number of Europeans who develop chronic liver disease or liver cancer by up to 7% before 2030 if we introduce a €1 MUP on alcohol, or we introduce complementary public health policies targeting alcohol consumption and obesity.

LBP-07

Validation of the R3-AFP model for risk prediction of HCC recurrence after liver transplantation in the SiLVER clinical trial

Federico Piñero¹, Quirino Lai², Charlotte Costentin³, Andreas Schnitzbauer⁴, Helena Degroote⁵, Edward Geissler⁶, Christophe Duvoux⁷.
¹Hospital Universitario Austral, Austral University, Liver Unit, Academic Department, Buenos Aires, Argentina; ²General Surgery and Organ Transplantation Unit, Sapienza University of Rome, Italy, Italy; ³Grenoble Alpes University; Institute for Advanced Biosciences, Research Center UGA/Inserm U 1209/CNRS 5309; ⁴Gastroenterology, hepatology and GI oncology department, Digidune, Grenoble Alpes University Hospital; La Tronche, France, France; ⁵HPB and transplant surgery, University Hospital Frankfurt, Germany, Germany; ⁶Department of Hepatology and Gastroenterology, Ghent University Hospital, Belgium, Belgium; ⁷University Hospital Regensburg, Regensburg, Germany, Germany; ⁸Department of Hepatology, Medical Liver Transplant Unit, Hospital Henri Mondor AP-HP, University of Paris-Est Créteil (UPEC), France
 Email: fpiñero@cas.austral.edu.ar

Background and aims: Hepatocellular carcinoma (HCC) recurrence risk after liver transplantation (LT) has been evaluated with different prediction models following pathology explant analysis. The inclusion of alpha-feto protein (AFP) in these models, such as the novel R3-AFP score (1), have significantly improved risk stratification of HCC recurrence post-LT. The SiLVER trial (NCT00355862) evaluated the efficacy of mTOR inhibitors (Sirolimus-Group B) compared to mTOR-free based immunosuppression (Group A) to reduce post-LT HCC recurrence (2). Here, we aimed to validate the prognostic and predictive discrimination power of R3-AFP scoring on the

POSTER PRESENTATIONS

Table: (abstract: LBP-06).

Country	Prediction scenario	Chronic liver disease			Liver cancer		
		Predicted absolute reduction in number of cases by-2030 (\pm SD)	2030 annual incidence (per 100,000 individuals) (\pm SD)	Reduced cases as % of expected cases under inaction scenario	Predicted absolute reduction in number of cases between 2022-2030 (\pm SD)	2030 Annual incidence (per 100,000 population) (\pm SD)	Reduced cases as % of expected cases under inaction scenario
France	Inaction	-	17.90(\pm 0.26)	-	-	17.34 (\pm 0.26)	-
	1€ MUP	7,632 \pm 731)	16.76 (\pm 0.25)	7.09	5,705 (\pm 698)	16.31 (\pm 0.25)	5.83
	0.7€ MUP	3,851 (\pm 738)	17.27 (\pm 0.26)	3.58	3,057 (\pm 703)	16.80 (\pm 0.25)	3.13
	0.7€ MUP, SSB tax and Volumetric tax	4,922 \pm 736)	17.11 (\pm 0.26)	4.57	3,866 (\pm 702)	16.66 (\pm 0.25)	3.95
Netherlands	Inaction	-	13.04 (\pm 0.22)	-	-	6.35 (\pm 0.16)	-
	1€ MUP	1,459 (\pm 163)	12.21 (\pm 0.22)	7.12	452 (\pm 111)	6.01 (\pm 0.15)	4.81
	0.7€ MUP	730 (\pm 165)	12.59 (\pm 0.22)	3.56	264 (\pm 112)	6.12 (\pm 0.15)	2.81
	0.7€ MUP, SSB tax and Volumetric tax	946 (\pm 164)	12.47 (\pm 0.22)	4.61	332 (\pm 112)	6.07 (\pm 0.15)	3.53
Romania	Inaction	-	19.52 (\pm 0.28)	-	-	21.51 (\pm 0.30)	-
	1€ MUP	2,459 (\pm 220)	18.28 (\pm 0.27)	7.28	1,764 (\pm 223)	20.38 (\pm 0.29)	5.14
	0.7€ MUP	1,091 (\pm 222)	18.94 (\pm 0.28)	3.23	920 (\pm 225)	20.89 (\pm 0.29)	2.68
	0.7€ MUP, SSB tax and Volumetric tax	1,449 \pm 222)	18.75 (\pm 0.28)	4.29	1,191 (\pm 224)	20.72 (\pm 0.29)	3.47

intention-to-treat population (ITT) included in the SiLVER trial (NCT00355862).

Method: We included the intention-to-treat (ITT) patient population from the SiLVER Study. Cox proportional hazard survival analysis was performed, estimating hazard ratios (HR) and 95% confidence intervals (95% CI). Discriminant function was evaluated using the Harrell's c-index. A competing risk regression analysis was also conducted estimating sub-HR. Calibration was conducted through expected versus observed events estimating the baseline hazard.

Results: Overall, 528 patients signed written informed consent of which 20 were excluded for the intention-to-treat analysis (Group A, n=256; Group B, n=252). The 5-year recurrence rate in the ITT population was 18.7% (95% CI 15.3-22.6; n=88 recurrences). The frequency distribution of the R3-AFP score was 42.6% low risk group (n=216), 35.7% (n=181) intermediate risk, 19.5% high risk group (n=99), and 2.2% very high risk group (n=11). The R3-AFP score correctly stratified HCC recurrence risk (Figure 1) (reference: low risk group): intermediate risk group SHR 1.80 (95% CI 1.02;3.18), high risk group SHR 4.20 (2.41;7.31), and very high risk group SHR 9.55 (3.66;24.92). Discrimination power for the R3_AFP model was 0.75 (95% CI 0.69;0.81) in the ITT population; lower in the mTOR group [Group B 0.67 (0.59-0.75) vs Group A 0.75 (CI 0.69-0.81); P=0.048]. No significant differences were observed between expected and observed events across R3-AFP strata.

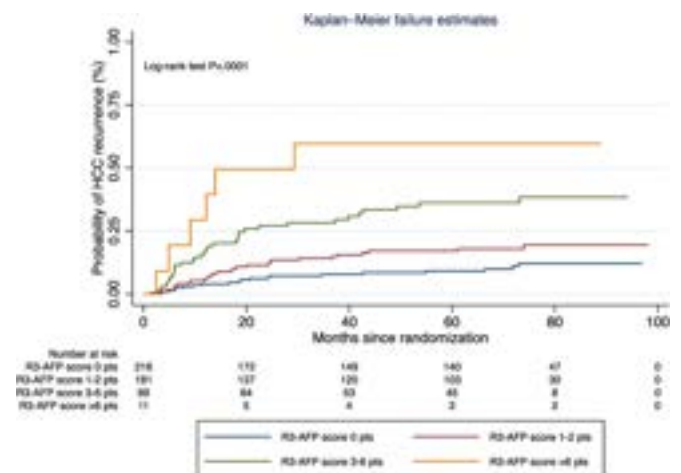


Figure:

Conclusion: The R3-AFP score has been validated in the ITT population of the SiLVER trial, a high-quality evidenced-based data, showing good performance. The model had lower discrimination of the risk of recurrence in exposed subjects with mTOR immunosuppression. This should lead to further hypothesis testing.

LBP-08

High prevalence of short telomeres in patients with idiopathic porto-sinusoidal vascular disorder

Alexander Coukos¹, Chiara Saglietti², Monika Haubitz³, Christine Sempoux¹, Jean-Marc Good², Thomas Greuter^{2,4}, Darius Moradpour¹, Lorenzo Alberio⁵, Gabriela Baerlocher³, Montserrat Fraga Christinet¹. ¹Lausanne University Hospital, Gastroenterology and hepatology, Lausanne, Switzerland; ²Lausanne University Hospital, Lausanne, Switzerland; ³Department for BioMedical Research of University of Bern (Mu35), Bern, Switzerland; ⁴GZO Spital Wetzikon, Wetzikon, Switzerland; ⁵Lausanne University Hospital, Hematology and central hematology laboratory, Lausanne, Switzerland Email: alexcoukos@gmail.com

Background and aims: Telomeres are repetitive DNA sequences on chromosomal ends which naturally shorten during mitosis, preventing loss of coding DNA. Monogenic loss-of-function mutations in telomere-maintenance genes cause excessive telomeric shortening, leading to cellular senescence and consequently systemic organ dysfunction, a condition referred to as short telomere syndrome (STS). One hepatic manifestation documented in STS is porto-sinusoidal vascular disorder (PSVD). Because the etiology of many cases of PSVD remains unknown, this study aimed to explore the extent to which short telomeres are present in patients with idiopathic PSVD.

Method: This single-center study included patients with idiopathic PSVD and characterized them in depth after histological review and confirmation. Telomere length in six peripheral blood leukocyte subpopulations was assessed by multicolor flow cytometry.

Results: In total, 28 patients were included of whom 19 (68%) had short (12/29) or very short (7/29) telomeres, while nine (32%) had telomere length in the middle part of the age-adjusted reference range (shown as percentiles) calculated from healthy individuals. Seventeen (61%) had clinically significant portal hypertension. The shortest telomeres were found in granulocytes compared to other cell subtypes. Short telomeres were more frequent in males ($p = 0.006$), in patients with portal hypertension ($p = 0.026$) as well as in patients with concomitant interstitial lung disease ($p = 0.001$), chronic kidney disease ($p = 0.002$) and erythrocyte macrocytosis ($p = 0.001$). Low serum albumin ($p = 0.004$), low platelets ($p = 0.048$),

hyperbilirubinemia ($p = 0.029$) and a dysmorphic liver on imaging studies ($p = 0.012$) were also associated with short telomeres.

Conclusion: Short telomeres were present at a remarkably high rate in all six cell lines in patients with idiopathic PSVD. This reinforces the hypothesis that they may play a role in the pathogenesis of vascular liver disease. Studies investigating the genetic basis in our patient cohort are ongoing.

LBP-09

Further decompensation as a new prognostic stage in cirrhosis. Results of a large multicenter cohort study supporting Baveno VII statements

Gennaro D'Amico¹, Guadalupe Garcia-Tsao², Alexander Zipprich³, Cándid Villanueva⁴, Juan Antonio Sorda⁵, Rosa M Morillas⁶, Matteo Garcovich⁷, Montserrat García-Retortillo⁸, Javier Martinez⁹, Paul Cales¹⁰, Mario D'Amico¹¹, Matthias Dollinger¹², Maria Garcia-Guix⁴, Esteban Gonzalez Ballerga⁵, Emmanuel Tsochatzis⁷, Isabel Cirera⁸, Agustin Albillos⁹, Guillaume Roquin¹⁰, Linda Pasta^{1,13}, Alan Colomo⁴, Nuria Cañete Hidalgo⁸, Jerome Boursier¹⁰, Marcello Dallio¹⁴, Antonio Gasbarrini¹⁵, Iacobellis Angelo¹⁶, Giulia Gobbo¹⁷, Manuela Merli¹⁸, Alessandro Federico¹⁹, Gianluca Svegliati-Baroni²⁰, Pietro Pozzoni²¹, Luigi Addario²², Luchino Chessa²³, Lorenzo Ridola²⁴, Andrew Burroughs⁷. ¹Azienda Ospedaliera Ospedali Riuniti Villa Sofia-Cervellomo, Gastroenterology, Palermo, Italy; ²Yale University School of Medicine, Digestive Disease Section, New Haven, United States; ³Jena University Hospitals, Internal Medicine IV, Jena, Germany; ⁴Hospital de la Santa Creu i Sant Pau, Gastroenterology Unit, Barcelona, Spain; ⁵Hospital de Clínicas "José de San Martín", Facultad de Medicina, Sección Hepatología-División Gastroenterología, Buenos Aires, Argentina; ⁶Hospital Germans Trias i Pujol, Liver Unit, Badalona, Spain; ⁷Royal Free Hospital, London, United Kingdom; ⁸Hospital del Mar, Parc de Salut MAR, Liver section, Servei de Digestiu, Barcelona, Spain; ⁹Hospital Universitario Ramon y Cajal, Universidad de Alcalá de Henares, Centro de Investigación Biomédica en Enfermedades hepáticas y Digestivas (CIBEREHD), Madrid, Spain; ¹⁰Centre Hospitalier Universitaire d'Angers; Laboratoire HIFIH, UPRES EA3859, SFR 4208, 13. Service d'Hépatogastroentérologie et d'Oncologie Digestive, Angers, France; ¹¹Ospedale

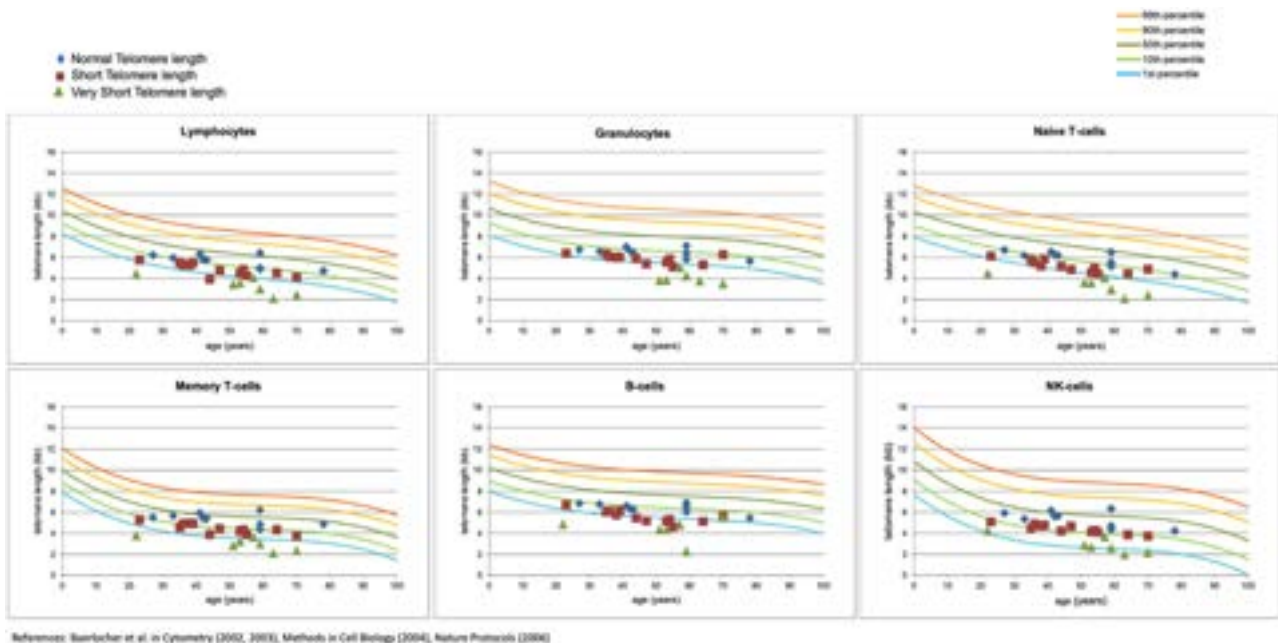


Figure: (abstract: LBP-08): Telomere length analysis. Each circle, square or triangle represents one patient, and the lines represent percentiles of the telomere length reference range calculated from over 400 healthy individuals.

POSTER PRESENTATIONS

Civico Di Cristina Benfratelli, Interventional Radiology Unit, Palermo, Italy; ¹²Klinikum Landshut, Department of Medicine I, Landshut, Germany; ¹³Casa di Cura Serena, Medicina, Palermo, Italy; ¹⁴University of Campania Luigi Vanvitelli, Department of Hepato-Gastroenterology, Department of Precision Medicine, Napoli, Italy; ¹⁵Catholic University of Sacred Heart, Fondazione Policlinico Universitario A. Gemelli IRCCS, Rome, Italy; ¹⁶Casa Sollievo della Sofferenza, Gastroenterology and Endoscopy, San Giovanni Rotondo, Italy; ¹⁷IRCCS Policlinico San Donato, Internal Medicine Unit, Milan, Italy; ¹⁸Università Sapienza, Translational and Precision Medicine, Italy; ¹⁹University of Campania Luigi Vanvitelli, 16. Department of Hepato-Gastroenterology, Department of Precision Medicine, Napoli, Italy; ²⁰Polytechnic University of Marche, Liver Injury and Transplant Unit, Ancona, Italy; ²¹Presidio Ospedaliero Azienda Socio Sanitaria Territoriale di Lecco, General Medicine Unit, Lecco, Italy; ²²Cardarelli Hospital, Hepatology Unit, Napoli, Italy; ²³Università degli Studi di Cagliari, Department of Medical Sciences and Public Health, Cagliari, Italy; ²⁴ASL Latina, Department of Translational and Precision Medicine-"Sapienza" University of Rome-. Gastroenterology Unit, Latina, Italy

Email: gedamico@libero.it

Background and aims: The development of a stage of "further" decompensation in cirrhosis is assumed to be associated with worse survival. However, this has been based on clinical observation rather than on scientific evidence. We investigated the incidence of further decompensation and its impact on mortality in cirrhosis

Method: Multicenter (Europe and Argentina) prospective cohort study. The cumulative incidence of further decompensation was assessed by competing risk analysis in 2028 patients presenting with their first decompensation of cirrhosis (variceal bleeding, ascites, hepatic encephalopathy or jaundice). At inclusion patients' characterization was based on MELD and Child-Pugh scores and on clinical stage defined as follows: stage 3, variceal bleeding alone; stage 4, any non-bleeding event (ascites encephalopathy or jaundice); stage 5, any combination of 2 or more events. Further decompensation was defined as any new ascites, encephalopathy, (re)bleeding or jaundice or complications of ascites (need of large volume paracentesis, spontaneous bacterial peritonitis, acute kidney injury-hepatorenal syndrome). The impact of further decompensation on mortality was assessed by the cause-specific Cox model.

Results: Etiology was viral in 31.5% (mostly untreated), alcoholic 38.6%, alcoholic/viral 10.7%, NASH 8.8%, autoimmune/cholestatic 5.2%. In a mean follow-up of 43 months, 1192 patients developed further decompensation and 649 died. Corresponding 5-year cumulative incidences were: further decompensation 52% and mortality 35%, respectively. The most common further decompensating event was ascites/complications of ascites. Five-year survival was significantly lower in patients with further decompensation compared to the 836 patients who did not develop further decompensation: 35% vs. 50%; $P < 0.0001$; median survival 273 vs. 767 days, $p < 0.0001$. This significant reduction in survival was observed independent of the stage of first decompensation, including patients whose first decompensation presented with two or more decompensating events. After variceal bleeding further decompensation decreased survival when occurred after 5 days from bleeding. Compared to first decompensation, the hazard ratio for death after further decompensation, adjusted for MELD and other prognostic indicators, was 2.05 ($p < 0.001$).

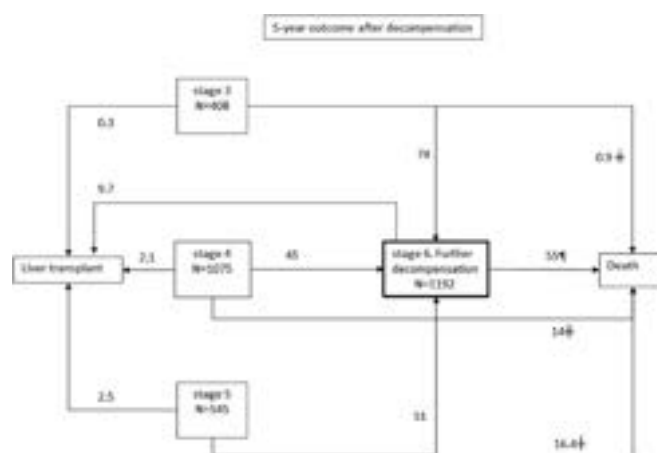


Figure: Summary of 5-year probability of outcome from each decompensated disease stage. Numbers next to the arrows represent the cumulative probability (%) of events from disease stages (3-4-5) at first decompensation or from further decompensation. After first decompensation, most patients develop further decompensation and most deaths occur after further decompensation. Mortality from each decompensation stage (\dagger) was significantly different from mortality after further decompensation (\S) ($p < 0.0001$ each).

Conclusion: In cirrhosis, further decompensation occurs in approximately 60% of patients after the first decompensating event and significantly increases mortality. We propose that further decompensation be considered a more advanced prognostic stage of cirrhosis, beyond first decompensation.

LBP-10

Prospective direct comparisons of four widespread non-invasive fibrosis tests (NITs) in outpatients with type-2 diabetes (T2D) using EPoS histological staging as reference

Olivier Deckmyn¹, Dominique Valla², Valentina Peta¹, Angélique Brzustowski³, Valérie Paradis², Pierre Bedossa⁴, Castera Laurent², Stanislas Pol⁵, Raluca Pais³, Vlad Ratziu³, Dominique Thabut⁶, Jean-François Gautier⁷, Thierry Poynard^{1,3,8}. ¹BioPredictive, Paris, France; ²Hospital Beaujon AP-HP, Clichy, France; ³Inserm, Paris, France; ⁴LIVERPAT, Paris, France; ⁵Cochin Hospital, Paris, France; ⁶University Hospitals Pitié Salpêtrière-Charles Foix, Paris, France; ⁷Lariboisière Hospital AP-HP, Paris, France; ⁸Faculty of Medicine Pierre et Marie Curie, Paris, France
Email: thierry@poynard.com

Background and aims: Very few prospective diagnostic studies have been published, comparing directly non-invasive liver tests (NITs) in T2D only, as well as using recent histological scores and intention to diagnose method. The main end point was to compare the diagnostic performance for the diagnosis of significant fibrosis stage of four NITs: a new FibroTest modified for T2D (FT-T2D), liver stiffness measurement (VCTE), Share-Ware-Elastography stiffness (SWE) and FIB4. The secondary aim was to compare the performance for the diagnosis of significant activity of two NITs: a new NashTest2 modified for T2D (NT2-T2D), and aspartate-aminotransferase (AST) the only NIT combined with VCTE in the FibroScan-AST score (FAST). The third aim was to compare the performance of three NITs for the diagnosis of steatosis $\geq 30\%$: a new SteatoTest2 (ST2-T2D), controlled attenuation parameter (CAP) available with VCTE and the hepatorenal gradient available with SWE (SWE-HR).

Method: The reference was a concomitant biopsy, blinded, centralized and scored using EPoS a new seven-tier fibrosis staging system which specifically identifies early versus advanced bridging as two separate stages with more specific bridging definitions than CRN score, and standard SAF/CRN scoring systems for Nash and steatosis (Pais, Hepatology 2022). Main end point was the binary AUROCs (bAUC) for the clinically significant features \geq EPoS-F3-stage (Bridging

Test	Comparator	Reliability and applicability		In intention to diagnose			Not taking into account reliability and applicability			Standard Error	P-Value
		Test	Comparator	AUC1 Test	AUC2 Comparator	AUC1 - AUC2	AUC1 Test	AUC2 Comparator	AUC1 - AUC2		
FT-T2D	FIB4	99.8%	99.5%	0.778	0.704	0.074	0.776	0.707	0.071	0.027	0.008
FT-T2D	SWE	99.8%	98.5%	0.778	0.795	-0.017	0.776	0.807	-0.029	0.027	0.289
FT-T2D	VCTE	99.8%	93.0%	0.778	0.758	-0.029	0.776	0.815	-0.037	0.029	0.195
NT2-T2D	AST	99.8%	99.8%	0.759	0.709	0.026	0.781	0.710	0.051	0.020	0.01
ST2-T2D	SWE-HR	99.8%	98.5%	0.748	0.718	0.030	0.749	0.729	-0.020	-0.039	0.606
ST2-T2D	CAP	99.8%	93.0%	0.748	0.655	0.093	0.749	0.700	-0.049	-0.042	0.240

Table: (abstract: LBP-10).

fibrosis), \geq SAF-A3-grade activity and \geq SAF-S3-grade steatosis. Obuchowski weighted-AUROC (wAUC) were also compared to take into account the spectrum effects. Intention to diagnose (ITD) was used to adjust the AUCs according to applicability and liability of NITs. Learning and validation subsets of T2D-modified NITs used a k-fold randomization.

Results: Between 2018 to 2022, 713 outpatients were investigated in four diabetes clinics (NCT03634098), and 402 with interpretable biopsy were included, median age 59 years, 63% male, 58% NASH, 39% bridging. Results are detailed in Table1 for the diagnosis of Bridging fibrosis. Due to lower applicability and liability the VCTE performance decrease by more than 5% vs the 3 other NITs when ITD method is used ($p < 0.05$). SWE, FT-T2D and VCTE AUROCs (0.795, 0.778 and 0.758) were not significantly different for Bridging ($p > 0.19$) and all three higher than FIB4 (0.704; $P < 0.01$). For the diagnosis of activity grades \geq SAF-A3-grade, the bAUC in ITD of NT2-T2D was 0.759, and 0.709 for AST alone. For the diagnostic of steatosis grades \geq SAF-S3-grade, the bAUC in ITD of ST2-T2D was 0.748, 0.718 for SWE-HR and 0.655 for CAP.

Conclusion: For the first time four fibrosis NITs were directly compared in ITD in a prospective study of T2D outpatients using a more specific definition of advanced fibrosis. SWE, new FT-T2D and VCTE performances were not significantly different for the diagnostic of Bridging ($p > 0.19$) and all three higher than FIB4 score.

LBP-11

Virological and clinical outcomes of patients with HDV-related compensated cirrhosis treated with Bulevirtide monotherapy: the retrospective multicenter European study (Save-D)

Elisabetta Degasper¹, Maria Paola Anolli¹, Victor de Lédighen², Sophie Metivier³, Mathias Jachs⁴, Thomas Reiberger⁴, Giampiero D'Offizi⁵, Christopher Dietz-Fricke⁶, George Papatheodoridis⁷, Maurizio Brunetto⁸, Gabriella Verucchi⁹, Alessia Ciancio¹⁰, Fabien Zoulim¹¹, Alessandra Mangia¹², Marie-Noëlle Hilleret¹³, Teresa Santantonio¹⁴, Nicola Coppola¹⁵, Adriano Pellicelli¹⁶, Bruno Roche¹⁷, Xavier Causse¹⁸, Louis Dalteroché¹⁹, Jérôme Dumortier²⁰, Nathalie Ganne-Carrié²¹, Frederic Heluwaert²², Isabelle Ollivier-Hourmand²³, Alessandro Loglio²⁴, Mauro Viganò²⁵, Alessandro Federico²⁶, Francesca Pileri²⁷, Monia Maracci²⁸, Matteo Tonnini²⁹, Jean-Pierre Arpurt³⁰, Karl Barange³¹, Eric Billaud³², Stanislas Pol³³, Anne Gervais³⁴, Anne Minello Franza³⁵, Isabelle Rosa³⁶, Massimo Puoti³⁷, Pietro Lampertico^{1,38}. ¹Division of Gastroenterology and Hepatology, Foundation IRCCS Ca' Granda Ospedale Maggiore Policlinico, Milan, Italy; ²Hepatology Department, Haut-Lévêque Hospital, Bordeaux, France; ³Hepatology Unit, CHU Rangueil, 31059, Toulouse, France; ⁴Medical University of Vienna, Division of Gastroenterology and Hepatology, Department of Internal Medicine III, Vienna, Austria; ⁵IRCCS Istituto Nazionale per le Malattie Infettive "L. Spallanzani", Rome, Italy; ⁶Klinik für Gastroenterologie, Hepatologie, Infektiologie und Endokrinologie Medizinische Hochschule Hannover, Hannover, Germany; ⁷Department of Gastroenterology, General Hospital of Athens "Laiko", Medical School of National and Kapodistrian

University of Athens, Athens, Greece; ⁸Hepatology Unit and Laboratory of Molecular Genetics and Pathology of Hepatitis Viruses, Reference Center of the Tuscany Region for Chronic Liver Disease and Cancer, University Hospital of Pisa, Pisa, Italy; ⁹Department of Medical and Surgical Sciences, Unit of Infectious Diseases, "Alma Mater Studiorum" University of Bologna, S. Orsola-Malpighi Hospital, Bologna, Italy; ¹⁰Department of Medical Sciences, University of Turin, Gastroenterology Division of Città della Salute e della Scienza of Turin, University Hospital, Turin, Italy; ¹¹INSERM U1052-Cancer Research Center of Lyon (CRCL), Lyon, France; ¹²Liver Unit, Fondazione IRCCS "Casa Sollievo della Sofferenza", San Giovanni Rotondo, Italy; ¹³Service d'hépatogastro-entérologie, CHU Grenoble-Alpes, Grenoble, France; ¹⁴Department of Medical and Surgical Sciences, Infectious Diseases Unit, University of Foggia, Foggia, Italy; ¹⁵Department of Mental Health and Public Medicine-Infectious Diseases Unit, University of Campania Luigi Vanvitelli, Naples, Italy; ¹⁶Liver Unit, San Camillo Hospital, Department of Transplantation and General Surgery, Rome, Italy; ¹⁷Hepato-Biliary Center, AP-HP Hôpital Universitaire Paul Brousse, Paris-Saclay University, Research INSERM-Paris Saclay Unit 1193, Villejuif, France; ¹⁸Hôpital de la Source Orleans, France; ¹⁹Service d'Hépatogastro-entérologie CHU de Tours, France; ²⁰Department of Digestive Diseases, Hospices Civils de Lyon, Edouard Herriot hospital, France; ²¹Claude Bernard Lyon 1 University, France; ²²AP-HP, Avicenne Hospital, Hepatology Department, Bobigny, France; ²³Centre Hospitalier Annecy Genevois, Annecy, France; ²⁴Department of Hepatogastroenterology, CHU de Caen Normandie, Caen, France; ²⁵Gastroenterology, Hepatology and Transplantation Division, ASST Papa Giovanni XXIII, Bergamo, Italy; ²⁶Division of Hepatology, Ospedale San Giuseppe, Milan, Italy; ²⁷Division of Hepatogastroenterology, Department of Precision Medicine, Università della Campania "Luigi Vanvitelli", Naples, Italy; ²⁸Division of Internal Medicine 2 and Center for Hemochromatosis, University of Modena and Reggio Emilia, Modena, Italy; ²⁹Institute of Infectious Diseases and Public Health, Università Politecnica delle Marche, Ancona, Italy; ³⁰Division of Internal Medicine, Hepatobiliary and Immunological Diseases, IRCCS Azienda Ospedaliero-Universitaria di Bologna, Bologna, Italy; ³¹Department of Gastroenterology, CH d'Avignon, Avignon, France; ³²Department of Gastroenterology, Toulouse University Hospital, Toulouse, France; ³³Université de Nantes, INSERM UIC 1413, Department of Infectious Diseases, CHU Hôtel Dieu, Nantes, France; ³⁴Assistance Publique des Hôpitaux de Paris, Hôpital Cochin, Liver department, Paris, France; ³⁵Assistance Publique des Hôpitaux de Paris, Hôpital Bichat Claude Bernard, Service des Maladies Infectieuses et Tropicales, Paris, France; ³⁶CHU Dijon, Service d'Hépatogastro-entérologie et oncologie digestive, Inserm EPICAD LNC-UMR1231, Université de Bourgogne-Franche Comté, Dijon, France; ³⁷Service d'hépatogastro-entérologie, Centre Hospitalier Intercommunal, Créteil, France; ³⁸ASST Grande Ospedale Metropolitano Niguarda, Division of Infectious Diseases, Milan, Italy; ³⁹CRC "A. M. and A. Migliavacca" Center for Liver Disease, Department of Pathophysiology and Transplantation, University of Milan, Milan, Italy
Email: elisabetta.degasper@policlinico.mi.it

Background and aims: Bulevirtide (BLV) has been conditionally approved by EMA for treatment of chronic compensated hepatitis D

virus (HDV) infection, however real-life data in large cohorts of cirrhotic patients are lacking.

Method: Consecutive compensated HDV cirrhotic patients starting BLV 2 mg/day since July 2019 were included in a retrospective multicenter real-life European study. Clinical, biochemical and virological features at BLV start and during treatment were collected. Virological response (HDV RNA undetectable or ≥ 2 -log decline vs. baseline), biochemical response (ALT < 40 U/L), combined response (biochemical + virological) and adverse events were assessed. HDV RNA was quantified locally. Liver-related events (hepatocellular carcinoma, decompensation, liver transplantation) were recorded.

Results: 176 patients receiving BLV monotherapy up to 96 weeks [median follow-up: 48 (8-96) weeks] were included: at BLV start, age was 50 (19-82) years, 59% men, ALT 77 (23-1,074) U/L, liver stiffness measurement (LSM) 18.3 (6.4-75.0) kPa (30% with LSM > 25 kPa), platelets 89 (17-330) G/L (80% with PLT < 150 G/L), 100% CPT score A, 9% HIV-positive, 46% with oesophageal varices, 12% with history of previous ascites, 6% with active HCC, 91% on NUC. Median HDV RNA and HBsAg levels were 5.38 (1.18-8.48) Log IU/ml and 3.7 (0.8-4.5) Log IU/ml, respectively. Rates of virological responses at W24, W48 and W96 were 48%, 66% and 77%, respectively; HDV RNA was undetectable in 16%, 33%, and 43% patients. Biochemical response was achieved by 60%, 69% and 73% at W24, W48 and W96, respectively, while rates of combined response were 28%, 48% and 58%. Patients with < 1 log HDV RNA decline vs baseline declined from 25% at W24 to 18% at W48. In the 15 HIV-positive patients, HIV-RNA persisted undetectable during treatment without significant changes in CD4 T-cell count; rates of virological response were similar to HIV-negative patients. Bile acids significantly increased, 10% patients reported mild and transient pruritus. Injection site reactions occurred in 3% of cases; 1 patient discontinued BLV due to a grade 3 maculopapular rash with mild eosinophilia. 4 patients were lost to follow-up and 3 discontinued due to primary non response. The W96 cumulative risk of de-novo HCC (7 cases) and decompensation ($n = 2$ ascites, $n = 1$ variceal bleeding) was 5.9% (95% CI 2-12%) and 2.4% (95% CI 1-5%), respectively. Six (3%) patients underwent liver transplantation ($n = 4$ for HCC, $n = 2$ for end-stage liver disease; BLV stopped at transplant) and 2 patients died of BLV-unrelated causes (pneumonia and intestinal infarction). The overall cumulative survival rate was 93% (95% CI 88-98%) at W96.

Conclusion: BLV 2 mg/day monotherapy up to 96 weeks was safe and effective in patients with HDV-related compensated cirrhosis. Virological and clinical responses increased over time. The risk of decompensation was very low.

LBP-12

Off-label Bulevirtide monotherapy for chronic hepatitis D virus infection in patients with decompensated liver disease

Christopher Dietz-Fricke¹, Elisabetta Degasperi², Pietro Lampertico², Mathias Jachs³, Thomas Reiberger³, Julia Grottenthaler⁴, Christoph Berg⁴, Toni Herta⁵, Florian van Bömmel⁵, Johannes Wiegand⁵, Thomas Berg⁵, Florian P Reiter⁶, Andreas Geier⁶, Kathrin Sprinzl⁷, Stefan Zeuzem⁷, Peter Buggisch⁸, Benjamin Maasoumy¹, Markus Cornberg¹, Heiner Wedemeyer¹, Katja Deterding¹. ¹Hannover Medical School, Dept. of Gastroenterology, Hepatology, Infectious Diseases and Endocrinology, Germany; ²University of Milan, Fondazione IRCCS Ca' Granda Ospedale Maggiore Policlinico, Italy; ³Department of Medicine III, Division of Gastroenterology and Hepatology, Medical University of Vienna, Austria; ⁴University Hospital Tuebingen, Tuebingen, Germany, Department of Gastroenterology, Gastrointestinal Oncology, Hepatology, Infectiology, and Geriatrics, Germany; ⁵Leipzig University Medical Center, Division of Hepatology, Clinic and Polyclinic for Gastroenterology, Hepatology, Infectiology, and Pneumology, Germany; ⁶University Hospital Würzburg, Division of Hepatology, Department of Medicine II, Germany; ⁷Goethe University Hospital, Internal Medicine Department, Germany; ⁸ifl-Institute for interdisciplinary medicine, Hamburg, Germany
Email: dietz-fricke.christopher@mh-hannover.de

Background and aims: Chronic hepatitis D virus infection is the most debilitating form of viral hepatitis causing severe hepatic damage consequently leading to liver cirrhosis. Bulevirtide (BLV) has been conditionally approved by the EMA for the treatment of chronic hepatitis D virus infection in patients with compensated liver disease. Its safety and efficacy on HDV viral load and ALT levels has been demonstrated for compensated patients in clinical trials and recently published real world cohorts. However, BLV data in the vulnerable collective of patients with decompensated cirrhosis are still lacking. We thus, aimed to report real-world data obtained from patients with decompensated HDV cirrhosis in whom BLV was used off-label.

Method: We collected anonymized and retrospective data from Austrian, Italian and German centers experienced in the use of BLV. Patients with HDV cirrhosis at Child-Pugh stages B and C or clinical signs of decompensated cirrhosis were included. Virologic response was defined by a decline in HDV-RNA levels by ≥ 2 log while virologic non-response was defined if HDV-RNA decline was < 1 log decline.

Results: We included 15 patients (Child-Pugh A $n = 1$, Child-Pugh B $n = 14$) with 10 patients showing ascites at BLV initiation. The patient with Child-Pugh A liver cirrhosis had history of large volume paracentesis due to ascites but resolution of ascites under ongoing diuretics at treatment initiation. However, given the uncontrolled CHD the patient was considered as decompensated following the Baveno VII recommendations. At baseline hypoalbuminemia was present in 9 patients (mean 33 ± 4.6 g/dL), hyperbilirubinemia (> 34.2 μ mol/l) in 6 patients (mean 36.1 ± 24.6 μ mol/l) and thrombocytopenia (platelets < 150 G/L) in all patients-indicating portal hypertension.

Virologic response was achieved after a mean of 23 weeks in 10 (66%) patients while viral non-response did not occur. ALT levels significantly decreased under BLV therapy (see figure) and normalized in 7 (47%). Under BLV treatment liver function improved from Child-Pugh B to Child-Pugh A in 4 cases. Ascites improved in 4 patients. Hepatic improvement was associated with virologic and biochemical response. In one case a worsening of liver function to Child-Pugh C occurred after off-label pegylated interferon was added to BLV treatment (data censored after start of interferon). Another case experienced further decompensation after TIPS insertion and incarceration of a hernia. In both cases decompensation was not attributed to BLV therapy. In 3 cases BLV was terminated at liver transplantation.

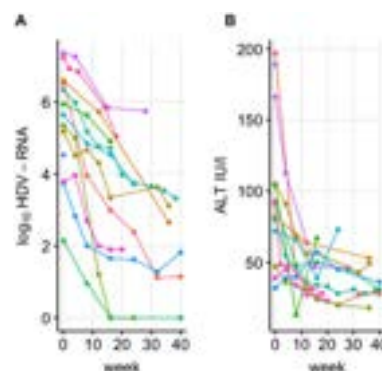


Figure 1. Decline in HDV-RNA (A) and ALT (B) in patients with decompensated liver disease under BLV treatment. Shown are individual data points from patients with complete data sets ($n = 13$). Viral response was achieved in 10 cases.

Conclusion: The off-label use of BLV in patients with decompensated cirrhosis and impaired liver function results in a decline in HDV-RNA and ALT levels. Improvement of liver function and cirrhosis recompensation may be achieved in selected patients. While some patients developed further decompensation, this was not related to the use of BLV. This case report series supports the antiviral efficacy of BLV also in decompensated cirrhosis. To investigate long term efficacy

of BLV on clinical end points and its safety profile in this highly vulnerable patient population with decompensated cirrhosis, prospective clinical trials are urgently needed.

LBP-13

Safety, pharmacokinetics and antiviral efficacy of freethiadine, a novel capsid assembly modulator, in healthy volunteers and patients with chronic hepatitis B virus infection

Yanhua Ding¹, Xiaojiao Li², Jia Xu³, Jixuan Sun¹, Yingjun Zhang⁴, Jing Zhu⁵, Yujie Chen⁴, Lin Luo⁶, Qingyun Ren⁶, Yunfu Chen⁶, Junqi Niu⁷. ¹Phase I Clinical Trial Center, The First Hospital of Jilin University, Changchun, China; ²Phase I Clinical Trial Center, The First Hospital of Jilin University, Changchun; ³Phase I Clinical Trial Center, The First Hospital of Jilin University, Changchun, China; ⁴Sunshine Lake Pharma Co., Ltd., Guangdong, China; ⁵Sunshine Lake Pharma Co., Ltd., Guangdong, China; ⁶Sunshine Lake Pharma Co., Ltd., Guangdong, China; ⁷Department of Hepatology, The First Hospital of Jilin University, Changchun, China
Email: dingyanh@jlu.edu.cn

Background and aims: Freethiadine is a novel capsid assembly modulator (CAM) developed by Sunshine Lake Pharma Co., Ltd. Here we report the safety, tolerability, pharmacokinetics (PK), and 28-day antiviral activity of freethiadine in two randomized, double-blinded phase I studies in healthy subjects and patients with chronic HBV infection (CHB).

Method: The studies were consisted of two parts. Part 1 was a double-blind, randomized, placebo-controlled single-ascending-dose (SAD, 50-600 mg), multiple-ascending-dose (MAD, 100 mg, 200 mg, or 300 mg, BID) and food effect (200 mg) study. Part 2 was a

double-blind, double-dummy, randomized, entecavir controlled, multi-dose escalation study in CHB patients. Patients were randomized 4:1 to freethiadine+ entecavir placebo or entecavir 0.5 mg+ freethiadine placebo across 4 multiple-dose cohorts: freethiadine 100 mg once a day (QD), 200 mg QD, 200 mg twice a day (BID), and 300 mg QD for 28 days.

Results: A total of 88 healthy subjects and 40 CHB patients were enrolled in the study. Freethiadine was safe and well tolerated both in healthy subjects and CHB patients. The paresthesia was occurred among both healthy subjects and patients when the freethiadine dose greater than 300 mg. Grade I or II alanine aminotransferase (ALT) elevation was the most common AE (12.5%-50%) among freethiadine treated patients, and the incidence and severity was not related to the dose. Only two grade III ALT elevation occurred at 200 mg QD and 300 mg QD cohorts, respectively. All the ALT elevation was correlated with the decline in the HBV DNA levels, which is "good flare". Absorption and elimination of HEC160208 and active metabolite HEC142106 occurred rapidly in plasma. In the SAD study, median Tmax of HEC160208 and HEC142106 was 1.75-3.0 h, 2.5-4 h, and t1/2 ranged from 0.71-2.02 h, 1.95-5.84 h, respectively. The exposure of HEC160208 and HEC142106 was proportional to dose and was not significantly affected by food intake. The HEC160208 exposure of 100 mg has exceeded that of the effective dose in the preclinical mouse model. In the MAD study, steady-state was attained on day 3, and there was no apparent plasma accumulation of HEC160208 and HEC142106 after 10-day dosing. (Racc <1.0). The exposure of both analytes was slightly higher in CHB patients than that in the healthy subjects. After 28 days of treatment, the mean maximum HBV DNA declines from baseline were -2.76, -3.47, -3.56, -2.89, and -2.55 log10 IU/ml for the 100 mg QD, 200 mg QD, 200 mg

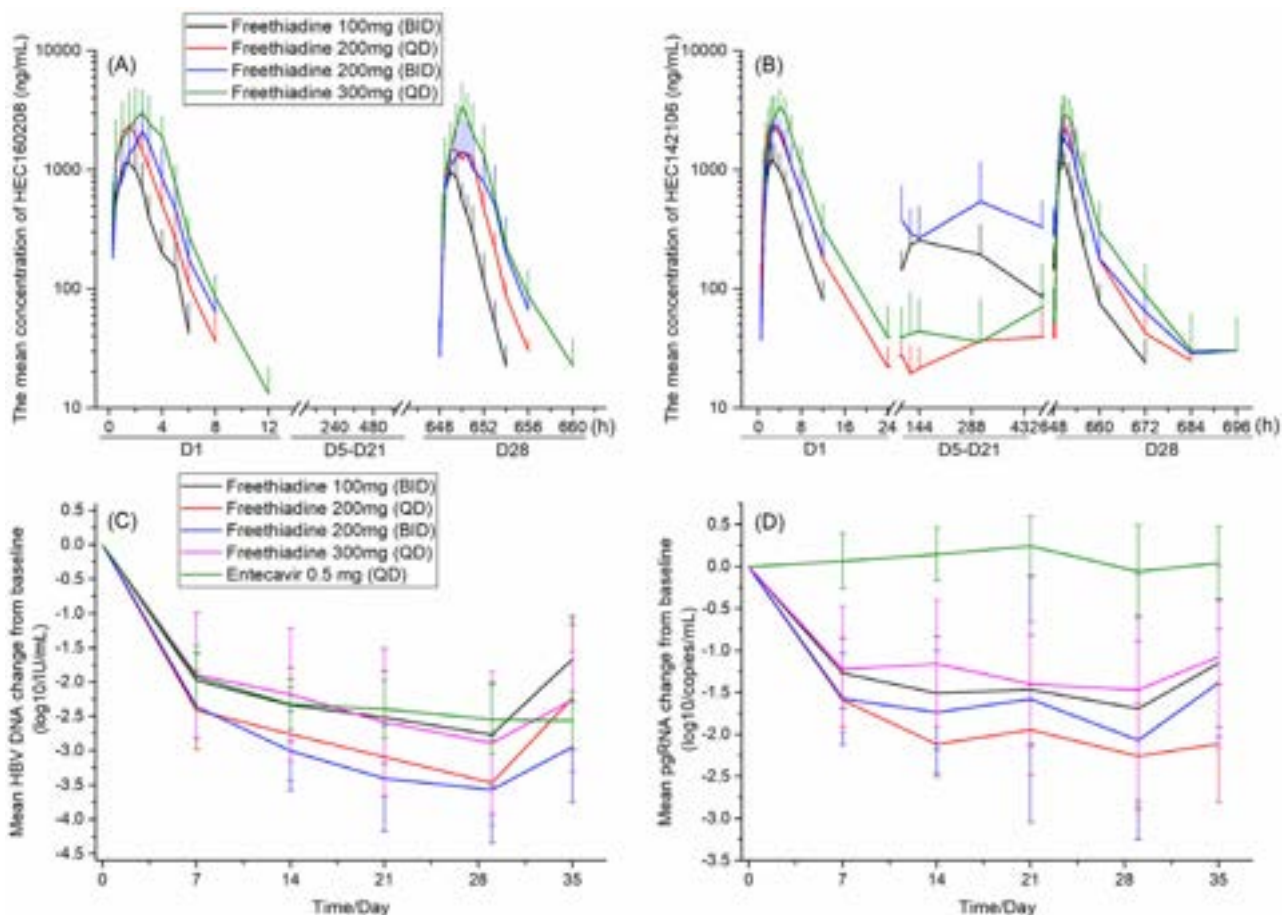


Figure: (abstract: LBP-13).

POSTER PRESENTATIONS

BID, and 300 mg QD of freethiadine or entecavir control cohorts, respectively; and the mean maximum pregenomic RNA (pgRNA) declines from baseline were -1.69, -2.26, -2.07, -1.47, and -0.06 log10 copies/ml, respectively. The numbers of patients whose HBV DNA level was reduced below the lower limit of quantification (LLOQ) after 28 days of administration were 3 (37.5%), 0, 3 (37.5%), 3 (37.5%), and 3 (37.5%), respectively. HBV DNA decrease did not differ substantially between HBeAg (-) and HBeAg (+) patients, however, the pgRNA decreased more in HBeAg (+) patients than in HBeAg (-) patients after freethiadine treatment, especially in 300 mg QD cohort. There were no significant changes in the levels of HBsAg, HBeAg, and HBcrAg. **Conclusion:** Freethiadine showed an acceptable safety profile and efficacious antiviral activity in CHB patients, 200 mg freethiadine (QD or BID) can be considered for further development in treating HBV infection.

LBP-14

Evaluation of 8 non-invasive models in predicting NAFLD severity and progression in a one-year prospective study based on MRI-PDFF

Aruhan Yang¹, Lei Zhang¹, Hong Chen¹, Guoyu Lv¹, Xiaoxue Zhu¹, Yanhua Ding¹. ¹First hospital of Jilin University, China
Email: arh20@mails.jlu.edu.cn

Background and aims: Although biopsy remains the gold standard for assessing NAFLD, several non-invasive models can provide useful estimates. The aim of this prospective study was to compare the accuracy of eight non-invasive methods to predict steatosis and disease progression.

Method: A total of 846 samples were collected, among which 236 samples were collected from participants with two examinations (baseline and 1 year). The liver fat content (LFC, measured by MRI-PDFF) decrease/increase by 20% from baseline was classified as the Improve/Progression group, and the others were referred to as the Keep group. Eight models (FAST, HSI, FLI, KANFLD, BAAT, LAP, Liver Fat Score, Liver Fat Equation) were calculated in agreement with previous studies, and their performances in diagnosing NAFLD and predicting progression were compared based on the MRI-PDFF.

Results: The 8 clinical models performed well in predicting different degrees of NAFLD in this cohort (healthy: N = 146, 17.3%; mild NAFLD: N = 400, 47.3%; moderate NAFLD: N = 257, 30.4%; severe NAFLD: N = 43, 5%), especially KANFLD (the highest AUC of diagnosis was 0.90). Within the whole cohort, the correlation analysis revealed that KANFLD was most strongly correlated with LFC ($r = 0.56$, $P < 0.01$, Figure 1), and other clinical models (FAST, liver fat score, BAAT, HSI, FLI, LAP, liver fat equation) also showed weaker but significantly positive correlations with LFC (correlation coefficients: 0.48, 0.48, 0.45, 0.43, 0.38, 0.35, 0.33, respectively; $P < 0.05$ for all). When the KANFLD score was above 2.935, the LFC was significantly higher (4.4% vs. 19.7%, $P < 0.001$). After 1 year of follow-up, FAST performed best in

predicting NAFLD progression (AUC = 0.84), correlation analysis showed that the association between the changes in FAST and LFC was the strongest ($r = 0.42$, $P < 0.01$), followed by KANFLD ($r = 0.39$, $P < 0.01$); when the change in FAST from baseline was lower than -0.012, the LFC significantly decreased (from 11.5% to 8.5%, $P < 0.05$), and when it was higher than -0.012, the LFC increased from 8.6% to 10.9% ($p < 0.05$).

Conclusion: Most non-invasive techniques are correlated with LFC and have acceptable accuracy in estimating the degree and progression of NAFLD, especially KANFLD. FAST has the best accuracy in predicting NAFLD progression.

LBP-15

Evidence of durable response to bepirovirsen in B-Clear responders: B-Sure first annual report

Adrian Gadano¹, Manuela Arbune², Masanori Atsukawa³, Shigetoshi Fujiyama⁴, Natalya Urievna Gankina Urievna Gankina⁵, Binu John⁶, Takuya Komura⁷, Masayuki Kurosaki⁸, Young Oh Kweon⁹, Seng Gee Lim¹⁰, Rosie Mngqibisa¹¹, Teerha Piratvisuth¹², Olga Sagalova¹³, Lawrence Serfaty¹⁴, Tatyana Stepanova¹⁵, Radoslava Tsrancheva¹⁶, Qing Xie¹⁷, Man-Fung Yuen¹⁸, Chelsea Macfarlane¹⁹, Stephen Corson²⁰, Jie Dong²¹, Helene Plein²², Geoff Quinn²³, Robert Elston^{23, 23}, Stuart Kendrick²³, Melanie Paff²⁴, Dickens Theodore²⁵. ¹Hospital Italiano de Buenos Aires, Buenos Aires, Argentina; ²Sf.Cuv. Parascheva Infectious Diseases Clinical Hospital, Galati, Romania; ³Nippon Medical School, Tokyo, Japan; ⁴Kumamoto Shinto General Hospital, Kumamoto, Japan; ⁵Krasnojarsk Regional Center of AIDS prevention, Krasnojarsk, Russian Federation; ⁶Miami VA Health System and University of Miami, Miami, United States; ⁷Kanazawa Medical Center, Ishikawa, Japan; ⁸Musashino Red Cross Hospital, Tokyo, Japan; ⁹Kyungpook National University Hospital, Daegu, Korea, Rep. of South; ¹⁰National University Health System, Singapore, Singapore; ¹¹Enhancing Care Foundation, Durban, South Africa; ¹²NKC Institute of Gastroenterology and Hepatology, Songkhla, Thailand; ¹³South Ural State Medical University, Chelyabinsk, Russian Federation; ¹⁴HUS-Hôpital de Hautepierre, Strasbourg, France; ¹⁵Modern Medicine Clinic, Moscow, Russian Federation; ¹⁶Alexandrovskaya University Hospital, Sofia, Bulgaria; ¹⁷Ruijin Hospital affiliated to Shanghai Jiao Tong University, Shanghai, China; ¹⁸Queen Mary Hospital, The University of Hong Kong, Hong Kong, China; ¹⁹GSK, Waltham, United States; ²⁰PHASTAR, Glasgow, United Kingdom; ²¹GSK, Shanghai, China; ²²GSK, Brentford, United Kingdom; ²³GSK, Stevenage, United Kingdom; ²⁴GSK, Collegeville, United States; ²⁵GSK, Durham, United States
Email: robert.c.elston@gsk.com

Background and aims: Bepirovirsen (BPV) is an investigational novel unconjugated antisense oligonucleotide for treatment of chronic hepatitis B virus (HBV) infection. Data from the Phase 2b B-Clear study (NCT04449029) indicated that a subset of participants (pts) achieved a response at end of BPV treatment, which was sustained for

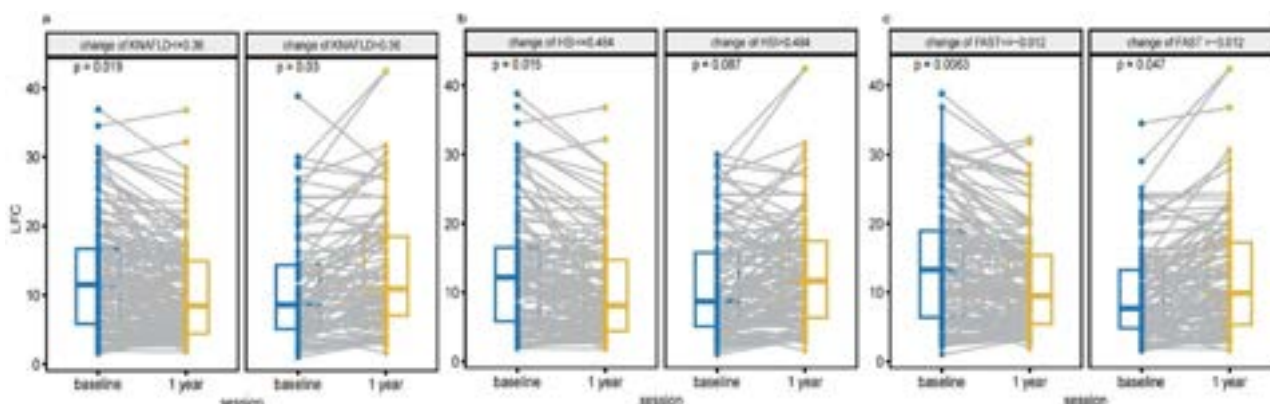


Figure: (abstract: LBP-14).

24 weeks' follow-up. This occurred in pts on and not on nucleos(t)ide analogue (NA) therapy (On-NA and Not-on-NA), in the absence of newly initiated antiviral therapy. Pts who achieved a partial or complete response at the end of study (EoS) visit were eligible for this long-term durability study-B-Sure (NCT04954859). Here we present preliminary data from the first annual review to examine the durability of response for B-Clear On-NA and Not-on-NA complete responders (hepatitis B surface antigen [HBsAg] <0.05 IU/ml and HBV DNA <lower limit of quantification) who enrolled into B-Sure.

Method: Not-on-NA pts will be followed up at Month 3, Month 6, and every 6 months thereafter for up to 36 months after B-Clear EoS. On-NA pts, if eligible, will cease NA 6 months after B-Clear EoS visit and be followed more intensively. Adverse events were recorded, and physical exams and blood tests were performed at each visit to assess safety and response. Durability of response was assessed:

- On-NA: Time from NA cessation to loss of complete response.
- Not-on-NA: Time from achieving a B-Clear complete response to loss of response.

Results: 13/16 On-NA and 12/14 Not-on-NA complete responders in B-Clear enrolled into B-Sure (Figure); 12 On-NA and 12 Not-on-NA pts remain in the study at the time of reporting. For On-NA pts (n = 13), 12 (92%) were male, with a mean age of 53.2 years; 6/13 (46%) had chronic HBV infection for ≥ 20 years, 10/13 (77%) were hepatitis B e antigen (HBeAg) negative and 9/13 (69%) had HBsAg ≤ 1000 IU/ml at B-Clear study baseline. 9/13 (69%) pts ceased NA as per protocol, 3/13 (23%) were not eligible to cease NA and 1/13 (8%) withdrew prior to NA cessation. 7/9 (78%) of those who ceased NA had complete data with ≥ 3 months of follow-up, and 6/7 (86%) maintained response 3 months post NA cessation. 4/9 (44%) had complete data with ≥ 6 months of follow-up post NA cessation, of whom 100% (4/4) maintained response. No pts restarted NAs. For Not-on-NA pts (n = 12), 7 (58%) were male with a mean age of 43.8 years; 3/12 (25%) had chronic HBV infection for ≥ 20 years, all were HBeAg negative and 7/12 (58%) had HBsAg ≤ 1000 IU/ml at B-Clear study baseline. 9/12 responders (75%) had complete data with ≥ 3 months of follow-up and 78% (7/9) maintained response 3 months after enrolling into B-Sure. 3/12 (25%) had complete data with ≥ 9 months of follow-up, of

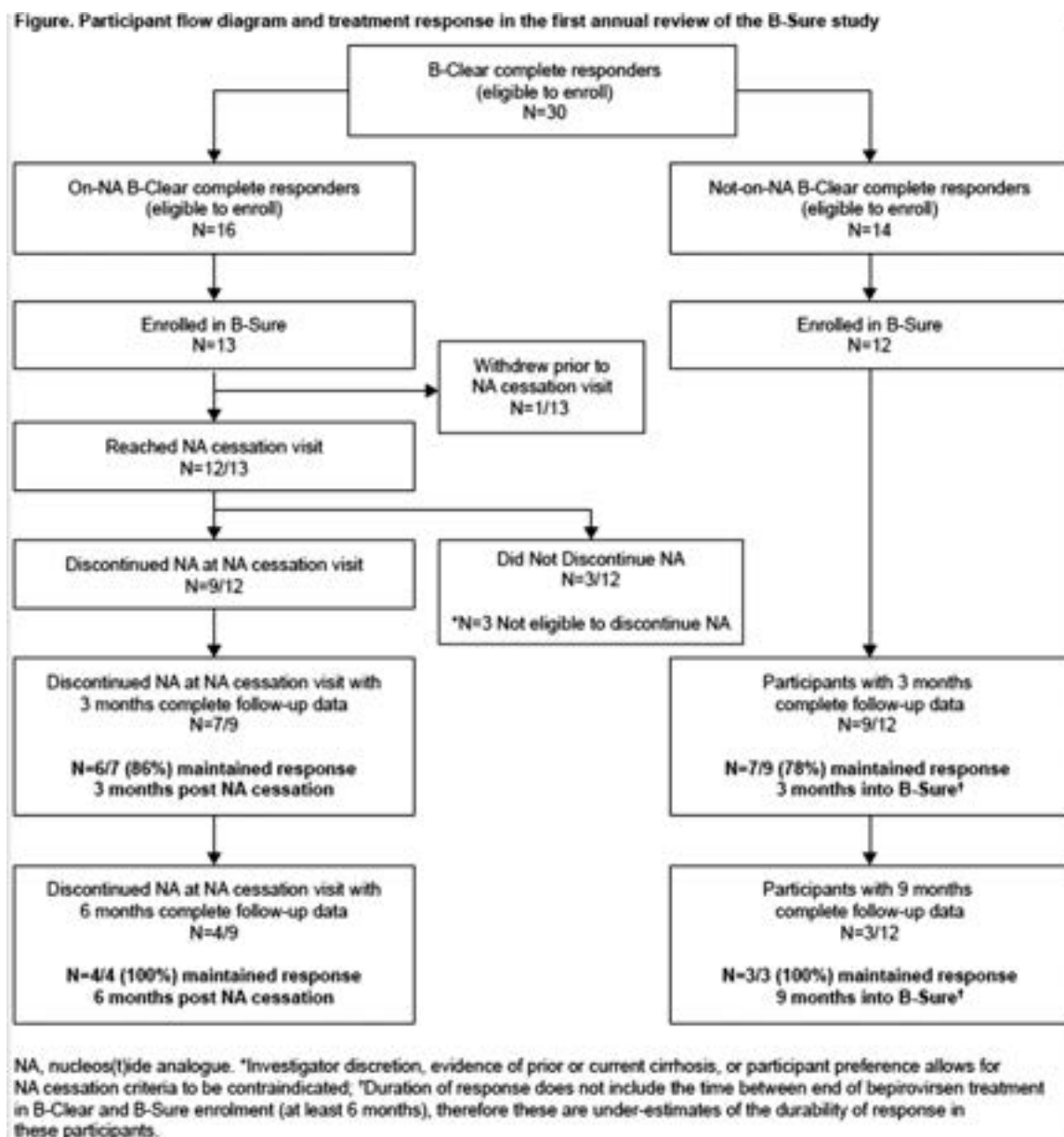


Figure: (abstract: LBP-15).

POSTER PRESENTATIONS

whom 100% (3/3) maintained response 9 months into B-Sure. There were no safety signals that suggested a latent adverse drug effect following use of BPV.

Conclusion: These data provide early evidence on the durability of response observed with BPV.

Funding: GSK (study 206882)

LBP-16

Hepatocellular carcinoma surveillance improves early detection and curative treatment in chronic hepatitis C patients treated with direct acting antivirals

Cassia Regina Guedes Leal¹, Carmem Ferguson Theodoro¹, Thais Guaraná¹, Jorge Strogoff-de-Matos¹, Rosângela Teixeira², Renata Perez³, Paulo de Tarso Aparecida Pinto⁴, Tatiana Guimaraes¹, Solange Artimos¹. ¹Antonio Pedro University Hospital, Fluminense Federal University, Brazil; ²Minas Gerais Federal University, Brazil; ³Federal University of Rio de Janeiro, Brazil; ⁴Hospital Federal dos Servidores do Estado, Brazil
Email: cassia.r.g.leal@gmail.com

Background and aims: Hepatocellular carcinoma (HCC) is the third leading cause of cancer mortality worldwide. HCC prognosis remains poor, partly because up to 70% of patients are diagnosed with advanced HCC at initial presentation. As with other cancers, surveillance programs aim to detect tumors at an early stage, facilitate curative-intent treatment, and reduce cancer-related mortality. The aim of this study was to evaluate the incidence of HCC and the impact of surveillance on early diagnosis in patients with chronic hepatitis C virus (HCV) treated with direct antiviral agents (DAAs).

Method: A cohort of 1075 HCV patients ≥ 18 years were treated with DAAs from 2015 to 2019 and followed until 2022. Ultrasonography was performed up to 6 months before DAAs and each 6 months thereafter for patients with advanced fibrosis (F3 and F4 METAVIR). HCC diagnosis was established based on the criteria of the European Association for the Study of the Liver and staging according to the Barcelona Clinic Liver Cancer (BCLC) system.

Results: Of the total, 51/1075 (4.7%) developed HCC in the median of 40 (IQR 25–58) months: 26/51 (51%) male, median age 60 (IQR 54–66) years, alpha-fetoprotein (AFP) 12.2 (IQR 6.1–18.8) ng/ml, 47/51 (92.1%) cirrhotic (78.7%; Child-Pugh (CP) A and 21.3% CP B), 8/51 (15.7%) without sustained virological response (SVR). Cumulative HCC incidence was 6.5%. Overall incidence was 1.46/100 patient-years (PY) (95% CI = 1.09–1.91), being 2.31/100 PY (95% CI = 1.70–3.06), 0.45/100 PY (95% CI = 0.09–1.32) and 0.20/100 PY (95% CI 0.01–1.01) in METAVIR F4, F3 and F2, respectively. According to BCLC, liver tumors were classified as follows: 0 (8/51, 15.6%), A (26/51, 51%), B (11/51, 21.6%), C (5/51, 9.8%) and D (1/51, 2%). Among patients with early HCC diagnosis, 71% received potentially curative treatment.

Conclusion: HCC still occurs after HCV treatment with DAAs, mainly in METAVIR F4 patients. According to our findings, screening favored early diagnosis in approximately 70% of patients, facilitating earlier initiation of potentially curative treatments thus improving the prognosis of these patients.

LBP-17

Artificial intelligence to measure fibrosis change on liver biopsy in MAESTRO-NASH a phase 3 52-week serial liver biopsy study in 966 patients with NASH treated with resmetirom or placebo

Stephen Harrison¹, Rebecca Taub², Dominic Labriola², Yayun Ren³, Elaine Chng³, Dean Tai³. ¹Pinnacle Research, United States; ²Madrigal Pharmaceuticals, RandD, United States; ³Histoindex, Singapore
Email: rebeccataub@yahoo.com

Background and aims: MAESTRO-NASH (NCT03900429) is an ongoing 54-month, Phase 3, registrational double blind, placebo-controlled non-cirrhotic NASH clinical trial to study the effect of once daily 80 mg or 100 mg resmetirom as compared with placebo in 966 patients with NASH and liver fibrosis. NASH resolution and fibrosis reduction end points on liver biopsy at 52 weeks were achieved at

both resmetirom doses, including at least a one stage reduction in fibrosis without worsening of NASH of 24%, 26% (mITT) at 80 and 100 mg doses compared with placebo (14%). As an exploratory end point, artificial intelligence slide reading technologies were employed to measure the effect on fibrosis on serial liver biopsy using both continuous and quantitative scoring.

Method: Fibrosis was estimated as a continuous and categorical variable using second harmonic generation (SHG) (qFibrosis)/two photon excited fluorescence of 768 paired biopsy samples from MAESTRO-NASH. A separate unstained slide was analyzed for qFibrosis (normalized by tissue area and then corrected for qSteatosis (tissue area-steatosis area)). Relative changes in 184 fibrosis parameters were determined.

Results: The analyses were based on a total of 768 slide pairs including a baseline and Week 52 slide that were received and met criteria for quality ($<10\%$ missing pairs; $<3\%$ excluded for quality). Based on a continuous qSteatosis score, the % change from baseline in steatosis was 80 mg, -36% ; 100 mg, -46% ; placebo, -10% , $p < 0.0001$ for both doses, the continuous change from baseline in corrected qFibrosis score was 80 mg, -22% ; 100 mg, -20% ; placebo, 3% , $p < 0.0001$ for both doses. The categorical qFibrosis stage aligned with pathologist scoring (F1, F2, F3) with the exception that qFibrosis estimated a high fraction $\sim 20\%$ as F4 stage fibrosis at baseline (F4 stage scored at baseline by central pathologists were excluded from this study). Based on categorical change in qFibrosis score, there was a significant improvement in fibrosis stage (1-stage or 2-stage improvement) at 80 and 100 mg relative to placebo, and less worsening of fibrosis in the resmetirom treatment groups compared with placebo (Table). The percentage showing improvement in qFibrosis (≥ 1 -stage) was higher than scored by pathologists, and identified 90% of resmetirom responders determined by pathologists. Significant correlations were observed between reduction in qFibrosis and reduction in PDFF, ALT, AST, and ELF.

Categorical change in qFibrosis stage		≥ 1 -stage improvement		≥ 2 -stage improvement		worsened	
		p value		p value		p value	
80 mg	58%	<0.0001	19%	<0.0001	11%	<0.0001	
100 mg	56%	<0.0001	25%	<0.0001	11%	<0.0001	
PBO	34%		7%		35%		

Conclusion: Measurements of fibrosis change using qFibrosis on either a continuous or categorical scale demonstrated a clear improvement and less worsening in fibrosis in resmetirom treated NASH patients as compared with placebo after 52 weeks of treatment.

LBP-18

ALC-000184, a capsid assembly modulator, dosed with entecavir for up to 28 weeks is well tolerated and resulted in substantial declines in surface antigen levels in untreated Hepatitis B e antigen positive subjects with chronic hepatitis B

Jinlin Hou¹, Yanhua Ding², Junqi Niu², Xieer Liang¹, Man-Fung Yuen³, Edward J. Gane⁴, Kosh Agarwal⁵, Min Wu⁶, Kha Le⁷, Meenakshi Venkatraman⁷, Christopher Westland⁷, Maida Maderazo⁷, Sushmita Chanda⁷, Leonid Beigelman⁷, Lawrence Blatt⁷, Tse-I Lin⁸, Matt McClure⁷, John Fry⁹. ¹Nanfeng Hospital, Southern Medical University, China; ²Jilin University, the First Hospital, China; ³University of Hong Kong, Hong Kong; ⁴University of Auckland, New Zealand; ⁵King's College, United Kingdom; ⁶Aligos Therapeutics (Shanghai) Co., Ltd, China; ⁷Aligos Therapeutics, United States; ⁸Aligos Belgium BV, Belgium; ⁹Consultant, United States
Email: jlhoumu@163.com

Background and aims: To evaluate the safety, pharmacokinetics (PK), and antiviral activity of

ALG-000184, an oral prodrug of ALG-001075, a novel, pan-genotypic capsid assembly modulator with picomolar potency.

Method: ALG-000184-201 is a multi-part, multi-center, double-blind, randomized, placebo-controlled study (NCT04536337). Single and multiple ALG-000184 daily doses have previously been shown in Parts 1-3 to be well tolerated for dosing durations of 1-28 days and have potent antiviral activity in untreated chronic hepatitis B (CHB) subjects. In Part 4, multiple cohorts are evaluating dosing with ALG-000184 (100 mg x 24 weeks in Cohort 1 and 300 mg x 48 weeks in Cohort 2) in combination with entecavir (ETV) in untreated hepatitis B e antigen positive (HBeAg+) CHB subjects. Previously, available data from Cohorts 1 and 2 have shown that ≤ 300 mg ALG-000184 + ETV for ≤ 28 weeks is well tolerated and lowers hepatitis B DNA and surface antigen (HBsAg) levels. Here we report newly emerging safety, PK, and antiviral activity data from Cohort 2.

Results: Fifteen subjects were enrolled, all of which were Asian, with 7 (47%) female, mean age 31.4 years and body mass index 22.2 kg/m². Baseline alanine aminotransferase (ALT) was elevated in 8 (53%) of subjects and all subjects were genotype B (33%) or C (67%). Mean (log₁₀) baseline HBV DNA, RNA and HBsAg levels were 8.1 IU/ml, 6.7 copies/ml, and 4.4 IU/ml, respectively. 300 mg ALG-000184 + ETV for up to 28 weeks has been well tolerated with no concerning safety findings or trends reported, including no serious or treatment emergent adverse events (TEAEs) leading to discontinuation. Three subjects have experienced Grade ≥ 3 TEAEs; 1 subject developed Grade 4 neutropenia that was deemed related to an upper respiratory tract infection and 2 subjects experienced aminotransferase elevations (Grade 4 ALT with Grade 2 or 3 aspartate aminotransferase (AST) elevations), both of which were considered by the study ALT Flare Committee to be related to antiviral activity. All of these events resolved or are improving despite continued dosing. The PK profile with longer term dosing is consistent with prior observations with shorter dosing durations. Substantial mean (SEM) DNA (6.4 (0.3) log₁₀ IU/ml) and RNA (4.7 (0.7) log₁₀ copies/ml) declines have been observed for subjects dosed x 28 weeks (N=5). Additionally, 4 (80%) of these subjects have exhibited continuous HBsAg declines of at least 1.1 log₁₀ IU/ml with a mean (SEM) decline of 1.4 (0.1) log₁₀ IU/ml; 2 of these 4 responders experienced declines of 1.6 and 1.7 log₁₀ IU/ml, respectively.

Conclusion: 300 mg ALG-000184 + ETV was well tolerated and had profound antiviral effects, including lowering HBsAg levels by up to 1.7 log₁₀ IU/ml among subjects dosed for 28 weeks. The observed HBsAg lowering effects indicate oral ALG-000184 may play an important role in combination regimens designed to achieve enhanced functional cure rates.

LBP-19

Assessing progress towards achieving regional hepatitis B control goal-nationwide serosurvey among children, Uzbekistan, 2022

Nino Khetsuriani¹, Dilorom Tursunova², Rano Kasimova³, Said Sharapov³, Brock Stewart¹, Renat Latipov⁴, Liudmila Mosina⁵, Bakhodir Yusupaliyev², Erkin Musabaev³. ¹Centers for Disease Control and Prevention (CDC), United States; ²Center for Sanitary-Epidemiological Welfare, Ministry of Health, Uzbekistan; ³Research Institute of Virology, Ministry of Health, Uzbekistan; ⁴World Health Organization Country Office for Uzbekistan, Uzbekistan; ⁵World Health Organization Regional Office for Europe, Denmark
Email: nck7@cdc.gov

Background and aims: Uzbekistan, a highly endemic country for hepatitis B virus (HBV), has adopted regional hepatitis B control and global hepatitis B elimination goals. Routine infant vaccination with hepatitis B vaccine (HepB), including a birth dose (HepB-BD), was introduced in the national immunization schedule in 2001. Since 2002, reported immunization coverage in Uzbekistan has been $\geq 90\%$ for ≥ 3 doses of HepB (HepB3) and $\geq 95\%$ for HepB-BD. However, the impact of vaccination and the progress towards achieving the European regional control target of $\leq 0.5\%$ HBV surface antigen

(HBsAg) prevalence in vaccinated age groups had not been assessed. To determine current HBsAg prevalence among children in Uzbekistan, we conducted a serosurvey in 2022.

Method: This nationwide serosurvey included primary school children (ages 6-10 years) and used a stratified, multi-stage cluster design. Participants' basic demographics and HepB immunization information (from clinic records) were obtained. Blood samples were tested for HBsAg using a WHO-prequalified rapid test (Bioline HBsAg WB, Abbott Diagnostics). Samples with positive and indeterminate results were tested for HBsAg by ELISA (Murex HBsAg Version3, Diasorin). Weighted proportions and adjusted 95% confidence intervals (CI) for HBsAg prevalence and for receipt of HepB3, HepB-BD, and timely HepB-BD (given within the first 24 hours of birth), were calculated.

Results: Of 4,119 children enrolled in classes selected from the 148 participating schools, blood was collected from 3,753 (91.1%) and immunization data were available for 3,833 (93.3%). Overall, national HBsAg prevalence was 0.20% (adjusted 95% CI, 0.09%-0.38%). Among children with available immunization data, 3,745 [97.7% (97.2%-98.1%)] received HepB3 and 3,635 [94.9% (94.1%-95.5%)] received HepB-BD. Timely HepB-BD was given to 3,349 [93.7% (92.9%-94.5%)] of 3,592 children with available HepB-BD vaccination age data.

Conclusion: Uzbekistan has most likely achieved the European region hepatitis B control target based on $\geq 90\%$ HepB-BD and HepB3 vaccine coverage and $< 0.5\%$ HBsAg seroprevalence among children. To further decrease HBsAg seroprevalence in Uzbekistan to a $\leq 0.1\%$ level consistent with the elimination of mother-to-child transmission of HBV, additional interventions should be considered, including improving antenatal screening for HBsAg and providing hepatitis B immunoglobulin to infants born to HBsAg-positive mothers and anti-HBV antiviral treatment to eligible HBsAg-positive pregnant women.

LBP-20

Continued treatment of early non-responder or partial virologic responders with bulevirtide monotherapy in patients with chronic hepatitis D through week 96 leads to improvement in virologic and biochemical responses

Pietro Lampertico^{1,2}, Heiner Wedemeyer³, Maurizia Brunetto⁴, Pavel Bogomolov⁵, Tatyana Stepanova⁶, Sandra Ciesek⁷, Annemarie Berger⁷, Dmitry Manuilov⁸, Qi An⁸, Audrey Lau⁸, Ben Da⁸, John F. Flaherty⁸, Renee-Claude Mercier⁸, Stefan Zeuzem⁹, Markus Cornberg³, Maria Buti¹⁰, Soo Aleman¹¹. ¹Foundation IRCCS Ca' Granda Ospedale Maggiore Policlinico, Division of Gastroenterology and Hepatology, Milan, Italy; ²CRC "A. M. and A. Migliavacca" Center for Liver Disease, University of Milan, Department of Pathophysiology and Transplantation, Milan, Italy; ³Klinik für Gastroenterologie, Hepatologie und Endokrinologie, Medizinische Hochschule Hannover, Hannover, Germany; ⁴Hepatology Unit, Reference Center of the Tuscany Region for Chronic Liver Disease and Cancer, University Hospital of Pisa and Department of Clinical and Experimental Medicine, Italy; ⁵State Budgetary Institution of Health Care of Moscow Region "Moscow Regional Research Clinical Institute After M.F. Vladimirsky", Moscow, Russian Federation; ⁶Limited liability company "Clinic of Modern Medicine", Moscow, Russian Federation; ⁷Institute for Medical Virology, German Centre for Infection Research, External Partner Site Frankfurt, University Hospital, Goethe University Frankfurt am Main, Frankfurt am Main, Germany; ⁸Gilead Sciences, Inc., Foster City, United States; ⁹University Hospital Frankfurt, Department of Medicine, Frankfurt am Main, Germany; ¹⁰Hospital Universitario Vall d'Hebron and CIBEREHD del Instituto Carlos III, Barcelona, Spain; ¹¹Karolinska University Hospital/Karolinska Institutet, Department of Infectious Diseases, Stockholm, Sweden
Email: pietro.lampertico@unimi.it

Background and aims: Bulevirtide (BLV), a novel entry inhibitor of hepatitis delta virus (HDV), is conditionally approved in the EU for treatment of chronic hepatitis D (CHD) based on surrogate end point results. In clinical studies, virologic responders (VR) to HDV therapy is

POSTER PRESENTATIONS

defined as achieving undetectability or a ≥ 2 -log₁₀ IU/ml decline in HDV RNA from baseline (BL). However, the optimal BLV treatment duration is unknown, and it is also unclear if patients who are early virologic non-responders (NR) will benefit from continued therapy. This analysis aimed to evaluate the efficacy of continued BLV monotherapy in those who were not VR after 24 weeks (W) of treatment.

Method: Data from the ongoing phase 3 study (MYR301; NCT03852719) was analyzed. MYR301 is an open-label, randomized study evaluating three cohorts: BLV 2mg (Arm B) and BLV 10mg (Arm C) for 144W, and a delayed treatment arm (Arm A). Only results from participants on treatment at 96W from Arm B + C were included in this analysis. NR and partial-responders (PR) were defined as HDV RNA declines of < 1 -log₁₀ IU/ml and ≥ 1 but < 2 -log₁₀ IU/ml, respectively. Rates of participants achieving biochemical response (alanine transaminase [ALT] within normal limits [WNL]), were compared between NR, PR, and VR.

Results: Participants with CHD (N = 94) were included (47 BLV 2mg; 47 BLV 10mg). BL characteristics included: 62% male, 85% white, 48% with cirrhosis, 61% taking concomitant nucleos (t)ide analogues and 55% with prior interferon exposure. Mean (SD) HDV RNA was 5.0 (1.3) log₁₀ IU/ml and median (Q1, Q3) ALT was 102 (65, 141) U/ml. At W24, 58 (62%) participants were VR of which 30 had ALT WNL, 22 were PR of which 12 had ALT WNL, and 14 were NR of which 2 had ALT WNL. (Table 1) Of the 36 NR or PR at W24 vs VR, mean (SD) baseline HDV RNA and median (Q1, Q3) ALT at W96 were as follows: VR [5.1 (1.7) log₁₀ IU/ml, 77 (58, 113) U/ml], PR [4.9 (1.4) log₁₀ IU/ml, 120 (52, 153) U/ml], and NR [4.4 (1.9) log₁₀ IU/ml, 156 (133, 196) U/ml]. Of 22 PR participants at W24, 18 became VR by W96 (11-BLV2 mg/7-BLV 10 mg); 15 with ALT WNL and 3 remained PR (3-BLV 10mg); 2 with ALT WNL. Of 14 NR participants at W24, 6 became VR (3-BLV2 mg/3-BLV10 mg) by W96, and 3 became PR (3-BLV2 mg), with 5 remaining NR. Mean (SD) HDV RNA decline from baseline at W96: VR [-3.6 (1.1) log₁₀ IU/ml], PR [-1.5 (0.3) log₁₀ IU/ml], and NR [-0.2 (0.5) log₁₀ IU/ml]. Median (Q1, Q3) ALT decline from baseline at W96: VR [-48 (-75, -12) U/ml], PR [-42 (-102, 9) U/ml], and NR [-83 (-102, -33) U/ml]. At W96, ALT had declined by $> 50\%$ from BL in 5 of the 6 NR (1 achieved ALT WNL).

Conclusion: Most patients who were PR (18 of 24; 75%) and a considerable portion who were NR (6 of 14; 43%) to BLV at 24W achieved VR by W96; with ALT improvements occurring in all groups including those who remained a NR. These results provide evidence for continuing BLV therapy despite early (W24) suboptimal virological responses in patients with CHD.

LBP-21

A global research priority agenda to advance public health responses to fatty liver disease

Jeffrey Lazarus^{1,2,3}, Henry Mark^{4,5}, Alina Allen⁶, Juan Pablo Arab^{7,8,9}, Carrieri Patrizia¹⁰, Mazen Noureddin¹⁰, Marcela Villota-Rivas¹, Jörn Schattenberg¹¹, Vincent Wai-Sun Wong¹², Zobair Younossi¹³.

¹Barcelona Institute for Global Health (ISGlobal), Hospital Clínic, University of Barcelona, Barcelona, Spain; ²University of Barcelona, Faculty of Medicine and Health Science, Barcelona, Spain; ³CUNY Graduate School of Public Health and Health Policy, New York, United States; ⁴European Association for the Study of the Liver (EASL), Geneva, Switzerland; ⁵Independent consultant, Derby, United Kingdom; ⁶Mayo Clinic, Division of Gastroenterology and Hepatology, Department of Internal Medicine, Rochester, United States; ⁷Western University and London Health Sciences Centre, Division of Gastroenterology, Department of Medicine, Schulich School of Medicine, London, Canada; ⁸Western University, Department of Epidemiology and Biostatistics, Schulich School of Medicine, London, Canada; ⁹Pontificia Universidad Católica de Chile, Department of Gastroenterology, School of Medicine, Santiago, Chile; ¹⁰Aix Marseille University, Inserm, IRD, SESSTIM, Sciences Economiques and Sociales de la Santé et Traitement de l'Information Médicale, ISSPAM, Marseille, France; ¹¹University Medical Centre Mainz, Metabolic Liver Research Program, I. Department of Medicine, Mainz, Germany; ¹²The Chinese University of Hong Kong, Hong Kong, Hong Kong; ¹³Inova, Center for Liver Disease, Falls Church, United States

Email: Jeffrey.Lazarus@isglobal.org

Background and aims: Over the past three decades the burden of non-alcoholic fatty liver disease has increased drastically, and globally an estimated 38% of adults and 1 in 10 children and adolescents have the condition. The implications of the disease are profound spanning health, social and economic consequences at both individual and population levels. This study aimed to develop an aligned, prioritised research agenda for the global fatty liver disease community of practice.

Method: Nine study co-chairs drafted initial research priorities which were reviewed by 40 core study members. Following a Delphi methodology, over two rounds a large panel reviewed the priorities, via Qualtrics XM, indicating agreement using a four-point Likert-scale ('agree', 'somewhat agree', 'somewhat disagree', and 'disagree') and providing written feedback. The core members revised the priorities between rounds. In R2, panellists also ranked the priorities within six domains: epidemiology, treatment and care, models of care, patient and community perspectives, education and awareness, and leadership and public health policy.

Table 1: Shift Table for Non- and Partial Responders at Week 24 Through Week 48 and 96

	BLV 2mg Week 24 HDV RNA			BLV 10mg Week 24 HDV RNA			BLV 2mg + 10mg Week 24 HDV RNA		
	NR	PR	VR	NR	PR	VR	NR	PR	VR
	n = 10	n = 12	n = 25	n = 4	n = 10	n = 33	n = 14	n = 22	n = 58
W48 HDV RNA									
Nonresponder	8 (80)	1 (8.3)	0 (0)	3 (75)	0 (0)	0 (0)	11 (78.6)	1 (4.6)	0 (0)
Partial Responder	1 (10)	0 (0)	2 (8)	0 (0)	5 (50)	1 (3)	1 (7.1)	5 (22.7)	3 (5.2)
Responder	1 (10)	11 (91.7)	23 (92)	1 (25)	5 (50)	32 (97)	2 (14.3)	16 (72.7)	55 (94.8)
W96 HDV RNA									
Nonresponder	4 (40)	1 (8.3)	0 (0)	1 (25)	0 (0)	0 (0)	5 (35.7)	1 (4.6)	0 (0)
Partial Responder	3 (30)	0 (0)	2 (8)	0 (0)	3 (30)	2 (6.1)	3 (21.4)	3 (13.6)	4 (6.9)
Responder	3 (30)	11 (91.7)	23 (92)	3 (75)	7 (70)	31 (93.9)	6 (42.9)	18 (81.8)	54 (93.1)

Figure: (abstract: LBP-20).



Figure: (abstract: LBP-21). Research priorities agenda for fatty liver disease.

Results: Of the 473 individuals invited to participate in R1, 344 (72.7%) completed the survey. The 344 R1 respondents were invited to participate in R2, with 288 (83.7%) completing the survey. The panel originated from 94 countries and are predominantly employed in the academic sector (66.6%), and work in the field of clinical research (79.4%). In R1, the study presented 31 initial priorities to the panel. In revisions ahead of R2 three priorities were removed, with key components of these being merged with others, leaving 28 for the panel to review in R2. Across rounds, consensus increased in all domains, with the mean percentage of 'agree' responses rising from 78.3 in R1 to 81.1 in R2. In R2, the mean level of combined agreement ('agree' + 'somewhat agree') across all priorities was 97.7% and five received unanimous combined agreement (Figure 1); the remaining 23 priorities exhibited >90% combined agreement. All but one of the priorities exhibited at least a super-majority of agreement (>66.7% 'agree'). Thirteen priorities had <80% 'agree', with reliance on 'somewhat agree' to achieve >90% combined agreement.

Conclusion: Adopting the multidisciplinary consensus research priorities agenda can deliver a step-change in understanding fatty liver disease, from the individual and societal harms to its prevention, identification, treatment, and care. The outcomes of this study should catalyse the global liver health community's efforts to advance and accelerate responses to this widespread and fast-growing public health threat.

LBP-22

Twelve-week treatment with BOS-580, a novel, long-acting Fc-FGF-21 fusion protein, leads to a reduction in liver steatosis, liver injury, and fibrosis in patients with phenotypic NASH: a randomized, blinded, placebo-controlled phase 2A trial

Rohit Loomba¹, Kris Kowdley², Jose Rodriguez³, Nomita Kim⁴, Alina Alvarez⁵, Linda Morrow⁶, Philip Yin⁷, Lakshmi Amaravadi⁸, Brenda Jeglinski⁹, Alicia Clawson¹⁰, Swapna Chowdhury¹¹, Craig Basson¹², Etienne Dumont¹³, Eric Svensson¹⁴, Tatjana Odrlija¹⁵.
¹UC San Diego, Medicine, La Jolla, United States; ²Liver Institute Northwest, N/A, Seattle, United States; ³Southwest General Health Care

Center, Medical Director/Principal Investigator, Fort Meyers, United States; ⁴Boston Pharmaceuticals, Research, Austin, United States; ⁵Century Research, LLC, Clinical, Miami, United States; ⁶ProSciento, Inc., Medical Affairs, San Diego, United States; ⁷Pemi River Health Solutions, LLC, N/A, Somerville, United States; ⁸Dewpoint Therapeutics, Preclinical Development and Translational Medicine, Natick, United States; ⁹Boston Pharmaceuticals, Clinical Operations, Cambridge, United States; ¹⁰Boston Pharmaceuticals, Research and Development, Biometrics, Cambridge, United States; ¹¹Boston Pharmaceuticals, Drug Metabolism and Pharmacokinetics, Cambridge, United States; ¹²Boston Pharmaceuticals, N/A, Needham, United States; ¹³Boston Pharmaceuticals, R and D, Phoenixville, United States; ¹⁴Boston Pharmaceuticals, Research and Development, Cambridge, United States; ¹⁵Boston Pharmaceuticals, Clinical Development, Cambridge, United States
 Email: roloomba@health.ucsd.edu

Background and aims: BOS-580 is a genetically engineered fusion of IgG1 Fc and fibroblast growth factor 21 (FGF-21) with specificity for FGF receptors 1c/2c/3c allowing for prolonged, balanced pharmacological effects. BOS-580 has a 21-day half-life that enables biweekly and monthly dosing. A growing body of evidence demonstrates that FGF-21 analogues can increase NASH resolution and improve fibrosis in patients with NASH. The aim of this study was to examine pharmacokinetics, safety and efficacy of multiple doses and dose regimens of BOS-580 in patients with phenotypic NASH.

Method: Inclusion criteria for this patient- and investigator-blinded, randomized, placebo-controlled Phase 2A trial were a BMI of 30-45 kg/m² hepatic magnetic resonance imaging proton density fat fraction (MRI-PDFF) of ≥10%, vibration controlled transient elastography liver stiffness measurement (VCTE-LSM) of 7.0 to 9.9 kPa, and serum aspartate transaminase (AST) >20 IU/L. Subjects were randomized into 5 dosing cohorts treated for 12 weeks: 75 mg every 4 weeks (Q4W), 75 mg every 2 weeks (Q2W), 150 mg Q4W, 150 mg Q2W and 300 mg Q4W, with a 4:1 ratio of BOS-580 to placebo per cohort. The primary end point was safety/tolerability and pharmacokinetics; exploratory efficacy end points were also evaluated.

	BOS-580					Placebo N=37
Baseline Characteristics (Enrolled Analysis Set)	75 mg Q4W N=8	75 mg Q2W N=14	150 mg Q4W N=15	150 mg Q2W N=15	300 mg Q4W N=13	
BMI kg/m ²	36.5	38.3	36.2	36.4	34.9	36.5
Hepatic MRI-PDFF (%)	24	22	21	21	24	19
AST IU/L	43.1	38.4	29.1	35.0	33.2	29.5
VCTE LSM score	8.4	8.2	8.4	8.4	8.1	8.1
Type 2 diabetes, %	25	57	40	47	46	43
Efficacy Biomarker Summary – Placebo Adjusted LS Means (modified FAS) at week 12	75 mg Q4W N=8	75 mg Q2W N=12	150 mg Q4W N=12	150 mg Q2W N=13	300 mg Q4W N=11	
MRI-PDFF: Relative Change from Baseline (CFB), %	-19*	-61***	-56***	-60***	-58***	
Super-responders: MRI-PDFF ≥ 50% Reduction Rate, %	22	72***	67***	72***	69***	
ALT Absolute CFB	-19	-31*	-18	-37**	-38**	
Pro-C3 Relative CFB, %	-11	-14*	-6	-24***	-26***	

*p < 0.05, ** p < 0.01, ***p < 0.001 (model adjusted for baseline value and treatment effects)
Pro-C3 – N-terminal type III collagen pro-peptide, ALT – alanine amino transferase, CFB – change from baseline, LS – Least Square

Figure: (abstract: LBP-22).

Results: 102 patients of both sexes, 26-72 years old, with phenotypic NASH were enrolled. Demographic and baseline disease characteristics were evenly balanced across cohorts, with a mean liver steatosis of 19-24% by MRI-PDFF, a mean AST of 29.1-43.1 IU/L and a mean liver stiffness of 8.1-8.4 kPa. BOS-580 was well-tolerated with only a 4.6% discontinuation rate due to treatment emergent adverse events, and with mild, transient gastrointestinal events reported more commonly at higher doses. No deleterious effect was seen on the serum low density lipoprotein. BOS-580 resulted in statistically significant hepatic MRI-PDFF reduction of up to 61% after 12 weeks of treatment. In dosing cohorts of 75mg Q2W to 300mg Q4W, 67% to 72% of patients achieved super-responder status (≥50% MRI-PDFF reduction). Further, multiple NASH biomarkers (ALT, AST, Pro-C3), high-density lipoprotein, and triglycerides significantly improved with a total monthly dose of 300mg.

Conclusion: Our results demonstrate that monthly dosing with BOS-580 can achieve clinically important reductions in liver fat and non-invasive biomarkers of liver injury and fibrosis in patients with phenotypic NASH.

LBP-23

Improving hepatitis B screening and linkage to care rates via the electronic medical record, provider engagement, and patient navigation in a large, urban health system

Anna Mageras¹, Eric Woods¹, Brooke Wyatt¹, Rebecca Roediger¹, Francina Collado¹, Tasnim Bhuiyan¹, Caroline Romano¹, Douglas T Dieterich¹. ¹Icahn School of Medicine at Mount Sinai, United States

Email: anna.mageras@mssm.edu

Background and aims: In March 2023, the United States CDC updated its screening guidelines for hepatitis B virus (HBV) from risk-factor-based to universal one-time screening for adults. The WHO recommends screening where prevalence is ≥2%. In NYC, HBV prevalence is 2.9%, and ~46% of New Yorkers with HBV are undiagnosed. To address this public health issue and in anticipation of the CDC's new guidelines, in October 2022 we implemented

universal one-time HBV screening for adults in our large, multi-center hospital system serving metro-NYC. We describe the process of implementing modifications to the electronic medical record (EMR). We also summarize initial changes in screening rates and outcomes from patient navigation for patients identified as HBsAg+.

Method: We met with leadership from population health, ambulatory, EMR IT, and laboratory teams to secure buy-in and to build the EMR modification and provider education materials. The screening consists of three lab orders: HBsAg, anti-HBs, and anti-HBc, in line with updated CDC guidance. In response to PCP concerns, we made several adjustments, including limiting the alert to adults 18-79 rather than 18+, turning off patient-facing alerts, and creating a new panel that orders all three labs in one step. To complement the EMR alert, we conducted outreach to PCPs in three of our five pilot clinics via presentations, feedback reports, broadcast and personalized emails, and a one-page tip sheet. We also implemented patient outreach and navigation via phone, patient portal, and PCP engagement for patients who tested HBsAg+, with the goal of connecting them to liver care.

Results: Since implementation of the EMR alert, the average HBV screening rate has increased from 4% at baseline in September 2022 to 23% in March 2023 across our pilot clinics that received our education (n = 3) and from 3% to 15% in clinics that did not (n = 2). From September 2022 to February 2023, we identified 207 HBsAg+ patients who were screened or had an encounter at one of our pilot clinics. Of these, 17 (8%) were screened for the first time during this period, and 190 (92%) had a previous HBsAg+ test on record. At the time of chart review, 62% of these patients were receiving care for HBV. Of the 78 who were not, 53% attended at least one liver appointment by April 21, 2023, largely due to patient navigation; 27% were still being followed by our patient navigators; and 20% declined care or were lost to follow-up.



Figure:

Conclusion: Policy changes, automatic prompts in the EMR, and outreach to providers can help promote and streamline universal HBV screening. More research is needed, but preliminary results indicate that provider education enhances the positive effect of EMR alerts on screening rates. This approach is replicable at low cost. Many patients with HBV are undiagnosed or diagnosed but not receiving liver care. Patient navigation and PCP engagement can help link them to life-saving care.

LBP-24

Safety and efficacy of anti-pre-S1 domain monoclonal antibody (HH-003) treatment in patients with co-infection of chronic hepatitis B virus (HBV) and hepatitis D virus (HDV): a single center, open-label, phase 2 trial

Xinrui Wang¹, Xiumei Chi¹, Yingyu Zhang¹, Yumei Gu², Long Xiao², Yonghe Qi², Liangfeng Zou², Jiaying Wen², Yin Zhang², Pan Chen², Cong Lei², Bin Ye², Jianhua Sui³, Wenhui Li³, Junqi Niu³. ¹First Hospital of Jilin University, China; ²Huahui Health Ltd., China; ³National Institute of Biological Sciences, China
Email: junqiniu@jlu.edu.cn

Background and aims: HH-003 is a human monoclonal antibody that targets the preS1 domain of the large envelope protein of HBV and HDV. It prevents the binding of preS1 with sodium taurocholate co-transporting polypeptide (NTCP), the cellular receptor for HBV and HDV, and effectively blocks viral infection and re-infection of hepatocytes. This open-label, phase 2 study (NCT05674448) aimed to evaluate the safety and efficacy of HH-003 in patients with chronic HBV and HDV co-infection.

Method: The study included nine participants (aged 18-70 years old) who were serum anti-HDV IgG positive and HDV RNA positive at screening and had a history of HBV for at least 6 months at screening. All participants received intravenous infusion of 20 mg/kg HH-003 once every two weeks for 24 weeks, with a 24-week follow-up. Virological response (a serum HDV RNA level below the limit of detection or a ≥ 2 log₁₀ IU/ml decline from baseline) and biochemical response (normalization of ALT, normal ALT was defined as ≤ 33 U/L for women and ≤ 41 U/L for men) to HH-003 treatment were assessed at week 24 and week 48. Serum HDV RNA level was measured using RoboGene HDV RNA Quantification kit 2.0.

Results: The median (min, max) HDV RNA and ALT levels at baseline were 3.48 (1.58, 5.40) log₁₀ IU/ml and 36.0 (21.0, 86.0) U/L, respectively. After HH-003 treatment, the median (min, max) changes of HDV RNA level from baseline at week 24 and week 48 were -2.18 (-3.88, 0.35) log₁₀ IU/ml and -1.98 (-3.64, 0.72) log₁₀ IU/ml, respectively. At week 24, 77.8% (7/9) of the participants achieved virological response; 3/5 (60%) of the participants with abnormal baseline ALT levels achieved ALT normalization, and the other 4 participants remained to have normal ALT levels (100%, 4/4); and 3/5 (60%) participants achieved combined response of both virological response and ALT normalization. At week 48, 66.7% (6/9), 2/5 (40%)

and 2/5 (40%) of participants achieved virological response, ALT normalization and combined response, respectively. One subject (11.1%) experienced treatment-related adverse events (AEs) of abdominal discomfort (Grade 1) and asthenia (Grade 2). No grade 3 or higher AEs or serious AEs occurred, and no participants discontinued treatment due to AEs.

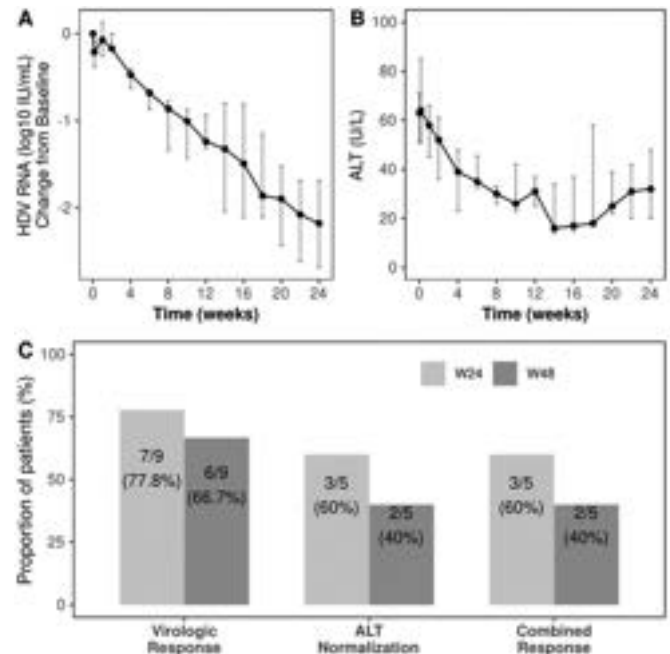


Figure: Efficacy outcomes from the study. (A) Serum HDV RNA level reduction during the HH-003 treatment period. Line plot with median and interquartile range (IQR) showing the log₁₀ change from baseline of the serum HDV RNA level. (B) Line plot with median and IQR showing the dynamics of ALT levels in 5 participants with abnormal baseline ALT levels. (C) The proportions of patients achieved virologic response, ALT normalization and combined response at week 24 and week 48.

Conclusion: HH-003 treatment at a dose of 20 mg/kg demonstrated significant decrease of HDV RNA level and ALT normalization, with a good safety profile in participants co-infected with HBV and HDV. HH-003 might provide a new treatment option for patients with HBV and HDV co-infection, and a large-scale study will be conducted to further demonstrate such a promising anti-viral effect of HH-003 in patients with HBV and HDV co-infection.

LBP-25

Concurrent nivolumab and external beam radiation therapy for patients with advanced hepatocellular carcinoma with vascular invasion: a phase 2, single-arm NEXTRAH trial

Joong-Won Park¹, Bo Hyun Kim¹, Hee Chul Park², Young-Hwan Koh³, Jung Yong Hong², Yuri Cho¹, Boram Park², Dong Hyun Sinn⁴, Tae Hyun Kim⁵. ¹National Cancer Center, Center for Liver and Pancreatobiliary Cancer Center, Korea, Rep. of South; ²Samsung Medical Center, Korea, Rep. of South; ³National Cancer Center, Department of Radiology, Korea, Rep. of South; ⁴Samsung Medical Center, Division of Gastroenterology, Department of Medicine, Korea, Rep. of South; ⁵National Cancer Center, Center for Proton Therapy, Korea, Rep. of South
Email: jwpark@ncc.re.kr

Background and aims: Nivolumab (NIV), a PD-1 inhibitor, was the first immune checkpoint inhibitor (ICI) to be used in the systemic treatment of advanced hepatocellular carcinoma (aHCC). ICIs have become the backbone of systemic therapy for HCC; however, their efficacy needs improvement in patients (pts) with far-aHCC with vascular invasion (VI). External beam radiation therapy (EBRT) could potentially enhance the effectiveness of immunotherapy. This study

POSTER PRESENTATIONS

aimed to investigate the efficacy and safety of concurrent therapy of NIV and EBRT in pts with aHCC with VI.

Method: In this phase 2, single-arm, multicenter, investigator-initiated trial, pts with Child-Pugh class A HCC with VI were treated with intravenous NIV (3 mg/kg every 2 weeks) and EBRT concurrently followed by maintenance NIV until progression or unacceptable toxicity. The primary end point was progression-free survival (PFS) and safety; secondary end points included overall survival (OS), time to progression (TTP), objective response rate (ORR), and disease control rate (DCR). (NCT04611165)

Results: Between January 2020 and June 2021, 50 pts were enrolled from two hospitals in South Korea: 47 (94.0%) had portal vein invasion (Vp) (Vp1/2, n = 21; Vp3, n = 23; Vp4, n = 3), and 13 (26.0%) and 2 (4.0%) had hepatic vein and inferior vena cava invasion, respectively. Also, 5 pts received prior systemic therapy. Pts received EBRT (proton beam RT, n = 26; intensity-modulated RT, n = 24), beginning 2-7 days after the first NIV dose; the median irradiation dose was 50 Gy (range, 21-66 Gy). The median number of NIV doses was 8.5 (interquartile range, 4-26), and 22 pts (44.0%) had at least one dose delay. After the follow-up (median: 29.3 months), the median PFS was 5.55 months (90% confidence interval [CI], 3.58-9.89). Median OS and TTP were 15.24 months (90% CI, 10.81-19.58) and 5.55 months (90% CI, 3.58-9.89), respectively. ORR and DCR were 36.0% and 74.0%, respectively. Any-grade adverse events (AE) and serious AEs were present in 48 (96.0%) and 9 pts (18.0%), respectively. Treatment-related AEs occurred in 40 pts (80.0%); pruritus (38.0%), nausea (10.0%), and pneumonitis (10.0%) were most commonly reported.

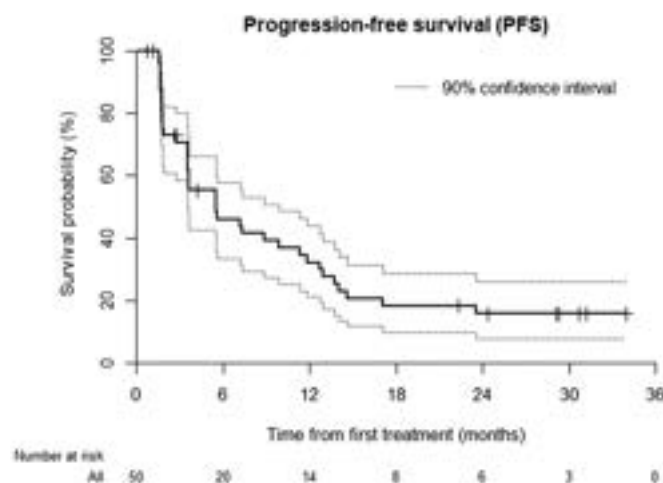


Figure:

Conclusion: Concurrent therapy of NIV and EBRT demonstrates a meaningful PFS and promising clinical outcomes in pts with aHCC with VI. The safety profile was overall acceptable.

LBP-26

Evaluation of non-invasive tests to identify precirrhotic fibrosis due to NASH in patients screened for the phase 3 REGENERATE and REVERSE studies of obeticholic acid

Rohit Loomba¹, Kris Kowdley², Quentin Anstee³, Mazen Nouredin⁴, Zobair Younossi⁵, Naim Alkhouri^{6,7}, Jerome Boursier⁸, Stephen Harrison⁹, Thomas Capozza¹⁰, Jing Li¹⁰, Christopher Gasink¹⁰, Mary Rinella¹¹. ¹University of California, San Diego, La Jolla, United States; ²Liver Institute Northwest and Elson S. Floyd College of Medicine, Washington State University, Seattle, United States; ³Translational and Clinical Research Institute, Faculty of Medical Sciences, Newcastle University, Framlington Place, Newcastle upon Tyne, United Kingdom; ⁴Division of Digestive and Liver Diseases, Cedars-Sinai Medical Center, Los Angeles, United States; ⁵Beatty Liver and Obesity

Research Program, Center for Liver Diseases, Inova Medicine, Falls Church, United States; ⁶The Texas Liver Institute, University of Texas Health San Antonio, San Antonio, United States; ⁷Arizona Liver Health, Chandler, United States; ⁸Angers University Hospital, Angers University, Angers, France; ⁹Pinnacle Clinical Research Center, San Antonio, United States; ¹⁰Intercept Pharmaceuticals, Inc., Morristown, United States; ¹¹University of Chicago, Pritzker School of Medicine, Chicago, United States

Email: roloomba@health.ucsd.edu

Background and aims: Liver biopsy is the historic basis to identify non-alcoholic steatohepatitis (NASH) fibrosis (F) stage but is limited by complications as well as pathologist read and sampling variability. However, non-invasive tests (NITs) are now widely used in clinical practice and society guidelines to identify and risk-stratify NASH F stage. Potential NASH therapies create a pressing need for NIT-based approaches to specifically identify appropriate patients (pts) with F2/3 (precirrhotic) fibrosis.

Method: Patients (pts) screened for the phase 3 trials of obeticholic acid (n = 6060) were examined based on values for FibroScan (FS), Enhanced Liver Fibrosis (ELF), Fibrosis-4 (Fib-4), direct bilirubin (DB), albumin (ALB), and platelet count (PLT) vs both original single-pathologist and consensus panel pathology reads to identify pts likely to have F2/F3 disease, while excluding F0, F1, and F4. The distribution of each NIT across the spectrum of histologic F stages was used to determine ideal cutoffs, which were then assessed for sensitivity (SENS), specificity (SPEC), and related parameters using NITs alone and in combination.

Results: Among all screened pts, F stage n was F0:658, F1:1160, F2:1088, F3:1619, and F4:1535 (REGENERATE only, n = F0:657, F1:1158, F2:1084, F3:1599, and F4:273). The lower bounds of Fib-4 (1.3), ELF (9.6), and FS (9.6) eliminated most F0/1 pts, while the upper bounds (Fib-4, 2.67; ELF, 11; FS, 18) discriminated between F3 and F4. Results were generally similar in single and consensus pathology reads (Table). Although single NITs had insufficient SPEC, use of 2 sequential tests, ie, Fib-4 (1.3-2.67) followed by either ELF (9.6-11) or FS (9.6-18) with additional exclusion of PLT <150 10³/μL, DB >0.5 mg/dL, and ALB <3.8 g/dL led to a SPEC of 91% for identification of F2/F3 pts (SENS:31, NPV:35, PPV:89, AUROC:75; for F3: SPEC:85, SENS:38, NPV:66, PPV:65, AUROC:74).

Conclusion: A combined NIT approach using Fib-4 followed by either ELF or FS identified F2/F3 pts with high SPEC and PPV. The addition of PLT, DB, and ALB upper bounds further increased SPEC, ensuring precise identification of pts who would be appropriate for therapies or studies in this population. While low SENS is a limitation, this approach reliably identified precirrhotic fibrosis without liver biopsy in almost 40% of F3 pts. This approach should be validated in an independent cohort of similar pts.

LBP-27

Evaluation of the hepatitis B virus liver reservoir with fine needle aspirates

Barbara Testoni^{1,2,3}, Armando Andres Roca Suarez^{1,2,3}, Arianna Battisti⁴, Marie-Laure Plissonnier^{1,2,3}, Marantha Heil⁵, Thierry Fontanges⁶, Francois Villeret⁶, Yasmina Chouik⁶, Massimo Levvero^{1,3,6,7}, Upkar Gill⁴, Patrick Kennedy⁴, Fabien Zoulim^{1,2,3,6}. ¹INSERM U1052, CNRS UMR-5286, Cancer Research Center of Lyon (CRCL), France; ²University of Lyon, Université Claude-Bernard (UCBL), Lyon, France; ³Hepatology Institute of Lyon, France; ⁴Barts Liver Centre, Immunobiology, Blizard Institute, Barts and The London School of Medicine and Dentistry, Queen Mary University of London, London, United Kingdom; ⁵Roche Molecular Diagnostics, Pleasanton CA, United States; ⁶Department of Hepatology, Croix Rousse hospital, Hospices Civils de Lyon, France; ⁷Department of Internal Medicine-DMISM and the IIT Center for Life Nanoscience (CLNS), Sapienza University, Rome, Italy

Email: fabien.zoulim@inserm.fr

	Criterion	Original Single Read (Patients Screened in REGENERATE + REVERSE) n=6060, (%)			Consensus Read (Patients Randomized in REGENERATE + REVERSE) n=2572, (%)		
		F2 n=1088	F3 n=1619	F4 n=1535	F2 n=565	F3 n=741	F4 n=1093
NITs	Fib-4 >2.7	59/1074 (5.5)	196/1595 (12.3)	485/1509 (32.1)	27/563 (4.8)	89/738 (12.1)	295/1090 (27.1)
	ELF >11.0	42/864 (4.9)	150/1289 (11.6)	261/911 (28.6)	22/547 (4.0)	84/727 (11.6)	275/1080 (25.5)
	FS >18	49/767 (6.4)	190/1143 (16.6)	685/1203 (56.9)	33/422 (7.8)	67/557 (12.0)	511/965 (53.0)
Additional Upper-bound Thresholds	PLT <150	40/1077 (3.7)	137/1599 (8.6)	466/1521 (30.6)	24/564 (4.3)	66/738 (8.9)	276/1093 (25.3)
	DB >0.5	34/1070 (3.2)	52/1587 (3.3)	113/1508 (7.5)	10/563 (1.8)	23/740 (3.1)	67/1092 (6.1)
	ALB <3.8	9/1079 (0.8)	23/1607 (1.4)	98/1527 (6.4)	3/565 (0.5)	7/740 (0.9)	50/1093 (4.6)

Abbreviations: ALB, albumin; DB, direct bilirubin; ELF, Enhanced Liver Fibrosis test; Fib-4, Fibrosis 4 score; FS, FibroScan; NIT, noninvasive test; PLT, platelet count.

Table: (abstract: LBP-22). Upper Bound Criteria Applied to Original and Consensus Pathology Reads, by Fibrosis Stage.

Background and aims: Finite duration of treatment associated with Hepatitis B surface antigen (HBsAg) loss is the current goal for improved therapeutic approaches against chronic hepatitis B virus (HBV) infection, as this indicates elimination or durable inactivation of intrahepatic covalently-closed circular (ccc)DNA. To assist drug development, it will be essential to define early predictive markers of HBsAg loss by assessing their value in reflecting intrahepatic cccDNA levels and transcriptional activity. In this context, fine needle aspirates (FNA) have recently emerged as a less invasive alternative to core liver biopsy (CLB), having already shown to be useful for the characterization of intrahepatic immune responses. The aim of this study was to optimize and validate the use of FNA vs CLB to evaluate the intrahepatic viral reservoir.

Method: Paired FNA/CLB samples were obtained from patients with hepatitis B e antigen (HBeAg)+ chronic hepatitis (n=4), HBeAg-chronic hepatitis (n=4) and HBeAg- chronic infection (n=1). One HBeAg+ patient was undergoing tenofovir treatment. HBV 3.5-kb RNA and cccDNA were quantified by droplet digital (dd)PCR.

Results: cccDNA was quantifiable in all but one FNA/CLB pair, showing the highest levels in untreated HBeAg+ subjects, with exception of the tenofovir-treated patient. Similarly, 3.5-kb RNA was detectable in all but one FNA sample and showed higher levels in HBeAg+ patients. When comparing cccDNA and 3.5-kb RNA quantification in FNA vs CLB samples, no statistically significant differences were identified.

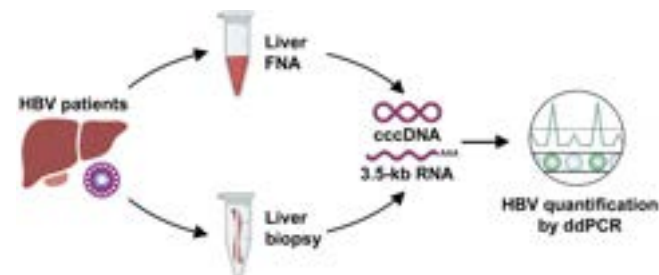


Figure:

Conclusion: These results demonstrate the possibility to quantify cccDNA and assess its transcriptional activity in chronic hepatitis B patients by combining FNA and ddPCR. Moreover, this supports the use of FNA in clinical trials to evaluate the intrahepatic viral reservoir during the development of new antivirals and immunomodulatory agents.

LBP-28

Phase 2a study of CM-101, a CCL24 neutralizing antibody, in patients with non-alcoholic steatohepatitis: a proof-of-concept study

Rifaat Safadi¹, John Lawler², Revital Aricha², Ilan Vaknin², Scott Friedman³, Adi Mor². ¹Hadassah Hebrew University Hospital, Israel; ²Chemomab Therapeutics, Ltd, Israel; ³Icahn School of Medicine, United States

Email: safadi@hadassah.org.il

Background and aims: CCL24 (eotaxin-2) is a chemokine that promotes cell trafficking and regulates inflammatory and fibrotic processes through the CCR3 receptor. CCL24 plays a central role in the development of hepatic fibrosis and liver injury (Segal-Salto M, 2020). Patients with non-alcoholic steatohepatitis (NASH) and advanced non-alcoholic fatty liver diseases (NAFLD) were noted to have elevated levels of CCL24 and CCR3 in liver and blood samples. CM-101 is a humanized IgG1 neutralizing monoclonal antibody to CCL24, which significantly reduced migration and activation of immune cells and fibroblasts, including hepatic stellate cells. CM-101 has been shown to reduce liver damage in three different experimental animal models of liver fibrosis and NASH (Segal-Salto M, 2020). The purpose of study is to evaluate the therapeutic potential of CM-101 in patients with NASH with fibrosis stages 1c, 2 and 3.

Method: This was a single country, multicenter, randomized, double-blind, placebo-controlled, phase 2a study. Patients with liver biopsy confirming NASH within 18 months of randomization or screening were randomized (2:1) to receive either CM-101 5mg/kg or placebo subcutaneously (SQ), every 2 weeks for 14 weeks (8 total administrations) and all patients had a follow-up visit 6 weeks after the end of

Figure 1A:
Proportion of patients reaching or surpassing threshold (number/% reduction) by fibrotic biomarkers

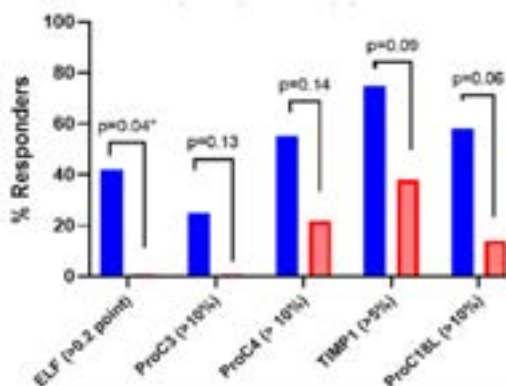


Figure 1B:
Proportion of patients who had improvements in at least 3 fibrotic parameters (PROC18L, ELF, PROC3, TIMP1, PROC4) at week 20

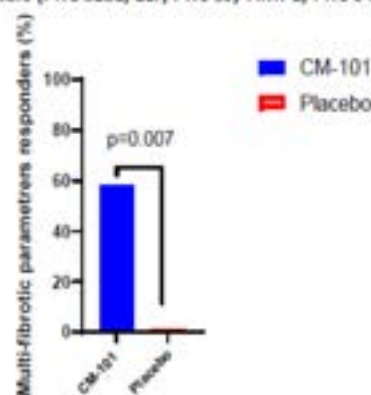


Figure: (abstract: LBP-28).

treatment (total study duration 20 weeks). The primary end point was safety and tolerability at 16 weeks. Secondary and exploratory end points included changes from baseline in various fibrotic and inflammatory serum biomarkers and liver stiffness as assessed by Fibroscan. PK and target engagement profile of CM-101, and the development of anti-drug antibodies (ADAs) were also assessed.

Results: 23 patients (14 CM-101; 9 Placebo) were randomized. The demographic and baseline characteristics were comparable between the groups, except more patients in the CM-101 group had a higher fibrosis stage (36% Stage F3 vs. 0% Stage 3), enhanced liver fibrosis (ELF) score (9.8 vs. 8.7, $p=0.001$), and liver stiffness (11.3 kPa vs. 8.1 kPa, $p=0.037$) at baseline than patients in placebo group, respectively.

CM-101 5mg/kg SQ every 2 weeks for 14 weeks was safe and well tolerated. Most adverse events (AEs) were mild with one unrelated serious adverse event. There were no significant injection site reactions, and no ADAs were detected at 20 weeks. CM-101 showed a favorable PK and target engagement profile that was consistent with other phase 1 studies. Compared to placebo-treated patients, a higher proportion of CM-101-treated patients showed improvement in liver fibrosis-related biomarkers (ProC-3, ProC-4, ProC-18, TIMP-1, ELF) (Fig 1A). At 20 weeks, 8 (60%) of CM-101-treated patients had improvements in at least 3 fibrotic biomarkers compared to 0 of the placebo-treated patients (Fig 1B). Among CM-101-treated patients, those with higher CCL24 levels at baseline showed greater reductions in fibrosis-related biomarkers than patients with lower CCL24 levels.

Conclusion: CM-101 5mg/kg administered SQ every 2 weeks for a relatively short duration of 14 weeks was safe and well tolerated and provided evidence supporting CCL24 as a potential therapeutic target in NASH. Neutralizing the pro-inflammatory and pro-fibrotic effects of CCL24 with CM-101 at higher doses and for prolonged duration should be further evaluated in a statistically powered, biopsy-based, randomized, placebo-controlled study.

LBP-29

Predictors of long-term mortality after HCV eradication among PLWH

Alessia Siribelli¹, Sara Diotallevi¹, Laura Galli¹, Giulia Morsica¹, Riccardo Lolatto¹, Costanza Bertoni¹, Emanuela Messina¹, Simona Bossolasco¹, Benedetta Trentacapilli¹, Caterina Uberti-Foppa², Antonella Castagna², Hamid Hasson¹. ¹San Raffaele Scientific Institute, Milan, Italy; ²Vita-Salute San Raffaele University, Italy
Email: siribelli.alessia@hsr.it

Background and aims: This study aimed to assess the long-term incidence and risk factors of death in HIV-HCV coinfecting people treated with direct acting antivirals (DAAs).

Method: Retrospective study in HIV-HCV coinfecting people, anti-retroviral-treatment experienced, followed at San Raffaele Hospital, who achieved sustained virological response (SVR) after DAAs. Biochemical and virological data were collected at baseline (BL), defined as end of DAA treatment; follow-up (FU) accrued since BL until death, lost-to FU or last visit. ALBI grade, which reflects the hepatic functional reserve, was calculated with the formula: $(\log_{10}\text{-bilirubin}[\mu\text{mol/L}] \times 0.66) + (\text{albumin}[\text{g/L}] \times -0.0852)$. Kaplan-Meier curves and the log-rank test were used to estimate cumulative probability of death for any cause according to some BL characteristics. Cox proportional hazard model was used to estimate adjusted hazard ratio (aHR) of death and the corresponding 95% confidence interval (95%CI); BL variables included in the model were: age, diabetes, HCC, α -fetoprotein (AFP), ALBI grade.

Results: Overall, 663 people analyzed; BL characteristics are reported in Table 1. During a median follow-up of 4.41 years (IQR = 3.5-5.5), 49 people died: 35% deaths were liver-related, 51% malignancies of which 16% liver cancers. The overall 3-, 5- and 7-year cumulative probabilities of death were 4.9% (95%CI = 3.2-6.7%), 8.0% (95%CI = 5.5-10.4%), 11.4% (95%CI = 7.8-14.9%), respectively. Cumulative probabilities of death were higher among older individuals (Figure1), in people with vs without cirrhosis (Figure2), with AFP ≥ 3.4 vs < 3.4 ng/ml (Figure3), with ALBI grade ≥ 2 vs 1 (Figure4), with HCC (log-rank $p=0.002$). At multivariate analysis, death was more likely in older people [aHR (5-year older) = 1.46, 95%CI 1.16-1.83, $p=0.0009$] and in people with diabetes [aHR = 2.98, 95%CI 1.55-5.71, $p=0.001$], ALBI grade ≥ 2 [aHR = 2.13, 95%CI 1.17-3.90, $p=0.014$] and AFP ≥ 3.4 ng/ml [aHR = 1.96, 95%CI 1.01- 3.84, $p=0.049$]; the effect of HCC on the risk of death was marginally significant [aHR = 2.69, 95%CI 0.90-8.05, $p=0.076$].

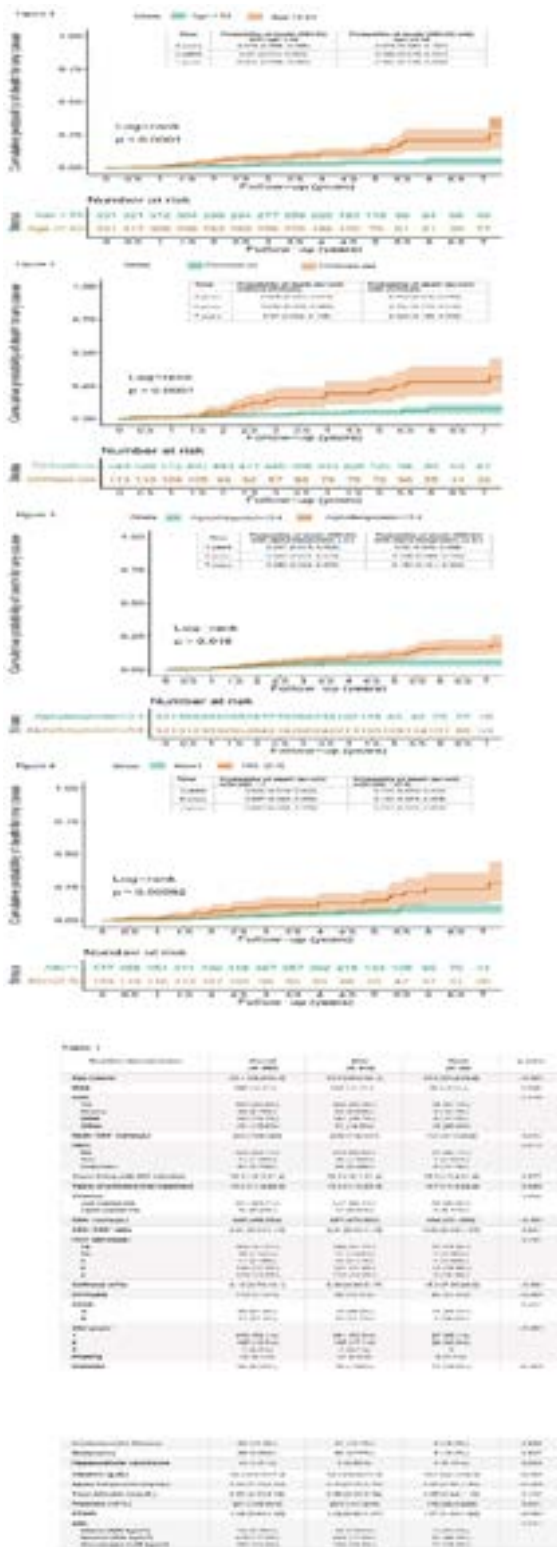


Figure:

Conclusion: HIV-HCV coinfecting people who achieved SVR after DAAs showed a higher risk of death in presence of cirrhosis, HCC, diabetes, ALBI grade ≥ 2 and AFP ≥ 3.4 ng/L, the latter as possible laboratory predictors of mortality. We observed a high number of liver and non-liver malignancies among died people suggesting that surveillance of non-liver events should be extended to all individuals, regardless of liver disease stage.

LBP-30-YI

A new risk model outperforms FIB-4 when predicting incident cirrhosis in the general population: a cohort study of 504,000 persons

Rickard Strandberg¹, Mats Talbäck², Niklas Hammar², Hannes Hagström^{1,3}. ¹Karolinska Institutet, Department of Medicine, Huddinge, Sweden; ²Karolinska Institutet, Institute of Environmental Medicine, Solna, Sweden; ³Karolinska University Hospital, Department of Upper GI, Huddinge, Sweden
Email: rickard.strandberg@ki.se

Background and aims: Non-alcoholic fatty liver disease (NAFLD) has a high prevalence in the general population, and the incidence of NAFLD-associated cirrhosis is increasing. The Fibrosis-4 score (FIB-4) is a diagnostic model used in patients with NAFLD to estimate the present degree of fibrosis, but the FIB-4 score is inadequate for predicting future events. The aim of this study was to develop a risk score allowing physicians to identify individuals at a high risk of developing cirrhosis. Correct identification would allow for early intervention and preventive measures.

Method: We used a large Swedish population-based cohort, free of known liver diseases other than possibly NAFLD, with available laboratory data, including biomarkers associated with liver disease, and national registry data. Using flexible parametric survival models, a 10-year risk model of cirrhosis or associated complications was created, employing non-liver death as a competing event. The new comprehensive risk score includes age, sex, body mass index (BMI), aspartate aminotransferase (AST), alanine aminotransferase (ALT), gamma-glutamyl transferase (GGT), cholesterol, platelet count, albumin, bilirubin, glucose, and triglycerides. The performance was assessed in terms of calibration (calibration curves), discrimination (time-dependent area-under-curve (AUC)), and utility (decision curve analysis). The model was compared to the FIB-4 score.

Results: We used data of 504,309 individuals that were followed over an average follow-up time of 25 years. During follow-up, 7604 liver-related outcomes were observed. The cumulative risk of liver cirrhosis at ten years was 0.22%. The new risk score achieved a 10-year AUC of 81% compared to the FIB-4 AUC of 73% (Figure). In total, 4525 individuals had a FIB-4 above the established high-risk cut-off (2.67). Among these, the 10-year positive predictive value (PPV) for incident cirrhosis was 4.6%. Among an equal 4525 individuals with the highest new score (corresponding to $>1.62\%$ predicted risk), the 10-year PPV was 7.2%. According to the decision curve analysis, the new score has a positive net benefit for risk thresholds up to 18%, and a higher net benefit than FIB-4 for all thresholds.

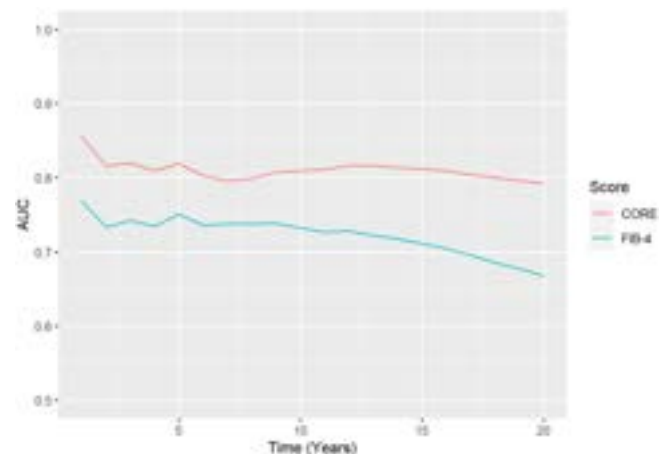


Figure:

Conclusion: The new risk score, the *Cirrhosis Outcome Risk Estimator* (CORE), based on a flexible modeling approach, and using biomarkers easily accessible in primary care, outperforms FIB-4 when predicting

POSTER PRESENTATIONS

liver-related outcomes in the general population. External validation is needed before use in primary care.

LBP-33-YI

Investigating the potential of the primary cilium as an immunomodulatory organelle in intrahepatic cholangiocarcinoma

Sara Teles¹, Scott Waddell¹, Kostas Gournopoulos¹, Kyle Davies¹, Philippe Gautier¹, Pleasantine Mill¹, Edward Jarman¹, Luke Boulter¹.
¹Institute of Genetics and Cancer, University of Edinburgh, MRC Human Genetics Unit, United Kingdom
 Email: sarapoteles@gmail.com

Background and aims: Primary cilia (PC) are important organelles that protrude from biliary epithelial cells to sense changes in bile. Although changes in PC have been observed in Intrahepatic Cholangiocarcinoma (iCCA), why these cancers suppress their cilia and how the lack of a functioning cilium benefits iCCA progression remains unexplored. Here, we investigate how PC loss shapes the immune microenvironment of iCCA to favour tumour progression.

Method: Using a combination of human iCCA tissue and two transgenic mouse models in which iCCA originates from either ciliated or unciliated cholangiocytes, we used bulk RNA sequencing to analyse the cell-intrinsic transcriptional changes resulting from PC-loss. By deriving organoid cultures from the same ciliated/unciliated cells, we have then functionally investigated how PC status in biliary cells affects the tumour immune microenvironment and how this influences iCCA progression.

Results: Human iCCA lack PC by immunohistochemical analysis; therefore, we developed an *in vivo* mouse model of iCCA in which PC are either lost or remain intact. In this model, iCCA does not develop when PC are present in biliary cells. However, when PC-loss is induced *in vivo* (through deletion of the essential cilia gene *Wdr35*), iCCA rapidly develops. Importantly, unciliated cells do not show increased rates of proliferation. Rather, bulk RNA sequencing showed that PC-loss induced the expression of progenitor transcription factors and immunoregulatory genes. Interestingly, in mice with unciliated iCCA we found lower levels of liver neutrophil infiltration. Using *in vitro* organoid cultures of ciliated and unciliated iCCAs and transwell assays, we found that PC-loss on cancer cells influences neutrophil recruitment and migration, indicating that loss of PC in iCCA has the potential to modulate local tumour immunity and avoid neutrophil-induced clearance.

Conclusion: PC-loss coordinates an inflammatory cell state that affects the recruitment of immune cells to the liver. By directly

modulating the chemotaxis and infiltration of neutrophils, PC-loss promotes an immunosuppressive tumour microenvironment, thereby favouring iCCA progression.

LBP-34

Modelling intrahepatic bile duct morphogenesis *in vitro* using synthetic hydrogels

Ludovic Vallier¹, Iona Thelwall², Kevin Chalut³, Carola Maria Morell², Lucia Cabriaes⁴.
¹Berlin Institute of Health, Berlin, Germany;
²Wellcome-MRC Cambridge Stem Cell Institute, United Kingdom;
³Altos Labs, Great Abington, United Kingdom;
⁴Lightcast Discovery Ltd, United Kingdom
 Email: igt20@cam.ac.uk

Background and aims: Cholangiopathies account for a third of adult liver transplantations, access to which is limited by a shortage of healthy donor organs. A promising alternative is the use of human induced pluripotent stem cell (hiPSC)-derived cholangiocytes in a therapeutic context. However, lack of knowledge regarding cholangiocyte development limits the generation of fully functional cells. To address this issue, we developed a culture system consisting of tuneable synthetic hydrogels capable of testing the influence of mechanical stimuli on cholangiocyte development, with the aim of generating fully functional cholangiocyte organoids.

Method: Novel 2D polyacrylamide hydrogels developed in the Chalut Lab (Labouesse *et al.* 2021) were optimised for the *in vitro* culture of hiPSC-derived hepatoblast-like-cells using established protocols (Hannan *et al.* 2013, Sampaziotis *et al.* 2017). Optimised parameters consist of seeding cells at a density of 500,000 cells/cm² onto collagen I-coated soft hydrogels. Once seeding was optimised, the hepatoblast-like-cells were differentiated into cholangiocyte-like cells and marker expression was verified. The 2D hydrogel was then used as the base of a novel sandwich culture consisting of two distinct hydrogels, both with a defined extracellular matrix. Production of the sandwich culture involves the differentiation of immature cholangiocyte-like cells on polyacrylamide and the subsequent application of a proprietary synthetic gel top layer. This provides the encapsulation required for 3D structure formation and enables cholangiocyte morphogenesis into tubular bile duct structures.

Results: We have developed a promising alternative to Matrigel in the form of a novel synthetic hydrogel which enables the production of luminal bile ducts *in vitro* from hiPSCs. Cholangiocytes cultured in this system express biliary markers (KRT7/SOX9) to the same or a greater level than that observed in iPSC-derived intrahepatic bile duct (IHBD) organoids. We found that collagen I-coated hydrogels provide

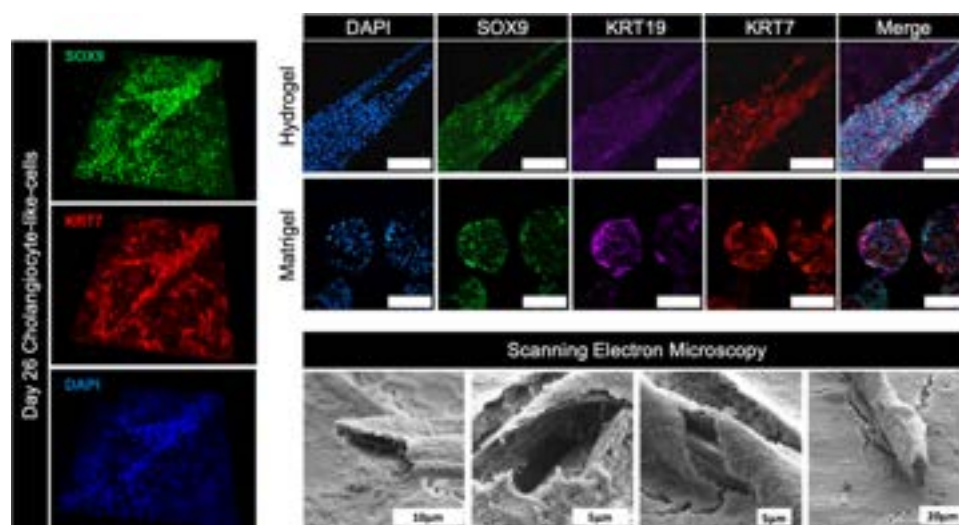


Figure: (abstract: LBP-34): Day 26 hiPSC-derived cholangiocyte-like-cells cultured within a synthetic hydrogel sandwich represented by immunostaining (300µm) and scanning electron microscopy.

an excellent substrate for cholangiocyte differentiation, with increased collagen correlated with enhanced biliary (KRT7/SOX9) and reduced hepatic (ALB/AFP) marker expression. Indicating a potential mechanism by which collagen I directs hepatoblast fate choice and subsequent differentiation. This is supported by *in vivo* results showing that foetal IHBDs are surrounded by a localised region of collagen I. We are currently using the hydrogel system as a model to study the role of extracellular matrix composition in the induction of mechanically activated pathways linked to cholangiocyte differentiation (TGF-beta Activin/Nodal and YAP-TAZ) with the end goal of elucidating a mechanism for extracellular matrix-driven hepatoblast zonation.

Conclusion: Overall, these results show that our synthetic hydrogel platform can be used to model bile duct development *in vitro*. Its tunable properties make the hydrogel a novel tool for the investigation of mechanical stimuli on cholangiocyte differentiation and enable the incorporation of good-manufacturing-process compliant reagents for cell therapy applications.

LBP-35

Long-term maintenance of response and improved liver health with maralixibat in patients with progressive familial intrahepatic cholestasis (PFIC): data from the MARCH-ON study

Alexander Miethke¹, Adib Moukarzel², Gilda Porta³, Joshue Covarrubias Esquer⁴, Piotr Czubkowski⁵, Felipe Ordóñez⁶, Manila Candusso⁷, Amal A. Aquil⁸, Robert H. Squires⁹, Etienne Sokal¹⁰, Daniel D'Agostino¹¹, Ulrich Baumann¹², Lorenzo D'Antiga¹³, Nagraj Kasi¹⁴, Nolwenn Laborde¹⁵, Cigdem Arkan¹⁶, Chuan-Hao Lin¹⁷, Susan Gilmour¹⁸, Naveen Mittal¹⁹, Fang Kuan Chiou²⁰, Simon P. Horslen⁹, Wolf-Dietrich Huber²¹, Tiago Nunes²², Anamaria Lascu²², Lara Longpre²², Douglas Mogul²², Raul Aguilar²², Pamela Vig²², Vera Hupertz²³, Regino Gonzalez-Peralta²⁴, Udem Ekong²⁵, Jane Hartley²⁶, Noemie Laverdure²⁷, Nadia Ovchinsky²⁸, Richard Thompson²⁹, ¹Cincinnati Children's Hospital Medical Center, Cincinnati, Ohio, United States; ²Hôtel Dieu De France Saint Joseph University Hospital, Beirut, Lebanon; ³Hospital Sirio Libanes, Sao Paulo, Brazil; ⁴Nois De Mexico SA De CV, Jalisco, Mexico; ⁵The Children's Memorial Health Institute, Gastroenterology, Hepatology, Nutritional Disorders and Pediatrics, Warsaw, Poland; ⁶Cardioinfantil Foundation-Lacardio, Bogota, Colombia; ⁷Ospedale Pediatrico Bambino Gesù Irccs, Lazio, Italy; ⁸University of Texas Southwestern Medical Center, Dallas, Texas, United States; ⁹UPMC Children's Hospital of Pittsburgh, Pediatrics, Pittsburgh, Pennsylvania, United States; ¹⁰Uclouvian, Cliniques Universitaires St Luc, Pediatric Hepatology, Brussels, Belgium; ¹¹Hospital Italiano De Buenos Aires, Buenos Aires, Argentina; ¹²Hannover Medical School, Pediatric Gastroenterology and Hepatology, Hannover, Germany; ¹³Hospital Papa Giovanni XXIII, Paediatric Hepatology, Gastroenterology and Transplantation, Bergamo, Italy; ¹⁴Medical University of South Carolina, Charleston, South Carolina, United States; ¹⁵Hôpital Des Enfants-CHU Toulouse, Toulouse, France; ¹⁶Koc University School of Medicine, Istanbul, Turkey; ¹⁷Children's Hospital Los Angeles, Los Angeles, California, United States; ¹⁸University of Alberta, Pediatrics, Alberta, Canada; ¹⁹University of Texas Health Science Center at San Antonio, San Antonio, Texas, United States; ²⁰Kk Women's and Children's Hospital, Singapore; ²¹Medical University of Vienna, Vienna, Austria; ²²Mirum Pharmaceuticals, Inc., Foster City, California, United States; ²³Cleveland Clinic Children's, Cleveland, Ohio, United States; ²⁴AdventHealth for Children and AdventHealth Transplant Institute, Pediatric Gastroenterology, Hepatology, and Liver Transplant, Orlando, Florida, United States; ²⁵Medstar Georgetown Transplant Institute, Medstar Georgetown University Hospital, Washington DC, United States; ²⁶Birmingham Women and Children's Hospital, Birmingham, United Kingdom; ²⁷Hopital Femme Mere Enfant, Hospices Civils De Lyon, Pediatric Hepato Gastroenterology and Nutrition Unit, Lyon, France; ²⁸New York University Grossman School of Medicine, New York, New York, United States; ²⁹Institute of Liver Studies, King's College

London, London, United Kingdom

Email: richard.j.thompson@kcl.ac.uk

Background and aims: Progressive familial intrahepatic cholestasis (PFIC) is a group of genetic disorders resulting in disrupted bile composition, cholestasis, and pruritus. Maralixibat (MRX) is a minimally absorbed ileal bile acid transporter (IBAT) inhibitor which prevents enterohepatic bile acid recirculation. In the 26-week placebo-controlled MARCH Phase 3 study, MRX at 570 µg/kg BID demonstrated significant improvements in pruritus, serum bile acid (sBA), bilirubin and growth in patients across the broadest range of PFIC types studied to date. MARCH-ON is an open-label long-term extension study for patients who completed the MARCH study. Here, we report on long-term maintenance of effect from MARCH-ON.

Method: Long-term maintenance of response was assessed for patients who were originally randomized to receive MRX in MARCH and continued with treatment in MARCH-ON (MRX-MRX group; n = 33). MRX response was assessed for patients who received PBO in the MARCH study and switched to open-label MRX in MARCH-ON (PBO-MRX group; n = 24). Assessments included: pruritus measured by 0-4 scale of ItchRO[Obs], sBA, bilirubin, and growth z-scores, as well as incidence of treatment-emergent adverse events (TEAEs). Baseline (BL) was defined as the start of MRX for each group.

Results: For the MRX-MRX group, the median (min, max) time on MRX was 394 days (108, 836). In total, 20 of 33 patients reached week 52 at time of analysis. Significant improvements observed in the first 26 weeks of the MARCH study were sustained from BL through week 52 in MARCH-ON for pruritus severity (-2.13, p < 0.0001), sBA (-200 µmol/L, p = 0.0004), bilirubin (-2.64 mg/dL, p = 0.0084), height z-score (+0.54, p < 0.0001), weight z-score (+0.44, p = 0.0010). In the PBO-MRX group, the median time on MRX was 256 days (29, 569). In total, 15 of 26 patients reached week 26 at time of analysis. Newly gained statistically significant reductions in pruritus and sBA levels were observed in the key efficacy end points from BL through Week 26 for pruritus (-1.05, p = 0.0017) and sBA (-141 µmol/L, p = 0.0003), in line with observations from the initial MARCH MRX group. Overall, there were no new safety signals identified. The most frequent TEAEs were GI-related with early onset of diarrhoea (44%) in line with the mechanism of IBAT inhibition, mostly mild and transient. In the MRX-MRX sub-group, fewer patients experienced diarrhoea (n = 2) in MARCH-ON supporting these effects are early and transient in nature.

Conclusion: Significant and sustained responses in pruritus, sBA, bilirubin as well as growth are observed with 52 weeks of MRX treatment across the broadest range of genetic PFIC types studied to date. These data suggest overall improved liver health with MRX treatment which can be maintained over time.

LBP-36

Oral vancomycin induces remission in PSC-IBD, which is associated with a reduction in bile salt hydrolase and colonic amine oxidase activity

Nabil Quraishi¹, James Ferguson¹, Ross McInnes², Jonathan Cheesbrough¹, Naveen Sharma¹, Rachel Cooney¹, Peter Rimmer¹, Willem van Schaik³, Tariq Iqbal⁴, Palak Trivedi⁴, ¹Queen Elizabeth Hospital Birmingham, Gastroenterology, Birmingham, United Kingdom; ²University of Birmingham, United Kingdom; ³University of Birmingham, Institute of Microbiology and Infection, Birmingham, United Kingdom; ⁴University of Birmingham, NIHR Birmingham BRC Centre for Liver and Gastrointestinal Research, Birmingham, United Kingdom
Email: nabilquraishi@gmail.com

Background and aims: Primary Sclerosing Cholangitis (PSC) is the classical hepatobiliary manifestation of inflammatory bowel disease (IBD). The strong association between gut and liver disease has fostered several pathogenic hypotheses, in which enteric dysbiosis is proposed to contribute. We conducted a phase 2A clinical trial of oral vancomycin (OV), a gut-restricted antibiotic, in patients (pts) with

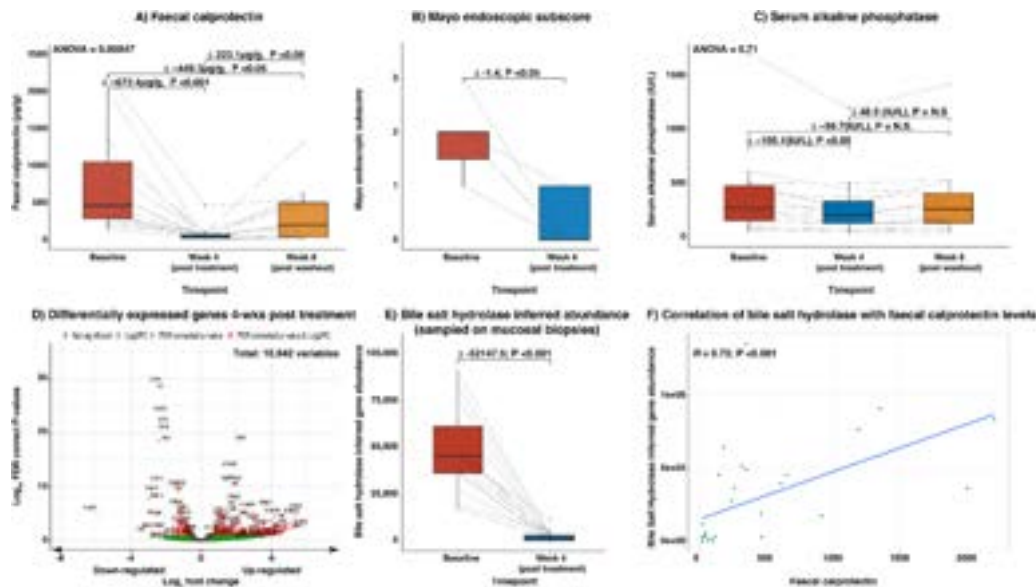


Figure: (abstract: LBP-36). Therapeutic effects and associated gene expression changes following OV treatment

PSC and active colitis. The overarching goal was to identify key mechanistic pathways associated with induction of treatment response.

Method: Study drug was administered at a dose of 125mg QID for 4 weeks (wk) followed by a 4wk washout (total study duration 8 wks). Lower gastrointestinal endoscopies were performed at 0 and 4 wks. Clinical assessment was performed and peripheral blood and stool laboratory tests obtained at 0, 4 and 8 wks. The primary outcome measure was to quantify the magnitude of composite treatment response at 4w, defined as a reduction in faecal calprotectin (fcal), Mayo endoscopic subscore and serum liver biochemistry. Important translational objectives included colonic mucosal profiling along with inferred metagenomics and colonic mucosal host RNA sequencing. The study was registered on clinicaltrials.gov (NCT05376228).

Results: In entirety, 15 patients were recruited to the study, all of whom completed the 4wk treatment course (11 men, 7 previously treated with at least one biological agent). At 4wks, all participants attained response with regards IBD activity (Fig. 1A+B), along with significant reductions in serum ALP (Fig 1C). No significant changes in bilirubin were observed. Paradoxically, a reduction in gut microbial diversity associated with improvement in IBD activity (Δ -1.25 [SD -1.15], $P = 0.001$), with the Shannon index positively correlating with fcal values ($R = 0.53$, $P = 0.002$). This was alongside significant shifts in beta diversity ($p < 0.001$). The latter was characterised by reduced abundance of *Lachnospiraceae*, *Blautia* and *Bacteriodes*, and enrichment of *Enterobacteriaceae*, *Veillonella* and *Escherichia*. Differential gene expression of host colonic mucosa demonstrated downregulation of 134 genes and upregulation of 298 genes following treatment with OV (Fig 1D). Reduction in IBD activity strongly correlated with downregulation in the enzymatic activity of several pathways, including copper containing amine oxidases and inferred microbial bile salt hydrolase (Fig 1E-F). No adverse safety events were observed during treatment. However, microbiological analyses captured the emergence of vancomycin resistant Enterococci in 6 pts as early as 1 wk into treatment. During washout, relapse in IBD activity and an increase in serum ALP was observed in 4 pts upon stopping OV therapy.

Conclusion: Oral vancomycin is associated with a reduction in colitis activity, serum ALT and ALP values in PSC-IBD. However, emergence of antimicrobial expression warrants further evaluation. Targeting specific bile acid and amine oxidase metabolic pathways may offer novel avenues for future therapeutic intervention in PSC-IBD.

Metagenomic, metatranscriptomic and metabolomic readouts from this study are ongoing.

LBP-37

Intestinal bacterial vesicles cause fibrosis progression and serum albumin levels reduction in cirrhosis

Atsunori Tsuchiya¹, Kazuki Natsui¹, Yui Natsui¹, Nobutaka Takeda¹, Shuji Terai¹. ¹Niigata University, Japan
Email: atsunori@med.niigata-u.ac.jp

Background and aims: Liver fibrosis progression causes portal hypertension and the formation of an edematous intestinal tract with impaired gut barrier function, resulting in bacteria and bacterial components invasion of the host. Lipopolysaccharides and pathogen-associated molecular patterns are well-known bacterial components. This study investigated the role of outer membrane vesicles (OMVs) of *Escherichia coli*, the representative pathogenic gut-derived bacteria in patients with cirrhosis, to assess cirrhosis pathogenesis.

Method: We analyzed the roles of OMVs in humans using human serum and ascites samples and the role of OMVs from *Escherichia coli* in mice using mouse liver-derived cells and a mouse cirrhosis model. The effects of OMVs in immune cells of the cirrhotic mouse liver were also investigated by single-cell RNA-sequencing.

Results: In vitro, OMVs activated inflammatory responses to macrophages and neutrophils especially, with upregulation of C-type lectin domain family 4 member E (Clec4e) and reduction in the albumin production from hepatocytes, but with a relatively little direct effect on hepatic stellate cells. In a mouse cirrhosis model, administration of OMVs led to increased liver inflammation, especially inducing the activation of macrophages, worsening fibrosis, and decreasing serum albumin levels. Albumin administration weakened these inflammatory changes. Human sample analysis showed increased antibodies against bacterial components such as ompA and CirA with a progressing Child-Pugh grade. OMVs were detected in ascites samples of patients with decompensated cirrhosis. The *Clec4e* reported in this study was not present in *Clec4f*-positive Kupffer cells but was abundant in *Cx3cr1*-positive, extrahepatic-derived macrophages that are *Mrc1*-negative and *Cd86*-positive by single-cell RNA-sequencing.

Conclusion: OMVs induce inflammation, fibrosis, and suppression of albumin production, affecting the pathogenesis of cirrhosis. Appropriate albumin administration could reduce these inflammatory changes. This study could pave the way for the future prevention and treatment of cirrhosis.

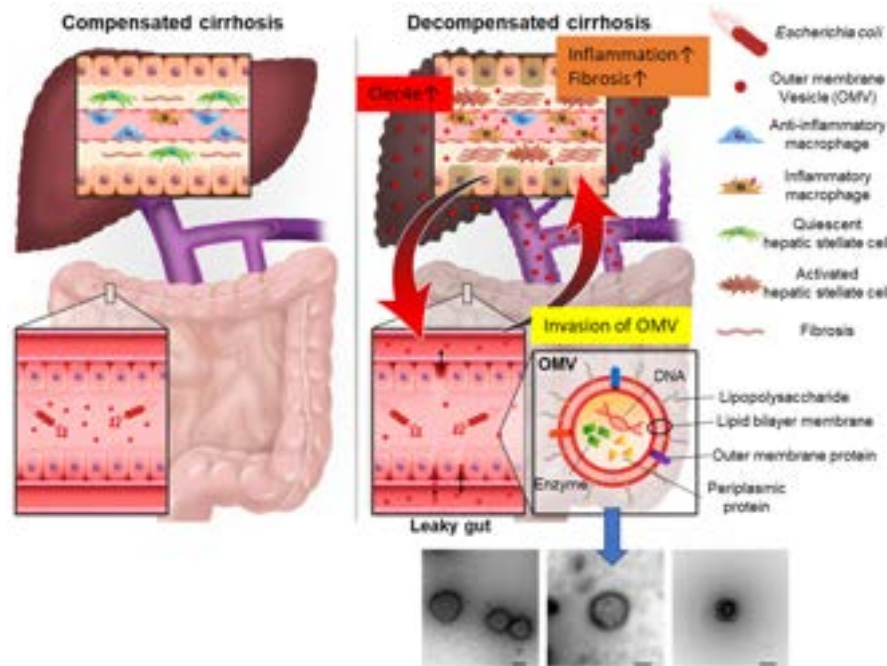


Figure: (abstract: LBP-37).

LBP-38

Preliminary safety and antiviral activity of AB-729 combination treatment with pegylated interferon alfa-2a in virally suppressed, HBeAg-negative subjects with chronic HBV infection

Man-Fung Yuen¹, Jeong Heo², Ronald G Nahass³, Grace Lai-Hung Wong⁴, Tatiana Burda⁵, Kalyan Ram Bhamidimarri⁶, Tsung-Hui Hu⁷, Tuan Nguyen⁸, Young-Suk Lim⁹, Chi-Yi Chen¹⁰, Stuart C Gordon¹¹, Jacinta Holmes¹², Wan-Long Chuang¹³, Anita Kohli¹⁴, Naim Alkhouri¹⁵, Kevin Gray¹⁶, Emily P. Thi¹⁷, Elina Medvedeva¹⁶, Timothy Eley¹⁶, Karen Sims¹⁸. ¹The University of Hong Kong, Gastroenterology and Hepatology, Hong Kong; ²Pusan National University Hospital, Gastroenterology and Hepatology, Korea, Rep. of South; ³ID Care, Hillsborough, United States; ⁴The Chinese University of Hong Kong, Medical Data Analytics Centre and Institute of Digestive Disease, Hong Kong; ⁵Arensia Exploratory Medicine, Chisinau, Moldova; ⁶University of Miami, Digestive Health and Liver Diseases, Miami, United States; ⁷Chang Gung Memorial Hospital, Internal Medicine, Taiwan; ⁸Research and Education Inc., San Diego, United States; ⁹Asan Medical Center, Gastroenterology, Seoul, Korea, Rep. of South; ¹⁰Chia-Yi Christian Hospital, Gastroenterology, Taiwan; ¹¹Henry Ford Hospital, Gastroenterology, Detroit, United States; ¹²St. Vincent's Hospital, Melbourne, Australia; ¹³Kaohsiung Medical University Hospital, Internal Medicine, Kaohsiung, Taiwan; ¹⁴Arizona Liver Health, United States; ¹⁵Arizona Liver Health, Chandler, United States; ¹⁶Arbutus Biopharma, Clinical Development, Warminster, United States; ¹⁷Arbutus Biopharma, Discovery, Warminster, United States; ¹⁸Arbutus Biopharma, Clinical Development, Warminster, United States
Email: ksims@arbutusbio.com

Background and aims: AB-729 is an N-Acetylgalactosamine (GalNAc)-conjugated single trigger RNA interference therapeutic that targets all HBV RNA transcripts, resulting in suppression of viral replication and all viral antigens. AB-729-201 is an ongoing Phase 2a study assessing 24 weeks of AB-729 followed by 12 or 24 weeks of pegylated interferon alfa-2a (IFN) with or without additional AB-729 doses in virally suppressed, HBeAg-negative CHB subjects. We report interim data through 12 weeks of IFN treatment for the first 12 subjects.

Method: Forty-three CHB subjects, virally suppressed on stable nucleos (t)ide analog (NA) therapy, were all enrolled to receive AB-729 60 mg every 8 weeks for 24 weeks (4 doses) during the lead-in

phase. After Week 24, the subjects were randomized to 1 of 4 sub-groups: A1 (24 weeks IFN + AB-729+NA), A2 (24 weeks IFN + NA), B1 (12 weeks IFN + AB-729 + NA) or B2 (12 weeks IFN + NA). After completing IFN ± AB-729 treatment, subjects continued NA therapy only for an additional 24 weeks and were then evaluated for NA discontinuation based on protocol criteria (ALT <2 x upper limit of normal, undetectable HBV DNA, confirmed HBsAg <100 IU/ml). Safety and antiviral assessments were obtained every 2-4 weeks. HBsAg quantification was assessed via Roche Cobas Elecsys HBsAg II quant II assay (lower limit of quantitation [LLOQ] = 0.05 IU/ml).

Results: The median subject age was 46 years, 72% were male, and 79% were Asian. To date, 32 of 43 subjects have been randomized to the 4 IFN sub-groups after completing the 24-week AB-729 lead-in period. The mean (standard error [SE]) baseline HBsAg level for all 43 subjects was 2.98 (0.07) log₁₀ IU/ml and the median (range) was 2.92 (2.7-3.4) log₁₀ IU/ml. The mean (SE) HBsAg decline observed at Week 24 was -1.65 log₁₀ (0.10, n = 34). All subjects had HBsAg declines of approximately 1 log₁₀ or more from baseline, and 28 of the 32 (88%) randomized subjects reached HBsAg <100 IU/ml. After 6 weeks of IFN treatment, mean HBsAg declines from baseline ranged from -1.53 to -2.49 log₁₀ across the 4 sub-groups (3-5 subjects/group), and after 12 weeks of IFN, mean HBsAg declines ranged from -0.74 to -2.20 log₁₀ (2-4 subjects/group). Three subjects had intermittent HBsAg <LLOQ, 2 during the IFN treatment period and 1 at the end of the AB-729 lead-in period. Three subjects have completed the NA follow-up period, and 1 subject met the criteria to stop NA therapy. AB-729 treatment has been well-tolerated with no serious adverse events (AEs) or AEs leading to AB-729 discontinuation. AEs during IFN treatment have been typical, with 4 subjects requiring IFN dose reduction or interruption due to neutropenia and 1 due to Grade 3 ALT elevation.

Conclusion: AB-729 treatment in virally suppressed CHB subjects was well tolerated and led to mean HBsAg declines of >1.6 log₁₀ after 24 weeks of treatment, comparable to other AB-729 studies. HBsAg levels <100 IU/ml were noted in 88% of the subjects. This interim data analysis suggests addition of IFN was well tolerated, and AB-729 + IFN appears to result in continued HBsAg declines in most subjects with 2 subjects reaching HBsAg <LLOQ during IFN treatment, but more data is needed to assess the overall impact on HBsAg responses.

Acute liver failure and drug induced liver injury

WEDNESDAY 21 TO SATURDAY 24 JUNE

TOP-087

Epigenetic modifications implicated in idiosyncratic drug-induced liver injury

Marina Villanueva¹, Romina De los Santos Fernández¹, Ismael Alvarez-Alvarez¹, Hao Niu¹, Camilla Stephens^{1,2}, A González-Jiménez¹, Gonzalo Matilla¹, Maria Isabel Lucena^{1,2}, Inmaculada Medina-Caliz¹, Raul J. Andrade^{1,2}. ¹Servicios de Aparato Digestivo y Farmacología Clínica, Hospital Universitario Virgen de la Victoria, Instituto de Investigación Biomédica de Málaga y Plataforma en Nanomedicina-IBIMA Plataforma BIONAND, Universidad de Málaga, Malaga, Spain; ²Centro de Investigación Biomédica en Red, Enfermedades Hepáticas y Digestivas (CIBERehd), Madrid, Spain
Email: lucena@uma.es

Background and aims: Drug-induced liver injury (DILI) is a complex disorder involving pharmacological, genetic, and environmental factors. Among these, genetic factors have been the most studied. Different Human Leucocyte Antigen (HLA) alleles and liver metabolism genes polymorphisms have been associated with an increased risk of DILI. However, the role of epigenetic modifications in DILI has been minimally investigated. Our study aimed to analyse the genome methylation status during an idiosyncratic DILI episode in a cohort of well-defined DILI cases from the Spanish DILI Registry.

Method: DNA from 32 well-characterized DILI cases enrolled in the Spanish DILI Registry and 32 healthy controls were extracted from peripheral blood samples by using the DNeasy Blood and Tissue Kit (Qiagen). For the study of genome-wide methylation analysis, high-quality genomic DNA samples (500 ng) were subjected to bisulfite treatment using the EZ-96 DNA Methylation kit (Zymo Research,

Irvine, CA) following the manufacturer's instructions. Subsequently, DNA methylation was analyzed by microarray assays using Infinium Methylation EPIC BeadChip Kit (Illumina, San Diego, CA). Then, whole-genome amplification and hybridization were performed using BeadChip, followed by single-base extension and analysis using the HiScan SQ module (Illumina) to assess the cytosine methylation states. The annotation of CpG islands (CpGIs) used the following categorization: (1) shore, for each of the 2-kb sequences flanking a CpGIs; (2) shelf, for each of the 2-kb sequences next to a shore; and (3) open sea, for DNA not included in any of the previous sequences or in CpGIs. DNA methylation for each CpG site was represented by beta values ranging from 0 to 1, corresponding to fully unmethylated and fully methylated. Finally, an analysis of differentially methylated regions between groups was performed.

Results: Control and DILI groups samples showed a similar density distribution of beta values. A total of 43861 CpG islands were identified (FDR ≤ 0.05) from which 213 manifested significant differential methylation (delta beta ≥ 0.1 and FDR ≤ 0.05) between groups with an overall tendency towards hypomethylation within the DILI cohort. Finally, candidate genes with the most significant differentially methylated CpGIs regions between groups were identified, resulting in 14 hypomethylated genes (*ZNF350-AS1*, *LOC349408*, *P2RY13*, *GPR109B*, *SUMO1B1*, *LOC285626*, *FAM200B*, *LOC284276*, *TEX28*, *STS*, *KLRK1*, *LOC101928100*, *TLR8*, *CSTA*) and one hypermethylated gene (*FAM163B*) in DILI group compared to the control group.

Conclusion: This exploratory analysis shows a general tendency towards hypomethylation in the DILI cohort compared to the control group. Further, deeper analysis must be conducted to unveil the relationship between DNA methylation and DILI phenotypes, severity, and outcome. Funding: PI19/00883, PEMP-2020-0127, PI21/01248, P18-RT-3364, PI-0310-2018, ISCIII CIBERehd, POSTDOC_21_00780, CD20/00083, CD21/00198.

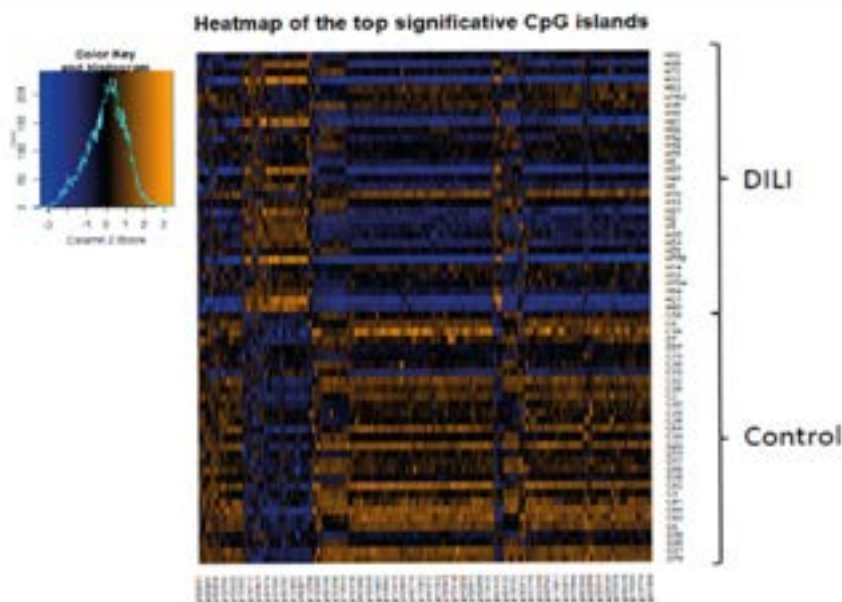


Figure 1: Heatmap of the top significant CpG islands. Significant CpG island hypermethylation and hypomethylation appear in orange and blue respectively. Differential distribution of significant CpG island methylation was observed between DILI and control groups (delta beta ≥ 0.1 and FDR ≤ 0.05).

Figure: (abstract: TOP-087).

TOP-092

Distinctive cytokine profiles in checkpoint inhibitor-induced liver injury, idiosyncratic drug-induced liver injury and autoimmune hepatitis: a potential mechanistic biomarker panel

Edmond Atallah^{1,2}, Stuart Astbury^{1,2}, Jane I. Grove^{1,2}, Ankit Rao³, Hester Franks^{3,4}, Poulam Patel^{3,4}, Guruprasad Aithal^{1,2}. ¹Nottingham University Hospitals NHS Trust and the University of Nottingham, National Institute for Health Research (NIHR) Nottingham Biomedical Research Centre, Nottingham, United Kingdom; ²University of Nottingham, Nottingham Digestive Diseases Centre, Translational Medical Sciences, School of Medicine, Nottingham, United Kingdom; ³Nottingham University Hospitals NHS Trust, Oncology, Nottingham, United Kingdom; ⁴University of Nottingham, Centre for Cancer Sciences, Translational Medical Sciences, Biodiscovery Institute, Nottingham, United Kingdom

Email: edmond.atallah@nottingham.ac.uk

Background and aims: Immune mechanisms underlie the development of acute liver injury in checkpoint inhibitor-induced liver injury (ChILI) which shares some clinical and histological features with idiosyncratic drug-induced liver injury (DILI) and acute autoimmune hepatitis (AIH). Currently, there are no biomarkers to differentiate between these three aetiologies in individuals presenting with acute liver injury. We aimed to characterise circulating cytokine profiles of well-phenotyped acute cases of ChILI, DILI and de-novo AIH and develop a classification model that distinguishes between the groups.

Method: Consecutive patients with acute liver injury were prospectively enrolled. All met the criteria defined by the DILI International Expert Working Group at the time of sampling. They were evaluated through formal causality assessment and then adjudicated by an independent panel as ChILI (n = 19), DILI (n = 18) or AIH (n = 7) based on International AIH Group criteria. Plasma cytokine profiling was performed using a 20-plex inflammatory panel (Luminex). Kruskal-Wallis test was used to compare cytokine levels between groups and corrected for multiple testing. Linear Discriminant Analysis (LDA) was performed for classification, dimension reduction, and data visualization.

Results: All cytokines except for GM-CSF were quantifiable and included in the analysis. There was a significant difference in the plasma levels of anti-inflammatory cytokine IL-10 (p < 0.0001) and pro-inflammatory cytokines CXCL10 (p = 0.006), IL-1 beta (p = 0.01), and CCL3 (p = 0.02) between the groups. Cytokines showed different linear discriminant coefficients separating the groups. Two dimensional LDA model, using 19 cytokines, classified patients into three types of liver injury with high diagnostic accuracy. IL-17A was the key cytokine associated with ChILI indicating a possible role of Th17 cells. IL-1 beta and CXCL10 which recruit T cells and amplify the inflammatory response in checkpoint-induced colitis, were important markers differentiating ChILI from DILI and AIH. CXCL8, a potent chemoattractant to neutrophils, distinguished AIH in combination with IFN gamma and IL-17A. IL-12p70 and TNF-alpha were the most important cytokines identifying DILI from other types of liver injury.

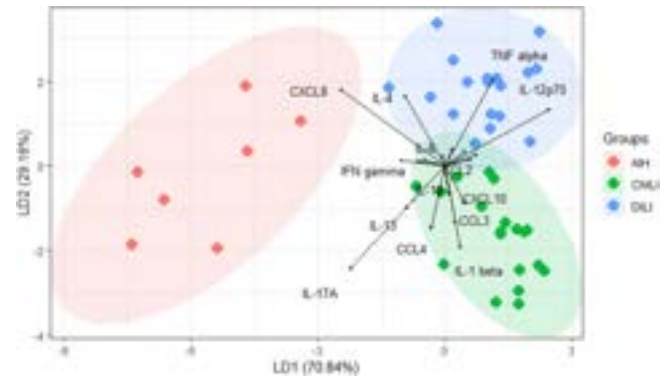


Figure:

Conclusion: Distinct cytokine profiles in ChILI, DILI and AIH point to key immunopathogenic pathways underlying each type of acute liver injury. The profile in ChILI highlights the contribution of pro-inflammatory subsets of CD4+ T cells producing IL-17A (characterizing Th17 subtype), similar to other immune-related organ toxicities. In AIH, CXCL8 release by monocytes and macrophages is distinctive, previously shown to correlate with serum IgG and macrophage accumulation in liver fibrosis. In DILI, IL12p70 stimulates the production of TNF-alpha (which previously showed prognostic value in acute DILI), emphasising the role of Th1 in response to antigenic stimulation.

Using cytokine profiles for LDA classification modelling revealed a high diagnostic accuracy in separating these aetiologies. If validated in a larger number of patients, an algorithm using cytokine profiles may assist in the diagnosis of these conditions.

TOP-093

Soluble and monocyte surface CD206 is a promising indicator of sepsis in patients with acute liver failure

Anna Cavazza^{1,2}, Evangelos Triantafyllou³, Roberto Savoldelli⁴, Salma Mujib^{1,2}, Ellen Jerome^{1,2}, Francesca Trovato^{1,2}, Florent Artru^{1,2}, Roosey Sheth^{1,2}, Rima Abdalla^{1,2}, Xiaohong Huang², Yun Ma², Francesco Dazzi⁴, Charalambos Gustav Antoniadis¹, William M. Lee⁵, Mark J W McPhail^{1,2}, Constantine Karvellas⁶. ¹Liver Intensive Therapy Unit, Institute of Liver Studies, King's College Hospital, London, United Kingdom; ²Institute of Liver Studies, Department of Inflammation Biology, Kings College London, United Kingdom; ³Section of Hepatology and Gastroenterology, Department of Metabolism, Digestion and Reproduction, Imperial College London, United Kingdom; ⁴School of Cardiovascular and Metabolic Medicine and Science, King's College London, London, United Kingdom; ⁵Division of Digestive and Liver Diseases, UT Southwestern Medical Center, Dallas, United States; ⁶Department of Critical Care Medicine and Division of Gastroenterology (Liver Unit), University of Alberta, Edmonton, Canada

Email: a.cavazza1@gmail.com

Background and aims: Acute liver failure (ALF) has a high mortality and need for emergency liver transplantation (LT). Deaths are mostly due to septic complications in part due to monocyte-macrophage dysfunction. The role of prophylactic antimicrobials is under debate as most infective complications occur late in the disease. A validated marker of immune dysfunction associated with sepsis is.

Method: Patients from the United States Acute Liver Failure Study Group (USALFG) were recruited and healthy volunteers as controls (HC) and ALF patients were also recruited from Kings College Hospital as a validation cohort. Patient serum samples were analysed for monocyte/macrophage activation markers secretory leukocyte protease inhibitor (SLPI), osteopontin (OPN), soluble Mer tyrosine kinase (sMerTK), CD163 (sCD163), mannose receptor (sMR/CD206) and programmed death ligand 1 (sPD-L1) by enzyme-linked

POSTER PRESENTATIONS

immunosorbent assay (ELISA). These were correlated to markers of illness severity and 21 day survival (LT was grouped with death). Validation of key markers CD155, CD163, HLA-DR, MerTK, programmed cell death protein 1 (PD1), PD-L1, and CD206 was performed on peripheral blood monocytes using flow cytometry and analysed using an R pipeline (cytokit) to generate unsupervised and unbiased clustering.

Results: Two hundred and twenty-four patients (79 (36%) male) with a median (range) age of 42 (17–81) and 34 HC were studied from USALFG. Eighty-seven ALF cases (39%) had drug induced liver injury (DILI), 46 (20%) indeterminate ALF, 60 (27%) with APAP-ALF, 15 (7%) autoimmune and 16 (7%) for other aetiologies as vascular or hypoxic hepatitis. All marker serum concentrations were significantly higher in ALF compared to controls ($p < 0.0001$). sMR/CD206 concentration was higher in patients with bacteraemia ($p = 0.002$) and infection ($p = 0.006$). In MELD-adjusted multivariate modelling sMR/CD206 and sCD163 after day 3 retained statistical significance for survival prediction. There were increases in surface expression of CD206 ($p < 0.001$) and PD-L1 ($p < 0.05$) on CD14+ monocytes from patients with ALF compared with controls. CD206% were higher in patients with sepsis compared to those without and correlated with SOFA score ($p = 0.018$).

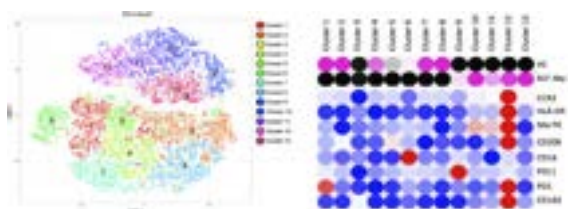


Figure: Surface expression on CD14+ monocytes in acute liver failure (ALF) and healthy controls (HC) measured by Flow Cytometry and analysed via Cytokit demonstrating 13 clusters with a clear division between healthy and ALF patient.

Conclusion: Soluble markers of macrophage activation are upregulated in patients with ALF that died compared to those who survived. sMR/cd206 serum concentrations were higher in patients with infections and those who died. In a validation cohort CD206 and PD-L1 were more highly expressed in ALF monocytes compared to controls. sMR/CD206 should be explored as a biomarker of sepsis in ALF.

THURSDAY 22 JUNE

THU-393

Non-invasive screening for histological features of autoimmune hepatitis and prognosis of patients with antinuclear antibody-positive drug-induced liver injury

Yanhong Gao¹, Feiyu Zhang¹. ¹The first hospital of Jilin University, China
Email: yanhong@mail.jlu.edu.cn

Background and aims: Although useful for distinguishing drug-induced liver injury (DILI) from autoimmune hepatitis (AIH), liver biopsy is an invasive examination, and the high prevalence of antinuclear antibody (ANA) positivity in cases of DILI may lead to excessive use of biopsy. Hence, we aimed to develop a non-invasive screening tool based on histological features for detection of AIH in ANA-positive DILI patients and analyzed their clinical outcomes.

Method: This retrospective study included patients who presented with suspected DILI, were ANA-positive, and underwent liver biopsy between January 2017 and December 2020. Two pathologists determined histological features of AIH. The follow-up period was 1 year after DILI onset.

Results: The final analysis included 93 ANA-positive DILI patients, of which 17 had AIH-like histology and 76 did not. Factors independently associated with AIH-like histology included globulin level (odds

ratio [OR] = 1.136, 95% confidence interval [CI]: 1.03–1.27; $p = 0.017$) and ANA titer $\geq 1:1000$ (OR = 6.363, 95% CI: 1.30–47.44; $p = 0.035$). The optimal cut-off value for globulin indicating AIH-like histology was 31.5 g/L. This globulin level in combination with ANA titer $\geq 1:1000$ provided a sensitivity of 100% and specificity of 57.9% for indicating histological features of AIH in ANA-positive DILI patients. During the 1-year follow-up, more patients developed AIH in the group with AIH-like histology than in the group without (31.2% vs 0, $p < 0.001$).

Table: Diagnostic performance of independently associated factors alone, in series, and in parallel.

	Sensitivity (%)	Specificity (%)	PPV (%)	NPV (%)	AUC	95% CI
ANA $\geq 1:1000$	59	82	42	90	0.702	0.574–0.830
Globulin ≥ 31.5 g/L	88	63	35	96	0.757	0.661–0.853
ANA $\geq 1:1000$ and Globulin ≥ 31.5 g/L	47	87	44	88	0.670	0.541–0.798
ANA $\geq 1:1000$ or Globulin ≥ 31.5 g/L	100	58	35	100	0.790	0.734–0.845

Statistical tests: Receiving-operating characteristic curve analysis.

Abbreviations: PPV: positive predictive value; NPV: negative predictive value; AUC: area under the curve; ANA, antinuclear antibody; CI: confidence interval.

Conclusion: For ANA-positive DILI patients who present with an ANA titer $\geq 1:1000$ or globulin ≥ 31.5 g/L, liver biopsy is indicated to determine the presence of histological features of AIH, and patients who then present with the histological features of AIH should be followed to detect the development of AIH.

THU-394

Outbreak of unexplained acute hepatitis in children: the role of viral infections

Yael Gozlan¹, Lital Goldberg¹, Orith Waisbourd-Zinman², Yael Mozar-Glazberg², Ronen Arnon³, Lior Hecht Sagie⁴, Michal Mandelboim¹, Merav Weil¹, Sara Dovrat¹, Orna Mor¹, Eyal Shteyer⁵. ¹Israeli Ministry of Health, Central Virology Laboratory, Israel; ²Schneider Children's Medical Center, Gastroenterology, Nutrition and Liver Diseases, Israel; ³Rambam Medical Center, Israel; ⁴Israeli Ministry of Health, Israel; ⁵Shaare Zedek Medical Center, The Juliet Keidan Institute of Pediatric Gastroenterology Institute, Jerusalem, Israel
Email: eyals@szmc.org.il

Background and aims: An increase in the number of cases of acute hepatitis of unknown etiology (AHUA) in children has been observed since October 2021. In view of the SARS-Cov-2 pandemic, adenovirus and adeno-associated virus 2 (AAV2) infections have been suggested as possible triggers in numerous cases. However, the causal relationship between AHUA and any potential etiology is still unclear. Our aim was to characterize the cohort of children with AHUA in Israel.

Method: Subsequent to the WHO/CDC announcement on the AHUA a national registry was established by the Israeli Ministry of health. Retrospective and prospective demographic, clinical data and laboratory results on the children compatible with the CDC criteria for AHUA were collected. In addition, when available, blood and stool were sent to the central virology laboratory (CVL).

Results: A total of 42 children were included in the registry, of them 21 females, median age of 39 months. Past SARS-Cov-2 exposure (infection or vaccination) was observed in 25 children. Median lab values were AST 1164 (IU/L), ALT 1082 (IU/L), total bilirubin 5 (mg/dL) and INR 1.12. Samples from 23 children were further assessed by the CVL. Adenovirus was found in 4/21 of cases. AAV2 was detected in 4/18. Past SARS-Cov-2 exposure (infection or vaccination) could be verified in 16/22 children. Interestingly, HHV6 infection or reactivation was identified in 13/22. Twelve children underwent liver biopsy

Patient number	AAV2	Adeno	SARS-Cov-2	HHV6	Any Virus
1					
2					
3					
4					
5					
6					
7					
8					
9					
10					
11					
12					
13					
14					
15					
16					
17					
18					
19					
20					
21					
22					
23					
Total positive	4/18 (22%)	4/21 (19%)	16/22 (73%)	13/22 (59%)	21/23 (91%)

Negative

Positive

Not tested

Figure 1: (abstract THU-394): Virological results in samples from 23 AUHA patients. Adeno, AAV2 and HHV6 were tested by RT-PCR in whole blood samples (adeno also in stool samples). Anti HHV6 IgG antibodies were measured by immunofluorescence in sera samples. All cases positive for HHV6 in whole blood, with high IgG titer (>1:600) or positive IgM were recorded as having HHV6 infection or reactivation. SARS-Cov-2 exposure status (infected or vaccinated) was retrieved from the Ministry of Health records.

of which 10 showed variable autoimmune features consisting of plasma cells and variable degree of interface hepatitis and two appeared as none-specific hepatitis. Six were treated with steroids. Two underwent liver transplantation.

Conclusion: In view of the SARS-Cov-2 pandemic, it may be that combination of reactivation or active infection with specific viruses is a trigger for this AHUA outbreak. In our cohort HHV6 is the most abundant cause.

THU-396

Determinants of steroid responsiveness in patients with severe acute hepatitis of indeterminate, autoimmune hepatitis and drug induced aetiologies

Mahdi Saeidinejad¹, Andrew Hall², Disha Jindal³, Shashank Ramakrishnan³, Su Lin⁴, Alberto Quaglia⁵, Fausto Andreola¹, Rajiv Jalan¹. ¹University College London, Liver failure Group, Institute for Liver and Digestive Health, Division of Medicine, London, United Kingdom; ²Royal Free London NHS Foundation Trust, Department of Cellular Pathology and Sheila Sherlock Liver Centre, United Kingdom; ³Royal Free London NHS Foundation Trust, Hepatology, United Kingdom; ⁴the First Affiliated Hospital, Fujian Medical University, Department of Hepatology, Hepatology Research Institute, Fuzhou, China; ⁵Royal Free Hospital and UCL Cancer Institute, Department of Cellular Pathology, London, United Kingdom
Email: mohammad.saeidinejad@nhs.net

Background and aims: Acute hepatitis (AH) due to autoimmune hepatitis (AIH), drug induced liver injury (DILI) and indeterminate acute hepatitis (IAH) have similar histological features. The role of corticosteroids (CS) in these situations is unclear. The aims of this real-world study were to determine the role of CS in patients with AH due to AIH, DILI and IAH. Furthermore, we aimed to identify prognostic factors and their value in predicting response to CS therapy.

Method: Patients admitted with AH due to AIH, DILI and IAH to Royal Free Hospital, between January 2010 to August 2022, who form part of an ongoing hospital database, the CARNATION cohort. Diagnosis was based on history, routine screening tests and liver biopsy. Response to CS was defined as survival at 90-days without the need for emergency liver transplantation (ELT). Univariate and Multivariate analyses were then performed to identify factors predictive of steroid responsiveness (SR).

Results: 129 patients with AH (76 IAH, 29 AIH, 24 DILI) were included of whom 76 had received CS (38 with IAH, 28 with AIH, 10 with DILI). CS was used more frequently in patients with AIH (96.6%) vs. 51.3% and 45.8% in IAH and DILI respectively. Transplant-free survival amongst patients who received CS was not different compared to those who did not (62.8% vs 51.0%; p = 0.18). 29.5% underwent ELT in the CS group compared to 43.1% in the latter (p = 0.11). The baseline MELD-Na (22.9 vs 24.0; p = 0.46) and the infection rates were similar between those that received steroids and those that did not (9.0% vs 7.8%; p = 0.70). SR was 67.9% in those with AIH, 60% in DILI, and 60.5% in IAH (p = 0.57). When comparing those with severe AH (n = 62) [total serum bilirubin of more than 5 times the upper limit of normal, and INR of more than 1.2], the overall SR was found to be lower at 54.8% but still not significantly different across the 3 etiologies (59.1% AIH, 50.0% DILI, 53.1% IAH; p = 0.27). All patients with non-severe AH were that were treated with CS were steroid responsive. In the multivariate analyses only the MELD-Na score was found to be independently predictive of SR.

Competing risk analysis of steroid responsiveness using the binary logistic regression model.

Variable	Univariate analysis			Multivariate analysis		
	HR	95% CI	P value	HR	95% CI	P value
Age	0.981	0.951–1.011	0.238			
MELD-Na	1.298	1.112–1.514	<0.001	1.308	1.043–1.641	0.020
ALF-OF	5.264	1.933–14.332	<0.001	1.516	0.308–7.458	0.609
Albumin	0.921	0.854–0.993	0.033	1.065	0.956–1.187	0.252

Figure:

Conclusion: The results show that administration of CS to patients with AIH, DILI or IAH did not improve the overall transplant free survival and SR was independent of etiology. The baseline MELD-Na score is the single best measure in predicting SR in patients with AH.

THU-397

Clinical and histological features of drug-induced liver injury: a retrospective study in biopsy-based cohort

Ting Zhang¹, Mengqi Li¹, Xingang Zhou², Hong Zhao¹, Gang Wan³, Wen Xie¹. ¹Center of Liver Diseases, Beijing Ditan Hospital, Capital Medical University, Beijing, China; ²Department of Pathology, Beijing Ditan Hospital, Capital Medical University, Beijing, China; ³Department of Biostatistics, Beijing Ditan Hospital, Capital Medical University, Beijing, China
Email: xiewen6218@163.com

Background and aims: This study aimed to describe the clinical and histological features of drug-induced liver injury (DILI) in a biopsy-based cohort.

Method: Patients diagnosed with DILI and underwent a liver biopsy were included in this retrospective study. We grouped the severity of DILI into 5 grades according to the Chinese guideline for DILI. The logistic regression analysis was performed to assess the associated clinical and histological factors for the severity of DILI.

Results: A total of 1070 hospitalized patients diagnosed with DILI between 2009 and 2012. Among them, 523 patients underwent a liver biopsy. Patients with pre-existing liver disease (n = 139), diagnosed with toxic liver injury (n = 19), undergone liver transplantation (n = 3), unqualified liver biopsy samples (n = 7) and followed up for less than 6 months (n = 14) were excluded. In addition, 40 patients could not be definitively diagnosed DILI were also excluded. Finally, 301 patients were included in this study. The leading single classes of implicated drugs were traditional Chinese medicines or herbal and dietary supplements (50%) and anti-infectious agents (8%). Only 8 (3%) patients with acute liver failure and no one died. Compared grades 3–4 group, grades 1–2 group with higher levels of biochemistry parameters and higher degrees of fibrosis stage, significant inflammation, cholestasis and ductular reaction. But granulomas were more often found in grades 1–2 group. Multivariable logistic regression analysis showed that grades 3–4 were still associated with higher degrees of fibrosis stage, cholangiolar cholestasis, ductular reaction and the presence of granulomas was associated with grades 1–2.

Table 1: Clinical and histological characteristics of DILI patients with different liver injury severity.

Characteristics	Grades 1–2 (n = 157)	Grades 3–4 (n = 144)	P value
Age at diagnosis, years	47 (35–55)	46 (35–54)	0.874
Females, n (%)	111 (70.7)	91 (63.2)	0.166
Implicated agents			0.161
Herbal and dietary supplements	70 (44.6)	79 (54.9)	
Western medicine	57 (36.3)	39 (27.1)	
Both	30 (19.1)	26 (18.1)	
ALT at onset (U/L)	517.0 (252.8–892.0)	685.0 (370.0–1120.1)	0.003
AST at onset (U/L)	251.5 (116.6–514.0)	497.4 (238.5–796.3)	<0.001
ALP at onset (U/L)	135.3 (97.9–175.5)	171.4 (132.9–239.8)	<0.001
TBIL at onset (μmol/L)	23.8 (15.5–41.8)	184.0 (122.5–276.4)	<0.001
ALB (g/L)	39.9 (37.6–42.9)	37.4 (33.5–41.3)	<0.001
Cr (μmol/L)	57.0 (51.0–71.0)	58.0 (51.0–68.0)	0.985
INR	0.97 (0.89–1.06)	1.02 (0.93–1.19)	0.006
PLT (×10 ⁹ /L)	192.0 (153.5–240.3)	195.8 (160.5–239.2)	0.447
Clinical pattern of liver injury, n (%)			0.372
Hepatocellular	115 (73.2)	95 (66.0)	
Cholestatic	15 (9.6)	16 (11.1)	
Mixed	27 (17.2)	33 (22.9)	
Granulomas, n (%)	9 (5.7)	2 (1.4)	0.045
Ductular reaction, n (%)	27 (17.2)	47 (32.6)	0.002
Cholangiolar cholestasis, n (%)	17 (10.8)	55 (38.2)	<0.001
IFS ≥ 1 points, n (%)	18 (11.5)	34 (23.6)	0.005
HAI ≥ 10 points, n (%)	23 (14.6)	43 (29.9)	0.001

All data are presented as n (%) or median (interquartile range).

DILI: drug-induced liver injury; ALT: alanine aminotransferase; AST: aspartate aminotransferase; ALP: alkaline phosphatase; TBIL: total bilirubin; ALB: albumin; Cr: creatinine; INR: international normalized ratio; PLT: platelet count; IFS: Ishak fibrosis score; HAI: histology activity index.

Conclusion: In this biopsy-based cohort of DILI, severer liver injury was related to higher degrees of fibrosis stage, cholestasis, and ductular reaction, whereas granulomas was associated with milder injury.

THU-398

Clinical characteristics of chronic drug-induced liver injury in mainland China: a multicenter retrospective cross-sectional study

Hong Zhao¹, Chengwei Chen², Yimin Mao³, Wen Xie¹. ¹Center of Liver Diseases, Beijing Ditan Hospital, Capital Medical University, Beijing, China; ²Liver Disease Center of Naval 905 Hospital, Shanghai, China; ³Division of Gastroenterology and Hepatology, Shanghai Institute of Digestive Disease, Renji Hospital, School of Medicine, Shanghai Jiao Tong University, Shanghai, China
Email: xiewen6218@163.com

Background and aims: To investigate the prevalence, clinical characteristics, and risk factors of chronic drug-induced liver injury (DILI) in mainland China.

Method: A multicenter, open, retrospective, non-interventional, epidemiological survey collected the baseline information, medical history, data of laboratory examinations and imaging, examinations and outcomes of the DILI patients from 308 medical centers in mainland China from 2012 to 2014.

Results: A total of 25,927 patients were enrolled in the study, including 22,556 cases with acute DILI and 3,371 cases with chronic DILI. The average age of patients with chronic DILI was higher than that of the acute DILI group (p < 0.0001). The proportion of male cases in the acute DILI group was significantly higher as compared to the chronic DILI group (p < 0.0001), while the chronic DILI had underlying liver diseases, significantly higher than the chronic DILI group (p < 0.0001). ALT, AST, AKP, TBIL, and INR levels in the chronic DILI group were higher than the acute DILI group (p < 0.0001). The percentage of patients with fatigue, jaundice, itch, and gastrointestinal symptoms in the chronic DILI group was higher than that in the acute DILI group (p < 0.0001). A large subset of chronic DILI group used Chinese herbal medicine or dietary supplements as compared to

the acute DILI group ($p < 0.0001$). In the chronic DILI group, the percentage of cholestatic liver injury was higher as compared to the acute DILI group ($p < 0.0001$). Multivariate logistic regression analysis showed that the independent risk factors of chronic DILI included gender (male, $p < 0.0001$) and history of underlying liver diseases ($p < 0.0001$).

Table 1: Demographics and clinical characteristics of DILI patients.

Characteristics	Acute DILI (N = 22556)	Chronic DILI (N = 3371)	P value
Age (y), mean \pm SD	45.19 \pm 17.12	48.00 \pm 16.65	<0.0001
Male (%)	11397 (51.51%)	1533 (46.27%)	<0.0001
History of liver disease	4832 (21.42%)	1229 (36.46%)	<0.0001
Cause of liver injury			<0.0001
Herbal medicines	5968 (26.46%)	1227 (36.40%)	
Western medications	15072 (66.82%)	1831 (54.32%)	
Herbal, Western medications and health products	1516 (6.72%)	313 (9.29%)	
Number of drugs for liver injury			<0.0001
1 drug	13491 (59.81%)	2154 (63.90%)	
2 drugs	4106 (18.20%)	618 (18.33%)	
≥ 3 drugs	4959 (21.99%)	599 (17.77%)	
Days from drug use to symptom appearance, median	33.00	51.00	<0.0001
Clinical symptoms and signs			
Jaundice	3895 (17.27%)	936 (27.77%)	<0.0001
Itching	729 (3.23%)	168 (4.98%)	<0.0001
Digestive symptoms (including inappetence, abdominal distension, nausea, vomiting)	8800 (39.01%)	1669 (49.51%)	<0.0001
Fever	1112 (4.93%)	163 (4.84%)	0.8127
Rash	463 (2.05%)	58 (1.72%)	0.2000
Feeble	8453 (37.48%)	1642 (48.71%)	<0.0001
Hemorrhagic tendency	28 (0.12%)	16 (0.47%)	<0.0001
Others (liver pain, arthralgia, hepatosplenomegaly)	4566 (20.24%)	1010 (30.13%)	<0.0001
No symptoms and signs	8472 (37.56%)	730 (21.66%)	<0.0001
Pattern of DILI			<0.0001
Hepatocellular	10626 (51.21%)	1672 (52.60%)	
Cholestatic	4091 (19.72%)	769 (24.19%)	
Mixed	6033 (29.07%)	738 (23.21%)	

Conclusion: Compared to acute DILI, patients with chronic DILI were older, with a high percentage of female patients. Moreover, liver function-associated indicators and clinical symptoms were severe. Among these, female gender and history of underlying liver diseases were independent risk factors of chronic DILI.

THU-399

Impact of plasma exchange and evolution of intensive care management in patients with acute liver failure in a liver transplant center over the past decade

David Toapanta¹, Octavi Bassegoda¹, Miriam Valdivieso¹, Fatima Aziz¹, Juliana Zapatero¹, Natalia Jimenez-Esquivel¹, Foix Valles¹, Helena Hernández Evole¹, Joan Cid¹, Enric Reverter¹, Miquel Lozano¹, Javier Fernandez¹. ¹Hospital Clínic de Barcelona, Barcelona, Spain
Email: bassegoda@clinic.cat

Background and aims: Acute liver failure (ALF) is a rare clinical syndrome characterized by an acute alteration in liver blood test, coagulopathy, and encephalopathy in patients without chronic liver disease. The most common causes are acetaminophen-induced liver injury (AILI) and drug-induced liver injury (DILI). ALF may progress to multiple organ dysfunction and need for an emergent liver

transplantation (LT). Plasma exchange (PE) improves transplant-free survival in patients with ALF, mainly in non-candidates to LT. PE was implemented in the standard care of those patients in the recent decade. Our goals were to determine the current management and outcomes of patients with ALF treated with PE in a real-life scenario.

Method: Retrospective cohort study of ALF patients admitted to the Liver Intensive Care Unit of Hospital Clínic de Barcelona during the period 2012–2022. We included all patients with a diagnosis of ALF defined as an acute alteration of liver blood tests, coagulopathy (INR > 1.5) and hepatic encephalopathy of any grade without previous chronic liver disease. Listing for emergent LT was applied according to local criteria. PE was initiated at the discretion of the clinical team, mainly when a contraindication for emergent LT was present, or the expected time-to-transplant was above 24 h as a bridge to LT.

Results: A total of 46 patients with ALF were included. The most common etiology was autoimmune hepatitis (26%), followed by DILI (20%) and acetaminophen-induced liver injury (15%). Most patients required organ support with mechanical ventilation (70%), vasoactive drugs (60%) and renal replacement therapy (36%). Neurological monitoring was performed with ultrasonography in 41% of the patients and with intracranial sensor in 28%. Most patients were listed for LT (70%) and 63% were transplanted. Overall, mortality was 30%. Of the total cohort, 35% received PE. Those patients requiring PE were more severely ill as assessed by SOFA score and only 31% were transplanted. Mortality of patients receiving PE was 43% compared to patients who did not receive PE (23%). In the subgroup of non-transplanted patients, mortality in patients who received PE was 54% vs. 45% in those who did not. PE was well tolerated with no serious adverse events.

Conclusion: Mortality of ALF in patients who are not candidates for LT remains high despite the use of PE. Autoimmune hepatitis has replaced AILI and DILI as the main causes of ALF in our environment in the last decade. Neurological monitoring is performed mainly using ultrasonography. More studies addressing the use of PE in ALF patients who are not candidates to emergent LT are needed.

THU-400

Clinical and histological features of porto-sinusoidal vascular disorder in drug-induced liver injury population: a retrospective study in biopsy-based cohort

Mengqi Li¹, Ting Zhang¹, Xingang Zhou², Hong Zhao¹, Gang Wan³, Wen Xie¹. ¹Center of Liver Diseases, Beijing Ditan Hospital, Capital Medical University, Beijing, China; ²Department of Pathology, Beijing Ditan Hospital, Capital Medical University, Beijing, China; ³Department of Biostatistics, Beijing Ditan Hospital, Capital Medical University, Beijing, China
Email: xiewen6218@163.com

Background and aims: Porto-sinusoidal vascular disorder (PSVD) has been introduced as a new entity to describe a group of vascular liver diseases with or without portal hypertension (PH)¹. Drug exposure is related to PSVD. However, the relationship between PSVD and drug-induced liver injury (DILI) is still unclear. This study aimed to describe the clinical and histological features of PSVD in DILI population.

Method: Patients diagnosed with DILI, underwent a liver biopsy at baseline and excluding those with pre-existing liver disease were screened for PSVD criteria in this retrospective study. Diagnosis of PSVD requires liver biopsy and the presence of (i) at least one specific feature for PH or one specific histological sign for PSVD or (ii) at least one unspecific feature for PH together with at least one unspecific histological sign for PSVD².

Results: Thirty-six patients with specific or unspecific clinical PH signs were enrolled in this study. Finally, 29 patients diagnosed with PSVD and 4 patients diagnosed with sinusoidal obstruction syndrome. Specific clinical PH signs and specific histological signs were found in 5 (17%) and 9 (31%) of 29 PSVD patients, respectively. Specific clinical PH signs including: (i) gastric, esophageal or ectopic

POSTER PRESENTATIONS

varices (n = 4); (ii) portal hypertensive bleeding (n = 1); (iii) porto-systemic collaterals at imaging (n = 1). Specific histological signs of PSVD including: (i) obliterative portal venopathy (n = 4); (ii) nodular regenerative hyperplasia (n = 5); (iii) incomplete septal fibrosis (n = 1). Patients with PSVD were mostly female (72%), with a median age of 47 years. Over half patients exposed to Chinese medicines or herbal and dietary supplements, 8 (28%) and 6 (21%) patients exposed to medicine or both of them, respectively. Five (17.2%) patients with persistent abnormalities in liver tests over 12 months.

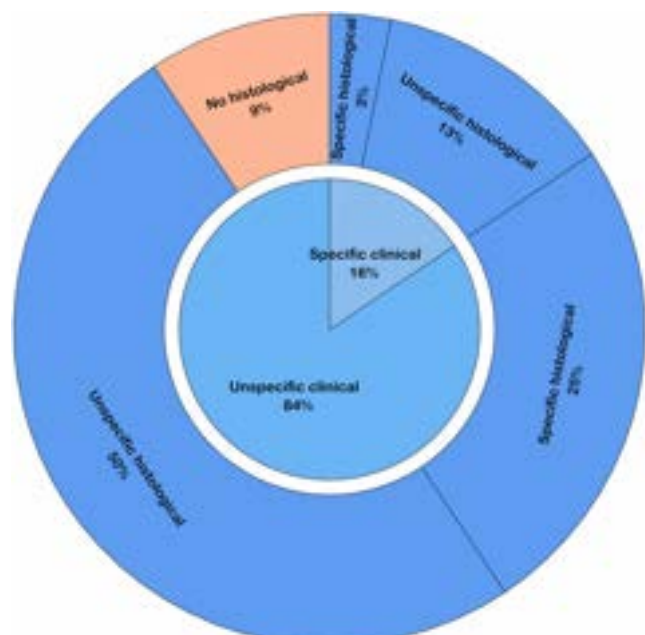


Figure: PSVD patients (blue background, n = 29) were stratified according to the presence of clinical PH signs and histological signs for PSVD. Red background indicates patients who are not meeting PSVD criteria (n = 3). Four patients diagnosed with sinusoidal obstruction syndrome is not shown in this figure.

Conclusion: It seems that PSVD is not rare in DILI patients. Therefore, clinicians and pathologists should pay more attention to PSVD patients in DILI population.

Reference

- De Gottardi A, Sempoux C, Berzigotti A. Porto-sinusoidal vascular disorder. *J Hepatol* 2022;77:1124–1135.
- de Franchis R, Bosch J, Garcia-Tsao G, Reiberger T, Ripoll C, Baveno VIII. Baveno VII-Renewing consensus in portal hypertension. *J Hepatol* 2022;76:959–974.

THU-401

Stanozolol-induced liver injury: a peculiar biochemical profile in a series of thirteen cases

Vinicius Nunes¹, Isadora Almeida¹, Maria Carolina Campos¹, Bárbara Freire¹, Marcelo Silva², Raymundo Parana Filho¹, Fernando Bessone³, Nélia Hernandez⁴, Eduardo Cancado⁵, Maria Schinoni¹. ¹Hospital Universitário Professor Edgard Santos, Brazil; ²Hospital Sao Roque, Argentina; ³Hospital Provincial del Centenario-University of Rosario School of Medicine, Argentina; ⁴Clinical Hospital, Uruguay; ⁵Hospital das Clínicas of University of São Paulo Medical School, Brazil
Email: isadora-lins@hotmail.com

Background and aims: Anabolic androgenic steroids (AAS) are synthetic derivatives of testosterone and stanozolol is a AAS 17 α -alkylated derivative, often used for the increase of physical strength. However, the AAS process of biotransformation involves the liver and has a large potential toxicity. Frequently, the use of ASS occurs concomitantly with other supplements or anabolic steroids, so it is

crucial to understand how the use of each drug presents clinically and laboratory. Also important is knowing other aspects such as latency period and prognosis, aiming to provide the best support for each case. The objective is to characterize patients with hepatotoxicity of stanozolol.

Method: Thirteen patients were evaluated by a group of specialists from the Latin American Dili Registry, configuring an epidemiologic, descriptive, prospective and observational study about hepatotoxic effect of Stanozolol between 2013 and 2022. The data were collected in Brazil (HUPES-BA and HC-USP), Argentina (Hospital Provincial Del Centenario- Rosário), and Uruguay (HC-UdelaR). We declare financial support from the Maria Emilia foundation.

Results: Nine reports of Stanozolol Induced Liver Injury were observed in Brazil, 02 in Argentina and 02 in Uruguay. All patients were males between 21 and 37 years old, and all of them reported use of AAS with the objective of muscular hypertrophy. About the symptoms latency period, the average was 63.2 days, and the average resolution time was 141 days. All patients presented with jaundice, pruritus and fatigue. The enzymatic pattern observed was a total bilirubin (TB) mean of 30.23 mg/dL, with 92.3% of patients presenting values higher than 9 mg/dL, a small increase of aminotransferases, which the aspartate transferase (AST) presented a mean value of 62.75 mg/dL, and the alanine transaminase (ALT), of 117.5 mg/dL. The alkaline phosphatase (ALP) was characterized by an increase in all cases with an average of 311.9 UI/L, and the gamma-glutamyl-transferase (GGT) was very close to normal, presenting an average of 52 UI/L, in which all cases presented values below 100 IU/L.

Subject	Age years	Sex	Latency period of time days	Duration days	TB mg/dL	AST U/L	ALT U/L	ALP U/L	GGT U/L
1	21	M	45	180	15.2	52	72	258	17
2	31	M	45	60	15	99	147	146	36
3	26	M	180	100	9.7	60	103	217	53
4	29	M	15	180	15.7	53	61	100	75
5	29	M	30	120	45	38	50	139	71
6	25	M	-	90	31	47	49	250	45
7	22	M	-	-	21	48	-	241	80
8	29	M	45	-	36	-	46	319	13
9	37	M	45	180	44.3	105	98	281	89
10	31	M	50	-	32	-	98	775	42
11	37	M	80	-	5, 1	-	355	253	51
12	36	M	99	-	38	-	104	689	52
13	26	M	62	218	49	-	228	387	22

Conclusion: Liver injury induced by stanozolol was found in a population of young men, who have aesthetic purpose. These patients have high levels of total bilirubin, modest aminotransferases elevations. We suppose that genetic mutations such as seen in familial intrahepatic cholestasis may be present. Further studies are needed to confirm this hypothesis.

THU-402

Systematic review: patients with pre-existing chronic liver disease are more vulnerable to the severe sequelae of drug induced liver injury

Georgia Zeng^{1,2}, Guy Eslick³, Martin Weltman^{1,2}. ¹Nepean Hospital, Gastroenterology and Hepatology, Australia; ²The University of Sydney, Nepean Clinical School, Australia; ³The University of Newcastle, NHMRC Centre of Research Excellence in Digestive Health, Australia
Email: georgiazeng@icloud.com

Background and aims: Drug-induced liver injury (DILI) is a leading cause of death from acute liver failure (ALF) as well as medication withdrawal from the market. The diagnosis and management of DILI in the context of preexisting chronic liver disease (CLD) remains a controversial and difficult area to navigate, given that the natural

history of certain hepatological conditions involves a spontaneous fluctuation of LFTs. Our systematic review sought to assess the current literature in regard to the diagnosis and prognosis of DILI in CLD patients, and evaluate whether patients with CLD are at higher risk of worse DILI outcomes.

Method: Studies with a minimum of 50 patients adhering to a systematic collection of all DILI cases available to the registry were identified from electronic databases PubMed and EMBASE through to 26 October 2022. Only studies inclusive of patients with pre-existing CLD were included. Data extraction from each study included DILI definition, causality assessment, severity assessment, types of pre-existing CLD included, predominant DILI agents implicated, and incidence of the following outcomes delineated by patients with and without pre-existing CLD where available: ALF, liver-related mortality, liver transplant and chronic DILI.

Results: Overall, 10 studies comprising 36,579 unique patients were included. 6,556 of these patients had CLD, and the most common aetiologies were viral hepatitis, non-alcoholic fatty liver disease and alcoholic liver disease. No studies adopted specialised algorithms proposed to define DILI in CLD patients, based on multiples of their baseline ALT or Bilirubin values rather than the ULN. Only 2 studies compared the spread of DILI agents between patients with and without CLD, of which the multicentre Spanish DILI registry found a significantly higher prevalence of antitubercular drugs in patients with CLD (21% of cases) vs without CLD (7.6% of cases). 6 of 9 studies reported significantly higher rates of mortality in DILI patients with vs without CLD, with adjusted HRs as high as 2.64 (95% CI 1.78–3.93, $p < 0.001$) in a multicentre Taiwanese study, and 2.72 (95% CI 2.33–3.19, $p < 0.001$) in a national population-based Thailand study. 6 studies compared rates of ALF, liver decompensation and/or severity of DILI between DILI patients with and without CLD, 3 of which returned significant results. For example, in a large-scale retrospective Chinese study comprising 25,927 DILI cases, patients with pre-existing CLD consisted of 64% of fatal cases, 29% of cases with jaundice, and only 21% of cases without jaundice. 3 of 4 studies concluded that DILI patients with CLD were not at higher risk of suffering from DILI chronicity.

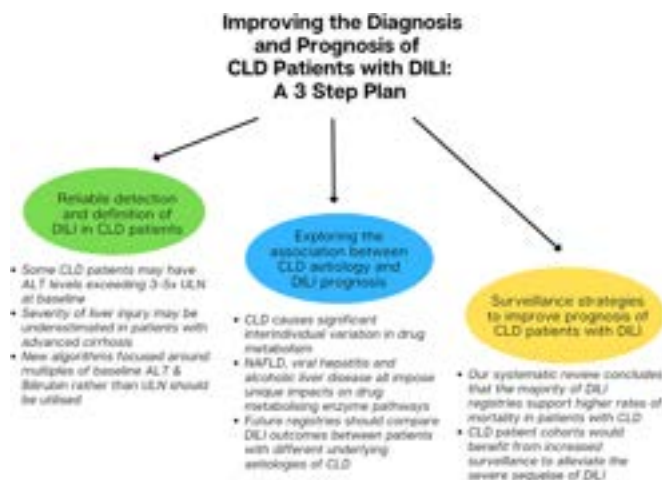


Figure: Improving the Diagnosis and Prognosis of CLD patients with DILI: A 3 Step Plan

Conclusion: Our systematic review demonstrates that a majority of DILI registries support higher rates of mortality in patients with CLD, with a stronger correlation between cirrhotic patients and poor outcomes. Future DILI registries should aim to fully characterize CLD patient cohorts regarding their demographics, clinical characteristics and spread of DILI agents. Our findings suggest that CLD patients who suffer DILI would stand to benefit from increased surveillance and a clear diagnostic strategy.

THU-403

Autoimmune hepatitis (AIH) or drug-Induced liver injury (DILI)-a diagnostic challenge

Yaakov Maor^{1,2}, Ali Abdallah^{1,3}, Leore Cohen Mendel⁴, Ehud Melzer^{1,2}, Stephen Malnick^{2,3}. ¹Kaplan Medical Center, Institute of Gastroenterology and Hepatology, Rehovot, Israel; ²The Hebrew University, Hadassah School of Medicine, Jerusalem, Israel; ³Kaplan Medical Center, Department of Medicine C, Rehovot, Israel; ⁴Kaplan Medical Center, Institute of Gastroenterology and Hepatology, Rehovot, Israel

Email: halishy@netvision.net.il

Background and aims: AIH and DILI share clinical, biochemical, serological and histopathological characteristics. DILI cause by several medications may simulate AIH, while certain drugs can induce bonae-fide AIH. Therefore, the diagnosis of AIH vs. DILI is often challenging.

Method: Patients evaluated for hepatitis with clinical, biochemical, serological, and liver biopsy with a presumptive diagnosis of AIH or DILI were included in a retrospective attempt to make a definitive diagnosis. All biopsies were reviewed for features compatible with either diagnosis or both. Conventional scores of AIH (simplified criteria) and DILI (RUCAM) were calculated.

Results: 20 patients were enrolled: 75% female; mean age 59 years (age >50 years in 75%). 50% were affected with the metabolic syndrome and 45% with autoimmune disorders. A potential hepatotoxic drug was identified in 90%, mainly statins. Pattern of injury was hepatic in 90%. Bilirubin >10 mg/dL occurred in 25%. IgG >1.5xULN was present in 65% and ANA/ASMA >1:80 in 40%. Histopathology considered typical of AIH in 70%; compatible with or atypical in 15% each. AIH simplified score was: probable (≥6 points) in 15% and definite (≥7 points) in 40%. Histopathology determined suspected of DILI in 55%, consider DILI in 25% and low probability in 20%. RUCAM scored possible (3–5 points) in 60% and probable (6–8 points) in 40%. 75% were treated with corticosteroids ± azathioprine, with 70% response rate.

Conclusion: Distinction between DILI and AIH is still problematic, reflected by significant overlap in immune serology and histopathologic features in HIA and DILI. The majority of patients received corticosteroid treatment for severe or protracted hepatitis. DILI may be the initiating event of a flare of AIH or still unrelated to liver injury in such instances.

THU-404

Gender differences in liver transplantation (LT) for acute liver failure (ALF) in a multicentre ALF-LT Spanish cohort

Isabel Conde^{1,2,3}, Sara Martinez¹, Andrea Bosca^{1,2}, Maria Senosiain⁴, Rosa María Martín Mateos⁵, Carolina Almohalla Alvarez⁶, Maria Luisa Gonzalez Dieguez⁷, Sara Lorente Perez⁸, Alejandra Otero⁹, Maria Rodriguez¹⁰, Jose Ignacio Herrero^{3,11,12}, Isabel Campos-Varela¹³, Ainhoa Fernandez¹⁴, Marina Berenguer^{1,2,3,15}, Victoria Aguilera Sancho^{1,2,3,15}. ¹Hospital Universitario y Politécnico La Fe, Valencia, Spain; ²Instituto de Investigación Sanitaria La Fe, Valencia, Spain; ³CIBERehd, Instituto Carlos III, Madrid, Spain; ⁴Hospital Universitario de Cruces, Bilbao, Spain; ⁵Hospital Universitario Ramón y Cajal, Madrid, Spain; ⁶Hospital Universitario Río Hortega, Valladolid, Spain; ⁷Hospital Universitario Central de Asturias, Oviedo, Spain; ⁸Hospital Clínico Universitario Lozano Blesa, Zaragoza, Spain; ⁹Complejo Hospitalario Universitario A Coruña, A Coruña, Spain; ¹⁰Hospital General Universitario de Alicante, Alicante, Spain; ¹¹Clínica Universidad de Navarra, Pamplona, Spain; ¹²Instituto de Investigación Sanitaria de Navarra, Pamplona, Spain; ¹³Hospital Universitari Vall d'Hebron, Barcelona, Spain; ¹⁴Hospital General Universitario Gregorio Marañón, Madrid, Spain; ¹⁵Universitat de València, Department of Medicine, Valencia, Spain

Email: icondemiel@gmail.com

Background and aims: ALF is a critical illness with high morbidity, improved by LT. There may be potential differences in

POSTER PRESENTATIONS

clinical presentation and outcome between men and women which we aimed to assess in this Spanish multicenter ALF-LT cohort.

Method: Baseline features, biochemical data, comorbidities, acute complications, early and late outcomes of an ALF-LT retrospective cohort from 11 hospitals (2001–2020) were collected.

Results: We included 217 adults ALF-LT (62% women) with an increasing proportion of women overtime (57% 2001–2005, 54% 2006–2010, 69% 2011–2015, 67% 2016–2020) but similar age (median: men 41, women 41.5yrs). Past history of alcohol, tobacco and drug use was higher in men ($p < 0.05$). Autoimmune and cryptogenic aetiologies were more frequent in women (31% vs 19% and 31 vs 20%) while HBV was more common in men (29% vs 10%) ($p = 0.007$). Kings College criteria as well as acute kidney injury (AKI) were present more frequently in men (14% vs 5% and 52% vs 29%, respectively). Renal function, ALT, platelets and MELD preLT were worse in men ($p < 0.05$). Early post-LT complications: AKI (73% vs 53%), and haemorrhage (26% vs 14%) were more frequent in men whereas rejection was more common in women (11% vs 22.5%) ($p < 0.05$). Later complications: arterial hypertension-AHT (36% vs 27%), dyslipidaemia (25% vs 11%), chronic kidney disease (24% vs 17%) and biliary complications (32% vs 21%) were all more frequent in men but without reaching statistical significance. AHT, pre-LT AKI and infection were independently associated with poor survival (HR 2.6, $p = 0.031$; HR 3.7, $p = 0.004$ and HR 2.5, $p = 0.03$, respectively) without gender differences. Causes of death, survival and reLT were similar in both groups.

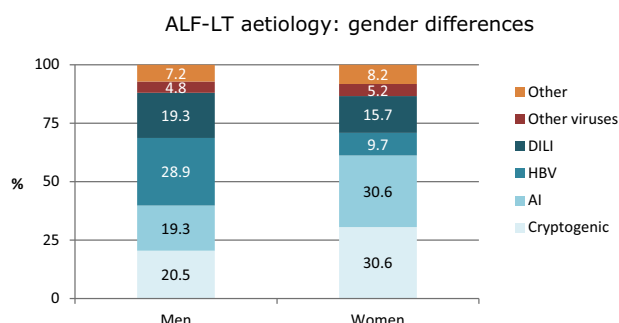


Figure:

Conclusion: Aetiology and history of toxic abuses were different between gender. At time of LT men were in worse clinical condition resulting in a higher rate of early post-LT complications, with the exception of rejection, yet long-term outcome was similar.

THU-405

CDK 4/6 inhibitors induced liver injury: 7 cases from REFHEPS registry

Lucy Meunier¹, Bénédicte Delire², Eleonora De Martin³, Yves Horsmans², Dominique Larrey¹. ¹CHU Montpellier, Hepatology, Montpellier, France; ²Cliniques Universitaires Saint-Luc, Gastroenterology, Belgium; ³Hôpital Paul Brousse, Centre hepato biliaire, France

Email: lucymeunier66@gmail.com

Background and aims: Cyclin-dependent kinase inhibitors (CDKIs) are the corner-stone of systemic therapy for patients with hormone-positive (HR+) HER2-negative metastatic breast cancer (MBC). As reported by large randomized clinical trials, grade 3 elevation of alanine and aspartate aminotransferases occurred in up to 11% and 6% of patients receiving ribociclib or abemaciclib. The mechanism of liver toxicity remains unclear.

Method: Seven cases have been retrospectively collected through the French-speaking hepatotoxicity network (REFHEPS).

Results: Of the 87 cases collected by REFHEPS between November 2021 and January 2023, 7 involved CDKIs: ribociclib (n = 5) and abemaciclib (n = 2). All were women, median age 63 yr-old (49–77), treated for metastatic breast cancer. All patients also had concomitant hormonal treatment: letrozole, fulvestran or anastrozole. The median time to onset of hepatitis after introduction of CDKIs was 46 (24–274) days. All liver events exhibited a hepatocellular profile with a CTCAE severity grade 3 (n = 4) or 4 (n = 3). Median peak of liver tests were: AST: 335 IU/L (262–1201); ALT: 698 IU/L (402–2523); ALP: 131 IU/L (87–423). Exhaustive work-up was performed in all patients including viral serologies, liver antibodies and imaging. Only 2 patients had positive anti-nuclear antibodies and one had a slightly elevated immunoglobulin G level (1.1N). Liver biopsy, performed in 3 patients, showed no fibrosis but centro-lobular hepatitis in favor of DILI. RUCAM score was between 3 and 9. For most patients, improvement was spontaneous after CDKI withdrawal, median xx 57.6 days (min:19; max:112). Three patients received steroids (0.5–1 mg/kg) introduced due to a lack of spontaneous resolution followed by complete resolution. No recurrence of hepatitis after stopping steroids or resuming anti-tumor treatment.

Conclusion: CDKIs are frequently used to treat metastatic breast cancer. A few DILI cases have been reported in the literature. The mechanism of toxicity is unknown. However, the interest of corticoids to treat such DILI cases has been outlined but its place remains unknown. Here we reported 7 DILI cases from the REFHEPS registry outlining the interest and potential limitations of steroid treatment. More data are clearly needed.

(abstract: THU-405): Patients' characteristics,

Case	Sex, age (years)	CDK 4/6	Concomitant medications	Delay treatment-DILI (days)	RUCAM score	Grade DILIN	Delay improvement (between stop drugs and grade 1) (days)	Steroids	Duration of steroids (days)	Delay DILI-steroids (days)
1	F, 49	Abemaciclib	Anastrozole	274	7	2	42	No	NA	NA
2	F, 77	Ribociclib	Fulvestran	24	9	1	34	No	NA	NA
3	F, 63	Ribociclib	Letrozole	77	8	1	112	Yes	15	88
4	F, 65	Ribociclib	Anastrozole	46	9	1	93	Yes	24	59
5	F, 61	Abemaciclib	Letrozole	46	8	1	19	No	NA	NA
6	F, 63	Ribociclib	Letrozole	27	8	1	NA	No	NA	NA
7	F, 71	Ribociclib	Letrozole/ pembrolizumab	52	3	3	46	Yes	76	1

THU-406

Exponential increase of paracetamol liver injury over the last decade in a Spanish referral center

Anna Pocurull¹, Helena Hernández Evole², Cristina Collazos¹, Elia Canga², Ana Martínez-Ibáñez³, David Toapanta³, Enric Reverter³, Xavier Forn¹. ¹Liver Unit, Hospital Clínic Barcelona. University of Barcelona. IDIBAPS. CIBEREHD., Spain; ²Liver Unit, Hospital Clínic Barcelona., Spain; ³Liver ICU, Liver Unit, Hospital Clínic Barcelona, IDIBAPS and CIBEREHD, Spain
Email: apocurull@gmail.com

Background and aims: Paracetamol is one of the most used analgesics worldwide. Despite the fact that paracetamol overdose accounts for most cases of acute liver failure in some countries, this was uncommon in Spain. Since we had the perception that more patients were admitted to our unit due to paracetamol overdose, we analyzed its incidence and characterized the clinical phenotype of patients admitted to our Liver Unit during the last decade.

Method: We retrospectively reviewed all admissions due to paracetamol-associated liver toxicity from January 2010 to August 2022. Demographic data, laboratory test, use of concomitant drugs and psychiatric comorbidities were registered. In addition, the severity of liver injury and the need for support therapy were analyzed.

Results: One hundred and five patients with a median age of 31 (22–34) years were included; 65% were women. From 2010 to 2015 the incidence remained stable with around 5 cases/year, whereas starting in 2016 the incidence increased progressively, reaching 20 cases in 2022. In most patients the overdose was taken with autolytic intention (93%) and was the first attempt (69%). Regarding psychiatric comorbidities, 29% had past medical history of depression, anxiety (25%), or borderline personality disorder (16%). The intake of other medications or drugs during the episode was common (55%): anti-inflammatories (37%), illicit drugs such as cocaine (22%) or benzodiazepines (22%). Regarding the severity of liver injury, 87% required ICU admission due to PT<40%, hepatic encephalopathy or metabolic acidosis. At admission, the median values of ALT and total bilirubin were 1177 (204–4509) IU/L and 1, 55 (0.89–2.5) mg/dl, respectively. Hepatotoxicity resolved with specific treatment (N-Acetylcysteine) in 87% patients; 4% required plasma exchange or renal replacement therapy. One patient (1%) required liver transplantation and six patients died (6%). Variables associated with acute liver failure were overdose with autolytic intent (84% vs 43%) and presence of psychiatric comorbidity (87% vs 69%) ($p < 0.05$).

Representation of paracetamol-induced liver injury in the time period

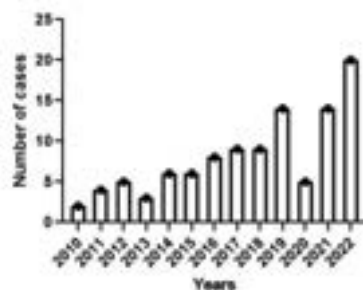


Figure:

Conclusion: The incidence of hepatitis caused by paracetamol has increased significantly in recent years in Spain. The profile of patients are young women with symptoms of anxiety and/or depression, who attempt suicide. Although most cases resolve with specific treatment, ICU admission is frequent.

THU-407

Liver transplantation in acute liver failure in Slovenia

Marjana Turk Jerovšek¹, Marija Ribnikar¹. ¹University medical centre Ljubljana, Department of gastroenterology, Ljubljana, Slovenia
Email: marjana.tjerovsek@gmail.com

Background and aims: Acute liver failure (ALF) is characterised by sudden onset of hepatic encephalopathy with concomitant coagulopathy, jaundice and multiorgan failure in a patient without previously known liver disease. Most prevalent causes of ALF in developed countries are paracetamol toxicity, drug induced liver injury (DILI), hepatitis B virus infection and autoimmunity. Viral hepatitis A, E and especially B are the main causes of ALF in Eastern countries. Patients with acute liver failure are transplanted urgently if criteria for urgent liver transplantation are met.

Method: 388 patients, of which two thirds' men and one third women, underwent liver transplantation in UMC Ljubljana, Slovenia, between 20.6.1995 and 31.12.2021. The average age at transplantation was 51 years. 31 (8,0%) patients, of which 9 men and 22 women, were transplanted urgently, due to acute liver failure. Their average age at transplantation was 39 years. 6 patients (1 man and 5 women) underwent emergency liver transplantation due to fulminant autoimmune hepatitis (19,4%), which is the most common indication for urgent liver transplantation in Slovenia. 4 patients (2 men and 2 women) each were urgently transplanted for drug-induced liver disease (12,9%) and Budd Chiari syndrome (12,9%) and 4 women for acute Wilsons disease (12,9%). 3 female patients (9,7%) were urgently transplanted due to fulminant hepatitis B. 1 man was urgently transplanted due to liver trauma and 1 female patient each due to mushroom poisoning and liver failure during pregnancy. We were unable to determine the cause of acute liver failure in 3 men and 4 women (22,6%). 41 (10,6%) of all patients and 3 (9,7%) of patients with acute liver failure were re-transplanted.

Results: 1 and 5-year survival of our liver transplanted patients is 84,1% and 76,1% respectively. 1 and 5-year survival of urgently transplanted patients with acute liver failure is 68,0%. 10 out of 31 urgently transplanted patients died, all of them in the first year after transplantation: 3 each because of infection and graft failure and 1 each because of gastric carcinoma and complication of liver transplant procedure. In 2 patients the cause of death is unknown.

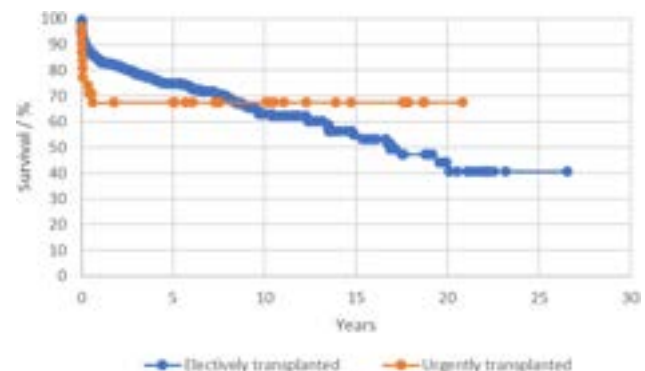


Figure:

Conclusion: Acute liver failure is a rare disease with poor prognosis and high mortality. For critically ill patients, urgent liver transplantation is currently the only effective method of treatment. Urgently transplanted patients are on average younger than electively transplanted patients. Unlike electively transplanted patients, women predominate among them. 1-year survival of urgently transplanted patients is worse than in electively transplanted, that reflects the severity and complexity of acute liver failure. Long-term survival is better due to younger age at transplantation and fewer comorbidities.

POSTER PRESENTATIONS

THU-408

Chemotherapy-induced hepatotoxic reactions in patients with acute myeloid leukemia: the overweight and obesity role in the pathogenesis

Igor Skrypnyk¹, Ganna Maslova¹, Roman Skrypnyk¹, Tetiana Lymanets¹. ¹Poltava State Medical University, Ukraine
Email: inskrypnyk@gmail.com

Background and aims: To investigate the frequency of development and nature of cytostatic-induced hepatotoxic reactions in patients with acute myeloid leukemia (AML) with overweight and obesity during remission induction chemotherapy (CT).

Method: We examined 25 patients with newly diagnosed acute leukemia (AL), of which 56% (14/25) were men, 44% (11/25) were women. Depending on the body mass index (BMI), patients were divided into groups: I (n = 10)-patients with AML and BMI of 18.5–24.9 kg/m²; II (n = 15)-patients with AML and BMI ≥25.0 kg/m². The biochemical blood analysis was evaluated twice: before and on the 56th day of CT, which included alanine-, aspartate-aminotransferases, gamma-glutamyltranspeptidase (GGT), alkaline phosphatase (ALP), total protein and total bilirubin.

Results: In patients with AML and normal BMI, CT conduction increased the risk of GGT (RR = 3.00; 95% CI = 1.14–7.91; p < 0.05) and ALP activity impairment (RR = 2.67; 95% CI = 0.98–7.22; p > 0.05). The presence of overweight and obesity in patients with AML of group II led to significant risk of increase the GGT (RR = 3.00; 95% CI = 1.46–6.14; p < 0.05) and ALP activity (RR = 4.00; 95% CI = 1.41–11.35; p < 0.05) during CT. GGT and ALP activity in the blood serum of group II patients after CT exceeded the baseline data in 2.4 times (p < 0.0001) and 1.6 times (p = 0.0007), respectively. After two courses of remission induction CT, the biochemical liver tests violations were recorded in 100% (15/15) of group II patients with overweight and obesity, of which cholestatic syndrome was detected in 20% (3/15) of patients and mixed syndrome-in 80% (12/15) of patients.

Conclusion: The remission induction CT of AML is accompanied by the risk of cytostatic-induced liver injury. In patients with AML, regardless of BMI, induction CT was associated with a risk of increased GGT and ALP activity. However, in patients with normal BMI, GGT and ALP activity increase was associated with hyperbilirubinemia, and in overweight and obese patients-with hypoproteinemia development. Moreover, the increased ALT activity after CT compared with the baseline data was observed in AML patients with high BMI. The presence of overweight, obesity and primary disorders of biochemical liver tests due to the oncohematological disease influence are the risk factors for hepatotoxic reactions development during CT.

THU-409

Clinical determinants of hospital mortality in liver failure: a comprehensive analysis of 62,717 patients

Tobias Eßing¹, Hans Bock¹, Christoph Roderburg¹, Tom Lüdde¹, Sven H Loosen¹. ¹University Hospital Düsseldorf, Department of Gastroenterology, Hepatology and Infectious Diseases, Germany
Email: Sven.Loosen@med.uni-duesseldorf.de

Background and aims: Liver failure (LF) is characterized by a loss of the synthetic and metabolic liver function and is associated with a high mortality. Large-scale data on recent developments and hospital mortality of LF in Germany are missing. A systematic analysis and careful interpretation of these data sets could help to optimize outcomes of LF.

Method: We used standardized hospital discharge data of the Federal Statistical Office to evaluate current trends, hospital mortality and factors associated with an unfavourable course of LF in Germany between 2010 and 2019.

Results: A total of 62,717 hospitalized LF cases were identified. Annual LF frequency decreased from 6,716 (2010) to 5,855 (2019) cases and was higher among males (60.51%). Hospital mortality was 38.08% and significantly declined over the observation period.

Mortality significantly correlated with patients' age and was highest among individuals with (sub)acute LF (47.5%). Multivariate regression analyses revealed pulmonary (OR_{ARDS}: 2.91, OR_{mechanical ventilation}: 8.49) and renal complications (OR_{acute kidney failure}: 2.05, OR_{hepatorenal syndrome}: 2.99) and sepsis (OR: 1.96) as factors for increased mortality. Liver transplantation reduced mortality in patients with (sub)acute LF. Hospital mortality significantly decreased with the annual LF case volume and ranged from 47.46% to 29.87% in low or high case volume hospitals, respectively.



Figure:

Conclusion: Although incidence rates and hospital mortality of LF in Germany have constantly decreased, hospital mortality has remained at a very high level. We identified a number of variables associated with increased mortality that could help to improve framework conditions for the treatment of LF in the future.

FRIDAY 23 JUNE

FRI-393

Serum proteomics in American adults with acute liver failure

Katharina Remih¹, Franziska Hufnagel¹, Valerie Durkalski-Mauldin², William M. Lee³, Zemin Su², Jody Rule³, Laura Krieg⁴, Isabel Karkossa⁴, Kristin Schubert⁴, Martin von Bergen⁴, Robert Fontana⁵, Pavel Strnad¹. ¹University Hospital RWTH Aachen, Clinic for Gastroenterology, Metabolic Disorders, and Internal Intensive Medicine, Aachen, Germany; ²Medical University of South Carolina, Department of Public Health Sciences, Charleston, United States; ³UT Southwestern Medical Center, Dallas, United States; ⁴Helmholtz Centre for Environmental Research, Department of Molecular Systems Biology, Leipzig, Germany; ⁵University of Michigan Medical Center, Division of Gastroenterology, Ann Arbor, United States
Email: pstrnad@ukaachen.de

Background and aims: Acute liver failure (ALF) indicates sudden hepatocellular dysfunction with coagulopathy and encephalopathy in patients without known liver disease. Liver transplantation represents the only effective treatment, but the decision for/against transplantation remains challenging. We used mass spectrometry to characterize day 1 proteomic profiles in adult ALF patients of varying aetiology to identify diagnostic and prognostic biomarkers.

Method: Serum proteomic patterns were compared in 200 and 119 (discovery/validation cohort) adult patients with ALF, ~50% of them acetaminophen (APAP)-related, as well as in 30 healthy controls without liver disease. The former were randomly selected from admission samples (<48 h) of the US ALF study group database. Non-survivors were defined as patients who passed away or required liver transplantation within 21 days. Ingenuity pathway analysis (Qiagen) was used to obtain mechanistic insights.

Results: In the discovery cohort, 187 proteins were detected in $\geq 70\%$ of subjects and most differed between ALF cases and controls. The key altered pathways were IL-6 signalling, acute phase response and prothrombin activation. 158 proteins differed between 95 APAP and 105 non-APAP cases. Three proteins reproducibly discriminated between the groups (AUROCs >0.9 in both cohorts) and were superior to other available markers.

In the discovery cohort, 46 proteins significantly differed between 21-day survivors and non-survivors. The most significantly enriched pathways were activated immune and acute-phase response which coincided with a better outcome. In particular, higher alpha1-antitrypsin (SERPINA1) and leucine-rich alpha-2 glycoprotein 1 (LRG1) levels were associated with better prognosis in the overall group (see figure, panel A). In both cohorts, they constituted the best discriminators (AUROCs >0.7) and were comparable to MELD score (see figure, panel B).

Conclusion: Unbiased proteomics may help identify a panel of new diagnostic and prognostic biomarkers with biological plausibility in ALF.

FRI-394

An in silico designed receptor antagonizing peptide targeting C-C motif chemokine receptor 8 attenuates monocyte/macrophage recruitment in vitro and in vivo

Eline Geervliet^{1,2}, Ralf Weiskirchen², Ruchi Bansal¹. ¹University of Twente, Medical cell biophysics, Enschede, Netherlands; ²RWTH Aachen, Institute of Molecular Pathobiochemistry, Experimental Gene Therapy and Clinical Chemistry, Aachen, Germany
Email: ekgeervliet@gmail.com

Background and aims: Acute liver injury is the most common cause of acute liver failure in the western world. Infiltrating monocytes/macrophages play a crucial role of liver inflammation, one of the hallmarks of acute liver injury. The macrophage compartment of the liver upon acute liver injury is augmented by the infiltrating monocytes driven by C-C motif chemokine receptor/C-C motif chemokine ligand (CCR/CCL) axis. Besides CCL2-CCR2, CCL1-CCR8 is involved in mediating monocyte recruitment which subsequently shapes the inflammatory microenvironment during liver injury. Several small molecular receptor-antagonists have been developed for CCR8 however failed in clinical translation possibly due to poor pharmacokinetic profile, serum stability, and lack of efficacy. Here, using in silico modelling approach, we have designed an antagonizing peptide for CCR8 (AP8) to inhibit liver inflammation and ameliorate acute liver injury.

Method: Efficacy of AP8 on CCL1-driven chemotaxis was examined in vitro in mouse RAW 264.7 macrophages and human THP-1 monocytes using transwell assays, and in vivo in an acute carbon tetrachloride (CCl₄)-induced acute liver injury mouse model. To assess intrahepatic monocyte infiltration in vivo, liver tissues were mechanically dissociated using Tissue Grinder, and the monocyte-derived macrophage (MoMF) population, characterized by CD11b and F4/80 expression levels, was analyzed using flow cytometry. Furthermore, effects of AP8 on disease progression (inflammation and fibrosis) were assessed using immunohistochemistry and mRNA analysis. The effects of AP8 were compared with R243, a selective CCR8 antagonist, in vitro and in vivo.

Results: AP8 showed favorable inhibition of CCL1-driven macrophage and monocyte chemotaxis in both murine RAW264.7 macrophages and human THP1 monocytes while R243 only showed reduced

infiltration of mouse macrophages and not human monocytes. In vivo in CCl₄-induced acute liver injury mouse model, flow cytometric analysis revealed a decrease in monocytes-derived macrophages (CD11b⁺⁺/F4/80⁺) following AP8 treatment, but not R243 treatment. Immunohistochemical analysis evidenced decreased inflammation (F4/80 expression), fibrosis (collagen-I and alpha-smooth muscle actin expression), and increased liver regeneration (Ki-67 and HNF4alpha expression) in the AP8 treated mouse livers. Our data shows effective amelioration of inflammation and fibrosis using a CCR8-antagonizing peptide.

Conclusion: Our CCR8-antagonizing peptide inhibited migration of macrophages/monocytes in vitro and in vivo and ameliorated inflammation and fibrosis in vivo in an acute liver injury mouse model.

FRI-395

E2F2 deficiency protects from acetaminophen-induced hepatotoxicity while E2F1 is required to prevent the devastating effects

Xabier Buque¹, Francisco Gonzalez-Romero¹, Maider Apodaka-Biguri¹, Maria Crespo², Mariana Mesquita^{3,4}, Igor Aurrekoetxea^{1,5}, Beatriz Gómez Santos¹, Igotz Delgado¹, Ane Nieva-Zuluaga¹, Mikel Ruiz de Gauna¹, Idoia Fernández-Puertas¹, Paul Gomez-Jauregui¹, Nerea Muñoz-Llanes¹, Natalia Sainz-Ramírez¹, Ainhoa Iglesias⁶, Francisco Javier Cubero^{3,7,8}, Guadalupe Sabio², Ana Zubiaga⁶, Patricia Aspichueta^{1,5,7}. ¹Department of Physiology University of the Basque Country UPV/EHU, Faculty of Medicine and Nursing, 48940 Leioa, Spain; ²Centro Nacional de Investigaciones Cardiovasculares Carlos III, 28029 Madrid, Spain; ³Institute of Biology, Department of Plant Biology, PPG BMM, University of Campinas (UNICAMP), 13083-970 Campinas, São Paulo, Brazil; ⁴Department of Immunology, Ophthalmology and ENT, Complutense University School of Medicine, 28040 Madrid, Spain; ⁵Biocruces Bizkaia Health Research Institute, Cruces University Hospital, 48903 Barakaldo, Spain; ⁶Department of Genetic, Physical Anthropology and Animal Physiology, Faculty of Science and Technology, University of Basque Country UPV/EHU, 48940 Leioa, Spain; ⁷National Institute for the Study of Liver and Gastrointestinal Diseases (CIBEREHD, Carlos III Health Institute), 28029 Madrid, Spain; ⁸Instituto de Investigación Sanitaria Gregorio Marañón (IISGM), 28009 Madrid, Spain
Email: patricia.aspichueta@ehu.eus

Background and aims: Acetaminophen (APAP) is one of the most commonly used pain relievers and antipyretics. APAP overdose, the leading cause of drug-induced hepatotoxicity in Western countries, entails a complex, time- and dose-dependent signaling network involving liver metabolism, immune response and liver regeneration. Available therapies are very limited; thus, new therapeutic targets need to be discovered. E2F1 and E2F2 proteins are cell cycle regulators involved in liver regeneration and mitochondrial metabolism. Additionally, they participate in the activation and maturation of T cells and macrophages. Therefore, the aims were: 1) to investigate if E2F1 and/or E2F2 are involved in APAP-induced liver injury and if so 2) to identify the mechanism.

Method: E2f1^{-/-}, E2f2^{-/-}, E2f1/E2f2 double knockout (DKO) and wild-type (WT) mice were used. CD45.1 WT mice were used for bone marrow (BM) transplant. APAP-induced liver injury was achieved through the intraperitoneal injection of 750 mg/kg or 360 mg/kg of APAP and mice were monitored up to 6, 24 and 48 h after overdose. Survival and metabolic studies, anatomopathological evaluation of necrosis and immune infiltrate, immunohistochemistry, and protein and lipid levels analysis were performed.

Results: Lack of E2F1 worsens APAP overdose while that of E2F2 has a protective effect. Accordingly, APAP-treated E2f1^{-/-} mice showed less survival and higher liver necrosis 24 h post-overdose. E2F2 deficiency ameliorated transaminases levels and improved the resolution of

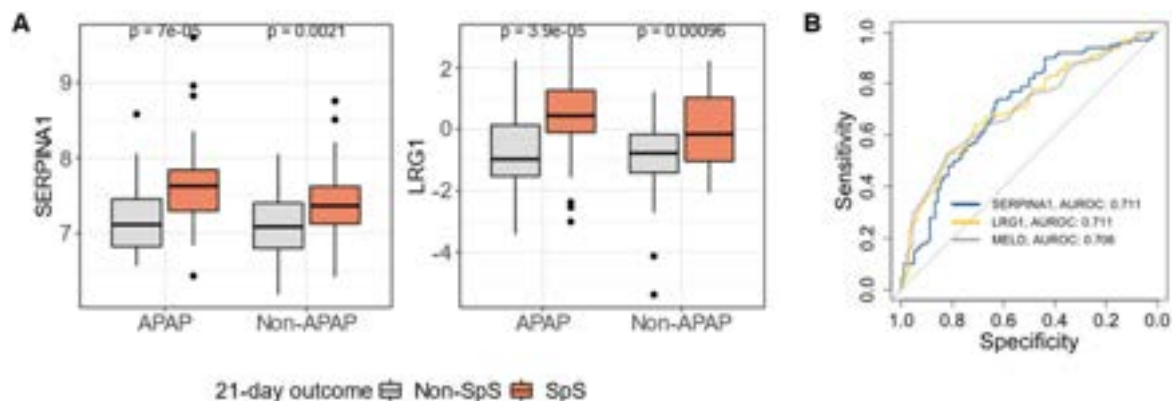


Figure: (abstract: FRI-393): A) The two strongest discriminating parameters for 21-day survival, SERPINA1 and LRG1, grouped by aetiology and survival status. Boxplots display median with first and third quartile and whiskers indicate smallest and largest nonoutlier observations. Outliers are depicted by black circles. APAP/non-APAP refers to the ALF aetiology (acetaminophen-related or not). SpS describes spontaneous survivors, non-SpS individuals who either died or required a liver transplant within 21 days of enrollment. B) Logistic regression analysis of SERPINA1 and LRG1 in comparison to the MELD-Score (discovery cohort).

liver necrosis by 48 h post-APAP. The anatomopathological evaluation post-APAP showed increased inflammatory component linked to necrotic areas in *E2f1*^{-/-} mice, with neutrophils as the main recruited cells, while in *E2f2*^{-/-} mice it was lower than that found in WT mice. The higher immune infiltrate in *E2f1*^{-/-} mice was reinforced with the immunofluorescence determination of CD45⁺, CD11b⁺ and F4/80⁺ cells in the whole liver, inflammation markers that also demonstrated the resistance conferred by *E2f2* deficiency. BM transplant showed that the protection of *E2f2*^{-/-} mice or vulnerability of *E2f1*^{-/-} mice were associated with the effect of its lack in liver rather than to changes in myeloid cell activity. Liver content of neutral lipids indicated a worse metabolic adaptation of *E2f1*^{-/-} mice to APAP overdose, which together with changes in mitochondrial complexes contributed to their susceptibility. Ultimately, APAP-treated DKO demonstrated similar phenotype to that of *E2f2*^{-/-} mice despite being deficient in both factors simultaneously showing the potent protective predominant role of *E2f2* deficiency over the negative *E2f1* deficient effect.

Conclusion: *E2f1* deficiency increases vulnerability to APAP-induced liver injury by altering liver metabolic adaptation. However, the inhibition of *E2f2* arise as a potential therapeutic approach.

FRI-396

Mesenchymal stem cell-derived small extracellular vesicles ameliorate liver injury via attenuating macrophage extracellular traps

Zhihui Li¹, Zhang Jing¹, Meng Shibo¹, Bingliang Lin¹. ¹Third Affiliated Hospital of Sun Yat-sen University, The department of infectious disease, Guangzhou, China

Email: lamikin@126.com

Background and aims: Acute liver failure (ALF) is characterized by massive hepatocyte necrosis and by systemic inflammation. The formation of macrophage extracellular traps (METs) has been associated with immune-mediated diseases. Small extracellular vesicles (sEVs) may act as mediators in the inhibition of inflammation by mesenchymal stem cells (MSCs). In this study, we aimed to investigate the mechanism of bone marrow MSC-derived sEVs (BMSC-sEVs) in treating mice with ALF.

Method: Small EVs and sEV-free BMSC concentrated medium were injected into mice with LPS/D-GalN-induced ALF to assess survival, changes in serology, liver pathology, and the yield of METs in different phases. The results were further verified in vitro in hydrogen peroxide injured L-02 and THLE-2 cells which were co-cultured with METs-induced macrophages THP-1. And Cl-amidine, an inhibitor of METs was used to evaluate the role and mechanism of BMSC-sEVs in METs-mediated liver injury.

Results: Treatment of BMSC-sEVs led to higher 24 h mouse survival rates and significant reductions in METs formation and liver injury compared to treatment with sEV-free concentrated medium. METs increased when macrophages were subjected to hypoxia/reoxygenation, and when METs were co-cultured with hepatocytes, apoptosis increased (Fig) and proliferation decreased, which were reversed by the inhibition of METs. Additionally, the Hippo/YAP pathway was activated in the METs-treated group.

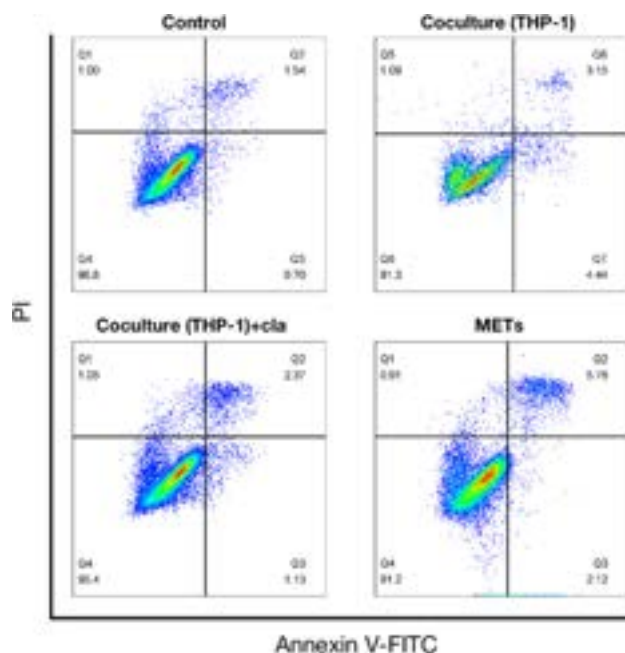


Figure:

Conclusion: Our results reveal that BMSC-sEVs play in suppressing METs formation and highlight the therapeutic potential of METs inhibition in reducing liver injury.

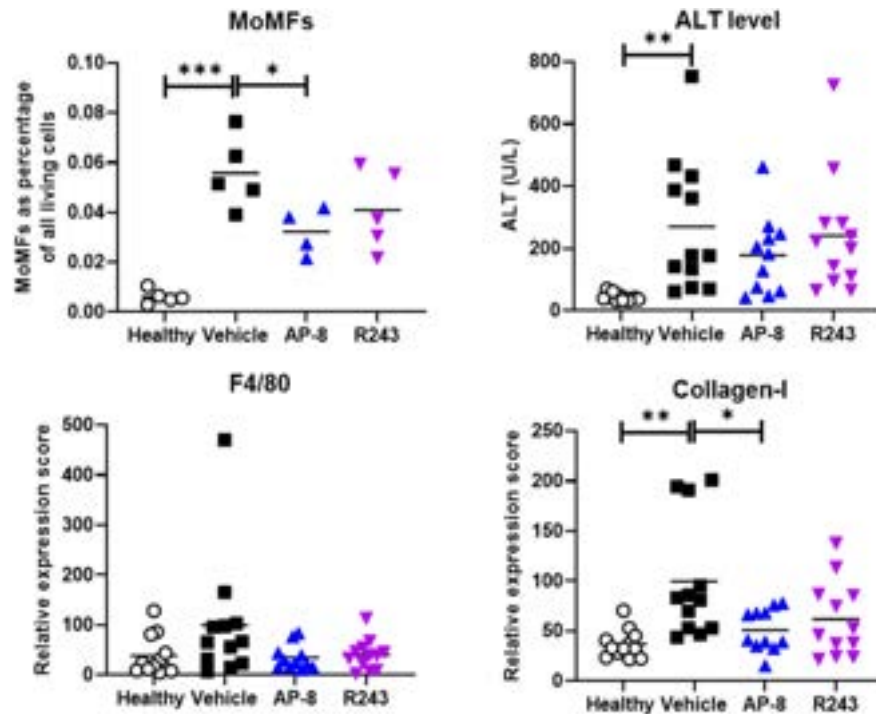


Figure: (abstract: FRI-394).

FRI-397

SRT-015, best-in-class apoptosis signal-regulating kinase 1 inhibitor, demonstrates preclinical efficacy in acute models of liver injury

Kathleen Elias¹, S. David Brown¹, Daniel Burge¹, Neil D. McDonnell¹, Artur Plonowski¹. ¹Seal Rock Therapeutics, United States
Email: kelias@sealrocktx.com

Background and aims: SRT-015, a best-in-class apoptosis signal-regulating kinase 1 (ASK1) inhibitor, has demonstrated preclinical efficacy in a chronic therapeutic DIO-NASH mouse model with biopsy verified steatosis and fibrosis. In vitro studies have demonstrated dose-dependent direct anti-apoptotic, anti-inflammatory and anti-fibrotic effects with SRT-015 treatment. Clinical safety was demonstrated and human pharmacokinetic profile was established in Phase 1 trials with SRT-015. Here we evaluate the efficacy of SRT-015 in two acute preclinical models of liver injury for alcoholic hepatitis (AH) and acetaminophen (APAP) overdose.

Method: C57BL/6 male mice were used for both models. In the acute AH model, pyrazole induces high cyp2E1 levels emulating the effect of alcohol and LPS administration the gut bacterial toxins. Cyp2E1 was induced by two consecutive days of pyrazole administration (150 mg/kg, i.p.). On day 3 LPS (4 mg/kg i.p.), vehicle or SRT-015 (1, 3, 10 mg/kg, BID p.o.) was administered (n = 6–9/group). Plasma ALT was measured 24 hr. post LPS treatment. APAP overdose was induced (300 mg, i.p.) and 1 hr. later SRT-015 (0.3–10 mg/kg, p.o.) or vehicle administered. Six hours after APAP treatment plasma ALT was determined and liver analyzed for mitogen-activated protein kinases (MAPK) including ASK1, p38 and JNK by Western blots.

Results: In the AH model, serum ALT level was increased significantly (p < 0.05; 6-fold) in pyrazole plus LPS group compared to vehicle control at 24 hr. SRT-015 dose-dependently decreased ALT (marker of liver injury) elevated by pyrazole plus LPS treatment in the AH model. SRT-015 treatment at 1, 3 and 10 mg/kg decreased ALT levels 63%, 71% and 80% respectively compared to pyrazole plus LPS alone. APAP treatment significantly increased ALT over 30-fold and SRT-015 treatment dose-dependently decreased ALT with 1, 3, and 10 mg/kg

treatments restoring ALT to control levels. Western blots demonstrated activation of phospho-JNK, phospho-ASK1 and phospho-p38 after APAP administration and all phospho-MAPKs were inhibited with SRT-015 treatment in a dose-dependent manner.

Conclusion: SRT-015 treatment significantly, and dose-dependently, decreased the liver injury marker ALT in two models of acute hepatotoxicity. These data support the advancement of SRT-015 to chronic AH models and suggest that SRT-015 is a promising therapeutic for both APAP overdose and AH.

FRI-398

Microbiome and metabolome analysis outlines circulatory predictors of poor outcomes in ALF

Jaswinder Maras¹, Sushmita Pandey¹, Neha Sharma¹, Nupur Sharma¹, Gaurav Tripathi¹, Babu Mathew¹, Manisha Yadav¹, Vasundhara Bindal¹, Sadam H Bhat¹, Rakhi Maiwall². ¹Institute of Liver and Biliary Sciences, Molecular and cellular medicine, New Delhi, India; ²Institute of Liver and Biliary Sciences, Department of Hepatology, New Delhi, India
Email: jassi2param@gmail.com

Background and aims: Acute liver failure (ALF) is severe hepatic dysfunction associated with early mortality. Exact mechanisms associated to severity and early mortality in ALF are obscure, but are thought to be driven by microbial and metabolic factors.

Method: Baseline plasma samples of 40 ALF patients and 5 healthy controls were subjected for albumin depletion followed by metabolome and meta-proteome (microbiome) analysis (labelled as training cohort). The results were validated on test cohort; plasma and paired one drop blood; in a 160 ALF patients using machine learning (ML). Albumin was depleted to enrich low abundant microbial peptide and metabolites. Circulating predictor of non-survival was identified and correlated with clinical parameters and outcome of ALF patients.

Results: Metabolomic profile of ALF-Non-Survival was distinct and showed significantly alteration in bile acid, sphingolipid, tryptophan metabolism, tyrosine metabolism and others already linked to inflammation, cell death, nutrient absorption, and response to stresses (p < 0.05). ALF-Non-Survival plasma showed significant increase in the bacterial diversity as shown by the Alpha and Beta

POSTER PRESENTATIONS

diversity indices ($p < 0.05$). ALF-Non-Survival were majorly linked to the phylum Proteobacteria, Firmicutes, Actinobacteria and others ($p < 0.05$) which documented significant increase in the bacterial functionality linked to energy, amino acids, xenobiotic metabolism and, others as compared to other groups ($p < 0.05$). Interestingly the increase in the bacterial taxa and functionality correlated with the metabolites Chenodeoxycholic acid, 4-(2-Aminophenyl)-2,4-dioxobutanoate and L-Tyrosine and others in ALF-NS ($R^2 < 0.7$). Multiomics signature-based probability of detection (POD) for non-survival in ALF was greater than 80% and correlated with clinical parameters ($R^2 > 0.85$). POD metabolites (AUC = 0.98) directly associated with early mortality ($p < 0.05$). Specific increase in L-Tyrosine, 4-(2-Aminophenyl)-2, 4-dioxobutanoate (linked to cell death and inflammation), Carnosine (linked to negative oxidative stress effect), Chenodeoxycholic acid (linked to bile acid synthesis), and alanyl-tyrosine (linked to removal of tyrosine) validated in different cohort five machine learning algorithms showed >98% accuracy/sensitivity/specificity for early mortality prediction.

Conclusion: Our findings demonstrated that changes in the plasma microbiome correlates to metabolome in ALF patients. Baseline increase in plasma metabolite signature could be offered as universal utility to serve as biomarker for ALF patients predisposed to early mortality.

FRI-399

Neddylaton inhibition recovers drug-induced liver injury through the stabilization of Tamm41

Claudia Gil-Pitarch¹, Marina Serrano-Macia¹, Jorge Simón Espinosa¹, Rubén Rodríguez Agudo¹, Sofia Lachiondo-Ortega¹, Maria Mercado-Gómez¹, Irene González-Recio¹, Naroa Goikoetxea¹, Teresa Cardoso Delgado¹, Luis Alfonso Martínez-Cruz¹, Ruben Nogueiras², Paula Iruzubieta³, Javier Crespo³, Steven Masson^{4,5}, Misti McCain⁵, Helen Louise Reeves^{4,5}, María Luz Martínez-Chantar¹, ¹CIC bioGUNE, Liver disease lab, DERIO, Spain; ²Department of Physiology, School of Medicine-Instituto de Investigaciones Sanitarias, University of Santiago de Compostela, Spain; ³Gastroenterology and Hepatology Department, Marqués de Valdecilla University Hospital, Clinical and Translational Digestive Research Group, IDIVAL, Spain; ⁴The Liver Unit, Newcastle-upon-Tyne Hospitals NHS Foundation Trust, Newcastle upon Tyne NE7 7DN, United Kingdom; ⁵Newcastle University Translational and Clinical Research Institute, The Medical School, Newcastle University, Newcastle upon Tyne, NE2 4HH, United Kingdom
Email: mlmartinez@cicbiogune.es

Background and aims: In Western countries, acute liver failure is a serious disorder, being the majority cases caused by drug-induced liver injury (DILI), commonly associated to acetaminophen (APAP) overdose. DILI does not have an effective late stage treatment. Neddylaton is an ubiquitin-like post-translational modification, usually associated to protein stabilization. It is upregulated in several liver diseases. The accumulation of Cullin-Ring E3 ligase (CRL) substrates induce cell-cycle arrest, senescence and apoptosis, thus, its proteolytic degradation is needed and occurs with posttranslational neddylaton of CRL impulsive by Nedd8-activating enzyme (NAE). MLN4924 is an anticancer small molecule, which is currently in phase I trials. MLN4924 inhibits NAE, therefore, blocks cullin neddylaton allowing CRL substrates accumulation and triggering cell-cycle arrest, senescence and apoptosis in cancer cells. Studying neddylaton role in DILI offers an attracting approach to improve DILI treatment. Tamm41 catalyzes the formation of CDP-diacylglycerol (CDP-DAG) which is central in phospholipid biosynthesis pathways in cells. Those are branched into several pathways, one of which chiefs to the synthesis of Cardiolipin (CL). CL is an

essential lipid for the activity of key mitochondrial enzymes that are involved in the cellular energy metabolism. Tamm41 has been identified when inhibiting neddylaton, thus, it is accurate to elucidate the relation Tamm41 might have with the neddylaton pathway, and, as a consequence, with a possible treatment for DILI.

Method: Nedd8 was measured immunohistochemically and in serum by ELISA assay in clinical DILI samples. The effects of APAP overdose and its treatment with the neddylaton inhibitor MLN4924 were evaluated in isolated mouse hepatocytes and pre-clinical three months mice models C57BL/6 and two BirA transgenic mice models, ^{Bio}NEDD8, and ^{Bio}UB. Serum and liver samples were cryopreserved, and part of the liver tissue was embedded in paraffin for histological procedures. Neddylaton was inhibited to study its implication in cell death, mitochondrial dynamics and respiration, redox balance, endoplasmic reticulum stress, proteome homeostasis and metabolic pathways. Tamm41 was silenced to study its effect and relation along with neddylaton pathway.

Results: Neddylaton was induced in DILI. Its inhibition reduced cell death and inflammation and promoted regeneration mitochondrial activity. The proteomic analysis of ^{Bio}NEDD8, and ^{Bio}UB transgenic mice liver reflected the stabilization of Tamm41. Tamm41 silencing resulted in the abolition of the positive effects caused by neddylaton inhibition.

Conclusion: Neddylaton was upregulated in DILI causing cell damage. Inhibiting neddylaton in DILI, returning it at the normal basal activity, restored the correct functioning of the cell by the stabilization of Tamm41.

FRI-400

Forward programming to produce hepatocytes organoids for cell based therapy

Fabian Bachinger¹, Ludovic Vallier². ¹Cambridge, Department of Hematology, Cambridge, United Kingdom; ²Berlin Institute of Health, BIH Centre for Regenerative Therapies, Berlin, Germany
Email: fb520@cam.ac.uk

Background and aims: Organ transplantation remains the only treatment for end stage liver diseases. Alternative therapies like hepatocyte cell transplantation have been developed in the recent years. However, availability and quality of primary hepatocytes represents a major limitation. Human induced pluripotent stem cells (hiPSCs) could provide an alternative source for the production of large quantity of hepatocytes in vitro. However current differentiation protocols are lengthy, complex, technically challenging and produce cells with foetal-like characteristics. The goal of this project is to create a rapid and robust approach to create high quality and large quantity of hepatocytes organoid with increased functional characteristics when compared to cells derived using directed differentiation in 2D.

Method: Here, we take advantage of Forward Programming (FoP), an approach relying on the overexpression of cell specific transcription factors, to generate hepatocytes for cell-based therapy. Factors to drive differentiation of hiPSCs to hepatocytes were identified by comparing primary cells with in vitro generate hepatocytes. The Opti-OX system was then used in hiPSCs to stably overexpress these transcription factors. Forward programming was further increased by optimising 3D culture conditions in suspension such as seeding density and media composition. Functionality was evaluated by direct comparison with directed differentiation derived and primary hepatocytes. Assays include CYP3A4 enzyme activity, qPCR, Immunofluorescence staining and flow cytometry for hepatocyte specific markers.

Results: Hepatocytes generated using FoP (FoP-Heps) display CYP3A4 activity 10-fold higher than cells generated using directed differentiation. Thus, FoP-Heps have detoxification property close to primary cells. Alb secretion and Urea cycle activity were also very similar between in vitro produced and freshly plated hepatocytes. qPCR analyses confirm expression of hepatocyte markers including

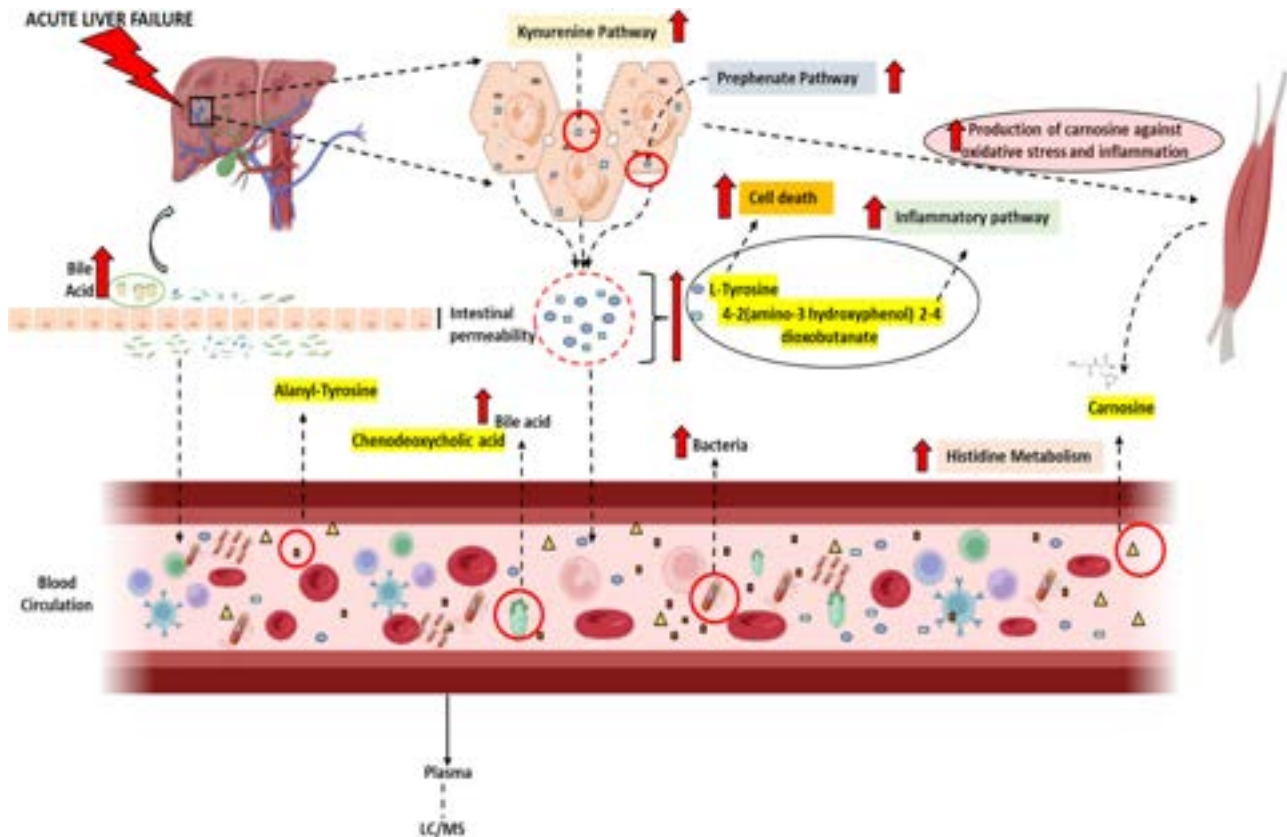


Figure: (abstract: FRI-398): Showing the baseline effect on metabolic pathway in acute liver failure patients.

Albumin, A1AT, PCK1, HNF4A and hFVII at values comparable to primary hepatocytes. Flow cytometry showed expression near homogenous expression of Albumin (90%), A1AT (99.8%) and ASGR1 (85%). Finally, FoP is a 2-step process taking 20 days compared to 30 days for directed differentiation while allowing the production of 10 hepatocytes from 1 hPSC.

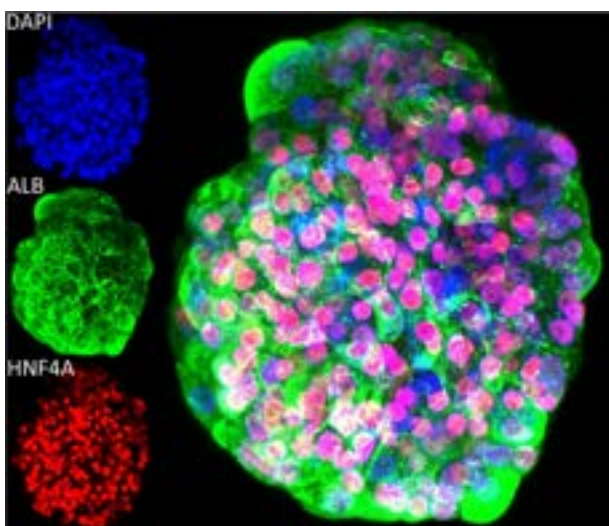


Figure 1: Hepatocytes derived in 3D suspension culture.

Conclusion: Forward Programming in 3D can be used to produce hepatocytes more rapidly and robustly than directed differentiation. In addition, FoP-Heps share key characteristics with their primary counterpart. Finally, this approach is compatible with GMP and large-scale production necessary for future cell-based therapies in the context of liver diseases.

FRI-401

Stress-driven suppression of the hippo pathway accelerates liver injury

Na Young Lee¹, Ari Kwon¹, Jae-Hyun Yu¹, Myeung Gi Choi¹, Ja Hyun Koo¹. ¹Seoul National University, Korea, Rep. of South
Email: jhkoo@snu.ac.kr

Background and aims: The Hippo pathway signals actively represses Yes-associated protein (YAP) and its homolog transcriptional coactivator with PDZ-binding motif (TAZ) to suppress overgrowth of organs and maintain homeostasis. Upon activation, YAP/TAZ translocate into the nucleus and bind to TEAD transcription factors to promote transcriptional programs for proliferation or mitochondrial quality control.

Method: YAP/TAZ activity was analyzed in hepatocytes from patients with cirrhosis using single-cell transcriptomic data. The impact on Hippo pathway regulation following hepatocyte stress was analyzed using RNA sequencing. Phos-tag immunoblotting, immunocytochemistry, and qRT-PCR were used to assess YAP activity. CRISPR-mediated knockout or knock-in cells were used for mechanistic studies. Mice with hepatocyte-specific disruption of Yap and Taz were used to examine their role in hepatocyte death upon damage.

Results: Here, we report that liver damage activates YAP/TAZ in hepatocytes that in turn contributes to promoting hepatitis. Hepatocyte stress suppressed phosphorylation of YAP, increased nuclear translocation and target gene expression of YAP/TAZ. In

POSTER PRESENTATIONS

addition, global changes in the transcriptome by cellular stress was significantly reversed by YAP/TAZ knockout. Mechanistically, the regulation was occurred through both Hippo-dependent and Hippo-independent pathway, largely requiring a phosphatase activity. Furthermore, hepatic deletion of YAP/TAZ in vivo suppressed liver injury and steatohepatitis progression.

Conclusion: These reveal a pathological role of YAP/TAZ in promoting steatohepatitis progression, which provides an insight into therapeutic intervention of the disease.

FRI-402

Dysregulated lipolysis increases intrahepatic concentrations of non-esterified fatty acids in chemotherapy-associated steatohepatitis

Martina Derler¹, Eva Waich², Elisabeth Ableitner², Julia Sturm², Patrick Starlinger³, Anton Stift³, Alice Assinger⁴, Marion Mussbacher².
¹Institute of Pharmaceutical Sciences, University of Graz, Department of Pharmacology and Toxicology, Graz, Austria; ²Institute of Pharmaceutical Sciences, University of Graz, Graz, Austria; ³Department of General Surgery, Division of Visceral Surgery, Medical University of Vienna, Vienna, Austria; ⁴Institute of Vascular Biology and Thrombosis Research, Medical University Vienna, Vienna, Austria
Email: martina.derler@uni-graz.at

Background and aims: Up to 50% of colorectal carcinoma patients receiving the chemotherapeutic drug irinotecan develop chemotherapy-associated steatohepatitis (CASH). Typical CASH symptoms include intrahepatic accumulation of lipids and hepatic inflammation. CASH impairs liver regeneration after surgical resection of hepatic metastasis and thereby drastically increases mortality. The biochemical mechanisms leading to CASH are still unknown, and treatment options are lacking. This project aims to investigate the effect of irinotecan on hepatocyte lipid metabolism.

Method: The murine hepatocyte cell line AML-12 was treated with increasing doses of irinotecan (10–60 μ M), and extra- and intracellular concentrations of non-esterified fatty acids (NEFA) were quantified. Additionally, the expression of enzymes involved in fatty acid oxidation, *de novo* lipogenesis, and lipolysis was analyzed on mRNA- and protein levels by quantitative PCR and western blotting, respectively. The content of adenosine triphosphate was investigated using high-performance liquid chromatography, and oxidative stress levels were determined by flow cytometry. For mechanistic experiments, AML-12 cells were treated with irinotecan in the presence and absence of 200 μ M oleic acid, the lipase inhibitor Atglistatin (40 μ M), and under serum-free conditions.

Results: Irinotecan treatment of AML-12 cells led to a significant accumulation of intracellular non-esterified fatty acids, whereas triglyceride and cholesterol levels remained unchanged. Protein expression of adipocyte triglyceride lipase (ATGL), which catalyzes the rate-limiting step of intracellular lipolysis, increased with rising doses of irinotecan by 7-fold. However, key proteins of *de novo* lipogenesis were reduced in irinotecan-treated AML-12 cells. Intracellular levels of adenosine triphosphate and mRNA of enzymes catalyzing fatty acid oxidation were significantly decreased upon irinotecan treatment. This was associated with elevated levels of oxidative stress and increased expression of the oxidative stress marker haemoxygenase-1. Despite increased oxidative stress and NEFA levels, mRNA levels of the peroxisomal biogenesis factor 2 (Pex2) were significantly decreased.

Conclusion: Irinotecan leads to a dysregulation of ATGL-mediated lipolysis, which results in a massive intracellular accumulation of NEFA. These metabolic changes might contribute to hepatocyte lipotoxicity and foster the pathogenesis of CASH.

FRI-403

Control compounds used to validate in vitro models of idiosyncratic drug-induced liver injury: a systematic review

Antonio Segovia-Zafra^{1,2}, Marina Villanueva¹, Ana Serras³, Gonzalo Matilla¹, Ana Bodoque-García¹, Daniel E. Di Zeo-Sánchez¹, Hao Niu¹, Ismael Alvarez-Alvarez¹, Sergej Godec⁴, Irina Milisav⁵, José Fernandez-Checa^{6,7}, Maria Isabel Lucena^{1,2}, Francisco Javier Cubero^{2,8,9}, Joana Miranda³, Leonard J Nelson¹⁰, Raul J. Andrade^{1,2}.
¹Servicios de Aparato Digestivo y Farmacología Clínica, Hospital Universitario Virgen de la Victoria, Instituto de Investigación Biomédica de Málaga y Plataforma en Nanomedicina-IBIMA Plataforma BIONAND, Universidad de Málaga, Málaga, Spain; ²Biomedical Research Network Center for Hepatic and Digestive Diseases (CIBERehd), Carlos III Health Institute, Madrid, Spain; ³Research Institute for Medicines (iMed.Ulisboa), Faculty of Pharmacy, Universidade de Lisboa, Lisbon, Portugal; ⁴Clinical Department of Anaesthesiology and Intensive Therapy, University Medical Center, Ljubljana, Slovenia; ⁵University of Ljubljana, Faculty of Health Sciences, University of Ljubljana, Ljubljana, Slovenia; ⁶Cell Death and Proliferation, Instituto de Investigaciones Biomédicas de Barcelona, CSIC, Barcelona, Spain; ⁷Liver Unit, Hospital Clínic I Provincial, IDIBAPS, Barcelona, Spain; ⁸University of Southern California Research Center for Liver Diseases, Keck School of Medicine, USC, Los Angeles, CA, USA, United States; ⁹Department of Immunology, Ophthalmology and ENT, Complutense University School of Medicine, Madrid, Spain; ¹⁰Instituto de Investigación Sanitaria Gregorio Marañón (IiSGM), Madrid, Spain; ¹⁰Institute for Bioengineering, The University of Edinburgh (UK), United Kingdom
Email: andrade@uma.es

Background and aims: Idiosyncratic Drug-Induced Liver Injury (DILI) encompasses the unpredictable damage that drugs, herbs, and dietary supplements may cause to the liver. When studying the prediction of DILI at preclinical stages, the choice of a validated system is decisive. The present study seeks to provide a list of both DILI positive and negative control compounds. This list arises from a systematic analysis of the existing literature, supported by clinical evidence collected in both national and international DILI registries and endorsed by a committee of experts from the ProEuroDILI Network (COST Action 17112).

Method: This systematic review was conducted following the Preferred Reporting Items for Systematic Reviews and Meta-Analyses (PRISMA) 2020 guidelines. Eligible literature published to June 1st, 2022 was identified through a search in PubMed, Embase, Web of Science, and Scopus. Only peer-reviewed original articles focused on studying the onset of DILI by using preclinical *in vitro* human models were included. The reliability of the studies was assessed using a modified version of the software-based “Toxicological data Reliability Assessment Tool” (ToxRTool). Drugs most commonly used as DILI-positive and negative controls in the literature were selected for in-depth analysis.

Results: The search strategy retrieved 2936 studies from the above-mentioned databases. After screening, 2885 studies were excluded, as they were duplicates or did not meet the inclusion criteria. 51 articles were finally included. Most studies were categorized as reliable without restrictions (58.6%). The mean number of drugs tested was 55 DILI-positive and 30 DILI-negative compounds. Diclofenac was the drug most used as DILI-positive control (88%), followed by troglitazone (80%) and flutamide (71%). Regarding DILI-negative controls, buspirone (49%), dexamethasone (41%), and diphenhydramine (35%) were the most tested compounds. Acetylsalicylic acid, fluoxetine, or warfarin were widely used as DILI-negative controls (33%, 25%, and 22%, respectively), but also as DILI-positive compounds (22%, 20%, and 16%). Moreover, up to 19% of the drugs used as DILI-negative controls had clinical hepatotoxicity cases reported within different DILI registries. The drug concentrations used varied remarkably. Although 49% of studies chose the drug concentrations based on the C_{max} values, the C_{max} assumed for the

same drug in different studies diverged. Most studies assessed drug effects in the short term (≤ 72 h; 71%). Cytotoxicity was the end point most evaluated (82%). Nevertheless, several studies included the assessment of functional parameters, such as biotransformation activity (20%), albumin (20%), or urea secretion (12%). A few studies included mechanistic end points such as cholestasis (24%) or mitochondrial damage (22%).

	COMPOUND	N° articles using it	
		as DILI positive (%)	as DILI negative (%)
COMPOUNDS MOST USED AS DILI POSITIVE CONTROLS	Diclofenac	45 (88.2%)	0 (0%)
	Troglitazone	41 (80.4%)	0 (0%)
	Flutamide	36 (70.6%)	0 (0%)
	Amiodarone	35 (68.6%)	0 (0%)
	Acetaminophen (APAP)/Paracetamol	33 (64.7%)	0 (0%)
	Ketocconazole	33 (64.7%)	0 (0%)
	Nefazodone	29 (56.9%)	0 (0%)
	Tamoxifen	29 (56.9%)	0 (0%)
	Chlorpromazine	27 (52.9%)	1 (1.9%)
	Isoniazid	27 (52.9%)	1 (1.9%)
COMPOUNDS MOST USED AS DILI NEGATIVE CONTROLS	Buspirone	3 (5.9%)	25 (49%)
	Dexamethasone	0 (0%)	21 (41.2%)
	Diphenhydramine	0 (0%)	18 (35.3%)
	Acetylsalicylic acid/Aspirin	11 (21.6%)	17 (33.3%)
	Isoproterenol	0 (0%)	17 (33.3%)
	Caffeine	0 (0%)	15 (29.4%)
	Propranolol	5 (9.6%)	15 (29.4%)
	Flumazenil	0 (0%)	14 (27.5%)
	Primidone	0 (0%)	14 (27.5%)
	Streptomycin	0 (0%)	14 (27.5%)

Figure:

Conclusion: This systematic study has shown a lack of consensus in terms of in vitro DILI modelling. Since no single system serves as a universal test for the multifactorial process of DILI, a portfolio of robust and well-characterized predictive platforms with a well-defined purpose is required. Moreover, there is a need for consensus about the reference drugs to be used for the DILI assay validations, including recommendations about the concentrations to test and criteria for interpreting the data. Funding: P119/00883, PEMP-2020-0127, PI21/01248, P18-RT-3364, PI-0310-2018, ISCIII CIBERehd, POSTDOC_21_00780, CD20/00083, CD2100198.

FRI-404

A systems medicine approach for the identification of potential prognostic biomarkers in patients with acute decompensation of cirrhosis

Estefania Huergo Iglesias¹, Sara Palomino¹, Ana Rosa López-Pérez¹, Núria Planell², Vincenzo Lagani³, Ferran Aguilar⁴, Patricia Sierra⁴, Paolo Caraceni⁵, Alberto Q. Farias⁶, Jonel Trebicka^{4,7}, Joan Clària^{4,8,9}, Pierre-Emmanuel Rautou¹⁰, David Gomez-Cabrero¹. ¹Navarrabiomed, Group of Translational Bioinformatic, Pamplona, Spain; ²CIMA Navarra University, Computational Biology, Spain; ³Ilia State University, Institute of Chemical Biology, Georgia; ⁴European Foundation for the Study of Chronic Liver Failure, Spain; ⁵University of Bologna, Department of Medical and Surgical Science, Italy; ⁶University of Sao Paulo School of Medicine, Department of Gastroenterology, Brazil; ⁷University of Münster, Department of internal medicine, Germany; ⁸Hospital Clínic-IDIBAPS, Biochemistry and Molecular Sciences, Spain; ⁹Universitat de Barcelona, Department of Biomedical Sciences, Spain; ¹⁰Université Paris-Cité, Inserm, Centre de recherche sur l'inflammation, France
Email: estefania.huergo.iglesias@navarra.es

Background and aims: Patients with acute decompensation (AD) of cirrhosis have a high short-term mortality due to a lack of a complete understanding of the pathophysiology of the disease and the wide heterogeneity of patients. Hence, it is necessary to better understand

the disease at a systems level. Therefore, the aim of this work was to understand at systems level the pathophysiology of AD cirrhosis by using a systems approach to integrate multi-omic profiling with clinical data.

Method: Clinical and omics data from three well-characterized cohorts of patients with AD cirrhosis -CANONIC (572 patients), PREDICT (766 patients) and ACLARA (580 patients)- were used to perform a multi-omic analysis applying a systems medicine framework to characterize AD (Figure), as part of the H2020 funded project DECISION. A multi-state survival analysis was performed using bootstrapping and permutation test to estimate confidence intervals and permuted p values for each feature. Non-Parametric Combination (NPC) analysis was conducted using custom gene-gene and gene-CpG maps (among others) and the STAtegRA R package. Network analysis was conducted using custom methods, FEM and Cytoscape available tools. MXM R package was used to identify subsets of variables with maximal predictive power.

Results: We conducted the five-step analysis described in the Method section in the PREDICT cohort. In the first step, we explored the coordination between omics, observing a low coordination in general, but metabolites and RNA-Seq as specific candidates. Secondly, we conducted an uni-omic analysis for each feature of each omic, that allowed us to identify, among thousands of features, statistically robust candidate biomarkers. However, we identified limited features of interest, so that we required to leverage over the multi-omic profiling of each individual. To this end, as a third step, we used an NPC analysis, so the number of features identified was increased. As a result, we gathered enough statistical power to conduct the fourth step: a network analysis. From this analysis, we identified systems-based feature combinations that are associated with ACLF, mortality and/or liver transplant. As a final step, using the identified features, we generated predictive models for prognosis in AD patients, which are being validated in the two additional cohorts, CANONIC and ACLARA.

Conclusion: Our study shows that, while AD patients are very heterogeneous explaining why classical statistical analysis are very limited in power, the use of multi-omic approaches can overcome partly such limitation. We observed that making use of feature-feature connections, systems medicine allows for increased power in the identification of disease mechanisms, but even more important, may allow for candidate biomarkers discovery.

This project has received funding from the European Union's Horizon 2020 research and innovation programme under grant agreement No 847949. This reflects only the author's view and the Commission is not responsible for any use that may be made of the information it contains.

FRI-405

Kelch-like ECH-associated protein-1 deletion rescues cell death associated with glutathione-glutathione peroxidase 4 knockdown in hepatocytes in acute models of liver injury

Julia Grube¹, Leticia Colyn¹, Chaochao Wang¹, Christian Trautwein¹. ¹University Hospital RWTH, Internal Medicine III, Aachen, Germany
Email: ctrautwein@ukaachen.de

Background and aims: Recently, acute liver injury (ALI) has been described to be mediated by ferroptosis in mice models. Ferroptosis is a type of cell death initiated by iron accumulation, reactive oxygen species (ROS) generation, and subsequent lipid peroxidation leading to membrane damage and cell death. The Kelch-like ECH-associated protein-1 (KEAP1)/erythroid 2-related factor 2 (NRF2) axis is of major relevance for ferroptosis, modulating the expression of genes associated with iron metabolism and inducing the cellular response to ROS through the activation of enzymes such as glutathione peroxidases (GPXs). Among them, GPX4 plays a crucial role in ferroptosis, as its inactivation leads to lipid peroxidation. Here, we sought to define the effect of NRF2 activation during acute liver injury in a model of ferroptosis.

POSTER PRESENTATIONS

Method: We generated a genetic model of ferroptosis by hepatocyte-specific deletion of GPX4 (GPX4^{deltahepa}). To study the activation of the NRF2 axis, we crossed GPX4^{deltahepa} mice with mice in which KEAP1 was specifically deleted in hepatocytes (KEAP1^{deltahepa}), generating GPX4^{deltahepa}/KEAP1^{deltahepa} mice. We performed acute models of liver injury–CCl₄ injection and bile duct ligation (BDL) for 48 hours.

Results: Hepatocyte-specific deletion of GPX4 results in increased liver injury associated with elevated serum transaminase levels and increased macrophage recruitment. Interestingly, histological analysis of GPX4^{deltahepa} livers showed no evidence of ferroptosis as indicated by immunohistochemical staining for 4-hydroxynonenal. They also showed no evidence of necroptosis or pyroptosis, but we found a strong increase in apoptosis. Deletion of KEAP1 in hepatocytes leads to activation of the NRF2 pathway, as confirmed by its upregulation and activation of target genes. In CCl₄-challenged GPX4^{deltahepa}/KEAP1^{deltahepa} mice, the damage observed in GPX4^{deltahepa} mice is reversed, as evidenced by serum transaminase levels and liver histology. KEAP1 deletion markedly inhibits apoptosis-mediated cell death as indicated by TUNEL assay, cleaved caspase-3 staining, and gamma-H2AX protein levels. We also observed an upregulation of the anti-apoptotic protein BCL2 in GPX4^{deltahepa}/KEAP1^{deltahepa} livers.

Conclusion: Our results indicate that in the GPX4^{deltahepa} mice challenged with CCl₄ injection and bile duct ligation for 48 hours, there is no evidence of ferroptosis, although we observed extensive tissue damage associated with increased apoptosis. Activation of the NRF2 pathway by deletion of KEAP1 rescues acute liver injury. This effect may be mediated by the upregulation of the anti-apoptotic protein BCL2.

FRI-406

Altered intestinal permeability in patients with drug-induced liver injury and other forms of acute liver injury: a sequential analysis of serum levels of LBP, CD14 and CD163

Daniel E. Di Zeo-Sánchez^{1,2}, Marina Villanueva¹, Alejandro Cueto-Sánchez¹, Jose Pinazo Bandera¹, Miren Garcia Cortes¹, Enrique del Campo Herrera¹, Ana Bodoque-García¹, Gonzalo Matilla¹, M Robles-Díaz^{1,2}, María Isabel Lucena^{1,2}, Raul J. Andrade^{1,2}, Camilla Stephens^{1,2}. ¹UGC Aparato Digestivo, Servicio de Farmacología Clínica, Instituto de Investigación Biomédica de Málaga-IBIMA, Hospital Universitario Virgen de la Victoria, Universidad de Málaga, Málaga, Spain, Spain; ²Centro de investigación en red en el área temática de enfermedades hepáticas y digestivas (CIBERehd), Madrid, Spain
Email: danieldzeo9@hotmail.com

Background and aims: The disruption of the intestinal barrier might be a major contributor to the pathogenesis of various liver disorders, including drug-induced liver injury (DILI), through impairment of hepatic immunotolerance. It has been speculated that pathogen-associated molecular patterns (PAMPs) may reach the liver as a consequence of an increase in intestinal permeability caused by alterations in the intestinal microbiota. Consequently, innate immune cells would initiate an inflammatory response that can be lethal to hepatocytes or trigger an adaptive immune response. LBP (lipopolysaccharide binding protein), CD14 and CD163 have been linked to intestinal permeability, as they play a key role in the innate immune response to bacterial endotoxins (e.g., LPS), by binding to them or by exerting an immunomodulatory role. Our aim was to conduct an exploratory study to assess the intestinal permeability status of DILI patients by quantification of LBP, CD14 and CD163 proteins in serum.

Method: Peripheral blood serum was collected from 8 healthy volunteers, 8 DILI patients and 8 patients with acute liver injury (ALI) other than DILI and stored at –80°C until analysis. The drugs responsible for toxic liver injury were antibiotics, antitumor drugs, dietary supplements and statins; whilst ALI cases were mostly viral hepatitis. Patients were followed from the detection of the acute episode (visit 1) until >30 days after detection (visit 3). Serum levels of LBP, CD14 and CD163 were measured by Luminex (RandD Systems) and results were statistically analyzed using Kruskal-Wallis, Dunn and Friedman tests.

Results: The concentration (mean ± standard deviation) of LBP, CD14 and CD163 proteins was >300-fold higher in DILI (LBP: $1.14 \times 10^7 \pm 4.3 \times 10^6$; CD14: $1.98 \times 10^6 \pm 5.8 \times 10^5$ and CD163: $2.8 \times 10^6 \pm 1.1 \times 10^6$ pg/ml) and ALI (LBP: $1.15 \times 10^7 \pm 5.1 \times 10^6$; CD14: $1.96 \times 10^6 \pm 6.8 \times 10^5$ and CD163: $3.2 \times 10^6 \pm 1.1 \times 10^6$ pg/ml) compared to healthy controls (LBP: $3.8 \times 10^4 \pm 9790$; CD14: 6369 ± 950 and CD163: 6273 ± 125 pg/ml) at visit 1 ($p < 0.001$). The levels of these proteins decreased significantly at visit 3, although they remained elevated compared to controls ($p < 0.05$). No significant differences were detected between DILI and ALI.

Conclusion: The elevated concentration of LBP and CD14 proteins detected in DILI patients could be indicative of increased translocation of bacterial products due to an altered intestinal permeability. This theory is further supported by the elevated levels of CD163 protein, which has been considered a marker of macrophage activation, associated with intestinal permeability and dysbiosis. Funding: CIBERehd-ISCiii, FEDER PI18/00901, PI19/00883, PI21/01248, UMA18-FEDERJA-193, PY18-3364, PEMP-0127-2020.

Systems medicine framework

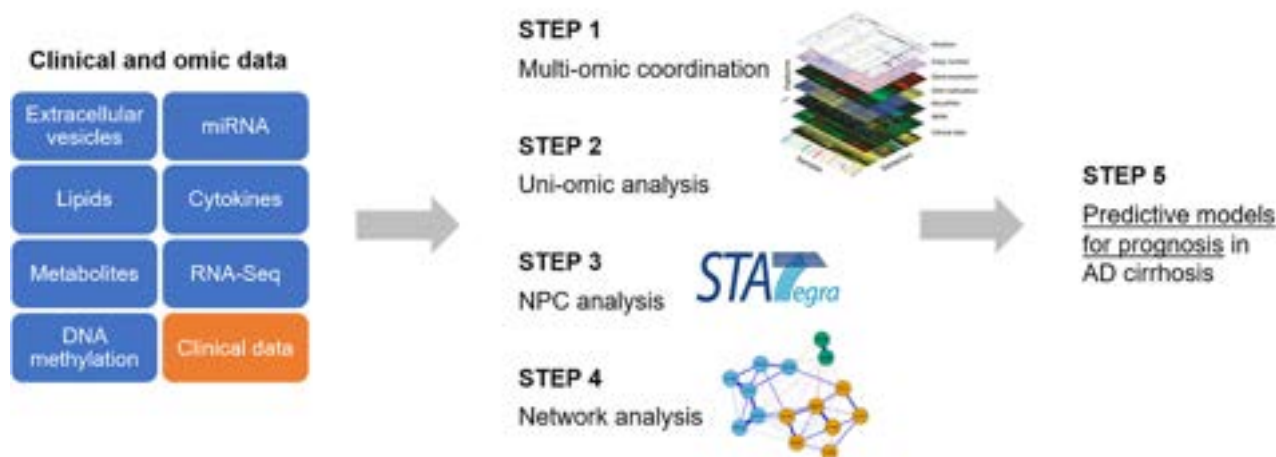


Figure: (abstract: FRI-404).

Alcohol-related liver disease

WEDNESDAY 21 TO SATURDAY 24 JUNE

TOP-073

AKR1B10 as a novel molecular driver of alcohol-associated hepatitis

Maria Hernandez-Tejero^{1,2,3,4}, Ana Clemente^{1,5}, Luma Melo¹, Samhita Ravi¹, Josep Maria Argemi⁶, Stephen Atkinson⁷, Juan Pablo Arab^{8,9}, Daniel Cabrera⁹, Paula Rivera⁹, Luis Antonio Diaz⁹, Francisco Idalsoaga⁹, Sheng Cao², Vijay Shah², Jaideep Behari^{1,10}, Gavin Arteel^{1,10}, Ramon Bataller^{1,11}. ¹Center for Liver Diseases, Division of Gastroenterology, Hepatology and Nutrition, University of Pittsburgh Medical Center, Pittsburgh, PA, USA, United States; ²Division of Gastroenterology and Hepatology, Mayo Clinic, Rochester, Minnesota, USA, United States; ³Division of Gastroenterology, Department of Medicine, Schulich School of Medicine, Western University and London Health Sciences Centre, London, Ontario, Canada, United States; ⁴Liver Unit, Hospital Clinic, Institut d'Investigacions Biomèdiques August Pi i Sunyer (IDIBAPS), Barcelona, Spain, Spain; ⁵Liver Unit, Digestive Department, Hospital General Universitario Gregorio Marañón, Complutense University of Madrid, CIBERehd, Madrid, Spain, United States; ⁶Internal Medicine Department, Hepatology Unit, Clínica Universidad de Navarra, Spain, Spain; ⁷Department of Metabolism, Digestive disease and Reproduction, Imperial College London, London, UK, United Kingdom; ⁸Division of Gastroenterology, Department of Medicine, Schulich School of Medicine, Western University and London Health Sciences Centre, London, Ontario, Canada, Canada; ⁹Departamento de Gastroenterología, Escuela de Medicina, Pontificia Universidad Católica de Chile, Santiago, Chile, Chile; ¹⁰Pittsburgh Liver Research Center, University of Pittsburgh, PA, USA, United States; ¹¹Liver Unit, Hospital Clinic, Institut d'Investigacions Biomèdiques August Pi i Sunyer (IDIBAPS), Barcelona, Spain, United States
Email: mhdeztejero@hotmail.com

Background and aims: Alcohol-associated hepatitis (AH) is a severe condition that needs novel targeted therapies. We recently showed by integrated multi-OMICS that severe AH is characterized by profound deregulation of glucose metabolism (Massey et al, Gastroenterology 2021). The polyol pathway is an alternative and potential harmful way to metabolize glucose and is governed by AKR1B10 and other aldose reductases. AKR1B10 metabolizes glucose to produce sorbitol that is oxidized by SORD to produce fructose. This study aimed at analyzing whether this pathway is deregulated in AH.

Method: 55 patients with probable and definite diagnosis of AH according to the NIAAA were included. We also included 10 healthy controls and 45 diseased controls (15 alcohol-associated cirrhosis, 15 NASH and 15 chronic hepatitis C). Hepatic gene expression profiling was assessed by DNA microarray. qPCR and RNAseq was performed to confirm results. To assess the expression of ductular reaction genes, microdissection of KT7 positive and negative areas was performed in 6 AH patients. Protein expression was assessed by IHC and western blotting. scRNAseq were performed in 12 patients including healthy controls, AH, PSC, alcohol-associated and NASH cirrhosis.

Results: AKR1B10 was found to be the most upregulated gene in livers with AH (>400-fold). The expression of SORD, another gene of the polyol pathway that metabolizes sorbitol, was downregulated by 2-fold compared to normal livers. AKR1B10 gene expression correlated with AST ($p=0.009$), bilirubin ($p=0.008$), and glucose ($p=0.01$) levels at admission in patients with AH. AKR1B10 expression also correlated with severity of liver disease according to MELD ($p=0.004$), portal hypertension ($p=0.01$), and increased the mortality at 180 days ($p=0.02$). AKR1B10 mRNA expression was increased in DR cells from patients with AH ($p=0.0059$). Density plots stratified by severity showed an inverse correlation between disease severity and the AKR1B10/SORD ratio. In addition, IHC indicates that AKR1B10 overexpression is predominantly in hepatocytes. scRNAseq studies demonstrated that AKR1B10 is expressed in hepatocyte and cholangiocyte cell populations compared. Figure 1.

Conclusion: The polyol pathway is dysregulated in AH and correlated with disease severity. Targeting key genes such as AKR1B10 and SORDs represents a potential novel therapy for AH. Further studies should evaluate the use of aldose reductase inhibitors in models of AH.

TOP-078

Pyroptotic MAITs link microbial translocation with severity of alcohol-related liver disease

Li-Ping Zhang¹, Hui-Fang Wang¹, Xing-Ran Zhai², Chun-Bao Zhou², Jin-Hong Yuan², Ye-Nv Ma², Zeng-Tao Yao², Shuo Huang², Wei-Zhe Li², Yan-Mei Jiao², Fu-Sheng Wang², Zhengsheng Zou³, Ji-Yuan Zhang², Qing-Lei Zeng¹. ¹The First Affiliated Hospital of Zhengzhou University, Department of Infectious Diseases and Hepatology, China; ²The Fifth Medical Center of Chinese PLA General Hospital, Treatment and Research Center for Infectious Diseases, China; ³The Fifth Medical Center of Chinese PLA General Hospital, Department of Liver Disease, Senior Department of Hepatology, China
Email: zengqinglei2009@163.com

Background and aims: Mucosal-associated invariant T cells (MAITs) are markedly reduced in patients with alcohol-related liver disease (ALD); however, the potential mechanism underlying MAITs loss

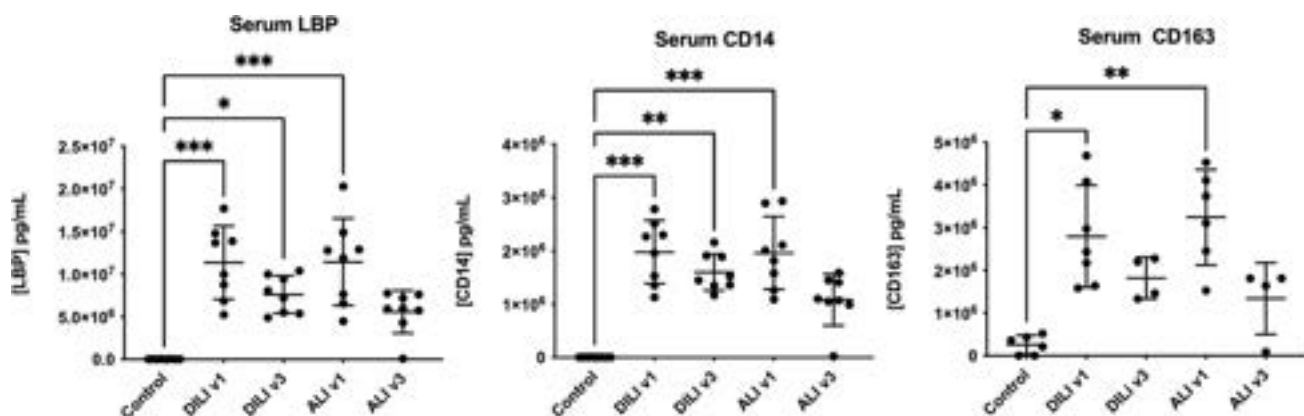


Figure: (abstract: FRI-406).

POSTER PRESENTATIONS

remains elusive. Hence, we aimed to explore what induced MAITs loss and its clinical significance.

Method: The characteristics of pyroptotic MAITs were evaluated in a cohort of patients with ALD, including 41 patients with alcoholic liver cirrhosis (ALC) and 21 patients with ALC complicated with severe alcoholic hepatitis (ALC+SAH).

Results: In patients with ALD, blood MAITs were significantly decreased, hyperactivated and displayed enhanced cell death through pyroptosis. The frequencies of pyroptotic MAITs increased with disease severity in patients with ALC and patients with ALC+SAH. These frequencies were negatively associated with the frequencies of MAITs and positively correlated with the levels of MAITs activation, plasma levels of intestinal fatty acid-binding protein (a marker of intestinal enterocyte damage), soluble CD14, lipopolysaccharide binding protein and peptidoglycan-recognition proteins (surrogate markers of microbial translocation). Pyroptotic MAITs were also found in the liver of patients with ALD. Interestingly, MAITs underwent further activation and pyroptosis *in vitro* under stimulation by *Escherichia coli* or direct bilirubin. Notably, blocking interleukin-18 signaling could reduced the activation and frequencies of pyroptotic MAITs.

Conclusion: The loss of MAITs in patients with ALD is, at least in part, due to cell death from pyroptosis and is closely associated with the severity of ALD. Such increased pyroptosis may be affected by dysregulated inflammatory responses to intestinal microbial translocation or direct bilirubin.

FRIDAY 23 JUNE

FRI-407

Platelets proteome dynamics and its association with liver severity in severe alcoholic hepatitis

Rupinder Kalra¹, Jaswinder Maras¹, Abhishak Gupta¹, Nupur Sharma¹, Gaurav Tripathi¹, Manisha Yadav¹, Babu Mathew¹, Vasundhra Bindal¹, Neha Sharma¹, Sushmita Pandey¹, Sadam H. Bhat¹. ¹Institute of Liver and Biliary Sciences, Molecular and Cellular Medicine, New Delhi, India
Email: jassi2param@gmail.com

Background and aims: Platelet activation mediates inflammation, oxidative stress, and contributes to disease severity in patients with SAH. Molecular cargo of platelet may differ between the healthy and SAH patients, which may be the reason for the increase in severity in SAH patients. Temporal change (Baseline, Day1, Day3 and Day7) in the molecular cargo in SAH patients is distinct and could help in stratifying patients with early mortality.

Method: Platelet proteomics was performed in (n = 20) SAH patients and (n = 20) controls at baseline, Day1, Day3, Day7 respectively. Weighted Protein Correlation Network Analysis (WPCNA) identified the temporal increase in SAH specific proteins clusters which were correlated to clinical parameters and outcome. Most prominent predictors of early mortality were identified and validated in a separate cohort of (n = 60) SAH patients.

Results: Platelet activation (PF4, TSP1 and p-selectin) were significantly higher in SAH patients as compared to controls ($p < 0.05$). Temporal proteomics evaluation identified 1236 proteins of them (baseline) 468 were differentially expressed (206-up, 262 down-regulated) in SAH as compared to controls ($p < 0.05$). Proteins cargo significantly increased were linked to platelet activation, ATP synthesis, oxidative phosphorylation and others whereas those significantly decreased were linked to Detoxification of Reactive Oxygen Species, Protein processing, Antigen Presentation and others ($p < 0.05$). Proteomic analysis at Day 1 (196 up- and 311 Dn), Day3 (279 up- and 469 Dn) and Day7 (207 up- and 562 Dn) showed significant change in DEP counts ($p < 0.05$, FC > 1.5, FDR < 0.01). Venn

integration identified 42 proteins commonly up- linked to platelet activation, degranulation, complement activation, dissolution of fibrin clot and others and 32 proteins downregulated linked to Detoxification of Reactive Oxygen Species, cGMP-PKG signalling pathway, Signalling by NGF and others ($p < 0.05$). WPCNA of platelets identified 18 proteins clusters ($p < 0.05$), which correlated to the severity indices (MELD, DF) and provided insight in to inflammation and severity of SAH patients ($p < 0.05$, $R^2 > 0.5$). Protein Family analysis showed linear decrease in the energy pathways (ATP-synthase, NADH-dehydrogenase), liver functions (coagulation) and others in SAH patients ($p < 0.05$, $R^2 > 0.5$). Blood transcriptome module (BTM) enrichment analysis showed that platelets in SAH patients are activated and carry inflammatory cargo of activated neutrophils, myeloid cells and monocytes, coagulation and TGF beta signalling and others ($p < 0.05$). Interestingly, proteins linked to TGF Beta such as Fibulin-5 (FBLN5), Peroxiredoxin-2 (PRDX-2) and others were temporally increased in SAH platelets. Validation experiments confirmed that platelets PRDX2 level increase with time showed direct correlation with the severity indices (MELD, mDF) and inhibit development of PDGF levels altering the molecular regeneration capacity of platelet in SAH patients.

Conclusion: Platelets in SAH are activated; energy deprived and carries inflammatory mediators and was able to stratify SAH patients with early mortality. Temporally these platelets accumulate PRDX2 which inhibit development of PDGF and regenerative support. Our proteomics study underlines PRDX2 as a novel target for therapeutic intervention for hyper-inflammation in SAH patients.

FRI-408

Characterization of fibrogenesis in severe alcohol-related hepatitis using a 3D model of coculture of organoids and fibroblasts from patients

Line Carolle Ntandja Wandji^{1,2}, Mohamed Bou Saleh², Cyril Sobolewski², Viviane Gnemmi³, Emmanuel Boleslawski⁴, Fabrice Bray⁵, Christian Rolando⁵, Philippe Mathurin^{1,2}, Laurent Dubuquoy², Alexandre Louvet^{1,2}. ¹CHU Lille, Service des maladies de l'appareil digestif et de la nutrition, Lille, France; ²Univ. Lille, Inserm, CHU Lille, U1286-INFINITE-Institute for Translational Research in Inflammation, Lille, France; ³CHU Lille, Service d'Anatomopathologie, France; ⁴CHU Lille, Service de Chirurgie Digestive et Transplantations, France; ⁵Univ. Lille, CNRS, USR 3290-MSAP-Miniaturisation pour la Synthèse, l'Analyse et la Protéomique, France
Email: carollewandji@yahoo.fr

Background and aims: Since few data are available on liver fibrogenesis during alcohol-related hepatitis (AH), the interplay between injured hepatocytes and fibrogenic cells needs to be studied into more details. Indeed, YAP-mediated impaired hepatocyte regeneration plays an important role in AH but its impact on fibrogenesis remains unknown. Our objectives were to characterize fibrosis during AH and to evaluate the impact of YAP in hepatocytes on the fibrogenic process observed in AH.

Method: Using PCR, immunohistochemistry and proteomic analysis, we characterized the molecular profile of fibrosis in liver explants from patients with AH not responding to steroids (n = 22) or alcohol-related cirrhosis (Cirrh, n = 24), and healthy livers (Ctrl, n = 15). From the explants, we also generated organoids which were cocultured with hepatic myofibroblasts to study their activation, their production of cytokines and their proliferation. We also transduced organoids from Cirrh liver with an active YAP and cocultured them with myofibroblasts to evaluate their contribution to fibrogenesis.

Results: In AH livers, standard histology and immunohistochemistry showed a specific intralobular fibrosis associated with specific markers (alpha-SMA, PDGFR alpha, COL1A1, lamininA2 etc.). PCR and proteomic analysis showed a specific extracellular matrix (ECM) signature (Figure 1) and an increased expression of fibroblast

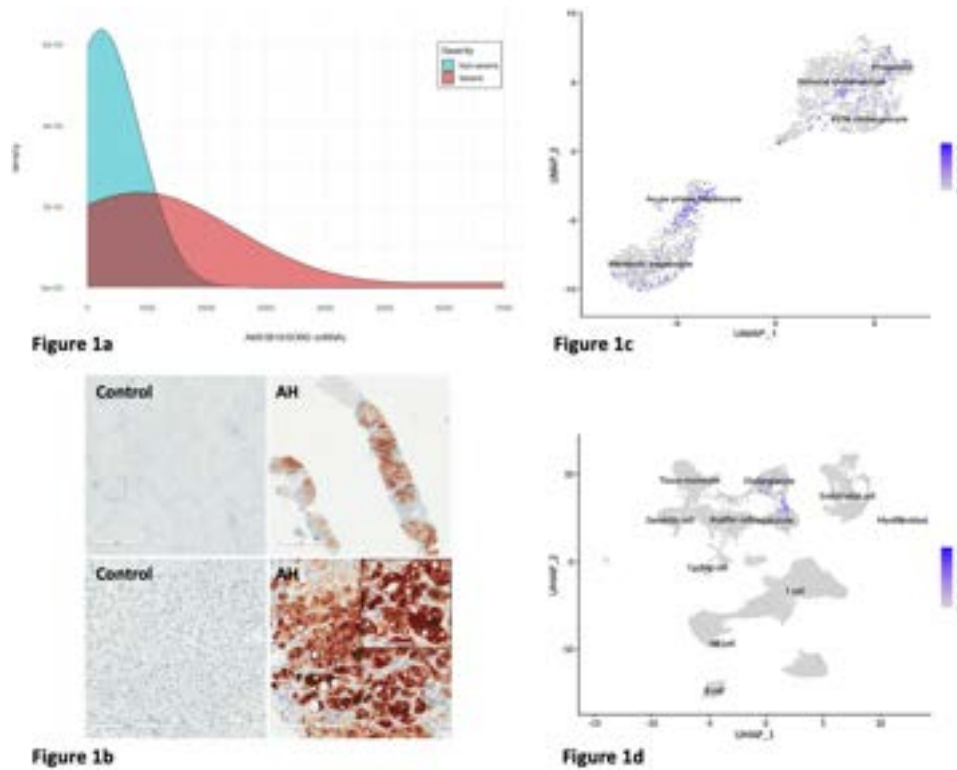


Figure 1: (abstract: TOP-073): (a) Density plot AKR1B10: SORD stratified by severity (MELD ≥ 21). (b) IHC results indicate that AKR1B10 is predominantly overexpressed in hepatocytes. (c) AKR1B10 is expressed in hepatocyte and cholangiocyte single cell populations. (d) AKR1B10 expression is increased in different hepatocyte and cholangiocyte profiles of liver diseases.

activation markers (alpha-SMA, PDGFR alpha), fibrillar collagens (COL1A1, COL3A1), lamininA2, cytokines (PDGF α , CCL5, MCP1), and a dysregulation of TIMP1 and MMP9. Ex vivo, the mRNA expression of alpha-SMA, PDGFR alpha, COL1A1, TIMP1, PDGF alpha, CCL5, MCP1 were higher in myofibroblasts cocultured with AH organoids as compared to fibroblasts cocultured with Cirrh organoids. Proliferation of myofibroblasts was also increased when cocultured

with AH organoids. Compared to non-transduced Cirrh organoids, transduction of YAP in Cirrh organoids led to a greater proliferation of myofibroblasts and increased alpha-SMA, PDGFR alpha, COL1A1, TIMP1, PDGF alpha, CCL5 and MCP1, a profile which mimics coculture with AH organoids.

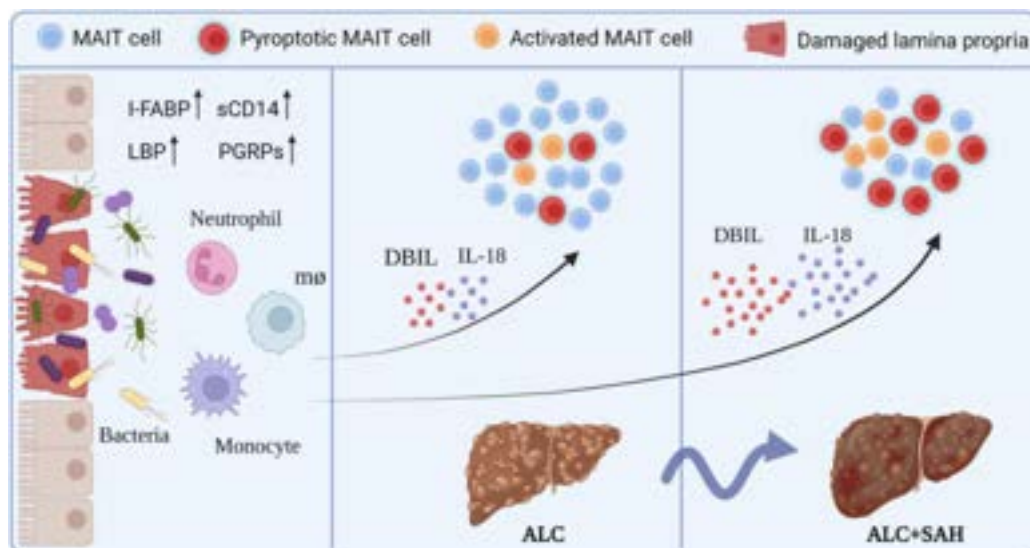


Figure: (abstract: TOP-078).

POSTER PRESENTATIONS

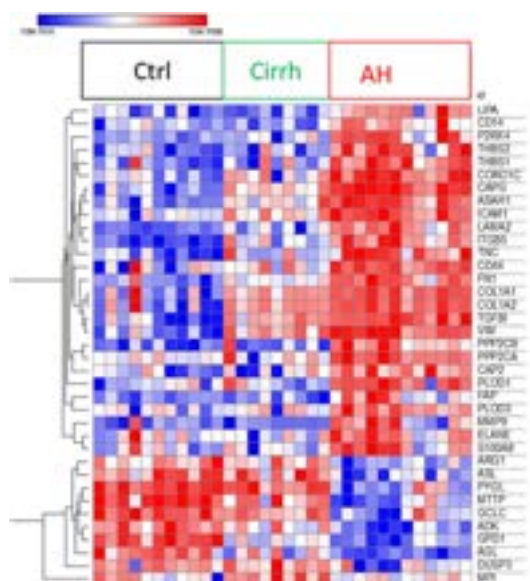


Figure:

Conclusion: AH is characterized by a specific fibrosis profile and organoids from AH patients induce activation, proliferation and release of inflammatory cytokines in myofibroblasts. Hepatocytic YAP appears to play an important role in the fibrogenesis during AH.

FRI-409

An increase in the number of activated regulatory T cells is associated with an improvement in liver function of patients with severe alcoholic hepatitis after steroid therapy

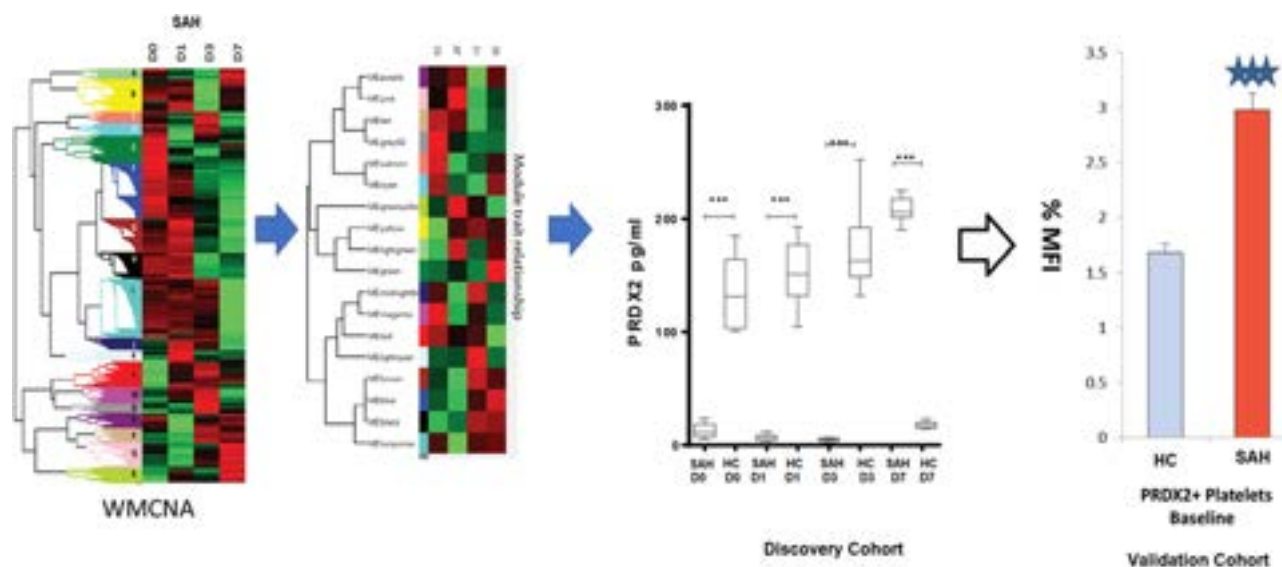
Soon Kyu Lee^{1,2}, Minwoo Kang², Ji Won Han^{2,3}, Jung Hyun Kwon^{1,2}, Soon Woo Nam^{1,2}, Jong Young Choi^{2,3}, Jeong Won Jang^{2,3}, Seung Kew Yoon^{2,3}, Pil Soo Sung^{2,3}. ¹Incheon St. Mary's Hospital,

College of Medicine, The Catholic University of Korea, Division of gastroenterology and hepatology, Department of Internal Medicine, Korea, Rep. of South; ²College of Medicine, The Catholic University of Korea, The Catholic University Liver Research Centre, Korea, Rep. of South; ³Seoul St. Mary's Hospital, College of Medicine, The Catholic University of Korea, Division of Gastroenterology and Hepatology, Department of Internal Medicine, Korea, Rep. of South
Email: pssung@catholic.ac.kr

Background and aims: Alcoholic liver disease is one of major cause of acute and chronic liver failure worldwide. Although steroid therapy is treatment of choice in severe alcoholic hepatitis, there has been limitation in the treatment of alcohol-related liver disease because of no improvement in the long-term survival after steroid therapy. Moreover, the role of regulatory T (Treg) cells, inhibiting T cell proliferation and cytokine production, in patients with alcoholic liver disease remains unclear. Here, we investigated the population and potential roles of activated Treg cells in patients with alcohol-related liver disease including severe alcoholic hepatitis using steroid treatment.

Method: A total of 30 patients with alcoholic liver disease were consecutively enrolled from two academic hospitals in our study. Among 30 patients, 11 patients had severe alcoholic hepatitis treated with steroid (steroid group) and the others (n = 19) had mild alcohol-induced liver injury without steroid treatment (no steroid group). Peripheral blood mononuclear cells (PBMCs) were isolated from patients at the time of enrollment and 7 days after treatment. Frequency of CD4⁺CD25⁺Foxp3^{high}CD45RA⁻ Treg cell was examined by flow cytometry and compared between the steroid and no steroid group. Moreover, we evaluated the population of Treg according to the steroid treatment response. Single cell RNA sequencing analysis using paired PBMCs was also performed and compared between patients with steroid responder and non-responder.

Results: Among 30 included patients, the steroid group (n = 11) had significant higher score of model for end-stage liver disease (MELD) than in the no steroid group (n = 19) (median MELD score, 24.0 vs.



Temporal change in platelet proteome profile of platelets in SAH patients

Figure: (abstract: FRI-407).

12.0, respectively; $p < 0.001$). Although initial frequency of Treg cells were marginally lower in the steroid group, the population of Treg cells were significantly increased in the steroid group ($p = 0.019$, Figure 1A). Of the steroid group, steroid responder ($n = 9$) showed significant increase in the population of Treg cells after steroid therapy ($p = 0.020$, Figure 1B). Moreover, there was significant positive correlation between the decrease in MELD score and increase in Treg cells ($R = 0.43$; $p = 0.019$). In the single cell RNA sequencing analysis using paired PBMCs (pre- and post- steroid therapy), we found that cytokine production and type I IFN gene signature in CD4 T cells were downregulated after steroid therapy, suggesting the possible protective roles of expanded activated Treg cells.

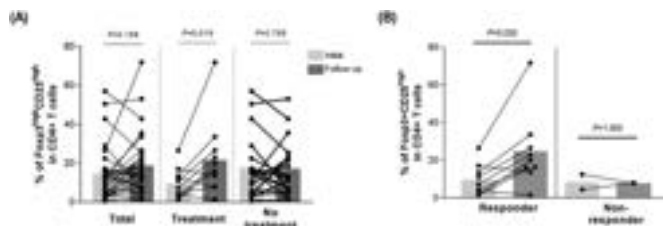


Figure: Changes in regulatory T cells according to steroid treatment (A) and response (B).

Conclusion: Our data suggest that an increase in the number of activated regulatory T cells is associated with an improvement in the liver function of patients with severe alcoholic hepatitis after steroid therapy.

Financial Support: This work was supported by the Research Foundation of Internal Medicine, The Catholic University of Korea (S.K.L.). This work was also supported by Basic Science Research Program through the National Research Foundation of Korea (NRF) funded by the Ministry of Education (No. 2021R111A1A01050954, S.K.L.). This work was partly supported by the Research Fund of Seoul St. Mary's Hospital, The Catholic University of Korea (P.S.S.).

FRI-410

Plasma lipidomics and meta-proteomics analysis classifies lipid species and microbial peptides associated with poor outcome in SAH patients

Jaswinder Maras¹, Manisha Yadav¹, Nupur Sharma¹, Gaurav Tripathi¹, Babu Mathew¹, Vasundhara Bindal¹, Neha Sharma¹, Sushmita Pandey¹.

¹Institute of Liver and Biliary Sciences, Molecular and Cellular Medicine, New Delhi, India

Email: jassi2param@gmail.com

Background and aims: Severe alcoholic hepatitis (SAH) has a high mortality and corticosteroid therapy non-response is seen in ~ 60% patients. Corticosteroid therapy is known to cause lipid profile abnormalities. Thus we speculated that lipidomics may represent a useful tool to characterise responders (R) and non-responders (NR) to corticosteroid therapy and outcome.

Method: Plasma lipidomics and metaproteome (metagenomics) was performed in 80 SAH (R = 55 and NR = 25) at baseline, day 4 and day 7 to identify signatures capable of early detection of nonresponse. Temporal change in lipidome was assessed by Weighted Lipid Correlation Network Analysis (WLCNA). Baseline Metaproteome and lipidome profiles were subjected to cross correlation network analysis followed by correlation with clinical parameters. Bacterial specific lipid species which could predict severity and outcome were identified and validated in a test cohort of ($n = 100$) SAH patients using Machine learning approach.

Results: Plasma samples showed significant alteration of lipidome and microbiome as indicated by multivariate PLS-regression analysis and alpha, beta diversity indices ($p < 0.05$). Significant reduction of lipid species and increase in bacterial taxa (baseline) were observed in NR ($p < 0.05$, LogFC > 1.5 , FDR < 0.01). Baseline plasma level of TG 48:4 was higher whereas level of PS and PE (known for maintaining

body cortisol level) were lower in NR ($p < 0.05$). Temporal analysis of lipidomic profile showed significant increase in lipid metabolism in R, whereas the NR showed specific increase in triglycerides already reported for promoting steatosis and inflammation ($p < 0.05$). NR specific Meta-proteomic signatures/functionality directly correlated with lipid species and clinical parameters; severity indices (mDF, MELD and others; $p < 0.05$). Baseline increase in TG 48:4 showed direct correlation with increased bacterial taxa; *Escherichia coli*, *Bacillales*, *Streptococcus*, *Enterobacteriaceae* and their functionality in NR ($r^2 > 0.5$, $p < 0.05$). Baseline reduction of PS and PE were associated *Lactobacillus*, *Nocardiopsaceae* and others along with their functionality in NR ($r^2 > 0.5$, $p < 0.05$). Lipidomic and metaproteomic signature based probability of detection of NR was $> 90\%$ ($p < 0.05$). Baseline decrease in PS ((PS a41:5, PS a43:6, PS a43:4, PS a43:5, PS a41:0) with (AUC > 0.89 , $p < 0.05$) predicted Non-response and segregated Non survivors (HR = 0.80 (0.75–0.90), $p < 0.05$) in SAH patients. Validation of 5 lipid species using 5 machine learning algorithms in the validation cohort ($n = 100$; R = 80, NR = 20) showed accuracy (99%), sensitivity/specificity $> (98\%)$ for NR detection in SAH.

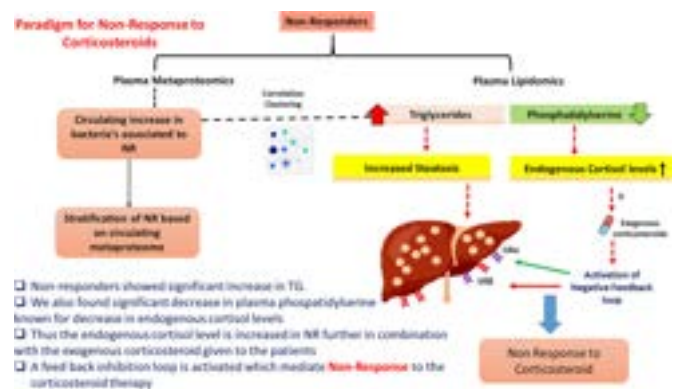


Figure:

Conclusion: Plasma sample of NR show significant reduction in lipid species and increase in bacterial taxa. We, report a core set of plasma lipidome and meta-proteome signature which could be used for early diagnosis of non-response and outcome prediction in SAH patients.

FRI-411

In-silico identification and ex-vivo validation in humans of distinct oncogenic potential of aldo-keto reductase AKR1B10 in hepatocellular carcinoma from alcohol induced liver injury

Michael Waters¹, Sukriti Sukriti², Chhagan Sharma³, Preeti Negi², Bhaumik Patel⁴, Michael Fuchs⁵, Shiv Kumar Sarin⁶, Puneet Puri⁷.

¹Washington University School of Medicine in St. Louis, Department of Radiation Oncology, St. Louis, United States; ²Institute of Liver and Biliary Sciences, Department of Molecular and Cellular Medicine, New Delhi, India; ³Institute of Liver and Biliary Sciences, Department of Pathology, New Delhi, India; ⁴Virginia Commonwealth University and Richmond VA Medical Center, Section of Medical Oncology, Department of Internal Medicine, Richmond, United States; ⁵Virginia Commonwealth University and Richmond VA Medical Center, Section of Gastroenterology, Hepatology and Nutrition, Department of Internal Medicine, Richmond, United States; ⁶Institute of Liver and Biliary Sciences, Department of Hepatology, New Delhi, India; ⁷Virginia Commonwealth University and Richmond VA Medical Center, Section of Gastroenterology, Hepatology and Nutrition, Richmond, United States

Email: puneet.puri@vcuhealth.org

Background and aims: Development of hepatocellular carcinoma (HCC) is complex. It is a major cause of cancer-related mortality with a minority diagnosed at an early stage. Chronic alcohol abuse, and hepatitis B and C viral (HBV and HCV) infections are major risk factors. However, pre-cancer alterations which also affect the prognosis are not well known. We aimed to investigate (i) the *in-silico*

POSTER PRESENTATIONS

transcriptional alterations among HCC patients induced by alcohol liver injury compared to those with hepatitis B and C, (ii) to identify the gene classifier for better prognosis of the disease and validate *ex-vivo* in human samples.

Method: We systemically interrogated The Cancer Genome Atlas (TCGA, n = 433) to search for genes that contribute to HCC. First, we compared the survival of HCC patients who had a history of alcohol abuse vs. Hepatitis B or C alone via Kaplan-Meier analysis. Next, we tested the differential gene expression utilizing dataset, GSE28619, containing healthy (n = 7) and alcohol associated cirrhosis (AAC, n = 15). Gene dysregulation was determined using the 'characteristic direction method' of the EnrichR algorithm. Using GEO database we performed a machine learning technique nearest-shrunken centroid analysis. Further, AKR1B10 expression was validated on human liver tissue from AAC (AAC, n = 5), hepatitis C related HCC (HCC-HCV, n = 5), alcohol cirrhosis related HCC (HCC-AC, n = 5) and normal tissue (control, n = 5) using immunohistochemistry (IHC).

Results: Patients with HCC due to chronic alcohol abuse had worse prognosis than patients with hepatitis B or C related infection (p = 0.011). Gene enrichment analysis showed 500 differentially expressed genes. The family of aldo-keto reductase (AKR) enzymes were statistically enriched in patients with alcohol associated hepatitis (AAH). Using machine learning, a singular gene classifier of AAH was identified as aldo-keto reductase AKR1B10. This is widely expressed in the gastrointestinal tract. However, it is virtually undetectable in normal liver tissue. Then we performed GSEx microarrays analysis between healthy and cirrhotic livers. AKR1B10 was the 5th most statistically upregulated gene. Further, we confirmed that AKR1B10 is upregulated in HCC using unbiased IHC samples from the Human Protein Atlas (Figure A). Additionally, AKR1B10 was an independent marker for poor patient survival in the large TCGA sample (n = 433). Importantly, in patients with HCC and an initial alpha fetoprotein (AFP) value of greater than 400, poor survival was associated with AKR1B10 expression (Figure B, red line). Alcohol associated HCC had higher AKR1B10 expression than those without a history of alcohol abuse (RR = 1.6, p = 0.0076, Figure C). We confirmed this in human liver tissues. There was no expression in controls and >2-fold increase in AAC. This was further increased in HCC-AC in contrast to minimal expression in HCC-HCV.

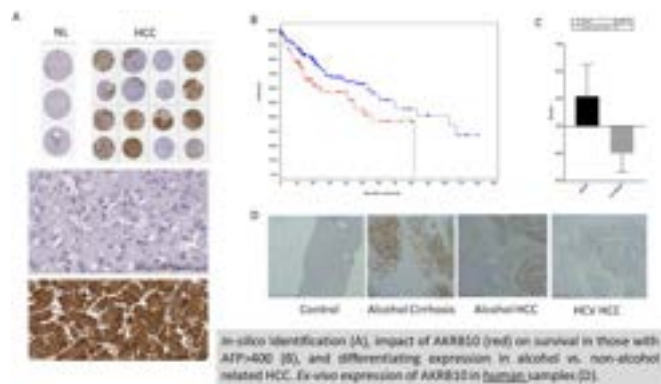


Figure:

Conclusion: Alcohol associated HCC are more aggressive than viral hepatitis infected patients. We identified a novel classifier AKR1B10, as precancerous marker of alcohol induced liver injury, alcohol associated cirrhosis and HCC. Additionally, AKR1B10 prognosticated HCC. This promising marker provides a platform to understand mechanism of alcohol induced hepatocarcinogenesis and merits further validation.

FRI-412

The beneficial effects of the diet withdrawal and physical exercise on steatohepatitis of DUAL etiology

Olga Estévez¹, Raquel Benedé^{1,2}, Hector Leal¹, Jeanne Fabre³, Johanna Reißing⁴, Marina Mazariegos¹, Tony Bruns⁴, Javier Vaquero^{5,6,7}, Rafael Bañares^{6,8,9}, Francisco Javier Cubero^{1,8,10}, Yulia Nevzorova^{1,8,10}. ¹Complutense University of Madrid, Immunology, Ophthalmology and ENT, Madrid, Spain; ²Complutense University of Madrid, Physiology, Genetics and Microbiology, Madrid, Spain; ³Polytech Angers, Génie Biologique et Santé, France; ⁴University Hospital RWTH Aachen, Internal Medicine III, Aachen, Germany; ⁵Centro de Investigación Biomédica en Red de Enfermedades Hepáticas y Digestivas (CIBERHED), Spain; ⁶Instituto de Investigación Sanitaria Gregorio Marañón, Madrid, Spain; ⁷Gregorio Marañón General University Hospital, Servicio de Aparato Digestivo, Madrid, Spain; ⁸Centro de Investigación Biomédica en Red de Enfermedades Hepáticas y Digestivas (CIBERHED), Spain; ⁹Hospital General Universitario Gregorio Marañón, Servicio de Aparato Digestivo, Spain; ¹⁰Instituto de Investigación Sanitaria Gregorio Marañón (IISGM), Spain
Email: olgaeste@ucm.es

Background and aims: Along with the increase of obesity and type 2 diabetes (T2D), steatohepatitis incidence is tremendously escalating and becoming a significant burden of liver-related outcomes. Dietary changes and physical activity are recommendable therapeutic strategies. Whether steatohepatitis is reversible remains a relevant clinical question and is a constant matter of debate.

In the present study, we used a synergistic DUAL murine model of NASH and alcohol consumption, and studied the biological impact of physical exercise and dietary changes on the progression of steatohepatitis and fibrosis.

Method: C57BL/6 male mice received 10% alcohol in sweetened drinking water together with a Western diet (DUAL model) for short (10 weeks) and long (23 weeks) period followed by either (i) the replacement with chow diet and normal water for 21 days; or (ii). chow diet/normal water plus treadmill sessions for 21 days. Metabolic syndrome (MS), serum parameters, liver and e-WAT (epididymal white adipose tissue, WAT) histology, were analysed in detail.

Results: Compared to the 10 weeks DUAL-fed mice, all animals in the diet withdrawal (DW) and withdrawal plus exercise (DW+EXER) groups showed significant decrease in body mass, liver and fat weight, remarkable improvement in liver and fat morphology, attenuated hepatic steatosis with reduced hepatic triglyceride (TG) content, diminished hepatic injury and inflammation. Nevertheless, as the long-term DUAL feeding (23 weeks) leads to the significant steatohepatitis and advanced fibrosis, the diet replacement with or without physical exercise resulted only in slightly decrease of the body and liver weight, faintly diminished hepatic steatosis and TG content in the liver and the significant improvement of serum parameters of liver damage. Importantly, long-term DUAL feeding, e-WAT cellular hypertrophy, central markers of the hepatic inflammation (CD45 and F4/80 levels) and fibrosis (alfa-SMA) were reversible only in the group of the diet withdrawal in combination with physical exercises.

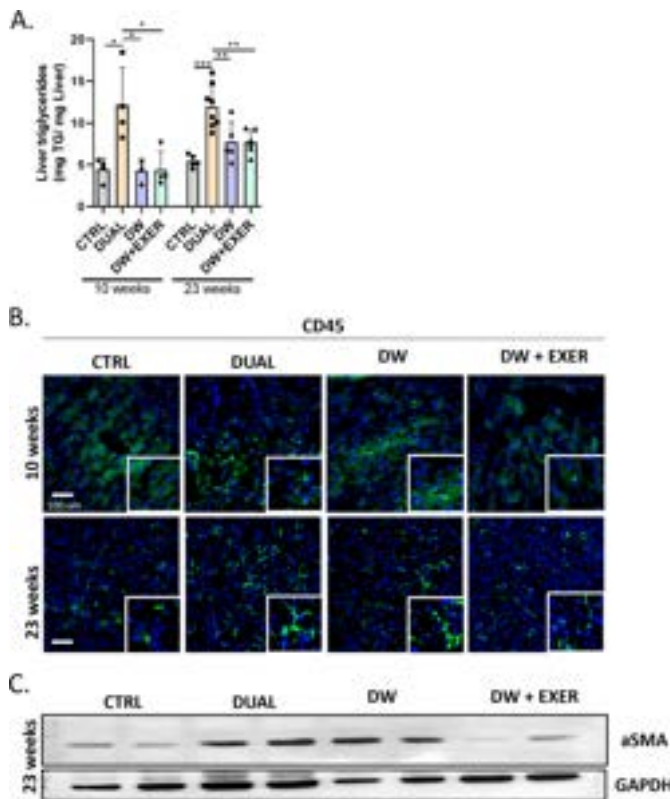


Figure: DUAL diet withdrawal only in combination with intensive physical activity attenuates hepatic inflammation and fibrosis even after long term DUAL feeding. DUAL mice manifest enhanced hepatic inflammation and fibrosis. (i) DUAL diet withdrawal for 21 days, (ii) DUAL diet withdrawal in combination with treadmill for 21 days. A. Quantification of hepatic triglycerides after 10 and 23 weeks feeding B. Illustrative CD45 staining in liver sections of mice fed for 10 and 23 weeks. Positive immune cells are stained in green. Nuclei are stained in blue using DAPI as a counterstain. Scale = 100 μ m C. α -SMA western blot using GAPDH as a loading control.

Conclusion: Dietary modification, alone or combination with physical exercisers in patients with the initial stages of steatohepatitis might be considered as an efficient non-pharmacological therapy, reducing body weight, hepatomegaly, steatosis and liver inflammation. However, only a combination of dietary changes and physical activity can lead to the clinical improvement at the advance stages of steatohepatitis.

FRI-413

When is the optimal time to collect baseline data for calculating the Lille score in severe alcoholic hepatitis?

Mina Ignat^{1,2}, Adelina Horhat³, Andreea Barb^{1,2}, Irina Dragomir¹, Andreea Fodor^{1,2}, Fischer Petra^{1,2}, Oana Nicoara-Farcu^{1,2,3}, Indre Madalina Gabriela^{1,2,3}, Vlad Taru^{1,2,3}, Corina Radu^{1,3}, Bogdan Procopet^{1,2,3}, Horia Stefanescu^{1,2}. ¹Regional Institute of Gastroenterology and Hepatology "Prof. Dr. O. Fodor," Cluj-Napoca, Romania; ²Liver Research Club, Hepatology, Cluj-Napoca, Romania; ³University of Medicine and Pharmacy "Iuliu Hatieganu," Cluj Napoca, Romania, 3rd Medical Clinic, Hepatology, Cluj-Napoca, Romania
Email: ignat.mina@gmail.com

Background and aims: Treatment of severe alcoholic hepatitis relies on corticosteroids. Lille score is used to identify patients with severe alcoholic hepatitis receiving corticosteroids, that respond or not to treatment. This model uses baseline data and the change in bilirubin level at day 7. However, many patients receive corticotherapy after several days of hospitalization because they need screening for

infections or treatment for a severe infection. In this time frame, the level of serum bilirubin can change in both ways compared with the level at admission time. There is no clear recommendation about the specific moment when baseline data needs to be collected in order to calculate the Lille score.

Our aim is to determine how important is the time interval between admission and first day of corticosteroids in the dynamics of Lille score and to evaluate the accuracy of different scores to predict short term mortality.

Method: We retrospectively analysed all consecutive patients with a history of alcoholism, suggestive liver chemistry, biopsy proven AH, Maddrey score >32, treated with corticosteroids, were included between January 2016–December 2022. Biological data was recorded at admission (T0) and prospectively at day 1 (T1), day 7 (T7) of corticosteroid therapy. We excluded patients who didn't receive corticosteroids because of uncontrolled infections, recent gastrointestinal hemorrhage. 40 mg Prednisone or 32 mg Methylprednisolone was given for 28 days for all patients.

Results: One hundred sixty-four patients were included, mean age was 52 \pm 9, 76.4% were males. 89.1% were decompensated (ascites 83.6%, hepatic encephalopathy 35.2%), 32.1% had infection at admission, 98% had an AHHS score >3. Out of all patients, 81.0% responded to the corticotherapy treatment, assessed by Lille score at day 7. The survival of these patients was 77.6% at one month, 69.7% at three months, 42.7% overall. Out of all patients, one hundred had the blood analysis required to assess both the Lille T0 and Lille T1. There are no significant differences regarding Meld score, Maddrey score and serum bilirubin at T0 compared to T1, $p > 0.05$. AUROC curve for survival at 1 month for Lille7 T0 was 0.84 ± 0.04 (95%CI: 0.74–0.93), Lille7 T1 0.85 ± 0.04 (95%CI: 0.75–0.93), Meld T0 0.73 ± 0.06 (95%CI: 0.61–0.85), Meld T1 0.76 ± 0.05 (95%CI: 0.66–0.87), Maddrey T0 0.62 ± 0.71 (95%CI: 0.48–0.76) and Maddrey T1 0.72 ± 0.06 (95%CI: 0.60–0.84). Lille T0 is significantly higher than Maddrey T0. AUROC for survival at 3 and 6 months is not significantly different between Lille T0 and Lille T1. Survival at one month in the group of patients who responded to corticotherapy according to Lille T1 was 83.0%, at three months 74.6% and at six months 72.4%. In comparison, the responders to Lille T0 survival at one month was 80.5%, at three months 72.2% and at six month 71.4%. The median follow-up duration was 13 months (varying between 0 and 78 months, range 78), 55% of the patients died at the end of the follow-up. Corticosteroids response assessed by Lille T1 predicts better overall survival than Lille T0, HR: 2.26 (95%CI: 1.19–4.29), $p = 0.01$, respectively HR: 2.03 (95%CI: 1.05–3.91), $p = 0.03$.

Conclusion: Therefore, our data showed that the time between admission and corticosteroid initiation does not significantly change the dynamic of Lille score and does not impact the prognostic and survival. However, further studies need to be done with larger number of patients.

FRI-414

Low doses of different hepatotoxins induce alcohol-related liver disease and drive hepatocellular carcinoma

Brisa Rodope Alarcón-Sánchez^{1,2}, Osiris German Idelfonso García², Verónica Rocío Vásquez-Garzón³, Pablo Muriel⁴, Julio Isael Pérez-Carreón², Saúl Villa-Treviño¹, Jaime Arellanes-Robledo^{2,5}. ¹Center for Research and Advanced Studies of the National Polytechnic Institute, Department of Cell Biology, Mexico City, Mexico; ²National Institute of Genomic Medicine-INMEGEN, Laboratory of Liver Diseases, Mexico City, Mexico; ³Faculty of Medicine and Surgery, 'Benito Juárez' Autonomous University of Oaxaca-UABJO, Laboratory of Fibrosis and Cancer, Oaxaca, Mexico; ⁴Center for Research and Advanced Studies of the National Polytechnic Institute, Laboratory of Experimental Hepatology, Mexico City, Mexico; ⁵National Council of Science and Technology-CONACYT, Directorate of Cátedras, Mexico City, Mexico
Email: brisa.alarcon@cinvestav.mx

Background and aims: Chronic alcohol abuse is one of the main causes of morbidity and mortality since promotes alcohol-related liver disease (ALD) worldwide. This condition may be attributed to multiple hits driving several liver alterations. Excessive ethanol intake promotes the production of reactive oxygen species (ROS) and increases both portal and systemic circulation of lipopolysaccharides (LPS), which exacerbate ROS and potentiate the liver damage. Since hepatocellular carcinoma (HCC) may be the late ALD stage, the synergistic effect of ethanol and diethylnitrosamine (DEN), a hepatic carcinogen, also has been tested. The aim of this work was to determine if the simultaneous administration of ethanol and low doses of LPS and DEN induces HCC as an *in vivo* multi-hit ALD model, as occurs in humans.

Method: C57BL/6J female mice were administered with ethanol and low doses of LPS and DEN. Firstly, after an ethanol adaptation period, mice were allowed to drink *ad libitum* a mixture of 20% (w/v) sucrose containing 20% ethanol for 18 weeks as the only source of drinking fluid, and DEN and LPS were dissolved in PBS and intraperitoneally injected twice a week. While DEN was administered at 7 mg/kg body weight (BW) for 15 weeks during ethanol consumption, LPS was administered at 1 mg/kg BW alongside the period of time of ethanol consumption. In addition to animals subjected to ethanol, LPS and DEN (ELD group), another group was administered with 20% sucrose as controls (C) or DEN plus 20% sucrose as DEN control (DEN). ELD groups were euthanized at 6, 9, 12, 15, 18 and 25 weeks; and C and DEN groups were euthanized at 18 and 25 weeks.

Results: We showed that ELD scheme interfered with BW gain and induced liver structural disarrangement, inflammatory infiltration, steatosis, and fibrosis, as illustrated in the figure (images from C, DEN and ELD groups treated for 18 weeks); which was accompanied by increased levels of the proliferation markers proliferating cell nuclear antigen (PCNA) and Ki-67, those of ethanol metabolism cytochrome P450 2E1 (CYP2E1) and alcohol dehydrogenase (ADH), that of hepatocarcinogenesis glutathione S-transferase P 1 (GSTP1), as well as, that of LPS-inducible myeloid differentiation primary response protein MyD88 (MYD88) and toll-like receptor 4 (TLR4), and that of inflammation interleukin-6 (IL6).

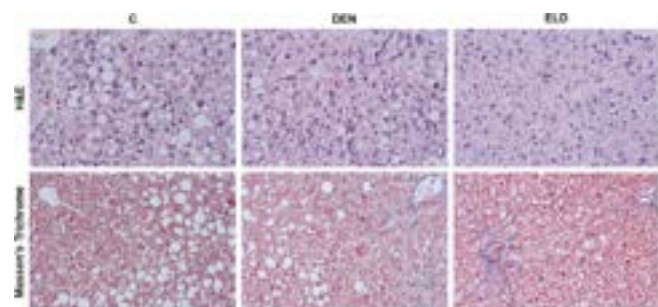


Figure:

Conclusion: Considering that ALD progression naturally occurs as the result of combined effects of multiples hits, we provide evidence showing that the simultaneous administration of ethanol, and low doses of LPS and DEN exacerbates ALD-associated alterations by inducing more deleterious effects on the liver and HCC as compared with those induced by DEN alone. Thus, here we introduce a promising multi-hit ALD model to better recapitulate ALD-associated pathogenesis and eventually, to identify therapeutic targets for the treatment of ALD stages.

FRI-415

Systemic dyslipidemia in Ldlr mice accelerates hepatic fibrosis after chronic-binge ethanol feeding

Constanze Hoebinger¹, Dragana Rajcic², Tim Hendrikx². ¹Medical University of Vienna, Department of Laboratory Medicine, Vienna, Austria, ²Medical University of Vienna, Department of Laboratory Medicine, Vienna, Austria

Email: constanze.hoebinger@meduniwien.ac.at

Background and aims: Chronic ethanol consumption is known to cause alcohol-associated liver disease, which poses a global health concern as almost a quarter of heavy drinkers develop severe liver damage. Alcohol-induced liver disease ranges from a mild, reversible steatotic liver to alcoholic steatohepatitis and irreversible liver fibrosis and cirrhosis, ultimately requiring liver transplantation. Although ethanol consumption is associated with dysregulated lipid metabolism, the impact of pre-existing dyslipidemia on the development of alcohol-related liver disease is still unknown. In this study, we investigated the contribution of pre-existing dyslipidemia and particularly hypercholesterolemia to the progression of alcohol-related liver disease.

Method: To address the influence of systemic dyslipidemia on ethanol-induced liver disease, chronic-binge ethanol feeding (NIAAA model) was applied to female C57BL/6J (wild type) mice and mice deficient for the low density lipoprotein receptor (Ldlr^{-/-}), which display a human-like lipoprotein profile with elevated cholesterol and triglyceride levels in circulation. Respective control groups were pair-fed with an isocaloric diet.

Results: Chronic-binge ethanol feeding did not alter systemic lipid levels in wild type mice. While increased systemic cholesterol levels in Ldlr^{-/-} mice were not affected by ethanol feeding, chronic-binge ethanol diet aggravated elevated plasma triglyceride levels in Ldlr^{-/-} mice. Despite higher circulatory triglyceride levels in Ldlr^{-/-} mice, hepatic lipid levels and the development of hepatic steatosis were not different from wild type mice after ethanol diet. Immunohistochemical assessment indicated a lower induction of infiltrating neutrophils in the livers of ethanol-fed Ldlr^{-/-} mice compared to wild type mice. In line, hepatic mRNA levels of the pro-inflammatory genes Ly6g, Cd11b, Ccr2, and Cxcl1 were reduced, indicating less inflammation in the livers of Ldlr^{-/-} mice. In contrast, Ldlr-deficient mice developed more liver fibrosis after ethanol diet than wild type mice, as indicated by increased levels of Sirius Red staining and higher expression of pro-fibrotic genes Tgfb and Col1a1. Ldlr^{-/-} and wild type mice had similar plasma ethanol levels and did not show differences in the hepatic mRNA levels of Adh1 and Cyp2e1, important for ethanol metabolism.

Conclusion: Our results show that chronic-binge ethanol feeding aggravates systemic dyslipidemia in Ldlr^{-/-} mice, resulting in an accelerated development of ethanol-induced hepatic fibrosis.

FRI-416

Dynamics of oxidized albumin and cognate metabolites are associated with severe inflammation in experimental model of alcohol related liver disease

Babu Mathew¹, Jaswinder Maras¹, Sadam H. Bhat¹, Nupur Sharma¹, Manisha Yadav¹, Gaurav Tripathi¹, Vasundhara Bindal¹, Neha Sharma¹, Sushmita Pandey¹, Abhishak Gupta¹, Shiv Kumar Sarin². ¹Institute of Liver and Biliary Sciences, Molecular and Cellular Medicine, New Delhi, India; ²Institute of Liver and Biliary Sciences, Hepatology, New Delhi, India

Email: jassi2param@gmail.com

Background and aims: Alcohol related liver diseases (ALD) result from progressive hepatocellular injury, inflammation and oxidative stress. Albumin therapy is often recommended for ALD patients to improve survival. Albumin exists in 3 major forms: reduced Human Mercaptoalbumin (HMA), oxidized Human Nonmercaptoalbumin 1 (HNA1) and oxidized Human Nonmercaptoalbumin 2 (HNA2). Due to increase in systemic oxidative stress in ALD, oxidation of HMA to

HNA1/HNA2 increases. However, the time at which the infused albumin (HMA) undergoes oxidative modification and changes in cognate circulating metabolites are not known. Our study aims to decipher the time dynamics of oxidized albumin and associated changes in the circulating metabolome in a rat model of ALD.

Method: ALD model was developed by feeding Lieber-DeCarli liquid diet (40% ethanol) to Long Evans rats for 28 weeks. Liver histology (ballooning, steatosis and neutrophil infiltration) and AST/ALT levels confirmed active ALD. HMA, *in-vitro* modified HNA1 and *in-vitro* modified HNA2 (2.5 g/kg) were injected intraperitoneally to the ALD rats (n = 3 each) at three time points: baseline, 24 hours and 48 hours. Plasma was collected at baseline, 5 minutes, 15 minutes, 30 minutes, 1 hour, 24 hours, 48 hours, 72 hours and post euthanasia. Oxidized albumin measurement and untargeted metabolomics was performed.

Results: At baseline (before injection), the ALD rats showed significant increase in HNA1 (42.61%) and HNA2 (24.99%). HMA infused ALD rats showed temporal increase in HMA levels (15%) (5 min to 72 hours) with a slight dip between 5 minutes and 1 hour. HNA1 levels decreased by 18% and there was no significant change in HNA2 levels. Untargeted metabolomics also showed temporal increase in histidine (anti-inflammatory), purine/pyrimidine, glutathione and pantothenate metabolism ($p < 0.05$) indicating the protective and anti-inflammatory activity of HMA. Interestingly, Infusion of HNA1 to ALD rats showed significant temporal increase (5 minutes to 72 hours) in HNA2 (10% to 32%) with simultaneous decrease in the HMA (10%) levels suggesting that HNA1 infusion increases the irreversible oxidation of HMA/HNA1 to HNA2. Metabolomics also showed temporal increase in spermidine synthesis (pro-inflammatory polyamines), ammonia recycling and phosphatidylcholine synthesis (pro-apoptotic phospholipids) ($p < 0.05$) documenting the pro-inflammatory and pro-apoptotic activity of HNA1. Unfortunately, HNA2 infused ALD rats died after 4 hours. We observed significant temporal increase of HNA2 (15%) (5 minutes to 4 hours) with significant and apparent decrease in HNA1 and HMA. Results of metabolomics analysis revealed an increase in fatty acid, amino-sugar, tryptophan, fructose, mannose and sphingolipid metabolism suggesting the increase of inflammatory metabolites in HNA2 infused ALD rats. The advanced oxidative state (AOS) of albumin was highest in HNA2 infused rats ($p < 0.05$).

Conclusion: Our results show that HMA infusion temporally decreases HNA1 levels with simultaneous increase in anti-inflammatory metabolites. HNA1/HNA2 infusion causes irreversible oxidation of albumin to HNA2 and increase in pro-inflammatory/pro-apoptotic metabolites in the circulation. Albumin modification time dynamics significantly correlate with their cognate plasma metabolite and could be used as putative indicators of increasing inflammation and severity over time.

FRI-417

Multi-omics analysis reveals the therapeutic effect and mechanism of the Chinese herbal JiGuCao capsule on acute alcoholic hepatitis in mice

Yue Chen¹, Hening Chen¹, Wenying Qi¹, Xu Cao¹, Ruijia Liu¹, Zao Xiaobin^{1,2}, Yong'an Ye^{1,3}, ¹Dongzhimen Hospital, Beijing University of Chinese Medicine, China; ²Key Laboratory of Chinese Internal Medicine of Ministry of Education and Beijing, Dongzhimen Hospital, Beijing University of Chinese Medicine, China; ³Institute of Liver Diseases, Beijing University of Chinese Medicine, China
Email: chen.yue123456@163.com

Background and aims: Alcoholic hepatitis (AH) is a kind of alcohol-related liver disease (ALD), caused by alcohol abuse, with high morbidity and mortality, which increases the risk of liver failure, liver

cirrhosis and hepatocellular carcinoma, and the current treatment methods are still limited. Its pathogenesis is closely related to inflammatory response, intestinal mucosal permeability changes, bile acid circulation disorders, and other mechanisms. Traditional Chinese medicine (TCM) has shown a therapeutic effect to treat AH. JiGuCao capsule (JGC) is a commonly used marketed TCM for the treatment of acute and chronic hepatitis. However, the therapeutic effect and mechanism of JGC in the prevention and treatment of AH are still unclear and need further study.

Method: A mouse model of AH was established with 14 days of 5% (v/v) ethanol liquid diet and a single dose of 31.5% (v/v) ethanol liquid diet gavage (Figure A). At the same time, the treatment group was given by gavage of an aqueous solution of JGC. The therapeutic effect of JGC on AH was determined by serological analysis of liver function and histopathological examination of hematoxylin-eosin (HE) and oil red (OR) staining. At the same time, transcriptomics and non-target metabolomics of liver tissues, and 16S ribosomal DNA sequencing (16S seq) of gut microbiota were used to investigate the protective effects of JGC on AH. The differently expressed genes (DEGs) and differently expressed metabolites (DEMs) between the model and the JGC groups were screened out to perform further enrichment analyses including the Gene Ontology (GO) and the Kyoto Encyclopedia of Genes and Genomes (KEGG).

Results: Compared with the model group, the intervention of JGC reduced serum levels of alanine aminotransferase and aspartate aminotransferase (Figure B). In histology and pathology, HE and OR staining showed that ethanol exposure significantly increased the number of steatosis and necrotic cells in the liver of the model group, and a large number of fat vacuoles appeared. Meanwhile, the villi structure of the small intestine was scattered, the cells were shed, and the small intestinal glands were increased. Compared with the model group, JGC alleviated hepatic steatosis and restored the integrity of the intestinal structure (Figure C). The enrichment analyses of DEGs showed that JGC may affect KEGG pathways of Bile secretion, retinol metabolism, fatty acid degradation, Gastric cancer and GO pathway of cellular response to interferon-beta, response to cytokine, symbiont-containing vacuole membrane, endoplasmic reticulum membrane, GTPase activity, GTP binding (Figure D-F). The enrichment analyses of DEMs showed that JGC could regulate amino acid metabolism, protein digestion and absorption, and ABC transporter pathways (Figure H-J). And in the gut microbiota level, the results of 16S seq showed that at the genus level, the JGC treatment restored the reduction of Lactobacillus content caused by alcohol, and increased the content of norank_f_Muribaculaceae and Prevotellaceae_UCG-001 (Figure K-L).

Conclusion: Histopathological and multi-omics analysis studies showed that JGC could have good preventive and therapeutic effect on AH. It could restore the normal function of the gut-liver axis by regulating the transport of bile acids and the ecological structure of intestinal flora. And JGC could effectively alleviate liver inflammation, restore the liver and intestinal injury caused by alcohol.

FRI-418

Strategies are needed to support people with alcohol use disorder and alcohol-related liver disease to take part in randomised clinical trials: results from the MIRAGE pilot trial of functional imagery training

Ashwin Dhanda^{1,2}, Victoria Allgar¹, Jackie Andrade¹, Lynne Callaghan¹, Benjamin Hudson³, Wendy Ingram¹, Angela King¹, Victoria Lavers⁴, Joe Lomax¹, Anne McCune⁵, Crispin Musicha¹, Richard Parker⁶, Christopher Rollinson⁷, Siobhan Creanor⁸.

POSTER PRESENTATIONS

¹University of Plymouth, Faculty of Health, Plymouth, United Kingdom;

²University Hospitals Plymouth NHS Trust, South West Liver Unit, Plymouth, United Kingdom; ³Royal Devon University Hospitals NHS Foundation Trust, United Kingdom; ⁴Unaffiliated, United Kingdom;

⁵University Hospitals Bristol and Weston NHS Foundation Trust, Department of Liver Medicine, United Kingdom; ⁶Leeds Teaching Hospitals NHS Trust, United Kingdom; ⁷University Hospitals Plymouth NHS Trust, Research Development and Innovation, United Kingdom;

⁸University of Exeter, Exeter Clinical Trials Unit, United Kingdom

Email: ashwin.dhanda@nhs.net

Background and aims: Treatment of alcohol use disorder (AUD) in people with alcohol-related liver disease (ARLD) reduces the risk of disease progression and mortality. However, there are no effective evidence-based therapies. Functional Imagery Training (FIT) is a novel therapy combining motivational interviewing techniques with imagery to strengthen motivation for behaviour change. We conducted a pilot trial of FIT to test whether people with AUD and ARLD could be recruited and retained in a trial and how well FIT could be delivered within the UK National Health Service (NHS).

Method: We conducted a multicentre randomised pilot trial of FIT with treatment as usual (TAU) versus TAU alone in patients with unplanned hospital admissions with AUD and ARLD. Primary outcomes were recruitment and retention rates. Secondary outcomes included self-reported alcohol use by timeline follow-back. Alcohol liaison nurses were trained to deliver FIT to participants who received the first session in hospital and a further 8 sessions over 6 months by phone. Follow-up of all participants was by phone for Days 28 and 90 and in-person at Day 180 (D180), the primary end point. To help retention, participants were asked to provide contact details for a nominated second person and offered a financial incentive at the final trial visit.

Results: Of 121 patients approached, 54 were recruited (45% recruitment rate) and randomised (TAU: 28; FIT+TAU: 26); mean

(SD) age 49 (11), 63% male, 52% had cirrhosis with mean MELD 24 (6.5). Non-participation was mainly due to ineligibility (n = 11), lack of interest (n = 17) and logistical challenges (n = 28). 14 (26%) participants were not retained to D180 due to death (n = 5) and withdrawal (n = 9). Of the remaining 40 participants, 23 (58%) attended the D180 visit. 9, 17 and 17 participants did not attend trial visits at Days 28, 90 and 180, respectively. Most alcohol liaison nurses delivered FIT with adequate fidelity. 50% of participants randomised to FIT+TAU received the first 2 sessions (considered an adequate dose of the intervention). Based on all available data, median alcohol use per week fell from 1568 g (range 788, 2128) pure ethanol at baseline to 0 g (0, 180) at D180 and from 1120 g (610, 1784) to 0 g (0, 196) in TAU and FIT+TAU groups, respectively.

Conclusion: This study demonstrates the importance and challenges of recruitment and retention. Although we showed that alcohol workers in the UK NHS could successfully deliver FIT to people with AUD and ARLD, low retention limited interpretation of clinical outcomes. The implemented retention plan was inadequate as participants frequently changed phone number or did not respond to calls. Robust strategies to support recruitment and retention of people with AUD and ARLD must be incorporated in future clinical trials to enable the evaluation of new interventions in this underserved patient population.

FRI-419

Supplementation of choline attenuates the onset of alcohol-related liver disease

Victor Sánchez¹, Anja Baumann¹, Franziska Kromm¹, Annette Brandt¹, Ina Bergheim¹. ¹University of Vienna, Department of Nutritional Sciences, Austria

Email: ina.bergheim@univie.ac.at

Background and aims: Alcohol-related liver disease (ALD) is still one of the most common liver diseases worldwide. Besides altering liver

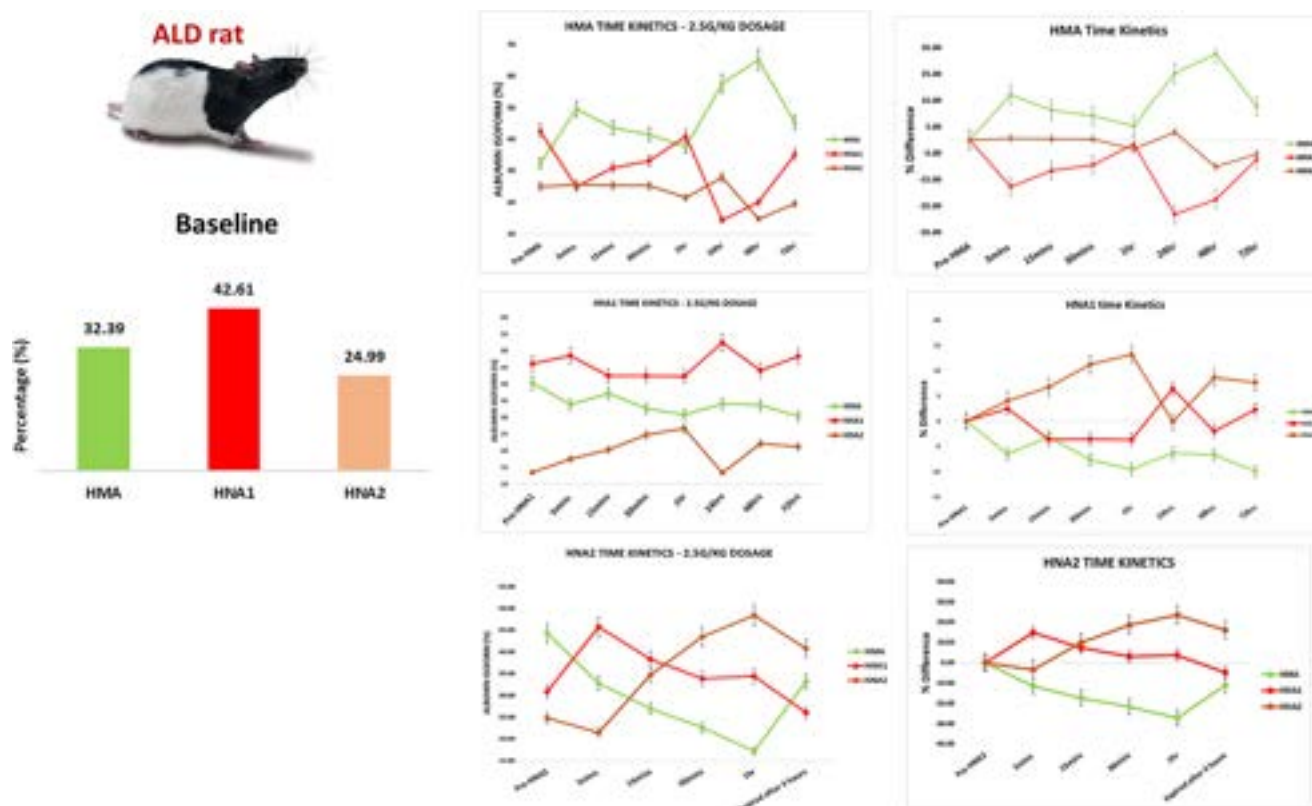


Figure: (abstract: FRI-416).

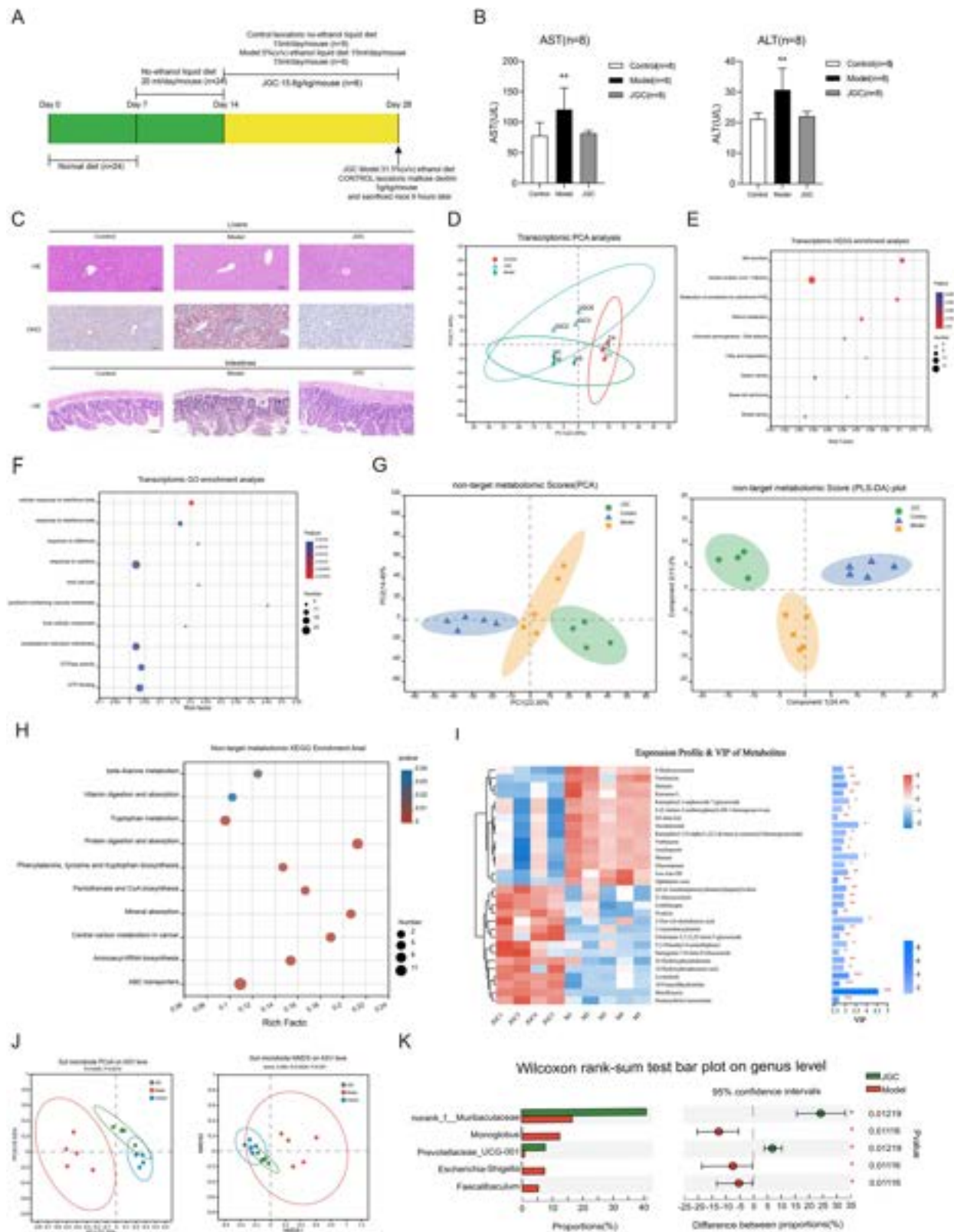


Figure: (abstract: FRI-417).

metabolism due to its metabolism, chronic elevated ethanol intake has also been shown to be accompanied with alterations of intestinal microbiota composition and intestinal barrier dysfunction. Despite intense research efforts, molecular mechanisms involved in the

damaging effects of ethanol on intestinal barrier function are not fully understood. Chronic alcohol intake has also been shown to be associated with alterations of choline metabolism in the liver. Here, we assessed the effects of an oral choline supplementation on the

POSTER PRESENTATIONS

development of a diet-induced ALD in C57BL/6J mice and determined associated molecular mechanisms.

Method: After an adaptation phase, female C57BL/6J mice (n = 8/group) were either pair-fed a liquid control diet (C), or a Lieber deCarli liquid diet (E, 5% ethanol) \pm 2.7 g choline/kg diet for 29 days. Markers of liver damage and intestinal permeability were determined. Additionally, effects of choline on ethanol-induced intestinal permeability were assessed *ex vivo* in an everted tissue sac model.

Results: As expected, chronic intake of ethanol was associated with the development of liver steatosis and early signs of inflammation as determined by liver histology, number of neutrophils, NOx concentration in liver tissue and ALT activity in plasma ($p < 0.05$ for all parameters compared to C-fed mice). Supplementing the ethanol diet with choline significantly attenuated the development of ALD with markers of inflammation, steatosis, number of neutrophils and NOx concentration in the liver all being significantly lower in E + choline-fed mice compared to E-fed mice ($p < 0.05$). The protective effects of choline were associated with significantly lower permeability of small intestinal tissue. In line with the *in vivo* findings, choline also significantly attenuated the ethanol-induced intestinal barrier dysfunction in small intestinal everted tissue sacs *ex vivo*, while the concomitant treatment with a choline oxidase inhibitor (diminonol) almost completely abolished these protective effects of choline.

Conclusion: Our results indicate that an oral supplementation of choline may attenuate the development of ALD in mice and that this at least in part is related to a protection against ethanol-induced intestinal barrier dysfunction.

FRI-420

Increased concentration of 4-hydroxyphenyllactic acid in patients with alcohol-related liver disease could promote the growth of *Lactobacillus* spp

Jin-Ju Jeong¹, Satya Priya Sharma¹, Raja Ganesan¹, Haripriya Gupta¹, Sung-Min Won¹, Ki Kwang Oh¹, Mi Ran Choi¹, Younglim Ham², Ki Tae Suk¹. ¹Institute for Liver and Digestive Diseases, Hallym University College of Medicine, Korea, Rep. of South; ²Department of Nursing, Daewon University College, Korea, Rep. of South
Email: ktsuk@hallym.ac.kr

Background and aims: Alcoholic liver disease (ALD) is caused by excessive alcohol consumption. It is increasing in prevalence. ALD is a progressive disease that is dangerous and can eventually lead to death. However, no specific treatment has been found to date. In the past decade, studies on the microbiome and metabolites have been conducted to develop disease mechanisms and medicines. Therefore, in this study, to identify metabolites and microorganisms related to alcoholic liver disease metabolites and microorganisms from feces of patients with alcoholic liver disease and healthy subjects will be analyzed. In addition, the correlation between the metabolite and intestinal bacteria that identified in this study will be analyzed.

Method: Stools were sampled from 17 healthy subjects, 26 subjects with alcoholic hepatitis, and 17 patients with more than alcoholic cirrhosis. Metabolites were analyzed using a Q-Exactive Plus Orbitrap MS-connected Ultimate-3000 UPLC system. The obtained data were analyzed using Metaboanalyst 5.0. For analysis of microbiome, the Illumina MiSeq platform was used. The obtained data was analyzed using the comparative microbiome taxonomic profiling analyzer of EZBioCloud. Based on metabolite and microbiome data, *Lactobacillus* spp. were pre-cultured in RCM media and subcultured to same media containing 4-HPA or containing SDW. After 2 days, colony forming unit was assessed by smearing on RCM agar medium.

Results: As alcoholic liver disease progressed, 4-HPA was increased. The family *Lactobacillaceae* was elevated in the microbiome of liver disease patients identified as having this substance. On the other hand, no increase in *Lactobacillaceae* was observed in patients without an increase of 4-HPA. Co-cultured with 4-HPA and

Lactobacillus spp. *in vitro*, colony forming units were increased compared to without 4HPA.

Conclusion: In this study, 4-HPA, a metabolite that is increased followed by the process of alcoholic liver disease, can increase the population of *Lactobacillus* spp. Research on the 4-HPA and correlation between the microbiome might be helpful to develop the mechanisms and treatments for alcoholic liver disease.

FRI-421

Granulocyte monocyte/macrophage apheresis for corticosteroid-nonresponsive or -intolerant severe alcohol-associated hepatitis: a nonrandomized controlled study

Ryosuke Kasuga¹, Po-sung Chu¹, Nobuhito Taniki¹, Rei Morikawa¹, Takaya Tabuchi¹, Fumie Noguchi¹, Karin Yamataka¹, Yuki Nakadai¹, Mayuko Kondo¹, Takanori Kanai¹, Nobuhiro Nakamoto¹. ¹Keio University School of Medicine, Division of Gastroenterology and Hepatology, Department of Internal Medicine, Japan
Email: pschu0928@icloud.com

Background and aims: Short-term mortality rate of patients with severe alcohol-associated hepatitis (SAH) remains as high as approximately 40–50%. Unmet needs exist in patients who are refractory to corticosteroids (CS) or are ineligible for early liver transplantation. In the current study, we aimed to investigate whether granulocyte and monocyte/macrophage apheresis (GMA) improves 180-day overall survival in CS-nonresponsive or CS-intolerant patients with SAH.

Method: This was a prospective, open-label, nonrandomized, historically controlled study conducted at a liver transplant center in Tokyo since October 2015. Lille model- and Model for End-stage Liver Disease (MELD) score-defined CS nonresponsive or CS-intolerant SAH patients who fulfilled inclusive criteria (leukocytosis over 10,000/ μ L, etc.) were enrolled. GMA was performed with Adacolumn[®], twice per week, for 5 to 10 times per session. Primary outcome was overall survival at 180 days. Secondary outcomes included changes in prognostic parameters, overall survival, cumulative rate of discharge and alcohol relapse. Correlations between cytokines or growth factors and prognostic parameters were also explored. Overall survival at 180 days was compared to SAH patients who were treated with CS and demonstrated nonresponse to CS in previous clinical trials (historical controls). Only patients who were not treated with any medication of interest other than CS, were pooled. This study was registered as UMIN000019351, and jRCT No. 032180221. This study was supported by grants-in-aid from Japan Society for the Promotion of Science (JSPS) KAKENHI (Grant Number 120K16999). Adacolumn was kindly provided by the manufacturer. The funders of the study had no role in study design, data collection, data analysis, data interpretation, or writing of this report.

Results: From October 2015 to December 2021, 13 GMA sessions were conducted on 11 patients. The Maddrey's Discriminant Function was 53.2 ± 17.7 at admission. The overall survival rate of the GMA group was 90.9% at 180 days, which was significantly better than that of the historical controls (51.7%) ($p = 0.0128$). Clinical parameters, including MELD scores, improved significantly ($p < 0.0001$). Estimated mortality risks using the Lille model and MELD scores at two and six months also significantly improved (both $p < 0.01$) and were internally validated. All patients recovered and discharged after a median of 25 days. The cumulative rate of first alcohol relapse was 35.9% per year. Four patients died from liver failure after alcohol relapse. No severe adverse events were observed. Granulocyte colony-stimulating factor levels were significantly inversely correlated with all prognostic scores surveyed after GMA (all $p < 0.05$).

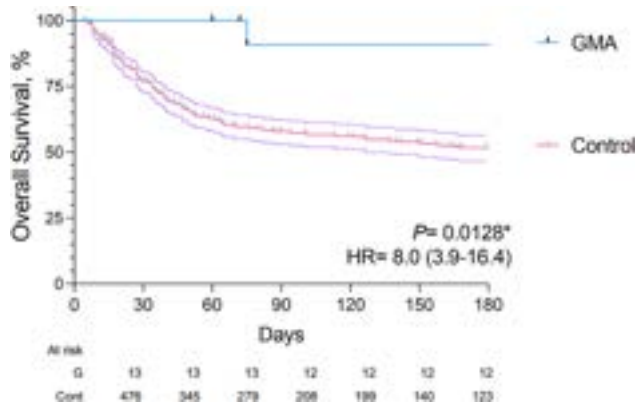


Figure:

Conclusion: Compared to historical controls, GMA significantly improved overall survival at 180 days in patients with CS-non-responsive or CS-intolerant SAH. As GMA has already been applied to other diseases with good safety profiles, immediate needs may be met as a salvage therapy following CS. Further investigations are warranted.

FRI-422

Diabetes increases risk of mortality in alcohol-related liver disease

Mark Theodoreson¹, Guruprasad Aithal^{2,3}, Michael Allison^{4,5}, Mayur Brahmanian^{6,7}, Ewan Forrest⁸, Hannes Hagström⁹, Alisa Likhitsup^{10,11}, Steven Masson¹², Anne McCune¹³, Neil Rajoriya¹⁴, Ian Rowe^{1,15}, Richard Parker¹. ¹Leeds Teaching Hospitals NHS Trust,

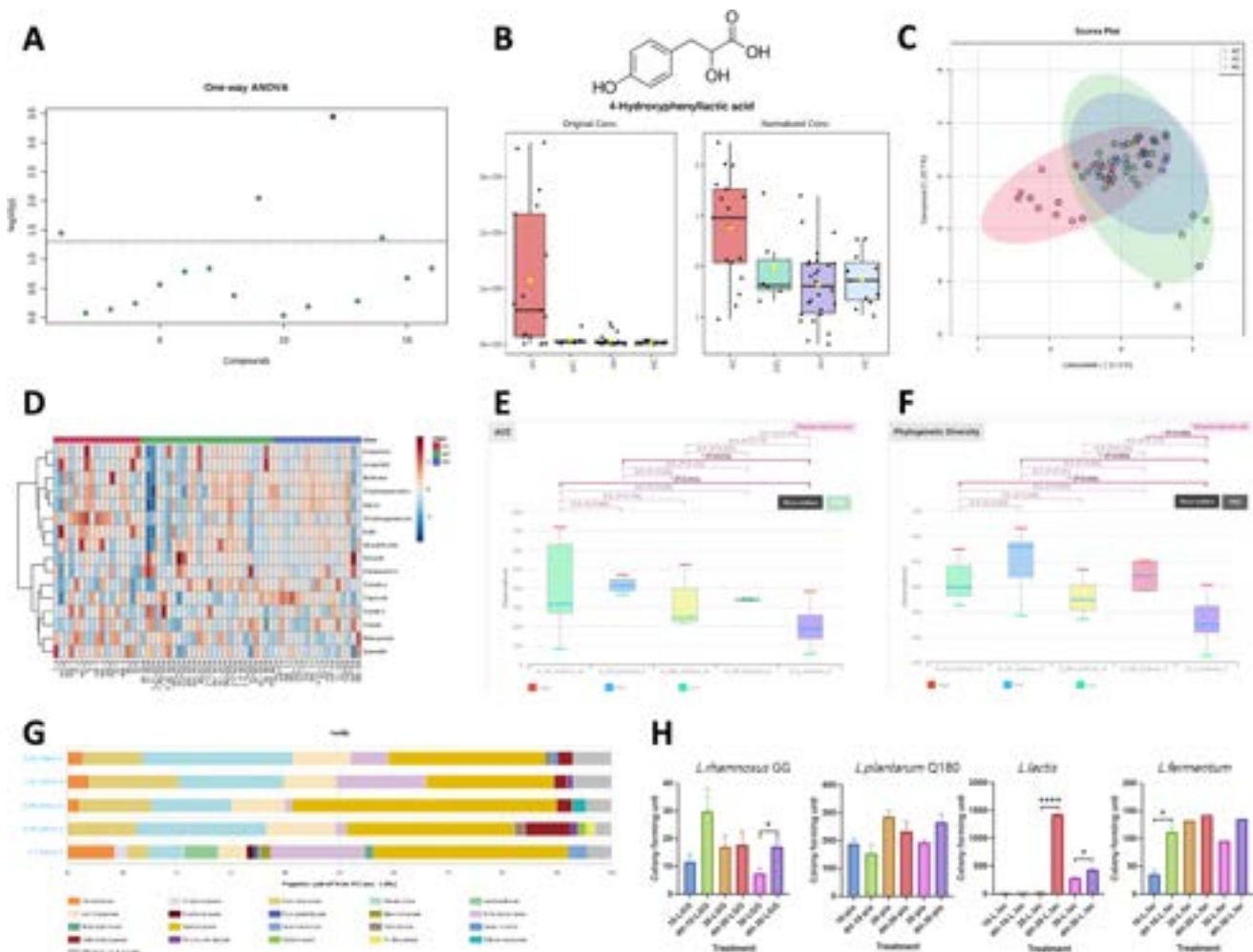


Figure: (abstract: FRI-420): A, one-way ANOVA and post-hoc tests with 16 phenolic compounds. B, significantly increased compound among 16 phenolic compounds. C, partial least squares discriminant analysis with HC (healthy control), AH (alcoholic hepatitis), and AC (alcoholic cirrhosis or cancer). D, hierarchical clustering heatmaps between 16 phenolic compounds and human subjects. E and F, ACE diversity and phylogenetic diversity based on microbiome of HC (healthy control) without 4-HPA, HC (healthy control) with 4-HPA, MD (cirrhosis) without 4-HPA, MD with 4-HPA, and sever (more than cirrhosis) with 4-HPA. G, relative abundances of cecal microbiome at Family level in different experimental groups. H, colony forming units of *Lactobacillus* spp.

POSTER PRESENTATIONS

Leeds Liver Unit, United Kingdom; ²NIHR Nottingham Biomedical Research Centre Nottingham University Hospitals NHS Trust, United Kingdom; ³University of Nottingham, United Kingdom; ⁴Liver Unit, Cambridge NIHR Biomedical Research Centre, United Kingdom; ⁵Cambridge University Hospitals NHS Foundation Trust, United Kingdom; ⁶Toronto General Hospital, Canada; ⁷University of Toronto, Canada; ⁸Queen Elizabeth Hospital, Glasgow, United Kingdom; ⁹Karolinska University Hospital, Sweden; ¹⁰St Luke's Hospital, Kansas City, United States; ¹¹University of Missouri School of Medicine, United States; ¹²The Freeman Hospital, Newcastle, United Kingdom; ¹³Bristol Royal Infirmary, United Kingdom; ¹⁴The Liver Unit, Queen Elizabeth Hospital, Birmingham, United Kingdom; ¹⁵University of Leeds, Leeds Institute for Medical Research, United Kingdom
Email: marktheo@doctors.org.uk

Background and aims: Diabetes Mellitus (DM) is a significant risk factor for metabolic associated fatty liver disease (MAFLD), and increases the risk of adverse outcomes. There have been multiple studies looking at the relationship between alcohol intake and the relative risk of developing diabetes, but few of these look specifically at the effect of DM on persons with alcohol-related liver disease (ArLD). This study explored the relationship between ArLD and DM.

Method: The WALDO study is an international multi-centre collaboration to gather a cohort of patients with biopsy proven ArLD and associated outcome data. The presence of DM at baseline or during follow-up was noted. Clinical events after index biopsy were noted retrospectively. Liver-associated clinical events (LACE) were defined as transplant, *de novo* decompensated cirrhosis or hepatocellular carcinoma. Mortality was sub-classified as liver-related or non-liver related. Risks for adverse outcomes was assessed with cox proportional hazards with the presence of diabetes treated as a time-dependent variable to reflect periods of time without or with diabetes. Analysis was done using the survival package in R.

Results: Seven hundred and four patients were included (median age 51.09 + standard error (SE) 0.44, 269 females, mean BMI 28.7, (range 16.3–48.9). During follow-up there were 215 episodes of LACE and 407 patients died (n = 380; 54.0%) and 47 had a liver transplant. At baseline 106 patients had DM (15.1%), and 246 (34.9%) had at least one previous decompensation episode. Median follow-up was 1591.5 days + SE 87.28, during which a further 51 patients (7.24%) developed DM (total diabetes n = 157 (22%)).

In univariable analysis DM was a significant risk factor for all-cause mortality (HR 1.38, 1.01–1.89, p = 0.041) and for incident cardiovascular disease (HR 2.29, 1.33–2.94, p < 0.001), and associated with increased risk of LACE, although this did not reach statistical significance (HR 1.48, 0.96–2.27, p = 0.074). In multivariable analysis controlling for fibrosis stage, decompensation at baseline, obesity and abstinence, DM remained significantly associated with all-cause mortality (HR = 2.08, 1.41–3.05, p < 0.001).

Univariate regression				Multivariate regression: death or transplant			
Outcome ¹	HR ²	95% CI ²	p-value	Characteristic ³	HR ²	95% CI ²	p-value
All cause death or transplantation	1.42	1.02, 1.86	0.036	Diabetes ⁴	2.08	1.41, 3.05	<0.001
Liver-related death or transplantation	1.35	0.94, 2.36	0.090	DM ⁵	0.89	0.36, 1.02	0.4
Non liver-related death	1.18	0.67, 2.09	0.5	Fibrosis grade	1.01	0.69, 1.26	>0.9
Liver-related clinical events	1.34	0.82, 2.16	0.2	Decompensation at baseline			
Hepatocellular carcinoma	0.87	0.18, 2.87	0.8	No	—	—	0.009
Cardiovascular events	2.30	1.02, 5.14	<0.001	Yes	1.79	1.22, 2.61	0.003
Non liver cancer	1.40	0.75, 2.62	0.3	Abstinence after biopsy	0.51	0.36, 0.72	<0.001

Figure: Cox-proportional hazard regression with diabetes as time dependent variable.

Conclusion: DM is a frequent co-morbidity in persons with ArLD and is associated with a higher risk of mortality. Clinicians managing those with ArLD should actively review diabetic status and ensure adequate treatment as required.

FRI-423

Pharmacological therapy for alcohol use disorder is effective and safe in patients with cirrhosis. Systematic review and meta-analysis

Jordi Gratacos^{1,2,3}, Pol Bruguera^{2,4,5}, Martina Perez¹, Ana Lopez Lazcano^{2,4}, Helena Hernández Evole¹, Ramon Bataller^{1,2,3,6}, Pere Ginès^{1,2,3,6}, Hugo Lopez^{2,4,5,6}, Elisa Pose^{1,2,3,6}. ¹Hospital Clínic de Barcelona, Liver Unit, Barcelona, Spain; ²Institut d'Investigacions Biomèdiques August Pi i Sunyer (IDIBAPS), Barcelona, Spain; ³Centro de Investigación Biomédica En Red en Enfermedades Hepáticas y Digestivas (CIBEREHD), Madrid, Spain; ⁴Hospital Clínic de Barcelona, Psychiatry, Barcelona, Spain; ⁵Centro de Investigación Biomédica En Red de Salud Mental (CIBERSAM), Madrid, Spain; ⁶Facultat de Medicina i Ciències de la Salut, Universitat de Barcelona, Barcelona, Spain
Email: EPOSE@clinic.cat

Background and aims: alcohol abstinence is the main prognostic factor in patients with alcohol-related liver disease. Most studies that have assessed the efficacy of pharmacological treatment for alcohol use disorder (AUD) have excluded patients with liver disease. The aim of this study was to perform a systematic review and meta-analysis on the efficacy and safety of pharmacological treatment for AUD in patients with cirrhosis.

Method: we retrieved all studies published in PubMed, Embase and Scopus until May 2022. PRISMA guidelines were used to design the study protocol, which was published in Prospero. We included randomized controlled trials (RCT), cohort studies and case-control studies using any pharmacological treatment for AUD in patients with cirrhosis. We used platform Rayyan[®] for the selection process, which was divided in a screening phase (evaluation of title/abstract) and an eligibility phase (full-text examination). Records were reviewed by four independent investigators divided in pairs. Data collection was performed by the same reviewers. The primary outcome was defined as percentage of alcohol abstinence (AA). Secondary outcomes were related to safety, amount of consumption and time to lapse/relapse. The meta-analysis was based on a random-effects model and heterogeneity was quantified using I².

Results: we identified 4095 studies after duplicates removal. Ten studies (4 RCT and 6 observational) met the inclusion criteria and none of the exclusion criteria. A total of 950 patients were included; 562 patients (59%) had a diagnosis of cirrhosis. The investigated treatments included baclofen (n = 6 studies), metadoxine (n = 2), acamprosate (n = 2), naltrexone (n = 1) and fecal microbiota transplantation (n = 1). Duration of treatment and follow-up ranged from 1 to 12 months. In the observational studies with no control group, abstinence rates varied from 51 to 85%. Two of the 4 RCT (1 on baclofen and 1 on metadoxine) found increased AA in the treatment groups. The random-effects model analysis conducted showed that the pharmacological treatment for AUD reduces the risk of active alcohol consumption with an overall increase in AA of 26% (risk ratio 0.74; CI 0.57–0.96; I² = 57%). Concerning individual treatments, we were only able to perform an analysis for baclofen, which did not reach significance (risk ratio 0.72; CI 0.46–1.13; I² = 76%). With respect to safety, none of the studies reported higher incidence of severe adverse events in the treatment groups.

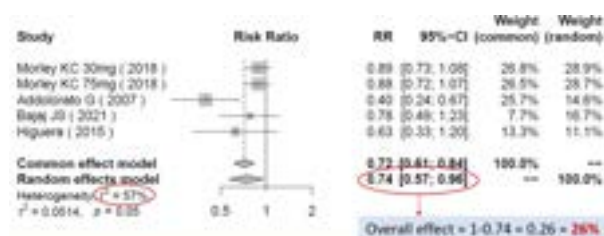


Figure: Random-effects model analysis of the relative risk of active alcohol consumption in patients with cirrhosis treated with pharmacological treatments for AUD or control therapy.

Conclusion: pharmacological treatment for AUD in patients with cirrhosis increases the probability of AA by 26% and has a good safety profile. Further prospective, high-quality studies are needed to establish a robust recommendation for the use of these treatments in patients with liver disease.

FRI-424

Binge drinking acutely induces fatty liver with increased liver stiffness which is readily reversed

Kristoffer Kjærgaard¹, Jeppe Yeoman¹, Anne Catrine Daugaard Mikkelsen¹, Peter Lykke Eriksen¹, Emilie Eifer Møller¹, Ann-Sophie Wietz¹, Lars Gormsen², Sara Heeboll³, Hendrik Vilstrup¹, Karen Louise Thomsen¹. ¹Aarhus University Hospital, Department of Hepatology and Gastroenterology, Denmark; ²Aarhus University Hospital, Department of Nuclear Medicine and PET, Denmark; ³Aarhus University Hospital, Department of Endocrinology and Internal Medicine, Denmark
Email: krikje@clin.au.dk

Background and aims: Alcohol-related liver disease is the leading cause of liver-related morbidity and mortality worldwide. Excessive alcohol consumption in a short period of time, also known as 'binge drinking', is a highly prevalent modus of alcohol intake. Binge drinking is often considered particularly harmful, however, the immediate effects on the development of a fatty liver representing the earliest alcohol-related liver injury, are not well established. The aim of this study was to investigate the acute effects of binge drinking on the liver and reversibility.

Method: We performed a cohort study of healthy adults attending a three-day music festival in June 2022 with the intention to binge drink. The participants were examined before, the day after, and 10 days after the festival. The participants were alcohol abstinent one week prior to the first visit and between the two last. Each visit included Magnetic Resonance Imaging (MRI) with measurement of liver fat content (Proton Density Fat Fraction; MRI-PDFF), liver stiffness (MR Elastography), and blood samples. During the festival, the participants were monitored with breathalyzer blood alcohol concentrations and app-based self-reported alcohol and food intake.

Results: Fifteen participants (9 male, 6 female) aged 35 ± 5 years with a BMI of 23.4 ± 2.7 kg/m² completed the study. The participants consumed on average 18.6 ± 5.6 units (186 ± 56 g alcohol) per day. Binge drinking induced a 2.5-fold increase in the hepatic fat fraction from 1.9% (IQR 1.6%-2.5%) to 4.6% (IQR 2.4%-5.7%; $p < 0.0001$) resulting in definitive steatosis ($>5\%$) in six participants. This was accompanied by an elevation of liver stiffness from 2.5 ± 0.3 kPa to 2.7 ± 0.3 kPa ($p = 0.04$). Also, binge drinking caused increased AST/ALT ratio and GGT, and a decrease in LDL-cholesterol. There was no change in plasma triglycerides or glucometabolic measurements. 10 days after binge drinking, all outcome measures were normalized.

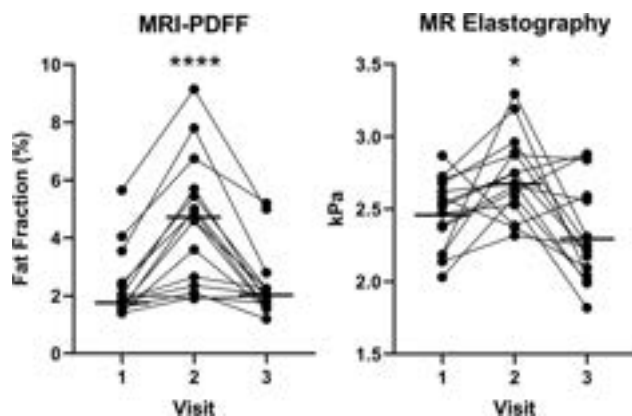


Figure:

Conclusion: In almost all of the healthy participants, a three-day bout of binge drinking caused unambiguous hepatic fat accumulation, which was accompanied by increased liver stiffness. This early alcohol liver injury was readily reversible upon only 10 days of alcohol abstinence. The study demonstrates a definite and potentially harmful fat accumulation in the liver caused by binge drinking. However, our findings imply that binge drinking is possibly not as dangerous as often assumed if binges are separated by a period of alcohol abstinence.

FRI-425

Disentangling the contributions of alcohol and alcohol-related liver disease towards dementia

Sixian Zhao¹, Linnea Widman¹, Hannes Hagström¹, Ying Shang¹. ¹Karolinska Institutet, Sweden
Email: ying.shang@ki.se

Background and aims: Previous studies have shown an association between alcohol use disorder (AUD) and dementia. However, both alcohol itself and alcohol-related liver disease (ALD) can have detrimental impacts on the brain, yet the relative weights of their contributions remain unknown. We aimed to disentangle the contributions of alcohol and ALD towards dementia by independently assessing the association between AUD alone or combined with ALD, and dementia.

Method: We identified patients with ALD or AUD from the DELIVER dataset, an ongoing nationwide register-based cohort including all patients diagnosed with chronic liver disease and up to ten matched controls from the general population in Sweden between 1987 and 2020. Three groups were identified through the linkage to the National Patient Register (NPR): AUD alone, ALD with co-existing AUD, and controls without any of these two diseases. The NPR and the Cause of Death Register were used to identify diagnoses of dementia. Cox regression models were used to assess the associations between AUD alone, or ALD, with dementia and dementia subtypes. Cumulative incidences were calculated accounting for competing risks of death.

Results: 128,884 individuals with AUD alone, 17,754 with ALD and 2,479,049 controls were identified. During a median follow-up of 8.9 years, 13,395 (10.4%), 2,187 (12.3%), and 138,925 (5.6%) dementia cases were identified in these groups. This translated into an increased dementia rate in the AUD alone group (adjusted HR [aHR] = 4.6, 95% CI 4.5–4.6), and a greater rate was observed in the ALD group (aHR = 8.6, 8.3–9.0) compared to the controls. AUD alone was also associated with a significantly increased rate of vascular (aHR = 2.3, 2.2–2.5) and Alzheimer's dementia (aHR = 1.4, 1.3–1.4), while ALD was associated with an increased rate of vascular (aHR = 2.7, 2.3–3.2) but not with Alzheimer's dementia (aHR = 0.9, 0.7–1.2). On average, the age at dementia diagnosis was younger in patients with AUD alone (67 years, IQR 56–76) and ALD (63 years, IQR 56–71) compared to controls (85 years, IQR 79–89). After stratifying by age at baseline, both AUD alone and ALD had disproportionately increased rates of dementia in the younger <40 yrs and 45–65 yrs groups. Both AUD and ALD had higher cumulative incidences of dementia, but not Alzheimer's or vascular dementia (Figure).

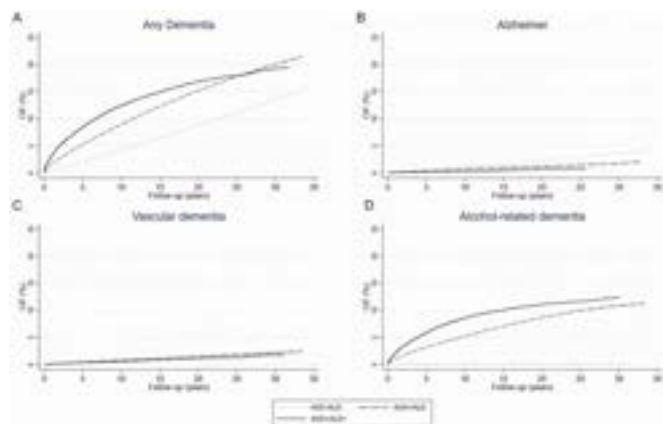


Figure: Cumulative incidence of dementia for AUD, ALD and controls from the general population.

Conclusion: AUD alone increased the risk of developing dementia, but additional ALD further exacerbates this risk. Dementia associated with AUD or ALD tended to be diagnosed at a younger age. These findings emphasize the importance of screening for cognitive impairment individuals with AUD to allow for earlier diagnoses and management of further cognitive decline and dementia. This may be of particular importance in younger patients.

FRI-426

Nucleoredoxin-dependent functioning is dysregulated by chronic alcohol consumption and is associated with the establishment of cellular senescence in the liver of aged mice

Osiris German Idelfonso García^{1,2}, Brisa Rodope Alarcón-Sánchez^{1,3}, Verónica Rocío Vásquez-Garzón^{4,5}, Saúl Villa-Treviño³, Pablo Muriel⁶, Héctor Serrano², Julio Isael Pérez-Carreón¹, Jaime Arellanes-Robledo^{1,5}. ¹National Institute of Genomic Medicine-INMEGEN, Mexico; ²Metropolitan Autonomous University-Iztapalapa Campus, Department of Health Sciences, Mexico; ³Center for Research and Advanced Studies of the National Polytechnic Institute-CINVESTAV-IPN, Department of Cell Biology, Mexico; ⁴Faculty of Medicine and Surgery, 'Benito Juárez' Autonomous University of Oaxaca-UABJO, Mexico; ⁵National Council of Science and Technology-CONACYT, Mexico; ⁶Center for Research and Advanced Studies of the National Polytechnic Institute-CINVESTAV-IPN, Department of Pharmacology, Mexico
Email: oidelfonso@inmegen.edu.mx

Background and aims: Aging, a natural process associated with abnormal oxidative stress production, involves several cellular and molecular changes that ultimately compromise the well-functioning of organs and systems in multicellular complex organisms. Aging is associated with a progressive and generalized deterioration of cellular functions, e.g., liver function is declined and involves alterations in hepatic structure, and function, thereby leading to the development of age-related liver disease. Aging also declines the liver metabolic capability and as a consequence, the efficiency to eliminate toxic agents is significantly decreased. These alterations are closely related with an increased production of reactive oxygen species (ROS) which is exacerbated by the chronic alcohol consumption; however, the underlying mechanisms had not been clarified. Nucleoredoxin (NXN) is both an oxidoreductase that targets ROS and a redox-sensitive enzyme that regulates key cellular processes through redox protein-protein interactions; however, the role of NXN during aging has not been investigated. Here, we aimed to determine the involvement of NXN in alcoholic liver disease (ALD) during aging in the mouse liver.

Method: ALD was recapitulated in 7-week-old (young) C57BL/6J female mice, 12-month-old (adult) and 18-month-old (aged) by the chronic ethanol consumption (20%) in 20% of sucrose for eight weeks and a single dose of lipopolysaccharide (1 mg/kg). We evaluated histological and cellular alterations, cellular senescence markers,

NXN protein level and NXN-dependent protein-protein interaction status, as well as, the gene expression profile changes.

Results: During aging, chronic alcohol consumption exacerbated liver structural disarrangement, steatosis and inflammatory infiltration which was accompanied by increased levels of proliferation markers namely proliferating cell nuclear antigen (PCNA) and Ki67, as well as, cellular senescence markers such as senescence-associated beta-galactosidase, H2A.X, Poly ADP ribose and interleukin 6. Interestingly, the level of oxidized proteins was significantly increased, and protein level of NXN and that of its interacting proteins FLII, MYD88, DVL and PP2A were also modified; as well as, the ratio of NXN/FLII interaction complex was significantly disrupted by the chronic alcohol consumption during aging. A RNA-seq analysis revealed that chronic alcohol consumption modified the expression of genes related with cell cycle arrest, oxidative stress regulator, induction of cellular senescence and lipid metabolism in aged mice.

Conclusion: Our results indicate that chronic alcohol consumption exacerbates both the structural and physiological damage, as well as, the cell proliferation and senescence in aged livers. Of note, the level of NXN redox-sensitive enzyme was decreased in the liver of mice subjected to ALD model during aging, but more interestingly, the interaction ratio of NXN-regulated proteins such as FLII was modified, likely, due to the increased protein oxidation induced by the ALD model. Thus, this evidence strongly suggests that ROS produced by the chronic alcohol consumption oxidize proteins and sensitize the liver cells and as a result, the NXN-dependent regulation is altered, a phenomenon that might accelerate the establishment of cellular senescence in the liver of aged mice.

FRI-427

Risk of alcohol-related liver disease in offspring of individuals with alcohol-related liver disease: a nationwide cohort study in Denmark

Peter Jepsen¹, Colin Crooks², Joanne Morling², Frederik Kraglund¹, Anna Emilie Kann³, Joe West², Gro Askgaard¹. ¹Aarhus Universitetshospital, Aarhus, Denmark; ²University of Nottingham, United Kingdom, ³Zealand University Hospital, Køge, Denmark
Email: gask@dadlnet.dk

Background and aims: Offspring of individuals with alcohol-related liver disease (ALD) may have an increased risk of ALD and therefore be potential candidates for screening for liver fibrosis. We compared the risk of ALD and the survival after ALD diagnosis in offspring of individuals with ALD to that of matched controls.

Method: We used nationwide healthcare registries to identify offspring of individuals diagnosed with ALD (ICD-10: K70.x) in Denmark from 1996 to 2018 and age- and gender-matched controls (20:1). Offspring and controls were followed for ALD diagnosis through 2018. We used landmark competing risk analyses to estimate the 10-year absolute and relative risk of ALD according to current age. To compare survival from ALD diagnosis between offspring and controls who developed ALD, we used Cox regression with adjustment for confounders of gender, age, and calendar year of ALD diagnosis.

Results: During the follow-up, ALD was diagnosed in 385 of 60,708 offspring and 2838 of 1,213,380 controls with an incidence rate ratio of 2.7 (95% CI 2.4–3.0). Offspring were slightly younger than controls at the time of ALD diagnosis (median age of 47 vs. 49 years) and the proportion who had cirrhosis at ALD diagnosis was similar in offspring and controls (57% vs. 56%). The 10-year absolute risk of ALD increased with age in both offspring and controls, peaking at 0.17% (95%CI: 0.09–0.28) for offspring aged 55 years and at 0.06% (95%CI 0.04–0.07) for controls aged 57 years (Figure 1, top). ALD was more frequent in offspring than controls at the younger ages, resulting in a very high relative 10-year risk before age 35 years, however, the absolute ALD risk was very low at these ages (Figure 1, bottom). There was no difference in ALD risk according to the gender of the offspring or the ALD parent, but offspring with both parents diagnosed with ALD had the highest risk [10-year absolute risk of 2.04% (95%CI: 0.17–9.40) at

age 57 years]. Survival after diagnosis of ALD was similar in offspring and controls, with an adjusted hazard ratio of 1.02 (95% CI 0.87–1.20).

Figure 1. Risk of alcohol-related liver disease (ALD) in offspring of individuals with ALD and age and sex-matched matched controls in Denmark from 1996 to 2018.

The top figure shows that the 10-year risk of ALD is 0.10% in offspring of individuals diagnosed with ALD compared to 0.04% in controls at the age of 50 years. The bottom figure shows that the relative risk for ALD in offspring of individuals with ALD compared to controls is 2.1 at age 50 years.

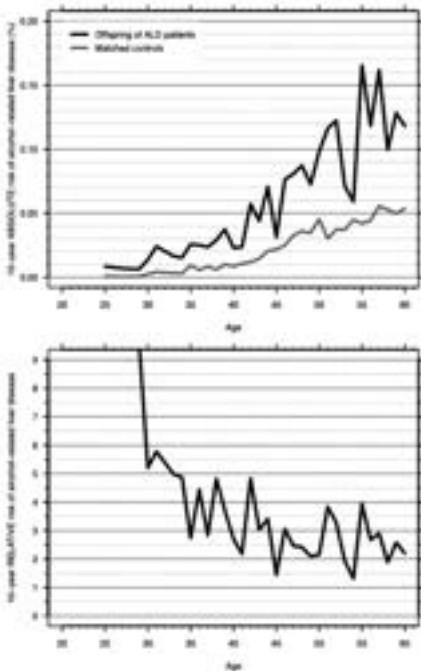


Figure:

Conclusion: Offspring of individuals with ALD had an increased relative risk of ALD, but their absolute risk was low. Their survival after ALD diagnosis was similar to that of controls. These findings indicate that screening may not be cost-effective; only 1 in 1000 offspring aged 50 years was diagnosed with ALD during the subsequent ten years.

FRI-428

US trends and contribution of metabolic syndrome in alcohol-associated liver disease from 1999 to 2018

Brian Lee¹, Jennifer Dodge¹, Norah Terrault¹. ¹University of Southern California, United States

Email: brian.lee@med.usc.edu

Background and aims: Mortality from alcohol-associated liver disease (ALD) has surged in recent years for unclear reasons. We aimed to examine the hypothesis that metabolic syndrome (MetS) may be an important contributor to ALD trends.

Method: Using the National Health and Nutrition Examination Survey (NHANES), an annual nationally-representative sample of the noninstitutionalized United States population, we assessed trends in MetS among ALD and non-ALD, in 4-year intervals (1999–2002, 2003–2006, 2007–2010, 2011–2014, 2015–2018). ALD was defined as average alcohol use >28 g/d in women and >42 g/d for men in the past 12 months, with AST or ALT >25 U/L in women and >35 U/L in men, excluding viral hepatitis. MetS was defined using National Cholesterol Education Program Adult Treatment Panel III criteria. High Fibrosis-4 (FIB-4) was defined as >2.67. Linear regression was used to assess prevalence of MetS among key subgroups and calculate absolute differences in prevalences with 95% confidence intervals. Multivariable logistic regression was used to assess odds of ALD associated with MetS adjusted for age, sex, race, alcohol intake.

Results: Among 36,349 respondents, 479 were with ALD (mean age 45, 70% male, 73% non-Hispanic White). The prevalence of ALD was stable throughout (1999–2002: 1.4% [95CI 1.1–1.8%]; 2015–2018: 1.4% [95CI 1.0–1.9%]). The prevalence of MetS among ALD increased (1999–2002: 36.4% [95CI 27.7–46.1%]; 2015–2018: 52.7% [95CI 38.6–66.3%]) vs. non-ALD (1999–2002: 30.4% [95CI 28.6–32.2%]; 2015–2018: 40.4% [95CI 38.0–42.9%]). Increases in MetS among ALD were observed among all demographic subgroups (age, sex, race) (Figure). Increases in MetS were driven by increases in high waist circumference, hypertension, and diabetes, not hypertriglyceridemia or low HDL. The prevalence of ALD with high FIB-4 increased significantly (1999–2002: 0.08% [95CI 0.03–0.2%]; 2015–2018: 0.25% [95CI 0.14–0.45%]; absolute difference: +0.17% [95CI +0.005 to +0.34%] $p = 0.04$), but was stable when excluding ALD with MetS (1999–2002: 0.06% [95CI 0.02–0.19%]; 2015–2018: 0.10% [95CI 0.03–0.29%], absolute difference: +0.04% [95CI –0.08 to +0.17%] $p = 0.52$). In multivariable regression, ALD was associated with female sex (aOR 1.73, $p = 0.004$), increasing alcohol use (aOR 1.97 per +10 g/day, $p < 0.001$), and MetS (aOR 1.93, $p < 0.001$). The association between ALD and alcohol use was 27% higher among those with MetS (interaction $p < 0.001$).

Conclusion: Between 1999–2018, while the national prevalence of ALD has been stable, the prevalence of ALD with advanced fibrosis has increased significantly, which was no longer apparent when cases with concomitant MetS were excluded. Thus, the rise in MetS among ALD may be an important contributor to the surge in ALD-related mortality observed in the last decade. Interventions to screen and treat MetS among patients with ALD may be relevant to clinicians and policymakers addressing the ALD epidemic.

FRI-429

Alcohol rehabilitation after alcoholic hepatitis is associated with reduced mortality: results of a 2012–2021 National retrospective study

Vincent Mallet^{1,2}, Eric Nguyen Khac^{3,4}, Lucia Parlati^{1,2,5}, Samir Bouam⁶, Anais Courtois⁴, Alexandre Louvet⁷, Marcq Ingrid⁴, Olivier Ganry⁸, Stanislas Pol^{1,2}, Philippe Sogni^{1,2}. ¹AP-HP, Centre, Groupe Hospitalier Cochin Port Royal, DMU Cancérologie et spécialités médico-chirurgicales, Service d'Hépatologie, Paris, France, France; ²Université Paris Cité, F-75006, Paris, France, France; ³Service d'Hépatogastro-Entérologie, CHU Amiens, Amiens 80054 Cedex 1, France; ⁴INSERM 1247 GRAP, CURS CHU Amiens site sud, Amiens 80054 Cedex 1, France; ⁵Institut Cochin, Université Paris Cité, CNRS, INSERM, F-75014, Paris, France, France; ⁶AP-HP, Centre, Groupe Hospitalier Cochin Port Royal, DMU PRIME, Unité d'Information Médicale, Paris, France, France; ⁷Service des maladies de l'appareil digestif, hôpital Claude-Huriez, Lille, France; ⁸Service de Santé Publique, CHU Amiens, Amiens 80054 Cedex 1, France

Email: vincent.mallet@aphp.fr

Background and aims: There is a lack of knowledge on the long-term prognosis of patients with alcoholic hepatitis. We measured multivariate risks and protective factors, including alcohol rehabilitation, after alcoholic hepatitis.

Method: We selected, among all patients recorded with alcohol use disorders in French hospitals in 2012–2021 (N = 1,438,236), those with alcoholic hepatitis. The primary exposure was alcohol rehabilitation ≥1 month after alcoholic hepatitis. The main outcome was death or liver transplantation. Adjusted hazard ratios were computed with Cox models with age as time scale, stratified on age at cohort inception, sex, severe comorbidities and deprivation.

Results: 65,814 (4.6%) patients were included. Median (interquartile range) age was 52.0 (44.0, 60.0) years and 71.5% were men. 7,141 (10.9%) patients underwent alcohol rehabilitation ≥1 month after alcoholic hepatitis. In-hospital death or liver transplantation were

POSTER PRESENTATIONS

recorded in 19,363 (29.4%) patients. Alcohol rehabilitation ≥ 1 month after alcoholic hepatitis was associated with death or liver transplantation ($p < 0.001$ with the log-rank test, see Figure). Alcohol rehabilitation [aHR 0.73, (95% CI 0.70, 0.77) $p < 0.001$] and liver disease progression to a liver-related complication [aHR 2.14, (95% CI 1.61, 2.84) $p < 0.001$] were protective and risk factors for death or liver transplantation, respectively.

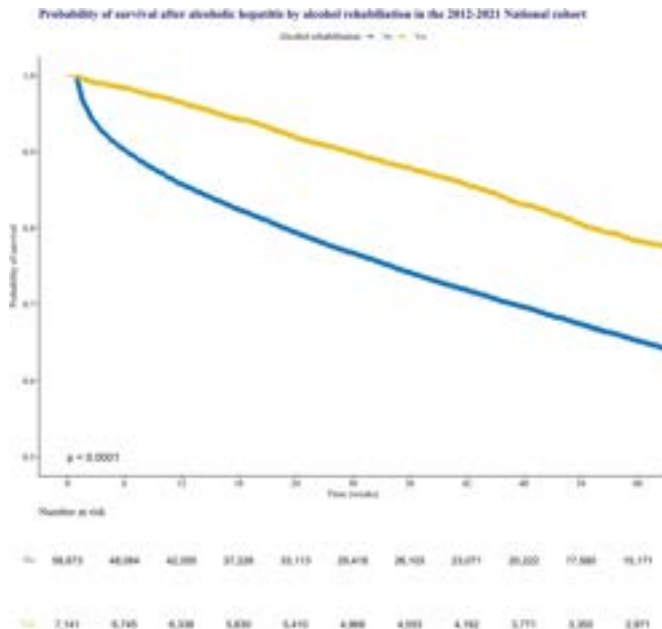


Figure:

Conclusion: Alcohol rehabilitation is the most critical clinical intervention to reduce mortality or liver transplantation from 1 month after alcoholic hepatitis. Currently only ~10% of patients have access to this treatment in France.

FRI-430

The role of HSD17B13 and MBOAT7 during alcohol detoxification: different effects on fibrosis and inflammation

Johannes Mueller¹, Vanessa Rausch¹, Phillippe Brosi², Sascha Müller², Peter Studer², Mathias Worni², Felix Sticke^{2,3}, Sebastian Mueller^{1,2}.

¹University of Heidelberg, Center for Alcohol Research, Germany;

²Viscera AG, Bern, Switzerland; ³University Hospital Zürich, Department of Gastroenterology and Hepatology, Switzerland

Email: sebastian.mueller@urz.uni-heidelberg.de

Background and aims: In genome wide association studies *PNPLA3*, *MBOAT7*, *TM6SF2* and *HSD17B13* were identified as important risk genes for the development of alcohol-related cirrhosis, however, their functions and molecular mechanisms are still incompletely understood. We here present first data on the role of these genotypes on liver stiffness (LS), steatosis (CAP) and inflammation during alcohol withdrawal.

Method: Patients with alcohol use disorders and heavy active alcohol consumption ($n = 550$) hospitalized for alcohol withdrawal were prospectively enrolled and genotyped for *PNPLA3* rs738409, *MBOAT7* rs626283, *TM6SF2* rs58542926 and *HSD17B13* rs72613567 variants. The Hardy-Weinberg-equilibrium was fulfilled for all loci. All patients had routine laboratory, abdominal ultrasound and measurement of liver stiffness (LS) and hepatic steatosis by controlled attenuation parameter (CAP) both using FibroScan platform (Echosens, Paris) at admission. For 415 patients, additional follow-up data after 6.3 days of alcohol withdrawal were available for analysis.

Results: Patients were predominantly male (72%), with a mean age of 51 (± 12) years, mean BMI of 25.3 kg/m² and mean alcohol consumption of 199 (± 147) g/day. At admission, no difference between the genotypes of the four genes was seen regarding age, BMI, gender, alcohol consumption or serum transaminase levels. Subjects with *MBOAT7* CC genotype had significantly higher LS values than those with the GG variant (22.5 kPa vs 10.4 kPa, $p < 0.0001$). The *HSD17B13* TA/TA variant had non-significantly lower levels of AST and LS. After detoxification, *PNPLA3* GG had significantly higher inflammation as reflected by higher AST levels ($p < 0.05$) and more steatosis (CAP 320 vs 280 dB/m, $p < 0.01$). *MBOAT7* CC carriers had significantly higher LS measurements (15 vs 9 kPa). *HSD17B13* TA/TA had significantly less inflammation (AST 69 vs 125 U/L) and lower LS (7 vs 12 kPa). The results were confirmed in a multivariate model using values after withdrawal. *HSD17B13* T and *PNPLA3* G alleles were

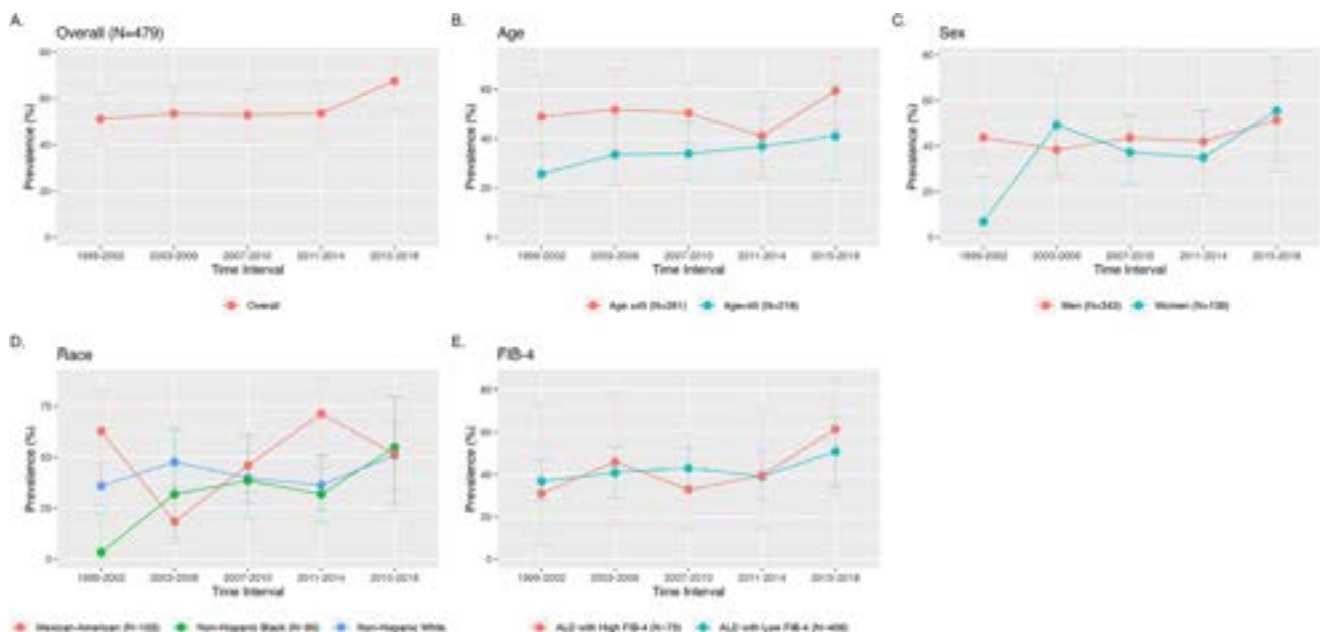


Figure: (abstract: FRI-428).

associated with increased inflammation (AST >50 U/L) (OR=0.53, $p < 0.001$ and OR=1.33, $p = 0.08$, respectively). Best association with steatosis (CAP >250 dB/m) was seen for *PNPLA3* G (OR=1.39, $p = 0.09$). *HSD17B13* T and *MBOAT7* C were both significantly associated with elevated LS (LS >6 kPa) (OR=0.57, $p < 0.001$ and OR=1.41, $p < 0.05$, respectively). No associations were seen for *TM6SF2*.

Conclusion: We found important differences between the studied genes during the alcohol detoxification phase. The *PNPLA3* G allele seems to be associated with steatosis and inflammation. The *MBOAT7* C allele seems to affect fibrosis without inflammation while *HSD17B13* TA appears to be protective against inflammation and fibrosis.

FRI-431

Patients with alcohol-related cirrhosis who recompensate on follow-up have a characteristic metabolomic profile with differential concentrations of lipid and amino-acid metabolites

Helena Hernández-Èvole¹, Jordi Gratacos¹, Emma Avitabile¹,
 Juanjo Lozano², Martina Perez¹, Julia Sidorova²,
 Alex Guillaumon Thierry³, Adria Juanola¹, Anna Soria¹, Isabel Graupera¹,
 Ana Belén Rubio¹, Marta Cervera¹, Marta Carol¹, Núria Fabrellas⁴,
 Pere Ginès^{1,4}, Elisa Pose¹. ¹Hospital Clínic de Barcelona, Liver Unit,
 Barcelona, Spain; ²Centro de investigación Biomédica en Red |
 Enfermedades Hepáticas y Digestivas, Spain; ³Facultat de Medicina-
 Universitat de Barcelona, Barcelona, Spain; ⁴Institut d'Investigacions
 Biomèdiques August Pi i Sunyer (IDIBAPS), Barcelona, Spain
 Email: hernandez.ievole@gmail.com

Background and aims: A notable proportion of patients with alcohol-related decompensated cirrhosis will experience resolution of clinical decompensations, which is a relevant phenomenon for prognosis of this population. The mechanisms and metabolic pathways involved in the recompensation of alcohol-related cirrhosis (ArC) are unknown. The aim of this study was to define the metabolomic profile of patients with ArC that will recompensate in the follow-up.

Method: Patients with ArC were selected from a prospective cohort collected between 2016 and 2020 and classified into 4 groups: 0) patients compensated at inclusion and during follow-up, 1) decompensated at inclusion but with subsequent recompensation, 2) decompensated at inclusion and during follow-up and 3) decompensated at inclusion who died the first 3 months of follow-up. Recompensation was defined as the absence of clinical decompensation without requiring specific treatment for ascites or encephalopathy during the year prior to the end of follow-up. Plasma samples were analyzed at baseline for metabolomic profile assessment by high-performance liquid chromatography-tandem mass spectroscopy.

Results: 63 patients with ArC were included: 18 in group 0, 15 in group 1, 15 in group 2 and 15 in group 3. Groups were comparable in terms of age and sex. Baseline MELD score was 8, 17, 16 and 27, respectively. Regarding alcohol follow-up, 11/18 (61%), 7/15 (47%) and 3/15 (20%) patients maintained abstinence at follow-up ($p = 0.04$). Median follow-up was similar between groups 1 and 2 (3.5 and 3.3 years). Patients in the 4 groups presented a differentiated metabolomic profile. When comparing group 1 and 2 (recompensated vs. decompensated patients) different concentrations in 32 metabolites were identified: 20 lipids were at higher concentrations in recompensated patients: 12 polyunsaturated fatty acids (docosahenoic acid and docosapanthenoic acid at concentrations 2.1 and 2.6 times higher ($p < 0.05$)) and 7 acylcarnitine and acylcholine metabolism compounds; 7 amino acids, including phenyl-lactate (3.1 times lower concentrations in the recompensated group ($p = 0.04$)); and 5 vitamins.

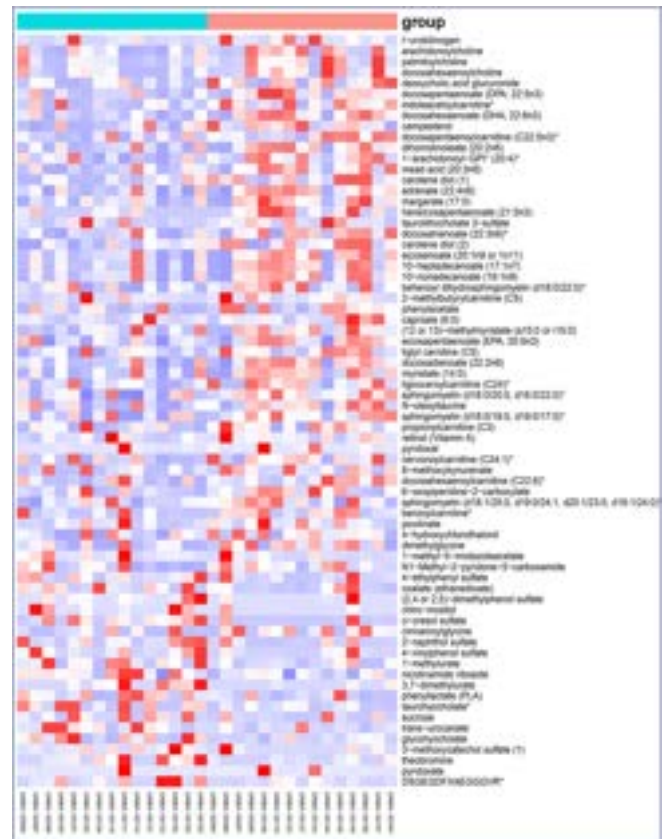


Figure: Heatmap representation of the top metabolites found at different concentrations in the group of patients recompensated during follow-up (group 1) vs those that remained decompensated (group 2).

Conclusion: Patients with ArC who were recompensated at follow-up presented a differentiated metabolomic regarding compounds involved in the metabolism of polyunsaturated fatty acids, acylcarnitines and amino acids such as phenyl-lactate. It is likely, therefore, that these metabolic pathways play a role in the recompensation of ArC.

FRI-432

A cost-comparison of the LiverPRO score with FIB-4, ELF, and FibroScan in 6,032 study participants

Katrine Prier Lindvig^{1,2,3}, Maria Kjærgaard^{1,2}, Katrine Thorhauge^{1,2},
Ellen Jensen^{1,2}, Johanne Kragh Hansen^{1,2}, Camilla Dalby Hansen^{1,2},
Stine Johansen^{1,2}, Mads Israelsen^{1,2}, Peter Andersen^{1,2}, Nikolaj Topp^{1,2},
Helle Lindholm Schnefeld^{1,2}, Sönke Detlefsen^{4,5}, Mathias Porselt⁶,
Nanna Kastrup⁷, Taus Holtug⁸, Aleksander Krag^{1,2}, Maja Thiele^{1,2}

¹Odense University Hospital, Department of Gastroenterology and Hepatology, Odense C, Denmark; ²University of Southern Denmark, Institute of Clinical Research, Odense C, Denmark; ³Evido, Taastrup, Denmark; ⁴Odense University Hospital, Department of Pathology, Odense C, Denmark; ⁵University of Southern Denmark, Department of Clinical Research, Faculty of Health Sciences, Denmark; ⁶Zealth, Copenhagen, Denmark; ⁷Aalborg University, Danish Center for Healthcare Improvements, Aalborg, Denmark
Email: katrine.prier.lindvig@rsyd.dk

Background and aims: Fatty liver disease is an increasing burden to the healthcare system. A key challenge is that most patients go undetected until the disease reaches its end stage. Therefore, an urgent need for cost-effective referral pathway from primary to secondary care is needed. LiverPRO is a diagnostic prediction model for liver fibrosis developed for primary care based on routine blood samples. We aimed to perform a cost analysis to assess the short-term

POSTER PRESENTATIONS

impact of implementing LiverPRO as a first-tier diagnostic test and compare it to other non-invasive tests.

Method: We conducted a prospective cohort study from 2017 to 2022. Participants were Danish residents with and without risk factors for alcohol-related liver disease (ArLD) and non-alcoholic fatty liver disease (NAFLD). The following referral pathways were evaluated: a) FIB-4 (>1.3) followed by FibroScan, b) ELF test (>9.8) followed by FibroScan, c) LiverPRO (>20%) followed by FibroScan or d) LiverPRO (>20%) followed by FibroScan, and if indeterminate then confirmation by ELF test (adapted from the EASL guideline). This cost analysis applies a hospital perspective and a mixed gross- and micro-costing approach. The analysis includes diagnosis-related costs for LiverPRO (€21 per test), FIB-4 (€7 per test), ELF (67€ per test), and FibroScan (€253 per test), targeting the identification of significant fibrosis ($\geq F2$), defined as TE>8 kPa. Costs for missed cases are not included. We reported the results as mean cost per patient on each pathway.

Results: This cost analysis is based on a study with 6,032 participants screened for chronic liver disease. Here, 48% were male, and the median age was 57 years (52–63 IQR). 30% were at risk of ArLD, 44% of NAFLD and 26% had no risk factors. The four pathways correctly classified patients according to the risk of significant fibrosis ($\geq F2$, defined as TE>8 kPa); a) at 65%, b) at 85%, c) at 93%, and d) at 95%, respectively (Figure). For advanced fibrosis ($\geq F3$, defined as TE>12 kPa) the pathways correctly classified; a) 65% b) 96% c) 95%, and d) 99%, respectively. According to the pathway, the mean cost per patient when diagnosing significant fibrosis ($\geq F2$) was a) € 97 b) € 103 c) € 36, and d) € 38 for the four pathways, respectively. The pathway c) consisting of LiverPRO followed FibroScan has the lowest cost compared to the other pathways.



Figure:

Conclusion: This cost analysis shows that using LiverPRO followed by FibroScan has the lowest cost compared to other pathways including FIB-4 and ELF. At the same time, LiverPRO followed by FibroScan correctly classifies 93% of patients with significant fibrosis. This is a notable increase compared to the pathways using FIB-4 and ELF as the initial tests.

FRI-433

Alcohol use disorder in patients undergoing bariatric surgery is associated with a worse prognosis

Edilmar Alvarado-Tapias^{1,2,3,4}, David Marti-Aguado^{2,5}, Concepción Gómez^{2,5}, Claudia Pujol^{1,4}, Ana Brujats^{1,4}, Rubén Osuna-Gómez⁴, Albert Guinart-Cuadra⁴, Josepmaria Argemi^{2,3,6}, Carlos Fernández-Carrillo^{2,3,7}, Meritxell Ventura Cots^{2,3,8}, Dalia Morales Arraez^{2,9}, Ana Clemente^{2,10},

Àngels Escorsell^{1,3}, Cándid Villanueva^{1,3}, Ramon Bataller^{2,11}.

¹Barcelona, Department of Gastroenterology, Hospital Santa Creu i Sant Pau, Institut de Recerca Sant Pau, Universitat Autònoma de Barcelona, Barcelona, Spain; ²Pittsburgh, Center for Liver Diseases, Division of Gastroenterology, Hepatology and Nutrition, Pittsburgh Liver Research Center, University of Pittsburgh Medical Center, Pittsburgh, PA, United States; ³Madrid, Centro de Investigación Biomédica en Red de Enfermedades Hepáticas y Digestivas (CIBERehd), Instituto de Salud Carlos III, Madrid, Spain; ⁴Barcelona, Inflammatory Diseases, Institut de Recerca de l'Hospital de la Santa Creu i Sant Pau, Biomedical Research Institute Sant Pau (IIB Sant Pau), Barcelona, Spain; ⁵Valencia, Digestive Disease Department, Clinic University Hospital, Biomedical Research Institute INCLIVA, Valencia, Spain; ⁶Pamplona, Liver Unit, Clínica Universidad de Navarra (CUN), Hepatology Program, Centro de Investigación Médica Aplicada (CIMA), Instituto de Investigación de Navarra (IdisNA), University of Navarra, Pamplona, Spain; ⁷Madrid, Liver Unit, Department of Gastroenterology and Hepatology, Hospital Universitario Puerta de Hierro-majadahonda, idiphisa, Madrid, Spain; ⁸Barcelona, Liver Unit, Hospital Universitari Vall d'Hebron, Vall d'Hebron Institute of Research (VHIR), Universitat Autònoma de Barcelona, Barcelona, Spain; ⁹Tenerife, Department of Gastroenterology, Hospital Universitario de Canarias, Tenerife, Spain; ¹⁰Madrid, Liver Unit, Department of Digestive Diseases, Hospital General Universitario Gregorio Marañón, Madrid, Spain; ¹¹Barcelona, Hospital Clinic de Barcelona, Universidad de Barcelona, Liver Disease department, Barcelona, Spain

Email: ealvaradot@santpau.cat

Background and aims: Alcohol use disorder has been described in patients undergoing bariatric surgery, but its impact on long-term outcomes is unknown. The aim of this study is to evaluate the prevalence, associated factors, and clinical impact of AUD prior to bariatric surgery.

Method: Prospective study of patients undergoing bariatric surgery and included in the LABS-2 (Long-term effect of Bariatric Surgery) registry. The study cohort was completed at 10 hospitals in the United States between 2006 and 2009 (Coordinated by University of Pittsburgh: ClinicalTrials.gov: NCT00465829). All cases with AUDIT performed prior to surgery and at least 7 years of follow-up after the bariatric procedure were included. AUD was defined as an AUDIT score ≥ 8 points. Cases with liver biopsy were histologically evaluated with the NASH-CRN system and Scheuer score to grade iron deposits. Survival analysis was performed with Kaplan-Meier curves and Cox regression adjusted for age, sex, BMI, smoking, diabetes, and cardiovascular events.

Results: A total of 2,271 patients were included (71% Y-De Roux, 25% gastric band, 4% other procedures), of which 16% had AUD prior to surgery. The factors associated with AUD were female gender (72.8% vs 27.2%; $p = 0.006$), age (40 ± 11 vs. 47 ± 11 years; $p < 0.001$), smoking (4.8% vs. 2.1%; $p = 0.005$) and the consumption of other drugs (15% vs. 4%; $p < 0.001$). Patients without AUD had higher prevalence of metabolic syndrome (57.1% vs. 44.1%; $p < 0.001$), arterial hypertension (73.4% vs. 60.3%; $p < 0.001$), diabetes (37.4% vs. 21.2%, $p < 0.001$), dyslipidemia (38.6% vs. 26.4%; $p < 0.001$), and cardiovascular events (10% vs. 5.1%; $p = 0.003$). Liver biopsy was performed in 286 subjects, 42% of whom had AUD. Patients with AUD had higher iron stores (41.7% vs. 22.6%; $p = 0.02$), with no differences in the presence of significant fibrosis (15.2% vs. 24.6%; $p = 0.17$) and steatohepatitis (21.7% vs. 32.5%; $p = 0.15$). Cases with AUD had a higher risk of mortality during follow-up (4.5% vs. 2.4%; log rank $p = 0.026$) (Figure 1). The factors associated with lower survival in Cox regression were: AUD (HR: 2.90 [95%CI 1.59–5.29] $p < 0.001$), age (HR: 1.04 [95%CI 1.01–1.07] $p = 0.002$), diabetes (HR: 2.22 [95%CI 1.30–3.79] $p = 0.003$), and BMI (HR: 1.03 [95%CI 1.01–1.06] $p = 0.001$).

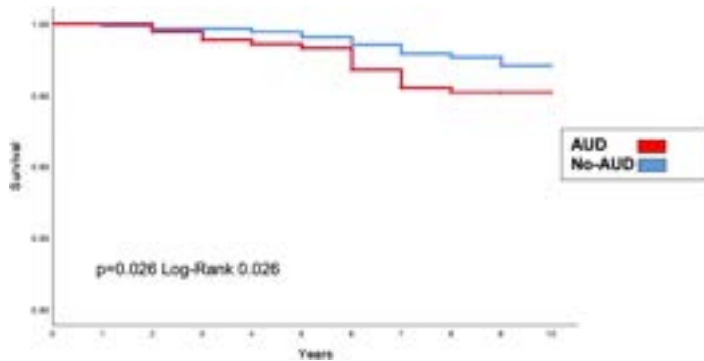


Figure:

Conclusion: The prevalence of AUD in patients undergoing bariatric surgery is high and is associated with increased long-term mortality.

FRI-434

Low sphingolipid levels indicate poor survival in patients with alcohol-related liver disease

Thit Mynster Kronborg¹, Qian Gao², Kajetan Trost², Henriette Ytting³, Malene Barfod O'Connell¹, Mikkel Werge³, Mira Thing¹, Lise Lotte Gluud¹, Søren Møller⁴, Thomas Moritz², Flemming Bendtsen³, Nina Kimer³. ¹Hvidovre University Hospital, Gastro Unit, Medical section, Denmark; ²Center for Basic Metabolic Research, Copenhagen University, Denmark; ³Hvidovre University Hospital, Gastro Unit, Medical Section, Hvidovre, Denmark; ⁴Hvidovre University Hospital, Clinical Physiology and Nuclear Medicine, Denmark
Email: thit.mynster.kronborg@regionh.dk

Background and aims: Alcohol-related hepatitis (AH) and alcohol-related cirrhosis are grave conditions with poor prognoses. Altered hepatic lipid metabolism may differentiate between different alcohol-related liver diseases. Therefore, assessment of individual lipidomic and/or metabolomic factors might help to predict short-term mortality. We aimed to investigate the influence of lipidomics and metabolomics on different stages of alcohol-related liver diseases and their impact on survival.

Method: Patients with newly diagnosed alcohol-related cirrhosis with current alcohol use (ALC-A), alcohol-related cirrhosis without current alcohol use (ALC) and AH were compared to each other and to liver-healthy individuals (HC). Circulating lipids and metabolites were analysed using high-performance liquid chromatography and mass spectrometry detection. Concentrations were measured as relative values compared to HC.

Results: Plasma samples from 207 patients were analysed; 40 patients with ALC; 95 patients with ALC-A; 30 patients with AH; and 42 HC. Lipidomics showed significant differences among patient groups and the healthy controls; most lipids decreased in patients compared to healthy. Nine of ten analysed free fatty acids differentiated the cirrhosis groups by increases with a relative change of 0.12–0.66 in the ALC group compared to the ALC-A group (p values <0.0005). For metabolomics, total bile acids increased significantly with a relative change of 19.73 in the ALC group, 31.29 in the ALC-A group and 80.38 in the AH group compared to HC (all p values <0.0001). Low sphingolipid (d42:1) and (d41:1) levels in the three patient groups had a high accuracy in predicting 90 days mortality (AUC = 0.922, 0.893; $p=0.007$, 0.008) and performed better than MELD score (AUC = 0.700, $p=0.19$).

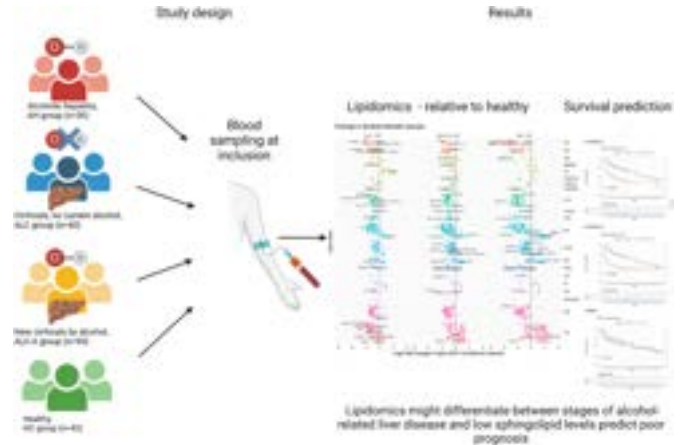


Figure:

Conclusion: Lipidomics classes decrease between stages of alcohol-related liver disease, and low sphingolipid levels predict poor prognosis.

FRI-435

Cause-specific mortality in patients with alcohol-related liver disease: a nationwide Danish cohort study

Anna Emilie Kann^{1,2,3}, Peter Jepsen², Lone Madsen¹, Joe West^{4,5}, Gro Askgaard^{1,2,3}. ¹Zealand University Hospital, Section of Gastroenterology and Hepatology, Køge, Denmark; ²Aarhus University Hospital, Department of Hepatology and Gastroenterology, Aarhus, Denmark; ³Bispebjerg and Frederiksberg Hospital, Center for Clinical Research and Prevention, Frederiksberg, Denmark; ⁴Nottingham University Hospitals NHS Trust and the University of Nottingham, NIHR Nottingham Biomedical Research Centre (BRC), United Kingdom; ⁵University of Nottingham, Population and Lifespan Sciences, United Kingdom

Email: aeka@regionsjaelland.dk

Background and aims: Knowledge of the pattern of causes of death is essential to prevent premature death in alcohol-related liver disease (ALD). We examined cause-specific mortality, including death due to specific cancers, in 15 years after diagnosis of ALD.

Method: We used the nationwide health registries to identify individuals diagnosed with ALD from 2002 to 2017 in Denmark and followed them for the underlying cause of death through 2019. We calculated the cause-specific mortality and investigated whether the pattern of cause-specific mortality differed by age (<60 and >60 years), gender, and ALD stage at diagnosis (cirrhotic and non-cirrhotic).

Results: The study included 23,385 individuals newly diagnosed with ALD with a median age of 58 years; 68% were men, and 64% had cirrhosis. During 110,322 person-years of follow-up, 15,692 (67%) died. Liver disease (Figure 1, red area) was the leading cause of death during the first five years after ALD diagnosis, and 26.0% (95%CI 25.5–26.6%) of patients died from liver disease within five years. Beyond five years of ALD diagnosis, cancer (orange and yellow area), alcohol abuse disorder (green area), and cardiovascular disease (blue area) became more important. The 10-year risk of death from cancer other than hepatocellular carcinoma (HCC) (orange area) was 8.5% (95%CI: 8.1–8.9%). HCC (yellow area) was the dominant cause of cancer death, followed by lung cancer, with 10-year risks of 2.5% (95%CI: 2.3–2.7%) and 1.9% (95%CI: 1.7–2.1), respectively. Alcohol abuse disorder (green area) continued to cause death even many years after ALD diagnosis, with a 10-year risk of 5.6% (95%CI 5.3–6.0). Death due to liver disease was similar according to age and gender but lower for those diagnosed with non-cirrhotic rather than cirrhotic ALD (10-year risk of death due to liver disease of 20.2% vs. 38.4%). Individuals aged >60 years were more likely to die due to extrahepatic causes

POSTER PRESENTATIONS

compared to younger individuals (10-year risk of death due to extrahepatic causes of 48% vs. 32%).

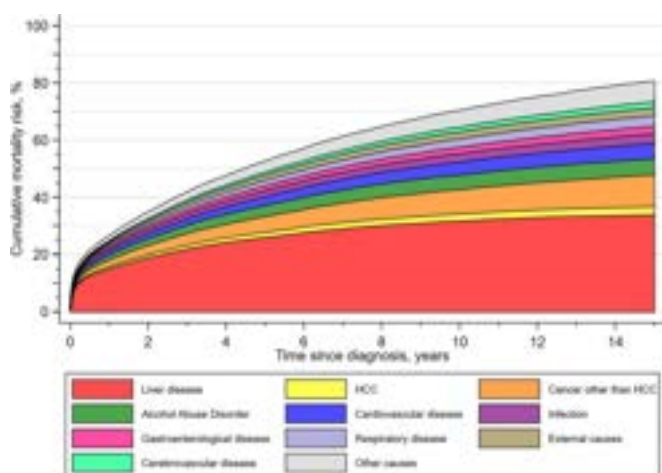


Figure: The cumulative risk of cause-specific death according to time since diagnosis of alcohol-related liver disease from 2002 to 2017 in Denmark, $n = 23,385$. Each color represents an underlying cause of death. The figure shows that liver disease is the leading cause of death in the first five years after diagnosis. Beyond five years, deaths due to cancer, alcohol abuse disorder, and cardiovascular disease rose.

Conclusion: In the first five years after the ALD diagnosis, liver disease caused the majority of deaths. Beyond five years, death caused by cancer, alcohol abuse disorder, and cardiovascular disease became more important. However, the risk of death due to specific cancers, including HCC, each contributed minimally to the total mortality in individuals with ALD.

FRI-436

Risk of primary liver cancer in alcohol-related cirrhosis-Danish and English cohort studies

Morten Daniel Jensen¹, Joe West^{1,2,3}, Peter Jepsen^{1,2}. ¹Aarhus University Hospital, Department of Hepatology and Gastroenterology, Aarhus N, Denmark; ²University of Nottingham, Lifespan and Population Health, School of Medicine, United Kingdom; ³Nottingham University Hospitals NHS Trust and the University of Nottingham, NIHR Nottingham Biomedical Research Centre (BRC), United Kingdom
Email: moje@clin.au.dk

Background and aims: Patients with alcohol-related cirrhosis (ALD cirrhosis) have an increased risk of primary liver cancer (PLC), i.e., hepatocellular carcinoma (HCC) or intrahepatic cholangiocarcinoma (iCCA). Screening for HCC may identify both cancers but is only recommended in England, not in Denmark. We set out to identify the risk and the high-risk-groups among patients with ALD cirrhosis in a Danish and English cohort.

Method: We included all Danish patients ($N = 20,265$) with ALD cirrhosis in the Danish National Patient Registry (1994–2021) and all English patients ($N = 16,763$) with ALD cirrhosis in the Clinical Practice Research Datalink (CPRD) (2000–2016). We computed incidence rates (IR) and cumulative incidence (CI) of PLC with death and transplantation as competing risks, stratifying by decompensation, age, and sex.

Results: The IR of PLC per 10,000 person-years was 66 (95% CI 61–71) in Denmark and 62 (95% CI 56–68) in England. The 5-year risk of PLC was 2.24% (95% CI 2.03–2.46) in Denmark and 2.18% (95% CI 1.95–2.43) in England. The 5-year risk of iCCA and HCC was, respectively, 0.04% (95% CI 0.02–0.07) and 2.20% (95% CI 2.00–2.42) in Denmark vs. 0.07% (95% CI 0.04–0.13) and 2.11% (95% CI 1.88–2.36) in England. In both countries, the risk of PLC was higher in men than in women and increased with increasing age; this pattern was seen for both iCCA and HCC. Men had a 5-year PLC risk of 2.92% (95% CI 2.63–3.23) in

Denmark and 2.80% (95% CI 2.48–3.15) in England, while men or women aged 70–79 year had a 5-year PLC risk of 3.91% (95% CI 3.04–4.94) in Denmark and 3.94% (95% CI 2.91–5.19) in England. No clear association was found with decompensation. In all patient subsets, HCC constituted the vast majority of PLCs (>96% of PLCs among men, >95% among women).

Conclusion: The risk of PLC is the same in Danish and English patients with ALD cirrhosis indicating that few PLCs are overlooked in Denmark, and that despite guidance recommending HCC screening in England this has not led to higher risks being observed. Male sex and older age were risk factors for both PLCs, while the effect of decompensation was uncertain. In both countries HCCs constituted >96% of PLCs, so the potential for overlooking iCCAs is likely to be small when discussions about moving from imaging-based to blood-based HCC surveillance are undertaken.

FRI-437

Beneficial effects of a screening programme for alcohol-related liver fibrosis with transient elastography in people with alcohol use disorder promoting alcohol abstinence

Emma Avitabile^{1,2}, Helena Hernández Evole¹, Jordi Gratacos^{1,2,3}, Pol Bruguera⁴, Lluís Ortega⁴, Anna Lligoña⁴, Martina Perez^{1,2,3}, Ana Belén Rubio^{1,2,3}, Ramon Bataller^{1,3}, Pere Ginès^{1,2,3,5}, Hugo Lopez⁴, Elisa Pose^{1,3,5}. ¹Hospital Clínic de Barcelona, Liver Unit, Barcelona, Spain; ²Universitat de Barcelona, Barcelona, Spain; ³Institut d'Investigacions Biomèdiques August Pi i Sunyer (IDIBAPS), Barcelona, Spain; ⁴Hospital Clínic de Barcelona, Psychiatry, Barcelona, Spain; ⁵CIBER-Center for Biomedical Research Network, Madrid, Spain
Email: EPOSE@clinic.cat

Background and aims: There are few screening programmes for detection of liver fibrosis in at-risk population of alcohol-related liver disease. The aims of this study were 1) to investigate risk factors of liver fibrosis in a population with high-risk alcohol consumption studied with Transient Elastography (TE); 2) to investigate the effect of the screening on alcohol consumption.

Method: Subjects attending the Addiction Unit of the Hospital Clínic of Barcelona for alcohol use disorder (AUD) between 2019 and 2022 were prospectively included (study cohort), excluding those with known liver disease or current alcohol consumption <21 or 14 SU/week in men and women, respectively, considering 1 SU = 10 g of alcohol. Subjects underwent a first visit in the Hepatology Clinic with collection of medical history and blood tests + TE with Liver Stiffness (LS) and a second visit to explain tests' results and for a brief intervention on healthy daily habits. Subjects with increased liver stiffness ($LS \geq 8$ kPa) underwent follow-up in the Hepatology Clinic. Abstinence was defined as a minimum of 2-months negative follow-up according to medical records and/or negative ethylglucuronide (ETG) in urine or discharge due to abstinence. Results were compared with a matched control cohort attending the Addiction Unit for AUD treated immediately before the study period between 2017 and 2019.

Results: 314/345 subjects (91%) accepted to enter the study cohort, 68% were men with average 70 SU/week of alcohol consumption. Prevalence of increased LS was 12% (38/315). Presence of diabetes, male gender and higher ferritin and GGT values were independently associated with increased LS at the multivariate analysis. At 6 months, 142/314 (45%) subjects were abstinent based on medical records ($n = 52$) or medical records and ETG ($n = 90$). There was a non-significant trend to higher abstinence between subjects with significant fibrosis (55% vs 44%, $p = 0.125$). The study and control cohort ($n = 148$) were comparable in terms of baseline characteristics. At 6 months follow-up, abstinence was higher in the study cohort (45% vs 32%, $p = 0.01$) and median consumption among active consumers was lower (18 vs 21 SU/week, $p = 0.008$). Factors independently associated with abstinence in the two cohorts considered together ($n = 463$) were older age ($OR = .97$ $p = 0.001$) and being part of the study cohort ($OR = 1.69$ $p = 0.01$).

Conclusion: a screening program of liver fibrosis in subjects with high-risk alcohol consumption and AUD appears to have an added beneficial effect to the alcoholological treatment for achievement of alcohol abstinence.

FRI-438

Epidemic within pandemic: alcohol-related hepatitis and COVID-19

Natalie Marlowe¹, David Lam², Suthat Liangpunsakul³. ¹DURECT Corporation, United States; ²Pharma Analytics, United States; ³Indiana University, United States

Email: natalie.marlowe@direct.com

Background and aims: We recently reported a steady increase in the total number of hospitalized alcohol-related hepatitis (AH) patients in the US; approximately 5.4% annually between 2015 and 2019. Alcohol consumption is a common coping mechanism for psychological distress. Alcoholic beverage sales increased significantly during the peak of the COVID-19 pandemic in the US. As a result, a rise in alcohol-associated liver disease cases was reported, however there is no published nationwide data on the prevalence of hospitalized AH cases in the US during the COVID-19 pandemic. In this study, we investigated the rate of AH hospitalizations in 2020 during the peak of the COVID-19 pandemic and its impact on patient outcomes and healthcare burden.

Method: We analyzed the US Nationwide Inpatient Sample data from 2019–2020. Patients with a primary or secondary diagnosis of AH were identified using International Classification of Diseases-10. We described associated comorbidities such as ascites, cirrhosis, hepatic encephalopathy (HE), acute renal failure (ARF), GI bleeding, pneumonia, and sepsis in AH patients, with or without COVID-19. The in-

hospital mortality, length of stay (LOS), and hospital charges during the study period were calculated and compared.

Results: We observed ~16% annual increase in cases of hospitalized AH patients from 136,620 in 2019 to 157,885 in 2020, a significant increase from an average of 5.4% per annum. The overall US hospitalizations declined by 8.7% in 2020. Men younger than 40 comprised the fastest growing AH group (23% increase) in 2020. There were 154,985 (98.2%) AH hospitalizations without COVID-19 and 2,900 (1.8%) AH with COVID-19. In-hospital mortality was 4.1% for AH+COVID (–) vs. 11.37% for AH+COVID (+) patients. Average LOS was 2.5 days longer for AH+COVID (+) patients (8.6 vs. 6.1 days). Mean hospital charges were 41.3% higher (\$93,670) for AH+COVID (+) patients compared to \$66,283 for AH+COVID (–) patients. The most common comorbidities in AH+COVID (–) patients were cirrhosis (38.9%), ascites (27.5%), ARF (24.7%), coagulopathy (17%), HE (14.7%), GI bleeding (11.1%), sepsis (10%) and pneumonia (1.5%). In contrast, pneumonia (275% increase) and sepsis (50% increase) were the most common comorbidities in AH+COVID (+) patients followed by GI bleeding (24%), ARF (37%), and HE (27.1%).

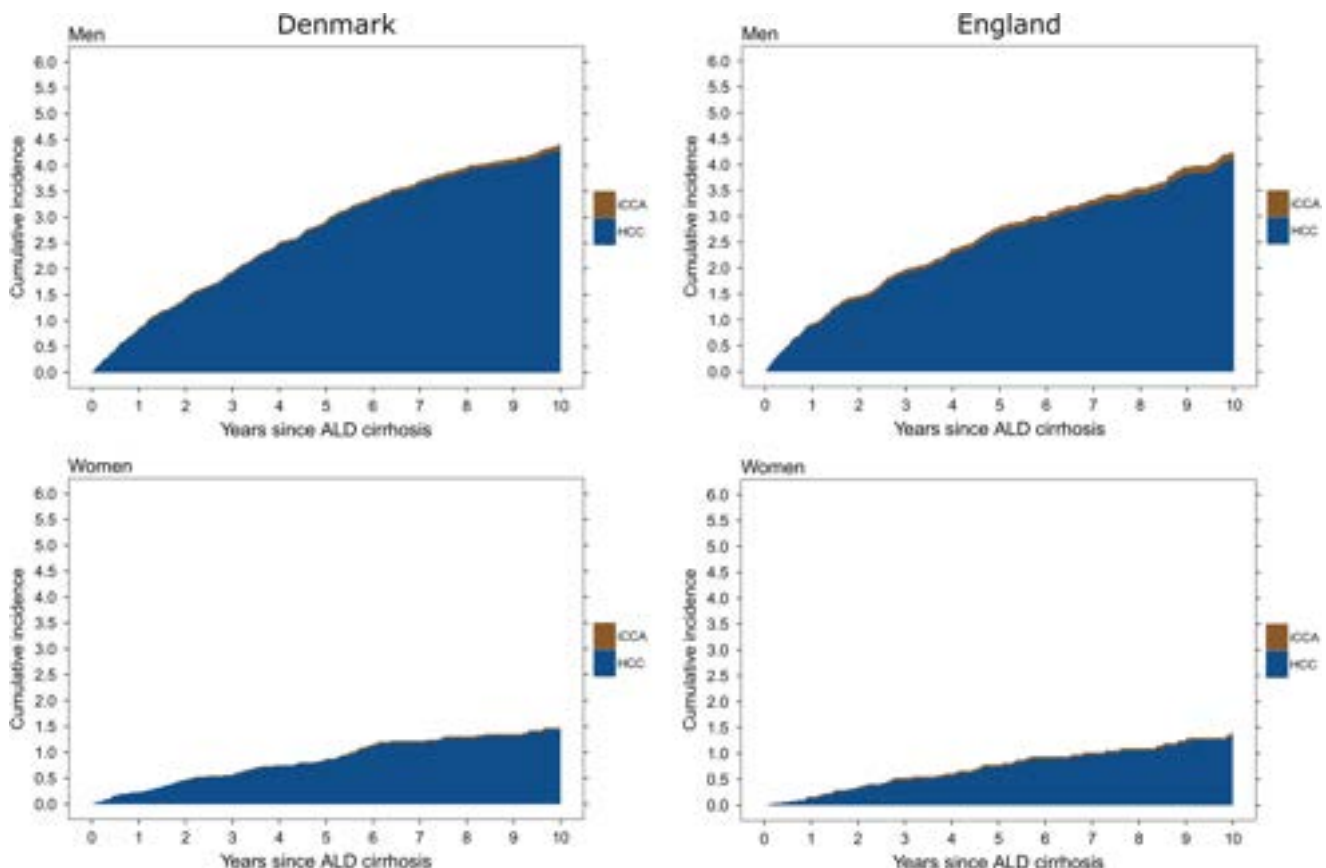


Figure: (abstract: FRI-436).

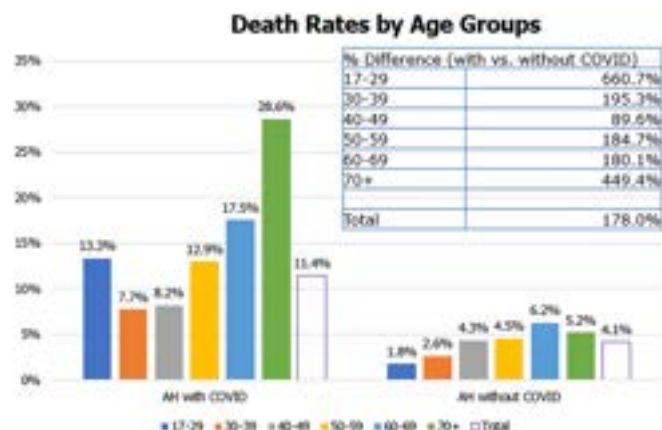


Figure:

Conclusion: Our study documented a significant increase in AH hospitalizations, in-hospital mortality, and healthcare cost and utilization among hospitalized AH patients, notably in those who were infected with SARS-CoV2. Our results underscore an unmet and urgent medical need to identify effective therapies for hospitalized AH patients.

FRI-439

Alcohol use disorder among patients admitted with non-alcohol related conditions: a retrospective cohort study in secondary care

Mohsan Subhani^{1,2}, Shamas Ul Haq³, Guruprasad Aithal^{1,2}, Stephen Ryder^{1,2}, Joanne Morling^{1,2,4}, ¹Nottingham Digestive Diseases Biomedical Research Centre (NDDC), School of Medicine, University of Nottingham, United Kingdom; ²NIHR Nottingham Biomedical Research Centre, Nottingham University Hospitals NHS Trust and the University of Nottingham, Nottingham, United Kingdom; ³Nottingham University Hospitals, United Kingdom; ⁴Division of Epidemiology and Public Health, Nottingham University Hospitals NHS Trust and the University of Nottingham, Nottingham, United Kingdom
Email: mohsan.subhani@nottingham.ac.uk

Background and aims: A substantial number of hospitalised patients drink alcohol harmfully. Only a proportion of those people at risk will have an ICD-10 diagnosis of alcohol-specific or alcohol-related disorders. We aim to determine the prevalence of alcohol use disorder (AUD) in patients admitted with non-alcohol related conditions and ascertain the shared high-risk characteristics.

Method: Retrospective cohort included adult patients admitted to Nottingham University Hospitals (NUH) between 1st-April-2019 to 31st-March-2020 with non-alcohol related disorders. Data were analysed to determine the epidemiology of alcohol use disorder (AUD), identify associated high-risk characteristics, and describe the distribution of AUD in non-alcohol related ICD-10 discharge diagnosis group as defined by an alcohol-attributable fraction.

Results: A total of 36,121 patients presented with a non-alcohol related condition of them 35,080 (97.1%) who had alcohol assessment by AUDIT-C score were included. The mean age of the cohort was 62.2 years (SD ± 20.4), 18,595 (53.0%) were male, and 24,939 (90.6%) were white. Based on AUDIT-C 5, 626 (16.0%) had AUD (increased risk n = 3,559, 63.3%, high risk n = 1,482, 26.3%, possible dependence n = 585, 10.4%). Patients with AUD compared to those without AUD were significantly younger (mean age difference 8.7 years ± 0.29, p < 0.001), were more likely to be male (p < 0.001), white (p < 0.001), not in a relationship (<0.001), admitted as an emergency (p = 0.048), and cared for by surgical specialities (p < 0.001). A significant (p < 0.001) higher proportion of patients with possible alcohol dependence compared to other AUD risk groups were from the most deprived areas (Table 1). General medicine, trauma and orthopaedics, general surgery, urology, and respiratory medicine were top five inpatient specialities of care for patients with AUD. Injury, poisoning, diseases

of musculoskeletal and connective tissues, neoplasms, and diseases of the digestive system were the most common ICD-10 diagnosis groups for patients with AUD.

Table 1: Characteristics of AUD individual risk groups compared to no AUD (low risk)

	Low risk (n=29,454)	Increased risk (n=3,559)	High Risk (n=1,482)	Possible dependence (n=585)	P
Age year (SD)	63.8 (20.48)	55.8 (19.0)	53.3 (17.8)	54.5 (14.7)	<0.001
Male	427 (79.8)	1,042 (79.3)	2,259 (83.5)	12,748 (83.3)	<0.001
Ethnicity					<0.001
White	20,907 (89.8)	3,528 (94.7)	1,672 (94.4)	432 (94.1)	
BAME	3,389 (10.2)	141 (5.3)	83 (5.6)	27 (5.9)	
Missing	8,178	890	347	126	
AUD quintiles					<0.001
1 (most deprived)	7,145 (26.4)	754 (21.1)	404 (29.8)	209 (38.8)	
2	4,905 (18.1)	565 (17.3)	249 (18.4)	116 (22.2)	
3	4,705 (17.4)	563 (17.3)	218 (16.1)	78 (14.9)	
4	4,485 (16.3)	992 (28.2)	251 (19.8)	58 (11.1)	
5 (least deprived)	5,856 (23.7)	789 (24.2)	289 (19.9)	68 (13.8)	
Missing	2,378	398	131	62	
Civil status					<0.001
In a relationship*	14,304 (50.1)	1,302 (49.3)	515 (45.1)	163 (34.1)	
Not in a relationship*	8,898 (40.8)	1,428 (50.5)	679 (56.8)	311 (65.9)	
Missing	5,252	729	288	113	
Mode of admission					<0.001
Emergency	16,732 (56.8)	1,820 (51.1)	857 (57.8)	439 (75.0)	
Other	12,722 (43.2)	1,739 (48.8)	625 (42.2)	146 (25.0)	
Speciality					<0.001
Medicine	14,967 (51.8)	1,386 (37.2)	580 (40.4)	354 (59.5)	
Surgery	15,943 (48.2)	2,186 (63.0)	856 (59.6)	227 (40.5)	
Other or unknown					
Length of stay (days)	4.0 (3-288)	3.0 (3-178)	3.0 (3-108)	4.8 (1-108)	<0.001

Data is n (%), mean (SD) or median (range).

AUDIT-C score: 0-4 (low risk), 5-7 (increased risk), 8-10 (high risk), 11-12 (alcohol dependent).

*In a relationship includes married, in a civil partnership or in a long-term relationship.

*Not in a relationship includes single, divorced, separated, dissolved civil partnership, widowed, or surviving civil partner.

Figure:

Conclusion: One in six admitted patients with non-alcohol related conditions had AUD. Majority of these patients had either increased or high-risk AUD and were cared for by surgical specialities. Efforts to identify AUD and unidentified liver disease early should be focused on areas of high burden which are outside the specialist wards and units.

FRI-440

Histological inflammation in severe alcohol-related hepatitis is the main pre-treatment factor associated to glucocorticoid response

Mialy Randrianarisoa¹, Laetitia Oertel², Pierre Mayer¹, Lucile Heroin¹, Simona Tripon^{1,3}, François Habersetzer^{1,3}, Lawrence Serfaty¹, Thomas Baumert^{1,3,4}, Antonio Saviano^{1,3}, ¹Service d'hépatogastroentérologie, Institut Hospitalo-Universitaire, Pôle hépato-digestif, Hôpitaux Universitaires de Strasbourg, Université de Strasbourg, France; ²Service d'anatomo-pathologie, Hôpitaux Universitaires de Strasbourg, Université de Strasbourg, France; ³Institut de recherche sur les maladies virales et hépatiques, Inserm UMR_S1110, Strasbourg, France; ⁴Institut Universitaire de France, France
Email: saviano@unistra.fr

Background and aims: Severe alcohol-related hepatitis is a condition associated with a significant mortality. Apart from liver transplantation, glucocorticoid is the only validated treatment. Treatment response is usually evaluated at day 7 by the Lille score. Clinical and histological pre-treatment features that could predict this response are unknown. The alcoholic hepatitis histological score, based on pre-treatment liver biopsy and developed to predict outcomes of patients with severe alcohol-related hepatitis, was not able to predict

glucocorticoid response and its prognostic value was not confirmed in an independent cohort.

The aim of this study was to characterize histological inflammation in severe alcohol-related hepatitis and to assess its predictive value of glucocorticoid response.

Method: This retrospective study included patients with histologically proven severe alcohol-related hepatitis treated with glucocorticoids at Strasbourg University Hospital, France, between 2014 and 2021. Pre-treatment liver biopsies stained with HandE were analyzed by QuPath v 0.3.2 to identify and quantify immune cells. Portal spaces, porto-lobular interfaces and lobules were annotated to describe the distribution of the immune cells.

The predictive value for glucocorticoids non-response (Lille score at day 7 >0.56) was evaluated by univariate and multivariate logistic regression analysis.

Results: Among the 61 patients included, 18 (29.5%) were non-responders and 43 (70.5%) were complete or partial responder. Most of the patients were cirrhotic in both groups (respectively 72.2% and 76.7%, $p = 0.962$). Liver disease was more severe in non-responders (median MELD 30 vs 24 $p < 0.001$; median Maddrey score 82.36 vs 61.74, $p = 0.003$). Total inflammatory cell infiltration was significantly lower in non-responders (median 3170 cells/mm², range 815–3906, $p = 0.018$) than in responders (median 3539 cells/mm², range 1779–5198).

The multivariate logistic regression analysis using pre-treatment clinical and histological variables, identified the following factors associated with glucocorticoids non-response: a high level of bilirubin (OR 1.02, CI 95% 1.01–1.03, $p = 0.016$), a high IGSII score (OR 1.19 CI 95% 1.07–1.46, $p = 0.012$) and a low total inflammatory infiltration (OR 38.9, 95% CI 2.54–3056, $p = 0.031$). Regarding the localization of the inflammation, portal immune cells were significantly lower in non-responders [1604/mm² (range 965–2370) vs 2273/mm² (range 1653–2766), $p = 0.012$] as well as in portal interface [341/mm² (range 269–397) vs 487/mm² (range 315–603), $p = 0.012$]. There was no difference between the two groups in terms of intralobular infiltration.

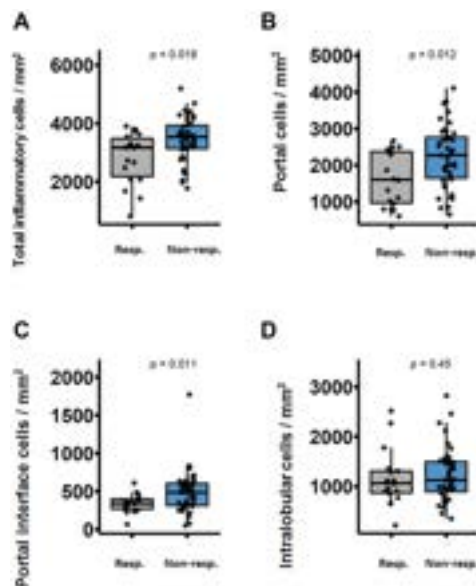


Figure:

Conclusion: Low histological inflammation is the strongest pre-treatment factor associated to glucocorticoids non-response in severe alcohol-related hepatitis. Automatic quantification of inflammatory cells from conventional HandE slides could be used for early detection of patients with a high risk of treatment failure in whom alternative medical therapies should be evaluated and early liver transplantation should be discussed.

FRI-441

The synergistic impact of food insecurity and alcohol use on mortality in adults with significant liver fibrosis

Ani Kardashian¹, Jennifer Dodge^{1,2}, Norah Terrault¹, Brian Lee¹.

¹Division of Gastrointestinal and Liver Diseases, University of Southern California, United States; ²Department of Population and Public Health Sciences, University of Southern California, United States

Email: ani.kardashian@med.usc.edu

Background and aims: Food insecurity is highly prevalent and associated with significant liver fibrosis. Food insecurity is also associated with adverse health behaviors, including heavy drinking, but the synergistic impact of the two on mortality among people with liver fibrosis is unknown.

Method: We performed a cross-sectional analysis of adult participants (age ≥20 years) with significant liver fibrosis from the National Health and Nutrition Examination Survey (NHANES) between 1999 and 2018. Fibrosis was defined using: NAFLD fibrosis score >0.675 (if subjects had NAFLD as defined by the U.S. Fatty Liver Index), AST-to-platelet ratio index >1.5, or Fibrosis-4 Index >2.67. Food insecurity was measured using the U.S. Department of Agriculture Food Security Survey Module. Alcohol use was self-reported in the prior 12 months and categorized as none versus any use. Mortality from all causes was ascertained through data linkage to the National Death Index through December 31, 2019. We used multivariable Cox proportional hazards regression to estimate hazard ratios (HRs) and 95% confidence intervals (CI) of all-cause mortality according to alcohol use and food security status. We further examined interactions between poverty and food security status/alcohol use given the known associations between these variables.

Results: In total, 1757 participants with significant fibrosis were included with mean follow-up of 6.4 years (SE: 0.10), of whom 443 (25%) were food insecure and 1080 (61%) reported any alcohol use. Participants with (vs. without) alcohol use were more likely to be younger (mean 66 vs 71 years) and male (62% vs 55%) and less likely to be living in poverty (11% vs 15%). Among those with alcohol use, all-cause age-standardized mortality per 1000 person-years was 22.6 among food secure and 30.4 among food insecure persons. In the multivariable model, mortality risk was elevated for food insecurity among participants with alcohol use (HR = 1.41, 95% CI: 1.002–1.98, $p = 0.049$) but not those without alcohol use (HR = 0.96, 95% CI: 0.68–1.37, $p = 0.84$; interaction $p = 0.11$). Furthermore, these effects differed by poverty. The combined effect of food insecurity and alcohol use (vs food secure without alcohol use) was 2.41-fold greater for those with poverty ($p = 0.01$). Among people without poverty, there was no difference in mortality among alcohol users by food security status (Figure).

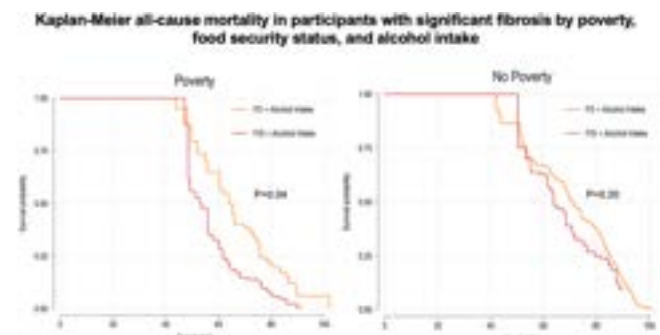


Figure:

Conclusion: Alcohol use disorder and food insecurity are comorbid conditions that have a more detrimental impact on liver health outcomes compared to either condition alone, particularly among people experiencing poverty. Greater efforts are needed to screen

POSTER PRESENTATIONS

low-income patients for food insecurity and alcohol use in clinical practice and refer them to appropriate resources.

FRI-442

Baclofen is effective on abstinence and improvement of Child-Pugh score in patients with cirrhosis: results of a meta-analysis

Gildas Fantognon¹, Jean-François Cadranel¹, Honoré Zougmore¹, Mourad Medmoun¹, Ryad Smadhi¹, Philippe Pulwermacher¹, Jean Rene Ngele Efole¹, Camille Barrault², Oumarou Nabi³. ¹GHPSO, CREIL, France; ²CH INTERCOMMUNAL de CRETEIL, Digestive Disease and Addiction Unit, Creteil, France; ³Washington University School of Medicine, United States
Email: honoretz87@gmail.com

Background and aims: Baclofen is one of the treatments recommended for abstinence (withdrawal) in patients (pts) with alcoholic cirrhosis (1). A few randomized and observational studies suggest a positive effect on abstinence and improvement of liver function in cirrhotic patients (2). However, despite obtaining marketing authorization in 2021, its impact on alcohol abstinence and liver function improvement remains debated. The aim of this meta-analysis was to evaluate the effect of baclofen in patients with alcoholic cirrhosis on abstinence and improvement of the Child Pugh score.

Method: Analysis studies on baclofen treatment in alcoholic cirrhotic patients published in extenso between January 1, 2020 and August 31, 2022. Randomized controlled studies and observational studies involving a large number of patients followed over a period of 12 months were included (for observational studies) were selected for analysis. The search for publications was based on a systematic search in MEDLINE, PubMed, Google Scholar, Web of Sciences, Academic Search Premier, Cochrane Library and SCOPUS. We have collected and analyzed the individual data of the patients included in the different studies to assess the effects of baclofen on abstinence and improvement of the Child Pugh score in patients with alcoholic cirrhosis. The size of the effects of baclofen on abstinence and Child Pugh score was assessed using relative risks (RR) and their 95% confidence intervals. We considered that there was improvement in the Child Pugh score when there was a change from a Child Pugh score from C at inclusion to stage A at the end of follow-up. Otherwise, it was considered no benefit. Assessment of bias and heterogeneity were using the I² and funnel plot. A p value <0.05 was considered statistically significant.

Results: Six studies were included in the final analysis, including four randomized trials (318 cirrhotic patients treated with baclofen and 147 patients treated with placebo) and two observational studies (100 pts). The median dose of baclofen was 30 mg per day.

In despite the high heterogeneity (I² = 79%), our results show a positive effect of baclofen on alcohol withdrawal and abstinence (RR 1.48, CI95% 1.25–1.76, p = 0.003 and 1.76, CI95% p = 0.0083 respectively). Similarly, baclofen showed a beneficial effect on improvement on the severity of liver injury as assessed by the Child Pugh score (RR 2.50, CI95% 1.48–4.18, p < 0.0001).

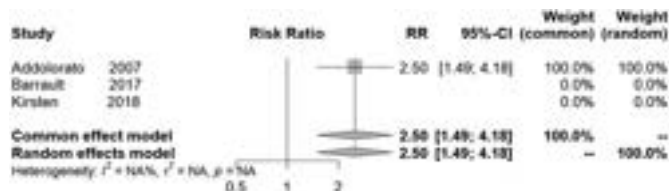


Figure:

Conclusion: Global improvement of the Pugh child.

This meta-analysis shows that baclofen is an interesting treatment for abstinence from alcohol consumption in patients with alcoholic cirrhosis and could improve liver functions in patients with alcoholic cirrhosis.

FRI-443

Hemoglobin is a short-term prognostic factor in decompensated alcohol-associated cirrhosis: a multicenter prospective study

José Ursic Bedoya¹, Claire Espérance², Safia Aouinti², Ludovic Caillio³, Magdalena Meszaros², Marie Pierre Ripault⁴, Laura Jaubert², Adrien Ardavan Prost³, Lucy Meunier², Stéphanie Faure², Cathy Soulayrac², Hélène Donnadiou², Boris Guiu², Nicolas Molinari², Jérôme Dumortier⁵, Georges-Philippe Pageaux². ¹CHU Montpellier, Montpellier, France; ²CHU Montpellier, France; ³CHU de Nîmes, France; ⁴CH Narbonne, France; ⁵Edouard Herriot Hospital, Lyon, France
Email: jose.ursicbedoya@chu-montpellier.fr

Background and aims: Acute decompensation of alcohol-associated cirrhosis can lead to acute-on-chronic liver failure development or death without liver transplantation (LT). LT can be avoided in some patients who spontaneously recover. Classic prognostic scores (such as Meld) are insufficient to discriminate between patients who recover and those needing LT. We aimed to identify new prognostic factors in the setting of acute decompensation (AD) of alcohol-associated cirrhosis.

Method: This prospective observational study included patients from two tertiary care centers (one with a LT team) and a secondary care center. Inclusion period ranged from 01/04/2018 to 30/09/2019 and patients were followed for a minimum of 12 months. Adults admitted for an AD of alcohol-associated cirrhosis, without hepatocellular carcinoma, previous TIPS placement or active viral hepatitis were included. Primary end points were overall and 3-month transplant-free survival (TFS).

Results: 131 patients were included (mean [SD] age, 58.4 [9.3] years; 96 men [73.3%]); median follow-up was 15 months. 3 and 12-month TFS were 74.8% and 64.1% respectively. Main etiologies for decompensation were alcohol-associated hepatitis (n = 52, 39.7%) and ascites flare (n = 35, 26.7%). Multivariate Cox regression identified baseline hemoglobin ([HR]: 0.558, [95% CI: 0.383; 0.813]) and Meld score ([HR]: 1.307, [95% CI: 1.171; 1.457]) as the variables associated with 3-month TFS. We constructed a score combining hemoglobin and Meld score with an AUROC of 0.91 (95%CI: 0.84; 0.98), showing higher prognostic performance than Meld, Meld-sodium and ACLF-AD scores. Our model was validated in an independent cohort of 49 patients.

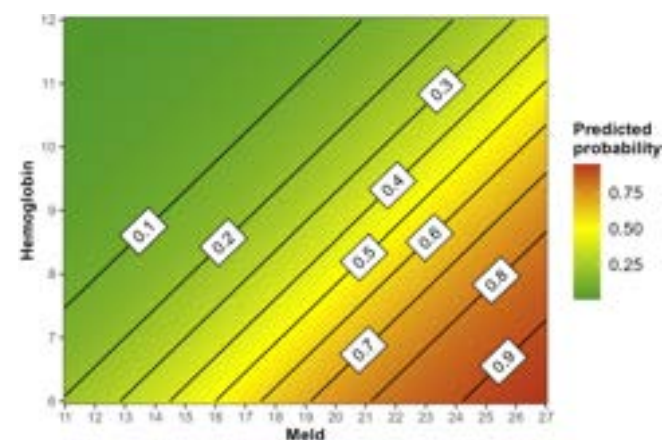


Figure: 3-month mortality or LT probability per the joint-effect score combining baseline Meld and hemoglobin.

Conclusion: Baseline hemoglobin shows potential short-term prognostic value in patients admitted for AD of alcohol-associated cirrhosis (Clinical Trials number 03508388).

FRI-444

Impact of heavy alcohol consumption on mitochondrial metabolism

Scott Minchenberg¹, Margery A. Connelly², Naga Chalasani³, Arun Sanyal⁴, Vijay Shah⁵, Z. Gordon Jiang¹, Eduardo Vilar Gomez³.
¹Beth Israel Deaconess Medical Center, Division of Gastroenterology and Hepatology, Boston, United States; ²LabCorp Corporate Office, Diagnostics Research and Development, Morrisville, United States; ³Indiana University School of Medicine, Division of Gastroenterology and Hepatology, Indianapolis, United States; ⁴VCU School of Medicine, Division of Gastroenterology and Hepatology, Richmond, United States; ⁵Mayo Clinic, Department of Internal Medicine, Rochester, United States
 Email: sminchen@bidmc.harvard.edu

Background and aims: Excessive alcohol consumption results in cumulative damage to mitochondria which has profound implications for cellular metabolism. Changes in mitochondria metabolism result in altered circulating metabolites, such as citrate and ketone bodies. We have previously demonstrated that high levels of circulating ketone bodies and citrate are associated with increased mortality. Herein, we hypothesize that excessive alcohol consumption and alcoholic hepatitis are associated with elevated ketone bodies and Krebs cycle metabolites due to mitochondria injury.

Method: Translational Research and Evolving Alcoholic Hepatitis Treatment (TREAT) was a prospective observational study of patients with alcoholic hepatitis (AH) (n = 196) and matched heavy drinkers (n = 169). Study participants were evaluated at baseline, 6 months, and 12 months. Metabolite levels were quantified from baseline plasma samples using nuclear magnetic resonance profiling. The relationship between metabolites and patient outcome was analyzed using multivariable regression and Cox proportional hazard models.

Results: Heavy drinkers have lower levels of citrate ($88.1 \pm 26.6 \mu\text{M}$), but higher levels of ketone bodies ($344 \pm 578 \mu\text{M}$) compared to healthy controls. Patients with AH have significantly increased levels of ketone bodies and citrate when compared to heavy drinkers (Figure). The increase in citrate and ketone body levels positively correlated with both Maddrey and MELD scores, suggesting liver injury in AH is directly linked to maladaptive mitochondria metabolism. In Cox proportional hazard models, the Citrate level is strongly associated with mortality at 90 days with HR ratio of 2.9 (95% CI 1.5–5.4, $p < 0.01$), while no significant association was observed with ketone bodies.

Variables	Heavy drinkers N = 169	Alcoholic hepatitis N = 196	P value*
Age, years	44.42 \pm 12.40	45.53 \pm 10.90	0.437
Gender (male), n (%)	110 (65)	117 (60)	0.28
ALT (U/L)	26.52 \pm 12.36	62.15 \pm 63.78	<0.001
AST (U/L)	28.45 \pm 10.65	136.75 \pm 83.50	<0.001
ALP (U/L)	76.52 \pm 31.14	188.0 \pm 137.07	<0.001
Creatinine (mg/dl)	0.88 \pm 0.27	1.01 \pm 0.91	0.170
Maddrey score	2.83 \pm 9.60	42.97	<0.001
MELD score	7.30 \pm 2.35	22.55 \pm 6.75	<0.001
Ketone bodies (KB)			
Total KB	344.1 \pm 577.7	608.5 \pm 517.6	<0.01
Beta-hydroxybutyrate	237.1 \pm 407.8	449.3 \pm 354.2	<0.01
Acetoacetate	71.3 \pm 124.4	64.5 \pm 85.9	0.29
Acetone	35.6 \pm 58.7	94.6 \pm 188.7	<0.01
Small molecule metabolites			
Glucose	92.2 \pm 80.9	104.7 \pm 43.4	<0.01
Citrate	88.1 \pm 26.6	166.3 \pm 196.0	<0.01

*Mann-Whitney U test for continuous and chi square for categorical.

Conclusion: Heavy alcohol use and AH are associated with elevated levels of ketone bodies, while an increase in circulating citrate level is associated with mortality in 90 days in AH, potentially indicative of mitochondrial biogenetic failure. Mitochondrial damage may trigger

a buildup of Krebs cycle metabolites that would shift acetyl-CoA to ketone body production. This study is the first to describe the changes in mitochondria metabolites in alcohol-related liver disease.

FRI-445

Recompensation following an episode of alcohol-associated hepatitis mostly occurs in the first year of follow-up and is related to Child-Pugh score, levels of GGT and platelets, and alcohol abstinence

Jordi Gratacos¹, Pilar Ruz-Zafra², Miriam Celada-Sendino³, Aina Martí-Carretero⁴, Claudia Pujol⁵, Rosa Martín-Mateos⁶, Víctor Echavarría⁷, Luis Frisanchó⁸, Sonia García-García⁹, Mónica Barreales Valbuena¹⁰, Javier Tejedor-Tejada¹¹, Sergio Vaquez Rodríguez¹², Nuria Cañete¹³, Carlos Fernández-Carrillo¹⁴, María Valenzuela¹⁵, David Martí-Aguado¹⁶, Diana Horta¹⁷, Marta Quiñones¹⁸, Vanesa Bernal Monterde¹⁹, Silvia Acosta-López²⁰, Tomás Artaza Varasa²¹, José Pinazo Bandera²², Carmen Villar²³, Ana Clemente²⁴, Esther Badia-Aranda²⁵, Conrado Fernández-Rodríguez¹⁸, Victoria Aguilera Sancho⁹, Pau Sancho-Bru²⁶, Joaquín Cabezas⁷, Meritxell Ventura Cots⁴, Santiago Tomé²⁷, Joan Caballería¹, Elisa Pose¹.
¹Hospital Clínic de Barcelona, Liver Unit, Barcelona, Spain; ²Virgen del Rocío University Hospital, Sevilla, Spain; ³Central University Hospital of Asturias, Oviedo, Spain; ⁴Vall d'Hebron University Hospital, Barcelona, Spain; ⁵Hospital de la Santa Creu i Sant Pau, Barcelona, Spain; ⁶Ramón y Cajal Hospital, Madrid, Spain; ⁷Marqués de Valdecilla University Hospital, Santander, Spain; ⁸Hospital Parc Taulí de Sabadell, Sabadell, Spain; ⁹La Fe University and Polytechnic Hospital, Valencia, Spain; ¹⁰University Hospital October 12, Madrid, Spain; ¹¹Hospital of Cabueñes, Gijón, Spain; ¹²Álvaro Cunqueiro Hospital, Vigo, Spain; ¹³Hospital del Mar, Barcelona, Spain; ¹⁴Puerta de Hierro Majadahonda University Hospital, Majadahonda, Spain; ¹⁵Hospital Universitari de Girona Doctor Josep Trueta, Girona, Spain; ¹⁶Hospital Clínic Universitari, Valencia, Spain; ¹⁷Hospital Universitari MútuaTerrassa, Terrassa, Spain; ¹⁸Hospital Universitario Fundación Alcorcón, Alcorcón, Spain; ¹⁹Miguel Servet University Hospital, Zaragoza, Spain; ²⁰Our Lady of Candelaria University Hospital, Santa Cruz de Tenerife, Spain; ²¹Hospital General Universitario de Toledo, Toledo, Spain; ²²Hospital Universitario Virgen de la Victoria, Málaga, Spain; ²³Salamanca University Hospital, Salamanca, Spain; ²⁴Gregorio Marañón General University Hospital, Madrid, Spain; ²⁵Burgos University Hospital, Burgos, Spain; ²⁶Institut d'Investigacions Biomèdiques August Pi i Sunyer (IDIBAPS), Barcelona, Spain; ²⁷Santiago Clinic Hospital CHUS, Santiago de Compostela, Spain
 Email: EPOSE@clinic.cat

Background and aims: several studies have recently described the phenomenon of resolution of clinical complications in patients with decompensated cirrhosis. There is currently no evidence regarding the incidence of this event following an episode of alcohol-associated hepatitis (AH), nor the factors associated to its occurrence.

Method: we collected data from a retrospective cohort of patients from 30 Spanish hospitals with a clinical diagnosis of AH between 2014 and 2021. We selected all patients that met the following criteria: 1) were alive after first hospitalization; 2) presented with a decompensation of cirrhosis at diagnosis or had a Model for End-stage Liver Disease (MELD) score >20. Recompensation was defined as: 1) compensated liver disease over the previous 3 months; 2) no specific treatment (diuretics, laxatives or rifaximin) over the previous 3 months; 3) improvement of liver function defined by MELD <12. We evaluated the percentage of recompensated patients at 1 and 3 years, and we performed a logistic regression to assess factors associated to recompensation.

Results: five hundred forty-eight patients were included. The majority were men (72%), with a median age of 52 years and a median MELD score of 22 at diagnosis. At 3-year follow-up, 105 patients (19%) met criteria for recompensation; of those, 74 patients (70%) already met the same criteria at 1-year follow-up. A lower Child-Pugh (CP) score (OR 1.66, CI [1.27–2.19]) at diagnosis, higher

POSTER PRESENTATIONS

levels of platelets (OR 1.04, CI [1.01–1.08]) and GGT (OR 1.07, CI [1.07–1.12]), and total alcohol abstinence during follow-up (OR 2.72, CI [1.48–5.00]), were the only factors associated to recompensation at 1 year. Baseline probability of recompensation at 1 year ranged from 6.6% in patients with Cp >9 and low platelets ($<75.5 \times 10^9/L$) and GGT ($<172 U/L$), up to 28.3% in patients with Cp <9 and high platelets and GGT levels.



Figure: Probability of recompensation at 1 year according to baseline Child-Pugh score and levels of platelets and GGT.

Conclusion: a significant percentage of patients diagnosed with AH achieve recompensation of cirrhosis, mainly during the first year after discharge. Recompensation is associated to alcohol abstinence, CP score and levels of platelets and GGT.

FRI-446

A prospective study of hepatic fibrosis evaluation in an alcohol withdrawal unit of an university hospital center: role of FIB-4 and elastometry. Fibr'addict study

Armand Abergel¹, Benjamin Buchard¹, Leon Muti¹, Dominique Boulrier¹, Maud Leautaud¹, Brigitte Chanteranne¹, Carine Nicolas¹, Sylvie Massoulie¹, Frédéric Faure¹, Anne Audrey Schmitt-Dischamp², Georges Brousse². ¹CHU Clermont-Ferrand, Medecine Digestive, Clermont-Ferrand, France; ²CHU Clermont-Ferrand, Service d'addictologie, Clermont-Ferrand, France
Email: aabergel@chu-clermontferrand.fr

Background and aims: Excessive alcohol consumption is the major cause of liver-related death and the leading cause of liver transplantation in France. Many patients are seen too late, at a decompensated stage. Early diagnosis of cirrhosis would allow early diagnosis for esophageal varices, screening for hepatocellular carcinoma and reinforcement of addictive behaviour care. This project is part of a process of screening for hepatic fibrosis, by elastography, in patients hospitalized in an addictology unit for alcohol withdrawal.

Method: 216 patients benefited from measurement of liver stiffness (LS) (Fibroscan®) upon entering in the unit (day 0 = D0). This measurement was repeated before the patients had left the unit (21 days on average). A LS>25 kPa ruled in advanced fibrosis (15 patients), and a LS<10 kPa ruled out advanced fibrosis (183 patients) (Legros et al. CGEH 2022). If the patients had a LS of between 10 and 25 kPa at D0, the status was determined by the second LS realised at the end of hospitalisation. If the patient had LS>10 kPa, they were considered to have advanced fibrosis (7 patients). Five patients had LS<10 kPa (no advanced fibrosis) and six patients had no second measurement, they were excluded from the analysis. Then 22

patients had an advanced fibrosis (F3 or F4 METAVIR) and 188 patients had no advanced fibrosis (FOF1F2). We also studied the diagnostic performance of FIB-4, prothrombin time and ASAT/ALAT>1 with the objective to reduce the number of LS measurements.

Results: In the total population (210 patients), mean age of the patients was 49±12 years and sex ratio was 2.81. The percentage of patients with a FIB-4 less than 2.6, a prothrombin time (expressed in %) higher than 85% and ASAT/ALAT<1 were respectively 78% (161/206), 83% (164/198), 58% (121/208). For the patients with an advanced fibrosis at D0, the mean LS was 34±18 kPa and the number of patients with CAP >275 kPa was 8/22 (36%). The average alcohol consumption over the last 5 years was 189 + 147 g/day. For the patients without advanced fibrosis, LS was 5 + 2 kPa and the CAP >275 was 35/188 (17%) at D0. The average alcohol consumption over 5 years was 206 + 162 g/day. For FIB-4 >2.6, sensitivity, specificity, positive predictive value and negative predictive value were respectively 77%, 85%, 38% and 97%. Negative predictive value were also excellent for prothrombin time<85% (97%) and ASAT/ALAT>1 (97%).

Conclusion: Ten percent (22/210) of patients admitted to an addictology unit had an advanced fibrosis. A FIB-4 less than 2.6 had an excellent negative predictive value to exclude advanced fibrosis and then could be able to reduce the number of LS measurements (up to 80% of the patients). The combination of FIB-4 and LS should be studied on a larger number of patients to validate this algorithm, preferably within the framework of a multicentre study. This study suggests that screening for advanced fibrosis should be performed in all hospital units for alcohol withdrawal.

FRI-447

The prevalence and prognostic impact of bariatric surgery in patients hospitalized with alcoholic liver disease

Louis Onghena^{1,2,3}, Sander Lefere^{2,3}, Laurissa Demeulenaere², Yves Van Nieuwenhove¹, Anja Geerts^{2,3}. ¹Ghent University Hospital, Department for Human Repair and Structure, Department of Gastrointestinal Surgery, Gent, Belgium; ²Ghent University Hospital, Liver Research Center Ghent, Ghent University, Ghent University Hospital, Gent, Belgium; ³Ghent University Hospital, Department of Internal Medicine and Paediatrics, Hepatology Research Unit, Gent, Belgium
Email: Louis.onghena@ugent.be

Background and aims: Patients with a history of bariatric surgery (BS) are susceptible to developing alcohol use disorder. We and others have previously shown that these patients can develop severe alcohol-related liver disease (ARLD), often at a younger age and despite lower cumulative alcohol intake when compared to ALRD patients without BS. However, there is still a paucity of data. Our aim was to describe the demographics and mortality of a hospitalized population diagnosed with alcohol-related liver disease, in relation to BS.

Method: We included patients hospitalized at the University Hospital in Ghent between 1/1/2018 and 31/12/2022 with ARLD. Data were retrieved retrospectively from the most recent hospitalization. Statistical analysis was performed using Mann-Whitney U and Chi² tests.

Results: 12.3% (35/284) of patients admitted with ARLD had a history of bariatric surgery, of which 28 (80.0%) underwent Roux-en-Y gastric bypass. Pre-BS BMI was 41.3 ± 5.6 on average, with a one-year post-BS BMI of 27.0 ± 4.7. Patients with a history of BS were predominantly female (77.1%), in contrast to the non-BS population (30.1%) (p < 0.0001) and despite being significantly younger (52.0 (45.0, 60.0) vs 63.0 (53.0, 69.0) years old) (p < 0.0001), had a similar survival (68.6%

vs 61.0%) and a higher likelihood of transplant listing (25.7% vs 14.2%) ($p = 0.085$). The cause of death was acute-on-chronic liver failure in 77.8% of BS patients, compared to only 15.9% of those without a history of BS ($p < 0.0001$). Conversely, and in keeping with the younger age, no BS patients died of non-hepatological causes or HCC. There were no differences in comorbidities (diabetes, ischemic heart disease), complications of liver disease (ascites, spontaneous bacterial peritonitis, esophageal varices, and hepatic encephalopathy), nor in BMI at the time of the latest hospitalization. ALT ($p = 0.043$) and AST ($p = 0.012$) were significantly elevated in the BS group, whereas the MELD score was comparable ($p = 0.727$). More than half of the BS cohort suffered from psychiatric illness, compared to a quarter of the non-BS population (51.4% vs 28.1%) ($p = 0.010$), paralleled by the number of patients currently treated with psychological counseling (51.4% vs 21.0%) ($p < 0.0001$). Alcohol abstinence was near identical with 57.6% vs 57.9%. The weekly amount of alcohol consumed during drinking periods (40.0 (25.0, 50.0) vs 50.0 (35.0, 79.0) units/week) ($p = 0.060$) and duration of use (8.0 (5.0, 15.0) vs 20.0 (10.0, 29.8) years) was significantly lower in the BS population ($p < 0.0001$). **Conclusion:** BS patients hospitalized with ARLD are predominantly young females with a lower cumulative alcohol consumption compared to those without prior BS. Despite this, mortality due to liver disease was higher. There is a need for prospective research to substantiate stricter pre-BS patient selection guidelines.

FRI-448

Prognostic role of serum alpha-1 antitrypsin levels for waitlist mortality in patients with alcohol-associated liver disease

Ronald Samuel¹, Basim Ali², Scott Berger², Richard Bui², Kadon Caskey², Cameron Goff², Norvin Hernandez², Seulgi Kim², Christo Mathew², Ankur Patel², Marguerite Poche², Prisca Pungwe², Anjiya Shaikh³, Vinh Tran², Ryan Ward², Ruben Hernaez¹, Saira Khaderi¹, Tzu-hao Lee¹, Fasiha Kanwal¹, George Cholankeril¹.
¹Baylor College of Medicine, Gastroenterology and Hepatology, United States; ²Baylor College of Medicine, United States; ³University of Connecticut, United States
Email: ronald.e.samuel1@gmail.com

Background and aims: Alcohol-associated liver disease (ALD) is the leading cause of end-stage liver disease, and is commonly associated with protein malnutrition. Although prevalent in ALD patients, the effect of serum zinc, ceruloplasmin and alpha-1 antitrypsin (A1AT), potential surrogates of protein nutritional deficiencies, on liver transplant (LT) waitlist dropout has yet to be examined. The primary aim of our study was to evaluate the variables and predictors of waitlist dropout among ALD patients listed for LT.

Method: A retrospective cohort study was performed of all adult patients (age > 18 years) added to the liver transplant waitlist at Baylor St Luke's Medical Center from January 2017 to August 2018. Patients with alcohol use as a primary or secondary etiology of liver disease were included. Multiple demographics, nutrition, alcohol, decompensation, and laboratory variables were collected using manual medical record review. Nutritional labs at waitlist date included albumin (low <2.5 g/dL), zinc (low <60 µg/mL), ceruloplasmin (low <20 mg/dL) and A1AT (low <100 mg/dL) levels. In patients with low ceruloplasmin and A1AT levels, 24 hour urine copper and A1AT phenotypes were obtained, and concomitant Wilsons Disease and genetic A1AT deficiency were excluded from the ALD cohort. Logistic regression was performed to assess the independent effect of nutrient deficiencies on waitlist dropout due to death or removal due to medical deterioration. The institutional review board of Baylor College of Medicine, Houston, Texas approved the research project. Data were analyzed using Stata version 13 (Stata Corp, College Station, TX).

Results: A total of 122 patients were listed with ALD, of which, 69% of patients were male and 61% were Caucasian, with median MELD at listing of 27 [IQR, 13–32]. With regards to hepatic decompensation, 66% had hepatic encephalopathy (HE), 84% had ascites, and 38% had a

history of gastroesophageal variceal bleeding and/or required variceal ligation. Overall, 16% of ALD patients died or were removed due to medical deterioration and median time from waitlisting to dropout was 56 days. At the time of listing, 14% of patients had low albumin ([mean] 3.1 g/dL). 70% of patients had low zinc (46.1 µg/mL), 19% had low ceruloplasmin (23.5 mg/dL), and 7% had low A1AT (149.6 mg/dL) levels. As a continuous predictor (increments of 1 mg/dL), higher A1AT levels was associated with reduced risk of waitlist dropout on univariate analysis (odds ratio [OR] 0.98, 95% confidence interval [CI]: 0.96–0.99) (Table 1). After adjusting for age, sex, and MELD score at listing, the association between serum A1AT level and waitlist dropout remained significant (adjusted OR 0.97, 95% CI: 0.95–0.996). As a categorical variable, low A1AT levels (<100 mg/dL) was observed to increased risk of dropout, but did not meet statistical significance (OR 3.32, 95% CI: 0.99–11.16) on univariate analysis. Serum ceruloplasmin and zinc levels, and deficiencies were also not found to be associated with waitlist dropout.

Table 1. Univariate and Multivariate Analysis of Continuous and Categorical Predictors of Waitlist Dropout Due to Medical Deterioration Among ALD Patients Listed for LT

Variable	Univariate		Multivariate	
	Odds Ratio (95% CI)	P-value	Odds Ratio (95% CI)	P-value
Continuous				
Zinc	0.98 (0.94 – 1.01)	0.17	0.98 (0.95 – 1.03)	0.32
Ceruloplasmin	0.94 (0.88 – 1.05)	0.37	0.98 (0.89 – 1.08)	0.69
A1AT	0.98 (0.96 – 0.99)	0.01	0.97 (0.95 – 0.996)	0.02
Albumin	0.86 (0.34 – 1.25)	0.54	0.81 (0.27 – 1.46)	0.3
Categorical				
Zinc < 60 µg/mL	2.51 (0.68 – 9.25)	0.17	1.96 (0.51 – 7.65)	0.32
Ceruloplasmin < 20 mg/dL	0.78 (0.21 – 2.93)	0.71	0.66 (0.17 – 2.55)	0.54
A1AT < 100 mg/dL	3.32 (0.99 – 11.16)	0.052	2.81 (0.77 – 18.2)	0.12
Albumin < 2.5 g/dL	2.71 (0.83 – 8.87)	0.1	2.48 (0.71 – 8.94)	0.16

Conclusion: Among patients with ALD listed for LT, A1AT levels were independently associated with waitlist dropout, and may have prognostic value in assessing the severity of liver disease for LT. Additional studies are needed to evaluate the effect of protein nutrition deficiency in patients with ALD to identify and intervene on those at risk for waitlist dropout.

FRI-449

Type VII collagen degradation biomarker (C7M): a new marker of alcohol-induced gut injury and bacterial translocation in steatotic liver disease

Emil Deleuran Hansen^{1,2}, Nikolaj Torp^{1,2}, Ida Lønsmann^{2,3}, Evelina Stankevici⁴, Stine Johansen^{1,2}, Camilla Dalby Hansen^{1,2}, Bjørn Stæhr Madsen¹, Helene Bæk Juel⁴, Katrine Lindvig^{1,2}, Katrine Thorhauge^{1,2}, Katrine Bech^{1,2}, Ellen Jensen^{1,2}, Peter Andersen¹, Ida Ziegler Spedtsberg^{1,2}, Johanne Kragh Hansen^{1,2}, Charlotte Wernberg², Ida Villesen^{1,2}, Morten Karsdal³, Maja Thiele^{1,2}, Torben Hansen⁴, Diana Leeming³, Mads Israelsen¹, Aleksander Krag^{1,2}.
¹Odense University Hospital, Department of Gastroenterology and Hepatology, Odense, Denmark; ²University of Southern Denmark, Institute of Clinical Research, Odense, Denmark; ³Nordic Bioscience A/S, Hepatic Research, Herlev, Denmark; ⁴University of Copenhagen, Novo Nordisk Foundation Center for Basic Metabolic Research, Copenhagen, Denmark
Email: emil.deleuran.hansen@rsyd.dk

Background and aims: The gut barrier is a treatment target in alcohol-related liver disease (ALD) and non-alcoholic fatty liver disease (NAFLD), but biomarkers to assess gut injury and bacterial translocation are lacking. Alcohol induces gut injury and bacterial translocation. Type VII collagen is abundant in the extracellular matrix (ECM) of the gut wall, which may be affected during gut injury. IL-6 is secreted by the Kupffer cells in response to microbial products. We aimed to investigate circulating markers of type VII collagen and IL-6 in response to acute alcohol intoxication as markers of gut injury and bacterial translocation.

POSTER PRESENTATIONS

Method: We performed a pathophysiological intervention study including 39 patients with three different hepatic phenotypes; healthy controls (HC), ALD and NAFLD. The intervention was 2.5 ml/kg of 40% ethanol in 9 mg/ml NaCl administered through a nasogastric tube for over 30 minutes. After the intervention, blood samples were collected simultaneously through the hepatic vein at eight-time points during a 180-minute study period. Markers of type VII collagen degradation (C7M) and formation (PRO-C7) were measured using competitive ELISA. IL-6 was measured using O-link technology.

Results: Mean age was 53 (± 11) years, 61.4% were males and the median transient elastography was 4.5 (3.9–5.0)/8.9 (5.9–11.0)/10.4 (9.5–11.4) kPa (HC/ALD/NAFLD). At baseline, the hepatic venous mean concentration of C7M was 7.8 (± 6.8)/16.6 (± 11.0)/10.9 (± 8.9) ng/ml (HC/ALD/NAFLD). A significant difference of C7M between ALD and HC was observed at baseline ($p = 0.026$). Baseline PRO-C7 was comparable between groups with a mean of 39.1 (± 27.3)/41.6 (± 30.2)/37 (± 26.6) ng/ml (HC/ALD/NAFLD), $p = 0.73$. In all groups, the hepatic venous concentration of C7M increased gradually during the first 90 minutes and decreased to near baseline values after 180 minutes (Figure). The area under the curve (AUC) for C7M was 1,659 ($\pm 1,225$)/3,330 ($\pm 1,460$)/2,456 ($\pm 1,729$) ng/ml (HC/ALD/NAFLD) during the 180 minutes (Figure). AUC^{ALD} for C7M was significantly higher than AUC^{HC} ($p = 0.0074$, 95% CI: 495–2846) but not AUC^{NAFLD} ($p = 0.15$, 95% CI: –350–2098). The difference between AUC^{NAFLD} and AUC^{HC} was not significant ($p = 0.22$, 95% CI: –513–2107). Hepatic and systemic IL-6 was significantly increased after 180 min (mean Normalized Protein eXpression (NPX) 0.62, 95% CI: 0.02–0.80, $p = 0.03$ and mean NPX 0.41, 95% CI 0.62, 95% CI: 0.24–1.01, $p < 0.001$, respectively). No change was observed in the hepatic venous concentration of PRO-C7 (Figure).

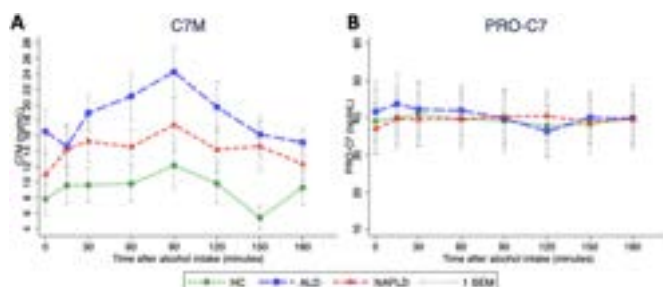


Figure: Change in hepatic A) C7M and B) PRO-C7 after alcohol intervention in patients with alcohol-related liver disease, non-alcoholic fatty liver disease and healthy controls.

Conclusion: Acute alcohol intake induces a rapid increase in hepatic type VII collagen degradation assessed by C7M, indicative of gut-driven ECM damage. The associated IL-6 increase, suggests elevated inflammatory activity from a potential increased bacterial translocation.

FRI-450

Implementation and outcomes of liver health check clinics in community alcohol services

Islam Nassar¹, Michael Griffiths¹, Susan Kemp¹, Douglas Macdonald¹.
¹Royal Free Hospital London, Hepatology, London, United Kingdom
 Email: islam.nassar@nhs.net

Background and aims: According to the English National Drug Treatment Monitoring Service, 3105 clients drinking more than 50 units of alcohol a week are engaged in community alcohol services

across Hertfordshire and North Central London. These services do not provide an assessment of liver disease. The earlier identification of cirrhosis in this group may facilitate detection of hepatocellular carcinoma (HCC) at a curable stage through surveillance and risk mitigation of complications of portal hypertension.

Method: As part of a National Cancer Program service evaluation, we implemented “Liver Health Check Clinics” (LHCC) in 9 community alcohol services in this region. These were delivered by clinician assistants who provided Fibroscan liver stiffness measurement (LSM) to pre-booked, self-booked and walk-in patients. Individuals with an LSM between 8.5 and 11.4 kPa were offered repeat elastography in 1 year. Those with an LSM > 11.4 were offered immediate blood tests including a full liver screen and onward referral to local hepatology services with a liver ultrasound before their first appointment. All patients were given an information sheet with their LSM and an explanation of its significance.

Results: 344 clients attended LHCC for assessment between 15/09/2022 and 27/01/2023. 60% were pre-booked and 40% were walk-ins. 100% gave a history of drinking at least 50 units of alcohol for at least 1 month. A further 120 clients were booked but did not attend (36%). Figure 1 shows the distribution of valid LSM results. 37 patients (10.8%) had LSM > 15 kPa and may benefit from long-term HCC surveillance. 24 patients (7%) met Baveno VI criteria for varices assessment (LSM > 20 kPa or platelets < 150), 15 (4.3%) patients had an LSM > 25 kPa predictive of a high risk of decompensation and 10 patients (3%) had biochemical evidence of decompensation (low albumin, raised bilirubin and/or INR). The cumulative non-attendance rate at the first booked liver ultrasound was 8%.

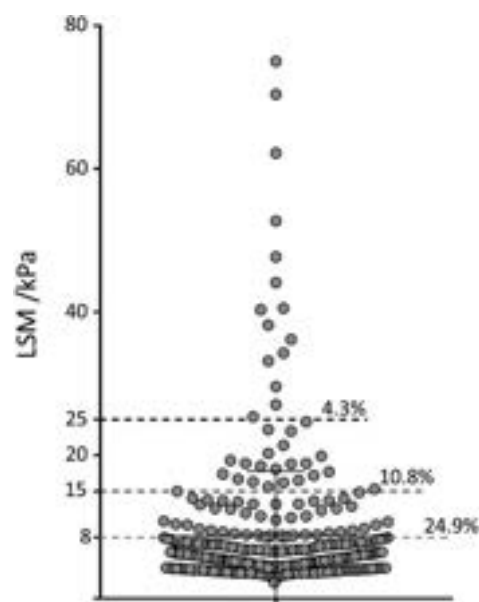


Figure 1: Distribution of LSM by Fibroscan of 344 clients assessed in Liver Health Check Clinics across 9 community drug and alcohol services. The percentage figure gives the proportions of those with a median kPa above the value shown by the dotted line

Conclusion: Although there is a substantial non-attendance rate in LHCC, these slots can be readily filled by walk-in clients. Subsequent engagement in follow-up ultrasound has been high. 11% of clients have an LSM with a high predictive value for cirrhosis and may benefit from long-term HCC surveillance. A significant minority have evidence of clinically significant portal hypertension requiring varices assessment and/or prophylactic beta blockade. The impact of LHCC assessment and feedback on harmful alcohol use and repeat LSM will be assessed prospectively.

FRI-451

Detrimental association between COVID-19 pandemic stages and alcoholic hepatitis admissions: a Canadian population-based study

Abdel-Aziz Shaheen¹, Mark G. Swain¹, Mayur Brahmanian¹, Juan G. Abraldes². ¹University of Calgary, Canada; ²University of Alberta, Canada
Email: az.shaheen@ucalgary.ca

Background and aims: Increased alcohol sales during the COVID-19 pandemic restrictions have led to a significant increase of alcoholic hepatitis (AH) admissions in Alberta early in the pandemic. We aimed to evaluate the impact of the COVID-19 pandemic on hospitalizations in patients with AH in Alberta, Canada.

Method: We used the definition of the National Institute of Alcohol Abuse and Alcoholism (NIAAA) to identify patients admitted with AH in the province of Alberta between March 2018 and March 2022. We divided admissions into three stages: pre-pandemic (March 2018–March 2020), first year of the pandemic (April 2020–March 2021), and second year of the pandemic (April 2021–March 2022). We calculated AH hospitalization monthly rates compared to overall hospitalizations. We compared demographic and clinical characteristics of AH admissions between the three pandemic stages.

Results: We identified 1,413 hospitalizations for AH (552 pre-pandemic, 462 during the first year, and 399 during the second year of the pandemic). Women admissions were similar during these stages (40.2%, 39.8%, and 45.1%, respectively, $p = 0.22$). AH admissions were more likely in younger patients (median age: 48, 44, and 44 years old, respectively, $p < 0.001$) and those living in rural areas (22.5%, 39.2%, and 31.8%, respectively, $p < 0.001$). Average MELD-Na was similar between the three stages (24, 25, and 25, respectively, $p = 0.39$). The hospitalization rates significantly increased during the first year of the pandemic (133/100,000 hospitalizations) and second year of the pandemic (102/100,000), compared to pre-pandemic (65/100,000) $p < 0.001$, Figure 1.

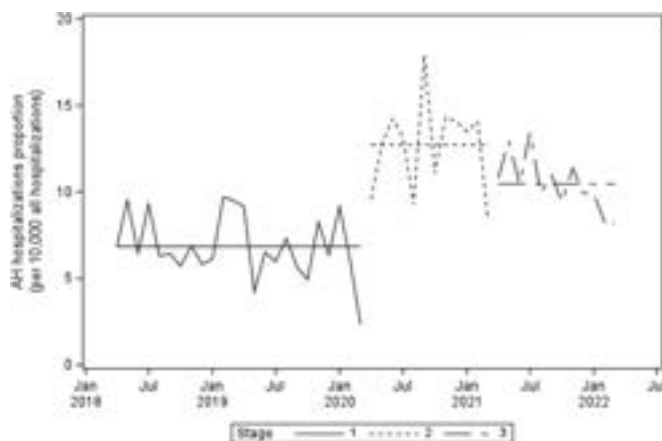


Figure: Monthly AH Hospitalization Rates to All-Hospitalizations Between 2018 and 2022 According to the Pandemic Stage

Conclusion: Since the beginning of the COVID-19 pandemic, AH admissions have particularly involved younger patients living in rural areas. Furthermore, admissions for AH peaked during the first year of the pandemic but remained elevated during the second year compared to pre-pandemic rates.

FRI-452

Cardiovascular events in patients with alcohol-related liver disease and the prognostic value of endotrophin assessed by PRO-C6

Ida Ziegler Spedtsberg^{1,2}, Ida Villesen¹, Stine Johansen^{1,2}, Johanne Kragh Hansen^{1,2}, Katrine Prier Lindvig^{1,2}, Peter Andersen¹, Nikolaj Torp^{1,2}, Mads Israelsen¹, Camilla Dalby Hansen^{1,2}, Katrine Thorhauge^{1,2}, Katrine Bech¹, Emil Deleuran Hansen^{1,2}, Sönke Dettelsen^{2,3}, Diana Leeming⁴, Morten Karsdal⁴, Aleksander Krag^{1,2}, Maja Thiele^{1,2}. ¹Odense University Hospital, Department of Gastroenterology and Hepatology, Odense, Denmark; ²University of Southern Denmark, Department of Clinical Research, Faculty of Health Sciences, Odense, Denmark; ³Odense University Hospital, Department of Pathology, Odense, Denmark; ⁴Nordic Bioscience A/S, Herlev, Denmark
Email: ida.katharina.ziegler.spedtsberg@rsyd.dk

Background and aims: Patients with alcohol-related liver disease (ALD) are at high risk of developing cardiovascular disease (CVD), however there is a lack of accurate biomarkers prognostic for cardiovascular events. Hence, a prognostic biomarker for early identification and risk stratification among these patients is needed. Fibrosis accumulation is a key pathophysiological process in both liver disease and CVD and can be measured by collagen formation. PRO-C3, a measure of type III collagen formation, strongly predicts fibrosis stage and risk of liver-related events in ALD patients. In contrast, PRO-C6, a type VI collagen formation marker, known as endotrophin, has been suggested to be a marker of cardiovascular events in patients with heart failure. However, the correlation between PRO-C6 and CVD events within ALD is not known. We, therefore, investigated the incidence of CVD in a cohort of ALD patients, and the prognostic value of PRO-C6.

Method: A prospective study of 459 patients with early, biopsy-proven ALD was collected. We obtained data on CVD, liver-related events, and all-cause mortality from patients' electronic medical records. At inclusion, PRO-C6, PRO-C3, and fibrosis stage by histology, along with a general panel of liver function tests were obtained. The following events defined CVD: coronary heart disease, cerebrovascular disease, peripheral arterial disease, hypertension, deep vein thrombosis, and pulmonary embolism. The risk of CVD according to liver fibrosis severity was evaluated using cumulative incidences and competing risk multivariable regression with all-cause mortality as competing risk. Furthermore, we evaluated the prognostic value of PRO-C6 on new CVD events.

Results: Included patients covered the full disease spectrum of ALD (F0-1/2/3-4 = 55.3%/22.8%/21.6%) and were followed for a median of 4.4 years (IQR 2.8–6.2). Patients in the CVD group were older; 61.5 ± 8.6 vs 55.5 ± 10.5 , $p = < 0.001$. Liver fibrosis stage, body mass index, and liver biochemistry did not differ between CVD vs. no-CVD patients. In total, 73 patients (15.9%) developed at least one CVD event during the follow-up period. Baseline PRO-C6 were significantly higher in patients who developed a CVD event as compared to patients who did not: 10.0 ng/ml (IQR 8.4–14.6) vs 9.2 ng/ml (IQR 7.2–12.7), $p = 0.05$. PRO-C3 did not differ between the two groups: 15.1 ng/ml (IQR 10.9–21.6) vs. 12.9 ng/ml (IQR 9.6–21.0), $p = 0.19$. A competing risk multivariable regression, with all-cause mortality as a competing risk, showed no correlation between CVD incidence and fibrosis stages. Furthermore, PRO-C6 did not show prognostic correlation with the development of a CVD event in the multivariable analysis.

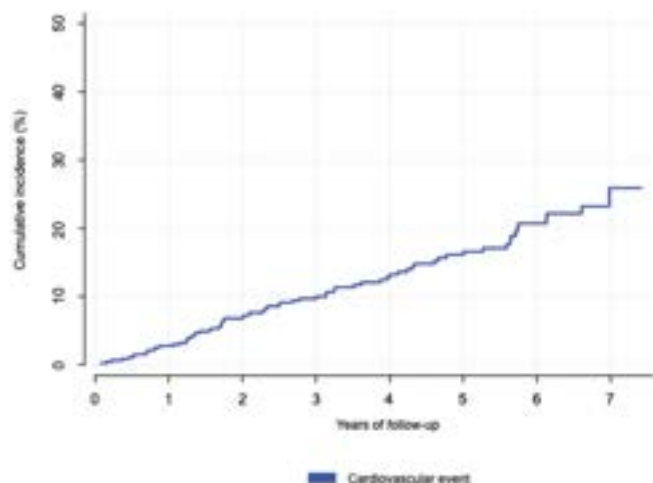


Figure:

Conclusion: ALD patients showed a marked risk of developing CVD. While those who developed CVD had a significantly higher PRO-C6 at baseline, PRO-C6 did not show good prognostic accuracy in the current population.

FRI-453

Bariatric surgery in alcohol dependence and alcohol-related liver disease

Thomas Williams^{1,2}, Andrew Palmer^{1,2,3}, Gerald Holtmann^{1,2}, Jason Connor^{2,3}, Paul Clark^{1,2,3}. ¹Princess Alexandra Hospital, Department of Gastroenterology and Hepatology, Brisbane, Australia; ²University of Queensland, School of Medicine, Brisbane, Australia; ³Princess Alexandra Hospital, Alcohol and Drug Assessment Unit, Brisbane, Australia
Email: thomasjwilliams42@gmail.com

Background and aims: Increased risk of alcohol dependence (AD) is recognised following bariatric surgery. Altered gastrointestinal anatomy and alcohol metabolism leads to more rapid increases and higher peaks of blood alcohol concentration. Such changes may enhance reward circuits, reinforcing alcohol ingestion and tolerance. Interactions of AD on liver disease has not been well-characterised using validated measures. We aimed to assess changes in AD and liver fibrosis, using validated tools, following bariatric surgery in patients reviewed within our quaternary Alcohol and Drug Assessment Unit (ADAU).

Method: Treatment seeking patients attending the ADAU with prior sleeve gastrectomy (SG) or Roux-en-Y gastric bypass (RYGB) were retrospectively identified. Patient demographics, comorbidities and surgical details were collected. Validated measures of AD, including Alcohol Use Disorders Identification Test (AUDIT) and brief Michigan Alcohol Screening Test (bMAST), were assessed pre- and post-surgery. FIB4 and APRI non-invasively assessed liver fibrosis before and after surgery.

Results: 20 patients with SG and 10 with RYGB were identified. Mean age at review was 49.0 years with 73.3% female. Mean reduction in body mass index (BMI) post-surgery was $14.5 \pm \text{SD } 9.2$ ($d = 1.5$, $p < 0.001$). Metabolic comorbidities were less frequent following surgery. Overall, mean AUDIT scores were low pre-operatively (10.2, SD 8.9), though 9 patients met criteria for AD (AUDIT score ≥ 13 in females, ≥ 15 in males). Mean AUDIT increased significantly post-surgery (18.1, SD 11.6; $d = 1.6$, $p < 0.001$). Interestingly, 29 patients met criteria for AD post-operatively. In those with pre-operative dependent-level AUDIT scores (mean AUDIT 22.5, SD 5.2), the mean AUDIT increased by 8.4 ($p < 0.05$). Patients with low risk AUDIT scores before surgery (mean 4.9, SD 2.6), observed more marked increases in mean AUDIT score post-surgery (mean change in AUDIT 26.8, $p < 0.001$). Changes in bMAST post-operatively reflected the AUDIT. Despite lower

metabolic risk after surgery, mean FIB4 increased (mean change 0.98, SD 1.8; $d = 0.5$, $p = 0.003$). The mean increase in APRI score was $0.41 \pm \text{SD } 0.83$ ($d = 0.49$, $p = 0.006$).

Conclusion: Post-bariatric surgery, significant increases in AD were observed in patients seeking treatment. While validated scores of dependence worsened in those with likely unrecognised AD, larger increases in dependent-level AUDIT score occurred in those with low pre-operative AUDIT-screened risk. Liver fibrosis scores increased for many despite reduction in metabolic risk factors, suggesting an alternate driver of disease progression. This suggests *de novo* AD may be important in explaining poor liver outcomes for some after surgery. Our work supports more intensive assessment and possibly lower thresholds of risk screening for AD and liver disease pre-bariatric surgery.

FRI-454

Risk factors for acute myocardial infarction in patients with alcohol-related liver cirrhosis-a nationwide register-based nested case-control study

Emma Celia Herting¹, Konstantin Kazankov¹, Peter Jepsen¹. ¹Aarhus University Hospital, Hepatology and Gastroenterology, Aarhus, Denmark
Email: ec.herting@gmail.com

Background and aims: Alcohol-related cirrhosis (ALD cirrhosis) predisposes patients to bleeding as well as to thrombosis. Its effect on acute myocardial infarction (MI) is weaker than its effect on other arterial or venous thromboses, and the reasons for this pattern are unclear. The aim of this study was to describe risk factors of MI amongst patients with ALD cirrhosis.

Method: This nationwide register-based nested case-control study included all Danish patients diagnosed with ALD cirrhosis in 2000–2019. Patients with first-time MI after the diagnosis of ALD cirrhosis were identified as cases. Per case, 10 ALD cirrhosis patients with no history of MI were selected as controls, using risk-set sampling. Controls were matched on time since cirrhosis diagnosis and calendar year. We used conditional logistic regression to study the association between risk factors and incidence rate ratio (IRR) of MI. Risk factors included gender, age, comorbidities, and events occurring less than 30 days before MI.

Results: 373 cases with MI were included and matched with 3,730 controls. The median age was 59.0 years in cases and 56.0 years in controls. 76.4% of cases and 65.2% of controls were male (adjusted IRR 1.65 [95% CI 1.27–2.15]). We identified the following risk factors for MI: history of atherosclerosis (26.5% of cases versus 11.0% of controls, aIRR 1.93 [95% CI 1.43–2.61]), history of cardiac ischemia (23.1% of cases versus 3.1% of controls, aIRR 6.99 [95% CI 4.93–9.90]), hospitalization for infection (aIRR 2.09 [95% CI 1.27–3.43]), recent surgery (aIRR 1.83 [95% CI 1.19–2.82]) or recent out-of-hospital treatment with antibiotics (aIRR 1.46 [95% CI 1.00–2.75]).

Figure: Associations between potential risk factors and incidence rate ratio of acute myocardial infarction

	Crude IRR	95% CI	Adjusted IRR	95% CI
Male	1.72	1.35–2.21	1.65	1.27–2.15
Age, pr year	1.04	1.03–1.06	1.03	1.02–1.04
Events in the previous 30 days				
Hospitalization of infection	2.69	1.74–4.15	2.09	1.27–3.43
Hospitalization of complication of liver disease				
Ascites	1.39	0.86–2.26	1.18	0.69–2.00
Spontaneous bacterial peritonitis	2.00	0.23–17.12	1.12	0.12–10.50
Gastrointestinal bleeding	2.11	1.18–3.75	1.42	0.74–2.75
Prescribed Antibiotics	1.83	1.30–2.58	1.46	1.00–2.14
Surgery	2.95	2.02–4.31	1.83	1.19–2.82
Comorbidities				
Atherosclerosis	3.12	2.40–4.06	1.93	1.43–2.61
Cardiac ischemia	10.58	7.62–14.68	6.99	4.93–9.90
Chronic obstructive pulmonary disease	2.89	2.13–3.92	2.20	1.58–3.08
Diabetes	1.67	1.29–2.16	1.15	0.86–1.55

Conclusion: Among patients the ALD cirrhosis, the incidence rate of MI was higher for those who had history of atherosclerosis or cardiac ischemia, were hospitalized because of infection, had surgery, or received antibiotics treatment in the community in the previous 30 days. Our findings contribute to the understanding of risk factors for MI in patients with ALD cirrhosis. They may have clinical implications e.g., for the decision to offer thromboprophylaxis.

FRI-455

Opportunistic cirrhosis casefinding in alcohol dependent inpatients through alcohol specialist nurse assessment and transient elastography: early detection in a high risk group

Ann Archer^{1,2}, Molly Thorpe¹, Saswata Roy¹, Charlotte E. Davies¹, Rosie Parnham¹, Grace Cameron¹, Lucy Krouma¹, Fiona Gordon¹, Kushala Abeysekera^{1,2}. ¹University Hospitals Bristol and Weston NHS Foundation Trust, Bristol, UK, Liver Medicine, Bristol, United Kingdom; ²University of Bristol, Population Health Science, Bristol, United Kingdom
Email: ann.archer@uhbw.nhs.uk

Background and aims: Europe has the highest per capita alcohol consumption and alcohol-related loss of disability adjusted life years compared with other WHO regions, with many countries seeing a rapid rise in alcohol related harms. Despite this, there is still widespread failure to recognise alcohol-related liver disease early before patients present with decompensation. Many patients with alcohol use disorder present frequently with unscheduled admissions to hospital, providing an opportunity for engagement with addiction and hepatology services. We sought to evaluate opportunistic testing for cirrhosis in this vulnerable patient group who often experience barriers to accessing healthcare.

Method: Our transient elastography (TE)-trained alcohol specialist nurses (ASNs) offered TE to patients with alcohol dependence and no previous diagnosis of cirrhosis. Those with elevated liver stiffness measurements (LSM) of ≥ 12 kPa were offered follow-up in hepatology clinic or assessed during their admission by a hepatologist. Paired t-test was used to assess mean differences between groups pre- and post- intervention.

Results: Between April and December 2022, 94 patients at the Bristol Royal Infirmary, UK were offered TE during emergency admissions by ASNs (23% F; median age 55 (IQR 18.5)). 27 people (30.8%) with LSM of ≥ 12 kPa (median IQR/M 11.5%) were identified as having probable alcohol related cirrhosis. Of these, 9 had LSM ≥ 25 kPa suggestive of clinically significant portal hypertension (CSPH). 27% (n = 25/94) of patients post-TE subsequently engaged with outpatient addiction services. Of those who had recorded alcohol consumption (n = 38/94), a trend towards lower units consumed post ASN review and TE

assessment was observed; pre admission mean alcohol consumption was 31 units/day (SD: 25.8) falling to 20.5 units/day (SD: 25; t (37) = 3.2; p = 0.003) post admission. Of the 94 patients screened, 4 patients died within the nine month period, 2 of whom had been identified with cirrhosis.

TE results for alcohol dependent inpatients without known cirrhosis April-December 2022

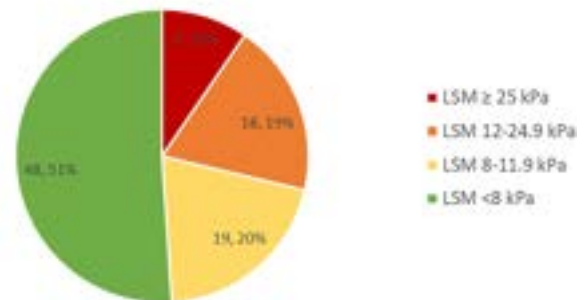


Figure:

Conclusion: Opportunistic testing for liver disease in people with alcohol use disorder is important and high yield to identify patients with cirrhosis and clinically significant portal hypertension. Crucially this is a socially disadvantaged patient cohort who experience barriers to accessing traditional healthcare. Prospective work is needed to establish whether diagnosis has a lasting impact on drinking behavior, engagement with addiction services, liver related morbidity and mortality.

FRI-456

Potential gut microbial biomarkers for detection of sarcopenia in alcohol-related liver disease patients

Haripriya Gupta¹, Sang Joon Yoon², Jin-Ju Jeong², Satya Priya Sharma², Raja Ganesan², Sung-Min Won², Ki Tae Suk^{2,3}. ¹Hallym University, Institute for Liver and Digestive Diseases, Korea, Rep. of South; ²Institute for Liver and Digestive Diseases, Hallym University, Korea, Rep. of South; ³Institute for Liver and Digestive Diseases, Hallym University College of Medicine, Department of Internal Medicine, Korea, Rep. of South
Email: ktsuk@hallym.ac.kr

Background and aims: Sarcopenia and alcohol-related liver disease (ALD) are closely related. Not only the liver, but excessive intake of alcohol also increases the catabolism of proteins under stress and inflammation conditions affecting function of skeletal muscles. Gut dysbiosis is thoroughly studied in ALD, however gut dysbiosis under sarcopenia condition in ALD is not well known. So, we aim to determine predictors of sarcopenia using gut microbiota and correlation with the sarcopenia indices in patients with ALD with or without sarcopenia.

Method: Total 177 subjects (healthy control (HC), sarcopenia control (SC) and ALD patients) were enrolled for this study. ALD patients were further categorized under non-sarcopenia (HC, n = 48 and ALD, n = 68) and sarcopenia groups (SC, n = 11 and S-ALD, n = 50) according to the appendicular skeletal mass (ASM) divided by height (meter) squared index. Liver function test, sarcopenia indices were performed, and stool microbiome analysis by 16S rRNA-based sequencing were examined through EzBioCloud Database.

Results: Analysis of variance of sarcopenia indices (subcutaneous, visceral, and appendicular skeletal muscle, ASM/Ht2 index) between the four groups (HC, SC, ALD and S-ALD) revealed significant decreased in S-ALD vs ALD group (p < 0.01). In gut microbiome analysis revealed significant shifts in the gut microbiome in sarcopenia group vs non-sarcopenia groups in ALD. Relative abundance of phylum *Bacteroides* and *Proteobacteria* was found to significantly decrease (p < 0.001) and increase (p < 0.05) respectively in S-ALD vs ALD group. Species *Phocaeicola dorei*, *Phocaeicola*

POSTER PRESENTATIONS

vulgatus, *Escherichia coli* and *Pantoea agglomerans* were found to be distinctive abundant in S-ALD group vs ALD group with LDA score >2 and AUC >0.60 ($p < 0.001$ and $q < 0.05$). Correlating all the four groups together, the aforementioned 4 species were shown to be significantly correlated with sarcopenia indices ($p < 0.05$).

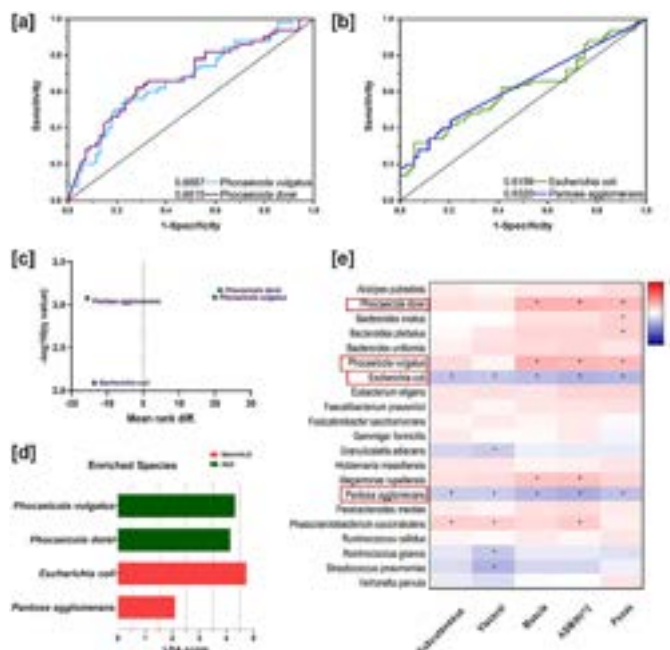


Figure: Identified distinctive gut microbiota in S-ALD vs ALD patients. (a) and (b) AUROC curves, (c) False Discovery Rate, (d) LDA score and (e) Spearman's rank correlation between identified distinctive gut microbiota and sarcopenia indices.

Conclusion: These findings provide preliminary data that *Bacteroides* abundance is severely impacted causing known pathobiont from *Proteobacteria* to grow in abundance. Aiming *Bacteroides* to *Proteobacteria* ratio might be beneficial for the ALD patients having sarcopenia complication which may improve quality of life.

FRI-457

Validation of the Lille 4 score on a cohort of romanian severe alcoholic hepatitis patients

Bumbu Andreea Livia¹, Adelina Horhat², Mina Ignat³, Horia Stefanescu⁴, Bogdan Procopet^{2,3}, ¹Iuliu Hațieganu University of Medicine and Pharmacy, Gastroenterology, Cluj-Napoca, Romania;

²University of Medicine and Pharmacy, Cluj Napoca, Romania; ³Regional Institute of Gastroenterology and Hepatology, Cluj Napoca, Romania;

⁴Regional Institute of Gastroenterology and Hepatology, Liver Unit and Clinical Ultrasound Department, Cluj Napoca, Romania

Email: andreea_bumbu@yahoo.com

Background and aims: Severe alcoholic hepatitis (sAH) has a high mortality rate. Corticoids are the only pharmacological means to improve short term survival, though burdened by their side effects. We aimed to validate the Lille 4 score on a population of sAH from our center in Cluj-Napoca, Romania.

Method: We enrolled 103 consecutive patients with a clinical suspicion of sAH (Maddrey DF>32). All patients underwent transjugular liver biopsy. The indication of prednisone was based on histological criteria, i.e. AHHS>6. The Lille 4 and Lille 7 scores were calculated and the correlation between these and the short (1 month) and medium/long term survival was analysed. Secondly, we analysed the benefit of subdividing the cut-off values into the intervals proposed by Mathurin *et al* in 2011- complete responders (Lille score ≤0.16), partial responders (Lille score 0.16–0.56) and null responders (Lille score ≥0.56).

Results: The bivariate analysis showed a high correlation between the responders at day 4 (Lille <0.45) and the ones at day 7 (Pearson coefficient 0.766, $p < 0.001$) and a very high correlation between the responders at day 7 and the ones at day 4 (Pearson coefficient 1, $p < 0.001$), respectively.

In the Lille 7 responder group, 12 patients (11.6%) died in the first month ($p = 0.047$), while in the Lille 4 responder group, 8 patients (7.7%) died in the first month ($p = 0.041$). The analysis of the Lille subgroups showed that out of 103 patients, 43 (41.74%) were situated in the complete responder group (Lille score ≤0.16), 39 (37.86%) in the partial responders group (Lille score 0.16–0.56) and 21 (20.38%) in the null responders group (Lille score ≥0.56), respectively. The mean survival of complete responders was 19.3 months (14.4–24.2; 95% CI), of partial responders was 18.6 months (12.6–24.7; 95% CI) and of null responders was 2.2 months (0.5–4.0; 95% CI) (Figure).

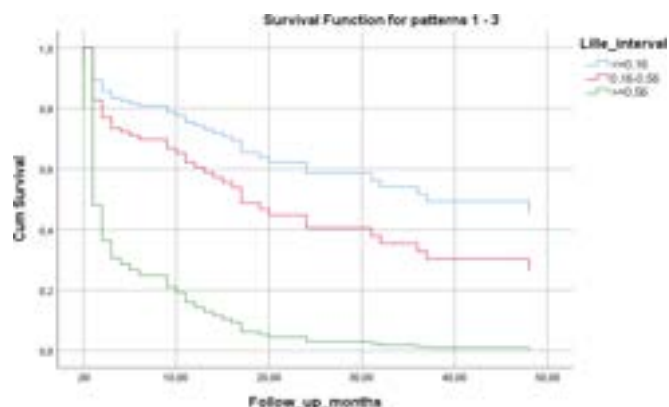


Figure:

Conclusion: The Lille 4 score is a good substitute for Lille 7, and its validation has the potential to lower the infectious and bleeding events rate. The responder status correlates with the short term survival, but doesn't influence the long term. The subdivision into the proposed intervals highlights a group of patients-the partial responders- that have a similar survival to the complete responders. The null responders have a significantly lower survival.

FRI-458

Evaluation of histological differences between cirrhosis due to alcoholic-related liver disease and non-alcoholic steatohepatitis using automated fibrosis phenotyping of liver histology

Masanori Fukushima¹, Hisamitsu Miyaaki¹, Yasuhiko Nakao¹, Ryu Sasaki¹, Satoshi Miuma¹, Shinji Okano², Kazuhiko Nakao¹.

¹Nagasaki University Graduate School of Biomedical Sciences, Department of Gastroenterology and Hepatology, Japan; ²Nagasaki University Graduate School of Biomedical Sciences, Department of Pathology, Japan

Email: ma-fukushima@nagasaki-u.ac.jp

Background and aims: Cirrhosis due to alcoholic-related liver disease (ALD) and non-alcoholic steatohepatitis (NASH) are different diseases with similar histopathology, and histological discrimination can be difficult. Although the distinction between ALD and NASH is defined by the amount of alcohol consumed, there is no sufficient consensus because of individual differences in the effects of alcohol. Therefore, it is desirable to establish new diagnostic criteria to objectively diagnose ALD and NASH. In recent years, digital analysis of pathology has become possible with whole slide imaging systems, which can convert pathology specimens into high-resolution digital images, enabling comprehensive quantitative analysis of pathological parameters using AI. The purpose of this study was to find histological differences between ALD and NASH by analysing more than 300 histological fibrosis phenotypic features.

Method: Thirty-six patients with cirrhosis due to ALD and 17 patients with cirrhosis due to NASH who underwent liver transplantation at Nagasaki University Hospital between January 2000 and December 2020 were included. Tissues of recipient-extracted livers were stained with SiriusRed and imported for digital pathology imaging. The FibroNest™ quantitative digital pathology platform (PharmaNest, Princeton, NJ, USA) was used to quantify the histological phenotype of fibrosis, including collagen amount and structure (12 traits), morphometric traits of the collagen fibres (13 traits), and architecture of fibrosis (7 traits). Each trait considers mean, variance, skewness, kurtosis and progression, for a total of over 300 parameters to compare differences in histological features between ASH and NASH.

Results: The 36 patients with ALD and 17 patients with NASH did not differ in terms of age, BMI, MELD score, or serum hyaluronic acid level. There were significantly more males in the ALD group. Analysis using FibroNest showed no significant differences in collagen amount, structure, and architecture of fibrosis between the two groups. However, morphometric traits of the collagen fibres were significantly different between the two groups. As for morphological traits, the NASH group was characterized by assembled collagen, which defined a complex skeleton with a high number of nodes and branches, were short in length, thin, and small in area. On the other hand, the ALD group had significantly more fine collagen than the NASH group. Using the Phenotypic Fibrosis Composite score (Ph-FCS) created from 350 quantitative fibrosis traits normalized to their maximum value in the group and then averaged, a diagnosis of ALD/NASH was possible with a sensitivity of 86% and specificity of 94% when the cut-off value was set at 4.35 (Figure).

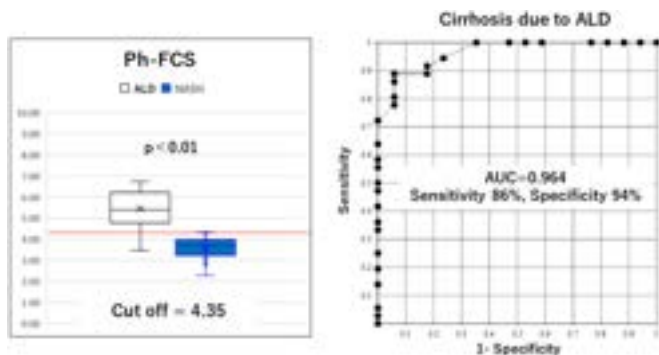


Figure:

Conclusion: The analysis of fibrosis patterns by digital pathology suggested the possibility of discriminating the histological diagnosis of ALD/NASH by differences in fibrosis morphology.

FRI-459

Radiomic data can define phenotypes of acute alcoholic hepatitis

Nawaz Safdar¹, Amy Hicks², Yun Chew², Craig Roe³, Sabina Choudhry⁴, Ashwani Singal⁵, Richard Parker². ¹University of Leeds, School of Medicine, Leeds, United Kingdom; ²Leeds Teaching Hospital Trust, Leeds Liver Unit, Leeds, United Kingdom; ³Leeds Teaching Hospital Trust, Radiology, United Kingdom; ⁴Avera Medical Group, Radiology, Sioux Falls, United States; ⁵University of South Dakota, Sioux Falls, United States

Email: richardparker@nhs.net

Background and aims: Alcohol associated-hepatitis (AAH) is an acute manifestation of alcohol-related liver disease with a 90-day mortality of ~30%. This study aimed to identify phenotypes of AAH based on radiological measures of hepatic volume and steatosis.

Method: Consecutive patients with a clinical diagnosis of AAH based on the NIAAA definition who had undergone computed tomography (CT) imaging of the abdomen within 10 days of admission were included. AAH phenotypes were defined using hepatic steatosis (HS),

calculated using a liver/spleen attenuation ratio, and adjusted liver volume (aLV) calculated as a ratio of observed: predicted liver volume using the formula published by Vauthey et al (2002). Radiological anthropometric data were collected using Hepatic VCAR (GE HealthCare, UK) and Vitrea (Canon, USA), and biochemical data were collected from electronic health records. Patients were assigned to three distinct phenotypes: small non-fatty (SNF), intermediate, and large fatty (LF) based on tertiles for HS and aLV (Figure 1). No specific study procedures were performed, and individual patient consent was not sought. All analyses were performed using R.

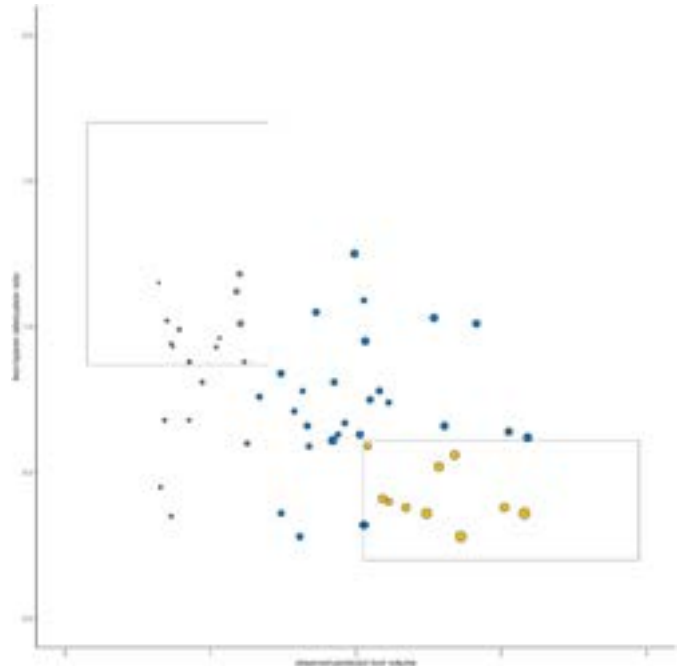


Figure:

Results: Fifty-six patients were included. The median patient age was 47 (IQR 41–53), of whom 62% were male. Twelve patients (21%) were categorised as having SNF livers, and 10 (18%) categorised as having LF livers. Thirty-four (61%) of patients had an intermediate phenotype. LV and HS varied considerably: SNF [LV: 1582 (1406–2086) cm³ and HS: 1.00 (0.94–1.13)], and LF [LV: 5112 (4564–6744) cm³ and HS: 0.39 (0.37–0.49)]. Patients with LF livers had significantly lower international normalised ratio (INR; 1.3 vs. 1.6 vs. 2.1 in LF vs. intermediate vs. SNF, respectively, ANOVA $p < 0.001$), significantly higher bilirubin (350 vs. 171 vs. 156 mmol/L in LF vs. intermediate vs. SNF respectively, ANOVA $p = 0.02$), and tended to have higher ALT, although this was not statistically significant (88 vs. 46 vs. 34 IU/ml in LF vs. intermediate vs. SNF, respectively). Overall survival was 73.2% at 90 days. Compared to the intermediate phenotype, both extremes of size and fat had worse mortality at 90 days: 40% and 33% in LF and SNF respectively vs. 21% in intermediate; this was not statistically significant (Log-rank $p = 0.31$). Infection was common and occurred more frequently in patients with LF livers: 75% of patients suffered infection vs. 52% and 26% in intermediate and SNF livers, respectively. Only a minority of patients received corticosteroids in this retrospective cohort, but response to treatment (Lille score < 0.45) was seen only with LF livers and not with other phenotypes.

Conclusion: Liver volume and steatosis assessed by CT varied significantly between patients admitted to hospital with acute AAH and were associated with clinical findings. A larger cohort is required to further investigate these findings.

FRI-460

New patient referrals and alcohol consumption data in an Irish hepatology outpatient setting

Aoife Moriarty¹, Paul Armstrong¹, Caroline Walsh¹, Jennifer Russell¹, Eleanor Ryan¹, Stephen Stewart¹. ¹Mater Misericordiae University Hospital, The Liver Centre, Dublin, Ireland
Email: aoifemoriarty@eril.ie

Background and aims: New patient referrals to specialist hepatology clinics are increasing. Alcohol remains a common problem for Irish healthcare. Concentrated efforts are required to establish which patients referred can be managed in primary care, thus improving specialist access for more complex cases. The aims of this prospective study were to evaluate new referrals to hepatology clinic in MMUH and to assess the impact of a hepatology nurse specialist. We also aimed to evaluate patterns of alcohol consumption in these new referrals and the correlation with phosphatidylethanol levels (PEth) testing.

Method: New patients to clinic were reviewed by a hepatology nurse specialist. A questionnaire was completed including referral details, basic demographics and alcohol consumption data. Bloods including PEth and transient elastography (TE) were performed. Following review by a consultant hepatologist, patients with alcohol or non-alcohol related steatosis with low TE scores (<6kPa) were discharged to their GP with lifestyle advice.

Results: 380 new patients were reviewed over 7 months, 53.75% male with a mean age 50.69 years (± 15.29). Mean BMI was 28.98 kg/m² (± 6.77) with a median TE score of 6.9kPa (IQR 5.63), and median CAP of 263.58 (IQR 90). 69.5% of referrals were made from primary care. 29% of patients were discharged following review at nurse led clinic. There was a 6% DNA rate of these patients at the subsequent doctor led clinic. 67.4% of patients consumed alcohol. The majority (18.4%) consumed alcohol on 2–3 occasions/week, with 11% drinking daily. Beer was most frequently consumed (39.2%), with the majority of patients (47.5%) drinking at home. Patients were separated into 3 groups; non-drinkers (33.68%), low risk drinkers (35%) and hazardous drinkers (31.32%), which was defined as >11units/week for females and >17units/week for males. Hazardous drinkers had statistically significantly higher PEth levels than non-drinkers and low risk drinkers (Kruskall Wallis $p < 0.05$) but no difference was observed in TE kPa, CAP or BMI. A strong correlation was observed between documented units of alcohol consumed and PEth levels (0.805 Spearman's rho $p < 0.001$). 2.1% of patients who reported never consuming alcohol had a positive PEth test, the majority (75%) at low levels (<50 ug/L).

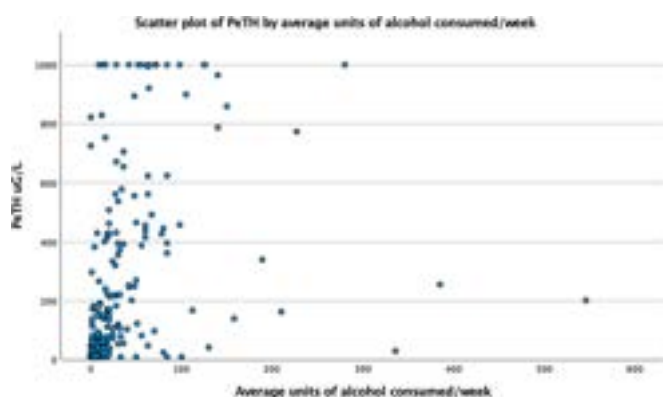


Figure:

Conclusion: Our study shows that the initial nurse led clinic is a useful adjunct in identifying which patients can be managed in a primary care setting after appropriate screening investigations, thus freeing up space in the doctor clinic to manage more advanced patients. Two thirds of our patients consume alcohol, with one third at hazardous levels with PEth testing being a useful tool in identifying

these patients. Equally, in patients who report alcohol abstinence, their history is generally very reliable without the need for further confirmatory PEth testing.

FRI-461

Carbohydrate-deficient transferrin is a suitable drinking marker for patients with metabolic dysfunction-associated fatty liver disease

Kazuyoshi Kon¹, Maki Morinaga¹, Akira Uchiyama¹, Hiroo Fukada¹, Toshifumi Sato¹, Shunhei Yamashina¹, Kenichi Ikejima¹. ¹Juntendo University School of Medicine, Department of Gastroenterology, Japan
Email: kazukon@juntendo.ac.jp

Background and aims: In 2020, an international expert group newly proposed the definition of metabolic dysfunction-associated fatty liver disease (MAFLD). MAFLD focuses on obesity and metabolic syndrome-related diseases, not exclude alcohol-related steatohepatitis; it is essential to objectively evaluate alcohol consumption as well as glycolipid metabolism in clinical practice. In this study, we examined the usefulness of measurement of carbohydrate-deficient transferrin/total transferrin ratio (%CDT) in patients with MAFLD.

Method: A total 121 patients who visited our hospital from September 2018 to November 2021 and were diagnosed with fatty-related liver disease, including alcohol-related liver disease and non-alcoholic fatty liver disease, were evaluated according to MAFLD diagnostic criteria of the International Consensus Panel. They were classified into a MAFLD group (n = 95) and a non-MAFLD group (n = 26). Controlled attenuation parameter (CAP) value of ≥ 220 dB/m was defined as fatty liver. ROC analysis was performed to evaluate the diagnostic usefulness of %CDT, mean corpuscular volume (MCV), and gamma-glutamyl transpeptidase (γ GT) as drinking markers for non-to light-drinkers (<210 g/week for men, <140 g/week for women) and heavy drinking (≥ 420 g/week). In addition, we analyzed the effects of alcohol consumption, age, gender, hepatic enzymes, lipids, blood glucose levels, CAP levels, and liver stiffness on each marker by multiple regression analysis.

Results: In the MAFLD group, the diagnostic power of non- to light-drinking by %CDT was higher than AUROC 0.78 (cut-off 1.78%: sensitivity 73%, specificity 76%), which was higher than AUROC 0.71 in MCV and AUROC 0.69 in γ GT. AUROC for %CDT was 0.78 (cut-off 2.08%: sensitivity 55%, specificity 88%), which was higher than 0.69 in AUROC for MCV or AUROC 0.66 in AUROC for γ GT. Even in the non-MAFLD group, the %CDT value remained high AUROC values, 0.88 for non- to light- drinking detection and AUROC 0.83 for heavy drinking, whereas other markers tended to increase in the non-MAFLD group more markedly than in the MAFLD group. (MCV: non- to light-drinker 0.90, heavy drinker 0.81, γ GT: non- to light-drinker 0.78, heavy drinker 0.74). In the multiple regression analysis, only alcohol consumption was an independent factor for %CDT in both the MAFLD and non-MAFLD groups. In contrast in γ GT, alcohol consumption was not a significant factor in either the MAFLD group or the non-MAFLD group, and serum triglycerides levels were detected as significant factors in the non-MAFLD group, and AST and triglycerides levels were detected as significant factors in the MAFLD group.

Conclusion: Measurement of %CDT showed high AUROC values in the detection of non- to light- drinkers and heavy drinkers regardless of MAFLD or non-MAFLD. MCV and γ GT values were affected by dyslipidemia and liver damage, and rather favorable AUROC values were shown in the non-MAFLD group. %CDT was shown to be a very useful marker for the objective evaluation of alcohol consumption in the diagnosis and treatment of MAFLD.

FRI-462

Early liver transplantation for acute alcoholic hepatitis in a spanish liver transplant center

Victoria Aguilera Sancho^{1,2,3}, Sonia García-García³, Sarai Romero Moreno², María García Eliz^{1,4}, Isabel Conde^{1,5}, Javier del Hoyo⁴, Carmen Castillo⁶, Sagrario Gutierrez⁶,

Marina Berenguer^{1,2,5}, ¹Instituto de Investigación Sanitaria La Fe de Valencia, Valencia, Spain; ²University of Valencia, Spain; ³La Fe University and Polytechnic Hospital, Hepatology and Liver Transplant Section, Valencia, Spain; ⁴La Fe University and Polytechnic Hospital, Valencia, Spain; ⁵La Fe University and Polytechnic Hospital, Hepatology and Liver Transplant Section, Valencia, Spain; ⁶La Fe University and Polytechnic Hospital, Social Work Department, Valencia, Spain
Email: toyagui@hotmail.com

Background and aims: Liver Transplantation (LT) for acute alcoholic hepatitis (AAH) has become an accepted treatment for selected patients. However, the inclusion in the waiting list and access to LT remains limited in our country.

Aims: (i) To describe the number of patients admitted due to AAH during 2015–2021 divided in 3 temporal cohorts and (ii) to evaluate access to LT and reasons for not been included.

Method: Patients admitted due to AAH during 2015–2021 were recorded and divided in 3 temporal cohorts (1:2015–2017, 2:2018–2019, 3:2020–2021). The demographics, social features, NIAAA criteria and severity of AAH assessed by Maddrey and MELD were recorded. Access to LT and reasons for not being included were recorded.

Results: 61 patients were admitted during these years (NIAAA probable criteria in 87%). There was a trend towards higher admissions in last cohort (1:33%, 2:16% and 3:51%). Mean age was 55 years, 75% were men, 73% were from Spain and rest were from foreign countries. Only 25% were married. Social risk was moderate-high in 77% of patients. 61% had cirrhosis at admission, median MELD was 21 and Maddrey 43. Treatment with corticoids was indicated in 38 (62%) but only 31 received treatment and 17 patients were considered non-responders at 7 day (Lille score). 24 patients (non-responders to corticoids (n = 17) and those who did not received them (n = 7)), were evaluated as potential early LT candidates for AAH. Reasons for not been included in the waiting list were: addiction risk (n = 8), high social risk (n = 4), improvement in liver function (n = 4), contraindication due to medical condition (n = 5). Only 1 patient (1.6%) was included on the waiting list due to AAH but died before LT and 2 patients were included after 6 months of abstinence. 1, 3 and 5 year survival was 69, 44 and 41%. High social risk and non-maintained abstinence were associated with mortality.

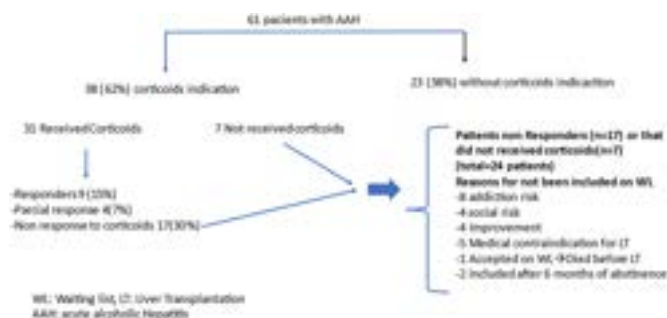


Figure:

Conclusion: Admissions due to AAH has increased during the last years, potentially related to COVID pandemic. Access to LT is very limited (<2%) at our center, mainly due contraindications related to social or addiction comorbidities. Both aspects should be managed intensively in order to improve the prognosis of those patients.

FRI-463

Identification of risk factors for alcohol relapse in liver transplant patients with alcohol-related liver disease

Dilara Turan¹, Fulya Günsar², Murat Harputluoglu³, Gökhan Kabaçam⁴, Hale Gokcan⁵, Murat Akyildiz⁶, Mesut Akarsu⁷, Gupse Adali⁸, Derya Ari¹, Ilker Turan², Nilay Danis⁷, Ulus Akarca², Esra Durmaz², Genco Gencdal⁶, Murat Aladag³, Murat Taner Gulsen⁹, Ozan Sarikaya², Volkan Yılmaz⁵, Zeki Karasu²,

Ramazan Idilman⁵, Meral Akdogan Kayhan¹, ¹Ankara Bilkent City Hospital, University of Health Science, Department of Gastroenterology and Hepatology, Turkey; ²Ege University, School of Medicine, Department of Gastroenterology and Hepatology, Turkey; ³Inonu University, School of Medicine, Department of Gastroenterology and Hepatology, Turkey; ⁴Yuksek İhtisas University, School of Medicine, Department of Gastroenterology and Hepatology, Turkey; ⁵Ankara University, School of Medicine, Department of Gastroenterology and Hepatology, Turkey; ⁶Koc University Hospital, School of Medicine, Department of Gastroenterology and Hepatology, Turkey; ⁷Dokuz Eylül University, School of Medicine, Department of Gastroenterology and Hepatology, Turkey; ⁸Umraniye Training and Research Hospital, University of Health Science, Department of Gastroenterology and Hepatology, Turkey; ⁹Gaziantep University, School of Medicine, Department of Gastroenterology and Hepatology, Turkey
Email: akdmeral@yahoo.com

Background and aims: Alcohol-related liver disease (ALD) is one of the most common causes of liver transplantation (LT). Although alcohol relapse after LT negatively impacts the graft and patient survival rates, predictors for alcohol relapse are not yet well defined. This study aimed to determine risk factors for alcohol relapse after LT.

Method: Patients with ALD who underwent LT from 9 different transplantation centres were assessed. Demographic and clinical features such as family support, alcohol consumption habits, educational level, whom the patient resided with, length of abstinence of alcohol before LT, marital status, age at transplantation, and smoking habits were evaluated and statistically analyzed. The chi-square test was used to evaluate categorical variables.

Results: A total of 124 patients with ALD, consisting of all males (100%) with mean age of 52.9 ± 9.6 years, were recruited for evaluation of the alcohol relapse. The mean follow-up time was 65 ± 54.2 months (range: 6 months–238 months). The mean MELD-Na score before LT was 21.6 ± 5.7. Twenty and eight patients reported consumption of alcohol following LT: all patients began drinking alcohol within the first 5 years of the posttransplant period (mean relapse time: 18.5 ± 3.2 months). Most patients had heavy alcohol consumption (53%, >210 g/day). There was no relationship between alcohol relapse and being a heavy drinker (p = 0.254). While fifty patients (40%) did not adhere to the “6-month rule” of alcohol abstinence before LT, it was found that their rate of alcohol relapse did not statistically increase after LT (p = 0.405). Approximately 30% of the patients reported strict adherence to alcohol abstinence during Ramadan time. Remarkably, marital status was related to higher rates of posttransplant alcohol abstinence success (p = 0.010).

Table 1: Risk factors of alcohol relapse after LT evaluated in patients (n = 124)

n, (%)	Relapse (n = 28)	No Relapse (n = 96)	p value
Age <50 years at Tx	11 (39.2)	29 (30.2)	0.248
Married	16 (57.1)	77 (80.2)	0.010
Social support	19 (67.8)	78 (81.2)	0.060
Family history of alcohol use	15 (53.5)	51 (53.1)	0.340
Smoker	20 (71.4)	53 (55.2)	0.110
Pre-LT abstinence <6 months	10 (35.7)	39 (40.6)	0.405
Alcohol consumption during Ramadan (Yes)	5 (17.8)	32 (33.3)	0.102
Donor (Living Liver Donor)	19 (67.8)	64 (66.6)	0.550

Conclusion: In our study, being married was linked to a lower rate of relapsing back to drinking. There was no increase in the rate of relapsing back to drinking among patients who had transplants without following the 6-month rule. The results of this study indicated that multifactorial predictors strongly influenced post-transplantation alcohol consumption among patients. All patients

POSTER PRESENTATIONS

should be comprehensively assessed in regard to multiple factors to determine whether or not the patient is eligible for LT.

FRI-464

Costs of hospital management of acute alcoholic hepatitis

Lucy Turner¹, Richard Parker¹, Kath Chapman². ¹Leeds Teaching Hospital Trust, Leeds Liver Unit, Leeds, United Kingdom; ²Leeds Teaching Hospital Trust, Finance, Leeds, United Kingdom

Email: richardparker@nhs.net

Background and aims: Alcoholic hepatitis is an acute manifestation of alcohol related liver disease (ARLD) with a high short-term mortality. Patients with AH are often very unwell and require significant healthcare resources.

Method: We used the ALLHEAL observational study of patients with ARLD to derive the cost of admissions to hospital with AH or other types of liver disease for individual patients. The cause of admission was recorded as per hospital discharge coding using ICD-10 codes. Validation of coded diagnoses was done by reviewing hospital records and laboratory values. Costs are reported in pounds sterling (£) with Euro (€, 1 GBP = 1.12 EUR) and US dollar (\$, 1 GBP = 1.22 USD) equivalent values. Hospital episode statistic (HES) reports for the NHS in England were used to estimate the costs of alcoholic hepatitis to the health service in England.

Results: Two hundred and sixteen patients recruited into ALLHEAL had a total of 2,947 hospital admissions over a five year period including 124 (4%) due to primary diagnosis of AH, and a further 183 admissions (6%) had AH as a secondary diagnosis. The average cost of a primary admission with alcoholic hepatitis was £3,880 (SD 3369) (€4377, \$4745). Secondary admissions with AH cost an average of £3461 (SD 2901), (€3904, \$4232). The average costs of non-AH admissions with ARLD was £1,004. HES data showed that in 2021–22 there were 2749 primary admissions to hospital in England with AH and 10,022 secondary admissions, with a clear increase in both types of admission over the past decade. Scaling up ALLHEAL costs based on HES data showed that costs to the health service in England in 2021–22 were £10,666,120 for primary admissions and £34,686,142 for secondary admissions.

Conclusion: Hospital admissions with AH are expensive, costing on average three times as much as admissions with other diagnoses. The cost to the health service is considerable: based on the admissions in this series, we estimate that the NHS in England spent a total of nearly £45 million on caring for patients with AH in the last financial year. Better treatments are urgently required to address this significant burden to the healthcare system.

FRI-465

Adverse childhood experiences as a background for alcoholic liver disease-cohort analysis of risk score in ALD and non-ALD cirrhosis patients in comparison with the control group

Karolina Sulejova¹. ¹University Hospital F.D. Roosevelt Banská Bystrica, Department of Internal Medicine Div Hepatology, Gastroenterology and Liver Transplantation, Banská Bystrica, Slovakia

Email: sulejovakarolina@gmail.com

Background and aims: The alcoholic liver disease represents the main cause of liver cirrhosis in the Slovak republic. An important position in the development of addiction has childhood trauma. Child abuse, neglect, and other traumatic experiences contribute to the development of risky patterns of behavior leading to the evolution of cirrhosis. The Adverse Childhood Experience Questionnaire is a rating scale evaluating the main risky domains for the development of addiction, and it could play as an indicator for cirrhosis development.

Method: In the following period, we evaluated adverse childhood experiences by the 10-item questionnaire in all patients enrolled in the local register of cirrhosis. The end point of this study was to assess the risk score for ALD and non-ALD groups in contrast with the cut-off value for the peril of addiction. According to the questionnaire, we tried to analyze the high-risk domain for the development of

alcoholic liver disease. Finally, we compared the ACE risk score in ALD, non-ALD, and control groups, which were represented by university students.

Results: ACE score in a cohort of patients with alcohol cirrhosis reached 3.21 points (2.88–3.54 points). In comparison, the ACE score in non-ALD cirrhosis was 1.26 points, and in the cohort of university students 1.32 points. The main domains of ACE for ALD were sexual and physical abuse, alcohol addiction, and depression in the family.

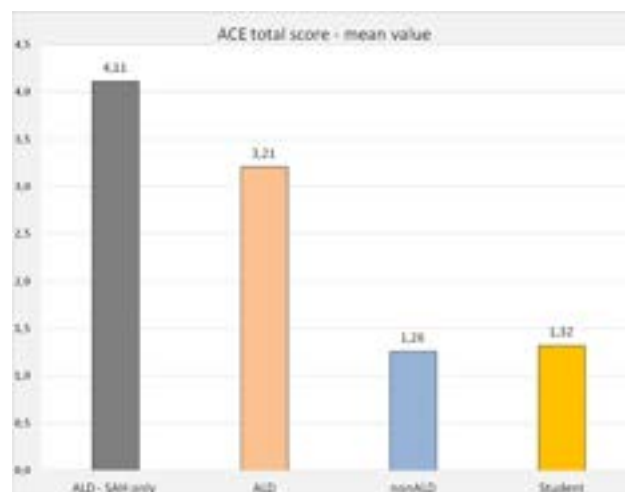


Figure:

Conclusion: The higher score in ACE-Q reflects grave childhood trauma which represents the risk for addiction and correlates with the prevalence of ALD-cirrhosis in our local register. We assume that a higher number of points from ACE-Q could predict the development of alcoholic hepatitis and alcoholic cirrhosis and simultaneously could be a useful predictive tool for recurrence of thy abuse after liver transplantation.

Cirrhosis and its complications ACLF and Critical illness

WEDNESDAY 21 TO SATURDAY 24 JUNE

TOP-040

Evaluation of albumin and midodrine versus albumin alone in the outcome of refractory ascites in patients with decompensated cirrhosis: a randomized controlled trial (NCT04816240)

Rakhi Maiwall¹, Priti Jain¹, Shiv Kumar Sarin¹, Manoj Kumar¹, Deepak Tempe¹, Shalini Thapar¹, Anupam Kumar¹, Vijayraghavan Rajan¹, Prashant Agrawal¹. ¹Institute of Liver and Biliary Sciences, New Delhi, India

Email: rakhi_2011@yahoo.co.in

Background and aims: Long term albumin has been recently shown to improve outcomes of uncomplicated ascites. Refractory ascites (RA) is a severe form of ascites wherein the hemodynamic alterations are further impaired and patients have marked vasodilatation and impaired renal perfusion. Midodrine acts on the alpha-adrenergic receptors, producing an increase in vascular tone and elevation of blood pressure. There are no studies on using combination of midodrine and albumin compared to albumin alone in improving liver related outcomes in RA. We studied efficacy of combining

midodrine with intravenous albumin (A-MIDO) versus albumin alone (A-PLAC) in 6-month mortality in RA.

Method: We conducted an open-label randomized controlled trial of 112 patients. A-MIDO group (55 patients) received albumin started at 80 gm/week for 2 weeks followed by 40 gm/week and midodrine started at 15 mg and increased up to 45 mg a day with target mean arterial pressure (MAP) of >75 and <90 mm Hg, while Group 2 (57 patients) received albumin and placebo. Competing risk survival analysis was performed with liver transplant (LT) and transjugular intrahepatic portosystemic shunt (TIPS) placement as competing events. Primary end point was survival free of LT and TIPS at 6 months and secondary end points were liver-related complications, impact on frailty and renal hemodynamics.

Results: Cirrhosis patients with RA [54 years age, 86.6% males, 48.2% alcohol] in both the groups were comparable at baseline; MELD Na [24.25 ± 5.85 vs. 25.95 ± 5.86; $p = 0.13$], MAP (mmHg) [72.18 ± 4.91 vs. 73.26 ± 5.51; $p = 0.23$], serum albumin (g/dL) [2.66 ± 0.39 vs. 2.69 ± 0.36; $p = 0.53$] and eGFR [79.68 ± 25.29 vs. 81.63 ± 26.51; $p > 0.05$]. Mean dosage of midodrine was 22.30 ± 5.15 mg at 6 months in A-MIDO. LT and TIPS free survival were significantly better in A-MIDO [74.5% vs 54.4%; $p = 0.01$]. On competing risk survival analysis, hazard ratio [2.29 (95% CI 1.09–4.48)]. Cumulative incidence of paracentesis induced circulatory dysfunction and therapeutic paracentesis were high in A-PLAC [20% vs. 35.1%; $p = 0.07$, 3.69 ± 1.90 vs. 5.16 ± 2.18; $p = 0.00$]. Liver related events were high in A-PLAC, hepatic encephalopathy [$p = 0.01$], acute variceal bleed [$p = 0.04$]. A significant decline in renal functions was seen in A-PLAC; hepatorenal syndrome (HRS)-acute kidney disease [18.2% vs. 7%; $p = 0.07$] while HRS-chronic kidney disease [10.9% vs. 26.3%; $p = 0.03$]. Similar results were observed in the per-protocol analysis.

Events in 6 months	A-MIDO	A-PLAC	p value
Number of hospitalizations (%)	35.1	60	0.03
MELD Na (mean ± SD)	20.92 ± 9.89	30.17 ± 10.09	0.00
Frailty index	1.91 ± 0.78	2.53 ± 0.57	0.00
Reintroduction of beta-blockers (%)	54.54	17.5	0.00
MAP at 6 months (mmHg)	77.47 ± 4.43	73.16 ± 5.18	0.00

Conclusion: The combination of Midodrine and albumin is better for LT and TIPS free survival and lesser liver related complications by improving hemodynamics and renal functions in RA.

TOP-049

Increased level of presepsin in patients with acutely decompensated cirrhosis predicts development of acute-on-chronic liver failure

Alberto Zanetto¹, Monica Mion², Alberto Ferrarese³, Sarah Shalaby¹, Giacomo Germani¹, Martina Gambato¹, Francesco Paolo Russo¹, Fabio Farinati¹, Daniela Basso², Patrizia Burra¹, Marco Senzolo¹.

¹Gastroenterology and Multivisceral Transplant Unit, Surgery, Oncology, and Gastroenterology, Padova University Hospital, Padova, Italy;

²Laboratory Medicine, Padova University Hospital, Padova, Italy; ³Unit of Gastroenterology, Borgo Trento University Hospital of Verona, Italy
Email: alberto.zanetto@yahoo.it

Background and aims: The clinical course of acutely decompensated cirrhosis (AD) is heterogeneous. Presepsin (PSP) is a soluble CD14-subtype biomarker that reflects Toll-like receptor activity as the immune response to endotoxemia and bacterial infections, and it has regulatory properties of the adaptive immune system. We conducted a prospective study to assess whether, in hospitalized patients with AD, plasmatic level of PSP could predict development of ACLF.

Method: Hospitalized patients with AD were prospectively recruited at admission and underwent determination of PSP

(chemiluminescent immunoassay). All patients were then followed for 1 year, and predictors of ACLF were assessed by Cox regression analysis.

Results: 99 patients with AD were included (male; 66%; median age: 61 years; 65% had alcohol-related cirrhosis). The main reasons for AD were bacterial infections and alcoholic hepatitis (52% and 22%, respectively). Median MELD and CLIF-C AD scores were 18 and 54, respectively. Median PCP was 674 U/L (308–1700). Thirty-six patients developed ACLF (median time from inclusion to development of ACLF was 88 days). Baseline level of PSP was significantly higher in patients who experienced ACLF vs those who did not (1253 [670–2562] vs 375 [245–722], respectively; $p < 0.0001$). Among patients who didn't develop ACLF, PSP was comparable between those who were re-hospitalized due to cirrhosis complications and those who were not re-hospitalized (432 vs 355, respectively). Cox regression analysis demonstrated that PSP was independently associated with development of ACLF (Table). AUROC of PSP was good and comparable to that of CLIF-C AD score (0.78 vs 0.79, respectively). A PSP value >660 U/L had 77% sensitivity and 70% specificity for the development of ACLF. In a sub-analysis including patients at lower risk of ACLF (i.e. CLIF-C AD score ≤50 and Child B), PSP was significantly higher in those who developed ACLF than in those who did not (1054 vs 250, respectively).

Table. Variables associated with development of ACLF (Cox-regression analyses).

Variables	HR	95%CI	P value
Univariate			
CLIF-C AD score (>54)	4.8	2.3-10.1	<0.0001
Presepsin, ng/L (>674)	3.9	1.9-8.5	<0.0001
MELD score (>18)	3.1	1.5-6.0	0.002
Child class C vs B	5.7	2.4-13.7	<0.0001
C-reactive protein, mg/dL (>21)	3.4	1.6-7.1	0.001
Infection (YES/NO)	1.8	0.93-3.45	0.08
Hemoglobin, mg/dL	0.9	0.8-1.2	0.8
Multivariate model #1			
Presepsin, ng/L (>674)	2.7	1.2-5.9	0.01
CLIF-C AD score (>54)	2.4	1.1-5.5	0.03
C-reactive protein, mg/dL (>21)	1.6	0.7-3.5	0.2
Child class C vs B	2.9	1.2-7.4	0.02
Multivariate model #2			
Presepsin, ng/L (>674)	2.5	1.1-5.6	0.02
CLIF-C AD score (>54)	3.1	1.4-6.8	<0.01
C-reactive protein, mg/dL (>21)	1.6	0.7-3.5	0.2
MELD score (>18)	1.5	0.7-3.1	0.3
Multivariate model #3			
Infection (YES/NO)	1.2	0.6-2.6	0.4
Presepsin, ng/L (>674)	2.5	1.1-5.6	0.02
CLIF-C AD score (>54)	3.2	1.5-7.2	0.003
MELD score (>18)	1.6	0.7-3.5	0.2

Figure:

Conclusion: PSP can be a useful, single and independent biomarker to identify trajectories of AD, even in patients who would be considered at lower risk of ACLF, if this is confirmed in larger cohorts.

FRIDAY 23 JUNE

FRI-339

Disparities in hospital outcomes among patients with end-stage liver disease with palliative care collaboration: a nationwide cohort analysis (2016–2020)

Sheza Malik¹, Mohammed Faisaluddin¹, Jay Bapaye¹, Ali Jaan¹, Yasir Rajwana². ¹Rochester General Hospital, United States, ²Stanford Medicine, United States

Email: sheza.malik@rochesterregional.org

Background and aims: Despite the very high symptom burden, palliative care (PC) services are underutilized in patients with end-stage liver disease (ESLD). In addition, previous studies have shown that there are significant racial disparities in PC utilization for these ESLD patients in the United States. Herein, we investigated the

POSTER PRESENTATIONS

disparities in the utilization of PC services among patients with ESLD hospitalized in the United States.

Method: We conducted a retrospective cohort analysis by utilizing Nationwide Inpatient Sample from 2016 to 2020. All patients greater than 18 years old admitted with ESLD, defined as having at least two hepatic decompensation events, were included in the analysis. A multivariate logistic regression model predicting referral to PC was created.

Results: The mean age of ESLD patients at the time seeking palliative care services was 62.25. PC consultation was performed in only 17% of ESLD patients. Hispanic patients were significantly less likely than White and Black patients to receive palliative care services (15.83% compared to 17.26% and 17.23% for White and Black patients respectively ($p < 0.01$). Our analysis also revealed that compared to Whites, Blacks, and other ethnicities, Hispanics are also less likely to be referred to other hospitals or skilled nursing facilities. This patient population also had significantly higher lengths of stay in the hospital (22 days in Hispanics versus 20 days in the White population, $p < 0.01$). Total hospitalization cost was also statistically significantly higher ($p < 0.01$) in Hispanics (76104 United States Dollars) compared to the White (66737 United States Dollars) and Black population (67209 United States Dollars). Furthermore, the mortality rate was significantly higher in the PC group than no-PC group among all racial groups (52.76% vs 13.95%, $p < 0.01$ for Whites, 55.45% vs 19.95%, $p < 0.01$ for Black and 55.19% vs 19.03%, $p < 0.01$ for Hispanics).

Conclusion: There are significant racial disparities in the use of palliative care services. Further research on the causes of racial disparities is needed to improve access to palliative care services for the vulnerable ESLD population.

FRI-340

ACLF grade is not independently associated with 1-year mortality after hospital discharge in cirrhotic patients admitted to ICUs in the Netherlands

Jubi de Haan¹, Fabian Termorshuizen^{2,3}, Nicolette de Keizer^{2,3}, Diederik Gommers¹, den Hoed Caroline⁴. ¹Erasmus University Medical Center, Department of Adult Intensive Care, Rotterdam, Netherlands; ²National Intensive Care Evaluation (NICE) foundation, Amsterdam, Netherlands; ³Amsterdam Public Health Institute, Amsterdam UMC, University of Amsterdam, Department of Medical Informatics, Amsterdam, Netherlands; ⁴Erasmus MC Transplant Institute, Erasmus University Medical Center, Department of Gastroenterology and Hepatology, Rotterdam, Netherlands
Email: j.dehaan@erasmusmc.nl

Background and aims: Patients with acute decompensated liver cirrhosis or Acute-on-chronic liver failure (ACLF) often require intensive care unit (ICU) admission for organ support. Nonetheless data addressing the outcomes of these patients remains scarce, is mainly limited to studies conducted in specialized liver transplant centres and has predominantly focused on short-term outcomes, such as ICU and hospital mortality. The aim of this study was to evaluate the influence of ACLF grade on the outcomes of cirrhotic patients admitted to all ICUs in the Netherlands.

Method: We conducted a nationwide observational cohort study using data from the Dutch ICU quality registry, the National Intensive Care Evaluation (NICE). Adult patients with an history of cirrhosis or first complications of cirrhotic portal hypertension admitted to all 82 ICUs in the Netherlands between 2012 and 2020 were included. Admission for elective or cardio-thoracic surgery or primary neurologic events were excluded. We identified 7779 cirrhotic patients; complete data to classify ACLF grade according to EASL-CLIF criteria was available in 2917 patients. The influence of ACLF grade on in-hospital mortality was evaluated using multivariate logistic regression (LR) to adjust for factors including demographics, GI bleeding, infection, APACHE IV probability and MELD score. Subsequently the influence of ACLF grade on 1-year mortality after hospital discharge among survivors of hospital admission was evaluated using unadjusted Kaplan-Meier (KM) survival curve and adjusted Cox proportional hazard model.

Results: In-hospital mortality rate according to ACLF grade is shown in figure 1A. The adjusted OR of in-hospital death among those with ACLF-1 vs no ACLF was 1.18 [95% CI 0.65–2.16], ACLF-2 vs no ACLF 1.92 [95% CI 1.16–3.16] and ACLF-3 vs no ACLF 1.99 [95% CI 1.2–3.3] ($p = 0.008$). In KM analysis among hospital survivors, a higher ACLF grade appeared to be associated with a lower survival following discharge ($N = 1318$) (Figure 1B; Logrank $p < 0.0001$). However, this association vanished after adjustment for factors including age, comorbidities, malignancy status, APACHE IV probability and MELD score ($p = 0.1715$), factors that appeared to have a more important influence on 1-year mortality than ACLF grade.

Figure: (abstract: FRI-339): Disparities in Hospital Outcomes ff End Stage Liver Failure Patients with Palliative Care Collaboration: A Nationwide Cohort Analysis (2016–2020).

	Whites (176950, 61.81%)	Blacks (47975, 16.76%)	Hispanics (38670, 13.51)	Others (16610, 3.71)	P Value
Age (Median, IQR)	64 (55–72)	62 (53–70)	61 (50–70)	62 (52–72)	<0.0001
Female	41.43%	43.10%	37.34%	40.11%	<0.0001
Palliative Care Consult	17.26%	17.23%	15.83%	17.86%	<0.0001
Do Not Resuscitate Status	61.97%	16.45%	13.79%	3.87%	<0.0001
In Hospital Mortality with Palliative Care Consult	52.76%	55.45%	55.19%	57.78%	<0.0001
In Hospital Mortality without Palliative Care Consult	13.95%	19.95%	19.03%	21.11%	<0.0001
Disposition					<0.0001
Routine	3.52%	3.93%	5.40%	3.43%	
Transferred To Other Hospital	30.84%	30.09%	23.63%	25.86%	
SNF/ICF Transfer	29.48%	28.33%	22.49%	24.80%	
Home Health Care	12.61%	10.47%	15.54%	12.40%	
LOS (Median, IQR)	20 (17–28)	21 (17–29)	22 (17–30)	21 (17–31)	<0.0001
Total Hospitalization Cost (Median, IQR)	66737.85 (40935.84– 111002.50)	67209 (43297.78– 115589.58)	76104.63 (4722.90– 131422.13))	78526.08 (48193.83– 145696.15)	<0.0001

Figure 1A

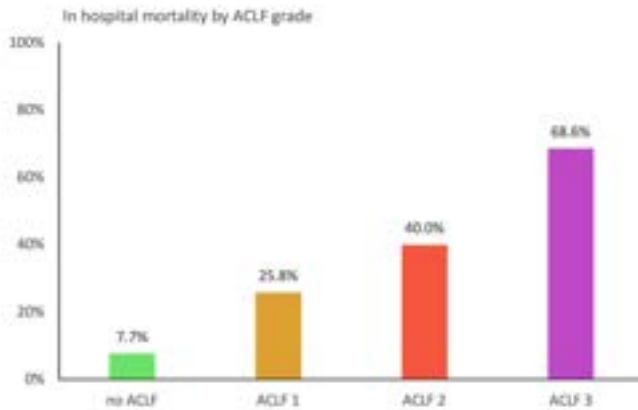


Figure 1B

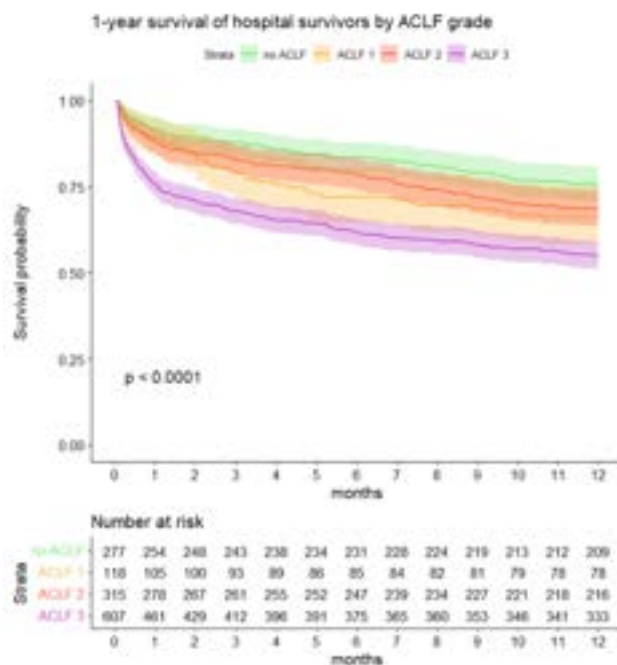


Figure:

Conclusion: In this nationwide cohort study ACLF grade was associated with in-hospital mortality of cirrhotic patients admitted to ICUs in the Netherlands. In those surviving hospital admission, ACLF grade was not an independent risk factor for 1-year mortality after hospital discharge.

FRI-341

Outcomes, clinical trajectories and risk factors of acute kidney injury (AKI) in critically-ill patients with liver cirrhosis

Martin Schulz¹, Georg Guttenberg², Wenyi Gu¹, Jan Mengers², Nora Ackermann², Frank Erhard Uschner¹, Maximilian Joseph Brol^{1,1}, Philip Ferstl², Michael Tischendorf², Christiana Graf², Salvatore Piano³, Paolo Angeli³, Stefan Zeuzem², Michael Praktiknjo¹, Alexander Zarbock⁴, Christoph Welsch², Hermann Pavenstaedt⁵, Kai-Henrik Peiffer¹, Jonel Trebicka^{1,6}. ¹Münster, Department of Internal Medicine B, Münster, Germany; ²Frankfurt, Department of Internal Medicine I, Frankfurt am Main, Germany; ³University of Padova, Unit of Internal Medicine and Hepatology, Dept. of Medicine, DIMED, Padova, Italy; ⁴University of Münster, Department of Anesthesiology, Intensive Care and Pain Medicine, Münster, Germany; ⁵University of Münster,

Department of Internal Medicine D, Münster, Germany; ⁶European Foundation for Study of Chronic Liver Failure, EF-Clif, Barcelona, Spain Email: jonel.trebicka@ukmuenster.de

Background and aims: In critically-ill patients with cirrhosis (CIC), AKI is a frequent and severe complication, associated with high mortality rates. This study aimed to assess the detailed impact of AKI in patients' clinical trajectory and identify risk factors for AKI development.

Method: In this observational study, data from 498 patients with liver cirrhosis and admission to IMC or ICU were retrospectively analysed. Risk factors for increased short-term mortality and AKI development were analysed by multivariable Cox regression. Decision tree analysis was performed to derive a risk stratification for AKI development. Clinical trajectories were visualized by Sankey plots dependent on AKI subtypes.

Results: At index IMC/ICU admission, AKI was observed in 208/498 CIC patients. Median age was 60 years, 71.5% of patients were male, 176/498 patients presented ACLF. AKI at index ICU admission was associated with a 28-day mortality of 43.3%. After IMC/ICU discharge, 21.4% of patients developed an AKI within a median of 30 days (IQR 13.8–93.3). Patients without full AKI resolution were observed as a highly vulnerable subgroup in case of AKI recurrence. In these patients, recurrent AKI was associated with a massive mortality increase compared to patients with regular AKI at readmission (90d-mortality 75.0% vs. 39.7%, $p < 0.05$). Multivariable Cox regression showed bilirubin (HR 1.06, 95%CI 1.01–1.10, $p < 0.05$) and tense ascites requiring paracentesis at ICU/IMC admission (HR 1.84, 95%CI 1.07–3.17, $p < 0.05$) are risk factors for AKI development. In decision tree analysis, bilirubin ≥ 6 mg/dl and tense ascites allowed a risk stratification into three distinct groups: Patients with none of these clinical features ($n=65$) showed a relatively low risk of AKI development (26.2%), while patients meeting one criterion (intermediate risk, $n=83$) or both criteria (high risk, $n=19$) developed AKI in 51.2% and 73.7%, respectively. Intermediate and high risk patients showed significantly higher mortality rates (90d-mortality 47.6% vs 12.9%, $p < 0.001$) and higher rate of renal replacement therapy (21.4% vs 9.7%, $p < 0.05$). High-risk patients also developed AKI significantly faster with a median time to AKI of 15 days ($p < 0.05$).

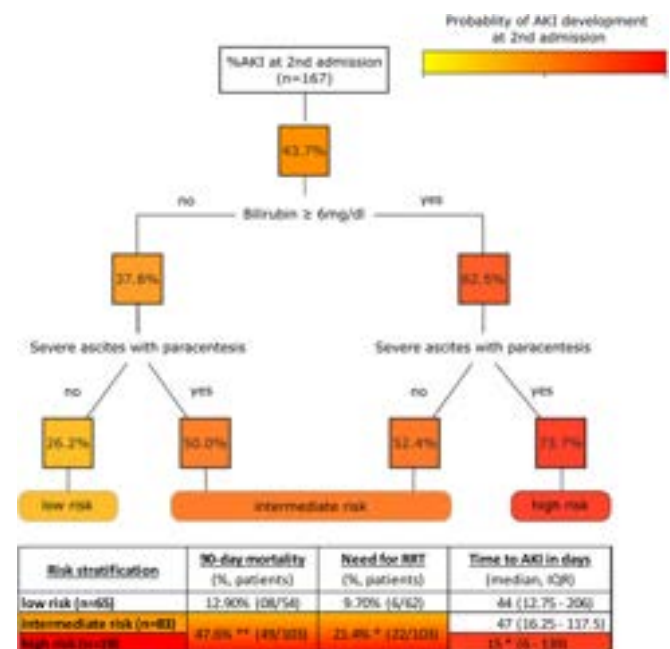


Figure:

Conclusion: Patients without full AKI resolution and persisting renal dysfunction emerge as a novel and profoundly vulnerable subgroup

POSTER PRESENTATIONS

in case of AKI recurrence as a second hit. Thus, full restoration of renal function should be closely monitored to identify recurrent AKI and initiate rapid treatment. Consequently, this data underscores the urgent clinical need for further evaluation of secondary prophylaxis for selected patients at risk.

FRI-342

VSIG4 as a biomarker for the diagnosis and prognosis of HBV-ACLF

Xi Liang¹, Peng Li², Jing Jiang², Jiaojiao Xin², Xin Chen³, Dongyan Shi², Jun Li². ¹Taizhou Central Hospital (Taizhou University Hospital), Precision Medicine Center, Taizhou, China; ²The First Affiliated Hospital, Zhejiang University School of Medicine, State Key Laboratory for Diagnosis and Treatment of Infectious Diseases, National Clinical Research Center for Infectious Diseases, National Medical Center for Infectious Diseases, Hangzhou, China; ³Zhejiang University School of Medicine, Institute of Pharmaceutical Biotechnology and the First Affiliated Hospital, Department of Radiation Oncology, Hangzhou, China Email: lijun2009@zju.edu.cn

Background and aims: Hepatitis B virus-related acute-on-chronic liver failure (HBV-ACLF) is a complex syndrome with high short-term mortality. This study aims to reveal the molecular basis and identify novel HBV-ACLF biomarkers.

Method: Transcriptome sequencing was performed using peripheral blood mononuclear cells (PBMCs) of HBV-ACLF patients in the derivation (n=20) and validation cohorts (n=50). Candidate biomarkers were confirmed in two external cohorts using enzyme-linked immunosorbent assay.

Results: Cellular composition analysis with PBMC transcriptomics from the derivation cohort showed that the proportions of monocytes, T cells and NK cells were significantly correlated with ACLF 28-day mortality. A significant upregulation of myeloid lineage modules and metabolic dysregulation with lipid, carbohydrate and energy metabolism were observed in ACLF nonsurvivors. External sequencing confirmed the above results. V-set and immunoglobulin domain-containing 4 (VSIG4) was the most robust predictor of ACLF patient survival (adjusted $p = 1.4 \times 10^{-6}$; 1.7×10^{-7} ; VIPred = 1.28/1.92; area under the receiver operating characteristic curve (AUROC) = 0.91/0.88) and was linked to T-cell activation/differentiation and inflammatory response. Plasma VSIG4 analysis externally validated its diagnostic value for ACLF patients (compared with chronic liver disease and healthy groups, AUROC = 0.983). The prognostic performance for 28-/90-day mortality (AUROCs = 0.769/0.767) was comparable to that of 5 commonly used scores (COSSH-ACLF IIs, 0.876/0.878; COSSH-ACLFs, 0.867/0.884; CLIF-C ACLFs, 0.840/0.835; MELD, 0.721/0.750; MELD-Na, 0.710/0.737). Risk stratification of the VSIG4 expression level (>122 µg/ml) specifically identified ACLF patients with a high risk of death. The generality of VSIG4 in other etiologies was validated.

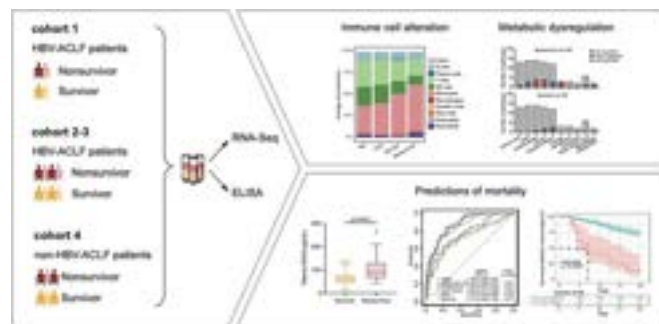


Figure:

Conclusion: This study reveals immune-metabolism disorder underlying poor ACLF outcomes. VSIG4, as a biomarker for the diagnosis and prognosis of HBV-ACLF, may be helpful in clinical practice.

FRI-343

The prognostic impact of each organ failure is different than that of acute-on-chronic liver failure according to the major clinical presentation in acutely decompensated cirrhosis

Jung Hee Kim¹, Sung-Eun Kim¹, Do Seon Song², Jang Han Jung¹, Hyoung Su Kim¹, Eileen Yoon³, Tae Hyung Kim⁴, Jung Hyun Kwon², Young Kul Jung⁴, Ki Tae Suk¹, Moon Young Kim⁵, Sang Gyune Kim⁶, Yoon Jun Kim⁷, Won Kim⁸, Jin Mo Yang², Jae Young Jang⁹, Dong Joon Kim¹. ¹Hallym University College of Medicine, Korea, Rep. of South; ²College of Medicine, The Catholic University of Korea, Korea, Rep. of South; ³Hanyang University College of Medicine, Korea, Rep. of South; ⁴Korea University Ansan Hospital, Korea, Rep. of South; ⁵Yonsei University Wonju College of Medicine, Korea, Rep. of South; ⁶Soonchunhyang University Bucheon Hospital, Korea, Rep. of South; ⁷Seoul National University College of Medicine, Korea, Rep. of South; ⁸Seoul Metropolitan Government Seoul National University Boramae Medical Center, Korea, Rep. of South; ⁹Soonchunhyang University College of Medicine, Korea, Rep. of South Email: sekim@hallym.or.kr

Background and aims: The acute-on-chronic liver failure (ACLF) is a major poor prognosis factor in acute decompensation (AD) of chronic liver disease (CLD) or liver cirrhosis (LC). Main pathogenic mechanism of AD has been speculated systemic inflammation and portal hypertension. The effects of not only ACLF but also each organ failure may be different depending on the major pathogenesis in AD patients, but studies for this have not yet been investigated. Therefore, we aimed to investigate whether significant differences of adverse outcomes (death or LT) show or not according to main clinical presentation in AD cirrhotic patients in prospective Korean Acute-On-Chronic Liver Failure (KACLiF) cohort. Also, we intend to reveal risk factor including ACLF and each organ failure for adverse outcomes.

Method: The prospective KACLiF cohort consisted of 1773 patients who were hospitalized with AD of CLD, from July 2015 to August 2018. We enrolled a total of 1,416 patients with AD after excluding non-LC patients. Patients were then regularly evaluated for 3 months outcomes (liver transplantation and death) at 1 year were also recorded.

Results: According to clinical presentation, patients were analyzed: gastrointestinal bleeding (GIB) (n=490), ascites (n=355), bacterial infection (n=103), hepatic encephalopathy (HEP) (n=178), and jaundice (n=290). The adverse outcomes rate for subgroups of AD were differed as followed; 28-day adverse outcome (total = 8.1%, GIB = 4.9%, ascites = 9.6%, bacterial infection = 13.6%, HEP = 10.1%, and jaundice = 8.3%; $p = 0.011$), 90-day adverse outcome (total = 13.5%, GIB = 8.4%, ascites = 15.2%, bacterial infection = 19.4%, HEP = 17.4%, and jaundice = 15.5%; $p = 0.001$), and 1-year adverse outcome (total 21.9%, GIB = 14.7%, ascites = 25.1%, bacterial infection = 31.1%, HEP = 27%, and jaundice = 23.8%; $p < 0.001$). After multivariate cox regression analysis, MELD was most important risk factor for adverse outcome in total or subgroup of AD patients if it were analyzed with ACLF. As a result of analysis with each organ failure as a variable other than ACLF, cardiac failure in GIB patients, coagulation failure in ascites patients, coagulation failure and brain failure in BI patients, liver failure in HEP patients, and MELD and DM in jaundice patients were the main factors.

Conclusion: According to main clinical presentation, cirrhotic patients with AD showed different 28-days, 90-days, and 1-year adverse outcomes. Although ACLF is a factor influencing the patient's adverse outcomes, the relevant organ failure may differ depending on the patient's major clinical presentation upon admission. Especially, AD patients with bacterial infection showed poorer adverse outcomes compared to patients with other clinical presentation. Each organ failure rather than ACLF tends to have a direct impact on the

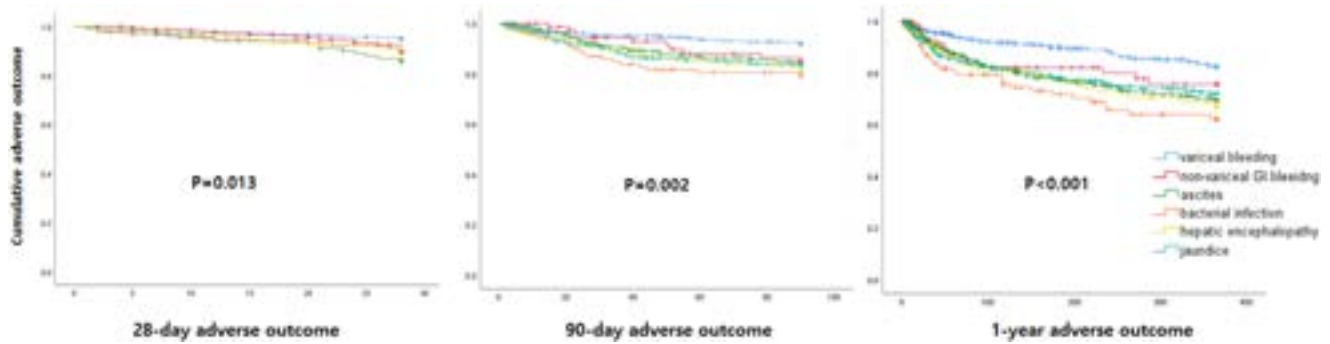


Figure 1: (abstract: FRI-343): Adverse outcome rate of each group in acutely decompensated cirrhosis

	Total	GIB	Ascites	BI	HEP	Jaundice
ACLF						
28-day adverse outcome	MELD	MELD	MELD preAD	MELD	MELD	MELD DM
90-day adverse outcome	MELD	MELD	MELD preAD	MELD	MELD	MELD DM
1-year adverse outcome	MELD	MELD	MELD Hb	MELD	MELD ACLF Hb	MELD DM Age
Each organ failure						
28-day adverse outcome	MELD Cardiac failure Coagulation failure	Cardiac failure	Coagulation failure	Coagulation failure Brain failure Respiratory failure WBC	Liver failure	MELD DM
90-day adverse outcome	MELD Cardiac failure Respiratory failure Coagulation failure	MELD-Na Albumin Cardiac failure Respiratory failure	Coagulation failure Na preAD	MELD Coagulation failure Brain failure Cardiac failure	Liver failure Respiratory failure	MELD DM
1-year adverse outcome	MELD Respiratory failure Coagulation failure	MELD-Na Albumin Cardiac failure Respiratory failure	MELD Coagulation failure	MELD Coagulation failure Brain failure Cardiac failure	Brain failure Respiratory failure Hb	MELD DM

Figure 2: (abstract: FRI-343): Risk factors for adverse outcomes in acutely decompensated cirrhosis patients

prognosis of cirrhotic patient with AD according to the main clinical presentation.

FRI-533

Incidence, risk factors and outcomes of acute kidney disease in cirrhosis patients with sepsis-related acute kidney injury

Rakhi Maiwall¹, Ashini Hidam¹, Neha Chauchan¹, Shiv Kumar Sarin¹.

¹Institute of Liver and Biliary Sciences, Department of Hepatology, New Delhi, India

Email: shivsarin@gmail.com

Background and aims: Cirrhosis patients frequently have sepsis related acute kidney injury (S-AKI). Persistence of kidney dysfunction in S-AKI is reported to have sustained inflammatory and procoagulant responses. Patients with acute kidney disease (AKD) in the context of sepsis may have worse outcomes compared to those with recovery. We aimed to investigate in a prospective cohort of patients with S-AKI the incidence, spectrum, risk factors, and outcomes of AKD.

Method: Prospective cohort of cirrhosis patients admitted to the liver intensive care unit with S-AKI (n = 254) were enrolled. AKD was

defined as acute or subacute damage and/or loss of kidney function for a duration between 7 and 90 days after AKI. A detailed biochemistry, urine sediment and neutrophil gelatinase-associated lipocalin (NGAL) was performed for all patients at enrolment and day 7. A urine microscopy score (UMS) was derived based on the observed quantification of renal tubular cells (RTC) and casts in the sediment. Our primary outcome was development of AKD. Secondary outcomes included need of dialysis, recovery from AKD and death. The stages of AKD at day 90 or last follow-up were defined in accordance with Levey et. al (Nephron 2022).

Results: Patients with S-AKI, mean age 45.6 ± 9.6 years, 91% males, mean MELD 27.3 ± 11.3, and CTP score 12.3 ± 1.6, 43% alcoholics, 44% obese, 29% diabetics, and 19% with grade 3 ascites were enrolled. The median urine NGAL was 1865.5 (1276.7–2863.5) ng/ml. Pneumonia was the most common infection in 67% and septic shock was seen in 58%. AKI stage at enrolment (KDIGO Stage 1:2:3 26%vs 33%vs 41%). The cause of AKI was acute tubular necrosis in 60% followed by hepatorenal syndrome in 24% and remaining had prerenal volume-responsive AKI. A total of 115 (45%) developed AKD at day 90. Patients

POSTER PRESENTATIONS

who developed AKD had significantly higher urine spot sodium (mEq/L) (27.6 ± 15.9 vs. 18.2 ± 8.7 ; $p < 0.001$), urine protein-to-creatinine ratio (2.0 ± 1.3 vs. 1.18 ± 0.89 ; $p < 0.001$), and NGAL at enrolment and day 7 (Figure). These patients also had higher UMS for granular casts and RTCs. On multivariate analysis, higher NGAL at enrolment (log transformed) (OR 2.9, 1.8–4.7), UMS (OR 3.2, 1.6–6.3), presence of metabolic syndrome (OR 1.9, 1.2–3.4) were risk factors for AKD. At last follow-up, 9% had stage 0, 4% had stage 1, 16% had stage 2, 18% had stage 3 AKD and 54% were on dialysis. In the proportion of patients with recovery ($n = 9$), 44% had stage C, 22% stage B and 33% stage A AKD. Development of AKD was an independent predictor of 90-day mortality (OR 6.4, 3.7–11.1)

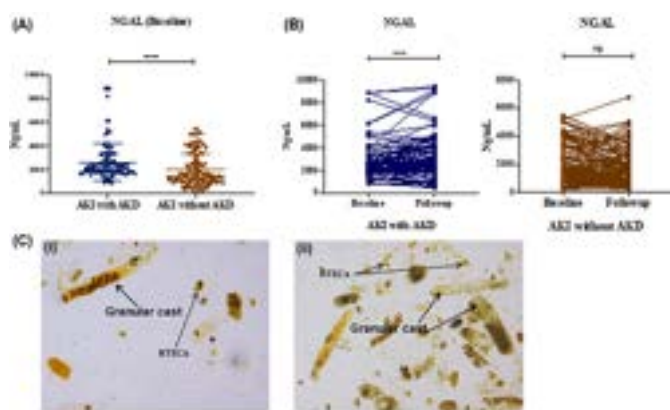


Figure:

Conclusion: Almost 60% of patients with S-AKI have acute tubular necrosis and one in two develops AKD. AKD after S-AKI is associated with worse outcomes, recovers in only 9%, and progresses to dialysis in one-half. Of patients with recovery only 33% have return to normal renal functions. Higher NGAL, urine sediment score and presence of metabolic syndrome predict risk of AKD in patients with S-AKI. Novel therapeutic modalities are an unmet need for preventing AKD in S-AKI.

FRI-534

Machine learning-based model is superior to CLIF-C ACLF score for predicting ICU mortality in critically ill patients with acute-on-chronic liver failure

Maike Rebecca Pollmanns¹, Bastian Kister², Samira Abu Jhaisha¹, Jonathan Frederik Brozat¹, Philipp Hohlstein¹, Tony Bruns¹, Lars Küpfer², Christian Trautwein¹, Alexander Koch¹, Theresa Hildegard Wirtz¹. ¹University Hospital RWTH Aachen, Medical Department III, Aachen, Germany; ²University Hospital RWTH Aachen, Institute for Systems Medicine with Focus on Organ Interaction, Aachen, Germany
Email: mpollmanns@ukaachen.de

Background and aims: Acute-on-chronic liver failure (ACLF) defines a highly heterogeneous syndrome characterized by acute decompensation in patients with pre-existing liver disease accompanied by multiple organ failure. Available prognostic scores predict overall mortality. The aim of the presented study was to establish a simply applicable scoring system that could reliably predict mortality of ACLF patients during intensive care unit (ICU) treatment.

Method: A retrospective analysis of 206 patients with ACLF who were admitted to the medical ICU at the University Hospital RWTH Aachen between 2015 and 2021 was conducted. To develop a machine-learning model for predicting ICU mortality a training and validation dataset were defined and model development was performed by logistic regression. Various metrics were assessed to evaluate the

calculated model and compare its predictive performance to existing scoring systems, including the chronic liver failure consortium (CLIF-C) ACLF score, the ACLF grade as well as CLIF-C OF, SOFA, MELD, APACHE-II, and SAPS score.

Results: The ICU mortality in this cohort was 60.2%. All evaluated scoring systems were able to distinguish between ICU survivors and non-survivors. The CLIF-C ACLF scoring system had the highest area under the receiver operating characteristics curve (AUROC) at 0.79 (95% CI) in the cohort. Machine learning resulted in seven different models using five up to thirteen features. The prognostic accuracy of CLIF-C ACLF score could be significantly improved by adding the number of organ failures, Horovitz quotient ($\text{FiO}_2/\text{PaO}_2$), FiO_2 and lactate (validation cohort AUROC 0.96, "model" in Fig. 1). Moreover, this model was superior to the existing 'gold-standard' CLIF-C ACLF score in predicting ICU mortality as well as 90-days transplant-free mortality.

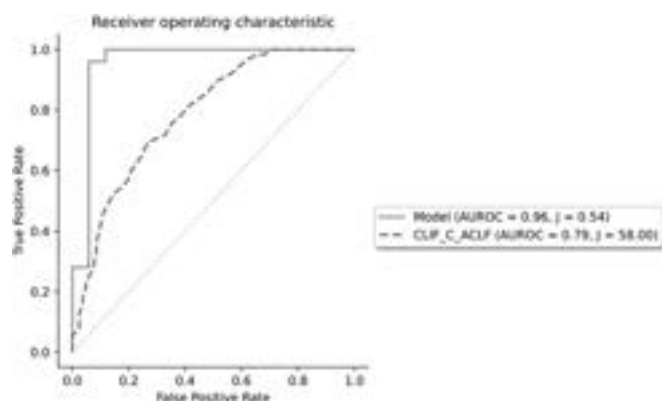


Figure: ROC curve analysis for the discrimination between ICU-survivors and non-survivors by our developed model including CLIF-C ACLF score, number of organ failures, Horovitz quotient ($\text{FiO}_2/\text{PaO}_2$), FiO_2 and lactate in comparison to CLIF-C ACLF score only. Abbreviations: AUROC, area under the receiver operating characteristic curve; J, Youden's J Index.

Conclusion: Our findings indicate that this novel model can effectively predict ICU mortality in critically ill patients with ACLF, highlighting its potential for practical use in clinical settings.

FRI-535

Albumin use in acute-on-chronic liver failure in a large national cohort

Nadim Mahmud¹, Tamar Taddei², David Kaplan¹, Elisabet Viayna³, Thomas Ardiles⁴, Marina Serper¹. ¹University of Pennsylvania, United States; ²Yale University, United States; ³Griñols, SA, Spain; ⁴Griñols, SA, United States
Email: marinas2@pennmedicine.upenn.edu

Background and aims: Acute-on-chronic liver failure (ACLF) is associated with high short-term mortality. Common ACLF triggers include hepatorenal syndrome (HRS) acute kidney injury (AKI) and as spontaneous bacterial peritonitis (SBP); conditions where albumin is indicated for treatment. Albumin use in ACLF hospitalizations has not been studied in detail in large cohorts. We aimed to investigate use of albumin in ACLF by severity and identify factors associated with its use in a large national cohort of patients with cirrhosis in the U.S. Veterans Health Administration Affairs (VHA).

Method: We identified all hospitalizations of patients with cirrhosis between 2008 and 2021 and classified them based on the EASL criteria from ACLF 0 (no ACLF) to 3 (severe ACLF) using validated methods. All inpatient albumin use was captured via inpatient pharmacy files; we also obtained demographic, comorbidity, and admission laboratory data. Average days of albumin administration were presented by length of hospital stay (LOS), stratified by ACLF grade. We subsequently fit multivariable logistic regression models for albumin use adjusting for characteristics at hospital admission: patient demographics, liver disease etiology, Child Pugh score, MELD-

Na, medical comorbidities, ACLF grade, and guideline-recommended albumin indication (HRS, SBP).

Results: Among 47,290 hospitalizations; 4.3% were ACLF-3, 6.6% ACLF-2, 12.1% ACLF-1, and 77.0% ACLF-0. Any albumin use was significantly associated with ACLF grade, for example 78.9% of ACLF-3 hospitalizations versus 22.8% of ACLF-0 ($p < 0.001$); these associations were also apparent when visualized as cumulative days of albumin use for hospitalizations of different LOS (Figure 1). In adjusted models, factors independently associated with lower odds of albumin use were: Black race (OR 0.78, 95% CI 0.72–0.84) and Hispanic ethnicity (OR 0.80, 95% CI 0.72–0.90) (relative to White race): congestive heart failure (OR 0.77, 95% CI 0.72–0.82), atrial fibrillation (OR 0.72, 95% CI 0.66–0.78), and diabetes (OR 0.72, 95% CI 0.67–0.76). Factors associated with higher use were: HRS-AKI (OR 2.48, 95% CI 2.16–2.85), SBP (OR 2.89, 95% CI 2.57–3.25), and ACLF grade [relative to ACLF-0]: (ACLF-1: OR 1.72, 95% CI 1.59–1.85; ACLF-2: OR 1.95 95% CI 1.78–2.15, ACLF-3: OR 4.25, 95% CI 3.73–4.84). Among liver disease etiologies, hepatocellular carcinoma was associated with higher albumin use (OR 1.22, 95% CI 1.13–1.32).

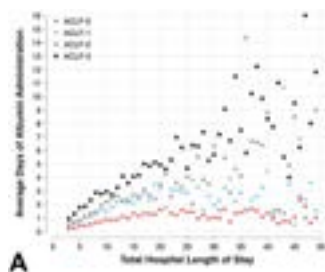


Figure 1: Albumin Use by ACLF Grade and Hospital Length of Stay

Conclusion: In this national cohort study, we show that inpatient albumin utilization is substantial in high-grade ACLF and in the setting of SBP and HRS-AKI. After adjusting for medical factors, we found variation in use by race/ethnicity suggesting practice variation and health inequity. These findings highlight the need to identify causes of practice variation to improve use of guideline recommended therapies; this is particularly important in ACLF, which carries very high mortality risk.

FRI-536

Microbial cell-free DNA next-generation sequencing of ascites in acutely decompensated cirrhosis patients: a proof-of-concept study

Beiling Li¹, Yanhang Gao², Yan Huang³, wei yuan⁴, Zuxiong Huang⁵, Qintao Lai¹, Qijun He¹, Ling Zhou¹, Miaoxia Liu¹, Jinjun Chen^{1,6}.

¹Hepatology Unit, Department of Infectious Diseases, Nanfang Hospital, Southern Medical University, Guangzhou, China, China; ²Department of Hepatology, The First Hospital of Jilin University, Jilin University, Changchun, China, China; ³Department of Infectious Diseases, Xiangya Hospital, Central South University, Changsha, China, China;

⁴Department of Liver Intensive Care Unit, Shanghai Public Health Clinical Centre, Fudan University, Shanghai, China, China; ⁵Department of Hepatology, Mengchao Hepatobiliary Hospital of Fujian Medical University, Fuzhou, China, China; ⁶Hepatology Unit, Zengcheng Branch, Nanfang Hospital, Southern Medical University, Guangzhou, China, China

Email: chjj@smu.edu.cn

Background and aims: Targeted anti-microbial treatment therapy in patients with spontaneous bacterial peritonitis (SBP) is currently not possible as pathogens are identified in only 5%–20% patients. Metagenome next-generation sequencing (mNGS) test can provide rapid diagnosis of a comprehensive spectrum of pathogens. The aim is to evaluate the performance of microbial mNGS of ascites and its clinical effect in the decompensated cirrhosis patients.

Method: Decompensated cirrhosis patients with ascites were prospectively recruited at 5 teaching hospitals between 2019 and 2020 (NCT04125654). Patients were underwent microbial mNGS detection of ascites and clinical characteristics as well as outcomes were recorded accordingly. The association between the microorganisms detected by mNGS and clinical outcomes was assessed.

Results: In this study, 165 decompensated cirrhosis patients with ascites were included. Twenty patients were diagnosed with SBP and 14 patients had positive ascites culture. By microbial mNGS of ascites testing, 149 microorganisms were detected in 52 (31.5%) patients, including bacteria (65.8%), fungi (4.0%), virus (30.2%). Fever was more frequent in patients with positive ascites mNGS detection than those without (30.8% vs.15.0% $p = 0.019$). The prevalence of new-onset SBP and acute kidney injury were much higher in the positive ascites mNGS group than the negative group (25.6% vs. 3.9%, $p < 0.001$; 30.8% vs. 14.2%, $p = 0.012$).

	Ascites mNGS positive (n = 52)	Ascites mNGS negative (n = 113)	P value
Age (years)-mean (SD)	54 (11)	53 (11)	0.818
Etiology of cirrhosis-n (%)			
HBV	31 (59.6)	70 (61.9)	0.973
Alcohol	9 (17.3)	18 (15.9)	
Alcohol plus Viral hepatitis (B or C)	2 (3.8)	4 (3.5)	
other	10 (27.3)	21 (18.5)	
Male- n (%)	41 (78.8)	86 (76.1)	0.698
Abdominal pain-n (%)	16 (30.8)	28 (24.8)	0.419
Ascites white blood cell ($\times 10^6/L$) - median (IQR)	160 (58–396)	161 (80–304)	0.838
Ascites neutrophil ($\times 10^6/L$)-median (IQR)	29 (15–109)	21 (14–75)	0.287
Ascites culture positive-n (%)	12 (23.1)	2 (1.8)	<0.001
Concomitant infection-n (%)			
Pneumonia-n (%)	23 (25.0)	38 (33.6)	0.265
Bacteremia-n (%)	5 (9.6)	3 (2.7)	0.053
Urinary tract infection-n (%)	2 (3.8)	2 (1.8)	0.420
Skin and soft tissue infection-n (%)	0 (0)	1 (0.9)	0.496
Laboratory measurements			
Bilirubin ($\mu\text{mol/L}$)-median (IQR)	86.9 (42.3–210.2)	70 (27.9–216.6)	0.203
INR -mean (SD)	1.9 (1.2)	1.7 (0.9)	0.242
Serum creatinine ($\mu\text{mol/L}$)-median (IQR)	71.0 (61.0–95.6)	81.8 (62.0–101.0)	0.405
Leukocytes counts ($\times 10^9/L$)-median (IQR)	6.8 (3.8–9.9)	5.3 (3.9–7.7)	0.126
C-reactive protein (mg/L)-median (IQR)	14.7 (8.8–35.6)	11.4 (6.3–23.7)	0.107
28-day mortality- n (%)	2 (3.8)	5 (4.4)	0.864

Conclusion: Microbial mNGS detection may improve the pathogen diagnosis of infected ascites in acutely decompensated cirrhosis. The positive detection by ascites mNGS was correlated with the progression of SBP and future studies need to be further validated.

FRI-537

Performances of the CLIF-consortium acute-on-chronic liver failure (ACLF) score are gender specific

Sophie-Caroline Sacleux¹, Thomas Mangana Del Rio², Philippe Ichai¹, Julien Vionnet², Audrey Coilly¹, Jean-Daniel Chiche², Faouzi Saliba¹, Constantine Karvellas³, Florent Artru^{2,4}, ¹Hopital Paul Brousse, France; ²Lausanne University Hospital, Switzerland; ³Department of Critical Care Medicine and Division of Gastroenterology (Liver Unit), University of Alberta, Edmonton, Canada; ⁴King's College Hospital, United Kingdom
Email: florent.artur@kcl.ac.uk

Background and aims: CLIF consortium acute-on-chronic liver failure (CLIF-C ACLF) score is the current gold standard for the

prediction of outcomes in ACLF. This score was derived from cohorts comprising mainly male participants, as women are underrepresented in studies on critically ill patients with ACLF. Our aim was to investigate whether the performance of CLIF-C ACLF is gender-specific in a large multicentric and international cohort of critically ill patients with ACLF.

Method: Three cohorts of consecutive patients with ACLF hospitalised in intensive care units (ICU) were included in the present study: Lausanne-Switzerland (2010 to 2020, n = 428), Paul Brousse-France (2017 to 2019, n = 200) and Edmonton- Canada (2001–2015, n = 308) cohorts. CLIF-C ACLF score was calculated using its original formula. Performances were evaluated by discrimination ability estimated by the area under the receiver operating characteristics (AUROC) curve and calibration.

Results: A total of 936 patients fulfilled the inclusion criteria: median age was 59 years (IQR 50–66 years), 268 (29%) were women, and 568 (61%) had alcohol-related cirrhosis. The main causes of admission were sepsis (n = 359, 33%) and bleeding (n = 243, 26%). On day 1, the median MELD score was 24, the median ACLF grade was 3, and the median CLIF-C ACLF score was 63. Forty-five patients (5%) underwent LT within the first 28 days of ICU admission. The 28-day transplant-free survival (TFS) was 56% and was not different between women (57%) and men (55%) ($p = 0.71$). The distribution of ACLF grades on day 1 between women and men was not different ($p = 0.31$), but there was a trend to an increased prevalence of ACLF grade 3 with 4 or more OFs in women vs. men (48.6% vs. 37.4%, $p = 0.09$). The AUROC of CLIF-C ACLF score on days 1 and 3 was greater in women (0.74 and 0.83) than in men (0.61 and 0.72) ($p = 0.002$ and $p = 0.006$, respectively). In sensitivity analyses, the AUROC of CLIF-C ACLF on days 1 and 3 remained greater in women at each of the three centers. Calibration according to the quintile of the population on days 1 and 3 had a maximum delta of 3% in women and 8% in men between observed and predicted 28-day TFS. We then explored whether variables included in the CLIF-C ACLF score had a different association with 28-day TFS in women vs. men. All the variables included in the CLIF-C ACLF score apart from leukocyte count and cerebral failure were associated with 28-day TFS in multivariable analyses in women. In men, leukocytes count, cerebral failure, and age were not associated with 28-day TFS. Besides, the probability of recovery was diminished in women. It was illustrated by a less dynamic course of organ failure (OF) as compared to men with 39% showing a different ACLF grade between days 1 and 3 vs. 49% in men ($p = 0.04$).

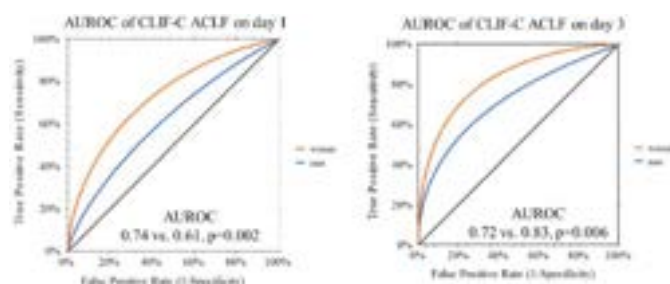


Figure: AUROC of CLIF-C ACLF on days 1 and 3 in women (orange) and men (blue)

Conclusion: CLIF-C ACLF score better predicts 28-day TFS of critically ill women with ACLF, likely due to a lower discriminant ability of age in men as well as a lower chance of recovery in women where ACLF is less dynamic. In women, based on its excellent performance, especially on day 3, CLIF-C ACLF allows identifying patients with the lowest chance of survival to adapt critical care management toward LT or withdrawal of intensive care. CLIF-C ACLF score should be optimised in men.

FRI-538

The risk factors for poor prognosis according to the clinical course after first acute decompensation in cirrhotic patients

Jung Hee Kim^{1,2}, Sung-Eun Kim^{1,2}, Do Seon Song³, Eileen Yoon⁴, Hyoung Su Kim^{1,2}, Jang Han Jung^{1,2}, Tae Hyung Kim⁵, Young Kul Jung⁵, Ki Tae Suk^{1,2}, Won Kim⁶, Jae Young Jang⁷, Dong Joon Kim^{1,2}. ¹Hallym University College of Medicine, Internal Medicine, Korea, Rep. of South; ²Institute for Liver and Digestive Diseases, Hallym University, Korea, Rep. of South; ³College of Medicine, The Catholic University of Korea, Korea, Rep. of South; ⁴Hanyang University College of Medicine, Korea, Rep. of South; ⁵Korea University Ansan Hospital, Korea, Rep. of South; ⁶Seoul Metropolitan Government Seoul National University Boramae Medical Center, Korea, Rep. of South; ⁷Soonchunhyang University College of Medicine, Korea, Rep. of South
Email: sekim@hallym.or.kr

Background and aims: The acute on chronic liver failure (ACLF) is well known poor prognosis in acute decompensation (AD) of chronic liver disease or liver cirrhosis. Recently the European Foundation for the Study of Chronic Liver Failure (EF-CLIF) consortium suggested that four clinical course within 3 months after first AD stratified the long term prognosis: stable decompensate cirrhosis (SDC), unstable decompensated cirrhosis (UDC) and pre-ACLF and ACLF. We verify the outcomes of these subgroups and analysis the initial factors for affecting these clinical course in Korean prospective cohort of AD.

Method: The prospective Korean Acute-On-Chronic Liver Failure (KACLIF) cohort consisted of 1773 patients who were hospitalized with AD of CLD, including either LC or non-cirrhotic CLD, from July 2015 to August 2018. We enrolled the first AD patient on LC after excluding as followed: previous history of decompensation (n = 902), previous diagnosis of HCC (n = 26) and non LC (n = 133). After exclusion, a total of 746 patients with AD were enrolled. Patients were then closely followed up and evaluated for 3 months outcomes (liver transplantation and death) at 1 year were also recorded.

Results: The subgroups consisted with SDC (n = 565), UDC (n = 29), Pre ACLF (n = 28) and ACLF (n = 124). The subgroups of AD stratified the 90 days and 1-year mortality as followed. (90 days' mortality: SDC = 5.3%, UDC = 10.3% and pre ACLF = 42.9%, 1year mortality: SDC = 13.5%, UDC = 34.5% and pre ACLF = 57.1%). And ACLF group showed favorable 90 days and 1year mortality (29.0% and 33.9%) compared with pre ACLF group. The initial factors that affected to occurrence of UDC or pre ACLF within 3 months were age [Odd ratio (OR) = 1.027, $p = 0.042$], non-variceal GI bleeding (OR = 3.031, $p = 0.008$), hepatic encephalopathy (HEP) (OR = 2.457, $p = 0.033$) and MELD (OR = 1.106, $p < 0.001$).

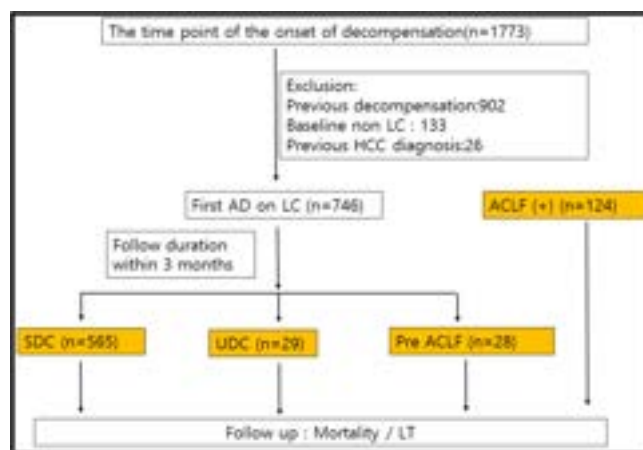


Figure 1: Flow chart of the study

	SDC (N=565)	UDC (N=29)	Pre-ACLF (N=28)	P value	ACLF (N=124)
Age (years)	54.7 ± 11.3	56.9 ± 14.0	54.7 ± 13.0	0.296	53.6 ± 10.2
Male (%)	412(72.9)	19(65.5)	18(64.3)	0.436	103(83.1)
Etiology				0.424	
Virus	62(11.0)	4(13.8)	4(14.3)		5(4.0)
Alcohol	398(70.4)	22(75.9)	20(71.4)		99(79.8)
Virus+Alcohol	61(10.9)	2(6.9)	3(10.7)		13(10.5)
AIH/PBV	16(2.8)	0	0		1(0.8)
Cryptogenic	287(50.9)	1(3.4)	1(3.6)		6(4.8)
AD					
Ascites	185(32.7)	9(31.0)	8(28.6)	0.867	32(25.8)
Bacterial infection	37(6.6)	5(17.2)	2(7.1)	0.091	14(11.3)
Varix bleeding	172(30.4)	8(27.6)	5(17.9)	0.352	28(22.6)
GI bleeding	37(6.6)	3(10.3)	6(21.4)	0.011	8(6.5)
HE	40(7.1)	5(17.2)	4(14.3)	0.062	38(30.6)
Jaundice	210(37.2)	8(27.6)	11(39.3)	0.559	61(49.2)
CKD	4(0.7)	1(3.4)	1(3.6)	1.00	11(8.9)
DM	120(21.2)	6(20.7)	6(21.4)	1.00	29(23.4)
HTN	120(21.2)	7(24.1)	8(28.6)	1.00	27(21.8)
PE					
Alcoholism	296(52.4)	11(37.9)	15(53.6)	0.310	84(67.7)
Bacterial infection	26(4.6)	3(10.3)	1(3.6)	0.354	13(10.5)
Varix bleeding	116(20.5)	8(27.6)	3(10.7)	0.281	19(15.3)

Table 1. Baseline characteristics of enrolled patients according to clinical course

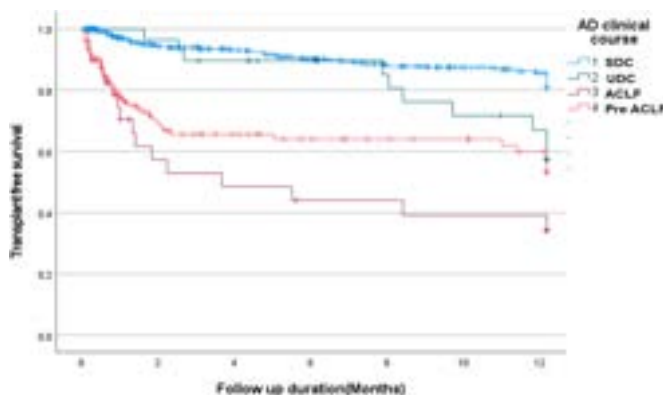


Figure 2: Clinical outcome according to clinical course

Conclusion: The prognostic groups of EF-CLIF are also verified in Asian cohort of cirrhosis. The accumulation of hepatic injury caused by recurrent symptom and progression to ACLF after first AD cause the dismal prognosis. Specially, the symptoms of first AD which were difficult to control and easily reproducible such as non-variceal bleeding and HEP are the sign of recurrent hepatic insult and should be care for prevention from the occurrence

FRI-539

Prediction of sepsis in patient of acute on chronic liver failure (ACLF)-a machine learning approach

Ashok Choudhury¹, Vinod Arora¹, Shiv Kumar Sarin¹, Vikash Dubey¹ and APASL ACLF Research Consortium Aarc Consortium¹. ¹Institute of liver and biliary sciences New Delhi, India
Email: doctor.ashokchoudhury@gmail.com

Background and aims: ACLF is syndrome rapid worsening liver failure with poor outcome. The survival is confounded by organ failure often with or without sepsis. Early sepsis identification is crucial. The machine learning using big data is could precisely and accurately predict the development of sepsis. Aim is to develop a machine learning based prediction model for development of sepsis among hospitalized patients of ACLF who had no sepsis at presentation.

Method: We analysed the prospective collected data from AARC registry. Clinical data, laboratory parameters and sepsis were serially noted. AI-modelling was done after appropriate mining, feature engineering, splitted randomly into train and test-sets (70:30). The models created on the train-set were (XGB), Random Forest, K-Nearest Neighbours Classifier, Decision Trees (DT), Logistic

Regression (LR), Adaptive Boosting (adaBoost) Model. We evaluated area under the curve (AUC), accuracy, sensitivity, specificity, and precision of models for predicting the outcomes in the test-set for any definite sepsis within first 7days of hospitalization who had none at baseline. AUC was the primary selection criteria; confusion matrix was used to compare AUCs between AI-models and calibration plot created to evaluate the observed and predicted risk.

Results: Of 4990 ACLF patients [mean age 44.8 ± 11.6 years, 86% male], sepsis at presentation was detected in 1180 (23.6%) patients. New onset sepsis developed in 9.4% (358) within first week and is considered as the event. Initial 54 features reduced to 45 after data cleaning and preparation and followed by selection of the top 14 features to prepare the basic model representing the sepsis development. The XGB-CV model had the best accuracy among other tested models for prediction in train-set: $0.94 \pm 5\%$, validation-set: $0.90 \pm 5\%$ and overall-dataset 0.86 with an AUROC of 0.954. The top five features critical for the XGB-CV model were baseline GGT, and day 4 parameters i.e., Heart rate, systolic and diastolic blood pressure and AARC score. New onset sepsis was associated with significantly higher 30-day mortality [56.4% versus 38.1%, OR = 2.07 (95 CI 1.77–3.61), $p = 0.01$].

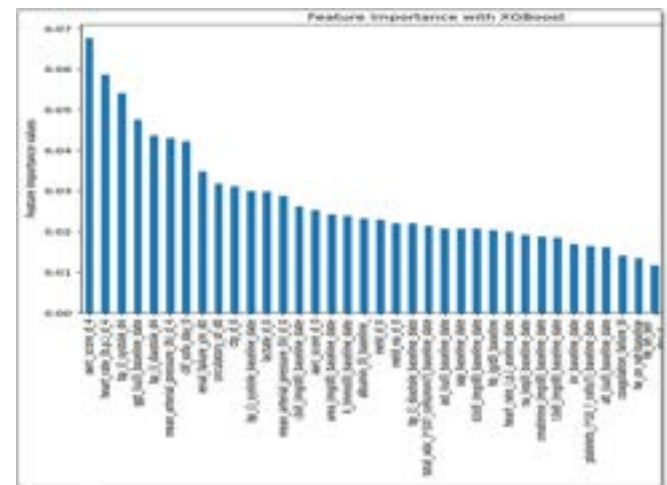


Figure:

Conclusion: New onset definite sepsis developed in one tenth of hospitalized ACLF patients within first week. The baseline GGT and fourth day AARC score along with simple heart rate and blood pressure dynamicity can predict sepsis. This may be a simple guide for decision regarding early prevention of sepsis and may improve survival.

FRI-540

Predictors of clinical courses in patients with acutely decompensated cirrhosis. An external validation of the PREDICT study

Enrico Pompili^{1,2}, Maurizio Baldassarre^{1,3}, Giorgio Bedogni^{1,4}, Giacomo Zaccherini¹, Giulia Iannone^{1,2}, Clara De Venuto^{1,2}, Francesco Palmese^{1,4}, Manuel Tufoni², Marco Domenicali^{1,4}, Paolo Caraceni^{1,2}. ¹Alma Mater Studiorum-University of Bologna, Department of Medical and Surgical Sciences, Bologna, Italy; ²IRCCS Azienda Ospedaliero-Universitaria di Bologna, Unit of Semeiotics, Liver and Alcohol-related diseases, Bologna, Italy; ³Alma Mater Studiorum-University of Bologna, Centre for Applied Biomedical Research (CRBA), Bologna, Italy; ⁴AUSL Romagna, Department of Primary Health Care, Internal Medicine, Frailty and Aging, Ravenna, Italy
Email: paolo.caraceni@unibo.it

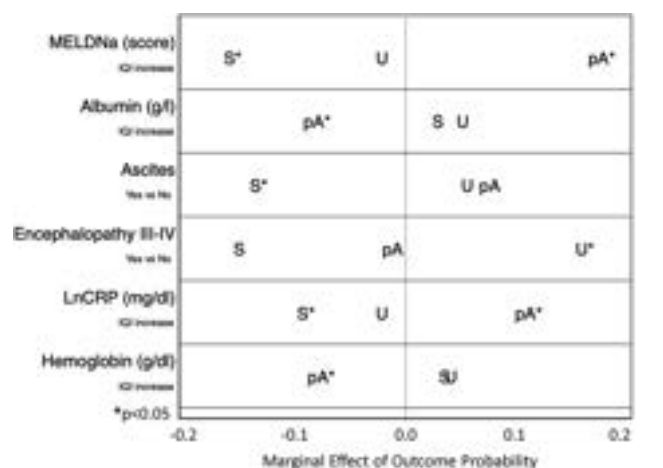
Background and aims: The PREDICT study recently showed that acutely decompensated (AD) cirrhotic patients without acute-on-chronic liver failure (ACLF) at admission present three different clinical trajectories and mortality rates: pre-ACLF, developing ACLF

POSTER PRESENTATIONS

within 90 days; Unstable Decompensated Cirrhosis (UDC), who were readmitted within 90-days or die without prior ACLF; and Stable Decompensated Cirrhosis (SDC), without ACLF or readmissions. This study aimed to i) validate the existence of three distinct trajectories in AD patients and compare their 1-year mortality rate; and ii) identify predictors for the occurrence of each trajectory.

Method: We performed a secondary analysis in a prospectively cohort of patients admitted to hospital for AD. Laboratory and clinical data at admission, development of ACLF and readmission up to 3 months and 1-year mortality were recorded. Patients were classified as pre-ACLF, UDC or SDC according to the PREDICT criteria. A pre-specified multinomial multivariable model (MNM) was used to evaluate the association between baseline features and the occurrence of pre-ACLF, SDC or UDC. Marginal estimates of the probability of pre-ACLF, SDC or UDC made by the MNM were calculated for one interquartile interval (IQI) increase for continuous predictors and for presence vs absence for binary predictors.

Results: Of the 311 patients included, 169 (55%) met the criteria for SDC, 57 (18%) for UDC, and 85 (27%) for pre-ACLF. The 1-year mortality was significantly different between the three groups: pre-ACLF 65%, UDC 46% and SDC 21% ($p < 0.001$). Marginal changes of the probability of pre-ACLF, SDC and UDC attributable to the predictors are reported in Figure 1. Among clinical parameters, the presence of hepatic encephalopathy was associated to UDC ($p = 0.043$), while the absence of ascites to SDC ($p = 0.017$). Among laboratory parameters, the increase in MELD-Na ($p = 0.000$) and C-Reactive Protein ($p = 0.009$) and the decrease in hemoglobin ($p = 0.004$) and albumin ($p = 0.008$) levels were associated to pre-ACLF.



S: Stable Decompensated Cirrhosis - U: Unstable Decompensated Cirrhosis - pA: pre-ACLF
Figure:

Conclusion: The present study confirms that patients with AD have 3 different clinical trajectories associated to different mortality rates. Besides severity of cirrhosis, the association with CRP supports the predominant role of systemic inflammation in ACLF development. Finally, HE is associated to the UDC trajectory highlighting the need of a better management of this complication after discharge.

FRI-541

Increased serum IL-6 and IL-8 are associated with echocardiographic signs of diastolic dysfunction in patients admitted for acutely decompensated cirrhosis

Andrei Voiosu^{1,2}, Ioana Doha^{1,2}, Victor Dragan¹, Mihaela Birligea¹, Paul Balanescu^{1,2}, Theodor Voiosu^{1,2}, Caterina Delcea^{2,3}, Ancuta Elena Vujan^{2,3}, Bogdan Mateescu^{1,2}, Cristian Baicus^{1,2}.
¹Colentina Clinical Hospital, Romania; ²Carol Davila University of Medicine and Pharmacy, Romania; ³Colentina Clinical Hospital, Cardiology, Romania
Email: andreivoiosu@gmail.com

Background and aims: We hypothesized that the inflammation underpinning many cases of acute decompensation (AD) in cirrhosis leads to impaired cardiac function increasing the risk of evolving towards Acute on Chronic Liver Failure (ACLF) or death. We aimed to explore the relationship between a panel of relevant inflammatory biomarkers and functional cardiac parameters in patients with AD of cirrhosis.

Method: This is a retrospective analysis of a prospective database of 70 patients with AD of cirrhosis who had echocardiography performed within 48 hours of admission and for whom follow-up was available. A single investigator examined all patients with according to a pre specified echocardiography protocol and measured parameters of systolic and diastolic function. Cardiac dysfunction was diagnosed by echocardiography according to current algorithms and cut-off values based on parameters available from the corresponding recorded examinations. We measured serum concentrations of inflammatory (IL-6, IL-8, TNF- α , CD206) and cardiac biomarkers (pro Brain Natriuretic Peptide -proBNP, Troponin T) from frozen samples stored in our biobank. Patients were divided into a low and a high-risk group by using a cut-off CLIF-C AD score of 50 [1]. We analyzed associations between the echocardiographic parameters of cardiac dysfunction, concentrations of biomarkers, CLIF-C AD score, and outcome.

Results: We included 70 patients (mean age 58 ± 10 years, 28 women) admitted for AD of cirrhosis and followed-up for 17 ± 7 months. 3 patients had ACLF at enrollment and the mean CLIF-C AD score was 47 ± 7 . 13 patients fulfilled the echocardiographic criteria for systolic dysfunction and 29 patients those for diastolic dysfunction, but there were no significant correlations with the concentrations of serum IL-6, IL-8, TNF- α or CD206. Of the echocardiographic parameters, increased left atrial volume and mitral A wave, both indicators of left ventricular diastolic dysfunction, positively associated with markers of inflammation: IL-6 ($r = 0.404$, $p < 0.001$), and, respectively, IL-8 ($r = 0.368$, $p = 0.002$). In univariate analysis, patients with higher CLIF-C AD score had higher levels of IL-6 ($r = 0.284$, $p = 0.02$) and IL-8 ($r = 0.307$, $p = 0.01$), but were not more likely to have cardiac dysfunction. 18/70 patients died during follow-up. Patients with higher concentrations of proBNP ($p = 0.01$), IL-6 ($p = 0.01$), IL-8 ($p = 0.008$), and higher CLIF-C AD score ($p = 0.02$) were more likely to die.

Conclusion: We found associations between inflammatory biomarkers and echocardiographic indicators of diastolic dysfunction. Cardiac dysfunction was not more prevalent in patients with AD of cirrhosis at higher risk of developing ACLF or death during follow-up. This work was supported by a grant of the Ministry of Research, Innovation and Digitization, CNCS-UEFISCDI project number PN-III-P1-1.1-PD-2021-0180, within PNCDI III.

Reference

1. Trebicka J, et al. *J Hepatol*. 2020;73 (4):842–854.

FRI-542

Different risk factors of clinical outcomes between variceal bleeding and non-variceal gastrointestinal bleeding in acutely decompensated cirrhosis

Ji Won Park¹, Sung-Eun Kim¹, Jung Hee Kim¹, Jang Han Jung¹, Hyoung Su Kim¹, Eileen Yoon², Young Kul Jung³, Ki Tae Suk¹, Moon Young Kim⁴, Won Kim⁵, Jae Young Jang⁶, Dong Joon Kim¹.
¹Hallym University College of Medicine, Korea, Rep. of South; ²Hanyang University College of Medicine, Korea, Rep. of South; ³Korea University Ansan Hospital, Korea, Rep. of South; ⁴Yonsei University Wonju College of Medicine, Korea, Rep. of South; ⁵Seoul Metropolitan Government Seoul National University Boramae Medical Center, Korea, Rep. of South; ⁶Soonchunhyang University College of Medicine, Korea, Rep. of South
Email: sekim@hallym.or.kr

Background and aims: Gastrointestinal bleeding (GIB) including variceal bleeding (VB) and non-variceal gastrointestinal bleeding

(NVB) is a major complication in patient with chronic liver disease, especially liver cirrhosis. Recent studies reported that there were no differences in clinical outcomes between VB and NVB. However, larger scale, multicenter, prospective studies were warranted to confirm these results because there was different pathogenic mechanism of development between VB and NVB. We aimed to investigate differences of clinical outcomes and risk factor in cirrhotic patients with GIB.

Method: The prospective Korean Acute-On-Chronic Liver Failure (KACLiF) cohort consisted of 1,773 patients who were hospitalized with acute decompensation of chronic liver disease, from July 2015 to August 2018. We enrolled a total of 490 cirrhotic patient with GIB after excluding non-cirrhotic patients. Patients were then regularly evaluated for adverse outcomes (liver transplantation and death) every 3 month during follow-up period.

Results: A total of 490 cirrhotic patient with GIB were included, 414 with VB and 76 with NVB. Patients with NVB had poorer underlying liver function than those with VB (bilirubin 4.49 ± 3.96 vs 2.86 ± 3.64 mg/dL, $p < 0.001$; Child-Pugh score 8 (5–14) vs 7 (5–15), $p < 0.001$; MELD 16.6 (7–41) vs 13.6 (7–54), $p = 0.004$; MELD-Na 19.2 (8–41) vs 15.3 (7–50), $p < 0.001$). Patients with VB and NVB had similar 28-day adverse outcome (death or liver transplantation) (4.6% vs 6.6%, $p = 0.460$), 90-day adverse outcome (7.5% vs 13.2%, $p = 0.101$), 1-year adverse outcome (18.4% vs 19.7%, $p = 0.177$). MELD was only one predictor for 28-day, 90-day, and 1-year adverse outcome in patients with VB if factors were analysed with ACLF. However, cardiac failure and/or respiratory failure were additional risk factors for 28-day, 90-day, and 1-year adverse outcomes in patients with VB if factors were analysed each statistically important organ failure. Compared to results in patients with VB, MELD was an important predictor for 28-day and 90-day adverse outcomes in patients with NVB.

Conclusion: Our results showed no statistically difference of adverse outcomes in cirrhotic patients with VB and NVB. However, there were differences of major predictor for short-term and long-term adverse outcomes between patients with VB and NVB.

FRI-543

Trajectory of outcome from acute-on-chronic liver failure is determined beyond 48 hours of admission to intensive care

Thomas Dixon¹, Laura White¹, Sherif Ghabina¹, Agnieszka Walecka¹, Phyllis Keen¹, Paul Bassett², Rajiv Jalan¹, Banwari Agarwal¹, Gautam Mehta^{1,3}. ¹Royal Free Hospital, United Kingdom; ²Statsconsultancy LTD, Amersham, United Kingdom; ³Roger Williams Institute of Hepatology, Foundation for Liver Research, London, United Kingdom
Email: thomasdixon@nhs.net

Background and aims: Acute-on-chronic liver failure (ACLF) represents the most severe form of acute decompensation of cirrhosis, associated with multi-organ failure and high mortality. The CLIF-C ACLF score has been shown as a predictor of outcome in Intensive Care Unit (ICU) settings, and to determine futility of ICU care in certain cases (Engelmann et al., 2018). Change in ACLF grade over time (between 3 and 7 days) has been noted to correlate with outcome (Gustot et al., 2015). The aim of this study was to determine if change in CLIF-C ACLF score from ICU admission baseline to day 2 and day 7 were predictive of survival up to 3 months.

Method: Data for consecutive patients admitted to Royal Free London ICU with a complication of cirrhosis, between 2016 and 2017, were contemporaneously maintained on a research database (Research Ethics committee: 21/NI/0175). Additional clinical metadata was entered retrospectively. CLIF-C ACLF scores were calculated at days 0, 2 and 7 following ICU admission, and survival assessed at ICU discharge and 3 months. Differences between CLIF-C ACLF score were compared using unpaired t-test. The relationship between CLIF-C ACLF Score, age, sex and survival at ICU discharge and 3 months were analysed by logistic regression.

Results: The cohort comprised of 102 patients with complete data available at baseline; 64% were males and a median age 55. 63 patients (62%) survived to ICU discharge. Baseline CLIF-C ACLF score was a significant predictor of ICU mortality and survival at 3 months. Change in CLIF-C ACLF score from baseline to day 7, but not day 2, was a significant predictor of survival at ICU discharge and 3-months (Table 1). Logistic regression for survival at 3 months demonstrated an odds ratio of 3.61 (1.04–12.5, $p = 0.04$) for 3-month mortality for every 10-point increase in CLIF-C ACLF score between days 0 and 7; changes at day 2 were not significant.

Conclusion: Although preliminary, the data presented here suggests that re-assessment of clinical status at day 2 following ICU admission is an insufficient time to determine prognosis in ACLF patients. The optimal duration is likely between 3 and 7 days. These data have implications for resource allocation in ICU care of liver patients and merit validation in larger cohorts.

FRI-544

Serum Cytokine and Chemokine profiles and disease prognosis in hepatitis B virus-related acute-on-chronic liver failure

Bingbing Zhu¹, Fangyuan Gao¹, Yuxin Li¹, Ke Shi¹, Yixin Hou¹, Jialiang Chen¹, Qun Zhang¹, Xianbo Wang¹. ¹Capital Medical University Affiliated Beijing Ditan Hospital, Center of Integrative Medicine, China
Email: wangxb@ccmu.edu.cn

Background and aims: Hepatitis B virus-related acute-on-chronic liver failure (HBV-ACLF) has significant morbidity and mortality and is associated with the induction of cytokines/chemokines, which might contribute to the pathogenesis of liver injury. This study aims to explore the cytokines/chemokines profiles of HBV-ACLF patients and develop a composite clinical prognostic model.

Method: We prospectively collected blood samples and clinical data of 107 HBV-ACLF patients admitted to the Beijing Ditan Hospital. The concentration of 40-plex cytokines/chemokines were measured by the Luminex assay in 86 survivors and 21 non-survivors. Discrimination between cytokine/chemokine profiles in different prognosis groups were analyzed using the multivariate statistical technique of principal component analysis (PCA) and partial least square discriminant analysis (PLS-DA). The immune-clinical prognostic model was obtained using multivariate logistic regression analysis.

Results: The PCA and PLS-DA method indicated that the cytokine/chemokine profiling could distinguish patients with different prognosis clearly. 14 cytokines including IL-1 β , IL-6, IL-8, IL-10, TNF- α , IFN- γ , CXCL1, CXCL2, CXCL9, CXCL13, CX3CL1, GM-CSF, CCL21 and CCL23 were significantly correlated with disease prognosis. Multivariate analysis identified CXCL2, IL-8, total bilirubin, and age as independent risk factors that constituted the immune-clinical prognostic model, which showed the strongest predictive value of 0.938 compared with the CLIF-C ACLFs (0.785), MELD (0.669), and MELD-Na (0.723) ($p < 0.05$ for all).

Conclusion: Serum cytokine/chemokine profiles correlated with 90-day prognosis of patients with HBV-ACLF. The composite immune-clinical prognostic model we proposed resulted in more accurate prognostic estimates than CLIF-C ACLFs, MELD, and MELD-Na.

FRI-545

Impaired pituitary-thyroid signaling and low free triiodothyronine indicate increased risk for ACLF and mortality in cirrhosis

Lukas Hartl^{1,2}, Benedikt Simbrunner^{1,2,3}, Mathias Jachs^{1,2}, Peter Wolf⁴, David JM Bauer^{1,2}, Bernhard Scheiner^{1,2}, Lorenz Balcar^{1,2}, Georg Semmler^{1,2}, Michael Schwarz¹, Rodrig Marculescu⁵, Michael Trauner¹, Matthias Mandorfer^{1,2}, Thomas Reiberger^{1,2,3}.

POSTER PRESENTATIONS

Table (abstract: FRI-543).

	Outcome at ICU Discharge						
	Alive		Dead		p Value	Logistic Regression: Age and Sex Adjusted Model	
	n	Mean \pm SD	N	Mean \pm SD		Odds Ratio (95% CI)	p Value
CLIF- C ACLF Score							
Day 0	63	50.2 \pm 9.6	39	60.6 \pm 11.1	p < 0.001	2.89 (1.75, 4.76)	p < 0.001
Day 7	20	53.2 \pm 9.5	15	64.7 \pm 6.5	p < 0.001	7.13 (1.93, 26.4)	p = 0.003
Change in CLIF-C ACLF Score							
Day 0 to Day 2	41	-1.4 \pm 8.0	27	0.4 \pm 9.6	p = 0.41	1.29 (0.71, 2.33)	p = 0.40
Day 0 to Day 7	19	-4.2 \pm 10.3	12	4.3 \pm 7.5	p = 0.02	4.42 (1.17, 16.7)	p = 0.03
Outcome at 3 months							
Alive	n	Mean \pm SD	Dead	Mean \pm SD	p Value	Odds Ratio (95% CI)	p Value
CLIF-C ACLF Score							
Day 0	53	49.6 \pm 10.2	44	59.9 \pm 10.7	p < 0.001	2.75 (1.69, 3.44)	p < 0.001
Day 7	16	53.8 \pm 10.5	16	64.0 \pm 6.9	p = 0.003	4.29 (1.36, 13.6)	p = 0.01
Change in CLIF-C ACLF Score							
Day 0 to Day 2	32	-1.3 \pm 7.3	31	1.0 \pm 9.2	p = 0.27	1.43 (0.77, 2.65)	p = 0.26
Day 0 to Day 7	16	-4.4 \pm 11.2	13	3.5 \pm 7.6	p = 0.04	3.61 (1.04, 12.5)	p = 0.04

Analysis comparing CLIF-C ACLF scores between patients alive and dead at each timepoint. The difference in scores at the given timepoint and change between timepoints was calculated using unpaired t-test. Logistic regression used for further analysis demonstrating effect of CLIF-C ACLF score on survival, representing the relative change in the odds of death for every 10-unit increase in CLIF-C ACLF Score.

¹Division of Gastroenterology and Hepatology, Department of Medicine III, Medical University of Vienna, Vienna, Austria; ²Vienna Hepatic Hemodynamic Lab, Division of Gastroenterology and Hepatology, Department of Medicine III, Medical University of Vienna, Vienna, Austria; ³Christian Doppler Lab for Portal Hypertension and Liver Fibrosis, Division of Gastroenterology and Hepatology, Department of Medicine III, Medical University of Vienna, Vienna, Austria; ⁴Division of Endocrinology, Department of Medicine III, Medical University of Vienna, Vienna, Austria; ⁵Department of Laboratory Medicine, Medical University of Vienna, Vienna, Austria
Email: thomas.reiberger@meduniwien.ac.at

Background and aims: A low free triiodothyronine (fT3) phenotype has been described in patients with advanced chronic liver disease (ACLD). While conversion, transport and metabolism of thyroid hormones is dependent on hepatic function, thyroid hormones in turn affect hepatic metabolism. We aimed to characterize the pituitary-thyroid axis and the prognostic value of low fT3 in ACLD. **Method:** Patients with ACLD, i.e. liver stiffness measurement (LSM) ≥ 10 kPa or HVPG ≥ 6 mmHg, undergoing hepatic venous pressure gradient (HVPG) measurement between 04/2007 and 09/2022 with available thyroid stimulating hormone (TSH) levels were considered. Patients with hepatocellular carcinoma (HCC), vascular liver disease, portal vein thrombosis, infections, liver transplantation (LT) or intake of thyroid hormones were excluded. Clinical stages were defined as: probable ACLD (pACLD): LSM ≥ 10 kPa and HVPG < 6 mmHg, S0: mild portal hypertension (PH; i.e. HVPG 6–9 mmHg), S1: clinically significant PH (CSPH) without varices, S2: CSPH with varices, S3: previous variceal bleeding, S4: previous non-bleeding hepatic decompensation and S5: further decompensation.

Results: A total of 648 ACLD patients (median age: 54.7 years; 65.9% male; main etiologies: alcohol-related 50.2% and viral liver disease 22.7%) were included. 316 were compensated (pACLD: n = 31; S0: n = 35; S1: n = 85; S2: n = 165), while 332 had decompensated ACLD (S3: n = 33; S4: n = 170; S5: n = 129). Median levels of TSH (p < 0.001) and C-reactive protein (CRP; p < 0.001) increased with progressive ACLD stages and fT3 (available in n = 298 patients; p < 0.001) declined, while free thyroxine (fT4) levels did not change significantly (available in n = 329 patients; p = 0.368; see Figure). 38 patients showed low fT3

levels with a higher prevalence among dACLD patients (cACLD: 7.0% vs. dACLD: 17.2%; p = 0.009) fT3 correlated with ACLD severity (Child score; rho = -0.52), portal hypertension (HVPG; rho = -0.30) endothelial dysfunction (von Willebrand factor antigen; rho = -0.36) and systemic inflammation (CRP; rho = -0.35). In multivariate linear regression analysis, CRP per mg/dL was associated with TSH (aB: 0.49; p < 0.001), as well as with fT3 (aB: -0.21; p = 0.016) after adjustment for HVPG, Child score and creatinine. Low fT3 was associated with a higher risk of acute-on-chronic liver failure (ACLF; aHR: 4.7; p = 0.004) and liver-related death (aHR: 5.5; p < 0.001), considering etiological cure, HCC, LT and non-liver-related death as competing risks.

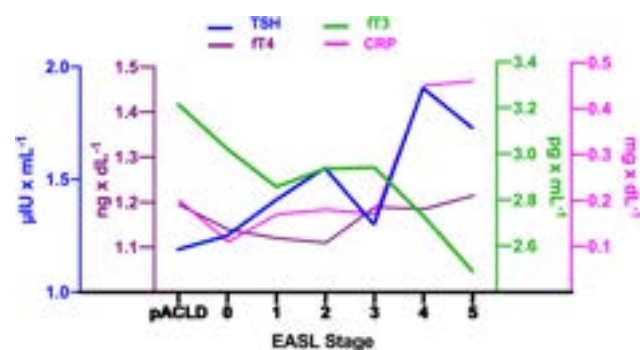


Figure:

Conclusion: The pituitary-thyroid axis is impacted by progressive severity of ACLD. Increasing TSH and declining fT3 levels in more advanced ACLD stages might be indicative of a low T3 (i.e. euthyroid sick) syndrome. In ACLD, low fT3 was associated with key disease driving mechanisms such as systemic inflammation. Importantly, low fT3 in patients with ACLD represents an independent risk factor for ACLF and liver-related death.

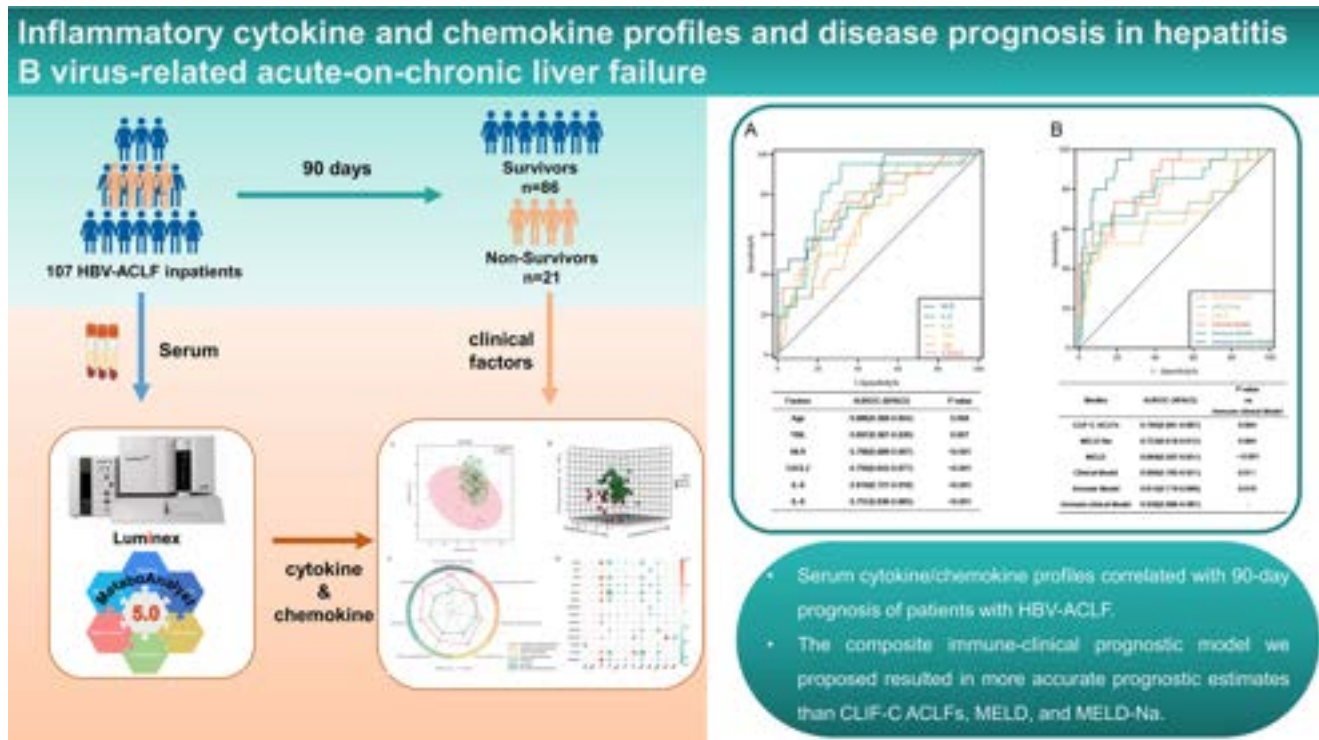


Figure: (abstract: FRI-544).

FRI-546

Nosocomial infections in cirrhosis are unpredictable and vary based on region of the world: CLEARED study

Jasmohan S Bajaj¹, Florence Wong², Qing Xie³, Patrick S. Kamath⁴, Mark Topazian⁵, Shiv Kumar Sarin⁶, Shiva Kumar⁷, Sebastián Marciano⁸, Fiona Tudehope⁹, Robert Gibson¹⁰, Adam Doyle¹¹, Stephen Riordan¹², Alberto Queiroz Farias¹³, Nabih Faisal¹⁴, Puneeta Tandon¹⁵, Marie Jeanne Lohoues¹⁶, Carlos Benitez¹⁷, Yongchao Xian¹⁸, Chuanwu Zhu¹⁹, Minghua Su²⁰, Yongfang Jiang²¹, Caiyan Zhao²², Lei Wang²³, Mingqin Lu²⁴, Ning-Ping Zhang²⁵, Hai Li²⁶, Xin Zheng²⁷, Hong Tang²⁸, Bin Xu²⁹, Zhiliang Gao³⁰, Minghua Lin³¹, Jinjun Chen³², Chenghai Liu³³, Peng Hu³⁴, Belimi Hibat Allah³⁵, Henok Fisseha³⁶, Aloysious Aravintan³⁷, Neil Rajoriya³⁸, Damien Leith³⁹, Danielle Adebayo⁴⁰, Diana Yung⁴¹, Wai-Kay Seto⁴², Helena Katchman⁴³, Abha Nagral⁴⁴, Anand Kulkarni⁴⁵, CE Eapen⁴⁶, Ajay Kumar Duseja⁴⁷, Anoop Saraya⁴⁸, Mohd. Rela⁴⁹, Anil Anora⁵⁰, Radha Krishan Dhiman⁵¹, Anil Chandra Anand⁵², Maria Sarai González-Huezo⁵³, Jose Luis Perez Hernandez⁵⁴, Godolfino Miranda Zazueta⁵⁵, Mauricio Castillo⁵⁶, René Malé Velazquez⁵⁷, Jose Antonio Velarde-Ruiz Velasco⁵⁸, Jacqueline Cordova⁵⁹, Ruveena Bhavani⁶⁰, Edith Okeke⁶¹, Dalia Allam⁶², Hiang Keat Tan⁶³, Sombat Treeprasertsuk⁶⁴, Busra Haktaniyan⁶⁵, Feyza Gunduz⁶⁶, Abdullah Emre Yildirim⁶⁷, Zeki Karasu⁶⁸, Enver Ucbilek⁶⁹, Haydar Adanir⁷⁰, Somaya Albhaisi⁷¹, Sumeet Asrani⁷², K. Rajender Reddy⁷³, Jawaid Shaw⁷⁴, Hugo Vargas⁷⁵, Scott Biggins⁷⁶, Paul J. Thuluvath⁷⁷, Andrew Keaveny⁷⁸, Peter Hayes⁷⁹, Aldo Torre⁸⁰, Ramazan Idilman⁸¹, Zhujun Cao³, Mario Álvares-da-Silva⁸², Jacob George⁸³, Hailemichael Desalegn⁵, Brian Bush¹, Leroy Thacker¹, Duarte Rojo Andres⁸⁴, Ashok Choudhury⁶. ¹Virginia Commonwealth University and Central Virginia Veterans Healthcare System, Richmond, USA, United States; ²University of Toronto, Toronto, Canada, Canada; ³Ruijin Hospital, Shanghai Jiao Tong University School of Medicine, Shanghai, China, China; ⁴Mayo Clinic School of Medicine, Rochester, USA, United States; ⁵St Paul's Hospital, Millennium Medical College, Addis Ababa, Ethiopia, Ethiopia; ⁶Institute of liver and biliary sciences New Delhi, India;

⁷Cleveland Clinic Abu Dhabi, United Arab Emirates; ⁸Hospital Italiano de Buenos Aires, Argentina, Argentina; ⁹Westmead Hospital, Sydney, Australia; ¹⁰John Hunter Hospital, Newcastle, Australia; ¹¹Royal Perth Hospital, Perth, Australia; ¹²Prince of Wales Hospital, Sydney, Australia; ¹³Hospital das Clínicas da Faculdade de Medicina da Universidade de São Paulo, Brazil; ¹⁴University of Manitoba, Winnipeg, Canada; ¹⁵University of Alberta, Edmonton, Canada; ¹⁶CHU de Cocody, Abidjan, Cote d'Ivoire, Côte d'Ivoire; ¹⁷Pontificia Catholic University of Chile, Santiago, Chile; ¹⁸The Third People's Hospital of Guilin, China; ¹⁹The Fifth People's Hospital of Suzhou, China; ²⁰The First Affiliated Hospital of Guangxi Medical University, China; ²¹The Second XiangYa Hospital of Central South University, China; ²²The Third Affiliated Hospital of Hebei Medical University, China; ²³Second Hospital of Shandong University, China; ²⁴The First Affiliated Hospital of Wenzhou Medical University, China; ²⁵Zhongshan Hospital, Fudan University, China; ²⁶Department of Gastroenterology, School of Medicine, Ren Ji Hospital, Shanghai Jiao Tong Medical University, China; ²⁷Department of Infectious Diseases, Union Hospital, Tongji Medical College, Huazhong University of Science and Technology, China; ²⁸Center of Infectious Disease, West China Hospital of Sichuan University, China; ²⁹Beijing Youan Hospital, Capital Medical University, China; ³⁰The Third Affiliated Hospital of Sun Yat-sen University, Guangzhou, China; ³¹Mengchao Hepatobiliary Hospital of Fujian Medical University, China; ³²Hepatology Unit, Department of Infectious Diseases, Nanfang Hospital, Southern Medical University, China; ³³Shuguang Hospital Affiliated to Shanghai University of Traditional Chinese Medicine, China; ³⁴Second Affiliated Hospital of Chongqing Medical University, China; ³⁵Mustapha Bacha University Hospital, Algiers, Algeria; ³⁶St Paul's Hospital Millennium Medical College, Addis Ababa, Ethiopia, Ethiopia; ³⁷NIHR Nottingham Biomedical Research Centre, Nottingham University Hospitals, United Kingdom; ³⁸Queen Elizabeth University Hospitals, Birmingham, United Kingdom; ³⁹Glasgow Royal Infirmary, United Kingdom; ⁴⁰Royal Berkshire Hospital, United Kingdom; ⁴¹Royal Infirmary of Edinburgh, United Kingdom; ⁴²Department of Medicine, School of Clinical Medicine, The University of Hong Kong, Hong Kong; ⁴³Tel-Aviv Sourasky Medical Center, Tel Aviv, Israel, Israel; ⁴⁴Jaslok Hospital, Mumbai, India; ⁴⁵Asian Institute of Gastroenterology, Hyderabad, India; ⁴⁶Department of Hepatology,

POSTER PRESENTATIONS

Christian Medical College, Vellore, India; ⁴⁷Deptt. of Hepatology, PGIMER, Chandigarh, India; ⁴⁸Deptt. of Gastroenterology and Human Nutrition, AIIMS, New Delhi, India; ⁴⁹Deptt. of Liver Transplant Surgery, Dr. Rela Institute and Medical Centre, Chennai, India; ⁵⁰Sir Ganga Ram Hospital, Delhi, India; ⁵¹Sanjay Gandhi Postgraduate Institute of Medical Research, Lucknow, India; ⁵²KIMS, Bhubaneswar, Odisha, India; ⁵³Centro Médico ISSEMYM, Mexico; ⁵⁴Hospital General de Mexico "Dr. Eduardo Liceaga", Mexico; ⁵⁵Instituto Nacional de Ciencias Médicas y Nutrición "Salvador Zubirán", Mexico City, Mexico; ⁵⁶Centro Médico la Raza, Mexico City, Mexico; ⁵⁷Instituto de la Salud Digestiva, Guadalajara, Mexico; ⁵⁸Hospital Civil de Guadalajara Fray Antonio Alcalde, Guadalajara, Mexico; ⁵⁹Hepatology, Hospital General Dr. Manuel Gea González, Mexico City, Mexico; ⁶⁰University of Malaysia, Kuala Lumpur, Malaysia, Malaysia; ⁶¹Jos University Teaching Hospital, Jos, Nigeria, Nigeria; ⁶²National Center for Gastrointestinal and Liver Disease, Khartoum, Sudan; ⁶³Singapore General Hospital, Singapore; ⁶⁴Chulalongkorn University and King Chulalongkorn Memorial Hospital, Bangkok, Thailand, Thailand; ⁶⁵University of Ankara, Turkey; ⁶⁶Marmara University, Istanbul, Turkey; ⁶⁷Gaziantep University, Turkey; ⁶⁸Ege University, Izmir, Turkey; ⁶⁹Mersin University, Mersin, Turkey; ⁷⁰Akdeniz University, Antalya, Turkey; ⁷¹Virginia Commonwealth University, Richmond, United States; ⁷²Baylor University Medical Center, Dallas, United States; ⁷³University of Pennsylvania, United States; ⁷⁴Richmond VA Medical Center, United States; ⁷⁵Mayo Scottsdale, United States; ⁷⁶University of Washington, United States; ⁷⁷Mercy Medical Center, Baltimore, United States; ⁷⁸Mayo Jacksonville, United States; ⁷⁹University of Edinburgh, Edinburgh, UK, United Kingdom; ⁸⁰Instituto Nacional de Ciencias Médicas y Nutrición Salvador Zubirán, Mexico City, Mexico; ⁸¹Ankara University School of Medicine, Ankara, Turkey, Turkey; ⁸²Hospital de Clínicas de Porto Alegre, Universidade Federal do Rio Grande do Sul, Porto Alegre, Brazil, Brazil; ⁸³Storr Liver Centre, The Westmead Institute for Medical Research and Westmead Hospital, University of Sydney, Sydney, Australia, Australia; ⁸⁴University of Pittsburgh, United States
Email: jasmohan.bajaj@vcuhealth.org

Background and aim: Define determinants, predictors, and variations in NI across a global population of cirrhosis inpatients.

Method: CLEARED Consortium prospectively recruited cirrhotic inpatients from 6 continents. Data were collected at baseline and patients followed during their hospitalization. Infections on admission, and NI (diagnosed >48 hrs after admission) were recorded. Comparisons were made between NI vs no-NI variables and between regions. Multivariable (MV) analysis for NI was performed using admission variables.

Results: 3884 patients from 95 centers identified 474 pts (12%) with NIs. Major NIs were respiratory (RTI 32%), UTI (18%), SBP (15%) and spontaneous bacteremia (11%). Most did not have an organism isolated (42%), then gram negative (29%), positive (16%) and fungal (6%). 16% had drug-resistant organisms (DRO) and 20% were 2nd infections. NI vs No-NI admission variables: NI pts were mostly female ($p = 0.05$), with alcohol as etiology (45% vs 40%, $p = 0.05$) and higher MELD-Na (26 vs 20, $p < 0.0001$). NI patients had ↑prior infections (28 vs 19%, $p < 0.0001$) and AKI (23 vs 15%, $p < 0.0001$), prior transplant listing (13 vs 9%, $p = 0.005$), admission lactulose use (48 vs 40% $p = 0.006$) and lower antivirals (14 vs 19% $p = 0.02$) use. NI pts had more often admissions due to infections (42 vs 32%, $p = 0.006$) and lower GI bleed (20 vs 26%, $p = 0.008$). Rest of the admission causes were similar. Of admission infections, sites were not different between those who developed NI or not. Outcomes: NI pts had higher mortality (32 vs 9%), ICU transfer (42 vs 15%), AKI development (59 vs 32%) [all $p < 0.001$]. MV analysis for NI had a low AUC (0.67) but was significant for ↑MELD-Na (OR 1.07, $p < 0.0001$) and infections in past 6 months (1.43, $p = 0.002$). Male gender (0.71, $p = 0.001$) was protective. Regional variations: Highest rate of NIs were in India, South America, Asia, and Europe (Fig A). Most common NIs were SBP, RTI and UTIs (Fig B). RTI was highest in Africa, Australia and Asia while UTIs were highest in Mexico and Turkey (Fig C). SBP was highest in China,

Turkey and India. Most pts in Africa did not have culture positivity followed by China, Europe and Australia. Gram negatives were higher in Asia and Turkey while Gram positives were relatively similar. Fungal infections were higher in China and Asia. DROs were highest in Asia, Mexico, and USA/Canada (Fig D) but similar overall since many regions did not have enough culture positive isolates.

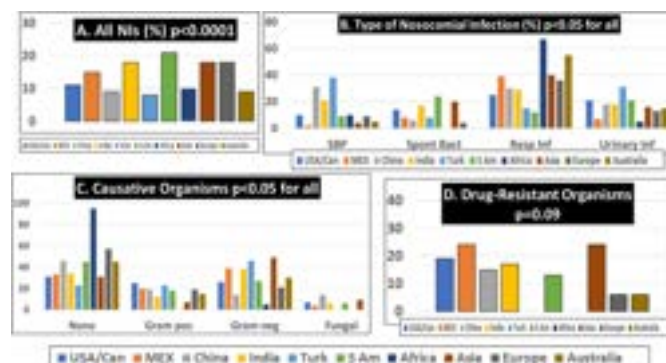


Figure:

Conclusion: In a global consortium of in-patients with cirrhosis, 12% developed NI, mostly women with alcohol cirrhosis, which led to poor outcomes and were difficult to predict. Most NIs were respiratory, UTI and SBP. NI sites, culture positivity rates and resultant DROs were substantially different across regions.

FRI-547

Metabolic biomarkers significantly enhance the prediction of HBV-related acute-on-chronic liver failure prognosis

Yan Zhang¹, Guohong Deng², Xian-bo Wang³, Xin Zheng⁴, Yan Huang⁵, Jinjun Chen⁶, Zhong-ji Meng⁷, Yanhang Gao⁸, Zhiping Qian⁹, Feng Liu¹⁰, Xiao-bo Lu¹¹, Yu Shi¹², Jia Shang¹³, Yan Huadong¹⁴, Zheng Yubao¹⁵, Weituo Zhang¹⁶, Lining Guo¹⁷, Hai Li¹.
¹Ren Ji Hospital, School of Medicine, Shanghai Jiao Tong University, China; ²Southwest Hospital, Third Military Medical University (Army Medical University), China; ³Beijing Ditan Hospital, Capital Medical University, China; ⁴Institute of Infection and Immunology, Union Hospital, Tongji Medical College, Huazhong University of Science and Technology, China; ⁵Hunan Key Laboratory of Viral Hepatitis, Xiangya Hospital, Central South University, China; ⁶Nanfang Hospital, Southern Medical University, China; ⁷Taihe Hospital, Hubei University of Medicine, China; ⁸The First Hospital of Jilin University, China; ⁹Shanghai Public Health Clinical Centre, Fudan University, China; ¹⁰Nankai University Second People's Hospital, China; ¹¹The First Affiliated Hospital of Xinjiang Medical University, China; ¹²The First Affiliated Hospital of School of Medicine, Zhejiang University, China; ¹³Henan Provincial People's Hospital, China; ¹⁴Shulan (Hangzhou) Hospital Affiliated to Zhejiang Shuren University Shulan International Medical College, China; ¹⁵the Third Affiliated Hospital of Sun Yat-sen University, China; ¹⁶Clinical Research Center, Shanghai Jiao Tong University School of Medicine, China; ¹⁷Precision Inc., United States
Email: haili_17@126.com

Background and aims: Acute-on-chronic liver failure (ACLF) is a clinical syndrome of high short-term mortality in patients with chronic liver disease. Early diagnosis and accurate prognosis are needed to improve disease management and survivals for ACLF patients. We aimed to discover novel ACLF biomarkers using metabolomics and assess if the biomarkers can be used to enhance ACLF diagnosis and prognosis.

Method: We performed a metabolomics profiling of 1,024 serum samples collected from HBV-related chronic liver disease patients with acute exacerbation at hospital admission in a multi-year and multi-center prospective study (367 ACLF and 657 non-ACLF). The samples were randomly separated into equal halves as a discovery set and a validation set. We identified metabolites associated with 90-

day mortality in the ACLF group and the progression to ACLF within 28 days in the non-ACLF group (pre-ACLF) using statistical analysis and random forest analysis. We developed diagnostic algorithms in the discovery set and assessed the findings in the validation set.

Results: ACLF significantly altered the serum metabolome, particularly in membrane lipid metabolism, steroid hormone metabolism, oxidative stress pathways, and energy metabolism. Numerous metabolites were significantly associated with 90-day mortality in the ACLF group and/or pre-ACLF in the non-ACLF group. We trained and validated machine learning algorithms for the prediction of ACLF 90-day mortality (area under curve, AUC: 0.87) and the diagnosis of pre-ACLF (AUC: 0.94). To translate our discoveries into practical clinical tests, we developed targeted assays on selected metabolites using liquid chromatography mass spectrometry (LCMS).

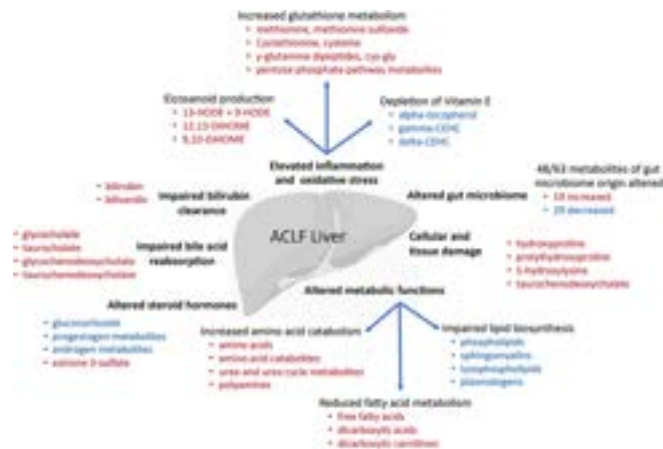


Figure:

Conclusion: Based on biomarkers uncovered by metabolomics analysis of a large cohort of HBV related ACLF and non-ACLF serum samples, we developed novel tests with improved accuracy for ACLF prognosis and early diagnosis. The in-depth analysis of metabolic perturbations caused by ACLF could provide new insights on ACLF pathogenesis and therapeutics development, and the novel ACLF tests could be used to improve the clinical management for ACLF patients.

FRI-548

Combination of CLIF-C ACLF and ammonia levels as a predictor of in-hospital outcomes in patients with acute-on-chronic liver failure

Sagnik Biswas¹, Manas Vaishnav¹, Shekhar Swaroop¹, Umang Arora¹, Shalimar Shalimar¹. ¹All India Institute of Medical Sciences, New Delhi, India

Email: drshalimar@gmail.com

Background and aims: The chronic liver failure consortium acute-on-chronic liver failure (CLIF-C ACLF) score performs significantly better than Child-Pugh-Turcotte (CTP), model for end-stage liver disease (MELD) and MELD-Na scores in predicting outcome in patients with ACLF. It also defines futility of care to enable withdrawal of support in patients with irreversible organ failures. Elevated ammonia levels have pleiotropic detrimental effects in multiple organ systems and constitute an independent risk factor to predict hospitalization due to liver related complications and mortality in cirrhotics. We explored the effect of addition of ammonia levels to existing prognostic scores in predicting outcomes in patients with ACLF.

Method: All consecutive ACLF patients with available ammonia values at admission evaluated between January 2011 to June 2022 were included. ACLF was defined as per the EASL-CLIF definition. Prognostic scores including CLIF-C ACLF, MELD-Na, CTP were calculated at baseline. A new model was generated which included CLIF-C ACLF and ammonia levels. Receiver operator characteristic

(ROC) curve was used to assess the performance of the prognostic model. Comparison of the area under ROC curves was performed using DeLong method.

Results: A total of 568 patients with ACLF were included, mean (\pm SD) age 42.4 ± 12.8 years, 456 (80.3%) males. Overall, 160 (28.2%) patients survived. Active alcohol consumption was the most common aetiology, both for the chronic liver disease and the acute insult (57.7% and 43.1% respectively). The mean (\pm SD) values of prognostic scores on day 1 were as follows: CTP (12.9 ± 1.5), MELD-Na (33.2 ± 6.3), CLIF-C ACLF (51.5 ± 10.0) and serum ammonia 108 ($82-140$) micromoles/L. The area under curve (AUC) for CLIF-C ACLF score was 0.75 (0.71–0.79) followed by CTP, MELD-Na, and ammonia at 0.71 (0.67–0.75), 0.64 (0.60–0.68) and 0.63 (0.59–0.67) respectively ($p = 0.02$). The model based on combination of CLIF-C ACLF and serum ammonia levels at admission had numerically highest AUC 0.76 (0.72–0.79), and performed significantly better than the CTP ($p = 0.050$), MELD-Na ($p = 0.001$) and serum ammonia ($p < 0.001$) alone, but was equivalent to CLIF-C ACLF score in predicting survival.

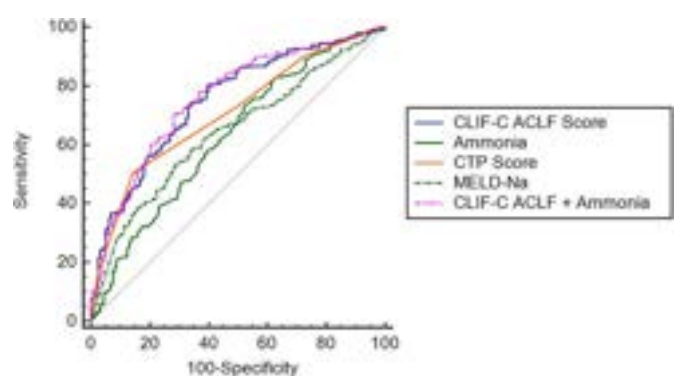


Figure: Receiver operating characteristic (ROC) curves of various prognostic variables and in-hospital mortality.

Conclusion: Addition of ammonia to CLIF-C ACLF score does not improve the overall diagnostic accuracy of CLIF-C ACLF score in predicting in-hospital mortality.

FRI-549

Soluble urokinase plasminogen activator receptor is a biomarker for outcome in decompensated liver cirrhosis and acute-on-chronic liver failure

Sven Lamatsch¹, Mohsin Hassan¹, Carlos de la Peña-Ramirez², Kai Kappert^{3,4}, Raphael Mohr¹, Münevver Demir¹, Minh Phan¹, Fausto Andreola⁵, Rhea Veelken^{6,7}, Niklas F Aehling⁶, Janett Fischer⁶, Raj Mookerjee⁵, Thomas Berg⁶, Rajiv Jalan⁵, Frank Tacke¹, Cornelius Engelmann¹. ¹Charité-Universitätsmedizin Berlin, corporate member of Freie Universität Berlin and HumboldtUniversität zu Berlin, Medizinische Klinik mit Schwerpunkt Hepatologie und Gastroenterologie, Berlin, Germany; ²EF CLIF, Barcelona, Spain; ³Charité-Universitätsmedizin Berlin, corporate member of Freie Universität Berlin and HumboldtUniversität zu Berlin, Institut für Laboratoriumsmedizin, Klinische Chemie und Pathobiochemie, Berlin, Germany; ⁴LABOR BERLIN-CHARITÉ VIVANTES GMBH, Fachbereich Laboratoriumsmedizin und Toxikologie, Berlin, Germany; ⁵University College London, Royal Free Campus, Liver Failure Group, Institute for Liver and Digestive Health, London, United Kingdom; ⁶Universitätsklinikum Leipzig, Klinik und Poliklinik für Onkologie, Gastroenterologie, Hepatologie, Pneumologie und Infektiologie Bereich Hepatologie, Leipzig, Germany; ⁷University Hospital of Leipzig, Division of Hepatology, Department of Medicine II, Germany

Email: cornelius.engelmann@charite.de

Background and aims: Liver cirrhosis represents a major health burden and decompensation may lead to acute-on-chronic liver failure (ACLF) with high morbidity and mortality. Reliable biomarkers predicting the course of the disease are urgently needed in order to

POSTER PRESENTATIONS

tailor treatment strategies. Expression of urokinase plasminogen activator receptor (uPAR, CD87) and the release of its soluble variant, the cleaved soluble uPAR (suPAR), showed to be related to systemic inflammation in liver disease. Therefore, we were seeking to evaluate suPAR as a predictive marker for the outcome in ACLF.

Method: In a retrospective study plasma suPAR concentrations were measured in two different academic centers in a derivation cohort (n = 178 (healthy controls (n = 6), compensated cirrhosis (n = 17), decompensated cirrhosis (n = 120) or ACLF (n = 35)) and a validation cohort (n = 197 (decompensated cirrhosis (n = 135) or ACLF (n = 62))). SuPAR levels were analyzed with suPARnostic® TurbiLatex (Nr. T004, suPARnostic, ViroGates, Birkerød, Denmark) on a Cobas c501/502 clinical chemistry analyzer (Roche Diagnostics Ltd., Burgess Hill, UK). Clinical data was obtained from patients medical records. Primary end point were death and disease dynamics during hospitalization.

Results: In the derivation cohort, 60.1% of patients were male, 36.5% female and in 3.4% no information on gender was provided. Alcohol related liver disease was the most common etiology before NASH and viral hepatitis. Median suPAR levels were significantly higher in patients with decompensated cirrhosis (13.7 ng/ml) and ACLF (20.0 ng/ml) compared to compensated cirrhosis (6.65 ng/ml) and healthy controls (1.9 ng/ml) (p < 0.001). Mortality during hospitalization was 13.7% in decompensated cirrhosis and 34.3% in ACLF. SuPAR levels showed a statistical significant correlation with other parameters indicating disease severity: Creatinine (r = 0.209, p < 0.012), Bilirubin (r = 0.473, p < 0.001), Albumin (r = -0.247, p < 0.02), INR (r = 0.323, p < 0.001), ALT (r = 0.273, p = 0.001) as well as disease severity scores such as MELD score (r = 0.486, p < 0.001) and CLIF-C ACLF score in ACLF patients (r = 0.454, p < 0.001) and duration of hospitalization (r = 0.361, p < 0.001). SuPAR levels ≥ 14.1 ng/ml were associated with a higher in hospital mortality (p = 0.020, sensitivity: 75.0%, specificity: 50.8%, AUC = 0.641), need for ICU treatment (p < 0.001) and 90 days mortality (p = 0.003) and in patients with decompensated cirrhosis higher suPAR levels indicated a higher risk of developing ACLF (p = 0.014). These findings were validated in our second cohort: higher suPAR levels indicated a higher 28 days mortality (p < 0.001) as well as 90 days mortality (p < 0.001) and in Cox-Regression a lower survival (p < 0.001, HR = 1.012).

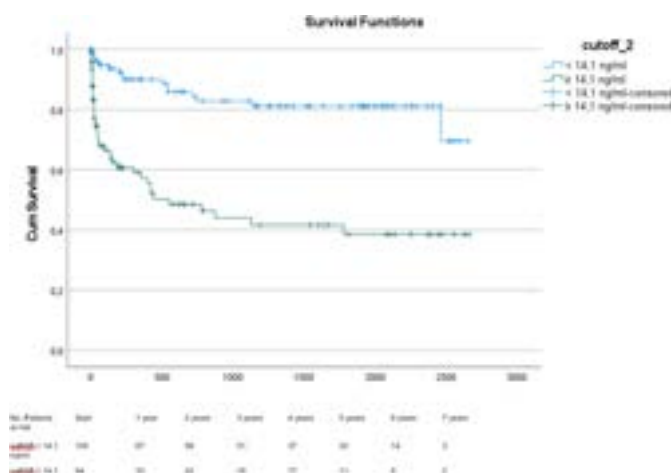


Figure:

Conclusion: SuPAR might be used as biomarker for outcomes in patients with ACLF and acute decompensated liver cirrhosis indicating disease severity.

FRI-550

ACLF course profiles over screening period in the phase IIb

DHELIVER study

Frederik Nevens¹, Dominique Thabut^{2,3}, Marika Rudler^{4,5}, Lannes Adrien⁶, Luc Lasser⁷, Vadim Brjalín⁸,

Georges-Philippe Pageaux⁹, Ewa Janczewska¹⁰, Pierluigi Toniutto¹¹, Javier Martinez¹², Thomas Reiberger¹³, Jordi Sánchez-Delgado¹⁴, Víctor Vargas¹⁵, Thierry Gustot¹⁶, Benjamin Maasoumy¹⁷, Henning Grønbaek¹⁸, Tony Bruns¹⁹, Christophe Bureau²⁰, Kalina Grivcheva Stadelova²¹, Desislava Pavlova²², Ivaylo Nikolov²³, Krum Katzarov²⁴, Ventseslav Draganov²⁵, Vanesa Bernal Monterde²⁶, Noelia Gordillo²⁷, Yelena Vainilovich²⁷, Mustapha Najimi^{27,28}, Virginie Barthel²⁷, Frederic Lin²⁷, Etienne Sokal^{27,29}. ¹University Hospital Gasthuisberg, KU Leuven, Hepatology, Belgium; ²Groupement Hospitalier APHP-Sorbonne Université, Hôpital de la Pitié-Salpêtrière, Unité de Soins Intensifs d'Hépatogastro-Entérologie, Paris, France; ³Sorbonne Université, INSERM, Centre de Recherche Saint-Antoine (CRSA), Institute of Cardiometabolism and Nutrition (ICAN), Paris, France; ⁴Groupement Hospitalier APHP-Sorbonne Université, Hôpital de la Pitié-Salpêtrière, Unité de Soins Intensifs d'Hépatogastro-Entérologie, Paris, France; ⁵Sorbonne Université, INSERM, Centre de Recherche Saint-Antoine (CRSA), Institute of Cardiometabolism and Nutrition (ICAN), Paris, France; ⁶CHU Angers, Hepatology Department, Angers, France; ⁷CHU Brugmann (Site Horta), Gastroenterology Service, Belgium; ⁸West Tallinn Central Hospital, Estonia; ⁹CHU Montpellier, Pôle Digestif, France; ¹⁰ID Clinic, Myslowice, Poland; ¹¹ASU Friuli Centrale, Hepatology and Liver Transplant Unit, Udine, Italy; ¹²University Hospital Ramón y Cajal, Hepatology, Madrid, Spain; ¹³Medical University Vienna, Department of Internal Medicine III, Division of Gastroenterology and Hepatology, Vienna, Austria; ¹⁴Hospital Parc Taulí Sabadell, Department Hepatology, Sabadell, Spain; ¹⁵Hospital Vall d'Hebron, Universitat Autònoma, Hepatology, Barcelona, Spain; ¹⁶C.U.B. Hôpital Erasme, Gastroenterology and Hepato-Pancreatology, Brussels, Belgium; ¹⁷Medical University Hannover, Clinic for Gastroenterology, Hepatology and Endocrinology, Hannover, Germany; ¹⁸Aarhus University Hospital, Department of Hepatology and Gastroenterology, Aarhus, Denmark; ¹⁹University Hospital Aachen RWTH, Internal Medicine III/ Gastroenterology and Hepatology, Aachen, Germany; ²⁰Hôpital Rangueil 1, Hepatology, Toulouse, France; ²¹PHI University Clinic of Gastroenterology, Skopje, Macedonia; ²²UMHAT Dr. Georgi Stranski, Gastroenterology Dept., Pleven, Bulgaria; ²³UMHAT Sveta Anna, Gastroenterology, Sofia, Bulgaria; ²⁴MMA-Sofia, Gastroenterology, Sofia, Bulgaria; ²⁵UMBAL Medica, Russe, Bulgaria; ²⁶Hospital Miguel Servet, Gastroenterology and Digestive, Zaragoza, Spain; ²⁷Cellaion, Belgium; ²⁸Laboratory of Pediatric Hepatology and Cell Therapy, Institute of Experimental and Clinical Research (IREC), UCLouvain, Brussels, Belgium; ²⁹Saint-Luc University Clinics, Belgium
Email: etienne.sokal@cellaion.com

Background and aims: Acute-on-chronic liver failure (ACLF) is a syndrome characterised by acute decompensation of cirrhosis associated with organ failures and high mortality. ACLF exhibits dynamic clinical course with final ACLF grade (G) defined 3 to 7 days after initial diagnosis in 81% of patients (Gustot, 2015). DHELIVER study is an ongoing Phase IIb RCT double-blinded POC trial that aims to demonstrate the efficacy of HepaStem® on overall survival in patients with persistent ACLF G1 and G2. The purpose of current analysis is to study evolution of ACLF during screening and to describe patients' characteristics.

Method: Consented patients were re-assessed at the end of screening period, 3 to 7 days after initial ACLF diagnosis (according to EASL-CLIF definition). Only patients with confirmed G1 and G2 were randomized.

Results: Up to 26-JAN-2023, 96 patients with ACLF (69 M/27 F), aged 52.5 years (range: 25–73), were screened in 23 sites in 11 European countries: 61 G1 and 35 G2. During screening (3 to 7-days) ACLF recovered or improved in 27 patients (28.1%), stable clinical course was in 57 patients (59.4%) and 12 patients worsened (12.5%). By ACLF grade: among G1, ACLF resolved in 39.3%, was stable in 49.2%, and worsened in 11.5% (9.8% to G2 and 1.6% died); while among G2, clinical course of ACLF was stable in 77.1%, worsened in 14.3% (2.9% to G3 and 11.4% died), and improved in 8.6% (2.9% to G0 and 5.7% to G1). Fifty-five patients (34 G1 and 21 G2) were enrolled; 41 (27 G1 and 14

G2) were screen failures, mostly because their condition resolved (61.0%, 24 G1 and 1 G2) or worsened/died (14.6%; 1 G1 and 4 G2 died, 1 G2 to G3). Enrollment criteria were not met for 10 patients (24.4%). The etiology of cirrhosis was mainly alcohol (88.5%). Other etiologies included NASH (2.1%), a combination of alcohol with viral (HCV or HBV) infection, hemochromatosis, or NASH (5.2%) or were unknown (4.2%). Patients with alcohol etiology were slightly younger compared to other etiologies (52.0 vs 56.3 years) and had more pronounced biochemical (e.g., total bilirubin: 20.2 vs 9.4 mg/dL) or hematological (e.g., WBC: 12.7 vs 10.0 G/L) alterations. Precipitating events of ACLF were mostly acute alcoholic hepatitis/active alcoholism (71.0%; 43.8% of them were on steroids) and bacterial infection (29.3%). Other trigger events were GI bleeding (3.1%), DILI (2.1%), or unknown (13.5%). Organ failures affected mainly the liver (68.8%), coagulation (46.9%), and kidney (8.3%). Most patients with G1 had liver failure (57.4%), primarily associated with mild or moderate hepatic encephalopathy (HE) (85.7%).

	Randomized		Screen failures	
N	55		41	
Age	52.0 ± 10.7		53.1 ± 9.5	
M/F	42/13		27/14	
	G1	G2	G1	G2
Initial ACLF grade	34	21	27	14
Stable	28 (82.4%)	19 (90.5%)	2 (7.4%)	8 (57.1%)
Improved	-	2 (9.5%)	24 (88.9%)	1 (7.1%)
Worsened	6 (17.6%)	-	1 (3.7%)	5 (35.7%)
T-BIL (mg/dL)	21.5 ± 10.5 ²		15.9 ± 9.0 ²	
WBC (G/L)	13.8 ± 7.7 ¹		10.4 ± 5.9 ²	
CRP (mg/L)	36.6 ± 26.1 ²		33.4 ± 38.6 ¹⁰	
INR	2.3 ± 0.7		2.5 ± 0.8 ⁴	
CLIF-ACLF score	49.8 ± 5.2		47.5 ± 8.0 ²	

*: information missing for x patients

Figure:

Conclusion: This prospective study confirms the variable and highly dynamic course of the disease in patients with ACLF G1 and G2 over the 3 to 7-day period post initial diagnosis. Improvement was most commonly observed in patients with ACLF G1 (39.3% vs 8.6% in G2). The most common etiology of cirrhosis was alcohol-related liver disease. Hepatic failure represented the most common type of organ failure, characterized by high level of bilirubin associated with HE.

FRI-551

Lower free and total serum cortisol levels are associated with higher risk of bacterial infection and acute-on-chronic liver failure in stable outpatients with advanced chronic liver disease

Lukas Hartl^{1,2}, Benedikt Simbrunner^{1,2,3}, Mathias Jachs^{1,2}, Peter Wolf⁴, David Jm Bauer^{1,2}, Bernhard Scheiner^{1,2}, Lorenz Balcar^{1,2}, Georg Semmler^{1,2}, Michael Schwarz¹, Rodrigo Marculescu⁵, Michael Trauner¹, Matthias Mandorfer^{1,2}, Thomas Reiberger^{1,2,3}.

¹Division of Gastroenterology and Hepatology, Department of Medicine III, Medical University of Vienna, Vienna, Austria; ²Vienna Hepatic Hemodynamic Lab, Division of Gastroenterology and Hepatology, Department of Medicine III, Medical University of Vienna, Vienna, Austria; ³Christian Doppler Lab for Portal Hypertension and Liver Fibrosis, Division of Gastroenterology and Hepatology, Department of Medicine III, Medical University of Vienna, Vienna, Austria; ⁴Division of Endocrinology, Department of Medicine III, Medical University of Vienna, Vienna, Austria; ⁵Department of Laboratory Medicine, Medical University of Vienna, Vienna, Austria

Email: thomas.reiberger@meduniwien.ac.at

Background and aims: We aimed to evaluate the prognostic value of free (f-Cort) and total serum cortisol (t-Cort) in a cohort of stable outpatients with advanced chronic liver disease (ACLD).

Method: We included consecutive outpatients with ACLD and hepatic venous pressure gradient (HVPG) measurement within the prospective VICIS (NCT03267615) study. Exclusion criteria were HVPG

<6 mmHg, hepatocellular carcinoma, vascular liver disease, occlusive portal vein thrombosis, a history of liver transplantation, evidence of infection and intake of corticosteroids. Competing risk regression was performed considering liver transplantation and death (or non-liver-related death, as appropriate) as competing events.

Results: In total, 151 patients (compensated ACLD: n = 61; decompensated ACLD: n = 90) were included. There was a strong correlation between f-Cort and t-Cort (Spearman's rho: 0.893). Lower levels of f-Cort and t-Cort independently predicted bacterial infections (f-Cort: aHR per ng/ml: 0.89; p = 0.014/t-Cort: aHR per µg/dL: 0.91, p = 0.003) and acute-on-chronic liver failure (ACLF; f-Cort: aHR per ng/ml: 0.84; p = 0.003/t-Cort: aHR per µg/dL: 0.90, p = 0.001). Youden's index determined f-Cort <4.8 ng/ml and t-Cort level <12.0 µg/dL as ideal cutoffs for the prediction of ACLF. Overall, 69/146 (47.3%) and n = 95/151 (62.9%) patients exhibited f-Cort <4.8 ng/ml and t-Cort <12 µg/dL, respectively. Patients with f-Cort <4.8 ng/ml tended to exhibit a more advanced clinical stage of ACLD (p = 0.095) and patients with t-Cort <12 µg/dL tendentially had more severe ACLD (CTP score: ≥12 µg/dL: 6.0 points vs. <12 µg/dL: 7.0 points; p = 0.053) and more pronounced portal hypertension (HVPG: ≥12 µg/dL: 15 mmHg vs. <12 µg/dL: 18 mmHg; p = 0.073). With low t-Cort (i.e. <12 µg/dL), the cumulative incidences of bacterial infections (p = 0.026), (further) decompensation (p = 0.028), and ACLF (p = 0.005) were significantly higher (Figure), with similar-but non-significant-trends observed for low f-Cort <4.8 ng/ml. Both f-Cort <4.8 ng/ml and t-Cort <12 µg/dL were independently linked to increased risk of bacterial infections (f-Cort <4.8 ng/ml: aHR: 2.11; 95%CI: 1.06–4.23; p = 0.034/t-Cort <12 µg/dL: aHR: 2.91; 95%CI: 1.12–7.00; p = 0.017), (further) decompensation (f-Cort <4.8 ng/ml: aHR: 2.23; 95%CI: 1.27–3.91; p = 0.005/t-Cort <12 µg/dL: aHR: 1.87; 95%CI: 1.06–3.30; p = 0.032) and ACLF (f-Cort <4.8 ng/ml: aHR: 2.45; 95%CI: 1.16–5.19; p = 0.019/t-Cort <12 µg/dL: aHR: 3.51; 95%CI: 1.35–9.10; p = 0.009).

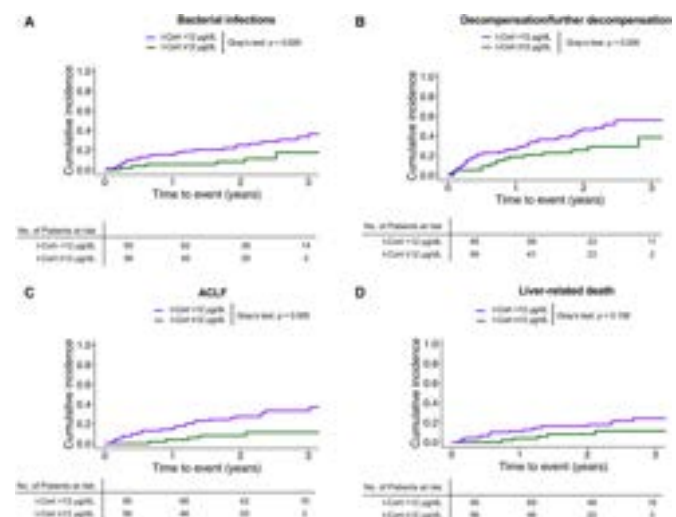


Figure:

Conclusion: Lower levels of both f-Cort and t-Cort are independently linked to bacterial infections and ACLF in patients with ACLD, possibly due to an impaired stress response. Moreover, f-Cort <4.8 ng/ml and t-Cort <12 µg/dL identify stable patients with ACLD with a particularly high risk of adverse outcomes.

FRI-552

Acute on chronic liver failure is associated with prolonged clot initiation in rotational thromboelastometry as compared to acute decompensation, but clot formation time and firmness are similar

Tian Yu Qiu¹, Louis Wang¹, Chin Kim Tan¹, Eugene Wong¹, Kenneth Lin¹, Andrew Kwek¹, James Weiquan Li¹, Tiing Leong Ang¹, Roshni Sahashiv², Louis Ng³, Prasanna Tirukonda⁴, Rahul Kumar¹.

POSTER PRESENTATIONS

¹Changi General Hospital, Gastroenterology and hepatology, Singapore;

²Changi General Hospital, Internal Medicine, Singapore; ³Changi General Hospital, Anaesthesia & Surgical Intensive Care, Singapore;

⁴Changi General Hospital, Diagnostic Radiology, Singapore

Email: rahul.kumar@singhealth.com.sg

Background and aims: Viscoelastic Test (VET) such as Rotational Thromboelastometry (ROTEM) is increasingly used in cirrhosis to guide blood product transfusion strategies as compared to conventional coagulation tests (CCT). Although ROTEM successfully reduced transfusion requirements, there is little clarity around changes in ROTEM parameters with severity of presentation i.e., Acute Decompensation (AD) or Acute on Chronic Liver Failure (ACLF). We aim to compare coagulation panel amongst AD and ACLF population using ROTEM.

Method: This is a single-center observational study conducted from August 2021 to December 2022 which included all patients admitted for AD or ACLF (defined based on EASL-CLIF classification). ROTEM, CCT and severity of liver disease (Child-Pugh score and MELD score) of both groups were collected and compared. Data was analyzed using standard statistical tests in SPSS.

Results: A total of 54 participants were included (38 in AD and 16 in ACLF group). The results are shown in Table 1. The mean age was 60.3 ± 10.5 years and 77.8% were males. Child-Pugh score and MELD scores among AD vs ACLF were (10.0 vs 10.5; $p = 0.227$) and (15.82 vs 23.25; $p = <0.001$) respectively. CCT showed marked derangements in PT (15.05 seconds (s) vs 18.20 s; $p = 0.012$) and aPTT (35.29 s vs 51.12 s; $p = <0.001$) but platelet and fibrinogen levels were comparable. ($p = NS$). Comparison of ROTEM parameters between groups showed initiation of clot formation was delayed in ACLF patients as evidenced by statistically significant prolongation of clotting time (CT) in INTEM (205.86 s vs 258.13 s; $p = <0.001$), EXTEM (73.39 s vs 91.06 s; $p = 0.022$) and FIBTEM (78.00 s vs 139.13 s; $p = 0.013$). However, interestingly clot formation time (CFT) in INTEM (132.83 s vs 165.44 s) and EXTEM (121.36 s vs 156.63 s) were similar between groups ($p = NS$), as was maximal clot firmness (MCF) in INTEM (48.75 millimeter (mm) vs 48.31 mm), EXTEM (50.25 mm vs 49.75 mm) and FIBTEM (11.69 mm vs 12.44 mm), ($p = NS$).

This data suggests that although there is a significant delay in clot initiation in ACLF patients, clot formation is not affected and the clot is as strong as in patients with AD. These findings have practical implications for ACLF patients undergoing either elective procedures or actively bleeding, as they should not be over transfused just to correct the delayed clot initiation. Another novel finding is although low fibrinogen levels were detected in AD, patients with ACLF had normal levels ($p = NS$). We cannot fully explain this finding mechanistically and it will require further exploration.

Table 1: Comparison of baseline characteristics, CCT and ROTEM parameters between AD and ACLF patients

Demographics	Normal values/ranges	All Patients (N=54)	AD (n=38)	ACLF (n=16)	P-value
Age, years ¹	-	60.32 (10.48)	59.03 (10.81)	63.38 (9.24)	0.170
Male ²	-	42 (77.78)	32 (84.21)	10 (62.50)	0.348
Organ Failures	-	-	-	-	-
Respiratory ³	-	2 (3.70)	1 (2.63)	1 (6.25)	<0.500
Brain ⁴	-	2 (3.70)	1 (2.63)	1 (6.25)	0.500
Liver ⁴	-	5 (9.26)	2 (5.26)	3 (18.75)	0.348
Cardiovascular ⁴	-	4 (7.41)	1 (2.63)	3 (18.75)	0.670
Coagulation ⁴	-	2 (3.70)	1 (2.63)	1 (6.25)	0.633
Renal ⁴	-	1 (1.85)	0 (0)	1 (6.25)	<0.003
Baseline laboratory results and CCT	-	-	-	-	-
Platelets ($\times 10^9/L$) ⁵	150-450	84.70 (52.23)	95.58 (57.82)	62.68 (38.54)	0.401
aPTT (sec) ⁶	24-34	39.98 (11.54)	35.29 (7.40)	51.12 (17.73)	<0.002
PT (sec) ⁶	9.5-12.5	15.05 (4.27)	15.05 (2.97)	18.20 (5.83)	0.012
Fibrinogen (g/L) ⁷	3.0-4.0	1.75 (0.93)	1.64 (0.726)	1.91 (1.31)	0.435
WBC ($\times 10^9/L$) ⁸	4-11	7.44 (5.24)	7.34 (5.25)	8.96 (5.13)	0.346
CRP (mg/L) ⁹	<3.0	38.86 (29.88)	36.94 (29.88)	52.96 (29.48)	0.538
Prothrombin (mg/L) ¹⁰	<0.5	0.86 (0.14)	0.51 (0.18)	1.37 (0.84)	0.049
MELD Score ¹¹	6-40	18.82 (6.12)	15.82 (5.88)	23.25 (11.75)	<0.002
Child-Pugh Score ¹²	5-15	10.00 (2.00)	10.00 (4.00)	10.50 (1.75)	0.217
ROTEM parameters	-	-	-	-	-
INTEM CT (sec) ¹³	181-264	223.94 (42.32)	205.86 (37.28)	258.13 (48.34)	<0.001
INTEM CFT (sec) ¹⁴	62-136	142.23 (39.78)	132.83 (36.56)	165.44 (22.35)	0.098
INTEM A5 (mm) ¹⁵	33-52	31.93 (8.48)	33.42 (7.93)	30.41 (9.88)	0.535
INTEM A10 (mm) ¹⁶	43-62	41.82 (9.11)	42.06 (8.42)	40.43 (10.52)	0.806
INTEM MCF (mm) ¹⁷	51-69	48.82 (8.93)	48.75 (8.36)	48.31 (10.38)	0.878
EXTEM CT (sec) ¹⁸	50-80	78.81 (25.98)	73.39 (21.23)	91.06 (17.12)	0.022
EXTEM CFT (sec) ¹⁹	46-149	121.36 (39.73)	121.36 (36.22)	156.63 (18.13)	0.094
EXTEM A5 (mm) ²⁰	32-52	34.73 (9.19)	35.08 (8.53)	33.94 (10.78)	0.682
EXTEM A10 (mm) ²¹	43-63	43.25 (9.78)	43.58 (8.96)	42.50 (11.52)	0.714
EXTEM MCF (mm) ²²	55-72	50.30 (9.37)	50.25 (8.67)	49.75 (11.28)	0.861
FIBTEM CT (sec) ²³	66-84	96.81 (33.98)	78.00 (34.24)	139.13 (33.88)	0.013
FIBTEM CFT (sec) ²⁴	5-30	9.32 (4.78)	9.94 (6.42)	9.80 (7.73)	0.962
FIBTEM A5 (mm) ²⁵	6-21	11.69 (5.32)	11.00 (4.82)	11.75 (8.48)	0.877
FIBTEM MCF (mm) ²⁶	6-21	11.82 (6.05)	11.69 (5.52)	12.44 (7.28)	0.718

Legend:

SD = mean (SD)

Q3 = median (Q3)

% = number (%)

Figure:

Conclusion: Our prospective exploratory study shows that in patients with ACLF as compared to AD, based on ROTEM parameters, although clot initiation is delayed, clot formation and strength of clot remains similar. Further studies are needed to validate our findings.

FRI-553

Even small amounts of alcohol consumption can worsen the prognosis in acutely decompensated patients with viral hepatitis

Jung Hee Kim¹, Sung-Eun Kim¹, Jang Han Jung¹, Hyoung Su Kim¹, Eileen Yoon², Jae Young Jang³, Dong Joon Kim¹. ¹Hallym University College of Medicine, Korea, Rep. of South; ²Hanyang University College of Medicine, Korea, Rep. of South; ³Soonchunhyang University College of Medicine, Korea, Rep. of South

Email: sekim@hallym.or.kr

Background and aims: Acute decompensation (AD), especially accompanied by dysfunction of other organs, is a common cause of death or liver transplantation (LT) in chronic liver disease (CLD). However, when comparing the aetiology of CLD, little is known about how aetiology affects the adverse outcomes of AD in CLD.

Method: The prospective Korean Acute-on-Chronic Liver Failure (KACLiF) cohort consisted of 1,501 patients who were hospitalized with AD of CLD, including either liver cirrhosis (LC) or noncirrhotic CLD, from July 2015 to August 2018. We compared their clinical characteristics and analysed 28-day/overall adverse outcomes according to the aetiology of CLD.

Results: There was a median follow-up of 8.0 months (1.0–16.0 months), the mean age was 54.7 years, and 74.5% of patients were male. Cirrhosis was confirmed in 93.2% of patients. The most common aetiology of CLD was alcohol-related CLD (n=1021), followed by viral hepatitis CLD (n=206), viral hepatitis with alcohol-related CLD (n=129), cryptogenic CLD (n=108) and autoimmune-related CLD (n=37). Viral hepatitis with alcohol-related CLD showed a poor liver function profile and a high frequency of acute-on-chronic liver failure (ACLF) (22.1%), with worse 28-day/overall adverse outcomes than other aetiologies. The difference in aetiology was a significant factor for 28-day adverse outcomes in multivariate analysis. In the subgroup analysis according to MELD, the differences in aetiology were stratified into 28-day adverse outcomes among patients with a high MELD score (≥ 15) ($p = 0.001$). Patients who

consumed alcohol or more than a small amount of alcohol (males, >20 g/day, females, >40 g/day) showed the most increased 28-day adverse outcomes of viral hepatitis with alcohol-related CLD. In addition, patients who did not drink or drank small amounts of alcohol showed increased overall adverse outcomes of viral hepatitis with alcohol-related CLD compared with viral hepatitis or alcohol-related hepatitis.

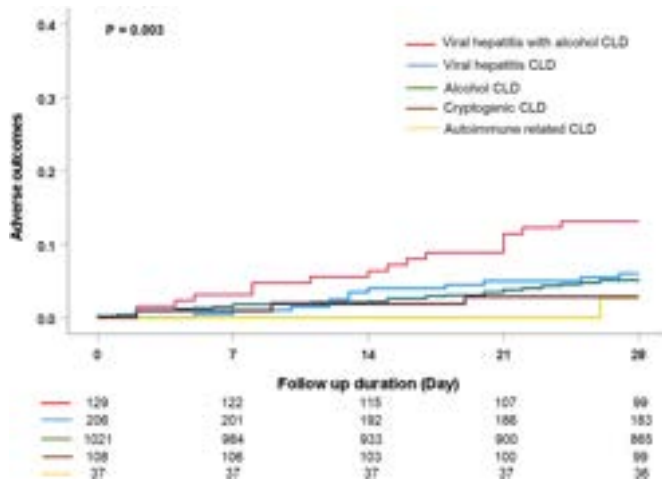


Figure 28: 28-days adverse outcome according to etiology of CLD

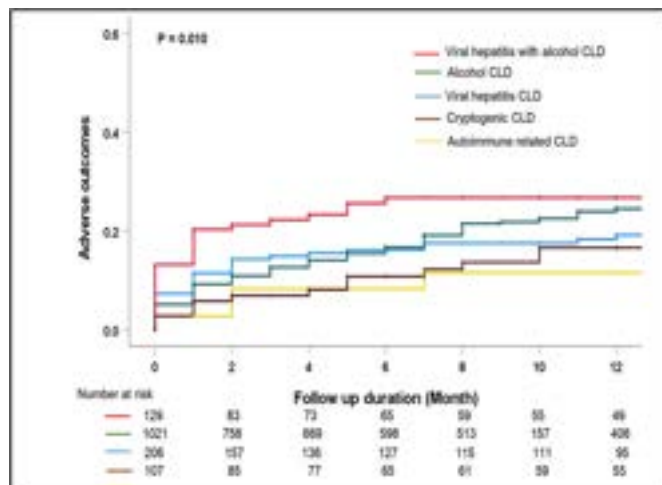


Figure 30: Overall adverse outcome according to etiology of CLD

	28 days adverse outcomes (%)				Overall adverse outcomes (%)			
	Viral	Alcohol	Viral related	p	Viral	Alcohol	Viral related	p
Current alcohol use								
No (n=389)	11/175 (6.2)	6/191 (3.1)	3/19 (1.5)	0.203	32/177 (18.1)	46/191 (24.1)	13/19 (6.8)	0.008
Yes (n=644)	109 (16.4)	43 (6.7)	13 (2.0)	0.004	82 (12.7)	18 (2.8)	27 (4.2)	0.201
Alcohol amount								
None -<40g (n=439)	12/183 (6.5)	10/196 (5.1)	6/19 (3.1)	0.108	34/183 (18.5)	72/196 (36.7)	17/19 (8.8)	0.008
More than 40g (n=205)	97 (47.4)	33 (16.1)	7 (3.4)	0.004	48 (23.4)	18 (8.7)	6 (2.9)	0.001

Table. Association with alcoholic intake and adverse outcomes

Conclusion: The aetiology of CLD is a valuable factor that affects short- and long-term adverse outcomes of AD in CLD, even among patients with high MELD scores. Thus, the aetiology of CLD, especially viral hepatitis with alcohol related CLD, should be considered when determining the priority of LT together with the MELD system for patients with AD of CLD. Additionally, patients with viral hepatitis should be careful even with small amounts of alcohol intake, which can cause aggravating adverse outcomes of AD.

FRI-554

High histamine levels associate with acute-on-chronic liver failure and liver-related death in patients with advanced chronic liver disease

Michael Schwarz^{1,2}, Benedikt Simbrunner^{1,2}, Mathias Jachs^{1,2}, Lukas Hartl^{1,2}, Bernhard Scheiner^{1,2}, Rafael Paternostro^{1,2}, David Jm Bauer^{1,2}, Matthias Pinter^{1,2}, Albert Stättermayer^{1,2}, Michael Trauner¹, Thomas Reiberger^{1,2}, Mattias Mandorfer^{1,2}.

¹Medical University of Vienna, Department of Internal Medicine III, Division of Gastroenterology and Hepatology, Austria; ²Medical University of Vienna, Department of Internal Medicine III, Division of Gastroenterology and Hepatology, Vienna Hepatic Hemodynamic Lab, Austria

Email: mattias.mandorfer@meduniwien.ac.at

Background and aims: Mast cells have been implicated in liver disease progression. The role of plasma histamine in advanced chronic liver disease (ACLD) is not fully understood, but may pose a potential target for pharmacological intervention.

Method: Patients (pts) included in the prospective Vienna Cirrhosis Study (VICIS) who underwent hepatic venous pressure gradient (HVPG) measurement (=baseline, BL) from April 2017 until March 2020 were considered. Inclusion criteria were portal hypertension (HVPG ≥6 mmHg) and/or a liver stiffness measurement by vibration-controlled transient elastography ≥10 kPa.

Results: Of the 251 included pts, 167 (66.5%) were male and median age was 58.5 years (IQR 49.8–67.0). The most common etiologies were alcohol-related liver disease (102 pts, 40.6%) and viral hepatitis (51 pts, 20.3%). Child-Turcotte Pugh (CTP) stages were: A 142 pts (56.6%), B 84 pts (33.5%), and C 25 pts (10.0%). A quarter of pts (67, 26.7%) had a model for end-stage liver disease (MELD) score ≥15 and half of pts were decompensated at BL (135 pts, 53.8%).

Median plasma histamine was 8.5 nmol/L (IQR 6.3–11.5) and 37.1% of patients had values above the upper normal limit (i.e., 9.9 nmol/L). Interestingly, histamine levels did not differ significantly across CTP, MELD, or HVPG strata. However, histamine concentrations showed weak positive correlations with markers of circulatory dysfunction (i.e., plasma renin and serum sodium).

During a median follow-up of 28.9 months, 69 patients developed acute-on-chronic liver failure (ACLF) or liver-related death. In univariate Cox proportional-hazards model, BL plasma histamine levels were predictive of overall mortality (hazard ratio [HR]: 1.021 per nmol/L; 95% confidence interval [95%CI]: 1.005–1.038; p = 0.010) as well as ACLF or liver-related death (HR: 1.023; 95%CI: 1.007–1.039; p = 0.004). When adjusting for either MELD, clinical stage, and serum albumin or CTP and serum sodium as well as age, sex, and HVPG, histamine levels remained associated with ACLF or liver-related death: CTP-based model: 1.033 (95%CI 1.014–1.053), p < 0.001; MELD-based model: 1.030 (95%CI 1.010–1.050), p 0.003 (Figure).

Conclusion: High plasma levels of histamine were linked to circulatory dysfunction and associated with increased risks of ACLF and liver-related death during follow-up. Further studies investigating the underlying mechanism (i.e., mast cell activation vs. decreased degradation) and the implications of histamine for hyperdynamic circulation and ACLF development are warranted.

FRI-555

Detection of 1,3-beta-D-glucan increases with the severity of decompensation stages in liver cirrhosis and is associated with lower survival in patients with acute on chronic liver failure

Adam Herber¹, Janett Fischer¹, Cornelius Engelmann², Niklas F Aehling¹, Rhea Veelken¹, Sirak Petros³, Lorenz Weidhase³, Thomas Berg¹, Florian van Bömmel¹. ¹Leipzig University Medical Center, Division of Hepatology, Department of Medicine II, Leipzig, Germany; ²Campus Charité Mitte/Campus Virchow-Klinikum, Department of Hepatology and Gastroenterology, Germany; ³University Hospital Leipzig, Medical Intensive Care Unit, Germany

Email: adam.herber@medizin.uni-leipzig.de

POSTER PRESENTATIONS

Background and aims: Increased intestinal permeability (IP) and translocation of pathogen associated molecular patterns (PAMPs) are factors contributing to the pathogenesis and outcomes of acute-on-chronic liver failure (ACLF). The polysaccharide 1,3- β -D-glucan (BDG) is a potential marker for increased IP. We have studied the correlation of BDG in patients with different stages of chronic liver disease.

Method: A total 230 individuals including 98 CLIF-ACLF patients (mean MELD score 27 ± 8 , ACLF grade 1: n = 59, grade 2: n = 23, grade 3: n = 16), 84 patients with decompensated cirrhosis with ascites (mean MELD score 16 ± 6), 24 with compensated cirrhosis (mean MELD 12 ± 6) (76% male, mean age 57 ± 9 years, 77% alcohol related liver disease), and 24 controls were prospectively enrolled. Blood samples from patients were collected during the hospital stay and stored at -20°C . BDG levels were measured in the serum (n = 230) and, if available, in corresponding duodenal fluids samples (n = 125) by Kinetic Turbidimetric Assay (FUJIFILM Wako, Japan, LOD = 2.57 pg/ml) and correlated with outcomes.

Results: BDG was more frequently detected in serum samples from ACLF patients (42/98, (43%)) than in patients with decompensated cirrhosis (23/84 (27%), $p = 0.03$), compensated cirrhosis (3/24, (12%), $p = 0.008$) or healthy controls (2/24 (8%), $p = 0.002$). The BDG-detection rate correlated with the ACLF grade (ACLF 1: 120/59 (34%), ACLF 2: 10/23 (43%) and ACLF 3: 12/16 (75%); ACLF 1 vs. ACLF 3 $p = 0.0004$). The mean serum BDG concentration was higher in ACLF 3 than in ACLF 1 patients (22.6 ± 19.1 vs. 16.2 ± 27.31 pg/ml, $p = 0.0003$). In contrast, in duodenal fluid samples the frequency of BDG detection was similar across all groups (79–100%). Within the ACLF group, mean 60-day, 90-day ($31.7 \pm 8.3\%$ vs. $59.5 \pm 6.9\%$; $p = 0.012$) and overall survival were significantly lower in patients with detectable BDG compared to those without BDG. In a multivariate Cox-regression analysis for 90-day mortality adjusted for ACLF grade and MELD, the detection of BDG in serum showed an OR of 19.0 (95% CI 4.0–90.9), $p = 0.0002$. In all patients, there was one microbiologically proven fungal infection in blood samples.

Conclusion: The serum BDG detection rate increases with increasing severity of chronic advanced liver disease and this serum marker is associated with significantly reduced survival in patients with ACLF. Serum BDG might be a marker of intestinal permeability and its potential for personalized patient management should be addressed in further studies.

FRI-556

Parvovirus B19 infection associated with adverse outcomes in decompensated cirrhosis patients

Changze Hong¹, Beiling Li¹, xiaojing wang², Yanhang Gao³, wei yuan⁴, Qinjun He¹, Xiaojin Lan¹, Qintao Lai¹, Wenfan Luo¹, Tingting Qi¹, Jinjun Chen^{1,5}. ¹Hepatology Unit, Department of Infectious Diseases, Nanfang Hospital, Southern Medical University, Guangzhou, China, China; ²Centre of Integrative Medicine, Beijing Ditan Hospital, Capital Medical University, Beijing, China, China; ³Department of Hepatology, The First Hospital of Jilin University, Jilin University, Changchun, China, China; ⁴Department of Liver Intensive Care Unit, Shanghai Public Health Clinical Centre, Fudan University, Shanghai, China., China; ⁵Hepatology Unit, Zengcheng Branch, Nanfang Hospital, Southern Medical University, Guangzhou, China, China
Email: chjj@smu.edu.cn

Background and aims: Cirrhotic patients are characterized by cirrhosis associated immune dysfunction and have a non-hepatotropic viral signature which correlates with clinical progression and poor outcomes. Human parvovirus B19 (B19V), a non-hepatotropic virus, is rarely reported in cirrhotic patients and its potential pathogenic role remains unknown. This study aims to assess the clinical characteristics and outcomes of B19V infection in decompensated cirrhosis.

Method: Acutely decompensated cirrhosis patients were recruited from two prospective, multi-center cohort study (from 2015 to 2020 and from 2021 to 2022, respectively). Demographics, laboratory data, antibiotic treatment and outcomes (death or transplant) were recorded. Metagenomic next-generation sequencing (mNGS) for plasma microbial cell-free DNA was performed in this study. According to the detection of plasma mNGS, patients with B19V or without any pathogens detectable (including only HBV detected) were included in analysis and were divided into “B19V positive” and “B19V negative” groups. Outcomes of patients with and without B19V infection were compared for transplant censored 28-day mortality by Log-rank test.

Results: Totally, 273 patients were enrolled. The mean age was 52 ± 11 years and male (81.3%) were predominant. HBV (71.1%) was the common etiology of cirrhosis. B19V were detectable in 10 (3.7%) patients by plasma mNGS testing, who were defined as the “B19V positive” group. Furthermore, 83 (30.4%) patients with complete

Patient characteristics	Univariate		MELD-based model		CTP-based model	
	HR (95% CI)	p	aHR (95% CI)	p	aHR (95% CI)	p
Age, per year	1.013 (0.994-1.034)	0.187	1.020 (0.998-1.041)	0.073	1.025 (1.001-1.047)	0.021
Sex, male vs. female (ref)	1.166 (0.698-1.948)	0.558	1.231 (0.710-2.137)	0.460	1.211 (0.704-2.085)	0.489
HVPG, per mmHg	1.069 (1.029-1.111)	<0.001	1.048 (0.999-1.100)	0.053	1.038 (0.991-1.088)	0.119
UNOS-MELD (2016), per point	1.056 (1.010-1.104)	0.017	1.024 (0.965-1.086)	0.434	-	
Decompensation, yes vs. no	1.898 (1.155-3.117)	0.011	0.992 (0.547-1.832)	0.980	-	
Albumin, per g/L	0.923 (0.885-0.962)	<0.001	0.961 (0.910-1.014)	0.149	-	
CTP A	1	Ref	-		1	Ref
CTP B vs. A	2.325 (1.380-3.918)	0.002	-		1.788 (0.980-3.261)	0.058
CTP C vs. A	3.933 (1.977-7.826)	<0.001	-		3.787 (1.688-8.495)	0.001
Sodium, mmol/L	0.931 (0.886-0.979)	0.006	-		0.995 (0.945-1.060)	0.884
Creatinine, per mg/dL	0.997 (0.747-1.331)	0.985	-		1.032 (0.725-1.469)	0.862
CRP, per mg/dL	1.280 (1.089-1.504)	0.003	1.264 (1.052-1.518)	0.012	1.303 (1.087-1.563)	0.004
Histamine, per nmol/L	1.023 (1.007-1.039)	0.004	1.030 (1.010-1.050)	0.003	1.033 (1.014-1.053)	<0.001

Figure: (abstract: FRI-554): Cox proportional-hazard models for ACLF or liver-related death. Univariate and multivariate models adjusted for MELD as well as for CTP are shown. Histamine was found to be an (independent) predictor of ACLF or liver-related death in the univariate model as well as in both multivariate models, which were adjusted for established prognostic indicators. HR = hazard ratio, aHR = adjusted hazard ratio, CI = confidence interval.

absence of pathogens and 28 (10.3%) only with HBV detectable were defined as the "B19V negative" group.

Compared to the "B19V negative" group, fever was more common in the "B19V positive" group (Figure A). The level of haemoglobin (73.8 ± 18.6 g/L vs 104.2 ± 25.3 g/L, $p < 0.001$) was significantly lower in the "B19V positive" group. Higher proportion of severe anaemia (Figure B) was observed in the "B19V positive" group, while the incidence of acute bleeding did not significantly differ between two groups (20.0% vs 14.4%, $p = 0.991$). Further, the percentage of unproven infection was significantly higher in "B19V positive" group compared to "B19V negative" group (60.0% vs 23.1%, $p = 0.048$). In "B19V positive" group, empirical antibiotic therapy was less effective (Figure C), and the resolution rate of infections was significantly lower (Figure C). Moreover, incidence of acute kidney failure was more frequent in "B19V positive" patients than that of the "B19V negative" (50.0% vs 14.4%, $p = 0.016$). Survival analysis showed that those with B19V infection had significantly higher 28-day mortality than those without B19V infection (Figure D).

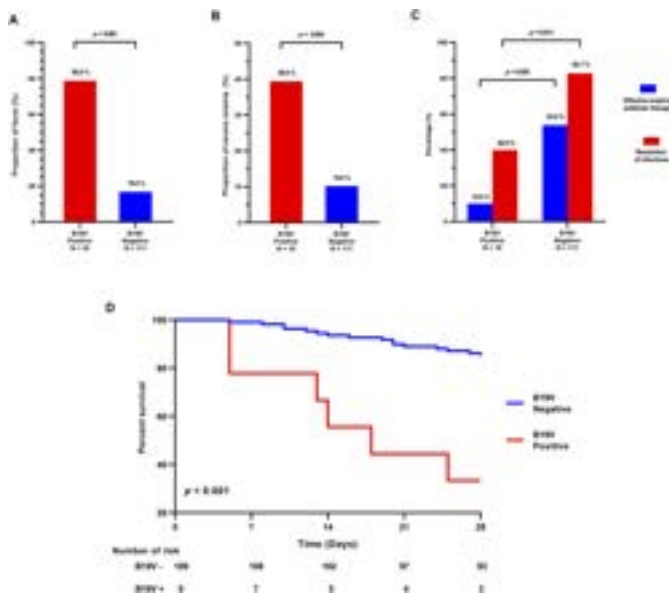


Figure:

Conclusion: B19V infection may have a pathogenic role in the adverse outcomes of cirrhotic patients, with clinical manifestations of recurrent fever, anemia and poor response of antibiotic therapy. This suggests that routine screening for B19V may benefit the management for the decompensated cirrhosis.

FRI-557

Real-world evidence of reversibility in patients with acute-on-chronic liver failure that survive hospitalization

Ahmed Elshabrawi^{1,2}, Kohilan Gananandan¹, Alexandra Phillips¹, Raj Mookerjee^{1,3}, Rajiv Jalan¹. ¹The Liver Failure Group, UCL Institute for Liver and Digestive Health, London, United Kingdom; ²Mansoura University, Endemic Hepatology and Gastroenterology, Mansoura, Egypt; ³Aarhus University Hospital, Department of Hepatology and Gastroenterology, Aarhus, Denmark
Email: r.jalan@ucl.ac.uk

Background and aims: Acute-on-Chronic Liver Failure (ACLF) is characterized by rapid deterioration of liver function and high short-term mortality rates. Although previous studies have hypothesized potential reversibility of ACLF, real-world data are lacking. In this study, we aimed to evaluate the clinical course and survival of hospitalized cirrhosis patients with ACLF in comparison to those with no ACLF.

Method: Consecutive patients with acute decompensation (AD) of cirrhosis with and without ACLF admitted to a single hepatology and transplantation center, between October 2018 and February 2021

were studied. Clinical and biochemical data, survival times and need for rehospitalization were collected at specified time points (index admission, discharge, 3, 6 and 12 months). ACLF was defined according to the EASL-CLIF criteria. The analyses were performed using data from the time of hospital discharge.

Results: 387 (67.4% males; mean age 58 years) cirrhosis patients were admitted with liver-related decompensation over the 29-month study period. Survivors were classified at discharge into ACLF group ($n = 48$) and no ACLF (AD) group ($n = 283$). Higher level of diuretic use at discharge was noted in the AD subgroup ($p = 0.039$) but no other significant differences were noted with regards to organ function parameters. During follow-up, serum albumin, bilirubin, INR, serum creatinine, severity of hepatic encephalopathy, portal hypertension related gastrointestinal bleeding and disease severity scores were similar in the two groups. There were no significant differences in the mean survival at 3, 6 and 12 months between the ACLF and the AD groups. Over the 12 months following discharge, there was no difference in the rate of re-hospitalizations with liver related complications between the ACLF group [0.35 (range, 0–5)] and the AD group [0.54 (range, 0–7)]; per patient, $p = 0.264$. To identify predictive factors of 90-day survival post-discharge of the whole cohort, univariate logistic regression analysis was conducted, showing that total serum bilirubin (OR = 0.996, 95% CI, 0.994–0.999; $p = 0.003$), INR (OR = 0.47, 95% CI, 0.231–0.954; $p = 0.037$), WBCs (OR = 0.91, 95% CI, 0.856–0.967; $p = 0.003$) and need for beta blockers at discharge (OR = 0.375, 95% CI, 0.168–0.834; $p = 0.016$), were significant predictors of survival, with only beta blockers remaining significant in a multivariate analysis ($p = 0.023$).

Conclusion: These real-world data show for the first time that patients surviving an episode of ACLF or AD are comparable in terms of re-hospitalizations and survival arguing strongly for the potential reversibility of ACLF. These data provide a strong rationale for rapid access of ACLF patients to intensive care to allow recovery and planning the need for liver transplantation.

FRI-558

Spur cells in liver cirrhosis are predictive of ACLF and liver-related mortality regardless of severe anaemia

Michele Bevilacqua¹, Leonardo De Marco², Roberta Stupia², Francesco Dima³, Filippo Cattazzo², Veronica Paon⁴, Donatella Ieluzzi⁴, Andrea Dalbeni², David Sacerdoti⁴. ¹Azienda Ospedaliera Universitaria Integrata, Verona, General Medicine C and Liver Unit, Verona, Italy; ²General Medicine C and Liver Unit, Italy; ³Laboratory section, AOUI Verona, Italy; ⁴Liver Unit, Italy
Email: bevilacqua.michele@yahoo.com

Background and aims: Chronic anaemia in advanced liver disease is a frequent finding that need to be carefully evaluated. The aim was to explore the clinical impact of spur cells anaemia, a rare form of non-immune haemolytic anaemia in which red blood cells are spiky-like and that is typically associated with end-stage cirrhosis with poor outcome in absence of etiological therapy.

Method: 119 consecutive patients (73.9% males; 43.7% alcoholic, 35.7% viral, 10.1% autoimmune, 10.9% metabolic) referring to our Liver Unit outpatient clinic were enrolled. Inclusion criteria were consistent with a diagnosis of liver cirrhosis of any aetiology and disease severity but without hepatocellular carcinoma. Patients with bone marrow diseases or nutrients deficiencies (iron, folates, vitamin B12) were excluded. In all patients a blood smear was performed in order to assess red blood cells morphology and quantify spur cells (achantocytes and echinocytes). A complete blood biochemical panel was recorded together with Child-Pugh (CPS) and MELD score. For each patients clinical data (acute decompensation and acute-on chronic liver failure, ACLF) and 1-year liver-related mortality were obtained. A cut-off of 5% of spur cell was considered as a threshold for clinical significance.

Results: 11 out of 119 patients (9.2%) had more than 5% of spur cells in blood smear, 7 out of 11 had alcoholic cirrhosis and 2 out of 11 had

POSTER PRESENTATIONS

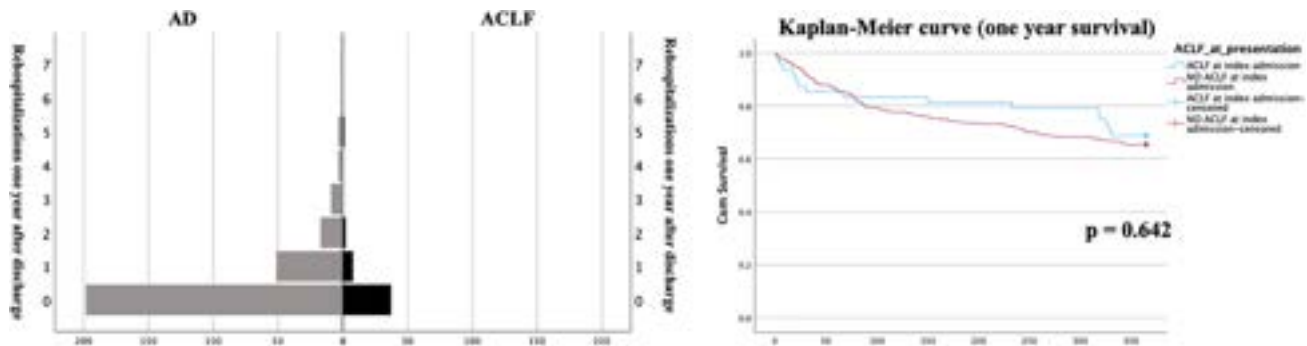


Figure: (abstract: FRI-557): Re-hospitalization and survival of patients with AD and ACLF post discharge

evidence of haemolysis; 33.6% (40/119) had more than 1%. In patients with more than 5% of spur cells, haemoglobin was lower compared with the other sub-group, while CPS, MELD score, prothrombin time, creatinine and unconjugated bilirubin were higher; no differences were shown in ferritin, folates, B12 vitamin, albumin and total bilirubin. Patients with more spur cells were more frequently decompensated, had more ascites (100% vs 55.1%, $p=0.002$) and hepatic encephalopathy (63.6% vs 20.8%, $p=0.008$). The median follow-up was 10 months (IQR 8–12 months). In multivariate Cox-regression analysis, CPS (HR 1.4 95% I.C.[1.2–1.7], $p=0.001$) and spur cells $>5\%$ (HR 3.4 95% I.C.[1.5–8.0], $p=0.005$), but not age, sex and MELD score, were independently related with ACLF development during follow-up. Similarly, the presence of more than 5% of spur cells (HR 3.3 95% I.C.[1.4–7.8], $p<0.001$), together with CPS and MELD score, was independently associated with 1-year liver-related mortality.

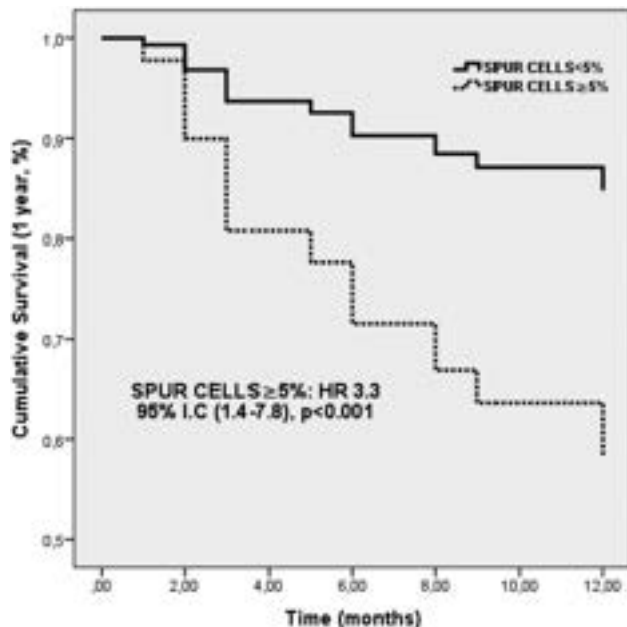


Figure:

Conclusion: Our results are consistent with a fairly high prevalence of spur cells in blood smear of cirrhotic patients. Despite not always associated with clinically overt haemolytic anaemia, the presence of spur red cells is associated *per se* with more severe disease, ACLF development and worse liver-related outcomes, underlining the role of blood smear in better stratifying prognosis and eventually prioritize patients for liver transplant.

FRI-559

Plasma thrombomodulin as a candidate biomarker for the diagnosis and prognosis of HBV-related acute-on-chronic liver failure

Xingping Zhou¹, Jinjin Luo¹, Xi Liang², Peng Li¹, Jiaojiao Xin¹, Jing Jiang¹, Dongyan Shi¹, Jun Li¹. ¹The First Affiliated Hospital, Zhejiang University School of Medicine, State Key Laboratory for Diagnosis and Treatment of Infectious Diseases, National Clinical Research Center for Infectious Diseases, National Medical Center for Infectious Diseases, Hangzhou, China; ²Taizhou Central Hospital (Taizhou University Hospital), Precision Medicine Center, Taizhou, China
Email: lijun2009@zju.edu.cn

Background and aims: Hepatitis B virus-related acute-on-chronic liver failure (HBV-ACLF) is a complicated syndrome with high short-term mortality. Effective biomarkers for early diagnosis and prognosis of HBV-ACLF are needed. This study aimed to assess the diagnostic and prognostic value of thrombomodulin (THBD) in HBV-ACLF patients.

Method: The expression of THBD during disease progression was evaluated analyzed through transcriptomics analysis. Plasma THBD levels in 393 subjects with HBV-ACLF ($n=213$), acute on-chronic hepatic dysfunction (ACHD, $n=50$), liver cirrhosis (LC, $n=50$), chronic hepatitis B (CHB, $n=50$) and normal controls (NC, $n=30$) from a prospective multi-center cohort were measured to validate the diagnostic and prognostic significance of THBD for HBV-ACLF patients by enzyme-linked immunosorbent assay (ELISA).

Results: THBD mRNA level was highly expressed in the HBV-ACLF group (compared with other groups, AUROC=0.887). High expression of THBD predicted poor prognosis for HBV-ACLF patients in 28/90 days (AUROCs=0.823/0.788). Functional analysis showed that THBD was significantly associated with complement activation and inflammatory signaling pathway. External validation confirmed its high diagnostic accuracy for HBV-ACLF patients (AUROC=0.931). Plasma THBD levels were correlated with organ failure, including coagulation and kidney failure. Plasma THBD levels showed a potential prognostic value for 28-day mortality (AUROC=0.702). Risk stratification of the THBD expression level (>8.4 ng/ml) specifically identified HBV-ACLF patients with a high risk of death.

Conclusion: This study reveals THBD could serve as a candidate biomarker for the diagnosis and prognosis of HBV-ACLF, which might play a crucial role in the coagulation and inflammatory response.

FRI-560

Frequency of ACLF and predictors of in-hospital mortality in cirrhotic patients in a tertiary care hospital of Pakistan

Marium Fatima Waqar¹, Sulhera Khan¹, Zeeshan Junejo¹. ¹Jinnah Postgraduate Medical Centre Karachi, Internal Medicine, Karachi, Pakistan
Email: sulherahussain@gmail.com

Background and aims: Acute on chronic liver failure (ACLF) is characterised by acute decompensation of the liver in patients with chronic liver disease (CLD). This condition presents as jaundice, deranged (international normalised ratio) INR or liver failure. To grade patients, we need to utilise liver-failure-adapted organ assessment scores such as the European Association for the Study of the Liver-Chronic Liver Failure (EASL-CLIF) criteria. Our study focuses on determining the frequency of ACLF in our population and correlating different scoring systems to predict in-hospital mortality.

Method: This study is conducted on cirrhotic patients admitted to Jinnah Postgraduate Medical Centre. The organ failure was assessed with the CLIF-C score. Demographics, baseline characteristics and laboratory investigations were recorded. The severity of cirrhosis was assessed by using the Child-Pugh (CTP), Model for End Stage Liver Disease (MELD) and MELD sodium (Na) scores.

Results: Out of 148 patients, 29.1% (n = 43) of participants met the diagnosis of ACLF according to the EASL-CLIF criteria. 55.4% of the participants were males. The in-hospital mortality rate of the enrolled cirrhotic patients was found to be 20.1% (n = 23). It was observed the mortality in the ACLF (23.3%, n = 10) group was twice that of the non-ACLF (12.4%, n = 13) group. The highest mortality was seen in the ACLF grade 3 group (100%, n = 6), whereas the combined mortality of ACLF grades 2 and 1 (10.8%, n = 4) was almost equivalent to the non-ACLF (12.4%, n = 13) group. The most common reason for admission was hepatic encephalopathy (44%). Renal (60.5%) and cerebral failure (23.8%) were identified as the most common organ failure in the ACLF and non-ACLF groups respectively. AUROC were 0.620 (CI95% 0.48–0.75), 0.646 (CI95% 0.52–0.77), 0.668 (CI95% 0.53–0.79) and 0.653 (CI95% 0.52–0.77) for MELD, MELD-Na, CLIF-C Organ Failure and CLIF-C ACLF scores, respectively. MELD, MELD-Na, and CLIF-C ACLF scores were independent predictors of mortality. Among these scores, the CLIF-C Organ Failure score was the strongest independent predictor of mortality (OR = 3.64, CI 95% = 2.34–5.65, p = 0.01). On ROC curve analysis, the maximum area (66.8%) under the curve was obtained for the CLIF consortium organ failure score (p = 0.01).

Parameters	Univariate analysis Odds Ratio (95% C.I)	Multivariate analysis Odds Ratio (95% C.I)
Blood Pressure	0.9 (0.92–0.99)	0.9 (0.8–1.0)
Diastolic		
Pulse	1.0 (1.0–1.06)	1.0 (0.9–1.0)
Total Bilirubin	1.1 (1.0–1.2)	1.0 (0.9–1.2)
PT	1.0 (1.0–1.1)	1.0 (0.8–1.1)
INR	2.8 (1.3–6.0)	1.7 (0.3–10)
Urea	1.0 (1.0–1.04)	1.0 (1.0–1.04)
Creatinine	5.0 (2.7–9.2)	3.7 (1.4–9.4)
MELD Score	1.3 (1.20–1.44)	1.2 (1.08–1.33)
CTP Grade B	3.9 (0.8–18.0)	62 (1.7–230)
CTP Grade C	5.8 (1.2–27.0)	9.5 (0.3–287)
Liver failure	6.6 (1.6–26.)	2.7 (0.01–86)
Cerebral failure	2.7 (1.3–5.8)	2.1 (0.5–8.8)
Circulation failure	10.0 (1.9–50.)	2.5 (2.2–285)
Use of	8.9 (2.3–35.)	1.0 (1.1–916)
Vasopressors		
MELD-Na Score	1.2 (1.16–1.36)	
CLIF-C ACLF Score	1.1 (1.06–1.17)	

Figure: Risk estimation of ACLF using binary logistic regression

Conclusion: It is important to promptly identify ACLF, as the patients identified early with two or more organ failures at presentation in resource-poor settings can be planned for aggressive management to reduce mortality. Upon analysis, it is seen that MELD Na, CLIF-C ACLF score, and EASL-CLIF organ failure score are superior to the MELD score and highly significant in predicting mortality in patients with ACLF.

Cirrhosis and its complications Experimental and pathophysiology

WEDNESDAY 21 TO SATURDAY 24 JUNE

TOP-042

Yaq-001, a non-absorbable, engineered carbon beads of controlled porosity impacts on gut dysbiosis, gut permeability, organ function and reduces mortality in rodent models of cirrhosis and ACLF

Jinxia Liu^{1,2}, Jane Macnaughtan¹, Yi Jin³, Frederick Clasen³, Francesco De Chiara¹, Ganesh Ingavle⁴, Paul Cordero¹, Junpei Soeda¹, Jude A. Oben¹, Jia Li⁵, I. Jane Cox⁶, Susan Sandeman⁴, Nathan Davies¹, Raj Mookerjee¹, Saeed Shoaie⁷, Rajiv Jalan¹, ¹UCL Institute for Liver and Digestive Health, Upper third floor, Royal Free Campus, Rowland Hill Street, Hampstead, London, NW3 2PF, United Kingdom; ²Department of Gastroenterology, Affiliated Hospital of Nantong University, Nantong, 226001, China; ³Centre for Host-Microbiome Interactions, Faculty of Dentistry, Oral and Craniofacial Sciences, King's College London, SE1 9RT, United Kingdom; ⁴Pharmacy and Biomolecular Sciences, University of Brighton, Moulsecoomb, Brighton, BN2 4GJ, United Kingdom; ⁵Department of Surgery and Cancer, Faculty of Medicine, Imperial College London, Sir Alexander Fleming Building, Imperial College Road, South Kensington, London, SW7 2AZ, United Kingdom; ⁶Roger Williams Institute of Hepatology, United Kingdom; ⁷Centre for Host-Microbiome Interactions, Faculty of Dentistry, Oral and Craniofacial Sciences, King's College London, SE1 9RT, United Kingdom
Email: r.jalan@ucl.ac.uk

Background and aims: Dysbiosis and translocation of bacterial lipopolysaccharide (LPS) stimulates a systemic inflammation in cirrhosis resulting in multiple organ dysfunction and acute on chronic liver failure (ACLF). Current strategies to target bacterial translocation in cirrhosis are limited to antibiotics with risk of resistance. Yaq-001 is a non-absorbable, engineered carbon bead that has been designed to adsorb small molecules such as ammonia and larger molecules such as LPS and bile acids from the gut. The aims of this study were to explore its therapeutic potential in models of cirrhosis and ACLF.

Method: Two rodent models of cirrhosis (4w, bile duct ligation, BDL) and ACLF (BDL+LPS). Eight groups: Sham (n = 36); Sham+Yaq-001 (n = 30); BDL (n = 36); BDL+Yaq-001 (n = 44); Sham+LPS (n = 9); Sham+LPS+Yaq-001 (n = 10); BDL+LPS (n = 16); BDL+LPS+Yaq-001 (n = 12). Yaq-001 was administered for 2-weeks prior to sacrifice. Portal pressure, organ function and transcriptome analysis of liver, colon, brain and kidney were performed. Stool in BDL rats was collected for 16 s microbiome study.

Results: *In vitro* studies: Yaq-001 exhibited rapid adsorption kinetics for endotoxin, ammonia and bile acids without exerting an antibiotic effect. *In vivo*, Yaq-001 supplementation resulted in a significant improvement in ALT, liver cell death (TUNEL stain), portal pressure, markers of systemic inflammation (TNFα, IL-8; white cell count) and renal function (creatinine) in BDL animals. ACLF animals treated with Yaq-001 had significantly better survival compared with controls, with significantly reduced ALT, portal pressure, brain water and creatinine. In addition to improvement in *in vivo* LPS sensitivity, ex-vivo LPS-induced reactive oxygen species production in both portal venous monocytes and Kupffer cell populations was diminished with Yaq-001 treatment. Transcriptomic analysis demonstrated a significant modulation of inflammation, cell death and senescence pathways in the liver, kidneys, brain and colon of Yaq-001-treated BDL rats compared to untreated controls. Abundance of *Family Porphyromonadaceae* and *Genus Barnesiella* were also significantly reduced with Yaq-001 treatment.

Journal of Hepatology **2023** vol. 78(S1) | S100–S1212

amino acids concentrations, liver multiplex immunofluorescence (IF) staining for the urea cycle enzymes (UCEs) and liver transcriptomics and metabolomics were studied.

Results: In WT mice, the AA-diet led to a significant increase in circulating ammonia levels ($p < 0.0001$), which was prevented by treatment with OP and TAK-242 (Fig.). Liver metabolomic analysis showed a distinct metabolic fingerprint in hyperammonemia with accumulation of metabolites related to the urea cycle, Krebs cycle and mitochondrial beta-oxidation. Comparative transcriptomics revealed that urea cycle-related pathways were downregulated in hyperammonemia, and oxidative stress related pathways were upregulated. IF confirmed downregulation of hepatic UCE expression in hyperammonemia, whereas the mitochondrial number was preserved. Hyperammonemia-induced changes in metabolomics, transcriptomics and IF were prevented by OP, TAK-242 and TLR4 deficiency. In hyperammonemia induced by OTC-deficiency and BDL, TAK-242 significantly reduced circulating ammonia levels.

Conclusion: These data point towards a novel mechanism of hyperammonemia-induced UCE dysfunction which is associated with a change in the metabolomic fingerprint, primarily involving mitochondrial metabolism. Inhibition of the TLR4 pathway protects against hyperammonemia and is a potential novel therapy for hyperammonemia associated with liver disease and UCE disorders.

THURSDAY 22 JUNE

THU-337

Factor VIII synthesis by adipose tissue stromal cells contributes to coagulopathy in chronic liver disease

Sarita Gupta¹, Kumaraswamy Parthasarathy², Archana Rastogi³, Perumal Nagarajan⁴, Shiv Kumar Sarin⁵, Viniyendra Pamecha², Sanal Madhusudana Girija^{1,1.6}. ¹New Delhi, Molecular and Cellular Medicine, New Delhi, India; ²Vasant Kunj, Hepato Pancreato Biliary Surgery, New Delhi, India; ³Institute of Liver and Biliary Sciences, Pathology, New Delhi, India; ⁴National Institute of Immunology, Small Animal Facility, New Delhi, India; ⁵Institute of Liver and Biliary Sciences, Hepatology, New Delhi, India; ⁶Institute of Liver and Biliary Sciences, Molecular and Cellular Medicine, New Delhi, India
Email: sanalmg@gmail.com

Background and aims: Adipose tissue also functions as an endocrine organ. Like bone-marrow, it's derived from embryonic mesenchyme and is a rich source of mesenchymal stem cells. Adipose tissue has more mesenchymal stromal stem cells (MSC) than bone marrow. Lungs, kidneys, and brain are affected in cirrhosis but we don't know

about adipose tissue. In cirrhosis, the risk of both thrombosis and bleeding increases, however, the risk of thrombosis is less appreciated. Factor VIII (F8) levels are raised in cirrhosis, not lowered, despite shrinking liver. Liver makes most of the F8, but we know little, how much extra-hepatic sources contribute to F8 levels. Bone marrow transplantation studies showed marrow MSCs could synthesize factor F8 and ameliorate bleeding in hemophilic mice. Considering the total adipose tissue mass in the human body the total contribution of F8 from adipose tissue could be significant. Here we compared the expression of F8 in adipose tissue in health and cirrhosis.

Method: Adipose tissue was harvested from 15 liver cirrhosis patients (recipients) and same number of healthy adults (donors) during Living Donor Liver Transplantation (LDLT). We adapted an MSC isolation protocol for liposuction samples. We confirmed F8 by immunohistochemistry (IHC)/immunofluorescence (IF), western-blot and flowcytometry. F8 'functional assay' was used to estimate F8 activity in plasma. Isolated MSC were transplanted to an immunodeficient F8 knock-out mouse model (factor VIII, *Prkdc^{scid}* double knock-out). One million MSC suspended in PBS (isolated from adipose tissue of cirrhosis patients or healthy controls) were i.v. administered to animals ($n = 9$, in each test group). C57BL and the double knock-out animals ($n = 5$, in each control group) were injected PBS. The blood was collected at baseline and after 10 days and 3–6 months post-transplantation. Animals were sacrificed, various tissues were preserved in formalin/liquid nitrogen. T-test/ANOVA was used to calculate the statistical significance.

Results: Of the 15 cirrhosis patients eleven were males and 4 were females. Mean age was 45.5 years (Range:11–59 years). Mean BMI was 23.2 kg/m². Mean MELD score was 22.2. Of the 15 donors, 2 were men and 13 were women. Mean age was 39.2 years (Range:19–50 years) and the mean BMI was 23.7 kg/m². We found higher expression of F8 in adipose tissue in cirrhosis compared to healthy. For the first time we demonstrated the contribution of F8 from adipose tissue to the body pool. Further we transplanted adipose derived MSC from healthy people and cirrhosis patients into F8 knock-out, immune-compromised mice. Transplanted cells seems to survive in these animals as shown by Real Time PCR in various tissues (Figure-1F-a) and IF (Figure-1F-b-e). F8 functional assay showed small but significant levels of F8 in all animals which received MSC treatment (Figure-1F-f). There is a small and insignificant increase in F8 in animals which received MSC from cirrhosis patients compared to the healthy controls.

Conclusion: We have demonstrated that adipose tissue contributes to F8 production, and this could be significant considering the total

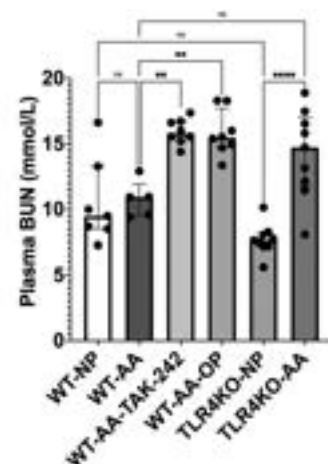
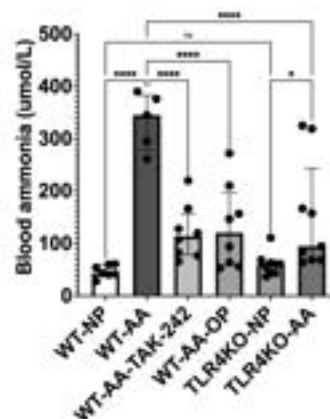
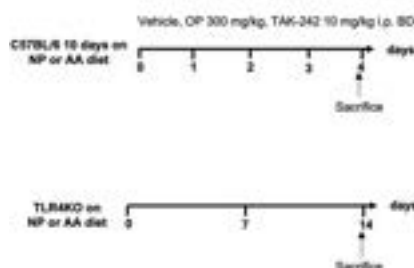


Figure: (abstract: TOP-046).

POSTER PRESENTATIONS

mass of adipose tissue in the human body. The MSC from adipose tissue upon transplantation to F8 knock-out animals produce F8. It is a less appreciated fact that chronic liver disease is thrombotic condition and the adipose tissue derived F8 could be a contributing factor in keeping delicate balance between bleeding and clotting in cirrhosis.

THU-338

ϵ -Lysine-melittin reduces pathological bacterial translocation and enhances gut immunity in experimental decompensated cirrhosis

Deepika Jakhar¹, Pinky Juneja¹, Aarti Sharma¹, Impreet Kaur¹, Dinesh Mani Tripathi¹, Lakshminarayanan Rajamani², Savneet Kaur¹.
¹Institute of Liver and Biliary Sciences, Molecular and Cellular Medicine, New Delhi, India; ²Singapore Eye Research Institute, Singapore
Email: savykaur@gmail.com

Background and aims: Pathological bacterial translocation from intestine to mesenteric lymph nodes (MLN) is an important

mechanism in development of systemic infections in liver cirrhosis. Melittin, major component of bee venom is cationic amphipathic peptide that has anti-microbial and cytolytic properties. We modified melittin by replacing alpha-lysine with ϵ -lysine at multiple sites to enhance its selective bactericidal properties and reduce its *in vivo* toxicity and evaluated effects of modified melittin on bacterial translocation, MLN immune responses and intestinal and liver inflammation in experimental cirrhosis with ascites.

Method: Rat models of cirrhosis were prepared by i.p injections of CCl₄ for 8–10 weeks. Melittin was administered i.p, 0.2 mg/kg, twice a week for 2 weeks in CCl₄ rats. CCl₄ rats given saline served as vehicle. Bacterial load was studied in MLNs. Intestinal permeability in ileum was assessed by immunohistochemistry of occludin protein. Immune cells were quantified in MLNs, portal and peripheral blood by flow cytometry. Gene expression of inflammatory markers in liver and ileum tissues was examined by RT-PCR.

Results: Modified melittin did not result in adverse effects in melittin treated CCl₄ rats. Bacterial load in MLNs of cirrhotic (<18 000 CFU/g of

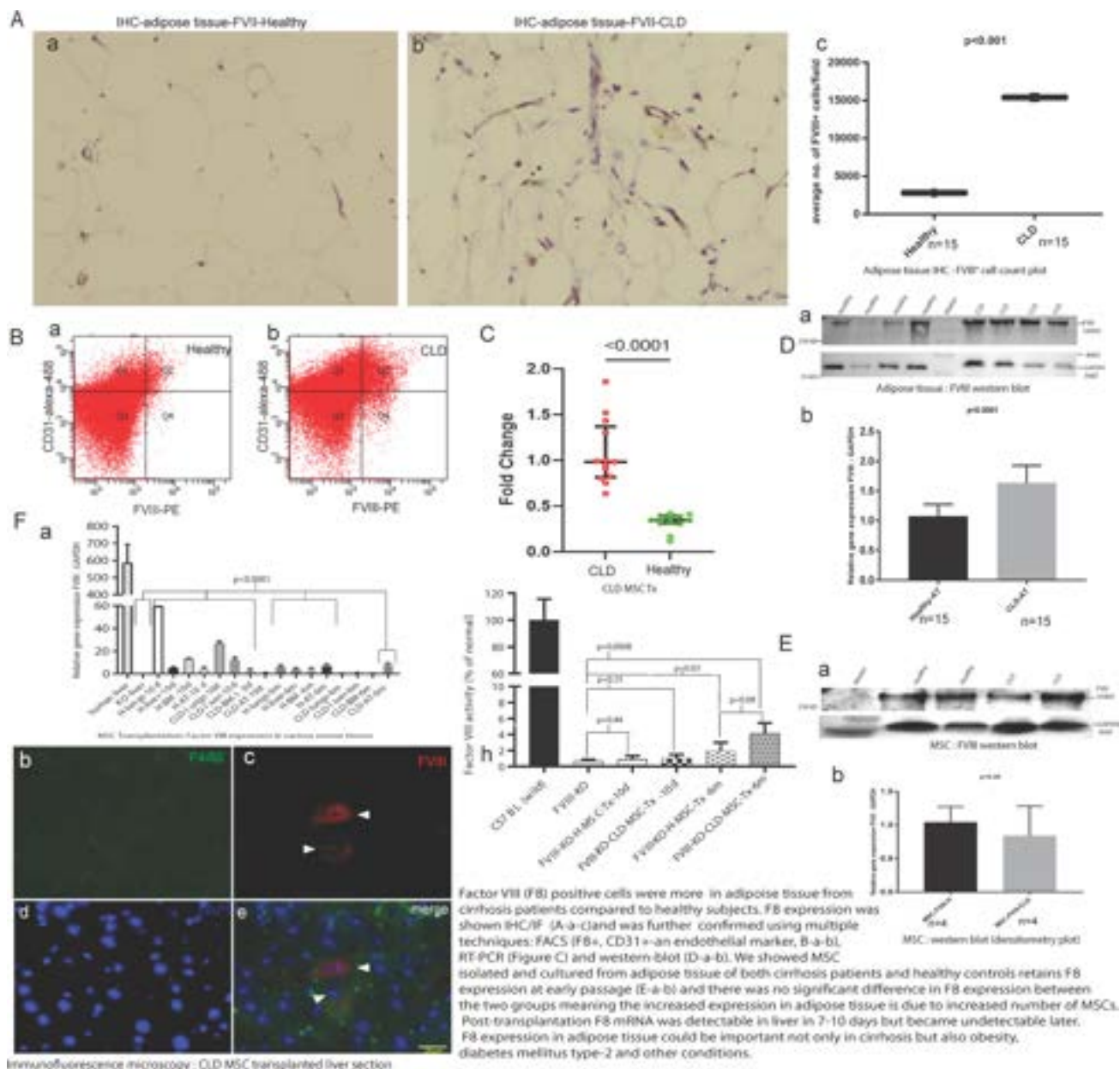


Figure: (abstract: THU-337).

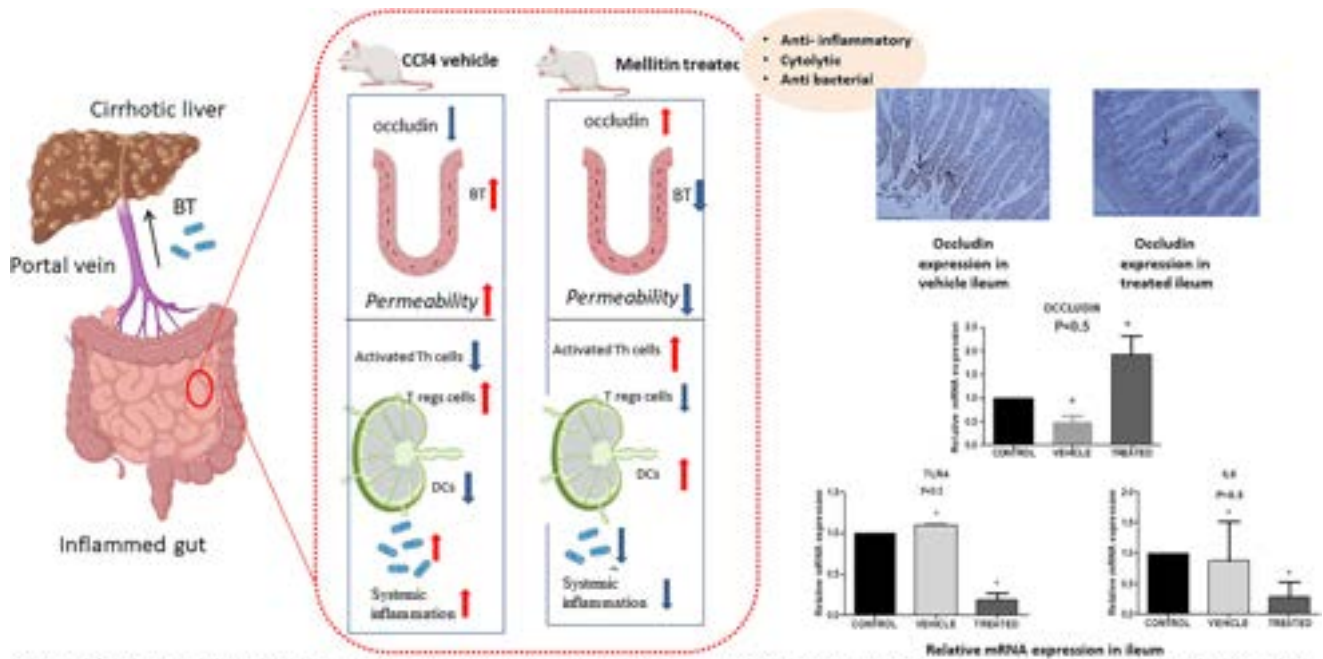


Figure: (abstract: THU-338).

tissue) was significantly reduced ($>10,000$ CFU/g) in MLNs of melittin-treated ($p < 0.01$) suggesting increased bacterial killing in MLNs. In treated rats, percentage of CD4⁺ (65.4 ± 0.6 vs 33.2 ± 0.7), CD8⁺ T (24.9 ± 1.3 vs 19.3 ± 1.5) and activated CD134⁺Th (34.6 ± 0.9 vs 30.1 ± 1.1) ($p < 0.05$) cells increased and CD25⁺Treg (3.20 ± 0.8 vs 56.1 ± 1.2 , $p < 0.05$) cells decreased compared to vehicle, decreased inflammatory monocytes (CD43-low) (33.5 ± 1.5 vs 44.2 ± 1.7 , $p < 0.05$) and increased dendritic cells (61.5 ± 0.3 vs 43.4 ± 0.5 , $p < 0.05$) in treated compared to vehicle. In portal and peripheral blood, there was increased CD8⁺T (23.57 ± 1.4 vs 19.10 ± 1.1) and CD134⁺Th (34.13 ± 1.9 vs 24.25 ± 1.7) ($p < 0.05$) in treated compared to vehicle. In treated rats, occludin protein expression significantly increased (3.2-fold, $p < 0.5$) in epithelial cells of intestinal villi and crypts compared to vehicle. A significant decrease in gene expression of pro-inflammatory markers such as IL6 and TLR4 in both ileum (IL6: 3.5-fold, $p < 0.5$, TLR4: 10 fold, $p < 0.5$) and liver (IL6: 8 fold, $p < 0.5$, TLR4: 9 fold, $p < 0.5$) of treated rats compared to vehicle. There was no change in liver fibrosis after melittin treatment (Fig).

Conclusion: In decompensated cirrhosis, treatment with modified melittin reduces bacterial load in MLNs by decreasing intestinal permeability and enhancing adaptive T cell immunity in MLNs. It also attenuates inflammation in both gut and liver. Modified ε-lysine melittin thus holds relevance as an emerging adjunct antimicrobial therapy for combating development of infections in cirrhosis.

THU-339

Combination of weekly albumin infusion, personalized nutrition and home-based exercise programme improves outcomes of patients with end stage liver disease (Al-Fit study)

Chandan Kedarisetty¹, Sasanka Vangara^{1,1}, Sridhar Reddy Chappidi², Malleswari Naga³, Rami Reddy Yalaka⁴, Sameer Godey⁴. ¹Gleneagles global hospital, Department of hepatology and liver transplant, Hyderabad, India; ²Gleneagles global hospital, Department of Radiology, Hyderabad, India; ³Gleneagles global hospital, Department of Nutrition, Hyderabad, India; ⁴Gleneagles global hospital, Department of Medical Gastroenterology, Hyderabad, India
Email: sasanka58v@gmail.com

Background and aims: Cirrhotic patients have progressive deterioration of liver functions and development of sarcopenia and frailty. Frailty has emerged as independent critical determinant of mortality and assessed by Liver Frailty index (LFI). We assumed improvement of LFI through weekly albumin supplementation, personalized nutritional counselling and monitored home based physiotherapy improves outcomes and quality of life in cirrhotic patients. We aimed to study the efficacy of combination therapy in improving physical performance assessed by LFI, reduction in decompensating events and improving quality of life.

Method: We randomized 60 cirrhotics with Model for end stage liver disease (MELD) score ≥ 15 in 1:1 ratio into 2 groups, A and B. Group A received combination therapy in the form of weekly once 20% 100 ml recombinant human albumin infusion, weekly diet recall ensuring calories 30–35 kcal/kg/day and proteins 1.2–1.5 g/kg/d and home-based rehabilitation exercises. Group B received only standard medical care. We assessed liver frailty index, MELD score, quality of life by chronic liver disease questionnaire (CLDQ) at baseline and at follow-up of 3 months.

Results: Mean age in the cohort was 49 ± 9.8 years, predominant etiology was alcohol related liver disease and more than 80% were male gender. Baseline LFI in Group A was 4.42 ± 0.4 vs. 4.3 ± 0.3 in Group B. There was a statistically significant reduction in LFI at 3 months compared to baseline in Group A (4.42 ± 0.4 to 4.3 ± 0.37), compared to an increase in Group B (4.3 ± 0.3 to 4.5 ± 0.45) ($p = 0.007$). The MELD score significantly reduced in Group A (17.5 ± 4.6 at baseline to 16.2 ± 2.6 at 3 months), compared to an increase in Group B (18 ± 3.2 at baseline to 19.7 ± 6.4 at 3 months) ($p = 0.009$). There was significant improvement of CLDQ score in Group A (23.7 ± 3.5 at baseline to 26.5 ± 4.4 at 3 months) compared to Group B (22.9 ± 2.7 at baseline to 21.7 ± 3.07 at 3 months) ($p = 0.00001$). There was no difference in number of hospital admissions in between the two groups ($p = 0.19$).

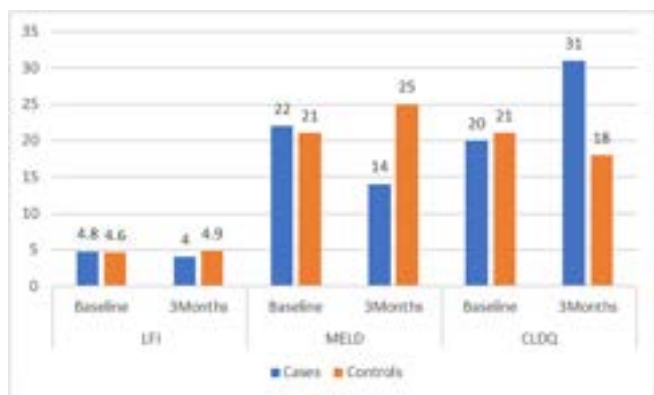


Figure:

Conclusion: Liver transplantation offers improved long-term survival for these patients but is negatively influenced by deceased donor availability and progression of disease in the wait-list. The combination of weekly albumin infusion, personalized nutritional counselling and monitored home-based physiotherapy is first kind of study in patients with high MELD score more than or equal to 15 to show significant improvement in liver frailty index, reduces MELD score and overall improves quality of life. My study trial enrolment details are as follows-CTRI No : REF/2023/02/063149.

THU-340

Imperfect maturation in erythroid progenitors leads to severe anemia in cirrhotic patients

Deepika¹, Chhagan Bihari², Jaswinder Maras¹, Rakhi Maiwall³, Anupam Kumar¹, Shiv Kumar Sarin^{1,3}, ¹Institute of liver and biliary sciences, Department of Molecular and cellular medicine, New delhi, India; ²Institute of liver and biliary sciences, Department of pathology, New delhi, India; ³Institute of liver and biliary sciences, Department of hepatology, New delhi, India

Email: dr.anupamkumar.ilbs@gmail.com

Background and aims: Anemia is seen in nearly >70% patients with cirrhosis. It is often non responsive to nutritional supplements known as refractory anemia. Therefore, to understand the unknown cause, we assessed the erythropoiesis process and associated alteration in bone marrow of cirrhotic patients.

Method: Flow cytometry was done to assess hematopoietic stem cells (HSCs) and erythroid population (EP) status in bone marrow (BM) of cirrhotic patients (N = 60) compared with Non cirrhotic portal fibrosis (N = 8) and healthy control (N = 3). Proteomics was done of pure CD71 erythroid population of cirrhotics to decipher the internal abnormalities supported by validation experiments Real Time-Polymerase chain reaction, colony assay and heme quantification. Cytokine array and ELISA were done to assess for erythropoietic stimulating agents (ESA), inflammatory cytokines and growth factors as an external factor affecting erythropoiesis.

Results: BM aspirates were collected from cirrhotic and NCPF patients having anemia with mean haemoglobin (8.73 ± 2.02 and 9.54 ± 1.02) with no nutritional deficiency and also from healthy control. We found significant decrease in CD34+ HSCs and intermediate [IEP; CD71+CD235a+], conversely early [EEP; CD71+CD235a-] and late [LEP; CD71- CD235a+] were significantly increased in cirrhotic and NCPF as compared to control ($p < 0.05$) [figure A], suggesting increase in stress induced erythropoiesis in both cirrhotic and non-cirrhotic (NCPF) injury. Unlike NCPF, cirrhotic BM EP showed significant ($p < 0.05$) decrease in expression of CD71+ Transferrin receptors (TfR1; for iron uptake) [Figure B] with increase in percentage of immature CD71+ erythroids (by 1.17%) in peripheral blood suggesting defective maturation of EP in cirrhosis. In compare to healthy control and NCPF, cirrhotic EP showed significant ($p < 0.05$) increase in protein associated with hypoxia, metabolism dysregulation and oxidative stress and decrease in proteins

associated with haemoglobin synthesis, ROS detoxification, Translation, mitochondrial activity ($p < 0.05$) [Figure C]. Further, cirrhotic EP showed decrease in intracellular heme and decreased expression of genes related to erythropoiesis and haemoglobin synthesis (>0.5 folds) [figure D, E]. They also showed significantly reduce number of erythroid colonies (BFU-E) as compared to control ($p < 0.05$). We found significant ($p < 0.05$) increase in inflammatory cytokines such as IL-5, TRAIL-R2, TGF- α and TGF- β in cirrhotic BM plasma. Surprisingly, ESA required facilitating normal erythropoiesis such as erythropoietin, transferrin and growth factors IL-3, IL-6, FLT3 and SCF were also significantly increased in cirrhosis as compared to NCPF and control [Figure F].

Conclusion: In cirrhosis, increased inflammatory cytokines in BM and altered erythroids intracellular physiological pathways involved in hemoglobin synthesis and erythroid cell development as well as decreased transferrin receptors leads to defective erythroid maturation.

THU-341

Study of epigenetic control of LSECTin in hepatic antigen presenting cells during experimental cirrhosis

Enrique Angel^{1,2}, Sebastian Martinez^{1,2}, Isabel Gómez-Hurtado^{2,3}, Paula Boix^{1,2}, Esther Caparrós^{1,2}, Rubén Francés^{1,2,3}, ¹Hepatic and intestinal immunobiology group, Miguel Hernandez University, Clinical Medicine Departament, San Juan, Spain; ²IIS Isabial. Hospital general universitario dr. Balmis, Alicante, Spain; ³Carlos III health institute, CIBERehd, Madrid, Spain

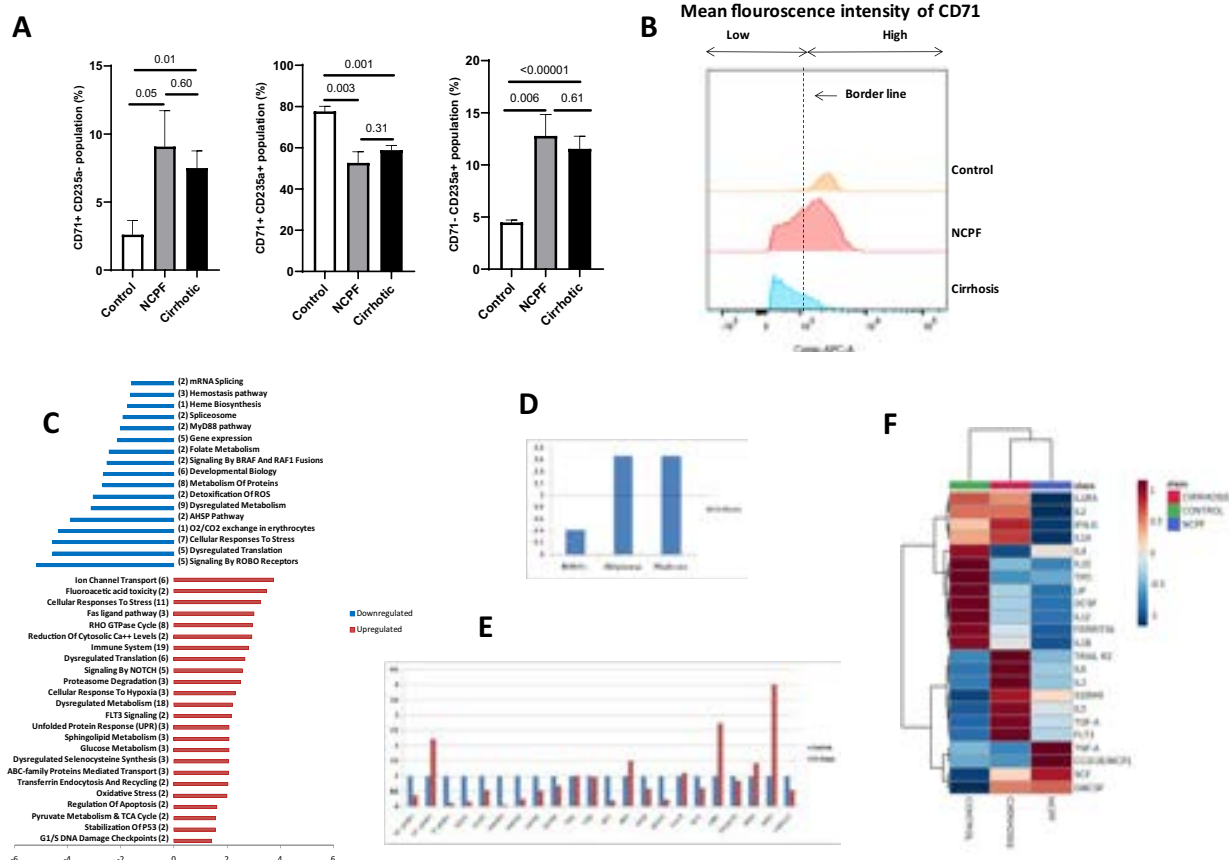
Email: eangel@umh.es

Background and aims: LSECTin, a C-type lectin that acts as Pattern Recognition Receptor and T-cell ligand, is expressed in Liver Sinusoidal Endothelial Cells (LSECs) and Kupffer Cells (KCs). The progressive reduction in the expression of LSECTin in animal models of experimental cirrhosis inhibits inflammatory response control associated to advanced chronic liver disease progression. The main aim of this work is to characterize the epigenetic control of LSECTin's expression during cirrhosis (attending to DNA methylation and histone proteins post-translational modifications, HPTMs) in order to evaluate new potential strategies that could contribute to the recovery of its expression.

Method: C57BL/6 mice were treated by oral gavage of carbon tetrachloride (CCl₄) or olive oil for 16 weeks, for cirrhotic and control groups, respectively. After laparotomy and liver perfusion, KCs and LSECs were isolated by cell sorting. DNA methylation analysis (Infinium Mouse Methylation BeadChip Array-Illumina) and chromatin immunoprecipitation followed by sequencing (ChIP-Seq) experiments were carried out in both APCs subpopulations.

Results: Analysis of DNA methylation allowed the identification of differentially methylated probes in pairwise comparisons using a Benjamini-Hochberg adjusted p value < 0.05 , distributed over gene body and proximal promoter of *Clec4g*, the gene that encodes LSECTin (Figure 1A). ChIP-Seq experiment for HPTMs associated to gene expression silencing showed a differential binding profile for all control vs CCl₄ comparisons (KCs, H₃K₂₇Me₃: 1099/300; H₃K₉Me₃: 11594/4571; LSECs, H₃K₂₇Me₃: 346/455; H₃K₉Me₃: 2573/5802). Specific peak profile of *Clec4g* flanking region for the aforementioned comparisons is depicted in Figure 1B.

Conclusion: The promoter region of LSECTin contains specific epigenetic marks in hepatic APCs during cirrhosis that include changes in DNA methylation and differences in the post-translational modification profile of histone proteins related to gene silencing, specifically H₃K₉Me₃ and H₃K₂₇Me₃.



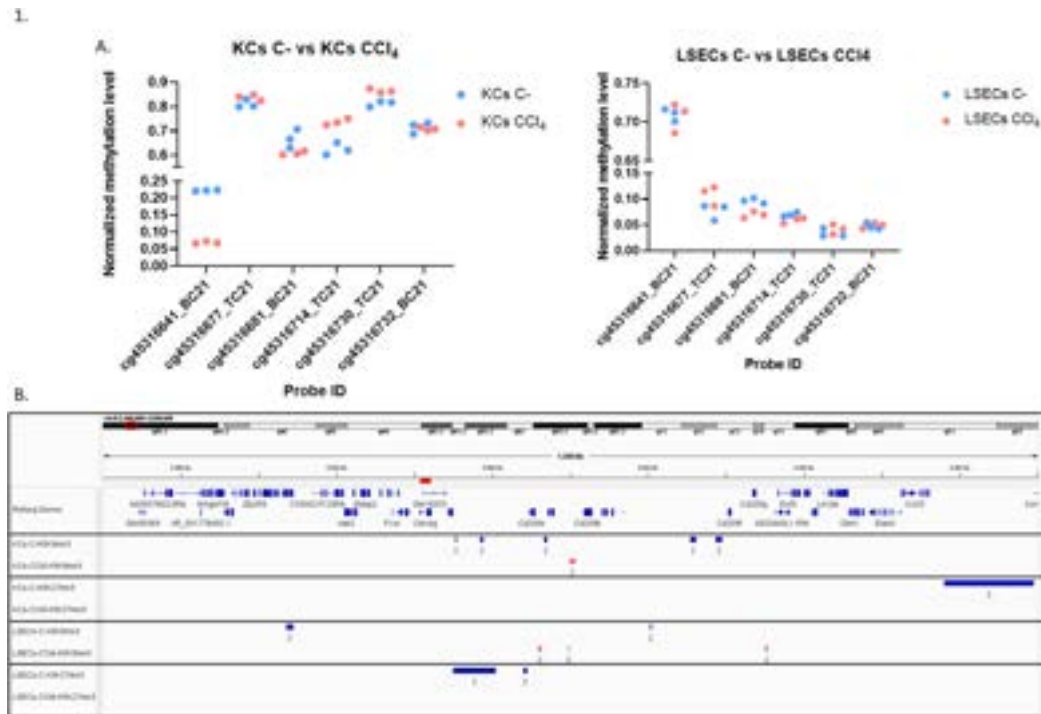


Figure: (abstract: THU-341).

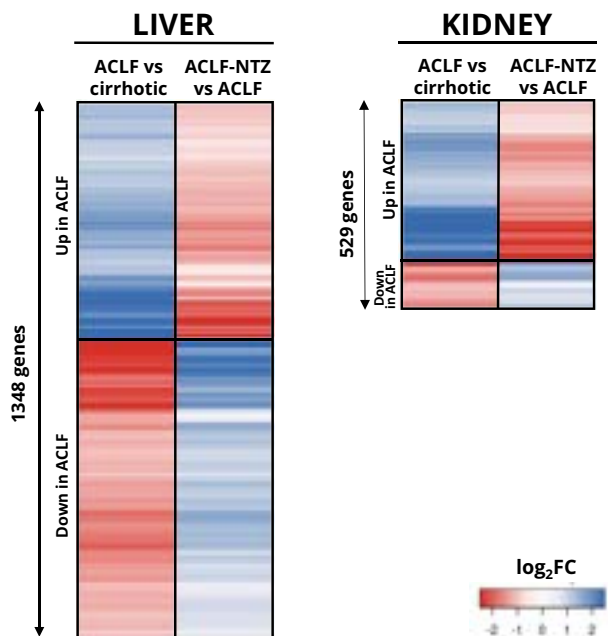


Figure: Heatmap displaying (\log_2) fold changes (FC) of genes differentially expressed in the liver and the kidney between ACLF and cirrhotic rats (adjusted $p < 0.01$ and $FC > 2$). Genes strongly induced by LPS injection (column 1, blue lines) were found to be repressed by NTZ treatment (column 2, red lines) and vice-versa in both liver and kidney.

Conclusion: A single oral administration of nitazoxanide rapidly counteracted LPS-induced systemic and tissue inflammation and protected against organ damage in a pre-clinical model of ACLF.

THU-343

Metabolic Derangements in Hematopoietic Stem and Progenitor Cells (HSPCs) underlie monocyte-macrophage dysfunction in cirrhosis

Deepanshu Maheshwari¹, Nidhi Nautiyal¹, Anupama Parasar¹, Rakhi Maiwall², Nirupma Trehanpati¹, Archana Rastogi³, Shiv Kumar Sarin^{1,2}, Anupam Kumar¹. ¹Institute of Liver and Biliary Sciences, Department of Molecular and Cellular Medicine, New Delhi, India; ²Institute of Liver and Biliary Sciences, Hepatology, New Delhi, India; ³Institute of Liver and Biliary Sciences, Department of Pathology, New Delhi, India

Email: dr.anupamkumar.ilbs@gmail.com

Background and aims: Myeloid-biased hematopoiesis play a key-role in promotion and resolution of injury and infection. Bioenergetic flexibility and metabolic adaptation in response to injury govern the balance between self-renewal and differentiation of hematopoietic stem and progenitor cells (HSPCs). In cirrhosis, this process gets dysregulated with poor resolution of infection and injury. We investigated the changes in energy metabolism of HSPCs and its impact on haematopoiesis to decipher the underlying cause of poor resolution of injury in cirrhosis.

Method: Cirrhosis was induced in C57Bl/6 mice ($n = 35$, 8–10 weeks) by i.p. injection of CCl₄ for 18 weeks till the development of decompensated cirrhosis. Mice were sacrificed at week 3 (W3), 6 (W6), 10 (W10) and 18 (W18) to study kinetic changes in liver bone marrow derived macrophages (BMDMs), their function and bone marrow (BM) haematopoiesis. Bioenergetics of HSPCs was determined using Extracellular Flux Analyzer. Mitochondrial properties were studied using MitoTracker dyes and MitoSOX assay. Glucose uptake (GU) was measured by NBDG-GU kit.

Results: Histology of liver showed inflammation with development of portal fibrosis at W3, bridging fibrosis at W6, cirrhosis at W10, ascites [SAAG 1.8 (1.21–2) g/dL] and jaundice by W18. With increase in liver injury there was a reduction in percentage ($p < 0.0001$) and phagocytic function ($p < 0.05$) of liver macrophages from W6 (Fig. 1A). Compared to age matched healthy animals, the cirrhotic animals showed significant loss of Long-term HSC ($p < 0.0001$) with increase in myeloid progenitor ($p < 0.0001$) from W6 (i.e., in

transition from fibrosis to cirrhosis and thereafter, Fig. 1B). Increase in myeloid progenitor in chronic liver injury was mainly contributed by neutrophil ($p < 0.0001$), with monocyte production being compromised ($p < 0.01$) (Fig. 1C). Bioenergetic analysis of HSPCs showed reduction in glycolysis ($p < 0.01$) due to compromised glucose uptake ($p < 0.0001$) (Fig. 1D) and increase in mitochondrial respiration (Fig. 1E) from W6. Interestingly while basal respiration was increased, there was a reduction in mitochondrial spare reserve ($p < 0.05$) with loss of total ($p < 0.0001$) and functional mitochondria. ($p < 0.0001$) in transition from fibrosis to cirrhosis and thereafter (Fig. 1E and F). In-vitro differentiation of HSPCs to BMDMs showed defects in their maturation ($p < 0.001$) and function ($p < 0.01$). These cells also showed metabolic defects with defective glycolysis and OXPHOS ($p < 0.01$).

Conclusion: Increased OXPHOS with loss of glycolysis disrupts the balance between HSC self-renewal and differentiation, leading to increased myelopoiesis and loss of Long-term HSC reserve in chronic liver injury. Further, increased mitochondrial dysfunction in HSPCs leads to production of defective myeloid cells particularly monocyte-macrophages in chronic liver injury. This may underlie for poor monocyte-macrophage driven resolution during chronic liver injury.

THU-344

Constant alcohol consumption exacerbates hepatic encephalopathy and leads to neuronal loss in rats with chronic liver disease

Farzaneh Tamnanloo^{1,2}, Xiaoru Chen¹, Mariana M. Oliveira¹, Mélanie Tremblay¹, Christopher F Rose^{1,2}. ¹CRCHUM, Hepato-neuro lab, Montréal, Canada; ²Université de Montréal, Medicine, Montréal, Canada

Email: farzaneh.tamnanloo@gmail.com

Background and aims: Hepatic encephalopathy (HE) is a debilitating neurological complication of chronic liver disease. Alcohol is a major etiological factor known to induce liver injury and disease. However,

excessive alcohol consumption has been shown to also induce atrophy of the cerebellum and cerebellar degeneration. To date, the role of alcohol in the development of HE remains unclear. Here we examined the effects of constant alcohol consumption on the neurological decline in rats with chronic liver disease induced following bile duct ligation (BDL).

Method: 5-week BDL rats and Sham-operated controls (Sham) were used. Starting day 7 after surgery, rats were gavaged twice a day (3 hours apart) with alcohol at a dose of 3 g/kg (51% v/v), 5 days per week, for 4 weeks. Motor coordination was assessed using Rotarod every week until week 5. At the end of the model (day 40), anxiety-like behavior was assessed using the open field (OF) and elevated plus maze (EPM). Upon sacrifice, brains were collected, and western blot and immunohistochemical (IHC) analyses were used to investigate the neuronal integrity as well as assess apoptosis and necroptosis pathways in the cerebellum.

Results: Alcohol worsened motor coordination performance in weeks 2, 3, 4, and 5 in BDL-alcohol rats ($p < 0.01$ vs respective shams). Anxiety-like behavior significantly increased in BDL-alcohol rats, with an increase in time spent in the closed arms of EPM and a decrease in time spent in the center of the open field ($p < 0.05$ vs respective shams). These impairments were associated with decreased neuronal markers of NeuN and SMI311 ($p < 0.01$ and $p < 0.05$, respectively), increased apoptotic markers of cleaved/pro-Caspase3 and Bax/Bcl2 ratio ($p < 0.001$ and $p < 0.01$ respectively), increased necroptosis markers of pRIP3 and pMLKL ($p < 0.01$ and $p < 0.001$, respectively), decreased total antioxidant capacity ($p < 0.001$) and increased oxidative stress marker of 4-HNE ($p < 0.05$) in the cerebellum of BDL-alcohol rats when compared to respective controls. IHC results confirmed the colocalization of apoptotic marker (cleaved Caspase3) and necroptosis marker (pMLKL) in the granular and Purkinje layer neurons of the cerebellum of BDL-alcohol rats.

Conclusion: Constant alcohol consumption exacerbates HE by worsening motor coordination impairment and increasing anxiety

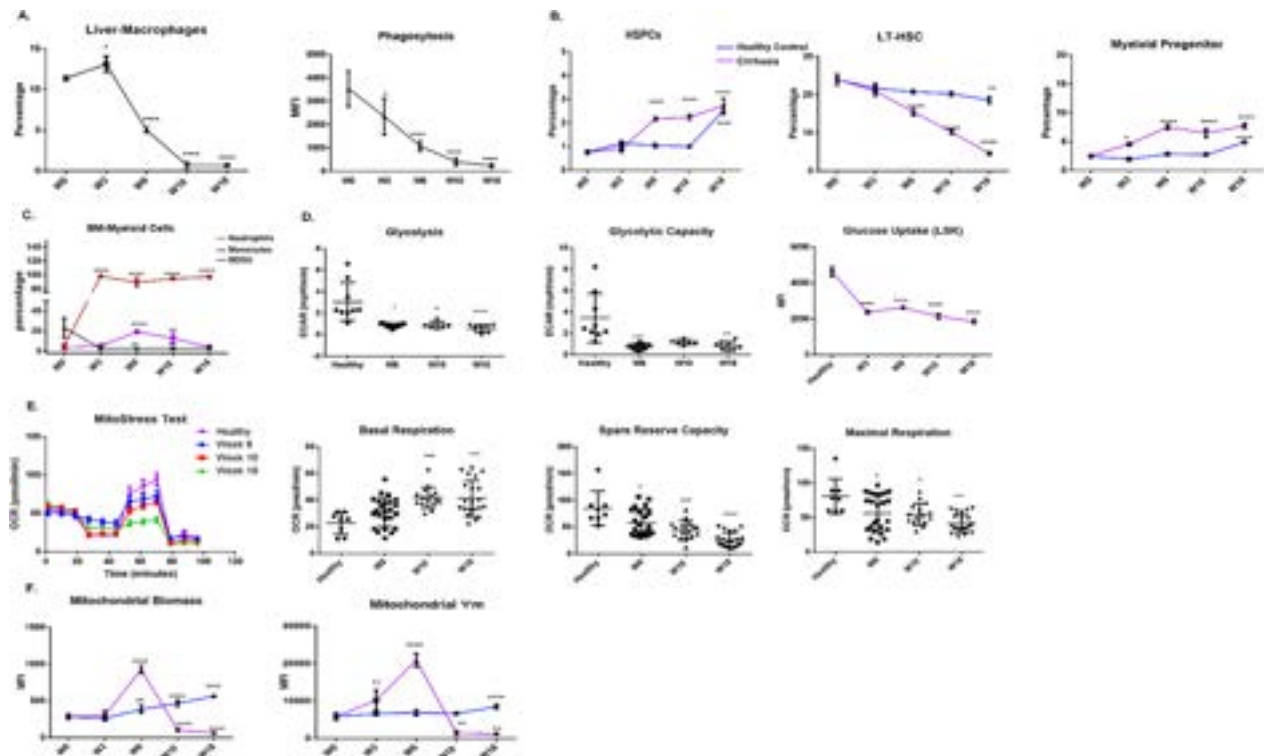


Figure 1: Metabolic Derangement in Hematopoietic Stem and Progenitor Cells (HSPCs) may underlie monocyte-macrophage dysfunction in cirrhosis: Kinetic changes in (A.) liver macrophages and their phagocytosis (B.) Hematopoietic Stem and Progenitor Cells (HSPCs), LT-HSCs and Myeloid progenitors and (D.) BM-Myeloid Cells (Neutrophils, Monocytes and MDSCs) during chronic liver injury. (D.) Changes in glycolysis, glycolytic capacity and glucose uptake and (E.) Real time changes in oxygen consumption rate of HSPCs during chronic liver injury. (F.) Changes in mitochondrial biomass and potential of HSPCs during chronic liver injury

Figure: (abstract: THU-343).

POSTER PRESENTATIONS

in BDL rats. Furthermore, our results show neuronal loss through apoptosis and necroptosis in the cerebellum of BDL-alcohol rats. Additionally, higher levels of oxidative stress marker of 4-HNE and decreased total antioxidant capacity in the cerebellum of BDL-alcohol rats suggest that oxidative stress is the triggering factor of apoptosis and necroptosis pathway leading to neuronal loss/injury. These results demonstrate the adverse effect of constant alcohol consumption on the development of HE and neuronal integrity in chronic liver disease.

THU-345

Targeting myeloid-derived suppressor cells in a carbon tetrachloride-induced murine model of chronic liver injury

Emilio Flint¹, Caner Ercan², Lucia Possamai³, Evangelos Triantafyllou³, Christine Bernsmeier¹, Emilio Flint¹, Caner Ercan³, Lucia Possamai⁴, Evangelos Triantafyllou⁴, Christine Bernsmeier^{1,2}. ¹University of Basel, Department of Biomedicine, Basel, Switzerland; ²University Hospital Basel, Institute of Medical Genetics and Pathology, Basel, Switzerland; ³Imperial College, Department of Metabolism, Digestion and Reproduction, London, United Kingdom ⁴Department of Biomedicine, University of Basel (CH); ⁵University Centre for Gastrointestinal and Liver Disease, Basel; ⁶Institute of Medical Genetics and Pathology, University Hospital Basel (CH); ⁷Department of Metabolism, Digestion and Reproduction, Imperial College London, UK
Email: emilio.flint@unibas.ch

Background and aims: Previously, we identified immunosuppressive monocytic myeloid-derived suppressor cells (M-MDSC) in the circulation of patients with cirrhosis and liver failure. These cells increased with disease severity and were associated with distinct impaired innate and adaptive immune responses, increased infection susceptibility and mortality. Impaired immune responses and M-MDSC expansion were reversed by TLR3 agonism *in vitro*. Thus, we aimed to identify MDSC in murine models of fibrosis and assess the

safety and efficacy of polyinosinic:polycytidylic acid (pl:pC) administration *in vivo*.

Methods: C57BL/6 mice were intraperitoneally (i.p.) administered carbon tetrachloride (CCl₄) for 6 weeks. To mimic an acute bacterial challenge, a group of CCl₄ mice was injected lipopolysaccharide (LPS) 24 hours prior to sacrifice. In another group, pl:pC (1 mg/Kg, i.p.) was administered 4 times for one week prior to sacrifice (A-B). Blood and liver cells were isolated and characterised with flow cytometry. Immunofluorescent stainings of CD11b+Gr-1+ identified MDSC in liver sections. Liver histopathology was evaluated on HandE or SiriusRed with Ishak Grade and Ishak Stage scores, plasma markers were quantified.

Results: CCl₄-treated mice displayed liver inflammation, fibrosis, increased plasma ALT levels and changes in frequency of myeloid cells in both the circulation and the liver. Phenotypically distinct polymorphonuclear (PMN)-MDSC and M-MDSC expanded in the blood (2-fold per ml, $p=0.001$, $p<0.0001$) and liver (7-fold per gram, $p<0.0001$ and $p<0.0001$) in the CCl₄ model (C). Moreover, LPS challenge significantly increased numbers of hepatic MDSC compared to saline-treated CCl₄ controls (C). MDSC expansion in the liver of CCl₄ mice was confirmed with immunofluorescent stainings (D). Both PMN-MDSC and M-MDSC expressed distinct markers Axl and Mertk, while M-MDSC expressed PD-L1. No changes in body weight were observed in CCl₄ mice with or without pl:pC (B), and pl:pC did not reduce MDSC numbers in the current therapeutic protocol. In addition, liver damage, function and necroinflammation (Ishak-Grade) were unvaried following pl:pC administration, while liver fibrosis (Ishak-Stage) was reduced ($p=0.0240$) (E).

Conclusion: We identified MDSC in the circulation and liver in murine models of fibrosis (CCl₄ and CCl₄ with LPS). Our data support the liver-related safety of pl:pC therapy, although MDSC numbers were unchanged. Yet, pl:pC alleviated fibrosis. Novel approaches targeting MDSC *in vivo* merit further evaluation.

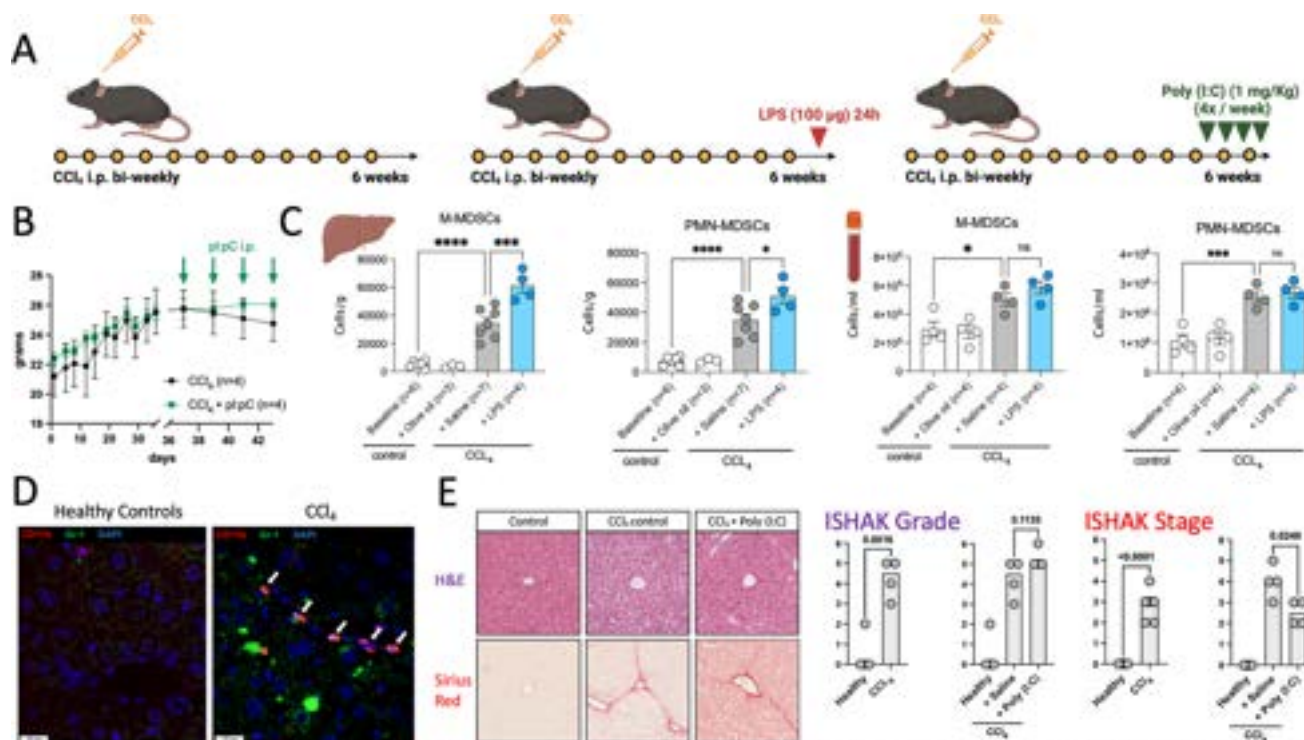


Figure: (abstract: THU-345).

THU-346

Cirrhosis alters receptor mediated clearance of therapeutic antibodies by hepatic sinusoidal endothelial cells

Bethany James¹, Louise Gliddon², Matthew Gardener², Chris J Weston¹, Patricia Lalor¹. ¹University of Birmingham, Centre for Liver and Gastroenterology Research and National Institute for Health Research (NIHR) Birmingham Biomedical Research Centre, Institute of Immunology and Immunotherapy, Birmingham, United Kingdom; ²Antibody Pharmacology, Biopharm Discovery, Glaxo Smith Kline Research and Development, Hertfordshire, United Kingdom
Email: bhj711@student.bham.ac.uk

Background and aims: Fully human or humanized monoclonal antibodies (mAbs) are increasingly used for immunotherapy; but the design of these molecules is complicated by the need to bypass normal antibody clearance mechanisms. The liver plays a key role in the internalisation and catabolic clearance of biological therapies via interactions with scavenger and Fc-receptors within the hepatic reticuloendothelial system. Liver sinusoidal endothelial cells (LSECs) express many of these receptors and play key roles in clearance of immune complexes and regulation of antibody pharmacokinetics. However, changes in the expression of key membrane receptors involved in antibody clearance in chronic disease are not well characterized and may impact on drug efficacy in target patients. Therefore, we wanted to investigate the impact of cirrhosis on the expression of key receptors by human LSEC and assess how this impacts on the uptake and clearance of varying formats of monoclonal antibodies.

Method: LSEC were isolated from diseased and normal human liver tissue; as well as use of whole liver for extraction of RNA and protein lysates. A novel recycling assay was designed using primary cells from both diseased and healthy livers in which the binding and internalisation of chimeric, human/humanised and bispecifics were visualised through immunofluorescence confocal imaging, flow cytometry and quantification of antibody within cells over 4 and 8 hours time periods via meso-scale discovery (MSD) assay. Furthermore, whole liver tissue wedges were used for antibody perfusion over a 4-hour period after which the wedges were either fixed for chromogen staining or mechanically digested to generate cell suspensions for flow cytometric analysis of antibody localisation. Fluorescence intensity and MFI was obtained using ImageJ and FlowJo and one-way ANOVA and student T tests were used to statistically analyse the data.

Results: Our results confirm that expression of three important receptors known for antibody clearance by human LSEC (CD32b, DC-SIGN and Mannose Receptor) is significantly altered at the protein level in cirrhosis. Importantly confocal imaging, MSD, flow cytometry and novel recycling assays on isolated diseased and healthy LSEC confirm that LSEC can bind and internalize therapeutic mAbs. We found that the binding capacity is altered on cells that originated from cirrhotic livers with immunofluorescent staining revealing a statistically significant difference between healthy and cirrhotic LSEC at 4 hours (Figure). Cells from cirrhotic livers also lacked the ability to process therapeutic biomolecules as evidenced by the retention of fluorescent signal at the 8-hour time point when compared to cells from donor tissue.

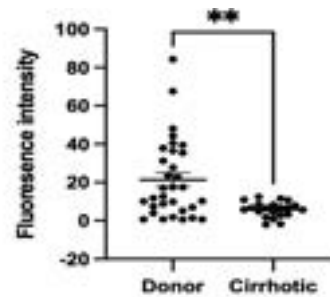


Figure 1: LSEC were isolated from either donor (n=32) or explanted cirrhotic livers (n=21). Once confluent these cells were seeded into 6 chamber ibids and were treated with a monoclonal antibody X for 4 hours. Here the cells were fixed with 4% PFA and permeabilised with 0.1% Triton before being stained with an Alexa fluor anti-mouse IgG 488 secondary. Fluorescence intensity was determined using ImageJ and statistical significance determined by an unpaired T test [p<0.0001]. Data shown as mean ± SEM. Each point corresponds to an individual liver.

Figure:

Conclusion: Our novel assays using human LSEC have demonstrated that changes in LSEC phenotype accompanying chronic disease may explain altered drug pharmacokinetics and toxicity observed in early trials. Therefore, future antibody development pathways should incorporate testing in models representative of the target patient demographic to address issues of poor kinetics, unexpected toxicity and poor predictive ability.

THU-347

Evaluation of the effect of glucocorticoids on cardiac chronotropic dysfunction in cirrhotic rats, do dopamine receptors also play a role?

Mohadese Shokrian Zeini^{1,2}, Maryam Shokrian Zeini^{1,2}, Qamar Niaz^{1,3}, Sania Mehreen⁴, Farahnaz Jazaeri¹. ¹Department of Pharmacology, School of Medicine, Tehran University of Medical Sciences, Tehran, Iran; ²Experimental Medicine Research Center, Tehran University of Medical Sciences, Tehran, Iran; ³Department of Pharmacology and Toxicology, Faculty of Bio-Sciences, University of Veterinary and Animal Sciences, Lahore, Pakistan; ⁴Department of Zoology, Faculty of Fisheries and Wildlife, University of Veterinary and Animal Sciences, Lahore, Pakistan
Email: fjazaeri@yahoo.com

Background and aims: Liver cirrhosis is defined by the regenerative nodules and fibrous septa formation, often causing a complication called cirrhotic cardiomyopathy (CCM) with chronotropic dysfunction. β -adrenergic receptors (β -ARs) are down-regulated in CCM. Glucocorticoids and the dopamine receptor's downstream signaling affect this pathway. Thus, we investigated the dexamethasone treatment effect on chronotropic dysfunction and the possible involved pathways in cirrhotic rats.

Method: Bile duct ligation (BDL) or Sham surgery was performed on male Wistar rats to induce cirrhosis or used as control groups and grouped as BDL/NS (normal saline) and BDL/dexamethasone [2.2 mg/kg/day through intramuscular injection, a short term treatment for the last three days of 4 weeks of BDL (28 days)], Sham/NS, and Sham/dexamethasone groups. *In vivo*, chronotropic responses and corrected QT (QTc) interval were studied through electrocardiography (ECG) before and after stimulation with different concentrations of isoproterenol, each concentration for 5 minutes. The tumor necrosis factor- α (TNF- α) and interleukin-1 β (IL-1 β) in heart ventricles were investigated through ELISA. Immunohistochemistry was performed to investigate the dopamine receptor D1 (DRD1) and D2 (DRD2) protein expression levels in the heart ventricles. Real-time polymerase chain reaction (real-time PCR) was conducted to investigate the expression of DRD1, DRD2, and Guanine nucleotide-binding protein G (olf) subunit alpha L (GNAL) receptors (relative to GAPDH) in the heart atria.

Results: The chronotropic responses decreased in BDL/NS and increased in BDL/dexamethasone group. The QTc interval and

POSTER PRESENTATIONS

ventricular TNF- α level were increased in BDL/NS and decreased in BDL/dexamethasone group. The IL-1 β level increased in BDL/NS group and was not affected in BDL/dexamethasone group. The atrial DRD1 mRNA expression level was not affected in BDL/NS group, while the DRD2 and GNAL mRNA expression levels were decreased in atria. The atrial DRD1 mRNA expression level was decreased in the BDL/dexamethasone group without affecting the DRD2 and GNAL mRNA expression levels in atria. The ventricular DRD1 and DRD2 protein expression levels were down-regulated in BDL/NS group, while the DRD1 protein expression level was up-regulated in the BDL/dexamethasone group without affecting the DRD2 protein expression level in ventricles.

Conclusion: Dexamethasone effectively treats the chronotropic hypo-responsiveness and decreases the QTc interval in CCM by

affecting the inflammation and the DRD1 expression level in the cirrhotic rat's hearts.

THU-348

Distinct changes in the inflammatory profile of patients with EASL-CLIF- versus APASL-acute-on-chronic liver failure

Mona-May Langer^{1,2}, Sabrina Guckenbiehl², Alina Bauschen², Gerald Denk¹, Christian M. Lange^{1,2}. ¹Department for Internal medicine II, LMU hospital, Munich, Germany; ²Department for gastroenterology and hepatology, University hospital Essen, Essen, Germany
Email: monamay.langer@med.uni-muenchen.de

Background and aims: Definitions of acute-on-chronic liver failure (ACLF) are heterogeneous. Whereas in APASL-definition the liver is the most important organ failure, EASL-CLIF- and NACSELD-definitions focus on extrahepatic organ failures. In the present study, we

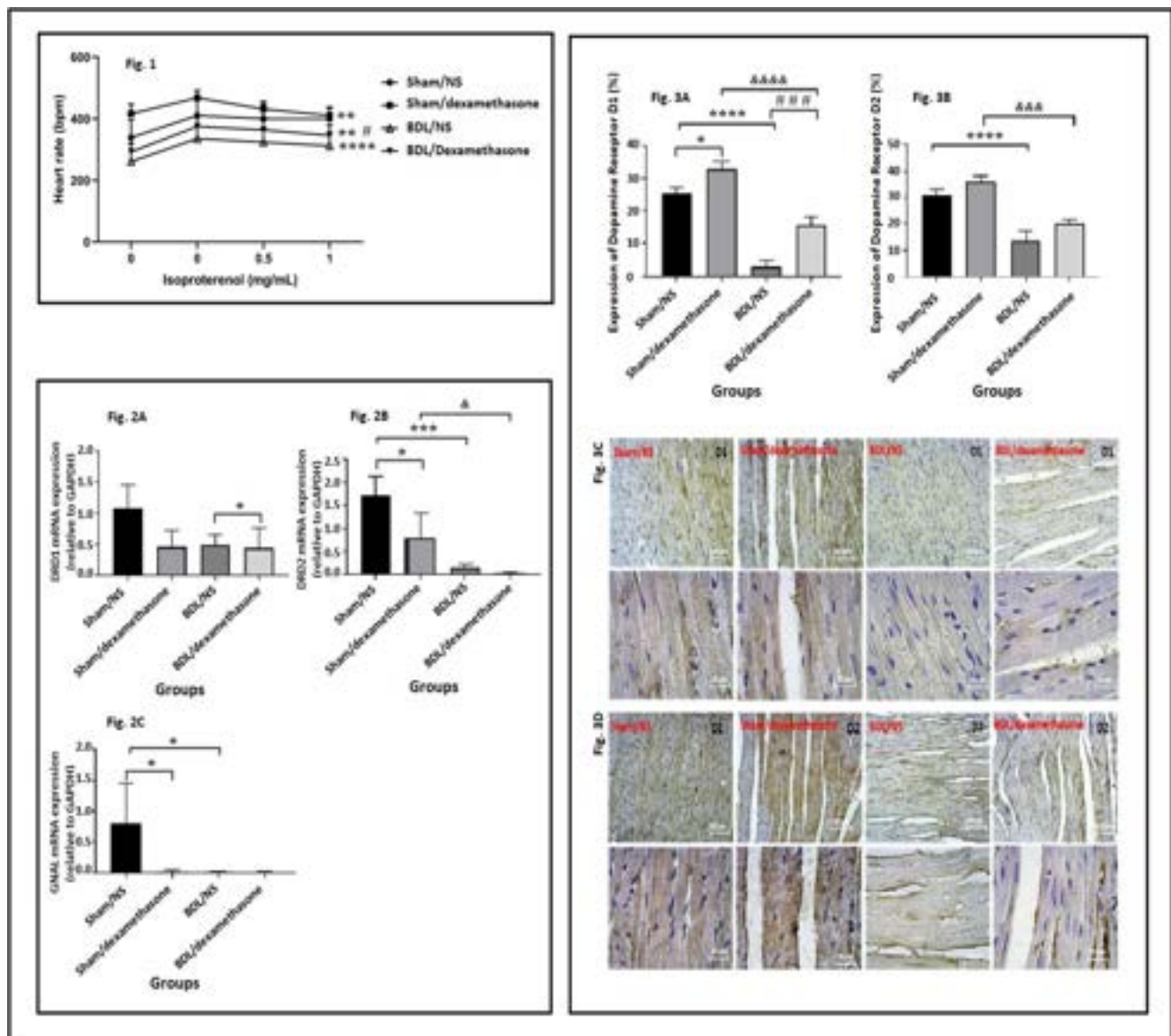


Figure: (abstract: THU-347): *In vivo* average heart beating rates (Fig. 1), DRD1, DRD2, and GNAL mRNAs expression in atria (Fig. 2), and DRD1 and DRD2 proteins expression in ventricles (Fig. 3) of Sham (Sham-operated) and BDL (cirrhotic) rats quantified through ECG, real-time PCR, and IHC, respectively. The data are shown after treatment with saline or dexamethasone (2.2 mg/kg/day) for 3 consecutive days. The average heart beating rates data were analyzed through two-way ANOVA with post-hoc Tukeys' test and the mRNAs and proteins expression data through one-way ANOVA with post-hoc Tukeys' test and presented as mean \pm SEM. Total 6 animals were included in each experimental group. Fig. 1: **p < 0.01 Sham/dexamethasone and BDL/dexamethasone groups compared to Sham/NS group; ****p < 0.0001 BDL/NS group compared to Sham/NS group; and #p < 0.05 BDL/dexamethasone group compared to BDL/NS group.

therefore determined associations between the presence and absence of ACLF and correlate these with inflammatory molecules, clinical parameters and outcome.

Method: 208 hospitalized patients with liver cirrhosis with or without ACLF were recruited from a prospective cohort study. 76 inflammatory molecules were quantified by proximity extension analysis assay (Olink, Uppsala, Sweden). Associations between inflammatory profiles and types of ACLF were determined. Moreover, surface expression profiles of immune cells were analyzed by flow cytometry.

Results: Of 208 patients, 127 had no ACLF at all, while 81 had any ACLF. Of patients with ACLF, 20 had ACLF based on the APASL-definition only, while 30 had ACLF exclusively based on the EASL-CLIF-definition. All 12 patients with NACSELD-ACLF also fulfilled the EASL-CLIF criteria. A differential expression of inflammatory molecules according to the type of ACLF was observed. Overall, patients with APASL-ACLF (but without EASL/NACSELD-ACLF) had rather moderate changes of inflammatory mediators compared to patients with acute decompensation without ACLF, whereas patients who met the EASL- or NACSELD-definition of ACLF showed signatures of substantial systemic inflammation. Furthermore, a differential increase of mediators between EASL-CLIF- and APASL-ACLF was observed, as for example FGF-19 and HGF were particularly increased in APASL-ACLF while VEGFA, FGF-23, TNF-beta or IL-17 are significantly upregulated in EASL-CLIF. Data on immune cell phenotypes will be presented.

Conclusion: Patients with APASL- versus EASL-CLIF-ACLF have partially distinct inflammatory profiles, which may point towards distinct pathophysiological mechanisms in different types of ACLF.

THU-349

Bacterial DNA translocation-induced systemic inflammation is associated with overt hepatic encephalopathy and predicts mortality in patients with cirrhosis

Kessarin Thanapirom^{1,2,3}, Sirinporn Suksawatamnuay^{1,2,3}, Salisa Wejnarnuarn^{1,2,3}, Panarat Thaimai^{1,2,3}, Nipaporn Siripon^{1,2,3}, Prooksa Ananchuensook^{1,2,3}, Supachaya Sriphoosanaphan^{1,3}, Sombat Treepasertsuk¹, Piyawat Komolmit^{1,2,3}. ¹Division of Gastroenterology, Department of Medicine, Faculty of Medicine, Chulalongkorn University and King Chulalongkorn Memorial Hospital, Medicine, Bangkok, Thailand; ²Liver Fibrosis and Cirrhosis Research Unit, Chulalongkorn University, Bangkok, Thailand; ³Excellence Center in Liver Diseases, King Chulalongkorn Memorial Hospital, Thai Red Cross Society, Bangkok, Thailand
Email: pkomolmit@yahoo.co.uk

Background and aims: There is mounting evidence that bacterial translocation (BT) and systemic inflammation play a key role in the pathogenesis of cirrhotic complications. However, the data on the relationship between BT, hepatic encephalopathy (HE), and mortality is limited. Therefore, we aimed to assess the association between bacterial DNA (bactDNA) translocation, inflammatory markers, ammonia level, and the presence of HE in patients with cirrhosis. In addition, we prospectively assessed the prognostic role of bactDNA translocation in predicting mortality and liver-related complication (LRC) within six months.

Method: Cirrhotic patients without bacterial infection were enrolled at Chulalongkorn University, Bangkok, Thailand, from June 2021 to October 2022. Grading of HE was classified by the West Haven Criteria and Psychometric hepatic encephalopathy score (PHES) \leq 5. BactDNA, lipopolysaccharide-binding protein (LBP), tumor necrosis factor-alpha (TNF-alpha), interleukin-6 (IL-6), soluble CD14 (sCD14), and venous ammonia were evaluated. LRC was a composite end point of bacterial infection, variceal bleeding, overt HE, or new onset ascites.

Results: Overall, 294 cirrhotic patients were enrolled. Of these, 92 (31.3%) and 58 (19.7%) had covert and overt HE, respectively. Patients

with overt HE had more bactDNA translocation (48.3% vs. 31.3%, $p = 0.02$), higher serum LBP ($13,480.0 \pm 9,469.3$ vs. $10,788.5 \pm 7,339.4$ ng/ml, $p = 0.01$), IL-6 (105.9 ± 302.2 vs. 10.9 ± 25.6 pg/ml, $p = 0.001$), and ammonia level (92.7 ± 41.3 vs. 62.2 ± 26.8 ug/dL, $p < 0.001$) than those without HE. While these tests revealed no differences between patients with covert HE and those without HE. Patients with bactDNA detection exhibited a greater white cell count, serum LBP, and IL-6 than those without bactDNA. During the 6-month follow-up, 40 patients (13.6%) died, and 65 patients (22.1%) developed at least one of the LRC. The multivariate Cox regression analysis showed bactDNA translocation (aHR = 2.14, 95%CI: 1.01–4.51, $p = 0.04$), MELD (aHR = 1.11, 95%CI: 1.07–1.16, $p < 0.001$), age (aHR = 1.07, 95%CI: 1.04–1.11, $p < 0.001$) and serum IL-6 (aHR = 1.002, 95%CI: 1.000–1.003, $p = 0.03$) were independent predictors of the 6-month mortality. Only the MELD score (aHR = 1.10, 95%CI: 1.06–1.15, $p < 0.001$) was an independent predictor of LRC development.

Conclusion: Apart from hyperammonemia, bactDNA translocation-related systemic inflammation is a potential pathophysiological mechanism of overt HE in patients with cirrhosis. In addition, the detection of bactDNA translocation and IL-6 elevation are independent predictors of 6-month mortality in patients with cirrhosis.

THU-350

Platelets from patients with decompensated cirrhosis display pro-inflammatory features

Simone Di Cola¹, Lucia Stefanini^{1,2}, Ludovica Lombardi¹, Stefano Fonte¹, Francesca Maiorca¹, Davide Pallucci¹, Ramona Marrapodi¹, Annamaria Sabetta¹, Marzia Miglionico¹, Roberto Cangemi¹, Marcella Visentini¹, Oliviero Riggio¹, Manuela Merli¹, Stefania Basili¹. ¹Department of Translational and Precision Medicine, Sapienza University, Rome, Italy, Italy; ²Istituto Pasteur Italia-Fondazione Cenci Bolognietti, Rome, Italy, Italy
Email: simone.dicola@uniroma1.it

Background and aims: Changes in platelet structure and function occur in chronic liver disease. These changes have also been implicated in progression of liver disease. Cirrhotic patients have a lower platelet count and a heightened risk of thrombosis. However, the functional state of circulating platelets in cirrhotic patients is debated and poorly understood. Thus, we aim to characterize the phenotypical and functional features of circulating platelets of cirrhotic patients.

Method: We here report the preliminary analysis of an ongoing interventional longitudinal study.

(PVTRIFA2017-EudraCT 2017-000488-34). We analyzed the platelet phenotype at baseline of patients with cirrhosis (Child-Pugh score B and C) in comparison to healthy donors matched by age and sex. Exclusion criteria were assumption of aspirin or other non-steroidal anti-inflammatory drugs at the time of enrollment. Phenotype, function, and immune interactions of platelets were studied by multiparameter flow cytometry within 1 hour from blood withdrawal. The study was approved by the Ethics Committee of the Hospital Umberto I (Rome, Italy).

Results: Decompensated cirrhotic patients had a significantly lower platelet count compared to healthy controls. The platelet size was larger than controls, but the immature platelet fraction (i.e. the fraction of platelets that are younger) was not increased, suggesting that there may be a higher platelet turnover, followed by a near-immediate platelet consumption. Circulating platelets from cirrhotic patients displayed higher levels of receptors implicated in immune-like functions (P-selectin, GPIIb, FcγRIIA) compared to controls and had a higher propensity to bind monocytes and lymphocytes in peripheral blood. Moreover, platelets from cirrhotic patients exhibited a higher platelet responsiveness to agonists of Immunoreceptor Tyrosine-based Activation Motif (ITAM)-coupled receptors, but a lower responsiveness to the thrombin-receptor agonist peptide (TRAP) signaling through G protein-coupled receptors (GPCRs) (Figure 1).

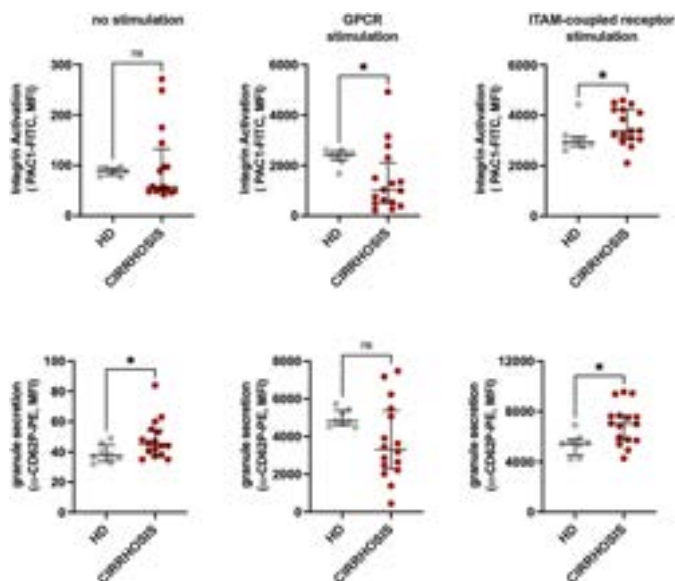


Figure: Activation of circulating platelets determined by multicolour flow cytometry. Citrated blood from healthy donors (HD, grey) or decompensated cirrhotic patients (cirrhosis, red) was diluted 1:10 and incubated with PAC1-FITC (that recognizes the active conformation of integrin α IIb β 3) and α -CD62P-PE (that is a marker of α granules secretion) in resting (no stimulation) or stimulated conditions with agonists specific for platelet-specific G protein-coupled receptor (GPCRs) or Immunoreceptor Tyrosine-based Activation Motif (ITAM)-coupled receptors. Samples were acquired on a BD Accuri C6 Plus and analysed with FlowJo version 10.8. Mann-Whitney test was performed for statistical analysis. * $p < 0.05$.

Conclusion: The study identified novel pro-inflammatory features that characterize platelets from decompensated cirrhotic patients. These may represent novel molecular targets to prevent thrombotic complications and potentially to decelerate the progression of liver disease.

THU-351

Single-cell RNA transcriptomics of peripheral blood mononuclear cells revealed altered gene expressions in monocyte and HLA variations in decompensated liver cirrhosis patients with sepsis

Nirupma Trehanpati¹, Rashi Sehgal¹, Pramod Gautam², Mojahidul Islam², Jayesh Kumar Sevak², Navkiran Kaur³, Gayatri Ramakrishna², Rakhi Maiwall², Shiv Kumar Sarin². ¹Institute of Liver and Biliary Sciences, Molecular and Cellular Medicine, New Delhi, India; ²Institute of Liver and Biliary Sciences, New Delhi, India; ³Amity University Noida, Noida, India
Email: trehanpati@gmail.com

Background and aims: Immune dysfunction and systemic inflammation are the hall marks of decompensated liver cirrhosis (DLC) patients, which gets aggravated with the development of sepsis. The molecular and cellular basis of rapid immune deterioration in cirrhotic patients is not well understood. We investigated immune responses in peripheral blood mononuclear cells (PBMCs) in DLC patients with sepsis using single-cell RNA (scRNA) transcriptomic.

Method: Twenty one DLC patients (age 42+7Yr, all males) with sepsis (n = 10) and without sepsis (n = 11) along with ten healthy controls were recruited. Isolated PBMCs from seven DLC patients were subjected to scRNA transcriptomics using BD Rhapsody (BD Biosciences, #633701). After quality control, raw fastq files were aligned to reference Human genome (GRCh38). Following normalization, a count matrix was generated and then using Seurat (v4.0), this count matrix was filtered and processed further for dimensionality reduction, batch correction, differential gene expression, clustering, gene set enrichment analysis (GSEA) and cell-type identification. Further, HLA DRB1 alleles typing was analysed in DLC patients by Sequence Specific Primer method in Luminex PCR.

Results: Cells with high proportion of mitochondrial and low proportion of ribosomal reads were removed. Single cell sequencing technology have revealed 10 clusters and 7 cell types with significant heterogeneity in monocytes. GSEA revealed, that in DLC patients, there was significant ($p > 0.05$) decrease in gene expression associated with O⁶-methylguanine-DNA methyltransferase (MGMT) mediated DNA damage reversal, Mitochondrial transcription termination and Melanin biosynthesis, but upregulated expression of genes belonging to lactose synthesis, hydroxycarboxylic-acid, FGFR1b and FGFR1c ligand binding and receptors compared to HC. Cluster pertaining to classical monocytes in DLC patients with sepsis, had significant down-regulation of genes related to NF- κ B signaling, TNF- α signaling, IL-17 signaling compared to without sepsis group. scRNA technology also revealed that along with decreased HLA-DR expression other HLA markers like HLA-A, HLA-B and HLA-DQA1 were also decreased in sepsis but with unique increased expression of HLA-DRB1, HLA-C, HLA-E, HLA-DRA, and HLA-DQA2. Genotyping of HLA-DRB1 by luminex assay revealed presence of HLADRB1*11 allele in DLC patients with sepsis (HLA-DRB1*07DRB1*11, HLA-DRB1*11 DRB1*14, HLA-DRB1*11 DRB1*13) than without sepsis.

Conclusion: Our study indicated possible reason for sepsis development in DLC patients due to defects in NF- κ B, TNF- α and IL-17 signaling in classical monocytes. Increased frequency of HLA-DRB1*11 in monocytes enhanced the potential of sepsis development in DLC patients.

THU-352

Role of extracellular vesicles in sarcopenia associated to chronic liver diseases

Simone Di Cola¹, Laura Barberi^{1,2,2}, Cristiana Porcu³, Lucia Lapenna¹, Stefano Fonte¹, Lorenzo Ridola¹, Antonio Musarò³, Manuela Merli¹.

¹Department of translational and precision medicine, Sapienza university of Rome, Italy, Italy; ²Sapienza University of Rome, Department of translational and precision medicine, Rome, Italy; ³2 DAHFMO, Unit of histology and medical embryology, Sapienza university of Rome, Italy

Email: simone.dicola@uniroma1.it

Background and aims: Sarcopenia is a condition of reduced skeletal muscle mass, quality and strength highly prevalent in patients with chronic liver disease and associated with adverse clinical outcomes. Its pathogenesis is multifactorial and mainly resulting from an imbalance between muscle protein synthesis and degradation; however, mechanisms underlying sarcopenia in liver disease are still not completely understood as the mediators of the liver-muscle axis have not yet been identified. Given the emerging role of extracellular vesicles (EVs) in mediating intercellular communication and the metabolic cross-talk between skeletal muscle and liver, we aimed to evaluate whether circulating EVs in liver disease could vehicle to skeletal muscle bioactive molecules, such as microRNAs, able to induce sarcopenia.

Method: Primary human muscle cells were exposed to EVs isolated from serum of healthy (H-EVs; n = 9) and cirrhotic individuals with sarcopenia (C-EVs; n = 13) at different times of muscle culture. Finally, they were examined, by immunofluorescence analysis, for their ability to differentiate in myotubes and, by western blotting, for the expression of markers of protein synthesis and degradation. Moreover, miRNA cargo of serum cirrhotic patients derived-EVs were analysed and compared with that of healthy subjects derived-EVs, examining the expression levels of some microRNAs involved both in liver disease and in muscle development.

Results: We showed that serum EVs were efficiently internalized by skeletal muscle cells and that EVs isolated from cirrhotic individuals were able to cause in vitro muscle atrophy. Indeed, they induced a decrease in muscle differentiation, as revealed by a reduced size of

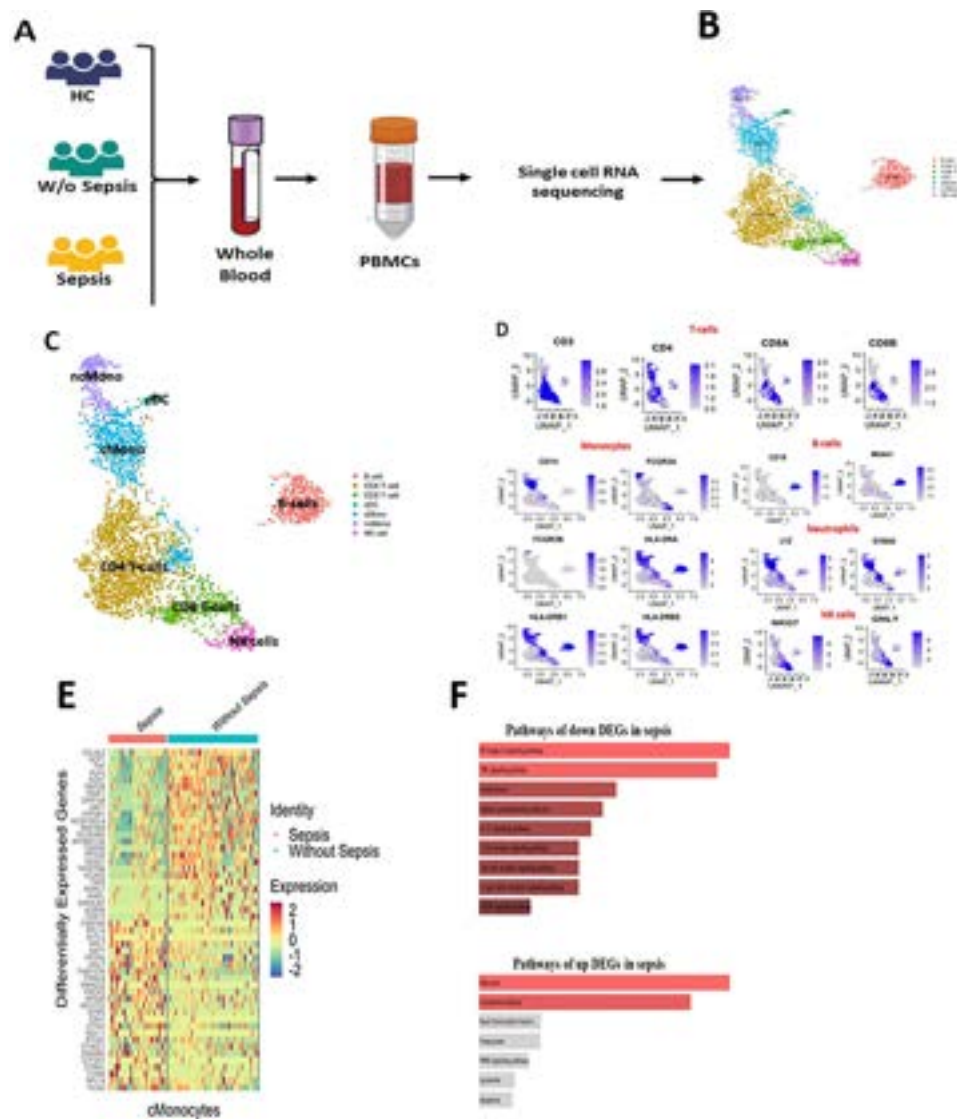


Figure: (abstract: THU-351).

myotubes in culture, and downregulated expression of myosin protein ($p < 0.05$), and an increase in protein degradation, as showed by an upregulation of Murf-1 and Atrogin-1 mRNA expression levels ($p < 0.05$), compared with serum EVs from healthy individuals. Moreover, EVs from cirrhotic patients exhibited significant higher expression levels ($p < 0.05$) of microRNAs, such as miR-223, -133a, -29a, -128a, -21, and -199a-3p, targeting the two most important signaling pathways in muscle tissue: the TGF- β /myostatin/BMP and PI3K/AKT/mTOR pathways, regulating protein synthesis and degradation respectively.

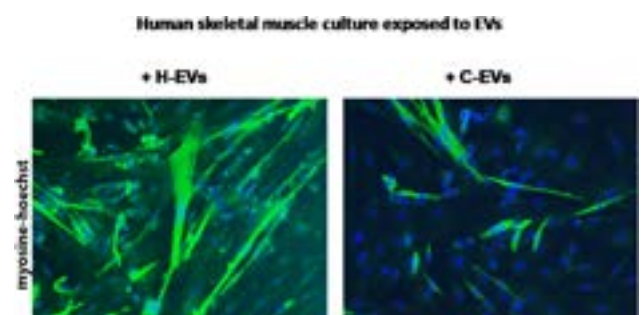


Figure:

Conclusion: Serum EVs in cirrhotic patients, likely released by damaged liver, could affect skeletal muscle homeostasis and mediate sarcopenic processes by delivering to muscle cells a specific miRNA cargo. Therefore, circulating EVs could be key players of the liver-muscle axis in sarcopenia associated to liver disease.

THU-353

Effects of β -adrenergic hyperstimulation, liver cirrhosis and acute-on-chronic liver failure (ACLF) on the small intestinal gut-vascular barrier (GVB)

Marco Felber¹, Reiner Wiest¹. ¹Institute for Visceral Surgery and Medicine, Gastroenterology, Bern, Switzerland
Email: marco.felber@unibe.ch

Background and aims: Acute on chronic liver failure (ACLF) is often characterized by precipitating events of which pathological bacterial translocation (BT) from the gut and/or bacterial infections have been proposed to be of particular pathophysiological relevance. In ACLF i) excessive adrenergic drive has been shown by markedly increased serum levels of norepinephrine (Jalan et al. (2015) *Liver international*) and ii) non-selective beta-blocker therapy appears to improve short-term mortality (Mookerjee et al. (2016) *Journal of Hepatology*). The only treatment in advanced ACLF is liver transplantation. ACLF patients even after transplantation present with up to 10% mortality within the first 60 months being most frequently caused by sepsis (Sundaram et al (2020) *Liver transplantation*). (Sundaram et al (2020) *Liver transplantation*). The gut-vascular-barrier (GVB) is fundamental for limiting access of pathological BT to the gut-liver-axis but has not been addressed as for changes induced by adrenergic drive and/or ACLF. Thus, we aimed to characterize the small intestinal GVB in terms of function, structure and integrity in dependency on beta-adrenergic stimulation, blockade (by propranolol) and/or presence of liver cirrhosis and ACLF.

Method: ACLF was induced in C57Bl/6 cirrhotic mice (bile-duct-ligation) via LPS i.p. and beta-adrenergic hyperactivity was induced by chronic intraperitoneal delivery of isoproterenol (by osmotic mini pump) for 7 days. Duodenal GVB-function was determined in-vivo by confocal laser endomicroscopy assessing extravasation of FITC-albumin. Endothelial intercellular junctions (VE-cadherin, claudin-5) were evaluated by immunofluorescence.

Results: Chronic beta-adrenergic hyperstimulation caused pathological increases in FITC-albumin extravasation into the duodenal lamina propria being even more pronounced in cirrhotic and ACLF mice. Moreover, propranolol-treatment ameliorated FITC-albumin-extravasation in beta-adrenergic stimulated mice. Changes in GVB-function induced by beta-adrenergic stimulation were associated with significant reductions in VE-cadherin and claudin-5 in duodenal capillaries.

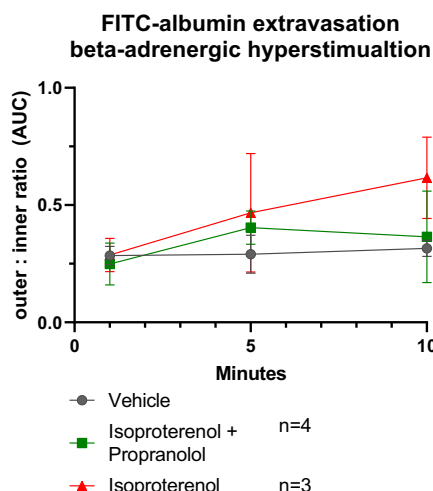


Figure:

Conclusion: Beta-adrenergic hyperstimulation modulates intercellular junctions impairing vascular barrier integrity and function of small intestinal GVB. This GVB-dysfunction may be a leading cause of pathological loss of albumin as well as pathological BT fueling the gut-liver-axis in ACLF.

THU-354

Identification of complication- dependent gut microbial biomarkers for early detection of decompensated cirrhosis

Ki Tae Suk¹, Satya Priya Sharma¹, Haripriya Gupta¹, Sung-Min Won¹, Jin-Ju Jeong¹, Raja Ganesan¹, Dong Joon Kim¹. ¹Institute for Liver and Digestive Diseases, Hallym University, Chuncheon, Korea, Rep. of South
Email: ktsuk@hallym.ac.kr

Background and aims: Change in gut microbiome is closely associated with liver cirrhosis progression from compensated to decompensated phase. Therefore, gut microbial compositional shift in cirrhosis progression is significantly important to identifying the potential biomarkers for two cirrhotic clinical phases. Here, we have compared the gut microbiome in compensated and decompensated cirrhosis patients based on the complications, to identify the gut composition specific gut microbial biomarkers. Additionally, we have evaluated cirrhosis-dependent gut microbial and metabolic markers.

Method: Stool samples were collected prospectively from 142 cirrhosis patients and 52 healthy controls. 16S-based Microbiome Taxonomic Profiling was performed to discover the gut microbial biomarkers based on cirrhosis severity progression and complications. Next, total 51 samples (control (n = 17) + cirrhosis patients ((n = 34)) were randomly selected for fecal samples metabolites profiling.

Results: Out of total 142 cirrhosis, 33% were females (n = 47) and overall mortality rate was 24% (n = 34), whereas higher mortality rate was found in male (74%) in comparison to female (26%). All 142 patients were classified in major two groups: compensated cirrhosis (n = 10), and decompensated cirrhosis (n = 132), decompensated cirrhosis group further classified based on the occurring and non-occurring decompensated-associated complications. A prominent difference in gut microbial composition has been observed in healthy controls, cirrhosis, and cirrhosis+ complications patients. Whereas 3 species found high in cirrhosis (*Clostridium clostridioforme*, *Bacteroides ovatus*, *Hungatella_uc*) compared to cirrhosis+ complications and combinedly showed ROAUC up to 0.807. Furthermore, 4 species found high in cirrhosis+ complications (*Bacteroides coprocola*, *Bacteroides coprophilus*, *Alistipes finegoldii*, *Parabacteroides goldsteinii*) and combinedly showed ROAUC up to 0.847. We have also identified, 10 species high in healthy control and 8 species high in cirrhosis. Additionally, 8 metabolites found high in healthy and 11 in cirrhosis. These microbial and metabolic biomarkers showed significant correlation with clinical markers.

Conclusion: We have identified multiple bacterial species and metabolites which has the potential to become biomarkers for the cirrhosis. Also, we discovered bacterial species which can be used to detected early stage of decompensated cirrhosis. However, further studies are required to establishment a robust pathophysiological mechanism between identified gut microbial species and liver cirrhosis.

THU-355

Pathophysiological biomarkers associated with resolution of ACLF in patients treated with the liver dialysis device, DIALIVE

Fausto Andreola¹, Banwari Agarwal^{1,2}, Rafael Bañares Cañizares^{3,4}, Faouzi Saliba⁵, María Pilar Ballester^{6,7}, Dana Tomescu^{8,9}, Daniel Martin¹⁰, Vanessa Stadlbauer¹¹, Gavin Wright¹², Mohammed Sheikh¹, Caroline Morgan¹³, Carlos Alzola¹⁴, Philip Lavin¹⁵, Daniel Green¹³, Rahul Kumar¹⁶, Sophie-Caroline Sacleux⁵, Gernot Schilcher¹¹, Sebastian Koball¹⁷, Andrada Tudor⁹, Jaak Minten¹⁸, Gema Domenech¹⁹, Juan Aragones¹⁹, Karl Oetti²⁰, Margret Paar²⁰, Katja Waterstradt²¹, Stefanie Bode-Boger²², Luis Ibañez Samaniego^{3,4}, Amir Gander²³, Jan Stange^{24,25}, Georg Lamprecht²⁶, Moises Sanchez²⁷, Raj Mookerjee¹, Andrew Davenport¹, Nathan Davies¹, Marco Pavesi²⁸, Agustín Albillos²⁹, Jeremy Cordingley³⁰, Hartmut Schmidt³¹, Juan Antonio Carbonell-Asins³², Vicente Arroyo²⁸, Javier Fernandez³³, Steffen Mitzner²⁴, Rajiv Jalan¹. ¹Institute for Liver and Digestive Health,

University College London, London, United Kingdom; ²Intensive Care Unit, Royal Free Hospital, London, UK, United Kingdom; ³Department of Gastroenterology, Gregorio Marañón General University Hospital, Spain, Spain; ⁴Health Research Institute Gregorio Marañón, Complutense University of Madrid, Spain, Spain; ⁵AP-HP Hôpital Paul Brousse, Centre Hépatobiliaire, INSERM Unit N° 1193, Université Paris-Saclay, France, France; ⁶INCLIVA Biomedical Research Institute, Hospital Clínico Universitario de Valencia, Spain, Spain; ⁷Digestive Disease Department, Hospital Clínico Universitario de Valencia, Spain, Spain; ⁸Carol Davila University of Medicine and Pharmacy, Romania, Romania; ⁹Fundeni Clinical Institute Bucharest, Romania, Romania; ¹⁰Peninsula Medical School, University of Plymouth, UK, United Kingdom; ¹¹Department of Internal Medicine, Division of Gastroenterology und Hepatology, Medical University of Graz, Austria, Austria; ¹²Basildon and Thurrock University Hospital, Mid and South Essex NHS Foundation Trust, Basildon, UK, United Kingdom; ¹³Yaqrit Ltd, United Kingdom; ¹⁴Etera

Solutions, United States; ¹⁵Boston Biostatistics Research Foundation, Inc, Framingham, MA, USA, United States; ¹⁶Changi General Hospital, Singapore, Singapore; ¹⁷University Hospital Rostock, Germany; ¹⁸FAKKEL-byba, Belgium; ¹⁹Medical Statistics Core Facility IDIBAPS-Hospital Clinic, Barcelona, Spain; ²⁰Division of Medicinal Chemistry, Otto Loewi Research Center, Medical University of Graz, Graz, Austria, Austria; ²¹MedInnovation GmbH, Germany; ²²Institut für Klinische Pharmakologie Magdeburg, Germany, Germany; ²³Tissue Access for Patient Benefit, Royal Free Hospital, United Kingdom; ²⁴University Hospital Rostock, Germany; ²⁵Fraunhofer IZI, Germany; ²⁶Department of Medicine II, Division of Gastroenterology and Endocrinology, Rostock University, Medical Center, Rostock, Germany; ²⁷IBM, Ireland; ²⁸European Foundation for the Study of Chronic Liver Failure (EF Clif), Barcelona, Spain; ²⁹Department of Gastroenterology and Hepatology, Hospital Universitario Ramón y Cajal, Madrid, Spain, Spain; ³⁰Perioperative Medicine-Critical Care, St. Bartholomew's Hospital, Barts Health NHS Trust, London, UK, United Kingdom; ³¹Department of Gastroenterology, Hepatology and Transplant Medicine, University Hospital Essen, 45147 Essen, Germany; ³²NCLIVA Biomedical Research Institute, Hospital Clínico Universitario de Valencia, Spain; ³³Liver ICU, Liver Unit, Hospital Clinic Barcelona, Spain
Email: f.andreola@ucl.ac.uk

Background and aims: Acute on chronic liver failure (ACLF) is characterized by severe systemic inflammation and high mortality rates. Its treatment is an urgent unmet need. DIALIVE is a novel liver dialysis device that aims to exchange dysfunctional albumin and remove damage and pathogen associated molecular patterns. In a recently completed clinical trial in patients with ACLF, its safety was confirmed and its use was associated with significantly faster resolution of ACLF (NCT03065699). The aim of this study was to evaluate pathophysiological factors associated with ACLF resolution in patients treated with DIALIVE or standard of care (SOC).

Method: 32 patients with ACLF grades 1-3a were included and randomized. Patients evaluated in the DIALIVE group had at least 3-treatment sessions. The main end point was resolution of ACLF at

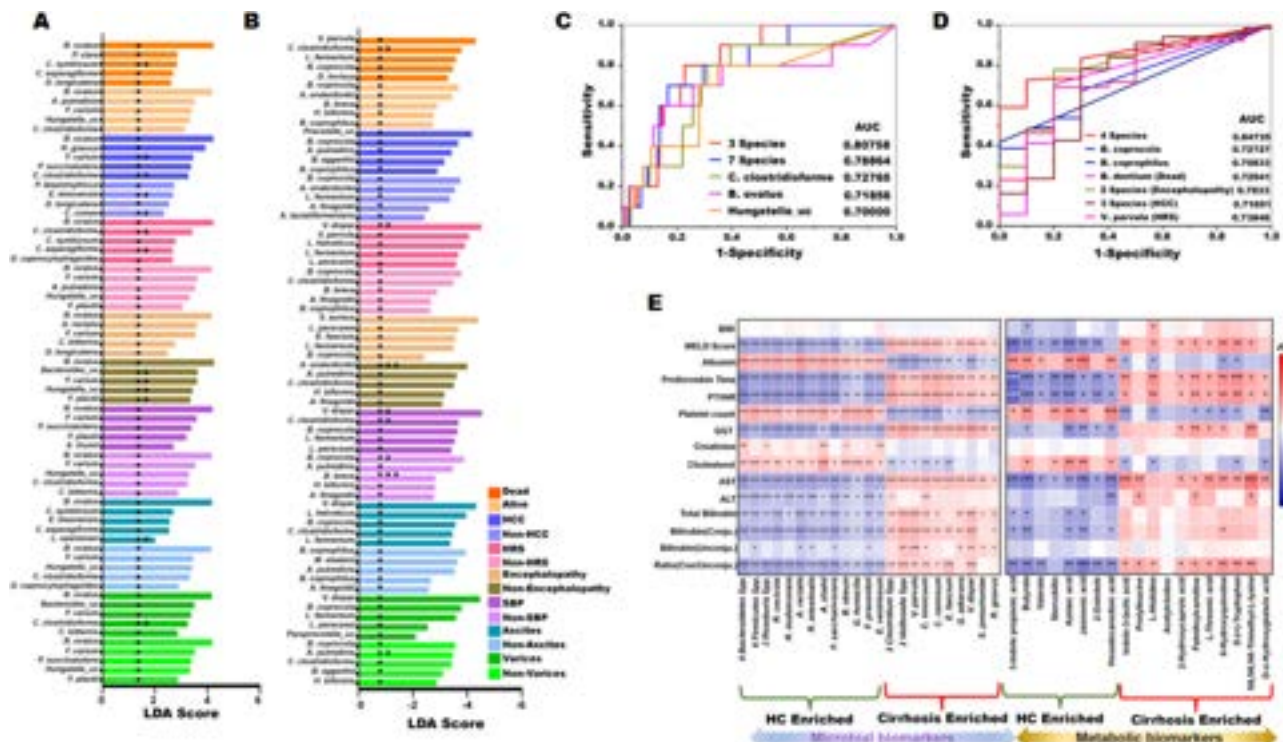


Figure: (abstract: THU-354): Figure (A) LDA score high in cirrhosis and, (B) LDA score high in complications, (C) cirrhosis-dependent species ROAUC (D) complications-dependent species ROAU, (E) Correlation between microbial and metabolic markers with clinical markers.

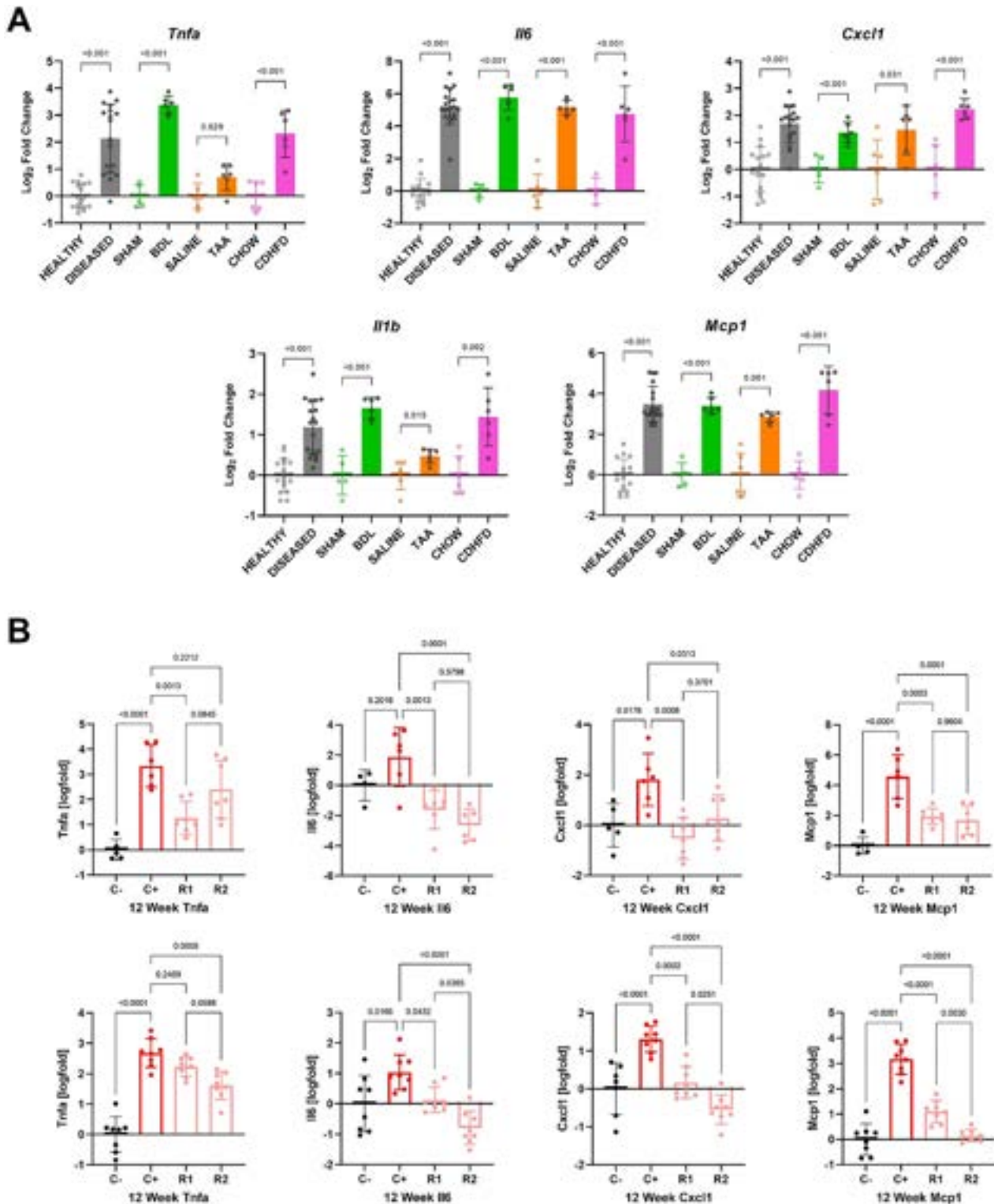


Figure: (abstract: THU-357).

animal models of different types of liver injury and (ii) systemic inflammation in ACLD patients with different liver disease aetiologies.

Method: Intrahepatic gene expression of TNF-alpha, IL-6, CXCL1, IL-1beta and MCP1 was investigated in rat cirrhosis models induced by thioacetamide (TAA, n = 12), choline-deficient high fat diet (CDHFD, n = 12), or bile duct ligation (BDL, n = 12). Inflammatory gene

expression was also analysed in two mouse models at 12 weeks of disease induction by TAA or carbon tetrachloride (CCl4) (i.e. peak fibrosis)-but also after regression for 1 (R1) or 2 (R2) weeks after withdrawing the toxic stimulus. In ACLD patients with different liver disease aetiologies, i.e., n = 226 alcohol-related liver disease (ALD), n = 40 non-alcoholic steatohepatitis (NASH), n = 21 cholestatic aetiologies (CHOL), systemic inflammation was assessed by white blood cell

count (WBC), CRP and IL-6 levels. Disease regression in human ACLD was explored in a subgroup of ALD patients (n = 181) with sustained abstinence.

Results: In diseased animals (C+), we observed a significant upregulation of intrahepatic proinflammatory genes across all aetiologies when compared to the respective healthy control group (C-) ($p < 0.05$ for all; Fig. 1A). Particularly intrahepatic IL-6 (log2 fold changes; TAA: 5.18; CDHFD: 4.75; BDL: 5.77; $p < 0.001$ for all) and MCP1 (TAA: 2.85; CDHFD: 4.18; BDL: 3.41; $p < 0.001$ for all) showed a pronounced upregulation. Similarly, in ACLD patients, there was a significant positive correlation between IL6 and MELD in ALD (Spearman's rho: 0.50, $p < 0.001$), NASH (r : 0.54, $p < 0.001$) and CHOL (r : 0.67, $p < 0.001$). For CRP, a comparable correlation was observed in ALD (r : 0.27, $p < 0.001$) and CHOL (r : 0.59, $p = 0.005$), but not in NASH (r : 0.08, $p = 0.618$). With regard to disease regression, we observed a significant decrease in intrahepatic inflammation during the regression period in the TAA and CCl4 models (Fig. 1B), with an immediate (R1) and sustained (R2) decrease of hepatic IL6 and CXCL1, but with a delayed (R2) decrease of TNF-alpha and MCP1. Accordingly, in abstinent ALD patients (n = 181), the duration of abstinence was negatively correlated to WBC (r : -0.26, $p < 0.001$), CRP (r : -0.23, $p = 0.002$) and IL-6 (r : -0.21, $p = 0.004$).

Conclusion: In animal models, the upregulation of hepatic proinflammatory genes follows a liver-injury-specific pattern. In ACLD patients, systemic inflammation is increased across all aetiologies of cirrhosis, and regresses gradually with sustained abstinence in ALD patients. In regressive toxic liver disease models, there is a time-dependent down-regulation of key proinflammatory genes.

THU-358

Extracellular vesicles carrying oxidation-specific epitopes as effectors in acute hepatic decompensation and acute-on-chronic liver failure-a pilot study

Benedikt Simbrunner¹, Taras Afonyushkin², Benedikt Hofer¹, Philipp Königshofer¹, Georg Semmler¹, Lorenz Balcar¹, Soreen Taqi², Michael Trauner¹, Matthias Mandorfer¹, Christoph Binder², Thomas Reiberger¹. ¹Division of Gastroenterology and Hepatology, Department of Medicine III, Medical University of Vienna, Vienna, Austria, Austria; ²Department of Laboratory Medicine, Medical University of Vienna, Austria, Austria
Email: thomas.reiberger@meduniwien.ac.at

Background and aims: Extracellular vesicles (EV) can act as mediators of intra- and extrahepatic cellular crosstalk. Oxidation-specific epitopes (OSE) may act as danger-associated molecular patterns (DAMPs) in the context of liver disease. This pilot study aimed to investigate whether circulating hepatocyte-derived EVs carrying OSE in patients with acute decompensation (AD) and acute-on-chronic liver failure (ACLF) are linked to liver injury/dysfunction and induce endothelial activation.

Method: Patients with AD (n = 9) and ACLF (n = 4) admitted at the University Hospital Vienna, Austria, were included. EVs were isolated from platelet poor plasma by differential centrifugation and characterized by flow cytometry. Annexin V (AnV) positivity and a size range of 0.2 to 1.1 μ m was used to define larger EVs. Antibodies recognizing hepatocyte-specific ASGPR1 protein and LR04 for the immunodominant OSE, malondialdehyde (MDA), were used to define EVs of hepatocellular origin carrying OSE (ASGPR1+ LR04+ EV). EVs from healthy individuals (n = 8) served as controls. Human umbilical vein endothelial cells (HUVEC) were stimulated with EVs isolated from patients and healthy controls, in the presence or absence of LR04 antibodies.

Results: Patients had a median MELD of 20 (14–24) points, 53% had male sex, and alcohol-related liver disease was the most common liver disease etiology (46%). ASGPR1+LR04+ EVs were significantly more frequent in patients with higher MELD ≥ 20 (vs. < 20) and in those with elevated ALT (vs. normal ALT values; both $p < 0.05$), while overall EVs of either hepatocyte origin or carrying MDA epitopes were

not significantly different across these patient strata. In contrast to EVs from healthy controls, EVs from patients with AD/ACLF robustly induced the expression of the cytokine IL-8 and the adhesion molecule VCAM in HUVECs (all $p < 0.001$; Figure). To assess whether this effect was primarily mediated by OSE-carrying EVs, HUVECs were stimulated with EVs either in the presence of LR04 or isotype control antibodies. Notably, the induction of VCAM and IL-8 expression in HUVECs was significantly blunted in the presence of LR04 antibodies (Figure).

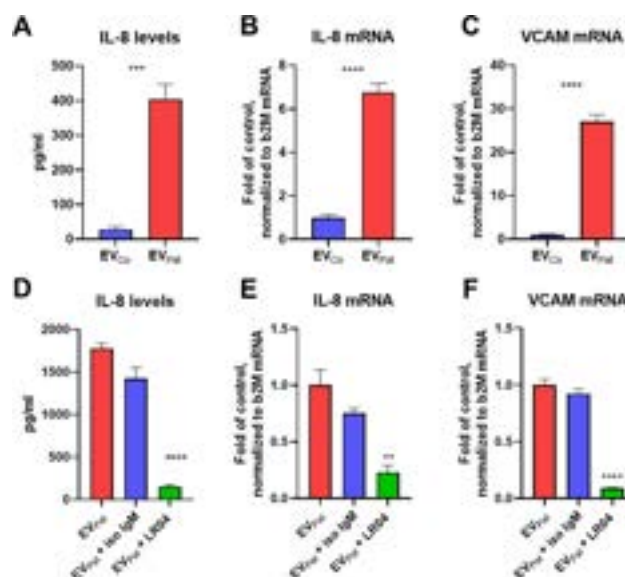


Figure:

Conclusion: Circulating OSE+ EVs from patients with AD/ACLF reflect liver dysfunction and liver injury and induce a pro-inflammatory state in ECs, suggesting them as propagators of systemic inflammation. Further studies should investigate the prognostic role of OSE+ MV in AD and ACLF and the therapeutic potential of OSE+MV-neutralizing antibodies.

THU-359

Multi-omics reveals the regulation mechanism of the Chinese herbal AnLuoHuaXian formula on reversing liver cirrhosis in the rat

Ruijia Liu¹, Xu Cao¹, Zao Xiaobin¹, Yijun Liang¹, Yong'an Ye^{1,2}. ¹Dongzhimen hospital, Beijing university of Chinese medicine, China; ²Beijing University of Chinese Medicine, Liver Diseases Academy of Traditional Chinese Medicine, China
Email: yeyongan@vip.163.com

Background and aims: Liver cirrhosis is a common disease that seriously endangers human health. The efficacy of the Chinese herbal AnLuoHuaXian formula (ALHX) in reversing liver cirrhosis is definite, but its specific mechanism of action is not yet perfected and needs further study, which is the purpose of this study.

Method: In this study, a rat model of liver cirrhosis was constructed by intraperitoneal injection of diethylnitrosamine for 12 weeks, with a gavage of ALHX granule aqueous solution starting at week 9. The therapeutic effects of ALHX in cirrhosis were investigated by basic situation analysis, histopathology, and serological analysis. Transcriptomics and non-target metabolomics of liver tissues, and 16S ribosomal DNA gene polymerase chain reaction analysis of gut microbiota were used to investigate the protective effects of ALHX on cirrhosis.

Results: Compared to the control, the hepatic and splenic indices were significantly higher in the model and significantly lower after the ALHX intervention. HE and Masson staining showed that the histopathological changes in the liver of ALHX rats were significantly

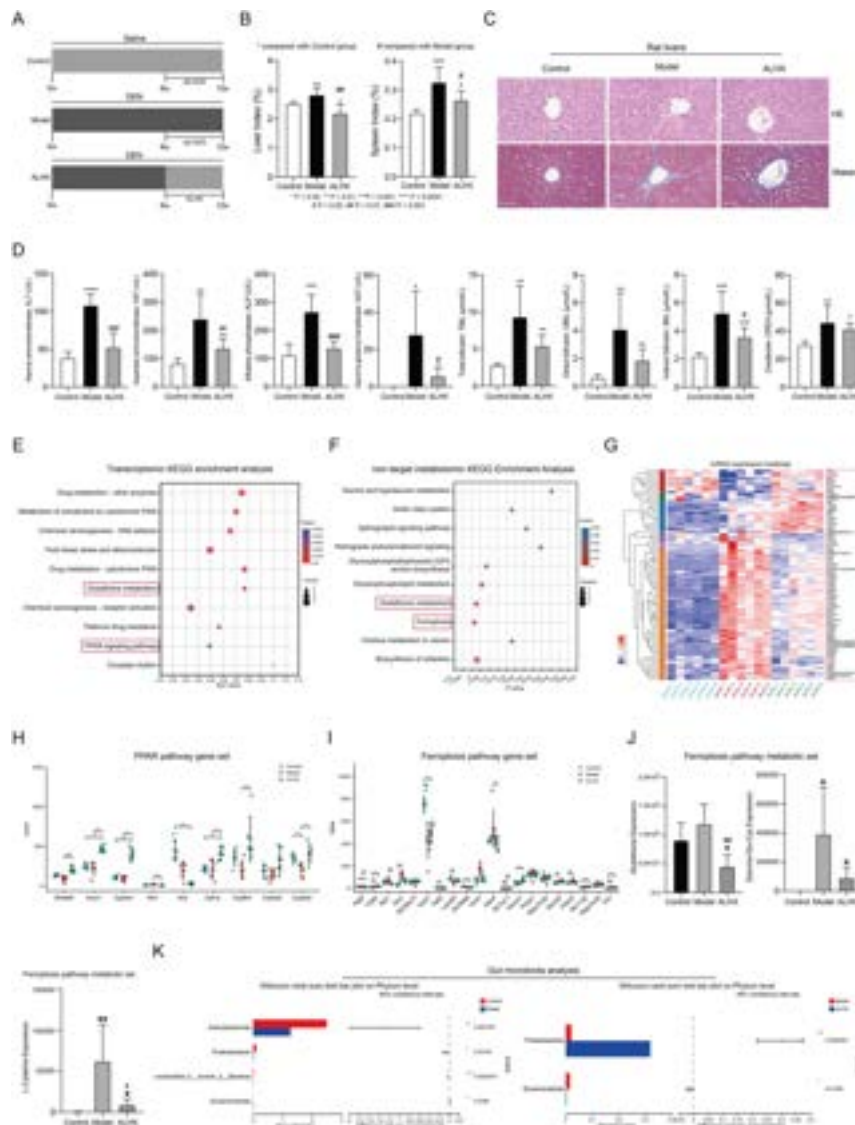


Figure: (abstract: THU-359).

better than those in the model, with less fibroplasia, hepatocyte inflammation, and necrosis, and less collagen deposition and heterotypic proliferation. Meanwhile, the serological indexes of the model were significantly reduced after ALHX intervention, especially the liver function of ALT, AST, ALP, and GGT were significantly improved. Transcriptomics and non-target metabolomics enrichment analyses indicated that ALHX inhibited rat cirrhosis possibly through regulation of Glutathione metabolism, Ferroptosis, and PPAR signaling pathways. In addition, the transcriptomic analysis also showed that ALHX could restore the abnormal expression trend of several genes to normal in model rat hepatocytes, such as *Slc7a11*, *Cyp4a3*, *Cyp8b1*, *Gsta2*, *Gsta3*, and *Gsta5*. The above findings were supported by differentially expressed genes in the PPAR and Ferroptosis pathway gene sets, and by three representative Ferroptosis pathway metabolites with significant intergroup variability. Moreover, gut microbiota analysis suggested that ALHX altered the overall structure of gut microbiota in cirrhotic rats, particularly proteobacteria and elusimicrobiota.

Conclusion: Multi-omics analysis showed that ALHX might effectively inhibit the progression of cirrhosis in rats by regulating Ferroptosis and PPAR signaling pathways, as well as the ecological structure of gut microbiota.

THU-360

MCC950 reduces glial cell activation and neuroinflammation in an animal model of thioacetamide-induced hepatic encephalopathy

Syed Afroz Ali¹, Ashok Kumar Datusalia¹. ¹National Institute of Pharmaceutical Education and Research-Raebareli (NIPER-R), Pharmacology and Toxicology, Lucknow, India
Email: ashok.datusalia@niperraebareli.edu.in

Background and aims: Hepatic encephalopathy (HE) a complex neurological disorder, characterized by increased levels of ammonia and inflammation resulting in glial cells activation and astrocyte swelling in individuals with liver disease. Despite past substantial investigations, the mechanisms regulating the neuroinflammation and pathogenesis of HE remains unclear reflecting higher mortality rates and unsuccessful therapeutic strategies. This study aims to explore the role of inflammasome signalling in HE and to investigate the effects of NLRP3 inhibitor (MCC950), against neuroinflammation and its associated mortality in an animal model of HE.

Method: The effects of MCC950 were evaluated in a rat model of acute liver failure induced HE. HE was induced by administering thioacetamide (TAA 300 mg/kg, 3 doses i.p., n = 10). The MCC950 was concurrently administered for 3 days to explore its effects in HE and various biochemical parameters (serum and plasma), BBB

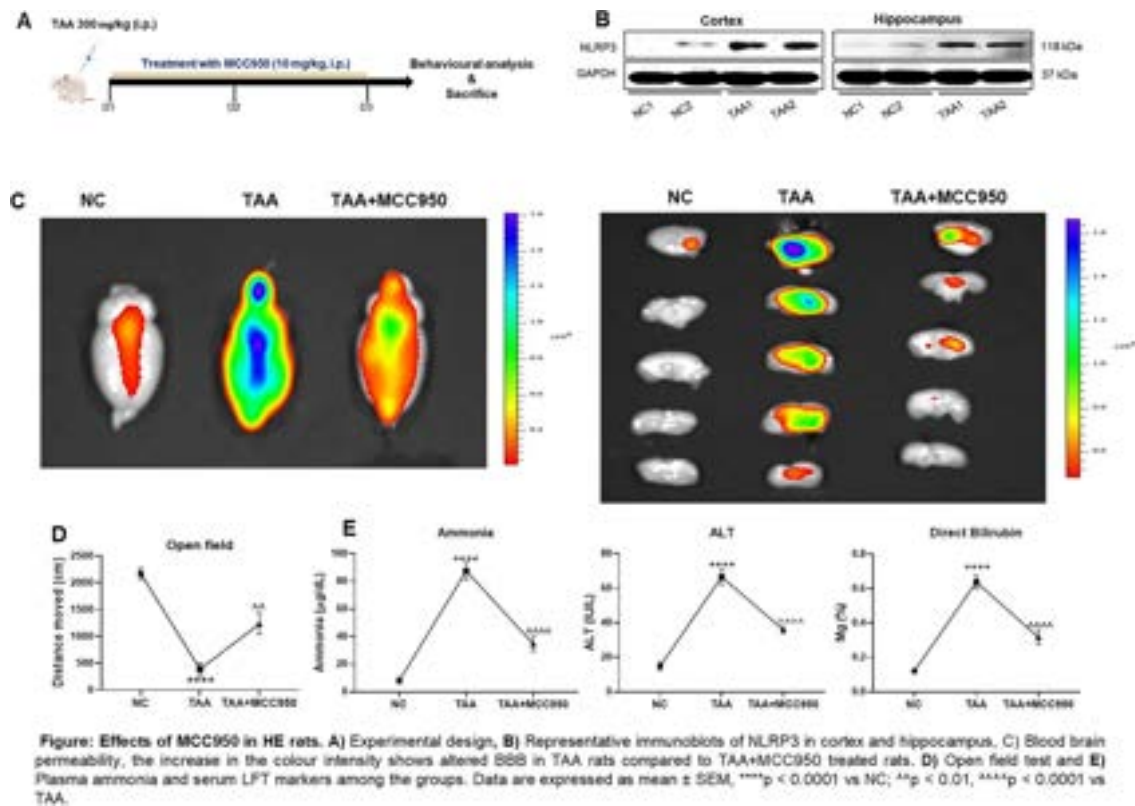


Figure: (abstract: THU-360).

permeability (IVIS), behavioural, molecular and histological changes in cortex and hippocampus (neuroinflammation and glial cell markers) and liver (inflammatory and fibrotic markers) were studied. **Results:** HE rats demonstrate reduced performance in the open field task, while MCC950 prevented the behavioural alterations. Plasma ammonia and serum LFT markers (ALT, AST, ALP, bilirubin and albumin) were induced in TAA rats and the treatment with MCC950 reduced the aberrations and prevented mortality. The increase in the levels of ammonia correlated well with the induced neuronal cell injury (BBB damage and astrocyte swelling), neuroinflammation (NLRP3 downstream) and hepatic cell death (Figure). Whereas, the treatment with MCC950 prevented BBB leakage, astrocyte swelling, hepatic cell death and induction of inflammation associated with IL-1 β , caspase-1, IL-18 and NF- κ B in cortex, hippocampus and liver. While on the other end treatment with MCC950 mitigated the microglial and astrocyte activation (IBA-1/GFAP) in cortex and hippocampus of TAA rats.

Conclusion: The findings from the current study for the first time demonstrated that treatment with MCC950 a direct inhibitor of NLRP3 inflammasome reduced hepatic injury, neuroinflammation, increased integrity of tight junction proteins and survival rate in HE rats. Altogether, these findings suggest that inhibition of NLRP3 inflammasome may be considered as a novel potential target for HE in the future.

THU-361

The pan-PPAR agonist lanifibranor decreases portal pressure in models of both hepatic and prehepatic portal hypertension

Anneleen Heldens^{1,2}, Christophe Casteleyn³, Louis Onghena^{1,2,4}, Milton Antwi^{1,2,5}, Benedicte Descamps⁶, Christian Vanhove⁶, Xavier Verhelst^{1,2}, Hans Van Vlierberghe^{1,2}, Lindsey Devisscher^{2,5}, Jean-Louis Junien⁷, Anja Geerts^{1,2}, Guillaume Wettstein⁷, Sander Lefere^{1,2}. ¹Ghent University, Internal Medicine and Pediatrics,

Ghent, Belgium; ²Ghent University Hospital, Liver Research Center Ghent, Ghent, Belgium; ³Ghent University, Morphology, Imaging, Orthopedics, Rehabilitation and Nutrition, Merelbeke, Belgium; ⁴Ghent University, Gastrointestinal Surgery, Ghent, Belgium; ⁵Ghent University, Basic and Applied Medical Sciences, Ghent, Belgium; ⁶Ghent University, Electronics and Information Systems, Ghent, Belgium; ⁷Inventiva, France Email: anneleen.heldens@ugent.be

Background and aims: Portal hypertension (PHT) can cause severe complications in patients with advanced chronic liver disease (ACLD). Studies have indicated that the pan-peroxisome proliferator-activated receptor (pan-PPAR) agonist lanifibranor reduces portal pressure in preclinical models of ACLD. However, as lanifibranor simultaneously improves the underlying fibrosis, the effect on PHT might be secondary. Angiogenesis and liver sinusoidal endothelial cell (LSEC) dysfunction play a major role in the pathogenesis of PHT. Using a combination of prehepatic and pre-cirrhotic PHT mouse models, we investigated the effect of lanifibranor on PHT, LSEC dysfunction, hepatic and splanchnic angiogenesis.

Method: Mice with prehepatic PHT (partial portal vein ligation; PPVL) and fibrotic mice with PHT (common bile duct ligation; cBDL) received daily lanifibranor (10 mg/kg or 30 mg/kg) or vehicle in a therapeutic setting for 7 or 14 days, respectively. The effect of lanifibranor on PHT, angiogenesis and LSEC was evaluated by analyzing hepatic and systemic hemodynamics, serum, hepatic and mesenteric histology, and hepatic, mesenteric and LSEC gene expression levels. Vascular corrosion casts of the venous mesenteric and hepatic vasculature were analyzed using μ CT.

Results: Portal pressure was substantially increased in vehicle-treated PPVL mice. 10 and 30 mg/kg lanifibranor reduced the portal pressure by 30–35% compared to vehicle-treated PPVL mice ($p = 0.0048$ and $p = 0.0008$ respectively), without affecting central venous pressure or heart rate. The portal pressure was increased to a lesser extent in the cBDL model, with a non-significant, but dose-dependent trend to decrease by 12–20% with lanifibranor. Lanifibranor significantly alleviated splenomegaly in both models.

Superior mesenteric artery blood flow was significantly increased in vehicle-treated PPVL mice but tended to decrease in PPVL mice treated with 30 mg/kg lanifibranor ($p=0.07$). Furthermore, the expansion of the venous mesenteric vasculature, as evaluated by μ CT, and the increased mesenteric vascular wall thickness (mVWT) caused by PHT were partially reduced by lanifibranor. PPVL did not induce distinct liver damage, with fibrosis, LSEC dysfunction or decreases in serum albumin being absent. In cBDL mice, high-dose lanifibranor treatment reduced fibrosis ($p=0.0001$) and restored the serum albumin to a level comparable to the sham-operated mice. Hepatic mRNA levels of inflammatory, fibrotic and angiogenic markers and cell adhesion molecules were significantly reduced in lanifibranor-treated cBDL mice compared to vehicle-treated cBDL mice. LSEC dysfunction was improved by lanifibranor treatment, whereas mVWT was not increased in this model.

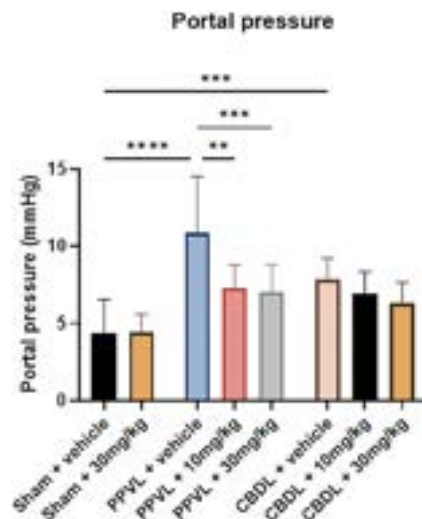


Figure: Portal pressure of sham-operated mice, PPVL mice and cBDL mice treated with vehicle, 10 mg/kg lanifibranor and 30 mg/kg lanifibranor.

Conclusion: Lanifibranor improves PHT, independently from fibrosis reduction, potentially through reducing the venous mesenteric vasculature expansion and intrahepatic angiogenesis, and ameliorating LSEC function.

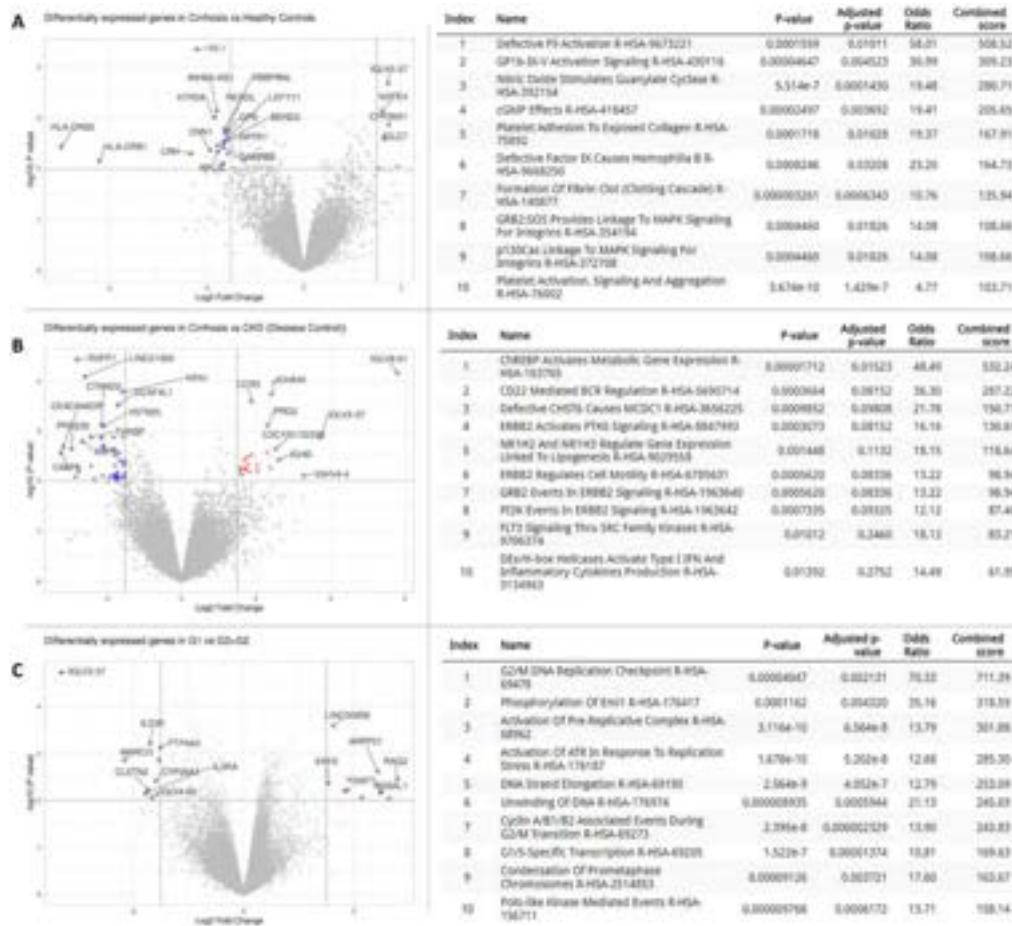


Figure 1. Functional enrichment of DGEs in all three comparisons. A. Between late-stage cirrhosis and healthy controls (HC). B. Between late-stage cirrhosis and disease controls (CKD). C. Between early-stage cirrhosis (G1) and late-stage cirrhosis (G2+G3). Top 20 DGEs are highlighted in the volcano plot. The enriched Reactome database terms are shown with distinct pathways being enriched

Figure: (abstract: THU-362).

THU-362

Whole transcriptomic analysis of bone marrow indicates distinct pathways to be at play in different stages of chronic liver disease patients

Pramod Gautam¹, Varun Suroliya², Shraddha Singh³, Prince Garg¹, Pooja Rao¹, Shruti Sureshan³, Rosmy Babu³, Shiv Kumar Sarin⁴, Chhagan Bihari³. ¹Institute of Liver and Biliary Sciences, Genome Sequencing Laboratory, New Delhi, India; ²Institute of Liver and Biliary Sciences, Genome Sequencing Laboratory, India; ³Institute of Liver and Biliary Sciences, 2Department of Pathology, India; ⁴Institute of Liver and Biliary Sciences, Department of Hepatology, New Delhi, India
Email: drcbsharma@gmail.com

Background and aims: Anemia is one of the common complications in liver cirrhosis. We have earlier highlighted the contribution of dyserythropoiesis (DE) in cirrhosis related anemia. We aimed to investigate the possible signatures of dyserythropoiesis in cirrhosis patients.

Method: here, we have studied the bone marrows of cirrhosis and controls. Patients were divided into four different groups: early-stage cirrhosis (ESC, n = 11), late-stage cirrhosis (LSC, n = 16), non-liver disease controls (C, n = 10) and disease controls (CKD, n = 4). The samples were sequenced with 2 × 150 bp approach using NEBNextUltra-II kit.

Results: Out of 525,569 and 1105 differential gene expression (DGE) in cirrhosis vs HC, cirrhosis vs CKD and ESC vs LSC respectively. Based on fold change (LogFC ± 1.5) we selected and 33 and 13 down- and upregulated gene in cirrhosis vs HC, 84 and 78 down- and upregulated gene in cirrhosis vs CKD and 19 and 17 down- and upregulated gene in ESC vs LSC respectively.

In LSC vs. HC group, taking all the DGEs combined, we observed regulatory pathways related to platelet activation, clotting and Nitric oxide stimulation to be enriched in cirrhosis using both Reactome and MGI database. When looked separately for up- and down-regulated genes, we observed retinoic acid signalling pathway to be significantly enriched among upregulated genes. While downregulated genes showed T-cell mediated immune.

In the comparison between LSC vs. CKD, we observed ERBB2 signalling pathways to be most enriched. Pathways enriched in upregulated genes included positive regulation of neutrophil extravasation and those enriched in downregulated genes included, antimicrobial immune response.

When compared LSC vs. ESC, we found cell-cycle checkpoints activation to be enriched. Terms enriched using MGI database included abnormal erythropoiesis, spleen hypertrophy and reticulocytosis. We found ERFE to be upregulated and BMP6 along with HMOX1 gene to be downregulated in this group. We also found high expression of ANGPTL4 (involved in iron homeostasis) in ESC. Importantly, GATA1 which is a crucial transcription factor in erythropoiesis was found to be moderately downregulated in LSC.

Conclusion: These findings indicate towards a possible mechanism involving retinoic acid signalling with ERFE suppressing hepcidin by inhibiting hepatic BMP/SMAD signalling via BMP subgroup. We believe that the possible role of retinoic acid in modulating erythropoiesis and could serve as a therapeutic target.

THU-363

Resection of mesenteric lymph nodes is associated with increased systemic immunosuppression in experimental cirrhosis following oral salmonella typhimurium challenge

Pinky Juneja¹, Deepika Jakhar¹, Aarti Sharma¹, Akash Kumar Mourya¹, Impreet Kaur¹, Shiv Kumar Sarin², Dinesh Mani Tripathi¹, Savneet Kaur³. ¹Institute of Liver and Biliary Sciences, Molecular and Cellular Medicine, New Delhi, India; ²Institute of Liver and Biliary Sciences, Department of Hepatology, vasant kunj, India; ³Institute of Liver and Biliary Sciences, Molecular and Cellular Medicine, vasant kunj, India
Email: savykaur@gmail.com

Background and aims: Mesenteric lymph nodes (MLN) are immune inductive sites that limit pathogens in gut, preventing their systemic spread. We studied the role of MLN in progression of endotoxemia and systemic inflammation in cirrhosis.

Method: Rat models of liver cirrhosis were prepared using ip CCl₄ administration for 8 wk. MLNs were resected from control (control MLNx) and CCl₄ (CCl₄ MLNx). Post MLN removal, they were allowed to reconstitute lymphatic vessels (LV) connection for next 4 wk. LV in gut were immunostained with LyVE1. Labelled *S. typhimurium* was gavaged and bacterial load was calculated after 48 h. Immune cells were quantified in blood at different time points within 0–48 h after bacterial challenge. Expression of inflammatory genes and proteins were quantified in MLN, gut, liver, spleen and blood after 48 h.

Results: In controls, bacteria were restricted to MLNs, with no bacterial growth seen in other organs and blood while in CCl₄, there was significant increase in bacterial load in lung, liver, spleen and blood at 48 h. Compared to control, there was an increase in percentage of activated CD134+ T cells (22 vs 41), CD25+ Treg (1.3 vs 3.2) and inflammatory cytokine (IL 6 = 2.5 fc, IFN gamma = 1.4 fc) in MLNs of CCl₄ at 48 h (p < 0.05 each). Increased percentage of CD134+ (32 vs 19) and CD25+ Treg (2.3 vs 1.8) was observed in blood of CCl₄ vs control. Surgical resection of MLNs from control resulted in regeneration of gut LV within 4 wk, however LV were not restored in CCl₄ MLNx. In contrast to control, there was enhanced bacterial growth in lung and blood of control MLNx 48 h after oral gavage of bacteria, similar to that observed in CCl₄. In gut and liver, there was increased expression of IL 6 (<5 fc) and IFN gamma (<2 fc) in control MLNx in comparison to control (p < 0.05 each). In blood of control MLNx vs control, inflammatory cytokines, activated CD134+ T cell (45 vs 30) and CD25+ Treg (4.1 vs 1.8) were increased (p < 0.05 each). In CCl₄ MLNx, there was reduced bacterial growth in all organs after bacterial challenge owing to failure of LV conduits restoration post MLN resection. In CCl₄ MLNx, there was significant increase in expression of defence promoting cytokine genes (IL 6 = 10.2 fc, IFN gamma = 3.1 fc, p < 0.05) in gut as compared to CCl₄. However, MLN resection in CCl₄ was associated with increased immunosuppressive Treg (5.9 vs 3.2) and decreased expression of IL 6 (<4 fc) and IFN gamma (<3 fc) in liver, spleen, and blood as compared to CCl₄ (p < 0.05 each).

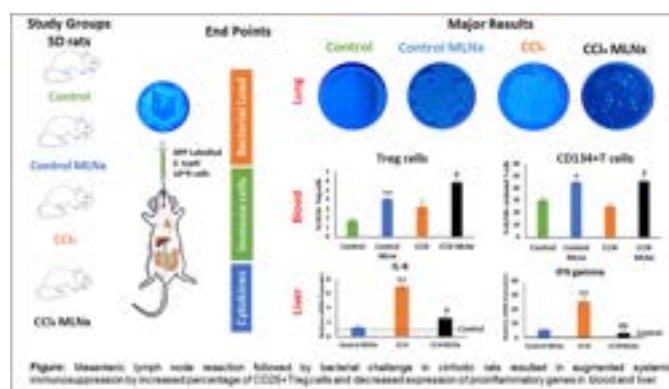


Figure:

Conclusion: In cirrhosis, MLNs mount an increased proinflammatory response to contain exogenous infection in gut, however an underlying immune dysfunction in MLNs fails to contain bacteria, condition that is immunologically similar to control without MLNs. Resection of MLNs in cirrhosis further aggravates systemic immunosuppression. The study provides first evidence of MLNs in maintaining systemic inflammatory responses to bacterial infection in cirrhosis.

THU-364

Glial transcriptional changes in experimental HE arise early and show similarities with established neuroinflammatory disorders

Wouter Claeys^{1,2,3,4}, Lien Van Hoecke^{1,2}, Clint De Nolf^{1,2}, Hannah Lernout^{1,5}, Griet Van Imschoot^{1,2}, Elien Van Wontergem^{1,2}, Daan Verhaege^{1,2}, Anja Geerts^{3,4,6}, Christophe Van Steenkiste^{7,8}, Roosmarijn Vandenbroucke^{1,2}. ¹VIB-UGent Center for Inflammation Research, Barriers in Inflammation, Zwijnaarde, Belgium; ²Ghent University, Department of Biomedical Molecular Biology, Zwijnaarde, Belgium; ³Ghent University, Liver Research Center Ghent, Ghent, Belgium; ⁴Hepatology Research Unit, Department of Internal Medicine and Paediatrics, Ghent, Belgium; ⁵Ghent Gut Inflammation Group, Department of Internal Medicine and Paediatrics, Ghent, Belgium; ⁶Ghent University Hospital, Department of Gastroenterology and Hepatology, Ghent, Belgium; ⁷Antwerp University, Department of Gastroenterology and Hepatology, Belgium; ⁸Maria Middelaers Hospital, Department of Gastroenterology and Hepatology, Ghent, Belgium
Email: wouter.claeys@ugent.be

Background and aims: Hepatic encephalopathy (HE) is a common complication of liver cirrhosis, associated with poor outcomes. Astrocytes, the primary ammonia-metabolizing cell type in the brain, and microglia, the resident brain macrophages, exhibit altered morphology in the experimental bile duct ligation (BDL) mouse model of HE. Signaling mechanisms underlying these morphological changes remain elusive however. We aim to characterize time-dependent transcriptional changes in glial cells in HE mice.

Method: 10–12 week old male C57Bl/6j mice (n = 6/group/timepoint) underwent BDL/sham surgery for 14 or 28 days. Microglia and astrocytes were isolated using FACS, followed by RNA sequencing. Gene set enrichment analysis (GSEA) and ingenuity pathway (IPA) upstream regulator analysis was performed. Transcriptomic profiles of astrocytes and microglia in the BDL model were compared to gene expression profiles in other acute or chronic neurological diseases.

Results: BDL induces an early and sustained response in microglia, with differential expression of 350 genes 14 days and 448 genes 28 days after induction, and a large overlap (226 genes) between both timepoints. At both timepoints, inflammatory signaling and chemotaxis pathways are significantly enriched. TNF signaling is the top predicted upstream regulator of microglial transcription at both timepoints, along with other cytokines. The microglial transcriptome in BDL mice significantly overlaps at both timepoints with acute LPS-induced changes (14 and 28 days p = 0.001 and 0.002, respectively) and Alzheimer's disease related 'disease-associated microglia' (14 and 28 days p = 0.001 and 0.02, respectively). In astrocytes, transcriptomic response is less strong, with 171 genes differentially expressed after 14 days, increasing to 495 after 28 days. As a consequence, pathway enrichment is limited at 14 days, while inflammatory signaling pathways are significantly enriched 28 days after BDL surgery. Comparative analysis with published transcriptomic responses shows significant overlap with both LPS-induced (p < 0.001 at both timepoints) and ischemia-induced (p < 0.001 at both timepoints) astrocyte subtypes. GM-CSF is the top upstream regulator at both timepoints. Corticoid receptor signaling is predicted to drive astrocyte transcription 14 days after BDL, while cytokines and interferon related signaling are mostly found at 28 days after injury.

Conclusion: Glial cells in BDL mice exhibit marked transcriptional changes, with striking similarities to transcriptional phenotypes in other, non-liver-related, brain pathologies. Inflammatory signaling is predicted to drive the observed changes. These data provides useful insights to unravel the sequence of cellular changes in HE and direct future research into the interplay in the neuroimmune compartment in this disease.

THU-365

Ascites CD8 T cells express a tissue-resident bystander phenotype that may contribute to disease pathogenesis in patients with decompensated liver cirrhosis

Christian Niehaus^{1,2,3}, Benedikt Strunz⁴, Benjamin Maasoumy^{1,5}, Heiner Wedemeyer^{1,5}, Niklas Björkström⁴, Anke Kraft^{1,2,3,5}, Markus Cornberg^{1,2,3,5}. ¹Hannover Medical School, Department of Gastroenterology, Hepatology and Endocrinology, Germany; ²Centre for Individualised Infection Medicine (CiIM), Germany; ³Twincore, Centre for Experimental and Clinical Infection Research, Germany; ⁴Karolinska Institutet, Karolinska University Hospital Huddinge, Center for Infectious Medicine (CIM), Department of Medicine Huddinge, Sweden; ⁵German Center for Infection Research (DZIF), Partner-site Hannover-Braunschweig, Germany
Email: niehaus.christian@mh-hannover.de

Background and aims: Liver cirrhosis is the end-stage of many chronic liver diseases. Patients with advanced cirrhosis often develop hepatic decompensation, which is accompanied by systemic inflammation and may ultimately result in acute-on-chronic liver failure. One of the most frequent consequences of hepatic decompensation is the accumulation of substantial amount of ascites in the peritoneal cavity. As liver cirrhosis affects immune cells both in peripheral blood and locally, in this study we aim to investigate the role of CD8⁺ T cells in the immune compartment ascites.

Method: Matched peripheral blood and ascites fluid were collected from 49 patients with decompensated cirrhosis. Phenotype and function of CD8⁺ T cells were analyzed using high-dimensional flow cytometry and obtained data were compared to each other as well as to healthy controls and compensated cirrhosis patients (n = 11).

Results: CD4⁺ as well as CD8⁺ T cells were decreased in the blood of patients with decompensated liver cirrhosis compared to healthy controls. Intriguingly, CD8⁺ T cells were enriched in the ascites of patients with liver cirrhosis whereas CD4⁺ T cells were diminished. This was also in line with a decreased CD4/CD8 T cell ratio in ascites compared to blood indicating a shift towards CD8⁺ T cells within the ascites T cell compartment. Interestingly, ascites-derived CD8⁺ T cells expressed an activated tissue-resident memory phenotype with high expression of tissue-homing markers. In addition, high-dimensional data analysis revealed unique ascites-specific (CXCR6⁺CD69⁺) clusters of late effector-memory CD8⁺ T cells that were rarely found in blood. Indeed, CXCR6⁺CD69⁺ CD8⁺ T cells were vastly activated, proliferative, and expressed markers of innate-like bystander inflammation. Remarkably, the frequency of ascites CXCR6⁺CD69⁺ CD8⁺ T cells correlated significantly with clinical parameters of disease severity (p = 0.01 for bilirubin, p = 0.004 for International Normalized Ratio). In line with this, peritoneal CD8⁺ T cells produced high levels of pro-inflammatory cytokines and cytolytic molecules following stimulation with the innate-like cytokines IL-12 + IL-18. Interestingly, the Janus kinase (JAK) inhibitor tofacitinib was effective in inhibiting the pro-inflammatory response by CXCR6⁺CD69⁺ CD8⁺ T cells.

Conclusion: CD8⁺ T cells are abundant in the ascites of patients with liver cirrhosis and exhibit a chronically activated bystander phenotype with innate like functions. Moreover, CD8⁺ bystander T cells in ascites may potentially contribute to disease progression in patients with decompensated cirrhosis, and JAK inhibitors could be a conceivable therapeutic option to inhibit hyperinflammation (similar to COVID-19) originating from CXCR6⁺CD69⁺ CD8⁺ T cells.

THU-366

Evaluation of myocardial inflammation and fibrosis in an experimental model of liver cirrhosis by quantitative cardiovascular MRI

Franziska Schneider^{1,2}, Alexander Isaak³, Marko Bulic⁴, Michael Praktijnjo⁵, Christian Strassburg^{1,2}, Oliver Weber⁶, Christoph Katemann⁶, Ulrike Attenberger³, Luetkens Julian³, Chang Johannes^{1,2}. ¹Department of Internal Medicine I, University

POSTER PRESENTATIONS

Hospital Bonn, Bonn, Germany, Germany;²Center of Cirrhosis and Portal Hypertension Bonn (CCB), University Hospital Bonn, Bonn, Germany, Germany;³Department of Diagnostic and Interventional Radiology, University Hospital Bonn, Bonn, Germany, Germany;⁴Department of Internal Medicine II, Heart Center, University Hospital Bonn, Bonn, Germany, Germany;⁵Department of Internal Medicine B, University Hospital Muenster, Muenster, Germany, Germany;⁶Philips GmbH Market DACH, Hamburg, Germany, Germany
Email: johannes.chang@ukbonn.de

Background and aims: Cardiac involvement in patients with end-stage liver disease is frequent. However, pathomechanisms contributing to the development of cirrhotic cardiomyopathy are not fully understood. Moreover, non-invasive biomarkers, including comprehensive imaging data with histopathological correlation are missing. The goal of this study was to explore the presence of cardiac involvement by multiparametric magnetic resonance imaging (MRI) in an experimental model of liver cirrhosis and correlate quantitative MRI biomarkers with parameters of fibrosis and inflammation of the heart-liver axis.

Method: Male Sprague-Dawley rats underwent bile-duct ligation (BDL) to induce cholestatic cirrhosis. Sham-operated rats served as controls. One group received combined liver and heart MRI after 3 weeks (BDL-3w), the other group after 5 weeks (BDL-5w). MRI scans were performed at 3-Tesla MRI. Myocardial function was assessed using cine imaging in standard axes. T1, T2, and extracellular volume fraction (ECV) values of the liver and the heart were assessed using quantitative MRI mapping techniques. After MRI, in-vivo portal pressure was measured. Gene expression studies and histological examinations were performed to evaluate fibrosis and inflammation of the heart and liver.

Results: Clinical and molecular parameters confirmed two distinct stages of liver cirrhosis, especially by portal pressure (4.56 ± 0.25 (sham) vs. 9.93 ± 0.39 (BDL-3w) or 13.29 ± 0.61 (BDL-5w) mmHg; $p < 0.0001$). Histopathological and molecular analyses revealed increased markers of cardiac inflammation and cardiac fibrosis/remodeling in BDL groups vs sham controls. Functional cardiac MRI analyses showed higher cardiac index, elevated left ventricular (LV) end-diastolic volume index and elevated LV mass in BDL groups. Myocardial T1, T2 and ECV values were elevated in BDL groups (T1: 946 ± 29 vs 952 ± 39 vs 987 ± 39 msec; $p = 0.014$; T2: 23 ± 4 vs 32 ± 3 vs 33 ± 4 msec; $p < 0.001$; ECV: 27 ± 3 vs 32 ± 3 vs 37 ± 5 ; $p < 0.001$; sham vs BDL-3w vs BDL-5w) and correlated with serum NT-proBNP levels and myocardial IL1b, CCL-3 and MMP-9. Interorgan correlations were found between quantitative myocardial imaging parameters and parameters of hepatic fibrosis, inflammation and portal pressure.

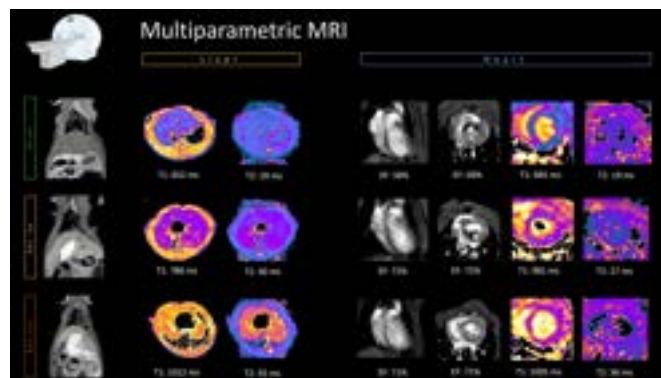


Figure:

Conclusion: Functional cardiac remodeling and elevation of inflammatory and fibrotic biomarkers of the myocardium were found in a preclinical model of cirrhosis. A marked increase in inflammatory gene expression suggests that hepatic cardiomyopathy is

predominantly driven by inflammation. Fibrotic myocardial alterations might play a role as another structural component. Quantitative cardiac MRI provides non-invasive, sensitive detection of cirrhotic cardiomyopathy, particularly diffuse myocardial edema/inflammation. This study may lay the groundwork for further clinical application of multiparametric cardio-hepatic MRI in cirrhosis.

THU-367

Peripheral blood metabolite associations with cardiac diastolic dysfunction in advanced chronic liver disease

Madeleine Gill^{1,2,3}, John O'Sullivan^{3,4}, Geoff McCaughan^{1,2,3}, Eugene Slaughter³, Ren Ping Liu³, Imre Hunyor^{3,4}, Stuart Moss⁴, Michele McGrady^{3,4}, Ian Wilcox^{3,4}, Avik Majumdar^{3,5,6}. ¹Royal Prince Alfred Hospital, AW Morrow Gastroenterology and Liver Centre, Camperdown, Australia; ²Centenary Institute, Camperdown, Australia; ³The University of Sydney, Faculty of Medicine and Health, Camperdown, Australia; ⁴Royal Prince Alfred Hospital, Cardiology, Camperdown, Australia; ⁵Austin Hospital, Liver Transplant Unit, Heidelberg, Australia; ⁶University of Melbourne, Parkville, Australia
Email: madeleine.gill@health.nsw.gov.au

Background and aims: Metabolomics offers the potential to comprehensively screen energetic and other changes in heart failure (HF), including cirrhotic cardiomyopathy (CCM). A burgeoning field in HF involves directly targeting the 'broken energetic machinery', which we aimed to explore with metabolomic screening in CCM, a type of HF with particular metabolic vulnerability.

Method: 47 patients with cirrhosis were included, with frozen plasma samples within six months of transthoracic echocardiogram (TTE), and 9 healthy controls. CCM and systolic dysfunction (SD) were defined by the 2020 CCM consortium criteria. Diastolic dysfunction (DD) was defined as any grade of diastolic impairment. Liquid chromatography tandem mass spectrometry (LC/MS-MS) was used to quantify more than 200 metabolites using two columns; hydrophilic interaction liquid chromatography (HILIC), and amide. Principal component analysis (PCA) was used to explore variation between patient groups. Linear and logistic regression with Benjamini-Hochberg adjustment were used for associations between metabolites, clinical traits and echocardiographic parameters.

Results: The median Model-for-End-Stage-Liver-Disease (MELD) was 16 (IQR 12–22), with median Child-Pugh Score of 10 (IQR 7–12). There were no differences in baseline characteristics of cirrhotic patients with CCM (n = 10) versus without (n = 37). When adjusted for age and sex, moderate to severe ascites was associated with lateral E/e' ($p = 0.006$) and medial E/e' ($p = 0.002$), volume-independent markers of DD. With respect to plasma metabolite profiles, there was clear separation between controls and cirrhotic patients on PCA, but there was no separation between patients with and without CCM. However, there were associations between several metabolites and TTE parameters, when analysed according to type of cardiac dysfunction (see table).

Pathway	Metabolites	Association	FC	Adjusted p value	Type of cardiac dysfunction
NAD	Nicotinate	Increased with medial e'	1.19	0.029	CCM
	Nicotinic acid		0.96	<0.001	SD
	NaAD_B	Decreased with IVRT	0.99	0.048	SD
	N-methyl-2-pyridone-5-carboxamide	Decreased with DT	1.26	0.04	CCM
		Increased with medial e'	1.19	<0.001	All
		Increased with TR velocity	1.39	0.04	CCM
ATP	Adenosine	Increased with medial E/e'	1.48	0.026	SD
	Adenosine diphosphate-ribose	Increased with DT	1.01	0.013	DD
Other					

(continued)

THU-369

Effect of fibrinogen substitution in hypofibrinogenaemic CTP class C patients on viscoelastic coagulation tests

Moritz Tobiasch¹, Anna Tobiasch², Volker Schäfer², Johannes Bösch², Mirjam Bachler³, Philipp Lichtenberger², Heinz Zoller⁴, Dietmar Fries². ¹Landeskrankenhaus Hall, Dept. of Medicine, Hall in Tirol, Austria; ²Medical University Innsbruck, Anaesthesiology and Intensive Care Medicine, Innsbruck, Austria; ³UMIT University for Health Sciences, Institute for Sports Medicine, Alpine Medicine and Health Tourism, Hall in Tirol, Austria; ⁴Medical University Innsbruck, Dept. of Medicine I, Austria

Email: moritztobiasch@gmail.com

Background and aims: Coagulation deficits in decompensated cirrhosis are complex and usually not reflected in classical coagulation group tests. Therapeutic interventions to optimize the coagulation function are thus difficult to guide. In hypofibrinogenaemic CTP class C patients, viscoelastic test parameters, single factor tests and group tests (INR, aPTT, thrombin time) were assessed in an in-vitro model of fibrinogen substitution.

Method: After obtaining informed consent of all participants, citrated plasma of 17 CTP class C patients with a fibrinogen level below or equal 150 mg/dL and 18 healthy control subjects was tested in classical group tests (prothrombin time/INR, activated partial thromboplastin time (aPTT), thrombin time (TT)), in single factor tests, and in viscoelastic tests (ExTest, InTest, FibTest) with and without addition of fibrinogen, hereby mimicking a therapeutic supplementation of fibrinogen. Fibrinogen levels were determined by Clauss' method and by immunoassay.

Results: Both classical coagulation group tests and viscoelastic test generally performed well in differentiating the CTP class C and the healthy control cohorts. Addition of fibrinogen had only marginal effects on the classical group tests (PT/Quick median absolute difference, -1.5% (IQR -11% to 2%)), whereas particularly FibTest parameters showed a clear and dose-dependent response to fibrinogen concentrations. Elevating the fibrinogen concentration with 200 mg/dL fibrinogen concentrate normalized FibTest clot firmness parameters A5, A10, A20, and maximum clot firmness (MCF) to normal levels (for MCF, R2 0, 38, $p < 0.0001$). The response to fibrinogen augmentation was markedly higher in hypofibrinogenaemic CTP class C patients than in healthy control subjects. All factors synthesized in the liver (F V, VII, IX, X, XI, XII, XIII, and alpha-2-antiplasmin) also showed clear correlations with FibTest parameters in both groups, whereas F VIII, and von Willebrand factor did not influence the response in CTP class C patients.

Conclusion: Viscoelastic tests might provide a better estimate of coagulation function in CTP class C patients than classical coagulation group tests. In hypofibrinogenaemic patients, a significant effect on coagulation function is plausible. With a high robustness in vitro, FibTest parameters might be valid surrogates for fibrinogen substitution in end-stage liver disease.

THU-370

The gene expression profile of skeletal muscle in end-stage liver disease patients undergoing assessment for liver transplantation with muscle wasting

Sophie Allen^{1,2}, Amritpal Dhaliwal^{2,3}, Jonathan Quinlan^{1,2}, Thomas Nicholson^{2,3}, Felicity Williams^{1,2,3}, Matthew Armstrong^{2,4}, Ahmed Elsharkawy^{2,4}, Simon Jones^{2,3,5}, Carolyn Greig^{1,2,5}, Gareth Lavery^{2,6}, Janet Lord^{2,3,5}, Leigh Breen^{1,2,5}. ¹University of Birmingham, School of Sport, Exercise and Rehabilitation Sciences, Birmingham, United Kingdom; ²University Hospitals Birmingham, National Institute for Health Research, Birmingham Biomedical Research Centre, Birmingham, United Kingdom; ³University of Birmingham, Institute of Inflammation and Ageing, Birmingham, United Kingdom; ⁴Queen Elizabeth Hospital Birmingham, Liver Unit, Birmingham, United Kingdom; ⁵University of Birmingham, MRC-Versus Arthritis Centre for Musculoskeletal Ageing Research, Birmingham, United Kingdom; ⁶Nottingham Trent University, Department of Biosciences, Nottingham, United Kingdom

Email: s.l.allen@bham.ac.uk

Background and aims: Sarcopenia, defined as a loss of muscle mass, strength and physical function is a common condition affecting end-stage liver disease (ESLD) patients. However, the molecular pathways which may underpin the progression of sarcopenia in ESLD are largely unclear. Therefore, the aim of this study was to characterize intracellular signaling pathways that may contribute to sarcopenia progression in ESLD patients with differing levels of muscle mass and physical function.

Method: Fasted muscle and blood samples were obtained from 23 decompensated ESLD patients (aged 54.7 ± 6.4 years, MELD 13.7 ± 4.6). Physical function and body composition assessments were also conducted. ESLD patients were divided into 3 clinically defined groups dependent on muscle mass and function; 1-adequate muscle mass and function ($n = 7$), 2-adequate muscle mass, inadequate function ($n = 5$) and 3-inadequate muscle mass and function ($n = 11$). The skeletal muscle transcriptome was determined by RNA-sequencing using a QuantSeq 2' kit (Lexogen, Austria) and sequenced on Illumina's NextSeq500. Transcripts were mapped to the human genome (hg38) and were analyzed using Ingenuity Pathway Analysis (Qiagen, UK).

Results: BMI and weight was significantly lower in patients with inadequate muscle mass and function compared to patients with adequate muscle mass and function ($p < 0.05$). Pathway analysis revealed a significant enrichment in canonical pathways related to mitochondrial dysfunction and oxidative phosphorylation in ESLD patients with inadequate muscle mass and function vs. patients with adequate muscle mass and function (Figure A), and patients with adequate muscle mass, with inadequate function (Figure B). A significant enrichment in canonical pathways related to oxidative stress and mTOR related signaling was also identified in patients with inadequate muscle mass and function compared to those with adequate muscle mass and inadequate function. Furthermore,

Canonical Pathway Analysis of End Stage Liver Disease Patients with Differing Levels of Muscle Mass and Function

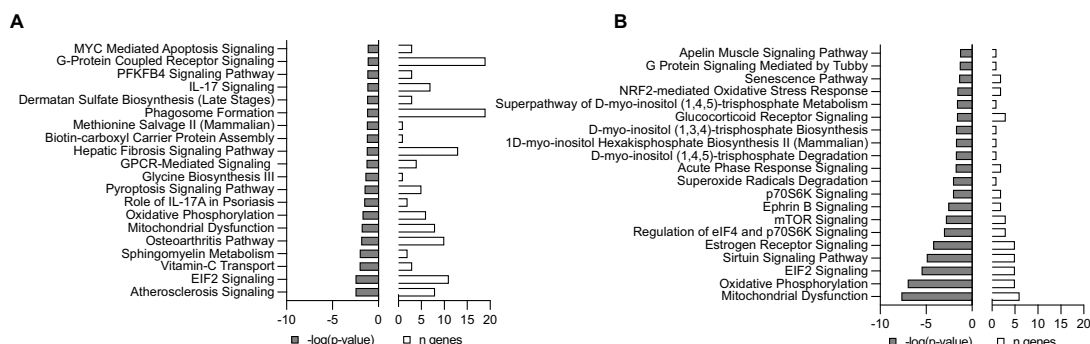


Figure: (abstract: THU-370).

RICTOR and LARP1 were identified as predictive, inhibited upstream regulators in ESLD patients with inadequate muscle mass and function vs. patients with adequate muscle mass and function, and adequate muscle mass and inadequate function.

Conclusion: Collectively, these findings highlight distinct signaling pathways which may underscore alterations in skeletal muscle mass and function in ESLD patients. These findings suggest a number of novel therapeutic targets for future interventions which aim to treat sarcopenia.

THU-371

Placement of a trans-jugular intrahepatic portosystemic shunt (TIPS) modifies the expression of proinflammatory cytokines in circulating monocytes exposed to lipopolysaccharide

Mirella Pastore¹, Francesco Vizzutti¹, Davide Roccarina¹, Nadia Navari¹, Benedetta Piombanti², Valentina Adotti¹, Valentina Cacciato², Fabrizio Fanelli³, Fabio Marra¹. ¹University of Florence, Italy; ²Azienda USL Toscana Centro, Italy; ³Azienda Ospedaliero-Universitaria Careggi, Italy
Email: fabio.marra@unifi.it

Background and aims: Recent data have indicated that decompensated cirrhosis is characterized by an imbalance in the innate immune system, leading to low-grade systemic inflammation. In particular, inflammatory cytokines secreted by monocytes and macrophages have been implicated in the pathogenesis of portal hypertension and its complications. Additionally, MerTK-expressing monocytes participate in the determination of severity of acute liver failure. Trans-jugular intrahepatic portosystemic shunt (TIPS) is currently used for the treatment of complications of portal hypertension, but whether portosystemic derivation results in changes in the biology of inflammatory cell is currently unknown.

Method: Fifteen patients with severe portal hypertension referred for TIPS placement were enrolled. During the TIPS procedure, blood from the portal and jugular vein was drawn, and at 4 weeks after TIPS placement a sample from a peripheral vein was repeated. Monocytes were isolated from peripheral blood mononuclear cells by adherence after Ficoll-Hypaque purification, and stimulated with LPS (1 µg/ml) for 2, 8 and 24 hours. Gene expression was evaluated by real-time PCR.

Results: Upon exposure to LPS, a significant increase in gene expression of IL-1β, IL-6, TLR4 and MERTK was observed in monocytes isolated from either the portal or the jugular vein. Basal and LPS-stimulated mRNA levels of these molecules were markedly lower in the post-TIPS compared to pre-TIPS, in particular after exposure to LPS. Expression of the anti-inflammatory cytokine, IL-10, was significantly increased after LPS stimulation for 2 and 8 hours. After TIPS, mRNA levels of IL-10 were reduced in unstimulated conditions but increased after LPS stimulation for 2 hours.

Conclusion: Reduction of portal pressure through TIPS placement is associated with reduced expression of pro-inflammatory mediators and modulation of anti-inflammatory IL-10. Increased portal pressure in cirrhotic patients may be a direct modulator of the complex changes in the inflammatory balance observed in these patients.

THU-372

Neurological dysfunction is improved after faecal microbiota transplantation in rats with bile duct ligated-induced chronic liver disease

Alexandre Bourgeois^{1,2}, Félix Veillette², Mariana Oliveira², Karine Dubois², Mélanie Tremblay², André Marette³, Chantal Bemeur^{1,2}, Christopher F Rose^{2,4}. ¹Université de Montréal, Nutrition, Montréal, Canada; ²Centre de recherche du CHUM (CRCHUM), Montréal, Canada; ³Université Laval, Québec, Canada; ⁴Université de Montréal, Médecine, Montréal, Canada
Email: alexandre.bourgeois.1@umontreal.ca

Background and aims: Hepatic encephalopathy (HE) is a complex neuropsychiatric syndrome arising from chronic liver disease (CLD). HE manifests with symptoms such as poor memory, impairment in

motor coordination, lethargy and coma. The gut microbiota has been shown to influence neurological functions via various mediators such as cytokines or bacterial metabolites, many studies have demonstrated the gut-brain axis is altered in liver disease. Faecal matter transplantation (FMT) in patients with cirrhosis has revealed beneficial effects yet many limitations of these studies render the results inconclusive. The aim of this study is to explore the impact of FMT on gut microbiota and the beneficial effects on neuro behaviour in bile-duct ligated (BDL) rats.

Method: Male Sprague-Dawley rats were randomly assigned to one of three groups; SHAM, BDL-VEH (vehicle) and BDL-FMT (who received FMT daily from pooled faeces from SHAM rats). After five weeks, behaviour tests were performed to evaluate short- and long-term memory (Novel Object Recognition), anxiety (Open Field and Elevated Plus Maze) and motor coordination (Rotarod). Plasmatic parameters such as cytokines, short chain fatty acids (SCFA) and liver impairment markers were measured by ELISA, LC-MS/MS and using Cobas respectively. Finally, faeces were collected for bacterial sequencing and SCFA analysis.

Results: FMT did not alter degree of liver disease in BDL rats. BDL-VEH developed a loss of short/long term memory and motor coordination compared to SHAM rats. However, alterations in neurological dysfunction were prevented in the BDL-FMT group. FMT did not impact microbiota α-diversity in BDL rats and β-diversity of microbiota was significantly different between all groups. The genera *Proteobacteria* UCO-001 significantly increased only in SHAM and BDL-FMT rats and *Clostridium* *Sensu Stricto* 1 significantly increased only in BDL-VEH compared to SHAMs. Finally, *Rombustia* was only present in SHAM. Plasma pro-inflammatory cytokines (TNF-α and IL-1β) increase in both BDL groups compared to the control group and no difference for the anti-inflammatory cytokine IL-10 was noted. Analysis of short-chain fatty acids in faeces and plasma showed a variation in propionate and butyrate between both BDL groups.

Conclusion: Our results demonstrate that FMT leads to improvement in memory and motor coordination in BDL rats. The microbiota profile was different between BDL-VEH and SHAM, and FMT lead to further alterations on microbiota. The fact that FMT did not normalize microbiota profile compared to SHAM, suggests BDL-FMT leads to a novel specific microbiota profile which in turn protects the brain. The effect of plasma SCFA needs to be further explored to define its impact on the brain and possible therapeutic application.

Cirrhosis and its complications Other clinical complications except ACLF

WEDNESDAY 21 TO SATURDAY 24 JUNE

TOP-041

Randomised controlled trial of intravenous versus oral iron in treatment of iron deficiency anaemia after variceal bleeding in patients with cirrhosis

Tabish Mohammad¹, Sanchit Sharma², Samagra Agarwal¹, Srikanth Gopi¹, Randeep Rana¹, Deepak Gunjan¹, Anoop Saraya¹. ¹All India Institute Of Medical Sciences, Gastroenterology and Human Nutrition Unit, New Delhi, India; ²Queen Elizabeth Hospital Birmingham, Gastroenterology, United Kingdom
Email: ansaraya@yahoo.com

Background and aims: There is limited evidence on the optimal strategy to correct iron deficiency anaemia after an episode of variceal bleeding (VB) in patients with cirrhosis. We evaluated the efficacy and safety of intravenous iron in this setting compared to oral iron therapy.

POSTER PRESENTATIONS

Table:(abstract: TOP-041).

Characteristics	Oral arm (n=39)	IV arm (n=41)	p value
Age (mean (SD) (years))	44.74 (12.17)	46.24 (11.67)	0.63
Male (n%)	33 (84.6%)	37 (90.2%)	
Etiology of cirrhosis			
Alcohol	20(51.3%)	21(51.2%)	0.374
NASH	6(15.4%)	7(17.1%)	
HBV	4(10.3%)	7(17.1%)	
HCV	2(5.1%)	3(7.3%)	
Under evaluation	7(17.9%)	3(7.3%)	
Child-Pugh classification			0.886
A	19(48.7%)	18(43.9%)	
B	13(33.3%)	16(39%)	
C	7(17.9%)	7(17.1%)	
CTP score (Median[IQR])	6 (6- 9)	8 (6-9)	0.588
MELD score (Median[IQR])	12.00 [9.00, 17.00]	12.00 [10.00, 17.00]	0.797
Baseline haemoglobin [mean (SD)] (g/dl)	8.13 (1.09)	8.36 (1.04)	0.335
Base line Ferritin (ng/dl) (Median[IQR])	42.00 [17.60, 72.00]	23.10 [15.00, 50.25]	0.146
Primary Outcome			<0.001
Rise in Haemoglobin (gram/dl) (Mean [SD])	1.62 (0.38)	3.63 (0.35)	
Secondary outcomes			
Resolution of anaemia (Hb>12gm/dl) n(%)	27.3	58.3	0.009
Restoration of iron stores (Ferritin>100ng/ml) n (%)	25.9	84.4	<0.001
Clinical outcomes			0.731
Mortality	5(13.5%)	3 (7.5%)	
ACLF	3(7.6%)	2 (4.8%)	
SBP	2(5.1%)	1(2.4%)	
Rebleed	4(10.2%)	4(9.7%)	
New onset ascites	2(5.1%)	1(2.4%)	
Improvement in quality-of-life questionnaire score (CLDQ)			
Abdominal symptoms. Change (median [IQR])	0.00 [2.00, 1.00]	4.00 [7.50, 1.50]	<0.001
Fatigue Change (median [IQR])	2.50 [8.50, 0.25]	16.00 [19.00, 9.50]	<0.001
Emotional. Change (median [IQR])	3.00 [9.00, 0.75]	16.00 [22.00, 8.00]	<0.001
Activity. Change (median [IQR])	1.00 [3.75, 0.75]	5.00 [9.00, 3.50]	<0.001
Systemic. Change (median [IQR])	1.00 [4.75, 1.00]	9.00 [10.50, 3.00]	<0.001
Worry. Change (median [IQR])	1.00 [2.00, 0.75]	2.00 [6.00, 0.00]	0.024
Change in hand grip strength at 12 weeks (Kg/m ²) {mean[SD]}	1.96(3.42)	2.90(3.63)	0.33
Adverse events	NA	0	<0.001
Infusion reaction	1(3.5%)	6(16.7%)	<0.001
Mild hypophosphatemia*	0	10 (27.8%)	
Moderate hypophosphatemia*	0	0	
Severe hypophosphatemia*	5(12.82%)	NA	
Oral intolerance			

Data is presented as n (%) for qualitative variables and median (IQR) for quantitative variables unless specified. List of abbreviations: VB-variceal bleed, NASH-non-alcoholic steatohepatitis; HBV-hepatitis B virus; hepatitis C virus; ACLF, acute on chronic liver failure; SBP, Spontaneous bacterial peritonitis, SD-standard deviation, IQR- Interquartile range.*Transient hypophosphatemia at 4 week of intervention (Mild: 2-2.5 mg/dL, Moderate: 1-2 gm/dL, Severe: <1gm/dL)

Method: In this single centre randomised controlled trial with superiority study design, eligible patients with cirrhosis with iron deficiency anaemia after VB were randomised to receive either intravenous iron (Ferric carboxymaltose, 2 doses, 7 days apart,

haemoglobin and weight-based dose calculation) or oral iron (Carbonyl iron, 100 mg elemental iron per day) for 3 months. The primary outcome was increase in haemoglobin in both arms at 3 months. Secondary outcomes included resolution of anaemia

(haemoglobin >12 g/dL), normalization of iron stores (ferritin >100 ng/dL), liver related outcomes and drug related adverse events. Changes in quality of life was assessed using Chronic Liver Disease Questionnaire at baseline and at 3 months.

Results: Eighty patients (Oral arm n = 39, IV arm n = 41, mean age 45.5 year, 87.5% males) of predominant non-viral aetiology (alcohol, NASH and HBV related 51%, 16%, 13% respectively) were included in this trial. Baseline characteristics including median CTP score 7.00 [IQR 6.00, 9.00], median MELD score 12.00 [IQR 10.00, 17.00] and degree of anaemia (8.25 ± 1.06 gm/dl) were comparable. The mean increase in haemoglobin in intravenous and oral arm was 3.63 ± 0.35 gm/dl and 1.62 ± 0.35 gm/dl respectively at 3 months (p value <0.001). Resolution of anaemia was seen in 58.3% and 27.3% in intravenous and oral arm (p value <0.009). Normalization of iron stores was seen in 84.4% and 25.9% in intravenous and oral arm respectively (p value <0.001). None of the patient developed drug related serious adverse event in any. There was a significant improvement in quality of life and functional status in intravenous arm.

Conclusion: Intravenous iron replacement is safe and more effective than oral iron in improving haemoglobin, iron stores and quality of life in patients with iron deficiency anaemia after episode of variceal bleed (CTRI/2022/11/47650).

TOP-044

Nutritional therapy improves minimal hepatic encephalopathy in cirrhosis by improvement in sarcopenia, proinflammatory cytokines and myostatin: a double blind randomized controlled trial

Sudhir Maharshi¹, Barjesh Sharma¹, Sanjeev Sachdeva², Bhawna Mahajan², Ashok Sharma³, Sushma Bara², Siddharth Srivastava⁴, Ajay Kumar², Ashok Dalal¹, Ujjwal Sonika¹. ¹G.B Pant Hospital, Gastroenterology, New Delhi, India, ²G.B Pant Hospital, New Delhi, India, ³G.B Pant Hospital, Radiology, New Delhi, India, ⁴G. B Pant Hospital, New Delhi, India
Email: sudhir.maharshi@gmail.com

Background and aims: Minimal hepatic encephalopathy (MHE) impairs health related quality of life (HRQOL), predicts development of overt hepatic encephalopathy (HE) and associated with poor prognosis. We assessed the effects of nutritional therapy on cognitive functions, HRQOL, anthropometry, endotoxins and inflammatory markers in patients of cirrhosis with MHE.

Method: In a double blind randomized controlled trial patient of cirrhosis with MHE were randomized to nutritional therapy (group I: 30–35 kcal/kg/day and 1.0–1.5 gram of protein/kg/day) and no nutritional therapy (group II: diet as patients were taking before) for 6 months. MHE was diagnosed based on psychometry hepatic

encephalopathy score (PHES). Anthropometry, ammonia, endotoxins, inflammatory markers, myostatin and HRQOL were assessed at baseline and after 6 months. Primary end points were improvement or worsening in MHE and HRQOL.

Results: A total 150 patients were randomized to group-I (n = 75, age 46.3 ± 12.5 years, 58 men) and group-II (n = 75, age 45.2 ± 9.3 years, 56 men). Baseline PHES (-8.16 ± 1.42 vs -8.24 ± 1.43 ; p = 0.54) was comparable in both the groups. Reversal of MHE was higher in group I (73.2% vs 21.4%; p = 0.001). Improvement in PHES (Δ PHES 4.0 ± 0.60 vs -4.18 ± 0.40 ; p = 0.001), HRQOL (Δ SIP 3.24 ± 3.63 vs 0.54 ± 3.58 ; p = 0.001), anthropometry, ammonia, endotoxins, cytokines and myostatin levels were also significantly higher in group I compared to group II. Overt HE developed in 6 patients in group I and 13 in group II (p = 0.04).

Conclusion: Nutritional therapy is effective in treatment of MHE and associated with improvement in nutritional status, HRQOL, ammonia, endotoxins, inflammatory markers and myostatin levels.

TOP-047

Efficacy of arginine glutamate injection for the treatment of hepatic encephalopathy and hyperammonemia in cirrhosis: a randomized controlled trial

Huaibin Zou¹, Ming Kong¹, Weiwei Kang¹, Rui Zhong¹, Xianshan Yang¹, Lili Feng¹, Yan Ren¹, Yuan Gao¹, Li Zhou¹, Shanshan Li¹, Li Wang², Zhongping Duan¹, Yu Chen¹. ¹Beijing Youan Hospital Capital Medical University, Beijing, 100069, China., China, ²School of Basic Medicine Peking Union Medical College, Beijing, 100730, China., China
Email: chybeyond1071@ccmu.edu.cn

Background and aims: Reducing blood ammonia is essential for treating cirrhotic patients with hepatic encephalopathy (HE). Arginine glutamate injection is a mixture that mainly works through two mechanisms of reducing blood ammonia and adjusting intestinal flora. Its efficacy for the treatment of HE has not been adequately studied. This study evaluated the therapeutic effects of arginine glutamate injection and L-ornithine L-aspartate (LOLA) on patients with HE.

Method: 108 patients with cirrhosis and HE aged 18–75 years were randomized to receive either intravenous infusions of arginine glutamate injection (experimental group, n = 54), 20 grams daily, or LOLA (control group, n = 54), 20 grams daily for 7 days (stratified factor: West-Haven grading). Standard of care treatment was given in both groups. The primary end point of the study was the improvement rate of HE in patients treated for 7 days. Secondary efficacy measures included the effective rate of ammonia reduction in patients treated for 7 days and the value and rate of ammonia

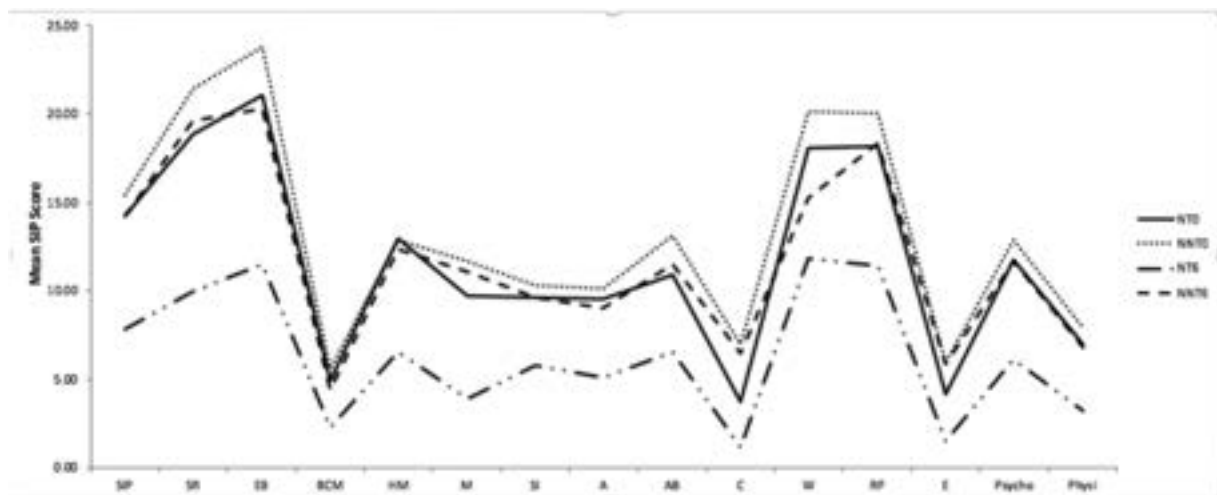


Figure: (abstract: TOP-044).

POSTER PRESENTATIONS

Table (abstract: TOP-047).

Drug group	N	FAS			p	PP			p
		Number of improvement (%)	Improvement rate difference (95% CI)			Number of improvement (%)	Improvement rate difference (95% CI)		
experimental group	54	48 (88.9)	-1.9% (-13.3%, 9.6%)		0.020	49	47 (95.9)	3.5% (-5.6%, 12.5%)	0.0015
control group	54	49 (90.7)				53	49 (92.4)		

Non-inferiority margin = -15.0%.

reduction from baseline at 4 h, 8 h, 24 h, and 7 d after initial administration.

Results: In the analysis of the FAS data set, after 7 days of treatment, the improvement rate of HE in the arginine glutamate injection group was 88.9%, and that in the LOLA group was 90.7%. The improvement rate of HE (non-efficacy threshold = -15.0%, $P=0.020$) and the reduction rate of blood ammonia were similar between the two groups. The serum ammonia level of the arginine glutamate injection group was lower than that of the LOLA group at all time points, especially at 4 h and 24 h. The serum ammonia level (4 h $p=0.011$, 24 h $p<0.001$), the decreased value of serum ammonia from baseline (4 h $p=0.023$, 24 h $p=0.005$), and the reduced rate of serum ammonia (4 h $p=0.011$, 24 h $p<0.001$) in the arginine glutamate injection group were significantly superior to that in the LOLA group. When there was no significant difference in blood ammonia reduction rate, the total treatment cost and the cost of reducing blood ammonia value by 1 unit/1% in the arginine glutamate injection group were significantly lower than LOLA, indicating that the economy of arginine glutamate injection was better. No significant difference in the incidence of adverse reactions was seen between the groups.

Conclusion: Compared with intravenous LOLA, arginine glutamate injection reduces blood ammonia faster and has a more significant effect in the early stage. Arginine glutamate injection has lower costs and more pharmacoeconomic advantages.

Results: 135 patients had diabetes (rifaximin + lactulose [$n=84$]; lactulose alone [$n=51$]), and 246 had no diabetes (rifaximin + lactulose [$n=152$]; lactulose alone [$n=94$]) at baseline. At baseline, 78.5% of patients with diabetes had mean MELD scores 11–24 (median, 13.0) and 69.1% without diabetes had MELD scores 11–24 (median, 12.3). Treatment with rifaximin + lactulose resulted in significantly lower percentage of patients with OHE episode vs lactulose alone during 6 months among those with (22.6% vs 51.0%; $p<0.001$) and without diabetes (17.1% vs 49.5%; $p<0.0001$). Rifaximin + lactulose reduced OHE recurrence risk by 64% (HR, 0.36; 95% CI, 0.20–0.65; number needed to treat [NNT], 3.5) vs lactulose alone during 6 months of treatment in patients with diabetes (Figure); reduction in risk among those without diabetes was 70% (HR, 0.30; 95% CI, 0.18–0.49; NNT, 3.3). Also, significantly fewer patients receiving rifaximin + lactulose vs lactulose alone had an HE-related hospitalization among those with (14.3% vs 29.4%; $p=0.01$) and without (10.5% vs 20.2%; $p=0.008$) diabetes. Patients with diabetes treated with rifaximin + lactulose had a 60% reduction in risk of first HE-related hospitalization during 6 months vs lactulose alone (HR, 0.40; 95% CI, 0.19–0.86; NNT=6.6); without diabetes, the risk reduction was 59% (HR, 0.41; 95% CI, 0.21–0.81; NNT=10.3). Comparing with vs without diabetes, rifaximin + lactulose arms had similar outcomes for rate of OHE episodes ($p=0.31$) and HE-related hospitalizations ($p=0.34$). Addition of rifaximin to lactulose was well tolerated.

WEDNESDAY 21 JUNE

WED-319

Rifaximin plus lactulose is more effective than lactulose alone for the prevention of overt hepatic encephalopathy in patients with or without diabetes

Jasmohan S Bajaj¹, Robert Wong², Zeev Heimanson³, Christopher Allen³, Robert Israel³, Arun Sanyal¹. ¹Virginia Commonwealth University and Central Virginia Veterans Healthcare System, Richmond, United States, ²Stanford University School of Medicine and Veterans Affairs Palo Alto Healthcare System, Palo Alto, United States, ³Salix Pharmaceuticals, Bridgewater, United States
Email: jasmohan.bajaj@vcuhealth.org

Background and aims: Rifaximin is approved for reduction in risk of overt hepatic encephalopathy (OHE) recurrence. Diabetes mellitus is a common comorbidity in patients with cirrhosis. Limited published data suggest that it may impact effectiveness of some OHE therapies. The aim was to evaluate the efficacy/safety of rifaximin + lactulose vs lactulose alone in patients with cirrhosis, with/without diabetes.

Method: Data were pooled from 2 randomized trials (1 phase 3 double-blind; 1 phase 4 open-label) of adults with cirrhosis and history of OHE within 6 months (in OHE remission). In phase 3 trial, patients received rifaximin 550 mg BID or placebo, with optional lactulose (2–3 soft stools/d) for 6 months; for phase 4 trial, rifaximin 550 mg BID + lactulose (2–3 soft stools/d) for 6 months. Patients were subgrouped post hoc by baseline diabetes (yes/no). Outcomes assessed included time to onset of OHE episode (Conn score ≥ 2) and time to first HE-related hospitalization.

Figure. Time to First Breakthrough Overt Hepatic Encephalopathy in Patients With Baseline Diabetes

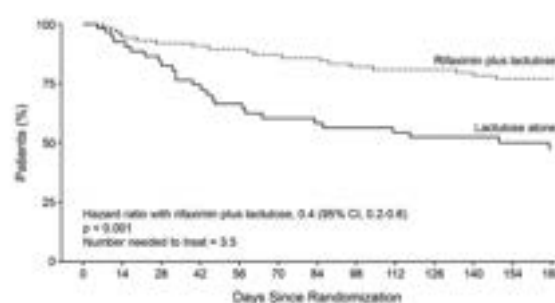


Figure:

Conclusion: Rifaximin + lactulose was more efficacious than lactulose alone for reducing the risk of OHE recurrence and HE-related hospitalization in adults regardless of diabetes status. Thus, both groups would benefit from addition of rifaximin to lactulose for reducing OHE recurrence risk. Also, although the sample size was small, diabetes may not impact rifaximin treatment outcomes; further studies are warranted.

WED-320

Real-world experience of long-term albumin treatment in a large cohort of patients with cirrhosis and ascites (Real-Answer study)

Giulia Iannone¹, Clara De Venuto¹, Salvatore Piano², Antonino Lombardo³, Davide Bitetto⁴, Stefania Gioia⁵, Giacomo Zaccherini¹, Roberta Gagliardi², Vincenza Calvaruso³, Enrico Pompili¹, Marta Tonon², Maurizio Baldassarre¹, Silvia Nardelli⁵, Pierluigi Toniutto⁴, Vito Di Marco³, Paolo Angeli², Paolo Caraceni^{1,6}. ¹Alma Mater Studiorum-University of Bologna, Department of Medical and Surgical Sciences, Bologna, Italy, ²University and Hospital of Padova- Unit of Internal Medicine and Hepatology, Department of Medicine-DIMED, Padova, Italy, ³UOC di Gastroenterologia, Dipartimento di Promozione della Salute, Materno Infantile, Medicina Interna e Specialistica (PROMISE), University of Palermo, Italy, ⁴Hepatology and Liver Transplantation Unit, University Academic Hospital of Udine, Udine, Italy, ⁵Sapienza University of Rome, Department of Translational and Precision Medicine, Rome, Italy, ⁶IRCSS Azienda Ospedaliero-Universitaria di Bologna, Unit of Semeiotics, Liver and Alcohol-related diseases, Bologna, Italy
Email: paolo.caraceni@unibo.it

Background and aims: Based on the results of the ANSWER randomized clinical trial, long-term albumin treatment (LTA) is now standard of care in patients with decompensated cirrhosis in many Italian liver units. However, several issues (i.e., better characterization of patients amenable to LTA, personalization of albumin infusion, clinical trajectories, stopping rules) should be addressed. Thus, this “real-life” study aimed to increase our knowledge on LTA.

Method: Patients with cirrhosis and ascites receiving albumin for at least one month were enrolled in a multicenter retrospective observational study. Data on patient’s characteristics, modalities of albumin treatment, clinical trajectories and outcomes were collected in 5 liver units across Italy.

Results: 326 patients (male 69%, median age 63) were included in the study from January 2016 to January 2022. Alcohol followed by NASH were the predominant etiologies. At baseline, median Child-Pugh score was 9, MELD 15, and MELD-Na 18; serum albumin concentration was 31 (27–35) g/dl. 36% of patients had grade 3 ascites and 27% refractory ascites. About 2/3 of them presented previous or ongoing other major complications of cirrhosis. LTA was started in hospital and then continued after discharge in 34% of patients, while in the outpatient clinic in the remaining cases. Albumin was infused in the outpatient clinic of the referral hospital in 45% of cases, in territorial services in 17% and at home in 38%. Median length of treatment was 401 (196–777) days and median weekly dose was about 40 g. Changes of doses during treatment were made in about 70% of cases. At last observation, albumin was still ongoing in 43% of patients, while it was interrupted due to clinical improvement in 22%, death in 17%, transplantation in 14%, and patient’s adherence/logistic barriers in 5%. In the 71 patients who stopped albumin for clinical improvement, median length of treatment was 257 (125–415) days, ascites returned to grade 0–1 in more than 95% of cases (20% of which had baseline diagnosis of refractory ascites), prognostic scores significantly improved (median Child-Pugh: 9 to 7, MELD 14 to 10, MELD-Na 18 to 13; $p < 0.001$) and median serum albumin concentration was 39 (IQR 35–44) g/L. At baseline, these patients were younger and more frequently had alcoholic cirrhosis. Finally, 15% of these patients re-started albumin infusion due to ascites re-accumulation.

Conclusion: These initial results of the Real-ANSWER study indicate that: 1. LTA is frequently added to diuretics as part of medical treatment of ascites in Italy; 2. adherence to treatment in real-life clinical practice is very high; 3. permanent interruption of LTA due to resolution of ascites and improvement of liver function can occur in almost 20% of cases, and 4. besides patients with uncomplicated ascites, also patients with refractory ascites can be responsive to LTA.

WED-321

Efficacy and safety of branched-chain amino acids supplementation on muscle cramps in patients with cirrhosis: a randomized double-blinded controlled trial

Tanongsak Chinaronchai^{1,2}, Thanapat Attakittmongkol¹, Supot Nimanong¹, Watcharasak Chotiyaputta¹, Phunchai Charatcharoenwitthaya¹, Tawesak Tanwandee¹, Siwaporn Chainuvati¹. ¹Siriraj Hospital, Mahidol University, Division of Gastroenterology, Department of Medicine, Bangkok, Thailand, ²Phang Nga Hospital, Department of Medicine, Phangnga, Thailand
Email: schain111@gmail.com

Background and aims: Patients with cirrhosis commonly experience muscle cramps, which are attributed to poor quality of life. The standard therapies, however, are not effective. This randomized controlled trial aimed to compare the efficacy and safety of branched-chain amino acids (BCAA) versus placebo for treating muscle cramps in cirrhotic patients.

Method: A total of 40 patients with cirrhosis who have experienced muscle cramps at least once per week were randomized to receive either a placebo ($n = 21$) or 12.45 grams of BCAA ($n = 19$) orally per day for 12 weeks. Patients were observed at 4-week intervals to monitor any changes in cramping and adverse events. Skeletal muscle index (SMI), handgrip strength, biochemical tests, and the chronic liver disease questionnaire (CLDQ) were assessed at enrollment and study completion. The primary outcome was a relative change in muscle cramp frequency from baseline.

Results: The mean age of the patients was 64.2 ± 9.4 years, with a female predominance of 67% and 90% were Child-Pugh A. Chronic hepatitis B or C was the primary cause of cirrhosis. The two groups were similar in baseline clinical characteristics, severity of liver disease, frequency and duration of muscle cramps, SMI, handgrip strength, and laboratory tests. At the end of the study, no significant difference in the percentage change of muscle cramps was observed between the BCAA group (-68.8% , 95% CI -100% to -46.4%) and the placebo group (-56.3% , 95% CI -75.0% to -20.0%) ($p = 0.235$). There were also no significant differences in the duration and severity of muscle cramps, SMI, hand grip strength, and CLDQ score between both two groups. However, a significant improvement in the activity and worry domains of the CLDQ score was observed in the BCAA group but not in the placebo group. In the subgroup of 30 participants having muscle cramps at least 3 times per week, BCAA supplementation showed a significant reduction in the muscle cramp frequency than the placebo group ($p = 0.010$) after the 12 weeks of treatment. Mild adverse events, including nausea or abdominal discomfort occurred in 31.6% and 23.8% of patients received BCAA and placebo, respectively ($p = 0.583$).

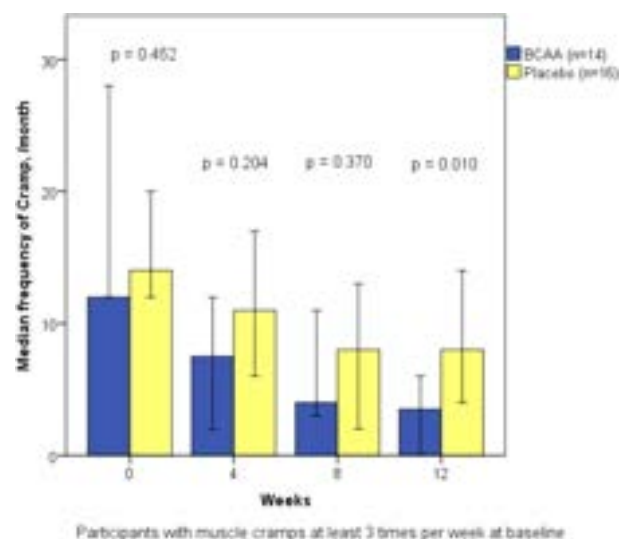


Figure:

POSTER PRESENTATIONS

Conclusion: A 12-week supplementation of BCAA significantly reduced the frequency of muscle cramps in cirrhotic patients who had cramping at least 3 times per week. However, there was no discernible improvement in skeletal muscle mass or function. Further studies with larger sample sizes and longer duration of BCAA supplementation are needed to validate these findings.

WED-322

Effects of nutritional therapy on Sarcopenia in patient with liver cirrhosis-a randomised controlled trial

Sudhir Maharshi¹, Shyam Sunder Sharma¹. ¹SMS Medical College and Hospital, Gastroenterology, Jaipur, India
Email: sudhir.maharshi@gmail.com

Background and aims: Sarcopenia has been associated with poor survival in patients with cirrhosis. Nutrition may have direct influence on sarcopenia and functional status. There are limited data on nutritional management in cirrhosis with sarcopenia. We assessed the effects of nutritional therapy on sarcopenia in cirrhotic patients.

Method: A randomized controlled trial conducted in a tertiary care setting on patients of cirrhosis with sarcopenia who were randomized to nutritional therapy (group A: 30–35 kcal/kg/day and 1.0–1.5 gram of protein/kg/day) and no nutritional therapy (group B: diet as patients were taking before) for 6 months. Sarcopenia was diagnosed based on computerized tomography psoas muscle index (PMI), hand grip strength (HG) and gait velocity (GV). Primary end points were improvement or worsening in sarcopenia. Secondary end points were improvement of other nutritional parameters and liver functions.

Results: 141 patients were randomized to group-A ($n = 70$, age 42.7 ± 10.1 yr, 58 men) and group-B ($n = 71$, age 42.1 ± 9.8 yr, 57 men). Baseline characteristics including age, body mass index (BMI), hemoglobin, mid arm circumference (MAC), hand grip, gait velocity and PMI were comparable in both the groups. Improvement in MAC (Δ MAC 2.78 ± 0.26 vs -2.13 ± 0.32 ; $p = 0.001$), hand grip strength (Δ HG 4.91 ± 1.4 vs -3.1 ± 0.73 ; $p = 0.001$), gait velocity (Δ GV 0.98 ± 0.20 vs -0.74 ± 0.32 ; $p < 0.01$), PMI (Δ PMI 3.5 ± 0.24 vs -2.7 ± 0.42 ; $p < 0.001$) was higher in group A compared to group B at the end of study. Liver functions assessed by Child Turcotte Pugh and Model for end stage liver disease also significantly improved in group A compared to group B, $p < 0.001$.

Conclusion: Nutritional therapy is effective in the improvement of sarcopenia and liver function in cirrhosis.

WED-323

Real-world treatment of decompensated liver cirrhosis in Italy: a propensity score-matched analysis of long-term versus acute albumin therapy

Wim Laleman¹, Jonel Trebicka², Giacomo Zaccherini³, Paolo Caraceni⁴, Dirk Steffen Schmidt⁵, Joana Rodrigues⁵, Kyle Rodney⁶, Sofia Schweiger⁷, Paolo Angeli⁸. ¹University Hospitals Leuven, Department of Gastroenterology and Hepatology, Section of Liver and Biliopancreatic Disorders, Leuven, Belgium, ²University of Münster, Department of Internal Medicine B, Münster, Germany, ³University of Bologna, Department of Medical and Surgical Sciences, Bologna, Italy, ⁴University of Bologna, Department of Medical and Surgical Sciences, Bologna, Italy, ⁵CSL Behring, Marburg, Germany, ⁶Adivo Associates LLC, California, United States, ⁷Adivo Associates LLC, Buenos Aires, Argentina, ⁸University of Padova, Department of Medicine, Unit of Internal Medicine and Hepatology, Padova, Italy
Email: wim.laleman@uzleuven.be

Background and aims: International guidelines recommend short-term albumin in specific acute conditions related to liver cirrhosis, but clinical trial data (e.g., ANSWER) show long-term albumin (LTA) treatment can be beneficial. We compared real-world outcomes in patients with decompensated cirrhosis receiving LTA or acute albumin therapy (non-LTA).

Method: A retrospective chart analysis was undertaken (Adivo Associates, funded by CSL Behring) to assess adults diagnosed with decompensated cirrhosis presenting ascites and treated in Italy with LTA (≥ 40 g per infusion per week) or non-LTA (administered at non-regular intervals). The observation period was from 1 Jan 2019 to 31 Dec 2021. In the LTA group, patients must have completed ≥ 3 months of LTA treatment by the start of the observation period. In the non-LTA group, patients must have received albumin for an acute complication at least once in the 12 months before the observation period. Data collection stopped if the patient received a transplant or switched treatment. The primary end point was the annualised therapeutic paracentesis rate. Propensity score matching (PSM), utilizing sex, Child-Pugh (CP) score and the presence of multiple comorbidities as covariates, was applied for the comparison of the two cohorts. The incidence rates of other cirrhosis-related complications were secondary end points. A negative binomial generalized linear model was used to adjust for the non-normality of the real-world data.

Results: The charts of 311 patients from 14 centres were screened and 125 matched pairs of LTA and non-LTA patients were analysed. In both cohorts, the mean age was 63.5 years, 64% were female, 14.4% had multiple comorbidities, and the mean CP score was 9.0. The mean standard difference between the cohorts for all three covariates included in the PSM model was 0.0% for all matched pairs (100% bias reduction). The mean annual number of therapeutic paracentesis episodes per patient was reduced by 47.8% in the LTA vs the non-LTA cohort (2.21 vs 3.97; $p < 0.001$; Figure). Statistically significant reductions in refractory ascites (44.2%, $p = 0.018$), spontaneous bacterial peritonitis (52.7%, $p = 0.009$), hepatorenal syndrome (62.6%, $p = 0.003$), hospital admissions (24.6%, $p = 0.050$) and length of stay for hospitalised patients (35.0%, $p = 0.015$) were also seen in the LTA cohort vs the non-LTA cohort. Hepatic encephalopathy did not show a statistically significant difference between the groups (13.1% reduction with LTA vs non-LTA, $p = 0.605$). Transplant and mortality rates were numerically lower in the LTA cohort (7% and 22%) than in the non-LTA cohort (12% and 26%) but were inconclusive due to the limited observation period.

Annualised rates of therapeutic paracentesis (numbers of episodes per patient per year).

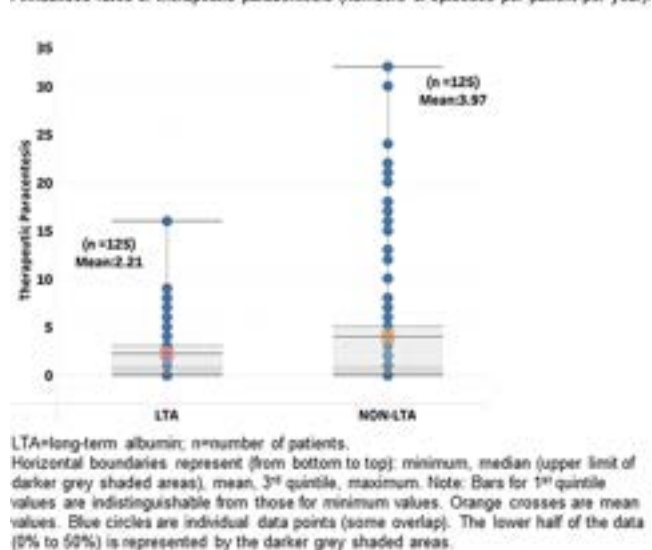


Figure:

Conclusion: These data provide further evidence of the benefits of LTA in patients with cirrhosis. LTA may reduce healthcare resource utilisation and has the potential to be cost-effective in real-world clinical practice.

WED-324

Potentially inappropriate medicine' use and nonadherence in hepatic encephalopathy: a retrospective real-world cohort study

Zhen Howe Hong^{1,2}, Stephanie Johnson³, Tina Ha⁴, Carolyn McIvor¹, Katherine Stuart⁵, Patricia Valery^{6,7}, Elizabeth Powell^{5,7}, Kelly Hayward^{5,7}. ¹Logan Hospital, Department of Gastroenterology and Hepatology, Meadowbrook, Australia, ²University of Queensland, Faculty of Medicine, St Lucia, Australia, ³Logan Hospital, Pharmacy Department, Meadowbrook, Australia, ⁴Princess Alexandra Hospital, Pharmacy Department, Woolloongabba, Australia, ⁵Princess Alexandra Hospital, Department of Gastroenterology and Hepatology, Woolloongabba, Australia, ⁶QIMR Berghofer Medical Research Institute, Herston, Australia, ⁷University of Queensland, Centre for Liver Disease Research, Woolloongabba, Australia
Email: zhenhowe.hong@health.qld.gov.au

Background and aims: Hepatic encephalopathy (HE) is a complex and debilitating complication of cirrhosis that may be precipitated by use of specific medicines and nonadherence with prophylaxis. We aimed to explore the association between 'potentially inappropriate medicine' use, nonadherence, and hospitalisation with HE in a real-world cohort.

Method: A random sample of 1,318 public hospital encounters among 326 CirCare participants (multi-site, prospective, observational study) with ≥ 1 admission between July-2017 and August-2019 were selected for review. Clinical and demographic information, comprehensive decompensation history, and medication data including adherence were abstracted from medical records. Encounters without medication documentation were excluded. A multinomial logistic regression model (adjusted for age, current infection, unplanned vs. elective presentation, and taking benzodiazepines, opioids and proton pump inhibitors (PPIs)) was used to calculate the odds of having covert (minimal, grade 1, or suppressed by medication) or grade 2/3 HE compared to no HE at admission. Adjusted odds ratios (OR) and 95% confidence intervals (CI) are reported.

Results: 354 of 1,318 encounters were selected, of which 245 had medication documentation and were included in the study (mean = 1.3 (standard deviation (SD) = 0.6) encounters among 184 patients). Mean age at encounter was 60 (SD = 11) years, and most encounters were unplanned presentations (75.1%) among males (69.4%) with decompensated cirrhosis (58.4%) in a tertiary hospital (69.4%). Nonadherence with ≥ 1 medicine was documented in 63 (25.7%) encounters. HE was identified in 69 (28.2%) encounters including 13 presentations of new HE. Among 56 encounters with chronic/recurrent HE, patients were prescribed lactulose in 50 (nonadherence rate 42.0%), rifaximin in 27 (nonadherence 7.4%), and other laxatives in 19 (nonadherence 21.5%). Lactulose was prescribed as a laxative in an additional 30 encounters (nonadherence 46.7%), including 8/13 with new HE (4/8 nonadherent). Nonadherence with HE prophylaxis occurred in 31.3% of admissions with grade 2/3 HE and 43.2% with covert HE. 47.8% of people with HE were nonadherent with ≥ 1 medicine compared to 17.0% without HE (chi-square $p < 0.01$). At least one 'potentially inappropriate medicine' was taken in 60/69 HE encounters (Figure). People taking benzodiazepines (OR = 3.75, 95%CI 1.50–9.35; $p < 0.01$) and those taking opioids (OR = 2.96, 95%CI 1.18–6.12; $p = 0.02$) were more likely to have grade 2/3 HE, and those taking PPIs (OR = 2.28, 95%CI 1.04–4.97; $p = 0.04$) were more likely to have covert HE, than people not taking these medicines. The indication was "unknown" for 30.2% of benzodiazepines, 33.3% of opioids, and 45.8% of PPIs.

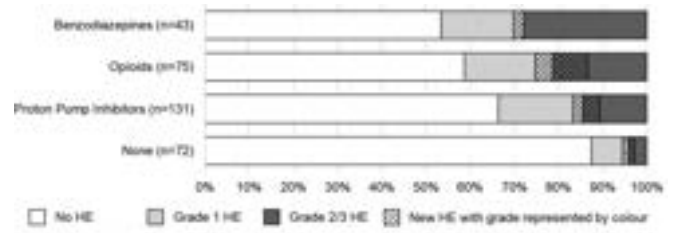


Figure: Proportion of (n) encounters in which patients took 'potentially inappropriate medicines' and were admitted to hospital with hepatic encephalopathy (HE). Textured portions of the bars represent presentations with new HE. Patients took 2 or more 'potentially inappropriate medicines' in 68 (27.8%) encounters.

Figure:

Conclusion: Nonadherence is common in HE, and people taking opioids and benzodiazepines are at higher risk of grade 2/3 HE. Further exploration of indication and potential alternative therapies is required.

WED-325

Atorvastatin reduces inflammation markers TNF- α , CD62L and MMP2 in a randomised trial

Thit Mynster Kronborg¹, Robert Schierwagen², Mette Lehmann Andersen³, Ane Soegaard Teisner³, Rasmus Hvidbjerg Gantzel⁴, Henning Grønbaek⁴, Lise hobolth¹, Søren Møller⁵, Flemming Bendtsen¹, Jonel Trebicka², Nina Kimer¹. ¹Hvidovre University Hospital, Gastro Unit, Medical section, Hvidovre, Denmark, ²Universitätsklinikum Münster (UKM), Medizinische Klinik B (Gastroenterologie, Hepatologie, Endokrinologie, Klinische Infektiologie), Germany, ³Herlev University Hospital, Gastroenterology and hepatology, Denmark, ⁴Aarhus University Hospital, Department of Hepatology and Gastroenterology, Denmark, ⁵Hvidovre University Hospital, Clinical Physiology and Nuclear Medicine, Denmark
Email: thit.mynster.kronborg@regionh.dk

Background and aims: In liver cirrhosis with portal hypertension, the mortality and risk of complications are high. Statins may have anti-inflammatory and anti-fibrotic effects in cirrhosis. Hence, statins can potentially reduce the risk of complications and mortality in patients with cirrhosis and portal hypertension. Therefore, we aimed to investigate the effects of Atorvastatin treatment on hospitalisations, mortality and systemic inflammation markers in cirrhosis.

Method: We performed a double-blind, randomised, placebo-controlled clinical trial in patients with liver cirrhosis and portal hypertension ≥ 10 mm Hg. Atorvastatin 10–20 mg was administered for six months. Invasive hemodynamics were measured at baseline and after six months. Inflammation and cellular markers were analysed in peripheral and liver vein blood samples by bead- and flow-cytometry-based multiplexed immunoassays at baseline and after six months.

Results: 78 patients were randomised. 38 were allocated to Atorvastatin and 40 to placebo. Fifty-eight patients completed six months of intervention. The number of liver-related complications and mortality was similar between groups. Atorvastatin did not significantly affect surrogate hemodynamic (HVPG-decrease 4.1% in Atorvastatin and 2.8% in placebo) or clinical parameters (MELD: 2.4% decrease in Atorvastatin and 7.3% increase in placebo). Interestingly, Atorvastatin significantly decreased the inflammation and extracellular matrix markers TNF- α , CD62L and MMP2 in the Atorvastatin group compared to the placebo group (p values; 0.005, 0.011 and 0.023).

Conclusion: Although six months of Atorvastatin treatment did not change clinical outcomes in this study, probably due to the small sample size, Atorvastatin has significant anti-inflammatory effects in cirrhosis.

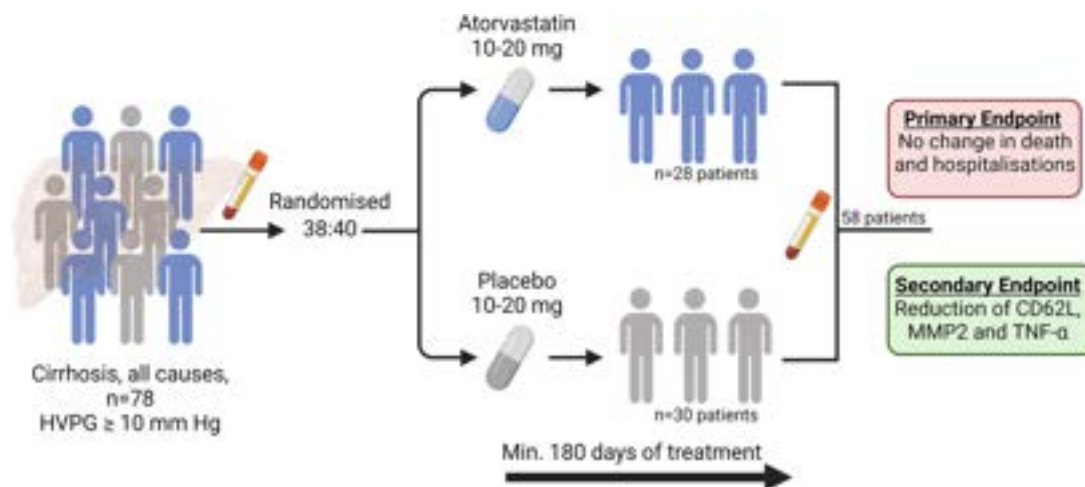


Figure: (abstract: WED-325).

WED-326

Impact of intrapulmonary vascular dilatations and hepatopulmonary syndrome on the clinical course of patients after transjugular intrahepatic portosystemic shunt insertion

Jim Benjamin Mauz¹, Hannah Schneider¹, Dominik Berliner², Anja Tiede¹, Lena Stockhoff¹, Jan Hinrichs³, Heiner Wedemeyer^{1,4}, Bernhard Meyer³, Karen Olsson^{5,6}, Benjamin Maasoumy^{1,4}, Tammo Lambert Tergast¹. ¹Hannover Medical School, Department of Gastroenterology, Hepatology and Endocrinology, Hannover, Germany, ²Hannover Medical School, Department of Cardiology and Angiology, Hannover, Germany, ³Hannover Medical School, Department of Interventional Radiology, Hannover, Germany, ⁴German Center for Infection Research (DZIF), Hannover-Braunschweig, Braunschweig, Germany, ⁵Hannover Medical School, Department of Respiratory Medicine, Hannover, Germany, ⁶German Center for Lung Research (DZL), Gießen, Germany
Email: mauz.jim@mh-hannover.de

Background and aims: Implantation of a transjugular intrahepatic portosystemic shunt (TIPS) is an established therapy of cirrhosis related complications such as ascites or variceal bleeding. In this setting, data on the impact of TIPS implantation on the clinical course of patients with intrapulmonary vascular dilatations (IPVD) and hepatopulmonary syndrome (HPS) are scarce and only few case reports and case series are available. Some authors suggested that TIPS insertion might exacerbate the hyperdynamic circulatory state that is present in patients with advanced liver disease and could therefore result in a higher incidence of hepatic or cardiac decompensation. Hence, this study aimed to investigate the impact of IPVD and HPS on the course of patients that underwent TIPS implantation.

Method: A number of 366 consecutive patients who received a TIPS between 2009 and 2021 were considered for this study. Contrast-enhanced echocardiography and blood gas analysis (BGA) were conducted to assess the presence of IPVD and HPS. Patients with Budd-Chiari syndrome, relevant lung disease, absence of liver cirrhosis or missing data regarding echocardiography or BGA were excluded from this study. Multivariable competing risk analysis was performed to assess longitudinal end points and adjusted for MELD score, age and refractory ascites as TIPS indication. Patients were followed up for one year after TIPS-insertion and analyzed end points were liver transplant (LTx)-free survival, hepatic decompensation or cardiac decompensation.

Results: Overall, 269 patients were included in the final analysis. A number of 138 patients had IPVD and 72 fulfilled HPS criteria. Patients with IPVD had lower MELD scores (12 ± 4 vs. 13 ± 4 , $p =$

0.028), while ascites as TIPS indication was less frequent than in those without IPVD (75% vs. 90%, $p < 0.001$). The alveolar-arterial oxygen gradient was higher in the IPVD group (29 ± 15 vs. 21 ± 17 , $p < 0.001$), while arterial-oxygen partial pressure was lower (80 ± 15 vs. 86 ± 17 , $p = 0.006$). Presence of IPVD was not associated with a lower LTx-free survival within one year after TIPS implantation (22% vs. 22%, HR: 1.26, 95%CI: 0.75–2.11, $p = 0.380$). However, IPVD were linked to cardiac decompensation (28% vs. 18%, HR: 1.78, 95%CI: 1.03–3.07, $p = 0.040$) and a numerically higher risk of hepatic decompensation (55% vs. 46%, HR: 1.37, 95%CI: 0.98–1.91, $p = 0.064$) in the follow-up. In those with HPS, LTx-free survival and hepatic decompensation did not differ from those without HPS or IPVD (26% vs. 22%, HR: 1.22, 95%CI: 0.68–2.19, $p = 0.510$, hepatic decompensation: 54% vs. 46%, HR 1.21, 95%CI: 0.82–1.78, $p = 0.340$). However, incidence of cardiac decompensation was numerically increased (32% vs. 18%; HR: 1.74, 95%CI: 0.97–3.13, $p = 0.061$).

Conclusion: Presence of IPVD or HPS increases the risk of cardiac decompensation but does not impact overall mortality after TIPS implantation.

WED-327

Efficacy and safety of nalfurafine hydrochloride for pruritus in patients with chronic liver disease in Japan

Tadamichi Kawano¹, Masanori Atsukawa¹, Akihito Tsubota², Kaori Shioda¹, Hiroki Ono¹, Tomomi Okubo¹, Taeang Arai¹, Korenobi Hayama¹, Keiko Kaneko¹, Norio Itokawa¹, Katsuhiko Iwakiri¹. ¹Nippon Medical School, Division of Gastroenterology and Hepatology, Tokyo, Japan, ²Jikei University School of Medicine, Core Research Facilities, Tokyo, Japan
Email: k-tadamichi@nms.ac.jp

Background and aims: Nalfurafine hydrochloride, a selective κ -opioid receptor agonist has been approved for treatment of pruritus in patients with chronic liver disease. However, not all patients respond to nalfurafine hydrochloride. The aim of this study was to clarify the efficacy and safety of nalfurafine hydrochloride.

Method: The subjects were patients with chronic liver disease complicated by pruritus who were treated with nalfurafine hydrochloride between May, 2015, and May, 2022. The degree of pruritus was evaluated based on the Visual Analog Scale (VAS) score and the Kawashima's pruritus score. Nalfurafine hydrochloride 2.5 μ g was orally administered once a day for 12 weeks. A decrease in the VAS score of ≥ 25 mm or the Kawashima's pruritus score of ≥ 1 scores was designated as relevant response. The former of ≥ 50 mm or the latter of ≥ 2 scores as remarkable response. The 332 patients who were

evaluated the efficacy at 12 weeks. The median time suffering from pruritus to administration of nalfurafine hydrochloride was 4 months. **Results:** The median VAS score improved from 70.0 mm before administration to 40.0 and 30.0 mm at 4 and 12 weeks of treatment, respectively. On multivariate analysis, shorter itching period and lower the fibrosis-4 (FIB-4) index value were extracted as the independent factors related to remarkable responder. On multivariate analysis, shorter itching period was extracted as the only independent factor related to relevant responder. The dose escalation (from 2.5 to 5.0 µg/day at 4 weeks of treatment) was performed in 24 patients. Of the 24 patients with dose escalation, 16, 8, and 8 had relevant response, remarkable response, and non-response, respectively.

Conclusion: This study suggested nalfurafine hydrochloride treatment markedly improves pruritus in patients with chronic liver disease. A short pruritus period and less-advanced fibrosis were associated with response to nalfurafine hydrochloride.

WED-328

Safety and efficacy of continuous infusion terlipressin in acute kidney injury-hepatorenal syndrome: the Infuse study

K. Rajender Reddy¹, Ethan Weinberg¹, Stevan Gonzalez², Manhal Izzy³, Douglas Simonetto⁴, Richard Frederick⁵, Raymond Rubin⁶, Zachary Fricker⁷, Grace Kim-Lee¹, Sherry Witkiewicz⁸, William Tobin⁸, Khurram Jamil⁹. ¹University of Pennsylvania, Division of Gastroenterology and Hepatology, Philadelphia, PA, United States, ²Simmons Transplant Institute, Baylor University Medical Center, Baylor Scott and White All Saints Medical Center, Hepatology, Dallas, TX, United States, ³Vanderbilt University Medical Center, Department of Gastroenterology and Hepatology, Nashville, TN, United States, ⁴Mayo Clinic, Rochester, MN, United States, ⁵California Pacific Medical Center, Hepatology and Liver Transplantation, San Francisco, CA, United States, ⁶Piedmont Healthcare, Piedmont Transplant Institute, Atlanta, GA, United States, ⁷Beth Israel Deaconess Medical Center, Harvard Medical School, Boston, MA, United States, ⁸International HealthCare, LLC, Norwalk, CT, United States, ⁹Mallinckrodt Pharmaceuticals, Scientific Affairs, Hampton, NJ, United States
Email: reddy@penmedicine.upenn.edu

Background and aims: Safety and efficacy of terlipressin for AKI-HRS may be greater with a continuous infusion strategy as opposed to bolus administration (CONFIRM; NCT02770716).

Method: An open-label study of continuous infusion terlipressin (INFUSE; NCT04460560) has been completed in 50 patients with cirrhosis and AKI-HRS. The cohort was enriched with those who were listed/in evaluation/eligible for liver transplantation (LT). Patients with MELD ≥ 35, ACLF-Grade 3, or serum creatinine (SCr) >5.0 mg/dL were excluded. Following a 0.5 mg bolus, terlipressin was administered as a continuous infusion from 2 to 8 mg/day based on SCr response and tolerability. Complete Response (CR): ≥ 30% decrease in SCr with EOT SCr ≤ 1.5, Partial Response (PR): ≥ 30% decrease in SCr with EOT SCr >1.5, Non-Response (NR): <30% decrease in SCr. Follow-up was up to 30 days post-treatment.

Results: (See table) There were no unexpected drug-related serious adverse events. One patient had hypoxic respiratory failure attributed to fluid overload and responded to diuretics. There were 3 deaths (2 progressive liver failure, 1 progressive renal failure). Midodrine and octreotide use prior to enrollment was in 37/50; 74%.

Table:

	All Patients	CR	PR	NR	p value
Mean age 57, 54% male	50	31/50 (62%)	8/50 (16%)	11/50 (22%)	
AKI Stage 1B/2/3	14/50 (28%) 20/50 (40%) 16/50 (32%)	9/31 (29%) 15/31 (48%) 7/31 (23%)	1/8 (12.5%) 3/8 (37.5%) 4/8 (50%)	4/11 (36%) 2/11 (18%) 5/11 (46%)	NS
Alcohol-Related Liver Disease	26/50 (52%)	18/31 (58%)	3/8 (37.5%)	5/11 (46%)	NS
NASH	15/50 (30%)	8/31 (26%)	4/8 (50%)	3/11 (27%)	
MELD, Baseline	26, 17–34	25, 18–34	27, 17–34	27, 17–33	NS
MELD, EOT	20, 11–32	18, 11–31	20, 14–29	23, 16–32	NS
SCr, Baseline	2.6, 1.5–4.9	2.3, 1.5–3.9	3.0, 2.3–4.4	2.8, 1.7–4.9	0.02
SCr, EOT	1.4, 0.8–4.9	1.2, 0.8–1.5	1.9, 1.7–2.4	2.6, 1.5–4.9	
Days of treatment	8, 1–14	7, 3–14	10, 3–14	4, 1–14	NS
Terlipressin dose (mg)	21, 3–87	21, 3–79	47, 5–87	13, 3–67	NS
Concurrent albumin dose (g)	150, 25–475	175, 50–400	125, 50–475	100, 25–188	0.037
RRT within 30 d	10/50 (20%)	1/31 (3%)	2/8 (25%)	7/11 (64%)	<0.001
Alive at 30 d	47/50 (94%)	30/31 (97%)	7/8 (87.5%)	10/11 (91%)	NS
Transplant candidates	40/50 (80%)	23/31 (74%)	8/8 (100%)	9/11 (82%)	NS
- Waitlist	5/40 (12.5%)	2/23 (9%)	1/8 (12.5%)	2/9 (22%)	
- Evaluation	23/40 (57.5%)	13/23 (57%)	5/8 (62.5%)	5/9 (56%)	
- Eligible	11/40 (27.5%)	8/23 (35%)	1/8 (12.5%)	2/9 (22%)	
LT	15/40 (37.5%)	9/15 (60%)	1/15 (7%)	5/15 (33%)	NS
SLKT	4/40 (10%)	1/4 (25%)	2/4 (50%)	1/4 (25%)	NS

Values are median, range unless otherwise stated.

Conclusion: A high CR of 62% was observed with continuous infusion terlipressin with a favorable safety profile. Fifteen underwent LT alone; 9/15 (60%) were CR, 1/15 (7%) PR, 5/15 (33%) NR, and 4 had simultaneous liver kidney transplants (SLKT). In patients with AKI-HRS, treatment with terlipressin was followed by LT alone in a high proportion of complete responders.

WED-329

Abstract withdrawn

WED-330

The effects of alfapump on ascites control and quality of life in patients with cirrhosis and recurrent or refractory ascites: pivotal trial results

Florence Wong¹, Hugo Vargas², K. Rajender Reddy³, Mangesh Pagadala⁴, Christine Pocha⁵, Vinay Sundaram⁶, Jasmohan Bajaj⁷, Jeroen Capel⁸, Patrick S. Kamath⁹. ¹University of Toronto, ON, Canada, ²Mayo Clinic, Phoenix, AZ, United States, ³University of Pennsylvania, PA, United States, ⁴Methodist Dallas Medical Center, TX, United States, ⁵Avera Medical Group, Sioux Falls, United States, ⁶Cedars-Sinai Comprehensive Transplant Center, Los Angeles, CA, United States, ⁷Richmond VA Medical Center, United States, ⁸Sequana Medical NV, Zürich, Switzerland, ⁹Mayo Clinic, Rochester MN, United States
Email: florence.wong@utoronto.ca

Background and aims: The standard of care for recurrent or refractory ascites (RA) in cirrhosis is repeat large volume paracentesis (LVP). The alfapump system, providing slow but continuous paracentesis (para) via a subcutaneous pump, has been shown to be a possible alternative in selected patients. The aim was to assess the effects of alfapump on ascites control and quality of life (QoL) in patients with cirrhosis and RA.

Method: Patients with cirrhosis and RA and TIPS contraindications or refusal who had required ≥ 2 paras in the 30 days prior were enrolled. Patients served as their own controls with ≥ 5 paras in 3 months (M) before pump implantation. Patients received post-implant prophylactic antibiotics and follow-up was ≥ 6 M. Data collected were demographics, albumin use, ascites control, safety, QoL and ascites symptoms using SF36 and Ascites Q questionnaires, respectively. The 3 M pre-pump and 4–6 M post-pump data were compared, after initial 3 M post-pump stabilization. Primary efficacy end point was reduction in para requirement; safety end points were pump system adverse events that resulted in intervention, explant or death.

Results: 40 patients with RA, mean age 64 ± 9 yrs, 65% men, mean MELD-Na 15 ± 4 , 48% alcohol-related cirrhosis received an alfapump. Efficacy: Para requirement decreased from 3.2 ± 1.5 to 0.2 ± 0.6 times/M ($p < 0.001$) from pre- to post- pump implant period, with 77% of patients having a $\geq 50\%$ reduction (Figure). Ascites volume removed by para fell from 54.2 ± 23.3 pre- to 2.8 ± 9.1 L/M post-pump ($p < 0.001$). Safety: 6 (17.6%) pumps were explanted, 3 due to pump site skin erosion and 3 due to bladder discomfort. There were 17 serious adverse events (SAEs) in 11 patients in the pre-, and 81 SAEs in 24 patients ($p < 0.001$) in the post-implant period, respectively. Six primary safety events post-implant were related to procedure, device or alfapump therapy. There was no AKI in the pre-, but 23 AKIs in the post-implant period (0–6 M), with 16/24 cases being stage 1, 5 stage 2, and 2 stage 3 AKI. Albumin use was 95 ± 105 g/M in the post-implant vs. 102 ± 127 g/M in the pre-implant period ($p = 0.38$), likely due to AKI treatment. There were 4 SBP SAEs and 1 UTI SAE. There were 5 deaths in the 6 M post-implant period, none related to device

or alfapump therapy, renal dysfunction or infection. QoL: Patients reported reductions in ascites related symptoms with an Ascites Q score of 32.2 ± 21.9 at 6 M post- vs. 51.0 ± 19.3 pre-implant (lower value = improvement) ($p < 0.001$). Physical but not mental component of SF36 improved (35.6 ± 9.3 pre-implant to 42.8 ± 8.5 at 6 M [$p < 0.001$]).

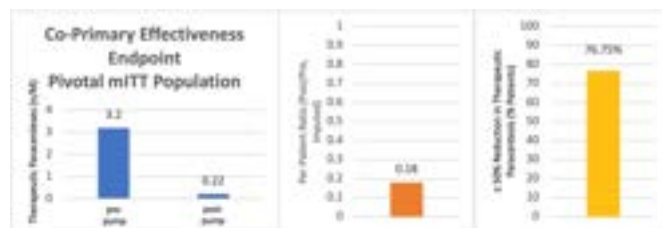


Figure:

Conclusion: The alfapump system was very effective in control of ascites, virtually eliminating the need for LVP. Patients with the alfapump need close monitoring for the development of AKI or infection, which must be treated promptly to prevent adverse outcomes. In carefully selected patients with RA, the alfapump is an alternative to repeat LVP.

WED-331

Quickstroop, an App-based strategy that takes <1 minute, predicts time to overt hepatic encephalopathy development and hospitalizations

Gowthami Kanagalingam¹, Dan Park¹, Bryan Badal¹, Andrew Fagan¹, Leroy Thacker¹, Jasmohan S Bajaj¹. ¹Virginia Commonwealth University, United States
Email: jasmohan.bajaj@vcuhealth.org

Background and aims: Prediction of overt hepatic encephalopathy (OHE) development needs to be refined beyond current clinical markers. Covert HE (CHE) diagnosis with QuickStroop (1st 2 runs of EncephalApp Off stage) takes <1 min vs the total EncephalApp. Both are comparable cross-sectionally but use of QuickStroop to predict OHE and hospitalizations is unclear. Aim: Determine the ability of QuickStroop to predict OHE and related hospitalizations, other hospitalizations and death in cirrhosis outpatients.

Method: Outpatients with cirrhosis underwent QuickStroop testing and were divided into CHE or not based on age, gender and education adjusted norms. Follow-up for OHE development (grade ≥ 2 needing Rx changes), OHE-related non-elective hospitalizations, all hospitalizations and death was performed. Demographics, cirrhosis details and medications were recorded. Cox proportional hazard models for CHE by QuickStroop for OHE and hospitalizations were created unadjusted and then adjusted for cirrhosis severity and complications.

Results: 250 pts (62.5 ± 8.2 years, 96% men, education median 12 years) were included. Median MELD-Na (range) was 11 (6, 37) with most pts with NAFLD (33%) then HCV (24%) and alcohol (18%). Prior OHE was seen in 33% (all on lactulose, 29% on rifaximin). 41% had ascites, 37% had varices and 24% were on non-selective beta-blockers (NSBB). Patients were followed a median of 7 (1–107) months from testing. The median time-to-event for those who developed OHE was 5 (1, 47) mths, HE-related hospitalizations was 5 (1, 47) months and all hospitalizations was 6 (1, 72) months post-testing. CHE: CHE on QuickStroop was found in 126 (50%) patients. MELD was higher (14.3 ± 6.4 vs 11.4 ± 5.1 , $p < 0.001$), with higher prior OHE (45% vs 23%, $p = 0.002$), higher ascites (51% vs 32%, $p = 0.003$) and lower albumin (3.3 ± 0.7 vs 3.5 vs 0.5 , $p = 0.001$) in CHE pts. Outcomes and cox hazards: 60% needed hospitalizations, 16% developed OHE, 10% needed OHE-related hospitalizations and 23% died. On unadjusted comparisons, CHE pts had higher risk of OHE development (24% vs 7%, $p = 0.003$), OHE-related hospitalizations (16% vs 5%, $p = 0.004$) and death (31% vs 5%, $p = 0.002$) but similar all-cause hospitalizations (62% vs 57%, $p =$

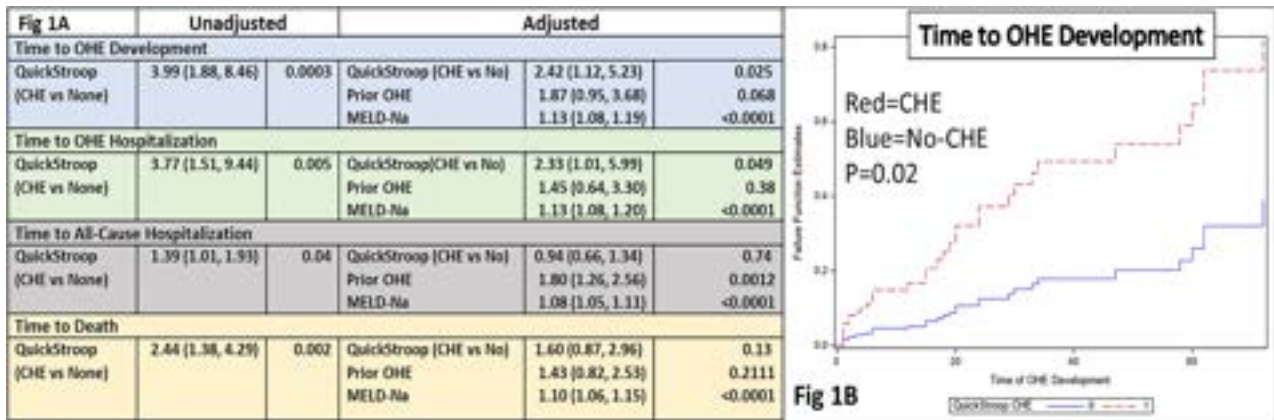


Figure: (abstract: WED-331).

0.45). This pattern was also seen in time-to-event analysis. After adjustment for other variables, CHE on Quickstroop remained significantly linked with lower time to OHE development and hospitalizations but not death or all-cause hospitalizations (Fig 1A/B). **Conclusion:** Using the Quickstroop, an App-based strategy providing CHE diagnosis within one minute, is associated with lower time to develop outcomes specific to Overt HE development.

WED-332

On-treatment factors predict recompensation in entecavir-treated hepatitis B patients with decompensated cirrhosis

You Deng¹, Huanwei Zheng², Xiang Huiling³, Yuemin Nan⁴, Jinhua Hu⁵, Qinghua Meng⁶, Hong Zhao¹, Qi Wang¹, Jilian Fang⁷, Jie Xu⁸, Xiaoming Wang⁹, Calvin Q Pan¹⁰, Hong You⁹, Xiaoyuan Xu¹¹, Wen Xie¹, Ji-Dong Jia⁹. ¹Beijing Ditan Hospital, Capital Medical University, China, ²Shijiazhuang Fifth Hospital, China, ³Tianjin Third Central Hospital, China, ⁴The Third Hospital of Hebei Medical University, China, ⁵The Fifth Medical Centre of Chinese PLA General Hospital, China, ⁶Beijing You-an Hospital, Capital Medical University, China, ⁷Peking University People's Hospital, China, ⁸Peking University Third Hospital, China, ⁹Beijing Friendship Hospital, Capital Medical University, China, ¹⁰Division of Gastroenterology and Hepatology, Department of Medicine, NYU Langone Medical Center, NYU School of Medicine, United States, ¹¹Peking University First Hospital, China
Email: jia_jd@ccmu.edu.cn

Background and aims: Recompensation is achievable in certain decompensated cirrhotic hepatitis B patients treated with nucleos (t) ide analogues (NAs). However, the prediction factors of recompensation are still unclear. Therefore, we aimed to develop a prognostic model for recompensation prediction in NA-treated hepatitis B patients with decompensated cirrhosis.

Method: In a multi-centre study enrolled decompensated chronic hepatitis B (CHB) patients with ascites and treated with entecavir for 120 weeks, clinical events, viral and biochemical tests were monitored every 12 weeks. The primary outcome was the rate of recompensation as defined by the Baveno VII definition and the criteria of stable improvement in liver function tests reported by us. Multivariate logistic regressions were used to identify the optimal prediction time and to build prediction models.

Results: Of the 320 recruited patients, 283 completed the 120-week entecavir treatment and follow-up, with 56.2% (159/283) of them achieving recompensation at week 120. Treatment week 24 was the optimal time to predict recompensation, with an albumin level of 34 g/L or greater being a reliable threshold for recompensation (AUROC: 0.676) at treatment week 120. Furthermore, a model based on platelet count, serum albumin, and sodium level (Brec-PAS models) at treatment week 24 offered better predictability (AUROC: 0.749) for recompensation at treatment week 120, outperforming the

MELD (AUROC: 0.629, $p = 0.002$) and FIB-4 scores (AUROC: 0.702, $p = 0.097$).

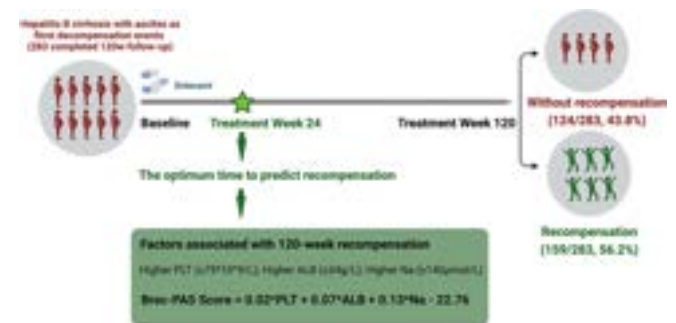


Figure:

Conclusion: At treatment week 24, the serum albumin level of 34 g/L or greater was a simple predictor, whereas Brec-PAS model was a more accurate predictor tool for 120-week recompensation in entecavir-treated CHB patients with decompensated cirrhosis.

WED-333

Temporal trajectory of the model for end-stage liver disease (MELD) score for prediction of mortality among patients with liver cirrhosis

Niv Zmora¹, Lian Bannon¹, Oren Shibolet¹, Liane Rabinowich¹. ¹Tel Aviv Sourasky Medical Center-Ichilov, Department of Gastroenterology and Hepatology, Tel Aviv-Yafo, Israel
Email: nivz@tlvmc.gov.il

Background and aims: The Model for End-Stage Liver Disease (MELD) score and its modification, the MELD-Na score, are important prognostic indicators for patients with liver cirrhosis, as predictors of 3-month survival as well as prioritization and organ allocation in liver transplantation. The scores provide a snapshot of mortality risk at a specific time-point, irrespective of the preceding course of liver disease. Our aim was to assess whether the trajectory in MELD-Na score over time affect mortality rates in patients with liver cirrhosis. **Method:** MELD-Na score was retrospectively applied to patients diagnosed with liver cirrhosis who died between the years 2004–2023 at the Tel-Aviv Sourasky Medical Center. Patients with at least 5 records of relevant blood tests required for MELD-Na score calculation (serum bilirubin, creatinine, sodium and international normalized ratio [INR]) within 2 years prior to death were included. The cumulative MELD-Na score was calculated for each patient throughout the study period using incremental area under the MELD-Na curve, and was correlated to patient survival for each MELD-Na score from 9 onwards.

POSTER PRESENTATIONS

Results: Within the study period there were 1,905 reported deaths among patients diagnosed with liver cirrhosis, of whom 982 were eligible for analysis, encompassing 13,136 calculated MELD-Na scores (average MELD-Na score 19.26 ± 6.88). Observed 3-month mortality rates for each MELD-Na score were higher than predicted by the published model (59.03% for scores in the range of 10–19; 84.14% for scores in the range of 20–29; and 97.27% for scores between 30–39). MELD-Na scores between 9–15 exhibited a statistically significant dependence on MELD-Na history (p values 0–0.05), with an inverse correlation between survival and cumulative MELD-Na scores (correlation coefficient range 0.07–0.20).

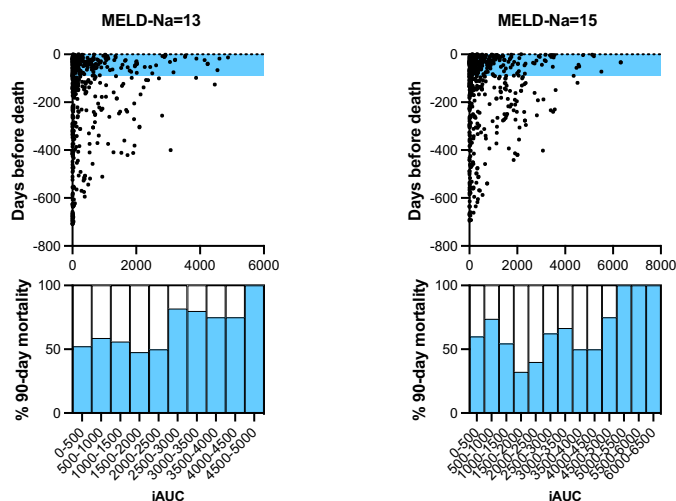


Figure: Top: Correlation between cumulative MELD-Na score to survival in instances where MELD-Na = 13 (left) and 15 (right). Blue fill denotes a 90-day mortality time frame; Bottom: percentage of 90-day mortality binned by iAUC values

Conclusion: In patients with cirrhosis and mild liver dysfunction, temporal trajectories in MELD-Na scores may aid in optimizing prediction of 90-day mortality.

WED-334

Smoking and obesity promote systemic inflammation in patients with compensated and decompensated cirrhosis

Benedikt Hofer^{1,2,3}, Benedikt Simbrunner^{1,2,3}, Georg Semmler^{1,2}, Michael Schwarz^{1,2}, Lorenz Balcar^{1,2}, Lukas Hartl^{1,2}, Mathias Jachs^{1,2}, Katharina Pomej^{1,2}, Rafael Paternostro^{1,2}, Theresa Müllner-Bucsics^{1,2}, Philipp Schwabl^{1,2,3}, Bernhard Scheiner^{1,2}, Michael Trauner¹, Matthias Mandorfer^{1,2}, Thomas Reiberger^{1,2,3}. ¹Medical University of Vienna, Division of Gastroenterology and Hepatology, Department of Internal Medicine III, Vienna, Austria, ²Medical University of Vienna, Vienna Hepatic Hemodynamic Laboratory, Division of Gastroenterology and Hepatology, Department of Internal Medicine III, Vienna, Austria, ³Medical University of Vienna, Christian Doppler Lab for Portal Hypertension and Liver Fibrosis, Vienna, Austria
Email: thomas.reiberger@meduniwien.ac.at

Background and aims: Cigarette smoking and obesity have been linked to systemic inflammation in patients with cardiovascular disease. The relative contribution of these two factors to the proinflammatory state in patients with advanced chronic liver disease (ACLD) remains unknown.

Method: ACLD patients with either compensated (cACLD, $n = 284$) or decompensated (dACLD, $n = 416$) disease and available information regarding smoking status and body mass index (BMI) were included. Blood markers of systemic inflammation (white blood cell count [WBC], C-reactive protein [CRP]) were evaluated in groups of “never-smokers” vs “ex-smokers” vs “active smokers” and in BMI strata “BMI < 25” vs “BMI 25–30” vs “BMI > 30”.

Results: Overall, 106 cACLD patients (37.3%) and 160 dACLD patients (38.5%) reported active smoking. 84 cACLD patients (29.6%) and 78 dACLD patients (23.5%; grade 3 ascites patients [$n = 84$] were excluded from all BMI analyses) presented with obesity (i.e., BMI > 30 kg/m²). In cACLD patients, median WBC increased according to smoking status (never: 4.3 vs ex: 5.1 vs active: 6.0 G/L; $p < 0.001$), with a significant difference between never-smokers and ex-smokers ($p = 0.025$) or active smokers ($p < 0.001$), as well as between ex-smokers and active smokers ($p = 0.009$). No significant difference was observed for CRP ($p = 0.649$). In dACLD, active smokers and ex-smokers demonstrated a significant increase in WBC (never: 4.4 vs ex: 4.8 vs active: 5.6 G/L; $p < 0.001$) and a clear trend for CRP (never: 3.9 vs ex: 4.9 vs active: 5.1 mg/L; $p = 0.176$). Importantly, the link between active smoking and increased WBC remained significant in both cACLD (< 0.001) and dACLD ($p < 0.001$) after adjusting for MELD in a multivariable linear regression model. With regard to obesity, BMI showed a significant positive correlation with CRP both in cACLD (Spearman's r : 0.17; $p = 0.004$) and dACLD patients (r : 0.11; $p = 0.039$). Accordingly, CRP was significantly higher in patients with BMI > 30 vs BMI 25–30 and BMI < 25 in cACLD patients (2.7 vs 1.6 and 1.8 mg/L; $p = 0.035$) and in dACLD patients (4.7 vs 3.3 and 3.2 mg/L; $p = 0.113$). Taking cACLD and dACLD together, active smokers with BMI > 30 ($n = 46$) showed significantly higher levels of systemic inflammation compared to never-smokers with BMI < 25 ($n = 79$): WBC (6.6 vs 4.3 G/L; $p < 0.001$), CRP (4.7 vs 2.2 mg/L; $p = 0.004$). WBC ($p = 0.134$) and CRP ($p = 0.145$) in ex-smokers with BMI 25–30 ($n = 72$) were not significantly different from never-smokers with BMI < 25 (Figure).

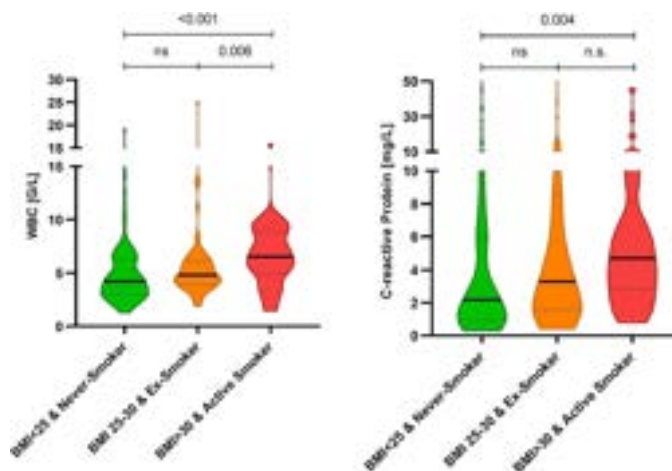


Figure:

Conclusion: In a large cohort of patients with compensated and decompensated cirrhosis, both active smoking and obesity promote a proinflammatory state. Thus, cessation of smoking should be encouraged in all ACLD patients, and weight loss in those with obesity.

WED-335

Association of polymorphisms in genes of the innate immunity with transplant-free survival of patients with decompensated liver cirrhosis

Niclas Selzer¹, Janett Fischer¹, Adam Herber¹, Niklas Aehling², Madlen Matz-Soja¹, Thomas Berg¹. ¹Division of Hepatology, Department of Medicine II, Leipzig University Medical Center, Germany, ²Internal Medicine III-Gastroenterology, University Hospital of Augsburg, Germany
Email: janett.fischer@medizin.uni-leipzig.de

Background and aims: Liver cirrhosis is associated with severe complications such as acute-on-chronic-liver-failure (ACLF), ascites as well as infections, especially spontaneous bacterial peritonitis (SBP). Several single nucleotide polymorphisms (SNP) have been

reported to affect innate immune responses. In previous studies, some SNPs in patients with liver cirrhosis were associated with altered patient survival, the occurrence of SBPs or cytokine response to bacteria. The aim of our study was to assess the impact of known SNPs in the genes of toll-like receptor 1, 2, 4, 5 and 6, the cluster of differentiation 14 (CD14), nucleotide-binding oligomerization domain-containing protein 2 (NOD2), the farnesoid-X receptor (FXR) and the Mannose-binding lectin 2 (MBL2) on disease progression and transplantation-free survival of patients with liver cirrhosis and ascites in a large, well-characterized cohort.

Method: In our study, we genotyped 409 patients with liver cirrhosis and ascites for 28 SNPs of the innate immune system. We then correlated the genotypes with clinical data from the time of inclusion and with the incidence of infections and survival over a period of 180 days after inclusion. Both the entire cohort and subgroups divided according to a low and high MELD-score (cut-off 17) and sex were examined.

Results: In the main cohort, the genotypes CT and TT of the *TLR4* SNP rs4986791 ($p = 0.039$; OR: 1.881) as well as the genotype CG of the *NOD2* SNP rs2066845 ($p = 0.025$; OR: 2.853) were significantly associated with a reduced transplant-free survival. Additionally, we found an association between CT and TT genotypes of the SNP *FXR* rs386377 and an increased occurrence of SBP ($p = 0.01$; OR: 2.986). Patients with the CC genotype of the *MBL2* SNP rs5030737 survived significantly shorter than other patients ($p = 0.037$; OR: 0.406). We observed more associations between variants and a worsened course of disease in the females compared to male patients (8,3% vs. 2,4%) as well as in the low-MELD subgroup compared to the high-MELD cohort (4,8% vs. 0%).

Conclusion: We identified several variants in the innate immune system that affect the clinical course of disease in patients with decompensated liver cirrhosis independently from other known risk factors. Thus, panels with different risk genotypes should be implemented into personalized medicine to identify patients with an increased risk of a severe course of the disease.

WED-336

Applicability of EASL clinical guidelines recommendations of empiric antibiotic treatment for spontaneous bacterial infections in patients with cirrhosis in South America

Melisa Dirchwolf^{1,2}, Marina Agozino³, Gonzalo Gomez Perdiguero⁴, Ivonne Giselle Duarte⁵, Maria Dolores Murga⁶, Fernando Bessone⁷, Sebastian Eduardo Ferretti⁸, Diego Arufe⁹, Andres Bruno¹⁰, Astrid Smud⁴, Diego Giunta⁴, Martín Elizondo¹¹, Hugo Fainboim¹², Adrian Gadano⁴, Julia Brutti¹³, Josefina Pages¹⁴, German Rojas¹⁵, Esteban Gonzalez Ballera¹⁵, Alina Zerrega¹⁶, Maria Garrido¹⁷, Natalie Vilcinskis Y Botteron¹⁸, Matias Machain¹⁹, Sebastián Marciano⁴. ¹Hospital Privado de Rosario, Argentina, ²Hospital Privado de Rosario, Liver Unit, Rosario, Argentina, ³Sanatorio Guemes, Argentina, ⁴Hospital Italiano de Buenos Aires, Argentina, ⁵Hospital 4 de Junio, Argentina, ⁶Hospital A.C. Padilla, Argentina, ⁷Hospital Provincial del Centenario, Argentina, ⁸Sanatorio Parque de Rosario, Argentina, ⁹Sanatorio Sagrado Corazón, Argentina, ¹⁰Hospital Argerich, Argentina, ¹¹Unidad Bi-Institucional de Trasplante Hepático: Hospital Militar HCFFAA y Hospital de Clínicas, Uruguay, ¹²Hospital de Infecciosas Francisco Javier Muñoz, Argentina, ¹³Hospital Aleman, Argentina, ¹⁴Hospital Universitario Austral, Argentina, ¹⁵Hospital de Clínicas José de San Martín, Argentina, ¹⁶Sanatorio Allende, Argentina, ¹⁷Hospital Central Ramon Carrillo, Argentina, ¹⁸Hospital Central de Mendoza, Argentina, ¹⁹Hospital Privado de la Comunidad de Mar del Plata, Argentina
Email: marinaagozino@hotmail.com

Background and aims: Clinical practice guidelines of major scientific societies are widely used to choose empiric antibiotic treatment for patients with cirrhosis. It is paramount to assess these recommendations' applicability in each epidemiological setting to guarantee optimal pathogen coverage. We aim to evaluate the applicability of the latest EASL clinical guidelines recommendations for empiric

antibiotic treatment for spontaneous bacterial infections according to the acquisition site.

Method: Cross-sectional study on the database of a multicenter prospective cohort study of patients with cirrhosis and bacterial infections in Argentina and Uruguay (NCT03919032). Only culture-positive spontaneous infections were included in this study: spontaneous bacterial peritonitis (SBP), spontaneous bacterial empyema (SBE), and spontaneous bacteremia (SB). We estimated the proportion of antibiotic susceptibility according to where the infection was acquired: community-acquired (CA), healthcare-associated (HCA), or nosocomial (NOS). Regarding applicability, approximately 80% coverage is advisable for empiric treatments in stable patients, and 90% for critically-ill patients.

Results: We included 154 patients: 74 (48%) SBP, 70 (45%) SB, and 10 (7%) SBE. Regarding the site of acquisition, 42% were CA, 34% NOS, and 24% HCA. Gram-positive and negative bacteria were isolated in 53% and 47% of the infections. The prevalence of multidrug-resistant organisms (MDROs) was 34%. Only cefepime and piperacillin-tazobactam offer rational coverage for CA and HCA infections, and imipenem or meropenem for NOS infections. Only meropenem or imipenem combined with vancomycin offer a coverage superior to 90% (table). When considering EASL recommendations for CA that include third generation cephalosporins or piperacillin-tazobactam, empiric coverage ranges from 43–81%; whereas for HCA or nosocomial infections the observed coverage with carbapenems with/without vancomycin ranges from 53–97%, depending on which antibiotic is considered even within the same antibiotic group.

Table: Proportion of isolations that were susceptible to selected antibiotics, according to the site of acquisition of the infection

	Community Acquired (n = 64)	HCA (n = 37)	Nosocomial (n = 53)
Ceftriaxone	34 (53%)	17 (46%)	18 (34%)
Cefepime	47 (75%)	23 (64%)	25 (49%)
Ceftazidime	27 (43%)	11 (31%)	16 (32%)
Piperacillin-tazobactam	52 (81%)	28 (76%)	31 (59%)
Imipenem or meropenem	53 (83%)	29 (78%)	36 (68%)
Imipenem or meropenem + Vancomycin*	63 (100%)	35 (97%)	49 (94%)
Ertapenem	47 (73%)	22 (59%)	28 (53%)

*available in 151 patients.

Conclusion: When considering EASL recommendations for empiric antibiotic treatment in spontaneous infections in cirrhosis according to the site of infection, we observed a wide range of coverage depending on which antibiotic is considered in this cohort of patients from South America. These findings demonstrate that all recommended regimens are not equivalent, even within antibiotic groups, which underlines the urgent need to tailor clinical practice guidelines to local epidemiology to optimize treatment efficacy.

WED-337

Progression of cirrhosis is not associated with clinically significant alterations in hemostasis assessed by thromboelastography

Alina Buliară¹, Bogdan Procopet^{1,2}, Daniela Matei^{1,2}, Horia Stefanescu³, Rares Craciun¹, Zeno Sparchez^{1,2}. ¹"Iuliu Hațieganu" University of Medicine and Pharmacy, Cluj-Napoca, Romania, ²"Prof. Dr. O. Fodor" Regional Institute of Gastroenterology and Hepatology, Cluj-Napoca, Romania, ³Regional Institute of Gastroenterology and Hepatology, Liver Unit and Clinical Ultrasound Department, Cluj Napoca, Romania
Email: bogdan.procopet@umfcluj.ro

Background and aims: Standard coagulation tests (SCTs) do not adequately reflect hemostasis in patients with cirrhosis. Thromboelastography (TEG) provides a more balanced overview of coagulation, assessing clotting factors (R-time), fibrinogen (K, alpha

angle), platelet function (maximum amplitude-MA), and fibrinolysis (Ly30). The current study investigated whether abnormal SCTs and liver disease severity are associated with alterations in TEG-based variables in patients with cirrhosis.

Method: Consecutive patients with liver cirrhosis and abnormal SCTs (at least one of International Normalized Ratio-INR >2, platelet count <50,000/ μ L, fibrinogen <200 mg/dL) were analyzed using native TEG. 19 (17.9%) patients underwent high-risk interventional procedures. The patients were divided according to liver disease severity (group 1-Child A and B, group 2-Child C). SCTs and TEG were compared between the two groups. The TEG abnormalities were assessed in relation to traditional cut-offs for interventional procedures.

Results: Of the 106 patients, 44 (41.5%) were included in group 1 and 62 (58.5%) in group 2. 65.1% of patients had a normal TEG. However, none of the remaining patients fulfilled the TEG-guided transfusion criteria. There were significant differences regarding INR-1.43 (1.25–1.61) vs. 2.57 (1.77–3.37) and fibrinogen levels-248 (189.5–306.5) vs. 155 (90.5–210.5) mg/dL between the two groups. In contrast, there were no significant differences regarding platelet count ($p=0.16$) or any of the TEG variables (R- $p=0.51$, K- $p=0.28$, alpha angle- $p=0.70$, MA- $p=0.72$, and Ly30- $p=0.74$). While there were significant differences in R time between patients with an INR below ($n=56$) or above ($n=50$) 2 (9.95 \pm 4.31 vs. 12.44 \pm 5.55, $p=0.01$), only two patients (4%) with an INR >2 exceeded the reference values for R. Patients with a platelet count below 50,000/ μ L ($n=36$) had a lower MA compared to those ($n=70$) exceeding the threshold value (42.38 \pm 13.85 vs. 55.02 \pm 14.10, $p<0.001$). The overall accuracy for the 50,000/ μ L platelet cut-off in predicting platelet dysfunction expressed by MA was 72.64%. Regarding fibrinogen, patients with a value above 200 mg/dL had a higher alpha angle (44.86 \pm 15.62 vs. 36.29 \pm 16.08, $p=0.01$). Nevertheless, only 4 (3.7%) patients had values below the reference range. There were no significant differences regarding the K-time ($p=0.40$). No periprocedural bleeding events were recorded.

Conclusion: There is no evidence of progressive worsening of the coagulation status with a more advanced liver disease based on native TEG analysis. Overall, SCTs have poor correspondence with TEG variables.

WED-338

Decreased platelet function is an independent predictor of liver-related and all-cause mortality in patients with advanced chronic liver disease

Benedikt Hofer^{1,2,3,4}, Ksenia Brusilovskaya^{1,3,4}, Benedikt Simbrunner^{1,2,3,4}, Beate Eichelberger⁵, Silvia Lee⁶, David JM Bauer^{1,2}, Mattias Mandorfer^{1,2}, Philipp Schwabl^{1,2,3,4}, Simon Panzer⁵, Thomas Reiberger^{1,2,3,4}, Thomas Gremmel^{6,7,8}.

¹Medical University of Vienna, Division of Gastroenterology and Hepatology, Department of Internal Medicine III, Vienna, Austria,

²Medical University of Vienna, Vienna Hepatic Hemodynamic Laboratory, Division of Gastroenterology and Hepatology, Department of Internal Medicine III, Vienna, Austria, ³Medical University of Vienna,

Christian Doppler Lab for Portal Hypertension and Liver Fibrosis, Vienna, Austria, ⁴Center for Molecular Medicine (CeMM) of the Austrian Academy of Sciences, Vienna, Austria, ⁵Medical University of Vienna,

Department of Blood Group Serology and Transfusion Medicine, Vienna, Austria, ⁶Medical University of Vienna, Department of Internal Medicine II, Vienna, Austria, ⁷Karl Landsteiner Society, Institute of Cardiovascular Pharmacotherapy and Interventional Cardiology, St. Pölten, Austria,

⁸Landesklinikum Mistelbach-Gänserndorf, Department of Internal Medicine I, Cardiology and Intensive Care Medicine, Mistelbach, Austria

Email: thomas.reiberger@meduniwien.ac.at

Background and aims: Patients with advanced chronic liver disease (ACLD) are at an increased risk of both bleeding and thromboembolic events. Thrombocytopenia due to portal hypertension (PH), as well as abnormal platelet activation and function, have been reported in ACLD. We aimed to assess whether alterations in platelet activation predict liver-related events.

Method: Within this prospective study, we included patients with ACLD undergoing a baseline measurement of the hepatic venous pressure gradient (HVPG). Platelet responsiveness was assessed by measuring surface expression of P-selectin by flow cytometry after stimulation with either the protease-activated receptor (PAR)-1 agonist TRAP (thrombin receptor activating peptide), the PAR-4 agonist AYPGKF or epinephrine.

Results: Overall, 107 ACLD patients (71% male; median age: 55.3 [IQR: 46.4–62.9] years; median HVPG: 18 [IQR: 12–21] mmHg) were included. During a median follow-up period of 25.3 (IQR: 15.7–31.2) months, 17 patients (15.8%) died. Of those deaths, 11 were considered liver-related. In univariable analysis, higher platelet surface expression of P-selectin in response to TRAP (HR per 100 MFI [median fluorescence intensity]: 0.92 [95%CI: 0.86–0.97]; $p=0.006$) or AYPGKF (HR per 10 MFI: 0.93 [95%CI: 0.87–0.99]; $p=0.034$) was significantly linked to a lower risk of all-cause mortality. In addition, a higher surface expression of P-selectin in response to TRAP was also associated with a reduced risk of liver-related mortality within the univariable analysis (HR per 100 MFI: 0.92 [95%CI: 0.85–0.99]; $p=0.026$). Importantly, the predictive role of TRAP-inducible P-selectin expression with regard to all-cause mortality remained significant in a multivariable model adjusted for MELD (model for end-stage liver disease) and HVPG (aHR: per 100 MFI: 0.93 [95%CI: 0.87–0.99]; $p=0.019$). Six patients presented with de novo portal vein thrombosis (PVT) during follow-up. Interestingly, higher P-selectin expression in response to epinephrine stimulation was significantly linked to a higher risk of developing PVT (HR per 10 MFI: 1.08 [95%CI: 1.03–1.14]; $p=0.004$), while no connection was found for other platelet activation parameters.

Conclusion: The assessment of platelet responsiveness provides additional prognostic information in ACLD patients on top of liver disease and PH severity. While higher PAR-1 and PAR-4 mediated platelet activation was linked to a decreased risk of liver-related and all-cause mortality, an increase in epinephrin-inducible platelet activation was associated with de novo PVT development.

WED-339

Thromboelastography-guided coagulopathy correction in cirrhotic patients decreases blood product transfusion: a systematic review and analysis

Hamed Komeilyan¹, Carmen Ching², Julie Zhu³. ¹Dalhousie University, Gastroenterology, Canada, ²Dalhousie University, Faculty of Medicine, Canada, ³Dalhousie University, Gastroenterology, Canada
Email: h.komeilyan@gmail.com

Background and aims: Patients with cirrhosis are a risk factor for coagulopathy and bleeding complications. Thromboelastography (TEG) guided therapy is available to rapidly assess and guide blood product transfusion in this population. This study aims to determine if TEG-guided therapy is able to decrease the administration of blood products and reduce adverse events such as bleeding and mortality compared to standard coagulation testing (SCT).

Method: We performed a systematic review and meta-analysis of literature in PubMed, EMBASE, and The Cochrane Library and pooled six randomized-controlled trials comparing thromboelastography versus standard coagulation testing in patients with cirrhosis. A total of six studies were pooled ($n=386$). Primary outcomes were mean platelet transfusion units and fresh frozen plasma (FFP) transfusion units. Secondary outcomes were mortality and bleeding events.

Results: Compared to SCT, there was a significant standard mean decrease in platelet ($p<0.00001$) and FFP ($p<0.00001$) administration compared to TEG perioperatively prior to a liver transplant. However, there was no significant difference in the pooled odds ratio between TEG and SCT in patients receiving both platelets and FFP (OR 1.40 [95% CI 0.61–3.23, $P=0.42$]). Recurrent variceal bleeding was significantly reduced in the TEG group compared to SCT for platelet transfusion (OR 0.05 [95% CI 0.01–0.20, $P<0.0001$]) or FFP transfusions (OR 0.18 [95% CI 0.05–0.63, $P=0.007$]). With regards to the 5-

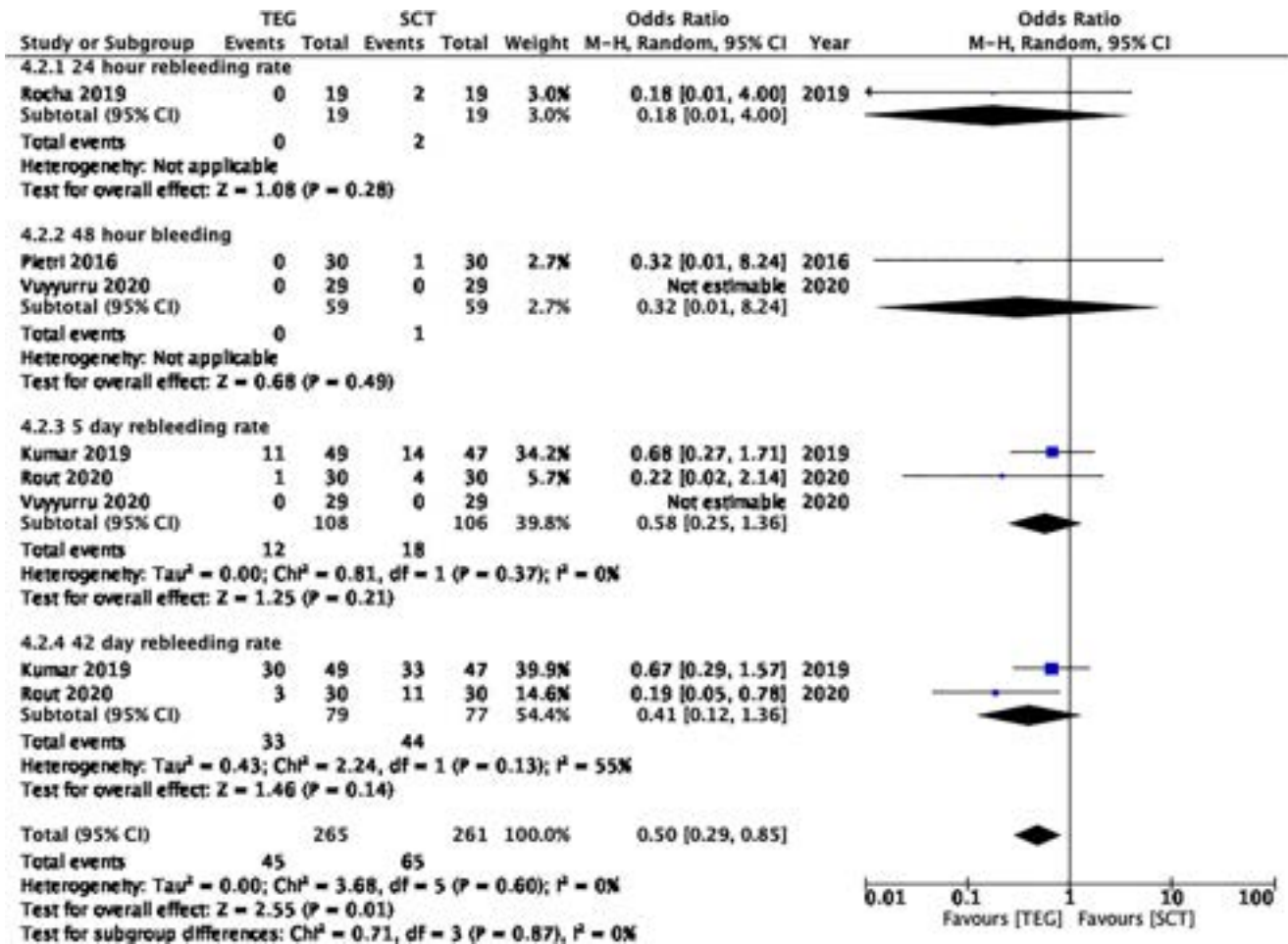


Figure: (abstract: 339).

day, 28-day, 42-day, and 90-day mortality, there was no significant difference between the pooled odds ratio between the TEG and SCT groups (OR 0.69 [95% CI 0.47–1.02, P = 0.06]). The 24-hour, 48-hour, 5-day, and 42-day rebleeding rates were significantly lower in TEG versus SCT groups (OR 0.50 [95% CI 0.29–0.85, p = 0.01]).

Conclusion: The use of TEG-guided therapy favors a reduction in platelet and FFP transfusion compared to SCT in patients with cirrhosis. Additionally, TEG-guided therapy is able to improve patient care by reducing the rebleeding rate of patients with cirrhosis compared to SCT. However, this same effect was not seen for mortality.

WED-340

An overview on microbial population in liver cirrhosis : changing paradigm in the known bacteriology of spontaneous bacterial peritonitis

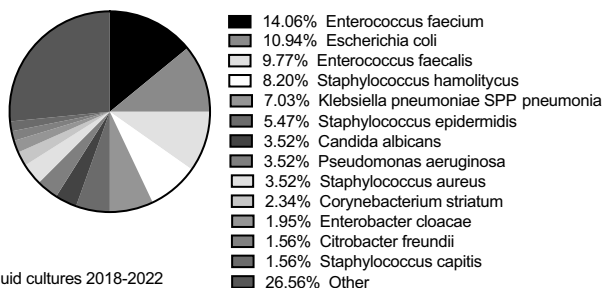
Shirin Demma¹, Bruno Mariani², Valerio Giannelli¹, Claudia Telesca¹, Roberto Villani¹, Adriano Pellicelli¹. ¹Azienda Ospedaliera San Camillo Forlanini, Dipartimento Interaziendale Trapianti POIT, Italy, ²Azienda Ospedaliera San Camillo Forlanini, Microbiology, Italy
Email: s.demma@ucl.ac.uk

Background and aims: Liver cirrhosis is a leading cause of death worldwide. Patients with cirrhosis have several biological and immunological alterations that predispose to the development of infections. The spread of multidrug resistant (MDR) infections has been blamed as responsible for the increase in mortality risk in cirrhosis. Therefore, improvement in the management of bacterial

infections represents an absolute priority for patients with cirrhosis. We aimed to examine the epidemiology and resistance phenotypes in cirrhotic patients admitted to our liver unit in order to analyse our microbial population and the prevalence of MDR bacteria.

Method: Ascitic fluid cultures from consecutive cirrhotic patients admitted to our liver unit in a tertiary centre in Rome (Italy) over a 4-year period (2018–2022) were analyzed to identify and explore the microbial population and the prevalence of MDR bacteria. Data on organisms culture and proportions of antibiotic resistance were collected. We then compared the results with the results of the ascitic fluid cultures collected over the previous 4-year period (2013–2017) to analyse the trend.

Results: In total 1219 ascitic fluid samples were identified. Organisms were cultured in 256 samples with *Enterococcus Faecium* as the most represented (14.06%), followed by *Escherichia Coli* (10.94%) and *Enterococcus Faecalis* (9.77%). In terms of resistance phenotypes, among the enterococci population, 14.75% were vancomycin resistant enterococci (VRE) and 1.63% were resistant to linezolid (LZD); 27.78% Enterobacteriaceae were extended-spectrum beta-lactamase (ESBL) and 11.11% were carbapenem resistant (CBPEN). All the *Acinetobacter Baumannii* identified were MDR and CLS-S. Comparing to the previous 4-year period, *Candida albicans* is less represented while the prevalence of *Acinetobacter Baumannii* is increasing. Enterococci was confirmed to be the most represented microbial population in our area.



Ascitic fluid cultures 2018-2022

Figure:

Conclusion: Interestingly, in our cohort, gram positive Enterococci were the most representative microbial population in ascitic fluid. This confirms the trend that has been demonstrated in the last years and represent a changing paradigm in the known bacteriology of spontaneous bacterial peritonitis (SBP). This might be related to the long-term quinolone administration, the overuse of extended spectrum antimicrobials or to the increase of invasive intervention. MDR Acinetobacter is a concern as resistance to colistin is increasing worldwide. Knowing the local microbial epidemiology and the resistance rate is fundamental in order to address the best antimicrobial empiric therapy where microbial characterization and antibiogram is not yet available.

WED-341

The combination of LACE index, MELD on discharge and a previous history of decompensation defines risk groups for early readmission in patients with liver cirrhosis

Yolanda Sánchez¹, Jose Miguel Rosales Zabal², Isabel Carmona³, Marta Casado⁴, Carlota Jimeno Mate⁵, Ana Torres², Paula Fernandez Alvarez³, Miren Garcia Cortes⁶, Alberto Garcia Garcia⁶, Paloma Alañón⁷, Maria Angeles Lopez Garrido⁸, Manuel Romero Gomez^{1,9}, Carmen Sendra¹⁰, Matias Estevez¹¹, Miguel Jiménez¹², Javier Ampuero^{1,9}. ¹Hospital Universitario Virgen del Rocío, Sevilla, Spain, ²Hospital Costa del Sol, Marbella, Spain, ³Hospital Universitario Virgen Macarena, Sevilla, Spain, ⁴Hospital Universitario Torrecárdenas, Almería, Spain, ⁵Hospital Universitario Valme, Sevilla, Spain, ⁶Hospital Universitario Virgen Victoria, Málaga, Spain, ⁷Hospital Universitario Reina Sofía, Córdoba, Spain, ⁸Hospital Universitario Virgen de las Nieves, Granada, Spain, ⁹Instituto de Biomedicina de Sevilla, Sevilla, Spain, ¹⁰Hospital Infanta Elena, Huelva, Spain, ¹¹Hospital Poniente, El Ejido, Spain, ¹²Hospital Regional, Málaga, Spain
Email: javi.ampuero@gmail.com

Background and aims: Reducing early (<30 days) hospital readmissions is a policy priority to improve the healthcare quality in liver

diseases. Thus, we aimed to: a) determine risk factors associated with 30-day hospital readmission in patients with liver cirrhosis; b) identify a subset of patients at risk of 90-day readmission and mortality; c) explore the usefulness of the model in the management of cirrhotic patients in the outpatient clinic.

Method: Multicenter and retrospective study including 885 patients with cirrhosis admitted to the Liver Unit and followed up 90 days after hospital discharge. We collected readmissions and all-cause mortality up to 90 days after discharge. In addition, LACE index was calculated, which comprises Charlson comorbidity index, the number of times in the Emergency Room 6 months before the admission, urgent versus scheduled admission, and length of the hospitalization.

Results: Finally, 818 patients were included in the study, of which 23.2% (190/818) and 42.4% (347/818) required a hospital readmission at 30 and 90 days, respectively, and 13.6% (111/818) died. The main reason for hospitalization was ascites (36%) followed by variceal bleeding (23%), while the leading cause of 30-day readmission was hepatic encephalopathy (35%). LACE index (OR 1.11 (IC95% 1.03–1.20); p = 0.006), MELD on discharge (OR 1.05 (IC95% 1.02–1.08); p = 0.003), and a history of a decompensated event (IC95% 0.99–2.00); p = 0.056) were independently associated with 30-day readmission. Further, according to 90% sensitivity and 90% specificity, this model predicted three risk groups of readmission and survival during the follow-up (Figure). Despite the time to the scheduled outpatient clinic after admission was similar between groups (45 ± 38 vs. 46 ± 40 vs. 50 ± 42 days; p = 0.593), 33% (30/91) of patients belonging to the high-risk group required a hospital readmission before going to the clinic versus 25.7% (148/575) and 14.7% (20/136) (p = 0.002) of intermediate- and low-risk groups, respectively.

Conclusion: The combination between the LACE index, MELD on discharge, and a previous history of decompensation identified different groups at risk of 30-day and 90-day readmission and mortality in patients with liver cirrhosis. This model should be considered for scheduling the outpatient clinic after hospitalization.

WED-342

Factors associated with inpatient albumin administration and center-level variation in a national cohort

Marina Serper¹, Tamar Taddei², David Kaplan¹, Thomas Ardiles³, Elisabet Viayna³, Nadim Mahmud¹. ¹University of Pennsylvania, United States, ²Yale University, United States, ³Grifols, United States
Email: marinas2@pennmedicine.upenn.edu

Background and aims: Guidelines recommend albumin administration in patients with cirrhosis complications including hepatorenal syndrome (HRS), spontaneous bacterial peritonitis (SBP), and in the evaluation and management of acute kidney injury. However, variation in albumin use is not well-characterized. We investigated

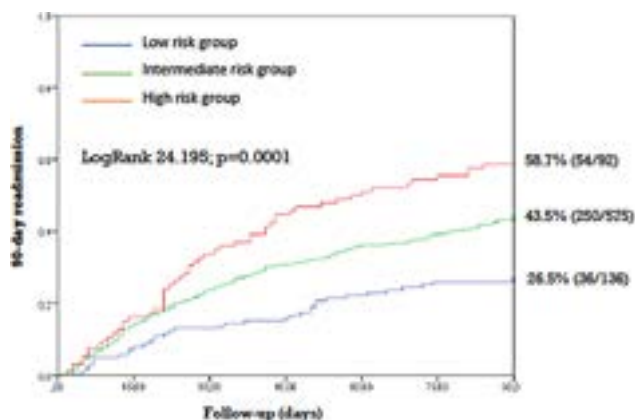
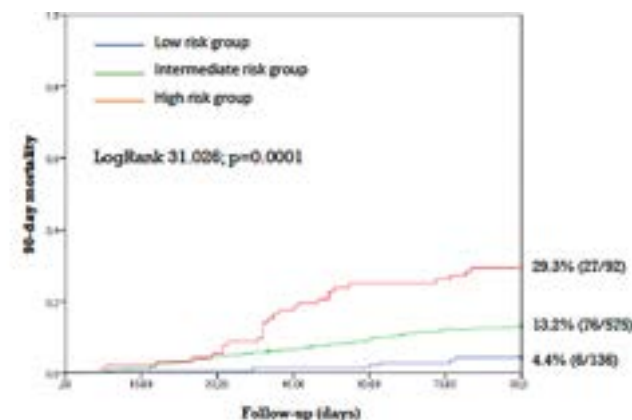


Figure: (abstract: WED-341).



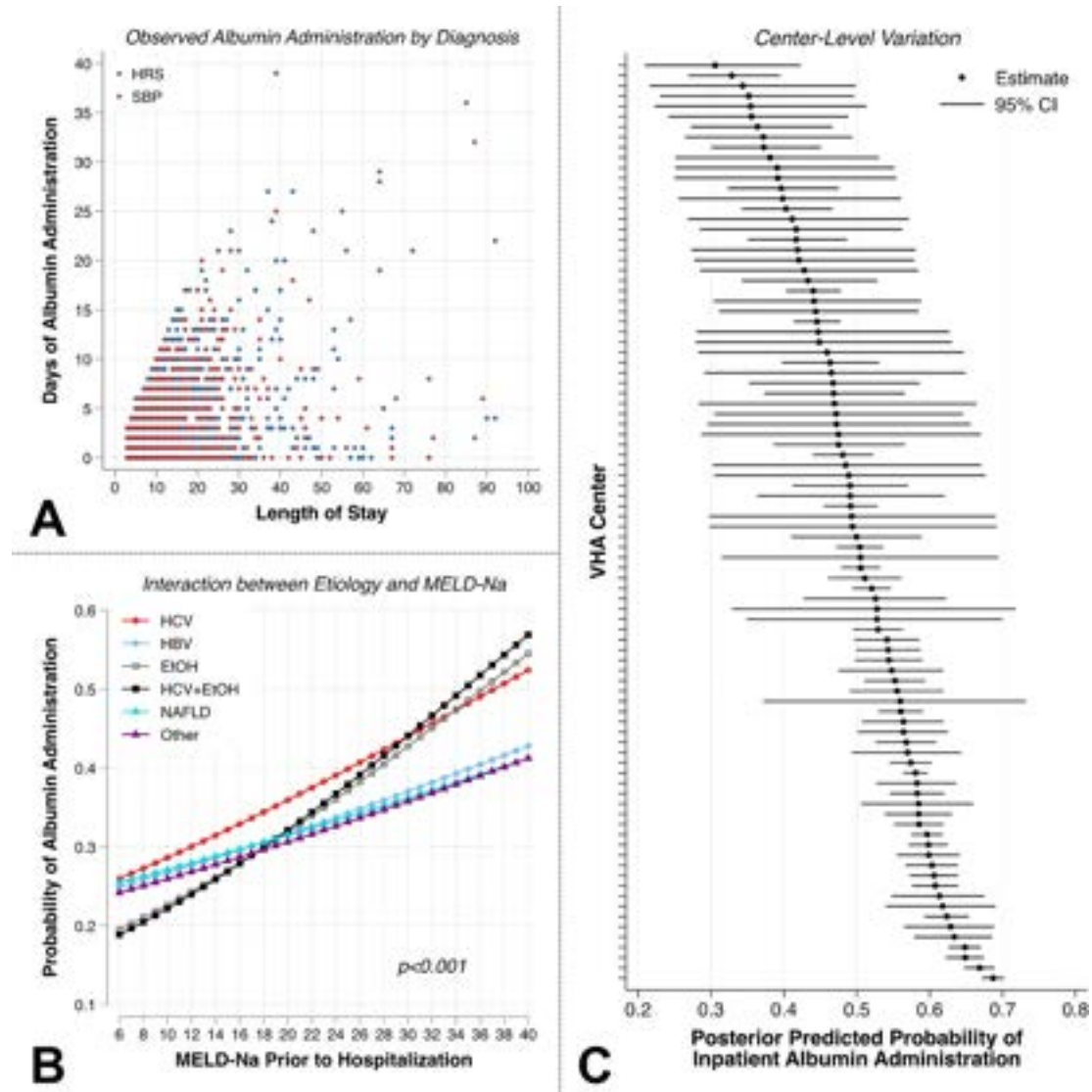


Figure: (abstract: WED-342).

inpatient albumin use, factors associated, and center-level variation in a cirrhosis cohort in the Veterans Affairs (VA) system across all 50 United States.

Method: We performed a retrospective cohort study using a well-characterized cohort of patients in the VA with cirrhosis. We identified all inpatient hospitalizations between 2008 and 2022 and ascertained all inpatient albumin use through via inpatient files. Hospitalizations were excluded for patients with a history of liver transplantation or if the length of stay (LOS) was ≤ 2 days. Patient baseline characteristics were collected immediately prior hospitalization. Hospitalizations were categorized as due to HRS, SBP, or other. To identify variables associated with inpatient albumin administration we used multivariable logistic regression with *a priori* modeling approaches. To explore variation in the probability of albumin administration across 90 VA centers we used mixed-effects logistic regression.

Results: The cohort included 49,611 hospitalizations among 11,149 patients. Albumin was administered in 14,882 (30.0%) hospitalizations; with a variation in days of albumin administered for different LOS in patients with HRS or SBP (Figure panel A). In multivariable logistic regression, higher odds of albumin use was associated with

increased age (OR 1.02 per year, 95% CI 1.01–1.02, $p < 0.001$), HRS (OR 4.30, 95% CI 3.84–4.81, $p < 0.001$), SBP (OR 4.13, 95% CI 3.74–4.56, $p < 0.001$), prior decompensation (OR 1.34, 95% CI 1.27–1.40, $p < 0.001$), and increased LOS (OR 1.01 per day, 95% CI 1.01–1.01, $p < 0.001$). Heart failure was associated with a reduced odds of albumin use (OR 0.65, 95% CI 0.61–0.68, $p < 0.001$). There was a significant interaction between MELD-Na and etiology of liver disease ($p < 0.001$), those with alcohol or hepatitis C-related cirrhosis were more likely to receive albumin at higher MELD-Na scores as compared to other etiologies (Figure panel B). In a mixed-effects logistic regression model adjusted for all variables included in the prior model and accounting for VA center as a random intercept, there was significant adjusted center-level variation in the probability of albumin use ($p < 0.001$; Figure panel C) which ranged from 31% to 69% holding all other clinical factors equal. Larger volume centers were more likely to use inpatient albumin.

Conclusion: In a large VA cohort of patients with cirrhosis, we identify key variables associated with inpatient albumin administration. Substantial center-level variation in albumin use suggests gaps in guideline-recommended care that warrants future studies.

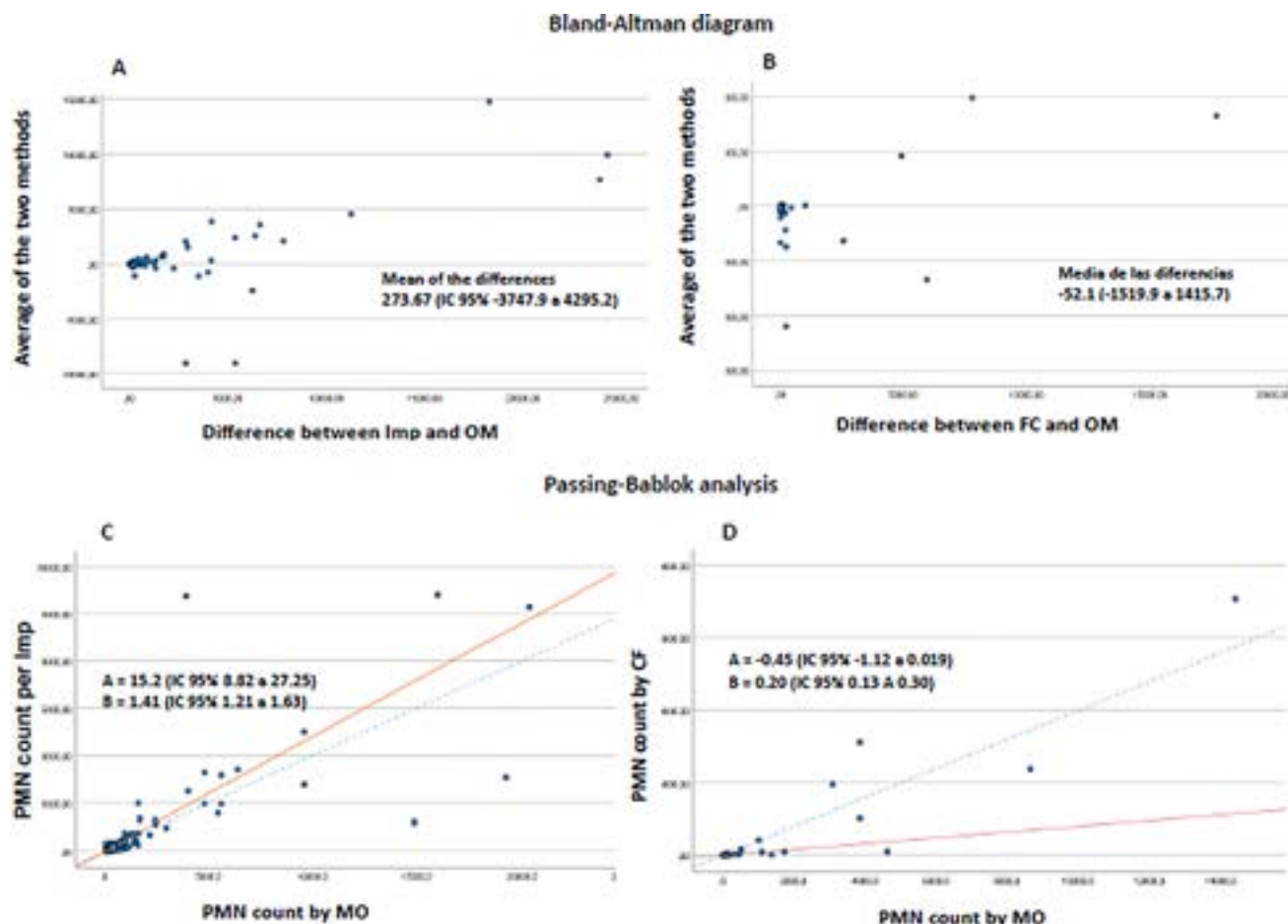


Figure: (abstract: WED-344).

WED-343

Serum PDL1 levels are associated with increased risk of bacterial infections in non-hospitalised patients with cirrhosis

Adria Juanola^{1,2,3}, Gabriel Mezzano¹, Simone Incicco⁴, Elisa Pose^{1,2,3}, Delia Blaya^{2,3}, Cristina Solé¹, Natalia Jimenez-Esquivel¹, Joaquín Andrés Castillo¹, Jordi Ribera^{2,3,5}, Xènia Almodovar², Martina Perez^{1,2,3}, Ana Belen Rubio Garcia^{1,2,3}, Marta Cervera^{2,3}, Marta Carol^{2,3}, Ruth Nadal^{1,3}, Anita Arslanow², Jordi Gratacos^{1,2,3}, Anna Soria^{1,2,3}, Núria Fabrellas^{2,3,6}, Paolo Angeli⁴, Manuel Morales-Ruiz^{2,3,5,6}, Mar Coll^{2,3}, Isabel Graupera^{1,2,3}, Salvatore Piano⁴, Elsa Solà⁷, Pere Ginès^{1,2,3,6}. ¹Liver Unit, Hospital Clínic De Barcelona, Barcelona, Catalonia, Spain, Spain, ²Institut d'Investigacions Biomèdiques August Pi i Sunyer (IDIBAPS), Barcelona, Catalonia, Spain, Spain, ³Centro de Investigación Biomédica en Red Enfermedades Hepáticas y Digestivas (CIBERED), Madrid, Spain, Spain, ⁴Unit of Internal Medicine and Hepatology (UIMH), Department of Medicine-DIMED, University of Padova, Padova, Italy, Spain, ⁵Biochemistry and Molecular Genetics Department, Hospital Clínic of Barcelona, Barcelona, Catalonia, Spain, Spain, ⁶Faculty of Medicine and Health Sciences, Universitat de Barcelona (UB), Barcelona, Catalonia, Spain, Spain, ⁷Institute for Immunity, Transplantation and Infection, Stanford University School of Medicine, Stanford, California, USA, United States
Email: juanola@clinic.cat

Background and aims: Infections, often recurrent, are a very common complication of cirrhosis and represent a frequent cause of hospitalization, renal failure, ACLF and death. Pathogenic factors responsible for bacterial infections remain largely unknown. Previous

data in patients hospitalized for complications of cirrhosis showed that high serum PDL-1 levels are associated with an increased risk of bacterial infections. However, it is not known whether serum PDL-1 levels also correlate with the risk of bacterial infections in decompensated but stable patients with cirrhosis that are not hospitalized. The present study was aimed at assessing the serum levels of PDL1 in stable outpatients with decompensated cirrhosis and its relationship with development of bacterial infections.

Method: Prospective cohort study of 110 patients with cirrhosis (76% men, 53% alcohol etiology, median MELD sodium 11). The serum levels of PDL1, which estimate the soluble form of PDL1 expressed in macrophages, were measured by ELISA. New bacterial infections were recorded during a follow-up period of one year.

Results: During follow-up, 36 patients (33%) developed at least one new episode of infection. The most frequent infections were respiratory tract infections (12, 33%), followed by SBP SBP (6, 17%), urinary infections (5, 14%), bacteremia (5, 14%), skin and soft tissue (2, 6%), colitis (2, 6%) and other (4, 10%). The serum levels of PDL1 in patients who developed infections were higher than those in patients who did not develop infections [135 (108–206) vs. 92 (81–145) pg/ml, respectively; $p = 0.030$]. In a multivariate analysis, the independent predictive factors of infection development were: MELD score and PDL1 levels [sHR 1.007 (1.001–1.012), $p = 0.017$].

Conclusion: In decompensated stable patients with cirrhosis, increased serum levels of PDL1 correlate with development of infections. These results, along with those previously reported, suggest that the activation of the PD1-PDL1 system represents a relevant factor in the pathogenesis of bacterial infections in cirrhosis.

WED-344

Validation of automatic cell counting based on impedanciometry and flow cytometry in ascitic fluid

Aitor Odriozola Herrán¹, Ángela Antón¹, Angela Puente Sanchez¹, Romina García Sardiña¹, David San Segundo Arribas¹, María Del Barrio Azaceta¹, Sara Alonso¹, Victor Echavarría¹, Andrea González¹, Carmen Ribes¹, Carlos Gutierrez¹, Marcos López-Hoyos¹, Antonio Cuadrado¹, Valeria Adam¹, Javier Crespo¹, Jose Ignacio Fortea¹. ¹Hospital Universitario Marqués de Valdecilla, Spain
Email: aodrihe94@gmail.com

Background and aims: The gold standard test for polymorphonuclear (PMN) cell count in ascitic fluid is manual counting by optical microscopy (OM). A few studies have found a good correlation between OM and the automatic counting based on impedance (Imp) and flow cytometry (FC). Our objective was to evaluate the accuracy of these techniques in PMN cell counting in ascitic fluid and in the diagnosis of spontaneous bacterial peritonitis (SBP) (>250/mm³ PMN).

Method: Prospective single-center study that included patients who underwent paracentesis between January 2020 and August 2022. Cell counts were performed in a Neubauer chamber (MO), DxH 900 Beackman Coulter (Imp), and AQUIOS CL (FC). The concordance between the techniques with OM was evaluated using the intraclass correlation coefficient (ICC) and the Bland-Altman (BA) and Passing-Bablok (PB) methods. The gold standard for the diagnosis of SBP was OM, obtaining the area under the curve (AUC) and the positive (PPV) and negative (NPV) predictive values.

Results: 330 paracenteses of 98 patients were included, 213 (64.5%) of them for diagnostic purposes. The origin of ascites was cirrhosis in 290 (87.9%). The ICC was 0.78 (95% CI, 0.70–0.83; $p < 0.001$) for Imp and 0.92 (0.88–0.94; $p < 0.001$) for FC. The BA diagram showed broader limits of agreement for Imp (Figures A and B) and the PB method showed systematic and proportional differences for Imp (i.e. Imp and MO are not comparable techniques), and only proportional differences for FC (Figures C and D) (i.e. need for calibration adjustment). 33 (10%) patients had SBP. The AUC, PPV and NPV for Imp were 0.96, 79.4% and 97.7%, and for FC 0.98, 100% and 94.8%.

Conclusion: Compared with impedance, flow cytometry showed greater concordance and reliability for the diagnosis of SBP, but its implementation in clinical practice requires evaluating whether a calibration adjustment is needed.

WED-345

Prevalence of minimal hepatic encephalopathy in patients with cirrhosis: a multicenter study

Simon Johannes Gairing^{1,2}, Chiara Mangini³, Lisa Zarantonello³, Stefania Gioia⁴, Elise Jonasson Nielsen⁵, Sven Danneberg⁶, Maria Magdalena Gabriel⁷, Alena Friederike Ehrenbauer⁷, Patricia Bloom⁸, Cristina Ripoll^{9,10}, Philippe Sultanik¹¹, Peter Galle^{1,2}, Joachim Labenz¹², Dominique Thabut¹¹, Alexander Zipprich^{9,10}, Anna Lok⁸, Karin Weissenborn⁷, Jens Marquardt⁶, Mette Munk Lauridsen⁵, Silvia Nardelli⁴, Sara Montagnese^{3,13}, Christian Labenz^{1,2}. ¹Department of Internal Medicine I, University Medical Center of the Johannes Gutenberg-University, Mainz, Germany, Germany, ²Cirrhosis Center Mainz (CCM), University Medical Center of the Johannes Gutenberg-University, Mainz, Germany, Germany, ³Department of Medicine, University of Padova, Padova, Italy, Italy, ⁴Department of Translational and Precision Medicine, Sapienza University of Rome, Rome, Italy, Italy, ⁵Department of Gastroenterology and Hepatology, Hospital of South West Jutland, Esbjerg, Denmark, Denmark, ⁶Department of Medicine I, University Hospital Schleswig-Holstein, Lübeck, Germany, Germany, ⁷Clinic for Neurology, Hannover Medical School, Hannover, Germany, Germany, ⁸Department of Medicine, Division of Gastroenterology, University of Michigan, Ann Arbor, MI, United States, United States, ⁹Department of Internal

Medicine IV, Jena University Hospital, Jena, Germany, Germany, ¹⁰First Department of Internal Medicine, Martin-Luther-University Halle-Wittenberg, Halle, Germany, Germany, ¹¹Service d'hépatogastroentérologie, Sorbonne Université, Hôpital Pitié-Salpêtrière Assistance Publique Hôpitaux de Paris, Paris, France, France, ¹²Department of Medicine, Diakonie Hospital Jung-Stilling, Siegen, Germany, Germany, ¹³Chronobiology Section, Faculty of Health and Medical Sciences, University of Surrey, Guildford, UK, United Kingdom
Email: sgairing@uni-mainz.de

Background and aims: Minimal hepatic encephalopathy (MHE) is associated with impaired quality of life, falls, and poorer prognosis. Reliable data on the prevalence of MHE in patients with cirrhosis is lacking with reported prevalence varying from 30% to 70%. Therefore, this study aimed to analyse the prevalence of MHE in a large multicentre cohort of patients with cirrhosis stratified by disease stage.

Method: This retrospective study analyzed data from patients recruited at 10 centers in Europe and the United States, all with experience in detecting MHE. Only patients without clinical signs of HE were included. MHE was detected with PHES according to local norms. Demographic, clinical, and laboratory characteristics were analyzed.

Results: In total, 1868 patients with cirrhosis were enrolled. Most patients were male (66.4%) with a median age of 60 years. Median MELD score was 11 (interquartile range (IQR) 9; 15) and Child-Pugh (CP) stages were as follows: CP A 46.2%, CP B 41.6%, CP C 12.2%. The most frequent etiologies were alcohol (43.2%) and viral hepatitis (23.4%). In the total cohort, MHE was detected by PHES in 650 (34.8%) patients. When excluding patients with a history of overt HE (OHE), the prevalence of MHE was 29.2%. In subgroup analyses of patients without a history of OHE stratified by CP stage, the prevalence of MHE in patients with CP A was low (20.6%), while it was higher in CP B or C (37.7% and 49.2%). In patients without a history of OHE with a MELD score <10, the prevalence of MHE was 22.2%. In contrast, in patients with a MELD score ≥20, the prevalence of MHE was high with 47.7%. Standardised ammonia levels (ammonia level/upper limit of normal of each center) correlated significantly, albeit weakly with PHES (spearman's rho = -0.16, $p < 0.001$). Age, sodium, creatinine, albumin, history of ascites, and history of OHE were associated with the presence of MHE in multivariable logistic regression analysis. After excluding patients with a history of OHE, age, sodium, creatinine, albumin, hemoglobin, and a history of ascites remained associated with MHE.

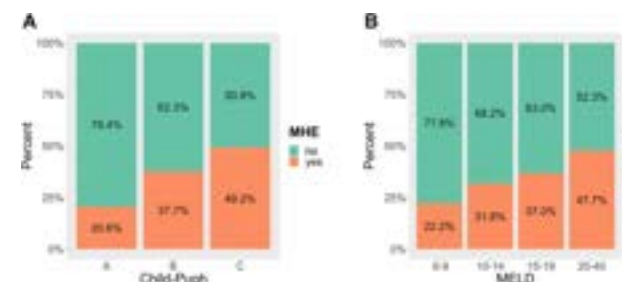


Figure: MHE prevalence in patients with cirrhosis without a history of OHE stratified by Child-Pugh stage (A) and MELD (B).

Conclusion: Roughly one-third of patients with cirrhosis were affected by MHE, but prevalence varied significantly by disease stage. These data may pave the way for more individualized MHE screening approaches.

WED-346

Vitamin D deficiency associates with gut dysbiosis, endotoxemia and the risk of infectious complications in patients with liver cirrhosis

Pei-Chang Lee¹, Kuei-Chuan Lee¹, Hsiao-Sheng Lu¹, Yu-Jen Chen¹, Tsung-Yi Cheng¹, Tsung-Chieh Yang¹, Jen-Jie Chiou², Chi-Wei Huang², Ueng-Cheng Yang², Yi-Hsiang Huang¹, Ming-Chih Hou¹. ¹Taipei Veterans General Hospital, Taiwan, ²National Yang Ming Chiao Tung University, Taiwan

Email: mchou@vghtpe.gov.tw

Background and aims: Vitamin D deficiency and gut dysbiosis are common problems in patients with liver cirrhosis and both would associate with poorer clinical outcomes. The impacts of vitamin D on gut barrier and microbiota have been demonstrated in cirrhotic rats, but few clinical studies have been reported. In this study, we aimed to investigate the association between vitamin D deficiency and gut microbiota, and the risk of infectious complications in patients with liver cirrhosis.

Method: From September 2018 to December 2020, 80 cirrhotic patients were prospectively enrolled in Taipei Veterans General Hospital. Serum level of 25-hydroxyvitamin D [25 (OH)D], cytokines, fecal microbiota and clinical characteristics were measured and analyzed. The associations between vitamin D deficiency and gut microbiota as well as the development of 1-year cirrhotic infectious complications were investigated.

Results: During the follow-up period of one year, total 41 infectious events and 91 hospitalizations were recorded. Decreased serum level of 25 (OH)D less than 15 ng/ml acceptably predicted development of 1-year infectious complications in these cirrhotic patients (AUROC: 0.818, 95% CI. 0.716–0.895, $p=0.001$). A significantly higher Child-Pugh score, neutrophil-to-lymphocyte ratio, prothrombin time, serum levels of lipopolysaccharides (LPS) and TNF-alpha, as well as lower serum albumin level were noted in patients with vitamin D deficiency. Besides, the richness and evenness of fecal microbiota were significantly reduced in vitamin D-deficient cirrhotic patients. A significant microbial dissimilarity could also be identified by unweighted UniFrac analysis according to the presence of vitamin D deficiency. In the feces of vitamin D-deficient cirrhotic patients, a significant prominence of genera *Streptococcus* and *Ruminococcus* *gnavus* were observed. In contrast, *Bacteroides* was significantly more prominent in patients with higher serum vitamin D. Moreover, the fecal abundance of *Streptococcus* was significantly positively correlated with serum LPS level, whereas, a significant negative correlation was noted between LPS and *Bacteroides*. Patients with vitamin D deficiency developed more infectious complications (60.7% vs. 11.5%, $p<0.001$) and more numbers of hospitalization (67 vs. 24, $p<0.001$) than cirrhotic patients with higher vitamin D. Furthermore, a higher serum 25 (OH)D >15 ng/ml independently decreased the risk of 1-year infectious complications in cirrhotic patients.

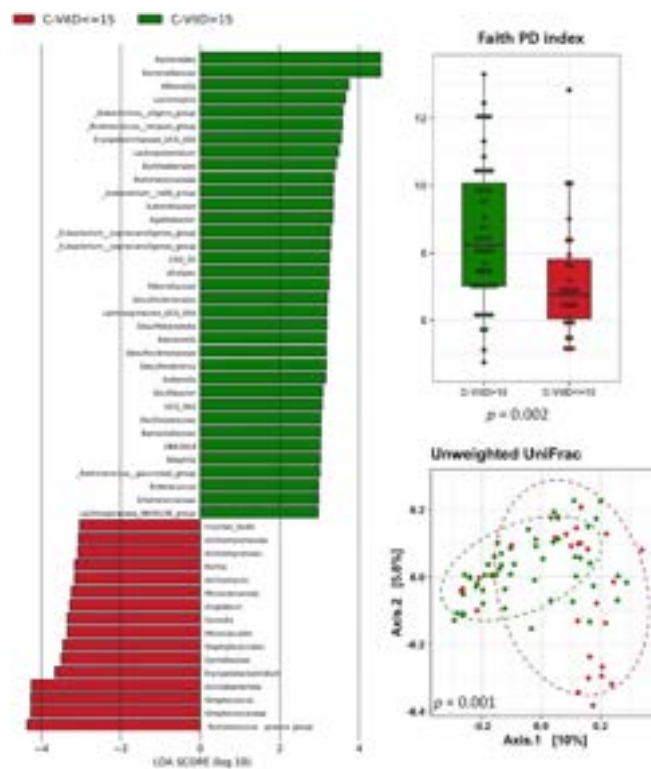


Figure:

Conclusion: Vitamin D deficiency was associated with significant gut dysbiosis, endotoxemia and significant increased risks of infectious complications in patients with liver cirrhosis. These findings potentiate to improve the outcomes of these patients by vitamin D supplementation and also gut microbial modification.

WED-347

Comparison of coagulation parameters as prognostic markers of decompensation and liver-related death in advanced chronic liver disease

Maria Pallozzi¹, Lucia Giuli¹, Francesco Santopaolo¹, Antonio Gasbarrini¹, Raimondo De Cristofaro², Maurizio Pompili¹, Francesca Romana Ponziani¹. ¹Fondazione Policlinico Universitario Agostino Gemelli IRCCS, Internal Medicine and Gastroenterology-Hepatology Unit, Rome, Italy, ²Fondazione Policlinico Universitario Agostino Gemelli IRCCS, Translational Medicine and Surgery Department, Rome, Italy
Email: mariapallozzi@yahoo.it

Background and aims: Liver cirrhosis has long been considered an acquired bleeding disorder but recent studies have demonstrated that the coagulation balance is associated with disease progression. In patients with advanced chronic liver disease (ACLD) plasma levels of many procoagulant factors (factor VIII [FVIII], von Willebrand Factor [VWF]) are reduced but also the levels of anticoagulant factors (a disintegrin and metalloprotease with thrombospondin 1 repeats number 13 [ADAMTS-13], protein C [PC]) are markedly decreased. A recent study demonstrated that FVIII/PC ratio correlates with the severity of liver disease and with worse liver outcomes [1]. We recently reported that ADAMTS-13/VWF ratio is useful to predict the development of portal vein thrombosis (PVT), but little is known about its role as marker of decompensated ACLD. Based on these previous results, we investigated the prognostic role of ADAMTS13/VWF ratio on the development of dACLD and compared it with FVIII/PC ratio [2].

Method: Consecutive outpatients with ACLD underwent clinical evaluation and were subjected to blood sampling for the assessment of laboratory tests and coagulation parameters. Data from ultrasound

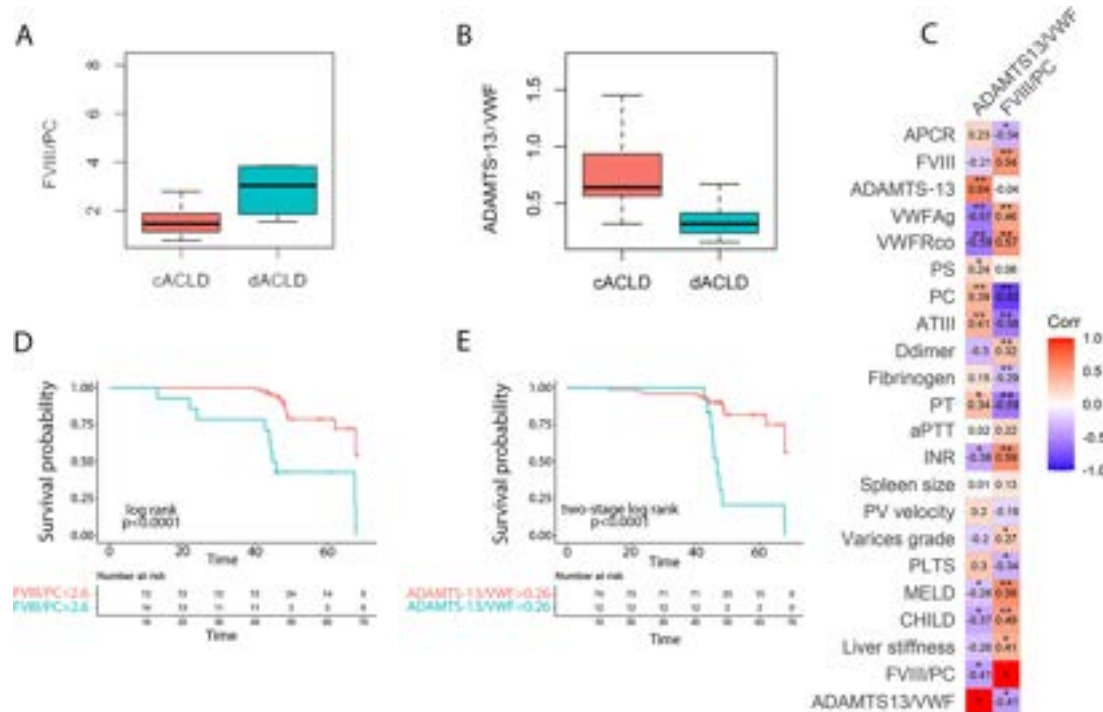


Figure: (abstract: WED-347).

examination and upper endoscopy were also recorded. We compared the FVIII/PC ratio and ADAMTS-13/VWF ratio between patients with compensated and decompensated ACLD and their correlation with the other variables. We finally analyzed survival probability of remaining free of decompensation/liver-related death, stratifying patients according to FVIII/PC ratio or ADAMTS-13/VWF ratio by using the median value of each index in decompensated patients as cut-off.

Results: We included 86 patients with ACLD (median age 66 (59–72.70) years; 65.47% male; etiology viral/nonviral 50%/50%; Child Pugh A/B/C 80.2%/15.1%/4.7% and median model for end-stage liver disease (MELD) 8 [7–9.20]), 20 (23.25%) developed dACLD after a median follow-up of 48.8 (48–57.30) months. Those patients showed a significantly higher FVIII/PC ratio and a lower ADAMTS-13/VWF ratio compared to their counterparts maintaining cACLD (FVIII/PC 2.62 [1.87–3.81] vs 1.44 [1.13–1.77], $p < 0.0001$ Figure 1A); ADAMTS-13/VWF 0.26 [0.22–0.41] vs 0.52 [0.16–0.62], $p < 0.0001$ Figure 1B). Both the indices correlated with liver disease severity according to Child Pugh score and MELD score (Figure 1C). FVIII/PC ratio showed the strongest correlation with clinical and coagulation parameters. Both FVIII/PC ratio or ADAMTS-13/VWF ratio had a good prognostic ability for ACLD decompensation/liver-related death ($p < 0.0001$, Figure 1D–E); however, when ADAMTS-13/VWF ratio was used the survival curves crossed after 40 months, underlining a limitation in the identification of patients with early events. Finally, the four patients who developed PVT during follow-up showed a lower ADAMTS-13/VWF ratio (0.23 [0.22–0.25] vs 0.58 [0.45–0.73], $p = 0.004$) or a higher FVIII/PC ratio (2.62 [2.45–2.82] vs 1.57 [1.2–2.09], $p = 0.02$) compared to their counterparts who did not experience PVT.

Conclusion: Coagulation parameters, historically used only for assessing bleeding risk in patients with ACLD, are instead harbingers of important prognostic information. Indeed, ADAMTS13/VWF ratio and FVIII/PC ratio correlate with liver disease severity and can predict liver-related death or decompensation in patients with ACLD.

WED-348

Development and external validation of a model to predict multi-drug resistant bacterial infections in patients with cirrhosis

Sebastián Marciano¹, Salvatore Piano², Virendra Singh³, Paolo Caraceni⁴, Rakhi Maiwall⁵, Carlo Alessandria⁶, Javier Fernandez⁷, Dong Joon Kim⁸, Sung-Eun Kim⁹, Elza Soares¹⁰, Mónica Marino¹¹, Julio Vorobioff¹², Manuela Merli¹³, Laure Elkrief¹⁴, Víctor Manuel Vargas Blasco¹⁵, Aleksander Krag¹⁶, Shivaram Singh¹⁷, Diego Giunta¹, Martín Elizondo¹⁸, Maria Margarita Anders¹⁹, melisa dirchwolf²⁰, Manuel Mendizabal²¹, Rinaldi Lesmana²², Claudio Toledo²³, Florence Wong²⁴, François Durand²⁵, Adrian Gadano¹, Paolo Angeli². ¹Hospital Italiano de Buenos Aires, Buenos Aires, Argentina, ²University of Padova, Italy, ³Postgraduate Institute of Medical Education and Research, India, ⁴University of Bologna, Italy, ⁵Institute of Liver and Biliary Sciences, India, ⁶University of Turin, Italy, ⁷Hospital Clinic, Spain, ⁸Hallym University College of Medicine, Korea, Rep. of South, ⁹Hallym Sacred Heart Hospital, Korea, Rep. of South, ¹⁰University of Campinas (UNICAMP), Brazil, ¹¹Hospital Dr. Carlos B. Udaondo, Armenia, ¹²Rosario University Medical School, Argentina, ¹³Sapienza University of Rome, Italy, ¹⁴Tours University Hospital, France, ¹⁵Hospital Vall d'Hebron, Spain, ¹⁶Odense University Hospital, Denmark, ¹⁷S.C.B. Medical College, India, ¹⁸Unidad Bi-Institucional de Trasplante Hepático, Hospital de Clínicas-Hospital Militar, Uruguay, ¹⁹Hospital Alemán, Argentina, ²⁰Hospital Privado de Rosario, Argentina, ²¹Hospital Universitario Austral, Argentina, ²²Dr. Cipto Mangunkusumo National General Hospital, Indonesia, ²³Hospital Valdivia, Chile, ²⁴University of Toronto, Canada, ²⁵Hospital Beaujon, France

Email: sebastian.marciano@hospitalitaliano.org.ar

Background and aims: Empirical antibiotic treatment for suspected infections in cirrhosis is crucial. We aimed to develop and validate a model to predict the individual probability of infections by multi-drug resistant organisms (MDRO) at the bedside in patients with cirrhosis to support the selection of appropriate empirical antibiotic treatment.

Figure. Calibration of the model in internal validation and predictors included in the model.

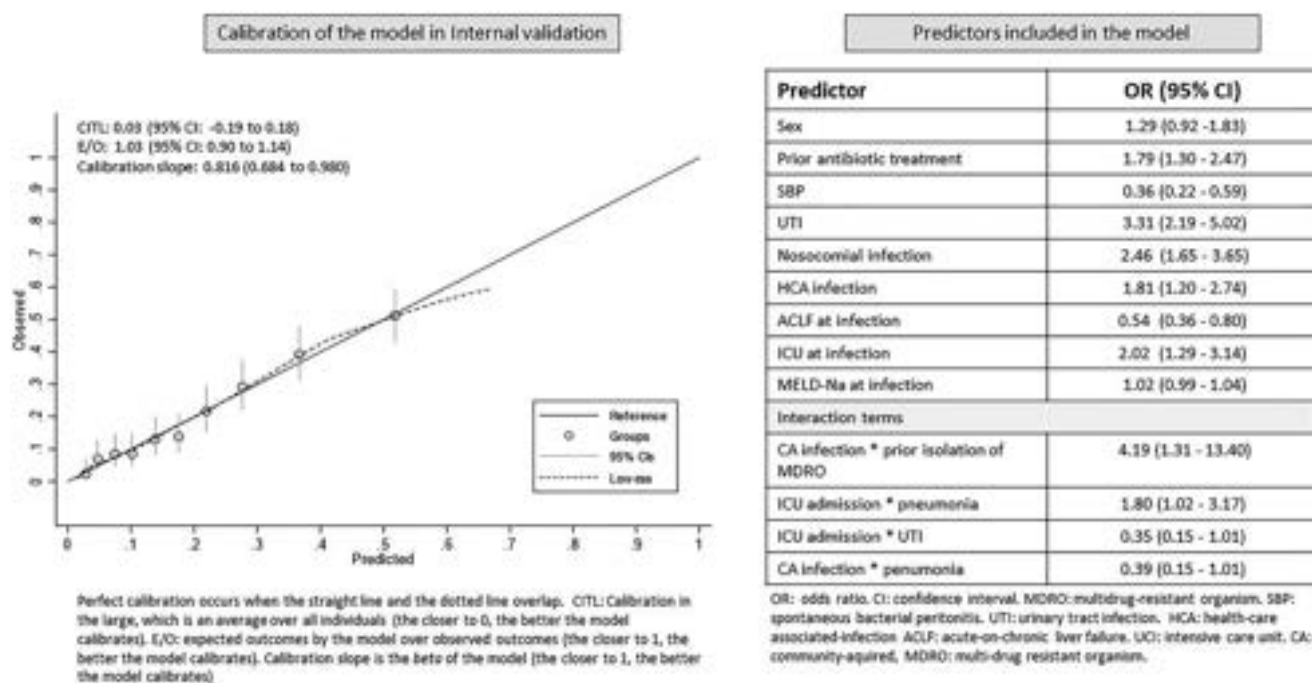


Figure: (abstract: WED-348).

Method: Cross-sectional study (NCT05641025) of consecutive inpatients with bacterial infections from two prospective studies. The Global transcontinental study was used for model development and internal validation (n=1,302), and a study from Argentina and Uruguay (n=472) was used for external validation. Infection by MDROs was defined as an infection caused by at least one bacteria with acquired resistance to at least one antibiotic of three different families. Multivariable logistic regression with backward stepwise selection of predictors of MDROs was used for model development. Bootstrapping was used for internal validation to adjust for optimism. The optimism-adjusted model was then applied to the external validation dataset. The model's performance diagnosis was explored by applying different cut-off points.

Results: The prevalence of infection by MDROs was 19% in the development and 22% in the external validation dataset. The most frequent etiologies of cirrhosis were alcohol and viral-related, and the most frequent infections were spontaneous bacterial peritonitis (SBP) and urinary tract infection (UTI). Half of the infections were community-acquired, and half were equally distributed among healthcare-associated and nosocomial origin. The model predictors are shown in the figure. Very good calibration was achieved in internal and external validation (Figure). Discrimination was adequate, as shown by the area under the receiver operating characteristic curve (AUROC) of 0.73 (95% CI: 0.69–0.76) in internal validation and 0.67 (95% CI: 0.62–0.74) in external validation. Regarding the clinical utility, when applying a probability cut-off point of 5% or 10%, a negative predictive value (NPV) of 98% (95% CI: 94%–99%) and 94% (95% CI: 91%–96%) was observed in the development dataset, respectively. In the external validation dataset, NPV values for the exact cut-off points were 93% (95% CI: 84%–98%) and 89%, respectively.

Conclusion: This easy-to-implement model achieved adequate performance for predicting infection by MDROs in patients with cirrhosis, offering costless bedside individualized risk estimates that might improve the selection of empiric antibiotics. Its high NPV suggests that it could be used as a rule-out tool, particularly in

patients at higher risk of infection by MDROs, to reduce the use of broad-spectrum antibiotics.

WED-349

Factors related to a shorter survival in patients with liver disease and followed by a specialized palliative care clinic

Fernando Xavier e Silva¹, Hemant A Shah², David Wong², Elizabeth Lee², Breffni Hannon³, Kirsten Wentlandt¹, Ebru Kaya¹.
¹University of Toronto, Department of Supportive Care-Palliative Care, Toronto, Canada, ²University of Toronto, Toronto Centre for Liver Disease (TCLD), Toronto, Canada, ³University of Toronto, Department of Supportive Care-Palliative Care-Princess Margaret Cancer Centre, Toronto, Canada
 Email: silva.fernandoxavier@gmail.com

Background and aims: Regardless of advances in tools to predict the survival among patients with advanced liver disease and increasing access to palliative care (PC) by this population, literature about their prognosis after referral to PC remains scarce. Considering the risk of rapid clinical deterioration for this population, better predictors of survival may enable more timely access to specialist PC services. This study aims to identify demographic and clinical factors presented at the time of referral to a PC clinic that are related to shorter survival.

Method: We retrospectively reviewed the charts of adult patients with advanced liver disease referred between May 2019 and May 2022 to a specialized PC clinic at a tertiary teaching hospital in Canada. Data collected included demographics, clinical presentation, and length of survival after referral to the clinic. Clinical factors included primary liver disease etiology; functional status (measured using the Palliative Performance Scale (PPS), a discrete numerical scale from 0% to 100%); the intensity of symptoms (using the Edmonton Symptoms Assessment System (ESAS), a discrete numerical scale from 0 to 10 used to grade intensity of common symptoms); candidacy for liver transplant; history of hepatic encephalopathy (HE); and comorbidities. The study was approved by our institutional

research ethics board. Multivariable regression analysis was used to identify variables associated with shorter survival.

Results: Fifty-four patients were included, 24 (44.4%) were female, the median age was 70 (mean 67.6) years, 6 patients (11.1%) were under 50 years and 30 (55.6%) were born outside of Canada. Primary liver disease aetiologies included the following: viral hepatitis (18, 33.3%); alcohol (17, 31.5%), non-alcoholic fatty liver disease (NAFLD; 8, 14.8%), and other (8, 14.8%). 53 (98.1%) patients had cirrhosis and 24 (44.4%) had hepatocellular carcinoma (HCC). 44 patients (81.5%) had more than 2 comorbidities and 20 patients (37%) had extrahepatic organ failure. 22 patients (40.7%) had a history of HE. Regarding functional status, none of the patients had a PPS of 30% or lower, 6 (11.1%) had a PPS of 40%; and 24 patients (44.4%) of 60% or more. The mean sum of ESAS scores for the 12 measured symptoms was 41 (median 35) out of a maximum of 120 points and fatigue was the symptom with the highest isolated score (6.4, median 7). The average survival from the first PC visit was 41.4 weeks (median of 28 weeks or 6.5 months) and 36 patients (66.7%) died within the study timeframe. On multivariable regression, male gender was the only factor statistically associated with shorter survival, with an average of 32.1 weeks (median of 24, compared with 45 weeks among women, $p = 0.02$) and the survival difference of 21 weeks was considered clinically relevant. Age, type of primary disease, diagnosis of HCC, HE or multiple comorbidities, extrahepatic organ failure, functional status, and severity of symptoms were not associated with the length of survival.

Conclusion: Male patients were more likely to die sooner than female patients in our study of patients with advanced liver disease followed in a PC clinic. Clarity on other prognostic factors for these patients is still needed and new prognostic markers should be explored. Given the size of this study, larger multicenter studies are needed to confirm the findings.

WED-350

Validation of thigh ultrasound for measurement of sarcopenia and fat mass in patient with cirrhosis: correlation with body composition analysis. Higher fat mass, lower muscle mass and reduced functional muscle

Reza Saeidi^{1,2}, Neasa McGettigan^{1,2}, Marion Hanley², Martina Morrin^{1,2}, John Ryan^{1,2}, Karen Boland^{1,2}, ¹RCSI Smurfit Building, Dublin, Ireland, ²Beaumont Hospital, Dublin, Ireland
Email: reza_saeidi@hotmail.com

Background and aims: Sarcopenia (low muscle mass, strength, and function) is associated with adverse outcomes in cirrhosis, including hepatic encephalopathy, ascites, infection, and increased hospitalisation. Sarcopenia is measured using cross-sectional CT scanning. Thigh ultrasound (TUS) may be a low-cost tool to identify sarcopenia in cirrhosis. We aim to validate anterior TUS for measurement of total muscle thickness (TMT) and superficial fat thickness (SF) in cirrhosis using bioelectrical impedance analysis (BIA) as a standard.

Method: Patients with cirrhosis were recruited from a tertiary hepatology clinic for this prospective cross-sectional study approved by the local ethics committee. Using thigh ultrasound, muscle mass using B-mode US was recorded. The right thigh muscle thickness was measured using bedside ultrasound. Point at one-half of the total distance from the top of the patella to the iliac crest were marked. Two readings were obtained by feather-weight technique where the probe was held without pressure on the thigh. Mean of measured anterior thigh muscle and superficial fat thickness were calculated. BIA was performed as the validation standard (SECA mBCA 525) using Sergi sarcopenia equation (PMID: 25103151). Validated functional muscle metrics (handgrip and sit-to-stand) and liver-frailty-indices (PMID: 28422306) were calculated. Descriptive statistics and comparisons between controls and patients was analysed in Stata with t-test/Whitney-Mann-test and Pearson-correlation. Using regression analysis, we constructed ROC curves for analysis of TUS.

Results: 69 patients {58% (40) alcohol liver disease, 25% (17) non-alcoholic steatohepatitis, 5% (4) viral, 4% (3) autoimmune and 7% (5) mixed aetiologies} were included. Additionally, 44 healthy controls (HC) were included. Most patients were male ($n = 39$, 56%), with mean age 58yrs (SD 10), mean Child-Pugh score 6 (IQR = 5–7) and MELD 10 (IQR = 7–12). 14 patients (20%) of patients had clinical ascites at recruitment and 38% ($n = 19$) were actively drinking alcohol. 23 (33%) male and 1 (3%) female patients with cirrhosis had sarcopenia based on BIA (SECA mBCA).

Using TUS, height-adjusted anterior muscle thickness was lower in cirrhotic cohort compared to HC (female: 1.33 vs 1.52 mm/m², SD 0.3 and 0.4 respectively, $p = 0.03$ and male: 1.31 vs 1.53 mm/m², SD 0.4 and 0.3 respectively, $p = 0.03$). BIA height-adjusted skeletal muscle mass positively correlated with TUS-measured TMT (male $r = 0.71$ and female $r = 0.43$, $P < 0.001$ and $p = 0.001$ respectively). TMT > 2.95 mm in men would exclude sarcopenia (sensitivity = 85%, specificity = 64%) with likelihood ratio of 2.4. Intra-rater reliability for TMT was good ($p < 0.001$). We report lower functional muscle strength and function in cirrhotic patients. Using functional testing, sit-to-stand time was lower in HCs (14.53 vs 9.08 secs, $p = 0.001$) and hand-grip strength higher in HC ($p < 0.001$) compared with patients. 13% ($n = 5$) of male and 30% ($n = 9$) of female were frail and frailty scores negatively correlated with TMT ($r = -0.4$, $p = 0.003$).



Figure:

Conclusion: TUS is a rapid and valid point-of-care test which can identify high-risk patients with systemic sarcopenia in cirrhosis. Furthermore, lower TMT is associated with increased frailty and reduced muscle function in cirrhosis. Further prospective studies are required to determine if this can be used with other biomarkers to identify patients who would benefit from intensive nutrition intervention.

WED-351

Goals of care and end-of-life for patients with advanced liver disease followed by a specialized palliative care clinic

Fernando Xavier e Silva¹, Elizabeth Lee², Hemant A Shah², David Wong², Breffni Hannon³, Kirsten Wentlandt¹, Ebru Kaya¹.
¹University of Toronto, Department of Supportive Care-Palliative Care, Toronto, Canada, ²University of Toronto, Toronto Centre for Liver Disease (TCLD), Toronto, Canada, ³University of Toronto, Department of Supportive Care-Palliative Care-Princess Margaret Cancer Centre, Toronto, Canada
Email: silva.fernandoxavier@gmail.com

Background and aims: Considering the life-limiting nature of advanced liver diseases and the suffering frequently experienced by patients diagnosed with these illness, palliative care (PC) has played an important role in their support, including the assessment of preferences regarding their care and during their end-of-life (EOL) period. This study aims to understand the frequency and possible

POSTER PRESENTATIONS

barriers to goals-of-care discussions (GOCd), the content of these preferences and how they are reflected on the dying process of these patients.

Method: The authors retrospectively reviewed the charts of adult individuals referred between May 2019 and May 2022 to a specialized PC clinic for patients with liver diseases at a tertiary teaching hospital in Canada and collected data regarding demographics, reason for referral, clinical characteristics including history of hepatic encephalopathy-HE and functional status (measured with Palliative Performance Scale-PPS, a discrete numerical scale from 0% to 100%), frequency and content of goals-of-care discussions (GOCd) during the first 3 appointments with PC, outcome from clinic, mortality and place of death. All personal identifiers were excluded and the study was approved by the research ethical board of the University of Toronto. Descriptive statistics was used to analyze data.

Results: 54 patients were included in the study, 30 (55.6%) were male, median age was 70 years and 24 (44.4%) had a preferred language other than English. GOCd were included in the motivations to refer 46 (85.2%) patients. History of HE was described in 22 (40.7%) patients. No patients had a PPS lower than 40% and 39 (72.2%) had a PPS between 40–60%. GOCd were not performed in the first visit of 11 (20.4%) patients and continued to be missed for 7 patients (13.0%) by the third visit. History of HE was the only barrier significantly related to the absence of GOCd at the first visit (OR 0.18, $p=0.02$) but not at the third meeting ($p=0.34$). Full medical management was preferred by 23 patients (42.6%) and 6 (11.7%) decided to exclusively receive comfort measures. Sixteen patients (29.6%) changed their preferences between the first and third visits, mostly (11, 92%) towards a more conservative choice. Most patients (30, 55.6%) decided for a “do not resuscitate” (DNR) status and 20 patients (37.0%) would want standard resuscitation procedures in the case of a cardiac arrest. 24 (44.4%) patients were able to discuss their preferred place of death, 17 (70.8% among them) would rather die at home and 4 (16.7%), in a hospital. For outcomes, 27 (50.0%) patients were referred either to a PC unit or to home visiting PC teams and 36 (66.7%) patients died. Information was available regarding place of death for 17 patients (47.2% of the dead). Among them, 8 (14.8%) patients died at the hospital, 5 (29.4%) at a PCU and 4 (23.5%) at home. Among the ones who discussed their preferences, at least 8 (33.3%) patients died in their place of choice, only 4 (16.7%) were known to die in a different place and data was missing for 10 (41.7%) of them.

Conclusion: GOCd and palliative planning were common reasons to refer patients to PC and HE was a significant initial barrier to this role. Most patients decided for a DNR status and for full medical management and these preferences tended to change towards comfort measures with time. Most patients would rather die at home when discussing the topic. Expanding the understanding about patients' preferences may help to increase the rates of goals-concordant care.

WED-352

Gender differences in the patient-reported outcomes and perception of ascites burden amongst outpatients with decompensated cirrhosis and ascites

Florence Wong¹, K. Rajender Reddy², Puneeta Tandon³, Jennifer Lai⁴, Guadalupe Garcia-Tsao⁵, Jacqueline O'Leary⁶, Scott W Biggins⁷, Hugo Vargas⁸, Leroy Thacker⁹, Jasmohan S Bajaj¹⁰. ¹University of Toronto, Medicine, Toronto, Canada, ²University of Pennsylvania, Medicine, Philadelphia, United States, ³University of Alberta, Medicine, Edmonton, Canada, ⁴University of California- San Francisco, Medicine, San Francisco, United States, ⁵Yale University, Medicine, New Haven, United States, ⁶Dallas VA Medical Center, Medicine, Dallas, United States, ⁷University of Washington, Medicine, Seattle, United States, ⁸Mayo Clinic, Scottsdale, Medicine, Phoenix, United States, ⁹Virginia Commonwealth University, Biostatistics, Richmond, United States, ¹⁰Virginia Commonwealth University, Internal Medicine, Richmond, United States

Email: florence.wong@utoronto.ca

Background and aims: The presence of ascites is a health burden to patients with decompensated cirrhosis. They have a poor quality of life (QOL), due to pain from abdominal distension, hernias and attendant frailty with need for repeat large volume paracentesis (LVP). Perception of these issues may be different between the genders. The aim of the study was to assess gender differences in the perception of ascites burden in patients with recurrent or refractory ascites.

Method: The North American Consortium for the Study of End-stage Liver Disease-3 (NACSELD3) prospectively enrolled outpatients with cirrhosis and large ascites who needed repeat LVPs. Data collected were demographics, laboratory results, co-morbidities, medications and frailty measurements. Self-reported questionnaires related to functional status (Duke Status Activity index), physical activities (Godin Leisure Activity Index), overall QOL (SF36, mental and physical), and ascites burden (ascites Q) were compared between genders.

Results: 241 men (60.4 ± 9.9 yrs) and 115 women (58.8 ± 10.7 yrs) of similar MELD (mean = 13) and Child-Pugh (mean = 7) scores were enrolled. Men had significantly more alcoholic cirrhosis (49% vs. 38%), while women had more NASH (29% vs. 23%) and autoimmune diseases (13% vs. 2%) ($p < 0.0001$). Both genders had similar co-morbidities and complications of cirrhosis. Both groups also had a history of median duration of ascites of 3 months ($p = 0.826$), as were the median number of LVPs ($p = 0.587$) and volume of their LVPs in the past 3 months ($p = 0.891$). Despite this, women felt a lot worse about their ascites (Figure) and had a significantly higher total Ascites Q score (67 ± 22 vs. 58 ± 22 , $p = 0.0001$) (higher value = feeling worse about their ascites), possibly related to their significantly higher median frailty index of 4.16 versus that of 3.95 in men ($p = 0.023$). 37% of women felt depressed compared to 25% ($p = 0.029$) and women scored lower on their emotional well-being ($p = 0.019$) and social functioning ($p = 0.032$) on SF36 questionnaire, even with 51% of men vs. 34% of women taking chronic beta blockers ($p = 0.003$). Despite this, women were able to conduct their daily activities as adequately as men as indicated by their equal scores on Duke Status Activity index ($p = 0.89$) and their Godin Leisure Activity Index ($p = 0.35$).

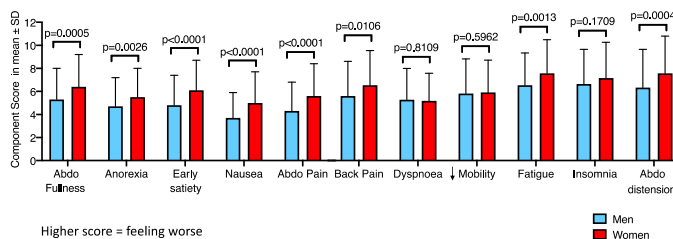


Figure:

Conclusion: The gender difference in the perception of ascites burden is not related to severity of physical illness. Although women felt worse about their ascites-related QOL and emotional health, and were more frail than men, this was not associated with impaired daily function or leisure activity. This may be related to other issues such as cultural/social conditioning, which should be considered when eliciting patient reported outcomes and managing the psychological aspects of ascites care for women.

WED-353

The role of renal impairment on rotational thromboelastometry (ROTEM) parameters in hospitalised patients with cirrhosis-a prospective cohort study

Louis Wang¹, Tianyu Qiu¹, Chin Kim Tan¹, Eugene Wong¹, Kenneth Lin¹, Andrew Kwek¹, James, WeiQuan Li¹, Tiing Leong Ang¹, Roshni Sahashiv², Louis Ng³, Prasanna Tirukonda⁴, Rahul Kumar¹.
¹Changi General Hospital, SingHealth, Gastroenterology, Singapore,
²Changi General Hospital, SingHealth, General Medicine, Singapore,
³Changi General Hospital, SingHealth, Anaesthesia, Singapore, ⁴Changi General Hospital, SingHealth, Diagnostic Radiology, Singapore
 Email: rahul.kumar@singhealth.com.sg

Background and aims: The use of ROTEM has allowed for better understanding of complex haemostatic processes involved in patients with cirrhosis compared to conventional clotting tests (CCT). Renal dysfunction (RD) is a common comorbidity in patients with cirrhosis, but its effect on ROTEM parameters in cirrhosis remains unknown. We conducted a novel study on how ROTEM parameters may be altered by the presence of RD among patients with cirrhosis.

Method: A total of 76 consecutively admitted patients with cirrhosis were prospectively recruited in this study. Patients were classified into 2 groups based on their estimated glomerular filtration rate (eGFR) by the CKD-EPI equation; no-RD (eGFR ≥ 90 , n = 36) and RD (eGFR < 90 , n = 40). ROTEM parameters (INTEM, EXTEM, FIBTEM and APTM), CCT (prothrombin time (PT), activated partial thromboplastin time (aPTT), fibrinogen, platelet) and Child- Pugh score were compared between the groups. Standard statistical tools were applied for group comparisons using Student's t-test and Mann-Whitney U test for parametric and non-parametric data, respectively.

Results: The mean age was 60.6 ± 10.0 years and 77.6% were male patients. For severity of liver cirrhosis, MELD scores were significantly higher in the RD group (RD 17.7 ± 7.2 vs non-RD 14.3 ± 6.7 , $p = 0.04$) likely owing to higher serum creatinine levels, while Child-Pugh score were similar (RD 9.4 ± 2.2 vs non-RD 9.0 ± 2.4 , $p = 0.4$). In figure 1, ROTEM parameters in the RD-group showed significantly higher clot amplitudes at A5, A10, A20 and A30 and lower clot formation time (CFT) across INTEM, EXTEM and APTM analyses ($p < 0.05$). The RD-group also had a significantly higher maximal clot firmness (MCF) for INTEM, EXTEM, APTM and FIBTEM ($p < 0.05$). Difference in clotting time (CT) was not statistically significant between the groups.

CCT showed significant differences in platelet (RD 95.9 ± 49.3 vs non-RD 73.2 ± 46.1 , $p = 0.04$) and aPTT (RD 41.1 ± 14.5 vs non-RD 34.7 ± 9.7 , $p = 0.03$), but no difference in PT (RD 15.6 ± 4.7 vs non-RD 14.5 ± 3.2 , $p = 0.22$) and fibrinogen (RD 2.0 ± 1.0 vs non-RD 1.6 ± 0.6 , $p = 0.07$).

Conclusion: The analysis of our data shows that kidney impairment is an important contributor towards the haemostatic processes in cirrhosis and results in an overall hypercoagulable state, as measured using ROTEM parameters. This was not apparent based on traditional clotting tests alone. This is a novel finding as there may be direct implications for patients undergoing procedures where decisions for prophylactic blood product transfusions were previously based on only traditional clotting parameters. By being in a more hypercoagulable state, patients with cirrhosis and renal dysfunction may require less transfusions and experience fewer transfusion-related complications. Further research is needed to elucidate the effect of platelet dysfunction from renal impairment on ROTEM parameters in cirrhosis, and how it contributes towards the complex interplay of various haemostatic mechanisms.

WED-354

Whole body clearance and production of ammonia quantified by constant ammonia infusion-the effects of cirrhosis and ammonia targeting treatments

Peter Lykke Eriksen¹, Lars Djernes², Hendrik Vilstrup¹, Peter Ott¹.
¹Aarhus University Hospital, Department of Hepatology and Gastroenterology, Aarhus, Denmark, ²Aarhus University Hospital, Department of Anaesthesiology and Intensive Care, Aarhus, Denmark
 Email: ple@clin.au.dk

Background and aims: Hyperammonaemia is a key pathological feature of liver disease and the most important driver of hepatic encephalopathy (HE). However, the relative role of increased ammonia production and reduced clearance is poorly understood, as is the action of ammonia targeting drugs to treat HE. To quantify whole body ammonia metabolism in healthy persons and cirrhosis patients and to validate the method by examination of the effects of glycerol phenylbutyrate and lactulose + rifaximin treatment.

Method: Ten healthy men and 10 male cirrhosis patients were investigated by a 90-minute constant ammonia infusion to achieve plasma ammonia steady-state. Whole body ammonia clearance was calculated as infusion rate divided by steady-state concentration increase and ammonia production as clearance times baseline

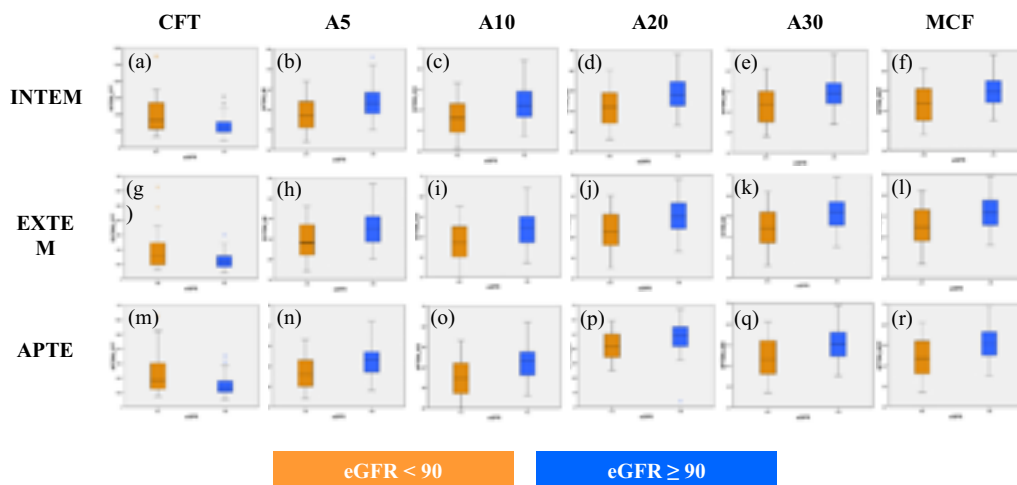


Figure 1 ROTEM parameters were significantly different between cirrhotic patients with or without renal dysfunction ($p < 0.05$). (a) INTEM CFT, (b) INTEM A5, (c) INTEM A10, (d) INTEM A20, (e) INTEM A30, (f) INTEM MCF, (g) EXTEM CFT, (h) EXTEM A5, (i) EXTEM A10, (j) EXTEM A20, (k) EXTEM A30, (l) EXTEM MCF, (m) APTM CFT, (n) APTM A5, (o) APTM A10, (p) APTM A20, (q) APTM A30, (r) APTM MCF.

Figure: (abstract: WED-353).

POSTER PRESENTATIONS

ammonia concentration. Participants were re-investigated after the ammonia targeting interventions.

Results: In healthy persons, ammonia clearance was 3.5 (3.1–3.9) L/min and production 49 (35–63) $\mu\text{mol}/\text{min}$. Phenylbutyrate increased clearance by 11% (4–19, $p=0.009$). Cirrhosis patients had a 20% decreased ammonia clearance of 2.7 (2.1–3.3) L/min ($p=0.02$) and a nearly tripled production of 131 (102–159) $\mu\text{mol}/\text{min}$ ($p<0.0001$). Lactulose + rifaximin reduced production by 20% (2–37%, $p=0.03$). The infusion was generally well-tolerated save one hyperammonaemic cirrhosis patient with possible bleeding who developed clinical HE that reverted upon infusion stop.

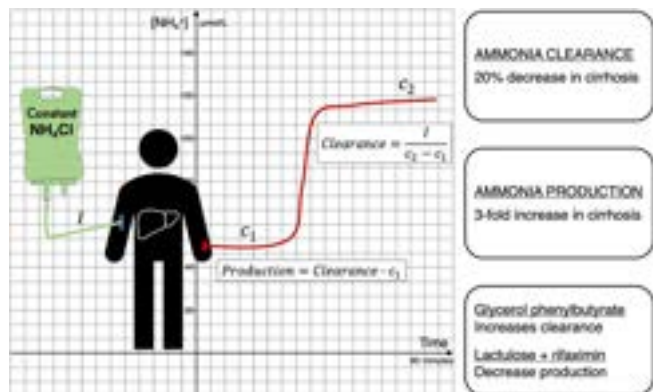


Figure:

Conclusion: Whole body ammonia clearance and production can be separately measured by the technique. The method identified lower clearance and higher production in cirrhosis patients, and showed that phenylbutyrate increases clearance while lactulose + rifaximin decreases production. The method can be used to examine a range of questions on normo-/pathophysiology and ammonia targeting treatment mechanisms.

WED-355

Prognostic significance of individual decompensating events in stable decompensated outpatients with cirrhosis using a multi-center cohort

Jasmohan S Bajaj¹, Guadalupe Garcia-Tsao², Puneeta Tandon³, Jennifer Lai⁴, Jacqueline O'Leary⁵, Hugo Vargas⁶, Scott Biggins⁷, Patrick S. Kamath⁸, Florence Wong⁹, Jawaid Shaw¹, Chimezie Mbachi², Jade Ikahihifo-Bender¹⁰, Leroy Thacker¹, K. Rajender Reddy¹⁰.

¹Virginia Commonwealth University, Richmond, United States, ²Yale University, New Haven, United States, ³University of Alberta, Canada, ⁴University of California San Francisco, United States, ⁵Dallas VA Medical Center, United States, ⁶Mayo Clinic Arizona, United States, ⁷University of Washington, United States, ⁸Mayo Clinic Rochester, United States, ⁹University of Toronto, Medicine, Canada, ¹⁰University of Pennsylvania, United States

Email: jasmohan.bajaj@vcuhealth.org

Background and aims: The type/prognostic significance of decompensating events in cirrhosis may be changing given changes in etiology and management of cirrhosis. Ascites, hepatic encephalopathy (HE) and prior variceal bleeding (VB) are considered decompensating events. Aim: to define the prognostic significance (specifically, 3- and 6-month hospitalization, transplant and mortality) in patients with "stable" decompensation.

Method: NACSELD3 (North American Consortium for the Study of End-stage liver Disease) is an ongoing study that enrolls outpatients with cirrhosis and follows them every 3 months (mos) for hospitalizations, transplant and death. Decompensating events prior to enrollment into the study were defined as ascites (requiring diuretics and/or LVP), hepatic encephalopathy (HE; grade ≥ 2 , on specific treatment) and variceal bleed (VB, controlled on EVL/NSBB). Those with alcohol as etiology had an AUDIT score <10 for at least 3

months and those with HCV etiology had achieved eradication. Outcomes (3and 6-month re-hospitalization, transplant and mortality) were compared among those without ascites but with HE \pm VB (group 1), those with ascites alone (group 2) and those with ascites and HE \pm VB (group 3). Multi-variable analyses were performed.

Results: 437 pts were included: MELD-Na 13.0 (6–33) 71% men, age 59.4 (10.22) with various etiologies (58% alcohol, 20% NASH, 10% HCV, 13% other); 56 were in group 1, 181 in group 2 and 200 in group 3. Only MELD-Na, pre-enrollment hospitalization and WBC count differed at baseline among groups. At 3 and 6 mos, we had data on total 397 pts and 332 pts respectively.

3-mo outcomes: Mortality rates (group 1 4%, group 2 3%, and group 3 3%, $p=0.89$) and transplant rates (0% vs 2% vs 4%, $p=1.0$) were not different among groups but significant differences in 3 and 6-mo hospitalization rates were noted (Figure). Most (81%) 3-mo hospitalizations were liver-related (21% GI bleed, 19% HE, 12% renal) and were not different among groups. 6-mo outcomes: Mortality rates (group 1, 17%, group 2, 9%, and group 3, 11%, $p=0.38$) and transplant rates (0% vs 6% vs 8%, $p=0.32$) were not different among groups. As per 3-mo outcomes, 6-mo hospitalizations were different among groups ((Figure); 62% were liver-related (17% HE, 10% GI bleed and 19% renal) and were not different among groups. None of the subjects had alcohol misuse during the follow-up.

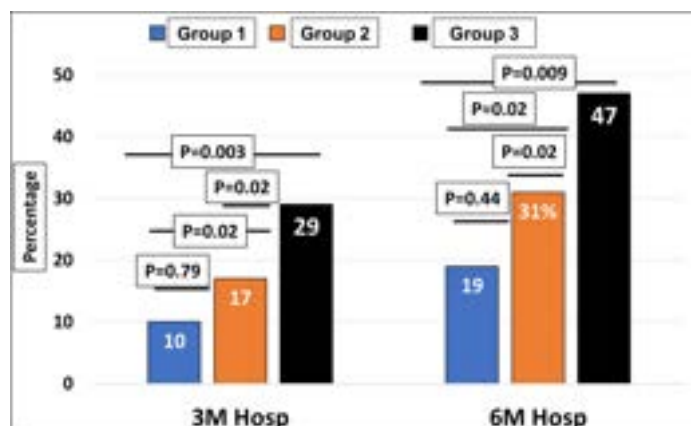


Figure:

MV hospitalization analysis: 3- mo: The only predictors were pre-enrollment hospitalizations (OR 2.95, 1.78–4.87, $p<0.001$) and pt group (overall $p=0.02$, OR 0.54 group 2 vs. 3 and OR 0.37 group 1 vs. 3). 6-mo: predictors were pre-enrollment hospitalizations (OR 1.97, 1.22–3.20, $p=0.006$) and pt group (overall $p=0.005$, OR 0.53 group 2 vs. 3 and OR 0.32 group 1 vs. 3).

Conclusion: In a multicenter cohort of North American outpatients with "stable" decompensated cirrhosis, a single decompensating event, regardless of type (ascites, HE or VB) has a better prognosis with respect to hospitalizations at 3 and 6 months compared to those with a combination of decompensating events.

WED-356

Classification of bleeding risk from invasive procedures in patients with cirrhosis: an expert consensus

Alix Riescher-Tuczkiwicz¹, Stephen H Caldwell², Erica Villa³, Pierre-Emmanuel Rautou^{1,4}. ¹Université Paris Cité, Inserm, Centre de recherche sur l'inflammation, UMR 1149, Paris, France, ²Division of Gastroenterology and Hepatology, University of Virginia Health System, Charlottesville, United States, ³Gastroenterology Unit, Department of Medical Specialties, University of Modena and Reggio Emilia and Azienda Ospedaliero-Universitaria di Modena, Modena, Italy, ⁴Service d'Hépatologie, AP-HP, Hôpital Beaujon, DMU DIGEST, Centre de Référence des Maladies Vasculaires du Foie, FILFOIE, ERN RARE-LIVER, Clichy, France

Email: perautou@yahoo.fr

Background and aims: Prevention of bleeding complications following invasive procedures in patients with cirrhosis is challenging. A first step in preventing such bleedings is to properly assess the risk of bleeding by considering the patient's history, the risk of the

procedure itself and the results of laboratory tests. Several classifications of the bleeding risk have been proposed in recent international guidelines. Several (AGA 2021, AASLD 2021, ISTH 2021, EASL 2022) used the same approach based on the frequency of major bleeding

		Procedure	Voting percentage	
			Low risk	High risk
Digestive endoscopy	ERCP	Without sphincterotomy	90%	10%
		With biliary or pancreatic sphincterotomy	12%	88%
		With papillary balloon dilatation without sphincterotomy	67%	33%
		With biliary or pancreatic stent placement without sphincterotomy	80%	20%
	Upper and lower	Mucosal resection	25%	75%
		Submucosal dissection	8%	92%
		Hemostasis with argon plasma coagulation	92%	8%
		Radiofrequency ablation	67%	33%
		Video-capsule	100%	0%
		Ultrasound without fine-needle aspiration	98%	2%
		Ultrasound with fine-needle aspiration	59%	41%
		Stricture dilatation (pneumatic or bougie)	32%	68%
		Stricture dilatation (balloon)	38%	63%
		Enteral stent deployment	77%	23%
	Upper	Cystogastrotomy	13%	87%
		Polypectomy < 1cm	76%	24%
		Polypectomy > 1cm	12%	88%
		Diagnostic (with or without biopsy)	98%	2%
		Variceal ligation	71%	29%
		Glue injection of gastric varices	54%	46%
		Peroral endoscopic myotomy	7%	93%
		Ampullary resection	6%	94%
		Percutaneous gastrostomy or jejunostomy placement	22%	78%
		Diagnostic balloon assisted enteroscopy	90%	10%
		Therapeutic balloon assisted enteroscopy	64%	36%
	Lower	Push enteroscopy	88%	12%
		Polypectomy < 1cm	78%	22%
		Polypectomy > 1cm	10%	90%
		Flexible sigmoidoscopy (with or without biopsy)	96%	4%
Cardiovascular		Diagnostic colonoscopy (with or without biopsy)	92%	8%
		Central venous catheter placement	81%	19%
		Peripherally inserted central catheter line placement	90%	10%
		Arterial line placement	73%	27%
		Central line removal	94%	6%
		Cardiac catheterization	82%	18%
		Transesophageal echocardiography	94%	6%
		Diagnostic coronary angiography	90%	10%
		Therapeutic coronary angiography	66%	34%
		Angiography or venography with intervention	60%	40%
		Inferior vena cava filter placement	87%	13%
	Hepatology	Percutaneous liver biopsy	33%	67%
		Transjugular liver biopsy	83%	17%
		Laparoscopic liver biopsy	46%	54%
		Hepatic venous pressure gradient measurement	92%	8%
		Portal recanalization	40%	60%
		Transjugular intrahepatic portosystemic shunt	38%	62%
		Transcatheter arterial chemoembolization or radioembolization	62%	38%
		Percutaneous ablation of liver cancer	40%	60%
		Cholecystostomy or percutaneous biliary drain placement	22%	78%
		Diagnostic paracentesis	98%	2%
	Pneumology	Therapeutic paracentesis	96%	4%
		Tunneled ascitic drain placement	59%	41%
		Thoracentesis	78%	22%
		Bronchoscopy without biopsy	96%	4%
		Bronchoscopy with biopsy	29%	71%
		Therapeutic bronchoscopy	26%	74%
		Intrathoracic organ biopsy	9%	91%
		Tunneled pleural drain placement	44%	56%
	Urology and nephrology	Prostate biopsy	25%	75%
		Cystoscopy	100%	0%
		Ureteroscopy	98%	2%
		Lithotripsy (kidney, bladder, ureter)	59%	41%
		Percutaneous kidney biopsy	10%	90%
		Transjugular kidney biopsy	61%	39%
		Nephrostomy tube placement	24%	76%
	Neurology	Lumbar puncture	41%	59%
		Epidural catheter placement	23%	77%
		Central nervous system procedure	2%	98%
	Gynecology	Colposcopy with cervical biopsy	79%	21%
		Diagnostic hysteroscopy	100%	0%
		Hysteroscopy with biopsy	64%	36%
Miscellaneous		Amniocentesis	38%	62%
		Dental cleaning	100%	0%
		Dental extraction	45%	55%
		Intra-articular puncture	65%	35%
		Intra-articular injection	77%	23%
		Lymph node percutaneous biopsy	83%	17%
		Nonliver intraabdominal solid-organ biopsy	15%	85%
		Skin biopsy	98%	2%
		Drainage catheter exchange	98%	2%

Consensus for a procedure to be at "low bleeding risk"

Consensus for a procedure to be at "high bleeding risk"

No consensus

Figure: (abstract: WED-356).

POSTER PRESENTATIONS

events following invasive procedures (threshold at 1.5%). Yet, these guidelines arrived at different conclusions highlighting the need for a broad consensus on this topic. The aim of this study was thus to establish a consensus of experts on the bleeding risk associated with invasive procedure in patients with cirrhosis.

Method: All international experts involved in recent guidelines on the management of invasive procedures in patients with cirrhosis were contacted, namely authors of the AASLD 2021, AASLD 2023, ACG 2020, AGA 2019, AGA 2021, AGA 2021, British Society of Gastroenterology 2020, and the ISTH 2022 guidelines, as well as panel and Delphi panel members of the EASL 2022 guidelines. All were invited to classify 80 procedures frequently performed in patients with cirrhosis as at “high risk” or “low risk” of bleeding. Procedures were considered at high-risk when the estimated bleeding risk is $\geq 1.5\%$ or when even minor bleeding may lead to severe consequences or death. The predetermined threshold considered as a consensus was 75%.

Results: Out of a total of 72 experts, 52 participated in the study (72%): 35 from Europe, 16 from the USA, 1 from Asia. Of those who specifically declined to respond, 1 was more laboratory oriented, 1 was no longer clinically active and 18 simply declined to respond. Out of the 80 procedures, a consensus could be reached for 51 procedures (64%): 16 procedures were classified as at “high risk,” 35 as at “low risk”; a consensus could not be reached for 29 procedures (Figure). Low-risk procedures were mainly diagnostic procedures, while high-risk procedures were mainly therapeutic procedures or procedures involving biopsy/sampling of a particularly high-risk sites (e.g., central nervous system).

Conclusion: A consensus was reached among clinically experienced experts who have published in the field of procedural bleeding risk in cirrhosis for 51 procedures: 16 procedures were classified as “high risk” and 35 as “low risk” for bleeding based on this collective clinical experience. While truly randomized and prospective studies that include various potential interventions would be necessary to be more definitive, this experience-based classification will be helpful to homogenize future study interpretation and in clinical decision making on invasive procedures in patients with cirrhosis.

WED-357

The role of prolonged albumin replacement therapy in correction of its structure and functional properties and management of ascites

Anastasia Turkina¹, Marina Maevskaya², Maria Zharkova², Vladimir Ivashkin¹. ¹Sechenov First Moscow University (Sechenov University), Department of Propaedeutics of Internal Disease, Gastroenterology and Hepatology, Russian Federation, ²Sechenov First Moscow University (Sechenov University), Vasilenko Clinic of Internal Diseases, Gastroenterology and Hepatology, Russian Federation
Email: daygawa@yandex.ru

Background and aims: Human serum albumin (Alb) undergoes posttranslational changes due to oxidative stress in cirrhotic patients (pts). It leads to “effective albumin” reduction. Alb infusions are widely used not only in short course but also in long term therapy. There is no information about the influence of prolonged Alb therapy on albumin structure and functions. Aim was to access the influence of 3 months albumin replacement therapy on albumin structure and functional properties and management of ascites.

Method: We included 50 eligible pts with decompensated cirrhosis and ascites. Pts were divided into 2 groups: albumin and control-age, gender and clinical presentation matched. Along with standard medical treatment (SMT), Alb group received albumin replacement therapy for 3 months (20%-200 ml per week). Control group-only SMT. On admission and after 3 months of therapy, we performed a standard examination and additionally assessed Alb properties by means of electronic paramagnetic resonance tests. We analyzed the following parameters: DR-an indicator of native albumin

conformation, BE -binding efficiency of albumin, RTQ-transport efficiency and DTE-detoxifying ability.

Results: The mean pts's age varied from 31 to 74 years; 2/3 of the patients were female. The main cause of cirrhosis was alcohol-62%. All patients initially had ascites. Only 48% (n=24) of pts had hypoalbuminemia (<32 g/l). Albumin structure (DR) and functions (BE, RTQ, DTE) were impaired totally in both groups. Those changes didn't depend on albumin serum level ($p < 0.001$). After 3 months of treatment in the Alb group, ascites resolved in 48.4% of pts (n=15) vs. 7% (n=1) in the control group ($p = 0.042$). Alb structure and functions also significantly improved in the Alb group vs. controls: DR 42.4% vs. 0%, BE 60.6% vs. 14.3%, RTQ 63.6% vs. 14.3%, DTE 60.6% vs. 28.6% ($p < 0.001$).

Conclusion: Albumin replacement therapy for 3 months induces reduction of ascites, improvement of Alb structure and functional properties. Native conformation and Alb functional properties can be an additional marker for the replacement therapy initiation and withdrawal.

WED-358

A multimodal treatment candidate for sarcopenia in men with decompensated cirrhosis: a randomized, placebo-controlled trial evaluating LPCN 1148

Benjamin Bruno¹, Josh Weavil¹, Jonathan Ogle¹, George Nomikos¹, Anthony DelConte^{1,2}, Nachaippan Chidambaram¹, Mahesh Patel¹, Jennifer Lai³, Arun Sanyal⁴. ¹Lipocine Inc, Salt Lake City, United States, ²Saint Joseph's University, Department of Food, Pharma, and Healthcare, Philadelphia, United States, ³University of California San Francisco, School of Medicine, San Francisco, United States, ⁴Virginia Commonwealth University, Division of Gastroenterology, Hepatology and Nutrition, Richmond, United States
Email: bjb@lipocine.com

Background and aims: Sarcopenia affects 30–70% of patients with liver cirrhosis and has been shown to negatively impact outcomes in cirrhosis, including increased hospitalizations, decompensation events (e.g. hepatic encephalopathy [HE] and infections), and deaths. Testosterone (T), a multimodal hormone influencing many organ systems, is low in the majority of cirrhotic men and is an independent predictor of mortality and decompensation events, including ascites, and HE. The aim of this study is to evaluate LPCN 1148, a novel, multimodal, orally available prodrug of T, for treatment of sarcopenia and decompensated cirrhosis. This abstract will present preliminary baseline characteristics for the study population.

Method: Men with cirrhosis and sarcopenia (confirmed by CT scan), who are waiting for a liver transplant, were eligible for this two-stage, randomized (1:1), blinded, placebo-controlled, proof-of-concept clinical trial. In the first stage, participants were assigned to receive either oral LPCN 1148 or placebo twice daily for 24 weeks. At week 24, the second stage open-label extension (OLE) portion of the study begins, where all participants receive LPCN 1148 from weeks 24–52. The primary end point is the change in skeletal muscle index (SMI) at week 24 with additional biochemical, clinical, functional, and PRO end points at 24 and 52 weeks.

Results: Enrollment is complete; at baseline participants (N=30, mean \pm SD for age: 58.8 ± 8.4 yrs, BMI: 29.0 ± 6.9 kg/m²) were sarcopenic (inclusion criterion, L3-SMI 46.4 ± 7.7 cm²/m²) with elevated markers of liver disease (MELD score 16.8 ± 4.2 ; ALP 147.6 ± 80.6 U/L, AST 45.1 ± 21.5 U/L; AST/ALT 1.69 ± 0.49). Etiology of cirrhosis was ALD (50.0%), followed by NASH (23.3%), hepatitis C (17.3%), PSC (6.7%), and ALD/hepatitis C (3.3%). Major decompensation events present at baseline were HE (72.4%), ascites (53.3%), and varices (46.7%). More than 80% of participants were categorized as frail or pre-frail by the Liver Frailty index. Participants were below the lower limit of normal for androgenic markers (calculated free T 53.5%, IGF-1 62.1%), albumin (56.7%), platelets (89.7%), hematological factors (hemoglobin 63.3%, hematocrit 66.7%), nutritional markers (pre-albumin 89.7%), bicarbonate (66.7%) and lymphocytes (43%).

Additionally, a large portion of participants were above the upper limits of normal for total bile acids (93%), SHBG (63.3%), luteinizing hormone (43.3%), B12 (70.0%), and ammonia (63.3%).

Conclusion: There are trends within this sarcopenic, decompensated cirrhotic population indicating dysfunction in other key physiologic areas, including hematologic, thrombotic, androgenic, metabolic, immunity, and frailty. Potentially related to the failing liver and reduced muscular mass, systemic ammonia levels are high in the majority of the study population which predisposes participants to episodes of overt HE.

WED-359

Clinical effectiveness of human albumin in liver cirrhosis: a meta-analysis update

Huijuan Zhou¹, Ziqiang Li¹, Yuhuan Liu², Daer Dili², Qing Xie¹. ¹Ruijin Hospital, Shanghai Jiao Tong University School of Medicine, China,

²Takeda (China) International Trading Co., Ltd, China

Email: xieqingrjh@163.com

Background and aims: Hyponatremia is a poor prognosis marker and independent predictor of mortality for patients with liver cirrhosis. Albumin infusions from volume expander (VE) treatment group are regarded as an effective strategy for the management of hyponatremia in cirrhosis. Hence, we examined the clinical effectiveness of albumin infusion to resolve hyponatremia and other complications as well as compare the effectiveness of diverse treatment groups in liver cirrhotic patients.

Method: A systematic literature search of PubMed and EMBASE for articles reporting clinical effectiveness of albumin infusion in cirrhotic patients was performed from inception till date. The key primary efficacy outcome was hyponatremia, and the key safety outcomes were peripheral edema, adverse events, and in-hospital mortality. For the main meta-analysis, the studies were pooled, and albumin infusion was compared with control (including VEs, vasoconstrictors, and inactive/standard medical therapy (I/SMT)). For subgroup meta-analysis, comparison was performed between

albumin infusion and other treatment groups. The odds ratio (OR) and mean difference (MD) estimated the outcome with a 95% confidence interval (CI). The study protocol was prospectively registered at PROSPERO (CRD42022372709).

Results: Twenty-two studies were included in the analysis. Pooled data showed an overall significant low incidence of hyponatremia (OR, 0.33; 95% CI [0.26–0.41]), severe infection (OR, 0.52 [0.29–0.94]), and post paracentesis circulatory dysfunction (PICD) (OR, 0.36 [0.21–0.61]) among albumin treated group compared to control. Among subgroup analysis, statistically significant improvement was observed with albumin infusion vs I/SMT (OR, 0.28 [0.22–0.36]), while favorable improvement was observed with VE (OR, 0.66 [0.38–1.17]) or vasoconstrictor (OR, 0.45 [0.05–3.75]). For PICD, improvement with albumin was significant compared to other VEs (OR, 0.31 [0.15–0.63]), but did not reach statistical significance with vasoconstrictor (OR, 0.63 [0.21–1.91]). Overall subgroup analysis showed albumin infusion lowered the odds of hyponatremia (OR, 0.33 [0.26 to 0.41]) and PICD (OR, 0.38 [0.21 to 0.69]) significantly. Pooled data showed comparable incidences of peripheral edema (OR, 0.97 [0.55, 1.70]) and overall adverse events (OR, 0.98 [0.92, 1.03]) between albumin and control groups. Comparable in-hospital mortality was observed with albumin vs other VE (OR, 1.02 [0.42 to 2.44]) and a favorable improvement when compared to the I/SMT group (OR, 0.58 [0.20 to 1.67]).

Conclusion: Albumin infusion may be beneficial for resolving hyponatremia, PICD and severe infection among cirrhotic patients. However, larger, multi-centered and double-blinded randomized controlled trials with longer follow-up periods are needed to generate more robust data.

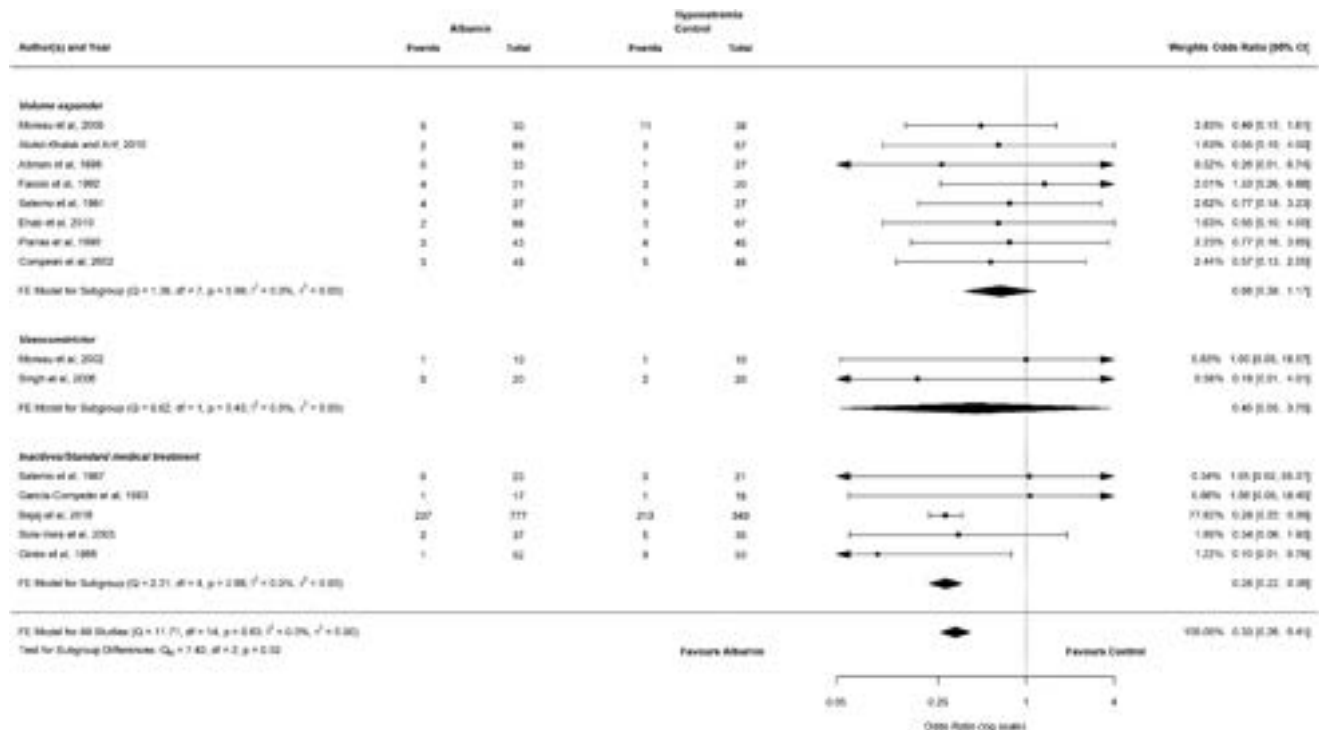


Figure 1: (abstract: WED-359): Forest plot comparing albumin with other treatment groups for hyponatremia

Abbreviations: CI, confidence interval; df, degrees of freedom; FE, fixed effect

WED-360

Effect of kidney injury and hemodynamic effect after moderate abdominal paracentesis: a randomized control study

Sakkarin Chirapongsathorn¹, Sanpolpai Khaoprasert¹, Anuchit Suksamai¹, Amnart Chaiprasert². ¹Phramongkutklao Hospital, Division of Gastroenterology and Hepatology, Department of Medicine, Bangkok, Thailand, ²Phramongkutklao Hospital, Division of Nephrology, Department of Medicine, Thailand
Email: sakkarin33@gmail.com

Background and aims: Patients with cirrhosis undergoing therapeutic paracentesis are at risk to develop kidney injury but not well evaluated in non-large volume paracentesis setting. The aims of this study are to determine the risk and consequence of acute kidney injury (AKI) and its progression in patients with decompensated cirrhosis after moderate paracentesis by use of a urine test measuring tissue inhibitor of metalloproteinases-2 (TIMP-2) and insulin-like growth factor-binding protein 7 (IGFBP7), both inducers of G1 cell cycle arrest and represent a key mechanism implicated in AKI and could predict AKI after paracentesis.

Method: A randomized, prospective cohort study was performed during December 2020 to December 2021. All outpatient decompensated cirrhosis with ascites were enrolled and randomized into 3 liters and 5 liters of paracentesis groups. Serial urine samples were analysed for [TIMP-2]*[IGFBP7] concentration before and after paracentesis. The primary outcome measure was kidney injury as defined by raising of Urine [TIMP2]*[IGFBP7] >2 (ng/ml)²/1000 after moderate paracentesis (<5 liters ascites removal).

Results: A total of 90 patients with decompensated cirrhosis with ascites were consecutive enrolled during study period. After screening, 54 patients analyzed, 29 patients underwent in 3 liters paracentesis group and 25 patients underwent in 5 liters paracentesis group. The mean of MELD score was 8 ± 1.2. Of the 17 (31%) patients develop kidney injury after moderate paracentesis. Urine TIMP2, IGFBP7>2, rising urine TIMP2 and rising urine TIMP2/urine Cr were significant higher in patients within 5 liters paracentesis group. Mean arterial pressure were statistically significant decline at 2 hours after paracentesis in both groups. The Urine [TIMP2]*[IGFBP7] predicted hemodynamic event with an area under the curve [95% confidence interval (CI)] of 0.82 [0.72–0.99], an optimal cut-off value of 3.4 (ng/ml)²/1000, a sensitivity 75%, and a specificity of 89%. For predicting severe AKI, hospital admission and death, Urine [TIMP2]*[IGFBP7] was not significantly discriminant. Five of these patients died within 90 days of follow-up.

Table 1: Primary outcome, secondary outcome and urine Biomarker data*

Variables	3 L group (n = 29)	5 L group (n = 25)	p value
Rising Urine TIMP2	3 (10.3%)	8 (32%)	0.049*
Rising Urine IGFBP7	8 (27.6%)	8 (32%)	0.723
Rising Urine TIMP2.IGFBP7	5 (17.2%)	7 (28%)	0.343
Rising Urine TIMP2/Urine Cr	12 (41.4%)	19 (76%)	0.010*
Rising Urine IGFBP7/Urine Cr	12 (41.4%)	13 (52%)	0.435
Rising Urine TIMP2.IGFBP7/ Urine Cr	9 (31%)	12 (48%)	0.202
TIMP2.IGFBP7>2	5 (17.2%)	12 (48%)	0.015*
Hemodynamic event	3 (10.3%)	5 (20%)	0.319
ΔMAP (120–0 mmHg)	–3.1 ± 3.7	–5.2 ± 4.3	0.065
Ascites release times (mins)	4 (3, 6)	6 (4, 6)	0.032*
Rapid decline of GFR	16 (55.2%)	14 (56%)	0.951
Admission within 3 months	7 (24.1%)	8 (32%)	0.520
Death within 3 months	3 (10.3%)	2 (8%)	0.767

*Value presented as n (%). P value corresponds to Independent t test or Pearson Chi-Square test.

Conclusion: Urine [TIMP2]*[IGFBP7] effectively identify patients with risk of kidney injury after moderate paracentesis but could not predict severe AKI. Below a cut-off of 3.4 (ng/ml)²/1000, the risk of

kidney injury is low. Kidney injury could occur even less than 5 liters of ascites release in decompensated cirrhosis was performed. Future studies should include a larger sample size to confirm these findings. The nation clinical registration number was TCTR20191116003.

WED-361

Clostridioides difficile infection in patients with liver cirrhosis

Olga Adriana Caliman-Sturdza¹. ¹Stefan cel Mare University, Faculty of Medicine and Biological Science, Suceava, Romania
Email: sturdza_olga@yahoo.com

Background and aims: Clostridioides difficile is an infectious agent associated with significant morbidity and mortality in patients with cirrhosis. Our aim is to identify variables that are predictive of poor outcomes and the risk of mortality in this patient population.

Method: We investigated the patients hospitalized in our department in 2022 with the diagnosis of Clostridioides difficile infection (CDI) and liver cirrhosis.

Results: Out of a total of 174 patients diagnosed with enterocolitis with Clostridioides difficile, 28 patients were known to have liver cirrhosis, 4 of viral B and C etiology and 24 of toxic etiology. 21.4% of cirrhotic patients received antibiotics before being diagnosed with CDI and 46.4% were under treatment with proton pump inhibitors. Decompensation of liver disease occurred in 71.4% patients, manifested by confusion, drowsiness, psychomotor agitation (32.1%), jaundice and ascites (39.3%). CDI had an unfavorable evolution towards sepsis with multiple organ failure in a percentage of 17.8% of patients with cirrhosis compared to 2.7% of non-cirrhotic patients, 7.15% developed upper digestive hemorrhage, 11.2% phenomena of hepatic encephalopathy with evolution towards coma. Cirrhotic patients who developed sepsis with Clostridioides difficile had hypoalbuminemia and severe anemia at admission. Mortality was 10.7% in patients with cirrhosis and CDI and only 1.3% in the group of non-cirrhotic patients. Recurrences occurred in 21.4% of cirrhotic patients, compared to 4.2% of non-cirrhotic ones. Diarrhea subsided after 6 days of oral treatment with vancomycin, while in non-cirrhotic patients normalization of intestinal transit was achieved after 3 days of treatment.

Conclusion: Patients with both Clostridioides difficile infection and liver cirrhosis have worse outcomes than patients without cirrhosis, included morbid complications, death and higher rates of hospital readmission. The incidence of CDI in cirrhotic patients is increasing and has become more common in the community. Risk factors of treatment with proton pump inhibitors and antibiotic exposure were associated with the diagnosis of CDI in cirrhosis patients. Hypoalbuminemia and anemia were found to be predictors of increased mortality in cirrhosis patients with CDI.

WED-362

The prevalence and prognostic impact of myosteatosis with and without sarcopenia and its association with age and severity of liver cirrhosis

Eleni Geladari¹, Theodoros Alexopoulos², Meropi Kontogianni³, Larisa Vasilieva⁴, Ilianna Mani⁵, Roxani Tenta³, Sofia Manioudaki⁶, Vasilis Sevastianos¹, Alexandros-Pantelis Tsigas³, Ioannis Vlachogiannakos², Alexandra Alexopoulou⁵. ¹Evangelismos General Hospital, 3rd Department of Internal Medicine and Liver Outpatient Clinic, Athens, Greece, ²Laiko General Hospital, Gastroenterology Department, Athens, Greece, ³School of Health Sciences and Education Harokopio University, Nutrition and Dietetics, Athens, Greece, ⁴Alexandra General Hospital, Gastroenterology, Athens, Greece, ⁵2nd Department of Internal Medicine and Research Laboratory, National and Kapodistrian University of Athens, Medical School, Hippokration General Hospital, Athens, Greece, ⁶Intensive Care Unit, Sismanogleio General Hospital of Athens, Greece
Email: alexandra61@med.uoa.gr

Background and aims: Myosteatosis (MS) is defined as increased fat infiltration in skeletal muscle and implies impaired muscle quality.

MS is different from sarcopenia but part of sarcopenia definition. MS may be considered as a precursor of sarcopenia. The aim of the study was to investigate the prevalence of MS either alone or with sarcopenia and its association with age and severity of liver disease.

Method: Skeletal muscle index (SMI) and MS measured by computed tomography at third lumbar vertebra, muscle strength evaluated by hand dynamometer and functionality by short physical performance battery (SPPB) were used to diagnose sarcopenia according to latest EWGSOP-2 criteria. MS was defined as muscle radiodensity <41 HU for dry body mass index <24, 9 kg/m² and <33 HU for ≥25 kg/m². Patients' demographics, severity of LC and 360-day mortality were recorded.

Results: 194 consecutive patients were included [age 61 (IQR 52–68); 66.5% male; MELD 10.5 (7.7–16); 60.3% with decompensated LC; 43.8%, 22.7% and 33.5% with alcoholic, viral and other etiology, respectively]. Patients were classified in four groups according to presence of MS and sarcopenia. Neither MS nor sarcopenia was diagnosed in 25.3% (group A), MS without sarcopenia in 30.9% (group B), sarcopenia according to handgrip and MS in 17.5% (group C) and sarcopenia according to handgrip, MS and low SMI in 26.3% (group D). MS was present in all but 3 cases with sarcopenia. There was a significant ascending order across the groups A, B, C and D in age [56 (50–63.5), 57.5 (51.2–66), 62.5 (57–69.5) and 67 (59–72.5) years, respectively, $p < 0.001$] and severity of LC as it was documented by the increasing rate of decompensated cirrhosis [32.7%, 58.3%, 73.5% and 80.4%, respectively, $p < 0.001$] and similarly by MELD ($p < 0.001$) and Child Pugh values ($p < 0.001$). In contrast, there was a significant descending order across the groups in SMI ($p < 0.001$) and SPPB ($p < 0.001$) values. Considering the Kaplan-Meier curve at 360 days, between groups B, C and D (no patient died in A), patients in group D had a higher mortality rate compared to B (log Rank $P = 0.001$) but not C (log Rank $P = 0.068$) (log Rank $P = 0.002$ in overall). In multivariable analysis adjusted for age and sex, mortality was 3.5 times higher in group D compared to B (as reference group) [HR 3.5 (95%CI 1.6–7.3), $P = 0.002$]. No difference was evident between groups B and C ($p = 0.530$).

Conclusion: In patients with LC, MS alone is present in earlier stage of LC and younger age and may imply a prodromal phase of muscle degeneration before the development of sarcopenia. MS is present in all but 3 patients with sarcopenia. Furthermore, sarcopenic patients with low SMI are older and have more advanced liver disease compared to sarcopenic with MS but normal SMI, implying that MS predates the decline of muscle strength and performance. Longitudinal data are required to draw solid conclusions about the significance of MS in patients with LC.

WED-363

Comparison of prognostic value of sarcopenia and MELD score in assessing 28 days and 3 months mortality in patients with cirrhosis of liver

Shivam Gupta^{1,1}. ¹Kalinga Institute of Medical Sciences, Gastroenterology and Hepatology, Bhubaneswar, India
Email: iamdrshivam@gmail.com

Background and aims: Sarcopenia in patients with cirrhosis of liver has been associated with increased mortality, sepsis, hyperammonemia, heart failure, increased length of stay and has been seen to be predictive of waiting list mortality, independent of the Model for End Stage Liver Disease (MELD) score and other possible confounders such as gender and refractory ascites. Sarcopenia and MELD are proven independent prognostic factors for cirrhosis of liver. However, MELD does not take into consideration nutritional and functional status of the patient and has inferior performance in predicting mortality in subgroup with lower MELD scores (≤ 15). Therefore, a prospective observational study is being carried out to compare sarcopenia and MELD score in assessing 28 days and 3 months mortality in patients with cirrhosis of liver and to study prevalence of sarcopenia in different etiologies of cirrhosis of liver. This study will

help in early and better prediction of mortality and therefore better listing of patients in need for liver transplant.

Method: This is an ongoing study on outpatients and inpatients ≥ 18 years of age and diagnosed with cirrhosis of liver. Patients with underlying co morbidities affecting nutrition such as human immunodeficiency virus, systemic malignancies, chronic kidney disease, neuromuscular disorders causing muscle wasting have been excluded. Also, patients with hepatic encephalopathy or hepatorenal syndrome where complete workup of sarcopenia was not possible have been excluded from this study. Evaluation of sarcopenia was based on combination of strength, assistance with walking, rising from a chair, climbing stairs and falls (SARC-F) questionnaire, hand grip strength test by dynamometer, transverse psoas muscle thickness evaluation for muscle quality and quantity by computerised tomography scan and physical performance by gait speed test. These patients with cirrhosis of liver and sarcopenia are then being followed up at 28 days and 3 months to record mortality.

Results: Out of 256 patients planned for recruitment in this study, 108 patients have been included in this interim analysis. Mortality is seen to be higher in patients with sarcopenia (21%) compared to cirrhotic patients without sarcopenia (11.1%). On assessing 28 days and 3-months mortality, sarcopenia was seen more in patients with lower MELD score (≤ 15) with higher mortality of 21%. Underlying etiology contributed significantly to development of sarcopenia with maximum sarcopenia seen in patients with Non-alcoholic fatty liver disease (NAFLD) followed by ethanol use related cirrhosis of liver.

Figure:

MELD score	Mean hand grip strength (Male)	Mean transverse psoas muscle thickness (Males)	Mean hand grip strength (female)	Mean transverse psoas muscle thickness (females)	Number of patients died	Percentage
	(Male)	(Males)	(female)	(females)		
≤ 15	15.97 kg	7.4 mm/m	11.8 kg	5.7 mm/m	11 (52)	21%
16–25	19.9 kg	8.4 mm/m	13.6 kg	6.9 mm/m	7 (38)	18%
≥ 26	16.2 kg	8.1 mm/m	13.4 kg	6.3 mm/m	6 (18)	33%

Conclusion: This interim analysis shows high prevalence of sarcopenia in cirrhosis with impact of sarcopenia on mortality seen to be more in patients with lower MELD score (< 15) and thus, sarcopenia is seen to be a better predictor of 28 days and 3 months mortality at lower MELD scores in patients with cirrhosis of liver. Interestingly, sarcopenia was seen to be more in patients with NAFLD than those with ethanol use related cirrhosis of liver.

WED-364

Activation of the kynurenine pathway potentially underlies neurodegeneration in patients with covert hepatic encephalopathy

Georgia Zeng^{1,2}, Shivani Krishnamurthy³, Ananda Staats Pires³, Anna Guller³, Nway Tun^{1,2}, Joga Chaganti⁴, Ian Lockart^{1,2}, Sara Montagnese⁵, Bruce Brew⁶, Gilles Guillemin³, Mark Danta^{1,2}, Benjamin Heng³. ¹St Vincent's Clinical School, Faculty of Medicine, Australia, ²St Vincent's Hospital, Gastroenterology, Australia, ³Macquarie University, Macquarie Medicine School, Australia, ⁴St Vincent's Hospital, Medical Imaging, Australia, ⁵University of Padua, Medicine, Italy, ⁶St Vincent's Hospital, Neurology and Immunology, Australia
Email: georgiazeng@icloud.com

Background and aims: Hepatic encephalopathy (HE) is a neuropsychiatric complication of liver disease, characterised by elevated systemic concentrations of ammonia and pro-inflammatory cytokines. These neurotoxins can cross the blood brain barrier and act synergistically to cause neuroinflammation, which can activate the kynurenine pathway (KP). This results in depletion of local tryptophan (TRP) reserves and the production of neuroactive KP metabolites. Specifically, 3-hydroxykynurenine (3-HK) and

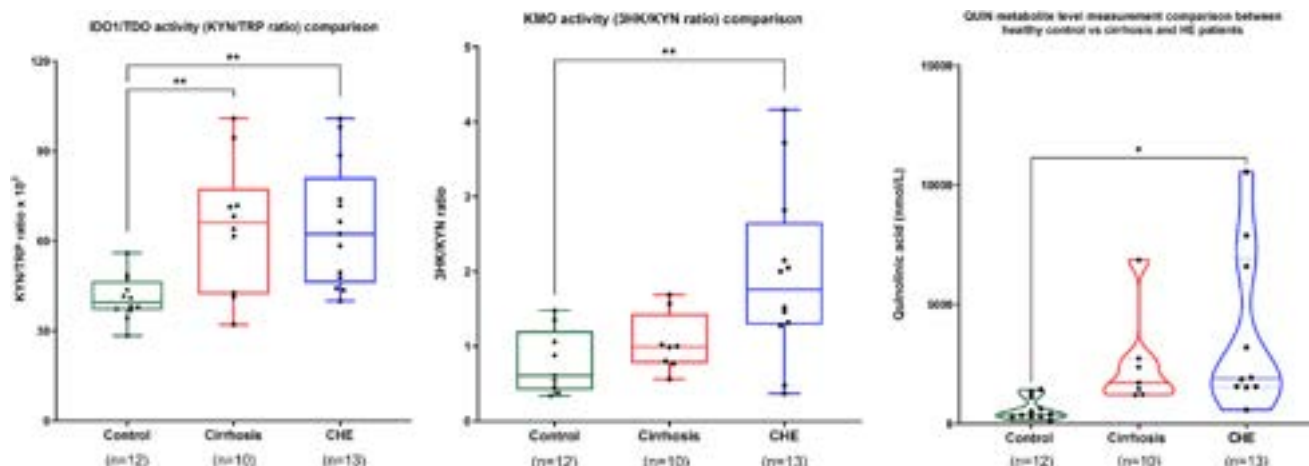


Figure: (abstract: WED-364): Comparison of KP metabolites between CHE patients, non-encephalopathic cirrhosis patients and healthy controls.

quinolinic acid (QUIN) cause astrocyte and neuronal death, while kynurenic acid (KYNA) is a NMDA receptor antagonist with neuroprotective effects. The aim of our study was to compare systemic KP activity between patients with covert HE (CHE), non-encephalopathic cirrhosis patients (NHE) and healthy controls.

Method: This was a single-centre prospective cohort study conducted between 2018–2021 at St Vincent's Hospital in Sydney. Overall, there were 13 CHE patients, 10 NHE patients and 12 healthy controls. Patients with cirrhosis were diagnosed with CHE if they scored ≤ -4 on the validated Psychometric Hepatic Encephalopathy Score. Plasma samples were obtained to determine the expression levels of KP enzymes, calculated by a ratio of metabolite product divided by its substrate. TRP, alongside upstream KP metabolites such as kynurenine (KYN), anthranilic acid (AA), KYNA, 3-HK and 3-hydroxyanthranilic acid (3-HAA) were quantified using high-performance liquid chromatography (HPLC) and ultra-HPLC. Downstream KP metabolites, QUIN and picolinic acid (PIC) were quantified using gas-chromatography/mass spectrometry.

Results: KP was highly activated in cirrhosis patients, especially those with CHE, in comparison to healthy controls, as demonstrated by higher KYN/TRP ratios representing elevation of the rate-limiting enzymes, indoleamine-2,3-dioxygenase (IDO-1) and tryptophan-2,3-dioxygenase (TDO). Following catabolism of TRP to KYN, the subsequent kynurenine 3-monooxygenase (KMO) enzyme demonstrated elevation in CHE patients only, skewing the pathway towards production of 3-HK. Levels of KYNA were higher in CHE patients compared to NHE patients and healthy controls. The activation of downstream KP pathways was evident through the higher production of QUIN and PIC metabolites at the final node of the pathway in cirrhosis patients, especially those with CHE.

Conclusion: The activation of KP in patients with cirrhosis results in the dysregulated production of neurotoxic metabolites. The higher levels in the CHE cohort suggest this is potentially contributing to neurodegeneration and clinical course. Dysregulation of the KP pathway appears to already be underway in cirrhosis patients who do not yet show any clinical signs of neurocognitive impairment. Therapeutic agents that modulate KP activity may be able to alleviate symptoms of patients with CHE.

WED-365

A virtual reality-driving test to predict car accidents in patients with cirrhosis

Simon Johannes Gairing^{1,2}, Eva Maria Schleicher^{1,2}, Leonard Kaps^{1,2}, Sophia Schulte-Beerbuehl^{1,2}, Kristina Steiner^{1,2}, Joachim Labenz³, Jörn Schattenberg^{4,5}, Peter Galle^{1,2}, Marcus-Alexander Wörns^{1,2,6}, Christian Labenz^{1,2}. ¹Department of Internal Medicine I, University

Medical Center of the Johannes Gutenberg-University, Mainz, Germany, ²Cirrhosis Center Mainz (CCM), University Medical Center of the Johannes Gutenberg-University, Mainz, Germany, ³Department of Medicine, Diakonie Hospital Jung-Stilling, Siegen, Germany, ⁴University Medical Center of the Johannes Gutenberg-University, Department of Internal Medicine I, Mainz, Germany, ⁵University Medical Center of the Johannes Gutenberg-University, Metabolic Liver Research Program, I. Department of Medicine, Mainz, Germany, ⁶Department of Gastroenterology, Hematology, Oncology and Endocrinology, Klinikum Dortmund, Germany, Germany
Email: sgairing@uni-mainz.de

Background and aims: Patients with cirrhosis and especially those with hepatic encephalopathy (HE) may have impaired driving skills and may be prone to car accidents. Currently, no sufficient tool is available to predict car accidents in these patients. This study aimed to evaluate the usefulness of a virtual reality-based application as a point-of-care tool to predict car accidents.

Method: A driving test using a virtual reality head-mounted-display (HTC Vive Pro eye) was developed to simulate five hazardous situations (e.g., a cyclist suddenly rides on the road). In this test, the car drives automatically on a straight street and events are triggered when an invisible hit box is passed. The patient has to react when he/she has recognized the hazardous situation. The time from triggering the event to pressing the handbrake is recorded as reaction time. Total reaction time (TRT) is defined as the combined reaction time to all five events. Car accidents were assessed retrospectively (previous 12 months) by interview at the day of enrollment. Minimal HE (MHE) was diagnosed using PHES. Patients were recruited in the outpatient clinic.

Results: In total, 112 patients with cirrhosis and 52 controls without cirrhosis were prospectively enrolled. Patients with cirrhosis were in median 61 years and median MELD was 10 (Child-Pugh A/B/C: 74/24/2%). MHE was detected in 14% (n=15). Regarding safety, no participant had to abort the test; mild forms of motion sickness were present in 16% (n=27). Patients with cirrhosis showed a worse median TRT compared to controls without cirrhosis (5.15 vs. 4.56 sec, $p < 0.001$). In patients with MHE, median TRT was significantly longer compared to patients without MHE (5.67 vs. 5.02 sec, $p = 0.01$). Seven patients reported a history of car accidents during the twelve months prior to study inclusion. Median TRT tended to be higher in patients with reported car accidents ($p = 0.099$). When patients who stopped driving for HE-related reasons or insecurity (n=14) were added to the group of patients with accidents (modelled end point), then a longer TRT was significantly associated with the modelled end point in univariable ($p < 0.001$) and multivariable analysis (OR 2.83, $p < 0.001$) after adjusting for age, MELD and PHES.

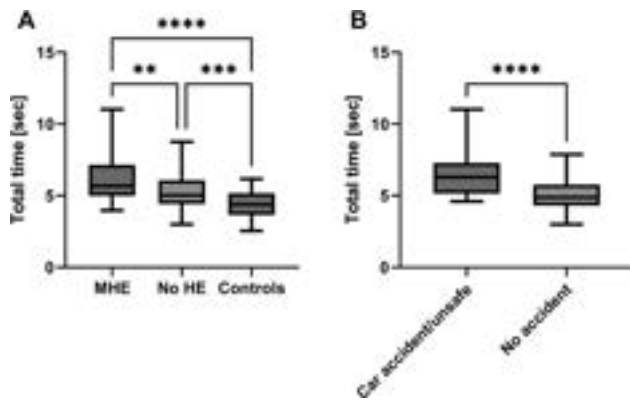


Figure: (A) TRT of patients with cirrhosis and MHE vs. without MHE vs. controls. (B) TRT of patients with the modelled end point (car accidents including patients not driving due to HE-related reasons or insecurity) vs. patients without car accidents. ** $p < 0.01$, *** $p < 0.001$, **** $p < 0.0001$.

Conclusion: Virtual reality may be helpful as a point-of-care tool for assessing the risk of future car accidents in patients with cirrhosis.

WED-366

The association between angiotensin converting enzyme inhibitor or angiotensin receptor blocker exposure and key cirrhosis-related outcomes

Roy Wang¹, Marina Serper², Tamar H Taddei³, David Kaplan², Nadim Mahmud². ¹Hospital of the University of Pennsylvania,

Philadelphia, United States, ²Hospital of the University of Pennsylvania, Hepatology, Philadelphia, United States, ³Yale University, Digestive Diseases, New Haven, United States
Email: royxwang88@gmail.com

Background and aims: Current guidelines caution against use of angiotensin converting enzyme inhibitors (ACEi) and angiotensin receptor blockers (ARB) in patients with decompensated cirrhosis. However, recent literature suggests ACEi/ARB may reduce fibrosis and mortality in patients with chronic liver disease or compensated cirrhosis. We explored the real-world association between ACEi/ARB and cirrhosis-related outcomes in a Veterans Affairs cohort.

Method: We performed a retrospective cohort study using an active comparator new user design of patients with cirrhosis newly initiated on ACEi/ARB or calcium channel blockers (CCB, comparator). Kaplan-Meier analysis was used to evaluate unadjusted associations with outcomes of mortality and—in a compensated cirrhosis subgroup—cirrhosis decompensation and hepatocellular carcinoma (HCC). Inverse probability treatment weighting (IPTW) was used to balance key confounders in Cox regression analysis. For the mortality outcome, subgroup analyses explored the impact of baseline Child-Turcotte-Pugh (CTP) class, diabetes, heart failure, and chronic kidney disease (CKD) stage on the primary association. Finally, cause-specific competing risk models were created to evaluate liver-related versus non-liver-related mortality.

Results: The cohort included 1,208 ACEi/ARB and 376 CCB new initiators. ACEi/ARB users were more likely to have higher body mass index (median 29.2 vs. 27.6, $p < 0.001$), non-alcoholic fatty liver disease (28.5% vs. 19.9%, $p = 0.03$), and metabolic comorbidities. In

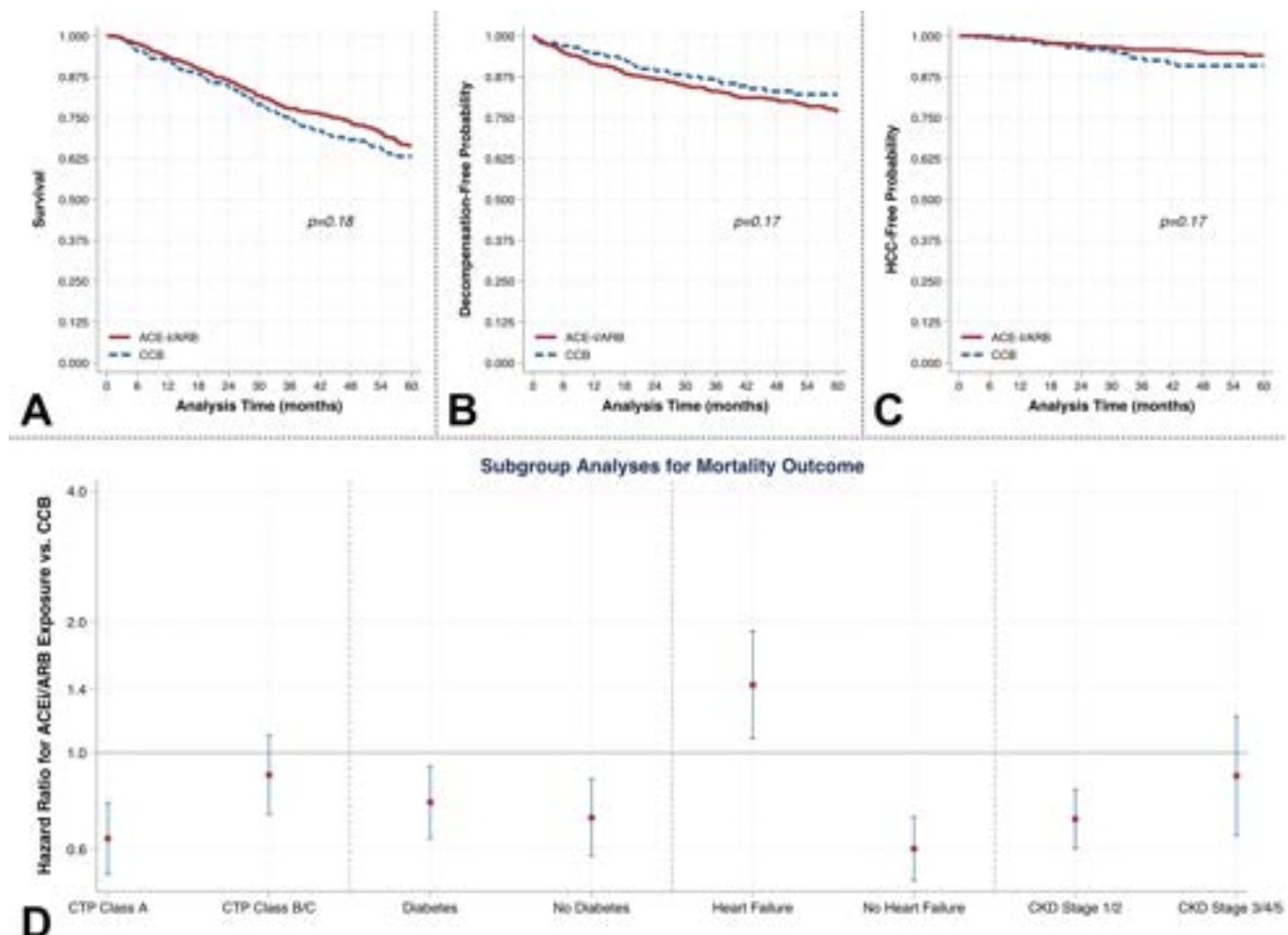


Figure: (abstract: WED-366).

POSTER PRESENTATIONS

unadjusted Kaplan-Meier analysis, ACEi/ARB exposure was not associated with reduction in mortality, cirrhosis decompensation, or incident HCC (each $p > 0.05$; Figure A/B/C). In IPTW Cox regression, ACEi/ARB exposure was associated with lower mortality (hazard ratio [HR] 0.74, 95% confidence interval [CI] 0.65–0.85, $p < 0.001$), increased hazard of cirrhosis decompensation (HR 1.29, 95% CI 1.01–1.65, $p = 0.04$), and no association with HCC (HR 0.88, 95% CI 0.57–1.37, $p = 0.58$). In subgroup analyses, the possible mortality benefit with ACEi/ARB exposure was isolated to patients with CTP class A, early-stage CKD, and an absence of heart failure (Figure D). In cause-specific competing risk models, ACEi/ARB exposure was associated with reduction in non-liver-related mortality (cause-specific hazard ratio [csHR] 0.58, 95% CI 0.47–0.71, $p < 0.001$) but not with liver-related mortality (csHR 0.90, 95% CI 0.75–1.09, $p = 0.29$).

Conclusion: ACEi/ARB exposure was associated with reduced mortality in patients with cirrhosis; however, this effect may be limited to CTP class A patients and those with early-stage CKD and no heart failure. Furthermore, this effect appears to be mediated through mitigation of non-liver-related mortality. Future research is needed to identify cirrhosis patient subgroups for whom the benefits of ACEi/ARB exposure exceed the risks.

WED-367

Liver nutrition clinic improves nutritional outcomes in patients with advanced cirrhosis

Kylie Matthews-Rensch¹, Elise Treleaven¹, Sharon Forbes¹, Dwayne Garcia¹, Joanne Mina², Olivia Cullen², Melanie Halford², Lucinda Vaux², Richard Skoien², Barbara Leggett², Enoka Gonsalkorala². ¹Royal Brisbane and Women's Hospital, Dietetics and Food Services, Herston, Australia, ²Royal Brisbane and Women's Hospital, Gastroenterology and Hepatology, Herston, Australia
Email: enokag@yahoo.com

Background and aims: Malnutrition and sarcopenia are recognised complications of cirrhosis and are associated with adverse patient outcomes. Current guidelines recommend nutrition assessments for all patients with advanced liver disease. The hepatology service at Royal Brisbane and Women's Hospital (RBWH) service a large catchment area spread over 170,000 km² in Queensland, Australia. The Liver Nutrition Clinic (LiNC) was developed to address nutrition requirements of patients with cirrhosis complications attending outpatient or inpatient hepatology services at RBWH. Here we describe the baseline characteristics and longitudinal nutritional outcomes of patients attending this specialist clinic.

Method: All patients attending LiNC were prospectively entered into a secure database and clinical, including nutritional and frailty, data were collected as part of routine clinical care. Descriptive statistics were used to describe demographics and interpret outcomes for patients attending LiNC between April 2021 to January 2023.

Results: Eighty-four patients (67% male, $n = 56$), median age 59 years (range 22–78 years) were included in this analysis. Indication (s) for referral were ascites (55%, $n = 46$), clinically significant weight loss (38%, $n = 32$), peripheral oedema (24%, $n = 20$), hepatic encephalopathy (14%, $n = 12$), and/or planned for liver transplant (12%, $n = 10$). About half (55%, $n = 46$) had more than one indication for referral. Chronic liver disease aetiology was alcohol (65%, $n = 55$), metabolic associated fatty liver disease (26%, $n = 22$), viral hepatitis (24%, $n = 20$) and other (12%, $n = 10$). Twenty-one patients had more than one aetiology (25%). Fifty-eight percent ($n = 49$) had ascites and 27% ($n = 23$) had peripheral oedema at baseline. Median values (range) for serology results were albumin 30 g/L (15–55), bilirubin 32 μ mol/L (3–422), and international normalized ratio 1.3 (0.4–4.8). The median MELD score was 12 (range 6–33). Liver frailty index (LFI) was available for 41 participants (49%) at baseline with 17% ($n = 7$) robust, 76% ($n = 31$) pre-frail and 7% ($n = 3$) considered frail. Baseline LFI was not available for 43 patients due to attendance via virtual appointment ($n = 21$), inadequate time or administrative issues ($n = 13$) or being too unwell or unsafe to complete the assessments ($n = 7$). Only 29% ($n =$

24) of patients were assessed as having adequate nutritional intake and 51% ($n = 43$) were well-nourished (per Subjective Global Assessment) at baseline, and this improved at 3- and 6-month follow-up per figure 1.

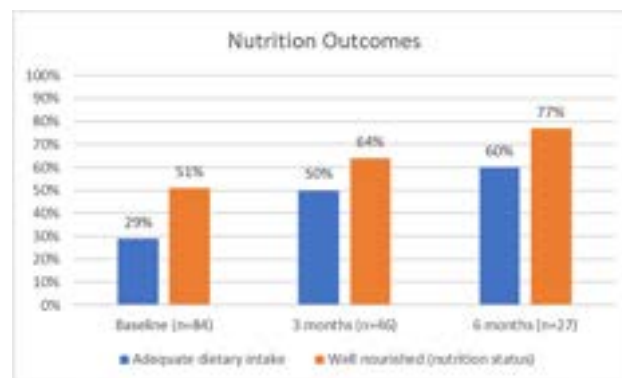


Figure: Nutrition Outcomes

Conclusion: Poor nutritional status (malnutrition) was a common finding in our cohort. Geographic spread and pandemic restrictions affected the ability to complete frailty assessment. This dedicated dietetic service for patients with cirrhosis complications improved dietary intake and nutritional status.

WED-368

Impact of allelic HLA divergence on the risk of bacterial infections in cirrhotic patients awaiting liver transplantation

Clementine Roger¹, Alessandra Mazzola², Romain Lhotte³, Maxime Mallet², Dominique Thabut², Jean Luc Taupin³, Filomena Conti². ¹Hôpital Paul-Brousse Ap-Hp, Villejuif, France, ²University Hospitals Pitié Salpêtrière-Charles Foix, Paris, France, ³Saint-Louis Hospital, Paris, France
Email: clementine9roger@gmail.com

Background and aims: Bacterial infections are frequent in cirrhotic patients and are associated with an increased risk of cirrhosis decompensation and death. The underlying immunologic mechanisms are not well known and the effect of allelic HLA divergence (AHLAD) on the risk of bacterial infections in humans has never been studied. However, higher AHLAD could bestow greater immunocompetence.

Method: We conducted an observational, retrospective, monocentric study. Cirrhotic patients awaiting liver transplantation (LT) in our center from 01/2019 to 02/2022 were included. The primary aim was to assess the impact of class I and class II AHLAD on the risk of bacterial infections. The secondary aim was the evaluation of the impact of AHLAD on the risk of cirrhosis complications.

Results: 269 cirrhotic patients listed for LT were included. The mean age was 56 years old (± 11) and the median MELD score was 14 (IQR 9–19). Overall, 153 bacterial infections were diagnosed in 98 patients. The cumulated incidence of bacterial infections was 36.4%. After multivariate analysis, a greater class II AHLAD was associated with reduced bacterial infections (beta coefficient -0.0057 ; IC 95% -0.011 ; -0.0001 ; $p = 0.034$) while there was no effect of class I AHLAD (beta coefficient 0.0126; $p = 0.074$). Independent risk factors of bacterial infections (multivariate analysis) included the realization of invasive procedures (beta coefficient 0.1426; $p < 0.001$), hospitalization in an intensive care unit (beta coefficient 0.5141; $p < 0.001$), antibiotic therapy within three months preceding the listing (beta coefficient 0.2014; $p = 0.046$), rifaximin intake (beta coefficient 0.2066; $p = 0.043$) and the occurrence of cirrhosis complications (beta coefficient 0.3266; $p = 0.002$). There was no effect of class I or II AHLAD on the risk of cirrhosis complications (OR 0.97; $p = 0.14$ and OR 1; $p = 0.63$ respectively).

Conclusion: This is the first time that the effect of AHLAD on the risk of bacterial infections was studied in humans. High class II AHLAD appears to be a protective factor from the risk of bacterial infections in cirrhotic patients awaiting LT. There was no impact of AHLAD on the risk of cirrhosis complications. Class II AHLAD could thus be considered as one of the immunological mechanisms underlying the risk of bacterial infections in this population.

WED-369

The impact of a massive transfusion protocol on the outcomes of patients with acute variceal bleeding: propensity score-matched analysis

Aryoung Kim¹, Byeong Geun Song¹, Myungji Goh¹, Dong Hyun Sinn¹, Wonseok Kang¹, Geum-Yon Gwak¹, Yong-Han Paik¹, Moon Seok Choi¹, Joon Hyeok Lee¹. ¹Department of Medicine, Samsung Medical Center, Sungkyunkwan University School of Medicine, Korea, Rep. of South
Email: dh.sinn@samsung.com

Background and aims: A goal-directed massive transfusion protocol (MTP) improved mortality and morbidity in trauma patients with hemorrhagic shock. However, whether MTP can improve outcomes for acute variceal bleeding is not known.

Method: A retrospective cohort of 218 consecutive patients with acute variceal bleeding who visited the emergency room between July 2014 and June 2022 were analyzed. Of those, 19 patients received MTP (8.7%). The 42-days mortality rate and treatment failures (death within 5 days, a 3 g/dL drop in hemoglobin within any 24 hours, and failure of endoscopic hemostasis within the first 24 hours) were compared by MTP use in overall cohort, subgroup stratified by systolic blood pressure (SBP) and the Model for End-Stage Liver Disease (MELD) score, and in 1:4 propensity score matched cohort. Matching variables were age, gender, initial SBP and the MELD score.

Results: In overall cohort, the 42-days mortality rate (42.1% vs 1.5%, $p < 0.001$), death within 5 days (26.3% vs 0%, $p < 0.001$), 3 g/dL hemoglobin drop within any 24 hours (21.1% vs 0.5%, $p < 0.001$), and failure of endoscopic hemostasis within the first 24 hours (15.8% vs 0%, $p < 0.001$) were higher in MTP group. MTP was associated with increased risk of mortality at 42-days (adjusted hazard ratio: 21.2, 95% confidence interval: 3.0–148.4). When stratified by initial SBP, the 42-days mortality rate was higher in MTP group in patients with SBP < 100 mmHg (46.2% vs 3.7%, $p < 0.001$), and in patients with SBP ≥ 100 mmHg (33.3% vs 0.7%, $p < 0.001$). When stratified by MELD score, the 42-days mortality rate was higher in MTP group in patients with MELD score ≥ 13 (47.1% vs 3.5%, $p < 0.001$). In 1:4 propensity matched cohort ($n = 56$; MTP = 14), the 42-days mortality rate was also higher in MTP group (42.9% vs 2.4%, $p < 0.001$).

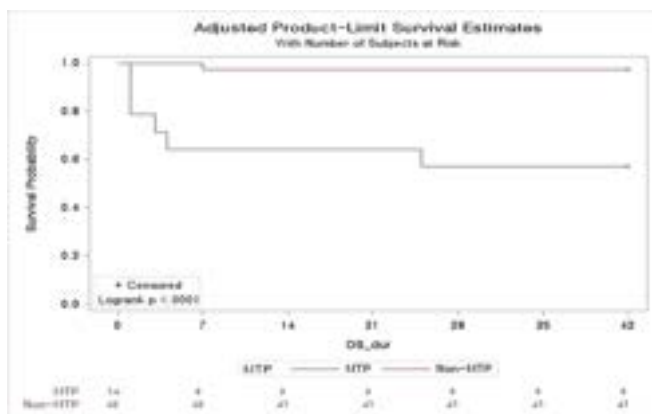


Figure: Kaplan-Meier curves of cumulative probability of 42-days mortality in patients receiving MTP compared to those who did not. (In the matched population)

Conclusion: In patients with acute variceal bleeding, goal-directed MTP was associated with poorer clinical outcomes, including

mortality and treatment failure rates. MTP use may not improve, or may even worsen, clinical outcomes in patients with acute variceal bleeding.

WED-370

Acute kidney injury related to metamizole in advanced chronic liver disease patients undergoing major orthopedic surgery

Lidia Canillas^{1,2,3}, Amalia Pelegrina^{2,3,4}, Elena Colominas⁵, Aina Salis³, César Jessé Enríquez-Rodríguez^{2,3}, Antonia Caro¹, Marc Puigvehí^{1,2}, Teresa Broquetas^{1,2}, Susana Coll^{1,2}, NURIA Cañete^{1,2}, Montserrat García-Retortillo^{1,2}, Xavier Bessa^{1,2,3}, Juan Carlos Álvarez⁶, Jose A. Carrión^{1,2,3}. ¹Hepatology section, Gastroenterology Department, Hospital del Mar, Barcelona, Spain, ²IMIM (Institut Hospital del Mar d'Investigacions Mèdiques), Barcelona, Spain, ³Departament de Medicina i Ciències de la Vida, Universitat Pompeu Fabra, Spain, ⁴General Surgery and Digestive Department Hospital del Mar, Barcelona, Spain, ⁵Pharmacy Department, Hospital del Mar, Barcelona, Spain, ⁶Anesthesiology Department, Hospital del Mar, Barcelona, Spain
Email: lidia.canillas.alaves@gmail.com

Background and aims: The use of metamizole and non-steroidal anti-inflammatory drugs (NSAIDs) is common after major orthopedic surgery, but they can lead to acute kidney injury (AKI) in patients with advanced chronic liver disease (ACLD).

Our objectives were to evaluate 1) the prevalence of patients treated with metamizole/NSAIDs and 2) the association with the development of complications (AKI or infections) during hospitalization.

Method: Retrospective, single-center study in patients with ACLD who underwent major orthopedic surgery (large joints and amputations) between 2010 and 2019. We recorded data about ACLD, comorbidities, analgesia, infection and type, development of AKI, hospital stay, and mortality. We defined severe infection if it required ICU admission, and multidrug-resistant microorganism (MDRM) if it presented resistance to ≥ 2 groups of antibiotics. Differences were compared with Chi-square or U-Mann Whitney tests, and the multivariate analysis was performed using binary logistic regression. Survival curves were contrasted with the Mantel-Cox test.

Results: Of 123 patients with ACLD who underwent major orthopedic surgery, 13 (11%) were excluded due to missing data. The median age (IQR) was 73 (62–82) years, 55% (61/110) were women, and 59 (75%) Child-Pugh A. The ACLD etiology was viral in 52 (47%) and alcohol in 40 (36%) patients. The hospital stay was 11 (5–18) days. Metamizole and/or NSAIDs were administered in 84 (76.4%) patients: 62 (56.4%) metamizole and 39 (35.5%) NSAIDs. Infection was observed in 43 (35%) patients: urinary tract (25/122; 21%), skin/prosthesis (16/122; 13%), and respiratory (14/122; 12%). Severe and MDRM infections were present in 12% (5/43) and 35% (15/43), respectively. Patients who developed infection were older (79 vs. 68 years; $p < 0.01$) and predominantly women (70% vs. 50%; $p = 0.04$). During admission, AKI was found in 25 (23%) patients: 20 (80%) AKI-I, 4 (16%) AKI-II, and 1 (4%) AKI-III. AKI was not associated with hypertension, diabetes, chronic kidney disease, Child-Pugh, or portal hypertension ($p = ns$). Patients with AKI were older (83 vs. 70 years; $p < 0.01$), had lower albumin values (3.6 vs. 4.1 g/dL; $p = 0.03$), higher prevalence of infection (60% vs. 31%; $p < 0.01$) and higher metamizole administration (88% vs. 42%; $p < 0.01$). In the multivariate analysis, the presence of AKI was related to age > 75 years [aOR 5.6 (1.7–17.9) $p < 0.01$] and metamizole [aOR 7.0 (1.8–27.2) $p < 0.01$]. Postoperative mortality at 30 days was higher in patients with AKI (20% vs. 6%, Log-Rank = 0.03).

Conclusion: In our cohort of patients with ACLD, the use of metamizole after major orthopedic surgery was very frequent and

POSTER PRESENTATIONS

was associated with the development of acute renal failure during admission. These data suggest the need to optimize perioperative management of patients with ACLD.

WED-371

Racial disparities in COVID-19 clinical outcomes among patients with cirrhosis in North America and Europe-an international registry study

Umar Hayat¹, Saba Afroz², Faisal Kamal³, Muhammad Haseeb⁴, Faisal Inayat⁵, Muhammad Kamal⁶, Andrew Moon⁷. ¹Geisinger Health, Internal medicine, division of gastroenterology, Wilkes-Barre, United States, ²Geisinger Health, Internal medicine, Wilkes-Barre, United States, ³Thomas Jefferson University hospital, Internal medicine, division of gastroenterology, Philadelphia, United States, ⁴Beth Israel Deaconess medical center, Internal medicine, Boston, United States, ⁵Jinnah hospital Lahore, Internal medicine, Lahore, Pakistan, ⁶Essen Health Care, Internal medicine, New York, United States, ⁷University of North Carolina, Division of Gastroenterology and Hepatology, Chapel Hill, United States Email: umarhayat216@gmail.com

Background and aims: Patients with decompensated cirrhosis have a higher risk of hospitalization, ICU admission, and death from COVID-19. The degree to which these outcomes vary with race and ethnicity is unclear.

Method: We used the SECURE-Liver and COVID-Hep international databases to explore disparities in COVID-19 outcomes among patients with cirrhosis. Patients were stratified by continent (North America and Europe). We defined race/ethnicity as white/non-Hispanic, black/non-Hispanic, and Hispanic for patients from North America. Given the low proportion of black patients in our European cohort, we defined race/ethnicity as white/non-Hispanic and non-white/non-Hispanic for Europe. Bivariate and multivariable logistic regression analyses were performed to determine the association between race/ethnicity and hospitalization, ICU admission, and death. Variables in the multivariable model included age, sex, CTP class, and comorbidity index (CI) (sum of obesity, hypertension, DM, CKD).

Results: Our cohort included 718 patients with cirrhosis and COVID-19 from North America (n = 290) and Europe (n = 428). In the North American subgroup, 51% of patients were white/non-Hispanic, 32% were black/non-Hispanic, and 17% were Hispanic. Black patients had a higher prevalence of comorbidities than white patients (CI 1.86 vs. 1.83, p = 0.007). Compared to white patients, a higher proportion of black patients were hospitalized (77% vs. 85%, p = 0.01), admitted to the ICU (27% vs. 40%, p = 0.05), and died (18% vs. 28%, p = 0.07) (Figure 1). Hispanic patients had the lowest proportions of clinical outcomes in all three groups. In the multivariable analysis, there were no statistically significant differences in the odds of clinical outcomes between white, black, and Hispanic patients. In the European cohort, 82% of patients were white/non-Hispanic, and 17% were non-white/non-Hispanic. White patients had a higher prevalence of comorbidities than non-white patients (CI; 1.63 vs. 1.31, p = 0.02). However, compared to white patients, a higher proportion of non-white patients were hospitalized (82% vs. 67%, p = 0.01) and admitted to the ICU (15% vs. 18%, p = 0.04), but fewer patients died (28% vs. 34%, p = 0.01) (Figure 1). In multivariable analyses, there were no statistically significant differences in the odds of clinical outcomes between the two groups.

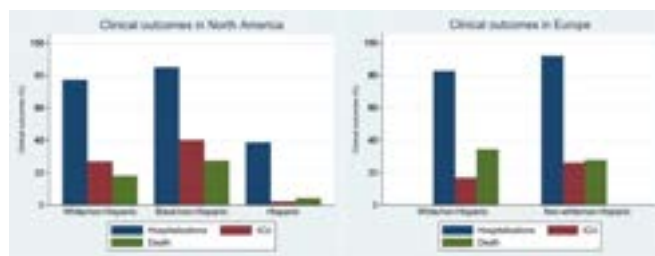


Figure: Clinical outcomes by race/ethnicity in North America and Europe

Conclusion: In conclusion, black patients in North America had a higher risk of hospitalization, ICU admission, and death than white patients. Similar findings were shown in the Europe subgroup; however, white patients had a higher risk of death than non-whites. There were no statistically significant differences for any outcomes after adjusting for potential confounders. The increased likelihood of poor outcomes in non-white patients, particularly in North America, may be driven by non-liver-related comorbidities.

WED-372

Effectiveness and safety of anticoagulant treatment in patients with liver cirrhosis and non-tumoral splenic-portal thrombosis

Nelson Daniel Salazar Parada¹, Elena Gómez Domínguez¹, Sara Pastor Royo¹, Nuria Del Val Huerta¹, Ana Martín Algibez¹, María Luisa Manzano Alonso¹, Maria Amo¹, Berta De las Heras¹, Inmaculada Fernández Vázquez¹. ¹Hospital Universitario 12 de Octubre, Gastroenterology and hepatology, Madrid, Spain Email: nnsdpdaniel@hotmail.com

Background and aims: Splenoportal axis thrombosis is a relatively common complication of liver cirrhosis, which can lead to liver function worsening, as well as morbidity and mortality increase after liver transplantation. Furthermore, if thrombosis is extensive, patients might not be able to receive a liver transplant. Although its treatment with anticoagulation is well established, its approaches are heterogeneous and there is not enough evidence about its effectiveness and safety in these patients.

The goal of the current study was to evaluate the effectiveness and safety of anticoagulant treatment in cirrhotic patients with non-tumoral thrombosis of the splenoportal axis in clinical practice.

Method: We retrospectively included all patients with liver cirrhosis and non-tumoral splenic-portal thrombosis who received anticoagulant treatment during 2017 to 2022 in our center. Six months into the treatment, the patient's response was assessed by partial or complete thrombosis recanalization on imaging tests (US/CT/MRI).

Results: A total of 91 cases were enrolled (64.84% male; median age: 60 ± 13.5 years). At the moment of thrombosis patients were in Child-Pugh classes A: 59.3% (n = 54); B: 28.5% (n = 26) and C: 12% (n = 11). Etiologies of cirrhosis included: alcohol-related liver disease 37.3% (n = 24), followed by chronic HCV infection 28.5% (n = 26), indeterminate 10.9% (n = 10) and MAFLD 5.49% (n = 5). Most common sites of thrombosis were the portal vein 53.8% (n = 49), followed by portal branches 15.3% (n = 14), and 7.6% (n = 11) in both territories. Most frequent type of anticoagulant treatment was low molecular weight heparin (78.2% patients), followed by 22.8% patients who received vitamin K antagonists. Global thrombosis recanalization was achieved in 55% patients (n = 50), being complete in 68% (n = 34) and partial in 32% (n = 16). Univariate and multivariate analysis did not show statistically significant association between response to treatment and baseline patient variables such as etiology, Child-Pugh class, MELD score, or thrombosis extent. During follow-up (42 ± 18.2 months), 13.1% patients (n = 12) died due to non-hemorrhagic complications of their liver disease; 8.7% (n = 8) presented

esophageal variceal bleeding, 0.9% (n = 1) presented bleeding due to portal hypertension gastropathy and 3.2% patients (n = 3) presented minor bleeding in other locations. No patient died due to hemorrhagic complications.

Conclusion: In our study, patients with liver cirrhosis and non-tumor splenic-portal thrombosis responded to anticoagulant treatment effectively. This treatment has achieved global thrombosis recanalization in more than half of cases, with an acceptable safety profile. Finally, in our analysis, we do not find some predictive factors of response to anticoagulation therapy.

WED-373

Normalisation of the psychometric hepatic encephalopathy score in a Nigerian population

Mansur Mohammed¹, Musa Muhammed Borodo², Shettima Kagu Mustapha³, ¹University Hospitals of Leicester NHS Trust, Leicester, United Kingdom, ²Aminu Kano Teaching Hospital, Medicine, Kano, Nigeria, ³Ahmadu Bello University Teaching Hospital, Medicine, Zaria, Nigeria

Email: mansurfm@gmail.com

Background and aims: Minimal hepatic encephalopathy (MHE) is part of the spectrum of hepatic encephalopathy (HE) with subtle cognitive and motor deficits, often not detected by routine clinical examination. The psychometric hepatic encephalopathy score (PHES) has been recommended as gold standard for the diagnosis of MHE, to allow for early diagnosis and treatment, and prevent progression to overt HE. Normalisation studies have been carried out in different countries to determine local norms and cut off values for diagnosis. This study aimed to construct normograms for the PHES test in the Nigerian population, calculate the cut off value for diagnosing MHE, and determine the prevalence of MHE among patients with liver cirrhosis.

Method: Two hundred apparently healthy subjects and 85 patients with liver cirrhosis but without overt hepatic encephalopathy were recruited. They all undertook the PHES test which include Number Connection Test-A (NCT-A), Number Connection Test-B (NCT-B), Digit Symbol Test (DST), Serial Dotting Test (SDT) and Line Tracing Test (LTT). The time taken for each subtest was converted to scores and summed up to give the final score of PHES. The cut off for abnormal PHES score was determined using results from the healthy subjects. Normal range of scores was taken as within mean \pm 2 SD. Abnormal PHES was set at PHES score less than -2 SD from the mean. Pearson's correlation coefficient was used to identify variables that confounded the PHES scores. These were then entered into multiple linear regression to construct formulas to remove the effect of these confounders and predict the PHES scores in the cirrhotic group. Using these formulas, PHES score was calculated in the cirrhotic patients and prevalence of MHE was determined. Chi square test was used to test for association between MHE and categorical variables and student t test for quantitative variables. Statistically significant variables ($p < 0.05$) were entered into logistic regression to identify independent predictors of MHE.

Results: The mean age of the cirrhotic patients was 40.5 ± 11.8 , with male to female ratio of 2.4. These were not significantly different from those of the controls. Age and education years were found to affect the PHES score ($p < 0.05$) while sex did not. The mean PHES in the cirrhotic group was -6 ± 3.7 (range -12 to 3). The cut off for diagnosis of MHE was calculated as < -5 . Hepatitis B was the predominant cause of liver cirrhosis (69.4%) while majority of the patients (62.4%) had decompensated cirrhosis (Child Pugh class B and C). Prevalence of MHE was 51.8%. Prothrombin time, albumin and Child Pugh class were significantly associated with MHE, while Child Pugh class and prothrombin time were independent predictors (O.R 9.3 and 19.5 respectively).

Table 1: Formulas for Predicting the PHES Score

PHES Test	Equation	SD
NCT-A	$42.37 + (0.565 \times \text{Age}) - (1.454 \times \text{Education Years})$	6.400
NCT-B	$100 + (0.677 \times \text{Age}) - (2.212 \times \text{Education Years})$	10.635
DST	$35 - (0.187 \times \text{Age}) + (0.457 \times \text{Education Years})$	3.156
SDT	$100 + (0.716 \times \text{Age}) - (1.162 \times \text{Education Years})$	9.610
LTT	$187 + (1.023 \times \text{Age}) - (1.918 \times \text{Education Years})$	19.932

Conclusion: This study constructed the Nigerian PHES normograms and determined a local cut-off value for MHE in Nigeria. It identified a high prevalence of MHE, underscoring the need for routine screening in patients with liver cirrhosis. Development of easily accessible online calculators using these normograms will aid easy and accurate diagnosis of MHE in clinical settings.

WED-374

Nutritional status of patients with advanced chronic liver disease: descriptive baseline of a prospective study

Estela Soria López¹, Laura Rey Fernández², Jorge Alberto Costa Fernandez³, Francisco Rivas Ruiz⁴, Jose Miguel Rosales Zabal¹, ¹Hospital Costa del Sol, Gastroenterology and Hepatology, Marbella (Málaga), Spain, ²Hospital Costa del Sol, Hospital Pharmacy and Nutrition Unit, Spain, ³Hospital Costa del Sol, Radiology Unit, Spain, ⁴Hospital Costa del Sol, Investigation Unit, Spain

Email: estelasoria89@gmail.com

Background and aims: Malnutrition in patients with advanced chronic liver disease is a prognostic factor, however, often forgotten in clinical practice. We analyzed the nutritional status of a prospective cohort in our healthcare area.

Method: Baseline descriptive analysis of a prospective study to assess nutritional status and evolution after starting oral supplementation. We included patients from day hospital (ascites unit) and hepatology consultation, identified as at risk or malnourished, with prior informed consent. After nutritional screening with Subjective Global Assessment (SGA), Malnutrition Universal Screening Tool (MUST) and Royal Free Hospital-Nutritional Prioritizing Tool (RFH-NPT), we performed anthropometry, dynamometry (hand pressure strength), blood tests, critical flicker frequency test (CFF), SF-36 health questionnaire and determination of the musculoskeletal index by measuring muscle mass at the L3 level by CT scan.

Results: 37 patients, 81% male. Median time in cirrhosis 2 years. Place of nutritional assessment: 27 day hospital, 9 nutrition consultation, 1 inpatient. Etiology: 1 HBV and 36 alcohol (6 mixed: 4 viral, 1 metabolic, 1 lymphoma). Portal hypertension data: 67.6% portal dilatation, 62.2% splenomegaly, 70% varicose veins. Decompensations: 89% ascites, 24% encephalopathy, 5.4% variceal upper gastrointestinal haemorrhage, 16% spontaneous bacterial peritonitis, 8% hepatorenal syndrome. Functional status: Child-Pugh (9A, 20B, 6C, 2 not listed for anticoagulation), median MELD 13, median MELD-Na 17.

ANALYTIC (medians)					
Lymphocytes	1641.138	Sodium 131mEq/L	Selenium 54mcg/L	Vitamin D 11.8ng/L	
Hemoglobin 10.5g/L	Creatinine 0.88mg/L	Potassium 4.4Eq/L	Magnesium 1.77mg/L	Albumin 3.9g/L	
Platelets 139,000/mL	Bilirubin 1.8uM	Zinc 43mcg/L	Phosphorus 3.5mg/L	Prealbumin 0.1mg/L	
ANTHROPOMETRY (medians)					
Body mass index 25	Arm circumference 25cm		Calf circumference 34cm		
Triceps skinfold 17mm	Heel-heel length 60cm		Clenched-fist length 17cm		
DYNAMOMETRY n=33					
21 patients (71%) decreased value >4 <30kg, M <30kg					
CARDIAC FLICKER FREQUENCY n=30					
Median 42.3 Hz		Pathologic (>38 Hz) → 5 patients			
MUSCULOSKELETAL INDEX n=35					
Median 50.22 cm ² /m ²					

Nutritional screening test

	MUST low risk	MUST medium risk	MUST high risk
SGA-A well nourished	1	0	0
SGA-B nutritional risk	4	1	2
SGA-C moderately malnourished	1	12	6
SGA-C severely malnourished	0	0	12
	RFH low risk	RFH medium risk	RFH high risk
SGA-A well nourished	0	0	1
SGA-B nutritional risk	1	2	4
SGA-C moderately malnourished	0	8	11
SGA-C severely malnourished	0	0	19

Nutritional diagnosis → 3 nutritional risk, 3 mild malnutrition, 21 moderate, 19 severe malnutrition

CHILD-PUGH		Moderate malnutrition (≥ 2 no Child)	Severe malnutrition		
Child-Pugh A	1	1			
Child-Pugh B	9	1			
Child-Pugh C	3	2			
DYNAMOMETRY		Nutritional risk	Mild malnutrition	Moderate malnutrition	Severe malnutrition
Reduced muscle force	2/3	3/3	14/19	8/8	
			~ 2 unmeasured	~ 2 unmeasured	
CFF		Moderate malnutrition	Severe malnutrition		
Pathologic <38Hz > 5 patients	3	2			

Correlation between dynamometry and musculoskeletal index (Pearson 0.815)

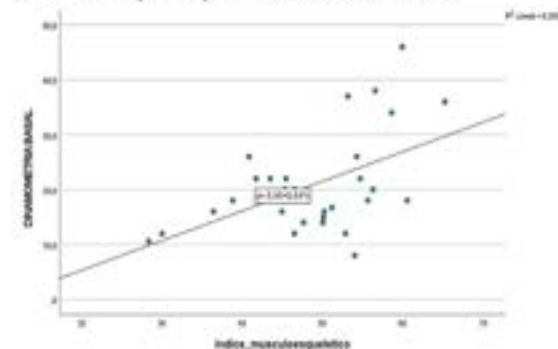


Figure:

Conclusion: Using several tools increases the reliability of nutritional risk assessment. RFH-NPT overestimates the risk of malnutrition in decompensated patients, compared to SGA and MUST, which are comparable. There are no differences in the distribution of malnutrition according to Child-Pugh. Micronutrient deficiency and frailty determined by dynamometry are frequent; sarcopenia is not, but there is a good correlation between dynamometry and CT. Malnutrition does not seem to influence CFF. Currently evaluating the impact of the implementation of a nutritional treatment.

WED-375

Experiences from a palliative care clinic specialized in liver diseases-utilisation, clinical characteristics of patients and outcomes

Fernando Xavier e Silva¹, Elizabeth Lee², Hemant A Shah², David Wong², Breffni Hannon³, Kirsten Wentland¹, Ebru Kaya¹.
¹University of Toronto, Department of Supportive Care-Palliative Care, Toronto, Canada, ²University of Toronto, Toronto Centre for Liver Disease (TCLD), Toronto, Canada, ³University of Toronto, Department of Supportive Care-Palliative Care-Princess Margaret Cancer Centre, Toronto, Canada
 Email: silva.fernandoxavier@gmail.com

Background and aims: Despite the significant global increase in liver disease over the last few decades and the high symptom burden for affected patients, access to palliative care (PC) is historically low and referrals happen late in the disease trajectory. Furthermore, the literature on PC in this area is sparse compared to other chronic diseases. This study aims to add to the evidence surrounding the utilization of PC services by this population, and to analyze the underlying reasons for referral as well as the morbidity and outcomes of referred patients.

Method: This study retrospectively reviewed charts of adult patients (18 years or older) with advanced-stage liver disease referred to a specialized PC clinic between May 2019 and May 2022. Data collected included type of primary liver disease, functional status (measured using the Palliative Performance Scale (PPS), a discrete numerical scale from 0% to 100%), and intensity of symptoms at the time of the first visit (using the Edmonton Symptoms Assessment System (ESAS), a discrete numerical scale from 0 to 10 used by patients to grade the intensity of common symptoms), candidacy for liver transplant, comorbidities, outcomes from the clinic (discharge, transfer for other modality of PC, continued care in the clinic, loss of follow-up or death during follow-up) and time and place of death. The study was approved by the research ethics board at University Health Network (UHN). Descriptive statistics were used to analyze data.

Results: Fifty-four patients were included, 30 (55.6%) were male and 70 years was the median age. Cirrhosis secondary to viral hepatitis was the most common diagnosis (18 patients, 33.3%) followed by alcohol-associated liver disease (17, 31.5%). A significant number of patients (24, 44.4%) also had hepatocellular carcinoma and 44 (81.5%) had more than two comorbidities. Forty (64.1%) patients were referred for both symptom management and palliative planning, and 5 patients (9.3%), for symptom management alone. Seven patients (13.0%) were candidates for a liver transplant, of whom 4 (57.1% of candidates) underwent transplantation. Regarding function, 33 patients (61.1%) had a PPS between 50–60% and none had a PPS of 30% or lower. Regarding their symptoms, the overall mean score per symptom on ESAS was 3.6 (median 3) (out of 10) and fatigue had the highest score (6.4, median 7), followed by lack of well-being (average 4.2, median 4) and lack of appetite (3.71, median 4). Patients were followed in the PC clinic for an average of 15.7 weeks (median of 10 weeks) with a mean of 4.6 (median of 3) visits. Outcomes from the clinic were related to clinical deterioration for 36 patients (66.7%) and 19 (35.4%) had their care transferred to home-visiting PC physicians (19, 35.4%) while 8 (14.8%) were referred to PC units. 36 patients (66.7%) died, with a mean survival of 31.2 weeks (median of 24 weeks).

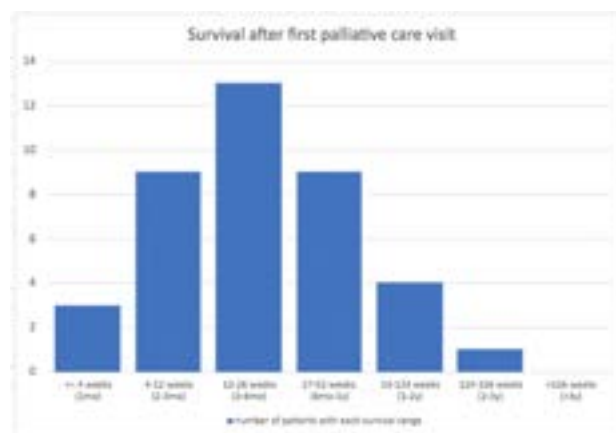


Figure:

Conclusion: Despite being referred for PC when presenting with an intermediate functional capacity and low symptom burden, patients

had high mortality and short follow-up and survival. More flexible criteria for PC referrals may be considered, possibly through a better understanding of prognostic factors for this population, to promote earlier referrals and better and longer support for patients and their families.

WED-376

Booster SARS-CoV-2 vaccination elicits robust antibody response to wild type but not Omicron subvariants BA.4/5 in patients with cirrhosis

Qian Zhu¹, Lu Wang¹, Xiaoxiao Hu¹, Dejuan Xiang¹, Ming-Li Peng¹, Dachuan Cai¹, Xiaofeng Shi¹, Hong Ren¹. ¹Institute for Viral Hepatitis, The Second Affiliated Hospital, Chongqing Medical University, China
Email: renhong0531@cqmu.edu.cn

Background and aims: Our aim is to determine immune efficacy of booster SARS-CoV-2 vaccination in cirrhotic patients who had received the 2-dose inactivated vaccines.

Method: We performed a longitudinal assessment in 48 patients with cirrhosis to continuously track the dynamics of SARS-CoV-2 specific antibodies and memory B cells after receiving the primary 2-dose series and booster dose. Neutralizing antibodies (NAbs) in serum samples were evaluated by capture chemiluminescence immunoassays. Neutralizing activity against Omicron subvariants BA.2.12.1, BA.4 and BA.5 was examined by pseudovirus neutralization assay.

Results: Serum neutralizing antibodies levels in cirrhotic patients were elevated in the early 15–45 days after primary series before rapidly declining and reaching a valley at around 165–195 days. After receiving the booster dose, the NAbs level was re-increased

significantly (0.1 µg/ml vs. 0.8 µg/ml, $p = 0.001$). 1 month after a booster dose, the serum geometric mean titer (GMT) against Omicron subvariants BA.2.12.1, BA.4 and BA.5 were 1.4-fold, 3.6-fold and 4.3-fold lower than titer against wild type (WT) strains respectively. Compared to 1 month after primary series, cirrhotic patients who received the booster dose did not show an evident improvement of neutralization activity against the Omicron subvariants BA.2.12.1 and BA.4 (BA.2.12.1, 1.9-fold; BA.4, 2.4-fold), and even exhibited a significant lower GMT against the Omicron subvariants BA.5 (3.3-fold, $p = 0.042$).

Conclusion: Booster SARS-CoV-2 vaccination elicits robust antibody response to wild type but not Omicron subvariants BA.4/5 in patients with cirrhosis. Repeated vaccination of inactivated SARS-CoV-2 vaccine might dampen neutralization activity against newly circulating strains.

WED-377

Poorer results in the clinical frailty scale are associated with covert and overt hepatic encephalopathy in patients with cirrhosis

Eva Maria Schleicher^{1,2}, Leonard Kaps^{1,2}, Jörn Schattenberg^{1,2}, Peter Galle^{1,2}, Marcus-Alexander Wörns³, Simon J. Gairing^{1,2}, Christian Labenz^{1,2}. ¹University Medical Center of the Johannes Gutenberg-University, Department of Internal Medicine I, Mainz, Germany, ²University Medical Center of the Johannes Gutenberg-University, Cirrhosis Center Mainz (CCM), Mainz, Germany, ³Klinikum Dortmund, Department of Gastroenterology, Hematology, Oncology and Endocrinology, Germany
Email: eva.schleicher@unimedizin-mainz.de

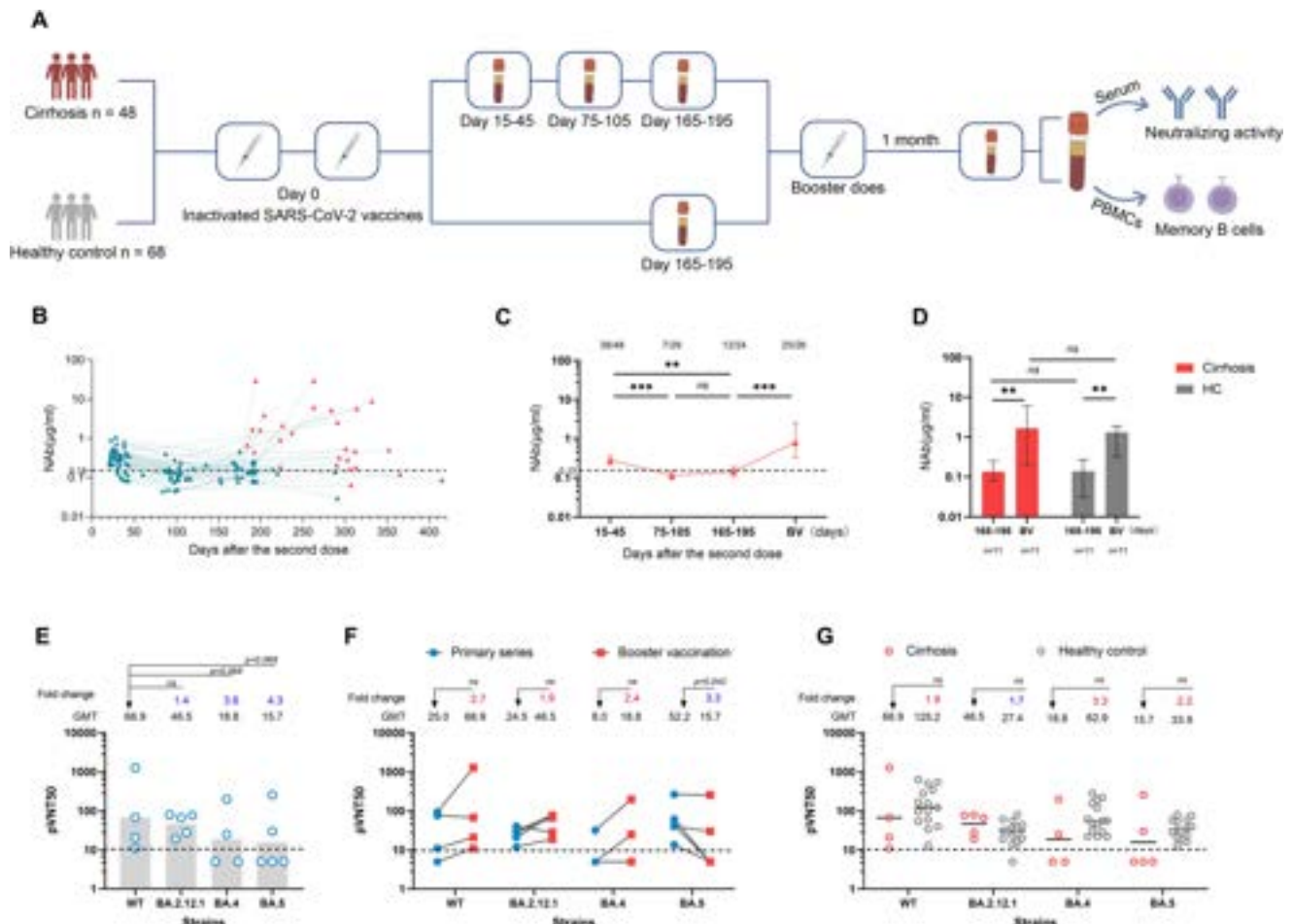


Figure: (abstract: WED-376).

Background and aims: Hepatic encephalopathy (HE) is associated with impaired quality of life, poor prognosis, and frequent hospitalizations in patients with liver cirrhosis. Frailty increases the vulnerability to internal and external stressors and may therefore be an indicator of a higher frequency of cirrhosis complications. We aimed to investigate the association of the rapidly applicable Clinical Frailty Scale (CFS) with covert HE (CHE) and overt HE (OHE) development in patients with cirrhosis.

Method: This study analyzed data from 228 outpatients or electively hospitalized patients with cirrhosis recruited at the Cirrhosis Center Mainz, Germany. Frailty was assessed using the CFS. Patients were examined for the presence of CHE at study inclusion using the West-Haven-Criteria (HE1) and the psychometric hepatic encephalopathy score (PHES). All patients were prospectively followed regarding the development of OHE.

Results: Patients had a median age of 60 years, and the predominant etiology of liver cirrhosis was alcoholism (32.5%), followed by viral hepatitis (19.7%). Median CFS was 3 (IQR 2; 3). 26 (11.4) patients were at least pre-frail (CFS >3) according to CFS. The majority of the patients were in a compensated state of cirrhosis (Child-Pugh A/B/C: 60.5%/30.3%/9.2%), and the median MELD at baseline was 10 (IQR 8; 14). CHE was detected in 71 patients (31.1%), and 33 (14.5%) had a history of OHE. In a multivariable logistic regression analysis that included the subcohort of patients without a history of OHE (n = 195), a higher CFS was independently associated with the presence of CHE at baseline (OR 1.7, 95% CI 1.1–2.6, p = 0.027), whereas age, MELD, sodium, albumin or a history of ascites were not. During a median follow-up of 436 days (IQR 191, 712), 42 (18.4%) patients developed an episode of OHE. In multivariable Cox regression analyses, a higher CFS was independently associated with the development of OHE in the total cohort (HR 2.1, 95% CI 1.5–2.9, p < 0.001) and the subcohort of patients without a history of OHE (HR 1.8, 95% CI 1.2–2.8, p = 0.008) after adjusting for age, MELD, sodium, albumin, CHE or a history of OHE (only in the model including the total cohort).

Conclusion: Frailty, as defined by the CFS, is associated with CHE and OHE development. The CFS appears to be a reliable tool to identify patients at higher risk of HE in whom intensified treatment and monitoring may be justified.

WED-378

Anemia in cirrhotic patients is a risk factor for esophagogastric variceal bleeding and mortality

Elena Santos Perez¹, Elba Llop¹, Marta López-Gómez¹, Marta Hernández Conde¹, Carlos Fernández-Carrillo¹, Esther Maderuelo¹, Jiacheng Cao¹, Natalia Fernández Puga¹, José Luis Martínez Porras¹, Javier Abad Guerra¹, Christie Perelló¹, Maria Trapero¹, Enrique Fraga¹, José Luis Calleja Panero¹. ¹Hospital Universitario Puerta de Hierro, Majadahonda (Madrid), Spain
Email: elenasantosperez8@gmail.com

Background and aims: In liver cirrhosis (LC), anemia has been related to a worsening of the hyperdynamic state associated with portal hypertension, its clinical impact being unknown. There is a lack of longitudinal studies analyzing anemia as a risk factor for relevant outcomes in LC, such as esophagogastric variceal bleeding (EGVB) and mortality.

Method: Cases and controls. A retrospective series of consecutive cases with LC and EGVB (January 2017–December 2021) with laboratory tests in the first year prior to the episode and a historical cohort of control patients with LC without EGVB during their prospective follow-up were included. Demographic, baseline laboratory and clinical data up to death were analyzed.

Results: 556 patients (61 cases, 495 controls) were selected. The mean follow-up time for cases was 24 months (SD 21.7) and for controls 92.3 months (SD 23.1). Given the known influence of age, sex and liver function (Child-Pugh) on variceal bleeding, a 3:1 matching was performed according to these variables, finally including 252 patients (51 cases, 151 controls). In multivariate analysis of the paired

data, the only independent factor associated with variceal bleeding was baseline haemoglobin (OR 2.57; p = 0.01). The prevalence of death in the overall cohort was 111 (20.2%). Cox proportional hazards analysis confirmed anemia (Hb < 12g/dL) as a baseline variable independently related to mortality (HR 2.0; CI 1.3–3.0; p = 0.002), as well as age (HR 1.03; CI 1.02–1.05; p < 0.001), liver function (Child Pugh B/C) (HR 1.8; CI 1.2–2.7; p = 0.03) and variceal bleeding (HR 6.7; CI 3.9–11.6; p < 0.001).

Conclusion: Anemia in cirrhotic patients should be considered as a risk factor for variceal bleeding, is globally associated with higher mortality and it is necessary to study whether it corresponds to a worse hyperdynamic state and to perform close monitoring when it appears.

WED-379

Prucalopride : a novel and safe usage for reducing incidence of hepatic encephalopathy in decompensated cirrhosis

Manasa Alla¹, Vinod Arora¹, Shantan Venishetty¹, Imran Khan¹, Shiv Kumar Sarin¹. ¹Institute of Liver and Biliary Sciences, New Delhi, India
Email: shivsarin@gmail.com

Background and aims: Prevention of recurring episodes of hepatic encephalopathy in cirrhotics is vital for improving morbidity and mortality. Previous studies have shown efficacy of lactulose and conflicting results with rifaximin in preventing breakthrough episodes in those with recurrent HE. Prucalopride remains a promising addition and study has been conducted to evaluate its safety and efficacy as a part of secondary prophylaxis in cirrhotic patients

Method: It was a retrospective data analysis with follow-up done at Institute of Liver and Biliary Sciences, New Delhi from Jan 2021–July 2022. Of 144 cirrhotics screened with HE, 78 cirrhotics with ≥2 prior episodes of overt HE despite receiving standard dosage of rifaximin (15–20 mg/kg/day) and lactulose in previous 6 months were analyzed. Patient then received prucalopride (1 mg/day) along with the standard therapy to maintain at least 3 soft stools/day. Number of overt HE episodes and adverse events over 6 months follow-up were recorded.

Results: 78 patients with the mean age 58.42 ± 12.32 years were analyzed. 20/78 (25.6%); 34/78 (43.6%); 24/78 (39.8%) were in CTP A, B and C class respectively. Mean CTP and MELD were 9.42 ± 1.56 and 19.86 ± 4.83 respectively. Alcohol {28/78 (35.9%)} was the most common aetiology of liver cirrhosis followed by NASH {25/78 (32.05%)}. Median number of HE episodes (/6 month) was 2 (0, 3) episodes and stool frequency (/day) at baseline were 1 (0, 2) respectively. 19/78 (24.3%) had presence of porto-systemic shunt. Mean duration of treatment for prucalopride was 90.23 ± 21.65 days. Median number of HE episodes; HE requiring hospitalization (/6 months) and stool frequency (/24 hours) with prucalopride was 1 (0, 2); 1 (1, 3), 3 (2, 5) respectively. Mean reduction in HE episode (/6month) with prucalopride was -0.8 ± 0.3, similarly mean increase in stool frequency (/Day) was noted (+1.2 ± 0.6). HE episode requiring ICU hospitalization was 1 (0, 2). >1 episode and >2 episode HE was seen in 17/78 (21.8%); 9/78 (11.5%) patients. Mortality at 6 months was found to be 12/78 (15.4%). 11/78 (14.1%) patients experienced bloating, abdominal discomfort and diarrhea (>6 episodes/d) was noted in 9/78 (11.5%) patients. 3/78 (3.8%) had worsening liver functions. No adverse events requiring discontinuation were noted. Limitation of the study was intestinal transit time could not be measured.

Conclusion: Our study showed that the addition of prucalopride reduced the incidence of hepatic encephalopathy in addition to lactulose and rifaximin and can be safely used in advanced cirrhotics.

WED-380

Surgical subtype predicts adverse outcomes and costs among non-alcoholic cirrhotic patients

Christopher Tait¹, Carolyn Catalano², Ankoor Patel², Carlos Minacapelli², You Li², Vinod Rustgi². ¹Rutgers Robert Wood Johnson Medical School, New Brunswick, United States, ²Rutgers Robert Wood Johnson Medical School, United States
Email: ct662@rwjms.rutgers.edu

Background and aims: Patients with cirrhosis are at increased risk of complications following surgery from multiple factors including portal hypertension and alterations in hemostasis. Gaps remain in our understanding of the cost and morbidity of cirrhotic patients who undergo surgery, particularly with respect to surgical subtype.

Method: We conducted a case-control study using the IBM Electronic health Record (EHR) MarketScan Commercial Claims (MSCC) databases from January 1st 2007 to December 31st 2017. Non-alcoholic cirrhotic patients who underwent surgery were identified based on ICD-9/ICD-10 codes for multiple surgical categories and matched with controls with cirrhosis who did not undergo surgery. Outcomes in the 6-month period following surgery were analyzed between matched groups and a cost analysis was performed. Cirrhotic patients were analyzed for adverse outcomes and cost for 9 different surgical subtypes.

Results: Mortality was increased in the cirrhotic patients undergoing surgery compared with the nonsurgical group (4.68% vs 2.38%, $P < 0.001$). Among surgical subtypes, mortality was highest in for gastrectomy (6.33%) and colectomy (6.00%), while lowest for total hip replacement (THR) (0%) and cholecystectomy (1.43%). The surgical cirrhotics had higher rates of adverse hepatic outcomes than the nonsurgical cirrhotics, including hepatic encephalopathy (HE) (5.00% vs 2.50%, $P < 0.0001$), spontaneous bacterial peritonitis (SBP) (0.64% vs 0.25%, $P < 0.001$), and higher rates of adverse nonhepatic outcomes. Among cirrhotics by surgical subtype (Figure 1), high rates of adverse hepatic outcomes were noted for colectomy and gastrectomy, with lower rates for total knee replacement (THR) and appendectomy. Healthcare utilization analysis revealed significantly increased costs in the surgical cohort (\$58,246 vs \$26,842, $P < 0.0001$), largely due to increased inpatient costs (\$34,446 vs \$10,789, $P < 0.0001$). Stratifying by surgical subtype, colectomy and gastrectomy had highest total costs (\$131,983 and \$109,796), with relative high costs from THR (\$98,742) and TKR (\$98,873).

Conclusion: Non-alcoholic cirrhotics undergoing surgery experienced worse mortality and adverse hepatic and nonhepatic outcomes. Gastrectomy and colectomy had the highest adverse event rates relative to other surgical subtypes. Claims and costs analysis showed significantly increased costs in the surgical group, largely due to the cost of more frequent and longer inpatient admissions.

WED-381

Analysis of surgical risk in patients with advanced chronic liver disease and major orthopedic surgery from a gender perspective

Lidia Canillas^{1,2,3}, Amalia Pelegrina^{2,3,4}, Elena Colominas⁵, Aina Salis³, César Jessé Enríquez-Rodríguez^{2,3}, Antonia Caro¹, Marc Puigvehí^{1,2}, Teresa Broquetas^{1,2}, Susana Coll^{1,2}, NURIA Cañete^{1,2}, Montserrat García-Retortillo^{1,2}, Xavier Bessa^{1,2,3}, Juan Carlos Álvarez⁶, Jose A. Carrión^{1,2,3}. ¹Hepatology section, Gastroenterology Department, Hospital del Mar, Barcelona, Spain, ²IMIM (Institut Hospital del Mar d'Investigacions Mèdiques), Barcelona, Spain, ³Departament de Medicina i Ciències de la Vida, Universitat Pompeu Fabra, Spain, ⁴General Surgery and Digestive Department Hospital del Mar, Barcelona, Spain, ⁵Pharmacy Department, Hospital del Mar, Barcelona, Spain, ⁶Anesthesiology Department, Hospital del Mar, Barcelona, Spain
Email: lidia.canillas.alaves@gmail.com

Background and aims: Improvements in medical care and increased life expectancy have raised the need for major orthopedic surgery in patients with advanced chronic liver disease (ACLD). However, the prevalence of women is underrepresented in the cohort of patients used to create the VOCAL-Penn surgical risk score. Our objective was to assess differences in the risk of surgery, postoperative complications, and mortality in patients with ACLD who underwent major orthopedic surgery from a gender perspective.

Method: Retrospective, single-center study in patients with ACLD who underwent major orthopedic surgery (large joints and amputations) between 2010 and 2019. Comorbidities, data on ACLD, estimated surgical risk, analgesic use with metamizole/non-steroidal anti-inflammatory drugs (NSAIDs), postoperative complications such as acute kidney injury (defined by *Kidney Disease Improving Global Guidelines*) and infections, hospital stay, and mortality were collected. Differences between gender were compared using the Fisher, Chi-square, or U-Mann Whitney tests, as appropriate. Survival curves were contrasted with the Mantel-Cox test.

Results: Of 123 patients, 13 (11%) were excluded from the analysis due to missing data. Women represented 55% (61/110) of the cohort. The median age (IQR) of women was 76 (66–83) years and of men 68 (58–79) ($p = 0.02$). No differences were found in body mass index, diabetes, and chronic kidney disease. However, women had a higher prevalence of hypertension (61% vs. 39%; $p = 0.03$) and a lower prevalence of chronic obstructive pulmonary disease (5% vs 18%; $p = 0.03$). The predominant etiology of ACLD was viral (57%) in women and alcohol (55%) in men ($p = 0.001$). No difference was found between gender in liver function (Child-Pugh A 41% vs. 39%), bilirubin, ASA scale, emergency of surgery, and estimated VOCAL-Penn surgical risk at 30, 90, and 180 days; while women showed lower values of albumin (3.8 vs. 4.1 g/dl; $p = 0.03$) and platelets (108 vs. $143 \times 10^9/L$; $p = 0.02$). There were no differences in the

Table (abstract: WED-380).

	Cholecystectomy	Appendectomy	Total knee replacement	Gastrectomy	Colectomy	Hernia repair (n = 264)	Total hip replacement
Patient Outcome	(n = 3,994)	(n = 1,984)	(n = 1,013)	(n = 1,058)	(n = 517)		(n = 61)
Death [n (%)]	57 (1.43)	51 (2.57)	24 (2.37)	67 (6.33)	31 (6.00)	8 (3.03)	0
Ascites [n (%)]	232 (5.81)	61 (3.07)	10 (0.99)	111 (10.49)	90 (17.41)	19 (7.20)	4 (6.56)
Hepatic Encephalopathy [n (%)]	52 (1.30)	21 (1.06)	13 (1.28)	137 (12.95)	26 (5.03)	2 (0.76)	1 (1.64)
Average Healthcare Costs (USD/patient)							
Total Cost	33,483	25,059	63,235	68,523	98,057	34,325	99,807
Inpatient Cost	14,361	8,961	43,872	42,772	66,746	8,365	75,768
Average Length of Stay [days]	2.11	1.43	5.01	9.86	10.47	1.43	9.97
Outpatient Cost	14,973	10,475	14,148	19,174	26,302	20,874	17,342

POSTER PRESENTATIONS

administration of metazole/NSAIDs or the development of AKI at postoperative admission. But, women developed more infections (48% vs. 25%, $p = 0.02$), especially in the urinary tract (24% vs. 6%, $p < 0.001$). No differences were found in the percentage of severe or nosocomial infections, neither related to multiresistant microorganisms. However, postoperative mortality at 30 days (13% vs. 4%; Log-Rank = 0.09) and 180 days (28% vs. 12%; Log-Rank = 0.04) was higher in women than in men.

Conclusion: Age and comorbidities differ in women with ACLD who underwent major orthopedic surgery. Although the VOCAL-Penn surgical risk score does not show significant differences in expected mortality between gender, the percentage of infections and observed mortality was higher in women. These data suggest the need to optimize perioperative management of patients with ACLD from a gender perspective.

WED-382

Availability and affordability of services affects outcome in hospitalized patients with cirrhosis-results from CLEARED consortium

Ashok Choudhury¹, Qing Xie², Patrick S. Kamath³, Mark Topazian⁴, Shiv Kumar Sarin¹, Peter Hayes⁵, Aldo Torre⁶, Hailemichael Desalegn⁴, Ramazan Idilman⁷, ZhuJun Cao², Shiva Kumar⁸, Adrian Gadano⁹, Alexander Prudence¹⁰, Patricia Zitelli¹¹, Chinmay Bera¹², Monica Dahiya¹³, Ponan Claude Regis Lah¹⁴, Marco Arrese¹⁵, Jin Guan¹⁶, Yingling Wang¹⁷, Man Su¹⁸, Xinrui Wang¹⁹, Feng Peng²⁰, Wei Wang²¹, Dedong Yin²², Yijing Cai²³, fuchen dong²⁴, Jing Liu²⁵, Libo Yan²⁶, Linlin Wei²⁷, Zhen Xu²⁸, haibing gao²⁹, Beiling Li³⁰, Yanyun Zhang³¹, Huan Deng³², Nabil Debzi³³, Suresh Vasan Venkatachalapathy³⁴, Rosemary Faulkes³⁵, Ewan Forrest³⁶, James Kennedy³⁷, Yan Yue James Fung³⁸, Liane Rabinowich³⁹, Mithun Sharma⁴⁰, Jatin Yegurla⁴¹, Dinesh Jothamani⁴², Ashish Kumar⁴³, Ashish Goel⁴⁴, Akash Roy⁴⁵, Dibya Lochan Praharaj⁴⁶, Araceli Bravo Cabrera⁴⁷, Oscar Morales Gutiérrez⁴⁸, Abraham Ramos Pineda⁴⁹, Lilian Torres Made⁵⁰, Francisco Félix Tellez⁵¹, Nik MA Nik Arsyad⁵², David Nyam⁵³, Yashwi Haresh Kumar Patwa⁵⁴, Liou Wei Lun⁵⁵, Salisa Wejnaruemarn⁵⁶, Busra Haktaniyan⁵⁷, Rahmi Aslan⁵⁸, Sezgin Barutcu⁵⁹, Alper Uysal⁶⁰, Tolga Kosay⁶¹, Dinc Dincer⁶², Mohammad Amin Fallahzadeh⁶³, Suditi Rahematpura⁶⁴, David Bayne⁶⁵, Natalia Filipek⁶⁶, Somya Sheshadri⁶⁷, Ricardo Cabello⁶⁸, Mario Álvares-da-Silva⁶⁹, Jacob George⁷⁰, Florence Wong¹², Brian Bush⁷¹, Leroy Thacker⁷¹, Jasmohan S Bajaj⁷¹.
¹Institute of liver and biliary sciences New Delhi, India, ²Ruijin Hospital, Shanghai Jiao Tong University School of Medicine, Shanghai, China, ³Mayo Clinic School of Medicine, Rochester, USA, ⁴United States, ⁵St Paul's Hospital, Millennium Medical College, Addis Ababa, Ethiopia, ⁶University of Edinburgh, Edinburgh, UK, ⁷United Kingdom, ⁸Instituto Nacional de Ciencias Médicas y Nutrición Salvador Zubirán, Mexico City, Mexico., ⁹Mexico, ¹⁰Ankara University School of Medicine, Ankara, Turkey, ¹¹Turkey, ¹²Cleveland Clinic Abu Dhabi, United Arab Emirates, ¹³Hospital Italiano de Buenos Aires, Argentina, ¹⁴Argentina, ¹⁵John Hunter Hospital, Newcastle, Australia, ¹⁶Hospital das Clínicas da Faculdade de Medicina da Universidade de São Paulo, Brazil, ¹⁷University of Toronto, Toronto, Canada, ¹⁸Canada, ¹⁹University of Alberta, Edmonton, Canada, ²⁰CHU de Cocody, Abidjan, Cote d'Ivoire, ²¹Côte d'Ivoire, ²²Pontificia Catholic University of Chile, Santiago, Chile, ²³The Third People's Hospital of Guilin, China, ²⁴The Fifth People's Hospital of Suzhou, China, ²⁵The First Affiliated Hospital of Guangxi Medical University, China, ²⁶The First Hospital of Jilin University, China, ²⁷The Second XiangYa Hospital of Central South University, China, ²⁸The Third Affiliated Hospital of Hebei Medical University, China, ²⁹Second Hospital of Shandong University, China, ³⁰The First Affiliated Hospital of Wenzhou Medical University, China, ³¹Department of Gastroenterology, School of Medicine, Ren Ji Hospital, Shanghai Jiao Tong University, China, ³²Department of Infectious Diseases, Union Hospital, Tongji Medical College, Huazhong University of Science and Technology, China, ³³Center of Infectious Disease, West China Hospital of Sichuan University, China,

²⁷Beijing Youan Hospital, Capital Medical University, China, ²⁸The Third Affiliated Hospital of Sun Yat-sen University, Guangzhou, China, ²⁹Mengchao Hepatobiliary Hospital of Fujian Medical University, China, ³⁰Hepatology Unit, Department of Infectious Diseases, Nanfang Hospital, Southern Medical University, China, ³¹Shuguang Hospital Affiliated to Shanghai University of Traditional Chinese Medicine, China, ³²Second Affiliated Hospital of Chongqing Medical University, China, ³³Mustapha Bacha University Hospital, Algiers, Algeria, ³⁴NIHR Nottingham Biomedical Research Centre, Nottingham University Hospitals, United Kingdom, ³⁵Queen Elizabeth University Hospitals, Birmingham, United Kingdom, ³⁶Glasgow Royal Infirmary, United Kingdom, ³⁷Royal Berkshire Hospital, United Kingdom, ³⁸Department of Medicine, School of Clinical Medicine, The University of Hong Kong, Hong Kong, ³⁹Tel-Aviv Sourasky Medical Center, Tel Aviv, Israel, ⁴⁰Asian institute of Gastroenterology, Hyderabad, India, ⁴¹Deptt. of Gastroenterology and Human Nutrition, AIIMS, New Delhi, India, ⁴²Deptt. of Liver Transplant Surgery, Dr. Rela Institute and Medical Centre, Chennai, India, ⁴³Sir Ganga Ram Hospital, Delhi, India, ⁴⁴CMC Vellore, India, ⁴⁵Sanjay Gandhi Postgraduate Institute of Medical Research, Lucknow, India, ⁴⁶KIMS BHUBANESWAR, India, ⁴⁷Centro Médico ISSEMYM, Mexico, Mexico, ⁴⁸Hospital General de Mexico "Dr. Eduardo Liceaga", Mexico, ⁴⁹Instituto Nacional de Ciencias Médicas y Nutrición "Salvador Zubirán", Mexico City, Mexico, ⁵⁰Instituto de la Salud Digestiva, Guadalajara, Mexico, ⁵¹Hospital Civil de Guadalajara Fray Antonio Alcalde, Guadalajara, Mexico, ⁵²University of Malaysia, Kuala Lumpur, Malaysia, ⁵³Jos University Teaching Hospital Jos, Nigeria, ⁵⁴Nigeria, ⁵⁵National Center for Gastrointestinal and Liver Disease, Khartoum, Sudan, ⁵⁶Singapore General Hospital, Singapore, ⁵⁷Chulalongkorn University and King Chulalongkorn Memorial Hospital, Bangkok, Thailand, ⁵⁸University of Ankara, Turkey, ⁵⁹Marmara University, Istanbul, Turkey, ⁶⁰Gaziantep University, Turkey, ⁶¹Ege University, Izmir, Turkey, ⁶²Mersin University, Mersin, Turkey, ⁶³Akdeniz University, Antalya, Turkey, ⁶⁴Baylor Dallas (Baylor University Medical Center), United States, ⁶⁵University of Pennsylvania, United States, ⁶⁶Mayo Scottsdale, United States, ⁶⁷University of Washington, United States, ⁶⁸Mercy Medical Centre, Baltimore, United States, ⁶⁹University of Pittsburgh, United States, ⁷⁰Hospital de Clínicas de Porto Alegre, Universidade Federal do Rio Grande do Sul, Porto Alegre, Brazil, ⁷¹Storr Liver Centre, The Westmead Institute for Medical Research and Westmead Hospital, University of Sydney, Sydney, Australia, ⁷²Virginia Commonwealth University and Central Virginia Veterans Healthcare System, Richmond, USA, United States
Email: doctor.ashokchoudhury@gmail.com

Background and aims: Treatment of inpatients with cirrhosis requires availability of several expensive interventions such as intensive care (ICU) and endoscopy, medications such as rifaximin, terlipressin and IV albumin. Also, the infrastructure and affordability of liver transplant (LT) and palliative care is needed for optimal management. These may vary in access and affordability globally. Aim: evaluate, access and affordability of important resources for inpatient cirrhosis management from Principal Investigators (PIs) from the Chronic Liver disease Evolution And Registry for Events and Decompensation-CLEARED consortium.

Method: CLEARED consortium enrolled in patients with cirrhosis admitted non-electively and followed them for 30-days post-discharge. All PIs were offered a survey regarding availability, access and affordability of their typical population with cirrhosis regarding important services (24 hr endoscopy, ICU care, palliative care), medications (somatostatin, octreotide, terlipressin, rifaximin and albumin). Sites across the world were compared with respect to the PI survey.

Results: We prospectively enrolled 3884 patients from 95 centers in all 6 continents. Of these according to the world bank definition, 34 were high-income, 39 upper middle and rest were low/low-middle income countries. Results summarized in figure. Insurance: Most insurances were national except for centers in India, USA and Mexico where >50% of patients were on private insurances. Services and

Table: Survey of principal investigators regarding availability and affordability for care of cirrhosis patients

Region	No of centre (n=95)	Availability of LT	>50% of pts can afford LT	24 hours Endoscopy service available?	Rifaximin Availability	Terlipressin Availability	>50% can afford Albumin	Palliative care available
China	24	16(67)	2(8)	23(96)	24(100)	23(96)	21(88)	7(26)
India	11	10(91)	0	11(100)	11(100)	11(100)	5(45)	4(36)
Middle East	9	6(67)	4(44)	9(100)	9(100)	9(100)	4(44)	6(67)
Rest of Asia	3	3(100)	2(67)	3(100)	2(67)	3(100)	3(100)	2(67)
North America	23	19(79)	15(65)	22(96)	23(100)	8(35)	16(70)	22(96)
Europe	6	3(50)	3(50)	6(100)	6(100)	6(100)	3(50)	6(100)
Australia	7	1(14)	6(86)	7(100)	7(100)	7(100)	5(71)	7(100)
Africa	5	1(20)	0	1(20)	3(60)	2(40)	1(20)	2(40)
South America	7	7(100)	3(42)	7(100)	7(100)	7(100)	3(43)	7(100)

*: includes USA, Canada, and Mexico, LT: liver transplantation, ICU: intensive care unit, Somatostatin and octreotide are medications needed for treating variceal hemorrhage,[] all figure in bracket indicate percentage

Figure: (abstract: WED-382).

Interventions: LT was available in most centers except in Africa. It was only accessible in remaining regions if insured. ICU was unaffordable in regions apart from North America, Australia, and some Asian and European sites. 24-hr endoscopy was available in all centers but not in Africa. Palliative care was least likely to be available in Indian, Chinese, and African sites. Medications: Rifaximin is available in most countries apart from a few in Asia and Africa but was unaffordable for majority of patients in Africa, South America, and Asia. In remaining sites, it was only affordable for 50% of patients. Somatostatin and octreotide were available at all sites except in Africa. This was largely affordable for patients in China, Australia, North America, and Asia but not the rest. Minority of patients in Indian, African, South American, and Middle Eastern sites could afford IV albumin. Terlipressin was not available in USA and Canada. In the remaining sites, Australian, Middle Eastern, Asian, and Chinese patients were more likely to afford terlipressin.

Conclusion: In a prospective global cohort of inpatients with cirrhosis, there are major differences in availability, access, and affordability of services, interventions, and medications needed for optimal inpatient cirrhosis care. In addition to cirrhosis-related variables, these factors should be considered when assessing cirrhosis outcomes.

WED-383

Serum ammonia levels do not correlate with overt hepatic encephalopathy severity and time to resolution in hospitalized patients with cirrhosis

Jasmohan S Bajaj¹, Nikolaos T. Pylasopoulos², Robert Rahimi³, Zeev Heimanson⁴, Christopher Allen⁴, Robert Israel⁴, Don Rockey⁵.

¹Virginia Commonwealth University and Central Virginia Veterans Healthcare System, United States, ²Rutgers New Jersey Medical School, United States, ³Baylor University Medical Center, United States, ⁴Salix Pharmaceuticals, United States, ⁵Medical University of South Carolina, United States

Email: jasmohan.bajaj@vcuhealth.org

Background and aims: Measuring ammonia levels is not considered a diagnostic or prognostic indicator for overt hepatic encephalopathy

(OHE) and, per guidelines, OHE is a clinical diagnosis. However, ammonia testing remains a common practice for the assessment of OHE severity/resolution in some practice settings. The current aim was to examine the relationship between ammonia levels and time to OHE resolution in hospitalized patients.

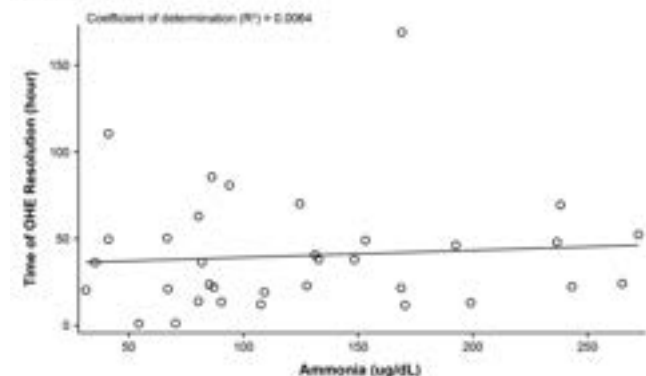
Method: Adults with cirrhosis and OHE (Hepatic Encephalopathy Grading Instrument score [HEGI], 2–3) were included in a phase 2, randomized, double-blind, placebo-controlled, 5-arm multicenter trial of investigational rifaximin soluble solid dispersion (SSD) immediate-release (IR) and sustained extended-release (SER) tablets. Patients were randomly assigned to placebo + lactulose (i.e., lactulose alone) or 1 of 4 rifaximin SSD groups: 1) IR 40 mg once daily (QD) + lactulose; 2) IR 40 mg twice daily (BID) + lactulose; 3) SER 80 mg QD + lactulose; or 4) SER 80 mg BID + lactulose. The primary efficacy end point was time to OHE resolution (HEGI score <2). Serum ammonia levels were measured daily and patients with an ammonia result at Day 1 were pooled (all treatment groups) and included in the analyses. A linear regression analysis (R^2) was conducted to assess the relationship between Day 1 ammonia levels and OHE severity and time to OHE resolution. The trial was terminated after a prespecified interim analysis and not restarted (COVID-19 – related issues). Published data showed that rifaximin SSD 40 mg BID + lactulose significantly reduced time to OHE resolution vs lactulose alone (21.1 h vs 62.7 h; $p = 0.02$; Bajaj JS, et al. doi: 10.1016/j.cgh.2022.05.042).

Results: 44 patients (median [range] age, 63 y [32–75 y]; 52.3% male) were included (6–13 per 5 groups [all of which included lactulose use]). The median baseline MELD score was 19.0, the median (range) serum ammonia level was 86.4 ug/dL (19.0–272.5 ug/dL), and 65.1% of patients had an HEGI score = 2. There was no relationship between Day 1 ammonia level and Day 1 HEGI score for overall population ($R^2 = 0.0255$) or when subgrouped by male ($R^2 = 0.0095$), female ($R^2 = 0.1179$), aged <65 y ($R^2 = 0.1264$), or aged ≥65 y ($R^2 = 0.0009$). Furthermore, there was no relationship between Day 1 ammonia level and time to OHE resolution for the overall population ($R^2 = 0.0064$; Figure) or when subgrouped by male ($R^2 = 0.0479$), female ($R^2 = 0.0052$), aged <65 y ($R^2 = 0.0780$), or aged ≥65 y ($R^2 = 0.0195$). There was also no significant difference between dosing regimens in

POSTER PRESENTATIONS

this analysis, despite the significant reduction in time to OHE resolution with rifaximin SSD 40 mg BID vs lactulose (Bajaj JS, et al.).

Figure. Lack of Correlation Between Time to OHE Resolution (HEG1 Score <2) and Serum Ammonia Level on Day 1 (N=44)



HEG1 = Hepatic Encephalopathy Grading Instrument; OHE = overt hepatic encephalopathy.

Figure:

Conclusion: This analysis of inpatients with cirrhosis and OHE found no relationship between serum ammonia levels and OHE severity or time to OHE resolution. These data reinforce the limited clinical utility of ammonia levels for the management and prognostication of inpatients with OHE.

WED-384

Six-fold increased rate of chronic kidney disease after acute kidney injury: a population-based cohort study of 46,946 patients with cirrhosis

Anna Cederborg^{1,2}, Linnea Widman³, Borje Haraldsson⁴, Björn Lindkvist^{2,5}, Ying Shang³, Axel Wester³, Hannes Hagström³, Hanns-Ulrich Marschall¹. ¹Institute of Medicine, Sahlgrenska academy, Gothenburg university, Department of clinical and molecular medicine, Gothenburg, Sweden, ²Department of Medicine, Sahlgrenska University Hospital, Gothenburg, Sweden, ³Karolinska Institutet, Sweden, ⁴Institute for neuroscience and physiology, Sahlgrenska Academy, Gothenburg university, Sweden, ⁵Institute of Medicine, Sahlgrenska academy, Gothenburg university, Sweden

Email: anna.cederborg@vgregion.se

Background and aims: Patients with cirrhosis have a high risk for acute kidney injury (AKI). The risk of developing subsequent chronic kidney disease (CKD) is not well known. Here, we investigated the risk for CKD after an episode of AKI in cirrhosis.

Method: Using Swedish national health registers, we identified all persons diagnosed with cirrhosis between 1988 and 2020. Cox regression was used to assess rates of incident CKD in patients with cirrhosis and an episode of AKI, compared to patients with cirrhosis without AKI. The cumulative incidence of CKD in both groups was calculated considering non-CKD related mortality as a competing event.

Results: We identified 46,946 patients with cirrhosis, 30,082 (64.1%) were men, and the median age was 63 years. The median time to follow-up for all patients was 2.1 (IQR 0.5–5.7) years. AKI was diagnosed in 2,873 (6.1%) patients, of whom 19.6% developed CKD, compared to 5.2% of patients without AKI. The incidence rate of CKD in patients with AKI compared to those without was 133.0 vs. 12.5 per 1,000 person-years (adjusted HR=6.5, 95%CI=5.9–7.2) and the cumulative incidence of CKD at 90 days was 9.1% and 0.6%, respectively. Furthermore, the kidney-related mortality rate was also considerably higher (adjusted HR=7.3, 95%CI=6.4–8.4) in patients with AKI.

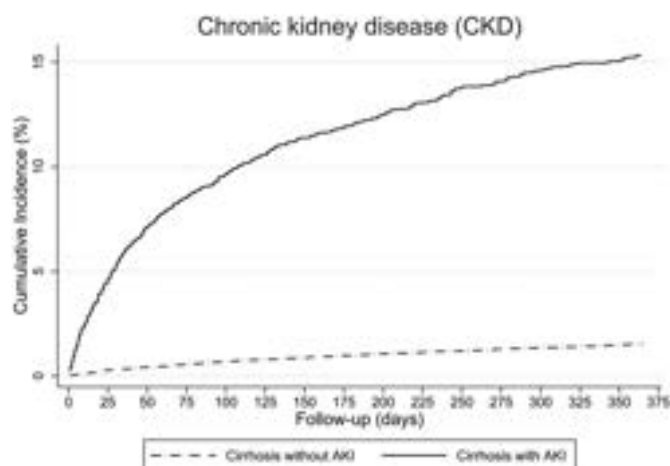


Figure:

Conclusion: Patients with cirrhosis and AKI have a more than six-fold increased rate of CKD, as well as a higher short-term kidney-related mortality compared to cirrhosis patients without AKI.

WED-385

Patients with liver cirrhosis and TIPS are prone to in-hospital falls

Nada Abedin¹, Moritz Hein¹, Christoph Welsch¹, Jörg Bojunga¹, Stefan Zeuzem¹, Georg Dultz¹. ¹Department of Internal Medicine I, University Hospital Frankfurt, Goethe University, Frankfurt am Main, Germany

Email: nada.abedin@kgu.de

Background and aims: In-hospital falls are associated with a high mortality in patients in general and especially in patients with chronic liver disease. Therefore, identifying patients at high risk and implementing safety measures is a major goal in the treatment of hospitalized patients with liver cirrhosis.

Method: In a cohort of hospitalized patients with liver cirrhosis between 2017 and 2019 at the department for gastroenterology at the University Hospital Frankfurt clinical data, treatment courses and follow-up data were assessed retrospectively and statistically analyzed using SPSS.

Results: In the analyzed period there were a total of 1985 hospitalizations of patients with liver cirrhosis. 80 falls were documented with respective complications. Median age significantly differed between the two groups (64 vs. 61 years on admission, $p < 0.001$) and in-hospital mortality was significantly higher in the group of patients with documented falls (27.5% vs. 8.9%, $p < 0.001$). There was no association of etiology and falling incident. 19.9% of the analyzed hospitalizations ($n=396$) included patients with an implanted TIPS. 63 of them fell during their hospital stay making up 78.8% of the patients with a documented falling incident. Reasons for admission in the fall-cohort were decompensation (37.5%), hepatic encephalopathy (32.5%), infection (22.5%) and others. While there was a significant difference in all of them, hepatic encephalopathy ($p=0.006$, OR 2.776, 95% CI) and implanted TIPS ($p < 0.001$, OR 3.146, 95% CI) were the two factors independently associated with in-hospital falls in the uni- and multivariate analysis.

Conclusion: Hospitalized patients with hepatic encephalopathy on admission and patients with a TIPS are at high risk for in-hospital falls. Given the associated increase in in-hospital mortality, these patients require specific safety measurements on admission and continuous monitoring.

WED-386

Correlation between mid-arm circumference and QRS alterations as markers of sarcopenia in patients with decompensated cirrhosis

Letitia Toma^{1,2}, Codruta Radu¹, Adriana Mercan-Stanciu^{1,2}, Teodora Isac^{1,2}, Mihai Dodot^{1,2}, Mircea Istrate^{1,2}, Razvan Rababoc^{1,2}, Elena Laura Iliescu^{1,2}. ¹Fundeni Clinical Institute, Internal Medicine, Bucharest, Romania, ²“Carol Davila” University of Medicine and Pharmacy, Bucharest, Romania
Email: letitia_toma@yahoo.com

Background and aims: Sarcopenia is a severe complication of liver disease, associated with a poor prognosis and decreased survival. Early identification and management may improve the patients' outcome. Sarcopenia affects muscle mass and function and may be diagnosed by measuring mid-arm circumference. Cardiac sarcopenia, reflected by electrocardiographic changes, is an important component in the pathogenesis of cirrhotic cardiomyopathy. The aim of this study is to evaluate the relationship between systemic sarcopenia estimated by mid-arm circumference and QRS amplitude and duration.

Method: We performed a cross-sectional observational study including patients with decompensated cirrhosis evaluated in our clinic between January 2022 and December 2022. Patients with cured hepatitis C virus infection or hepatitis B virus infection undergoing treatment with nucleoside analogues and undetectable viremia were considered eligible. Patients with history of cardiovascular disease, malignancies, malabsorption, alcohol-related liver disease, deposit diseases or acute decompensation were excluded from the trial. A total of 161 patients were included and divided into 2 groups, according to Child Pugh classification. We evaluated mid upper arm circumference (MUAC), serum levels of albumin, total cholesterol, INR, as well as QRS mean amplitude and duration in all limb and precordial leads. QRS hypovoltage was defined as less than 0.5 mV in one limb lead and less than 1 mV in one precordial lead.

Results: We included 108 patients with Child B cirrhosis and 53 patients with Child C cirrhosis, with a female predominance in both groups (59.25% and 66.03% respectively). There was no statistically significant difference in age between the groups (56.24 ± 21.32 years versus 59.22 ± 18.3 years, $p = 0.8$). We noted decreased MUAC in Child C patients, both male and female, compared to Child B patients, as well as decreased QRS amplitude and increased QRS duration within the subgroups (Table). Hypovoltage was present in 9 Child B patients (8.33%) and 41 Child C patients (77.35%). Sarcopenia defined by MUAC was noted in 28 Child B patients (25, 92%) and 49 Child C patients (92.45%). Low MUAC correlated with low QRS amplitude in male ($p = 0.02$, CI 95%) and female patients ($p = 0.01$, CI 95%) and also with increased QRS duration ($p = 0.03$ and $p = 0.02$ respectively).

Figure: Table: Differences in clinical, biologic and electrocardiographic parameters in Child B and Child C in the male and female population

	Male		P value	Female		P value
	Child B N = 44	Child C N = 18		Child B N = 64	Child C N = 35	
Albumin (g/dL)	3.01 \pm 0.52	2.73 \pm 1.12	<0.01	3.22 \pm 0.82	2.45 \pm 0.98	<0.01
Total Cholesterol (mg/dL)	167.88 \pm 45.18	97.21 \pm 62.46	<0.01	154.29 \pm 28.32	102.29 \pm 38.13	<0.01
INR	1.37 \pm 0.53	1.98 \pm 1.09	<0.01	1.64 \pm 0.28	2.02 \pm 0.87	<0.01
MUAC (cm)	25.12 \pm 5.29	21.44 \pm 4.12	0.03	26.73 \pm 3.98	20.15 \pm 4.73	0.02
QRS -A (limbs) (mV)	0.92 \pm 0.36	0.61 \pm 0.41	0.02	0.89 \pm 0.22	0.77 \pm 0.35	0.03
QRS- A (precordial) (mV)	2.14 \pm 0.76	1.13 \pm 0.19	0.04	1.98 \pm 0.57	1.01 \pm 0.42	0.03
QRS- D (ms)	92.27 \pm 7.82	115.28 \pm 10.61	0.01	96.35 \pm 9.17	122.24 \pm 11.85	0.02

Conclusion: MUAC as well as QRS amplitude and duration may serve as markers for sarcopenia in decompensated cirrhosis. The accessibility of these parameters makes them easy to use in clinical practice.

WED-387

Uromodulin serum levels are associated with poorer prognosis in patients with cirrhosis and hepatorenal syndrome

Eva Maria Schleicher^{1,2}, Simon J. Gairing^{1,2}, Darko Castven³, Charlotte Sophie Hock¹, Henrike Dobbermann³, Raffael Schlüter³, Sophia Heinrich⁴, Leonard Kaps^{1,2}, Peter Galle^{1,2}, Julia Weinmann-Menke¹, Marc Nguyen-Tat¹, Jens Marquardt³, Christian Labenz^{1,2}. ¹University Medical Center of the Johannes Gutenberg-University, Department of Internal Medicine I, Mainz, Germany, ²University Medical Center of the Johannes Gutenberg-University, Cirrhosis Center Mainz (CCM), Mainz, Germany, ³University Hospital Schleswig-Holstein, Lübeck, Department of Medicine I, Germany, ⁴Hanover Medical School, Clinic for Gastroenterology, Hepatology and Endocrinology, Germany
Email: eva.schleicher@unimedizin-mainz.de

Background and aims: Hepatorenal syndrome (HRS) is associated with a dismal prognosis in patients with cirrhosis. Biomarkers to identify patients with poor response to therapy with terlipressin and albumin are urgently needed. Uromodulin is a kidney-specific protein and a reliable, early biomarker of impaired renal function. This study aimed to evaluate the predictive value of serum levels of Uromodulin (sUMOD) in patients with cirrhosis and HRS treated with vasopressors.

Method: This study analyzed data of 81 patients with HRS treated with terlipressin and albumin, 39 patients with cirrhosis without kidney injury and 33 patients with cirrhosis with prerenal acute kidney injury (AKI) treated at the Cirrhosis Center Mainz, Germany. sUMOD were analyzed by ELISA and clinical data were collected. Patients with HRS treated with terlipressin were prospectively followed for the composite end point of hemodialysis-/liver transplantation-free survival (HD/LTx-free survival).

Results: Of the 81 patients with HRS, 40 had HRS type 1 and 41 HRS type 2. In the cohort of patients with HRS treated with terlipressin, median sUMOD were 100 ng/ml (interquartile range (IQR) 64; 144). sUMOD differed significantly between patients with HRS compared to patients with no AKI ($p = 0.001$), but not between patients with HRS and prerenal AKI ($p = 0.872$). There was a non-significant trend for lower sUMOD in patients with HRS type 2 compared to type 1 (type 2 vs. 1: 99 vs. 106 ng/ml, $p = 0.094$). Patients with sUMOD in the lowest quartile had significantly lower rates of complete response of HRS after treatment with terlipressin ($p = 0.044$). During follow-up, a total of 75 patients with HRS reached the end point of HD/LTx-free survival. In multivariable Cox regression analysis, sUMOD in the lowest quartile (<64 ng/ml) (HR 1.747, 95% CI 1.013–3.011, $p = 0.045$) and MELD (HR 1.081, 95% CI 1.047–1.116, $p < 0.001$) were independently associated with HD/LTx-free survival during follow-up. In logistic regression analysis, sUMOD in the lowest quartile were independently associated with 90-days HD/LTx-free survival (OR 3.957, 95% CI 1.033–15.163, $p = 0.045$) after adjusting for MELD (OR 1.179, 95% CI 1.081–1.286, $p < 0.001$).

Conclusion: sUMOD may be a valuable biomarker to identify patients with HRS treated with terlipressin and poor prognosis.

WED-388

24-Hour urinary creatinine excretion (UCE) a marker of muscle mass is associated with mortality in critically ill patients with cirrhosis

Jaya Benjamin¹, Pallavi Dua¹, Harshita Tripathi¹, Puja Bhatia¹, Varsha Shasthry¹, Saniya Khan¹, Rakhi Maiwall², Guresh Kumar³, Yogendrakumar Joshi¹, Shiv Kumar Sarin². ¹Institute of Liver and Biliary Sciences, Clinical Nutrition and Hepatology, New Delhi, India, ²Institute of Liver and Biliary Sciences, Hepatology, New Delhi, India, ³Institute of Liver and Biliary Sciences, Department of Biostatistics, New Delhi, India
Email: jayabenjaminilbs@gmail.com

Background and aims: Loss of muscle mass is a common feature in cirrhosis which may adversely affect the clinical outcomes in the ICU.

POSTER PRESENTATIONS

Assessment of muscle mass is a challenge in the critically ill cirrhotics (CIC). The 24 hour urine creatinine excretion (UCE) reflects muscle mass and is a simple method in the ICU settings. To study the relationship of UCE at ICU admission with mortality in critically ill cirrhosis Patients.

Method: In this prospective observational study, CIC meeting the inclusion (age 18–65 yrs, likely ICU stay >24 hours) and exclusion criteria (patients with chronic kidney disease, malignancy, acute kidney injury, anuria or on dialysis) were enrolled. Total duration of ICU stay and mortality were noted. Urinary creatinine concentration was assessed by kinetic modified Jaffe Method. UCE was determined by multiplying the urinary creatinine concentration with the 24 hour urinary volume and expressed in gm/24 hours. An average of first 3 days UCE after admission was taken for analysis. Value of UCE was divided into tertiles (T), and mortality was compared between tertiles using chi-square test. The association of UCE with mortality was analyzed using Kaplan-Meier graph and log-rank test across tertiles.

Results: Altogether, 104 CICs [male-76%; age-48.8 ± 10 yrs; BMI 23.6 ± 4.6 kg/m²; etiology: alcohol-60%, NASH-15%, others-16%; CTP-10.7 ± 1.5; MELD-27.6 ± 8.1; SOFA-9.5 ± 2.8; APACHE-18.2 ± 6.9; MV- 48 (46%)] were studied. The mean UCE (gm/24 hours) was 0.77 ± 0.4 (range 0.33–2.7) and UCE categorization on the basis of tertiles was T1-≤0.57, T2-0.58–0.82, T3- >0.82. Overall, mortality was seen in 62 (59.6%) patients, which was significantly different between tertiles of UCE [T1:T2:T3 = 26 (41.9%) : 23 (37.1%) : 13 (20.9%); p = 0.030]. Patients in the lowest UCE tertile had an increased mortality compared to those in the highest UCE tertile as depicted in Kaplan Meier graph (fig1).

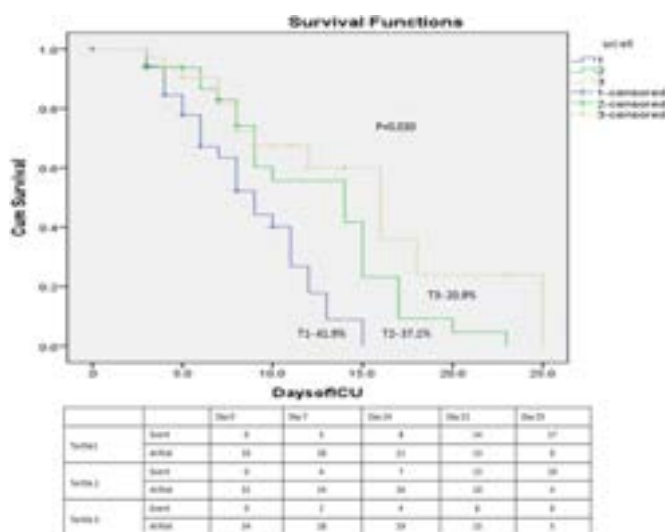


Figure 1: Association of Urinary Creatinine Excretion (UCE) with Mortality in Critically Ill Cirrhotics (CIC)

Figure:

Conclusion: In critically ill patients with cirrhosis low urinary creatinine excretion is associated with higher mortality, thereby underscoring the role of muscle mass as a risk factor for mortality and UCE as a relevant marker.

WED-389

Rotational Thromboelastometry (ROTEM) reduces need for pre-emptive transfusion in low-moderate risk procedure in cirrhosis: a randomized controlled trial

Chin Kim Tan¹, Louis Ng², Eugene Wong³, Kenneth Lin³, Andrew Kwek³, James, Weiquan Li³, Tiing Leong Ang³, Louis Wang³, Tianyu Qiu³, Roshni Sahashiv⁴, Tirukonda Prasanna Sivanath⁴, Rahul Kumar³. ¹Changi General Hospital, Department of Gastroenterology and Hepatology, Singapore, ²Changi General Hospital, Department of Respiratory Medicine, Singapore, Singapore, ³Changi

General Hospital, Department of Gastroenterology and Hepatology, Singapore, Singapore, ⁴Changi General Hospital, Department of Radiology, Singapore, Singapore
Email: ckimg87@yahoo.com

Background and aims: Viscoelastic tests (VET) like Rotational Thromboelastometry (ROTEM) assess global hemostasis in cirrhosis. We aimed to assess whether ROTEM-guided blood product transfusion results in lower blood product requirement in patients with cirrhosis undergoing elective invasive procedures as compared to standard of care (SOC) based on conventional coagulation tests (CCT).

Method: This is a planned scheduled interim analysis of a single center randomized controlled trial. Patients with cirrhosis and coagulopathy requiring blood product transfusion based on CCT undergoing elective invasive procedure were recruited. Patients were randomized in a 1:1 ratio to receive blood products by either ROTEM-guidance or standard of care (SOC). The primary outcome was the difference in blood products (fresh frozen plasma (FFP) or platelets) transfused between the groups. The secondary outcome was procedure related bleeding or complications within 7 days of the procedure. Haybittle-Peto rule was applied for the interim analysis with p < 0.001 taken as statistically significant.

Results: From August 2021 to January 2023, 40 patients were recruited (20 in each group). The mean age was 57.4 ± 9.3 years. Most patients underwent large volume paracentesis (n = 23, 57.5%) followed by microwave ablation of liver tumor (n = 5, 12%). Other procedures were hepatic venous pressure gradient measurement (n = 4, 10%) and percutaneous liver biopsy (n = 3, 7.5%). More than half of the patients had Child Pugh C liver cirrhosis (n = 24, 64%) with a mean MELD score of 17.38 ± 6.14. Mean platelet count was 75 ± 51 × 10⁹/L, mean prothrombin time (PT) was 16.2 ± 2.9 seconds, mean INR 1.55 ± 0.31 and mean activated partial thrombin time was 39.9 ± 12.01 seconds. There was no difference in the baseline demographics, CCT (platelet count, PT, INR and APTT), ROTEM parameters, Child-Pugh and MELD score between the two groups. Overall, 8 (40%) patients in ROTEM-group required pre-emptive blood products compared to all (100%) in SOC group (p < 0.001), Figure 1. The volume of FFP (63 mls ± 160 mls vs 325 mls ± 500 mls, p < 0.001) and platelet (70 mls ± 98 mls vs 110 mls ± 137 mls p = 0.048) transfused were lower in the ROTEM group. None of the patients included in the study had clinically significant bleeding events. One patient (5%) in the SOC group developed allergic reaction but none developed transfusion associated lung injury.

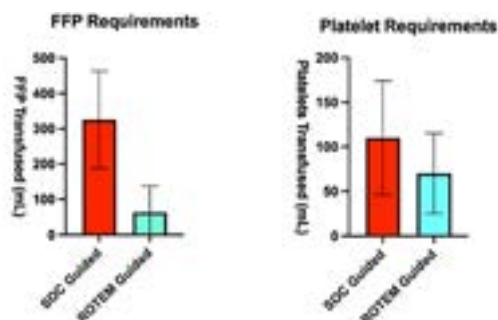


Fig 1: Comparison of Blood product requirements: FFP and Platelets

Abbreviations: FFP, Fresh Frozen Plasma, ROTEM, Rotational Thromboelastometry, SOC, Standard of Care

Figure: Fresh frozen plasma (FFP) and platelet transfusion in ROTEM-guided group and standard of care (SOC) group.

Conclusion: ROTEM-guided transfusion strategy significantly reduces the need for FFP transfusion in patients with cirrhosis undergoing elective procedure without any increased risk of bleeding events. It has important implication as it can reduce transfusion associated adverse events. Trial registration number: NCT05698134.

WED-390

Long-term cellular immune response to COVID-19 vaccination in patients with chronic liver disease

Mariana Moura Henrique¹, Carolina Santos Palma¹, André L. Simão¹, Ana Godinho-Santos¹, Miguel Cardoso¹, Diogo Fernandes¹, Sofia Carvalhana², Miguel Moura², João Gonçalves¹, Helena Cortez-Pinto^{2,3}, Rui E. Castro¹. ¹Research Institute for Medicines (iMed.Ulisboa), Faculty of Pharmacy, Universidade de Lisboa, Lisbon, Portugal, ²Departamento de Gastrenterologia, Centro Hospitalar Universitário Lisboa Norte, Lisbon, Portugal, ³Clínica Universitária de Gastrenterologia, Faculdade de Medicina, Universidade de Lisboa, Lisbon, Portugal
Email: ruieduardocastro@ff.ulisboa.pt

Background and aims: Patients with chronic liver disease (CLD), particularly those with cirrhosis, typically present with immune dysregulation, which may lead to a higher risk of adverse outcomes after SARS-CoV-2 infection and a defective immune response after COVID-19 vaccination. Because patients with CLD were not included in COVID-19 vaccine licensing studies, data on effectiveness in this vulnerable population is lacking. Our aim was to evaluate cellular immune responses of CLD patients to COVID-19 vaccines.

Method: Blood from Portuguese CLD patients and healthy volunteers receiving the mRNA-1273, BNT162b2, ChAdOx1 and Ad26.COV2.S vaccines were collected prior to vaccination, six months after vaccination, and one year after vaccination (after 3rd dose). Immunophenotyping of peripheral blood mononuclear cells was performed by flow cytometry with acquisition on a four-laser spectra analyzer, using a panel composed of twenty-two surface markers and a viability dye. After gating, a total of twenty-eight different immune cell subsets were identified.

Results: Prior to and at six months after vaccination, the number of CD4⁺ T cells was lower in vaccinated patients comparing to vaccinated healthy individuals. During the first six months following vaccination, naïve CD8⁺ T cells decreased more in CLD patients comparing to healthy individuals, while plasmablasts increased in healthy individuals but not in CLD patients, suggesting a defective production of these antibody secreting B cells in vaccinated patients. In turn, one year after vaccination, the subsets of T and Natural Killer cells were found increased in both groups, suggesting that the booster dose is critical for inducing a strong cellular immune response. Curiously, cirrhotic patients presented with more CD27⁺ B cells comparing to non-cirrhotic patients. Finally, regarding COVID-19 infection, variations in the percentage of gated cells before and one year after vaccination were similar in almost all cell sub-types, except for TEMRA CD8⁺ T cells, which showed a more prevalent decrease in non-infected patients.

Conclusion: Patients with more advanced stages of CLD display impaired cellular immune responses to COVID-19 vaccination. Notwithstanding, impaired responses are largely recovered after the administration of a third dose of the vaccine. Studying the response of patients with CLD to recent SARS-CoV-2 variants should elucidate whether novel COVID-19 vaccines are needed.

WED-391

The relation of serum nesfatin-1 levels with disease severity and complications in patients with liver cirrhosis

Özlem Kandemir Alibakan¹, Hasan Eruzun², Yasemin Gökden³, Yücel Arman¹, Tufan Tükek⁴. ¹Prof. Dr. Cemil Taşçıoğlu City Hospital, Internal Medicine, İstanbul, Turkey, ²Ondokuz Mayıs University, School of Medicine, Gastroenterology, Samsun, Turkey, ³Prof. Dr. Cemil Taşçıoğlu City Hospital, Gastroenterology, İstanbul, Turkey, ⁴İstanbul University, School of Medicine, Internal Medicine, İstanbul, Turkey
Email: hasaneruzun@gmail.com

Background and aims: Nesfatin-1 is an anorectic polypeptide that has important roles in the regulation of food intake and energy homeostasis. With the hypothesis that common problems such as cachexia and malnutrition in patients with cirrhosis might be due to

the increase in nesfatin-1 protein, we examined the levels of nesfatin-1 peptide in patients with cirrhosis and its relationship with the severity of the disease.

Method: Fifty-one patients with cirrhosis and thirty healthy volunteers were included in the study. Serum samples were collected from the groups and serum nesfatin-1 levels were compared using ELISA. Child-Pugh stages and multifactorial end-stage liver disease (MELD) scores of patients with cirrhosis were calculated and their relationship with nesfatin-1 was examined. In addition, the relationship between the complications of cirrhosis and nesfatin-1 was investigated.

Results: Nesfatin-1 levels were found to be significantly higher in the patients with cirrhosis than in the control group ($p = 0.001$). Patients with cirrhosis were grouped as compensated and decompensated and compared with the control group. It was determined that the significant difference between these three groups ($p = 0.001$) was due to the elevation of nesfatin-1 in the compensated cirrhosis group ($p = 0.01$). When patients with cirrhosis were classified according to Child-Pugh stages and MELD scores, there was no significant relationship between these groups and nesfatin-1 levels.

Nesfatin-1 (ng/ml)	Control A (n = 30)	Compensated cirrhosis B (n = 20)	Decompensated cirrhosis C (n = 31)	A-B-			
				C p value	A-B p value	A-C p value	B-C p value
Median	7.2 (6– 10.1)	11.9 (10.2– 14.8)	10.4 (6.6–12.6)	0.001	0.010	0.077	0.218
BMI		28.01 (± 4.09)	26.9 (± 4.27)				0.38

Figure:

Conclusion: Nesfatin-1 may be involved in the maintenance of compensation with its antioxidant, anti-inflammatory, and anti-apoptotic effects. The decrease in serum nesfatin-1 levels in decompensated cirrhosis compared with compensated cirrhosis may be due to the defense mechanism and insufficient production.

Cirrhosis and its complications Portal Hypertension

WEDNESDAY 21 TO SATURDAY 24 JUNE

TOP-043

Natural history of patients with NAFLD-associated compensated advanced chronic liver disease stratified according to severity of portal hypertension

Rafael Paternostro¹, Wilhelmus Kwanten², Benedikt Hofer¹, Georg Semmler¹, Ali Bagdadi², Irina Luzko³, Virginia Hernandez-Gea³, Isabel Graupera³, Juan Carlos Garcia Pagan³, Dario Saltini⁴, Federica Indulti⁴, Filippo Schepis⁴, Lucile Moga⁵, Pierre-Emmanuel Rautou⁵, Elba Llop⁶, Luis Téllez⁷, Agustín Albillos⁷, Jose Ignacio Fortea⁸, Angela Puente⁸, Giulia Tosetti⁹, Massimo Primignani⁹, Alexander Zipprich¹⁰, Élise Vuille-Lessard^{11,12}, Annalisa Berzigotti¹¹, Madalina Gabriela Taru¹³, Vlad Taru¹³, Bogdan Procopet¹³, Christian Jansen¹⁴, Michael Praktikjnjo¹⁵, Wenyi Gu¹⁵, Jonel Trebicka¹⁵, Luis Ibañez¹⁶, Rafael Bañares¹⁶, Jesús Rivera¹⁷, Juan Manuel Pericàs¹⁷, Joan Genesca¹⁷, Edilmar Alvarado-Tapias¹⁸, Cándid Villanueva¹⁸, Hélène Larrue¹⁹, Christophe Bureau¹⁹, Wim Laleman²⁰, Alba Ardevol Ribalta²¹, Helena Masnou²¹, Thomas Vanwolleghem², Michael Trauner¹, Mattias Mandorfer¹, Sven Francque², Thomas Reiberger¹. ¹Medical University of Vienna, Austria; ²University of Antwerp, Belgium; ³University of Barcelona,

POSTER PRESENTATIONS

Spain; ⁴Azienda Ospedaliero-Universitaria di Modena and University of Modena and Reggio Emilia, Italy; ⁵Hôpital Beaujon, France; ⁶Hospital Puerta del Hierro, Spain; ⁷Hospital Universitario Ramón y Cajal, Spain; ⁸Marqués de Valdecilla University Hospital, Spain; ⁹University of Milan, Italy; ¹⁰Friedrich-Schiller-Universität Jena, Germany; ¹¹Inselspital-University of Bern, Switzerland; ¹²Inselspital, Bern University Hospital, University of Bern, Switzerland, Department of Visceral Surgery and Medicine, Switzerland; ¹³Hepatology Department and "Iuliu Hatieganu" University of Medicine and Pharmacy, Romania; ¹⁴University Hospital Bonn, Germany; ¹⁵University Hospital Muenster, Germany; ¹⁶Hospital General Universitario Gregorio Marañón, Spain; ¹⁷Vall d'Hebron Hospital Universitari, Spain; ¹⁸Hospital de la Santa Creu i Sant Pau, Spain; ¹⁹Toulouse university hospital, France; ²⁰Hepatology, University Hospitals Leuven, and Department of Liver and Biliopancreatic disorders, KU Leuven, Belgium; ²¹H.Germans Trias i Pujol, Spain
Email: rafael.paternostro@meduniwien.ac.at

Background and aims: Non-alcoholic fatty liver disease (NAFLD) is a leading cause of advanced chronic liver disease (ACLD). Portal hypertension (PH) drives decompensation and is best diagnosed by hepatic venous pressure gradient (HVPG). However, in NAFLD-ACLD decompensation may occur at lower HVPG thresholds than in other ACLD etiologies. Here we investigate the clinical course of strictly compensated NAFLD-ACLD patients (NAFLD-cACLD) according to severity of PH.

Method: In this European multicentre study, NAFLD-cACLD patients were characterized by HVPG at baseline. Patients with any previous decompensation, hepatocellular carcinoma and portal vein thrombosis were excluded. First occurrence of hepatic decompensation (ascites, hepatic encephalopathy, variceal bleeding) or liver-related death defined the composite study end point. Fine and Gray competing risk regression models were used for time-to-event outcome analyses.

Results: 342 patients with NAFLD-cACLD with a median MELD of 8 (7–9) points and a median HVPG of 11 mmHg (11–15) were included; 244 (71.3%) had diabetes. NAFLD diagnosis was made via liver biopsy in 281 (82.2%) and clinical in 61 (17.8%) patients.

CSPH (HVPG ≥ 10 mmHg) was present in 210/342 patients (61.4%) including 71 patients with severe PH (HVPG ≥ 16 mmHg; PH16; 20.8%). Median BMI was 31.7 kg/m² (28.0–35.8), with a significantly lower BMI in the CSPH group (31.5 vs. 32.6 kg/m², $p = 0.011$). During a median follow-up of 41.5 (28–66) months, 85 (24.9%) patients developed liver-related events: 36 (10.5%) ascites, 23 (6.7%) hepatic encephalopathy, 16 (4.7%) variceal bleeding and 10 (2.9%) liver-related death.

CSPH (vs. <10 mmHg; subdistribution hazard ratio-SHR: 4.81, $p < 0.001$) and PH16 (vs. <10 mmHg; SHR: 6.44, $p < 0.001$) represented significant risk factors for developing decompensation or liver-related death. Importantly, NAFLD-cACLD patients developed decompensation even without CSPH with a rate of 1.5% within the first year (Y1) and 3.3% within Y2. Variceal bleeding did, however, not occur in patients without CSPH. With increasing severity of PH, i.e. with HVPG 10–15 and ≥ 16 mmHg, respectively, the cumulative incidence rates for developing first hepatic decompensation gradually increased at Y1: 2.2%/8.7%, at Y2: 10.7%/13.5%, and at Y5 36.3%/50.3% (Figure).

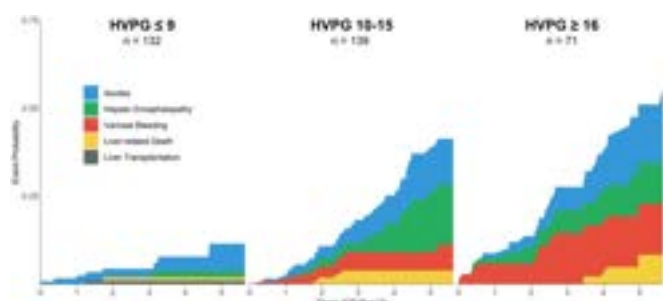


Figure: Stacked incidence curves for the respective first liver-related events during follow-up, stratified according to severity of portal hypertension.

Conclusion: CSPH is strongly linked to the incidence of hepatic decompensation in NAFLD-cACLD. Decompensation, however, may also occur, albeit at low rates, at HVPG <10 mmHg, suggesting an underestimation of PH severity by HVPG. Nevertheless, HVPG represents an important risk stratification tool in NAFLD-cACLD patients.

TOP-045

The effect of precipitating factors for hepatorenal syndrome on response to terlipressin treatment: a subgroup analysis of a pooled North American database

Kevin Moore¹, Zunaira Zafar², Nikolaos T. Pylsopoulos³, Khurram Jamil⁴. ¹UCL Institute of Liver and Digestive Health, Royal Free Hospital, University College London, London, United Kingdom; ²St. Mary Medical Center, Langhorne, PA, United States; ³Rutgers University, New Jersey Medical School, Newark, NJ, United States; ⁴Mallinckrodt Pharmaceuticals, Hampton, NJ, United States
Email: kevin.moore@ucl.ac.uk

Background and aims: Hepatorenal syndrome (HRS) type 1 is a potentially reversible form of acute kidney injury. Terlipressin is approved for the treatment of adult patients (pts) with HRS and rapidly worsening kidney function. This study assessed the efficacy of terlipressin in patient subgroups based on their precipitating factors (PFs) for HRS in a pooled dataset.

Method: Pooled data from 3 North American placebo-controlled Phase III clinical studies (OT-0401, REVERSE, and CONFIRM) of terlipressin to treat pts with HRS type 1 (N = 564), was evaluated for the effect of PFs on efficacy outcomes including renal replacement therapy (RRT) at Day 90, HRS reversal (serum creatinine [SCr] ≤ 1.5 mg/dL up to 24 hours after the last dose of study drug; SCr values obtained posttransplant or post-RRT were excluded), overall survival, and transplant-free survival (TFS) at Day 90. Significance was determined using a Fisher's exact test.

Results: The most common PF for HRS was hypovolemia due to large volume paracentesis or diuretic therapy (25.2%), followed by infection (18.3%) and gastrointestinal (GI) bleeding (6.2%); no PFs were reported in 50.3% of pts. The incidence of RRT by Day 90 was numerically lower in the terlipressin group versus placebo (overall, 32.2% [109/338] vs 41.2% [93/226]), with the largest difference among those pts with GI bleeding (26.3% vs 43.8%). HRS reversal was higher in the terlipressin versus placebo group, with a significant improvement among pts with no PF or PFs of hypovolemia or infection. Overall survival at Day 90 in pts with GI bleeding was numerically higher in the terlipressin group versus placebo (47% vs 19%; $p = .152$) and was otherwise similar for the remaining PF subgroups. TFS at Day 90 was numerically higher for the terlipressin group among pts with GI bleeding and hypovolemia (Figure).

Conclusion: Treatment with terlipressin leads to greater HRS reversal and less need for RRT compared with placebo. Across subgroups, HRS reversal in response to terlipressin was significantly greater among pts with no PFs or PFs of infection or hypovolemia.

TOP-048

Predictors and management of post-banding ulcer bleeding in cirrhosis: a systematic review and meta-analysis

Maria De Brito Nunes¹, Matthias Knecht², Reiner Wiest², Jaume Bosch¹, Annalisa Berzigotti². ¹Department for BioMedical Research of University of Bern (Mu35), Bern, Switzerland; ²Department of Visceral Surgery and Medicine, Bern, Switzerland
Email: maria.debritorodriguesnunes@unibe.ch

Background and aims: Esophageal varices endoscopic band ligation (EBL) is an endoscopic procedure aimed at eradicating esophageal varices in patients with cirrhotic portal hypertension, by ligating

Figure: (abstract: TOP-045): Efficacy Outcomes by Precipitating Factors (PFs) for Hepatorenal Syndrome (HRS) for Terlipressin (Terli) versus Placebo (Pbo)

Possible PFs	Infection n = 103			Gastrointestinal Bleeding n = 35			Hypovolemia n = 142			No PFs identified or reported n = 284		
N = 564												
Parameter, n (%)	Terli n = 59	Pbo n = 44	p value	Terli n = 19	Pbo n = 16	p value	Terli n = 83	Pbo n = 59	p value	Terli n = 177	Pbo n = 107	p value
HRS Reversal	24 (40.7)	8 (18.2)	.018	4 (21.1)	1 (6.3)	.347	30 (36.1)	11 (18.6)	.025	61 (34.5)	17 (15.9)	<.001
Renal Replacement Therapy by Day 90	22 (37.3)	20 (45.5)	.425	5 (26.3)	7 (43.8)	.311	29 (34.9)	25 (42.4)	.386	53 (29.9)	41 (38.3)	.154
Overall Survival on Day 90	30 (50.8)	24 (54.5)	.842	9 (47.4)	3 (18.8)	.152	46 (55.4)	33 (55.9)	1.000	89 (50.3)	63 (58.9)	.178
Transplant-Free Survival at Day 90	8 (13.6)	5 (11.4)	1.000	2 (10.5)	0	.489	16 (19.3)	6 (10.2)	.163	32 (18.1)	18 (16.8)	.873

them with rubber rings (bands). According to current international guidelines, EBL of esophageal varices plays an important therapeutic role in three settings: a) the prevention of a first VH as an alternative to non-selective beta-blockers (NSBB) in patients with contraindications or who cannot tolerate these drugs; b) to achieve hemostasis in combination with vasoactive drugs (somatostatin, octreotide or terlipressin) in patients with acute VH; and c) to prevent recurrent bleeding. In the latter case, patients are treated both with NSBB and EBL. Post-banding ulcer bleeding (PBUB) is an understudied complication of this procedure. The aims of this systematic review with meta-analysis were: to review the reported incidence of PBUB in patients with cirrhosis and varices treated with EBL in primary and secondary prophylaxis or urgent treatment for acute variceal bleeding; to identify predictors of PBUB; and to ascertain strategies to prevent and manage bleeding after PBUB.

Method: A systematic review of articles in English published in 2006–2022 was conducted using the Preferred Reporting Items for Systematic Reviews and Meta-analyses (PRISMA) guidelines. Searches were made in the following electronic databases: Google

Scholar, Medline (OVID interface), Embase (OVID interface), PubMed, Cochrane Library, Cochrane Central Register of Controlled Trials (CENTRAL), clinicaltrials.gov, EU clinical Trials. An independent extraction of articles using predefined data fields and quality indicators was used. Random effects meta-analysis was used to determine the incidence, mean interval and predictors of PBUB in cirrhosis. Treatment of PBUB were assessed with qualitative analysis due to the heterogeneity of procedures employed to control bleeding. **Results:** Eighteen studies (9034 patients) were included. The incidence of PBUB was overall 5.5% (95% CI, 4.3–7.1%). The mean time for it to occur was 11 days (95% CI 9.94–11.97). Model for End-stage Liver Disease score (OR 1.162, 95% CI 1.047–1.291, p 0.005) and endoscopic band ligation done in emergency setting (OR 4.09, 95% CI 2.99–8.05, p < 0.001) independently predicted PBUB. Patients were treated with a variety of drugs (vasoactive drugs such as somatostatin, octreotide or terlipressin, endovenous proton pump inhibitors) and/or endoscopic procedures (EBL, argon plasma coagulation, esophageal variceal obliteration with sclerotherapy or cyanoacrylate injection, epinephrine injection, hemoclip) and Transjugular

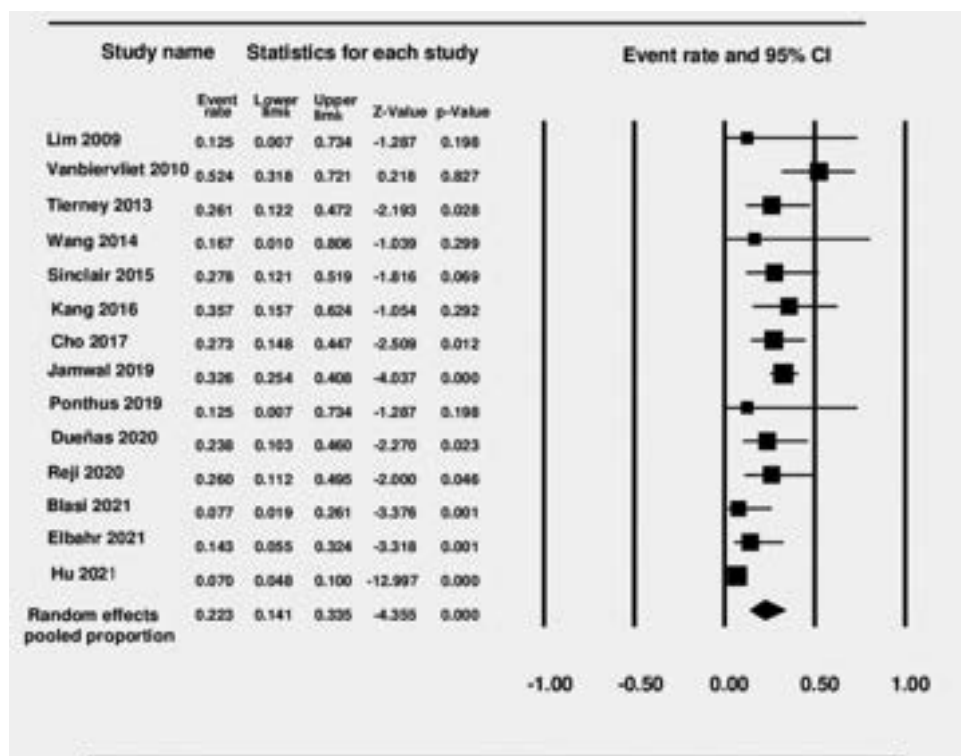


Figure: (abstract: TOP-048): Mortality associated to PBUB

POSTER PRESENTATIONS

Intrahepatic Portosystemic Shunt (TIPS) for severe bleeding. Refractory bleeding was treated with self-expandable metallic stents and oesophageal balloon tamponade. Treatments had a limited success, as shown by a mortality after PBUB of 22.3% (IC 95%, 14.1–33.6%) (Figure).

Conclusion: Patients more prone to develop PBUB are those with high MELD score, and EBL performed in an emergency context. PBUB carries a severe prognosis with a high mortality despite the variety of treatments used, which calls for prospective, specifically designed studies to improve outcomes of this severe iatrogenic complication. The best therapeutic strategy to address PBUB remains to be ascertained.

SATURDAY 24 JUNE

SAT-325

Outcome of sucralfate vs proton pump inhibitor vs sucralfate and proton pump inhibitor combination post endoscopic esophageal variceal band ligation-A randomized controlled trial

Arun Vaidya¹, Mayur Satai¹, Abu Aasim Ansari¹, Shashank Pujalwar¹, Gautam Jain¹, Tanmay Laxane¹, Shruti Mehta¹, Aditya Kale¹, Akash Shukla¹. ¹Seth GS Medical college and KEM Hospital, Mumbai, Department of Gastroenterology, India
Email: drakashshukla@yahoo.com

Background and aims: Proton pump inhibitor (PPI) and mucoprotectant like sucralfate are commonly used post variceal band ligation. However, data is sparse in literature on outcome of using them alone or in combination. Therefore, we conducted this trial with the aim to study the outcome of using combination of sucralfate and PPI vs sucralfate alone vs PPI alone vs no treatment post endoscopic variceal band ligation in terms of presence of band ulcers, chest pain, ulcer related bleeding and mortality.

Method: We conducted a single center, single blind randomized trial and included patients above 18 years undergoing esophageal variceal band ligation. Patients already on PPI or sucralfate, pregnant, on anticoagulation, having acute kidney injury or chronic kidney disease and pre-existing esophageal ulcers on endoscopy were excluded. Using simple randomization technique, patients were randomized in 4 arms: Sucralfate plus PPI combination, PPI alone, Sucralfate alone and no treatment. Patients were given these medications for 14 days. We repeated endoscopy after 14 days. Primary end point was post band ulcer bleed and ulcer bleed related mortality at day 28. Secondary end point was to evaluate post band chest pain and presence of band ulcer in each arm.

Results: We randomized 200 patients (50 patients in each arm). Mean age was 43.93 ± 12.8 years. Males were 157 (78.5%). Post band ulcers were seen in 65 (32.5%) patients with mean of maximum ulcer size was 5 mm. Band related chest pain and ulcer bleed were present in 24 (12%) and 2 (1%) patients respectively. Ulcer bleed related mortality at day 28 was 0.5%. There was no significant difference in presence of post band ulcer, chest pain, bleeding or mortality in any trial arm. Serum albumin level was not associated with presence of band ulcer ($p = 0.766$).

Figure:

Parameters	Sucralfate + PPI (n = 50)	Sucralfate alone (n = 50)	PPI alone (n = 50)	No treatment (n = 50)	p value
Post Band ulcer	17 (34%)	15 (30%)	16 (32%)	17 (34%)	0.969
Chest Pain	5 (10%)	5 (10%)	7 (14%)	7 (14%)	0.568
Ulcer Bleed	1 (2%)	1 (2%)	0	0	0.356
Ulcer bleed related mortality at Day 28	1 (2%)	0	0	0	0.389

Conclusion: Addition of sucralfate, PPI or sucralfate plus PPI combination post variceal band ligation did not reduce post band ulcer bleed or bleed related mortality.

SAT-326

TIPS increases muscle mass in patients with decompensated cirrhosis

Theresa Bucsics^{1,2}, Katharina Lampichler^{2,3}, Jakob Kittinger³, Maria Schoder³, Konstantin Vierziger⁴, Lukas Hartl^{1,2}, Lukas Reider³, Florian Wolf³, David JM Bauer^{1,2}, Mathias Jachs^{1,2}, Georg Semmler^{1,2}, Rafael Paternostro^{1,2}, Philipp Schwabl^{1,2,5}, Lorenz Balcar^{1,2}, Katharina Pomej^{1,2}, Vinzent Karner¹, Michael Trauner¹, Matthias Mandorfer^{1,2}, Thomas Reiberger^{1,2,5}. ¹Medical University of Vienna, Department of Internal Medicine III, Division of Gastroenterology and Hepatology, Wien, Austria; ²Medical University of Vienna, Vienna Hepatic Hemodynamic Laboratory, Department of Internal Medicine III, Division of Gastroenterology and Hepatology, Wien, Austria; ³Medical University of Vienna, Department of Biomedical Imaging and Image-guided Therapy, Wien, Austria; ⁴Klinik Favoriten-Wiener Gesundheitsverbund, Department of Radiology, Wien, Austria; ⁵Medical University of Vienna, Christian Doppler Laboratory for Portal Hypertension and Liver Fibrosis, Wien, Austria
Email: thomas.reiberger@meduniwien.ac.at

Background and aims: Transjugular intrahepatic portosystemic shunt (TIPS) is used to treat complications of portal hypertension (PH). Sarcopenia is prevalent and associated with poor outcomes in patients with decompensated cirrhosis; however, it may potentially improve after TIPS. We systematically evaluated the evolution of (i) muscle mass and (ii) sarcopenia in patients undergoing TIPS.

Method: Retrospective analysis of the Vienna TIPS cohort. Transversal psoas muscle thickness at the 3rd lumbar vertebra (TPMT) was assessed at CT prior to TIPS, at 3–18 months (FU1) and >18 months (FU2) after TIPS by two independent radiologists. Sarcopenia was defined by height-corrected TPMT <12 mm/m (men) or <8 mm/m (women).

Results: 199 patients with cirrhosis were included (age 55.7 ± 11.0 years; 69.3% men; median MELD 11; Child-C: 12.6%), with 132 (66.3%) undergoing TIPS for ascites. Inter-rater agreement of TPMT readings was excellent ($\kappa = 0.766$ –0.975). Median TPMT at baseline was 13.4 (IQR: 11.1–15.4) mm/m in men and 12.0 (9.6–13.3) mm/m in women. Sarcopenia was found in 42.7% and correlated with older age (57.7 ± 9.6 vs 53.8 ± 11.7 years, $p = 0.012$), male sex (50.4% vs 22.7% in women, $p < 0.001$), alcohol-related liver disease, (49.6% in ALD vs 29.4% in other etiologies, $p = 0.006$) and Child-C cirrhosis (72.0% vs 36.4% in Child-A/B, $p < 0.001$). Pre-TIPS portal pressure gradient did not differ between patients with vs. without sarcopenia (20 ± 5 mmHg vs 20 ± 6 mmHg, $p = 0.472$).

Pre-TIPS sarcopenia was further associated with higher risk for post-TIPS overt hepatic encephalopathy (OHE; 56.5% vs 35.1%, log-rank $p = 0.024$) and persistent ascites (48.2% vs 24.6%, $p < 0.001$), but not variceal re-bleeding (3.5% vs 5.3%, $p = 0.630$) and was not identified as an independent risk factor for post-TIPS complications in multivariable analysis.

TPMT improved significantly after TIPS at FU1, with a median relative increase of +18.7% ($p < 0.001$) at FU1. Sarcopenia resolved in 47.4% of patients with an available CT scan at FU1 and in 72.2% at FU2.

Transplant-free survival (TFS) was significantly shorter in patients with sarcopenia at baseline (median: 21.8 vs 65.9 months; $p < 0.001$) as well as in those with sarcopenia at FU1 (TFS after FU1: 4 vs 59 months, $p < 0.001$). When corrected for age, Child-Pugh score, and alcohol-related etiology, sarcopenia at FU1 remained an independent risk factor for mortality afterwards (HR: 6.055, 95% CI: 1.466–25.009, $p = 0.013$).

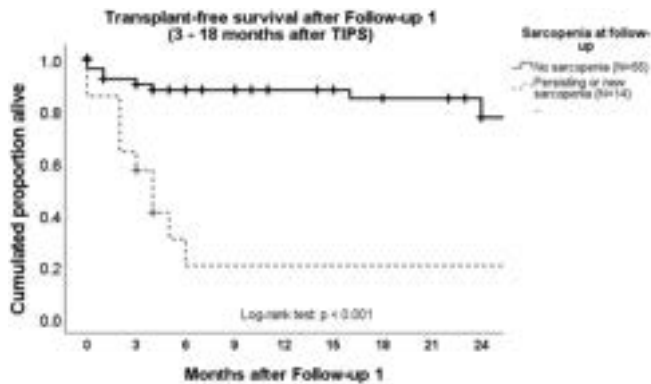


Figure:

Conclusion: Sarcopenia resolves in a considerable share of patients with cirrhosis after TIPS, which is linked to a clear survival benefit. Patients who do not resolve sarcopenia after TIPS remain at considerable risk of mortality and thus should be timely listed for liver transplantation.

SAT-327

Accuracy of spleen stiffness measurement for the diagnosis of clinically significant portal hypertension in patients with advanced chronic liver disease: an individual patient meta-analysis

Elton Dajti^{1,2}, Federico Ravaioli^{1,2}, Romanas Zyklus³, Laure Elkrief⁴, Pierre-Emmanuel Rautou⁵, Ivica Grgurevic⁶, Horia Stefanescu⁷, Masashi Hirooka⁸, Fraquelli Mirella⁹, Matteo Rosselli¹⁰, Jason Pik Eu Chang¹¹, Alberto Borghi¹², Thomas Reiberger¹³, Elba Llop¹⁴, Sebastian Mueller¹⁵, Giovanni Marasco², Annalisa Berzigotti¹⁶, Agostino Colli⁹, Davide Festi², Antonio Colecchia¹. ¹University of Modena and Reggio Emilia, Dipartimento Chirurgico, Medico, Odontoiatrico e di Scienze Morfologiche con interesse Trapiantologico, Oncologico e di Medicina Rigenerativa, Italy; ²University of Bologna, Italy; ³Lithuanian University of Health Sciences, Kaunas, Lithuania; ⁴Service d'Hépatogastroentérologie, CHU de Tours, France; ⁵Université de Paris, AP-HP, Hôpital Beaujon, Service D'Hépatologie, Italy; ⁶University Hospital Dubrava, University of Zagreb School of Medicine and Faculty of Pharmacy and Biochemistry, Croatia; ⁷Regional Institute of Gastroenterology and Hepatology, Liver Unit and Clinical Ultrasound Department, Cluj Napoca, Romania; ⁸Ehime University Graduate School of Medicine, Shitsukawa 454, Toon, Ehime, 791-0295, Japan; ⁹Fondazione IRCCS Ca' Granda Ospedale Maggiore Policlinico, Milano, Italy; ¹⁰UCL Institute for Liver and Digestive Health and Sheila Sherlock Liver Centre, Royal Free Hospital and UCL, London, United Kingdom; ¹¹Singapore General Hospital, Singapore, Singapore; ¹²Internal Medicine Department, Faenza Hospital, Italy; ¹³Medical University of Vienna, Austria; ¹⁴Universidad Autónoma de Madrid, Spain; ¹⁵University of Heidelberg, Germany; ¹⁶Inselspital, Bern University Hospital, Switzerland
Email: e_dajti17@hotmail.com

Background and aims: The identification of patients with clinically significant portal hypertension (CSPH) is of utmost prognostic and therapeutic relevance in patients with compensated advanced chronic liver disease (cACLD). Spleen stiffness measurement (SSM) has been proposed as a direct surrogate of portal hypertension and an accurate non-invasive test for CSPH diagnosis. However, the diagnostic performance and the cut-offs used are very heterogeneous in current literature. Our aim was to perform a systematic review with individual patient data (IPD) meta-analysis to establish the diagnostic performance of SSM and SSM-based algorithms, as measured by different elastography techniques, for the diagnosis of CSPH.

Method: We systematically researched MEDLINE, Ovid Embase, Scopus, and Cochrane Library electronic databases for any study

published up to June 2020 and that reported data on hepatic venous pressure gradient (HVPG) and SSM in adult patients. After receiving IPD data, patients with liver stiffness measurement (LSM) <10 kPa, previous decompensation or missing data were excluded. The diagnostic accuracy of the Baveno VII Criteria and the combined Baveno VII-SSM criteria was assessed using a random effect bivariate model. Sensitivity analyses for cACLD definition, center, etiology, and obesity, were conducted. The methodological quality of the included studies was assessed using QUADAS-2 tool.

Results: Of the 44 eligible articles, 17 studies (14 full-texts, 3 abstracts) were included in the meta-analysis. Six hundred patients from six studies were included in the transient elastography cohort. The Baveno VII and the Baveno VII-SSM criteria with a dual cut-off of 21 and 50 kPa were validated, showing adequate (>90%) negative (NPV) and positive predictive values (PPV) in the whole cohort and in all sensitivity analyses. The combined Baveno VII-SSM criteria with a single cut-off (40 kPa) was the most performant in ruling-in CSPH with PPV >90%, while it could rule-out safely CSPH only in viral etiology. The SSM-based algorithms significantly reduced the rate of patients in the "grey zone" from 48% (Baveno VII criteria) to 32% and 9%, respectively. Similar cut-offs showed adequate performance also in the two-dimensional shear-wave elastography (SWE) cohort, compromising 225 patients from five studies. Available data was insufficient to evaluate the performance of SSM assessed by point-shear-wave-elastography.

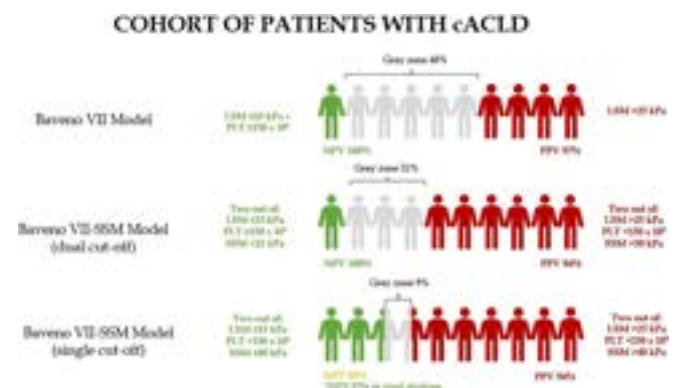


Figure:

Conclusion: The combined Baveno VII-SSM models are highly performant non-invasive algorithms to diagnose CSPH, and were validated in this large, multicenter, international study. Importantly, they significantly reduce the rate of patients in the "grey zone." These criteria can be used in clinical practice to best identify patients that could benefit from carvedilol treatment to reduce the risk of first decompensation.

SAT-328

Effects of renin angiotensin system inhibition on renal function and the clinical course of patients with decompensated liver cirrhosis and ascites

Tammo Lambert Tergast¹, Marie Griemsmann¹, Heiner Wedemeyer¹, Markus Cornberg¹, Benjamin Maasoumy¹. ¹Hannover Medical School, Department of Gastroenterology, Hepatology and Endocrinology, Germany
Email: tergast.tammo@mh-hannover.de

Background and aims: Patients with decompensated liver cirrhosis and ascites are at a high risk of developing acute kidney injury (AKI). Studies have suggested that inhibition of the Renin-Angiotensin System (RAS) has certain nephro- and hepatoprotective effects in patients with liver fibrosis and early stages of liver cirrhosis. However, data in patients with decompensated cirrhosis are scarce. This study aimed to investigate the clinical impact of Angiotensin converting

POSTER PRESENTATIONS

enzyme antagonists and Angiotensin II receptor inhibitors (RAS-Inhibitors) in individuals with decompensated liver cirrhosis.

Method: All hospitalized patients with liver cirrhosis and ascites that underwent paracentesis at Hannover Medical School between 2012 and 2018 were considered for this study. Overall, 667 patients were included of whom 41 (7%) had reported intake of RAS-Inhibitors at baseline. End points were incidences of AKI and severe AKI (i.e. AKI grade III^b) within 28-days and long-term need for hemodialysis as well as liver transplant (LTx-) free survival. Patients without RAS-inhibitors were matched via propensity score matching (PPSM) with individuals with RAS-inhibitor intake in a 3:1 manner. Factors included in the matching were glomerular filtration rate, age, mean arterial pressure, leukocyte count, platelet count and presence of type 2 diabetes mellitus. Competing risk analysis was used to analyze longitudinal end points.

Results: After PPSM, 117 patients remained in the No RAS-Inhibitor group and were compared with 39 patients with RAS-inhibitor intake. Baseline characteristics were comparable between both groups and standardized mean differences (SMD) indicated successful matching (SMDs <0.10). Within 28-days, incidence of AKI did not differ between both groups (HR: 0.92, 95%CI 0.49–1.74, P=0.81). Furthermore, no case of severe AKI was observed in the RAS-Inhibitor group and a significantly increased incidence of severe AKI was observed in those without RAS-Inhibitor intake within 28-days (p < 0.001). Progressive AKI was numerically higher in patients without RAS-Inhibitor intake (RAS-Inhibitor: 25% vs. No RAS-Inhibitor: 46%, P = 0.14). In the long-term follow-up, need for hemodialysis in patients with RAS-Inhibitor intake was significantly decreased compared to patients without RAS-Inhibitors (HR: 0.22, 95%CI: 0.05–0.91 P = 0.03, Figure 1). Furthermore, LTx-free survival was comparable between those with and without RAS-Inhibitor intake (HR: 0.83, 95%CI: 0.48–1.45, P=0.52). Last, incidence of hepatocellular carcinoma did not differ significantly between patients with or without RAS-Inhibitor intake (HR: 0.81, 95%CI 0.17–3.72 P = 0.71).

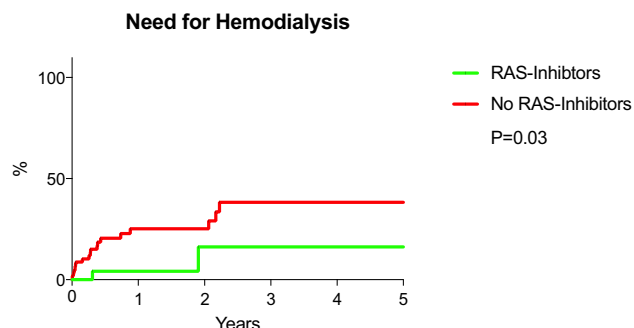


Figure 1: Need for hemodialysis in patients with or without RAS-Inhibitor intake.

Conclusion: RAS-Inhibitor intake is associated with a decreased incidence of severe acute kidney injury and need for hemodialysis in patients with decompensated liver disease.

SAT-329

Adoption of a clinical assessment service in hepatology

Gioia Bratos¹, William Ovenden¹, Arjuna Singanayagam¹, Daniel Forton¹, Metin Yalcin¹, Sarah Hughes¹, Sarah Clark¹. ¹St George's Hospital, United Kingdom
Email: sarah.clark@stgeorges.nhs.uk

Background and aims: The Hepatology Clinical Assessment Service (CAS) was established as a new service at St Georges Hospital in April 2020 during the COVID19 pandemic. It is a novel way to assess new patients referred to the liver outpatient clinic with a view to streamlining the patient pathway, pre-investigation patients prior to a clinic appointment, avoiding inappropriate clinic appointments, rejecting inappropriate referrals and improving the efficiency of the

clinic. Hepatology CAS is a weekly consultant-led clinic supported by the Clinical Nurse Specialist (CNS) and the Patient Pathway Coordinator (PPC), the clinic happening virtually without the patient being present at the time of the triage and assessment. On average, every week 35 patients are referred to the Liver Clinic by their GPs or by other clinicians internally or externally to the hospital.

Method: Once the patient's referral has been assessed, the CNS requests the investigations, communicates with the patient and dictates a clinical letter to patient and referrer, while the PPC prioritises the appointments based on their clinical needs. Following this assessment most of the patients then attend a face-to-face appointment, although some patients can be managed entirely virtually if clinically appropriate. With the introduction of the community non-alcoholic fatty liver pathways GP, at a similar time to this service, referrals are rejected if this pathway has not been followed.

Results: Since CAS has been introduced there have been several positive outcomes: in 2021, 18% of the referrals were appropriately repatriated to primary care with advice; 30% of the referrals were managed without needing a face to face appointment; the waiting time reduced from 8 weeks to 5 weeks for a clinical review, and from 16 weeks to 15 weeks for a follow-up appointment; from 2020 to 2022 the proportion of patients discharged after the first clinical review has increased from 16% to 29%;

Table 1: Comparison of patients over 6 weeks that were seen and discharged before and after the introduction of CAS.

	2020		2022	
		%		%
Total 'New' appts	190	100	181	100
Total pts seen ¹	134	71	141	78
Total DNAs ²	56	29	40	22
Breakdown of patients seen ¹				
Total pts seen	134	100	141	100
Of pts seen & F/Up	113	84	100	71
Of pts seen & Di/C'd	21	16	41	29
Breakdown of DNAs ²				
Total DNAs	56	100	40	100
DNA & Reschedule	33	59	25	62.5
DNA & Di/C'd	23	41	15	37.5

Conclusion: Hepatology CAS has impacted extremely positively on our service. Following the introduction of the Hepatology CAS service specialist treatment is instigated more quickly, patients can be discharged following their first face to face visit as all information is to hand, it has eliminated unnecessary follow-up and has resulted in a clear and concise pathway to refer the patients into the service, with the diagnostic tests being performed at an earlier stage.

SAT-330

Diabetes impairs the hemodynamic response to non-selective betablockers in compensated cirrhosis and predisposes for hepatic decompensation

Rafael Paternostro¹, Mathias Jachs¹, Lukas Hartl¹, Benedikt Simbrunner¹, Bernhard Scheiner¹, David Jm Bauer¹, Philipp Schwabl¹, Georg Semmler¹, Michael Trauner¹, Mattias Mandorfer¹, Thomas Reiberger¹. ¹Medical University of Vienna, Austria
Email: rafael.paternostro@meduniwien.ac.at

Background and aims: Non-selective betablockers (NSBB) reduce the risk of hepatic decompensation in patients with compensated advanced chronic liver disease (cACLD). The prevalence of metabolic

comorbidities (MetC) in cACLD patients is increasing. We aimed to investigate the impact of MetC on (i) the hemodynamic effects of NSBB and (ii) hepatic decompensation in cACLD.

Method: cACLD patients undergoing paired hepatic venous pressure gradient (HVPG) measurements before/under NSBB-therapy were considered for this study. MetC, i.e. obesity, dyslipidemia, and diabetes (DM) were recorded. Hepatic decompensation and liver-related mortality were evaluated.

Results: Ninety-two patients were included (Child-A n=80, 87%; Child-B n=12, 13%). MetC were found in 34 (37%) patients: n=19 (20.7%) had obesity, n=14 (15.2%) dyslipidemia, and n=23 (34.8%) DM. The median baseline-HVPG of 18 (IQR: 15–21) mmHg decreased to a median of 15 (IQR: 9–12) mmHg under NSBB. HVPG-response (decrease $\geq 10\%$ or to ≤ 12 mmHg) was achieved in n=60 (65.2%) patients. Interestingly, patients with DM (OR: 0.35, p=0.021) and higher BMI (OR: 0.89 per kg/m², p=0.031) were less likely to achieve HVPG-response. During a median follow-up of 2.3 (0.5–4.2) years, 18 (19.5%) patients experienced first hepatic decompensation. Child-B (adjusted subdistribution hazard ratio, aSHR: 4.3 [95%CI: 1.5–12.2], p=0.006), HVPG-response (aSHR: 0.3 [95%CI: 0.1–0.9], p=0.037), and DM (aSHR: 2.8 [95%CI: 1.1–7.2], p=0.036) were independently associated with hepatic decompensation (Table).

Table: (A) Univariate and (B) multivariate competing risk regression analysis modeling the risk for hepatic decompensation during follow-up. Diagnosis of hepatocellular carcinoma, removal of the primary aetiological factor, and non-liver-related death were considered competing events

Model for hepatic decompensation	Univariate regression model			Multivariate regression model		
	SHR	95% CI	p value	aSHR	95% CI	p value
CTP stage B (vs. A)	3.420	1.330–8.80	0.011	4.325	1.536–12.175	0.006
HVPG-Response (vs. Non-response)	0.279	0.107–0.728	0.009	0.313	0.105–0.934	0.037
Age, per year	1.070	1.010–1.140	0.021	1.040	0.978–1.105	0.210
Diabetes mellitus, vs. no diabetes mellitus	5.280	1.870–14.900	0.002	2.772	1.071–7.175	0.036
Dyslipidemia, vs. no dyslipidemia	2.030	0.548–7.530	0.290	–	–	–
Arterial hypertension, vs. no arterial hypertension	0.940	0.309–2.860	0.910	–	–	–
Obesity, vs. normal weight	1.110	0.362–3.390	0.860	–	–	–

Conclusion: In cACLD patients DM and a higher BMI impair the HVPG-response to NSBB. Furthermore, DM-independent from hepatic function and lack of HVPG-response-increases the risk for hepatic decompensation. Thus, DM seems to promote first hepatic decompensation by hemodynamic and non-hemodynamic mechanisms.

SAT-331

Preoperative transjugular intrahepatic portosystemic shunt and in-house mortality in patients with liver cirrhosis undergoing surgery

Felix Piecha¹, Joscha Vonderlin², Friederike Fröhhaber¹, Julia-Kristin Graß³, Ann-Kathrin Ozga⁴, Aenne Harberts¹, Daniel Bente¹, Peter Huebener¹, Matthias Reeh³, Christoph Riedel⁵, Peter Bannas⁵, Jakob R. Izbicki³, Gerhard Adam⁵, Samuel Huber¹, Ansgar W. Lohse¹, Johannes Kluwe¹. ¹University Medical Center

Hamburg-Eppendorf, I. Department of Medicine, Germany; ²Charité-Universitätsmedizin Berlin, Department of Hepatology and Gastroenterology, Germany; ³University Medical Center Hamburg-Eppendorf, Department of General, Visceral and Thoracic Surgery, Germany; ⁴University Medical Center Hamburg-Eppendorf, Institute of Medical Biometry and Epidemiology, Germany; ⁵University Medical Center Hamburg-Eppendorf, Department of Diagnostic and Interventional Radiology and Nuclear Medicine, Germany
Email: f.piecha@uke.de

Background and aims: Liver cirrhosis is associated with an increased surgical morbidity and mortality. Portal hypertension and the surgery type have been established as critical determinants of postoperative outcome. We aim to evaluate the hypothesis that preoperative placement of a transjugular intrahepatic portosystemic shunt (TIPS) in patients with liver cirrhosis is associated with a lower in-house mortality after surgery.

Method: A retrospective database search for the years 2010–2020 was carried out. We identified 64 patients with liver cirrhosis who underwent surgery within three months after TIPS-placement and 131 cirrhosis patients who underwent surgery without prior TIPS (control). Surgeries were categorized into low-risk and high-risk procedures. The primary end point was postoperative in-house mortality.

Results: In both the TIPS and the control cohort, most patients presented with a Child-Pugh B stage (37/64, 58% vs. 70/131, 53%) at the time of surgery, but the median MELD score was higher in the TIPS cohort (14 vs. 11 points). Low-risk and high-risk procedures amounted to 47% and 53% in both cohorts. In-house mortality was lower in the TIPS cohort (12/64, 19% vs. 53/131, 41%), also when further subdivided into low-risk (0/30, 0% vs. 11/61, 18%) and high-risk (12/34, 35% vs. 42/70, 60%) surgery. We analyzed the influence of high-risk surgery, preoperative TIPS-placement, age, sex, baseline creatinine, presence of ascites, chronic liver failure consortium-acute decompensation (CLIF-C AD), American Society of Anesthesiologists (ASA) and model for end-stage liver disease (MELD) scores on in-house mortality by multivariable Cox proportional hazards regression. Preoperative TIPS-placement was associated with a lower rate (hazard ratio 0.42, 95%-confidence interval 0.18–0.93) for postoperative in-house mortality.

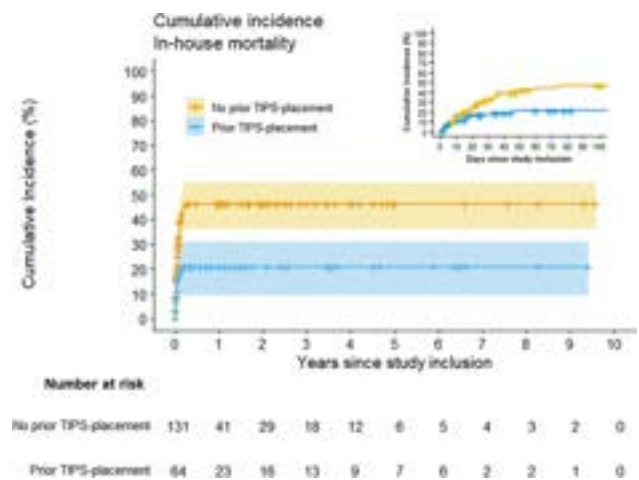


Figure:

Conclusion: A preoperative TIPS might be associated with reduced postoperative in-house mortality in patients with liver cirrhosis, especially after high-risk surgical procedures.

SAT-332

Indocyanine green clearance reflects various pathophysiological mechanisms and independently predicts liver-related events in ACLD

Mathias Jachs¹, Lukas Hartl¹, Benedikt Simbrunner¹, Lorenz Balcar¹, Georg Semmler¹, David Jm Bauer¹, Benedikt Hofer¹, Michael Schwarz¹, Albert Stättermayer¹, Matthias Pinter¹, Michael Trauner¹, Thomas Reiberger¹, Mattias Mandorfer¹. ¹Medical University of Vienna, Austria

Email: mattias.mandorfer@meduniwien.ac.at

Background and aims: Indocyanine green (ICG) clearance, determined by venous sampling, has shown a promising diagnostic/prognostic utility for clinically significant portal hypertension (CSPH)/hepatic decompensation in compensated advanced chronic liver disease (cACLD), while the prognostic utility of pulse dye densitometry (PDD)-derived values conveniently measured via a finger clip has primarily been evaluated in the context of hepatectomy or decompensated cirrhosis.

Method: For this retrospective evaluation, patients with ACLD (defined by LSM ≥ 10 kPa) enrolled in the prospective Vienna Cirrhosis Study (VICIS, NCT03267615) who underwent same-day measurements of the hepatic venous pressure gradient (HVPG) and ICG clearance between 2017 and 2022 were included. ICG retention rate at 15 minutes (R15) was assessed in vivo by PDD. Long-term follow-up data on first hepatic decompensation (cACLD) and the incidence of acute-on-chronic-liver failure (ACLF) or liver-related mortality (decompensated ACLD [dACLD]) was recorded and analysed by competing risk regression.

Results: Two-hundred and sixty-one patients were included: Median age: 56.0 years; 62.8% male; etiology: 55.2% ALD, 18.0% viral, 18.1% NAFLD/cryptogenic, while 10.7% other; Child-Turcotte-Pugh stage A: 49.6%, B: 36.8%, C: 13.8%. The median HVPG was 17 (IQR: 11–20) mmHg. The median ICG-R15 was 24.1 (10.4–41.3) %. Among cACLD patients (n = 115, CSPH prevalence: 62.4%), ICG-R15 correlated moderately with HVPG (Spearman's rho: 0.458, $p < 0.001$) and yielded a suboptimal diagnostic accuracy for CSPH (AUROC: 0.687 [95% CI: 0.585–0.789]), while a strong correlation with the model for end-stage liver disease (MELD) score (rho: 701, $p < 0.001$) was found. ICG-R15 also correlated with biomarkers of endothelial dysfunction (von Willebrand factor antigen [VWF]) and inflammation (CRP, IL-6, procalcitonin [PCT]), as shown in the Figure. In dACLD (n = 146), similar correlations were found, however, ICG-R15 correlated only weakly with HVPG (rho: 0.189, $p = 0.023$). ICG-R15 additionally correlated with renin/mean arterial pressure, i.e., biomarkers of circulatory dysfunction. ICG-R15 was independently associated with hepatic decompensation in cACLD patients in competing risk regression (adjusted subdistribution Hazard Ratio [aSHR]: 1.045 [95%CI: 1.006–1.090] per %, $p = 0.024$; adjusted for liver stiffness, MELD, and albumin levels). Furthermore, ICG-R15 was an independent predictor for the composite end point ACLF/liver-related mortality in dACLD (aSHR: 1.070 [95%CI: 1.030–1.100] per %, $p < 0.001$; adjusted for CLIF-C ACLF-D score).

Conclusion: ICG-R15 by PDD correlated with portal hypertension and systemic inflammation as key disease-driving mechanisms in cACLD. Although its diagnostic value for CSPH is insufficient for clinical application, it predicted first hepatic decompensation, even after adjusting for other non-invasive parameters. Moreover, ICG-R15 was independently predictive of ACLF/liver-related death in dACLD.

SAT-333

A multimodal deep learning network for non-invasive prediction of the hepatic decompensation risk in compensated cirrhotic people: a multicentre cohort study (CHESS1701)

Qian Yu¹, Yi Zhou², Yuxiang Lai², Xiaolong Qi³, Shenghong Ju¹. ¹Department of Radiology, Zhongda Hospital, School of Medicine, Southeast University, China; ²School of Computer Science and Engineering, Southeast University, China; ³Center of Portal Hypertension, Department of Radiology, Zhongda Hospital, School of Medicine, Southeast University, China

Email: jsh@seu.edu.cn

Background and aims: Assessing the risk of portal hypertension (PHT)-related decompensation aids the prophylactic strategy to improve prognosis of the compensated cirrhotic population. Conventional imaging methods are inadequate to assess this risk, and the usage of specialized screening tools (such as liver stiffness measurement (LSM)) is still limited. Hence, we aimed to develop a multimodal artificial intelligence decompensation prediction system (AIDE) that integrates computed tomography (CT) image-type and clinical context-type information to predict the hepatic decompensation risk non-invasively.

Method: 1,045 compensated cirrhotic patients from seven tertiary medical centres who underwent baseline contrast-enhanced CT imaging were enrolled with a median follow-up of 33 months. A total of 615 patients from the first five centres were treated as the training and validation cohorts, while 430 from other two centres comprised the external test cohort. AIDE's performance was evaluated using concordance index (C-index) and time-dependent area under the curve (tAUC). The risk stratification performance was assessed by Kaplan-Meier analysis and compared with the Baveno VII performance. The classification ability of baseline clinically significant PHT (CSPH) was assessed in 430 persons with or without CSPH to explore the biological mechanisms of AIDE.

Results: In the external test cohort, AIDE achieved a C-index of 0.84 (95% confidence interval (CI): 0.80–0.87) and a 3-year tAUC of 0.87 (0.83–0.92), outperformed the conventional models (Figure 1). The 3-year decompensation rates were 1% (3/230), 25% (47/188), and 59% (23/39) in the low-, moderate-, and high-risk groups, respectively ($p < 0.05$). AIDE reduced the proportion of patients in the grey zone of Baveno VII by 63% and achieved an AUC of 0.82 (0.76–0.89) for CSPH diagnosis; the PHT progression mechanisms might be captured by the AIDE.

Conclusion: AIDE provided an accurate decompensation risk assessment in compensated cirrhotic patients. It could help guide the prophylactic strategies when HVPG/LSM are not available.

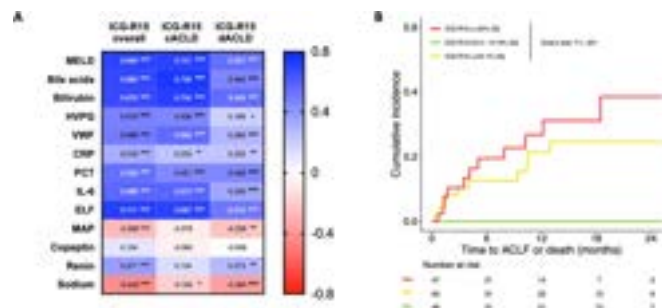


Figure:

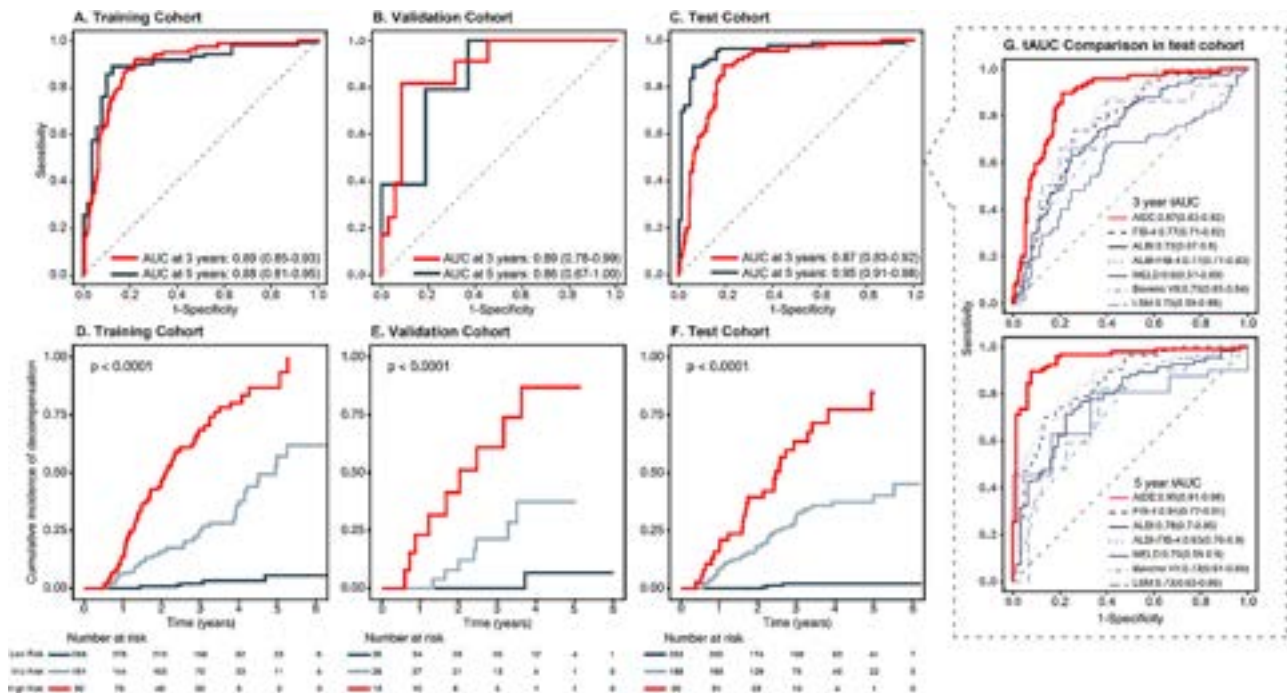


Figure: (abstarct: SAT-333): Performance of the AIDE in predicting the decompensation risk. (A–C) The time-dependent AUC of AIDE at 3 years and 5 years. (D–F) Risk stratification by Kaplan-Meier analysis in the training, validation, and test cohorts. (G) Comparing time-dependent AUC of AIDE to those of other models.

SAT-334

TIPS under-dilation strategy with new controlled expansion endoprosthesis: a hemodynamic and imaging confirmation of its feasibility

Dario Saltini^{1,2}, Cristian Caporali^{2,3}, Federica Indulti^{1,2}, Marcello Bianchini^{1,2}, Federico Casari^{2,3}, Francesco Prampolini^{2,3}, Davide Felaco^{2,3}, Tomas Guasconi¹, Biagio Cuffari¹, Alberto Zanetto^{1,4}, Gian Piero Guerrini⁵, Nicola De Maria^{1,5}, Erica Villa¹, Antonio Colecchia¹, Fabrizio Di Benedetto^{2,5}, Filippo Schepis^{1,2}.

¹Gastroenterology Unit, University of Modena and Reggio Emilia and Azienda Ospedaliero-Universitaria di Modena, Italy; ²TIPS team, Azienda Ospedaliero-Universitaria di Modena, Italy; ³Interventional Radiology Unit, Azienda Ospedaliero-Universitaria di Modena, Italy;

⁴Gastroenterology and Multivisceral Transplant Unit, Azienda Ospedale-Università di Padova, Italy; ⁵Hepato-Pancreato-Biliary Surgery and Liver Transplantation Unit, University of Modena and Reggio Emilia, Azienda Ospedaliero-Universitaria di Modena, Italy

Email: fschepis@unimore.it

Background and aims: The use of small caliber (<8 mm) transjugular intrahepatic portosystemic shunt (TIPS) is a promising approach to reduce shunt-related complications. Its feasibility with the new controlled expansion stent-grafts (GORE® VIATORR® CX 8–10 mm or VCX) has not yet been explored. Our aim was twofold: to investigate whether VCX self-expands over time when under-dilated to <8 mm at TIPS placement; to compare VCX under-dilated to 6 mm versus first generation 8 and 10 mm VIATORR® TIPS stent-grafts (VTS).

Method: For the first aim, we prospectively enrolled consecutive patients with cirrhosis who received under-dilated TIPS between June 2020 and September 2022 at our tertiary referral Center in Modena, Italy. All patients underwent hemodynamic measurements a) immediately before and after TIPS placement, b) 6–7 days and c) ≥1 month after the procedure. We measured average pressure values in different sites along the TIPS: portal-vein tract (PV), intra-parenchymal tract (IP), hepatic-vein tract (HV) and inferior vena cava (IVC). A subgroup of patients underwent serial CT scans within 24 h (T0), at 6–7 days (T1) and at ≥1 month after TIPS (T2). Average maximal inner

diameter of endoprosthesis was measured at 5 standard sites: PV, PVW, IP, HVW and distal HV. For the second aim, we retrospectively enrolled consecutive patients with cirrhosis who received under-dilated TIPS to 6 mm between January 2015 and September 2022 and underwent a CT scan >1 month after TIPS. Average maximal inner diameter of stent-graft was measured at PVW, IP, and HVW and compared between VCX and VTS-8 or VTS-10. Percentage variations from the dilation diameter were also assessed.

The institutional review board gave approval to collect prospective and retrospective clinical, hemodynamic, and CT data.

Results: For the first aim, 64 patients underwent hemodynamic assessments: 25, 29 and 10 received TIPS under-dilated to 5, 6 and 7 mm, respectively. A significant drop of pressure was observed while crossing PVW and HVW in all under-dilated groups (Figure 1A). Forty-three of these patients underwent CT scans: 17, 19 and 7 were dilated to 5, 6 and 7 mm, respectively. PVW and HVW sites maintained under-dilation overtime (Figure 1B). No TIPS dysfunction occurred during a mean follow-up period of 363 days. For the second aim, 20 patients were enrolled in the VCX, VTS-8 and VTS-10 mm groups, respectively (N = 60). VCX maintained the dilation diameter at PVW and HVW similarly to VTS-8 but significantly better than VTS-10 mm. VCX self-expansion at IP site was significantly inferior than VTS-10 mm (Figure 1C).

Conclusion: Under-dilation TIPS strategy performed with VCX is feasible. Reduced self-expansion in comparison to first generation VTS positively impact the strategy application. Evaluation of clinical outcomes after applying this strategy are awaited.

Figure 1A Average pressure at each standard site in hemodynamic assessment time points (immediate post-TIPS, 6-7 days and ≥ 1 months after TIPS)

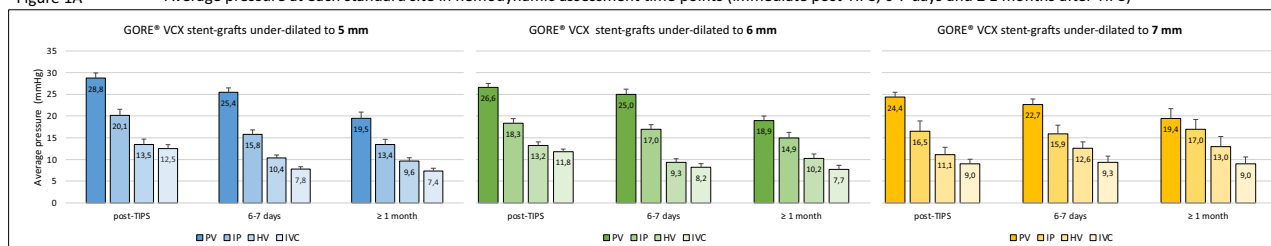


Figure 1B Average maximal inner diameters at each standard site in CTs time points (T0, T1 and T2)

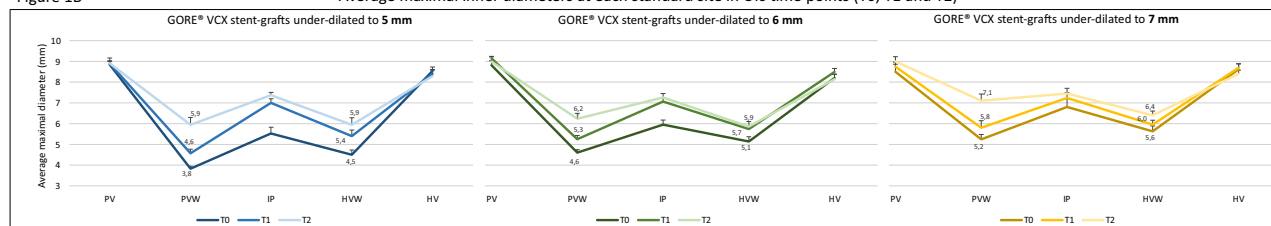
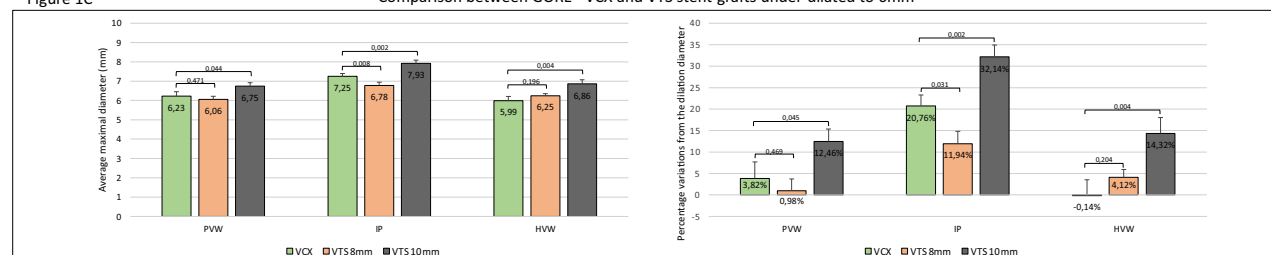


Figure 1C Comparison between GORE® VCX and VTS stent-grafts under-dilated to 6mm



Bars represent mean \pm SE

HVW, hepatic vein wall; HV, hepatic vein lumen; IP, TIPS intra-parenchymal tract; IVC, inferior vena cava lumen; PV, portal vein lumen; PVW, portal vein wall; VCX, VIATORR® CX 8-10mm stent-grafts; VTS, VIATORR® TIPS stent-grafts.

Figure: (abstract: SAT-334).

SAT-335

Is elastography needed for diagnosing cACLD and stratifying CSPH risk?

Georg Semmler^{1,2}, Lukas Hartl^{1,2}, Mathias Jachs^{1,2}, Benedikt Simbrunner^{1,2}, Benedikt Hofer^{1,2}, Lorenz Balcar^{1,2}, Michael Schwarz^{1,2}, Laurenz Fritz^{1,2}, Anna Schedlbauer^{1,2}, Katharina Stopfer^{1,2}, Daniela Neumayer^{1,2}, Jurij Maurer^{1,2}, Robin Szymanski^{1,2}, Bernhard Scheiner^{1,2}, Michael Trauner^{1,2}, Thomas Reiberger^{1,2}, Mattias Mandorfer^{1,2}. ¹Medical University of Vienna, Division of Gastroenterology and Hepatology, Department of Internal Medicine III, Vienna, Austria; ²Medical University of Vienna, Vienna Hepatic Hemodynamic Lab, Division of Gastroenterology and Hepatology, Department of Internal Medicine III, Vienna, Austria
Email: mattias.mandorfer@meduniwien.ac.at

Background and aims: Compensated advanced chronic liver disease (cACLD) identifies the population at risk for liver-related complications and the presence of clinically significant portal hypertension (CSPH) defines the target population for preventing hepatic decompensation. While liver stiffness measurement (LSM) by vibration-controlled transient elastography (VCTE) has enabled non-invasive identification of these conditions, its availability is mostly restricted to tertiary care. As the reliance on VCTE/referral pathways may impede the identification of cACLD/CSPH in the community, we developed a routine laboratory-based algorithm to identify cACLD patients (by FIB-4) and to subsequently rule-in/rule-out CSPH (by the von Willebrand factor/platelet count ratio [VITRO]).

Method: FIB-4/LSM cohort: To determine a FIB-4 cut-off that reflects cACLD, all patients with (suspected) compensated chronic liver disease undergoing FIB-4+LSM at the Medical University Vienna from 2007 to 2022 were characterized and followed for the development of hepatic decompensation. HVPG cohort: To determine VITRO cut-

offs for ruling-in/ruling-out CSPH, cACLD patients (as diagnosed by FIB-4) undergoing hepatic venous pressure gradient (HVPG) measurement were analyzed.

Results: FIB-4/LSM cohort: 5646 patients were followed for a median of 54 months during which 248 (4.4%) developed first hepatic decompensation. 1785 (32%) had a LSM ≥ 10 kPa, which corresponded to a FIB-4 of >1.7 . Importantly, both LSM (AUC 0.894) and FIB-4 (AUC 0.900) were similarly accurate in predicting hepatic decompensation within the subsequent 2 years. FIB-4 >1.7 identified patients at risk for first hepatic decompensation (cumulative incidence at 5 years: 11.9%), while in those below this threshold, risk was negligible (cumulative incidence at 5 years: 0.07%, Figure-panel A). HVPG cohort: 393 cACLD patients (as defined by a FIB-4 >1.7) were included. Among patients with FIB-4 ≥ 1.7 , CSPH prevalence was 61.8% (n = 201/325). VITRO exhibited an excellent performance for diagnosing CSPH (AUC 0.844), which was comparable to LSM (AUC 0.854; DeLong test: p = 0.746) and comparable to the ANTICIPATE model (AUC 0.894; DeLong test: p = 0.073, Figure-panel B). A VITRO <1.0 ruled-out (prevalence: 12.0%; negative predictive value [NPV] 87.2%; sensitivity 97.5%) CSPH, while it was ruled-in (prevalence: 40.9%; positive predictive value [PPV] 91.0%; specificity 90.3%) by VITRO ≥ 2.5 . Importantly, the diagnostic indices were comparable to the Baveno VII cut-offs of LSM ≤ 15 kPa and PLT ≥ 150 G/L (prevalence: 10.8%; NPV 94.3%; sensitivity: 99.0%) and LSM ≥ 25 kPa (prevalence: 43.4%; PPV 90.8%; specificity: 89.5%).

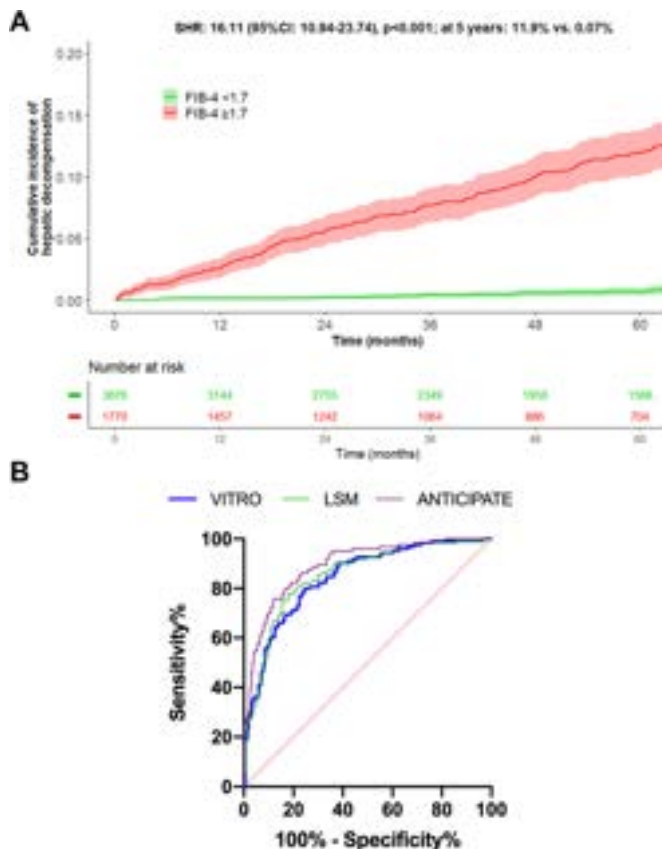


Figure:

Conclusion: FIB-4 >1.7 and VITRO ≥2.5 identify cACLD (defined by risk rather than stage, as endorsed by Baveno VII) and CSPH with a similar diagnostic accuracy as LSM-based criteria, questioning the need for VCTE. Simple laboratory tests which are available in primary/secondary care may broaden the access to risk stratification and early intervention.

SAT-336

Systemic inflammation remains a critical determinant of the dynamic component of portal hypertension in abstinent patients with alcohol-related cirrhosis

Benedikt Hofer^{1,2,3,4}, Benedikt Simbrunner^{1,2,3,4}, Kerstin Zinöber^{1,2,3}, Georg Semmler^{1,2}, Philipp Königshofer^{1,3,4}, Thomas Sorz^{1,3,4}, Vlad Taru^{1,3}, Michael Trauner¹, Philipp Schwabl^{1,2,3,4}, Matthias Mandorfer^{1,2}, Thomas Reiberger^{1,2,3,4}. ¹Medical University of Vienna, Division of Gastroenterology and Hepatology, Department of Internal Medicine III, Vienna, Austria; ²Medical University of Vienna, Vienna Hepatic Hemodynamic Laboratory, Division of Gastroenterology and Hepatology, Department of Internal Medicine III, Vienna, Austria; ³Medical University of Vienna, Vienna, Christian Doppler Lab for Portal Hypertension and Liver Fibrosis, Vienna, Austria; ⁴Center for Molecular Medicine (CeMM) of the Austrian Academy of Sciences, Vienna, Austria. Email: thomas.reiberger@meduniwien.ac.at

Background and aims: Portal hypertension (PH) drives disease progression in cirrhosis even after removal/suppression of the primary aetiological factor. While the static component of PH is reflected by the degree of liver fibrosis, the assessment of dynamic contributors to PH is particularly challenging. We assessed the impact of hepatic/systemic inflammation on the dynamic component of PH in (i) rodent models of cirrhosis regression and in (ii) abstinent patients with cirrhosis due to alcohol-related liver disease (ALD).

Method: Male C57BL/6J mice were exposed to carbon tetrachloride or thioacetamide for 12 weeks to induce cirrhosis before allowing for regression by discontinuing the toxic stimulus for one (R1, n = 15) or

two (R2, n = 15) weeks. ALD patients with sustained abstinence (>1 month) undergoing same-day hepatic venous pressure gradient (HVPG) and liver stiffness measurement (LSM) were included. The static component of PH (histological collagen proportionate area [CPA; %] in animals; LSM in patients) was used in a linear model to predict portal pressure (PP). Factors affecting the dynamic component of PH (i.e., the discrepancy between the true PP and the PP predicted by LSM/CPA) were explored using the respective linear model's residuals (Figure).

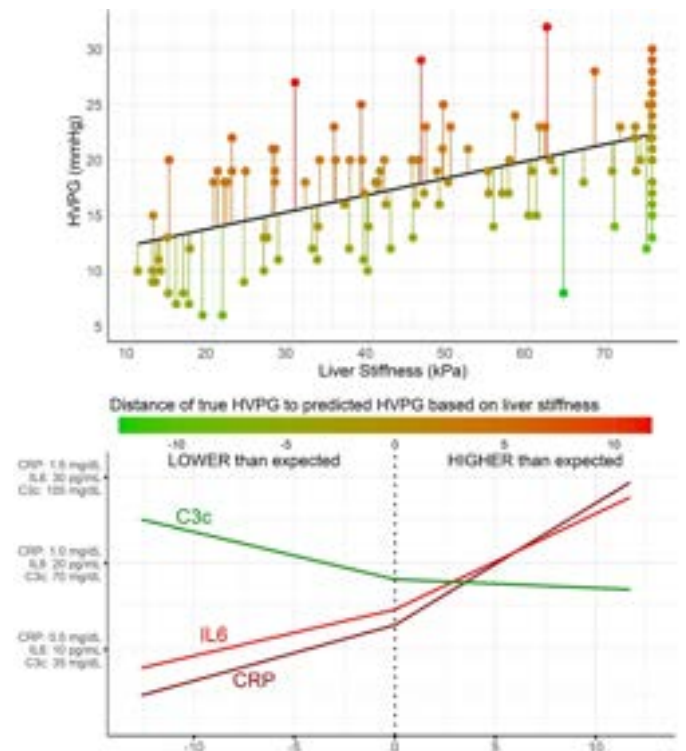


Figure:

Results: In animals, CPA demonstrated a significant positive relationship with PP (beta: 0.20; p <0.001). Hepatic inflammatory gene expression was linked to higher-than-expected PP. Specifically, TNF-alpha (r: 0.46, p = 0.012), CXCL1 (r: 0.36, p = 0.054), IL1-beta (r: 0.46, p = 0.012) and MCP1 (r: 0.35, p = 0.058) were positively correlated with the model's residuals. The impact of intrahepatic inflammation was significantly more pronounced in R2 than R1 animals. In addition to the animal models, 130 ALD patients (median abstinence: 6 [IQR: 10] months) with a median HVPG of 19 (IQR: 8) mmHg and a median LSM of 49 (IQR: 44) kPa were included. In the linear model, LSM showed a significant positive relationship with HVPG (beta: 0.15; p <0.001). Systemic inflammation was significantly upregulated in patients with higher-than-expected HVPG, as demonstrated by a positive correlation of the model's residuals to CRP (Spearman's r: 0.19, p = 0.026) and IL-6 (r: 0.16, p = 0.066). In contrast, complement factors C3c (r: -0.32, p = 0.005) and C4 (r: -0.21, p = 0.059) were lower in patients with higher-than-expected HVPG. While the negative correlation of C3c was only found in short-term abstinence (≤6 months), the impact of systemic inflammation was notably more pronounced in long-term abstinence (>6 months).

Conclusion: In animal models of regressive cirrhosis, increased intrahepatic inflammatory gene expression was linked to more pronounced dynamic PH. Similarly, systemic inflammation, as evident from increased CRP and IL-6 and consumption of complement factor C3c, drives the dynamic PH component in abstinent ALD patients.

SAT-337

Robust identification of patient subgroups in acute decompensated cirrhosis

Sara Palomino¹, Estefanía Huergo¹, Eva Uson², Cristina Sanchez², Vincenzo Lagani³, Narsis Kiani⁴, Nuria Planell¹, Unai Gurbindo¹, Jonel Trebicka⁵, Alberto Q. Farias⁶, Paolo Caraceni⁷, Pierre-Emmanuel Rautou⁸, David Gomez-Cabrero¹. ¹Navarrabiomed, Unit of Translational Bioinformatics, Pamplona, Spain; ²European Foundation for the Study of Chronic Liver Failure, Barcelona, Spain; ³Iliia State University, Institute of Chemical Biology, Georgia; ⁴Karolinska Institute, Algorithmic Dynamics lab, Sweden; ⁵University of Münster, Department of internal medicine, Münster, Germany; ⁶Hospital das Clínicas da Universidade de São Paulo, Department of Gastroenterology, Brazil; ⁷University of Bologna, Department of Medical and Surgical Science, Bologna, Italy; ⁸Université Paris-Cité, Inserm, Centre de recherche sur l'inflammation, France
Email: sarapalominoecheve@gmail.com

Background and aims: Understanding patient heterogeneity is essential to better comprehend the mechanisms underlying complex diseases and improve clinical decisions. Therefore, it is necessary to characterize patient diversity by identifying possible sub-types of patients and the clinical features that define them. Classical clustering methods allow patient stratification; however, the intricate nature of clinical data makes the development of more versatile and robust approaches necessary. Here, we developed a tool called *ClustAll* to identify patient subgroups in individuals with acute decompensation of cirrhosis (AD).

Method: In this study, part of the H2020 funded project DECISION, we developed and applied *ClustAll*, an unsupervised clustering strategy capable of identifying all possible robust ways of stratifying a population while addressing high dimensional data, missing values, and correlated features. For each resulting stratification, the subgroups identified by *ClustAll* were statistically characterized, and the minimal model was found using MXM. Subgroup associations with disease outcomes (ACLF, transplant or death) were explored using survival Kaplan-Meier curves. Then, a supervised classifier was trained to predict the groups obtained by *ClustAll* into additional independent cohorts.

Results: *ClustAll* was first applied to stratify AD patients from the European multicenter PREDICT cohort (n = 766). 74 clinical variables collected at hospital admission were included in the analysis. Five different robust stratifications were identified. Based on clinical expertise, one of the stratifications was selected for further exploration, defining three sub-groups of AD patients: 306 patients were assigned to Cluster 1, presenting the highest rates of organ dysfunction, clinical events, and precipitating events; Cluster 2 (n = 118) included the highest percentage of diabetic patients (51%) and of patients with suffering from hepatic encephalopathy (HE) (89%); Cluster 3 (n = 342) revealed a cluster with similar patterns to Cluster 2, but not afflicted by HE. Regarding the outcomes, patients in Cluster 1 had a poorer outcome (ACLF, transplant requirement or death) compared to the other groups. Cluster 2 and Cluster 3 had similar prognoses. This patient clustering was validated in two independent international cohorts of AD patients (CANONIC, n = 572 and ACLARA, n = 580) as well as in follow-up visits of PREDICT cohort (n = 725). The resulting clustering was robust in all three cohorts, and survival significantly differed in the subgroups identified.

Conclusion: Using a data driven approach, our analysis of three large international prospective cohorts of AD patients robustly identified three clusters of patients with different clinical features and short term outcomes. *ClustAll* may help improve the characterization of AD complexity.

SAT-338

Clinical profile of porto-sinusoidal vascular disorder : experience from tertiary referral hospital in India

Love Garg¹, Akash Shukla¹, Kashmira Kawli², Arun Vaidya², Aditya Kale², Shashank Pujalwar². ¹Seth GS Medical College and KEM hospital, Mumbai, Gastroenterology, Mumbai, India; ²Seth GS Medical College and KEM hospital, Mumbai, India
Email: drakashshukla@yahoo.com

Background and aims: Porto-sinusoidal vascular disorder (PSVD) is recently described clinical entity encompassing non cirrhotic portal fibrosis, idiopathic portal hypertension, non cirrhotic intrahepatic portal hypertension and various overlapping histologic patterns. We decided to study clinical profile of patients with PSVD at our center. **Method:** Prospectively maintained liver clinic database was reviewed to identify 125 patients meeting the inclusion criteria of PSVD proposed in Baveno VII guidelines. Demography, clinical features, endoscopic, radiological and histological findings and associated conditions were noted.

Results: Median age of cohort was 34 years. Females were 80 (64%). Median duration of symptoms at the time of diagnosis was 8 months. Common presentations were gastrointestinal bleed in 59 (47.2%), symptomatic splenomegaly in 45 (36%), transient ascites following bleed in 25 (20%), incidentally detected in 21 (16.8%) patients. Hemogram showed pancytopenia in 101 (80.8%) patients. Portal hypertension was seen in 120 patients (96%). End stage liver disease (ESLD) developed in 18 (14.4%) patients with median follow-up of 110 months (range 30–150 months). Significant ascites was seen in 16 (12.8%) and spontaneous hepatic encephalopathy in 3 (2.4%) patients. Autoantibodies seen in 41 patients {ANA- 29 (23.2%) and ASMA-12 (9.6%)}. IgG elevation was seen in 36 (28.8%) cases. Imaging revealed collaterals and splenomegaly in 113 (90.4%) and 103 (82.4%) patients respectively. Portal vein thrombosis and splenic vein thrombosis was present in 18 (14.4%) and 3 (2.4%) patients respectively. Specific biopsy findings like obliterative portal venopathy, nodular regenerative hyperplasia and incomplete septal fibrosis were seen in 19 (15.2%), 2 (1.6%), 6 (4.8%) patients and combination of obliterative portal venopathy and nodular regenerative hyperplasia in 1 (0.8%). Table 1 shows associated conditions with PSVD. Pancytopenia and IgG elevation was seen significantly more commonly in males than female patients (32 v/s 69 and 7 v/s 29, p value <0.05 for both). Splenomegaly was significantly more common in <35 years age group than >35 years (57 v/s 46, p value <0.005). Devascularization and shunt surgery was performed in 2 patients for refractory bleed. Transjugular intrahepatic portosystemic shunt (TIPS) was performed in 3 patients for recurrent GI bleed and 3 patients for ascites, out of which 2 patients had favourable outcomes.

Table 1: Conditions associated with porto-systemic vascular disorder

Associated disorders	Number of patients	Percentage
Immunological (Autoimmune hepatitis)	7	5.6%
Myeloproliferative disorder	1	0.8%
Hodgkin's lymphoma	1	0.8%
Prothrombotic disorders	10	8%
Protein S deficiency	1	0.8%
Protein C + S deficiency	4	3.2%
Antiphospholipid antibody	2	1.6%
JAK 2 mutation	2	1.6%
Factor V mutation	1	0.8%

Conclusion: PSVD is female predominant entity with varied clinical and histological manifestations. PSVD can present without portal hypertension. Portal vein thrombosis is common. Prothrombotic disorders and autoimmune disorders are less common than reported in western. A proportion of patients developed ESLD (End stage liver disease) with median follow-up of 110 months.

SAT-339

Impact of rifaximin use post-discharge of an overt hepatic encephalopathy (OHE) hospitalization on the annual rates of OHE-related inpatient stays

Arun Jesudian¹, Patrick Gagnon-Sanschagrin², Zeev Heimanson³, Rebecca Bungay², Jingyi Chen⁴, Annie Guérin², Ankur Dashputre⁵, Brock Bumpass⁵, Danellys Borroto⁵, George Joseph⁵. ¹Weill Cornell Medicine, New York, United States; ²Analysis Group, Inc., Montreal, Canada; ³Salix Pharmaceuticals, Bridgewater, United States; ⁴Analysis Group, Inc., Boston, United States; ⁵Bausch Health Companies Inc., Bridgewater, United States
Email: brock.bumpass@bauschhealth.com

Background and aims: Overt hepatic encephalopathy (OHE) is a severe neurologic manifestation of cirrhosis, with a wide range of symptoms related to loss of brain function, cognitive impairment, and confusion. Healthcare resource use (HRU) in OHE is substantial, with OHE recurrence as a significant driver. Thus, a key element of OHE treatment is preventing recurrence. Among patients with an initial OHE hospitalization in a real-world setting, literature on the impact of rifaximin use post-discharge on rates of OHE-related inpatient (IP) stays is limited.

Method: Adults (18–64 years) with an OHE index hospitalization were identified from the MarketScan[®] Commercial claims database (Q4/2015–Q2/2020). Patients were classified into two mutually exclusive cohorts based on treatment following index hospitalization: rifaximin treated (with/without lactulose) and not rifaximin treated. Patients were further classified into four subgroups based on decreasing quality of care (QOC): Type 1 (highest QOC) received rifaximin with no gap in treatment following index hospitalization; Type 2 received rifaximin within 30 days post-discharge; Type 3 received only lactulose within 30 days post-discharge; Type 4 (lowest QOC) received no treatment. The impact of rifaximin use on annual rates of OHE-related IP stays were described and compared by cohort, by QOC subgroup, and by treatment received pre-index hospitalization, accounting for differences in patient characteristics.

Results: At baseline, patients in the rifaximin treated cohort (N = 1,452; Type 1: N = 1,138, Type 2: N = 314) and not rifaximin treated cohort (N = 560; Type 3: N = 337, Type 4: N = 223) had similar demographic characteristics. Specifically, mean age of rifaximin treated and not rifaximin treated patients were 54.2 and 55.2 years, respectively, and 39.3% and 42.7% were female, respectively. Following the index hospitalization, the annual rate of OHE-related IP stays was 59% lower for the rifaximin treated cohort compared to the not rifaximin treated cohort (0.72 vs. 2.04; adjusted incidence rate ratio [IRR] 0.41, $p < 0.01$). Decreasing QOC (from Type 1 to Type 4) after the index hospitalization resulted in higher annual rates of OHE-related IP stays; more specifically, the annual rate for Type 1 was 0.6 whereas it ranged as high as 1.4 for Type 4. Compared to Type 1; the IRRs were 1.61 (Type 2), 2.60 (Type 3), and 2.90 (Type 4) (all $p < 0.01$; Figure). Regardless of whether patients received treatment with rifaximin, lactulose only, or neither prior to the index hospitalization, annual rates of OHE-related IP stays were numerically lower in Type 1 (0.6–0.7) compared to Type 2 (1.1–1.2), Type 3 (1.3–3.7), and Type 4 (1.2–2.6).

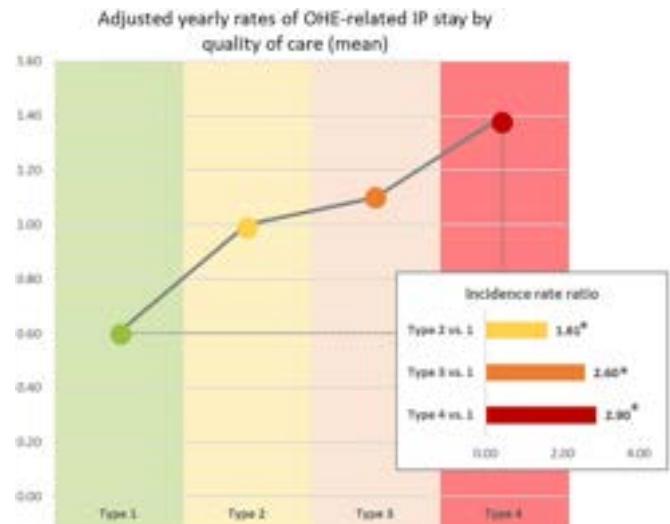


Figure: *Significant at the 5% level Notes: [1] An incident rate ratio greater than 1 indicates that the rate of OHE-related IP stays in patients with Type 2, 3, or 4 care is greater than those of patients with Type 1 care. [2] The four subgroups represent decreasing quality of care and are defined as follows: Type 1 received rifaximin without any gap in treatment following hospitalization; Type 2 received rifaximin within 30 days post-discharge; Type 3 received lactulose within 30 days post-discharge; Type 4 received no treatment.

Conclusion: Patients receiving rifaximin without any gap in treatment following an index OHE hospitalization had lower annual rates of OHE-related IP stays compared with patients who did not receive rifaximin.

SAT-340

MELD-sarcopenia and clinically significant portal hypertension as independent risk factors in the evolution of liver cirrhosis

Elba Llop^{1,2,3}, Marta Hernández Conde^{1,2}, Marta López-Gómez^{1,2}, Christie Perelló^{1,2}, Carlos Fernández-Carrillo^{1,2}, Javier Abad^{1,2}, Jesús Rivera^{1,2}, José Luis Martínez Porras^{1,2}, Natalia Fernández Puga^{1,2}, Maria Traperó^{1,2}, Enrique Fraga¹, José Luis Calleja Panero^{1,2,2,2,3}. ¹Hospital Universitario Puerta de Hierro Majadahonda, Gastroenterología y Hepatología, Spain; ²IDIPHISA, Spain; ³CIBERhd, Spain
Email: elballop@gmail.com

Background and aims: Clinically significant portal hypertension (CSPH) and MELD-sarcopenia score have been related to the prognosis of liver cirrhosis. Our aim was to evaluate the relationship between both in the evaluation of hepatic decompensation and mortality.

Method: Single-center prospective study that included consecutive patients with liver cirrhosis who underwent baseline laboratory tests, anthropometric and impedance measurements, sarcopenia assessment (by CT scan (SMI <50 cm²/m² in men and <39 cm²/m² in women) or Handgrip (<19.5 kg) and measurement of hepatic venous pressure gradient (HVPG) or Fibroscan[®] for the evaluation of clinically significant portal hypertension (CSPH; HVPG ≥10 mmHg or Fibroscan[®] ≥25 KPa in the rest). Exclusion criteria were HIV coinfection, hepatocellular carcinoma outside the Milan criteria and TIPS. Hepatitis C had to be cured, hepatitis B controlled with treatment and patients had to demonstrate abstinence of at least 6 months (through AUDIT). Clinical follow-up was carried out until December 2022.

Results: From January 2016 to December 2019, 196 patients were included with a mean follow-up of 47 months (SD 20). Mean age 63 years (SD 10), 67.9% males and predominant HCV etiology 52.6%, CHILD-PUGH A/B/C was 83.2%/5.1%/1.5%. Mean MELD was 9.4 (SD 2.7) and 32.7% had sarcopenia, the mean MELD-sarcopenia was 12.6 (5.1).

46.4% had HPTCS. The presence of sarcopenia showed low correlation with MELD ($r = 0.2$, $p = 0.02$). No correlation was found between CSPH and sarcopenia, both in patients with HVPG measurements ($n = 60$) and in the overall cohort ($r = 0.1$; $p = 0.5$, $r = 0.05$; $p = 0.5$). During follow-up, 51 (26%) decompensated, 38 (19.4%) died, and 18 (9.3%) underwent liver transplant. Competing risk analysis showed that both CSPH and MELD-sarcopenia were independent predictors of risk of hepatic decompensation during follow-up (SHR 2.2 (CI95 1.2–4.0; $p = 0.01$); SHR 1.07 (CI95 1.02–1.1; $p = 0.01$) respectively). Likewise, MELD-sarcopenia was an independent predictor of mortality (SHR 1.1 (95 CI 1.02–1.14); $p < 0.01$), although CSPH showed a SHR 1.9 (CI95 0.93–3.9, $p = 0.07$). In the subgroup of CHILD A patients, only CSPH was a predictor of hepatic decompensation (SHR 2.6 (CI95 1.3–5.4; $p = 0.03$); however, MELD-Sarcopenia obtained a SHR 1.1 (CI95 1–1.12), $p = 0.07$. **Conclusion:** MELD-sarcopenia and CSPH are two independent factors that determine the course of liver cirrhosis. The measurement of both is relevant to know the prognosis of the patient.

SAT-341

Spleen stiffness assessed by point shear-wave elastography predicts portal hypertension better than liver elastography

Vaclav Smid¹, Karel Dvorak^{1,2}, Barbora Nováková^{1,3}, Aleš Kuběna³, Jaromír Petrtyl¹, Radan Bruha¹. ¹General University Hospital in Prague, Charles University, 4th Internal Department, Czech Republic; ²Regional Hospital Liberec, Department of Gastroenterology and Hepatology, Liberec, Czech Republic; ³General University Hospital in Prague, Charles University, Institute of Medical Biochemistry and Laboratory Diagnostics, Czech Republic
Email: vaclav.smid@vfn.cz

Background and aims: Severity of portal hypertension is a crucial prognostic factor in patients with liver cirrhosis. The spleen stiffness as compared with liver stiffness might better assess the more advanced stages of portal hypertension. The aim of our study was to assess the usefulness of spleen elastography in the evaluation of portal hypertension in cirrhotic patients and to evaluate the relationship between spleen stiffness measurement and hepatic venous pressure gradient (HVPG).

Method: We examined 138 patients (84 men, 54 women), average age 60.1 ± 12.1 years, with liver cirrhosis (81 etylic, 15 viral hepatitis, 14 NAFLD, 18 other aetiology). Diagnosis of cirrhosis was confirmed by liver biopsy and/or by ultrasound-based elastography. Every patient underwent standard biochemistry and blood count, abdominal ultrasound and elastography of liver and spleen using point shear-wave elastography (pSWE). HVPG was afterwards measured in every patient.

Results: Clinically significant portal hypertension (HVPG ≥ 10 mmHg) was diagnosed in 110 patients. The average HVPG was 16.07 ± 7.4 mmHg (median 16.0). The average liver stiffness was 2.7 ± 0.55 m/s (median 2.72), stiffness of the spleen was 3.14 ± 0.47 m/s (median 3.22). HVPG correlated with pSWE liver stiffness measurement ($p = 0.001$, $\eta^2 = 0.122$, “medium effect size”) as well as with pSWE spleen stiffness measurement ($p < 0.001$, $\eta^2 = 0.219$, “large effect size”). However, the liver stiffness correlation worked significantly only for patients with alcoholic liver disease ($p < 0.001$, $\eta^2 = 0.132$, “medium effect size”) but not for a non-alcoholic aetiology ($p = 0.248$, $\eta^2 = 0.010$, “no effect size”). On the contrary, the HVPG correlated with spleen stiffness pSWE measurement independently of aetiology-dependence works for both groups and for both groups statistically in the same way ($p < 0.001$, $\eta^2 = 0.131$, “medium effect size”) for an alcoholic aetiology; $p = 0.001$, $\eta^2 = 0.093$, “medium effect size” for a non-alcoholic aetiology). We also analysed our data using a Cox’s regression model (average follow-up period was 43.2 months) and the spleen pSWE emerged as an independent predictor of survival ($p = 0.0408$, RR = 1.79 per IQR, CI = (1.024, 3.14), whereas liver pSWE did not ($p = 0.300$).

Conclusion: Spleen stiffness measured using pSWE correlates positively with HVPG independently of aetiology in contrast with

liver stiffness. Spleen stiffness also predicts overall survival and may represent a useful additional non-invasive method in the evaluation of portal hypertension in cirrhotic patients. Supported by: MH CZ-DRO-VFN00064165 and KNLVR 180310.

SAT-342

Suppression of the pituitary-adrenal axis in stable outpatients with advanced chronic liver disease increases with disease severity and may be linked to systemic inflammation and bile acids

Lukas Hartl^{1,2}, Benedikt Simbrunner^{1,2,3}, Mathias Jachs^{1,2}, Peter Wolf⁴, David Jm Bauer^{1,2}, Bernhard Scheiner^{1,2}, Lorenz Balcar^{1,2}, Georg Semmler^{1,2}, Michael Schwarz¹, Rodrig Marculescu⁵, Michael Trauner¹, Mattias Mandorfer^{1,2}, Thomas Reiberger^{1,2,3}. ¹Division of Gastroenterology and Hepatology, Department of Medicine III, Medical University of Vienna, Vienna, Austria; ²Vienna Hepatic Hemodynamic Lab, Division of Gastroenterology and Hepatology, Department of Medicine III, Medical University of Vienna, Vienna, Austria; ³Christian Doppler Lab for Portal Hypertension and Liver Fibrosis, Division of Gastroenterology and Hepatology, Department of Medicine III, Medical University of Vienna, Vienna, Austria; ⁴Division of Endocrinology, Department of Medicine III, Medical University of Vienna, Vienna, Austria; ⁵Department of Laboratory Medicine, Medical University of Vienna, Vienna, Austria
Email: thomas.reiberger@meduniwien.ac.at

Background and aims: Adrenal dysfunction has been described in patients with liver cirrhosis during acute decompensation or infection. Impaired hypothalamus-pituitary signaling may play a role in the adrenal dysfunction of these patients. Mechanistically, elevated bile acid (BA) levels, chronic inflammation and altered cholesterol homeostasis may all impact on adrenal function. We aimed to characterize the pituitary-adrenal axis in a cohort of stable outpatients with advanced chronic liver disease (ACLD).

Method: Consecutive outpatients with ACLD who underwent hepatic venous pressure gradient (HVPG) measurement between June 2018 and March 2020 included in the prospective VICIS (NCT03267615) study were analyzed. Exclusion criteria were HVPG < 6 mmHg, occlusive portal vein thrombosis, vascular liver disease, hepatocellular carcinoma, a history of liver transplantation, intake of corticosteroids and evidence of infection at the time of characterization. Patients were stratified into 6 clinical stages: S0: subclinical portal hypertension (PH; HVPG 6–9 mmHg), S1: clinically significant portal hypertension (HVPG ≥ 10 mmHg) without varices, S2: presence of varices, S3: previous variceal bleeding, S4: previous non-bleeding decompensation and S5: further decompensation.

Results: Overall, 151 patients were included, 61 of which had compensated ACLD (S0: $n = 17$; S1: $n = 15$; S2: $n = 29$), while 90 patients were decompensated (S3: $n = 7$; S4: $n = 50$; S5: $n = 33$). Median levels of ACTH (from S0: 38.0 pg/ml to S5: 20.0 pg/ml; $p = 0.001$), cortisol binding globulin (from S0: 52.0 μ g/ml to S5: 38.9 μ g/ml; $p < 0.001$) and total serum cortisol (t-Cort; from S0: 14.9 μ g/dL to S5: 9.2 μ g/dL; $p = 0.023$) decreased with progressive clinical stages. While median levels of free serum cortisol (f-Cort; from S0: 6.6 ng/ml to S5: 5.7 ng/ml; $p = 0.379$) were non-significantly different across the clinical substages, there was a numerically higher share of patients with particularly low f-Cort levels (i.e. < 5.0 ng/ml) with increasing ACLD severity (from S0: 28.6% to S5: 45.5%; $p = 0.169$). Importantly, there was a significant increase of C-reactive protein (CRP) and BA throughout the clinical substages (see Figure), while no difference in total cholesterol and high-density lipoprotein (HDL) cholesterol was found. Both CRP ($\rho = -0.293$; $p < 0.001$) and BA ($\rho = -0.186$; $p = 0.025$) negatively correlated with ACTH. In multivariate linear regression analysis, CRP ($p = 0.024$), but not BA levels ($p = 0.859$) were independently associated with ACTH (adjusted for HVPG, Child-Pugh score, creatinine and cholesterol).

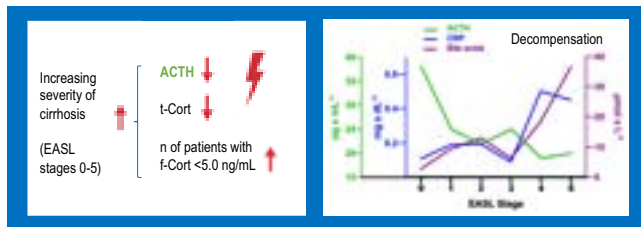


Figure:

Conclusion: With increasing cirrhosis severity, the pituitary-adrenal axis is progressively suppressed in stable outpatients with ACLD. Mechanistically, elevated levels of BA and systemic inflammation in ACLD may explain this clinically relevant suppression of ACTH-cortisol signaling.

SAT-343

Role of non neoplastic portal vein thrombosis in natural history of patients with cirrhosis and hepatocellular carcinoma

Sarah Shalaby¹, Marco Grasso¹, Alessandro Vitale², Enrico Pizzirani³, Alberto Zanetto¹, Paolo Feltracco⁴, Paolo Simioni⁵, Patrizia Burra¹, Umberto Cillo², Marco Senzolo¹. ¹Multivisceral Transplant Unit, Department of Surgery, Oncology and Gastroenterology, Padua University Hospital, Padua, Italy; ²Hepatobiliary Surgery and Liver Transplantation Unit, Department of Surgery, Oncology and Gastroenterology, Padua University Hospital, Padua, Italy; ³Institute of Radiology, Department of Medicine, Padua, Italy; ⁴Section of Anesthesiology and Intensive Care, Department of Medicine, Padua, Italy; ⁵General Internal Medicine, Hemorrhagic and Thrombotic Diseases Unit, Department of Medicine, Padua, Italy
Email: sarahshalaby18@gmail.com

Background and aims: Hepatocellular carcinoma (HCC) increases the risk of non-neoplastic portal vein thrombosis (PVT) in cirrhosis. However, data on its natural history and prognostic role in HCC-patients are lacking

Method: Cirrhotic HCC-patients undergoing laparoscopic ablation were consecutively enrolled (2015–2018) and followed until transplantation or up to 36months. HCC and PVT (baseline and incident) characteristics, and their evolution in the first 12months, were reviewed by a single radiologist. PVT evolution was categorized according to changes in occlusion (cut-off 20%) and extension to other segments as: 'complete/progressive': partial-PVT progressing to complete, complete-PVT not improving or, PVT extending to other segments; 'partial/ameliorated': partial-PVT improving or remaining stable, complete-PVT improving. Variables associated with presence of PVT and evolution patterns were analyzed, as well as its impact on survival.

Results: Seven-hundreds-fifty patients were included, 88 with PVT (78.4% partial, 43.2% extended to mesenteric and/or splenic vein). On multivariate analysis, presence of PVT was associated with pre-treatment total-tumor-volume (TTV) (OR1.10, $p < .0001$) and clinically-significant portal hypertension (OR2.90, $p = .0046$). During follow-up, 46 incident PVT occurred, 27/46 (58.7%) in the presence of viable tumor. Among total 115 PVT diagnosed in presence of HCC, 83 had available radiological follow-up (77.1% partial, 41% extended to the mesenteric and/or splenic vein), and 22 were anticoagulated. The 'complete/progressive' evolution pattern was associated with occlusive PVT at diagnosis and absence of anticoagulation in all PVT; whereas to Child C score and non-response to HCC treatment in non-anticoagulated patients. Overall survival was lower in presence of PVT, specifically for 'complete/progressive' PVT [HR3.9, $p < 0.001$]. A higher cumulative risk of death emerged for 'complete/progressive' PVT, both for HCC-related ($p < 0.001$) and non-HCC-related ($p < 0.001$) death.

Conclusion: Non neoplastic PVT in HCC seems to be characterized by a higher risk of progression when not anticoagulated, correlated with

the HCC activity. Complete/progressive PVT is an independent factor associated with mortality, regardless of HCC evolution.

SAT-344

To study effect of the combination of midodrine and tolvaptan versus tolvaptan alone in patients with severe hyponatremia in cirrhosis-an open label RCT (TOLMINA Trial-NCT05060523)

Srinivasa Reddy Golamari^{1,2}, Shiv Kumar Sarin¹, Manoj Kumar Sharma¹, Jaya Benjamin¹. ¹Institute of liver and biliary sciences, hepatology, NEW DELHI, India; ²Institute of liver and biliary sciences, hepatology, delhi, India
Email: srinivasareddygolamari@gmail.com

Background and aims: Decreased effective circulating volume secondary to splanchnic vasodilatation plays a central role in the pathogenesis of hyponatremia in patients with cirrhosis. Vaptans have shown promise in increasing serum sodium levels in hyponatremia. Vasoconstrictor therapy may improve the diminished effective circulating volume, which in turn would reduce vasopressin release, thereby allowing for more urinary electrolyte-free water excretion. There is no data on combination of vasoconstrictors and tolvaptan till now. Therefore, the current study reports analysis of the efficacy and safety of tolvaptan and midodrine versus tolvaptan alone in patients with cirrhosis and hyponatremia.

Method: Patients [$n = 135$] with severe chronic hyponatremia (< 120 meq/L) who did not respond to albumin infusion [40 gm/day for 48 hours] were randomized to receive Midodrine plus Tolvaptan ($n = 70$) or Tolvaptan alone ($n = 65$) for 7 days with a follow-up of 1 month. Tolvaptan was administered as 15–30 mg/d for 7 days and midodrine as 5–15 mg/d to achieve a target Mean Arterial Pressure of ~ 80 mmHg. Primary end point was improvement in serum sodium to 125 mEq/L within 1 week.

Results: 135 patients were included; 85.2% males. Baseline parameters in the two groups were comparable. Grade 3 ascites was seen in 45 (65%) cases in group A and 35 (53%) in group B. There was significant difference in improvement in serum sodium levels from day 1 to day 7 in group A compared to group B ($p = 0.007$). The proportion of patients in group A who improved serum sodium at day 7 was higher, 60/75 (80%) compared to group B 42/65 [$p = 0.001$]. Absolute Change in Serum sodium levels increase at day 5 and 7 was significant in group A $p = 0.001$ ([OR] 4.7021; 95% CI: 3.554–5.432, $p = 0.001$ ([OR] 6.11; 95% CI: 5.238–7.142.5). Urinary sodium excretion significantly increased in both groups after treatment at 7 days as compared to baseline respectively ($p = 0.003$, $p = 0.01$). Absolute change in urine sodium was significantly increased in group A than group B ($p = 0.05$). Plasma renin activity and pro b-type natriuretic peptide (PRO BNP) significantly decreased in both groups at day-7 compared to baseline respectively. ($p = 0.027$, $p = 0.023$). Renal resistivity index significantly decreased in group A at day7 compared to group B ($p = 0.03$). Absolute change in renal resistivity index was also significant in group A than B ($p = 0.027$). Mean arterial pressure (MAP) in group A was higher than group B ($p = 0.004$). Twenty-four-hour urine output was significantly higher in group A than B ($p = 0.03$) when compared to baseline. Mortality was high in group B at 7 and 28 days [$p = 0.005$ ([OR] 6.281; 95% CI: 1.354–29.9, $p = 0.003$ ([OR] 2.121; 95% CI: 0.8–5.5]. Overall adverse events occurred in 30.2% of group A and 24% in group B ($p = 0.39$). Development of acute kidney injury/Hepatic encephalopathy at day 7 and day 28 in group A [16.7%, 12.75%] and B [9.7%, 6%] were not different.

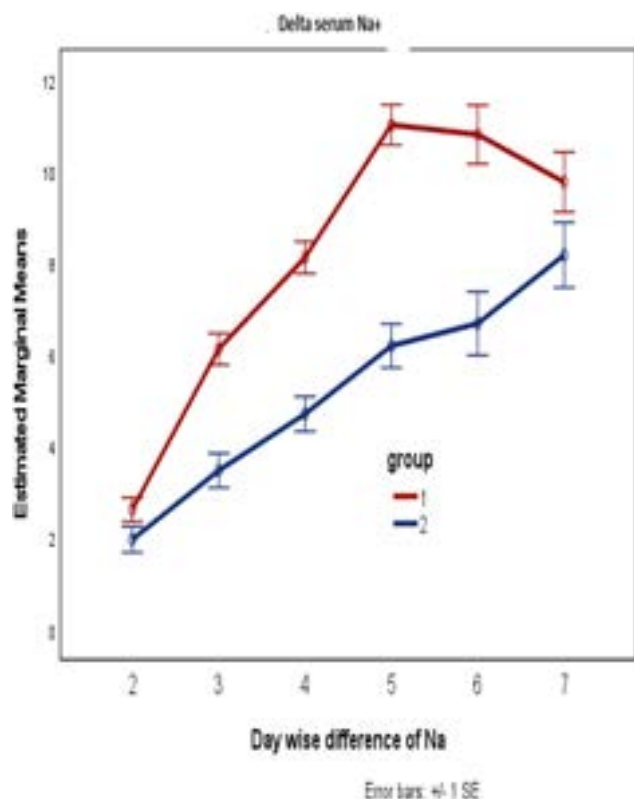


Figure:

Conclusion: Our results clearly demonstrate that combination of tolvaptan and midodrine is superior to Tolvaptan monotherapy in the treatment of severe hyponatremia in cirrhosis patients with ascites.

SAT-345

Bacterial translocation has an early onset in cirrhosis and induces a selective inflammatory response

Benedikt Simbrunner¹, Esther Caparrós², Teresa Neuwirth³, Philipp Schwabl¹, Philipp Königshofer¹, David Jm Bauer¹, Rodrig Marculescu⁴, Michael Trauner¹, Bernhard Scheiner¹, Georg Stary³, Mattias Mandorfer¹, Thomas Reiberger^{1,1}, Rubén Francés². ¹Division of Gastroenterology and Hepatology, Department of Medicine III, Medical University of Vienna, Vienna, Austria, Austria; ²CIBEREHD, Instituto de Salud Carlos III, Madrid, Spain, Spain; ³CeMM Research Center for Molecular Medicine of the Austrian Academy of Sciences, Austria; ⁴Department of Laboratory Medicine, Medical University of Vienna, Austria, Austria
Email: thomas.reiberger@meduniwien.ac.at

Background and aims: Bacterial translocation (BT) is considered to play an important role in advanced chronic liver disease (ACLD) by promoting systemic inflammation, portal hypertension, and circulatory dysfunction.

Method: Patients with ACLD (n=249) and absence of acute decompensation or infections undergoing hepatic venous pressure gradient (HVPG) measurement were classified according to EASL stages of compensated and decompensated (c/d) ACLD (cACLD: S0 : HVPG 6–9 mmHg, S1-2 : HVPG ≥10 mmHg/varices; dACLD: S3 : previous variceal bleeding, S4 : one previous non-bleeding decompensation; S5 : 2 or more previous decompensation events). BT biomarkers (lipopolysaccharide, LPS; lipoteichoic acid, LTA; bacterial DNA, bactDNA) and markers of systemic inflammation and circulatory dysfunction were evaluated. Furthermore, T-cell subsets were characterized by flow cytometry in small intestinal biopsies in additional 7 ACLD patients and 4 controls.

Results: The main cohort had a median HVPG of 18 (12–21) mmHg and 56% had dACLD. BT markers were significantly elevated in patients with ACLD compared to healthy controls (n=40; p<0.001): The median LPS levels were 0.04 (0.02–0.06) in controls vs. 0.64 (0.30–1.06) EU/ml, LTA 4.53 (3.58–5.97) vs. 43.2 (23.2–109) pg/ml, and bactDNA was detected (≥5 pg/ml) in 5% of controls vs. 41% of patients with ACLD, respectively. Surprisingly, BT markers were similar across the clinical stages of ACLD and not linked to HVPG, systemic hemodynamics, or clinical events during follow-up. LPS was correlated with TNF α and IL-10 (Spearman's r = 0.523, p<0.001; r = 0.143, p=0.024). The presence of bactDNA was associated with elevated LPS (0.54, 0.28–0.95, vs. 0.88, 0.32–1.31 EU/ml, p=0.001) and TNF-α levels (15.3, 6.31–28.1, vs. 20.9, 13.8–32.9, pg/ml). Patients with ACLD displayed a decreased CD4 : CD8-ratio and higher TH1-cells in their intestinal mucosa than liver-healthy controls.

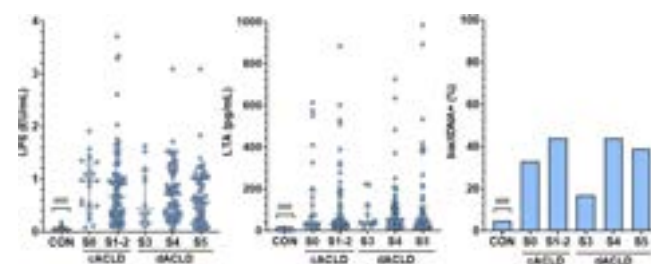


Figure:

Conclusion: BT occurs in early clinical stages of ACLD and linked to a systemic inflammatory response reflected by TNF-α and IL-10. Surprisingly, BT markers were not associated with portal hypertension, circulatory dysfunction, and clinical events in patients with stable ACLD. Changes of the intestinal mucosa immune cell composition may be mechanistically involved in pathological BT of patients with ACLD and should be further investigated by future studies.

SAT-346

Efficacy of long term albumin therapy in treatment of decompensated cirrhosis

Deepanshu Khanna^{1,2}, Premashis Kar¹, Pabitra Sahu¹. ¹Max Super Speciality Hospital, Vaishali, Ghaziabad, India; ²Max Super Speciality Hospital, Vaishali, Gastroenterology, Ghaziabad, India
Email: drdeepanshukhanna@gmail.com

Background and aims: Decompensated liver cirrhosis has a poor prognosis, with a median overall survival of 2–4 years, which is worse than for many oncological disorders. These patients are highly susceptible to infections due to increased systemic inflammation leading to kidney failure and death. Aim was to study the efficacy of albumin in reducing episodes of decompensation, preventing bacterial infection, kidney dysfunction and mortality.

Method: Study involved patients with Child B or C cirrhosis with albumin level below 30 g per litre, who were administered 20% human albumin weekly with standard medical treatment for 3 months and compared with age and sex matched controls who received only standard medical treatment. The primary end point was 6 month mortality, and the secondary end points were reduction in infections, kidney dysfunction, ascites recurrence, hepatic encephalopathy, gastrointestinal bleed and complications of cirrhosis.

Results: From September 2021 to January 2023, 88 cases and 86 controls were taken and followed up for 6 months. Overall 6-month survival was not statistically significant between groups (95.1% vs 91.9%; p=0.330). Incidence of Recurrence of ascites (30.7% v/s 75.6%, P<0.001), Kidney dysfunction (6.8% v/s 24.4%, P<0.001) hepatic encephalopathy (18% vs 40%, P<0.001), Spontaneous bacterial peritonitis (3.4% vs 25.6%, P<0.001) were significantly less in cases as compared with controls, however infections (8% vs 11.6%, P=

0.603) and Gastrointestinal bleed (14.8% vs 17.4%, $P = 0.632$) was not statistically significant.

End point	Case	Control	P value
Mortality	4.9%	8.1%	0.330 (NS)
Recurrence of ascites	30.7%	75.6%	<0.001
Refractory ascites	6.8%	16.3%	0.050
Kidney dysfunction	6.8%	24.4%	<0.001
Hepatic encephalopathy	18%	40%	<0.001
Infections	8%	11.6%	0.603 (NS)
SBP	3.4%	25.6%	<0.001
GI Bleed	14.8%	17.4%	0.632 (NS)

NS- Not significant

Conclusion: Long-term Human albumin acts as a disease modifying treatment in patients with decompensated cirrhosis.

SAT-347

Recently validated non-invasive tests for liver fibrosis assessment have great performance in identifying NASH patients at risk for decompensation

Vlad Taru^{1,2,3}, Madalina Gabriela Taru^{2,4,5}, Bobe Petrushev², Rusu Ioana², Horia Stefanescu², Andreea Fodor², Mina Dana Ignat², Fischer Petra², Oana Nicoara-Farcu^{1,2}, Monica Platon^{6,7}, Bogdan Procopet^{1,2}, ¹"Iuliu Hatieganu" University of Medicine and Pharmacy, Internal Medicine, Cluj-Napoca, Romania; ²Regional Institute of Gastroenterology and Hepatology "Octavian Fodor", Hepatology, Cluj-Napoca, Romania; ³Medical University of Vienna, Medicine III-Division of Gastroenterology and Hepatology, Vienna, Austria; ⁴"Iuliu Hatieganu" University of Medicine and Pharmacy, Biochemistry and Molecular Biology, Cluj-Napoca, Romania; ⁵University of Bologna, Medical and Surgical Sciences, Bologna, Italy; ⁶"Iuliu Hatieganu" University of Medicine and Pharmacy, Medical Imaging, Cluj-Napoca, Romania; ⁷Regional Institute of Gastroenterology and Hepatology "Octavian Fodor", Medical Imaging, Cluj-Napoca, Romania
Email: vlad.taru@lirec.ro

Background and aims: Non-alcoholic fatty liver disease (NAFLD) has become a substantial burden worldwide, with alarmingly increasing prevalence. NAFLD may progress to non-alcoholic steatohepatitis

(NASH), NASH-related cirrhosis, and hepatocellular carcinoma. Scientific efforts concentrate on developing non-invasive tests (NITs) to predict clinically significant portal hypertension (CSPH) and reduce the need for invasive, costly investigations. The vibration-controlled transient elastography (VCTE) has become part of many algorithms, including the recent Baveno VII criteria. A new model (ANTICIPATE-NASH) was proposed to identify CSPH in obese patients. Other NITs, such as Agile 3+ and Agile 4, were recently validated for predicting advanced fibrosis and cirrhosis in patients with NAFLD/NASH. Still, their performance in assessing CSPH has not been tested yet. This study aimed to evaluate the performances of Agile3+ and Agile 4 in identifying CSPH in patients with NAFLD/NASH.

Method: Seventy-six consecutive patients with biopsy-proven NAFLD/NASH were included. Hepatic venous pressure gradient (HVPG) was assessed using a 7F-balloon catheter, and a value ≥ 10 mmHg was considered CSPH. LS was measured by VCTE and fibrosis was assessed histologically using the Metavir scoring system. The statistical analysis was performed in MedCalc v20, using AUROC analysis to assess the performance of NITs and DeLong protocol for comparison of NITs. Differences in classification between NITs were tested using McNemar's test. Continuous variables are expressed as median (interquartile range), and a p value <0.05 was considered statistically significant.

Results: The median HVPG was 7 (4–13) mmHg, and 27 (35.5%) patients had CSPH. The liver histology fibrosis scoring identified 1 (1.3%), 10 (13.2%), 18 (23.7%), 15 (19.7%) respectively 32 (42.1%) patients as F0, F1, F2, F3, respectively F4. The performance of VCTE in identifying CSPH was excellent (AUC = 0.95, 95% CI: 0.86–0.99, $p < 0.001$). The ANTICIPATE-NASH score had a slightly lower but still excellent performance (AUC = 0.935, 95% CI: 0.84–0.98, $p < 0.001$). Agile 3+ had the best performance in identifying CSPH (AUC = 0.96, 95% CI: 0.89–0.99, $p < 0.001$) and was significantly better only compared to FIB-4 ($p = 0.04$) and FIB-4+ ($p = 0.02$). The Baveno VII criteria for CSPH had excellent rule-out (Se = 96%, NPV = 96.3%) and rule-in (Sp = 100%, PPV = 100%) performance, with 21 (33.9%) patients left unclassified. Agile 3+ was superior to the Baveno VII criteria in identifying patients with CSPH, with 15 (24.2%) patients still in the "grey zone," and no significant difference in classification (3.17%, CI: -5.59–11.94, $p = 0.22$).

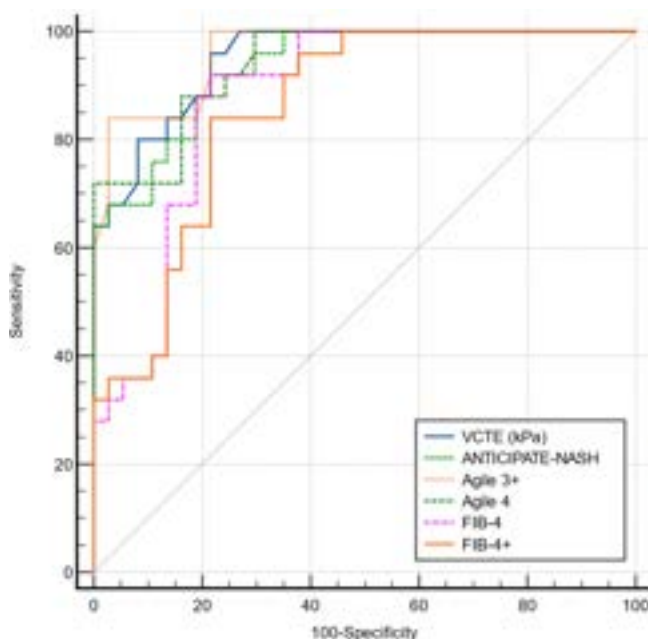


Figure: (abstarct: SAT-347).

Performance of NITs in identifying NASH patients with CSPH			
Variable	AUC	SE	95% CI
VCTE	0.95	0.0235	0.862 to 0.989
ANTICIPATE-NASH	0.935	0.0281	0.843 to 0.982
Agile 3+	0.961**	0.0204	0.879 to 0.994
Agile 4	0.941*	0.0266	0.851 to 0.985
FIB-4	0.878	0.0433	0.770 to 0.947
FIB-4+	0.855	0.0464	0.743 to 0.932

*vs FIB-4plus, **vs FIB-4; $p < 0.05$; other comparisons $p > 0.05$

NITs	Grey zone (n, %total)
BAVENO VII	21 (33.9%)
ANTICIPATE-NASH	19 (30.6%)
Agile 3+	15 (24.2%)
Agile 4	16 (25.8%)

POSTER PRESENTATIONS

Conclusion: Newly developed NITs to assess liver fibrosis in NAFLD/NASH patients, such as Agile 3+ and Agile 4, show good performance in identifying patients with CSPH at risk for decompensation.

SAT-348

Earlier diagnosis of hepatorenal syndrome-acute kidney injury with updated guidelines-review of the Confirm trial

Richard Frederick¹, Florence Wong², Hugo Vargas³, Chris Pappas⁴, Khurram Jamil⁵. ¹California Pacific Medical Center, Department of Transplant, San Francisco, CA, United States; ²University of Toronto, Department of Medicine, Toronto, ON, Canada; ³Mayo Clinic Hospital, Phoenix, AZ, United States; ⁴Orphan Therapeutics, LLC, Longboat Key, FL, United States; ⁵Mallinckrodt Pharmaceuticals, Hampton, NJ, United States

Email: todd.frederick@sutterhealth.org

Background and aims: In 2015, the International Club of Ascites (ICA) published revised consensus recommendations for the diagnosis of acute kidney injury (AKI) and hepatorenal syndrome (HRS) based on a change in serum creatinine (SCr) rather than a required threshold of SCr of 2.5 mg/dL in patients with cirrhosis, to facilitate earlier treatment of HRS Type 1 (HRS-1). Patients receiving vasoconstrictor-based treatment for HRS-AKI respond better and have higher rates of HRS reversal if treatment is started at lower SCr. This study estimated the effect of using the updated ICA-AKI diagnostic criteria on diagnosis and timing of HRS treatment in patients who were enrolled in CONFIRM-a large, prospective, randomized (terlipressin vs placebo) clinical trial.

Method: 2015 HRS-AKI criteria were retrospectively applied to available individual patient's pre-enrollment serial SCr data from CONFIRM. The number of days between meeting current ICA HRS-AKI criteria (for both Stage 1b and Stage 2) and old HRS-1 criteria were determined to estimate the impact of the new criteria on potential earlier treatment. In addition, SCr at HRS-AKI diagnosis using the ICA 2015 criteria was compared to SCr at diagnosis of HRS-1 using the 2007 diagnostic criteria to estimate the effect of the new criteria on SCr at the potential start of vasoconstrictor therapy.

Results: Of 300 patients included in CONFIRM, 297 and 215 subjects had data available for this analysis (Stage 1b and 2, respectively). Compared with the traditional diagnostic criteria used for CONFIRM: the diagnosis of HRS-AKI could be made a median of 4 and 2 days earlier for Stage 1b and Stage 2, respectively; and the absolute median SCr was 1.0 mg/dL and 0.4 mg/dL lower at the time of diagnosis of AKI-HRS Stage 1b and 2, respectively (Figure).

	Stage 1b (n = 297)	Stage 2 (n = 215)	P value*
HRS-1 vs HRS-AKI criteria*			
Change in median time to diagnosis	4 days	2 days	<.0001
Change in median SCr at diagnosis	1.0 mg/dL	0.4 mg/dL	<.0001

*T-test for the change between the 2 diagnostic criteria.

Conclusion: Applying the new 2015 ICA AKI-based criteria for HRS-AKI is estimated to result in earlier diagnosis and treatment of patients by approximately 2–4 days, depending on use of Stage 1b or 2. The SCr at initiation of treatment would be 0.4–1.0 mg/dL lower with use of the updated criteria. Using the new ICA HRS-AKI diagnostic criteria will allow for earlier treatment at lower SCr and the potential for better clinical outcomes.

SAT-349

Predicting esophageal varices and varices needing treatment in patients with compensated advanced chronic liver disease using Baveno VI Criteria, CHESS-ALARM score, FIB-4 score, and recently proposed FIB-5 score

Fares Mashal¹, Nimy John^{1,2}, Shakshi Sharma³, Mauricio Garcia Saenz De Sicilia¹, Abhilash Perisetti⁴, Ragesh Babu Thandassery¹. ¹University of Arkansas for Medical Sciences, Medicine, Division of Gastroenterology, Little Rock, United States; ²UCLA David Geffen School of Medicine, Medicine, Division of Digestive Diseases/Gastroenterology, Los Angeles, United States; ³University of Arkansas for Medical Sciences, Institute of Aging, Little Rock, United States; ⁴Veteran Affairs Medical Center, Medicine, Division of Gastroenterology, Kansas City, United States
Email: doc.ragesh@gmail.com

Background and aims: FIB-5 score (FIB-4 and Liver Stiffness, Fibrosis-5 Risk Prediction (fib5.net)) was proposed recently to predict complications of portal hypertension in a US Veteran Cohort. We aim to validate the FIB-5 score in general population with compensated advanced chronic liver disease (cACLD) and compare it with other non-invasive scores for predicting the presence of esophageal varices (EV) and varices needing treatment (VNT).

Method: We studied Baveno VI criteria (BC = liver stiffness >20 kPa and platelet count <150 × 10⁹ cells/L), expanded BC (liver stiffness >25 kPa and platelet count <110 × 10⁹ cells/L), CHESS-ALARM score (Model = 0.033 × Age - 0.598 × Male - 0.018 × Platelet + 0.032 × liver stiffness), aspartate transaminase platelet count ratio (APRI), FIB-4 score and FIB-5 score in predicting presence of EV and varices needing treatment (VNT), in a cohort of patients with clinical cACLD, in Mid-West United States (Jan 2015–Dec 2021).

Results: 424 patients were studied, mean age 59.2 ± 12.5 years, 57.3% females, 78.3% Caucasian and 14.9% African American. Most common causes of cACLD were non-alcohol associated fatty liver disease (NAFLD, 55.3%), chronic hepatitis C (32.7%) and alcohol (23.1%). EV were present in 126 (29.7%) and VNT in 32 (7.5%). 221 patients (52%) met BC, and 173 (40.7%) met expanded BC.

Among patients with EV seen on EGD, 87.7% met BC, and 77.4% met expanded BC. Of all patients who had VNT (n = 32), 85.7% met expanded BC. BC (p < 0.001), expanded BC (p < 0.001), CHESS-ALARM score (p < 0.001, at cut off >0.37) and FIB-5 score (p < 0.001, at cut off >0.75) independently correlated with presence of EV on logistic regression analysis.

The predictive accuracy (AUROC) for EV on EGD was highest for FIB-5 score (0.88, CI = 0.83 to 0.94), followed by CHESS-ALARM score (0.82, CI = 0.76 to 0.86), FIB-4 (0.80, CI = 0.76 to 0.85), APRI (0.76, CI = 0.72 to 0.81), and the lowest for MELD-Na (0.66, CI = 0.60 to 0.72). FIB-5 score at 0.75 had a sensitivity of 73% and specificity of 80% to predict EV. Similarly, the AUROC for predicting VNT on EGD was highest for FIB-5 score (0.85, CI = 0.81 to 0.88), followed by CHESS-ALARM score (0.79, CI = 0.72 to 0.86), FIB-4 (0.78, CI = 0.72 to 0.85), APRI (0.73, CI = 0.66 to 0.81), and the lowest for MELD-Na (0.66, CI = 0.58 to 0.74). FIB-5 score at 1.5 had sensitivity of 81% and specificity of 80% to predict VNT.

Conclusion: Newly proposed FIB-5 score has higher predictive accuracy than most other non-invasive scores for identifying EV and VNT in patients with cACLD. We validate the accuracy of FIB-5 score in predicting EV and VNT in a general (non-veteran) population with cACLD (predominantly from NAFLD).

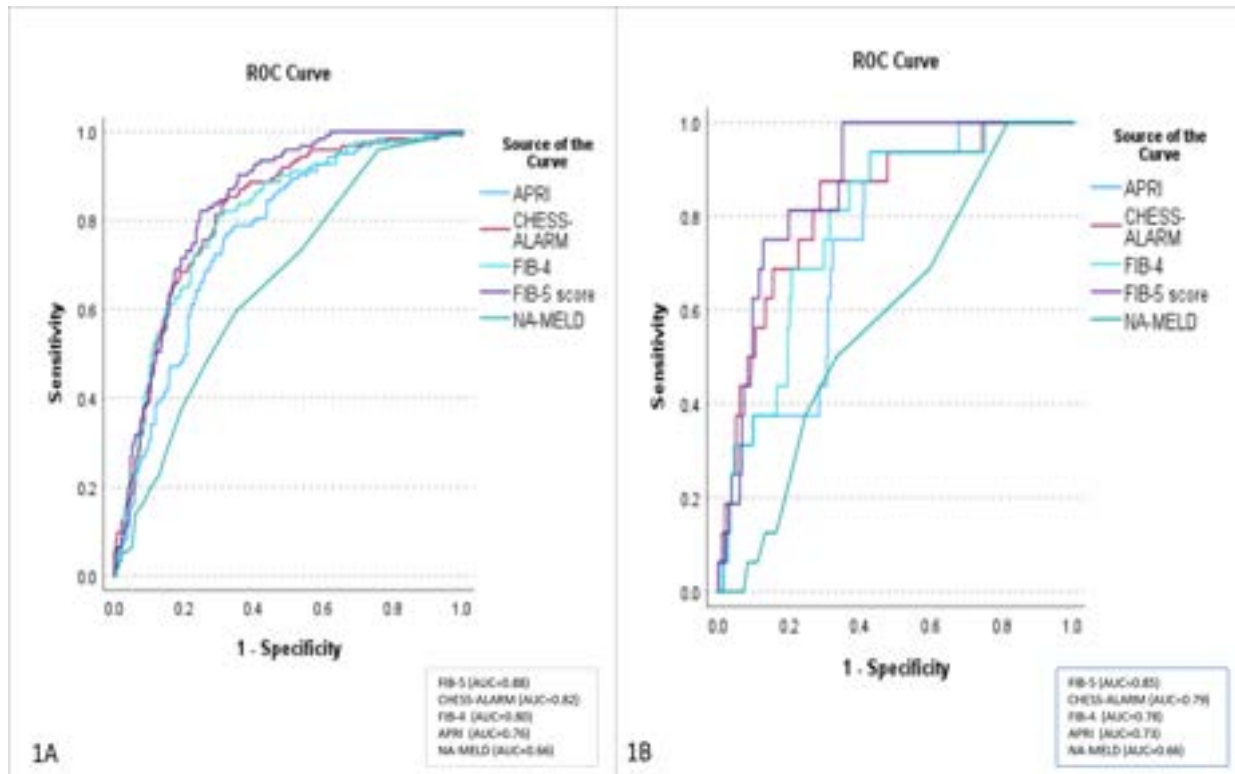


Figure: (abstarct: SAT-349): Comparison of non-invasive scores for predicting esophageal varices and varices needing treatment.

SAT-350

Hepatic venous pressure gradient predicts further decompensation in cirrhosis patients with acute esophageal variceal bleeding

Manas Vaishnav¹, Sagnik Biswas¹, Shekhar Swaroop¹, Arnav Aggarwal¹, Piyush Pathak¹, Abhinav Anand¹, Shalimar¹. ¹All India Institute of Medical Sciences, New Delhi, India
Email: drshalimar@yahoo.com

Background and aims: Portal hypertension is the major driver in the transition from compensated to decompensated cirrhosis. However, the role of hepatic venous pressure gradient (HVPG) in predicting further decompensation in cirrhosis decompensated with acute variceal bleeding (AVB) is not known. We aimed to evaluate the role of HVPG in predicting the risk of further decompensation in cirrhosis patients with AVB.

Method: In a prospective study, 190 patients with cirrhosis with esophageal (n = 103) or gastric AVB (n = 87) were included. HVPG was measured on the day of the AVB, within 8 hours of endotherapy. Decompensating events occurring after 42-day of AVB were considered further decompensation. Multivariate analysis was performed to assess factors associated with further decompensation.

Results: The median age of the study cohort was 45 years with 81.6% male. The predominant etiology of cirrhosis was alcohol in 82 (43.2%), chronic hepatitis B in 27 (14.2%), and chronic hepatitis C in 18 (9.5%). Overall, 53 (27.9%) patients developed further decompensation during a median follow-up duration of 274 days following AVB. New-onset/worsening ascites and GI bleeding were the most common decompensating event in 30 (15.8%). On the multivariate model, HVPG was an independent predictor of any further decompensation in esophageal AVB patients but not in gastric variceal bleeding patients. HVPG cut-off of ≥ 16 mmHg predicted further decompensation in the esophageal AVB cohort with a sensitivity and specificity of 66.7% and 57.5% respectively. Patients with HVPG ≥ 16 mmHg compared to <16 mmHg had higher cumulative probability of

further decompensation: GI bleed (log-rank p=0.013) and new-onset/worsening ascites (log-rank p=0.023). There were no differences in hepatic encephalopathy and jaundice (Figure 1). However, HVPG was not an independent predictor of mortality in the entire, esophageal or gastric AVB cohorts.

Conclusion: HVPG measured during an episode of acute variceal hemorrhage from esophageal varices predicts further decompensating events in patients with liver cirrhosis. For patients with gastric varices, no similar relationship with HVPG could be established. Further studies, including a dynamic evaluation of HVPG in relation to impending decompensation, would shed more light on this matter.

SAT-519

Ultrasound predictors of hemodynamic TIPS dysfunction: friends or foes?

Andreea Fodor¹, Rares Craciun¹, Oana Nicoara-Farcu¹, Fischer Petra¹, Mina Ignat¹, Ionel-Andrei Motofelea¹, Roxana Buda², Corina Radu¹, Zeno Sparchez¹, Horia Stefanescu³, Bogdan Procopet¹. ¹Prof Dr Octavian Fodor Regional Institute of Gastroenterology and Hepatology, Romania; ²Iuliu Hatieganu University of Medicine and Pharmacy, Romania; ³Regional Institute of Gastroenterology and Hepatology, Liver Unit and Clinical Ultrasound Department, Cluj Napoca, Romania
Email: andreea.fodor11@gmail.com

Background and aims: Although the role of non-invasive tools, namely ultrasound (US) parameters, in the assessment of transjugular intrahepatic portosystemic shunt (TIPS) dysfunction has widely been studied, there is insufficient data regarding clear criteria applicable in current practice.

We primary aimed at evaluating the performance of US parameters for detection of hemodynamic TIPS dysfunction, in the absence of clinical symptoms suggestive for dysfunction. Secondly, we assessed the role of spleen and liver stiffness measured by 2D shear wave elastography (2D SWE) and Fibroscan in predicting hemodynamic dysfunction (HD).

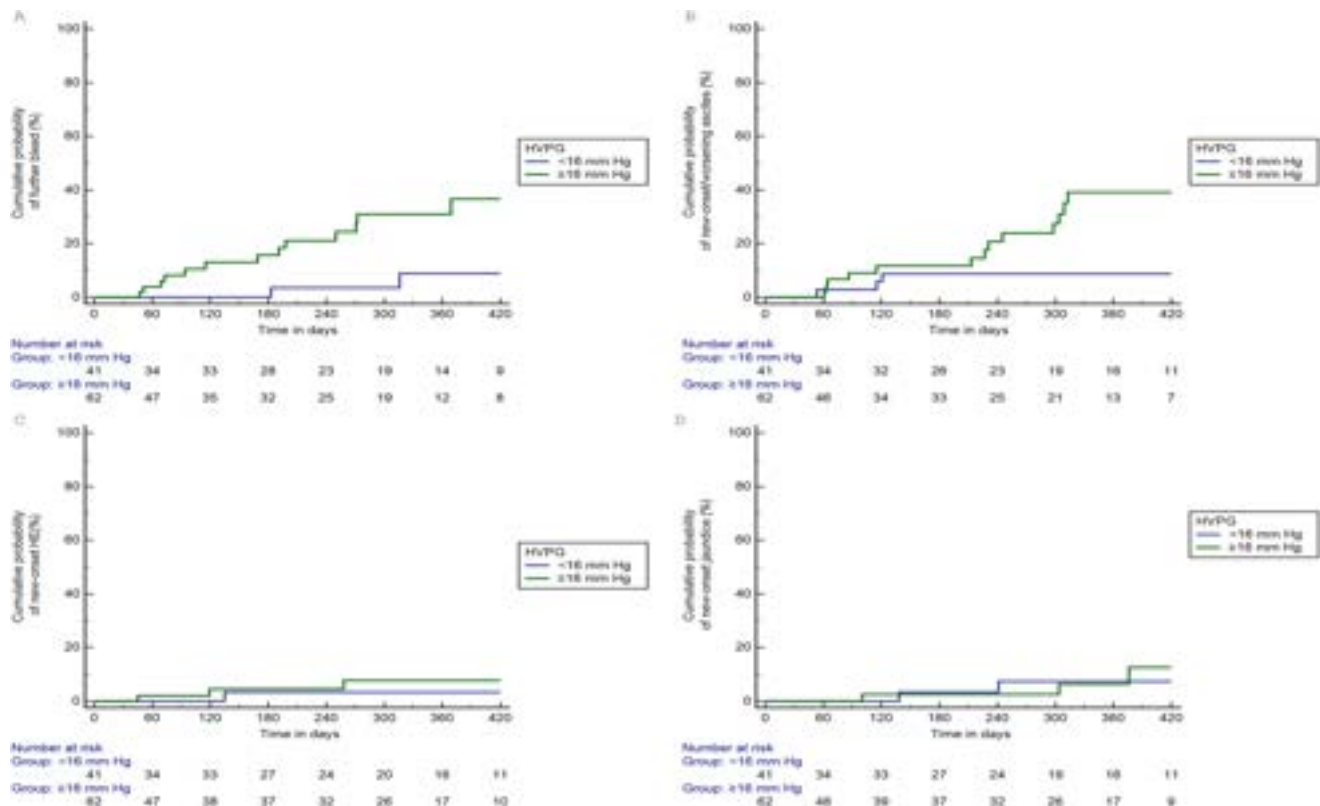


Figure 1: (abstract: SAT-350): Cumulative probability of individual further decompensation in esophageal AVB group based on HVPG: (a) GI bleeding (log-rank p = 0.013), (b) Ascites (log-rank p = 0.023), (c) HE (log-rank p = 0.217), (d) jaundice (log-rank p = 0.812).

Method: All consecutive patients treated with TIPS for portal hypertension-related complications and systematic hemodynamic TIPS revision at 6 weeks after the procedure have been included. Clinical dysfunction was defined as recurrence of variceal bleeding or inadequate control of ascites, whereas HD was defined as revision portal pressure gradient (PPG) ≥ 12 mmHg. Subgroup analysis was performed on available elastography measurements (initial and at revision) of spleen (delta SSM) and liver (delta LSM).

Results: 86 eligible patients with paired US parameters at TIPS placement and first TIPS revision were analyzed. Recurrent variceal bleeding was the main indication for TIPS placement (82.5%), while 17.5% had refractory ascites. 6 weeks clinical dysfunction rate was 18.6%. Two patients presented with recurrence of PHT-related bleeding and 14 had no clinical improvement of ascites. Median initial and post-TIPS PPG were 16 mmHg (14–19) and 7 mmHg (5.5–8), respectively. A decrease higher than 50% in PPG was achieved in 74.4% of cases. Median 6 weeks systematic PPG was 10 mmHg (7–14). HD occurred in 37 cases (43%). Portal vein velocity had an AUROC of 0.71 for a cut-off of 40.5 cm/s ($p < 0.001$) in detecting HD, with a sensitivity of 0.84 and specificity of 0.50. In subgroup analysis ($n = 30$), the percentage change in delta 2D SWE SSM predicted HD with a modest AUROC of 0.77 for a cut-off of 40% ($p = 0.03$). However, percentage change in delta LSM in both 2D SWE and Fibroscan, exhibited low performance in discriminating HD (see Figure).

non-invasive marker (cut-off, %)	AUROC	accuracy (%; 95% CI)	p
delta 2D SWE SSM (40%)	0.77 (0.59 – 0.95)	79.0 (60.3 – 97.6)	0.03
delta Fibroscan SSM (40%)	0.58 (0.40 – 0.77)	76.3 (59.7 – 88.5)	0.38
delta 2D SWE LSM (30%)	0.47 (0.26 – 0.69)	59.2 (39.8 – 76.7)	0.83
delta Fibroscan LSM (30%)	0.58 (0.43 – 0.76)	80.4 (66.1 – 90.6)	0.27

Figure:

Conclusion: Doppler US and elastography surveillance cannot replace systematic TIPS revision for diagnosing hemodynamic TIPS dysfunction.

SAT-520

Efficacy of Simvastatin plus non-selective beta blocker in improving survival of cirrhotic patients with variceal bleed: a systematic review and meta analysis

Jemimah Andrea Fajardo¹, Gian Paulo Alberto Soliman¹, Sarah Jean Bellido¹, ¹St. Luke's Medical Center Quezon City, Medicine, Quezon City, Philippines
Email: jemimahpfajardo@gmail.com

Background and aims: Around 60% of patients with decompensated liver cirrhosis have esophageal varices with a high propensity to bleed which is the major cause of death in these patients. Pharmacological treatment in addition to endoscopic intervention has been documented to prevent variceal bleeding. Initial studies exploring the addition of simvastatin, a readily accessible and safe medication, to beta blockers in cirrhotic patients with index variceal bleeding have shown potential benefits in terms of liver generation of



Figure 1: (abstract: SAT-520): Forrest plot on Simvastatin plus non selective beta blocker versus non selective beta blocker alone for survival.

nitric oxide and hepatic endothelial dysfunction. We therefore assessed the efficacy of simvastatin with a non-selective beta blocker in improving survival for cirrhotic patients with variceal bleed through a systematic review and meta-analysis.

Method: A comprehensive systematic search through Pubmed, Cochrane and Google scholar was performed to include clinical studies that examined the use of statin with a beta blocker in improving survival in cirrhotic patients. Two reviewers independently screened and reviewed all abstracts and full text papers available. An inclusion and exclusion criteria was made which was a basis for selection of included studies. The Cochrane Risk of Bias tool was used to assess possible bias in each article. Data was analyzed using RevMan 5.4 and GRADEPro. The dichotomous outcomes were analyzed using relative risk with a confidence interval of 95% and the primary outcome pertained to improvement in survival, with a secondary outcome of rebleeding also noted.

Results: The study included 3 randomized control trials with 361 patients with variceal bleeding. There was significant survival benefit among patients given simvastatin therapy with a risk ratio of 0.43 (95% confidence interval 0.26–0.73; p value (probability value)= 0.002). A secondary outcome of rebleeding was also studied and showed a trend towards benefit with a risk ratio of 0.72. However, the results were not statistically significant (95% confidence interval; 0.47–1.09; p value = 0.12).

Conclusion: Among cirrhotic patients with variceal bleeding, the addition of simvastatin provides a significant benefit in survival, but not in rebleeding. However, there remains a need for larger studies with more participants to strengthen this evidence, and a deeper look into its safety profile in cirrhotic patients specifically.

SAT-521

Validation and refinement of the Baveno VII criteria for risk stratification in compensated advanced chronic liver disease after HCV-cure

Georg Semmler^{1,2}, Sonia Alonso Lopez^{3,4,5}, Monica Pons⁶, Sabella Lens⁷, Elton Dajti⁸, Marie Griemsmann⁹, Alberto Zanetto¹⁰, Lukas Burghart^{1,11}, Stephanie Hametner-Schreil¹², Lukas Hartl^{1,2}, Adriana Ahumada³, Sergio Rodriguez-Tajes⁷, Paola Zanaga¹⁰, Michael Schwarz^{1,2,11}, Clara Uson⁴, Mathias Jachs^{1,2}, Anna Pocurull⁷, Maria Luisa Manzano Alonso¹³, Dominik Ecker¹², Daniel Riado¹⁴, Beatriz Mateos Muñoz, Michael Gschwantler¹¹, Francesco Paolo Russo¹⁰, Francesco Azzaroli⁸, Benjamin Maasoumy⁹, Thomas Reiberger^{1,2}, Xavier Forn⁷, Joan Genesca^{6,16}, Rafael Bañares^{3,4,5}, Mattias Mandorfer^{1,2}. ¹Medical University of Vienna, Division of Gastroenterology and Hepatology, Department of Internal Medicine III, Vienna, Austria; ²Medical University of Vienna, Vienna Hepatic Hemodynamic Lab, Division of Gastroenterology and Hepatology, Department of Internal Medicine III, Vienna, Austria; ³Hospital General Universitario Gregorio Marañón, Liver Unit, Madrid, Spain; ⁴Instituto De Investigación Sanitaria Gregorio Marañón (IISGM), Madrid, Spain; ⁵Universidad Complutense de Madrid, Madrid, Spain; ⁶Vall d'Hebron University Hospital, Vall d'Hebron Institut of Research (VHIR), Vall d'Hebron Barcelona Hospital Campus, Universitat Autònoma de Barcelona, Liver Unit, Barcelona, Spain; ⁷Hospital Clínic, Universitat

de Barcelona, Liver Unit, Barcelona, Spain; ⁸University of Bologna, Department of Medical and Surgical Sciences (DIMEC), Bologna, Italy; ⁹Hannover Medical School, Department of Gastroenterology, Hannover, Germany; ¹⁰Padua University Hospital, Gastroenterology and Multivisceral Transplant Unit, Department of Surgery, Oncology, and Gastroenterology, Padua, Italy; ¹¹Klinikum Ottakring, Department of Internal Medicine IV, Vienna, Austria; ¹²Ordensklinikum Linz Barmherzige Schwestern, Department of Internal Medicine IV, Linz, Austria; ¹³Hospital Universitario 12 De Octubre, Liver Unit, Madrid, Spain; ¹⁴Hospital Universitario Fundación Alcorcón, Gastroenterology Unit, Madrid, Spain; ¹⁵Hospital Universitario Ramón y Cajal, Liver Unit, Madrid, Spain; ¹⁶Centro de Investigación Biomédica En Red de Enfermedades Hepáticas y Digestivas (CIBERehd), Instituto de Salud Carlos III, Madrid, Spain
Email: mattias.mandorfer@meduniwien.ac.at

Background and aims: Baveno VII has established criteria for excluding clinically significant portal hypertension (CSPH) after HCV-cure in compensated advanced chronic liver disease (cACLD), and thus, identifying patients who may be discharged from portal hypertension surveillance (post-treatment liver stiffness measurement (LSM) <12kPa and platelet count (PLT) >150G/L). In contrast, post-treatment LSM values ≥25kPa indicate CSPH and a substantial risk of hepatic decompensation, despite HCV-cure.

However, the long-term prognostic value of these criteria has yet to be independently validated and determinants of decompensation in the gray zone (i.e., in patients meeting none of these criteria) have yet to be identified.

Method: We retrospectively analyzed cACLD patients with paired LSM and PLT before and after HCV-cure by interferon-free therapies from 7 European regions. Fine and Gray competing risk regression models adjusted for clustered data with respective cumulative incidence curves were used to study risk of hepatic decompensation across risk strata. Factors associated with hepatic decompensation in the gray zone were studied using backward elimination. Development of hepatocellular carcinoma and death were considered as competing risks.

Results: 2347 cACLD patients (mean age 60 ± 12 years, 60% male, 21% obese, and 21% diabetes) were followed for a median of 6.0 years during which 65 patients (2.8%) developed hepatic decompensation. In the subgroup of patients who have not been analyzed previously (n = 1527), Baveno VII criteria for excluding CSPH identified patients at a negligible risk of decompensation (at 6 years: 0.5%), while those for ruling-in CSPH identified a high-risk population (at 6 years: 11.4%; Figure-panel A). In the overall study population, decompensation in gray zone patients was uncommon (2.0%, incidence rate 0.4/100 patient years) and was associated with diabetes (adjusted subdistribution hazard ratio (SHR): 2.61 (95%CI: 1.70–4.00), p < 0.001) and post-treatment γ-glutamyltransferase (γ-GT; SHR: 1.38 (95%CI: 1.11–1.73), p = 0.003) independently of LSM, PLT, and albumin. Diabetes or elevated γ-GT identified a subset of gray zone patients (39%) at higher risk (at 6 years: 3.6%; Figure-panel B).

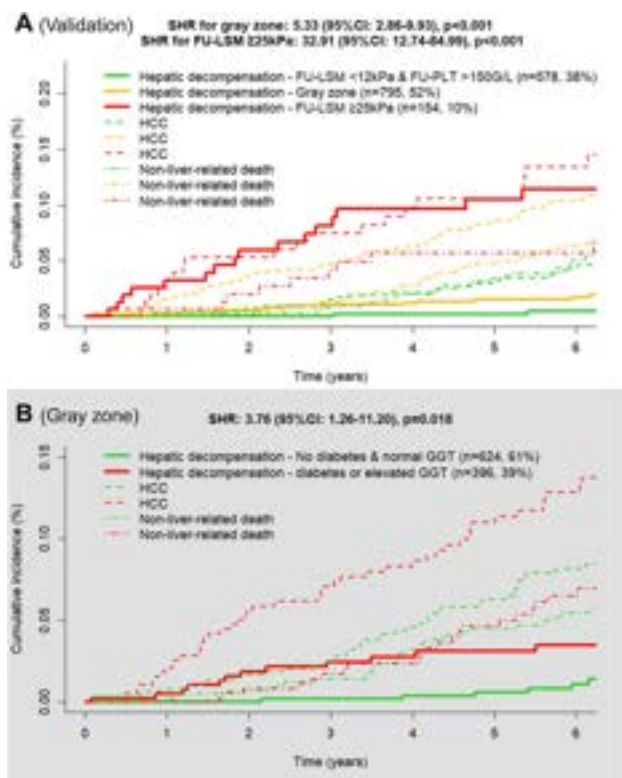


Figure:

Conclusion: Baveno VII criteria for excluding/ruling-in CSPH in HCV-cured patients accurately stratify decompensation risk and may guide patient management. The increased risk of hepatic decompensation in gray zone patients with diabetes and/or elevated γ -GT highlights the importance of managing cofactors. Notably, gray zone patients without diabetes and with normal γ -GT had a negligible risk of hepatic decompensation, despite LSM values of 12–25 kPa and/or thrombocytopenia.

SAT-522

Real-world practice of pre-emptive tipps: an Asia perspective based on Singapore nationwide variceal bleeding audit

Yu Jun Wong^{1,2}, Margaret Teng³, Alyssa Sim⁴, Marianne De Roza⁵, Junhui, Garrett Kang⁶, Guan Sen Kew³, Jia Hong Koh³, Jonathan Kuang⁴, Htay Myat Thet⁷, En Xian Sarah Low⁷, Pooi Ling Loi⁸, Kai Lim⁸, Xuhui Teoh⁹, Jing Liang Ho¹⁰, Gabriel Cher⁹, Kenny Sze⁹, Andrew Kwek¹, Guan Wee Wong¹¹, Wei Lyn Yang⁴, Jason Pik, Eu Chang⁸. ¹Changi General Hospital, Gastroenterology and Hepatology, Singapore, Singapore; ²Duke-NUS Medical School, Singapore, Singapore; ³National University Hospital (NUH)-Singapore, Singapore, Singapore; ⁴Tan Tock Seng Hospital, Singapore, Singapore; ⁵Sengkang General Hospital, Singapore, Singapore; ⁶Changi General Hospital, Singapore, Singapore; ⁷Ng Teng Fong General Hospital, Singapore, Singapore; ⁸Singapore General Hospital, Gastroenterology and Hepatology, Singapore, Singapore; ⁹Khoo Teck Puat Hospital/Dental Department, Gastroenterology and Hepatology, Singapore, Singapore; ¹⁰Woodlands Hospital, Singapore, Gastroenterology and Hepatology, Singapore; ¹¹Ng Teng Fong General Hospital, Gastroenterology and Hepatology, Singapore, Singapore
 Email: wongyujun1985@gmail.com

Background and aims: The Baveno-VII consensus recommends pre-emptive transjugular intrahepatic portosystemic shunt (pTIPSS) in acute variceal bleeding (AVB) patients with high-risk of rebleeding, ie: Child-Turcotte-Pugh (CTP) class C < 14 , or CTP class B > 7 with active bleeding. Data on the real-world adoption and practice on pTIPSS remains limited, particularly from Asia. To understand the real-world

practice on pTIPSS, we aimed to determine: (1) the proportion of patients eligible for pTIPSS, (2) the proportion of patients who underwent pTIPSS based on a Singapore nationwide AVB audit.

Method: We performed a nationwide audit to retrospectively review all adult cirrhosis patients consecutively admitted for AVB from January 2015 to December 2020. Individual patient data on baseline characteristics and clinical outcomes were reviewed and extracted using unified data frame. Eligibility for pTIPSS was based on Baveno-VII consensus; implementation of pTIPSS was based on institutional protocol. We compare the clinical outcomes (5-day rebleeding, 6-week mortality and 1-year mortality) between (1) patients eligible for pTIPSS (vs not eligible), and (2) patients who were eligible and underwent pTIPSS (vs. eligible but no pTIPSS).

Results: This nationwide acute variceal bleeding audit included 910 adult cirrhosis patients with AVB from all 7 public hospitals in Singapore. The mean age was 61 years, 73.7% were male, with ethnicity distribution similar to the general Singapore population. The mean (\pm SD) MELD score was 13 (\pm 6). The mean CTP score was 7 (\pm 1.3), among which 42.2% were CTP-A, 52.1% were CTP-B and 5.7% were CTP-C. At baseline, 18.0% had prior variceal bleeding, 28.7% had ascites requiring diuretics, 34.5% had prior HE, 23.7% had HCC and 18.9% had PVT. Among 14.3% of hospitalized AVB patients who fulfil the eligibility for pTIPSS, only 1.8% underwent pTIPSS. Patients eligible for pTIPSS (vs. not eligible for pTIPSS) had a significantly shortened median (IQR) time to rebleeding [4 (1–15) days vs. 18 (2–111) days, $p=0.025$], a higher risk of early rebleeding (19% vs 6%, $p<0.0001$) and death at 6 weeks (30% vs 11%, $p<0.0001$) and 1 year (45% vs 25%, $p<0.0001$), respectively. Yet, only 44% of pTIPSS were performed within 72 hours of AVB. Low uptake of pTIPSS were similar between transplant and non-transplant centers (6.8% vs 3.5%, $p=.357$). Patients who underwent pTIPSS were more likely to have prior AVB (69% vs 18%, $p<0.001$), lower baseline MELD score (11.6 vs 13.5, $p=0.02$), lower serum bilirubin (25 vs 41, $p<0.001$) and lower AST (47 vs 87, $p<0.001$). pTIPSS patients were more likely to be intubated (63% vs 37%, $p=0.025$), had early endoscopy <12 hours (100% vs 80.2%, $p=0.03$), and had active bleeding during endoscopy (50% vs 17.8%, $p=0.003$).

Among patients eligible for pTIPSS, those who underwent pTIPSS (vs. no pTIPSS) had a lower risk of 6-week mortality (17% vs 30%), but a higher risk of HE at 1-year (67% vs 21%, $p<0.001$), with a similar risk of early rebleeding within 5 days (17% vs 19%) and 1-year mortality (50% vs 44%).

Conclusion: The Singapore nationwide AVB audit showed that one in seven hospitalized AVB patients were eligible for pTIPSS, but only 1.8% underwent pTIPSS. Future work is needed to identify the barrier for timely pTIPSS implementation among high-risk AVB patients.

SAT-524

Sequential BAVENO VI plus dedicated spleen stiffness measurement or a novel spleen-centered algorithm significantly enlarges non-invasive ruling out of high risk varices: results from an international derivation-validation cohort study

Emma Vanderschueren^{1,2}, Angelo Armandi^{3,4}, Wilhelmus Kwanten^{5,6}, Luisa Vonghia^{5,6}, Merle Marie Werner³, Talal Merizian³, Georg Semmler⁷, Thomas Reiberger⁷, Thomas Vanwolleghem^{5,6}, David Cassiman^{1,2,8}, Sven Francque^{5,6}, Jörn Schattenberg³, Wim Laleman^{1,2,8}. ¹University Hospital Leuven, Department of Gastroenterology and Hepatology, Leuven, Belgium; ²Catholic University of Leuven, Department of Chronic Diseases, Metabolism and Aging (CHROMETA), Leuven, Belgium; ³University Medical Center of the Johannes Gutenberg University, Metabolic Liver Disease Research Program, I. Department of Internal Medicine, Mainz, Germany; ⁴University of Turin, Division of Gastroenterology and Hepatology, Department of Medical Sciences, Turin, Italy; ⁵University of Antwerp (UA), Laboratory of Experimental Medicine and Paediatrics (LEMP)-Gastroenterology and Hepatology, Antwerp, Belgium; ⁶Antwerp

University Hospital (UZA), Department of Gastroenterology and Hepatology, Antwerp, Belgium; ⁷Medical University of Vienna, Vienna Hepatic Hemodynamic Lab, Division of Gastroenterology and Hepatology, Department of Internal Medicine III, Vienna, Austria; ⁸Universitätsklinikum Münster, Department of Gastroenterology and Hepatology, Münster, Germany
Email: emma.vanderschueren@student.kuleuven.be

Background and aims: The BAVENO VI criteria, combining liver stiffness measurement (LSM <20 kPa) and platelet count ($>150 \times 10^9/L$), have set the stage for non-invasive assessment of patients with compensated advanced chronic liver disease (cACLD) who can safely avoid screening endoscopy at the cost of <5% missed varices needing treatment (VNTs). Attempts to expand these two parameters (expanded BAVENO VI) to save a higher proportion of endoscopies resulted in a relevant loss of negative predictive value. For this reason, we aimed to evaluate the potential additive value of spleen stiffness measurement (SSM) using spleen-dedicated vibration-controlled transient elastography (FibroScan[®] Expert 630, EchoSens) and in addition, to test a novel spleen-centered algorithm combining spleen size and SSM.

Method: We first analyzed in a single-center fashion (Leuven) all consecutive patients with ACLD (LSM ≥ 10 kPa) from 2020 till 2022 undergoing LSM/SSM and had available reports on upper endoscopy, abdominal ultrasound (spleen size, i.e. craniocaudal diameter) and platelet count. VNTs were defined as grade II or III esophageal varices or varices of any size with red spots. Different models were built in this derivation cohort (see Figure 1). Subsequently, these were tested in an external validation cohort (Mainz, Antwerp) with a higher prevalence of VNTs as this was the downfall of the expanded BAVENO VI criteria.

Results: The derivation cohort included 201 patients (123 men, mean age 58 years, 85.1% Child A-14.9% Child B). Overall prevalence of VNTs was 11.9% (comparable to the ANTICIPATE study). In the derivation

cohort, BAVENO VI criteria could spare 33.8% of screening endoscopies which could be doubled to 66.2% by applying sequential BAVENO VI/SSM-criteria (using a SSM cut-off at 43kPa) (Figure 1). A newly developed simple 'spleen size and stiffness' algorithm could save even more patients (71%) from undergoing endoscopy. All applied algorithms missed less than 5% of VNT.

The validation cohort included 176 patients (104 men, mean age 58 years, 70.4% Child A-29.6% Child B). The prevalence of VNTs amounted to 34.7%. Applying the BAVENO VI criteria in this cohort spared a lower amount of screening endoscopies (8.5%). Adding SSM tripled the gain to 27%. The 'spleen stiffness and size' model equally avoided 31% of screening endoscopies, all at the cost of less than 5% of VNT being missed.

Conclusion: The sequential BAVENO VI plus dedicated SSM (<43 kPa) or the more simplified spleen-centred algorithm (size and stiffness) can safely and more extensively "rule out" VNT than the BAVENO VI criteria alone.

SAT-525

Detection of candida species in hospitalized patients with decompensated liver cirrhosis and ascites indicates an unfavorable clinical course and outcome

Marie Griemsmann¹, Tammo Lambert Tergast¹, Michael P. Manns¹, Heiner Wedemeyer¹, Markus Cornberg¹, Benjamin Maasoumy¹.

¹Medical School Hannover, Germany

Email: griemsmann.marie@mh-hannover.de

Background and aims: Long hospital stays, invasive procedures and antibiotic treatment are major risk factors for fungal colonisation in patients with decompensated liver cirrhosis. However, the general impact of fungal colonisation on outcome and clinical course in patients with decompensated liver cirrhosis has not been investigated, so far. Therefore, we aimed to evaluate the predictive value of the detection of candida species for the further clinical outcome in patients with decompensated liver cirrhosis.

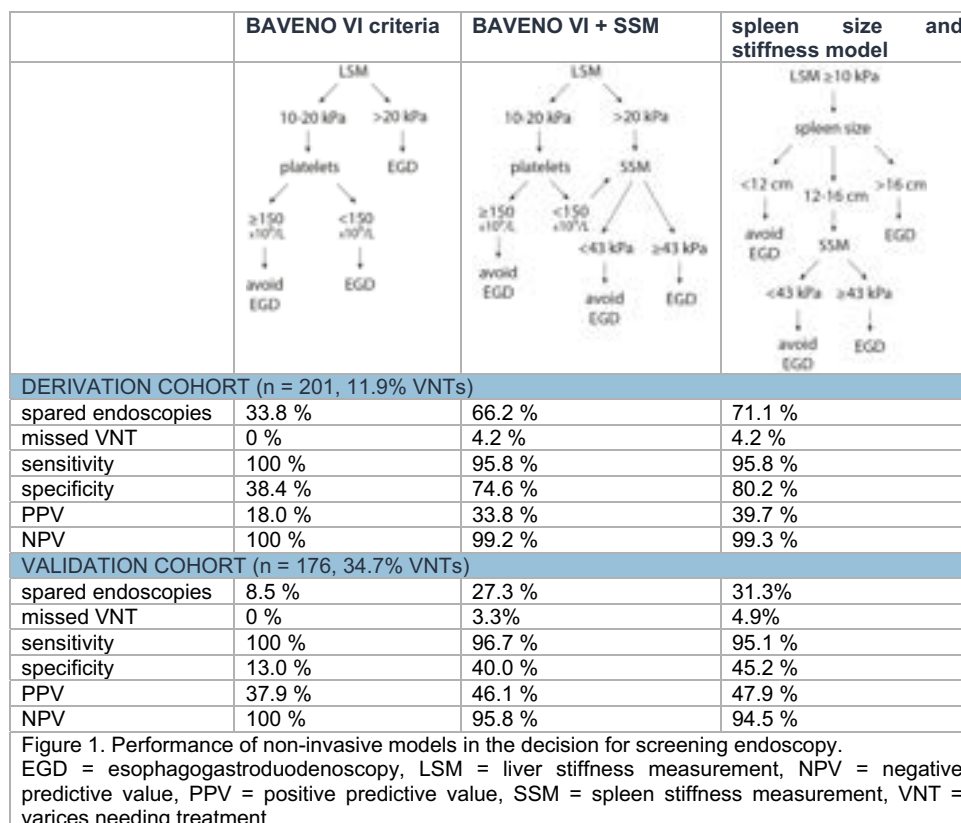


Figure: (abstract: SAT-524).

POSTER PRESENTATIONS

Method: Overall, 1314 patients, in whom a paracentesis was performed in Hannover Medical School between 2012 and 2018, were retrospectively screened for liver cirrhosis and ascites. After applying in- and exclusion criteria, 667 consecutive patients of the Hannover Ascites Cohort were eligible for further analysis. Patients were followed up for incidence of acute kidney injury (AKI), acute-on-chronic liver failure (ACLF) and death. Multivariate competing risk analysis was performed to adjust for potential confounders (e. g. the MELD score).

Results: Candida species were detected in 81 patients (12%). In the baseline characteristics some significant differences were shown. In the group of patients with detection of candida species was associated with a higher MELD score (22 vs. 18, $p < 0.001$), proportion of female patients (48% vs. 34%, $p = 0.014$) and incidence of diabetes (36% vs. 23%, $p = 0.011$). Of note, most of the detected candida species were candida albicans and were located in urine and respiratory aspirations. Incidence of AKI and incidence of ACLF was significantly higher in the group of patients with detected candida species. Even after adjusting to several confounders spotted candida species was a significant risk factor for development of AKI and ACLF ($p = 0.013$, HR = 1.57; $p = 0.009$, HR = 1.84, respectively).

In the univariate competing risk analysis a significant association between detection of candida species and 90-day mortality ($p < 0.001$) was identified. The 90-day mortality remained significantly influenced by detection of candida species after adjusting to confounders in multivariate competing risk analysis with liver transplantation as competing risk ($p = 0.033$, HR = 1.66).

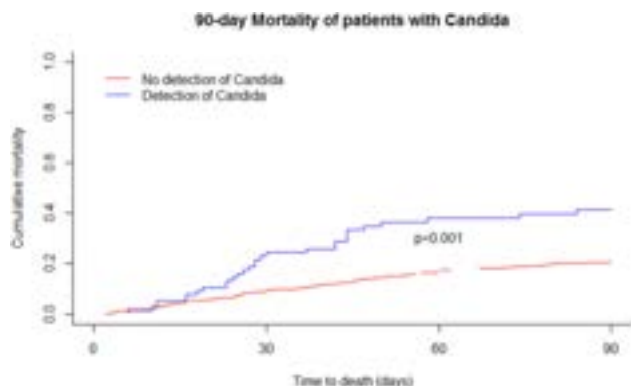


Figure:

Conclusion: Detection of candida species is linked to an impaired short-term mortality and development of severe complications in patients with liver cirrhosis. Further studies may assess if treatment of candida colonisation influences the clinical course and survival in this patient collective or the detection on candida can be used to identify patients that require specific measures to prevent cirrhosis-associated complications.

SAT-526

Clinical utility of liver and spleen elastography in the management of patients living with liver disease

Carmen Lara Romero¹, María Del Barrio², María Del Carmen Rico¹, Belen Pino¹, Manuel Romero Gomez¹. ¹Liver and Digestive Diseases Unit, Virgen del Rocío University Hospital; SeLiver Group, Biomedicine Institute of Seville (HIVR/CSIC/US), Medicine Department, University of Seville, CIBEREHD, Seville, Spain; ²Gastroenterology and Hepatology Department, Clinical and Translational Research in Digestive Diseases, Valdecilla Research Institute (IDIVAL), Marqués de Valdecilla University Hospital., Santander, Spain
Email: carmenlararomero@gmail.com

Background and aims: Portal hypertension (PH) is responsible for the progression of liver diseases and the development of complications. In patients with liver elastography <10 kPa, advanced liver

disease is ruled out according to Baveno VII consensus. Our aims are a) To analyze the prevalence of portal hypertension and porto-sinusoidal vascular disease (PSVD) in patients with liver disease; b) Identify non-invasive parameters of suspicion of PSVD and/or hidden PH; c) To Assess the clinical impact of the presence of elevated spleen stiffness in the development of complications.

Method: Prospective cohort of 276 consecutive patients seen in a hepatology consultation who underwent liver and splenic transient elastography (Fibroscan 630, Echosens, France). Thresholds for advanced disease were spleen stiffness measurement (SSM) >45 kPa and Liver stiffness measurements (LSM) >10 kPa. It was evaluated: hepatic, renal, metabolic function, concomitant treatment, ultrasound, endoscopy, liver histology and portal hemodynamic. Statistical analysis: t-student, ANOVA, Chi-square, Spearman's coefficient, U-Mann-Whitney, Wilcoxon, logistic regression, and linear correlation.

Results: SSM >45 kPa in 23 cases of 154 with LSM <10 kPa (14.9%) versus 56 of 122 with LSM >10 kPa (45.9%); $p < 0.001$). The predictive parameters of SSM >45 kPa in patients with LSM <10 kPa are collected in the table (platelets, INR, Child-Pugh and MELD3.0). In the multivariate analysis, the platelet count and MELD 3.0 were independently related to SSM >45 kPa and LSM <10 kPa. The rate of decompensation (hepatic encephalopathy, ascites, or variceal bleeding) was 1.5% in patients with LSM <10 kPa and SSM <45 kPa (2/131), versus 13% (3/23) in patients with LSM <10 kPa and SSM >45 kPa, 15.4% (10/65) in patients with LSM >10 kPa and SSM <45 kPa and 44% (24/54) in patients with LSM >10 kPa and SSM >45 kPa; $p < 0.0001$.

Table: Univariate and multivariate analysis

Variable	Univariate analysis			Multivariate analysis	
	SSM ≤ 45 kPa (n = 129)	SSM >45 kPa (n = 23)	p	HR (IC95%)	p
Platelets	240 \pm 83	173 \pm 112	<0.001	0,982 (0,973–0,991)	=0,008
INR	0,99 \pm 0,18	1,13 \pm 0,29	<0.073		
MELD 3.0	6,93 \pm 0,98	8,75 \pm 2,93	<0.055	1,335 (1,002–1,778)	P = 0,048
Child-Pugh	5,0 \pm 0,0	5,75 \pm 1,36	<0.082		

Conclusion: The SSM can detect up to 15% of cases of occult PH/PSVD in patients with LSM <10 kPa and SSM >45 kPa. In patients with LSM <10 kPa, a decrease in platelet count or an increase in MELD 3.0 should lead to suspicion of PH. The presence of altered SSM is associated with an increased risk of liver events. The implementation of SSM will improve the management of patients with liver disease.

SAT-527

Secondary prevention of variceal bleeding is often imperfect: a national, population-based cohort study of 5,018 patients

Hannes Hagström¹, Ying Shang¹, Elliot Tapper², Axel Wester¹, Linnea Widman¹. ¹Karolinska Institutet, Sweden; ²University of Michigan, United States
Email: hannes.hagstrom@ki.se

Background and aims: Secondary prevention of variceal bleeding is important to improve prognosis, but uptake of guidelines is unknown in a real-world setting. Here, we determined the proportion of patients receiving appropriate beta-blocker treatment and repeat upper endoscopy after a first episode of variceal bleeding within a reasonable timeframe.

Method: Population-based registers were used to identify all patients with a first episode of variceal bleeding in Sweden, 2000–2020. Cross-linkage between registers was performed to receive information on the cumulative incidence of patients with a dispensation of beta-blockers within 30 days and repeat upper endoscopy within 120 days from baseline. Overall mortality was investigated using Cox regression.

Results: In total, 5,018 patients were identified, with a median age of 62 years (IQR = 54–71). Of patients not on previous beta-blocker

therapy, the cumulative incidence of a dispensation of beta-blockers within 30 days was 54.3%. The cumulative incidence of repeat endoscopy was 34.5% within 120 days. Overall mortality was high, with 71.2% of patients dying after variceal bleeding during the full follow-up period (median 1.8 years). We observed an improved overall mortality during the later years of the study period (adjusted hazard ratio for the 2016–2020 period compared to the 2000–2005 period: 0.84, 95%CI=0.75–0.93). Patients with beta-blockers and repeat upper endoscopy had better overall survival compared to those without, respectively.

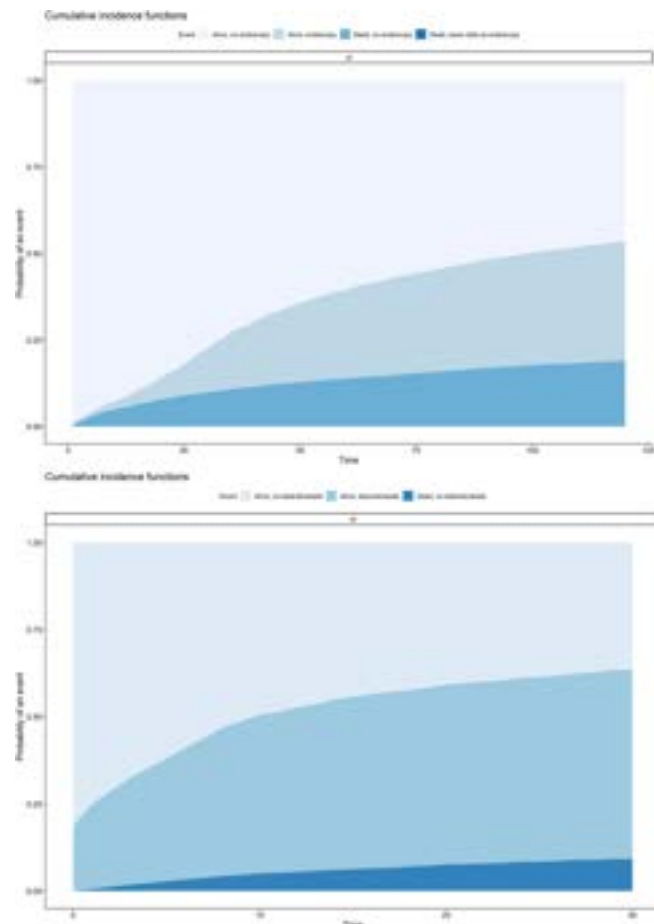


Figure: Probabilities of repeat upper endoscopy within 120 days after bleeding (top panel) and dispensation of beta-blockers 30 days after bleeding (bottom panel).

Conclusion: Secondary prevention of variceal bleeding has not been widely undertaken, with many patients not receiving guideline-supported interventions within a reasonable timeframe. This highlights a need to raise awareness on appropriate prevention strategies to clinicians and patients.

SAT-528

Terlipressin has acute effects on systemic inflammation markers in patients with cirrhosis and ascites

Nikolaj Torp^{1,2}, Mads Israelsen^{1,2}, Emil Deleuran Hansen^{1,2}, Stine Johansen^{1,2}, Camilla Dalby Hansen^{1,2,2}, Emilie Dahl³, Bjørn Stæhr Madsen¹, Johanne Kragh Hansen^{1,2}, Katrine Prier Lindvig^{1,2}, Katrine Thorhauge^{1,2}, Katrine Bech¹, Ida Villesen¹, Ellen Jensen^{1,2}, Ida Ziegler Spedtsberg^{1,2}, Peter Andersen¹, Annette Fialla¹, Boye Jensen², Maja Thiele^{1,2}, Sabine Klein⁴, Robert Schierwagen⁴, Jonel Trebicka^{4,5}, Aleksander Krag^{1,2}. ¹Odense University Hospital, Department of Gastroenterology and Hepatology, Odense, Denmark; ²University of

Southern Denmark, Faculty of Health Science, Odense, Denmark; ³Copenhagen University Hospital Herlev, Department of Gastroenterology, Denmark; ⁴University of Münster, Department of Internal Medicine B, Germany; ⁵European Foundation for the Study of Chronic Liver Failure, Spain
Email: aleksander.krag@rsyd.dk

Background and aims: Terlipressin is widely used in the management of variceal bleeding and hepatorenal syndrome. However, terlipressin increases the risk of intestinal ischemia, respiratory failure and possibly sepsis and septic shock. The complications are all associated to systemic inflammation, where IL-6 is a pivotal marker. IL-6 is associated to a poor prognosis in patients with cirrhosis, but the immediate effect of terlipressin on IL-6 and other systemic inflammation markers is unknown. We therefore aimed to investigate the acute impact of terlipressin on markers of systemic inflammation in patients with cirrhosis and ascites.

Method: We included 25 stable patients with cirrhosis and ascites from a 2:2:1 cross-over randomized controlled trial of terlipressin with dobutamine as a cardioselective control. The intervention was administered in two treatment periods with A) dobutamine followed by terlipressin (n = 10), B) terlipressin followed by both terlipressin and dobutamine and C) placebo (n = 5). Serial blood and urine samples were available before treatment (baseline) and during both treatment periods. We used the Luminex MAGPIX platform to measure changes of inflammatory markers in blood and urine (CCL2, CCL3, CCL4, CXCL10, IL-1alpha, IL-1beta, IL-1RA, IL-6, IL-10 and IL-18). Urine measurements were corrected for changes in glomerular filtration rate (GFR) as assessed by ⁵¹Cr-labeled clearance. All measurements were log-transformed to normalize data.

Results: Mean age was 57 (± 9 years), majority were male (68%) with alcohol-related cirrhosis (92%) as the dominant etiology. Baseline WBC = $6.1 \times 10^9/L$ [5.0–7.7], CRP = 6 mg/L [2–10] and MELD-Na = 10 [9–14]. Before treatment, CRP correlated positively with blood IL-6 (p = 0.040) while WBC did not (p = 0.384). Relative to placebo and before treatment periods, terlipressin increased blood IL-6 (p < 0.001) and urine IL-6 (p < 0.001), while dobutamine did not (Figure). Terlipressin also led to increased levels of inflammasome activation markers IL-1alpha (p < 0.001) and IL-1beta (p < 0.01) in the urine, whereas dobutamine treatment only increased urine IL-1alpha (p < 0.05). A significant decrease of differing systemic inflammatory chemokines was observed in blood (CCL2, p < 0.001 and CXCL10, p < 0.001) and urine (CCL3, p < 0.001 and CCL4, p < 0.01) following terlipressin. As expected, GFR improved in treatment periods with only terlipressin (+18.8 ml/min/1.73 m², 95% CI: +5.7 to +32.0, p < 0.01). However, the changes in blood systemic inflammation markers were not associated with the effect of terlipressin on GFR.

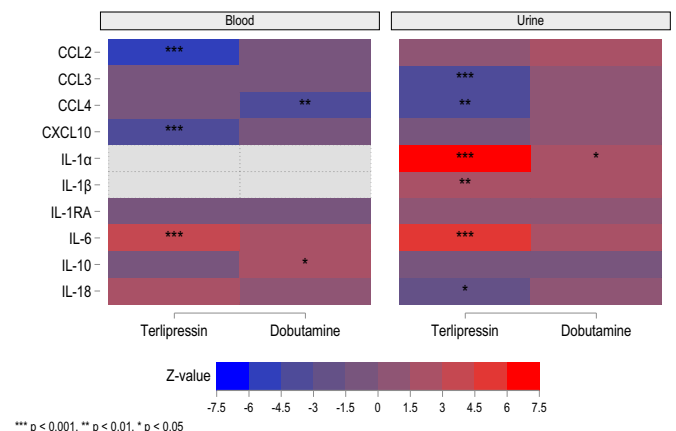


Figure: Heatmap of the effect of terlipressin and dobutamine on systemic inflammatory markers in blood and urine. Z-value changes are relative to placebo and before treatment periods.

Conclusion: Terlipressin induces a rapid changes in systemic inflammation marker, including an increase in IL-6. This increase may likely be a result of intestinal ischemia, since cardioselective dobutamine did not elicit this effect. We did not observe an association between systemic inflammatory changes and the effect of terlipressin on renal function.

SAT-530

Individualized portal pressure gradient threshold based on liver function categories in preventing rebleeding after TIPS

Yifu Xia¹, Jun Tie², Guangchuan Wang^{3,4}, Yuzheng Zhuge⁵, Hao Wu⁶, Hui Xue⁷, Jiao Xu², Feng Zhang⁵, Lianhui Zhao^{1,3}, Guangjun Huang³, Mingyan Zhang³, Bo Wei⁶, Peijie Li⁷, Wei Wu⁸, Chao Chen⁸, Chengwei Tang⁶, Chunqing Zhang^{1,3}. ¹Shandong Provincial Hospital Affiliated to Shandong University, China; ²National Clinical Research Center for Digestive Diseases and Xijing Hospital of Digestive Diseases, China; ³Shandong Provincial Hospital Affiliated to Shandong First Medical University, China; ⁴Department of Biostatistics, School of Public Health, Shandong University, China; ⁵Affiliated Drum Tower Hospital of Nanjing University Medical School, China; ⁶West China Hospital, China; ⁷First affiliated hospital of xi'an Joao Tong university, China; ⁸The First Affiliated Hospital of Wenzhou Medical University, China
Email: zhangchunqing_sdu@163.com

Background and aims: The evidence in Portal pressure gradient (PPG) <12 mmHg after transjugular intrahepatic portosystemic shunt (TIPS) for preventing rebleeding mostly comes from observations in uncovered stents era. Moreover, association between Child-Pugh classes and post-TIPS hepatic encephalopathy (HE) has indicated that tolerance of PPG reduction depends on liver function.

We aimed to investigate the optimal PPG for covered TIPS and explore the optimal threshold tailored to the Child-Pugh classes to find individualized PPG to balance rebleeding and overt HE.

Method: This multicenter retrospective study analyzed rebleeding, OHE, and mortality of patients associated with post-TIPS PPGs (8, 10, 12, and 14 mmHg) in the entire cohort and among different Child-Pugh classes. Propensity score matching (PSM) and competing risk analyses were performed for sensitivity analyses.

Results: We included 2100 consecutively screened patients undergoing TIPS. In all patients, PPG <12 mmHg reduced rebleeding after TIPS ($p=0.022$). In Child-Pugh class A, none of the PPG thresholds were discriminative of clinical outcomes. In Child-Pugh class B, 12 mmHg ($p=0.022$) and 14 mmHg ($p=0.037$) discriminated rebleeding, but 12 mmHg showed a higher net benefit. In Child-Pugh class C, PPG <14 mmHg had a lower rebleeding incidence ($p=0.017$), and exhibited more net benefit than 12 mmHg.

might be suitable for patients in Child-Pugh class B, while <14 mmHg might be optimal for patients in Child-Pugh class C.

SAT-531

Serum procalcitonin and interleukin-6 predict acute-on-chronic liver failure following transjugular intrahepatic portosystemic shunt implantation in patients with refractory ascites

Lukas Sturm¹, Michael Schultheiss¹, Laura Stolz¹, Marlene Reincke¹,
Patrick Huber¹, Robert Thimme¹, Dominik Bettinger¹. ¹Medical Center
University of Freiburg, Germany
Email: lukas.sturm.med@uniklinik-freiburg.de

Background and aims: As acute-on-chronic liver failure (ACLF) is associated with high morbidity and mortality, early identification of patients who are at risk for developing ACLF is crucial. However, risk factors for ACLF in connection with transjugular intrahepatic portosystemic shunt (TIPS) implantation are only sparsely investigated. Therefore, the present study aimed to evaluate the predictive relevance of inflammatory markers in the context of ACLF development following TIPS implantation.

Method: Sixty-nine patients allocated to TIPS implantation due to refractory ascites were included and blood samples were obtained prior to TIPS placement. Serum levels of high-sensitive c-reactive protein (hsCRP), procalcitonin (PCT) and interleukin-6 (IL-6) were determined. The development of ACLF and death within 90 days after TIPS implantation were recorded. Inflammatory markers were evaluated as predictors of ACLF using uni- and multivariable Fine and Gray competing risk regression models, considering death as competing risk.

Results: Twenty-two patients (31.9%) developed ACLF within 90 days after TIPS implantation, thereof 86.4% ACLF grade 1 and 13.6% ACLF grade 2. ACLF was lethal in 27.3% of cases. Patients developing ACLF had significantly elevated plasma levels of PCT (0.12 [0.09–0.24] ng/ml vs. 0.08 [0.00–0.12] ng/ml, $p = 0.004$) and IL-6 (30.5 [20.2–41.9] pg/ml vs. 21.4 [13.3–39.2] pg/ml, $p = 0.048$) prior to TIPS implantation in comparison to patients without ACLF, while there was no significant difference in levels of hsCRP. Competing risk regression analyses showed that besides the Freiburg Index of Post-TIPS Survival (FIPS; SHR 2.848, 95% CI 1.167–6.948, $p = 0.021$) and elevated serum creatinine (SHR 1.675, 95% CI 1.146–2.450, $p = 0.008$), levels of PCT (SHR 1.129, 95% CI 1.018–1.253, $p = 0.022$) and IL-6 (SHR 1.002, 95% CI 1.001–1.004, $p = 0.015$) were independent predictors of ACLF. ROC-analyses confirmed a high discriminatory performance especially of PCT in the prediction of ACLF (PCT: AUROC 0.715 [0.594–0.836]; IL-6: AUROC 0.648 [0.514–0.782]).

Conclusion: The present results indicate that besides impaired renal function, an inflammatory status predisposes for ACLF development following TIPS implantation in patients with refractory ascites. In this context, the inflammatory markers PCT and IL-6 can help to identify patients at high risk of developing ACLF.

SAT-532

Refractory hepatic hydrothorax is associated with Increased mortality compared to cirrhosis and refractory ascites

Allison Chin¹, Dustin Bastaich², Bassam Dahman², David Kaplan³,
Tamar Taddei⁴, **Binu John**⁵. ¹Florida International University, United
States; ²Virginia Commonwealth university, United States; ³University of
Pennsylvania, Philadelphia, United States; ⁴Yale School of Medicine and
VA Connecticut Healthcare System, West Haven, CT, United States;
⁵University of Miami and Miami VA, United States
Email: binu.john@gmail.com

Background and aims: Refractory hepatic hydrothorax (RH) requiring therapeutic thoracentesis is a serious complication of cirrhosis. Undrained effusions can lead to pulmonary atelectasis, while thoracentesis (particularly multiple), can be complicated by life threatening hemo- or pneumothorax. Patients with RH on the liver transplant list do not receive standardized MELD exemption points because of inadequate evidence to suggest increase mortality. The



Figure:

Conclusion: Different PPG standards may be required for patients with different liver function categories. A PPG threshold <12 mmHg

aim of this study was to examine liver-related death associated with RH compared to participants with refractory ascites (RA).

Method: This was a retrospective cohort study of patients with cirrhosis from the Veterans Health Administration. Eligibility criteria included patients with RH or RA who underwent at least one therapeutic thoracentesis or paracentesis respectively. The primary outcome was LRD, with non-liver-related-death or liver transplantation as competing risk.

Results: Of 120,952 participants with cirrhosis in the VOCAL cohort, 2,225 met study inclusion criteria. On multivariable analysis, hepatic hydrothorax was associated with a 4.0-fold increased adjusted hazard of LRD compared to refractory ascites (95% CI 3.15–5.07, $p < 0.0001$). This association of increased LRD with RH was observed across varying levels of MELD-Na from <10 (aHR 3.23, 95% CI 2.10–4.95, $p < 0.0001$), 10–15 (aHR 4.39, 95% CI 2.78–6.93, $p < 0.0001$), 15–25 (aHR 4.38, 95% CI 2.96–6.50, $p < 0.0001$), and ≥ 25 (aHR 5.81, 95% CI 2.97–11.34, $p < 0.0001$). Compared to participants requiring a single thoracentesis, LRD was similar for those requiring 2–3 (aHR 1.33, 95% CI 0.75–2.35, $p = 0.33$), but higher with ≥ 4 thoracentesis (aHR 2.80, 95% CI 1.52–5.16, $p = 0.001$). There was no association between number of paracentesis and LRD among participant with RA.

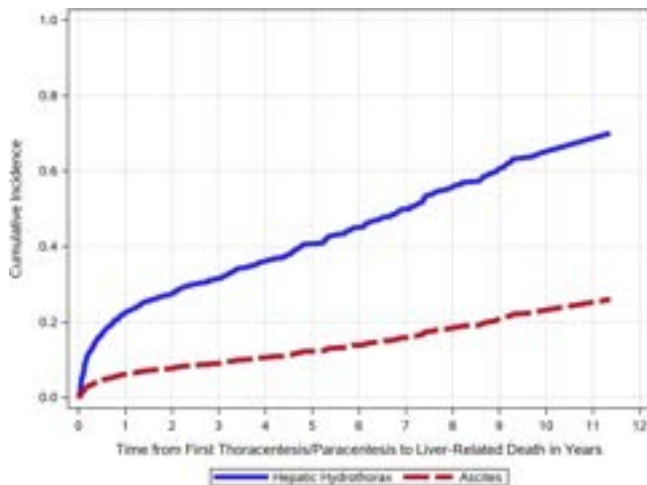


Figure: Cumulative incidence frequency for adjusted hazard ratio of liver-related death with transplantation and non-liver-related death as competing risk. Note: The cumulative incidence was estimated from the Fine-Gray competing risk model.

Conclusion: RH is associated with significantly higher LRD compared to participants with ascites across varying levels of MELD. Consideration should be given for a standard MELD exemption in participants with RH listed for transplantation.

SAT-533

Validation of Baveno-VII criteria regarding non-invasive diagnosis of clinically significant portal hypertension

Byeong Geun Song¹, Aryoung Kim¹, Myungji Goh¹, Wonseok Kang¹, Geum-Yon Gwak¹, Yong-Han Paik¹, Moon Seok Choi¹, Joon Hyeok Lee¹, Seung Woon Paik¹, Dong Hyun Sinn¹. ¹Samsung Medical Center, Korea, Rep. of South
Email: sinndhn@hanmail.net

Background and aims: Baveno VII consensus introduced the criteria of clinically significant portal hypertension (CSPH) by non-invasive tools (NITs) using liver stiffness measurement (LSM) and platelet. We aimed to validate the Baveno VII criteria to predict the risk of adverse liver related events in patients with compensated advanced chronic liver disease (cACLD).

Method: We conducted a retrospective cohort study of 1,966 patients with cACLD. Patients were grouped into four subgroups (CSPH excluded ($n = 619$), grey zone (low probability of CSPH ($n = 699$), high probability of CSPH ($n = 207$)), and CSPH included ($n = 441$))

according to Baveno VII consensus. Risk of decompensation and HCC was estimated using a Fine and Gray competing risk regression analysis, with liver transplantation and death as competing events.

Results: Among 1,966 patients, 178 and 176 patients developed decompensation and HCC over a median follow-up of 3.06 (range, 1.03–6.00) years, respectively. Patients with CSPH had substantially higher risk of decompensation compared to those without CSPH (18%, 21%, 22% vs. 0.69%, 1.1%, 1.4% at 1-year, 2-year, 3-year, respectively). Patients with CSPH had 8-fold higher risk of decompensation (standardized hazard ratio (sHR) 8.00, 95% confidence interval (CI) 4.00–16.0). Also, patients with CSPH had higher risk of HCC compared to those without CSPH (sHR 3.14 (95% CI 1.96–5.04)), yet considerable proportion of patients without CSPH also developed HCC (2.4% at 3-year). Restricted cubic spline curves showed linear relationship between LSM and risk of decompensation. Among patients within the grey zone, alcoholic liver disease, high prothrombin time, high bilirubin, and low albumin was associated with higher risk of decompensation.

Conclusion: Baveno VII criteria for CSPH using NITs can stratify the risk of decompensation and liver related events.

SAT-534

Pressure response to TIPS does not depend on stent diameter

Martin Rössle¹, Dominik Bettinger², Robert Thimme³, Michael Schultheiss⁴. ¹University Hospital Freiburg, Gastroenterology, Freiburg, Germany; ²University Hospital Freiburg, Gastroenterology, Germany; ³University Hospital Freiburg, Gastroenterology, Freiburg, Germany; ⁴University Hospital Freiburg, Gastroenterology, Freiburg, Germany
Email: martin-roessle@t-online.de

Background and aims: In patients receiving the transjugular intrahepatic portosystemic shunt (TIPS) a greater reduction of the portosystemic pressure gradient (the difference between the portal and right atrial pressure) may harbour a higher risk of shunt-induced complications such as liver failure and hepatic encephalopathy. Prediction of the stent diameter necessary to reach the treatment goal (6–12 mmHg) may reduce the risk of overtreatment with its respective consequences.

Method: We evaluated immediate post-TIPS pressures and stent diameters in 208 patients with liver cirrhosis receiving a TIPS for refractory ascites (69.7%) or variceal bleeding (30.3%). Diameters were determined by planimetry from the angiographic image. Clinical and hemodynamic factors (portal vein diameter, portal vein flow velocity, hepatic resistance) possibly related to response to TIPS were determined before the intervention. Patients were divided into groups with post-TIPS pressure gradients of ≥ 6 mmHg (low risk; group 1, $n = 155$) or < 6 mmHg (high risk; group 2, $n = 53$).

Results: Mean post-TIPS pressure gradients, relative reduction of the pre-TIPS gradient, and specific reduction of the pre-TIPS gradient per mm of stent diameter were 10.2 ± 2.3 mmHg, $50.0 \pm 12.5\%$, and $7.1 \pm 2.1\%$ per mm in group 1 and 4.5 ± 1.5 mmHg ($p < 0.001$), $73.6 \pm 11.1\%$ ($p < 0.001$), and $10.1 \pm 2.0\%$ per mm in group 2 ($p < 0.001$), respectively. The stent diameters did not correlate with the reduction of the gradient ($r = 0.17$) and the pressure changes in group 1 and group 2 were achieved with similar diameters (7.2 ± 1.0 vs 7.4 ± 0.9 mm, $p = 0.999$). The right atrial pressures, a measure of the preload, increased in group 1 and group 2 by 4.1 ± 3.1 mmHg and 5.0 ± 2.9 mmHg ($p = 0.042$), and the portal pressures decreased by 6.64 ± 3.9 mmHg and 8.6 ± 4.4 mmHg ($p = 0.002$), respectively. Prediction of the appropriate stent diameter was not possible.

Conclusion: In most patients, pressure response to TIPS was achieved with real diameters of < 8 mm and was not correlated to the measured stent-diameter. The stent diameter was not predictable and a greater response (group 2, ≤ 6 mmHg) was associated with a greater increase in the right atrial (increased preload) and greater decrease in the portal pressure (decreased afterload) suggesting that systemic hemodynamics and cardiac function may play a role in the response to TIPS.

SAT-535

Single-centre experience of spleen stiffness measurement across the spectrum of chronic liver disease

Sarah Romero¹, Alexander Thompson¹, Jessica Howell¹, Marno Ryan¹, Swee Lin Chen Yi Mei¹, Catherine Croagh¹, Barbara Demediuk¹, David Iser¹, Tim Papaluca¹, Paul Desmond¹, Jacinta Holmes¹. ¹St Vincent's Hospital Melbourne, Department of Gastroenterology, Melbourne, Australia
Email: s.romero.md@gmail.com

Background and aims: Onset of clinically significant portal hypertension (PH) is a critical clinical event, predicting liver-related events and death in cirrhosis¹. However, HVPG is invasive and inaccessible, and current non-invasive tools are suboptimal. Liver stiffness measurement (LSM) >25 kPa has been suggested to be sufficient to rule in clinically significant PH (CSPH), but LSM <25 kPa remains indeterminate. Spleen stiffness measurement (SSM) correlates strongly with HVPG, where SSM >40kPa rules in CSPH²; therefore SSM may be superior to detect CSPH where current algorithms remain indeterminate. However, SSM remains suboptimal due to lack of data regarding optimal procedural technique, quality metrics, and validation with the dedicated spleen probe. We report procedural success and limitations, and clinical correlates of SSM across the spectrum of chronic liver disease (CLD).

Method: Prospective, single-centre study of SSM (100hz) for CLD from January 1 to December 31, 2022, under ultrasound guidance, with paired LSM. Demographics and clinical parameters of PH were collected. Outcomes included: SSM success [10 valid SSM, representing >60% of total SSM, with IQR <30%]; SSM correlation with parameters of PH; factors associated with SSM failure.

Results: 63 patients underwent SSM; 87% (n = 55) had cirrhosis, 62% male, median age 62 yrs [IQR 51–68], median body mass index (BMI) 28 [IQR 24–32]. Child-Pugh A/B/C status was present in 77/16/7% of cirrhotics, respectively, with a median Meld-Na of 10 [IQR 8–14]. Aetiology of liver disease included: viral (35%), alcohol (32%), MAFLD (17%), other (16%). Varices were present on gastroscopy or abdominal imaging in 37% (n = 20). 11% (n = 7) had ascites at time of SSM. SSM was successful in 70% (n = 44); median stiffness 42.6 kPa. SSM failure was due to failure to meet quality criteria or failure to return SSM. Maximum SSM (100 kPa) was reached in 7% (n = 3) and 27% (n = 12) had SSM >75 kPa. SSM was significantly higher in patients who met criteria for CSPH (LSM >25 kPa), 61.3 vs 25.6 kPa (p = 0.001), and in patients with thrombocytopaenia (Table). Interestingly, SSM met criteria for CSPH in patients with LSM >15 kPa (median SSM 58.3 kPa (Table)). SSM was significantly higher in patients with non-viral vs viral CLD aetiology (46.6 vs 27.1 kPa, p = 0.044) and in those with varices (90.4 vs 29.1 kPa, p < 0.0001). SSM failure was more common if LSM <25 kPa (p = 0.047). SSM correlated only moderately with platelet count (r² = 0.304, p < 0.001), LSM (r² = 0.190, p = 0.006) and Meld-Na (r² = 0.235, p = 0.002). SSM procedural success was not affected by age, BMI or ascites.

Table:

			P value
SSM (kpa)	LSM <15: 22.3	LSM >15: 58.3	0.0001
	LSM <25: 25.6	LSM >25: 61.3	0.0010
	Plt >150: 26.1	Plt <150: 61.4	0.0012
	Plt >100: 38.2	Plt <100: 90.4	0.0073

Conclusion: In this real-world cohort with mixed liver disease aetiology (treated and untreated), LSM >25 kPa alone was not sufficient to exclude probable CSPH, based on SSM threshold of 40kPa. Furthermore, SSM was significantly higher in non-viral CLD. SSM could not be obtained in 30%. These data have significant implications for wider applicability of LSM in CLD to predict for CSPH. SSM should be considered an adjunct to existing tools for CSPH screening, however further data is required to identify optimum

quality criteria, factors associated with SSM failure and optimal SSM cut-offs for degrees of PH according to CLD aetiology, particularly non-viral subgroups.

References

1. Ripoli C. *Gastroent* 2007; 133:481.
2. Colecchia A. *Gastroent* 2012; 143:646.

SAT-536

Adverse outcomes following transjugular intrahepatic portosystemic shunt placement in relation to the underlying cause of portal hypertension

Adriaan Van der Meer¹, Michelle Spaan¹, Adriaan Moelker², Willemijn Dijkstra¹, Ellen Werner¹, Diederik Bijdevaate², Tychon Geeraedts², Milan Sonneveld¹, Sandra Coenen¹, Dave Sprengers¹, Robert De Man¹, Rael Maan^{1,3}, Sarwa Darwish Murad^{1,3}. ¹Erasmus MC University Medical Center Rotterdam, Gastroenterology and Hepatology, Netherlands; ²Erasmus MC University Medical Center Rotterdam, Radiology, Netherlands; ³Erasmus MC Transplant Institute, Netherlands
Email: s.darwishmurad@erasmusmc.nl

Background and aims: A variety of non-cirrhotic liver diseases, predominantly Budd-Chiari syndrome (BCS) and portal vein thrombosis (PVT), can lead to portal hypertension (PH) with the need for transjugular intrahepatic portosystemic shunt (TIPS). In comparison to cirrhosis-related PH (CPH), non-cirrhotic PH (NCPH) differ in underlying pathophysiological conditions, e.g. in hypercoagulability and residual liver function. Therefore, the aim of this study was to assess TIPS thrombosis and hepatic encephalopathy (HE) in patients with NCPH in comparison to patients with CPH.

Method: Occurrence of TIPS thrombosis (i.e. in-stent or in proximity of TIPS) and HE was assessed in a retrospective mono-center cohort, which included all consecutive patients with PH who received a TIPS with a covered stent between 2007 and 2021. End points were assessed as time-to-event data in Kaplan Meier and Cox proportional hazard analyses, and compared those with NCPH and CPH. Patients were censored at the time of liver transplantation or death.

Results: Overall, 385 patients with PH received a TIPS of which 55 (14.3%) had NCPH and 330 (85.7%) had CPH. Among patients with NCPH, 28 (51%) were male, median age was 51 (range 19–75) years, 26 (47%) had Budd-Chiari syndrome (BSC), 13 (24%) had portal vein thrombosis, and 16 (29%) had other causes of PH. Among patients with cirrhosis, 222 (67%) patients were male, the median age was 57 (range 15–84) years, and the etiology of cirrhosis was viral hepatitis/auto-immune or cholestatic liver disease/(non)alcoholic steatohepatitis or cryptogenic/other in 12/11/71/6%, respectively. Patients with NCPH patients were significantly younger (p = 0.005) and more frequently female (p = 0.019). NCPH patients developed significantly more TIPS thrombosis than CPH patients (22% vs 8.5%) with 1- and 5-y cumulative incidence of 19.1% (95%CI 13.3–24.9) and 33.2% (95%CI 23.7–42.7) versus 7.1% (95%CI 5.5–8.7) and 12.1% (95%CI 9.4–14.8) (p = 0.002). Likewise, the need for re-intervention at 1 and 5 y in NCPH was 33.6% 95%CI 26.4–40.8) and 52.8% (95%CI 43.6–62.0) versus 22.0% (95%CI 19.3–24.7) and 35.4% (95%CI 31.6–39.2) in CPH (p = 0.026). BCS patients had the highest 3-year incidence of TIPS thrombosis of 39.6% (95% CI 28.3–50.9) compared to 19.2% in PVT (95%CI 6.6–31.8) and 6.2% for other NCPH (95%CI 0.1–12.3), despite the fact that 92.3% used anticoagulants. HE was more prevalent in CPH (47% vs 31%) with 1- and 5-year cumulative incidence of 46.7% (95%CI 43.6–49.8) and 58.9% (95%CI 55.4–62.4) versus 29.1% (95%CI 22.5–35.7) and 43.6% (95%CI 34.4–52.8) in NCPH (p = 0.022).

Conclusion: Post-TIPS complications in patients with PH differ according to the etiology, with a higher risk of TIPS thrombosis in those with NCPH, in particular BCS, despite anticoagulation and a higher risk of HE in those with CPH. Importantly, post-TIPS HE is not uncommon following TIPS in NCPH.

SAT-537

Validation of a discrete event simulation model evaluating the cost-effectiveness of long-term albumin administration in real-world UK patients with recurrent ascites

Kris Bennett¹, Elisabet Viayna², Duncan Stacey³, Matthew Cramp¹.

¹University Hospitals Plymouth NHS Trust, South West Liver Unit, Plymouth, United Kingdom; ²Grifols S.A., Sant Cugat del Valles, Spain;

³Grifols UK Ltd., Cambridge, United Kingdom

Email: kbennett6@nhs.net

Background and aims: The development of cirrhotic ascites is associated with significant complications and costs. We previously developed a discrete event simulation (DES) model to assess the cost-effectiveness of long-term albumin (LTA; 40 g twice/week for 2 weeks, 40 g/week thereafter) in addition to standard medical treatment (SMT) in a UK patient cohort, based on patient characteristics and healthcare resource use (HCRU) from Hospital Episode Statistics (HES) and outcomes from the ANSWER trial. We estimated that treating 30/100 eligible patients with LTA may save up to £264,589/year. We aimed to validate our model and the HES inputs, by performing a detailed notes-based audit of patients undergoing large-volume paracentesis (LVP) for cirrhotic ascites at University Hospitals Plymouth NHS Trust (UHP).

Method: All patients undergoing LVP at UHP between March 2016-June 2018 were identified by OPCS procedure code (T46). Patients were excluded if ascites was not due to cirrhosis or there was insufficient follow-up data. Demographics, cirrhosis aetiology/severity, and 12-month rates for complications and HCRU, was collected by audit of patient records. Patients with recurrent ascites were considered eligible for LTA. The cost-effectiveness of LTA in this cohort was assessed using the previously developed DES by simulating the clinical and economic impact of treating 50% of the cohort with LTA+SMT vs SMT only. Clinical complications and HCRU were transformed into costs using NHS tariffs. Reductions in event probabilities associated with LTA were based on ANSWER trial data.

Results: 87 patients underwent an index LVP for cirrhotic ascites during the study period. 56 were considered ineligible for LTA due to early death (7), rapid ascites resolution (27) or refractory ascites (RA; 22), leaving a sample of 31 patients with recurrent ascites. Patients were predominantly male with alcohol-related liver disease and a median MELD score of 17. 12-month HCRU and complication rates were similar to our HES analysis; on average patients had 4 paracenteses, 5 in- and 10 out-patient encounters. 12-month mortality was 32%, 4 patients were transplanted and 8 developed RA. Hyponatraemia was the most common complication (18/31), followed by HRS (10/31). Our model estimates that treating 15/31 patients with LTA+SMT would avoid 28 inpatient encounters, 2 cases of RA and 3 deaths at 12-months, with an estimated cost-saving of £1,746/patient (Fig. 1).

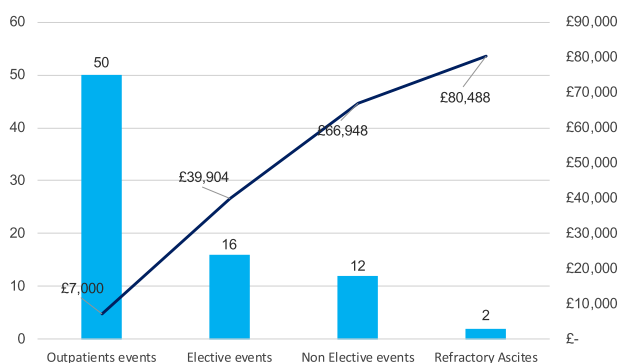


Figure 1. Main events avoided and associated costs savings when adding long-term albumin to standard medical treatment to 15 patients with recurrent ascites out of a cohort 31 patients

Conclusion: This detailed audit of patients with recurrent ascites validates our previous analysis; we found similar HCRU and event rates to previous HES data inputs and this DES model supports the conclusion that treating patients with recurrent ascites with LTA improves survival and leads to cost-savings through reduction of HCRU and complications.

SAT-538

Application of updated diagnostic criteria for cirrhotic cardiomyopathy: evaluation of its clinical impact in liver transplantation candidates

Maxim Khalenkov¹, Francis Voet¹, Michel De Pauw², Sander Lefere¹, Helena Degroote¹, Xavier Verhelst¹, Anja Geerts¹,

Hans Van Vlierberghe¹, Sarah Raevens¹. ¹Ghent University, Gastroenterology and Hepatology, Belgium; ²Ghent University, Cardiology, Belgium

Email: sarah.raevens@ugent.be

Background and aims: Cirrhotic cardiomyopathy (CCMP) is a liver-related cardiac complication that can occur in patients with cirrhosis, and mainly manifests as diastolic dysfunction (DD). Diagnostic criteria were first established by the Montréal consensus in 2005, however, they substantially lacked specificity. With the application of tissue Doppler imaging, the evaluation of DD has significantly evolved, and diagnostic criteria have been revised since 2019. The prevalence and the clinical impact of DD in liver transplantation (LT) candidates are not well studied.

In this single-center retrospective study, we aimed to estimate the prevalence of DD, applying the 2019 criteria, in our population of LT candidates. We assessed the impact of DD on waitlist mortality and post-LT outcome and explored if DD can improve after LT.

Method: Demographic, clinical, echocardiographic and outcome data of 522 adult patients on the waitlist for LT between 01/01/2005 and 31/03/2017 in the Ghent University Hospital were analyzed. DD was diagnosed based on the diagnostic criteria established in 2019, using tricuspid regurgitation velocity and e' lateral. Data were analyzed using SPSS.

Results: DD was diagnosed in 5.7% of our patients evaluated for LT. Patients with DD were significantly older compared to patients without DD (mean age 65y versus 60y, $P < 0.001$). Other demographic data and clinical characteristics, e.g. etiology and severity of the underlying liver disease, were similar between LT candidates with and without DD. Numerically, more patients with DD (21.1%) died on the waitlist compared to patients without DD (8.9%), although these results did not reach statistical significance. Patients who died on the waitlist were significantly older, had more severe liver disease, and more frequently had pulmonary comorbidities. A similar amount of LT candidates without DD underwent LT as LT candidates with DD (85.4% versus 73.6% respectively). The mean follow-up time in patients with and without DD was 1395 and 988 days ($p = 0.44$) respectively. Post-LT survival was similar in both groups: 14.3% of patients with DD and 15.2% of patients without DD died during follow-up. Pulmonary comorbidities and lower e' lateral were more frequently seen in deceased patients. Follow-up echocardiographic data post-LT were available in 10 patients who were diagnosed with DD before LT: only 1 of them fulfilled the diagnostic criteria of DD post-LT.

Conclusion: This large cohort study indicates that the prevalence of DD among LT candidates is rather low. Our data suggest that the presence of DD could potentially impact waitlist outcome, but does not affect post-LT survival.

SAT-539

Baveno VII algorithm can avoid endoscopic surveillance in patients with cirrhosis

Jinjun Chen¹, Haiyu Wang¹, Jiankang Song¹, Biao Wen¹, Yuanjian Zhang¹. ¹Hepatology Unit, Department of Infectious Diseases, Nanfang Hospital, Southern Medical University, Guangdong Provincial Key Laboratory of Viral Hepatitis Research, Guangdong Provincial Clinical Research Center For Viral Hepatitis, Guangzhou, China
Email: chjj@smu.edu.cn

Background and aims: Baveno VI criteria combined with spleen stiffness measurement (SSM) ≤ 40 kPa (Baveno VII algorithm) can safely rule out high-risk varices (HRV) and avoid esophagogastroduodenoscopy (EGD) screening. With a prospective cohort of cirrhosis patients having paired EGDs assessments, the present study aimed to validate the performance of Baveno VII algorithm in avoiding endoscopic surveillance in cirrhosis patients.

Method: The present study was a prospective study. Patients with cirrhosis were enrolled from April 2019 to February 2020 for endoscopic screening analysis (NCT04123509; NCT04890730). Endoscopic surveillance was performed and recorded in studied patients from June 2020 to April 2022. Liver and spleen transient elastography and EGD were performed within one month. Patients were followed up every 6 months at the clinic, and liver related events including clinical significant ascites, variceal bleeding, overt hepatic encephalopathy, HCC development and death were documented.

Results: Overall 715 patients with compensated cirrhosis were enrolled into screening analysis, of which 287 patients with paired EGDs were further analyzed. At screening, 153 (21.4%) patients had HRVs. Baveno VII algorithm with HRV missing rate at 2.0% (3/153) can avoid more EGDs than Baveno VI criteria (52.0% vs 32.7%, $p < 0.001$). Of the 287 patients, 27 patients were HRVs, Baveno VII algorithm can avoid 61.3% (176/278) endoscopic screening without (0/27) missing HRV. The distribution of varices at baseline in the 287 patients was as follows: no EV: 111 (38.7%), low-risk varices (grade 1 EV without red sign): 149 (51.9%), and high-risk varices: 27 (9.4%). During 17 (12–24) months follow-up, of the 111 patients without EV at baseline, 35 (31.5%) progressed to low-risk varices at follow-up. In the 149 patients with low-risk varices, varices disappearance of varices at

follow-up was found in 19 patients, and 7 cases progressed to HRV. Of the remaining 27 patients with HRV at baseline, 3 regressed to low-risk varices and 24 remained as HRV at follow-up. Eventually, the distribution of varices at follow-up were as follows: no EV: 95 (33.1%), low-risk varices: 161 (56.1%), and HRV: 31 (10.8%). At follow-up, 31 HRV was eventually diagnosed and 27 found in patients with consecutive unfavored Baveno VII status, 3 in worsening Baveno VII status and 1 in consecutive favored Baveno VII status. Baveno VII algorithm spared 63.8% (183/287) EGDs surveillance and only one HRV was missed (3.2%, 1/31). Baveno VII algorithm can avoid more EGDs than Baveno VI criteria both at screening (61.3% vs 40.8%, $p < 0.001$) and surveillance (63.8% vs 50.5%, $p = 0.001$). In the whole 715 patients, after 33 months of follow-up, Baveno VII algorithm could be a predictive model to detect patients with low risk of decompensation.

Conclusion: We have validated that the Baveno VI criteria and Baveno VII algorithm (Baveno VI criteria combined with SSM ≤ 40 kPa) both can safely avoid EGDs surveillance. Baveno VII algorithm is able to avoid more unnecessary EGDs surveillance than Baveno VI criteria in compensated liver cirrhosis patients. The Baveno VII algorithm was able to rule out HRVs safely with HRV missing rate (missed/total) $< 5\%$, and over a half of EGD procedures were spared at both screening and surveillance. As well as Baveno VII algorithm was developed to detect cirrhotic patients with low risk of decompensation.

SAT-540

Symptoms from refractory ascites: contributions from both abdominal pressure and the patient

Nikhilesh Mazumder¹, Sardar Ansari², Elliot Tapper¹, Anna Lok¹. ¹University of Michigan Hospital, Gastroenterology and Hepatology, Ann Arbor, United States; ²University of Michigan Hospital, Emergency Medicine, Ann Arbor, United States
Email: mazumde@med.umich.edu

Background and aims: Ascites significantly impairs quality of life among patients with cirrhosis. Large volume paracentesis (LVP) can relieve patient symptoms. However, data are limited regarding both the threshold at which a patient experiences symptoms and potential

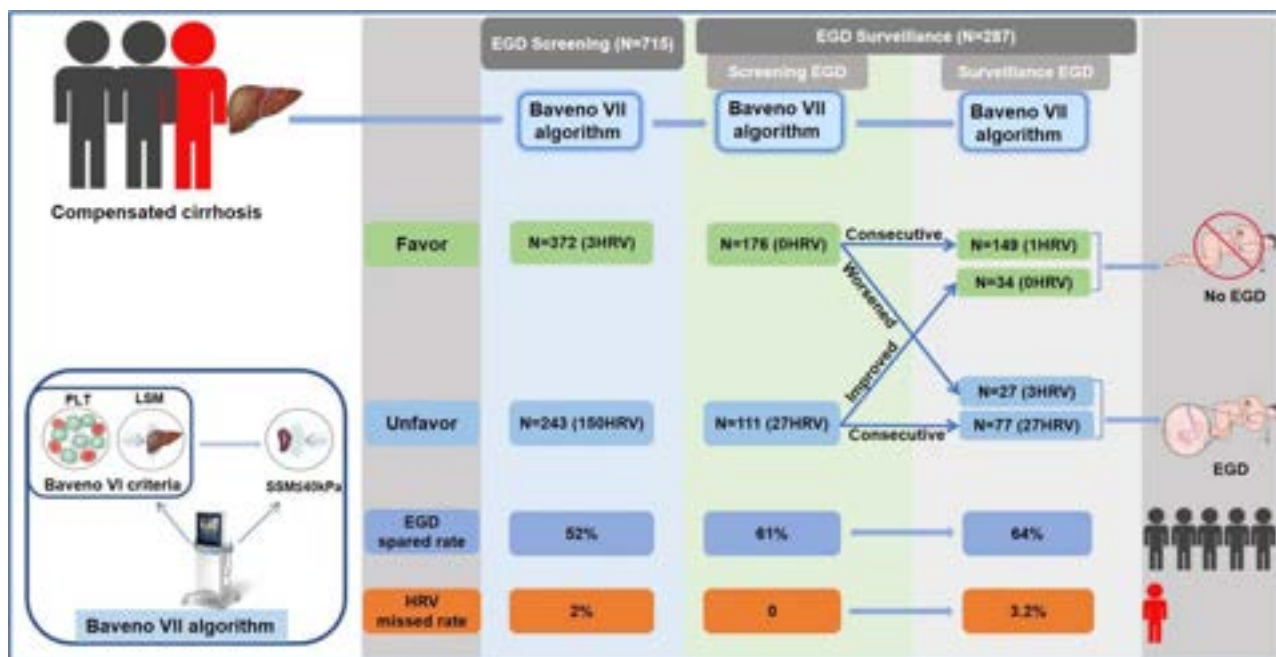


Figure: (abstract SAT-539).

for relief. The objective of this study was to delineate predictors of patient relief and persistence of symptoms after paracentesis.

Method: Patients with cirrhosis undergoing outpatient, therapeutic paracentesis were included. An open-ended manometer was used to measure ascites pressure at 1.5L increments during the procedure. The Ascites Symptom Index-7 (ASI-7), a validated PRO measure that rates seven domains impacted by ascites, was assessed before and at the end of the procedure (0: no symptoms, 35: maximal symptoms). Each component of ASI-7 was also examined separately. Relation between patient-specific responses to ASI-7 and ascites pressure was determined using a random-effects linear mixed model.

Results: 61 LVPs were performed on 21 unique patients (median 2 per patient, IQR 1–3). Opening pressure was 10.7 cmH₂O (IQR 8–13), which dropped to a median of 0 cmH₂O (IQR 0–5) after an average of 7.1 L (SD 2.1L) was removed per procedure. Median ASI-7 score pre-procedure dropped from 25 (IQR 20.5 to 27.5) to 7 (IQR 1–11) immediately after the procedure. Opening pressure was significantly associated with pre-LVP total ASI-7 score ($p=0.04$). By univariate regression, opening pressure had the strongest association with difficulty moving ($\beta=0.12$, $p=0.0016$), bloating/discomfort ($\beta=0.06$, $p=0.05$), and dyspnea while walking ($\beta=0.09$, $p=0.07$). An ASI-7 score focused on these three questions was more predictive of opening pressure ($p=0.03$) and closing pressure ($p=0.04$) than the full survey. Random effects linear modeling suggests that each patient had a unique pressure-symptom relationship ($p<0.001$). Regression trendlines by patient are plotted denoting the pressure-symptom relationship (Figure). This model also suggests that at abdominal pressure of zero, patients had residual symptoms even using the focused score (7.5 [max 15], 95% CI [5.4, 9.7], $p<0.006$)

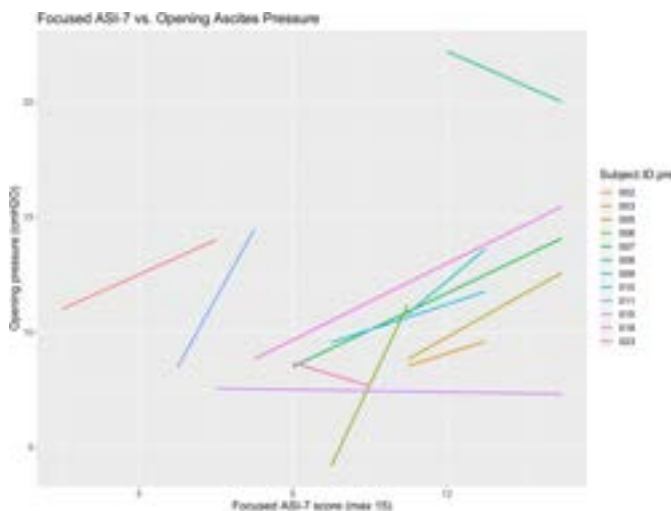


Figure:

Conclusion: Cirrhosis patients seeking relief from ascites-related discomfort typically present with abdominal pressure 10.7 cmH₂O which correlated with specific portions of the ASI-7 score. Each patient had a unique but typically direct relationship between the amount of discomfort experienced and abdominal pressure. However, residual discomfort was reported despite removing attaining zero pressure from ascites. Understanding this relationship will guide when and how much ascitic fluid should be drained for each patient to maximize symptom relief.

SAT-541

A retrospective evaluation of the effectiveness and safety of palliative long-term abdominal drains for the management of refractory ascites in patients with end-stage liver disease, in comparison with large volume paracentesis

Rodrigo Motta¹, Senamjit Kaur², Bryony Butler², Victoria Wharton², Jane Collier², Francesca Saffioti². ¹University of Oxford, Translational Gastroenterology Unit, Nuffield Department of Medicine-Experimental Medicine, United Kingdom; ²Oxford University Hospitals NHS Foundation Trust, United Kingdom
Email: francesca.saffioti@ouh.nhs.uk

Background and aims: Long term abdominal drains (LTAD) are a cost-effective palliative measure to manage malignant ascites in the community, but their use in patients with end-stage liver disease (ESLD) and refractory ascites (RA) is not routine practice.

We aimed to retrospectively evaluate effectiveness and safety of LTAD in palliative patients with ESLD and RA followed-up at our UK tertiary centre, in 2018–2022, and assess survival and the incidence of peritonitis, acute kidney injury (AKI), drain related complications and relevant hospitalisations, in comparison with a group of palliative patients with ESLD undergoing regular large volume paracentesis (LVP).

Method: Data was collected retrospectively from patients' electronic health records. Fisher's exact tests and Mann-Whitney U Test were used to compare qualitative and quantitative variables, respectively. Significance was set at $p<0.05$. Kaplan-Meier survival estimates were generated to stratify outcomes according to type of drain.

Results: Thirty patients had LTAD (35 drains, 1–2 litre drained per week). There were no peri-operative complications. Drain displacement occurred in 4 cases (11%), catheter blockage in 2 (6%). Symptoms of shortness of breath and abdominal pain resolved in 70% and anorexia in 50% of patients, following LTAD insertion. Nineteen patients only underwent regular LVP (median drain frequency 21 days).

Median follow-up (with LTAD in place/undergoing LVP), age, Child-Pugh score, liver disease aetiology, baseline renal function, ascitic protein, and presence of hepatocellular carcinoma were not significantly different between the LTAD and LVP cohort (Table 1). Prophylactic antibiotics were more frequently prescribed in the patients with LTAD ($p=0.012$), but the incidence of peritonitis did not differ between the two groups ($p=0.46$). Despite a similar use of diuretics, the incidence of AKI was significantly higher in the LVP group ($p=0.014$). Ascites/drain related hospital admissions occurred more frequently in the LVP cohort ($p=0.004$).

Survival was similar in the two groups (log-rank $p=0.71$). End point-free survival was significantly shorter in the LVP group ($p=0.004$, $p<0.001$, $p=0.018$ for first ascites/drain related hospitalisation, AKI and drain related complications, respectively).

Conclusion: The use of LTAD for the management of RA in palliative patients with ESLD is effective and relatively safe compared to LVP, and may reduce hospital admissions and health resource utilisation. A randomised controlled trial comparing LVP and LTAD is currently recruiting in the UK, to confirm these retrospective findings.

POSTER PRESENTATIONS

Table 1. Comparison of baseline characteristics and outcomes between the LTAD and the LVP cohort.

	LTAD	LVP	p value
Baseline characteristics			
Age, years (SD)	71 (11)	66 (12)	0.07
Child-Pugh score (IQR)	9 (2)	9 (2)	0.48
Aetiology (NASH/ArLD/viral/other)	9/12/2/7 (30%/40%/7%/23%)	3/10/1/5 (16%/53%/5%/26%)	0.69
HCC	5 (16.6%)	4 (21%)	0.46
Proteins in ascites ≤15 g/L	14 (47%)	9 (53%)	0.76
Prophylactic antibiotics	25 (81%)	8 (44%)	0.012
Previous peritonitis	2 (7%)	5 (28%)	0.86
T2DM	12 (40%)	8 (42%)	1.00
AKI	8 (23%)	11 (61%)	0.014
Baseline creatinine	104 (68)	84 (143)	0.44
Use of diuretics	23 (66%)	12 (63%)	1.00
Outcomes			
Median follow-up	77 (191)	64 (132)	0.45
Ascites /drain related admissions	11 (31.4%)	17 (73.7%)	0.004
Time to first hospitalisation (days)	44 (93)	7.5 (35)	0.002
AKI	8 (23%)	11 (61%)	0.014
Drain-related complications	14 (40%)	11 (73%)	0.06
Patients with peritonitis	5 (17%)	5 (28%)	0.46
Total n. of peritonitis episodes	10 (28%)	5 (26%)	0.98
Drain-related complications	14 (40%)	11 (73%)	0.06
Cellulitis	4 (11%)	2 (11%)	1.00
Site leakage	12 (34%)	2 (11%)	0.10
Bleeding of drain site	2 (6%)	1 (6%)	1.00
Hypotension	6 (17%)	4 (23%)	0.711

Abbreviations: LTAD, Long term abdominal drains; LVP, large volume paracentesis; SD, standard deviation, IQR, interquartile range; NASH, non-alcoholic fatty liver disease; ArLD, alcohol-related liver disease; HCC, hepatocellular carcinoma; T2DM, type 2 diabetes mellitus; AKI, acute kidney injury.

Table: (abstract SAT-541).

SAT-542

Coagulation profile in adult patients with porto-sinusoidal vascular disease

Sidharth Harindranath¹, Ankita Singh¹, Kashmira Kawli¹, Aditya Kale¹, Akash Shukla¹. ¹King Edward Memorial Hospital, Gastroenterology, Mumbai, India

Email: drakashshukla@yahoo.com

Background and aims: Porto-sinusoidal vascular disease is a recently described clinical entity that includes non-cirrhotic portal fibrosis, idiopathic portal hypertension, non-cirrhotic intrahepatic portal hypertension and various overlapping histological patterns.

The proposed aetiologies of this conditions is wide including autoimmune conditions, genetic disorders and thrombophilic states. We decided to study the clinical profile and prevalence of thrombophilic conditions in patients with PSVD at our centre.

Method: It was a single centre prospective study conducted over a period of 12 months. 69 consecutive patients were identified meeting the inclusion criteria of PSVD as defined by the recent BAVENO VII guidelines. Clinical, biochemical, and imaging findings were recorded. Thrombophilia profile was done in all patients which included analysis for MTHFR mutation, prothrombin gene mutation, factor V Leiden mutation, JAK2 mutation, estimation of level of homocysteine, Anti-thrombin III, protein C, protein S, APLA and ACLA

antibody levels and flow cytometry for PNH. Bone marrow aspiration with biopsy was done where indicated.

Results: Forty patients (58%) were male with a median age of 37 years (18–61). Common presentations were gastrointestinal bleed in 27 (39.1%), symptomatic splenomegaly in 27 (39.1%) and transient but clinically significant ascites in 20 (28.9%) patients. Twenty two patients (31.8%) were incidentally detected. Evidence of portal hypertension was seen in 62 (89.1%) patients. Portal vein thrombosis was seen in 13 (18.8%) patients. Superior mesenteric vein and splenic vein thrombosis was seen in 4 (5.7%) and 3 (4.3%) patients respectively. Twenty three patients (33.3%) had one or more thrombophilic disorders. Four patients (5.7%) had more than two thrombophilic disorders. Anti-phospholipid antibodies was the most common thrombophilic condition seen in 16 (69.5%), followed by MTHFR mutation in 8 (34.7%), low protein S in 6 (26%), low protein C in 5 (21.7%), prothrombin mutation in 5 (21.7%), JAKV617F mutation in 3 (13%), hyperhomocysteinemia, lupus anticoagulant and antithrombin III deficiency in 1 (4.3%) patient each. Symptomatic splenomegaly was seen significantly more commonly in males than in females ($p = 0.003$). MTHFR mutation was seen more commonly in patients who presented later (age > 35 years). Patients with one or more thrombophilic disorders had a higher incidence of splanchnic venous thromboses like superior mesenteric vein and/or splenic vein thrombosis ($p = 0.034$) and had a higher chance of presenting with variceal bleeding ($p = 0.07$).

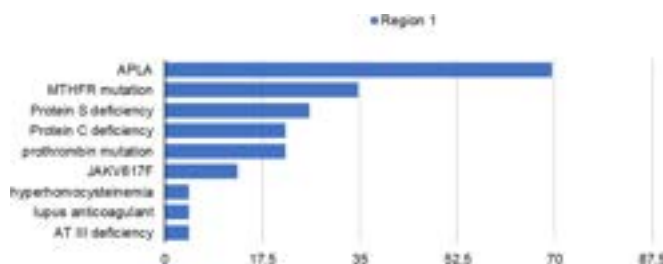


Figure:

Conclusion: PSVD is a distinct and all encompassing clinical entity with varied clinical manifestations. Association of prothrombotic conditions with this disorder has been established. One or more thrombophilic states can be seen in upto 30% of patients. These patients had a higher chance of presenting with splanchnic venous thrombosis and variceal bleeding. Hence all adult patients with PSVD should undergo thrombophilic workup as presence of thrombophilic risk factor like anti-phospholipid antibodies and JAK2 mutation may require additional therapy.

SAT-543

Continuous terlipressin infusion improves muscle function but not muscle mass in patients with cirrhosis and portal hypertension

Ryma Terbah^{1,2}, Darren Wong^{1,2}, Paul Gow^{1,2}, Avik Majumdar^{1,2}, Brooke Chapman^{1,2,3}, Adam Testro^{1,2}, Marie Sinclair^{1,2}. ¹Austin Health, Department of Gastroenterology and Liver Transplant Unit, Melbourne, Australia; ²The University of Melbourne, Department of Medicine, Melbourne, Australia; ³Austin Health, Department of Nutrition and Dietetics, Australia
Email: rterbah@hotmail.com

Background and aims: Sarcopenia is highly prevalent in patients with cirrhosis and is associated with increased morbidity and mortality both pre- and post-liver transplant. It tends to progress with increasing severity of liver disease and has few treatment options. We have previously shown that terlipressin, a vasopressin analogue, can improve handgrip strength (HGS), but there remains little data on the impact of terlipressin on muscle mass and function.

Method: In this single-centre, prospective study, a continuous infusion of terlipressin 3.4 mg daily was given for 12 weeks to adult

patients with cirrhosis, diuretic-refractory ascites, and sarcopenia. Muscle function was assessed using three HGS measurements in the non-dominant hand and the Liver Frailty Index (LFI). Muscle mass was evaluated using dual x-ray absorptiometry (DEXA) appendicular lean mass (APLM) and CT skeletal muscle index (SMI) at the level of the L3 vertebra. Assessments were performed at baseline and at the end of treatment.

Results: Twenty-three patients have completed study to date. The majority were male ($n = 15$, 65%) and the median age was 62 years (IQR 57–64 years). The most common aetiology of cirrhosis was alcohol ($n = 9$, 39.1%), followed by NASH ($n = 7$, 30.4%), chronic hepatitis C ($n = 4$, 17.4%), cryptogenic ($n = 2$, 8.7%), and chronic hepatitis B and delta co-infection ($n = 1$, 4.3%). The median MELD score at enrolment was 16 (12.5–17.5). Muscle function improved after terlipressin therapy. The maximum HGS recording increased from 27.5 kg (21.2–31.6 kg) to 28.4 kg (21.8–34.2 kg), $p = 0.012$, and the mean HGS increased from 25.9 kg (20–29.6 kg) to 27.8 kg (20.9–31.8 kg) $p = 0.021$. There was also a significant improvement in the liver frailty index from 4.25 (3.88–4.50) to 4.02 (3.69–4.28), $p = 0.01$. The SMI increased slightly from 46 cm²/m² (42–54 cm²/m²) to 47 cm²/m² (42–51 cm²/m²), however this was not significant ($p = 0.2$). DEXA APLM decreased from 7.53 kg/m² (6.22–8.30 kg/m²) to 7.09 kg/m² (6.04–7.78 kg/m²) but was not significant ($p = 0.07$). Of the APLM, the DEXA lower limb lean mass decreased from 16.54 kg (14.14–19.96 kg) to 15.58 kg (14.06–17.72 kg) ($p = 0.008$), but the lean mass in the upper limb, which is less affected by peripheral oedema, increased from 5.13 kg (4.52–5.54 kg) to 5.22 kg (4.64–5.59 kg) ($p = 0.4$).

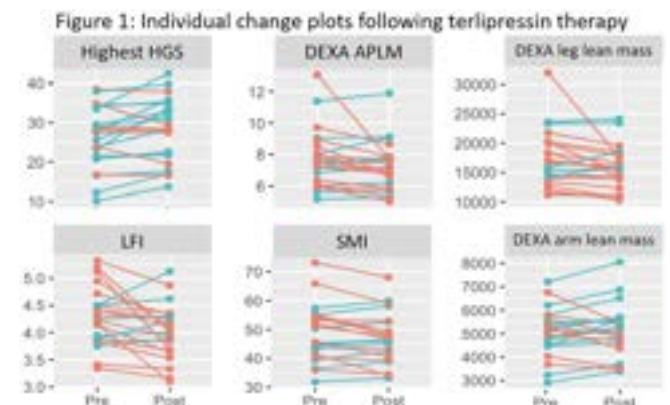


Figure 1:

Conclusion: In a sick cohort of cirrhotics for whom muscle function tends to steadily decline, 12 weeks of terlipressin therapy significantly improved muscle function and reduced frailty. While not statistically significant in this small cohort, the trend towards improvement in SMI and DEXA arm lean mass warrants further investigation with larger and longer studies, given muscle mass tends to take longer to increase than improvements in muscle function. This study provides a promising new therapy for sarcopenia in the sickest cohort of chronic liver disease patients.

SAT-544

Predicting the efficacy of splenic embolization on refractory ascites using a computational model of portal hypertension

Nikhilesh Mazumder¹, Filip Jezek², Elliot Tapper¹, Daniel Beard². ¹University of Michigan Hospital, Gastroenterology and Hepatology, Ann Arbor, United States; ²University of Michigan, Department of Molecular and Integrative Physiology, Ann Arbor, United States
Email: mazumde@med.umich.edu

Background and aims: Ascites is the most common cause of decompensation among patients with cirrhosis and carries a high morbidity and mortality rate. When refractory, splenic artery

POSTER PRESENTATIONS

embolization is often offered to patients not eligible for liver transplantation or transjugular intrahepatic portosystemic shunt (TIPS) creation, however its effect on ascites volume varies among patients. The objective of this study was to utilize a computational model of portal hypertension to simulate the effect of splenic embolization on portosystemic gradient (PSG) and ascites volume in different patients.

Method: We developed model of isolated portosplanchnic hemodynamics. This model consists of resistive components in series (intestinal arteries and veins, liver, hepatic vein) and a model of ascites generation (adapted from Levitt and Levitt. *BMC Gastroenterol.* 2012). We then modeled portosystemic collateral shunts with a diameter proportional to its pressure gradient. With increasing luminal diameter, larger amounts of portal flow is shunted, altering the hemodynamics. We then gradually increased intrahepatic resistance to model the progression of liver disease and simulated the steady state ascites volume at each stage. Splenic artery (SA) embolization was simulated by dropping portal inflow by 40% and the resulting effect on portosystemic gradient (PSG) and steady state ascites volume was compared across various levels of portosystemic collateralization.

Results: Representative cases comparing a no-shunt to a shunt case are displayed in the Figure with an end stage marked by the orange line. As liver disease progressed, patients with increased shunting (Fig. A, open red boxes) had a more gradual rise in PSG compared to patients without any shunting (Fig. A, open blue circles). At the same liver resistance (orange line), the end stage of disease resulted in a PSG of 25 vs 18 mmHg. Similarly, patients with shunts had lower ascites volumes at all stages (Fig. B, red crosses) with end stage patients attaining a steady state volume of 6L compared to 12L in the patients without collaterals. PSG was reduced by the same percentage regardless of shunt status, but the absolute drop was greater in patients with fewer shunts (Fig. A). Most notably, in patients with more portosystemic shunting splenic embolization was less effective at improving ascites volume compared to the no shunt case (Fig. C) with an average drop in steady state ascites volume of 3.5 vs 9.6 L.

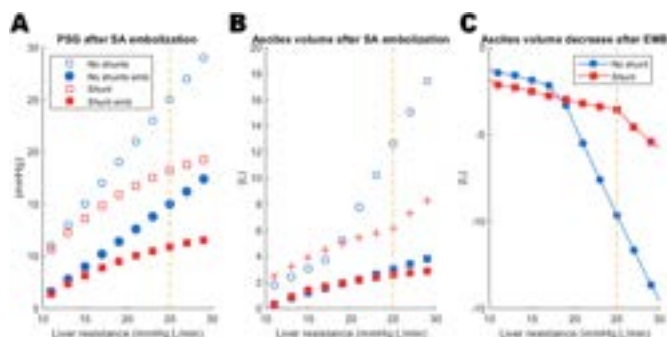


Figure:

Table 1. (abstract: SAT-545): Development of GI cancer in the Lactulose only, Rifaximin only, and Lactulose plus Rifaximin cohorts in the follow-up period.

Development of Cancer:						
	Total	Lactulose only	Rifaximin only	Lactulose only vs Rifaximin only	Lactulose plus rifaximin combination therapy	Lactulose only vs Rifaximin only vs Lactulose plus rifaximin
Patient Characteristics	n=12,409	n=5,244	n=2,502	p-value	n=4,663	p-value
Total GI Cancers [n (%)]	1,114 (8.98)	350 (6.67)	168 (6.71)	0.9470	596 (12.78)	<0.0001
colon [n (%)]	69 (0.56)	36 (0.69)	7 (0.28)	0.0243	26 (0.56)	<0.0001
rectum and anus [n (%)]	23 (0.19)	10 (0.19)	7 (0.28)	0.4334	6 (0.13)	<0.0001
esophagus [n (%)]	25 (0.20)	14 (0.27)	2 (0.08)	0.0900	9 (0.19)	<0.0001
stomach [n (%)]	23 (0.19)	16 (0.31)	0	0.0025	7 (0.15)	<0.0001
pancreas	38 (0.31)	11 (0.21)	6 (0.24)	0.7916	21 (0.45)	<0.0001
liver and intrahepatic bile duct [n (%)]	981 (7.91)	288 (5.49)	146 (5.84)	0.5389	547 (11.73)	<0.0001
other GI organs/peritoneum [n (%)]	43 (0.35)	14 (0.27)	7 (0.28)	0.9193	22 (0.47)	<0.0001

Conclusion: We developed a computational model for portal hypertension that demonstrates varying trajectories dependent on the quantity of portosystemic shunting. This model also shows the importance of portosystemic shunting on the severity of ascites and the effectiveness of splenic artery embolization. Such computational models may provide an explanation for heterogenous effects of this intervention in patients with ascites. Future work should seek to fit computational models to individual patients in order to personalize care of portal hypertension.

SAT-545

Administration of Lactulose, Rifaximin, or combination therapy for hepatic encephalopathy is associated with a reduction in gastrointestinal cancers

Ankoor Patel¹, You Li², Carlos Minacapelli², Carolyn Catalano², Vinod Rustgi². ¹Rutgers-Robert Wood Johnson Medical School, Medicine, New Brunswick, United States; ²Rutgers-Robert Wood Johnson Medical School, Gastroenterology and Hepatology, United States Email: ahp60@rwjms.rutgers.edu

Background and aims: Patients with cirrhosis are frequently administered rifaximin and/or lactulose for prevention and treatment of hepatic encephalopathy (HE). Both rifaximin and lactulose theoretically have anti-cancer effects. The risk of GI cancers in patients with cirrhosis on lactulose, rifaximin, and/or combination therapy has not been evaluated.

Method: A retrospective cohort study was conducted using the Truven Health MarketScan® Commercial Claims database from 2007 to 2017. Patients with cirrhosis were identified using ICD-9/10 codes. An index date was defined for each participant as the earliest date of cirrhosis diagnosis. A baseline period for each participant was defined as the twelve months prior to the first medication date while the study follow-up period represented the period from the first medication date to the last medication date. Patients with history of any cancer before the first medication date were excluded from the study. Student's t tests were used to compare all continuous measures of age and duration of medication. Wald Chi-square tests were performed to test the associations between the study groups.

Results: The rifaximin only cohort had the lowest risk of developing colon cancer (rifaximin only vs lactulose plus rifaximin vs lactulose only (0.28% vs 0.56% vs 0.69%; $p < 0.0001$), esophageal cancer (0.08% vs 0.19% vs 0.27%; $p < 0.0001$), and stomach cancer (0.0% vs 0.15% vs 0.31%; $p < 0.0001$).

Conclusion: Colon, esophageal, and gastric cancers had an incidence reduction in the rifaximin only cohort compared to the lactulose only and lactulose plus rifaximin cohorts. Further studies are required to understand the mechanisms by which rifaximin may exert anti-cancer properties.

SAT-546

Use and impact of transjugular intrahepatic portosystemic shunt: a twelve-year nationwide study in Germany

Wenyi Gu¹, Yasmin Zeleke², Hannah Hortlik², Louisa Schaaf², Frank Erhard Uschner¹, Martin Schulz¹, Michael Tischendorf¹, Kai-Henrik Peiffer², Maximilian Joseph Brol¹, Markus Kimmann¹, Thomas Vogl², Michael Köhler¹, Carsten Meyer³, Alexander Gerbes⁴, Martin Rössle⁵, Wim Laleman⁶, Alexander Zipprich⁷, Christian Steib³, Michael Praktikjnjo¹, Jonel Trebicka¹. ¹University Hospital Muenster, Germany; ²University Hospital Frankfurt, Germany; ³University Hospital Bonn, Germany; ⁴University Clinic Munich LMU, Germany; ⁵Medical Centre University of Freiburg, Germany; ⁶University Hospitals Leuven, Germany; ⁷Jena University Hospital, Germany
Email: jonel.trebicka@ukmuenster.de

Background and aims: Portal hypertension (PHT) is the driver of many complications in liver cirrhosis. The number of cirrhosis cases as well as diagnosis of PHT-driven complications have increased over time. Transjugular intrahepatic portosystemic shunt (TIPS) placement is the most effective treatment of PHT. The aim of this study was to analyze the use and impact of TIPS placement in patients with different portal hypertensive complications during the last decade in a German nationwide study.

Method: We analyzed 14,598 admissions of patients for TIPS insertions in Germany from 2007 to 2018 using the DRG system. 1,987,888 admissions of cirrhotic patients did not have TIPS placement and were compared in the analysis as a control group. All diagnoses and procedures were coded according to ICD-10-CM and OPS code. The data were analyzed focusing on the number of admissions and in-hospital mortality in patients admitted for TIPS.

Results: The number of admissions of patients received TIPS insertion increased from 439 in 2007 to 2,037 in 2018. The vast majority ([88.7%] 12,948) of patients received TIPS in the observational 14 years had cirrhosis. The survival of cirrhotic patients with ascites and HRS increased significantly from TIPS insertions by 6.1% and 24.4%, respectively, compared to patients without TIPS. In cirrhotic patients with gastrointestinal bleeding, TIPS significantly decrease their in-hospital mortality with concomitant ascites or hepatorenal syndrome (HRS). 22.6% of patients with TIPS insertion developed hepatic encephalopathy (HE). However, compared to cirrhotic patients without TIPS, TIPS improved the survival of patients with HE grades-1 and -2 as comorbidity by 10% and 33%, respectively. In the logistic regression, higher HE grade (-3 and -4), as well as infection and circulatory diseases (including any forms of diseases of the circulatory system excluded ischemic heart diseases) are found independently associated with in-hospital death in patients with TIPS. Furthermore, TIPS and TIPS revision were independently associated with improved in-hospital survival in cirrhotic patients (Figure).

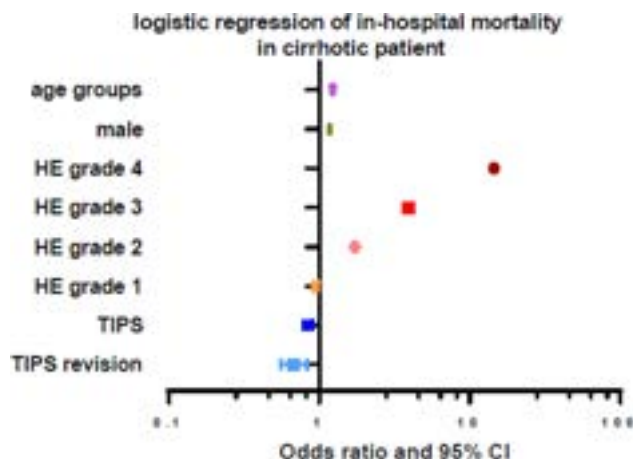


Figure: Logistic regression of in-hospital mortality in 2,000,836 admissions of patients with liver cirrhosis

Conclusion: Our nationwide population-based study demonstrates that TIPS insertion is more frequently used, and it improves outcomes, especially in patients with ascites and HRS. In gastrointestinal bleeding, the effect is significant only when ascites and/or HRS is present. TIPS is beneficial with regard to better survival despite lower HE grades, while higher grade HE, infection and circulatory diseases seem to be associated with risk of in-hospital mortality.

SAT-547

Spontaneous portosystemic shunts (SPSS) regress after transjugular intrahepatic portosystemic shunt (TIPS) implantation

Theresa Bucsics^{1,2}, Katharina Lampichler^{2,3}, Maria Schoder³, Lukas Reider³, Konstantin Vierziger⁴, Lukas Hartl^{1,2}, David Jm Bauer^{1,2}, Mathias Jachs^{1,2}, Georg Semmler^{1,2}, Rafael Paternostro^{1,2}, Philipp Schwabl^{1,2,5}, Lorenz Balcar^{1,2}, Katharina Pomej^{1,2}, Michael Trauner¹, Mattias Mandorfer^{1,2}, Thomas Reiberger^{1,2,5}. ¹Medical University of Vienna, Department of Internal Medicine III, Division of Gastroenterology and Hepatology, Wien, Austria; ²Medical University of Vienna, Vienna Hepatic Hemodynamic Laboratory, Department of Internal Medicine III, Division of Gastroenterology and Hepatology, Wien, Austria; ³Medical University of Vienna, Department of Biomedical Imaging and Image-Guided Therapy, Wien, Austria; ⁴Klinik Favoriten-Wiener Gesundheitsverbund, Department of Radiology, Vienna, Austria; ⁵Medical University of Vienna, Christian-Doppler Laboratory for Portal Hypertension and Liver Fibrosis, Wien, Austria
Email: thomas.reiberger@meduniwien.ac.at

Background and aims: The impact of transjugular intrahepatic portosystemic shunt (TIPS) on the evolution of spontaneous portosystemic shunts (SPSS) has not been systematically evaluated.

Method: Ninety-one patients with paired contrast-enhanced CT scans pre and post TIPS were included. The presence of small (S-SPSS, 3–8 mm) and large SPSS (L-SPSS, ≥8 mm) as well as total cross-sectional diameter and area of all SPSS were evaluated. A semiquantitative visual SPSS score was applied: (Coll-0) no, (Coll-1) one S-SPSS, (Coll-2) 2–3 S-SPSS; (Coll-3) ≥4 S-SPSS or 1 L-SPSS.

Results: Median total SPSS diameter and area significantly decreased after TIPS from 14 mm [10–19] to 6 mm [3–10; $p < 0.0001$] and from 69.9 cm² [33.8–523.1] to 15.7 cm² [7.1–412.3; $p < 0.0001$], respectively. The proportion of patients with pre-TIPS L-SPSS decreased from 45.1% (n = 41/91) to 19.8% (18/91; $p < 0.001$), and the proportion of patients with Coll-3 from 85.7% to 51.6% ($p < 0.001$). Patients with persisting L-SPSS (or a post-TIPS visual SPSS score of 3) showed a significantly shorter transplant-free survival than those with only few S-SPSS or improvement of SPSS (median 30.0 vs 84.0 months, log-rank $p = 0.011$ and median 53.0 vs 115.0 months, $p = 0.037$, respectively).

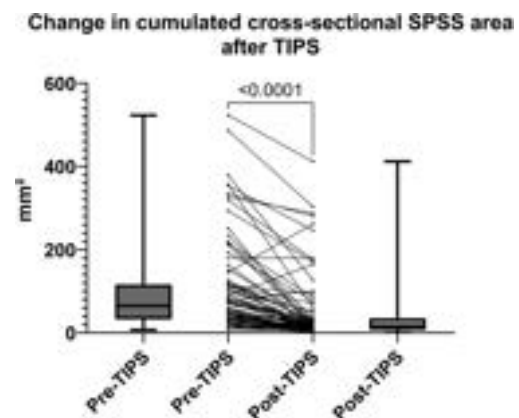


Figure:

POSTER PRESENTATIONS

Conclusion: TIPS implantation ameliorates the extent of SPSS. While large SPSS regress in a considerable number of patients, their persistence after TIPS is linked to an increased risk of mortality.

SAT-548

Predicting post-TIPSS mortality: external validation of the FIPS score in a Canadian cohort

Shamir Malik¹, Arash Jaber², Sebastian Mafeld², Bettina Hansen³, Morven Cunningham⁴, Jordan J. Feld⁴, Scott K Fung⁴, Aliya Gulamhusein⁴, Keyur Patel⁴, David Wong⁴, Gideon Hirschfield⁴, Ann T Ma⁴. ¹Faculty of Medicine, University of Toronto, Canada; ²JDMI, University Health Network, Toronto, Canada; ³Institute of Health Policy, Management and Evaluation, University of Toronto, Canada; ⁴Toronto Centre for Liver Disease, University Health Network, Toronto, Canada
Email: ma.ann.thu@gmail.com

Background and aims: The Model for End-Stage Liver Disease (MELD) score was originally developed to predict mortality post-transjugular intrahepatic portosystemic shunt (TIPSS) insertion. A new prognostic score, the “Freiburg index of post-TIPSS survival” (FIPS) score, has emerged and includes age, serum creatinine, bilirubin and albumin. Preliminary data suggest FIPS outperforms MELD in predicting mortality in certain European and Asian cohorts, while a recent US Veterans Affairs (VA) study did not. We aimed to validate its use in a single-centre cohort in Canada.

Method: This retrospective cohort study included patients who underwent TIPSS insertion between 2010 and 2021 at the University Health Network in Toronto. Prognostic scores including MELD, MELD-Na and FIPS were obtained within 3 months prior to TIPSS insertion. Patients were followed for up to 12 months post-TIPSS. Patients who were lost to follow-up within the first 90 days post-TIPSS were excluded. The performance of prognostic scores at 90 days post-TIPSS was assessed by area under the receiver operating characteristic curve (AUROC).

Results: A total of 129 patients were included (median age 58, 46% male). The indication for TIPSS placement was refractory ascites in 64%, variceal bleeding in 26%, hydrothorax in 5%, hepatorenal syndrome in 4% and portal vein thrombosis in 1%. TIPSS insertion was done in an emergent setting in 19%. The main etiologies of liver disease were alcohol in 46%, autoimmune in 16% and non-alcoholic fatty liver disease in 15%. The median [P25-P75] MELD, MELD-Na and FIPS scores before TIPSS were 15 [12–17], 16 [13–19] and 0.30 [–0.24–0.69], respectively. At 90 days, 6 patients had died (7%), while none had undergone liver transplant. The performance of all prognostic scores to predict 90-day mortality was poor (AUROC 0.54, 0.47 and 0.60 for MELD, MELD-Na and FIPS, respectively). However, using the FIPS cut-off of 0.92 as reported in the original derivation cohort, patients with a high FIPS score had significantly poorer 90-day survival compared to those with a low FIPS score (84% vs 97% respectively, $p = 0.04$) (Figure).

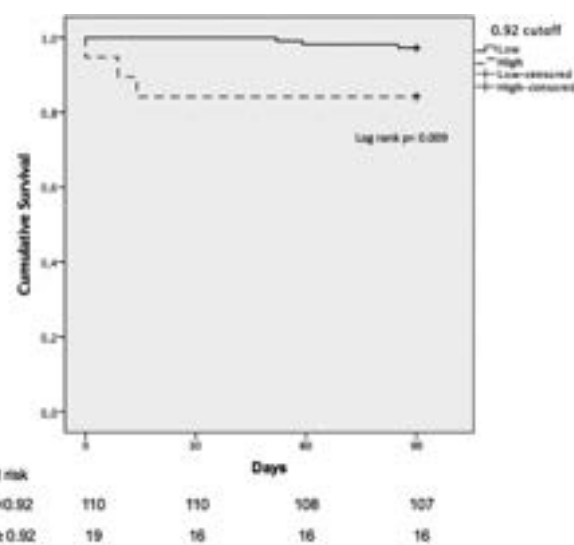


Figure: 90-day survival post TIPSS of patients with high FIPS (≥ 0.92 , dashed line) and low FIPS (< 0.92 , solid line).

Conclusion: The FIPS score failed to outperform traditional risk scores in predicting post-TIPSS survival in this single-centre Canadian cohort. However, the use of a single FIPS cut-off point was useful in identifying patients at higher risk of mortality. The recent VA study presented important results in a specific population, and further validation of the FIPS score in large, diverse cohorts is still required.

SAT-549

Clinical practice results of the use of intrahepatic portosystemic shunt for the treatment of refractory hepatic hydrothorax

Elena Tenorio González¹, Enrique Pérez-Cuadrado Robles¹, Rocio González-Grande², Miguel Jiménez-Pérez². ¹Georges-Pompidou European Hospital, AP-HP, Paris, France; ²Regional University Hospital, Málaga, Spain
Email: etengo89@gmail.com

Background and aims: Technical advances and accumulated experience in the placement of intrahepatic portosystemic shunt (TIPS) in patients with endoscopically uncontrolled gastrointestinal bleeding have allowed their use in other less predominant indications for which there is less data. Refractory hepatic hydrothorax (RHH) is defined as that which either does not respond to treatment with diuretics at maximum doses (spironolactone 400 mg/day and furosemide 160 mg/day) or develops complications derived from their use, and therefore requires periodic thoracentesis for its control. We analyzed the results obtained in terms of clinical success and survival in patients with RHH treated at a tertiary hospital.

Method: Single center cohort retrospective study. Patients who required TIPS placement due to RHH between January 2011 and December 2019 was included, with the last prospective review of the status of the patients being in August 2022. Baseline analytical data and clinical and radiological follow-up data were analyzed at 1, 3, 6, and 12 months after TIPS placement, as well as until death or liver transplantation (if this occurred). Matching techniques were performed for the descriptive analysis of the results, taking into account the cases lost due to loss of follow-up, transplantation or exitus.

Results: Among 83 patients who required TIPS placement during this period of time, 7 were due to HRH. Only one patient required posterior thoracentesis during the first month after TIPS placement due to persistent severe hydrothorax. No patient required further thoracentesis to control hydrothorax after 3, 6, or 12 months (Table 1). However, it should be noted that all the patients had previous ascites, and the ascites resolved in 4 of them (57.1%) during the first year of follow-up. 85.7% of patients ($n = 6$) required, however, associated diuretics to control hydrothorax. It should be noted that at 6 months

Table 1 (abstract: SAT-549).

	Clinical and radiologic (chest X-ray) follow-up							
	1 month		3 months		6 months		12 months	
	Frequency	Percentage	Frequency	Percentage	Frequency	Percentage	Frequency	Percentage
No hydrothorax	0	0	1	16.7	3	75	2	66.7
Mild hydrothorax	0	0	4	66.7	1	25	1	33.3
Moderate hydrothorax	6	85.7	1	16.7	0	0	0	0
Severe hydrothorax	1	14.3	0	0	0	0	0	0
Survival rate								
After liver transplantation	0	0	0	0	1	14.3	1	14.3
Without liver transplantation	7	100	7	100	5	71.4	4	57.1

the best results are observed due to maximum improvement in hyperdynamic circulation thanks to the TIPS. Thus, there is a 12-month survival of 71.4%, being 57.1% without the need for liver transplantation and 14.3% thanks to transplantation.

Conclusion: These data allow us to corroborate that the placement of TIPS is effective and safe in the treatment of RHH, with a gradual improvement in hydrothorax during the first year of follow-up, which is accompanied by an improvement in ascites when associated and, with it, of their MELD score, sometimes avoiding the need for transplantation and increasing their survival.

SAT-550

Detection of minimal hepatic encephalopathy: standardization of psychometric hepatic encephalopathy scale for Israeli population

Nave Firestein¹, Niv Zmora^{2,3,4}, Nir Bar^{2,3}, Oren Shibolet^{2,3}, Helena Katchman^{2,3}. ¹Barzilai Medical Center, Israel; ²Tel Aviv University, Israel; ³Tel Aviv Sourasky Medical Center, Israel; ⁴Tel Aviv Sourasky Medical Center-Ichilov, Department of Gastroenterology and Hepatology, Tel Aviv-Yafo, Israel
Email: hkatchman@gmail.com

Background and aims: Minimal hepatic encephalopathy (MHE) is a subclinical form of hepatic encephalopathy (HE) that leads to decreased quality of life and increased incidence of overt HE in cirrhotic patients. Psychometric hepatic encephalopathy scale (PHES) is the gold standard for MHE diagnosis, but its use requires adjustment to population-specific norms of performance. The aim of this study was to construct and validate a set of normal values for PHES in an Israeli population.

Method: PHES tests (NCT-A, NCT-B, DST, SDT and LTT) were performed on 189 healthy volunteers and 63 cirrhotic patients, and possible confounding factors, including age, gender and years of education, were assessed. Linear regression models were computed on the healthy cohort to generate confounder-adjusted equations for each of the PHES components. Reference values were then calculated for the cirrhotic patients with suspected MHE and Z-scores determined. Flicker and ICT tests were also performed in cirrhotic patients and their correlations with PHES results were evaluated.

Results: Age was correlated with all 5 components of PHES and education level was only correlated with NCT-A, NCT-B and DST results. No correlation between gender and test results was noted in our population. Adjusted Z-scores were calculated (figure 1A) and found to be in closest correlation to Chinese scores (figure 1B). Among 45 cirrhotic patients without previous overt HE, MHE was diagnosed in 22 (49%), 17 (38%) and 22 (49%) patients using PHES, ICT or Flicker respectively. There was a statistically significant agreement on MHE diagnosis between Flicker and ICT tests and PHES results (figure 1C). In addition, PHES results correlated to patients' MELD-Na scores (figure 1D).

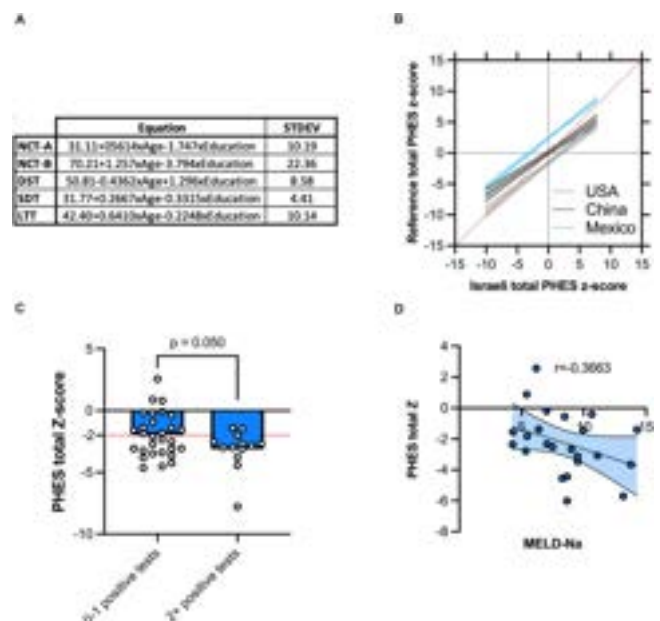


Figure: Calculation of adjusted Z-scores (A) and evaluation of PHES for Israeli population. Correlation to other national PHES norms (B), other MHE tests (C) and MELD-Na score (D).

Conclusion: Norms for PHES tests were generated and validated, demonstrating a good diagnostic capability, a fair agreement with ICT and Flicker tests and a correlation to liver disease severity.

SAT-551

Impact of non-selective beta-blockers on first and further hepatic decompensation after transjugular intrahepatic portosystemic shunt insertion

Anja Tiede¹, Jim Benjamin Mauz¹, Lena Stockhoff¹, Hannah Schneider¹, Bernhard Meyer², Heiner Wedemeyer^{1,3}, Markus Cornberg^{1,3,4}, Jan Hinrichs², Tammo Lambert Tergast¹, Benjamin Maasoumy^{1,3}. ¹Hannover Medical School, Department of Gastroenterology, Hepatology and Endocrinology, Hannover, Germany; ²Hannover Medical School, Department of Diagnostic and Interventional Radiology, Hannover, Germany; ³German Center for Infection Research (DZIF), Braunschweig, Germany; ⁴Center for Individualised Infection Medicine (CIIM), c/o CRC Hannover, Hannover, Germany
Email: tiede.anja@mh-hannover.de

Background and aims: Treatment with non-selective beta-blockers (NSBB) is linked to a lower risk of hepatic decompensation in patients with liver cirrhosis and portal hypertension. These positive effects of NSBB do not directly correlate with the decrease of portal pressure and are even present if portal pressure remains unaffected. So far, little is known about the impact of NSBB therapy on the outcome of patients after insertion of a transjugular intrahepatic portosystemic

POSTER PRESENTATIONS

shunt (TIPS). In this study we aimed to investigate the role of NSBB treatment in preventing first and further hepatic decompensation after TIPS.

Method: A number of 366 consecutive patients receiving a TIPS between 2009 and 2021 were considered. Patients with Budd-Chiari syndrome, absence of liver cirrhosis, history of liver transplantation (LTx), cystic fibrosis, or those receiving a rescue TIPS were excluded. First and further hepatic decompensation (HD) were assessed according to the Baveno VII criteria. After evaluating the impact of NSBB intake at TIPS insertion on the occurrence of periinterventional HD, patients were followed up for one year after hospital discharge with continuous reassessments of NSBB status. Link between NSBB intake and development of HD as well as LTx-free survival was tested using multivariable competing risk and cox regression analysis, adjusting for FIPS score, TIPS indication refractory ascites and Cholinesterase (CHE).

Results: Overall, 176 (57.3%) of the included 307 patients received NSBB therapy prior to TIPS insertion. Patients in the NSBB group had lower FIPS- (-0.25 vs -0.15 , $p = 0.001$) and MELD scores (11 vs 13 , $p = 0.008$) and a higher CHE (2.63 vs 2.13 , $p < 0.001$). Refractory ascites for TIPS indication was more common in the no-NSBB group (94.7% vs 71.0% , $p < 0.001$).

In the periinterventional period, NSBB therapy at TIPS insertion had no significant impact on the development of first or further HD (first: $n = 34$, NSBB/no-NSBB $16/18$; $p = 0.21$; further: $n = 77$, $38/39$, $p = 0.10$). Most common first and further HD was hepatic encephalopathy (HE, $n = 18$) and acute kidney injury ($n = 46$), respectively.

At time of discharge, 132 patients (43.0%) still received NSBB therapy, 37 of whom stopped NSBB therapy before end of follow-up. After discharge, ascites ($n = 66/127$ first HD) and HE ($n = 55/119$ further HD) were the respective predominant HD. While NSBB therapy was associated with a lower risk for first and further HD in univariable competing risk analysis (first: HR 0.625 , $p = 0.01$; further: HR 0.588 , $p = 0.005$), this did not remain statistically significant in multivariable analysis (HR 0.787 , $p = 0.23$; HR 0.729 , $p = 0.12$). NSBB intake was also not linked to a higher LTx-free survival in multivariable analysis (HR 0.610 , $p = 0.16$).

Conclusion: NSBB therapy at TIPS insertion and its (dis-)continuation afterwards has no significant impact on the development of first and further hepatic decompensation after TIPS.

SAT-552

Audit assessing real-world incidence of adverse events and mortality rate in patients receiving Terlipressin for hepatorenal syndrome at Royal Free hospital

Naz Kanani Alviri¹, Fatema Jessa¹, David Patch². ¹Royal Free Hospital, Pharmacy, London, United Kingdom; ²Royal Free Hospital, Hepatology, London, United Kingdom

Email: naz.kanani@nhs.net

Background and aims: Hepatorenal Syndrome-Acute Kidney Injury (HRS-AKI) involves an acute onset of renal dysfunction on a background of decompensated cirrhosis and ascites, and is associated with high mortality. Terlipressin (TRL), a synthetic vasopressin analogue, is widely used in the management of HRS-AKI to cause vasoconstriction of the splanchnic circulation and improve renal perfusion. In September 2022, the European Medicines Agency issued an alert regarding a higher than previously known risk of respiratory failure and a new risk of sepsis associated with TRL. An audit was carried out in Royal Free Hospital (RFH) in London with the aim of assessing the real-world incidence of adverse events and mortality rate in patients who received TRL for HRS-AKI.

Method: All patients initiated on TRL for HRS-AKI between April 2018 and October 2022 at RFH were investigated retrospectively. Data from electronic dispensing records, clinical documentation, prescription charts and discharge letters were used to determine diagnosis of HRS-AKI, the incidence of respiratory failure, respiratory distress,

sepsis and mortality rate within 90 days of receiving the first dose of TRL.

Results: A total of 37 patients received TRL. The mean age was 52.8 years with a Male:Female ratio of 25:12. Within 90 days of the first dose of TRL, respiratory failure was reported in 19% (7), respiratory distress in 14% (5), and sepsis in 11% (4) of patients. Additionally, cardiac rhythm abnormalities were seen in 5% (2). A total of 46% (17) patients experienced adverse reactions; in which 90-day survival was 41% (7). Overall, a mortality rate of 49% (18) was observed. 8% (3) underwent liver transplantation.

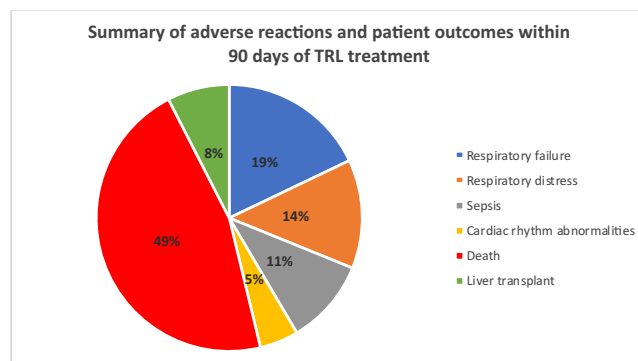


Figure:

Conclusion: Almost half of patients receiving TRL for hepatorenal syndrome experienced adverse reactions within 90 days of the first dose. High mortality was observed at a similar incidence to that in recently published research. Limitations of the audit include varying treatment duration, dosing, method of administration and concomitant human albumin solution. Additionally, severity of clinical presentation and multimorbid state differed within the patient group. Therefore, a larger sample is required to estimate causality, and safety of TRL. Due to risk of sepsis, respiratory failure and respiratory distress, it is advised to monitor patients for signs of infection and stabilise any respiratory symptoms prior to initiating TRL.

SAT-553

Collagen-proportionate area determined by semiautomated histomorphometry correlates with HVPG across different liver disease etiologies

Thomas Sorz^{1,2,3}, Benedikt Simbrunner^{1,2,3,4}, Kerstin Zinöber^{1,3,4}, Georg Semmler^{1,4}, Philipp Königshofer^{1,3,4}, Christopher Kaltenecker⁵, Benedikt Hofer^{1,2,3,4}, Behrang Mozayani⁵, Vlad Taru^{1,3}, Renate Kain⁵, Michael Trauner¹, Matthias Mandorfer^{1,4}, Philipp Schwabl^{1,2,3,4}, Thomas Reiberger^{1,2,3,4}. ¹Medical University of Vienna, Department of Medicine III, Division of Gastroenterology and Hepatology, Vienna, Austria; ²Center for Molecular Medicine (CeMM), Vienna, Austria; ³Medical University of Vienna, Christian Doppler Lab for Portal Hypertension and Liver Fibrosis, Vienna, Austria; ⁴Medical University of Vienna, Department of Medicine III, Vienna Hepatic Hemodynamic Laboratory, Vienna, Austria; ⁵Medical University of Vienna, Department of Pathology, Vienna, Austria
Email: thomas.sorz@meduniwien.ac.at

Background and aims: Liver fibrosis represents the main static component of portal hypertension (PH). The gold-standard of sinusoidal PH evaluation in advanced chronic liver disease is the measurement of the hepatic venous pressure gradient (HVPG). Digital histomorphometry allows quantification of collagen proportionate area (CPA) on liver biopsies. We aimed (i) to assess the correlation between CPA and HVPG across different etiologies and (ii) to compare the diagnostic performance of CPA and liver stiffness measurement (LSM) for clinically significant portal hypertension (CSPH).

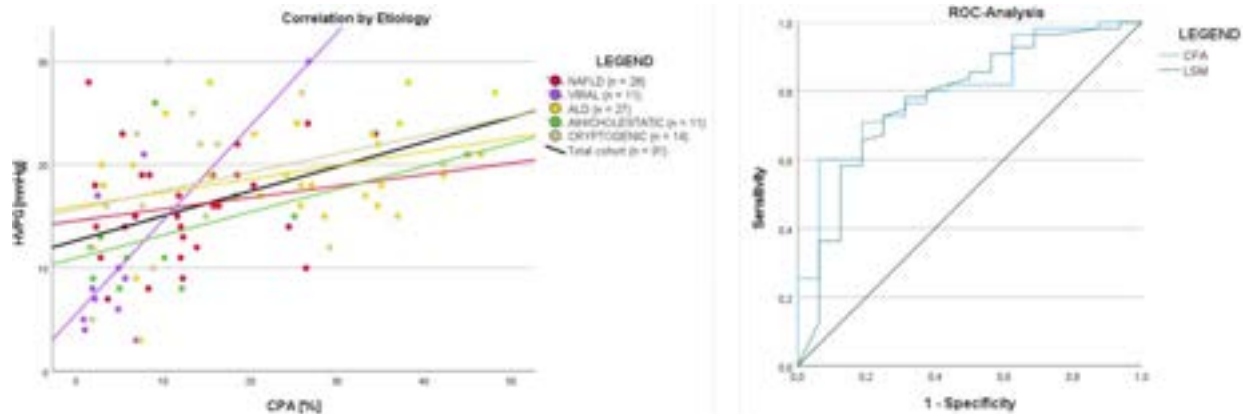


Figure: (abstract: SAT-553).

Method: Patients undergoing liver biopsy with available data on same-day measurement of HVP were included in this study. The biopsies were stained with picro-sirius-red (PSR) and digitalized with a slide scanner. HALO software (Indica Labs) was used for CPA morphometry. The data for HVP, LSM, enhanced liver fibrosis (ELF) score, platelet count, MELD and Child-Pugh score were extracted from medical records. Correlations were analyzed using Spearman's Rho (r) coefficient. The performance of CPA to diagnose CSH was evaluated via ROC analysis and optimal cutoffs were determined by Youden's index.

Results: 91 patients with a median HVP of 17 (IQR: 10) mmHg ($n = 72$, 79.1% had CSH) and a median CPA of 12.1 (IQR: 20) % were included. The liver disease etiologies were: alcohol-related liver disease (ALD; $n = 27$, 29.7%), non-alcoholic fatty liver disease (NAFLD; $n = 28$, 30.8%), viral hepatitis ($n = 11$, 12.1%), cryptogenic fibrosis ($n = 14$, 15.4%) and AIH/cholestatic liver disease ($n = 11$, 12.1%). CPA significantly correlated with HVP ($r = 0.494$, $p < 0.001$), LSM ($r = 0.478$, $p < 0.001$), ELF ($r = 0.433$, $p < 0.001$) and MELD ($r = 0.356$, $p < 0.001$). Importantly, the correlation coefficient of CPA-to-HVP was distinct for the various etiologies: $r = 0.185$ for ALD, $r = 0.545$ for viral hepatitis, $r = 0.149$ for NAFLD, $r = 0.420$ for AIH/cholestatic liver disease and $r = 0.335$ for cryptogenic liver disease. LSM (available in $n = 71$) showed a similarly high correlation with HVP ($r = 0.410$, $p < 0.001$). CPA diagnosed CSH with an area under the curve (AUC) of 0.801 ($p < 0.001$), with a Youden's index-based CPA cutoff at 12.24% (sensitivity: 60%, specificity: 93.75%). LSM yielded a similar AUC of 0.770 ($p = 0.003$) for diagnosis of CSH and had a sensitivity of 72.7% and a specificity of 75% using a cut-off at 23.5 kPa.

Conclusion: CPA is a valuable and investigator-independent diagnostic tool for quantification of the static component of PH across different liver disease etiologies. While CPA showed a higher specificity for CSH diagnosis than LSM, the requirement of invasive liver biopsy limits the broad applicability of CPA.

SAT-554

Impact of new ESC/ERS diagnostic criteria for pulmonary hypertension in cirrhotic patients with portal hypertension on the frequency of portopulmonary hypertension

Hiroki Ono¹, Masanori Atsukawa¹, Kaori Koyano¹, Yuta Hasegawa¹, Tadamichi Kawano¹, Tomohide Tanabe², Yuji Yoshida³, Tomomi Okubo³, Taeng Arai¹, Korenobi Hayama³, Norio Itokawa¹, Katsuhiko Iwakiri¹. ¹Nippon Medical School Hospital, gastroenterology and hepatology, Bunkyo City, Japan; ²Nippon Medical School Musashi Kosugi Hospital, gastroenterology, Kawasaki, Japan; ³Nippon Medical School Chiba Hokusoh Hospital, Inzai, Japan
Email: h-ono0@nms.ac.jp

Background and aims: Portopulmonary hypertension (PoPH) is categorized as pulmonary arterial hypertension (PAH), which belongs

to group 1 of the clinical classification of pulmonary hypertension (PH). In addition, PoPH is defined as PAH associated with portal hypertension. So far, conventional PoPH was defined as a mean pulmonary artery pressure (mPAP) ≥ 25 mmHg, pulmonary vascular resistance (PVR) > 3 Wood units (WU), and pulmonary arterial wedge pressure (PAWP) ≤ 15 mmHg according to the previous diagnostic criteria, whereas in 2022, the European guideline for pulmonary hypertension revised the hemodynamic definition of pulmonary hypertension in pre-capillary PH by lowering the mPAP to > 20 mmHg and the PVR to > 2 WU. Thus, the purpose of this study is to determine how the diagnosis of PoPH according to the new guideline may change among cirrhotic patients with portal hypertension who underwent hepatic venous catheterization and right heart catheterization that we have previously reported.

Method: One hundred eighty-six patients with liver cirrhosis and portal hypertension were subjected and underwent right heart catheterization in this analysis.

Results: The patients comprised 138 males and 48 females, with a median age of 59 (range, 35–80) years. The etiologies of liver cirrhosis were alcoholic liver disease ($n = 61$), chronic hepatitis B virus infection ($n = 11$), chronic hepatitis C virus infection ($n = 91$), autoimmune hepatitis ($n = 2$), primary biliary cholangitis ($n = 4$), non-alcoholic steatohepatitis ($n = 7$), and others ($n = 10$). The median Child-Pugh score was 8 (range, 5–13) points. The numbers of patients with Child-Pugh class A, B, and C were 53, 92, and 41, respectively. The median mPAP, PVR and PAWP were 12.9 mmHg (range, 6.6–40.8), 0.8 WU (range, 0.1–4.5) and 7.5 mmHg (range, 2.2–15.4) respectively. For both diagnostic criteria, many of the 186 patients were below the cut-off values for both mPAP and PVR, respectively (conventional, $n = 184$; new, $n = 182$). Two (1.1%) patients had conventional PoPH. In addition, two patients that were not diagnosed as PoPH by the conventional diagnostic criteria were included in the PoPH range by the new diagnostic criteria. For each diagnostic criteria, there were no patients that met only one criterion of mPAP and PVR, and were divided into two groups. mPAP and PVR were significantly but weakly correlated ($p = 7.44 \times 10^{-5}$, $r = 0.286$).

Conclusion: With the new diagnostic criteria of PoPH, there were patients that were not diagnosed with PoPH by conventional diagnostic criteria, resulting in an increase in the number of patients diagnosed with PoPH from 1.1% to 2.2% in this cohort. In particular, it is possible that the change in the cut-off value of PVR was particularly important, since patients with a PVR of 2 to 3 WU were newly diagnosed.

SAT-555

Correlation of lymphangiogenesis and inflammation in patients with ACLD

Florian Offensperger¹, Lukas Sturm^{1,2}, Elahe Salimi Alize¹, Patrick Huber¹, Marlene Reincke¹, Maïke Hofmann¹, Robert Thimme¹, Michael Schultheiss^{1,2}, Dominik Bettinger¹. ¹Medical Center University of Freiburg, Department of Medicine II, Freiburg, Germany; ²Berta-Ottenstein-Program, Faculty of Medicine, University of Freiburg, Germany

Email: florian.offensperger@uniklinik-freiburg.de

Background and aims: Lymphangiogenesis plays a major role in fluid homeostasis but its role in the development of ascites is not well studied. There is emerging inflammation during hepatic decompensation, whereas the interaction of lymphangiogenesis and inflammation is poorly understood. Therefore, the aim of our study was to analyze the role of inflammation in the context of lymphangiogenesis in patients with advanced chronic liver disease (ACLD).

Method: Markers of lymphangiogenesis (Vascular endothelial growth factor-D, VEGF-D, and VEGF-C, sVEGF-R3 as main markers of lymphangiogenesis growth factors) and inflammation (IL-6) were analyzed in healthy controls (n=38), patients with compensated ACLD (cACLD, n=27) and in patients with decompensated ACLD (dACLD, n=35) with recurrent ascites. Patients with dACLD were allocated to TIPS implantation and markers of lymphangiogenesis were analyzed before and after TIPS implantation as well as in the portal vein and in peripheral veins.

Results: There was a significant increase in IL-6 along patients with cACLD and dACLD (3.8 vs. 33.3 pg/ml, $p < 0.001$). VEGF-C was significantly lower in patients with ACLD compared to healthy individuals (2825 vs. 1172 pg/ml, $p < 0.001$) and VEGF-R3 was significantly higher in ACLD (165119 vs. 134081 pg/ml, $p < 0.001$). VEGF-D did not differ between patients with ACLD and healthy donors, but was higher in cACLD than in dACLD (985 vs. 381 pg/ml, $p = 0.004$). Further, only VEGF-D showed an increase after compared to before TIPS implantation (467 vs. 381 pg/ml, $p = 0.040$). Importantly, no differences in lymphangiogenesis markers in the portal vein and the peripheral vein were observed. Only moderate correlation was observed between IL-6 and VEGF-C ($r = -0.475$, $p < 0.001$) and VEGF-R3 (0.348, $p < 0.001$).

Conclusion: Inflammation increased in patients with dACLD compared to cACLD. However, there was no concomitant increase in overall lymphangiogenesis. Correlation of lymphangiogenesis and inflammation was only moderate indicating that other co-factors may influence lymphangiogenesis in patients with ACLD.

SAT-556

Current prognosis of gastric variceal bleeding in France: preliminary results from a multicenter prospective cohort of 87 cirrhotic patients

Delphine Weil-Verhoeven^{1,2}, Jean Paul Cervoni¹, Frédéric Oberti³, Alexandre Louvet⁴, Louis D'alteroche⁵, Stéphanie Faure^{6,7}, Marianne Latournerie⁸, Nicolas Carbonell⁹, Caroline Jezequel¹⁰, Claire Billioud¹¹, Faouzi Saliba¹², Charlotte Bouzbib¹³, Florence Tanne¹⁴, Isabelle Ollivier-Hourmand¹⁵, Hiriart Jean-Baptiste¹⁶, Faiza Chermak¹⁷, Sophie-Caroline Sacleux¹², Laure Elkrief⁵, Agnès Rode¹⁸, Gerster Théophile¹⁹, Isabelle Mabile-Archambeaud²⁰, Eric Nguyen Khac²¹, Ludivine Legros¹⁰, Lannes Adrien³, Marie-Angèle Robic²², Patrick Borentain²³, Maxime Desmarests²⁴, Dominique Thabut¹³, Vincent Di Martino^{1,2}, Marika Rudler¹³, Christophe Bureau²². ¹CHU Jean Minjoz, Service d'Hépatologie et Soins Intensifs Digestifs, Besançon, France; ²Université de Franche-Comté, EA 4266, Besançon, France; ³CHU d'Angers, Service d'Hépatogastro-entérologie et oncologie digestive, Angers, France; ⁴CHU de Lille, Service des maladies de l'appareil digestif, Lille, France; ⁵CHU de Tours, Unité Mixte d'Urgence d'Hépatogastro-entérologie, Tours, France; ⁶CHU Saint-Eloi, Service d'hépatologie-gastroentérologie, Montpellier, France; ⁷CHU Saint Eloi Montpellier, Liver Unit, Montpellier, France; ⁸CHU François Mitterrand, Hépatogastroentérologie et cancérologie digestive, Dijon, France; ⁹AP-HP, Hôpital Saint-Antoine, Gastro-entérologie Et Hépatologie, Paris, France; ¹⁰CHU de Rennes, Service d'Hépatologie, Rennes, France; ¹¹CHU Croix Rousse, Service d'hépatogastroentérologie, Lyon, France; ¹²AP-HP Hôpital Paul-Brousse, Centre Hépatobiliaire, Villejuif, France; ¹³Groupe Hospitalier Pitié-Salpêtrière, Service d'Hépatogastro-Entérologie, Paris, France; ¹⁴CHRU de Brest, Service d'hépatologie-gastroentérologie, Brest, France; ¹⁵CHU de Caen, Service d'hépatologie-gastroentérologie, Caen, France; ¹⁶CHU de Bordeaux, Service d'Hépatogastro-entérologie et oncologie digestive, Bordeaux, France; ¹⁷Centre Hospitalier Universitaire de Bordeaux, Service d'hépatogastroentérologie, Bordeaux, France; ¹⁸CHU Croix Rousse, Service d'imagerie médicale, Lyon, France; ¹⁹CHU Grenoble Alpes, Service d'Hépatogastroentérologie, Pôle Digidune, La Tronche, France; ²⁰CHU Hôtel Dieu, Institut des Maladies de l'Appareil Digestif, Nantes, France; ²¹CHU d'Amiens, Service d'hépatogastroentérologie, Amiens, France; ²²CHU de Toulouse, Service d'Hépatologie, Toulouse, France; ²³AP-HM, Hôpital de La Timone, Service d'Hépatologie, Marseille, France; ²⁴CHU Jean Minjoz, uMETH, Centre d'investigation Clinique 1431, Besançon, France

Email: dweil@chu-besancon.fr

Background and aims: Gastric variceal bleeding (GVB) accounts for 10% of portal hypertension related bleedings. Its prognosis is poorer than that of esophageal variceal bleeding, with 1-year mortality up to 43%. This analysis aimed to evaluate the prognosis of GVB in the Transjugular Intrahepatic Portosystemic Shunt (TIPS) era.

Method: We analyzed some preliminary data from an ongoing randomized controlled trial (NCT03705078) that aims to determine the relevance of preemptive TIPS in the management of GVB. Consecutive cirrhotic patients admitted for GVB in 18 university hospitals between 2019 and 2022 were randomized after a first glue obliteration (GO) into a group receiving preemptive TIPS (pTIPS) and another group treated by iterative GO. The primary end point was 1-year survival without rebleeding. The secondary objectives were to analyze the factors associated with GVB and to determine the survival at day 42 (D42) and at 1 year. Analyses were performed using univariate and multivariate Cox models.

Results: 87 cirrhotic patients were followed up to 1 year after GVB. Among them, 84% had alcoholic cirrhosis, 80% were male, with a mean age of 59 years. Cirrhosis was decompensated in 81% of patients (Child-Pugh score B/C). The median MELD score was 14; 5% of patients had hepatocellular carcinoma. Type 2 gastroesophageal varices were the most frequent source of bleeding (55%) followed by type 1 isolated gastric varices (IGV, 52%), and type 2 IGV (1%). Concomitant esophageal varices were present in 51% of cases; band ligation was performed simultaneously with GO in 19% of patients. A complication of the initial GO was observed in 17% of the procedures, including 9% of per procedure bleeding and 7% of glue migration. A total of 41 patients received a TIPS within 72 hours after the initial GO. The overall survival and the survival without rebleeding in the whole cohort were respectively 94% and 86% at D42 and 84% and 65% at 1 year. In univariate analysis, death or rebleeding at 1 year was associated with the MELD score (HR = 1.12; CI95%: 1.03–1.23, $p = 0.01$) and the Maddrey score (HR = 1.04; CI95%: 1.00–1.07, $p = 0.005$) calculated on admission, and with an active bleeding at the time of initial GO (HR = 4.05; CI95%: 1.63–10.1, $p = 0.003$). In multivariate analysis, only the MELD score was associated with death or recurrent bleeding at 1 year (HR = 1.12; CI95%: 1.03–1.23, $p = 0.01$).

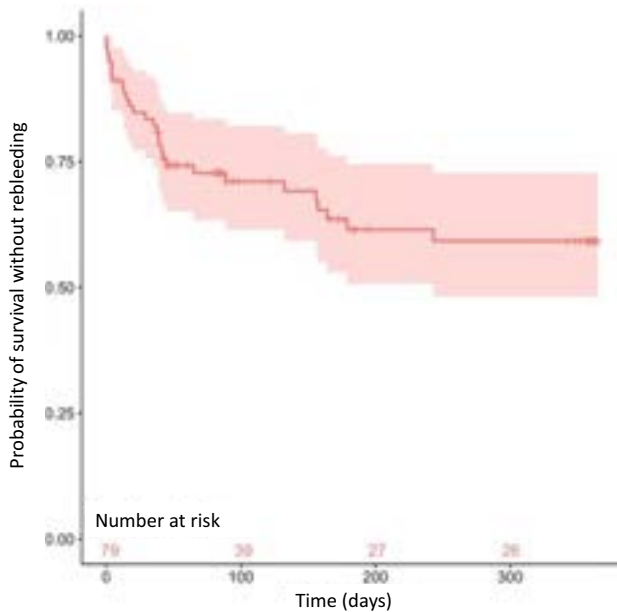


Figure: 1-year survival without rebleeding

Conclusion: The prognosis of GVB treated in expert centers in France between 2019 and 2022 appears to be better than that reported in the literature. The impact of pTIPS on this prognosis will be assessed through the final analysis of the RCT.

SAT-557

MELD 3.0 score in prediction of varices and comparison with its previous versions in patients undergoing esophago-gastro-duodenoscopy for variceal screening or band ligation

Bader Faiyaz Zuberi¹, Faiza Sadaqat Ali¹, Amanullah Abbasi¹, Tazeen Rasheed¹. ¹Dow University of Health Sciences, Medicine/ Gastroenterology, Pakistan
Email: faiza.sadaqat@duhs.edu.pk

Background and aims: For assessing and predicting complications of chronic liver disease, different prognostic scores have been formulated. In a recent validation study MELD 3.0, incorporating serum Albumin (Alb) and female gender, correctly making 8.8% subjects to a higher tier to be eligible for liver transplant especially in women, and lower waiting list deaths in comparison with MELDNa.⁴ Although the importance of MELD 3.0 is validated in liver organ transplant allocation, its use for predicting variceal bleed is not yet studied. Aims of this study are to estimate value of MELD 3.0 for predicting small and large varices using AUROC. To compare MELD, MELD Na and MELD 3.0 score values with presence of varices in patients undergoing variceal screening or band ligation.

Method: Cross-sectional ongoing study and is being conducted in Gastroenterology ward and endoscopy unit of Civil hospital Karachi and OMI Hospital, from August 2022 till Jan 2023 on 74 patients of either gender of age between 18 and 60 years undergoing screening endoscopy. Patients with severe cardio-respiratory or psychiatric disease, splenic or portal vein thrombosis, hepatocellular carcinoma, primary biliary cirrhosis, INR ≥ 5 were excluded from study. Online free calculator was used for calculation of all three scores.⁵ Normal distribution of quantitative variables was checked by Kolmogorov-Smirnov (KS) test and value of ≤ 0.05 determined that variable is not normally distributed. Frequencies of qualitative variables were compared by χ^2 test. Means \pm SD of quantitative variables was compared by Student's t-test or ANOVA. AUROC plots were generated for all MELD variants for presence of both small and large varices separately. Sub-group analysis for gender and stage of varices was also done.

Results: Out of Seventy-four patients, 42 (56.8%) were males and 32 (43.2%) were females. Mean age for males was 45.19 ± 9.70 and that for females was 48.19 ± 17.74 years, without statistically significant difference. Significant differences among gender were found between serum sodium levels and MELD Na scores. Varices were found in 66 out of 74 patients as 22 (29.7%) as Small, 42 (56.8%) Large and 2 (2.7%) Gastric varix. Presence of varices correlated positively and significantly with all three MELD score variants with p values of $< .001$. ROC curves were plotted for all three variants of MELD for absence of varices, small varices and large varices. AUC were also calculated for all three variants and options. MELD and MELD Na performed slightly better than MELD 3.0 in prediction of absence of varices with all having significantly high AUCs. For prediction of small varices MELD Na performed the best while simple MELD was non-significant. For prediction of large varices MELD Na performed the best. Details are given in Table 1. ROC Curves are plotted in Figure 1

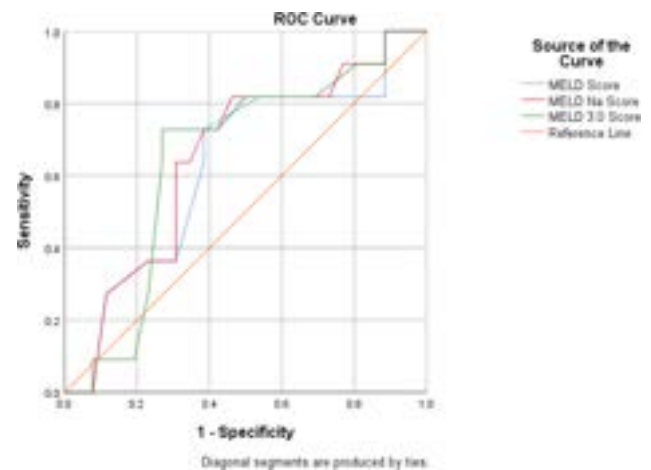


Figure: 1

Table 1: Area under Curve and their significance of MELD variants

Variables	Varices Absent		Small Varices		Large Varices	
	AUC	Sig.	AUC	Sig.	AUC	Sig.
MELD Score	.875	.001*	.626	.089	.704	.003*
MELD Na Score	.875	.001*	.652	.040*	.726	.001*
MELD 3.0 Score	.871	.001*	.649	.044*	.722	.001*

*. Significant values ≤ 0.05
AUC: Area Under Curve

Conclusion: MELD and MELD Na performed slightly better than MELD 3.0 in prediction of presence of all types of varices. For prediction of small varices MELD Na performed the best while simple MELD was non-significant

SAT-558

Study the effect of serum YKL-40 as a risk of variceal bleeding in Egyptian cirrhotic patients

Abdelfattah Hanno¹, Mohamed Ahmed², Reham Aboelwafa³, Essam Bedewy², Aly Elkady². ¹Alexandria University, Tropical Medicine, Alexandria, Egypt; ²Alexandria University, Tropical Medicine, Alexandria, Egypt; ³Alexandria University, Clinical and chemical pathology, Alexandria, Egypt
Email: dr_afhanno@yahoo.com

Background and aims: Chronic liver disorders are mostly resulted from HCV infection globally. Esophageal and gastric varices are common in cirrhotic patients due to concomitant portal hypertension. Variceal hemorrhage is a major decompensating event with high morbidity and mortality. The YKL-40 protein is classified as an inflammatory protein that is linked to a variety of factors in

POSTER PRESENTATIONS

expressing the severity of hepatic fibrosis, including the hepatic venous pressure gradient. The aim of the work was to assess the value of serum YKL-40 as a risk of variceal bleeding in cirrhotic Egyptian patients.

Method: This prospective controlled research was done on 60 HCV induced liver cirrhosis patients visiting the Tropical Medicine Department at the Main University Hospital in Alexandria. Participants were divided into two groups. Group I consisted of thirty patients having grade I, II oesophageal varices (bleeder and non-bleeder). Group II included thirty patients with grade III, IV oesophageal varices (bleeder and non-bleeder). Moreover, all participants in groups I and II had post-viral liver cirrhosis. All were due to chronic HCV infection and all of them received treatment for HCV and had a negative Polymerase Chain Reaction for HCV. Serum YKL-40 was measured by ELISA. Patients with sepsis, other causes of liver cirrhosis, portal vein thrombosis, diabetes mellitus, malignancies, acute liver failure and rheumatoid arthritis were excluded from the study.

Results: Table 1 showed that serum YKL-40 was statistically significantly higher in patients who suffered from bleeding varices in group I and II ($p = 0.028^*$) and ($p = 0.010^*$) respectively. Also serum YKL-40 was able to discriminate bleeder from non bleeder patients in group I at a cut of value of (>102.5 ng/dl) with sensitivity of 76.92% and specificity of 52.94%. Additionally, serum YKL-40 was able to discriminate bleeder from non bleeder patients in group II at a cut of value of (>160.1 ng/dl) with sensitivity of 75.0% and specificity of 57.14%. Moreover, a positive correlation between serum YKL-40 and spleen size in patients who suffered from bleeding varices in both groups was found, however there was a negative correlation between serum YKL-40 and platelets count in bleeder patients also in both groups.

	Group I (n = 30)		Group II (n = 30)	
	Non bleeder (n = 17)	Bleeder (n = 13)	Non bleeder (n = 14)	Bleeder (n = 16)
Serum YKL-40				
Min.-Max.	74.0–118.7	85.40–135.2	97.50–180.4	109.1–189.4
Mean \pm SD.	99.51 \pm 14.88	115.7 \pm 16.35	140.2 \pm 35.27	166.2 \pm 25.33
Median (IQR)	102.5 (88.1–112.4)	114.5 (104.9–133.8)	158.5 (101.4–170.7)	175.9 (150.1–185)
U (p)	U = 58.00*, ($p = 0.028^*$)		U = 51.00*, ($p = 0.010^*$)	

IQR: Inter quartile range; SD: Standard deviation; U: Mann Whitney test
p: p value for comparing between Non bleeder and Bleeder

*: Statistically significant at $p \leq 0.05$

Conclusion: serum YKL-40 would be useful in prediction of esophageal varices bleeding risk in cirrhotic patients

SAT-559

Progression of portal hypertension in PBC: doppler ultrasound velocity as a non-invasive assessment

Aiymkul Ashimkhanova^{1,2}, Damesh Orazbayeva³, Aibar Agynbay⁴, Marzhan Zhanasbayeva⁴, Kulpash Kaliaskarova^{2,4}, Gaukhar Kurmanova¹, Nataliya Satlikova⁵, Irina Ten⁶, Raima Kapiyeva⁷. ¹Al-Farabi Kazakh National University, School of Medicine and Health, Almaty, Kazakhstan; ²GastroHepatoTransplant Group, Astana, Kazakhstan; ³National Research Oncology Center, Radiology, Astana, Kazakhstan; ⁴National Research Oncology Center, Oncohepatology and Gastroenterology, Astana, Kazakhstan; ⁵UMC, Republican Diagnostic Center, Department of Internal Medicine, Astana, Kazakhstan; ⁶UMC, National Research Center for Maternal and Child Health, Interventional Radiology, Astana, Kazakhstan; ⁷MEDICAL CENTRE HOSPITAL OF PRESIDENT'S AFFAIRS ADMINISTRATION OF THE REPUBLIC OF KAZAKHSTAN, Radiology, Astana, Kazakhstan
Email: ashimkhanova.a@kaznu.kz

Background and aims: Primary biliary cholangitis is one of the most common autoimmune diseases worldwide with a female prevalence after age of 45–50's. The natural history of the development of portal hypertension in PBC patients is still not well known. Doppler ultrasound can be routinely used modality to assess non-invasively portal venous system with the additional advantage of determining velocity and flow direction. It has been observed during routine clinical practice that signs of portal hypertension by Doppler ultrasound in Primary biliary cholangitis patients occur faster before the synthetic dysfunction of the liver can be observed or the progression into cirrhosis is established. In order to assess this hypothesis, we decided to analyse the role of ultrasound Doppler characteristics in 23 patients with confirmed diagnosis of primary biliary cholangitis.

Method: Patients admitted from 2018 to 2020 at National Research Oncology Center, Liver Unit were retrospectively analyzed. The chief specialist was a single person assessing the Doppler measurements to keep the validity of the results. Criteria of diagnosis for primary biliary cholangitis: positive AMA- M2 antibodies, Liver histology signs and ALP/GGT elevation together with bilirubinemia and transaminasemia

Results: Out of 23 patients, female to male ratio was 21:2, AMA-M2 negative, but gp210 and sp100 antibodies positive patients were observed in 6 female patients with confirmatory features of bile duct inflammation and concurrent ALT/AST elevation. Among them there were 3 patients with an Overlap syndrome with IgG increase more than 20 g/L and gamma globulin fraction of more than 20% together with AMA-M2 high titers, and increase of ALT/AST more than 300 IU/ml. Mean age for the onset of disease was 47 ± 8.98 years, mean ALP of $475. \pm 289.92$ IU/ml, GGTp mean was 315 ± 228.49 IU/ml, mean cholesterol was 6.7 mmol/l ± 2.67 mmol/L, total bilirubin of 33.51 ± 35.17 mcmmol/L, direct bilirubin of 26.11 sd ± 32.29 mcmmol/L. Ultrasound Doppler characteristics for this cohort was following: mean portal vein size of 1.14 ± 0.2 cm, mean velocity was 21 ± 12.87 cm, V.lialalis diameter mean of 0.8 ± 0.28 cm, with a velocity of 21.31 ± 7.9 cm, the diameter of hepatic artery propria was 0.42 ± 0.06 cm, with a mean velocity of 98.57 ± 25.28 cm, mean IR of 0.67 ± 0.05 , splenic artery diameter of 0.56 cm ± 0.1 , with an increased velocity of 125 ± 31.5 cm, IR 0.64 ± 0.07 , the averaged area of the spleen was calculated to be 66.94 cm² ± 37.15 and with the following platelet average of 229×10^9 /L ± 93 , WBC average 5.31×10^9 /L ± 1.34 and a mean hemoglobin of 112 g/L ± 27 . Other synthetic function tests measured by total protein (mean = 75.68), albumin (mean = 36.93), fibrinogen (mean = 2.97), INR (mean = 1.07) were not affected despite high inflammatory signs within the liver parenchyma.

Conclusion: According to the results of the Doppler measurements of portal system among patients with confirmed primary biliary cholangitis, there is a tendency in increasing velocity of splenic artery as a first sign of portal hypertension progression in patients without confirmed cirrhosis, Ishak fibrosis stage 3/6. Another finding is the splenomegaly which appears also earlier. Baveno-VII classification stratification might not be ideal for PBC patients, and Portal pressure gradient measurement needs to be applied to stratify these category of patients for future interventions.

SAT-560

Clinical features and analysis of serum BMP9 levels in patients with portal pulmonary hypertension

Ruihua Zhang^{1,2}, Tengfei Li¹, Yu Tian², Xiaoyu Wen¹. ¹First Hospital of Jilin University, Department of Hepatology, China; ²First Hospital of Jilin University, Center of Infectious Diseases and Pathogen Biology, China
Email: 15804301609@163.com

Background and aims: Portal pulmonary hypertension (POPH) is a serious complication of portal hypertension with low morbidity and high mortality. Bone morphogenetic protein 9 (BMP9), a member of the bone morphogenetic protein family, can protect endothelial integrity and maintain vascular homeostasis. It has been reported

Fibrosis Stellate cell biology

WEDNESDAY 21 TO SATURDAY 24 JUNE

TOP-036

Liver cell-type specific molecular signatures marking transition from advanced fibrosis to cirrhosis in human non-alcoholic steatohepatitis

Martin Rønn Madsen¹, Mathias Møllerhøj¹, Mikkel Werge², Mikkel Christensen-Dalsgaard¹, Sanne Veidal³, Lise Rudkjær¹, Elisabeth Galsgaard³, Lise Lotte Gluud², Henrik B. Hansen¹. ¹Gubra, Hørsholm, Denmark; ²Hvidovre Hospital, Hvidovre, Denmark; ³Novo Nordisk A/S-site Måløv, Måløv, Denmark
Email: mam@gubra.dk

Background and aims: Hepatic fibrosis is the strongest predictor of morbidity and mortality in non-alcoholic steatohepatitis (NASH), establishing fibrosis as a critical therapeutic target in this disease. To improve treatment outcomes in NASH, the specific roles and molecular signaling mechanisms of hepatic cell types in the progression of fibrosis must be clarified. Here, we developed a transcriptomic map at cellular resolution, defining molecular signatures of parenchymal and non-parenchymal cell types across all stages of fibrosis in human NASH.

Method: Bulk RNA sequencing (RNAseq) was performed on snap-frozen liver biopsies obtained from a patient cohort of 40 obese individuals with NASH (stages F0-F4, n = 4–10 per fibrosis stage) or no/mild NAFLD (macrovesicular steatosis) without fibrosis (control group, n = 7). Paired single-nucleus (sn) RNAseq analysis was performed on a subset of biopsies (control, NASH F0-1, NASH F2-3, NASH F4; n = 4 per group). Cell type deconvolution of differentially expressed genes in bulk RNAseq samples was based on corresponding snRNAseq data.

Results: The transcriptomics platform enabled for paired bulk and single-nucleus (sn) RNAseq analysis on small percutaneous/transjugular human liver biopsies (≤5 mg tissue). The number of differentially expressed genes increased progressively with disease severity. Transcriptome signatures were clearly separated from NASH patients with cirrhosis (fibrosis stage 4), demonstrating perturbations in genes associated with extracellular matrix remodeling and the immune system. Bulk RNAseq data were cross-referenced to public bulk RNAseq data sets for further data validation. snRNAseq yielded data from 33,764 nuclei after quality control, recovering all major liver cell types in both control and disease samples based on cell-specific marker genes. Subclustering of snRNAseq datasets revealed multiple subtypes of hepatic stellate cells (HSCs) relevant in the progression of fibrosis.

Conclusion: We report a state-of-the-art integrative transcriptomics pipeline mapping molecular changes in liver non-parenchymal cell types covering the entire spectrum of fibrosis in NASH patients. Distinct HSC subpopulations and transcriptional programs may play important roles in the transition from advanced fibrosis to cirrhosis in human NASH.

that the BMP9 signaling pathway is involved in the pathogenesis of pulmonary arterial hypertension, and POPH is a sub-group of pulmonary arterial hypertension (PAH). While, it is unclear whether BMP9 is involved in the pathogenesis of POPH. The aim of this study is to collect the clinical data of POPH patients, and to compare the expression levels of BMP9 in POPH and other different forms of PAH.

Method: From January 2018 to July 2022, a total of 3348 patients with liver cirrhosis or portal hypertension were screened underwent Doppler echocardiography in the First Hospital of Jilin University. Finally, 45 patients were considered to have POPH. The clinical data of these patients were collected. Serum samples from 10 patients with POPH, 9 patients with PAH caused by left heart disease, 9 patients with PAH caused by pulmonary disease, and 9 healthy individuals were detected by enzyme-linked immunosorbent assay (ELISA) to detect BMP9 levels.

Results: 1) The prevalence rate of POPH in patients with portal hypertension or liver cirrhosis was rare (1.34%). The basic information of 45 POPH patients selected were listed here, the average age was 60.29 ± 12.10 years old, 40% were female, hemoglobin: 95.96 ± 29.67 g/L, platelet: 83.96 ± 51.67 × 10⁹/L, albumin: 28.50 ± 5.66 g/L, creatinine: 91.28 ± 69.34 μmol/L, prothrombin time: 17.46 ± 5.83 s, partial pressure of CO₂: 31.31 ± 4.51 mmHg, the most common cause of cirrhosis was alcohol, and the most common complication of cirrhosis patients was gastrointestinal bleeding. 2) The expression levels of BMP9 in each group were detected, and the results were as follows: POPH group: 2.345 ± 0 pg/ml (compared with 17.6 ± 8.1 pg/ml in healthy group, p < 0.0001); PAH caused by left heart disease: 14.9 ± 5.7 pg/ml (compared with 2.345 ± 0 pg/ml in POPH group, p = 0.0002); PAH caused by pulmonary disease: 12.6 ± 7.0 pg/ml (compared with 2.345 ± 0 pg/ml in POPH group, p < 0.0001); Healthy control group: 17.6 ± 8.1 pg/ml.

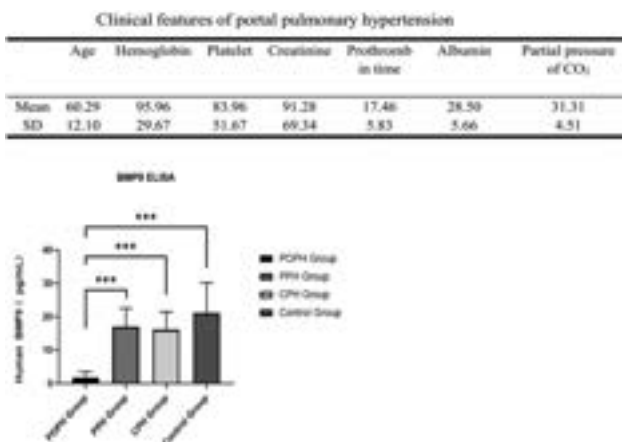


Figure:

Conclusion: 1) Compared with healthy control group, BMP9 in POPH patients was significantly decreased, and the decrease in BMP9 was considered to be related to the pathogenesis of POPH. 2) Compared with patients with PAH caused by left heart disease or by pulmonary disease, BMP9 in POPH group was significantly decreased. Thus, the application of BMP9 is helpful to distinguish POPH from PAH caused by common clinical cardiopulmonary diseases.

TOP-037

Does sex influence the development of sarcopenia in liver fibrosis?

Katia Sayaf¹, Ilaria Zanotto², Daniela Gabbia², Gaia Gherardi³, Rosario Rizzuto³, Sara De Martin², Francesco Paolo Russo¹. ¹University of Padova, Department of surgery, oncology and gastroenterology, Italy;

²University of Padova, Department of pharmaceutical and pharmacological sciences, Italy; ³University of Padova, Department of biomedical sciences, Italy

Email: francescopaolo.russo@unipd.it

Background and aims: Sarcopenia is a debilitating condition affecting 60–70% of patients with liver disease. Interestingly, the incidence of sarcopenia shows sex dimorphisms. In this condition, muscle atrophy is linked to a progressive loss of skeletal muscle function and strength, and correlated to an increased mortality. However, the mechanisms underlying liver-associated sarcopenia, and the role of sex in its development are still poorly understood. In this study, we investigated sex dimorphism in the development and resolution of sarcopenia in a murine model of liver fibrosis and regeneration.

Method: Progressive stages of liver fibrosis were induced in female and male mice by injecting increasing doses of carbon tetrachloride (CCl₄, from 0.17 to 0.72 ml/Kg*bw) for 12 weeks. At the end of the treatment, an 8-week washout period was set to allow liver regeneration. Muscle function and strength were evaluated by the grid hanging and the grip strength test. Mice were sacrificed after 6 and 12 weeks of CCl₄-treatment, and after the washout period. Masson's trichrome stain was used to assess liver fibrosis, while hematoxylin and eosin staining was used to calculate the cross-sectional area (CSA) of muscle quadriceps fibers. Muscle pAkt and p4EBP1 protein expression was assessed by western blot, and mRNA expression of *Musa*, *Atrogin-1*, *Murf-1*, and *Snip3* by qRT-PCR. Plasma levels of TNF were measured by means of multiplexed bead-based immunoassay.

Results: After 6 and 12 weeks of CCl₄-treatment, mice developed a progressive liver fibrosis that was associated to a significant loss of muscle force in both sexes, as demonstrated by the poor performances on the grid hanging and the grip strength test ($p < 0.05$), and by the reduced CSA of quadriceps fibers ($p < 0.001$). pAkt and p4EBP1 levels, promoters of muscle protein synthesis, were not affected by fibrosis development. However, atrophy-related ubiquitin ligases (*Musa*, *Atrogin-1*, *Murf-1*, and *Snip3*), responsible for the breakdown of muscle proteins, were significantly upregulated in fibrotic mice with respect to controls, especially in females ($p < 0.05$). Plasma levels of TNF, responsible for the hepatic-induced muscle damage, were higher in fibrotic mice than in controls. After the washout period, males recovered their physical force and CSA, although liver fibrosis was still present, whereas females were characterized by an amelioration of liver histology and a decrease in the plasma levels of TNF, which was not accompanied by a recovery of muscle function.

Conclusion: CLD-associated sarcopenia is due to an increase of muscle protein degradation, more evident in females, whereas muscle protein synthesis is not affected by liver fibrosis in both sexes. Furthermore, the severity of sarcopenia is not correlated to the severity of liver fibrosis.

WEDNESDAY 21 JUNE

WED-215

Dual alpha-v/beta-6 and alpha-v/beta-1 integrin inhibitor bexotegast attenuates profibrogenic gene expression of myofibroblasts in human liver explant tissue with biliary fibrosis

Steve Ho¹, Chris Her¹, Richard Ahn¹, Vikram Rao¹, Jessie Lau¹, Mahru An¹, Scott Turner¹, Martin Decaris¹, Johanna Schaub¹. ¹Pliant Therapeutics, United States

Email: jschaub@pliantrx.com

Background and aims: Bexotegast (PLN-74809), a dual inhibitor of TGF-beta-activating integrins alpha-v/beta-6 and alpha-v/beta-1 currently in clinical development for the treatment of primary sclerosing cholangitis (PSC), has previously been shown to reduce fibrosis in the MDR2^{-/-} mouse model of biliary fibrosis. To examine the effects of bexotegast on individual cell populations in the fibrotic human liver, we combined the precision cut liver slice (PCLivS) platform, a physiologically relevant ex vivo model system, with 10x single nuclei RNA sequencing (snRNA-Seq) to characterize the response of unique cell populations in fibrotic PSC and primary biliary cholangitis (PBC) PCLivS to bexotegast.

Method: Liver explants were collected from patients with PSC ($n = 3$) and PBC ($n = 1$) at the time of transplant. PCLivS were generated and cultured for 2 days in the presence of bexotegast or vehicle (DMSO). A TGF-beta receptor 1 kinase inhibitor (ALK5i; R-268712) was also evaluated as a control. Single nuclei were isolated from two pooled slices per treatment and processed for single nuclear barcoding using 10x Chromium Next GEM 3' HT kits. Resulting libraries were sequenced, processed using Cell Ranger, and analyzed using Seurat. Custom annotation of cell types was performed using gene markers established from recently published data sets. Differential gene expression was determined using a non-parametric Wilcoxon rank sum test. Pathway enrichment analysis was performed with Enrichr.

Results: snRNA-Seq analysis of human PCLivS identified unique cell populations, including cholangiocytes, mesenchymal cells, hepatocytes, endothelial cells, and leukocytes. Within the overall mesenchymal cell population, we observed clusters of RGS5-high cells and PDGFRA-high cells, identified as hepatic stellate cells (HSCs) and myofibroblasts, respectively, with the latter myofibroblast cluster having the highest level of type 1 collagen (*COL1A1*) expression. Differential gene expression analysis comparing bexotegast or ALK5i treatment to vehicle showed significant reductions in type I collagen (*COL1A1*) expression in myofibroblasts (FDR < 0.05), with bexotegast approximately 80% as effective as ALK5i. Gene expression pathways most downregulated by bexotegast in myofibroblasts were "collagen fibril organization" (GO:0030199) and "extracellular matrix organization" (GO:0030198), driven by reduced expression of genes such as *COL7A1*, *BGN*, and *FBLN1*.

Conclusion: Treatment of human PCLivS with biliary fibrosis with dual alpha-v/beta-6 and alpha-v/beta-1 integrin inhibitor bexotegast resulted in clear reductions in profibrogenic gene expression within myofibroblasts. The similar degree of effect of bexotegast compared to ALK5i demonstrates the importance of the integrin-TGF-beta activation pathway in fibrotic biliary disease. These data demonstrate the utility of combining single nuclei transcriptomics with fibrotic human PCLivS to evaluate the mechanism of action of novel anti-fibrotic therapies.

WED-216

TLC-3595, a selective acetyl-CoA carboxylase 2 (ACC2) inhibitor, improves steatosis and fibrosis in murine models of NASH via pleiotropic mechanisms

Archana Vijayakumar¹, Eisuke Murakami¹, Ryan Huss¹, Natalie Sroda¹, Atsuyuki Shimazaki², Ippei Morita², Hideaki Kato², Manami Nakai², Naoki Ohyabu², Mani Subramanian¹, Robert Myers¹. ¹OrsoBio, Inc, Palo Alto, United States; ²Shinogi and Co. Ltd., Osaka, Japan
Email: archana@orsobio.com

Background and aims: TLC-3595 is a potent ($IC_{50} = 14$ nM), systemically distributed, allosteric inhibitor of acetyl-CoA carboxylase 2 (ACC2i) that is 76-fold selective over ACC1. By increasing fatty acid oxidation, TLC-3595 has potential for the treatment of metabolic diseases including type 2 diabetes and NASH. Here, we report the pleiotropic benefits of TLC-3595 *in vitro* and in murine models of NASH and fibrosis.

Method: Hepatocyte (HepG2 and H4IIE), hepatic stellate (LX2), or adipocyte (3T3L1) cell lines were treated with TLC-3595 (or a tool compound) for 24–72 hours *in vitro*. High-fat diet (HFD)-fed, diet-induced obese (DIO) mice, Fatty Liver Shionogi-Lep^{ob}/Lep^{ob} (FLS-ob/ob) mice, or choline-deficient, L-amino acid-defined HFD (CDAHFD)-fed mice were treated with TLC-3595 (5–60 mg/kg BID) or the nonselective, liver-targeted ACC inhibitor firsocostat (FIR, 0.5–1.5 mg/kg BID) for 4–8 weeks. Liver fibrosis was quantified based on picosirius red-positive (PSR⁺) area and hepatic hydroxyproline (HYP) content.

Results: *In vitro*, TLC-3595 or a tool ACC2i dose-dependently reduced apoptosis (27% lower caspase 3/7 activity) and gluconeogenesis (39%) in hepatocytes, decreased procollagen 1 secretion (20%) in LX2 cells, and increased adiponectin in the supernatant (25%) and decreased lipid droplet size (40%) in differentiated adipocytes. In FLS-ob/ob mice, TLC-3595 treatment for 4 weeks increased plasma adiponectin (51%; $p < 0.0001$) (Fig. A). Additionally, TLC-3595 increased *Fgf21* mRNA expression (4 to 15-fold) in skeletal muscle and intact FGF21 levels (1.5-fold) in plasma of FLS-ob/ob mice after a single or repeat doses (10 days to 4 weeks). These changes were associated with significant reductions in liver HYP (58%) and PSR⁺ area (38%) in FLS-ob/ob mice after 4 weeks of TLC-3595 treatment. In the CDAHFD mouse model, TLC 3595 treatment for 8 weeks significantly reduced liver triglyceride (TG; 20%), hepatic PSR⁺ area (28%, Fig. B), and HYP content (36%) vs. vehicle. In contrast, FIR did not increase plasma adiponectin in FLS-ob/ob mice (Fig. A) but caused greater liver TG reduction (31%) without impacting hepatic PSR⁺ area (Fig. B) or HYP in CDAHFD mice. Lastly, in DIO mice, TLC-3595 reduced liver TG by 35% ($p < 0.05$) without effects on plasma TG, unlike FIR, which decreased liver TG by 66% while increasing plasma TG by 168% after 4 weeks of treatment (Fig. C–D).

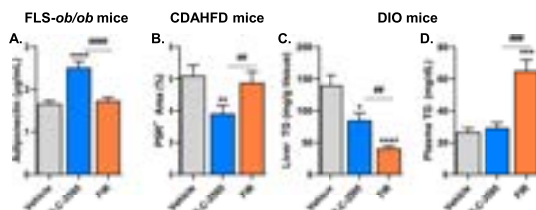


Figure A. Plasma adiponectin levels in FLS-ob/ob mice. **B.** Fibrosis assessed by hepatic PSR⁺ area in CDAHFD-fed mice. **C.** Liver and plasma TG levels in DIO mice treated with vehicle, TLC-3595 (5–45 mg/kg BID) or firsocostat (FIR, 0.5–1.5 mg/kg BID) for 4–8 weeks. * $p < 0.05$, ** $p < 0.01$, *** $p < 0.001$, **** $p < 0.0001$ vs. vehicle; * $p < 0.05$, ** $p < 0.01$, *** $p < 0.001$, **** $p < 0.0001$ vs. FIR.

Figure:

Conclusion: TLC-3595 has beneficial effects on steatosis and fibrosis in NASH via multiple mechanisms, including direct effects in hepatocytes, hepatic stellate cells, adipocytes, and skeletal muscle, without causing hypertriglyceridemia as seen with nonselective ACC inhibitors. These data support the development of TLC-3595 in patients with NASH.

WED-217

Spatial lipidomics reveal dysregulated sphingolipid metabolism in liver fibrosis

Aleksandra Gruevska¹, Fiona Oakley², Jack Leslie², Derek A Mann², Matthew Hoare³, Zoe Hall¹. ¹Division of Systems Medicine, Imperial College London, London, United Kingdom; ²Newcastle Fibrosis Research Group, University of Newcastle, Newcastle-upon-Tyne, United Kingdom; ³Early Cancer Institute, University of Cambridge, Cambridge, United Kingdom
Email: zoe.hall@imperial.ac.uk

Background and aims: Liver fibrosis (LF) represents a major health problem worldwide due to its increasing prevalence and the lack of effective treatments. Although detailed molecular mechanisms are still unclear, during development of fibrosis, specific lipid pathways are re-wired in the liver and may represent candidate therapeutic targets. This is especially relevant for NASH-induced LF where increased hepatic storage of potentially lipotoxic species occurs. The aim of this study is to uncover the complex metabolic adaptations in LF and identify key lipid markers of hepatic fibrosis.

Method: Animal models of liver fibrosis included western diet + CCl₄, bile duct ligation (BDL) and chronic CCl₄ treatment (all in C57BL/6 male mice). To verify findings in the animal models, background cirrhotic tissue from patients with fatty liver-associated hepatocellular carcinoma (HCC) undergoing liver resection or transplant were analyzed. Lipids were extracted from bulk liver tissue (mice and human) and analysed using liquid chromatography-mass spectrometry (LC-MS) to study metabolic changes. Key lipid-gene transcript correlations were evaluated by performing RNA sequencing on the same set of samples. Pathway analysis and integration of the transcriptomics and lipidomics data was done. Mass spectrometry imaging (MSI) on cryosectioned human liver tissue was used to evaluate the spatial distribution of key altered lipids/metabolites.

Results: RNA sequencing of whole liver samples from mice ($n = 5$ per group) revealed upregulation of glycosphingolipid metabolism in the fibrotic groups compared to their control groups. Differential gene expression showed an increased expression of the enzymes implicated in ceramide production and these results were confirmed using bulk tissue lipidomics, demonstrating higher amounts of hexose ceramides (HexCer) and sphingomyelins (SM) in the three animal models employed relative to control. Specific lipids such as SM (34:1), SM (42:2), HexCer (34:1) and HexCer (42:2) were able to discriminate fibrotic groups from control. In the human samples ($n = 7$), pathway analysis and the integration of the transcriptomics and lipidomics data showed strong positive correlation between SM (34:1) lipid abundance and gene expression for transforming growth factor (TGF) beta 1 and bone morphogenetic protein (BMP) receptor 1—both implicated in pro-fibrotic signalling. In addition, spatial lipidomics by MSI revealed a dramatic increase of SM (34:1) and hexose ceramides in fibrotic regions of human cirrhosis (Figure).

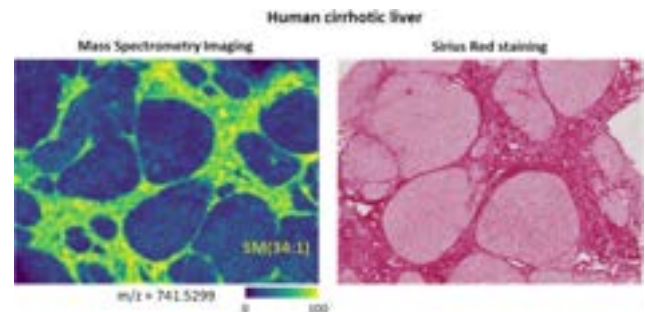


Figure:

Conclusion: Overall, these results have identified several prominent lipid markers for hepatic fibrosis and suggest that altered sphingolipid metabolism is a key process occurring during fibrogenesis.

POSTER PRESENTATIONS

Targeting these metabolic pathways could be a novel strategy to resolve fibrosis.

WED-218

Cyclophilin inhibition exhibits preventive and curative antifibrotic effects via extracellular matrix remodelling

Sara Campinoti^{1,2,3}, Una Rastovic^{1,2,3}, Lai Wei^{1,2}, Nicola Harris^{1,2}, Bruna Almeida^{1,2}, Omolola Ajayi^{1,2}, Caoimhe Kerins⁴, Fiona Kenny², Sandra Phillips^{1,2}, Ane Zamalloa⁵, Rosa Miquel⁵, Yoh Zen⁵, Krishna Menon⁵, Eileen Gentleman⁴, Tanya Shaw², Nigel Heaton⁵, Daren Ure⁶, Shilpa Chokshi^{1,2}, Luca Urbani^{1,2}, Elena Palma^{1,2}. ¹The Roger Williams Institute of Hepatology, Foundation for Liver Research, London, United Kingdom; ²King's College London, Faculty of Life Sciences and Medicine, London, United Kingdom; ³equal contribution, United Kingdom; ⁴King's College London, Centre for Craniofacial and Regenerative Biology, London, United Kingdom; ⁵Institute of Liver Studies, King's College London, London, United Kingdom; ⁶Hepion Pharmaceuticals, Edison, United States
Email: e.palma@researchinliver.org.uk

Background and aims: Fibrosis is caused by persistent liver damage and inflammation and is a central driver for disease progression in chronic liver disease. It is characterised by excessive activation of hepatic stellate cells (HSCs) and altered extracellular matrix (ECM) deposition and remodelling ultimately affecting liver function. Despite enormous research efforts, there are no approved anti-fibrotic drugs. Inhibition of cyclophilins, peptidyl-prolyl isomerases that facilitate protein folding and regulate several biological processes, has been proven beneficial in various disorders, including liver diseases, but the mechanism of action requires further elucidation. Here, we firstly investigate the role of cyclophilins in HSC transdifferentiation, ECM production, composition and 3D organisation and secondly, we tested the efficacy of a pan-cyclophilin inhibitor (rencofilstat) currently in clinical development for NASH, using patient-derived *in vitro* and *ex vivo* models of liver fibrosis.

Method: Patient-matched Precision Cut Liver Slices (PCLS) and primary HSCs were prepared from human liver specimens and exposed to mechanical or chemical insults to induce fibrogenesis, in the presence/absence of 5 μ M rencofilstat together (preventive approach) or after the insults (curative approach). Fibrosis and cell activation in HSCs and PCLS were assessed by gene (RNAseq, Quantigene) and protein expression analysis (proteomics, immunofluorescence), and secretion of fibrotic and inflammatory markers by ELISA/Luminex. ECM deposition upon stimulation was characterised for biochemical composition and fibre orientation in cell-derived matrix (CDM) via immunofluorescence, confocal imaging and proteomics. Stiffness of PCLS upon treatment was assessed by atomic force microscopy (AFM).

Results: Rencofilstat profoundly and consistently reduced expression and secretion of pro-fibrogenic markers in both models, independently of insult and treatment regime. Remarkably, cyclophilin inhibition significantly reduced HSC activation and consequent ECM deposition and induced qualitative and quantitative changes in ECM composition (proteomic analysis on CDM and PCLS). The order of organisation of matrix fibres was affected by rencofilstat resulting in significantly less organised bundles, indicating remodelling towards a less stiff 3D matrix structure, which was in line with the AFM analysis performed on PCLS that showed decreased stiffness upon cyclophilin inhibition.

Conclusion: This study confirms the key role of cyclophilins in liver fibrosis and inflammation in patient-derived 3D and multicellular models revealing the remarkable potential of cyclophilin inhibition as anti-fibrotic therapy in relevant models of human disease. We also provide novel insights regarding rencofilstat's mechanism of action in the remodelling of the ECM in liver fibrosis, demonstrating a direct consequence on tissue stiffness.

WED-219

Hepatic stellate cell-derived extracellular matrix to model aetiology- and patient-specific matrix remodelling and fibrosis progression

Lai Wei^{1,2}, Sara Campinoti^{1,2}, Bruna Almeida^{1,2}, Fiona Kenny³, Rosa Miquel⁴, Tanya Shaw³, Shilpa Chokshi^{1,2}, Luca Urbani^{1,2}. ¹The Roger Williams Institute of Hepatology, United Kingdom; ²King's College London, Faculty of Life Sciences and Medicine, United Kingdom; ³King's College London, Centre for Inflammation Biology and Cancer Immunology, United Kingdom; ⁴King's College Hospital, Institute of Liver Studies, United Kingdom
Email: luca.urbani@researchinliver.org.uk

Background and aims: Liver fibrosis is characterised by aberrant accumulation of extracellular matrix (ECM) secreted by activated hepatic stellate cells (HSCs). Several factors (aetiology, pro-fibrogenic insults, and fibrotic stage) influence the ECM composition, organisation and quantity in fibrosis. However, mechanisms underpinning distinct remodelling processes that affect the ECM biochemical and biophysical properties are elusive, primarily due to the lack of relevant *in vitro* models. Typically, stellate cells are immortalised cells, such as LX-2, and whilst easy to use and unexpensive, they are not patient-specific and the immortalisation process alters their original characteristics. Here, we present the study of the activation potential, metabolic status and specific ECM deposition of patient-derived HSCs as an *in vitro* model to investigate ECM remodelling in chronic liver disease.

Method: Primary human HSCs were isolated from liver tissue collected from patients with different fibrotic stages (METAVIR score): F0 (no fibrosis) to F4 (cirrhosis). Cell activation was induced using different combinations of pro-fibrotic stimuli typically found in non-alcoholic fatty liver disease and steatohepatitis: TGF β , IL-6, free fatty acids, high glucose and insulin. Cell activation towards myofibroblasts was determined by gene and protein expression analysis. The metabolic activity of activated cells was determined with Seahorse real-time cell metabolic analysis. ECM deposited was characterised for biochemical composition and fibre orientation by decellularisation of cell-derived matrix (CDM) followed by immunofluorescence and confocal imaging and compared to standard LX-2.

Results: Human HSCs were successfully isolated and cultured from liver tissue with different METAVIR fibrotic scores. Upon administration of pro-fibrotic stimuli, HSCs showed clear increased gene and protein expression of activation markers (α SMA, SOX9, collagens), increased proliferation, and high deposition of ECM. Matrix deposition showed remarkable differences between LX-2 and primary HSCs, suggesting substantial limitations in the use of the immortalised HSC line. Various combinations of insults and the fibrotic score of the liver tissue of origin generated different levels of cell activation, metabolic activity and ECM deposition with striking differences in both composition and structure, indicating the suitability of our model to mimic patient- and aetiology-specific fibrotic features.

Conclusion: Here we present the potential of personalised patient-derived cells to investigate ECM remodelling in different fibrotic settings. Our study reveals that patient-derived HSCs, but not LX-2 cells, maintain a unique capacity to produce a highly bundled ECM upon induction of fibrosis. In particular, the use of the CDM analysis allows for mechanistic studies in the field of ECM deposition and remodelling upon different stimuli, an aspect often overlooked in fibrotic models. The information on fibrillar quantity and alignment between patients and upon different pro-fibrotic insults provides new crucial information on the molecular mechanisms of ECM deposition in chronic liver disease and could pave the way to the discovery of novel therapeutic strategies.

WED-220

Selective RNF41 restoration in hepatic macrophages from thioacetamide-induced fibrotic mice reduces liver fibrosis and inflammation

Alazne Moreno-Lanceta^{1,2}, Mireia Medrano-Bosch², Yilliam Fundora^{1,3}, Meritxell Perramón^{1,4}, Jessica Aspas³, Marina Parra-Robert⁴, Sheila Baena³, Constantino Fondevila^{1,3}, Elazer Edelman^{5,6}, Wladimiro Jiménez^{1,2,4}, Pedro Melgar-Lesmes^{1,2,5}.
¹Institut d'Investigacions Biomèdiques August Pi-Sunyer (IDIBAPS), Spain; ²Department of Biomedicine, School of Medicine, University of Barcelona, Spain; ³Liver Transplant Unit, Institut Clínic de Malalties Digestives i Metabòliques, Hospital Clínic, Spain; ⁴Biochemistry and Molecular Genetics Service, Hospital Clínic Universitari, Spain; ⁵Institute for Medical Engineering and Science, Massachusetts Institute of Technology, United States; ⁶Cardiovascular Division, Brigham and Women's Hospital, Harvard Medical School, United States
 Email: pmelgar@ub.edu

Background and aims: Macrophages play a crucial role during the progression of chronic liver disease. They actively participate in the response to liver damage and in the balance between fibrogenesis and regression. Indeed, macrophage activation is a prognostic of survival in patients with liver cirrhosis. RNF41 E3 ubiquitin ligase has been associated to negative regulation of pro-inflammatory signals and M2 macrophage polarization in muscle injury, but its role in liver fibrosis remains unclear.

Method: RNF41 expression was quantified using real-time PCR in CD11b+ macrophages isolated from the liver of cirrhotic (n = 12) and healthy subjects (n = 8), and from fibrotic (n = 6) and healthy mice (n = 6). Fibrosis was induced in mice with i.p. injections of thioacetamide (200 mg/Kg) twice a week for 9 weeks. Macrophage selective RNF41 induction was achieved with i.v. (50 µg/Kg) injection of dendrimer-graphite nanoparticles delivering a plasmid encoding RNF41 (RNF41-DGNP) or control scrambled plasmid every 3 days for 9 days (n = 12). The therapeutic effect of RNF41 restoration on fibrosis, liver function, and inflammation was evaluated via Real-time PCR and histological techniques.

Results: RNF41 expression was significantly lower in macrophages isolated from the liver of cirrhotic patients regardless of cirrhosis aetiology (1.1 ± 0.2 vs 0.3 ± 0.1 , fold change (fc), $p < 0.001$), and from the liver of fibrotic mice (1.0 ± 0.1 vs 0.5 ± 0.1 fc, $p < 0.001$). Selective restoration of macrophage RNF41 in fibrotic mice using RNF41-DGNP promoted remarkable hepatic repair with 56% reduction in liver fibrosis area, and recovery of parenchymal structure. In concert, macrophage RNF41 restoration reduced the hepatic expression of pro-inflammatory genes and increased the expression of anti-inflammatory genes, denoting a beneficial macrophage switch on liver fibrosis. These anti-fibrotic and anti-inflammatory effects translated into a significant reduction in liver injury (AST: 592.6 ± 93.9 vs. 243 ± 46.15 U/L, $p < 0.01$; ALT: 182.7 ± 22.54 vs. 91.09 ± 12.51 U/L, $p < 0.01$). RNF41-DGNP therapy similarly orchestrated fibrosis regression at cellular level with reduced hepatic stellate cell activation, highlighted by a decrease in the hepatic expression of collagen-I (1.0 ± 0.1 vs. 0.5 ± 0.1 fc, $p < 0.001$), alpha-SMA (1.0 ± 0.1 vs. 0.6 ± 0.1 fc, $p < 0.001$) and TIMP-1 (1.0 ± 0.1 vs. 0.5 ± 0.1 fc, $p < 0.001$). These effects were attributed to a reduction in the hepatic expression of macrophage pro-fibrogenic factors (TGF-beta, PDGFB, and OSM). RNF41-DGNP also promoted an increase in the expression of the collagenase MMP-9, suggesting an active participation of macrophage RNF41 on extracellular matrix remodelling.

Conclusion: RNF41 plays a major role in the regulation of macrophages in hepatic inflammation and fibrosis. This study highlights the potential of macrophage RNF41 as a novel therapeutic target for patients with cirrhosis.

WED-221

Therapeutic effect of recombinant human Cytochrome c against mouse liver fibrosis and stellate cell activation via ROS scavenger function and activation of JAK-STAT1 pathway

Norifumi Kawada¹, Duc Pham Minh¹, Le Thi Thanh Thuy¹, Hai Hoang¹.
¹Osaka Metropolitan University, Department of Hepatology, Graduate School of Medicine, Japan
 Email: kawadanori@omu.ac.jp

Background and aims: Cytochrome c (CYGB) is a gas-binding hexa-coordinate globin that was originally discovered in the cytoplasm of hepatic stellate cells (HSCs) and has been demonstrated to play a crucial role in maintaining HSCs in a quiescent status. Here we show the promising therapeutic effects of extracellular 6-His tagged recombinant human CYGB (6His-CYGB) against mouse liver fibrosis and activated human HSCs.

Method: Mice with Cygb deficiency or those (TG) with specific overexpression of Cygb in HSCs underwent BDL or CDAA diet-induced liver fibrosis. Synthesized 6His-CYGB was tested for its bio-distribution and function in human HSCs (HHStECs) and for its therapeutic effects against advanced liver fibrosis in mice induced by TAA, CCl₄, or DDC. RNA-Seq, single-cell RNA-Seq and pathway analysis were performed in non-treated or 6His-CYGB-treated HHStECs and liver tissues exposed to CCl₄ or CCl₄/6His-CYGB.

Results: Cygb deficiency or overexpression in mice caused marked deterioration or amelioration of liver inflammation and fibrosis, respectively, in both BDL and CDAA-induced liver injuries. In cultured HHStECs, exogenous 6His-CYGB (~80 µg/ml) was found to be endocytosed and accumulated in endosomes via the clathrin-mediated pathway and gave rise to the attenuated production of reactive oxygen species (ROS), fibrosis-related gene sets including Col 1A1, and alpha-SMA. Besides its ROS-scavenger function, exogenous 6His-CYGB induced interferon (IFN)-gamma secretion by HHStECs via activating TANK-binding kinase 1, resulting in the activation of JAK-STAT1 pathway. Memolotinib, a JAK1/2 inhibitor, canceled these effects of 6His-CYGB. To assess whether these biological functions of 6His-CYGB was created by the heme holding in CYGB's 3D conformation, we replaced the iron center of the heme with cobalt ions (Co-CYGB). As results, Co-CYGB administration failed to exhibit all 6His-CYGB effects, including the activation of IFN-gamma pathway and the suppression of COL1A1 and alpha-SMA in HHStECs. In vivo analyses revealed that intravenously injected 6His-CYGB through mouse tail vein reached the liver and, surprisingly, accumulated in sinusoidal cells, dominantly in HSCs and liver sinusoidal endothelial cells (LSECs), but not in Kupffer cells. Administration of 6His-CYGB (2 mg/kg, twice a week) protected mouse liver from ROS-induced DNA damage and histological fibrosis aggravation in TAA, CCl₄ or DDC models without any adverse events. We annotated 25 non-parenchymal cell populations in our single-cell RNA-Seq data set obtained from CCl₄-mice treated with 6His-CYGB compared with 22 clusters in CCl₄ single exposure and identified unique HSC and LSEC subpopulations that responded to fibrosis regression and extracellular matrix degradation pathways.

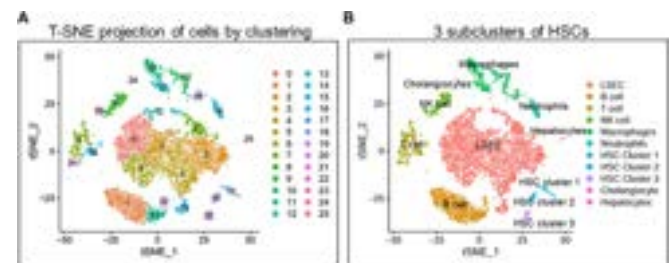


Figure 1. Six weeks of CCl₄ treatment with recombinant human CYGB tail vein injection twice a week at the final 4 weeks revealed 25 non-parenchymal cell populations (A) including 3 sub-clusters of HSCs (B) with inactivated phenotype which response to extracellular matrix degradation pathway.

Figure:

Conclusion: Recombinant extracellular 6His-CYGB exhibits a promising anti-fibrotic property for chronic liver diseases.

WED-222

Hepatic proteomic analysis identifies proteins linked to hepatic sympathetic neuronal degeneration and disorganization which promotes liver fibrosis in bile duct ligation murine model

Sadam H Bhat¹, Nupur Sharma¹, Csaba Adori², Anupama Parasar³, Babu Mathew¹, Manisha Yadav¹, Hami Hemati^{4,5}, Neha Sharma¹, Gaurav Tripathi¹, Sushmita Pandey¹, Vasundhara Bindal¹, Nilesh Patil⁶, Vinayendra Pamecha⁷, Savneet Kaur¹, Roshan Koul⁸, Manoj Kumar⁹, Jaswinder Maras¹, Shiv Kumar Sarin⁹. ¹Institute of liver and biliary sciences, Molecular and cellular medicine, India; ²Karolinska institutet, Neuroscience, Sweden; ³Institute of liver and biliary sciences, Center for comparative medicine, India; ⁴University of Kentucky, Toxicology, United States; ⁵University of Kentucky, Department of Toxicology and Cancer Biology, Lexington, United States; ⁶Institute of Liver and Biliary Sciences, Liver Transplant and Hepato Pancreato Biliary Surgery, India; ⁷Institute of liver and biliary sciences, Liver transplant and hepato pancreato biliary surgery, India; ⁸Institute of liver and biliary sciences, Neurology, India; ⁹Institute of liver and biliary sciences, Hepatology, India
Email: shivsarini@gmail.com

Background and aims: Hepatic sympathetic nerves (HSN) are critically involved in hepatic metabolism. These nerve fibres innervate around hepatic artery, portal vein, and bile duct. Disorganization or degeneration of the HSN is known to alter hepatic metabolism, however, its role in progression of liver disease and the associated molecular changes are not fully elucidated. Our aim is to identify liver proteins that are altered after hepatic sympathetic neuronal damage and are associated with the progression of liver injury.

Method: Liver-specific sympathetic neuronal damage/denervation [sympathectomy (Sx)] was performed by intraportal injection of 6-OHDA hydrobromide on 8–10-week-old male Sprague Dawley rats. Study groups were divided as Group-1 (GR-1), control rats with intact HSN (Veh; n = 9); Group-2 (GR-2) sympathectomized rats (Sx; n = 12); Group-3 (GR-3) Bile duct ligation vehicle with intact HSN; (BDL/Veh; n = 9); and Group-4 (GR-4) sympathectomized rats with BDL (BDL/Sx; n = 9), respectively. All groups were subjected to histological, confocal microscopy, plasma AST/ALT, and proteomic analysis at baseline, Day-7 (D7), D15, and D30.

Results: Liver-specific sympathectomy was validated in GR-2 and GR-4 by observing the change in urine colour (orange red), ptosis (droopy eyelid) and absence of sympathetic nerves marker (tyrosine hydroxylase; TH) in the liver samples. Mild steatosis and inflammation were observed in GR-2 at D7 and D15 with no significant difference in AST and ALT levels when compared to GR-1. Liver histology analysis showed significant increase in liver fibrosis in GR-4 as compared to GR-3 (p < 0.05). Interestingly, the level of fibrosis was significantly higher at D15 in GR-4 and it was comparable to the fibrosis seen in D30 in GR-3 (p < 0.05). Concordantly, we found significant increase in the AST and ALT values in GR-4, as compared to GR-3 (p < 0.05). In GR-3, we observed a significant progressive disorganization of sympathetic nerves that correlated with the severity of fibrosis and inflammation. PLS-DA (Partial least squares-discriminant analysis) analysis of the liver proteome showed clear differences between the study groups. 462 proteins were differentially expressed (227 upregulated and 235 downregulated) in GR-4 as compared to GR-3, showing significant activation of both the fibrogenic (TNFR2, Wnt, FGF) and inflammatory (NLRP3, MAPK, PDGF) pathways (p < 0.05). Interestingly, several hepatic secretory proteins [Annexin A2 (Anxa2), Butyrylcholinesterase (Bche), Fibroblast growth factor 5 (Fgf5), Hepatoma-Derived Growth Factor (HdGF), and Paraoxonase 3 (Pon3)] showed temporal increase in expression (FC > 2, FDR < 0.01, p < 0.05) in GR-4 and significantly correlated with the severity of fibrosis (R² > 0.7, p < 0.05) in GR-4, suggesting that upregulation of these secretory proteins due to sympathetic neuronal damage could be associated with the progression of liver fibrosis in GR-4.

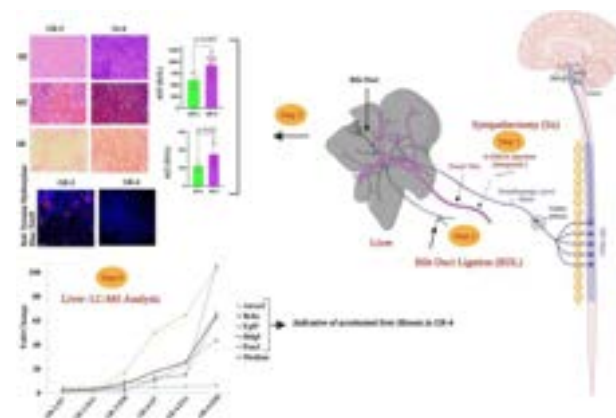


Figure: Graphical abstract

Conclusion: Hepatic sympathetic denervation promotes fibrosis and liver injury. Elevated levels of the secretory proteins, Anxa2, Bche, Fgf5, HdGF, and Pon3 after hepatic sympathetic neuronal damage/denervation are an indicative of accelerated liver fibrosis in a rat model of bile duct ligation.

WED-223

Functional and mechanistic role of lncRNA-C1 in cholestatic liver diseases

Joan Blázquez Vicens¹, Alberto Tinahones Ruano¹, Jorge Cañas¹, Luigi Borzacchiello^{1,2}, Alba Capelo¹, Marcos Fernandez Fondevila³, Begoña Porteiro³, Mason Bunyan-Woodcraft⁴, David Fernández Ramos⁴, Maria Jesus Perugorria Montiel⁵, Juan Carlos Garcia Pagan⁶, Jesus Maria Banales⁵, Piotr Milkiewicz⁷, Małgorzata Milkiewicz⁷, Bruno Sangro⁸, Luis Bujanda⁵, Matías A Avila⁴, Ana María Aransay⁴, José M. Mato⁴, Juan Turnes⁹, Beatriz Pelacho¹⁰, Ruben Nogueiras³, María Luz Martínez-Chantar⁴, Ashwin Woodhoo¹, Marta Varela-Rey¹. ¹Gene Regulatory Control in Disease Laboratory. CiMUS-USC, Xunta de Galicia, Spain; ²Università Degli Studi Della Campania "Luigi Vanvitelli," Italy; ³Molecular Metabolism Laboratory. CiMUS-USC (Ciberobn), Spain; ⁴Liver metabolism Laboratory, CIC bioGUNE-CIBERhd, Spain; ⁵Department of Liver and Gastrointestinal Diseases, Biodonostia Health Research Institute-Donostia University Hospital, University of the Basque Country (UPV/EHU), National Institute for the Study of Liver and Gastrointestinal Diseases (CIBERhd), Spain; ⁶Barcelona Hepatic Hemodynamic Laboratory, Liver Unit, Hospital Clinic Barcelona, IDIBAPS, CIBERhd, University of Barcelona, Spain; ⁷Translational Medicine Group, Pomeranian Medical University, Szczecin, Poland; ⁸Liver and Internal Medicine Unit, Medical University of Warsaw, Poland; ⁹Instituto de Investigaciones Sanitarias de Navarra-IdiSNA. CIBERhd. Hepatology Unit, Navarra University Clinic, Spain; ¹⁰Servicio de Digestivo del Complejo Hospitalario Universitario de Pontevedra (CHUP), Spain; ¹¹Insuficiencia Cardíaca. Grupo de Investigación. Cima, Spain
Email: martavarela.rey@usc.es

Background and aims: Liver fibrosis is characterized by complex cellular responses of several hepatic cell types. Long non-coding RNAs (lncRNA) are a class of non-coding RNAs that can interact with DNA, RNA and proteins to regulate global gene expression patterns. They are remarkably versatile regulators, influencing multiple biological processes and playing key roles in the pathogenesis of several disorders. Their function in liver fibrosis however remains largely unexplored.

Method: We have studied the expression of lncRNA-C1 in samples from patients with primary biliary cirrhosis (PBC) and primary sclerosing cholangitis (PSC), in mice models of cholestasis, NAFLD and toxic-induced fibrosis by CCl₄, and in several hepatic cell types after liver injury. Finally, we have performed functional analysis by *in vivo* and *in vitro* targeting of lncRNA-C1.

Results: We have observed that lncRNA-C1 was significantly upregulated in liver samples from patients with primary biliary cirrhosis (PBC) and primary sclerosing cholangitis (PSC), and that its expression was consistently elevated in three different mice models of cholestasis, including bile duct ligation (BDL), mice fed with a cholic acid diet, and MDR2-KO mice. In addition, levels of this lncRNA were also upregulated in other mice models of hepatic fibrosis, including toxic-induced fibrosis by CCl₄ (6 weeks), or mice fed with methionine-choline deficient diet (MCDD), methionine-choline deficient and high fat diet (MCDD-HFD), choline deficient and high fat diet (CD-HFD), and high fructose and high fat diet (HF-HFD). *In vivo* hepatic targeting of lncRNA-C1 exacerbated liver damage after BDL (as seen by elevated levels of transaminases and enhanced number of necrotic areas), increased NOS2 expression and decreased FXR levels. Using primary cells isolated from MDR2-KO mice, we found that, lncRNA-C1 was upregulated in hepatocytes and in hepatic stellate cells (HSC). Furthermore, both primary hepatocytes isolated from BDL mice, and activated HSC (including LX-2 cells or primary human HSC treated with TGF- β , or HSC isolated from MCDD, CD-HFD, CCl₄ mice models) showed increased levels of lncRNA-C1. Surprisingly, when lncRNA-C1 was silenced in TGF- β -treated LX2 cells, phosphorylation levels of Smad2, and the mRNA expression levels of col1a1, col1a2 and acta2 were increased, suggesting an antifibrotic role of lncRNA-C1. Finally, in cholestatic mice models, we observed a positive correlation between the levels of lncRNA-C1 in serum and the hepatic levels of col1a1 and col1a2 mRNA, suggesting the potential role of lncRNA-C1 as non-invasive biomarker for hepatic fibrosis.

Conclusion: Altogether, our data suggest that lncRNA-C1 could play a protective role during liver fibrosis development, and that lncRNA-C1 could represent a clinically relevant novel target in liver fibrosis.

WED-224

Evaluation of anti-fibrotic compounds effect in 3D human NASH model using quantitative digital pathology

Radina Kostadinova¹, Simon Ströbel¹, Louis Petitjean², Agnieszka Pawlowska Pawlowska¹, Li Chen², Francisco Verdeguer¹, Mathieu Petitjean². ¹InSphero AG, Liver disease discovery, Schlieren, Switzerland; ²PharmaNest, Princeton, NJ, United States
Email: radina.kostadinova@insphero.com

Background and aims: Non-alcoholic steatohepatitis (NASH) is a progressive and severe liver disease characterized by lipid accumulation, inflammation and, later, fibrosis. The development of novel anti-fibrotic therapies has been hindered, in part, by the limitations of existing fibrosis analysis techniques of the histology samples from *in vivo* and *in vitro* preclinical models. The novel digital pathology quantitative AI platform, FibroNest, was used previously to generate automatic, and direct fibrosis end points to quantify fibrosis severity and compound treatment response in clinical NASH samples. Here, we established an algorithm for quantification of fibrosis in an *in vitro* 3D human liver microtissue (hLiMT) NASH model using FibroNest imaging.

Method: The NASH hLiMT model consists of primary human hepatocytes, Kupffer cells, liver endothelial cells and hepatic stellate cells (HSC). Upon exposure to defined lipotoxic and inflammatory stimuli such as free fatty acids and LPS in media containing high levels of sugar and insulin the 3D NASH model displayed key disease pathophysiological features within 10 days of treatment. Quantifiable markers were established for anti-NASH drug efficacy testing such as secretion of pro-collagen type I/III and TIMPs/MMPs as well as quantification of fibrosis using FibroNest platform based on the Sirius Red staining of histology slides. Next generation sequencing (NGS) was also used for the assessment of the gene expression changes and pathways perturbation in the NASH model upon compounds treatment.

Results: The FibroNest algorithm for NASH hLiMTs was first validated using reference anti-fibrotic compounds, ALK5i and anti-TGF- β

antibody. The quantification of fibrosis using the “phenotypic fibrosis quantitative score” demonstrated that both reference compounds decreased the deposition and degradation of fibrosis. An efficacy study extended the evaluation to include clinical compounds, Firsocostat, Selonsertib, and Resmitemon, and a combination of Firsocostat and Selonsertib. When the anti-fibrotic effects of these were evaluated using the same panel of end points, there was a disconnect between the functional assays with gene-expression data and the phenotypic quantification of fibrosis using FibroNest. With few exceptions, none of the clinical single drugs or the combination of Firsocostat and Selonsertib decreased the secretion of pro-collagen type I and III, TIMPs or MMPs. Of the clinical compounds, only 10 μ M Selonsertib decreased the pro-collagen type I secretion on day 7. By contrast, the quantification of fibrosis using FibroNest platform demonstrated that all the tested clinical compounds had antifibrotic effects, which were in accordance with clinical observations.

Conclusion: In summary, the use of NASH hLiMTs and FibroNest imaging combined with transcriptomics and functional assays represents a promising drug discovery tool for the evaluation of the efficacy of different modalities of anti-fibrotic drug candidates and their combinatorial treatment.

WED-225

Bulk and single cell RNA sequencing profiling of human hepatic stellate cells and the potential biomarkers for liver cirrhosis

Xu Liu^{1,2}, Heming Ma^{1,2}, Qingtian Guan³, Huan Wang⁴, Guangyi Wang⁵, Yanhang Gao^{1,2}, Guoyue Lv⁵, Junqi Niu^{1,2}. ¹First Hospital of Jilin University, Department of Hepatology, Changchun, China; ²First Hospital of Jilin University, Center of Infectious Diseases and Pathogen Biology, China; ³First Hospital of Jilin University, Bioinformatics Laboratory, Changchun, China; ⁴Union Hospital, Tongji Medical College, Huazhong University of Science and Technology, Department of Infectious Diseases, Wuhan, China; ⁵First Hospital of Jilin University, Department of Hepatobiliary and Pancreatic Surgery, Changchun, China
Email: junqiniu@jlu.edu.cn

Background and aims: Liver cirrhosis, which presents with the distortion of hepatic architecture, is a significant global health burden. However, its exact mechanisms remain incompletely established. Hepatic stellate cells (HSCs) participate in the core regulation of fibrotic occurrence and reversion. Here, we used single-cell and bulk RNA sequencing (RNA-seq) to analyze the changes in the transcriptional patterns of patient-derived HSCs, revealing the diagnostic and therapeutic targets for cirrhosis.

Method: Primary HSCs were isolated from human liver tissues by recirculating perfusion. Bulk mRNA-seq of HSCs was performed by two comparative schemes [scheme A: Group_Cir (n=9) versus Group_Noncir (n=6); scheme B: Group_Act (n=7) versus Group_Fre (n=7)]. The dysregulated mRNAs of HSCs induced by hepatic cirrhosis were identified, and enrichment analyses were depicted. Protein-protein interaction (PPI) networks were constructed to search for candidates, which were verified by quantitative real time PCR. Then, the upstream transcription factors (TFs) were predicted using the KnockTF database. Cells from seven livers were obtained for single-cell RNA sequencing (scRNA-seq) and myofibroblastic HSCs were identified and analyzed. Ligand-receptor interactions in scRNA-seq were applied to predict the intercellular crosstalk.

Results: In the bulk RNA-seq, we observed 3828 and 2262 differentially expressed genes (DEGs) in scheme A and B, respectively.

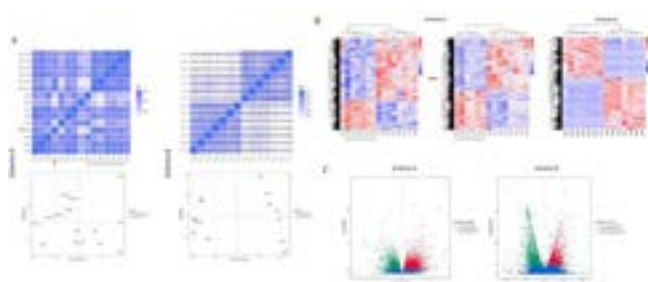


Figure 1. Distinct transcriptional patterns in HSCs during activation.

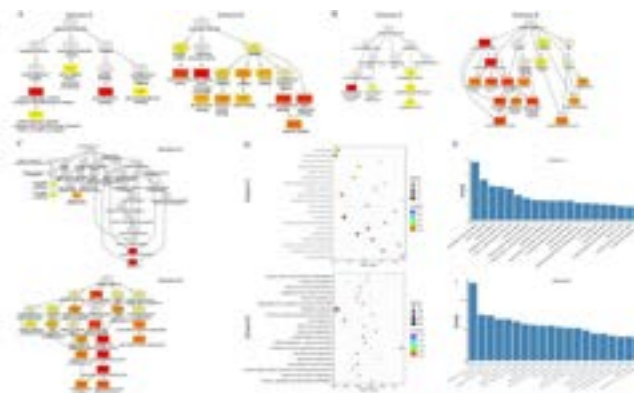


Figure 2. Enrichment analyses of DEGs.

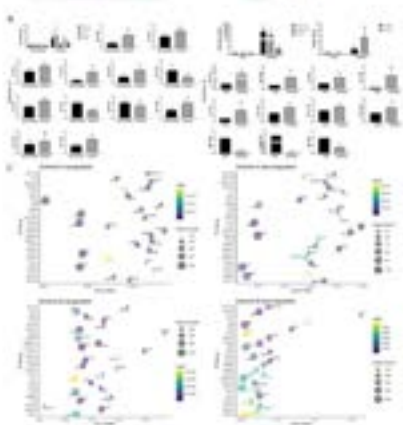


Figure 3. Screening of hub genes and key upstream TFs associated with hepatic fibrosis.

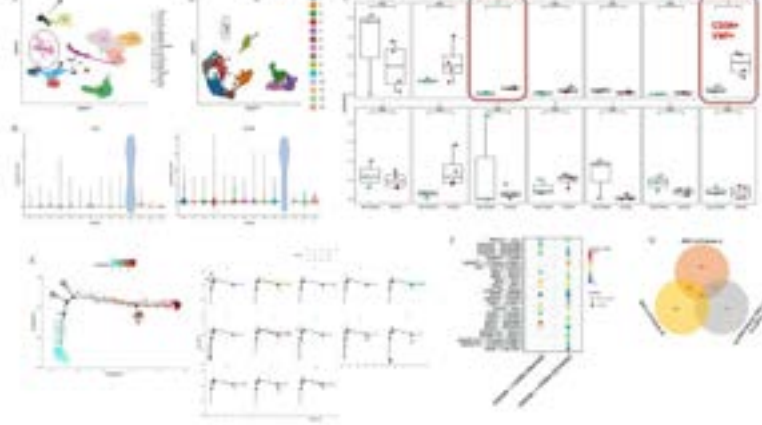


Figure 4. Single-cell transcriptomic analyses of myofibroblastic HSCs.

Figure: (abstract: WED-225).

According to the functional annotations of these two schemes, the DEGs were significantly enriched in 'focal adhesion', 'retinol metabolism', and 'formation, assembly, or degradation of collagen or extracellular matrix'. By PPI analysis, CAV1, ESR1, APP, SHC1, BCR, and LPL were screened as hub genes. Through the TFs-DEGs networks, POU5F1, ZFX, RARA, and MXD3 were considered the most important TFs that significantly regulate our DEGs. The scRNA-seq revealed myofibroblastic HSCs were at the end stage of differentiation and were regulated by cirrhosis-related endothelial cells through key ligand-receptor pairs, including PDGFs-PDGFRs, ANGPTL4-SDC2/SDC4/ITGA5+ITGB1, and NAMPT-ITGA5+ITGB1. Finally, we found that 38 upregulated genes of myofibroblastic HSCs in scRNA-seq were shared in bulk RNA-seq.

Conclusion: Our study offers multiple sequencing data; reveals the changing characteristics of human HSCs; and investigates potential targets associated with liver cirrhosis. It therefore sheds light on the molecular mechanisms underlying liver cirrhosis and provides information for its detection and treatment.

WED-226

Novel natural killer cell immunotherapy through synthesized Neuroligin-4 peptides improved liver fibrosis

Baker Saffouri¹, Johnny Amer¹, Ahmad Salhab¹, Rifaat Safadi¹.

¹Hadassah-Hebrew University Hospital, Liver Institute, Jerusalem, Israel
Email: johnnyamer@hotmail.com

Background and aims: NK cells lose their antifibrotic potential in advanced liver fibrosis particularly in patients with non-alcoholic fatty liver disease (NAFLD). Neuroligin-4 (NLGN4) receptor, a postsynaptic neuroinhibitory signalling, recently found overexpressed on NK cells and influence their killing potentials in NAFLD patients with advanced liver fibrosis. NLGN4 and its ligand β -neurexin (β -NRXN) expressed on activated hepatic stellate cells

(HSCs) showed to exert a synergistic inhibitory effect on NK cells. β -NRXN overexpression in activated HSCs indicated its role in fibrogenesis. Herein, we developed a newly synthesized NLGN4 peptides to assess their effects on NK cells and HSCs activities in an in vitro and in vivo liver fibrosis model.

Method: Three synthesized peptides were used and incubated for two hours at concentration of 2, 4, 8 μ g/ml with LX2 cells prior to co-cultures with NK cells for 24-hours. NK cells were obtained from NAFLD patients with F3/F4 scores. Flow cytometry was used for assessing NK cell activity through CD107a; lysosomal-associated membrane protein-1 and LX2 activations through α -Smooth muscle actin (α SMA expressions). For the in vivo study, C57/Bl mice were i.p injected with CCl₄-induced liver fibrosis (0.5 μ l/g body weight) and synthesized peptides (8 μ g/mice) twice a week for 6 weeks. Serum and livers were assessed for pro-inflammatory cytokines and histopathological staining, respectively.

Results: In an in vitro setting, HSCs pre-incubated with NLGN4 peptides, reduced their activations (α SMA expressions 1.53 and 1.55-folds in peptide 1 and peptide 2 respectively, $P < 0.001$) with a further prominent reduction in α SMA expressions following incubations with NK cells (2.85 and 2.3-folds in peptide 1 and peptide 2, respectively, $P < 0.001$). Moreover, the studied peptides downregulated expressions of both NLGN4 and β -NRXN in liver extracts isolated from CCl₄ liver fibrosis mice model. NLGN4 peptides showed a delayed progressions of liver fibrosis through improving liver histological findings of inflammatory and fibrotic lesions and reducing liver injury enzymes (ALT). Fibrotic markers (α SMA, Collagen, CREB and MMP4) assessed via western blot and RT-PCR were also alleviated following treatment with peptides, and these results were associated with elevated NK cells activations assessed by the CD107a and F-actin expressions through the flow cytometry and confocal microscopy, respectively.

Conclusion: Interruption of NK/myofibroblast cellular synapse by targeting the NLGN4/ β -NRXN axis with NLGN4 peptides achieved a synergistic antifibrotic effects through (1) cytotoxic NK cells stimulation against myofibroblasts; either directly via NLGN4 inhibition and indirectly by blocking the NK inhibitor β -NRXN, (2) directly inhibit β -NRXN of myofibroblasts and decreased their activation. Thus, immunotherapy targeting the NLGN4/ β -NRXN axis represent a potential novel immune therapeutic strategy in NK cell-mediated diseases.

WED-227

Multimodal decoding of the mesenchymal landscape of human biliary fibrosis

David Wilson¹, Neil Henderson¹. ¹Centre for Inflammation Research, University of Edinburgh, United Kingdom
Email: d.h.wilson@ed.ac.uk

Background and aims: Primary Biliary Cholangitis (PBC) is a fibrosing cholangiopathy of the liver that is increasing in prevalence globally. Currently, there are no effective antifibrotic therapies available with which to treat patients with liver fibrosis. In end-stage disease, transplantation is the only treatment option, however, less than 10% of global transplantation needs are met. Therefore, effective antifibrotic therapies are urgently required. To advance our understanding of human liver fibrosis and to inform design of antifibrotic therapies, we have used multimodal single cell genomics approaches to generate single-cell, pan-lineage atlases of human primary biliary cholangitis and mouse models of biliary fibrosis.

Method: To deepen our understanding of the cellular and molecular mechanisms driving human biliary fibrosis, and to inform design of effective antifibrotic therapies, we performed single nuclei RNA sequencing (snRNA-seq) of healthy and PBC explant livers to generate a single-cell, multi-lineage atlas of human biliary fibrosis. Following this, we established a single-nuclei pan-lineage atlas of mouse biliary fibrosis and used this mouse model to interrogate the function of corollary subpopulations observed in both human and mouse biliary fibrosis.

Results: We uncovered multiple, disease-associated mesenchymal and cholangiocytes subpopulations in human biliary fibrosis and using newly generated markers we have comprehensively characterised the topography of these subpopulations in the human biliary fibrotic niche. Moreover, ligand-receptor analysis of pathogenic mesenchymal subpopulations has identified a distinct set of putative therapeutic targets, which we are currently functionally interrogating using genetic approaches in mouse biliary injury models, and small molecule approaches in human biliary, multi-lineage organoids.

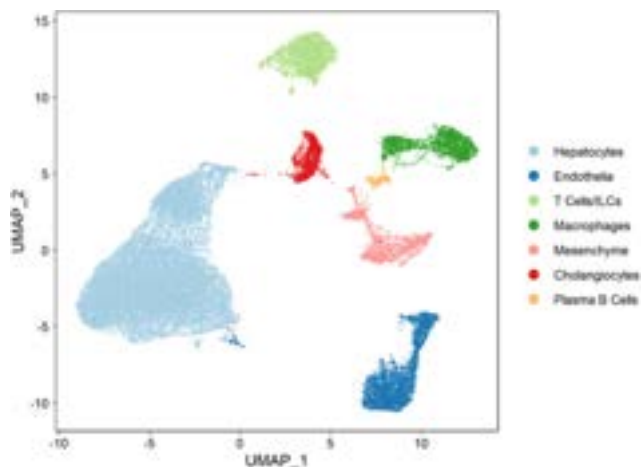


Figure: UMAP delineating a single-nuclei pan-lineage atlas of healthy and PBC human liver (n = 10) showing major cell lineage cluster annotations.

Conclusion: Multimodal single cell genomic approaches, in conjunction with functional interrogation of corollary cellular subpopulations in mouse models of biliary fibrosis, have allowed us to uncover novel cell states and unanticipated aspects of biliary fibrogenesis. Our ongoing work is currently assessing the feasibility and tractability of these newly identified therapeutic targets to treat patients with biliary fibrosis.

WED-228

Composition of the bile salt pool critically modulates liver fibrosis-towards humanization of murine models of liver disease

Jingguo Li^{1,2}, Sebastian Zimny¹, Dennis Koob¹, Ralf Wimmer¹, Gerald Denk¹, Biguang Tuo², Simon Hohenester¹. ¹Ludwig Maximilian University of Munich, Department of Medicine II, University Hospital, LMU Munich, Germany, Germany; ²Department of Gastroenterology, Affiliated Hospital of Zunyi Medical University, China, China
Email: simon.hohenester@med.uni-muenchen.de

Background and aims: Accumulation of hydrophobic bile salts is believed to promote liver fibrosis in human cholestatic liver disease. An important difference between mice and man in regard to liver pathophysiology is their different composition of the bile salt pool with hydrophilic bile salts predominating in mice, and hydrophobic bile salts such as (glyco-) chenodeoxycholate ((G)CDC) in man. We have previously shown that humanization of the bile salt pool by GCDC-feeding is crucial for development of liver fibrosis in chronic hepatocellular cholestasis and hypothesized that direct activation of hepatic stellate cells (HSC) may be involved. Here, we further explored the capability of various bile salts to activate HSC in vitro and tested the role of a humanized bile salt pool in development of CCl₄-induced liver fibrosis.

Method: C57BL/6 mice were fed a control diet or a diet enriched with GCDC (0, 1% w/w) for 6 weeks to humanize their bile salt pool. For the last 4 weeks, mice were treated with CCl₄ (0.93 g/kg) 3 times per week. Liver fibrosis was quantified by hydroxyproline measurement and Sirius red staining. The human HSC line LX2 was stimulated with bile salts in standard culture medium at a slightly acidic pH (7.3) to account for the acidic microenvironment known to be present in the perisinusoidal space. Activation of cells was quantified by Western blotting for α SMA (normalized for GAPDH).

Results: LX2 were stimulated with GCDC (100–500 μ M), CDC, taurocholate (TC) and deoxycholate (DC) at 10–100 μ M, respectively. Among those, only GCDC (minimal concentration 100 μ M) and CDCA (minimal concentration 10 μ M) specifically led to an increase in α SMA expression by 1.9 ± 0.4 - and 1.4 ± 0.1 -fold respectively, compared to control (n = 4, p < 0.05). In vivo, CCl₄ led to development of liver fibrosis, as expected. Supplementation with GCDC aggravated this phenotype, as evidenced by liver hydroxyproline (CCl₄+GCDC vs. CCl₄+Control: 383.6 ± 35.4 vs. 284.6 ± 68.5 , n = 5, p < 0.05), sirius red staining ($9.5\% \pm 3.3\%$ vs. $5.9\% \pm 0.7\%$, n = 5, p < 0.05) and α SMA expression (0.9 ± 0.3 vs. 0.5 ± 0.1 , n = 4, p < 0.05). ALT serum levels were unaltered by GCDC feeding in both control and CCl₄-treated animals, excluding a direct co-toxic effect of GCDC. Identical results in regard to liver fibrosis were seen when unconjugated CDCA was used. In control animals without CCl₄-treatment, bile salt feeding was without pro-fibrotic effects.

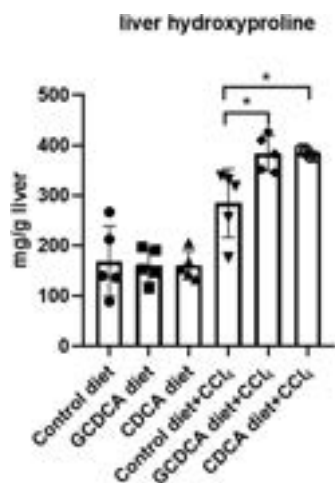


Figure:

Conclusion: Our data add to the growing body of evidence, that human, hydrophobic bile salts can directly activate hepatic stellate cells to promote liver fibrosis. Composition of the bile salt pool in mice may impact on the fibrotic phenotype not only in cholestasis, but on development of liver fibrosis in general. This way of ‘humanization’ of murine models should thus be further explored when studying liver pathophysiology or exploring novel pharmacological therapies in chronic liver disease.

WED-229

Reactive oxygen species-mediated hepatic stellate cell activation via PI3K in liver cancer

Qi Ruan^{1,2}, Lu Cao², Haotian Yang², Leslie Burke², Kim Bridle², Darrell Crawford², Xiaowen Liang^{1,2}. ¹University of Queensland Diamantina Institute, Australia; ²Gallipoli Medical Research Foundation, Australia

Email: x.liang@uq.edu.au

Background and aims: One of the standard treatments of unresectable hepatocellular carcinoma (HCC) is transarterial chemoembolization (TACE), using cisplatin or doxorubicin. However, chemotherapy is considered as a “double-edged sword” through activating hepatic stellate cells (HSCs) which can promote tumour growth and chemoresistance. With a better understanding of the molecular mechanism mediated HSC activation in response to chemotherapy, novel potential targets could be revealed for improving the treatment efficacy of liver cancer.

Method: Cancer associated fibroblasts (CAFs) in HCC patients with or without TACE treatment were analysed using a single cell RNA sequencing dataset. The effect of chemotherapeutic drugs on HSC activation was examined in two *in vitro* models, mixed-cell spheroids and treatment of conditioned medium (CM) of cisplatin- or doxorubicin-pretreated Huh7 cells in LX2 cells. LX2 cells were transfected by a pFRET HSP33 plasmid for monitoring reactive oxygen species (ROS) levels of LX2 cells cultured in Huh7-CM. RNA sequencing was conducted to profile gene expression of primary HSCs cultured in Huh7 CM. Three *in vivo* models of HCC were used to validate these results, including orthotopic HCC mouse model, HCC mouse model with fibrosis background induced by thioacetamide acid, and spontaneous HCC model using 11 month-Mdr2 knockout mice. Chemotherapeutic drugs, cisplatin or doxorubicin, were given a total of four doses. Tumour tissues were collected for immunofluorescence staining and western blot. Finally, tumour samples from TACE-treated or untreated patients were collected and stained for the expressions of alpha-smooth muscle actin (SMA) and PI3K p110 alpha.

Results: The proportion of activated CAFs showed a huge increase from 28.3% to 72% of alpha-SMA positive subpopulation and 7% to 27.8% of COL1A1 positive subpopulation in liver cancer patients after

TACE treatment. Using two *in vitro* models, LX2 cells were activated by cisplatin-pretreated Huh7 cells but not doxorubicin, with a significant increase in the expression of activation markers. Cisplatin CM obviously increased ROS in LX2 cells, indicating ROS might mediate HSC activation in response to platinum-based drug. Furthermore, RNA sequencing revealed that PI3K pathway contributes to HSC activation among a total of 55 upregulated and 47 downregulated genes. The key genes such as PIK3R3 and PIK3C2B were significantly increased in HSCs cultured in cisplatin CM. Consistent with *in vitro* results, PI3K pathway related-molecules were significantly increased and its downstream molecules, AKT and ERK, were activated in the tumour tissues of HCC-bearing mice treated by cisplatin. Finally, the expressions of alpha-SMA and PI3K were increased in patient liver tumour samples after TACE treatment.

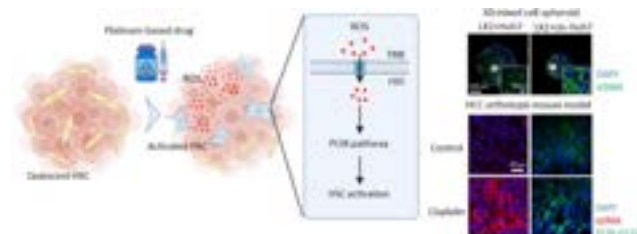


Figure:

Conclusion: Liver cancer patients with TACE or chemotherapy had a higher level of HSC activation. We have confirmed HSCs can be activated through paracrine factors from cisplatin- but not doxorubicin-treated liver cancer cells through a ROS-mediated pathway. Finally, we concluded that the activation of PI3K pathway contributes to ROS mediated-HSC activation in response to platinum-drug treatment. Understanding the HSC activation mechanism induced by chemotherapy could provide potential therapeutic targets as a complement to chemotherapy against liver cancer.

WED-230

Hepatic stellate cells from zone 1 do not transform into myofibroblasts but engage in capillarization in preclinical models of liver fibrosis

Muhammad Ashfaq-Khan¹, Julian Fischer¹, Fabian Schwiering¹, Dieter Groneberg^{1,2}, Andreas Friebe¹. ¹Universität Würzburg, Germany; ²Fraunhofer Institut für Silicatforschung ISC, Germany

Email: andreas.friebe@uni-wuerzburg.de

Background and aims: Hepatic stellate cells (HSC) reside in the sinusoids of the liver lobule. Recently, two different types of HSC have been described in mice which are located either close to the central vein or near the portal field. We here identify a novel subgroup of HSC. These PDGFRβ-positive cells are found in zone 1 (thus named zone 1-HSC) of the lobule and form a subpopulation of the portal field-associated HSC. In this project, we identified the origin and function of zone 1-HSC in mice.

Method: Mice expressing Cre recombinase under the control of the smooth muscle myosin heavy chain (Myh11) promoter (SMMHC-CreER^{T2}) in combination with the tdTomato reporter were used to identify and trace zone 1-HSC under physiological and pathophysiological conditions. Two different models of hepatic fibrosis, CCl₄ and a Western diet in combination with cholesterol and fructose, were used. Immunofluorescence analysis was performed using confocal microscopy.

Results: Using SMMHC-Cre-induced tdTomato expression in combination with zone-specific antibodies (anti-GS and anti-NGFR), we identify a subtype of HSC in zone 1 of the liver lobule. Under physiological conditions, tdTomato-labeled cells remain in zone 1 even 1 year after reporter induction. Short time induction shows progenitor cells near the canal of Hering in close association with OPN/SOX9- and CK19-positive cells.

After induction of hepatic fibrosis (CCl₄ and Western diet), zonation is lost as zone 1-HSC migrate into zones 2 and 3. Surprisingly, zone 1-HSC do not become myofibroblasts (as shown by lack of α SMA and col1 α 1 expression) but rather appear to engage in the capillarization of sinusoids. As expected, regular HSC (not tdTomato-labeled by SMMHC-Cre) can be shown to engage in the fibrotic reaction as α SMA-expressing myofibroblasts.

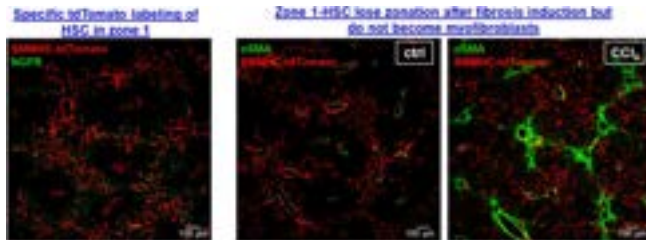


Figure:

Conclusion: Our data allow to differentiate HSC into the regular central HSC that become myofibroblasts under fibrotic conditions, and zone 1-HSC which do not transform into myofibroblasts in two different fibrosis models. Thus, HSC are not a group of cells that are uniformly involved in fibrosis but rather subdivide into mediators of capillarization and myofibroblast precursors.

WED-231

Role of the hepatocyte Epidermal Growth Factor Receptor (EGFR) pathway on the cellular interactome within the liver fibrotic niche

Ester Gonzalez-Sanchez^{1,2}, Javier Vaquero^{1,2}, Daniel Caballero-Díaz^{1,2}, Jan Grzelak², Esther Bertran^{1,2}, Josep Amengual², Juan García-Sáez^{3,4}, Pilar Valdecantos^{5,6}, Angela Martinez Valverde^{5,6}, Aranzazu Sanchez^{3,4}, Blanca Herrera^{3,4}, Isabel Fabregat^{1,2}. ¹CIBER de Enfermedades Hepáticas y Digestivas-

CIBEREHD, Spain; ²Bellvitge Biomedical Research Institute-IDIBELL, L'Hospitalet, Barcelona, Spain; ³Faculty of Pharmacy, Complutense University of Madrid (UCM), Madrid, Spain; ⁴Health Research Institute of the 'Hospital Clínico San Carlos' (IdISSC), Madrid, Spain; ⁵'Alberto Sols' Biomedical Research Institute, Spanish National Research Council and Autonomous University of Madrid (IIBM, CSIC-UAM), Madrid, Spain; ⁶Biomedical Research Networking Center in Diabetes and Associated Metabolic Disorders of the Carlos III Health Institute (CIBERDEM-ISCIII), Madrid, Spain
Email: ifabregat@idibell.cat

Background and aims: Liver fibrosis is the consequence of chronic liver injury in the presence of an inflammatory component. Although the main executors of this activation are known, the mechanisms that lead to the inflammatory process that mediates the production of profibrotic factors are not well characterized. The Epidermal Growth Factor Receptor (EGFR) signaling in hepatocytes is essential for the regenerative process of the liver; however, its potential role in regulating the fibrotic niche is not yet clear.

Method: Our group generated and validated a mouse model that expresses an inactive truncated form of the EGFR in hepatocytes (Δ EGFR mice). Here, we have analyzed the role of the hepatocyte EGFR pathway in the fibrotic niche cell interactome in WT and Δ EGFR mice subjected to CCl₄-induced liver fibrosis.

Results: The analysis of the *in vivo* model indicated that the hepatocyte-specific EGFR activity may be contributing to the proinflammatory response, activated due to the liver damage. Indeed, the absence of EGFR activity in hepatocytes induces changes in the pattern of immune cells in the liver, with a notable change in the population of macrophages that display a bias toward an M2 phenotype more related to fibrosis resolution, as well as an increase in the population of lymphocytes related to eradication of the damage. The hallmarks of liver fibrosis are attenuated in CCl₄-treated Δ EGFR mice when compared to WT mice, coinciding with a faster resolution of the fibrotic process and an ameliorated damage. *In vitro* studies have revealed that hepatocytes may directly regulate the macrophage phenotype by inducing the secretion of specific factors,

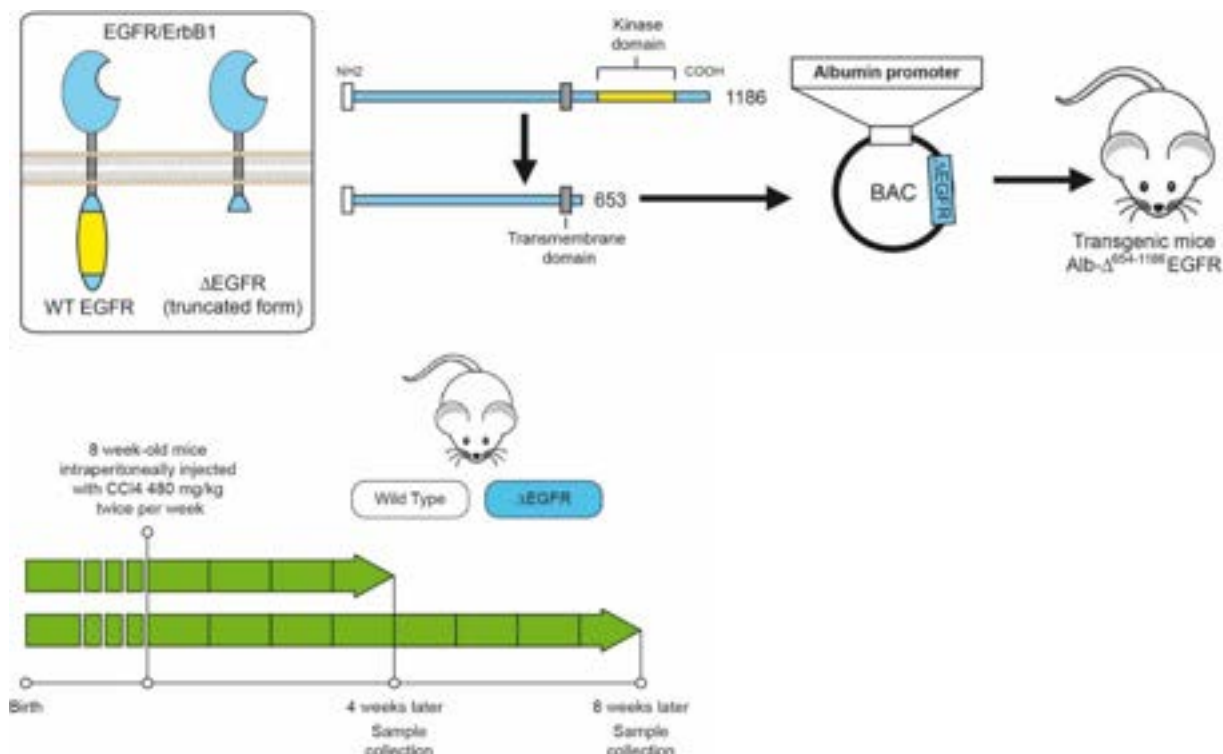


Figure: (abstract: WED-231): Transgenic model Alb- $\Delta^{654-1186}$ EGFR (Δ EGFR) mice (up) and experimental model of CCl₄-induced liver fibrosis (bottom).

POSTER PRESENTATIONS

whose expression depends on the activation of the EGFR pathway. Transcriptomic and proteomic studies, currently being performed, will allow to elucidate the specific molecular mechanisms regulated by EGFR that are responsible for the observed changes in the hepatocyte secretory phenotype.

Conclusion: EGFR inactivation specifically in hepatocytes leads to a profound alteration in the liver inflammatory response in experimental fibrosis, with a clear immune cell switch into a pro-restorative phenotype. Besides supporting a pro-fibrogenic role for EGFR activity, our study provides new mechanistic insights on EGFR kinase-dependent actions during chronic liver damage.

This work has been supported by the Ramon Areces Foundation: 20th National Competition for Scientific and Technical Research in Life and Matter Science (2020), grant C1VP20A6593. We help the initial contribution of Drs. Lluís Montoliu and Jose Carlos Segovia in the generation of the transgenic mice.

WED-232

Discovery of novel small molecule inhibitors of HDAC6 that suppress liver fibrosis

Maria Teresa Borrello¹, Dusan Ruzic², Fiona Oakley¹, Katarina Nikolic², Jelena Mann¹, Derek Mann¹. ¹Biosciences Institute, 4th Floor, William Leech Building, Newcastle University, Medical School, Newcastle Fibrosis Research Group, Newcastle upon Tyne, United Kingdom; ²University of Belgrade, Faculty of Pharmacy, Department of Pharmaceutical Chemistry, Belgrade, Serbia
Email: jelena.mann@newcastle.ac.uk

Background and aims: Liver fibrosis is a dynamic process characterized by deposition of scar tissue within hepatic parenchyma. At a molecular level, fibrosis is associated with perturbations in expression of histone deacetylases, therefore specific HDAC inhibitors (HDACis) could have a role as therapeutic agents for liver fibrosis. HDAC6, a microtubule-associated deacetylase, is increased in expression in fibrotic liver. Recent studies have shown that HDAC6 enzyme could be selectively targeted, mostly because of its cytoplasmic localisation. Selective HDAC6i have shown promise in diverse number of fibrotic diseases, which led us to investigate novel HDAC6i as potential therapeutic agents for liver fibrosis.

Method: Structure-based molecular modelling studies were conducted in order to rationalise selective HDAC6 inhibitory profiles. The biological activities of the hydroxamic acid derivatives DR-3 and FDR-2 were profiled in an enzymatic assay and their anti-fibrotic potential evaluated in *in vitro* and *in vivo* human and murine models.

Results: The novel compounds FDR-2 and DR-3 were found to be nM inhibitors of HDAC6 enzymatic activity with high selectivity towards HDAC6 over HDAC1/8. Biological and biochemical evaluation demonstrated that DR-3 and FDR-2 were capable of suppressing the activation of primary rat hepatic stellate cells, significantly decreasing the expression of profibrogenic markers. Both compounds markedly reduced TGF- β 1-induced SMAD3 activation. Finally, the compounds demonstrated anti-fibrotic pharmacological activities at 5 μ M in human precision cut liver slices (hPCLS). hPCLS retain structure and cellular composition of the native human liver and represent a state-of-art preclinical model to study liver fibrosis. The antifibrotic activity of DR-3 and FDR-2 in hPCLS was assessed by Picrosirius Red, α -smooth muscle actin staining and soluble ELISAs. Both FDR2 and DR-3 blunted the progression of fibrosis in hPCLS with no obvious signs of toxicity.

Conclusion: Combining structural analyses and molecular modelling efforts, we generated a series of novel, highly selective HDAC6 inhibitors named DR-3 and FDR-2. Both compounds demonstrate synthetic accessibility, high potency and interesting preliminary pharmacological profile, including low toxicity in hPCLS. These results emphasised the important role that HDAC6 inhibition plays in liver fibrosis. This evidence was further confirmed by the attenuation of TGF- β 1-dependent fibrogenesis in hepatic stellate cells as well as reduction in histological and protein markers of

fibrosis in human PCLS after culturing with compounds DR-3 and FDR-2. Overall, this work provides robust evidence for HDAC6 inhibitors as potential therapeutic tools for the treatment of liver fibrosis and paves the way for the development of novel lead compounds.

WED-233

MCPIP1 inhibits hepatic stellate cell activation in autocrine and paracrine manner

Natalia Pydyn¹, Anna Ferenc¹, Katarzyna Trzos¹, Piotr Major¹, Mateusz Wilamowski¹, Tomasz Hutsch², Andrzej Budzyński¹, Jolanta Jura¹, Jerzy Kotlinowski¹. ¹Jagiellonian University, Poland; ²Veterinary Diagnostic Laboratory ALAB Bioscience, Poland
Email: j.kotlinowski@uj.edu.pl

Background and aims: Hepatic fibrosis is characterized by enhanced deposition of extracellular matrix (ECM) which results from the wound-healing response to the chronic, repeatable injury of any etiology. Upon injury hepatic stellate cells (HSCs) activate and secrete ECM proteins, forming a scar tissue, which results in liver dysfunction. Monocyte-chemoattractant protein-induced protein 1 (MCPIP1) encoded by *ZC3H12A* gene is a protein which possesses anti-inflammatory activity. It is an RNase that degrades a wide plethora of transcripts for example coding for proinflammatory cytokines like IL-1 β or IL-6. MCPIP1 overexpression reduces liver injury in septic mice. Also, mice with deletion of *Mcpip1* in liver epithelial cells, develop features of primary biliary cholangitis. In this study, we analyzed MCPIP1 level in human fibrotic livers and hepatic cells isolated from murine fibrotic livers. We also investigated MCPIP1 impact (coculture of murine primary cells and *Mcpip1* in vivo overexpression) on HSCs activation.

Method: We analyzed MCPIP1 level in patients' fibrotic livers and hepatic cells isolated from fibrotic murine livers. We used both CCl₄ treated mice and livers from *Mcpip1* knock-out animals (*Mcpip1*^{fl/fl}/flAlbCre). Paracrine effect of *Mcpip1* on HSCs activation was studied by coculture of *Mcpip1* KO or WT primary hepatocytes with HSCs. Silencing and overexpression of *ZC3H12A* in LX-2 cell line was used for analysis of autocrine effects of MCPIP1. *In vitro* experiments were conducted on primary HSCs, cholangiocytes and hepatocytes. To overexpress *Mcpip1* *in vivo*, we used AAV8 vectors encoding GFP (control) or *Mcpip1* injected to tail vein at the dose of 1×10^{11} cfu.

Results: MCPIP1 level is induced in patients' fibrotic livers in comparison to non-fibrotic counterparts. Similarly, both mRNA and protein *Mcpip1* levels were induced in primary HSCs isolated from murine fibrotic livers in comparison to control cells. *Mcpip1* KO hepatocytes were characterized by increased expression of Ctgf protein in comparison to control cells. High level of Ctgf produced by *Mcpip1* KO hepatocytes resulted in enhanced activation of HSCs cocultured with these cells. Overexpression of MCPIP1 in LX-2 cells led to decreased mRNA expression of HSCs activation markers e.g. *Acta2*, *Tgfb*, *Col1a1* and α -SMA protein level. Contrary, MCPIP1 silencing in LX-2 cells resulted in their increased activation status. *In vivo* overexpression of *Mcpip1* in corn-oil treated mice reduced hepatic expression of *Tgfb1*, *Acta2*, *Mmp3*, *Col3a1* and amount of IL-6 and *Tgfb* proteins, although did not impact degree of fibrosis after CCl₄ administration.

Conclusion: MCPIP1 is induced in human fibrotic livers and regulates activation of HSCs cells in both autocrine and paracrine manner. Our results indicate that MCPIP1 could have a potential role in development or resolution of liver fibrosis.

Acknowledgments: This study was supported by National Science Centre, grant number K/PBM/000672 and 2021/42/E/NZ5/00169.

WED-234

The proto-oncogene Bmi1 is a novel regulator of the activated hepatic stellate cell phenotype

Kim Su^{1,2}, Elliot Jokl¹, Karen Piper Hanley^{1,3}. ¹University of Manchester, Diabetes, Endocrinology and Gastroenterology, Manchester, United Kingdom; ²Blackpool Victoria Hospital, Gastroenterology, Blackpool, United Kingdom; ³University of Manchester, Wellcome Trust Centre for Cell-Matrix Research, Manchester, United Kingdom
Email: kim.su@nhs.net

Background and aims: Epigenetic regulation of gene expression has been implicated in liver fibrosis and is an important mechanism underlying hepatic stellate cell (HSC) activation. Polycomb repressor complexes (PRC) are a key class of epigenetic regulators. Whilst PRC2 components have been implicated in HSC activation, the role of PRC1 in liver fibrosis has not been explored. The proto oncogene B-cell specific Moloney murine leukemia virus integration site 1 (Bmi1) is a key component of the PRC1 complex. Bmi1 is implicated in hepatocellular carcinomas (HCC) and cholangiocarcinomas (CCA) but its role in liver fibrosis and HSC biology is unknown. We have utilized *in vivo* and *ex vivo* murine models to examine the role of Bmi1 in liver fibrosis.

Method: The murine *Schistosomiasis mansoni* (*S. mansoni*) model of liver fibrosis was used for *in vivo* detection of BMI1 by immunoblotting. HSCs were extracted by enzyme mediated perfusion of isolated mouse livers and activated on tissue culture. The small molecule inhibitor PTC-209 was used to inhibit BMI1 in *ex vivo* culture activated HSCs. BMI1, mono-ubiquitinated Histone 2A (H2AK119ub), fibrosis markers and HSC activation markers were assessed with immunocytochemistry (ICC), immunoblotting and qPCR. HSC proliferation and cell cycle analysis were conducted using immunoblotting for proliferating cell nuclear antigen (PCNA) and propidium iodide flow cytometry. Statistical analyses were carried out using Student's t-test (Graphpad Prism 8).

Results: *In vivo* expression of BMI1 is significantly increased in *S. mansoni* infected livers versus uninfected controls ($p < 0.05$). *Ex vivo* HSC culture reveals BMI1 is upregulated in activated HSCs (aHSCs) at day 7 compared to quiescent HSCs (qHSCs) at day 0 ($p < 0.01$). This is associated with increased expression of alpha-smooth muscle actin, (Asma), collagen I (Col1a1), Yes associated protein 1 (Yap1) and SRY-Box Transcription Factor 9 (Sox9), all established markers of the aHSC phenotype. ICC staining confirms nuclear localisation of BMI1 in the aHSC. PTC-209 mediated BMI1 inhibition in aHSCs was associated with reduced levels of BMI1 protein in HSCs and reduced levels of H2AK119ub, reflecting diminished PRC1 ubiquitin ligase activity. BMI1 inhibition diminished the profibrotic phenotype of aHSCs. Significant reduction in protein and mRNA levels of collagen I ($p < 0.01$), a fibrillar collagen that is a hallmark of liver fibrosis was detected. Markers of HSC activation were also diminished, with reduced levels of platelet derived growth factor receptor-beta (PDGFRB) protein ($p < 0.01$) and reduced transcript levels of Pdgfrb ($p < 0.001$) and Asma ($p < 0.01$). These observations are unlikely due to diminished cell survival, as no significant changes in PCNA or cell cycle kinetics were detected at PTC-209 doses utilized in this study.

Conclusion: In this study, we provide proof-of-concept data demonstrating *ex vivo* inhibition of BMI1 abrogates the profibrotic phenotype of activated HSCs. Moreover, we have identified a potentially new target linked to epigenetic mechanisms in the ongoing search for anti-fibrotic therapies in chronic liver disease.

WED-235

3D engineered perihepatic endothelial cell implants reduce fibrosis and inflammation, boosting liver regeneration in fibrotic hepatectomized mice

Mireia Medrano-Bosch¹, Alazne Moreno-Lanceta^{1,2}, Blanca Simón-Codina¹, Laura Macias-Muñoz², Elazer Edelman^{3,4}, Wladimiro Jiménez^{1,2,5}, Pedro Melgar-Lesmes^{1,2,3}. ¹School of

Medicine, University of Barcelona, Department of Biomedicine, Barcelona, Spain; ²Institut d'Investigacions Biomèdiques August Pi-Sunyer (IDIBAPS), Centro de Investigación Biomédica en Red de Enfermedades Hepáticas y Digestivas (CIBERehd); Spain; ³Institute for Medical Engineering and Science, Massachusetts Institute of Technology, United States; ⁴Cardiovascular Division, Brigham and Women's Hospital, Harvard Medical School, United States; ⁵Biochemistry and Molecular Genetics Service, Hospital Clinic Universitari, Spain
Email: pmelgar@ub.edu

Background and aims: Endothelial cells (ECs) display a myriad of protective effects that contribute to the minimization of liver injury and the restoration of hepatic function. Embedding healthy ECs in a 3D collagen-based scaffold shields their immunogenicity and maximizes their protective roles. Indeed, a previous study has shown that matrix-embedded endothelial cells (MEEC) can protect the liver against ischemic injury. Here, we evaluate whether perihepatic implantation of MEECs might be of therapeutic interest in the context of fibrosis with liver resection.

Method: Fibrosis was induced in BALB/c mice ($n = 12$) by i.p. injection of CCl₄ twice weekly for 8 weeks. Acellular matrices or MEECs were implanted between the median and right lobe in fibrotic mice with partial hepatectomy (40% resection, HP40). After 7 days, serum and hepatic samples were collected for fibrosis (Sirius Red staining) and liver function analysis. The expression of genes associated with extracellular matrix turnover, hepatic stellate cell (HSC) activation, or inflammation were quantified by Real-time PCR. Liver restoration rate, proliferating cell nuclear antigen (PCNA) immunostaining and the expression of different growth factors were also studied.

Results: Perihepatic implantation of MEECs in HP40 fibrotic mice promoted a 27% reduction in hepatic fibrosis area and significant improvement in liver function (2-fold reduction in transaminases-ALT, 139 ± 19.5 vs 60 ± 10.4 U/L, $p < 0.01$; AST, 608 ± 105 vs 253 ± 37 U/L, $p < 0.01$). HSC activation was similarly mitigated with concomitant 2-fold reduction in expression of extracellular matrix turnover genes (Collagen I, 1.0 ± 0.1 vs 0.65 ± 0.1 , fold change (fc), $p < 0.01$; alpha-SMA, 1.1 ± 0.1 vs 0.5 ± 0.1 fc, $p < 0.01$; TIMP1, 1.0 ± 0.1 vs 0.6 ± 0.1 fc, $p < 0.05$). MEECs also promoted a significant down-regulation of macrophage-derived HSC activators and pro-inflammatory genes, and a parallel increased expression of anti-inflammatory genes. Beneficial anti-fibrotic and anti-inflammatory effects of MEECs implantation in HP40 fibrotic mice were associated with restoration of liver mass (7.0 ± 0.1 g/body weight, BW vs. 7.9 ± 0.1 g/BW, $p < 0.05$). Indeed, tissue preservation correlated with induced cell growth as the number of proliferating cells in livers from mice implanted with MEECs was three times higher than in mice receiving acellular implants (PCNA positive cells, $5.3 \pm 0.3\%$ vs. $15.4 \pm 1.5\%$, $p < 0.001$). This hepatic proliferation correlated with an upregulation of hepatocyte growth factor expression (1.0 ± 0.1 vs 1.7 ± 0.2 fc, $p < 0.001$) but not with insulin growth factor 1 induction (1.0 ± 0.1 vs 1.1 ± 0.1 fc).

Conclusion: 3D engineered perihepatic ECs implants reduce fibrosis and inflammation and induce hepatic regeneration in fibrotic mice with hepatectomy. This study emphasizes the therapeutic potential of MEECs to improve the recovery of patients with fibrosis and liver resection.

WED-236

Artificial Intelligence analysis of liver biopsies in pre-cirrhotic NASH: qFibrosis explained

Dean Tai¹, Elaine Chng¹, Kutbuddin Akbary¹, Yayun Ren¹, Pol Boudes². ¹HistoIndex Pte Ltd, Singapore; ²Galectin Therapeutics, United States
Email: akbary.kutbuddin@histoindex.com

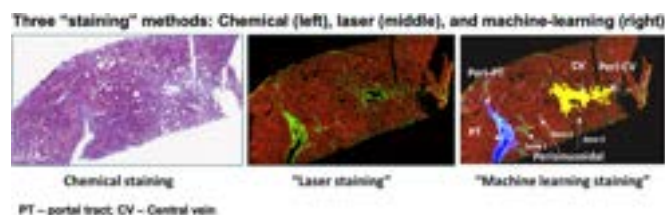
Background and aims: Liver histopathology is a primary outcome for non-alcoholic steatohepatitis (NASH) candidate drugs registration. Besides biopsy size, tissue homogeneity, and staining quality, intra and inter observer variability confound the interpretation of available semi-quantitative scales for fibrosis. We designed an innovative

POSTER PRESENTATIONS

processing and analysis of digitized liver tissue and submit it to artificial intelligence analysis to provide a more sensitive and fully quantitative analysis of fibrosis.

Method: Unstained tissue obtained from liver biopsy are digitized using a proprietary system and submitted to two detection methods (Genesis[®]200): a second harmonic generation (SHG) microscopy to identify collagen and a laser two-photon excited fluorescence (TPEF) microscopy to identify hepatocytes. A fully automated machine-learning (ML) image analysis processes information. Algorithms identify portal, septal and fibrillar collagen and exclude portal tracts and central veins pixels, as well as sinusoidal spaces, and extract multiple features of tissue fibrosis. Finally, for each biopsy tissue, a fully quantitative value, qFibrosis, is obtained. Quantitative and semi-quantitative results are compared.

Results: A total of 17 collagen features were selected by ML for the qFibrosis equation, among which, the most important features (with largest coefficients) are number of intersections and number of short and aggregated fiber in the overall tissue region. qFibrosis has open-ended ranges, but typical values are between 0 and 3.7 in pre-cirrhotic NASH (F0-F3) patients, with higher values representing increasing severity of fibrosis. The correlation of qFibrosis values correlate with semi-quantitative fibrosis scores and are 0.761, 0.882, and 1.491 for F1, F2, and F3, respectively.



Conclusion: The combination of digitization, laser imaging and machine learning allows for a quantitative analysis of fibrosis on unstained liver biopsy tissue. This methodology can improve the evaluation of NASH candidate treatments and offers advantages to address liabilities of current methods. By capturing and quantifying important morphological features, it is more precise and more amenable to detecting changes. With further validation data, qFibrosis could provide liver biopsy information that are more clinically relevant to support diagnosis and treatment decisions.

WED-237

Advancement of artificial intelligence in digital pathology: from exploratory end point to primary end point in non-alcoholic steatohepatitis clinical trials

Dean Tai¹, Kutbuddin Akbary¹, Yayun Ren¹, Elaine Chng¹. ¹HistoIndex Pte Ltd, Clinical Research, Singapore

Email: Dean.Tai@histoindex.com

Background and aims: Improvements in liver histology is the current accepted surrogate end point for accelerated approval for access to treatment before the impact on clinical outcomes are known in patients with non-alcoholic steatohepatitis (NASH). Recent clinical data has demonstrated the regression of NASH as a dynamic and heterogeneous process. Depending on the effects of different disease-modifying drugs, fibrosis may regress differently, with variations in morphological and architectural features across zonal regions. Hence, a histological system developed based on changes in untreated individuals does not account well for changes after an intervention. To address this, sponsors and regulatory agencies are working to explore the use of artificial intelligence (AI) in digital pathology to facilitate accurate fibrosis assessment. qFibrosis has been used in the past in phase 2 trials to help stratify patient inclusion criteria for

successful phase 3 trials. The most recent development is the US Food and Drug Administration (FDA) approving the use of qFibrosis as a primary end point in a NASH phase 2 study.

Method: Using a stain-free second harmonic generation and two-photon excitation fluorescence (SHG/TPE) imaging technology, qFibrosis is an AI-based tool which offers a reproducible and quantitative way to assess liver fibrosis on a continuous scale. It is a knowledge-based machine learning tool capable of automatically identifying and differentiating portal tracts and central veins, as well as to quantify collagen characteristics such as length, width, and area to provide an objective assessment on fibrosis patterns including peri-portal fibrosis, bridging fibrosis, of which these are key morphological features defined in NASH fibrosis system.

Results: qFibrosis models have demonstrated correlation with histologically determined NASH scores, with significant correlation observed for qFibrosis ($r = 0.776$) whereas the correlation between central pathologists' ranges from between 0.57 to 0.81 in retrospective studies. Furthermore, qFibrosis provides additional insights such as identification of the most potent fibrosis response in baseline F3 patients in some trials. Increasingly, qFibrosis is included in prospective studies, first as exploratory end point to supplement analysis done by pathologists (NCT03900429), then as a secondary end point in a NASH phase 2b study (NCT04906421), and most recently as a primary end point in another phase 2 NASH study (NCT05519475).

Conclusion: qFibrosis has the potential to provide a quantitative understanding of subtle morphological changes due to treatment-induced fibrosis regression, allowing it to be more sensitive to change within the timeframes of typical phase 2 and 3 NASH trials. This can be used for better stratification of patient inclusion criteria, which is crucial for efficacy evaluation during drug development, as well as for diagnosis once the drug is approved. This clearly demonstrates the utility of AI in digital pathology in a real-world clinical setting.

WED-238

Repeatability and reproducibility assessment and its acceptable standard error of means for qFibrosis system in multi-site NASH clinical trials

Jason Pik Eu Chang¹, Claudia Filozof², Dean Tai³, Kutbuddin Akbary³, Yayun Ren³, Elaine Chng³, Feng Liu⁴, Lai Wei⁵, David E Kleiner⁶, Arun Sanyal⁷. ¹Singapore General Hospital, Gastroenterology and Hepatology, Singapore; ²Labcorp Drug Development, Israel; ³HistoIndex Pte Ltd, Singapore; ⁴Peking University Hepatology Institute, Peking University People's Hospital, China; ⁵Hepatopancreatobiliary Center, Beijing Tsinghua Changgung Hospital, China; ⁶National Cancer Institute, National Institutes of Health, United States; ⁷Stravitz-Sanyal Institute of Liver Disease and Metabolic Health, VCU School of Medicine, United States

Email: akbary.kutbuddin@histoindex.com

Background and aims: Accurate quantification of fibrosis is critical in clinical trials in NASH. In recent years, the application of digital pathology with artificial intelligence (AI), including qFibrosis has gained increased attention due to the potential to quantify fibrosis features from liver biopsies with better inter-/intra observer agreements as compared to conventional reads. Our group has recently reported the inter-system (repeatability) and intra-system (reproducibility) of qFibrosis. In this study, we aim to describe an acceptable standard error of means for the qFibrosis system in NASH clinical trials.

Method: The study included 41 core biopsies with confirmed NASH, of which 9, 9, 13 and 10 samples were staged F1, F2, F3 and F4, respectively. Scanning was conducted with 3 Genesis200[®] machines, using second harmonic generation/two-photon excitation fluorescence (SHG/TPEF) microscopy on unstained slides. 3 repeated scans were conducted for each sample by each machine (reproducibility) and by three different machines (repeatability) at different time points, and a qFibrosis continuous value (qFC) is generated based on an AI algorithm for each sample per scan. The standard error of means

(SEM) was determined by 2 methods: 1) cohort based: taking the qFC for each patient (the median of 9 scans); 2) sample based: taking the 9 scans for each patient; with the same fibrosis stages.

Results: The SEM for F1, F2, F3, F4 are 0.1924, 0.1917, 0.3595, 1.1038 respectively using cohort-based method. And the SEM for F1, F2, F3, F4 are 0.1334, 0.1081, 0.1417, 0.3464 respectively using sample-based method. Note that the SEM values are progressively larger for higher stage of fibrosis using the cohort-based method, this is due to the fact the qFC is generally larger for higher stage of fibrosis. This is not the case for sample-based method, as the SEM is dependent on system repeatability and reproducibility instead of the value of qFC.

Conclusion: In our recent efforts in establishing repeatability and reproducibility in the advent of AI digital pathology, there is still a gap in determining the acceptable SEM for these quantitative measurements. This study aims to summarize different approaches to determine SEMs and their results. The group intends to further investigate impact of SEM on the result of assessment in NASH clinical trials with additional approaches such as Obuchowski index and report these findings to the clinical trials community.

WED-239

The anti-HIV drug Rilpivirine downregulates migration and proliferation of activated hepatic stellate cells: relevance for the purpose of drug repurposing in liver fibrosis

Ana Benedicto^{1,2}, Isabel Fuster-Martínez^{1,2}, Aleksandra Gruevska^{1,2}, Eduardo Carbonell¹, Alessandra Caligiuri³, Fabio Marra³, Elena Muñoz⁴, Dimitri Dorcaratto⁴, Juan V. Esplagues^{1,2,5}, Ana Blas-García^{2,5,6}, Nadezda Apostolova^{1,2,5}. ¹Department of Pharmacology, University of Valencia, Valencia, Spain; ²FISABIO, University Hospital Dr. Peset, Valencia, Spain; ³Department of Experimental and Clinical Medicine, University of Florence, Florence, Italy; ⁴Department of Surgery, Liver, Biliary, and Pancreatic Unit, Biomedical Research Institute INCLIVA, Hospital Clínico University of Valencia, Valencia, Spain; ⁵Biomedical Research Networking Center in Hepatic and Digestive Diseases (CIBERehd), Valencia, Spain; ⁶Department of Physiology, University of Valencia, Valencia, Spain

Email: nadezda.apostolova@uv.es

Background and aims: Liver fibrosis, a common denominator in most liver diseases, lacks specific pharmacological treatment. Rilpivirine (RPV), a widely used anti-HIV drug, has shown antifibrotic properties in several murine models of hepatic injury. Specifically, it reduces the activation of hepatic stellate cells (HSCs) and induces cell death in activated HSCs. Nevertheless, the exact mechanisms behind these actions are still unknown.

Method: Primary human HSCs were activated with the profibrogenic cytokine TGF-beta or with PDGF-beta and co-treated with clinically

relevant concentrations of RPV for 48h. For RNA sequencing transcriptomic analysis, mRNAs libraries were obtained using total RNA, their size was assessed and sequencing was performed through a single read of 75 cycles (1 × 75 bp). After differential gene expression analysis, over-representation analysis was performed using the databases Gene Ontology (GO), KEGG pathways and Reactome. Then, we validated the implication of RPV on PDGF-beta-induced chemotaxis and cell proliferation (transwell chemoattraction assay in Boyden chamber and counting the cells with trypan blue). The involvement of several protein kinases downstream of PDGF was analysed by Western Blot.

Results: In the transcriptomic analysis, 2309 genes were differentially expressed by RPV's treatment. When analyzing the pathways and processes changed, RPV showed several effects in accordance with the previous published studies, including downregulation on collagen biosynthesis and upregulation of apoptosis. Nonetheless, in the comparison of RPV at highest concentration + TGFbeta vs TGFbeta novel pathways were revealed, being the top 5 downregulated reactome pathways with highest strength of the enrichment: "unwinding of DNA," "Smooth Muscle contraction," "XBP1 (S) activates chaperone genes," "Signaling by PDGF" and "Collagen biosynthesis and modifying enzymes"; and the top upregulated: "OAS antiviral response," "keratan sulfate degradation," "STING mediated induction of host immune responses," "interferon α/β signaling" and "stabilization of p53." Similar results were obtained when analysing GO terms. Downregulation of the activated cell migration capacity and the PDGF signaling pathway stood out in the different analysis. These findings were validated in PDGF- treated HSCs in which RPV inhibited both PDGF-beta-induced chemotaxis and cell proliferation. Moreover, RPV downregulated PDGF downstream signaling pathways of AKT and JNK, but not of p38 and ERK1/2.

Conclusion: RPV reduces the PDGF-beta-induced chemotaxis and proliferation of HSCs, which may be relevant for in the antifibrotic properties of this drug already shown in mouse models of hepatic fibrosis. These finding might shed more light on the HSCs pathophysiology and give hints for novel pharmacological targets of chronic liver diseases.

WED-240

Is the fibrosis phenotype in pre- and post-menopausal F2/F3 women the same?

Isabel Fernández-Lizaranzu¹, Emilio Gomez-Gonzalez¹, Helena Pastor², Rocío Gallego-Durán², Rocío Montero-Vallejo², Louis Petitjean³, Mathieu Petitjean³, Manuel Romero Gomez².

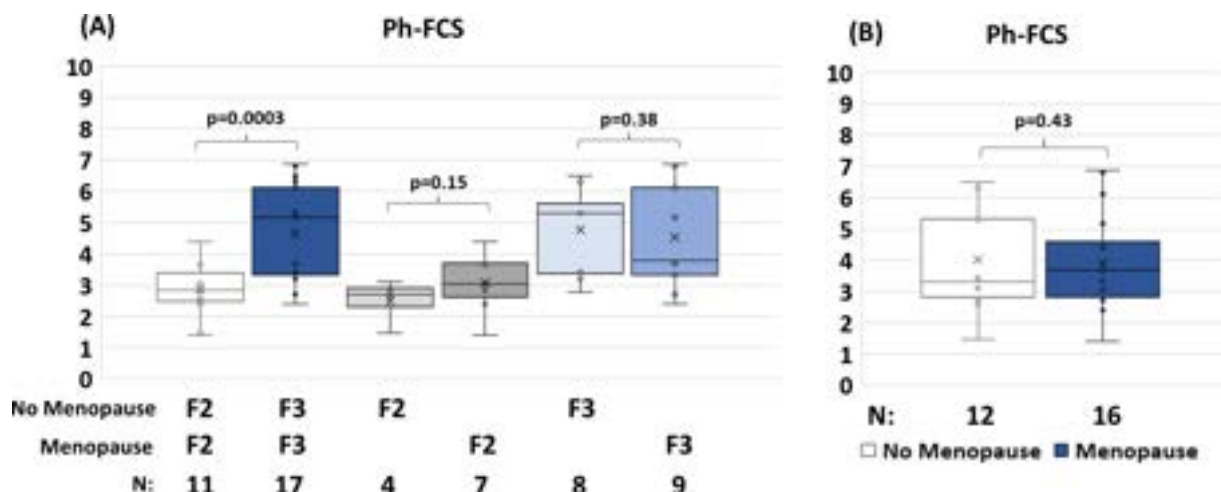


Figure: (abstract: WED-240): Phenotypic Fibrosis Severity Score (Ph-FCS) and qFTs of different groups under analysis

POSTER PRESENTATIONS

¹Interdisciplinary Physics Department, Virgen del Rocío University Hospital; SeLiver Group, Biomedicine Institute of Seville (HUVR/CSIC/US), Medicine Department, University of Sevilla; CIBEREHD, Seville, Spain; ²Liver and Digestive Diseases Unit, Virgen del Rocío University Hospital; SeLiver Group, Biomedicine Institute of Seville (HUVR/CSIC/US), Medicine Department, University of Sevilla; CIBEREHD, Seville, Spain; ³PharmaNest, Princeton, NJ, United States
Email: ifernandez14@us.es

Background and aims: While several teams have hypothesized that the hepatic phenotype of pre- and post-menopausal women should be different, current histological methods (semi-quantitative categorical stages) do not have the analytical sensitivity to address the question. Here we use high-resolution, single-fiber digital pathology quantitative pathology and AI (FibroNest™) to distinguish different phenotypes of fibrosis between pre- and post-menopausal patients with moderate (F2/F3 stages) fibrosis.

Method: This study was performed on a retrospective cohort of 28 biopsy-proven patients recruited between 2010 and 2018 at seven different Spanish hospitals. The overall cohort consisted of female patients with two different stages of fibrosis, 11 (39%) were F2 and 17 (61%) were F3, 16 (57%) had menopause and 12 (43%) didn't have it, a median age of 56 (±11) years. FFPE liver biopsies were stained with Masson Trichrome, scanned using 20X light microscopy and quantified using FibroNest™ for the Phenotypic Quantification of Fibrosis and its associated features. This method provides a continuous phenotypic Fibrosis Composite Severity (Ph-FCS) scores that ranges from 1 to 10 fibrosis severity observed in the liver. The Ph-FCS were evaluated at different groups: F2, F3, Menopause, No Menopause, F3-No menopause (N = 8), F3-Menopause (N = 9), F2-No menopause (N = 4), F2-Menopause (N = 7).

Results: F2 cases had lower Ph-FCS than F3 cases with a significant difference between them independently of the menopause state (Student's t-Test $p = 0.0003$) (Figure, A). When F2/F3 cases were compared considering the menopause stage, there was no significant difference between pre-/post-menopause ($p = 0.15$ for F2 and $p = 0.38$ for F3) (Figure, B). Yet, we found 55 phenotypes that changed significantly in both cases (pre-/post-menopause), among them perimeter and filled to area ratio of assembled collagen phenotypes. We found 16 phenotypes changed significantly for only post-menopause cases and 75 phenotypes changed significantly only for pre-menopause cases.

Conclusion: Quantitative Digital Pathology analysis, using FibroNest™, was able to distinguish severity groups in concordance with NASH CRN stages in this limited cohort, as reported elsewhere. In each severity group and in aggregate we do not find statistically significant differences in fibrosis severity between pre- and post-menopausal women. It was also able to identify specific differences in the progression of fibrosis between pre- and post-menopausal women.

WED-241

Amelioration of CCl₄ induced hepatic fibrosis in-vitro and in-vivo by bone marrow derived mesenchymal stromal cells lysate loaded nanostructured lipid carriers

Sabeen Malik¹, Sana Awan², Tehreem Malik³. ¹The University of Lahore, Institute of Molecular Biology and Biotechnology, Lahore, Pakistan; ²Kinnaird College for Women, Department of Zoology, Lahore, Pakistan; ³Rehbar Medical and Dental College, Lahore, Pakistan
Email: sabeen004@gmail.com

Background and aims: Bone marrow mesenchymal stromal cells (BMSCs) are considered a novel strategy to treat hepatic fibrosis. BMSCs lysate was encapsulated in nanostructured lipid carriers (NLC) to deliver cellular contents and regulatory elements of BMSCs at the injury site. This study was designed to evaluate the therapeutic potential of BMSCs lysate loaded NLC (BMSCs-L-NLC) in carbon tetrachloride (CCl₄) induced liver fibrosis *in-vitro* and *in-vivo*.

Method: NLC was prepared by using the nano-template engineering method. CCl₄ induced hepatotoxicity in hepatocytes (*in-vitro*) and

rats (*in-vivo*) was used to evaluate the therapeutic potential of BMSCs-L-NLC.

Results: NLC preparation and loading with BMSCs lysate was confirmed via size and morphology analysis, and ELISA of lysate proteins. *In-vitro*, BMSCs-L-NLC treatment increased the viability of injured hepatocytes, elevated antioxidants (superoxide dismutase (SOD), glutathione reductase (GR), ascorbate peroxidase (APX) and catalase (CAT)) and alleviated liver markers (alanine aminotransferase (ALT), alkaline phosphatase (ALP), and lactate dehydrogenase (LDH)) in hepatocytes secretome. *In-vivo*, rats exposed to CCl₄ developed liver injury characterized by a significant increase in liver enzymes, apoptosis, and decreased liver markers expression and proliferation. Treatment with BMSCs-L-NLC enhanced liver state effectively. It significantly decreased the elevated liver enzymes (bilirubin, ALT, ALP, and LDH), apoptosis (measured via p53, Bax, Caspase-3 expression), and immunosuppression of annexin V and increased liver markers (measured via ALB, AFP, and IGF-1), proliferation (measured via Ki-67, PCNA and TOP2A expression), antioxidants and immunoexpression of liver marker ALB. Histopathological studies confirmed the therapeutic effects of BMSCs-L-NLC.



Figure:

Conclusion: BMSCs-L-NLC could restore liver structure and function in CCl₄-induced liver fibrosis *in-vitro* and *in-vivo* by ameliorating the toxicity of CCl₄ and improving liver functioning as indicated by biochemical, histological, immunohistochemical, and gene expression results.

WED-242

Characterizing the long-term stability of human pluripotent stem cell-derived non-parenchymal liver cells

Ingrid Wilhelmsen^{1,2}, Mikel Martinez¹, Justyna Stokowiec¹, Aleksandra Aizenshtadt¹, Stefan Krauss^{1,2}. ¹University of Oslo, Institute of Basic Medical Sciences, Hybrid Technology Hub, Oslo, Norway, ²Oslo University Hospital, Institute of Clinical Medicine, Department of Immunology, Oslo, Norway
Email: ingrid.wilhelmsen@medisin.uio.no

Background and aims: There is a significant need for predictive and stable *in vitro* human liver models for disease modelling and drug testing. Hepatic stellate cells (HSCs) and liver sinusoidal endothelial cells (LSECs) are important non-parenchymal cell (NPC) components of a variety of such models, particularly models involving hepatic fibrosis. However, the use of primary human HSCs and LSECs is significantly limited by the availability of donor material and rapid loss of cell-specific phenotype and functionality during isolation and *in vitro* culture. Recently published approaches to obtaining pluripotent stem cell- (PSC-) derived HSCs and LSECs offer an attractive alternative to primary human material; yet, the suitability of PSC-derived HSCs and LSECs for extended *in vitro* modelling has not been characterized. In this study, we aimed to describe changes in cell-specific phenotype and functionality of PSC-derived HSCs and LSECs during long-term *in vitro* culture.

Method: PSC-derived HSCs and LSECs (differentiated from hESC line H1 and iPSC lines WTC-11, WTSli28-A and WTSli013-A) were cultured *in vitro* for 14 days post-differentiation. Cell-specific phenotypes were evaluated by cell morphology, immune fluorescence, gene- and protein expression. Functionality was assessed in HSCs by their capacity for intracellular storage of vitamin A and response to pro-fibrotic stimuli induced by TGF-beta 1 and in LSECs by nitric oxide- and factor VIII secretion as well as endocytic uptake of bioparticles and acetylated low density lipoprotein. Notch pathway inhibition by treatment with DAPT and co-culturing HSCs and LSECs were separately tested as options for enhancing long-term stability and maturation of the PSC-derived NPCs.

Results: Both cell types exhibited significant changes in their phenotype and functionality during the long-term culture, acquiring signs of activation and decline in functionality. Notch pathway inhibition modestly improved the stability of both PSC-derived HSCs and LSECs in a cell line-dependent manner. Long-term co-culturing of PSC-derived HSCs and LSECs showed signs of improved HSC function as judged by vitamin A storage and responsiveness to pro-fibrotic stimuli.

Conclusion: PSC-derived HSCs and LSECs show a deteriorating phenotype and functionality during extended post-differentiation culture. Choice of PSC line and a limited experimental timeframe is crucial when designing *in vitro* platforms involving PSC-derived HSCs and LSECs. While Notch inhibition offers a promising approach to extend post-differentiation monoculture, co-culturing PSC-derived HSCs and LSECs could be used for both prolonged phenotypic and functional stability as well as HSC maturation.

WED-243

3D Extracellular matrix human liver hydrogels for the investigation of genetic variants in hepatic stellate cells

Elisabetta Caon¹, Philipp Schwabl¹, Luca Frenguelli¹, Hannah Evans¹, Margarita Papatheodoridi¹, Zalihe Keskin-Erdogan², Nicola Mordan², Jonathan Knowles², Giuseppe Mazza¹, Massimo Pinzani¹, Krista Rombouts¹. ¹University College of London, Royal Free Campus, Regenerative Medicine and Fibrosis Group, Institute for Liver and Digestive Health, United Kingdom; ²University College of London, Royal Free Campus, Biomaterials and Tissue Engineering Division, Eastman Dental Institute, United Kingdom
Email: elisabetta.caon.17@ucl.ac.uk

Background and aims: Liver fibrosis is a crucial pathophysiological step in chronic liver diseases (CLD). Activated hepatic stellate cells (HSCs) are the key mediators of fibrogenesis and, therefore, research has been focusing on identifying and addressing pro-fibrogenic mechanisms in HSCs for the development of new drug candidates to treat fibrogenic liver diseases. This process has been hampered by the lack of appropriate *in vitro* models. In addition, only recently attention has been given to the importance of genetic polymorphisms for the onset of CLD, with numerous new variants being discovered, although their molecular role is still largely unclear. In this project, the synergic impact of the PNPLA3 I148M and TM6SF2 E156K SNP variants on the pro-fibrogenic behaviour of HSCs has been investigated, utilizing a newly developed platform of 3D hydrogels obtained from the decellularized extracellular matrix (ECM) of healthy and diseased human livers.

Method: Healthy or cirrhotic decellularized human liver ECM 3D scaffolds were lyophilized and solubilized to yield liver ECM solution. The ECM solution was mixed with a nanocellulose-based gelling agent to form hydrogels for culturing primary human HSCs WT or mutant for the PNPLA3 I148M and TM6SF2 E156K genetic variants in a 3D setting. Following evaluation of the ECM hydrogels mechanical properties by Dynamic Mechanical Analysis (DMA) and SEM, cell behaviour of HSCs cultured in ECM hydrogels and treated with/without TGFβ1/Endothelin-1 was investigated using various molecular biology techniques.

Results: Hydrogels made with human liver ECM proved to be mechanically stable and with a stiffness comparable to that of healthy human livers. Both healthy and cirrhotic ECM liver hydrogels supported HSC viability and responsiveness to pro-fibrogenic agents such as TGFβ1, with an increase in COL1A1, TIMP1 and TGFβ1 gene expression. Furthermore, HSCs showed similar behaviour when cultured in an established model of 3D ECM scaffolds or ECM hydrogels and featured a less activated phenotype (lower expression of ACTA2, COL1A1, TIMP1 and higher CYGB) compared to 2D plastic culture. HSCs carrying the PNPLA3 I148M and TM6SF2 E156K variants showed an increased basal contraction and activation (increased COL1A1 and TIMP1) compared to WT HSCs. This effect was strongly increased by the presence of cirrhotic ECM.

Conclusion: This study introduces and provides a technical characterization of liver ECM hydrogels as high throughput 3D cell culture models recapitulating the cellular microenvironment of normal or fibrotic human liver, to be employed in unravelling the pro-fibrogenic behaviour of HSCs in presence of different genetic variants and their role in the progression of CLD.

WED-244

Analysis of alpha adrenoblocker as antifibrotic and hepatoprotective agent in a Wistar rat model of cirrhosis

Mariana Yazmin Medina Pizaño¹, María de Jesús Loera Arias¹, Roberto Montes de Oca Luna¹, Odila Saucedo Cárdenas¹, Javier Ventura Juárez², Martín Muñoz Ortega³. ¹Autonomous University of Nuevo Leon, Histology, Monterrey, Mexico; ²Autonomous University of Aguascalientes, Morphology, Aguascalientes, Mexico; ³Autonomous University of Aguascalientes, Chemistry, Aguascalientes, Ags., Mexico
Email: mariana93medina@gmail.com

Background and aims: Liver cirrhosis is a major public health problem and a significant source of morbidity and mortality. Cirrhosis is the histological development of regenerative nodules surrounded by fibrous bands in response to chronic liver injury. In the liver, damage-activated stellate cells or hepatic myofibroblasts play a key role in the initiation and progression of the disease. The liver has a cellular compartment with neuroendocrine characteristics composed of progenitor cells and hepatic stellate cells. There is increasing evidence that the sympathetic and parasympathetic nervous systems influence this cellular compartment. Evaluation of the effects of alpha and beta adrenoblockers on a murine cirrhosis model concludes that the reduction of type I collagen after the treatment is achieved by reducing the profibrotic activities of TGF-β, a decrease in fibrotic tissue and increase of liver function. In this study, we aimed to analyze tamsulosin's antifibrogenic and hepatoprotective capacity in a Wistar rat model of cirrhosis.

Method: Wistar rats were injected twice per week with thioacetamide to induce liver cirrhosis. Rats were treated with tamsulosin, an alpha adrenoblocker, five times per week, and samples were taken after 4 weeks. The serum was collected and tested for the activity levels of aminotransferases (AST or GOT and ALT or GPT) and alkaline phosphatase (ALP). Collagen deposition was analyzed on HandE, Masson's trichrome, and Sirius red staining. The expression of molecular markers of collagen deposit and hepatoprotective effect were evaluated by RT-qPCR (collagen I, PPARγ, α-SMA, Nrf2 and HO-1). To study the interaction between stellate cells and tamsulosin, a stellate cell line (LX2) was co-cultured using viability assays (calcein-AM and SYTOX Green), and oxidative stress was analyzed at 24 h using dihydroethidium (DHE). The activation of HSCs was observed by Oil Red O Staining and the migratory response of HSCs by scrape wound healing assay.

Results: Masson's trichrome and Sirius red staining showed a significant decrease in collagen deposition with tamsulosin treatment compared to controls. Liver sections of the control group exhibited normal lobular architecture, whereas liver sections of the thioacetamide-intoxicated group exhibited typical architectural

POSTER PRESENTATIONS

distortions with regenerative nodules surrounded by proliferative connective tissue; co-treatment with tamsulosin improved the architecture of liver parenchyma. Study results indicated that the activity of the aminotransferases (AST and ALT) and ALP increased significantly in thioacetamide-treated rats compared to control animals. However, tamsulosin showed a decrease in activity. Treatment with tamsulosin regulates the oxidative stress through mRNA expression of hepatoprotector markers (Nrf2, PPAR γ and HO-1) and decrease the expression of collagen I and α -SMA. Tamsulosin treatment significantly inhibits the LX2 cell proliferation activation and migration (without affecting its viability).

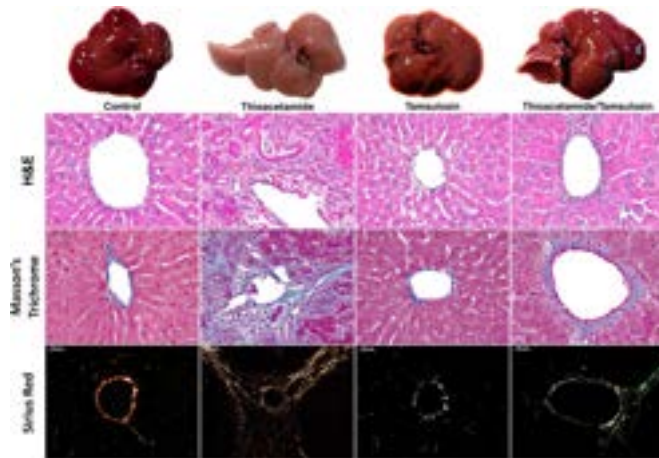


Figure:

Conclusion: The present study demonstrated that tamsulosin may enhance hepatic efficiency in Wistar rats by a decrease of collagen synthesis and an increase of liver function. Therefore, tamsulosin retards the proliferation, activation, and migration of LX2 cells without inducing cytotoxicity and oxidative stress.

WED-245

MicroRNA-29b involves in the progression of NAFLD to liver fibrosis

Qihua Duan¹, Qiaozhu Su². ¹Institute for Global Food Security, School of Biological Sciences, Queens University Belfast, Belfast, United Kingdom; ²Institute for Global Food Security, School of Biological Sciences, Queens University Belfast, United Kingdom
Email: q.su@qub.ac.uk

Background and aims: Liver fibrosis, a pathological consequence of multiple injurious insults in liver, is the late stage of Non-alcoholic fatty liver disease (NAFLD) that can lead to liver failure. MicroRNAs (miRNAs) are small non-coding RNAs that can regulate their target mRNAs and impact diverse cellular processes by complementary base-pairing the 3'-UTR of the target mRNAs. MiR-29 family has been implicated in the pathogenesis of pulmonary fibrosis and cardiac fibrosis, however, its role in liver fibrosis is unclear. In this study, we investigated the mechanism of miR-29b in the progression of NAFLD to liver fibrosis.

Method: In vivo, a mouse model was established by feeding high-fat diet (HFD) and treating the mice with miR-29 mimics. In vitro, the Murine hepatocytes cell line AML12, and Hepatic stellate cells (HSC) are used treated with inflammatory cytokine TNF α and free fatty acid Palmitic acid (PA), Hedgehog Inhibitors MDB5 and/or miR-29b mimics.

Results: Q-RT-PCR analysis revealed that HFD induced liver injury from NAFLD to liver fibrosis, which was associated with the significant decrease of miR-29b in the liver tissues of the HFD

feeding mice. Treated the mice with nanoparticles encapsulated with miR-29b mimics significantly improved liver fibrosis and enhanced insulin sensitivity. In vitro, TNF α or PA treatment inhibited miR-29b in the mouse hepatocytes, AML-12, whereas, incubation with a hedgehog inhibitor MDB5 upregulated miR-29b expression, suggesting the crucial role of miR-29b in Hedgehog pathway and liver fibrosis. Moreover, upregulated cellular miR-29b by transient transfection improved expression of genes involved in mitochondrial energy homeostasis and fatty acid β -oxidation. mRNA levels of PPAR α and CPT1 α were increased in AML12 cells treated with miR29 mimics ($p < 0.001$).

Conclusion: Novel findings from demonstrate the essential role of miR-29b in preventing the progression of NAFLD to liver fibrosis.

WED-246

Novel Pathways implicated in the seladelpar-mediated reductions of established liver fibrosis are identified from RNA-SEQ data using plex search and two independent mouse pharmacology datasets

Edward Cable¹, Doug Selinger², Yun-Jung Choi¹, Charles McWherter¹. ¹Cymabay Therapeutics Inc., Newark, United States, ²Plex Research, Inc, Cambridge, United States
Email: ecable@cymabay.com

Background and aims: Seladelpar is a selective peroxisome proliferator delta (PPARD) agonist that reduced established liver fibrosis in the Amylin-diet NASH and CCl₄ chemical injury models. In each model, an induction period for fibrosis is followed by a treatment period during which the fibrotic stimuli is maintained. End points include evaluation of fibrosis and RNA-seq analysis. The aim of our analysis is to uncover novel aspects of seladelpar's anti-fibrotic mechanism using liver RNA-seq datasets from these models together with the Plex AI-analytical platform to search relevant large public data bases. Unlike bioinformatics methods that insinuate biological importance with the magnitude of change, Plex allows the use of an omics data set as a search query in a search engine interface against aggregated data from publicly available databases. The search results can suggest novel associations as hypotheses not evident in bioinformatic evaluation of the original omics data set.

Method: RNA-seq from the livers of mice treated in the Amylin-diet model (43w induction, 12w Tx; [n = 12 (V), n = 11 (Tx)] and CCl₄ (5w induction, 3w Tx; [n = 20]) were analyzed and the top 100 differentially expressed genes were used as query gene lists in Plex's search platform (www.plexresearch.com). Liver tissue samples were obtained after sacrifice at 2 (Amylin diet) and 24 hours (CCl₄) post last dose. Plex queries with the RNA-seq data sets identified enrichment of the differentially expressed genes in multiple data domains. Gene family results were obtained by this analysis.

Results: The lipocalin family members (transporters of small hydrophobic molecules) were reduced in both models with amongst the highest observed scores. Lipocalins have not been associated with PPARD but levels are correlated with fibrosis. Decreases in lipocalin-2 have been accompanied by decreased inflammation in disease models. In addition, the clade A serpin protease inhibitors were reduced in both models whereas serpins from clades B-D were minimally changed. The reduction of serpin

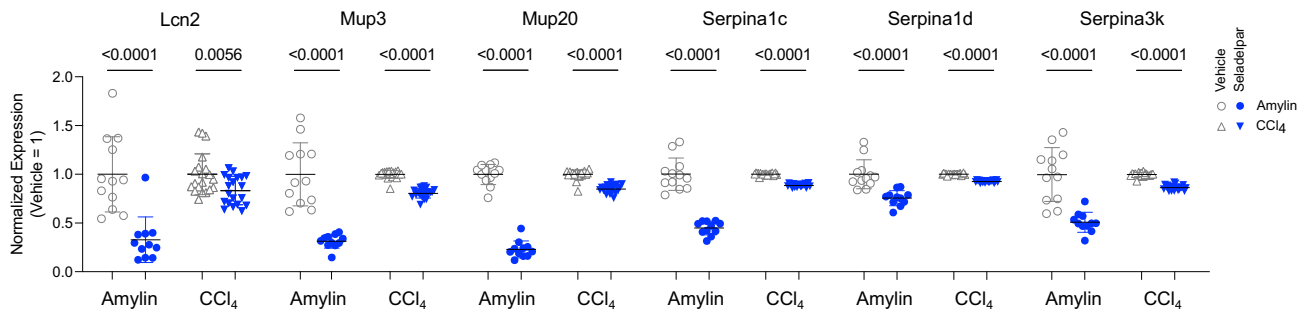


Figure: (abstract: WED-246).

protease inhibitors could implicate proteolytic fibrolysis contributing to the decrease in fibrosis. Seladelpar treatment also led to decreases in protein families related to hedgehog signaling, intracellular chloride channels, glutathione reductase transferases, and rhodopsin-like GPCRs, gene families that have been previously associated with fibrosis. Shown in the graph below are the three highest expressing genes in the lipocalin and serpin families.

Conclusion: The use of a novel search platform along with transcriptomics data sets produced consistent findings for two different fibrosis models. The results identified several pathways to investigate for their role in the reduction of fibrosis by seladelpar observed in mice. Understanding the roles of these pathways will assist in our understanding of the relevance of mechanisms for human disease.

WED-247

Cathepsin D expressed in hepatocytes does not participate in the development of liver fibrosis after chronic CCl₄ administration

Paloma Ruiz-Blazquez^{1,2}, Maria Fernandez-Fernandez^{1,2}, Valeria Pistorio^{3,4}, Susana Núñez², M. Carmen Garcia-Ruiz^{1,2,5,6}, José Fernandez-Checa^{1,2,5,6}, Anna Moles^{1,2,5}. ¹Instituto de Investigaciones Biomédicas de Barcelona (IIBB-CSIC), Spain; ²Centro de Investigación Biomédica en Red de Enfermedades Hepáticas y Digestivas (CIBERehd), Spain; ³Sorbonne Université, Inserm, Centre de Recherche Saint-Antoine (CRSA), France; ⁴University of Naples Federico II, Italy; ⁵Institut d'Investigacions Biomèdiques August Pi i Sunyer (IDIBAPS), Spain; ⁶USC Research Center for ALPD, United States
Email: anna.moles.fernandez@gmail.com

Background and aims: During liver fibrosis, proteolytic activity is timely regulated in infiltrating and resident cells depending on the cellular demands. Proteolytic modification of certain substrates such as growth factors, chemokines and extracellular matrix proteins among others, results in important changes in inflammation, apoptosis, extracellular matrix remodeling and autophagy paving the way for fibrosis development, progression and reversion. Despite our growing understanding of the roles played by lysosomal proteases in liver fibrosis, our knowledge of their specific targets and signaling networks remains still limited. Thus, the aim of this study was to analyze cathepsin D (CtsD) cell-specific role in hepatocytes during liver fibrosis.

Method: We generated a novel knock-out mouse strain by breeding Albumin-Cre (hepatocytes) mice with CtsD floxed mice. CtsD^{ΔHep} mice was validated by CtsD WB in primary mouse hepatocytes and dual IF (F4/80-CtsD) in liver sections. Fibrosis was established by chronic administration of CCl₄ twice a week for 8 weeks or bile duct ligation for 14 days in CtsD^{F/F} and CtsD^{ΔHep} mice. Liver damage was determined by serum ALT. CtsD deletion was assessed by enzymatic activity assay, WB, IF and RTPCR. Fibrosis was analysed by Sirius Red staining, liver hydroxyproline, α-SMA IHP and α-SMA, Col1A1 and TGF-β RTPCR. Liver inflammation was determined by NIMP and F4/80 IHP and TNF-α, CCL3 and CCL4 RTPCR.

Results: CtsD cell-specific deletion in hepatocytes was validated by CtsD WB in primary mouse hepatocytes and dual IF (F4/80-CtsD) in liver section from CtsD^{F/F} and CtsD^{ΔHep} mice. Of note, CtsD expression remained unaffected in liver non-parenchymal cells. Next, fibrosis was established for 8 weeks by CCl₄ administration. CtsD deletion in CtsD^{ΔHep} livers was confirmed by CtsD IHP and gene expression. CtsD deletion in hepatocytes did not affect liver damaged (ALT) and liver fibrosis as determined by Sirius red staining, α-SMA IHP and hepatic α-SMA, Col1A1 and TGF-β gene expression. Furthermore, liver inflammation was also not significantly affected in CtsD^{ΔHep} mice after CCl₄ as assessed by NIMP and F4/80 IHP and TNF-α, CCL2 and CCL3 gene expression. In agreement, no significant changes in liver damage, fibrosis and inflammation were observed after 14 days BDL between CtsD^{F/F} and CtsD^{ΔHep} mice supporting our results in the CCl₄ model.

Conclusion: CtsD expressed in hepatocytes does not play an essential role in liver fibrosis development.

WED-248

Myeloperoxidase from neutrophil granulocytes accomplish destruction of Schistosoma mansoni eggs

Ricarda Sölter¹, Verena von Buelow¹, Dorothee Dreizler¹, Grit Stampa¹, Thomas Quack², Christoph G. Grevelding², Max Moescheid², Annette Tschuschner¹, Heike Mueller¹, Martin Roderfeld¹, Elke Roeb¹. ¹Justus-Liebig-University and University Hospital UKGM, Gastroenterology, Giessen, Germany; ²Institute for Parasitology, Justus-Liebig-University and University Hospital UKGM, Giessen, Germany
Email: Ricarda.N.Solter@med.uni-giessen.de

Background and aims: Schistosomiasis is a highly relevant parasitic diseases with worldwide over 200 million affected people. Schistosoma parasite pairs occur in the mesenteric veins and produce eggs. These eggs can be flooded into different organs like the liver and lead to a chronic inflammation, causing liver portal hypertension and fibrosis. These hepatic eggs can be removed by immune cells after the treatment with Praziquantel, but neither a precise cellular mechanisms nor molecular processes of this elimination have been described so far.

Method: Male C57BL/6 mice were infected with 100 cercariae of the species *Schistosoma mansoni*. Histologic grading, myeloperoxidase (MPO)- and CD11b-immunohistochemistry were conducted to determine the inflammation and involved immune cells. Furthermore, *S. mansoni* eggs were cultivated in vitro with active and inactivated MPO for 48 hours, and stained stained with Calcein, Hoechst, and SytoxOrange afterwards to determine their vitality.

Results: *S. mansoni* is able to induce a typical hepatic granulomatous inflammation in infected mice. About 20% of the analyzed eggs, however, appeared destroyed and partly entered by immune cells. These immune cells were CD11b-positive. The nuclear shape of the CD11b+ cells match that of neutrophil granulocytes. MPO-immunohistochemistry showed several MPO-expressing cells within the granulomas and also next to destroyed *S. mansoni* eggs. Moreover, the

POSTER PRESENTATIONS

in vitro cultivation of *S. mansoni* eggs with MPO significantly reduced their viability compared to the control eggs cultivated with heat-inactivated MPO.

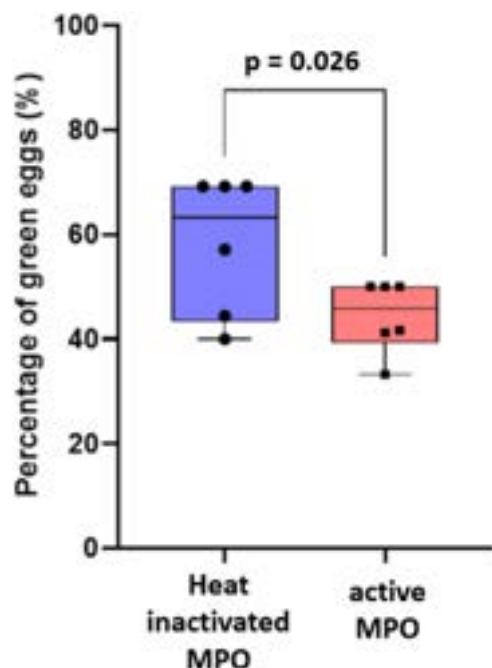


Figure:

Conclusion: Our results suggest that neutrophil granulocyte derived MPO is able to devitalize and to remove *S. mansoni* eggs from mouse liver *in vivo* and *in vitro*.

WED-249

Identification of pseudo-immune tolerance for chronic hepatitis B patients : development and validation of a non-invasive prediction model

Shuo Li^{1,2}, Zhiguo Li³, Xiaoke Li^{1,2}, Xiaobin Zao^{1,2}, Yufeng Xing⁴, Yong'an Ye^{1,2}. ¹Dongzhimen Hospital, Beijing University of Chinese Medicine, China; ²Institute of Liver Diseases, Beijing University of Chinese Medicine, China; ³Beijing Fengtai Hospital of Integrated Traditional and Western Medicine, China; ⁴Shenzhen Traditional Chinese Medicine Hospital, China
Email: yeyongan@vip.163.com

Background and aims: Patients with chronic hepatitis B (CHB) in the immune tolerant (IT) phase were thought to have no or slight inflammation or fibrosis in the liver. Indeed, some patients with normal ALT levels still experience liver fibrosis. This study aimed to develop and validate a non-invasive model for identifying pseudo-immune tolerance of CHB by predicting significant liver fibrosis.

Method: This multi-center study enrolled a total of 445 IT-phase patients who had undergone liver biopsy for the training cohort (n = 289) and validation cohort (n = 156) during different time periods. A risk model (IT-3) for predicting significant liver fibrosis (Ishak fibrosis score ≥ 3) was developed using high-risk indicators that were identified using multivariate stepwise logistic regression. Next, an online dynamic nomogram was created for the clinical usage. The receiver operating characteristic (ROC) curve and the area under the ROC curve (AUC) were used to assess the discrimination of the model. Calibration curves were used to evaluate the models' calibration. The

clinical practicability of the model was evaluated using decision curve analysis and clinical impact curves.

Results: Aspartate aminotransferase (AST), hepatitis B e-antigen (HBeAg) and platelet (PLT) were included in the IT-3 model. The IT-3 model showed good calibration and discrimination both in the training and validation cohorts (AUC = 0.888 and 0.833, respectively). At a cut-off value of 106 points, the sensitivity and specificity were 91.7% and 70.2%, respectively. The decision curve analysis and clinical impact curves indicated that the IT-3 model had good clinical application.

Conclusion: The IT-3 model proved an accurate non-invasive method in predicting significant liver fibrosis for CHB patients with pseudo-immune tolerance, which can help to formulate more appropriate treatment strategies.

WED-250

The anti-fibrotic efficacy of Adelmidrol depends in the level of hepatic PPAR γ

Huanyu Xiang¹, Jing Xiao¹, Zilin Sun¹, Zongyi Liu¹, Junhao Zhang¹, Hongyan Xiang¹, Hong Ren¹, Peng Hu¹, Ming-Li Peng¹. ¹The Second Affiliated Hospital, Chongqing Medical University, Key Laboratory of Molecular Biology for Infectious Diseases (Ministry of Education), Institute for Viral Hepatitis, Department of Infectious Diseases, Chongqing, China
Email: peng_mingli@hospital.cqmu.edu.cn

Background and aims: Effective anti-inflammatory therapy is beneficial to delay the progression of liver fibrosis. Adelmidrol, a potent anti-inflammatory small-molecule compound, has been reported to treat inflammatory diseases like arthritis and colitis. The study is aimed to investigate the effect of adelmidrol on hepatic fibrosis.

Method: Experimental liver fibrosis was induced by chronic CCl₄ exposure or choline-deficient, L-amino acid-defined, high-fat diet (CDAA-HFD). Histopathological signs and serum markers were used to evaluate the pharmacological activity of adelmidrol.

Results: Firstly, adelmidrol had different anti-fibrotic effects in these two liver fibrotic models. In the CCl₄ model, serology and liver pathology showed adelmidrol significantly improved liver injury and fibrosis by significantly reducing ALT, AST, and the deposition of extracellular matrix. While adelmidrol exhibited limited anti-fibrotic effect in CDAA-HFD-induced fibrosis, instead, aggravated the hepatic steatosis and TG content. Secondly, the inconsistencies of expression trend in liver PPAR γ were observed in both models. The CCl₄ injury led to the continuous decrease of hepatic PPAR γ levels, and the CDAA-HFD diet induced the increased PPAR γ level. Long-time adelmidrol administration significantly increased hepatic PPAR γ levels of both models. Interestingly, GW9662 (a specific PPAR γ antagonist) pretreatment prevented the up-regulation of PPAR γ induced by adelmidrol in both models, which counteracted the anti-fibrotic effect of adelmidrol in the CCl₄ model, and reversed the aggravating steatosis effect of adelmidrol in the CDAA-HFD model. Thirdly, liver RNA-Seq analysis and immunohistochemistry demonstrated adelmidrol markedly inhibited the activation of hepatic macrophages and stellate cells (HSCs) in the CCl₄ model, and *in vitro* and *in vivo* experiments confirmed adelmidrol aggravated steatosis in hepatocytes by activating the PPAR γ /CD36 pathway in the CDAA-HFD model.

Conclusion: Adelmidrol significantly up-regulates the level of PPAR γ in liver tissue, which is mainly expressed in hepatocytes, macrophages, and HSCs. The anti-fibrotic effect of adelmidrol finally depends on the synergistic interactions among hepatocytes,

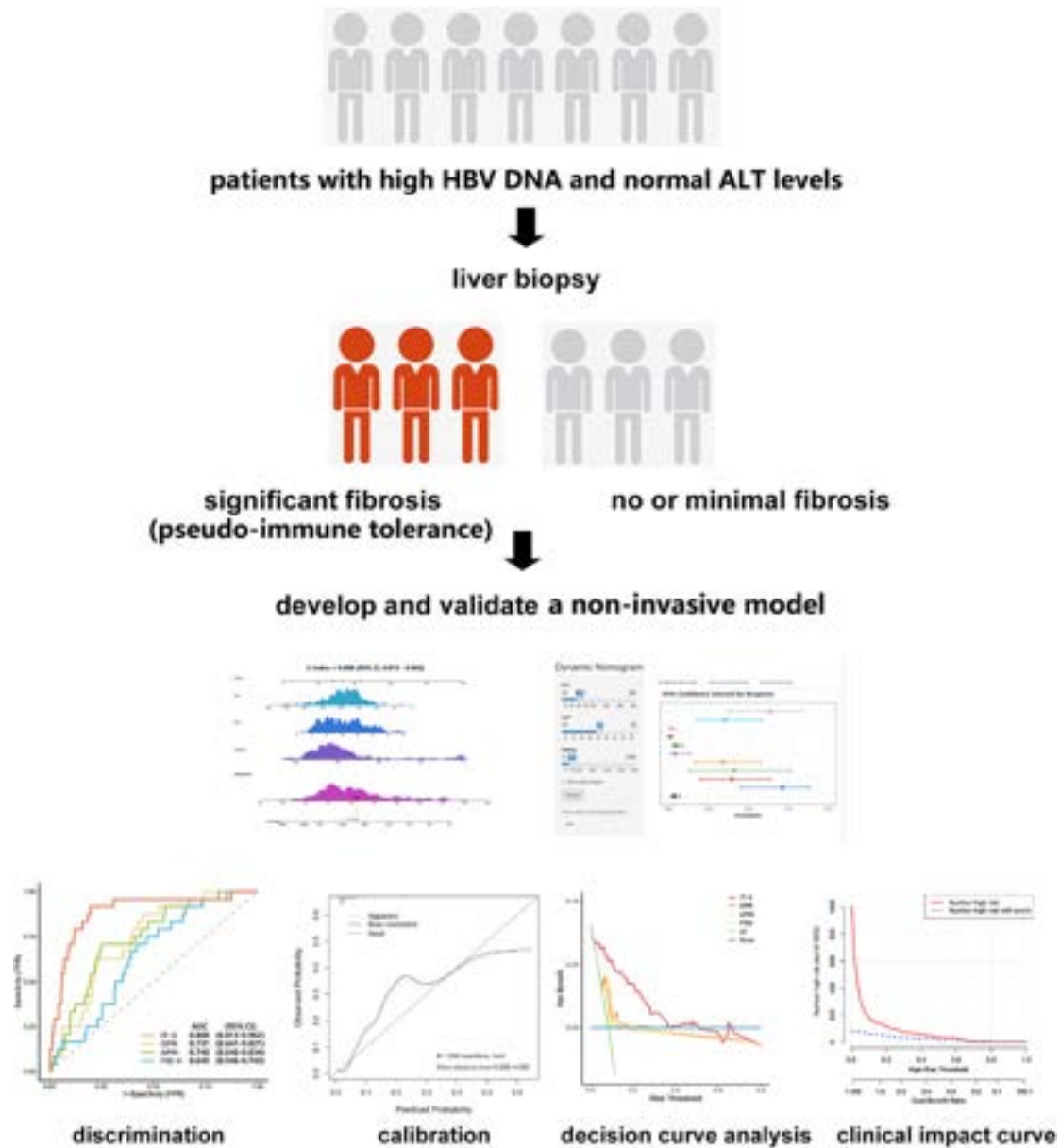


Figure: (abstract: WED-249).

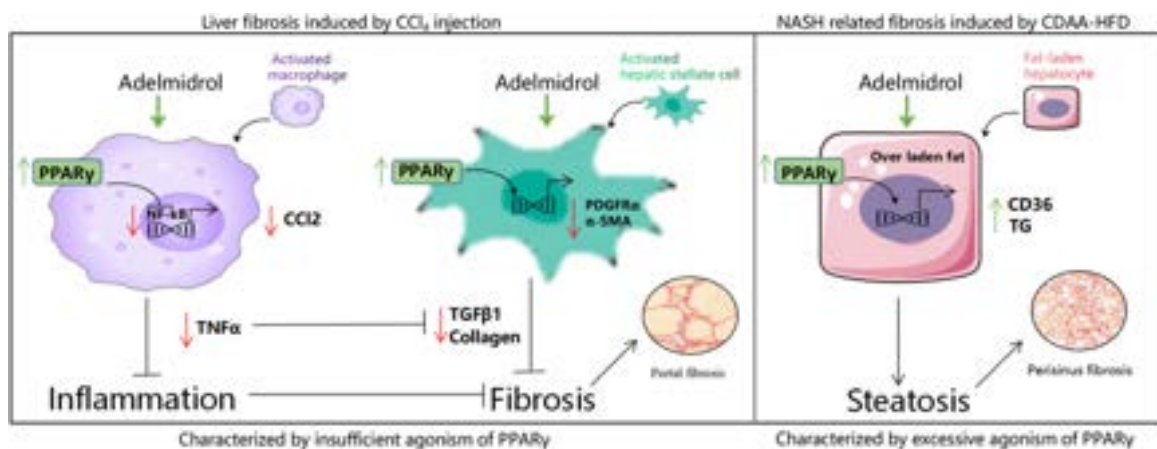


Figure: (abstract: WED-250).

POSTER PRESENTATIONS

macrophages, and HSCs in different pathological states. For liver injury characterized by insufficient agonism of PPAR γ , adelmirdrol tends to inhibit macrophage and HSCs activation to improve fibrosis. Conversely, it may aggravate steatosis.

Gut microbiota and liver disease Liver-organ crosstalk

WEDNESDAY 21 TO SATURDAY 24 JUNE

TOP-038

Gut viral and bacterial alterations modulate the presence and dynamics of minimal hepatic encephalopathy at baseline and longitudinally

Thananya Jinato¹, Andrew Fagan², Masoumeh Sikaroodi¹, Patrick Gillevet¹, Jasmohan S. Bajaj², ¹George Mason University, United States; ²Virginia Commonwealth University, United States
Email: jasmohan.bajaj@vcuhealth.org

Background and aims: Minimal hepatic encephalopathy (MHE) is associated with an altered gut-brain axis. However, most recent data are focused on bacteria but viruses, especially phages could affect brain dysfunction in cirrhosis. Aim: Determine linkage of cognitive function with MHE and bacteria and viruses cross-sectionally and longitudinally.

Method: Outpts with cirrhosis underwent cognitive testing using psychometric hepatic encephalopathy score (PHES) to diagnose MHE using local norms cross-sectionally. A subset was followed over time and MHE dynamics were determined over time. Stool was collected for metagenomics at all time points. Bacteria and viruses were evaluated and linked with MHE/no at baseline and over time using DESeq2. Correlation networks between cognitive testing, viruses and bacteria were created and compared using R.

Results: Clinical: Cross-sectional: 138 cirrhosis pts; 46% MHE, 52% prior HE, (50 HCV, 49 alcohol, 23 both and rest NAFLD). MHE pts were older (62 vs 58, $p=0.04$) but had similar prior HE (51% vs 53%) and MELD (10.7 vs 10.9) as no-MHE pts. PPI (40 vs 40), lactulose (40 vs 31) and rifaximin use (27 vs 24) were similar between groups. Longitudinal: 36 pts were followed for 9 \pm 4 mths, when testing was repeated. 23 had MHE at baseline. Over time, MHE status changed in 9 pts; 5 pts developed new MHE and 4 resolved their MHE. Rest were stable from an MHE perspective. α -diversity: Cross-sectional:

Shannon index for bacteria (2.6 ± 0.5 vs 2.5 ± 0.8 , $p=0.8$) and viruses (1.2 ± 0.6 vs 1.3 ± 0.6 , $p=0.8$) was similar in MHE vs no-MHE. Chao1 for bacteria was similar (79.4 ± 20.0 vs 82.8 ± 20.1 , $p=0.4$) but higher in MHE vs no-MHE for viruses (19.6 ± 8.9 vs 14.5 ± 9.6 , $p=0.03$). Longitudinal: Shannon for resolved (2.6 ± 0.6 vs 2.8 ± 0.3 developed MHE, $p=0.9$) for bacteria and viruses (1.4 ± 0.8 vs 1.1 ± 0.7 developed, $p=0.5$). Chao1 for resolved (86.6 ± 21.8 vs 88.2 ± 17.9 developed MHE, $p=0.9$) for bacteria and viruses (20.6 ± 12.8 vs 14.6 ± 12.2 developed, $p=0.3$). Individual taxa: Cross-sectional: No-MHE had higher commensals (*Lachnospiraceae*, *Ruminococcus*, *Anaerostipes* and *Eubacterium* spp) while potential pathobionts (*Escherichia*, *Klebsiella*) and lactate producers (*Streptococcus* and *Lactobacillus* spp) were higher in MHE pts (FigA). CrAssphage and Siphoviridae were lower and *Streptococcus Javan* and *Azobacteroides* phage were higher in MHE pts. Longitudinal: Commensals were \uparrow in resolved MHE (*Ruminococcaceae* and *Lachnospiraceae* spp) while pathobionts were \uparrow in MHE developers (*Enterococcus*, *Enterobacteraceae* spp). *Bacteroides* phage were lower and *Lactobacillus* phage LfeSau and Phage-DP 2017a was higher in those whose MHE resolved vs those who developed it (FigB). Correlation network characteristics: MHE pts had \uparrow network heterogeneity (1.08 vs 0.94) and centralization (0.20 vs 0.13) than no-MHE pts. Resolved MHE pts had \uparrow network heterogeneity (0.65 vs 0.53) and centralization (0.29 vs 0.18) than those who developed MHE.

Conclusion: In addition to bacteria, changes in viruses such as phages linked with *Streptococcus* and *Lactobacillus* are associated with MHE at baseline and in those followed over time for MHE resolution and those who developed new-onset MHE. Viral-bacterial correlation characteristics with cognitive function are also different between MHE and no-MHE and change over time. Viral and bacterial interactions are important to study in the modulation of brain function in cirrhosis.

TOP-039

Tissue resident NK NTCP-transplanted to immunosuppressed mice exhibiting liver fibrosis and fed with high fat diet (HFD) alleviate intestinal fibrosis

Johnny Amer, Ahmad Salhab, Rifaat Safadi, Hadassah Hebrew University Hospital, Liver Institute, Jerusalem, Israel
Email: johnnyamer@hotmail.com

Background and aims: NOD-scld *IL2r γ ^{null}* (NSG) mouse is one of the most widely used immunosuppressed mouse strains. We adapted this model as it exhibits absent T, B, and NK cells and allowed us to study the effects of transplanted NK cells expressing or not expressing the sodium taurocholate co-transporting polypeptide (NTCP); a transmembrane protein highly expressed in human hepatocytes that mediates the transport of bile acids.

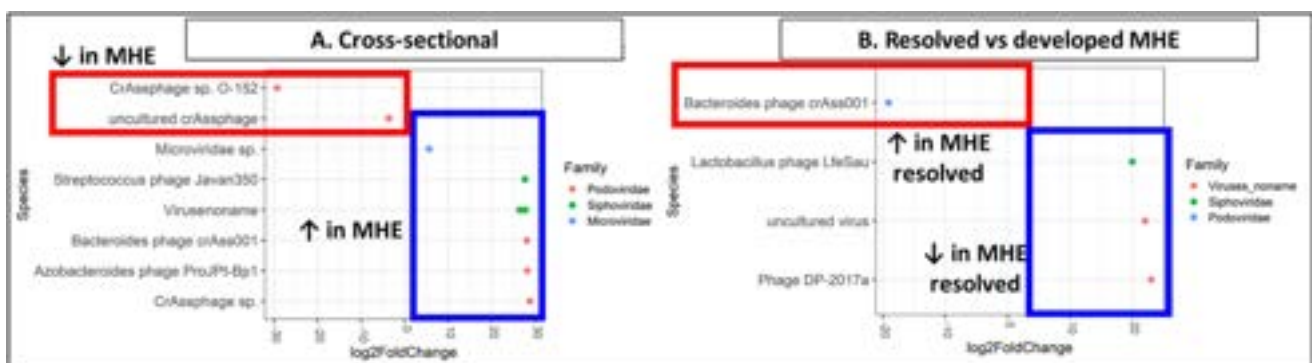


Figure: (abstract: TOP-038).

Method: Tissue resident (tr) NK cells obtained from livers of naïve C. B-17 scid (having NK cells while lacking T and B cells) were sorted according to NTCP expressions and transplanted to the CCl₄-induced liver fibrosis immunosuppressed mice fed with HFD. Inflammatory (HandE staining, and pro-inflammatory panel of cytokines), fibrosis (Sirius red staining, α -smooth muscle actin, collagen, and fibronectin) and metabolic (BAs, cholesterol, triglyceride, glucose tolerance test (GTT) and fasting blood sugar (FBS)) profiles were assessed.

Results: Our data showing trNK^{NTCP+} displaying higher expressions of exhaustion markers of PD-1, TIGIT and LAG-3 as compared to their trNK^{NTCP-} counterparts. Moreover, these populations showed a reduction in their activation markers profile of NKp46, NKp30 and CD107a expressions. HandE staining from non-treated mice (NT) intestines showed swelled cells with and large necrotic areas of high infiltrating inflammatory cells with steatosis while mice transplanted with trNK^{NTCP+} showed a delayed in these histological findings with a significant reduction in micro- and macrovascular steatosis. Sirius Red staining in NT demonstrated increased collagen deposition in perisinusoidal areas; transplantation with trNK^{NTCP+} resulted in a remarkable reduction in the fibrous dense tissue of the stained area and significant inhibitions in α SMA and Col III in the trNK^{NTCP-} transplanted mice (1.8-fold and 3.1-fold, respectively; $p < 0.0002$) as compared to NT mice. These results were associated with reductions in pro-inflammatory (TNF- α , IL-1b, IL-6 and IL-10) and pro-fibrotic (IL-4 and MCP-1) cytokines and amelioration lipid profile in the mice group receiving the trNK^{NTCP+} while further significant reductions were obtained following the trNK^{NTCP-} transplantations ($p < 0.05$). Moreover, IL-2 and INF- γ showed substantial increase in the mice receiving the trNK^{NTCP-} cells.

Conclusion: Our data clearly indicate effects of transplanted trNK^{NTCP-} in intestinal fibrosis amelioration and improving intestine histology of inflammation and fibrosis sections.

THURSDAY 22 JUNE

THU-225

Impact of human gut microbiota from PSC patients on a mouse model of biliary disease

Petra Hradicka^{1,2,3}, Henrik Rasmussen^{3,4}, Georg Schneditz^{1,2,3}, Kristian Holm^{1,2,3}, Jørgen Bjørnholt^{3,5}, Espen Melum^{1,2,3,6,7}, Johannes R. Hov^{1,2,3,6}. ¹Oslo University Hospital, Rikshospitalet, Norwegian PSC Research Centre, Oslo, Norway; ²Oslo University Hospital, Rikshospitalet, Research Institute of Internal Medicine, Oslo, Norway; ³University of Oslo, Institute of Clinical Medicine, Faculty of Medicine, Oslo, Norway; ⁴Oslo University hospital, Rikshospitalet, Department of comparative medicine, Oslo, Norway; ⁵Oslo University Hospital, Rikshospitalet, Department of microbiology, Oslo, Norway; ⁶Oslo University Hospital, Rikshospitalet, Department of transplantation medicine, Oslo, Norway; ⁷University of Oslo, Hybrid Technology Hub-Centre of excellence, Faculty of medicine, Oslo, Norway
Email: petra.hradicka@medisin.uio.no

Background and aims: The gut microbiota composition differs between primary sclerosing cholangitis (PSC) and healthy controls (HC). Transfer of PSC microbiota to mice with biliary disease has previously been reported to cause more severe disease with Th₁₇ activation, associated with bacterial translocation of *Klebsiella pneumoniae*, *Enterococcus gallinarum* and *Proteus mirabilis*. In the present study, we further investigated the direct role of PSC microbiota in a gnotobiotic mouse model.

Method: Stool samples from HC (n = 4) and PSC patients (n = 3) were collected into a sterile pot containing an anaerobic generator. Fecal microbiota transplant (FMT) was prepared anaerobically and stored

in 10% glycerol solution at -80°C. Germ-free 8-week old gender matched C57BL/6J mice were kept in individually ventilated cages and divided into 2 groups: HC-microbiota group colonized by FMT from HC (n = 10) and PSC-microbiota group colonized by FMT from PSC patients (n = 11). Mice were colonized for 3 weeks, after which cholestatic disease was induced in all animals by feeding 0.1% 3,5-diethoxycarbonyl-1,4-dihydrocollidine (DDC)-enriched diet for 2 weeks. Animals were then sacrificed and samples for plasma biochemistry, cytokine tissue analysis and microbiota profiling by 16S rRNA sequencing were collected. Mesenteric lymph nodes were cultured.

Results: PSC-microbiota mice had an increased inflammatory response, e.g., increased levels of TNF- α and IL-17 in liver tissue ($p < 0.05$) accompanied by increased relative liver weight ($p < 0.01$), suggesting disease worsening. There were no significant differences in plasma liver enzymes between the experimental groups. Mesenteric lymph node cultures were mainly positive for *Escherichia coli* and *E. faecalis*, which were found in both groups. Microbiota profiling of mucosa and fecal/cecal material showed distinct clustering of the experimental groups, using both unweighted UniFrac and Jaccard distance analysis ($p < 0.01$ and $p < 0.001$, respectively). Differential abundance testing identified several altered genera, including significant decreases in *Akkermansia* and *Anaerostipes* in the PSC-microbiota group, which are observed to be depleted in PSC and ulcerative colitis (Figure).

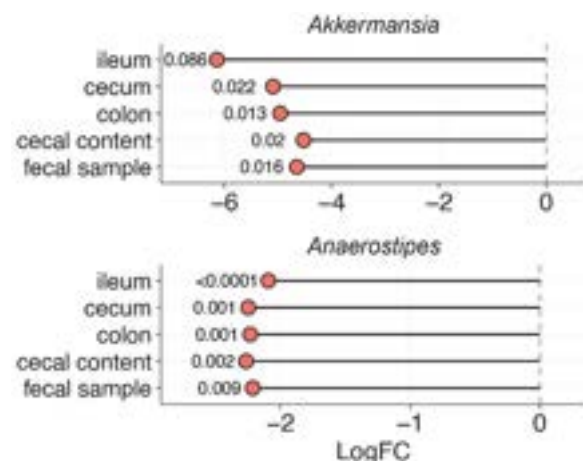


Figure: Differential abundance test showing log fold change (LogFC) in bacterial genera significantly decreased in PSC-microbiota group in various sample types. p values are displayed for each sample type.

Conclusion: We demonstrated an association between PSC microbiota and increased liver inflammation in the gnotobiotic DDC model. In addition, differences in microbiota composition in PSC and HC colonized mice were observed, while microbial translocation was common irrespective of microbiota source. Further experiments are necessary to verify the effect on disease severity and whether these can be linked to bacterial translocation or other mechanisms.

THU-227

Pasteurized Akkermansia muciniphila inhibits fibrosis progression in mouse cirrhosis model and induces changes in the gut microbiome

Sung-Min Won¹, Jin-Ju Jeong¹, Satya Priya Sharma¹, Raja Ganesan¹, Haripriya Gupta¹, Mi Ran Choi¹, Ki Kwang Oh¹, Young Lim Ham², Ki Tae Suk¹. ¹Institute for Liver and Digestive Diseases, Rep. of South Korea; ²Daewon Univ Coll, Dept Nursing, Rep. of South Korea
Email: ktsuk@hallym.ac.kr

POSTER PRESENTATIONS

Background and aims: Cirrhosis is the final stage of chronic liver disease, and the gut microbiome acts as one of the key factors in the development and progression of disease. There is evidence that some probiotic microorganisms contribute to the recovery of gut dysbiosis in patient with cirrhosis and help treatment of complications due to cirrhosis. We identified the specific relative abundance of *Akkermansia muciniphila* in the gut microbiome of patients with cirrhosis and evaluated the molecular mechanisms and effects of live or pasteurized *Akkermansia muciniphila* on the gut microbiome in a mouse model of liver cirrhosis.

Method: 57 healthy controls and 93 cirrhotic patients were enrolled for microbiome analysis. Six-week-old male C57BL/6J mice were divided into 4 groups (n = 5/group; control, 3,5-Diethoxycarbonyl-1,4-Dihydrocollidine diet-fed [DDC, 0.05%], and 2 DDC diet-fed + *Akkermansia muciniphila* [10^9 CFU/200 μ l for 8 weeks; live *Akkermansia muciniphila*, pasteurized *A. muciniphila*]). The gut microbiome of mice was initialized by administering antibiotics cocktail (ampicillin [100 mg/kg], vancomycin [50 mg/kg], metronidazole [100 mg/kg], neomycin [100 mg/kg], amphotericin B [1 mg/kg]) before strain treatment. The weight, pathology, molecular analysis, and microbiome analysis were examined.

Results: The significant relative abundance differences of *akker-mansia muciniphila* in the gut microbiome of healthy and cirrhosis patients was identified. In a cirrhosis model in which liver damage with fibrosis was induced over 8 weeks by feeding mice DDC diet, supplementation with *akker-mansia muciniphila* inhibited disease progression. In particular, supplementation with pasteurized *A.*

muciniphila effectively ameliorated the decrease in tumor necrosis factor- α and liver fibrosis markers more effectively than supplementation with live strains. In gut microbiome analysis, shifts in alpha and beta diversity and microbial composition were observed in pasteurized *A. muciniphila* group compared to live *A. muciniphila* group.

Conclusion: The significant relative abundance differences of *akker-mansia muciniphila* in the gut microbiome of healthy and cirrhosis patients was identified. In a cirrhosis model in which liver damage with fibrosis was induced over 8 weeks by feeding mice DDC diet, supplementation with *akker-mansia muciniphila* inhibited disease progression. In particular, supplementation with pasteurized *A. muciniphila* effectively ameliorated the decrease in tumor necrosis factor- α and liver fibrosis markers more effectively than supplementation with live strains. In gut microbiome analysis, shifts in alpha and beta diversity and microbial composition were observed in pasteurized *A. muciniphila* group compared to live *A. muciniphila* group.

THU-228

Investigating the correlation of a poly-metabolic risk score to clinical features in non-alcoholic fatty liver disease patients throughout a faecal microbiota transplant clinical trial

Nadeen Habboub¹, Benjamin H. Mullish¹, Celia Moore¹, Maria Lanoria¹, Benjamin Challis², Roberta Forlano¹, Mark Thursz¹, Marc-Emmanuel Dumas^{1,3}, Pinelopi Manousou¹. ¹Imperial College

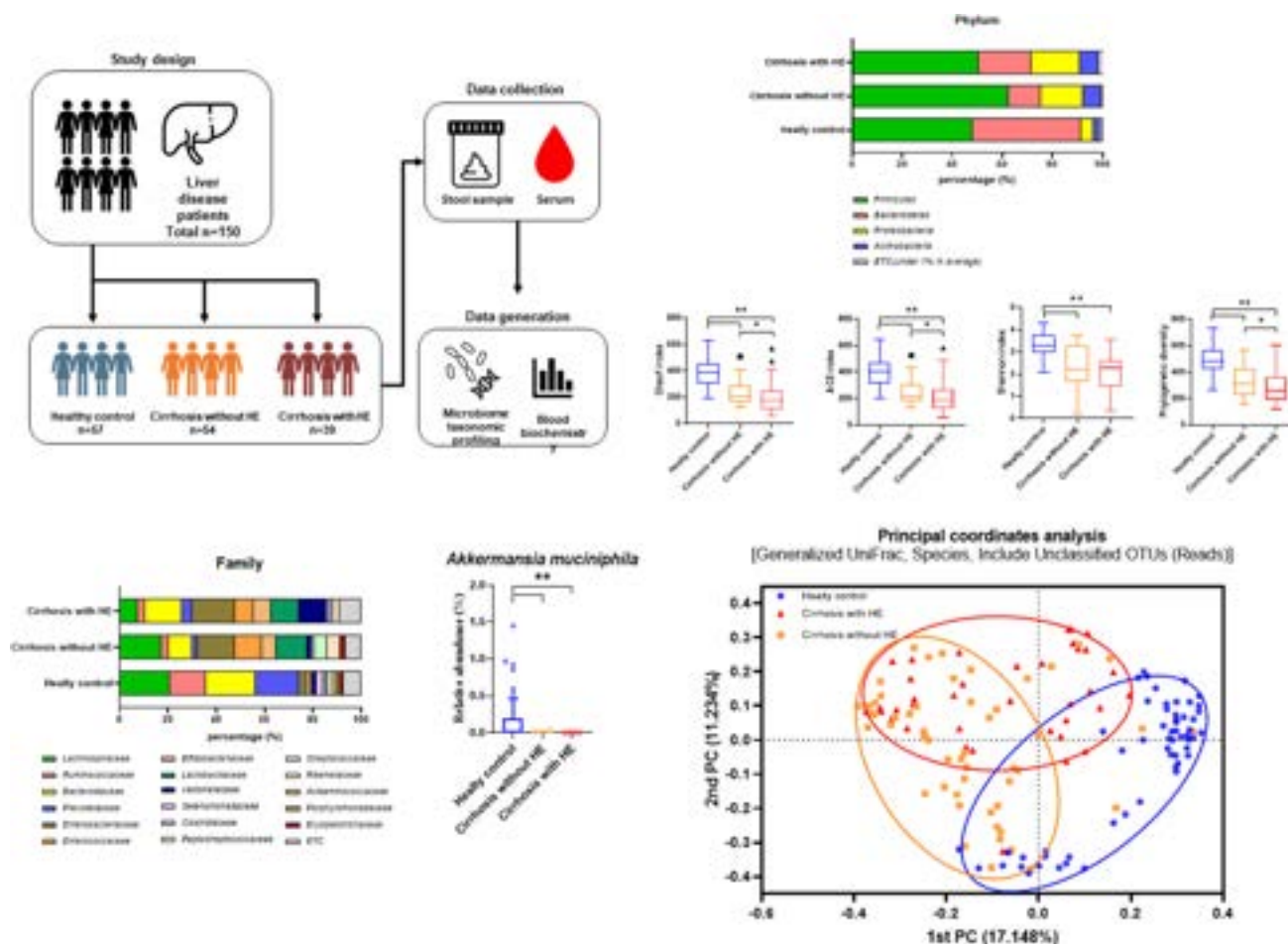


Figure: (abstract: THU-227).

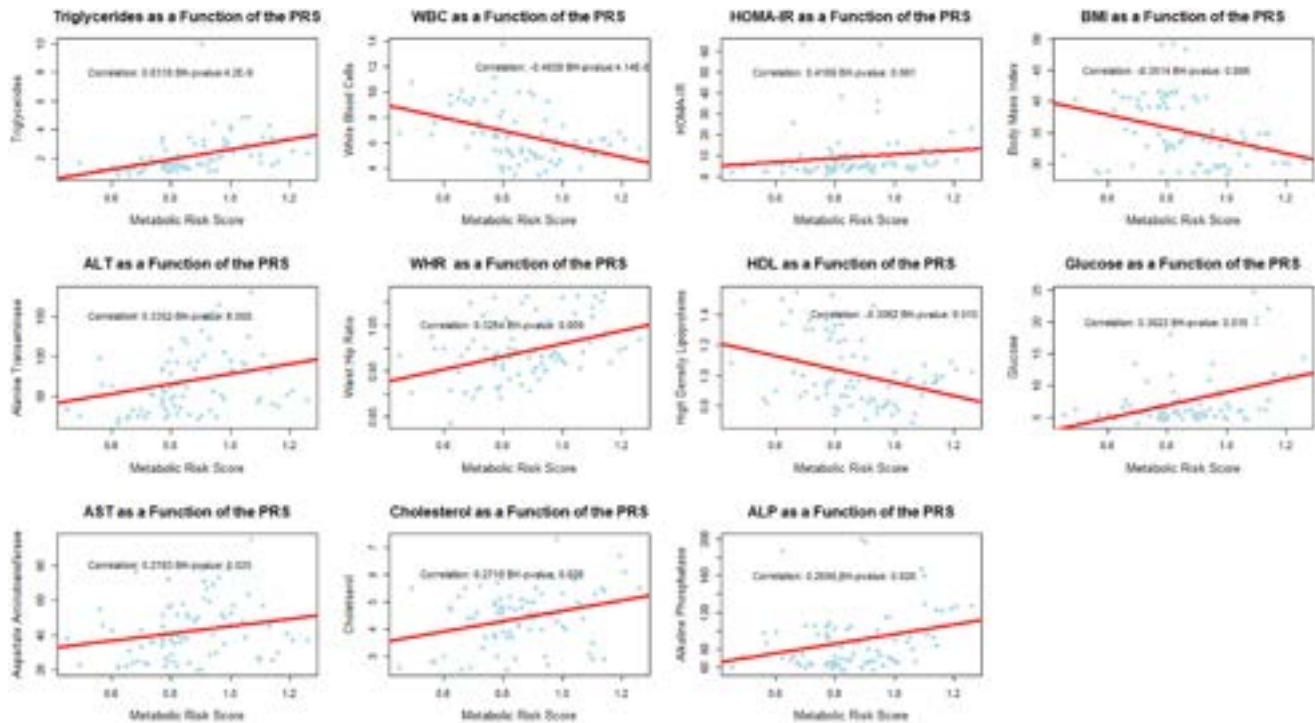


Figure 1. Significant correlations between the poly-metabolic risk score and key clinical parameters in NAFLD.

Figure: (abstract: THU-228).

London, Metabolism, Digestion and Reproduction, United Kingdom;
²AstraZeneca, Biopharmaceuticals Research and Early Development,
 Translational Science and Experimental Medicine, United Kingdom;
³Imperial College London, Heart and Lung Institute, United Kingdom
 Email: nh819@ic.ac.uk

Background and aims: Gut microbiota changes contribute to the pathogenesis and progression of non-alcoholic fatty liver disease (NAFLD) by increasing intestinal permeability and facilitating the translocation of gut microbiome-modulated metabolites and bacterial products to the liver. Faecal microbiota transplant (FMT) may restore pre-morbid microbiome-metabolome interactions and mitigate NAFLD. We aimed to develop a plasma metabolite scoring model that distinguished NAFLD from healthy patients, and which allowed longitudinal tracking of the impact of FMT upon NAFLD patients' metabolism in a clinical study. Furthermore, we aimed to examine whether this 'polymetabolic risk score (PRS)' correlates with clinical parameters of the NAFLD/NASH FMT recipients throughout the clinical trial.

Method: Untargeted ¹H-NMR spectroscopy was used to obtain metabolic profiles of plasma samples from biopsy-proven NASH patients (n = 54) and NAFLD patients (n = 213) recruited from the specialist NAFLD clinic, St Mary's Hospital (London, UK) and healthy controls (n = 534), selected from the AIRWAVE population study, to build a polymetabolic scoring model by OPLS-DA multivariate analysis (0 = Healthy, 1 = NAFLD/NASH). Plasma samples from NAFLD patients (n = 13) were collected serially (approximately fortnightly, week 0–24) throughout an ongoing longitudinal trial in which they received up to three healthy donor capsulised FMT. Fasted plasma samples from the trial's FMT recipients collected thus far (n = 82) were examined by ¹H-NMR spectroscopy and scored based on their full metabolic profiles. The NAFLD FMT recipients calculated polymetabolic risk scores were compared to their clinical features at each timepoint of the trial using Spearman correlation; p values were adjusted using the Benjamini-Hochberg method.

Results: Triglycerides (p = 4.2E-9), HOMA-IR (p = 0.001), ALT (p = 0.008), waist-hip ratio (p = 0.009), glucose (p = 0.015), AST (p = 0.025), cholesterol (p = 0.026) and ALP (p = 0.026) showed significant positive correlations to the PRS towards the NAFLD phenotype, while WBC (p = 4.14E-5), HDL (p = 0.015), and unexpectedly, BMI (p = 0.006) showed significant negative correlations to the PRS. In contrast, weight (p = 0.306), insulin (p = 0.103), creatinine (p = 0.115), albumin (p = 0.366), bilirubin (p = 0.366), LDL (p = 0.366), GGT (p = 0.398), C-reactive Protein (p = 0.572) and HbA1c (p = 0.672) did not exhibit correlation with the PRS thus far throughout the trial.
Conclusion: We have demonstrated that the pre-calculated ¹H-NMR plasma PRS developed for predicting the NAFLD phenotype strongly correlates to routinely-measured hepatic enzymes and common clinical markers of dysmetabolism measured longitudinally throughout the trial. This gives further insight into the potential contribution of the gut microbiome to metabolic perturbations in NAFLD. This also shows potential for a multi-profile risk assessment based on clinical parameters and the plasma ¹H-NMR PRS.

THU-229

Identifying the role of gut-vascular barrier associated macrophages in liver cirrhosis

Lena Smets¹, Maria Viola¹, Hannelie Korf¹, Frederik Nevens²,
 Guy Boeckxstaens¹, Schalk van der Merwe^{1,2}. ¹KULeuven, CHROMETA,
 Belgium; ²UZ Leuven, Belgium
 Email: lena.smets@kuleuven.be

Background and aims: During cirrhosis where progressive liver dysfunction prevails, there is a simultaneous breach in intestinal barrier integrity. Failure of either the intestinal epithelial- and/or gut-vascular barrier (GVB) allows pathological bacterial translocation to the circulation and liver, driving a gut-liver crosstalk that perpetuates systemic inflammation and hepatic injury. The mechanisms for intestinal barrier failure during cirrhosis remain incompletely understood. In this project, we investigated the importance of

specialized macrophages in maintaining vascular barrier integrity and consequently in protecting the host against pathological bacterial translocation during the development of experimental cirrhosis.

Method: Liver cirrhosis was induced in genetically modified mice by subcutaneous injection of CCL₄ for 20 weeks. Bacterial translocation was evaluated in ileal loop experiments by injecting fluorescent E.coli bioparticles into closed-off ileal loops of animals with progressive cirrhosis, followed by the microscopic fluorescein quantification in the liver. We performed single-cell transcriptomics of the lamina propria macrophage population from cirrhotic and control animals.

Results: Exposing Cx3cr1CreERT2.Rosa26-LSL-YFP mice (a state-of-the-art tool to identify intestinal long-lived GVB-associated macrophages) to CCL₄, resulted in a decrease and/or possible dysfunction of YFP⁺ cells lining the vasculature. The loss or dysfunction of YFP⁺ macrophages coincided with the breach in intestinal barrier integrity and bacterial translocation to the cirrhotic liver. In addition, we established a causal link between the absence of GVB-associated macrophages and the breach of GVB integrity. Hereto, we used tamoxifen injected Cx3cr1CreERT2.Rosa26-IDTR mice to allow the specific depletion of long-lived macrophages by the injection of diphtheria toxin. Following depletion of these macrophages, bacterial translocation to the circulation was evaluated using ileal loop experiments. The data revealed that even at early disease time points (with intact barrier integrity), elevated fluorescein signal in the liver sections of long-lived macrophage-depleted mice could be detected, pointing towards an accelerated vascular barrier breach. Currently, we are mapping the single cell transcriptomes of these long-lived GVB-associated macrophages along with all other lamina propria myeloid cells in experimentally induced cirrhosis versus control animals, to pinpoint the reason for their defective functionality in supporting vascular barrier integrity.

Conclusion: We provide novel insights into the role of long-lived GVB-associated macrophages in supporting intestinal barrier integrity and in bacterial translocation in an experimental model of liver cirrhosis.

THU-230

Altered gut microbiome and stool bile acids in sarcopenia in cirrhosis

Benard Aliwa^{1,2}, Angela Horvath^{3,4}, Nicole Feldbacher^{3,4}, Julia Traub⁵, Günter Fauler⁶, Vanessa Stadlbauer^{3,4}. ¹Medical university of Graz, Gastroenterology and Hepatology, Graz, Austria; ²University of Nairobi, Food Science, Nutrition and Technology, Kenya; ³Medical University of Graz, Gastroenterology and Hepatology, Austria; ⁴Centre of Biomarker Research in Medicine (CBmed), Austria; ⁵University Hospital Graz, Clinical Medical Nutrition, Austria; ⁶Medical University of Graz, Austria
Email: benard.aliwa@medunigraz.at

Background and aims: Sarcopenia in cirrhosis is associated with low quality of life and high mortality risk. The pathogenesis is not fully understood yet. We previously showed that secondary bile acids (sec-BAs) such as deoxycholic acid (DCA) and lithocholic acid (LCA) were significantly elevated in serum samples of cirrhotic patients with sarcopenia compared to cirrhotic patients without sarcopenia. Since sec-BAs are produced by the gut microbiome, we hypothesize that stool BAs composition differs between cirrhotic patients with and without sarcopenia and is related to stool microbiome composition and abundance of genes involved in BAs transformation.

Method: Sarcopenia was diagnosed according to the European working group on sarcopenia in older people. Fecal BAs composition by ultra-high-performance liquid chromatography-tandem mass spectrometry (UPLC-MS/MS) in cirrhotic patients with (n = 78) and without (n = 38) sarcopenia. Microbiome composition was analyzed by 16S rDNA sequencing and stool BAs gene abundances were analyzed by qPCR.

Results: We observed that cholic acid (CA) and cholic acid to chenodeoxycholic acid (CA: CDCA) were significantly reduced in the stool of cirrhotic patients with sarcopenia compared to cirrhotic

patients without sarcopenia (p = 0.02 and p = 0.03, respectively). Compared to cirrhotic patients without sarcopenia, the ratios of deoxycholic acid to cholic acid (DCA: CA) and lithocholic acid to chenodeoxycholic acid (LCA: CDCA) were significantly elevated in the stool of cirrhotic patients with sarcopenia (p = 0.014 and p = 0.042, respectively) indicating an enhanced transformation of primary to secondary bile acids by the gut microbiome. Furthermore, bacterial species linked to sarcopenia in cirrhosis (*Bacteroides fragilis*, *Blautia marseille*, and *Sutterella* spp) clustered together and correlated positively with DCA: CA and LCA: CDCA indicating that *Bacteroides fragilis*, *Blautia marseille*, and *Sutterella* spp may individually or collectively enhance the transformation of primary to secondary BAs. Despite alterations in BAs composition in stool, the gene abundances of bile salt hydrolase (BSH) and 7 alpha-dehydroxylase (7 alpha-HSDH) were comparable between cirrhotic patients with and without sarcopenia.

Conclusion: Changes in BAs composition occur in sarcopenic cirrhotic and are linked to compositional changes in the gut microbiome; however, we observed no difference in BAs transforming genes between sarcopenic and non-sarcopenic microbiomes in cirrhosis. Thus, the study demonstrated a potential functional gut microbiome-host interaction linking sarcopenia with the changes in the gut microbiome and stool BAs profiles pointing towards a potential mechanistic interplay in understanding sarcopenia pathogenesis.

THU-231

The gut (and its microbiota)-liver axis in liver disease associated with alpha-1-antitrypsin deficiency

Francesco Annunziata, Nunzia Pastore. Telethon Institute of Genetics and Medicine, Pozzuoli, Italy
Email: f.annunziata@tigem.it

Background and aims: Alpha-1-Antitrypsin Deficiency (AATD) is an inherited genetic disorder caused by mutations in the *SERPINA1* gene. The most common variant is the Z allele (ATZ), which leads to improper protein folding causing retention of the polymeric ATZ protein in the hepatocytes inducing a cascade of hepatotoxic events resulting in chronic liver inflammation, fibrosis, cirrhosis and increased risk of hepatocellular carcinoma (HCC). Despite the common genetic mutation, patients suffer from different onset and severity of the liver disease; of note, most of the patients with the homozygous ATZ mutation will never develop any liver disease. The reason for this phenotypic variability is unknown. Several studies have been carried out to investigate the involvement of genetic and environmental modifiers and their influence on the expression and severity of the liver disease among patients. The aim of our study is to investigate the gut-liver axis in AATD, focusing in particular on the gut functionality and the possible connection between AATD-associated liver disease and the gut microbiota as modifier of the liver phenotype.

Method: Methods for the characterization of the gut and its functionality: Bulk- and single cell-(sc)RNA sequencing. Immunoblots and Immunostainings. Organoid forming assays. Methods for the analysis of the intestinal microbiota composition: Metagenomic sequencing.

Results: PiZ mice (an AATD mouse model) show a reduction in body weight compared to age-matched controls. We hypothesized defects in gut functionality and nutrient absorption. Interestingly, we found high ATZ mRNA and protein levels in the intestine of PiZ mice, particularly in the ileum, the region where the majority of microbes resides. Single cells RNA (scRNA)-sequencing analysis revealed that ATZ mRNA is expressed in all the intestinal cell types. We confirmed this data by co-immunostaining for human ATZ and cell-specific markers. Of note, we found ATZ polymers in Goblet, Enteroendocrine and Paneth cells, responsible for the secretion of the gut protective mucus layer, of hormones reflecting dietary intake, of factors necessary for stem cell function, and molecules with antimicrobial

properties. In addition, we observed differences between WT and PiZ intestinal crypts-derived organoids, with the latter showing impaired differentiation, likely due to accumulation of the toxic polymeric ATZ. Lastly, from metagenomic analyses we observed that WT and PiZ mice have a well distinguished intestinal microbiota composition with many bacterial strains up-regulated in PiZ mice demonstrated to be increased in many liver diseases.

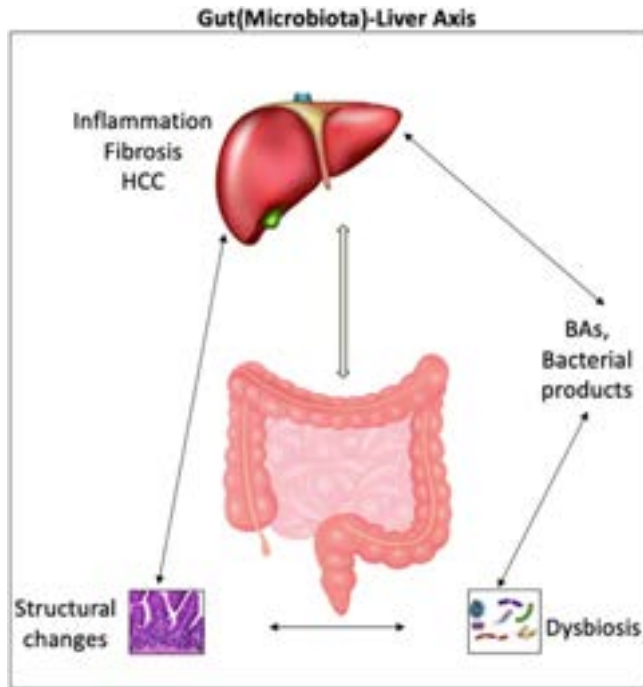


Figure:

Conclusion: Our preliminary data suggest that ATZ expression and accumulation in intestinal cells may affect the gut and its microbiota, thus affecting the continuous bidirectional crosstalk between gut and liver and being a candidate for the different onset and severity of liver disease in AATD.

THU-232

Intestinal dysbiosis exacerbates gut barrier dysfunction via inhibiting FXR-FGF15 in intra-abdominal sepsis

Shuwen Qian¹, Xiaomei Wang², Qiaohao Hou², Zehua Su³, Haobing Shi³, Lijun Liao³, Xiangrui Wang³. ¹Yangpu Central Hospital affiliated to Tongji University, Shanghai, China; ²Shanghai East Hospital, School of Medicine, Tongji University, Shanghai, China; ³Shanghai East Hospital, School of Medicine, Tongji University, China
Email: Shuwen_Qian@tongji.edu.cn

Background and aims: Intestinal barrier dysfunction due to intestinal dysbiosis is considered a major cause of initiation and development of intra-abdominal sepsis and multiple organ dysfunction. Farnesoid X receptor (FXR) plays an important role in enteroprotection, but the exact mechanism is still unclear. This study was to determine whether intestinal dysbiosis aggravate intestinal barrier impairment by inhibiting FXR-FGF15 in intra-abdominal and its probable mechanism.

Method: Caecal ligation and puncture (CLP) and fecal microbiota transplanted (FMT) from septic mice constructed a model of intestinal flora dysbiosis, intestinal FXR and FGF15 expressions and the gut barrier function were examined and compared. INT-747, an agonist of FXR, was assessed whether improve the phenotype of CLP mice or gut barrier. The relevance of intestinal epithelial cell-specific deletion of MyD88 (MyD88^{ΔIEC}) on FXR-FGF15 axis as well as microbiota and barrier were studied. The role of probiotics on FXR

was also discussed. Intestinal flora was analyzed by 16S rRNA metagenomic sequence.

Results: In intra-abdominal sepsis mice model, FXR and FGF15 in ileum displayed significantly decreased, along with cholestasis, impairment barrier function and flora dysbiosis. Upregulation of FXR by INT-747 and significantly improved survival, barrier function and other phenotypes in septic mice. In FMT, septic intestinal flora activated intestinal myd88 expression and reduced intestinal FXR and FGF15 expression. After myd88 knockdown in intestinal epithelial villi, the index of FXR was elevated, ZO-1 was improved, IL-6 and IL-1 β were reduced, and the abundance and diversity of flora were increased. Strikingly, Probiotics boost FXR-FGF axis to improve intestinal function.

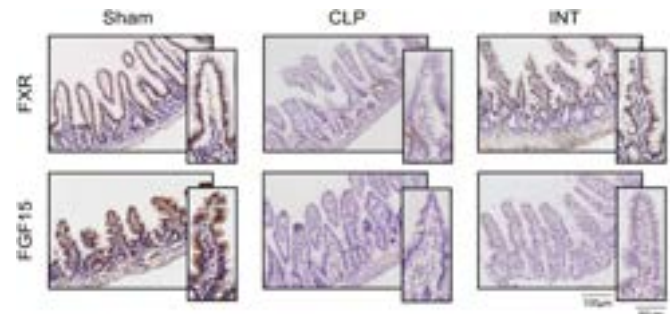


Figure:

Conclusion: Intestinal dysbiosis triggers over activation of MyD88 in intestinal epithelial cells in intra-abdominal septic mice, and subsequent inhibited the FXR-FGF15 signalling associated with gut barrier function deteriorated.

THU-233

Viral like particle analysis shows changes with PPIs and may be more sensitive than metagenomics to study PPI modulation of virome in cirrhosis

Marcela Peña Rodríguez^{1,2}, Masoumeh Sikaroodi³, Patrick Gillevet³, Jasmohan S. Bajaj⁴. ¹University of Guadalajara, Mexico; ²Laboratory for the Diagnosis of Emerging and Reemerging Diseases (LaDEER), Microbiología y Patología, Guadalajara, Mexico; ³George Mason University, United States; ⁴Virginia Commonwealth University, United States

Email: jasmohan.bajaj@vcuhealth.org

Background and aims: In addition to bacteria, gut microbiota has viruses, which could impact outcomes in cirrhosis. Current cirrhosis studies have analyzed metagenomics but not direct viral like particle (VLP) analysis. These could reflect changes with proton pump inhibitor (PPI) therapy. Aim: Determine the changes in VLPs in cirrhosis vs controls, changes with addition/removal of PPI and compare VLP to metagenomics.

Method: Healthy controls (not on PPI) and cirrhotic outpatients underwent stool collection. A group of cirrhotics on PPI underwent PPI withdrawal for 14 days while in another group not on PPI Omeprazole 40 mg was added for 14 days. Stools were collected at baseline and day 14 for PPI addition and removal. Demographics, medications, cirrhosis details and PPI use were recorded. Virome analysis: Stool analysis was performed using VLP enrichment. Only abundant contigs were analyzed, those with at least 100 (transcripts per million) tpm in the dataset and with a threshold of at least 5 tpm mapped to the contig by Kallisto and at least 5 tpm present in 3% of samples. Mean log₁₀ scaled abundances were analyzed for control vs cirrhosis and between controls and pts with cirrhosis \pm PPI use. A subset was sent for metagenomics in addition to VLP and viruses detected by both techniques were compared. α diversity and DESeq2, using raw read counts. A p value <0.05 and a log₂ fold change >2 was

VLP analysis *p<0.05	Cross-sectional Study				Longitudinal trials			
	Cirrhosis vs controls		Within cirrhosis PPI use?		PPI addition		PPI withdrawal	
	Cirrhosis	Control	Yes	No	Pre PPI	Post	On PPI	Off PPI
Shannon Mean±SD	1.53 ± 0.76	2.06 ± 0.67*	1.67 ± 0.71	1.56 ± 0.81	1.44 ± 0.88	1.66 ± 0.87	1.19 ± 1.20	1.12 ± 0.91
Observed Mean±SD	12.40 ± 6.88	17.85 ± 7.38*	13.72 ± 7.12	12.89 ± 7.34	10.43 ± 6.80	14.13 ± 7.36	10.50 ± 10.00	8.29 ± 6.65
Chao1 Mean±SD	19.26 ± 15.06	26.58 ± 12.82*	21.22 ± 14.64	19.76 ± 15.27	14.21 ± 9.77	20.09 ± 11.17	14.13 ± 15.35	12.84 ± 11.64
Viruses higher on DESeq2	-Bacteriophage sp. sp. cat28548 -crAss-like viruses sp. cat8522 -unclassified Gokushovirinae sp. cat28993 -Drulisvirus sp. cat27004 -CrAssphage sp. sp. cat26877 -unclassified Siphoviridae sp. cat16818 -unclassified Microviridae sp. cat27563 -CrAssphage sp. sp. cat21691 -Bacteroides phage crAss001 sp. Cat27059	-Bacteroides phage -Phage DP-2017a sp. cat27141 -Bacteroides phage crAss001 sp. cat27327 cat17738	-Siphoviridae sp. cat16818 - Human mastadenovirus A sp. cat27160 -Bacteroides phage crAss001 sp. cat27059 -Human mastadenovirus A sp. cat28854 not classified sp. cat10396 -crAss-like viruses sp. cat8522 cat21723 & cat13435	-Microviridae sp. cat27563 -crAss-like viruses (sp. cat7034, cat28533, cat25161, cat1539, cat7055, cat27132, cat8628, cat32032 cat29880)	-cat28842 Bacteroides phage - crAss001 sp. cat27161 -Gokushovirus WZ-2015a sp. Cat4053	None	-Tomato mottle mosaic virus sp. -crAss-like viruses sp. Cat24225	None

Figure: (abstract: THU-233).

considered statistically significant. Metagenomics to VLP: compared with LeFSe.

Results: Clinical data: 110 subjects (20 controls and 90 cirrhosis) were enrolled. Controls (60.8±6.9 years, 13 men) and cirrhotic outputs (62.1±7.0 yrs, 72 men with 15 HCV, 29 alcohol, 12 both, 17 NAFLD and 3 other etiologies) had similar demographics. 38 had HE, 41 ascites and 38 were on omeprazole 31 ± 17 mg/day. PPI users had similar MELD (11.7 ± 5.4 vs 11.0 ± 6.3, p = 0.52), HE pts (37% vs 46%, p = 0.38) and lower ascites (29% vs 52%, p = 0.006) than non-users. 27 cirrhotics (14 on and 13 not on PPI had) both VLP and metagenomics done. PPI trials: 8 compensated pts (age 58 yrs) underwent addition and 8 other compensated pts (age 59 yrs) underwent PPI withdrawal and addition respectively over 14 days. No clinical changes were found. VLP changes (Fig): Cirrhotics had lower viral α-diversity. No change in PPI cross-sectionally or before/after addition or withdrawal was seen on viral α-diversity. DESeq2 showed higher Bacteroides phages in controls and higher Siphoviridae, Gokushovirinae and Drulisviruses (Enterobacterial phages) in cirrhotics. PPI linked with higher Siphoviridae, mastadenovirus and lower CrAss-like viruses and Microviridae. PPI addition reduced Bacteroides phage and some crasslike viruses while removal reduced other CrAss-like viruses. VLP vs metagenomics: Metagenomics did not differentiate between PPI use but VLP showed that crAss-like viruses cat8522, Przondovirus spp, unclassified Siphoviridae and Podoviridae sp. ctf10 were higher in the PPI group while Microviridae, Gokushovirinae, Bacteroidesphages were higher in no-PPI group.

Conclusion: Viral-like particle analysis shows important phage and eukaryotic viral changes in patients with cirrhosis vs controls and especially those with PPI use. A direct comparison of these analysis with metagenomics shows that VLP may be more sensitive to the role of PPIs in cirrhosis.

THU-234

Edible exosomes oral administration restores gut homeostasis and reduces systemic ammonia level in rodent model

P. Debishree Subudhi¹, Jitendra Kumar¹, Anupama Parasar¹, Shivani Gautam¹, Ashmit Mittal¹, Varun Suroliya², Shruti Sureshan², Dinesh Mani Tripathi¹, Chhagan Bihari³, Shiv Kumar Sarin⁴, Sukriti Sukriti¹. ¹Institute of Liver and Biliary Sciences, Molecular and

Cellular Medicine, New Delhi, India; ²Institute of Liver and Biliary Sciences, Genome Sequencing Laboratory, India; ³Institute of Liver and Biliary Sciences, Department of Pathology, India; ⁴Institute of Liver and Biliary Sciences, Department of Hepatology, India
Email: sukritibiochem@gmail.com

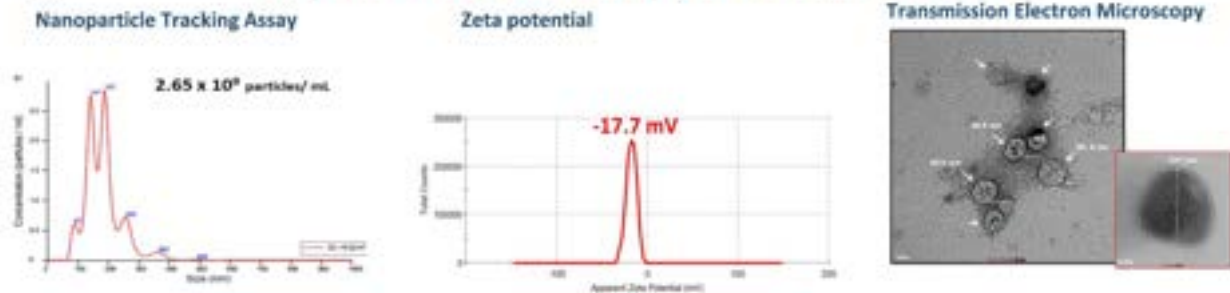
Background and aims: Elevated plasma ammonia is attributed to hepatic dysfunction and gut dysbiosis along with systemic inflammation. There is an urgent need of agents which can reinstate the gut commensals and reduce ammonia levels. We investigated the effects of Carrot Edible Exosomes (CEE) on gut microbiome and hepatic injury.

Method: CEE were fractionated from black carrots [*Dacus carota*] by differential ultracentrifugation and characterized by transmission electron microscopy and nanoparticle tracking assay. Proteomics was performed to evaluate cargoes. Stability, viability were assessed using *in-vitro* stomach/intestine like digestion and also by co-culture with hepatocytes. Prophylactic oral administration of CEE was done in Thioacetamide (TAA) induced acute hyperammonemia model, compared with vehicle and lactulose. Behavioral, biochemical markers of hepatic injury, ammonia, intestinal permeability and liver histology were investigated. Gut microbiota were assessed by 16s metagenomics.

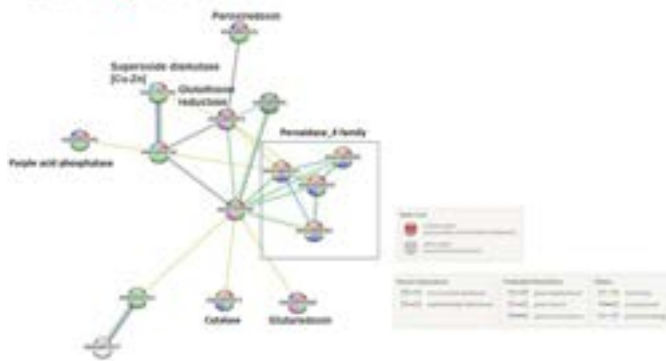
Results: The size of CEE ranges (52 nm–331 nm) with concentration of $2.65 \times 10^9 \pm 0.65/\text{ml}$ with zeta potential $-17.7 \pm 2.4 \text{ mV}$. Total 647 proteins were identified as CEE cargoes, highly enriched with superoxide dismutase, ferritin and aspartate aminotransferase. After stomach like *in-vitro* digestion, no changes in concentration were found with particle size reduced (p=0.02) with intact zeta potential. Upon CEE co-culture with hepatocytes after LPS injury, ornithine transcarbamylase (otc; p=0.0004) and Argininosuccinate synthetase (ass; p=0.0331) were upregulated and IL-1b and Caspase3 (p<0.001) mRNA levels reduced within 30 mins than controls. CEE administration in TAA compared to vehicle and lactulose reduced the plasma ammonia levels [Vehicle-145.3 ± 43.6; CEE-92.2 ± 23.2; lactulose-124.8 ± 12.5 μmol/L (p=0.03)], ALT and bilirubin (p=0.006; p=0.007). CEE improved sensory motor activity (p<0.001), hepatic necrosis and inflammation. ZO-1 expression was

Figure

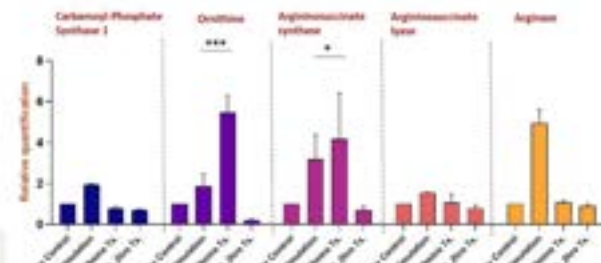
A. Size, concentration and stability of Carrot Edible Exosomes



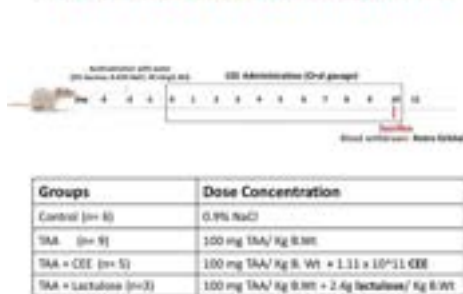
B. Cargoes of CEE



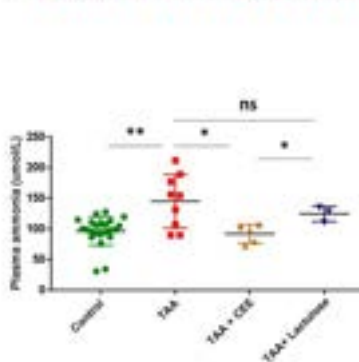
C. Co-culture of CEE with hepatocytes



D. Schematic CEE administration



E. Plasma ammonia Levels



F. Beta diversity by 16S Sequencing

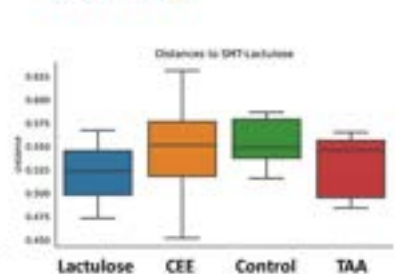


Figure: (abstract: THU-234).

higher in CEE than lactulose or vehicle ($p < 0.001$). CEE enhanced abundance of Firmicutes [Peptococcaceae, Lachnospiraceae, Ruminococcaceae ($p < 0.001$)] provides energy to maintain gut epithelia, aid in SCFA production. CEE increased growth of *Desulfovibrio* responsible for acetic acid levels and reduced inflammation by producing α -synuclein protein.

Conclusion: CEE potentiate the hepatic urea cycle and lower plasma ammonia levels in acute hyperammonemic rodent model. The CEE carry strong hepatoprotective cargoes which help restore the gut homeostasis and restore gut permeability and can be considered as therapeutic nutritional tools.

THU-235

Microbiota-targeted interventions in the gut-liver axis for chronic liver disease of DUAL etiology

Raquel Benedé^{1,2}, Olga Estévez¹, Hector Leal¹, Salvador Iborra^{1,3}, Ana Redondo^{1,3}, José María Herranz^{4,5}, Alexander Tyakht⁶, Viktoria Odintsova⁶, Beatriz Gómez Santos⁷, Patricia Aspichueta^{5,7,8}, Johanna Reißing⁹, Tony Bruns⁹, Andreea Ciudin^{10,11}, Juan M. Pericas^{5,12}, Javier Vaquero^{5,13,14}, Christian Trautwein⁹, Christian Liedtke⁹, Rafael Bañares^{1,5,13,14}, Matías A. Avila^{4,5,15}, Francisco Javier Cubero^{1,5,13}, Yulia Nevzorova^{1,5,13}. ¹Complutense

POSTER PRESENTATIONS

University School of Medicine, Department of Immunology, Ophthalmology and ENT, Madrid, Spain; ²Faculty of Biology, Complutense University Madrid, Department of Physiology, Genetics and Microbiology, Madrid, Spain; ³12 de Octubre Health Research Institute (imas12), Madrid, Spain; ⁴CIMA, University of Navarra, Hepatology Program, Pamplona, Spain; ⁵Centro de Investigación Biomédica en Red de Enfermedades Hepáticas y Digestivas (CIBEREHD), Instituto de Salud Carlos III, Madrid, Spain; ⁶Atlas Biomed Group-Knomx LLC, London, United Kingdom; ⁷University of Basque Country UPV/EHU, Department of Physiology, Faculty of Medicine and Nursing, Leioa, Spain; ⁸Biocruces Health Research Institute, Barakaldo, Spain; ⁹University Hospital RWTH Aachen, Department of Internal Medicine III, Aachen, Germany; ¹⁰Vall d'Hebron University Hospital, Vall d'Hebron Institute for Research (VHIR), Endocrinology Department, Barcelona, Spain; ¹¹Universitat Autònoma de Barcelona, Barcelona, Spain; ¹²Vall d'Hebron University Hospital, Vall d'Hebron Institute for Research (VHIR), Liver Unit, Internal Medicine Department, Barcelona, Spain; ¹³Instituto de Investigación Sanitaria Gregorio Marañón (IISGM), Madrid, Spain; ¹⁴Hospital General Universitario Gregorio Marañón, Servicio de Aparato Digestivo, Madrid, Spain; ¹⁵Instituto de Investigaciones Sanitarias de Navarra IdiSNA, Pamplona, Spain
Email: yulianev@ucm.es

Background and aims: Emerging evidence highlights the role of gut microbiome in chronic liver disease (CLD). In the present work, we used our recently published DUAL preclinical model of steatohepatitis and fibrosis and aimed to analyse the relevance of the liver-gut-microbiome crosstalk in order to define potential therapeutic circuits in DUAL model.

Method: C57BL/6 male mice received 10% alcohol in drinking water together with a Western diet (WD) for 10 and 23 weeks (DUAL model). Liver and gut tissue histology, hepatic inflammation, intestinal permeability and 16S rRNA microbiome profiling were analysed. Feeding of 10 weeks was used to evaluate the effects of microbiota modulation after: (i) Short-term (10 days) oral administration of antibiotics and (ii) Fecal matter transplantation (FMT) from healthy donor.

Results: 23 weeks DUAL feeding resulted in reduction of colon length accompanied by a significant decrease in the height of colonic crypts. The rate of apoptosis in intestinal epithelial cells (IEC) exceeded the rate of compensatory proliferation in colon. Pathological IEC shedding resulted in gap formation in the epithelium and decreased expression of tight junctions (occluding, ZO1). These changes were accompanied by degradation of mucus layer and by the accumulation of giant inflammatory foci in the colon submucosal layer formed by CD3+ T and B220+ B lymphocytes. Consistently, gut permeability, translocation of microbial products (LPS) to the circulation significantly increased and overexpression TLR2/4/9 was detected in the DUAL livers. Microbiome profiling of DUAL animals revealed decreased alpha diversity, elevated proportions of Gram-negative Bacteroidaceae and lower presence of other commensal taxa. Similarly, 16S rRNA sequencing of stool samples from obese patients with mild alcohol consumption revealed reduced overall microbiota diversity and increase in gram-negative LPS producing Bacteroides. Short-term oral application of antibiotics to 10 weeks DUAL-fed mice markedly improved hepatic steatosis, attenuated liver damage, lowered serum transaminases, decreased CD45 and F4/80 positive infiltrates, decreased the expression of TLR2/4/9 and reduced collagen accumulation in the liver. The implementation of FMT resulted in decreased accumulation of triglycerides in the liver, reduction in hepatic inflammation and fibrosis.

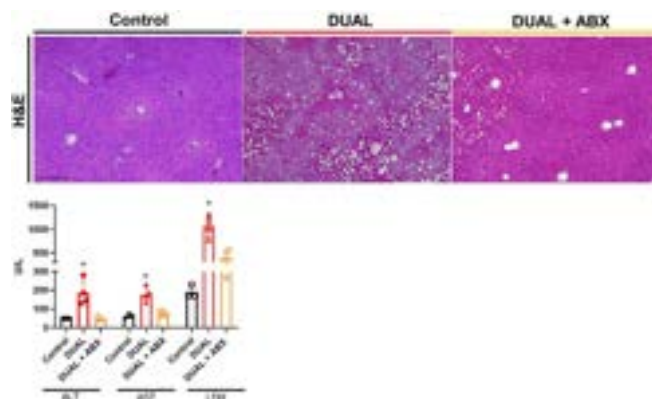


Figure:

Conclusion: Dysbiosis is a critical factor in the regulation of steatohepatitis/fibrosis of DUAL etiology. Gut-based early therapeutic interventions could be beneficial to halt CLD development.

THU-236

The novel class of microbially conjugated bile salts activate the main host bile salt receptors FXR and TGR5

Ümran Ay¹, Martin Lenicek², Raphael Haider³, Arno Classen⁴, Hans van Eijk⁵, Carsten Hoffmann³, Carsten Bolm⁴, Steven Olde Damink^{1,5}, Frank Schaap^{1,5}. ¹University Hospital RWTH Aachen, Surgery, Germany; ²Institute of Medical Biochemistry and Laboratory Diagnostics, Czech Republic; ³University Hospital Jena, Molecular Cell Biology, Germany; ⁴RWTH Aachen University, Organic Chemistry, Germany; ⁵Maastricht University Medical Centre, Surgery, Netherlands
Email: uay@ukaachen.de

Background and aims: A new class of bile salt metabolites comprising bile salts that are N-amidated with non-canonical amino acids by gut microbes, was recently reported. The function of these microbial bile salt conjugates (MBSCs) and their relevance for human (patho)physiology is unresolved. Initial disease associations were made for Crohn's disease and dysbiotic states. Here, we sought to determine if MBSCs can activate the main host bile salt receptors FXR and TGR5, and assessed their entrance into the circulation.

Method: N-amidates of cholic acid (CA) and chenodeoxycholic acid (CDCA) and leucine, tyrosine and phenylalanine were synthesized, and assayed for binding to FXR and TGR5 using coactivator and G_{sa} recruitment assays, respectively. Activation of FXR by MBSCs, and requirement for an uptake transporter, was further studied by reporter assays in 293 embryonic kidney cells, and in HuH7 hepatoma cells using a transcriptional read-out. For initial explorations, levels of aforementioned MBSCs were determined using LC-MS in relevant patient cohorts in chyme and blood samples, including mesenteric venous blood.

Results: CDCA-based MBSCs elicited dose-dependent recruitment of SRC1 coactivator peptide to the ligand-binding domain of FXR, with Tyrosine-CDCA having the highest affinity (EC₅₀ = 2.8 µM). Treatment of HuH7 cells with CA- or CDCA-based MBSCs resulted in elevated mRNA levels of FXR target genes (e.g. *SHP*, *OSTβ*), in a manner dependent on the bile salt uptake transporter NTCP. Both intestine- and liver-predominant FXR isoforms (α4 and α2, resp.) were activated by MBSCs in luciferase reporter assays, provided that a bile salt uptake

transporter (ASBT or NTCP) was present. MBSCs were also ligands of TGR5 as evidenced by dose-dependent recruitment of the stimulatory G_{sa} subunit in a nanoBRET assay. CDCA-based MBSCs displayed higher affinity than their CA-based counterparts. Moreover, MBSCs induced downstream activation of a cAMP-driven reporter in an TGR5-dependent manner. Using a LC-MS assay with nanomolar range sensitivity, MBSCs were readily detected in chyme of patients with intestinal failure ($n=12$), where MBSCs comprised a minor fraction (up to 40 ppm) of total bile salts. MBSCs could not be detected in matched systemic blood of these patients, or in systemic blood of patients with morbid obesity ($n=8$) or PSC ($n=6$), or mesenteric and portal blood of patients with a pancreatic malignancy with/without cholestasis ($n=6$).

Conclusion: MBSCs are agonists of FXR and TGR5, and substrates for the intestinal and hepatic bile salt uptake transporters. Initial pilot data indicates that absorption and entry into the host circulation of MBSCs, is unsubstantial. Degradation of MBSCs by host carboxypeptidases and bacterial bile salt hydrolases may contribute to this. Follow-up studies are required to unravel the function of MBSCs and their relevance for human disease.

THU-237

The bile acid chenodeoxycholic acid increases muscle insulin sensitization via FOXO1

Aileen Shiqi Zhong¹, Maria Corliand¹, Raphael Chevré², David Castano Mayan¹, Blake Cochran³, Bert Groen⁴, Kerry Ann Rye³, Hong Chang Tan⁵, Roshni Rebecca Singaraja¹. ¹National University of Singapore, Singapore; ²Agency for Science technology and Research, Singapore; ³University of New South Wales, Australia; ⁴University of Amsterdam, Netherlands; ⁵Singapore General Hospital, Singapore
Email: mdcrrs@nus.edu.sg

Background and aims: CYP8B1 acts in the bile acid (BA) synthesis pathway to generate 12 α -hydroxylated BAs which were associated with insulin resistance in humans. We identified the first carriers of mutations in CYP8B1, a bile acid (BA) synthesis gene. These carriers showed increased circulatory primary BA cholic acid (CA):chenodeoxycholic acid (CDCA) ratio and peripheral insulin sensitivity. In vitro, CDCA increased glucose uptake in myotubes. However, it's unclear whether CDCA alone increases insulin sensitization and if skeletal muscle-mediated mechanisms contribute in vivo.

Method: We generated *Cyp8b1*^{-/-} and *Cyp2c70*^{-/-} mice with increased circulatory CDCA.

Results: *Cyp8b1*^{-/-} mice showed increased insulin sensitivity and muscle insulin signaling, while β -cell insulin secretion was decreased and hepatic glucose metabolism remained unchanged. Muricholic acids (MCAs) were also increased in *Cyp8b1*^{-/-} mice. In mice, *Cyp2c70* generates MCAs from CDCA. To exclude contributions by MCAs to insulin sensitivity, we generated *Cyp2c70*^{-/-} mice with almost absent MCAs. These mice showed increased circulatory CDCA, increased insulin sensitivity and increased muscle-specific glucose uptake, despite the near absent MCAs. *Wild-type* mice administered CDCA reproduced these phenotypes, confirming that CDCA increases muscle insulin sensitization. In *Cyp8b1*^{-/-}, *Cyp2c70*^{-/-}, and CDCA-administered *wild-type* mice, muscle Insulin receptor expression increased, as did activity of its transcription factor Forkhead Box O1 (FOXO1). The CDCA-mediated increase in muscle insulin signaling was attenuated by inhibition of FOXO1.

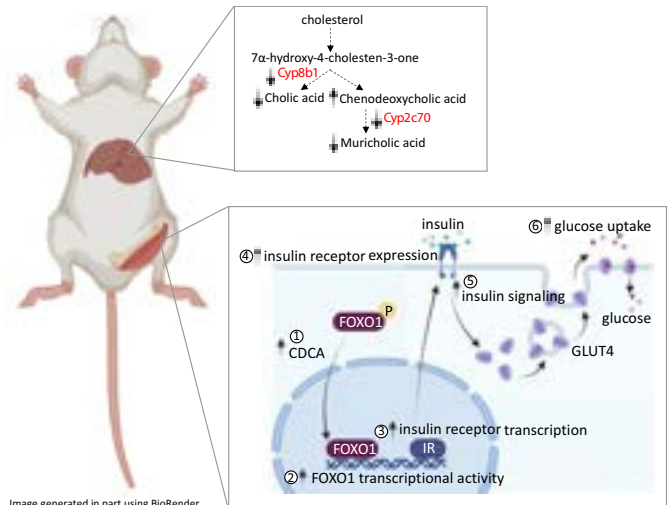


Figure:

Conclusion: Our study demonstrates that CDCA signals in skeletal muscle through the FOXO1 pathway to increase whole organism insulin sensitization.

THU-238

Characterization of pattern recognition receptor expression for regulating myeloid cell responses in the gut-liver axis in non-alcoholic fatty liver disease and cholangiopathies

Alix Bruneau, Simon Wdowinski, Linda Hammerich, Burcin Özdirik, Michael Sigal, Münevver Demir, Frank Tacke. Charité Universitätsmedizin Berlin, Department of Hepatology and Gastroenterology, Berlin, Germany
Email: alix.bruneau@hotmail.fr

Background and aims: The gut-liver axis is a key pathogenic circuit in the progression of liver diseases. Changes in the composition of the gut microbiota in patients with Primary Sclerosing Cholangitis (PSC) and Non-Alcoholic Fatty Liver Disease (NAFLD) have been reported, suggesting a role of microbiota in their pathogenesis. Microbial signals can be recognized by immune cells in the circulation and in the liver via Pattern Recognition Receptors (PRRs), mainly Toll-like receptors (TLRs). Here, we characterized PRR/TLR expression patterns on immune cells of these patients in order to understand relevant (dys)regulations and determine their potential as therapeutic targets.

Method: We performed multiplex immunofluorescence staining on liver and colon samples of patients as well as mouse models of PSC and NAFLD. A panel with 16 different antibodies was used to characterise TLR expression on immune cells of PSC/NAFLD patients as well as in the *mdr2*^{-/-} PSC-like model (in the presence or absence of dysbiosis) as well as in mice subjected to western diet (NAFLD model). In parallel, we developed a 26-colour panel for full spectrum flow cytometry on peripheral immune cells isolated from patients. This study included 140 samples divided in 4 cohorts: healthy donors, PSC, NAFLD and inflammatory bowel disease.

Results: We observe unique variations in TLR9 expression in myeloid populations for NAFLD and PSC patients compared to controls in both liver and peripheral blood. Moreover, in PSC a decrease in lymphoid cell populations can be observed, which is associated with an overexpression of several PRRs, as well as bile acid and chemokine receptors. PRR/TLR expression data correlate with parameters indicating disease severity and/or progression, supporting their potential as novel biomarkers.

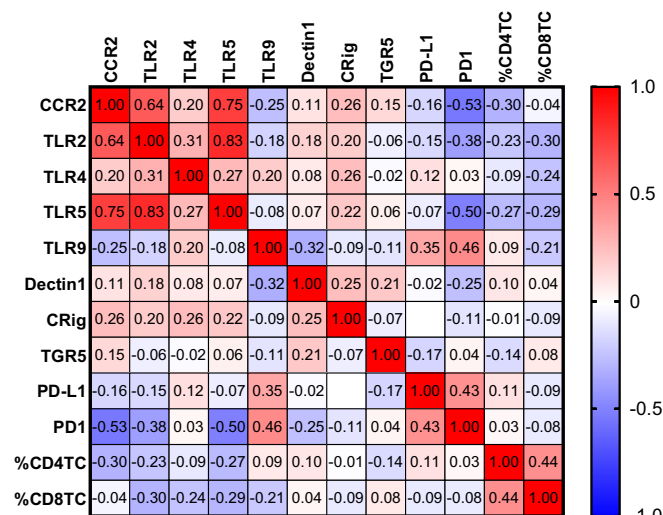


Figure: Heat map for markers expression in classical monocytes (CD14+; CD16low) across 40 PSC patients (Spearman r correlation)

Conclusion: Our results indicate that specific modulation of PRRs in immune cells occurs for PSC and NAFLD patients. These data provide the basis to establish early non-invasive markers for those pathologies and might become potential therapeutic targets for the treatment of chronic liver diseases.

THU-239

Gut microbial proteomic changes from commensal bacteria are associated with development of first decompensation in cirrhosis

Katarzyna Tyc, Xixian Jiang, Jinze Liu, Jasmohan S. Bajaj, Virginia Commonwealth University, United States

Email: jasmohan.bajaj@vcuhealth.org

Background and aims: Prediction of who will develop their first decompensating event in cirrhosis is difficult using clinical biomarkers. Microbiota composition is related to cirrhosis change but proteomics could offer a deeper understanding. Aim: Determine impact of inferred microbial proteomics in differentiating between compensated cirrhotic patients who remain stable versus those that develop their first decompensation.

Method: Compensated outpatients with cirrhosis underwent stool collection and were followed over time for development of their first decompensation. Demographics, cirrhosis severity and medications were collected at baseline and over time. Stool was analyzed for deep

metagenomics and inferred proteomics linked with specific taxa were evaluated at baseline between groups who remained stable over time vs decompensated as well as pre/post were analyzed using MetaWIBELE. Microbially-associated proteins with absolute log fold change greater than 1 between groups, MetaWIBELE priority score >0.9 and p value <0.05 were selected and characterized proteins were closely investigated.

Results: We enrolled 68 patients with compensated cirrhosis, of whom 19 decompensated on follow-up for 429 (391) days. The 19 who decompensated developed ascites (n = 10), hepatic encephalopathy (HE, n = 6) or both (n = 3). At baseline, there was no difference in age (59 vs 59 yrs), MELD (8.9 vs 9.2, p = 0.87), albumin level (3.8 vs 3.5, p = 0.62), or medication use (PPI, statins and opioids). Both groups were followed for a similar time period 435 (429) vs 426 (321) days. Inferred Protein analysis: **Baseline comparison:** We found 3,120 proteins significantly different between groups (158 down/2962 up in unstable vs stable). Fig. 1A shows the top 10 proteins and linked bacterial species. Several proteins related to cell-wall integrity (blue color), and virulence/anti-bacterial resistance (red color) were seen in those who ultimately decompensated. Proteins related to bio-energetics (yellow highlights) in commensals belonging to Firmicutes were over-represented in those who remained stable. **Pre and post-1st decompensation:** We found 3,086 proteins changed over time (8 up/3,078 down in post compared to pre). Fig. 1B shows the *E.coli* and *S.pyogenes* expressing sulfur-reducing enzymes and resistance-associated proteins were higher post-decompensation. Commensal Firmicutes-associated proteins involved in energy metabolism were higher at baseline.

Conclusion: Inferred microbial proteomics in patients with compensated cirrhosis show significant difference that span several important processes such as bioenergetics, cell wall, and antibiotic resistance between those who ultimately developing their first decompensation as well as after the development of decompensation compared to their baseline. Microbial function through proteomics could be promising to predict first decompensation in stable outpatients with compensated cirrhosis.

THU-240

Altered levels of secondary bile acids in enterohepatic circulation impairs liver regeneration in a rat model of partial hepatectomy

Impreet Kaur¹, Rajnish Tiwari¹, Pinky Juneja¹, Ashwini Vasudevan¹, Akash Kumar Mourya¹, Michael Trauner², Shiv Kumar Sarin³, Dinesh Mani Tripathi¹, Savneet Kaur¹. ¹Institute of Liver and Biliary

1A: Baseline Comparison of those who remained stable vs decompensated later : Data presented as Inferred protein comparison Protein (organism)	
Higher in those who remained stable	Higher in those who decompensated in the future
Enoyl-CoA hydratase/isomerase family protein (Firmicutes CAG 114)	Chitinase (Dorea)
Serine hydroxymethyltransferase (Firmicutes bacterium CAG 114)	Xanthine phosphoribosyltransferase (Bacteroides cellulosilyticus CAG 158)
Methionine adenosyltransferase (Ruminococcaceae bacterium KLE1738)	IS110 family transposase (Eubacterium)
SIS domain protein (Firmicutes bacterium CAG 114)	Inner membrane ABC transporter permease protein ycp (Clostridiaceae)
GTPase Der (Firmicutes bacterium CAG 114)	UDP-N-acetylmuramoyl-L-alanyl-D-glutamate-2,6-diaminopimelate ligase (Bacteroides cellulosilyticus)
Homoserine kinase (Firmicutes bacterium CAG 114)	Site-specific integrase (Subdoligranulum sp.)
DNA-binding protein (Bacteroides uniformis)	Autoinducer 2 sensor kinase/phosphatase luxQ (Anaerostipes hadrus)
Phosphate import ATP-binding protein PstB (Firmicutes bacterium CAG 114)	UDP-3-O-acetylglucosamine N-acetyltransferase (Bacteroides uniformis)
Proline-4-oxo-5-oxo-6-oxo-7-oxo-8-oxo-9-oxo-10-oxo-11-oxo-12-oxo-13-oxo-14-oxo-15-oxo-16-oxo-17-oxo-18-oxo-19-oxo-20-oxo-21-oxo-22-oxo-23-oxo-24-oxo-25-oxo-26-oxo-27-oxo-28-oxo-29-oxo-30-oxo-31-oxo-32-oxo-33-oxo-34-oxo-35-oxo-36-oxo-37-oxo-38-oxo-39-oxo-40-oxo-41-oxo-42-oxo-43-oxo-44-oxo-45-oxo-46-oxo-47-oxo-48-oxo-49-oxo-50-oxo-51-oxo-52-oxo-53-oxo-54-oxo-55-oxo-56-oxo-57-oxo-58-oxo-59-oxo-60-oxo-61-oxo-62-oxo-63-oxo-64-oxo-65-oxo-66-oxo-67-oxo-68-oxo-69-oxo-70-oxo-71-oxo-72-oxo-73-oxo-74-oxo-75-oxo-76-oxo-77-oxo-78-oxo-79-oxo-80-oxo-81-oxo-82-oxo-83-oxo-84-oxo-85-oxo-86-oxo-87-oxo-88-oxo-89-oxo-90-oxo-91-oxo-92-oxo-93-oxo-94-oxo-95-oxo-96-oxo-97-oxo-98-oxo-99-oxo-100-oxo-101-oxo-102-oxo-103-oxo-104-oxo-105-oxo-106-oxo-107-oxo-108-oxo-109-oxo-110-oxo-111-oxo-112-oxo-113-oxo-114-oxo-115-oxo-116-oxo-117-oxo-118-oxo-119-oxo-120-oxo-121-oxo-122-oxo-123-oxo-124-oxo-125-oxo-126-oxo-127-oxo-128-oxo-129-oxo-130-oxo-131-oxo-132-oxo-133-oxo-134-oxo-135-oxo-136-oxo-137-oxo-138-oxo-139-oxo-140-oxo-141-oxo-142-oxo-143-oxo-144-oxo-145-oxo-146-oxo-147-oxo-148-oxo-149-oxo-150-oxo-151-oxo-152-oxo-153-oxo-154-oxo-155-oxo-156-oxo-157-oxo-158-oxo-159-oxo-160-oxo-161-oxo-162-oxo-163-oxo-164-oxo-165-oxo-166-oxo-167-oxo-168-oxo-169-oxo-170-oxo-171-oxo-172-oxo-173-oxo-174-oxo-175-oxo-176-oxo-177-oxo-178-oxo-179-oxo-180-oxo-181-oxo-182-oxo-183-oxo-184-oxo-185-oxo-186-oxo-187-oxo-188-oxo-189-oxo-190-oxo-191-oxo-192-oxo-193-oxo-194-oxo-195-oxo-196-oxo-197-oxo-198-oxo-199-oxo-200-oxo-201-oxo-202-oxo-203-oxo-204-oxo-205-oxo-206-oxo-207-oxo-208-oxo-209-oxo-210-oxo-211-oxo-212-oxo-213-oxo-214-oxo-215-oxo-216-oxo-217-oxo-218-oxo-219-oxo-220-oxo-221-oxo-222-oxo-223-oxo-224-oxo-225-oxo-226-oxo-227-oxo-228-oxo-229-oxo-230-oxo-231-oxo-232-oxo-233-oxo-234-oxo-235-oxo-236-oxo-237-oxo-238-oxo-239-oxo-240-oxo-241-oxo-242-oxo-243-oxo-244-oxo-245-oxo-246-oxo-247-oxo-248-oxo-249-oxo-250-oxo-251-oxo-252-oxo-253-oxo-254-oxo-255-oxo-256-oxo-257-oxo-258-oxo-259-oxo-260-oxo-261-oxo-262-oxo-263-oxo-264-oxo-265-oxo-266-oxo-267-oxo-268-oxo-269-oxo-270-oxo-271-oxo-272-oxo-273-oxo-274-oxo-275-oxo-276-oxo-277-oxo-278-oxo-279-oxo-280-oxo-281-oxo-282-oxo-283-oxo-284-oxo-285-oxo-286-oxo-287-oxo-288-oxo-289-oxo-290-oxo-291-oxo-292-oxo-293-oxo-294-oxo-295-oxo-296-oxo-297-oxo-298-oxo-299-oxo-300-oxo-301-oxo-302-oxo-303-oxo-304-oxo-305-oxo-306-oxo-307-oxo-308-oxo-309-oxo-310-oxo-311-oxo-312-oxo-313-oxo-314-oxo-315-oxo-316-oxo-317-oxo-318-oxo-319-oxo-320-oxo-321-oxo-322-oxo-323-oxo-324-oxo-325-oxo-326-oxo-327-oxo-328-oxo-329-oxo-330-oxo-331-oxo-332-oxo-333-oxo-334-oxo-335-oxo-336-oxo-337-oxo-338-oxo-339-oxo-340-oxo-341-oxo-342-oxo-343-oxo-344-oxo-345-oxo-346-oxo-347-oxo-348-oxo-349-oxo-350-oxo-351-oxo-352-oxo-353-oxo-354-oxo-355-oxo-356-oxo-357-oxo-358-oxo-359-oxo-360-oxo-361-oxo-362-oxo-363-oxo-364-oxo-365-oxo-366-oxo-367-oxo-368-oxo-369-oxo-370-oxo-371-oxo-372-oxo-373-oxo-374-oxo-375-oxo-376-oxo-377-oxo-378-oxo-379-oxo-380-oxo-381-oxo-382-oxo-383-oxo-384-oxo-385-oxo-386-oxo-387-oxo-388-oxo-389-oxo-390-oxo-391-oxo-392-oxo-393-oxo-394-oxo-395-oxo-396-oxo-397-oxo-398-oxo-399-oxo-400-oxo-401-oxo-402-oxo-403-oxo-404-oxo-405-oxo-406-oxo-407-oxo-408-oxo-409-oxo-410-oxo-411-oxo-412-oxo-413-oxo-414-oxo-415-oxo-416-oxo-417-oxo-418-oxo-419-oxo-420-oxo-421-oxo-422-oxo-423-oxo-424-oxo-425-oxo-426-oxo-427-oxo-428-oxo-429-oxo-430-oxo-431-oxo-432-oxo-433-oxo-434-oxo-435-oxo-436-oxo-437-oxo-438-oxo-439-oxo-440-oxo-441-oxo-442-oxo-443-oxo-444-oxo-445-oxo-446-oxo-447-oxo-448-oxo-449-oxo-450-oxo-451-oxo-452-oxo-453-oxo-454-oxo-455-oxo-456-oxo-457-oxo-458-oxo-459-oxo-460-oxo-461-oxo-462-oxo-463-oxo-464-oxo-465-oxo-466-oxo-467-oxo-468-oxo-469-oxo-470-oxo-471-oxo-472-oxo-473-oxo-474-oxo-475-oxo-476-oxo-477-oxo-478-oxo-479-oxo-480-oxo-481-oxo-482-oxo-483-oxo-484-oxo-485-oxo-486-oxo-487-oxo-488-oxo-489-oxo-490-oxo-491-oxo-492-oxo-493-oxo-494-oxo-495-oxo-496-oxo-497-oxo-498-oxo-499-oxo-500-oxo-501-oxo-502-oxo-503-oxo-504-oxo-505-oxo-506-oxo-507-oxo-508-oxo-509-oxo-510-oxo-511-oxo-512-oxo-513-oxo-514-oxo-515-oxo-516-oxo-517-oxo-518-oxo-519-oxo-520-oxo-521-oxo-522-oxo-523-oxo-524-oxo-525-oxo-526-oxo-527-oxo-528-oxo-529-oxo-530-oxo-531-oxo-532-oxo-533-oxo-534-oxo-535-oxo-536-oxo-537-oxo-538-oxo-539-oxo-540-oxo-541-oxo-542-oxo-543-oxo-544-oxo-545-oxo-546-oxo-547-oxo-548-oxo-549-oxo-550-oxo-551-oxo-552-oxo-553-oxo-554-oxo-555-oxo-556-oxo-557-oxo-558-oxo-559-oxo-560-oxo-561-oxo-562-oxo-563-oxo-564-oxo-565-oxo-566-oxo-567-oxo-568-oxo-569-oxo-570-oxo-571-oxo-572-oxo-573-oxo-574-oxo-575-oxo-576-oxo-577-oxo-578-oxo-579-oxo-580-oxo-581-oxo-582-oxo-583-oxo-584-oxo-585-oxo-586-oxo-587-oxo-588-oxo-589-oxo-590-oxo-591-oxo-592-oxo-593-oxo-594-oxo-595-oxo-596-oxo-597-oxo-598-oxo-599-oxo-600-oxo-601-oxo-602-oxo-603-oxo-604-oxo-605-oxo-606-oxo-607-oxo-608-oxo-609-oxo-610-oxo-611-oxo-612-oxo-613-oxo-614-oxo-615-oxo-616-oxo-617-oxo-618-oxo-619-oxo-620-oxo-621-oxo-622-oxo-623-oxo-624-oxo-625-oxo-626-oxo-627-oxo-628-oxo-629-oxo-630-oxo-631-oxo-632-oxo-633-oxo-634-oxo-635-oxo-636-oxo-637-oxo-638-oxo-639-oxo-640-oxo-641-oxo-642-oxo-643-oxo-644-oxo-645-oxo-646-oxo-647-oxo-648-oxo-649-oxo-650-oxo-651-oxo-652-oxo-653-oxo-654-oxo-655-oxo-656-oxo-657-oxo-658-oxo-659-oxo-660-oxo-661-oxo-662-oxo-663-oxo-664-oxo-665-oxo-666-oxo-667-oxo-668-oxo-669-oxo-670-oxo-671-oxo-672-oxo-673-oxo-674-oxo-675-oxo-676-oxo-677-oxo-678-oxo-679-oxo-680-oxo-681-oxo-682-oxo-683-oxo-684-oxo-685-oxo-686-oxo-687-oxo-688-oxo-689-oxo-690-oxo-691-oxo-692-oxo-693-oxo-694-oxo-695-oxo-696-oxo-697-oxo-698-oxo-699-oxo-700-oxo-701-oxo-702-oxo-703-oxo-704-oxo-705-oxo-706-oxo-707-oxo-708-oxo-709-oxo-710-oxo-711-oxo-712-oxo-713-oxo-714-oxo-715-oxo-716-oxo-717-oxo-718-oxo-719-oxo-720-oxo-721-oxo-722-oxo-723-oxo-724-oxo-725-oxo-726-oxo-727-oxo-728-oxo-729-oxo-730-oxo-731-oxo-732-oxo-733-oxo-734-oxo-735-oxo-736-oxo-737-oxo-738-oxo-739-oxo-740-oxo-741-oxo-742-oxo-743-oxo-744-oxo-745-oxo-746-oxo-747-oxo-748-oxo-749-oxo-750-oxo-751-oxo-752-oxo-753-oxo-754-oxo-755-oxo-756-oxo-757-oxo-758-oxo-759-oxo-760-oxo-761-oxo-762-oxo-763-oxo-764-oxo-765-oxo-766-oxo-767-oxo-768-oxo-769-oxo-770-oxo-771-oxo-772-oxo-773-oxo-774-oxo-775-oxo-776-oxo-777-oxo-778-oxo-779-oxo-780-oxo-781-oxo-782-oxo-783-oxo-784-oxo-785-oxo-786-oxo-787-oxo-788-oxo-789-oxo-790-oxo-791-oxo-792-oxo-793-oxo-794-oxo-795-oxo-796-oxo-797-oxo-798-oxo-799-oxo-800-oxo-801-oxo-802-oxo-803-oxo-804-oxo-805-oxo-806-oxo-807-oxo-808-oxo-809-oxo-810-oxo-811-oxo-812-oxo-813-oxo-814-oxo-815-oxo-816-oxo-817-oxo-818-oxo-819-oxo-820-oxo-821-oxo-822-oxo-823-oxo-824-oxo-825-oxo-826-oxo-827-oxo-828-oxo-829-oxo-830-oxo-831-oxo-832-oxo-833-oxo-834-oxo-835-oxo-836-oxo-837-oxo-838-oxo-839-oxo-840-oxo-841-oxo-842-oxo-843-oxo-844-oxo-845-oxo-846-oxo-847-oxo-848-oxo-849-oxo-850-oxo-851-oxo-852-oxo-853-oxo-854-oxo-855-oxo-856-oxo-857-oxo-858-oxo-859-oxo-860-oxo-861-oxo-862-oxo-863-oxo-864-oxo-865-oxo-866-oxo-867-oxo-868-oxo-869-oxo-870-oxo-871-oxo-872-oxo-873-oxo-874-oxo-875-oxo-876-oxo-877-oxo-878-oxo-879-oxo-880-oxo-881-oxo-882-oxo-883-oxo-884-oxo-885-oxo-886-oxo-887-oxo-888-oxo-889-oxo-890-oxo-891-oxo-892-oxo-893-oxo-894-oxo-895-oxo-896-oxo-897-oxo-898-oxo-899-oxo-900-oxo-901-oxo-902-oxo-903-oxo-904-oxo-905-oxo-906-oxo-907-oxo-908-oxo-909-oxo-910-oxo-911-oxo-912-oxo-913-oxo-914-oxo-915-oxo-916-oxo-917-oxo-918-oxo-919-oxo-920-oxo-921-oxo-922-oxo-923-oxo-924-oxo-925-oxo-926-oxo-927-oxo-928-oxo-929-oxo-930-oxo-931-oxo-932-oxo-933-oxo-934-oxo-935-oxo-936-oxo-937-oxo-938-oxo-939-oxo-940-oxo-941-oxo-942-oxo-943-oxo-944-oxo-945-oxo-946-oxo-947-oxo-948-oxo-949-oxo-950-oxo-951-oxo-952-oxo-953-oxo-954-oxo-955-oxo-956-oxo-957-oxo-958-oxo-959-oxo-960-oxo-961-oxo-962-oxo-963-oxo-964-oxo-965-oxo-966-oxo-967-oxo-968-oxo-969-oxo-970-oxo-971-oxo-972-oxo-973-oxo-974-oxo-975-oxo-976-oxo-977-oxo-978-oxo-979-oxo-980-oxo-981-oxo-982-oxo-983-oxo-984-oxo-985-oxo-986-oxo-987-oxo-988-oxo-989-oxo-990-oxo-991-oxo-992-oxo-993-oxo-994-oxo-995-oxo-996-oxo-997-oxo-998-oxo-999-oxo-1000-oxo-1001-oxo-1002-oxo-1003-oxo-1004-oxo-1005-oxo-1006-oxo-1007-oxo-1008-oxo-1009-oxo-1010-oxo-1011-oxo-1012-oxo-1013-oxo-1014-oxo-1015-oxo-1016-oxo-1017-oxo-1018-oxo-1019-oxo-1020-oxo-1021-oxo-1022-oxo-1023-oxo-1024-oxo-1025-oxo-1026-oxo-1027-oxo-1028-oxo-1029-oxo-1030-oxo-1031-oxo-1032-oxo-1033-oxo-1034-oxo-1035-oxo-1036-oxo-1037-oxo-1038-oxo-1039-oxo-1040-oxo-1041-oxo-1042-oxo-1043-oxo-1044-oxo-1045-oxo-1046-oxo-1047-oxo-1048-oxo-1049-oxo-1050-oxo-1051-oxo-1052-oxo-1053-oxo-1054-oxo-1055-oxo-1056-oxo-1057-oxo-1058-oxo-1059-oxo-1060-oxo-1061-oxo-1062-oxo-1063-oxo-1064-oxo-1065-oxo-1066-oxo-1067-oxo-1068-oxo-1069-oxo-1070-oxo-1071-oxo-1072-oxo-1073-oxo-1074-oxo-1075-oxo-1076-oxo-1077-oxo-1078-oxo-1079-oxo-1080-oxo-1081-oxo-1082-oxo-1083-oxo-1084-oxo-1085-oxo-1086-oxo-1087-oxo-1088-oxo-1089-oxo-1090-oxo-1091-oxo-1092-oxo-1093-oxo-1094-oxo-1095-oxo-1096-oxo-1097-oxo-1098-oxo-1099-oxo-1100-oxo-1101-oxo-1102-oxo-1103-oxo-1104-oxo-1105-oxo-1106-oxo-1107-oxo-1108-oxo-1109-oxo-1110-oxo-1111-oxo-1112-oxo-1113-oxo-1114-oxo-1115-oxo-1116-oxo-1117-oxo-1118-oxo-1119-oxo-1120-oxo-1121-oxo-1122-oxo-1123-oxo-1124-oxo-1125-oxo-1126-oxo-1127-oxo-1128-oxo-1129-oxo-1130-oxo-1131-oxo-1132-oxo-1133-oxo-1134-oxo-1135-oxo-1136-oxo-1137-oxo-1138-oxo-1139-oxo-1140-oxo-1141-oxo-1142-oxo-1143-oxo-1144-oxo-1145-oxo-1146-oxo-1147-oxo-1148-oxo-1149-oxo-1150-oxo-1151-oxo-1152-oxo-1153-oxo-1154-oxo-1155-oxo-1156-oxo-1157-oxo-1158-oxo-1159-oxo-1160-oxo-1161-oxo-1162-oxo-1163-oxo-1164-oxo-1165-oxo-1166-oxo-1167-oxo-1168-oxo-1169-oxo-1170-oxo-1171-oxo-1172-oxo-1173-oxo-1174-oxo-1175-oxo-1176-oxo-1177-oxo-1178-oxo-1179-oxo-1180-oxo-1181-oxo-1182-oxo-1183-oxo-1184-oxo-1185-oxo-1186-oxo-1187-oxo-1188-oxo-1189-oxo-1190-oxo-1191-oxo-1192-oxo-1193-oxo-1194-oxo-1195-oxo-1196-oxo-1197-oxo-1198-oxo-1199-oxo-1200-oxo-1201-oxo-1202-oxo-1203-oxo-1204-oxo-1205-oxo-1206-oxo-1207-oxo-1208-oxo-1209-oxo-1210-oxo-1211-oxo-1212-oxo-1213-oxo-1214-oxo-1215-oxo-1216-oxo-1217-oxo-1218-oxo-1219-oxo-1220-oxo-1221-oxo-1222-oxo-1223-oxo-1224-oxo-1225-oxo-1226-oxo-1227-oxo-1228-oxo-1229-oxo-1230-oxo-1231-oxo-1232-oxo-1233-oxo-1234-oxo-1235-oxo-1236-oxo-1237-oxo-1238-oxo-1239-oxo-1240-oxo-1241-oxo-1242-oxo-1243-oxo-1244-oxo-1245-oxo-1246-oxo-1247-oxo-1248-oxo-1249-oxo-1250-oxo-1251-oxo-1252-oxo-1253-oxo-1254-oxo-1255-oxo-1256-oxo-1257-oxo-1258-oxo-1259-oxo-1260-oxo-1261-oxo-1262-oxo-1263-oxo-1264-oxo-1265-oxo-1266-oxo-1267-oxo-1268-oxo-1269-oxo-1270-oxo-1271-oxo-1272-oxo-1273-oxo-1274-oxo-1275-oxo-1276-oxo-1277-oxo-1278-oxo-1279-oxo-1280-oxo-1281-oxo-1282-oxo-1283-oxo-1284-oxo-1285-oxo-1286-oxo-1287-oxo-1288-oxo-1289-oxo-1290-oxo-1291-oxo-1292-oxo-1293-oxo-1294-oxo-1295-oxo-1296-oxo-1297-oxo-1298-oxo-1299-oxo-1300-oxo-1301-oxo-1302-oxo-1303-oxo-1304-oxo-1305-oxo-1306-oxo-1307-oxo-1308-oxo-1309-oxo-1310-oxo-1311-oxo-1312-oxo-1313-oxo-1314-oxo-1315-oxo-1316-oxo-1317-oxo-1318-oxo-1319-oxo-1320-oxo-1321-oxo-1322-oxo-1323-oxo-1324-oxo-1325-oxo-1326-oxo-1327-oxo-1328-oxo-1329-oxo-1330-oxo-1331-oxo-1332-oxo-1333-oxo-1334-oxo-1335-oxo-1336-oxo-1337-oxo-1338-oxo-1339-oxo-1340-oxo-1341-oxo-1342-oxo-1343-oxo-1344-oxo-1345-oxo-1346-oxo-1347-oxo-1348-oxo-1349-oxo-1350-oxo-1351-oxo-1352-oxo-1353-oxo-1354-oxo-1355-oxo-1356-oxo-1357-oxo-1358-oxo-1359-oxo-1360-oxo-1361-oxo-1362-oxo-1363-oxo-1364-oxo-1365-oxo-1366-oxo-1367-oxo-1368-oxo-1369-oxo-1370-oxo-1371-oxo-1372-oxo-1373-oxo-1374-oxo-1375-oxo-1376-oxo-1377-oxo-1378-oxo-1379-oxo-1380-oxo-1381-oxo-1382-oxo-1383-oxo-1384-oxo-1385-oxo-1386-oxo-1387-oxo-1388-oxo-1389-oxo-1390-oxo-1391-oxo-1392-oxo-1393-oxo-1394-oxo-1395-oxo-1396-oxo-1397-oxo-1398-oxo-1399-oxo-1400-oxo-1401-oxo-1402-oxo-1403-oxo-1404-oxo-1405-oxo-1406-oxo-1407-oxo-1408-oxo-1409-oxo-1410-oxo-1411-oxo-1412-oxo-1413-oxo-1414-oxo-1415-oxo-1416-oxo-1417-oxo-1418-oxo-1419-oxo-1420-oxo-1421-oxo-1422-oxo-1423-oxo-1424-oxo-1425-oxo-1426-oxo-1427-oxo-1428-oxo-1429-oxo-1430-oxo-1431-oxo-1432-oxo-1433-oxo-1434-oxo-1435-oxo-1436-oxo-1437-oxo-1438-oxo-1439-oxo-1440-oxo-1441-oxo-1442-oxo-1443-oxo-1444-oxo-1445-oxo-1446-oxo-1447-oxo-1448-oxo-1449-oxo-1450-oxo-1451-oxo-1452-oxo-1453-oxo-1454-oxo-1455-oxo-1456-oxo-1457-oxo-1458-oxo-1459-oxo-1460-oxo-1461-oxo-1462-oxo-1463-oxo-1464-oxo-1465-oxo-1466-oxo-1467-oxo-1468-oxo-1469-oxo-1470-oxo-1471-oxo-1472-oxo-1473-oxo-1474-oxo-1475-oxo-1476-oxo-1477-oxo-1478-oxo-1479-oxo-1480-oxo-1481-oxo-1482-oxo-1483-oxo-1484-oxo-1485-oxo-1486-oxo-1487-oxo-1488-oxo-1489-oxo-1490-oxo-1491-oxo-1492-oxo-1493-oxo-1494-oxo-1495-oxo-1496-oxo-1497-oxo-1498-oxo-1499-oxo-1500-oxo-1501-oxo-1502-oxo-1503-oxo-1504-oxo-1505-oxo-1506-oxo-1507-oxo-1508-oxo-1509-oxo-1510-oxo-1511-oxo-1512-oxo-1513-oxo-1514-oxo-1515-oxo-1516-oxo-1517-oxo-1518-oxo-1519-oxo-1520-oxo-1521-oxo-1522-oxo-1523-oxo-1524-oxo-1525-oxo-1526-oxo-1527-oxo-1528-oxo-1529-oxo-1530-oxo-1531-oxo-1532-oxo-1533-oxo-1534-oxo-1535-oxo-1536-oxo-1537-oxo-1538-oxo-1539-oxo-1540-oxo-1541-oxo-1542-oxo-1543-oxo-1544-oxo-1545-oxo-1546-oxo-1547-oxo-1548-oxo-1549-oxo-1550-oxo-1551-oxo-1552-oxo-1553-oxo-1554-oxo-1555-oxo-1556-oxo-1557-oxo-1558-oxo-1559-oxo-1560-oxo-1561-oxo-1562-oxo-1563-oxo-1564-oxo-1565-oxo-1566-oxo-1567-oxo-1568-oxo-1569-oxo-1570-oxo-1571-oxo-1572-oxo-1573-oxo-1574-oxo-1575-oxo-1576-oxo-1577-oxo-1578-oxo-1579-oxo-1580-oxo-1581-oxo-1582-oxo-1583-oxo-1584-oxo-1585-oxo-1586-oxo-1587-oxo-1588-oxo-1589-oxo-1590-oxo-1591-oxo-1592-oxo-1593-oxo-1594-oxo-1595-oxo-1596-oxo-1597-oxo-1598-oxo-1599-oxo-1600-oxo-1601-oxo-1602-oxo-1603-oxo-1604-oxo-1605-oxo-1606-oxo-1607-oxo-1608-oxo-1609-oxo-1610-oxo-1611-oxo-1612-oxo-1613-oxo-1614-oxo-1615-oxo-1616-oxo-1617-oxo-1618-oxo-1619-oxo-1620-oxo-1621-oxo-1622-oxo-	

Sciences, Molecular and Cellular Medicine, New Delhi, India; ²Medical University of Vienna, Wien, Austria; ³Institute of Liver and Biliary Sciences, Department of Hepatology, New Delhi, India
Email: savykaur@gmail.com

Background and aims: Liver is exposed to gut-derived components via portal vein that regulates host metabolism and tissue homeostasis. Here, we aim to explore gut microbiota-associated metabolites during liver regeneration in response to 70% partial hepatectomy (PHx).

Method: Liver regeneration was studied in PHx and compared to gut microbiota-modulated PHx, achieved by 3-week antibiotic (Abx) treatment prior to PHx (Abx+PHx). Sham without Abx served as controls and were compared to Abx+controls. Relative abundance of dominant gut phyla was evaluated in faeces by RT-PCRs. Primary hepatocytes and liver sinusoidal endothelial cells (LSECs) were isolated by collagenase perfusion. Liver regeneration was assessed by proliferating cell nuclear antigen (PCNA) in liver tissues by immunohistochemistry and cell cycle gene expression in primary hepatocytes by RT-PCRs. Untargeted metabolomics of portal and peripheral serum was performed and differentially abundant metabolites (DAMs) were identified between different study groups. In vitro effects of few DAMs were studied on viability and proliferation of hepatocytes and secretory factors of LSECs.

Results: We observed reduction in bacterial phyla, *Firmicutes* (2-fold), *Actinobacteria* (2.4-fold) and *Bacteroidetes* (2.3-fold) ($p < 0.0001$ each) post Abx treatment in controls and PHx. Compared to controls ($13.4 \pm 3.2\%$) PHx showed an increase ($44.6 \pm 6.9\%$); ($p < 0.001$) in PCNA positivity in livers that correlated with cell cycle genes involved in hepatocyte proliferation at day 2 post-PHx. In Abx-treated PHx, there was reduced PCNA ($9 \pm 3\%$); ($p < 0.001$) and cyclins' gene expression in hepatocytes as compared to PHx (cyclin B1 = 8-fold, cyclin D1 = 4-fold, cyclin E = 20-fold; $p < 0.0001$ each). In both portal and peripheral serum, we obtained about 800 total metabolites each, where we identified 224 DAMs between PHx and controls while 189 DAMs between Abx+PHx vs PHx in portal serum at day 2 post-PHx. 70 common metabolites showed exactly opposite levels between PHx vs controls and Abx+PHx vs PHx in portal serum. 3-hydroxysebacic acid

and secondary bile acids such as deoxycholic (DCA) and lithocholic acid (LCA) were enhanced in PHx vs controls while decreased in Abx+PHx vs PHx. In vitro treatment with DCA ($10 \mu\text{M}$) significantly enhanced PCNA-positivity in hepatocytes ($52.6 \pm 7.3\%$ vs $32.4 \pm 7.9\%$, $p < 0.05$) and secretion of angiocrine factors, HGF ($122.06 \pm 9.7 \text{ pg/ml}$ vs $77.8 \pm 7.2 \text{ pg/ml}$) and Wnt 2 ($74.5 \pm 6.8 \text{ pg/ml}$ vs $57 \pm 5.3 \text{ pg/ml}$); ($p < 0.001$ each) in LSECs as compared to DMSO treatment.

Conclusion: We report that altered levels of secondary bile acids such as DCA in portal serum or enterohepatic circulation in Abx-treated rats lead to impaired hepatocyte proliferation, angiocrine factor secretion by LSECs and hence liver regeneration post 70% PHx. The study underscores a crucial role of secondary bile acids in liver regeneration through varied cellular mechanisms.

THU-241

Gut-liver crosstalk in hepatocellular carcinoma and non-selective beta-blockers: is there a link?

Tasnim Mahmoud¹, Olfat Hammam², Mahmoud Khattab³, Aiman El-Khatib³, Yasmeen Attia⁴. ¹The British University in Egypt, Pharmacology and Biochemistry, Egypt; ²Theodor Bilharz Research Institute, Pathology, Egypt; ³Faculty of Pharmacy, Cairo University, Pharmacology and Toxicology, Egypt; ⁴The British University in Egypt, Pharmacology, Egypt
Email: yasmeen.attia@bue.edu.eg

Background and aims: The bidirectional relationship between the gut and liver orchestrated by the portal vein and dubbed the "gut-liver axis" is becoming increasingly recognized. The interest in its impact on disease onset and severity has also surged recently. Microbial dysbiosis, intestinal permeability, and compromised tight junctional proteins are manifestations in the gut that hugely provoke immune remodeling in the liver. Likewise, hepatocellular carcinoma (HCC) and its ensuing alterations on the liver microenvironment were found to govern the inflammatory milieu in the gut. An intriguing bridge linking both edges of the gut-liver axis seems to be presented in the toll-like receptor 4 (TLR4) signaling. Non-selective beta blockers (NSBBs) are known for their protective effect against intestinal permeability and dysbiosis, especially in cirrhotic patients.

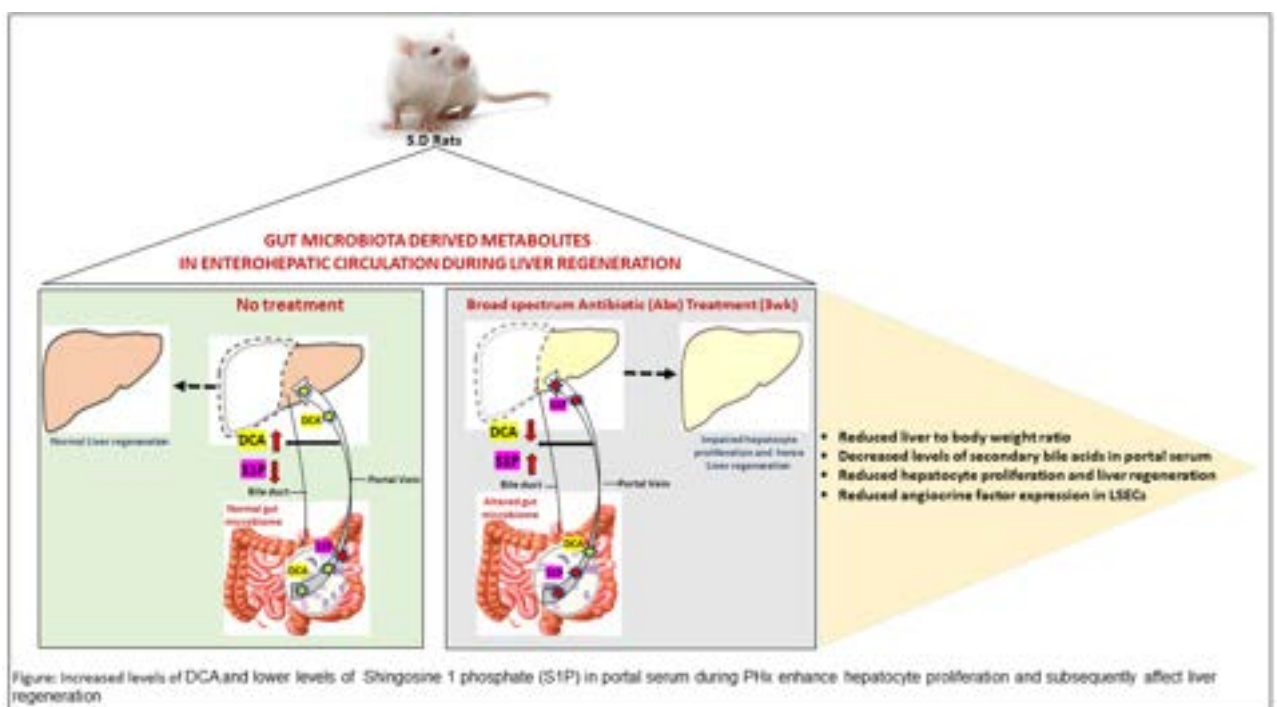


Figure: (abstract: THU-240).

POSTER PRESENTATIONS

Moreover, an established role for NSBBs in cancer was alluded to by the overexpression of beta receptors in solid tumors. Thus, the present study sought to unleash the likely gut barrier dysfunction in an experimental model of HCC and whether a protective role exists for carvedilol (CAR), a NSBB, on both gut- and liver-related disruptions via modulating the TLR4 signaling.

Method: Male Sprague Dawley rats received weekly intraperitoneal injections of 50 mg/kg of diethyl nitrosamine (DEN) for 16 weeks. Daily treatment with CAR started at week 18 for a period of 4 weeks, at a dose of 10 mg/kg/day, p.o. After sacrifice, livers, ileums, and colons were collected for further analysis. Histopathological examination was performed on harvested tissues. TLR4, occludin, and claudin-1 intestinal immunoreactivities were investigated using immunohistochemistry. Liver and intestinal phosphorylated nuclear factor kappa B (p-NF-kB) along with hepatic TLR4 were also estimated using ELISA.

Results: Our findings showed epithelial hyperplasia apparent as elongated crypts along with increased inflammatory infiltrates in the intestinal sections of the DEN-treated group. These results were coupled with increased pleomorphic hepatocytes with a high nuclear-to-cytoplasmic ratio in the livers of the control untreated group. These effects were, however, abrogated by CAR treatment. The DEN-treated group also demonstrated increased TLR4 hepatic levels along with surged p-NF-kB, as compared to normal animals. These effects paralleled an increase in TLR4 intestinal immunoreactivity and NF-kB levels along with altered occludin and claudin-1 levels. CAR treatment was capable of reversing both the hepatic and intestinal changes observed in the untreated DEN-treated group with significant reductions in TLR4 levels (Fig. 1) and restoration of tight junctional protein expression.

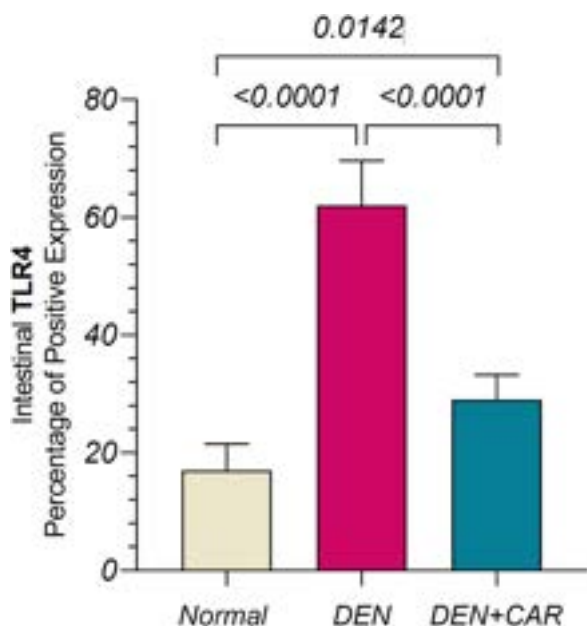


Figure: Effect of CAR treatment on intestinal immunohistochemical expression of TLR4 in normal, DEN-treated, and DEN+CAR-treated groups. Data are analyzed using one-way ANOVA followed by Tukey's for multiple comparisons. Data are presented as mean ± S.D. P values less than 0.05 are considered statistically significant.

Conclusion: These findings, therefore, suggest a likely protective role of CAR in the gut-liver crosstalk in an HCC setting.

THU-242

Phascolarctobacterium as a predictor for survival in cirrhotic patients

Rosa Haller¹, Stefan Fürst¹, Johannes Woltsche¹, Lukas Gulden¹, Jakob Schwarzl¹, Julia Traub¹, Nicole Feldbacher^{1,2}, Benard Aliwa^{1,3},

Tobias Madl⁴, Günter Fauler⁵, Angela Horvath^{1,2}, Vanessa Stadlbauer^{1,2}. ¹Medical University of Graz, Institute of Gastroenterology and Hepatology, Graz, Austria; ²CBmed GMBH, Graz, Austria; ³University of Nairobi, Department of Food Science, Nutrition and Technology, Kenya; ⁴Medical University of Graz, Gottfried Scharz Research Center, Graz, Austria; ⁵Medical University of Graz, Clinical Institute of Medical and Chemical Laboratory Diagnostics, Graz, Austria Email: rosa.haller@medunigraz.at

Background and aims: Previously we linked zonulin, a marker for intestinal permeability, to an increased risk of mortality in cirrhosis and subsequent microbiome analysis identified *Phascolarctobacterium* to be associated with improved zonulin levels and better survival over 36 months. We aim to verify the role of *Phascolarctobacterium* in liver cirrhosis.

Method: Stool, serum and urine samples from 92 cirrhotic patients (62 ± 11 years, 24 female) were obtained. *Phascolarctobacterium* abundance was extracted from 16s rRNA sequencing data. Kaplan-Meier survival analysis, group comparisons and correlation analysis were performed.

Results: A higher abundance (>50 counts per 8000 sequences) of *Phascolarctobacterium* was associated with a higher chance of survival over 36 months (log rank mantel cox, p=0.027). In accordance with the previous analysis, higher abundance of *Phascolarctobacterium* was associated with better liver function (higher total protein (p=0.025), higher fibrinogen levels (p=0.0011) lower international normalized ratio (p=0.016), lower bilirubin levels (p=0.009)) and better intestinal permeability (lower zonulin levels (p=0.047)), but not with etiology (p=0.29). In addition to the previous study we found higher *Phascolarctobacterium* abundance in men (p=0.011), higher age (p=0.0055), patients with higher neutrophil (p=0.031), monocyte (p=0.044) and thrombocyte counts (p=0.0096) and lower lymphocyte counts (p=0.028).

Higher *Phascolarctobacterium* abundance was associated with changes in the metabolome (lower stool succinate and glucose, higher serum glucose, urine acetoacetate and phenylalanine; all p < 0.05) and bile acids (lower total primary bile acids, total glucosyl-co-deoxycholic acid and a lower ratio of 12α hydroxylated bile acids to non 12α hydroxylated bile acids, all p < 0.05) in stool.

Conclusion: Higher *Phascolarctobacterium* abundance in the gut microbiome of cirrhotic patients is again linked to better survival, better hepatic function and decreased intestinal permeability in this validation cohort. *Phascolarctobacterium* is associated with stool, serum and urine metabolomic changes, as well as changes in stool bile acid composition, indicating a potential role of *Phascolarctobacterium* in short chain fatty acid, glucose, amino-acid and bile acid metabolism in cirrhosis. Increasing *Phascolarctobacterium* could therefore be a therapeutic target to modulate the gut-liver axis.

THU-243

Long-term benefit of direct-acting antivirals on gut dysbiosis and microbial translocation in HCV-infected patients with and without HIV coinfection

Natthaya Chuaypen, Thananya Jinato, Pisit Tangkijvanich. Faculty of Medicine, Chulalongkorn University, Biochemistry, Bangkok, Thailand Email: pisittkvn@yahoo.com

Background and aims: Emerging evidence indicate that direct-acting antivirals (DAAs) could alleviate gut dysbiosis in patients with hepatitis C virus (HCV) infection who achieve sustained virological response (SVR). However, limited data are available regarding the long-term effect of DAAs on gut microbial composition, short-chain fatty acids (SCFAs) and microbial translocation in patients with chronic HCV infection.

Method: A prospective longitudinal study of 50 patients with HCV monoinfection and 19 patients with HCV/HIV coinfection received DAAs were conducted. Fecal specimens collected at baseline and at

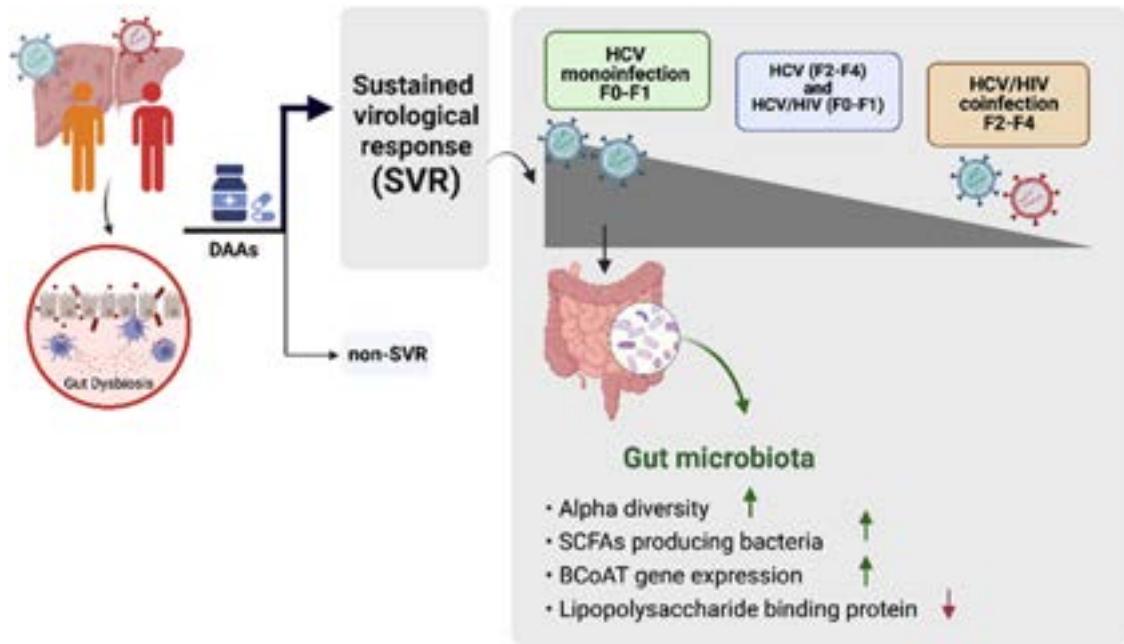


Figure: (abstract: THU-243).

week 72 after treatment completion (FUw72) were analyzed for gut microbiota by 16S rRNA sequencing and estimation expression of butyryl-CoA:acetateCoA transferase (BCoAT) in microbiota using real-time PCR. Plasma lipopolysaccharide binding protein (LBP) and intestinal fatty acid binding protein (I-FABP) were quantified by ELISA assays.

Results: In this study, SVR rates in mono- and coinfecting patients were comparable (94% vs.100%). The improvement of gut dysbiosis and microbial translocation was found in responders but was not in non-responders. Among responders, significant restoration of alpha-diversity, BCoAT and LBP were consistently observed in HCV-monoinfected patients with low-grade fibrosis (F0-F1), while HCV/HIV-coinfecting patients exhibited partial improvement at FUw72. Plasma I-FABP was not declined significantly in responders. Treatment-induced microbiota changes were associated with increasing abundance of SCFAs-producing bacteria, including *Blautia*, *Fusicatenibacter*, *Subdoligranulum* and *Bifidobacterium*.

Conclusion: Our results provided a perspective regarding long-term effect of successful DAAs in restoration of gut dysbiosis and microbial translocation. However, early initiation of DAAs possibly required an alteration in gut microbiota, especially enhanced SCFAs-producing bacteria, toward the reduction of HCV-related complications.

THU-244

The intestinal immune barrier is associated with bile acid pool modifications in mice suffering from non-alcoholic steatohepatitis

Simon Peschard¹, Margaux Nawrot¹, Olivier Molendi-Coste¹, Emmanuelle Vallez¹, Amandine Descat², Véronique Touche¹, Joel Haas¹, Anne Tailleux¹, David Dombrowicz¹, Bart Staels¹, Sophie Lestavel¹. ¹Univ. Lille, Inserm, CHU Lille, Institut Pasteur de Lille, U1011, EGID, Lille, France; ²Univ. Lille, PSM-ULR7365 GRITA, Lille, France
Email: simon.peschard@univ-lille.fr

Background and aims: Obesity and insulin resistance are usually associated with metabolic liver injuries such as non-alcoholic steatohepatitis (NASH). To go deeper into the alterations of the gut-liver crosstalk in this pathology, we used a well characterized diet-

induced NASH mouse model to study the intestinal immune barrier and the intra-caecal bile acid (BA) composition.

Method: Eight-week-old C57BL/6J male mice were fed for 24 weeks with a high fat/high sucrose diet supplemented with cholesterol to induce histological NASH and impaired glucose sensitivity, and were compared to their littermate controls under chow diet. Liver and gut samples were collected for histological analysis. Immunophenotyping was performed on alive cells purified from the lamina propria of the small intestine. A panel of 18 antibodies was used to identify immune cell subtypes by flow cytometry (Fortessa X20). Results were analyzed using FlowJo software. Caecal content of NASH and control mice were collected, freeze-dried prior to bile acid extraction and dosage by tandem mass spectrometry.

Results: As expected, liver of mice under NASH diet were consistent with histological features of the human disease, with hepatic steatosis, inflammation and fibrosis in a context of obesity. Serum alanine aminotransferase levels and oral glucose intolerance were also induced by the diet. Despite no histological remodeling of the small intestine, the intestinal immunological barrier was found altered in NASH animals. In particular, a decrease of CD8⁺ T lymphocyte proportions was found and regardless of TCR and CD8 subtypes. Proportions of B lymphocytes and myeloid-derived cells seem not to be affected by the diet. NASH mice display an overall increase of BA with an increase of primary to secondary BA ratio. More interestingly, BA described as functional regulators of immune cells such as isodeoxycholic acid, leucine-, phenylalanine- or tyrosine-conjugated cholic acid were also found increased in the intestine of NASH mice.

Conclusion: We have shown that in parallel to diet-induced histological features of NASH, intestinal immunity and bile acid homeostasis are altered. Whether specific BA could modulate the intestinal immune barrier in NASH remains to be elucidated, as well as the importance of these data and the molecular mechanisms involved in the intestine that may participate to the hepatic histological development of NASH.

THU-245

Identification of gut microbiota signature for differentiating between viral- and non-viral related hepatocellular carcinoma

Natthaya Chuaypen, Thananya Jinato, Pisit Tangkijvanich, Faculty of Medicine, Chulalongkorn University, Biochemistry, Bangkok, Thailand
Email: pisittkvn@yahoo.com

Background and aims: Altered gut microbiota have been associated with the development of hepatocellular carcinoma (HCC). In this report, our aim was to identify gut microbiota signature in differentiating between viral-related HCC (Viral-HCC) and non-hepatitis B-, non-hepatitis C-related HCC (NBNC-HCC).

Method: Fecal samples obtained from 16 healthy controls, 33 patients with Viral-HCC (17 and 16 patients with HBV and HCV infection, respectively) and 18 patients with NBNC-HCC were analyzed using 16S rRNA sequencing. Bioinformatic analysis was performed with the dada2 pipeline in R program. The 16 of significantly different genera from top 50 relative abundance were used to classify between Viral- and NBNC-HCC by using Random Forest machine learning algorithm.

Results: The mean age of patients with NBNC-HCC was significantly older than the Viral-HCC group. However, there was no significant difference between groups regarding sex, biochemical parameters, alpha-fetoprotein level, presence of cirrhosis and tumor stage. The HCC group showed reduced alpha-diversity and altered gut microbial composition compared with healthy controls. Within the top 50 relative abundance, there were 11 genera such as *Faecalibacterium*, *Agathobacter* and *Coprococcus* significantly enriched in the Viral-HCC subgroup, while 5 genera such as *Bacteroides*, *Streptococcus* and *Erysipelatoclostridium* were significantly increased in the NBNC-HCC subgroup (Table). Based on their distinct signatures, a high diagnostic accuracy to classify the HCC subgroups was achieved with an area under the curve (AUC) of 0.90 by Random Forest classifier. Compared to the Viral-HCC subgroup, we also demonstrated significant reduction of fecal butyrate levels but increased plasma surrogate markers of microbial translocation in patients with NBNC-HCC.

Figure: Top 50 relative abundance at the genus level

	Viral-HCC		NBNC-HCC		p values
	Median	IQR	Median	IQR	
<i>Bacteroides</i>	0.085	0.099	0.123	0.076	0.029
<i>Faecalibacterium</i>	0.081	0.063	0.031	0.061	0.004
<i>Streptococcus</i>	0.005	0.027	0.026	0.086	0.035
<i>Agathobacter</i>	0.028	0.034	0.000	0.023	0.014
<i>Prevotella</i>	0.000	0.057	0.000	0.000	0.049
<i>Ruminococcus gnavus</i> group	0.002	0.023	0.028	0.038	0.001
<i>Coprococcus</i>	0.012	0.030	0.000	0.009	0.022
<i>Subdoligranulum</i>	0.017	0.029	0.000	0.000	<0.001
<i>Parabacteroides</i>	0.003	0.006	0.010	0.021	0.034
<i>Ruminococcus gauvreauii</i> group	0.004	0.011	0.000	0.002	0.041
<i>Lachnospiraceae ND3007</i> group	0.005	0.010	0.000	0.003	0.006
<i>Erysipelotrichaceae UCG-003</i>	0.001	0.014	0.000	0.000	0.016
CAG56	0.002	0.010	0.000	0.000	0.001
<i>Holdemanella</i>	0.000	0.013	0.000	0.000	0.048
<i>Erysipelatoclostridium</i>	0.000	0.001	0.005	0.013	0.001
<i>Lachnospiraceae UCG-004</i>	0.004	0.006	0.000	0.004	0.010

Conclusion: Our result demonstrated that gut dysbiosis was distinct regarding different etiological factors of HCC. Additionally, the NBNC-HCC subgroup appeared to have reduced fecal butyrate but increased microbial translocation compared with viral-related HCC. The gut microbiota signature might serve as a potential biomarker for the diagnosis and therapeutic options for HCC.

THU-246

Pemaifibrate modulates microbiota profile in a dietary model of fatty liver in rat

Roger Bentanachs^{1,2}, Lluïsa Miró^{3,4}, Cristina Rosell-Cardona^{3,4}, Concepció Amat^{3,4}, Marta Alegret^{1,2,5}, Núria Roglans^{1,2,5}, Anna Pérez-Bosque^{3,4}, Juan Carlos Laguna^{1,2,5}. ¹University of Barcelona, School of Pharmacy and Food Sciences, Pharmacology, Toxicology and Therapeutic Chemistry, Spain; ²Institute of Biomedicine of the University of Barcelona, Spain; ³University of Barcelona, School of Pharmacy and Food Sciences, Biochemistry and Physiology, Spain; ⁴Institute of Nutrition and Food Safety of the University of Barcelona, Spain; ⁵CIBER de Fisiopatología de la Obesidad y Nutrición, Instituto de Salud Carlos III, Spain
Email: alegret@ub.edu

Background and aims: Non-alcoholic fatty liver disease (NAFLD) is a prevalent and progressive disease with no drug available for its prevention or treatment. Therefore, the aim of this study was to analyze the effect of pemaifibrate on the microbiota profile in a dietary model of NAFLD, namely feeding a high-fat, high-fructose rat diet, described previously (Velázquez et al., Mol. Nutr. Food Res 2022, 2101115).

Method: The study has been conducted in female Sprague-Dawley rats, that were randomly distributed into 3 groups (n = 8): (1) control (CT; standard rodent chow); (2) high-fat diet with 10% w/v fructose in drinking water (HFHFr); (3) HFHFr plus pemaifibrate at 1 mg/Kg/day (PEMA). The experimental design consisted in feeding the rats with the HFHFr diet or standard rodent chow for three months. Rats from the PEMA group were fed with the high fat diet supplemented with the drug pemaifibrate for the last month. Hepatic triglycerides (TG) were determined at the end of experimental period. Fecal microbiota profile was analyzed by using 16S rRNA sequencing.

Results: NAFLD induced by HFHFr produced profound changes in the microbiota profile (Figure 1A), which were partially attenuated by PEMA treatment. Specifically, HFHFr rats showed an increase in Phylum Firmicutes and a reduction in Phylum Bacteroidetes, increasing the ratio between them (F/R ratio). PEMA treatment attenuated the effects on Firmicutes and F/R ratio (both p < 0.05). Furthermore, changes in Firmicutes abundance as well as F/R ratio correlated positively with liver TG concentration (Figure 1B). Within the phylum Firmicutes we find families such as Clostridiaceae, which contain genera associated with inflammatory processes. This bacterial family was increased in HFHFr animals and decreased in PEMA-treated rats (both, p < 0.05).

Conclusion: In our dietary model of NAFLD in rat, pemaifibrate treatment was able to modulate the microbiota profile. Some of these changes correlate with the reduction of liver TG. This work was supported by grants PID2020-112870RB-I00, funded by CIN/AEI/10.13039/501100011033 and 2021SGR-00345.

THU-247

Culturomics study of gut microbiota in NASH patients and healthy controls

Babacar Mbaye¹, Patrick Borentain², Matthieu Million¹, René Gerolami^{1,2}. ¹IHU Méditerranée Infection, Aix-Marseille Université, Marseille, France; ²CHU Timone. Assistance Publique Hopitaux de Marseille, Hepatologie, Marseille, France
Email: rene.gerolami@ap-hm.fr

Background and aims: The gut microbiota has been extensively studied in patients with NASH. Metagenomic studies have suggested a dysbiotic signature characterised by an increase in *Proteobacteria* at the phylum level, *Enterobacteriaceae* and *Lactobacillaceae* at the family level and *Clostridium*, *Escherichia* and *Lactobacillus* at the genus level. No large-scale bacterial culturomic studies have been published to date. In this study, we report the results of metagenomic and culturomic analysis of the gut microbiota in 41 NASH patients and 24 controls.

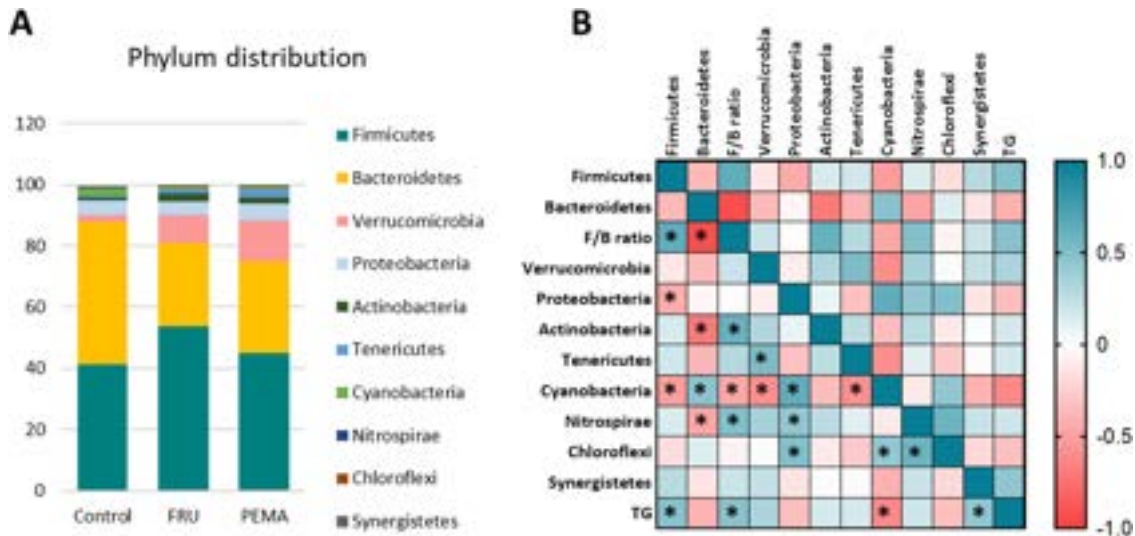


Figure: (abstract: THU-246): Phylum distribution (A) and correlation between the top ten Phylum taxa and hepatic TG (B). * Indicates significant correlation (p < 0.05).

Method: Sequencing of 16S rRNA amplicons was performed on fecal samples from all patients using the Illumina MiSeq instrument. Bacterial culturing was performed on fecal samples from 14 NASH patients and 11 controls using COS and YCFA (Yeast Casitone Fatty Acids Broth with Carbohydrates) agar plates, under anaerobic and aerobic conditions. In a second approach, we used a liquid enrichment step with sterile rumen juice and defibrinated sheep blood. Each sample was inoculated for 30 days. On day 1, day 3, day 7, day 10, day 15, day 21 and day 30, the contents of the flask were sampled, followed by ten 10-fold serial dilutions and inoculation onto COS and YCFA agar. All colonies in each sample were identified by MALDI-TOF mass spectrometry. Unidentified colonies were subjected to genome sequencing to decipher new putative species.

Results: Analysis of the cultures identified 1446 bacterial strains, representing 371 different species including 5 new species. Seven bacterial species were significantly enriched in NASH and five in controls (Figure). Three strains were found only in NASH: *Enterocloster boltea*, *Facklamia hominis* and *Streptococcus constellatus*. In contrast, *Lentilactobacillus parabuchneri*, *Lactocaseibacillus casei* and *Phascolarctobacterium faecium*, which are known to be associated with health, were only found in controls. *Lactobacillus gasseri* and *Limosilactobacillus fermentum*, a species capable of producing ethanol, were found to be enriched in NASH. Only *L. fermentum* and *L. gasseri* (enriched in NASH), *P. faecium* and *Alistipes communis*

(enriched in controls) were significantly different between NASH and controls in both culturomic and metagenomic analyses.

Conclusion: Here, we have confirmed a microbial signature associated with NASH, in particular bacteria known to produce ethanol. Culturomics has the unique advantage of providing bacterial strains which can be stored and subsequently analyzed. Further studies will evaluate their metabolic properties, including ethanol and triglyceride production *in vitro*, to confirm their role in the pathophysiology of NASH.

THU-248

Oral microbiome signature associated with liver graft dysfunction

Shruti Sureshan, Rosmy Babu, Varun Suroliya, Prince Garg, Pooja Rao, Viniyendra Pamecha, Chhagan Bihari, Shiv Kumar Sarin. *Institute of Liver and Biliary Sciences, India*
Email: drcbsharma@gmail.com

Background and aims: Stool and saliva dysbiosis in patients with cirrhosis incites changes in bacterial defences and higher risk for bacterial infections. As most of the studies have been conducted on gut microbiome from stool samples, here we profiled the salivary microbiome in pre- and post- LT patients along with their living donors to identify oral microbiome signature associated with early graft dysfunction.

Method: Saliva samples of cirrhosis patients between the age group 18–65 years admitted for living donor liver transplant and their

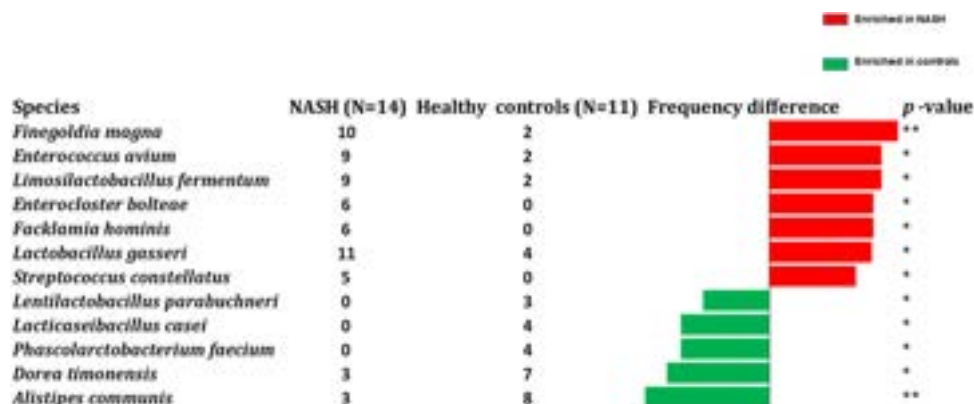


Figure: (abstract: THU-247): Bacterial species with a significant frequency difference between 14 NASH and 11 controls by culturomics

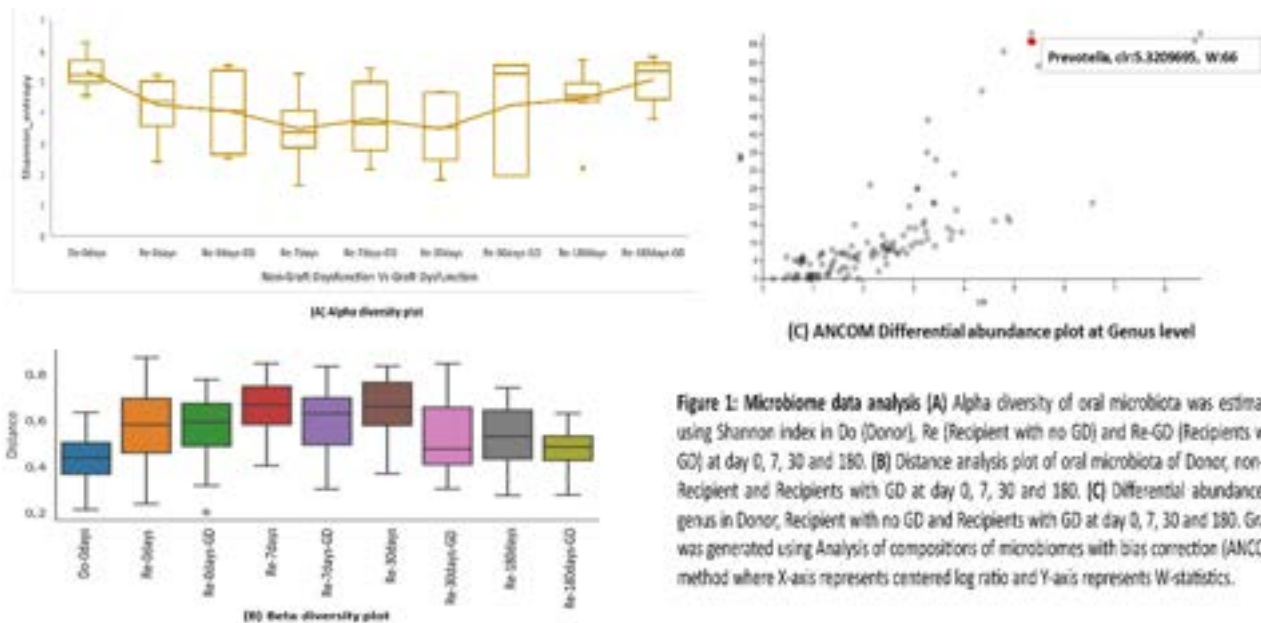


Figure: (abstract: THU-248).

donors were collected at different time-point with the informed consent. V3-V4 Amplicon sequencing was performed on Illumina MiSeq instrument and microbiome analysis was performed using QIIME pipeline. Patient with Acute Liver Failure/Acute-on-chronic liver failure, pregnant, cancer, surgical liver complications post LT, on pro/symbiotic were excluded from the study.

Results: A total of 47 participants, 21 donors (Do) (32.4 ± 9 years) and 27 recipients (Re) (46.6 ± 10 years) were selected for this study. Recipient saliva samples were collected at 4 time-points: before transplant ($n = 27$), post-transplant 7 days, 30 days, and 180 days. On follow-up nine recipients had graft dysfunction (GD) based on transaminitis and biopsy proven rejections and the remaining 18 patients were noted as non-GD. Any of the donor did not have any complications after LT.

Alpha diversity was higher ($p < 0.00003$, Fig. 1A) and beta diversity was lower at 180 days compared to baseline in GD recipient ($p < 0.05$, Fig. 1B). Differential abundance of family Prevotellaceae was high in patients with GD at baseline with a decreasing trend till 30 days and eventually increasing by 180 days. At genus level, the abundance of *Prevotella* was consistently higher across all time points, and *Lactocaseibacillus*, a probiotic was higher at baseline but was reduced after 7 days in GD recipients ($p < 0.05$, Fig. 1C).

Conclusion: Oral bacteria was significantly altered at both genus and family level within 180 days in GD recipients in comparison to non-GD recipients. Abundance of *Prevotella* were noted to be elevated and could be a potential bacterial signature to identify liver GD.

FRIDAY 23 JUNE

Hepatocyte biology

FRI-381

Insulin determines TGF- β effects on HNF4 α transcription in liver injury and hepatocyte epithelial-to-mesenchymal transition

Rilu Feng¹, Chenhao Tong¹, Tao Lin¹, Hui Liu², Chen Shao², Yujia Li¹, Carsten Sticht³, Kejia Kan⁴, Stefan Munker^{5,6}, Hanno Nieß^{7,8}, Roman Liebe^{9,10}, Matthias Ebert^{11,12,13}, Hua Wang¹⁴, Huiguo Ding¹⁵, Honglei Weng¹, Steven Dooley¹. ¹Department of Medicine II, Section Molecular Hepatology, University Medical Center Mannheim, Medical Faculty Mannheim, Heidelberg University, Mannheim, Germany; ²Department of Pathology, Beijing You'an Hospital, Affiliated with Capital Medical University, Beijing, China; ³NGS Core Facility, Medical Faculty Mannheim, Heidelberg University, Mannheim, Germany; ⁴Department of Surgery, Medical Faculty Mannheim, Heidelberg University, Mannheim, Germany; ⁵Department of Medicine II, Liver Centre Munich, University Hospital, Campus Großhadern, LMU Munich, Germany; ⁶Liver Centre Munich, University Hospital, Ludwig-Maximilians-University, Munich, Germany; ⁷Department of General, Visceral, and Transplant Surgery, Ludwig-Maximilians-University Munich, Munich, Germany; ⁸Biobank of the Department of General, Visceral and Transplant Surgery, Ludwig-Maximilians-University, Munich, Germany; ⁹Clinic of Gastroenterology, Hepatology and Infectious Diseases, Heinrich Heine University, Düsseldorf, Germany; ¹⁰Department of Medicine II, Saarland University Medical Center, Saarland University, Homburg, Germany; ¹¹Department of Medicine II, University Medical Center Mannheim, Medical Faculty Mannheim, Heidelberg University, Mannheim, Germany; ¹²Mannheim Institute for Innate Immunoscience (MI3), Medical Faculty Mannheim, Heidelberg University, Mannheim, Germany; ¹³Clinical Cooperation Unit Healthy Metabolism, Center of Preventive Medicine and Digital Health, Medical Faculty Mannheim, Heidelberg University, Mannheim, Germany; ¹⁴Department of Oncology, The First Affiliated Hospital of Anhui Medical University, Hefei, China; ¹⁵Department of Gastroenterology and

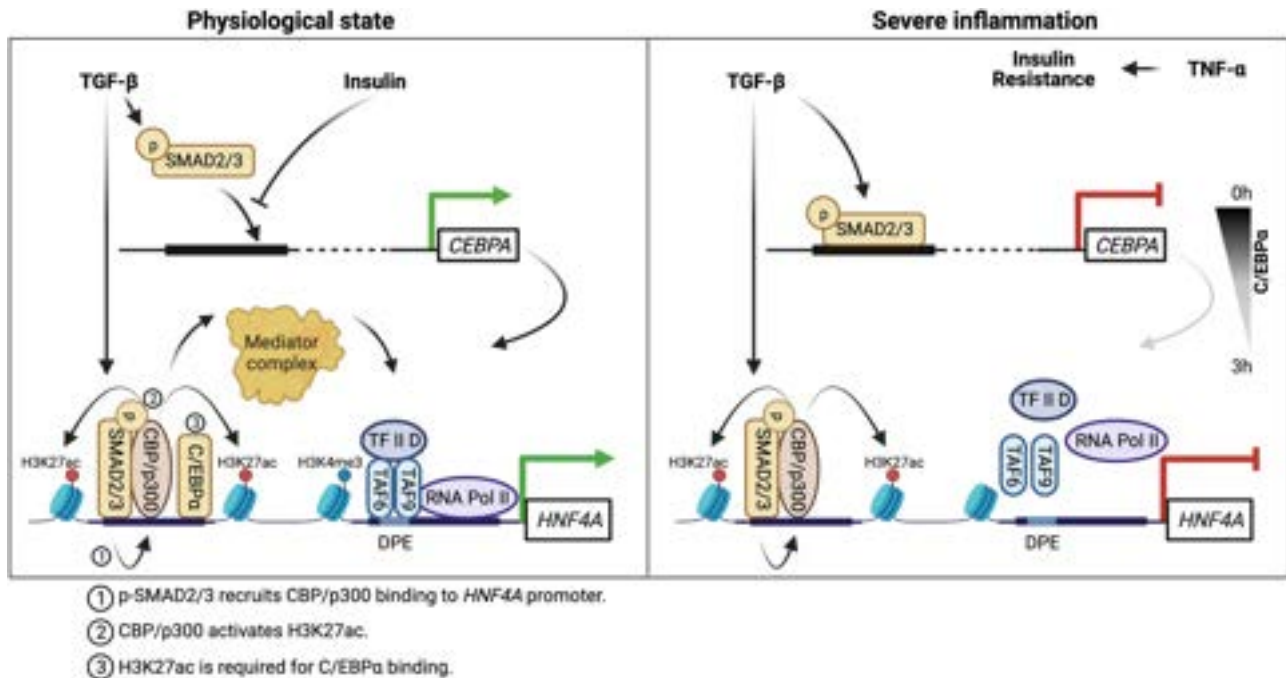


Figure: (abstract: FRI-381).

Hepatology, Beijing You'an Hospital, Affiliated with Capital Medical University, Beijing, China
Email: steven.dooley@medma.uni-heidelberg.de

Background and aims: Loss of hepatic HNF4 α expression is frequently observed in end-stage liver disease (ESLD) and associated with loss of vital liver functions and thus increases mortality. Details of how HNF4 α is suppressed are largely unknown to date. It has been proposed that TGF- β inhibits HNF4 α via SMAD2/3 complex and thus initiates hepatocyte epithelial-to-mesenchymal transition (EMT) *in vitro*. However, many patients express hepatic HNF4 α despite the presence of high levels of TGF- β . To address this conundrum, we scrutinized how TGF- β regulates HNF4A transcription in different disease conditions.

Method: Expression of hepatic transcription factors was examined in 98 HBV-infected patients. The effects of TGF- β on HNF4A transcription and EMT were investigated *in vitro*.

Results: HNF4A transcription requires both SMAD2/3 and C/EBP α binding to the HNF4A promoter. Although SMAD2/3 binding does not directly influence HNF4A transcriptional activity, SMAD2/3-recruited acetyltransferase CBP/p300 is essential for C/EBP α binding. *In vivo*, 67 patients positive for hepatic HNF4 α express both p-SMAD2 and C/EBP α , whereas 22 patients negative for HNF4 α expression lack either p-SMAD2 or C/EBP α . Interestingly, TGF- β -activated SMAD2/3 represses CEBPA transcription. Thus, long-term TGF- β stimulation results in C/EBP α depletion, which eventually inhibits HNF4 α expression. Insulin inhibits SMAD2/3 binding to the CEBPA, but not the HNF4A promoter. Maintaining insulin concentrations in culture medium not only sustains HNF4 α expression, but also inhibits TGF- β -induced hepatocyte EMT, because insulin inhibits SMAD2/3 binding to the promoters of core EMT transcription factor SNA11. ESLD patients lacking HNF4 α usually demonstrate insulin resistance.

Conclusion: Insulin signalling is crucial to maintain HNF4 α expression in hepatocytes.

FRI-382

3D digital histopathology: a new methodology for morphological characterization of the human liver

Mathieu de Langlard^{1,2}, Olivier Trassard^{2,3}, Messina Antonietta^{2,4}, Nassima Benzoubir^{2,4}, Anne Dubart-Kupperschmitt^{2,4}, Jean-Charles Duclos-Vallée^{2,4}, Catherine Guettier^{2,4,5}, Irene Vignon-Clementel^{1,2}, Dirk Drasdo^{1,2}. ¹Inria Saclay, Palaiseau, France; ²Fédération Hospitalo-Universitaire Hépatinov, Hôpital Paul Brousse, Villejuif, France; ³UMS44 Inserm-Paris-Saclay University, Le Kremlin-Bicêtre, France; ⁴UMR_S1193 Inserm-Paris-Saclay University, Villejuif, France; ⁵Pathology Unit, Bicêtre University Hospital, Assistance Publique-Hôpitaux de Paris, Le Kremlin-Bicêtre, France
Email: mathieu.de-langlard@inria.fr

Background and aims: 2D histopathology is a common technic for the diagnosis and study of diseases of the liver tissue as many of these diseases are directly linked to structural disorders at the micro- and mesoscale. However, the complexity of the liver organization calls for richer and more consistent data representation, hence for spatially resolved 3D visualization and analysis of histological images. This analysis, called here 3D histopathology, would enable better understanding and earlier diagnosis of liver disorders.

Method: A tissue of approximately 14 mm × 9 mm × 9 mm is taken from a patient liver from a surgical specimen removed for liver cell adenoma at the Centre Hépatobiliaire/Paul-Brousse Hospital. After fixation and paraffin inclusion, 300 serial sections of 3 μ m thick are individually labelled with the antibodies anti-EpCAM for the bile ducts, and anti-CD31 for the vessels, and stained with haematoxylin for the nuclei. Due to the physical sectioning, misalignment and deformation of the tissue occur, hence the first step of the image analysis pipeline is the registration of the 300 images. The reconstructed tissue volume is further segmented for the sinusoids, hepatocyte nuclei, biliary ducts, portal venules, hepatic arteries and central venules, and post-processed. Besides, the liver primary units, called lobules, are automatically reconstructed using the morphological watershed algorithm.

Results: The vascular system and the bile ducts at the micro- and mesoscale were reconstructed and visualized in 3D. The topology of the vascular and biliary trees was described using the so-called

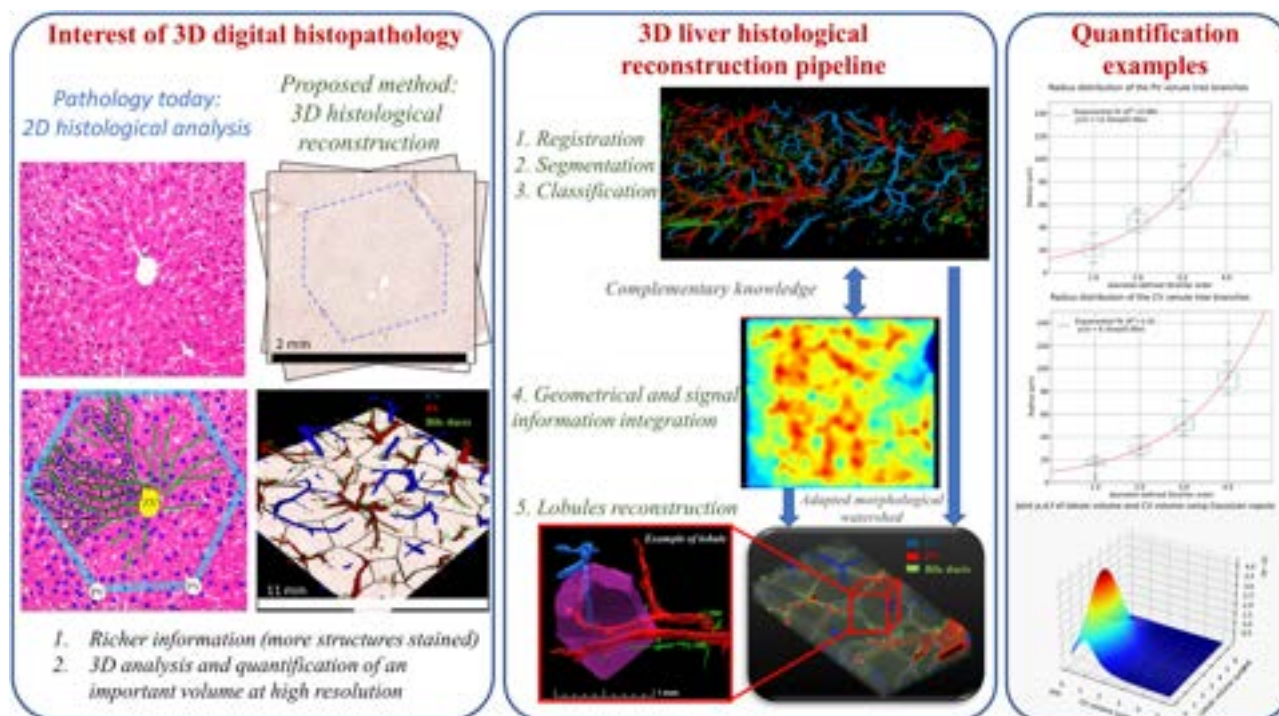


Figure: (abstract: FRI-382): Pipeline of the proposed 3D digital histopathology approach.

diameter-defined Strahler system. The morphology of the vascular and biliary trees was then computed, i.e. the mean diameter and length of the segments with respect to their order. The mean radius of the segments with respect to the Strahler order follows an exponential law (for the central and portal venules), which is coherent with the literature for larger liver vessels and other organs (e.g. heart and lungs). Moreover, a statistically representative number of entire lobules were automatically reconstructed. The sinusoids cross-section orientation significantly correlates with the reconstructed lobule borders: the sinusoids are rather radially directed in the pericentral region and orthoradially oriented at the periportal regions, where the center is chosen to be the closest central venules.

Conclusion: For the first time, a large human liver tissue volume is reconstructed in 3D and morphologically quantified from a stack 2D histological images i.e. from the micro- to the mesoscale. Such visualization at the micro- and mesoscale have not yet been obtained in the field of 3D imaging at the microscale, hence highlighting the innovation of this work. We proposed several quantification criteria which were evaluated on a healthy tissue which can serve as *benchmark*. This new digital histology approach can be readily applied to pathological cases where spatial and morphological abnormalities could be analyzed more consistently in three dimensions and bring new information on detailed morphological alterations of liver structures according the different liver disease stages.

FRI-383

Magnesium content decreases and transient receptor potential melastatin-subfamily member 7 expression increases in hepatocytes as liver inflammation and cirrhosis worsen in liver transplant candidates

Simona Parisse¹, Michela Fratini², Francesco Luigi Gambaro³, Alessandra Gianoncelli⁴, Emil Malucelli⁵, Giulia Andreani⁶, Giuliana Aquilanti⁴, Flaminia Ferri¹, Ilaria Carlomagno⁴, Monica Mischitelli¹, Quirino Lai⁷, Gianluca Mennini⁷, Massimo Rossi⁷, Irene Pecorella³, Cira Di Gioia³, Gloria Isani⁶, Stefano Iotti⁵, Stefano Ginanni Corradini¹. ¹Sapienza University of Rome, Department

of Translational and Precision Medicine, Italy; ²Institute of Nanotechnology-CNR, Department of Physics, Italy; ³Sapienza University of Rome, Department of Radiological Sciences, Oncology and Pathology, Italy; ⁴Elettra-Sincrotrone Trieste S.C.p.A, Italy; ⁵University of Bologna, Department of Pharmacy and Biotechnology, Italy; ⁶Alma Mater Studiorum-University of Bologna, Department of Veterinary Medical Sciences, Italy; ⁷Sapienza University of Rome, Department of General and Specialistic Surgery, Italy
Email: simona.parissee@gmail.com

Background and aims: It has been proposed that low magnesium (Mg) intake or depletion could be implicated in the pathogenesis and progression of chronic liver disease. A major Mg cellular transport mechanism is Transient Receptor Potential Melastatin-subfamily member 7 (TRPM7) channel, also involved, in experimental studies, in hepatic necrosis, inflammation and fibrosis. The aim of this study is to measure, for the first time in human liver cirrhosis, the Mg content of the liver and in hepatocytes and the expression of TRPM7 in these cells, correlating these variables with indices of liver inflammation and disease prognosis.

Method: We analyzed 58 biopsies of cirrhotic livers and 16 of healthy donor livers before ischemia obtained at liver transplantation (LT). Atomic absorption spectrometry (AAS) and synchrotron-based X-ray microscopy (SAXM) were used to estimate the Mg content in the liver and within hepatocytes, respectively. Hepatocyte intracellular expression of TRPM7 was evaluated by immunohistochemistry and expressed as the percentage of stained hepatocytes per 500 cells. Delta-MELDNa was calculated as: ((MELDNa at the time of transplant-MELDNa at the time of listing)/time elapsed between listing and transplant expressed in days).

Results: At AAS Mg median content was significantly ($p < 0.001$) lower in cirrhosis [117.2 (IQR 110.5–132.9) $\mu\text{g/g}$] compared to healthy livers [162.8 (IQR 155.9–169.8) $\mu\text{g/g}$]. All cirrhosis samples were clearly positive for cytosolic expression of TRPM7 in hepatocytes, whereas this was barely detectable in normal liver tissue. In cirrhotic patients the following correlations were present after adjustment for confounding factors in different multiple linear regression models: (a) inverse correlations between liver Mg content measured with AAS

and both MELDNa ($B = -0.102$ 95% CI -0.207 to 0.005 ; $p < 0.05$) and serum AST activity ($B = -0.824$ 95% CI -1.560 to -0.288 $p < 0.01$) at LT; (b) direct correlations between the percentage of hepatocytes intensely stained for TRPM7 and both MELDNa ($B = 0.297$ 95% CI 0.175 – 0.578 ; $p < 0.01$) and serum AST activity ($B = 3.256$ 95% CI 0.758 – 6.208 $p < 0.05$) at LT; (c) direct correlation between the percentage of hepatocytes intensely stained for TRPM7 and Delta-MELDNa ($B = 0.436$; 95% CI 0.179 – 0.670 ; $p < 0.01$). To test whether the severity of cirrhosis prognosis correlated with the Mg content within hepatocytes, the latter was measured in 15 cirrhotic liver samples using SXRM and confirmed the inverse correlation between Mg in hepatocytes and MELDNa a LT ($r = -0.531$; $p < 0.05$).

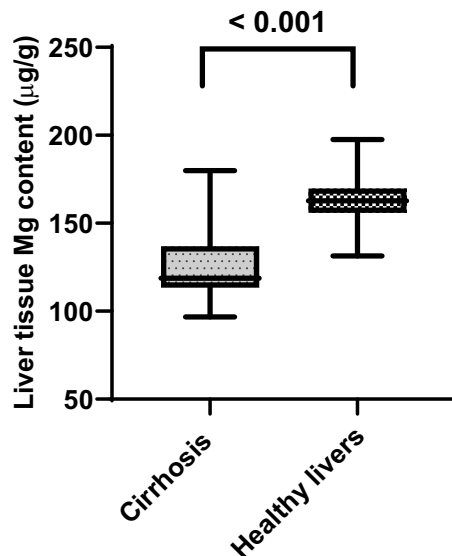


Figure:

Conclusion: The more severe the liver inflammation and the prognosis of liver cirrhosis, the more severe the magnesium depletion and the higher the expression of TRPM7 in hepatocytes. The latter could represent an attempt to restore intracellular Mg, but be one of the causes of disease progression.

FRI-384

Three-dimensional single-cell digital atlas of liver tissue architecture

Dilan Martinez¹, Valentina Maldonado¹, Cristian Perez¹, Valeria Candia¹, Hernan Morales-Navarrete², Fabián Segovia-Miranda¹. ¹Universidad de Concepción, Department of Cell Biology, Chile; ²University of Konstanz, Department of Systems Biology of Development, Germany
Email: fabiansegovia@udec.cl

Background and aims: The liver is an organ that performs a wide variety of functions that are highly dependent on its complex 3D structure. Geometrical models (digital representations of tissues) represent a versatile technique for characterizing 3D tissues as well as obtaining quantitative insights into structure-function relationships. Till date, these models are incomplete due to experimental limitations in acquiring multiple (>4) fluorescent channels at once. Indeed, geometrical models have been restricted to few tissue (sinusoids and bile canaliculi) and cellular components (nuclei and hepatocytes), excluding important cellular populations such as stellate and Kupffer cells. Here, we aimed to generate a “3D single-cell atlas of liver tissue architecture,” i.e., a full 3D geometrical model that includes all the main tissue and cellular components simultaneously.

Method: We overcame the technical constraints by using deep tissue immunostaining, multiphoton microscopy, deep learning techniques, and 3D image processing. As a proof of concept, we used the 3D atlas

to describe the morphological changes that occur in the mouse liver during post-natal early development and adulthood.

Results: We described how liver tissue architecture progressed from postnatal day one to adulthood by a novel set of morphometric cellular and tissue parameters. Our analysis revealed unknown details about the spatial organization of different liver cell types. Unexpected spatiotemporal patterns of non-parenchymal cells and hepatocytes with differing in size, number of nuclei, and DNA content were uncovered. We also provided information regarding the remodeling of the bile canaliculi and sinusoidal networks.

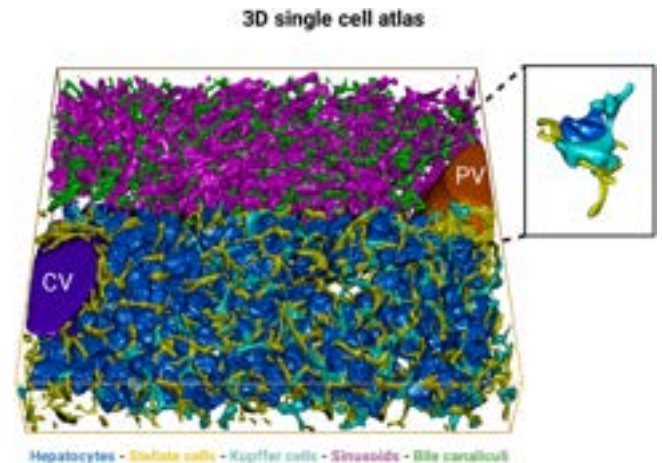


Figure: 3D single-cell atlas of liver tissue architecture: Central vein (dark blue), portal vein (orange). Upper part: sinusoids (magenta), bile canaliculi (green). Lower part: nuclei (not visible), hepatocytes (blue), stellate cells (yellow) and Kupffer cells (light blue).

Conclusion: These findings revealed novel characteristics of liver heterogeneity and have important implications for both the structural organization of liver tissue and its functional features. 3D single-cell atlas will provide a powerful tool for understanding liver tissue architecture, under both physiological and pathological conditions.

FRI-385

Multimic profiling associated with lipid remodeling in senescent primary human hepatocytes

Sin-Tian Wang¹, Wei-Chia Chen¹, Li-Chi Chi¹, Yi-Hsuan Tsai¹, Kung-Chia Young^{1,2}. ¹National Cheng Kung University, Department of Medical Laboratory Science and Biotechnology, Taiwan; ²National Cheng Kung University, Institute of Basic Medicine, Taiwan
Email: t7908077@mail.ncku.edu.tw

Background and aims: Metabolic associated fatty liver disease (MAFLD), also as non-alcoholic fatty liver disease, is characterized by the excessive lipid accumulation in liver with pathological progress, from simple steatosis, steatohepatitis, cirrhosis, to hepatocellular carcinoma. The development of MAFLD is long-term affected by multiple factors, including aging. However, the pathogenic changes in normal human hepatocyte during aging remained uncovered. In this study, we investigated the lipid remodelling from young to senescent primary hepatocytes by multimic analysis.

Method: First, we characterized the lipid metabolism of primary human hepatocytes (PHH) with the expression of senescent biomarkers. Next, we analysed the changes of metabolic gene expression and lipid contents by transcriptomic and lipidomic analysis. Finally, we investigated the pathogenic mechanism of lipid remodeling in aging by PHHs and animal model treated with senolytic or senomorphics agents.

Results: The PHHs were monitored for the expression of senescent biomarkers of p16, p21 and p53, then classified into three stages by different passages, including young (passage (P)3 to P5), early

senescence (P7 to P9) and late senescence (P11 to P13). With transcriptomic analysis by mRNA-sequencing, the differentially upregulated/downregulated genes in senescent PHH were determined, revealing the genes (P4 vs. P8 and P8 vs. P12) in six categories, namely development processes, multicellular organismal process, cellular anatomical entity, structural molecule activity, binding and molecular function regulator activity; the genes (P4 vs. P8) in four categories, namely reproduction, cellular process, protein-containing complex and catalytic activity; and the genes (P8 vs. P12) in two categories, namely metabolic process and transporter activity. With lipidomic analysis, the results showed the differentially contents of lipids from young to senescent PHH, including lipid class of cholesteryl ester (CE), phosphatidylcholine (PC), PC O-ether-linked PC, phosphatidylethanolamine, phosphatidylinositol, and sphingomyelin. In senescent PHH, the lipid contents were increased as compared to young hepatocytes, including triglyceride (TG; by 10 folds), free cholesterol (FC; by 3 folds) and cholesteryl ester (CE; by 2 folds). Additionally, it was confirmed in the liver of 50~62 weeks-old female mice by accumulation of excessive lipids with lipid quantification and oil red staining.

Conclusion: In conclusion, the transcriptional and lipidomic profiling associated with lipid accumulation in aging PHH were deciphered.

FRI-386

Tick-tock-Uncovering new aspects of circadian-regulated liver metabolism by kinetic modeling

Christiane Körner^{1,2}, Madlen Matz-Soja^{1,2}, Fritzi Ott^{1,2}, Eugenia Marbach-Breitück², Rolf Gebhardt², Thomas Berg³, Nikolaus Berndt⁴. ¹Division of Hepatology, Department of Medicine II, Leipzig University Medical Center, Laboratory for Clinical and Experimental Hepatology, Leipzig, Germany; ²Rudolf-Schönheimer-Institute of Biochemistry, Faculty of Medicine, Leipzig University, Leipzig, Germany; ³Clinic of Gastroenterology, Hepatology, Infectious Diseases and Pneumology, Germany; ⁴Institute of Computer-Assisted Cardiovascular Medicine, Charité-Universitätsmedizin Berlin, Corporate Member of Freie Universität Berlin and Humboldt-Universität zu Berlin, Berlin, Germany
Email: christiane.rennert2@medizin.uni-leipzig.de

Background and aims: The circadian rhythm is a decisive regulator for metabolic homeostasis especially in the liver. The importance of diurnal control is highlighted by the increased risk of liver diseases, obesity and metabolic syndrome due to disturbance of circadian rhythms. However, time resolved *in vivo* studies of liver metabolism are rare and molecularly resolved, kinetic models can be used for metabolic phenotyping based on proteomic data, enabling linking circadian rhythmicity of protein abundances to metabolic regulation. We aim to investigate whether hepatic metabolism is regulated by central circadian mechanisms or nutrition availability in plasma.

Method: We investigated the rhythmicity of liver metabolism in male C57BL/6N mice in transcriptomic and proteomic data using liver samples isolated throughout a day. We incorporated the proteomic data of each time point in kinetic models to identify circadian rhythms of metabolic pathways. Additionally, we correlated plasma metabolite profiles with metabolic liver functions and validated the model predictions with biochemical assays.

Results: Our analysis revealed clusters of typical regulated expressions of various metabolic genes. The kinetic models showed circadian rhythms for lipid metabolism, ethanol detoxification and partly carbohydrate metabolism in the liver. However, gluconeogenic capacity, fructose and urea synthesis capacity were obviously not underlying circadian regulation. We could show a correlation between plasma fatty acid concentrations and fatty acid liver

metabolism. Concerning detoxification capacities, ethanol utilization capacity was highly associated with plasma glucose concentrations, but no significant correlations with plasma metabolites could be found for urea synthesis and ammonia uptake capacities.

Conclusion: The model helps to better understand whether circadian rhythms are intrinsic and independent of nutrient availability or follow diurnal dietary patterns. By accounting for the circadian regulatory properties of all enzymes, our model integrates the accumulated knowledge from decades of biochemical research and allows quantitative predictions of system behavior as a function of circadian rhythmicity.

FRI-387

Dickkopf-1 inhibitor enhances the anti-tumor effects of sorafenib through inhibition of PI3K/Akt/Wnt signaling in hepatocellular carcinoma

Sang Hyun Seo^{1,2}, Kyung Joo Cho³, Hye Jung Park³, Hye Mi Kim⁴, Jae Seung Lee^{3,5}, Hye Won Lee^{3,5}, Beom Kyung Kim^{3,5}, Jun Yong Park^{3,5}, Do Young Kim^{3,5}, Sang Hoon Ahn^{3,5}, Seung Up Kim^{3,5}. ¹Department of Internal Medicine, Graduate School of Medical Science, Brain Korea 21 Project, Yonsei University College of Medicine, Rep. of South Korea; ²Yonsei Liver Center, Severance Hospital, Rep. of South Korea; ³Yonsei Liver Center, Severance Hospital, Rep. of South Korea; ⁴Department of Microbiology and Immunology, Yonsei University College of Medicine, Rep. of South Korea; ⁵Department of Internal Medicine, Institute of Gastroenterology, Yonsei University College of Medicine, Rep. of South Korea
Email: skukorea@yuhs.ac

Background and aims: Sorafenib prolongs overall survival in patients with advanced hepatocellular carcinoma (HCC). Dickkopf-1 (DKK1) is frequently overexpressed in HCC. This study investigated whether the inhibition of DKK1 enhances anti-tumor efficacy of sorafenib in patients with advanced HCC.

Method: The high expression of DKK1 level in HCC was confirmed by TCGA datasets, IF stain and ELISA in human tissues. HCC cells were treated with sorafenib and/or WAY-262611, which is an inhibitor of DKK1, to identify the additional efficacy of DKK1 inhibition on proliferation, migration, invasion, apoptosis. Transgenic mouse models using hydrodynamic injection were also used. The mice were orally injected with sorafenib (32 mg/kg), WAY-262611 (16 mg/kg), or sorafenib/WAY-262611 for 10 days.

Results: DKK1 was significantly overexpressed in patients with HCC, compared with healthy subjects and those with chronic liver diseases, but without HCC (all $P < 0.05$). DKK1 expression was also high in transgenic mouse models (all $P < 0.01$). Sorafenib combined with WAY-262611 significantly inhibited the cell viability, migration, and invasion by altering apoptosis in HCC cells, compared with sorafenib alone (all $P < 0.05$). In addition, we found that sorafenib combined with WAY-262611 inhibited p110 α , phospho-Akt (all $P < 0.05$), active β -catenin (all $P < 0.05$), phospho-Ser9-GSK-3 β , whereas phospho-Tyr216-GSK-3 β increased *in vitro* and *in vivo*, compared with sorafenib alone. Moreover, sorafenib combined with WAY-262611 increased cleaved Caspase-3 ($p < 0.01$), but decreased the Ki67 ($p < 0.05$) and EMT markers, compared with sorafenib alone.

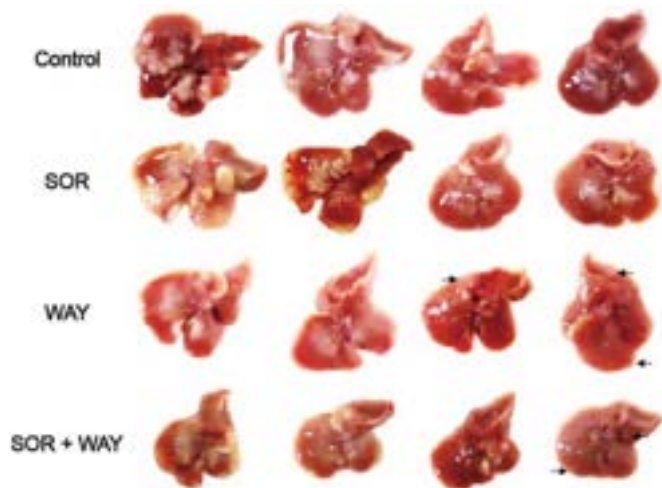


Figure:

Conclusion: Inhibition of DKK1 significantly enhanced anti-tumor efficacy of sorafenib through inhibition of PI3K/Akt/Wnt signaling, which might be a novel therapeutic strategy in HCC.

FRI-388

Liver spheroids engrafted in the anterior chamber of the eye-a novel platform to study hepatic physiology and pathology

Francesca Lazzeri-Barcelo¹, Nuria Vilarnau², Barbara Leibiger¹, Volker Lauschke², Ingo Leibiger¹, Per-Olof Berggren¹, Noah Moruzzi¹.

¹Karolinska Institute, Molecular Medicine and Surgery, Stockholm, Sweden; ²Karolinska Institutet, Physiology and Pharmacology, Stockholm, Sweden

Email: francesca.lazzeri.barcelo@ki.se

Background and aims: The tools for liver research have hugely advanced in the last decades, but the field still contends with two important limitations; the de-differentiation of primary hepatocytes outside the liver, and longitudinal *in vivo* imaging at cellular resolution. Liver spheroids are the current gold standard for *in vitro* liver studies, but lack the complexities of the natural microenvironment. The anterior chamber of the eye (ACE) of mice can be used as a transplantation site, where the cornea acts as a natural window, through which microtissues engrafted on the iris can be imaged by confocal microscopy. In this work, we aim to establish and characterise a platform for non-invasive *in vivo* longitudinal imaging of mouse liver spheroids engrafted in the ACE and explore its suitability for different areas of liver research.

Method: Mouse liver spheroids were generated *in vitro* and transplanted into the ACE of recipient mice, where they engrafted and were imaged by confocal microscopy. Fluorescent probes were administered intravenously during *in vivo* imaging to identify cells and structures. *Ex vivo* techniques such as immunofluorescence, transmission electron microscopy, RNA *in situ* hybridization and RNA sequencing were used to characterise the engrafted liver spheroids. To investigate the functions of the engrafted spheroids, hepatic fat accumulation was induced by feeding transplanted recipient mice a high-fat-high-fructose diet (HFHFrd) or control diet for 12 weeks.

Results: Transplanted liver spheroids engraft on the iris and become vascularised and innervated. *In vivo* imaging of liver spheroids in the eye shows functional vascular and bile canaliculi networks and active hepatic LDL uptake. *Ex vivo* characterisation demonstrates that the liver spheroids recapitulate hepatic markers and architectural features of the liver. Lipid droplet staining confirmed fat accumulation in the ACE-liver spheroids of mice fed a HFHFrd in comparison to control animals, suggesting that engrafted liver spheroids can mirror and report on endogenous liver function.

Longitudinal *in vivo* imaging of liver spheroids engrafted in the anterior chamber of the eye

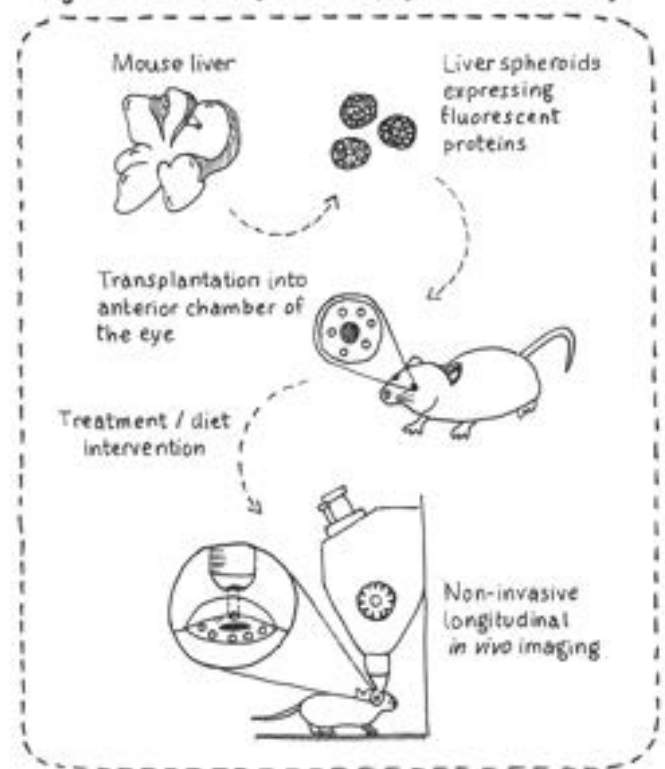


Figure:

Conclusion: We have established and characterised a platform for intraocular non-invasive imaging of liver-like tissue, opening the way for longitudinal study of liver functions. Our data show ACE-engrafted liver spheroids retain overall differentiation and functionality status post-transplantation. This liver spheroid ACE imaging platform therefore has potential to facilitate the longitudinal study of liver pathophysiology in both pre-clinical and basic research.

FRI-389

With-in patient comparison of single-cell versus single-nucleus sequencing on human transjugular liver biopsies

Lukas Van Melkebeke^{1,2}, Jef Verbeek^{1,2}, Dóra Bihary^{3,4}, Markus Boesch¹, Hannelie Korf¹, Diether Lambrechts^{3,4}, Schalk van der Merwe^{1,2}. ¹KU Leuven, Laboratory of Hepatology, Belgium; ²University hospitals Leuven, Gastro-enterology and Hepatology, Belgium; ³KU Leuven, Laboratory for Translational Genetics, Belgium; ⁴VIB, Center for Cancer Biology, Belgium

Email: lukas.vanmelkebeke@kuleuven.be

Background and aims: RNA sequencing at single cell level has advanced discoveries in translational research. In patients with advanced liver disease, with ascites or coagulation defects, transjugular liver biopsy (TJB) is the only safe way to obtain liver tissue. The ability to successfully apply single-cell (scRNA-seq) or single-nucleus RNA-sequencing (snRNA-seq) using TJB has the potential to uncover unique pathways and targets for therapy in advanced liver diseases.

Method: A protocol was developed for scRNA-seq and snRNA-seq on TJB. A within-patient comparison was made between both techniques in 3 patients with alcohol-related cirrhosis. The analysis was performed using R (v4.1.2). All samples were anchor integrated using Seurat (v4.1.1). Doublets were identified using DoubletFinder (v2.0.3).

Results: In total 31,055 single nuclei and 6,160 single cells were isolated from TJBs, with a significantly higher number of nuclei than cells per sample. All major cell types including hepatocytes, cholangiocytes, mesenchymal, endothelial, NK/T-, myeloid, and B-

POSTER PRESENTATIONS

cells could be identified (Figure 1). Furthermore, these cell types could be subtyped into 17 different known subclusters. Cell composition differed significantly between both techniques with significantly higher percentages of hepatocytes ($p < 0.05$) and sinusoidal endothelial cells ($p < 0.05$), and significantly lower percentages of NK/T-cells ($p < 0.05$), endothelial cells ($p < 0.01$), vascular smooth muscle cells ($p < 0.05$), hepatic artery endothelial cells ($p < 0.05$) and monocytes ($p < 0.05$) in snRNA-seq compared to scRNA-seq. In absolute numbers, there was a significantly higher number of hepatocytes ($p < 0.05$) in snRNA-seq. In a direct comparison of snRNA-seq and scRNA-seq, long non-coding RNA was upregulated in snRNA-seq, and mitochondrial and ribosomal RNA were upregulated in scRNA-seq. Importantly, stress-related genes (e.g. heat shock proteins) were also upregulated in scRNA-seq. Based on the gene signature of scRNA-seq, we could correctly identify the cell type of 96.9% of the nuclei and vice versa for 96.7% of the cells. gProfiler was used to compare functional pathways (gene ontology) between cell types. The top upregulated functional pathways calculated for one cell type using one technique were highly significantly upregulated in the corresponding cell type with the other technique.

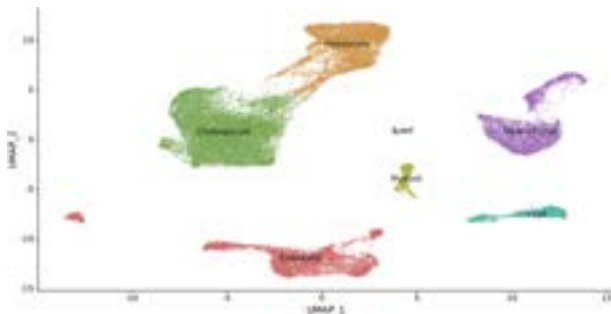


Figure 1: UMAP of the integrated dataset

Conclusion: We describe a working protocol enabling the use of scRNA-seq and snRNA-seq on TJBs, allowing the application of these techniques in advanced liver disease. Furthermore, using a within-patient comparison of both techniques, we found that both techniques recover hepatic cell types at a different composition. Importantly, the gene signature and top upregulated functional pathways of the cell types were highly comparable between the two techniques.

FRI-390

Accumulation of apical bulkheads and hepatocyte rosettes as adaptive responses upon impaired bile flow in liver diseases

Carlotta Mayer¹, Sophie Nehring², Michael Kücken³, Urska Repnik⁴, Sarah Seifert¹, Aleksandra Sljukic¹, Julien Delpierre¹, Hernan Morales-Navarrete¹, Sebastian Hinz⁵, Mario Brosch⁶, Brian K. Chung^{7,8}, Tom Hemming Karlsen^{7,8}, Meritxell Huch¹, Yannis Kalaidzidis¹, Lutz Brusch³, Jochen Hampe^{2,6}, Clemens Schafmayer⁵, Marino Zerial¹. ¹Max Planck Institute of Molecular Cell Biology and Genetics, Dresden, Germany; ²University Hospital Carl-Gustav-Carus, Department of Medicine I, Gastroenterology and Hepatology, Dresden, Germany; ³Technische Universität Dresden, Center for Information Services and High-Performance Computing, Germany; ⁴Christian-Albrechts-Universität zu Kiel (CAU), Central Microscopy, Department of Biology, Germany; ⁵University Hospital Rostock, Department of General Surgery, Germany; ⁶Technische Universität Dresden (TU Dresden), Center for Regenerative Therapies Dresden (CRTD), Germany; ⁷Oslo University Hospital Rikshospitalet, Norwegian PSC Research Center, Department of Transplantation Medicine, Clinic of Surgery, Inflammatory Medicine and Transplantation, Norway; ⁸Oslo University Hospital and University of Oslo, Research Institute of Internal Medicine, Clinic of Surgery, Inflammatory Diseases and Transplantation, Norway
Email: zerial@mpi-cbg.de

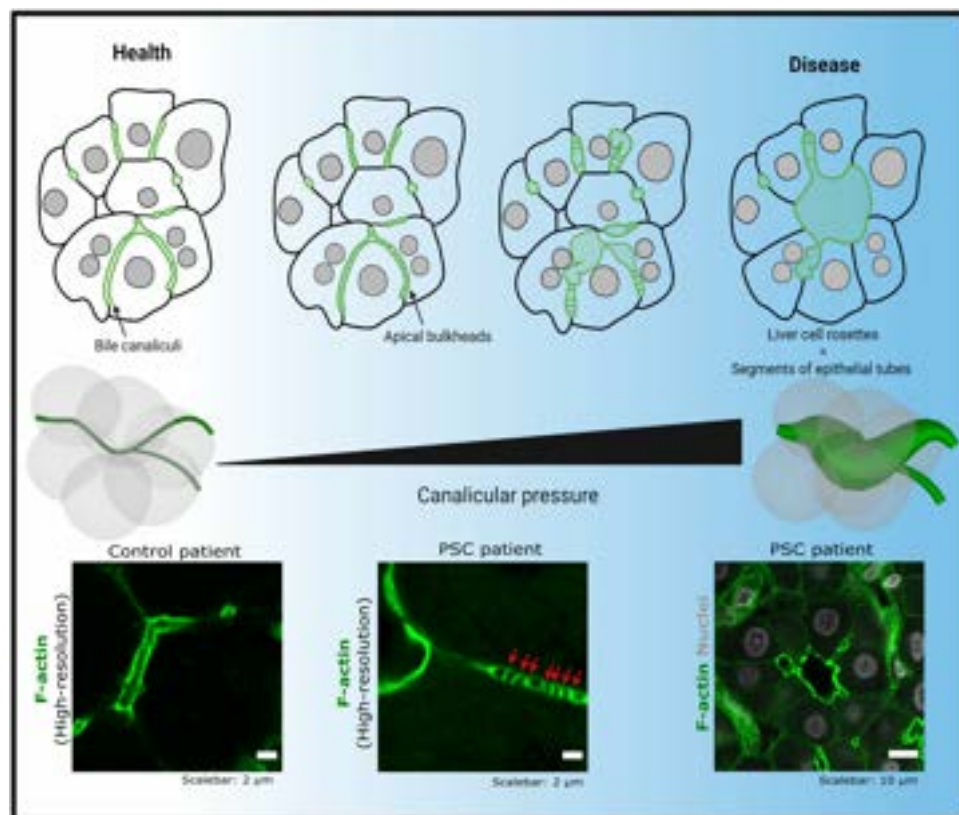


Figure: (abstract: FRI-390).

Background and aims: Hepatocytes form a network of bile canaliculi that dynamically respond to the signaling activity of bile acids and to changes in bile flow. During embryonic development hepatocytes assemble specialized structures, termed apical bulkheads, that enforce the elongation of bile canaliculi.

Method: We hypothesized that apical bulkheads protect bile canaliculi against impaired bile flow and increased canaliculi pressure in the adult liver.

Results: We found that hepatocytes accumulate apical bulkheads in liver tissue from patients with primary sclerosing cholangitis (PSC) and different mouse models, suggesting that apical bulkheads are an adaptive response of adult hepatocytes towards changes in bile flow. We assessed the underlying molecular mechanism in primary hepatocytes and 3D organoids *in-vitro* and determined that high-pressure conditions can induce abnormally dilated and rearranged bile canaliculi that are characterized by the absence of apical bulkheads. We found morphologically similar structures in patients with PSC, that resemble so-called liver cell rosettes described in other liver diseases. Using 3D reconstruction of the bile canaliculi network in PSC patients and mathematical modeling to infer canaliculi pressure, we found that the formation of liver cell rosettes positively correlates with canaliculi pressure and occurs already early in PSC progression.

Conclusion: Our results reveal a novel protective mechanism against impaired bile flow and highlight the role of canaliculi pressure in the pathogenesis of liver diseases with potential implications for diagnosis and treatment.

FRI-391

Long-term effects in primary human hepatocytes (PHH) after exogenous exposure to human intestinal microbiome secretome peptides

Natalia Sanchez-Romero^{1,2}, Pilar Sainz de la Maza Arnal^{1,2}, Maria Jesus Lozano Limones^{1,2}, Mario Fernández Sanz¹, Alvaro Blanes Rodriguez¹, Sandra Melitón Barbancho¹, Sara Borrego Bernal¹, Pedro Baptista^{1,3,4,5}. ¹Health Research Institute of Aragón (IIS Aragón), Zaragoza, Spain; ²Cytes Biotechnologies SL, Spain, Spain; ³Department of Biomedical and Aerospace Engineering, Carlos III University of Madrid, Madrid, Spain; ⁴ARAID Foundation, Zaragoza, Spain; ⁵CIBERehd, Spain

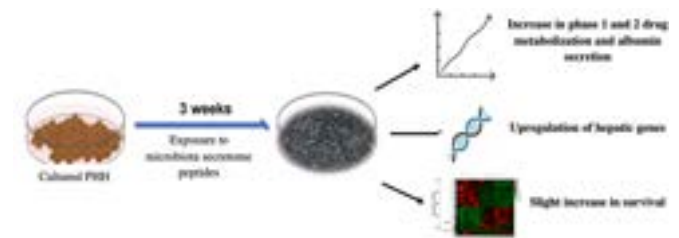
Email: nsanchez@cytesbiotech.com

Background and aims: The human intestinal microbiome's effects on the liver are finally starting to be unveiled in health and disease. If its action in the origin of several diseases is already well-known, its outcomes on liver maturation and function are still recognized to a lesser extent. Notably, the potential effects in the liver of the peptides generated by the gut enzymes' activity on the microbiome's secreted proteins are entirely unknown. Hence, we sought to determine their role in hepatic function and metabolism maintenance and induction in cultured PHH *in vitro* for up to 3 weeks.

Method: Several synthetic peptides were produced after an *in-silico* digestion of the whole secretome of the human intestinal microbiome when exposed to all the known gut enzymes. Preliminary work with selected synthetic peptides identified four peptides capable of inducing hPSC-derived hepatocyte differentiation and functionalization. Then, cryopreserved PHH (Cytes Biotechnologies) were thawed and plated in 24-well collagen I coated plates and cultured in Human Hepatocyte Maintenance Medium (Cytes Biotechnologies) with each one of these four peptides shown to be active in the preliminary screening. After three weeks, PHH (from 6 distinct donors) were tested for cell viability (Presto Blue), morphology, albumin secretion, drug metabolism (bupropion, midazolam, phenacetin, 7-OH coumarin), and gene expression (ALB, HNF4a, CYP3A4, CYP2C9, CYP2B6, GAPDH). In addition, cell morphology was observed by phase-contrast microscopy, albumin secretion was quantified by ELISA, and metabolites were quantified by LC-MS/MS

and normalized to cell viability and gene expression determined by RT-qPCR and RNA seq.

Results: After three weeks in culture, PHH exposed to each peptide showed a slight increase in survival compared to control. Cell morphology was kept constant in all conditions, but PHH exposed to the microbiome's peptides showed higher expression of CYP3A4, CYP2C9, CYP2B6, and upregulation of ALB and HNF4a. We also showed that these peptides stimulation caused a significant increase in albumin secretion, when compared with control. Likewise, we determined that these peptides could significantly increase phase 1 and 2 drug metabolism *in vitro*, even after three weeks of *in vitro* culture of PHH. Finally, RNAseq analysis showed an increase in hepatic, survival and drug metabolism genes, when compared with unstimulated controls.



Graphical abstract: Primary human hepatocytes were isolated by using a 2 steps perfusion protocol. Hepatocytes were cultured in 24 well coating plates for 3 weeks in Cytes Biotechnologies maintenance medium (control) and exposed to each microbiome secretome peptide (B2, B3, B4, B20). During the experiment, morphology and cell viability showing a slight increase in survival was checked through the time. At the end of experiment, drug metabolism by LC-MS, albumin secretion by ELISA kit, and gene expression by RT-PCR and RNA-seq were determined showing an increase in phase 1 and 2 metabolism, in albumin secretion, as well as an upregulation of hepatic genes.

Figure:

Conclusion: Considering that PHH lose their metabolic function quite rapidly (within days) *in vitro*, the long-term maintenance of PHH survival and function by these microbiome's secretome peptides is, in our view, quite significant. Additional efforts are needed to unravel these mechanisms. However, it already hints at the potential that the unexplored protein fraction of the human intestinal microbiome secretome might have in hepatocyte homeostasis, function and regulation and its potential role in biotechnological and possible therapeutic applications.

FRI-392

Integrated metabolomic and transcriptomic analyses implicate specific metabolic pathways in crocin-induced apoptosis of HCC cells

Amr Amin. UAE University, United Arab Emirates

Email: a.amin@uaeu.ac.ae

Background and aims: Saffron, the golden spice, is known for its wide spectrum of health-promoting characteristics including but not limited to its potent anticancer effects. Saffron is really the stigmas of the beautiful flower of *Crocus sativus*. Among more than a hundred others, crocin is a major constituent of saffron that is responsible for its yellow color. Crocin's therapeutic effects are well documented. However, the molecular mechanisms underlying crocin's anti-cancer effect remains unclear.

Method: This study investigated the impact of crocin, a water-soluble carotenoid and saffron's secondary metabolite, on the HCC cell line HepG2 using integrated metabolomic (HPLC-MS) and transcriptomic analyses (RNAseq).

Results: Up-regulated genes were enriched with double-strand break repair via homologous recombination which included RAD51, RAD51C, BRCA2, XRCC2 and XRCC3. The down-regulated genes were involved in positive regulation of I-kappaB kinase/NF-kappaB signaling, angiogenesis and wound healing. TNF- α , TNF receptor 1 (TNFR1) and NF- κ B-p65 were also reduced after treatment with crocin. Most dysregulation of metabolites we reported was centered on several biomarkers for liver stress, including lipidomic profile and indicators of antioxidant status. The highest up- and down-regulated

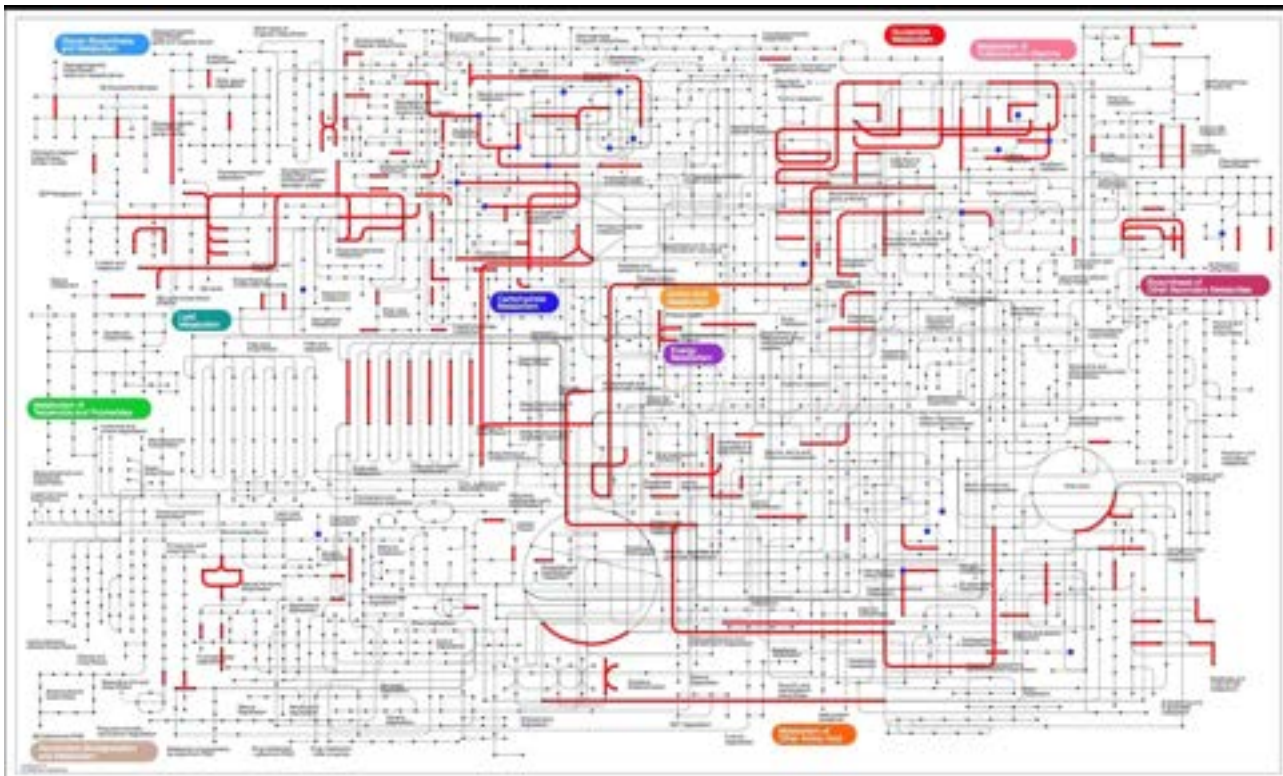


Figure: (abstract: FRI-392).

metabolites were dopamine glucuronide and L-carnitine intermediate molecules, respectively.

Conclusion: The dual omics datasets describe routes to widespread protein destabilization and DNA damage from crocin-induced oxidative stress in HepG2 cells.

Immune-mediated and cholestatic disease Clinical aspects

WEDNESDAY 21 TO SATURDAY 24 JUNE

TOP-061

Long-term prospective follow-up of a primary biliary cholangitis (PBC) multicenter cohort treated with Obeticholic Acid (OCA).

Interaction effect of triple therapy with fibrates

Elena Gómez-Domínguez¹, Esther Molina², Luisa García-Buey³, Marta Casado⁴, Marina Berenguer⁵, Isabel Conde⁶, Miguel Angel Simón⁷, Pedro Costa-Moreira⁸, Guilherme Macedo⁸, Rosa M. Morillas⁹, José Presa¹⁰, Francisco Jorquera¹¹, Javier Ampuero¹², Jose Manuel Sousa-Martin¹³, Antonio Oliveira Martin¹⁴, Manuel Hernández Guerra¹⁵, Juan Ignacio Arenas¹⁶, Arsénio Santos¹⁷, Armando Carvalho¹⁸, Juan Isidro Uriz Otano¹⁹, Maria Luisa Gutierrez Garcia²⁰, Elia Perez-Fernandez²¹, Conrado Fernandez-Rodriguez²². ¹Hospital

Universitario 12 de Octubre, Spain; ²Hospital Universitario de Santiago de Compostela, Spain; ³Hospital Universitario de La Princesa, Spain; ⁴Hospital de Torrecardenas, Spain; ⁵Hospital Universitario La Fe, Spain; ⁶Hospital Universitario La Fe, Spain; ⁷Hospital Universitario Lozano Blesa, Spain; ⁸Centro hospitalar Univeritario São João, Porto, Portugal; ⁹Hospital Germans Trias i Pujol, Spain; ¹⁰Servicio de Medicina Interna. Centro Hospitalar De Trás-Os-Montes E Alto Douro., Portugal; ¹¹Service of Gastroenterology, Complejo Asistencial Universitario de León, IBIOMED and CIBERRehd, León, Portugal; ¹²Hospital Universitario Virgen del Rocío, Spain; ¹³Hospital Universitario Virgen del Rocío, Spain; ¹⁴Service of Gastroenterology. La Paz University Hospital, Madrid, Spain; ¹⁵Hospital Universitario de Canarias, Tenerife, Spain; ¹⁶Hospital Universitario de Donostia, Spain; ¹⁷Centro Hospitalar e Universitário de Coimbra, Portugal, Spain; ¹⁸Centro Hospitalar e Universitário de Coimbra, Portugal; ¹⁹Hospital Universitario de Navarra, Pamplona, Spain; ²⁰Hospital Universitario Fundación Alcorcón, Spain; ²¹Hospital Universitario Fundación Alcorcón., Instituto de Investigación, Spain; ²²Hospital Universitario Fundación Alcorcón, Spain
Email: conrado.fernandez@salud.madrid.org

Background and aims: About one third of patients with primary biliary cholangitis (PBC) have a suboptimal response to ursodeoxycholic acid (UDCA) and have a worse prognosis. Although clinical trials have shown varying degrees of response to second line therapies, there are few data on their long-term effectiveness and safety. Our aim was to determine the long-term effect of second-line therapies on liver function, POISE response and GLOBE-PBC and 5-yr-UK-PBC scores in a multicentre cohort of patients with PBC who did not respond to UDCA according to Paris II criteria.

Method: Prospective, multicenter, real practice study cohort of Paris II UDCA non-responders from 17 hospitals who received obeticholic acid (OCA) or OCA plus fibrates. End points were effect on

biochemical, liver function, GLOBE-PBC and 5yr-UK-PBC scores and response to POISE criteria at 12, 24 and 36 months and liver-related survival and safety.

Results: One hundred and ninety-one patients were included; median follow-up 26.6 months (IQR 16.1–36.9). There was a reduction in alkaline phosphatase (ALP), GGT, aminotransferases and GLOBE-PBC score ($p < 0.01$) and an increase in serum albumin levels ($p = 0.012$) (Fig. 1). By intention-to-treat (ITT), 40.1% (95% CI 32.9–47.8) achieved POISE response at 12 months. Triple therapy was associated with POISE response (Adjusted aRR = 0.63, 95% CI 0.43–0.93, $p = 0.02$). Compared to POISE responders at 12 months, late-responders had a longer time from diagnosis ($p = 0.007$) and lower albumin levels ($p = 0.009$) (Fig. 1). Liver-related events occurred more frequently in patients with cirrhosis ($p < 0.001$). Within this group, events were limited to those patients with abnormal platelets value and serum albumin below 1.3 times the normal value.



Figure 1. POISE response rate over time, factors associated to early and late POISE response and effect on serum albumin

Figure:

Conclusion: This study shows long-term improvement in biochemistry, liver function and Globe-PBC in patients on second line treatment. POISE response was associated with earlier stages of disease and triple therapy. Treatment was safe in patients with early-stage cirrhosis.

TOP-062

Change in serum bile acids correlates with improvement in itch in patients with primary biliary cholangitis receiving linerixibat

Eleni Karatza¹, Fernando Carreño², Sumanta Mukherjee², Linda Casillas², James Fettiplace³, Megan McLaughlin², Brandon Swift⁴. ¹The University of North Carolina at Chapel Hill, NC, United States; ²GSK, Collegeville, PA, United States; ³GSK, London, United Kingdom; ⁴GSK, Durham, NC, United States
Email: brandon.x.swift@gsk.com

Background and aims: Pruritus (itch) affects up to 3/4 of patients with primary biliary cholangitis (PBC) over the course of their illness. Bile acids (BA) are an important pathophysiological mediator of cholestatic pruritus. Linerixibat, a selective small-molecule inhibitor of the ileal bile acid transporter, reduced circulating BA levels and improved itch in patients with PBC.¹ Here, we analyse the relationship between linerixibat dose and change in total serum BA (TSBA) over time and explore correlation between change in TSBA and change in itch.

Method: Data from Phase 1/2 studies of healthy volunteers or patients with PBC were used to develop a population dose-pharmacodynamic (k-PD) model to characterise the linerixibat dose-TSBA relationship. Simulations were performed to explore the effect of linerixibat dose and regimen on daily TSBA profiles. Individual Bayesian parameter estimates for subjects in GLIMMER, a Phase 2b study of linerixibat in patients with PBC and moderate to severe pruritus (NCT02966834),¹ were used to derive the area under the TSBA concentration-curve (AUC_{0-24}). These post hoc estimates of AUC_{0-24} were correlated with itch reported on a 0–10 numerical rating scale (NRS). In GLIMMER, 4 weeks single-blind placebo (baseline = Week 4) was followed by a randomised, double-blind

12-week treatment period with linerixibat or placebo (to Week 16), and a further 4 weeks single-blind placebo (to Week 20).¹ Mean worst daily itch (MWDI) and monthly itch score (MIS) were calculated as described previously.¹ Itch responders were defined as having a ≥ 2 point improvement in itch score from baseline.

Results: The final population k-PD model successfully described the effect of linerixibat on TSBA in PBC. Linerixibat treatment resulted in a rapid dose-dependent decrease in TSBA AUC_{0-24} ; the reduction in TSBA AUC_{0-24} reached steady-state after approximately 10 days. Baseline TSBA concentrations did not correlate with change from baseline in MIS at Week 16 ($r = -0.13$, $p = 0.14$). At Week 16, there was a moderate correlation between change in TSBA AUC_{0-24} and change in MIS from baseline ($r = 0.27$, $p = 0.002$), which dissipated during the placebo washout period (Week 20; $r = 0.011$, $p = 0.91$). Change in TSBA AUC_{0-24} strongly correlated with improvement in MWDI score from baseline over the 12-week treatment period ($r = 0.52$, $p < 0.0001$; Figure). A $\geq 30\%$ decrease in TSBA AUC_{0-24} was approximately 64% associated with an itch response.

Figure. Individual Bayesian estimate of TSBA change from baseline AUC_{0-24} correlates with change in mean worst daily itch

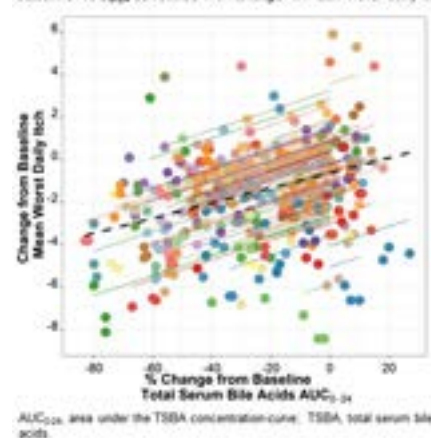


Figure:

Conclusion: Linerixibat treatment leads to rapid and dose-dependent reductions in TSBA. Baseline TSBA levels do not correlate with on-treatment change in NRS itch score, suggesting they do not predict linerixibat response. Change in TSBA over the double-blind treatment period correlates significantly with, and can be predictive of, improvement in itch in patients with PBC.

Reference

1. Levy C, et al. *Clin Gastroenterol Hepatol* 2022; S1542-3565(22)01021-7.

TOP-063

Seladelpar treatment resulted in correlated decreases in serum IL-31 and pruritus in patients with primary biliary cholangitis (PBC): post-hoc results from the phase 3 randomized, placebo-controlled ENHANCE study

Andreas E. Kremer¹, Marlyn J. Mayo², Gideon Hirschfield³, Cynthia Levy⁴, Christopher Bowlus⁵, David Jones⁶, Charles McWherter⁷, Yun-Jung Choi⁷. ¹University Hospital Zürich, Department of Gastroenterology and Hepatology, Zürich, Switzerland; ²University of Texas SW Medical Center, Division of Digestive and Liver Diseases, United States; ³University Health Network, Toronto Centre for Liver Disease, Toronto, Canada; ⁴University of Miami Miller School of Medicine, Division of Digestive Health and Liver Diseases, Miami, United States; ⁵University of California Davis, Department of Internal Medicine, Sacramento, United States; ⁶Newcastle University, Clinical and Translation Research Institute, Newcastle upon Tyne, United Kingdom; ⁷Cymabay Therapeutics, Inc., Newark, United States
Email: andreas.kremer@usz.ch

Effects of seladelpar on serum IL-31 and pruritus NRS in patients with PBC

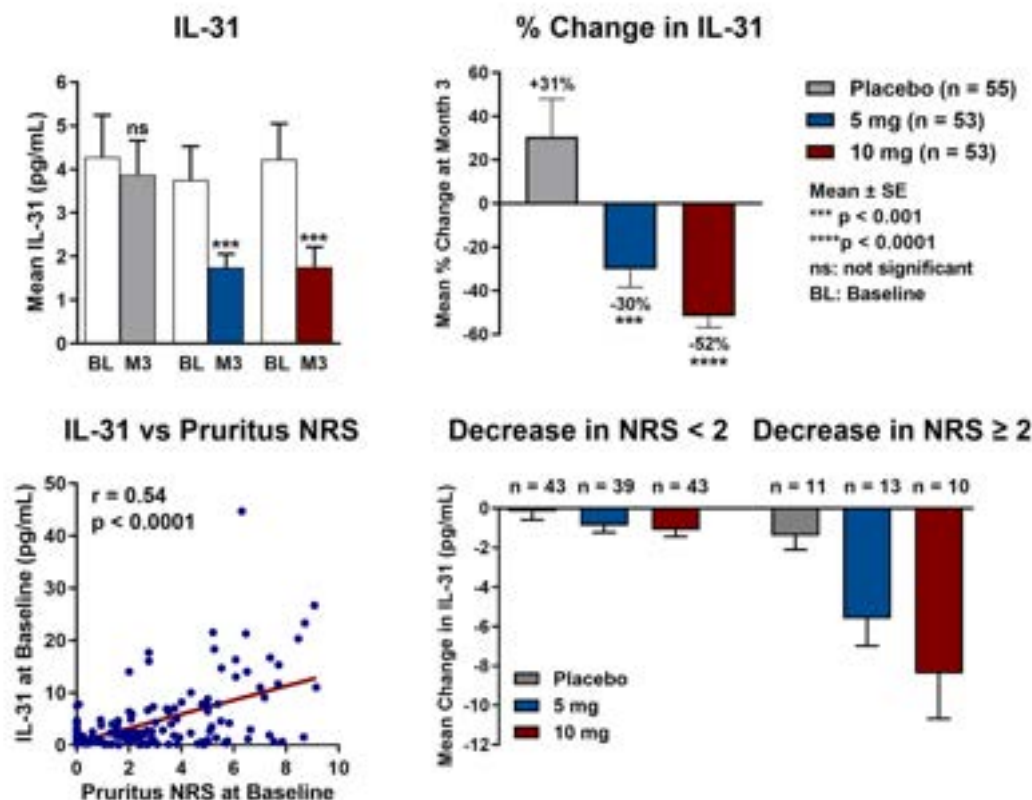


Figure:

Background and aims: Pruritus is a debilitating symptom impacting the quality of life for many people living with PBC. Interleukin-31 (IL-31) is a cytokine reported to be mechanistically relevant to pruritus and its treatment, including those with cholestasis. Treatment with seladelpar, a selective PPAR- δ agonist, is associated with significant improvement in pruritus in PBC. Here we report the effect of seladelpar on serum IL-31 levels and its association with pruritus in patients with PBC.

Method: IL-31 levels were quantified in serum samples from the ENHANCE study of seladelpar (EudraCT 2018-001171-20) in patients with PBC who received daily oral doses of placebo (n = 55), seladelpar 5 mg (n = 53) or 10 mg (n = 53) for 3 months. Serum IL-31, bile acids and their correlation with patient-reported pruritus numerical rating scale (NRS, 0–10) were assessed.

Results: Baseline IL-31 levels positively correlated with pruritus NRS ($r = 0.54$, $p < 0.0001$). Patients with NRS ≥ 4 had significantly higher baseline median [IQR] IL-31 compared to patients with pruritus NRS < 4 (7.6 pg/ml [1.2, 14.5] vs 1.2 pg/ml [0.3, 2.8], $p < 0.0001$). At baseline, IL-31 was also correlated with serum total bile acids ($r = 0.54$, $p < 0.0001$) and ALP ($r = 0.44$, $p < 0.0001$). Seladelpar treatment strongly decreased mean IL-31 levels from baseline to Month 3: seladelpar 5 mg (3.8 to 1.7 pg/ml, $p < 0.001$), 10 mg (4.2 to 1.7 pg/ml, $p < 0.001$) compared to placebo (4.3 to 3.9 pg/ml, not significant). A substantial dose-dependent % decrease in IL-31 was observed with seladelpar treatments: seladelpar 5 mg (–30%, $p < 0.001$) and 10 mg (–52%, $p < 0.0001$) compared to placebo (+31%). Patients with a clinically meaningful improvement in pruritus NRS (≥ 2 decrease) demonstrated greater dose-dependent reductions in IL-31 from baseline compared to those without pruritus improvement. We also observed significant correlations between changes in IL-31 vs pruritus NRS ($r = 0.54$, $p < 0.0001$) and ALP ($r = 0.40$, $p < 0.01$), but neither with ALT nor AST, in the seladelpar 10 mg group. Changes in

IL-31 and total bile acids correlated in the seladelpar 10 mg group ($r = 0.63$, $p < 0.0001$).

Conclusion: Seladelpar dose-dependently decreased IL-31 in patients with PBC. Reduction in serum IL-31 correlated with pruritus improvement. These results suggest that IL-31 may have a role in pruritus in patients with PBC. It may also be a biomarker related to the anti-pruritic effects of seladelpar.

WEDNESDAY 21 JUNE

WED-251

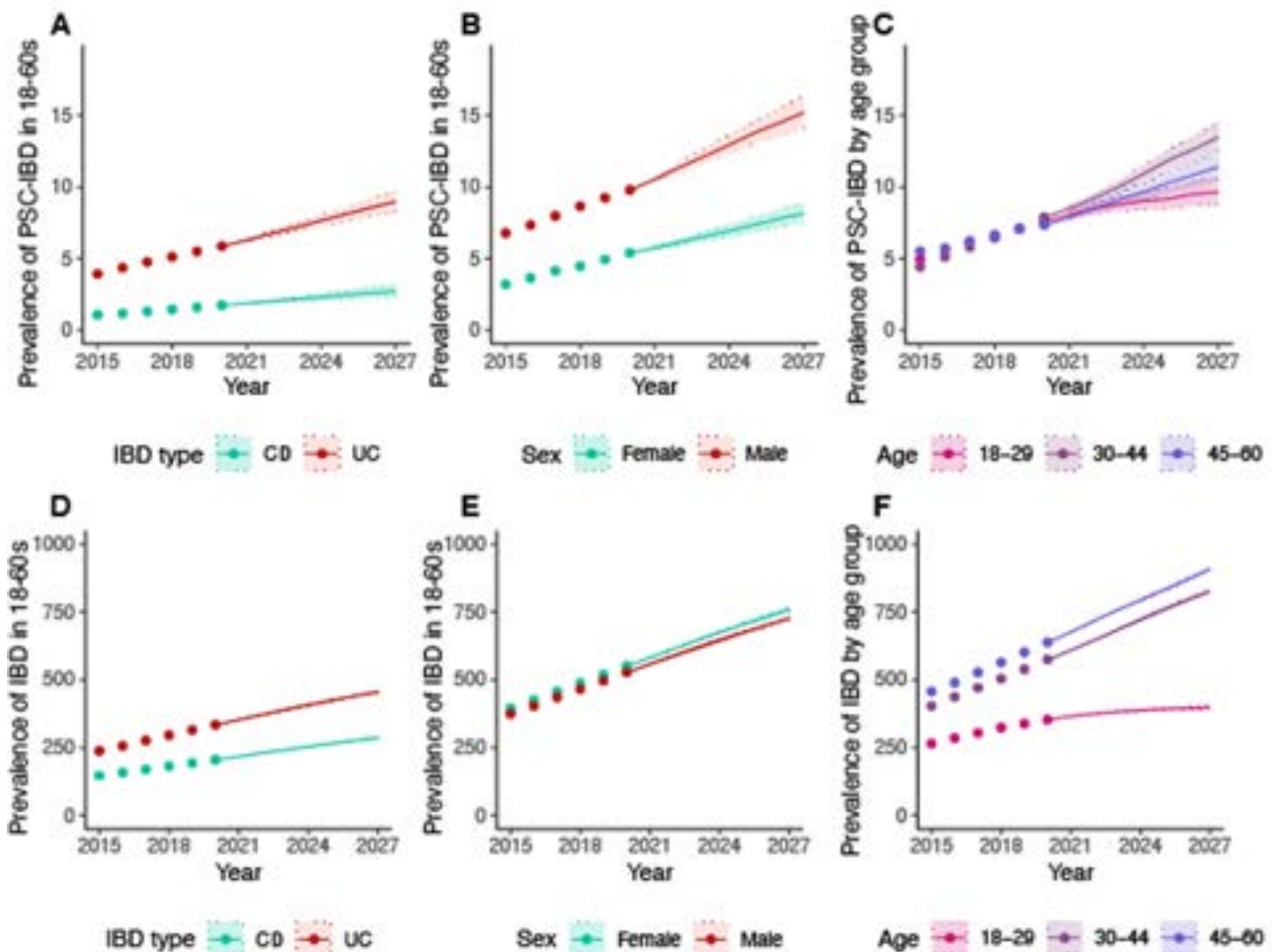
Predicting the current and future prevalence of primary sclerosing cholangitis with inflammatory bowel disease (PSC-IBD): a nationwide population-based study

Hannah Crothers¹, James Ferguson¹, Tariq Iqbal², Nabil Quraishi¹, Rachel Cooney¹, Katherine Reeves¹, Palak Trivedi². ¹University Hospitals Birmingham, United Kingdom; ²University of Birmingham, National Institute for Health Research (NIHR) Birmingham Biomedical Research Centre (BRC), Birmingham, United Kingdom
Email: p.j.trivedi@bham.ac.uk

Background and aims: Primary sclerosing cholangitis (PSC) is a leading indication for transplantation and a major risk factor for colorectal cancer in patients (pts) with inflammatory bowel disease (IBD). However, the scale of unmet need is not well defined, and it is not known how the epidemiology of PSC is changing as that of IBD evolves.

Method: We quantified the prevalence of PSC-IBD in 18 to 60-year-olds using nationwide population-based health administrative data across the whole of England (start: 1st Jan 2015). Incidence and

Figure 1: Current and Future Prevalence of PSC-IBD and IBD Alone Across England



Observed (dots) and forecasted (solid lines) adjusted prevalence with 95% prediction intervals (shading and dotted lines, respectively) for PSC-IBD (A-C) and IBD alone (D-F).

Figure:

mortality models were fitted and combined with population projections from the Office for National Statistics to forecast prevalence with 95% prediction intervals (PIs) from 2020 to 2027. Prevalence estimates were censored at the point of death or transplantation.

Results: We identified 1550 individuals with PSC and prior diagnosis of IBD on 1st Jan 2015, yielding a point prevalence of 5.0 per 100,000 population. An additional 12% were diagnosed with IBD in the 5 years following PSC presentation, yielding an estimated adjusted point prevalence of 5.6. Comparatively, point prevalence of IBD alone was 384.3. The prevalence of PSC-IBD increased to 7.6 in Jan 2020, and for IBD alone to 538.7. The average annual percentage change (AAPC) was 8.8% for PSC-IBD and 7.0% for IBD alone. The region with peak PSC-IBD prevalence was the East of England (9.4) and lowest in the Southwest (6.4). Reciprocally for IBD alone, peak prevalence was observed in the Northeast (585.2) and the lowest in the West Midlands (482.6). The group of PSC-IBD pts estimated to have the largest growth during this time were men compared to women (AAPC 11.1% and 7.6%, respectively), PSC with Crohn's disease (CD) over PSC with ulcerative colitis (UC) (10.3% and 8.4%), and pts aged 30–44y (18–29y: 8.8%, 30–44y: 12.3%, 45–60y: 5.9%). By contrast for IBD alone, the AAPC for

men and women, CD and UC, and across age groups were all similar, falling between 5.9% and 7.3%.

The prevalence of PSC-IBD in year 2027 is forecasted to increase to 11.7 per 100,000 (95% PI: 10.8–12.7) yielding an estimated 3683 people living with the condition (Fig. 1A–C). This increases to 4125 when including pts diagnosed with IBD after PSC. The largest group of people living with PSC-IBD in 2027 are estimated to be men (15.2 per 100,000; 14.1–16.4), with PSC-UC (9.0; 8.3–9.7), and aged 30–44y (13.5; 12.5–14.6). In turn, the number of people aged 18–60 years living with IBD alone is estimated to increase to 233,603 in 2027 (Fig. 1D–F). The largest group of individuals with IBD alone are estimated to be women (758.7 per 100,000; 95% PI: 750.3–767.4), with UC (455.7; 451.0–460.4), and those aged 30–44y (908.7; 900.3–916.5).

Conclusion: The rate of growth in PSC-IBD is not explained by that of IBD alone and unique with regards areas of heightened prevalence. Additionally, our data provides nationwide estimates reflecting the current and future landscape of PSC-IBD, which may be used to inform health technology assessments, service evaluation, and allow policy makers to develop strategies for high-quality and cost-effective care in rare liver disease.

WED-252

Maralixibat leads to significant reductions in pruritus and improvements in sleep for children with progressive familial intrahepatic cholestasis: data from MARCH-PFIC

Richard Thompson¹, Douglas Mogul², Tiago Nunes², Will Garner², Pamela Vig², Alexander Miethke³. ¹King's College London, Institute of Liver Studies, London, United Kingdom; ²Mirum Pharmaceuticals, Inc., Foster City, California, United States; ³Cincinnati Children's Hospital Medical Center, Cincinnati, Ohio, United States
Email: richard.j.thompson@kcl.ac.uk

Background and aims: Progressive Familial Intrahepatic Cholestasis (PFIC) is a collection of disorders in bile formation leading to intrahepatic cholestasis, chronic liver disease, and severe pruritus with markedly reduced quality of life from several domains including sleep. MARCH-PFIC was a phase 3, 26-week randomized trial of maralixibat (MRX), an ileal bile acid transporter (IBAT) inhibitor, that achieved its primary and key secondary end points of improvements in pruritus and serum bile acids for patients with PFIC. Here, we further characterize the pruritus response and changes in sleep in the MARCH-PFIC trial.

Method: Key inclusion criteria for MARCH-PFIC were genetically-confirmed PFIC and ItchRO (Obs) >1.5 (moderate-to-severe pruritus). Participants were randomized to receive MRX 570 µg/kg BID or placebo (PBO). The primary analysis evaluated pruritus as assessed by the caregiver using ItchRO (Obs) 0–4 scale; as well as by physician using the Clinician Scratch Scale (CSS). Sleep was assessed using the Exploratory Diary Questionnaire (EDQ[Obs]). Responses for pruritus and sleep were determined as the average in weekly score using a mixed-effects model with recurrent measurements for Change from Baseline (CFB) through Week 26.

Results: 64 patients [nt-BSEP (n = 31), FIC1 (n = 13), MDR3 (n = 9), TJP2 (n = 7), and MYO5B (n = 4)] were randomized to MRX (n = 33) or PBO (n = 31). Baseline characteristics were well-balanced as previously reported. Baseline pruritus score was 2.9 vs 2.7 for MRX and PBO. From Baseline to Week 26, the proportion (SE) of pruritus assessments ≤1 was greater in MRX [0.62 (0.06)] vs PBO [0.28 (0.06)] groups and the difference was significant [delta (95% CI): 0.34 (0.19, 0.50)]. From Weeks 15–26, the median proportion of reported days with 0–1 pruritus was 95% for MRX and 9% for PBO (p = 0.0005). Pruritus response from Weeks 15–26 using ItchRO (Obs) was greater in the MRX group when measured in the morning [delta (95% CI): -1.17 (-1.71, -0.64)], evening [delta: -1.13 (-1.67, -0.60)], or max daily [delta: -1.17 (-1.71, -0.63)]. Pruritus response measured with the CSS was greater in MRX [delta: -1.8 (-2.2, -1.53)] vs PBO [delta: -0.7 (-1.1, -0.3)] groups and the difference was significant [delta: -1.1 (-1.7, -0.6); p < 0.0001]. The CFB in sleep was greater in MRX [delta: -1.74 (-2.15, -1.33)] vs PBO [delta: -0.55 (-0.99, -0.11)] groups and the difference was significant [delta: -1.19 (-1.78, -0.60); p = 0.0002]. Throughout the study, there was a strong correlation between pruritus and sleep (spearman r = 0.93; p < 0.0001) and for CFB for pruritus and sleep (r = 0.93; p < 0.0001).

Conclusion: MRX was associated with complete or near-complete resolution of pruritus in the majority of patients with PFIC and the effect was independent of how it was measured, or who made the assessments. Changes with pruritus were strongly correlated with changes in sleep, suggesting that use of MRX may yield meaningful improvements in this domain of quality of life.

WED-253

Dominant strictures in patients with primary sclerosing cholangitis: comparison between old and new definition

Andrea Tenca¹, Hannu Kautiainen², Mathias Thylin³, Lauri Puustinen¹, Nina Barner-Rasmussen¹, Kalle Jokelainen¹, Martti Färkkilä¹. ¹Helsinki University Central Hospital, Finland; ²Medcare, Finland; ³Porvoo Hospital, Finland
Email: ante14@hotmail.it

Background and aims: Patients with primary sclerosing cholangitis (PSC) may develop a dominant stricture (DS) in up to 50% of the cases.

DS is associated with an impaired prognosis and its presence in the hilum should always be regarded as a warning sign for cholangiocarcinoma (CC). The traditional definition of DS (TDS, i.e., a narrowing ≤1 mm in the common hepatic duct, CHD, 2 cm within the bifurcation and ≤1.5 mm in the common bile duct, CBD) has been recently replaced by a new definition (NDS) which combines patient's symptoms and signs of cholestasis, elevation of alkaline phosphatase (P-ALP) and P-bilirubin and response to the endotherapy (i.e., dilatation and/or stenting). However, the impact of the NDS definition in disease course of PSC has not been evaluated.

Method: In this longitudinal prospective cohort study, all PSC patients referred for endoscopic retrograde cholangio-pancreatography (ERCP) to confirm diagnosis or to screening biliary dysplasia have been recruited between October 2021–2022. Symptoms of cholestasis and laboratory tests before and after ERCP were collected. Cholangiographic images were scored by using Helsinki score and the presence of TDS and NDS was reported. In addition, need for dilatation or stenting and data of brush cytology findings were also collected. Variables were presented as median and interquartile range (IQR) or mean and standard deviation (SD) when ordinal and as number and percentage (%) when nominal. Fisher's exact test, Chi-squared test and Mann-Whitney tests were used when appropriate.

Results: Overall, 248 patients underwent ERC for confirmation of diagnosis in 28 (11%) or screening for biliary dysplasia in 216 (89%). TDS was detected in 62 (25%) and NDS in 43 (17%) patients, respectively; in the remaining 143 patients no DS was observed. Patients with NDS had more symptoms (NDS 17, 40% vs TDS 1, 2%, p < 0.001). P-ALP, NDS 288 IU/l (IQR 233–419) vs TDS 94 IU/l (IQR 74–129), and P-bilirubin, NDS = 17, µmol/l (IQR 11–28) vs TDS 13; (IQR 9–17), were elevated in patients with NDS compared with those with TDS. Helsinki-score showed more advanced bile duct disease in patients with NDS, 10 (SD 2.1); vs TDS 8 (SD 2.4), p < 0.001. As expected, patients with NDS needed more dilatation, NDS 35; (81%) vs TDS 37; (60%), p < 0.001 and stenting, NDS 9 (21%) vs TDS 3 (5%), p < 0.001. After endotherapy P-ALP decreased more in patients with NDS, 258 IU/l (IQR 211–354) vs TDS 114 IU/l (IQR 77–192), p = 0.001. Biliary dysplasia was detected more frequently in patients with NDS (9%) vs TDS (5%), p = 0.004.

Conclusion: According to the new definition, DS is frequent in patients with PSC and associated with increased signs of cholestasis, more advanced bile duct disease and more frequent prevalence of biliary dysplasia.

WED-254

Mitochondrial dysfunction and lipid alterations in primary sclerosing cholangitis

Guri Fossdal^{1,2,3}, Peder Rustøen Braadland^{1,4}, Johannes R. Hov^{1,4}, Eystein Husebye³, Trine Folseraas^{1,4}, Tom Hemming Karlsen^{1,4}, Rolf Berge³, Mette Vesterhus^{1,2,3}. ¹Oslo Universitetssykehus HF, Rikshospitalet, Norwegian PSC Research Center, Norway; ²Haralds plass Diakonale Sykehus, Department of Medicine, Bergen, Norway; ³University of Bergen, Department of Clinical Science, Bergen, Norway; ⁴University of Oslo, Institute of Clinical Medicine, Oslo, Norway
Email: mette.vesterhus@uib.no

Background and aims: Liver diseases commonly present with indices of mitochondrial dysfunction, yet little is known about this in primary sclerosing cholangitis (PSC). By analysing circulating and liver-resident molecules that indirectly reflect mitochondrial dysfunction, we aimed to comprehensively characterize the degree of this deficit in PSC, and whether this was PSC specific or corresponded to the degree of cholestasis.

Method: In this cross-sectional study, we included 190 non-transplant PSC patients (NoPSC biobank, Norway) and 100 healthy controls (mean age ± SD: 41 ± 14.1 and 42.4 ± 6.6, respectively) who had donated blood, and explanted liver tissue extracts from 24 PSC patients and 18 non-cholestatic liver disease controls (AIH and ARLD). Using mass spectroscopy, we profiled fatty acids, carnitine and

acylcarnitines, and metabolites in the tryptophan-kynurenine-nicotinamide (Trp-Kyn-NAD) pathway.

Results: Compared to healthy controls, we found that PSC patients had increased palmitate (C16:0) but reduced levels of long-chain saturated fatty acids (SFAs) and higher levels of all measured monounsaturated fatty acids (MUFAs) in the circulation. Notably, these characteristics were more pronounced in PSC patients with cholestasis (bilirubin levels \geq ULN [$25 \mu\text{mol/L}$]). Several n-3 polyunsaturated fatty acids were elevated in PSC but were similar among cholestatic and non-cholestatic patients. We found reduced acylcarnitine ratios C2/C5 and C2/C3 in PSC, indicating deficits in mitochondrial fatty acid oxidation, and larger deficits in cholestatic patients. Levels of intermediates in the tryptophan-kynurenine pathway indicated reduced NAD biosynthesis, which is compatible with impaired energy supply to mitochondria in PSC. While not as apparent as in plasma, explanted liver tissue from PSC patients with high bilirubin at time of surgery also showed evidence of decreased long-chain SFAs and elevated MUFAs. However, fatty acid profiles were overall similar between livers from PSC and non-cholestatic liver disease patients, suggesting that the observed indications of mitochondrial biosynthesis in PSC may not be conditional on cholestasis.

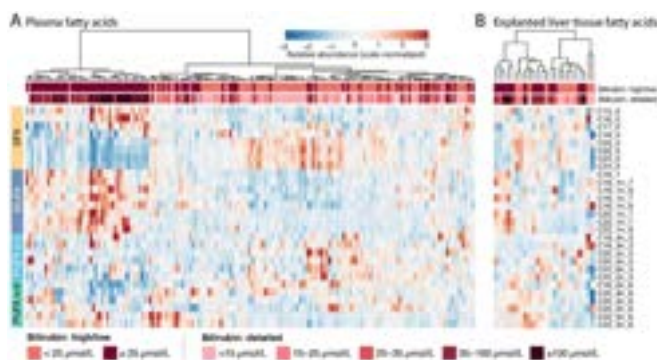


Figure: Fatty acid profiles in PSC patients with various levels of cholestasis

Conclusion: Using indirect measures of mitochondrial dysfunction in blood, we find that mitochondrial dysfunction is prominent in PSC and worsens with disease progression and increasing cholestasis. The important but unresolved question is whether impaired mitochondrial function is mainly a marker of liver disease and severity, or an underlying disease driver that could be targeted therapeutically.

WED-255

The socioeconomic status, epidemiology, and outcomes of people living with primary sclerosing cholangitis-inflammatory bowel disease in Ontario, Canada: a two-decade analysis

Kristel Leung^{1,2}, Wenbin Li¹, Bettina Hansen^{1,2,3}, Abdel Aziz Shaheen⁴, Aliya Gulamhusein², Jennifer Flemming^{5,6}, Gideon Hirschfield².

¹Institute of Health Policy, Management and Evaluation, Toronto, Canada; ²Toronto Centre for Liver Disease, University Health Network, University of Toronto, University Health Network, Canada; ³Erasmus MC, Rotterdam, Netherlands; ⁴University of Calgary, Division of Gastroenterology and Hepatology, Department of Medicine and Community Health Sciences, Canada; ⁵Institute for Clinical Evaluative Sciences (ICES), Canada; ⁶Queen's University, Division of Gastroenterology, Department of Medicine, Kingston, Canada
Email: k.leung333@gmail.com

Background and aims: Understanding the total disease burden of primary sclerosing cholangitis (PSC) with inflammatory bowel disease (IBD) in the diverse province of Ontario (population ~15 million) is important to anticipate healthcare needs and improve outcomes.

Method: A population-based cohort of individuals with PSC-IBD was derived using health administrative data at the Institute for Clinical

Evaluative Sciences in Ontario from 2002 to 2018. Patients were excluded if transplant occurred prior to PSC diagnostic code use or had competing liver disease diagnoses for other autoimmune liver diseases, hemochromatosis, alpha-1-antitrypsin deficiency, and/or Wilson disease. We described individual (age, sex) and census dissemination area-level demographics (household income, ethnic diversity, material deprivation, residential instability, and financial dependency). We also described incidence/prevalence (standardized to the 2011 Canadian population) and transplant-free survival (censored December 31, 2021). Changes in incidence and prevalence over time were evaluated using joinpoint regression.

Results: There were 888 incident cases of PSC-IBD identified: 62% were male, with median age at PSC diagnosis of 47 yrs. (IQR 32–62 yrs.). The majority were long-term residents/citizens (92%) and resided in non-rural areas (87%) at diagnosis, with an equal distribution diagnosed in areas of varying ethnic diversity. Patients identified tended to be more from areas of higher income (49.7% in two highest quintiles) and lower material deprivation (49.6% in two lowest quintiles). This disparity was also reflected in residential instability and financial dependency indices. The overall age and sex-adjusted incidence and prevalence rate of PSC-IBD in Ontario was 0.46 (95% CI 0.43–0.49) and 5.5 (95% CI 5.4–5.6) per 100,000 person-years respectively. Incidence increased at a 1.60 average annual percent change (APC). Prevalence increased at a 4.84 average APC 2002–2015; from 2015 to 2018, prevalence increased slightly less at a 2.44 average APC. Patients who are diagnosed with IBD prior to PSC have worse clinical outcomes, with twice the rate of death/transplant compared to vice versa (Figure), with 5-year transplant-free survival from PSC diagnosis of 68% vs. 90% (log-rank p value <0.001). Increasing age at diagnosis and long-term residence in Ontario were also significantly associated with increased rates of death/transplant in PSC-IBD.

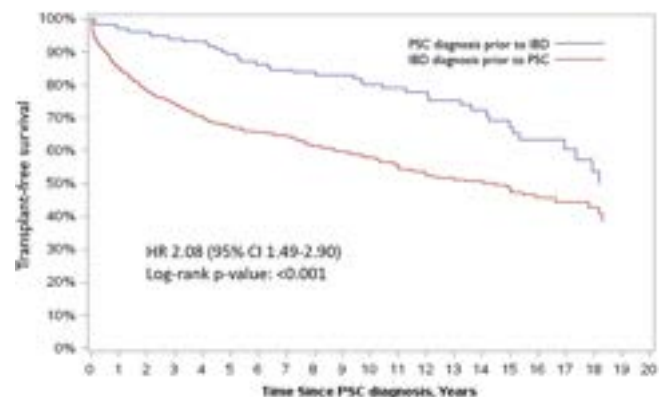


Figure:

Conclusion: There is a clear gradient favouring PSC-IBD diagnosis in those with higher socioeconomic status on a background of steadily increasing incidence and prevalence in Ontario. Transplant-free survival is significantly worse in those diagnosed with IBD prior to PSC compared to those diagnosed with PSC first.

WED-256

Baseline characteristics and risk profiles of 1111 patients with primary biliary cholangitis (PBC) in need of second-line therapy

Gideon Hirschfield¹, Kris Kowdley², Andreas E. Kremer³, John M. Vierling⁴, Christopher Bowlus⁵, Cynthia Levy⁶, Marlyn J. Mayo⁷, Daria B. Crittenden⁸, Mary Standen⁸, Ke Yang⁸, Yun-Jung Choi⁸, Charles McWherter⁸. ¹Toronto Centre for Liver Disease, University Health Network and Division of Gastroenterology and Hepatology, Toronto, Canada; ²Liver Institute Northwest, Seattle, United States; ³University Hospital Zürich, Zürich, Switzerland; ⁴Baylor College of Medicine, Houston, United States; ⁵University of California Davis School of Medicine, Sacramento, United States; ⁶Schiff Center for Liver

POSTER PRESENTATIONS

Diseases, University of Miami Miller School of Medicine, Miami, United States; ⁷University of Texas Southwestern, Dallas, United States; ⁸CymaBay Therapeutics, Newark, United States
Email: gideonhirschfield@gmail.com

Background and aims: Ursodexocholic acid (UDCA) is the first-line treatment for primary biliary cholangitis (PBC). Up to 40% of patients receiving UDCA have an alkaline phosphatase (ALP) $\geq 1.67 \times \text{ULN}$ and are usually considered for second-line therapy to prevent progression. Cohort studies confirm that targeting normal ALP and bilirubin are better treatment goals. We examined patients who screen failed due to elevated ALP $< 1.67 \times \text{ULN}$ to further characterize this population, including presence of additional risk factors for progression.

Method: In four clinical trials with seladelpar from 2015 to 2022, 1111 patients with PBC were screened at 197 clinical sites in 27 countries after treatment with UDCA for ≥ 12 months, or intolerance to UDCA. ALP levels of $\geq 1.67 \times \text{ULN}$ were required for enrollment. We compared the baseline characteristics and risk profiles of patients enrolled (ALP $\geq 1.67 \times \text{ULN}$) to those who screen failed due to ALP $\geq \text{ULN}$, but $< 1.67 \times \text{ULN}$. We stratified using proportions with Enhanced Liver Fibrosis (ELF) values ≥ 10.0 or bilirubin levels $> 0.6 \times \text{ULN}$. The relationship of ELF and liver stiffness assessed with FibroScan® was confirmed when available.

Results: The 1111 screened patients were predominantly female (94%) with a mean (SD) age of 57 ± 9.5 years. Studies enrolled 54% of screened patients ($n = 603$) (EN cohort) with a duration of PBC of 8 ± 6.5 years and on a UDCA dose of 15 ± 3.9 mg/kg/day (92% were on UDCA). Overall, 26% of patients ($n = 284$) screen failed due to ALP $> \text{ULN}$, but $< 1.67 \times \text{ULN}$ (SF Cohort). The most common reasons for screen failure in the remaining 20% of patients were ALT and AST $> 3 \times \text{ULN}$, ALP $< 1 \times \text{ULN}$, and EGFR < 60 . Meaningful differences in baseline values in the EN and SF cohorts were in ALP, GGT and ALT. Higher-risk bilirubin levels were present in 51.1% and 42.0% of EN and SF cohorts, respectively. Elevated risk based on ELF was identified in 43.2% of the EN and 27.2% of the SF cohorts. Liver stiffness was assessed in 66% of EN patients, and a mean liver stiffness of 9.7 kPa correlated with ELF ($r = 0.50$, $p < 0.001$).

Parameter	EN (N=603)	SF (N=284)	Total (N=1111)
Mean (SD)			
ALP (U/L)	303.6 (123.58)	140.9 (39.02)	275.8 (162.24)
Total Bilirubin (mg/dL)	0.7 (0.32)	0.7 (0.36)	0.8 (0.34)
$> 0.6 \times \text{ULN}$, n (%)	308 (51.1)	119 (42.0)	575 (51.8)
GGT (U/L)	246.0 (213.83)	117.2 (85.46)	226.5 (255.24)
ALT (U/L)	46.7 (22.33)	30.8 (15.79)	47.2 (35.45)
ELF	9.9 (1.03)	9.5 (0.90)	9.9 (1.06)
≥ 10.0 , n (%)	223 (43.2)	65 (27.2)	377 (40.8)
Liver Stiffness (kPa)	9.7 (6.38)	NA	NA

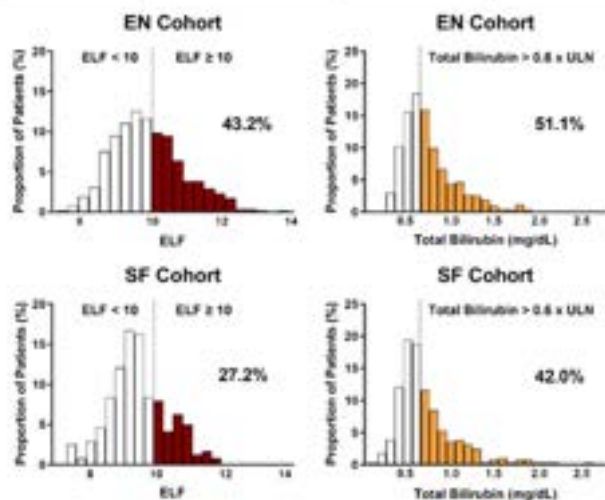


Figure:

Conclusion: We found that in this large international cohort of UDCA treated PBC patients, clinical risk factors for disease progression were common in patients achieving ALP levels $> \text{ULN}$, but $< 1.67 \times \text{ULN}$. Consideration should be given to including this population in clinical research of second-line therapies with a goal of normalization of ALP.

WED-257

Impact of maralixibat on cholestatic pruritus in adults aged 16 years and older with Alagille syndrome

Gideon Hirschfield¹, Douglas Mogul², Marshall Baek², Pamela Vig², Binita M. Kamath³. ¹University of Toronto, Toronto Centre for Liver Disease, University Health Network, Toronto, Ontario, Canada; ²Mirum Pharmaceuticals, Inc., Foster City, California, United States; ³The Hospital for Sick Children and the University of Toronto, Division of Gastroenterology, Hepatology and Nutrition, Toronto, Ontario, Canada
Email: gideon.hirschfield@uhn.ca

Background and aims: Alagille syndrome (ALGS) is an inherited multisystem disorder that is predominantly characterized by bile duct paucity with cholestasis, as well as variable abnormalities in the heart, eyes, face, skeleton, kidneys, and vasculature. Maralixibat (MRX), an inhibitor of the ileal bile acid transporter, was recently approved by the FDA and EMA for the treatment of cholestatic pruritus in patients with ALGS ≥ 1 year of age and ≥ 2 months of age, respectively. Data in ALGS has primarily been focused on paediatric patients, however adults with ALGS who survive with their native liver may require treatment for cholestasis and pruritus. We report here for the first time on the efficacy and safety of MRX in adults aged 16 years and older with ALGS transitioning to adult care, and adults that initiate treatment.

Method: Individuals with ALGS were included if they received at least one dose of MRX ≥ 16 years of age within the MRX clinical development program. Pruritus [assessed with ItchRO (Obs), a 0–4 scale with ≥ 1 -point reduction considered clinically meaningful] and serum bile acids (sBA) were assessed at Baseline, average of two values both before and after 16 years, and at end of study. Changes in sBA and pruritus were measured using t-tests.

Results: 14 individuals met inclusion criteria. 11 began treatment at 16 years of age with a median (min, max) age of 13 (11, 15) years at start of therapy and duration of therapy of 3.7 (1.5, 5.9) years with the oldest patient taking MRX at 21 years; 3 patients began MRX ≥ 16 years and were followed for a mean of 3.1 years. All patients received the daily dose appropriate for their weight, with an adult maximum dose of 28.5 mg/day. For individuals that started MRX < 16 years of age, Baseline mean (SE) ItchRO (Obs) was 2.5 (0.21), and significantly decreased to 0.8 (delta = -1.7 ; $p = 0.002$), meaning minimal to no itch, prior to age 16 years; pruritus response was durable with no significant change before and after age 16 years (delta = -0.2 ; $p = 0.2$), or to end of therapy (delta = 0.2 ; $p = 3$). Baseline mean sBA was 130 $\mu\text{mol/L}$, and significantly decreased to 52 $\mu\text{mol/L}$ (delta = -79 ; $p = 0.03$) prior to age 16 years; the reduction was durable with no significant change before and after age 16 years (delta = -7 ; $p = 0.3$), or to end of therapy (delta = 3 ; $p = 0.4$). The three individuals that started MRX ≥ 16 years had improvements in pruritus from baseline (delta in ItchRO[Obs] of -2.8 , -0.6 , and -1.0). One patient had a large decrease in sBA (delta = $-112 \mu\text{mol/L}$) and two had small increases in sBA (delta = 8 and 11 $\mu\text{mol/L}$). MRX was generally well tolerated with the same safety and tolerability profile observed across the program previously reported.

Conclusion: MRX was effective, durable and well tolerated in ALGS patients aged 16 years and older, providing critical data for patients who transition to adulthood while on therapy. These data support an ongoing role for treatment in adults with ALGS that survive with their native livers into adulthood.

WED-258

Non-adherence to standard pharmacotherapy in autoimmune hepatitis is associated with over-the-counter medication and steroid treatment. Results from the ERN online survey

Ewa Wunsch¹, Linda Krause², Ansgar W. Lohse^{3,4}, Christoph Schramm^{4,5}, Bernd Löwe⁵, Natalie Uhlenbusch⁵, Romée Snijders^{4,6}, José Willemse⁷, Piotr Milkiewicz^{1,4,8}, Tom Gevers^{4,6}. ¹Pomeranian Medical University in Szczecin, Department of Translational Medicine, Poland; ²University Medical Centre Hamburg-Eppendorf, Institute of Medical Biometry and Epidemiology, Germany; ³University Medical Centre Hamburg-Eppendorf, Department of Medicine, Germany; ⁴RARE-LIVER European Reference Network, Germany; ⁵University Medical Centre Hamburg-Eppendorf, Department of Psychosomatic Medicine and Psychotherapy, Germany; ⁶Maastricht University Medical Center, Department of Internal Medicine, Netherlands; ⁷Dutch Liver Patients Association, Netherlands; ⁸Warsaw Medical University, Liver and Internal Medicine Unit, Poland
Email: ewa.wunsch@gmail.com

Background and aims: Adherence to treatment is of particular importance to achieving therapy goals in autoimmune hepatitis (AIH), however, several factors can affect medication intake by patients. The aim of this study was to assess adherence to treatment and related factors in AIH among a large, transnational group of patients with autoimmune liver disease (AILD).

Method: A European cross-sectional online survey was conducted in patients with AIH and in a comparison group of patients with primary biliary cholangitis (PBC) and primary sclerosing cholangitis (PSC). Standard prescribed medication was defined as the use of steroids, azathioprine, and other immunosuppressants in AIH; ursodeoxycholic acid in PBC and PSC; and over-the-counter (OTC) medication as non-prescribed drugs and diet supplements, based on patients' statements. Adherence to prescribed treatment was inferred from the patients' anonymous answers to questions about the regularity of prescribed treatment intake and defined as skipping their medication less than three times a month and never reducing or stopping their medication by themselves. Multivariable logistic regression analyses were used to identify potentially modifiable factors associated with adherence to treatment while adjusting for known confounders.

Results: A total of 1102 patients with AILD (80% female, mean age 48 ± 14 years) who took prescribed pharmacotherapy for their liver disease were included in the analysis: 444 patients with AIH (85% female, mean age 47 ± 15 years) and 653 patients from the comparison group (77% female, mean age 48 ± 13 years). Based on the applied definition, patients with AIH were the most non-adherent group (47%), in comparison to those suffering from PBC (29%), and PSC (38%). In the multivariable logistic regression models (Figure), OTC medication use was identified as one common important factor negatively associated with treatment adherence in all patients, most relevant for the AIH group. Among standard treatments, steroids but not azathioprine were negatively associated with adherence in the AIH group.

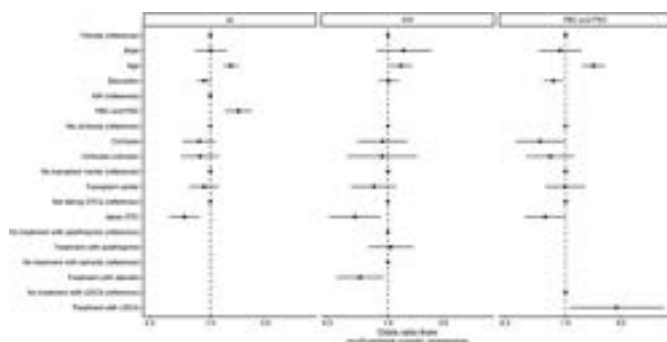


Figure: Variables influencing adherence to treatment in all patients, the study group (AIH) and in the control group (PBC and PSC).

Conclusion: This anonymous survey revealed high non-adherence in patients with AIH, particularly in those treated with steroids. OTC medication intake may reflect low treatment confidence in standard treatment and should be carefully assessed in patients with AILD in a clinical setting.

WED-259

Vibration-controlled transient elastography predicts clinical outcomes in patients with autoimmune hepatitis

Narmeen Umar¹, Christina Plagiannakos², Ellina Lytvyak¹, Mark G. Swain³, Lawrence Worobetz⁴, Catherine Vincent⁵, Jennifer Flemming⁶, Andrew L. Mason¹, Gideon Hirschfield², Bettina Hansen², Aldo J. Montano-Loza¹. ¹University of Alberta, Canada; ²University Health Network, Canada; ³University of Calgary, Canada; ⁴University of Saskatchewan, Canada; ⁵University of Montreal, Canada; ⁶Queen's University, Canada
Email: montanol@ualberta.ca

Background and aims: Autoimmune hepatitis (AIH) is a heterogeneous liver disease that varies widely in clinical response and prognosis. The assessment of liver fibrosis in a non-invasive manner during follow-up seems fundamental to predicting disease prognosis and evaluating the effectiveness of therapies. In this study, we aimed to investigate the usefulness of vibration-controlled transient elastography (VCTE) in prognosis in a large cohort multicentric study of patients with AIH across Canada.

Method: We evaluated 761 patients with AIH who had a simplified international score ≥6 from the Canadian Network for Autoimmune Liver Diseases (CaNAL). All patients had at least one reliable liver stiffness measurement taken by VCTE. The primary end point was the time to adverse outcomes defined as death or liver transplantation. Hazard ratios (HR) for adverse outcomes were determined using a Cox regression univariate and multivariate analysis.

Results: 566 were female (74%) and the median age at diagnosis was 45 years (IQR 28–58). 564 patients (76%) were Caucasians. The first VCTE was performed with a median of 35.7 months (IQR 2.9–111.6) after AIH diagnosis. The median value of the VCTE was 8.80 kPa (IQR 5.8–17.3). The liver stiffness measurement value was significantly associated with clinical adverse outcomes (HR 1.05, 95%CI 1.04–1.07; $p < 0.001$). Considering the first VCTE as time zero, liver stiffness was independently associated with clinical outcomes (HR 1.03, 95% CI 1.02–1.04, $P < 0.001$), after adjustment for age (HR 1.04, 95% CI 1.02–1.06, $P < 0.001$), female sex (HR 0.83, 95% CI 0.57–2.00, $P = 0.8$), cirrhosis at diagnosis (HR 0.87, 95% CI 0.56–1.98, $P = 0.8$), and time from AIH diagnosis to first VCTE (HR 0.99, 95% CI 0.98–0.99, $P < 0.001$, Figure 1a). Patients were classified into low, moderate, and high-risk groups for adverse outcomes based on VCTE cut-off values: <8 kPa (reference group, $n = 331$), ≥8 and <14 kPa ($n = 184$, HR 2.98, 95% CI 1.25–7.15, $P = 0.01$) and ≥14 kPa ($n = 246$, HR 7.36, 95% CI 3.38–16.00, $P < 0.001$). The adverse event-free survival curves according to the low, medium and high-risk groups are presented in Figure 1b (Log Rank 0.001).

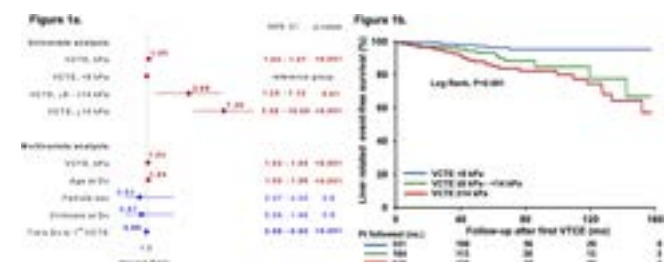


Figure: Parameters associated with adverse outcomes in AIH.

POSTER PRESENTATIONS

Conclusion: Without reference to the type of treatment or biochemical response, liver stiffness measurement by VCTE is an important tool to predict adverse outcomes in AIH. VCTE should be considered as a tool for stratification and potential surrogate end points in clinical practice and controlled trials.

WED-260

RESIST criteria accurately rule-out high-risk esophageal varices in patients with primary biliary cholangitis and compensated advanced chronic liver disease

Vincenza Calvaruso¹, Ciro Celsa¹, Laura Cristofori², Miki Scaravaglio², Luigi Capodicasa¹, Luca Cadamuro¹, Gabriele Di Maria¹, Vito Di Marco¹, Alessio Gerussi², Federica Malinverno², Pietro Lampertico^{3,4}, Nora Cazzagon⁵, Marco Marziani⁶, Umberto Vespasiani Gentilucci⁷, Pietro Andreone⁸, Ana Lleo⁹, Cristina Rigamonti^{10,11}, Edoardo Giovanni Giannini¹², Maurizio Russello¹³, Ester Vanni¹⁴, Federica Cerini¹⁵, Gabriele Missale¹⁶, Maurizia Brunetto¹⁷, Grazia Niro¹⁸, Giovanni Vettori¹⁹, Antonino Castellaneta²⁰, Domenico Alvaro²¹, Valeria Pace Palitti²², Francesco Bellanti²³, Pietro Invernizzi², Calogero Camma¹, Marco Carbone². ¹University of Palermo, UOC di Gastroenterologia, Dipartimento di Promozione della Salute, Materno Infantile, Medicina Interna e Specialistica (PROMISE), Palermo, Italy; ²Fondazione IRCCS San Gerardo dei Tintori, Division of Gastroenterology, Center for Autoimmune Liver Diseases, Department of Medicine and Surgery, University of Milano-Bicocca, Monza, Italy; ³Foundation IRCCS Ca' Granda Ospedale Maggiore Policlinico, Division of Gastroenterology and Hepatology, Milan, Italy; ⁴CRC "A. M. and A. Migliavacca" Center for Liver Disease, Department of Pathophysiology and Transplantation, University of Milan, Milan, Italy; ⁵Department of Surgery, Oncology and Gastroenterology, University of Padova, Padova, Italy; ⁶Department of Gastroenterology, Università Politecnica delle Marche, Ancona, Italy; ⁷Internal Medicine and Hepatology, University Campus Bio-Medico of Rome, Rome, Italy; ⁸Unit of Internal Medicine and Metabolic Medicine, University Hospital Modena and Reggio Emilia, Modena, Italy; ⁹Department of Biomedical Sciences, Humanitas University, Milan, Italy; ¹⁰Division of Internal Medicine and Hepatology, Department of Gastroenterology, Humanitas Clinical and Research Center IRCCS, Rozzano, Italy; ¹¹Department of Translational Medicine, Università del Piemonte Orientale, Novara, Italy; ¹²Azienda Ospedaliero-Universitaria Maggiore della Carità, Novara, Italy; ¹³Gastroenterology Unit, Department of Internal Medicine, University of Genoa, IRCCS-Ospedale Policlinico San Martino, Genoa, Italy; ¹⁴Liver Unit, Arnas Garibaldi, Catania, Italy; ¹⁵Gastroenterology Unit, Città della Salute e della Scienza, Turin, Italy; ¹⁶Division of Hepatology, Ospedale San Giuseppe MultiMedica IRCCS, Università degli Studi di Milano, Milan, Italy; ¹⁷Infectious Diseases and Hepatology Unit, Azienda Ospedaliero-Universitaria di Parma, Parma, Italy; ¹⁸Department of Clinical and Experimental Medicine, Hepatology and Liver Physiopathology Laboratory and Internal Medicine Unit, University of Pisa, Pisa, Italy; ¹⁹Gastroenterology Unit, Fondazione Casa Sollievo Della Sofferenza IRCCS, San Giovanni Rotondo, Italy; ²⁰Department of Gastroenterology, Santa Chiara Hospital, Azienda Provinciale Per I Servizi Sanitari (APSS), Trento, Italy; ²¹Gastroenterology Unit, Policlinico di Bari Hospital, Bari, Italy; ²²Department of Translational and Precision Medicine, University La Sapienza, Rome, Italy; ²³Hepatology Unit, Santo Spirito Hospital, Pescara, Italy; ²⁴Department of Medical and Surgical Sciences, University of Foggia, Foggia, Italy
Email: vincenza.calvaruso@unipa.it

Background and aims: Non-invasive criteria to identify patients with Primary Biliary Cholangitis (PBC) and compensated Advanced Chronic Liver Disease (cACLD) who can avoid esophagogastroduodenoscopy (EGD) are lacking. Aim of this study was to evaluate the diagnostic performance of RESIST criteria to rule out high-risk esophageal varices (HRV) in patients with PBC related cACLD.

Method: Data of patients with PBC and cACLD from 24 centres belonging to "Italian PBC registry," were captured. All patients who performed an EGD for evaluation of signs of portal hypertension were analyzed. Patients were classified as RESIST low risk if platelets were $>120 \times 10^9/L$ and serum albumin >3.6 g/dL or RESIST high risk if platelets were $<120 \times 10^9/L$ or serum albumin <3.6 g/dL. Outcomes were the presence of HRV at EGD. The decision curve analysis (DCA) of non-invasive criteria were calculated. RESIST criteria were compared with elastography-based criteria (Baveno VI, Expanded Baveno VI, and Baveno VII criteria).

Results: The cohort consisted of 204 Child-Pugh class A patients. At EGD 101 patients (49.5%) had no varices, 67 (32.8%) had low-risk varices and 36 (17.6%) had HRV. Liver stiffness by Fibroscan was available in 159 patients (78%). The correctly spared endoscopies (true negative) for HRV were: 95% (96/101), 84% (42/50), 86.1% (68/79) and 81.8% (18/22) respectively by RESIST, Baveno VI, Expanded Baveno VI, and Baveno VII criteria. DCA demonstrates the highest net benefit of RESIST criteria compared to elastography-based criteria in ruling out HRV (Figure).

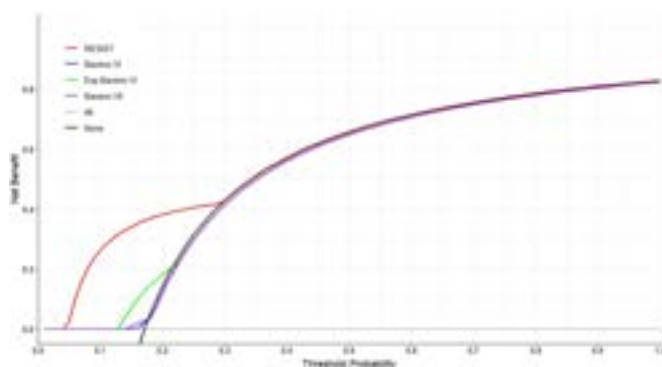


Figure:

Conclusion: Biochemical-based RESIST criteria are useful to easily rule out HRV in patients with PBC and compensated Advanced Chronic Liver Disease.

Table: (abstract: WED-261).

Feature (median)	Gliadin IgA			F-actin IgA		
	Negative	Positive	p	Negative	Positive	p
PLT (ths/ul).	243 (24–875).	253 (40–1233).	0.73.	249 (24–875).	203 (42–1233).	0.002.
Haemoglobin (g/dl).	14.1 (8.1–18.0).	13.4 (8.4–17.7).	<0.001.	14.1 (8.1–18.0).	12.4 (8.8–16.2).	<0.001.
BIL (mg/dl).	0.8 (0.2–45.4).	1.1 (0.2–25.0).	0.02.	0.8 (0.2–45.4).	1.9 (0.2–18.7).	<0.001.
ALP (IU/L).	212 (37–1515).	254 (46–1464).	0.008.	220 (37–1515).	309 (45–1468).	0.009.
AST (IU/L).	52 (14–831).	65 (10–402).	0.02.	53 (12–831).	78 (10–498).	<0.001.
ALB (g/dl).	4.4 (2.1–5.8).	4.1 (2.3–5.6).	<0.001.	4.4 (2.2–5.8).	3.7 (2.1–5.1).	<0.001.
INR.	1.0 (0.3–3.0).	1.0 (0.8–2.1).	0.07.	1.0 (0.3–3.0).	1.1 (0.8–3.0).	<0.001.
MELD (points).	7.0 (6.4–39.9).	7.7 (6.4–30.0).	0.01.	7.0 (6.4–40.0).	10.3 (6.4–31.4).	<0.001.
Mayo Risk (points).	−0.8 (−3.2–4.3).	−0.4 (−2.7–4.9).	<0.0001.	−0.7 (−3.2–4.3).	0.2 (−2.9–4.9).	<0.001.

WED-261

Clinical significance of F-actin IgA and gliadin IgA antibodies in primary sclerosing cholangitis

Ewa Wunsch¹, Małgorzata Milkiewicz², Gary Norman³, Piotr Milkiewicz¹. ¹Pomeranian Medical University in Szczecin, Department of Translational Medicine, Poland; ²Pomeranian Medical University in Szczecin, Department of Medical Biology, Poland; ³Werfen, Research and Development, San Diego, United States
Email: ewa.wunsch@gmail.com

Background and aims: Both gliadin IgA and F-actin IgA antibodies, primary detected in sera of patients with gluten sensitive enteropathy, have been postulated to correlate with disease severity in PSC. We aimed to assess the frequency of examined autoantibodies in PSC and define their potential value as predictors of progressive disease course and poor outcome in a large, well-defined cohort of PSC patients.

Method: Enzyme-linked immunosorbent assay (Werfen, San Diego, USA) was applied for detection of gliadin IgA and F-actin IgA antibodies in sera of 623 patients with PSC (age range 16–73, 65% male, 22% cirrhotic) and 305 gender- and age-matched healthy controls. Poor PSC outcome was defined as liver transplantation and/or liver-related death during a median follow-up of 19 months.

Results: Both gliadin and F-actin antibodies were more frequent in PSC than in healthy controls (28.9% vs 12.8% and 12.0% vs 2.9%, respectively; $p < 0.0001$ for both). Examined autoantibodies were associated with poor liver function and risk scores (Table). F-actin antibody was associated with cirrhosis (RR = 2.48, 95%CI = 1.9–3.3, $p < 0.001$). Significant associations between gliadin and F-actin antibodies and poor outcome were found (Chi2 = 6.4, HR = 1.6, 95%CI = 1.1–2.4, $p = 0.01$ and Chi2 = 32.1, HR = 5.5, 95%CI = 3.1–10.0, $p < 0.001$, respectively).

Conclusion: Gliadin IgA and F-actin IgA antibodies identify a subgroup of PSC patients at risk of more aggressive course, poor outcome and may be of prognostic value in PSC.

WED-262

Clinicopathological features and prognosis of early primary biliary cholangitis with clinically significant portal hypertension

Qi Zheng¹, Bin Wang², Ruimin Lai¹, Huaying Lai¹, Xiaoyu Lin¹. ¹The First Affiliated Hospital, Fujian Medical University, Hepatology Research Institute, Fuzhou, China; ²Fujian Medical University, China
Email: zhengqi0825@sina.com

Background and aims: Early primary biliary cholangitis (PBC) may progress to clinically significant portal hypertension (CSPH) before the development of cirrhosis. This study assessed different pathological features and explored the correlation between liver histopathologic features and long-term prognosis in early PBC patients with CSPH.

Method: Patients with PBC were prospectively enrolled in the study. All the patients were performed to clarify the prevalence, characteristics, pathologic features and prognosis. The independent risk factors for CSPH were identified and selected using logistic regression analysis, and the correlation between baseline pathological features and prognosis was evaluated by COX regression analysis in PBC patients.

Results: A total of 180 PBC patients were included in this study, and 108 had liver biopsy (71 patients with pathological stage I to II, 2 patients between pathological stage II and stage III). Features of CSPH were showed in 45% (81/180) of PBC patients at assessment, and 21.1% (15/71) of patients with early PBC. During median follow-up 4 (IQR 1.1–6.3) years, 19.2% (15/78) developed CSPH, 18.0% (16/89) hepatic decompensation events, 1.7% (3/180) liver transplantation events, and 17.8% (32/180) deaths. Prolonged prothrombin time (PT) and low platelet counts were associated with the presence of CSPH in early PBC ($p = 0.034$, $p = 0.017$, respectively). The 1-, 3- and 5-year cumulative survival rates of PBC patients with baseline CSPH features were 81.4%, 72.5%, and 65.2%, respectively, and CSPH was an

important risk factor for adverse outcomes (HR 7.942, $p < 0.001$). Perisinusoidal fibrosis and nodular regenerative hyperplasia (NRH) were the common histopathological features of early PBC with CSPH.

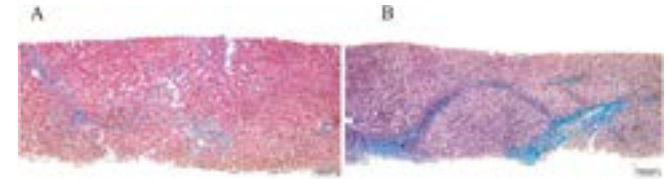


Figure: Pathological features of perisinusoidal fibrosis and NRH in patients with early PBC. A: Perisinusoidal fibrosis with Masson staining (x50). B: NRH with Masson staining (x50)

Conclusion: In early PBC, the event rates for features of CSPH were substantial. Comorbid CSPH at baseline evaluation indicated an increased risk for subsequent adverse outcomes. Hence, early identification of CSPH was crucial, and perisinusoidal fibrosis and NRH served as the valuable histological features of CSPH in early PBC.

WED-263

A two-step algorithm avoids corticosteroids in two-thirds of cancer patients with severe immune-mediated hepatitis due to immune checkpoint inhibitors

Mar Riveiro Barciela^{1,2,3}, Ana Barreira^{1,2}, María-Teresa Salcedo⁴, Ana Callejo-Pérez⁵, Eva Muñoz-Couselo⁵, Patricia Iranzo⁵, Carolina Ortiz-Velez⁵, Susana Cedrés⁵, Nely Díaz-Mejía⁵, Juan Carlos Ruiz-Cobo^{1,2}, Rafael Morales⁵, Juan Aguilar-Company⁵, Ester Zamora⁵, Mafalda Oliveira⁵, María-Teresa Sanz-Martínez^{6,7,8}, Lluís Viladomiu¹, Mónica Martínez-Gallo^{6,7,8}, Enriqueta Felip⁵, Maria Buti^{1,2,3}. ¹Liver Unit, Internal Medicine Department, Hospital Universitari Vall d'Hebron, Vall d'Hebron Barcelona Hospital Campus, Barcelona, Spain; ²Universitat Autònoma de Barcelona, Department of Medicine, Barcelona, Spain; ³CIBERehd, Instituto Carlos III, Barcelona, Spain; ⁴Human Pathology Department, Hospital Universitari Vall d'Hebron, Vall d'Hebron Barcelona Hospital Campus, Barcelona, Spain; ⁵Oncology Department, Hospital Universitari Vall d'Hebron, Vall d'Hebron Barcelona Hospital Campus, Barcelona, Spain; ⁶Immunology Division, Hospital Universitari Vall d'Hebron, Vall d'Hebron Barcelona Hospital Campus, Barcelona, Spain; ⁷Translational Immunology Group, Vall d'Hebron Research Institute (VHIR), Vall d'Hebron Barcelona Hospital Campus, Barcelona, Catalonia, Spain; ⁸Department of Cell Biology, Physiology and Immunology, Autonomous University of Barcelona (UAB), Barcelona, Spain
Email: mar.riveiro@gmail.com

Background and aims: Preliminary data suggest some patients with immune-mediated hepatitis (IMH) may recover after immune checkpoint inhibitors (ICI) discontinuation. Our primary aim was to assess the performance of a 2-step algorithm for management of severe IMH, based on ICI temporary discontinuation (first step) and in case of lack of improvement, indication of corticosteroids based on the degree of necroinflammation at biopsy (second step).

Method: Prospective study that included all subjects with grade-3/4 IMH, after excluding alternative diagnosis. Study protocol: ICIs were discontinued in all patients (Step 1). After 48–72 hours, a new blood test including extended peripheral immunophenotyping was performed. Those who showed a 20% drop in AST/ALT levels were maintained without ICI until grade-1 hepatitis or normalization, when ICI were restarted. In the case of absence of improvement in transaminases, a liver biopsy was performed within 24–48 hours (Step 2); Indication for corticosteroids was severe necroinflammation at biopsy, or mild or moderate necroinflammation but progressive worsening at analytical values in the following days.

Results: From January/2020 to November/2022, 94 patients were assessed, and 59 (62.7%) were excluded, with cancer progression as the most common alternative diagnosis. Thirty-five individuals with grade-3/4 IMH were included: 54% women, median age 61 years,

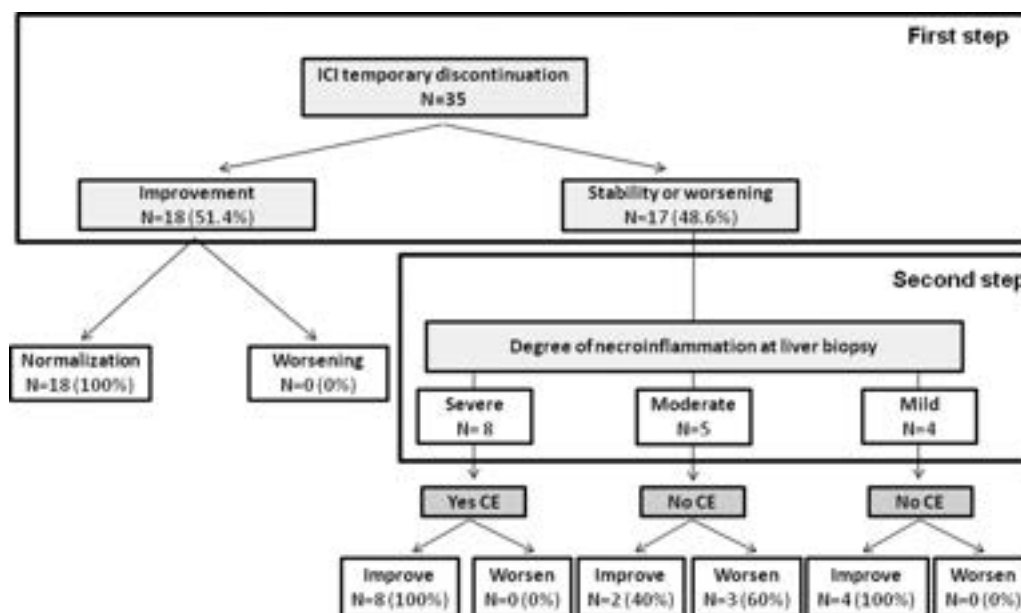


Figure: (abstract: WED-263)

31.4% lung cancer and 25.7% melanoma. ICI: 68.5% anti-PD1/anti-PD-L1, 22.8% combined, 8.6% anti-CTLA-4; CTCAE severity: 27 grade-3, 8 grade-4; DILI severity score: 28 mild, 6 moderate, 1 severe. Overall, 24/35 (68.6%) patients benefited from avoidance of corticosteroids: 18 (51.4%) according to the first step (ICI discontinuation), and 6 (17.1%) to the second step (necroinflammation degree). No patient with mild necroinflammation required corticosteroids, since all presented progressive transaminases normalization. However 3/5 subjects with moderate necroinflammation required corticosteroids during follow-up due to lack of analytical improvement in the following days. Results of the algorithm are shown in the Figure. Liver biopsy mainly impacted on patients with grade-3 IMH, sparing corticosteroids in 6/11 non-improved patients with just ICI discontinuation. Patients requiring corticosteroids had a significant increase in HLA-DR expression on CD8+ lymphocytes ($p = 0.002$), in central memory CD4+ ($p = 0.065$), and a lower effector-memory CD4+ ($p = 0.014$).

Conclusion: A two-step algorithm including discontinuation of immunotherapy and liver biopsy allows avoidance of corticosteroids in almost 70% of patients with severe immune-mediated hepatitis.

WED-264

Impact of the metabolic profile on the response to ursodeoxycholic acid in patients with primary biliary cholangitis: results of the ColHai registry

Alvaro Diaz Gonzalez¹, Andrea González Pascual¹, Judith Gómez-Camarero², Elena Gómez Domínguez³, María Carlota Londoño⁴, Mercedes Vergara Gómez⁵, Javier Ampuero⁶, Javier Martínez⁷, Diana Horta⁸, Adolfo Gallego⁹, Javier Salmerón¹⁰, Montserrat García-Retortillo¹¹, Rosa M. Morillas¹², Raul J. Andrade¹³, Juan Turnes¹⁴, Moises Diago¹⁵, Ismael El Hajra Martínez¹⁶, Merce Roget Alemany¹⁷, Manuel Hernández Guerra¹⁸, Nerea Quintans¹⁹, Margarita Sala²⁰, Nuria Domínguez²¹, Ana Arencibia Almeida²², Javier Crespo¹, Ana Barreira²³, Magdalena Salcedo²⁴, Mar Riveiro Barciela²³. ¹Departamento de Gastroenterología y Hepatología. Hospital Universitario Marqués de Valdecilla. Grupo de Investigación Clínica y Traslacional en Enfermedades Digestivas. Instituto de Investigación Valdecilla (IDIVAL), Santander, Spain; ²Burgos University Hospital, Burgos, Spain;

³University Hospital October 12, Madrid, Spain; ⁴Hospital Clínic de Barcelona, Barcelona, Spain; ⁵Hospital Parc Taulí de Sabadell, Sabadell, Spain; ⁶Virgen del Rocío University Hospital, Sevilla, Spain; ⁷Ramón y Cajal Hospital, Madrid, Spain; ⁸Hospital Universitari MútuaTerrassa, Terrassa, Spain; ⁹Hospital de la Santa Creu i Sant Pau Church, Barcelona, Spain; ¹⁰Hospital Universitario Clínico San Cecilio, Granada, Spain; ¹¹Hospital del Mar, Barcelona, Spain; ¹²Germans Trias i Pujol Hospital, Badalona, Spain; ¹³Hospital Universitario Virgen de la Victoria, Málaga, Spain; ¹⁴Complejo Universitario Hospitalario de Pontevedra, Spain; ¹⁵Consortium General University Hospital of Valencia, València, Spain; ¹⁶Puerta de Hierro Majadahonda University Hospital, Majadahonda, Spain; ¹⁷Consorci Sanitari de Terrassa, Spain; ¹⁸Hospital Universitario de Canarias, La Laguna, Spain; ¹⁹Álvaro Cunqueiro Hospital, Vigo, Spain; ²⁰Hospital Universitario Josep Trueta, Spain; ²¹Hospital Infanta Cristina, Spain; ²²Hospital Universitario Nuestra Señora de la Candelaria, Spain; ²³Hospital Vall d'Hebrón, Spain; ²⁴Hospital General Universitario Gregorio Marañón, Spain

Email: diazg.alvaro@gmail.com

Background and aims: A high prevalence of metabolic pathology has been described in patients with primary biliary cholangitis (PBC). However, its impact on the evolution of these patients is controversial. To describe the prevalence and the impact of the metabolic profile on the response and evolution in patients with PBC.

Method: Retrospective study from the Spanish ColHai registry in which patients who met the following criteria were included: (a) Diagnosis of PBC; (b) Treated with ursodeoxycholic acid (UDCA); (c) Minimum follow-up of 1 year; (d) Registered metabolic profile. Patients with variant syndromes were excluded. Response to UDCA was assessed using the Paris II criteria, prognosis using the GLOBE scale (≤ 0.3 vs > 0.3) and liver fibrosis using FIB-4.

Results: A total of 802 patients were included, 90.6% women with a median age of 54.4 years. Considering the metabolic profile, 69.2% had hypercholesterolemia, 62% overweight/obesity, 27.9% arterial hypertension (AHT), 14% type 2 diabetes mellitus (DM2), 8.3% HBP and DM2 (AHT + DM2), and 14% hypertriglyceridemia (hyperTAG). At baseline, GGT values were higher in patients with AHT (228 UI/L vs 168 UI/L, $p = 0.001$) and in those with dyslipidemia (204 UI/L vs 155 UI/L, $p = 0.002$).

One year after starting UDCA, 437 patients (60.3%) had a response according to Paris II, 461 (63%) GLOBE ≤ 0.3 and 469 (63.8%) FIB4 ≤ 1.45 . GGT values persisted higher in patients with dyslipidemia (64 vs 48 UI/L, $p = 0.004$) and DM2 (79 UI/L vs 56 UI/L, ($p = 0.06$)). Presence of DM2 (OR 2.25; IC95 1.42–3.58), AHT (OR 2.62; IC95 1.84–3.74) and AHT + DM2 (OR 2.81; IC95 1.57–5.01) were associated with greater risk of fibrosis in the univariate analysis. In the multivariate analysis, the presence of AHT (OR 2.66; IC95 1.46–4.88) and AHT + DM2 (OR 3.12; IC95 1.23–7.91) were independently associated with an increased risk.

On the other hand, presence of DM2 (OR 1.98; IC95 1.13–3.48), AHT (OR 2.54; IC95 1.65–3.91) and AHT + DM2 (OR 2.24; IC95 1.12–4.50) were associated with a worse prognosis (GLOBE > 0.3). In the multivariate analysis, the presence of AHT (OR 2.37; IC95 1.41–3.99) and AHT + DM2 (OR 2.56; IC95 1.19–5.45) independently predicted a dismal prognosis. However, the presence of hypercholesterolemia, hyperTAG, or overweight/obesity was not associated with a worse prognosis by means of GLOBE score or FIB-4.

Conclusion: The metabolic profile impacts the evolution of patients with PBC. The concomitant presence of AHT + DM2 represents the scenario with the highest risk of unfavorable evolution. However, the isolated presence of AHT is also independently associated with a worse prognosis. Finally, the presence of hypercholesterolemia did not negatively impact the risk of these patients.

WED-265

Chronic pruritus is associated with altered nerve fiber function and anatomy in patients with cholestatic hepatobiliary diseases

Miriam Düll^{1,2,3}, Hannah Kleinlein^{1,2,3}, Konstantin Agelopoulos⁴, Victoria Leibl³, Peter Dietrich^{1,2,5}, Markus F. Neurath^{1,2}, Sonja Ständer⁴, Barbara Name^{3,6,7}, Andreas E. Kremer^{1,2,8}.
¹Department of Medicine 1, University Hospital and Friedrich-Alexander-University Erlangen-Nürnberg, Germany; ²Deutsches Zentrum Immuntherapie DZI, Erlangen, Germany; ³Institute of Physiology and Pathophysiology, Friedrich-Alexander-University Erlangen-Nürnberg, Germany; ⁴Department of Dermatology and Center for Chronic Pruritus, University Hospital Münster, Germany; ⁵Institute of Biochemistry, Emil-Fischer-Zentrum, Friedrich-Alexander-University Erlangen-Nürnberg, Germany; ⁶Research group Neuroscience, Interdisciplinary Centre for Clinical Research within the faculty of Medicine at the RWTH Aachen University, Germany; ⁷Institute of Physiology, University Hospital of the RWTH Aachen University, Germany; ⁸Department of Gastroenterology and Hepatology, University Hospital Zürich, Zürich, Switzerland
Email: miriam.duell@uk-erlangen.de

Background and aims: Chronic pruritus as a symptom of cholestatic liver diseases represents a major unmet clinical need. The underlying pathophysiological mechanisms are only partially elucidated. Sensory C-nerve fiber endings in the skin act as pruritoceptors and can be activated by previously identified mediators of hepatic pruritus such as lysophosphatidic acid. We therefore assessed C-fiber function in patients with cholestatic liver disorders with and without chronic pruritus.

Method: We included 56 clinically well-characterized patients with cholestatic liver diseases consisting of PBC ($n = 22$), PSC ($n = 17$) and other causes of cholestasis ($n = 17$). Pruritus was evaluated using validated questionnaires including a numeric rating scale (NRS). Patients underwent testing of skin nerve fiber function including an electrical stimulation protocol using sine-wave stimuli on the forearm and dorsum of the foot to selectively activate C-fibers in the skin. We additionally obtained skin punch biopsies at the forearm to analyze histology and intraepidermal nerve fiber density (IENFD).

Results: Patients were divided into those with significant chronic pruritus as defined of a mean itch rating of NRS ≥ 3 (pruritus high; $n = 26$) and those without clinically significant pruritus (pruritus low, NRS < 3 ; $n = 30$). Both patient groups were comparable regarding age, liver and kidney function tests, disease entity and stage of liver

disease including proportion of patients with liver cirrhosis. Singular sine-wave stimulation (0.025–0.4 mA) of the skin caused a dose-dependent pain sensation in both, the pruritus low and high group (Figure 1), in a comparable range of healthy subjects. Intriguingly, in addition to pain, solely the high pruritus group experienced a dose-dependent itch sensation (Figure 1B). This difference occurred both at the level of the forearm and the forefoot. Similarly, a prolonged electrical sine-wave stimulation of 60 s resulted in a significant itch sensation only in the high pruritus group. Adaptation was observed to pain but not itch intensity. In skin biopsies, the mean IENFD was strongly reduced ($p < 0.001$) in patients with cholestatic liver diseases (5.1 IENF/mm) compared to age- and sexed-matched healthy controls (12.3 IENF/mm), with a trend towards lower IENFD in patients in the high pruritus group (4.7 IENF/mm) compared to patients with low-intensity pruritus (6.1 IENF/mm).

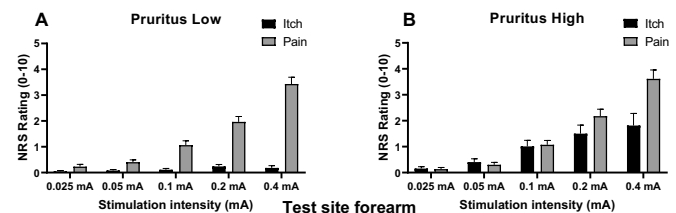


Figure 1:

Conclusion: Patients with chronic cholestatic pruritus exhibit functional changes in sensory C-fiber function to which altered intraepidermal nerve fiber anatomy could contribute.

WED-266

Vitamin D associates with clinical outcomes in patients with primary sclerosing cholangitis

Maryam Ebadi, Elora Rider, Catherine Tsai, Sarah Wang, Ellina Lytyvak, Andrew L. Mason, Aldo J. Montano-Loza. University of Alberta, Medicine, Edmonton, Canada
Email: montanol@ualberta.ca

Background and aims: Primary sclerosing cholangitis (PSC) is a chronic cholestatic liver disease characterized by progressive biliary inflammation and fibrosis. Given the importance of vitamin D in the modulation of inflammatory and immune-mediated pathways, vitamin D status may impact the PSC course. The objectives of this study were to identify the prevalence of severe vitamin D deficiency in patients with PSC and to investigate its association with cirrhosis progression, hepatobiliary malignancies and liver-related events (liver transplantation or mortality).

Method: Patients with a diagnosis of PSC ($n = 354$), followed by our autoimmune liver disease clinic were included. Patients with vitamin D levels < 25 nmol/L were defined as severely deficient. In addition, patients were divided into three groups regarding longitudinal vitamin D deficiencies as always deficient, less than 50% of the time-points deficient, and never deficient. The types of hepatobiliary malignancies included were cholangiocarcinoma, hepatocellular carcinoma, and gallbladder cancer. Univariate and multivariate analyses were conducted using the Cox proportional hazards regression models.

Results: The mean vitamin D level was 59 ± 2 nmol/L, and 63 patients (18%) had a severe vitamin D deficiency. Patients with a severe vitamin D deficiency were 2.5 times more likely to experience hepatobiliary malignancies (HR 2.55, 95% CI, 1.02–6.40, $p = 0.046$). However, this association was no longer significant when adjusting for the bilirubin level (HR 1.86, 95% CI, 0.65–5.31, $p = 0.25$). Of 316 patients without cirrhosis at diagnosis, 151 (44%) developed cirrhosis during follow-up. Serum vitamin D level as a continuous variable was only associated with cirrhosis development in univariate analysis (HR 0.99, 95% CI, 0.99–0.999, $p = 0.02$). There was no association between severe vitamin D deficiency at presentation and the risk of developing

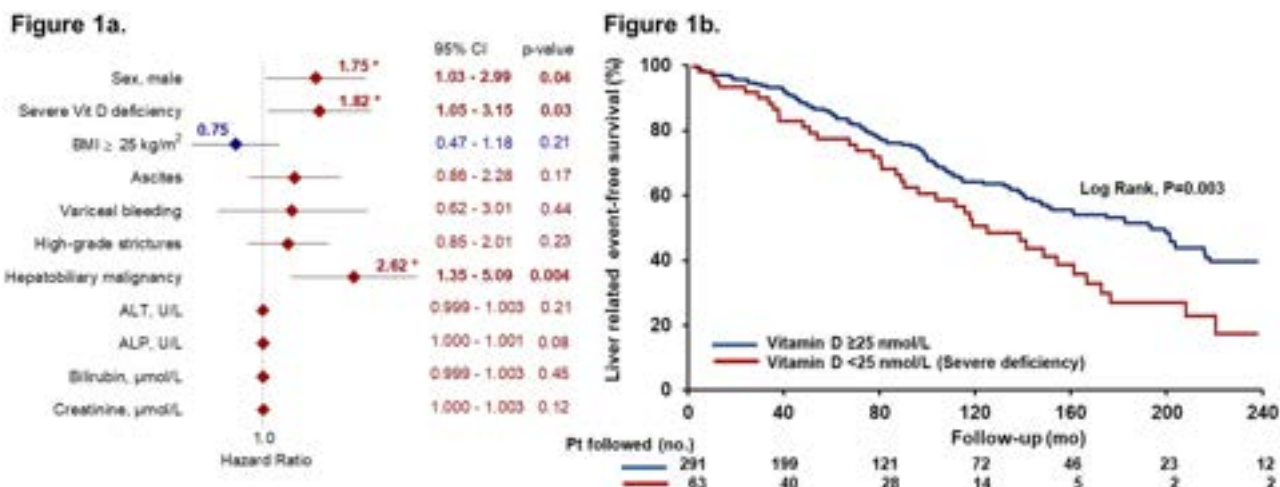


Figure: (abstract: WED-266): Parameters Associated with Liver-Related Events in PSC.

cirrhosis. Over a median follow-up period of 153 months (95% CI, 130–177), 24 deaths were attributed to liver-related disease and 137 patients underwent liver transplantation. Severe vitamin D deficiency at diagnosis (HR 1.82, 95% CI, 1.05–3.15, $p=0.03$) was independently associated with a higher risk of liver-related events (Figure 1a). Liver-related event-free survival was shorter in patients with severe deficiency (119 months; 95% CI, 81–156 vs. 185 months; 95% CI, 146–224, $p=0.003$; Figure 1b). Patients with persistent severe vitamin D deficiencies at all time points (10% of the population) had more than two-fold higher risk of liver-related events after adjusting for confounding predictors (HR 2.26, 95% CI, 1.17–4.37, $p=0.02$).

Conclusion: Severe vitamin D deficiency presented in 18% of patients with PSC at diagnosis and was associated with a higher frequency of liver-related events and hepatobiliary malignancies. Persistent severe vitamin D deficiency was common among 10% of the patients and was associated with a two-times-higher risk of adverse events.

WED-267

Modulation of alkaline phosphatase levels by obeticholic acid in clinical trials and cultured human hepatocytes

Alan Bonder¹, Nicholas Procaccini², Mary Erickson², Erik Ness², Antonio Civitarese², Kris Kowdley³. ¹Beth Israel Deaconess Medical Center, Harvard Medical School, Boston, United States; ²Intercept Pharmaceuticals, Inc., San Diego, United States; ³Liver Institute Northwest and Elson S. Floyd College of Medicine, Washington State University, United States

Email: erik.ness@interceptpharma.com

Background and aims: Obeticholic acid (OCA), a potent farnesoid X receptor (FXR) agonist, was approved in 2016 as a second-line treatment for primary biliary cholangitis (PBC) in combination with ursodeoxycholic acid (UDCA) based on reduction of serum alkaline phosphatase (ALP) and total bilirubin levels. However, data from trials of OCA monotherapy in patients with non-alcoholic steatohepatitis (NASH) have shown 15–20% stable mean increases in ALP without mean elevation of other liver biochemical markers including gamma-glutamyl transferase (GGT), aspartate aminotransferase (AST), and alanine transaminase (ALT), indicating that ALP fluctuations may be independent of cholestasis or inflammation, and may occur by an unknown mechanism. Importantly, ALP is anchored to the cell membrane by glycosylphosphatidylinositol, which may be cleaved by phospholipase D (PLD), thus releasing ALP into the plasma. We investigated whether OCA affected ALP or PLD gene expression in human hepatocytes *in vitro*.

Method: Human sandwich-cultured hepatocytes were treated up to 48 hours with 0.1% dimethyl sulfoxide (DMSO; vehicle) or 0.1–

100 μM of OCA. Using quantitative PCR, mRNA concentrations were determined for each treatment group relative to the expression of a control gene (GAPDH).

Results: Cultured human hepatocytes exposed to OCA for 48 hours showed no significant changes in relative levels of ALP mRNA compared to the vehicle control; however, hepatocytes displayed dose-dependent increases in PLD mRNA levels. The highest dose of OCA (100 μM) showed a statistically significant increase in PLD expression compared with the vehicle (Figure).

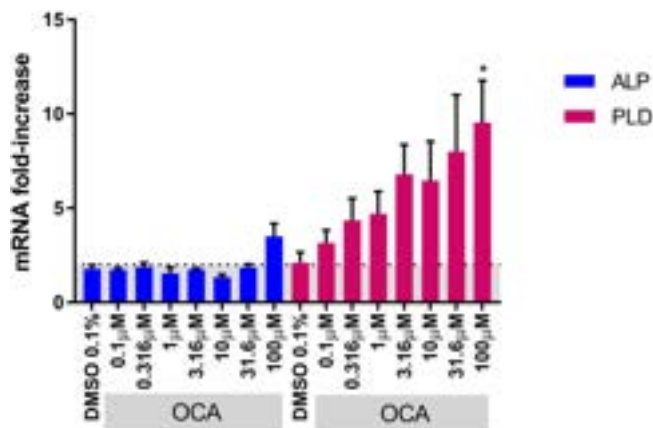


Figure: Assessment of ALP and PLD gene expression levels in human hepatocytes. After 48 hours of OCA exposure, hepatocytes exhibited no significant increases in ALP mRNA levels compared with vehicle, but dose-dependent increases in PLD mRNA levels were observed. ALP indicates alkaline phosphatase; DMSO, dimethyl sulfoxide; OCA, obeticholic acid; PLD, phospholipase D. Data are mean ± SD. Statistics were performed using a 2-way unpaired Student's *t* test. $n=3$ per treatment group. Shaded area represents a 2-fold increase vs internal control. * $p<0.05$ compared with DMSO 0.1% (vehicle).

Conclusion: These results support that the approximate 15–20% stable mean increase in plasma ALP levels observed after administration of OCA in NASH clinical trials, in the absence of mean increases in other liver biochemical markers, is not suggestive of liver injury. The likely mechanism of action elevating plasma ALP is via increased expression of PLD, which may in turn release ALP from the cell surface into the bloodstream. This potential mechanism of action may attenuate the observed mean reduction of ALP believed to reflect improved hepatic function in people living with PBC.

WED-268

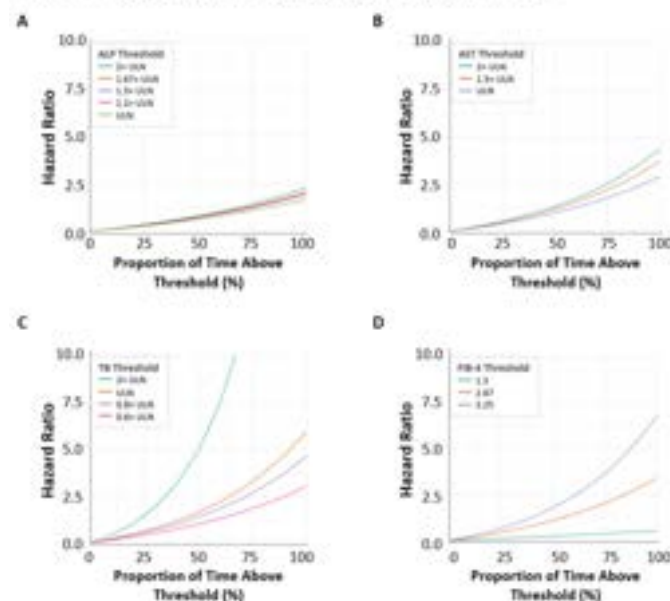
Risk of death, liver transplant or hepatic decompensation in primary biliary cholangitis increases with increased duration and degree beyond established clinical thresholds for hepatic biomarkers and fibrosis scores

Kris Kowdley¹, Tracy Mayne², Erik Ness², Darren Wheeler², Radhika Nair², Nicholas Procaccini², Leona Bessonova², Joanna MacEwan³, Alina Levine³, Gideon Hirschfield⁴. ¹Liver Institute Northwest and Elson S. Floyd College of Medicine, Washington State University, United States; ²Intercept Pharmaceuticals Inc, Morristown, United States; ³Genesis Research, Hoboken, United States; ⁴Toronto Centre for Liver Disease, University of Toronto, Division of Gastroenterology and Hepatology, Toronto, Canada
Email: erik.ness@interceptpharma.com

Background and aims: Current primary biliary cholangitis (PBC) risk scores use biomarkers from a single point in time to predict clinical outcomes. Recent data showed higher rates of liver transplant or death associated with serum alkaline phosphatase (ALP) and total bilirubin (TB) maintained below current PBC treatment guideline thresholds (ALP < 1.67× upper limit of normal [ULN] and TB < ULN). We aimed to confirm these results and assess additional serum biochemistries and liver fibrosis scores (fibrosis-4 [FIB-4], aspartate aminotransferase [AST] to platelet ratio index [APRI]) and duration of elevations as predictors of the risk of clinical outcomes.

Method: A cohort of patients ≥18 years old with ≥1 inpatient or ≥2 outpatient PBC diagnosis claims separated by ≥30 days (baseline) between January 1, 2014 and April 1, 2022 was created using the Komodo Health database merged with national lab data. Those with ≥2 measures of ALP, TB, AST, alanine aminotransferase (ALT), albumin (ALB), or platelets separated by >1 day were included in the analysis. Patients with a history of hepatic decompensation, liver transplant, major comorbidities, or prescribed obeticholic acid or fibrates (second-line [2L] therapies) were excluded. Survival analysis examined the proportion of follow-up time that liver biochemistries exceeded limits of normal/specific thresholds as a time-dependent covariate on time to first occurrence of hospitalization for hepatic decompensation, liver transplant, or death. Patients were censored at initiation of 2L treatment, end of insurance enrollment, or end of follow-up.

Figure 1. Incremental risk of negative outcomes in real-world sample patients with primary biliary cholangitis by the proportion of time that liver biochemistries (A) alkaline phosphatase, (B) aspartate aminotransferase, (C) total bilirubin and (D) fibrosis-4 score were above thresholds.



Results: A total of 3929 patients (87.8% female; mean [SD] age 59 [12.7] years) met eligibility criteria; 77.7% had a history of UDCA use, 8.4% had baseline cirrhosis, and the mean (SD) duration of follow-up was 3.0 (2.1) years. For ALP and AST, all results above ULN were associated with increased risk of negative outcomes and risk increased as time above ULN increased (Figure 1A, B). This was also observed for TB > 0.6 × ULN (Figure 1C) and FIB-4 > 2.67 (Figure 1D). Similar associations were observed for ALT, albumin, platelets, and APRI.

Conclusion: Liver biochemistries and fibrosis scores at thresholds lower than those in current PBC treatment guidelines were associated with an increased risk of hospitalization for hepatic decompensation, liver transplant, or death. Risk of negative outcomes increased as time above each threshold increased. These data suggest that risk of hepatic events should be evaluated using measures over time. Guidelines should consider revising treatment recommendations to incorporate chronic elevations at levels meaningfully below current static thresholds to improve clinical outcomes in people living with PBC.

WED-269

Accuracy of controlled attenuation parameter (CAP) measurement for the detection of steatosis in autoimmune liver diseases

Silja Steinmann^{1,2}, Johannes Hartl^{1,2}, Sören Alexander Weidemann³, Füssel Katja¹, Claudia Kroll¹, Ansgar W. Lohse^{1,4,5}, Christoph Schramm^{1,4,5,6}. ¹University Medical Centre Hamburg-Eppendorf (UKE), 1st Department of Medicine, Hamburg, Germany; ²European Reference Network for Hepatological Diseases (ERN-RARE LIVER), Hamburg, Germany; ³University Medical Centre Hamburg-Eppendorf (UKE), Institute of Pathology with the Sections Molecular Pathology and Cytopathology, Hamburg, Germany; ⁴European Reference Network for Hepatological Diseases (ERN-RARE LIVER), Hamburg, Germany; ⁵University Medical Centre Hamburg-Eppendorf (UKE), Hamburg Centre for Translational Immunology (HCTI), Hamburg, Germany; ⁶University Medical Centre Hamburg-Eppendorf (UKE), Martin Zeitz Center for Rare Diseases, Hamburg, Germany
Email: sfk.steinmann@outlook.com

Background and aims: Concurrent fatty liver disease represents an emerging challenge in the care of people with autoimmune liver diseases (AILD). Therefore, we here aimed to validate controlled-attenuation parameter (CAP) as a non-invasive tool to detect hepatic steatosis in people with AILD. **Method:** People with AILD (AIH, PBC, PSC, or variant syndromes) who underwent liver biopsy at the University Medical Center Hamburg-Eppendorf between 2015 and 2020 were included. The diagnostic performance of CAP to determine biopsy-proven hepatic steatosis (>5%) was assessed by calculating area under the receiver operating characteristic (AUROC) curves. Optimal cut-offs to detect hepatic steatosis were determined by Youden's index. In AIH, the impact of disease activity was explored by assessing changes of CAP upon resolution of hepatic inflammation during follow-up.

Results: 433 people with AILD (AIH: 218, PBC: 51, PSC: 85, AIH/PBC: 63, AIH/PSC: 16) were included. Histologically proven steatosis was present in 90 individuals (20.7%). Steatosis was less frequently observed in PSC (14%) than in other AILD. CAP strongly correlated with grade of steatosis ($\rho = 0.39$) and BMI ($\rho = 0.53$). In PBC and PSC, ROC curves defined an AUROC of 0.81 and 0.93 for detecting steatosis at an optimal cut-off of 276 (sensitivity: 0.71; specificity: 0.82) and 254 (sensitivity: 0.91, specificity: 0.85) dB/m, respectively. In AIH, the diagnostic performance of CAP was significantly lower (AUROC: 0.72). However, resolution of hepatic inflammation under treatment was associated with a significant increase of CAP levels (median +38.0 dB/m) and considerably improved diagnostic accuracy (AUROC: 0.85; cut-off: 288 dB/m; sensitivity: 0.67, specificity: 0.90).

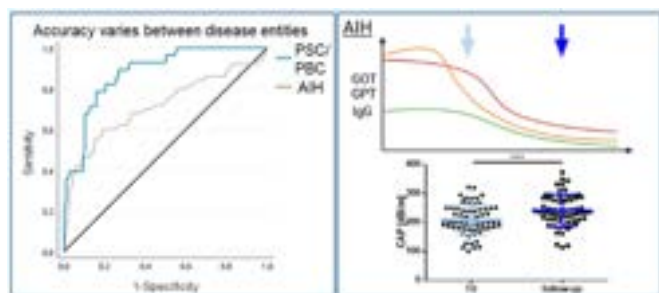


Figure:

Conclusion: In PBC and PSC, hepatic steatosis can be reliably detected by applying disease-specific thresholds of CAP. In AIH, the diagnostic accuracy of CAP is moderate at diagnosis, but improves after acute hepatitis has resolved.

WED-270

Risk of decompensated cirrhosis in patients with primary biliary cholangitis under first, second and third-line therapies

Ana Lucena¹, Esther Molina², Manuel Hernández Guerra³, Marina Berenguer⁴, Elena Gómez Domínguez⁵, Marta Casado⁶, Francisco Jorquera⁷, Rosa M. Morillas⁸, Luisa García-Buey⁹, Miguel Angel Simon¹⁰, Maria Carlota Londoño¹¹, Jose manuel Sousa-Martin¹, Conrado Fernández-Rodríguez¹², Javier Martinez¹³, Judith Gómez-Camarero¹⁴, Antonio Oliveira Martin¹⁵, Nerea Quintans¹⁶, Diana Horta¹⁷, Álvaro Díaz-González¹⁸, Indhira Perez Medrano¹⁹, Carmen Álvarez-Navascués²⁰, Montserrat García-Retortillo²¹, Javier Ampuero^{1,22}. ¹Hospital Universitario Virgen del Rocío, Sevilla, Spain; ²Hospital Universitario Clínico, Santiago de Compostela, Spain; ³Hospital Universitario de Canarias, Tenerife, Spain; ⁴Hospital Universitario La Fe, Valencia, Spain; ⁵Hospital Universitario 12 de Octubre, Madrid, Spain; ⁶Hospital Universitario Torrecárdenas, Almería, Spain; ⁷Complejo Asistencial de León, León, Spain; ⁸Hospital Germans Trias i Pujol, Badalona, Spain; ⁹Hospital Universitario La Princesa, Madrid, Spain; ¹⁰Hospital Clínico, Zaragoza, Spain; ¹¹Hospital Clinic, Barcelona, Spain; ¹²Hospital Universitario Alcorcón, Alcorcón, Spain; ¹³Hospital Universitario Ramón y Cajal, Madrid, Spain; ¹⁴Hospital Universitario de Burgos, Burgos, Spain; ¹⁵Hospital Universitario La Paz, Madrid, Spain; ¹⁶Hospital Universitario Álvaro Cunqueiro, Vigo, Spain; ¹⁷Hospital Mutua, Terrasa, Spain; ¹⁸Hospital Universitario Marqués de Valdecilla, Santander, Spain; ¹⁹Complejo Hospitalario de Pontevedra, Pontevedra, Spain; ²⁰Hospital Universitario Central de Asturias, Oviedo, Spain; ²¹Hospital del Mar, Barcelona, Spain; ²²Instituto de Biomedicina de Sevilla, Sevilla, Spain

Email: javi.ampuero@gmail.com

Background and aims: About 25% of patients with primary biliary cholangitis (PBC) inadequately respond to ursodeoxycholic acid (UDCA) and, thus, require a second-line therapy. In this setting, patients with cirrhosis receiving obeticholic acid (OCA) and fibrates have been poorly represented to date. Therefore, we aimed to: (a) assess the risk of decompensation in PBC cirrhotic patients receiving first, second and third-line treatments; (b) determine risk factors associated with the occurrence of a decompensation event in patients taking OCA.

Method: Multicenter and retrospective study from the COLHAI registry (belonging to the Spanish Association for the Study of the Liver), including 272 PBC patients showing liver cirrhosis, which was defined by liver biopsy, ultrasound, or transient elastography (>16.9 kPa). Patients were classified according to receiving first (UDCA), second (UDCA and OCA or fibrates), and third-line therapies (UDCA and OCA and fibrates). Outcomes were decompensation events and mortality during the follow-up from the beginning of each treatment.

Results: We included patients with UDCA (n = 173), UDCA+OCA (n = 37), UDCA + fibrates (n = 39), and UDCA + OCA + fibrates (n = 23). Baseline features of the patients are shown in Table. Decompensation by 100-person-years was: (a) UDCA, 2.73 (events = 47; follow-up: 10.1 years); (b) UDCA+OCA, 11.1 (events = 10; follow-up: 2.5 years); (c) UDCA+OCA additionally including those with triple therapy, 12.1 (events = 17; follow-up: 2.42 years); (d) UDCA+fibrates 5.8 (events = 8; follow-up: 3.54 years); (e) UDCA + fibrates additionally including those with triple therapy, 6.83 (events = 15; follow-up: 3.59 years). Serum levels of bilirubin (OR 2.43 (IC95% 1.09–5.46; p = 0.031), albumin (OR 0.09 (IC95% 0.01–0.66; p = 0.018), and presence of type 2 diabetes mellitus (OR 11.35 (IC95% 1.94–66.36; p = 0.007) were independently associated with the occurrence of a decompensation event in PBC patients with OCA (ROC 0.89 (IC95% 0.80–0.98; p = 0.0001)). Fifteen patients taking OCA discontinued the drug (7 due to disease progression and 8 to adverse events).

Characteristic	UDCA (n=173)	UDCA + OCA (n=40) (including double and triple therapy)	UDCA + Fibrates (n=42) (including double and triple therapy)
Female sex	86.7% (150/173)	85.0% (34/40)	95.2% (38/42)
Age, years ± SD	68.3 ± 13.1	61 ± 11.3	60.5 ± 11.9
Obesity (BMI ≥ 30 kg/m ²)	23.1% (40/173)	27.5% (11/40)	22.4% (14/42)
Arterial Hypertension	37.6% (65/173)	32.5% (13/40)	27.1% (11/42)
Type 2 Diabetes Mellitus	30.2% (52/173)	18.3% (7/40)	16.7% (7/42)
Dyslipidemia	30.1% (52/173)	48.3% (19/40)	45.2% (19/42)
AST ± SD (U/L)	70 ± 121	58 ± 81	55 ± 41
ALT ± SD (U/L)	64 ± 91	50 ± 48	48 ± 38
GGT ± SD (U/L)	300 ± 212	338 ± 118	178 ± 126
Alkaline phosphatase ± SD (U/L)	287 ± 382	252 ± 181	340 ± 141
Bilirubin ± SD (mg/dL)	1.05 ± 1.45	1.38 ± 0.97	1.54 ± 1.13
Albumin ± SD (g/dL)	3.98 ± 0.13	4.04 ± 0.44	4.06 ± 0.43
Creatinine ± SD (mg/dL)	0.80 ± 0.28	0.75 ± 0.28	0.69 ± 0.17
Platelet count ± SD (x 10 ⁹ /L)	170 ± 79	172 ± 90	190 ± 90
INR ± SD	1.08 ± 0.12	1.09 ± 0.1	1.05 ± 0.12
Decompensated cirrhosis	0% (0/173)	13.3% (5/40)	6.7% (2/42)
Transient elastography (kPa)	29.5 ± 14.3	24.5 ± 17.5	26.4 ± 18.4
Overlap syndrome	16.2% (28/173)	23.3% (9/40)	29% (12/42)

Figure:

Conclusion: Patients with cirrhosis secondary to PBC under double and triple therapy were at a relatively high risk of decompensation, particularly those receiving OCA, probably because they were sicker at the beginning of the treatment. Serum bilirubin and albumin levels, as well as the presence of diabetes mellitus, predicted the risk of decompensation in patients with OCA.

WED-271

Improved survival with regular surveillance imaging in patients with primary sclerosing cholangitis

Natassia Tan^{1,2}, Natalie Ngu^{2,3}, Thomas Worland⁴, Tanya Lee⁵, Tobie Abrahams⁵, Keval Pandya⁶, Elliot Freeman¹, Nicholas Hannah^{7,8}, Kathryn Gazelakis⁹, Richie Madden¹⁰, Kate Lynch¹⁰, Zina Valaydon⁹, Siddharth Sood^{7,8}, Anouk Dev^{2,3}, Sally Bell^{2,3}, Alexander Thompson^{5,8}, John Nik Ding^{5,8}, Amanda Nicoll^{2,11}, Ken Liu⁶, Paul Gow^{4,8}, John Lubel^{1,2}, William Kemp^{1,2}, Stuart Roberts^{1,2}, Ammar Majeed^{1,2}. ¹The Alfred, Melbourne, Australia; ²Monash University Clayton Campus, Clayton, Australia; ³Monash Medical Centre, Clayton, Australia; ⁴Austin Hospital, Heidelberg, Australia; ⁵St. Vincent's Hospital Melbourne, Fitzroy, Australia; ⁶Royal Prince Alfred Hospital, Camperdown, Australia; ⁷The Royal Melbourne Hospital, Parkville, Australia; ⁸University of Melbourne, Parkville, Australia; ⁹Western Health, St Albans, Australia; ¹⁰Royal Adelaide Hospital, Adelaide, Australia; ¹¹Eastern Health, Box Hill, Australia

Email: natassiapintan@gmail.com

Background and aims: The benefits of regular surveillance imaging for cholangiocarcinoma (CCA) in patients with primary sclerosing cholangitis (PSC) are unclear. Hence, we aimed to evaluate the impact of regular magnetic resonance imaging with cholangiopancreatography (MRCP) on outcomes of patients with PSC in Australia, where the practice of MRCP surveillance is variable.

Method: We evaluated MRCP surveillance and outcome data from a multicentre, retrospective cohort of PSC patients from 9 tertiary liver centres in Australia. An inverse probability of treatment weighting (IPTW) approach was used to balance groups across potentially confounding covariates to achieve a standardized difference of less than 0.10. IPTW-weighted Cox proportional hazard models was conducted to assess the risk of death in those undergoing regular surveillance compared to those who were not. A competing risk analysis was conducted whereby liver transplant (LT) was considered a competing risk for death. IPTW-weighted Kaplan-Meier method was used to estimate survival time from diagnosis of PSC and CCA diagnosis.

Results: A total of 298 PSC patients with 2,117 person-years (median 6, interquartile range 3–11 years) of follow-up were included. Two hundred and twenty patients (73.8%) had undergone MRCP surveillance. Forty-six patients (15.4%) had a liver transplant and 35 (11.7%) died during the follow-up period. Patients who had regular surveillance were younger at diagnosis, more likely to have dominant strictures and higher alkaline phosphatase at last follow-up. Eleven patients (5%) in the surveillance group and 2 (2.6%) in the non-surveillance group developed CCA ($p = 0.560$). IPTW was performed with age of diagnosis, sex, Model for End-Stage Liver Disease score, presence of cirrhosis or dominant stricture, liver transplant, and serum alkaline phosphatase level at follow-up as covariates. Regular surveillance was significantly associated with 62% reduced risk of death on multivariate weighted Cox analysis ($p = 0.005$). Improved survival was also demonstrated on weighted Kaplan-Meier curves ($p = 0.009$) as shown below. The cumulative incidence of death was significantly lower in the surveillance group with LT as a competing event ($p = 0.017$). However, survival post CCA diagnosis was not significantly different between both groups ($p = 0.74$). Patients who had surveillance of less than one scan a year ($N = 41$) had comparable survival ($p = 0.231$) compared to patients who had surveillance at least yearly ($N = 172$).

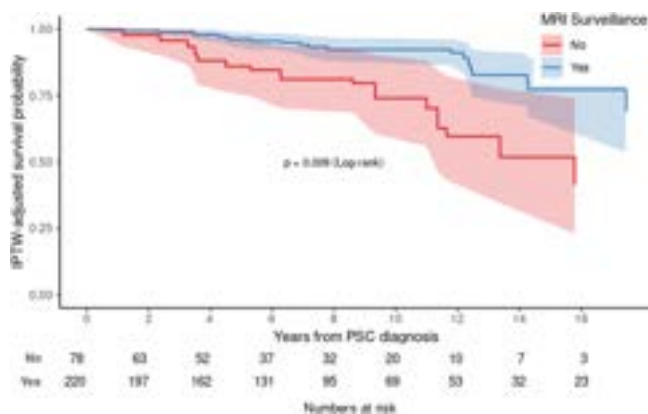


Figure: Kaplan-Meier curve estimating survival probability from PSC diagnosis

Conclusion: In this large multicentre retrospective cohort study that employed IPTW to minimize selection bias, regular MRCP surveillance is associated with improved overall survival in PSC patients, however there was no difference in survival after CCA. Further prospective studies are needed to determine the optimal interval of surveillance imaging and follow-up in patients with PSC.

WED-272

Relative enhancement and spleen volume predict clinical outcomes in primary sclerosing cholangitis

Laura Cristofori^{1,2}, Cesare Maino³, Paolo Marra^{4,5}, Alberto Savino^{1,2}, Ilaria Ripamonti^{1,2}, Marta La Milia^{4,5}, Davide Bernasconi⁶, Miki Scaravaglio^{1,2}, Alessio Gerussi^{1,2}, Alberto Rossi^{1,2}, Eugenia Vittoria Pesatori^{1,2}, Luisa Pasulo⁴, Stefano Fagioli^{4,5}, Pietro Invernizzi^{1,2}, Davide Ippolito^{3,5}, Sandro Sironi^{4,5}, Marco Carbone^{1,2}. ¹Fondazione IRCCS San Gerardo dei Tintori, Department of Medicine and Surgery-University of Milano Bicocca, Monza, Italy; ²European Reference Network on Hepatological Diseases (ERN RARE-LIVER), Italy; ³Fondazione IRCCS San Gerardo dei Tintori, Department of Radiodiagnostics, Italy; ⁴ASST Papa Giovanni XXIII Hospital, Bergamo, Italy; ⁵University of Milano Bicocca, School of Medicine and Surgery, Italy; ⁶University of Milano Bicocca, Bicocca Bioinformatics Biostatistics and Bioimaging Centre-B4, Italy
Email: l.cristofori@campus.unimib.it

Background and aims: Magnetic resonance cholangiopancreatography (MRI-MRCP) assessment in primary sclerosing cholangitis (PSC) is currently based on qualitative or semi-quantitative parameters and has high inter-observer variability. In this study, we aimed to explore the predictive performance of quantitative and reproducible MRI-MRCP features, reflecting hepato-biliary function and portal hypertension, to enhance risk stratification in PSC.

Method: This is a retrospective cohort study of PSC patients with at least one complete gadoxetate disodium-enhanced MRI available from 2015 to 2021. Patients with overlapped chronic liver disease and a follow-up shorter than 6 months were excluded. The composite clinical end point was liver-related death, liver transplantation (LT), or hepatic decompensation. Signal intensities were measured in each liver segment. Mean relative enhancement and spleen volume were calculated for each exam. Liver stiffness measurement (LSM), Mayo risk score (MRS), Amsterdam Oxford model (AOM) and blood test within one month from MRI-MRCP were collected. Cox proportional hazards regression was used for the time-to-event analysis. Multivariable model has been internally validated using k-fold cross-validation.

Results: The study cohort included 71 patients. 43 (60.6%) were male, median age at diagnosis of 29 years [IQR 21–45.5], 44 (62.0%) had concomitant IBD, and median follow-up of 614 days (IQR 402–1090). 13 (14.3%) patients reached the outcome (7 LT, 1 liver-related death, 5 hepatic decompensation). At the univariate analysis, spleen volume, spleen cranio-caudal diameter, platelets count, LSM, MRS, AOM, and RE were predictive of outcomes and were taken forward. At the multivariable analysis, the RE and the spleen volume were the only independently associated with the occurrence of adverse event with an HR of 0.29 (per unit, CI 95% 0.09–0.98, $p = 0.047$) and 1.13 (per 50 cm³, CI 95% 1.07–1.21, $p < 0.0001$), respectively and a C-statistic of 0.89. The model was internally validated and outperformed the MRS and AOM in our cohort (C-statistic of 0.82 vs 0.74 and 0.76, respectively). The discriminative power of the score on survival is shown in figure 1 (mean value of the score as cut-off).

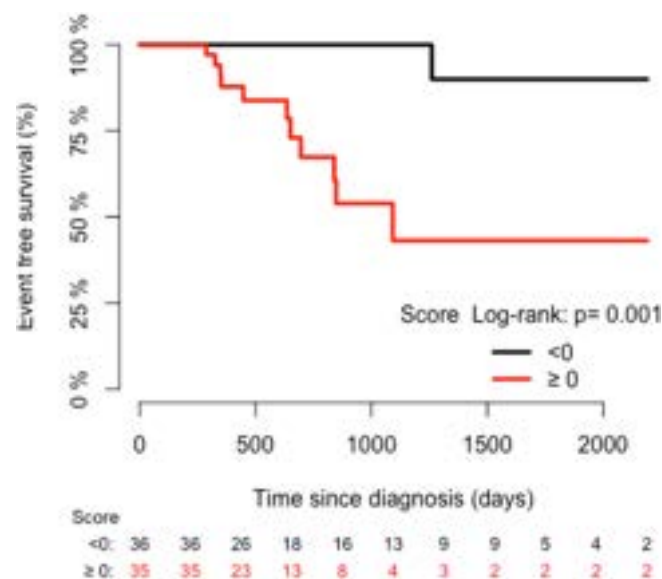


Figure:

Conclusion: Relative enhancement and spleen volume are quantitative, reproducible, simple MRI-metrics, which provide complementary information in predicting event-free survival in PSC.

WED-273

Hepatic steatosis in patients with autoimmune hepatitis: relationship with corticosteroid treatment and long-term outcome

Sarah Flatley¹, Asha Dube¹, Victoria Gordon², Barbara Hoeroldt¹, Laura Harrison¹, Elaine Wadland¹, Dermot Gleeson¹. ¹Sheffield Teaching Hospitals NHS Foundation Trust, United Kingdom; ²University Hospitals Coventry and Warwickshire NHS Trust, United Kingdom
Email: s.flatley@nhs.net

Background and aims: We have previously reported (Gut 2010;52: 431) an association between worsening steatosis and corticosteroid treatment in autoimmune hepatitis (AIH). Here, we aimed to assess further, associations of steatosis with corticosteroids, fibrosis progression and long-term outcome.

Method: Retrospective/prospective single centre audit of patients with AIH (1999 IAHG criteria) and followed to death, transplant, loss to follow-up or 31/12/21. Necroinflammatory (NI) score, fibrosis stage (both Ishak) and steatosis grade were assessed by one histopathologist (AKD). Steatosis was graded by percent of hepatocytes containing fat (0: <5%, 1: 5–33%, 2: 34–66%, 3: >67%). Steatohepatitis was defined as hepatocyte ballooning ± neutrophils in zone 3 and graded using Brunt criteria.

Results: 354 patients (81% women, age (median (range)) 55 (2–82) yr, 96% receiving steroids) had an evaluable diagnostic liver biopsy (biopsy 1) and were followed up for 10 (0–47) years. 242 (68%) had a follow-up biopsy (biopsy 2) after 26 (3–174) months. On biopsy 1, 89 (25%) had steatosis (Grade 1, 2 and 3: 70, 18 and 1 respectively) and 6 (2%) had steatohepatitis. Patients with steatosis (vs those without) were older (58 vs 49 years, $p < 0.001$), had higher BMI (29.1 vs 27.3, $p = 0.04$), and more were diabetic (15% vs 7%, $p = 0.02$). They had a lower NI score (9.4 vs 11.5, $p < 0.001$) and AIH histology grade (3.1 vs 3.9, $p < 0.001$) but similar IAHG diagnostic score and fibrosis stage. On biopsy 2, 117 (48%) had steatosis and 9 (4%) steatohepatitis. Steatosis

had appeared/worsened in 83 patients (34%), overall grade increasing from (0.3 (0–3) to 0.6 (0–3), $p < 0.001$). Worsening steatosis was positively associated with age ($p = 0.002$), initial prednisolone dose ($p < 0.001$), BMI ($p = 0.005$), and weight gain ($p = 0.05$) but was unrelated to diabetes or biopsy interval. Steatosis (biopsy 1, 2 or change between biopsies) was unrelated to: (a) NI score or % in histological remission (NI score <4) on biopsy 2, (b) fibrosis score on biopsy 2, or (c) fibrosis progression between biopsies 1 and 2. 89 patients died (15 liver-related, 72 non-liver, 2 cause unknown) and 7 underwent liver transplantation. All-cause 10- and 20-yr death/transplantation rates were $16 \pm 2\%$ and $45 \pm 4\%$ respectively. We confirmed independent associations of death/transplantation rate with older age, cirrhosis at diagnosis, failure of ALT normalisation by 12 months, and with diabetes (onset anytime), which we recently reported (Flatley Gut 2022; 71: A74). All-cause death/transplantation rate was associated with steatosis at diagnosis on univariate ($p = 0.03$), but not on multivariate analysis; there was no association with worsening steatosis.

Conclusion: Steatosis is present at diagnosis in 25% of AIH patients and worsens during steroid treatment. However, steatosis is not associated with histological remission or fibrosis progression and shows no independent association with long-term outcome.

WED-274

Antibodies against multiple post-translationally modified proteins aid in diagnostic work-up of autoimmune hepatitis and associate with complete biochemical response to treatment

Anna Stoelinga¹, Michelle van den Beukel², Adriaan Van der Meer³, Stef van der Meulen², Lu Zhang², Maarten Tushuizen¹, Leendert Trouw², Bart Van Hoek¹. ¹Leiden University Medical Center (LUMC), Department of Gastroenterology and Hepatology, Leiden, Netherlands; ²Leiden University Medical Center (LUMC), Department of Immunology, Leiden, Netherlands; ³Erasmus MC, Department of Gastroenterology and Hepatology, Rotterdam, Netherlands
Email: a.e.c.stoelinga@lumc.nl

Background and aims: 'Autoimmune liver disease' (AILD) includes autoimmune hepatitis (AIH), primary biliary cholangitis (PBC) and primary sclerosing cholangitis (PSC). Inflammation occurs in both AIH and cholestatic liver disease. During sustained inflammation and oxidative stress post-translational modifications (PTMs) can be generated. In rheumatoid arthritis, autoantibodies against PTMs are used as diagnostic and prognostic markers, respectively. We studied the presence of six anti-PTM antibodies in patients with AILD and non-AILD.

Method: Patients with AILD were eligible for inclusion. Serum samples were taken simultaneously with routine laboratory assessments. Antibodies against six PTMs (nitration (NT), Cit, acetylation (AL), advanced glycation end-products (AGE), CarP and malondialdehyde-acetaldehyde adducts (MAA)) were tested in collected sera of patients with AILD, and compared to patients with non-AILD and healthy controls (HC). Levels and positivity were correlated with clinical and biochemical features in a well-defined cohort of untreated AIH patients. Differences in levels of anti-PTM antibodies between HCs, AILD and non-AILD were assessed. Analyses of correlation between anti-PTM antibody levels and clinical variables were done.

Results: Anti-PTM IgG antibody levels were measured in 106 patients with AILD, 101 patients with non-AILD and 100 HCs in two academic hospitals in the Netherlands. Anti-PTM antibodies were more often detectable in sera from AILD patients compared with HCs (anti-AL: 18.9% vs 5.0%, anti-AGE: 36.8% vs 4.0%, anti-CarP: 47.2% vs 5.0% and

anti-MAA: 67.9% vs 2.0%). Patients with AILD more frequently harboured at least one type of anti-PTM antibody compared to non-AILD and HCs (AILD: 81.2%, non-AILD: 58.4% and HCs: 20%). The AILD group was dissected into AIH, PBC and PSC. Patients with AIH harboured significantly more anti-MAA, anti-CarP and anti-AGE antibodies compared to non-AILD patients (anti-MAA: 77.3% vs 26.7%, anti-CarP: 63.6% vs 27.7% and anti-AGE: 48.5% vs 17.5%, all $p < 0.001$, respectively). Patients with AIH harboured anti-PTM antibodies more often compared to other subgroups of AILD. In untreated AIH (N=58), time to complete biochemical response (CBR) was associated with anti-MAA, anti-CarP, anti-AGE and anti-AL antibodies. Significantly more patients with at least three anti-PTM antibodies attained CBR at 12 months of treatment (13 vs 3 $p = 0.01$).

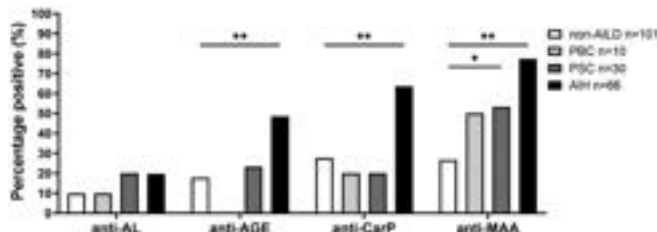


Figure: The association between the presence of anti-PTM antibodies and the three major autoimmune liver diseases

Conclusion: Anti-PTM antibodies are frequently present in AILD. The presence of anti-AGE, anti-CarP and anti-MAA antibodies correlates with the presence of AIH within this cohort. In AIH, harbouring at least three positive anti-PTM antibody responses is positively associated with CBR. Determination of anti-PTM antibodies in liver disease may have diagnostic and prognostic value.

WED-276

Collagen proportionate area is associated with adverse clinical outcomes and allows risk stratification of patients with autoimmune hepatitis

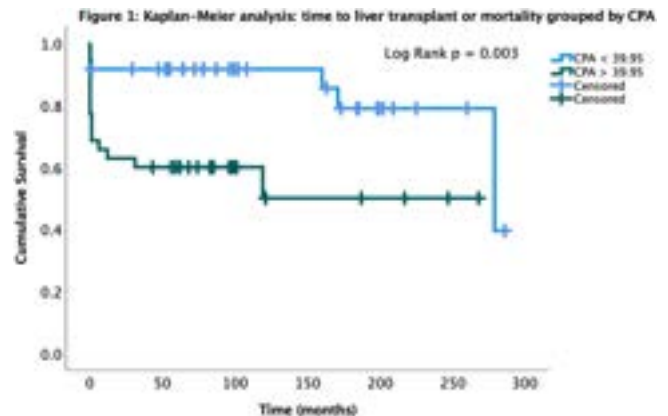
Neil Halliday^{1,2}, Andrew Hall^{2,3}, Alessio Gerussi⁴, Najeeha Siddiqi¹, Jennifer Watkins^{1,3}, Aileen Marshall^{1,2}, Alberto Quaglia^{1,3}, Douglas Thorburn^{1,2}. ¹University College London, UCL Institute for Liver and Digestive Health, London, United Kingdom; ²Royal Free London NHS Foundation Trust, Sheila Sherlock Liver Centre, United Kingdom; ³Royal Free London NHS Foundation Trust, Department of Cellular Pathology, London, United Kingdom; ⁴University of Milano-Bicocca, Division of Gastroenterology and Center for Autoimmune Liver Diseases, Milan, Italy. Email: neilhalliday@doctors.org.uk

Background and aims: The diagnosis of autoimmune hepatitis (AIH) remains reliant on histological assessment of the liver. However, AIH-specific scoring systems for histological stage have not been determined and are complicated by the coexistence of fibrosis and parenchymal collapse. Novel, reproducible predictors of clinical outcomes are required for risk stratification and prognostication in patients with AIH. Collagen proportionate area (CPA) represents a reproducible, quantitative measure of collagen deposition and also captures the presence of collapse due to the increased density of extracellular matrix proteins. CPA is predictive of clinical outcomes in other liver diseases, hence we sought to determine whether CPA was reflective of fibrosis stage and clinical outcomes in AIH.

Method: Patients from a single centre, with definite or probable AIH were identified; demographics, clinical features and outcomes were recorded and liver biopsies re-reviewed by 2 independent pathologists. CPA was measured on all biopsies and correlated with clinical outcomes by Kaplan-Meier analysis and Cox proportional hazard modelling.

Results: 71 patients with a median follow-up of 78 months (IQR 29–163) were included. CPA correlated with Ishak stage (Spearman Rank $p < 0.001$). Lower CPA was associated with improved liver transplant-free survival in Kaplan-Meier analysis (figure 1) (Log rank $p = 0.003$),

however Ishak stage was not ($p = 0.25$). Receiver operator curve analysis identified an optimum CPA cut off of 34.0% which provided a sensitivity of 71% and specificity of 60% for the prediction of transplantation or all-cause mortality. CPA was associated with an elevated hazard of transplant or all-cause mortality in univariate Cox-proportional hazard models (HR 1.04, 95% CI 1.01–1.06, $p = 0.003$), but not in multivariate analysis (HR 1.14, 95% CI 0.99–1.33, $p = 0.08$). However, in multivariate analysis CPA was associated with an increased hazard of all-cause mortality, transplant or decompensation (HR 1.13, 1.04–1.23, $p = 0.005$).



Conclusion: Increasing CPA was associated with adverse patient outcomes in AIH. Although true CPA may be overestimated due to parenchymal collapse in AIH, it still provided a quantitative measure that correlated with important clinical outcomes and was more strongly associated with transplant free survival than Ishak fibrosis stage. CPA represents a potentially useful, reproducible tool for prognostication and risk stratification in AIH.

WED-277

Patient reported gaps between current practice and new practice guidelines for primary sclerosing cholangitis

Annika Bergquist¹, Martine Walmsley², David Tornai³, Nora Cazzagion⁴, Angela Leburgue⁵, Anna Mrzljak⁶, Henrike Lenzen⁷, Marco Carbone⁸, Joao Madaleno⁹, Ana Lleo¹⁰, Norman Junge⁷, Christoph Schramm¹¹. ¹Karolinska University Hospital and Karolinska Institutet, European Reference Network on Hepatological Diseases (ERN RARE-LIVER), Sweden; ²PSC Support UK, European Reference Network on Hepatological Diseases (ERN RARE-LIVER), United Kingdom; ³University of Debrecen, European Reference Network on Hepatological Diseases (ERN RARE-LIVER), Hungary; ⁴University of Padua, European Reference Network on Hepatological Diseases (ERN RARE-LIVER), Italy; ⁵Association Albi European Reference Network on Hepatological Diseases (ERN RARE-LIVER), France; ⁶University Hospital Center Zagreb, European Reference Network on Hepatological Diseases (ERN RARE-LIVER), Croatia; ⁷Hannover Medical School, European Reference Network on Hepatological Diseases (ERN RARE-LIVER), Germany; ⁸University of Milano-Bicocca, European Reference Network on Hepatological Diseases (ERN RARE-LIVER), Italy; ⁹CH Univ Coimbra, European Reference Network on Hepatological Diseases (ERN RARE-LIVER), Portugal; ¹⁰Humanitas University, European Reference Network on Hepatological Diseases (ERN RARE-LIVER), Italy; ¹¹Martin Zeitz Center for Rare Diseases, University Medical Center Hamburg Eppendorf, European Reference Network on Hepatological Diseases (ERN RARE-LIVER), Germany. Email: annika.bergquist@ki.se

Background and aims: Management and follow-up strategies for primary sclerosing cholangitis (PSC) vary. A new European practice guideline for management of PSC was recently published. The aim of the present study was to assess patient reported quality of care and

POSTER PRESENTATIONS

identify gaps in current practice in Europe in relation to the new guidelines.

Method: Data was collected via an online survey hosted on the EU Survey platform in 11 languages between October 2021 and January 2022. Questions were asked about the disease, symptoms, treatment, investigations, and quality of care. Responses were received from participants in 36 countries around the world and included transplanted and non-transplanted respondents. Only responses from non-transplanted individuals were analysed in detail (n = 798). They were reviewed against the recommendations in the EASL guidelines for management of PSC. Respondent ages were grouped as follows: Children: aged 7–15 years, young adults: 16–25 years, adults: 26–60 years, seniors: 61+ years. Selection of response to open ended answers (quotes) was used to support and give examples of the findings.

Results: In total, 798 non-transplanted people with PSC from 33 countries responded. Eighty-six % of respondents reported having had at least one symptom. Twenty-four percent had never undergone an elastography, 8% had not had a colonoscopy. Of responders with IBD, 15% had a colonoscopy less frequently than every 2 years. Nearly half (49%) had never undergone a bone density scan. Ursodeoxycholic acid (UDCA) was used in 90–93% in France, Netherlands, and Germany, and 49–50% in the United Kingdom and Sweden. Itch was common (60%), and 50% of those had received any medication. Antihistamines were taken by 27%, cholestyramine 21%, rifampicin 13%, and bezafibrate 6.5%. Forty-one % had been offered participation in a clinical trial or research. The majority (91%) reported that they were confident with their care although half of the individuals reported need for more information on disease prognosis and diet. *Quote: "I would like to know the vital prognosis and life expectancy for these diseases because on the internet the data is old and frightening."* Responder ERN431, France

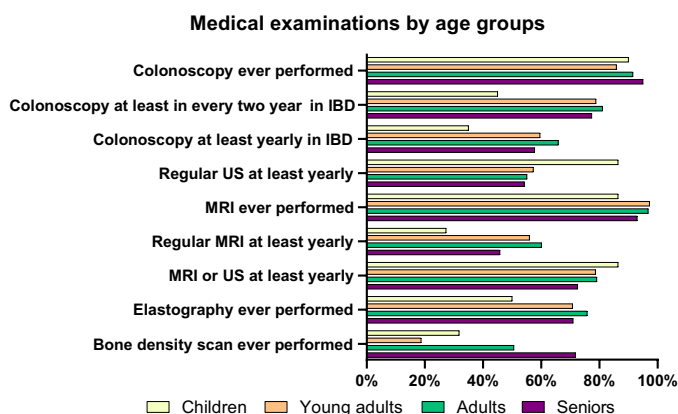


Figure: Examinations performed per age group

Conclusion: Our findings suggest that current practice needs to change if the new EASL clinical practice recommendations are to be universally followed. Identified areas of improvement are prognostication and disease monitoring with more widespread use of elastography, bone density scan, and appropriate treatment for itch.

WED-278

The changing clinical phenotype of autoimmune hepatitis across the millennium. A 40 year cohort study in Bologna, Italy

Marco Ferronato¹, Chiara De Molo², Marco Lenzi¹, Luigi Muratori¹.

¹IRCCS Azienda Ospedaliero Universitaria di Bologna, Center for the Study and Treatment of Autoimmune Diseases of the Liver and Biliary System, Bologna, Italy; ²IRCCS Azienda Ospedaliero Universitaria di Bologna, Interventional, Diagnostic and Therapeutic Ultrasound Unit, Department of Organ Insufficiency and Transplantation, Bologna, Italy
Email: marco.ferronato@studio.unibo.it

Background and aims: Autoimmune hepatitis (AIH) is a liver disease with heterogeneous clinical expression, diagnosed at any age and at any latitude. We aim to evaluate modifications of the clinical-epidemiological phenotype of AIH patients from 1980 to our days in Italy.

Method: Single-center observational retrospective study, among 507 AIH patients. Patients were divided into 4 subgroups according to the decade of diagnosis: 1981–1990, 1991–2000, 2001–2010 and 2011–2020. We collected clinical, laboratory and immunological features at diagnosis and assessed the response to treatment 6–12 months thereafter. We defined AIH presentation as "acute" when an increase in transaminases of at least 10-fold the UNL and/or a bilirubin greater than 5 mg/dl is observed, with or without jaundice. Clinical progression is defined as cirrhosis development in non-cirrhotic AIH patients and clinical decompensation and/or HCC development in compensated autoimmune cirrhosis.

Results: Mean age at diagnosis increased among each decade (31.44, 32.96, 39.99, 49.63 years, $p < 0.001$). Acute disease onset progressively increased (39.0% [N = 16/41], 47.3% [N = 44/93], 42.0% [N = 73/174], 52.4% [N = 88/168], $p = 0.014$) and the ratio of cirrhosis at diagnosis decreased (36.5% [N = 19/52], 16.1% [N = 15/93], 10.8% [N = 17/158], 8.7% [N = 14/161], $p < 0.001$). Complete response rates rose between 1981 and 2000 and 2001–2020 (39.3% [N = 46/117], 74.7% [N = 233/312], $p < 0.001$) and clinical progression during follow-up decreased (54.3% [N = 19/35], 29.9% [N = 26/87], 16.9% [N = 27/160], 10.6% [N = 15/142], $p < 0.001$). Anti-nuclear antibodies positivity at diagnosis increased (40.7% [N = 22/54], 52.0% [N = 53/102], 73.7% [N = 123/167], 79.3% [N = 134/169], $p < 0.001$), while positivity for anti-LKM and for anti-LC1 became less frequent (20.8%, 19.4%, 16.0%, 4.3% [$p < 0.001$] and 20.8%, 14.1%, 6.9%, 5.3% [$p = 0.005$] respectively). IgG level at diagnosis progressively decreased (17.40, 17.50, 13.80 and 13.00 g/l, $p < 0.001$).

Conclusion: In the new millennium in Italy at the time of diagnosis the typical AIH patient is older, more often presents with acute hepatitis, cirrhosis is less frequent and complete response to treatment is more commonly achieved. These epidemiological changes can be due to a better understanding of the spectrum of manifestations of AIH, especially the acute onset, together with a larger availability of standardized assays for autoantibody detection. In addition, they may also reflect the constant population ageing. In addition to the classical onset in young women with manifestations of advanced liver disease and high immunoglobulins, AIH can manifest in the context of acute hepatitis, among elderly patients or in more elusive contexts.

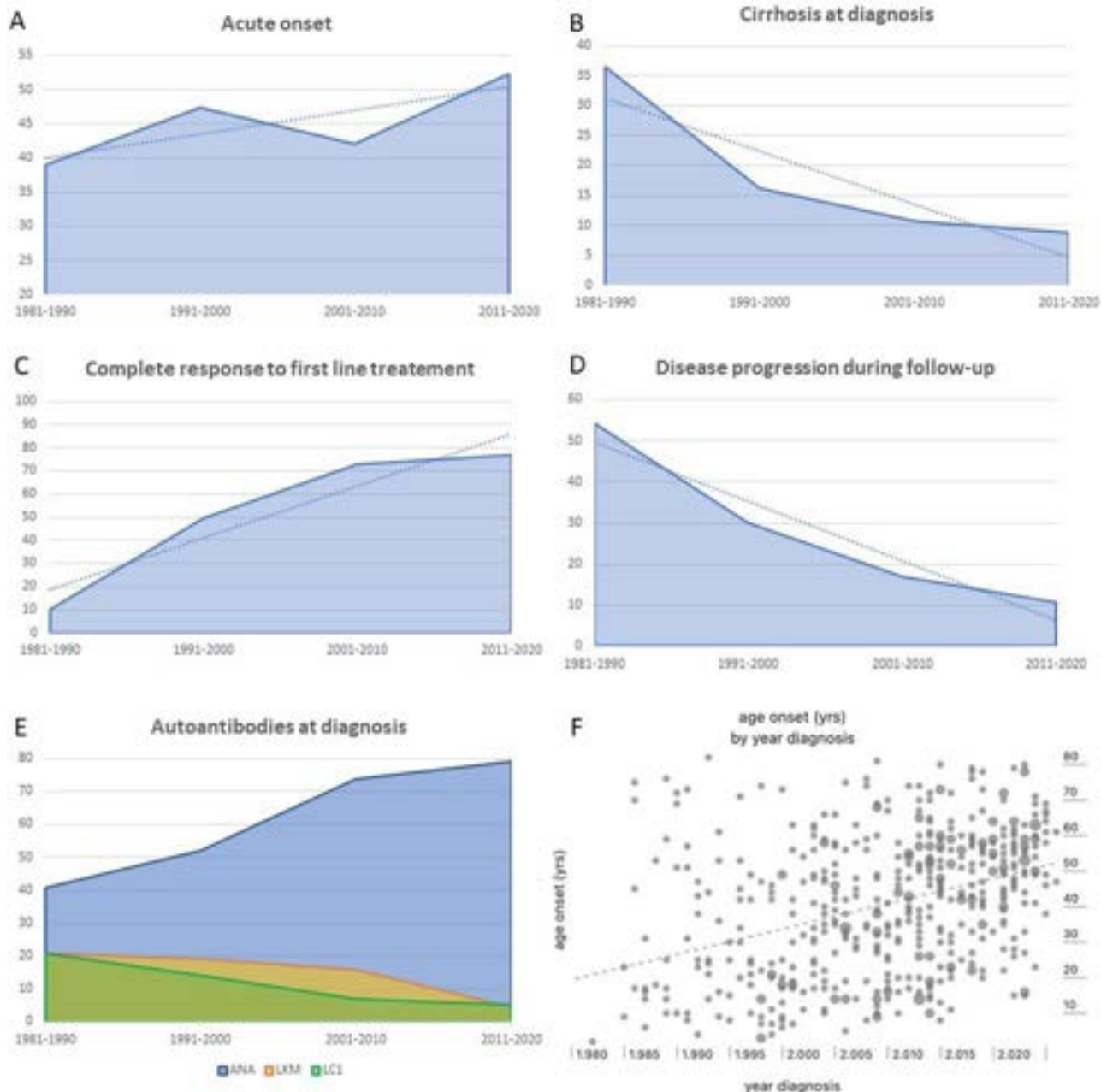


Figure: (abstract: WED-278): (A) Acute disease onset among each decade, showing an increasing trend ($p = 0.014$). (B) Cirrhosis at diagnosis among each decade, showing a clear decreasing trend ($p < 0.001$). (C) Patients with complete response rates after one year with first line treatment, showing a clear increasing trend ($p < 0.001$). (D) Patients with disease progression among each decade, showing a decreasing trend ($p < 0.001$). (E) Autoantibodies at diagnosis showing an increase of ANA positivity ($p < 0.001$) and a decrease of anti-LC1 and anti-LKM ($p < 0.001$ and $p = 0.005$ respectively). (F) Progressive increase of age at diagnosis among each decade ($R = 0.381$, $p < 0.001$).

WED-279 Clinical characteristics, hospitalization, and mortality outcomes of Coronavirus Disease 2019 in primary sclerosing cholangitis liver transplant patients

Stela Celaj¹, Vibhu Chittajallu², Scott Martin³, Jaime Perez³, Emad Mansoor². ¹Division of Gastroenterology, Hepatology and Nutrition, University of Pittsburgh Medical Center, Pittsburgh, Pennsylvania, United States; ²Division of Gastroenterology and Liver Disease, University Hospitals Cleveland Medical Center, Case Western Reserve University, Cleveland, Ohio, United States; ³Clinical Research

Center, University Hospitals Cleveland Medical Center, Cleveland, Ohio, United States
Email: celajs@upmc.edu

Background and aims: It remains unclear whether the outcomes of liver transplant (LT) patients with COVID-19 differ based on the etiology of liver disease. Primary sclerosing cholangitis (PSC) patients are particularly of interest given the autoimmune nature of disease, and the associated cholangiopathy, which has been independently described during COVID-19 infection. Therefore, we sought to study the outcomes of PSC LT patients with COVID-19.

Method: We used a large healthcare research network (TriNetX) to compile the electronic medical records of LT patients (age ≥ 18 years)

POSTER PRESENTATIONS

with PSC and confirmed COVID-19 (PSC cohort) from 75 healthcare organizations in the USA, between 1 January-31 December 2020. LT patients of other etiologies (non-PSC cohort) with COVID-19 were also identified during the same time. We studied the risk of hospitalization (composite outcome of inpatient or critical care services), mortality, thrombosis (composite outcome of deep vein thrombosis, acute pulmonary embolism, stroke or myocardial infarction) and intensive care unit (ICU) (requiring mechanical ventilation or extracorporeal membrane oxygenation) within 90 days of COVID-19 diagnosis. We performed 1 : 1 propensity score matching (PSM) using a greedy nearest-neighbor matching algorithm to account for potential confounding variables.

Results: We identified 78 PSC LT patients and 1370 non-PSC LT patients with COVID-19. PSC LT patients were younger than the non-PSC cohort (50.5 ± 14.7 vs 57.4 ± 13.7 , $p < 0.001$). Though most of the comorbidities (hypertension, chronic kidney disease, nicotine dependence, heart failure, alcohol related disorders, chronic lower respiratory diseases and ischemic heart disease) were equally distributed among the two groups, the percentage of diabetes and cerebrovascular diseases statistically differed between the cohorts. Therefore, PSM was performed for demographics, comorbidities (including body mass index) as well as immunosuppression regimen. Following PSM, the PSC and non-PSC cohorts were relatively balanced ($n = 74$ each cohort). PSC LT patients were more likely to experience symptomatic COVID-19 infection with hypoxemia, fever, nausea, emesis, diarrhea and abdominal pain when compared to non-PSC LT patients. Mean values of alkaline phosphatase were also higher in the PSC cohort compared to non-PSC (223 vs 140 U/L, $p = 0.03$), whereas the rest of liver enzymes were similar among the groups. However, when looking at COVID-19 outcomes, we found no significant difference in mortality, hospitalization, thrombosis or ICU care between PSC and non-PSC LT patients (as seen in the Figure).

Outcomes	Before Matching				After Matching			
	PSC (n=78)	non-PSC (n=1370)	OR (95% CI)	P value	PSC (n=74)	non-PSC (n=74)	OR (95% CI)	P value
Mortality	10 (12.8)	114 (8.3)	0.67 (0.30 to 1.45)	0.36	10 (13.5)	10 (13.5)	1.0 (0.39 to 2.64)	1
Thrombosis	10 (12.8)	102 (7.4)	0.64 (0.42 to 0.98)	0.038	10 (13.5)	10 (13.5)	1.0 (0.39 to 2.64)	1
Hospitalization	24 (30.8)	668 (48.8)	1.42 (1.07 to 1.89)	0.16	23 (31)	30 (40.5)	1.32 (0.76 to 2.31)	0.33
ICU Care	10 (12.8)	123 (8.9)	0.67 (0.37 to 1.24)	0.203	10 (13.5)	10 (13.5)	1.0 (0.39 to 2.64)	1

Figure:

Conclusion: To our knowledge, this is the largest study to date looking at PSC LT patients outcomes with COVID-19 in the USA. We found that though PSC LT patients were more likely to experience symptomatic COVID-19, reassuringly they did not carry a higher risk of mortality, hospitalization, thrombosis or ICU care requirement compared to LT patients of other liver disease etiologies.

WED-280

INTEGRIS-PSC phase 2a study: evaluating the safety, tolerability, and pharmacokinetics of bexotegast (PLN-74809) in participants with primary sclerosing cholangitis

Gideon Hirschfield¹, Palak Trivedi^{2,3}, Cynthia Levy^{4,5}, Christoph Schramm⁶, Kris Kowdley⁷, Michael Trauner⁸, Richard Pencek⁹, Hardean Achneck⁹, Eric Lefebvre⁹. ¹University of Toronto, Toronto Centre for Liver Disease, Toronto, ON, Canada; ²University of Birmingham, 1. National Institute for Health and Care Research Birmingham Biomedical Research Centre, Centre for Liver and Gastroenterology Research, United Kingdom; ³University Hospitals Birmingham Queen Elizabeth, Liver Unit, Birmingham, United Kingdom; ⁴University of Miami, Division of Digestive Health and Liver Diseases, Miami, FL, United States; ⁵University of Miami, Schiff Center for Liver Diseases, Miami, FL, United States; ⁶University Medical Center Hamburg-Eppendorf, Department of Medicine, Martin Zeitz Center for Rare Diseases, Hamburg Center for Translational Immunology,

Hamburg, Germany; ⁷Liver Institute Northwest, Seattle, WA, United States; ⁸Medical University of Vienna, Wien, Austria; ⁹Pliant Therapeutics, South San Francisco, United States
Email: rpencek@pliantrx.com

Background and aims: Transforming growth factor beta (TGF-beta) signaling is a key driver of liver fibrosis. In primary sclerosing cholangitis (PSC), integrins over-expressed on injured cholangiocytes (alpha-v/beta-6) and myofibroblasts (alpha-v/beta-1) regulate TGF-beta activity. Bexotegast (PLN-74809) is an oral, once-daily, dual-selective inhibitor of integrins alpha-v/beta-6 and alpha-v/beta-1 in development for the treatment of PSC and idiopathic pulmonary fibrosis (IPF). The primary objective of the present study is to assess the safety and tolerability of bexotegast in participants with PSC. Additional end points include pharmacokinetics and exploratory biomarkers of fibrosis.

Method: INTEGRIS-PSC is an ongoing, randomized, placebo-controlled 12-week Phase 2a study evaluating the safety and tolerability of multiple doses of bexotegast in participants with PSC (EudraCT: 2020-001428-33, NCT04480840). The study uses an ascending dose model (Figure): dosing cohorts (~28 participants/cohort) are enrolled and evaluated in a sequential manner with an independent data safety monitoring board review before proceeding to higher dosing cohorts. Entry criteria include established diagnosis of large duct PSC with evidence of hepatic fibrosis based on biopsy, ELF ≥ 7.7 , transient elastography >8 kPa or magnetic resonance elastography >2.4 kPa and stable disease in participants with IBD. Randomization to bexotegast or placebo (3 : 1) is stratified by UDCA use. At the time of abstract submission, enrollment of the 40 mg cohort was completed and was ongoing for the 80 and 160 mg cohorts. An additional cohort of 320 mg is planned.

Results: INTEGRIS-PSC is ongoing and blinded. As of the last safety review, 64 participants were randomized. Participants were mean 45 years old with a duration of PSC of 9 years, 78% male, and 61% with IBD. Mean (SD) baseline liver chemistries were: ALP: 273 (146) U/L, ALT: 84 (61) U/L, bilirubin: 0.8 (0.4) mg/dL. 13% (each) had history of fatigue and pruritus. 49 participants completed the study, 13 were ongoing and 2 discontinued due to adverse events (COVID, Insomnia). Most reported adverse events on blinded study drug were Grade 1 or 2 severity (93%). The most common were: pruritus (14%), fatigue (13%), headache (11%), abdominal pain (6%), cholangitis (6%), COVID (6%), nausea (6%) and upper abdominal pain (6%). 2 participants experienced serious adverse events: one had a grade 3 event of ascending cholangitis, and another had grade 3 events of concurrent abdominal pain with cholecystitis; all serious events resolved, were not considered related to study medication and both participants continued in the study.



Figure:

Conclusion: The INTEGRIS-PSC phase 2a study evaluating the safety, tolerability, and pharmacokinetics of bexotegast in participants with primary sclerosing cholangitis continues without modification by the Data Safety Monitoring board. Results from this study are expected in 3Q2023.

WED-281

Peri-procedural complications in people with primary sclerosing cholangitis undergoing endoscopic retrograde cholangiopancreatography-evaluating a high-volume programme

Kristel Leung^{1,2,3}, Yasi Xiao³, Jeff Mosko^{3,4}, Aliya Gulamhusein^{1,3}, Bettina Hansen^{2,5}, Gary May^{3,4}, Gideon Hirschfield^{1,3}. ¹University Health Network, Toronto, Canada; ²Institute of Health Policy, Management and Evaluation, Toronto, Canada; ³University of Toronto, Gastroenterology and Hepatology, Medicine, Toronto, Canada; ⁴St. Michael's Hospital, Gastroenterology, Medicine, Toronto, Canada; ⁵Erasmus MC, Epidemiology, Biostatistics, Rotterdam, Netherlands
Email: k.leung333@gmail.com

Background and aims: Endoscopic retrograde cholangiopancreatography (ERCP) is an important component of the care for people living with primary sclerosing cholangitis (PSC). Frequently it is performed to address complex biliary concerns, including obstruction, source control for infection, or evaluation for biliary malignancy. We sought to characterize the peri-procedural course for people living with PSC undergoing ERCP in a high-volume therapeutic endoscopy centre at a single-centre hospital receiving quaternary care referrals from the province of Ontario, Canada.

Method: Using hospital procedural codes to find ERCPs from April 2011 to July 2021, patients who underwent ERCP with PSC were identified. Procedure-related complications (up to 90 days post-procedure) and clinical characteristics information was retrospectively collected. Mixed model logistic regression was performed to evaluate factors associated with post-ERCP complications.

Results: In 78 patients who underwent 271 ERCPs, two-thirds were male and median age at ERCP was 45 years (IQR 31–59 years). In 39% (89) of ERCPs, patients had been diagnosed with liver cirrhosis. Jaundice (152, 59%), abdominal pain (133, 52%), and subjective fevers (88, 34%) were the most common patient-reported indications. Procedural indication was biliary obstruction in 86%, cholangitis in 38%, and malignancy concerns in 20%. Biliary cannulation was successful in 251 ERCPs (97%). Pancreatic duct cannulation occurred in 6.6% (17), while preferential contrast injection into the cystic duct occurred in 32 ERCPs (12%). Balloon dilatation was completed in 61% of cases, while stent insertion, removal, and biliary brushings was performed in 31%, 25%, and 39% respectively. Technical success with satisfactory biliary drainage and flow post-ERCP was reported in 92%. Post-ERCP, biliary blockage, post-ERCP cholangitis, and post-ERCP pancreatitis was reported in 66 (29%), 45 (20%), 11 (4.9%) cases respectively. No perforations occurred. In 1% of cases, post-ERCP bleed, cholecystitis, or respiratory complications occurred. There were 5 deaths in the post-ERCP follow-up period. Post-ERCP hospitalization occurred in 86 cases (37%), with 28 (14%) for an ERCP-related complication, and 8 (9.3%) for liver failure. Repeat ERCP at the same centre within 90 days occurred in 88 (32%) of cases. Male sex (OR 2.79, 95%CI 1.38–6.07), cirrhosis (OR 1.92, 95% CI 1.06–3.50) and stent insertion were associated with post-ERCP complications on univariable analysis (OR 2.37, 95% CI 1.34–4.22); only stent insertion (OR 2.82, 95% CI 1.31–6.05) was significantly associated on multivariate analysis.

Conclusion: For people living with PSC, ERCP remains an important component of their complex care; procedural morbidity and mortality occur but at relatively infrequent rates.

WED-282

Analysis of safety in maralixibat-treated participants with progressive familial intrahepatic cholestasis: data from MARCH-PFIC

Alexander Miethke¹, Adib Moukarzel², Gilda Porta³, Joshue Covarrubias Esquer⁴, Piotr Czubkowski⁵, Felipe Ordoñez⁶, Manila Candusso⁷, Amal A. Aql⁸, Robert H. Squires⁹, Etienne Sokal¹⁰, Daniel D'Agostino¹¹, Ulrich Baumann¹², Lorenzo D'Antiga¹³, Nagraj Kasi¹⁴, Nolwenn Laborde¹⁵, Cigdem Arkan¹⁶, Chuan-Hao Lin¹⁷, Susan Gilmour¹⁸, Naveen Mittal¹⁹, Fang Kuan Chiou²⁰, Simon P. Horslen⁹, Wolf-Dietrich Huber²¹, Susan David-Feliciano²², Elaine Chien²², Douglas Mogul²², Will Garner²², Tiago Nunes²², Anamaria Lascau²², Pamela Vig²², Vera Hupertz²³, Regino Gonzalez-Peralta²⁴, Udem Ekong²⁵, Jane Hartley²⁶, Noemie Laverdure²⁷, Nadia Ovchinsky²⁸, Richard Thompson²⁹.
¹Cincinnati Children's Hospital Medical Center, Cincinnati, Ohio, United States; ²Hotel Dieu De France Saint Joseph University Hospital, Beirut, Lebanon; ³Hospital Sirio Libanes, Sao Paulo, Brazil; ⁴Nois De Mexico SA De CV, Jalisco, Mexico; ⁵The Children's Memorial Health Institute, Gastroenterology, Hepatology, Nutritional Disorders and Pediatrics, Warsaw, Poland; ⁶Cardioinfantil Foundation-Lacardio, Bogota, Colombia; ⁷Ospedale Pediatrico Bambino Gesù Irccs, Lazio, Italy; ⁸University of Texas Southwestern Medical Center, Dallas, Texas, United States; ⁹UPMC Children's Hospital of Pittsburgh, Pediatrics, Pittsburgh, Pennsylvania, United States; ¹⁰Uclouvian, Cliniques Universitaires St Luc, Pediatric Hepatology, Brussels, Belgium; ¹¹Hospital Italiano De Buenos Aires, Buenos Aires, Argentina; ¹²Hannover Medical School, Pediatric Gastroenterology and Hepatology, Hannover, Germany; ¹³Hospital Papa Giovanni XXIII, Paediatric Hepatology, Gastroenterology and Transplantation, Bergamo, Italy; ¹⁴Medical University of South Carolina, Charleston, South Carolina, United States; ¹⁵Hôpital Des Enfants-CHU Toulouse, Toulouse, France; ¹⁶Koc University School of Medicine, Istanbul, Turkey; ¹⁷Children's Hospital Los Angeles, Los Angeles, California, United States; ¹⁸University of Alberta, Pediatrics, Alberta, Canada; ¹⁹University of Texas Health Science Center at San Antonio, San Antonio, Texas, United States; ²⁰Kk Women's and Children's Hospital, Singapore; ²¹Medical University of Vienna, Vienna, Austria; ²²Mirum Pharmaceuticals, Inc., Foster City, California, United States; ²³Cleveland Clinic Children's, Cleveland, Ohio, United States; ²⁴AdventHealth for Children and AdventHealth Transplant Institute, Pediatric Gastroenterology, Hepatology, and Liver Transplant, Orlando, Florida, United States; ²⁵Medstar Georgetown University Hospital, Medstar Georgetown Transplant Institute, Washington DC, United States; ²⁶Birmingham Women and Children's Hospital, Birmingham, United Kingdom; ²⁷Hopital Femme Mere Enfant, Hospices Civils De Lyon, Pediatric Hepato Gastroenterology and Nutrition Unit, Lyon, France; ²⁸Children's Hospital at Montefiore, Bronx, New York, United States; ²⁹King's College London, Institute of Liver Studies, London, United States
Email: alexander.miethke@cchmc.org

Background and aims: Maralixibat (MRX) is a novel, minimally absorbed, orally administered inhibitor of the ileal bile acid transporter (IBAT) that interrupts the enterohepatic circulation of bile acids to improve cholestatic pruritus. MARCH-PFIC, a 26-week randomized Phase 3 study, is the largest and most genetically inclusive clinical trial of Progressive Familial Intrahepatic Cholestasis (PFIC) to date, and achieved primary and key end points of reduction in cholestatic pruritus, serum bile acids (sBA), improved bilirubin, and growth. Here, we provide a detailed analysis of safety data observed in the study.

Method: Treatment-emergent adverse events (AEs) and laboratory data from MARCH-PFIC were analysed.

Results: 93 PFIC patients were randomized to MRX 570 µg/kg twice daily (n = 47) or placebo (PBO; n = 46). Median (min, max) treatment exposure was 183 (10, 203) days. AEs included diarrhea (57.4% vs 19.6%), and abdominal pain (25.5% vs 13%) for MRX vs PBO, respectively. Diarrhea was mostly grade 1, transient, with a median duration of 5.5 days; there were no severe or serious events. One

POSTER PRESENTATIONS

patient with mild diarrhea discontinued therapy. Abdominal pain was also mostly mild and transient and, in nearly all instances, was concurrent with diarrhea. There were no clinically meaningful changes observed in either groups from baseline in transaminase levels. Transaminase AEs were observed in 17% and 6.5% of MRX and PBO patients, respectively. Among the 8 MRX patients with transaminase elevations, 6 had resolution of the elevation without drug interruption; 2 patients had ongoing stable elevation even after drug interruption ($n = 1$) or dose reduction ($n = 1$) and both ultimately resumed prior maximum dose. No patients discontinued MRX due to transaminase elevation. Bilirubin increase was less common in MRX vs PBO (14.9% vs 19.6%). FSV deficiency, which was reported as an adverse event, was also less common in MRX vs PBO (27.7% vs 34.8%). Fractures were seen in 6.4% of MRX and in 0% of PBO; none were considered related as all had clear alternative causes for fracture, including pre-existing vitamin D deficiency which were stable or improved on MRX. Serious AEs were reported in 10.6% of MRX and 6.5% of PBO patients; none were deemed related (except 1 event of mild bilirubin increased in MRX); all resolved without any dose modifications.

Conclusion: The MARCH-PFIC study is the largest PFIC study conducted across PFIC types. MRX was well-tolerated, with GI effects being the most frequent event but generally mild and self-limiting. FSV deficiency and bilirubin increase were more frequently seen in the PBO group.

WED-283

Investigating the cholestatic pruritus of primary sclerosing cholangitis (ItCh-PSC): a study of patients participating in the consortium for autoimmune liver disease (CALiD)

Richard Dean¹, Maryam Yazdanfar¹, Joseph Zepeda¹, Cynthia Levy², Stuart C. Gordon³, Lisa Forman⁴, Craig Lammert⁵, David N. Assis⁶, Daniel Pratt⁷, Usha Gungabissoon⁸, Ashleigh McGirr⁹, Sumanta Mukherjee¹⁰, Megan McLaughlin¹⁰, Christopher Bowlus¹.
¹University of California Davis, Sacramento, United States; ²Schiff Center of Liver Disease and Division of Gastroenterology and Hepatology, University of Miami, Miami, United States; ³Henry Ford University, Detroit, United States; ⁴University of Colorado, Denver, United States; ⁵Indiana University, Indianapolis, United States; ⁶Yale University, New Haven, United States; ⁷Massachusetts General Hospital, Boston, United States; ⁸GSK, London, United States; ⁹GSK, Mississauga, Canada; ¹⁰GSK, Collegeville, United States
 Email: clbowlus@ucdavis.edu

Background and aims: Primary sclerosing cholangitis (PSC) is a chronic cholestatic liver disease that causes significant impairments to quality of life. Compared with other cholestatic liver diseases, pruritus has not been well studied in patients with PSC. The aim of this study was to determine the prevalence, severity and treatment patterns for pruritus among patients with PSC.

Method: Patients with PSC were identified from a multicentre, retrospective cohort study of the Consortium for Autoimmune Liver Disease (CALiD). Electronic medical records were searched for keyword terms "itch" and "pruritus" to identify "pruritus" encounters. The severity of pruritus was graded for each pruritus encounter as absent, mild, moderate or severe based on descriptors in the medical record. Medications and endoscopic retrograde cholangiopancreatography (ERCP) planned to treat pruritus was recorded.

Patients with more than one pruritus encounter were categorised according to the encounter with the maximum severity of pruritus.

Results: A total of 724 patients were included in the study. Pruritus terms were recorded in 1178 encounters from the medical records of 372 (51.4%) patients. Patients with a pruritus encounter ($N = 372$, 51.4%) compared with those without ($N = 352$, 48.6%) had a lower frequency of small duct PSC (4% vs 8%, $p = 0.02$) but were comparable in terms of inflammatory bowel disease (IBD), cirrhosis, hepatic decompensation, and baseline laboratories, except for international normalised ratio (INR) 1.2 ± 0.4 vs 1.2 ± 0.4 , $p = 0.02$). Among those with a pruritus encounter, the maximum pruritus severity was graded as mild in 142 (38.2%), moderate in 140 (37.6%), severe in 77 (20.7%), and pruritus was recorded as absent in 13 (3.5%) patients. IBD diagnosis, PSC type, cirrhosis and hepatic decompensation did not differ by the maximum severity of pruritus (Table). However, baseline alkaline phosphatase (ALP), aspartate transaminase (AST) and total bilirubin were greater in those with more severe itch. Anti-pruritic medication usage among patients with any degree of itch included bile acid-binding resins (36.5%), hydroxyzine (22.6%), rifampin (11.4%) and sertraline (9.7%). Two or more medications were used by 46.7% of patients with severe itch. ERCP was planned in 13 (2.5%), 34 (8.4%), 27 (17.3%) encounters with mild, moderate and severe pruritus, respectively.

Table. Baseline clinical and laboratory values by maximum itch severity¹

	Absent ² N=13	Mild N=142	Moderate N=140	Severe N=77	p-value
IBD Diagnosis					0.69
Total IBD UC/CD/IC	7 (54%) 7/0/0	76 (54%) 60/15/1	76 (54%) 56/19/2	42 (55%) 34/6/2	—
None	6 (46%)	41 (29%)	37 (26%)	26 (34%)	—
Unknown	0%	25 (18%)	27 (19%)	15 (19%)	—
PSC Type					0.51
Large duct	11 (85%)	91 (64%)	87 (62%)	51 (66%)	—
PSC/ACH	0%	6 (4%)	14 (10%)	5 (6%)	—
Small duct	1 (8%)	6 (4%)	5 (4%)	2 (3%)	—
Unknown	1 (8%)	39 (27%)	34 (24%)	19 (25%)	—
Cirrhosis	2 (15%)	33 (23%)	36 (26%)	16 (21%)	0.54
ALP	186 (119–392)	171 (94–299)	236 (139–481)	246 (156–435)	0.02
AST	52 (34–65)	40 (27–66)	57 (35–108)	53 (32–88)	0.003
ALT	58 (36–84)	45 (28–76)	60 (32–136)	63 (38–87)	0.06
Total bilirubin, mg/dL	0.9 (0.5–1.4)	0.8 (0.6–1.4)	1.1 (0.7–2.4)	1.0 (0.6–2.2)	0.03
INR	1.1 (1.0–1.2)	1.0 (1.0–1.2)	1.0 (1.0–1.2)	1.0 (1.0–1.1)	0.87
Haemoglobin	13.3 (12.3–13.8)	13.6 (12.2–14.5)	13.2 (11.3–14.2)	13.1 (11.6–14.6)	0.49
Platelets	296 (266–366)	229 (149–300)	212 (147–281)	219 (148–302)	0.12

¹Only patients with an itch encounter included. ²Itch recorded as being absent. Continuous variables represented by median (IQR). Comparisons by Chi-square and Kruskal-Wallis.

AILD, autoimmune hepatitis; ALP, alkaline phosphatase; ALT, alanine transaminase; AST, aspartate transaminase; CD, Crohn's disease; IBD, inflammatory bowel disease; IC, indeterminate colitis; INR, international normalised ratio; IQR, interquartile range; PSC, primary sclerosing cholangitis; UC, ulcerative colitis.

Conclusion: Pruritus in patients with PSC is not well documented but is frequent and often severe. Patients who experience severe pruritus have more severe liver disease and frequently require multiple anti-pruritic medications and ERCP. These results establish the clinical significance of pruritus in PSC and support the need for prospective studies to accurately ascertain itch prevalence and the unmet need for therapies to treat pruritus among patients with PSC.

WED-284

Spleen stiffness measurement predicts decompensation risk in primary biliary cholangitis

Giulia Francesca Manfredi^{1,2}, Carla De Benedittis², Francesca Baorda^{1,2}, Davide Di Benedetto^{1,2}, Michela Burlone², Rosalba Minisini¹, Mario Pirisi^{1,2}, Cristina Rigamonti^{1,2}. ¹Università degli Studi del Piemonte Orientale, Department of Translational Medicine, Novara, Italy; ²AOU Maggiore della Carità, Division of Internal Medicine, Novara, Italy
Email: cristina.rigamonti@uniupo.it

Background and aims: Primary biliary cholangitis (PBC) is a slowly progressive cholestatic disease, which may lead to portal hypertension (PH) and its complications even in a pre-cirrhotic stage. Spleen stiffness measurement (SSM) by vibration-controlled transient elastography (VCTE) is predictive of PH. We aimed to investigate in PBC patients the prognostic value of SSM in stratifying the risk of decompensation and SSM ability to identify those at low probability of high-risk varices.

Method: Monocentric study of 88 PBC patients, who underwent VCTE for liver stiffness measurement (LSM) and SSM with a spleen dedicated module. Demographic and clinical features at baseline and at the time of VCTE examination were recorded. Screening for varices with esophagogastroduodenoscopy (EGDS) was performed according to Baveno VI guidelines and proposed to all patients with SSM >40 kPa, independently of LSM.

Results: Among the 88 patients (95% women, median age 62 years, median disease duration 40 months, 14% cirrhotic, 94% on monotherapy with ursodeoxycholic acid, 6% on combination therapy with obeticholic acid); median LSM was 6.3 kPa (IQR 4.7–8.9), being ≥ 10 kPa in 15/88 (17%). Median SSM was 22.4 kPa (IQR 19–29.5), resulting >40 kPa in 15/88 (17%). None of the subjects with SSM ≤ 40 kPa who underwent EGDS had esophageal varices, regardless of LSM value and platelet count. Varices were found in 11/13 (85%) patients with SSM >40 kPa who underwent EGDS (2 patients refused endoscopy); high-risk varices were found in 2/11 patients. LSM was <10 kPa in 2/11 (18%) patients with varices and SSM >40 kPa. During a median follow-up of 10 months (IQR 9–26) after VCTE examination, 4 (4%) patients developed liver decompensation. Stratifying the 88 patients based on the LSM value (LSM <10 kPa vs. LSM ≥ 10 kPa), the probability of liver decompensation was significantly higher among patients with LSM ≥ 10 kPa (21% vs. 0% at 12 months, 41% vs 0% at 24 months, $p < 0.0001$). Similarly, stratification upon SSM value (SSM ≤ 40 kPa vs. SSM >40 kPa), showed a probability of decompensation of 21% at 12 months for patients with SSM >40 kPa vs. 0% for those with SSM ≤ 40 kPa ($p < 0.0001$) and a probability of decompensation of 48% vs 0% at 24 months ($p < 0.0001$). LSM ≥ 10 kPa and SSM >40 kPa demonstrated 100% sensitivity in predicting the risk of liver decompensation.

Conclusion: Both LSM and SSM predict risk of decompensation in PBC patients. SSM >40 kPa is predictive of presence of varices and might be used in combination with LSM and platelet count to improve prediction of complications related to portal hypertension.

WED-285

Rechallenge with anti-PD1 monotherapy after checkpoint inhibitor hepatitis is associated with low rates of recurrence: a single centre study

Nicola Jones¹, Dominique Parslow², Stewart Macdonald³, Lucy Walker³. ¹University Hospitals Plymouth, Oncology, Plymouth, United Kingdom; ²University Hospitals Plymouth, Oncology, United Kingdom; ³South West Liver Unit, Plymouth, United Kingdom
Email: lucy.walker34@nhs.net

Background and aims: Immune checkpoint inhibitors are now widely used in numerous Oncology indications and the management of checkpoint inhibitor-induced liver injury (ChILI) is becoming routine in the practice of Oncologists and Hepatologists alike. Management of these patients is guided by the Oncology society

guidelines at national and regional levels and include guidance regarding rechallenge of patients with ChILI. There is growing consensus that the use on anti-PD1 monotherapy is a safe approach, however, overall there is very little data within the public domain to support these guidelines and decisions.

Method: We performed a retrospective analysis of all patients who had developed ChILI between November 2016 and December 2022, including grade of index hepatitis by indication and regimen, rechallenge practice and outcome of rechallenge.

Results: 21 cases of ChILI were identified to have been treated in our center since November 2016. Of these 19% were treated for primary lung cancer and 81% melanoma. The majority of index hepatitis was grade 3 (71% overall; lung ca 50%; melanoma 70.6%), grade 4 14%, grade 2 10% and grade 1 5%. Ipilimumab/Nivolumab combination therapy caused the majority of ChILI events (66.7%) and 100% of the grade 4 events. Rechallenge was initiated in 38% of patients and 100% of these received anti-PD-1 monotherapy. Of these 50% had successful rechallenge and remain alive and on treatment, 25% had treatment withdrawn due to disease progression and 25% had recurrent ChILI. Of those with a successful rechallenge, 25% had a grade 2 index hepatitis and 50% had a grade 3 index hepatitis, compared to those with recurrent ChILI, where 100% had grade 3 index hepatitis.

Conclusion: Based on our data, rechallenge with single agent anti-PD1 inhibitors should be considered in patients up to grade 3 of index hepatitis. However the higher the grade of the index hepatitis, the greater the likelihood of developing recurrent ChILI.

WED-286

Transient elastography measurements of spleen stiffness are associated with treatment response to ursodeoxycholic acid in primary biliary cholangitis

Ilkay Ergenc¹, Hasan Yapici², Caglayan Keklikkiran³, Yusuf Yilmaz^{1,3,4}. ¹Marmara University School of Medicine, Gastroenterology and Hepatology, Istanbul, Turkey; ²Marmara University School of Medicine, Turkey; ³Rize Recep Tayyip Erdoğan University Faculty of Medicine, Gastroenterology and Hepatology, Turkey; ⁴Marmara University Institute of Gastroenterology, Turkey
Email: ergencilkay@gmail.com

Background and aims: The biochemical response criteria fail to predict disease progression in up to 20% of patients with Primary Biliary Cholangitis (PBC).¹ Recent evidence has suggested a prognostic role of portal pressure in PBC.² Alterations in the biomechanical properties of the spleen can be quantified by transient elastography (TE) and represent a reliable surrogate marker of portal pressure. This cross-sectional study investigated the association between Spleen Stiffness Measurements (SSMs) by TE and biochemical response to UDCA.

Method: Patients with PBC who had undergone at least two outpatient visits over the last 12 months were deemed eligible. Diagnosis and clinical management were per the European Association for the Study of Liver PBC guidelines. Biochemical response to UDCA was determined according to the Paris II criteria. A single experienced gastroenterologist performed all SSMs by TE (FibroScan® Expert 630; Echosens). The diagnosis of cirrhosis was established histologically or based on clinical and laboratory findings combined with characteristic radiological features.

Results: A total of 107 patients with PBC (101 women and 6 men; mean age at diagnosis: 45.9 \pm 11 years) were included in the study. The median duration of follow-up after UDCA treatment was 4.6 years (range, 1–7.75 years). All patients had at least one positive diagnostic serological marker of PBC, and 60 (56.1%) had undergone liver biopsy at the time of diagnosis. On histopathological examination, 19 patients (33.3%) had no fibrosis, 25 (43.9%) F1 fibrosis, 8 (14.0%) F2 fibrosis, 2 (3.5%) F3 fibrosis, and 3 (5.3%) F4 fibrosis according to Metavir scoring system. Fifteen patients met the diagnostic criteria for cirrhosis. We identified 28 (26.2%) patients who were

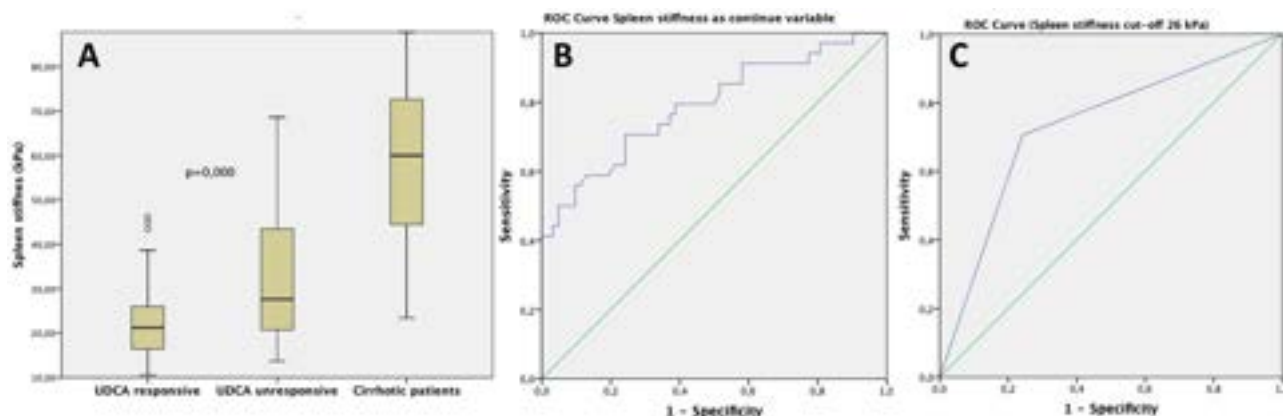


Figure: (abstract: WED-286): SSMs according to the presence of cirrhosis and response to UDCA treatment (panel a) and ROC curve analysis of SSMs in predicting response to UDCA (continuous variable, panel b; dichotomized according to the optimal cut-off, panel c).

unresponsive to UDCA treatment according to the Paris II criteria. Mean SSMs in patients with cirrhosis, unresponsive to UDCA without cirrhosis, and responsive to UDCA without cirrhosis were 60.6 ± 21.8 kPa, 32.8 ± 15.3 kPa, and 22.6 ± 8.5 kPa, respectively. After the exclusion of cirrhotic patients, SSMs were significantly higher in patients who did not respond to UDCA (32.9 ± 15 kPa) than in those who did (22.6 ± 9 kPa; $p < 0.001$). In receiver operating characteristic (ROC) curve analysis, the optimal cut-off value for SSMs in identifying patients who did not respond to UDCA was 26 kPa (sensitivity, 70.6%; specificity, 75.8%; area under the curve, 0.732).

Conclusion: Cross-sectional SSMs by TE are significantly higher in patients with PBC who did not respond to UDCA treatment than in those who did. Longitudinal studies are required to establish the prognostic role of elevated SSMs in PBC.

WED-287

Associations between patient-reported outcomes, liver inflammation and fibrosis in patients with primary sclerosing cholangitis

Emilie Eifer Møller¹, Henning Grønbaek¹, Søren Peter Jørgensen¹, Rasmus Hvidbjerg Gantzel¹, Anders Mellemkjaer¹, Lars Bossen¹.
¹Aarhus University hospital, Hepatology and Gastroenterology, Aarhus, Denmark
 Email: emimol@rm.dk

Background and aims: Primary sclerosing cholangitis (PSC) is a chronic liver disease characterized by hepatic inflammation and biliary fibrosis leading to cholangitis and cirrhosis. Patients with PSC have impaired quality of life (QoL); however, the relationship between QoL, liver fibrosis stage, and liver inflammation remains unclear. We aimed to investigate the associations between QoL, liver fibrosis, and inflammation.

Method: We prospectively included patients with PSC followed at the Department of Hepatology and Gastroenterology, Aarhus University Hospital, Denmark. The QoL was quantified using the general EQ-5D-5L questionnaire and the newly developed PSC-specific PSC PRO instrument. Liver fibrosis was estimated using FibroScan and liver inflammation by the macrophage-specific biomarker sCD163.

Results: Seventy-one patients were included with a median age of 44 years (IQR: 31–56). Forty-five (63.4%) were male and 60 (84.5%) had concomitant inflammatory bowel disease. The overall QoL expressed with the EQ-5D-5L utility score was similarly high in patients with PSC and the general population ((mean \pm SD) 0.86 ± 0.13 vs. $0.90 \pm$

0.16). The PSC PRO total score was similar across fibrosis stages ($p = 0.164$). However, patients with F4-fibrosis tended to report lower QoL on the EQ-5D-5L visual analog scale (VAS) than patients with F0-F3-fibrosis ($p = 0.08$). Notably, patients with previous hospitalization due to episodes of cholangitis reported significantly higher median PSC PRO total score (20.8 (11.8–64.5) vs. 13.9 (8.9–26.3), $p = 0.047$) and lower median EQ-5D-5L ((71 (IQR: 56–81.5) vs. 85 (75–91), $p = 0.017$)) than patients with no previous episodes of cholangitis. Finally, we observed a significant correlation between sCD163 and PSC PRO total score ($R = 0.36$, $p = 0.003$), and a weak trend towards a negative correlation between sCD163 and EQ-5D-5L VAS score ($R = -0.20$, $p = 0.099$).

Conclusion: In this cohort, patients with PSC generally reported a high QoL. There was no association between QoL and the stage of liver fibrosis. However, patients with previous episodes of cholangitis reported a lower QoL. Further, liver inflammation determined by sCD163 levels was associated with low QoL. This may suggest that inflammation is more important than fibrosis, when looking at the effect on QoL in PSC patients.

WED-288

Non-invasive evaluation of progression to primary biliary cholangitis in patients with positive antimitochondrial antibodies

Alvaro Diaz Gonzalez^{1,2}, Marta Alonso-Peña², Maria Monte^{3,4}, Christie Perelló⁵, Paula Iruzubieta^{1,2}, Marina Cobreros^{1,2}, Juan Irure⁶, Marcos López-Hoyos⁶, José Luis Calleja Panero⁵, Jose Marin^{3,4}, Javier Crespo^{1,2}.
¹Marqués de Valdecilla University Hospital, Gastroenterology and Hepatology Department, Clinical and Translational Research in Digestive Diseases Group, Santander, Spain; ²Research Institute Marques de Valdecilla (IDIVAL), Clinical and Translational Research in Digestive Pathology Group, Santander, Spain; ³University of Salamanca, Experimental Hepatology and Drug Targeting (HEVEPHARM), SALAMANCA, Spain, Salamanca, Spain; ⁴Carlos III National Institute of Health, Center for the Study of Liver and Gastrointestinal Diseases (CIBERehd), Madrid, Spain; ⁵Department of Gastroenterology and Hepatology, Hospital Universitario Puerta de Hierro Majadahonda, Majadahonda, Spain; ⁶Marques de Valdecilla University Hospital, Immunology Department, Santander, Spain
 Email: diazg.alvaro@gmail.com

Background and aims: Only a small percentage of people with positive antimitochondrial antibodies (AMA+) develop primary

biliary cholangitis (PBC). However, there is no tool to predict who will do so and what their management should be. Here, we aim to evaluate the usefulness of serum bile acid (BA) profile as a non-invasive follow-up and predictive tool in AMA+ patients.

Method: Bicerter ambispective study in AMA+ individuals identified in the ETHON cohort (Spanish population-based cross-sectional study) between 2015 and 2017 in Cantabria and Madrid (Spain). Twenty BA species and 7 α -hydroxy-4-cholesten-3-one (C4) were analyzed in serum samples by mass spectrometry (HPLC-MS/MS), both at inclusion and follow-up. Patients with a diagnosis of PBC at inclusion were excluded

Results: Fifty-four AMA+ individuals were identified, of whom 38 (73%) were women with a median age of 49.5 years. None had alterations in liver biology. Baseline liver stiffness was normal (4.5 kPa). Of the initial cohort, 47 (87%) continued follow-up and 6 (12.7%) developed PBC over a median of 5.3 years. The BA profile of non-progressors (NOPROG) vs those who progressed to PBC (PROG) during follow-up was assessed at both baseline and progression. At baseline, PROG individuals had a higher concentration of non-12 α -hydroxylated BAs (non-12aOH) (PROG 2.49 vs NOPROG 1.45 μ M; $p=0.04$) and glycoconjugated BAs (PROG 1.75 vs NOPROG 1.03 μ M; $p=0.06$ at the limit of significance), as well as lower percentage distribution of cholic acid (CA) family with respect to NOPROG (9.9 vs 17.1% $p=0.02$). At follow-up, PROG patients presented higher values in 12aOH (PROG 1.75 vs NOPROG 0.69 μ M; $p=0.01$), non-12aOH (PROG 2.00 vs NOPROG 0.84 μ M; $p=0.04$), glycoconjugated (PROG 1.86 vs NOPROG 0.69; $p=0.05$) and free (PROG 1.05 vs NOPROG 0.49 μ M; $p=0.07$ at the limit of significance) BAs concentrations. In paired analysis, PROG patients had increased concentration and percentage of CA family ($p=0.02$ and $p=0.04$, respectively) and deoxycholic acid family ($p=0.07$ at the limit of significance), an increase that was also reflected in the concentration of 12aOH BAs. Moreover, the concentration of non-12aOH BAs in PROG patients remained elevated and stable ($p=0.91$). On the other hand, in NOPROG subjects, the profile of all BAs remained stable during follow-up, showing no alterations in serum BA concentrations or in their percentage distribution

Conclusion: AMA+ individuals without progression to PBC show a stable and non-pathological serum BA profile, whereas those who progress show significant changes in the BA profile. Patients who progress show significantly higher non-12aOH BAs values at baseline than those who do not progress, which may be a useful early biomarker for the development of PBC.

WED-289

Does fibrosis regression in autoimmune hepatitis require histological as well as biochemical remission?

Sarah Flatley¹, Asha Dube¹, Barbara Hoeroldt¹, Laura Harrison¹, Elaine Wadland¹, Dermot Gleeson¹. ¹Sheffield Teaching Hospitals NHS Foundation Trust, United Kingdom
Email: s.flatley@nhs.net

Background and aims: Prevention of fibrosis progression, an important aim of autoimmune hepatitis (AIH) treatment, is associated with histological remission. Complete biochemical remission (CBR) has been proposed as the best surrogate marker for histological remission (Hartl, J Hepatol 2018), although it may be less reliable in patients with cirrhosis (Laschtowitz, JHep Rep 2021). We aimed to

assess the association of biochemical and histological remission with fibrosis regression, in cirrhotic and non-cirrhotic AIH patients.

Method: Retrospective/prospective single centre audit of patients with AIH (1999 IAIHG Criteria) presenting 1998–2020. All patients had a liver biopsy at diagnosis and a follow-up biopsy once in CBR (defined as normal ALT, AST, and IgG), after (median (range)) 27 (12–123) months of immunosuppressive treatment. Biopsies were assessed by one histopathologist (AKD) using a predesigned proforma. Histological remission was defined as Ishak histological activity index (HAI) ≤ 3 and fibrosis regression as Ishak decrease of ≥ 1 .

Results: Of 90 patients who had an evaluable biopsy in CBR (79% women, age 56 (7–75), follow-up 7 (2–23) years), only 36 (40%) were also in histological remission. Fibrosis regressed in 27 (30%), progressed in 33 (37%) and was unchanged in 30 patients (33%). Patients achieving histological remission were more likely to have fibrosis regression (50% vs 18%, $p<0.001$) than those with persisting histological activity. Fibrosis stage increased in patients with persisting histological activity (2 (0–6) to 3 (0–6), $Z=-2.277$, $p=0.023$) but did not change in patients achieving histological remission (3 (0–6) to 2 (0–6), $Z=-1.170$, $p=0.242$). On regression analysis, only achieving histological remission was independently associated with fibrosis regression (OR 4.22, 95% CI 1.6–11.4). Cirrhosis (Ishak stage 5–6) was present in 12 patients at diagnosis, developing in a further 6 on follow-up biopsy. Rates of histological remission did not differ between patients with and without cirrhosis at diagnosis (50% vs 42.3%, $p=0.617$) or on follow-up biopsy (35.7% vs 44.7%, $p=0.531$). Patients with cirrhosis showed a similar association between histological remission and fibrosis regression as the overall group (Table, not significant due to small sample size).

Conclusion: Only 40% of patients with AIH in CBR achieved histological remission, with similar rates in those with and without cirrhosis. Fibrosis regressed in 30% overall and more (50%) if histological remission was achieved. CBR is not an adequate surrogate marker for histological remission in cirrhotic or non-cirrhotic AIH patients. These data support a role for follow-up biopsy to assess response and guide further treatment of AIH.

Table: (abstract: WED-289)

		No cirrhosis (n = 72)			Cirrhosis either biopsy (n = 18)		
		Regressed	Same	Progressed	Regressed	Same	Progressed
Histological remission	Yes	13 (42%)	9 (29%)	9 (29%)	5 (63%)	0 (0%)	3 (37%)
	No	7 (17%)	19 (46%)	15 (37%)	2 (20%)	2 (20%)	6 (60%)

WED-290

Predictive models of treatment benefit in patients with autoimmune hepatitis and decompensated cirrhosis at diagnosis

Pinelopi Arvaniti^{1,2}, Sergio Rodríguez-Tajes^{1,3}, Marlene Padilla⁴, Olivas Ignasi¹, Álvaro Díaz-González⁵, Isabel Conde⁶, Beatriz Mateos Muñoz⁷, Diana Horta⁸, Rosa M. Morillas^{3,9}, Maria Torner⁹, Mar Riveiro Barciela¹⁰, Juan Carlos Ruiz-Cobo¹⁰, Indhira Perez Medrano¹¹, Carmen Álvarez-Navascués¹², Inmaculada Castello¹³, Ana Arencibia Almeida¹⁴, Judith Gómez-Camarero¹⁵, Elena Gómez Domínguez¹⁶, Magdalena Salcedo¹⁷, Carmen Vila¹⁸, Sara Lorente¹⁹, Vanesa Bernal Monterde²⁰, Eva Fernandez Bonilla²⁰, Francisca Cuenca Alarcon²¹, Cumali Efe²², Maria Alejandra Gracia Villamil²³, George Dalekos², Maria Carlota Londoño^{1,3}. ¹Liver Unit, Hospital Clinic, Institut d'Investigació Biomèdica August Pi i Sunyer (IDIBAPS), Barcelona, Spain; ²Department of Medicine and Research Laboratory of Internal Medicine, Expertise Center of Greece in Autoimmune Liver Diseases, ERN RARE-LIVER, University Hospital of Larissa, Greece, Greece; ³Centro de Investigación Biomédica en Red en Enfermedades Hepáticas y Digestivas (CIBEREHD), Spain; ⁴Unidad de Autoinmunidad Hepática Sección de Hepatología y Trasplante Hepático, Hospital Italiano de Buenos Aires, Argentina, Spain; ⁵Gastroenterology and Hepatology Department, Clinical and Translational Research in Digestive Diseases Group, Valdecilla Research Institute (IDIVAL), Marqués de Valdecilla University Hospital, Santander, Spain; ⁶Unit of Hepatology and Liver Transplantation, University Hospital La Fe. Institute of Sanitary Investigation, La Fe, Valencia, Spain; ⁷Servicio de Aparato Digestivo. Hospital Universitario Ramón y Cajal, CIBEREHD, IRYCIS, Madrid, España, Spain; ⁸Servicio de Aparato Digestivo. Hospital Universitario Mutua de Terrassa. Terrassa, España, Spain; ⁹Department of Hepatology, Hospital Germans Trias i Pujol. Institute of Investigation Germans Trias i Pujol (IGTP), Badalona, Spain; ¹⁰Unit of Hepatology, Department of Internal Medicine, University Hospital Vall de Hebron, Barcelona, Spain; ¹¹Servicio de Aparato Digestivo, Complejo Hospitalario Universitario de Pontevedra, Pontevedra, España, Spain; ¹²Servicio de Aparato Digestivo. Hospital Universitario Central de Asturias. Oviedo, España, Spain; ¹³Servicio de Aparato Digestivo. Hospital General Universitario de Valencia, Spain; ¹⁴Servicio de Aparato Digestivo. Hospital Universitario Nuestra Señora de la Candelaria. Santa Cruz de Tenerife, España, Spain; ¹⁵Servicio de Aparato Digestivo. Hospital Universitario de Burgos. Burgos, España, Spain; ¹⁶Servicio de Aparato Digestivo. Hospital Universitario 12 de Octubre. Madrid, España, Spain; ¹⁷Sección de Hepatología, Servicio de Aparato Digestivo. Hospital General Universitario Gregorio Marañón, CIBEREHD. Madrid, España, Spain; ¹⁸Servicio Digestivo (Endumsalut), Hospital Universitario Quirón Dexeus, Barcelona, España, Spain; ¹⁹Servicio de Hepatología, Hospital Clínico Lozano Blesa, Universidad de Zaragoza, Zaragoza, España, Spain; ²⁰Servicio de Aparato Digestivo, Hospital Universitario Miquel Servet, Zaragoza, España, Spain; ²¹Servicio de Aparato Digestivo. Hospital Clínico San Carlos, Madrid, España, Spain; ²²Department of Gastroenterology, Gazi Yaşargil Education and Research Hospital, Diyarbakir, Turkey; ²³Unidad de Autoinmunidad Hepática Sección de Hepatología y Trasplante Hepático, Hospital Italiano de Buenos Aires, Argentina, Argentina
Email: peni.arvaniti@gmail.com

Background and aims: One third of patients with autoimmune hepatitis (AIH) have already advanced fibrosis or cirrhosis at diagnosis. Although treatment administration is strongly recommended in this group, there are no established guidelines about the management of patients with AIH and decompensated cirrhosis at diagnosis. The aim of this study was to assess the efficacy and safety of immunosuppressive treatment in AIH-related decompensated cirrhosis and to establish predictive models of favorable outcome and treatment response.

Method: This is a multicenter retrospective study of 134 patients with AIH and decompensated cirrhosis at diagnosis confirmed by

liver biopsy. Competing risk analysis was used to determine cumulative incidence of survival (liver transplantation, LT was considered a competing event). Predictive models of transplant-free survival, and recompensation were calculated with Cox regression analysis. A decision tree analysis was used to determine the patients who will benefit from treatment.

Results: Eighty five patients (63%) were female, with median age of 58 years old (IQR: 48–68) and median follow-up of 28 months (IQR: 5–65). One hundred twenty five (93%) had ascites and 54 (40%) had hepatic encephalopathy (HE) at diagnosis. Thirteen (10%) patients did not receive treatment; all of them died or required LT. Treated patients (n = 121, 90%) had higher levels of ALT (333 vs. 42, p < 0.001), modified hepatic activity index (mHAI) (9 vs. 3, p < 0.001) and of bilirubin (7 vs. 2.7, p = 0.001). Cumulative incidence of mortality was significantly higher in untreated patients (36% vs. 54%, p = 0.002). The most efficient predictive model of transplant-free survival (AUC: 0.75; 95% CI: 0.66–0.83) included the absence of HE and MELD-Na score at diagnosis. Using decision tree analysis, patients with HE ≥ grade 2 and MELD-Na > 23.5 (Figure) had higher probability of dying or requiring a LT after treatment initiation. In the remaining patients, a decrease in MELD-Na ≥ 5.5 points after 4 weeks of treatment had a negative predictive value for death of 100%. Sixty two (51%) patients recompensated. Factors associated with recompensation were the absence of HE (OR: 0.193 p < 0.001, 95%CI: 0.0, 084–0, 441) and serum sodium levels (OR: 1,111, p = 0, 03, 95%CI: 1,013–1,234) at diagnosis. During follow-up, 26 patients stopped treatment, 20 during the first 4 weeks, and 18 due to non-response. HE ≥ grade 2 was associated with treatment withdrawal.

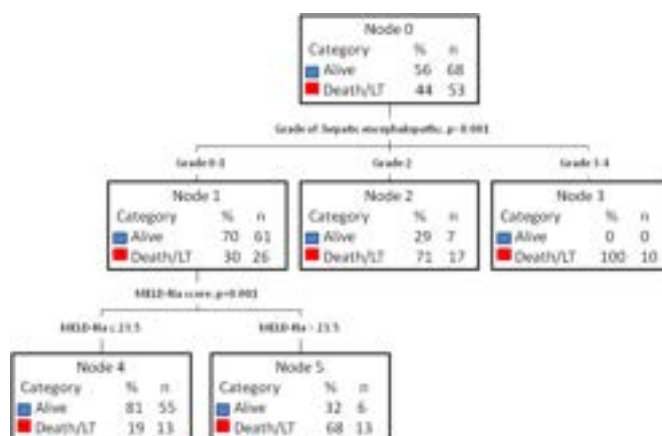


Figure:

Conclusion: Patients with AIH-related decompensated cirrhosis and active disease can benefit from treatment initiation. The grade of HE at diagnosis is strongly associated with outcome, cirrhosis recompensation and treatment withdrawal. The grade of HE, the value of MELD-Na score at diagnosis and the reduction of MELD-Na during the first 4 weeks of treatment can guide treatment decisions and predict transplant-free survival.

WED-291

Anti-Saccharomyces cerevisiae antibodies predict severe liver disease and advanced fibrosis in patients with primary sclerosing cholangitis and inflammatory bowel disease

Lian Bannon¹, Niv Zmora¹, Roie Tzadok¹, Haim Leibovitzh¹, Ehud Zigmond¹. ¹Tel Aviv Sourasky Medical Center-Ichilov, Department of Gastroenterology and Hepatology, Tel-Aviv Sourasky Medical Center, Sackler Faculty of Medicine, Tel-Aviv University, Tel-Aviv, Tel Aviv-Yafo, Israel

Email: liandhn@gmail.com

Background and aims: Primary Sclerosing Cholangitis (PSC) Risk Estimate Tool (PRESTo) is a novel prognostic tool, which is used to predict hepatic decompensation in patients with PSC. Anti-Saccharomyces cerevisiae antibody (ASCA) is one of the main serological markers used in Inflammatory Bowel Diseases (IBD) which is more prevalent in Crohn's disease (CD) and is associated with a more aggressive IBD phenotype. Nevertheless, data on the association between ASCA and adverse liver outcomes in PSC-IBD is limited. We aimed to explore whether ASCA is associated with liver disease severity, predicted by the PRESTo score, and with the degree of liver fibrosis measured by Transient Elastography (TE) in PSC-IBD patients.

Method: We conducted a retrospective study on adult patients with PSC-IBD, at a single tertiary center in Tel Aviv, Israel, between 2010 and 2023. Medical records were reviewed for baseline demographics, clinical data, including IBD subtype, PSC and IBD disease duration, blood tests assessed at the last documented visit and serum ASCA. Severity of liver disease was assessed at the last documented visit using (1) the PRESTo score (risk of decompensation at 5 years [%]), which is composed of serum levels of bilirubin, albumin, alkaline phosphatase, aspartate aminotransferase, sodium, hemoglobin, platelets concentrations, patient's age and PSC duration, and (2) Degree of liver fibrosis measured by TE (FibroScan, measured in Kpa). Univariate (Student's t-test) and multivariable linear regression model adjusted for gender, IBD subtype, IBD duration and PSC duration was used to assess associations between ASCA and outcomes of PRESTo score and degree of liver fibrosis.

Results: The cohort comprised of 102 subjects with PSC-IBD. Fifty-six (54.9%) were males, mean age was 50.2 years (SD 17.05), 57 patients were diagnosed with ulcerative colitis (UC) and 45 with CD. The mean age of IBD and PSC diagnosis was 31.2 years (SD 15.6) and 39.5 years (SD 17.07), respectively. ASCA data was available for 59 (57.8%) subjects. Six of 30 (20%) patients with UC and 14 of 28 patients (50%) with CD had positive ASCA. PRESTo score was available for 51 (50%) subjects and TE measurements were available for 43 (42.1%) patients. In the univariate analysis both the PRESTo score ($p=0.017$) and TE measurements ($p=0.018$) were significantly higher in those with positive ASCA (Figure 1). In the multivariable model, ASCA positivity was still significantly associated with higher PRESTo scores (Estimate = 22.27, 95% CI 2.88–41.67, $p=0.026$) and a higher TE measurements (Estimate 2.80, 95% CI 0.19–5.41, $p=0.036$), even after adjustment for IBD subtype, IBD and PSC duration.

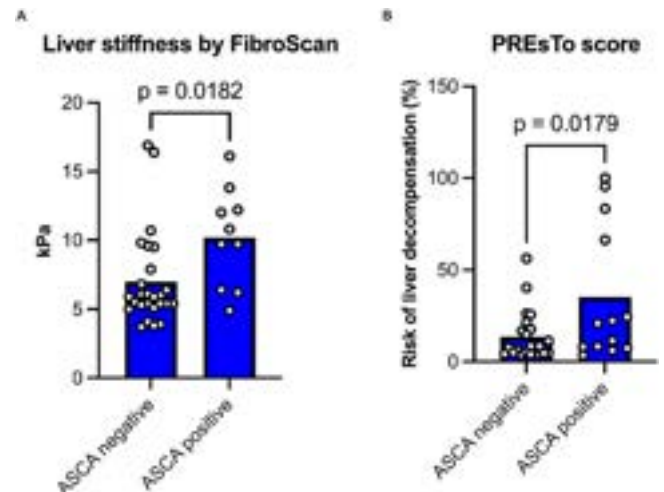


Figure:

Conclusion: In subjects with IBD with concomitant PSC, the presence of serum ASCA may be used to predict 5-years liver decompensation and degree of liver fibrosis. Further studies are warranted to explore the biological mechanism underlying this association

WED-292

Increased risk of osteoporotic fracture in patients with autoimmune hepatitis

Jihye Lim¹, Ye-Jee Kim², Seon-Ok Kim², Jonggi Choi³. ¹Yeouido St. Mary's Hospital, Internal Medicine, Seoul, Rep. of South Korea; ²Asan Medical Center, Rep. of South Korea; ³Asan Medical Center, Gastroenterology, Liver Center, Rep. of South Korea
Email: jkchoi0803@gmail.com

Background and aims: Chronic liver disease is a recognized risk factor for osteoporosis and fragility fractures. Especially, patients with autoimmune hepatitis (AIH) are thought to be more vulnerable to loss of bone mass in several aspects. From an epidemiologic perspective, AIH is a female-dominant disease, particularly in postmenopausal women who have an increased risk of developing osteoporosis. In addition, glucocorticoids, the most common cause of secondary osteoporosis, are frequently used. Few large-scale studies are published regarding the association between AIH and risk of osteoporotic fracture. This study aimed to determine the risk of developing an osteoporotic fracture in patients with AIH.

Method: We used claims data from the Korean National Health Insurance Service (NHIS) between 2007 and 2020. Patients with AIH ($n=7062$) were matched with controls ($n=28,122$) using a ratio of 1 : 4, based on age, sex, and duration of follow-up. Osteoporotic fractures, included fractures of the vertebral, hip, distal radius, and proximal humerus. Prescription of glucocorticoid or other immunosuppressive agent for 30 consecutive days after the diagnosis of AIH was used to assess medication utilization. The incidence rate (IR) and incidence rate ratio (IRR) of osteoporotic fracture were compared between the two groups and their associated factors were also evaluated. We performed subgroup analysis for the patients with AIH whose follow-up was at least ≥ 2 years to determine the association between the cumulative use of glucocorticoid or immunosuppressive agents during the initial 2 years and the risk of osteoporotic fractures.

Results: During a median follow-up period of 5.4 years, 712 osteoporotic fractures occurred in patients with AIH with an IR of 17.5 per 1,000 person-years (PYs) while 1,922 osteoporotic fractures with an IR of 11.6 per 1,000 PYs in the controls. Patients with AIH showed a significantly higher risk of osteoporotic fractures than matched controls, with an IRR of 1.24 (95% confidence interval, 1.10–1.39, $p<0.01$) in the multivariable analysis. Vertebral fractures were significantly higher among the patients with AIH when compared to the controls in unadjusted (IRR: 1.66) and adjusted analyses (IRR:

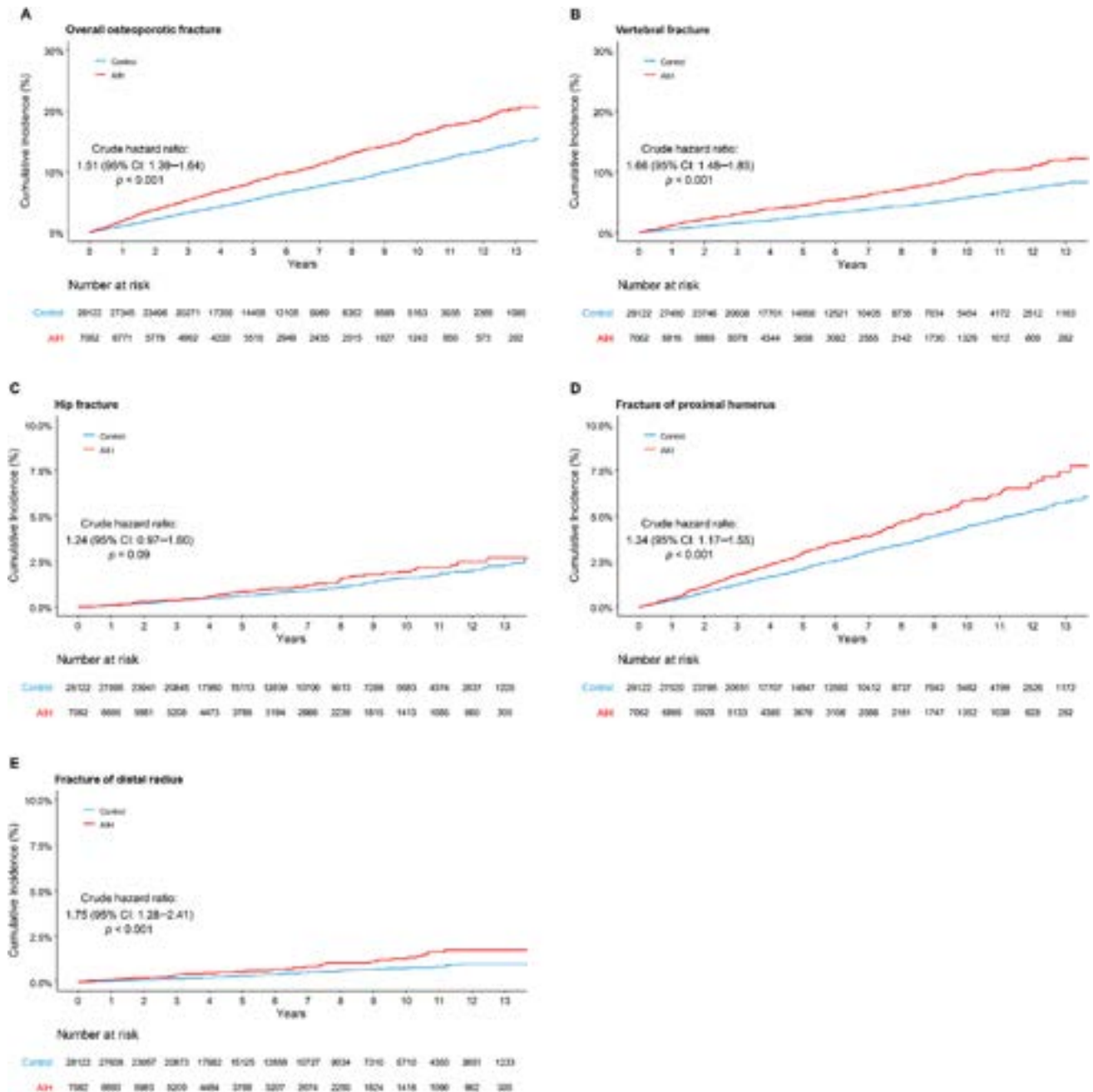


Figure: (abstract: WED-292): Cumulative risks of osteoporotic fractures in patients with autoimmune hepatitis and the control group. Overall osteoporotic fracture, (B) Vertebral fracture, (C) Hip fracture, (D) Fracture of proximal humerus, and (E) Fracture of distal radius.

1.31). Patients with AIH appeared to have a higher risk of hip (IRR: 1.24), proximal humerus (IRR: 1.34), and distal radius (IRR: 1.75) fracture than the controls in the unadjusted analysis, whereas this risk did not significantly differ after adjustment. Female sex, older age, history of stroke, presence of cirrhosis, and use of glucocorticoids were associated with an increased risk of osteoporotic fractures. In the two-year landmark analysis, long-term use of glucocorticoid had an increased risk of osteoporotic fracture in a dose-dependent manner (4% as per 10% increase in the duration of glucocorticoid use). **Conclusion:** In conclusion, the risk of osteoporotic fracture was significantly increased in the AIH patients. Female sex, old age, presence of cirrhosis, longer use of glucocorticoids increased the risk of fracture. Considering the morbidities from osteoporotic fracture,

recognition of these risk factors and early diagnosis and intervention may be crucial in the care of patients with AIH.

WED-293

Prognostic value of serum ALP levels during additional treatment in Japanese patients with primary biliary cholangitis treated with ursodeoxycholic acid and bezafibrate

Akihito Takeuchi¹, Kosuke Matsumoto¹, Atsumasa Komori², Masanori Abe³, Tadashi Namisaki⁴, Kazuhito Kawata⁵, Masashi Ninomiya⁶, Hideki Fujii⁷, Atsushi Takahashi⁸, KANG Jong-Hon⁹, Masaaki Takamura¹⁰, Mie Arakawa¹¹, Satoru Joshita¹², Ken Sato¹³, Takako Nomura¹⁴, Keisuke Kakisaka¹⁵, Akira Kaneko¹⁶, Kentaro Kikuchi¹⁷, Tsutomu Masaki¹⁴, Takeji Umemura¹², Akira Honda¹⁸, Hiromasa Ohira⁸,

Norifumi Kawada⁷, Hitoshi Yoshiji⁴, Satoshi Mochida¹⁹, Atsushi Tanaka¹, ¹Teikyo University School of Medicine, Japan; ²National Hospital Organization (NHO) Nagasaki Medical Center, Japan; ³Ehime University Graduate School of Medicine, Japan; ⁴Nara Medical University, Japan; ⁵Hamamatsu University School of Medicine, Japan; ⁶Tohoku University Graduate School of Medicine, Japan; ⁷Osaka Metropolitan University Graduate School of Medicine, Japan; ⁸Fukushima Medical University School of Medicine, Japan; ⁹Teine Keijinkai Hospital, Japan; ¹⁰Niigata University Graduate School of Medical and Dental Sciences, Japan; ¹¹Oita University, Japan; ¹²Shinshu University School of Medicine, Japan; ¹³Gunma University Graduate School of Medicine, Japan; ¹⁴Kagawa University School of Medicine, Japan; ¹⁵Iwate Medical University, Japan; ¹⁶Minoh City Hospital, Japan; ¹⁷Teikyo University Mizonokuchi Hospital, Japan; ¹⁸Tokyo Medical University Ibaraki Medical Center, Japan; ¹⁹Saitama Medical University, Japan
Email: a-tanaka@med.teikyo-u.ac.jp

Background and aims: Treatment response in primary biliary cholangitis (PBC) is important in predicting long-term prognosis. The standard of care for PBC is ursodeoxycholic acid (UDCA), and various indices have been reported to evaluate the response to UDCA monotherapy. On the other hand, obeticholic acid (OCA) or bezafibrate (BZF) are used in the real world for patients who exhibited incomplete response to UDCA, but no clinical indices have been demonstrated for predicting the long-term outcome in patients with combination treatment. In this study, we investigated the association of ALP levels during additional BZF treatment with long-term outcomes in Japanese patients with PBC treated with UDCA and BZF.

Method: We took advantage of a retrospective cohort, consisting of 799 PBC patients (male/female = 120/679, age at initiation of treatment 58.9 ± 11.1 years) attending 19 centers in Japan. Date of birth and gender, date, presence of symptoms and biochemical test findings (ALP, total bilirubin, albumin) at baseline, treatment protocol (UDCA and/or BZF), serum ALP at 6 and 12 months of UDCA or additional BZF treatment, and the final follow-up date and outcomes (liver transplantation (LT) and all-cause death) were recorded in all patients. Using this cohort, the association of ALP levels at 6 and 12 months of treatment with outcomes was examined by Kaplan-Meier method and Cox proportional hazards model, along with other covariates.

Results: Among 799 patients, 619 and 180 patients were treated with UDCA monotherapy and UDCA/BZF combination therapy, respectively. All patients with combination therapy received UDCA first, followed by BZF. In the analysis of all 799 patients (observation period 7.4 ± 5.1 years, death/LT = 24/3), ALP levels at 12 months of treatment (UDCA or additional BZF; $1.5\times$, $1.67\times$, and $2\times$ ULN) and at 6 months ($2\times$ ULN) were significantly associated with outcome, along with gender, presence of symptoms and albumin at baseline. In the analysis of 180 patients with a combination treatment of UDCA and BZF (observation period 6.8 ± 4.6 years, death/LT = 7/0), ALP levels at 12 months ($2\times$ ULN) and at 6 months ($1.5\times$, $1.67\times$, and $2\times$ ULN) of additional BZF treatment along with age and albumin at baseline were significantly associated with outcome. C-statistics were 0.968 ($2\times$ ULN at 12 months), 0.968 ($1.5\times$ ULN at 6 months), 0.968 ($1.67\times$ ULN at 6 months) and 0.975 ($2\times$ ULN at 6 months). In the figure, we demonstrate LT-free survival adjusted by clinical covariates according to serum ALP level $2\times$ ULN at 6 and 12 months of additional BZF in patients treated with combination treatment.

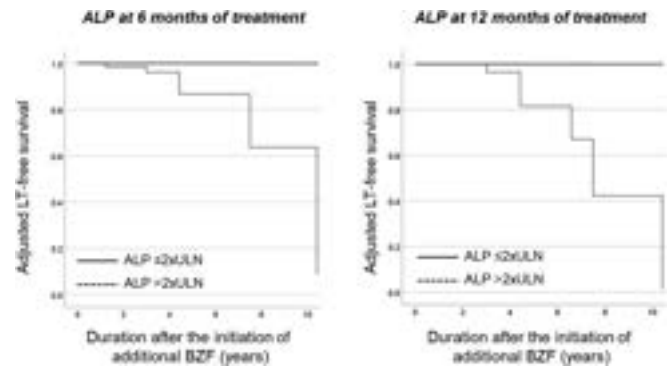


Figure:

Conclusion: In patients treated with a combination of UDCA and BZF, serum ALP values at 6 or 12 months of additional BZF treatment are significantly associated with long-term outcome, and are of value as prognostic tools.

WED-294

A novel web-based online nomogram to predict advanced liver fibrosis in patients with autoimmune hepatitis-primary biliary cholangitis overlap syndrome

Zhiyi Zhang¹, Jian Wang^{2,3}, Yun Chen⁴, Yiguang Li⁵, Li Zhu⁶, Huali Wang⁷, Yilin Liu¹, Chuanwu Zhu⁶, Jie Li^{1,2,3,4}, Rui Huang^{1,2,3,4}, Chao Wu^{1,2,3,4}, Yuanwang Qiu⁵. ¹Department of Infectious Diseases, Nanjing Drum Tower Hospital Clinical College of Traditional Chinese and Western Medicine, Nanjing University of Chinese Medicine, Nanjing, Jiangsu, China; ²Department of Infectious Diseases, Nanjing Drum Tower Hospital, The Affiliated Hospital of Nanjing University Medical School, Nanjing, Jiangsu, China; ³Institute of Viruses and Infectious Diseases, Nanjing University, Nanjing, Jiangsu, China; ⁴Department of Infectious Diseases, Nanjing Drum Tower Hospital, Clinical College of Nanjing Medical University, Nanjing, China; ⁵Department of Infectious Diseases, The Fifth People's Hospital of Wuxi, Wuxi, Jiangsu, China; ⁶Department of Infectious Diseases, The Affiliated Infectious Diseases Hospital of Soochow University, Suzhou, Jiangsu, China; ⁷Department of General Practice, Nanjing Second Hospital, Nanjing University of Chinese Medicine, Nanjing, Jiangsu, China
Email: qywang839@126.com

Background and aims: Patients with autoimmune hepatitis-primary biliary cholangitis (AIH-PBC) overlap syndrome have a worse prognosis compared to AIH or PBC alone and accurately predicting the severity and dynamically monitoring the progression of disease are therefore essential. We aimed to develop a nomogram-based model to predict advanced liver fibrosis in patients with AIH-PBC overlap syndrome.

Method: A total of 121 patients with AIH-PBC overlap syndrome were retrospectively included and randomly assigned to a development set and a validation set. Backward stepwise multivariate regression's best model with the lowest AIC was employed to create a nomogram. Diagnose accuracy was evaluated using the area under the receiver operator characteristic curve (AUROC), calibration analysis, and decision curve analysis (DCA) and was compared with aspartate aminotransferase-to-platelet ratio (APRI) and fibrosis index based on four factors-4 (FIB-4) score.

Results: The median age of patients was 53.0 years (IQR: 46.0–63.0), and female patients accounted for 95.0%. Platelets, globulin, total bilirubin, and prothrombin time were associated with advanced fibrosis ($\geq S3$) and used to construct an AIH-PBC overlap syndrome fibrosis (APOSF)-nomogram (available online at <https://ndth-zzy.shinyapps.io/APOSF-nomogram/>). The AUROCs of APOSF-nomogram were 0.845 (95% CI: 0.754–0.936) and 0.843 (95% CI: 0.705–0.982) in the development set and validation set respectively, which was significantly better than APRI and FIB-4. Calibration revealed that the estimated risk fits well with biopsy-proven observation. DCA

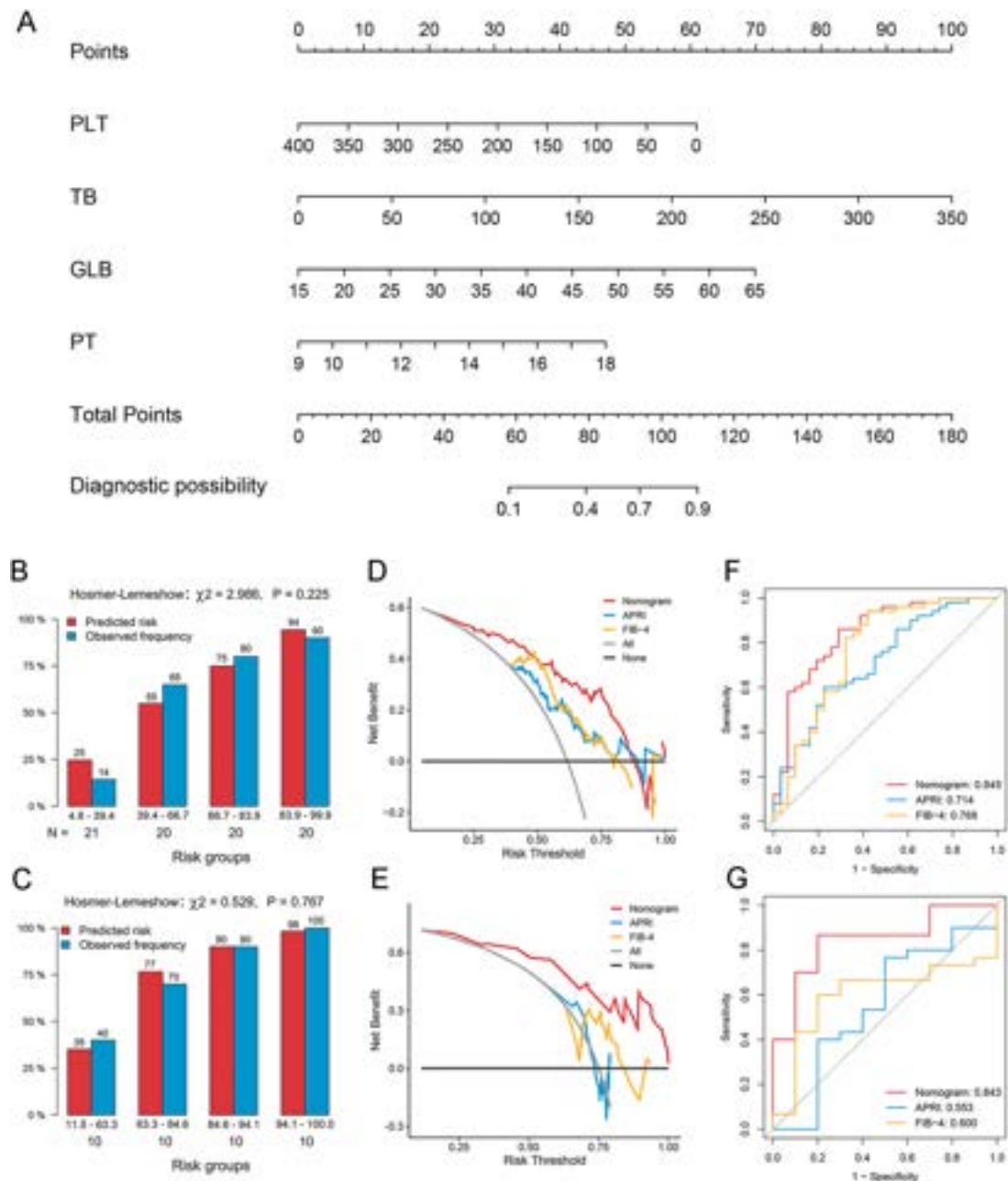


Figure: (abstract: WED-294): Nomogram-based model to predict advanced liver fibrosis in patients with AIH-PBC overlap syndrome

outperformed APRI and FIB4 in terms of net benefit, demonstrating clinical utility.

Conclusion: This novel non-invasive web-based online APOSF-nomogram provided a convenient tool for identifying advanced fibrosis in patients with AIH-PBC overlap syndrome.

WED-295

Presence of metabolic associated liver disease in autoimmune hepatitis is associated with advanced liver fibrosis

Alvaro Urzúa¹, Daniela Simian¹, Giselle Arevalo¹, Consuelo Palomo¹, Jaime Poniachik¹. ¹University of Chile Clinical Hospital, Gastroenterology Section, Santiago, Chile
Email: dralvarourzua@gmail.com

Background and aims: Metabolic associated liver disease (MAFLD) is one of the most frequent causes of chronic liver disease worldwide. Steatohepatitis is a major risk factor for the development of fibrosis

and its progression. MAFLD is very common and is present in other causes of chronic liver damage, such as autoimmune hepatitis (AIH). There is scarce information of the role of MAFLD in fibrosis in patients with AIH. We describe the frequency of steatosis, steatohepatitis, and fibrosis in AIH liver biopsies and the impact of steatosis and steatohepatitis on fibrosis severity.

Method: Observational and retrospective study of liver biopsies performed, prior to initiation of immunosuppressive therapy, between 2015 and 2018. Presence of steatosis, steatohepatitis and fibrosis was recorded. Alcohol and other etiologies of liver disease were excluded. Clinical data was obtained from electronic charts. Descriptive analysis was performed using media and median, comparative analysis was performed with chi 2 and exact Fisher test, $p < 0.05$ was considered statistically significant.

Results: 131 biopsies were analyzed for the presence of steatosis, steatohepatitis, and fibrosis with its staging, 76% were female, mean age 56 (15–83) years. Steatosis was present in 27%, steatohepatitis in

14% and advanced fibrosis (>F3) in 60%. Presence of steatosis and steatohepatitis were risk factors for advanced fibrosis (OR 2.97, CI 95% 1.22–7.21 $p=0.016$). We performed a sub analysis to compare patients with and without steatosis, steatohepatitis, and advanced fibrosis, including 66 patients with complete clinical data (diabetes mellitus, hypertension, body mass index, bilirubin, platelet count, INR and mortality). Steatosis and steatohepatitis were more frequent in obese patients ($p=0.0003$ and 0.019). Mortality was higher in patients with steatosis (47% vs 14% $p=0.011$). All patients with steatohepatitis had advanced fibrosis (>F3).

Figure:

N = 66	With steatosis n = 15	Without steatosis n = 51	P value
Female venter	12 (80)	41 (80)	0.973
Age (median; min-max)	53 (29–72)	58 (20–83)	0.357
IMC (mediana; min-max)	31.2 (23.5–43.15)	25.4 (19–44.4)	0.0001
Co-Morbidities			
Diabetes	4 (27)	9 (18)	0.440
Hipertensión	6 (40)	11 (22)	0.151
Lab Tests (median; min-max)			
Bilirubin	1.3 (0.2–3.1)	1.4 (0.3–33)	0.481
INR	1.2 (1–2.08)	1.2 (0.9–2.28)	0.759
Platelets	133000 (60000–260000)	175000 (58000–491000)	0.085
Mortality	7 (47)	7 (14)	0.011

Conclusion: In this cohort of AIH liver biopsies, steatosis and steatohepatitis were risk factors for advanced fibrosis. All patients with steatohepatitis had advanced liver fibrosis and mortality was higher in patients with steatosis. In patients with AIH, MAFLD should be treated to avoid progression to fibrosis.

WED-296

Improving the diagnosis of primary biliary cholangitis through immunology protocols

Mario de Bonis Encinosa¹, Javier Rodríguez Jiménez¹, Carmen Iglesias Sobrino¹, Hildo Rodríguez Santos¹, Cristina Suárez Montesdeoca¹, Paula Moreno Martín¹, Elisaul Suarez Zambrano¹, Esther Rodríguez Candelaria¹, Itahisa Marcelino-Rodríguez², Delia Almeida González³, Francisco Andrés Pérez Hernández¹, Ana Arencibia Almeida¹.
¹University Hospital of Nuestra Señora de la Candelaria, Gastroenterology and Hepatology Service, Santa Cruz de Tenerife, Spain; ²University of La Laguna, Preventive Medicine and Public Health Area, San Cristóbal de La Laguna, Spain; ³University Hospital of Nuestra Señora de la Candelaria, Immunology Laboratory, Santa Cruz de Tenerife, Spain
Email: mario.dbencinosa@gmail.com

Background and aims: The diagnosis of primary biliary cholangitis (PBC) relies largely on the detection of antinuclear antibodies (ANA) and antimitochondrial antibodies (AMA) by indirect immunofluorescence (IIF). The primary aim of this study was to analyse the role of autoimmunity in the diagnosis of PBC. The secondary aim was to analyse differences in diagnosis rates between AMA-positive and AMA-negative patients, and to propose an immunological diagnostic algorithm designed to recruit the largest number of patients who meet PBC laboratory criteria.

Method: A descriptive observational study was conducted between 2015 and 2020. Patients with alkaline phosphatase (ALP) levels exceeding the upper limit of normal (ULN) and any PBC-specific antibody were followed up.

Results: 635 positive antibody determinations were recorded in 274 patients. From these, 89% were AMA-positive and 96% ANA-positive.

Furthermore, 234 (85%) patients were AMA-ANA positive, whilst 30 (12%) were AMA-negative, but ANA-positive. The staining pattern obtained (by IIF on HEP-2 cells) was reticular mottled cytoplasmic pattern (AC21) in 219 patients, multiple nuclear dots (AC6) in 40 patients and punctate nuclear envelope (AC12) in 21 patients. Immunoblot was performed on 182 patients resulting in 179 subjects testing positive: 145 for AMA-M2, 117 for BPO, 55 for Gp210, 47 for Sp100, and 17 for PML; additionally, of these 145 AMA-M2 patients, 18 were AMA-negative, and all ANA-positive. 55.8% of the sample had a clinical diagnosis of PBC: 96% AMA-positive (147) and 4% AMA-negative (6); $p<0.001$. 99.3% ANA-positive (152) and 1% ANA-negative (1); $p<0.001$. 121 patients had no diagnosis; 80% AMA-positive (97) and 20% AMA-negative (24); $p<0.001$; 92% ANA-positive (112) and 7% (9) ANA-negative. The sensitivity of AMA was 96% and that of ANA was 99%. 147 AMA-positive patients (60.2%) were diagnosed with PBC whilst 97 (39.8%) were undiagnosed; ($p<0.001$). The Gastroenterology Department diagnoses a higher number of patients with PBC in relation to AMA request ($p<0.001$) followed by Primary Care and Rheumatology. Statistically significant differences were observed between undiagnosed and diagnosed patients for AMA ($p<0.001$), ANA ($p=0.007$), immunoblot ($p=0.004$), Gp210 ($p=0.001$), AMA-M2 ($p=0.027$), Sp100 ($p=0.005$) and chronicity of ALP, altered GGT and AST ($p<0.001$).

Conclusion: Although AMA are present in 90–95% of patients with PBC, IIF based on HEP-2 is more sensitive to detect autoantibodies associated with the disease than IIF in rodent tissue (99.3% vs. 96%). In cases where PBC is suspected, the most efficient action to take is to combine IIF on HEP-2 with specific autoantibody detection using immunoblotting. The immunology laboratory can approach the diagnosis of PBC through the standardization of algorithms, especially in patients whose autoimmunity was requested by other medical departments besides Gastroenterology.

WED-297

The devastating impact of severe pruritus in primary biliary cholangitis

Helen Smith¹, Megan McLaughlin², Sugato Das³, Andrea Ribeiro⁴, Philip Troke¹, Andreas E. Kremer⁵, David Jones⁶. ¹GSK, United Kingdom; ²GSK, United States; ³GSK, India; ⁴GSK, Spain; ⁵University of Zürich, Switzerland; ⁶Newcastle University, United Kingdom
Email: helen.t.smith@gsk.com

Background and aims: Pruritus associated with primary biliary cholangitis (PBC) affects sleep and, social and emotional wellbeing. The impact of itch severity on quality of life (QoL) using the EuroQol-5-Dimension 5-Level (EQ-5D-5L) health utility score was explored and quantified in a post hoc analysis of the Phase 2b GLIMMER study of lincicibat for the treatment of pruritus in PBC (NCT02966834). Pruritus (particularly severe pruritus) was previously found to have a significant negative impact on QoL and health utility: mean (standard deviation [SD]) baseline (BL) utility was 0.69 (0.23); patients with mild or moderate pruritus at BL had similar utilities (0.75 [0.17] and 0.76 [0.17], respectively) whereas patients with severe pruritus at BL had notably worse utility (0.49 [0.28]). Here we look in detail at factors impacting QoL in patients with PBC and pruritus.

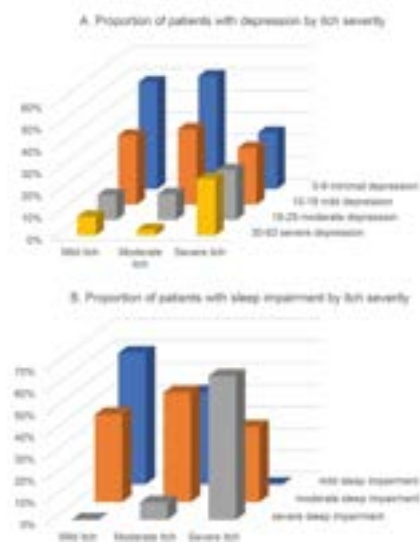
Method: Patients in GLIMMER completed the EQ-5D-5L and Beck Depression Inventory (BDI-II) at BL, which followed a 4-week single-blind placebo run-in period. EQ-5D-5L is a generic, standardised and simple health-related QoL instrument. Scores range from 1 “perfect health” to 0 “death.” BDI is a 21-item, self-rated scale that evaluates key symptoms of depression. Patients were classified as having mild (<4, BL all mild were ≥ 3 to <4), moderate (≥ 4 to <7) or severe pruritus (≥ 7 to 10) using the mean worst daily itch score. Sleep disturbance severity was based on the same numerical rating scale thresholds as those used for pruritus.

Results: There were striking associations between itch severity, sleep disturbance and health utility, and between itch severity, depression and health utility. Overall mean (SD) health utility was highest in

POSTER PRESENTATIONS

those with mild sleep impairment 0.83 (0.126). Those with severe sleep impairment had a much lower score and those with severe itch and severe sleep disturbance even lower (0.52 [0.30] and 0.47 [0.31], respectively). Interestingly, no patients with mild itch had severe sleep impairment and no patients with severe itch had mild sleep impairment. As might be expected, health utility was lower with worse depression; from 0.81 (0.18) with minimal depression to 0.39 (0.31) for those with severe depression; amongst those with moderate or severe depression the incremental impact of severe pruritus on health utility was striking, with utilities of 0.32 and 0.26, respectively. In mild and moderate itch, the distribution of depression severity was similar, with over 80% having minimal or mild depression. However, in the group with severe itch, 49% had moderate or severe depression.

Figure: Presence and severity of depression and sleep disturbance by itch severity



Conclusion: Pruritus in PBC significantly impacts QoL. Severe sleep disturbance and moderate and severe depression were far more common in patients with severe pruritus. In patients suffering with both severe pruritus and moderate to severe depression, health utility was severely impaired.

WED-298

Variation in maintenance therapy practices in a large U.S. cohort of patients with autoimmune hepatitis

Therese Bittermann¹, Ranganath Kathawate², James Lewis¹, Cynthia Levy³, David Goldberg³. ¹University of Pennsylvania, United States; ²Wayne State University, United States; ³University of Miami, United States

Email: therese.bittermann@pennmedicine.upenn.edu

Background and aims: The overarching goals of treating autoimmune hepatitis (AIH) are to induce remission and prevent disease progression while minimizing corticosteroids (CS) due to side effects. Data on maintenance therapy for AIH are largely derived from clinical trials or studies from tertiary care centers. "Real-world" data in a representative population are limited. We sought to determine patient factors associated with the use of CS-sparing and CS monotherapy regimens among patients receiving maintenance therapy for AIH.

Method: Retrospective cohort study of adults (≥ 18 years) with incident or prevalent AIH identified using a validated algorithm in the Optum® Clinformatics® Deidentified Data Mart, a U.S. health insurance database. All patients were followed 2 years: the first year served as a washout period to exclude instances of the induction phase of treatment and the second year served as the observation

period during which the dominant maintenance AIH regimen was assessed. Dominant regimen was defined as that received >6 months during observation year. All patients in the cohort were required to have filled ≥ 1 prescription of any drug (AIH-related or not) during the observation period. Separate multivariable logistic regression models investigated patient factors independently associated with a dominant maintenance regimen of (i) azathioprine (AZA) or mycophenolate mofetil (MMF) monotherapy (vs AZA/MMF with prednisone [Pred]) and (ii) Pred monotherapy (vs AZA/MMF \pm Pred).

Results: Among 3,591 AIH patients, 2,330 (64.9%) had ≥ 1 prescription for an AIH drug during the observation year. Patients who did not receive AIH treatment were largely similar to those receiving treatment. Dominant regimens during the observation period included: 41.5% AZA monotherapy, 13.4% AZA with Pred, 10.9% Pred monotherapy, 3.7% MMF monotherapy, 1.8% MMF with Pred, 1.6% Bud monotherapy, 0.3% tacrolimus (Tac) mono, 0.2% Tac with Pred, and 8.5% other regimens. Factors independently associated with decreased AZA/MMF monotherapy (vs AZA/MMF with Pred) as a dominant regimen included: male sex (OR 0.7; $p = 0.007$), age 18–39 years (OR 0.6 vs age 40–59 years; $p = 0.025$), Hispanic ethnicity (OR 0.6 vs White; $p = 0.021$), osteoporosis (OR 0.5; $p < 0.001$), and other autoimmune disease (OR 0.7; $p < 0.001$). Factors associated with increased use of Pred monotherapy as a dominant regimen included: age ≥ 70 (OR 2.7 vs age 40–59 years; $p < 0.001$) and history of other autoimmune disease (OR 2.0; $p < 0.001$).

Conclusion: Less than half of patients receiving AIH therapy in a large, diverse insurance-based cohort were treated with AZA or MMF monotherapy as their dominant regimen. Older patients ≥ 70 years were more likely to receive Pred monotherapy, which may be suboptimal in this group.

WED-299

Burden, impact and variability of pruritus in primary sclerosing cholangitis (PSC) over time: a prospective observational study

Nasir Hussain^{1,2}, Benjamin Hirschfield², James Ferguson^{1,2}, Nadir Abbas^{1,2}, Usha Gungabissoon³, Khushpreet Bhandal², Emma Burke², Diana Hull², Penelope Rogers², Sumanta Mukherjee³, Andrea Ribeiro³, Martine Walmsley⁴, Paula Hanford⁴, Megan McLaughlin⁴, Linda Casillas³, Palak Trivedi^{1,2}. ¹University of Birmingham, National Institute for Health Research (NIHR) Birmingham Biomedical Research Centre (BRC), Birmingham, United Kingdom; ²University Hospitals Birmingham, Liver Unit, Birmingham, United Kingdom; ³GlaxoSmithKline, United States; ⁴PSC Support, United Kingdom

Email: nxh100@student.bham.ac.uk

Background and aims: Pruritus is a recognised symptom of PSC, although the prevalence, persistence and impact on quality of life (QoL) are unknown. The aims of this study are to (A) quantify the proportion of patients (pts) with PSC who experience pruritus, (B) identify factors associated with symptom intensity, and (C) determine the association between pruritus and overall health related QoL. **Method:** Pts with a diagnosis of PSC (age > 16 years; non-transplant) were invited to complete specific QoL tools: 5D itch, itch numerical rating scale (NRS), chronic liver disease questionnaire (CLDQ) and the EQ-5D-5L. Measures were obtained at 0, 3, 6, 9 and 12 months, alongside clinical and laboratory data. This multicentre, prospective observational study began recruitment in Aug '21. Follow-up is ongoing, and interim results are presented herein.

Results: Between Aug '21 and Nov '22, we accrued data from 184 pts. The majority had large duct disease ($n = 166$), were men ($n = 105$), with a median age of 41yrs (IQR 29–57), a history of inflammatory bowel disease (IBD, $n = 156$; 134 with quiescent activity) and a median MELD score of 7 (IQR 6–8). (A) Observing the cohort in its entirety, median baseline 5D itch score was 8 (IQR 5–12), with 92 pts. reporting any degree of itch according to the NRS. The latter included 23 pts. who reported itch despite taking anti-pruritic therapy. (B) 5D itch scores negatively correlated with age, positively correlated with

Figure 1: Baseline factors associated with pruritus intensity

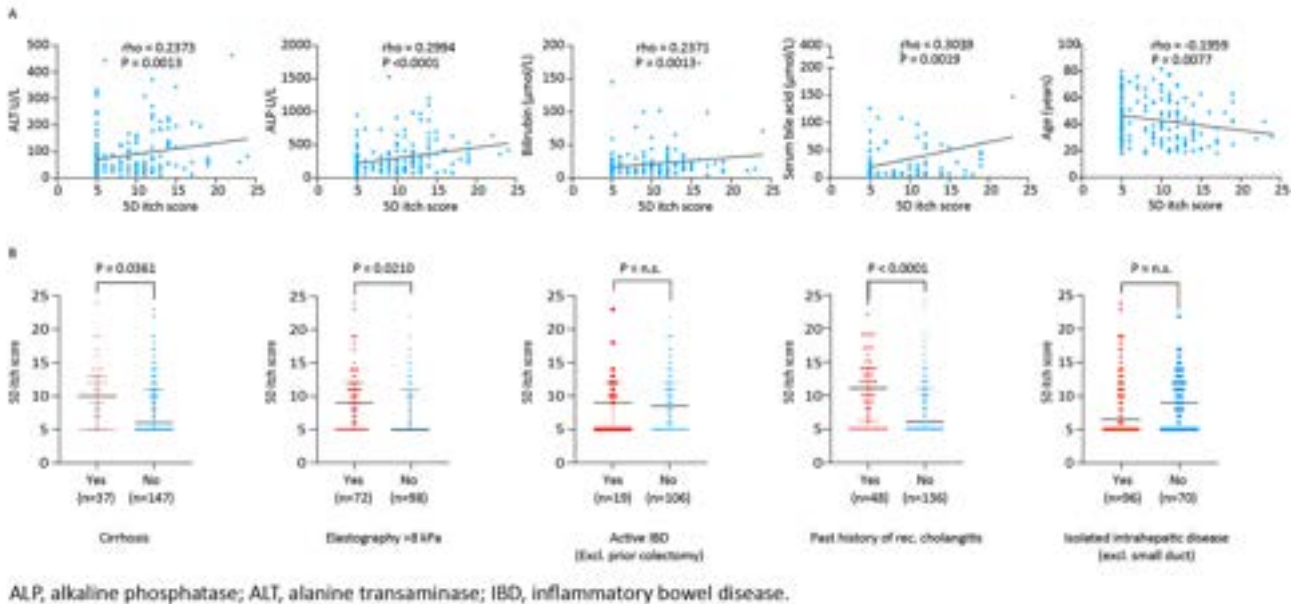


Figure: (abstract: WED-299)

serum bilirubin, ALT, ALP and bile acid values, and was greater in pts with previous episodes of acute cholangitis, those with advanced fibrosis, and people with cirrhosis (Fig). No significant differences in 5D itch score were seen according to the presence/activity of IBD or extent of ductal disease (Fig). (C) The median baseline NRS score was 1 (IQR 0–3), with 37 pts (20%) scoring >4 . According to the NRS, symptom severity associated with significantly poorer health utility: mean (SD) CLDQ scores in patients with no, mild, moderate, and severe itch were 5.6 (1.0), 5.1 (1.2), 4.4 (1.2) and 3.6 (1.3), respectively. Mean EQ-5D scores for no, mild, moderate, and severe itch were 77.0 (17.1), 72.9 (19.0), 64.1 (22.1) and 47.3 (16.4), respectively. At time of writing, 72/184 pts undertook repeat assessment over 12 months. In 42/72 pts (58%) with baseline pruritus, 28 reported unchanged or worsening itch over time (including 9/28 pts who were taking symptom-specific therapy).

Conclusion: Pruritus is commonly reported yet under-treated in PSC, has a propensity to persist over time, and with negative connotations on QoL. Those with a history of recurrent cholangitis, advanced fibrosis and cirrhosis have the greatest need for anti-pruritic therapy and must be prioritised for symptom-directed interventional trials.

WED-300

Variation in the presentation pattern of primary biliary cholangitis (PBC) in Spain according to the diagnostic period: data from the Spanish registry of cholestatic and autoimmune liver diseases (COLHAI)

Sergio Rodríguez-Tajes¹, Álvaro Díaz-González², Mercedes Vergara Gómez³, Judith Gómez-Camarero⁴, Javier Ampuero⁵, Beatriz Mateos Muñoz, Diana Horta⁷, Javier Salmerón⁸, Inmaculada Castello⁹, Rosa M. Morillas¹⁰, Manuel Hernández Guerra¹¹, Carmen Álvarez-Navascués¹², Javier Martínez⁶, Ismael El Haja Martínez¹³, Raul J. Andrade¹⁴, Montserrat García-Retortillo¹⁵, Ana Barreira¹⁶, Mar Riveiro Barciela¹⁶, Magdalena Salcedo¹⁷, Maria Carlota Londoño^{1,18,19}. ¹Hospital Clínic de Barcelona, Barcelona, Spain; ²Marqués de Valdecilla University Hospital, Santander, Spain; ³Hospital Parc Taulí de Sabadell, Sabadell, Spain; ⁴Burgos University Hospital, Burgos, Spain; ⁵Virgen del Rocío University Hospital, Sevilla, Spain; ⁶Ramón y Cajal Hospital, Madrid, Spain; ⁷Hospital Universitari MútuaTerrassa, Terrassa, Spain; ⁸Universidad de Granada, Granada, Spain; ⁹Consortium General University Hospital of Valencia, Valencia, Spain; ¹⁰Germans Trias i Pujol Hospital, Badalona,

Spain; ¹¹Hospital Universitario de Canarias, La Laguna, Spain; ¹²Central University Hospital of Asturias, Oviedo, Spain; ¹³Puerta de Hierro Majadahonda University Hospital, Majadahonda, Spain; ¹⁴University of Malaga, Málaga, Spain; ¹⁵Hospital del Mar, Barcelona, Spain; ¹⁶Vall d'Hebron University Hospital, Barcelona, Spain; ¹⁷Gregorio Marañón General University Hospital, Madrid, Spain; ¹⁸Institut d'Investigacions Biomèdiques August Pi i Sunyer (IDIBAPS), Barcelona, Spain; ¹⁹CIBEREHD, Spain

Email: mlondono@clinic.cat

Background and aims: The incidence and prevalence of PBC has increased within the last years. This is most likely a result of earlier diagnosis and greater disease awareness. It is currently uncertain if this results in modifications to the pattern of presentation and treatment response. Therefore, the aim of the study was to assess the impact of the diagnostic period (P) in the characteristics of PBC at diagnosis and treatment response.

Method: Retrospective analysis of 795 patients with PBC included in COLHA registry. The inclusion criteria were: (1) diagnosis of PBC made after 1997 (when ursodeoxycholic acid, UDCA, was approved), (2) UDCA treatment for at least 1 year. Patients with variants forms (overlap syndromes) of PBC and other concomitant liver diseases were excluded. The cohort was divided in 3 periods according to the date of PBC diagnosis: P1 before April 2008, P2 between May 2008 and November 2013, and P3 after December 2013.

Results: Most of the patients were female (n = 713, 91%), with a median age of 55 years, 223 (28%) with autoimmune comorbidities. At diagnosis, patients from P3 had lower levels of alkaline phosphatase (ALP), transaminases, bilirubin, and total cholesterol than patients from P1 and P2 (Table). The proportion of patients with liver biopsy and ALT $\geq 2 \times \text{ULN}$ was lower in patients from P3 (44% vs. 31% vs. 24%, $p < 0.001$ y 49% vs. 43% vs 36%, $p = 0.012$, respectively). The mean time from diagnosis to UDCA initiation was lower in patients from P3 (9.8 vs. 4.3 vs. 2.9 months; $p = 0.006$). After 1 year of UDCA treatment, patients from P3 had lower transaminases, GGT, and bilirubin (Table). There was a trend towards a higher response rate (according to Paris-II criteria) in patients from P3, but the difference was not statistically significant (58% vs. 60% vs. 62%, $p = 0, 754$).

POSTER PRESENTATIONS

Variable	Period 1	Period 2	Period 3	p value
Age (years)	54 (23-87)	55 (20-86)	56 (30-88)	0.309
At diagnosis				
ALP (x ULN)	1.97 (1-20.7)	1.77 (1-18.7)	1.68 (1-15.7)	0.036
AST (U/L)	52 (17-957)	47 (14-362)	41 (12-727)	<0.001
ALT (U/L)	66 (8-683)	58 (12-427)	46 (7-489)	<0.001
GGT (U/L)	213 (21-1660)	215 (13-1363)	200 (12-1957)	0.336
Bilirubin (mg/dL)	0.6 (0.2-14.6)	0.5 (0.1-13.1)	0.5 (0.2-13)	0.011
Cholesterol (mg/dL)	224 (92-1847)	217 (76-651)	212 (103-1128)	0.011
Creatinine (mg/dL)	0.86 (0.4-2.5)	0.70 (0.4-2.1)	0.70 (0.2-2.5)	<0.001
1 year after UDCA				
ALP (x ULN)	1.17 (0.29-12.6)	1.25 (0.25-13)	1.22 (0.22-9.53)	0.180
AST (U/L)	31 (12-230)	30 (12-448)	27 (10-121)	<0.001
GGT (U/L)	65 (13-1402)	80 (6-1366)	59 (8-849)	0.016
Bilirubin (mg/dL)	0.6 (0.15-8.4)	0.5 (0.17-15.3)	0.5 (0.02-14)	0.021

Data are median (range)

Figure:

Conclusion: PBC is currently diagnosed with lower levels of ALP, transaminases, and bilirubin. The time from diagnosis until treatment initiation is shorter. However, these differences do not appear to influence treatment response

WED-301

Health-related quality of life and medication adherence in adult patients after liver transplantation due to autoimmune hepatitis: a pilot, single centre study

Maciej K. Janik¹, Joanna Łącz¹, Joanna Raszeja-Wyszomirska¹, Piotr Milkiewicz^{1,2}. ¹Medical University of Warsaw, Department of Hepatology, Transplantology and Internal Medicine, Poland; ²Pomeranian Medical University, Translational Medicine Group, Poland
Email: mjanik24@gmail.com

Background and aims: It has been shown that patients with autoimmune hepatitis (AIH) are prone to impaired HRQoL including increased incidence of depression, anxiety and fatigue. Here, we analyse HRQoL in patients with AIH who underwent liver transplantation (LT-AIH).

Method: We have enrolled 53 liver transplant recipients (74% women, mean age 45 ± 15 years) with AIH. Patients less than six months after LT and those with cholestatic variants of AIH were excluded. HRQoL assessment included following questionnaires: (i) Short Form-12 (SF-12) on physical (PCS) and mental (MCS), (ii) PHQ-9 for depression; (iii) GAD-7, STAI-1 (state) and STAI-2 (trait) for anxiety; (iv) MFIS for fatigue and (v) VAS (visual analogue scale) for self-assessed adherence. Data before and after LT was available in 24 patients. Healthy subjects, non-transplanted cirrhotic and non-cirrhotic patients with AIH, all matched in terms of age and gender served as controls.

Results: The mean time after LT was 4.9 ± 2.6 years. In paired observation before and after LT, all aspects of HRQoL, namely physical and mental component of SF-12, fatigue, anxiety (all $p < 0.01$) as well as depression ($p = 0.016$) showed a significant improvement. Compared to healthy controls, only physical scale of HRQoL was impaired in liver recipients ($p = 0.002$), whereas all others were comparable. LT-AIH group when compared to non-cirrhotic AIH showed a significantly better scores in anxiety assessment (both as a state (STAI-1) and a trait (STAI-2) with $p < 0.01$). Finally, when analysing liver recipients and patients with AIH-related cirrhosis, LT-AIH patients had better physical HRQoL, lower fatigue (physical, psychical and total) (all $p < 0.05$) and lower anxiety ($p < 0.001$, for both STAI domains). VAS for self-assessed adherence to medication in LT-AIH group showed correlation with depression i.e. the better adherence the lower depression scores in PHQ-9 ($\rho = -0.43$, $p = 0.002$) and lower anxiety estimated by GAD-7 ($\rho = -0.31$, $p = 0.02$).

Conclusion: Patients after LT-AIH have a comparable HRQoL to healthy controls, except for the impaired physical domains. Liver recipients had better HRQoL than matched subjects with AIH, both

cirrhotic and non-cirrhotic. Lower adherence to medication was associated with depression and anxiety, this issue needs a special clinical attention. A multicentre prospective study is required to confirm these findings.

WED-302

Autoimmune hepatitis (AIH) in Greece: first results from the Hellenic autoimmune liver diseases study group of the Hellenic association for the study of the liver (HASL)

Nikolaos Gatselis^{1,2}, Christos Triantos³, George Papatheodoridis⁴, Pinelopi Arvaniti^{1,2}, Katerina Antoniou^{1,2}, Efthymios Tsounis³, Margarita Papatheodoridi⁴, Demetrios N. Samonakis⁵, Themistokis Vasileiadis⁶, Ioannis Ketikoglou⁷, Emmanouil Manesis⁷, Dimitrios Christodoulou⁸, Alexandra Alexopoulou⁹, Ioannis-Georgios Koskinas⁹, Spyridon Michopoulos¹⁰, Mairi Koulentakis⁵, Evangelos Cholongitis¹¹, Elena Vezali¹², Emmanouil Sinakos¹³, Melanie Deutsch⁹, Nikolaos Papadopoulos¹⁴, Adonis Protopapas¹⁵, Athina Chounta¹⁶, Konstantinos Thomopoulos³, Vasileios Lekakis⁴, Maria Tsafaridou⁵, Anna Samakidou^{1,2}, Stella Gabeta^{1,2}, George Koukoulis¹⁷, Eirini Rigopoulou^{1,2}, Kalliopi Zachou^{1,2}, Dina Tiniakos¹⁸, George Dalekos^{1,2}. ¹General University Hospital of Larissa, Department of Medicine and Research Laboratory of Internal Medicine, National Expertise Center of Greece in Autoimmune Liver Diseases, Larissa, Greece; ²General University Hospital of Larissa, European Reference Network on Hepatological Diseases (ERN RARE-LIVER), Larissa, Greece; ³University Hospital of Patras, Division of Gastroenterology, Department of Internal Medicine, Patras, Greece; ⁴General Hospital of Athens "Laiko", Academic Department of Gastroenterology, Medical School, National and Kapodistrian University of Athens, Athens, Greece; ⁵University Hospital of Heraklion, Department of Gastroenterology and Hepatology, Heraklion, Greece; ⁶Papageorgiou Hospital, Aristotle University of Thessaloniki, 3rd Department of Internal Medicine, Thessaloniki, Greece; ⁷Liver Unit Euroclinic, Athens, Greece; ⁸University Hospital of Ioannina, Division of Gastroenterology, Department of Internal Medicine, Ioannina, Greece; ⁹Hippokraton General Hospital of Athens, 2nd Department of Internal Medicine, Medical School of National and Kapodistrian University of Athens, Athens, Greece; ¹⁰Alexandra General Hospital, Department of Gastroenterology, Athens, Greece; ¹¹General Hospital of Athens "Laiko", 1st Department of Internal Medicine, Medical School, National and Kapodistrian University of Athens, Athens, Greece; ¹²"Hygeia" Hospital of Athens, Department of Hepatology, Athens, Greece; ¹³Hippokraton Hospital, 4th Department of Internal Medicine, Aristotle University of Thessaloniki, Thessaloniki, Greece; ¹⁴Army Share Fund Hospital of Athens, 1st Department of Internal Medicine, Athens, Greece; ¹⁵Hepatogastroenterology Unit, First Propaedeutic Department of Internal Medicine, Aristotle University of Thessaloniki, Thessaloniki, Greece; ¹⁶University Hospital "ATTIKON", Hepatology Unit, 4th Dep. of Internal Medicine, National and Kapodistrian University of Athens, Athens, Greece; ¹⁷University of Thessaly, Department of Pathology, Faculty of Medicine, School of Health Sciences, Larissa, Greece; ¹⁸Areataieon Hospital, Department of Pathology, Medical School, National and Kapodistrian University of Athens, Athens, Greece
Email: gatselis@me.com

Background and aims: AIH is an acute or chronic inflammatory disease of the liver, affecting people from all ethnic groups irrespective of age and sex. The Hellenic Autoimmune Liver Diseases Study Group of HASL was established in 2016, aiming to evaluate patients' characteristics, treatment practices and outcome, determine the unmet needs of patients, and develop and implement improved treatment approaches.

Method: We included data from 691 patients (518 females, 75%; mean age: 47.5 years) who were recorded in our database till 11/2022.

Results: There was a mean delay till diagnosis of 26.8 ± 60 months. One fifth of patients (20.4%) were initially evaluated by physicians other than Internists/General practitioners, Gastroenterologists or Pediatricians. At first evaluation, 441/691 (63.3%) patients were asymptomatic, 149/691 (21.6%) had general symptoms, while only 102/691 (14.8%) had icteric hepatitis. Extrahepatic autoimmune diseases were diagnosed in 34%. Cirrhosis was present in 153/691 (22.1%), with decompensation in 41/153 (26.8%). During follow-up, 541/691 (78.3%) received corticosteroids, 278/691 (40.2%) azathioprine and 282/691 (40.8%) mycophenolate mofetil (MMF). In 72/691 (10.4%) patients, immunomodulatory treatment changed between azathioprine and MMF. At last evaluation ($n=587$ patients), 81.6% had complete biochemical response (CBR) on treatment, 13.5% insufficient response, 2.4% relapse and 2.4% no-response.

Conclusion: AIH is frequently misdiagnosed because of its heterogeneity, resulting in diagnosis delay and increased cirrhosis incidence. Approximately 1/5 of patients did not achieve CBR on treatment suggesting the need for strict follow-up and potential new therapies. Large databases will aid better understanding and management of AIH in Greece. [on behalf of the Hellenic Autoimmune Liver Diseases Study Group of HASL]

WED-303

May symptom combinations at initial diagnosis of primary biliary cholangitis implicate distinct natural history?

Atsumasa Komori¹, Yuki Kugiyama², Junko Hirohara³, Toshiaki Nakano³, Atsushi Tanaka⁴. ¹National Hospital Organization Nagasaki Medical Center, Clinical Research Center, Omura, Japan; ²National Hospital Organization Nagasaki Medical Center, Hepatology, Japan; ³Kansai Medical University, The Third Department of Internal Medicine, Japan; ⁴Teikyo University School of Medicine, Department of Medicine, Japan
Email: atsuriko1027@yahoo.co.jp

Background and aims: It is generally appreciated that pruritus and jaundice, a hallmark cholestatic symptoms of primary biliary cholangitis (PBC), precede clinically significant portal hypertension (CSPH) in disease progression. Meanwhile, CSPH, esophagogastric varix in particular, may emerge as a sole initial symptom of PBC, in the absence of either pruritus or jaundice. The pattern of combination of liver-related symptoms, in conjunction with age, at initial diagnosis of PBC is a clue for a greater understanding of natural history and trajectories of disease progression in PBC. We analysed the association between symptom combinations of PBC and age at initial diagnosis in large nationwide Japanese PBC cohort.

Method: We performed a cross-sectional study using the nationwide registry in Japan, a cohort study of patients with PBC that has been conducted almost every 3 years by the Intractable Hepato-Biliary Diseases Study Group for Research on Measures for Intractable Disease, which is supported by Health Labour Science Research Grants in Japan. Patients who met at least 2 of the following criteria were diagnosed as having PBC: biochemical evidence of chronic cholestasis; positive AMA in sera; histologic features compatible with PBC. Prevalence and age distribution of patients with liver-related symptoms at diagnosis, comprising of pruritus (P), jaundice (≥ 2 mg/dl of total serum bilirubin: TSB) (J), esophagogastric varix (V), and ascites (A), were analysed.

Results: A total of 2985 patients (mean age 60.4 years) from 14th, 15th and 16th registry ($n=632$, 2005–9; $n=1096$, 2008–12; $n=1244$, 2011–16) were enrolled for study. The mean age of patients with P at

diagnosis (58.8; $n=521$, 17.5%) was significantly younger than those with V (64.7; $n=201$, 6.7%) ($p < 0.0001$) or A (67.1; $n=95$, 3.2%) ($p < 0.0001$), but not than those with J (61.0; $n=160$, 5.4%) ($p = 0.6247$). In 16th registry, patients presenting P and/or J with CSPH (either P/V, P/V/A, P/J/V, P/J/V/A, J/V or J/V/A: stringently cholestatic PBC with CSPH, $n=44$) were significantly younger than those with V or V/A, but without P/J (CSPH-only PBC, $n=49$) (59.9 vs 68.5, $p = 0.00134$). The median TSB and platelet count (PLT, $\times 10^4/\text{microL}$) of CSPH-only PBC were 1.0 and 12.0, respectively; 13 (26.5%) were larger than 15.0 in PLT, suggesting possible inclusion of non-advanced chronic liver disease.

Conclusion: The age distribution of CSPH among PBC patients might be bimodal, reflecting two distinct trajectories toward CSPH in the natural history of PBC, that is, with or without overt cholestasis.

WED-304

Prevalence of celiac disease in adult patients with cryptogenic liver disease

Aditya Vikram Pachisia¹, Ankit Agarwal¹, Shubham Mehta¹, Alka Kumari¹, Anam Ahmed¹, Shubham Prasad¹, Vignesh Dwarkanathan², Sonu Sharma¹, Sambuddha Kumar¹, Prasenjit Das³, Rimlee Dutta³, Shalimar Shalimar¹, Vineet Ahuja¹, Govind Makharia¹. ¹All India Institute Of Medical Sciences, Gastroenterology, New Delhi, India; ²All India Institute Of Medical Sciences, Community Medicine, New Delhi, India; ³All India Institute of Medical Sciences, Pathology, India
Email: avpafmc@gmail.com

Background and aims: In addition to the small intestine, liver also gets affected in them. The spectrum of liver disease in CeD may vary from hypertransaminasaemia, cirrhosis and autoimmune liver diseases. A recent systematic review, including studies with a small number of patients, has shown that 4.6% of patients with cryptogenic cirrhosis have CeD.

Method: Consecutive patients with cryptogenic liver disease with a spectrum ranging from cryptogenic hypertransaminasaemia to cryptogenic cirrhosis were recruited prospectively. All of them were screened for CeD using IgA anti-tissue transglutaminase antibody (anti-tTG ab) and if anti-tTG Ab was found positive, they were subjected to anti-endomysial antibody (AEA) testing and duodenal mucosal biopsy examination. Liver biopsies and corresponding duodenal biopsies of patients with cryptogenic cirrhosis and CeD were subjected to IgA/anti-tTG colocalization studies. For assessment of the prevalence of CeD in cryptogenic cirrhosis, 235 patients were required.

Results: Of 264 patients recruited, 232 had cryptogenic cirrhosis and 32 had cryptogenic hypertransaminasaemia. Of 232 with cryptogenic cirrhosis, 16 had high anti-tTG Ab mean (SD) fold rise of 16.9 (10.5) folds and 11 of them had biopsy-proven CeD, suggesting a prevalence of 4.7%. Of 11 patients with cryptogenic cirrhosis with CeD, AEA was positive in 9. IgA/anti-tTG Ab colocalization was demonstrated in 7/8 liver biopsies from cryptogenic cirrhosis with CeD. All patients with cryptogenic cirrhosis with CeD were started on a gluten-free diet (GFD). Till the writing of this abstract, 6 patients completed a follow-up of 6 months, and all of them had a trend towards improvement in liver functions (CTP score and Meld Na). Two out of 32 patients with cryptogenic hypertransaminasaemia had high anti-tTG Ab and 1 had biopsy-proven CeD

Figure: Individual patient characteristics with Cryptogenic liver cirrhosis with CoD (N=16/330)

Site	Age	CSM	UGB	Incision	HE	CTF	Mean TTC No	Act TTC No	ASA	Modified Mann grade	Liver Injury TTC No	Abut Ab contaminated No	Ductal Injury TTC No	Spectrum Of (Ca)
1	26M	24	Y	N	N	8	17	26	yes	3c	yes	yes	yes	Definite
2	26M	30.2	Y	Y	N	7	19	22	yes	3a	yes	yes	yes	Definite
3	30M	11.6	N	Y	N	7	11.3	25	no	3c	yes	yes	yes	Definite
4	26F	22.6	N	Y	N	8	6.8	26	yes	3c	NO	no	yes	Definite
5	40F	11	N	N	N	9	7.6	26	yes	2	yes	yes	yes	Definite
6	30M	25.6	Y	Y	N	7	7.6	25	no	3c	NO	no	yes	Definite
7	19F	22.6	N	Y	N	8	7.3	26	yes	3c	NO	yes	yes	Definite
8	26M	30.5	N	N	N	5	14.4	21	yes	3c	yes	yes	yes	Definite
9	32M	28	N	N	N	8	6.4	25	yes	3c	yes	no	yes	Definite
10	30F	16.2	N	Y	N	8	16.9	20	yes	3a	no	no	yes	Definite
11	40F	13	N	N	N	5	8.2	25	yes	3c	yes	yes	yes	Definite
12	36M	38.2	N	Y	N	11	24.3	2.2	no	0	NO	no	yes	Potential
13	46M	14.2	N	N	N	7	17.6	2	no	0	NO	yes	yes	Potential
14	40M	47.5	Y	N	N	8	16.7	2.8	no	0	NO	yes	yes	Potential
15	28M	23.3	Y	Y	N	7	8.8	3.4	no	0	NO	no	yes	Potential
16	24F	12.4	N	N	N	8	6.4	2.2	no	1	NO	yes	yes	Potential

SI no- Serial number, LSM-liver stiffness measurement, UGIB- upper gastrointestinal bleeding, HE- Hepatic encephalopathy, CTP-Child-Turcotte-Pugh, MELD-Na- Model of end-stage liver disease, ITG- Tissue transglutaminase, AEA- anti-endomysial antibody, IgA- immunoglobulin A, CaD- celiac disease, MD- not done

Figure:

Conclusion: Approximately 4.7% of patients with cryptogenic cirrhosis have biopsy-proven CeD which is substantially higher than the prevalence of CeD in the general population. Hence all patients with cryptogenic cirrhosis should be screened for CeD.

WED-305

Budesonide is associated with less weight gain than Prednisolone amongst patients with autoimmune hepatitis: results from long term follow-up in routine clinical care

Josh Orpen-Palmer¹, Thea Rodig¹, Alexander Grayston¹, Shannon Devlin¹, Michael Johnston², Jude Morris³, Shouren Datta⁴, Helen Cairns⁵, Ewan Forrest¹, Stephen Barclay¹. ¹Glasgow Royal Infirmary, Glasgow, United Kingdom; ²Royal Alexandra Hospital, United Kingdom; ³Queen Elizabeth University Hospital, United Kingdom; ⁴The New Victoria Hospital, United Kingdom; ⁵Gartnavel General Hospital, United Kingdom

Email: josh.orpen-palmer@ggc.scot.nhs.uk

Background and aims: The survival benefit of corticosteroid therapy in the management of autoimmune hepatitis is well recognised. Budesonide (Bude), an option in patients without cirrhosis, undergoes 90% first pass hepatic clearance with potentially fewer systemic effects than Prednisolone (Pred). A registration trial demonstrated fewer side effects, including lower rates of weight gain, with Bude vs Pred. However, data on the amount of weight gained was not reported and the comparative effects on weight in routine clinical practice over longer durations are unknown.

Method: A retrospective chart review of patients attending 5 Scottish hospitals with a diagnosis of autoimmune hepatitis was performed using a list prospectively kept to facilitate audit. Data was obtained from electronic health records supplemented by historic case notes. Patients diagnosed in paediatric care, with cirrhosis at diagnosis, not treated with steroids or treated with both regimens were excluded. Data on BMI, Diabetes, Diabetic medication and routine biochemistry were collected at diagnosis, end of steroid therapy and last known encounter. Comparison of changes in BMI from baseline to end of steroid therapy and end of follow-up were compared using a two-sample t-test.

Results: 291 patients were identified of whom 56 were excluded (35 cirrhosis, 13 paediatric and 8 receiving both regimens). Of 110 patients reviewed to date, 39/110 (39.4%) receiving Bude and 71/110 (64.5%) Pred. Mean age at diagnosis (57.5 and 52.8 $p=0.11$), BMI at diagnosis (27.1 vs 28.7 $p=0.22$), and diabetes at diagnosis (1/39 (2.56%) and 5/71 (7.04%), $p=0.42$) were similar between both groups. Mean ALT at diagnosis was significantly higher in those receiving Pred (318 vs 744 $p<0.01$). Median follow-up time was 49 months. Pred was associated with significantly increases in BMI at the end of steroid treatment (mean 1.49 (± 2.63) vs (0.35 ± 2.66), $p=0.03$), and a trend towards increased BMI at end of follow-up (1.20 (± 4.02), budesonide -0.24 (± 3.60), $p=0.06$). 2/71 Pred treated patients developed diabetes and 2/5 with existing diabetes required escalation of treatment whilst on steroids. Neither complication was seen in Bude treated patients.

Change in Body Mass Index at end of steroid therapy according to steroid regimen

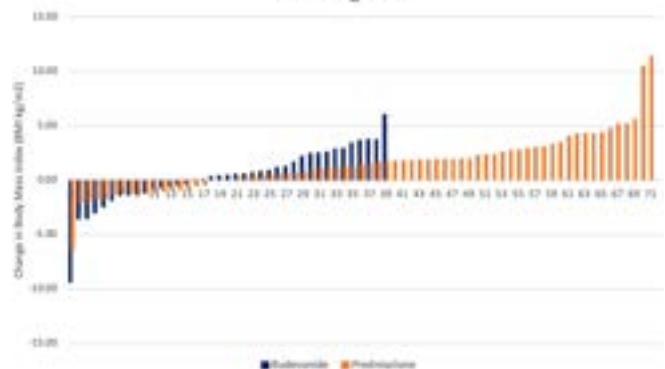


Figure:

Conclusion: In a multi-centre retrospective cohort study, Bude demonstrated reduced rates of BMI gain, de-novo diabetes and deterioration in diabetic control compared with Pred. Weight gained tended to persist overtime, though changes in BMI at end of follow-up did not reach statistical significance in this interim data set. Further data will be presented.

WED-306

Unexpected high incidence of AMA positive primary biliary cholangitis in a northern Italian region

Davide Bitetto¹, Ezio Fornasiere¹, Elisa Fumolo¹, Annarosa Cussigh², Sara Cmet², Pierluigi Toniutto¹. *¹Hepatology and Liver Transplantation Unit, University of Udine, Udine, Italy; ²Clinical Pathology, Azienda Ospedaliero Universitaria Friuli Centrale, Udine, Italy*
Email: davide_bitetto@yahoo.it

Background and aims: Primary Biliary Cholangitis (PBC) is probably underdiagnosed. This is due to the absence of clinical symptoms in the early phase of the disease and the low attention attributed to the mild alteration of cholestatic liver function tests. Anti-mitochondrial antibodies (AMA) are a specific diagnostic marker of PBC and its widespread use of auto-antibody test panels in non-hepatological settings allows incidental findings of AMA patients.

Method: This is a case finding study. The study population consists of all subjects with AMA positive reports in a whole northern Italian region. The study period ranges from August 2018 to January 2023. All the AMA essays of this region are performed in the same laboratory. Clinical and biochemical information of all subjects were retrospectively collected since first appearance of AMA positivity by consulting medical reports.

Results: In a region of 521117 inhabitants, 261 tested positive for AMA for the first time, 83% of them were female with a median age 62 years (range 25–92). The overall yearly incidence was 11.13 cases per 100 000 persons. Out of these, 76 matched criteria for AMA positive PBC, 69 of which were female (91%), with an overall yearly incidence

of 3.24 cases per 100 000 persons, 0.6 cases per 100 000 males and 5.7 cases per 100 000 females. Only 73% of patients were referred to a Liver Unit and started UDCA treatment, out of these 70% underwent stadiation with transient elastography or liver biopsy. Stage III-IV liver fibrosis were present in 5% of them.

Conclusion: The present study found an unexpected high incidence of AMA positive PBC. This could be explained by the availability of all AMA reports of a whole region.

WED-307

Norucholic acid for the treatment of primary sclerosing cholangitis: baseline data from a phase III trial

Michael Trauner¹, Peter Fickert², Palak Trivedi³, Gerald Denk⁴, Martti Färkkilä⁵, Michael Dill⁶, Gerda Elisabeth Villadsen⁷, Christoph Berg⁸, Kristin Kaasen Jørgensen⁹, Marcel Vetter¹⁰, Tobias Müller¹¹, Beat Müllhaupt¹², Christoph Schramm¹³, Christian Strassburg¹⁴, Heike Bantel¹⁵, Tobias Böttler¹⁶, Ulrich Beuers¹⁷, Alexandre Louvet¹⁸, Emina Halilbasic¹, Michael Stiess¹⁹, Markus Proels¹⁹, Michael P. Manns¹⁵. ¹Medical University of Vienna, Division of Gastroenterology and Hepatology, Department of Internal Medicine III, Vienna, Austria; ²Medical University of Graz, Department of Medicine, Graz, Austria; ³University of Birmingham, NIHR Birmingham Biomedical Research Centre, Birmingham, United Kingdom; ⁴University Hospital LMU, Department of Medicine II, Munich, Germany; ⁵University of Helsinki and Helsinki University Hospital, Department of Gastroenterology, Helsinki, Finland; ⁶University Hospital Heidelberg, Division of Gastroenterology, Heidelberg, Germany; ⁷Aarhus University Hospital, Department of Hepatology and Gastroenterology, Aarhus, Denmark; ⁸University Hospital Tübingen, Department of Gastroenterology, Hepatology and Infectiology, Tübingen, Germany; ⁹Akershus University Hospital, Dept. of Gastroenterology, Lørenskog, Norway; ¹⁰Friedrich-Alexander-University Erlangen-Nürnberg, Department of Medicine 1, Erlangen, Germany; ¹¹Charité Universitätsmedizin Berlin, Department of Hepatology and Gastroenterology, Berlin, Germany; ¹²University Hospital Zürich, Swiss-Hepato-Pancreato-Biliary Center and Department of Gastroenterology and Hepatology, Zürich, Switzerland; ¹³University Medical Centre Hamburg-Eppendorf, Department of Medicine and Martin Zeitz Centre for Rare Diseases, Hamburg, Germany; ¹⁴University Hospital Bonn, Department of Internal Medicine I, Bonn, Germany; ¹⁵Hannover Medical School, Department of Gastroenterology, Hepatology and Endocrinology, Hannover, Germany; ¹⁶University Hospital Freiburg, Department of Medicine II, Freiburg, Germany; ¹⁷Amsterdam UMC, Locatie AMC, Department of Gastroenterology and Hepatology, Amsterdam, Netherlands; ¹⁸CHRU de Lille, Services des maladies de l'appareil digestif, Lille, France; ¹⁹Dr. Falk Pharma GmbH, RandD, Freiburg, Germany
Email: michael.trauner@meduniwien.ac.at

Background and aims: Primary sclerosing cholangitis (PSC) is a devastating inflammatory/fibro-obliterative bile duct disease lacking effective medical therapy. The role of ursodeoxycholic acid (UDCA) in the therapy of PSC remains unclear. Norucholic acid (NCA) is a side chain-shortened C23 homologue of UDCA which undergoes cholehepatic shunting and has potent anti-cholestatic, anti-inflammatory and anti-fibrotic properties in preclinical mouse models of cholestatic liver injury with features of PSC. NCA was effective in reducing serum Alkaline Phosphatase (ALP) levels in a phase II trial. In the ongoing Phase III trial the efficacy and safety of 1500 mg/d of oral NCA and Placebo will be compared in the treatment of PSC.

Method: Patients with PSC, ALP >1.5 × ULN and bilirubin ≤4 mg/dL of either sex at the age of 16–75 years, were randomized to a 192-weeks treatment period followed by an open-label extension treatment. Randomized patients received either NCA or Placebo. Stable concomitant UDCA therapy was allowed. The primary efficacy end point was prespecified as partial normalization of ALP levels to <1.5 × ULN and no worsening of overall Nakanuma disease stage at week 96 compared to baseline in the Intention to treat population. For this

purpose, the trial has been designed as a double-blind, randomized, multi-centre trial conducted in the form of a parallel group comparison.

Results: 77 sites from 17 European countries participated in the trial. 417 patients were screened, 303 were randomized and 302 received at least one treatment dose. Median age was 39 years, 71.5% were male, median BMI was 24.1, 78.8% were on UDCA, and 64.2% had inflammatory bowel disease, of which 89.2% had ulcerative colitis. Location of PSC-typical alterations were reported for both intra- and extra-hepatic bile ducts in 48.3% and median duration of PSC was 5.0 years. Median (IQR) laboratory parameters were: bilirubin 0.78 mg/dl (0.54, 1.19), albumin 4.4 mg/dl (4.2, 4.6), INR 1.0 (1.0, 1.1), platelets 235 × 10³/cmm (182 × 10³, 298 × 10³), ALP 310 U/L (230, 437), GGT 274 U/L (159, 514). ELF and liver stiffness by transient elastography were 9.9 (9.2, 10.9) and 9.85 kPa (7.05, 14.40), respectively. Stage F4 liver stiffness was present in 25.4% of the patients. In 16.5% of all patients, clinical signs of liver cirrhosis were reported with a median (IQR) Child-Pugh score of 5.4 (5.0, 6.0). Median (IQR) values for Quality of Life at baseline were 168 (149, 182) for the Chronic Liver Disease Questionnaire (CLDQ) and 20 (15, 28) score points in the PBC-40 questionnaire (PSC adapted) for the domain fatigue.

Conclusion: Baseline characteristics of patients included in this Phase-3 trial NUC-5/PSC represent the typical distribution for a PSC population with active and advanced disease. The investigation of this trial population over a long-term period of 4 years appears adequate to study long-term clinical efficacy of NCA in PSC.

WED-308

Clinical, demographic, laboratory characteristics and disease progression of autoimmune hepatitis patients, asymptomatic at diagnosis, in a tertiary medical center in Israel

Fadi Kinaani¹, Lian Bannon², Majd Khader², Inbal Hour², Moshe Leshno³, Oren Shibolet^{2,3}, Ehud Zigmond^{1,3}. ¹Tel Aviv Sourasky Medical Center-Ichilov, Gastroenterology, Tel Aviv, Israel; ²Tel Aviv Sourasky Medical Center-Ichilov, Gastroenterology, Tel Aviv, Israel; ³Tel Aviv University, Israel
Email: zigmond@u.tlv.ac.il

Background and aims: Autoimmune hepatitis (AIH) is a rare chronic, inflammatory disease with variable presentation, ranging from a mild subclinical course to severe acute icteric disease rarely associated with fulminant hepatic failure. Asymptomatic patients are usually identified following an incidental finding of elevated liver enzymes in blood tests done for various reasons. We investigated the demographics, laboratory tests, liver histology features and disease progression in patients with asymptomatic versus symptomatic presentation of AIH.

Method: Clinical, demographic, laboratory and liver histology data were collected from electronic medical records of patients diagnosed with AIH followed in the hepatology outpatient clinic of a tertiary referral medical center in Israel between 2010 and 2021. Patients with features of overlap variants were excluded.

Results: One hundred and twenty-eight patients with AIH with a median follow-up time of 4.6 years since AIH diagnosis were included. Fifty one percent of the patients were asymptomatic at presentation. Asymptomatic patients were older at diagnosis (50.7 vs. 41.2 years, OR 1.031, p < 0.01), had higher female predominance (86% vs. 67%, p < 0.05) and among the Jewish population were more frequently from Ashkenazi ethnicity (73% vs. 41%, p < 0.01). The body mass index (BMI) tended to be higher among asymptomatic patients (27.1 vs. 24.4, p = 0.058). Liver enzymes and total bilirubin at diagnosis were lower among asymptomatic patients (ALT-271 vs. 826 U/L, p < 0.0005; AST-261 vs. 743 U/L, p < 0.001; total bilirubin 1.7 vs. 8, p < 0.005). Analysis of pathological reports of liver biopsies performed at diagnosis revealed that only 27% of the asymptomatic patients had no fibrosis (F0 stage) as compared to 45% among the symptomatic patients (OR 0.37, p < 0.05).

POSTER PRESENTATIONS

Interestingly, a higher proportion of asymptomatic patients progressed to liver cirrhosis as compared with the symptomatic group (37% vs. 21%, $p < 0.03$).

Conclusion: Our data demonstrates differences in demographic and laboratory parameters between patients with symptomatic and asymptomatic presentation of AIH and an increased progression rate to cirrhosis in patients who were asymptomatic at diagnosis. These findings may support screening for liver enzyme elevation in people at high risk to develop AIH.

WED-309

Prevalence and risk factors of osteoporosis in patients with primary biliary cholangitis in Chinese population

Jialiang Chen¹, Yao Liu¹, Yufei Bi¹, Guiqin Zhou¹, Xiaojing Wang¹, Xianbo Wang¹. ¹Beijing Ditan Hospital affiliated to Capital Medical University, Center of Integrative Medicine, China
Email: wangxb@ccmu.edu.cn

Background and aims: Osteoporosis has been considered the metabolic bone disease associated with primary biliary cholangitis (PBC), which increases the risk of fractures and mortality in patients with PBC. However, there is a lack of epidemiological data on the prevalence of osteoporosis in patients with PBC from China and even the Asia-Pacific region. This study aimed to assess the prevalence and risk factors for osteoporosis in Chinese population with PBC

Method: The clinical data including bone mineral density information of patients with PBC from January 2013 to December 2021 from a tertiary hospital in China were retrospectively collected and analyzed. We defined individuals with T scores of -2.5 or less in any sites (L1 to L4, femoral neck, or total hip) as having osteoporosis based on dual-energy X-ray absorptiometry.

Results: A total of 1272 patients were diagnosed as PBC; 268 (21.1%; 236 women [88.1%]; mean [SD] age, 56.7 [10.6] years; 163 liver biopsies [60.8%]) had a qualified x-ray absorptiometry image at baseline. The prevalence of osteoporosis was 45.5% (95% CI, 39.5%–51.7%) among total population, 34.4% (95% CI, 18.6%–53.2%) among men and 47.0% (95% CI, 40.5%–53.6%) among women, respectively. Osteoporosis was associated with age, fatigue, previous

glucocorticoid therapy, menopausal status, body mass index, splenomegaly, gastroesophageal varices, ascites, Mayo risk score, histological stage, alanine aminotransferase, albumin, bilirubin, platelets and international normalized ratio (INR). Multivariate regression analysis identified older age, higher Mayo risk score, lower body mass index, gastroesophageal varices and previous glucocorticoid therapy as the independent risk factors for osteoporosis.

Conclusion: Osteoporosis is very prevalent in Chinese population with PBC. Age, body mass index, severity of the disease and previous glucocorticoid therapy are the main risk factors for osteoporosis in PBC.

WED-310

Symptom burden in people living with primary biliary cholangitis does not associate with transient elastography measures

Inbal Hourli¹, Madeline Cameron¹, Jonelle Pallotta¹, Aliya Gulamhusein¹, Kristel Leung¹, Gail Wright², Bettina Hansen^{1,3,4}, Gideon Hirschfield¹. ¹Toronto General Hospital, University Health Network, Toronto Centre for Liver Disease, Toronto, Canada; ²Canada PBC Society, Canada; ³Erasmus MC University Medical Center, Department of Epidemiology and Biostatistics, Rotterdam, Netherlands; ⁴University of Toronto, IHPME, Canada
Email: inbalhourio@gmail.com

Background and aims: The symptom burden for people living with primary biliary cholangitis (PBC) significantly impacts quality-of-life. Risk-assessment tools for disease prognosis include importantly transient elastography, a now well-demonstrated surrogate for patient outcome. We sought to evaluate whether a validated symptom burden score (PBC-40) correlated with elastography measures in a large cohort from a dedicated PBC clinic programme.

Method: The PBC-40 scores from people living with PBC cared for at the Toronto Centre for Liver Disease between 2018 and 2022 were correlated with clinical, demographic and laboratory data collected as standard of care.

Results: 243 patients (55% of the clinic cohort; $n = 440$) completed a total of 558 questionnaires. Mean age at questionnaire was 59.5 years (SD 10.74), 94% were female, and mean time from diagnosis was 10

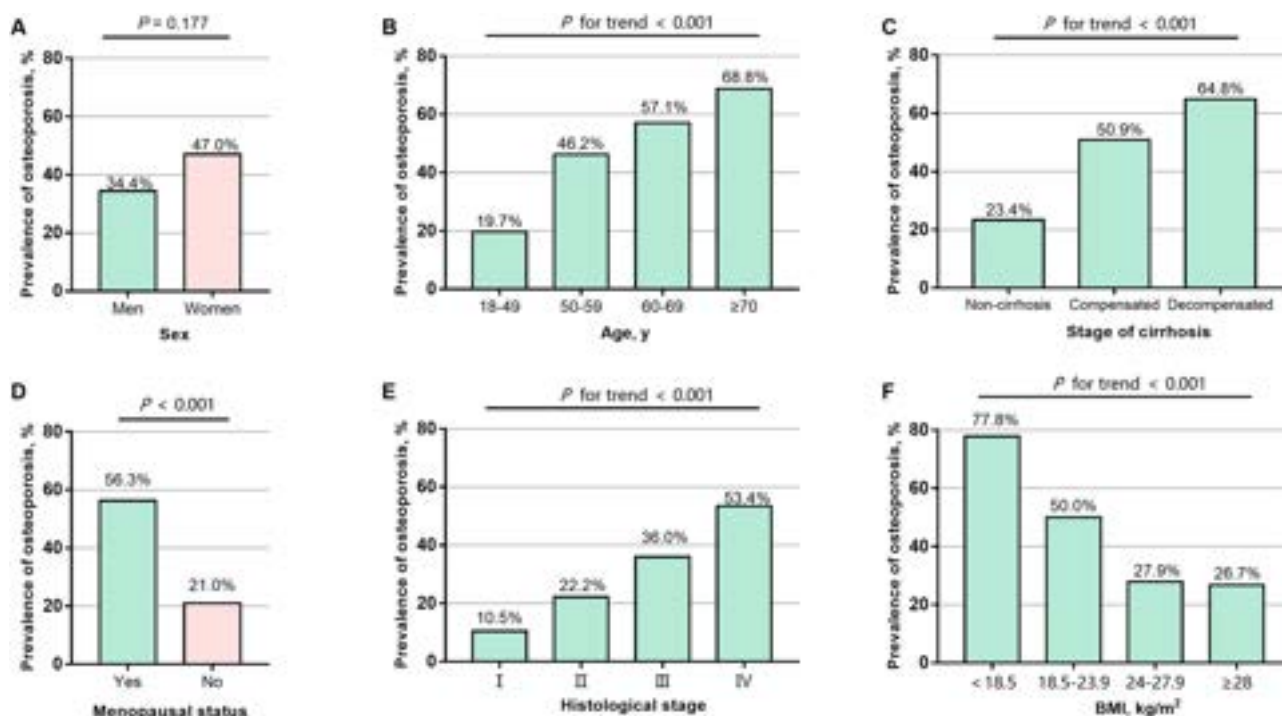


Figure: (abstract: WED-309): Prevalence of osteoporosis in Chinese population with primary biliary cholangitis.

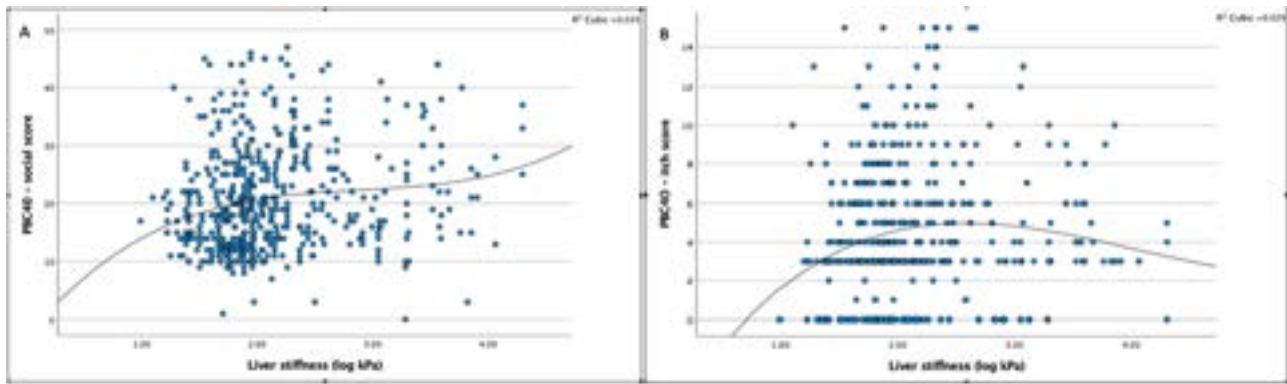


Figure: (abstract: WED-310)

years (SD 7.4). Mean ALP was 177 U/L (SD 125) and AMA was positive in 87.3%. The mean time on ursodeoxycholic acid (UDCA) treatment was 120 months (SD 85.5).

Elastography results were available for 93% of participants, with 61.1% < 8 kPa, 24.6% between 8 and 15 kPa and 14.2% > 15 kPa. In the PBC-40 questionnaire, mean symptom score was 14.11/35 (SD 4.99), fatigue score was 26.12/55 (SD 11.31), itch score was 4.34/15 (SD 3.35), cognitive function score was 11.17/30 (SD 5.9), social score was 20.54/50 (SD 9.01), and emotional score was 6.76/15 (SD 3.28). Logistic regression did not show association between liver stiffness and total PBC-40 score. There was association between the itch and social sub-scores and liver stiffness of higher than 8 kPa, OR of 1.09 (1.03–1.15, $p = 0.001$) (Fig. A); 1.05 (1.03–1.07, $p < 0.001$) (Fig. B).

Conclusion: Symptom burden is significant for people living with PBC but is not a facet of disease severity as evaluated by elastography. Independent approaches to reducing symptoms for people living with PBC are needed alongside disease modifying therapy.

WED-311

Drug-induced autoimmune hepatitis or drug-induced liver injury with autoimmune features: two faces of the same coin?

Pinelopi Arvaniti^{1,2}, Olivas Ignasi¹, Sergio Rodriguez-Tajes¹, Anna Pocurull¹, Helena Hernández Evole¹, Xavier Fornis¹, Maria Carlota Londoño¹. ¹Liver Unit, Hospital Clinic of Barcelona, Institute of Biomedical Investigations August Pi and Sunyer (IDIBAPS), CIBERehd, University of Barcelona, Barcelona, Spain; ²Department of Medicine and Research Laboratory of Internal Medicine, Expertise Center of Greece in Autoimmune Liver Diseases, ERN RARE LIVER, University Hospital of Larissa, Greece
Email: peni.arvaniti@gmail.com

Background and aims: The exposure to certain drugs and/or toxics can trigger liver immune response and unmask a previously unknown or induce de novo autoimmune hepatitis (DI-AIH). However, acute or chronic exposure to the same drugs can also cause drug-induced liver injury with autoimmune features (DILI-AI). Up to now, there are no standardized criteria to differentiate these two entities and the existence of distinct characteristics from idiopathic AIH (i-AIH) is a matter of debate. Therefore, the aims of the current study were to: (1) determine the prevalence of drug exposure among patients diagnosed with AIH, (2) describe the characteristics of DI-AIH and DILI-AI and (3) compare these two entities with i-AIH.

Method: This was a single center retrospective study of 295 patients diagnosed with AIH confirmed by a liver biopsy. Patients were categorized in 3 groups: (1) DILI-AI: patients consuming drugs/toxics known to be associated with DILI-AI and sustained complete biochemical response (CBR) after immunosuppressive treatment withdrawal, (2) DI-AIH: same characteristics, but without an attempt to stop treatment or presenting a relapse after treatment discontinuation and (3) i-AIH: cases without a clear trigger.

Results: Sixty-nine percent of patients ($n = 203$) were female with a median age of 53 years (interquartile range [IQR]: 39–63). Twenty-three percent ($n = 69$) were consuming drugs/toxics at diagnosis, 29 (42%) statins. Eleven patients (4%) were categorized as DILI-AI, 58 (20%) as DI-AIH (in 50 of them treatment was never stopped, while 8 relapsed after treatment withdrawal) and 226 (76%) as i-AIH. Patients with drug exposure (DILI-AI/DI-AIH) were older (58 vs. 52, $p = 0.05$), had higher ALT (867 vs. 555, $p = 0.034$) and faster CBR (3 vs. 5 meses; $p = 0.01$) than patients with i-AIH. In contrast, patients with i-AIH had higher rates of portal/peritportal fibrosis (62% vs. 47%; $p = 0.03$) and established cirrhosis (17% vs. 4%; $p = 0.008$) at diagnosis. No difference in the type of presentation (acute vs. insidious) or in the rate of CBR was noticed, but patients with DILI-AI/DI-AIH had lower levels of ALT and IgG at 12 months of follow-up than patients with i-AIH. Among patients with drug exposure, those with DILI-AI had higher ALT (1334 vs. 734, $p = 0.03$), lower IgG (12 vs. 17; $p = 0.003$) and lower simplified score (5 vs. 6; $p = 0.012$) than patients with DI-AIH. No differences were detected in the time of drug exposure or in the rate of CBR.

Conclusion: Drugs/toxics can trigger AIH in a significant number of patients. The differences between these entities were subtle, but treatment withdrawal was attempted in a minority of cases. Consequently, patients with DILI-AI can be mis-diagnosed being exposed to side effects of unnecessary long lasting treatment regimens.

WED-312

To assess response to steroids and validate SURFASA score in Indian autoimmune hepatitis patients

Harsh Gandhi¹, Shubham Jain¹, Pravin Rathi¹, Sanjay Chandnani¹, Anuraag Jena¹. ¹B.Y.L. Nair Charitable Hospital, Gastroenterology, Mumbai, India
Email: harshgandhi345@gmail.com

Background and aims: In Autoimmune hepatitis (AIH) patients response to steroids and optimal timing of liver transplantation is still a clinical dilemma. In clinical practice to assess response to steroids we monitor bilirubin, SGOT, SGPT, INR and look for signs of worsening in form of ascites or encephalopathy. Recently, a SURFASA score was introduced to identify patients who are not responding to steroids at day 3. The aims of study are: (1) To assess the response to steroids at day 3 from start of treatment. (2) To validate SURFASA score in Indian AIH patients.

Method: It is an interim analysis of an observational prospective study of 45 patients of AIH divided into: (1) Acute AIH (2) Acute severe (AS-AIH) and (3) Acute on chronic liver failure (ACLF) AIH (according to APASL guideline). Response to steroids was assessed at day 3.

Results: 51.1% (23) patients presented as Acute AIH, 28.8% (13) as ACLF and 20% (9) as AS-AIH. Patients (9) who succumbed belonged to ACLF group. Traditional scores such as CTP and MELD were accurate in

POSTER PRESENTATIONS

predicting response to steroids ($p < 0.001$). The cutoff of SURFASA score is < -2.8 in our patients.

Parameters	Improved(n=36)	Death(n=9)	P value
D0-CTP	9 (8-10)	12(12-13)	<0.001
D3-CTP	8.5 (8-9)	12.5(12-14)	<0.001
D0-MELD,mean(SD)	19.6 (2.8)	29.5(7.2)	0.001
D3-MELD,mean(SD)	17.7 (2.5)	31.3 (7)	<0.001
$\Delta\%3$ -bilirubin	-0.1[-0.2(-0.01)]	0.05(-0.1-0.1)	0.003
$\Delta\%3$ -INR	-0.1(-0.4-0.3)	0.1(-0.04-0.7)	<0.001
SURFASA score	-4.7[-5.1(-4.1)]	-2.8[-3.14(-1.2)]	<0.001

Figure:

Conclusion: Patients with Acute and AS-AIH responded to steroids. However, only 30% ACLF AIH patients responded to steroids. SURFASA score and traditional scores (CTP and MELD) are accurate in predicting response to steroids and transplant free survival. Threshold of SURFASA score is different in our population group and so the score needs further validation.

WED-313

The natural history and prognosis of primary sclerosing cholangitis: a multi-center, retrospective cohort study in China

Mingxia Shi¹, Li Yang², Qiuxiang Lin³, Xiaowei Liu⁴, Lu Zhou⁵, Yanhang Gao⁶, Yonghong He⁷, Huihong Yu⁸, Yong-Jian Zhou⁹, Yingmei Tang¹⁰, Yiling Yi¹¹, Ying Sun¹², Min Lian¹³, Xiong Ma¹⁴. ¹Renji Hospital, School of Medicine, Shanghai Jiao Tong University, Shanghai, China, Shanghai Institute of Digestive Disease, China; ²Department of Gastroenterology, West China Hospital, Sichuan University, Chengdu, China; ³Mengchao Hepatobiliary Hospital of Fujian Medical University, Fuzhou, China, Department of Hepatology, China; ⁴Xiangya Hospital of Central South University, Changsha 410008, Hunan, China, Department of Gastroenterology, China; ⁵General Hospital, Tianjin Medical University, Tianjin, China, Department of Gastroenterology and Hepatology, China; ⁶First Hospital of Jilin University, Department of Hepatology, China; ⁷Southwest Hospital, Third Military Medical University, Chongqing 400038, People's Republic of China, Department of Gastroenterology, China; ⁸The Second Affiliated Hospital of Chongqing Medical University, Department of Gastroenterology, China; ⁹Guangzhou First People's Hospital, Department of Gastroenterology, China; ¹⁰the Second Affiliated Hospital of Kunming Medical University, Gastroenterology Department, China; ¹¹First Affiliated Hospital of China Medical University, ShenYang, China, Department of Gastroenterology, China; ¹²the Fifth Medical Center of PLA General Hospital, Department of Liver Disease, Senior Department of Hepatology, China; ¹³Renji Hospital,

School of Medicine, Shanghai Jiao Tong University, Shanghai Institute of Digestive Disease, Shanghai, China, Division of Gastroenterology and Hepatology, Key Laboratory of Gastroenterology and Hepatology, Ministry of Health, State Key Laboratory for Oncogenes and Related Genes, China; ¹⁴Renji Hospital, School of Medicine, Shanghai Jiao Tong University, Shanghai Institute of Digestive Disease, 145 Middle Shandong Road, Shanghai 200001, China, Division of Gastroenterology and Hepatology, Key Laboratory of Gastroenterology and Hepatology, Ministry of Health, State Key Laboratory for Oncogenes and Related Genes, China

Email: maxiongmd@hotmail.com

Background and aims: Contemporary population-based cohorts describing the natural history and prognosis of primary sclerosing cholangitis (PSC) in Asia are scarce. This study aimed to clarify the disease characteristics and long-term outcomes in patients with PSC, and to compare the prognostic value of the Mayo risk score (MRS), UK-PSC score, and the Amsterdam-Oxford model (AOM) in a real-world clinical setting.

Method: We performed a retrospective outcome analysis of patients with PSC referred to 12 centers in China from January 2010 to December 2022. Clinical and laboratory data were collected until the last visit or time of liver transplantation or death. The discriminatory performance of the prognostic scores was assessed with concordance statistics at diagnosis.

Results: Of the 536 patients in the cohort, 371 met the primary end point, with a mean age of 43.2 ± 13.9 years, of whom 201 (54.2%) were male, 42.4% with inflammatory bowel disease (IBD). The diagnosis was large duct PSC in 251 (67.7%), PSC with features of autoimmune hepatitis in 61 (16.4%) and small-duct PSC in 59 (15.9%). Cholangiocarcinoma occurred in 1.6%. During a median follow-up of 42.3 (interquartile range 22.7–67.5) months, 16 patients underwent liver transplantation, and 18 patients died. Overall transplant-free survival was 90% at 5 years and 84% at 10 years. At diagnosis, the concordance statistic for the MRS was 0.689 (95% confidence interval [CI] 0.601–0.777), 0.686 (95% CI 0.612–0.760) for the UK-PSC score, 0.693 (95% CI 0.613–0.774) for the AOM.

Conclusion: In this large multicenter cohort of patients with PSC in China, patients with PSC are increasingly being diagnosed with a milder phenotype. All prognostic scores developed for PSC (MRS, UK-PSC, and AOM) demonstrated comparable discriminating performance for liver transplantation or death.

WED-314

Elevated GGT levels as predictor of non-response to ursodeoxycholic acid in patients with primary biliary cholangitis

Flor M. Fernandez-Gordón Sánchez¹, Elena Gómez Domínguez¹, Ana Martín Algibez¹, Inmaculada Fernández Vázquez¹. ¹Hospital Universitario 12 de Octubre, Spain
Email: florfgs@hotmail.com

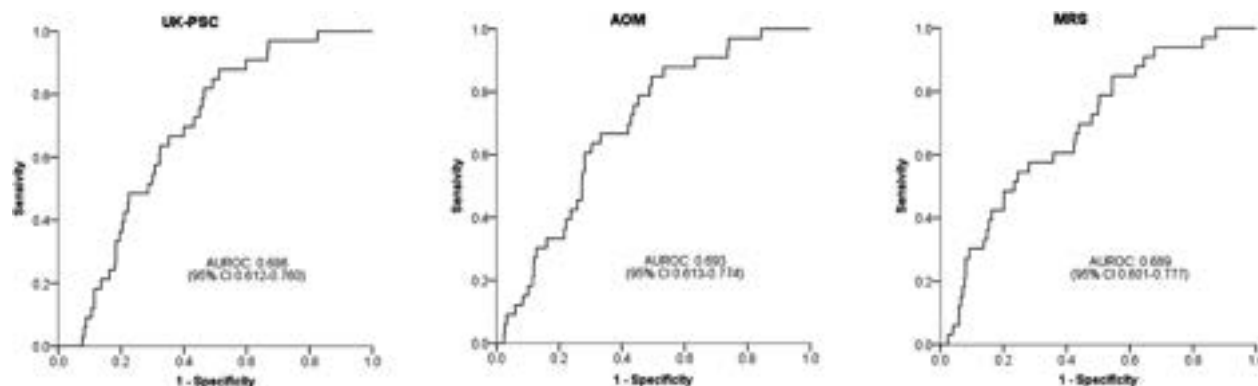


Figure: (abstract: WED-313)

Background and aims: Isolated gamma glutamyl transferase (GGT) values as predictor of response to ursodeoxycholic acid (UDCA) in patients with primary biliary cholangitis (PBC) are not yet well defined. We aimed to analyze the predictive value of GGT elevation at diagnosis and after one year of treatment with UDCA in patients with PBC; we aimed to establish a cut-off point to identify patients who are candidates to second-line therapies.

Method: This single center retrospective cohort study included two cohorts of patients diagnosed with PBC treated with UDCA, according to response to UDCA. Non-response was defined according to the Paris II Criteria. The study was developed between 2014 and 2022. Clinical and analytical variables at baseline and at one year of treatment were compared. ANOVA test and Youden Index were used to define optimal cut-off points in the ROC curve.

Results: 179 patients were included, mean age 60 years (51–71.5), 89.38% women, 152 UDCA responders and 27 non-responders. Liver biopsy was required in a higher percentage in non-responders (74.07 vs 34.67, $p < 0.001$). Non-responders were younger, mean age 51 years ($p < 0.001$), and had higher GGT values at diagnosis [195.00 vs 93.00, $p < 0.008$] and at one year of follow-up [127.00 vs 41.00, $p < 0.001$]. In addition, the alkaline phosphatase (AF) values in the UDCA non-responder group were significantly higher at diagnosis [210.00 vs 122.00, $p < 0.001$] and at one year of follow-up [197.00 vs 102.00, $p < 0.001$]. GGT levels ≥ 219 U/l (S 66.7%, E 88.9%, AUC-ROC 0.7778) and AF ≥ 164 U/l (S 61.9%, E 80%, AUC-ROC 0.7095) were established as cut-off points indicative of non-response after one year of treatment with UDCA. Fig. 1.

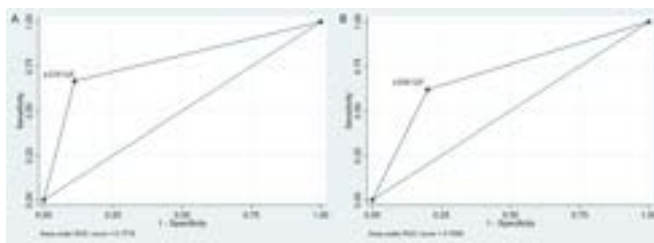


Figure: GGT (A) and AF (B) cut-off points for non-response at one year of treatment with UDCA.

Conclusion: Elevated baseline GGT levels and after one year of UDCA treatment were associated with a worse response. This study may help to identify patients with PBC who are potential candidates to second-line treatment.

WED-315

Celiac disease in patients with autoimmune hepatitis is associated with a milder liver disease course and a better chance of immunosuppressive treatment withdrawal

Francesco Pezzato^{1,2}, Erica D'Ovidio^{1,2}, Lisa Perini^{1,2,3}, Emanuela Bonaiuto^{1,2}, Paolo Rollo^{1,1}, Francesco Paolo Russo^{1,2}, Anna D'Odorico^{1,2}, Fabiana Zingone^{1,2}, Annarosa Floreani^{4,5}, Nora Cazzagon^{1,2}. ¹University of Padova, Department of Surgery, Oncology and Gastroenterology, Italy; ²Padova University Hospital, Gastroenterology Unit, Padova, Italy; ³Company Health Authority n. Serenissima 3, Mira, Italy; ⁴University of Padova, Padova, Italy; ⁵Ospedale Sacro Cuore Don Calabria, Negrar di Valpolicella, Italy
Email: pezzatofrancesco94@gmail.com

Background and aims: Celiac Disease (CD) is 3-times more frequent in people with Autoimmune Hepatitis (AIH) than in the general population. In paediatric patients with AIH, CD is associated with a milder course of AIH and higher chances of immunosuppressive therapy withdrawal. Our aim is To assess the frequency of CD in AIH, and to analyse the features and the long-term response to immunosuppressive treatment in patients with AIH associated with CD (AIH-CD) compared to patients without CD (AIH-non-CD).

Method: A retrospective cohort study including all consecutive people with an established diagnosis of AIH in adulthood was performed. Exclusion criteria were the presence of overlap syndromes or concomitant liver diseases. Decompensation-free survival was calculated according to Kaplan-Meier estimates; data were censored at the date of the last visit or the occurrence of cirrhosis decompensation.

Results: 166 consecutive people (80% female, median age 52) diagnosed with AIH between 1990 and 2021 and followed-up for a median of 63 (24–125) months at the Gastroenterology Unit of the University Hospital of Padova were included. At diagnosis, 18% of patients were cirrhotic; 9 patients (5.4%) had a histologically confirmed diagnosis of CD. People with AIH-CD were treated with significantly lower doses of prednisone at 2 years from diagnosis (2.5 vs 5 mg/day $p = 0.007$) and at 3 years from diagnosis were more likely to have interrupted steroids (83% vs 31%, $p = 0.007$) compared to AIH-non-CD. During the follow-up, immunosuppressive therapy withdrawal was more frequent in AIH-CD compared to AIH-non-CD (44% vs. 13%, $p = 0.01$) while the need for immunosuppressive therapy reintroduction was similar ($p = n.s.$). We did not find any difference regarding cirrhosis development, cirrhosis decompensation, liver-related deaths or the number of relapses between people with AIH-CD and AIH-non-CD.

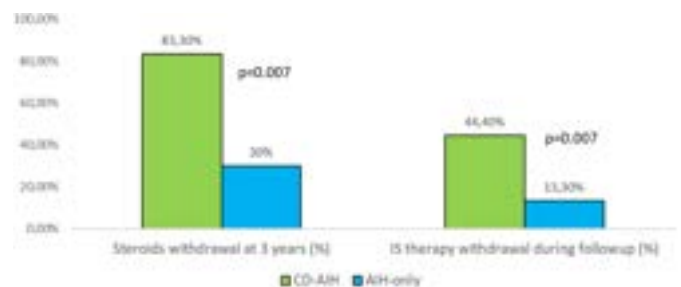


Figure:

Conclusion: In our cohort, CD is present in 5.4% of people with AIH. In people with AIH-CD, we observed a milder course and a higher possibility of immunosuppressive therapy withdrawal compared to AIH-non-CD.

WED-316

Outcome and prognostic factors of primary biliary cholangitis in South Korea

Kyung Ahkim¹, Hwa Young Choi², Moran Ki², Eun Sun Jang³, Sook-Hyang Jeong³. ¹INJE University Ilsan Paik Hospital, Internal Medicine, Goyang-si, Korea, Rep. of South; ²National Cancer Center, Korea, Rep. of South; ³Seoul National University Bundang Hospital, Korea, Rep. of South
Email: kakim@paik.ac.kr

Background and aims: This study aimed to analyze changes in liver biochemistry after UDCA treatment and their prognostic impacts in patients with primary biliary cholangitis (PBC) using the Korean National Health Insurance System database.

Method: PBC patients who were diagnosed between 2010 and 2014 and had taken national health screening before and after PBC diagnosis were included. The Korean National health screening biennially includes aspartate aminotransferase (AST), alanine aminotransferase (ALT), and gamma-glutamyl transferase (GGT), but not alkaline phosphatase. Liver biochemistry measured 1–2 years before and 1–3 years after PBC diagnosis was regarded at baseline and after UDCA treatment. Adherence to UDCA treatment was assessed by calculating the medication possession ratio. Transplant-free survival was analyzed according to age, sex, UDCA treatment, and liver biochemistry using Kaplan-Meier and Cox regression analyses.

Results: A total of 1,449 patients (female 1,237, mean age 57.8) was included. The proportions of abnormal AST, ALT and GGT significantly

POSTER PRESENTATIONS

decreased from 64.3%, 66.7, and 90.8% at baseline to 25.2%, 25.0%, and 64.0% after UDCA treatment, respectively. The 5-year transplant-free survival rate was 92.2%. Old age, male, low adherence to UDCA, abnormal AST, and AST/ALT > 1 were associated with poor prognosis among baseline characteristics. Abnormal AST, AST/ALT > 1, and abnormal GGT were also associated with poor prognosis among features after UDCA treatment.

Table 1: Cox regression analysis of risk factors for death or liver transplantation

	All-cause death or liver transplantation	
	Hazard ratio (95% confidence interval)	
	Univariable	Multivariable
Sex (vs. female)		
male	2.17 (1.49–3.17)	2.14 (1.45–3.17)
Age (by 10-year increase)	2.11 (1.81–2.48)	1.90 (1.63–2.23)
MPR of UDCA (≥80% vs. <80%)	1.78 (1.36–2.33)	1.89 (1.45–2.47)
Baseline liver biochemistry		
AST>ULN (vs. ≤ULN)	2.14 (1.41–3.24)	2.16 (1.47–3.16)
AST/ALT>1 (vs. ≤1)	2.59 (1.79–3.73)	2.16 (1.47–3.16)
GGT>ULN (vs. ≤ULN)	1.11 (0.60–2.05)	0.88 (0.46–1.71)
Posttreatment liver biochemistry		
AST>ULN (vs. ≤ULN)	4.30 (2.73–6.76)	4.35 (2.67–7.07)
AST/ALT>1 (vs. ≤1)	1.75 (1.00–3.07)	1.84 (1.02–3.29)
GGT>ULN (vs. ≤ULN)	2.01 (1.16–3.47)	1.50 (0.83–2.74)

MPR, medication possession ratio; UDCA, ursodeoxycholic acid; AST, aspartate aminotransferase; ULN, upper limit of normal; ALT, alanine aminotransferase; GGT, gamma-glutamyl transferase

Conclusions: The poor prognostic factors in PBC patients were old age, male, low adherence to UDCA, baseline AST/ALT > 1 indicating advanced fibrosis, abnormal AST and GGT after UDCA treatment indicating insufficient UDCA response.

WED-317

The association between cholestatic biochemical markers and clinical symptoms in patients with non-end-stage primary sclerosing cholangitis

Tim Middelburg¹, Nahid Mostafavi², Seval Akbulut¹, Annika Bergquist³, Olivier Chazouilleres⁴, Astrid Kemgang⁴, Hanns-Ulrich Marschall⁵, Stephen Pereira⁶, Lars Aabakken⁷, Cyriel Ponsioen¹. ¹Amsterdam UMC, Locatie AMC, Gastroenterology and Hepatology, Amsterdam, Netherlands; ²Amsterdam University Medical Center, Biostatistics Unit, Gastroenterology and Hepatology, Amsterdam, Netherlands; ³Karolinska University Hospital, Gastroenterology and Hepatology, Sweden; ⁴Hospital Saint-Antoine Ap-Hp, Hepatology, Paris, France; ⁵Sahlgrenska University Hospital, Department of Medicine, Gastroenterology and Hepatology, Gothenburg, Sweden; ⁶Institute of Liver and Digestive Health, University College London and Sheila Sherlock Liver Centre, Royal Free Hospital, London, United Kingdom; ⁷Rikshospitalet, Gastroenterology and Hepatology, Norway
Email: t.e.middelburg@amsterdamumc.nl

Background and aims: In primary sclerosing cholangitis (PSC) the absence of validated surrogate end points impedes treatment development. We aimed at assessing the correlation between biochemical markers of cholestasis and clinical symptoms in order to evaluate their construct validity as surrogate end points.

Method: Cholestatic biochemical markers and clinical symptoms measured by the simple cholestatic complaint score were collected from non-end-stage PSC patients who participated in the DILSTENT trial. The association between each biochemical marker and clinical symptom from baseline to 12 months post-intervention was explored using univariate and multivariate mixed-effect ordinal logistic regression analysis. Measures of associations were expressed as Odds Ratio (OR). Correlation was determined by using Spearman's rank correlation and was expressed as r .

Results: Data from 65 patients was included. The median level of alkaline phosphatase (ALP), bilirubin, gamma-glutamyltransferase (GGT), aspartate aminotransferase (AST) and the proportion of patients with a high levels of complaints decreased during follow-up. The levels of ALP, bilirubin and AST were significantly associated with pruritus levels (OR 1.01 ($p < 0.001$), OR 1.02 ($p = 0.009$), OR 1.01 ($p = 0.004$) respectively) in univariate analysis. Only ALP remained significant in multivariate analysis (OR 1.01, $p < 0.001$). ALP, bilirubin, GGT and AST were not significantly associated with fatigue, right upper quadrant pain or fever. A significant correlation was found between relative change in ALP and change in pruritus from baseline to month 3 post-intervention ($r = 0.34$; $p = 0.02$)

Conclusion: ALP is significantly associated with the most exigent symptom of cholestasis, i.e. pruritus. Our results corroborate the hypothesis that ALP has construct validity as a marker of cholestatic itch, thereby supporting its role as potential surrogate end point for clinical trials.

WED-318

Exploring the impact of ursodeoxycholic acid therapy on COVID-19 in a real-world setting

Christophe Corpechot¹, Marie Verdoux², Marie Frank-Soltysiak³, Lamiae Grimaldi², Jean-Charles Duclos-Vallée⁴. ¹Saint-Antoine Hospital, Assistance Publique-Hôpitaux de Paris, Sorbonne University, Reference Center for Inflammatory Biliary Diseases and Autoimmune Hepatitis, Paris, France; ²Bicêtre Hospital, Assistance Publique-Hôpitaux de Paris, Paris-Saclay University, Department of clinical research, France; ³Bicêtre Hospital, Assistance Publique-Hôpitaux de Paris, Paris-Saclay University, Department of medical information, France; ⁴Paul-Brousse Hospital, Assistance Publique-Hôpitaux de Paris, Inserm UMR-S 1193, Paris-Saclay University, University Hospital Federation HepatinoV, Villejuif, France

Email: christophe.corpechot@aphp.fr

Background and aims: Very recently, Brevini et al. demonstrated that ursodeoxycholic acid (UDCA)-mediated ACE2 downregulation reduces susceptibility to SARS-CoV-2 infection in vitro, in vivo and in human biliary and pulmonary organoids ex situ perfused (1). They also observed an association between UDCA therapy and positive clinical outcomes following COVID-19. Given the potentially important implications of this finding, the therapeutic value of UDCA in this infectious setting must to be confirmed. Our aim was to investigate the association between UDCA exposure and the occurrence of hospitalization for COVID-19.

Method: We designed a case-control study in the source population of adult patients followed up at the Assistance Publique-Hôpitaux de Paris (APHP), Paris Hospitals Group, France, through their medical records (APHP health data registry) and pre-diagnosed with primary biliary cholangitis (PBC) or primary sclerosing cholangitis (PSC). Liver transplant patients were excluded. Cases were patients hospitalized >24 h for COVID-19 as the primary diagnosis between 2020/03/01 and 2020/12/31 (1st stay of the first hospitalization if multiple stays). Controls were patients from the same source population, not hospitalized for COVID-19 as the primary diagnosis over the same period, secondarily matched on PBC/PSC, age, sex and index date (date of case admission). Exposure was defined by UDCA use prior to index date. The confounding factors, including age, severity of liver disease, autoimmune hepatitis, diabetes, cardiovascular disorders, obesity, alcoholism, chronic obstructive pulmonary disease, renal failure, chronic inflammation of gastrointestinal tract, and hospitalization prior to pandemics, were controlled for by a risk score.

Results: Among 1401 patients with PBC or PSC, 1330 (94.9%) were given UDCA therapy. Out of the 7 cases and 1394 unmatched controls identified during the study period, 6 (85.7%) and 1324 (95.0%) were exposed to UDCA. The matching yielded to 6 cases and 52 matched controls. Comparison of exposure between cases ($n = 5$, 83.3%) and matched controls ($n = 48$, 92.3%), using a conditional logistic regression model estimated a crude and adjusted odds ratio (95%

confidence interval, CI) of 0.84 (0.07–9.86) and 2.67 (0.11–63.93) respectively. Non-significant results were also obtained from the full unmatched population adjusted for age, sex, PBC/PSC and above-mentioned confounding factors (Table below).

Table Odds Ratios (95% CI) of UDCA exposure for hospitalization due to Covid-19.

Population	Exposed cases	Exposed controls	Unadjusted OR	Adjusted OR
Complete	6 (85.7%)	1324 (95.0%)	0.32 (0.04–2.67)	0.25 (0.03–2.25)
Matched	5 (83.3%)	48 (92.3%)	0.84 (0.07–9.86)	2.67 (0.11–63.93)

Conclusion: In this real-world data study, we could not establish evidence of an association between UDCA use and the occurrence of hospitalized COVID-19, a result that does not support a protective effect of UDCA against SARS-CoV2 infection. However, the high exposure to UDCA in this population as well as the limited number of cases resulted in a lack of statistical power that precludes any definitive conclusion. Larger studies are therefore warranted.

Reference

1. Brevini *et al.*. *Nature*. 2022 Dec 5. doi:. Epub ahead of print. PMID: 36470304.

Immune-mediated and cholestatic Experimental and pathophysiology

WEDNESDAY 21 TO SATURDAY 24 JUNE

TOP-060

Bacteriophage therapy against pathological *Klebsiella pneumoniae* that determine the clinical course of primary sclerosing cholangitis

Masataka Ichikawa¹, Nobuhiro Nakamoto¹, Sharon Kred-Russo², Eyal Weinstock², Iddo Nadav Weiner², Efrat Khabra², Noa Ben-Ishai², Dana Inbar², Noga Kowalsman², Ron Mordoch², Julian Nicenboim², Myriam Golemb², Naomi Zak², Takahiro Suzuki¹, Kentaro Miyamoto¹, Toshiaki Teratani¹, Sota Fujimori¹, Yoshimasa Aoto³, Mikiko Konda³, Naoki Hayashi³, Po-Sung Chu¹, Nobuhito Taniki¹, Rei Morikawa¹, Ryosuke Kasuga¹, Takaya Tabuchi¹, Shinya Sugimoto¹, Yohei Mikami¹, Atsushi Shiota^{4,5}, Merav Bassan², Takanori Kanai¹. ¹Keio University School of Medicine, Division of Gastroenterology and Hepatology, Department of Internal Medicine, Shinjuku-ku, Tokyo, Japan; ²BiomX Ltd, Ness Ziona, Israel; ³JSR-Keio University Medical and Chemical Innovation Center (JKIC), JSR Corp., Shinjuku-ku, Tokyo, Japan; ⁴Department of Microbiology and Immunology, Keio University, Shinjuku-ku, Tokyo, Japan; ⁵Microbiopharm Japan, Co. Ltd., Japan
Email: ichikawa_mstk_19@yahoo.co.jp

Background and aims: Primary sclerosing cholangitis (PSC) is a cholestatic liver disease characterized by progressive biliary inflammation and fibrosis with a frequent complication of inflammatory bowel disease (IBD). We recently reported that specific gut microbiota, *Klebsiella pneumoniae* (Kp), *Proteus mirabilis* (Pm), and *Enterococcus gallinarum* (Eg), were frequently present in faecal samples from patients with PSC+IBD and the combination of these three gut bacteria contributed to the pathogenesis of the hepatobiliary phenotype. As a mechanism of pathogenesis, these bacteria translocated to mesenteric lymph nodes (MLN) and contributed to subsequent T helper 17 (TH17) cell induction in the liver. However, it remains unclear whether the abundance or combination of these microbiota is associated with the clinical outcome of PSC, and whether certain bacteria might serve as therapeutic targets. As a

therapeutic tool for targeting specific gut microbiota, we developed a lytic bacteriophage cocktail specifically targeting PSC-derived Kp strains, which demonstrated a sustained suppressive effect in vitro.

Method: We collected faecal samples from 45 PSC patients, either complicated with IBD (n = 34) or without IBD (n = 11) and investigated whether carriage of each bacterium or its combination could affect the clinical course. Germ-free (GF) mice and specific pathogen free (SPF) mice were inoculated with PSC-derived Kp and administered with the phage cocktail, and Kp levels in faecal samples were measured. 16 s rRNA metagenome analysis was used to examine the effect of phage cocktail on the overall gut microbiota composition of faecal samples. Furthermore, to examine the effect of phage cocktail on experimental hepatobiliary injuries, Kp-colonized mice were given phage cocktail or vehicle orally or intravenously three times a week during 3,5-diethoxycarbonyl-1,4-dihydrocollidine (DDC) feeding for three weeks.

Results: We detected abundant Kp and Eg in faecal samples from 45 patients with PSC regardless of intestinal complications (Kp: PSC, 82% vs. PSC+IBD, 82%; Pm: PSC, 21% vs. PSC+IBD, 9%; and Eg: PSC, 73% vs. PSC+IBD, 76%). Carriers of both Kp and Eg (n = 28) exhibited higher serum ALP levels and poorer transplant-free survival compared to non-carriers (n = 17). Colonization of PSC-derived Kp in hepatobiliary injury-prone mice enhanced liver Th17 cell responses and exacerbated hepatobiliary injury through bacterial translocation to MLN. Oral administration of the phage cocktail reduced intestinal Kp levels in Kp-colonized mice by 2 log without inducing off-target dysbiosis. Furthermore, oral and intravenous administration of phage cocktail reduced Kp levels in hepatobiliary injury-prone SPF mice, and attenuated liver Th17 numbers, hepatobiliary inflammation, and fibrosis progression. Of note, the amount of Kp in the MLN significantly correlated with the degree of fibrosis in the phage-treated mice, suggesting that a direct targeting of the translocated Kp may be a more appropriate therapeutic approach.

Conclusion: Our results identified a clear association between specific gut microbiota Kp and the clinical course of PSC, and revealed that targeting a single Kp pathogen with a strain-specific phage cocktail is promising for the treatment of PSC.

TOP-064

Development of an in vitro bile-duct-on-a-chip-platform using patient-derived cholangiocytes

Anna Katharina Frank^{1,2,3,4,5}, Henry Hoyle^{1,2,4,5}, Kayoko Hirayama-Shoji^{4,6}, Mathias Busek^{4,6}, Aleksandra Aizenshtadt⁴, Fotios Sampaziotis^{7,8,9,10}, Tom Hemming Karlsen^{1,2,5,11}, Stefan Krauss^{4,6}, Espen Melum^{1,2,4,5,11}. ¹Norwegian PSC Research Center, Department of Transplantation Medicine, Division of Surgery, Inflammatory Diseases and Transplantation, Oslo University Hospital Rikshospitalet, Oslo, Norway; ²Research Institute of Internal Medicine, Division of Surgery, Inflammatory Diseases and Transplantation, Oslo University Hospital Rikshospitalet, Oslo, Norway; ³Scientia Fellowship, European Union's Horizon 2020 research and innovation program under the Marie Skłodowska-Curie grant agreement No 801133, Norway; ⁴Hybrid Technology Hub, Institute of Basic Medical Science, University of Oslo, Oslo, Norway; ⁵Institute of Clinical Medicine, Faculty of Medicine, University of Oslo, Oslo, Norway; ⁶Department of Immunology and Transfusion Medicine, University of Oslo, Oslo, Norway; ⁷Wellcome Trust-Medical Research Council Cambridge Stem Cell Institute, Jeffrey Cheah Biomedical Centre, University of Cambridge, Cambridge, United Kingdom; ⁸Department of Surgery, University of Cambridge, Cambridge, United Kingdom; ⁹Department of Medicine, University of Cambridge, Cambridge, United Kingdom; ¹⁰Cambridge Liver Unit, Cambridge University Hospitals NHS Foundation Trust, Cambridge, United Kingdom; ¹¹Section of Gastroenterology, Department of Transplantation Medicine, Division of Surgery, Inflammatory Diseases and Transplantation, Oslo University Hospital Rikshospitalet, Oslo, Norway
Email: anna.frank@medisin.uio.no

POSTER PRESENTATIONS

Background and aims: Primary sclerosing cholangitis (PSC) is a progressive bile duct-based liver disease without medical treatment options. Cholangiocytes are the main target of destruction in PSC, yet the exact mechanisms that lead to cholangiocyte damage are not fully understood. A lack of representative disease models available is currently hindering advances in our understanding of PSC development and progression. Current *in vitro* bile-duct models are limited to the use of murine cholangiocytes and do not offer the inclusion of bile or other disease relevant cell types, such as immune cells. We aimed to develop a representative, robust and simplified *in vitro* model of a human bile duct that allows us to interrogate the cross-function between cholangiocytes and other disease-relevant components on a cellular level.

Method: Cholangiocytes were isolated from the bile ducts of PSC and healthy control patients undergoing routinely performed endoscopic retrograde cholangiopancreatography (ERCP) and propagated as organoids using previously established culture conditions. Cholangiocytes were then seeded into a perfused channel surrounded by a collagen/laminin mixture that resembles the *in vivo* environment within the bile ducts. Cells were grown for approximately 7 days before channel confluency was reached and then analyzed by fluorescent microscopy.

Results: We developed a robust and scalable *in vitro* platform that resembles the *in vivo* architecture of a bile duct (Fig. 1A and B). We optimized the chip design and materials for high-throughput analysis, advanced microscopy and drug screening compatibility and adjusted the channel size and coating mixture to maximize physiological resemblance. We further designed a fluidic system that allows incorporation of internal fluidics (bile/blood) to the system without the use of tubing. The chip design supports the stable growth of patient-derived cholangiocytes in form of a 3-dimensional gravity perfused bile-duct-like channel. Cholangiocytes grown in the chip form a confluent monolayer channel, express key markers of cellular identity and exhibit strong cell-cell contacts (Fig. 1C).

Conclusion: In this proof-of-concept study we provide a robust fluidic platform for culturing patient-derived cholangiocytes in a tubular structure resembling the *in vivo* architecture of a bile duct. The flexible chip design supports the inclusion of other disease-relevant components, such as bile or relevant immune cells, and can be used in future studies to model various aspects of cholangiopathies *in vitro*. The use of patient-derived cells further offers possibilities for personalized drug testing approaches.

FRIDAY 23 JUNE

FRI-330

Phenotypic diversity and regeneration in a model of Alagille syndrome recapitulate patient heterogeneity

Linde Sevenants¹, Stefaan Verhulst², Franziska Hildebrandt³, Johan Ankarklev³, Leo van Grunsven², Noémi K. M. Van Hul¹, Emma Andersson¹. ¹Karolinska Institute, Cell and Molecular Biology, Stockholm, Sweden; ²Vrije Universiteit Brussel, Liver Cell biology research group, Brussels, Belgium; ³Stockholm University, Department of Molecular Biosciences, Stockholm, Sweden
Email: noemi.van.hul@ki.se

Background and aims: Alagille syndrome (ALGS) is caused by a mutation in *JAG1* or *NOTCH2* and is characterized by bile duct paucity. There is a high phenotypic variability in disease presentation and a genotype-phenotype correlation is lacking. An estimated 60–75% of children with cholestatic ALGS will need a liver transplantation (LT), while others will spontaneously recover their biliary system. We use our *Jag1^{Ndr/Ndr}* model recapitulating hallmark features of ALGS to (1) characterise disease presentation, (2) to identify biomarkers predicting the disease course, and (3) to study mechanisms driving bile duct recovery.

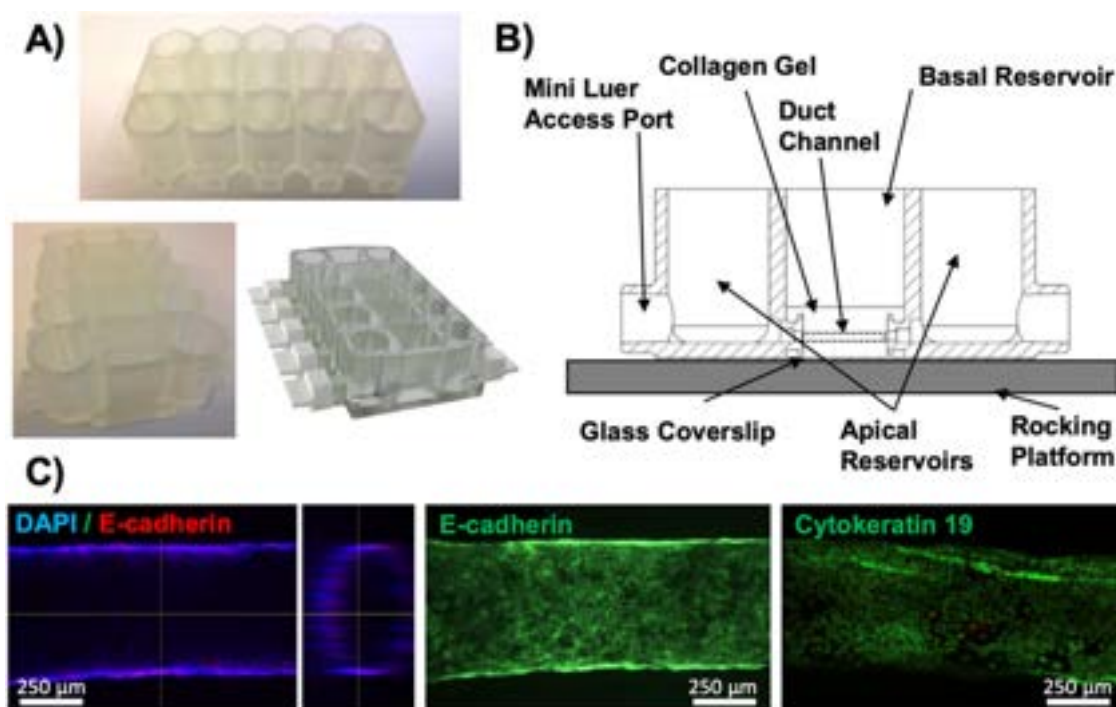


Figure: (abstract: TOP-064): The bile-duct-on-a-chip platform. A) Photos and a schematic of the chip. B) A cross section showing the compartments in the chip design. C) Fluorescent staining of cholangiocytes within the bile-duct-chip showing formation of a tubular structure through nuclear staining (DAPI) with expression of key proteins such as E-cadherin and Cytokeratin 19.

Method: Outbred *Jag1^{+/+}* and *Jag1^{Ndr/Ndr}* mice were sacrificed at P30. Plasma was analyzed for liver function (BR, BA, ALP, ALT). IHC was done on liver sections for early biliary marker SOX9, myofibroblast marker aSMA and proliferation marker Ki67. Spatial transcriptomics (ST) was performed on 4 liver sections from regenerating mice and 4 sections from mice with severe condition.

Results: All *Jag1^{Ndr/Ndr}* pups display strong cholestasis at birth. At P30, three phenotypic groups can be distinguished: mice with (1) a mild phenotype with bile ducts and clear plasma (15 out of 47 mice, representing patients with recovered bile ducts), (2) intermediate severity phenotype with ongoing regeneration and bile infarcts (BIs) (21/47 mice), and (3) regeneration-incompetent mice with severe jaundice and large BIs (11/47 mice, representing patients in need of LT). The BIs in regenerating livers (3–10% of liver surface, preliminary data), were infiltrated by aSMA⁺ cells and lined by SOX9⁺ hepatocytes implying ongoing biliary reprogramming in these areas. aSMA⁺ BI (up to 16% of surface) were predominant in severe *Jag1^{Ndr/Ndr}* mice, and SOX9⁺ hepatocytes around the BIs were sparser and scattered. Finally, there was a strong proliferative response in intermediate mice (increase in Ki67⁺ cells), but not in severe mice. ST sequencing data of regenerating and severe livers with an estimated 200 spatial spots covering BIs (each spotted array is 100 mm in diameter, and contains mRNA captured from 10 to 60 cells) is currently being analyzed.

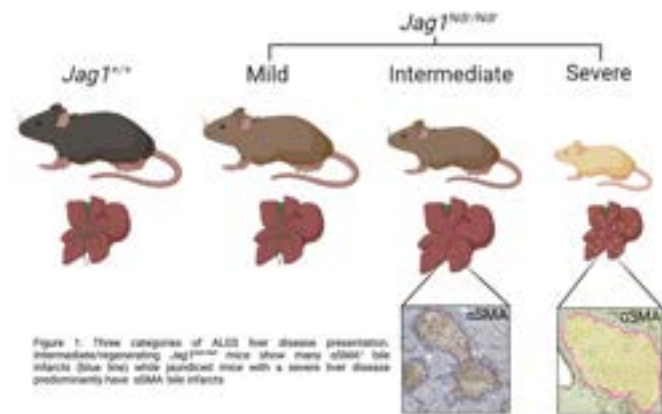


Figure:

Conclusion: *Jag1^{Ndr/Ndr}* mice recapitulate a broad spectrum of liver disease in ALGS at P30. The data indicate a lack of reparative response in severe mice. We hypothesize that aSMA⁺ BIs act as signaling centers for hepatocyte conversion and biliary regrowth. Using ST, we are investigating the molecular landscape of the BI microenvironment.

FRI-331

Identification of potential targets amenable to novel therapeutics to treat symptoms in primary biliary cholangitis

Aaron Wetten^{1,2}, Ben Barron-Millar², Laura Ogle², George Mells³, Steven Flack³, Vinod Hegade⁴, Richard Sandford³, John Kirby², Jeremy Palmer², Sophie Brotherston², Laura Jopson^{1,2,2}, John Brain², Graham Smith⁵, Steve Rushton⁶, Rebecca L. Jones⁴, Simon Rushbrook⁷, Douglas Thorburn⁸, Stephen Ryder⁹, Gideon Hirschfield^{10,11}, David Jones^{1,2}, Jessica Dyson^{1,2}. ¹Newcastle Freeman Hospital, High Heaton, United Kingdom; ²Newcastle University, Translational and Clinical Research Institute, United Kingdom; ³University of Cambridge, Dept of Human Genetics, United Kingdom; ⁴Saint James Hospital, Liver Unit, United Kingdom; ⁵Newcastle University, Bioinformatics Support Unit (BSU), United Kingdom; ⁶Newcastle University, School of Natural and Environmental Science, United Kingdom; ⁷Norwich Medical School, University Department of Hepatology, United Kingdom; ⁸Royal Free Hospital, Liver Unit, United Kingdom; ⁹Queen's Medical Centre, NIHR Nottingham Biomedical Research centre, United Kingdom; ¹⁰Queen Elizabeth Hospital Birmingham, United Kingdom; ¹¹University of Toronto, Toronto Centre for Liver Disease, Toronto, Canada
Email: aaron.wetten@nhs.net

Background and aims: Primary Biliary Cholangitis (PBC) is a progressive autoimmune cholestatic liver disease. Symptoms of pruritus, fatigue and cognitive impairment are common and have a significant negative impact on patients' quality of life. The PBC-40 is a validated, disease-specific, patient-reported outcome measure with well described and validated cut-offs for 'clinically significant' symptoms. The biological mechanisms underpinning these symptoms are poorly understood. The UK-PBC consortium recently published data on an inflammatory proteome associated with disease response. This study further explored the link between the proteome and symptoms in PBC.

Method: An exploratory cohort used O-link serum proteomics of 20 inflammatory markers previously associated with the pathogenesis of PBC were performed on 289 fully-characterised PBC patients from the UK-PBC nested cohort. They were compared to clinically significant symptoms, as assessed using the PBC-40. A validation cohort, using 6 of the markers showing positive associations and a further 5 biologically linked markers, was undertaken using a custom-made multiplex on a symptom heavy cohort of 160 PBC patients (identified from the BANC, RITPBC and UK-PBC cohorts) and 40 healthy controls.

Results: In both the exploratory and validation cohorts, younger age was associated with more severe fatigue (exploratory $p=0.016$; validation $p=0.003$), and cognitive symptoms (exploratory $p<0.001$;

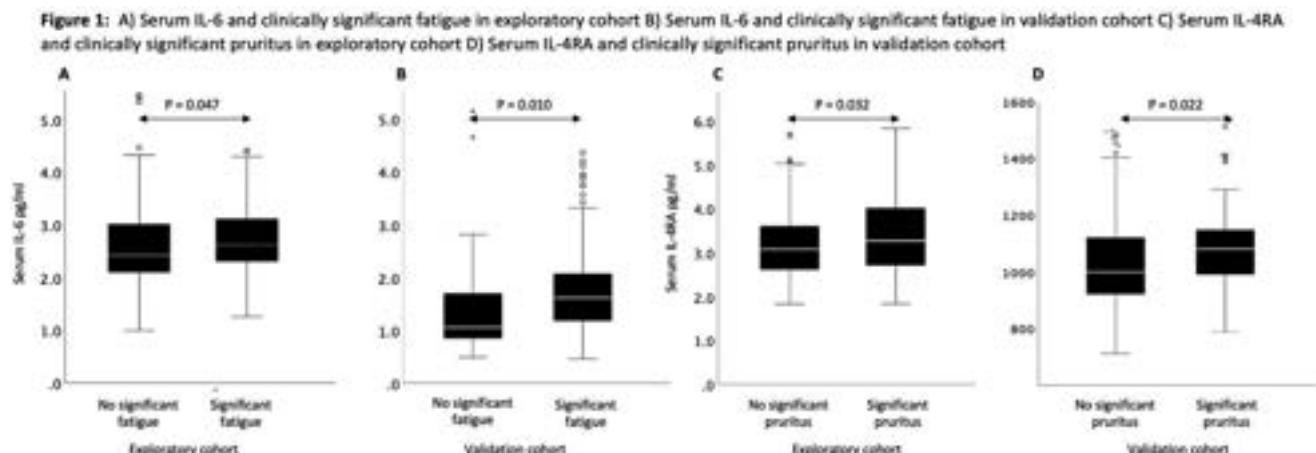


Figure: (abstract: FRI-331).

POSTER PRESENTATIONS

validation $p < 0.001$), but not pruritus. Interleukin-6 (IL-6) was positively associated with clinically significant fatigue, as compared with not clinically significant fatigue, in both studies (exploratory: median 2.63 (IQR 0.80) pg/ml vs 2.42 (0.89), $p = 0.047$; validation: 1.62 (0.89) vs 1.06 (0.86); $p = 0.01$) [Figure 1A and 1B]. Interleukin-4 Receptor Alpha (IL-4RA) was associated with clinically significant pruritus, as compared with not clinically significant pruritus in both cohorts (exploratory: 3.27 (1.30) pg/ml vs 3.09 (1.01), $p = 0.032$; validation: 1081 (173) vs 1000 (200); $p = 0.022$) [Figure 1C and 1D].

Conclusion: Pruritus treatments are effective in some, but not all, patients whilst there are no effective treatments for fatigue or cognitive symptoms. The development of novel therapeutics targeting symptoms remains a significant unmet need in PBC. IL-6 was consistently elevated in two distinct PBC groups with clinically significant fatigue. Elevated IL-6 has previously been implicated in chronic fatigue, skeletal muscle fatigability and mitochondrial dysfunction. With established IL-6 blockade therapies available, this may present a new therapeutic strategy for fatigue. IL-4RA demonstrated a positive association for clinically significant pruritus across both groups. A trial of Dupilumab, an IL-4RA receptor antagonist, is ongoing and may prove to be an effective treatment for cholestatic pruritus.

FRI-332

Anti-nucleosome antibodies as an important marker to distinguish between autoimmune hepatitis and drug-induced liver injury

Mirjam Kolev¹, Guido Stirnimann¹, Henning Nilius², Juliette Schlatter², Michèle Freiburghaus¹, Michael Nagler², Michael Horn², Nasser Semmo¹. ¹Inselspital, Bern University Hospital, University of Bern, Department of Visceral Surgery and Medicine, Bern, Switzerland; ²Inselspital, Bern University Hospital, University of Bern, Department of Clinical Chemistry, Bern, Switzerland
Email: nasser.semmo@insel.ch

Background and aims: Antinuclear antibodies (ANA) are positive in 70–100% of patients with autoimmune hepatitis (AIH) and in 22–33% of patients with drug-induced liver injury (DILI), yet little is known about their antigen-specificity. Differentiation between AIH and DILI is often difficult, especially in DILI cases with ANA positivity but no need for immunosuppression. Since treatment strategies differ, correct classification is important. Our aim was to investigate the antigen-specificity of ANA in AIH and DILI patients and to model their value in the classification of the two diseases.

Method: Samples were obtained from the Hepatology Biobank of the University Hospital Bern, Switzerland, from patients with AIH ($n = 54$) or DILI ($n = 29$) who were ANA positive at diagnosis or during follow-up. ANA testing was performed with indirect immunofluorescence (IIF), followed by pattern specific antibody testing with enzyme-linked immunosorbent assays (ELISA) according to the International Consensus on Antinuclear Antibody Pattern; e.g. anti-DNA, -histone and -chromatin/nucleosome, when a homogenous pattern was detected. Based on the descriptive results, we built a random forest model with the variables of significance.

Results: The median (IQR) age at diagnosis was 57 years (43.50, 67.75) in the AIH versus 58 years (40, 65) in the DILI group. In the AIH group, 74% were women, in the DILI group 65.5%. The median level of immunoglobulin G was higher in the AIH group (22.20 g/l (14, 31.2)) than in the DILI group (10.5 g/l (9.5, 14.7)) ($p < 0.001$). The most frequent ANA patterns in AIH were homogeneous in 76% and fine-speckled in 69%. In DILI patients, the most frequent ANA patterns were fine-speckled in 90% and homogenous in 48%. In AIH patients, anti-nucleosome antibodies were detected in 37% of patients compared to 7% in DILI patients ($p < 0.01$), anti-histone antibodies in 30% in AIH compared to 3% in DILI ($p < 0.01$). 26% of AIH and 34% of DILI patients remained non-specific after ELISA testing. The Figure shows the mean depth in the random forest model for anti-nucleosome and established AIH-related antibodies. The smaller the

mean value, the higher the significance of the variable in the classification of the two diseases.

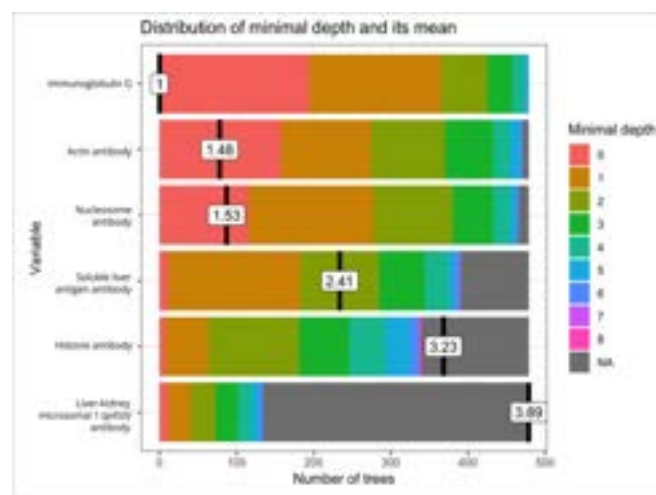


Figure:

Conclusion: Our data shows a significantly higher positivity of anti-nucleosome and anti-histone antibodies in patients with AIH compared to DILI patients. The random forest model shows that anti-nucleosome antibodies are almost as important as the established anti-actin antibody in the classification of AIH and DILI. Therefore, anti-nucleosome antibodies may be able to help distinguish between the two diseases. External validation is the next step to confirm this relationship.

FRI-333

Combination of intestinal bile salt uptake inhibition with pharmacological repression of bile salt synthesis improves liver health in cholestatic mice

Roni Kunst¹, Esther Vogels¹, Isabelle Bolt¹, Ronald Oude-Elferink¹, Stan van de Graaf¹. ¹Amsterdam UMC, Tytgat Institute for Liver and Intestinal Research, Netherlands
Email: k.f.vandegraaf@amsterdamumc.nl

Background and aims: Intestine-restricted inhibitors of the apical sodium-dependent bile acid transporter (ASBT or IBAT) are approved as treatment against cholestasis but also associated with symptoms such as diarrhea and abdominal pain. Furthermore, blocking ASBT alone might be less effective in severe cases of cholestasis. We hypothesize that therapeutic interventions that lower bile salt synthesis provide an effective complementary treatment strategy. Here, we test combination therapies of intestinal ASBT inhibition in combination with obeticholic acid (OCA), cilofexor and NGM282 in a mouse model for cholestasis induced liver injury.

Method: Wild type male C57Bl6J/OlaHsd mice were fed a 0.05% 3,5-diethoxycarbonyl-1,4-dihydro-collidine (DDC)-diet and received daily oral gavage with either 10 mg/kg OCA, 30 mg/kg Cilofexor, 10 mg/kg GSK2330672 (ASBT inhibitor; ASBTi) or a combination. Alternatively, wild type male C57Bl6J/OlaHsd mice were injected with control AAV8 or AAV8-NGM282, a non-tumorigenic analogue of FGF19 to repress bile salt synthesis. While being fed a DDC diet, mice received daily oral gavage with ASBTi or placebo control.

Results: Combination therapy of OCA, Cilofexor and NGM282 with ASBTi effectively reduced fecal bile salt excretion. NGM282+ASBTi further lowered plasma bile salt levels compared to ASBTi monotherapy. Cilofexor+ASBTi and NGM282+ASBTi treatment reduced plasma alanine transaminase and aspartate transaminase levels. Gene expression analysis indicated dampening of inflammatory and fibrotic processes in Cilofexor+ASBTi and NGM282+ASBTi treated mice, and this was confirmed by histology.

Conclusion: Combination therapy of repressed bile salt synthesis and intestinal bile salt uptake is an effective treatment strategy to reduce liver injury while dampening the ASBTi-induced colonic bile salt load in a pre-clinical cholestasis model.

FRI-334

Cholestatic liver disease is alleviated by colitis-induced inhibition of bile acid synthesis

Wenfang Gui¹, Mikal Jacob Hole², Antonio Molinaro³, Karolina Edlund⁴, Kristin K. Jørgensen^{5,6}, Huan Su¹, Brigitte Begher-Tibbe⁴, Nikolaus Gaßler⁷, Carolin V. Schneider¹, Uthayakumar Muthukumarasamy⁸, Antje Mohs¹, Lijun Liao^{1,9}, Julius Jäger¹, Christian Mertens¹, Ina Bergheim¹⁰, Till Strowig⁸, Jan G. Hengstler⁴, Johannes R. Hov², Hanns-Ulrich Marschall³, Christian Trautwein¹, Kai Markus Schneider¹. ¹University Hospital RWTH Aachen, Medicine III, Aachen, Germany; ²Norwegian PSC Research Center, Section of Gastroenterology and Research Institute of Internal Medicine, Division of Surgery, Inflammatory Diseases and Transplantation, Oslo University Hospital and University of Oslo, Norway; ³Department of Molecular and Clinical Medicine/Wallenberg Laboratory, Sahlgrenska Academy, University of Gothenburg, Sweden; ⁴Leibniz Research Centre for Working Environment and Human Factors, Technical University Dortmund, Dortmund, Germany; ⁵Norwegian PSC Research Centre, Department of Transplantation Medicine, Oslo University Hospital, Rikshospitalet, Norway; ⁶Department of Gastroenterology, Akershus University Hospital, Lørenskog, Norway; ⁷Institute for Legal Medicine, Section Pathology, University Hospital Jena, Jena, Germany; ⁸Helmholtz Centre for Infection Research, Braunschweig, Germany and Hannover Medical School, Hannover, Germany; ⁹Department of Anesthesiology and Pain Management, Shanghai East Hospital, School of Medicine, Tongji University, Shanghai, China; ¹⁰Department of Nutritional Sciences, Molecular Nutritional Science, University of Vienna, Vienna, Austria
Email: kmschneider@ukaachen.de

Background and aims: Primary sclerosing cholangitis (PSC) is a chronic cholestatic liver disease characterized by inflammation and progressive fibrosis of the biliary tracts. The intriguing and strong epidemiological link between PSC and inflammatory bowel disease (IBD) is known for decades, but the mechanisms by which colitis affects cholestatic liver disease remain incompletely understood.

Method: To study the effects of colitis on liver injury, inflammation, fibrosis, and bile acid metabolism in cholestatic liver disease, we established acute and chronic mouse models of PSC-IBD by

administering dextran sodium sulfate (DSS) to *Mdr2*^{-/-} mice. The pathophysiological consequences of colitis treatment on WT and *Mdr2*^{-/-} mice were studied based on transcriptomic analyses, histology, flow cytometry, Matrix Assisted Laser Desorption imaging of spatial BA distribution as well as comprehensive BA profiling using UPLC-MS/MS, including the BA synthesis marker C4 (7 α -hydroxy-4-cholesten-3-one). By treating *Mdr2*^{-/-} mice with lipopolysaccharide (LPS) and studying the impact of LPS on co-cultured human primary hepatocytes and Kupffer cells, we also investigated whether LPS could phenocopy the effects of bacterial translocation that occurs during colitis induction. Finally, we generated *Mdr2*^{-/-}*Nemo*^{thepa} mice to explore whether hepatocytic NF-kappaB signaling plays a role in inflammation-mediated changes in bile acid metabolism.

Results: DSS treatment induced intestinal inflammation, barrier impairment, and bacterial translocation in WT and *Mdr2*^{-/-} mice. Impaired barrier function was linked to bacterial translocation inducing an increased hepatic inflammatory response but was surprisingly associated with ameliorated liver injury and hepatocellular apoptosis in both acute and chronic DSS treated *Mdr2*^{-/-} mice. Most interestingly, biliary septal fibrosis was improved in *Mdr2*^{-/-} mice with chronic colitis induction. Inflammatory pathways and specifically hepatic NF-kappaB activation inversely correlated with bile acid synthesis reducing hepatic bile acid accumulation, thereby alleviating cholestatic liver injury and fibrosis. Importantly, LPS was sufficient to activate this protective circuit in-vitro and in-vivo, while the absence of NF-kappaB signaling in *Mdr2*^{-/-}*Nemo*^{thepa} mice strongly exacerbated cholestasis.

Conclusion: Here, we identify an unexpected colitis-driven and hepatocytic NF-kappaB-dependent protective circuit in cholestatic liver disease. Our findings may have important implications for the treatment of individuals with PSC suffering from concomitant colitis.

FRI-335

Non-invasive imaging method demonstrates anti-fibrotic efficacy of a dual integrin alpha-v/beta-6 and alpha-v/beta-1 inhibitor in a rat model of biliary fibrosis

Johanna Schaub¹, Yingying Ning², Iris Y. Zhou², Nicholas Rotile², Avery Boice², Jessie Lau¹, Peter Caravan², Scott Turner¹. ¹Pliant Therapeutics, United States; ²Massachusetts General Hospital and Harvard Medical School, United States
Email: jschaub@pliantrx.com

Background and aims: There is an unmet need for antifibrotic treatments which can prevent, halt or reverse hepatic fibrosis in

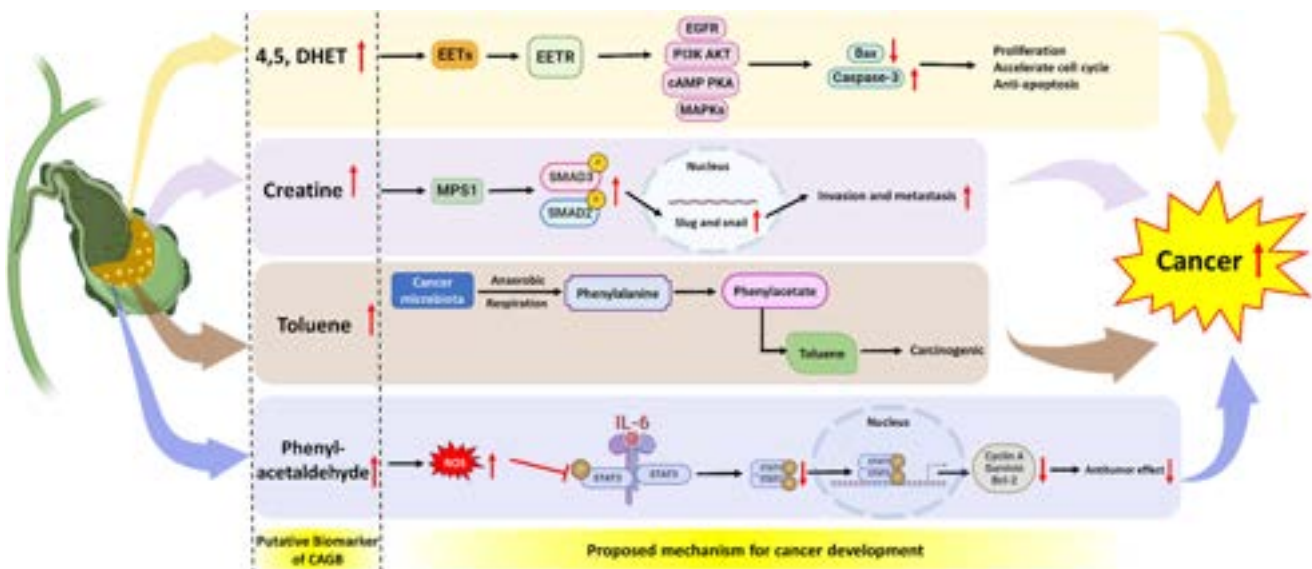


Figure: (abstract: FRI-344): Putative biomarkers and their proposed mechanism for CAGB

POSTER PRESENTATIONS

chronic liver diseases; however, drug development efforts have been hampered by a lack of non-invasive methods to measure fibrosis. In primary sclerosing cholangitis, integrins overexpressed on injured cholangiocytes (alpha-v/beta-6) and myofibroblasts (alpha-v/beta-1) are attractive therapeutic targets because they bind and activate latent TGF-beta, a key driver of liver fibrosis. Here, we used molecular MRI with CM-101, a type I collagen probe that directly measures fibrosis, and PET with an alpha-v/beta-6 probe to provide a non-invasive readout of anti-alpha-v/beta-6 and alpha-v/beta-1 antagonism in a rat model of biliary fibrosis.

Method: Liver fibrosis was induced in rats by ligation of the common bile duct (BDL). The selective integrin alpha-v/beta-6 and alpha-v/beta-1 antagonist PLN-169 was dosed orally 4–17 days post-BDL. MRI with CM-101 and PET with a ^{68}Ga -DOTA-alpha-v/beta-6 cysteine knot probe were performed on days 6 and 18 post-BDL. On day 18, livers were collected for histological and molecular analysis. Sirius Red was used to stain collagen and fibrosis assessment was performed measuring collagen proportional area (CPA) in ImageJ and with Fibronectin (PharmaNest). Gene expression changes were measured using the NanoString platform.

Results: Bile duct ligation significantly increased the levels of integrin alpha-v/beta-6 in the liver 18 days post-surgery as assessed by ex vivo gene expression ($>10\times$, $p < 0.05$) and by in vivo alpha-v/beta-6 PET imaging ($2.6\times$, $p < 0.05$). BDL resulted in severe fibrosis with $22\times$ increase in CPA and a significant increase in Phenotypic Fibrosis Composite Score (Ph-FCS) (both $p < 0.0001$). Treatment with PLN-169 significantly reduced hepatic accumulation of the alpha-v/beta-6 PET probe (34% , $p < 0.05$) and markedly attenuated histological measures of fibrosis with $>50\%$ decrease in CPA ($p < 0.0001$) and decreases in multiple phenotypic measures of fibrosis. MRI with CM-101 showed a significant increase in liver-to-muscle contrast to noise ratio (delta-CNR) in BDL animals compared to sham animals on day 18 ($4.5\times$, $p < 0.0001$) as well as a significant decrease in BDL animals with PLN-169 treatment (45% , $p < 0.05$). Delta-CNR significantly increased in vehicle-treated animals from day 6 to day 18 ($>2.0\times$, $p < 0.05$) but not in PLN-169-treated animals. Importantly, delta-CNR correlated with the direct measurement of collagen from digital pathology (CPA, $r = 0.65$, $p < 0.001$).

Conclusion: PET imaging for alpha-v/beta-6 and molecular MRI of collagen can non-invasively assess target expression, target engagement, and treatment response of an integrin alpha-v/beta-6 and alpha-v/beta-1 antagonist in a rat model of biliary fibrosis. This study raises the possibility that non-invasive methods may be valuable for evaluating treatment responses in liver fibrosis and supporting drug development in this field.

FRI-336

Blockade of IL-18 via long-acting IL-18 binding protein attenuates experimental diet-induced cholestatic disease

Dong-Hyun Kim¹, Jin Joo Park², Mi-Hyun Park², Kyungsun Lee², Jaekyu Han², Susan Chi², Moo Young Song², Seung Goo Kang^{2,3}, Sang-Hoon Cha², Yong-Hyun Han¹. ¹Laboratory of Pathology and Physiology, College of Pharmacy, Kangwon National University, Korea, Rep. of South; ²AprilBio Co., Ltd., Korea, Rep. of South; ³Division of Biomedical Convergence, College of Biomedical Science, Kangwon National University, Korea, Rep. of South
Email: yhhhan1015@kangwon.ac.kr

Background and aims: Primary sclerosing cholangitis (PSC) is defined as a cholestatic liver disease characterized by multiple segmental strictures in the hepatic bile ducts. Eventually, chronic biliary inflammation drives liver fibrosis and cirrhosis, and there are no clinically effective therapeutic drugs to cure PSC disease. IL-18 binding protein (IL-18BP) is a secretory protein and acts as a high affinity neutralizer for IL-18. Here, we developed SAFA-IL-18BP (APB-R3), a long-acting version of IL-18BP that covalently attached to an anti-serum albumin Fab (SAFA), and evaluated whether blockade of

IL-18 via APB-R3 reduce PSC-induced injury markers such as bile ductal reactions, fibrosis, and senescence.

Method: To establish diet-induced PSC model, we provided 3,5-diethoxycarbonyl-1,4-dihydrocollidine (DDC) diet to mice. Mice were intraperitoneally injected with APB-R3 at a dose of 10 mg/kg in a volume of 5 ml/kg thrice a week from day 0 to day 20 of feeding period.

Results: We first found that expression of hepatic IL-18 and IL-18BP was enhanced in DDC diet-induced PSC conditions. We observed that administration of APB-R3 effectively decreased key indicators related with hepatobiliary disease such as plasma ALP and GGT activities as well as bile acid levels. Bile ductular reactions were also inhibited by APB-R3 injection. Furthermore, APB-R3 significantly suppressed periductal fibrosis and transcriptional activations of hepatic pro-fibrotic genes. Finally, we revealed that APB-R3 decreased senescence-associated secretory phenotype (SASP) markers such as TGF β , IL-1 β , MMP3 and p27.

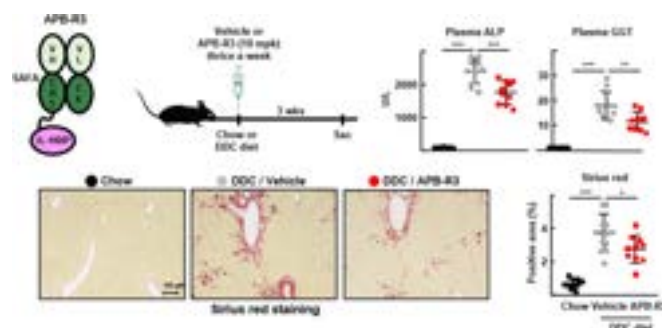


Figure:

Conclusion: The long-acting IL-18BP, APB-R3, effectively ameliorates DDC diet-induced biliary injuries in rodent PSC model. These pre-clinical results suggest that APB-R3 can be potential leading therapeutic drug to relieve PSC disease, and our results warrant further clinical trial studies.

FRI-344

Proteomics and metabolomics of bile reveal molecular insights and classify signatures predictive of carcinoma of gallbladder

Jaswinder Maras¹, Nupur Sharma¹, Sadam H. Bhat¹, Babu Mathew¹, Manisha Yadav¹, Gaurav Tripathi¹, Vasundhara Bindal¹, Neha Sharma¹, Sushmita Pandey¹, Hani Hemati^{2,3}, Deepika Bohra⁴, Rashmi Rana⁴, Sanyam Falari⁵, Viniyendra Pamecha⁵. ¹Institute of liver and biliary sciences, Molecular and cellular medicine, New Delhi, India; ²University of Kentucky, Department of toxicology and cancer biology, Lexington, United States; ³University of Kentucky, Department of Toxicology and Cancer Biology, Lexington, United States; ⁴Sir ganga ram hospital, Department of research, New Delhi, India; ⁵Institute of liver and biliary sciences, Department of liver transplant and hepato pancreato biliary surgery, New Delhi, India
Email: jassi2param@gmail.com

Background and aims: Carcinoma of the gall bladder (CAGB) has poor prognosis. Bile concentrated in the gallbladder (GB) is expected to recapitulate molecular (proteome/metabolome) alteration which may provide critical pathophysiological insight linked with the development of CAGB. Reliable biomarker-based assays with high sensitivity and specificity for detection of this cancer are a clinical need.

Method: In this cross-sectional study, 127 patients admitted at ILBS (CAGB, n = 37; Gallstone (GS), n = 60; Healthy liver donor (HC), n = 30) were classified into training and test cohort. In training cohort, bile samples (n = 87) were collected from patients undergoing cholecystectomy for GS disease and grouped as GS (n = 40) and patients undergoing surgery for CAGB were grouped as CAGB (n = 17); we also collected healthy liver donor samples (n = 30). Whereas in the test

cohort, both bile (T1, n = 20) and plasma (T2, n = 20) samples were analysed and validated using machine learning (ML) approach.

Results: Bile samples were screened for proteomics/metabolomics signatures capable of early detection of cancer in GB anomalies. Bile of CAGB showed distinct proteomic (217up- and 258 downregulated; FC>1.5) and metabolomic (111 up- and 505 downregulated; FC>1.5) profiles compared to GS or HC ($p < 0.05$, FDR<0.01). Partial least square discriminant analysis (PLS-DA) and unsupervised hierarchical clustering showed clear segregation of CAGB from other groups. CAGB bile was significantly enriched for proteins/metabolites linked to inflammation (complement and coagulation cascade, arachidonic acid metabolism, bile acid, tryptophan, and sphingolipid signaling, ferroptosis and others), alternate energy pathways (pentose phosphate pathway, amino acid metabolism, lipid metabolism, and others). Proteins/metabolites decreased were associated to glycolysis, cholesterol metabolism, PPAR, RAS and RAP1 signaling glutathione, pyruvate, histidine, purine metabolism, oxidative phosphorylation and others. Integration analysis revealed strong correlation ($r^2 > 0.5$, $p < 0.05$) between significant proteins/metabolites and clinical parameters and showed alteration of pathways linked to lipid metabolism, platelet activation, amino acid metabolism and others ($p < 0.05$). Metabolite/protein signature based probability of detection for CAGB was >90% ($p < 0.05$) with AUC>0.94. Validation of top four metabolite panel: Toluene, 5, 6-DHET, Creatine and Phenyl acetaldehyde using five machine-learning algorithms in n = 40 samples from T1 and T2 showed highest accuracy (99%) and sensitivity/specificity (>98%) for CAGB detection.

Conclusion: Bile proteome/metabolome alteration provides key molecular insight in development of CAGB. We put forward a core set of bile signatures which may offer universal utility for early detection of CAGB.

FRI-345

Serum proteomics reveals association of CCL24 with key aspects of primary sclerosing cholangitis

Raanan Greenman¹, Tom Snir¹, Avi Katav¹, Omer Levi¹, Revital Aricha¹, John Lawler², Douglas Thorburn³, Massimo Pinzani⁴, Ilan Vaknin¹.

¹Chemomab Ltd., Israel; ²Chemomab Inc., Clinical Operations, United States; ³Royal Free Hospital School Of Medicine, London, United Kingdom; ⁴UCL Institute of Immunity and Transplantation, London, United Kingdom

Email: raanan@chemomab.com

Background and aims: CCL24, also known as Eotaxin-2, is a pro-inflammatory, pro-fibrotic chemokine overexpressed in livers of patients with primary sclerosing cholangitis (PSC), predominantly in areas of evident biliary injury. CCL24 blockade, using a monoclonal antibody, was shown to interfere with core pathways that induce PSC pathophysiology in pre-clinical models. Here, we further demonstrate the role of CCL24 in PSC and its association with disease related pathways through the analysis of proteomic data from the serum of patients with PSC and from an in-vitro model.

Method: Sera from healthy controls (n=30) and patients with PSC (n = 45) were analyzed using the Olink proximity extension assay (PEA) of 3072 proteins. Individuals' demographics, enhanced liver fibrosis (ELF) scores and alkaline phosphatase (ALP) levels were documented. To evaluate the direct effect of CCL24 on hepatic cells, an LX2 hepatic stellate cell (HSC) line was stimulated with CCL24 and subsequently blocked by a neutralizing monoclonal antibody (CM-101). Conditioned media underwent proteomic profiling using a proteomic chip (L-507; RayBiotech). Data was analyzed using bioinformatic and computational tools.

Results: The serum proteomics data was stratified according to 3 comparisons: (1) healthy controls vs. patients with PSC, (2) fibrosis severity as defined by ELF score (9.8 cutoff) in patients, and (3) serum levels of CCL24 in patients. These stratifications identified differentially expressed proteins (DEP; by Welch two sample t-test), that were used for pathway enrichment analysis. This analysis found enriched

pivotal pathways such as HSC activation/hepatic fibrosis, Th1/Th2 activation and granulocyte adhesion, that were activated in patients with PSC, patients with severe fibrosis and patients with elevated CCL24. Moreover, CCL24 levels were significantly correlated with serum proteins frequently associated with inflammation, fibrosis and vascularization (e.g., CXCL10, collagens, and VEGFA) in patients with ALp >1.5 ULN.

In-vitro, CCL24 stimulated HSC manifest a set of upregulated proteins that are commonly elevated in serum of patients with severe PSC. This CCL24 dependent altered protein expression was blocked following treatment with CM-101.

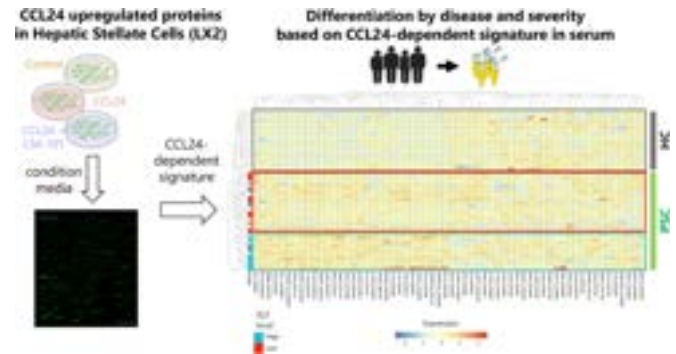


Figure:

Conclusion: This study provides novel insights into the role of CCL24 in PSC and its association with disease-related pathways and severity. We identified a potential CCL24 related signature in PSC that supports the ongoing phase 2 study of CM101 in patients with PSC.

FRI-346

Combination of Ileal bile acid transporter inhibitor and a non-steroidal Farnesoid X receptor agonist for reversal of cholestatic liver injury in Cyp2c70 KO mice with a humanized bile acid composition

Caroline Klindt-Morgan¹, Jennifer Truong¹, Ashley Bennett¹, Kimberly Pachura¹, Diran Herebian², Ertan Mayatepek², Saul J. Karpen¹, Paul Dawson¹. ¹Emory University School of Medicine and Children's Healthcare of Atlanta, Department of Pediatrics, Atlanta, United States; ²Heinrich-Heine University, Department of General Pediatrics, Neonatology, and Pediatric Cardiology, Medical Faculty, Heinrich-Heine-University, Düsseldorf, Germany, Dusseldorf, Germany
Email: cklindt@emory.edu

Background and aims: Cyp2c70 has been identified as the key enzyme in mice for synthesis of hepatoprotective 6-hydroxylated muricholates. Cyp2c70 knockout (2c70 KO) mice have a more hydrophobic human-like bile acid (BA)-composition and develop signs of cholestatic liver injury. Preventive monotherapy with an ileal BA transporter (IBAT) inhibitor reduces hepatic BA burden and alleviates liver injury in these mice. However, it is unclear if there is an intrahepatic BA threshold for onset of liver injury and if short-term complementary therapies designed to reduce the hepatic BA pool can reverse the hepatotoxicity in this model. The non-steroidal Farnesoid-X-Receptor (FXR) agonist Cilofexor inhibits BA-synthesis and has been shown to reduce fibrosis in a model for NASH in rats.

Method: 12-week-old male and female 2c70 KO and wild type (WT) mice (C57Bl/6J) were fed chow or a diet containing an IBAT inhibitor (0.006% SC-435) and/or an FXR agonist (0.015% Cilofexor) for 14 days. Upon sacrifice, livers were collected for histology, immunohistochemistry, RT-PCR and gas-liquid chromatography. Blood samples were analyzed for serum biochemistry.

Results: By the age of 12 weeks, female 2c70 KO mice exhibited cholestatic liver injury as indicated by elevated serum liver injury markers (AST and ALT) and histological evidence of liver inflammation and fibrosis. Therapy with SC-435 as well as Cilofexor

POSTER PRESENTATIONS

significantly reduced ALT and AST levels (e.g. AST decreased by >86% and 79% respectively compared to chow) after 14 days of treatment without significant additional effect in combination. Liver BAs were significantly reduced in all treatment groups as compared to chow. RT-PCR analysis showed a reduction of inflammatory markers in the Cilofexor and Cilofexor + SC-435 groups in comparison to chow (e.g. Tgf-beta reduced by >73% and 76% and Interleukin-1 beta reduced by >81% and 76% respectively). Fibrosis as indicated by Sirius Red staining showed a tendency for decrease especially after combination therapy without reaching significance (reduction of 62% in Cilofexor + SC-435 as compared to chow).

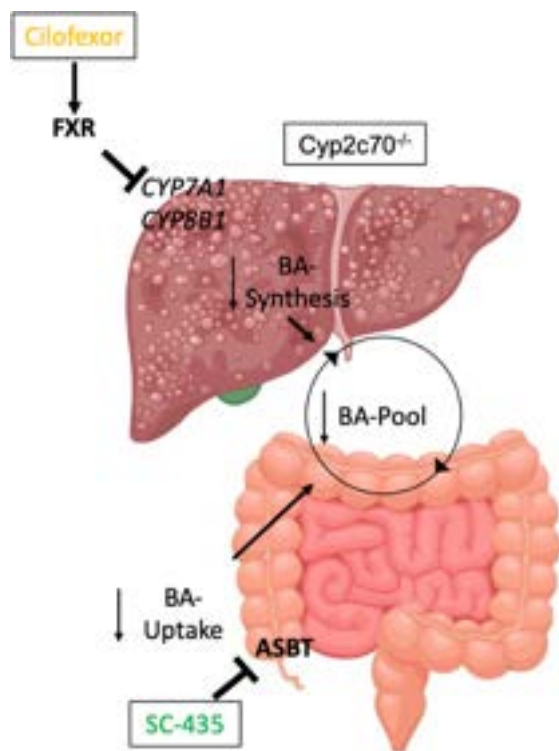


Figure:

Conclusion: Short term therapy with an IBAT inhibitor after onset of liver injury in *2c70 KO* mice can reduce liver injury but is insufficient for a complete rescue. The therapeutic benefit associated with short term combined administration of Cilofexor and SC-435 shows a tendency for a synergistic effect in reducing inflammation but has no significant effect on fibrosis.

FRI-347

Production of reactive oxidant species and fatty acid uptake is increased in regulatory T-cells in autoimmune hepatitis, and associated with down-regulation of markers linked to suppressor function

Scott Davies¹, Naomi Richardson¹, Grace Wootton¹, Ye Htun Oo^{1,2}, Palak Trivedi^{1,2}. ¹University of Birmingham, National Institute for Health Research (NIHR) Birmingham Biomedical Research Centre (BRC), Birmingham, United Kingdom; ²University Hospitals Birmingham, Liver Unit, United Kingdom
Email: p.j.trivedi@bham.ac.uk

Background and aims: Autoimmune hepatitis (AIH) is characterised by a breach in liver immune tolerance. Inflammatory triggers are largely unknown, but dysregulated activity and function of regulatory T cells (Tregs) are proposed to contribute. In this study, we evaluated metabolic functions of Tregs in patients with AIH with evidence of well-controlled disease, alongside expression of functional markers in liver-infiltrating cell populations.

Method: Peripheral blood mononuclear cells (PBMCs) were isolated from patients (pts) with AIH. Tregs were characterized according to the following profile: CD4⁺ CD25^{hi}, CD127^{lo}. Cells were then labelled with fluorescent dyes reporting the production of reactive oxidant species (ROS), fatty acid uptake and mitochondrial activity. All cells were analysed by flow cytometry whilst acquiring median fluorescence intensity values. Control blood samples were obtained from patients with haemochromatosis (HFE) undergoing venesection without evidence of liver disease. Disease control PBMCs were also obtained from individuals with primary biliary cholangitis (PBC) and alcohol-induced liver disease (ALD).

Results: Firstly, peripheral blood was obtained from 5 patients with AIH (median age 50, 60% men, median ALT and bilirubin values 36 U/L and 19 micromol/L, respectively). Circulating Tregs displayed higher production of ROS compared to that of patients with haemochromatosis. This observation was coupled with increased fatty acid uptake and reduction in mitochondrial mass (Fig 1A-C). Next, protein expression of functional markers was evaluated in Tregs derived from a separate cohort of AIH patients (median age 37.5, 43% men, median ALT and bilirubin values 46 U/L and 12.5 mg/dL, respectively). These included reductions in CD39 expression and lower values for CTLA-4 and FOXP3, as compared to HFE (Fig 1D-F). Such changes were not observed in peripheral blood Tregs obtained from patients with PBC and ALD.

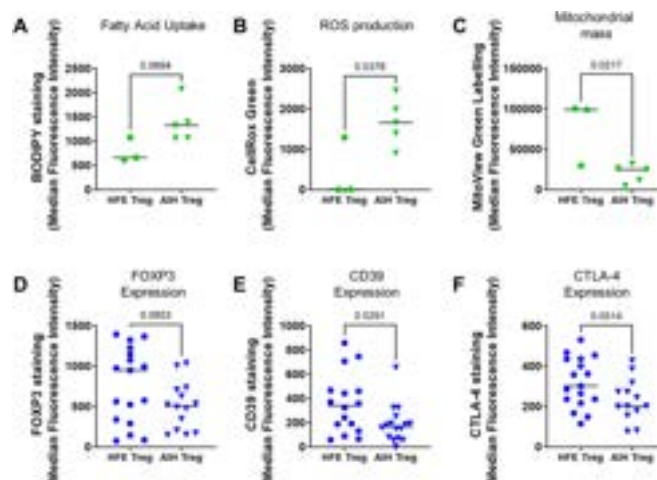


Figure:

Conclusion: In AIH, mitochondrial dysfunction and heightened fatty acid oxidation may lead to generation of ROS, reducing the suppressive activity of Tregs. Mitigating ROS production may rescue the immunosuppressive activity of Tregs and requires exploration as part of cell therapy trials to promote long-term immune tolerance.

FRI-348

The cell cycle protein Cyclin E1 mediates pro-inflammatory signals in a mouse model of acute hepatitis and in primary macrophages

Christian Penners¹, Anna Verwaayen¹, Antje Mohs¹, Alexander Jans¹, Julia Hennings¹, Matthias Bartneck¹, Christian Trautwein¹, Roland Sonntag¹, Christian Liedtke¹. ¹University Hospital RWTH Aachen, Department of Medicine III, Germany
Email: cliedtke@ukaachen.de

Background and aims: Cyclin E1 is a regulatory subunit of cyclin-dependent kinase 2 (CDK2) and mediates the transition from quiescence into the S-Phase of the cell cycle. We previously identified unexpected essential functions of Cyclin E1 for liver fibrogenesis as well as for initiation and progression of hepatocellular carcinoma. However, the effector cells of Cyclin E1 in the liver have not yet been fully identified. In particular, the potential role of Cyclin E1 in liver

resident and circulating immune cells is poorly investigated. Therefore, in the present study we aimed to investigate the role of Cyclin E1 in immune cells during acute liver inflammation.

Method: For our study we used constitutive Cyclin E1 knockout (*Ccne1*^{-/-}) mice and Wildtype (WT) controls in a C57BL/6 background. Acute liver injury was induced using the established Concanavalin A (ConA) model of immune-mediated hepatitis; mice were sacrificed after 24 hours. Explanted livers were investigated by histological analysis, FACS, qPCR and ELISA. Bone marrow-derived macrophages (BMDM) were isolated from *Ccne1*^{-/-} and WT mice and analyzed for differentiation, cell cycle activity and pro-inflammatory polarization. *In vitro* knockdown of *Ccne1* was performed using the macrophage cell line J774A.1 and anti-*Ccne1* siRNA encapsulated in lipid nanoparticles (LNP).

Results: Surprisingly, *Ccne1*^{-/-} mice showed improved survival after ConA-treatment, which was associated with significantly reduced liver necrosis compared to WT controls. In addition, loss of *Ccne1* was related to down-regulation of pro-inflammatory mediators such as interleukin-6 (IL6), tumor necrosis factor alpha (TNF), and CC-chemokine ligand 2 (CCL2), which are typically expressed in macrophages. We thus tested the impact of *Ccne1* deletion in pro-inflammatory polarized BMDMs. Importantly, *Ccne1*^{-/-} BMDMs also revealed reduced IL6 expression in comparison to WT controls. Of note, *Ccne1*^{-/-} BMDMs did not show any changes in cell cycle progression or in myeloid progenitor cell to macrophage differentiation. These findings were validated in an interventional approach. To this end pro-inflammatory polarized J774A.1 cells were treated with anti-*Ccne1* siRNA-LNPs, which was sufficient to significantly reduce IL6 expression.

Conclusion: In this study we provide evidence for a novel, pro-inflammatory function of Cyclin E1, which is fully independent from its canonical role as a cell cycle mediator. This involves the transcriptional up-regulation of interleukin-6 via Cyclin E1 in macrophages. Our data suggest that interventional inhibition of Cyclin E1 could be a promising approach for treatment of acute immune-mediated hepatitis.

FRI-349

Depletion of excess liver copper ameliorates liver damage in a mouse model of chronic cholestatic liver disease

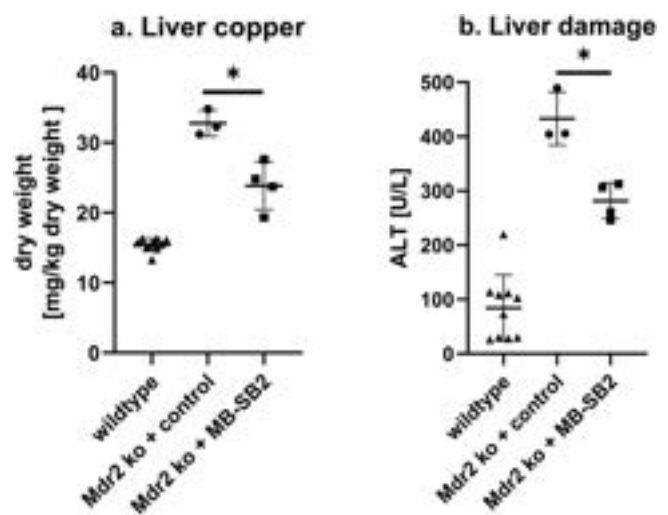
Dennis Koob¹, Judith Nagel², Jingguo Li^{1,3}, Sebastian Zimny¹, Ralf Wimmer¹, Gerald Denk¹, Martin Roderfeld⁴, Elke Roeb⁴, Svetlana Lutsenko⁵, Hans Zischka^{2,6}, Simon Hohenester¹. ¹University Hospital LMU, Department of Medicine II, Munich, Germany; ²Technical University of Munich, Department of Toxicology and Environmental Hygiene, Munich, Germany; ³Affiliated Hospital of Zunyi Medical University, Department of Gastroenterology, Zunyi, China; ⁴Justus Liebig University, Gastroenterology/Center for Internal Medicine, Gießen, Germany; ⁵John Hopkins Medical Institute, Department of Physiology, Boston, United States; ⁶Helmholtz Center Munich, Institute of Molecular Toxicology and Pharmacology, Munich, Germany
Email: dennis.koob@med.uni-muenchen.de

Background and aims: Disturbed copper (Cu) homeostasis in the liver, as seen in Wilson's disease, can cause liver damage. Cu accumulation also occurs in cholestatic liver disease, though to a lesser extent. In primary sclerosing cholangitis, Cu accumulation, i.e. orcein staining as a component of the Nakanuma score, even seems to predict poor transplant-free survival. We hypothesize that Cu accumulation might not only be a consequence of cholestasis, but also modulate the course of disease. We aimed to investigate the role of Cu accumulation in animal models of cholestasis and identify potential treatment targets.

Method: Hepatic Cu content was determined in wild type and Mdr2ko animals on FVB, BL6 or BALBc background as well as in Atp7b/Mdr2 (BL6) double knockout mice (DKO). Mice were fed a control or Cu-enriched diet or treated with the potent Cu chelator methanobactin (MB)-SB2. The hepatocyte cell line HepG2 was stably transfected with Ntcp to allow for bile salt uptake and was stimulated

with glycochenodeoxycholate (GCDc) and/or Cu (5–10µM, each). Cell survival and apoptosis were assessed, as well as the recently described cell death mode cuproptosis.

Results: While liver Cu was not different between Mdr2ko and wt mice on FVB background, we found a 1.5 ± 0.2-fold increase in Cu levels in Mdr2/BALBc (15.4 ± 0.9 vs. 24.5 ± 2.8 mg/kg in wt/BALBc vs. Mdr2/BALBc, n = 5, p < 0.05). This was associated with more advanced liver fibrosis (liver hydroxyproline 167.5 ± 31.7 vs. 252.8 ± 56.6 µg/g, Mdr2/BL6 vs. Mdr2/BALBc, n = 7, p < 0.05). In DKO, liver Cu was increased 1.5 ± 0.3 -fold (vs. Mdr2/BL6), again associated with a trend towards increased liver hydroxyproline. Feeding a Cu-enriched diet led to an increase in liver Cu in Mdr2/FVB, but not in wt FVB, again associated with a 2.2 ± 0.3-fold increase in liver hydroxyproline. Treatment of Mdr2/BALBc mice with MB-SB2 over 4 weeks was able to decrease excess liver Cu content (Figure 1a). This was associated with a marked amelioration of liver damage (ALT, Figure 1b). In HepG2, both GCDc and Cu were non-toxic in the concentrations applied in metabolic assays. Combination of both stimuli, however, led to a marked impairment of cell survival. While caspase-3/-7 assays excluded apoptosis, detection of DLAT-oligomers via Western blotting indicated presence of cuproptosis upon co-stimulation with Cu+GCDc. This was supported by the finding that preload of HepG2 with lipioic acid, intended to prevent cuproptosis, indeed improved cell survival (66.8 ± 13.9 vs. 83.8 ± 11.3% for Cu/GCDc vs. Cu/GCDcA/lipioic acid, n = 6, p < 0.05).



Conclusion: Hepatic copper deposition in Mdr2 ko mice is associated with more advanced liver fibrosis, mimicking the human phenotype in PSC. Effective copper chelation by use of MB-SB2 ameliorated liver damage in Mdr2 ko animals. On a cellular level, bile salts and Cu act synergistically to cause cell death, potentially via the route of cuproptosis.

FRI-350

Genetic predisposition for liver inflammation and response to anti-cholestatic therapy in experimental sclerosing cholangitis

Ramesh Kudira¹, Srikanth Pasula¹, Annika Yang vom Hofe¹, Liva Pfulher¹, Manavi Singh¹, Jennifer Kasten², Anas Bernieh², Cory Kostrub³, Pamela Vig³, Ty Troutman⁴, Alexander Miethke¹. ¹Cincinnati Children's Hospital Medical Center, Pediatric Gastroenterology, United States; ²Cincinnati Children's Hospital Medical Center, Pediatric Pathology and Laboratory Medicine, United States; ³Mirum Pharmaceuticals, United States; ⁴Cincinnati Children's Hospital Medical Center, Allergy and Immunology, United States
Email: alexander.miethke@cchmc.org

Background and aims: Genetic deletion of the phospholipid floppase MDR2 causes sclerosing cholangitis from biliary

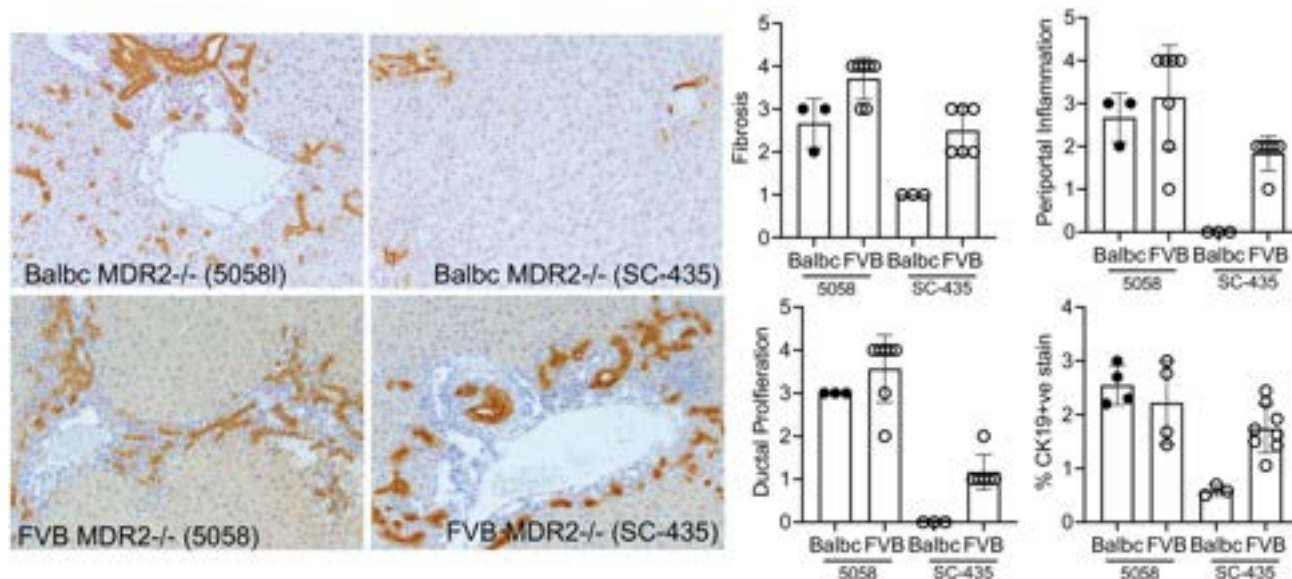


Figure: (abstract: FRI-350).

precipitation of unopposed bile acid microcrystals. FVB background mice with such deletion are prone to HCC, whereas BALB/c background mice with the same deletion display accelerated fibrosis. Here we examine treatment response differences between MDR2^{-/-} mice in FVB or BALB/c backgrounds receiving SC-435, a minimally absorbed inhibitor of IBAT-mediated intestinal bile acid reuptake. This may have clinical relevance for identifying novel injury pathways to be targeted in combination with current anti-cholestatic therapies.

Method: In 30-day-old female MDR2^{-/-} mice, sclerosing cholangitis phenotype and treatment response to SC-435 admixed to chow were compared between FVB and BALB/c backgrounds using serum biochemistries, liver histomorphology, and flow cytometry.

Results: At 30 days of life, serum ALT and ALP levels were higher in MDR2^{-/-} mice in FVB background compared with BALB/c, accompanied by more severe periportal inflammation and ductal proliferation. When mice were treated with SC-435 from days 30–45, greater ALT level reduction compared with median levels of age- and strain-matched MDR2^{-/-} mice receiving 5058 chow occurred in BALB/c background (Δ ALT: –93% vs –37% in BALB/c vs FVB mice; $p < 0.0001$). ALP only improved in BALB/c mice (Δ ALP: –63% vs +62%, $p < 0.0001$). The differences were corroborated by liver histomorphology scoring on a 0 to 4+ scale and CK19 immunohistochemistry with image analysis to determine the biliary mass (Figure). 30-day-old MDR2^{-/-} mice in FVB background had higher frequencies of CD3⁺ cells and lower frequencies of CD11b⁺F4/80^{low} monocytes compared to BALB/c. Following treatment with SC-435, BALB/c background mice had significantly higher frequencies of anti-inflammatory Ly6C^{neg} monocytes (4.5 vs 0.43% of CD45⁺ cells, $p = 0.002$) and regulatory T cells (4.0 vs 1.4% of CD45⁺ cells, $p = 0.009$) relative to FVB mice.

Conclusion: Genetic traits underlying distinct injury responses in mice of different backgrounds control liver inflammation and response of bile duct epithelial injury to IBAT inhibitor treatment in experimental sclerosing cholangitis. Single-cell ATACseq studies on purified liver infiltrating myeloid and lymphocyte populations are underway to interrogate chromatin accessibility and underlying genetic variants contributing to the strain-dependent immune response differences.

FRI-351

In vitro modulation of fibrogenesis and inflammation in patient-derived cholangiocyte organoids

Anna Katharina Frank^{1,2,3,4,5}, Yuliia Boichuk^{1,2}, Jan Tchorz⁶, Myriam Duckely⁶, Fotios Sampaziotis^{7,8,9,10}, Espen Melum^{5,11,12,13,14}, Tom Hemming Karlsen^{1,5,12,14}. ¹Norwegian PSC Research Center, Department of Transplantation Medicine, Division of Surgery, Inflammatory Diseases and Transplantation, Oslo University Hospital Rikshospitalet, Oslo, Norway; ²Research Institute of Internal Medicine, Division of Surgery, Inflammatory Diseases and Transplantation, Oslo University Hospital Rikshospitalet, Oslo, Norway; ³Scientia Fellowship, European Union's Horizon 2020 research and innovation program under the Marie Skłodowska-Curie grant agreement No 801133, Norway; ⁴Hybrid Technology Hub, Institute of Basic Medical Science, University of Oslo, Oslo, Norway; ⁵Institute of Clinical Medicine, Faculty of Medicine, University of Oslo, Oslo, Norway; ⁶Novartis Institutes for BioMedical Research, Novartis Pharma AG, Basel, Switzerland; ⁷Wellcome Trust-Medical Research Council Cambridge Stem Cell Institute, Jeffrey Cheah Biomedical Centre, University of Cambridge, Cambridge, United Kingdom; ⁸Department of Surgery, University of Cambridge, Cambridge, United Kingdom; ⁹Department of Medicine, University of Cambridge, Cambridge, United Kingdom; ¹⁰Cambridge Liver Unit, Cambridge University Hospitals NHS Foundation Trust, Cambridge, United Kingdom; ¹¹Norwegian PSC Research Center, Department of Transplantation Medicine, Division of Surgery, Inflammatory Diseases and Transplantation, Oslo University Hospital Rikshospitalet, Oslo, Norway; ¹²Research Institute of Internal Medicine, Division of Surgery, Inflammatory Diseases and Transplantation, Oslo University Hospital Rikshospitalet, Oslo, Norway; ¹³Hybrid Technology Hub, Institute of Basic Medical Science, University of Oslo, Oslo, Norway; ¹⁴Section of Gastroenterology, Department of Transplantation Medicine, Division of Surgery, Inflammatory Diseases and Transplantation, Oslo University Hospital Rikshospitalet, Oslo, Norway
Email: anna.frank@medisin.uio.no

Background and aims: Cholangiocytes represent the main target in the disease process in primary sclerosing cholangitis (PSC), yet there is scarce knowledge on their role in the progression and resolution. Cholangiocyte senescence and senescence-associated secretion of inflammatory and fibrogenic mediators into the surrounding liver tissue are suggested as potential drivers of PSC. By obtaining a highly secretive phenotype, cholangiocytes could participate in modulating disease progression through recruitment and activation of immune

cell populations. We aimed to interrogate the inflammatory and fibrogenic capacity of patient-derived cholangiocytes after prolonged 3D cell culture.

Method: Human cholangiocytes were isolated from extrahepatic bile duct brushings of PSC patients undergoing endoscopic retrograde cholangiopancreatography (ERCP) and propagated as organoids using previously established culture conditions. Organoids were treated for 5 days with a defined cocktail of inflammatory and fibrogenic cytokines (TNF α , IL-17, IL-6 and TGF- β). Treatment was performed with single cytokines at different concentrations and the complete cocktail mix. After treatment, senescence and secretion of inflammatory and fibrogenic mediators were assessed by microscopy and multiplex ELISA measuring a large panel of in total 26 inflammatory and fibrogenic analytes.

Results: Cholangiocyte organoids derived from the diseased bile ducts of PSC patients showed no evidence of cellular senescence and low levels of secretion of inflammatory or tissue-remodelling mediators under normal culture conditions. Treatment with a well-defined cocktail of inflammatory and fibrogenic cytokines, all of which have previously been shown to be present at high levels in diseased livers, lead to a change in cholangiocyte morphology towards a fibroblast-resembling phenotype, loss of organoid formation and upregulation of senescence-associated markers such as SA- β -Gal and PAI1. Cholangiocytes further obtained an activated and highly secretive phenotype, demonstrated by increased secretion of pro-inflammatory and tissue-remodelling mediators (IL-8, CXCL1, CXCL10, CCL2, MIF, S100A8/12, MMP9 and MMP2 among others) into the cell culture medium compared to untreated cells.

Conclusion: We here demonstrate that patient-derived cholangiocytes cultured as organoids, when brought into a disease-resembling in vitro environment, increase their secretion of mediators that are associated with immune-modulation and tissue remodelling. This highlights that cholangiocytes are not only a target during biliary disease, but likely also actively participate in modulating and driving disease progression. Our data show the potential of patient-derived cholangiocyte organoids as a powerful tool for unravelling disease-associated cellular mechanisms in PSC.

FRI-352

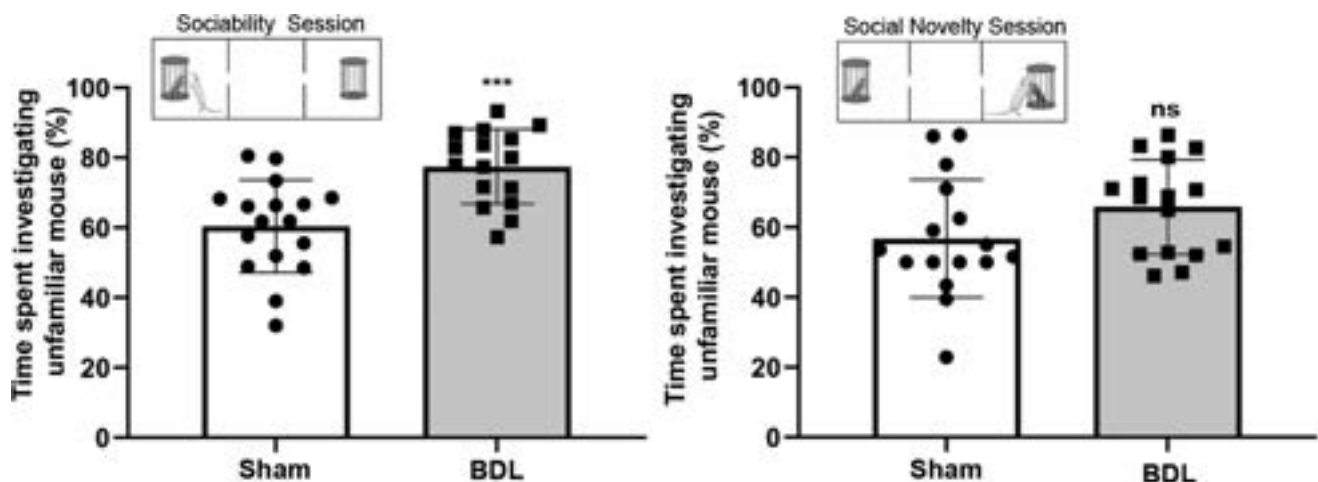
Cholestatic liver disease enhances sociability and leads to significant adaptive changes in amygdala neural circuits regulating social behavior in mice

Wagdi Almishri¹, Mark G. Swain^{1,2}. ¹Snyder Institute for Chronic Diseases, Medicine, Calgary, Canada; ²University of Calgary Liver Unit, Department of Medicine, Canada
Email: waalmish@ucalgary.ca

Background and aims: Social dysfunction is common in patients with cholestatic liver diseases (CLD). However, it is unclear whether this results from direct brain effects, or from the psychological impact, of CLD. The psychological aspects of disease are absent in an animal model; therefore, a strong behavioral phenotype suggests an organic basis for behavioral changes. Therefore, we examined the impact of CLD on social behavior in an animal model.

Method: Bile duct ligated (BDL) and sham control mice were studied 10 days post-surgery (model of CLD; male C57BL/6 mice; Jackson, 8–10 wks) to determine CLD impact on sociability and social memory (measured using automated 3 chamber sociability test). Mice from 5 separate cohorts of BDL/sham mice (n = 5–7/cohort) were studied. Additional cohorts of BDL/sham mice (n = 6/grp) were sacrificed at day 10 and the amygdala removed (key brain region regulating social behavior) and analyzed by RNAseq. Differentially expressed genes (DEG) between sham and BDL mice were then subjected to Ingenuity Pathway Analysis[®] (IPA; Qiagen) to determine CLD-related changes in social behavior-regulating amygdala neural pathways (neurotransmitters: glutamate, GABA; neuromodulators: dopamine, oxytocin). IPA z scores indicate predicted directionality of gene expression changes (–ve vs +ve).

Results: BDL mice showed enhanced sociability, reflected by a significant increase in social interactions during the sociability test phase (time investigating an unfamiliar juvenile mouse vs an inanimate object (Figure; left panel), compared to sham mice. Both sham/BDL mice had intact social memory in the novelty test phase (Figure; right panel). RNAseq showed increased numbers of DEGs in the amygdala of BDL vs sham mice (>3000 DEGs). IPA[®] analysis



3 Chamber Social Test: Sociability (propensity to investigate an unfamiliar mouse; left panel) and Social Novelty (propensity to investigate an unfamiliar vs familiar mouse; right panel) were both measured in BDL/sham mice during 10 min observation sessions. BDL mice exhibited enhanced sociability (**p=0.0003) and intact social novelty compared to sham mice (n=16 and 17 mice/grp). Data expressed as (%): (i) Sociability = % time spent investigating unfamiliar mouse + entire time spent engaged in investigation of either cage, and (ii) Social Novelty = % time spent investigating unfamiliar mouse + entire time spent engaged in investigation unfamiliar and familiar mouse.

Figure: (abstract: FRI-352).

POSTER PRESENTATIONS

revealed significant changes in genes in amygdala neural signaling pathways regulating social behavior in BDL vs sham mice. Specifically, significant alterations were observed in genes encoding the Canonical Pathway for Brain Oxytocin Signaling ($z = -1.64$; $p < 1.79 \times 10^{-3}$) and CREB Signaling in Neurons (positively regulated by glutamate signaling; $z = -1.943$; $p < 2.02 \times 10^{-3}$) pathways. Additionally, IPA® Upstream Regulator analysis predicted significant changes in numerous upstream transcriptional regulators for DEGs in BDL vs sham mice, including activity of upstream regulators for genes regulating dopaminergic ($z = 3.309$; $p < 1.02 \times 10^{-35}$), GABAergic ($z = -1.509$; $p < 1.69 \times 10^{-26}$), and glutaminergic ($z = -2.87$; $p < 2.87 \times 10^{-7}$) neural pathways.

Conclusion: Cholestatic mice demonstrate enhanced sociability with significant changes in amygdala gene expression profiles within neural pathways critically regulating social behavior. These findings suggest adaptive changes occur in brain neural pathways in CLD to preserve sociability and are consistent with clinical observations that social isolation leads to poor clinical outcomes.

FRI-353

Oxazolone-mediated bile duct inflammation reveals specific natural killer T cell-dependent inflammatory pathways

Markus Jördens^{1,2,3,4}, Kathrine Sivertsen Nordhus^{1,2,4}, Jonas Øgaard^{1,2}, Tom Lüdde³, Tom Hemming Karlsen^{1,2,4,5}, Brian K. Chung^{1,2,4}, Espen Melum^{1,2,4,5,6}. ¹Oslo University Hospital and Institute of Clinical Medicine, University of Oslo, Norwegian PSC Research Center, Norway; ²Oslo University Hospital, Rikshospitalet, Research Institute of Internal Medicine, Norway; ³University Hospital

Düsseldorf, Medical Faculty, Heinrich Heine University Düsseldorf, Department of Gastroenterology, Hepatology and Infectious Diseases, Germany; ⁴University of Oslo, Institute of Clinical Medicine, Norway; ⁵Oslo University Hospital, Rikshospitalet, Section for Gastroenterology, Department of Transplantation Medicine, Division of Surgery, Inflammatory Diseases and Transplantation, Norway; ⁶University of Oslo, Hybrid Technology Hub-Centre of Excellence, Institute of Basic Medical Sciences, Faculty of Medicine, Norway
Email: markus.joerdens@med.uni-duesseldorf.de

Background and aims: Primary sclerosing cholangitis (PSC) is an inflammatory bile duct disease characterized by cholangiocyte destruction. We modelled the inflammatory process by performing intrabiliary injection oxazolone which induces cholangitis driven by natural killer T (NKT) cells—a subset of innate-like lymphocytes enriched in liver that rapidly secrete inflammatory mediators upon recognition of CD1d-restricted lipid antigens. To examine the molecular granularity driving NKT-dependent biliary inflammation, we assessed livers from oxazolone-treated mice at multiple time-points by spatial transcriptomics and compared differential gene expression in biliary regions.

Method: Livers from male 10–12-week old C57Bl/6 wild-type (WT), were harvested at 1, 3, and 7 days after intrabiliary oxazolone or DMSO (vehicle) injection and processed for spatial transcriptomics (10X Genomics, USA). Similarly, livers from matched *Cd1d*^{-/-} animals (lack both CD1d and NKT cells) and *Ja18*^{-/-} mice (lack only Type I NKT cells) were harvested 3 days post-treatment. Spatial transcripts of all mice were aligned by Space Ranger and cluster analysis and differential gene expression was analyzed using Loupe Browser

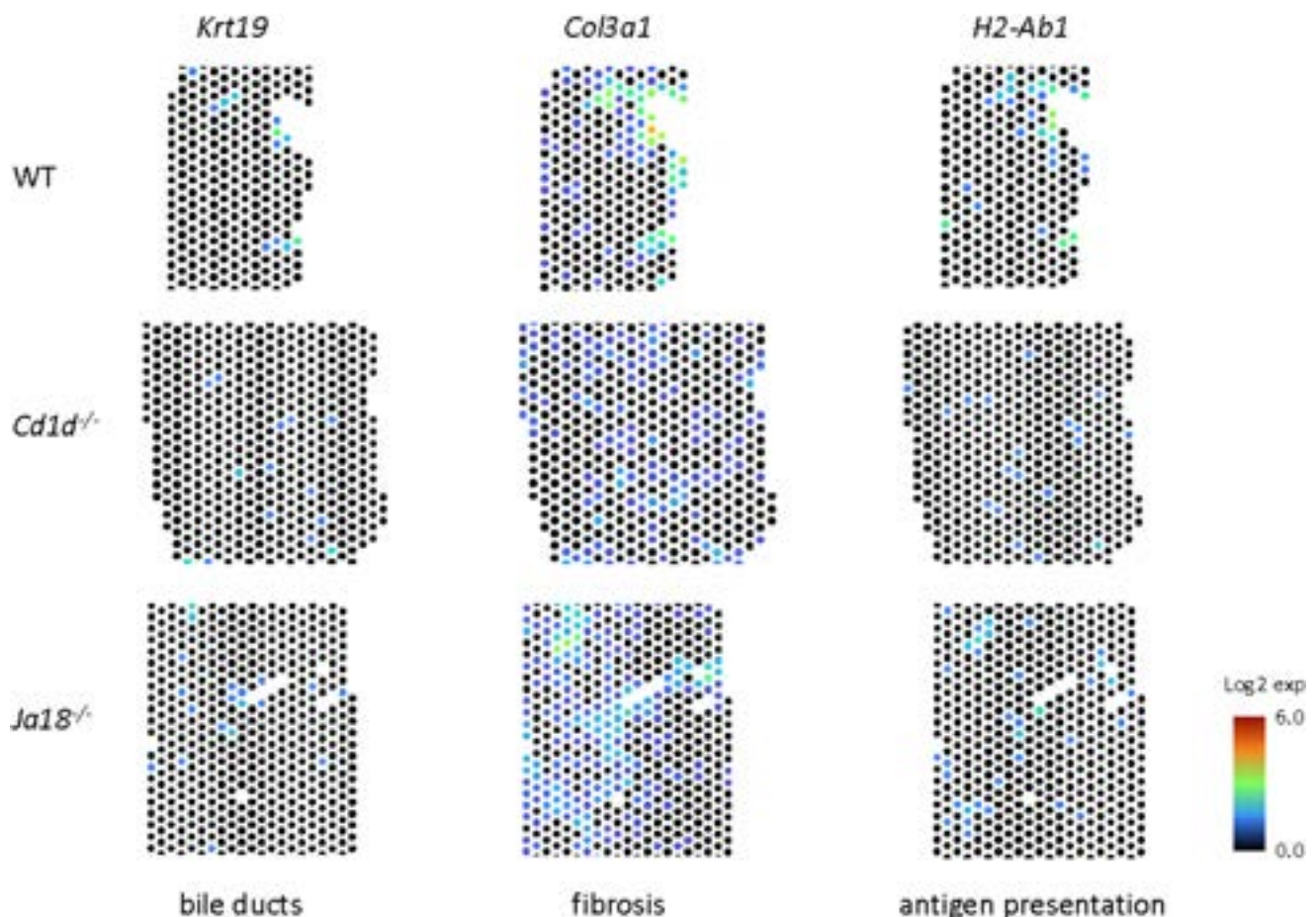


Figure 1: (abstract: FRI-353): Localization of markers for bile ducts (*Krt19*), fibrosis (*Col3a1*) and antigen presentation (*H2-Ab1*) in liver tissue of WT, *Cd1d*^{-/-} and *Ja18*^{-/-} mice 3 days after oxazolone injection. Log2 expression values are shown

(10X Genomics). Gene pathway enrichment was determined using STRING analysis.

Results: Differential gene analysis of biliary regions defined by spatial transcriptomics as cytokeratin 19 (Krt19) positive and confirmed by histological assessment showed no significant gene upregulation 1 day post-oxazolone versus DMSO ($p < 0.05$, Benjamini-Hochberg corrected), 124 genes 3 days post-oxazolone and zero genes after 7 days post-oxazolone. Genes upregulated on day 3 predominantly related to drug metabolism (*Cyp1a2*, *Cyp2b10*, *Cyp2c29*, *Aox3*), complement activation (*C8g*, *C9*, *Mbl1*, *Mbl2*, *Hc*) and acute phase response (*Saa1*, *Saa2*, *Saa3*, *Orm2*, *Serpina3n*, *Crp*) pathways indicating oxazolone-induced inflammation peaks at day 3 and resolves by day 7. NKT cells had a marked effect on biliary gene expression as transcripts relating to MHC class II antigen processing (*Cd74*, *H2-Ab1*) and collagen organization (*Col1a2*, *Col1a1*, *Col3a1*, *Serpinh1*) were significantly upregulated in WT animals 3 days post-oxazolone compared to both *Cd1d*^{-/-} ($n = 3$) and *Ja18*^{-/-} ($n = 3$).

Conclusion: Spatial transcriptome analysis of oxazolone-induced bile duct inflammation revealed a distinct pattern relating to antigen presentation and fibrosis that was both temporal and NKT cell-dependent. The identified pathways could be of relevance as future treatment targets for inflammatory bile duct disorders such as PSC.

FRI-354

The significance of patatin-like phospholipase domain-containing protein-3 I148M genetic variant in autoimmune hepatitis

Kalliopi Azariadi^{1,2}, Angeliki Lyberopoulou^{1,2}, Pinelopi Arvaniti^{1,2}, Kalliopi Zachou^{1,2}, Nikolaos Gatselis^{1,2}, George Dalekos^{1,2}. ¹General University Hospital of Larissa, Department of Medicine and Research Laboratory of Internal Medicine, National Expertise Center of Greece in Autoimmune Liver Diseases, Larissa, Greece; ²General University Hospital of Larissa, European Reference Network on Hepatological Diseases (ERN RARE-LIVER), Larissa, Greece
Email: gatselis@me.com

Background and aims: Autoimmune hepatitis (AIH) is a relatively rare autoimmune disease with a strong genetic background. The concurrence of non-alcoholic fatty liver disease (NAFLD) in AIH possibly signifies a more severe disease. The patatin-like phospholipase domain-containing protein 3 (PNPLA3) I148M (rs738409 C/G) variant is well established genetic modifier of NAFLD. Our aim was to investigate the significance of the PNPLA3 I148M variant in AIH.

Method: Two-hundred patients with AIH followed in our Centre were evaluated while a hundred healthy subjects served as controls. Genotyping was performed with in-house allelic discrimination end point polymerase chain reaction (PCR).

Results: The I148M variant was present in 95/200 (47.5%) AIH patients compared to 47/100 (47%) healthy controls ($p = 1.000$). Patients with GG/CG genotypes were more likely to suffer from at least one metabolic risk factor (GG/CG 74.4% vs CC 61%, $p = 0.038$) and to present with decompensated cirrhosis at diagnosis (GG/CG 6.3% vs CC 1%, $p = 0.039$). Simple steatosis was present in 35/186 (18.8%) and steatohepatitis in 14/186 (7.5%) patients with available liver biopsy without correlation with the PNPLA3 genotype. The stage of fibrosis and grade of inflammation didn't correlate with any genotype. Response to treatment was also independent of the presence of the I148M variant. On Kaplan-Meier analysis homozygosity for the G allele correlated with reduced survival free of decompensation ($p = 0.006$), cirrhotic events (decompensation, liver transplantation, hepatocellular carcinoma) ($p = 0.001$) and liver related death or liver transplantation ($p = 0.011$) in treated patients.

Conclusion: The PNPLA3 I148M variant in AIH patients is associated with increased risk of advanced disease at diagnosis and reduced survival free of cirrhotic events and liver related death or liver transplantation, regardless of the presence of NAFLD. This signifies a potential role for the PNPLA3 I148M variant as a new AIH biomarker

allowing to identify patients with increased risk to disease progression.

FRI-355

Temporal characteristics of cell compartments in immune-mediated cholestatic disease

Markus Jördens^{1,2,3,4}, Kathrine Sivertsen Nordhus^{1,2,3}, Kristian Holm^{1,2,3}, Jonas Øgaard^{1,2}, Tom Lüdde⁴, Tom Hemming Karlsen^{1,2,3,5}, Brian K. Chung^{1,2,3}, Espen Melum^{1,2,3,5,6}. ¹Oslo University Hospital and Institute of Clinical Medicine, University of Oslo, Norwegian PSC Research Center, Norway; ²Oslo University Hospital, Rikshospitalet, Oslo, Research Institute of Internal Medicine, Norway; ³University of Oslo, Institute of Clinical Medicine, Norway; ⁴University Hospital Düsseldorf, Medical Faculty, Heinrich Heine University Düsseldorf, Department of Gastroenterology, Hepatology and Infectious Diseases, Germany; ⁵Oslo University Hospital, Rikshospitalet, Section for Gastroenterology, Department of Transplantation Medicine, Division of Surgery, Inflammatory Diseases and Transplantation, Norway; ⁶Faculty of Medicine, University of Oslo, Hybrid Technology Hub-Centre of Excellence, Institute of Basic Medical Sciences, Norway
Email: markus.joerdens@med.uni-duesseldorf.de

Background and aims: Primary sclerosing cholangitis (PSC) and primary biliary cholangitis (PBC) are progressive liver disorders featuring peribiliary immune infiltration and cholangiocyte destruction with limited treatment options. The pathogenic interactions between immune cells and cholangiocytes remain unclear but can represent novel treatment targets. Using NOD.c3c4 mice that exhibit spontaneous bile duct inflammation as a model of PSC and PBC, we characterized the immunobiliary pathogenesis by defining the gene expression localized to the biliary microenvironment and examined whether progression from early to late disease correlated with alterations in the biliary immune compartment.

Method: Liver tissue from 10-, 20- and 40-week NOD.c3c4 mice ($n = 2-4$ per age group) were harvested and analyzed by spatial transcriptomics and single-cell RNA sequencing (scRNA-seq; 10X Genomics, USA). Transcriptomes were processed using Space Ranger (spatial) or Cell Ranger (scRNA-seq). Unsupervised k-means clustering and differential gene expression analysis was performed in Loupe Browser (10X Genomics). Relative cell abundances were estimated from spatial transcriptomes using scRNAseq profiles and CIBERSORTx and CARD deconvolution analyses.

Results: Spatial transcriptomes from 10-, 20- and 40-week NOD.c3c4 mice clearly demonstrated high expression of hepatocyte markers in histologically-defined parenchymal regions (*Muc9*, *Muc12*, *Muc17*, *Cyp2C67*, *Cyp2E1*) and cholangiocyte markers in biliary regions (*Tspan8*, *Krt19*, *Epcam*). The non-cholangiocyte markers demonstrating the highest differential expression in biliary regions were related to inflammation (*S100a6*, *Crip1*, *Cd24*, *Cd63*). Differential gene expression analysis of 10- and 20-week biliary regions (age-matched combined) showed four significant genes whereas comparisons between 10- and 40-week biliary regions showed 420 genes ($p < 0.05$, Benjamini-Hochberg corrected) with strongest upregulated expression in 40-week animals associated with cell proliferation (*Cd24a*, *Prom1*, *Dmbt1*, *Ccnd1*) and chronic inflammatory response (*Gja1*, *Camp*, *Mdk*). Deconvolution of spatial transcriptomes into immune cell types revealed biliary infiltration of granulocytes (*S100a9*, *S100a8*, *Il1b*), plasmacytoid dendritic cells (*Siglech*), monocytic phagocytes (*Lyz2*, *Clec4a3*, *Clec4a1*), dendritic cells (*Xcr1*), B cells (*Cd79a*, *Cd79b*, *Cd19*) and T cells (*Cd3g*, *Cd3e*, *Nkg7*) in all age groups.

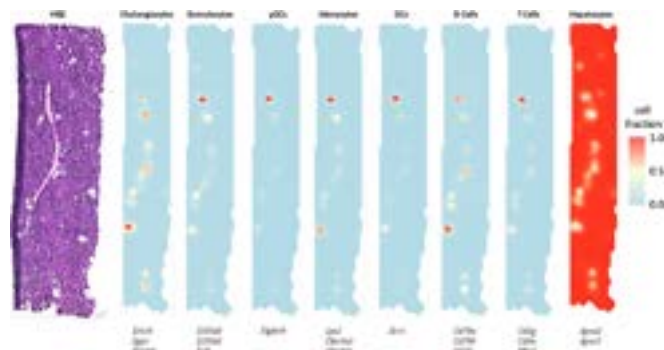


Figure 1: Hematoxylin and eosin (HandE) staining of 10-week NOD.c3c4 liver (left) and localization of indicated immune cell types in biliary regions (cholangiocytes) of the same tissue section using CARD deconvolution of spatial transcriptomes (right). Exemplar lineage markers and relative cell fractions are shown.

Conclusion: Spatial transcriptomics combined with scRNA-seq demonstrates that disease progression is driven by a defined and time-dependent molecular signature in biliary regions of NOD.c3c4 mice. These findings may point to immune pathways amenable to novel treatment approaches in PSC and PBC patients.

FRI-356

HSD17B13 inhibitors are hepatoprotective and anti-inflammatory in a mouse model of autoimmune hepatitis

Manuel Roqueta-Rivera¹, Yaohui Nie¹, Jordan Butts¹, Mary Chau¹, Kelsey Garlick¹, Archie C. Reyes¹, Jonathan Lloyd¹, Joshua Klaene¹, Yat-Sun Or¹, Bryan Goodwin¹. ¹Enanta Pharmaceuticals, Inc., Biology, Watertown, United States
Email: mroqueta@enanta.com

Background and aims: Genome wide association studies identified a loss of function gene variant (rs72613567:TA) for 17-beta hydroxysteroid dehydrogenase 13 (HSD17B13), a lipid droplet-associated protein linked to decreased risk for chronic liver diseases. Delayed onset of autoimmune hepatitis (AIH) has also been observed in TA variant carriers. HSD17B13 inhibitors (HSDi), previously shown to be anti-inflammatory *in vivo* with modulation of sphingolipids, were evaluated in a mouse model of AIH for anti-inflammatory and hepatoprotective effects.

Method: Distinct chemical series of HSDi of sub-micromolar potency were tested in a concanavalin A (ConA) model of acute hepatitis. Mice were pretreated with HSDi by oral gavage, followed by intravenous delivery of ConA. Liver, spleen, and plasma were collected at 6 hours post-ConA injection. Hepatoprotection was assessed using plasma ALT. Inflammatory gene markers were evaluated in liver and spleen by qPCR. Cytokines and chemokines were measured in plasma by mesoscale immunoassay. The HSDi effect on sphingolipids was

measured in mouse liver and primary human hepatocytes by mass spectrometry.

Results: HSDi from distinct chemical series were hepatoprotective and anti-inflammatory. Splenomegaly due to ConA was observed across all groups. However, elevation of plasma ALT and cytokines (TNF, IL1b, CXCL9) by ConA was attenuated by HSDi. In addition, HSDi decreased inflammatory gene markers (*Nlrp3*, *Il1*, *Il6*, *Ccl2*) in liver. The influx of T-cells (*Cd8*) to liver was not altered by HSDi, however, markers of immune cell activation (*Cd69*, *S1pr4*) and mediators of cell death (*FasL*) were decreased. In line with a favorable anti-inflammatory and anti-apoptotic profile, liver ceramides (d18:0/16:0 and d18:1/24:1) were decreased in HSDi-treated livers. The modulation of these ceramides was confirmed in HSDi-treated primary human hepatocytes.

Conclusion: We have identified potent and selective HSDi that decrease ceramide levels *in vitro* and *in vivo*. The hepatoprotective effects by HSDi in an acute T-cell driven liver injury model of AIH may be partially mediated by the modulation of bioactive lipids responsible for cytotoxic immune cell activation.

FRI-357

Differential activation of regulatory CD4⁺ T cells via the JAK-STAT-pathway in Primary sclerosing cholangitis

Leona Dold¹, Sandra Kalthoff¹, Leonie Frank¹, Taotao Zhou¹, Pia Esser¹, Philipp Lutz¹, Christian Strassburg¹, Ulrich Spengler¹, Bettina Langhans¹. ¹University Hospital Bonn, Department of Internal Medicine I, Bonn, Germany
Email: Leona.Dold@ukbonn.de

Background and aims: Primary sclerosing cholangitis (PSC) is an autoimmune cholestatic liver disease of unknown aetiology. Regulatory CD4⁺ T cells (Tregs) are important for induction/maintenance of self-tolerance and inhibition of autoimmunity. In PSC a low number of Tregs has been reported. However, their functionality is still unclear. Activation of the JAK-STAT (Janus kinase-signal transducer and activator of transcription) pathway plays a pivotal role in modulating T cell functions. Here, we analyzed cytokine-induced activation of different STAT proteins in Tregs from patients with PSC.

Method: 51 PSC-patients (37 with inflammatory bowel disease (IBD), 14 without IBD; all without acute cholangitis or colitis) and 36 healthy controls were enrolled in our study. We measured cytokines in serum via bead-based immunoassays. Using multiparameter phospho-flow cytometry we analyzed ex vivo frequencies of Foxp3⁺CD25⁺CD127^{low}CD4⁺ Tregs and phosphorylation of STAT1/3/5/6 in Tregs after *in vitro* stimulation with recombinant IFN-gamma, IL-6, IL-2, and IL-4, respectively, and correlated the results to clinical data.

Results: Frequencies of peripheral Tregs were significantly reduced in PSC patients compared to healthy controls ($p = 0.0028$). In line, serum

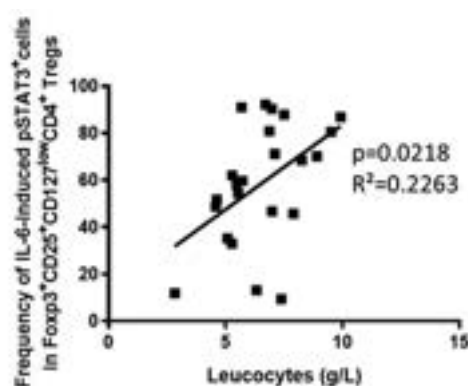
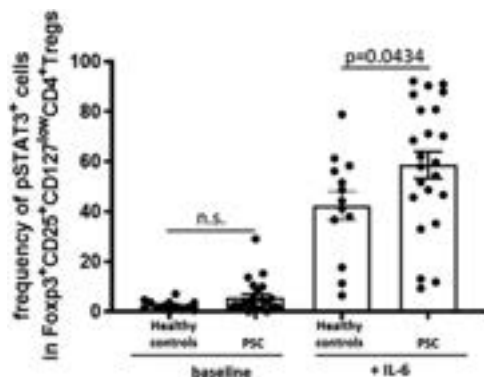


Figure: (abstract: FRI-357).

levels of IFN- γ , IL-6, IL-2 and IL-4 were markedly higher in PSC patients than in healthy controls ($p < 0.05$ each). While none of these cytokines affected activation of STATs 1/5/6, IL-6 stimulation induced enhanced phosphorylation of STAT3 in Tregs of PSC patients (Figure 1A). Unlike to commonly proposed markers for PSC progression (bilirubin, alkaline phosphatase, MELD-score), the frequency of IL-6-induced phospho-STAT3⁺ Tregs correlated to the leukocyte counts in PSC (Figure 1B).

Conclusion: Our data indicate differential JAK-STAT activation of CD4⁺ Tregs in PSC. The correlation between IL-6-induced phospho-STAT3⁺ Tregs and leukocyte counts may reflect triggering of this pathway in response to an infection.

FRI-358

scRNA transcriptomics reveal the role of cholangiocytes and neutrophils cross talk in PKHD1-KO mice

Zehra Syeda¹, Romina Fiorotto¹, Shakila Taleb¹, Tory Bauer-Pisani¹, Dejian Zhao¹, Mario Strazzabosco¹. ¹*Yale School of Medicine, United States*

Email: mario.strazzabosco@yale.edu

Background and aims: Congenital hepatic fibrosis (CHF) and Caroli disease (CD) are caused by mutation in Polycystic kidney hepatic disease 1 gene (PKHD1) and lead to biliary malformations, cholangiocyte dysfunction and portal fibrosis. PKHD1 encodes for fibropolycystin (FPC), a protein expressed in cilia, plasma membrane and centromeres of cholangiocytes. FPC is involved in multiple cellular functions from polarity and cell matrix interactions to differentiation. This study was designed to investigate the relationships among the cell types present in the pericyclic infiltrate in Pkhd1-KO mice at single cell level, to better understand the pathophysiology of CHF/CD.

Method: We isolated single cells from liver portal tract of 3 months old Pkhd1-KO and WT mice. Transcriptomics profiling of 16,383 single cells, yielded molecular definitions for cell types present in samples. Datasets were analyzed by Seurat and CellPhoneDB package in R.

Results: ScRNA seq analysis revealed 9 distinct populations in the portal tract of WT and Pkhd1-KO. Interestingly, a second population of cholangiocytes, having higher expression of chemokines (Cxcl5, Cxcl2) along with other features of "reactive cholangiocytes," was exclusively present in Pkhd1-KO together with classical cholangiocytes. Gene ontology analysis in reactive cholangiocytes showed an enrichment of genes involved in the recruitment of neutrophils and activation of innate immune responses and suggested the potential involvement of microbial components. Among 4 different subpopulations of T cells identified (i.e. CD4⁺, CD8⁺, CD4/CD8 double negative and NKT), CD8⁺ and Double Negative T Cells (DNT) are present only in KO sample. DNT cells have previously shown a critical role in perpetuating inflammation. CellPhoneDB analysis showed that Cxcl5 and Cxcl1 play a major role in cross talk and recruitment of neutrophils by cholangiocytes. Cxcl16 attracts T cells and is expressed by cholangiocytes and macrophages in Pkhd1-KO. Neutrophils secrete Csf1 that promotes macrophage polarization. Neutrophils and macrophages express Ccl6, a chemoattractant for macrophages and T cells. Ccl8 is expressed by Macrophages and provide signals for naive T cell activation and survival by binding to Cd28 on CD4⁺ and CD8⁺ T cells. IL17a is expressed by DNT cells in Pkhd1-KO. The IL17a receptor is expressed by neutrophils. IL-1 β is highly expressed by neutrophils and macrophages in Pkhd1-KO. The receptor Il1r1 is expressed by DNT cells.

Conclusion: This study shows a complex signaling network originating from cholangiocytes and amplified by the recruited neutrophils and then T cells and macrophages in Pkhd1-KO. Many of the identified signals are druggable and therefore their blockade may bear therapeutic advantages to improve inflammation and progression to fibrosis in Pkhd1-KO model. The role of microbial population is of particular interest.

FRI-359

Golexanolone, a GABA receptor-modulating steroid antagonist, improves peripheral inflammation, fatigue, locomotor gait, motor incoordination and short-term memory in rats with cholestasis and hepatic encephalopathy due to bile duct ligation

Paula Izquierdo-Altarejos¹, Yaiza Arenas¹, Mar Martinez-Garcia¹, Carla Gimenez-Garzo¹, Gergana Mincheva¹, Magnus Doverskog², Marta Llansola¹, Vicente Felipo¹. ¹*Centro de Investigacion Principe Felipe, Valencia, Spain;* ²*UmeCrine Cognition AB, Sweden*

Email: vfelipo@cipf.es

Background and aims: Cholestasis may appear in patients with primary sclerosing cholangitis, primary biliary cholangitis, or drug-induced liver injury. Patients with cholestasis may show fatigue and other symptomatic alterations that severely reduce their quality of life. Patients with liver disease may also eventually show hepatic encephalopathy, with cognitive and motor impairment. Rats with bile-duct ligation (BDL) are a common animal model both of cholestatic liver disease as well as of hepatic encephalopathy. Current management and treatment of cholestatic liver disease include secondary bile acids like ursodeoxycholic acid, UDCA. The licensed therapies are exclusively used to slow or prevent disease progression but have no impact on symptomatic alterations such as fatigue. There are presently no licensed or effective medications for the management of symptomatic alterations such as fatigue in PBC or any other liver disease but immunomodulatory treatments have been proposed. Golexanolone (GR3027), reduces GABAergic tone by reducing the potentiation of GABA_A receptors activation by neurosteroids such as allopregnanolone. We have recently shown that golexanolone reduces peripheral inflammation and neuroinflammation and improves cognitive and motor function in rats with chronic hyperammonemia. The aims of this study were to assess if golexanolone treatment reduces peripheral inflammation and improves fatigue and cognitive and motor function in BDL rats.

Method: Rats were subjected to bile duct ligation. One week after surgery golexanolone was administered daily using intra-gastric probes to BDL and sham-operated controls. To assess the effects on peripheral inflammation several interleukins were analyzed in plasma. Fatigue was analyzed in the treadmill, motor coordination in the motorater, locomotor gait in the Catwalk, and short-term memory in the Y maze. These analyses were performed after 2–4 weeks of treatment with golexanolone.

Results: BDL increases the plasma levels of the pro-inflammatory interleukins TNF α , IL-6, IL-17 and IL-18. Golexanolone reverses the increases in these interleukins. BDL induces fatigue in the rats, motor incoordination in the motorater test and alters locomotor gait analyzed in the Catwalk. Golexanolone reverses these changes. BDL impairs short-term memory in the Y maze. Golexanolone improves this impairment.

Conclusion: Golexanolone reduces peripheral inflammation in BDL rats. This is associated with improvement in fatigue, locomotor gait and coordination, and short-term memory. Golexanolone may have beneficial effects to treat symptomatic alterations such as fatigue, and motor-, and cognitive impairment in patients with cholestatic liver disease, or hepatic encephalopathy.

FRI-360

Elevated JAG1-NOTCH Signaling is Associated with Fibrosis Stages in Patients with PSC

Michael Trauner¹, Kaiyi Zhu², Jun Xu², William Barchuk², Lisa Boyette², Timothy R. Watkins², Andrew Billin², Sharlene Lim², Vlad Malkov², Christopher Bowlus³. ¹*Medical University of Vienna, Austria;* ²*Gilead Sciences, Inc., United States;* ³*University of California Davis, United States*

Email: jun.xu@gilead.com

Background and aims: The canonical NOTCH signaling pathway is a fate-determinant factor for intrahepatic bile duct epithelium during liver organogenesis. Null mutations in the NOTCH ligand JAG1 or the

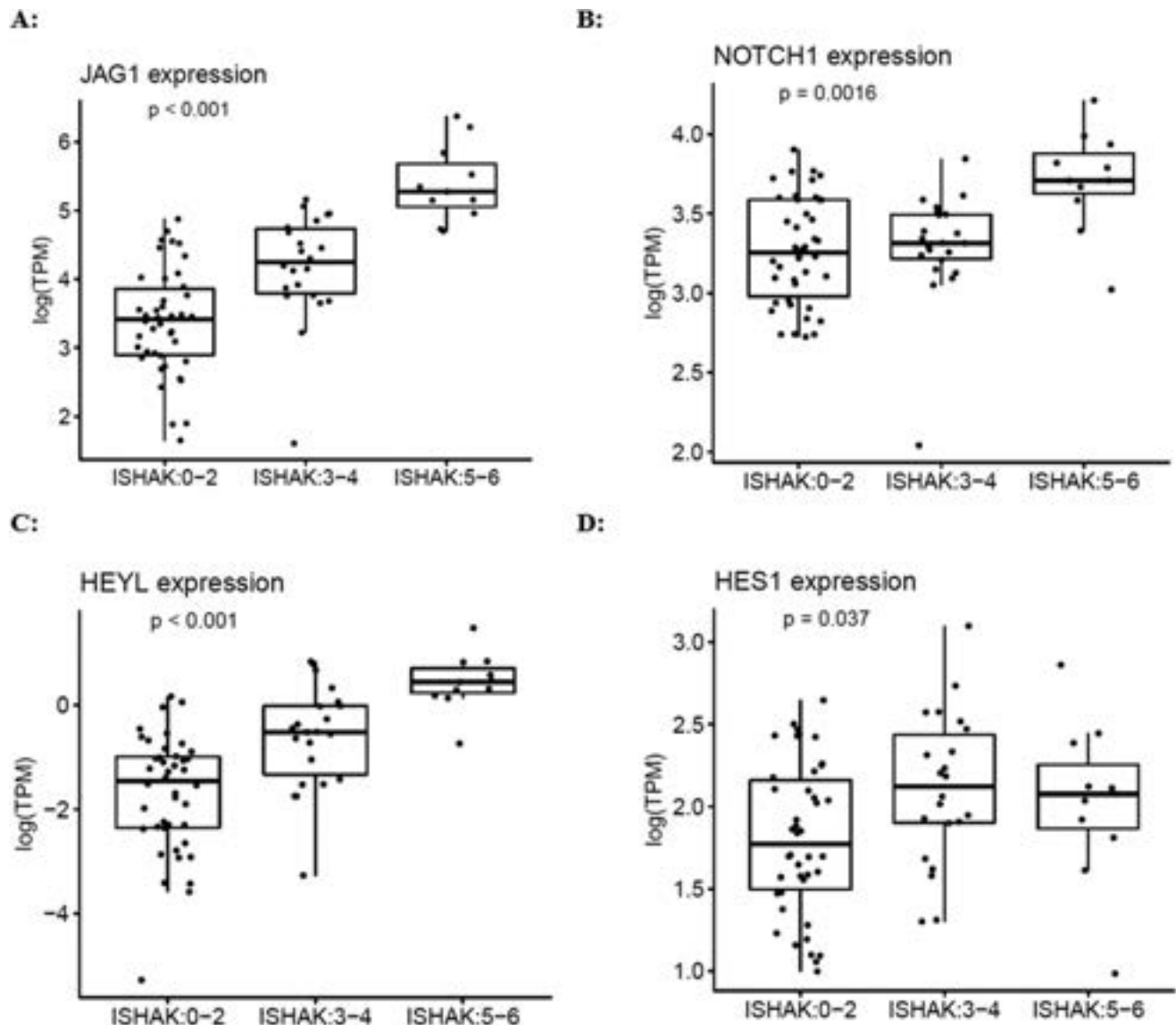


Figure: (abstract: FRI-360): Associations between JAG1-NOTCH Signaling and Ishak Fibrosis Stages in PSC

NOTCH2 receptor are associated with Alagille syndrome characterized by bile duct paucity. The ductular reaction is commonly observed in liver histology from patients with primary sclerosing cholangitis (PSC) or other cholestatic diseases, but the contribution of NOTCH signaling to abnormal bile duct proliferation driving biliary fibrosis is unknown. The aim of the study is to evaluate hepatic NOTCH signaling in patients with PSC.

Method: The study population comprised participants in a phase 2b, placebo-controlled trial of simtuzumab in PSC (NCT01672853). A transcriptomic analysis was performed on baseline liver biopsy samples. Fibrosis was staged according to the Ishak classification by a central pathologist. Mild fibrosis was defined by Ishak 0–2, moderate fibrosis by Ishak 3–4 and cirrhosis by Ishak 5–6. RNA-sequencing data was quantified in log2 transcripts per million (TPM). P values were derived by Kruskal-Wallis (KW) test, Wilcoxon test or Spearman correlation.

Results: A total of 75 PSC patients with mild (n = 42) and moderate (n = 22) fibrosis and cirrhosis (n = 11) were included with a median (IQR) expression of *JAG1*, the canonical ligand for NOTCH signaling, of 3.41 (2.89, 3.86), 4.25 (3.79, 4.74) and 5.28 (5.50, 5.68), respectively.

JAG1 expression levels were significantly associated with fibrosis stages with the highest levels in the cirrhosis cohort (KW p < 0.001) (Figure 1A). The hepatic expression of *NOTCH1* was greater in the cirrhosis cohort [3.71 (3.63, 3.88)] compared to mild [3.25 (2.89, 3.86)] and moderate [3.32 (3.22, 3.50)] fibrosis cohorts (KW P = 0.0016) (Figure 1B). *NOTCH2* expression levels did not differ by different fibrosis stages (KW p = 0.068). In concordance with the elevated ligand expression of *JAG1*-NOTCH-responsive genes *HEYL* and *HES1* were increased in PSC with cirrhosis cohort compared to the mild and moderate cohorts (KW p < 0.05) (Figure 1 C and D). In addition, *JAG1* (Wilcoxon p < 0.001), *HES1* (Wilcoxon p = 0.015) and *HEYL* (Wilcoxon p < 0.001) were elevated in patients with Enhanced Liver Fibrosis (ELF) score ≥ 9.8. In the liver of PSC patients, *JAG1* expression was positively correlated with *SOX9* ($\rho = 0.73$, p < 0.001), which determines cholangiocyte fate during liver development and negatively correlated with newly generated hepatocyte markers (PMID: 34792289), *ALDOB* ($\rho = -0.42$, p < 0.001), *ASGR1* ($\rho = -0.38$, p < 0.001) and *SERPINA1* ($\rho = -0.28$, p = 0.014).

Conclusion: JAG1-NOTCH signaling in PSC increases with fibrosis stages. The spatial expression pattern of *JAG1* in the liver, cellular

interactions, and non-invasive tests to monitor elevated NOTCH signaling in PSC patients warrant further investigation.

FRI-361

Pyroptosis plays a key role in primary biliary cholangitis of humans and mice

Linxiang Huang¹, Wang Zilong¹, Zheng Jiarui¹, Zhicheng Liu¹, Bo Feng¹.

¹Peking University People's Hospital, China

Email: fengbo@pkuph.edu.cn

Background and aims: Primary biliary cholangitis (PBC) is a progressive, non-suppurative, destructive intrahepatic cholestatic disease, which is considered to be an immunological disorder with both environmental and genetical participation. Around 40% PBC patients were reported to have an incomplete response to the first-line treatment, ursodeoxycholic acid (UDCA), leading to a poor prognosis and lack efficient treatment. Pyroptosis, a newly discovered cell death pathway, characterized by gasdermin-mediated programmed necrosis, was proved to be involved in many liver diseases. However, if pyroptosis is involved in the pathogenesis of PBC remains unclear. In this study, we aim to investigate the involvement of pyroptosis in PBC patients and mice and explore the potential of pyroptotic pathway as a possible treatment target.

Method: Liver tissue samples were collected from liver biopsy of six PBC patients with no history of other liver diseases from Hepatology Department of Peking University People's Hospital. Samples from control individuals with normal liver histology were collected from patients with no evidence of other liver diseases. Twenty female C57BL/6 mice of 4–6 months old were evenly divided into PBC group and control group. PBC mice were induced with two doses of 2-nonynoic acid (2OA-BSA) and polycytidylic acid (poly I: C) for total 12 weeks. Immunocyte type correlation analysis was performed on the GSE119600 dataset of Gene Expression Omnibus (GEO) database with whole blood samples from PBC patients (n=90) and non-liver disease controls (n=47). Immunohistochemistry (IHC) staining of gasdermin D (GSDMD) in liver samples of PBC patients and mice, and

the expression levels of GSDMD and its classical pathway were determined in the PBC mice model.

Results: The immunocyte type correlation analysis reported that the expression of key transcription factors of M1 macrophages-NOS2, IRF5, PTGS2 were significantly higher in PBC patients than that of control group ($p < 0.05$, Fig. A). The expression levels of GSDMD in liver samples of PBC patients were significantly improved. Noteworthily, the IHC staining of GSDMD in the PBC liver sections showed a distribution pattern of macrophage (Fig. B). For the 2OA-induced PBC mice model, pyroptosis pathway was upregulated than control mice. Both the mRNA ($p < 0.05$, Fig. C) and protein levels ($p < 0.05$, Fig. D) of GSDMD significantly increased compared to normal controls, determined by qrt-PCR and western blotting, respectively. Besides, the qrt-PCR showed that the expression levels of all key elements of classical pyroptosis pathway (i.e., NLRP3-Caspase-1-GSDMD, Fig. C) was significantly higher than control ($p < 0.05$). IHC staining also revealed improved GSDMD and Caspase-1 expression in PBC mice, especially around the portal area (Fig. E).

Conclusion: Pyroptosis plays a key role in PBC patients and 2OA-BSA induced PBC mice, possibly macrophages being the most important executors. Inhibition of the pyroptosis pathway might be a potential target for the future treatment of PBC.

FRI-362

Molecular signatures of treatment response in autoimmune hepatitis

Bastian Engel¹, Zhaoli Liu^{2,3}, Finn C. Derben¹, Björn Hartleben⁴, Geffers Robert⁵, Cheng-Jian Xu^{2,3}, Elmar Jaecel¹, Richard Taubert¹.

¹Hannover Medical School, Gastroenterology, Hepatology and Endocrinology, Hannover, Germany, ²TWINCORE, a joint venture between the Helmholtz Centre for Infection Research (HZI) and Hannover Medical School (MHH), Hannover, Germany, Germany; ³Centre for Individualised Infection Medicine (CiiM), a joint venture between the Helmholtz Centre for Infection Research (HZI) and Hannover Medical School (MHH), Hannover, Germany, Germany; ⁴Hannover Medical

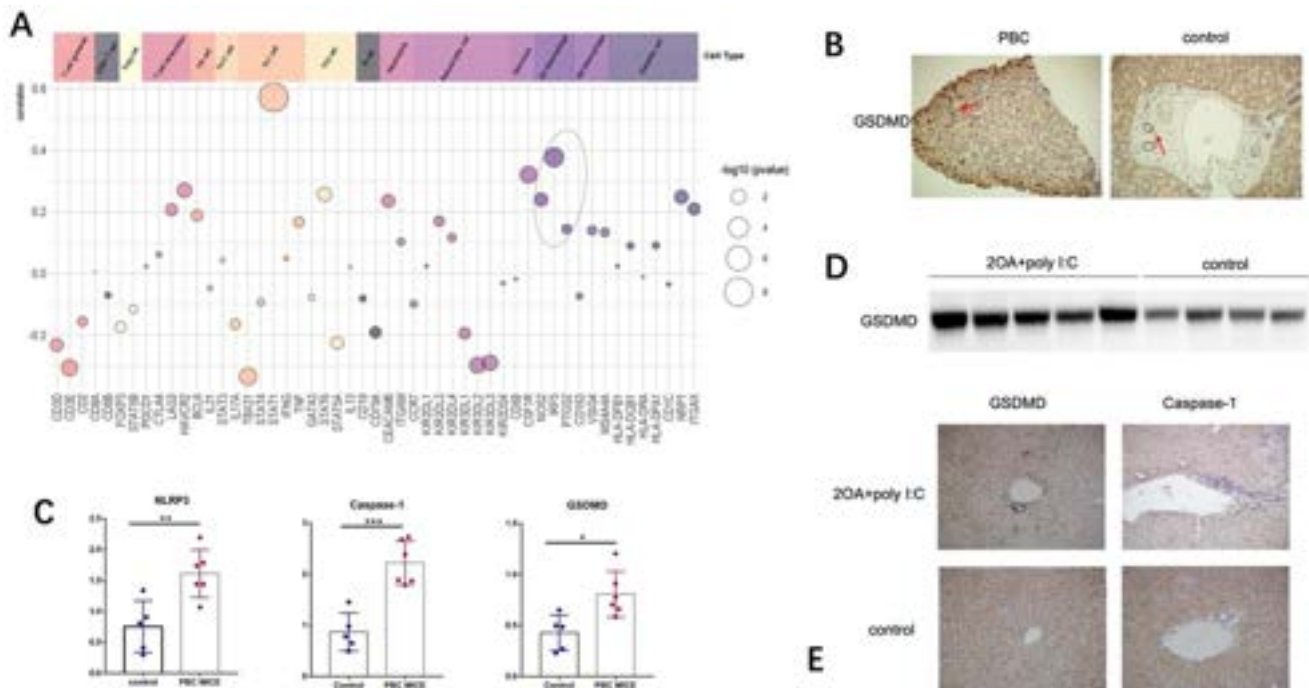


Figure: (abstract: FRI-361): Figure A. immunocyte type correlation analysis. Figure B. Representative immunohistochemistry stained sections of GSDMD in liver tissues of PBC patients and control. Figure C. Hepatic mRNA levels of NLRP3-Caspase-1-GSDMD pathway. Figure D. Hepatic protein expression of GSDMD. Figure E. Representative immunohistochemistry stained sections of GSDMD and Caspase-1 in WT and PBC mice model. * $p < 0.05$, ** $p < 0.01$, *** $p < 0.001$.

POSTER PRESENTATIONS

School, Institute for Pathology, Germany; ⁵Helmholtz Centre for Infection Research, Research Group Genome Analytics, Germany
Email: Engel.Bastian@mh-hannover.de

Background and aims: Autoimmune hepatitis (AIH) is a chronic inflammatory liver disease that needs long-term immunosuppression. Biochemical remission (BR), defined by normalisation of IgG and transaminases, is the treatment goal and is associated with a favourable clinical outcome. Recently, it was proposed by the international AIH group to report outcomes at six and twelve months. Our exploratory analysis aims to investigate different molecular signatures between patients with BR at twelve months (BR12) and incomplete response at twelve months (IR) to immunosuppressive therapy using baseline biopsies.

Method: Forty AIH patients from Hannover Medical School (Hannover, Germany) were enrolled in this study; 20 with BR12 and 20 with IR. RNA was extracted from formalin-fixed, paraffin-embedded liver tissue and was sequenced using Illumina HighSeq 6000. Bulk RNA sequencing data were processed using nf-core/rnaseq pipeline. Further downstream analyses were performed using DESeq2 in R. Two samples from the IR group were excluded due to insufficient number of reads ($n = 1$) and sex mismatch ($n = 1$).

Results: Patients with BR12 had lower IgG (median 1.1 vs. 1.7 times upper limit of normal (xULN), $p = 0.006$) and higher AST (median 24.0 vs. 11.6 xULN, $p = 0.045$) but not ALT values (20.7 vs. 11.1 xULN, $p = 0.133$) than patients with IR. Other clinical variables did not differ, including histological inflammation (median mHAI 7 vs. 9 points, $p = 1.000$) and fibrosis stage (median Ishak F 1 vs. 2, $p = 0.326$). Top 20 principal components calculated from the gene expression were significantly correlated with group, sex, and age. Hence, we adjusted the molecular expression data for sex and age.

Compared to patients with IR, patients with BR12 showed higher expression of innate immunity related genes, such as Toll like receptor 4 (TLR4), interferon gamma receptor 2 (IFNGR2), colony-stimulating factor 3 receptor (CSF3R), sialic acid binding Ig like lectin 1 (SIGLEC1), and protein tyrosine phosphatase receptor type J (PTPRJ), suggesting that pro-inflammatory pathways are more prominent in BR12. In addition, the expression of CR1 (complement receptor 1) and LIL2RB (leukocyte immunoglobulin-like receptor B2) was higher in patients with BR12. These genes are involved in regulatory T cell (Treg) formation and Treg-mediated down-regulation of the immune response. The down-regulated genes were not linked to immunological processes but enriched in the muscle function pathway.

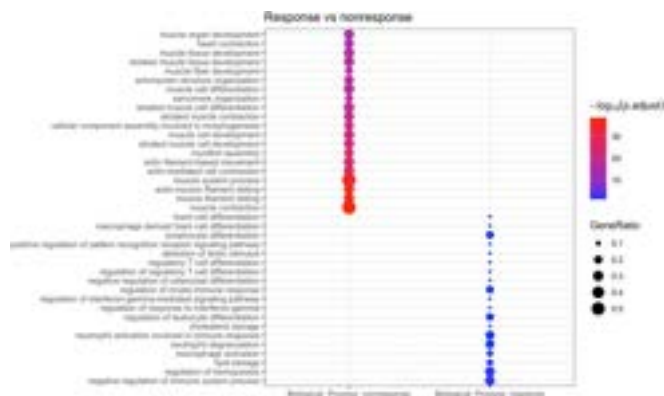


Figure:

Conclusion: BR12 was associated with pro-inflammatory pathways of innate immunity and with genes related to Treg differentiation. SIGLEC1-positive macrophages are involved in the regulation of immune homeostasis in multiple autoimmune diseases, and low CR1 is associated with poorer prognosis in systemic lupus erythematosus.

Overall, our study confirms the notion that patients with more severe disease respond better or faster to treatment.

FRI-363

Loss of innate and adaptive effector lymphocytes is associated with diminished globe score prognosis in patients with primary biliary cholangitis

Hussain Syed¹, Greg Vallée¹, Bishoi Aziz¹, Ning Sun¹, Mohamed Osman², Ellina Lytyvak¹, Hin Hin Ko³, Mark G. Swain⁴, Lawrence Worobetz⁵, Jennifer Flemming⁶, Cynthia Tsien⁷, Angela Cheung⁸, Aliya Gulamhusein⁹, Karim Qumosani¹⁰, Catherine Vincent¹¹, Julian Hercun¹¹, Tianyan Chen¹², Dusanka Grbic¹³, Kevork Peltekian^{14,15}, Mary Erickson¹⁶, Bettina Hansen^{9,17}, Aldo J. Montano-Loza¹, Gideon Hirschfield⁹, Andrew L. Mason¹. ¹Division of Gastroenterology and Hepatology, University of Alberta, Canada; ²Division of Rheumatology, University of Alberta, Canada; ³Division of Gastroenterology, University of British Columbia, Canada; ⁴Division of Gastroenterology and Hepatology, University of Calgary, Canada; ⁵Department of Medicine, University of Saskatchewan, Canada; ⁶Medicine and Public Health Sciences, Queen's University, Kingston, Canada; ⁷Department of Medicine, University of Ottawa, Ottawa, Canada; ⁸Department of Medicine, University of Ottawa, Ottawa, Canada; ⁹Toronto Centre for Liver Disease, University Health Network, Toronto, Canada; ¹⁰Western University, Department of Medicine, London, Canada; ¹¹Centre Hospitalier De l'Université de Montréal, Département De Médecins, Montréal, Canada; ¹²McGill University Health Centre, Department of Medicine, Division of Gastroenterology and Hepatology, Montréal, Canada; ¹³Université de Sherbrooke, Sherbrooke, Canada; ¹⁴Dalhousie University, Division of Digestive Care and Endoscopy, Halifax, Canada; ¹⁵Victoria Building @ the QEII Health Sciences Centre, Halifax, Canada; ¹⁶Intercept Pharmaceuticals, Inc., United States; ¹⁷Erasmus University Medical Center, Gastroenterology and Hepatology, Rotterdam, Netherlands
Email: am16@ualberta.ca

Background and aims: Patients with primary biliary cholangitis (PBC) have an increased risk of infectious diseases and cancers, and higher prevalence of alleles encoding genes in the interleukin (IL)-12 pathway. The prognostic role of immunodeficiency has been assessed by the Canadian Network of Autoimmune Liver Disease using the neutrophil to lymphocyte ratio (NLR) as a surrogate for lymphopenia in ~2,000 PBC patients. A high NLR following 12 months of ursodeoxycholic acid was found to be an independent risk factor for decreased liver transplant free survival. Herein we assess the immune subsets linked with adverse prognosis and whole blood transcriptional differences in PBC patients with and without lymphopenia.

Method: 140 PBC peripheral blood samples from CaNAL patients were used for flow cytometry to quantify subsets of B cells (CD19, IgD, CD27), T cells (CD3, CD4, CD8, CD27, CD45RA), NK (natural killer) and NK-like T cells (CD16, CD56). PBC Globe scores were assessed as categorical variables for adverse prognosis. An RNAseq database of whole blood RNA from 86 PBC patients in the POISE study was sorted by 50% highest versus lowest NLR calculated by transcripts per million of FCRGR3B (CD16b) divided by CD3e. Differential gene expression and gene set enrichment analyses by NLR were conducted using DESeq2 and gProfiler packages.

Results: PBC patients with reduced transplant free survival scores had decreased CD4, CD8, NK and NK-like T cells (Figure). Study of individual subsets revealed that all CD8 subsets (Naïve, central and effector memory, terminally differentiated) and terminally differentiated CD4T cells were associated with reduced prognosis. Transcriptional profiling showed that the high NLR patients with lymphopenia had activation of several proinflammatory pathways including NFkappaB signalling, IL-1, IL-6 and IL-8 and type I interferon production pathways, whereas IL-12 production pathway was found to be deregulated with upregulation of both activation and inhibitory transcripts.

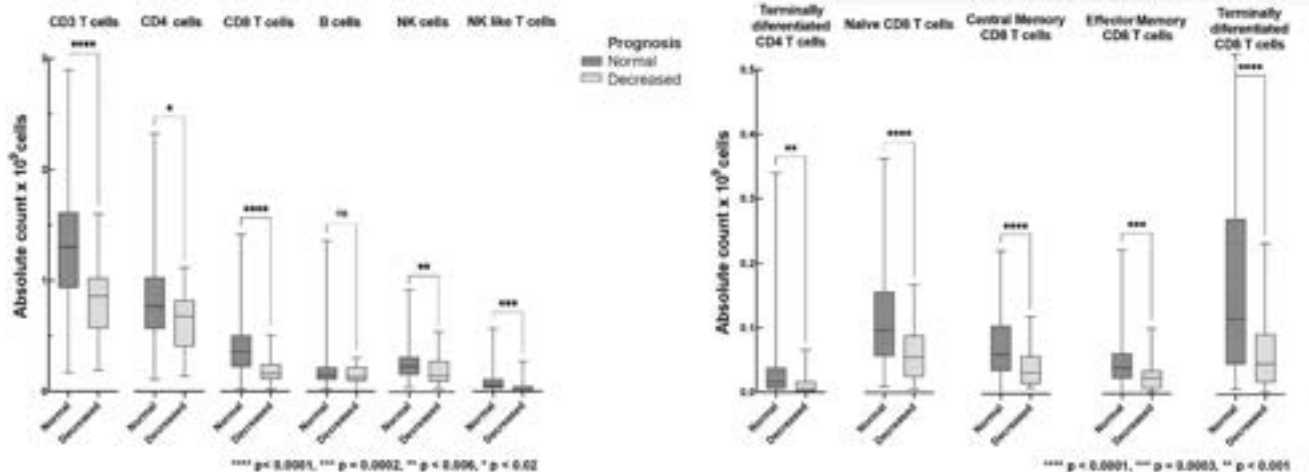


Figure: (abstract: FRI-363).

Conclusion: PBC patients with reduced transplant free survival scores had diminished innate and adaptive effector lymphocyte subsets and activated proinflammatory cytokine pathways. The decreased effector NK, CD4 and CD8 T-cells may reflect a degree of immune deficiency but the cause of loss is unknown. Further study of regulatory T cell function regarding IL-12 modulation of down-stream interferon-gamma pathways will be required to link lymphopenia and proinflammatory cytokine production with progressive liver disease.

FRI-364

The role of bile salts in cholestasis associated pruritus

Frank Wolters¹, Dagmar Tolenaars¹, Rudi de Waart¹, Arthur Verhoeven¹, Michel van Weeghel², Stan van de Graaf¹, Ulrich Beuers^{1,3}, Ronald Oude-Elferink¹. ¹Amsterdam University Medical Centers, University of Amsterdam, Tytgat Institute for Liver and Intestinal Research, Amsterdam, Netherlands; ²Amsterdam UMC, University of Amsterdam, Core Facility Metabolomics, Amsterdam, Netherlands; ³Amsterdam University Medical Centers, University of Amsterdam, Department of Gastroenterology and Hepatology, Amsterdam, Netherlands
Email: f.wolters@amsterdamumc.nl

Background and aims: Although it has repeatedly been reported that there is no good correlation between circulating bile salt levels and itch scores, the present dogma in the field remains that bile salts may act as pruritogens in cholestasis. The present treatment modalities of cholestatic pruritus, a major and poorly understood symptom, lack efficacy and would benefit greatly from a molecular rationale. At this moment, the effect of inhibiting MRGPRX4 in cholestatic patients with itch is studied in a clinical trial after the group of Meixiong et al. reported that bile salts and their conjugates activate this receptor, where deoxycholate was the most potent agonist. Our study aimed to evaluate bile salts as agonists of known pruriceptors (TRPA1, TRPV1, TRPV3, TRPV4, MRGPRX4) at (patho) physiological concentrations.

Method: Unconjugated and conjugated bile salts were tested for pruriceptor activation (intracellular free Ca²⁺ assays) on transduced HEK293T-rTTA3 cells (with and without the various receptor cDNAs). These assays were all done in the absence of albumin. Plasma concentrations were determined in 45 cholestatic patient samples and in 15 healthy controls by means of HPLC-MS.

Results: Most conjugated bile salts correlated with pruritus. Unconjugated bile salts did not, were not significantly elevated compared to controls, but were much more potent agonists to itch

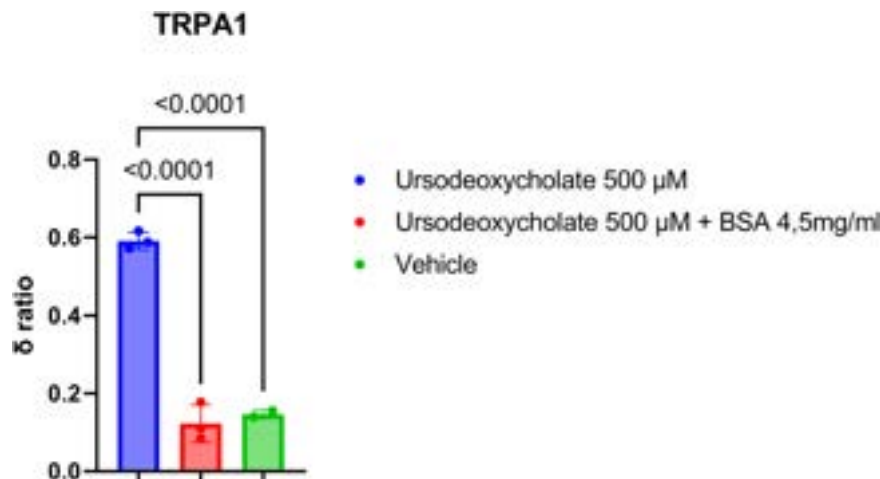


Figure:

POSTER PRESENTATIONS

receptors than their conjugated forms. The order of sensitivity to bile salts was TRPA1>MRGPRX4>TRPV3>TRPV4>TRPV1. Activation of all receptors only occurred in supra-pathophysiological levels. When incubations were done in the presence of 4.5% albumin (physiological plasma concentration) activation was virtually completely abrogated. **Conclusion:** Although most conjugated bile salts correlate with cholestatic pruritus, they do not activate itch receptors at pathophysiological concentrations. Given the extensive binding to albumin, it is highly unlikely that bile salts produce significant activation of this set of pruriceptors. In vitro evidence for bile salts as a pruritogens is therefore still lacking.

FRI-365

Spatial transcriptomics reveals shared gene and cellular composition in recurrent and primary sclerosing cholangitis

Mikal Jacob Hole^{1,2,2,3}, Kristian Holm^{1,2,3}, Jonas Øgaard^{1,3}, Peder Rustøen Braadland^{1,2,3}, Espen Melum^{1,2,3,4,5}, Johannes R. Hov^{1,2,3,4}, Brian K. Chung^{1,3}. ¹Research Institute of Internal Medicine, Oslo University Hospital, Rikshospitalet, Oslo, Norway, Norway; ²Institute of Clinical Medicine, University of Oslo, Oslo, Norway, Norway; ³Oslo University Hospital and University of Oslo, Norwegian PSC Research Center, Department of Transplantation Medicine, Norway; ⁴Section of Gastroenterology, Department of Transplantation Medicine, Division of Surgery, Inflammatory Diseases and Transplantation, Oslo University Hospital, Rikshospitalet, Norway, Norway; ⁵Hybrid Technology Hub-Centre of Excellence, Institute of Basic Medical Sciences, Faculty of Medicine, University of Oslo, Norway, Norway
Email: m.j.hole@studmed.uio.no

Background and aims: Primary sclerosing cholangitis (PSC) is an autoimmune biliary disease with up to 30% recurrence (rPSC) following liver transplantation. Whether rPSC represents the same disease process as PSC is unclear, therefore we investigated if genes and cell types differ in rPSC liver explants compared to PSC and alcoholic liver disease (ALD).

Method: Spatial transcriptomics (Visium, 10X Genomics) was performed on snap-frozen liver explant tissue from rPSC (n = 7), PSC (n = 5) and ALD (n = 3). Sequenced transcripts were aligned and grouped using Space Ranger; k-means clustering and significant differential expression ($p < 0.05$, Benjamini-Hochberg corrected) of highly expressed genes (greater than one read per RNA capture spot) was analyzed in Loupe Browser (10X Genomics). Relative cell abundances were estimated using spatial transcriptomes and conditional autoregressive-based deconvolution (CARD) analysis (Figure 1). Differential cell abundances accounting for dependency of spots from the same liver sample was tested using linear mixed modeling (glmer package in R).

Results: Data-driven analysis of spatial transcriptomes from all fifteen liver samples identified two clusters that closely corresponded to histopathologically defined parenchymal and fibrotic tissue regions. Expectedly, the parenchymal cluster was enriched for known hepatocyte markers (*CYP2E1*, *C9*, *CYP2A6*), while genes relating to collagen deposition (*COL1A2*, *COL4A2*, *COL6A1*) and immune inflammation (*IGKC*, *CD74*, *C7*) were enriched in fibrotic regions. Gene analysis of rPSC and PSC parenchyma revealed only 51 differentially regulated genes whereas 226/277 (82%) genes were detected at similar levels. By contrast, rPSC vs. ALD parenchyma showed 93 differentially expressed genes and 258/351 (74%) detected at similar levels, suggesting that the rPSC parenchyma was transcriptionally more similar to PSC than ALD. Differential analysis of fibrotic regions between rPSC and PSC showed 539/719 (75%) expressed at similar levels whereas rPSC vs. ALD displayed similar expression of 876/993 (88%) genes. Estimated cellular composition using deconvolution of spatial transcriptomes showed similar proportions of different cell types in rPSC and PSC parenchyma. In contrast, increased mast cells (6-fold), plasma B cells (10-fold) and dendritic cells (3-fold) were seen in rPSC parenchyma vs. ALD. In fibrosis, rPSC and PSC vs. ALD showed similar proportions of immune infiltrate except a modest increase of plasma B cells (1.1-fold) in ALD, suggesting fibrotic pathways overlap irrespective of disease etiology.

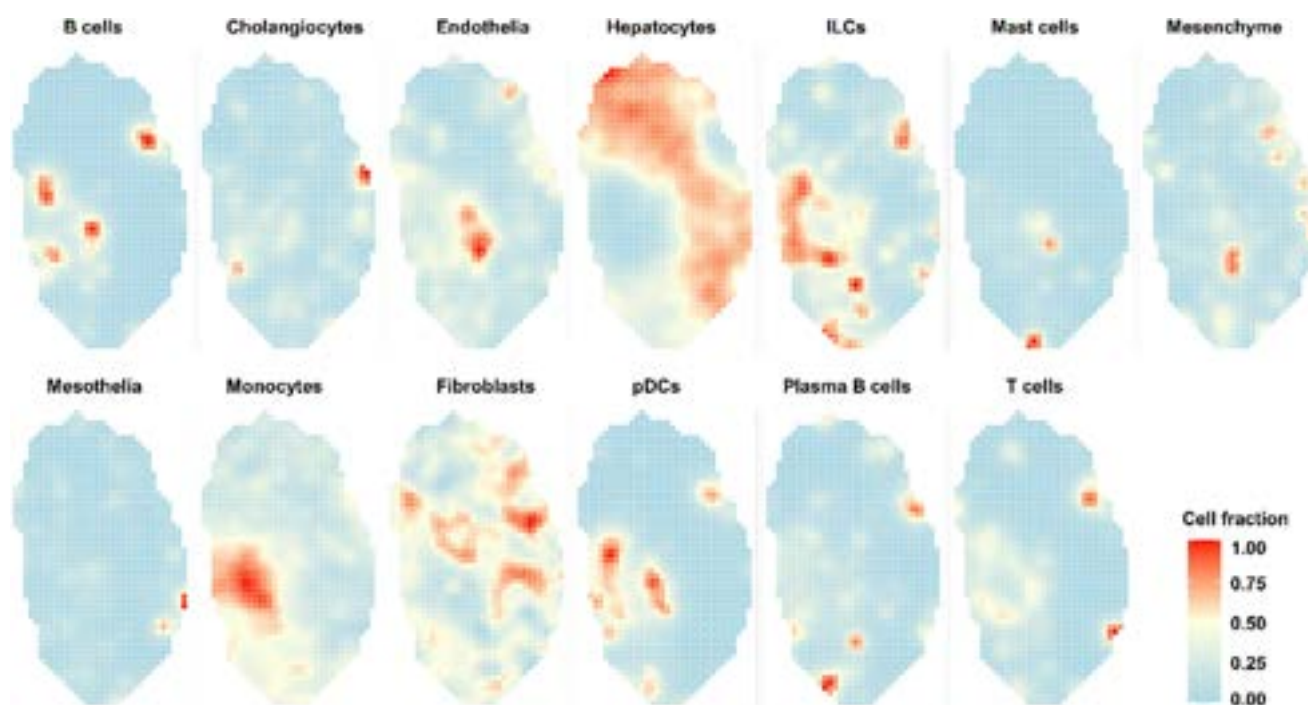


Figure: (abstract: FRI-365): Representative gene deconvolution (CARD) showing major immune cell types localize to regions of fibrosis; ILCs: innate lymphoid cells, pDCs: plasmacytoid dendritic cells.

Table 1A

CD107a ⁺ CD56 ^{high} NK	Baseline	+K562	+LPS	+K562+LPS	+Pam ₃ Cys	+K562+Pam ₃ Cys
Healthy controls	12.9%	62.1%	25.9%	72.6%	32.2%	74.5%
AIH	9.0%	56.5%	24.5%	68.4%	20.3%	64.8%
PSC	4.5%*	42.5%*	5.3%*	45.7%*	5.7%*	43.8%*

Table 1B

CD107a ⁺ CD56 ^{dim} NK	Baseline	+K562	+LPS	+K562+LPS	+Pam ₃ Cys	+K562+Pam ₃ Cys
Healthy controls	5.8%	36.3%	7.6%	40.9%	9.7%	42.8%
AIH	5.0%	37.0%	8.7%	41.9%	7.1%	39.4%
PSC	2.9%*	22.4%*	3.3%*	22.4%*	3.7%*	22.8%*

*p<0.05: PSC vs. healthy control and PSC vs. AIH

Table

Conclusion: We find that the liver parenchymal transcriptome and cellular composition in rPSC appears to more closely resemble PSC than ALD. Although this aligns with the presumed shared etiology between rPSC and PSC, the findings from fibrotic areas were more ambiguous. Nevertheless, our study underscores the potential utility of spatial analyses in delineating molecular features and potential targets in liver diseases and prompts replication in larger cohorts.

FRI-366

Cytotoxic activity of peripheral NK cells is decreased in primary sclerosing cholangitis

Jessica Wolf¹, Leona Dold¹, Sandra Kalthoff¹, Taotao Zhou¹, Pia Esser¹, Philipp Lutz¹, Christian Strassburg¹, Ulrich Spengler¹, Bettina Langhans¹. ¹University Hospital Bonn, Department of Internal Medicine I, Germany
Email: Leona.Dold@ukbonn.de

Background and aims: Primary sclerosing cholangitis (PSC) is a chronic inflammatory liver disease associated with progressive obliterative fibrosis of intra- and extrahepatic bile ducts which can lead to biliary cirrhosis and bile duct cancer. Although the cause of this disease is still unclear, it has been proposed that microbial triggers may lead to altered immune cell activation. Since natural killer (NK) cells regulate immune response and can kill altered cells, they are potential key features in autoimmune disorders. Here, we analysed frequency and cytotoxicity of peripheral NK cell subsets in PSC.

Method: We enrolled 12 patients with PSC (8 with inflammatory bowel disease (IBD), 4 without IBD), 15 patients with autoimmune hepatitis (AIH; all budesonide-treated) as disease control, and 12 age- and sex-matched healthy controls. Using multi-colour flow cytometry, we analysed frequencies of CD56^{high} and CD56^{dim} NK cell subsets ex vivo and studied their cytotoxic activity (CD107a assay) at baseline and after *in vitro* stimulation with K562 target cells and Toll-like receptor ligands (LPS, Pam₃Cys).

Results: Frequencies of NK cells subsets did not differ between PSC (7.1% CD56^{high}, 88.8% CD56^{dim}) and healthy controls (6.5% CD56^{high}, 90.5% CD56^{dim}) whereas a shift towards CD56^{high} was found in AIH (22.7% CD56^{high}, 74.6% CD56^{dim}). Unlike AIH, fractions of CD107a⁺ NK cells with cytotoxic activity in PSC were substantially reduced both in CD56^{high} (Table 1A) and CD56^{dim} (Table 1B) NK cell subsets at

baseline and after *in vitro* stimulation (K562 cells). Importantly, added TLR ligands LPS and Pam₃Cys as well as their combination with K562 cells did not increase CD107a⁺ NK cells (Table 1A, 1B).

Conclusion: The frequency of NK cells was not altered in PSC. However, a substantially reduced cytotoxic activity was found in CD56^{high} and CD56^{dim} NK cell subsets which was not overcome by stimulation with tumour cells or TLR ligands. This deficit in NK cell cytotoxic activity may play a role in PSC-related inflammation.

FRI-367

The effect of the combination of metformin with propionic acid on the indicators of oxidative stress in liver tissue of rats with type 2 diabetes mellitus

Olena Khokhliuk¹, Nataliia Shulha², Yuliia Klys³, Yulia Osadchuk³, Larysa Natrus³. ¹Bogomolets National Medical University, Medical Faculty №2, Kyiv, Ukraine; ²Bogomolets National Medical University, Medical Faculty №4, Kyiv, Ukraine; ³Bogomolets National Medical University, Department of Modern Technologies of Medical Diagnostics and Treatment, Kyiv, Ukraine
Email: natalishulha.ua@gmail.com

Background and aims: The main mechanism of type 2 diabetes mellitus (T2DM) contributing to liver damage is the activation of oxidative stress (OS), accompanied by excessive formation of reactive oxygen species in the mitochondria and depletion of the antioxidant defense system. Therefore, the aim was to investigate the effect of combined administration of metformin with propionic acid (PA) on the degree of oxidative damage in liver of rats with an experimental model of T2DM.

Method: Male Wistar rats were divided: (1) control, (2) T2DM, the group with experimentally induced T2DM by high-fat diet (HFD) for 3 months followed by a single injection of streptozotocin (STZ, 25 mg/kg); and T2DM groups that received the following (14 days, orally): (3) metformin (60 mg/kg), (4) PA (60 mg/kg), and (5) PA + metformin. The rate of generation of superoxide radicals (SR) by mitochondria in liver tissue samples was studied by electron paramagnetic resonance, by spectrophotometer were analyzed 8-oxoguanine, gas-liquid chromatography studies the composition of fatty acids (FAs). We have identified the nine most informative fatty acids (denoted as 100%), and calculated relative combination of saturated fatty acids (SFA), unsaturated fatty acids (USFA); and polyunsaturated fatty acids

POSTER PRESENTATIONS

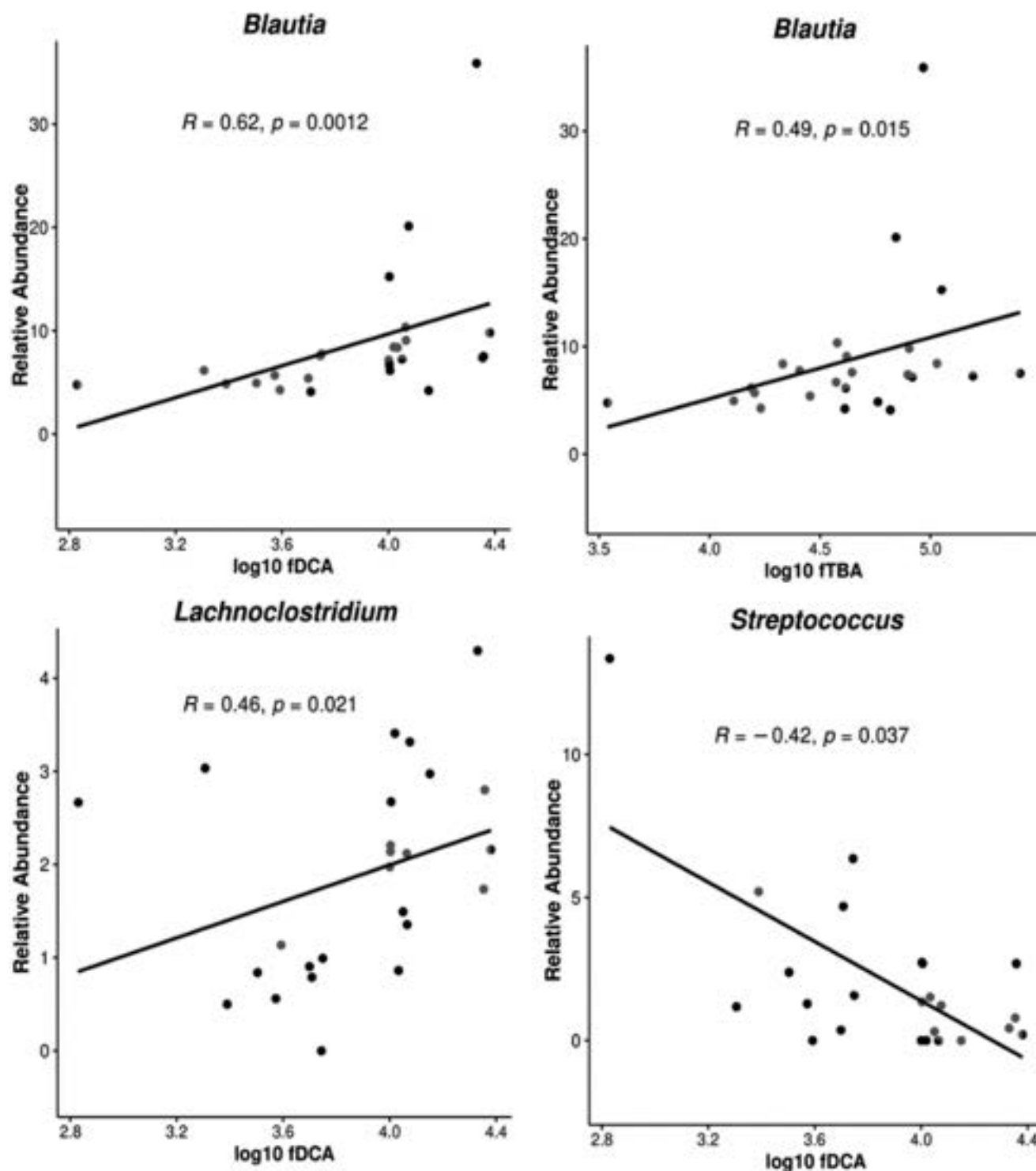


Figure: (abstract: FRI-368).

(PUFA). Statistical differences between groups were evaluated by ANOVA followed by Tukey post-hoc test.

Results: The effect of the combined administration of metformin with propionate on the indicators of OS was evaluated by the study of liver tissue.

SR in the liver tissue on the background of diabetes was increased by 3 times compared to the control group ($p < 0.01$). The introduction of

metformin and PA led to a decrease of SR by 25% ($p < 0.01$), the use of combined treatment contributed to a decrease in the generation of SR by 36.5% in liver tissue ($p < 0.01$). The level of 8-oxoguanine in T2DM exceeded its content in the control group by 2.3 times ($p < 0.01$). The use of metformin, PA and simultaneous use of these drugs led to a decrease in this indicator by 27.1%, 16.9% and 31.7%, respectively ($p < 0.01$). The modeling of T2DM led to significant changes in the content

of fatty acids in the tissues of experimental animals compared to intact animals: a 1.3-fold increase in SFA ($p < 0.05$), due to a 1.3-fold decrease in USFA ($p < 0.05$), and a 1.8-fold decrease in PUFA ($p < 0.05$). Combined administration of metformin and propionate to rats with T2DM leads to changes in the redistribution of fatty acids. It increases the content of USFA and PUFA to $43.78 \pm 2.4\%$ and $32.02 \pm 3.8\%$ and decreases the content of SFA to $56.22 \pm 2.9\%$.

Conclusion: Our study demonstrated that PA and its combination with metformin have beneficial effects on the indicators of OS in liver tissue of rats with T2DM. In our opinion, PA may be considered one of the promising substances for correcting damages of hepatocytes diabetic.

FRI-368

Associations of fecal bile acids, diet, and intestinal microbes with markers of disease progression in primary sclerosing cholangitis disease

Connie Chan¹, Mateus Lemos², Peter Finnegan², William Gagnon³, Richard Dean¹, Joseph Zepeda¹, Maryam Yazdanfar¹, Marie-Claude Vohl⁴, Joshua Korsenik⁵, Olivier Barbier³, Maria Marco², Christopher Bowlus¹. ¹University of California Davis, Gastroenterology and Hepatology, United States; ²UC Davis, Food Science and Technology, United States; ³Université Laval, CHU de Québec Research Center, Canada; ⁴Université Laval, NUTRISS, Canada; ⁵Brigham and Women's Hospital, Gastroenterology, United States
Email: clbowlus@ucdavis.edu

Background and aims: Primary Sclerosing Cholangitis (PSC) disease progression is variable and associated with changes in bile acids (BA) and intestinal dysbiosis. The objective of this study was to elucidate relationships between diet, intestinal microbes, and fecal bile acids with markers of PSC progression.

Method: Stool and blood was collected from patients with early-stage, large duct PSC for measurements of bile acids (BA; LC-MS/MS) and fecal 16S rRNA DNA sequencing. Dietary intake of alcohol, fats, protein, and fiber was estimated from food frequency questionnaires. Healthy controls (HC) included individuals who had participated in a diet supplement clinical trial and had received placebo.

Results: A total of 25 patients with PSC (58.3% male, 70.8% with IBD) with a median [IQR] age 53.8 [43.2–65.4] years, alkaline phosphatase 174.5 [109.5–359.5] IU, and total bilirubin (TB) 17.1 [12.0–20.5] micromol/L, and 10 HC were enrolled. Unconjugated fecal BA (fDCA) was lower in PSC than HC ($p < 0.05$). No differences in other fecal BA were found. Among patients with PSC, fDCA, but no other BA, was negatively associated with TB after adjusting for IBD status and UDCA use ($B = -0.45$, $p = 0.006$). No fecal BA were associated with serum alkaline phosphatase. Surprisingly, fDCA was associated with greater serum C4 ($B = 4.5$, $p = 0.02$). Serum FGF19 was not associated with fDCA or C4. Alcohol intake, but not intake of fats, protein, or fiber, was associated with higher fDCA levels ($B = 423.6$, $p = 0.04$) and lower serum bilirubin ($B = -0.07$, $p < 0.001$). Microbiota analysis revealed correlations between fDCA and increasing abundance of *Blautia* and *Lachnospirillum* ($r = 0.62$, $p = 0.001$ and $r = 0.46$, $p = 0.02$, respectively) and decreasing *Streptococcus* ($r = -0.42$, $p = 0.04$) (Figure 1). *Blautia* also correlated with total fecal BA ($r = 0.49$, $p = 0.01$).

Conclusion: In early-stage PSC, decreasing fDCA was associated with increasing TB but did not appear to be mediated through FXR. fDCA was associated with alcohol use and microbes involved in bile acid transformation which may lead to new avenues for treatment.

FRI-369

CD44 reduces fibrosis development in chronic cholestatic liver injury in Mdr2 knock-out mice

Franziska Ihli¹, Fabian Delugré¹, Sophia Bernatik¹, Köhnke-Ertel Birgit¹, Carolin Mogler², Simone Jörs¹, Fabian Geisler¹, Roland M. Schmid¹, Ursula Ehmer¹. ¹Klinikum rechts der Isar, Technische Universität München, Internal Medicine II, Munich, Germany; ²Technische Universität München, Institute of Pathology and Unit of Comparative Experimental Pathology, Germany
Email: ursula.ehmer@tum.de

Background and aims: In cholestatic liver injury, chronic inflammation is associated with the emergence of ductular reactions around the portal triad. In different animal models of liver injury, the expression of the cellular adhesion molecule CD44 in biliary epithelial cells/ductular reactions has been linked to fibrosis. However, the functional relevance of CD44 in the development of fibrosis remains unclear. To determine whether CD44 could present a potential target to reduce fibrosis in chronic cholestatic liver injury, we investigated the functional role of CD44 in *Mdr2*^{-/-} mice.

Method: Livers of *Mdr2*^{-/-}; *Cd44*^{-/-} double knock-out (DKO) mice and age-matched *Mdr2*^{-/-} control mice were analyzed at different time points by histopathology. Protein expression of Ki67, CK19 and YAP was quantified by immunohistochemistry.

Results: At 6 months of age, ductular reactions in *Cd44*-deficient *Mdr2*^{-/-} mice were more prominent in than in control mice but comprised a significantly lower number of CK19-positive biliary cells per area. Importantly, DKO livers showed higher levels of fibrosis in comparison to *Cd44*-proficient controls. By immunohistochemistry, cells in the periportal areas of DKO mice expressed lower levels of YAP-a CD44 downstream target-in comparison KO mice (56% vs. 68%, $p = 0.023$).

Conclusion: In the *Mdr2*^{-/-} model of chronic cholestatic liver injury, CD44 protects against fibrosis development. While previous reports suggested that CD44 could contribute to liver fibrosis, our data indicate that CD44 instead has a protective role in chronic cholestatic liver injury. Here, we were able to show that loss of CD44 leads to a lower expression of YAP in ductular reactions as a potential mediator of this phenotype. YAP is a pro-proliferative transcriptional co-factor that is expressed biliary epithelial cells and contributes to their differentiation. In the *Mdr2*^{-/-} model, loss of *Cd44* and reduced levels of YAP translate into lower levels of CK19-expressing cells-indicating that these cells might be essential in mitigating liver damage and consecutive liver fibrosis upon chronic cholestatic liver injury.

FRI-370

Results of pharmacological treatment of Mcpip1 knock-out mice which develop symptoms of primary biliary cholangitis

Katarzyna Trzos^{1,2}, Natalia Pydyn¹, Joanna Koziel³, Magdalena Pilarczyk-Zurek³, Jolanta Jura¹, Jerzy Kotlinowski¹. ¹Jagiellonian University, Faculty of Biochemistry, Biophysics and Biotechnology, Department of General Biochemistry, Kraków, Poland; ²Jagiellonian University, Doctoral School of Exact and Natural Sciences, Faculty of Biochemistry, Biophysics and Biotechnology, Department of General Biochemistry, Kraków, Poland; ³Jagiellonian University, Faculty of Biochemistry, Biophysics and Biotechnology, Department of Microbiology, Kraków, Poland
Email: kat.trzos@doctoral.uj.edu.pl

Background and aims: Primary biliary cholangitis (PBC) is a chronic autoimmune liver disease that results from slow, progressive destruction of the intrahepatic bile ducts. PBC progression leads to the development of fibrosis, cholestasis, liver cirrhosis. *Mcpip1*/fAlbCre mice which are characterized by deletion of the *Zc3h12a* gene (encoding *Mcpip1* protein) in liver epithelial cells and develop a number of typical PBC symptoms, such as presence of antimitochondrial (AMA) and antinuclear antibodies, total bile acids elevated, increased activity and alkaline phosphatase. *Mcpip1*/fAlbCre mice are also characterised by bile duct pathology which includes

POSTER PRESENTATIONS

hyperplasia of the intrahepatic bile ducts, bile duct epithelium disruption and fibrosis, resulting in lumen obstruction and bile duct destruction. The main goal of this project is to define the dynamics of PBC-like disease development in those mice after administration of first- and second-line therapy commonly used in patients suffering with PBC. The study was enriched with the use of a probiotic (*Lactobacillus rhamnosus*), since there is a growing number of evidence of a huge role that gut microbiota plays in PBC development and progression.

Method: Mcpip1fl/flAlbCre knock-out male mice and Mcpip1fl/fl control male mice at 6 weeks of age were randomly divided into five groups for drug treatment. Control group received corn oil, other groups received consecutively Lakcid (*L. rhamnosus*, 10^9 CFU per day) suspended in water, ursodeoxycholic acid (UDCA, 15 mg/kg body mass per day) diluted in corn oil, UDCA diluted in corn oil and Lakcid suspended in water, UDCA and obeticholic acid (OCA, 10 mg/kg body mass per day) both diluted in corn oil. After 6 weeks of treatment, the mice were sacrificed, and the collected material analysed by, amongst other, detailed serum liver tests, ELISA tests for the presence of anti-PDC-E2 autoantibodies, histological stainings (hematoxylin and eosin, picro Sirius red) and qPCRs.

Results: After 6-weeks of treatment we detected significant proliferation of cholangiocytes and fibrosis in livers from Mcpip1 knock-out mice, together with high serum level of total IgM, total bile acids and anti-PDC-E2 autoantibodies. Livers isolated from Mcpip1 knock-out mice were also characterized by high expression of Tgfb1, Il1b, Ngp and Ngf. There were no changes in serum levels of ALT, AST, bilirubin, cholesterol and LDH between Mcpip1fl/fl and Mcpip1fl/flAlbCre mice. Mcpip1fl/flAlbCre treated with Lakcid had reduced amount of total bile acids in the serum and decreased proliferation of cholangiocytes. Additionally, they had reduced amount of PDC-E2 autoantibodies to the level observed in Mcpip1fl/fl counterparts. Although Lakcid administration did not ameliorate liver fibrosis, mice from this group were chosen for further multiomic analysis of liver (next generation sequencing, mass spectrometry) that are currently ongoing. Treatment with UDCA or with UDCA+OCA also reduced serum levels of TBA in Mcpip1fl/flAlbCre mice but had no effect on cholangiocytes' proliferation nor gene expression in the livers.

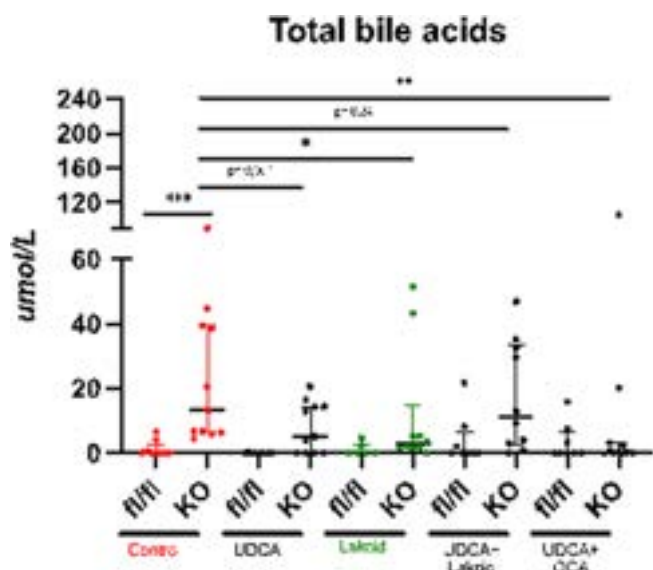


Figure:

Conclusion: Treatment of Mcpip1fl/flAlbCre mice with Lakcid had beneficial effects on PBC symptoms that are normally observed in these animals. We hope that analysis of Mcpip1fl/flAlbCre may shed a new light on the pathology of PBC development.

Acknowledgments: This study was supported by scientific grant awarded by Polpharma Scientific Foundation to dr Jerzy Kotlinowski.

FRI-371

The role of Type II and III Interferons in primary biliary cholangitis

Yooyun Chung^{1,2,3}, Phoebe Tsou^{2,3,4}, Michael Heneghan^{1,2}, Antonio Riva^{2,4,5}, Shilpa Chokshi^{2,4,5}. ¹Institute of Liver Studies, King's College Hospital, London, United Kingdom; ²Faculty of Life Sciences and Medicine, King's College London, London, United Kingdom; ³Joint First Authors, United Kingdom; ⁴The Roger Williams Institute of Hepatology, Foundation for Liver Research, London, United Kingdom; ⁵Joint Senior Authors, United Kingdom

Email: a.riva@researchinliver.org.uk

Background and aims: Primary biliary cholangitis (PBC) has a variable disease course with limited treatment options. There is a need for targeted therapeutic agents and prognostic biomarkers which would allow personalised risk stratification and management. Type I interferons (IFNs) have shown to play a role in murine PBC; however, little is known regarding their involvement and the role of type II/III IFNs in PBC patients. The aim of this investigation was to explore the involvement of IFNs in PBC.

Method: Plasma samples from 64 PBC patients between 2012 and 2022 were compared to 10 healthy controls (HC). PBC subgroups were 24 ursodeoxycholic acid (UDC) responders (UDCR) according to the Paris criteria, 18 UDC non-responders (UDCNR), 22 end stage PBC prior to liver transplantation (ESPBC). Luminex multiplex ELISA was used to quantify concentrations of 28 pro/anti-inflammatory cytokines including Type II and III IFNs and D-lactate was also measured.

Results: The majority of PBC patients were female (n = 62, 97%) with a mean age of 55 years. UDCR and UDCNR were mostly non-cirrhotic patients with 4 early cirrhotic patients in UDCR and 5 in UDCNR. ESPBC represented a distinct group with significantly higher liver prognostic scores compared to UDCR and UDCNR. All PBC subgroups had upregulation of CCL2, IL-7 and IL-8 compared to HC. IFN-gamma levels became progressively detectable as disease progressed to UDCNR and ESPBC (Chi-sq p = 0.007). IFN-gamma levels were not significantly different between UDCR and HC. However, the IFN-gamma levels became increasingly upregulated in UDCNR (p = 0.0262) and ESPBC (p = 0.0012) when compared to UDCR. The difference in IFN-gamma levels between UDCR and UDCNR was also maintained on excluding cirrhotic patients (p = 0.0056). In ESPBC, elevated IFN-gamma was accompanied by increased CXCL10. ESPBC expressed several predominantly pro-inflammatory cytokines including IL-6 and TNF-alpha compared to HC. Interestingly, IFN-lambda3, but not IFN-lambda2, was elevated in ESPBC when compared to all other subgroups, hinting at differential gut mucosal involvement. Using D-lactate, as an established marker of bacterial translocation, we found levels were equally elevated in all PBC subgroups compared to HC.

Conclusion: Type II and Type III Interferons are associated with PBC. IFN-gamma increased as disease progressed suggesting contributions from NK and/or T cells in the immunopathogenesis and may serve as a potential biomarker. IFN-lambda3 may have a role in advanced disease that is distinct to IFN-lambda2 and warrants further exploration. The increased gut permeability and bacterial translocation in PBC may indicate the gut microbiome as a potential therapeutic target.

SATURDAY 24 JUNE

Liver development and regeneration

SAT-353

Liver innervation is dysregulated in a mouse model of Alagille syndrome

Elisabeth Verboven¹, Noémi K. M. Van Hul¹, Simona Hankeova¹, Csaba Adori¹, Ewa Ellis¹, Björn Fischler¹, Emma Andersson¹.

¹Karolinska Institute, Stockholm, Sweden

Email: elisabeth.verboven@ki.se

Background and aims: The liver is richly innervated, which is often overlooked despite the key roles of nerves in liver function. Liver innervation is enriched in the periportal area, where both mesenchyme and bile ducts are extensively innervated. In Alagille syndrome (ALGS), caused by mutations in Notch components, bile ducts do not develop properly, with severe consequences for liver function. Although Notch is well known for its role in development of the nervous system, it is not yet known whether liver innervation is affected in ALGS, and whether disturbed innervation might further aggravate liver function. The aim of this study is to determine how liver innervation interacts with and regulates bile duct development and homeostasis.

Method: I performed whole mount immuno-stainings for cholangiocytes and nerves in livers from wild-type and *Jag1^{Ndr/Ndr}* mice (a model of ALGS). To test the function of liver innervation, wild-type mice were treated with the dopaminergic and noradrenergic neurotoxin 6-hydroxydopamine for nerve depletion. Lightsheet microscopy allowed visualization of the three-dimensional neural and biliary expansion throughout the liver, with analysis using Imaris software. Patient liver biopsies were analyzed with immunofluorescence to validate observations in humans.

Results: Preliminary timecourse data of the developing liver confirmed that innervation is first established in the hilar region of the liver, followed by outgrowth of the nerves into the periphery from postnatal day 6 (P6) on. In *Jag1^{Ndr/Ndr}* livers, innervation was strongly reduced and mislocalized during development. The absence of liver nerves is physiologically relevant for patients with Alagille syndrome, and is not an indirect consequence of cholestasis, as we confirmed loss of innervation in biopsies from patients with ALGS, but not in progressive familial intrahepatic cholestasis (PFIC). Ablation of peripheral nerves in wild-type mice at P1 by injection of a neurotoxin did not compromise bile duct development.

Conclusion: We show that in addition to bile duct development, liver innervation is also impaired in ALGS. We developed and validated a method for postnatal denervation, showing that liver nerves are not required for bile duct development at this postnatal stage. The physiological consequences of dysregulated innervation in ALGS will be further investigated to identify how denervation impacts this

cholangiopathy. Further research is ongoing to also investigate how bile ducts and nerves interact during development and to define the regulatory mechanisms that each exerts on the other.

SAT-354

A novel organoid model of human liver bud development

Charlotte Grey-Wilson¹, Sabitri Ghimire¹, Ludovic Vallier^{1,2,3}, Anna Osnato¹, Carola Maria Morell¹. ¹University of Cambridge, United Kingdom; ²Berlin Institute of Health (BIH), BIH Centre for Regenerative Therapies (BCRT), Charité- Universitätsmedizin, Berlin, Germany; ³Max-Planck-Institut für molekulare Genetik, Berlin, Germany

Email: cg697@cam.ac.uk

Background and aims: Understanding the mechanisms controlling the development of human liver is challenging due to technical and ethical limitations. Of particular interest, the process by which the human liver bud first arises from the foregut and the subsequent specification of the hepatoblasts, remains to be fully uncovered. To address these major questions, we decided to develop a novel 3D culture system allowing the differentiation on human induced Pluripotent Stem Cells (hiPSCs) into self-organising human liver buds.

Method: To generate a new model of liver bud development, we first tested popular foregut induction conditions across different hiPSC systems to develop and optimise a new protocol for the generation of hepatoblast and hepatocytes *in vitro*. This novel system uses a foregut induction step which has not been previously described in the context of liver development *in vitro*. Following 2–3 weeks of hepatic induction, cells are then dissociated into clumps and seeded in Matrigel to form liver bud organoids in conditions previously used to maintain primary hepatoblast organoids (pHBOs). When passaged sequentially, organoids persist as hiPSC-derived HBOs (iHBOs) which can be passaged similar to pHBOs. iHBOs were then tested for their ability to differentiate into hepatocytes and cholangiocytes.

Results: We first developed and optimised a protocol to drive differentiation of hiPSCs into a population of foregut cells containing progenitor (s) for pancreas, liver and extra-hepatic biliary cells. The resulting cells were then grown in 3D culture conditions known to support organoid formation. These cells rapidly self-organise into complex budding structures which appear to recapitulate the initial organogenesis of the liver bud *in vitro*. This includes the formation of a “bud” consisting of cell expressing HNF4A/ALB/AFP, extra-hepatic biliary cells expressing CK19 and also potential pancreato-biliary progenitors marked by PDX1. Thus, these organoids are composed of multiple cell types produced during the early hepato-biliary specification from the foregut. Finally, we decided to demonstrate the functional relevance of this 3D structure by deriving HBOs from *in vitro* generated liver bud. For that, liver bud organoids underwent serial passaging. We rapidly observed the formation of self-renewing organoids containing homogeneous population of cells expressing hepatoblast markers. These human iHBO were able to self-renew for an additional 8 passages while maintaining their morphological characteristics and initial results also suggest iHBO have a capacity to differentiate into cholangiocytes and hepatocytes.

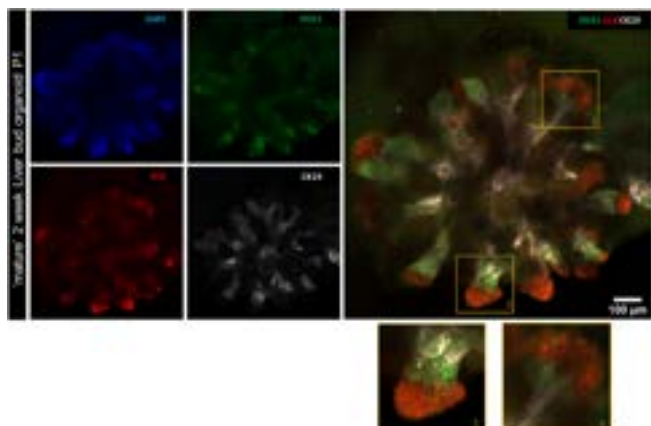


Figure: Two-week old liver bud organoids generated from hiPSCs.

Conclusion: Taken together, these results show that our model of liver bud development provides a new platform not only to study hepatobiliary lineage specification *in vitro* but also to produce cell types with a clinical interest.

SAT-355

Tunable host senescence determines the success of hepatocyte transplantation in a mouse model of liver injury

Victoria Gadd¹, Sofia Ferreira-Gonzalez¹, Wei-Yu Lu², Tak Yung Man¹, Alastair Kilpatrick¹, Ian Smith¹, Rhona E. Aird¹, Daniel Rodrigo-Torres¹, Stuart J. Forbes¹. ¹University of Edinburgh, Centre for Regenerative Medicine, United Kingdom; ²University of Edinburgh, Centre for Inflammation Research, United Kingdom
Email: victoria.gadd@ed.ac.uk

Background and aims: Hepatocyte transplantation has shown promise for genetic diseases but has mixed efficacy for acute and severe liver injury. One reason for this is poor function of donor hepatocytes in recipient liver. Hepatocyte senescence is a key feature of many liver diseases. We have sought to model this using Ah^{cre}Mdm2^{fl/fl} mice, where genetic induction results in excision of hepatocyte Mdm2 (negative regulator of p53), leading to hepatocellular senescence and liver injury. We have used this model to determine the effects of host liver senescence upon human and mouse hepatocyte engraftment and function.

Method: Freshly isolated mouse, or human cryopreserved hepatocytes, were injected into the spleen of Ah^{cre}Mdm2^{fl/fl} (immune competent and deficient strains) mice. Engraftment kinetics, donor cell and host liver function were assessed.

Results: Senescence-driven liver injury could be induced in Ah^{cre}*Mdm2^{fl/fl} mice in controlled and predictable levels through excision of hepatocyte Mdm2. Host senescence and injury was a requirement for donor hepatocyte engraftment and repopulation, but too much was inhibitory to this. Mice with moderate senescence (30–50%) demonstrated up to 95% engraftment of transplanted mouse hepatocytes after 8 weeks. Human hepatocyte engraftment was also dependent upon host senescence in Ah^{cre}*Mdm2^{fl/fl}Rag2^{−/−}Il2rg^{−/−} mice where 1 mg/ml of human albumin was detected in the serum of chimeric mice after 16 weeks. Histological features of injury (senescence, ductular reaction and fibrosis) were negatively associated with the level of hepatocyte engraftment. Importantly, in some Ah^{cre}Mdm2^{fl/fl} mice (2/13), despite initial engraftment, transplanted hepatocytes failed to provide long-term functional support. Previously healthy donor hepatocytes acquired p21 expression and failed to expand, suggesting that host senescence had been transferred to donor cells in a paracrine manner. Further modelling using high levels of induced host senescence (>90%) resulted in rapid host-mediated paracrine senescence in donor cells. Paired proteomic and transcriptomic analysis of healthy vs senescent hepatocytes reveal a unique senescent signature associated with paracrine

senescence. Inhibition studies are underway to assess the effects on host-mediated paracrine senescence and donor hepatocyte function. To test this hypothesis, pre-treatment of senotherapeutic drug ABT737 in host mice with high levels of senescence (>65%) improved proliferation in donor cells after 1 week.

Conclusion: Host liver senescence provides a required non-competitive niche for donor hepatocytes to repopulate the recipient liver. However, host-mediated paracrine senescence can impair donor hepatocyte function. Targeting paracrine senescence may be a way to improve donor hepatocyte function, optimise therapy and guide translation into the clinics.

SAT-356

Liver regeneration is regulated by intestinal sirtuin-1

Sian Seaman¹, Mar Moreno-Gonzalez¹, Mark Philo², Naiara Beraza¹.

¹Quadram Institute, Gut Microbes and Health Institute Strategic Programme, Norwich, United Kingdom; ²Quadram Institute, Analytical Science Unit, Norwich, United Kingdom
Email: naiara.beraza@quadram.ac.uk

Background and aims: Sirtuin1 (SIRT1) is recognised as a master regulator of bile acid (BA) metabolism in both the liver and the intestine. In the liver, SIRT1 has previously been hailed as crucial for successful liver regeneration by regulating BA metabolism through FXR. However, despite these findings and the recent interest in the gut-liver axis, the role of intestinal SIRT1 in liver regeneration remains undefined.

Method: We performed partial hepatectomy (PHx) on intestinal-specific SIRT1 knockout mice (SIRT1^{int-KO}) to stimulate liver regeneration. Samples were collected at intervals post-PHx and analysed via quantitative polymerase chain reaction (qPCR) to determine gene expression, immunoblotting and immunohistochemistry (IHC) to determine protein expression and liquid chromatography-mass spectrometry (LC-MS) to characterize the bile acid pool in both the liver and intestine.

Results: Liver weight: body weight ratio in SIRT1^{int-KO} mice was comparable to that found in wildtype (WT) mice at 10 days post-PHx. However, SIRT1^{int-KO} mice exhibited profuse liver injury at 24 hrs post-PHx associated with BA accumulation, suggesting increased hepatocellular death due to BA toxicity. Additionally, SIRT1^{int-KO} mice presented signs of impaired hepatocyte proliferation through decreased expression of cell cycle proteins, cyclin D1 and delayed expression of cyclin E and A compared to WT mice. Further IHC analysis of pHistone-H3 showed significantly decreased presence of mitotic hepatocytes in SIRT1^{int-KO} livers compared to WT mice at 48 hrs post-PHx. This reduced hepatocyte proliferation correlated with increased abundance of senescent hepatocytes shown by IHC analysis of P21 and qPCR analysis of P16 and P21. Remarkably, IHC analysis of cytokeratin-19 (CK-19), a liver progenitor cell (LPC) marker, revealed SIRT1^{int-KO} livers had increased presence of LPCs in the parenchyma at 48 hrs post-PHx, denoting activation and expansion of the stem cell compartment to repopulate the liver as an alternative form of liver regeneration. Further study of intestinal BA metabolism regulation revealed that SIRT1^{int-KO} mice exhibited a dysregulation of intestinal SIRT1 downstream targets, farnesoid x receptor (FXR) and fibroblast growth factor-15 (FGF15), during the regenerative process compared to WT mice.

Conclusion: We define intestinal SIRT1 as a key regulator of the regenerative response in the liver. Our results point towards intestinal BA metabolism factors, FXR and FGF15, as mechanistic mediators of the effects of intestinal SIRT1 in regulating hepatocyte proliferation during liver regeneration. Overall, our results shed light into the mechanisms regulating the liver regenerative response and highlights the importance of intestinal-derived signals to control liver regeneration.

SAT-357

IGF1 specifically rescues peripheral intrahepatic biliary organoids from a mouse model of Alagille syndrome

Afshan Iqbal¹, Noémi K. M. Van Hul¹, Lenka Belicova¹, Agustin Corbat¹, Simona Hankeova^{1,2}, Emma Andersson¹. ¹Karolinska Institute, Cell and Molecular Biology, Solna, Sweden; ²Genentech, South San Francisco, United States
Email: afshan.iqbal@ki.se

Background and aims: Patients with Alagille syndrome (ALGS) display peripheral intrahepatic bile duct paucity. Intriguingly, some patients and the *Jag1^{Ndr/Ndr}* mouse model for ALGS can de novo generate their biliary system. We have shown that this occurs via distinct architectural mechanisms in the hilum and periphery. IGF1, a trophic factor for biliary cells, is downregulated in patients and *Jag1^{Ndr/Ndr}* mice, making it an interesting possible therapeutic target for ALGS. Here, we investigated hilar and peripheral bile ducts from *Jag1^{Ndr/Ndr}* mice, after recovery, to address biliary heterogeneity and mechanisms of recovery, and investigate potential therapeutic approaches.

Method: To investigate molecular differences in hilar and peripheral bile ducts, intrahepatic cholangiocyte organoids (ICOs) were derived from hilar and peripheral regions of adult *Jag1^{+/+}* and *Jag1^{Ndr/Ndr}* mouse livers (hICOs, and pICOs respectively, 3 cell lines from each region and genotype, 12 total). Region-specific ICOs were analyzed using RNA sequencing, live imaging, proliferation analysis (EdU assay), live/dead staining (CalceinAM/PI) and immunofluorescence. Organoids were treated with IGF1 to test whether this positively modulates organoid growth or survival.

Results: *Jag1^{Ndr/Ndr}* hICOs and pICOs were functionally and molecularly distinct from one another and from corresponding *Jag1^{+/+}* ICOs. *Jag1^{Ndr/Ndr}* hICOs were significantly ($p < 0.0036$) smaller than *Jag1^{+/+}* hICOs and *Jag1^{Ndr/Ndr}* pICOs ($p < 0.0020$). Both *Jag1^{Ndr/Ndr}* hICOs and pICOs were far less ($p < 0.0001$) proliferative than corresponding *Jag1^{+/+}* ICOs. Bulk RNA sequencing analysis of regional ICOs revealed downregulated cell cycle-associated genes in *Jag1^{Ndr/Ndr}* ICOs corroborating decreased proliferation. IGF1 treatment of regional ICOs specifically rescued survival and growth of *Jag1^{Ndr/Ndr}* pICOs ($p < 0.0464$), while hICOs were not significantly affected. RNA sequencing analysis revealed that *Jag1^{Ndr/Ndr}* hICOs were the most divergent ICOs and enrichment analysis demonstrated expression of a hepatocyte signature with activated IGF1 signaling pathway components. Finally, Notch components *Jag2* and *Nrarp* were specifically downregulated in *Jag1^{Ndr/Ndr}* hICOs.

Conclusion: *Jag1^{Ndr/Ndr}* hilar and peripheral ICOs are molecularly distinct from one another and from corresponding *Jag1^{+/+}* ICOs. *Jag1^{Ndr/Ndr}* ICOs are growth-impaired, but cell cycle can be rescued in pICOs by IGF1. IGF1 furthermore improves survival of *Jag1^{Ndr/Ndr}* pICOs and is thus a potential therapeutic target for ALGS. Hilar *Jag1^{Ndr/Ndr}* ICOs are Notch-off and express a hepatocyte-like signature, associated with active Igf1 production/signaling, and are less benefitted by IGF1 treatment.

SAT-358

Endothelial autophagy is not required for liver regeneration after partial hepatectomy in mice with fatty liver

Adel Hammoutene^{1,2}, Marion Tanguy^{1,2}, Mélanie Calmels¹, Riccardo Pravisani³, Chantal Boulanger¹, Valérie Paradis^{2,4}, Hélène Gilgenkrantz², Pierre-Emmanuel Rautou^{1,2,5}. ¹Université Paris Cité, PARCC, INSERM, F-75015 Paris, Paris, France; ²Université Paris-Cité, Inserm, Centre de recherche sur l'inflammation, UMR 1149, Paris, France, France; ³Service de chirurgie hépatobiliaire et pancréatique, Hôpital Beaujon, AP-HP, Clichy, France, France; ⁴Service d'Anatomie Pathologique, Hôpital Beaujon, Assistance Publique-Hôpitaux de Paris, Clichy, France, France; ⁵Service d'Hépatologie, AP-HP, Hôpital Beaujon, DMU DIGEST, Centre de Référence des Maladies Vasculaires du Foie, FILFOIE, ERN RARE-LIVER, Clichy, France, France
Email: amsadel@hotmail.com

Background and aims: Patients with metabolic associated fatty liver disease (MAFLD) have impaired liver regeneration following liver resection. Liver endothelial cells play a key role in liver regeneration. Autophagy is a cellular conserved process involved in the degradation of dysfunctional material. In non-alcoholic steatohepatitis (NASH), liver endothelial cells display a defect in autophagy, thus contributing to NASH progression. We aimed in this study to determine the role of endothelial autophagy in liver regeneration following liver resection in MAFLD.

Method: We analyzed the effect of the defect in endothelial autophagy on liver regeneration by using mice deficient in endothelial autophagy (*Atg5^{lox/lox}-VECadherinCre⁺*; $n = 13$) and littermate controls (*Atg5^{lox/lox}*, $n = 15$) mice, fed a high fat diet (HFD) for 16 weeks. Mice were subjected to 2/3 partial hepatectomy (removal of 70% of liver parenchyma) and liver regeneration was assessed by histology and western blot at two time points (40 and 48 hours after liver resection). We confirmed our finding using two other models of MAFLD.

Results: At the two time points of the liver regeneration process (40 and 48 hours), deficiency in endothelial autophagy had no impact on liver/body weight ratio, plasma AST, ALT and albumin concentration. Compared to control mice, *Atg5^{lox/lox}-VECadherinCre⁺* mice had similar liver protein expression of proliferation markers (proliferating cell nuclear antigen, PCNA) and cell-cycle markers (Cyclin D1 for G1/S phases and BrdU incorporation for S phase; phospho-Histone H3 for G2/M phases). Deficiency in endothelial autophagy did not affect either liver apoptosis as assessed by cleaved-Caspase-3 liver protein expression. Same results were observed in two other models of MAFLD, namely a model of simple steatosis (5 mice deficient in *ApoE/Atg5^{lox/lox}-VECadherinCre⁺* vs. 5 *ApoE/Atg5^{lox/lox}*), and model of NASH (5 *Atg5^{lox/lox}-VECadherinCre⁺* mice fed a methionine and choline deficient diet vs. 5 *Atg5^{lox/lox}* mice fed the same diet) (data not shown).

Study workflow: role of endothelial autophagy in liver regeneration after partial hepatectomy in mice with fatty liver

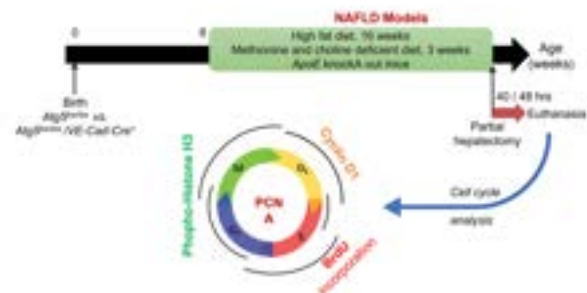


Figure:

Conclusion: Our results demonstrate that endothelial autophagy is not required for liver regeneration after partial hepatectomy in mice in the MAFLD setting. The defect in endothelial autophagy occurring

POSTER PRESENTATIONS

in NASH does not account for the impaired liver regeneration associated with MAFLD.

SAT-359

Transcriptomics confirm the establishment of a liver-immune dual-humanized mouse model after transplantation of a single type of human bone marrow mesenchymal stem cell

Suwan Sun^{1,2}, Hui Yang¹, Jiaojiao Xin¹, Heng Yao¹, Jing Jiang¹, Dongyan Shi¹, Jun Li¹. ¹The First Affiliated Hospital, Zhejiang University School of Medicine, State Key Laboratory for Diagnosis and Treatment of Infectious Diseases, National Clinical Research Center for Infectious Diseases, National Medical Center for Infectious Diseases, Hangzhou, China; ²The First Affiliated Hospital, Zhejiang University School of Medicine, Department of Endocrinology and Metabolic Disease, Hangzhou, China
Email: lijun2009@zju.edu.cn

Background and aims: Human bone marrow mesenchymal stem cells (hBMSCs) are important for developing a dual-humanized mouse model to clarify disease pathogenesis. We aimed to elucidate the characteristics of hBMSC transdifferentiation into liver and immune cells.

Method: A single type of hBMSCs was transplanted into immunodeficient *Fah^{-/-} Rag2^{-/-} IL-2R γ ^{-/-} SCID* (FRGS) mice with fulminant hepatic failure (FHF). Liver transcriptional data from the hBMSC-transplanted mice were analysed to identify transdifferentiation with traces of liver and immune chimerism.

Results: Mice with FHF were rescued by implanted hBMSCs. Human albumin/leukocyte antigen (HLA) and CD45/HLA double-positive hepatocytes and immune cells were observed in the rescued mice during the initial 3 days. The transcriptomics analysis of liver tissues from dual-humanized mice identified two transdifferentiation phases (cellular proliferation at 1–5 days and cellular differentiation/maturation at 5–14 days) and ten cell lineages transdifferentiated from hBMSCs: human hepatocytes, cholangiocytes, stellate cells, myofibroblasts, endothelial cells and immune cells (T/B/NK/NKT/Kupffer cells). Two biological processes, hepatic metabolism and liver regeneration, were characterized in the first phase, and two additional biological processes, immune cell growth and extracellular matrix regulation, were observed in the second phase. Immunohistochemistry verified that the ten hBMSC-derived liver and immune cells were present in the livers of dual-humanized mice.

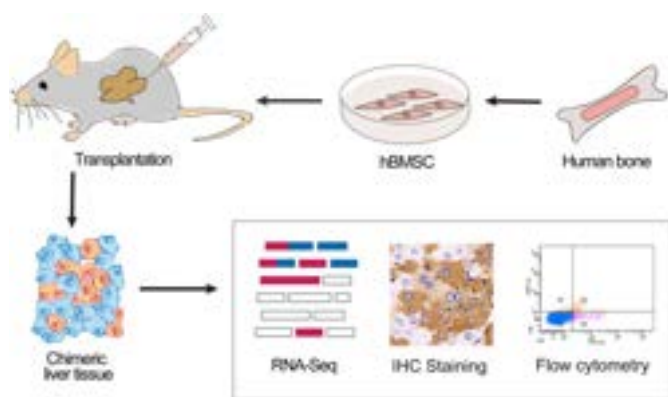


Figure:

Conclusion: A syngeneic liver-immune dual-humanized mouse model was developed by transplanting a single type of hBMSC. Four biological processes linked to the transdifferentiation and biological functions of ten human liver and immune cell lineages were identified, which may help to elucidate the molecular basis of this dual-humanized mouse model for further clarifying disease pathogenesis.

SAT-360

Skin-decellularized matrix-derived microgels accelerate 3D cultures of functional primary hepatocyte spheroids in vitro

Ashwini Vasudevan¹, Shreemoyee De², Neetu Singh², Shiv Kumar Sarin³, Dinesh Mani Tripathi³, Savneet Kaur³. ¹Institute of Liver and Biliary Sciences, Molecular and Cellular Medicine, New Delhi, India; ²Indian Institute of Technology Delhi, India; ³Institute of Liver and Biliary Sciences, India
Email: savykaur@gmail.com

Background and aims: Tissue extracellular matrix (ECM) plays a major role in providing a suitable niche for cell growth and differentiation. Skin tissue ECM is extremely dynamic with inherent properties such as enhanced wound healing and regeneration in response to tissue damage. In the current study, we explored the skin matrix vis-a-vis liver matrix for *in vitro* cultures of primary hepatocytes.

Method: Skin decellularized matrix (SDCM) was prepared by carefully excising dorsal skin tissues from adult rats, and tissues were decellularized with TritonX-100 and SDS. Liver decellularized matrix (LDCM) was prepared by perfusing rat livers with detergents. Tissue acellularity post-decellularization was confirmed with HandE staining and DNA quantification and intact matrix components were studied by proteomic analysis using LC-MS. Rodent primary hepatocytes were isolated by collagenase perfusion method. Viable hepatocytes were mixed with digested matrices and 1% alginate, and encapsulation was performed with CaCl₂ solution to form microgels containing cells. Stiffness of the cell microgels was assessed by Young's modulus. Encapsulated hepatocytes were cultured in microgels for up to 21 days, studied by scanning electron microscopy (SEM) and their viability, gene expression and functions were assessed.

Results: Proteomic analysis of the decellularized matrices revealed 16 types of collagens predominantly Collagen I, III, IV and VI, and upregulated expression of elastin and laminin in SDCM as compared to LDCM. Microgels with the LDCM showed increased compressive stress ($\Sigma 2.4$ Pa) when compared to SDCM ($\Sigma 0.98$ Pa). SEM analysis confirmed the encapsulation of hepatocytes as 3D spheroids in the microgels. There was significant increase in viability of hepatocytes cultured on both SDCM and LDCM microgels at days 7, 15 and 21 in comparison with those on collagen. On day 21, >2-fold increase ($p < 0.05$) in viability was observed in hepatocytes on SDCM microgels in comparison to those on LDCM. Hepatocytes grown on SDCM microgels also showed a significant increase in the expression of hepatocyte-specific genes including Alb, ASGR1, HNF4-alpha in comparison to those cultured on LDCM microgels and collagen on both day 15 and day 21. Albumin and urea secretion in culture supernatants from hepatocytes on SDCM microgels showed a significant increase on all days (On day 21: $\Sigma 1250$ mg/dl albumin and $\Sigma 50$ g/dl urea) in comparison to those on LDCM ($\Sigma 750$ mg/dl albumin and $\Sigma 30$ g/dl urea on day 21) and collagen ($\Sigma 150$ mg/dl albumin and $\Sigma 10$ g/dl urea on day 21) ($p < 0.05$).

Conclusion: Hepatocytes cultured with the SDCM microgels grow as 3D spheroids and show significantly improved viability and functionality for 3 weeks in comparison to LDCM. SDCM thus forms a better and lucrative alternative to decellularized liver matrix for maintaining long-term cultures of hepatocytes.

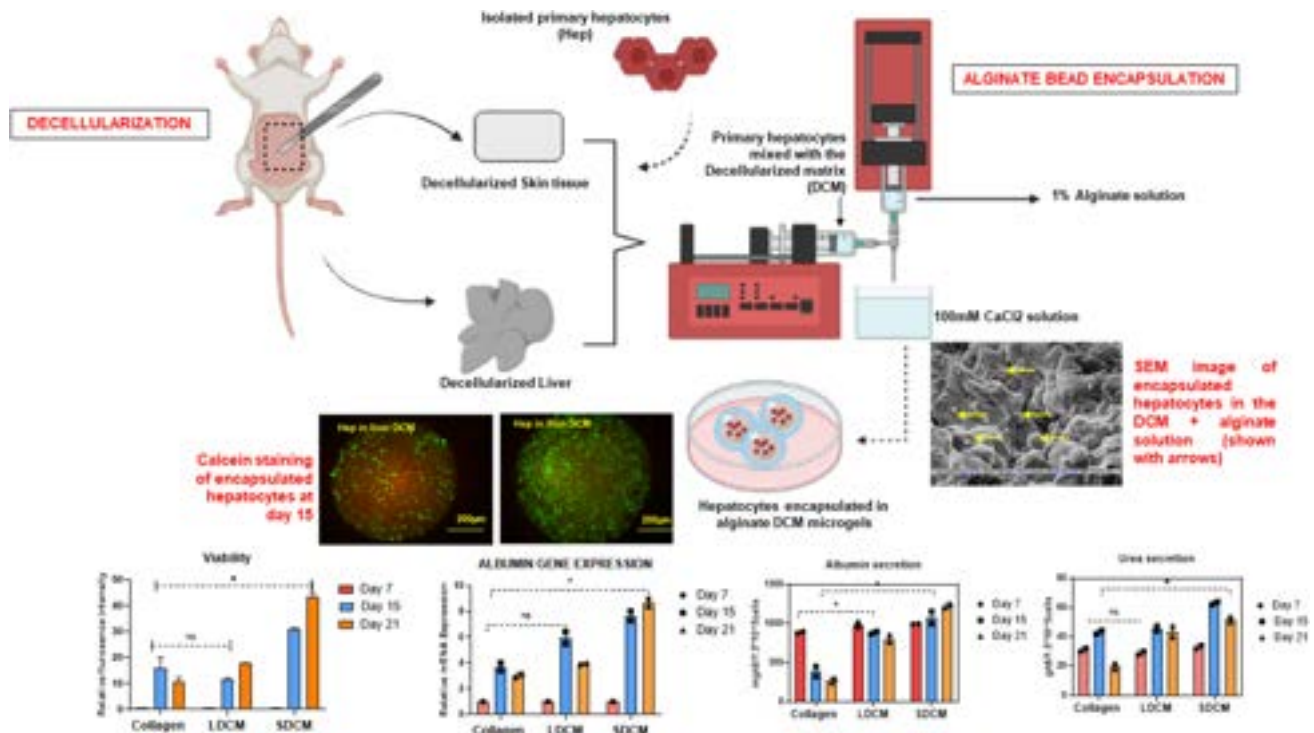


Figure: (abstract: SAT-360).

SAT-361

Autophagy regulates the generation and differentiation of chemically derived hepatic progenitors (CdHs)

Hayoon Kim^{1,2}, Myounghoi Kim¹, Elsy Soraya Salas Silva¹, Tae Hun Kim¹, Jiyeon Byeon¹, Michael Adisasmita¹, Min Kim¹, Ji Hyun Shin¹, Dongho Choi¹. ¹Research Institute of Regenerative Medicine and Stem Cells, Seoul, Korea, Rep. of South; ²Hanyang University College of Medicine, Korea, Rep. of South
Email: crane87@hanyang.ac.kr

Background and aims: Stem cell therapies have been proposed as a novel therapeutic strategy as an alternative to tissue transplantation for patients with liver diseases. To improve this, we have developed human chemically derived hepatocytes (hCdHs) that can be proliferated into hepatocytes (hCdH-Heps) and cholangiocytes in previous research. Moreover, we corroborated the successful engraftment of hCdHs in the mouse liver. However, despite its efficacy, the overall reprogramming mechanisms of CdHs during the generation and differentiation remain unclear. Autophagy, a self-degradation process, is a well-known pathway in cell reprogramming. Thus, we aimed to reveal autophagic activity throughout the whole reconstruction process of CdHs from generation to differentiation.

Method: Human and mouse primary hepatocytes (hPHs, mPHs) were cultured in reprogramming media containing HGF, A83-01, and CHIR99021 (HAC) for 7 days to generate human and mouse chemically derived hepatic progenitors (hCdHs, mCdHs). mPHs and hPHs maintained in basal media without HAC were used as a control. mCdHs were treated with bafilomycin A1 (Sigma-Aldrich, B1793) to inhibit autophagy flux. To induce differentiation of mCdHs and hCdHs into hepatocyte-like cells, mCdHs and hCdHs were cultured in hepatic differentiation medium, which contains oncostatin M, dexamethasone, and HGF. Then, expressions of major autophagy markers during CdHs generation and differentiation, such as p62 and LC3BII, were analyzed by western blotting and qPCR.

Results: mCdHs were generated from mPHs in the reprogramming medium, which contains HAC. It was primarily confirmed by observing cells expressing epithelial morphology. Also, mRNA expression of hepatic progenitor markers, such as Sox9, EpCAM,

Ck19, CD90, CD44, and AFP, increased in mCdHs compared to mPHs. Furthermore, protein expression of two autophagy markers, p62 and LC3BII, was elevated while mCdHs were generated from mPHs, indicating that autophagy was suppressed. mCdHs on day 12, after the generation, expressed lower protein levels of p62 and LC3BII, which means the recovery of autophagy to the basal level. Moreover, bafilomycin A1, an autophagy inhibitor, accelerated the growth of mCdHs during the generation. However, there was no increase in the mRNA expression levels of hepatic progenitor markers except Sox9 in the presence or absence of bafilomycin A1. Also, during the differentiation of mCdHs into mCdH-Heps, cells expressed a continuously decreasing protein level of p62 and LC3BII from the early phase, which suggests that autophagy activity decreased. Lastly, hCdHs were also generated from hPHs by the HAC reprogramming medium. hCdHs showed epithelial morphology and increased gene levels of hepatic progenitor markers. Interestingly, autophagy was inhibited during generation and downregulated to the basal level during differentiation into hepatocyte-like cells in hCdHs as well as in mCdHs.

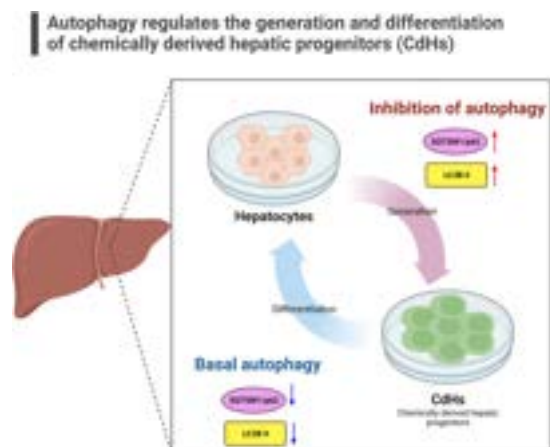


Figure:

POSTER PRESENTATIONS

Conclusion: In conclusion, all these findings indicate that autophagy regulates the generation of CdHs and the differentiation of CdHs into CdH-Heps.

This research was supported by the National Research Foundation of Korea (2022R1A2C2004593), and the Korean Fund for Regenerative Medicine funded by Ministry of Science and ICT, and Ministry of Health and Welfare (21A0401L1).

SAT-362

Development of intrahepatic bile ducts during liver progenitor cell-driven liver regeneration is associated with epithelial cell adhesion molecule function

Eun Young Cho¹, Tae-Young Choi^{2,3}, Azra Memon², Donghun Shin⁴, Hoon Gil Jo¹. ¹Wonkwang University, Department of Internal Medicine, School of Medicine, Iksan, Korea, Rep. of South; ²Digestive Disease Research Institute of Wonkwang University, Department of Pathology, Iksan, Korea, Rep. of South; ³Graduate School of Wonkwang University, Department of Biomedical Science, Iksan, Korea, Rep. of South; ⁴McGowan Institute for Regenerative Medicine, University of Pittsburgh, Department of Developmental Biology, Pittsburgh, United States
Email: choity76@wku.ac.kr

Background and aims: Epithelial cell adhesion molecule (EpCam) is a membrane glycoprotein involved in multiple functions, including cell-cell adhesion, proliferation, maintenance of undifferentiated states. During liver injury, EpCam-positive cells are associated with a population of cells within ductular reactions, thought to contain liver progenitor cells (LPCs). In this study, we aimed to analyze EpCam function, which might be involved with developing intrahepatic bile duct during LPC-driven liver regeneration.

Method: Using transgenic and mutant zebrafish (figure A), we examined the roles of EpCam on LPC-driven liver regeneration. These zebrafish assessed liver size; liver marker expression was analyzed by immunostaining, in situ hybridization, and quantitative PCR. Moreover, we used in vivo dye to visualize the development of intrahepatic bile ducts.

Results: After severe hepatocyte injury in the epcam mutants, we showed that the developing intrahepatic bile ducts were impaired, but not the regenerating liver size, indicating that LPC-driven liver regeneration proceeded; however, the maturation of intrahepatic bile ducts are impaired. Intriguingly, after BODIPY staining to visualize intrahepatic bile ducts, most of the biliary structure disconnected in the liver throughout (figure B-G), supporting the findings that epcam is associated with the developing intrahepatic bile duct during LPC-driven liver regeneration.

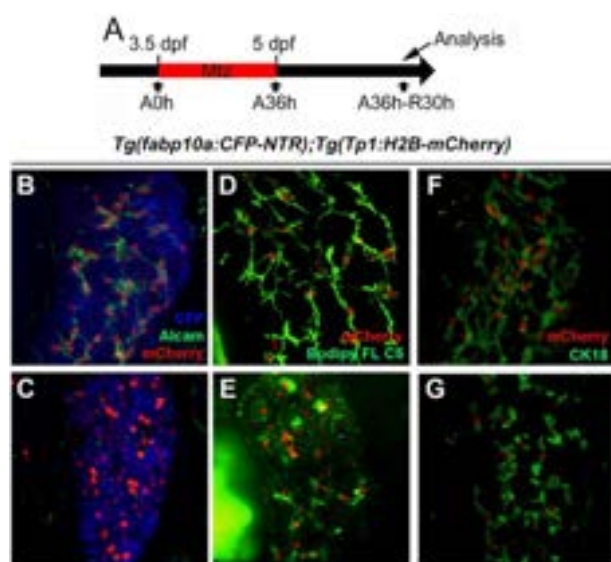


Figure:

Conclusion: These findings suggest that epcam positively regulates liver development, in particular, structure of intrahepatic bile duct, and play a potential role for bile duct epithelial cells to commit itself to a particular cell type during a regenerative response.

SAT-363

Excessive proliferation after extended hepatectomy compromises liver function in mice

Maxime De Rudder¹, Isabelle Leclercq¹, Alexandra Dili^{1,2}. ¹Institute of Experimental and Clinical Research, Laboratory of Hepato-Gastro-Enterology, Woluwe-saint-Lambert, Belgium; ²CHU UCLouvain-Namur, Department of Surgery, Yvoir, Belgium
Email: maxime.p.derudder@uclouvain.be

Background and aims: Small-for-size syndrome (SFSS) is a post-extended hepatectomy liver failure. After an extended hepatectomy, high portal pressure leads to vascular damage and induces hyperproliferation of hepatocytes and disruption of the lobule arrangement in the liver remnant. Both factors are thought to be major culprits leading to the SFSS. Previously, we showed that mice exposed to an hypoxic environment after extended hepatectomy had higher survival rates compared to mice in normoxia (~70% vs ~35% respectively). With survival, hypoxia triggered early endothelial cell proliferation and subsequently a denser sinusoidal network with larger sinusoids, rescue of the disturbed perfusion found after a SFSS-setting hepatectomy, and recruitment of endothelial progenitor cells. Our first aim was to assess whether rescue of the sinusoidal network alone increases survival after a SFSS-setting hepatectomy. Surprisingly, hypoxia decreased hepatocyte proliferation but improved liver function. Thus, we investigated epithelial-to-mesenchymal transition (EMT) process in hepatocytes following a SFSS-setting hepatectomy.

Method: We removed 80% of the total liver to induce SFSS. Granulocyte-colony stimulation factor (G-CSF) was administered 3 times intraperitoneally to replicate hypoxia's effects on the vascular network. Vascular diameter and density were assessed on CD31 staining. Recruitment of endothelial progenitors was assessed using Cdh5-Cre^{ERT2} × mTmG mice. Liver function was evaluated by ELISA for circulating factor V, circulating albumin by colorimetric test and hepatocyte glycogen content by PAS staining. EMT was evaluated by expression of E-Cadherin, Hes1 and Notch1 by immunofluorescence, and gene expression of HNF4A and Snai1 by qPCR.

Results: Administration of G-CSF increased vascular diameter and density and induced the recruitment of endothelial progenitors in regenerating livers compared to non-treated animals but did not positively impacted survival. We thus shifted our focus on the hepatocyte population. After a SFSS-setting hepatectomy, a large portion of the hepatocytes enters the cell cycle at the same time (around 50% at POD3). High proliferation was associated with significantly decreased circulating albumin and factor V, two proteins heavily produced by the liver. PAS staining revealed that only 30% of hepatocytes were PAS+, compared to 60% in mice kept in hypoxia. HNF4A, a master regulator of hepatocyte phenotype, was down-regulated in normoxia and its expression was inversely correlated with Snai1, a regulator of EMT. Concordantly, the epithelial marker E-Cadherin was faintly stained (Figure). We explored through which pathway EMT is induced in hepatocytes. Notch1 intracellular domain exhibited a nuclear staining in hepatocytes of mice kept in normoxia while none was found in hypoxia. Similarly, Hes1, a target of the Notch pathway, was more expressed in normoxia compared to hypoxia.

Conclusion: In this study, we found that rescue of vascular damage after a SFSS-setting is not sufficient to increase survival. Extravagant engagement in the cell cycle in hepatocytes was associated with decreased function of the liver remnant. We found that a large portion of the proliferative hepatocytes engaged in an EMT process through the Notch1/Hes1 pathway. Thus, we think that EMT engagement after a SFSS-setting hepatectomy disrupts the balance

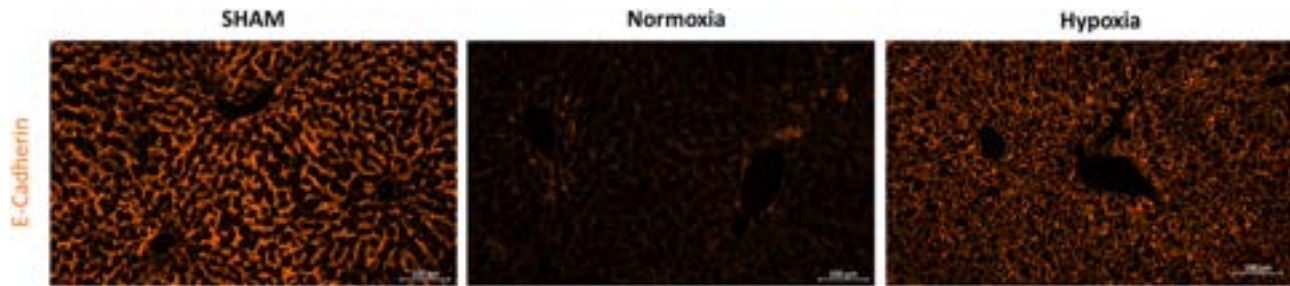


Figure: (abstract: SAT-363).

between function and proliferation in the remnant, leading to organ failure.

SAT-364

Conditioned medium from human allogeneic liver-derived progenitor cells protects against LPS-induced endothelial hyperpermeability via shingosine-1 phosphate

Audrey Ginion¹, Marine Angé¹, Pauline De Berdt², Mustapha Najimi^{2,3}, Etienne Sokal^{2,3}, Sandrine Horman¹. ¹Pole of Cardiovascular Research, Institut de Recherche Expérimentale et Clinique, Université catholique de Louvain, Brussels, Belgium; ²Cellaion, Mont-Saint-Guibert, Belgium; ³Laboratory of Pediatric Hepatology and Cell Therapy, Institute of Experimental and Clinical Research (IREC), Université catholique de Louvain, Brussels, Belgium
Email: mustapha.najimi@cellaion.com

Background and aims: Stem cells are recognized as an important tool for the treatment of several disease processes and injured tissues. Intravenous administration of mesenchymal stem cells, the stromal progenitor cells found within the bone marrow, has been shown to benefit a variety of disease models, including sepsis. The underlying mechanism results from direct interaction with the vascular endothelium and/or secretion of soluble factors. Human allogeneic liver-derived progenitor cells (HALPCs), currently under clinical development for the treatment of ACLF, display unique paracrine anti-inflammatory, immunomodulatory and regenerative features. This study tested the impact of conditioned medium derived from HALPCs (CM-HALPC) on microvascular permeability, a determinant factor in the pathophysiology of sepsis. Underlying mechanisms were also investigated.

Method: Conditioned media from HALPCs were generated and kept frozen until analysis. Human dermal microvascular endothelial cells (HDMECs) were incubated with non-conditioned medium or CM-HALPC mixed with EGM-2 MV (1:1) for 24 hours prior to treatment with E. coli lipopolysaccharide (LPS 055:B5, 50 µg/ml). Functional endothelial permeability was measured by in vitro transwell assay, and quantification of cellular junctions (IEJs) in the plasma membrane was assessed by VE-Cadherin (VE-Cad) immunofluorescence.

Results: Preincubation of HDMECs with CM-HALPC preserved VE-Cad organization and protected endothelial barrier function against LPS injury. Since ELISA analysis revealed the presence in CM-HALPC of sphingosine-1-phosphate (S1P) and hepatocyte-growth factor (HGF), two factors known to be involved in the regulation of vascular permeability, we tested their contribution to the protective effect. Addition of a pharmacological antagonist of S1P to CM-HALPC was associated with the loss of the barrier-protective function. However, when HDMECs were treated with CM-HALPC supplemented with an anti-HGF antibody, the protective effect of the conditioned medium was not affected.

Conclusion: These results demonstrate that CM-HALPC protects against LPS-induced hyperpermeability and preserves IEJs integrity, in part via S1P. These data have implications for the potential

therapeutic use of those cells also in disease conditions characterized by compromised vascular integrity.

SAT-365

Lineage tracing of hepatic stellate cells with ultrasound-guided in utero nano-injection

Jingyan He¹, Lenka Belicova¹, Sandra De Haan¹, Noémi K. M. Van Hul¹, Stefaan Verhulst^{1,2}, Michael Ratz¹, Emma Andersson¹. ¹Karolinska Institutet, Department of Cell and Molecular Biology (CMB), Solna, Sweden; ²Vrije Universiteit Brussel, Liver Cell Biology Research Group, Belgium
Email: emma.andersson@ki.se

Background and aims: Hepatic stellate cells (HSCs) are essential mesenchymal cells in the liver and contribute to fibrosis upon liver injury. HSCs express both mesenchymal and neural markers, and current lineage tracing studies have demonstrated contribution of Mesp1- and Wnt1-expressing mesodermal/mesenchymal cells to liver, as well as Wnt1- and Gfap-expressing cells. However, some of these studies have been contradicted by others. Thus, a definitive origin of HSCs and their relationship with other hepatic mesenchymal cells is still unclear. Traditional lineage tracing with Cre mouse models is powerful but has inevitable limitations for hybrid cell types.

To circumvent this limitation, we developed a novel Cre-independent method to trace HSC lineages and their clonal relationships with other mesenchymal cells.

Method: A diverse lentivirus barcode library was injected into the amniotic cavity (AC) or exocoelomic cavity (ExC) of mice at embryonic day (E)7.5 to target the neural crest or mesoderm, respectively. By using clonal TRacing and gene EXpression via scRNA-seq (Trex) and IF staining, E9.5–12.5 embryos were analyzed to trace the HSC trajectory, ≥E16.5 livers were analyzed to resolve clonal relations.

Results: In utero nano-injection with lentivirus results in successful transduction of septum transversum mesenchyme (STM) and intrahepatic mesenchymal cells, including HSCs.

Conclusion: Ultrasound-guided in utero nano-injection is a powerful Cre-independent method to lineage trace HSCs in the liver. It requires fewer mice, is faster and cheaper compared to using genetically engineered mice. By using this technique and Trex, we are now investigating the developmental trajectory of HSC lineages.

SAT-366

Autologous skeletal myoblast cell-sheet transplantation for liver regeneration

Keisuke Toya¹, Yoshito Tomimaru¹, Shogo Kobayashi¹, Akima Harada¹, Kazuki Sasaki¹, Yoshifumi Iwagami¹, Daisaku Yamada¹, Takehiro Noda¹, Hidenori Takahashi¹, Ryota Dhijimatsu², Shigeru Miyagawa¹, Yuichiro Doki¹, Hidetoshi Eguchi¹. ¹Graduate School of Medicine, Osaka University, Japan; ²Center for Comprehensive Genomic Medicine, Okayama University Hospital, Japan
Email: ktoya@gesurg.med.osaka-u.ac.jp

Background and aims: There have been no established effective therapies for liver failure. Here, we focused on autologous skeletal myoblast cell-sheet transplantation, which is proved to improve

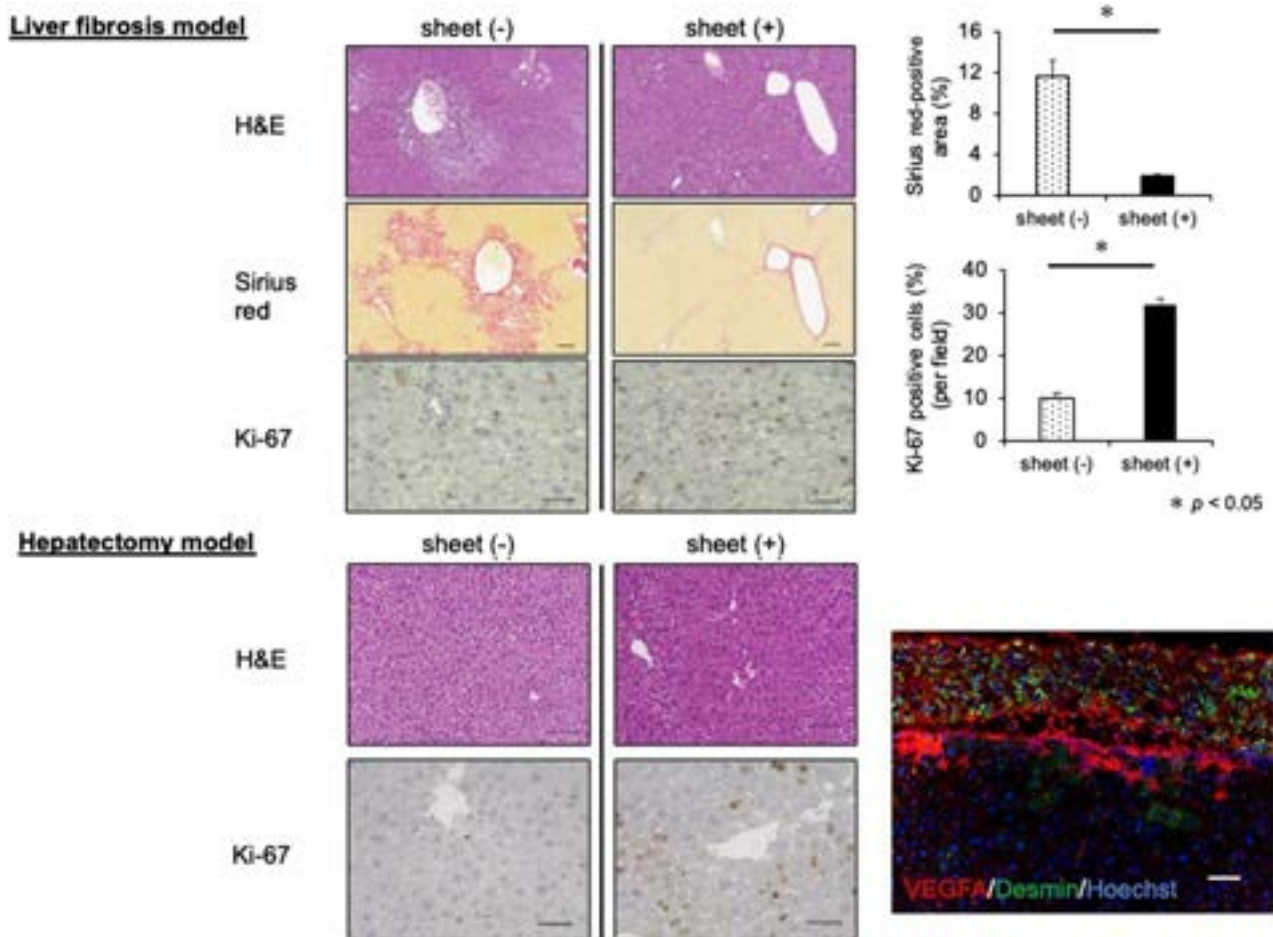


Figure: (abstract: SAT-366).

cardiac function in patients with heart failure, for the treatment of liver failure. Thus, in this study, we preclinically assessed the effect of the sheet transplantation on liver failure model mice.

Method: We assessed two liver failure model C57BL/6 mice; one was liver fibrosis mouse induced by intraperitoneal administration of thioacetamide (TAA), the other was 70% partial hepatectomy model mouse. The mice received the autologous skeletal myoblast cell-sheet transplantation. In fibrosis model, the effect of the sheet transplantation was examined in terms of the extent of the fibrosis judged by Sirius red and Masson trichrome staining and the expression of a hepatocyte proliferation marker, Ki-67, and liver fibrosis markers, Acta2 and Col1 α -1, in the liver tissues after the transplantation with comparison to the control receiving sham surgery. In hepatectomy model, the effect was examined the remnant liver to body weight ratio and the expression of Ki-67 and a marker for angiogenesis, CD31. Furthermore, immunohistochemical analysis for VEGFA, which myoblast cells secreted, was assessed to investigate the mechanism for liver regeneration of myoblast cell sheet.

Results: In the TAA model, the liver tissue was analyzed 3-week and 5-week after the myoblast cell-sheet transplantation. The percentage of Ki-67-positive cells was significantly higher in the sheet transplantation group than in the control group. Sirius red and Masson trichrome staining showed that liver fibrosis is less severe in the transplantation group than the control group. Furthermore, mRNA expression levels of Acta2 and Col1 α -1 were significantly lower in the transplantation group than the control group. In the hepatectomy model, the remnant liver to body weight ratio 2 days after hepatectomy and sheet transplantation was significantly higher in the sheet group than that in the control group. The percentage of

Ki-67-positive cells was significantly higher in the sheet group than in the control group at the same time. Moreover, the expression of CD31 in the remnant liver was significantly increased in the sheet group. Additionally, VEGFA was overexpressed at the sheet and the remnant liver near the sheet.

Conclusion: These results suggested that the autologous skeletal myoblast cell-sheet transplantation significantly improved the liver fibrosis and accelerated liver regeneration in the mice models. The sheet transplantation has the potential to be a clinically therapeutic option for liver regeneration.

SAT-367

Role of GATA4 in the modulation of hepatic progenitor cell fate

Laura Villamayor^{1,2}, Noelia Arroyo³, Silvia Calero^{1,2}, Pedro Miguel Rodriguez^{4,5,6}, Elena Carceller-Lopez¹, Malgorzata Milkiewicz⁷, Piotr Milkiewicz^{8,9}, Jesus Maria Banales^{4,5,6,10}, Anabel Rojas^{2,3}, Angela Martinez Valverde^{1,2}. ¹Institute of Biomedical Research "Alberto Sols" (CSIC-UAM), Madrid, Spain; ²Network Biomedical Research Center for Diabetes and Associated Metabolic Diseases (CIBERdem), Madrid, Spain; ³Andalusian Molecular Biology and Regenerative Medicine Centre (CABIMER), University Pablo de Olavide, Universidad de Sevilla, Consejo Superior de Investigaciones Científicas (CSIC), Seville, Spain; ⁴Department of Liver and Gastrointestinal Diseases, Biodonostia Health Research Institute, Donostia University Hospital, University of the Basque Country (UPV/EHU), San Sebastián, Spain; ⁵National Institute for the Study of Liver and Gastrointestinal Diseases (CIBERehd, Carlos III Health Institute), Madrid, Spain; ⁶IKERBASQUE, Basque Foundation for Science, Bilbao, Spain; ⁷Department of Medical Biology, Pomeranian

Medical University in Szczecin, Szczecin, Poland; ⁸Liver and Internal Medicine Unit, Department of General, Transplant and Liver Surgery, Medical University of Warsaw, 02-097, Warsaw, Poland; ⁹Translational Medicine Group, Pomeranian Medical University, 70-204, Szczecin, Poland; ¹⁰Department of Biochemistry and Genetics, School of Sciences, University of Navarra, Pamplona, Spain
Email: laura.villamayor.coronado@gmail.com

Background and aims: Primary biliary cholangitis (PBC) and primary sclerosing cholangitis (PSC) are biliary diseases characterized by the damage of mature cholangiocytes, diffuse inflammation and fibrosis of the bile ducts. PSC patients have a higher risk to develop cholangiocarcinoma (CCA) while patients PBC more likely develop hepatocellular carcinoma (HCC). In PBC and PSC, the epithelial-mesenchymal transition (EMT) inducers are essential for disease progression and fibrosis development. Another feature of both diseases is the presence of ductular reaction (DR) due to the activation of hepatic progenitor cells (HPCs), known as oval cells (OCs) in rodents. Interestingly, HPC proliferation has been involved in progression of the duct lesions in PSC towards CCA. The zinc finger transcription factor GATA4 is a master driver of liver organogenesis and cancer development. Until now, it was known that *Gata4* expression in the liver was restricted to endothelial and hepatic stellate cells (HSCs). However, we detected the expression of *Gata4* in OCs in culture, as well as in OCs located in the oval niche in mice. On that basis, our aim was to unravel the role of *Gata4* as modulator of OCs fate in the context of PBC and PSC progression.

Method: OCs in culture were exposed to TGF- β or hypoxia (1% O₂ saturation) and the correlation between EMT and *Gata4* and *Hif2a* expression levels were determined by qPCR and Western blot. A step further, we silenced *Gata4* in OCs in culture by infection with *shGata4* lentiviral particles to study a possible essential role like occur during liver development. Moreover, we analyzed the expression levels of GATA4 in liver samples from PSC and PBC patients by qPCR.

Results: Our results showed that OCs express the transcription factor *Gata4* *in vitro* and *in vivo*. Surprisingly, OCs are sensitive to hypoxia that promotes EMT in these cells in parallel with GATA4 down-regulation. This was accompanied by the loss of cell identity monitored by reduction in the OC specific marker A6. Similar relationship between EMT, loss of cell identity and *Gata4* down-regulation was found upon treatment of OCs with TGF β . Silencing *Gata4* in OCs led to a loss of OCs viability since we did not obtain viable clones with *Gata4* downregulation, suggesting that *Gata4* might be essential for preserving OCs viability and survival. Moreover, the expression levels of GATA4 in liver samples from PSC and PBC patients revealed a significant decrease in PSC patients and a decrease trend in PBC patients.

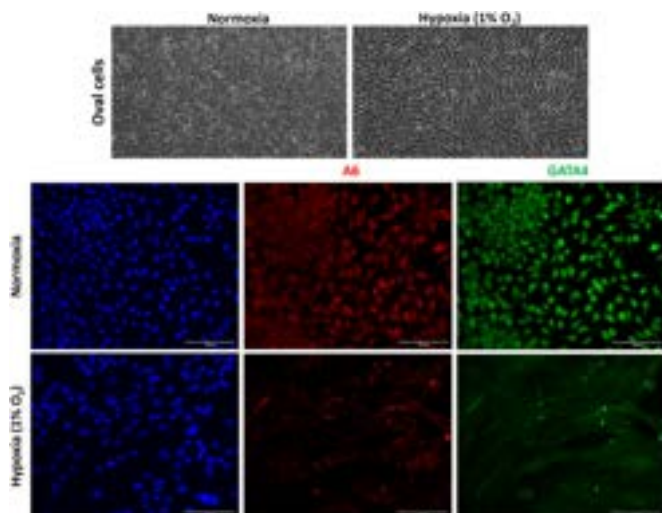


Figure:

Conclusion: Given the progenitor nature of OCs, the role of GATA4 in liver development and tumor suppression, and our data showing a correlation between *Gata4* expression and EMT in OCs, our results suggest that GATA4 could be a *bona fide* modulator of OC fate.

SAT-368

Rescue mechanism of hHIL-6 after partial hepatectomy

Julia Ettich¹, Hendrik Weitz¹, Melissa Nowak², Friedrich Reusswig³, Tobias Buschmann², Kristina Vogel¹, Juergen Scheller¹. ¹Institut für Biochemie und Molekularbiologie II, Germany; ²Institut für Molekulare Medizin III, Germany; ³Research Group Experimental Vascular Medicine, Germany
Email: jscheller@hhu.de

Background and aims: Previous reports show interleukin-6 (IL-6) is critically involved in liver regeneration after partial hepatectomy (PHx) comprising both IL-6 classic- and trans-signaling. However, the exclusive impact of IL-6 classic-signaling for liver regeneration after PHx is unknown due to the necessity of the IL-6R, which generates PHx-induced soluble IL-6R (sIL-6R) by disintegrin and metallo proteases enabling also IL-6 trans-signaling.

Method: Acute liver injury in mice investigates liver regeneration following surgical removal of 70% of the liver. RNA-sequencing analyzed the gene expression profile of liver tissue pre PHx, 6 h, and 24 h post PHx and were verified by RT-PCR. Serum protein levels (AST, ALT, Bilirubin, alkaline phosphatase) were analyzed. H/E-staining of liver sections and cytokine ELISAs were performed.

Results: IL-6R deficient mice after PHx resulted in significantly impaired survival. Elevated liver transaminases, accompanied by an elevation in cholestasis, and delayed bile acid synthesis affected liver regeneration following PHx. While the capacity for regeneration itself showed no effect, a delay in cell cycle gene expression and reduced proliferation supported with reduced SAA1 was given. Histopathology revealed a delayed lymphocyte infiltration in correlation with more necrotic areas of in IL6R-deficient mice following PHx. Application of human Hyper-IL-6 (hHIL-6), a fusion protein of sIL-6R and IL-6, rescued the impaired survival following PHx via IL-6 trans-signaling. To further investigate the role of hHIL-6 during regeneration, IL-6R deficient mice were analyzed in transcriptomic analysis. Besides the gene expression profiling, hHIL-6 treated animals displayed a significant increase in SAA1 activity already pre-PHx, indicating a sufficient and restored STAT3 activation. Within 24 h post PHx liver transaminases were significantly reduced, cholestasis marker stayed at moderate level and hHIL6-treated mice revealed reduced necrotic areas accompanied by an increase in proliferation.

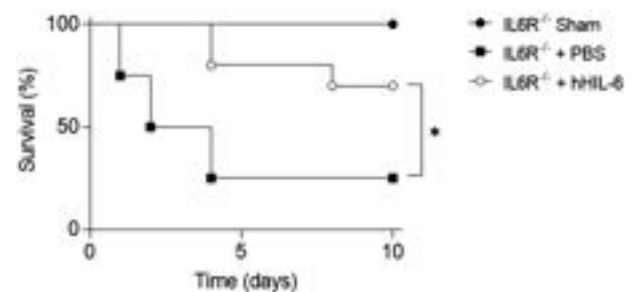


Figure:

Conclusion: IL-6R deficient mice can be rescued via synthetic hHIL-6 due to the protection of intrahepatic cholestasis-induced hepatocyte death during liver regeneration.

SAT-369

Hepatic progenitor cell activation through the interaction of mesenchymal stem cells and liver sinusoidal endothelial cells

Su Jung Park¹, Jin Suk Lee¹, Mi Ra Lee¹, Han Seul Ki^{1,2}, Soon Koo Baik^{1,2}, Moon Young Kim^{1,2}. ¹Yonsei University Wonju College of Medicine, Regenerative Medicine Research Center, Wonju-si, Korea, Rep. of South; ²Yonsei University Wonju College of Medicine, Department of Internal Medicine, Division of Gastroenterology and Hepatology, Wonju-si, Korea, Rep. of South

Email: drkimmy@yonsei.ac.kr

Background and aims: The hepatic progenitor cell (HPC) is an innate stem cell in the liver and the main cell in liver regeneration. Induce that the proliferation and regenerative activity of HPC is the main issue in the liver regeneration field. Liver sinusoidal cells (LSECs) inactivation and stabilization are essential in accelerating the regression of fibrosis and inhibiting the progression of cirrhosis. LSEC also has been known to activate HPC through the Wnt- β -catenin signaling. However, the method to stabilize LSECs is not yet established. Therefore, we investigated the functional recovery of LSECs through mesenchymal stem cells (MSCs) and whether it can induce HPCs activation.

Method: To evaluate the stabilization of LSEC by MSC, the recovery of fenestrae of LSECs was confirmed by Scanning Electron Microscope (SEM) after co-culture. Changes in various factors affecting the stabilization of LSEC were also confirmed by real-time polymerase chain reaction and Western blot. The specific cell markers of the isolated mouse LSECs and MSCs were confirmed by FACS. In addition, HPCs were cultured using the culture soup obtained by co-culture of LSECs and MSCs, and the activities of HPCs were analyzed.

Results: In human-derived MSC and LSEC co-culture, LSEC showed recovery of fenestrae with increased expression of VEGF, eNOS, HGF, Wnt2, and Wnt9b in LSEC compared with control. Also, when LSECs and MSCs isolated from mice were co-cultured, the expression of VEGF and HGF, which play an important role in maintaining the morphology of LSEC, increased. The expression of Wnt9b, which acts as an angiocrine factor in liver regeneration, was also increased.

In the culture of HPC, when the soup obtained from LSEC during LSEC and MSC co-culture was added, an increase in HPC activity was observed compared to the control group. The proliferation of stem progenitor cells was doubled in both 24 and 48 hours compared to the control group. Also, the expression of VEGF and Wnt2 increased in HPC at 24 hours, and the expressions of HGF, VEGF, and Wnt9b increased at 48 hours.

Conclusion: MSC showed the property that can induce stabilization (undifferentiated) LSEC. Stabilized and functionally recovered LSEC by MSC also induced the proliferation and increased the activity of HPCs and which suggests a possibility that MSC-based recovery of LSEC in hepatic fibrosis can be helpful in the promotion of liver regeneration through HPC activation.

Background and aims: Viral infections of the liver with hepatotropic viruses, such as the hepatitis B virus, are most often successfully cleared by the adaptive immune response, in particular virus-specific CD8 T cells. Persistent infection occurs when antigen-specific immunity fails to eliminate virus-infected hepatocytes, the reasons of which are still unclear. In this project, we investigate the contribution of a novel form of metabolic T cell activation termed auto-aggressive T cells and its relevance to control of virus infection in hepatocytes.

Method: We used time-lapse cytotoxicity assays measuring cell impedance to determine the ability of antigen-specific CD8 T cells to engage in combination with auto-aggressive CD8 T cells in a synergistic fashion to achieve killing of virus-infected hepatocytes. We established cocultures of primary murine hepatocytes with conventional effector CD8 T cells and auto-aggressive CD8 T cells, and measured antigen-specific killing compared to auto-aggressive killing of hepatocytes.

Results: As expected, antigen-specific CD8 T-cells efficiently killed virus-infected hepatocytes within 12 hours. Conversely, high effector to target ratio (>10) of auto-aggressive T-cells exerted antigen independent *in vitro* hepatocyte killing. Strikingly, co-incubation of cytotoxic effector CD8 T cells and auto-aggressive CD8 T cells at effector to target ratios that would not elicit any hepatocyte killing by a single T cell population, led to efficient killing of hepatocytes. This demonstrated different pathways leading to hepatocyte killing that rely on synergistic effector functions exerted by conventional antigen-specific CD8 T cells and auto-aggressive CD8 T cells. Remarkably, we identified soluble factors secreted by conventional T cells that initiated auto-aggression by CD8 T cells.

Conclusion: Our results demonstrate that cytotoxic CD8 T cells and auto-aggressive CD8 T cells have a synergistic activity in eliciting killing of virus-infected hepatocytes. This unravels novel means of cooperation among T cells with effector functions. Future experiments will characterize how conventional effector CD8 T cells engage auto-aggressive CD8 T cells in a synergistic killing of virus-infected hepatocytes in a "swarm hunting" fashion.

TOP-053

Rheostat function of liver sinusoidal endothelial cells and macrophages limiting antiviral CD8 T cell immunity in the liver

Anna Fürst¹, Sutirtha Chattopadhyay¹, Hannah Wintersteller¹, Dirk Wohlleber¹, Miriam Bosch¹, Percy A. Knolle¹. ¹Institute of Molecular Immunology, Germany

Email: anna.fuerst@tum.de

Background and aims: Hepatitis B virus (HBV) infection can be controlled by strong antiviral CD8 T cell immunity. However, in persisting HBV infection virus-specific CD8 T cells are scarce and lack effector functions. We aimed at investigating the local influence of liver sinusoidal endothelial cells (LSECs) and liver macrophages on antiviral CD8 T cell immunity against virus-infected hepatocytes.

Method: We used hepatotropic recombinant adenoviruses to transfer ovalbumin or HBV 1.3 overlength genomes into hepatocytes leading to either acute-resolving or persistent hepatocyte infection. We transferred virus-specific CD45.1⁺ CD8 T cells before infection to study T cell immunity against infection with hepatotropic viruses. Liver tissue sections were analyzed for localization of T cells by volumetric confocal microscopy. Virus-specific T cells were co-cultured with LSECs and liver macrophages *in vitro*, and their phenotype and function were analyzed by flow cytometry and mass spectrometry imaging.

Results: During persistent viral infection, dysfunctional virus-specific CD8 T cells had a significantly shorter distance to and larger cumulative surface contact area with LSECs and liver macrophages compared to fully functional CD8 T cells after resolved infection. Remarkably, CD8 T cells engaging in close contact with LSECs or liver macrophages *ex vivo* upregulated CXCR6 expression, a marker previously described for tissue-resident T cells. Consequently,

Liver immunology

WEDNESDAY 21 TO SATURDAY 24 JUNE

TOP-050

"Swarm hunting" of virus-specific CD8 T cells together with auto-aggressive CD8 T cells to achieve efficient killing of virus-infected hepatocytes

Ariane Eceiza Tenreiro¹, Michael Dudek¹, Dirk Wohlleber¹, Percy A. Knolle¹. ¹Institute of Molecular Immunology, Germany

Email: percy.knolle@tum.de

dysfunctional CD8 T cells during persistent infection expressed higher CXCR6 levels compared to fully functional CD8 T cells after resolved infection. Moreover, co-culture with LSECs led to augmented protein kinase A phosphorylation and caused inhibition of T cell receptor signaling in CXCR6⁺CD8 T cells pointing towards increased cAMP signaling as cause of T cell dysfunction during persistent hepatotropic infection. Mass spectrometry imaging of LSECs and CD8 T cells further identified changes in lipid and metabolite profiles associated with the distinct functional properties of virus-specific CD8 T cells.

Conclusion: Our results identify close physical interaction between virus-specific CD8 T cells and LSECs and liver macrophages as initial event in regulating loss of T cell function. Future work will aim at elucidating the exact molecular mechanism determining the metabolite-induced regulation of T cell function and their consequences for anti-viral immunity in the liver.

SATURDAY 24 JUNE

SAT-371

AAV-HBV mouse model replicates immune exhaustion patterns of chronic HBV patients at single-cell level

Ren Zhu¹, Qinglin Han², Nadia Neto³, Zhiyuan Yao⁴, Qun Wu², Dries de Maeyer⁵, Koen Van der Borght⁵, Matthias Beyens⁵, Ellen Van Gulck³, George Kukolj⁴, Podlaha Ondřej⁴, Chris Li⁴, Isabel Najera⁴. ¹Janssen, Infectious Disease Translational Discovery, China; ²Janssen, Infectious Disease Translational Discovery, China; ³Janssen, Infectious Disease Translational Discovery, Belgium; ⁴Janssen, Infectious Disease Translational Discovery, United States; ⁵Janssen, DTMP, Belgium
Email: rzhu7@its.jnj.com

Background and aims: Chronic hepatitis B viral infection (CHB) can lead to a state of immune exhaustion or dysfunction preventing the resolution of infection. AAV-HBV transduction leads to persistent HBV replication in immune-competent mice; comprehensive characterization of the liver immune microenvironment is however lacking. This study investigated the intrahepatic immune profile of AAV-HBV-transduced mice at the single cell level and compared these data to data of a human CHB dataset¹ across clinical stages of CHB.

Method: Liver immune cells were isolated from 4 to 5-week-old male C57/BL6 mice with AAV-HBV (n = 5), AAV control vector (n = 5) 24-weeks post-transduction or naïve (n = 5) mice. Cells were loaded on to a 10× Genomics platform (5' capture protocol) for single-cell RNA sequencing analysis. Downstream analysis was performed using

custom R scripts that utilized the Seurat, CellChat, and CellPhoneDB packages. The mouse model data was compared with a human CHB dataset¹, using the bioinformatics packages described above.

Results: A total of 107,925 high quality mouse immune cells were captured from the 15 samples, covering all major immune cell populations (Ts, Bs, NKs, DCs, monocytes and neutrophils) and hepatocytes. Pre-exhausted CD8⁺ T cells with self-renewing capacity (Tpex, TCF1⁺), and terminally exhausted CD8⁺ T cells (Tex, TCF1⁻) were identified in the AAV-transduced mice. The terminally exhausted CD8⁺ T cells (expressing PD-1, LAG-3, TIGIT) were significantly enriched in the AAV-HBV mouse group. Deconvolution of cell-to-cell signaling pathways identified CD4⁺ Th1 cells (Pdc1lg2-Pdcd1 pathway) and mature B- cells (H2k1-Cd8a/b1 pathway) as major signal senders to CD8⁺ Tex cells, while resident regulatory T cells contributed to the Pvr-Tigit interaction with CD8⁺ Tex. We performed analogous single cell analyses across the Immuno-Tolerant (IT), Immuno-Active (IA), and HBV resolver (CR) patients as well as healthy donors of the human CHB dataset¹. The immune cell population composition as well as ligand/receptor expression patterns observed in AAV-HBV mice were consistent with observations from IT and IA CHB patients (Figure 1).

Conclusion: Enrichment for exhausted CD8⁺ T cells was observed in the livers of AAV-HBV mice by expression of immune checkpoint marker genes (PD-1, LAG-3, TIGIT). We also observed immune cell crosstalk which may be driving or maintaining T cell exhaustion. The exhausted CD8 gene and pathway profiles were comparable between mouse AAV-HBV and the human CHB samples from Zhang et al¹. These data support the use of the AAV-HBV mouse model in the study of liver immune tolerance mechanisms induced by HBV.

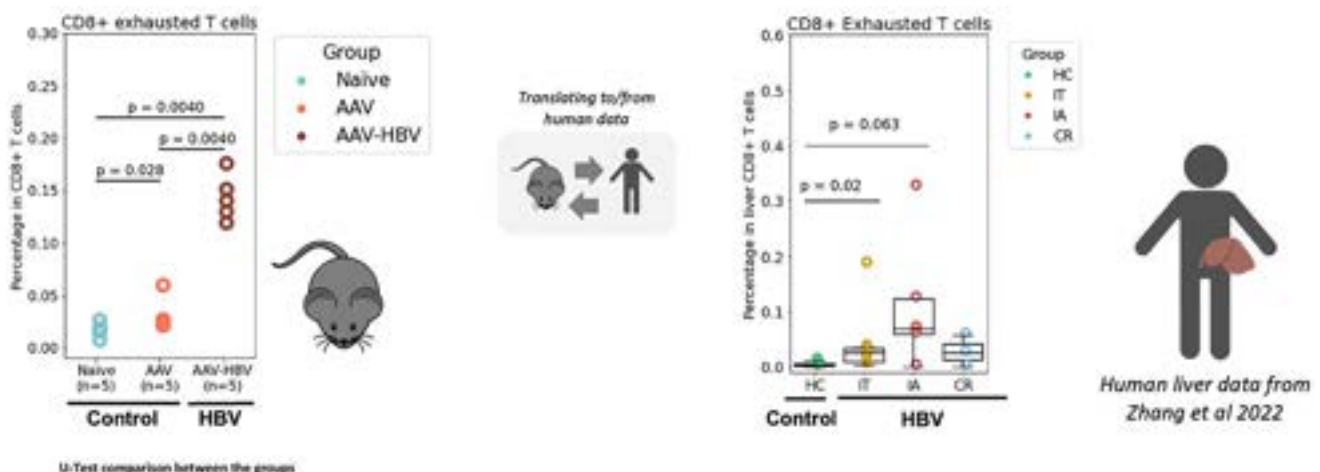
Reference

- Zhang et al. (2023). Single-cell RNA sequencing reveals intrahepatic and peripheral immune characteristics related to disease phases in HBV-infected patients. *Gut*.

SAT-372

Developing highly pure, functional GMP grade Treg for the treatment of autoimmune liver disease

Naomi Richardson^{1,2}, Grace Wootton^{1,2}, Amber Bozward^{1,2}, Ye Htun Oo^{1,3}. ¹University of Birmingham, Centre for Liver and Gastrointestinal Research, Institute of Immunology and Immunotherapy, United Kingdom; ²University of Birmingham, Advanced Therapies Facility, United Kingdom; ³Queen Elizabeth Hospital Birmingham, Liver Medicine, United Kingdom
Email: y.h.oo@bham.ac.uk



Background and aims: Autoimmune liver diseases (AILD) are immune mediated liver diseases causing chronic damage to hepatocytes and biliary tissue. Regulatory T cells (Treg) are crucial to maintain peripheral immune tolerance, reduce inflammation and promote tissue repair. Our previous trial (AUTUMN) showed that >25% of natural Treg cells from autoimmune hepatitis (AIH) patients' blood effectively home to the liver and readily respond to IL-2 via STAT-5 signaling. We have now developed a platform to generate Good Manufacturing Practice (GMP) grade autologous Treg cells with potential to treat AILD and reduce reliance on immunosuppressive drugs.

Method: The isolation of highly pure, functional Treg cells from peripheral blood is achieved using Miltenyi Prodigy to enrich CD25⁺ T cells, before careful cell sorting using the MACSQuant Tyto to remove CD8⁺ T cells and gain CD4⁺CD25⁺CD127^{low} bona fide Treg cells at >95% purity. Isolated Treg can be expanded *in vitro*, according to our optimized protocol, to achieve therapeutic doses of cells within 4 weeks (>1 × 10⁹ Treg cells). Treg expansion optimisation involved testing different medias, IL-2 concentrations, stimulation types and duration, seeding densities, culture vessels and mTOR inhibition. Measuring lactate enables effective monitoring of cell number throughout expansion without need for intervention.

Results: Treg cells manufactured at GMP grade retain their immunosuppressive phenotype, including expression of CTLA-4, CD39, FoxP3 as well as liver homing chemokine receptor CXCR3 and ratio of naïve:memory. Th1 and Th17 markers including Tbet, CCR6, CD161 are not increased after expansion. Treg final product is functional, suppresses CD4 conventional cells, and exhibits TSDR demethylation-albeit with slightly reduced potency compared to Treg cells prior to expansion.

Conclusion: We have developed a robust, reproducible protocol to manufacture high quality therapeutic GMP grade Treg cells, which will be applied in our upcoming ReSolving Primary biliary cholangitis with Regulatory T cell and Interleukin-2 GMP immunotherapy (SPRING) trial. SPRING trial will deliver 1) autologous GMP-Treg cells, 2) low-dose IL-2 or 3) GMP-Treg + low dose IL-2 to PBC patients, to directly compare the efficacy and immunological changes in blood and liver tissue of these novel treatments. This platform is readily transferable to any autoimmune or autoinflammatory disease in which GMP-Treg therapy is a viable treatment option.

SAT-373

ILT2 as a biomarker of impaired natural killer cells expressing excess lipid peroxidation in patients with hepatocellular carcinoma

Toshihiro Sakata^{1,2}, Sachiyo Yoshio¹, Masaaki Mino¹, Shiori Yoshikawa¹, Taiji Yamazoe¹, Taizo Mori¹, Eiji Kakazu¹, Taketomi Akinobu², Tatsuya Kanto¹. ¹National Center for Global Health and Medicine, Japan; ²Hokkaido University, Japan
Email: toshihiro0514sakata@gmail.com

Background and aims: Overall response rates of systemic therapies against advanced hepatocellular carcinoma (HCC) remain unsatisfactory despite the introduction of immune checkpoint inhibitor (ICI) to the clinic. Thus, exploring for new immunotherapy targets is indispensable. Natural killer (NK) cells play a pivotal role in immune surveillance against hepatocellular carcinoma (HCC). We previously identified some of signature NK cell receptors in HCC patients, ILT2 as an inhibitory and NKp46 as a stimulatory receptor, respectively. We aimed to explore potential targets for immune intervention by revealing NK cell function-related phenotypes in HCC patients.

Method: We enrolled 17 HCC patients who underwent liver tumor resection. We examined peripheral NK cells (pNK) and intrahepatic NK cells from cancerous (Ca-NK) and noncancerous liver tissues (NCa-NK). To evaluate the impact of aging on NK phenotypes, we also examined pNK from 42 healthy volunteers (HVs) whose age were at a range from 21 to 82 years old. We analyzed 39 surface markers on NK

cells by mass cytometry. We separated ILT2+NKp46-, ILT2-NKp46- and NKp46+CD56dimNK cells and cultured them in the presence of K562 cells or Daudi cells as targets for cytotoxicity and ADCC assay. Cytotoxicity/ADCC assay was performed with ILT2+NKp46-CD56dimNK cells with or without anti-ILT2 neutralizing antibody or antioxidant compounds. We evaluated whether HLA-G, which is a ligand of ILT2, were expressed or not in cancerous and noncancerous liver tissues.

Results: The expression levels of activating NK cell markers, Siglec7, CD160 and NKp46, were decreased with aging. In contrast, an increasing trend with aging was observed for inhibitory receptors, ILT2, PD-1, LAG-3, Siglec10, TIGIT and KIR2DL2L3, and maturation marker CD57, respectively. In comparison of phenotypes of CD56dimNK cells between age-matched HCC patients and HVs, ILT2, CD69, CX3CR1, CD49a and CD200R in patients were significantly higher, while DNAM-1 and 2B4 were lower in HCC patients. ILT2+CD56dimNK cells, which were enriched in cancer tissue, were NKp46-negative and highly positive for C11-BODIPY581/591 as a marker of lipid peroxidation. ILT2+NKp46-CD56dimNK cells exhibited lesser capacity of cytotoxicity and ADCC compared with ILT2-NKp46- and NKp46+CD56dimNK cells, the capacity of which was partially restored by ILT2 blockade or antioxidant compounds. The level of HLA-G expression was more in cancerous liver than those in noncancerous lesions.

Conclusion: ILT2+CD56dimNK cells in the HCC liver were functionally impaired with upregulation of lipid peroxidation. ILT2 could be a biomarker of NK cells as a target for immune or antioxidant intervention in HCC patients.

SAT-374

Interplay between hepatitis B virus replication and intrahepatic expression of VISTA and TIM-3 immune checkpoint markers in chronic hepatitis B patients

Kim Thys¹, Marianne Tuefferd¹, Thomas Derenne¹, Marjolein Crabbe², Clement Laloux³, Alfonso Blazquez¹, Jeroen Aerssens¹, Cheng-Yuan Peng⁴. ¹Janssen Pharmaceutica, Translational Biomarkers Infectious Diseases, Beerse, Belgium; ²Janssen Pharmaceutica, Statistics and Decision Sciences, Beerse, Belgium; ³PharmaLex, Friedrichsdorf, Hessen, Germany; ⁴China Medical University Hospital, Taichung, China
Email: mtueffe1@its.jnj.com

Background and aims: Host immune characterization of chronic hepatitis B (CHB) patients is usually limited to an assessment of the peripheral compartment as a consequence of the challenges to access samples from the site of the viral infection, the liver. However, the routine measurement of viral and immune markers in blood (serum hepatitis B virus [HBV] DNA, hepatitis B surface antigen [HBsAg], hepatitis B e-antigen [HBeAg], and alanine aminotransferase [ALT]) to monitor disease progression may not fully capture the dynamics and relationship between the host and virus in the liver.

Method: Core liver biopsies collected from 28 treatment naïve CHB patients, 5 HBeAg positive and 23 HBeAg negative, were characterized using Nanostring GeoMx[®] Digital Spatial Profiler technology. CD45-positive cells, HBsAg-positive hepatocytes, and HBsAg-negative hepatocytes were assessed for the expression of 72 proteins, including 16 immune checkpoint markers: 10 immune checkpoint receptors (PD-1, CTLA4, LAG-3, TIM-3, VISTA, GITR, ICOS, CD27, 4-1BB, and CD40) and 6 ligands (PD-L1, PD-L2, VISTA, B7-H3, OX40L, and CD80). For each liver biopsy, pools of 100 selected cells per cell type population were analyzed as areas of interest (AOIs). Up to 24 AOIs were collected per biopsy, resulting in a total of 732 AOIs analyzed. Linear models were applied comparing markers expression between HBsAg-positive and HBsAg-negative hepatocytes on one hand, and liver protein expression association with serum viral marker on a second hand. Significant associations after multiple testing correction are reported.

Results: Of the 72 proteins, CD45RO, GZMB, and CD44 showed significantly higher expression in HBsAg-positive hepatocytes than

HBsAg-negative hepatocytes, highlighting clearly different hepatocyte activation states. Four (CD80, GITR, PD-L1, and PD-L2) of the 16 immune checkpoint markers in the panel were not detected in any of the AOIs analyzed. PD-1 was detected in CD45-positive cells, but not significantly associated with any viral marker. VISTA and TIM-3 were significantly upregulated in CD45-positive cells collected in biopsies from HBeAg-positive CHB patients, but also in HBeAg-negative patients with high HBV DNA (>20,000 IU/ml) and/or high HBsAg (>1000 IU/ml) levels (false discovery rates: VISTA <5%; TIM-3 <10%). Upregulation of CTLA-4 was observed in intrahepatic CD45-positive cells from CHB patients with high HBV DNA and/or high HBsAg. Interestingly, TIM-3 overexpression was also observed in hepatocytes from patients with high peripheral HBsAg levels and high HBV DNA. Expression of OX40L, B7-H3, and IDO-1 in hepatocytes was negatively correlated with peripheral ALT levels, while no markers in CD45 cells were significantly associated with ALT levels.

Conclusion: Multiparametric profiling of immune checkpoint and activation markers in the livers of CHB patients highlights the interrelation between the HBV replication state and the host response.

SAT-375

Kupffer cell activation enhances systemic anti-bacterial immunity

Christian Zwicker^{1,2}, Anneleen Remmerie^{1,2}, Tinne Thoné^{1,2}, Liesbet Martens^{1,2}, Bavo Vanneste^{1,2}, Fleur Parmentier^{1,2}, Christopher Anderson^{2,3}, Charlotte Scott^{1,2}. ¹Laboratory of Myeloid Cell Biology in Tissue Damage and Inflammation, VIB-UGent Center for Inflammation Research, Ghent, Belgium; ²Department of Biomedical Molecular Biology, Faculty of Science, Ghent University, Ghent, Belgium; ³Unit for Cell Clearance in Health and Disease, VIB-UGent Center for Inflammation Research, Ghent, Belgium
Email: christian.zwicker@irc.vib-ugent.be

Background and aims: Tissue resident macrophages are regarded as highly plastic cells able to rapidly respond to changes in their local microenvironment. However, we have recently shown that in a mouse model of non-alcoholic fatty liver disease Kupffer Cells (KCs), the resident macrophages of the liver, were gradually lost and did not exhibit an activated phenotyping questioning the plasticity of KCs in the liver. Given, that KCs have been proposed to have a crucial function in systemic immune surveillance, we sought to investigate whether these cells are able to respond to an acute bacterial infection.

Method: To investigate KC activation during systemic infection, we challenged mice with a sublethal dose of soluble LPS or the gram-negative pathogen *Salmonella enterica* serovar Typhimurium (S. Tm) and assessed KC fate and gene expression profiles. To manipulate the KC response to whole bacteria or purified bacterial components, we made use of the Clec4f-Cre mouse allowing KCs to be specifically targeted.

Results: Single cell RNA-sequencing and quantitative PCR revealed that KCs can mount an acute but temporally restricted pro-inflammatory response (*Il1b*, *Il6*, *Tnf* and *A20*) to free LPS peaking as early as 30 min post challenge and returning to baseline about 10 h later. Importantly, this tight regulation was crucial as mice lacking *A20* specifically in KCs (Clec4f-Cre *A20*^{fl/fl}) which are unable to regulate this response, were highly susceptible to LPS and showed severe inflammation and mortality only 6–8 h after LPS challenge. This exaggerated response enhanced KC death in Clec4f-Cre *A20*^{fl/fl} mice and just inhibiting KC death by removing RIPK3 (Clec4f-Cre × *A20*^{fl/fl} × RIPK3^{fl/fl}) could rescue KCs and significantly reduce mortality. However, while KC-specific loss of *A20* in Clec4f-Cre *A20*^{fl/fl} mice was detrimental for host survival after challenge with soluble LPS, these mice exhibited strongly reduced bacterial load in liver and spleen after infection with pathogenic *S. Tm* compared with WT controls suggesting that hyperactivated KCs may promote systemic pathogen clearance. This protective effect was associated with

increased monocyte and neutrophil infiltration in livers of Clec4f-Cre *A20*^{fl/fl} mice.

Conclusion: We show that KCs are able to respond to an acute microbial insult, however, the exact nature of this response (protective vs pathogenic) strongly depends on the stimulus. While the response to free LPS needs to be tightly controlled to prevent excessive inflammation and to ensure host survival, recognition of whole bacteria by activated KCs enhances microbicidal cell recruitment and promotes pathogen clearance. Understanding the mechanisms underlying macrophages responses to microbes and microbial components may allow us to develop novel therapeutic strategies to activate these cells specifically and thereby improve patient outcomes in infectious diseases.

SAT-376

Osteopontin serves as a potential regulator of T cell immunity in patients with hepatocellular carcinoma

Tengfei Si¹, Zhenlin Huang¹, Shirin Elizabeth Khorsandi², Wayel Jassem³, Abid Suddle³, Ragai Mitry¹, Mark J W McPhail¹, Xiaohong Huang¹, Francesca Trovato¹, Salma Mujib³, Salvatore Napoli³, Ellen Jerome³, Yun Ma¹, Nigel Heaton¹. ¹Institute of Liver Studies, King's College London, United Kingdom; ²the Roger Williams Institute of Hepatology, United Kingdom; ³King's College Hospital, United Kingdom
Email: yun.ma@kcl.ac.uk

Background and aims: Osteopontin (OPN) is a secreted acidic protein which highly expressed in patients with hepatocellular carcinoma (HCC). Its involvement in the tumour invasion and metastasis has been defined recently. In our previous study we have found that it has a close association with PD-L1 in HCC setting, but little is known about its role in regulating the host cellular immunity. Through multiple assays and *in vitro* investigation, we aimed to define the interactions between OPN and the T cell mediated anti-tumour immunity.

Method: Blood samples were collected from patients with HCC (n = 40) for peripheral blood mononuclear cells (PBMCs) and plasma collection. Hepatic mononuclear cells (HMCs) were harvested from liver perfusate (n = 5) of pre-transplant donor graft, among which T cells were further isolated for 72-hour *in vitro* culture with different concentrations of OPN (0, 1 µg/ml, 5 µg/ml, 10 µg/ml). OPN and Th1 type cytokine (IFN-γ/TNF-α) levels were measured through enzyme-linked immunosorbent assay (ELISA). Cell phenotyping was conducted using flow cytometry. In addition, patients' RNA-seq data was used to analyse the association between the expression of OPN in tumour tissues and patients' prognosis after sorafenib treatment.

Results: Higher percentages of circulating CD4^{pos}CD25^{pos}CD127^{low/neg} (p = 0.0026) and CD4^{pos}CD25^{pos}CD39^{pos} (p = 0.0004) two Tregs subsets were observed in patients with elevated plasma OPN level, whereas the number of peripheral CXCR3^{pos} CD8 T cells significantly decreased (p = 0.0002). After 72-hour *in vitro* culture, hepatic T cells from OPN-5 µg/ml group (8.724% vs 3.224%, p = 0.043) and OPN-10 µg/ml group (10.85% vs 3.224%, p = 0.0007) had higher portion of CD4^{pos}CD25^{pos} Tregs compared to OPN-0 µg/ml group. The percentage of Ki67^{pos} CD8 T cells decreased (p < 0.05) along with the increasing OPN concentrations in cell culture medium and the production of Th1 type cytokines IFN-γ (p = 0.027)/TNF-α (p = 0.0005) from T cells was also reduced with the upregulation of OPN. RNA-seq data revealed that patients with no response to sorafenib were accompanied with higher OPN expression in tumour compared to those who responded to treatment (TPM 974.7 vs 473.2, p = 0.012).

Conclusion: Overexpression of OPN could negatively regulate T cell immunity, featured by promoting the proliferation of Tregs, down-regulating the percentages of inflammatory T cells and inhibiting their ability of producing Th1 type cytokines. Targeting OPN in HCC may reverse the immunosuppression by restoring the T cell mediated anti-tumour immunity thus improving patients' prognosis.

SAT-377

Comprehensive phenotypic and molecular characterization of B lymphocytes in patients affected by intrahepatic cholangiocarcinoma

Giulia Milardi¹, Barbara Franceschini¹, Guido Costa¹, Cristiana Soldani¹, Paolo Uva², Davide Cangelosi², Barbara Cassani¹, Guido Torzilli¹, Matteo Donadon³, Ana Lleo⁴. ¹IRCCS Humanitas Research Hospital, Italy; ²IRCCS Istituto Giannina Gaslini, Italy; ³Università del Piemonte Orientale, Italy; ⁴Humanitas University, Italy
Email: giulia.milardi@st.hunimed.eu

Background and aims: Intrahepatic cholangiocarcinoma (iCCA) is a heterogeneous biliary tract cancer whose incidence is increasing worldwide. Due to the aggressive evolution of the disease, there is an urgent need for diagnostic and therapeutic alternatives. The immune infiltrate is a key component of the tumour microenvironment (TME), but remains poorly characterized, limiting development of successful immunotherapies. While there are many aspects related to T lymphocytes that are undergoing extensive studies, the effect exerted by B cells in iCCA development and progression is still controversial and no characterization has been performed. Herein, we aimed to define phenotypic and functional properties of B lymphocytes in the TME of iCCA, with the goal of finding new mechanisms important for cancer initiation and/or progression.

Methods: We used high-dimensional single-cell technologies to characterize the B-cell compartments of iCCA tissues, comparing these with their tumor-free tissues and circulating counterparts. We further performed gene expression analysis and cellular assays to define the B cell-specific role in iCCA tissues and investigate whether and how liver TME impact on B cell biology.

Results: Single-cell RNA-sequencing analysis of CD20⁺ cells in iCCA patients (n = 6) identified four main subclusters of B and revealed an up-regulation of genes involved in neutrophil degranulation, cellular response to stress, GPCR binding and a downregulation of B cell activation/inflammatory genes in intratumoral compared to adjacent non-malignant tissue; suggesting an immunosuppressive role of B cells in iCCA TME. Multicolour flow cytometry analysis of B cells isolated from iCCA patients (n = 13) highlighted a higher frequency of naïve B cells respect to the memory phenotype. A reduction in B-cell effector functions was also detected. Immunohistochemical analyses showed that B cells, when infiltrate the tumour, create cellular aggregates similar to tertiary lymphoid structures.

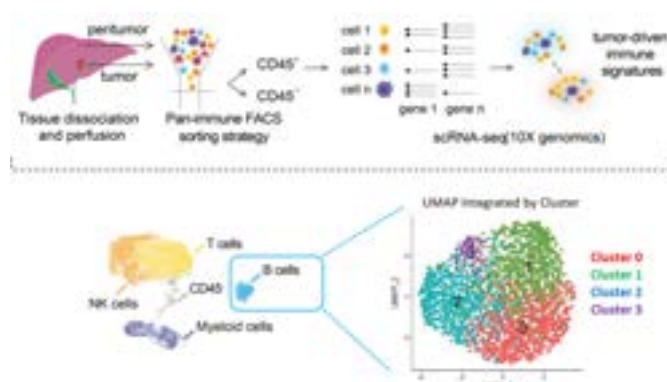


Figure: The present work was partially funded by the Associazione Italiana per la Ricerca sul Cancro (IG AIRC 2019-ID 23408 to A. Lleo).

Conclusion: Overall, these data suggest that iCCA tissue contain various B cells subtypes probably with an immunosuppressive role. However, a comprehensive characterization of B cell property, organization and crosstalk with other cells of iCCA milieu will elucidate mechanisms of tumour progression/control, exploitable for the development of novel immunotherapeutic approaches.

SAT-378

The *Ninj1*/*Dusp1* axis contributes to liver ischemia reperfusion injury by regulating macrophage activation and neutrophil infiltration

Shun Zhou¹, Yuanchang Hu¹. ¹First Affiliated Hospital of Nanjing Medical University, Hepatobiliary Center and Research Unit of Liver Transplantation and Transplant Immunology, Nanjing, China
Email: hand2399@njmu.edu.cn

Background and aims: Liver ischemia and reperfusion (IR) injury represents a major risk factor in both partial hepatectomy and liver transplantation. Nerve injury-induced protein 1 (*Ninj1*) is widely recognized as an adhesion molecule in leukocyte trafficking under inflammatory conditions, but its role in regulating innate immune during liver IR injury remains unclear.

Method: Myeloid *Ninj1* deficient mice were generated by bone marrow chimeric models using *Ninj1* knockout (KO) mice and wild type (WT) mice. In vivo, liver partial warm ischemia model was applied. Liver injury and hepatic inflammation were investigated. In vitro, primary Kupffer cells (KCs) isolated from *Ninj1* KO and WT mice were used to explore the function and mechanism of *Ninj1* in modulating KCs inflammation upon LPS stimulation.

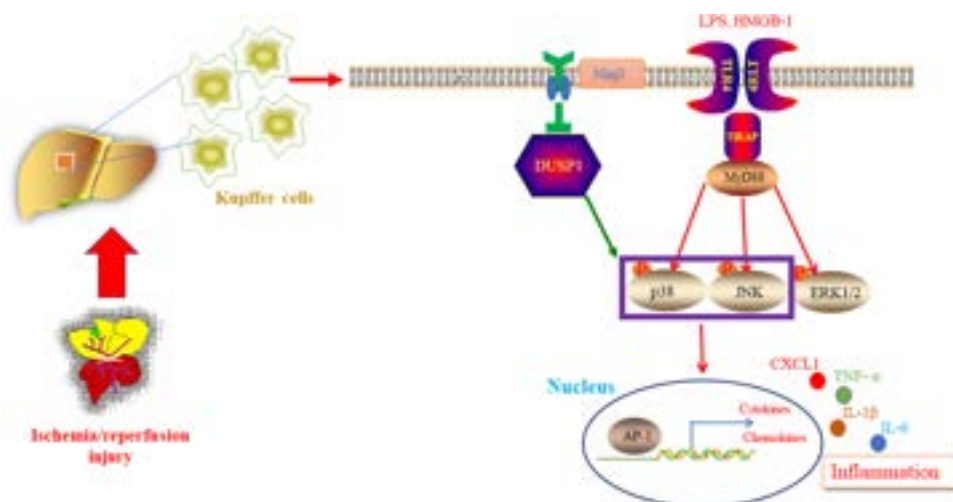


Figure: (abstract: SAT-378).

Results: Ninj1 deficiency in KCs protected mice against liver IR injury during the later phase of reperfusion, especially in neutrophil infiltration, intrahepatic inflammation, and hepatocyte apoptosis. This prompted ischemia-primed KCs to decrease proinflammatory cytokine production. In vitro and in vivo, using small interfering RNA against Dual specificity Phosphatase 1 (DUSP1), we found that Ninj1 deficiency diminished the inflammatory response in KCs and neutrophil infiltration through DUSP1-dependent deactivation of the JNK and p38 pathways. Sivelestat, a neutrophil elastase inhibitor, functioned similarly to Ninj1 deficiency, resulting in both mitigated hepatic IR injury in mice and a more rapid recovery of liver function in patients undergoing liver resection.

Conclusion: Ninj1/Dusp1 axis contributes to liver IR injury by regulating the proinflammatory response of KCs, and influences neutrophil infiltration, partly by subsequent regulation of CXCL1 production post-IR.

SAT-379

The decrease of HCV-specific neutralizing antibody responses after DAA therapy is associated with weak envelope-specific CD4 T cell immunity

Jana Gawron¹, Jill Werner¹, Lara Kelsch¹, Dorothea Bankwitz², Maike Hofmann¹, Robert Thimme¹, Thomas Pietschmann², Tobias Böttler¹. ¹University Hospital Freiburg, Department of Medicine 2, Freiburg, Germany; ²Institute for Experimental Virology, TWINCORE, Hannover, Germany
Email: jill.werner@uniklinik-freiburg.de

Background and aims: Despite the development of direct-acting antiviral agents (DAA) against hepatitis C virus (HCV) infections, the need for an effective vaccine remains. Many vaccines rely on the emergence of neutralizing antibodies (nAbs). Here, we aimed to get a more detailed understanding of the longevity and persistence of HCV-specific nAbs after DAA-mediated viral clearance and its relation to the CD4 T cell response, particularly follicular T helper cells (Tfh), targeting the HCV-envelope proteins in a longitudinal patient-based study.

Method: Neutralizing antibodies, B cells and Tfh cells were analyzed in human blood in a longitudinal cohort of 27 patients infected with HCV genotype 1a, 1b or 3a. Samples were collected before DAA therapy, at the end of therapy (EOT) and up to one year after end of therapy. HCV-specific secretion of IL-2, INF γ and IL-21 by CD4 T cells were analyzed by flow cytometry after stimulation with *in silico* predicted, genotype-matched envelope proteins. nAbs were analyzed by co-incubation of Huh 7.5 cells with patient IgGs and HCV luciferase reporter viruses. Infectivity was assessed by luminescence measurements.

Results: nAb levels remained stable with some inter-patient variability between baseline and 5-to-7-months post EOT and uniformly decreased thereafter. Longitudinal analyses of bulk B or Tfh cells revealed no changes in frequencies of these populations. Envelope-specific CD4 T cells were detectable in 87.5% of patients, with low frequencies of cytokine expressing CD4 T cells. While the frequency of IL-21 producing HCV-envelope-specific CD4 T cells correlated with the nAb response at baseline, no changes were observed in the longitudinal analysis of HCV-envelope-specific CD4 T cells after viral clearance.

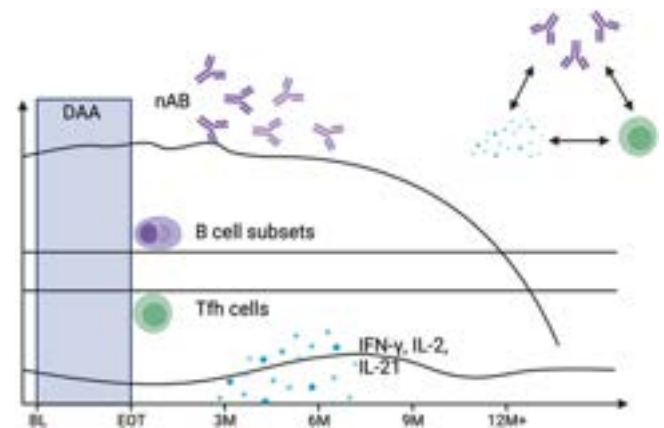


Figure:

Conclusion: A weak envelope-specific CD4 T cell response during chronic HCV infection might contribute to the failure to maintain nAb levels after DAA mediated viral clearance.

SAT-380

Epigenetic conversion of CD4⁺ T cells to stable and functioning induced regulatory T cells via cyclin-dependent kinase inhibition and CD28 signal deprivation in patients with primary biliary cholangitis

Vincenzo Ronca^{1,2,3,4,5}, Scott Davies^{1,2}, Kayani Kayani^{1,2,4}, Norihisa Mikami⁴, Masaya Arai⁴, Yamami Nakamura⁴, Natsumi Okamoto⁴, Jason White⁴, Naomi Richardson^{1,2}, Naganari Ohkura⁴, Pietro Invernizzi^{3,5}, Shimon Sagakuchi⁴, Ye Htun Oo^{1,2,5}. ¹Institute of Immunology and Immunotherapy, University of Birmingham, Birmingham, UK, United Kingdom; ²NIHR Birmingham Biomedical Research Centre, University of Birmingham and University Hospitals Birmingham NHS Foundation Trust, Birmingham, UK, United Kingdom; ³Division of Gastroenterology, Center for Autoimmune Liver Diseases, Department of Medicine and Surgery, University of Milano Bicocca, 20900 Monza, Italy, United Kingdom; ⁴Laboratory of Experimental Immunology, WPI Immunology Frontier Research Center, Osaka University, Suita, Japan, Japan; ⁵European Reference Network on Hepatological Diseases (ERN RARE-LIVER), United Kingdom
Email: v.ronca@bham.ac.uk

Background and aims: Primary biliary cholangitis (PBC), is a chronic, autoimmune liver disease. Regulatory T cells (Treg) are a subset of CD4⁺ T lymphocytes whose activity is driven by the expression of a key transcription factor, Forkhead box P3 (FOXP3). A reduction in Treg frequency and functionality has been proposed as an underlying pathogenic mechanism of PBC. We aimed to characterise the natural Treg (nTreg) epigenetic profile in PBC patients. Additionally, we set out to induce functional and stable Treg cells (SF-iTregs) from PBC-derived effector CD4 cells in vitro, via cyclin-dependent kinase (CDK8/19) inhibition.

Method: CD4⁺ T cells were magnetically enriched from peripheral blood mononuclear cells (PBMCs) of PBC patients. CD4⁺T cells were activated by CD3⁺ activator beads and TCR stimulation without CD28 co-stimulatory signal, and cultured in presence of IL-2 and AS2863619 (CDK8/19 inhibitor). FoxP3, CTLA4 and Helios expression of SF-iTregs was assessed via flow cytometry and by bisulphite sequencing pre- and post-activation in presence of Th1 polarising cytokines. nTregs and SF-iTregs suppressive function was investigated by measuring CellTrace Violet dye-labelled effector T-cells proliferation co-culturing them with SF-iTregs at different dilution. nTregs and SF-iTregs Foxp3 gene locus for STAT5 binding, H3K27ac, and chromatin status was characterized by Chromatin immunoprecipitation followed by sequencing (ChIP-seq) and assay for transposase-accessible Chromatin sequencing (ATAC-seq).

Results: Deprivation of CD28 signal and chemical inhibition of cyclin-dependent kinase 8/19 of CD4 T cells is instrumental to induce DNA hypomethylation in Treg signature genes. Our protocol allowed us to obtain above 90% of FOXP3 expressing cells with a 100-fold increase in the cell number over 2 weeks. ATAC-seq and ChIP-seq confirmed that Treg specific epigenetic changes in the SF-iTregs were comparable to nTreg at the baseline. To resemble the liver inflammatory environment of PBC, we cultured nTreg and SF-iTregs in Th1-conditioned media containing IL-12 and IFN- γ for 6 days, demonstrating a better lineage stability in SF-iTregs compared with nTregs. In addition, SFiTreg maintain suppressive function in inflamed environment.

Conclusion: We apply a novel technique to generate abundant, functional induced regulatory T cells from peripheral conventional CD4+T cells in patients with primary biliary cholangitis. This approach would facilitate the production on a large scale of phenotypically stable, functional induced Tregs from antigen-experienced disease-mediating T cells to apply as GMP cellular therapy in PBC.

SAT-381

Intermediate monocytes and associated chemokines allow differentiation of idiosyncratic drug-induced liver injury (DILI) and autoimmune hepatitis (AIH)

Stuart Astbury¹, Edmond Atallah¹, Amber Bozward², Natalia Krajewska^{2,3}, Grace Wootton², Jane I. Grove¹, Ye Htun Oo², Guruprasad Aithal¹. ¹University of Nottingham, Nottingham Digestive Diseases Centre, Nottingham, United Kingdom; ²University of Birmingham, United Kingdom; ³University of Würzburg, Germany
Email: stuart.astbury@nottingham.ac.uk

Background and aims: About 30% of AIH cases can present acutely and up to 9% of DILI cases share clinical, serological, and histological features with AIH. Distinguishing patients with DILI from AIH is of critical importance as the management of these two conditions differs substantially. Characterising different immune cell types may reveal different mechanisms underlying these conditions. These may have a clinical application as biomarkers to differentiate both types of liver injury.

Method: Patients with acute liver injury were enrolled prospectively. Following adjudication by an independent panel, patients were assigned to DILI (n = 13) or AIH (n = 6) groups according to criteria set by the DILI International Expert Working Group or International AIH Group respectively. These were compared with age-matched controls (n = 20).

Patients were sampled at time of liver injury, all AIH cases were steroid naive. Whole blood was stained using the Maxpar Direct Immune Profiling assay and analysed using a Helios mass cytometer. FlowSOM was used to identify cell populations from the 30 antibody panel, with monocyte clusters defined according to existing criteria of classical (CD14++CD16-), intermediate (CD14++CD16+) and non-classical (CD14+CD16++). The diffcyt R package was used to make pairwise comparisons between groups, with all p values adjusted for multiple comparisons.

Inflammatory cytokines were measured in plasma using the Human ProcartaPlex 20-plex Inflammation panel. Cytokines were compared between groups and correlated with immune cell subsets.

Results: We observed a significant decrease in classical monocyte frequency in AIH compared to both DILI and healthy controls (adjusted p < 0.001). Intermediate monocytes were significantly increased in AIH compared to DILI. Plasma CCL2 was negatively correlated with classical monocytes (Rho = -0.46, p = 0.04) and positively correlated with intermediate monocytes (Rho = 0.5, p = 0.028). Plasma CCL2, CCL3, CCL8, CXCL10, TNF- α and IL-17A were significantly increased in AIH compared to DILI.

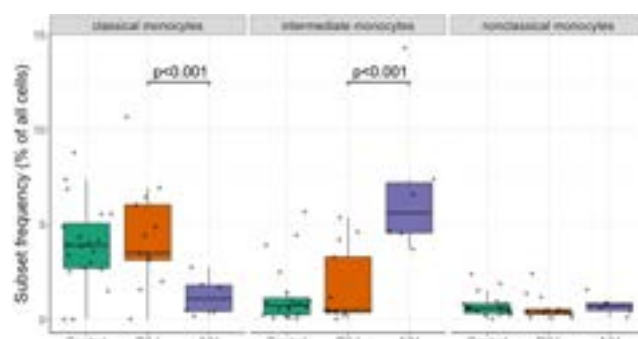


Figure:

Conclusion: Our results indicate the potential use of monocyte subtypes as a marker to distinguish between DILI and AIH. The significant increase in intermediate monocytes and monocyte chemoattractant protein 1 (MCP1/CCL2), MCP2/CCL8, monocyte inflammatory protein α (MIP-1 α /CCL3), and hepatic homing chemokine CXCL10 highlight the role of intermediate monocytes as mediators of liver injury in acute AIH compared to DILI. The significant increases in proinflammatory cytokines: TNF- α and IL-17 indicate that both Th1/Th17 adaptive immune pathways are involved. Hepatic inflammation in idiosyncratic DILI is characterised by a Th1 dominant mechanism compared to AIH. Further work with liver infiltrating monocytes is required to dissect the innate and adaptive immune crosstalk in the pathogenesis of both diseases.

SAT-382

TIGIT inhibits the cytotoxic effects of NK cells towards biliary epithelial cells in autoimmune hepatitis

Amber Bozward^{1,2,3,4}, Rémi Fiancette^{1,2}, Scott Davies^{1,2}, Grace Wootton^{1,2,3,4}, Ye Htun Oo^{1,2,3,4}. ¹University of Birmingham, Institute of Immunology and Immunotherapy, Birmingham, United Kingdom; ²NIHR Birmingham Biomedical Research Centre, University of Birmingham, Birmingham, United Kingdom; ³Centre for Rare Diseases, European Reference Network on Hepatological Diseases (ERN RARE-LIVER) Centre, Birmingham, United Kingdom; ⁴Birmingham Advanced Cellular Therapy Facility, University of Birmingham, Birmingham, United Kingdom

Email: a.g.bozward@bham.ac.uk

Background and aims: Natural killer (NK) cells play an important role in autoimmune hepatitis (AIH) and are enriched in the liver, accounting for 25–40% of total intrahepatic lymphocytes. The interaction of checkpoint inhibitor, TIGIT, with its ligands, CD155 and CD112, has been shown to inhibit NK cytotoxicity in an oncological environment. However, little is known regarding the role of TIGIT⁺NK cells in autoimmune hepatitis.

Method: TIGIT⁺NK cell phenotype was investigated using 16 colour flow cytometry analysis of peripheral blood mononuclear cells (AIH = 12, PBC = 5, PSC = 2, NASH = 2, ALD = 1, healthy volunteers = 10) and liver infiltrating lymphocytes (PBC = 2, AIH/PSC/PVT = 1, AIH = 1, NASH = 1, ALD = 2, non-cirrhotic donor = 4). Immunohistochemistry was applied to investigate localisation of NK cells in explanted liver tissue. Coculture experiments were performed with peripheral blood TIGIT⁺NK cells from AIH patients with either biliary epithelial cells (BEC) isolated from explant livers or sorted dendritic cells (DCs) and monocytes.

Results: NK cells were significantly upregulated in diseased livers compared to AIH blood (p = < 0.0001). Immunohistochemistry staining demonstrated that CD56⁺NK cells localise around the bile ducts and hepatocytes in AIH. TIGIT expression in AIH liver also localised around bile ducts and hepatocytes. TIGIT ligand CD112 is expressed on both hepatocytes and BEC and the other TIGIT ligand, CD155 is expressed predominantly on hepatocytes. Flow cytometry staining demonstrated that TIGIT⁺NK cells in AIH patients express liver homing chemokine receptor, CXCR3 (7.53% \pm 22.18), biliary homing

chemokine receptor, CCR6 ($10.95\% \pm 65.45$) and integrin, VLA-4 ($56.15\% \pm 59.52$). These cells also expressed tissue residency marker CD69 ($13.48\% \pm 52.92$). Coculturing co-inhibitory TIGIT⁺NK cells with BEC did not lead to apoptosis/necrosis of BEC, despite their expression of cytotoxic molecules (granzymes A, B, K, perforin). Intrahepatic DC's and monocytes in AIH also express TIGIT ligands, CD112 and CD155; within DC's this expression was predominantly on myeloid DCs ($p < 0.0001$ and $p = 0.0096$ respectively compared to pDCs). Coculturing TIGIT⁺NK cells with DCs and monocytes could mount a bi-directional T cell and antigen presenting cell immune response in both subsets.

Conclusion: We have shown that TIGIT⁺NK cells are present in AIH liver. We also demonstrated the localisation of TIGIT ligands CD112 and CD155 in AIH livers. TIGIT⁺NK cells express liver homing, biliary homing, and tissue resident phenotype. Our results indicate that TIGIT⁺NK cells lack cytotoxicity towards biliary epithelial cells and could mount a tolerogenic immune response in AIH. TIGIT⁺NK cells therefore may contribute to resolving inflammation in AIH.

SAT-383

Liver sinusoidal scavenger cells eliminate betaherpesvirus from the blood stream

Anett Kristin Larsen¹, Javier Sánchez Romano¹, Jaione Simón-Santamaria¹, Kim Erlend Mortensen², Ingelin Kyrrestad¹, Eirik Lænsman¹, Anne-Lotte Vada Hatlegjerde¹, Bård Smedsrød¹, Hans Hirsch³, Christine Hanssen Rinaldo⁴, Peter McCourt¹, Karen Kristine Sørensen¹. ¹UiT The Arctic University of Norway, Department of Medical Biology, Norway; ²University Hospital of North Norway, Department of Gastrointestinal Surgery, Norway; ³University of Basel, Department Biomedicine Transplantation and Clinical Virology, Switzerland; ⁴University Hospital of North Norway, Department of Microbiology and Infection Control, Norway
Email: anett.k.larsen@uit.no

Background and aims: The liver sinusoidal endothelial cells (LSECs) are pivotal as scavengers of circulating large molecules and nanoparticles. Hence, we hypothesize that LSECs, in collaboration with Kupffer cells, are key contributors to the cellular arm of the anti-viral innate immune system as virus scavengers. Most viruses taken up by LSECs will likely be eliminated through the effective degradative endolysosomal apparatus, but some viruses may escape. Murine LSECs have been shown to serve as a latent reservoir for murine betaherpesvirus (MuHV-1), but the permissivity of these specialized endothelial cells is less clear with regards to human betaherpesvirus 5 (HHV-5). The aim of this study was to reveal the role of the liver in blood clearance of betaherpesviruses, determine the capability of LSECs to scavenge larger enveloped viral particles, and investigate cellular effects following viral internalization. In addition, we compared if LSECs handle host-pathogenic viruses and similar non-pathogenic viruses differently.

Method: Murine models (C57Bl/6) were used to investigate blood clearance and organ distribution of HHV-5 and MuHV-1. Furthermore, liver tissue was obtained from patients undergoing hepatic resections. LSECs were isolated from the non-parenchymal liver cell fraction using MACS Microbeads, challenged with viruses, immunolabelled and imaged using different microscopy techniques. Primary LSECs of human and murine origin were used to investigate cellular uptake mechanisms, intracellular transport of endocytosed virus, susceptibility to infection as well as immune responses following viral challenge.

Results: HHV-5 and MuHV-1 were efficiently cleared from blood within 30 min in the mouse model and high uptake of viral particles in liver and spleen was confirmed. Association of HHV-5 with fenestrated human LSECs was verified using super-resolution light microscopy (see figure), whereas internalization of viral particles was confirmed using transmission electron microscopy. Internalized viruses colocalized with LAMP-1 positive structures already at 2 h post challenge. Early and late viral proteins were detected 24 and 72 h

post challenge, respectively. Secretion of the cytokines TNFalpha and IL-6 following challenge with MuHV-1 was superior to levels detected following HHV-5-challenge in the murine model system. The latter confirmed that LSECs are capable of internalizing and degrading non-pathogenic viruses without eliciting an immune reaction.

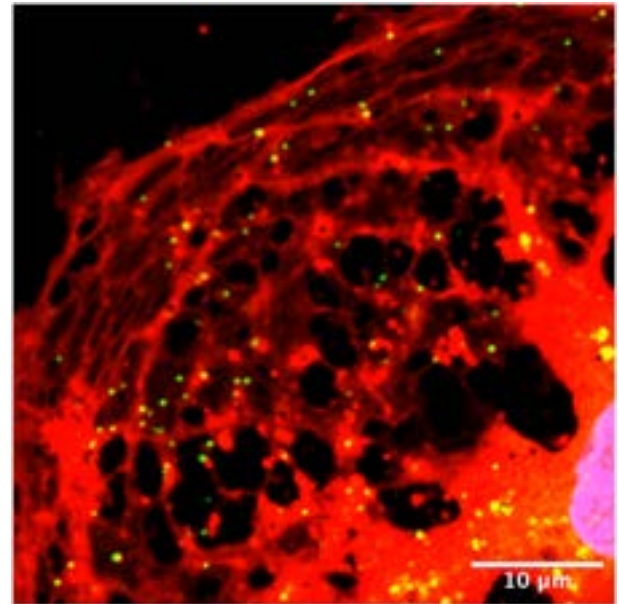


Figure:

Conclusion: The presented work confirms the essential role of the liver in elimination of betaherpesviruses from the circulation, with shared viral scavenging between LSECs and Kupffer cells. Human LSEC are permissive for HHV-5 infection, introducing the possibility of these cells contributing to latency.

SAT-384

Immune characterization of the melanocortin-4-receptor mouse model for non-alcoholic steatohepatitis using mass cytometry and imaging mass cytometry

Fabienne Birrer¹, Tess Brodie¹, Tural Yarahmadov¹, Deborah Stroka¹. ¹University of Bern, Inselspital, Bern University Hospital, Department of Visceral Surgery and Medicine, Bern, Switzerland
Email: fabienne.birrer@unibe.ch

Background and aims: Dysregulated liver immune responses are critical in liver diseases, including non-alcoholic fatty liver disease (NAFLD), non-alcoholic steatohepatitis (NASH) and cirrhosis. Histological features of NASH are liver steatosis, inflammation, hepatocyte ballooning and fibrosis. There are many animal models used to study NAFLD and NASH, which are either genetically modified, chemically- or diet induced. The melanocortin-4-receptor knock out (MC4R-KO) mouse fed a western type diet (WD) is one of the models with the highest similarities to human NASH. However, the model was established only in 2019 and characterization, especially immune cell characterization, is not completed yet. Mass cytometry (MC) is a well-established method to phenotype cells in suspension by labelling them with metal tagged antibodies. Imaging mass cytometry (IMC) is a new high multiplexing imaging technology that provides complex cellular phenotyping on single cell level and interrelationships in spatial context at the same time. In this project, we aim to better characterize the MC4R NASH mouse model and describe a specific immune profile found during disease progression by using MC for phenotyping cells in suspension and IMC for cell localization and community building.

Method: We used the MC4R-KO mouse model to study NAFLD and NASH. MC4R-KO and wild-type mice were fed either a WD or normal

diet for 25 weeks. By immunohistochemistry stainings (IHC), we characterized liver tissue using the following parameters: micro- and macro vesicular steatosis (oil red and haematoxylin/eosin (HE)); fibrosis (sirius red; score 0–4); hepatocyte ballooning and Mallory–Denk bodies (HE; yes/no); inflammation (HE; degree 0–2); hepatic crown-like structures (hCLS) HE; counts per 20x visual field). Parameters were scored by a pathologist. The immune cell composition was assessed in the liver and spleen, using a 32 target MC panel. To characterize the immune cell distribution in the liver, we used a 20 target IHC antibody panel in mouse formalin fixed paraffin embedded tissues.

Results: To define the liver condition of our experimental groups, we assessed the main parameters used for clinical diagnosis in patients. The livers of MC4R-KO mice on a WD had massive steatosis, fibrosis, inflammation and hepatocyte ballooning. There were hCLS in all MC4R-KO WD livers. The MC4R-KO on normal diet only exhibited massive steatosis but no other signs of NASH. The identified immune populations were B-cells, T-cell subsets, NK cells, infiltrated and liver resident myeloid cells, neutrophils and liver sinusoidal endothelial cells. There were several differences between controls, NAFLD and NASH in immune cell numbers in liver and spleen samples. The spatial distribution of immune cells in the livers of NAFLD and NASH mice by IHC showed structural and cell population differences between conditions.

Conclusion: Previously, the MC4R-KO mouse model has been described as a model that closely resembles human NASH. With our data, we can confirm that this model leads to the following conditions: healthy control group (WT on normal diet), NAFLD (MC4R-KO on normal diet) and NASH (MC4R-KO on WD). With this data we can study the immune cell changes during disease progression. Additionally, IHC data provides information about immune cell localization during disease progression. This helps to understand tissue architecture and cell communications in the liver, as well as important cell contributions in diseased states.

SAT-385

The effect of testosterone on human T cells in health and autoimmune liver disease

Lara Henze¹, Stephanie Stein¹, Jasper Meyer¹, Tobias Poch¹, Jenny Krause¹, Christian Casar^{1,2}, Dakyung Lee¹, Johannes Fuß^{3,4}, Thomas Renne⁵, Dorothee Schwinge¹, Christoph Schramm^{1,6,7}.
¹University Medical Center Hamburg-Eppendorf, I. Department of Medicine, Germany; ²University Medical Center Hamburg-Eppendorf, Bioinformatics Core, Germany; ³University of Duisburg-Essen, Institute of Forensic Psychiatry and Sex Research, Germany; ⁴University Medical Center Hamburg-Eppendorf, Institute for Sex Research, Sexual Medicine and Forensic Psychiatry, Germany; ⁵University Medical Center Hamburg-Eppendorf, Institute for Clinical Chemistry and Laboratory Medicine, Germany; ⁶University Medical Center Hamburg-Eppendorf, Hamburg, Hamburg Center for Translational Immunology, Germany; ⁷University Medical Center Hamburg-Eppendorf, Martin Zeitz Centre for Rare Diseases, Germany
 Email: la.henze@uke.de

Background and aims: Females are more prone to develop autoimmune diseases, including primary biliary cholangitis (PBC). The underlying mechanisms are still unknown. We here aimed to unravel the effects of testosterone on T cell phenotype and function, and how this may contribute to the pathogenesis of PBC.

Method: Two unique clinical cohorts were analyzed: I) Female and male individuals with PBC compared to age and sex matched healthy controls and II) transgender men receiving gender-affirming testosterone treatment. *Ex vivo* multi-color flow cytometry, *in vitro*

conversion assays and CITE-single cell sequencing were used to characterize T cells and to identify changes upon *in vivo* testosterone treatment.

Results: Immunophenotyping revealed increased TH1 cell numbers and reduced Tregs to TH17 cell ratio in female individuals with PBC compared to healthy controls. The shift towards pro-inflammatory immune responses was supported by significant increase of *in vitro* TH1 conversion rates in female individuals with PBC. Importantly, female people with PBC presented with lower serum testosterone levels compared to healthy female age matched controls. Reduced TNF α and IFN γ release by testosterone treated T cells confirmed a direct effect of testosterone on immune cell regulation. Moreover, we analyzed single cell T cell transcriptomes in the transgender cohort after high dose *in vivo* testosterone treatment and identified significant changes in CD4 as well as CD8 T cell subset composition.

Conclusion: Together these data suggest that testosterone has a regulatory effect on T cells in health and autoimmunity and that this may contribute to the pathogenesis of PBC.

SAT-386

CXCL9 does not ameliorate murine macrophage activation syndrome hepatitis

Tamir Diamond^{1,2}, Michelle Lau², Jeremy Morrisette³, Niansheng Chu², Edward Behrens^{1,2}. ¹University of Pennsylvania, Pediatrics, Philadelphia, United States; ²Children's Hospital of Philadelphia, Pediatrics, Philadelphia, United States; ³University of Pennsylvania, Immunology, United States
 Email: diamondt@chop.edu

Background and aims: Macrophage activation syndrome (MAS) is a cytokine storm syndrome characterized by systemic inflammation, multiorgan dysfunction and hepatitis. It is a known cause for liver failure in pediatric population. Interferon gamma (IFN γ) is a main mediator of disease in MAS. Its downstream Chemokine (C-X-C motif) ligand 9 (CXCL9) is a clinically established biomarker to measure disease activity. In previous published studies of murine MAS-like disease model through TLR9 stimulation by CpG DNA as well as human clinical data showed correlation of CXCL9 levels to hepatitis. However, its biological role in pathogenesis of MAS-hepatitis through its leukocyte receptor C-X-C motif chemokine receptor 3 (CXCR3) has not been studied to date. This study aimed to determine this relationship using a *cxcl9*^{-/-} (cxcl9 KO) murine model of MAS.

Method: MAS was induced in *cxcl9* KO and WT C57BL/6 mice using established method of repeated TLR9 stimulation by CpG (50mcg) on days 0, 2, 4, 7 and 9 with sacrifice at day 10. Immunopathology was assessed in various methods: (1) Peripheral blood samples to assess for cytopenia were collected on day 0 and sacrifice. (2) Serum was collected at sacrifice to measure alanine aminotransferase and serum cytokines (INF γ , Ferritin and sIL2r). (3) Spleen and liver leukocytes were extracted using established methods to assess the hepatic inflammatory milieu. (4) Livers were fixed in 4% formalin for 24 hours and stained with haematoxylin and eosin for histological review.

Results: MAS features developed in both *cxcl9*-ko and WT groups with anemia, leukopenia, lymphopenia, hepatosplenomegaly, elevated sIL2r and ferritin. Features of MAS such as weight loss, splenomegaly, serum ferritin, sIL2r did not differ between groups. Mice from *cxcl9*-ko group had significantly larger livers (Fig 1A) but comparable serum ALT (Fig 1B). There was no significant difference in degree of hepatitis histologically or in hepatic leukocyte count by flow cytometry. *Cxcl9*-ko resulted in larger percentage of hepatic T-cells with reduction in NK cells and trend towards reduction in inflammatory monocytes (figure 1C). However, expression of CXCR3+

on these populations did not differ in these groups (figure 1D) suggesting alternative mechanism of hepatic immune recruitment in MAS-hepatitis.

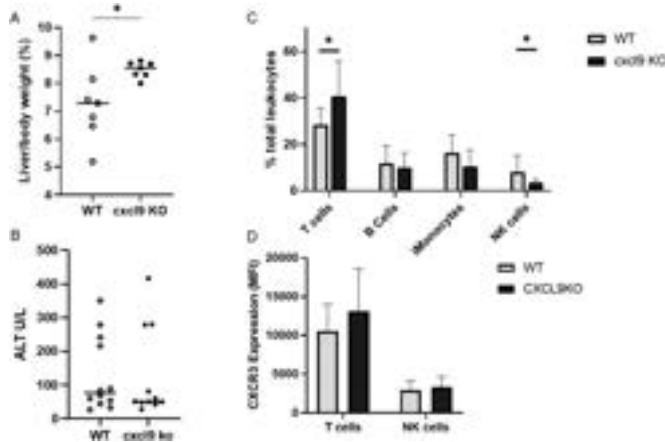


Figure:

Conclusion: Cxcl9 deficiency does not alter phenotype of hepatitis in murine model of MAS. Evaluation of alternative pathways of immune recruitment in MAS-hepatitis should be investigated. Cxcl9 is a useful biomarker to monitor IFN γ activity but is unlikely to be a therapeutic target for MAS-hepatitis.

SAT-387

Characterisation of invariant natural killer T cells in human hepatic biopsies

Elena Jiménez-Martí^{1,2}, Maria Aguilar Ballester², Gema Hurtado-Genovés², Luis Sabater Ortí^{2,3}, Marina Garcés Albir⁴, Dimitri Dorcaratto⁴, Sergio Martínez-Hervás^{5,6,7}, Herminia González-Navarro^{1,2,7}. ¹University of Valencia, Biochemistry and Molecular Biology, Valencia, Spain; ²INCLIVA Institut d'Investigació Sanitària, Valencia, Spain; ³Hospital Clínic Universitari, Department of Surgery, Valencia, Spain; ⁴Hepatobiliary and Pancreatic Unit, General and Digestive Surgery Department, Valencia, Spain; ⁵Hospital Clínic Universitari, Servicio de Endocrinología y Nutrición, Valencia, Spain; ⁶University of Valencia, Departamento de Medicina, Valencia, Spain; ⁷CIBER de Diabetes y Enfermedades Metabólicas asociadas (CIBERDEM), Spain
Email: herminia.gonzalez@uv.es

Background and aims: Previous studies in human and mouse models have shown discrepant effects of hepatic NKT sublineages in complications associated with metabolic dysfunction-associated liver disease (MALD). In the present investigation the characterization of iNKT sublineages were done in human hepatic samples from patients undergoing surgical procedures for hepatic tumor or cyst resection.

Method: Human hepatic biopsies from patients were obtained from the Hospital Clínic Universitario de Valencia. Other relevant clinical data was also collected. Patients were grouped in low and high hepatic triglyceride (TG)-content groups for comparisons. Hepatic analysis consisted of collagen percentage area with Masson trichrome stained cross-sections, and TG content by a biochemical in vitro assay and determination of NAS score determined in Hematoxylin-Eosin stained cross-sections. Resident hepatic NKT subtypes in fresh samples were analyzed by flow cytometry using different markers for detection of NKT subsets including nNKT and iNKT and additional markers to define and analyse iNKT1, iNKT2, iNKT17 and iNKTreg. Gene expression analysis of different fibrosis and cancer markers was

performed by RT-qPCR and data was relativised to low TG-content patient group.

Results: Consistently, increased classic NAS score, glucose levels and BMI were observed in the high TG-content patient group compared with low TG-content patients consistent with an augmented MALD. By contrary collagen was reduced in patients with high hepatic TG content. Interestingly, TG content was inversely correlated with the intrahepatic CD3⁺ CD56⁺ NKT cells percentage. No significant differences were observed in NK and NKT cells between patients with low and high TG content. Likewise, similar levels were observed in the percentages of iNKTreg (CD3⁺ Va18J24⁺ Foxp3⁺ Tbet⁻), iNKT1 (CD3⁺ Va18J24⁺ Tbet⁺ PLZF⁺ ROR⁻), iNKT2 (CD3⁺ Va18J24⁺ Tbet⁻ PLZF⁺ ROR⁺) and iNKT17 (CD3⁺ Va18J24⁺ Tbet⁻ PLZF⁺ ROR⁺) between patients' groups but iNKT17 and iNKT2 were discretely decreased. Gene expression analysis of genes related with fibrosis including MMP9, COL1A1, TIMP1 and ACTA2 were similar between patients' groups but SOX9, was significantly enhanced in patients with high TG content.

Conclusion: The present data indicate that patients with exhibiting augmented MALD, display increased SOX9 expression and a mild no significant decrease in iNKT17 and iNKT2. In addition, the inverse correlation between intrahepatic CD3⁺ CD56⁺ NKT and intrahepatic TG accumulation suggest a protective role of NKT in advanced hepatic diseased patients.

SAT-388

Mast cell activation index as a novel prognostic marker in a pan-analysis of gastrointestinal cancers

Nataliya Rohr-Udilova¹, Matthias Pinter¹, Erika Jensen-Jarolim^{2,3}, Michael Trauner¹, Rodolfo Bianchini^{2,3}. ¹Medical University of Vienna, Internal Medicine III, Gastroenterology and Hepatology, Wien, Austria; ²Institute of Pathophysiology and Allergy Research, Center of Pathophysiology, Infectiology and Immunology, Wien, Austria; ³The Interuniversity Messerli Research Institute, University of Veterinary Medicine Vienna, Medical University of Vienna, University of Vienna, Comparative Medicine, Vienna, Austria
Email: nataliya.rohr-udilova@meduniwien.ac.at

Background and aims: Mast cells are key components of the allergic response, as they release mediators and cytokines when activated due to allergen binding. There is growing evidence supporting the role of mast cell activation in cancer, thus contributing to the novel field of Allergooncology. Machine learning algorithms can be used to quantify bulk gene expression data from tumours, including activated and resting mast cells (1, 2). Drawing from the preceding data on liver cancer, we hypothesized that mast cells could play a special role in the development of gastrointestinal cancers in general. To this end, we propose a novel marker, the mast cell activation index (MCAI), to evaluate the role of mast cells in GI cancers.

Method: Gene expression data from 1675 patients with GI cancers, including hepatocellular carcinoma, cholangiocarcinoma, esophageal carcinoma and adenocarcinomas of the pancreas, rectum, stomach and colon (TCGA), were evaluated using a machine learning algorithm (1) and compared to 7673 patients with non-GI cancers (2). The mast cell activation index (MCAI) was calculated as a ratio of activated mast cells to total mast cells. Based on the MCAI value, patients were stratified into three groups: i) MCAI = 0 (low, n = 712, zero mast cell activation), ii) 0 < MCAI < 1 (medium, n = 168, partial activation) and iii) MCAI = 1 (high, n = 795, full activation). The results were correlated with clinical characteristics such as overall survival (OS) and progression-free survival (PFS) using the Log-Rank Mantel-Cox test.

Results: Mast cell activation was found to be a favorable prognostic marker for GI cancers. The median PFS was 3 times longer in the high

POSTER PRESENTATIONS

MCAI group compared to the low MCAI group, with the medium MCAI group being in between (Low: 644 d, 95%CI 504–783 d; Medium: 1003 d, 95% CI 545–1460 d; High: 1929 d, 95% CI 1317–2540 d, $p < 0.0001$, Fig. 1A). The differences in OS were much less pronounced (Low: 1372 d, 95%CI 1162–1581 d; Medium: 2532 d, 95% CI 653–4411 d; High: 1849 d, 95% CI 1478–2220 d, $p = 0.03$, Fig. 1B). In contrast, a high MCAI was associated with worse OS and PFS outcomes in non-GI cancers ($p < 0.0001$, Fig. 1C, D).

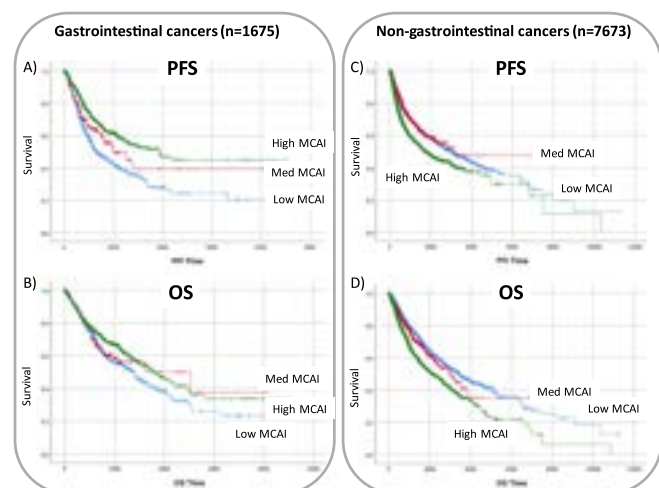


Figure 1: Kaplan-Meier survival curves of cancer patients stratified according to the intratumoral mast cell activation index (MCAI).

Conclusion: Our pan-analysis of seven gastrointestinal cancers using a novel marker-mast cell activation index (MCAI)-showed that gastrointestinal tumour patients with fully active mast cells had a longer progression-free survival. This suggests that mast cell activation has a protective effect in GI cancers and merits further exploration. It is possible that mast cells may offer new therapeutic opportunities for treating gastrointestinal tumours.

References

1. Newman AM, Liu CL, Green MR *et al.* *Nat Meth* 2015; 12: 453–457.
2. Thorsson V, Gibbs DL, Brown SD *et al.* *Immunity*. 2018 Apr 17;48 (4):812–830.

SAT-389

The ascitic environment in cirrhosis upregulates the expression of the immune checkpoint CD155 on peritoneal macrophages

Joseph Delo^{1,2}, Daniel Forton^{1,2}, Evangelos Triantafyllou³, Arjuna Singanayagam^{1,2}. ¹St George's University of London, United Kingdom; ²St George's Hospital, United Kingdom; ³Imperial College London, United Kingdom

Email: joseph.delo@gmail.com

Background and aims: Peritoneal macrophages from the ascites of patients with decompensated cirrhosis (DC) are known to have impaired phagocytic and anti-microbial function. This is most profound in those with accompanying organ-failure (acute-on-chronic liver failure; ACLF). CD155 (poliovirus receptor) binds the inhibitory receptors TIGIT and CD96 on T cells and NK cells. CD155 on macrophages can mediate a transition to an M2-like, immunosuppressive, phenotype in tumour-associated macrophages. It has also been shown, in the context of other chronic diseases, to impair macrophage ability to activate T cells during antigen-presentation. A soluble form of CD155 is also produced by cells, which can inhibit NK cells. We hypothesised that peritoneal macrophages from patients with DC would express more CD155, and that this might be a result of chronic exposure to bacterial products translocating from the gut into the ascites.

Method: Peripheral blood mononuclear cells (PBMC) and peritoneal mononuclear cells from patients with DC ($n = 11$) were assessed for

surface expression of CD155 on monocytes or macrophages by flow cytometry analysis. Peritoneal cells from patients with end-stage renal disease undergoing Continuous Ambulatory Peritoneal Dialysis (CAPD) were used as a control ($n = 5$). The concentration of soluble CD155 in ascitic fluid from DC patients, with or without ACLF, was determined by ELISA. Healthy control PBMCs were cultured in ascites, or in media with various Toll-Like Receptor (TLR) agonists, for 48 hours, and the surface expression of CD155 assessed.

Results: More peritoneal CD14+CD16- macrophages from the ascites of patients with DC expressed CD155 than those from CAPD controls (58.64 versus 26.09%, $p = 0.0365$, figure A). The concentration of soluble CD155 in ascites was higher in patients with ACLF compared to those without ACLF. Patients with DC had higher levels of CD155 on their peritoneal macrophages compared to their peripheral monocytes, indicating that the ascitic environment may influence CD155 expression. Indeed, culturing healthy PBMCs with ACLF ascites upregulated monocyte CD155 expression more than culture media alone or non-ACLF ascites ($p = 0.0245$, figure B). Similar upregulation of CD155 on monocytes was seen after culturing healthy PBMCs with lipopolysaccharide (LPS; a TLR-4 agonist).

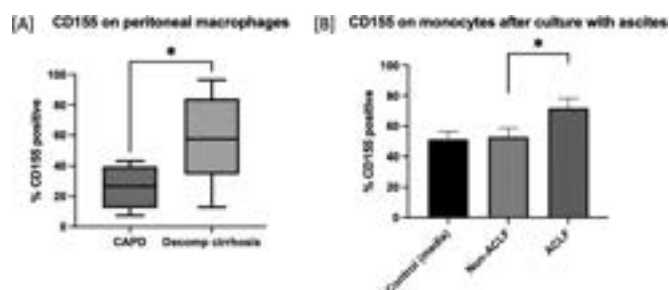


Figure:

Conclusion: The high expression of CD155 on peritoneal macrophages from patients with decompensated cirrhosis might in part explain their immunosuppressive phenotype and why patients are so susceptible to spontaneous bacterial peritonitis. This increase in CD155 expression is particular to the peritoneum, and not seen in the periphery, and can be induced by exposure to ascites and LPS, suggesting that bacterial translocation may be responsible.

SAT-390

Distinct immunometabolic signatures in circulating immune cells define disease outcomes in acute-on-chronic liver failure

Rita Furtado Feio de Azevedo¹, Markus Boesch¹, Silvia Radenkovic^{1,2,3,4}, Marie Wallays¹, Lukas Van Melkebeke^{1,5}, Bram Boeckx^{6,7}, Gino Philips^{6,7}, Lena Smets¹, Wim Laleman^{1,5}, Philippe Meersseman⁸, Alexander Wilmer⁸, David Cassiman^{1,3}, Hannah Van Malenstein^{1,5}, Joan Clària⁹, Frederik Nevens^{1,1,5}, Jef Verbeek^{1,5}, Richard Moreau¹⁰, Vicente Arroyo¹¹, Dieter Lambrechts^{6,7}, Bart Ghesquière^{3,4}, Hannelie Korf¹, Schalk van der Merwe^{1,5}. ¹Laboratory Hepatology, KU Leuven, CHROMETA Department, Leuven, Belgium; ²Mayo Clinic, Department of Clinical Genomics, Rochester, United States; ³VIB Center for Cancer Biology, Metabolomics Expertise Center, Leuven, Belgium; ⁴KU Leuven, Metabolomics Expertise Center, Department of Oncology, Leuven, Belgium; ⁵UZ Leuven, Department of Gastroenterology and Hepatology, Leuven, Belgium; ⁶VIB Center for Cancer Biology, Department of Human Genetics, Leuven, Belgium; ⁷KU Leuven, Laboratory for Translational Genetics, Department of Human Genetics, Leuven, Belgium; ⁸UZ Leuven, Department of Internal Medicine, Leuven, Belgium; ⁹Universitat de Barcelona, Hospital Clínic-IDIBAPS, CIBERehd, Barcelona, Spain; ¹⁰Université de Paris Cité, Centre de Recherche sur l'Inflammation (CRI) UMRS1149, Clichy, France; ¹¹EASL-CLIF Consortium, Barcelona, Spain

Email: rita.azevedo@kuleuven.be

Background and aims: Acute-on-chronic liver failure (ACLF) is a devastating syndrome characterized by multiple organ failure and

high short-term mortality. The pathophysiology of ACLF is on the one side linked to elevated systemic inflammation that precipitate organ dysfunction and on the other side, immune dysfunction and increased susceptibility to bacterial infections. However, this immunological paradox is poorly understood and it is unclear how these aspects are associated with disease outcome. Here we map the single cell transcriptome of circulating cells from ACLF patients and we interrogated how specific immunometabolic signatures are linked to disease outcome.

Method: We performed single-cell transcriptomics of PBMCs from healthy (n = 3), acute decompensated (n = 3) and ACLF patients (n = 9). We further validated these findings in an independent cohort using bulk-sequencing, metabolomics and functional assay approaches.

Results: The data revealed two distinct classical monocyte (cMon) states that were uniquely linked to either ACLF-recovery (ACLF-R) or -non-recovery (ACLF-NR). Characteristic markers include VIM, LGALS2 and TREM1 for ACLF-NR cMon and RETN, S100A8/P and LGALS1 for ACLF-R cMon. Additionally, ACLF-NR cMon featured inflammation- and stress response transcriptional traits, while ACLF-R cMon were hallmarked by transcripts involved in stress tolerance, IFN signaling, superoxide scavenging, oxidative phosphorylation and refractory functionality. Interestingly, we observed a common stress-induced tolerant state, oxidative phosphorylation program, blunted activation and functionality also among lymphoid populations in ACLF-R compared to ACLF-NR patients.

Conclusion: This study uncovers unique cellular states and their underlying metabolite fingerprints that underlie disease outcome in ACLF patients. The data further provide important insights in disease pathogenesis and can act as foundation for larger studies to identify and validate targets for therapies.

SAT-391

RIPK3-mediated XBP1-Foxo1 axis controls NOD1 function and Calcineurin/TRPM7-induced cell death in liver inflammatory injury

Xiaoye Qu^{1,2}, Tao Yang³, Xiao Wang³, Dongwei Xu^{2,3}, Michael Ke¹, Jun Li⁴, Longfeng Jiang⁴, Qiang Xia², Douglas Farmer¹, Bibo Ke³. ¹The Dumont-UCLA Transplant Center, Division of Liver and Pancreas Transplantation, Surgery, Los Angeles, United States; ²Renji Hospital, Shanghai Jiaotong University School of Medicine, Liver Surgery, China; ³The Dumont-UCLA Transplant Center, Division of Liver and Pancreas Transplantation, Surgery, Los Angeles, United States; ⁴The First Affiliated Hospital, Nanjing Medical University, Infectious Diseases, China
Email: bke@mednet.ucla.edu

Background and aims: RIPK3 is a central player in triggering necroptotic cell death. However, whether macrophage RIPK3 may regulate NOD1-dependent inflammation and Calcineurin/TRPM7-induced hepatocyte death in oxidative stress-induced liver inflammatory injury remains elusive.

Method: A mouse model of hepatic ischemia/reperfusion injury (IRI), the primary hepatocytes, and bone marrow-derived macrophages were used in the myeloid-specific RIPK3 knockout (RIPK3^{M-KO}) and RIPK3-proficient (RIPK3^{FL/FL}) mice.

Results: RIPK3^{M-KO} diminished IR stress-induced liver damage with reduced serum ALT/AST levels, macrophage/neutrophil infiltration, and proinflammatory mediators compared to the RIPK3^{FL/FL} controls. IR Stress activated RIPK3, IRE1α, XBP1, NOD1, NF-κB, Foxo1, Calcineurin A, and TRPM7 in ischemic livers. Conversely, RIPK3^{M-KO} depressed IRE1α, XBP1, NOD1, Calcineurin A, and TRPM7 activation with reduced serum TNF-α levels. Moreover, Foxo1^{M-KO} alleviated IR-

induced liver injury with reduced NOD1 and TRPM7 expression. Interestingly, chromatin immunoprecipitation (ChIP) coupled with massively parallel sequencing (ChIP-Seq) revealed that macrophage Foxo1 colocalized with XBP1 and activated its target gene *Zc3h15*. Activating macrophage XBP1 enhanced *Zc3h15*, NOD1, and NF-κB activity. However, disruption of macrophage *Zc3h15* inhibited NOD1 and hepatocyte Calcineurin/TRPM7 activation, with reduced ROS production and LDH release after macrophage/hepatocyte co-culture. Furthermore, adoptive transfer of *Zc3h15*-expressing macrophages in RIPK3^{M-KO} mice augmented IR-triggered liver inflammation and cell death.

Conclusion: Macrophage RIPK3 activates the IRE1α-XBP1 pathway and Foxo1 signaling in IR-stress livers. The XBP1-Foxo1 interaction is essential for modulating target gene *Zc3h15* function, which is crucial for the control of NOD1 and Calcineurin-mediated TRPM7 activation. XBP1 functions as a transcriptional coactivator of Foxo1 in regulating NOD1-driven liver inflammation and Calcineurin/TRPM7-induced cell death. Our findings underscore a novel role of macrophage RIPK3 in stress-induced liver inflammation and cell death, implying the potential therapeutic targets in liver inflammatory diseases.

SAT-392

Phenotypical and functional sub-classification of Kupffer cells and liver monocyte-derived macrophages in mice

Hiroyuki Nakashima¹, Azusa Kato¹, Bradley Kearney¹, Masahiro Nakashima¹, Hiromi Miyazaki², Seigo Ito³, Manabu Kinoshita¹. ¹National Defense Medical College, Immunology and Microbiology, Tokorozawa, Japan; ²National Defense Medical College Research Institute, Division of Biomedical Engineering, Tokorozawa, Japan; ³Self-Defense Force Iruma Hospital, Department of Internal Medicine, Iruma, Japan
Email: hiro1618@ndmc.ac.jp

Background and aims: The macrophages in the liver are critical components of systemic defense mechanisms. F4/80^{high} Kupffer cells (KCs) are the most recognized liver macrophages, which efficiently contribute to the innate immune system. F4/80^{low} monocyte-derived macrophages (MoMφs) are other essential macrophages that modulate liver immune functions. In this study, we aimed to achieve a detailed subclassification of each population and its possible implications in the pathogenesis of an experimental non-alcoholic steatohepatitis model.

Method: Male C57BL/6 mice were subjected to the experiments, and liver non-parenchymal cells were isolated with collagenase digestion and analyzed by flow cytometry. F4/80^{high} and F4/80^{low} macrophage populations were identified, and their subclassifications were analyzed using uniform manifold approximation and projection (UMAP).

Results: KCs were classified into CD163 (+) or (-) population, and liver capsular macrophages co-existed in the same F4/80^{high} cells. CD163 (+)KCs had higher phagocytic and bactericidal activities and more complex cellular structures than CD163 (-) KCs. These three populations were eliminated by clodronate liposome treatment. F4/80^{low} MoMφs were divided into four populations according to Ly6C and MHC class II expression. The number of these monocyte-derived cells decreased in the chemokine receptor CCR2 knock-out mice. In high-fat- and cholesterol-diet-fed mice, the number of MHC class II positive pro-inflammatory MoMφs was specifically increased and considered to be the critical cell cluster for the progression of the non-alcoholic steatohepatitis model.

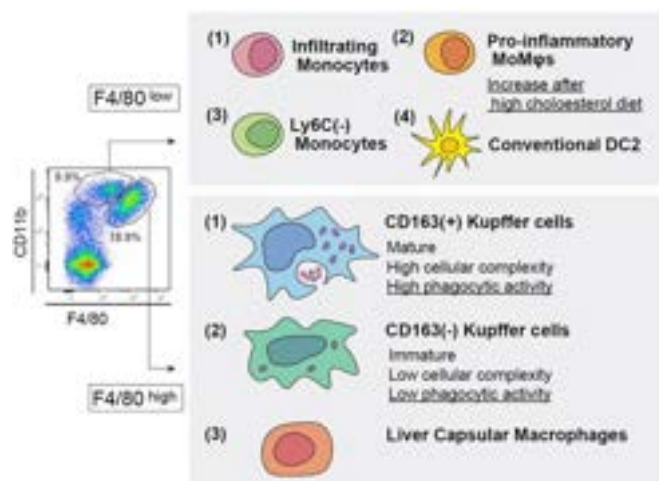


Figure:

Conclusion: CD163 expression effectively differentiated functional subclassification of Kupffer cells. F4/80^{low} pro-inflammatory MoMφs were the crucial effectors in accelerating inflammatory reactions in the liver. Our detailed subclassification and gating strategy can contribute to a better understanding of the complex immunological mechanisms in the liver.

Liver transplantation and hepatobiliary surgery

WEDNESDAY 21 TO SATURDAY 24 JUNE

TOP-051

Neoadjuvant PD-1 blockade with Pembrolizumab combined with Lenvatinib therapy in patients with hepatocellular carcinoma beyond Milan criteria before liver transplantation (PLENTY): a single-site pilot randomized controlled trial

Zicheng LV^{1,2}, Qiang Xia^{3,4}, Hao Feng^{1,3}. ¹Shanghai Engineering Research Center of Transplantation and Immunology, China; ²Shanghai Engineering Research Center of Transplantation and Immunology, China; ³Shanghai Renji Hospital, Dept. of Liver Surgery, China; ⁴Shanghai Renji Hospital, Dept. Liver Surgery, China
Email: surgeonfeng@live.com

Background and aims: Liver transplantation (LT) has become the most effective treatment for hepatocellular carcinoma (HCC); however, the high recurrent rate after LT remains a clinical challenge, especially for those exceeding the Milan criteria. Recently, there have been no approved standardized neoadjuvant or adjuvant therapies for hepatocellular carcinoma before LT. Therefore, we aim to investigate whether programmed death receptor 1 (PD-1) blockade plus lenvatinib as a neoadjuvant therapy before LT allows safely administered and effectively reduces post-LT recurrence for those patients with hepatocellular carcinoma beyond Milan criteria.

Method: In this prospective, randomized, open-label, pilot study, patients with hepatocellular carcinoma exceeding the Milan criteria were randomly assigned (1:1) to receive 200 mg of pembrolizumab every 3 weeks until approximately 6 weeks before LT and combined with lenvatinib 8 mg orally once daily until 1 week before LT (PLENTY group) or to receive routine treatments (control group) before LT. Patients were randomly assigned to the two groups by computer-generated random number codes concealed in opaque envelopes. The primary end point of the study was the recurrence-free survival after LT. Secondary end points were objective response rate, overall

survival, and adverse events. This trial is registered with ClinicalTrials.gov (NCT04425226).

Results: Between February 3, 2020, and September 5, 2021, 22 patients were enrolled and randomly assigned: 11 to the PLENTY group and 11 to the control group. The 12-month tumor-specific recurrence-free survival after LT was significantly improved in the PLENTY group (62.5%, 95%CI 24.49–91.48) compared to the control group (37.5%, 95%CI 8.52–75.51) (log-rank $p = 0.0028$). The objective response rate in the PLENTY group was 30% (95%CI 6.67–65.2) and 60% (95%CI 26.2–87.8) when determined by RECIST 1.1 and mRECIST, respectively. In the PLENTY group, the disease control rate was 100% (95%CI 69.15–100) according to both RECIST 1.1 and mRECIST; Six patients had significant tumor necrosis (60%, 95%CI 26.2–87.8), including three who had complete tumor necrosis (30%, 95%CI 6.67–65.2) at histopathology. No acute allograft rejection after LT occurred in either group. No grade 4 or 5 adverse events were observed. Grade 3 adverse effects were observed in 30% (3/10) of patients in the PLENTY group.

Conclusion: Neoadjuvant pembrolizumab plus lenvatinib before LT appears to be safe and feasible in hepatocellular carcinoma patients; it would be a potential therapeutic option for patients exceeding the Milan criteria, associated with significantly better recurrence-free survival. Our findings support further studies of neoadjuvant immunotherapy in combination with TKIs in the bridging treatment for hepatocellular carcinoma.

TOP-052

Graft steatosis and donor diabetes mellitus additively increase the risk of retransplantation and death in adult liver transplantation -data from the Eurotransplant registry

Milan Sonneveld¹, Fatemeh Parouei¹, Caroline den Hoed¹, Jeroen de Jonge¹, Morteza Salarzadei¹, Robert Porte¹, Harry LA Janssen¹, Marieke van Rosmalen², Serge Vogelaar², Adriaan Van der Meer¹, Rael Maan¹, Sarwa Darwish Murad¹, Wojciech Polak¹, Willem Pieter Brouwer¹. ¹Erasmus MC, Netherlands; ²Eurotransplant, Netherlands

Email: m.j.sonneveld@erasmusmc.nl

Background and aims: Presence of severe steatosis in the donor graft has been associated with an increased risk of adverse outcomes after liver transplantation. Recent studies indicate that presence of other metabolic risk factors increases the risk of advanced liver disease among patients with hepatic steatosis. Presence of metabolic risk factors in the donor may therefore confer additive risk for graft failure after transplantation. We studied the association between graft steatosis and metabolic risk factors in the donor with recipient outcomes after liver transplantation.

Method: We analysed data from all consecutive first adult full-graft DBD liver transplantations performed in the Eurotransplant region between 2010 and 2020. Presence of graft steatosis was assessed through review of individual donor imaging reports. Presence of diabetes mellitus (DM), hypertension (HT) and dyslipidaemia was assessed through review of individual donor medical history reports. The association between graft steatosis and metabolic risk factors in the donor with retransplantation-free survival of the recipient was assessed through the Kaplan-Meier method and multivariable Cox regression models, adjusted for Eurotransplant donor risk index (ET-DRI), donor and recipient sex, recipient age, and recipient labMELD.

Results: We studied 12174 transplantations. Median donor age was 56 (IQR 45–67), median donor BMI was 26 (24–28), median cold ischemia time (CIT) was 506 (403–610) minutes, median ET-DRI was 1.49 (1.24–1.76) and median recipient labMELD was 16 (10–26). Graft steatosis was detected in 2689 (22.1%), and diabetes mellitus, hypertension and dyslipidaemia was present in 1245 (10.2%), 5056 (41.5%) and 524 (4.3%) of donors. In univariable analysis, presence of graft steatosis (Hazard Ratio [HR] 1.247, $p < 0.001$), and presence of DM (HR 1.274, $p < 0.001$), HT (HR 1.144, $p < 0.001$), and higher BMI (HR 1.014, $p < 0.001$) in the donor were associated with impaired

retransplantation-free survival, whereas donor dyslipidaemia was not (HR 1.019, $P=0.810$). In multivariable Cox regression analysis, graft steatosis (adjusted HR [aHR] 1.197, $p<0.001$) and donor DM (aHR 1.157, $p=0.004$) were independently associated with an increased risk of retransplantation or death in the recipient, whereas hypertension, dyslipidemia and donor BMI were not. When compared to donors without graft steatosis and DM, the risk of recipient retransplantation or death was increased for grafts from donors with DM alone (aHR 1.155, $p=0.019$), or steatosis alone (aHR 1.199, $p<0.001$) and highest for grafts obtained from donors with both steatosis and DM (aHR 1.362, $p<0.001$). Observed retransplantation-free survival at 1, 5 and 10 years was 79%, 65% and 48% among recipients of a non-steatotic graft from a non-diabetic donor, compared to 69%, 53% and 29% for recipients of a steatotic graft from a diabetic donor ($p<0.001$).

Conclusion: Graft steatosis and donor DM additively increase the risk of retransplantation or death in adult DBD liver transplantation. Future studies should focus on methods to assess and improve the quality of these high risk grafts. Until such time, caution should be exercised when considering these grafts for transplantation.

TOP-059

Two-year follow-up of liver grafts from COVID-19 donors

Margherita Saracco¹, Donatella Cocchis², Francesco Tandoi², Federica Rigo², Renato Romagnoli², Silvia Martini¹. ¹AOU Città della Salute e della Scienza di Torino, Gastrohepatology Unit, Italy; ²AOU Città della Salute e della Scienza di Torino, General Surgery 2U, Liver Transplantation Center, Italy
Email: margherita.saracco@gmail.com

Background and aims: SARS-CoV-2 infections complicated by thrombosis and secondary sclerosing cholangitis were reported; however, solid non-lungs transplantation from COVID-19 donors showed excellent early results, but medium/long-term data are lacking. We aimed to describe the outcome of our LT patients (pts) who received a graft from COVID-19 donors.

Method: We consecutively enrolled all pts transplanted in our Center from 11/2020 to 03/2022 who received a liver graft from COVID-19 donors. Pts underwent protocol liver biopsy and magnetic resonance cholangiopancreatography (MRCP) after at least 1 year from LT. Follow-up was closed in January 2023.

Results: In the study period, among 213 adult LTs, 12 (5.6%) received a COVID-19 donor (11 active and 1 resolved COVID-19)¹. Recipients' and donors' characteristics are reported in table 1. None of the pts developed COVID-19 after LT. Two recipients tested SARS-CoV-2 RNA positive in nasopharyngeal swab immediately before LT and one was treated with sotrovimab on day-1 after LT. Eleven pts underwent end-to-end biliary anastomosis and 1 biliodigestive anastomosis. One pt underwent successful hepatic artery thrombectomy at day-1. Eleven pts underwent protocol MRCP (median time from LT 573 days, IQR 290–648), which showed: no visible abnormalities in 8, 1 donor-recipient's bile duct size discrepancy, and 2 caliber changes <50% at anastomotic level (without cholestasis and which were not treated). Ten pts underwent liver biopsy (median time from LT 557 days, 391–682) which showed 1 acute rejection (RAI 4/9) successfully treated with steroids and no signs of rejection, biliopathy or fibrosis in the other 9. After a median time from LT of 669 days (344–737) 11 pts are alive and 1 died after 320 days for hepatocellular carcinoma recurrence.

Table 1: Pts' and donors' characteristics at liver transplant

	Recipients n = 12	Donors n = 12
Age, years	61 [56–65]	59 [52–63]
Sex, male	9 (75%)	8 (67%)
Body mass index, kg/m ²	27 [24–28]	25 [24–27]
Hepatocellular carcinoma	9 (75%)	NA
Model for end stage liver disease at LT	10 (8–14)	NA
SARS-CoV-2 vaccination before LT	4 (33%)	1 (8%)
SARS-CoV-2 IgG positive before LT	12 (100%)	1 (8%)
SARS-CoV-2 RNA swab positive at LT	2 (17%)	2/3 (67%)
SARS-CoV-2 RNA BAL positive at LT	NA	9/9 (100%)
Donor risk index	2 (1.6–2.2)	
SARS-CoV-2 RNA PCR negative on liver biopsy	11/11, 100%	
Hypothermic machine perfusion	3 (25%)	
Normothermic machine perfusion	1 (8%)	

¹The COVID-19 resolved donor was not tested.

Conclusion: After a median time from LT of 1.8 years, 11/12 pts who received a liver graft from COVID-19 donors are alive, without evidence of SARS-CoV-2 RNA transmission. Protocol MRCP and liver biopsy did not show signs of biliopathy or fibrosis supporting the safe utilization of COVID-19 donors to expand the donor pool and reduce the waiting list mortality.

Reference

1. Peghin M, Grossi PA. COVID-19 positive donor for solid organ transplantation. *J Hepatol.* 2022 Oct; 77(4):1198–1204.

THURSDAY 22 JUNE

THU-477

Defective efferocytosis by aged macrophages promotes STING signaling mediated inflammatory liver injury

Haoran Hu¹, Zhuqing Rao¹, Xuyu Cheng¹, Jian Xu¹, Dongming Wu¹, Ping Wang¹, Haoming Zhou¹, Feng Cheng¹. ¹The First Affiliated Hospital of Nanjing Medical University, China
Email: docchengfeng@njmu.edu.cn

Background and aims: Timely efferocytosis of apoptotic cells is a key mechanism for avoiding excessive inflammation and tissue injury. MerTK (c-mer proto-oncogene tyrosine kinase), a member of the TAM (Tyrro3, Axl, and MerTK) family, plays an essential role in the regulation of efferocytosis. We previously found that aging promoted macrophage STING (stimulator of interferon genes) activation to aggravate inflammatory liver injury. Here, we investigated the alteration of efferocytosis by aged macrophages and its role in regulating macrophage STING signaling and ischemic liver injury.

Method: Young (8 weeks) and aged (100 weeks) STING myeloid-specific Cre mice and wild-type mice were subjected to a model of liver ischemia and reperfusion. Efferocytosis by macrophages was analyzed in vivo and in vitro macrophages co-cultured with apoptotic Jurkat cells. The MerTK CRISPR activation plasmid, ADAM17 (a disintegrin and metalloproteinase 17) siRNA and N-acetylcysteine were used to conduct rescue experiments.

Results: Aged macrophages exhibited impaired efferocytosis with decreased MerTK activation, which was reversed by treatment with the MerTK CRISPR activation plasmid. Increased MerTK cleavage by ADAM17 due to enhanced ROS levels contributed to defective MerTK-mediated efferocytosis by aged macrophages. MerTK activation by suppressing ADAM17 or ROS improves aged macrophage efferocytosis, leading to reduced liver inflammation and IR injury. Moreover, increased apoptotic hepatocytes, DNA accumulation, and

POSTER PRESENTATIONS

macrophage STING activation were observed in aged livers post-IR. Improvement in efferocytosis by aged macrophages via MerTK activation suppressed STING activation and inflammatory liver injury.

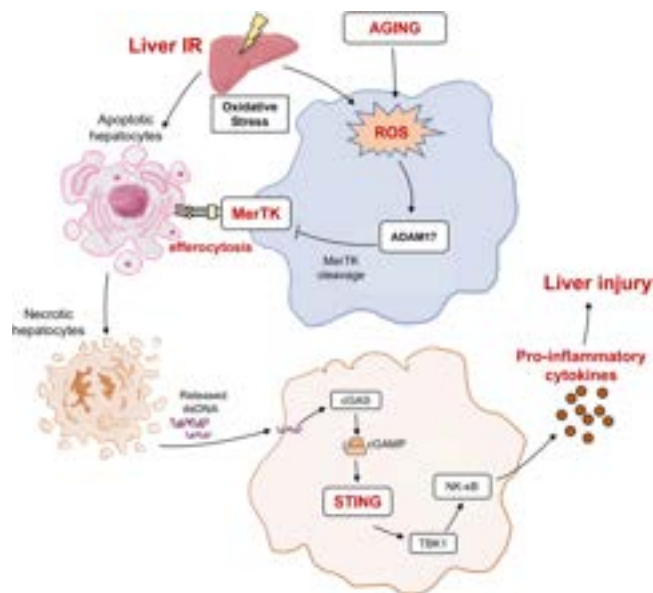


Figure:

Conclusion: Our study demonstrates that aging suppresses MerTK-mediated macrophage efferocytosis to promote macrophage STING activation and inflammatory liver IR injury, suggesting a new mechanism and potential therapy to promote inflammation resolution and efferocytosis in aging.

THU-478

C105SR, a novel non-peptidic small-molecule cyclophilin inhibitor with potent mitoprotective and hepatoprotective properties in the context of hepatic ischemia/reperfusion injury

Amel Kheyr^{1,2}, Nazim Ahnou^{1,2}, Hakim Ahmed-Belkacem^{1,2}, Bijan Ghaleh^{2,3}, Jean-François Guichou^{4,5}, Didier Morin^{2,3}, Jean-Michel Pawlotsky^{1,6}, Fatima Teixeira-Clerc^{1,2}. ¹INSERM U955, Équipe « Virus, Hépatologie, Cancer », Créteil, France; ²Université Paris-Est, Créteil, France; ³INSERM U955, Équipe « Pharmacologie et Technologies pour les Maladies Cardiovasculaires », Créteil, France; ⁴CNRS UMR5048, INSERM U1054, Centre de Biochimie Structurale (CBS), Montpellier, France; ⁵Université de Montpellier, Montpellier, France; ⁶DMU de Biologie et Pathologie, Département Prévention, Diagnostic et Traitement des Infections, Créteil, France

Email: fatima.clerc@inserm.fr

Background and aims: Mitochondrial permeability transition pore (mPTP) opening is critical in mediating cell death during hepatic ischemia/reperfusion injury. Blocking mPTP opening by inhibiting cyclophilin D (CypD) is a promising pharmacological approach for the treatment of ischemia/reperfusion injury. Here, we show that diastereoisomers of a new class of small-molecule cyclophilin inhibitors (SMCypls) bear properties making them credible candidates for hepatic ischemia/reperfusion injury therapeutic development.

Method: Derivatives of the original SMCypl were synthesized and evaluated for their ability to inhibit CypD peptidyl-prolyl cis-trans isomerase (PPIase) activity and for their mitoprotective properties, assessed by measuring mitochondrial swelling and calcium retention capacity in mouse liver mitochondria. The ability of the selected compounds to inhibit mPTP opening was evaluated in cells subjected to hypoxia/reoxygenation using a calcein/cobalt assay. Their ability to inhibit cell death was evaluated in cells subjected to hypoxia/reoxygenation by measuring LDH release, propidium iodide staining

and cell viability with a MTT assay. The best performing compound *in vitro* was selected for *in vivo* efficacy evaluation in a mouse model of hepatic ischemia/reperfusion injury.

Results: The two best compounds at inhibiting CypD PPIase activity and mPTP opening, C105 and C110, were selected. Their SR diastereoisomers carried the activity of the racemic mixture and exhibited mitoprotective properties superior to those of the known macrocyclic cyclophilin inhibitors cyclosporin A and alisporivir. C105SR was more potent than C110SR to inhibit mPTP opening and prevent cell death in a model of hypoxia/reoxygenation. Finally, C105SR substantially protected against hepatic ischemia/reperfusion injury *in vivo* by reducing hepatocyte necrosis and apoptosis.

Conclusion: We identified a novel cyclophilin inhibitor with strong mitoprotective and hepatoprotective properties both *in vitro* and *in vivo* that represents a promising candidate for cellular protection in hepatic ischemia/reperfusion injury.

THU-479

Application of human chemically-derived hepatic progenitors organoids (hCdHO) in regenerative medicine, hepatotoxic and disease modeling

Elsy Soraya Salas Silva¹, Yohan Kim², Tae Hun Kim¹, Myounghoi Kim¹, Daekwan Seo³, Valentina M. Factor⁴, Ji Hyun Shin¹, Dongho Choi¹.

¹Hanyang University, General Surgery, Seoul, Korea, Rep. of South; ²Max Planck, Institute of Molecular Cell Biology and Genetics, Germany;

³Psonagen Inc, United States; ⁴National Institutes of Health, United States

Email: crane87@hanyang.ac.kr

Background and aims: Chemically derived hepatic progenitors (hCdHs), reprogrammed from human primary hepatocytes (hPHs) were recently reported by our research group, which presented differentiation characteristics of both hepatocytes and cholangiocytes. The high percentage of EpCAM expression and other stemness markers allow to our hCdHs be a great source for organoid generation and longer culture maintenance. Our aim is to demonstrate the hCdH organoids (hCdHO) potency as a regenerative medicine, hepatotoxic test, and modeling disease tool.

Method: hCdHs and hPHs were embedded on Matrigel with organoid medium to generate hCdHOs and liver organoids (hLOs) respectively.

Results: Our hCdHO showed a high expression in stemness markers compared with hLOs and higher organoid rate generation. We performed hepatic differentiation of organoids, termed hCdHO_DM and hLO_DM, and as we expected hCdHO_DM presented elevated expression of hepatic markers as well as functional markers, similar to those of hLOs. To address their regenerative capacity, the hCdHO were transplanted into FRG mice. The group that received the hCdHO transplant survived longer (for more than 100 days) than hLOs and control groups. In addition, the markers of liver damage decreased, and albumin and A1AT levels increased. We demonstrated the hCdHO_DM exhibit elevated drug sensitivity versus hPH and hCdHs. Finally, we developed a model of alcohol damage in organoids, where we observed that hCdHO_DM increased the activation of transcription factors and lipogenic-associated enzymes and inflammatory cytokines levels. Gene set enrichment analysis (GSEA) indicated that ethanol-treated hCdHO_DM showed strong induction of alcoholic metabolic process and fatty acid metabolism, reflected in lipid accumulation and loss of mitochondrial membrane potential



Figure:

Conclusion: These results show the potency of hCdHs in organoid generation, culture maintenance, and hepatic differentiation. hCdHO display an efficient repopulation in liver disease mice model, are more sensitive for hepatotoxic tests, and recapitulate alcohol-related liver disease features. This work was supported by Korean Fund for Regenerative Medicine funded by Ministry of Science and ICT, and Ministry of Health and Welfare (21A0401L1) and National Research Foundation of Korea (2022R1F1A1073058).

THU-480

In vitro model of liver ischemia/reperfusion injury identifies iRhom2 as new target of disease

Giovanni Zito¹, Matteo Calligaris², Vitale Miceli¹, Claudia Carcione², Chiara Gatto¹, Simone Scilabra², Duilio Pagano¹, Pier Giulio Conaldi¹.
¹IRCCS ISMETT, Regenerative Medicine, Palermo, Italy; ²Fondazione Ri. MED, Italy

Email: gzito@ismett.edu

Background and aims: Ischemia/reperfusion injury (IRI) represents one of the leading causes of primary-non function acute liver transplantation failure. IRI activates an inflammatory cascade from the resident Kupffer cells leading to neutrophils recruitment and apoptosis of the parenchyma. In the last decade, the pro-inflammatory protein iRhom2 has emerged as a central regulator of TNF release, one of the most prominent cytokines activated during IRI. However, no data described iRhom2 in liver IRI yet. Thus, our study focused on the evaluation of the primary role of iRhom2 in an in vitro model of liver IRI.

Method: IRI was tested on primary macrophages and hepatic cells. In vitro cold ischemia was performed with 2% O₂ exposition in preservation medium. Warm reperfusion was performed at 1, 4 and 24 hrs. Cold ischemia and reperfusion effects on wt and iRhom2 KD cells were evaluated by ELISA, qPCR and ATP analysis. Shotgun proteomics was performed to compare wt and iRhom2 KD cells undergoing IRI.

Results: We found a positive association between iRhom2 expression and IRI in patients undergoing liver transplantation. Furthermore, iRhom2 transcripts are present in pre-reperfusion donor allografts, but its expression did not change in non-damaged livers, indicating iRhom2 as a mediator of the ischemic injury, rather than being a predictive risk factor of the injury. Next, we investigated the role of iRhom2 in IRI by using an in vitro model of IRI applied to M1 pro-inflammatory macrophages. In line with the in silico analysis, iRhom2 expression was enhanced by IRI during the early timepoints of macrophages reperfusion. These results showed that iRhom2 is

involved in the progression of re-perfusion damage also the in vitro IRI model we established in the lab. These findings prompted us to further dissect iRhom2 function in vitro IRI context. For this purpose, we silenced iRhom2 in primary macrophages prior to IRI protocol. iRhom2 silencing was effective at all the timepoints analyzed. Furthermore, we found that iRhom2 KD reduced release of TNF and other IRI-related pro-inflammatory proteins, such as IL-18 and HMGB1. Interestingly, iRhom2 silencing accelerated macrophage recovery during re-perfusion, as shown by increased cell viability and reduced cytotoxicity in comparison with the control primary macrophages. Altogether, these data indicated that iRhom2 contributed to the progression of damage following IRI in vitro, not only by regulating pro-inflammatory cytokine secretion, but also by modulating cell survival. Interestingly, iRhom2 KD macrophages promoted a faster and better recovery of human hepatocyte-like cells compared to controls, when cells were co-cultured using a Transwell permeable supports and applied to the in vitro model of IRI. This suggested that iRhom2 silencing in macrophages could impair release of paracrine factors that contributed to IRI induction. Interestingly, proteomic approach revealed, among others, 7 proteins which are up-regulated during cold ischemia, such as ORM1, ORM2, AZGP1, LRG1, A1BG, CP, HPX. Interestingly, we found that the same proteins are strongly down-regulated in the secretome of macrophages undergoing IRI when iRhom2 was silenced. To note, their levels in the cell lysate were not affected by iRhom2 silencing.

Conclusion: Taken together, these data suggest that iRhom2, in response to IRI, could regulate secretion of these proteins post-transcriptionally, by a mechanism that might be independent from TNF pathway.

THU-481

HBV re-infection or de-novo infection in the course of liver transplantation in patients chronically infected with HBV, HBV/HDV, or HCV

Daniele Lombardo¹, Giuseppina Raffa¹, Irene Cacciola¹, Lucio Caccamo², Maria Francesca Donato², Giovanni Raimondo¹, Teresa Pollicino¹.
¹University of Messina, Clinical and Experimental Medicine, Messina, Italy; ²Fondazione IRCCS Ca' Granda Ospedale Maggiore Policlinico, Surgery, Italy

Email: tpollicino@unime.it

Background and aims: Long-term anti-HBV prophylaxis has been highly effective in reducing the rate of HBV recurrence in HBsAg-positive patients or de novo infection in HBsAg-negative liver transplant recipients of anti-HBc positive hepatic grafts. However, HBV reinfection still occurs in several patients. Aim. To verify HBV reinfection in HBsAg-positive/HDV-negative and HBV/HDV coinfecting patients as well as de novo infection in HBsAg-negative liver transplant (LT) recipients during the LT procedures.

Method: Virological analyses were performed on sera and hepatic tissues (native liver, pre- and post-perfusion allograft biopsies) from 21 LT patients (10 HCV-positive/HBsAg-negative, 5 HBsAg positive and 6 HBV/HDV positive). Moreover, liver biopsies from 6/21 cases (2 HCV-positive, 2 HBsAg positive and 2 HBV/HDV positive) obtained at 3 years post-LT were also analysed. Six of the 21 LT patients received anti-HBc positive liver graft.

Results: At the end of surgery, 2/5 HBsAg-positive patients, 2/6 HBV/HDV co-infected patients, and 2/10 HCV-infected patients showed HBV DNA (range: 6×10^{-4} – 1×10^{-3} copies/cells) and HBV cccDNA (range: 2×10^{-5} – 2×10^{-3} copies/cell) in the liver. All these patients received anti-HBc positive liver graft. Moreover, liver biopsies from all these patients at 3 years post-LT were HBV DNA positive despite the persistent HBsAg negativity, showing the presence of occult HBV infections (OBI). Furthermore, tissues from HBV/HDV positive patients were also positive for HDV RNA, which was not detected at the end of LT. Sequencing analysis of HBV DNA isolated from native livers and allografts revealed that the viruses present in liver biopsies 3 years after LT were viral strains of the donors. Of note, an HBV

POSTER PRESENTATIONS

positive LT patient showed HBV genotype D sequences in the native liver, whereas HBV genotype A was identified in the allograft both at the end of LT and 3 years after LT.

Conclusions: (1) OBI in anti-HBc positive liver graft persists over time both in HBsAg positive and negative recipients after LT. (2) HDV infects the transplanted liver subsequently to LT (3) HBV sequences persisting in transplanted liver are of donor origin.

THU-482

The impact of statin utilization on mortality in liver transplant recipients independent of underlying cardiovascular risk

Megan Ghai¹, Pooja Rangan¹, Rohit Nathan², Karn Wijarnpreecha², Mark Wong², Moises Nevah Rubin², Michael Fallon², Ma Ai Thanda Han². ¹University of Arizona College of Medicine Phoenix, Internal Medicine, Phoenix, United States; ²University of Arizona College of Medicine Phoenix, Gastroenterology and Hepatology, Phoenix, United States

Email: megan.b.ghai@gmail.com

Background and aims: Liver transplant recipients (LTRs) have a 55.3% risk of developing coronary artery disease within five years of transplant. However, statins are under-prescribed in LTRs despite this known risk. Studies reviewed showed only 23–41% of LTRs with obstructive coronary artery disease were initiated on a statin. It has been hypothesized that the concern for developing drug-induced liver injury in LTRs results in physician hesitancy to prescribe statins, though the estimated rate of statin-induced liver injury is only 1 in 100,000. This study aims to characterize the use of statins and its impact on mortality in LTRs.

Method: A retrospective analysis of adult LTRs from January 2012 through March 2022 at a single-center was performed. The population was split into two cohorts, those who had not been prescribed a statin versus those who had been prescribed a statin. Descriptive statistics, including patient demographics and comorbidities were produced. Lifetime major adverse cardiovascular events (MACE), as defined by myocardial infarction, cerebrovascular accident, congestive heart failure, and coronary revascularization, were calculated. Chi-squared and Fisher's exact tests and Wilcoxon Rank Sum tests were used to assess categorical and continuous variables, respectively. Multivariate logistic regression was used to assess the impact of statin use on mortality while controlling for lifetime MACE and known comorbidities of cardiovascular disease.

Results: Included were 776 LTRs ages 18–76 years, of whom 566 (72.9%) were not prescribed a statin and 210 (27.1%) were prescribed a statin (table 1). Demographic data and comorbidities are presented in Table 1. Prevalence of lifetime composite MACE was higher LTRs prescribed a statin (no statin = 26.68% vs statin = 46.19%, $p < 0.001$). However, mortality was lower in those with statin use (no statin = 27.24% vs statin = 13.33, $p < 0.001$). The adjusted odds of death in LTR taking a statin were significantly less than those not taking a statin (aOR = 0.33, 95% CI [0.18, 0.54], $p < 0.001$).

Table 1: Descriptive Statistics & Severity

		Liver Transplant Recipient without a prescribed statin	Liver Transplant Recipients with a prescribed statin	P-value
Liver Transplant Recipients		566	210	
Patient Characteristics				
Sex, n(%)	Female	215 (37.99)	70 (33.33)	$p = 0.232$
	Male	351 (62.01)	140 (66.67)	
Mean Age, years(standard deviation)		54.44 (10.9)	59.36 (7.51)	$p < 0.001$
Race, n(%)	White	309 (54.59)	118 (56.19)	$p = 0.489$
	Black	21 (3.71)	5 (2.38)	
	Hispanic	165 (29.15)	68 (32.38)	
	Asian	20 (3.53)	3 (1.43)	
	Native American	41 (7.24)	14 (6.67)	
	Multiracial	10 (1.77)	2 (0.95)	
Comorbidities				
Diabetes Mellitus, n(%)		123 (21.77)	100 (47.62)	$p < 0.001$
Hypertension, n(%)		457 (80.74)	201 (95.71)	$p < 0.001$
Hyperlipidemia, n(%)		155 (27.39)	181 (86.19)	$p < 0.001$
Chronic Kidney Disease, n(%)		356 (62.90)	158 (75.24)	$p = 0.001$
Severity				
Myocardial Infarction, n(%)		28 (4.95)	24 (11.43)	$p = 0.001$
Cerebrovascular accident, n(%)		26 (4.59)	18 (8.57)	$p = 0.033$
Congestive Heart Failure, n(%)		113 (19.96)	68 (32.38)	$p < 0.001$
Coronary Revascularization, n(%)		13 (2.30)	43 (20.48)	$p < 0.001$
Composite MACE, n(%)		151 (26.68)	97 (46.19)	$p < 0.001$
Mortality, n(%)		152 (27.24)	28 (13.33)	$p < 0.001$

Conclusion: We have demonstrated that mortality is reduced in LTRs taking a statin in comparison those not taking a statin. The prevalence of lifetime composite MACE was higher in LTRs taking statins, suggesting that LTRs who have had a MACE are more likely to be prescribed a statin. These results indicate that statin use is an independent predictor of mortality in LTRs, irrespective of underlying cardiovascular risk. Future studies that stratify patients based on their known cardiovascular risk will allow us to clarify these results further.

THU-483

Quantification of remnant liver ischaemia after hepatectomy for hepatocellular carcinoma (HCC) using advanced 3D software analysis and its impact on disease recurrence

Acidi Belkacem¹, Mohammed Ghallab¹, Omar Ali², Nassiba Beghdadi¹, Nicolas Golse¹, Marc Antoine Allard¹, Antonio Sa Cunha¹, Daniel Azoulay¹, René Adam¹, Daniel Cherqui¹, Eric Vibert¹. ¹Chb-Centre Hépatobiliaire, Villejuif, France; ²Inserm 1193, Villejuif, France
Email: gacem05@hotmail.com

Background and aims: Many patients with HCC are not candidates for resection. Those amenable to curative surgical resection, still have a poor prognosis with recurrence reported up to 70% at 5 years either by dissemination or de novo tumours with 15% of patients presenting with distant recurrence. Risk factors related to disease biology have been well studied. When it comes to surgical technique impacting oncologic outcomes this is still not the case. Some authors have shown superiority of anatomic resection (AR), other data have suggested that nonanatomic resection (NAR) had comparable outcomes. Few recent reports have examined the clinical relevance of remnant liver ischemia (RLI) after partial hepatectomy and its impact on patients' oncologic outcomes. Our aim was to objectively measure RLI volume after resection of HCC by processing medical imaging by advanced 3D software package (Synapse 3D). The primary outcome was the impact of the RLI volume on HCC recurrence (HR). Secondary outcomes were the impact of NAR vs AR on the presence or absence of RLI and oncologic outcomes

Method: We retrospectively analysed 239 medical records of patients who had surgery for HCC at our Hospital between 2012 and 2020. RLI was investigated on early postoperative computed tomographic scans. The detection of RLI was assisted by pre-existing tools within the medical imaging software to automatically detect hypodense

areas within the liver and quantified the total volume of RLI areas in millilitres.

Results: Among 239 patients (median follow-up 60 months, 30-day mortality 1.3% Laparoscopic surgery in 36%, AR was performed in 69% of patients. RLI was detected in 71% of patients, median volume of 11.5 ml (6–34.5). Univariate analysis showed that at 6 months, HR was 6% in the RLI group vs 0% in the group without RLI ($p = 0.036$). At 1 year this was 16% and 5% of HR respectively ($p = 0.041$). There was significantly less RLI in the AR group 23% compared to the NAR group 77% ($p < 0.01$). Multivariate analysis showed the presence of RLI (2.18 (1.56; 3.06); $p < 0.001$) and the NAR (RR 2.55 (1.84–5.55); $p < 0.01$) were independent risk factors for HR. To identify the cut-off, point for RLI volume, a ROC curve analysis was done showing it to be 82mls with an AUC of 0.86.

Conclusion: Based on the results of this study, RLI has a significant impact on disease recurrence after surgery for HCC. Surgical technical refinements, surgical planning with 3D software and adjuncts like fluorescence-guided liver surgery to avoid significant RLI.

THU-484

Inequity in access to liver transplantation for critically ill patients with cirrhosis across U.S. transplant centers

Thierry Artzner¹, David Goldberg², Constantine Karvellas³, Sumeet Asrani⁴. ¹Hôpitaux Universitaires de Strasbourg, France; ²University of Miami, United States; ³University of Alberta, Canada; ⁴Baylor Medical Center Dallas, United States
Email: thierry.artzner@gmail.com

Background and aims: Liver transplantation (LT) is the most effective treatment for critically ill patients with decompensated cirrhosis. Some European studies have suggested that access to LT for this category of patients varies across transplant centers. We used UNOS data to examine whether this was also the case across U.S. LT centers at the national and regional levels.

Method: We included adult patients who received a primary, single LT between 2011 and 2020 using data from the Scientific Registry of Transplant Recipients (SRTR). We distinguished five (non exclusive) categories of patients who received LT: (i) non-critically ill patients with cirrhosis, (ii) critically ill patients with cirrhosis, (iii) patients

with MELD scores >35 at LT who were not critically ill, (iv) patients with hepatocellular carcinoma (HCC), and (v) patients transplanted with Status 1A at listing. Critically ill patients with cirrhosis were defined as being in the ICU at the time of LT with one or more of the following characteristics: (i) grade III/IV hepatic encephalopathy, (ii) mechanical ventilation, (iii) dialysis, (iv) vasopressors. We assessed the correlation between the total number of LTs in each center and the number of LTs for each category of patients.

Results: A total of 56,572 patients received a first, single LT over the study period in 109 LT centers, of which 45,512 (median: 82.7%, IQR: 77.8%–86.2%) had cirrhosis and were not critically ill, 4,459 (median: 5.5%, IQR: 3.1%–7.7%) had cirrhosis and were critically ill, 4,898 had a MELD score at LT >35 without being critically ill (median: 8.5%, IQR: 5.8%–11.4%), 20,461 (median: 36.7%, IQR: 32.1%–42.1%) had HCC, and 1,512 (median: 2.4%, IQR: 1.6%–4%) were transplanted with Status 1A. The total number of patients transplanted in each center correlated most strongly with the number of non-critically ill patients with cirrhosis (correlation coefficient = 0.98, panel A). By contrast, the number of critically ill patients with cirrhosis was most poorly correlated with the total number of patients transplanted in each center (correlation coefficient = 0.45, panel C). The correlation coefficient between the total number of patients transplanted and the number of patients transplanted for others indications was higher: 0.72 for patients transplanted with MELD scores >35 (panel B), 0.55 for patients with Status 1A, and 0.92 for patients transplanted with HCC.

Panel D illustrates the variability in LT activity across centers and among each UNOS region for critically ill patients with cirrhosis.

Conclusion: This study shows that the size of transplant centers correlates poorly with the number of critically ill patients with cirrhosis receiving LT and that there is more variability in LT for this indication than for other indications for which there is greater consensus (patients transplanted with HCC, MELD >35 or Status 1A). It shows that there is both national and regional variability in this LT activity.

This study corroborates European observations and illustrates the lack of practical consensus concerning the role of LT in this indication.

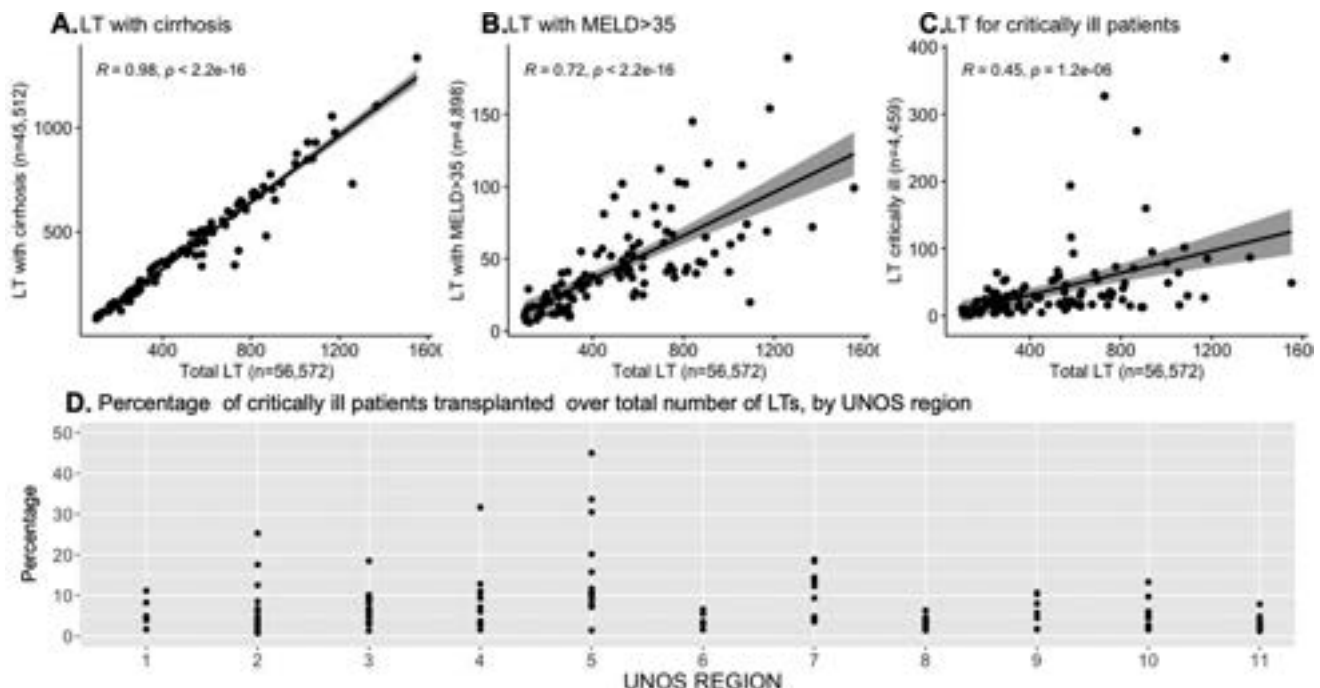


Figure: (abstract: THU-484).

POSTER PRESENTATIONS

In practice, it highlights inequities in access to this life-saving treatment for this subgroup of patients.

THU-485

Polycystic disease: a cumbersome benign indication for transplantation

Alberto Calleri¹, Bruna Lavezzo², Luigi Biancone³, Renato Romagnoli⁴, Silvia Martini¹. ¹Gastrohepatology Unit, AOU Città della Salute e della Scienza di Torino, Turin, Italy, Italy; ²Anesthesia and Intensive Care Unit 2, AOU Città della Salute e della Scienza di Torino, Turin, Italy, Italy; ³Division of Nephrology Dialysis and Transplantation, Department of Medical Sciences, AOU Città della Salute e della Scienza di Torino, Turin, Italy, Italy; ⁴General Surgery 2U, Liver Transplantation Center, AOU Città della Salute e della Scienza di Torino, Turin, Italy, Italy
Email: alberto.calleri.md@gmail.com

Background and aims: polycystic liver disease (PCLD), usually associated with polycystic kidney disease (PCKD), is a benign condition that potentially leads to abdominal fullness and portal hypertension (PH), burdened by increased risk of cyst-related infection and bleeding. Liver transplantation (LT) or simultaneous liver-kidney transplantation (SLKT) remains the only curative treatment for severe polycystic disease. We aimed at describing pre- and post-LT characteristics of patients (pts) who underwent LT/SLKT for PCLD/PCKD.

Method: Pts who underwent LT or SLKT for PCLD or PCKD in our Center from January 1st, 2010 to September 30th, 2022 were enrolled. Follow-up was closed on December 31st, 2022.

Results: In the study period 1754 LTs were performed. Sixty-three LTs for PCLD (3.6%) have been carried out, of which 45 (71%) were SLKT. 48 (76%) pts were female, median age 52 years [IQR 48–56], median BMI 24 kg/m² [23–26]. Median serum creatinine (sCr) was 5.7 mg/dL [4.1–7.8] and median estimated-glomerular filtration rate (eGFR) was 11 ml/min [7–17] in pts affected by kidney failure who received SLKT (29/45 on pre-LT dialysis); median eGFR of pts listed for LT alone of 78 ml/min [68–94]. 58/63 (92%) pts underwent LT for abdominal fullness with sarcopenia (median liver weight 3950 g [2450–6750]; median largest cyst size 7 cm [5–9]); while 19/63 (30%) showed refractory ascites. Nine pts (2%) had pre-transplant cyst interventions. Of note, 10/63 (16%) were known to be pre-LT colonized by multidrug-resistant (MDR) bacteria. Median surgery duration was 357 min [307–456] for LT and 405 min [355–462] for SLKT with a median number of 7 [3–16] red blood units needed. The Piggy-back technique was possible in 18/63 (29%) and 9 pts (14%) underwent temporary porto-cava shunt while only 6 pts (10%) received venous-venous bypass. Among 48 pts listed for SLKT, 7 (15%) underwent a delayed kidney transplantation within 24 h and 3 (6%) were then listed for sequential kidney transplant due to the complexity of LT-surgery. Forty-one pts (65%) were extubated within the first 48-hours and the median ICU stay was 5 days [3–9]. Two pts had primary non-function and underwent re-LT after 3 days while only 1 pt had hepatic artery-thrombosis solved surgically. Moreover, 28 pts (44%) underwent early post-transplant surgical revisions. After a median 4.3 years [1.8–7.8] of follow-up: 59/63 (94%) were alive while 3 pts died for sepsis 3 weeks after transplant (1 LT and 2 SLKT) and 1 pt died for HHV8-induced hemophagocytic syndrome 3 years after SLKT.

Conclusion: PCLD/PCKD is an insidious benign disease for which high-complex surgical procedure such as transplantation is the ultimate solution. In our cohort 16% of pts were pre-transplant colonized by MDR bacteria and post-LT early surgical revisions were needed in 44% of cases. Nevertheless, the expertise of a high-volume transplant Centre allowed to achieve a 3-year survival rate of 94%.

THU-486

De novo cancers after liver transplantation: a French nationwide cohort

Ilias Kounis¹, Christophe Desterke¹, Paul Landais¹, Eric Vibert¹, Didier Samuel¹, Cyrille Feray¹. ¹INSERM 1193, France
Email: cyrille.feray@gmail.com

Background and aims: *De novo* cancer (DNC) following liver transplantation (LT) have been reported as one of the major causes of post-transplant mortality. Everolimus is frequently prescribed to patients presenting *de novo* cancer after LT and those who are at risk of cancer recurrence. With this study we aimed to estimate the cancer burden after LT at a nationwide level and to evaluate the potential role of everolimus in *de novo* cancer occurrence.

Method: The French national health data system (SNDS), linked with the national hospital database (PMSI), contains information on at least 99% of the French population, concerning ICD-10 codes, medical procedures (MP), prescribed drugs and vital status. 8658 patients having received LT for hepatocellular carcinoma (n=3902) or decompensated cirrhosis were identified from 2009 to 2019. Algorithms combining ICD and MP identified post-transplant invasive neoplasia at different sites. Cox models including competitive risk, everolimus as time-dependent exposure (tmerge function) and propensity score (weightit pkg) analysed cancer incidence, mortality.

Results: With a median follow-up of 4.6 [2.2, 6.8] years after LT, 1119 (13%) patients developed DNC, of which 232 (2.7%) dysmyelopoiesis, 216 (2.5%) head and neck, 213 (2.5%) skin cancer, 184 (2.1%) metastatic cancer, 180 (2.1%) lung cancer, 100 (1.2%) lymphoma, 88 (3.3%) colorectal cancer, 87 (1.0%) prostate cancer and 50 (0.6%) bladder cancer. Age, tobacco, alcohol, diabetes and cancer before LT were significantly associated to DNC for most studied sites. 5-year survival after DNC was poor: 40% for dysmyelopoiesis or skin, 30% for colorectal or lymphoma, 25% for prostate, 20% for lung, head and neck and metastasis. During the follow-up, 2588 (30%) patients were exposed to everolimus including 997 before the detection of any cancer. In all cases both using landmark analysis or time-dependent exposure, everolimus was associated neither to a lower incidence nor to a better survival after occurrence (Figure).

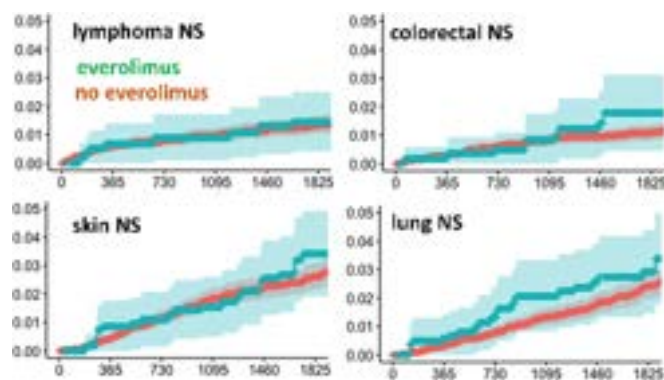


Figure:

Conclusion: DNC occur in at least 13% of adults after LT. Systematic screening is clearly insufficient in view of the poor survival observed after their detection. More surprisingly, the antitumoral action of everolimus recipients to prevent *de novo* malignancies was not observed for any cancer including skin cancers.

THU-487

Assessment of silent coronary artery disease with functional and anatomic tests in liver transplantation: analysis of the diagnostic and prognostic capacity of a risk-adapted protocol

Giulia Pagano¹, Pablo Ruiz², Jordi Colmenero², Sergio Rodriguez-Tajes², Judit Mestres², Julia Martinez-Ocon², Salvatore Brugaletta², Gonzalo Crespo². ¹Hospital Clinic, Liver Transplant, Spain; ²Hospital Clinic, Spain
Email: gpagano@clinic.cat

Background and aims: Cardiovascular (CV) risk burden of liver transplant (LT) candidates is increasing, and CV events (CVE) are a main cause of post-LT death, thus identifying LT candidates at high CV risk is key to improve outcomes. The best strategy to assess silent coronary artery disease (CAD) before LT is controversial. We aimed to evaluate the performance of a risk-adapted protocol that uses functional (stress tests) and anatomical (coronary artery calcification score [CACS] by CT, and CT angiography [CTCA]) explorations, to diagnose pre-LT CAD and predict post-LT CVE.

Method: Single-center, retrospective analysis with patients considered for LT between July 2015 and September 2020. In a pre-specified clinical protocol depending on the accumulation of risk factors, primary CAD assessment included a) no specific test; b) CACS followed by CTCA; or c) stress test. Invasive coronary angiography (ICA) was performed according to the results of non-invasive tests. We investigated the variables, including the diagnostic tests and the clinical risk factors comprised in the CAD-LT score, associated with the presence of significant lesions in ICA; as well as the association between diagnostic tests and the incidence of CVE 2 years after LT.

Results: 634 candidates were evaluated and 351 underwent LT. CACS was performed as primary test in 244 (39%), stress tests in 81 (13%, most dobutamine stress echocardiography [DSE]), and in 309 cases (49%) no specific explorations were indicated. 122 patients eventually underwent ICA. In patients undergoing CACS, the prevalence of CACS = 0 (absence of calcifications) was 22%, while severe coronary calcifications (CACS ≥ 400) were found in 26%. Most DSE (61%) were non-diagnostic, and very few stress tests resulted positive. The prevalence of significant lesions in ICA was 23%, and it was not associated with either CACS, CTCA findings or stress tests results. In contrast, the incremental presence of CV risk factors in a modified CAD-LT score predicted the presence of significant lesions in ICA ($p < 0.001$). Among LT recipients, the 2-year cumulative incidence of CVE was 12%. Patients without specific exploration indications for silent CAD presented the lowest incidence (7%) of CVE, while those with pre-LT CACS ≥ 400 ($p < 0.001$) had the highest incidence (37%). In the adjusted multivariate analysis, pre-transplant CACS ≥ 400 and the indication of stress test were independent predictors of post-LT CVE (Figure).

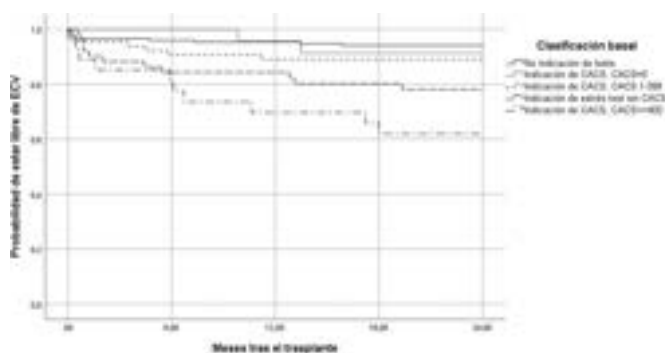


Figure:

Conclusion: A high (≥ 400) CACS identifies LT candidates at the highest risk of post-LT CVE, despite being poorly associated with the presence of CAD before LT, probably highlighting its value as a biomarker of systemic atherosclerosis. Stress tests are of limited value

due to a high rate of unreliable results. The accumulation of clinical risk factors using calculators like the CAD-LT score can be useful to identify LT candidates with more risk of significant lesions in ICA.

THU-488

Sex-based differences and comparative predictive value of MELD 3.0 in simultaneous liver-kidney transplantation waitlist outcomes after standardization of listing criteria in the United States

Emily Leven¹, Ditian Li², Emilia Bagiella², Lauren Grinspan³. ¹Icahn School of Medicine at Mount Sinai, Gastroenterology, New York, United States; ²Icahn School of Medicine at Mount Sinai, Department of Population Health Science and Policy, New York, United States; ³Recanati/Miller Transplantation Institute, New York, United States
Email: emily.leven@mountsinai.org

Background and aims: In liver transplantation (LT) in the United States (U.S.), women experience longer waitlist times and higher mortality than men, in part because of the use of a creatinine-based organ allocation score (Model of End-stage Liver Disease-Sodium, or MELD), which underestimates renal dysfunction in women. The newly proposed MELD 3.0 incorporates sex and mitigates LT waitlist disparities in models. In 2017, the United Network for Organ Sharing (UNOS) implemented a new policy requiring either a need for renal replacement therapy or reduced glomerular filtration rate (GFR) for simultaneous liver-kidney (SLK) listing; prior to this, no standardized criteria existed. The impact of this policy on sex-based waitlist disparities has not been reported. We aimed to 1) compare waitlist outcomes by sex before and after SLK listing criteria standardization; and 2) examine the predictive value of the difference in MELD vs. calculated MELD 3.0 at SLK listing on waitlist outcomes.

Method: Publicly available UNOS data were used. Pre- and post-groups included adult SLK listings from 2013 to 2016 and 2018–2021, respectively. 2017 listings (SLK policy change year) were excluded. Data were censored at 3 years. Cox proportional hazards and competing risk analyses were used to compare pre- and post- waitlist outcomes (death, transplantation, delisting due to improvement, delisting due to illness) between sexes and time groups and to estimate the predictive value of MELD vs. MELD 3.0 on waitlist outcomes.

Results: 2633 men (61.1%) and 1676 women (38.9%) were listed pre-policy change; 2610 men (57.6%) and 1921 women (42.4%) were listed post-policy change. Controlling for age, ethnicity, transplant indication, height, and listing MELD, women were less likely than men to undergo transplantation pre-policy change (hazard ratio [HR] = 0.87, 95% confidence interval [CI] = 0.77–0.99, $p = 0.03$). Women post-policy change were significantly more likely to undergo transplantation compared to women in the pre- group ($p = 0.02$); sex-based differences in likelihood of transplantation were no longer significant post-intervention, though there was an increased chance of transplantation for women vs. men in the post- group (HR = 1.11, 95% CI = 0.98–1.23, $p = 0.10$) (Figure). A one-point deficit in MELD vs. MELD 3.0 at SLK listing was associated with a 2% lower chance of transplantation (HR = 0.98, 95% CI = 0.97–0.99, $p = 0.002$).

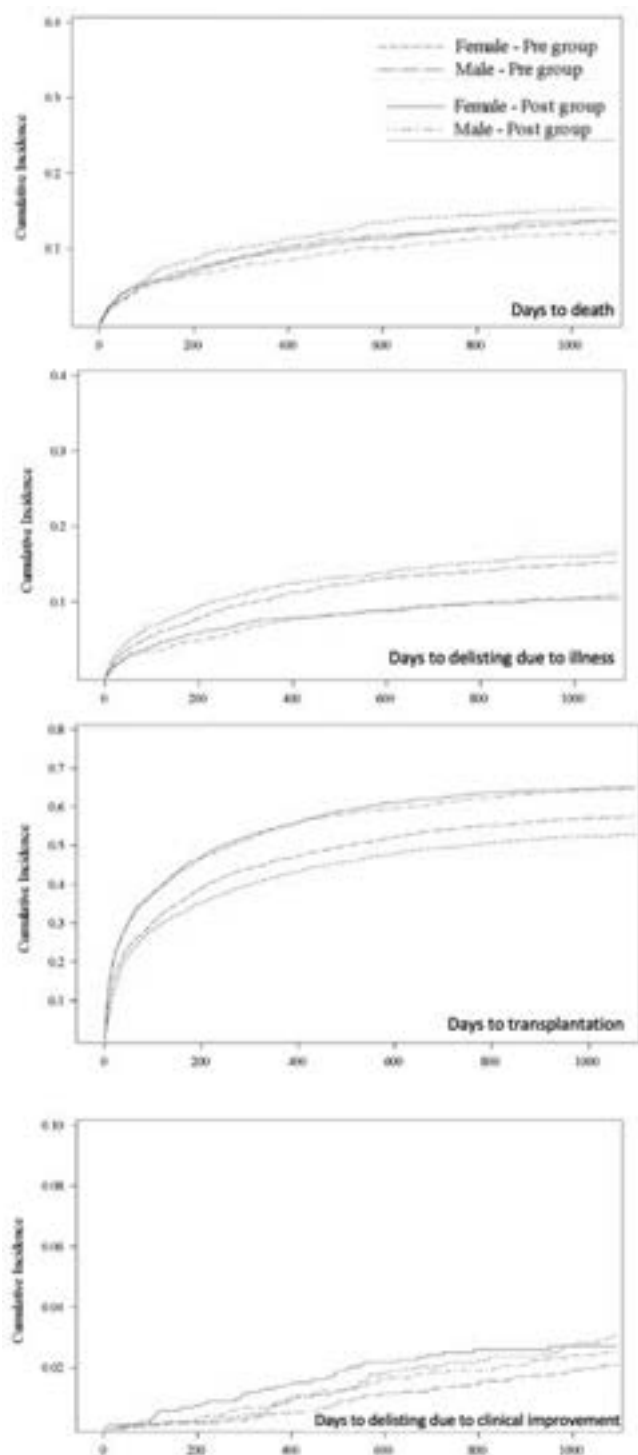


Figure: Competing risk analyses for waitlist outcomes by sex and time group.

Conclusion: Accounting for sex in SLK listing and allocation may reduce health disparities. GFR-based standardization of SLK listing in the U.S. was associated with better chances of transplantation for women and with the mitigation of decreased female vs. male transplantation patterns in this population. The use of MELD 3.0 may also contribute to equity in SLK waitlist outcomes.

THU-489

Increased left ventricular dimensions are the new risk factor for acute kidney injury after living donor liver transplantation (cardio-renal interaction)

Dheepak V¹, Lalita Mitra^{2,3}, ¹Institute of Liver and Biliary Sciences, Organ Transplant Anaesthesia and Critical Care, India; ²homi Bhabha Cancer Hospital and Research Centre, India; ³Institute of Liver and Biliary Sciences, Organ Transplant Anaesthesia and Critical Care, New Delhi, India

Email: dheepak22@gmail.com

Background and aims: Acute kidney injury (AKI) is a common complication of liver transplant surgery, resulting in lengthy intensive care unit/hospital stays and considerable morbidity with the development of chronic renal failure in liver transplant recipients. AKI after liver transplantation is caused by a variety of factors, including recipient's hepatic decompensation, poor donor graft quality, intraoperative hemodynamic instability, blood loss and blood product transfusions. The cardiac dysfunction could also mediate impairment in renal function (Cardio-renal syndrome). We prospectively evaluated the possible associations between perioperative N-terminal pro B-type natriuretic peptide (NT-proBNP) levels, transthoracic echocardiograph findings and post-transplant AKI in patient undergoing living donor liver transplantation.

Method: Seventy adult cirrhotic patients without endogenous heart or renal disease were included. AKI was defined as increase in serum creatinine by 0.3 mg/dL or more within 48 hours (or) increase in serum creatinine to 1.5 times baseline or more within the last 7 days. Serum NT-proBNP levels were measured immediately after induction of anaesthesia and also at the end of the surgery. We analysed the relationship between NT-proBNP levels, preoperative echocardiographic findings and post-transplant AKI.

Results: The overall incidence of AKI was 38.57%. However, the majority (77.78%) of patients had stage 1 AKI, and none of our patients had stage 3 AKI or required renal replacement therapy during the first week following LT. The patients who developed AKI had significantly higher left ventricular end-diastolic dimension (LVEDD = 49.37 ± 4.48 mm vs 45.6 ± 4.01 mm, p = 0.0005) and left ventricular end-systolic dimension (LVESD = 28.7 ± 3.46 mm vs 26.3 ± 3.44 mm, p = 0.006) in the 2d echocardiography and also had a higher intra-procedural transfusion of platelets. Other echocardiographic parameters were comparable between both groups. In multivariate logistic regression analysis, left ventricular end diastolic dimension [odds ratio (OR): 1.168, 95% confidence interval (CI): 1.011–1.349; p = 0.035] and left ventricular end systolic dimension (OR: 1.196, 95% CI: 1.002–1.428; p = 0.048) were found to be independently associated with the development of AKI. There was a moderately significant correlation between baseline NT-proBNP level and MELD score and amount of ascites drained intraoperatively. There was no significant association between perioperative NT-proBNP levels and post-transplant AKI.

Parameters	Beta coefficient	Standard error	P value	Odds ratio	Odds ratio Lower bound (95%)	Odds ratio Upper bound (95%)
LV ED D (mm)	0.155	0.074	0.035	1.168	1.011	1.349
LV ES D (mm)	0.179	0.090	0.048	1.196	1.002	1.428
SDPC (unit)	0.978	0.555	0.078	2.659	0.895	7.897

Figure: Multivariate logistic regression to identify independent factors associated with the development of AKI.

Conclusion: We confirmed that post-transplant AKI in patients with cirrhosis is related to cardio-renal interactions. The enlarged left ventricle during systole and diastole indicates the state of hyperdynamic circulation with increased cardiac output and blood volume along with decreased systemic vascular resistance. This results in the state of effective hypovolemia and along with latent cardiac dysfunction in cirrhosis causes renal hypoperfusion and abnormal

neurohumoral regulation resulting in renal vasoconstriction and acute kidney injury.

THU-490

Effect of glucagon-like peptide-1 receptor agonists and sodium-glucose cotransporter-2 inhibitors on post-liver transplant mortality and major adverse cardiovascular events

Kelli Kosako Yost¹, Paul Gomez¹, Pooja Rangan¹, Michael Fallon¹, Rohit Nathan¹, Moises Nevah Rubin¹, Mark Wong¹, Karn Wijarnpreecha¹, Ma Ai¹, Thanda Han¹. ¹University of Arizona College of Medicine-Phoenix, United States
Email: kellikosakoyost@gmail.com

Background and aims: Glucagon-like peptide-1 receptor agonists (GLP-1 RA) and Sodium-glucose cotransporter-2 inhibitors (SGLT2i) have shown to have cardiovascular benefit, promote weight loss, and improve glycemic control in patients with type 2 diabetes mellitus (T2DM). Although there is some data of these medications on post-heart and kidney transplant populations, there is no data on their effect on cardiovascular events and mortality in post-transplant population, especially the post-liver and post-simultaneous liver/kidney transplant populations. The aim of our study was to determine the effect of GLP1 RA and SGLT2i on post-liver and post-simultaneous liver/kidney transplant recipients on major adverse cardiovascular events (MACEs) and overall mortality.

Method: A retrospective chart review in a single hospital system reviewing any adult age ≥ 18 -year-old with either solitary liver or simultaneous liver and kidney transplant from January 2012 to March 2022 was completed. GLP1RA or SGLT2i usage was determined. Demographic, clinical characteristics, and outcomes were compared between the two groups. MACE events included myocardial infarction, coronary revascularization (percutaneous intervention, stent placement, coronary artery bypass graphing), cerebrovascular event, or congestive heart failure. The Mann-Whitney test and Fisher's exact or Chi-square test was used for continuous and categorical variables respectively and multivariate logistic regression was used to evaluate for significant differences in outcomes between the two groups.

Results: Of the 776 patients included, 33 (4.25%) were on a SGLT2i or a GLP1 RA. Patients' demographics and comorbidities are shown in the table. Hypertension ($p < 0.001$), hyperlipidemia ($p < 0.001$), and BMI at transplant ($p = 0.021$) were all statistically significant comorbidities between the two groups on univariate analysis. On multivariate analysis, the use of an SGLT2i or a GLP1 RA was associated with significantly lower mortality rate (OR 0.28, CI 95% 0.08–0.97, $P = 0.045$) and number of MACEs (OR 0.32, CI 95% 0.13–0.79, $P = 0.014$) after controlling for age at transplant, BMI at transplant, sex, hypertension, T2DM at listing, hyperlipidemia, chronic kidney disease, and tobacco use.

Demographics	Total patients	Patients on SGLT2i or GLP1 RA	Patients not on SGLT2i or GLP1 RA	P-value
Total patients, n (%)	776	33 (4.25%)	743 (95.75%)	
Age at Transplant, Mean \pm SD		58.43 \pm 7.64	58.65 \pm 10.42	0.2132
Male	495 (63.77%)	16 (48.48%)	269 (36.20%)	0.152
Race/Ethnicity				0.252
White	421 (55.03%)	16 (48.48%)	411 (55.32%)	
Black	28 (3.71%)	0 (0%)	28 (3.76%)	
Asian	23 (3.00%)	0 (0%)	23 (3.10%)	
Hispanic/Latino	233 (30.03%)	12 (36.36%)	221 (29.74%)	
American Indian	35 (4.51%)	3 (9.09%)	30 (4.04%)	
Multiracial	12 (1.55%)	0 (0%)	12 (1.62%)	
BMI at Transplant, Mean \pm SD		30.92 \pm 5.38	28.91 \pm 5.76	0.021*
Smoking	294 (37.89%)	14 (42.42%)	280 (37.69%)	0.5161
Diabetes Mellitus at listing	223 (28.71%)	28 (84.85%)	195 (26.28%)	< 0.001*
Hypertension	638 (82.20%)	32 (96.97%)	606 (81.95%)	0.046*
Hyperlipidemia	336 (43.30%)	26 (78.79%)	310 (41.72%)	< 0.001*
Myocardial Infarction (MI)	33 (4.25%)	0 (0%)	33 (4.44%)	0.568
Chronic Kidney Disease (CKD)	214 (27.59%)	17 (51.52%)	197 (26.69%)	0.149
Cerebral Vascular Accident (CVA)	44 (5.67%)	3 (9.09%)	41 (5.50%)	1.000
Congestive Heart Failure (CHF)	181 (23.32%)	9 (27.27%)	172 (23.28%)	0.590
Coronary Revascularization	36 (4.64%)	4 (12.12%)	32 (4.29%)	0.389
Avg MACE	248 (31.96%)	7 (21.21%)	241 (32.44%)	0.176
Mortality	188 (24.24%)	3 (9.09%)	175 (23.58%)	0.057

*Statistically significant

Figure:

Conclusion: This study shows that, after controlling for comorbidities, the use of an SGLT2 inhibitor or a GLP1 agonist post-liver or post-

liver/kidney transplant was associated with decreased mortality and decreased number of MACEs. Although this was a small cohort of patients on these medications, this proves promising to this patient population and warrants further studies.

THU-491

Deep learning prediction modeling of major adverse cardiovascular events following liver transplantation

Ahmed Abdelhameed¹, Cui Tao^{1,2}, Liu Yang³. ¹The University of Texas Health Science Center at Houston, School of Biomedical Informatics, United States; ²University of Texas Health Science Center at Houston, United States; ³Mayo Clinic, United States
Email: ahmed.m.abdelhameed@uth.tmc.edu

Background and aims: Major adverse cardiovascular events (MACE) are among the leading causes of morbidity and mortality following liver transplantation (LT). The aim was to develop and validate deep learning models' ability to predict post-transplantation MACE among patients undergoing LT

Method: Using data from Optum's de-identified Clinformatics® Data Mart Claims Database, we identified patients who received LT between January 2007 and March 2020 and built multiple predictive models for the risk of developing any of the post-transplantation MACE, including myocardial infarction, atrial fibrillation, pulmonary embolism, heart failure, cardiac arrest, and stroke, as an outcome. A MACE is primarily predicted using the Bidirectional Gated Recurrent Units (BiGRU) deep learning sequence processing model in different prediction interval lengths up to 5 years after the LT index date, using patients' demographics and retrospective diagnosis, medications, and procedures claim data recorded back to 3 years before the LT index date. The performance of the deep learning model against other machine learning models such as Logistic Regression (LR), Random Forest (RF), and Light Gradient-boosting Machine (LGBM) was assessed using a cohort of 18304 liver transplant recipients (mean age 57.4 years [SD 12.76]; 11146 [60.9%] men and 7158 [39.1%] women). Models' optimization was done using five-fold cross-validation on 80% of the cohort (training set) and the performance of the models is assessed using the remaining 20% (testing set) based on the area under the receiver operating characteristic curve (AUC-ROC) and the area under the precision-recall curve (AUC-PR).

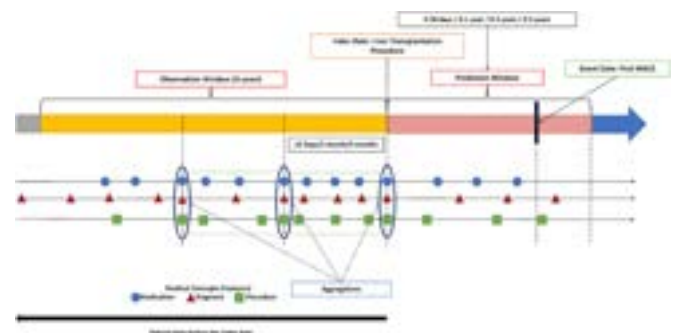


Figure:

Results: Using different prediction intervals (0–30 days, 0–1 year, 0–3 years, and 0–5 years) after the LT index date and compared to the three machine learning models, the top-performing model was the deep learning model, BiGRU, achieved an AUC-ROC of 0.833 (95% confidence interval [CI], 0.8127–0.8522) and AUC-PR of 0.560 (95% CI 0.5205–0.6058) for a 30-day prediction interval after LT.

Conclusion: Using patient longitudinal claims data, deep learning systems can efficiently model and predict outcomes following liver transplantation. This model will help clinicians to identify high-risk candidates for further risk stratification or other management strategies to improve liver transplant outcomes.

THU-492

The growing prevalence and impact of type 2 diabetes among liver transplant candidates in the United States

Zobair Younossi^{1,2,3}, Katherine Eberly^{1,3}, Reem Al Shabeeb^{1,3}, Ameeta Kumar^{1,3}, Pamela Brandt^{1,2}, Nagashree Gundu Rao^{1,4}, Janus Ong⁵, Kenneth Cusi⁶, Saleh Alqahtani^{7,8}, Maria Stepanova^{1,2,9}.
¹Inova Health System, Department of Medicine, United States; ²Beatty Liver and Obesity Research Program, Inova Health System, United States; ³Inova Health System, Medicine Service Line, United States; ⁴Inova Health System, Division of Endocrinology, United States; ⁵University of the Philippines, College of Medicine, Philippines; ⁶University of Florida, Division of Endocrinology, Diabetes and Metabolism, United States; ⁷Johns Hopkins University, Division of Gastroenterology and Hepatology, United States; ⁸King Faisal Specialist Hospital and Research Center, Liver Transplant Center and Biostatistics, Epidemiology and Scientific Computing Department, Saudi Arabia; ⁹Center for Outcomes Research in Liver Disease, United States
 Email: zobair.younossi@inova.org

Background and aims: Type 2 diabetes (T2D) and superimposed NAFLD can negatively impact outcomes of patients with chronic liver disease (CLD). The aim of this study was to assess the impact of pre-transplant T2D on the outcomes of liver transplantations (LT).

Method: We used Scientific Registry of Transplant Recipients (SRTR) 2008–2020 to collect data for all adult patients ≥18 years of age who received a liver transplant in the U.S. The study outcome was time to post-transplant mortality (cut-off date March 2, 2022).

Results: A total of 86,153 LTs were included: mean age 56 ± 11 years, 71% Caucasian, 66% male, 5.0% re-transplants. Acute liver failure accounted for 4.2% of LTs. Of those transplanted with a CLD, 2% had chronic hepatitis B, 20% chronic hepatitis C, 17% NASH, 24% alcoholic liver disease; 25% also had hepatocellular carcinoma (HCC). Of all LT recipients, 26% had history of pre-transplant T2D; this rate increased from 22% (2008) to 28% (2019). Similar trends were observed in subgroups with acute liver disease (from 10% to 15%), those with HCC (from 26% to 38%), and CLD patients without HCC (from 22% to 27%). During follow-up (median = 61 months, IQR = 30–103 months), 26% of LT recipients died and 5.4% had a graft failure; the cumulative mortality rates were 23% in acute liver disease, 30% in HCC, and 25% in non-HCC subgroups. The 5-year mortality rates were higher in LT

recipients with vs. without pre-transplant T2D: 28% vs. 21% in acute liver disease, 27% vs. 24% in HCC, and 24% vs. 20% in non-HCC (all $p < 0.01$). In multivariate survival analysis, pre-transplant T2D was independently associated with a higher risk of post-LT mortality in all subgroups: adjusted hazard ratio (aHR) = 1.26 (1.22–1.30) in all LT patients, aHR = 1.30 (1.05–1.62) in acute liver disease, aHR = 1.20 (1.13–1.28) in HCC, and aHR = 1.28 (1.23–1.34) in non-HCC (all $p < 0.02$). Other risk factors included an earlier calendar year for LT, older age, higher MELD score, lack of college education, coverage by Medicare or Medicaid, and being on life support before LT ($p < 0.01$). However, there was no association between pre-LT T2D and greater the risk of graft failure (one-sided $p > 0.05$).

Conclusion: There is a growing burden of T2D among liver transplant candidates in the United States. The presence of pre-transplant T2D is independently associated with an increased risk of post-transplant mortality in all LT subgroups.

THU-493

The evolution of the muscle compartment from the listing to six-month post-transplantation: a longitudinal monocentric study

Delorme Alicia^{1,2}, Alexis Goffaux³, David De Azevedo⁴, Colin Dumont¹, Guillaume Henin³, Marie Philippart¹, Frédéric Braem¹, Olga Ciccarelli⁵, Pierre Trefois⁶, Nicolas Lanthier^{7,8}, Géraldine Dahlqvist¹. ¹Clinique Universitaire Saint-Luc, Hepatology and Gastroenterology, Bruxelles, Belgium; ²Clinique Universitaire Saint-Luc, Hepatology, Bruxelles, Belgium; ³Clinique Universitaire Saint-Luc, Laboratory of Hepatology and Gastroenterology, Bruxelles, Belgium; ⁴Clinique Universitaire Saint-Luc IREC/CARD, Cardiovascular Disease, Bruxelles, Belgium; ⁵Clinique Universitaire Saint-Luc, Abdominal Surgery and Liver Transplant Department, Bruxelles, Belgium; ⁶Clinique Universitaire Saint-Luc, Radiology, Belgium; ⁷Cliniques universitaires Saint-Luc (UCLouvain), Service d'Hépatogastroentérologie, Bruxelles, Belgium; ⁸Université Catholique de Louvain, Laboratory of Hepato-Gastroenterology, Institut de Recherche Expérimentale et Clinique, Brussels, Belgium
 Email: alidelorme0206@gmail.com

Background and aims: Body composition of the cirrhotic patient plays an important role in his prognosis. Skeletal muscle mass (sarcopenia), malnutrition, frailty (liver frailty index LFI) and

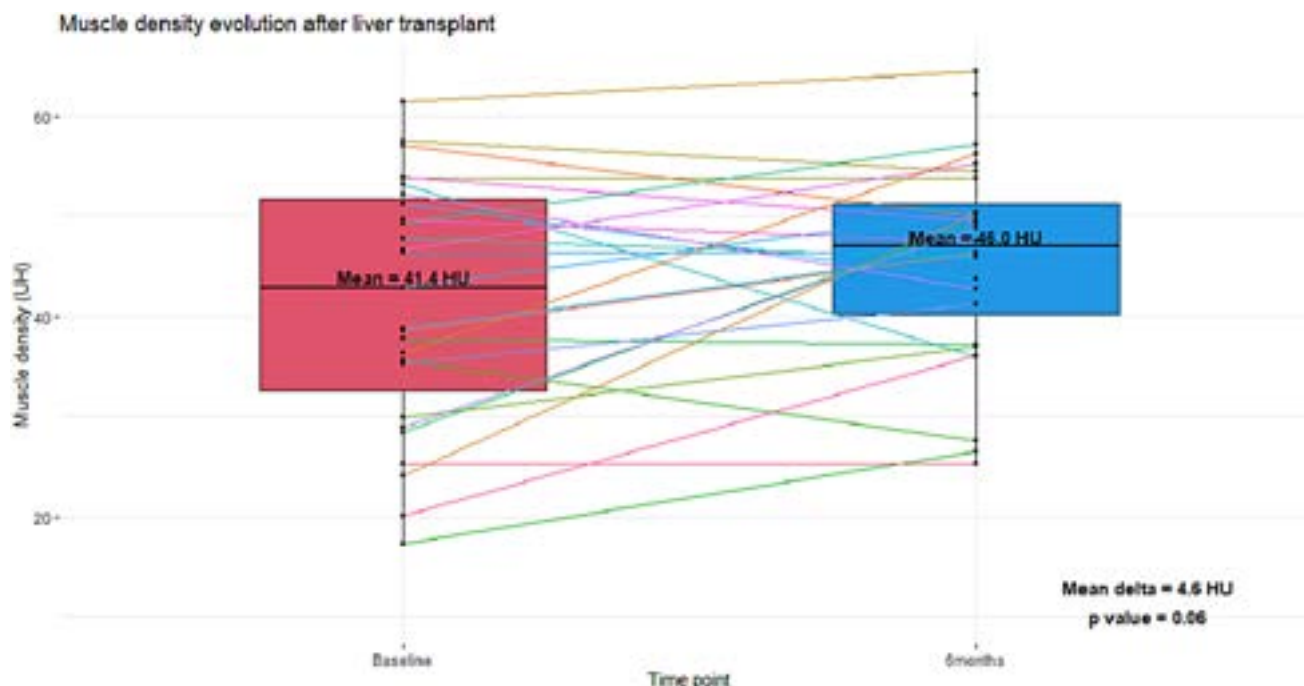


Figure: (abstract: THU-493).

myosteotosis are associated with worse outcome in cirrhotic patients. The aim of this study was to determine the best muscle-related predictor of morbidity and mortality on the waiting list and after LT and to evaluate the evolution of all muscle-related parameters up to six months post-transplant.

Method: This single-center prospective observational study screened adult patients who were candidates for liver transplantation from June 2021 to September 2022. Each candidate received a functional and nutritional assessment during its pre-transplant evaluation. Muscle quantity and quality were assessed using an abdominal CT scan at the third lumbar level (L3). Sarcopenia was defined as skeletal muscle mass index (SMI) $<39 \text{ cm}^2/\text{m}^2$ in females and $<50 \text{ cm}^2/\text{m}^2$ in males. Myosteotosis was assessed by skeletal muscle radiodensity attenuation (SM-RA), with cut-offs of SM-RA $<41 \text{ HU}$ for patients with a BMI $<24.9 \text{ kg}/\text{m}^2$ and $<33 \text{ HU}$ for patients with a BMI $\geq 25 \text{ kg}/\text{m}^2$. Frailty was defined using the Liver Frailty Index (LFI). Time-to-event analysis was performed using Kaplan-Meier method to investigate the impact of functional variables on outcome. One-year survival was determined for patients who underwent liver transplant during this period. Univariate and multivariate Cox proportional hazard regressions were computed to identify predictors of morbidity and mortality on the waiting list for LT.

Results: 103 patients were screened, 84 were placed on the Eurotransplant LT waiting list and 49 were transplanted during the study period. The mean age was 54 years and 67.7% were males. The primary etiology of liver disease was alcohol and 38% had a hepatocellular carcinoma. The one-year patient survival probability on the waiting list was $76.9 \pm 7.2\%$. This probability was significantly reduced in patients with myosteotosis compared with patients with higher SM-RA values ($43 \pm 17\%$ vs $95 \pm 4\%$, $p < 0.001$). Compared with other muscle characteristics, myosteotosis was the strongest predictive factor of mortality. 28 patients had a full 6-months post-LT assessment. Of those liver transplanted patients, 57.7% were frail and 40.7% had myosteotosis before LT. At 6 months post-LT, 53.8% were frail and only 25% had myosteotosis. SMI was not different before and after LT. Compared with pre-LT data, muscle density increased with a mean delta of 4.6 HU ($p = 0.06$) (Figure). The 5 chairs stand test significantly improved after LT (11.6 sec vs 9.0 sec ($p = 0.013$)). The other parameters (handgrip, LFI, ...) remained stable.

Conclusion: Myosteotosis is significantly associated with negative pre-transplant outcomes. After LT, patients improve in muscle strength but not in muscle quantity or quality evaluated by CT-scan.

THU-494

Endothelial glycocalyx damage marker Syndecan-1 measured during hypothermic oxygenated machine perfusion can predict early allograft dysfunction after liver transplantation

Laurin Rauter¹, Judith Schiefer², Pierre Raeven², Thomas Öhlinger², Marija Spasic¹, Effimia Poupouridou¹, Jule Dingfelder¹, Andreas Salat¹, Zoltan Mathe¹, Georg Gyöeri¹, Thomas Soliman¹, Dagmar Kollmann¹, Gabriela Berlakovich¹. ¹Medical University of Vienna, Department of General Surgery, Division of Transplantation, Austria; ²Medical University of Vienna, Department of Anesthesia, Intensive Care Medicine and Pain Medicine, Austria
Email: laurin.rauter@meduniwien.ac.at

Background and aims: During liver transplantation, the graft has to endure an ischemic phase and additional injury after reperfusion (IRI), especially mediated by reactive oxygen species (ROS). The endothelial glycocalyx covers the luminal side of the vascular endothelium and regulates vascular permeability, modulates adhesion of leucocytes onto the vascular wall and transduces mechanical shear stress. It is very sensitive to ROS and therefore degraded during graft preservation and reperfusion. Hypothermic oxygenated machine perfusion (HOPE) is a preservation strategy that can reduce IRI-inflicted graft injury compared to static cold storage (SCS). We aimed to measure glycocalyx degradation after HOPE or

SCS alone, to evaluate its viability-assessment potential for liver transplantation.

Method: We measured glycocalyx degradation via ELISA for its main component Syndecan-1, in samples from 77 liver transplant patients. 37 grafts were directly transplanted after SCS, 40 grafts additionally underwent HOPE with the Organ Assist® perfusion system, prior to liver transplantation.

Results: Sdc-1 concentrations in the graft effluent are significantly lower after HOPE [466 (350–1073)] compared to SCS alone [4011 (3382–4683)] ($p < 0.001$). Further, Sdc-1 concentrations regenerate faster towards baseline levels on postoperative day 1 [HOPE: 362 (232–880) vs. SCS: 1017 (637–1900) $p < 0.001$], indicating a shorter glycocalyx shedding period. Regarding viability assessment, Sd1-concentrations in the perfusate were elevated in EAD patients after 60 minutes of HOPE compared to non-EAD patients [429 (260–556) vs. 896 (419–1681) $p = 0.018$]. Additionally ROC-analysis indicated a significant discriminatory value of Sdc-1 concentration after 60 minutes of HOPE regarding the occurrence of EAD with an AUC of 74% ($p = 0.018$, sensitivity 66.7% and specificity 84.6%).

Conclusion: HOPE reduces the duration of glycocalyx shedding, evident by Sdc-1 release in recipient serum after liver transplantation. Sdc-1 concentration during HOPE can predict early allograft dysfunction. Therefore, Sdccc-1 could be a potential viability assessment marker in liver transplantation.

THU-495

Use of von Willebrand factor antigen for surgical decision making in patients with hepatocellular carcinoma

David Pereyra^{1,2}, Lindsey Gregory³, Aidan Mullan³, Anna Kern¹, Jule Dingfelder², Hubert Hackl⁴, Thomas Grünberger⁴, Rory L. Smoot³, Sean Cleary³, David M. Nagorney³, Mark Truty³, Susanne Warner³, Cornelius Thiels³, Michael Kendrick³, Georg Gyöeri², Patrick S. Kamath⁵, Gabriela Berlakovich², Julie Heimbach⁶, Patrick Starlinger^{1,3}. ¹Medical University of Vienna, Department of General Surgery, Division of Visceral Surgery, Austria; ²Medical University of Vienna, Department of General Surgery, Division of Transplantation Surgery, Austria; ³Mayo Clinic Rochester, Department of Surgery, Division of Hepatobiliary and Pancreatic Surgery, United States; ⁴HPB Center, Viennese Health Network, Clinic Favoriten and Sigmund Freud Private University, Department of Surgery, Austria; ⁵Mayo Clinic Rochester, Division of Gastroenterology and Hepatology, United States; ⁶Mayo Clinic Rochester, Department of Surgery, Division of Transplantation Surgery, United States
Email: david.pereyra@meduniwien.ac.at

Background and aims: Potential treatment modalities for hepatocellular carcinoma (HCC) are widely varied. Many affected patients undergo transplant or resection with curative intent. While current guidelines aim to clarify appropriate patient selection for liver resection (LR) or transplantation (LTx), both modalities carry significant risk of adverse perioperative outcomes that warrant improvement. We previously reported on von Willebrand factor antigen (vWF-Ag) as a predictor of both post-hepatectomy liver failure (PHLF) and early mortality on the waiting list for LTx. Herein, we explore the use of vWF-Ag as a tool for perioperative decision-making in patients with HCC.

Method: Included patients were diagnosed with HCC within Milan criteria and underwent either LR or listing for LTx at Medical University of Vienna (MUV) and Mayo Clinic Rochester (MCR) between 2004 and 2022. VWF-Ag was evaluated prior to LR or at time of listing for LTx, respectively. The previously evaluated cut-offs at 182% and 291% vWF-Ag were used to divide the cohort into low- ($\leq 182\%$), intermediate- (183%–291%) and high-risk ($> 291\%$) groups. Clinical course and overall survival (OS) were prospectively documented and retrospectively analyzed (chi-squared, Kaplan-Meier).

Results: In total, 443 patients were included: 106 patients underwent LR (MUV: 72, MCR: 34); 337 patients were listed for LTx (MUV: 214, MCR: 123), of those 199 underwent LTx (MUV: 124, MCR: 75).

POSTER PRESENTATIONS

Patients in intermediate- and high-risk groups undergoing LR displayed significantly higher incidences of PHLF (low = 4.0%, intermediate = 27.5%, high = 53.3%, $p < 0.001$). Furthermore, post-operative OS was significantly reduced in both these cohorts (median in months: low = 95.5, intermediate = 46.7, high = 13.7, $p = 0.006$). As previously reported for a cohort of all-comers listed for LTx, HCC patients with increased vWF-Ag had reduced survival on the waiting list ($p = 0.01$). Yet, no difference in post-LTx OS was observed when comparing risk groups according to vWF-Ag (median in months: low = not reached, intermediate = 130.4, high = 116.6, $p = 0.343$). Similarly, OS from listing was comparable between vWF-Ag risk groups (median in months: low = 108.7, intermediate = 131.8, high = 90.0, $p = 0.390$).

Conclusion: Herein, we present an international bicentric evaluation of vWF-Ag as a perioperative decision-making tool for patients with HCC. Patients with high vWF-Ag prior to LR show an increased risk for PHLF and reduced OS and therefore seem to derive limited benefit from surgery. Furthermore, increased vWF-Ag is associated with poor outcome while on the LTx waiting list. Because no difference in post-LTx OS was observed between risk groups according to vWF-Ag, patients presenting with HCC and high vWF-Ag values may benefit from a vWF-Ag risk adjusted LTx listing process. We conclude that vWF-Ag can optimize LR and LTx decision-making for patients with HCC.

THU-496

Incidence and risk factors for de-novo NAFLD after liver transplantation: real-world data

Lea Guetzlaff¹, Alejandro Campos-Murguía¹, Emily Bosselmann¹, Anna Katharina Baumann¹, Björn Hartleben², Elmar Jaeckel³, Richard Taubert¹, Katharina Luise Hupa-Breier¹. ¹Hannover Medical School, Gastroenterology Hepatology, and Endocrinology, Germany; ²Hannover Medical School, Pathology, Hannover, Germany; ³University of Toronto, Ajmera Transplant Center, Canada
Email: hupa.katharina@mh-hannover.de

Background and aims: Non-alcoholic fatty liver disease (NAFLD) is not only a leading indication for liver transplantation (LT), but also a frequent complication after LT in patients, who developed graft dysfunction. However, the overall incidence of de-novo NAFLD after LT and its risk factors even in patients without graft dysfunction are unknown. This is the first study to describe the incidence and risk factors of de-novo steatosis and steatohepatitis in a unique cohort of surveillance and indication biopsies from patient after LT.

Method: This was a retrospective single-center study in a post-LT cohort with surveillance (svLbx) and indication biopsies (indLbx). Patients with NAFLD as primary indication for LT were excluded. Risk factors were analyzed with univariate and multivariate analyses. P values < 0.05 were considered as statistical significant.

Results: After applying the in- and exclusion criteria, we analyzed 255 representative biopsies from patient after LT, where 21% ($n = 54$) of patient had NAFLD, in which already 43% ($n = 23$) had non-alcoholic steatohepatitis (NASH) (Figure 1). Interestingly, the incidence of de-novo NAFLD in svLbx was with 18% nearly similar compared to the overall cohort. PSC as primary disease is associated with significant decreased risk of de-novo steatosis after LT. On the multivariate analyses, BMI after LT and Diabetes mellitus are independent risk factors for development of NAFLD and NASH (OR: 1.09, $p = 0.006$ for BMI, OR: 1.68, $p = 0.033$ for diabetes). Furthermore, transaminases were significantly higher in NAFLD and NASH patient compared to control group, although transaminases were still in the normal range. Therefore, even borderline elevations of transaminases should raise suspicion of graft injury including NAFLD, especially in patients with other risk factors.

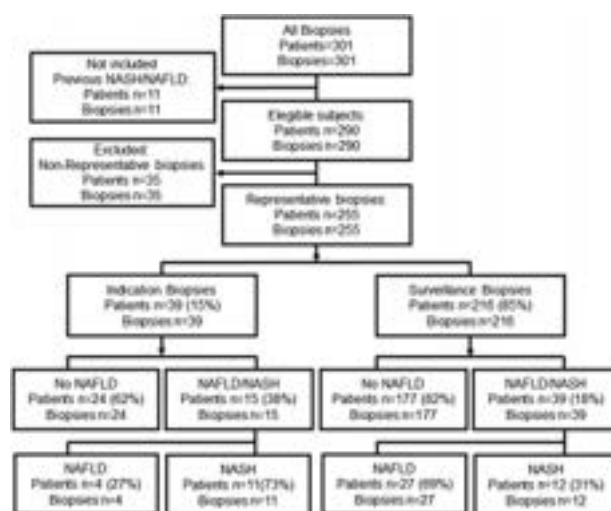


Figure:

Conclusion: To date, this is the first study representing the actual incidence of de-novo NAFLD in the overall post-LT cohort. It demonstrates that de-novo steatosis and steatohepatitis are common findings after LT even in patients without clinical signs of graft dysfunction and therefore supports the indication for post-LT biopsies on a regular basis even without signs of graft dysfunction.

THU-497

Long-term outcomes following donation after cardiac death (DCD) liver transplantation in primary sclerosing cholangitis (PSC)

Arul Suthanathan¹, Nadir Abbas^{1,2}, Graham Caine^{1,2}, James Ferguson^{1,2}, Thamara Perera¹, Palak Trivedi^{1,2}. ¹University Hospitals Birmingham, Liver Unit, United Kingdom; ²University of Birmingham, National Institute for Health Research (NIHR) Birmingham Biomedical Research Centre (BRC), Birmingham, United Kingdom
Email: p.j.trivedi@bham.ac.uk

Background and aims: Liver transplantation is the only life-extending intervention for individuals with PSC. Whilst donation after brain death (DBD) is the practice of choice, patients may endure prolonged waitlist times due to young age. Equally, outcome data following DCD transplantation are conflicting, particularly with regards long-term follow-up. We have previously published data showing that post-transplant outcomes among PSC patients transplanted with a DCD liver were no different to that of DBD recipients at 1 year (*J Hepatol.* 2017; PMID:28690174). In the current study, we seek to validate prior observations through a contemporary PSC transplant cohort, in parallel to long-term evaluation of graft loss and re-graft-free survival among patients with a minimum 5 years since their first transplant.

Method: Long-term outcomes following DCD transplantation in PSC (DCD-PSC) were compared to DBD recipients (DBD-PSC). (A) First, we validated 1y-outcomes presented from our previous study (liver transplants performed 2006–2016) with a contemporary cohort transplanted 2016–2020. (B) Next, we evaluated long-term outcomes in the combined cohort of patients (transplanted 2006–2020), alongside (C) 5y-outcomes specifically in the 2006–2016 cohort, including for non-PSC patients (DCD-nonPSC).

Results: (A) In the 2016–2020 cohort, 1y-risk of death-censored graft loss was not significantly greater in the DCD-PSC vs DBD-PSC group (odds ratio [OR]: 2.6; 95% CI: 0.96–7.0), nor was the risk of all-cause mortality (1.14; 0.39–3.38) or re-graft-free survival (2.66; 0.79–8.89). (B) In the combined 2006–2020 cohort, a total of 17 patients experienced graft loss in the DCD-PSC group, compared to 30 in the DBD-PSC group (Fig. 1A); 88% of the DCD-PSC graft losses occurred within five years of transplantation vs. 60% in the DBD-PSC group.

Figure 1: Post-transplant outcomes stratified by donor type and underlying disease aetiology

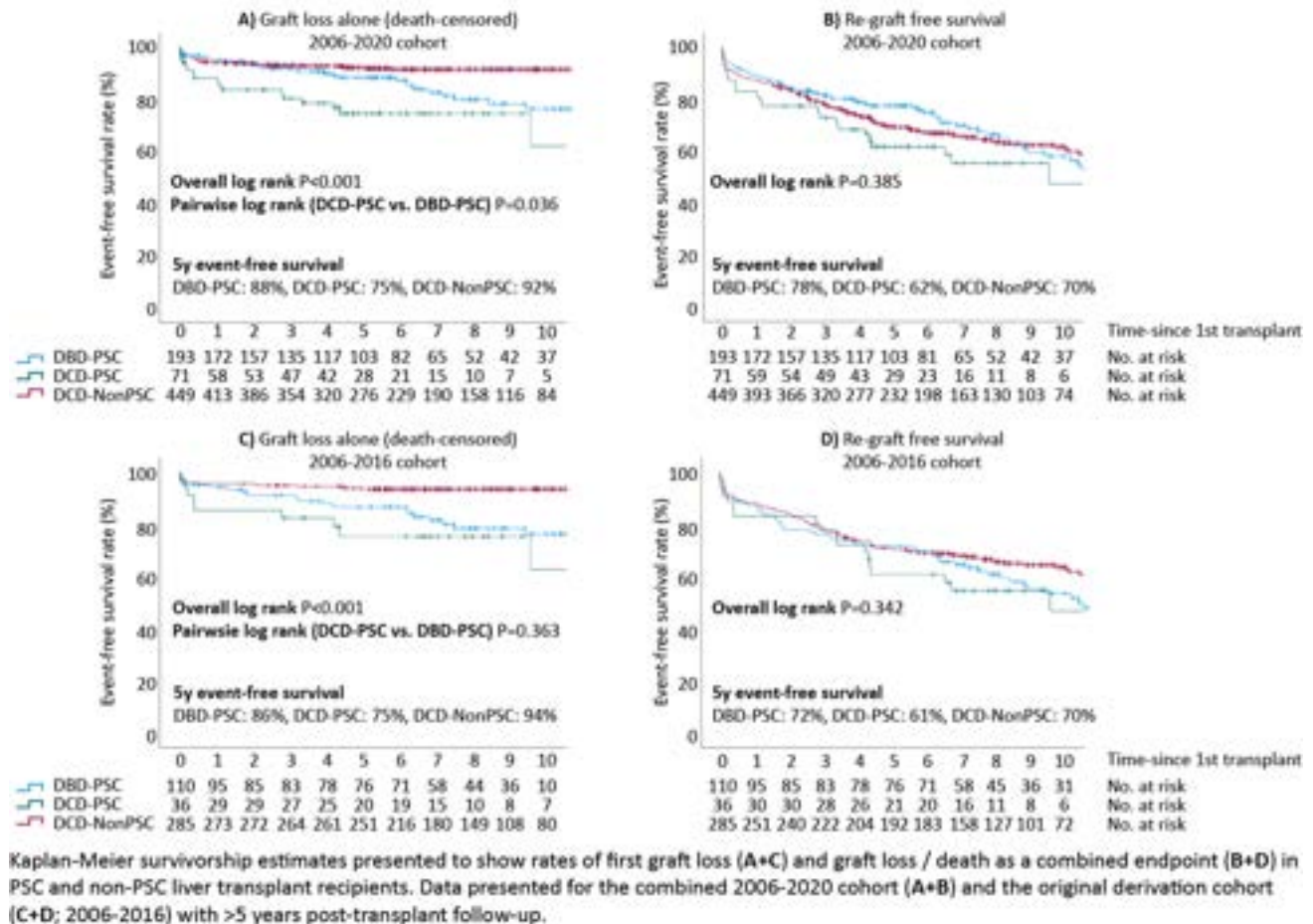


Figure 1: (abstract: THU-497).

However, overall re-graft-free survival was not significantly different between PSC groups, and both were inferior to DCD-nonPSC (Fig. 1B). (C) On restricting analysis to patients with a minimum 5 y since first transplant, the risks of death-censored graft loss (hazard ratio [HR]: 1.44; 0.66–3.14), all-cause mortality (0.62; 0.29–1.34) and re-graft-free survival (1.14; 0.66–1.97) were not significantly greater for DCD-PSC vs. DBD-PSC (Fig. 1C+D).

Conclusion: In an era of organ shortage, re-graft-free survival rates are not significantly different for PSC patients transplanted with a DCD vs. DBD liver. Given the heightened risks of graft loss in PSC compared to non-PSC patients, improved understanding of high-risk combinations of donor-recipient factors is essential to maximise outcomes following transplantation.

THU-498

Evaluation of a delayed liver transplant strategy for patients listed for hepatocellular carcinoma treated with resection or thermo-ablation as a bridge to liver transplantation; the DELTAS-HCC study

Catherine Lamarque¹, Lauriane Segaux¹, Armand Aberger², Philippe Bachellier³, Faiza Chermak⁴, Audrey Coilly⁵, Filomena Conti⁶, Thomas Decaens⁷, Sebastien Dharancy⁸, Vincent Di Martino⁹, Jérôme Dumortier¹⁰, Claire Francoz¹¹, Jean Gugenheim¹², Jean Hardwigsen¹³, Fabrice Muscarì¹⁴, Sylvie Radenne¹⁵, Ephrem Salame¹⁶, Thomas Uguen¹⁷, José Ursic Bedoya¹⁸, Corinne Antoine¹⁹, Vincent Leroy¹, Nadia Oubaya¹, Christophe Duvoux¹. ¹Henri Mondor Hospital APHP- Paris Est

University, France; ²CHU Estaing, France; ³Hopitaux Universitaires Strasbourg, France; ⁴Bordeaux University Hospital, France; ⁵Centre Hépatobiliaire, Hôpital Paul Brousse, France; ⁶APHF, France; ⁷HOPITAL ALBERT MICHALLO, France; ⁸HOPITAL CLAUDE HURIEZ, France; ⁹CHU Jean Minjoz, France; ¹⁰HOPITAL EDOUARD ERRIOT, France; ¹¹Beaujon University Hospital, France; ¹²Department of Digestive Surgery, Archet Hospital, University of Nice-Sophia Antipolis, France; ¹³Aix Marseille University, Department of General Surgery and Liver Transplantation, Hôpital la Timone, France; ¹⁴Toulouse University Hospital, France; ¹⁵Hospices Civils de Lyon, France; ¹⁶CHU Trousseau, France; ¹⁷HOPITAL PONTCHAILLOU, France; ¹⁸CHU Montpellier, France; ¹⁹Agence de biomedecine, France
Email: catherine.lamarque@yahoo.fr

Background and aims: To maximize utility and prevent premature liver transplantation (LT), a delayed transplant strategy (DS) was adopted in France in 2015 in patients listed for any single hepatocellular carcinoma (HCC) treated with surgical resection (SR) or thermo-ablation (TA) during the waiting phase, postponing LT until recurrence. It is crucial to make sure that pre and post-LT outcomes of patients entering DS are not negatively impacted. The purpose of this study was to evaluate this DS.

Method: Study population: patients listed for HCC in France between 2015 and 2018, with an AFP score ≤ 2 . After data extraction from the national LT database, Cristal, 2025 patients were classified according to 6 groups: single tumor entering DS, single tumor not entering DS (NDS), multiple tumors (MT), other loco-regional therapies (LRT) with no DS, untreatable HCC (UH) and T1 tumors (T1). 18-months

POSTER PRESENTATIONS

Kaplan-Meier estimates of drop-out before LT and 5-year post-LT recurrence and survival rates were compared.

Results: The patients' features are shown in the table. Pre-LT drop-out probabilities were 13, 18, 21, 22 and 25% in DS, LRT and MT, UH, NDS and T1, respectively ($p = 0.05$), significantly lower in DS, and higher in T1. Post-LT 5-year survival and recurrence rates did not differ among groups.

	DS N = 341 (16.8%)	NDS N = 74 (3.7%)	MT N = 238 (11.7%)	LRT N = 879 (43.4%)	UH N = 346 (17.1%)	T1 N = 147 (7.3%)	p
MELD (median)	8.47	10.25	8.95	9.93	15.54	13.21	<0.0001
Tumor size (cm) (median)	2.5	2.55	2.4	3.0	2.3	1.5	0.0005
Number of tumor (median)	1.0	1.0	2.0	2.0	2.0	1.0	0.006
AFP (ng/ml) (median)	7.95	7.00	9.25	9.30	5.71	7.00	1
Time from treatment to LT (days) (median)	910	285	666	442		717	<0.0001

This study benefited from a grant of Agence de la Biomédecine, the French Organ Sharing Organization.

Figure:

Conclusion: The DELTAS HCC study shows that: DS can be considered in around 20% of HCC candidates (DS and NDS groups), DS in patients amenable to curative treatments pre-LT has no negative impact on pre- and post-LT outcomes, DS has the potential to redistribute organs to patients in more urgent need and can reasonably be pursued. The unexpected high drop-out in T1 patients seems related to a combination of purely MELD-based driving rules, with a 15 median MELD at listing, hampering bridging treatments and access to LT. It calls for revision of allocation rules in this subgroup.

THU-499

Use and outcomes of hepatitis B virus positive grafts for renal or heart transplantation in the US (1999–2021)

Ashwani Singal¹, K. Rajender Reddy², Mindie Nguyen³, Zobair M. Younossi⁴, Paul Yien Kwo³, Yong-Fang Kuo⁵. ¹University of South Dakota-Sioux Falls, Sioux Falls, United States; ²University of Pennsylvania, Philadelphia, United States; ³Stanford University, Stanford, United States; ⁴Fairfax, Fairfax, United States; ⁵UTMB Health-University of Texas Medical Branch at Galveston, Galveston, United States
Email: ashwanisingal.com@gmail.com

Background and aims: The gap between demand and supply for solid organ transplants continues to widen, requiring strategies to expand the donor pool. The use of hepatitis B virus (HBV) positive grafts in liver transplantation without impacting the graft and patient survival has been reported. However, the outcomes of kidney transplant (KT) or heart transplant (HT) recipients with HBV positive grafts from deceased donors is not known.

Method: We examined the outcomes of recipients undergoing KT or HT with HBV positive grafts (hepatitis B surface antigen and/or HBV nucleic acid test [NAT] positive) from deceased donors using the UNOS database (01/1999 to 06/2021). Propensity score matching (1:5) was done for KT recipients of HBV positive with HBV negative grafts for transplant year, recipient demographics, donor age, and serum creatinine at transplant. Similar matching (1:10) was done among HT recipients for transplant year and recipient demographics.

Results: Among 189,898 potential donors, 448 (0.24%) were HBV positive with 996 kidneys and 448 hearts available for transplantation. Of these, 352 kidneys (35.3%) and 56 hearts (12.5%) were transplanted, with 332 kidneys and 53 hearts in HBV negative recipients. Although, use of HBV positive kidney and heart grafts increased over time ($p < 0.001$), 60% of kidneys and 94% of heart grafts were discarded in 2020. Among KT recipients of HBV positive and negative grafts, 10-yr. graft survival rates were similar at 47.1% and 49% (log rank $P = 0.353$), and respective patient survival rates were 58% and 59% ($p = 0.999$). Similarly, among HT recipients of HBV positive and negative grafts, 10-yr. graft survival rates were 41.9% and 38.9% for graft survival ($p = 0.471$), and 54.3% and 61.2% for patient

survival ($p = 0.277$). Outcomes were similar in subgroups with HBV grafts matched with HBV negative grafts based on HBsAg, NAT, and anti-HBc serology (Figure).

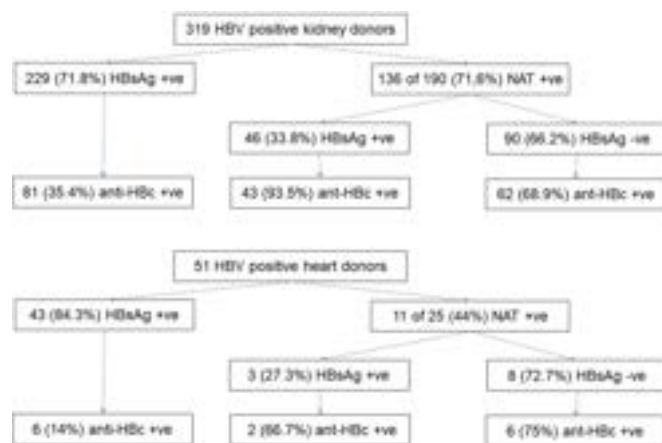


Figure: Hepatitis B surface antigen (HBsAg), nucleic acid test (NAT), and core antibody (anti-HBc) status of hepatitis B positive donor kidneys (A) and hearts (B).

Conclusion: These observations wherein that use of HBV positive donors for KT or HT did not impact the recipient graft or patient survival, suggest that it is a reasonable strategy to expand the donor pool and lower the waitlist mortality rate among candidates waiting for kidney or heart transplant.

THU-500

Donor outcomes incidence after living-donor liver transplantation: meta-analysis and systematic review

Jieling Xiao¹, Rebecca Wenling Zeng¹, Wen Hui Lim¹, Darren Jun Hao Tan¹, Cheng Han Ng¹, Margaret Teng², Eunice Tan², Daniel Huang², Mohammad Shadab Siddiqui³, Alfred Kow², Mark Muthiah². ¹Yong Loo Lin School of Medicine, National University of Singapore, Singapore; ²National University Health System, Singapore; ³Division of Gastroenterology, Department of Internal Medicine, Virginia Commonwealth University, United States
Email: margaret.tenglp@gmail.com

Background and aims: Liver transplantation remains a critical means of treatment for end stage liver disease which has increased steadily in the recent decades. The scarcity of liver grafts has prompted developments in living donor liver transplantations (LDLT) with previous literature illustrating similar outcomes in recipients as compared to deceased donor transplants. However, there are concerns regarding living donor morbidity and mortality which has yet to be examined comprehensively. This study aims to provide estimates of the incidence of various outcomes in living liver donors.

Method: In this meta-analysis, Medline and Embase were searched from inception to July 2022 for articles assessing incidence of outcomes in LDLT donors. Analysis of incidence was done using a generalised linear mixed model with Clopper-Pearson intervals in terms of incidence rate per 10,000 person-days. With regards to risk factors, binary variables were analysed with generalised linear model while meta regression with logit transformation was done for continuous variables.

Results: Of 5074 abstracts, 182 articles involving 60,152 living liver donors were included. The overall pooled incidence rate of complications in LDLT donors was 29.23 (CI: 23.42 to 36.48) per 10,000 person-days. The incidence rate of complications in liver donors in study conducted before and in 2010 was 40.77 (CI: 30.32 to 54.82) while that on study conducted after 2010 was 22.84 (CI: 16.79 to 31.07) per 10,000 person days. The incidence rate of major complications was 5.32 (CI: 4.10 to 6.90) while the incidence rate of

donor mortality was 0.05 (CI: 0.02 to 0.12) per 10,000 person-days. The complications with the highest incidence rate in LDLT donors were respiratory complications (IR: 6.28, CI: 4.40 to 6.95), followed by wound-related (IR: 5.95, CI: 4.64 to 7.62) and biliary complications (IR: 5.59, CI: 4.49 to 6.95) per 10,000 person-days. Additionally, the incidence rate of cardiovascular complications was lowest amongst the subgroups of complications at 0.81 (CI: 0.41 to 1.62) per 10,000 person-days. Duration of ICU stay was significantly associated with greater complications rate in liver donors while preoperative liver volume, donation volume and liver remnant were not.

Conclusion: This study presents the incidence of post-LDLT outcomes in liver donors illustrating the high incidence of respiratory, wound-related and biliary complications. While significant advancements in recent decades have contributed towards decreased morbidity in living liver donors, targeted measures and continued efforts are warranted to ensure the safety and quality of life of liver donors post LDLT.

THU-501

Access to liver transplant for women in Spain: a national registry analysis

Marta Tejedor Bravo¹, Fernando Neria², Gloria de la Rosa³, Carolina Almohalla Alvarez⁴, Andrea Bosca⁵, Yilliam Fundora⁶, Francisco Sánchez-Bueno⁷, Marina Berenguer⁵. ¹Hospital Universitario Infanta Elena, Gastroenterology and Hepatology, Spain; ²Universidad Francisco de Vitoria, Madrid, Spain; ³Organización Nacional de Trasplantes, Madrid, Spain; ⁴Comité científico del Registro Español Trasplante Hepático, Spain; ⁵La Fe University and Polytechnic Hospital, València, Spain; ⁶Hospital Clínic de Barcelona, Barcelona, Spain; ⁷Hospital Clínico Universitario Virgen de la Arrixaca, El Palmar, Spain
Email: marina.berenguer@uv.es

Background and aims: Gender inequities in liver transplantation (LT) have been documented recently in several studies. Providing national data is crucial as poorer access to liver transplantation for women than men might be explained by different analytical approaches or different national contexts. Our aim was to describe the recipient profile over time in Spain, particularly regarding potential sex-related differences in access to LT.

Method: All adult patients registered in the RETH-Spanish Liver Transplant Registry from 2000 to 2018 for LT were included. Baseline demographics, presence of hepatocellular carcinoma (HCC), cause and severity of liver disease, time on the waiting list (WL), access to transplantation, and reasons for removal from the WL were assessed.

Results: 9427 patients were analyzed (77.6% men, 55.3 ± 8.6 years of age). Mean MELD score was reported for 3404 patients (36.1%), and was 16.5 ± 5.8. Women were less likely to receive a transplant than men (OR 0.84, 95% CI 0.73, 0.97) and more likely to be excluded for deterioration (HR 1.21, 95% CI 1.02, 1.44), despite similar liver disease severity (MELD score 16.6 ± 5.8 vs 16.5 ± 5.8 respectively, N.S) and only a slightly longer mean time on the WL (244 ± 398 days for women vs 213 ± 324 for men, p = 0.001). In recent years, this difference in access to LT was less significant (before 2011 women's HR for exclusion was 1.51 [95% CI 1.01, 2.26] vs 1.17 [95% CI 0.97, 1.41] after 2011) and could be attributed to overall shorter mean WL times after 2011 (398 ± 602 vs 154 ± 217 days respectively, p < 0.001). When analyzed by MELD, WL times were similar by sex for patients with scores under 16 or above 20, but women had significantly longer mean WL times than men with MELD scores 16–20 (270 ± 267 vs 211 ± 207 days respectively, p < 0.001). Women were shorter (170.5 ± 9.7 vs 158.5 ± 9.8 cm) but had a similar BMI compared to men. In women, the main indications for transplant were cholestatic liver diseases, autoimmune hepatitis and NASH, whilst in men it was alcohol (p < 0.001). Women had less HCC than men (27.1 vs 16.6%, p < 0.001).

Conclusion: Shorter WL times contribute to a more equal access to LT by sex, as it prevents women from deteriorating while waiting and therefore being excluded from the list.

THU-502

Body composition and MAFLD are associated with prognosis after resection of intrahepatic cholangiocarcinoma

Isabella Lurje¹, Deniz Uluk², Sandra Pavicevic², Minh Phan¹, Timo Auer³, Dominik Modest⁴, Frank Tacke¹, Johann Pratschke², Georg Lurje². ¹Charité-Universitätsmedizin Berlin, Department of Hepatology and Gastroenterology, Campus Charité Mitte | Campus Virchow-Klinikum, Berlin, Germany; ²Charité-Universitätsmedizin Berlin, Department of Surgery, Campus Charité Mitte | Campus Virchow-Klinikum, Germany; ³Charité-Universitätsmedizin Berlin, Department of Radiology, Germany; ⁴Charité-Universitätsmedizin Berlin, Department of Hematology, Oncology, and Tumor Immunology, Germany
Email: isabella.lurje@charite.de

Background and aims: Body composition alterations are frequent in patients with cancer or chronic liver disease. We investigated the impact of disease etiology and body composition after surgery for intrahepatic cholangiocarcinoma (iCCA), a rare and understudied cancer entity in European cohorts.

Method: Computer tomography-based assessment of body composition at the level of the third lumbar vertebra was performed in 173 patients undergoing curative-intent liver resection for iCCA. Muscle mass and -quality as well as subcutaneous and visceral adipose tissue quantity were determined semi-automatically. Sarcopenia, sarcopenic obesity, myosteatosis, visceral and subcutaneous obesity were correlated to clinico-pathological data.

Results: Fifty-eight patients (34%) had metabolic (dysfunction)-associated fatty liver disease (MAFLD). Patients with MAFLD had a higher incidence of sarcopenic (p = 0.006), visceral (p < 0.001) and subcutaneous obesity (p < 0.001). At the same time, patients with MAFLD had longer disease-free survival than patients without liver disease or with fibrosis (median: 38 months vs. 12 months, p = 0.025). Sarcopenia was associated with higher postoperative morbidity (intraoperative transfusions [p = 0.027], Clavien-Dindo ≥ IIIb complications [p = 0.030], postoperative comprehensive complication index, CCI [p < 0.001]). Inferior overall survival was noted in patients with subcutaneous obesity (median: 35 vs. 23 months, p = 0.042) and myosteatosis (33 vs. 23 months, p = 0.020). Multivariable analysis confirmed only clinical parameters (lymph node invasion, CCI > 40) as independently prognostic for overall survival.

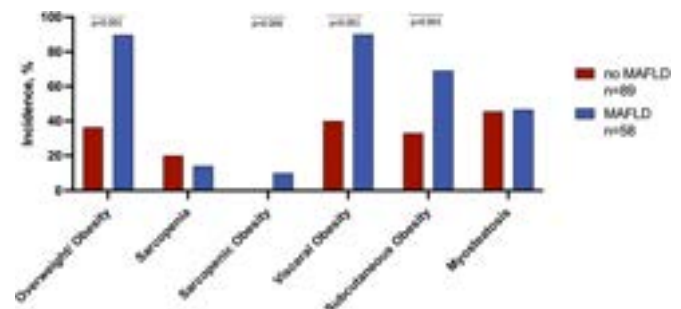


Figure:

Conclusion: This study evidenced a high prevalence of MAFLD in iCCA, suggesting its potential contribution to disease etiology. While being associated with body composition phenotypes regarded as pathological, MAFLD may be associated with improved disease-free survival in patients undergoing surgery for iCCA.

THU-503

Cytomegalovirus reactivation is associated with lower hepatocellular carcinoma recurrence rates after liver transplantation

Victoria Aguilera Sancho^{1,2,3}, Sarai Romero Moreno⁴, Isabel Conde^{1,3,5}, Ángel Rubín^{1,5,6}, Cristina Dopazo⁷, Antonio Cuadrado⁸, Carmen Bernal⁹, Sheila Pereira¹⁰, Magdalena Salcedo¹¹, Sara Lorente Perez¹², Ana Sánchez Martínez¹³, Javier Zamora¹⁴, Sonia Pascual¹⁵, Esteban Fuentes Valenzuela¹⁶, Laura Martínez-Arenas⁵, Jose Ignacio Herrero¹⁷, Marina Berenguer¹⁸, Manuel Rodríguez-Perálvarez^{3,14}. ¹La Fe University and Polytechnic Hospital, Hepatology and Liver Transplant Section, Valencia, Spain; ²Instituto de Investigación Sanitaria La Fe de Valencia, Valencia, Spain; ³CIBERehd Instituto de Salud Carlos III, Spain; ⁴La Fe University and Polytechnic Hospital, Hepatology and Liver Transplant Section, Valencia, Spain; ⁵Instituto de Investigación Sanitaria La Fe de Valencia, Valencia, Spain; ⁶Ciberehd, Instituto Carlos III, Spain; ⁷Hospital Universitario Vall d'Hebron, Barcelona, Spain; ⁸Hospital Universitario Marqués de Valdecilla, Department of Gastroenterology and Hepatology, Santander, Spain; ⁹Hospital Universitario Virgen del Rocío, Hepato-Biliary-Pancreatic Surgery, Sevilla, Spain; ¹⁰Hospital Universitario Virgen del Rocío, Hepato-Biliary-Pancreatic Surgery Unit and Liver Transplantation, Sevilla, Spain; ¹¹Hospital General Universitario Gregorio Marañón, Department of Hepatology and Liver Transplantation, Madrid, Spain; ¹²Hospital Clínico Universitario Lozano Blesa, Department of Hepatology and Liver Transplantation, Zaragoza, Spain; ¹³Hospital Universitario Virgen de la Arrixaca, Liver Transplantation Unit, Murcia, Spain; ¹⁴Hospital Universitario Reina Sofía, Department of Hepatology and Liver Transplantation, Córdoba, Spain; ¹⁵Hospital General Universitario Alicante, Department of Hepatology and Liver Transplantation, Alicante, Spain; ¹⁶Hospital Universitario Río Hortega, Unit of Hepatology and Liver Transplantation, Valladolid, Spain; ¹⁷Clínica Universitaria de Navarra, Liver Unit, Pamplona, Spain; ¹⁸La Fe University and Polytechnic Hospital, Hepatology and Liver Transplant Section, Valencia, Spain
Email: toyagui@hotmail.com

Background and aims: CMV reactivation (rCMV) may impact morbidity and mortality after liver transplantation (LT). Immune modulation occurring after rCMV could decrease HCC recurrence rates after LT. Aims: To assess the effect of early rCMV LT-patients with HCC in a multicenter cohort.

Method: We included LT patients with HCC (2010–2015) in a multicenter cohort involving 11 Spanish institutions. Exclusion criteria were: age <18, re-LT, mortality within the first 12 months, and combined organ transplantation. Variables: (i) Donor (D) and recipient (R) demographics, (ii) related with rCMV (reactivation after LT prior to HCC recurrence) DR CMV mismatch, preemptive therapy, CMV disease, (iii) related to HCC: bridging, downstage, vascular invasion, baseline AFP. Prophylaxis with valganciclovir was used in high-risk patients while a preemptive approach was used in low-risk patients.

Results: Out of 621 LT, 543 (87% men, median age 58 [range: 20.5–71.5]) fulfilled inclusion criteria; the main etiology was alcoholic liver disease (n = 313, 50%) followed by hepatitis C (n = 299, 48%) and hepatitis B (n = 57, 9%). MELD at LT was 13 (6–40). Most patients met Milan criteria (87%) or up to seven criteria (97%) before LT; 111 patients (21%) were included after downstaging and 63% received locoregional therapy either for bridging or downstaging. On explant, 11% of patients had microvascular invasion. Median serum AFP at inclusion and at transplantation were 75 ng/ml (range 1–5245) and 64 ng/ml (range 1–764), respectively. High-risk CMV mismatch (D +/R-) occurred in 11% of patients. rCMV occurred in 185 patients (30%); 115 (65%) started early treatment and 25 (14.5%) developed CMV disease. Overall, 81 patients (13%) had HCC recurrence after a median of 2, 6 years (0.3–9.6). In the multivariate Cox regression analysis, microvascular invasion [HR 4.03 (p: 0, 0001)], absence of rCMV (HR: 2, 307, p = 0.028), moderate or poor histological

differentiation (HR 2.049, p: 0.03) and MELD (HR 1.094, p 0.005) were associated with HCC recurrence. Survival at 1, 3 and 5 and 7 yrs post-LT were in HCC recurrence vs non HCC recurrence: 85%, 61%, 30% and 14% and 99%, 91%, 86% and 81% respectively.

Conclusion: In a Spanish multicenter series, the absence of rCMV was associated with increased risk of HCC recurrence after controlling for well-established prognostic features.

THU-504

The influence of immunosuppression and recipient geography on non-melanoma skin cancer risk after liver transplantation

Therese Bittermann¹, James Lewis¹, David Goldberg². ¹University of Pennsylvania, United States; ²University of Miami, United States
Email: therese.bittermann@pennmedicine.upenn.edu

Background and aims: Immunosuppression (IS) after liver transplantation (LT) is associated with an increased solid cancer risk, of which the most common is non-melanoma skin cancer (NMSC). The optimal approach to IS management in those at the highest risk for *de novo* NMSC has not been determined, nor has the impact of recipient geography.

Method: Using a merged dataset of Medicare healthcare claims linked to U.S. national transplant registry data, we identified a retrospective cohort of adult first liver-alone transplant recipients who were alive with their native allograft at 1-year post-LT. Patients with a prior history of NMSC were excluded. *De novo* NMSC incidence was computed overall and by latitude of residence at transplant. Patient characteristics were described. Multivariable Cox regression evaluated the association of clinical characteristics, latitude and time-updating maintenance IS regimen with *de novo* NMSC.

Results: The 10,413 LT recipients in the cohort were 62.6% male, 69% non-Hispanic White (NHW) and with median age 60 years. In total, 891 (8.6%) developed *de novo* NMSC, yielding an overall incidence of 23 per 1,000 person-years (PY). Median time from LT to NMSC was 2.6 years (IQR: 1.7–3.9). NMSC incidence increased at lower latitudes: from 17 per 1,000 person-years (PY) for patients residing at $\geq 40^\circ$ to 25 per 1,000 PY for those $< 30^\circ$ (Northern). In multivariable analyses, factors independently associated with *de novo* NMSC included: female sex (hazard ratio [HR] 0.6 vs male; p < 0.001), NHW race/ethnicity (HR 7.8; p < 0.001), age ≥ 60 years (HR 2.0 vs < 60 years; p < 0.001), lower latitude of residence (HRs of 1.4 and 1.8 for $< 30^\circ$ and $30-39^\circ$ vs $\geq 40^\circ$; p < 0.001) and calcineurin inhibitor plus anti-metabolite (CNI + antiM) maintenance IS (HR 1.5 vs CNI alone; p = 0.003 overall). The interaction of IS with latitude was non-significant (p = 0.967). There was a possible interaction of IS with age (p = 0.096). In stratified analyses, IS was not associated with NMSC for patients < 60 years (p = 0.355), but was so in patients ≥ 60 years (p = 0.002), in whom CNI + antiM and mechanistic target of rapamycin inhibitor regimens were associated with increased NMSC (HRs 1.5 and 1.4, respectively, vs CNI alone; p = 0.002 overall).

Conclusion: *De novo* NMSC is a frequent occurrence among LT recipients with modifiable and non-modifiable risk factors. An individualized approach to post-LT IS has the potential to reduce *de novo* NMSC post-LT.

THU-505

Perfusate composition of transplanted and not transplanted livers during normothermic machine perfusion

Jule Dingfelder¹, David Pereyra¹, Laurin Rauter¹, Sertac Kacar¹, Gerd Silberhumer¹, Andreas Salat¹, Zoltan Mathe¹, Thomas Soliman¹, Dagmar Kollmann¹, Georg Gyoeri¹, Gabriela Berlakovich¹. ¹Medical University of Vienna, Department of General Surgery, Division of Transplantation, Vienna, Austria
Email: jule.dingfelder@meduniwien.ac.at

Background and aims: Dynamic changes in perfusate composition during normothermic machine perfusion (NMP) can reflect on the synthesis capability of the graft and extent of preservation injury. Components of the perfusate are either flushed out of the liver during

perfusion or produced by the liver or endothelial cells. Our aim was to compare perfusate composition during NMP of transplanted livers (tx) with not transplanted livers (non-tx).

Method: During NMP of 27 livers, blood gas analysis (BGA) of perfusate and bile was performed, as well as perfusate analysis for thrombocytes, leukocytes, van Willebrand factor activity (vWF), factor XIII activity (FXIII), fibrinogen, bilirubin, sodium, alkaline phosphatase (AP), alanine-aminotransferase (ALT), aspartate-aminotransferase (AST) gamma-glutamyl transferase (gGT) and lactate dehydrogenase (LDH). Liver and bile duct biopsies were taken before and after perfusion. Viability assessment was performed between hours 2 and 4 and included lactate clearing, decreasing perfusate glucose, perfusate and bile pH, bile glucose and bile production.

Results: In total 31 livers underwent NMP, 20 were transplanted following viability assessment while 11 livers did not meet the criteria for transplantation. The two groups did not differ in donor age ($p = 0.06$) and BMI ($p = 0.197$), but WIT was significantly longer ($p = 0.016$) and gGT was higher ($p = 0.005$) in the non-tx group. BGA of perfusate showed lower sodium and bicarbonate (60 minutes, $p = 0.011$) levels in non-tx livers after 30 ($p = 0.001$) and 60 ($p = 0.05$) minutes. The pH was higher in tx livers at 0 ($p = 0.012$), 30 ($p = 0.001$), and 60 ($p = 0.024$) minutes. Non-tx livers presented with higher FXIII activity at 5 min ($p = 0.041$), 60 min ($p = 0.07$), 120 min ($p = 0.084$), and 240 min ($p = 0.069$). FXIII act was increasing in non-tx livers but remained mostly stable in tx livers. Bilirubin (5 min, $p = 0.02$), AP (5 min, $p = 0.027$; 60 min, $p = 0.049$), AST (5 min, $p = 0.02$; 60 min, $p = 0.04$; 120 min, $p = 0.008$; 240 min, $p = 0.014$), ALT (5 min, $p = 0.07$; 60 min, $p = 0.08$; 120 min, $p = 0.009$; 240 min, $p = 0.043$), gGT (5 min, $p = 0.002$; 60 min, $p = 0.013$), LDH (5 min, $p = 0.05$; 60 min, $p = 0.011$; 120 min, $p = 0.009$) was significantly higher in non-tx livers. Fibrinogen levels trended higher in tx livers (not significantly) and were increasing over the course of the perfusion in both groups.

Conclusion: Decisions regarding viability assessment were confirmed by damage marker composition in perfusate. Interestingly, FXIII in perfusate was significantly higher in non-tx livers and presented with different dynamics. Fibrinogen was increasing over the course of perfusion in all livers. Transplanted livers presented with higher fibrinogen levels, maybe indicating a higher regenerative capacity.

THU-506

Risk factors associated with surgical morbidities of laparoscopic living liver donors

Jinsoo Ryu¹, Gyu-Seong Choi¹, Jong Man Kim¹, Jae-Won Joh¹.

¹Samsung Medical Center, Department of Surgery, Korea, Rep. of South Email: jsrrules@gmail.com

Background and aims: This study analyzed incidence and risk factors for surgical morbidities of laparoscopic living donors. Although laparoscopic living donor program has been safely established in leading centers, donor morbidities have not been sufficiently discussed.

Method: Laparoscopic living donors operated during May 2013 to June 2022 were reviewed. Donors' complications were reviewed, and factors related to bile leakage and biliary stricture were analyzed using multivariable logistic regression method.

Results: A total of 636 donors underwent laparoscopic living donor hepatectomy. Open conversion rate was 1.6%. Thirty-day complication rate was 16.8%. (n=107) Grade IIIa and IIIb complication occurred in 4.4% (n=28) and 1.9% (n=12), respectively. The most common complication was bleeding (n=38, 6.0%). Fourteen donors (2.2%) required reoperation. Portal vein stricture, bile leakage and biliary stricture occurred in 0.6% (n=4), 3.3% (n=21), and 1.6% (n=10) of cases. Readmission rate and reoperation rate was 5.2% (n=33) and 2.2% (n=14), respectively. Risk factors related to bile leakage were two hepatic arteries in liver graft (OR = 13.836, CI = 4.092–46.789, $P < 0.001$), division-free margin < 5 mm from main duct (OR = 2.624, CI = 1.030–6.686, $P = 0.043$) and estimated blood loss during

operation (OR = 1.002, CI = 1.001–1.003, $P = 0.008$) while Pringle maneuver (OR = 0.300, CI = 0.110–0.817, $P = 0.018$) was protective for leakage. Regarding biliary stricture, only bile leakage was the only significant factor (OR = 11.902, CI = 2.773–51.083, $P = 0.001$).

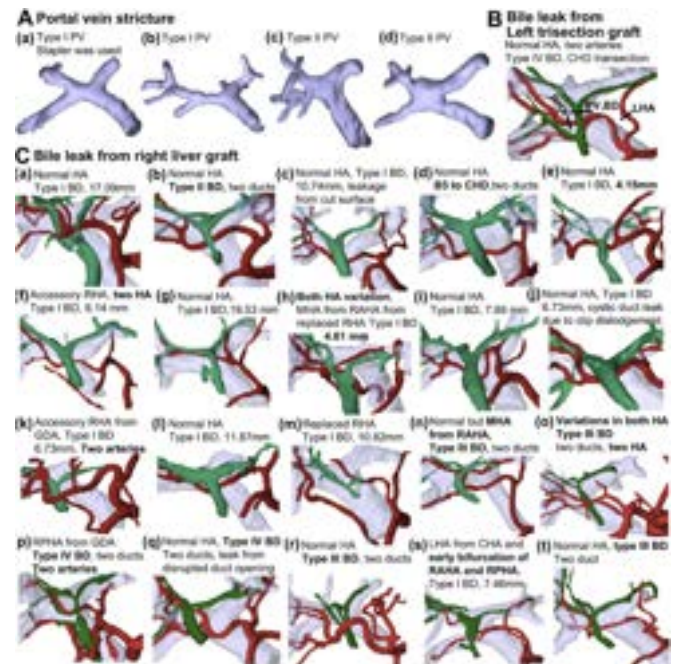


Figure: 3D reconstructed models of donors who experienced portal vein stricture or bile leakage after laparoscopic living donor hepatectomy. (A) Portal vein stricture cases. Two type I portal veins and two type II portal veins. (B) Bile leakage after left trisection graft donation. Right and left hepatic artery was divided at the black line marked, while bile duct was divided at the common hepatic duct level. Portal vein was divided at the common trunk of left and right anterior portal vein. (C) Bile leakage cases after right liver graft donation. Type and number of hepatic artery and bile duct variation are summarized. In type I bile duct cases, length of right hepatic duct common channel is measured. The leakage points are also summarized for cases with reoperation. The bold descriptions emphasize the possible risks for bile leakage.

Conclusion: Laparoscopic living donor showed excellent safety for majority of the donors and critical complications were resolved with proper management. To minimize bile leakage, cautious surgical manipulation should be made on donors with complex hilar anatomy.

THU-507

Clinical impact and treatment of veno-occlusive disease/sinusoidal obstruction syndrome (VOD/SOS) after liver transplant (LT): the role of transjugular intrahepatic porto-systemic shunt (TIPS)

Michela Triolo¹, Mauro Viganò¹, Francesca Poggi¹, Luisa Pasulo¹, Leonardi Filippo¹, Maria Grazia Lucà¹, Massimo De Giorgio¹, Claudia Iegri¹, Michele Colledan², Aurelio Sonzogni³, Paolo Marra^{4,5}, Stefania Camagni², Domenico Pinelli², Stefano Fagioli¹. ¹Papa Giovanni XXIII Hospital, Gastroenterology and Transplant Hepatology, Bergamo, Italy; ²Papa Giovanni XXIII Hospital, Department of Organ Failure and Transplantation, Gastroenterology, Hepatology and Liver Transplantation, Italy; ³Bolognini Hospital, Seriate, ASST Bergamo est, Department of Pathology, Italy; ⁴Papa Giovanni XXIII Hospital, Department of Diagnostic Radiology, Bergamo, Italy; ⁵University of Milano-Bicocca, Medicine, Italy Email: mik.triolo@gmail.com

Background and aims: veno-occlusive disease/sinusoidal obstruction syndrome (VOD/SOS) after liver transplantation (LT) is a rare complication, and best treatment and long-term outcome is still

POSTER PRESENTATIONS

undefined. Aim of this monocentric retrospective study is to evaluate the management and outcome of VOD/SOS after LT.

Method: between November 1997–2022, 1123 adult patients underwent LT. In patients who developed portal hypertension with ascites and/or hydrothorax after LT, the diagnosis of VOD/SOS was established by liver biopsy and measurements of hepatic venous pressure gradient (HVPG).

Results: 35/1123 (3%) patients [74% males, median age 51 (18–70) yrs, all treated with steroids plus tacrolimus (94%), plus tacrolimus and mycophenolic acid (3%) or plus cyclosporin and mycophenolic acid (3%)] had histologically proven VOD/SOS diagnosis. All patients presented with ascites, associated with hydrothorax in 4 (11%) cases. In 28/35 (80%) HVPG was measured at diagnosis of VOD/SOS. Median HVPG was 14 (7–34) mmHg. Median time of VOD/SOS after LT was 47 (20–220) days. In 6 (17%) patients VOD/SOS developed 24 (13–201) days after acute cellular rejection (ACR), whereas 2 (6%) patients had concomitant ACR and VOD/SOS occurrence. Ten (28%) patients showed spontaneous clinical improvement after a median time of 41 days (17–259), 2 (6%) were treated with defibrotide and 23 (66%) underwent TIPS. HVPG and Meld-Na at VOD/SOS diagnosis were significant higher in patients treated with TIPS compared to those which experienced spontaneous clinical improvement (19 vs 12.5, $p < 0.001$ and 14 vs 10, $p = 0.002$). After TIPS placement, the median HVPG was reduced to 8 mmHg (2–15), 17 (89%) patients resolved ascites \pm hydrothorax after a median time of 3 months, 3 (16%) patients developed porto-systemic encephalopathy which resolved with medical therapy in 2 cases and with TIPS caliber reduction in the other one. Two (10%) patients needed TIPS enlargement within one year due to stent dysfunction and ascites relapse. Overall, during a median follow-up of 62 months, 3 (16%) patients needed re-OLT, 1 (3%) for tipstis, 1 (3%) for hepatic arteria thrombosis and 1 (3%) for delayed dysfunction of graft. The 1, 3, 5 and 10-yr survival of patients having VOD/SOS spontaneous improvement were 100%, 100%, 87% and 73% compared with 95%, 91%, 63% and 29% of those treated with TIPS, respectively ($p = 0.016$).

Conclusion: VOD/SOS is a rare (3%) post LT complication associated with ACR in nearly 25% of cases. Among patients with high HVPG (median 19 mmHg) and without an early spontaneous clinical improvement, TIPS could be a safe and effective treatment option in our case series.

THU-508

Reassessing BCLC stage at transplant to predict risk of mortality and HCC recurrence in HCC liver transplant recipients

Cameron Goff¹, Ronald Samuel¹, Nicole Rich², Jihanne Benhammou³, Ponnadai Somasundar⁴, Abbas Rana¹, Hashem El-Serag¹, Fasiha Kanwal¹, George Cholaneril¹. ¹Baylor College of Medicine, Houston, United States; ²UT Southwestern Medical Center, Dallas, United States; ³Peter Morton Medical Building-UCLA Medical Center, Los Angeles, United States; ⁴Boston University School of Medicine, Boston, United States

Email: george.cholaneril@bcm.edu

Background and aims: The Barcelona Clinic Liver Cancer (BCLC) staging system is widely used for prognostication and treatment-decision making for patients with hepatocellular carcinoma (HCC) at time of diagnosis. However, progression in BCLC stage and change in performance status for HCC liver transplant (LT) recipients is not routinely reassessed at LT, and could predict risk of HCC recurrence and post-LT mortality. The aim of this study is to evaluate BCLC stage at LT as an independent predictor for post-LT mortality and HCC recurrence.

Method: Using the United Network for Organ Sharing (UNOS) database, we retrospectively analyzed all adult T2 HCC exception patients who received LT in the United States from January 1, 2012, to July 1, 2022. BCLC stage at LT was determined for all patients using calculated Child Pugh Score, ECOG Performance Status Scale from reported Karnofsky performance status, and explant pathology at

the time of transplant. Due to poor data quality, performance status of 1 was not used for classification. Cox Hazards regression analyses performed to analyze BCLC as a predictor for mortality, and logistic regression was used to analyze BCLC as a predictor for HCC recurrence.

Results: The study population consisted of 18,534 HCC LT recipients, of which 19.5% (3,808) remained at BCLC stage 0–A and 11.8% (2,188) were BCLC stage B at time of LT. 29.8% of HCC recipients progressed to BCLC stage C and 39.3% ($n = 7,279$) progressed to BCLC stage D at LT. In recipients with BCLC stage D at LT, 59.1% had ECOG 3–4 and 79.1% were Child Pugh C at time of LT. In addition, 45.7% ($n = 3,295$) recipients with BCLC stage D at LT had ECOG 0–1 at listing, of which 46.6% ($n = 1,536$) progressed to ECOG 3–4 at LT. On multivariate analyses accounting for recipient characteristics (age, sex, race and ethnicity), hepatic decompensation, laboratory MELD-Na and AFP at listing, wait time, and donor characteristics, BCLC stage C (Hazard Ratio (HR): 1.48, $p < 0.001$) and stage D (HR: 1.39, $p < 0.001$) at LT were significant predictors for post-LT mortality. For post-LT HCC recurrence, on multivariate analyses, BCLC stage B [Odds Ratio (OR): 1.40, $p = 0.004$], stage C (OR: 1.86, $p < 0.001$), and stage D (OR: 1.42, $p < 0.001$) were also significant predictors of recurrence.

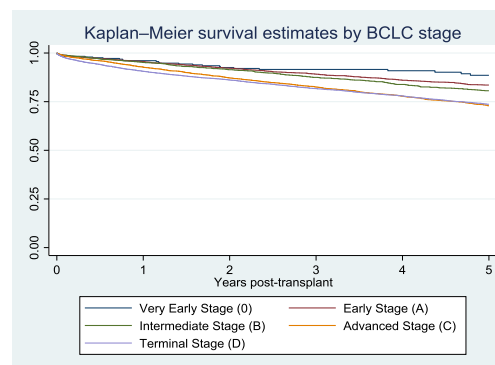


Figure:

Conclusion: These results suggest that BCLC stage should be reassessed at LT to prognosticate risk of post-LT mortality and HCC recurrence. This can aid clinicians in determining optimal surveillance strategies for disease monitoring and recurrence.

THU-509

Outcomes in patients with new-onset atrial fibrillation after liver transplantation using the national readmission database

Induja Nimma¹, Anand Maligreddy², Denise Harnois¹, Rohan Goswami³. ¹Mayo Clinic Florida, Gastroenterology and Hepatology, Jacksonville, United States; ²Mayo Clinic Arizona, Cardiovascular Medicine, Scottsdale, United States; ³Mayo Clinic Florida, Cardiology and Heart Transplant, Jacksonville, United States
Email: nimma.induja@mayo.edu

Background and aims: Atrial fibrillation (AF) increases morbidity and mortality in patients undergoing liver transplantation (LT). Outcomes data is limited on readmission in patients with new-onset AF (NOAF) after LT. We reviewed 90-day outcomes in patients utilizing the National Readmission Database (NRD).

Method: Retrospectively reviewed all adults undergoing LT between 2016 and 2019 using the NRD. Patients readmitted within 90 days were selected based on ICD-10 procedure code for LT (0FY00Z0). Patient data were abstracted from NRD, and descriptive statistics were used to determine significance with a p value of < 0.05 . All statistical analysis was performed using the Stata version 17.0 (StataCorp LLC, College Station, TX, USA).

Results: 31,557 patients underwent LT during our review period, with 8,449 patients (28%) readmitted within 90 days of the index transplantation hospitalization. 222 patients (2.6%) were found to

have NOAF, with 67 (43.2%) being female. The median age of NOAF LT patients was 63 (58–67) compared to those without NOAF, which was 58 (50–64) $p < 0.01$. Comparing NOAF to those without NOAF, we found an increased average hospital length of stay (12 days vs. 6 days), $p < 0.01$ (95% CI 6.2–7.1). Similarly, the average cost of care was greater in NOAF, 87,010.23 vs. 44,033.59 (US Dollars), $p = 0.02$ (95% CI 11,932–138,860). NOAF was also associated with increased inpatient mortality 13 deceased (6%) vs. 52 deceased (0.7%) using a multivariate mixed effect logistic regression analysis, $p < 0.01$ (OR 7.6, 95% CI 3–19).

Conclusion: Based on NDR data, patients in the US who undergo LT and are readmitted within 90 days have increased hospital costs and length of, as well as significantly increased risk of death if they develop new-onset AF. This data highlights risk models' potential benefit in predicting NOAF risk after LT. This may prevent adverse outcomes and increased patient mortality in this population.

THU-510

Liver Transplantation outcomes in patients following COVID-19 infection

Dinesh Jothamani¹, Mullai Ezhili¹, Radhika Venugopal¹, Hemalatha Ramachandran¹, Sathish Srinivasan¹, Ramya Paramashivam¹, Mohamed Rela¹. ¹Dr Rela Institute and Medical Centre, India
Email: dinesh.jothamani@relainstitute.com

Background and aims: COVID-19 can be associated with deleterious effects in patients with underlying chronic liver disease. However, the clinical impact of COVID-19 in patients who undergo LT following recovery from the infection is unclear. This study aimed to compare patients who underwent LT following recovery from COVID-19 to those underwent LT without COVID-19.

Method: A retrospective study of patients who underwent LT following recovery from COVID-19 illness between January 2020 and December 2021 carried out and compared with MELD matched LT recipients without COVID in a 1:1 ratio. Demographics, clinical presentation, post-operative events, allograft dysfunction and laboratory parameters at week 1, month 1 and 3 compared between the groups. Data analysis done using SPSS v24.

Results: 35 patients underwent LT after COVID illness with a median time of 94 (IQR 58–153) days. Most common etiology was NASH (N = 31.4% vs 37.14%). Mean age 51.23 vs 52.26, $p = 0.620$, MELD at the time of LT (18.03 vs 18.03, $P = 1$). Post-operative variables showed ventilator days (mean 3.2 ± 5.346 vs 2.17 ± 0.707 $p = 0.95$), ICU (11.14 ± 7.826 vs 8.23 ± 7.42 days, $P = 0.097$) and hospital stay (mean, 18.34 ± 7.82 vs 11.14 ± 6.28 , days; $P = 0.045$) between COVID-LT and non-COVID-LT groups. Post-operative events showed ACR (5.7% vs 8.6% $P = 1$), AKI (37.1% vs 25.7%, $P = 0.44$), early allograft dysfunction (17.1% vs 22.9%, $P = 0.766$), pleural effusion (25.7% vs 5.7%, $P = 0.045$) between two groups, respectively.

Conclusion: Patients who recovered from COVID-19 illness had comparable outcome following LT akin to those with no COVID in MELD matched recipients.

THU-511

Long-term outcome following liver transplantation for chronic liver disease in intensive care unit: the French nationwide experience

Magdalena Meszaros¹, Faouzi Saliba², Claire Francoz³, Christophe Duvoux⁴, Filomena Conti⁵, François Faitot⁶, Pauline Houssel-Debry⁷, Jean Hardwigsen⁸, Marie-Noëlle Hilleret⁹, Claire Vanlemmens¹⁰, Ephrem Salamé¹¹, Nassim Kamar¹², Jean Gugenheim¹³, Armand Abergel¹⁴, Claire Perignon¹⁵, Laurence Chiche¹⁶, Maryline Debette Gratién¹⁷, Jean-Yves Mabrut¹⁸, Sebastien Dharancy¹⁹, Jérôme Dumortier²⁰, Georges-Philippe Pageaux²¹, Florent Artru^{7,22}. ¹Hospital Center University De Montpellier, Montpellier, France; ²Hôpital Paul-Brousse Ap-Hp, Villejuif, France; ³Hospital Beaujon AP-HP, Clichy, France;

⁴Henri-Mondor University Hospital, Créteil, France; ⁵University Hospitals Pitié Salpêtrière-Charles Foix, Paris, France; ⁶Hôpital de Haute-pierre-Hôpitaux Universitaires de Strasbourg, Strasbourg, France; ⁷CHU Rennes-Pontchaillou Hospital, Rennes, France; ⁸Hôpital Nord, Marseille, France; ⁹Chu Grenoble Alpes, La Tronche, France; ¹⁰Besançon Regional University Hospital Center, Besançon, France; ¹¹Chru Hospitals of Tours, Tours, France; ¹²Hospital Center University De Toulouse, Toulouse, France; ¹³Hospital L'archet, Nice, France; ¹⁴Site Estaing Clermont-Ferrand University Hospital, Clermont-Ferrand, France; ¹⁵University Hospital Center of Caen, Caen, France; ¹⁶Hospital Center University De Bordeaux, Bordeaux, France; ¹⁷CHU Dupuytren 1, Limoges, France; ¹⁸Hôpital de la Croix-Rousse-HCL, Lyon, France; ¹⁹Hospital Center University De Lille, Lille, France; ²⁰Edouard Herriot Hospital, Lyon, France; ²¹Hospital Center University of Montpellier, Montpellier, France; ²²King's College Hospital, United Kingdom
Email: m-meszaros@chu-montpellier.fr

Background and aims: Long-term outcomes of patients with chronic liver disease (CLD) who undergo liver transplantation (LT) in the intensive care unit (ICU) have been poorly reported. We aimed to investigate it and to evaluate the impact on organ utility.

Method: The study was allowed by the French LT organism (Agence de la Biomédecine). All patients with CLD who underwent LT alone between 2008 and 2013 in France were retrospectively included. Data were extracted from the CRISTAL national database. Patients ≤ 18 years old or who underwent LT in the context of unknown liver disease, secondary malignancy of the liver or primary non-function of the graft were excluded from the analyses. We evaluable organ failure was defined by EASL CLIF-OF criteria.

Results: 5532 patients fulfilled the inclusion criteria including 5236 (94.7%) with CLD and 296 (5.3%) transplanted in the context of fulminant hepatitis (FH). Among them, 708 patients with CLD (12.8%) and 253 (4.6%) with FH were transplanted while in ICU with a median follow-up of 6.1 years. The main causes of LT for CLD-ICU patients were alcohol-related ($n = 288$, 40.7%) and viral-related cirrhosis ($n = 148$, 20.9%). Their median age was 54 years old with a median MELD score of 30.8. At the time of LT, 42% were under mechanical ventilation, 31.2% had renal failure (22.0% treated with renal replacement therapy), 63.3% had liver failure and 43.4% had coagulation failure. The 5-year survival was 64.3% in CLD-ICU patients vs. 78.1% in patients with CLD transplanted outside of ICU (CLD-non-ICU, $p < 0.0001$) and 72.6% in patients with FH ($p = 0.09$). In CLD-ICU patients, 169/246 deaths (68.7%) occurred within the 1st year following LT. After the 1st year, the annual risk of death was 3.5% vs. 3.1% ($p = 0.4$) in CLD-ICU and CLD-non-ICU respectively. At the time of LT in CLD-ICU patients, factors independently associated with 5-year survival in multivariable analyses were age ($p = 0.04$), MELD score ($p = 0.05$), mechanical ventilation ($p = 0.002$), and liver failure ($p = 0.04$). There was a trend toward an independent association of 5-year survival with the timeframe of LT (with better survival observed when LT was performed in the two last years (68% vs. 61.8%, $p = 0.06$). Causes of death were different between CLD-ICU vs. CLD-non-ICU patients ($p < 0.0001$) with infection being the leading cause of death (37.2% vs. 20.5%) and cancer being less frequent (9.5% vs. 20.8%).

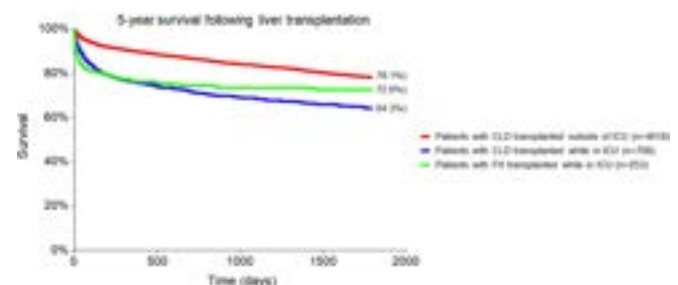


Figure: 5-year survival following liver transplantation according to the presence of chronic liver disease and intensive care hospitalization.

POSTER PRESENTATIONS

Conclusion: CLD-ICU patients had a poorer 5-year survival rate as compared to CLD-non-ICU patients. This was explained by an increased mortality risk at 1 year with infection being the main driver of mortality. After 1-year the annual risk of death was not different. Research should focus on predictors of early mortality as well as on the prevention of infectious events in these patients to improve organ utility.

THU-512

Validation of MELD3.0 in two centres from different continents

Marta Tejedor Bravo¹, José Bellón², Margarita Fernández-de la Varga³, Peregrina Peralta⁴, Eva Montalvá³, Nazia Selzner⁴, Marina Berenguer³. ¹Hospital Infanta Elena, Valdemoro, Spain; ²Instituto de Investigación Sanitaria Gregorio Marañón, Madrid, Spain; ³La Fe University and Polytechnic Hospital, València, Spain; ⁴Toronto General Hospital, Toronto, Canada
Email: marina.berenguer@uv.es

Background and aims: A new scoring system, MELD3.0, has been proposed to stratify patients on the liver transplant (LT) waiting list (WL), as it seems to reduce the historical disadvantage of women in accessing LT. Our aim was to validate MELD3.0 in our populations.

Method: a 2 centre retrospective review of medical charts of all adult patients included in the LT WL between 2015 and 2019 was conducted. Variables related to patient's demographics, liver function, etiology of liver disease and survival were collected.

Results: 619 patients were included, 61% were male, mean age 56 years. Mean MELD at inclusion was 18.00 ± 6.88 , MELDNa 19.78 ± 7.00 , MELD3.0 20.39 ± 7.25 (MELD3.0 only available for 548 patients). AUC to predict mortality on the WL was 0.8791 (95% CI 0.81965, 0.93850) for MELD, 0.9212 (95% CI 0.87571, 0.96661) for MELDNa and 0.9439 (95% CI 0.91160, 0.97611) for MELD3.0. MELDNa and MELD3.0 were better predictors than MELD ($p=0.06$ and $p=0.04$ respectively). In women, AUC for MELD was 0.8348 (95% CI 0.74380, 0.92575), for MELDNa 0.8732 (95% CI 0.78544, 0.96104) and for MELD3.0 0.9166 (95% CI 0.86975, 0.96345), differences for the comparison between AUC in women vs men for all 3 scores were non-significant. Better survival was found in the European cohort, attributable to shorter WL times (212 ± 426 vs 649 ± 821 days respectively, $p<0.001$) and less severely ill patients (patients on pressors or intubated at the time of LT were 0.7 vs 4.4% and 0 vs 5.3% respectively, $p<0.05$ for both comparisons), although no differences in postLT survival were observed. In particular, no differences in postLT survival between women and men were found. Etiology of liver disease was significantly different between the two cohorts, with a predominance of alcohol (56%) and virus related (34%) liver disease in the European one, and alcoholic (35%) and non-alcoholic (24.6%) fatty liver disease, followed by viral (18%) and primary sclerosing cholangitis (14.7%), being the leading causes in the Canadian cohort.

Conclusion: MELD3.0 has been validated in centers with significant heterogeneity and offers the highest mortality prediction for women on the WL without disadvantaging men.

THU-513

Pre-transplant mycophenolate mofetil may be associated with reduced intrahepatic cholangiopathy in ABO-incompatible liver transplantation

Jinsoo Rhu¹, Gyu-Seong Choi¹, Jong Man Kim¹, Jae-Won Joh¹. ¹Samsung Medical Center, Korea, Rep. of South
Email: jsrrules@gmail.com

Background and aims: Intrahepatic cholangiopathy is a life-threatening sequela of ABO-incompatible liver transplantation. We analyzed the clinical impact of pre-transplant administration of mycophenolate mofetil in reducing intrahepatic cholangiopathy in ABO-incompatible liver transplantation.

Method: Patients who underwent living donor liver transplantation between 2010 and April 2022 were included. Pre-transplant mycophenolate mofetil was started in November 2020. A comparison between patients who experienced intrahepatic cholangiopathy and who did not among ABO-incompatible transplantation was performed. Recipients of ABO-incompatible transplantations were categorized based on donor surgery into open, laparoscopy without pre-transplant mycophenolate mofetil, and laparoscopy with pre-transplant mycophenolate mofetil groups. Cox analysis of intrahepatic cholangiopathy was performed.

Results: A total of 234 ABO-incompatible transplantations were included. Intrahepatic cholangiopathy occurred in 1.1% ($n=1/94$), 13.3% ($n=12/90$) and 2.0% ($n=1/50$) of patients who received an ABO-incompatible liver with open surgery, laparoscopic donor surgery without pre-transplant mycophenolate mofetil and laparoscopic donor surgery with pre-transplant mycophenolate mofetil. ($p=0.001$) Multivariable analysis showed that transplantations involving a donor who underwent a laparoscopic hepatectomy and a recipient who did not receive pre-transplant mycophenolate mofetil were associated with a higher risk of intrahepatic cholangiopathy (HR = 13.449, CI = 1.710–105.800, $P=0.02$) compared to transplantations from donors who underwent open surgery. Transplantations involving a donor who underwent laparoscopic donor surgery and a recipient who received pre-transplant mycophenolate mofetil resulted in no increased risk compared to transplantations from donors who underwent open surgery. (HR = 5.307, CI = 0.315–89.366, $P=0.25$)

Conclusion: Laparoscopic donor hepatectomy was a risk factor for intrahepatic cholangiopathy in ABO-incompatible liver transplantation while pre-transplant mycophenolate mofetil was related to risk reduction of intrahepatic cholangiopathy.

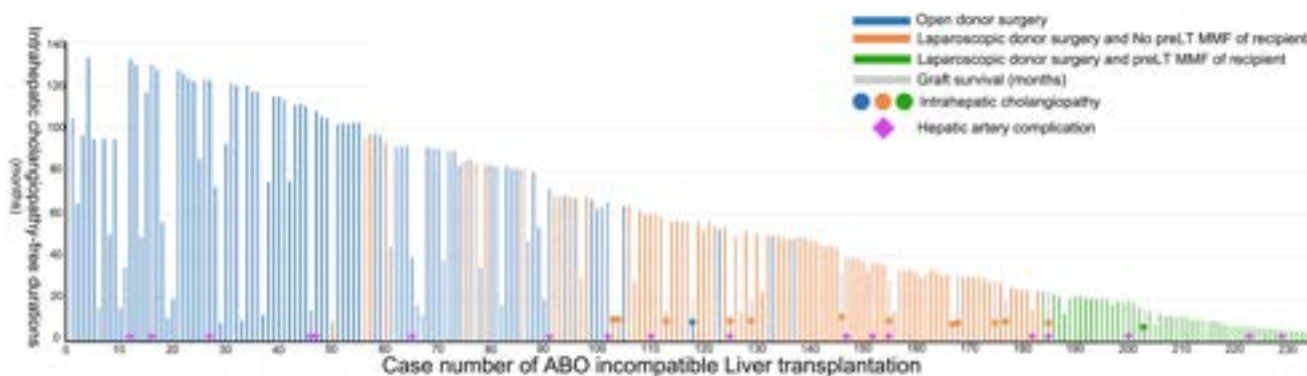


Figure: (abstract: THU-513): Intrahepatic cholangiopathy-free survival according to the case number of ABO-incompatible living donor liver transplantation cases as demonstrated in different groups.

THU-514

Prevalence of renal dysfunction is higher in patients that receive a liver transplant for non-alcoholic steatohepatitis

Rubén Sánchez-Aldehuelo^{1,2,3,4}, Margarita Papatheodoridi^{1,2}, Agustín Albillos^{3,4}, Emmanouel Tsochatzis^{1,2}. ¹Royal Free Hospital, London (United Kingdom), United Kingdom; ²Institute for Digestive and Liver Health, University College London (UCL), United Kingdom; ³Hospital Universitario Ramón y Cajal, Madrid (Spain), Instituto Ramón y Cajal de Investigación Sanitaria (IRYCIS), Spain; ⁴Universidad de Alcalá, Spain
Email: ruben.sanchez.aldehuelo@gmail.com

Background and aims: Renal dysfunction (RD) is common among liver transplant (LTx) recipients and is associated with worse long-term outcomes. In patients with non-alcoholic steatohepatitis (NASH), additional well-known risk factors for developing RD are present prior to LTx such as diabetes mellitus, hypertension or obesity. We aimed to: i) Investigate the prevalence of pre-LTx RD; ii) Assess the development of RD post-LTx and iii) Identify predictors of RD in such patients.

Method: Retrospective analysis of prospectively collected data of patients that received a LTx at the Royal Free Hospital (London, United Kingdom) between 01/1995 and 04/2022. Patients were considered as NASH cirrhosis if registered as such in the National Database records or if diagnosed with cryptogenic cirrhosis and a BMI ≥ 30 kg/m² or BMI ≥ 25 kg/m² and diabetes. Patients who died during LTx or early after were excluded. RD was defined as glomerular filtration rate (GFR) < 60 ml/min/1.73 m². Demographic and clinical features were collected from clinical records. A cohort of non-NASH cirrhotic patients transplanted from 01/1995 to 09/2013 was also considered for the aim of the study.

Results: NASH was the primary etiology of cirrhosis in 140/2090 (6.7%) LTx performed. Sixteen patients (11.4%) were excluded because of early post-LTx death and 14 (10%) were lost to follow-up (FU). Finally, 124 patients were included (76.6% males; mean age 59.2 ± 6.8 years; median FU 49.47 months [22.85–102.35]). Diabetes was present in 75% and hypertension in 34.7% pre-LTx. RD was present in 60% and 65.8% at 1 year and at FU respectively. In the multivariate analysis (Figure) we found age, pre-LTx RD, creatinine, presence of varices, ascites and gastrointestinal (GI) bleeding as predictors of RD at 1 year. The NASH group showed a lower GFR compared with other etiologies of cirrhosis (56 vs 63; $p < 0.001$ and 63 vs 55 ml/min; $p < 0.001$) at 1 year and FU, respectively. In the logistic regression, NASH was associated with a higher risk of RD during post-LTx FU (OR = 2.511; $p < 0.001$). After propensity-score matching (PSM) adjustment for age, sex and presence of diabetes and hypertension, no differences for RD at 1 year or at the end of FU were found between NASH and PSM non-NASH LTx recipients (47.5% vs 40.3%; $p = 0.24$ and 50.8% vs 50.8%; $p = 1$, respectively).

	One year OR (95% CI)	P	Last FU OR (95% CI)	P
Age	1.08 (1.02-1.15)	0.01	1.03 (0.99-1.06)	0.075
Sex	0.64 (0.25-1.65)	0.35	0.71 (0.46-1.11)	0.13
BMI	0.99 (0.90-1.09)	0.84	1.01 (0.97-1.06)	0.61
Renal dysfunction preLTx	4.17 (1.82-9.55)	<0.001	15.52 (7.08-34.06)	<0.001
Hypertension	0.86 (0.37-1.99)	0.73	0.84 (0.56-1.27)	0.40
Diabetes mellitus	2.14 (0.88-5.14)	0.09	1.22 (0.76-1.91)	0.44
Varices	1.64 (1.01-2.65)	0.05	1.04 (0.83-1.31)	0.74
Ascites	2.84 (0.99-8.07)	0.05	1.45 (0.88, 2.51)	0.14
GI bleeding	3.10 (1.31-7.36)	0.01	1.10 (0.74, 1.62)	0.64
Hepatic encephalopathy	2.13 (0.93-4.91)	0.08	0.89 (0.60, 1.32)	0.56
MELD	1.01 (0.95, 1.08)	0.75	1.00 (0.98, 1.03)	0.63
Cr at LTx	1.03 (1.01-1.05)	0.002	1.02 (1.01-1.03)	<0.001
Renal sparing regime	1.46 (0.66, 3.22)	0.35	1.12 (0.76, 1.67)	0.55

OR: odds ratio; 95% CI: 95% confidence interval; BMI: body mass index; Cr: creatinine.

Figure: Multivariate analysis showing predictors of renal dysfunction at 1 year and last FU in patients with NASH cirrhosis

Conclusion: RD at 1 year and FU is higher in patients transplanted with NASH-cirrhosis compared to other etiologies. Several pre-LTx factors may predict the development of RD in this group of patients.

THU-515

Comparing clinical outcomes of robot-assisted versus open hepatectomy for liver cancer: a systematic review and meta-analysis

Muhammed Elfaituri¹, Ala Khaled¹, Ahmed BenGhatnash², Ahmed Elfaituri¹, Hazem Faraj¹, Ahmed Msherghi¹. ¹University of Tripoli, Faculty of Medicine, Tripoli, Libya; ²National Heart Centre, Tajoura, Libya
Email: dr.muhammed.khaled.elfaituri@gmail.com

Background and aims: Liver cancer is a major contributor to cancer-related deaths worldwide. Surgical management of liver tumors remains a challenge, with both open hepatectomy and robot-assisted hepatectomy being commonly used. This systematic review and meta-analysis compare the clinical outcomes of these two surgical techniques.

Method: A comprehensive search of electronic databases, including PubMed, Embase, and the Cochrane Library, was conducted to identify eligible studies comparing robot-assisted and open hepatectomy for liver tumors. The search was conducted up to January 2023. The primary outcome measures were operative time, blood loss, length of hospital stay, and overall complications. The meta-analysis was performed using R version 4.0.3 and the metafor and meta packages.

Results: Seven studies with a total of 368 patients who underwent robot-assisted hepatectomy and 648 patients who underwent open hepatectomy met the inclusion criteria and were included in the meta-analysis. The results showed that robot-assisted hepatectomy was associated with longer operative time (SMD 1.65, 95% CI 0.53 to 2.75, $p < 0.01$, $I^2 = 98$) but lower blood loss (SMD -0.39, 95% CI -0.55 to -0.25, $p < 0.01$, $I^2 = 0$) compared to open hepatectomy. Length of hospital stay was also significantly shorter in the robot-assisted group (SMD -1.7, 95% CI -2.7 to -0.43, $p < 0.01$, $I^2 = 98$). There was no significant difference in the need for blood transfusions between the two groups (RR 1.02, 95% CI 0.38 to 2.71, $p = 0.98$, $I^2 = 60\%$). Resection margins and overall complication rates did not show significant differences between the two approaches (SMD -0.08, 95% CI -0.25 to 0.102, $p = 0.4$, $I^2 = 0$ and RR 0.77, 95% CI 0.56 to 1.05, $p = 0.1$, $I^2 = 6\%$, respectively).

Conclusion: This systematic review and meta-analysis suggest that robot-assisted hepatectomy is associated with longer operative time, but shorter hospital stays, and lower blood loss compared to open hepatectomy for liver tumors. Further high-quality studies are needed to confirm these findings and assess the long-term outcomes of the two surgical techniques.

THU-516

Association between waiting time and post-transplant survival in recipients with hepatocellular carcinoma outside Milan criteria after downstaging with locoregional therapy

Zoljargal Lkhagvajav¹, Elliott Haut², Uurtsaikh Baatarsuren³, Betsy King². ¹Onom foundation-ОНОМ САИ, Ulaanbaatar, Mongolia; ²The Johns Hopkins University School of Medicine, Baltimore, United States; ³Onom foundation-ОНОМ САИ, Ulaanbaatar, Mongolia[NT1]
Email: zoljargal.l@onomfoundation.org

Background and aims: Prior studies show conflicting results on the association between waiting time and post-transplant survival among patients with hepatocellular carcinoma (HCC). We aimed to assess the association between waiting time and post-transplant survival in recipients with HCC outside Milan criteria after downstaging with locoregional therapy and identify factors that are associated with higher post-transplant survival.

Method: Using the Scientific Registry of Transplant Recipients (SRTR) database, we retrospectively analyzed 5-years post-transplant survival of all adult patients who had HCC outside Milan criteria and received liver transplantation (LT) between January 1, 2010, and December 31, 2021, after downstaging with LRT and with information about their tumor size and number. According to their waiting time,

POSTER PRESENTATIONS

recipients were divided into three groups: <6 months, 6–12 months, and >12 months. Kaplan-Meier method and a log-rank test were used to assess survival. Univariable and multivariable Cox regression was used to identify factors associated with post-transplant mortality.

Results: A total of 479, 439, and 307 recipients were included in the waiting time group of <6 months, 6–12 months, and >12 months respectively. We conclude that there is no statistically significant difference among the three waiting time groups in terms of post-transplant survival (HR 1.4; 95% CI 1.03–1.91; $p = 0.03$; HR 1.17; 95% CI 0.83–1.66; $p = 0.37$ and log-rank $p = 0.12$). Waiting time of <6 months prior to LT put the patients at a significantly higher risk of mortality compared to a waiting time of 6–12 months (HR, 1.4; 95% CI 1.03–1.91; $p = 0.03$). Being in the higher median serum alpha-fetoprotein (AFP) level groups (HR, 1.37; 95% CI 1.02–1.79 and HR, 1.37; 95% CI 1.02–1.79) was associated with a higher risk for post-transplant mortality.

Table 2. Univariate and multivariate Cox regression analysis for 5-year survival in recipients with HCC Outside Milan Criteria After Downstaging with Locoregional Therapy

Variable	Univariable		Multivariable	
	HR (95% CI)	p-value	HR (95% CI)	p-value
Study groups (ref. 6–12 months)				
<6 months	1.35 (1.00–1.82)	0.04	1.4 (1.03–1.91)	0.03
>12 months	1.28 (0.91–1.80)	0.15	1.17 (0.83–1.66)	0.37
Age (years)	1.02 (1.00–1.04)	0.01	1.02 (1.00–1.04)	0.04
Sex (ref. male)	1.25 (0.87–1.45)	0.25	1.22 (0.88–1.70)	0.26
BMI (kg/m ²)	1.01 (0.98–1.03)	0.60		
Race (ref. white)				
African American	0.93 (0.60–1.42)	0.75		
Hispanic	0.77 (0.54–1.13)	0.19		
Asian	0.94 (0.58–1.53)	0.81		
Other	1.49 (0.74–3.03)	0.26		
Total tumor size (cm)	1.02 (0.97–1.06)	0.33	1.02 (0.97–1.08)	0.42
Tumor number (N)	1.04 (0.93–1.16)	0.46		
Etiology of HCC (ref. alcoholic cirrhosis)				
Unknown	2.31 (1.08–4.94)	0.03	2.35 (1.09–5.05)	0.03
Chronic liver disease	2.86 (1.22–5.77)	0.01	2.70 (1.24–5.91)	0.01
Metastasis	2.03 (0.71–5.81)	0.18	2.03 (0.71–5.81)	0.18
Other	2.17 (0.89–5.30)	0.09	2.13 (0.86–5.18)	0.10
LRT type (ref. RFA)				
Chemoembolization	0.94 (0.44–2.00)	0.87		
Both	1.09 (0.45–2.64)	0.84		
Number of total LRT - Median (IQR)	1.11 (0.63–1.33)	0.23	1.14 (0.64–1.57)	0.17
MELD (ref. 6–10)				
11–20	1.03 (0.80–1.34)	0.80	1.02 (0.78–1.33)	0.91
21–30	0.72 (0.38–1.37)	0.32	0.58 (0.28–1.08)	0.12
31–40	2.63 (1.54–4.50)	0.000	2.10 (1.04–3.99)	0.03
Median AFP (ref. 0–20)				
20–400	1.37 (1.21–2.04)	0.03	1.37 (1.02–1.79)	0.03
400+	2.28 (0.80–2.89)	0.03	2.35 (1.08–5.11)	0.03
Need of life support - n (ref. no)				
Yes	2.87 (1.28–6.48)	0.01	2.83 (1.21–6.64)	0.02
Dialysis within a week before LT (ref. no)				
Yes	2.62 (1.43–4.80)	0.002	2.29 (1.01–5.57)	0.046
Insurance (ref. public)				
Private	0.72 (0.56–0.92)	0.01	0.77 (0.60–1.03)	0.055
Donor age (years)	1.00 (0.99–1.01)	0.52		
Non-heartbeat donor (ref. no)	0.86 (0.53–1.41)	0.56		
COT (hours)	1.02 (0.97–1.07)	0.37		

BMI, body mass index; HCC, hepatocellular carcinoma; IQR, interquartile range; LRT, locoregional therapy; MELD, model for end-stage liver disease; AFP, alpha-fetoprotein; LT, liver transplantation; COT, cold ischemia time

Conclusion: To our knowledge, there hasn't been any study that measured the association between waiting time and post-transplant survival among recipients who presented HCC outside Milan criteria and downstaged through LRT before receiving LT. Thus, we aimed to evaluate the association among these patients and find factors that are associated with post-transplant survival. Our findings show that a waiting time of <6 months was associated with 1.4 times increased hazard of mortality compared to a waiting time of 6–12 months. We found that a higher median serum AFP level is associated with a higher risk for post-transplant mortality. Although, the generalizability of this study is affected by the small size of the study population and the selection criteria. As we included patients who were responsive to LRT and successfully downstaged within Milan criteria, it can be implied that these patients had good tumor biology and the result of the current study could not be generalized to all patients who present with HCC outside Milan criteria. Our study indicates that it is important to consider the tumor biology for post-transplant survival and serum AFP level can be used as an indicator for tumor biology and subsequently an indicator for post-transplant survival. The result is consistent with the existing literature that the higher serum AFP level is associated with a higher risk for mortality after LT among patients with HCC. Further research is needed to

assess the association with a bigger sample size, possibly in another country where the HCC patients are diagnosed at a more progressed stage and the prevalence of HCC outside Milan criteria is higher.

THU-517

CMV reactivation after liver transplantation (LT) in HIV infected is similar to non-HIV patients: a single center comparative study

Sonia García-García¹, Isabel Terol Cháfer¹, Víctor Argumánez Tello¹, Carmen Vinaixa^{1,2}, Javier Maupoey¹, Marino Blanes Julia¹, Angela Carvalho Gomez¹, Marina Berenguer Haym^{1,2,3}, Victoria Aguilera Sancho^{1,2}. ¹Hospital Universitario y Politécnico La Fe, Valencia, Spain; ²CIBERehd, Instituto Carlos III, Madrid, Spain; ³Universidad de Valencia, Facultad de Medicina, Spain
Email: soniagg1995@hotmail.com

Background and aims: Cytomegalovirus (CMV) reactivation after liver transplant (LT) has been associated with poor outcomes. There is no evidence of a higher rate of CMV reactivation or disease in HIV-infected patients. Our aim was to describe the CMV reactivation, primary infection and need of antiviral treatment in HIV-infected LT patients, compared to non-HIV-infected LT patients.

Method: We included patients who underwent LT from June 2004 to December 2020 in a single LT center. Each HIV-infected patient was matched to 2 non-HIV infected controls by age, sex, liver disease etiology, and date of LT. Pre-LT baseline features, HIV related variables, and post-LT outcomes related to CMV were recorded. Patients at donor/recipient (D/R) mismatch high risk (D +/R -) were given prophylaxis with valganciclovir. The rest of the patients were followed with a "preemptive" strategy and received early treatment based on clinical criteria.

Results: A total of 156 LT recipients were included (52 HIV-infected and 104 non-HIV-infected). Baseline characteristics were similar in both groups (see figure 1), except for age and body mass index, which were lower in HIV-infected patients. Mean follow-up post-LT was 7.5 years in the HIV group vs 8.2 years in the non-HIV group. CMV reactivation occurred in 10 (20%) in HIV vs 24 (24%) in non-HIV and CMV disease occurred in 2 (2%) non-HIV and 1 (2%) HIV ($p = 0.521$ and 0.687). The need for preemptive treatment was 11.5% in the HIV group and 14% in the non HIV group ($p = 0.8$).

Mean CMV viral load (VL) at reactivation was 2518 in HIV-patients and 5453 in non-HIV ($p = 0.47$); and mean high CMV VL was 5435 in HIV and 9263 in non-HIV ($p = 0.36$). Time to reactivation was 6, 8 weeks in the HIV-patients group and 8 weeks in non-HIV patients. Factors significantly associated with CMV reactivation were D/R mismatch ($p = 0.006$) and recipient's age ($p = 0.037$). Factors such as HIV condition, CD4 count, MELD and hepatocarcinoma were not associated with CMV reactivation ($p = 0.85$).

	HIV (n = 52)	Non HIV (n = 104)	p
Age at LT (mean) (years, range)	48 (33-60)	52 (25-70)	0.002
Sex (Men) (%)	88%	87%	0.866
HCV	92%	86%	0.266
HCC	33%	40%	0.350
BMI at LT (mean)	24.8	27.1	0.0016
MELD at LT (mean)	18	17	0.21
Diabetes preLT	22%	18%	0.625
Arterial hypertension preLT	10%	13%	0.489
Dislipidemia preLT	8%	5%	0.466

Figure:

Conclusion: In the post-LT setting, CMV reactivation in HIV-infected patients was similar to non-HIV patients. Variables associated with reactivation were D/R mismatch and recipient's age. Preemptive strategies seem to be effective in both groups.

THU-518

Development of metabolic disorders in transplant recipients

Gizem Erdemir¹, Hale Gokcan², Aysegül Gürsoy Çoruh³, Basak Gulpinar³, Zeynep Melekoğlu Ellik⁴, Mesut Gümüşsoy⁵, Serkan Duman⁶, Emin Bodakçi², Ramazan Idilman². ¹Ankara University School of Medicine, Internal Medicine, Turkey; ²Ankara University School of Medicine, Gastroenterology and Hepatology, Turkey; ³Ankara University School of Medicine, Radiology, Turkey; ⁴Karaman Training and Research Hospital, Gastroenterology and Hepatology, Turkey; ⁵Gaziantep Şehitkamil Public Hospital, Gastroenterology and Hepatology, Turkey; ⁶Mersin Toros Public Hospital, Gastroenterology and Hepatology, Turkey
Email: halesumer@yahoo.com

Background and aims: Metabolic syndrome (MS) is the most common long-term complication after liver transplantation. The aim of this study was to assess the prevalence and risk factors for metabolic syndrome (MS) and its component after living donor liver transplantation (LDLT).

Method: A total of 114 adult patients listed for liver transplantation (LT) between 2005 and 2021 with a minimum follow-up of one year were included. Demographics, laboratory and computed tomography data were collected pre and post-transplant.

Results: Mean age was 56.0 ± 11.5 and 63% were male. LDLT was performed on 88 (77%) patients. Forty-six (40%) patients were smokers. HBV infection (36%) was the main indication. The majority of the patients (n = 101, 89%) were on tacrolimus-based treatment. Median follow-up period after LT was 7.5 year (range 1–20 year). In post-transplant period; BMI was 27.8 kg/m², 29.7% of them were obese. Thirty-two (28%) patients developed new-onset DM (NODAT), 60.1% hypertension, 40.7% hyperlipidemia, and 51.3% MS (Table 1). The post-transplant median atherosclerotic cardiovascular disease (ASCVD) risk score was 16.5. Sixteen patients (14%) had a history of a cardiac event post-transplant. The mean posttransplant HbA1C, waist and hip circumference were 6.22 ± 1.57, 104.2 ± 15.3 and 109.4 ± 12.5 respectively. Post-transplant hypertension, diabetes,

antihypertensive and antidiabetic drug use, ASCVD score and BMI were higher in post-transplant MS. Posttransplant median visceral adipose tissue (VAT), subcutaneous tissue (SAT), total fat area (TFA) and VAT/SAT were 146.8 cm² (12.6–484.4), 169.3 cm² (22.7–527.5), 348.1 cm² (40.9–744.8) and 0.76 (0.1–4.2). In the MS present group, the median VAT, VAT/SAT and TFA were 171.7 cm² (29.9–484.4), 0.82 (0.23–4.21) and 400.8 cm² (62.3–744.8) respectively, which were higher than in the non-metabolic syndrome group 103.0 cm² (12.6–340.8), 0.63 (0.1–4.2) and 314.4 cm² (40.9–653.4) (p = 0.002, p = 0.06, and p = 0.005). SAT in the MS and non-MS group were 201.6 cm² (32.4–527.5) and 156.1 cm² (22.7–448.7) respectively (p = 0.06).

Conclusion: Metabolic disorders are frequent complications after liver transplantation and a high VAT, VAT/SAT and TFA are at increased risk for developing MS. The high incidence of MS and its components in our sample highlights the importance of closely and carefully monitoring for development of MS and its complications.

THU-519

Tailored immunosuppression with LCPT extended release Tacrolimus based on NFAT-regulated gene expression

Judith Kahn¹, Eva Matzhold², Petra Ofner-Kopeinig³, Peter Schlenke², Peter Schemmer⁴. ¹General, Visceral and Transplant Surgery, Graz, Austria; ²Department of Blood Group Serology and Transfusion Medicine, Graz, Austria; ³Institute for Medical Informatics, Statistics and Documentation, Graz, Austria; ⁴General, Visceral, and Transplant Surgery, Graz, Austria[NT2]
Email: judith.kahn@medunigraz.at

Background and aims: There is a narrow therapeutic window for immunosuppression (IS) with calcineurin (CNI) inhibitors. The immunosuppressive effect of CNIs differs between individuals. Therefore, the drugs' trough levels do not reflect IS and should be replaced by pharmacodynamic monitoring. Since nuclear factor of activated T-cells (NFAT)-depending gene expression correlates with cyclosporine induced IS, this study was designed to evaluate the effect of LCP extended release tacrolimus (Tac) on NFAT regulated residual gene expression (RGE).

Method: Gene expressions of interleukin-2, interferon-γ and granulocyte-macrophage colony-stimulating factor and three reference genes were measured with droplet digital polymerase chain reaction (ddPCR) in whole blood samples at day 2, 7, 14, month 1 and 6 until 1

Figure: Table 1. Demographics and laboratory data of pre and post transplant period

	Pre-transplant	Post-transplant
Weight (kg) mean±SD	73.9±14.8	80.2±15.2
BMI (kg/m ²) mean±SD	25.7±4.6	27.8±5.0
Obesity n, (%)	11(9.7)	28(24.7)
Hypertension n, (%)	12(10.6)	68 (60.1)
Diabetes Mellitus n, (%)	28(24.7)	54(47.7)
Hyperlipidemia n, (%)	13(11.5)	46(40.7)
Coronary artery disease n, (%)	8(7.07)	16(14.1)
Metabolic syndrome n, (%)	15(13.2)	58(51.3)
Glucose (mg/dL) (median-range)	104 (69-260)	113 (66-289)
Cholesterol (mg/dL) (median-range)	128 (39-246)	172 (85-350)
Triglyceride (mg/dL) (median-range)	97 (11-449)	155 (46-514)
ASCVD risk score (median-range)	7(0.2-41.89)	13.6 (0.1-63.8)
Anti-lipidemic drug use n, (%)	3 (2.6)	11 (9.6)
Anti-hypertensive drug use n, (%)	10 (8.7)	52 (45.6)

Table 2. Comparison of post-transplant patients with and without metabolic syndrome in terms of pre-transplant clinico-demographic data

Patient characteristics	Metabolic Syndrome Present n:59	Metabolic Syndrome Absent n:55
Sex: Male [n (%)]	42 (71.1)	27 (49)
Age, years mean±SD	60.4±7.38	51.9±13.57
BMI (kg/m ²) mean±SD	26.6±4.27	24.4±4.93
Hypertension n, (%)	11 (18.6)	1 (1.81)
Anti-hypertensive drug use n, (%)	10 (16.9)	1 (1.81)
Diabetes mellitus n, (%)	21 (35.59)	7 (12.7)
Anti-diabetic drug use n, (%)	21 (35.59)	5 (9.09)
Smoking n, (%)	30 (50.8)	16 (29)
ASCVD risk score [median (range)]	12.5 (0.9-41.8)	5.8 (0.1-22.7)
VAT (cm ²) [median (range)]	171.7 (29.9-484.4)	103.0 (12.6-340.8)
SAT (cm ²) [median (range)]	201.6 (32.4-527.5)	156.1 (22.7-448.7)
Total Fat Area (cm ²) [median (range)]	400.8 (62.3-744.8)	314.4 (40.9-653.4)
VAT/SAT [median (range)]	0.82 (0.23-4.21)	0.63 (0.1-4.2)

Table: (abstract: THU-518).

year after LT in 23 patients transplanted between February 2019 and June 2020. The RGE after Tac intake was calculated as $c_{peak}/c_0 \times 100$, where c_0 is the adjusted number of transcripts at the Tac predose level and c_{peak} is the number of transcripts at peak level. IS consisted of LCPT extended-release Tac introduced directly after LT, mycophenolic acid, and a corticosteroid-taper for 3 months.

Results: Tac peak levels and NFAT-RGE showed a strong inverse correlation ($r = -0.8$). Our descriptive analysis shows that although patients show a Tac trough level within the targeted therapeutic window, low RGE can result in a higher risk for infection. Mean individual trough effect of Tac on the 3 target genes with all timepoints pooled was 33% (26–56%) in patients without infection and 81% (53–95%) in patients with infection ($p < 0.011$), mean individual peak effect was 48% (44–64%) in patients without infection and 91% (90–94%) in patients with infection ($p < 0.001$).

Conclusion: Tailored IS monitored with NFAT-RGE is promising to decrease infectious complications by optimization of the IS level in LT recipients on LCP extended release Tac.

THU-520

Long-term survival after liver transplantation in patients with common variable immunodeficiency

Ina Andersen^{1,2}, Henrik Reims³, Krzysztof Grzyb³, Børre Fevang^{1,4}, Espen Melum^{2,5,6}, Pål Aukrust^{1,7,8}, Kristine Wiencke², Ingvild Nordøy^{1,7}, Pål-Dag Line^{8,9}, Silje Jørgensen^{1,7}. ¹Section of Clinical Immunology and Infectious Diseases, Department of Surgery, Inflammatory Medicine and Transplantation, Oslo, Norway; ²Section of Gastroenterology, Department of Surgery, Inflammatory Medicine and Transplantation, Oslo, Norway; ³Oslo universitetssykehus HF, Rikshospitalet, Department of Pathology, Oslo, Norway; ⁴Centre of Rare Diseases, National Advisory Unit on Rare Disorders, Oslo, Norway; ⁵Norwegian PSC research centre, Department of Surgery, Inflammatory Medicine and Transplantation, Oslo, Norway; ⁶Hybrid Technology Hub Centre of Excellence, Institute of Basal Medical Sciences, Oslo, Norway; ⁷Research Institute of Internal Medicine, Department of Surgery, Inflammatory Medicine and Transplantation, Oslo, Norway; ⁸Institute of Clinical Medicine, Faculty of Medicine, University of Oslo, Oslo, Norway; ⁹Division of Transplant Surgery, Department of Surgery, Inflammatory Medicine and Transplantation, Oslo, Norway
Email: inaand@ous-hf.no

Background and aims: A considerable proportion of patients with common variable immunodeficiency (CVID) have inflammatory and

autoimmune complications. This can include liver disease with development of nodular regenerative hyperplasia (NRH) leading to portal hypertension and end-stage liver disease. We sought to assess the long-term outcome after liver transplantation (LTX) of patients with CVID.

Method: Information was retrieved from the Nordic liver transplant registry and the patients' medical records at Oslo University Hospital (OUH) until December 31st 2021.

Results: Between 2009 and 2021, six patients with CVID underwent LTX at OUH. Patient characteristics and indications for LTX are summarized in table 1. All patients had NRH in the explanted liver and none was hepatitis C positive. All patients received our standard initial immunosuppression after LTX which includes prednisolone, tacrolimus and mycophenolate. Table 1 gives an overview of complications and outcome after LTX. Five of the six patients are still alive after an observational time of 4–12 years with median survival 7.5 years. Of the three patients who underwent LTX due to hepatopulmonary syndrome, one is currently well without need for extra oxygen therapy 4 years after LTX, one underwent a lung-transplantation 6 years after LTX due to relapse of pulmonary shunt-related respiratory failure and one is deceased. Patient 2 died suddenly and unexpectedly 6 years after LTX without signs of liver failure, infection or chronic respiratory failure. Two patients (Patient 1 and 4) have developed signs of increased portal vein pressure including one case of severe upper gastrointestinal bleeding, but no other complications of chronic liver disease have been noted. Four patients have had a graft biopsy, all with findings of de-novo NRH. All patients who are still alive have slightly elevated transaminases and/or cholestatic markers. All six patients have had bacterial infections post-LTX, but based on small numbers it's difficult to conclude if there are more infectious complications in CVID post-LTX compared to other liver recipients. Airway and GI infections may be CVID related, whereas urinary tract infections are not, and none of these infections resulted in severe morbidity or death following LTX. Overall survival rate was 83% after 4–12 years post-transplant observation, which is comparable with overall post LTX survival in the Nordic countries for conventional transplant indications.

Conclusion: Our report shows that CVID patients may obtain overall survival fully comparable to conventional indications for LTX. These patients have a dismal prognosis without transplant. Hence, CVID with severe liver failure should not be considered a contraindication to LTX.

Patient no.	Age at LTx	Sex	CVID-related complications	Year of LTx	Cause of LTx	MELD-Na	Infections				Vascular complications	Miscellaneous	Rejection	Survival (years)
							Viral	Bacterial	Fungal					
1	55-59	F	Recurrent airway infections, bronchiectasis, lymphoid hyperplasia, splenomegaly, duodenal IEL, thrombocytopenia, leucopenia	2009	Acute portal vein thrombosis and liver failure	16	CMV reactivation 2.5 months post LTx	Recurrent CD colitis, Recurrent UTI, S. aureus, Pseudomonas, Shigella, Pneumonia, Erythema due to MRSA	No	No	Benign gastric non-breeding esophageal varices 8.5 years post LTx	-	No	12
2	50-54	M	Recurrent airway infections, bronchiectasis, lymphoid hyperplasia, splenomegaly, lymphopenia	2011	Respiratory failure due to hepatopulmonary shunting	24	No	Pneumonia, CD colitis, UTI due to enterococcus sp.	No	PJP pneumonia, Candida esophagitis	No	-	No	Deceased By post-LTx
3	50-54	M	Recurrent airway infections, bronchiectasis, lymphoid hyperplasia, splenomegaly, duodenal IEL, thrombocytopenia	2011	Respiratory failure due to hepatopulmonary shunting	7	Ulcerative CMV disease of the GI tract	Salmonella septicemia, Recurrent bacterial airway infections - S. aureus, H. influenza, ESBL, Klebsiella and E. coli, Intestinal CD, H. influenza, sinusitis, S. aureus UTI, Postoperative zoon infection	No	Candida esophagitis, Pulmonary aspergillosis twice (once treated), C. glabrata in BAL after lung TS (treated)	Postoperative lung embolus, Pulmonary arteriovenous malformations	Long transplant 6 years post LTx due to respiratory failure, Squamous cell carcinoma and prostate cancer	No	11
4	40-44	F	Recurrent airway infections, bronchiectasis, lymphoid hyperplasia, splenomegaly, duodenal IEL, thrombocytopenia, lymphopenia, anaemia	2013	Cirrhosis with liver failure	28	Intestinal non-viral infection	Recurrent bacterial vaginosis, Intestinal Campylobacter (acute), Recurrent UTI, Salmonella, sinusitis, Post-ERCP cholangitis, Airway infection with Moraxella catarrhalis	Intestinal C. parvum	No	Varicella zoster 7 years post LTx	Daughter of patient S. heterozygous for variant in TNFAIP3 gene	No	9
5	50-54	F	Recurrent airway infections, bronchiectasis, lymphoid hyperplasia, splenomegaly, duodenal IEL, thrombocytopenia, leucopenia, lymphopenia	2017	Cirrhosis with liver failure	22	Ulcerative CMV disease of the esophagus, shingles	Neutropenic septicemia due to H. influenza pneumonia, CD colitis	No	Candida esophagitis	Embolization of splenic artery due to suspected splenic steal syndrome, Acute upper GI bleed with hypotensive shock, 2 years post LTx	Mother of patient S. heterozygous for variant in TNFAIP3 (RAI 3) gene	Borderline	4
6	50-54	F	Recurrent airway infections, bronchiectasis, lymphoid hyperplasia, splenomegaly, duodenal IEL, thrombocytopenia, GILD	2018	Respiratory failure due to hepatopulmonary shunting	11	CMV reactivation 5 months post LTx	Recurrent UTI and airway infections	No	No	No	-	No	9

Figure: (abstract: THU-520): LTx, liver transplantation; CVID, common variable immunodeficiency; MELD-Na, Model For End-Stage Liver Disease; IEL, intraepithelial lymphocytosis; CMV, cytomegalovirus; CD, *Clostridium difficile*; UTI, urinary tract infection; MRSA, methicillin-resistant *Staphylococcus aureus*; PJP, *Pneumocystis jirovecii* pneumonia; ESBL, extended spectrum betalactamase; ERCP, endoscopic retrograde cholangiopancreatography; GI, gastrointestinal; RAI, rejection activity index; GILD, granulomatous lymphocytic interstitial lung disease.

THU-521

Porto-pulmonary hypertension in patients considered for liver transplantation: a cohort study

Ilaria Curro¹, Declan Lewis², Tasneem Pirani³, Robert Loveridge³, Varuna Aluvihare⁴, Krishna Menon⁵, William Bernal³, Christopher Willars³, Mark McPhail³, Julia Wendon³, Georg Auzinger³, Sameer Patel³. ¹King's College Hospital, Department of Critical Care, United Kingdom; ²Institute of Liver Studies, King's College Hospital, Department of Hepatology, United Kingdom; ³Liver Intensive Therapy Unit, King's College Hospital, Consultant in Critical Care, United Kingdom; ⁴Institute of Liver Studies, King's College Hospital, Consultant Transplant Hepatologist, United Kingdom; ⁵Institute of Liver Studies, King's College Hospital, Consultant Transplant Surgeon, United Kingdom

Email: declan.lewis@nhs.net

Background and aims: Porto-pulmonary hypertension (PoPH) is a rare cardiovascular complication of portal hypertension and carries significant morbidity and mortality both in the pre- and post-liver transplant (LT) groups. The aim of this study is to assess the efficacy of therapeutic interventions and outcomes in PoPH patients in transplanted and non-transplanted cohorts.

Method: Retrospective review of health records of adult patients with PoPH in a large tertiary centre over an 18-year period.

Results: Records of twenty adult patients diagnosed with PoPH between January 2005 and December 2022 were analysed. Mean age was 48.8 years (SD: ± 10.2); male 14 (70%); MELD and UKELD scores were 16.1 (SD ± 7.1) and 53.5 (SD ± 5.3) respectively; 18 (90%) had cirrhosis; 6 (30%) carried a dual diagnosis of PoPH and hepatopulmonary syndrome. Ten (50%) patients had severe PoPH at diagnosis (mean pulmonary artery pressures (mPAP) >45 mmHg); 7 (35%)

moderate (35–44 mmHg); and 2 (10%) mild (25–34 mmHg). MPAP before initiation of monotherapy was 46.1 mmHg (SD ± 12.3), decreasing to 39.8 mmHg (SD ± 11.7) post-treatment (6.3% reduction; $p < 0.05$). MPAP prior to dual therapy was 51.8 mmHg (SD ± 6.1) decreasing to 35.9 mmHg (SD ± 15.5) post-treatment (15.9% reduction; $p < 0.05$). Normalization of mPAP was achieved in 1 (5%) patient following initiation of pharmacological therapy; 8 (47%) patients improved to mPAP <35 mmHg. Overall, 13 (65%) patients were assessed for LT; five (25%) patients were deemed too unwell for formal transplant assessment; transplantation was not indicated in two (10%) patients due to relative preservation of native liver function. Twelve patients were listed (two were de-listed due to the development of contraindications). One patient was declined for transplant due to prohibitive underlying cardiovascular risk factors. Median transplant free survival was 19 months (IQR 8–28); median survival in transplanted group was 33 months (IQR 19–54), with 1 year survival 69.2% and 71.4%, respectively. No patients died on the waiting list.

Conclusion: Dual therapy strategies appear to be superior to monotherapy for reduction in mean pulmonary artery pressures in patients with PoPH. However, despite improvement in pulmonary haemodynamics post initiation of pharmacological therapy, outcomes in both transplanted and non-transplanted cohorts remain suboptimal. Further studies are required to assess the impact of dual versus monotherapy on post-transplant outcomes.

THU-522

Liver transplantation in patients with cystic fibrosis: 30 years of experience in Australia and New Zealand

Thomas Wilson¹, Toni Illhardt¹, Michael Fink^{2,3}, Robert Jones², Anastasia Volovets⁴, Mandy Byrne², Mark Oliver^{1,3}, ¹The Royal Children's Hospital Melbourne, Parkville, Australia; ²Austin Hospital, Heidelberg, Australia; ³University of Melbourne, Parkville, Australia; ⁴Royal Prince Alfred Hospital, Camperdown, Australia
Email: tom.wilson3@rch.org.au

Background and aims: Liver transplantation has emerged as an effective treatment strategy in patients with Cystic Fibrosis-related liver disease (CFLD) who develop features of hepatic decompensation or intractable variceal bleeding. We aimed to review the outcomes of patients within our region who had undergone liver transplantation for CFLD.

Method: We utilised the Australia and New Zealand Liver and Intestinal Transplant Registry (ANZLITR) to retrospectively review data from all patients in Australia and New Zealand who had undergone liver transplantation for CFLD, including those who underwent liver transplantation as a component of a multi-organ transplantation.

Results: A total of 54 patients (25 children and 29 adults) underwent liver transplantation for CFLD in Australia and New Zealand between January 1989 and July 2022. Mean age at time of transplantation was 12.2 ± 4.3 years and 28.5 ± 6.0 years for the paediatric and adult groups, respectively. Thirty-six patients (67%) underwent isolated liver transplantation (22 of 25 children (88%); 14 of 29 adults (48%)). Eighteen patients (33%) underwent liver transplantation as a component of a multi-organ transplantation (combined liver-heart-lung in 8, combined liver-lung in 5, combined liver-pancreas in 4, and combined liver-pancreas-kidney in 1). Three patients underwent re-transplantation for liver graft failure. Causes of death following transplantation included pulmonary disease (12 patients), sepsis (2 patients), intra-abdominal haemorrhage (1 patient), and multi-organ failure (1 patient). The overall 5-year survival rate for the children was 92.0% (95% confidence interval [CI]: 71.6–97.9%) versus 66.2% (95% CI: 44.8–80.9%) for the adults. The 5-year survival rate for those who underwent isolated liver transplantation was 82.6% (95% CI: 65.3–91.8%) versus 67.7% (95% CI: 38.3–85.3%) for those undergoing multi-organ transplantation. Survival at 5- and 10-years after transplantation for the entire group was 78.1% (95% CI: 63.8–87.3%) and 71.0% (95% CI: 54.3–82.5%), respectively.

Conclusion: Liver transplantation remains a viable treatment option in children and young adults with CFLD. Survival outcomes are comparable to those previously reported in the literature, with superior survival rates observed among both children and those undergoing isolated liver transplantation.

THU-523

Which is the best therapy for not transplantable patients with multinodular early HCC?

Alessandro Vitale¹, Fabrizio Romano², Fabio Farinati¹, Franco Trevisani³, Umberto Cillo¹, ¹Azienda Ospedale Università di Padova, Italy; ²Università Milano Bicocca, Italy; ³Università di Bologna, Italy
Email: alessandro.vitale@unipd.it

Background and aims: The 2022 version of the BCLC staging system recommends a treatment stage migration from liver transplantation (LT) directly to trans-arterial chemo-embolization (TACE) in patients with multinodular early stage HCC, when LT is not feasible. We sought to compare the effectiveness of liver resection (LR), percutaneous radiofrequency ablation (PRA), and TACE in patients with not transplantable but potentially resectable multinodular early HCC.

Method: Only multinodular not transplantable early stage (2 or 3 nodules ≤ 3 cm) HCC patients were considered. LR patients were obtained from the HE.RC.O.L.E.S. register, whereas PRA and TACE patients were obtained from the ITA.LI.CA register. Since the aim of

this study was to compare the effectiveness of three potential treatments in resectable patients, the statistical method “matching-adjusted indirect comparison” (MAIC) was used to match the PRA and TACE groups to the LR group.

Results: Between 2008 and 2020, 655 HCC cirrhotic patients were enrolled: 303 in LR, 204 in PRA, and 148 in TACE groups. Age, sex, Charlson Comorbidity index, Child-Pugh grade, MELD, platelets count, etiology of cirrhosis, number, and diameter of nodules, and alpha-fetoprotein were weighted by MAIC to create two PRA and TACE pseudo-populations balanced with the LR group. After MAIC, 1–3–5 years OS was 88%, 71%, 56% for LR (median survival 67 months), 97%, 63%, 22% for PRA (median survival 53 months), and 88%, 58%, 32% for TACE (median survival 41 months) ($p < 0.001$). At Cox multivariable weighted regression, the survival benefit of LR over alternative treatments was confirmed: LR group as the reference; PRA (hazard ratio 1.44; 95% confidence interval 1.19–1.84; $p = 0.0045$); TACE (hazard ratio 1.70; 95% confidence interval 1.25–2.31; $p = 0.0007$).

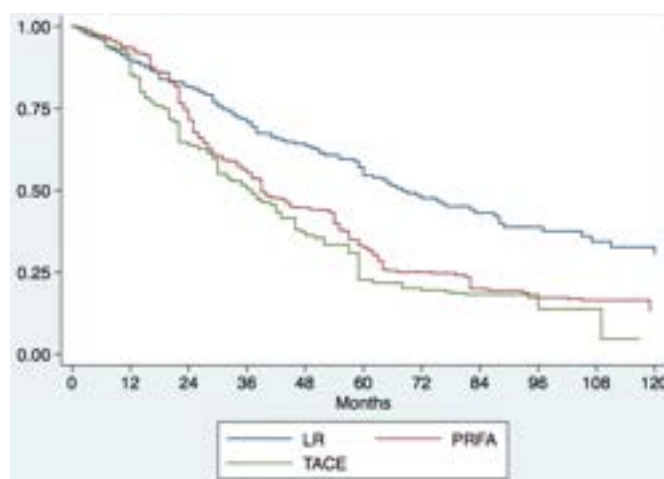


Figure: Comparison of survival curves.

Conclusion: In multinodular early, not transplantable HCC, LR should be the first option, followed by PRA and TACE only when LR is not feasible.

THU-524

Management in hepatology: cost analysis of two opposite options for pretransplantation evaluation

Irene Peñas Herrero¹, Gloria Sánchez Antolín¹, Carmen Alonso Martín¹, Félix García Pajares¹, Carolina Almohalla Alvarez¹, Beatriz Burgueño¹, Sandra Izquierdo Santervás², Isabel Ruiz Núñez¹, Jorge Ruiz Rodríguez¹, Alicia San José Crespo¹, Cristina Martínez Cuevas¹, Esteban Fuentes Valenzuela¹, Soledad Sañudo García³, ¹Hospital Universitario Río Hortega, Hepatology Unit, Valladolid, Spain; ²Hospital Clínico Universitario, Gastrointestinal and Hepatology Department, Valladolid, Spain; ³Hospital Universitario Río Hortega, Admission and Clinical Documentation Department, Valladolid, Spain
Email: ipenash@saludcastillayleon.es

Background and aims: Pretransplantation evaluation before a liver transplant is a critical step in every liver transplant program. It establishes the indication of liver transplant in every patient, and it detects any contraindication that risk the life of patients or the survival of liver graft. This evaluation can be done as an inpatient manner or in an outpatient clinic. In our tertiary hospital, from 2011 the pretransplantation evaluation is done in the outpatient setting with an specific hepatology clinic. It includes at least 2 onsite visits. The aim of our study is to compare the cost associating to the

pretransplantation evaluation between conventional inpatient hospitalization and in an outpatient setting.

Method: Retrospective, single-center, observational comparison between the cost of pretransplantation evaluation as an inpatient manner before 2011 vs the cost of the same evaluation in an external clinic specifically dedicated to pretransplantation evaluation. We used in both periods the valid costs in 2022 to avoid introducing a bias.

Results: In total, 1789 patients were evaluated, 78.53% were male, mean age of 56.1 years (SD 7.08). The most frequent etiology of cirrhosis was alcohol-related in 54.16% of patients. Cirrhosis due to HCV infection was the second most frequent etiology in 23.53% of patients. The most common cause for referring the patient was decompensated cirrhosis and hepatocellular carcinoma in 42.29% and 37.28%, respectively. Pretransplantation evaluation as an inpatient manner implies a length of hospitalization of a mean of 22.97 days (SD 11.75), with a cost of 9388.75 euros by patient. In outpatient clinic, pretransplantation evaluation results in a mean of 5.1 (SD 3.64) visits of every patient, 2.2 (SD 1.67) of them were onsite visits. The total cost for every patient, including 2 morning stays in a day-hospital was 843.83 euros by patient.

Conclusion: Liver pretransplantation evaluation in an outpatient setting and with an specific clinic reduce cost of it in a significant manner. It contributes to a better sustainability of sanitary system. Also, it cuts down iatrogenic complications, nosocomial infections, as avoiding long hospital stays. Also, it allows to preserve the usual liver transplantation activity in periods with a high stress in hospital occupancy without interfering with other diseases, like recent example of SARS-CoV-2 pandemia.

THU-525

Primary sclerosing cholangitis as an indication for liver transplantation. Results and conditioning factors: relationship with associated intestinal pathology

Ainhoa Fernandez¹, Miguel Cova¹, Sergio Rodriguez-Tajes², Maria Senosiain³, Isabel Conde⁴, Rosa Martin-Mateos⁵, Maria Luisa Gonzalez Dieguez⁶, Sonia Pascual⁷, Emilio Fabrega⁸, Alejandra Otero⁹, Cristina Corchado¹⁰, Laura Benitez Gutierrez¹¹, Mario Romero¹, Jordi Colmenero², Javier Bustamante³, Marina Berenguer⁴, Fernando Diaz¹, Luis Menchen Viso¹, Rafael Bañares¹, Magdalena Salcedo¹. ¹General University Gregorio Marañón Hospital, Madrid, Spain; ²Hospital Clínic, Barcelona, Spain; ³Hospital Universitario de Cruces, Bilbao, Spain; ⁴Hospital Universitario y Politécnico La Fe, Valencia, Spain; ⁵Hospital Ramón y Cajal, Madrid, Spain; ⁶Hospital Universitario Central de Asturias, Oviedo, Spain, Spain; ⁷Hospital General Universitario Dr. Balmis de Alicante, Spain; ⁸Marqués de Valdecilla University Hospital, Idival, Spain; ⁹Complejo Hospitalario Universitario A Coruña, Spain; ¹⁰Complejo Hospitalario Universitario de Badajoz, Spain; ¹¹Research Institute and University Hospital Puerta de Hierro, Spain

Email: afyunquera@gmail.com

Background and aims: Liver transplantation (LT) for primary sclerosing cholangitis (PSC) is conditioned by recurrence of PSC and the course of inflammatory disease (IBD). OBJECTIVES: 1) to analyse the incidence of PSC recurrence and its conditioning factors 2) to analyse the course of IBD after LT and 3) to determine the impact of both (PSC recurrence and IBD) on LT outcomes in southern European population.

Method: Retrospective multicentre study of LT indicated by PSC during 1991–2022. Recurrence of PSC was defined as cholangiopathy with patent hepatic artery and no ischaemic history. IBD activity was assessed by Mayo endoscopic index and histology. Factors associated with recurrence of PSC and outcomes after LT were determined by regression analysis.

Results: 143 patients with LT for PSC were included (68.3% male, median age at LT 46 (37–53), 28 (19.6%) of them with recurrence of PSC after median 4.17 (2–6.99). Before HT, 81 (55.9%) patients had IBD, (66 ulcerative colitis [UC]), with colectomy in 10 patients. In

univariate analysis the absence of IBD was associated with a lower risk of recurrence of CEP, OR 0.17 (0.04–0.80). Gender, age, type of donation, immunosuppression (90.6% receiving tacrolimus + mycophenolate), UDCA treatment, study period (before/after 2012), IBD treatment, and colectomy before or after LT were not associated with recurrence. Recurrence of PSC was more frequent in UC vs Crohn's (64.3% vs 3.6%, $p = 0.02$) and was associated with the development of cholangitis (OR 7.43 (2.87–19.25)), graft liver disease (OR 13.5 (3.31–54.90)), portal hypertension (PHT) (OR 11.84, (3.36–42.41)), and retransplantation (11 vs.4 patients, OR 16.17 (4.61–56.72)). In post-LT, de novo IBD was diagnosed in 10 cases (6.9%). The presence of colonic endoscopic activity was more frequent after LT (52.4% vs. 38.4%, $p = 0.7$) with need for therapeutic escalation in 24.7%. Recurrence of PSC was not associated with endoscopic or histological activity, nor with changes in IBD treatment. 22/143 (15.6%) patients died during follow-up (40.9% due to complications of PSC or IBD). In univariate analysis, age at LT (HR: 1.034 (0.99–1.072)), cholangiocarcinoma (HR 5.763 (1.672–19.861)), PTH (HR 2.843 (1.02–7.92)) and infectious complications (HR 2.376 (0.880–6.365)) were associated with lower survival in univariate analysis, whereas in multivariate only PTH was significant (HR 3.8 (1.3–11.6), $p = 0, 015$).

Conclusion: The frequency of recurrence of PSC after LT in our country is similar to that described in other series and is associated with worse LT outcomes. The presence of IBD, especially UC, is associated with recurrence of PSC. We observed worse control of IBD after LT, but it was not associated with recurrence of PSC.

THU-526

Liver transplant recipients with autoimmune hepatitis in the Swiss transplant cohort study have a higher risk of graft loss and vascular complications

Aurélié Rosat¹, Benedetta Terziroli², Linard Hoessly³, Susanne Stampf⁴, Michael Koller⁵, Nicolas Goossens⁴, Montserrat Fraga Christinet¹, Annalisa Berzigotti⁵, Nasser Semmo⁵, Beat Müllhaupt⁶, David Semela⁷, Markus Heim³, Simon Brunner⁸, Manuel Pascual¹, Darius Moradpour¹, Julien Vionnet¹. ¹Lausanne University Hospital, Switzerland; ²Epatocentro Ticino, Switzerland; ³University of Basel, Switzerland; ⁴Geneva University Hospitals, Switzerland; ⁵Inselspital, Switzerland; ⁶Universitätsspital Zürich, Switzerland; ⁷Kantonsspital St Gallen, Switzerland; ⁸Kantonsspital Graubünden, Switzerland

Email: aurelie.rosat@chuv.ch

Background and aims: Data suggest that patients transplanted for autoimmune hepatitis (AIH) have a higher post-liver transplantation (LT) mortality as compared to other liver diseases. Our aim was to compare patient and graft survival of patients transplanted for AIH included in the Swiss Transplant Cohort Study (STCS) with those of patients transplanted for other indications.

Method: All adult patients who underwent a first LT from May 2008 to December 2020 and who consented to participate in the STCS were classified into seven categories according to their initial indication to LT: AIH, alcohol-related liver disease (ARLD), viral liver disease (VLD), primary biliary cholangitis (PBC), primary sclerosing cholangitis (PSC), non-alcoholic steatohepatitis (NASH) and other. Patients with AIH were selected based on clinical, immunological and histopathological criteria; patients with unequivocal etiology were classified in the respective categories, patients with mixed or other diagnoses being classified as "other." Primary outcomes were graft and patient survival; secondary outcomes were post-transplant vascular, biliary and infectious complications. Cumulative incidence of graft loss and death were calculated in the different categories and compared with AIH. The p value was adjusted according to the Bonferroni method. A Cox proportional hazards model was used to investigate the effect of AIH on complications.

Results: A total of 880 LT recipients were included: 23 transplanted for AIH, 254 for ARLD, 303 for VLD, 38 for PBC, 49 for PSC, 61 for NASH, and 152 for other indications. In the AIH group, 65.2% ($n = 15$)

POSTER PRESENTATIONS

were women, the median age was 49 (IQR 39–58) years, follow-up time 3.36 (1.69–5.20) years, and MELD score 20 (15–32); graft loss and death rates were 34.8% (n=8) and 21.7% (n=5), respectively. There was no significant difference in death rates between AIH and other groups but graft loss was significantly higher in AIH patients ($p=0.002$) (Figure). Eighteen (78.3%) AIH patients had a relevant complication, 77.8% (n=14), 44.4% (n=8) and 27.7% (n=5) of them having a vascular, biliary or infectious complication, respectively. In the multivariate analysis, AIH was independently associated with a higher risk of complications (HR 1.693, 95% CI 1.024–2.799, $p=0.040$), along with pre-LT MELD score (HR 1.013, 95% CI 1.002–1.024, $p=0.017$), living donation (HR 3.165, 95% CI 2.069–4.841, $p<0.005$), and rejection (HR 3.452, 95% CI 2.487–4.791, $p<0.005$).

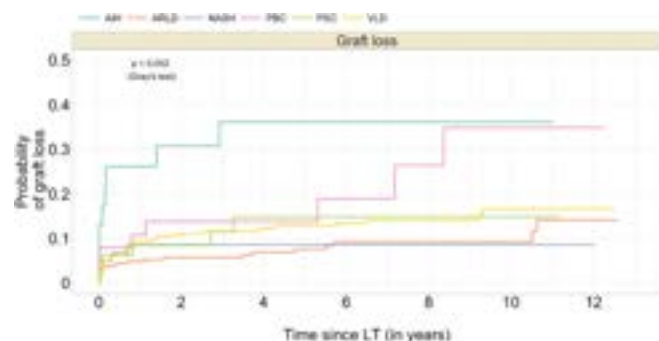


Figure:

Conclusion: Patients transplanted for AIH have a higher risk of early graft loss compared to other etiologies, likely explained by a higher rate of vascular complications.

THU-527

Primary sclerosing cholangitis recurrence after liver transplantation: a nationwide survey in Italy

Maria Cristina Morelli¹, Martina Gambato², Silvia Martini³, Paola Carrai⁴, Pierluigi Toniutto⁵, Valerio Giannelli⁶, Maria Francesca Donato⁷, Ilaria Lenci⁸, Luisa Pasulo⁹, Chiara Mazzarelli¹⁰, Alberto Ferrarese¹¹, Maria Grazia Rendina¹², Antonio Grieco¹³, Alfonso Galeota Lanza¹⁴, Gianluca Svegliati-Baroni¹⁵, Nicola De Maria¹⁶, Laura Mameli¹⁷, Simona Marengo¹⁸, Patrizia Burra¹⁹. ¹IRCCS Azienda Ospedaliero-Universitaria di Bologna, Italy; ²Internal Medicine Unit for the treatment of Severe Organ Failure, Bologna, Italy; ³Multivisceral Transplant Unit, Padua University Hospital, Padua, Italy; ⁴Gastrohepatology Unit, AOU Città della Salute e della Scienza di Torino, University of Torino, Turin, Italy; ⁵Hepatobiliary Surgery and Liver Transplantation Unit, University of Pisa Medical School and Hospital, Pisa, Italy; ⁶Hepatology and Liver Transplant Unit, Department of Medical Area, Udine University Hospital, Udine, Italy; ⁷San Camillo Hospital, Department of Transplantation and General Surgery, Rome, Italy; ⁸Gastroenterology and Hepatology Division, Foundation IRCCS Ca' Granda Ospedale Maggiore Policlinico, Milan, Italy; ⁹Hepatology and Transplant Unit, Fondazione Policlinico Tor Vergata, Rome, Italy; ¹⁰Gastroenterology and Transplant Hepatology Department, Papa Giovanni XXIII Hospital, Bergamo, Italy; ¹¹Gastroenterology and Hepatology Department, Liver Unit, ASST Grande Ospedale Metropolitano Niguarda, Milan, Italy; ¹²Unit of Gastroenterology, Borgo Trento University Hospital of Verona, Verona, Italy; ¹³Gastroenterology Unit, Department of Emergency and Organ Transplantation, University of Bari, Bari, Italy; ¹⁴Liver Transplant Medicine Unit, Gastroenterological Area, Department of Gastroenterological, Endocrine and Metabolic Sciences, Fondazione Policlinico Universitario Gemelli, Catholic University of the Sacred Heart, Rome, Italy; ¹⁵Liver Unit, Cardarelli Hospital, Naples, Italy; ¹⁶Liver Injury and Transplant Unit, Polytechnic University of Marche, Ancona, Italy; ¹⁷Gastroenterology Unit, Department of Medical Specialties, University of Modena and Reggio Emilia and Azienda Ospedaliero-Universitaria di

Modena, Modena, Italy; ¹⁷Liver and Pancreas Transplant Center, Azienda Ospedaliera Brotzu, Cagliari, Italy; ¹⁸Department of Internal Medicine, Gastroenterology Unit, Ospedale Policlinico San Martino, Genova, Italy; ¹⁹Multivisceral Transplant Unit, Padua University Hospital, Padua, Italy Email: mariacristina.morelli@aosp.bo.it

Background and aims: Primary sclerosing cholangitis recurrence (rPSC) after liver transplantation (LT) occurs at a variable rate among different studies from different geographical areas; moreover, the impact of rPSC on patient and graft survival has not been fully defined. We aimed to investigate the rate and impact of rPSC after LT in an Italian cohort.

Method: In April 2022, we conducted a nationwide survey of LT in PSC over the past 15 years, including 85% of Italian LT centers. Participating centers were instructed to define rPSC according to established Mayo criteria and were asked to report rPSC rates at 1, 5 and 10 years. In addition, we explored the effect of rPSC on graft and patient survival.

Results: From January 2007 to December 2021, 445 patients with PSC were listed for LT and 411 underwent LT. The median age at LT was 46 years (18–73), with a prevalence of males of 70% (287/411). rPSC was diagnosed in 81 patients (20%), 24% in the first year, 64% in the first three years, and 91% in the first five years. The prevalence of rPSC varied among centers according to surveillance procedures; the one center that performed protocol liver biopsies reported a higher prevalence than those that did not (24% vs. 15%). rPSC was more frequent in recipients with inflammatory bowel disease (66%) than in recipients with isolated PSC. Recurrence was symptomatic in 69% of the cases, and the main symptoms were cholangitis (66%), pruritus (86%) and jaundice (60%). The overall post-LT mortality was 15% (66/441): 24 patients died in the first year (50% from surgical complications and 25% from infection); 33 patients died between 1 and 5 years (36% rPSC, 21% recurrence of occult CCA) and 9 patients after 5 years (56% cancer, 44% rPSC).

22 out of 81 (27%) patients with rPSC were retransplanted, with an overall survival of 72%; three developed early recurrence one year after the second LT.

Conclusion: In our Country, the rate of rPSC was 20% at five years after liver transplantation. Recurrent PSC was a major cause of long-term mortality and the leading cause of retransplantation.

THU-528

Statins and metformin after liver transplantation: a nationwide cohort

Cyrille Feray¹, Christophe Desterke¹, Nathalie Goutte¹, Daniel Azoulay¹, Eric Vibert¹, Didier Samuel¹, Paul Landais¹. ¹INSERM 1193, Villejuif, France Email: cyrille.feray@gmail.com

Background and aims: LT is the treatment for decompensated cirrhosis or liver cancer. Along with immunosuppressants, drugs such as statins, oral antidiabetics, aspirin, proton pump inhibitors and many others are prescribed over the long term. We studied, in the total population of French 8658 liver transplanted recipients between 2009 and 2018, the influence of non-immunosuppressive drugs on survival and other outcomes.

Method: The French health insurance SNDS database, linked with the national hospital database (PMSI), contains information on at least 99% of the French population: all ICD-10 codes, medical procedures (MP) and prescribed drugs and the vital status. The drugs were evaluated as a time dependent covariate in a cox model using propensity score adapted to studied drug and to the outcome. Outcome on other relevant events were defined by algorithm combining ICD and MP.

Results: Among the 10 most prescribed drugs, statin and oral antidiabetic (OAD) were associated to a favorable survival (HR for statin: 0.53–0.85 $p=0.0003$, HR for OAD: 0.51–0.89 $p<0.005$) (Figure). Statins were associated to less hepatic events and better survival after cardiovascular, renal and infectious events. OAD were associated to less kidney, hepatic and infectious events. None of them

were associated neither to the incidence of *de novo* cancer nor the recurrence of liver cancer. A dose-dependent action was established for both. Hydrophilic more than lipophilic statins and metformin more than other OAD were associated to a better survival. Multivariate analysis showed that the action of statin and OAD were independent each other and to other drugs (including immunosuppression) and was not synergic.

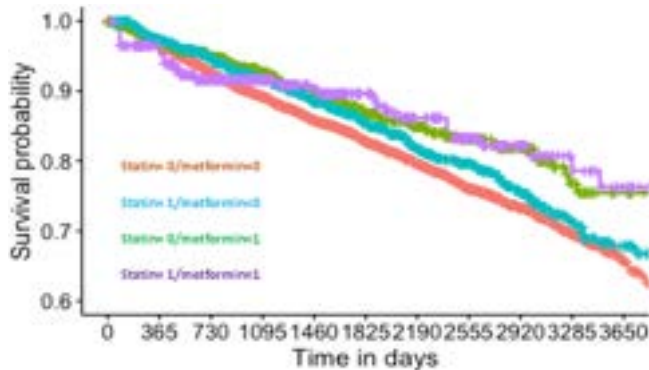


Figure:

Conclusion: In conclusion. Statins and OAD were associated to a favorable effect on survival and important outcomes such as hepatic, cardiovascular and infectious events. The dose-effect observed and the specificity of drug (hydrophilic statins and metformin) suggest that these drugs are directly involved and that their prescription should be extended in the population of patients liver transplanted for cirrhosis or liver cancer.

THU-529

The GALAD score allows early detection of recurrent hepatocellular carcinoma after orthotopic liver transplantation

Magdalena Hahn¹, Adam Herber¹, Janett Fischer¹, Sebastian Rademacher², Daniel Seehofer², Sebastian Ebel³, Timm Denecke³, Thomas Berg¹, Florian van Bömmel¹. ¹Leipzig University Medical Center, Division of Hepatology, Department of Medicine II, Leipzig, Germany; ²Leipzig University Medical Center, Department of Visceral, Transplant, Thoracic and Vascular Surgery, Leipzig, Germany; ³Leipzig University Medical Center, Department of Diagnostic and Interventional Radiology, Leipzig, Germany
Email: magdalena.hahn@medizin.uni-leipzig.de

Background and aims: Recurrence of hepatocellular carcinoma (HCC) after orthotopic liver transplantation (OLT) has an unfavourable prognosis. The potential of novel HCC biomarkers for prediction and early detection of HCC recurrence after OLT is not established. We have assessed the value of the GALAD score for detection and prediction of HCC recurrence after OLT.

Method: In this retrospective monocentric study all patients who underwent OLT due to HCC between 2010 and 2020 in one University Hospital were included. Inclusion criteria were diagnosis of HCC by radiologic or histologic criteria before OLT, availability of serum for biomarker measurement before OLT, 6, 12 and 24 months after OLT, follow-up for at least two years or until HCC recurrence after OLT and written informed consent. AFP, alpha-fetoprotein-L3 (AFP-L3) and des-carboxy-prothrombin (DCP) were measured by μ TASWako i30 test system. The GALAD score was calculated as previously published.

Results: A total of 77 patients was enrolled. The mean observation time was 68 ± 44 (range 2–144) months. HCCR was diagnosed in 20 patients after a mean period of 32 ± 30 (1–104) months. The median recurrence free survival after OLT was 135 months (95% CI: 126, 144 months). The GALAD score before OLT was associated with the number of HCC nodules ($p = 0.009$), with HCC grading ($p = 0.025$) and total HCC diameter in the explanted liver ($p = 0.004$). GALAD score correlated negatively with the time between first diagnosis of HCC recurrence and

OLT ($p = 0.047$). Regular determination of the GALAD score within the first two years after OLT showed a positive score (cut-off value of -1.55) in 8 of the 9 patients with HCC recurrence. GALAD score became positive on average 2.13 ± 3.5 (0–10) months before radiological diagnosis of HCC recurrence. The mean GALAD score was higher before OLT in patients with early HCC recurrence diagnosed within 6 months of OLT ($n = 4$), as compared to those with late or no HCC recurrence or (2.23 ± 2.1 (0.84–4.61) vs -0.97 ± 2.6 (-5.88–11.21); $p = 0.02$).

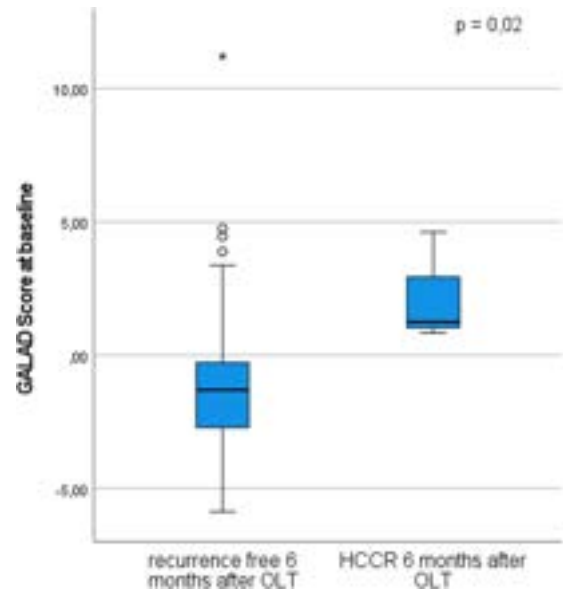


Figure:

Conclusion: The GALAD score may be a useful tool to improve the prediction and early diagnosis of HCC recurrence after OLT.

THU-530

Post reperfusion syndrome in liver transplant after normothermic perfusion: experience of a reference center

Luciano Beltrão Pereira¹, Alice Loughnan¹, Yamen Jabri¹, Lucy Dancy¹, Fionnuala Schwartz¹, Wayel Jassem¹, Juliana Pereira¹, Gudrun Kunst¹, Zoka Milan¹. ¹King's College Hospital, Institute of Liver Studies, United Kingdom
Email: lpereiras@me.com

Background and aims: Post reperfusion syndrome (PRS) is defined as severe haemodynamic instability, with a greater than 30% drop below the anhepatic mean arterial blood pressure (MAP) within 5 minutes of reperfusion sustained for at least 1 minute. It is an important factor in graft survival, morbidity and mortality. Therefore diminishing PRS is essential and the type of donor liver storage could affect it such as preserving the organ in specialised cold storage (CS) reaching 4°C, conventional method, or with normothermic machine perfusion (NMP), modern method, which may reduce ischemic reperfusion liver damage because of its continuous normothermic perfusion of the donor liver.

Method: This was a retrospective case controlled study. Patients were recruited between January 2011 and December 2013. A total of 22 patients were included; 11 patients received a NMP Organ OX perfused liver (OX), and 11 patients formed a control group, who received liver grafts from CS. Recipient and donor demographics were evenly matched between patients (Table 4). The primary outcome was the incidence of PRS with secondary outcomes being inotrope, blood product and fluid requirements. Data was examined for normality, and compared using Fisher exact test or Mann-Whitney.

Results: PRS occurred in 54% ($n = 6$) of the CS group compared to 18% ($n = 2$) of the OX group, $p = 0.183$. The percentage drop in MAP was significantly lower for the OX (15.8%) compared with the CS group

POSTER PRESENTATIONS

(40%) $p = 0.007$ (Figure 2). Total amount of adrenaline used was lower in the OX group compared with the CS group, $p = 0.088$. Total amount and number of patients on noradrenaline was similar between the groups. Total fluids administered was less for the OX group (5090 mls) compared with the CS group (7419 mls) $p = 0.365$. The OX group received less blood products in the post reperfusion phase compared to the CS group, however this was also not statistically significant.

Donor parameters	OX	CS	p Value
Donor Sex M/F	7/4	5/6	0.9
Donor age	60.7	57.4	0.63
Donor BMI	25 (22-28.6)	24.6 (16.6-32)	0.57
Inotropic Support	7/32	9/12	0.66
Liver Steatosis			
normal	7	6	0.9
mild	3	4	0.73
Mild - moderate	1	1	1
moderate	0	0	1
Severe	0	0	1

Table 1: Recipient demographics and characteristics

BMI: Body Mass Index; M: male; F: female

Conclusion: A reduced incidence of PRS in patients receiving NMP compared to CS livers was observed, with improved haemodynamics and lower adrenaline requirements.

THU-531

Comorbidities and complications of patients hospitalized for liver transplantation evaluation, transplant and post-LT: a fourteen-year nationwide study in Germany

Wenyi Gu¹, Louisa Schaaf², Hannah Hortlik², Yasmin Zeleke², Maximilian Joseph Brol¹, Andreas Schnitzbauer², Wolf Bechstein², Alexander Queck², Michael Tischendorf¹, Andreas Pascher¹, Michael Praktijn¹, Martin Schulz¹, Frank Erhard Uschner¹, Florian Rennebaum¹, Jonel Trebicka¹. ¹University Hospital Muenster, Department of Internal Medicine B, Germany; ²University Hospital Frankfurt, Germany
Email: jonel.trebicka@ukmuenster.de

Background and aims: Liver transplantation (LT) is so far the only cure for end-stage liver disease or progressive acute liver failure (ALF), hepatocellular carcinoma (HCC), as well as other chronic liver diseases. However, LT bears also morbidities and mortality, even post-LT. Different comorbidities may follow, and further increase mortality and morbidity. We investigated the outcomes in hospitalized patients, evaluated for LT and in the post-LT patients in Germany in this study over a period of 14 years.

Method: This German nationwide study investigated 10,787 patients hospitalization for LT evaluation, 14,745 on the waiting list, 12,836 underwent LT and 142,809 admissions of patients after LT on related comorbidities and complications between the year of 2005 and 2018. All data were based on the diagnosis related groups (DRG) system with ICD-10 and procedure key (OPS) codes.

Results: The number of admissions for LT evaluation or waiting list increased approximately three times over the observational years from 2005 to 2018. Balance between LT evaluation and LT waiting list entering reached in 2014. LT number decreased by 2.3% overtime, while waiting-list mortality rate increased by 5%. By contrast, the in-hospital mortality rate decreased over the observational period, especially in ALF patients with a drop by 16%. Interestingly, admissions of post-LT patients for complications almost doubled, driven mainly by complications of immunosuppression (e.g. respiratory diseases, infections, acute kidney injury [AKI], malignant diseases, gastritis and diarrhea), which nearly tripled (from 2,748 to 7,290). Importantly, post-LT patients with AKI and biliodigestive anastomosis showed the highest in-hospital-mortality rate of 20% and 18% of all complications, respectively.

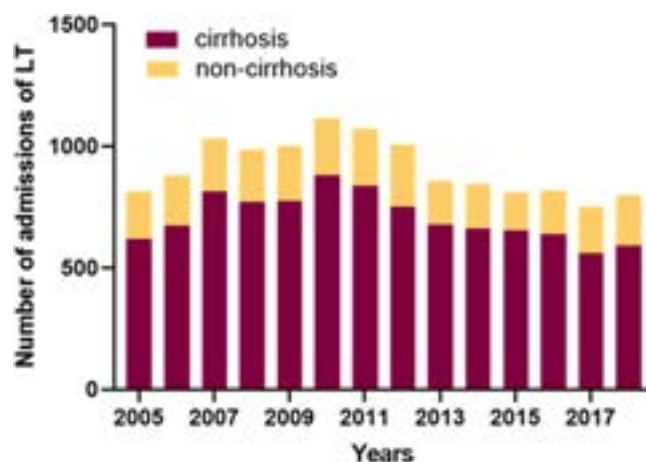


Figure: Number of admissions of liver transplantation patients during the observational year of 2005 to 2018.

Conclusion: In conclusion, the drop of LT leads most probably to the increased in-hospital mortality of patients on the waiting-list. Interestingly, in-hospital mortality decreased in LT patients. An important finding of this study is that post-LT comorbidities requiring hospitalization increased over the observational period. AKI and biliodigestive anastomosis are associated with highest in-hospital mortality and should be addressed.

THU-532

Long-term benefit of mTOR inhibitors for dropping calcineurin inhibitors in liver transplant recipients

Yael Milgrom¹, Ashraf Imam¹, Alaa Jammal¹, Suha Shabaneh¹, Johnny Amer¹, Asher Shafrir¹, Muhammad Massarwa¹, Wadi Hazou¹, Abed Khakayla¹, Rifaat Safadi¹. ¹Hadassah-Hebrew University Hospital, Liver Institute, Jerusalem, Israel
Email: johnnyamer@hotmail.com

Background and aims: Dropping the calcineurin inhibitors (CNI) with an antimetabolite (azathioprine or mycophenolate mofetil (MMF)) or mTOR inhibitor (mTORi) became common practice to protect renal function in liver transplant recipients (LTR). We retrospectively assessed our real-life experience in a trans sectional study 2020–2022.

Method: Long-term follow-up of CNI drop in 169 LTR compared in 4 regimens (study groups): CNI drop that needed an addition of mTORi ($n = 44$, 26%), MMF (58, 34%), both mTORi and MMF (7, 4%) or no additional therapeutic regimen (60, 36%). ANOVA, Hochberg Multiple Comparisons, Chi-Square Tests used for the comparison analysis.

Results: After post-transplant follow-up of 10.9 ± 8.7 years, the used immunosuppression included steroids in 38.9% of LTR, CNI; usually tacrolimus (81.7%) but also cyclosporine-A (6.5%), MMF in 38.9% and mTORi in 30.2% (usually everolimus in 24.9%, but also sirolimus in 5.3%). All 4 regimens (study groups) share a similar means and distributions of ages, gender, ethnicity, smoking, BMI, post-transplant follow-up, etiologies (except of significantly higher HCV and PBC in mTORi and MMF groups, respectively), HCC, incidence of impaired glucose homeostasis, hypertension, hematology, liver enzymes, eGFR, LDL, HDL, TG, HbA1c, and the incidence for using some medications (glucose lowering agents, cyclosporin-A, and UDCA). Comparing to MMF, mTORi group found with significantly increased serum fasting glucose, lower total bilirubin, increased incidence of using statins, decreased number of immunosuppressants, decreased incidence of steroids (without impact on daily dosages) and of prograf (with reduced dosages and trough levels), and lower death rates along the study follow-up 2020–2022 (2.3% in mTORi, 14.3% in mTORi and MMF, 6.9% in MMF, and none in the no additional therapeutic regimen).

Conclusion: Comparing to MMF, the long term CNI drop with mTORi was safer than MMF in LTR needed an additional therapeutic CNI

sparing. Although mTORi introduced for LTR with higher risk factors (high HCV background and worse metabolic homeostasis of glucose and lipid), it allowed better CNi drop to achieve similar renal outcomes with lower bilirubin levels and favorable survival.

THU-533

Sarcopenia at listing for liver transplantation is a negative predictor for post-transplant survival, but not for graft survival

Guido Stirnimann¹, Anja Beugger¹, Federico Storni¹, Vanessa Banz¹, Annalisa Berzigotti¹, Verena Obmann². ¹Inselspital, Bern University Hospital, Department of Visceral Surgery and Medicine, Bern, Switzerland; ²Inselspital, Bern University Hospital, Department of Radiology, Bern, Switzerland
Email: guido.stirnimann@insel.ch

Background and aims: Sarcopenia is a common finding in patients listed for liver transplantation (LT), independent of the underlying liver disease. Sarcopenia has a known influence on wait-list mortality and is associated with an unfavourable outcome after LT including longer intensive care and hospital stay, short-term mortality, higher incidence of infections, and higher overall health care cost. To date, data on the influence of sarcopenia on patient long-term and graft survival is scarce.

Method: In this retrospective tertiary care center analysis, patients with first LT only between 2012 and 2022 and a CT scan ± 3 months before/after listing for LT were included. CT slides were analyzed with sliceOmatic, TomoVision, Canada. Total skeletal muscle area was measured at lumbar level L3 and normalized by height to obtain skeletal muscle index (SMI). Sarcopenia was defined by gender-specific cut-offs ($<50 \text{ cm}^2/\text{m}^2$ in males and $<39 \text{ cm}^2/\text{m}^2$ in females). Survival was visualized with Kaplan Meier survival curves and assessed with the Breslow (generalized Wilcoxon) test.

Results: In total, 161 patients were included (male = 113, 70.2%). Mean age at listing was $55.8 (\pm 11.8)$ years. 59 (36.6%) patients were sarcopenic (mean age 57.6 ± 10.9 years), 102 (63.4%) were not sarcopenic (mean age 54.8 ± 12.3 years). Mean wait-list time was 10.1 (± 7.9) for sarcopenic and 9.9 (± 8.2) months for non-sarcopenic patients. Mean post-LT follow-up time was 49.3 (± 36.5 ; range 0–131) for sarcopenic and 59.8 (± 33.4 ; range 0–130) months for non-sarcopenic patients, respectively. Mean SMI was $43.3 (\pm 5.0)$ in the sarcopenic group and $54.3 (\pm 10.0) \text{ cm}^2/\text{m}^2$ in the non-sarcopenic group. Kaplan Meier survival curve is displayed in the figure. Overall post-LT survival was significantly shorter for sarcopenic patients compared to non-sarcopenic patients (94.1 (± 7.5) versus 107.8 (± 4.6) months, $p = 0.039$ Breslow (generalized Wilcoxon) test). Pre-transplant sarcopenia did not have a relevant effect on graft survival ($p = 0.65$).

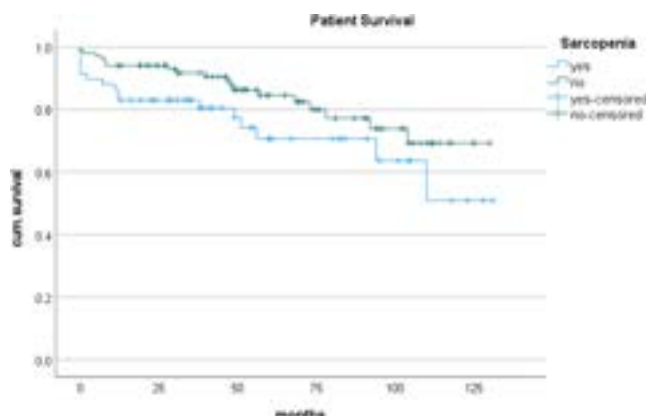


Figure: Post-transplant survival based on pre-transplant nutritional status.

Conclusion: Sarcopenia at listing for LT is a negative predictor for post-transplant survival, but not for graft survival. To what extent counteracting sarcopenia in this patient population improves post-transplant outcome remains to be elucidated.

THU-534

Safety of coronary angiography with consecutive dual antiplatelet therapy in patients with liver cirrhosis and esophageal varices as part of an evaluation for liver transplantation

Moritz Passenberg¹, Aycan Bogazliyan¹, Alexandra Frey¹, Hartmut Schmidt¹, Roxane Authorsen-Grudmann¹, Katharina Willuweit¹, Jassin Rashidi-Alavijeh¹. ¹University of Duisburg-Essen, Medical Faculty, Department of Gastroenterology, Hepatology and Transplant Medicine, Essen, Germany
Email: jassin.rashidi@uk-essen.de

Background and aims: For patients with advanced liver cirrhosis, liver transplantation is the only curative therapeutic option most cases. Inclusion on the waiting list for liver transplantation usually requires extensive evaluation examinations, which in many cases include coronary angiography. Depending on the findings, this may lead to the placement of a stent with subsequent use of dual antiplatelet therapy. To date, there are only limited data on the influence of dual antiplatelet therapy on bleeding events and transplant-free survival.

Method: Clinical data from 228 patients with liver cirrhosis who underwent coronary angiography with or without stenting were collected and statistically analyzed.

Results: Of 228 patients who underwent coronary angiography, 21 (9%) had a bleeding event within 6 months after the intervention, whereas 207 (91%) did not have a bleeding event during the same period. After multivariate analysis, the occurrence of bleeding events was significantly associated with the laboratory parameters INR (HR 15.96 [2.57, 99.10]; $P = 0.003$), albumin (HR 0.42 [0.19, 0.93]; $P = 0.033$), and the placement of a stent after coronary angiography (HR 2.68 [1.07, 6.74]; $P = 0.036$). However, neither platelet count nor the presence of esophageal varices showed an independent and significant association with bleeding events. Furthermore, an analysis was performed to determine the impact of stent placement on the occurrence of ACLF; here, stent placement (HR 2.94 [1.2, 7.18]; $P = 0.018$) was shown to be an independent risk factor for the occurrence of ACLF, in addition to the parameters bilirubin (HR 1.12 [1.03, 1.21]; $P = 0.009$) and hemoglobin (HR 0.81 [0.65, 0.99]; $P = 0.042$).

Conclusion: The performance of coronary angiography with stent placement and consecutive antiplatelet therapy in patients with liver cirrhosis is significantly associated with bleeding events during the period of taking this medication. However, the occurrence of bleeding events is not dependent on the presence of esophageal varices or the extent of thrombocytopenia. Despite increased bleeding events, stenting was not associated with a significantly more frequent occurrence of ACLF or worsening of transplant-free survival.

THU-535

Incidence of de novo tumors after liver transplantation (LT) in HIV infected is similar to non-HIV patients: a single center comparative study

Isabel Terol Cháfer¹, Carmen Vinaixa¹, Sonia García¹, Víctor Argumáñez Tello¹, Marina Berenguer^{1,2}, Victoria Aguilera Sancho¹. ¹La Fe University and Polytechnic Hospital, València, Spain; ²Facultat de Medicina i Odontologia, Departament de Medicina, València, Spain
Email: vinaixa.carmen@gmail.com

Background and aims: De novo tumors and cardiovascular diseases are one of the leading causes of death after LT. Our aim was to describe the incidence of de novo tumors in a HIV-infected LT patients and compared to non-HIV-infected LT patients.

Method: We conducted a retrospective study based on a prospectively maintained database including patients who underwent liver transplantation (LT) from June 2004 to December 2020 in a single LT center. HIV-infected patients were matched to 2 non-HIV infected controls each by age, sex, liver disease etiology, and date of LT. Pre-LT baseline features, HIV related variables, and post-LT outcomes were recorded.

POSTER PRESENTATIONS

Results: A total of 156 LT recipients were included (52 HIV-infected and 104 non-HIV-infected). Baseline characteristics were similar in both groups, except for age and body mass index, which were lower in HIV-infected patients. Mean follow-up post-LT was 7, 5 years in the HIV group vs 8, 2 years in the non-HIV group. Incidence of de novo tumors was 17% in HIV patients vs 12% in non-HIV, pNS. The mean time of appearance de novo tumors since LT was similar in both groups (6, 25 years in HIV-infected patients vs 6, 18 years in non-HIV infected, pNS) (see graph 1). Approximately one third of patients in each group died during follow-up, leading to similar overall survival between groups. De novo tumors were the leading cause of death in both groups (5 HIV patients and 8 on-HIV patients). Smoking after LT was the only factor significantly associated to development of de-novo tumors (p 0, 008).



Figure:

Conclusion: In the post-LT setting, incidence of de-novo tumors in HIV-infected patient was similar to non-HIV patients. Smoking after LT was associated to development of de novo tumors. Larger prospective studies are warranted to validate these results.

THU-536

Biliary strictures in liver transplant recipients: novel strategies for identifying therapeutic targets of biliary fibrosis

Alex Bofill^{1,2}, Pablo Ruiz³, Yilliam Fundora⁴, Carla Montironi⁵, Manuel Morales-Ruiz⁶, Andres Cardenas⁷. ¹Institute of Digestive Diseases, GI Unit, Spain; ²ICMDM, GI Unit, Barcelona, Spain; ³Institute of Digestive Diseases, Liver Unit, Spain; ⁴Institute of Digestive Diseases, HBP Surgery, Spain; ⁵Pathology Department, Spain; ⁶Biochemistry and Molecular Genetics Department, Spain; ⁷Institute of Digestive Diseases, GI/Liver Unit, Spain
Email: acardena@clinic.cat

Background and aims: Biliary anastomotic strictures (BAS) are the most common biliary complication in liver transplant (LT) recipients. The mechanisms of BAS fibrosis are unknown; but overexpression of transforming growth factor beta-1 (TGF-β1) and interleukin-6 (IL-6) is described in animal models. Per-oral digital cholangioscopy (POCS) allows direct visualization of the bile duct and adequate sampling of the biliary epithelium to evaluate factors associated with BAS. We aimed to determine gene expression of TGF-β1 and IL-6 from POCS and from surgical bile duct samples as a potential therapeutic target for local therapies. In addition, confirm the role of POCS for classifying BAS. We present preliminary data of this study.

Method: Prospective and single-center study of patients that developed BAS after LT. Biliary samples were obtained with POCS performing biopsies of the anastomotic stricture, and from surgical bile duct samples. Samples were preserved in RNAlater for subsequent processing and purification of mRNA. Gene expression of TGF-β1 and IL-6 was quantified by quantitative real-time PCR.

Results: Twenty-two recipients have been included, 82% male, median age 62 y (IQR 58–67). The underlying etiology that led to LT was cirrhosis due to alcohol, MAFLD, HCV and HCC. All patients

received a cadaveric organ. The median period from LT to POCS or surgery was 12.7 months (IQR 5–48). POCS was successfully performed in 18 patients (4 of them had surgery). Of all patients treated 12 had BAS pattern A (scar), and 6 pattern B (sloughing, ulcer). Molecular studies (mRNA expression of TGF-β1 and IL-6) have been performed in 13 (4 had insufficient RNA) Figure. 2/18 had mild pancreatitis (11%).

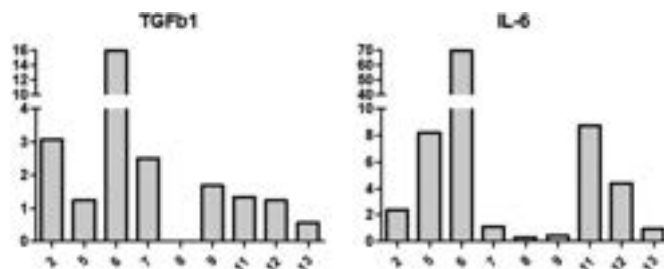


Figure:

Conclusion: Preliminary results indicate mRNA expression of TGF-β1 and IL-6 in BAS of LT recipients. Overexpression of TGF-β1 and IL-6 are potential therapeutic targets for local endoscopic therapy of BAS.

THU-537

Coronary computed tomography angiography in pre-liver transplant cardiac work-up

Chiara Manuli¹, Margherita Saracco¹, Bruna Lavezzo², Alessandro Depaoli³, Fabrizio D'Ascenzo⁴, Renato Romagnoli⁵, Silvia Martini¹. ¹Gastrohepatology Unit, AOU Città della Salute e della Scienza, University of Turin, Italy; ²Anesthesiology and Intensive Care Unit, AOU Città della Salute e della Scienza, University of Turin, Italy; ³Department of Imaging Diagnostics and Radiotherapy, AOU Città della Salute e della Scienza, University of Turin, Italy; ⁴Cardiology Unit, AOU Città della Salute e della Scienza, University of Turin, Italy; ⁵General Surgery 2U, Liver Transplantation Center, AOU Città della Salute e della Scienza, University of Turin, Italy
Email: chiara.manuli@gmail.com

Background and aims: Controversies persist around the optimal screening of pre-liver transplant (LT) candidates for coronary artery disease (CAD). Dobutamine-stress-echocardiography (DSE) is used in many centers, but real-life studies demonstrated its poor performance. Coronary-computed-tomography-angiography (CCTA) is emerging as a promising non-invasive tool to detect CAD; therefore, we aimed to describe its role in the pre-LT setting.

Method: All patients (pts) who underwent CCTA during the pre-LT work-up from 01/01/2022 to 31/12/2022 in our Centre were included. Pts with previous CAD or with cardiac symptoms underwent per-protocol cardiac catheterization (CATH) and were not included in the study. CCTA was performed in pts with at least one major cardiovascular risk factor (age >65 years, insulin-dependent diabetes, NASH-cirrhosis, severe peripheral vascular disease, previous stroke). Significant CAD (S-CAD) was defined as ≥50% stenosis in major-vessels (left main, left anterior descending or right coronary artery) or ≥70% stenosis in moderate-sized vessels. Pts with S-CAD or non-diagnostic CCTA underwent CATH.

Results: During the study period, 122 pts underwent pre-LT work-up in our Centre. CCTA was performed in 42/122 (34%) pts, who represent our study population. Median age was 65 years (IQR 60–68), 24/42 (57%) pts had diabetes (22 insulin-dependent), 16/42 (38%) had NASH-cirrhosis, 3/42 (7%) peripheral vascular disease, 4/42 (10%) previous stroke. As additional risk factors, 19/42 (45%) suffered from arterial hypertension, 9/42 (21%) dyslipidemia and 15/42 (36%) were active smokers.

CCTA identified S-CAD in 17/42 (40%) pts and was non-diagnostic in 2/42 pts (5%); 15 of these 19 pts (79%) underwent CATH; in 2/19 (10.5%) CATH was not performed after careful evaluation with

cardiology specialist and the remaining 2/19 (10.5%) were excluded from LT for extra-cardiac reasons.

CATH showed S-CAD needing revascularization in 8/15 pts (53%): 7/8 pts (88%) underwent percutaneous coronary intervention (PCI) (one complicated by myocardial infarction), 1/8 (12%) required surgical-bypass. After PCI, the median duration of dual-antiplatelet therapy (DAPT) was 1 month (IQR 1–4.5). After revascularization, 1 patient underwent uneventful LT, 3 were listed for LT, 1 was still in DAPT at the end of the study period, 1 died and 2 were excluded from LT for extra-cardiac reasons.

To date, among the 23 pts without S-CAD on CCTA, 14 (61%) underwent LT without early cardiological events.

Conclusion: During a 1-year study period, 42/122 (34%) pts evaluated for LT listing at our Centre had at least one major cardiovascular risk factor and underwent CCTA which identified S-CAD in 17/42 (40%). 8 pts underwent successful revascularization and the median duration of DAPT was 1 month.

THU-538

Safety and efficacy of glucagon-like peptide-1 receptor agonists and sodium-glucose co-transporter-2 inhibitors compared with the standard of care in a cohort of liver transplanted patients: a retrospective study

Aida Rebiha¹, Alessandra Mazzola¹, Philippe Sultanik², Dominique Thabut², Olivier Scatton³, Olivier Bourron⁴, Filomena Conti¹. ¹APHP-Pitié-Salpêtrière Sorbonne University, Liver Transplant Unit, Hepato-Gastroenterology, France; ²APHP-Pitié-Salpêtrière Sorbonne University, Hepato-Gastroenterology, Paris, France; ³APHP-Pitié-Salpêtrière Sorbonne University, Hepatobiliary and Liver Transplantation Surgery, Paris, France; ⁴APHP-Pitié-Salpêtrière Sorbonne University, Diabetology, Paris, France
Email: alessandra.mazzola3@gmail.com

Background and aims: Few data on the safety and efficacy of the use of Glucagon-like peptide-1 receptor agonists (GLP-1RAs) and sodium-glucose co-transporter-2 inhibitors (iSGLT2) are available after liver transplantation (LT). The aims of this study were to evaluate the safety and the efficacy of this treatment 6 months after LT compared to the standard of care treatment.

Method: We performed a retrospective monocentric comparative study on 36 liver recipients with post and/or pre-transplant diabetes treated with GLP1-RAs and/or iSGLT2 after LT. A control group of recipients receiving the standard of care therapy, matched (1:2) according to the time of LT, sex, age and causes of chronic liver disease was performed to compare clinical and biological outcomes. The effectiveness was defined as: glycated hemoglobin (Hb1Ac) target <7% and fasting glycaemia ranged to 0.8–1.3 g/l at 6 months. Side effects were collected. Comparison of the 2 groups was performed using Chi-2.

Results: A total of 36 LT adult patients between 2019 and 2022 were treated in our center with GLP-1RAs and/or iSGLT2 after LT. The majority of patients were male (88.8%, n = 34) with a mean age of 58.91 years old (±8.4). The median MELD score was 14 (IQR 10–21). The most common etiology of liver disease was alcohol in 52.7% of patients (n = 19) and NASH in 44.4% (n = 16). Pre-transplant diabetes was reported in 47.2% of patients (n = 17). After LT 63.9% of patients (n = 23) have GLP1-RAs and 61.1% (n = 22) iSGLT2 therapy. Patients were comparable for clinical and biological characteristics to the control group. Non-serious adverse event was reported in patients receiving GLP1-RAs and/or iSGLT2 treatment. 16.6% (n = 6) of patients had moderate side effects: 4 patients developed gastrointestinal disorders. The hypoglycemia rate was similar between the two groups (p = 0.1). Fasting glycaemia target was achieved in 78.1% (n = 25) and in 61.8% (n = 34) of patients in the GLP1-RA and/or iSGLT2 group compared to the control group (p = 0.1). Hb1Ac <7% was achieved for 81.2% (n = 26) and 75.9% (n = 41) of patients in GLP1-RAs and/or iSGLT2 group and in the control group (p = 0.5), respectively. Fast and slow acting insulin withdrawals were statistically significantly

different between the 2 groups, especially in the sub-group of patients with post-transplant diabetes receiving GLP1-RAs and/or iSGLT2 treatment (s) (p < 0.001, p < 0.001).

Conclusion: In our study performed on liver transplant recipients with a higher rate of NASH and alcoholic diseases, the use of GLP1-RAs and SGLT2 treatments for diabetes was safe. The effectiveness was similar to the standard of care with a remarkable benefit of insulin withdrawal in a subgroup of patients with post-transplant diabetes. Futures prospective studies are needed to evaluate the benefit of the GLP1-RAs and SGLT2 treatments on long-term cardiovascular events, obesity, liver steatosis and mortality.

THU-539

Influence of marginal organs on the drug metabolism in liver transplantation

Laura Büttow^{1,2}, Dominik Schröter^{1,2}, Uta Dahmen¹, Peter Schlattmann¹, Utz Settmacher¹, Hans-Michael Tautenhahn¹. ¹Jena University Hospital-Hospital Lobeda, Jena, Germany; ²Erlä Kröner Graduate School for Medical Students "JSAM", Jena University Hospital, Jena, Germany
Email: hans-michael.tautenhahn@med.uni-jena.de

Background and aims: Metabolic zonation is a phenomenon of the liver that describes the differential distribution of functions between liver lobules. One important liver function is drug degradation, which is realized by cytochrome P450 enzyme (CYP). Alteration of CYP expression and activity is being studied in marginal donor livers to better characterize these high-risk organs and improve the transplant selection process to allow for better risk assessment in the allocation process. We hypothesize that marginal organ factors influence drug metabolism in donor livers of transplanted patients.

Method: The first step of the study is to investigate the influence of marginal organs on drug metabolism, by comparing the steatosis severity, the donor age, and the CIT to the CYP expression and activity. The measurements will be correlated with changes in reperfusion and ischemia-reperfusion-injured grafts. Second, to evaluate the LiMax assay as a CYP 1A2 point-of-care diagnostic, in vivo and in vitro CYP measurements will be correlated. Experimental results will be correlated with patient outcome, particularly the prevalence of delayed graft function, and validated clinical chemistry parameters. 40 patients undergoing liver transplantation at Jena University Hospital in 2022 who gave informed consent will be studied. For an exploratory approach, 10 subjects per independent variable are needed. With the tissue samples we perform an H.E. staining for the morphological analysis of the donor organs. CYP expression will be visualized using an indirect immunohistochemistry more specifically CYP 1A2, CYP 3A4, CYP 2C19. Additionally, fluorescence assay is performed to measure CYP 1A2 activity in vitro, and a breath assay (LiMax) to measure CYP activity in vivo.

Results: The CYP enzymes are expressed pericentral in the lobules. Steatosis, age, and CIT are three interrelated factors influencing the CYP expression pattern. We assume that the CYP activity is altered by the reperfusion and the IRI.

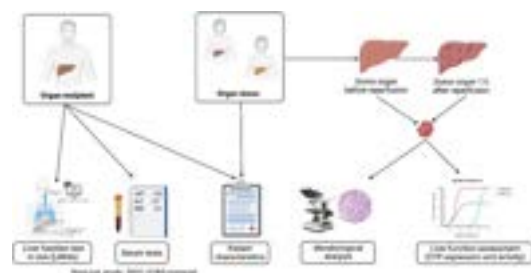


Figure:

Conclusion: It is likely that LiMax can be used to better predict liver regeneration after transplantation.

THU-540

A multi-center, stratification-randomized, double-blind, placebo-controlled, phase III clinical trial of topical recombinant human thrombin for intraoperative hemostasis

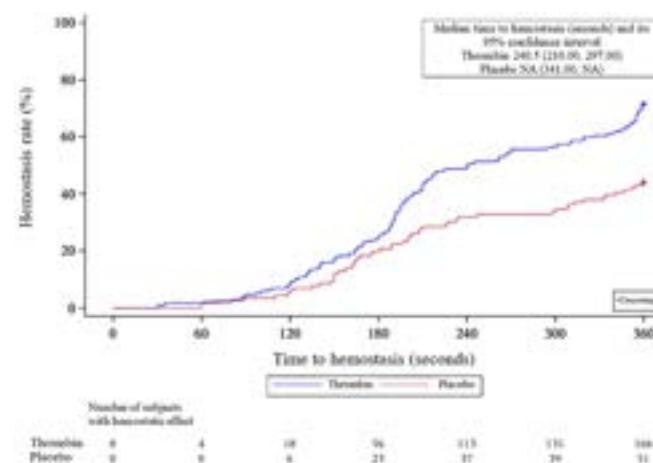
Sheng Yan¹, Jun Yu², Chaoyong Tu³, Chengyou Du⁴, Jia Luo⁵, Jingfeng Liu⁶, Tian-Qi Liu⁷, Qiang Liu⁸, Jun Liu⁹, Xuehua Li¹⁰, Lianchen Wang¹¹, Zheping Fang¹², Weimin Yi¹³, Yajin Chen¹⁴, Qinglong Li¹⁵, Yong Ni¹⁶, Jincai Wu¹⁷, Changjiang Qin¹⁸, Yuanlong Gu¹⁹, Zheng Lu²⁰, Zengjun Lun²¹, Lixue Du²², Gang Chen²³, Qichang Zheng²⁴, Ling Zhu²⁵, Kejian Sun²⁶, Weiqing Han⁵. ¹The Second Hospital of Zhejiang University School of Medicine, China; ²The First Hospital of Zhejiang University School of Medicine, China; ³Lishui Central Hospital, China; ⁴The First Affiliated Hospital of Chongqing Medical University, China; ⁵Hunan Cancer Hospital, China; ⁶Mengchao Hepatobiliary Hospital of Fujian Medical University, China; ⁷Jiangbin Hospital of Guangxi Zhuang Autonomous Region, China; ⁸Liuzhou People's Hospital, China; ⁹Guizhou Provincial People's Hospital, China; ¹⁰Liaocheng People's Hospital, China; ¹¹The Third People's Hospital of Hainan Province, China; ¹²Taizhou Hospital of Zhejiang Province, China; ¹³Hunan Provincial People's Hospital, China; ¹⁴Sun Yat-sen Memorial Hospital of Sun Yat-sen University, China; ¹⁵The Second Xiangya Hospital of Central South University, China; ¹⁶Shenzhen Second People's Hospital, China; ¹⁷Hainan Provincial People's Hospital, China; ¹⁸Huaihe Hospital of Henan University, China; ¹⁹The Third People's Hospital of Wuxi, China; ²⁰The First Affiliated Hospital of Bengbu Medical College, China; ²¹Zaozhuang Municipal Hospital, China; ²²Shaanxi Provincial People's Hospital, China; ²³The First People's Hospital of Kunming, China; ²⁴Union Hospital Affiliated to Tongji Medical College of Huazhong University of Science and Technology, China; ²⁵Wuhan Central Hospital, China; ²⁶Zibo Central Hospital, China
Email: shengyan@zju.edu.cn

Background and aims: Thrombin is a local hemostatic drug commonly used during surgical interventions and can promote blood coagulation by bypassing the initial enzymatic step of the coagulation pathway. Topical recombinant human thrombin is a potentially safer substitute for plasma-derived thrombin and has demonstrated hemostatic activity in a Phase I/II study. This study was designed to evaluate the hemostatic effect of human recombinant thrombin for capillary and venule errhysis after hepatectomy and for any conditions when conventional surgical hemostasis is ineffective or inapplicable.

Method: A total of 510 subjects are expected to be enrolled at 33 study sites in China by the end of the study. Enrolled subjects were randomized to the thrombin group and the placebo group in a 2:1 ratio. An interim analysis was conducted after about 70% of the subjects had completed the observation, and O'Brien Fleming spending function was used to control the total α level at a two-sided significance level of 5%. If the results of the interim analysis supported efficacy, the study was to be terminated early. The primary efficacy end point was the hemostasis rate within 6 min of the evaluable bleeding point. Safety analysis was performed within one month after operation and positive rates of antidrug antibody (ADA) and neutralizing antibody were evaluated.

Results: At the interim analysis, a total of 348 subjects had been randomized and received the study drug, 232 in the thrombin group and 116 in the placebo group, with balanced and comparable demographics and baseline characteristics between the two groups. The hemostasis rate at 6 minutes was 71.6% (95% CI [65.75%, 77.36%]) in the thrombin group and 44.0% (95% CI [34.93%, 53.00%]) in the placebo group, respectively. After adjusting for stratification factors, the difference in hemostasis rate was 27.6% (95% CI [16.92%, 38.36%]), with a significant difference between groups ($p < 0.0001$). The median time to hemostasis was 240.5 s (95% CI [210.00, 297.00]) in the thrombin group and NA (95% CI [341.00, NA]) in the placebo group, respectively. No grade ≥ 3 drug-related adverse events and no drug-related deaths were reported from the study. No recombinant human

thrombin-induced immunologically-enhanced ADA or immunologically-induced ADA was detected after topical use in subjects.



Note: NA indicates that the median time to hemostasis was not reached 6 minutes after administration.

Figure: Hemostasis time curve of evaluable bleeding points

Conclusion: Topical recombinant human thrombin has a significant hemostatic effect for capillary and venule errhysis during surgical operation and has shown good safety and immunogenicity.

THU-544

Liver transplantation for alcohol-related-liver disease in the era of acute on chronic liver failure-single center experience

Dinesh Jothimani¹, Evangeline Simon¹, Hemalatha Ramachandran¹, Rajesh Rajalingam¹, Ilankumaran Kaliamoorthy¹, Gomathy Narasimhan¹, Mohamed Rela¹. ¹Dr. Rela Institute and Medical Centre, India
Email: dinesh.jothimani@relainstitute.com

Background and aims: Liver transplantation (LT) is curative in patients with end stage liver disease (ESLD). Alcohol related liver disease (ALD) is a leading indication for LT. Acute on chronic Liver failure (ACLF) is an increasingly recognised condition requiring LT.

Method: A retrospective analysis of patients who underwent LT from October 2018 to September 2022 was carried out. Patients were stratified as ACLF and ESLD. Demographics, transplant indication, modality (deceased vs Living donor) and survival between the groups were studied.

Results: 114 (19.1%) out of 594 adult patients underwent LT for ALD during the study period; 26 (22.8%) were ACLF and 88 (77.1%) were ESLD. Mean age (52.0 vs 29.31, years, $P = 0.13$), MELD (22.0 vs 20.6, $P = 0.231$), diabetes (19.2% vs 22.7%, $P = 0.793$), LDLT (92.3% vs 97.7%, $P = 0.223$) did not differ between the groups. Spontaneous bacterial peritonitis (34.6% vs 15.9%, $P = 0.05$), was significantly higher in the ACLF group. Post-operative parameters such as ICU stay (9.08 vs 8.32, $P = 0.733$), hospital stay (17.62 vs 18.16, $P = 0.862$) in days, did not differ between the groups. One and three year post-transplant patient survival was 83.3% vs 95.0%, $P = 0.054$ and 72.9% vs 95.0%, $P = 0.014$ between ACLF and ESLD, respectively. Sepsis was significantly higher in the ACLF group (42.3% vs 21.6%, $P = 0.044$) and was the most common cause of death in both groups. Recidivism showed no difference (3.8% vs 3.4%, $P = 1.0$).

Conclusion: Compared to ESLD, ACLF patients have lower but acceptable over-all survival in the predominant LDLT set up. Efforts to overcome septic complications in these patients should be implemented.

THU-545

Liver transplantation as treatment option for cholangiocellular carcinoma

Gabriela Berlakovich¹, Georg Gyoeri¹, David Pereyra¹, Jule Dingfelder², Thomas Soliman¹. ¹Medical University of Vienna, Division of Transplantation, Vienna, Austria; ²University of Vienna, Division of Transplantation, Vienna, Austria
Email: gabriela.berlakovich@meduniwien.ac.at

Background and aims: The treatment of choice for cholangiocarcinoma is surgery and the most important predictor of outcome is a complete margin-negative resection (R0) with an adequate future liver remnant. This goal is only achieved in 60%-80% of cases with a recurrence rate over 50%. The 90-day postoperative mortality is up to 10% in experienced centers in Europe and ~48% of patients who die are dying from post-hepatectomy liver failure. Disappointingly, long-term survival following radical resection remains low, ranging from 20% to 40% at 5 years. On the basis of the anatomical site of origin, cholangiocarcinoma is classified into intrahepatic (iCCA), perihilar (pCCA) and distal (dCCA). Surgery is a potential curative option for all subtypes. However, most patients (~70%) are diagnosed at late stages due to lack of specific symptoms.

Method: Review.

Results: Liver transplantation for pCCA was initially determined to be contraindicated due to a high rate of recurrence (~50%). However, a multicenter retrospective study analyzed 216 patients with early-stage, unresectable pCCA treated with neoadjuvant chemoradiotherapy and followed by liver transplantation showing 5-year disease-free survival of 72%, in the standard group. Several predictors of a patient dropping out before liver transplantation were identified: mass size >3 cm, positive or suspicious intraluminal brushing or biopsy, elevated CA 19-9 ≥500, and higher MELD score ≥20. The drop-out rate was nearly one third of these already highly selected patients. Of those transplanted, the recurrence rate was 20%. Despite selection and neoadjuvant treatment R1 was diagnosed in 47% of explanted livers. Liver transplantation for iCCA might be of great value for patients with cirrhosis and small tumors. 5-year survival following transplantation in patients with small, incidental iCCA (<2 cm) was 65%. In larger iCCA transplantation is reserved for unresectable cases and should only be performed under strict clinical protocols.

Conclusion: Liver transplantation could be a cure for CCA (1) upfront in patients with very early iCCA (single tumor ≤2 cm) in a cirrhotic liver. (2) Highly selected pCCA patients with a single small tumor <3 cm and treated in a specific protocol with neoadjuvant chemoradiation may be candidates and (3) patients with advanced iCCA in a noncirrhotic liver may become transplant candidates if the disease remains stable after neoadjuvant therapy. In any case, the number of patients with cholangiocarcinoma eligible for liver transplantation is very small.

THU-546

Liver transplantation in patients with schistosomiasis in a reference hospital in Sao Paulo, Brazil

Martina Zannini¹, Patricia Zitelli², Javier Fernandez³, Alberto Farias⁴, Miquel Sanz⁵, Isabel Requejo¹, Laia Zamora¹, Laura Lorenzo¹, Miriam Valdivieso¹, Eva Centelles¹, Foix Valles⁶, Susana Nieto¹. ¹Nurse in Liver Unit ICU Hospital Clinic de Barcelona, Spain; ²Investigation nurse at Hospital das Clinicas de Sao Paulo, Brazil; ³Head of the Liver unit ICU, Spain; ⁴Hepatologist at Hospital das Clinicas de Sao Paulo, Brazil; ⁵Nurse coordinator of the Liver unit ICU, Spain; ⁶Research nurse in Liver unit ICU Hospital Clinic de Barcelona, Spain
Email: zannini@clinic.cat

Background and aims: Schistosomiasis is a parasitic disease caused by a trematode which belongs to the *Schistosoma* genus. Globally, this illness causes a huge amount of morbimortality (around 240.000 people die every year). Although schistosomiasis is unusual in Europe, globalization increases the risk of facing imported cases in our continent. Hepatosplenic schistosomiasis causes presinusoidal

portal hypertension requiring pharmacological, endoscopic or surgical treatment. LT is indicated in refractory cases. LT is a common reality in decompensated hepatosplenic schistosomiasis in Brazil, where the illness is endemic. The aim is to describe prevalence and outcome of patients with schistosomiasis transplanted in Hospital das Clinicas, Universidad de Sao Paulo between years 2010–2021.

Method: Retrospective, descriptive analysis on patients with liver disease caused by *Schistosoma mansoni* requiring LT. Clinical records of 1354 liver transplant patients were reviewed.

Results: Among the investigated population, 24 had an infection by this trematode (2% of the total series of LT). The mean age was 54, 63 ±10, 64 years and 58% were men. In 67% of cases schistosomiasis was associated with other concomitant etiologic factor. Portal vein thrombosis after LT occurred in 33%, whereas portal thrombosis before LT were not relevant. One-year survival rate of LT patients with hepatosplenic schistosomiasis was 75%, figure slightly higher than that observed in the non-schistosomiasis group (72%; p = 1330).

Conclusion: Schistosomiasis was an infrequent cause of LT in Hospital das Clinicas de Sao Paulo. Prognosis of patients requiring LT is good with survival rates similar to those observed in other LT recipients.

Liver tumours Clinical aspects except therapy

WEDNESDAY 21 TO SATURDAY 24 JUNE

TOP-065

Multidimensional genomic analysis of cell-free DNA for early detection of hepatocellular carcinoma

Ju Dong Yang¹, Poching Liu², Manaf Alsudaney³, Naomy Kim³, Perla Hernandez³, Monserrat Marquez³, Patricia Torres³, Hirsch Trivedi³, Walid S Ayoub³, Alexander Kuo³, Marc Friedman³, Jonathan Steinberger³, H. Gabriel Lipshutz³, Jun Gong³, Arsen Osipov³, Andrew Hendifar³, Kamya Sankar³, Tsuyoshi Todo³, Irene Kim³, Georgios Voidonikolas³, Todd Brennan³, Steven Wisel³, Justin Steggerda³, Anatoly Ulyanov², Jason Guo², Jonathan Randall², Moin Ahmad², Kang Lu⁴, Qianqian Song⁴, Pei Wang⁴, Yayun Wang⁴, Mengfan Li⁴, Dandan Cao⁴, Chenyu Ma⁴, Zongkui Shi⁴, Kambiz Kosari³, Nicholas Nissen³, Hai Yan². ¹Cedars Sinai Medical Center, United States; ²Genetron Health, Inc., United States; ³Cedars-Sinai Medical Center, United States; ⁴Genetron Health, Inc., China
Email: judong.yang@cshs.org

Background and aims: Early detection of cancer is imperative to improve dismal outcomes of hepatocellular carcinoma (HCC). Conventional imaging techniques and serologic markers based surveillance have suboptimal accuracy. Recently, several blood-based cell-free DNA (cfDNA) platforms have emerged for early detection of cancers including HCC. However, it still needs to be better understood what type of biomarkers provide the most valuable information for the detection of HCC. In this study, we conducted multidimensional genomic profiling of plasma cell-free (cfDNA) to analyze HCC gene mutations, DNA methylation, copy number variation (CNV), the 5 prime end motif on cfDNAs, and serum protein biomarkers in a phase 2 case-control study.

Method: We applied Mutation Capsule (MC) Screening technology and conducted RACEseq to profile mutations and methylation alterations simultaneously in target genomic regions, and sWGS for CNV and 5 prime end motif analysis. For mutations, we targeted frequently mutated regions of frequently mutated genes. Methylation alterations were predicted by a methylation model we developed

POSTER PRESENTATIONS

using the methylation values of 19 genes. For analytical modeling, GLM was performed for individual genomic feature-based model construction in the training cohort. Tenfold cross-validation was used in parameter optimization. The probability score of each genomic and serologic feature for each sample was generated by base models, in which a higher score represented a higher probability for cancer.

Results: We analyzed blood samples from a cohort of 175 patients, including 87 HCC patients and 88 non-HCC patients with liver cirrhosis. Individual panels have various accuracy for HCC detection: AUC of 0.849 (95% CI: 0.791–0.907) for mutation, 0.914 (95% CI: 0.870–0.958) for methylation, 0.896 (95% CI: 0.848–0.945) for CNV, 0.768 (95% CI: 0.698–0.838) for 5 prime end motif, 0.839 (95% CI: 0.779–0.899) for serum protein markers (AFP, AFPL3%, DCP). An integrated model, which combined the biomarkers of mutation, methylation, CNV, 5 prime end motif, and protein markers exhibited a consistently strong screening potential, achieving an AUC of 0.971 (95% CI: 0.946–0.997), 93.1% sensitivity and 94.3% specificity. The sensitivity increased with HCC stages: 100% (5/5) for BCLC stage 0, 89.4% (42/47) for stage A, 93.8% (15/16) for stage B, and 100% (19/19) for stage C, respectively. When stratified by etiology, the performance remains excellent: AUC of 0.964 (95% CI: 0.910–1.000), 93.5% sensitivity, 90.9% specificity in alcohol-associated HCC, AUC of 1 (95% CI: 1.000–1.000), 100% sensitivity, 100% specificity in non-alcoholic steatohepatitis associated HCC, AUC of 0.934 (95% CI: 0.861–1.000), 72.7% sensitivity, 93.5% specificity in viral hepatitis associated HCC.

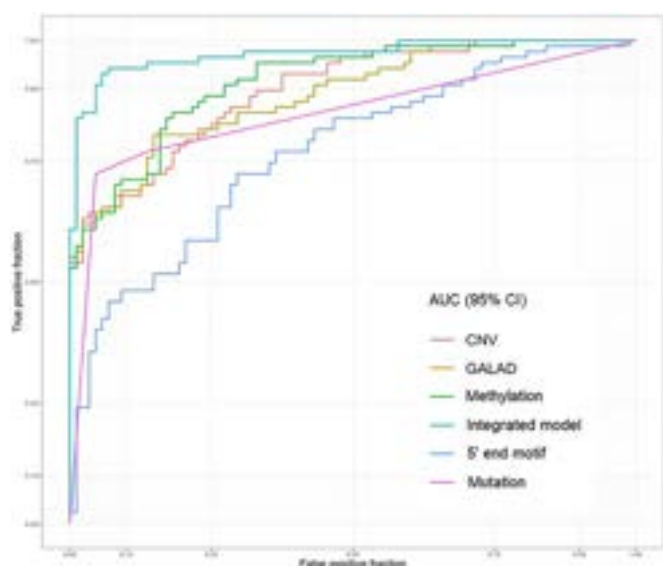


Figure:

Conclusion: Liquid biopsy demonstrates outstanding performance in early detection of HCC with superior performance via multiomics approach. External validation is in progress in a larger phase 2 study.

TOP-068

Deep learning-based model in pre-operative computed tomography for prediction of hepatocellular carcinoma recurrence after curative surgery

Rex Wan-Hin Hui¹, Keith Wan Hang Chiu², I-Cheng Lee^{3,4}, Chenlu Wang⁵, Ho Ming Cheng¹, Lok-Ka Lam¹, Lung Yi Loey Mak¹, Nam-Hung Chia⁶, Chin-Cheung Cheung⁷, Yi-Hsiang Huang^{3,4}, Man-Fung Yuen¹, Philip Yu⁵, Wai-Kay Seto¹. ¹Department of Medicine, School of Clinical Medicine, The University of Hong Kong, Hong Kong, Hong Kong; ²Department of Radiology and Imaging, Queen Elizabeth Hospital, Hong Kong, Hong Kong; ³Institute of Clinical Medicine, Faculty of Medicine, National Yang Ming Chiao Tung University, Taiwan, Taiwan; ⁴Division of Gastroenterology and Hepatology, Taipei Veterans General Hospital, Taiwan, Taiwan; ⁵Department of Mathematics and Information Technology, The Education University of Hong Kong, Hong Kong, Hong Kong

Kong; ⁶Department of Surgery, Queen Elizabeth Hospital, Hong Kong, Hong Kong; ⁷Department of Surgery, Tuen Mun Hospital, Hong Kong, Hong Kong
Email: huirex@connect.hku.hk

Background and aims: Curative surgery is a first-line treatment for early-stage hepatocellular carcinoma (HCC), yet recurrence within 5 years post-resection occurs in over 70% of patients. Early recurrence, particularly within the first year, is associated with worst prognosis. Current risk scores cannot accurately predict recurrence. While histological microvascular invasion (MVI) predicts recurrence, it is only ascertained from surgical specimens and cannot provide pre-treatment prognostication. We developed a deep learning-based model using pre-operative computed tomography (CT) for prediction of early first-year recurrence.

Method: A residual-network deep learning-based model was developed through the training-validation-testing approach. The model utilised both pre-operative CT and clinical data (age, sex, comorbidities and baseline blood tests) to predict HCC recurrence. Chinese patients with resected histology-confirmed HCC were recruited from 5 Hong Kong centers. Patients were randomly divided in a 8:2 ratio to training and internal validation cohorts. The model was then externally tested in an independent cohort from Taiwan. Area-under-curve (AUC) with positive and negative predictive values (PPV/NPV) of the model were calculated, and the AUC of the model was compared with MVI from resected specimens by Delong's test. The 1-year recurrence risk prediction by the model and MVI were compared by survival analysis, with Kaplan Meier curves plotted.

Results: This interim analysis included 1306 patients (83.1% male, age at CT 62.2 ± 10.8 years, median follow-up 5.3 [2.8–8.3] years), with 391 patients (29.9%) developing recurrence within the first year. 564 (43.2%), 141 (10.8%) and 601 (46.0%) patients were included in the training, internal validation and external testing cohorts respectively, and the model was trained for 200 epochs. In the internal validation cohort, the deep learning-based model achieved AUC of 0.783 (95% CI 0.643–0.821; PPV 70.5%; NPV 79.6%) for predicting HCC recurrence at 1-year, which was significantly better than MVI (AUC 0.546 [95% CI 0.446–0.649]; PPV 43.2%; NPV 66.7%) ($p=0.04$). In the external testing cohort, the deep learning-based model achieved AUC of 0.709 (95% CI 0.546–0.762; PPV 47.8%; NPV 81.0%) for HCC recurrence at 1-year, which was numerically higher than MVI (AUC 0.614 [0.525–0.670]; PPV 34.5%; NPV 86.8%). In both the validation and external testing cohorts, the deep learning-based model had better discriminative ability on 1-year recurrence risk when compared with MVI (Fig 1: 70.5% vs 43.2% and 47.8% vs 34.5% respectively, both $p < 0.05$).

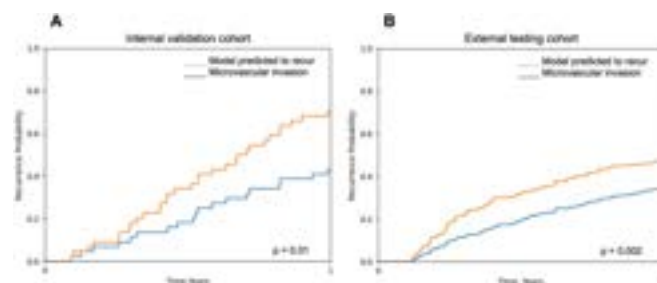


Figure:

Conclusion: A deep learning-based model on pre-treatment CT can accurately predict HCC recurrence within the first year after surgery, outperforming MVI in risk stratification. Our deep learning-based model will be developed, and has potential to become a novel tool for pre-treatment prognostication of short- and long-term outcomes in HCC.

FRI-273

Validation of the CRAFTY score in patients with hepatocellular carcinoma treated with atezolizumab and bevacizumab

Bernhard Scheiner^{1,2,3}, Riccardo Sartoris⁴, Antonio D'Alessio³, Claudia Fulgenzi^{3,5}, Katharina Pomej^{1,2}, Lorenz Balcar^{1,2}, Mohamed Bouattour⁶, Sabrina Sidali⁶, Vera Himmelsbach⁷, Fabian Finkelmeier⁷, Kornelius Schulze⁸, Johann von Felden⁸, Florian Hucke⁹, Kateryna Shmanko¹⁰, Alexander Siebenhüner^{11,12}, Joachim C. Mertens¹³, Sara De Dosso^{14,15}, Matthias Ebert^{16,17}, Andreas Teufel^{17,18}, Dirk-Thomas Waldschmidt¹⁹, Iuliana Pompilia Radu^{20,21}, Anja Krall²², Michael Trauner¹, Jean-François Dufour²³, Henning Wege^{24,25}, Arndt Weinmann¹⁰, Jörg Trojan⁷, Rudolf E. Stauber²², Markus Peck-Radosavljevic⁹, Wei-Fan Hsu²⁶, Arndt Vogel²⁷, Maxime Ronot^{4,28}, David J. Pinato^{3,29}, Matthias Pinter^{1,2}. ¹Medical University of Vienna, Division of Gastroenterology and Hepatology, Department of Internal Medicine III, Austria; ²Medical University of Vienna, Liver Cancer (HCC) Study Group Vienna, Division of Gastroenterology and Hepatology, Department of Internal Medicine III, Austria; ³Imperial College London, Department of Surgery and Cancer, United Kingdom; ⁴APHP Nord, Hôpital Beaujon, Department of Radiology, United Kingdom; ⁵University Campus Bio-Medico, Department of Medical Oncology, Italy; ⁶APHP Nord, Hôpital Beaujon, Department of Digestive Oncology, France; ⁷University Hospital Frankfurt, Department of Gastroenterology, Hepatology and Endocrinology, Germany; ⁸University Medical Center Hamburg-Eppendorf, 1. Department of Internal Medicine, Gastroenterology and Hepatology, Germany; ⁹Klinikum Klagenfurt am Wörthersee, Internal Medicine and Gastroenterology (IMuG), Hepatology, Endocrinology, Rheumatology and Nephrology including Centralized Emergency Department (ZAE), Austria; ¹⁰University Medical Center of the Johannes Gutenberg University Mainz, Department of Internal Medicine I, Germany; ¹¹University Hospital Zurich and University Zurich, Department of Medical Oncology and Hematology, Switzerland; ¹²Cantonal Hospital Schaffhausen, Department of Medical Oncology and Hematology, Switzerland; ¹³University Hospital Zurich and University Zurich, Department of Hepatology and Gastroenterology, Switzerland; ¹⁴Oncology Institute of Southern Switzerland, Ente Ospedaliero Cantonale, Department of Medical Oncology, Switzerland; ¹⁵Università della Svizzera italiana (USI), Faculty of Biomedical Sciences, Switzerland; ¹⁶University Medical Center Mannheim, Medical Faculty Mannheim, Heidelberg University, Department of Internal Medicine II, Germany; ¹⁷Medical Faculty Mannheim, Heidelberg University, Clinical Cooperation Unit Healthy Metabolism, Center for Preventive Medicine and Digital Health Baden-Württemberg (CPDBW), Germany; ¹⁸University Medical Center Mannheim, Medical Faculty Mannheim, Heidelberg University, Department of Internal Medicine II, Division of Hepatology, Germany; ¹⁹University of Cologne, Department of Gastroenterology and Hepatology, Germany; ²⁰University of Bern, Hepatology-Department of Biomedical Research, Switzerland; ²¹Inselspital, University of Bern, University Clinic for Visceral Surgery and Medicine, Switzerland; ²²Medical University of Graz, Division of Gastroenterology and Hepatology, Department of Internal Medicine, Austria; ²³Centre for digestive diseases, Lausanne, Switzerland; ²⁴Klinikum Esslingen, Cancer Center Esslingen, Germany; ²⁵University Medical Center Hamburg-Eppendorf, Department of Internal Medicine, Gastroenterology and Hepatology, Germany; ²⁶China Medical University Hospital, Center for Digestive Medicine, Department of Internal Medicine, Taichung, Taiwan; ²⁷Hannover Medical School, Department of Gastroenterology, Hepatology and Endocrinology, Germany; ²⁸Université Paris Cité, CRI INSERM U1149, France; ²⁹University of Piemonte Orientale, Department of Translational Medicine, Division of Oncology, Italy

Email: matthias.pinter@meduniwien.ac.at

Background and aims: We recently developed the C-reactive protein (CRP) and alpha-fetoprotein (AFP) in Immunotherapy (CRAFTY) score in patients with hepatocellular carcinoma (HCC) undergoing immune checkpoint inhibitor (ICI) therapy. As CRAFTY was developed in patients undergoing different ICI-based regimens, the score

requires validation in patients treated with atezolizumab and bevacizumab (AB), the current standard of care in systemic first-line treatment for advanced HCC.

Method: AB-treated patients with HCC at 15 centers in Europe and Asia between 12/2018 and 01/2023 were included. CRAFTY was derived from serum CRP and AFP values prior to AB initiation by adding one point each for CRP ≥ 1 mg/dL and AFP ≥ 100 ng/ml resulting in the following categories: 0 points = CRAFTY-low, 1 point = CRAFTY-intermediate, 2 points = CRAFTY-high. The prognostic (overall survival (OS) and progression-free survival (PFS)) and predictive ability (best radiological response) of the CRAFTY score were assessed using uni- and multivariable analyses.

Results: Overall, 274 patients (66.1 ± 11.0 years; male: $n = 224$, 82%) were included, of which 208 (76%) had cirrhosis. Most patients had BCLC C ($n = 198$, 72%). While 97 patients (35%) had CRAFTY-low, $n = 113$ (41%) and $n = 64$ (23%) had CRAFTY-intermediate and CRAFTY-high, respectively.

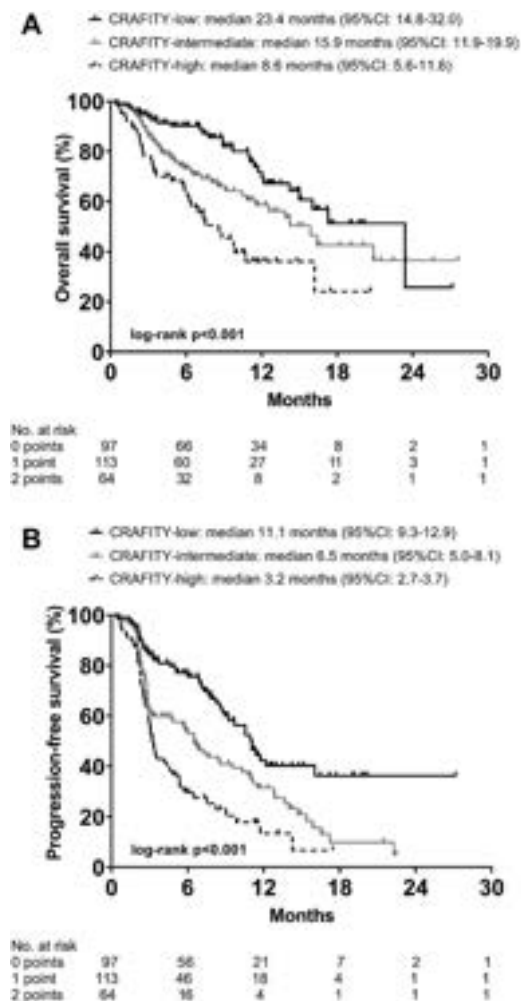


Figure: Comparison of overall (A) and progression-free survival (B) across CRAFTY score

Median OS (Panel A) and PFS (Panel B) were significantly worse in patients with higher CRAFTY scores (OS: low: 23.4 (95%CI: 14.8–32.0) vs. intermediate: 15.9 (95%CI: 11.9–19.9) vs. high: 8.6 (95%CI: 5.6–11.6) months, $p < 0.001$; PFS: low: 11.1 (95%CI: 9.3–12.9) vs. intermediate: 6.5 (95%CI: 5.0–8.1) vs. high: 3.2 (95%CI: 2.7–3.7) months, $p < 0.001$). Upon multivariable analyses, CRAFTY was independently associated with OS (aHR: intermediate vs. low: 1.51 (95%CI: 0.92–2.48), $p = 0.103$; high vs. low: 2.56 (95%CI: 1.52–4.33), p

POSTER PRESENTATIONS

<0.001) as well as PFS (aHR: intermediate vs. low: 1.77 (95%CI: 1.21–2.59), $p=0.003$; high vs. low: 2.90 (95%CI: 1.91–4.39), $p<0.001$). CRAFTY was also significantly associated with radiological response (complete/partial response (CR/PR)/stable disease (SD)/progressive disease (PD), which was evaluable in 245 patients (89%): low: $n=34$ (38%)/ $n=45$ (50%)/ $n=11$ (12%) vs. intermediate: $n=37$ (37%)/ $n=28$ (28%)/ $n=34$ (34%) vs. high: $n=12$ (21%)/ $n=18$ (32%)/ $n=26$ (46%); $p<0.001$). Disease control rates (DCR) were 88% vs. 66% vs. 54% ($p<0.001$), respectively. Upon multivariable logistic regression, a higher CRAFTY score was independently associated with a lower probability of disease control (aOR: intermediate vs. low: 0.25 (95%CI: 0.11–0.55), $p=0.001$; high vs. low: 0.15 (95%CI: 0.06–0.35), $p<0.001$).

Conclusion: The CRAFTY score identifies AB treated patients with a favourable prognosis and response and may help with patient counselling.

FRI-274

Baveno VI and VII criteria are not suitable for screening of large size esophageal varices and clinically significant portal hypertension in patients with HCC

Manon Allaire¹, Bertille Campion¹, Edouard Larrey¹, Mathilde Wagner¹, Marika Rudler¹, Charles Roux¹, Lorraine Blaise², Nathalie Ganne-Carrié², Dominique Thabut¹. ¹Hôpital Pitié Salpêtrière, France; ²Hôpital Avicenne, France
Email: allama5@hotmail.fr

Background and aims: Baveno VI and VII criteria are used in patients with cirrhosis to rule-out large size varices (EV) and rule-in/out CSPH. Their diagnostic performance is still unclear in patients with HCC.

Method: All Child-Pugh A cirrhotic patients with HCC with endoscopy, liver stiffness measurement (LSM) and platelet count within 6 months were retrospectively included and classified according to the BCLC stage in 2 centers. Favorable Baveno VII criteria were defined by LSM ≤ 20 kPa and Plt ≥ 150 G/l, favorable Baveno VI criteria if LSM ≤ 15 kPa and Plt ≥ 150 G/l. Clinical significant portal hypertension (CSPH) was defined by a HVPG ≥ 10 mmHg or the presence of EV regardless the size.

Results: 185 Child-Pugh A cirrhotic patients were included in the study (male 87%, median age 63 years, etiology of cirrhosis alcohol/metabolic syndrome/hepatitis C/hepatitis B in 46%/36%/20%/31% of cases and mixed for 33% of patients). Esophageal varices (EV) were present in 44% of patients (23% large size EV) and HVPG ≥ 10 mmHg in 41.7% (mean HVPG 8 mmHg). Median platelet count and elastometry were $148 \times 103/\text{mm}^3$ and 25 kPa respectively, 50% had platelet count $<150 \times 103/\text{mm}^3$.

In the cohort, 46% of patients were classified as BCLC-0/A, 28% as BCLC-B and 26% as BCLC-C, and 18% had received prior treatment for HCC. A multinodular and infiltrative form was present in 52% and 15% of patients respectively, with a location in the right liver in 78% of cases. Compared to BCLC-0-A HCC (21 kPa), elastometry was higher in BCLC-B (25 kPa, $p=0.005$) and BCLC-C (27 kPa, $p<0.001$) patients. There was no difference in platelet count between the different groups. In patients with favorable Baveno VI criteria, 7.8% in the whole cohort (Se 93%, PNV 82%), 11.1% of BCLC-0-A (Se 89%, PNV 89%) and 10.0% of BCLC-C patients (Se 91%, PNV 90%) had large EV. Among the patients with HVPG <10 mmHg, i.e. without CSPH, 5.7% had large size EV and 17.1% small EV. CSPH was present in 26.7% of patients with favorable Baveno VII criteria in the whole cohort and in 23.5% of those of the BCLC-0/A subgroup. Specificity of LSM ≥ 25 kPa to rule-in CSPH was of 63%.

Conclusion: Favorable Baveno VI criteria are not appropriate to rule-out the presence of high-risk EV and Baveno VII criteria to rule-in/out CSPH in HCC patients.

FRI-275

Multi-omic large scale risk prediction for hepatocellular carcinoma

Jan Clusmann¹, Kai Markus Schneider¹, Christian Trautwein¹, Carolin V. Schneider¹. ¹RWTH Aachen University, Department for Gastroenterology, Metabolic Disorders and Internal Intensive Medicine, Aachen, Germany
Email: janclusmann@ukaachen.de

Background and aims: Hepatocellular carcinoma (HCC) is the third-leading cause of cancer-related death worldwide and a crucial public health concern. Many patients with HCC are only diagnosed at advanced tumor stages, with low to no chance of curative treatment. Meanwhile, high-risk populations for liver cancer are well known. This highlights the urgent need for improved risk stratification, especially as multi-omics pave the way for personalized medicine.

Method: In a systematic approach we analyzed the population-based UK Biobank with $n>500,000$ subjects. We assessed population characteristics, electronic health records, death registers, lifestyle, physical and biological measures as well as single nucleotide polymorphisms (SNPs) associated with risk of HCC for $\sim 500,000$ subjects (508 with HCC) and nuclear magnetic resonance based (NMR) metabolomics for 106,000 subjects. We train several machine learning algorithms on the different data modalities, to assess relevance for risk stratification (Figure 1A).

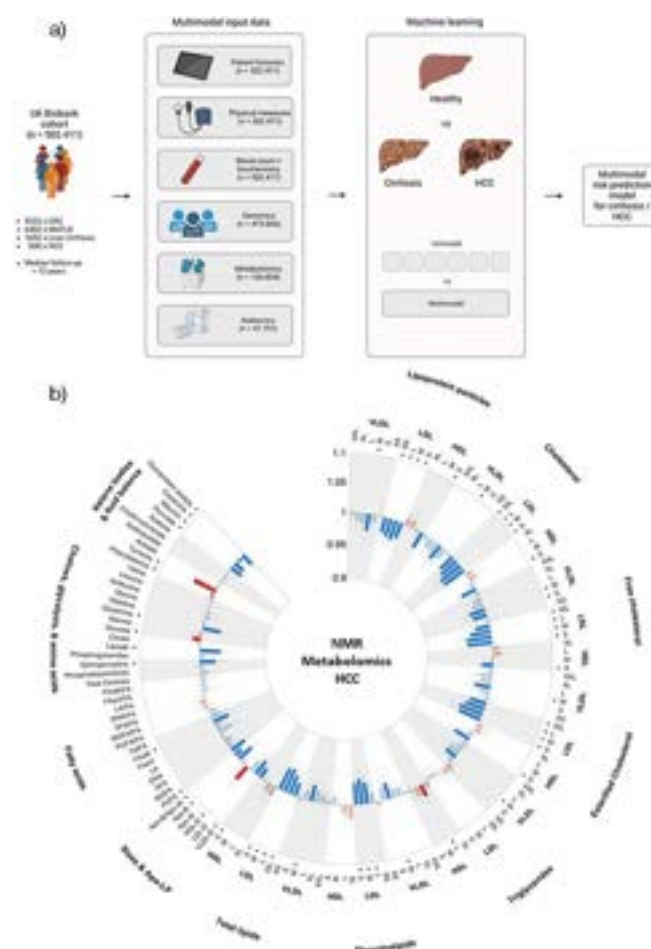


Figure: a) Study design for multimodal risk prediction of HCC (Created with BioRender.com). b) Associations of metabolic biomarkers with development of HCC. Hazard ratios (with 95% confidence intervals) are presented per 1-SD higher metabolic biomarker on the natural log scale, stratified by age, sex, body mass index and previous diagnosis of liver cirrhosis. *False discovery rate-controlled $p<0.01$. DHA, docosahexaenoic acid; FA, fatty acids; FAW3/6, omega-3/6 fatty acids; HDL, high-density

lipoprotein; IDL, intermediate-density lipoprotein; LA, linoleic acid; LDL, low-density lipoproteins; LP, lipoprotein; MUFA/PUFA, mono-/polyunsaturated fatty acids; SFA, saturated fatty acids; VLDL, very low-density lipoprotein; (Code adapted from Diego J Aguilar-Ramirez).

Results: Preliminary results show robust validation for known single nucleotide polymorphisms (in TM6SF2, PNPLA3, GCKR, HLA-DP/DQ), risk factors (e.g., male sex and older age), and diagnosis commonly associated with HCC (e.g., cirrhosis). Linear regression models of NMR-metabolomics show a broad spectrum of significant alterations in metabolomic profiles for patients with HCC, even when stratified for liver cirrhosis (Figure 1B). Current benchmarking experiments comparing 25 different classifiers reveal decision-tree based models as highest performing models. As a next step, we are currently building a decision-tree based classifier, step-by-step integrating the multimodal data predicting HCC.

Conclusion: Our study shows significant changes in metabolomic profiles, as well as risk factors in several data modalities for individuals with HCC. Multimodal risk prediction models for HCC may assist clinicians in improving risk stratification.

FRI-276

Macrotrabecular-massive pattern is associated with aggressive factors, but it is not an independent predictor of tumor recurrence and overall survival in patients with hepatocellular carcinoma treated with liver resection

Ezequiel Mauro¹, Carla Fuster², Joana Ferrer³, Berta Caballol¹, Marco Sanduzzi Zamparelli¹, Jordi Bruix¹, Josep Fuster³, María Reig¹, Alba Díaz², Alejandro Forner¹. ¹Hospital Clínic de Barcelona, Liver Oncology Unit, Liver Unit, Barcelona Clínic Liver Cancer (BCLC) Group, IDIBAPS, CIBEREHD, University of Barcelona, Barcelona, Spain; ²Hospital Clínic de Barcelona, Liver Oncology Unit, Pathological Unit, Barcelona Clínic Liver Cancer (BCLC) Group, IDIBAPS, CIBEREHD, University of Barcelona, Barcelona, Spain; ³Hospital Clínic de Barcelona, Liver Oncology Unit, Unit, Hepatobiliopancreatic and Liver Transplant Department, Barcelona Clínic Liver Cancer (BCLC) Group, IDIBAPS, CIBEREHD, University of Barcelona, Barcelona, Spain
Email: aforner@clinic.cat

Background and aims: The assessment of recurrence risk after liver resection (LR) is critical, particularly with the advent of effective adjuvant therapy. The presence of macrotrabecular-massive histological pattern (MTM: trabeculae >6 cells thick and whose pattern represents >50% of the tumor) has been recently associated with an increased risk of tumor recurrence and decreased overall survival (OS) after LR in patients with hepatocellular carcinoma (HCC). The aim of the study was to describe the subgroup of patients with HCC-MTM, as well as to evaluate its association with aggressive recurrence and OS after LR.

Method: Retrospective study in which all BCLC-0/single-A patients treated with LR between February 2000 and November 2020 were included. The main clinical variables were recorded at the time of admission, surgery and during follow-up. Histological features were evaluated by two independent pathologists. Aggressive recurrence was defined as those that exceeded the Milan criteria at the 1st recurrence.

Results: A total of 218 patients were included (30% BCLC 0 and 70% BCLC A), the median (interquartile range) age and tumor size were 63 years (54–69) and 28 mm (19–42), respectively. The prevalence of MTM and microvascular invasion and/or satellitosis (mVI/S) was 7.8% and 39%, with a kappa index between the two pathologists of 0.81 and 0.77. The presence of the MTM histological pattern was significantly associated with a higher prevalence of mVI/S (82.4% vs. 35.8%, $p < 0.001$), Edmonson Steiner grade III-IV (82.4% vs 36.8%, $p < 0.001$), and higher AFP values [185 (7–664) vs 6 (3–20) ng/ml, $p < 0.001$]. The median follow-up to the 1st recurrence was 34 (14–59) months and 127 (58%) patients experienced HCC recurrence. The recurrence free survival was 51 (41–61) months. The prevalence of aggressive recurrence was 35% (44/127, advanced stage in 20). The

median follow-up was 49 (23–85) months, with a 5-year OS of 81%. The presence of MTM was not significantly associated with recurrence [HR: 1.57 (0.84–2.92), $p:0.154$] or with aggressive recurrence [HR: 1.57 (0.53–4.43), $p:0.154$], and the presence of mVI/S was the only independent predictor of aggressive recurrence [HR: 3.31 (1.74–6.29), $p < 0.001$]. Regarding OS, in the univariate analysis the presence of MTM was associated with a higher risk of death [HR: 2.50 (1.19–5.29), $p:0.016$], but after adjusting for AFP and mVI/S, it was not a predictor of OS [HR: 1.32 (0.49–3.52), $p:0.573$]. The presence of mVI/S was the only independent predictor of mortality [HR: 2.23 (1.27–3.91), $p:0.005$].

Conclusion: The MTM pattern is significantly associated with clinical and histological features of poor prognosis (worse degree of differentiation, mVI/S, and elevated AFP values), but it does not represent an independent predictor for recurrence/OS. Finally, the presence of mVI/S was the only independent risk factor of aggressive recurrence or lower OS rate.

FRI-277

GALAD score outperforms aMAP and ALBI scores in the 5- and 10-year prediction of hepatocellular carcinoma (HCC) development in patients with compensated advanced chronic liver disease (cACLD): a 12-year prospective study

Valentina Baldaccini¹, Sara Ascari¹, Rosina Maria Critelli¹, Letizia Pesole², Simone Lasagni¹, Sergio Coletta², Calogero Claudio Tedesco², Giuseppe Pasculli², Rossella Donghia², Filippo Semellini¹, Erica Villa¹, Gianluigi Giannelli². ¹Gastroenterology, Chimomo, Italy; ²National Institute of Gastroenterology "S. De Bellis" Research Hospital, Italy
Email: erica.villa@unimore.it

Background and aims: Several scores for hepatocellular carcinoma (HCC) prediction have been derived from the analysis of prospective or retrospective patients' cohorts, among these aMAP and ALBI scores. In this study, we have tested the performance of GALAD score alone for predicting 5-year and 10-year HCC risk score from the analysis of a cohort of patients with cACLD of any etiology prospectively enrolled since 2011 vs. aMAP and ALBI scores.

Method: A cohort of 545 patients with cirrhosis was recruited and their GALAD score was calculated. The patients were followed up for a median of 3.60 years at 5 years, and 5.58 years at 10 years. A Cox proportional hazard regression model was used to analyse the predictive ability of GALAD, aMAP and ALBI scores towards the development of HCC at 5 and 10 years.

Results: The results of the study showed that GALAD were all significant predictors of HCC at 5 (HR = 1.373, $p < 0.001$), aMAP (HR = 1.097, $p < 0.001$), and ALBI (HR = 0.162, $p = 0.074$) and at 10 years (HR = 1.315, $p < 0.001$), aMAP (HR = 1.072, $p < 0.001$), and ALBI (HR = 0.389, $p = 0.042$) respectively. Their direct comparison at the same time points showed that GALAD outperformed the other two for the prediction both at 5 and at 10 years (Figure).

Conclusion: We have shown in this study that GALAD score outperforms two other already validated and commonly used scores (aMAP and ALBI) for HCC prediction both at 5 and at 10 years. One possible explanation for GALAD advantage resides in the specific GALAD composition, i.e. the inclusion of AFP as well as AFP-L3 and DCP, whose alteration, especially on the long-term, can be of relevant gain vs. scores including biochemical parameters, more related with liver function than with carcinogenic risk thus opening new opportunities for the clinical management and the decision making of patients with cACLD.

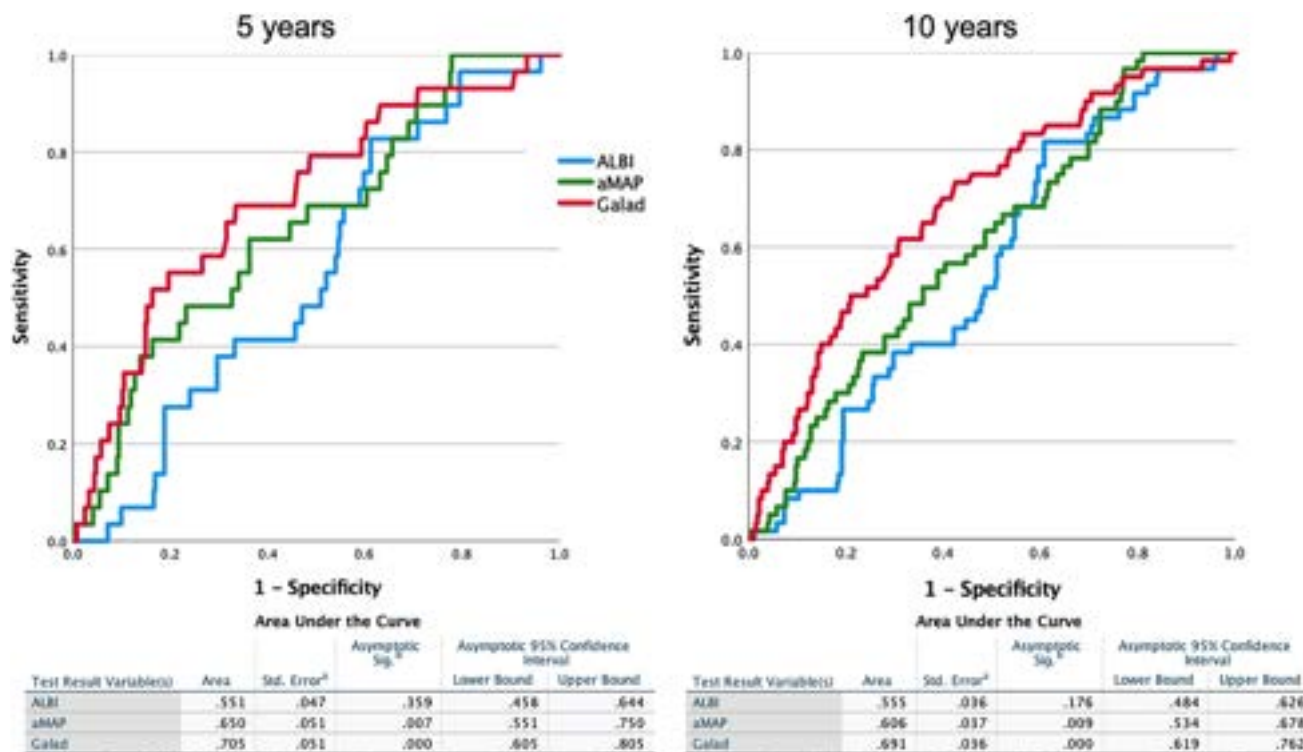


Figure: (abstract: FRI-277).

FRI-278

Alternative surveillance using CT/MR improves clinical outcomes by detecting early-stage hepatocellular carcinoma in High-risk patients with chronic hepatitis B

Su Jong Yu¹, Dong Ho Lee², Heejin Cho¹. ¹Seoul national university hospital, Internal Medicine, Korea, Rep. of South; ²Seoul national university hospital, Radiology, Korea, Rep. of South
Email: dhlee.rad@gmail.com

Background and aims: This study aimed to evaluate the outcome of alternative hepatocellular carcinoma (HCC) surveillance using CT/MR compared to that of US only in chronic hepatitis B (CHB) patients.

Method: We enrolled consecutive CHB patients undergoing regular HCC surveillance, classifying into two groups: US only group and alternative surveillance group. The risk estimation for HCC in CHB (REACH-B) score was calculated to categorize high and low risk. Outcomes included 10-year overall survival (OS), Size and Barcelona Clinic Liver Cancer (BCLC) stage of HCC, and OS after HCC diagnosis.

Results: A total of 2024 patients were enrolled with 1012 patients in each group. In alternative surveillance group, all of 1012 patients underwent contrast enhanced CT (median number, 3; IQR, 1–6; range, 1–24) instead of scheduled US for HCC surveillance during the follow-up. Contrast enhanced MR was done in 222 patients (median number, 1; IQR, 1–2; range, 1–10). There was no significant difference in OS (96.0% in US only vs. 96.8% in alternative surveillance; $P = 0.379$). In both groups, HCC occurred in 66 patients. Medium size of HCC in alternative surveillance was significantly smaller than US only (1.6 cm vs. 2.1 cm; $P < 0.001$). The rate of BCLC 0 stage HCC was also significantly higher in alternative surveillance than US only (71.2% [47/66] vs. 42.4% [28/66]; $P = 0.003$). OS after HCC diagnosis in alternative surveillance group was significantly better than that in US only group (83.0% vs. 67.0%; $P = 0.025$). In high risk group including 970 patients, alternative surveillance provided significantly better OS (97.3% vs. 93.6%; $P = 0.029$) and OS after HCC diagnosis (83.0% vs. 60.6%; $P = 0.010$) than US only. However, there was no significant difference in both OS ($p = 0.202$) and OS after HCC diagnosis ($p = 0.937$) in 1054 patients with low risk.

Conclusion: Alternative surveillance using CT/MR enabled the detection of HCC in earlier stage with smaller size than US only, and had a potential to improve OS after HCC diagnosis, especially for patients with high risk.

FRI-279

Presence of esophageal varices regardless their size is associated with overall survival in patients with advanced HCC treated with Atezolizumab/Bevacizumab

Philippe Sultanik¹, Edouard Larrey¹, Bertille Campion¹, Manon Evain¹, Christine Brochet², Héloïse Giudicelli¹, Mathilde Wagner³, Jérôme Denis², Marika Rudler¹, Dominique Thabut¹, Manon Allaire¹. ¹Hôpital Pitié-Salpêtrière, Liver Unit, Paris, France; ²Hôpital Pitié-Salpêtrière, Biochemical Department, France; ³Hôpital Pitié-Salpêtrière, Radiology Department, France
Email: philippe.sultanik@aphp.fr

Background and aims: Portal hypertension (PHT) and hepatocellular carcinoma (HCC) are 2 closely related complications of cirrhosis. The presence of PHT is associated with higher mortality with locoregional treatments of HCC. Our objectives were to investigate whether PHT parameters were associated with progression-free survival (PFS) and overall (OS) in HCC patients (pts) treated with Atezolizumab/Bevacizumab (Atezo/Beva).

Method: Data from all pts treated with Atezo/Beva were collected prospectively since August 2020. OS and PFS were assessed using Kaplan Meier. Progression was defined as a composite (progression and/or side effects/hepatic decompensation requiring discontinuation). The influence of baseline characteristics on events during follow-up was assessed by Cox model.

Results: Data from 75 pts treated with Atezo/Beva were analyzed prospectively (median age 65 years, 21% women, 81% cirrhotic pts). Risk factors for cirrhosis were viral infection (57%), excessive alcohol consumption (47%) and metabolic syndrome (35%). 37% had a mixed cause of cirrhosis. At inclusion, 74% of the pts were Child-Pugh A and 49% had esophageal varices (EV) (25% large size EV). On the day of treatment, 65% of pts were BCLC-C and 52% were treatment-naïve for

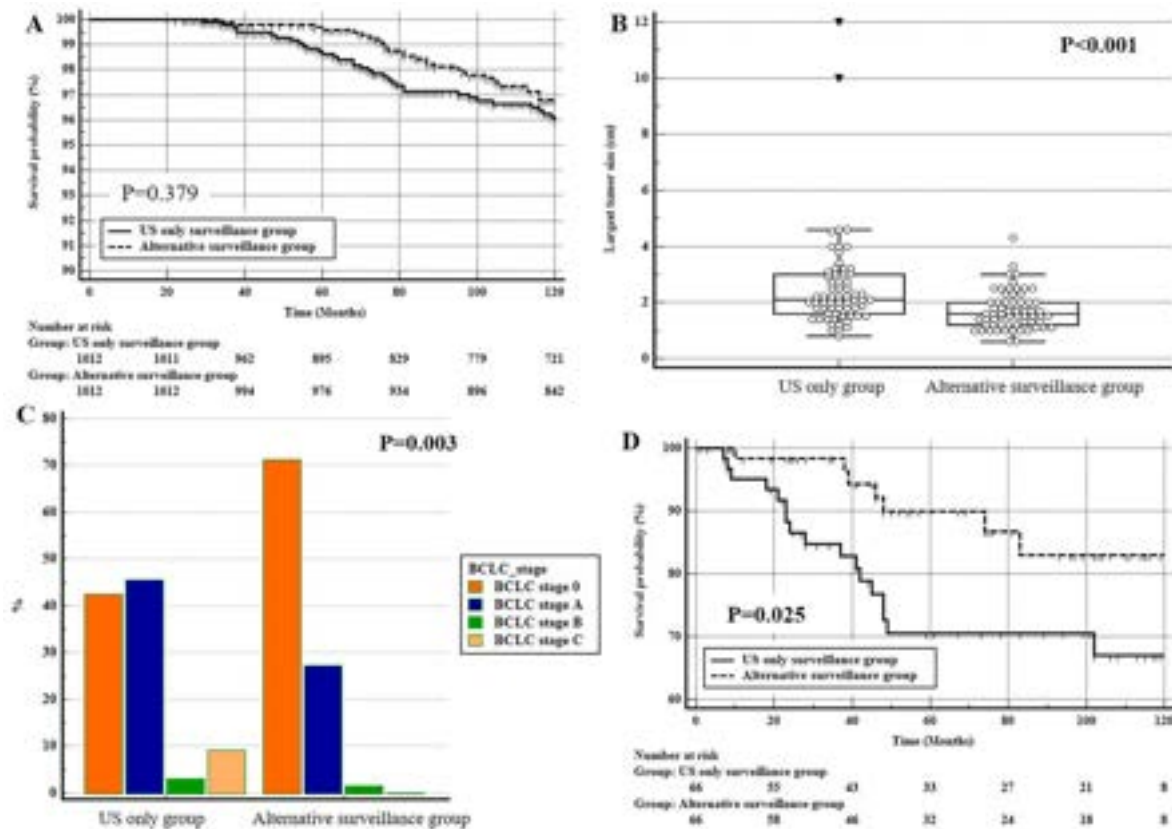


Figure: (abstract: FRI-278): (A) Overall survival in total of 2024 patients with 1012 patients in each group. (B) Size of HCC in total of 132 patients who had HCC. HCC was occurred in 66 patients of both two groups. (C) Distribution of BCLC stage of HCC at the time of diagnosis in total of 132 patients who had HCC. (D) Overall survival after HCC diagnosis in 132 patients who had HCC.

HCC. HCC was multi-nodular in 68%, with a median size of 59 mm for the largest lesion, 33% had infiltrating HCC and 47% vascular invasion. At inclusion, median bilirubin was 14 μ M, INR 1.14, albumin 35 g/L, platelets 170,000/mm³, MELD score 9.0, PIVKA 3.358 and AFP 207 ng/ml. Of the patients, 15% had an ALBI score of 3 and 18% had thrombocytopenia <100,000/mm³. Median follow-up was 13 months, 33% of pts had a response to treatment (regression or stability). The PFS was 30% at 12 months. In univariate analysis, the presence of ≥ 3 HCC lesions (HR = 1.4, 95% CI [0.6–3.2], $p = 0.02$), platelet count (HR = 1.01, 95% CI [1.01–1.1], $p = 0.03$), albumin level (HR = 0.9, 95% CI [0.89–0.99], $p = 0.04$), PIVKA (HR = 1.01, 95% CI [1.01–1.1], $p = 0.003$), AFP (HR = 1.01, 95% CI [1.01–1.1], $p = 0.003$) and the presence of large EV (HR = 2.2, 95% CI [1.2–4.2], $p = 0.02$) were associated with PFS. Only the presence of large EV was associated with PFS in multivariate analysis (HR = 3.5, 95% CI [1.5–8.3], $p = 0.005$). OS was 54% at 12 months. Death was related to HCC in 59%, liver failure in 15%, sepsis in 15% and other causes in 11%. In univariate analysis, BMI (HR = 1.1, 95% CI [1.02–1.2], $p = 0.01$), presence of ≥ 3 HCC lesions (HR = 1.1, 95% CI [0.4–2.2], $p = 0.001$), ALBI grade (HR = 1.9, 95% CI [1.2–3.3], $p = 0.01$), PIVKA (HR = 1.01, 95% CI [1.01–1.1], $p < 0.001$), AFP (HR = 1.01, 95% CI [1.01–1.1], $p = 0.001$), presence of EV regardless the size (HR = 2.2, 95% CI [1.2–4.2], $p = 0.02$) were associated with OS. Only the presence of EV regardless of the size was associated with OS in multivariate analysis (HR = 2.2, 95% CI [1.1–6.9], $p = 0.03$). During the follow-up, 8% of pts presented an acute variceal bleeding (AVB): 60% of them had a history of AVB, 60% small size EV and 40% large size EV at the pre-treatment endoscopy. Primary prophylaxis for AVB was started only in pts with large size EV according to Baveno VI recommendations. None of the pts died secondary to AVB.

Conclusion: The presence of EV regardless of their size is associated with OS in patients with advanced HCC treated with Atezo-Beva. Among the patients who presented AVB under treatment, 60% had small size EV, motivating the implementation of an AVB prophylaxis with beta-blockers in all patients with EV regardless of their size.

FRI-280

A machine learning enabled score based on large varices predicts 5- and 10-year hepatocellular carcinoma (HCC) development in a 12-year prospective cohort of patients with compensated advanced chronic liver disease

Sara Ascarì¹, Rodolfo Sardone², Fabio Castellana², Filippo Schepis¹, Valentina Baldaccini¹, Filippo Semellini¹, Alessandra Pivetti¹, Lorenza Di Marco¹, Barbara Lei¹, Nicola De Maria¹, Francesco Dituri², Gianluigi Giannelli², Erica Villa¹. ¹Gastroenterology, Chimomo, Modena, Italy; ²S. De Bellis Research Hospita, National Institute of Gastroenterology, Italy
Email: erica.villa@unimore.it

Background and aims: Most scores for HCC prediction can assess at most 3- or 5-year HCC risk, as the observation period of the derivative cohort is usually short. We aimed to develop a 5- and 10-year HCC risk score from a prospective cohort of patients with compensated advanced chronic liver disease (cACLD) of any aetiology followed up for 12 years.

Method: 545 patients with cACLD, HCC-free, prospectively enrolled from 2011 to 2022, using a convenience sampling, underwent at enrolment upper g.i. endoscopy, liver ultrasound/elastography, HVPG measurement, lab tests. Cox proportional models were used to assess the association between esophageal varices, adjusted for all the selected covariates, and HCC incidence. Random Survival Forest (RSF), a machine learning (ML) prediction model, was used as a

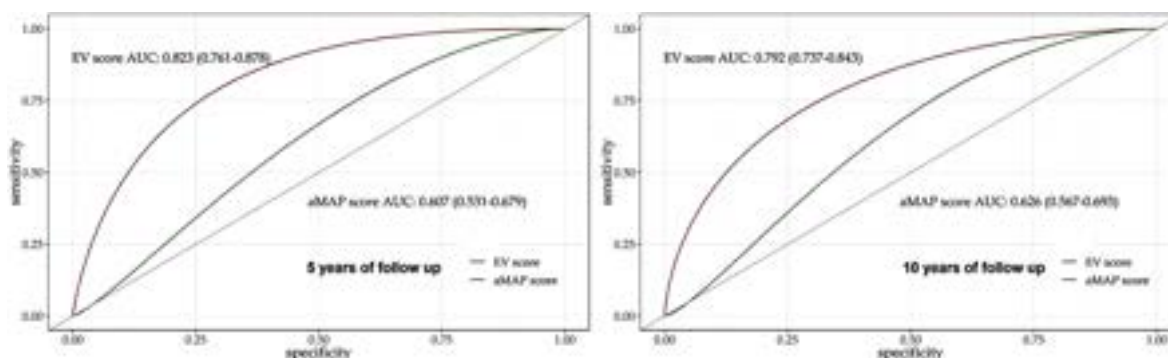


Figure: (abstract: FRI-280).

sensitivity analysis to test prediction power of the same covariates, considering all the possible interactions and non-linear relationships with HCC incidence as the outcome.

Results: Median f-up time was 5.9 years. We observed 78 incident HCCs (14.3%). In the fully adjusted Cox proportional models after the adjustment for covariates, patients with large esophageal varices had 4 times the risk of developing HCC (HR:4.02; 95% C.I.: 2.42–6.68) than patients with small/without varices. The covariates, viral aetiology (HR 2.61;95% C.I.: 1.57–4.35), LSM (for each kPa) (HR: 1.01;95% C.I. 1.01–1.03, male sex (HR:1.94 C.I. 95%: 1.10–3.41), were also meaningfully associated with HCC risk. As a sensitivity analysis we performed the RSF selection algorithm to rank all the variables of the Cox models, according to their prediction power (using minimal depth metric) for the incidence of HCC. Large esophageal varices had the best prediction power for HCC, followed by LSM, viral aetiology, BMI, albumin, and age at the enrolment. Interestingly, RSF prediction power was in line with the magnitude of association with Cox model, but ML further identified BMI and albumin as related and excluded sex. The score built with the RSF-selected variables (Esophageal Varices [EV] score) had excellent discrimination and calibration in assessing both 5- (AUROC 0.823) and 10-year (AUROC 0.792) HCC risk irrespective of aetiology, with a significantly better overall performance at both time points than aMAP score, built on the same data (figure).

Conclusion: The machine learning approach, used to build this score, allowed us to identify large varices as the most important predictor for HCC risk (underlining the critical pathogenetic role of long-standing and severe portal hypertension in HCC development). This score also obtained better prediction for 5- and 10-year HCC development than aMAP score (i.e. the best score so far for HCC prediction independently from aetiology) tested in the same dataset. The proposed score is highly reliable. Being based on routine clinical data of the patients with CACLD it can be easily applied worldwide.

FRI-282

Validation of serum biomarker panels for early HCC detection: results from a large prospective European and Latin American multicenter study

Boris Beudeker¹, Siyu Fu¹, Domingo Balderramo², Angelo Z. Mattos³, Enrique Carrera⁴, Javier Diaz-Ferrer⁵, Jhon Prieto⁶, Marco Arrese⁷, Arndt Vogel⁸, Jesus Maria Banales⁹, Jeffrey Oliveira¹, Anthony Grooshuismink¹, Gertine Oord¹, Robert De Man¹, Jose Debes¹⁰, Andre Boonstra¹. ¹Erasmus MC, Gastroenterology and hepatology, Rotterdam, Netherlands; ²Hospital Privado Universitario de Córdoba, Argentina; ³Federal University of Health Sciences of Porto Alegre, Brazil; ⁴Hospital Eugenio Espejo, Ecuador; ⁵Hospital Nacional Edgardo Rebagliati Martins, Peru; ⁶Centro de Enfermedades Hepáticas y Digestivas (CEHYD), Colombia; ⁷Facultad de Medicina, Chile; ⁸Medizinische Hochschule Hannover, Germany; ⁹Biodonostia Health Research Institute, Spain; ¹⁰University of Minnesota, United States
Email: b.beudeker@erasmusmc.nl

Background and aims: HCC is a major cause of cancer death. Guidelines recommend routine 6-month ultrasonography surveillance for high-risk patients, but its effectiveness in early-stage HCC detection is limited. PIVKA-II, AFP, and the GALAD panel of serum biomarkers are linked to HCC, but inconsistent use in guidelines limits their value.

Method: In a multi-center study, 2045 patient samples were retrospectively or prospectively collected from 7 countries and analyzed for cancer diagnosis and liver disease etiology. The performance of multivariable models based on AFP and PIVKA were tested for early stage HCC detection, low AFP HCC, 12 months pre-diagnostic HCC (n=92, range 9–15 months), and compared to cirrhosis and other liver tumors.

Results: The GALAD model showed excellent ability to differentiate HCC from liver cirrhosis in the prospective Latin American cohort (n = 288), with an AUC of 87.9. A novel multivariable model was developed to detect early-stage HCC with low AFP levels, by combining sex, age, AFP, and PIVKA-II (also called GAAD), with an AUC of 87.3. Both GALAD and GAAD effectively differentiated low AFP HCC from cirrhosis in both European and Latin American patients, with AUCs of 82.8 and 81.6, respectively. Aiming to improve and recalculate the GALAD model in early HCC cirrhotic cases performed similarly to the original. 12 Months prior to HCC diagnosis, GAAD differentiated cirrhosis (n = 193) from pre-diagnostic HCC (n = 92) (p < 0.0001), with 59% sensitivity and 85% specificity in those who would develop an advanced HCC in 9–15 months. In addition, GAAD differentiated non-cirrhotic HCC (n = 243) from other malignant and benign liver tumors with an AUC of 91.9, and it was 100% sensitive and specific in hemangioma cases (n = 64).

Conclusion: The GALAD model has proven to be robust in early stage HCC and diverse patient populations, and its performance remains consistent even when recalculated using different patient cohorts. Our findings warrant its consideration for inclusion in international guidelines for HCC diagnosis and surveillance. With high accuracy, sensitivity, and specificity, the GAAD models has the potential to revolutionize the routine HCC surveillance and diagnosis, in both high-risk cirrhotic and non-cirrhotic cases patients and in low AFP early stage HCC.

FRI-283

A novel AFP-M2BPGi score has better performance than CRAFTY score in predicting survival for patients with viral hepatocellular carcinoma undergoing immunotherapy

Pei-Chang Lee¹, Chijung Wu¹, Kuo-Wei Huang², Chieh-Ju Lee¹, I-Cheng Lee¹, Ming-Chih Hou¹, Yi-Hsiang Huang¹. ¹Taipei Veterans General Hospital, Taiwan; ²Taipei City Hospital Yang-Ming branch, Taiwan
Email: yhhuang@vghtpe.gov.tw

Background and aims: CRAFTY score has been developed to predict the clinical outcomes of patients who received immune checkpoint inhibitors (ICI) for unresectable hepatocellular carcinoma (HCC).

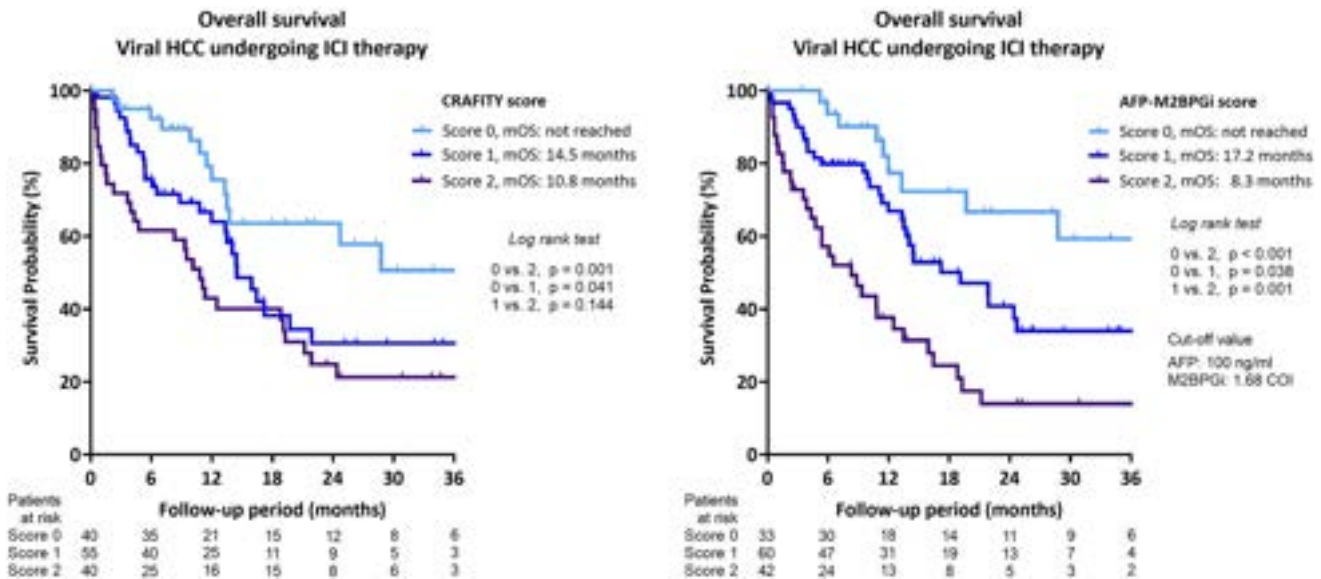


Figure: (abstract: FRI-283).

However, it remains uncertain about the performance of CRAFITY score in patients with viral HCC undergoing ICI-based therapy. Serum Mac-2 binding protein glycosylation isomer (M2BPGi) is a novel biomarker reflecting liver fibrosis for chronic hepatitis B and C. In this study, we aimed to investigate the role of serum M2BPGi in predicting the survival of ICI-treated viral HCC.

Method: From May 2017, 243 consecutive patients had received ICI-based immunotherapy for unresectable HCC in Taipei Veterans General Hospital. The prognostic value of baseline variables, including M2BPGi, on overall survival was analyzed.

Results: During the follow-up period, 140 patients died and the median overall survival (OS) was 13.9 months (95% confidence interval [CI]: 10.6–17.2). Patients with baseline low CRAFITY score had the significantly longest median OS (not yet reached) than the others. However, the OS could not be significantly differentiated between CRAFITY-intermediate and CRAFITY-high patients (median OS: 13.3 vs. 9.5, $p = 0.105$), particularly in patients with viral HCC (median OS: 14.5 vs. 11.1, $p = 0.241$). Among patients with viral HCC, blood samples had been prospectively collected from 135 patients at baseline for measuring M2BPGi. A serum level of M2BPGi greater than 1.68 COI acceptably predicted OS in these patients (AUROC: 0.629, hazard ratio: 2.599, 95% CI: 1.594–4.238, $p < 0.001$). Combined with baseline serum alpha-fetoprotein level (AFP ≥ 100 ng/ml), a new score including AFP and M2BPGi was developed. Patients who fulfilled no criterion (0 points) had the longest median OS (not yet reached), followed by those fulfilling 1 point (17.2 months, 95% CI: 7.6–26.8), and patients meeting both criteria (8.3 months, 95% CI: 3.8–12.8) ($p = 0.038$, <0.001 , and 0.001 for score 0 vs. 1, 0 vs. 2, and 1 vs. 2). Besides, the new AFP-M2BPGi scoring model had a higher homogeneity value (21.85 vs. 11.21) and lower corrected Akaike information criterion value (582.76 vs. 593.41) compared to the CRAFITY score.

Conclusion: A new AFP-M2BPGi score would be superior to CRAFITY score to predict survival in patients receiving ICI-based immunotherapy for viral HCC. This new score may have better clinical application for HCC patients in areas endemic for viral hepatitis.

FRI-284

Implication of patients experience in the liver cancer multidisciplinary approach

Gemma Iserte^{1,2,3}, Eva Palou⁴, Neus Llarch^{1,2,3,5}, Jessica Farre⁴, Maria Angeles García-Criado^{1,2,3,6}, Joana Ferrer^{1,2,3,7}, Alba Díaz^{1,2,3,8}, Marta Burrel^{1,2,3,6}, Montse Brañas⁹, Antonia Murcia⁹,

María Reig^{1,2,5,10}, Joan Escarrabill⁴. ¹BCLC group. Fundació Clinic per a la Recerca Biomèdica-IDIBAPs, Barcelona, Spain, Spain; ²CIBERhd, Madrid, Spain; ³Liver Oncology Unit. Institut de Malalties Digestives i Metabòliques. Hospital Clinic of Barcelona, Barcelona, Spain, Spain; ⁴Patient Experience and Cronicity Department. Hospital Clinic of Barcelona, Barcelona, Spain, Spain; ⁵University of Barcelona, Barcelona, Spain, Spain; ⁶Radiology Department, Hospital Clinic of Barcelona, Barcelona, Spain, Spain; ⁷Liver Oncology Unit. Hepatobiliopancreatic Surgery and Liver and Pancreas Transplant Department. ICDMD. Hospital Clinic of Barcelona, Spain, Spain; ⁸Pathology Department, Hospital Clinic of Barcelona, Barcelona, Spain, Spain; ⁹Institut de Malalties Digestives i metabòliques. Hospital Clinic of Barcelona, Barcelona, Spain, Spain; ¹⁰Liver Oncology Unit. Liver Unit, Hospital Clinic of Barcelona, Barcelona, Spain, Spain

Email: escarrabill@clinic.cat

Background and aims: The three pillars of the Quality of Health Care are efficacy, safety and patients experience (PE). Additionally, it has been demonstrated that the multidisciplinary approach is associated to better outcome. The last version of BCLC staging system includes the chapter on 'clinical decision-making' showing the multiparametric approach used by physicians when selecting treatments including patient perspective. Aim: to evaluate PE in the BCLC group.

Method: The project was divided into 3 parts: 1) The Patient Experience Team (PExT) and professionals from BCLC map the patient journey, the stakeholder map, and identify the patient's archetype; 2) based on the information from part 1, the PExT designed questions. The BCLC nurses, according the archetypes, invited patients for the focal groups/interviews and 3) PExT did the focal groups/interviews. All the interventions were recorded and verbatim transcription was analyzed through MAXQDA software.

Results: A total of 11 patients and 3 caregivers of patients who died due to liver cancer were invited. Eleven patients participated in 3 focal groups and 3 caregivers were interviewed. In the focal groups 91 concepts were identified and were grouped into 23 categories and 6 meta-categories (Figure 1). The most frequent meta-categories were related to the information received, the contact with professionals, the impact of cancer in their life and the support received. The majority of patients did not need to look further information on the internet, they found that the information at diagnosis was clear, precise and enough but they would like to have more time to clarify doubts. The patients were aware of the role of the different professionals and saw them as a coordinated group but some of

POSTER PRESENTATIONS

them requested more information regarding the 'clinical decision process.' The majority of patients agreed that the diagnosis had affected their lives and most of them commented that the best support was their family despite of the fact that some received external support. In the caregivers interviews the good coordination between the Hospital and palliative home care teams was mentioned. However, they raised the difficulties that they had to openly speak about death with their relatives due to the cultural barrier and the need of support for caregivers in this regard. The PE can be positive even in situations where outcomes worsen, such as in the case of the end of life.

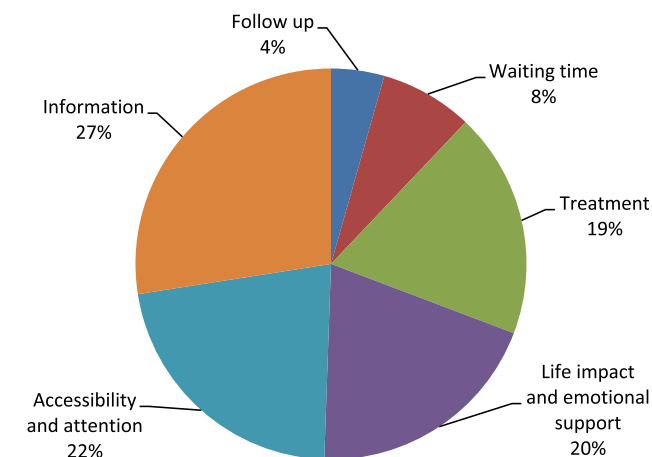


Figure:

Conclusion: Patients and caregivers are interested on aspects related to contact with professionals and the support received. Thus, the evaluation of PE helps the BCLC team to promote Value-based Health Care. In addition, this study reinforces the need of information given during the follow-up visits or organizing activities not only with patients but also for caregivers as well as developing the PROMs/PREMs to effectively implement 'shared-decision making'.

FRI-285

Management of varices but not anticoagulation is associated with improved outcome in patients with hepatocellular carcinoma and macrovascular tumour invasion

Lorenz Balcar^{1,2}, Arpad Mrekva³, Bernhard Scheiner^{1,2}, Katharina Pomej^{1,2}, Tobias Meischl^{1,2,4}, Mattias Mandorfer¹, Thomas Reiberger¹, Michael Trauner¹, Dietmar Tamandl³, Matthias Pinter^{1,2}, ¹Medical University of Vienna, Division of Gastroenterology and Hepatology, Department of Internal Medicine III, Vienna, Austria; ²Medical University of Vienna, Liver Cancer (HCC) Study Group Vienna, Vienna, Austria; ³Medical University of Vienna, Department of Radiology, Vienna, Austria; ⁴Hanusch Krankenhaus, 3rd Medical Department (Hematology and Oncology), Vienna, Austria
Email: lorenz.balcar@meduniwien.ac.at

Background and aims: The value of bleeding prophylaxis and anticoagulation in patients with hepatocellular carcinoma (HCC) and macrovascular tumour invasion (MVI) is unclear. We evaluated the impact of anticoagulation on thrombosis progression, bleeding events, and overall mortality, and assessed the efficacy of adequate management of varices as recommended for patients with cirrhosis.

Method: HCC patients with MVI who had Child-Turcotte-Pugh A-B7 were included between Q4/2002 and Q2/2022. Localization of the tumour thrombus and changes at 3–6 months were evaluated by two radiologists. Univariable and multivariable logistic/Cox regression analyses included time-dependent variables (i.e., anticoagulation, systemic therapy, non-selective beta blocker treatment). The occurrence of portal-hypertension-related complications was recorded.

Results: Of 124 patients included (male: n = 110, 89%), MVI involved the main portal vein in 47 patients (38%), and 49 individuals (40%) had additional non-tumorous thrombus apposition. Fifty of 80 patients (63%) with available endoscopy had varices. Twenty-four individuals (19%) received therapeutic anticoagulation and 94 patients (76%) were treated with effective systemic therapies. The use of therapeutic anticoagulation did not significantly affect the course of the malignant thrombosis at 3–6 months. Systemic therapy (aHR: 0.26 [95%CI: 0.16–0.40]) but not anticoagulation was independently associated with reduced all-cause mortality. In patients with known variceal status, adequate management of varices was independently associated with reduced risk of variceal bleeding (aHR: 0.12 [95%CI: 0.02–0.71]). In the whole cohort, non-selective beta blockers were independently associated with reduced risk of variceal bleeding or death from any cause (aHR: 0.69 [95%CI: 0.50–0.96]).

Conclusion: Adequate bleeding prophylaxis and systemic anti-tumour therapy but not anticoagulation were associated with improved outcomes in patients with HCC and MVI.

FRI-286

Phenotypic characteristics of primary liver cancer in a large French cohort of patients with viral chronic liver disease followed-up before and after viral eradication: an ANRS study

Alina Pascale¹, Sonia Tamazirt¹, Clovis Lusivka-Nzinga², Samuel Nilusmas², Meriem Djebbar¹, Fabien Zoulim³, Thomas Decaens⁴, Nathalie Ganne-Carrié⁵, Georges-Philippe Pageaux⁶, Vincent Leroy⁷, Laurent Alric⁸, Jean-Pierre Bronowicki⁹, Marc Bourliere¹⁰, Albert Tran¹¹, Stanislas Pol¹², Philippe Mathurin¹³, Veronique Loustaud-Ratti¹⁴, Sophie Metivier⁸, Armand Aberger¹⁵, Victor de Ledinghen¹⁶, Dominique Thabut¹⁷, Louis Dalteroché¹⁸, Tarik Asselah¹⁹, Olivier Chazouillères²⁰, Paul Cales²¹, Moana Gelu-Simeon²², Dominique Roulot⁵, Marianne Zioli⁵, Maïte Lewin¹, Fabrice Carrat², Pierre Nahon^{5,23}, Jean-Charles Duclos-Vallée^{1,24}. ¹CHU Paul Brousse, APHP, France; ²INSERM UMR-S 1136 CHU Saint Antoine, APHP, France; ³CHU Lyon, France; ⁴CHU Grenoble, France; ⁵CHU Avicenne, APHP, France; ⁶CHU Montpellier, France; ⁷CHU Henri Mondor, France; ⁸CHU Toulouse, France; ⁹CHU Nancy, France; ¹⁰CHU Marseille, France; ¹¹CHU Nice, France; ¹²CHU Cochin, APHP, France; ¹³CHU Lille, France; ¹⁴CHU Limoges, France; ¹⁵CHU Clermont-Ferrand, France; ¹⁶CHU Bordeaux, France; ¹⁷CHU Pitié-Salpêtrière, APHP, France; ¹⁸CHU Tours, France; ¹⁹CHU Beaujon, APHP, France; ²⁰CHU Saint Antoine, APHP, France; ²¹CHU Angers, France; ²²CHU Guadeloupe, France; ²³INSERM U1138, France; ²⁴INSERM U1193, Université Paris-Saclay, France
Email: alina_pascale@yahoo.com

Background and aims: Liver cancer is the third leading cause of cancer death and the sixth most commonly diagnosed cancer worldwide. In patients with viral chronic liver disease, the risk of liver cancer diminishes significantly after viral eradication but it does not become null. Our study aims to describe the phenotypic characteristics of primary liver cancer occurring in a large cohort of patients with viral chronic liver disease, followed-up before and after viral eradication or control.

Method: 406 patients with viral chronic liver disease included in the French cohort LICAVIR (partially prospective), who developed a liver cancer, were analyzed. Epidemiological, radiological, histological data were recorded and assessed. Among them, 380 (93.5%) patients had centrally revised radiological data and 128 (31.5%) had centrally revised histological data. The median follow-up was 61 months [IQR: 40–74]. Statistical analysis was performed using SAS software version 9.4 (SAS Institute Inc., Cary, North Carolina).

Results: Most patients were males: 312 (77%) with median age of 61.8 years. 368 patients (90%) had hepatitis C virus (HCV) infection, 33 (8%) had hepatitis B virus (HBV) infection and 5 (1%) were coinfectants. The main cofactors for chronic liver disease were: excessive alcohol consumption (37%), diabetes (25%), arterial hypertension (35%). 361

patients (89%) had cirrhosis, among whom 82% had a Child-Pugh A score and a median MELD score of 8.5 [IQR: 7–11]. 28% of cirrhotic patients had a prior history of liver decompensation. The median time between cirrhosis and liver cancer diagnosis was 72 months [IQR: 37–126]. 78% of liver cancers were diagnosed during regular surveillance. 385 patients (97.8%) developed hepatocellular carcinoma (HCC), 7 patients (1.7%) developed cholangiocarcinoma and 2 (0.5%) patients had hepato-cholangiocarcinoma. At diagnosis, 243 of liver cancers (62%) were single tumors, with a mean diameter of 28.5 mm, while 67 (17%) were associated with portal vein thrombosis or invasion and 22 (6%) were metastatic (27% of lung metastasis). Among HCV-infected patients, 126 developed liver cancer after achieving sustained virological response (SVR) and were compared to 215 patients who developed it before SVR. Multinodular HCC were more frequent in HCV-infected patients (43% vs 33%, $p < .0001$), while single tumors were more frequent in patients who achieved SVR (66% vs 56%, $p = 0.0075$). The median time between SVR and liver cancer diagnosis was 23 months [IQR: 9–36]; 96% of liver cancers occurred within 5 years after SVR. Multiple treatments were performed: among 364 curative treatments-189 (51%) percutaneous tumor ablations, 112 (31%) liver resections and 63 (17%) liver transplantations; among 501 palliative treatments-217 (43%) trans-arterial chemoembolizations and 128 (26%) systemic therapies. During follow-up, 110 patients died.

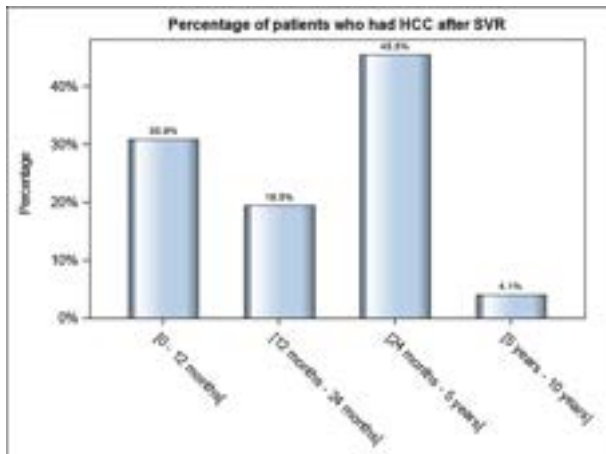


Figure:

Conclusion: In our large cohort of patients with viral chronic liver disease, followed-up before and after viral eradication or control, liver cancers developed mostly in cirrhotic liver. The most frequent type of

liver cancer was HCC, which in more than half of patients was a single tumor, detected during a surveillance program. There was no significant phenotypical difference between HCC occurring before or after SVR, except for the multinodular type, which seemed to be more frequent before SVR. In our cohort, most of liver cancers (96%) occurred within the five first years after SVR.

FRI-287

Predicting cardiovascular risk in patients with HCC receiving tyrosine kinase inhibitors: comparison of two different scores

Bernardo Stefanini¹, Francesco Tovoli¹, Alessandro Granito¹, Franco Trevisani², Tiziana Pressiani³, Andrea Casadei Gardini⁴, Rodolfo Sacco⁵, Fabio Piscaglia¹. ¹Division of Internal Medicine, Hepatobiliary and Immunoallergic Diseases, IRCCS Azienda Ospedaliero-Universitaria di Bologna, Bologna, Italy, Italy; ²Semeiotica Medica, Azienda Ospedaliero-Universitaria di Bologna, Bologna, Italia., Italy; ³Medical Oncology and Hematology Unit, Humanitas Clinical and Research Center, IRCCS Humanitas Research Hospital, Rozzano (Milan), Italy, Italy; ⁴Department of Oncology, IRCCS San Raffaele Scientific Institute Hospital, Milan, Italy, Italy; ⁵Gastroenterology Unit, Azienda Ospedaliero-Gastroenterology and Digestive Endoscopy Unit, Foggia University Hospital, Foggia, Italy, Italy
Email: bernardo.stefanini@gmail.com

Background and aims: Antineoplastic agents targeting the VEGF-VEGFR pathway increase the risk of major adverse cardiac and cerebrovascular events (MACE). In the HCC setting these agents include bevacizumab (as part of the first-line combination treatment) and TKIs. The European Society of Cardiology proposed a risk stratification algorithm for cardio-oncology (ESC-2022), never been tested in HCC. The CARDIOSOR score has been also proposed (Carballo-Folgo, 2021) but lacks external validation in predicting MACE in sorafenib-treated patients.

Method: Retrospective analysis of the ARPES and ITA.LI.CA databases to test the ESC-2022 and CARDIOSOR abilities in predicting MACE in sorafenib-treated HCC patients (2010–2018 timeframe). Evolutive events after sorafenib start (including the occurrence of MACE) were available for all patients. Competing-risk regressions for each score were performed to address the study aim.

Results: This study included 815 patients, 28 suffered at least one MACE (3.4%). The four-tier ESC classification showed an sHR 1.42, ($p = 0.015$) per every risk-class (1-year risk 1.7%, 2.1%, 4.3%, and 8.0% in the low, medium, high, and very-high-risk tiers, respectively). The dichotomous CARDIOSOR scale identified a high-risk group with a 4-fold increased risk of MACE (sHR 4.12, $p = 0.007$; 1-year risk 3.2% and 13.1%). Both score had similar predictive ability (Akaike information criterion 360 and 366, respectively).

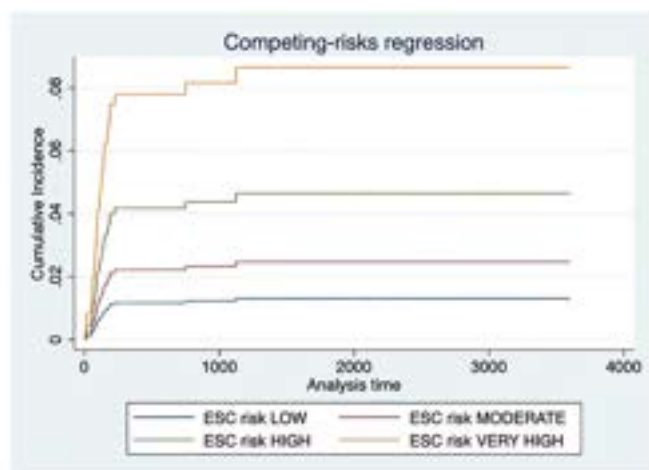
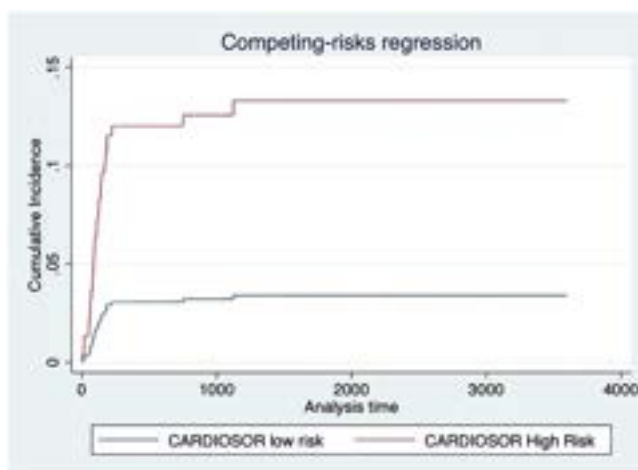


Figure: (abstract: FRI-287).

POSTER PRESENTATIONS

Conclusion: The risk of MACE in patients receiving TKI for HCC was non-negligible. Both scores discriminated this probability accurately, with different perks and pitfalls. These tools will be useful in the near-future to identify high-risk patients, candidate for anti-VEGF-free regimens (i.e. tremelimumab-durvalumab).

FRI-288

A prospective multicenter study to examine the impact of acquired and genetic predictors on Hepatocellular carcinoma risk in patients with advanced NAFLD: first report

Serena Pelusi¹, Cristiana Bianco¹, Luisa Ronzoni¹, Alessandro Cherubini¹, Ilaria Marini¹, Francesco Malvestiti¹, Roberta D'Ambrosio¹, Anna Ludovica Fracanzani¹, Annalisa Cespiati¹, Giorgio Soardo^{2,3}, Stephanie Pivet², Luca Miele⁴, Antonio Liguori⁴, Elisabetta Bugianesi⁵, Chiara Rosso⁵, Salvatore Petta⁶, Grazia Pennisi⁶, Umberto Vespasiani Gentilucci⁷, Federica Tavaglione⁷, Alessandro Federico⁸, Francesco Paolo Russo⁹, Paola Zanaga⁹, Mario Masarone¹⁰, Daniele Prati¹, Luca Valenti¹. ¹IRCCS Ca' Granda Ospedale Maggiore Policlinico Milano, Italy; ²University of Udine, Department of Medicine, Italy; ³Italian Liver Foundation AREA Science Park, Italy; ⁴Università Cattolica del Sacro Cuore, Department of Internal Medicine, Roma, Italy; ⁵University of Torino, Department of Medical Sciences, Division of Gastroenterology, Torino, Italy; ⁶University of Palermo, Palermo, Italy; ⁷University Campus Bio-Medico of Rome, Roma, Italy; ⁸University of Campania, Napoli, Italy; ⁹University of Padova, Padova, Italy; ¹⁰University of Salerno, Salerno, Italy
Email: serenapelusi@libero.it

Background and aims: In parallel with the diabetes pandemic, hepatocellular carcinoma (HCC) is increasingly being diagnosed in non-alcoholic fatty liver disease (NAFLD), often at a late stage. Aim was to estimate the impact of acquired and genetic factors on HCC incidence in a prospective multicenter cohort of patients with advanced NAFLD.

Method: Inclusion criteria were NAFLD diagnosis, age 45–75 years, fibrosis stage F3–F4, determined histologically or by non-invasive assessment (stiffness >7.9 kPa by Fibroscan and FIB-4 ≥ 1.3), regular 6-months surveillance. Clinical parameters were collected and the cohort was genotyped for rs738409C>G in *PNPLA3*, rs58542926C>T in *TM6SF2*, rs1260326C>T in *GCKR*, rs641738C>T in *MBOAT7* and rs72613567:TA in *HSD17B13* genes. In 276 subjects with complete genetic data, variants were combined to calculate a polygenic risk score (PRS-5). Time of progression to HCC was evaluated by Kaplan-Meier's estimates of cumulative incidence rates and p values were adjusted for confounding factors.

Results: We enrolled 429 individuals (59% male) with median follow-up of 46 months (IQR 34–53). Of these, 213 (49%) showed overt cirrhosis; diabetes was present in 196 (45%), whereas 231 (53%) had hypertension. Twelve patients developed HCC during follow-up. Of these, 11 had cirrhosis and 1 showed F3 fibrosis at liver biopsy. The cumulative 5-year incidence of HCC was 3.7% (95%CI, 2–6%), 1.2% (95%CI, 0.5–2.5%) in the first year. We registered 6 HCC-related deaths, median survival after HCC diagnosis was 17.5 months (IQR 2–24). At Kaplan-Meier analysis, time of progression to HCC was not influenced by diabetes, sex or hypertension but it was faster in patients with cirrhosis ($p = 0.006$; fig. 1) and in those homozygous for the *GCKR* P446 variant (Wilcoxon, $p = 0.02$). At multivariable Cox regression, considering sex, age, diabetes, platelets count, albumin and FIB-4, higher FIB-4 and lower albumin were correlated with faster progression to HCC ($p = 0.01$; $P = 0.005$). In this cohort the best FIB-4 cut-off to identify HCC risk was 4.09 (Sn100%, Sp83%, AUC 0.92). Carriage of *PNPLA3* I148M and PRS-5 were associated with cirrhosis ($p = 0.007$; $p = 0.003$) but not with HCC risk.

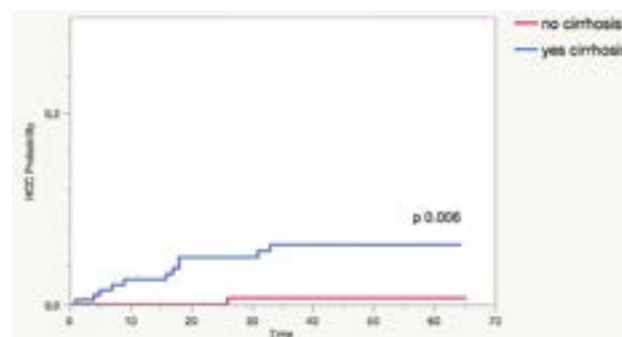


Figure:

Conclusion: In a multicenter prospective cohort of advanced NAFLD, HCC 5-year incidence was 3.7%, median survival was 17 months. Non-invasive markers of liver fibrosis are useful to identify patients at increased risk of HCC. A longer follow-up is needed to clarify the impact of genetic factors on HCC in advanced NAFLD.

FRI-289

Sex disparities in presentation and outcome of hepatocellular carcinoma: results of a nationwide study in France

Charlotte Costentin^{1,2}, Mélanie Minoves³, Sylvain Kotski³, Nathalie Goutte⁴, Olivier Farges⁵, Thomas Decaens^{1,2}, Zuzana Macek-Jílková^{1,2}, Sébastien Bailly³. ¹Centre Hospitalier Universitaire de Grenoble, Hepatology, gastro-enterology and digestive oncology, La Tronche, France; ²Institute for Advanced Biosciences, INSERM U1209/CNRS UMR 5309, Grenoble, France; ³Centre Hospitalier Universitaire de Grenoble, HP2 Laboratory, Grenoble Alpes University, INSERM U1300, La Tronche, France; ⁴Hôpital Paul-Brousse Ap-Hp, Paris XI University, INSERM UMRS-1193, DHU Hépatinov and centre hépatobiliaire, Villejuif, France; ⁵Hospital Beaujon AP-HP, Hepatobiliary surgery department, Clichy, France
Email: charlotte.costentin.pro@gmail.com

Background and aims: Men are disproportionately affected by hepatocellular carcinoma (HCC) compared to women across the globe. A growing body of evidence also suggests differences in risk factors as well as prognosis. Our aim was to assess sex disparities in HCC in France, leveraging the national French Healthcare Database (PMSI).

Method: Incident cases of HCC were identified between 2009 and 2012. We only retained patients with 1) at least one hospital stay more than 3 months before the diagnosis and 2) one rolling year of follow-up from the first hospital stay preceding the diagnosis to ensure a minimum depth into the patient's history. Etiology was ascertained according to ICD-10 codes.

Results: We identified 26,117 patients (5,458 women and 20,659 men). Women were older at the time of HCC diagnosis (mean 73 years vs 68 years; $p < 0.01$). The underlying etiology was unclassified in 50.8% of cases in women, while alcohol was retained as the only etiology in 50.1% of cases in men. From patient with unclassified etiology ($n = 8664$; including 2772 women and 5892 men), metabolic comorbidities and in particular diabetes were less frequent in women than in men (diabetes 22.7% and 36.4% respectively; $p < 0.01$). Cirrhosis was less often documented in women (45.9% vs. 62.7% in men; $p < 0.01$), and less often recognized before diagnosis HCC (24.0% vs 28.7% in men; $p < 0.01$). At the time of diagnosis, liver complications were less frequent in women than in men (ascites: 19.3% vs 23.6%; hepatic failure: 12.9% vs 16.2%; hepatorenal syndrome 1.3% vs 2.4%; varice banding 2.6% vs 4.6%; $p < 0.01$). Women less often than men received treatment with curative intent (resection, radio-frequency or transplantation: 16.9% vs 20.2%). However, in univariate analysis, 12-month survival was higher for women than for men ($p = 0.026$).

Conclusion: In a large cohort of patients with HCC identified from the national French Healthcare Database, notable differences were

observed between women and men in terms of risk factors and severity of the underlying liver disease. Interestingly, women experienced higher 12-month survival.

FRI-290

Artificial intelligence assisted qFibrosis as a pathological “biomarker” to evaluate disease severity in patients with hepatocellular carcinoma

Chih-Yang Hsiao¹, Yayun Ren², Elaine Chng², Kutbuddin Akbary², Dean Tai², Kai-Wen Huang¹. ¹National Taiwan University Hospital, Surgery, Taiwan; ²HistoIndex Pte Ltd, Singapore
Email: cyhsiao1102@gmail.com

Background and aims: Hepatocellular carcinoma (HCC) is highly heterogeneous in both intra-tumoral and inter-patient features and its manifestations in its pathology. Tumor grade is a comprehensive index that is subjectively judged by a pathologist, which does not reflect the local regional differences of tumor cells and different disease characteristics relating with its pathological heterogeneity. Our hypothesis is that collagen features of pathology in HCC analyzed by artificial intelligence assisted qFibrosis could be used as a pathological “biomarker” to evaluate disease severity.

Method: Tumor specimen from 201 patients with HCC who underwent curative treatment were scanned by the second harmonic generation (SHG) microscopy (HistoIndex Pte. Ltd., Singapore). Digital image analysis generated 33 collagen parameters. Patients were grouped into tumor grades ≤ 2 and tumor grades ≥ 3 groups. Collagen features of tumor specimen between the two groups were compared, and the features with most significant differences were selected. A combined index was built using the selected collagen features. The usefulness of the combine index to predict survival outcome and the correlation between the combine index and tumor grade were tested. Leave-one-out cross-validation method was utilized.

Results: Total of 5 collagen features has been selected by sequential selection methods to build a combine index model. In addition, the value of each collagen features is shown in the radar map (Figure A), so that the dynamics of the extracellular matrix can be visualized instead of just a single number, tumor grade. These collagen features are further illustrated (Figure B) to help researchers to visualize and investigate the histopathological relevance for further disease studies and treatment efficacy evaluations. With specific cut-off values, the combine index model was significant in distinguishing patients with

tumor grades ≤ 2 and ≥ 3 ($p < 0.05$), as well as in distinguishing patients with long-term survival and early death ($p < 0.05$). Moreover, it can be seen in the radar map that the features that are relevant include intersections of collagen strings, ratio between distributed and aggregated collagens. This implies the physical characteristics of extracellular matrix (ECM) is correlated to long-term survival of the patients.

Conclusion: Pathological heterogeneity of HCC could be profiled by artificial intelligence assisted qFibrosis. Selected collagen features of HCC could be used as a pathological “biomarker” that has the potential to be a parameter to evaluate disease severity in patients with HCC. Quantitative measurements and the new visualization tools like radar map better reveals dynamic of ECM with other cell types, enhances disease studies and drug development programs in the future.

FRI-291

Cryptogenic non-cirrhotic HCC: clinical, prognostic and immunologic aspects of an emerging HCC etiology

Boris Beudeker¹, Rael Guha¹, Kalina Stoyanova¹, Jan Ijzermans², Robert De Man¹, Dave Sprengers¹, Andre Boonstra¹. ¹Erasmus MC, Gastroenterology and hepatology, Rotterdam, Netherlands, ²Erasmus MC, Surgery, Rotterdam, Netherlands
Email: p.a.boonstra@erasmusmc.nl

Background and aims: The incidence of hepatocellular carcinoma (HCC) in non-cirrhotic livers is increasing. In order to better understand this trend, we conducted a comprehensive study to investigate the characteristics of HCC in non-cirrhotic livers in detail.

Method: Data was analyzed of 2304 HCC cases diagnosed at a large referral center in the Netherlands between 2009 and 2020, and 1654 cases with a complete medical record were included for analysis. Patient characteristics, liver disease etiologies, post-diagnosis survival rates, genetic risk factors, and immune profiles were analyzed.

Results: Of the 1654 included HCC cases, 371 (22%) were non-cirrhotic. The incidence of non-cirrhotic HCC rose by 61% between 2009 and 2020, with 39% of cases diagnosed in the absence of underlying liver disease classified as cryptogenic non-cirrhotic HCC. Cryptogenic non-cirrhotic HCC cases were similar to non-cirrhotic NAFLD HCC cases in terms of patient characteristics, but had more advanced tumors, a higher prevalence of symptoms (such as significant weight loss) at the time of diagnosis, and shorter survival times. Overall survival of non-cirrhotic cryptogenic HCC was dismal

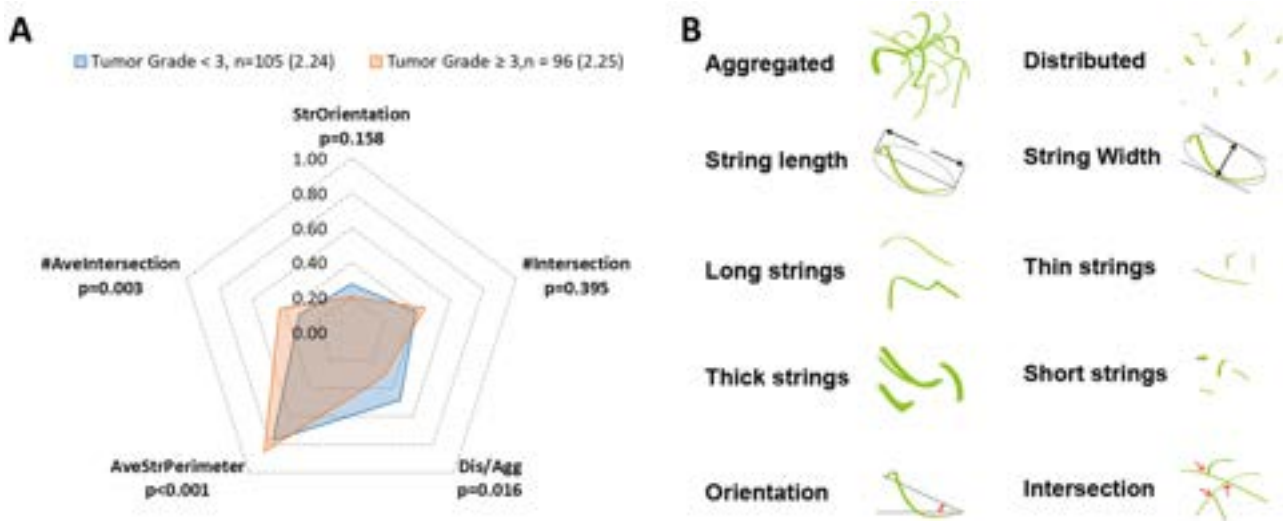


Figure: (abstract: FRI-290): (A) Radar map showing 5 parameters: total orientation of strings (StrOrientation), total number of intersections (#Intersection), the ratio of distributed collagen area and aggregated collagen area (Dis/Agg), average perimeter for one string (AveStrPerimeter) and average number of intersections within each string; (B) graphical illustration of how collagen strings are defined and measured.

POSTER PRESENTATIONS

compared to viral and non-viral causes of HCC (figure 1). In a multivariable analysis, cryptogenic etiology was found to be an independent negative prognostic factor ($p=0.037$), along with intermediate and advanced tumor stage and older age. More advanced stages of cryptogenic HCC were associated with higher levels of circulating interleukin-6. Analysis of a balanced sub-cohort of non-cirrhotic cryptogenic and NAFLD HCC cases revealed comparable immune profiles and HCC risk gene phenotypes.

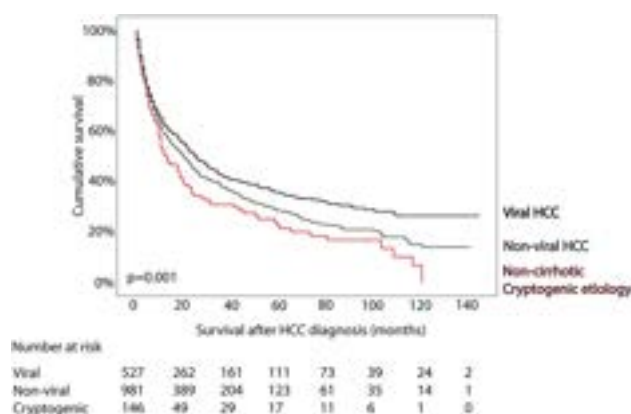


Figure 1: Survival proportion after the diagnosis of de novo hepatocellular carcinoma (HCC) in patients with viral hepatitis-related HCC in cirrhotic or non-cirrhotic liver, non-viral related HCC in cirrhotic and non-cirrhotic liver and in those with cryptogenic HCC.

Conclusion: These findings suggest that cryptogenic non-cirrhotic HCC may represent a unique HCC etiology, with more aggressive traits such as advanced tumors and a pro-inflammatory immune protein signature in the blood. These observations made us postulate that cryptogenic non-cirrhotic HCC may be a group of patients with "burned-out" NAFLD. Further research is needed to identify risk factors and guide better clinical management.

FRI-292

Add-on benefits of AFP-L3, PIVKA-II and GALAD score to ultrasound plus AFP for surveillance of hepatocellular carcinoma

Supot Nimanong¹, Tawesak Tanwandee¹, Panchai Charatcharoenwithaya¹, Siwaporn Chainuvati¹, Watcharasak Chotiyaputta¹. ¹Division of Gastroenterology, Department of Medicine, Siriraj Hospital, Mahidol University, Thailand
Email: supotgi@gmail.com

Background and aims: Combination of abdominal ultrasound (US) and alpha-fetoprotein (AFP) is widely recommended as a surveillance tool for hepatocellular carcinoma (HCC). Lens culinaris-agglutinin-reactive fraction of AFP (AFP-L3) and protein induced by vitamin K absence or antagonist-II (PIVKA-II) are potential biomarkers for small HCC detection. This study was aimed to determine the add-on benefits of AFP-L3, PIVKA-II and GALAD score to routine use of US plus AFP for HCC surveillance.

Method: This prospective study enrolled patients with cirrhosis or high risk non-cirrhotic chronic hepatitis B (HBV). US and three biomarkers were measured and GALAD score was calculated. Triple phase computed tomography (CT) or dynamic magnetic resonance imaging (MRI) was performed in all patients who had new liver nodule larger than 1 cm or abnormal biomarkers (cutoff: 20 ng/ml for AFP, 10% for AFP-L3, and 40 mAU/ml for PIVKA-II). All patients were followed at 6-month for the missed lesions.

Results: Among 1003 enrolled patients, the mean age was 60 years, 56% were men, 72% had cirrhosis (95% were Child A). The major etiologies of chronic liver disease were HBV (79%), hepatitis C (12%), and alcohol (3%). HCC was diagnosed in 33 patients (3.3%) with the median size of 1.85 cm and all of lesions were within Milan criteria. Among three biomarkers, PIVKA-II showed the highest sensitivity (51.5%) followed by AFP-L3 (24.2%) and AFP (9.1%) for detecting small HCC. The sensitivity and specificity of US plus AFP were 54.5% and 97.5% respectively, whereas the combination of triple markers with US increased the sensitivity to 87.9% but decreased the specificity to 94.6%. The area under the curve (AUC) of US plus AFP and combination of triple markers with US were 0.961 and 0.944 respectively. GALAD score had lower sensitivity than triple markers (48.3% vs 57.6%), and the addition of GALAD score to US did not provide more sensitivity than combined triple markers with US (86.2% vs 87.9%).

Conclusion: Routine use of US plus AFP appears to be suboptimal for detecting small HCC. The addition of AFP-L3 and PIVKA-II to US plus AFP increase the sensitivity for HCC detection at an early stage. GALAD score does not provide superior sensitivity than using of triple markers.

Performance of tools for HCC surveillance

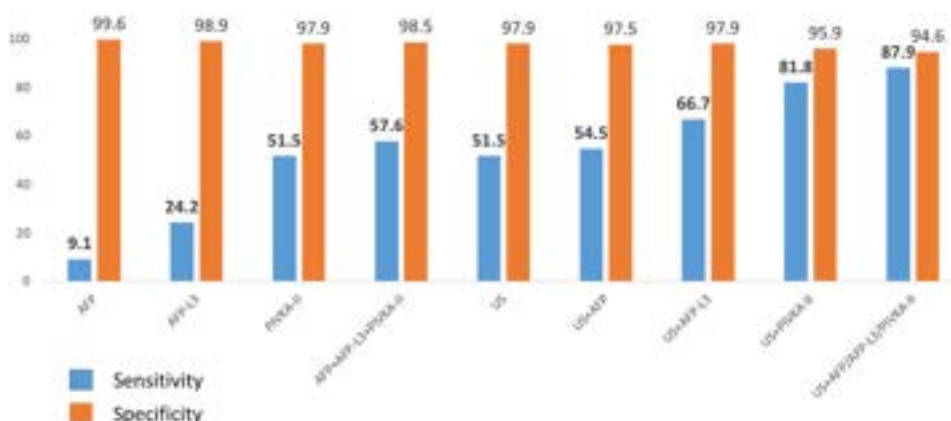


Figure: (abstract: FRI-292).

FRI-293

Addition of des-gamma-carboxy prothrombin to standard of care is effective for HCC surveillance among high-risk patients

Grishma Hirode^{1,2,3}, Hooman Farhang Zangneh¹, Orlando Cerocchi¹, Lima Awad El-Karim⁴, Korosh Khalili⁴, Harry LA Janssen^{1,5}, Bettina Hansen^{1,6,7}, Jordan J. Feld^{1,2,3}. ¹Toronto Centre for Liver Disease, Toronto General Hospital, University Health Network, Toronto, Canada; ²The Toronto Viral Hepatitis Care Network (VIRCAN), Toronto, Canada; ³Institute of Medical Science, University of Toronto, Toronto, Canada; ⁴Joint Department of Medical Imaging, University Health Network, Toronto, Canada; ⁵Department of Gastroenterology and Hepatology, Erasmus University Medical Center, Rotterdam, Netherlands; ⁶Department of Epidemiology, Biostatistics, Erasmus University Medical Center, Rotterdam, Netherlands; ⁷Institute of Health Policy, Management and Evaluation, University of Toronto, Toronto, Canada
Email: grishma.hirode@gmail.com

Background and aims: Despite regular surveillance, several patients are diagnosed with hepatocellular carcinoma (HCC) at an advanced stage. An understanding of the effectiveness of current methods and the development of novel strategies are required to improve early-stage HCC diagnosis. We aim to analyze the utility of each specific biomarker from a study evaluating ultrasound (US) alone compared to US plus serum biomarkers (BM) for HCC surveillance.

Method: Prospective study of patients with cirrhosis or high-risk HBV infection (REACH-B score ≥ 9) randomized to HCC surveillance with US alone (Group A) or US and BM (Group B) measuring alpha-fetoprotein (AFP), des-gamma-carboxy prothrombin (DCP) and lectin-reactive fraction of AFP (AFP-L3). For all analyses using Group B data, any BM levels above the specified thresholds (AFP >100 ng/ml, DCP >2 ng/ml, AFP-L3 $>10\%$) or a positive US result triggered further imaging for HCC confirmation. US or AFP is the current standard method of surveillance. We examined the incremental value of adding DCP, AFP-L3, or both to US and AFP by comparing sensitivity and specificity between groups; US and AFP was used as the reference group.

Results: Among 603 patients in Group A (mean age at baseline 58 ± 9.8 years, 72% male, 64% with cirrhosis at baseline), 35 patients were diagnosed with HCC (30 early-stage, 5 advanced) with a sensitivity of 80% and specificity of 35% for the detection of early-stage HCCs using US alone. Among 605 patients in Group B (mean age at baseline 58 ± 9.9 years, 72% male, 63% with cirrhosis at baseline), 27 patients were diagnosed with HCC (22 early-stage, 5 advanced). US or AFP had a sensitivity of 78% and specificity of 35% (Figure). The addition of DCP to AFP and US yielded higher sensitivity (81%, $p=0.32$) but slightly lower specificity (34%, $p=0.01$) whereas the addition of AFP-L3 to AFP and US did not change the sensitivity (78%) and resulted in lower specificity (32%, $p<0.001$). The overall sensitivity and specificity for Group B using US or BM were 81% ($p=0.32$) and 31% ($p<0.001$), respectively; that is with the addition of both DCP and AFP-L3 to US or AFP. There was no significant difference in sensitivity or specificity between the two study arms. Among the individual biomarkers, AFP-L3 had both low sensitivity and specificity.

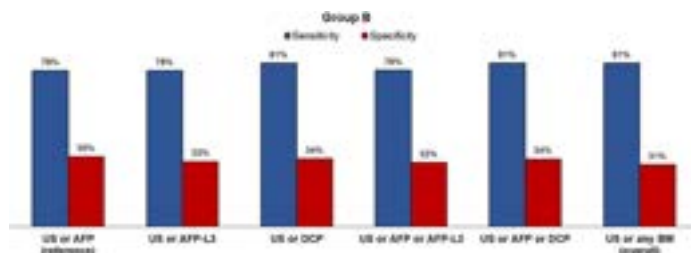


Figure:

Conclusion: In this large study, US and DCP was the most sensitive while US and AFP was the most specific for an early diagnosis of HCC. The addition of DCP to the existing standard of care using US plus AFP

would optimize sensitivity and specificity. Lower AFP thresholds may also be beneficial for enhanced HCC surveillance.

FRI-294

A radiogenomics study for hepatocellular carcinoma: distinct transcriptome patterns underlying different radiomics phenotypes in early recurrence

Weijia Liao¹, Liying Ren², Dongbo Chen², Tingfeng Xu¹, Bigeng Zhao¹, Zhipeng Zhou³, Yong He⁴, Junxiong Yu⁵, Minjun Liao⁶, Hongsong Chen². ¹Laboratory of Hepatobiliary and Pancreatic Surgery, Affiliated Hospital of Guilin Medical University, China; ²Peking University People's Hospital, Peking University Hepatology Institute, Beijing Key Laboratory of Hepatitis C and Immunotherapy for Liver Disease, China; ³Department of Radiology, Affiliated Hospital of Guilin Medical University, China; ⁴Department of Radiology, the Second Affiliated Hospital of Guilin Medical University, China; ⁵Department of Anesthesiology, Affiliated Hospital of Guilin Medical University, China; ⁶Guangdong Provincial Key Laboratory of Gastroenterology, Department of Gastroenterology and Hepatology Unit, Nanfang Hospital, Southern Medical University, China
Email: liaoweijia288@163.com

Background and aims: The prognosis of early-recurrence (within 2 years) hepatocellular carcinoma (HCC) remains poor. We aim to explore the biological pathway underlying the radiomics phenotypes.

Method: The datasets involved in this study were collected from Guilin Medical University and The Cancer Genome Atlas dataset, with contrast-enhanced CT images and corresponding transcription data. Low and high radiomics phenotypes based on the rad-score were determined to predict early recurrence. Radiomics features were annotated with biological pathways. Then, the most relevant gene modules underlying the radiomics phenotypes were identified and radiomics hub genes were selected.

Results: Rad-score constructed by 6 radiomics features illustrated a predictive value for HCC early recurrence in both training (AUC: 0.915, 95% CI: 0.796–1.033) and external validation datasets (AUC: 0.794, 95% CI: 0.731–0.858). Patients with high risk radiomics phenotype were prone to early recurrence. Early recurrence related radiomics features were associated with metabolism, proliferation and immune-related pathways. Further, the red module was considered as the most relevant radiomics gene module, in which the 6 hub genes (ACACA, ACLY, ATRNL1, FADS2, MPV17L, ZNF492) were determined, and the model fitted by the hub genes had the ability to predict early recurrence (AUC: 0.724, 95% CI: 0.509–0.930). There were significant correlations among radiomics features, hub genes, immune cell infiltration, metabolism and immune-related key genes.

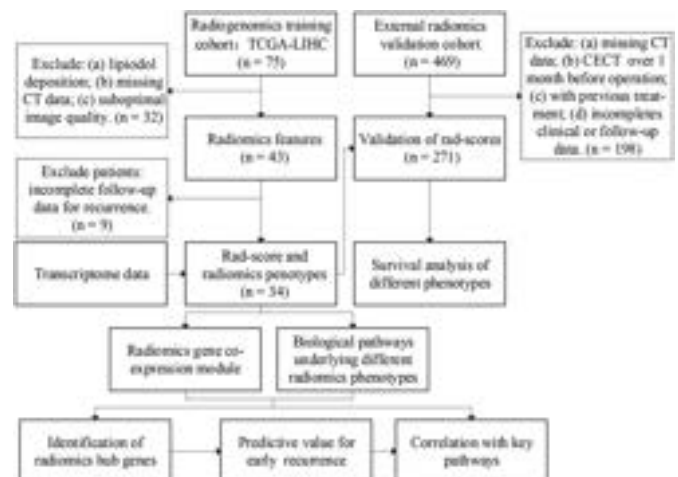


Figure 1: Flowchart of the study cohorts.

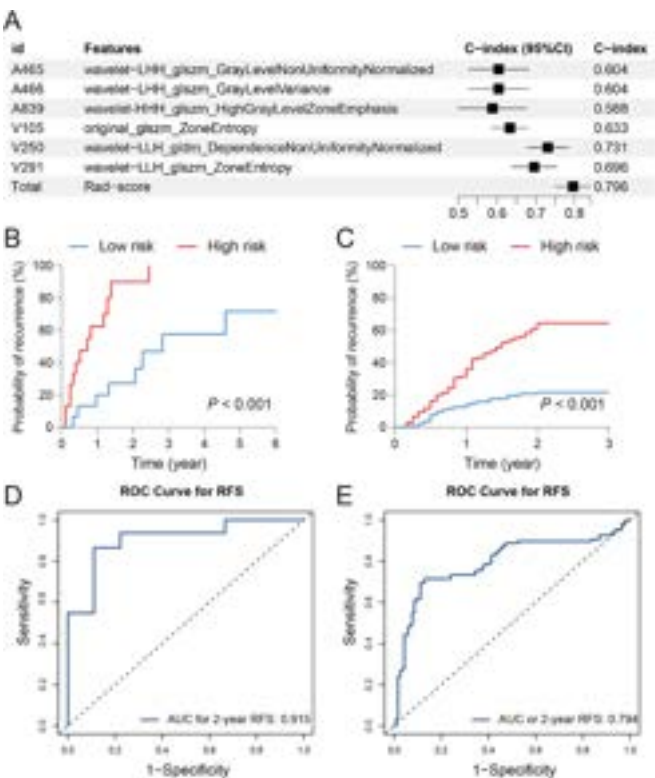


Figure 2: Construction and validation of the rad-score for the early recurrence of HCC.

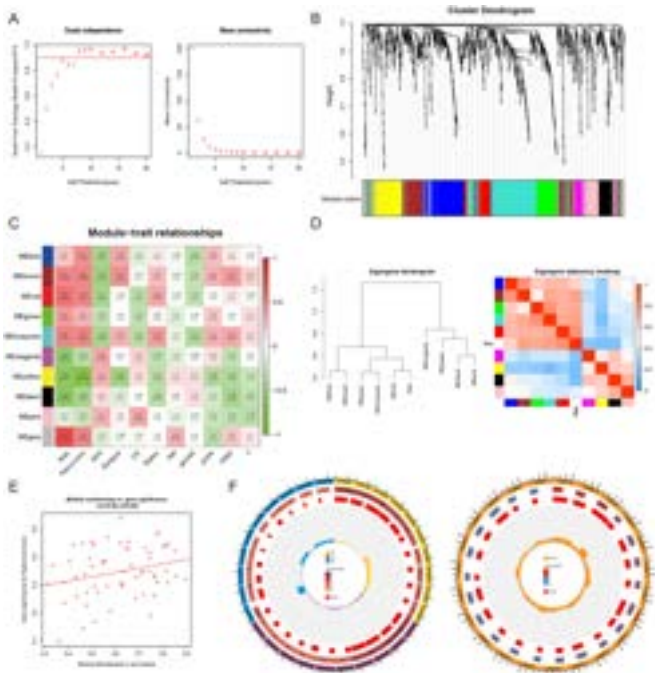


Figure 3: Weighted Correlation Network analysis (WGCNA) of the radio-mics gene modules.

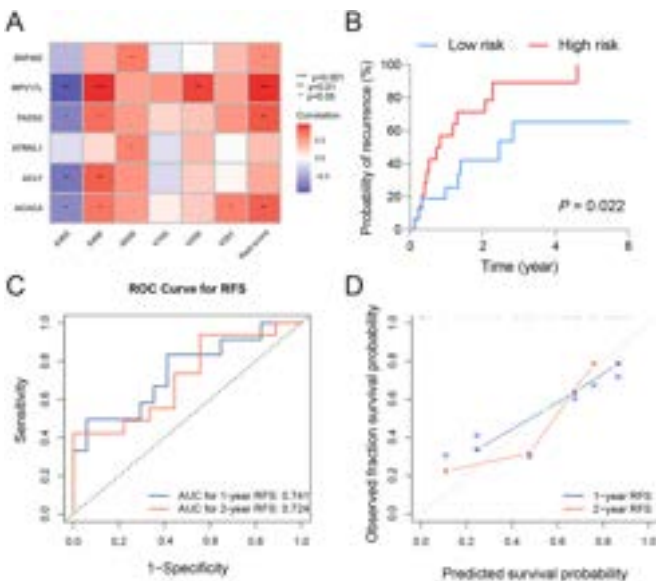


Figure 4: Radiomics hub genes and their predictive value for early recurrence.

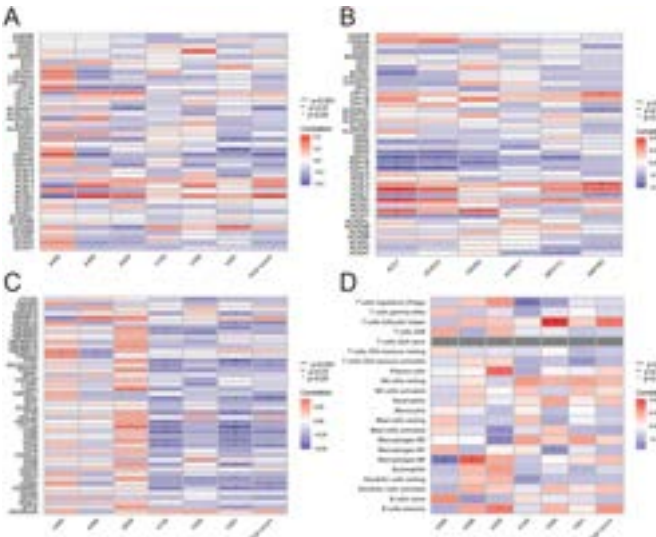


Figure 4: Function and mechanisms related to radiomics features and hub genes.

Conclusion: Rad-score derived from enhanced CT of HCC could effectively predict early recurrence. Metabolic, proliferative and immune-related pathways varied in low and high radiomics phenotypes, in which the hub genes might play an important role.

FRI-295

Transversal psoas muscle thickness measurement is associated with response and survival in patients with hepatocellular carcinoma undergoing immunotherapy

Bernhard Scheiner^{1,2,3}, Katharina Lampichler⁴, Katharina Pomej^{1,3}, Lucian Beer⁴, Lorenz Balcar^{1,3}, Riccardo Sartoris⁵, Mohamed Bouattour⁶, Sabrina Sidali⁶, Michael Trauner¹, Martina Scharitzer⁴, Dietmar Tamandl⁴, David J. Pinato^{2,7}, Maxime Ronot^{5,8}, Matthias Pinter^{1,3}. ¹Medical University of Vienna, Division of Gastroenterology and Hepatology, Department of Internal Medicine III, Austria; ²Imperial College London, Department of Surgery and Cancer, United Kingdom; ³Medical University of Vienna, Liver Cancer (HCC) Study Group Vienna, Division of Gastroenterology and Hepatology, Department of Internal Medicine III, Austria; ⁴Medical University of Vienna, Department of Biomedical Imaging and Image-Guided Therapy, Austria; ⁵APHP Nord, Hôpital Beaujon, Department of Radiology, France; ⁶APHP Nord, Hôpital Beaujon, Department of Digestive Oncology, France; ⁷University of Piemonte Orientale, Department of Translational Medicine, Division of Oncology, Italy; ⁸Université Paris Cité, CRI INSERM U1149, France
Email: matthias.pinter@meduniwien.ac.at

Background and aims: Sarcopenia is a common problem in patients with hepatocellular carcinoma (HCC) and may be diagnosed using clinical or imaging-based assessments. This study aimed to evaluate the prognostic and predictive value of transversal psoas muscle thickness (TPMT) measurement at baseline in patients with HCC undergoing immunotherapy.

Method: Patients with HCC treated with PD- (L)1-based therapies between 06/2016 and 10/2022 at the Vienna General Hospital (n = 80) and the Hôpital Beaujon Clichy (n = 96) were included. TPMT at the level of the third lumbar vertebrae was measured independently by two radiologists in the Vienna cohort to evaluate inter-reader reliability and by one radiologist in the Clichy cohort. Clinical outcomes were evaluated in the pooled cohort. TPMT <12 mm/m in men and <8 mm/m in women indicated sarcopenia.

Results: Overall, 176 patients (age: 66.3 ± 11.7 years; male: n = 143, 81%) were included, of which 131 (74%) had cirrhosis. Most patients had BCLC C HCC (n = 121, 69%).

Inter-reader agreement for the diagnosis of sarcopenia based on TPMT was 90% and Cohen's Kappa showed a 'strong agreement' (κ = 0.80 (95%CI: 0.66–0.93)). Sarcopenia was present in 59 patients (34%) and predominantly observed in men (n = 56 (39%) vs. women: n = 3 (9%), p = 0.001). Sarcopenia was associated with shorter overall (median OS, 8.0 (95%CI:4.1–11.9) vs. 24.7 (95%CI:19.1–30.4); p < 0.001, Figure A) and progression-free survival (median PFS, 5.0 (95%

CI:0.8–9.2) vs. 9.7 (95%CI:6.0–13.4), p = 0.003), and an independent predictor of overall (HR:1.80 (95%CI:1.10–2.95)) and progression-free mortality (HR:1.54 (95%CI:1.03–2.30)) in multivariable analyses. Radiological response was evaluable in 161 subjects (91.5%). Objective response rate per mRECIST in patients with and without sarcopenia was 20% and 39%, respectively (p = 0.011). Outcomes were worst in patients with sarcopenia and elevated serum C-reactive protein (Figure B).

Conclusion: Evaluation of sarcopenia using TPMT measurement is reliable and identifies HCC patients with a dismal prognosis and response to immunotherapy.

FRI-296

The efficacy of direct-acting antivirals for chronic hepatitis C in patients with the active oncological disease

Maria Dąbrowska¹, Jerzy Jaroszewicz¹, Marek Sitko², Janocha-Litwin Justyna³, Dorota Zarebska-Michaluk⁴, Ewa Janczewska⁵, Beata Lorenc⁶, Magdalena Tudrujek⁷, Anna Parfieniuk-Kowerda⁸, Jakub Klapaczynski⁹, Hanna Berak¹⁰, Łukasz Socha¹¹, Beata Dobracka¹², Dorota Dybowska¹³, Włodzimierz Mazur¹⁴, Robert Flisiak⁸. ¹Medical University of Silesia, Department of Infectious Diseases and Hepatology, Poland; ²Jagiellonian University, Kraków, Poland; ³Medical University Wrocław, Poland; ⁴Jan Kochanowski University, Kielce, Poland; ⁵Medical University of Silesia, Bytom, Poland; ⁶Medical University of Gdańsk, Poland; ⁷Medical University of Lublin, Poland; ⁸Medical University of Białystok, Poland; ⁹Central Clinical Hospital of the Ministry of Internal Affairs and Administration, Poland; ¹⁰Hospital for Infectious Diseases in Warsaw, Poland; ¹¹Pomeranian Medical University, Szczecin, Poland; ¹²MED-FIX Medical Center, Poland; ¹³Faculty of Medicine, Collegium Medicum Bydgoszcz, Nicolaus Copernicus University, Poland; ¹⁴Specialist Hospital in Chorzów, Medical University of Silesia, Katowice, Poland
Email: jerzy.jr@gmail.com

Background and aims: The introduction of direct-acting antivirals (DAA) has revolutionized HCV infection treatment and extended possibilities for patients with active malignancies. Data on the safety and efficacy of DAA in this group is limited but often crucial to undertake oncologic therapy. We investigated patients with active solid malignant tumor (SMT), hematologic disease (HD), and hepatocellular carcinoma (HCC) treated with DAA.

Method: A total of 203 patients with active oncological disease (SMT n = 62, HD n = 67, HCC n = 74) were evaluated and compared to 12,930 subjects without any history of malignancy. All subjects were treated with DAA between 2015 and 2020 and included in the national real word evidence project EPITER.

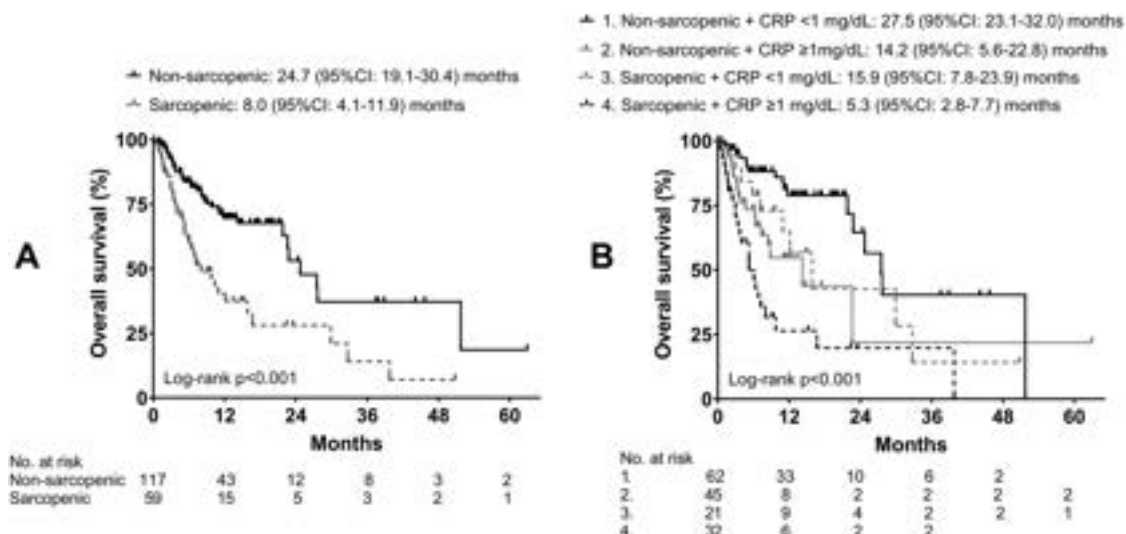


Figure: (abstract: FRI-295).

Results: The proportion of patients suffering from malignancies among chronic hepatitis C patients was lower than in the general population of Poland (any malignancy 1.5% vs 3.1%; HD 0.26% vs 0.49%, data: National Registry of Cancers). The distribution of genotypes was comparable in patients with and without malignancies, while HCV-viral load was significantly higher in hematologic patients (HD = 6.2 vs SMT = 5.7 vs HCC = 5.8 log10 IU/ml, $P < 0.001$). Likewise, the rate of extrahepatic symptoms was more frequent in HD patients (17.2% vs. SMT = 10.3%, HCC = 8.2%, without = 7.8%, $p = 0.04$). Patients with HCC had higher ALT activity (81 IU/l vs. SMT = 59.5 IU/l, HD = 52 IU/l, controls = 58 IU/l $p < 0.001$) and more often F4 fibrosis (86.11% vs. SMT = 23.3%, HD = 28.8%, controls = 24.4%, $p < 0.001$). DAAs were well tolerated with the need for premature discontinuation in 9.4% of HCC patients, only 2.9% of HD and no SMT patients compared to 1.1% in the general population. Sustained virologic response rates were 89.55% in HD, 90.32% in SMT and 77.03% in HCC (ITT analysis), and in 93.6% HD, 90.16% SMT and 80.6% in HCC after exclusion of non-virologic failures.

Conclusion: A lower proportion of active malignancies among patients with chronic hepatitis C than the general population might suggest shortfalls in HCV screening or DAA uptake. Importantly, we claim the high effectiveness and safety profile of the DAAs therapy in solid tumor and hematologic malignancies subjects. Patients with HCC remain to be a challenging group not only considering the severity of their liver disease but also struggling to achieve SVR.

FRI-297

Abbreviated magnetic resonance imaging for secondary surveillance of recurrent hepatocellular carcinoma after curative treatment

Sun Kyung Jeon¹, Dong Ho Lee¹, Bo-Yun Hur¹, Juil Park², Se Woo Kim¹, Junghoan Park¹. ¹Seoul National University Hospital, Korea, Rep. of South; ²Severance hospital, Korea, Rep. of South
Email: dhlee.rad@snu.ac.kr

Background and aims: Given the high hepatocellular carcinoma (HCC) recurrence rate even after a long recurrence-free year following HCC treatment and the risk of developing de novo secondary HCC, long-term continued secondary surveillance (i.e., follow-up after HCC treatment) is needed. However, there is no consensus regarding the ideal imaging modality for the secondary surveillance of HCC. Recently proposed abbreviated magnetic resonance imaging (AMRI) protocols can be a promising imaging modality, however, little is known about the performance of AMRI for secondary surveillance of HCC. This study aimed to evaluate the detection performance of abbreviated MRI (AMRI) for secondary surveillance of HCC after curative treatment, including surgical resection or radiofrequency ablation (RFA).

Method: This retrospective study analysed 243 patients who underwent secondary surveillance for HCC using gadoteric acid-enhanced MRI after more than two year of disease-free period following curative treatment, including surgical resection or RFA, between January 2015 and December 2017 in tertiary academic center. Four abdominal radiologists with different experience level in liver imaging independently reviewed non-contrast AMRI (NC-AMRI) (T2-weighted, T1-weighted, and diffusion-weighted images), hepatobiliary phase AMRI (HBP-AMRI) (T2-weighted, diffusion-weighted, and HBP images), and full-sequence MRI sets. HCC was confirmed based on either histopathological confirmation or imaging-based diagnosis. Per-lesion sensitivity, per-patient sensitivity and specificity for HCC detection were compared among three image sets using generalized estimating equation.

Results: A total of 42 recurrent HCCs were confirmed in the 39 patients. The per-lesion and per-patient sensitivities did not show significant differences among the three image sets for all reviewers ($p \geq 0.358$): per-lesion sensitivity, 59.5–83.3%, 59.5–85.7%, and 59.5–83.3% for NC-AMRI, HBP-AMRI, and full-sequence MRI, respectively, and per-patient sensitivity: 53.9–83.3%, 56.4–85.7%, and 53.9–83.3%

for NC-AMRI, HBP-AMRI, and full-sequence MRI, respectively. Per-patient specificity was not significantly different among the three image sets for all reviewers (95.6–97.1%, 95.6–97.1%, and 97.6–98.5% for NC-AMRI, HBP-AMRI, and full-sequence MRI, respectively; $p \geq 0.117$).

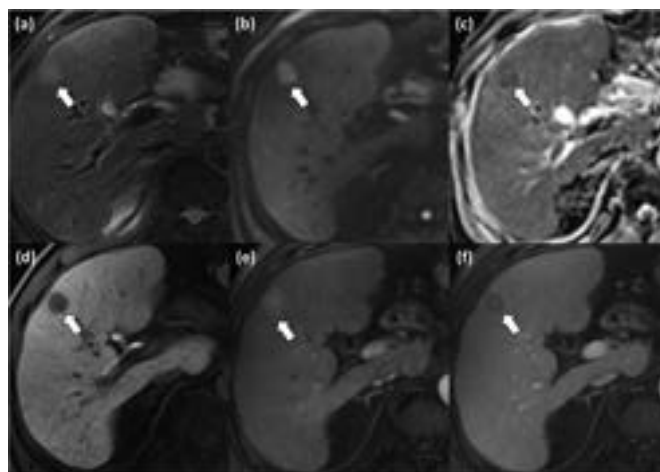


Figure: A case of recurrent HCC 33 months after left lateral sectionectomy in a 66-year-old man, which was detected by reviewers on NC-AMRI (a-c), HBP-AMRI (a-d), and full-sequence MRI (a-f).

Conclusion: NC-AMRI and HBP-AMRI had comparable detection performance to that of full-sequence gadoteric acid-enhanced MRI during secondary surveillance for HCC after more than 2-year disease free interval following curative treatment. Based on its good detection performance, short scan time, and lack of contrast agent-associated risks, NC-AMRI can be a promising option for the secondary surveillance of HCC, and further prospective validation is needed.

FRI-298

A new biomarker panel for differential diagnosis of cholangiocarcinoma: results from an exploratory analysis

Bruno Köhler¹, Marta Bes², Henry LY Chan³, Juan Ignacio Esteban Mur⁴, Teerha Piratvisuth⁵, Wattana Sukeepaisarnjaroen⁶, Tawesak Tanwandee⁷, Anika Mang⁸, David Morgenstern⁹, Magdalena Swiatek-de Lange⁸, Farshid Dayyani¹⁰. ¹University Hospital Heidelberg, Germany; ²Instituto de Salud Carlos III, Spain; ³The Chinese University of Hong Kong, Hong Kong; ⁴Hospital Universitari Vall d'Hebron, Spain; ⁵Songklanagarind Hospital, Thailand; ⁶Srinagarind Hospital, Thailand; ⁷Siriraj Hospital, Thailand; ⁸Roche Diagnostics GmbH, Germany; ⁹Roche Diagnostics Operations, United States; ¹⁰University of California in Irvine, United States
Email: magdalena.swiatek-de_lange@roche.com

Background and aims: Accurate diagnosis of cholangiocarcinoma (CCA) can be challenging due to unclear diagnostic imaging criteria and difficulty obtaining adequate tissue biopsy. Although serum cancer antigen 19-9 and carcinoembryonic antigen have been proposed as potential diagnostic aids, they have insufficient sensitivity and specificity. This exploratory analysis aimed to identify individual and combinations of serum tumour biomarkers that could distinguish CCA from hepatocellular carcinoma (HCC) and benign chronic liver disease (CLD) controls using samples obtained from a previously published study.

Method: This prospective, multicentre, case-control study included patients ≥ 18 years who were at high risk of HCC. Serum and ethylene diamine tetraacetic acid-plasma samples were collected prior to any treatment and a confirmed diagnosis of HCC or CCA. A panel of 14 electrochemiluminescence immunoassays or enzyme-linked immunosorbent assays were used; 14 biomarkers were subjected to

univariate analysis and 13 to multivariate analysis (per selected combinations and exhaustive search).

Results: Overall, 55 CCA (22 intrahepatic CCA; 11 perihilar CCA), 306 HCC and 733 CLD control samples were analysed. The biomarkers with the best individual performance were alpha-fetoprotein and matrix metalloproteinase-2 (MMP-2) (area under the curve [AUC] 86.6% and 84.4%, respectively) for distinguishing CCA from HCC, and tissue inhibitor of metalloproteinase-1 (TIMP-1) for distinguishing CCA from CLD (AUC 94.5%) and HCC + CLD (AUC 88.6%). MMP-2 and TIMP-1 combination was the best performing two-marker panel (Table), with AUC >90% for all comparisons. Carbohydrate antigen 19-9 (CA 19-9) and carcinoembryonic antigen (CEA) performed relatively poorly as individual biomarkers (Table).

Table: Performance of individual biomarkers and of the TIMP-1 and MMP-2 two-biomarker panel for distinguishing CCA from HCC and/or benign CLD controls.

	CCA vs HCC.	CCA vs benign CLD.	CCA vs HCC + benign CLD.
Individual biomarkers (univariate analysis).			
AFP.	86.6 (81.4–91.8).	53.2 (44.1–62.2).	63.0 (55.4–70.6).
CA19-9.	67.5 (58.2–76.8).	78.4 (70.6–86.2).	75.2 (67.1–83.2).
CEA.	60.5 (50.7–70.3).	48.3 (38.9–57.7).	51.9 (42.5–61.3).
MMP-2.	84.4 (78.9–89.9).	72.4 (64.6–80.2).	75.9 (68.9–82.9).
TIMP-1.	74.5 (68.2–80.8).	94.5 (92.1–96.9).	88.6 (85.3–91.9).
Two-biomarker panel (multivariate analysis).			
TIMP-1 and MMP-2.	91.8 (88.3–95.3).	97.9 (96.6–99.2).	95.6 (93.7–97.6).

All results shown as AUC, % (95% CI).

Conclusion: MMP-2 and TIMP-1 are promising non-invasive biomarkers that could rapidly provide additional diagnostic information to help differentiate CCA from HCC and CLD.

FRI-299

CRAFITY score is associated with overall survival in patients with hepatocellular carcinoma treated with transarterial chemoembolisation

Rhea Veelken^{1,1}, Anne Olbrich¹, Aaron Schindler¹, Sabine Lieb¹, Janett Fischer¹, Sebastian Ebel², Timm Denecke², Thomas Berg¹, Florian van Bömmel¹. ¹University Hospital of Leipzig, Division of Hepatology, Department of Medicine II, Germany; ²University Hospital of Leipzig, Department of Diagnostic and Interventional Radiology, Germany
Email: rhea.veelken@medizin.uni-leipzig.de

Background and aims: The CRAFITY score is based on alpha fetoprotein (AFP ≥100 ng/ml) and C-reactive protein (CRP ≥1 mg/dL), and it stratifies patients by the likelihood of increased overall survival (OS) and treatment response to subsequent immunotherapy containing systemic treatment for hepatocellular carcinomas (HCC). We aimed to investigate the association of the CRAFITY score with survival and treatment response to transarterial chemoembolisation (TACE).

Method: A total cohort of 546 patients with HCC was treated with TACE as first-line therapy at our center between 2010 and 2020. Patients were retrospectively enrolled in our study if follow-up was documented over at least 3 months, and if CRP and AFP were available from baseline. We investigated the association of baseline variables on overall survival using Kaplan-Meier estimation and a Cox regression model.

Results: A total of 113 patients was included in the analysis (15 (13%) female). All patients suffered from HCC (BCLC stages A (n = 64), B (n = 37), C (n = 10) and D (n = 2)) with a median age of 63 years (range 31–85 years). Eighty-eight (78%) patients had compensated liver cirrhosis, 25 (22%) patients showed no clear signs of liver cirrhosis on imaging. Patients with a GRAFITY score 0 (n = 67) had the longest median OS of 46.82 (range, 0–140) months followed by patients with

1 point (n = 38), who had a median OS of 24.71 (range, 0–121) months and patients with 2 points (n = 8), who had a median OS of 19.38 (range, 0–67) months (p < 0.001) (Figure). In Cox regression analyses, the CRAFITY score 1 was associated with significantly increased risk of mortality with a hazard ratio (HR) of 2.4 (95% CI 1.23–4.55, p = 0.01). Moreover, patients with a CRAFITY score of 2 had a 6 times higher risk of mortality (HR = 5.9 [95% CI 2.44–14.14] p < 0.001) compared to patients with a score of 0. Interestingly, 62% of the responders at week 12 had a CRAFITY score of 0 and 33% of the responders at week 12 had a CRAFITY score of 1.

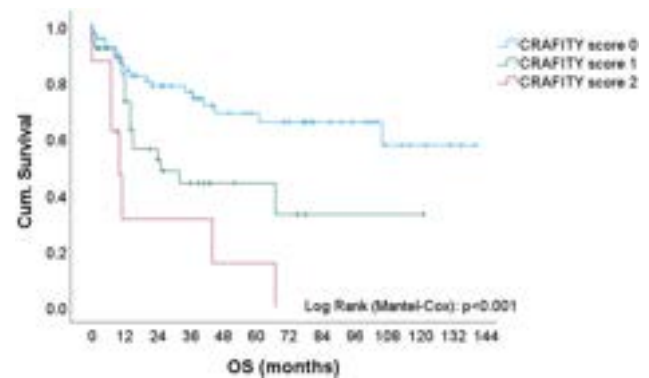


Figure: Kaplan-Meier estimation for overall survival according to the CRAFITY score

Conclusion: The CRAFITY score is a potential tool for the identification of patients who benefit from TACE. The potential of the CRAFITY score for the personalisation of multimodal treatment of HCCs needs to be assessed in future studies.

FRI-300

Development, clinical validation and implementation of a novel algorithmic score (GAAD) for the detection of early-stage hepatocellular carcinoma

Teerha Piratvisuth¹, Jinlin Hou², Tawesak Tanwandee³, Thomas Berg⁴, Arndt Vogel⁵, Jörg Trojan⁶, Enrico de Toni⁷, Masatoshi Kudo⁸, Anja Eiblmaier⁹, Hanns-Georg Klein¹⁰, Johannes Kolja Hegel¹¹, Kairat Madin¹², Konstantin Kroeniger¹², Ashish Sharma¹³, Henry Ly Chan¹⁴. ¹Prince of Songkha University, Thailand; ²Southern Medical University, China; ³Mahidol University, Thailand; ⁴Universitätsklinikum Leipzig, Germany; ⁵Medizinische Hochschule Hannover, Germany; ⁶Goethe Universität Frankfurt, Germany; ⁷Ludwig Maximilian University of Munich, Germany; ⁸Kindai University, Japan; ⁹Microcoat Biotechnologie GmbH, Germany; ¹⁰Zentrum für Humangenetik und Laboratoriumsdiagnostik, Germany; ¹¹Labor Berlin Charité Vivantes Services GmbH, Germany; ¹²Roche Diagnostics GmbH, Germany; ¹³Roche Diagnostics International AG, Switzerland; ¹⁴The Chinese University of Hong Kong, Hong Kong
Email: teerha.p@psu.ac.th

Background and aims: Protein induced by vitamin K absence-II (PIVKA-II) and alpha-fetoprotein (AFP) are serum biomarkers that can support the diagnosis of hepatocellular carcinoma (HCC). The GAAD algorithm is a novel in vitro diagnostic combining quantitative measurements of Elecsys[®] PIVKA-II assay and Elecsys AFP assay, plus age and gender to generate a semi-quantitative result. This study aimed to establish and train the algorithm coefficients, and clinically validate clinical performance of the GAAD algorithm in differentiating HCC and benign chronic liver disease (CLD), across different regions and aetiologies.

Method: Participants aged ≥18 years were prospectively enrolled across China, Hong Kong Special Administrative Region, Spain, Germany, Japan and Thailand for Algorithm development and clinical validation studies. The HCC group had a first-time diagnosis of HCC confirmed by imaging or biopsy. The CLD control group had an

POSTER PRESENTATIONS

absence of HCC confirmed by imaging ≤ 12 months before, and diagnosis of cirrhosis or non-cirrhotic liver disease (viral or non-viral). Serum samples were analysed using the Elecsys PIVKA-II and AFP assays on a cobas e 601 analyser. The established cut-off for the detection of HCC was a GAAD score of 2.57 (range 0–10). Cut-off for detection of HCC in the Elecsys AFP assay was 20 ng/ml.

Results: In the HCC group (n = 366) and CLD control group (n = 303), 176 (48.1%)/136 (44.9%) were from China, 142 (38.8%)/124 (40.9%) from Europe and 48 (13.1%)/43 (14.2%) from Asia-Pacific, respectively. In the HCC group, 287 (78.4%) had cirrhosis, of which 222 (60.7%) had viral liver disease aetiology, and 174 (47.6%) had early-stage HCC (Barcelona Clinic Liver Cancer [BCLC] 0 and A). In the control group, 112 (37%) had cirrhosis including 76 (25.1%) with viral disease. GAAD performed well for differentiating both early- and all-stage HCC from benign disease controls across disease aetiologies and regions (Figure). Sensitivity for detecting early- and all-stage HCC, respectively, was 67.4% and 81.9% in cirrhotic CLD (specificity, 86.6%) and 79.5% and 87.3% in non-cirrhotic CLD (specificity, 97.9%); all sensitivity rates were higher than for AFP alone. Sensitivity was similar across China (67.3% for early-stage HCC/77.3% for all-stage HCC), Europe (76.9%/90.8%) and Asia-Pacific (72%/81.3%), with $>85\%$ specificity for CLD controls for all regions; all sensitivity rates were higher than for AFP alone. Two independent workflow options: (a) website solution with user login and manual data entry and (2) an automated integrated solution via the NAVIFY® Algorithm suite were implemented for the GAAD algorithm.

Figure. Clinical performance of GAAD for detection of (A) early-stage HCC vs benign disease control according to disease aetiology; (B) all-stage HCC vs benign disease control according to disease aetiology; (C) early-stage HCC vs benign disease control according to region; (D) all-stage HCC vs benign disease control according to region.

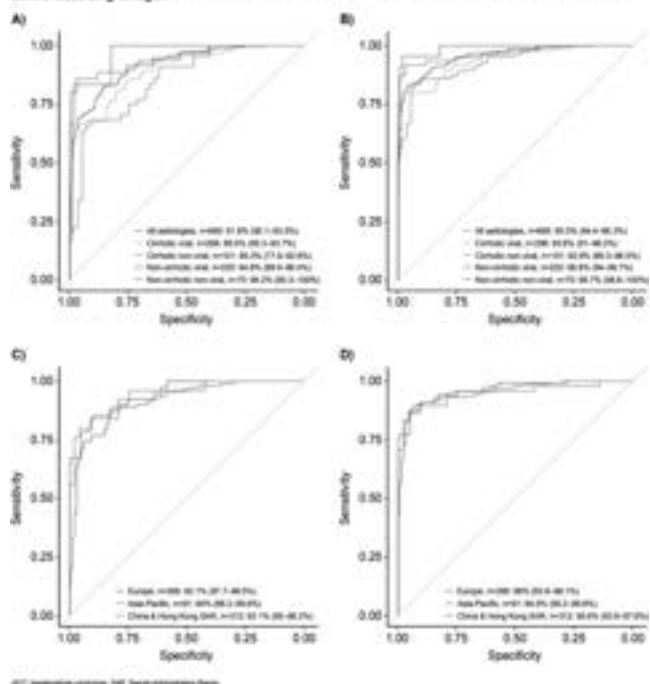


Figure:

Conclusion: The GAAD algorithm, combining PIVKA II and AFP, plus age and gender, demonstrated good clinical performance in differentiating HCC and benign CLD, across all regions and aetiologies.

FRI-301

Gadoxetic acid-enhanced MRI-based risk scoring system development and validation for the recurrence-free survival of a single hepatocellular carcinoma after curative surgery

Bohyun Kim¹, So Hyun Park², Joon-Il Choi¹. ¹Seoul St. Mary's Hospital, College of Medicine, The Catholic University of Korea, Korea, Rep. of South; ²Gil Medical Center, Gachon University College of Medicine, Korea, Rep. of South

Email: baboojum@naver.com

Background and aims: To develop and validate risk scoring systems using gadoxetic acid-enhanced liver MRI features and clinical factors that predict recurrence-free survival (RFS) of a single hepatocellular carcinoma (HCC).

Method: Consecutive 295 patients with treatment-naïve single HCC who underwent curative surgery and preoperative gadoxetic acid-enhanced MRI were retrospectively enrolled from two centers. Cox proportional hazard models developed risk scoring systems whose discriminatory powers were validated using external data and compared to the Barcelona Clinic Liver Cancer (BCLC) or American Joint Committee on Cancer (AJCC) staging systems using Harrell's C-index.

Results: Independent variables—tumor size (per cm; hazard ratio [HR], 1.07; 95% confidence interval [CI]: 1.02–1.13; $p=0.005$), targetoid appearance (HR, 1.74; 95% CI: 1.07–2.83; $p=0.025$), radiologic tumor in vein or tumor vascular invasion (HR, 2.59; 95% CI: 1.69–3.97; $p<0.001$), the presence of a nonhypervascular hypointense nodule on the hepatobiliary phase (HR, 4.65; 95% CI: 3.03–7.14; $p<0.001$), and pathologic macrovascular invasion (HR, 2.60; 95% CI: 1.51–4.48; $p=0.001$)—with tumor markers (AFP ≥ 206 ng/ml or PIVKA-II ≥ 419 mAU/ml) derived pre- and post-operative risk scoring systems. The risk scores showed comparably good discriminatory powers in the validation set (C-index, 0.75–0.82) and outperformed the BCLC (C-index, 0.61) and AJCC staging systems (C-index, 0.58; $p<0.05$). The preoperative scoring system stratified the patients into low-, intermediate-, and high-risk for recurrence, whose 2-year recurrence rate was 3.3%, 31.8%, and 85.7%, respectively.

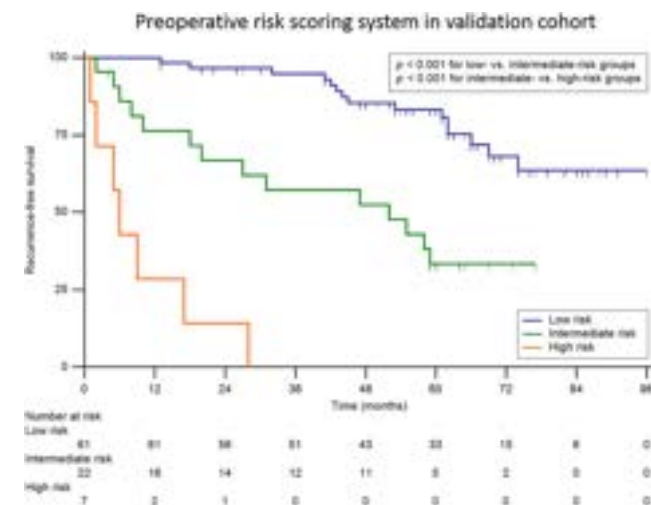


Figure:

Conclusion: The developed and validated pre- and postoperative risk scoring systems can estimate RFS after surgery for a single HCC.

FRI-302

The apparent diffusion coefficient values predict prognosis and Ki67 expression in intrahepatic cholangiocarcinoma on diffusion-weighted magnetic resonance imaging

Daiki Hokkoku¹, Kazuki Sasaki¹, Shogo Kobayashi¹, Yoshifumi Iwagami¹, Daisaku Yamada¹, Yoshito Tomimaru¹, Takehiro Noda¹, Hidenori Takahashi¹, Yuichiro Doki¹, Hidetoshi Eguchi¹. ¹Osaka University, Graduate School of Medicine, Department of Gastroenterological Surgery, Suita, Japan
Email: hokkoku-daiki@gmail.com

Background and aims: Intrahepatic cholangiocarcinoma (ICC) is a primary liver cancer with high aggressiveness and an extremely poor prognosis. A poor prognosis with a 5-year survival rate is about 40% after radical resection. Previous reports have indicated that lymph node metastasis and multiple tumors are poor prognostic factors in ICC. However, definite evidence regarding the lymph node dissection for ICC does not exist at present. Therefore, selecting the poor prognosis group and the group that does not require lymph node dissection based on preoperative imaging is necessary. Diffusion-weighted image (DWI) of magnetic resonance imaging (MRI) is a promising functional imaging tool for detecting and characterizing tumors. In biologic tissue, the DWI signal is derived from the motion of water molecules. The apparent diffusion coefficient (ADC) values were calculated based on water protons experiencing different restrictions to diffusion inside cellular compartments. In hepatocellular carcinoma and breast cancer, it has been reported that ADC values obtained from DWI-MRI, especially minimum ADC values (ADC_{min}), are associated with prognosis and Ki67, but there have been few reports focusing on ADC values in ICC. The aim of this study is to investigate the correlation of ADC_{min} and Ki67 expression in ICC.

Method: A total of 39 ICC cases confirmed by surgical pathology were analyzed retrospectively. Subjects underwent MRI at 1.5 or 3.0 T and calculated their minimum ADC_{min} using DWI MRI (b:0, 50, 200, 1000, 1500 seconds/mm²). Patients were divided into ADC_{min} high group and ADC_{min} low group. The cut-off value for ADC_{min} was obtained using the receiver operating characteristic curve. We compared clinicopathological factors between two groups. Immunohistochemical analysis of Ki67 expression in tumor tissues was performed, and its expression was determined as low (less than 10% immunopositive cells) or high (more than 10% immunopositive cells). We evaluated the relationship between the ADC_{min} and Ki67 expression.

Results: The overall survival rate of the ADC_{min} low group was significantly lower than that of the ADC_{min} high group (p = 0.0404). Univariate analysis revealed that CEA (>5 ng/ml), CA19-9 (>35 U/ml), microvascular invasion, lymph node metastasis, and low ADC_{min} were prognostic factors. Multivariate analysis identified low ADC_{min} as an independent prognostic factor (p = 0.0202). Furthermore, the ADC_{min} low group more frequently expressed high levels of Ki67 than the ADC_{min} high group (75.0% vs. 26.1%, p = 0.0038).

Correlation between ADC_{min} and Ki67 expression in tumor tissues

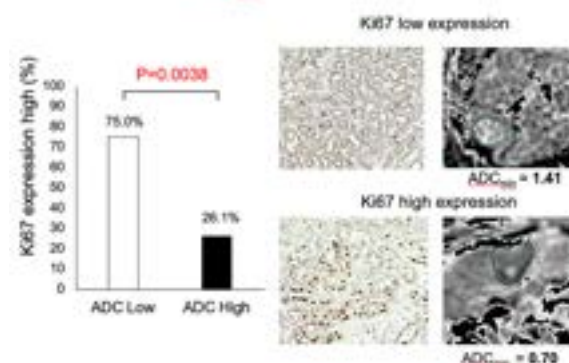


Figure:

Conclusion: Low ADC_{min} was an independent prognostic factor of ICC and correlated with Ki67 expression.

FRI-303

The Kupffer phase of Sonazoid-enhanced ultrasound as the major imaging feature for diagnosing hepatocellular carcinoma in at-risk individuals

Hyo-Jin Kang¹, Jeong Min Lee¹, Jeong Hee Yoon¹, Jeongin Yoo¹. ¹Seoul National University Hospital, Radiology, Seoul, Korea, Rep. of South
Email: jmsn@snu.ac.kr

Background and aims: Sonazoid has different physiologic characteristics from blood-pool ultrasound contrast agents, but there has been no consensus about the diagnostic criteria of HCC. We aimed to investigate whether the Kupffer phase (KP) can be used as a major feature without lowering specificity for diagnosing HCC in high-risk individuals.

Method: Participants at risk of HCC with treatment-naïve solid hepatic lesions (≥ 1 cm) who underwent PFB-US from March 2019 to June 2022 were prospectively recruited. Three radiologists reviewed the enhancement pattern in the arterial phase, washout time and degrees, and echogenicity in the KP. All malignancies were pathologically confirmed. The pooled per-lesion diagnostic performance for diagnosing HCC using five different diagnostic criteria were compared by McNemar test: Criteria 1) any APHE with hyper-enhancement (APHE) with hypoechogenicity in KP, Criteria 2) nonrim APHE with hypoechogenicity in KP, Criteria 3) following criteria 2, but exclude early (<60 s postcontrast) and marked washout, Criteria 4) nonrim APHE with mild and late (≥ 60 s postcontrast) washout within 5 min, Criteria 5) nonrim APHE with mild and late washout within 5 min or hypoechogenicity in KP. Criteria 4 was identical to the diagnostic criteria of blood-pool agent-enhanced ultrasound.

Results: In total, 204 individuals with 213 lesions (mean size 32.5 ± 3.2 mm; HCC [n = 122], non-HCC malignancies [n = 21], and benign [n = 46]) were evaluated. For HCC diagnosis, the specificity of criteria 1 and 2 were significantly lower (42.9% and 72.2%) than criteria 3 (91.9%, p < .001) and 4 (p < .001). The sensitivity (63.7%) of criteria 5 was higher than criteria 3 (61.5%) and 4 (63.4%), and specificity (94.1%) of criteria 4 was higher than criteria 3 (91.9%) and 5 (91.9%), but both fail to meet the statistical significance (p = .59 and .93).

Criteria	Definition for HCC	Sensitivity	Specificity	Accuracy
1	any APHE + KP defect	48.1 (82.1, 89.4)	42.9 (34.9, 48.8)	57.8 (83.8, 71.2)
2	nonrim APHE + KP hypoechogenicity	81.7 (77.3, 85.5)	72.2 (66.4, 77.4)	77.6 (74.2, 80.8)
3	nonrim APHE + KP hypoechogenicity (exclude early/marked washout)	61.5 (50.3, 68.5)	91.9 (85.1, 94.8)	74.5 (70.9, 77.8)
4	nonrim APHE + mild and late washout within 5 min*	63.4 (58.2, 68.3)	94.1 (90.7, 96.8)	78.5 (73.8, 79.8)
5	nonrim APHE + mild and late washout within 5 min, or KP hypoechogenicity	63.7 (58.5, 68.5)	94.9 (88.1, 96.5)	79.7 (72.3, 79.8)
P values				
1 vs. 4		<.001	<.001	.801
2 vs. 4		<.001	<.001	.64
3 vs. 4		.59	.31	.41
5 vs. 4		.93	.31	.74

* Same as the diagnostic criteria of blood-pool agent-enhanced ultrasound

† Data are percentage with 95% CI in parentheses

Figure:

Conclusion: Precluding early or marked washout and including nonrim APHE reinforced the specificity when KP was used as a major feature for diagnosing HCC. The KP imaging can be alternative to the 2–5 min postcontrast imaging without significant change in diagnostic performance.

FRI-304

It takes a team for HCC: improvement of outcome with the multidisciplinary ambulatory for systemic therapy

Andrea Dalbeni¹, Alessandra Auriemma², Marco Vicardi¹, Andrea Ruzzenente³, Alfredo Guglielmi³, Michele Milella², David Sacerdoti¹. ¹AOU Verona, University of Verona, Medicine Department, Liver Unit, Italy; ²AOU Verona, University of Verona, Oncology, Italy; ³AOU Verona, University of Verona, Surgery Department, Italy

Email: andrea.dalbeni@aovr.veneto.it

Background and aims: Hepatocellular carcinoma (HCC) is the major cause of liver-related death worldwide. In the last years, a new approach with tyrosine kinase inhibitors (TKIs) and immune checkpoint inhibitors (ICIs) started to gain attention in HCC setting. With these new therapies multidisciplinary team (MDT) discussion becomes necessary due to increased curative treatments, frequency of stage migration, higher treatment rates and reduced mortality. In Verona Hospital, in addition to MDT discussion, a LIVER-MDT ambulatory was created, to our knowledge the first in the Italian health system, with an oncologist, an hepatologist, a surgeon, and an internist. Aim of this study was to verify if the LIVER-MDT ambulatory is useful to reduce adverse effects and mortality compared to a traditional ambulatory (ELEVATOR cohort, Liver cancer 2022).

Method: we collected data from patients attending the LIVER-MDT ambulatory. Major and minor adverse effects (MAE and mAE) and antitumoral doses were collected. Death and progression free survival (PFS) were also recorded.

Results: Among 834 patients evaluated at the MDT discussion from 2021, 40 patients were referred to the LIVER-MDT ambulatory to start systemic treatment. Median age was 69.5 (53–82), 82.5% were male. Cirrhosis etiology was 45% viral (HCV/HBV), 37.5% MAFLD and 10% alcohol. Compared to ELEVATOR cohort, less MAE were recorded (20% vs 32.7%, $p < 0.01$). In addition, MAE strictly due to the systemic therapy developed in 7.5%. No patients developed uncontrolled and resistant arterial hypertension or heart failure during the treatment. 32.5% died, with a median PFS of 8.85 ± 6.03 (median in ELEVATOR 6.4). Only 15% of patients needed a reduction of antitumoral drug dose, compared to 50% in ELEVATOR.

Conclusion: LIVER-MDT ambulatory improves the outcome of HCC patients on systemic therapy, reducing MAEs and mAEs, in particular cardiovascular complications, and seems the best approach for the increasing number of HCC patients.

FRI-305

Developing an aptamer biomarker model for the diagnosis of hepatocellular carcinoma

Mikkel Breinholt Kjær¹, Stine Karlsen Oversoe¹, Søren Fjelstrup², Daniel Miotto Dupont², Jens Kelsen¹, Jørgen Kjems², Henning Grønbaek¹. ¹Aarhus University Hospital, Department of Hepatology and Gastroenterology, Denmark; ²Aarhus University, Interdisciplinary Nanoscience Centre (iNANO), Department of Molecular Biology and Genetics, Denmark

Email: mikj@clin.au.dk

Background and aims: Hepatocellular carcinoma (HCC) is the fourth leading cause of cancer-related death globally and most tumors are detected at late stages of disease. The current screening method for HCC in risk populations relies on abdominal ultrasound. While ultrasound exhibits acceptable sensitivity for detection of HCC at any stage, the sensitivity to detect early stages of disease is less so. Coupled with the fact that the chance of cure diminishes with later stages of disease warrants novel methods for detection of HCC, herein biomarkers of early-stage HCC.

Thus, the aim of this study is to explore the clinical potential of aptamer technology to distinguish patients with HCC regarding early and late-stage disease.

Method: In this study we utilize APTA-SHAPE, an unbiased biomarker discovery platform based on aptamer technology. Aptamers are short

chemically stabilized RNA strands often termed “chemical antibodies.” The aptamers form defined 3D shapes capable of specific recognition of a biological target. Through consecutive trainings with plasma from patients with HCC we build a library specifically able to detect thousands of plasma molecules in HCC. In subsequent analysis, aptamers associated with disease stage in HCC are identified and the protein targets of these aptamers are identified by mass spectrometry.

Data for this study was generated by aptamer analysis performed on plasma samples from a cohort of 104 HCC patients and 24 healthy controls collected at the Department of Hepatology and Gastroenterology, Aarhus University Hospital from 2016 to 2018. The material was divided to generate a training set and a validation set for the constructed models. Disease severity groups were defined by TNM staging or Barcelona Clinic Liver Cancer (BCLC) score.

Results: An aptamer-based model for detection of HCC defined by TNM-staging was able to discriminate between healthy and early-stage disease (TNM stages 1A, 1B and 2) with an AUC in the validation set of 0.85 (95% CI: 0.73–0.97). Furthermore, the model was able to discriminate between healthy and late-stage disease (TNM stages 3A, 3B, 4A and 4B) with an AUC of 0.93 in the validation set (95% CI: 0.84–1.00). A second model based on BCLC scores were able to discriminate between healthy controls and patients with early (stages 0, A or B) or late-stage disease (stages 3 and 4) with AUCs of 0.8 (95% CI: 0.64–0.95) and 0.94 (95% CI: 0.87–1.00).

Conclusion: The APTA-SHAPE technology is a promising and unbiased tool to identify novel biomarkers for HCC. We developed a model capable of identifying HCC patients as well as grouping patients with regards to their disease stage and severity of disease. Future studies will aim to identify the protein plasma biomarkers discovered in this study.

FRI-306

The association between alcohol consumption and the risk of hepatocellular carcinoma according to glycemic status: a nationwide population-based study

Eun Ju Cho¹, Goh Eun Chung², Jeong-Ju Yoo³, Yuri Cho⁴, Dong Wook Shin⁵, Yoon Jun Kim¹, Jung-Hwan Yoon¹, Kyungdo Han⁶, Su Jong Yu⁷. ¹Seoul National University College of Medicine, Korea, Rep. of South; ²Seoul National University Hospital Healthcare System Gangnam Center, Korea, Rep. of South; ³Soonchunhyang University Bucheon Hospital, Korea, Rep. of South; ⁴National Cancer Center, Korea, Rep. of South; ⁵Samsung Medical Center, Sungkyunkwan University School of Medicine, Korea, Rep. of South; ⁶Soongsil University, Korea, Rep. of South; ⁷Seoul National University College of Medicine, Department of Internal Medicine and Liver Research Institute, Korea, Rep. of South

Email: ydoctor2@snu.ac.kr

Background and aims: Alcohol and diabetes are known risk factors for hepatocellular carcinoma (HCC), however, it is unclear whether the association between alcohol consumption and HCC risk differs by fasting serum glucose level and diabetes. We investigated the dose-response relationship between alcohol consumption and the risk of HCC according to glycemic status.

Method: We included patients who underwent general health checkups in 2009 linked with death certificate data using the Korean National Health Insurance Service Database. Cox proportional hazard regression analysis was performed to estimate the relationship between alcohol consumption and HCC risk according to glycemic status.

Results: A total of 39,798 patients newly diagnosed with HCC were observed in the 8.3 years median follow-up period. Mild-to-moderate alcohol consumption increased the risk of HCC in all glycemic status (normoglycemia: hazard ratio [HR], 1.06; 95% CI, 1.02 to 1.10; prediabetes: HR, 1.14; 95% CI, 1.09–1.20 and diabetes: HR, 1.23; 95% CI, 1.17–1.29). Heavy alcohol consumption also increased the risk of HCC in all glycemic statuses (normoglycemia: HR, 1.39; 95% CI, 1.32–1.44; Prediabetes: HR, 1.60; 95% CI, 1.51–1.71, and diabetes: HR,

2.01; 95% CI, 1.89–2.14). The increased risk in mild-to-moderate or heavy alcohol consumption was the greatest in the diabetes group, followed by prediabetes and normoglycemia (P for interaction <0.001).

Conclusion: Mild-to-moderate alcohol consumption was associated with an increased risk of HCC in all glycemic status groups. The increased risk of HCC was the highest in the diabetes group, suggesting that more intensive alcohol abstinence is required for patients with diabetes.

FRI-307

Combined hepatocellular-cholangiocarcinoma : epidemiological, radiological and survival data from a retrospective single-center study

Guillaume Henin¹, Ivan Borbath¹, Bénédicte Delire¹. ¹Cliniques Universitaires Saint-Luc, Hepato-gastro-enterology, Belgium
Email: ghenin1993@gmail.com

Background and aims: Combined hepatocellular-cholangiocarcinoma (cHCC-CCA) is a rare primary liver malignancy with a poor prognosis and very few available data in terms of pathophysiology, risk factors, imaging features and no current consensus in terms of treatment recommendations. Therefore, our aims were to assess the risk factors, imaging-pathology correlation and survival of these patients in a real-life cohort.

Method: All patients with histologically-confirmed or with imaging-based suspicion of cHCC-CCA (classified Li-Rads M) treated between 2016 and 2021 were screened in a retrospective single-center study. Other histological subtypes of liver tumor in the absence of radiological suspicion of mixed tumor by magnetic resonance imaging (MRI) were excluded. MRI data of transplanted patients were not recorded considering the artifacts due to waiting treatments. All data were recorded based on medical records.

Results: Among 761 screened patients, 69 were included among which 38 patients (55.1%) had a cHCC-CCA lesion (cHCC-CCA group). A hepatocellular carcinoma was confirmed in 18 patients (HCC group-26.1%) and a cholangiocarcinoma in 9 patients (CCA group-13.0%). 4 patients had a benign tumor (5.8%). In terms of risk factors for the onset of cHCC-CCA, alcohol-related liver disease and pre-existing liver lesions were correlated to this risk (OR 4.67, $p=0.024$ and OR 4.16, $p=0.043$ respectively). In terms of imaging diagnostic accuracy in the HCC-CCA group ($N=26$, liver transplant recipients excluded in this analysis), 17 patients had a positive MRI for HCC-CCA (65.4%) and 9 had a negative MRI (34.6%). In the non-HCC-CCA group (HCC, CCA, benign tumors and non-histologically investigated patients- $N=735$), 31 patients had a positive MRI (4.2%) and 704 had a negative MRI (95.8%) (Sensitivity=0.65; Specificity=0.96; positive predictive value=0.35 (PPV); negative predictive value=0.99 (NPV); $p<0.0001$). In terms of tumor biomarkers profiles, there was no significant differences between the 3 histological subtypes of malignant lesions (cHCC-CCA, HCC, CCA) for CA19.9 ($p=0.43$), AFP ($p=0.28$) and DCP ($p=0.22$). In terms of survival analysis, no significant differences were observed in terms of overall survival between histological subgroups (cHCC-CCA : 44.77; CCA : undefined; HCC : 37.61 months- $P=0.81$). No significant differences were also observed in the cHCC-CCA group depending on treatment modality (liver directed therapy : 44.8; systemic treatment : 26.86 months- $p=0.06$).

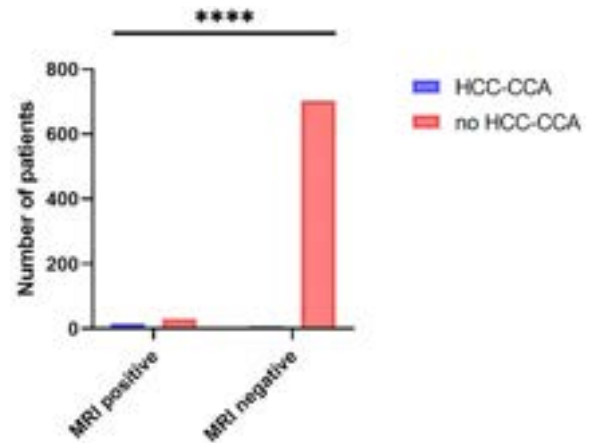


Figure:

Conclusion: We highlighted alcohol-related liver disease and pre-existing liver tumor prior to histological diagnosis as risk factors for the onset of cHCC-CCA (OR 4.67, $p=0.024$ and OR 4.16, $p=0.043$). We also highlighted an excellent NPV of liver MRI for the diagnosis of cHCC-CCA but a poor PPV (PPV=0.35; NPV=0.99- $p<0.0001$) confirming the necessity to perform a tumor biopsy in case of diagnostic uncertainty. Further well-conducted prospective studies are required to establish systemic treatment guidelines, systemic treatment regimens being currently chosen based on expert opinion.

FRI-308

Predictors of extrahepatic recurrence after transarterial chemoembolization as first-line therapy for hepatocellular carcinoma

Elisa Pinto¹, Filippo Pelizzaro¹, Alessandro Vitale¹, Edoardo Giannini², Franco Trevisani³, Fabio Farinati¹. ¹University of Padua, Italy; ²University of Genova, Italy; ³University of Bologna, Italy
Email: pintoelisa93@gmail.com

Background and aims: The literature regarding the risk of progression to extrahepatic disease and clinical factors associated with the development of metastases in patients with hepatocellular carcinoma (HCC) treated with transarterial chemoembolization (TACE) is sparse. We aimed to assess the incidence of extrahepatic recurrence and to identify clinically relevant risk factors for the development of metastases in patients with HCC treated with TACE as first-line treatment.

Method: From the Italian Liver Cancer (ITA.LI.CA) database, data of 981 HCC patients undergoing TACE as first-line treatment were retrieved and retrospectively analyzed. Incidence of extrahepatic recurrence was compared between two groups according to the diameter of the largest liver lesion at the time of TACE (HCC ≤ 3 cm vs. HCC >3 cm). Multivariate Cox regression was used to identify predictor of extrahepatic recurrence.

Results: During a median follow-up of 27.0 months (IQR, 13.2–49.0) the overall recurrence rate was 75.4%. Only 78/981 patients (8.0%) had an extrahepatic tumor localization at first recurrence (5.4% in the ≤ 3 cm group and 10.7% in the >3 group; $p=0.002$), while the overall extrahepatic recurrence rate was 26.0% (21.2% and 31.0% patients in the ≤ 3 cm and >3 cm groups, respectively; $p=0.0006$) (Figure 1). Compared to those with larger tumors, patients with HCC ≤ 3 cm had a significantly longer recurrence-free survival (12.0 [95% CI 10.7–13.3] vs. 9.7 [95% CI 8.2–11.2] months; $p=0.02$) and overall survival (52.5 [95% CI 45.5–59.4] vs. 34.7 [95% CI 30.7–38.7] months; $p<0.0001$). HCC size ≥ 3 cm, multifocality and AFP levels were independent predictors of extrahepatic recurrence.

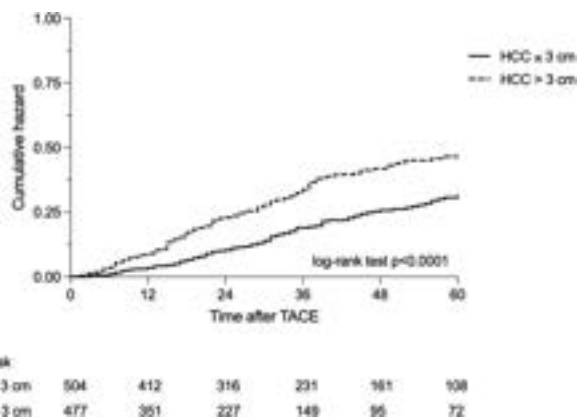


Figure 1: Cumulative hazard of extrahepatic recurrence among patients with HCC ≤ 3 cm and > 3 cm treated with first-line TACE.

Conclusion: Although the majority of patients treated with TACE do not develop metastases during their lifespan, knowledge of risk factors for extrahepatic recurrence (HCC size, multifocality, AFP levels) may help to assess patient prognosis and to identify patients deserving closer follow-up in order to start early systemic therapy.

FRI-309

Associations of pathologic features with integrated genomic and clinical characteristics of cholangiocarcinoma

Keun Soo Ahn¹, Koo Jeong Kang², Tae-Seok Kim², Yong Hoon Kim².

¹Keimyung University Dongsan Hospital, Surgery, Korea, Rep. of South;

²Keimyung University Dongsan Hospital, Korea, Rep. of South

Email: ahnksmd@gmail.com

Background and aims: Pathologically, cholangiocarcinoma (CCA) can be divided as two pathological subtype; large duct type and small duct type. It represents different origin and carcinogenesis of CCA. However, its clinical impact and molecular characteristics are not well known yet, and we evaluated clinical and molecular features according to pathological subtype.

Method: On 3 different cohort (Korea; Keimyung University Dongsan Hospital, USA; Mayo clinic, TCGA), 107 cases of CCA were included which had available clinical and molecular data (RNA sequencing with mutation). For Korea and USA data, we performed next generation RNA sequencing and RNA expression, variants and fusions were analyzed. For TCGA data, we downloaded clinical and genetic information from TCGA serve. We analyzed clinical and molecular features for them.

Results: On large duct type, frequency of extrahepatic CCA (Klatskin and distal bile duct ca), periductal infiltrating type, history of cholangitis or IHD stone, and N1 stage were significantly high compared to small duct type. In addition, level of serum CEA and CA 19-9 were significantly high in large duct type. In small duct type, history of hepatitis was significantly frequent than large duct type. In both type, frequency of mass forming type was similar. Patients with large duct type showed significant poor disease-free and overall survival than those with small duct type. On multivariate analysis, large duct type, lymph node metastasis and vascular invasion were independent poor prognostic factors. On mutation analysis, KRAS, PIK3CA gene mutation was common in large duct type, whether IDH1/2 mutation and FGFR2 fusion were common in small duct type. On pathway analysis, inflammation related, AKT, Wnt and KRAS related signalling were enriched in large duct type, while metabolism and EMT related pathways were enriched in small duct type.

Conclusion: Two pathological subtypes of intrahepatic CCA with distinct clinical, biological and prognostic differences were identified. Therefore, molecular characteristic of CCA can be predicted based on pathological subtype, and it may lead to more rational targeted approaches to treatment.

FRI-310

Classification of microvascular invasion of hepatocellular carcinoma: correlation with prognosis and MR imaging

Dong Ho Lee¹, Haeryoung Kim², Yoon Jung Hwang³, Jae Seok Bae³.

¹Seoul National University Hospital, Radiology, Korea, Rep. of South;

²Seoul National University College of Medicine, Korea, Rep. of South;

³Seoul National University Hospital, Korea, Rep. of South

Email: dhlee.rad@gmail.com

Background and aims: This study aimed to evaluate the prognostic value of classification of microvascular invasion (MVI) in hepatocellular carcinoma (HCC) and to analyze the radiologic features predictive of MVI.

Method: Total 506 consecutive patients with surgically resected solitary HCCs were enrolled for this study. We retrospectively reviewed the histological and MR imaging features of MVI. Univariable and multivariable logistic regression analyses were performed to identify factor associated with the degree of MVI. Kaplan-Meier curves were calculated to assess prognostic impact of MR imaging features on overall survival (OS) and beyond-Milan recurrence-free survival (RFS).

Results: We identified MVI-positive HCCs with invasion of ≥ 5 vessels or those with ≥ 50 invaded tumor cells were significantly associated with decreased OS ($p < 0.001$ and 0.001 , respectively). Based on these findings, the number of invaded vessels and the number of invaded tumor cells were decided to be reliable risk factors, and we classified HCCs into three group; severe MVI (presence of all two risk factors; $n = 110$), mild MVI (presence of one or none of the risk factors; $n = 85$), and no MVI ($n = 311$). OS and beyond Milan RFS in severe MVI group were significantly poorer than that in mild or no MVI group ($p < 0.001$). On multivariate analysis, severe MVI was a significant independent predictive factor for OS and beyond Milan RFS. For MRI findings, non-smooth tumor margin (OR, 2.224; $p = 0.023$) and satellite nodule (OR, 3.264; $p < 0.001$) were independently associated with severe-MVI group in multivariate analysis. Both non-smooth tumor margin and satellite nodule were associated with worse 5-year OS rate and beyond-Milan RFS rate ($P_s \leq 0.039$).

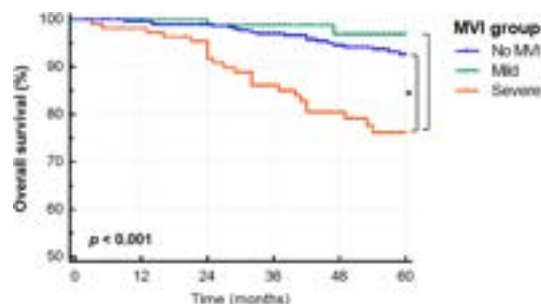


Figure: Overall survival of hepatocellular carcinoma patients, stratified by MVI classification.

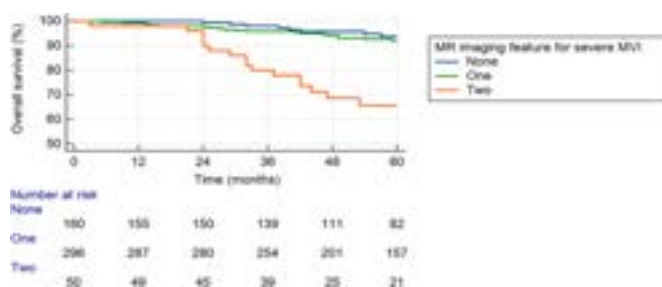


Figure: Overall survival of hepatocellular carcinoma patients, stratified by MR imaging feature for severe MVI.

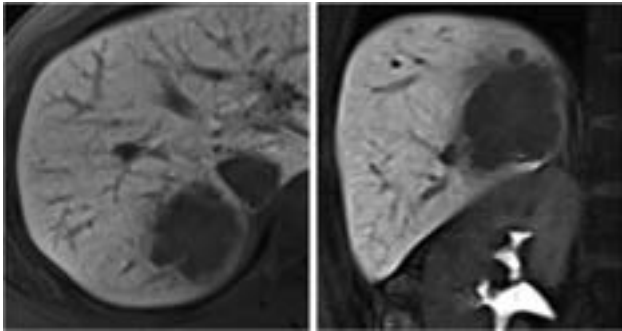


Figure: A representative example of gadoxetic acid-enhanced MRI obtained from a 47-year-old woman with hepatocellular carcinoma with severe-MVI. On the axial image of hepatobiliary phase, there is a tumor with a non-smooth margin (arrows) in segment 7 of the liver. On coronal image, there is a satellite nodule (arrowhead) at the superior aspect of the tumor. After surgical resection, severe MVI was identified by pathological examination. Twenty-five months after surgical resection, this patient experienced recurrence with inferior vena cava invasion, and died 42 months after resection.

Conclusion: Our study revealed the histologic risk classification of MVI according to the number of invaded microvessels and invading carcinoma cells is valuable for predicting prognosis in HCC patients. Non-smooth tumor margin and satellite nodules were significantly associated with both severe MVI and poor prognosis.

FRI-311

Liver function is a predictor of survival in patients with hepatocellular carcinoma in best supportive care

Claudia Campani¹, Laura Bucci², Martina Rosi¹, Valentina Adotti¹, Tancredi Li Cavoli¹, Umberto Arena¹, Franco Trevisani², Fabio Marra¹ and Ita.Li.Ca. Study Group². ¹University of Florence, Italy; ²University of Bologna, Italy
Email: fabio.marra@unifi.it

Background and aims: The prognosis of patients with hepatocellular carcinoma (HCC) is very variable, and the relative contribution of tumor burden and liver dysfunction to survival is uncertain. Median overall survival (OS) of patients managed with best supportive care is around 3–6 months, although longer values may be observed in clinical practice. Aim of this study was to identify the factors linked to tumor or liver dysfunction associated with survival in patients with HCC treated with BSC.

Method: We retrospectively evaluated the clinical characteristics of 1414 patients who had an indication for BSC recorded in the Ita.Li.Ca. database between 2000 and 2020. We analyzed both patient and tumor characteristics to identify predictors of OS.

Results: Median age was 69y and 76% of patients were male. Etiology included chronic viral infection (68.3%), alcohol use disorder (30.9%) and non-alcoholic steatohepatitis (8.3%). 67.4% of patients had a performance status 0–1 and 41.4% were in Child-Pugh B class. Median MELD was 13. 60% of patients had a multifocal HCC with a median number of 3 lesions and a median size of 33 mm. 533 patients had vascular invasion. Median alpha-fetoprotein was 49.25 ng/ml. 111 patients were classified as BCLC-A, 148 as BCLC-B, 791 as BCLC-C and 325 as BCLC-D (12 unknown). No differences in terms of OS were observed considering the etiology of liver disease or the presence of cirrhosis. Among comorbidities, obesity ($p < 0.001$), hypercholesterolemia ($p = 0.036$) and hypertriglyceridemia ($p = 0.034$) were associated with lower OS. Absence of symptoms (6 vs 10 months, $p < 0.001$), lack of vascular invasion (9.1 vs 5.03, $p < 0.001$), and absence of metastasis (8.167 vs 4.733 $p < 0.001$) were associated with a better OS. Median OS in BCLC-A (14.37 months) patients was longer than in stages B (9.20) or C (7.13). Survival progressively declined according to severity of liver function using three different scores (CPS, ALBI, pALBI, $p < 0.001$). Women tended to survive longer 23 vs. 19 months, $p = 0.053$). Comparing patients surviving more or less than 12 months

(398 vs. 1016), age, size of lesions, albumin, bilirubin, alpha-fetoprotein, and MELD were significantly different. At Cox univariate analysis presence of cirrhosis (HR: 1.201 CI 95%CI 0.998–1.445 $p = 0.052$), number of lesion (HR: 1.02 CI 95%CI 1.01–1.04 $p = 0.013$), median size (HR: 1.02 CI 95%CI 1.01–1.03 $p < 0.001$), vascular invasion (HR: 1.80 CI 95%CI 1.59–2.02 $p < 0.001$), metastasis (HR: 1.48 CI 95%CI 1.28–1.72 $p < 0.001$), ALBI grade (ALBI 2 HR: 1.25 CI 95%CI 1.04–1.50 $p = 0.015$ ALBI 3 HR: 1.75 CI 95%CI 1.43–2.14 $p < 0.001$), pALBI grade (pALBI 2 HR: 0.99 CI 95%CI 0.824–1.202 $p = 0.960$ pALBI 3 HR: 1.49 CI 95%CI 1.25–1.78 $p < 0.001$), MELD (HR: 1.04 CI 95%CI 1.04–1.05 $p < 0.001$) and CPS (HR: 1.13 CI 95%CI 1.10–1.165 $p < 0.001$) were significantly associated with OS. Using different models to avoid colinearity ALBI, pALBI, and CPS maintained an independent prognostic role on OS (ALBI HR 1.58 CI 1.26–1.98 $p < 0.001$, pALBI 1.22 CI 1.01–1.49 $p = 0.43$, CPS 1.12 CI 1.85–1.16 $p < 0.001$).

Conclusion: In a large series of patients with HCC in BSC, parameters of liver function are strongly associated with survival.

FRI-312

Similar recurrence after curative treatment of HBV-related HCC regardless of HBV replication activity

Mi Na Kim¹, Beom Kyung Kim², Heejin Cho³, Myungji Goh⁴, Su Jong Yu³, Dong Hyun Sinn⁴, Soo Young Park⁵, Seung Up Kim². ¹Yonsei University College of Medicine, Department of Internal Medicine, Seoul, Korea, Rep. of South; ²Yonsei University College of Medicine, Korea, Rep. of South; ³Seoul National University College of Medicine, Korea, Rep. of South; ⁴Sungkyunkwan University School of Medicine, Korea, Rep. of South; ⁵Kyungpook National University Hospital, Korea, Rep. of South
Email: kskorea@yuhs.ac

Background and aims: Antiviral therapy (AVT) is required for patients with newly diagnosed hepatitis B virus (HBV)-related hepatocellular carcinoma (HCC), if HBV DNA is detectable. We compared the risk of recurrence according to HBV replication activity at curative treatment of HBV-related HCC.

Method: Patients with HBV-related HCC who received surgical resection or radiofrequency ablation between 2013 and 2018 were enrolled in this retrospective cohort study. Patients were categorized into two groups according to HBV replication activity at curative treatment of HBV-related HCC (group 1: patients who met AVT indication for HBV-related HCC due to detectable HBV DNA, but did not meet AVT indication for HBV if without HCC; group 2: patients who met AVT indication for HBV regardless of HCC).

Results: In the entire cohort ($n = 911$), HCC recurred in 303 (33.3%) patients during a median follow-up of 4.7 years. After multivariate adjustment for the key covariates, group 2 showed a statistically similar risk of HCC recurrence (adjusted hazard ratio [aHR] = 1.18, 95% confidence interval [CI] = 0.85–1.64; $P = 0.332$) compared to group 1. In addition, group 2 showed statistically similar risks of early (<2 years) (aHR = 1.31, 95% CI = 0.88–1.95), and late (≥ 2 years) (aHR = 0.83, 95% CI = 0.45–1.55) recurrence compared to group 1. Propensity score matching and inverse probability of treatment weighting analysis also yielded similar risks of HCC recurrence between the two groups (all $P > 0.05$, log-rank tests).

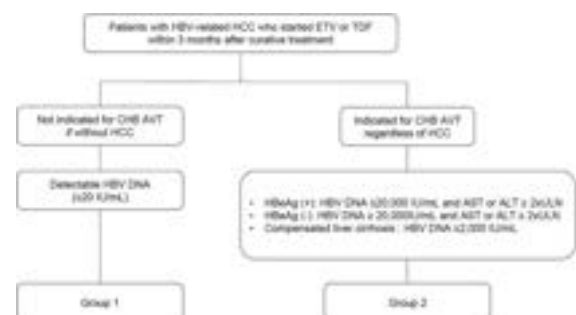


Figure: Definitions of groups according to HBV replication activity

Conclusion: The risk of HCC recurrence in patients who received curative treatment for newly diagnosed HBV-related HCC was comparable, regardless of HBV replication activity at curative treatment of HCC.

FRI-313

Loss of mucosal tolerance to glycoprotein 2 isoform 1 is a novel diagnostic biomarker for cholangiocarcinoma without underlying PSC

Chang-sheng Xia¹, Marcin Krawczyk^{2,3}, Chun Di¹, Łukasz Krupa⁴, Beata Kruk³, Wacław Hołósko⁵, Piotr Milkiewicz^{6,7}, Huizhang Bao¹, Xiao He¹, Daming Liu¹, Chunhong Fan¹, Abdullah Nasser⁸, Steffi Lopens^{8,9}, Peter Schierack^{9,10}, Dirk Roggenbuck^{8,9,10}, Yudong Liu¹¹. ¹Department of Clinical Laboratory, Peking University People's Hospital, Beijing, China; ²Department of Medicine II, Saarland University Medical Center, Homburg, Germany; ³Laboratory of Metabolic Liver Diseases, Medical University of Warsaw, Warsaw, Poland; ⁴Department of Gastroenterology and Hepatology with Internal Disease Unit, Medical Department, University of Rzeszów, Rzeszów, Poland; ⁵Department of General, Transplant and Liver Surgery, Medical University of Warsaw, Warsaw, Poland; ⁶Liver and Internal Medicine Unit, Medical University of Warsaw, Warsaw, Poland; ⁷Translational Medicine Group, Pomeranian Medical University, Szczecin, Poland; ⁸Medipan GmbH, R/D Department, Dahlewitz, Germany; ⁹Institute of Biotechnology, Faculty Environment and Natural Sciences, Brandenburg University of Technology Cottbus-Senftenberg, Senftenberg, Germany; ¹⁰Faculty of Health Sciences Brandenburg, Brandenburg University of Technology Cottbus-Senftenberg, Senftenberg, Germany; ¹¹The Key Laboratory of Geriatrics, Beijing Institute of Geriatrics, Beijing Hospital, Beijing, China
Email: marcin.krawczyk@uks.eu

Background and aims: Cholangiocarcinoma (CCA) is a very aggressive tumor with dismal prognosis. In our previous studies we showed that the anti-glycoprotein 2 (anti-GP2) IgA and antineutrophil-cytoplasmic antibodies to proteinase 3 (PR3-ANCA) are predictive for CCA development in patients with primary sclerosing cholangitis (PSC). Here we investigate these antibodies in two independent cohorts of patients with CCA without underlying PSC and in patients with other hepatobiliary tumors.

Method: The PR3-ANCA, IgA and IgG to large (anti-GP2₁) and short (anti-GP2₄) GP2 isoforms were measured in sera of prospectively collected patients with hepatobiliary-tumors and in controls. The discovery (118 Chinese patients) and validation (38 Polish patients) cohorts with CCA without PSC were compared with patients with pancreatic ductal adenocarcinoma (PDAC, n=49), patients with hepatocellular carcinoma (HCC, n=45), patients with benign pancreatic neoplasms (BPN, n=21). The control cohort consisted of 75 healthy individuals.

Results: Among testes antibodies, anti-GP2₁ IgA was the most prevalent one in the CCA cohorts (Chinese cohort: 65/118, 52.6%; Polish cohort: 17/38, 44.7%) and its levels were significantly elevated as compared to other cohorts included in the analysis, except the PDAC patients. The anti-GP2₄ IgA levels were, in turn, significantly higher in the individuals with CCA patients as compared to HC and

PDAC patients. Neither of the IgA autoantibody correlated with the CCA differentiation or CA19-9 in serum. Among analyzed autoantibodies, the anti-GP2₁ IgA demonstrated the best diagnostic performance for the differentiation of CCA from disease controls and HC (AUC = 0.82, 95% CI 0.77–0.86, p < 0.01). Logistic regression including GGT, patients age and anti-GP2 IgG₄ as confounders showed that anti-GP2₁ IgA was an independent predictor of CCA occurrence.

Conclusion: Analysis of patients with hepatobiliary tumors demonstrated that the anti-GP2₁ IgA is prevalent in patients with cholangiocarcinoma. Mucosal loss of tolerance in the form of anti-GP2₁ IgA distinguishes patients with CCA from ones with hepatocellular carcinoma and benign pancreatic neoplasms.

FRI-314

Baseline cirrhosis in addition to the aMAP score, increased the risk of developing hepatocellular carcinoma in patients with hepatitis B

Supakorn Chaiwiriawong¹, Pimsiri Sripongpun¹, Naichaya Chamroonkul¹, Apichat Kaewdech¹. ¹Prince of Songkla University, Thailand
Email: apichatka@hotmail.com

Background and aims: Hepatocellular carcinoma (HCC) is a major global problem impacting patients' survival with liver diseases. With a few external validation studies, the aMAP score (age, male sex, and ALBI score) was recently developed to predict the risk of HCC development. We aim to externally validate this score in patients with chronic hepatitis B (CHB) infection as well as study the additional predictive factor for HCC development.

Method: We identified all CHB patients who were followed up between January 2007 and December 2021 at our hospital. Patients with CHB infection who were over the age of 18 were eligible. The exclusion criteria were being diagnosed with HCC within 6 months of the baseline visit, coinfection with another viral infection, or other causes of chronic liver disease. Baseline data from the initial diagnosis was retrieved and tracked until the occurrence of HCC.

Results: There were 866 eligible patients among the 902 CHB patients who were followed up on, with a median follow-up time of 7.7 years. Ninety-two (10.62%) patients developed HCC. HCC patients had significantly higher age, male sex, HBeAg-negative status, cirrhosis, total bilirubin, aspartate aminotransferase (AST), and alanine aminotransferase (ALT) levels than non-HCC patients. Serum albumin and platelet count were lower in HCC patients than in non-HCC patients. Multivariate analysis showed that the presence of cirrhosis at baseline [aHR 14.9 (5.62, 39.49), p < 0.001] and a high aMAP score at baseline [aHR 2.94 (1.38, 6.26), p = 0.005] were associated with HCC development. The cumulative incidence of HCC in patients with cirrhosis and a high aMAP score is higher than in patients with medium or low aMAP score and non-cirrhotic patients, as shown in the figure.

Conclusion: Cirrhosis status at the initial diagnosis of CLD is the strongest predictive factor for HCC development. Patients with cirrhosis and high aMAP were at the highest risk of developing HCC in the future. This group of patients should undergo intensive surveillance.

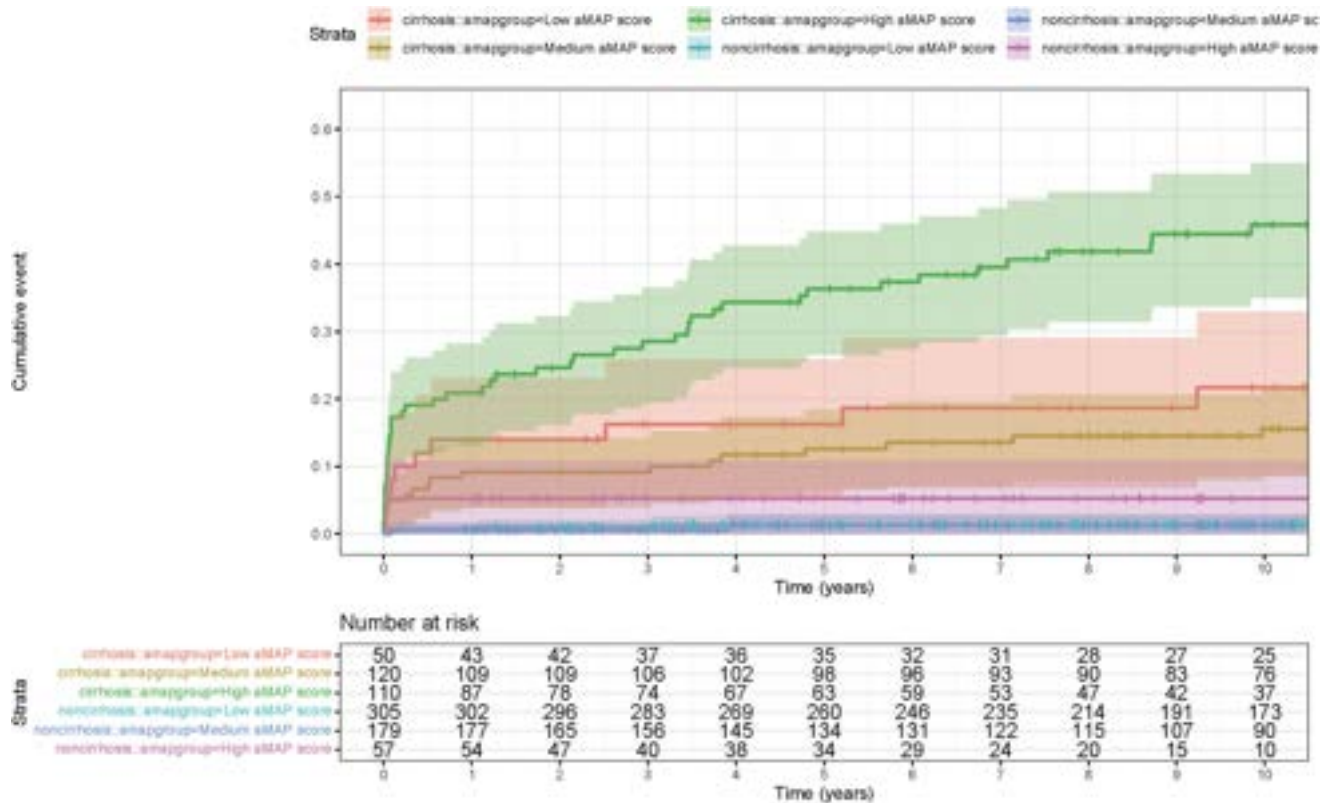


Figure: (abstract: FRI-314): Cumulative probability of development of HCC according to the combination of cirrhosis and aMAP score among CHB patients.

FRI-315

Comparative study of scoring systems predicting outcome of transarterial chemoembolization for hepatocellular carcinoma: a nationwide cohort study

Myeong Jun Song¹, Hae Lim Lee¹, Seok-Hwan Kim¹. ¹*the Catholic university of Korea, Korea, Rep. of South*
Email: mjsong95@catholic.ac.kr

Background and aims: Several scoring systems have been proposed to predict the outcome of transarterial chemoembolization (TACE) in patients with hepatocellular carcinoma (HCC). However, the application of the albumin-bilirubin (ALBI) grades to TACE candidates is poorly validated. Evaluation of the applicability of prognostic factors for patients performing TACE is necessary. We aimed to develop new scoring system including ALBI grade.

Method: 3,069 patients with unresectable HCC, child class A/B and ECOG 0-1 performing TACE were included from national cohort of the Korean Central Cancer Registry between 2008 and 2017. Patients were randomly divided into training (n = 1,507) and validation cohort (n = 1,562). A prognostic model was developed and validated. We compared with previous scoring models.

Results: In entire cohort, the patient's mean age was 62 years. The patients were hepatitis B virus (57.1%) and child class A (83.2%). The prognostic model of TACE was "largest tumor diameter+ tumor number, AFP, and ALBI grade," which consistently outperformed other currently available models in both training and validation datasets. Patients were assigned points according to sum of tumor burden (≤ 5 , 5-10, ≥ 10), AFP or ALBI grade. Patients were divided into four risk groups based on their TACE-prognostic (TP) scores: A, B, C and D. The median survival for the groups A, B, C and D was 80.1, 53, 35.2 and 19.4 months, respectively.

Conclusion: This new TP scoring system may prove a favorable tool to stratify ideal candidates of TACE and predict OS with favorable performance and discrimination. Further external validation is needed.

FRI-316

Liver Frailty Index is associated with progression-free survival in patients with advanced HCC treated with Atezolizumab/Bevacizumab

Philippe Sultanik¹, Edouard Larrey¹, Manon Evain¹, Bertille Campion¹, Amandine Ait Oufella¹, Héloïse Giudicelli¹, Mathilde Wagner², Dominique Thabut¹, Manon Allaire¹. ¹*Hôpital Pitié-Salpêtrière, Liver Unit, Paris, France;* ²*Hôpital Pitié-Salpêtrière, Radiology Department, Paris, France*
Email: philippe.sultanik@aphp.fr

Background and aims: Prognostic factors of response to immunotherapy (IT) for advanced hepatocellular carcinoma (HCC) are not all established. Sarcopenia is associated with poor prognosis in patients (pts) under tyrosine kinase inhibitors, but its impacts on pts treated with IT is not known. The Liver Frailty Index (LFI) is a simple bedside tool for sarcopenia evaluation and is closely related to morbidity-mortality in cirrhotic pts awaiting for liver transplantation. Our objective was to investigate whether LFI was associated with progression-free survival (PFS) and overall (OS) in advanced HCC pts treated with Atezolizumab/Bevacizumab (Atezo-Beva).

Method: From all pts treated with Atezo-Beva in our center, we performed a prospective study with baseline LFI measurement from January 2022. Baseline sarcopenia was asserted using BMI, albumin (ALB) and LFI (as continuous [LFI_c] and categorical [LFI_{gr}] variable-defined as frail [LFI > 4.5] or no-frail [LFI < 4.5] pts). Progression was defined as a composite (progression and/or side effects/hepatic decompensation requiring discontinuation). OS and PFS were assessed using Kaplan Meier. The influence of baseline characteristics on events during follow-up was assessed by Cox model.

Results: 23 pts treated with Atezo-Beva had a baseline LFI measurement from January to August 2022, 74% men, median age at 68 years. 17 (77%) pts had cirrhosis (heavy drinking 62%, NASH 43%, HCV 33%, HBV 10%, mixed causes 48%). At inclusion, Child-Pugh class was A for 45%, B for 45% and C for 10%, with a median MELD score at

POSTER PRESENTATIONS

11_[8-15]. On the day of treatment, HCC characteristics were a median size of CHC at 60_[40-76] mm for the largest lesion, infiltrative for 19% and vascular invasion for 38% pts. Pts' characteristics were: BMI 25.7_[23.9-28.2] kg/m², bilirubin 17_[10-33] μM, INR 1.25_[1.13-1.41], ALB 31_[26-36] g/l, creatinine 74_[66-87] μM, platelets 133_[91-202] G/mm³, AFP 126_[11-2525] ng/ml, ALBI score : 1 in 14%-2 in 48%-3 in 38%, LFI_c 4.25_[3.99-4.68]. Overall, 10 (43%) pts displayed frailty (LFI_{gr} frail). The median follow-up was 5.3_[1.9-6.8] months. Median PFS was 5.9 months, and 11 (48%) pts were alive without progression. In Cox univariate analysis, platelets ($p = 0.01$), AFP ($p = 0.03$), LFI_c ($p = 0.01$) and being LFI_{gr} frail ($p = 0.02$) were associated with PFS. Overall, 9 (69%) no-frail and 2 (20%) frail pts (median PFS at 4.2 months) were alive without progression, log-rank = 0.01 (Figure). AUROC of LFI_c for PFS was 0.77. Only LFI_c (aHR 4.49, $p = 0.01$) and LFI_{gr} frail (aHR 4.66, $p = 0.03$) were associated with PFS in multivariate analysis. Overall, 9 (39%) pts died, 10 (77%) no-frail pts and 4 (40%) frail pts (median PFS at 5.6 months) were alive, log-rank = 0.09. In multivariate analysis, platelets (aHR 1.01, $p = 0.04$) and ALB (aHR 0.79, $p = 0.03$) associated with OS but not LFI.

Liver Frailty Index & Progression-free Survival

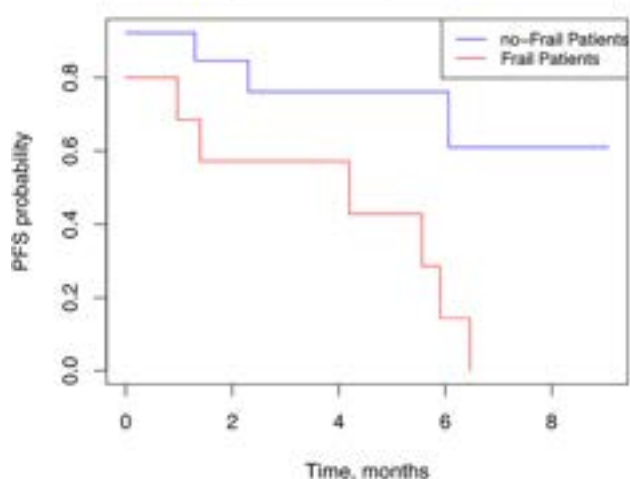


Figure:

Conclusion: The Liver Frailty Index is an easy tool for sarcopenia assessment which is associated with PFS in patients with advanced HCC treated with Atezo-Beva. Sarcopenia screening and treatment including nutritional and physical strengthening should be performed for all patients.

FRI-317

Characterization of the imaging signature of hepatocellular carcinoma with enhancement pattern mapping

Newsha Nikzad¹, David Fuentes², Millicent Roach², Tasadduk Chowdhury², Matthew Cagley², Mohamed Badawy², Manal Hassan², Khaled Elsayes², Laura Beretta², Eugene Koay², Prasun Jalal¹. ¹Baylor College of Medicine, Houston, United States; ²MD Anderson Cancer Center, Houston, United States
Email: newshanikzad@gmail.com

Background and aims: Limited methods exist to accurately characterize risk of malignant progression of liver lesions in patients undergoing surveillance for hepatocellular carcinoma (HCC). Enhancement pattern mapping (EPM) measures voxel-based root mean square deviation (RMSD) and improves the contrast to noise ratio (CNR) of liver lesions on standard of care imaging. This study investigates the utilization of EPM to differentiate between malignant versus non-malignant lesions.

Method: Patients with liver cirrhosis undergoing MRI surveillance were studied retrospectively. Controls ($n = 99$) were patients without lesions during surveillance. Cases ($n = 48$) were defined as patients with LI-RADS 3 and 4 lesions who developed HCC within the study

period. RMSD measured with EPM was compared to the signal from MRI arterial and portovenous phases. EPM signals of liver parenchyma between cases and controls were compared.

Results: With EPM, RMSD of 0.37 was identified as a quantitative cutoff for distinguishing HCC from background cirrhotic parenchyma on pre-diagnostic scans with an AUC of 0.83 (CI: 0.73–0.94). EPM RMSD signals of background parenchyma in cases and controls were similar (case EPM: 0.22 ± 0.08 , control EPM: 0.22 ± 0.09 , $p = 0.8$).

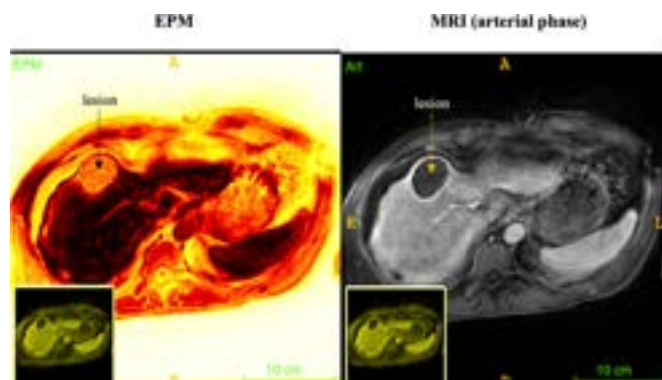


Figure:

Conclusion: EPM differentiates between HCC and non-cancerous parenchyma in a surveillance population. Future directions may involve applying EPM for early detection of HCC and risk stratification of indeterminate lesions.

FRI-318

Initial treatment response and short-term mortality of spontaneous bacterial peritonitis in cirrhotic patients with hepatocellular carcinoma

Chang Hun Lee¹, Hye Jin Kang¹, Seung Young Seo¹, Seong-Hun Kim¹, Sang Wook Kim¹, Seung Ok Lee¹, Soo Teik Lee¹, In Hee Kim¹. ¹Research Institute of Clinical Medicine of Jeonbuk National University-Biomedical Research Institute of Jeonbuk National University Hospital, Internal Medicine, Jeonju, Korea, Rep. of South
Email: ihkimmd@jbnu.ac.kr

Background and aims: This study aimed to investigate the initial treatment response and short-term mortality of spontaneous bacterial peritonitis (SBP) in cirrhotic patients with hepatocellular carcinoma (HCC) compared with those without HCC.

Method: A total of 245 patients with liver cirrhosis diagnosed with SBP between January 2004 and December 2020 were included. Of these, 107 (43.7%) were diagnosed with HCC.

Results: Overall, the rates of initial treatment failure, 7-day and 30-day mortality were 91 (37.1%), 42 (17.1%), and 89 (36.3%), respectively. While the baseline CTP score, MELD score, culture-positive rate, and rates of antibiotic resistance did not differ between both groups, patients with HCC had a higher rate of initial treatment failure than those without HCC patients (52.3% vs. 25.4%, $p < 0.001$). Similarly, 30-day mortality was also significantly higher in patients with HCC (53.3% vs. 23.2%, $p < 0.001$). In the multivariate analysis, HCC, renal impairment, CTP grade C, and antibiotic resistance were independent factors for initial treatment failure. Furthermore, HCC, hepatic encephalopathy, MELD score, and initial treatment failure were independent risk factors for 30-day mortality, with statistically significant poor survival outcomes in patients with HCC and initial treatment failure ($p < 0.001$ and $p < 0.001$, respectively).

Conclusion: HCC is an independent risk factor for initial treatment failure and high short-term mortality in patients with cirrhosis with SBP. It has been suggested that more attentive therapeutic strategies are required to improve the prognosis of patients with HCC and SBP.

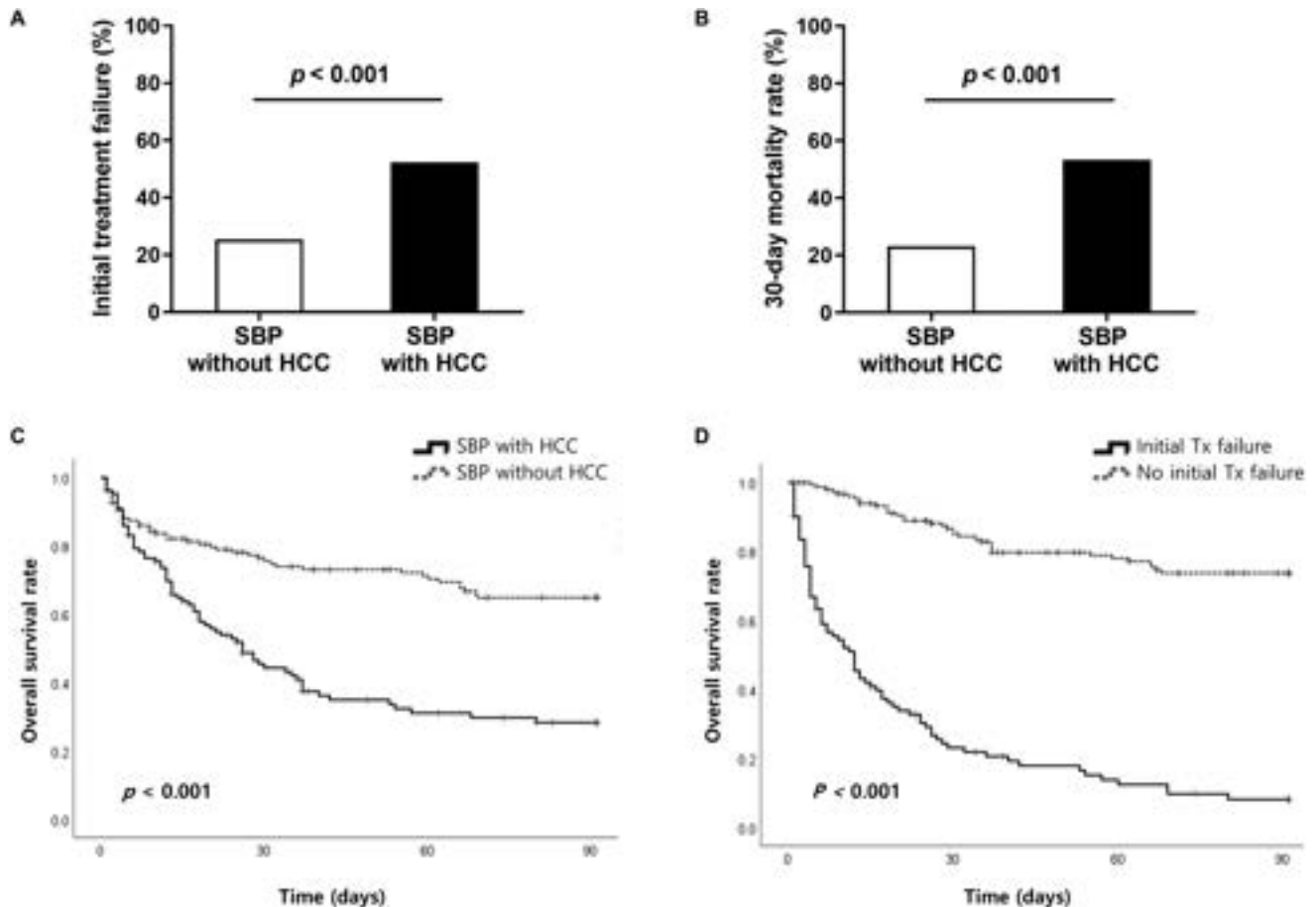


Figure: (abstract: FRI-318).

FRI-319 **Effect of different radiologic modalities for surveillance of hepatocellular carcinoma on survival of high risk cirrhotic patients**

Ahmed El Sabagh¹, Islam Mohamed^{1,2}, Megha Bhongade¹, Nikita Rao¹, Eunji Jo³, Susan Hilsenbeck³, Prasun Jalal¹. ¹Baylor College of Medicine, Houston, United States; ²Ain Shams University, Medicine, Cairo, Egypt; ³Dan L Duncan Comprehensive Cancer Center at Baylor St. Luke's Medical Center, Houston, United States
 Email: ahmed.elsabagh@bcm.edu

Background and aims: European association for the study of the liver (EASL) recommends that patients with high risk of developing hepatocellular carcinoma (HCC) undergo regular surveillance with ultrasonography (US) every 6 months. However, compared to cross-sectional imaging modalities -Computed tomography (CT) and Magnetic resonance imaging (MRI)-US has lower efficacy for detection of early HCC. To our knowledge, there are no studies evaluating the overall survival and receipt of curative treatment for patients who received surveillance using the different imaging modalities.

Method: We retrospectively reviewed all patients who were diagnosed with HCC at Baylor Saint Luke's Medical Center Hospital between January 2011 and June 2021. Patients who underwent regular surveillance were identified. Data retrieved from electronic medical records and radiology reports included demographic and laboratory features, surveillance modality, tumour characteristics, treatments received and survival data. We estimated survival using the Kaplan-Meier method and compared the different modalities

using the Log Rank test. We used univariate and multivariate Cox model to evaluate factors affecting survival.

Results: A total of 183 patients developed HCC while on biannual surveillance program (115 with MRI, 34 with CT and 34 with US). Patients were similar regarding with respect to age, sex, comorbid diseases. However, our cohort showed statistically significant differences regarding race and ethnicity, with more African American and Hispanic population undergoing surveillance with US. The initial survival analysis showed that compared to other modalities MRI had statistically significant association with longer survival (p value = 0.034). However, cox-multivariate regression model with adjustment for race, ethnicity, MELD score and total tumor size at time of diagnosis shows that surveillance modality has no statistically significant association with survival (MRI: HR 1.80, p value = 0.095) (CT: HR 0.71, p value = 0.26).

Conclusion: For cirrhotic patients with high risk for HCC, surveillance with MRI or CT was not associated with higher survival rate compared. This result shed the light on importance of adherence to surveillance irrespective of modality. Additionally, racial and ethnic disparities may affect the access to the HCC surveillance.

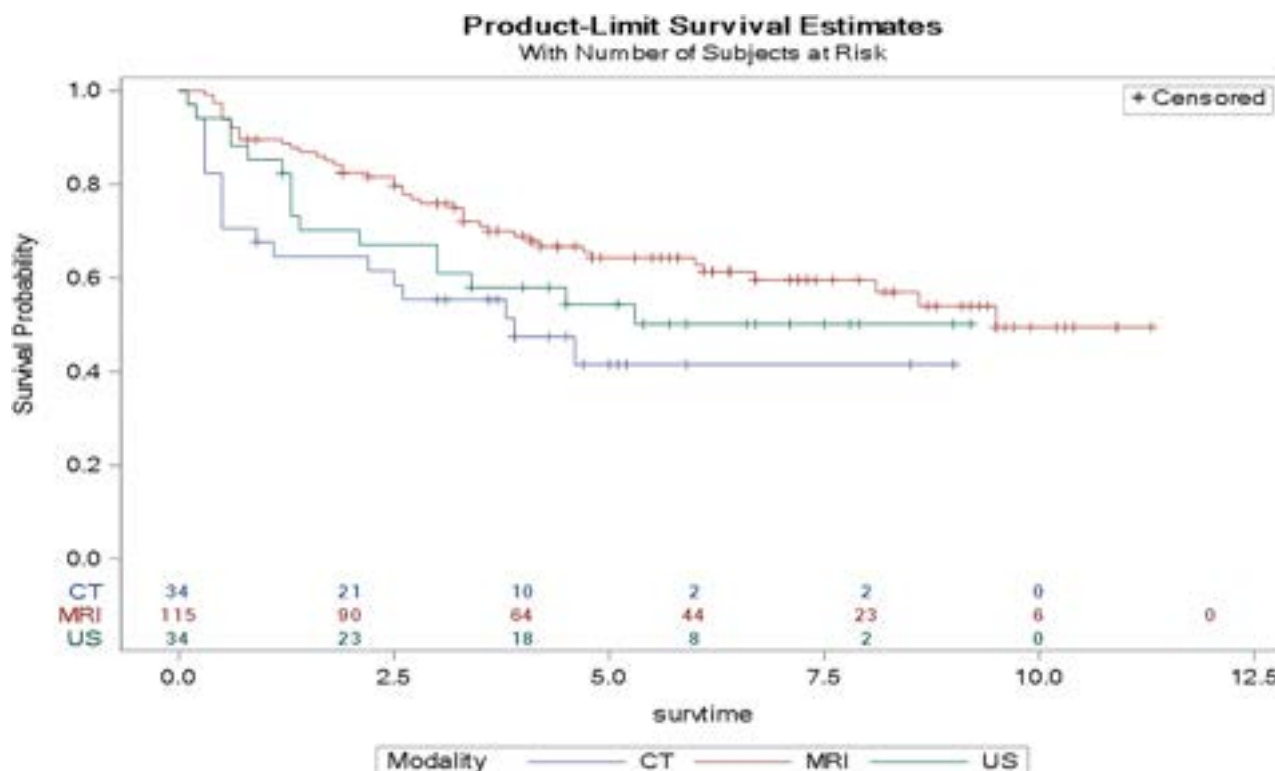


Figure: (abstract: FRI-319).

FRI-320

Comparison of clinical manifestations and outcomes between non-viral-related and viral hepatitis-related hepatocellular carcinoma

Sih-Han Liao¹, Shang-Chin Huang², Tung-Hung Su³, Shih-Jer Hsu³, Jia-Horng Kao³, ¹National Taiwan University Cancer Center, Taipei, Taiwan; ²National Taiwan University Hospital Bei-Hu Branch, Taipei, Taiwan; ³National Taiwan University Hospital, Taipei, Taiwan
Email: winterreise0810@gmail.com

Background and aims: After the provision of hepatitis B vaccination and antiviral therapy, the incidence and mortality of viral-related HCC, including hepatitis B (HBV) or C (HCV) virus, have improved. In contrast, the disease burden of non-viral HCC increased. Here we investigated the differences of clinical manifestations and outcomes between non-viral HCC and viral-related HCC.

Method: From 1996 to 2016, a total of 2,781 patients with complete information were identified from the Cancer Registry Database and Integrated Medical Database of National Taiwan University Hospital. Based on the information of viral hepatitis profiles, the patients were categorized into five groups as follows: group 1, non-viral HCC (triple negative for HBsAg, anti-HCV, and anti-HBc); group 2, occult HBV-HCC (only positive for anti-HBc); group 3, HBV-HCC (positive for HBsAg and negative for anti-HCV); group 4, HCV-HCC (positive for anti-HCV and negative for HBsAg); group 5, dual infection-HCC (both positive for HBsAg and anti-HCV). Overall survivals were examined using Kaplan-Meier method. Prognostic factors were explored using Cox proportional hazards regression model.

Results: The proportions of women were more in the group of non-viral HCC (48.0%) and HCV-HCC (45.3%) than other three groups ($p < 0.0001$). The median age at diagnosis were older in the non-viral HCC group than the groups of viral-related HCC ($p < 0.0001$). The maximal tumor size was larger in the non-viral HCC group ($p < 0.0001$). The baseline AFP level of the non-viral HCC group was significantly lower than the groups of viral-related HCC ($p = 0.01$). The estimated 1-, 3-, and 5-year overall survival rates were 42.5%, 20.5%, and 8.2% for non-

viral HCC group; 20.9%, 24.9%, and 8.7% for occult HBV-HCC group; 55.9%, 28.1%, and 13.3% for HBV-HCC group; 63.1%, 31.5%, and 13.0% for HCV-HCC group; 63.4%, 33.0%, and 16.1% for dual infection-HCC group. The BCLC stage could be used to predict the prognosis for HCC with various etiologies, including non-viral and viral-related HCC (all log-rank $p < 0.0001$). In the multivariable analysis of overall survival for all patients, four independent prognostic predictors were identified, including HCV-HCC group, advanced BCLC stage, larger tumor size, and higher FIB-4 score.

Variable	HR	95% CI	p value
Sex (Men vs. Women)	1.20	0.93-1.56	0.16
Age (per year increase)			
BMI (others vs. normal)			
Underweight (BMI<18.5 kg/m ²)	1.03	0.61-1.73	0.93
Overweight (BMI≥24 kg/m ²)	0.98	0.80-1.21	0.85
Alcohol consumption (others vs. no abuse)			
Quit	0.91	0.69-1.20	0.49
Abuser	0.91	0.64-1.28	0.57
Group (others vs. group 1, n = 73)			
Group 2 (n = 481)	0.58	0.32-1.05	0.07
Group 3 (n = 1400)	0.72	0.41-1.28	0.27
Group 4 (n = 715)	0.48	0.26-0.88	0.02
Group 5 (n = 112)	0.64	0.30-1.41	0.27
BCLC stage (others vs. stage 0+A)			
Stage B	2.25	1.63-3.10	<.0001
Stage C	9.10	6.47-12.71	<.0001
Stage D	15.33	9.90-23.73	<.0001
Tumor size (per 1 cm increase)	1.06	1.04-1.08	<.0001
Fibrosis-4 score (per 1 increase)	1.07	1.05-1.09	<.0001

Figure: Multivariable Cox proportional hazards regression model for overall survival

Conclusion: The patients of the non-viral HCC were older and more women. The baseline AFP level of the patients with non-viral HCC was lower. Additionally, the overall survival of the patients with non-viral HCC was significantly worse than that of the patients with HCV-HCC, but was similar as that of the patients with other etiologies.

FRI-321

Impact of obesity on outcome of hepatocellular carcinoma in an Asian cohort: when should we consider obesity treatment?

Wei-Lun Liou^{1,2}, Kaina Chen¹, Ravishankar Asokkumar¹, Chee-Kiat Tan¹. ¹Singapore General Hospital, Singapore; ²Singapore General Hospital, Gastroenterology and Hepatology, Singapore
Email: liouweilun@gmail.com

Background and aims: Obesity is associated with increased risk of hepatocellular carcinoma (HCC) development. There is however conflicting data on impact of obesity on HCC outcome and prognosis. We studied the influence of obesity on clinical characteristics of HCC and on survival in a cohort of Asians.

Method: The study cohort comprised of patients with HCC seen in our centre from 2005 to 2020. We studied and compared HCC characteristics and survival between the non-obese group (body mass index: BMI <27.5) and the obese group (BMI >27.5). Survival analysis was censored on 28 November 2022.

Results: There were 271 HCC patients in this study, 202 (74.8%) were male. 73 (27%) patients were obese. Median age of the patients was 65 (IQR 14). Non-alcoholic steatohepatitis (NASH) or cryptogenic cirrhosis was more common in the obese group (47.9% vs 32.8%, $p = 0.02$). Tumours median diameter was significantly larger in the non-obese group (25 mm vs 21 mm, $p = 0.045$). There was no statistically significant difference in Barcelona Clinic Liver Cancer (BCLC) staging: BCLC 0/A, 130 patients (65.7%) in non-obese group vs 49 patients (67.1%) in obese group, $p = 0.83$. HCC treatment modality was similar between the two groups (curative 61.1% vs 64.4%, non-curative 20.2% vs 21.9%, palliative 18.7% vs 13.7%, $p = 0.55$). For the cohort of patient receiving curative treatment, there was no significant difference in HCC recurrence rate between the two groups (65.3% vs 74.5%, $p = 0.28$). 1, 5, 10-year survival were similar between the two groups (non-obese group 75%, 43%, 23% vs obese group 82%, 51%, 23%, $p = 0.59$). Multivariable analysis confirmed that patient's BMI had no influence on overall survival (Hazard ratio 1.09, 95% C.I. 0.78–1.51). Patients with underlying NASH or cryptogenic cirrhosis had worse survival outcome than patients with HCC of other aetiologies (1, 5, 10-year survival of 73%, 32%, 9% vs 80%, 52%, 30%, $p < 0.001$). HCC secondary to NASH or cryptogenic cirrhosis was also a predictor for poorer survival (hazard ratio 1.76, 95% C.I. 1.31–2.37).

	1 Year (%)	5 Years (%)	10 Years (%)	p value
Overall	77	45	23	-
BMI				
<27.5	75	43	23	0.59
>27.5	82	51	23	
Aetiology				
NASH/Cryptogenic	73	32	9	<0.001
Others	80	52	30	
Resection				
BMI <27.5	96	68	56	0.91
BMI >27.5	100	89	48	
Ablation				
BMI <27.5	92	57	21	0.59
BMI >27.5	93	62	20	

Figure: Comparison of 1, 5, 10-year survival of patients with hepatocellular carcinoma.

Conclusion: In this cohort of Asian patients with HCC of all etiologies, obesity does not affect the outcome of HCC nor patients' survival. Patients with NASH or cryptogenic cirrhosis had poorer outcome than patients with HCC of other aetiology. Early preventive measures and therapeutic interventions to treat obesity remain vital to prevent development of non-alcoholic fatty liver disease which carries poorer HCC outcome.

FRI-322

Collagen proportionate area (CPA) measurement of liver parenchyma and hepatocellular carcinoma (HCC) can predict HCC recurrence after liver resection

Federico Ravaioli^{1,2}, Mattia Riefolo², Chiara Sicuro¹, Benedetta Rossini², Elton Dajti², Matteo Serenari², Matteo Cescon², Maria Antonietta D'Errico², Antonio Colecchia¹, Francesco Vasuri². ¹Gastroenterology Unit, Department of Medical Specialties, University Hospital of Modena, University of Modena and Reggio Emilia, Modena, Italy; ²IRCCS Azienda Ospedaliero-Universitaria di Bologna, Bologna, Italy, Department of Medical and Surgical Sciences (DIMEC), University of Bologna, Bologna, Italy
Email: f.ravaioli@unibo.it

Background and aims: Hepatocellular carcinoma (HCC) is a frequent complication in patients with advanced chronic liver disease (ACLD) with an HCC recurrence (HCC-r) rate of around 70% after liver resection (LR) at five years. Previous studies have found several predictive variables for HCC-r mainly related to the primary tumour characteristics (such as degree of histological differentiation and extent of vascular invasion, satellite nodules, size and the number of nodules) or related to the stage of liver disease and the degree of portal hypertension (as Metavir score, liver (LSM) and spleen stiffness (SSM) measurements). Collagen proportionate area (CPA) measurement is a quantitative automated method for estimating fibrous tissue in liver biopsies by determining the collagen deposition percentage of the total biopsy area. Recently it has been proposed as a reliable tool to predict hepatic decompensation and mortality in patients with ACLD. Thus, we aimed to evaluate the predictive role of CPA in HCC-r after curative LR.

Method: From a cohort of 175 patients with primary HCC eligible for LR prospectively enrolled and followed for at least 30 months or until HCC-r, we analysed the biopsy specimen sampled obtained during LR surgery of 54 patients with a 3:2 ratio of HCC-r. For each patient, ten images of liver sections stained with Sirius red for collagen fibres were acquired from the non-neoplastic liver parenchyma adjacent to the tumour (liver-CPA; Fig. 1A) and HCC tissue (HCC-CPA; Fig. 1B) with an AxioCam 305 colours mounted on a Zeiss AxioScope AX10 microscope, attached to a close-up copy stand with flicker-free backlight. Liver biopsy specimens were reviewed centrally by an expert pathologist. CPA was measured by free public-domain software developed by the National Institutes of Health (NIH-ImageJ). For analyses, the median CPA values were evaluated. Logistic regression analyses were performed to evaluate the prediction of HCC-r.

Results: 35 out of 54 (65%) patients developed HCC-r, 25 (46.3%) patients developed an early (≤ 24 months) HCC-r, and 10 (18.5%) patients developed late (> 24 months) HCC-r. Patients were mainly males (88.9%), with a median age at HCC diagnosis of 73 [68–85] years; the prevalent etiology was viral (81.5%). 47 (87%) median MELD score was 8 (7–9). 98.15% was Child-Pugh A with median alpha-fetoprotein values of 6 (3–38) ng/ml. Liver and HCC-CPA were significantly higher in patients with HCC-r than those without HCC-r (Fig. 1). Liver-CPA significantly correlates with LSM ($R = 0.703$; $p = 0.05$). Among all variables evaluated, HCC-r was significantly predicted by liver-CPA (OR 2.672 [95%CI 1.142–6.255] $p = 0.002$) and HCC-CPA (OR 1.0002 [95%CI 1.000–1.0004]; $p = 0.021$), number of HCC nodules (OR 2.489 [95%CI 1.876–7.071]; $p = 0.054$), microvascular invasion (OR 3.611 [95%CI 1.088–11.039]; $p = 0.036$), and macrovascular invasion (OR 8.609 [95%CI 1.014–73.024]; $p = 0.048$).

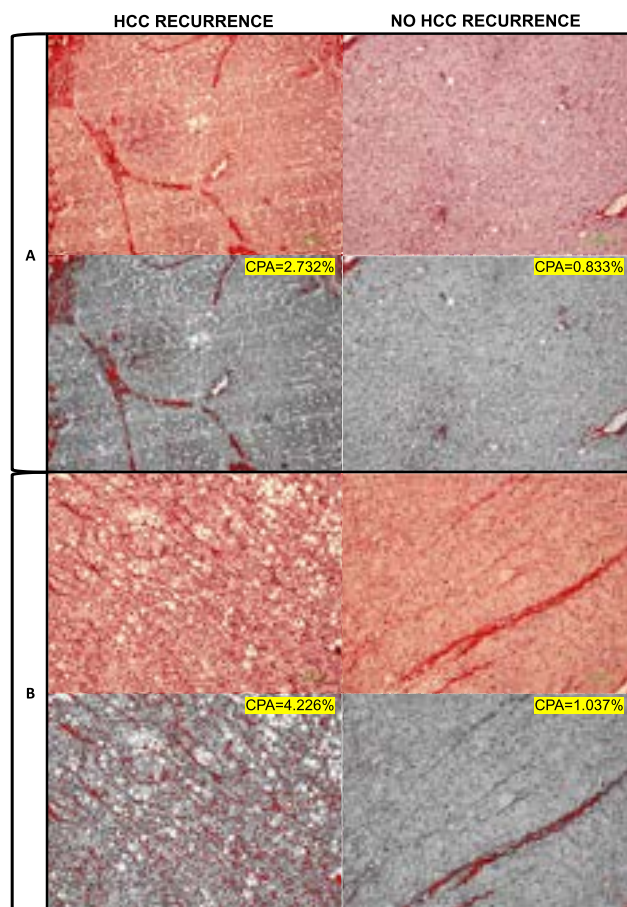


Figure:

Conclusion: CPA is a good quantitative and automated method for estimating fibrosis tissue, and together with already known predictive factors (such as histological differentiation and extent of invasion, satellite nodules, size and the number of nodules, Metavir score, LSM and SSM) can predict the recurrence of HCC after liver resection. Further studies should confirm our results to recommend adding CPA to the standard pathological analysis of liver resected HCC patients.

FRI-323

Exploration of a holistic management procedure for liver cancer surveillance to improve the early diagnosis of liver cancer in Chinese population

Yong Li¹, Ligong Lu¹, Qing Yang¹, Manhua Zhong¹, Xiaofeng Wang¹, Linfang Li¹, Yanhong Chen¹, Xiaolei Zhou¹, Chao Yang¹, Jie Dong¹.

¹Zhuhai people's hospital (zhuhai hospital affiliated with jinan university), Zhuhai, China

Email: lu_ligong@163.com

Background and aims: China accounts for nearly half of all new hepatocellular carcinoma (HCC) cases and death worldwide each year, and over 80% of them suffer from chronic hepatitis B (CHB). In China, up to 80% of the HCC cases are diagnosed at an advanced stage, lost the chance of radical treatment. The 5-year survival rate is only 12.1%. Therefore, it is urgent to enhance HCC screening in China and improve the level of early diagnosis. Accordingly, here we aim to develop a stratified management procedure of HCC screening and surveillance for CHB patients at Zhuhai People Hospital.

Method: CHB patients, without previous HCC diagnosis, visiting the Department of Hepatology and Infectious Disease were recommended for enrollment by the attending physician since Jan 2022. We have established a digital platform and procedure that can collect and synthesize all-round information of enrolled patients, including comprehensive medical history, as well as laboratory and imaging examination results. Dashboards were generated for dedicated liver disease management. Each enrolled patient first took an initial HCC screening (step 2 in the figure), including abdominal ultrasound, and serum tests for AFP and PIVKA-II. Patients with abnormal results will follow standard HCC diagnostic work-up, while other patients who are not currently suspected of HCC will be classified into different risk groups (step 3 in the figure) according to local guidelines, in-house standards (Zhuhai model), and published risk stratification models (such as aMAP). These patients were thereafter matched with a risk-dependent follow-up plan for HCC surveillance. The early diagnosis rate of HCC defined as stage Ia, Ib, and IIa according to the Chinese National Liver Cancer (CNLC) standards, was evaluated and compared to the historical baseline as 30% using one-side binomial test.

Results: 2071 patients were enrolled in 2022. So far, 8 patients have been diagnosed with HCC during either initial screening or surveillance follow-up, of which 7 (87.5%) were at an early stage (CNLC Stage Ia), showing a significant increase as compared to baseline (p value = 0.001). A total of 2030 CHB patients were risk-

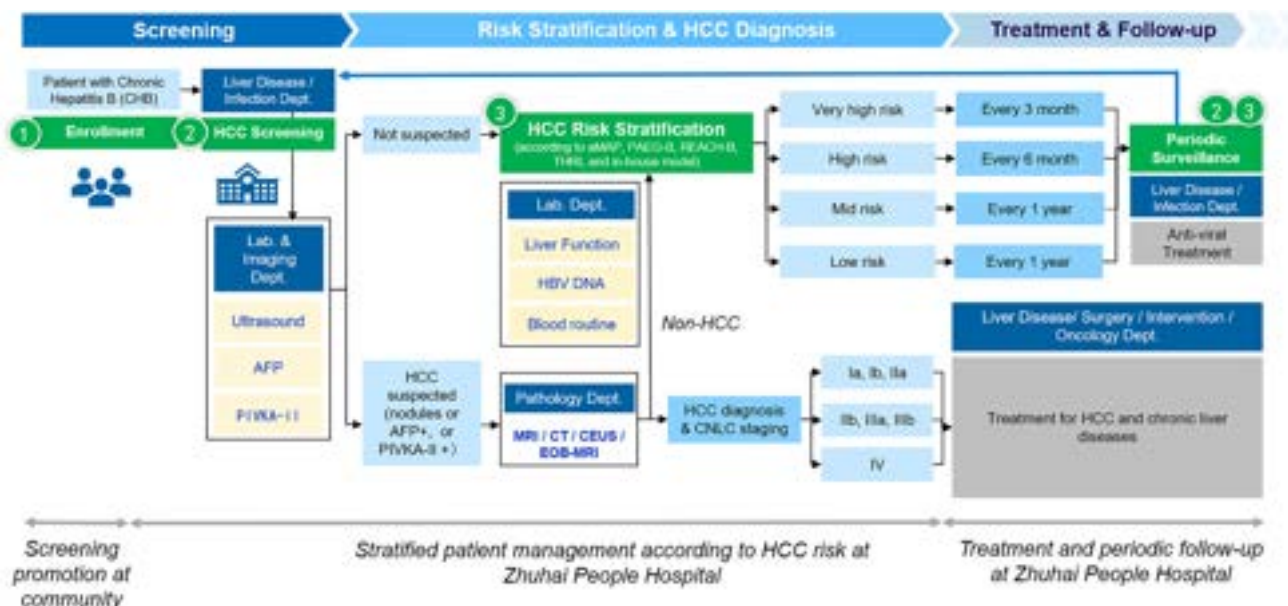


Figure: (abstract: FRI-323): We have established a digitalized management system for HCC screening and surveillance at our hospital.

stratified, 14.2% of whom were classified as high-risk for HCC, and subsequently matched with a well-designed periodic surveillance plan. Our management system has also enabled a significant increase in patient compliance to 71%.

Conclusion: The standardized screening and management system established has so far significantly improved the early diagnosis rate of HCC among the enrolled patients. The stratified management strategy embedded has also considerably improved the management efficiency and follow-up compliance of high-risk patients. The established system warrant further validation and promotion.

FRI-324

Chemerin protein in hepatocellular carcinomas is related to disease severity in European patients

Christa Büchler¹, Kirsten Utpatel², Katja Evert², Oliver Treeck³, Florian Weber². ¹Regensburg University Hospital, Department of Internal Medicine, Germany; ²Regensburg University Hospital, Institute of Pathology, Germany; ³Regensburg University Hospital, Department of Gynaecology and Obstetrics, Germany
Email: christa.buechler@klinik.uni-regensburg.de

Background and aims: The chemoattractant protein chemerin is protective in experimental hepatocellular carcinoma (HCC), and high expression in HCC tissues of Asian patients leads to a better prognosis. In the present study, immunohistochemistry was used to find out whether higher chemerin in HCC is associated with less severe disease in European patients.

Method: Chemerin and chemokine like receptor 1 (CMKLR1) protein expressions were determined by immunohistochemistry in HCC tissues of 383 patients.

Results: Chemerin protein expression was low in 24%, medium in 49% and high in 27% of the tissues. Chemerin protein in the HCC tissues relates positively to T-stage, vessel invasion, higher histologic grade, Union for International Cancer Control (UICC) stage and tumour size. Chemokine like receptor 1 (CMKLR1) is a functional chemerin receptor. CMKLR1 protein was low expressed in 36%, medium expressed in 32% and high expressed in 32% of the HCCs. Tumour CMKLR1 was positively related to T-stage, vessel invasion, higher histologic grade and UICC stage. Associations of tumour chemerin and CMKLR1 protein with steatosis, inflammation and fibrosis were not observed. In summary, chemerin as well as CMKLR1 protein, were positively related to disease severity of European HCC patients. This is in contrast to Asian patients where higher tumour chemerin was protective.

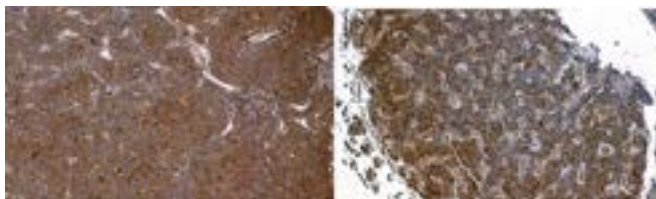


Figure: Chemerin (left) and its receptor CMKLR1 (right) in the liver

Conclusion: Current analysis provides evidence for ethnicity-related differences of HCC expressed chemerin and HCC severity.

FRI-325

Prognostic value of simple non-invasive tests for the risk stratification of HCC development in patients with cirrhosis due to non-alcoholic fatty liver disease

Amina Abdulle¹, Angelo Armandi¹, Gian Paolo Caviglia¹, Chiara Rosso¹, Daphne D'Amato¹, Gabriele Castelnovo¹, Nuria Pérez Diaz del Campo¹, Kamela Gjini¹, Irene Poggiolini¹, Marta Guariglia¹, Giorgio Maria Saracco¹, Elisabetta Bugianesi¹.

¹University of Turin, Turin, Italy, Italy

Email: amina.abdulle.md@gmail.com

Background and aims: Hepatocellular Carcinoma (HCC) represents a major clinical event in the cirrhotic population, leading to a significant incidence of morbidity and mortality. The aim of our study is to assess the prognostic value of simple non-invasive tests (NITs) for the stratification of the risk of HCC development in a Non-Alcoholic Fatty Liver Disease (NAFLD) cirrhotic population on long-term follow-up (FU).

Method: A total of 122 patients with NAFLD-cirrhosis (median age: 62 years; males 52.5%; median BMI 30.5 kg/m²; prevalence of type-2 diabetes: 57.4%) were retrospectively analyzed. Cirrhosis diagnosis was achieved by either liver histology, instrumental findings and/or clinical evidence of portal hypertension. Clinical and biochemical data were collected at the time of diagnosis; the following NITs were calculated: FIB-4, AST to Platelet Ratio Index (APRI) gamma-glutamyl transpeptidase-to-platelet ratio (GPR), BARD.

Results: During a median FU of 6 (IQR 3.2–9.3) years, 13 (10.7%) patients developed HCC. Baseline FIB-4 (HR = 1.27, 95%CI 1.03–1.58, p = 0.027) and GPR (HR = 1.44, 95%CI 1.11–1.85, p = 0.005) values resulted significantly associated to HCC occurrence. Conversely, no association was observed for APRI and BARD. Conventional FIB-4 cut-off values allowed a proper patients' stratification into 3 risk categories with different HCC incidence: FIB-4 < 1.3 = 0/18 (0%), FIB-4 between 1.3–3.25 = 7/73 (9.6%), and FIB-4 > 3.25 = 6/31 (19.4%) (Log-rank test: p = 0.009). Likewise, the cumulative HCC incidence according to GPR tertiles risk groups was: 3/41 (7.3%), 4/40 (10.0%) and 6/41 (14.6%) (Log-rank test: p = 0.041).

Conclusion: Baseline FIB-4 could stratify patients with NAFLD-cirrhosis on long-term FU according to their individual risk of HCC development. In such patients, this simple NITs may be useful to optimize tailored HCC surveillance strategies.

The research has been supported by the Italian Ministry for Education, University and Research (MIUR) under the programme "Dipartimenti di Eccellenza 2018–2022" Project code D15D18000410001

FRI-326

Exploration of the lack of systematic surveillance for hepatocellular carcinoma for patients with non-alcoholic fatty liver disease

Theresa Hydes^{1,2}, Connor Henry Blake^{1,2}, Mohamed Kassab², Charmaine Matthews², Vinay Kumar², Elizabeth Baggus^{1,2}, Nick Stern², Daniel Cuthbertson^{1,2}, Daniel Palmer¹, Philip Johnson¹, Tim Cross^{1,2}. ¹University of Liverpool, United Kingdom; ²Liverpool University NHS Hospitals Foundation Trust, United Kingdom

Email: therasa@doctors.org.uk

Background and aims: Non-alcoholic fatty liver disease (NAFLD) is emerging as a leading cause of hepatocellular carcinoma (HCC). We aimed to compare the frequencies of HCC detected in those not under systematic surveillance for people with NAFLD vs. other aetiologies of liver disease, to explore possible underlying reasons and determine impact on survival.

Method: A prospective dataset of 623 patients with HCC seen at a large hospital trust in Northwest England from 2007 to 2022 was examined. A diagnosis of NAFLD was made based on radiological evidence of steatosis or cryptogenic cirrhosis in the presence of the metabolic syndrome, without significant alcohol intake or other causes of chronic liver disease. Group comparisons were made using

POSTER PRESENTATIONS

Mann Whitney *U*-test where data was continuous and Chi-squared test was used to compare categorical data.

Results: Within this cohort 76.2% ($n=475$) of patients were male, with a median age of 68 years. In total, 30.3% ($n=189$) had NAFLD, 31.9% ($n=199$) alcohol-related liver disease, and 19.6% ($n=122$) hepatitis C infection. People with NAFLD HCC were less likely to have been enrolled in HCC surveillance (25.4% vs. 43.3% for other aetiologies of liver disease, $p<0.0001$) and more likely to have a diagnosis of HCC based on symptoms (Table 1). We explored why people with NAFLD HCC presented outside of surveillance. Fewer people with NAFLD were known to secondary liver services prior to developing HCC (26.0% vs. 48.3% of people without NAFLD, $p<0.0001$). We also noted more people with NAFLD developed HCC without pre-existing cirrhosis (33.9% vs. 14.8% without NAFLD, $p<0.0001$). Patients with NAFLD HCC presented with a greater median diameter of their largest tumour (43 vs. 30 mm, $p=0.0009$). While there was an observation that a lower frequency of patients with NAFLD met Barcelona Clinic Liver Cancer (BCLC) staging 0/A (NAFLD 32.6% vs. non-NAFLD HCC 37.6%, $p=0.2419$) and were less likely to receive curative treatment (resection/transplant/ablation) (NAFLD 31.2% vs. non-NAFLD HCC 38.7%, $p=0.0802$), no significant difference was detected between the groups. Patients with NAFLD HCC had similar severity of liver disease than people with non-NAFLD HCC according to the model for end stage liver disease (MELD) score (9.8% vs. 9.4% had a MELD ≤ 6 , $p=0.8766$), although patients with NAFLD HCC were less likely to have ascites (20.6% vs. 28.5%, $p=0.0406$) and displayed lower median levels of bilirubin (13 vs. 18 mg/dl, $p<0.0001$). Performance status was comparable (performance status 0, 64.6% NAFLD vs. 63.5% for people without NAFLD, $p=0.8830$), despite people with NAFLD being older (median age 75 vs. 65 years, $p<0.0001$) and more likely to have cardiovascular disease (37.7% vs. 21.1%, $p=0.0002$). Overall median survival was comparable between groups (NAFLD HCC 484 days vs. non-NAFLD HCC 475 days, $p=0.8489$).

Indication	NAFLD (%) N=189	Non-NAFLD aetiology of liver disease (%) N=411
HCC Surveillance	16.9	33.9
Abnormal liver biochemistry	26.8	24.4
Rising Alpha fetoprotein	5.5	8.5
Incidental finding on other imaging	25.1	14.7
Abdominal pain	8.2	5.4
Weight loss	6.0	2.3
Clinical ascites	0.5	3.6
Hepatomegaly	1.1	0.5
Anaemia	1.1	0.5
Variceal bleed	3.3	1.0
Other	6.0	5.1

Table 1: Clinical indications for imaging resulting in a diagnosis of HCC.

Conclusion: Patients with NAFLD are more likely to present with HCC outside of surveillance because they are not known to secondary care, or do not have cirrhosis at the time of HCC diagnosis. While patients with NAFLD do not appear to be significantly disadvantaged in terms of overall survival, there may be scope to optimise outcomes for this group via implementation of more widespread screening for advanced NAFLD in the community and the development of better HCC risk stratification models.

FRI-327

Aetiology and outcomes of cirrhosis and hepatocellular carcinoma in Blantyre, Malawi

Alexander Stockdale^{1,2}, Benno Kreuels^{3,4,5}, Isaac Shawa^{2,6}, Niza Silungwe², Karen Chetcuti⁴, Elizabeth Joekes^{2,7}, Blessings Mbale², Jane Mallewa^{4,5}, Egbert Tannich³, Christina Weiler-Normann⁸, Marc Luetgehetmann⁸, Peter Finch⁵, Emma Thomson⁹, Anna Maria Geretti¹⁰, Melita Gordon^{1,2}. ¹University of Liverpool, Liverpool, United Kingdom; ²Malawi-Liverpool-Wellcome Trust Clinical Research Programme, Blantyre, Malawi; ³Bernhard Nocht Institute for Tropical Medicine, Hamburg, Germany; ⁴Kamuzu University of Health Sciences (KUHeS), Blantyre, Malawi; ⁵Queen Elizabeth Central Hospital, Blantyre, Malawi; ⁶University of Derby, United Kingdom; ⁷Royal Liverpool University Hospital, United Kingdom; ⁸University Medical Center Hamburg-Eppendorf, Hamburg, Germany; ⁹Centre For Virus Research, Bearsden, United Kingdom; ¹⁰University of Rome "Tor Vergata", Italy

Email: a.stockdale@liverpool.ac.uk

Background and aims: Age-standardised mortality from liver disease is highest in African countries. We studied the aetiology and outcomes of patients with cirrhosis and hepatocellular

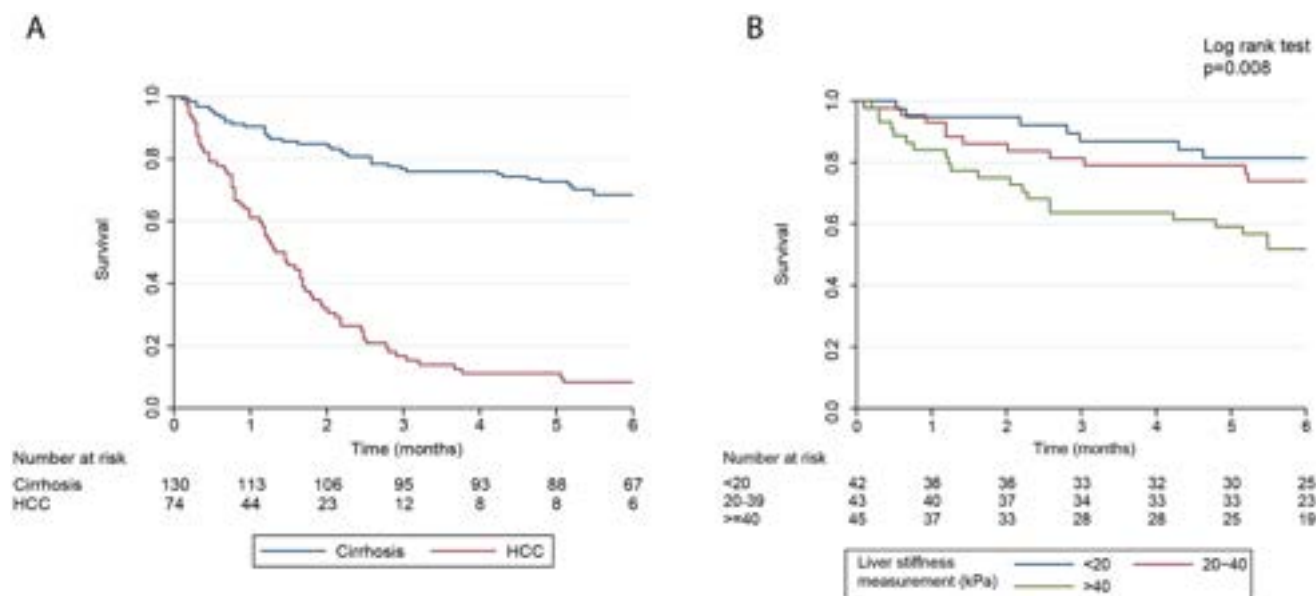


Figure (abstract: FRI-327): Kaplan Meier curve. A: All participants; B: Cirrhosis stratified by liver stiffness

carcinoma (HCC) presenting to a tertiary hospital in southern Africa, to identify interventions to address liver-related mortality.

Method: We prospectively screened 708 patients over 18 months using transient elastography (>12 kPa) and ultrasound, diagnosing 138 patients with cirrhosis and 78 with HCC. We excluded patients with non-liver-related disease. We estimated population attributable fractions (PAF) using randomly-sampled community controls (n = 3258 for hepatitis B; n = 120 for other exposures) using binomial logistic regression with robust standard errors, with PAF represented by 1- the ratio between the logit of the baseline likelihood and a zero exposure scenario. We tested for hepatitis B (HBsAg), anti-HCV and HCV RNA, anti-HDV, HDV RNA, HEV IgG and RNA, HIV, autoimmune serology, schistosomiasis Ag and PCR in cases and controls.

Results: Patients with HCC were median 40 (IQR 35–50) years old; tumour size was 13.2 cm (IQR 10.2–17.3) with median survival 40 days (95% CI:30–51). Hepatitis B (HBsAg) was attributable for 25.5% (95% CI 17.1–33.1) of cirrhosis and 73.2% (61.0–81.6) of HCC cases. HIV was the second most important cause with PAF 23.6% (13.5–32.5) for cirrhosis and 20.2 (7.4–31.2) for HCC; the association persisted after adjusting for HBV/C co-infection. Hepatitis C was attributable for <5% of liver disease; 6% with cirrhosis had autoimmune liver disease, and no active hepatitis D or E was diagnosed. Alcohol and smoking were attributable for 14.0% (–2.3–27.7) and 23.6% (8.4–36.3) of cases of HCC respectively, but were not associated with cirrhosis. Schistosomiasis was diagnosed in cirrhosis patients by urine antigen (30.4%) or PCR (36.2%); 12.5% had ultrasound signs of *S. mansoni*. Liver stiffness (hazard ratio 1.13 (1.05–1.20) per 5 kPa increase, $p < 0.001$) and presence of ascites (HR 9.09 (2.80–29.5), $p < 0.001$) were predictors of 6-month cirrhosis mortality.

Conclusion: Hepatitis B and HIV are the principal causes of liver disease in southern Malawi. Patients with HCC are diagnosed at an advanced stage, with a dismal prognosis. There is an urgent need for community HBV screening and treatment programmes to address liver-related mortality.

FRI-328

Survival outcomes of patients with non-alcoholic fatty liver disease-related HCC: a retrospective cohort study

Anders Møllemejkær¹, Josefine Lahn², Linda Skibsted Kornerup², Gerda Elisabeth Villadsen², Henning Groenbaek². ¹Aarhus University Hospital, Dept. of Gastroenterology and Hepatology, Aarhus N, Denmark; ²Aarhus University Hospital, Gastroenterology and Hepatology, Aarhus N, Denmark

Email: anders.møllemejkær@clin.au.dk

Background and aims: Non-alcoholic fatty liver disease (NAFLD) is emerging as a leading cause of hepatocellular carcinoma (HCC) in many Western countries. The aim of this study was to compare survival outcomes of NAFLD-related HCC by other etiologies in Danish patients with newly diagnosed HCC.

Method: We retrospectively included all patients diagnosed with HCC at the tertiary liver center at Aarhus University Hospital, Denmark in 2018 and 2019. Data was derived from patients' electronic records and follow-up was carried out until death or December 1st, 2022. To identify cases of NAFLD-related HCC, a strict definition was applied, comprising either: 1) previous NAFLD diagnosis, 2) evidence of steatosis on biopsy, ultrasonography, or computer tomography, or 3) presence of three or more features of the metabolic syndrome. Further, patients with alternative causes of HCC or current or previous record of alcohol abuse were excluded from the case definition.

Results: A total of 133 patients diagnosed with HCC were identified. Of these, 29 (21.8%) fulfilled our criteria for NAFLD-related HCC. Remaining etiologies included alcohol (n = 67, 50%), viral hepatitis B and C (n = 22, 17%), cholestatic liver disease (n = 4, 3%) and other or unknown etiology (n = 15, 11%). Patients with NAFLD-related HCC were older (median 76 vs. 67 years, $p < 0.001$), fewer had cirrhosis (41% vs. 73%, $p = 0.001$), and fewer were smokers (7% vs. 38%, $p =$

0.002) compared to non-cases. Barcelona Clinic Liver Cancer (BCLC) stages was similar in the two groups ($p = 0.49$). The Kaplan-Meier plot (Fig. 1) revealed no differences in the survival functions ($p = 0.46$) or median survival time between NAFLD-related HCC cases (19.8 months) and non-cases (17.8 months). The proportional hazards model adjusted for BCLC stage and age showed no difference in hazards rates between the two groups (Hazard Ratio (HR) = 1.20, 95% CI: 0.74–1.95, $p = 0.47$).

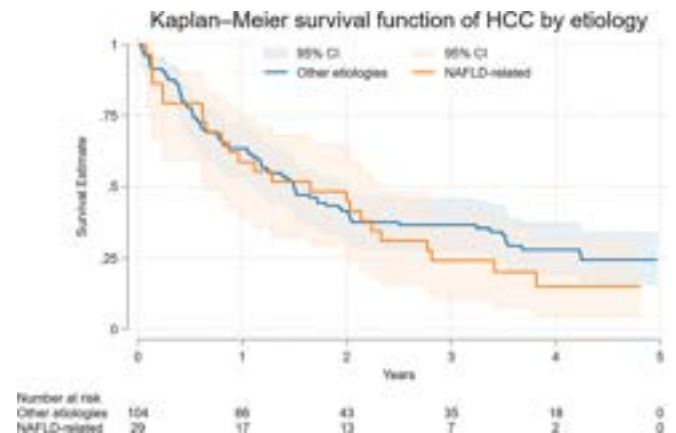


Figure 1: Kaplan-Meier plot of the survival function for patients with newly diagnosed HCC by etiology.

Conclusion: NAFLD-related HCCs were more often diagnosed in older patients and in patients without cirrhosis compared to other etiologies. However, disease stage at diagnosis and overall prognosis was comparable in patients with and without NAFLD-related HCC. Larger cohort studies are needed to substantiate these findings.

FRI-329

Targeted surveillance for hepatocellular carcinoma is cost effective in Australia: evidence from a microsimulation study

Barbara de Graaff¹, Le Tuan Anh Nguyen¹, Lei Si², John Lube^{3,4}, Nicholas Shackel⁵, Kwang Chien Yee⁶, Mark Wilson⁷, Jane Bradshaw⁷, Kerry Hardy⁷, Andrew Palmer¹, Christopher Leigh Blizzard¹.

¹University of Tasmania, Menzies Institute for Medical Research, Hobart, Australia; ²Western Sydney University, School of Health Sciences, Campbelltown, Australia; ³Alfred Hospital, Gastroenterology Department, Melbourne, Australia; ⁴Monash University, School of Medicine, Melbourne, Australia; ⁵Launceston General Hospital, Launceston, Australia; ⁶University of Tasmania, School of Medicine, Hobart, Australia; ⁷Royal Hobart Hospital, Gastroenterology Department, Hobart, Australia

Email: barbara.degraaff@utas.edu.au

Background and aims: In Australia and many other Western countries, hepatocellular carcinoma (HCC) is one of the fastest increasing causes of cancer mortality. Recently published Australian Consensus Guidelines recommend HCC surveillance for all patients with liver cirrhosis and high-risk groups living with non-cirrhotic chronic hepatitis B (CHB) (i.e. Aboriginal and Torres Strait Islanders aged <50 years, Asian males >40 years, Asian females >50 years, people born in sub-Saharan Africa aged >20 years). The aim of this study was to assess the cost-effectiveness of these recommendations.

Method: A microsimulation model was developed. Three strategies were evaluated: biannual ultrasound scan (USS), biannual USS+ alpha-fetoprotein (AFP), and usual care (i.e. no formal surveillance). A hypothetical cohort aged 40–80 years with one of the conditions: non-cirrhotic CHB, compensated cirrhosis (CC) or decompensated cirrhosis (DC), was simulated. Face, internal and external validity were assessed. One-way, probabilistic sensitivity analyses were conducted. To account for uncertainties, scenario and threshold analyses were carried out. Scenarios included surveillance of each

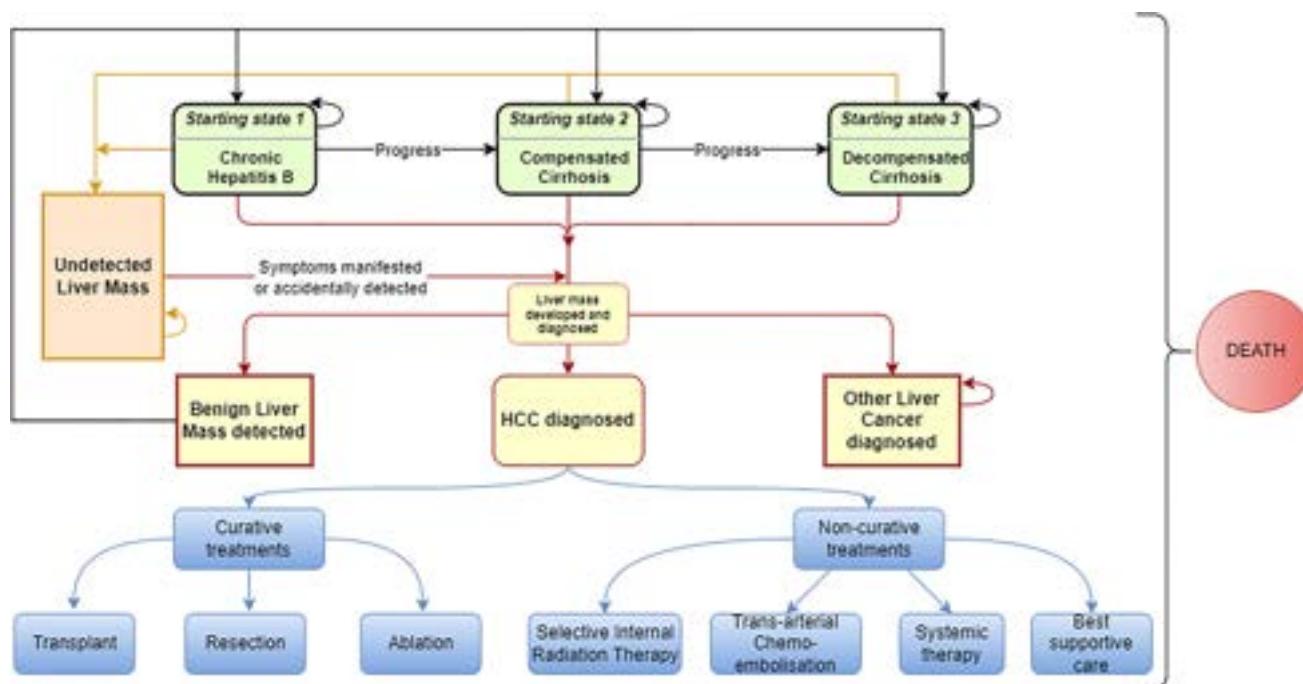


Figure 1: (abstract: FRI-329): Structure of the state-transition individual-level model.

disease individually (CHB, CC, DC), reduced sensitivity of USS due to central adiposity and real-world adherence rates.

Results: The validation analyses indicated that the model is highly accurate in terms of reflecting observed real-world data. For a range of HCC surveillance scenarios for combined CHB, CC and DC patients, USS + AFP was the most cost-effective with an incremental cost-effectiveness ratios (ICER) compared to usual care less than the willingness-to-pay threshold of A\$50,000 per quality-adjusted life year (QALY). Whilst USS alone was also cost-effective, it was dominated by USS+AFP. When evaluating cost-effectiveness by groups, surveillance was cost-effective in CC and DC groups (ICERs <\$30,000), but not for CHB alone (ICERs >\$100,000). Central adiposity decreased the performance of USS, however USS ± AFP surveillance remained cost-effective.

Conclusion: HCC surveillance using USS ± AFP for combined target populations is cost-effective. Surveillance limited to CC and DC groups is also cost-effective. Whilst surveillance for CHB patients alone was not cost-effective, this may be due to an important limitation of this model. As there is a lack of published data for model parameters on CHB and Indigenous status, region of birth, age and sex, our model was simplified and assumed that HCC risk was the same for all CHB patients. Our model will be updated with these data as they become available. Nonetheless, HCC surveillance based on Australian recommendations for all three groups is highly likely to be cost-effective in the Australian setting.

Liver tumours Experimental and pathophysiology

WEDNESDAY 21 TO SATURDAY 24 JUNE

TOP-066

PD1-negative CD45RA effector-memory CD8 T-cells are essential for response to checkpoint inhibition in advanced hepatocellular carcinoma

Sarah Cappuyns^{1,2,3,4}, Gino Philips^{3,4}, Vincent Vandecaveye^{5,6}, Bram Boeckx^{3,4}, Rogier Schepers^{3,4}, Thomas Van Brussel^{3,4}, Ingrid Arijis^{3,4}, Aurelie Mechels^{3,4}, Ayse Bassez^{3,4}, Francesca Lodi^{3,4}, Joris Jaekers⁷, Halit Topal⁷, Baki Topal⁷, Orian Bricard^{3,4}, Junbin Qian^{8,9}, Eric Van Cutsem^{1,2}, Chris Verslype^{1,2}, Diether Lambrechts^{3,4}, Jeroen Dekervel^{1,2}. ¹University Hospitals Leuven, Digestive Oncology, Department of Gastroenterology, Belgium, ²Katholieke Universiteit Leuven, Laboratory of Clinical Digestive Oncology, Department of Oncology, Belgium, ³Katholieke Universiteit Leuven, Laboratory for Translational Genetics, Department of Human Genetics, Belgium, ⁴Vlaams Instituut voor Biotechnologie, Centre for Cancer Biology, Leuven, Belgium, ⁵University Hospitals Leuven, Department of Radiology, Belgium, ⁶Katholieke Universiteit Leuven, Laboratory of Translational MRI, Department of Imaging and Pathology, Belgium, ⁷University Hospitals Leuven, Hepatobiliary- and pancreas Surgery, Department of Abdominal Surgery, Belgium, ⁸Zhejiang University School of Medicine, Zhejiang Provincial Key Laboratory of Precision Diagnosis and Therapy for Major Gynaecological Diseases, Women's Hospital, China, ⁹Zhejiang University School of Medicine, Institute of Genetics, China
Email: sarahcappuyns@hotmail.com

Background and aims: Checkpoint inhibitors (CPI) have dramatically changed the treatment landscape of advanced HCC (aHCC). While PD1-expressing CD8 T-cells have repeatedly been linked to response to CPI, their role in aHCC is controversial. Using single-cell profiling,

we aimed to characterize the intra-tumoural and peripheral immune context of aHCC patients treated with CPI to identify features associated with response and/or resistance.

Method: Both pre-treatment tissue biopsies and serial peripheral blood mononuclear cell (PBMC) samples of aHCC patients (n=37) treated with systemic therapy were subjected to single-cell transcriptome (scRNAseq) and T-cell receptor sequencing (scTCRseq). Patients (n=30) treated with PD (L)1 inhibition were stratified according to clinical response and various single-cell readouts were correlated with response and clinical outcome.

Results: Tumours with durable response were enriched for PDL1-expressing CXCL10+ macrophages and, based on cell-cell interaction, expressed high levels of CXCL9/10/11 to attract peripheral CXCR3+ effector-memory T-cells (CD8 T_{EM}) into the tumour. Furthermore, based on TCR sharing and pseudotime trajectory analysis, CD8 T_{EM} preferentially differentiated into clonally-expanded PD1-negative, CD45RA effector-memory CD8 T-cells (CD8 T_{EMRA}) with pronounced cytotoxicity. In contrast, in non-responders, CD8 T_{EM} remained frozen in their effector-memory state. Finally, in responders, CD8 T_{EMRA} displayed a high degree of T-cell receptor sharing with blood, consistent with their patrolling activity.

Conclusion: In conclusion, we propose a novel paradigm, where response to checkpoint inhibition in aHCC is driven by clonally expanded, cytotoxic CD45RA effector-memory CD8 T-cells, characterized by a high degree of TCR sharing with peripheral blood and present in the tumour prior to therapy. PDL1-expressing CXCL10+ macrophages are positioned as essential gatekeepers in the TME, interacting with the peripheral T-cell compartment to ensure effective T-cell recruitment into the TME.

TOP-069

Interleukin 10-mediated signaling dampens antitumor immunity and promotes liver metastasis

Tao Zhang^{1,2}, Ahmad Mustafa Shiri^{1,2}, Tanja Bedke^{1,2}, Jöran Lücke^{1,2,3}, Dimitra E. Zazara^{4,5}, Anastasios Giannou^{1,2,3}, Samuel Huber^{1,2}.

¹University Medical Center Hamburg-Eppendorf, Section of Molecular Immunology und Gastroenterology, I. Department of Medicine, Germany, ²University Medical Center Hamburg-Eppendorf, Hamburg Center for Translational Immunology (HCTI), Germany, ³University Medical Center Hamburg-Eppendorf, Department of General, Visceral and Thoracic surgery, Germany, ⁴University Medical Center Hamburg-Eppendorf, Division for Experimental Feto-Maternal Medicine, Department of Obstetrics and Fetal Medicine, Germany, ⁵University Medical Center Hamburg-Eppendorf, University Children's Hospital, Germany
Email: s.huber@uke.de

Background and aims: Liver metastasis is one of the most common causes of cancer-associated mortality. A presence of liver metastasis was reported to be responsible for an immunosuppressive micro-environment and a diminished immunotherapy efficacy. As a master regulator of the immune system, interleukin-10 (IL-10) targets both innate and adaptive immune cells and orchestrates immunosuppressive functions. Interestingly, IL-10 is upregulated in both human and murine liver metastasis. We aimed here to decipher the source, regulation and function of IL-10 in liver metastasis. Our long-term aim is to improve the outcome of patients with liver metastasis.

Method: To induce spontaneous or forced liver metastasis on mice, murine cancer cells (MC38) were injected into cecum or spleen, respectively. Cell-specific IL-10 and IL-10 receptor (IL-10R) deficient mice were used to identify source and target of IL-10 during metastasis formation. PD-L1 deficient mice were used to test the role of this check point. 3–4 weeks post injection, livers were harvested and metastatic burden including liver weight and number of metastatic sites were analyzed. Immune composition characterization was performed in IL-10-reporter mice using flow cytometry. To investigate the underlying mechanisms, hepatic myeloid cells were sorted for RNA sequencing. Hepatic CD8+ T cells were

cocultured with MC38 to measure changes in antitumor immunity using flow cytometry.

Results: In our liver metastasis mouse models, IL-10 blockade as well as IL-10 deficient mice were protected from metastasis formation. Furthermore, by using IL-10 reporter mice, we could demonstrate that Foxp3+ regulatory T cells (Tregs) are the major cellular source of IL-10 in the liver metastatic sites. Deletion of IL-10 expression in Foxp3+ Tregs led to reduced liver metastatic sites, a finding that underlines the importance of this cytokine during metastasis formation. Ablation of IL-10R on myeloid cells, but not DCs, resulted in less liver metastatic burden, suggesting that IL-10 signaling in myeloid cells regulated liver metastasis formation. Nevertheless, Tregs themselves were shown to respond to IL-10 by highly boosting its production, which in turn triggered monocytes to upregulate the immune checkpoint mediator PD-L1. Accordingly, deletion of PD-L1 let to decreased liver metastasis. Coculture with hepatic infiltrating CD8+ T cells and MC38 cells showed that the PD-L1/PD-1 axis attenuates the CD8-dependent cytotoxicity against metastatic lesions.

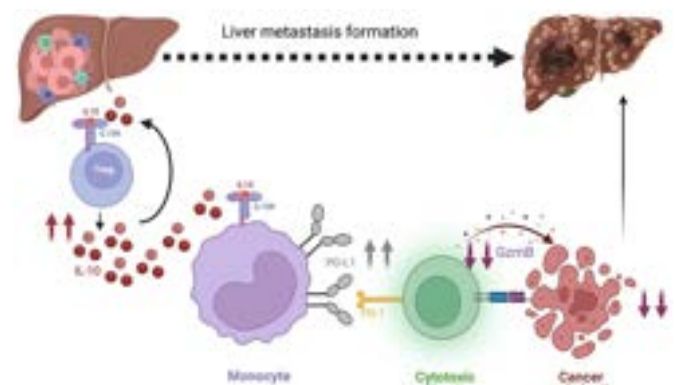


Figure:

Conclusion: Our data provides evidence that Treg- produced IL-10 upregulates PD-L1 expression in monocytes, which in turn reduces CD8+ T cell infiltration and related antitumor immunity, thereby promoting liver metastasis formation. These findings highlight the potential therapeutic benefit of a novel combined anti-IL-10R and anti-PD-L1 approach against liver metastasis.

TOP-070

Constitutive signaling from an engineered IL-21 receptor programs long-lived effector TCR-T cells for HCC therapy

Wei Zhu¹, Zhiming Zhang¹, Jinzhang Chen¹, Xiaolan Chen¹, Xuan Huang¹, Weikang Xu¹, Xuan Yi¹, Xinyu Lu¹, Sha Wu², Yongyin Li¹, Jinlin Hou¹, ¹Nanfang Hospital, Southern Medical University, China, ²School of Basic Medical Sciences, Southern Medical University, China
Email: jlhoumu@163.com

Background and aims: Strategies to improve T cell therapy efficacy in solid tumours such as hepatocellular carcinoma (HCC) are urgently needed. The common cytokine receptor γ chain (γ_c) family cytokines such as IL-2, IL-7, IL-15 and IL-21 play fundamental roles in T cells development, differentiation and effector phase. The aim of this study is to determine the effect of IL-21 combination in T cell therapy against HCC and investigate optimized strategies to utilize the effect of IL-21 signal in T cell therapy.

Method: The contributions of IL-7, IL-15 and IL-21 in human alpha fetoprotein (AFP) specific TCR engineered T cells (TCR-T) against HCC were evaluated in vitro and in vivo. The phenotypic and transcriptome alteration in AFP-specific TCR-T cells was further determined by flow cytometry and RNA sequencing. A novel IL-21 receptor transmitting IL-21 signal without exogenous IL-21 supplement was designed and expressed in AFP-specific TCR-T cells. The antitumor function of TCR-T cells expressing novel IL-21 receptor (IL-21R-TCR-T)

POSTER PRESENTATIONS

was evaluated *in vitro* and *in vivo*, the phenotypic and transcriptome alteration induced by engineered IL-21 receptor was investigated by flow cytometry and single-cell RNA sequencing.

Results: The antitumor function of AFP-specific TCR-T cells was augmented by exogenous IL-21 both in coculture assay and xenograft model. IL-21 enhanced TCR-T cells proliferation capacity both after CD3/CD28 and tumor antigen stimulation. Phenotypic analysis revealed that IL-21 promoted memory differentiation, downregulated PD-1 expression and alleviated apoptosis in TCR-T cells after activation. IL-21R-TCR-T showed upregulated STAT3 phosphorylation level compared with conventional TCR-T in the absence of IL-21. Superior antitumor function and proliferation capacity after activation was found in IL-21R-TCR-T cells compared with conventional TCR-T cells *in vitro* and *in vivo*. Phenotypic analysis revealed that IL-21R-TCR-T cells showed lower apoptosis level, less differentiated and exhausted phenotype and higher effector function after repetitive tumor antigen stimulation.

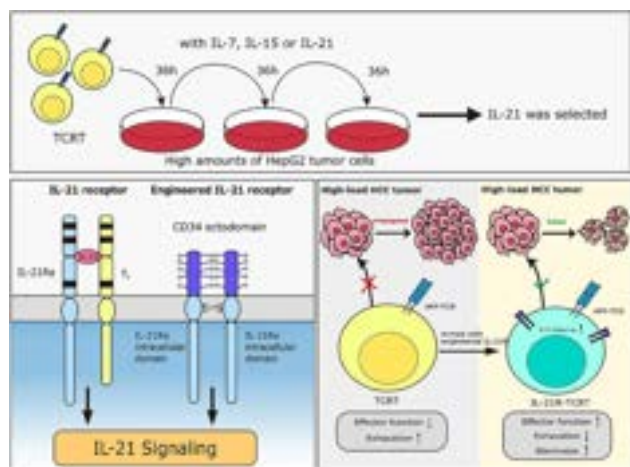


Figure:

Conclusion: We designed a novel IL-21 receptor which programs long-lived effector TCR-T cells and avoids side effects induced by systemic utilization of IL-21. The novel IL-21 receptor creates new opportunities for next generation TCR-T cells against HCC.

TOP-072

Antitumoral activity of the G9a inhibitor EZM8266 in hepatocellular carcinoma: potential for combination with immune checkpoint inhibitors

Maite G Fernandez-Barrena^{1,2}, José María Herranz^{1,2}, Elena Adan-Villaescusa¹, Borja Castello¹, Felipe Prosper^{3,4}, Bruno Sangro^{5,6}, Maria Arechederra^{1,6,7}, Carmen Berasain^{1,7}, Jennifer Totman⁸, Veronica Gibaja⁸, Matias A Avila^{1,6,7}. ¹CIMA-University of Navarra, Hepatology Program, PAMPLONA, Spain, ²Carlos III Health Institute, National Institute for the Study of Liver and Gastrointestinal Diseases, CiberEHD, Madrid, Spain, ³CIMA, CCUN, University of Navarra, Hemato-Oncology Program, PAMPLONA, Spain, ⁴Instituto de Investigación Sanitaria de Navarra, Hemato-Oncology Program, Spain, ⁵Liver Unit, Clínica Universidad de Navarra, CCUN, Hepatology Unit, Spain, ⁶Instituto de Investigación Sanitaria de Navarra, IdiSNA, Spain, ⁷Carlos III Health Institute, National Institute for the Study of Liver and Gastrointestinal Diseases, CiberEHD, Madrid, Spain, ⁸Epizyme, An Ipsen Company, United States
Email: maavila@unav.es

Background and aims: Advanced hepatocellular carcinoma (HCC) treatment has radically changed with the advent of immune-checkpoint inhibitors (ICIs). Still, a significant proportion of patients show innate or acquired resistance to ICI-based therapies. Therefore, new strategies to overcome resistance and increase efficacy are

needed. Epigenetic alterations are increasingly recognized to participate in hepatocarcinogenesis. Moreover, these mechanisms are known to repress the expression of chemokines that promote tumor lymphocyte infiltration, as well as that of immunogenic neoantigens, such as cancer testis antigens (CTAs). As we previously showed, one attractive epigenetic target in HCC is the histone-methyltransferase G9a. In this study, we tested the *in vitro* and *in vivo* anti-HCC activity of EZM8266, a highly specific G9a inhibitor with favorable pharmacokinetic properties.

Method: We performed a comprehensive transcriptomic analysis of 180 epigenetic modifiers and validated *in silico* the upregulation of G9a expression in a combined cohort including 292 HCC tissue samples, and explored its association with the different immune tumor tissue signatures. We examined the effects of EZM8266 on the growth of human (Hep3B, HuH7, PLC/PRF5, HepG2, SNU449) and mouse (PM299L) HCC cell lines. We performed colony formation, migration, invasion and anchorage-independent growth assays. EZM8266 was tested on the basal and IFN γ -triggered expression of CXCL9 and CXCL10 chemokines and CTAs in HCC cells. The effects of EZM8266 on the growth of PM299L cells orthotopically implanted in immunocompetent mice, alone and in combination with α -PD1 antibodies, were also evaluated.

Results: G9a is consistently overexpressed in HCCs, positioned as one of the most highly deregulated epigenetic modifiers in HCC patients and most prominently in the “non-inflamed” transcriptomic subclasses. EZM8266 inhibited HCC cells proliferation and all malignant traits tested *in vitro*. EZM8266 induced the expression of CTAs, CXCL9 and CXCL10, potentiating the effect of IFN γ on these chemokines. *In vivo*, EZM8266 inhibited the growth of PM299L cells, and enhanced the effects of α -PD1 resulting in a remarkable antitumoral activity. No signs of systemic or liver toxicity were observed.

Conclusion: G9a is confirmed as an effective druggable target in HCC. Pharmacological inhibition of G9a with EZM8266 antagonizes HCC cells growth and leverages the efficacy of ICIs. Our findings provide strong support for the combination immunotherapy with epigenetic drugs such as EZM8266 for HCC treatment.

SATURDAY 24 JUNE

SAT-211

Oncostatin M promotes a pro-tumorigenic inflammatory response in NASH-related HCC

Beatrice Foglia¹, Salvatore Sutti², Jessica Nurcis¹, Chiara Rosso³, Marina Maggiora¹, Claudia Bocca¹, Patrizia Carucci⁴, Silvia Gaia⁴, Elisabetta Bugianesi³, Emanuele Albano², Maurizio Parola¹, Stefania Cannito¹. ¹University of Torino, Clinical and Biological Sciences, Torino, Italy, ²University Amedeo Avogadro of East Piedmont, Health Sciences and Interdisciplinary Research Center for Autoimmune Diseases, Novara, Italy, ³University of Torino, Medical Sciences, Torino, Italy, ⁴Città della Salute e della Scienza University-Hospital, Division of Gastroenterology, Torino, Italy
Email: beatrice.foglia@unito.it

Background and aims: Oncostatin M (OSM) is a pleiotropic cytokine belonging to the interleukin (IL)-6 family that acts on a large variety of cells involving two distinct heterodimeric receptor complexes: leukemia inhibitory factor receptor beta (LIFRbeta) and OSM receptor beta (OSMRbeta) that is the receptor able to mediate the most relevant biological effects of OSM in mice. OSM has been proposed to contribute to the progression of chronic liver diseases, hepatocellular carcinoma (HCC) development and metastasis. High levels of OSM were found in cirrhotic patients with different etiology carrying HCC. In particular we observed that OSM serum levels are significantly higher in patients carrying non-alcoholic steatohepatitis (NASH)-related HCC, as compared to those with viral etiologies, and their

increase parallels the disease progression from simple steatosis to HCC. Noteworthy, OSM serum levels are significantly higher in patients with intermediate/advanced HCC and correlate with poor survival. This work discusses the role of OSM in relation to the development of HCC in a NASH background.

Method: We investigated the role of OSM in NASH-related HCC taking advantage of: a) cohort of NASH patients with HCC; b) human THP1 macrophage cell lines exposed to human recombinant OSM (hrOSM); c) Wild type (wt) mice fed with a control diet (CSAA) or a lipogenic diet (CDAA) for 24 weeks in order to reproduce the non-alcoholic fatty acid disease (NAFLD)/NASH pathogenic phenotype (CSAA-CDAA protocol); d) Wild type (wt) and OSMRbeta knock out (OSMRbeta^{-/-}) mice treated with a protocol of NASH-related liver carcinogenesis (DEN/CDAA protocol).

Results: In patients with NASH-related HCC, OSM is expressed in cancer cells in relation to CD68+ macrophages infiltrating tumour. In *in vitro* experiments, conducted on human THP1 macrophages exposed to hrOSM, we found that OSM is able to promote an M2 pro-tumorigenic phenotype, which is due to the activation of STAT3 and PI-3K/Akt signaling pathways. Accordingly, OSM expression, which was found increased in NASH-related liver tumours of wt mice during the progression of NAFLD/NASH towards HCC, correlates with F4/80 gene expression. This data suggests an interplay between OSM and macrophages recruitment/functions in the tumor microenvironment. In particular, wt mice treated with the DEN-CDAA protocol show a stronger promotion of the M2 phenotype compared with the M1 and in these mice OSM transcript levels correlate better with M2 macrophage polarization markers. As OSMRbeta is fundamental for the activation of the OSM-related STAT3 and PI-3K/Akt signaling pathways, the OSMRbeta^{-/-} murine model was employed to exploit the role of OSM in this regard. In this respect, the data obtained in the OSMRbeta^{-/-} murine models shows that the livers of these animals develop smaller tumours. This event appears to be due to: i) a decreased amount of M2 Tumor Associated Macrophages (TAMs) in the nodules as revealed by the reduction of transcription levels of CD163, PDL1, CD206 and CCR2 compared with wt mice; ii) a impairment of the angiogenic process as shown by lower transcript levels of VE-cadherin, VEGFR2 and CD105 compared with wt mice.

Conclusion: Experimental data highlight a pro-carcinogenic contribution for OSM in NASH, by promoting pro-tumorigenic inflammation, suggesting a possible role for the OSM-OSMRbeta axes as therapeutic target for NASH-related HCC.

SAT-212

Novel platinum-based chemotherapeutic agents halt cholangiocarcinoma progression through the induction of inter-strand DNA breaks, preventing DNA repair mechanisms

Irene Olaizola¹, Mikel Odriozola², Maitane Asensio^{3,4}, Paula Olaizola^{1,4}, Ivan Rivilla^{2,5}, Amanda Guimaraes², Francisco J. Caballero¹, Elisa Herraes^{3,4}, Oscar Briz^{3,4}, Pedro Miguel Rodrigues^{1,4,5}, María Jesús Perugorria^{1,4,6}, Luis Bujanda^{1,4}, Jose Marin^{3,4}, Fernando Pedro Cossio², Jesus Maria Banales^{1,4,5,7}. ¹Department of Liver and Gastrointestinal Diseases, Biodonostia Health Research Institute-Donostia University Hospital - University of the Basque Country (UPV/EHU), Spain, ²Department of Organic Chemistry I, Center of Innovation in Advanced Chemistry (ORFEO-CINQA), Faculty of Chemistry, University of the Basque Country (UPV/EHU) and Donostia International Physics Center (DIPC), Spain, ³Experimental Hepatology and Drug Targeting (HEVEPHARM), Institute of Biomedical Research of Salamanca (IBSAL), University of Salamanca, Spain, ⁴National Institute for the Study of Liver and Gastrointestinal Diseases (CIBERehd, "Instituto de Salud Carlos III"), Spain, ⁵IKERBASQUE, Basque Foundation for Science, Spain, ⁶Department of Medicine, Faculty of Medicine and Nursing, University of the Basque Country (UPV/EHU), Spain, ⁷Department of Biochemistry and Genetics, School of Sciences, University of Navarra, Spain
Email: jesus.banales@biodonostia.org

Background and aims: Cholangiocarcinoma (CCA) comprises a heterogeneous group of biliary malignant tumors characterized by dismal prognosis. The first-line treatment for advanced CCA [cisplatin (CisPt) and gemcitabine] is considered palliative due to the high chemoresistance of this cancer, barely impacting on patients' overall survival. Here, we aimed to design, synthesize and study a new generation of platinum (Pt)-derived chemotherapeutic drugs that produce inter-strand DNA breaks (vs classical single-strand breaks induced by CisPt and related compounds) and thus, prevent the development of DNA repair mechanisms in cancer cells.

Method: Ten Pt-derivatives (Aurki-Pt#s) were designed and synthesized. Atomic Force Microscopy (AFM) and Transmission Electron Microscopy (TEM) were used to characterize the binding of Aurki-Pt#s to DNA. The antitumoral effect of the two best candidates (Aurki-Pt#1 and #2) was evaluated by measuring the viability of human CCA cells (EGI-1 and HUCCT1), newly generated CisPt-resistant EGI-1 CCA cells, normal human cholangiocytes (NHC) and cancer-associated fibroblasts (CAFs). The DNA damage induced by Aurki-Pt#1 and #2 was assessed using the comet assay. To ascertain the internalization mechanism of Aurki-Pt#1 and #2, substrate competition studies through flow cytometry and accumulation studies using HPLC-MS/MS were carried out. Finally, the effect of Aurki-Pt#1 and #2 was also tested *in vivo* on a subcutaneous xenograft model of CCA.

Results: Aurki-Pt#s induced inter-strand DNA breaks, and the subsequent DNA fragmentation, contrary to CisPt. Aurki-Pt#1 and #2 significantly reduced CCA cell viability. Both compounds triggered increased DNA damage in CCA cells when compared to CisPt, augmenting the reactive oxygen species levels and being more effective when inducing apoptosis *in vitro*. Additionally, Aurki-Pt#1 and #2 decreased the proliferative capacity of those CCA cells that survived. Importantly, Aurki-Pt#1 and #2 also promoted cell death in CisPt-resistant CCA cells. Moreover, Aurki-Pt#1 and Aurki-Pt#2 caused CCA spheroid shrinkage. On the contrary, Aurki-Pt#1 and #2 did not induce a lethal effect in NHC in culture, but promoted cell cycle arrest. Besides, Aurki-Pt#1 and Aurki-Pt#2 had an impact on the survival of CAFs. Aurki-Pt#1 and #2 were transported into cells through OCT1, OCT3, CTR1 and OATP1A2, which did not transport CisPt. Finally, Aurki-Pt markedly hampered tumor growth on a subcutaneous xenograft model of CCA in comparison with CisPt or vehicle control.

Conclusion: This new generation of Pt-derived chemotherapeutic drugs selectively diminishes CCA cell viability through the induction of inter-strand DNA breaks, and has an impact on its tumor microenvironment, representing a promising therapeutic tool for naïve or CisPt-resistant CCA tumors.

SAT-213

Dynamic evolution of the serum metabolome reflects human hepatocarcinogenesis

Johann von Felden¹, Tim Rose², Lorenz Adlung¹, Manuela Peschka¹, Thorben Fruendt¹, Ismail Labgaa³, Philipp Haber⁴, Carolin Zimpel⁵, Darko Castven⁵, Arndt Weinmann⁶, Teresa Garcia-Lezana⁴, Moritz Waldmann¹, Thomas Renne¹, Hannah Voß¹, Manuela Moritz¹, Dorian Orlikowski¹, Helmut Schlüter¹, Myron Schwartz⁴, Jan Baumbach⁷, Ansgar W. Lohse¹, Samuel Huber¹, Henning Wege¹, Jens Marquardt⁵, Augusto Villanueva⁴, Josch Pauling², Kornelius Schulze¹. ¹University Medical Center Hamburg Eppendorf, Germany, ²Technical University Munich, Germany, ³Lausanne University Hospital (CHUV), Switzerland, ⁴Mount Sinai, United States, ⁵University Medical Center Schleswig Holstein, Germany, ⁶University Medical Center Mainz, Germany, ⁷University Hamburg, Germany
Email: j.von-felden@uke.de

Background and aims: Liver cancer is associated with rising incidence and mortality rates. Mechanisms of hepatocarcinogenesis are poorly understood and current tools for early detection of hepatocellular carcinoma (HCC) remain suboptimal. The aim of this

POSTER PRESENTATIONS

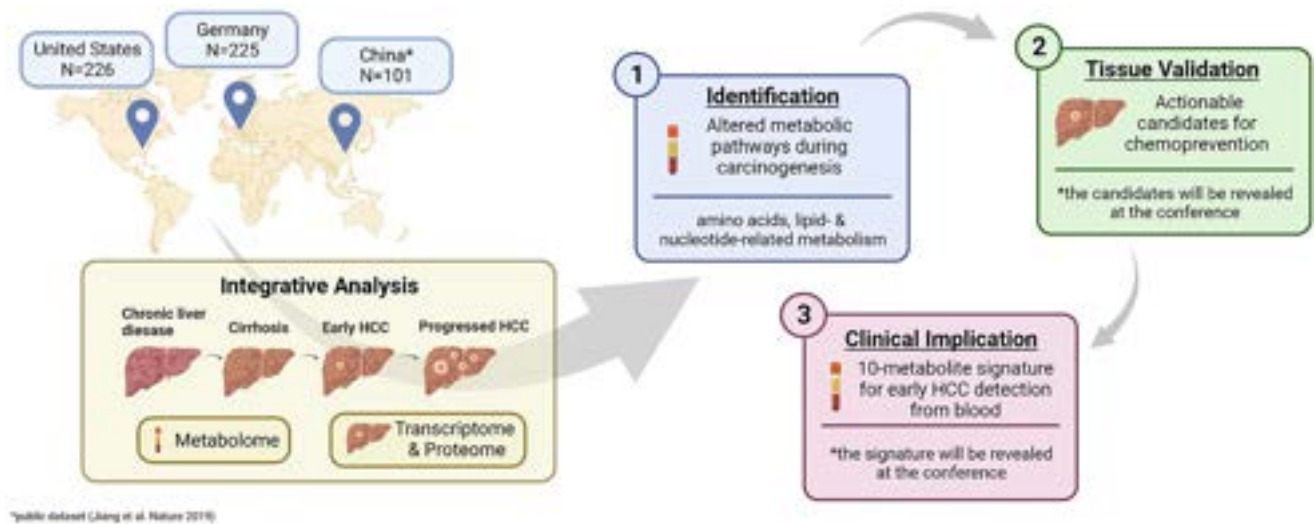


Figure: (abstract: SAT-213).

study was to confirm that the human serum metabolome undergoes significant alterations during hepatocarcinogenesis.

Method: This global, multicenter study included a total of N = 552 patients and n = 691 biospecimens from United States, Germany, and China. We performed targeted metabolomics by ultra-high pressure liquid chromatography coupled to tandem mass spectrometry in sera of N = 406 patients across the spectrum of hepatocarcinogenesis. Deregulated metabolites and respective pathways were identified by differential abundance, unsupervised biclustering using MoSBI, lipid network analysis with LINEX2, and pathway enrichment analysis. Findings were validated by mRNA sequencing and proteome profiling of primary HCC tissue and adjacent non-tumoral tissue in two independent cohorts (n = 285 specimens), including a publicly available dataset (Jiang et al. Nature 2019). Finally, we performed a phase 2 biomarker case-control study for early-stage HCC detection using blood samples (N = 375).

Results: Aspartic acid, glutamic acid, taurine, and hypoxanthine were among the top differentially abundant metabolites in the serum across chronic liver disease, cirrhosis, early HCC, and progressed HCC, independent of sex, age, and etiology (all $p < 2 \times 10^{-16}$, n = 406). Unsupervised biclustering (FDR < 0.05), lipid network analysis (>1.5-log2 fold change, FDR < 1×10^{-5}), and pathway enrichment analysis (up to 30% impact, FDR = 1.43×10^{-2}) further confirmed alterations in amino acids, lipid-, and nucleotide-related pathways. In tissue, these

pathways were significantly deregulated on gene expression and protein abundance levels in two independent datasets, including upregulation of *DUT*, *GMPS*, *NME6*, and *RRM2* (purine metabolism and/or nucleotide metabolism), *BCAT1* and *PYCR2* (biosynthesis of amino acids), and *NEU1* (sphingolipid metabolism) (all FDR < 0.05, n = 285). Finally, a phase 2 biomarker case-control study yielded high accuracy for a 10-metabolite signature from serum to discriminate between early HCC and cirrhotic controls (AUC 92%, n = 330).

Conclusion: Our findings demonstrate that serum metabolome profiling reflects deregulated metabolites and pathways during human hepatocarcinogenesis and identifies actionable candidates for chemoprevention. In addition, this liquid biopsy approach accurately detects early-stage HCC.

SAT-214

TAK1 deficiency promotes liver injury and tumorigenesis via ferroptosis and macrophage cGAS-STING signaling

Haoming Zhou¹, Wantong Su¹, Qi Wang¹, Xun Wang¹, Ling Lu¹. ¹The First Affiliated Hospital of Nanjing Medical University, Hepatobiliary Center, China

Email: lvling@njmu.edu.cn

Background and aims: Oxidative stress-mediated ferroptosis and macrophage-related inflammation play an important role in various

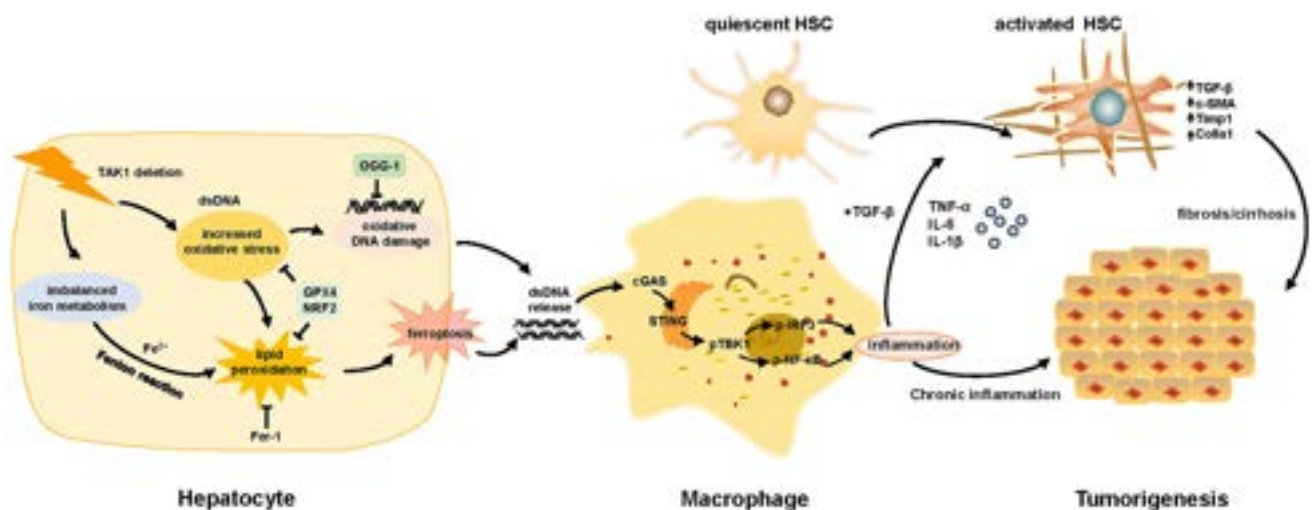


Figure: (abstract: SAT-214).

liver diseases. Here, we explored if and how hepatocyte ferroptosis regulates macrophage STING activation in the development of spontaneous liver damage, fibrosis, and tumorigenesis.

Method: We used TAK1 deficiency-induced liver spontaneous damage, fibrosis, and tumorigenesis model to investigate hepatocyte ferroptosis and its impact on macrophage STING signaling. Primary hepatocytes and macrophages were used for *in vitro* experiments.

Results: Significant liver injury and increased numbers of intrahepatic M1 macrophages were found in hepatocyte-specific TAK1-deficient (TAK1^{ΔHEP}) mice, peaking at 4 w and gradually decreasing at 8 w and 12 w. Meanwhile, activation of STING signaling was observed in livers from TAK1^{ΔHEP} mice at 4 w and had decreased at 8 w and 12 w. Treatment with a STING inhibitor promoted macrophage M2 polarization and alleviated liver injury, fibrosis, and tumor burden. TAK1 deficiency exacerbated liver iron metabolism in mice with a high-iron diet. Moreover, consistent with the results from single-cell RNA-Seq dataset, TAK1^{ΔHEP} mice demonstrated an increased oxidative response and hepatocellular ferroptosis, which could be inhibited by ROS scavenging. Suppression of ferroptosis by ferrostatin-1 inhibited the activation of macrophage STING signaling, leading to attenuated liver injury and fibrosis and a reduced tumor burden. Mechanistically, increased intrahepatic and serum levels of 8-OHdG were detected in TAK1^{ΔHEP} mice, which was suppressed by ferroptosis inhibition. Treatment with 8-OHdG antibody inhibited macrophage STING activation in TAK1^{ΔHEP} mice.

Conclusion: Hepatocellular ferroptosis-derived oxidative DNA damage promotes macrophage STING activation to facilitate the development of liver injury, fibrosis, and tumorigenesis. Inhibition of macrophage STING may represent a novel therapeutic approach for the prevention of chronic liver disease.

SAT-215

Targeting the E2F/MCM axis in cholangiocarcinoma halts disease progression in experimental models by rewiring lipid metabolism

Mikel Ruiz de Gauna¹, Ane Nieva-Zuluaga¹, Maider Apodaka-Biguri¹, Francisco González-Romero¹, Nerea Muñoz-Llanes¹, Paul Gomez-Jauregui¹, Natalia Sainz-Ramírez¹, Kendall Alfaro-Jiménez¹, Beatriz Gómez Santos¹, Xabier Buque¹, Igor Aurrekoetxea^{1,2}, Igotz Delgado¹, Idoia Fernández-Puertas¹, Ainhoa Iglesias³, Pedro Miguel Rodríguez^{4,5,6}, Diego Calvisi⁷, Ana Zubiaga³, Jesus Maria Banales^{4,5,6,8}, Patricia Aspichueta^{1,2,5}.

¹University of the Basque Country (UPV/EHU), Faculty of Medicine and Nursing, Department of Physiology, Leioa, Spain, ²Biocruces Health Research Institute, Cruces University Hospital, Barakaldo, Spain, ³University of Basque Country (UPV/EHU), Faculty of Science and Technology, Department of Genetic, Physical Anthropology and Animal Physiology, Leioa, Spain, ⁴Department of Liver and Gastrointestinal Diseases, Biodonostia Health Research Institute, Donostia University Hospital, University of the Basque Country (UPV/EHU), San Sebastian, Spain, ⁵National Institute for the Study of Liver and Gastrointestinal Diseases (CIBERehd, Instituto de Salud Carlos III), Spain, ⁶IKERBASQUE, Basque Foundation for Science, Bilbao, Spain, ⁷Institute for Pathology, Regensburg University, Regensburg, Germany, ⁸Department of Biochemistry and Genetics, School of Sciences, University of Navarra, Pamplona, Spain

Email: patricia.aspichueta@ehu.eus

Background and aims: Cholangiocarcinoma (CCA) comprises a heterogeneous group of biliary cancers with dismal prognosis. E2F1 and E2F2, transcription factors that regulate cell cycle and metabolism, are upregulated in metabolic associated fatty liver disease (MAFLD), which is a risk factor of CCA. E2F1/2 drive MAFLD-related hepatocellular carcinoma (HCC) development, sustaining a pro-carcinogenic lipid-rich environment. Minichromosome maintenance (MCM) proteins, helicases involved in DNA replication and cell cycle, are recognized targets of E2Fs that have been linked to different cancers. Thus, the aims were: 1) to evaluate the involvement of the E2F/MCM axis in CCA, and 2) to investigate the potential therapeutic

regulatory value of E2F/MCM axis in the rewiring of the cancer lipid metabolism.

Method: *Akt1* and *Yap* or *Taz* were overexpressed in the liver of wild type (WT) or *E2f1*^{-/-} mice as models of CCA. CCA cancer associated fibroblasts (CAFs) were isolated from patients. Triglyceride (TG) concentration was measured in liver samples of the mouse models of CCA and in cell lines *in vitro*. Cell viability, proliferation, spheroid growth and fatty acid oxidation (FAO) rate were measured in EGI1 and HUCCT1 CCA cell lines in the presence or absence of ciprofloxacin (CPX), an antibiotic that inhibits the MCM2-7 helicase activity. The effect on CCA cell viability, proliferation and spheroid growth of an inhibitor of E2F activity (HLM006474) was also tested. Data from human CCA tumours from the TCGA-CHOL cohort were analysed.

Results: Expression (mRNA) of E2F1 and E2F2 was upregulated in human CCA tumours, patient-derived CAFs, and in cellular and mouse models of CCA compared to controls; consequently, expression levels of MCM2-7 were also found elevated, and correlated positively with E2F1/2 expression. Experimental overexpression of *Akt1* and *Yap*, or *Akt1* and *Taz*, in *E2f1*^{-/-} mice resulted in significantly reduced tumour development compared to WT mice. The upregulation of E2F1/2 and MCM2-7 in CCA cells and tumours in mice was accompanied by increased TG content. Inhibition of MCM activity in human CCA cells with CPX induced a dose-dependent decrease in tumour cell viability, proliferation and spheroid growth. CPX also reduced the TG content and the FAO of CCA cells (EGI1) *in vitro*, which we had previously shown to be highly dependent on FAO for proliferation, and incubation with HLM006474 also decreased CCA cell viability, proliferation and spheroid size *in vitro*. Combination of CPX and HLM006474 induced a higher reduction of CCA cell viability *in vitro* than CPX or HLM006474 alone, suggesting that E2F activity promotes CCA progression not only by modulating MCM expression.

Conclusion: The E2F/MCM axis is upregulated in CCA and is required for tumour cell survival and proliferation, potentially by affecting, among other mechanisms, the increased TG content, FAO rate and the tumour microenvironment, arising as a novel target for therapy in this cancer.

SAT-216

MAP17 promotes an epithelial-mesenchymal-amoeboid transition in hepatocellular carcinoma by switching one-carbon metabolism

Claudia Gil-Pitarch¹, Iker Uriarte², Esther Bertran³, Natalia Hermán-Sánchez⁴, José Manuel García-Heredia^{5,6,7}, Rubén Rodríguez Agudo¹, Naroa Goikoetxea¹, Sofia Lachiondo-Ortega¹, Maria Mercado-Gómez¹, Irene González-Recio¹, Teresa Cardoso Delgado¹, Maria Vivanco⁸, Luis Alfonso Martínez-Cruz¹, Cesar Augusto Martín⁹, Rafael Artuch¹⁰, Mario Fernández¹¹, Manuel Gahete Ortiz¹², Isabel Fabregat^{3,13,14}, Matías A. Avila^{2,15}, Amancio Carnero¹⁶, María Luz Martínez-Chantar¹. ¹CIC bioGUNE, Liver disease lab, DERIO, Spain, ²CIMA, University of Navarra, Spain, ³Bellvitge Biomedical Research Institute (IDIBELL), Spain, ⁴Maimonides Institute for Biomedical Research of Cordoba (IMIBIC), Spain, ⁵Universidad de Sevilla, Spain, ⁶Grupo del CIBER de cáncer (CIBERONC), agencia estatal consejo superior de investigaciones científicas, instituto de biomedicina de sevilla (IBIS), Spain, ⁷Instituto de Biomedicina de Sevilla (IBIS), Spain, ⁸CIC bioGUNE, basque research and technology alliance, Spain, ⁹Department of molecular biophysics, biofísica institute (university of basque country and consejo superior de investigaciones científicas (UPV/EHU, CSIC), Spain, ¹⁰Clinical biochemistry department, Institut de Recerca Sant Joan de Déu, CIBERER and MetabERN Hospital Sant Joan de Déu, Spain, ¹¹Cancer Epigenetics and Nanomedicine Laboratory, Nanomaterials and Nanotechnology Research Center (CINN-CSIC), Spain, ¹²Department of Cell Biology, Physiology, and Immunology (University of Córdoba), Reina Sofia University Hospital and CIBERobn, Córdoba, Spain, ¹³CIBER Enfermedades hepáticas y digestivas (CIBERehd), Spain, ¹⁴Department of physiological sciences II, University of Barcelona, Spain, ¹⁵IdiSNA, Navarra institute for health research, Pamplona, Spain, ¹⁶Instituto de

POSTER PRESENTATIONS

Biomedicina de Sevilla (IBIS), Hospital Universitario Virgen del Rocío, Universidad de Sevilla, Consejo Superior de Investigaciones Científicas, Sevilla, Spain
Email: mlmartinez@cicbiogune.es

Background and aims: Epithelial-mesenchymal transition (EMT), a key process during embryonic development, promotes cell migration and resistance to apoptosis during tumour invasion and metastasis. In hepatocellular carcinoma (HCC) an amoeboid behaviour tends to increase the aggressiveness and metastatic capacity of epithelial tumours. MAP17 is a 17 kDa membrane protein expressed during embryogenesis, absent in most adult organs. The presence of MAP17 correlates with an inflammatory environment, hypoxia and increased reactive oxygen species (ROS). MAP17 has been identified in several types of cancer, including HCC. Modulation of EMT and amoeboid behaviour via MAP17 offers an attractive approach to prevent metastasis.

Method: Two HCC patient cohorts were used to characterise MAP17 levels. *In vitro*, expression of MAP17 was measured in mesenchymal and epithelial hepatoma cells, and its levels were modulated to study cell proliferation, drug resistance, mitochondrial dynamics, metabolic rewiring, and proteome homeostasis. *In vivo*, the role of MAP17 in the metastatic capacity was evaluated using orthotopic HCC mouse models.

Results: A positive correlation between MAP17 and mesenchymal markers, RAC/RHO family genes and markers of amoeboid movement was established in 751 HCC patients by *in silico* studies and by mRNA expression analysis in 246 HCC patients. MAP17 overexpression in 3D epithelial cell experiments led to the formation of rosette invadopodia, proinvasive structures with high metastatic capacity. MAP17 overexpression *in vitro* induced a reprogramming of energy metabolism in hepatoma cells with epithelial phenotype, increasing mitochondrial dynamics and Warburg effect-mediated lactic acidosis, which support a tumour microenvironment conducive to cancer cell proliferation. ROS generation was increased as a protective mechanism to avoid apoptotic and senescence processes. Rewiring of the one-carbon metabolic pathway was identified, proving an accelerated metabolism of the cell. There was a faster methionine degradation fuelling the folate cycle, which is the source of purines and pyrimidines, supporting a higher proliferative state. Thus, MAP17 could be involved in the methionine cycle, specially affecting the folate cycle. Accordingly, overexpression of MAP17 in PLC/PRF/5 cells led to the formation of multiple tumour foci when orthotopically implanted in the mouse liver. MAP17 silencing in hepatoma cells with mesenchymal phenotype led to the opposite results, regressing the tumour phenotype and slowing down the cell metabolism and proliferation.

Conclusion: Modulation of MAP17 in epithelial and mesenchymal HCC cells leads to the reprogramming of the transitional genes that define each phenotype. Our findings have identified the metastatic potential of MAP17 in liver cancer, as it triggers the mesenchymal phenotype and amoeboid behaviour in HCC.

SAT-217

Deciphering the cellular and molecular determinants of immunotherapy resistance in NASH-associated hepatocellular carcinoma by single-cell analysis

Lingyun Zhang^{1,2}, Yiling Zhang¹, Wenshu Tang¹, Zhewen Xiong¹, Xiaoyu Liu¹, Zhixian Liang¹, Weiqin Yang¹, Alfred Sze-Lok Cheng¹. ¹The Chinese University of Hong Kong, School of Biomedical Sciences, Hong Kong. ²The Chinese University of Hong Kong, Hong Kong
Email: alfredcheng@cuhk.edu.hk

Background and aims: Non-alcoholic steatohepatitis (NASH) has become a prominent risk and the fastest growing cause of hepatocellular carcinoma (HCC). Although immune checkpoint blockade (ICB) therapy, such as anti-programmed cell death-ligand 1 (anti-PD-L1) has exhibited effect in a subset of HCC patients, recent studies unveiled that NASH limited anti-tumor surveillance in ICB-

treated HCC. Here we aimed to delineate the mechanisms underlying ICB resistance in NASH-HCC at single-cell resolution.

Method: Orthotopic NASH-HCC mouse models were established through intrahepatic inoculation of liver cancer cell line in NASH mouse induced by methionine-and choline-deficient diet (MCD) or choline-deficient, L-amino acid-defined, high-fat diet (CDAHFD). Multi-color flow cytometry and single-cell RNA-sequencing (scRNA-seq) were utilized to dissect the liver and tumor immune micro-environment upon anti-PD-L1 treatment.

Results: Both MCD-HCC and CDAHFD-HCC mouse models showed no response to anti-PD-L1 therapy. Compared to control liver, multi-color flow cytometry demonstrated that CD11b⁺F4/80⁺CD206⁺M2 macrophages accumulated in NASH and further increased in liver and tumor upon anti-PD-L1 treatment. Notably, significantly positive correlations were identified among hepatic, intratumoral M2 macrophages and tumor weight. Moreover, tumor-infiltrating PD-1-expressing CD8⁺ T cells positively correlated with tumor weight and intratumoral M2 macrophages. Furthermore, scRNA-seq analysis of tumor-infiltrating immune cells demonstrated remarkably distinct pattern of monocyte/macrophage subclusters compositions which enriched in NASH-HCC development and anti-PD-L1 resistance.

Conclusion: The results provide insights into the importance of monocyte/macrophage reprogramming in ICB-resistance in NASH-HCC. Further investigation is warranted to determine the molecular determinants of these subclusters and identify potential targeted strategy for immunotherapeutic enhancement.

Acknowledgements: This study is supported by the RGC GRF (14120621), CRF (C4045-18W) and Li Ka Shing Foundation.

SAT-218

Differential hepatoprotective effects of semaglutide and lanifibranor in the GAN diet-induced obese and biopsy-confirmed mouse model of NASH with advanced fibrosis and HCC

Malte H. Nielsen¹, Susanne Pors¹, Jacob Nøhr-Meldgaard¹, Andreas Nygaard Madsen¹, Mathias Bonde Møllerhøj¹, Denise Oró¹, Mogens Vyberg², Henrik B. Hansen¹, Michael Feigh¹. ¹Gubra, Hørsholm, Denmark, ²Center for RNA Medicine, Aalborg University, Department of Clinical Medicine, Aalborg, Denmark
Email: mni@gubra.dk

Background and aims: Non-alcoholic steatohepatitis (NASH) increases the risk for the development of liver fibrosis which may progress to cirrhosis and hepatocellular carcinoma (HCC). Semaglutide (glucagon-like-receptor (GLP)-1 agonist) and lanifibranor (pan-peroxisome proliferator-activated receptor agonist) are currently in late-stage clinical development for NASH. The present study aimed to evaluate the efficacy of semaglutide and lanifibranor monotherapy on disease progression in the translational Gubra Amylin NASH (GAN) diet-induced obese (DIO) and biopsy-confirmed mouse model of advanced fibrosing NASH and HCC.

Method: Male C57BL/6J mice were fed the GAN diet high in fat, fructose, and cholesterol for 54 weeks prior to treatment intervention. Only animals with liver biopsy-confirmed NAFLD Activity Score (NAS ≥ 5) and advanced fibrosis (stage F3) were included and stratified into study groups. DIO-NASH-HCC mice received vehicle (SC, QD, n = 16), semaglutide (SC, QD, 30 nmol/kg, n = 15), or lanifibranor (PO, QD, 30 mg/kg, n = 15) for 14 weeks. Vehicle-dosed chow-fed C57BL/6J mice (SC, QD, n = 9) served as lean healthy controls. Untreated DIO-NASH-HCC mice (n = 10) were terminated at baseline. Tumor histopathological classification was performed by a clinical histopathologist. Within-subject (pre-to-post) change in non-alcoholic fatty liver disease (NAFLD) Activity Score (NAS), fibrosis stage, and collagen deposition (PSR % area) was evaluated using automated deep learning-based image analysis (GHOST). Other end points included terminal blood biochemistry and quantitative histomorphometry.

Results: DIO-NASH-HCC mice demonstrated progressive HCC burden over the 14-week study period. Tumors showed consistent

architectural and cytologic features of HCC with a marked loss of reticulin-stained fibers. Both semaglutide and lanifibranor significantly improved individual histopathological NAS ≥ 2 point, supported by beneficial changes in quantitative histological markers of steatosis (lipids and hepatocytes with lipid droplets) and inflammation (number of inflammatory foci, galectin-3). While both compounds did not improve fibrosis stage, lanifibranor significantly reduced individual pre-to-post quantitative fibrosis levels after 14 weeks. Notably, though, both compounds reduced histological marker of fibrogenesis (α -SMA). In contrast, semaglutide, but not lanifibranor, completely prevented progression in macroscopic tumor numbers, accompanied by reduced quantitative histological markers of proliferation (Ki67) and progenitor cell activation (CK19).

Conclusion: Consistent with recent clinical trials, lanifibranor and semaglutide improves NASH, while only lanifibranor promoted fibrosis regression in GAN DIO-NASH-HCC mice. Notably, semaglutide also improves HCC burden in the model. Deep learning-based image analysis is advantageous to assess within-subject changes in histopathological scores and quantitative fibrosis histology following drug treatment. Collectively, our data highlights the suitability of GAN DIO-NASH-HCC mice for profiling novel drug therapies targeting NASH with advanced fibrosis and HCC.

SAT-219

Capillarization of tumor endothelial cells within tumor associated with T cell exclusion in an autochthonous mouse HCC model

Pin-Hung Lin¹, Tai-Chung Tseng², Hung-Chih Yang², Ian Liao³.

¹National Taiwan University College of Medicine, Taiwan, ²National Taiwan University Hospital, Taiwan, ³National Yang Ming Chiao Tung University, Taiwan

Email: tctsenghvb@gmail.com

Background and aims: Liver sinusoidal endothelial cells (LSEC) is featured by the presence of fenestrae and lack of basal lamina and tight junctions between cells, which is different from the capillary EC. Such unique characteristics make LSEC where the surveillance and infiltration of T cells occurs. Recent studies have shown that persistent inflammation in liver results in sinusoidal capillarization, which is featured by overexpression of CD31, CD34, plasmalemmal vesicle associated protein-1 (PLVAP), and collagen IV, a major component of basal lamina. However, little is known about whether sinusoidal capillarization is present in hepatocellular carcinoma (HCC) and how it affects the T cell infiltration.

Method: We generated a spontaneous HCC mouse model via transposon-based delivery of oncogenes and CRISPR/Cas9-mediated knockout of tumor suppressor genes to transform primary hepatocytes through hydrodynamic injection (HDI). In addition, the oncogene was conjugated with a tumor antigen (OVA₂₅₇₋₂₆₄), a fluorescence protein for intravital imaging, and a secretory HiBiT for tumor marker.

Results: In our autochthonous mouse HCC model, the HiBiT level was first shown to correlate well with the tumor cell number and size *in vitro* and *in vivo*, respectively. We then found that the serum HiBiT level remained stable and the tumor size increased slowly within 3–5 weeks after HDI (early tumor, <100 μ m in diameter) but increased rapidly after week 7 (advanced tumor). The IHC staining showed that T cells were present within the early tumor but were excluded at the border of advanced tumor. The transferred OT-I T cells were shown to infiltrate into the tumor from the LSEC surrounding the early tumor using intravital imaging. In contrast, these cells were shown to be stay mostly at the peripheral part, but not the core of advanced tumor using clear tissue imaging ($n=8$, $P<0.01$). We then studied the difference between tumor endothelial cells (TEC) and LSEC, the key to affect T cell infiltration. We found that TEC expressed more CD31, CD34, and PLVAP than LSEC, and the specific component of basement membrane, collagen IV, was only present around the TEC in advanced tumor, but not LSEC via clear tissue imaging. In human HCC, we also

found that the increased expression of CD34 and PLVAP was present in TEC, but not LSEC, of human HCC either using IHC of human samples or RNAseq data of TCGA database. All these data suggest that the capillarization of TEC in HCC, which may be the key to block T cell infiltration into advanced tumor.

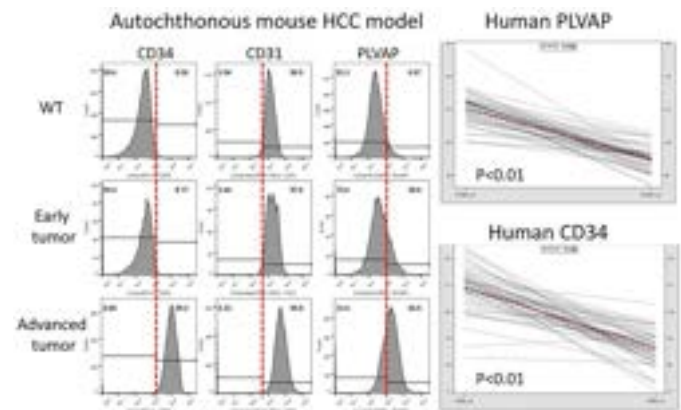


Figure:

Conclusion: Capillarization of tumor endothelial cells in HCC is not only present in our HCC model and human HCC samples. As our intravital imaging shows that the tumor-specific T cells infiltrate into the tumor from the surrounding LSEC, but not the capillarized TEC, it is critical to design a new strategy to delay or reverse the TEC development, which facilitates the T cell infiltration and improves immunotherapy response in HCC.

SAT-220

Anti-CD122 antibody restores specific CD8⁺ T cell response in non-alcoholic steatohepatitis and prevents hepatocellular carcinoma growth

Stéphanie Lacotte¹, Florence Slits¹, Beat Moeckli¹, Andrea Peloso², Stéphane König³, Matthiew Tihi², Sofia El Hajji¹, Laura Rubbia-Brandt², Christian Toso^{1,2}. ¹University of Geneva, Surgery, Geneva, Switzerland, ²Hôpitaux Universitaires de Genève (HUG), Genève, Switzerland, ³University of Geneva, Geneva, Switzerland

Email: stephanie.lacotte@unige.ch

Background and aims: Non-alcoholic steatohepatitis (NASH) can lead to hepatocellular carcinoma (HCC). Although immunotherapy is used as first-line treatment for advanced HCC, the impact of NASH on anticancer immunity is only partially characterized. We aimed at assessing the tumor-specific T cell immune response in the context of NASH in a mouse model of recurrent HCC.

Method: We engineered an HCC cell line (RIL-175) with cytoplasmic expression of ovalbumin (OVA). C57BL/6N mice fed a high-fat (HFD) or a control diet (ND) for 35 weeks were injected with 1.5×10^5 RIL-175-LV-OVA-GFP cells into the portal vein. The immune cell subsets and their phenotype were assessed in the blood, in the liver and in the tumors. A dataset of human gene expression in healthy liver, NASH, NASH-adjacent to HCC and HCC was also analyzed.

Results: After 35 weeks of HFD, the mice were obese and developed severe steatosis with inflammation. We observed an increase of the CD8⁺ T cell subset in the livers of HFD-fed mice, which corresponded to an expansion of the population of CD44⁺ CXCR6⁺ PD-1⁺ CD8⁺ T cells known to promote NASH lesions. 14 days after injection of RIL-175-LV-OVA-GFP cells, HFD-fed mice had a higher percentage of peripheral OVA-specific CD8⁺ T cells than ND-fed mice (8.31 vs 3.67%; $p=0.010$), but these cells did not prevent HCC growth as the tumors were larger in HFD-fed mice (620 vs 1603 mm³, $p=0.051$). In the liver, OVA-specific CD44⁺ CXCR6⁺ CD8⁺ cells were present at similar levels in ND- and HFD-fed mice, but the expression of PD-1 was higher in HFD-fed mice suggesting lowered immune activity (MFI 12605 vs. 16083, $p=0.0159$). Treating mice with an anti-CD122

POSTER PRESENTATIONS

antibody, which reduced the number of CXCR6⁺ PD-1⁺ cells, we restored OVA-specific CD8 activity (MFI 16406 vs. 10516, $p = 0.0571$), and reduced HCC growth compared to untreated HFD-fed mice ($p = 0.0286$). The human dataset confirmed that NASH-affected livers, NASH tissues adjacent to HCC and HCC in patients with NASH exhibited similar expression of a panel of genes.

Conclusion: The immune system is altered and fails to prevent HCC growth in HFD-fed mice. This effect is primarily linked to a higher representation of CD44⁺ CXCR6⁺ PD-1⁺ CD8⁺ T cells. Treatment with anti-CD122 antibody reduces the number of these cells and prevents HCC growth.

SAT-221

Metabolic rewiring by increased mitochondrial respiration drives immunosuppression in liver cancer

Naroa Goikoetxea^{1,2}, Leire Egia-Mendikute³, Miren Bravo¹, Marina Serrano-Macia¹, Teresa Cardoso Delgado¹, Iraia Ladero⁴, Elena Molina⁴, Sofia Lachiondo-Ortega¹, Rubén Rodríguez Agudo¹, Janire Castelo⁵, Diego Barriales⁵, Begoña Rodríguez Iruretagoyena¹, Eva Santamaria⁶, Maria Mercado-Gómez¹, Irene González-Recio¹, Mercedes Rincón⁷, Matías A Avila^{2,6,8}, Juan Anguita⁵, Natalia Elgueza⁴, Asís Palazón³, María Luz Martínez-Chantar^{1,2}. ¹Liver Disease Lab, Centre for Cooperative Research in Biosciences CIC bioGUNE, Basque Research and Technology Alliance, Derio, Spain, Spain, ²CIBERERHD, Spain, ³Cancer Immunology and Immunotherapy Lab, Centre for Cooperative Research in Biosciences CIC bioGUNE, Basque Research and Technology Alliance, Derio, Spain, Spain, ⁴Animal Health Department, NEIKER-Instituto Vasco de Investigación y Desarrollo Agrario, Derio, E-48160 Bizkaia, Spain., Spain, ⁵Inflammation and Macrophage Plasticity Lab, Centre for Cooperative Research in Biosciences CIC bioGUNE, Basque Research and Technology Alliance, Derio, Spain, Spain, ⁶Instituto de Investigaciones Sanitarias de Navarra-IdiSNA, Pamplona, Spain, Spain, ⁷Department of Medicine, Immunobiology Division, University of Vermont, Burlington, VT, 05405, USA, United States, ⁸Hepatology Program, Cima-University of Navarra, Pamplona, Spain, Spain
Email: ngoikoetxea@cicbiogune.es

Background and aims: Recent evidence supporting the need of a mitochondria-based metabolism for tumor growth prompted us to study the role of MCJ, an endogenous negative regulator of mitochondrial complex I, in the context of hepatocellular carcinoma (HCC). The tumor microenvironment imposes various metabolic regulations to hamper the antitumor immunity of infiltrating immune cells, therefore, modulating the metabolic rewiring may help recover the antitumor immune potential. This work aims to prove increased malignancy in mitochondria-based tumors and to analyze the differential immune response driven by metabolic changes.

Method: Two different experimental models of HCC were used. Firstly, Wt and whole-body *Mcj*^{-/-} mice were treated with diethylnitrosamine (DEN) for 5, 8 or 12 months. Secondly, C57/BL6 mice were injected with MYC-luc;sgp53 plasmid combination and *Mcj* was specifically silenced in the hepatocytes. Tumor progression, liver metabolism, mitochondrial activity and tumor infiltrating cells were assessed in both models.

Results: An *in silico* approach using UALCAN revealed reduced *Mcj* expression in patients at stage IV HCC. *In vivo*, the absence of MCJ increased tumorigenesis and mortality after DEN treatment. A strong oxidative phenotype was confirmed in *Mcj*^{-/-} tumors, as mitochondrial respiration was significantly higher, with increased intracellular ATP, NAD⁺, and NADPH levels. Examination of immune cells infiltrating the tumor showed a reduction in effector T lymphocytes (CD44⁺ CD62L⁻) and neutrophils (GR1⁺CD11b⁺) in *Mcj*^{-/-} mice. Serum and liver cytokine analysis showed a decrease in inflammatory IFN γ and TNF in *Mcj*^{-/-} mice. Significantly increased PDL-1 levels in *Mcj*^{-/-} mice indicated possible immunosuppression. On the other hand, liver-specific silencing of *Mcj* enhanced tumorigenesis in the

MYC-luc;sgp53 model, along with reduced inflammatory IFN γ and TNF and increased PDL-1. Interestingly, 20% of *Mcj*-silenced mice developed brain metastases. Mechanistically, increased expression of ectoenzymes *Cd39* and *Cd73* was found in *Mcj*^{-/-} mice, along with higher hepatic adenosine levels, which may promote immunosuppression in T cells via adenosine receptor signaling cascades.

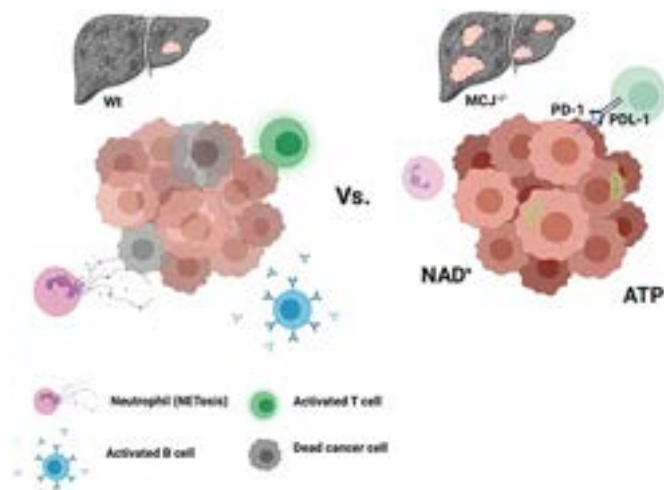


Figure:

Conclusion: Overall, decreased MCJ levels in the liver, which are also seen in advanced HCC patients, promote oxidative respiration and lead to metabolic rewiring that impedes antitumor immune potential via ATP-ectoenzyme-adenosine signaling and promotes tumorigenesis and even metastasis. Therefore, measurement of MCJ levels along with characterization of glycolytic versus oxidative respiration could help determine the most appropriate treatment, such as blockade of the adenosine axis in combination with immunotherapy.

SAT-222

Drug screening for hepatocellular carcinoma: automating and miniaturizing organoid assays for drug screening

Tijmen Booij¹, Sandro Nuciforo², David Keller¹, Eva Riegler², Diego Calabrese³, Markus Heim². ¹ETH Zurich, NEXUS Personalized Health Technologies, Zurich, Switzerland, ²University of Basel, Department of Biomedicine, Basel, Switzerland, ³University Hospital Basel, Histology Core Facility, Basel, Switzerland
Email: booij@nexus.ethz.ch

Background and aims: The past decades have shown an enormous increase in the popularity of using organoids for *in vitro* drug evaluation due to their improved physiological relevance. This is in turn expected to reduce the number, and size, of *in vivo* studies required to select drugs. Due to technological restraints and practical limitations, drug screens with patient-derived organoids have traditionally been performed on a small scale, and these experiments are often used to validate results from earlier *in vitro* drug screens. To enable large-scale drug screens with hepatocellular carcinoma (HCC) organoids derived from patient biopsies, we aimed to automate and miniaturize the drug screening methodology.

Method: The core facility NEXUS Personalized Health Technologies of ETH Zurich operates a lab-automation platform (HighRes Biosolutions). Using this platform, we optimized the liquid handling of organoids and eliminated the requirement for the use of animal-derived hydrogels for 3D culturing. Instead, we optimized the culture conditions with GrowDex and GrowDex-T (UPM Biomedicals), which could be pre-mixed with organoids and dispensed into 1536 well plates using a Certus Flex (Fritz Gyger AG). Using acoustic dispensing technology (Beckman), we could dispense test compounds in nanoliter range to eliminate the requirement for pipette tips. Drug efficacy was measured using cell viability measurement (CellTiterGlo

3D, Promega) and the developed methodology was evaluated in two patient-derived HCC organoid lines.

Results: Here we report the development of a robust organoid high-throughput drug screening platform for hepatocellular carcinoma organoids that is compatible with 1536 well plates and uses the nanocellulose based hydrogel GrowDex-T rather than its animal-derived alternatives as a matrix. We used the newly developed methodology to screen a library of approximately 1'200 FDA-approved drugs in a technical duplicate, and additionally screened a panel of 1'250 novel chemicals in a biological duplicate (performed more than one year apart). For both screens we report high reproducibility and robustness. Furthermore, due to the miniaturization to 1536 well plate format and the elimination of animal-derived matrices, no pipette tips are required at any step in the screening procedure, thereby dramatically reducing the experimental cost and improving assay quality.

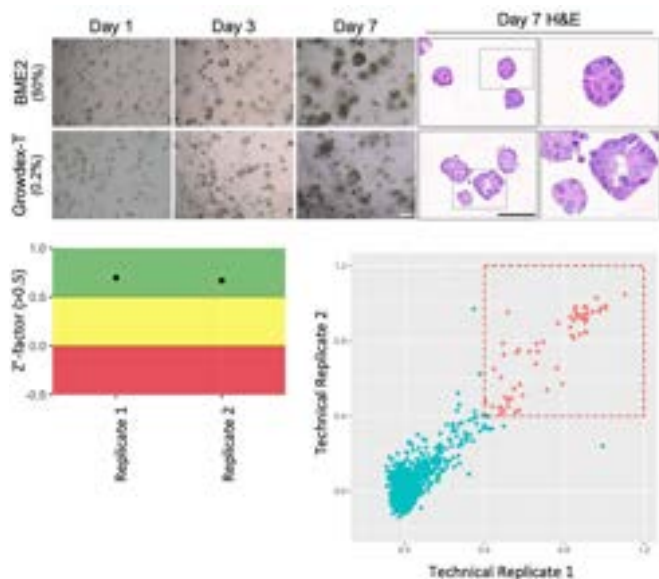


Figure:

Conclusion: We have developed a screening platform for HCC that uses biopsy-derived organoids in a 1536 well plate format. The developed methodology is automation-compatible and vastly the costs of testing drugs while delivering high-quality and robust screening results.

SAT-223

Therapeutic potential of targeting protein hyper-SUMOylation in cholangiocarcinoma

Paula Olaizola^{1,2}, Irene Olaizola¹, Marta Fernandez de Ara¹, Maite G Fernandez-Barrena^{2,3,4}, Laura Alvarez³, Mikel Azkargorta^{2,5}, Colm O'Rourke⁶, Pui-Yuen Lee-Law^{1,7}, Luiz Miguel Nova-Camacho⁸, Jose Marin^{2,9}, María Luz Martínez-Chantar^{2,10}, Matías A Avila^{2,3,4}, Patricia Aspichueta^{2,11,12}, Felix Elortza^{2,5}, Jesper Andersen⁶, Luis Bujanda^{1,2}, Pedro Miguel Rodríguez^{1,2,13}, María Jesús Perugorria^{1,2,14}, Jesus Maria Banales^{1,2,13,15}. ¹Department of Liver and Gastrointestinal Diseases, Biodonostia Health Research Institute-Donostia University Hospital- University of the Basque Country (UPV/EHU), Spain, ²National Institute for the Study of Liver and Gastrointestinal Diseases (CIBERehd, "Instituto de Salud Carlos III"), Spain, ³Hepatology Program, CIMA, University of Navarra, Spain, ⁴Instituto de Investigaciones Sanitarias de Navarra (IdiSNA), Spain, ⁵Proteomics Platform, CIC bioGUNE, CIBERehd, ProteoRed-ISCIII, Bizkaia Science and Technology Park, Spain, ⁶Biotech Research and Innovation Centre (BRIC), Department of Health and Medical Sciences, University of Copenhagen, Denmark, ⁷Department of Gastroenterology and Hepatology, Radboud University Nijmegen Medical Center, Netherlands,

⁸Osakidetza Basque Health Service, Donostialdea IHO, Donostia University Hospital, Department of Pathology, Spain, ⁹Institute of Biomedical Research of Salamanca (IBSAL), University of Salamanca, Spain, ¹⁰Liver Disease Laboratory, CIC bioGUNE, Basque Research and Technology Alliance (BRTA), Spain, ¹¹Department of Physiology, Faculty of Medicine and Nursing, University of the Basque Country (UPV/EHU), Spain, ¹²Biocruces Bizkaia Health Research Institute, Cruces University Hospital, Spain, ¹³IKERBASQUE, Basque Foundation for Science, Spain, ¹⁴Department of Medicine, Faculty of Medicine and Nursing, University of the Basque Country (UPV/EHU), Spain, ¹⁵Department of Biochemistry and Genetics, School of Sciences, University of Navarra, Spain Email: jesus.banales@biodonostia.org

Background and aims: cholangiocarcinoma (CCA) comprises a heterogeneous group of malignant tumors with dismal prognosis. Alterations in post-translational modifications (PTMs), including SUMOylation, result in abnormal protein dynamics, cell disturbances and disease. Here, we investigate the role of SUMOylation in CCA development and progression.

Method: levels and function of SUMOylation, together with response to S-adenosylmethionine (SAME) and ML792 (SUMOylation inhibitors) or CRISPR/Cas9 against *UBE2I* were evaluated *in vitro*, *in vivo* and/or in patients with CCA. The impact of SUMOylation in CCA cells on tumor-stroma crosstalk was assessed performing co-culture experiments with CCA-derived cancer-associated fibroblasts (CAFs), human endothelial cells and monocytes. Proteomic analyses were carried out by mass spectrometry.

Results: the SUMOylation machinery was found overexpressed and overactivated in human CCA cells and tumors, correlating with poor prognosis. Most SUMOylated proteins found upregulated in CCA cells, after SUMO1-immunoprecipitation and further proteomics, participate in cell proliferation, survival or cell homeostasis. Genetic (CRISPR/Cas9-*UBE2I*) and pharmacological (SAME and ML792) inhibition of SUMOylation reduced CCA cell proliferation and impeded colony formation *in vitro*. Moreover, both SAME and ML792 induced apoptotic cell death in CCA cells *in vitro*. SUMOylation depletion (SAME, ML792 or CRISPR/Cas9-*UBE2I*) halted tumorigenesis in subcutaneous models of CCA *in vivo*. Furthermore, SUMOylation deficiency in CCA cells reduced cancer-associated fibroblast and endothelial cell proliferation and impaired macrophage polarization towards an anti-inflammatory M2-like phenotype.

Conclusion: Aberrant protein SUMOylation contributes to cholangiocarcinogenesis by promoting cell survival and proliferation. Moreover, SUMOylation impacts the CCA-stroma crosstalk. Impaired SUMOylation halts CCA growth and, thus, may represent a potential new therapeutic strategy for patients with CCA.

SAT-224

Cytokine levels and circulating DNA profiling in plasma as biomarkers of response to immunotherapy in hepatocellular carcinoma

Elena Vargas Accarino¹, Monica Higuera¹, María Bermúdez¹, Monica Pons¹, Maria Torrens¹, Ana María Aransay², Jose Ezequiel Martín², Xavier Merino³, Beatriz Minguez¹. ¹Vall d'Hebron University Hospital, Liver Unit, Spain, ²CIC bioGUNE, Spain, ³Vall d'Hebron University Hospital, Radiology Department, Spain Email: bminguez@vhebron.net

Background and aims: Immune checkpoint inhibitors (ICIs) have revolutionized the therapeutic landscape for advanced hepatocellular carcinoma (HCC). The combinations anti-PD-L1 antibody (atezolizumab) and VEGF-neutralizing antibody (bevacizumab) and anti-PD-L1 antibody (durvalumab) and anti-CTLA-4 (tremelimumab) have become first line options. Our aim was to identify potential serological markers of response to ICIs.

Method: Prospective cohort of 25 patients treated with ICIs (Nivolumab (n = 14), Atezolizumab/Bevacizumab (n = 8), Durvalumab/Tremelimumab (n = 2) and Lenvatinib/Pembrolizumab

(n = 1)). Plasma samples were collected at the beginning and after 3 months of ICI treatment. 24 inflammatory cytokine levels were analyzed by ELISA as well as the levels of circulating cell free DNA (cfDNA), circulating tumor DNA (ctDNA) and percentage of TERT mutation by ddPCR, at baseline and after 3 months of treatment. Basal cfDNA profiling from 21 of these patients was analyzed by Onco-500 TruSight.

Results: 84% of patients were male, median age was 71 years and 76% were BCLC-C at the beginning of ICIs treatment. 76% had underlying liver disease, being HCV infection the most frequent etiology (52%). Median follow-up was 17 months. 8% presented complete radiological response (CR), 20% partial radiological response (PR), 44% stable disease (SD) and 28% radiological progression (PD) as best radiological outcome (RECIST 1.1). Baseline CTLA-4 levels were significantly higher in patients presenting radiological progression [mean (SD)] [76.55 (150.84) in PD and 0.15 (0.67) pg/ml in no PD] ($p < 0.05$). 3 months post-treatment, MCP-1 levels were significantly lower in patients presenting PD [49.25 (25.73)] than in patients presenting CR/PR/SD [73.73 (86.34) pg/ml] ($p < 0.05$) and TNF- α levels were significantly higher in those patients [110.4 (239.7) vs 49.9 (189.43) pg/ml] ($p < 0.05$). Baseline cfDNA levels were significantly different between patients presenting radiological response (CR/PR) [2.3 (0.58) ng/ul] vs patients (SD/PD) [8.95 (6.89) ng/ul]. These differences were also present after 3 months under therapy [CR/PR 2.12 (0.92) vs SD/PD 10.1 (10) ng/ul]. Higher levels of cfDNA than 3.04 ng/ul were associated with a poorer overall survival ($p < 0.005$). ctDNA levels after 3 months of treatment were also significantly different [0.55 (0.35) in CR/PR and 4.34 (5.5) ng/ul in SD/PD] ($p < 0.005$). Regarding sequencing of baseline cfDNA patients with radiological response (CR/PR) had significantly more copy number variation (CNV) than those without it (97 vs 1) ($p < 0.05$). Pathogenic mutations in CTNNB1 were present in 100% of patients showing PD, but only in 53% of those presenting stable disease or radiological response, and patients presenting PD had significantly more pathological mutations in CDKN2A (67% vs 7%) ($p < 0.05$).

Conclusion: Basal levels of cfDNA, CTLA-4, CDKN2A mutations and CNV are significantly different between patients with and without radiological response to ICIs treatment. Levels of MCP-1, TNF- α and total amount of cfDNA and ctDNA after three months of ICIs treatment are significantly different in patients presenting radiological response. Analysis of cfDNA and cytokines could help to identify HCC patients benefiting more of immunotherapies. Deeper molecular analysis are currently ongoing.

SAT-225

Fibroblast growth factor 19 cooperates with Myc to promote liver carcinogenesis

José Ursic Bedoya^{1,2}, Guillaume Desandré², Carine Chavey², Pauline Marie², Benjamin Riviere¹, Anthony Lozano², Eric Assenat^{1,2}, Urszula Hibner², Damien Gregoire². ¹CHU Montpellier, Montpellier, France, ²Institute of Molecular Genetics of Montpellier, CNRS-UMR 5535, Montpellier, France
Email: jose.ursicbedoya@chu-montpellier.fr

Background and aims: Increased expression of the fibroblast growth factor (FGF19), a hormone whose physiological function is the regulation of bile acids and glucose homeostasis, is a hallmark of a sub-group of aggressive hepatocellular carcinoma (HCC). Analogs have been developed to mimic the hepatoprotective metabolic effects of FGF19, while being theoretically devoid of its oncogenic effects. FGF19 analogs, as well as inhibitors of its signaling, are under investigation for treatment of metabolic disorders and HCC, respectively. Our work investigates oncogenic cooperation between FGF19, or its analogs, and pathways frequently mutated in HCC.

Method: We performed hydrodynamic gene transfer (HGT) in C57BL/6J mice to combine overexpression of FGF19, FGF15, FGF21, FGF19 analog (aldafermin) or constitutively active FGFR4 mutant (FGFR4^{V547L}) with oncogenic events commonly found in HCC (p53

inactivation, MYC overexpression, Wnt/ beta-catenin pathway activation). Sequential HGT experiments were used to transfect distinct sets of hepatocytes. Tumors were analyzed by RT-qPCR, RNA-seq, immunohistochemistry (IHC) and phospho-proteome assays. In addition, tumors were dissociated to establish cell lines, which were used for orthotopic xenografts. Transcriptomic datasets from patients with NASH and healthy controls were analyzed to detect Myc pathway activation.

Results: We report that while FGF19 is by itself a weak oncogene, it efficiently cooperates with several oncogenic events characteristic of HCC, such as activation of the Wnt/beta-catenin pathway or increased Myc expression. Sequential HGT experiments demonstrate that FGF19 cooperates with Myc in a non-cell autonomous, paracrine fashion. Transcriptomic and IHC analyses show that FGF19+ tumors display increased neoangiogenesis. Oncogenic cooperation was also observed when Myc was co-expressed with FGF15, FGF21 or FGFR4^{V547L}. Surprisingly, similar results were obtained with a plasmid coding for aldafermin, notwithstanding the reported lack of oncogenic activity of this analog. Human datasets from NASH patients display frequent Myc pathway activation compared to healthy controls.

Conclusion: Our findings indicate that FGF19/FGFR4 pathway activation cooperates with Myc to promote aggressive HCC. Moreover, we suggest that aldafermin might keep oncogenic properties in this context. Since Myc pathway is often deregulated in patients with NASH or cirrhosis, our results suggest a precautionary approach with regard to the potential adverse effects of FGF analogs in these patients.

SAT-226

KLF5 upregulation is a common event in cholangiocarcinoma, acting as an oncogene and constituting a bad prognostic factor

Pedro Miguel Rodrigues^{1,2,3}, Oihane Erice¹, Ana Landa-Magdalena¹, Nuno Paiva¹, Maite G Fernandez-Barrena^{2,4}, Paula Olaizola^{1,2}, Ainhoa Lapitz¹, Colm O'Rourke⁵, Jesper Andersen⁵, Diego Calvisi⁶, Mikel Azkargorta^{2,7}, Felix Elortza^{2,7}, Ibai Goicoechea⁸, Charles Lawrie^{3,8}, Luis Bujanda^{1,2}, María Jesús Perugorria^{1,2,9}, Jesus Maria Banales^{1,2,3,10}. ¹Biodonostia Health Research Institute, Department of Liver and Gastrointestinal Diseases, San Sebastian, Spain, ²National Institute for the Study of Liver and Gastrointestinal Diseases (CIBERehd, "Instituto de Salud Carlos III"), Spain, ³Ikerbasque, Basque Foundation for Science, Spain, ⁴CIMA-University of Navarra, Division of Hepatology, Spain, ⁵Biotech Research and Innovation Centre (BRIC), Department of Health and Medical Sciences, University of Copenhagen, Denmark, ⁶Institute of Pathology, University of Regensburg, Germany, ⁷CIC bioGUNE, CIBERehd, ProteoRed-ISCIII, Bizkaia Science and Technology Park, Proteomics Platform, Spain, ⁸Biodonostia Health Research Institute, Molecular Oncology group, Spain, ⁹University of the Basque Country UPV/EHU, Department of Medicine, Faculty of Medicine and Nursing, Spain, ¹⁰School of Sciences, University of Navarra, Department of Biochemistry and Genetics, Spain
Email: pedro.rodrigues@biodonostia.org

Background and aims: Cholangiocarcinoma (CCA) comprises a heterogeneous group of malignant tumors with poor prognosis. Krüppel-like factors (KLF) are a family of transcription factors involved in large variety of biological processes, including organogenesis, differentiation and cellular homeostasis. Here, we investigated the role of KLF5 in cholangiocarcinogenesis and evaluated the therapeutic potential of its inhibition during CCA tumorigenesis.

Method: KLF5 expression was determined in human CCA tissues [Copenhagen (n = 210), TCGA (n = 36), Job (n = 78), TIGER-LC (n = 90) and San Sebastian cohorts (n = 12)] and cell lines. KLF5^{-/-} CCA cells were generated by CRISPR/Cas9. Proteomic analyses were carried out by mass spectrometry and the functional effects of KLF5 genetic ablation or chemical inhibition with ML264 were evaluated *in vitro* and *in vivo*.

Results: KLF5 expression was upregulated in human CCA tissues from 5 different patient cohorts compared to surrounding normal liver tissue. High KLF5 levels correlated with lymph node invasion and worse overall survival. In vitro, KLF5 protein and mRNA levels were found upregulated in human CCA cells compared to normal human cholangiocytes. Proteomic analysis of KLF5^{-/-} CCA cells revealed that most of the altered pathways are related with the modulation of cell cycle, proliferation, survival and migration. In agreement, KLF5^{-/-} CCA cells displayed decreased cell proliferation, colony formation and migration while promoting cell cycle arrest at G1/S and apoptosis in vitro, when compared with CCA control cells. Instead, no signs of tumor development were evident after subcutaneous or orthotopic injection in a xenograft animal model of CCA. Likewise, pharmacological inhibition of KLF5 with ML264 hampered CCA cells proliferation and migration in vitro and blocked tumor growth in vivo in distinct animal models. Lastly, both genetic and pharmacological inhibition of KLF5 sensitized CCA cells to chemotherapy-induced apoptosis in vitro, and the combination of the standard of care chemotherapy (gemcitabine + cisplatin) and ML264 completely halted CCA tumor growth in mice.

Conclusion: Increased KLF5 is a general event in CCA, contributing to cancer progression by promoting cell survival and proliferation, as well as, chemoresistance. KLF5 inhibition with ML264 may represent a potential therapeutic strategy for CCA.

SAT-227

NLRP3 and IL-1, but not IL-18, are drivers of hepatocellular carcinoma in two independent murine models

Mona Peltzer¹, Antje Mohs¹, Jan G. Hengstler², Serena Pelusi³, Luca Valenti^{3,4}, Carolin V. Schneider¹, Kai Markus Schneider¹, Christian Trautwein¹. ¹University Hospital RWTH Aachen, Department of Internal Medicine III, Aachen, Germany, ²Leibniz Research Centre for Working Environment and Human Factors, Toxikologie/ Systemtoxikologie, Dortmund, Germany, ³Biological Resource Center, Fondazione IRCCS Ca' Granda Policlinico, Milan, Italy, ⁴Department of Pathophysiology and Transplantation, Università degli Studi Milano, Milan, Italy
Email: mpeltzer@ukaachen.de

Background and aims: Hepatocellular carcinoma (HCC) occurs as a consequence of malignant transformation of hepatocytes frequently triggered during chronic inflammation. The NLR Family Pyrin Domain containing 3 (NLRP3) inflammasome plays a crucial role in inflammation related liver disease but its contribution to hepatocyte malignant transformation remains unclear. After the two-step activation of the NLRP3 inflammasome by Pathogen-/Damage-associated molecular patterns (PAMPs/DAMPs), secretion of the pro-inflammatory cytokines Interleukin 1 beta (IL-1beta) and Interleukin 18 (IL-18) is initiated. In the present study, we aimed to understand the role of the NLRP3 inflammasome and its downstream targets (IL-1beta and IL-18) in inflammation- and primary sclerosing cholangitis (PSC) -related hepatocarcinogenesis.

Method: Prevalence of NLRP3, Interleukin 1 receptor (IL1R) and Interleukin 18 receptor (IL18R) as well as inherited variants determining alterations in protein sequence were analyzed in HCC patients. In mice, HCC was induced by the N-nitrosodiethylamine/ carbon tetrachloride (DEN/CCl₄) model in wild-type (WT), *Nlrp3*^{-/-}, *Il1r*^{-/-} and *Il18r*^{-/-} mice. To study PSC related carcinogenesis, *Nlrp3*^{-/-} mice were crossed to multidrug resistance gene 2 (*Mdr2*) knockout mice (*Mdr2*^{-/-}/*Nlr3*^{-/-}) and were analyzed at the age of 64 weeks. In both models, tumor development, immune cell infiltration and proliferation were analyzed.

Results: Analysis of human data sets revealed an overexpression of inflammasome-related proteins in HCC tissue and an overrepresentation of inflammasome-associated protein-coding variants. In two murine tumor models (DEN/CCl₄ and genetic modified *Mdr2*^{-/-}) NLRP3 deletion reduced tumor burden and inflammation compared to their respective controls. Reduced inflammation was evidenced by

decreased immune cell infiltration via FACS, especially monocyte-derived macrophages and neutrophils. In addition, NLRP3 deletion significantly reduced proliferation in both models, as demonstrated by Western Blot analysis and stainings. To further dissect the downstream pathway, *Il1r*^{-/-} and *Il18r*^{-/-} mice were treated with DEN/CCl₄. Interestingly, tumor bearing *Il1r*^{-/-} but not *Il18r*^{-/-} mice showed a reduced tumor burden and inflammation, mainly of monocyte-derived macrophages and neutrophils. Surprisingly, whereas in tumor-bearing *Nlrp3*^{-/-} mice CD8⁺/PD1⁺ T cells were downregulated in tumor-bearing *Il1r*^{-/-} mice these cells were upregulated. Thus, the deletion of NLRP3 or IL1R, but not of IL18R showed protective effects for HCC development.

Conclusion: Our results demonstrate that in human HCC tissue NLRP3, IL-1R and IL18R is overexpressed and an overrepresentation of inflammasome-associated protein-coding variants are present. In two independent murine models NLRP3 and IL-1, but not IL-18 were identified as driver of malignant hepatic tumor development.

SAT-228

Infiltrating suppressive myeloid cells dominate the pediatric hepatoblastoma tumor immune microenvironment

Danielle Krijgsman¹, Lianne Kraaijer², Meggy Verdonshot¹, Jeanette Leusen³, Weng Chuan Peng², Yvonne Vercoulen¹. ¹UMC Utrecht, Center for Molecular Medicine, Utrecht, Netherlands, ²Princess Máxima Center for Pediatric Oncology, Utrecht, Netherlands, ³UMC Utrecht, Center for Translational Immunology, Utrecht, Netherlands
Email: y.vercoulen@umcutrecht.nl

Background and aims: Pediatric hepatoblastoma is a rare disease, affecting approximately 1/million children. Pediatric liver tumors likely originate from immature hepatocyte precursors and show low mutational burden. Until now, the pathobiology of pediatric liver cancer is poorly understood due to their low incidence. Currently, pediatric hepatoblastoma patients are treated with chemotherapeutics followed by tumor resection. Although this treatment results in a clinical response in most patients, it associates with high toxicity. Better understanding of the pathogenesis and effects of chemotherapy in pediatric hepatoblastoma is crucial to optimize treatment decisions. In adult liver cancer, the immune system plays a pivotal role in tumor development and progression. Tumor-associated macrophages (TAM) and myeloid-derived suppressor cells (MDSC) potentially suppress the immune system while supporting tumor growth. We here set out to investigate the role of the myeloid immune infiltrate in pediatric hepatoblastoma.

Method: Tissue samples of pediatric hepatoblastoma were included from pre-treatment biopsies, and post-chemotherapeutic resections containing both tumor tissue and adjacent normal tissue. A custom developed antibody panel was used for high-plex imaging mass cytometry (Hyperion). Data analysis for single-cell spatial profiling was performed, using the 'MATISSE' pipeline which identified both immune cell subsets, and tumor cells. Spatial neighborhood analysis was performed using CytoMap.

Results: Principal Component Analysis revealed that while lymphocyte markers associate with normal tissue, myeloid markers associate with tumor, regardless of treatment. T cell markers CD8a and CD4, and pro-inflammatory proteins IFNγ and NFκB were significantly elevated in normal tissue compared to tumor. Moreover, chemotherapy induced an increased expression of CD68 (macrophages) and HLA-DR (MHC-II) in the tumor. We identified diverse myeloid populations: The abundance of macrophage cluster 1, and a cluster of cytotoxic (CD8⁺) T cells and Macrophages was increased in the tumor upon chemotherapy. Detailed characterization revealed that these macrophages were suppressive, reflected by high expression of CD163, iNOS, and arginase. Moreover, chemotherapy reduced CD33 expression reflecting maturation of infiltrating macrophages upon treatment. Finally, neighborhood analysis revealed that overall, the immune cells avoided tumor and stromal cells, while lymphocytes

POSTER PRESENTATIONS

and myeloid cells clearly interacted, suggesting immune cell exclusion.

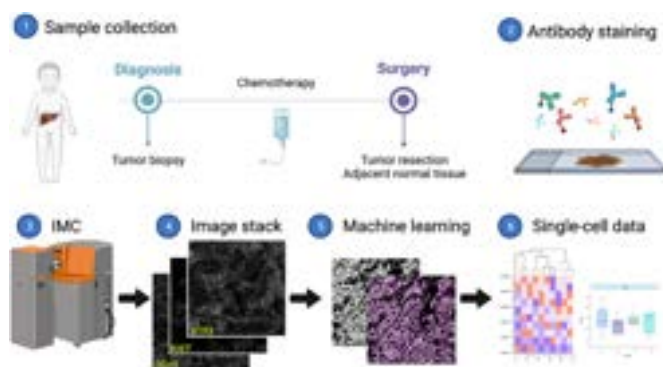


Figure:

Conclusion: We demonstrate here the first in-depth immune infiltrate characterization of pediatric hepatoblastoma and reveal that the myeloid compartment dominates the immune infiltrate in the tumor compared to normal tissue. Moreover, the infiltrating macrophages numbers increased upon chemotherapy and showed a suppressive phenotype upon chemotherapy, indicating that the chemotherapy itself modulates the immune microenvironment in the tumor. The low numbers of infiltrating lymphocytes and reduced expression of pro-inflammatory proteins, and low interaction between immune cells and tumor indicate an immune-cold tumor microenvironment in hepatoblastoma. Our results suggests that these tumors will likely not benefit from T-cell directed therapeutic strategies and that the myeloid compartment would serve as a more relevant target for alternative treatments to chemotherapy.

SAT-229

Fatty Acid Synthase expression promotes the malignant features of cholangiocarcinoma cells and predicts shorter survival in patients

Giulia Lori¹, Chiara Raggi¹, Benedetta Piombanti¹, Mirella Pastore¹, Elisabetta Rovida¹, Jesper Andersen², Monika Lewinska², Amalia Gastaldelli³, Fabio Marra¹. ¹University of Florence, Italy, ²University of Copenhagen, Denmark, ³CNR, Italy
Email: fabio.marra@unifi.it

Background and aims: Cancer cells are exposed to a metabolically challenging environment with scarce availability of nutrients, and alterations in lipid metabolism may affect the cellular response to drugs. We hypothesize that fatty acids (FA) modulate the biology of cholangiocarcinoma (CCA) cells and the development of stemness features.

Method: CCA cells (HuCCT-1 or CCLP1) were treated with monounsaturated FAs (132 μ M oleic or 100 μ M palmitoleic acid). Self-renewal ability was tested with a colony formation assay. Cancer stem cell (CSC)-enriched spheres were obtained growing cells in anchorage-independent conditions and selective medium. Five-year overall survival (OS) was analyzed in 34 patients with CCA sub-grouped based on fatty acid synthase (FASN) expression. Desaturation index and triglyceride de novo synthesis were performed by lipidomic analysis. NSG mice were injected with CCLP1 spheres and treated with the FASN inhibitor orlistat (240 mg/Kg). Tumor volume was measured with Vevo LAZR-X imaging station. RTPCR array on tumor masses was performed using the QuantiNova LNA PCR Panel.

Results: Exposure of CCA cell lines to FAs increased cell proliferation and activated growth and survival pathways, including AKT and ERK1/2. Exposure to FA made CCA cells less sensitive to the toxic effects of chemotherapeutic agents, and modulated the expression of ABC transporters involved in drug resistance. The colony forming ability of CCA cells was increased by FAs, and was associated with upregulation of genes controlling epithelial-mesenchymal transition

and stemness. Expression levels of genes involved in lipid metabolism were upregulated in CSC-enriched spheres as well as the percentage of desaturated TGs. FASN inhibition by orlistat decreased cell proliferation and CSC or EMT markers. In a xenograft model of CCA, tumor volume was significantly lower in mice treated with orlistat. Accordingly, expression of genes involved in cell proliferation was downregulated while the one of tumor suppressor genes increased. In a series of CCA patients, the expression of FASN correlated with OS.

Conclusion: FA promote malignant features of CCA and increase CSC markers. FASN expression levels correlate with survival in patients with CCA and promote CCA growth in mice. Lipid metabolism could be a new target to block CCA progression.

SAT-230

Positive effects of PARP-1 inhibition in KRAS-mutated intrahepatic cholangiocarcinoma is mediated by CHK1 kinase

Darko Castven¹, Friederike Keggenhoff², Stojan Stojkovic¹, Diana Becker², Jovana Castven¹, Carolin Zimpel¹, Beate Straub², Harald Langer¹, Patrizia Hähnel², Thomas Kindler², Jörg Fahrner³, Colm O'Rourke⁴, Lichun Ma⁵, Xin W. Wang⁵, Timo Gaiser⁶, Matthias Matter⁷, Christian Sina¹, Stefanie Derer¹, Stephanie Roessler⁸, Bernd Kaina², Jesper Andersen⁴, Peter Galle², Jens Marquardt¹. ¹Universitätsklinikum Schleswig-Holstein, Campus Lübeck, Lübeck, Germany, ²University medicine at the Johannes Gutenberg University in Mainz, Mainz, Germany, ³Technical University of Kaiserslautern, Kaiserslautern, Germany, ⁴Biotech Research and Innovation Centre, København, Denmark, ⁵National Cancer Institute, NIH, Bethesda, United States, ⁶UNIVERSITÄTSMEDIZIN MANNHEIM, Mannheim, Germany, ⁷Universitätsspital Basel, Basel, Switzerland, ⁸Heidelberg University, Heidelberg, Germany
Email: castvendarko@gmail.com

Background and aims: Intrahepatic cholangiocarcinoma (iCCA) is the second most common primary liver cancer with an increasing incidence over recent years. Due to the complexity of iCCA pathogenesis and the pronounced genetic heterogeneity treatment options are still limited. Activating KRAS mutations are among the most abundant genetic alterations in iCCA and are associated with early recurrence, poor response to chemotherapy, and reduced overall survival, highlighting the need for novel therapeutic approaches. Poly (ADP-ribose)polymerase-1 (PARP-1) is frequently observed to be upregulated in iCCA. Evidence indicate potential therapeutic relevance for PARP-1 inhibition in iCCA that preferentially affects KRAS-mutated cancers, but exact mechanisms remain unknown.

Method: PARP-1 depletion was generated by siRNA and CRISPR/Cas9-mediated knockdown/knockout in KRAS-mutated and non-mutated iCCA cell lines. Functional assessment of PARP-1 knockout and inhibition of tumorigenic potential was analyzed by viability assay and colony and sphere formation. RNA sequencing was employed to further decipher PARP-1 regulation. To investigate the impact of PARP-1 deficiency in KRAS-driven tumorigenesis, PARP-1 knockout mice were combined with an inducible KRAS-driven mouse model using hydrodynamic tail vein injection. Molecular analyses including transcriptome profiling were employed to further investigate molecular mechanisms.

Results: Significant upregulation of PARP-1, as well as enrichment of genes related to PARP-1 activation, was observed in iCCA tissue and KRAS-mutated cell lines. Knockout of PARP-1 in KRAS-mutated cells led to a reduction in colony and sphere formation. Moreover, KRAS-mutated cell lines showed higher sensitivity to PARP-1 inhibition. In vivo PARP-1 deficiency considerably impaired biliary carcinogenesis and induced a shift from dominant iCCA towards HCC phenotype in a KRAS-dependent manner. Transcriptome analyses of CRISPR/Cas9 PARP-1 knockout clones and in vivo tumors revealed differential expression of DNA damage response pathways (e.g. CHK1) as well as cellular pathways affected by PARP-1, (inflammation, oxidative stress,

cell death signaling). The most prominent candidate regulating PARP1 in KRAS cell lines and tumors appeared to be CHK1 kinase, further validated by qRT-PCR, western blot, and drug-screening assays.

Conclusion: Together, these findings suggest an unrecognized prognostic and therapeutic role of PARP-1 in iCCA patients with oncogenic KRAS signaling and unveil the potential mechanism of PARP-1 regulation by CHK1 kinase.

SAT-231

Sortilin-driven cancer secretome enhances self-renewal and metastasis of hepatocellular carcinoma via de novo lipogenesis

Kwan Shuen Chan¹, Kwan Yung Au¹, Bernice Leung¹, Cheuk Yan Wong¹, Clive Yik Sham Chung², Regina Cheuk Lam Lo³.
¹The University of Hong Kong, Pathology, School of Clinical Medicine, LKS Faculty of Medicine, Hong Kong, ²The University of Hong Kong, School of Biomedical Sciences, LKS Faculty of Medicine, Hong Kong, ³The University of Hong Kong, Pathology, School of Clinical Medicine, LKS Faculty of Medicine; State Key Laboratory of Liver Research (The University of Hong Kong), Hong Kong
Email: kristykc@hku.hk

Background and aims: De novo lipogenesis (DNL) is a key metabolic pathway to fuel tumorigenesis. Increased free fatty acid uptake and DNL is consistently observed in chronic liver disease and genes related to DNL are universally upregulated in hepatocellular carcinoma (HCC). Yet, the upstream regulatory events triggering DNL in HCC remains to be delineated. Sortilin (*SORT1*) is reported as a regulator to transport a wide range of proteins intra/extracellularly. Association between sortilin and lipid metabolism has been established as reported by genome-wide association studies and animal models. In the present study, we aimed at investigating the functional roles of sortilin-driven cancer secretome in HCC.

Method: Sortilin expression in HCC and paired non-tumoral liver tissues was compared using The Cancer Genome Atlas Liver Hepatocellular Carcinoma dataset and public dataset (GSE89377). Conditioned medium collected from stable sortilin-overexpressing HCC cells was deployed to study the effect of sortilin-driven secretome in HCC using in vitro and in vivo assays. Proteomic profiling of sortilin-driven secretome was analyzed using liquid chromatography-tandem mass spectrometry.

Results: Sortilin was overexpressed in HCC. Overexpression of sortilin was correlated with poorer survival outcome. Functional studies showed that sortilin-driven secretome conferred self-renewal ability and metastatic potential in HCC cells. Fatty acid metabolism was highlighted as a potential molecular pathway associated with sortilin-driven secretome by proteomic profiling. Lipid content and fatty acid synthase (FASN) was increased in HCC cells treated with sortilin-driven secretome. The enhanced tumorigenic phenotypes endowed by sortilin-driven secretome were partially abrogated by co-administration of FASN inhibitor C75. Stabilization of FASN upon treatment with sortilin-driven secretome might be mediated through O-GlcNAcylation.

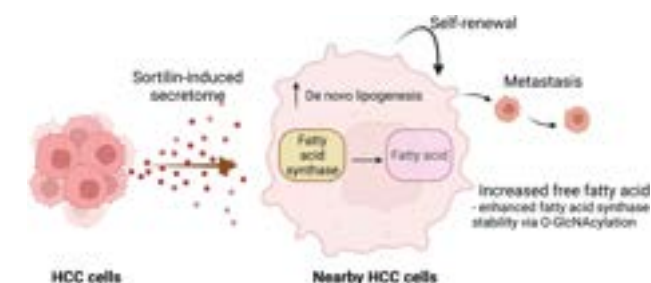


Figure:

Conclusion: Our study uncovered the role of sortilin in contributing to hepatocarcinogenesis via modulation of cancer secretome and deregulated lipid metabolism.

SAT-232

Identification and experimental validation of druggable epigenetic targets in hepatoblastoma

Alex Claveria-Cabello¹, José María Herranz², Elena Adan-Villaescusa¹, Maria U Latasa¹, Maria Arechederra^{1,2,3}, Iker Uriarte², Antonio A Pineda^{4,5}, Pedro Berraondo^{5,6}, Bruno Sangro^{2,3,7}, Jose Marin^{2,8}, María Luz Martínez-Chantar^{2,9}, Sergio Ciordia¹⁰, Fernando Corrales^{2,10}, Jessica Zucman-Rossi¹¹, Emilie Indersie¹², Stefano Cairo^{13,14}, Montserrat Domingo-Sabat¹⁵, Carmen Berasain^{1,2}, Maite G Fernandez-Barrena^{1,2}, Matías A Avila^{1,2,3}. ¹Program of Hepatology, CIMA, University of Navarra, Hepatology Program, Spain, ²Centro de Investigación Biomédica en Red, CIBERehd, Instituto de Salud Carlos III, Madrid, Spain, ³Instituto de Investigaciones Sanitarias de Navarra, IdiSNA, Pamplona, Spain, ⁴Molecular Therapies Program, CIMA, Universidad de Navarra, Pamplona, Spain, ⁵Centro de Investigación Biomédica en Red de Cáncer (CIBERONC), Spain, ⁶Program of Immunology and Immunotherapy, CIMA-University of Navarra, Pamplona, Spain, ⁷Liver Unit, Clínica Universidad de Navarra, Pamplona, Spain, ⁸Experimental Hepatology and Drug Targeting (HEVEPHARM) Group, University of Salamanca, IBSAL, Salamanca, Spain, ⁹Liver Disease Laboratory, Center for Cooperative Research in Biosciences (CIC bioGUNE), Basque Research and Technology Alliance, Spain, ¹⁰Centro Nacional de Biotecnología (CNB), CSIC, Madrid, Spain, ¹¹Centre de Recherche des Cordeliers, Sorbonne Université, Inserm, Université de Paris; Functional Genomics of Solid Tumors laboratory, Équipe labellisée Ligue Nationale contre le Cancer, Labex OncoImmunology; Hôpital Européen Georges Pompidou, APHP, Paris, France, ¹²Xentech, Evry, France, ¹³Champions Oncology, Inc., United States, ¹⁴Xentech, France, ¹⁵Program for Predictive and Personalized Medicine of Cancer, Germans Trias i Pujol Research Institute (PMPPC-IGTP), Badalona, Spain
Email: maavila@unav.es

Background and aims: Hepatoblastoma (HB) is the most frequent childhood liver cancer. Surgical resection is the mainstay treatment which frequently is preceded by neoadjuvant chemotherapy (cisplatin or doxorubicin). However, patients with aggressive tumors have limited therapeutic options; therefore, a better understanding of HB pathogenesis is needed to improve treatment. HB have a very low mutational burden; however, epigenetic alterations are increasingly recognized. We aimed to identify epigenetic regulators consistently dysregulated in HB and to evaluate the therapeutic efficacy of their targeting in clinically relevant models.

Method: We performed a comprehensive transcriptomic analysis of 180 epigenetic genes. Data from fetal, pediatric, adult, peritumoral (n = 72) and tumoral (n = 91) tissues were integrated. Selected epigenetic drugs were tested in HB cells. The most relevant epigenetic target identified was validated in primary HB cells, HB organoids, a PDX model, and a genetic mouse model. Transcriptomic, proteomic and metabolomic mechanistic analyses were implemented.

Results: Altered expression of genes regulating DNA methylation and histones modifications was consistently observed in association with molecular and clinical features of poor prognosis. The histone methyl-transferase G9a was markedly upregulated in tumors with epigenetic and transcriptomic traits of increased malignancy. Pharmacological targeting of G9a significantly inhibited HB cells, organoids and PDX's growth. Development of HB induced by oncogenic forms of β -catenin and YAP1 was ablated in mice with hepatocyte-specific deletion of G9a. We observed that HB undergo significant transcriptional rewiring in genes involved in amino acids metabolism and ribosomal biogenesis. G9a inhibition counteracted these pro-tumorigenic adaptations. Mechanistically, G9a targeting potentially repressed the expression of c-MYC and ATF4, master regulators of HB metabolic reprogramming.

POSTER PRESENTATIONS

Conclusion: HB display a profound dysregulation of the epigenetic machinery. Among them, G9a is upregulated in association with tumor aggressiveness. Pharmacological targeting of G9a potentially quells HB growth. Inhibition of G9a abrogates the c-MYC and ATF4-mediated metabolic reprogramming that supports cancer cell survival. Pharmacological targeting of key epigenetic effectors exposes metabolic vulnerabilities that can be leveraged to improve the treatment of these patients.

SAT-233

Tumor-extrinsic Axl expression shapes an inflammatory microenvironment independent of tumor-cell promoting Axl signaling

Kristina Breitenacker¹, Denise Heiden¹, Gerhard Weber¹, Iros Barozzi¹, Thomas Grünberger², Patrick Starlinger^{3,4}, Wolfgang Mikulits¹.

¹Center for Cancer Research, Comprehensive Cancer Center, Medical University of Vienna, Vienna, Austria, ²Department of Surgery, HPB Center, Viennese Health Network, Clinic Favoriten and Sigmund Freud Private University, Vienna, Austria, ³Department of General Surgery, Division of Visceral Surgery, Medical University of Vienna, Vienna, Austria, ⁴Department of Surgery, Division of Hepatobiliary and Pancreatic Surgery, Mayo Clinic, Rochester, United States
Email: kristina.breitenacker@meduniwien.ac.at

Background and aims: Signaling of the receptor tyrosine kinase Axl activated by its ligand Gas6 is a major driver of cancer progression. In hepatocellular carcinoma (HCC), patients show upregulation of Axl expression correlating with vascular invasion and poor prognosis. In pre-malignant stages of HCC, Gas6/Axl is crucially involved in developing hepatic fibrosis. Although recent insights into the role of Gas6/Axl in liver disease, a deep understanding of tumor-intrinsic and tumor-extrinsic functions of Axl in HCC is lacking. In this study, we focused on Axl in HCC development by employing novel mouse models and translating experimental data into the HCC patient situation.

Method: Liver tumors were induced by diethylnitrosamine (DEN) and carbon tetrachloride (CCl₄) in systemic Axl^{-/-} and in Axl^{Δhep/Δhep} mice lacking Axl expression in hepatocytes. Oncogenic-transformed p19^{ARF}^{-/-} hepatocytes were used to study tumor-intrinsic Axl expression. Invasive abilities of cells were examined *in vitro* and *in vivo*. Mouse tumors were subjected to immune cell profiling by FACS and immunohistochemistry. HCC patient samples (n=47) were analyzed by multiplex immunohistochemistry.

Results: DEN/CCl₄-induced liver tumor burden of systemic Axl^{-/-} mice was enhanced showing higher proliferation rates including lower infiltration of cytotoxic CD8⁺ T cells and granzyme B⁺ cells. PD-L1 levels did not vary between Axl^{-/-} and Axl^{+/+} tumors indicating alternative escape mechanisms. Interestingly, livers of CCl₄-treated Axl^{-/-} mice were increasingly infiltrated with pro-inflammatory monocytes and neutrophils prior to tumor formation, potentially fostering tumor-promoting inflammation and therefore enhancing tumorigenesis. Most notably, tumor burden and infiltration of CD8⁺ T cells did not differ between Axl^{Δhep/Δhep} and Axl^{fl/fl} mice suggesting that hepatocyte-intrinsic Axl expression does not alter proliferation and cytotoxic immune cell infiltration. However, we observed that tumor-intrinsic Axl expression augments invasive abilities *in vitro* and decreases overall survival of mice by increasing pulmonary metastasis. The Axl-driven invasive phenotype was

accompanied by upregulation of Snai1/Snai2 and downregulation of E-Cadherin indicating changes in epithelial plasticity.

Conclusion: In an inflammatory setting, tumor-extrinsic Axl expression shapes the liver immune environment which curbs cancer development. Tumor-intrinsic Axl expression promotes the cancer-progressive phenotype of HCC by fostering cell invasion and reprogramming of epithelial organization. These findings highlight the versatile functions of Axl in tumor-stroma interaction which are highly relevant for anti-cancer strategies.

SAT-234

Immunotherapy resistance in NASH-HCC is driven by the dysfunctional liver microenvironment of NASH

Daniel Geh¹, Erik Ramon Gil¹, Maja Laszczewska¹, Amy Collins¹, Saimir Luli¹, Rainie Cameron¹, Fiona Oakley¹, Jack Leslie¹, Helen Louise Reeves^{2,3}, Derek A Mann¹. ¹Newcastle University-Newcastle Fibrosis Research Group, Biosciences Institute, Faculty of Medical Sciences, United Kingdom, ²Newcastle University-Translational and Clinical Research Institute, Faculty of Medical Sciences, United Kingdom, ³Freeman Hospital-Hepatopancreatobiliary Multidisciplinary Team, Newcastle upon Tyne Hospitals NHS Foundation Trust, United Kingdom
Email: daniel.geh@newcastle.ac.uk

Background and aims: There is growing evidence suggesting that anti-programmed death ligand 1 (PDL1)/anti-vascular endothelial growth factor (VEGF) combination therapy in hepatocellular carcinoma (HCC) with underlying non-alcoholic steatohepatitis (NASH) is less effective compared to other aetiologies. Previous work suggests that a subgroup of exhausted CD8⁺PD1⁺EOMES⁺CXCR6⁺ T cells is responsible in the context of anti-PD1 monotherapy. We aim to explore this further in the context of anti-PDL1/VEGF combination therapy.

Method: C57BL/6J mice were fed either a western diet to induce NASH or fed control diet (lean mice) followed by either intrahepatic or subcutaneous implantation of tumours (Hep 53.4 line). After 2 weeks of tumour growth mice were treated with either anti-PDL1/VEGF or IgG isotype control. Tumour burden was measured and immune characterisation conducted using flow cytometry.

Results: NASH mice with intrahepatic tumours had a poor response to anti-PDL1/VEGF therapy compared to lean mice (figure 1a-c). Analysis showed an influx of CD8⁺T cells into anti-PDL1/VEGF treated intrahepatic tumours but with a preferential recruitment of CD8⁺PD1⁺EOMES⁺CXCR6⁺ T cells in NASH intrahepatic tumours (figure 1d-e). On the other hand, both NASH and lean mice with subcutaneous tumours had a good response to anti-PDL1/VEGF therapy (figure 2a-c). Analysis demonstrated an influx of CD8⁺T cells into the subcutaneous tumours of anti-PDL1/VEGF treated mice. Unlike in the intrahepatic tumours, the proportion of recruited CD8⁺PD1⁺ cells were similar in NASH and lean mice (figure 2 d-e).

Conclusion: In our model of NASH-HCC intrahepatic tumours have a poor response to anti-PDL1/VEGF therapy whereas subcutaneous tumours have a good response. This was likely due to a higher proportion of exhausted CD8⁺PD1⁺EOMES⁺CXCR6⁺ T cells being recruited into intrahepatic tumours due to their expansion in the pre-cancerous NASH hepatic microenvironment. This suggests that the NASH hepatic microenvironment is the key determinant to treatment response in NASH-HCC.

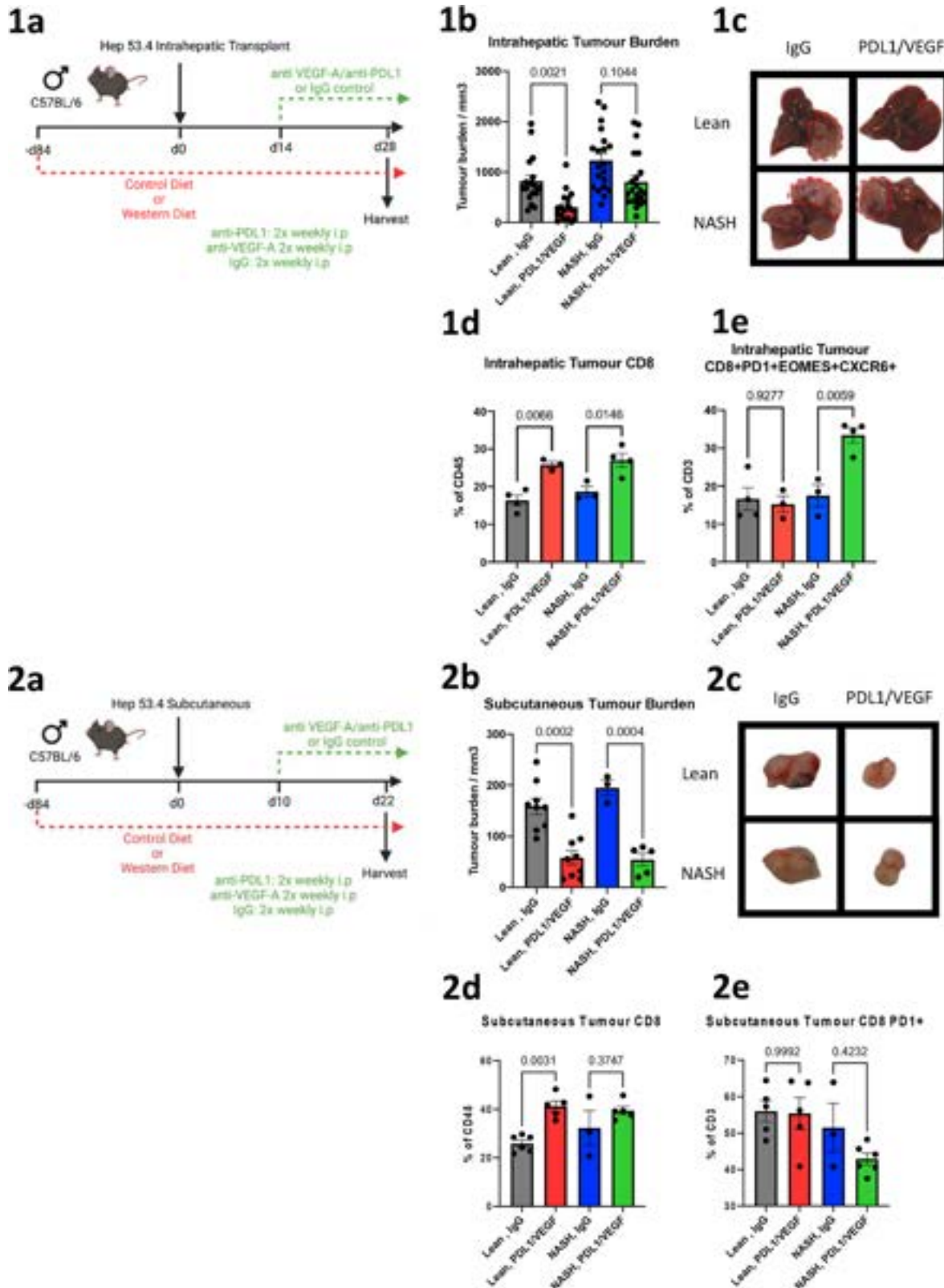


Figure: (abstract: FRI-234).

POSTER PRESENTATIONS

SAT-235

PSMP inhibits HCC progression by regulating the polarization of tumor-associated macrophages via the PI3K/Akt pathway

Shaoping She¹, Liying Ren¹, Dongbo Chen¹, Hongsong Chen¹. ¹Peking University People's Hospital, Peking University Hepatology Institute, Beijing Key Laboratory of Hepatitis C and Immunotherapy for Liver Diseases, China

Email: chenhsong@bjmu.edu.cn

Background and aims: Hepatocellular carcinoma (HCC) is one of the malignant tumors with high morbidity and high mortality, which is prone to metastasis and recurrence and has a poor prognosis. PC3 secreted microprotein (PSMP) or microprotamine (MSMP) is a novel chemotactic cytokine discovered through genome-wide bioinformatics analysis and chemoattractant platform screening, which can act as a CCR2 ligand to recruit peripheral blood monocytes and lymphocytes. Our previous study found that PSMP was significantly highly expressed in human and mouse liver fibrosis/cirrhosis tissues induced by different causes. PSMP can promote the progression of liver fibrosis by regulating the infiltration, activation and polarization of macrophages. However, the relationship between PSMP and the development and prognosis of HCC remains unclear.

Method: The expression of PSMP was detected in two independent HCC patients cohorts and its correlation with patients' prognosis was analyzed. *In vivo*: In PSMP knockout and wild-type mice, two mouse HCC cell lines (Hepa1-6, H22) were used to construct the subcutaneous tumorigenesis models and the liver orthotopic tumorigenesis models; In nude mice, two human HCC cell lines (BEL-7402, BEL-7405) were used to construct the subcutaneous tumorigenesis models. The direct effects of PSMP on the polarization of macrophages (human THP-1 cell line and mouse bone marrow-derived macrophages (BMDMs) were studied *in vitro*. In addition, we performed RNA sequencing of BMDMs from WT and PSMP gene knockout mice.

Results: Through the detection of clinical HCC patient samples, we found that PSMP is downregulated in human HCC tissues, and its expression level is positively correlated with the prognosis of HCC patients. *In vivo*, we found that knockout of PSMP promotes subcutaneous and liver orthotopic tumor growth in mice; Overexpression of PSMP inhibits the formation of subcutaneous tumors in nude mice. Further, knockout of PSMP significantly inhibits the infiltration of CD8⁺ tumor-infiltrating lymphocytes (TILs) and promotes the infiltration and polarization of M2-type tumor-associated macrophages (TAMs) in mice. *In vitro*, we found that PSMP could directly promote M1-polarization and inhibit M2-polarization of human THP-1 cells and mouse BMDMs. In addition, analysis of RNA sequencing results showed that PSMP may mediate the polarization of macrophages by regulating the PI3K/Akt signaling pathway.

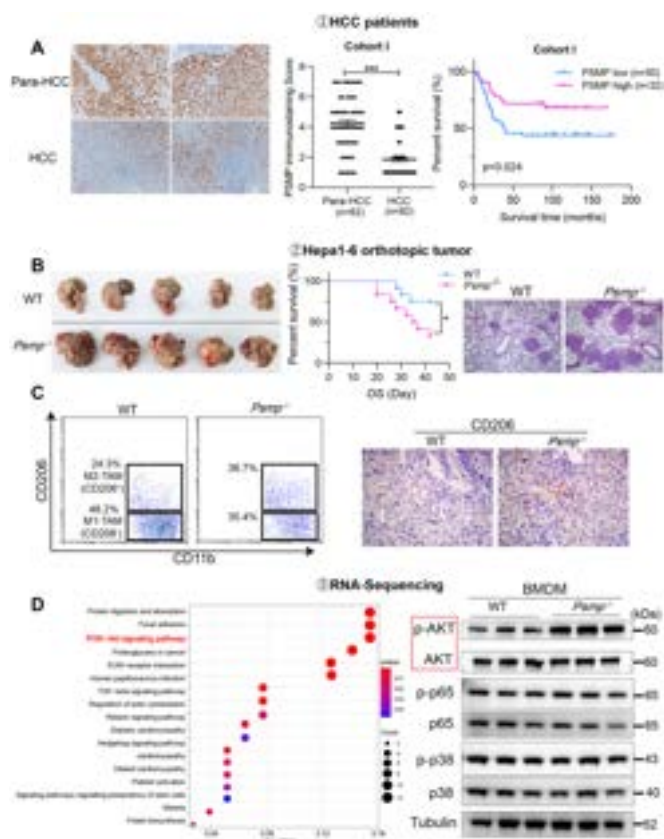


Figure:

Conclusion: Taken together, PSMP may inhibit the M2 polarization of tumor-associated macrophages through the PI3K/Akt signaling pathway, and then promote the anti-tumor immune response of CD8⁺ T cells, and ultimately inhibit the progression of HCC. The results are expected to clarify the role and mechanism of PSMP in the liver tumor microenvironment for the first time, which has important theoretical significance, and may also provide new targets for the treatment of HCC, with potential application value.

SAT-236

Macrophage STING signaling promotes NK cell to suppress colorectal cancer liver metastasis via 4-1BBL/4-1BB co-stimulation

Haoming Zhou¹, Yu Sun¹, Haoran Hu¹, Jian Xu¹, Yiyun Gao¹, Xinyu Zhan¹, Shun Zhou¹, Weizhe Zhong¹, Dongming Wu¹, Ping Wang¹, Lianbao Kong¹, Zhuqing Rao¹. ¹The First Affiliated Hospital of Nanjing Medical University, China
 Email: zhuqingrao_njmu@163.com

Background and aims: Macrophage innate immune response plays an important role in tumorigenesis. However, the role and mechanism of macrophage STING signaling in modulating tumor microenvironment to suppress tumor growth at secondary sites remains largely unclear.

Method: STING expression was assessed in liver samples from patients with colorectal cancer (CRC) liver metastasis. Global or myeloid STING-deficient mice, myeloid NLRP3-deficient mice, and wild-type mice were subjected to a mouse model of CRC liver metastasis by intrasplenic injection of murine colon carcinoma cells (MC38). Liver non-parenchymal cells including macrophages and NK cells were isolated for flow cytometry analysis. Bone marrow-derived macrophages pretreated with MC38 were co-cultured with splenic NK cells for *in vitro* studies.

Results: Significant activation of STING signaling were detected in adjacent and tumor tissues and intrahepatic macrophages. Global or

myeloid STING-deficient mice had exacerbated CRC liver metastasis and shorten survival, with decreased intrahepatic infiltration and impaired antitumor function of NK cells. Depletion of NK cells in WT animals increased their metastatic burden, while no significant effects were observed in myeloid STING-deficient mice. STING activation contributed to the secretion of IL-18 and IL-1 β by macrophages, which optimized antitumor activity of NK cells by promoting the expression of 4-1BBL in macrophages and 4-1BB in NK cells, respectively. Moreover, MC38 treatment activated macrophage NLRP3 signaling, which was inhibited by STING depletion. Myeloid NLRP3 deficiency increased tumor burden and suppressed activation of NK cells. NLRP3 activation by its agonist effectively suppressed CRC liver metastasis in myeloid-STING deficient mice.

Conclusion: We demonstrated that STING signaling promoted NLRP3-mediated IL-18 and IL-1 β production of macrophages to optimize the anti-tumor function of NK cells via the co-stimulation signaling of 4-1BBL/4-1BB.

SAT-237

A patient-derived hepatocellular carcinoma multicellular spheroid system modeling the tumor microenvironment for drug development and precision medicine

Emilie Crouchet¹, Nuno Almeida¹, Sarah Durand¹, Sara Cherradi¹, Antonio Saviano^{1,2}, Fabio Giannone^{1,2,3}, Emanuele Felli^{1,2,3}, Patrick Pessaux^{1,2,3}, François H.T. Duong¹, Thomas Baumert^{1,2}, Catherine Schuster¹. ¹Université de Strasbourg, Inserm, Institut de Recherche sur les Maladies Virales et Hépatiques UMR_S1110, Strasbourg, France, ²Hôpitaux Universitaires de Strasbourg, Service d'hépatogastroentérologie, Strasbourg, France, ³Institut hospitalo-universitaire (IHU), Institute for Minimally Invasive Hybrid Image-Guided Surgery, Strasbourg, France
Email: ecrouchet@unistra.fr

Background and aims: Hepatocellular carcinoma (HCC) is the third leading and fastest rising cause of cancer-related death worldwide. Despite recently approved therapies, the response to treatments remains limited and prognosis of patients with advanced HCC is poor. Preclinical and high-throughput screening of approved drugs or candidate compounds for treatment of HCC is hampered by the absence of tractable model systems recapitulating heterogeneity of HCC tumors and tumor microenvironment.

Method: We established a patient-derived multicellular spheroid model based on liver tumor resections following enzymatic and mechanical dissociation. Cells were grown in 3D in presence of growth factors and autologous patient-derived serum to maintain cell phenotypes. Characterization of the tumorspheroid cellular populations was performed by flow cytometry. As a proof of concept, we treated patient-derived spheroids with FDA approved anti-HCC compounds and assessed treatment response by measuring cell viability and by assessing the effect of drugs on the key signaling pathways by single cell RNA-Seq (scRNA-Seq) and Western blot analysis. Moreover, the 3D tumorspheroid system was used in preclinical proof-of-concept studies to understand the mechanism of action of approved and investigational therapeutics.

Results: The model was successfully established in a highly reproducible manner, independently from the donors and from cancer etiology. The spheroids maintained a high cellular viability during at least 8 days and include epithelial cancer cells as well as all major cell populations that are present in the tumor microenvironment (TME), such as myofibroblasts, immune cells (macrophages and T cells) and endothelial cells. Cell type proportions were variable between spheroids representing the different HCC existing subtypes and patient heterogeneity. We observed differential responses to FDA HCC approved drugs (targeted- and immune-based treatments) between donors. Moreover, treatment response could be correlated to the proportion of the different cell types present in the patient derived spheroids. Finally, using scRNA-Seq we show that the 3D tumorspheroid system enables to study the effect of therapeutics on

TME including T cell responses, which offers new perspectives for preclinical drug evaluation compared to the liver organoid model based on epithelial cell differentiation.

Conclusion: Our patient-derived spheroid model may be used to predict clinical treatment response in patients enabling precision medicine. The 3D tumorspheroid system is a powerful tool to monitor anti-tumor treatment responses and uncover the mechanism of action of novel compounds in research and development. Collectively, this model will accelerate clinical translation of personalized liver cancer therapies based on functional screening including the TME.

SAT-238

Liquid biopsy protein biomarkers of cholangiocarcinoma risk, early diagnosis and survival mirroring tumor cells

Ainhoa Lapitz¹, Mikel Azkargorta^{2,3}, Piotr Milkiewicz⁴, Paula Olaizola¹, Ekaterina Zhuravleva⁵, Marit M. Grimsrud⁶, Christoph Schramm⁷, Ander Arbelaziz¹, Colm O'Rourke⁵, Adelaida La Casta¹, Malgorzata Milkiewicz⁸, Tania Pastor¹, Mette Vesterhus⁶, Raul Jimenez-Aguero¹, Michael Dill⁹, Angela Lamarca¹⁰, Juan Valle¹⁰, Rocio IR Macias^{3,11}, Laura Izquierdo-Sánchez¹, Ylenia Pérez Castaño¹, Francisco J. Caballero^{1,12}, Ioana Riaño¹, Marcin Krawczyk¹³, Cesar Ibarra¹⁴, Javier Bustamante¹⁴, Luiz Miguel Nova-Camacho¹⁵, Juan Falcon-Perez^{2,3}, Felix Elortza^{2,3}, María Jesús Perugorria^{1,3}, Jesper Andersen⁵, Luis Bujanda^{1,3}, Tom Hemming Karlsen⁶, Trine Følseaa⁶, Pedro Miguel Rodrigues^{1,3}, Jesus Maria Banales^{1,3}. ¹Biodonostia Health Research Institute, Spain, ²CIC bioGUNE, Spain, ³National Institute for the Study of Liver and Gastrointestinal Diseases (CIBERehd), Spain, ⁴Medical University of Warsaw, Poland, ⁵Biotech Research and Innovation Centre, Denmark, ⁶Oslo University Hospital, Norway, ⁷European Reference Network Hepatological Diseases (ERN RARE-LIVER), Germany, ⁸Pomeranian Medical University in Szczecin, Poland, ⁹Heidelberg University Hospital, Germany, ¹⁰The Christie NHS Foundation, United Kingdom, ¹¹University of Salamanca, Spain, ¹²University of the Basque Country, Medicine, Spain, ¹³Saarland University Medical Centre, Germany, ¹⁴Cruces University Hospital, Spain, ¹⁵Donostia University Hospital, Spain
Email: ainhoa.lapitz@biodonostia.org

Background and aims: Cholangiocarcinoma (CCA), heterogeneous biliary tumors with dismal prognosis, lacks accurate early-diagnostic methods, especially important for individuals at high-risk (i.e., primary sclerosing cholangitis (PSC)). Here, we searched for protein biomarkers in serum extracellular vesicles (EVs).

Method: EVs from patients with isolated PSC (n = 45), concomitant PSC-CCA (n = 44), PSC who developed CCA during follow-up (PSC to CCA; n = 25), CCAs from non-PSC etiology (n = 56), hepatocellular carcinoma (n = 34) and healthy individuals (n = 56) were characterized by mass-spectrometry. Diagnostic biomarkers for PSC-CCA, non-PSC CCA or CCAs regardless etiology (pan-CCAs) were defined and validated by ELISA. Their expression was evaluated in CCA tumors at single-cell level. Prognostic EV-biomarkers for CCA were investigated.

Results: High-throughput proteomics of EVs identified diagnostic biomarkers for PSC-CCA, non-PSC CCA or pan-CCA, and for the differential diagnosis of intrahepatic CCA and HCC, that were cross-validated by ELISA using total serum. Machine learning-based algorithms disclosed CRP/FIBRINOGEN/FRIL for the diagnosis of PSC-CCA (local disease (LD)) vs isolated PSC (AUC = 0.947; OR = 36.9), and when combined with CA19-9, overpowers CA19-9 alone. CRP/PIGR/VWF combination allowed the diagnosis of LD non-PSC CCAs vs healthy individuals (AUC = 0.992; OR = 387.5). Noteworthy, CRP/FRIL accurately diagnosed LD pan-CCA (AUC = 0.941; OR = 89.4). Levels of CRP/FIBRINOGEN/FRIL/PIGR showed predictive capacity for CCA development in PSC before clinical evidences of malignancy. Multi-organ transcriptomic analysis revealed that serum EV-biomarkers were mostly expressed in hepatobiliary tissues, and scRNA-seq and immunofluorescence analysis of CCA tumors showed their presence mainly in malignant cholangiocytes. Multivariable analysis

POSTER PRESENTATIONS

unveiled EV-prognostic biomarkers, with COMP/GNAI2/CFAI and ACTN1/MYCT1/PF4V associated negatively or positively to patients' survival, respectively.

Conclusion: Serum EVs contain protein biomarkers for the prediction, early diagnosis and prognosis estimation of CCA detectable using total serum, representing a tumor cell-derived liquid biopsy tool for personalized medicine.

SAT-239

Neutrophil degranulation and ageing as potential therapeutic targets in hepatocellular carcinoma?

Daniel Geh¹, Erik Ramon Gil¹, Maja Laszczewska¹, Amy Collins¹, Saimir Luli¹, Rainie Cameron¹, Fiona Oakley¹, Helen Louise Reeves^{2,3}, Derek A Mann¹, Jack Leslie¹. ¹Newcastle University-Newcastle Fibrosis Research Group, Biosciences Institute, Faculty of Medical Sciences, Newcastle upon Tyne, United Kingdom, ²Newcastle University-Translational and Clinical Research Institute, Faculty of Medical Sciences, Newcastle upon Tyne, United Kingdom, ³Freeman Hospital-Hepatopancreatobiliary Multidisciplinary Team, Newcastle upon Tyne Hospitals NHS Foundation Trust, Newcastle upon Tyne, United Kingdom
Email: daniel.geh@newcastle.ac.uk

Background and aims: Neutrophils are recognised to play a vital role in hepatocellular carcinoma (HCC) progression through pro-tumour functions such as creating an immunosuppressive tumour micro-environment. This makes them potential therapeutic targets. Aims; 1. To characterise neutrophil phenotype and heterogeneity in HCC using patient samples and an *in vivo* model. 2. Manipulate HCC specific neutrophil changes in our *in vivo* model in order to develop novel neutrophil directed therapies for HCC.

Method: *Patient study.* Circulating neutrophils were isolated from HCC and chronic liver disease patients using density centrifugation. *In vivo model.* C57BL/6J mice underwent orthotopic tumour implantation. Both patient and mouse neutrophils were characterised using flow cytometry and functional assays.

Results: HCC patient blood samples were identified as having an increase in low density (LD) CD16^{high} neutrophils compared to healthy controls. Flow cytometry analysis revealed LD CD16^{hi} neutrophils as being more activated, degranulated and aged compared to normal density (ND) neutrophils as demonstrated by differing expression of CXCR2, CXCR4, CD11b, CD62L, CD10 and CD66b. In addition, LD CD16^{hi} neutrophils expressed markers associated with pro-tumour neutrophils such as CD36 and LOX-1. Tumour bearing mice also developed an increase in LD neutrophil frequency compared to controls with their phenotypic features being highly conserved compared to human. Functionally LD neutrophils were less phagocytic, had reduced migration to CXCL2 and had increased basal reactive oxygen species (ROS) production but a blunted stimulated ROS response further supporting them as being aged and degranulated neutrophils. This highlights circulating LD neutrophils and neutrophil ageing and degranulation as potential therapeutic targets. We used TGF- β and JAK2/STAT3 inhibition in our *in vivo* model in order to test this. ALK5 (TGF- β receptor 1) inhibition failed to significantly impact tumour burden however did significantly reduce the frequency of circulating LD neutrophils, increase the frequency of tumour associated neutrophils and increase CD62L expression indicating reduced ageing/degranulation (figure 1a-f). JAK2 inhibition significantly reduced tumour burden and altered neutrophil phenotype with an increase in neutrophil CD62L expression (figure 2a-d).

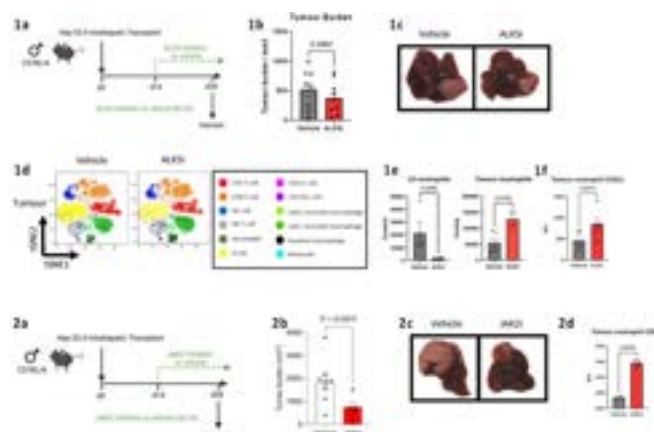


Figure:

Conclusion: We have identified an increase in frequency of circulating LD neutrophils with a degranulated, aged and pro-tumour phenotype in HCC that are highly conserved between HCC patients and tumour bearing mice. Inhibition of the TGF- β and JAK2/STAT3 pathway using ALK5 and JAK2 inhibitors resulted in alterations of neutrophil phenotype suggesting reduced degranulation and ageing. Further studies investigating these therapeutic agents in combination with immune checkpoint inhibitors is warranted.

SAT-240

Carbohydrate restriction inhibits tumor progression in a hepatocellular carcinoma mouse model

Merve Erdem¹, Sraddha Bharadwaj², Ana Izcue², Frank Schaap³, Eray Sahin⁴, Thorsten Cramer¹. ¹University Hospital RWTH Aachen, Molecular Tumor Biology, Department of General, Visceral and Transplantation Surgery, Aachen, Germany, ²University Hospital RWTH Aachen, Institute of Molecular Medicine, Aachen, Germany, ³Maastricht University, Department of Surgery, NUTRIM School of Nutrition and Translational Research in Metabolism, Netherlands, ⁴Acibadem Mehmet Ali Aydinlar University, Department of Biostatistics and Medical Informatics, School of Medicine, Turkey
Email: merdem@ukaachen.de

Background and aims: Hepatocellular carcinoma (HCC) is characterized by robust therapy resistance and poor prognosis. Dietary approaches and modifications are actively investigated regarding their impact on tumor metabolism and potential inhibitory effects on cancer progression. Dietary carbohydrate restriction (DCR) is considered to have an anti-tumor effect, conceivably due to the reduced glucose supply to cancer cells. We investigated different DCR approaches in a therapy-resistant HCC mouse model to analyze the effect of dietary carbohydrate restriction on tumor growth.

Method: We used a transgenic mouse model of hepatocellular carcinoma (HCC), termed ASV-B. These mice develop HCC via the T oncogene of SV40. In this study, ASV-B mice were placed under two different DCR regimens, precisely a "low carb high fat" (LCHF, ketogenic diet) and a "low carb high protein" (LCHP) chow. The consequences of the different DCR approaches on the composition of the tumor immune microenvironment, bile acids in blood and the gut microbiome were analyzed.

Results: Both DCR approaches significantly reduced tumor growth in ASV-B mice. However, the effect of LCHF and LCHP diets were variable in subsequent analyses, suggesting different underlying molecular mechanisms for the tumor-inhibiting effects. In the tumor micro-environment, the ketogenic diet resulted in significant accumulation of interleukin-17-producing lymphocytes, while no such observation was made in the LCHP diet group. In this group, on the other hand, enhanced oxidative stress was observed in tumor cells, contrary to LCHF diet feeding. In line, the anti-oxidant N-acetyl cysteine reversed the tumor-inhibiting effect of LCHP diet but not of LCHF diet. The

systemic effects of diet application were further investigated at different levels. In the gut microbiome, carbohydrate restricted-diet highly modified the bacterial composition, where fat and protein content had modest impact. Additionally, bile acid composition also changed upon diet even though total bile acid amount was not significantly affected.

Conclusion: The effect of dietary intervention is especially intriguing due to the fact that ASV-B mice demonstrate resistance to various therapeutic approaches, e.g. sorafenib and conventional chemotherapy drugs such as etoposide and doxorubicin. These results also suggest that macronutrient composition, especially carbohydrate availability, is crucial for murine HCC progression. With the safe use of diets in the clinical application, dietary interventions may provide a promising approach especially in the adjuvant setting.

SAT-241

Efficacy of HBV-TCR T cell therapy to eliminate circulating HBV-HCC cells in immunosuppressed whole blood

Meiyin Lin^{1,2}, Sebastian Chakrit Bhakdi^{3,4}, Damien Tan², Andrea Pavesi^{2,5}, Joycelyn Lee^{6,7}, David Tai^{6,7}, Antonio Bertoletti^{1,8}, Anthony Tan¹. ¹Duke-NUS Medical School, Emerging Infectious Diseases, Singapore, Singapore, ²Institute of Molecular and Cell Biology (IMCB), Singapore, Singapore, ³Mahidol University, Department of Pathobiology, Faculty of Science, Bangkok, Thailand, ⁴X-ZELL Biotech Pte Ltd., Singapore, Singapore, ⁵National University of Singapore, Mechanobiology Institute, Singapore, ⁶National Cancer Centre Singapore, Division of Medical Oncology, Singapore, Singapore, ⁷Duke-NUS Medical School, Oncology Academic Programme, Singapore, Singapore, ⁸Agency for Science, Technology and Research (A*STAR), Singapore Immunology Network, Singapore, Singapore
Email: anthony.tan@duke-nus.edu.sg

Background and aims: Recurrence of Hepatitis B virus-related hepatocellular carcinoma (HBV-HCC) after liver transplant (LT) is mediated by circulating tumour cells (CTCs) and exacerbated by the immunosuppression required to prevent graft rejection. In a murine model of HBV-HCC, we have shown the ability of HBV-TCR T cells to prevent HCC cell seeding and subsequent tumour development, demonstrating its potential use in a prophylactic setting. However, it is unclear whether HBV-targeting T cell therapy can eliminate HBV-HCC CTCs in the blood of immunosuppressed liver-transplanted patients.

Method: Here we first developed a microscopy-based assay to quantify CTCs in whole blood. The assay was then utilised to evaluate the cytolytic ability of our previously developed immunosuppressive drug-resistant HBV-TCR T cells (IDRA HBV-TCR) against HBV-HCC CTCs by quantifying the number of spiked HepG2.215 (an HCC cell line) targets recovered after an overnight culture with whole blood containing autologous IDRA HBV-TCR T cells in the presence of Tacrolimus and MMF to mimic the immunosuppressive peripheral blood of LT patients.

Results: Using 6 HCC cell lines (HepG2.215, Hep3B, SNU354, SNU368, SNU387 and SNU475) and the peripheral blood of patients with advanced metastatic liver cancer (n=5), we optimised and validated an immunofluorescence panel containing seven markers: pan-Cytokeratin, vimentin, glypican-3, alpha-fetoprotein, CD34, CD45 and DRAQ5, that can effectively differentiate HCC-CTCs from immune cells. In the presence of immunosuppressants, conventional HBV-TCR T cells had reduced effector function while IDRA HBV-TCR T cells were robustly activated by the spiked HCC cells to produce TNF α and IFN γ . More importantly, we observed a dose-dependent clearance of spiked HepG2.215 targets with a reduction of 60–80% of the targets using 20,000 IDRA HBV-TCR cells/ml of blood.

Conclusion: Our results demonstrate the ability of IDRA HBV-TCR T cells to effectively eliminate HBV-HCC CTCs in the presence of immunosuppressive drugs and support their use as prophylaxis against HCC relapse after LT.

SAT-242

RBCK1 promotes cancer stemness and sorafenib resistance by restoring Numb/Notch1 axis independently of its ubiquitin ligase activity in hepatocellular carcinoma

Peng Chen¹, Zheyu Dong¹, Jian Ruan², Junling Chen¹, Yuxin Zhou¹, Xinxin Liao³, Yongfa Tan⁴, Chuanjiang Li⁴, Yuhao Wang¹, Huajin Pang⁵, Chunhua Wen¹, Yuchuan Jiang⁶, Xiaoqing Li⁷, Bo Li⁸, Aihetimu Aimaier⁷, Li Lin⁹, Jian Sun¹, Jiajie Hou^{10,11}, Libo Tang¹, Jinlin Hou¹, Yongyin Li¹. ¹State Key Laboratory of Organ Failure Research, Guangdong Provincial Key Laboratory of Viral Hepatitis Research, Department of Infectious Diseases, Nanfang Hospital, Southern Medical University, Guangzhou, China, China, ²Department of Medical Oncology, The First Affiliated Hospital, Zhejiang University School of Medicine, and Key Laboratory of Cancer Prevention and Intervention, Ministry of Education, Hangzhou, China, China, ³Department of Anesthesiology, Nanfang Hospital, Southern Medical University, Guangzhou, China, China, ⁴Department of Hepatobiliary Surgery, Nanfang Hospital, Southern Medical University, Guangzhou, China, China, ⁵Division of Vascular and Interventional Radiology, Department of General Surgery, Nanfang Hospital, Southern Medical University, Guangzhou, China, China, ⁶Department of General Surgery, The First Affiliated Hospital, Jinan University, Guangzhou, China, China, ⁷Department of Pathology, Nanfang Hospital and School of Basic Medical Sciences, Southern Medical University, Guangzhou, China, China, ⁸Department of Hepatobiliary Surgery, The Affiliated Hospital of Guizhou Medical University, Guiyang, Guizhou, China, China, ⁹Department of Oncology, Nanfang Hospital, Southern Medical University, Guangzhou, China, China, ¹⁰Cancer Centre, Faculty of Health Sciences, University of Macau, Macau SAR, China, China, ¹¹MOE Frontier Science Centre for Precision Oncology, University of Macau, Macau SAR, China, China
Email: yongyinli@foxmail.com

Background and aims: Drug resistance of hepatocellular carcinoma (HCC) is primarily attributed to cancer stem cells (CSCs). RBCK1, a component of linear ubiquitin chain assembly complex, has been reported to participate in the progression of HCC; however, its role and the underlying mechanisms in regulating the therapeutic response of HCC remain poorly understood. Herein, we investigated the role of RBCK1 in regulating sorafenib resistance and the CSC properties of HCC.

Method: The association between RBCK1 expression and the therapeutic response was evaluated by half-maximal inhibitory concentration of sorafenib and patient-derived xenografts models. The role of RBCK1 in promoting sorafenib resistance and the CSCs properties of HCC was investigated *in vitro* and *in vivo*. The underlying mechanism of RBCK1 in regulating Numb/Notch1 axis was explored using mass spectrometry, co-immunoprecipitation and western blot.

Results: Upregulated RBCK1 expression was associated with sorafenib resistance in HCC patients and mouse models. Functional studies revealed that RBCK1 promoted sorafenib resistance of HCC cells independently of its ubiquitin ligase activity, and acted as an oncogene that sustained the CSC properties of HCC. Gene set enrichment analysis and serials of assays confirmed that Notch1 signaling was necessary for RBCK1 mediated sorafenib resistance and CSC properties of HCC. Notably, RBCK1 competed with Notch1 for Numb binding, thereby impairing Numb-mediated Notch1 lysosomal degradation, but exerted no significant effects on Numb ubiquitin degradation. Further study indicated that the A64 and Q65 residues of RBCK1 were proven as the key pockets for the oncogenic effects by forming hydrogen bonds with K78 residue of Numb.

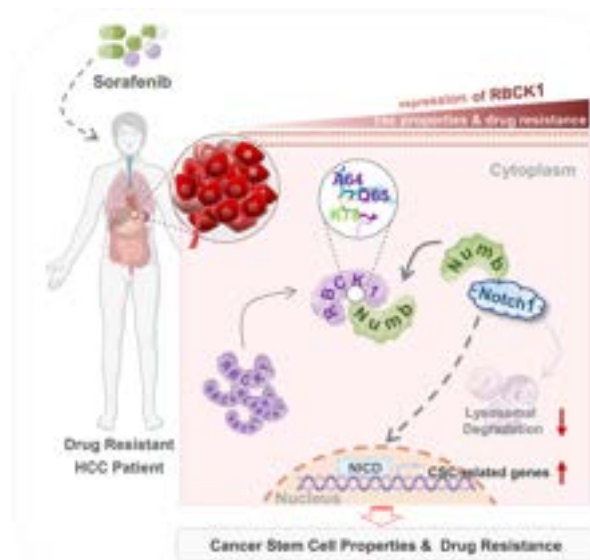


Figure:

Conclusion: RBCK1 is critical in promoting CSC properties of HCC to drive sorafenib resistance through Notch1 signaling, independently of its ubiquitin ligase activity. Our study highlights that RBCK1 is a potential target to reverse sorafenib resistance of HCC, and pave the way for RBCK1-targeted drugs development.

SAT-243

Pegozafermin inhibits NASH-induced hepatocellular carcinoma in the STAMTM mouse model

Maya Margalit¹, Moti Rosenstock¹, Leo Tseng², Taishi Hashiguchi³, Yuka Shirakata³, Hank Mansbach². ¹89bio Inc., Rehovot, Israel, ²89bio Inc., San Francisco, CA, United States, ³SMC Laboratories Inc., Japan
Email: mayamargalitmd@gmail.com

Background and aims: Pegozafermin (PGZ), a long-acting glycoPEGylated recombinant human FGF21 analog, led to marked histological and other liver-related benefits, as well as cardiometabolic benefits, with favorable safety and tolerability, in a Phase 1b/2a study in NASH. PGZ does not activate FGFR4, and is not mitogenic. NASH- associated HCC, previously viewed as a complication of cirrhotic NASH, is increasingly diagnosed in pre-cirrhotic NASH. In the STAMTM model, which recapitulates the human NASH-HCC sequence; HCC appears at ~16 weeks of age and develops universally at ~20 weeks of age. In HCC prevention studies in this model, treatment typically begins between 6 and 12 weeks of age. PGZ led to significant improvements in features of NASH, including liver histology, liver transaminases and various metabolic parameters in STAMTM mice. The objective of this study was to evaluate its effect on development of HCC in this model.

Method: STAMTM mice (12 or 13 weeks old, male, N=20 per group) were treated by vehicle, pegozafermin (previous name BIO89-100), (0.3 mg/kg, 1.0 mg/kg or 3.0 mg/kg) 3 times a week or a positive control, sorafenib (30 mg/kg once daily) for 9 weeks, starting at Week 12 (N=16 per group) or Week 13 (N=4 per group). Sorafenib slows tumor progression and decreases tumor burden in HCC mouse models. All surviving animals were sacrificed at 20 or 21 weeks of age. At time of sacrifice, number of surviving animals, liver weight, liver weight/body weight ratio and the number of visible tumor nodules on the surface of the liver in surviving mice were assessed.

Results: PGZ led to a dose-dependent decrease in the number of macroscopic tumor nodules; the mean (\pm SD) number of visible tumor nodules per mouse was 9 ± 7 , 10 ± 4 , 7 ± 4 , 2 ± 2 and 5 ± 4 in the vehicle, PGZ 0.3 mg/kg, PGZ 1.0 mg/kg and sorafenib groups, respectively (Figure 1; $p < 0.05$ for PGZ 3 mg/kg). A decrease in liver

weight and liver/body weight ratio was observed in PGZ-treated animals; mean liver weight and liver/body weight ratios were 2391 ± 473 mg and 9.6 ± 2.2 ; 2498 ± 1120 mg and 11.0 ± 4.6 ; 1802 ± 391 mg and 7.8 ± 1.7 ; 1252 ± 210 mg and 6.2 ± 1.1 ; and 2013 ± 916 mg and 8.4 ± 3.8 for the vehicle, PGZ 0.3 mg/kg, PGZ 1.0 mg/kg and sorafenib groups, respectively ($p < 0.05$ for liver weight and liver/body weight ratio for PGZ 3 mg/kg). Survival was 4/20, 4/20, 9/20, 8/20 and 12/20 in the vehicle, PGZ 0.3 mg/kg, PGZ 1.0 mg/kg and sorafenib groups, respectively; effect on survival was not statistically significant with either PGZ or sorafenib treatment.

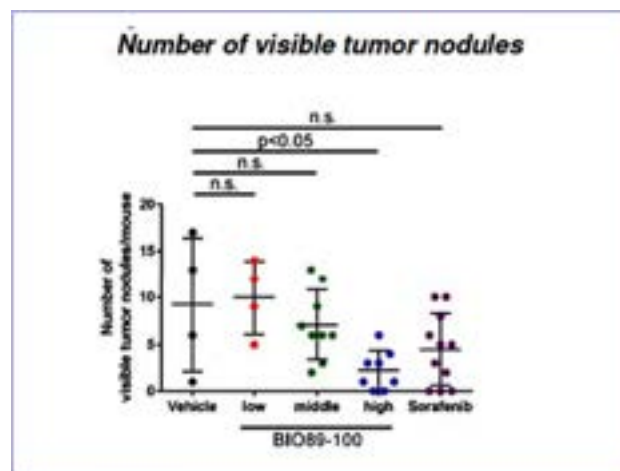


Figure: Number of visible tumor nodules in STAMTM male mice treated with vehicle, pegozafermin or sorafenib

Conclusion: In STAMTM mice, PGZ treatment led to a decrease in the development of HCC tumor nodules and tumor burden, that was comparable to that achieved with sorafenib. These data suggest that in addition to its beneficial effects on NASH and fibrosis and significant metabolic benefits, which render PGZ a promising treatment for NASH, should these pre-clinical data translate to human use, reducing the risk of HCC may be an additional benefit of PGZ treatment. The mechanism of this anti-tumor effect remains to be elucidated. PGZ is currently being studied in the ENLIVEN Phase 2b clinical trial in NASH.

SAT-244

Silencing CNNM4 in cholangiocarcinoma inhibits tumoral progression by means of non-canonical ferroptosis

Maria Mercado-Gómez¹, Alvaro Eguilero Giné¹, Miren Bravo¹, Mikel Azkargorta^{2,3}, Marina Serrano-Macia¹, Naroa Goikoetxea¹, Irene González-Recio¹, Sofia Lachiondo-Ortega¹, Claudia Gil-Pitarch¹, Marta Romero^{3,4}, Judit Domenech Omella⁵, Rubén Rodríguez Agudo¹, Leidy Estefanía Zapata-Pavas¹, Patricia Peña-San Felix¹, Paula Olaizola^{3,6}, Pedro Miguel Rodrigues^{3,6,7}, Luis Alfonso Martínez-Cruz¹, Angela Lamarca^{8,9}, Víctor Moreno¹⁰, Jesus Maria Banales^{3,6,7,11}, Teresa Cardoso Delgado¹, Felix Elortza^{2,3}, Matías A Avila^{3,12}, Francisco Javier Cubero^{3,13,14}, Cesar Augusto Martín¹⁵, Miguel Angel Merlos Rodrigo¹⁶, Diego Calvisi¹⁷, Jose Marin^{3,4}, María Luz Martínez-Chantar^{1,3}. ¹CIC bioGUNE, Basque Research and Technology Alliance (BRTA), Liver Disease Lab, Derio, Spain, ²CIC bioGUNE, Basque Research and Technology Alliance (BRTA), Proteomics Platform, Derio, Spain, ³Centro de Investigación Biomédica en Red de Enfermedades Hepáticas y Digestivas (CIBERehd), Carlos III National Institute of Health, Madrid, Spain, ⁴University of Salamanca, IBSAL, Experimental Hepatology and Drug Targeting (HEVEPHARM) Group, Salamanca, Spain, ⁵KU Leuven, Laboratory of Protein Phosphorylation and Proteomics, Dept. Cellular and Molecular Medicine, Leuven, Belgium, ⁶Biodonostia Health Research Institute-Donostia University Hospital, University of the Basque Country (UPV/EHU), San Sebastian, Spain, ⁷IKERBASQUE, Basque Foundation for

Science, Bilbao, Spain, ⁸Fundación Jiménez Díaz University Hospital, Department of Oncology-OncoHealth Institute, Madrid, Spain, ⁹The Christie NHS Foundation, Manchester; Division of Cancer Sciences, University of Manchester, Department of Medical Oncology, Manchester, United Kingdom, ¹⁰Hospital Universitario Fundación Jiménez Díaz, START Madrid-FJD, Madrid, Spain, ¹¹University of Navarra, Department of Biochemistry and Genetics, School of Sciences, Pamplona, Spain, ¹²Hepatology Programme, CIMA, Idissa, Universidad de Navarra, Pamplona, Spain, ¹³Complutense University School of Medicine, Department of Immunology, Ophthalmology and ENT, Madrid, Spain, ¹⁴Instituto de Investigación Sanitaria Gregorio Marañón (IISGM), Madrid, Spain, ¹⁵Instituto Biofisika (UPV/EHU, CSIC), Universidad del País Vasco, Departamento de Bioquímica, Bilbao, Spain, ¹⁶Mendel University in Brno, Department of Chemistry and Biochemistry, Brno, Czech Republic, ¹⁷Institute of Pathology, University of Regensburg, Regensburg, Germany
Email: mlmartinez@cicbiogune.es

Background and aims: Cholangiocarcinoma (CCA) is a heterogeneous neoplasm of biliary ducts that represents the second most common primary hepatic cancer, after hepatocellular carcinoma. Due to its aggressiveness, late diagnosis and immunoregulatory capacity of the disease, CCA outcomes are poor, with a median overall survival of less than 12 months. Currently, the only curative treatment is surgical resection, but this only applies to 25% of cases and despite this tumoral recurrence is frequent. For that reason, the study of new therapies is of utmost importance. Recent studies show that the isocitrate dehydrogenase 1 (*IDH1*) inhibitor, used to treat patients with irresectable iCCA harboring *IDH1* mutations, reduces cell proliferation, invasion and metastasis by promoting, ferroptosis, a programmed cell death caused by iron-dependent lipid peroxidation. **Method:** In this study, we analyze the role of CNNM4 (*Cyclin and CBS Domain Divalent Metal Cation Transport Mediator 4*), a Mg^{2+} effluxer, that is overexpressed in CCA *in silico*, at transcriptional levels and also in human biopsies.

Results: Silencing CNNM4 in CCA human cell lines, EGI-1 and TFK-1, which show high expression of CNNM4, not only increases intracellular Mg^{2+} but also reduces cellular proliferation and sensitizes cells to chemotherapeutic drugs. Key metastasis steps (intravasation, extravasation and invasion in other organs) were also slowed down when CNNM4 is silenced, as seen by 3D spheroid experiments and *in ex ovo* and *in ovo* chicken embryo chorioallantoic membrane assay. Proteomic analysis reveals a metabolic shift into a less glycolytic phenotype in CNNM4-silenced cells, also indicating a role of this transporter in the Warburg effect. Alteration of iron metabolism after CNNM4 modulation in both cell lines is associated with a decrease of NUPR-1 levels, a ferroptosis inhibitor, that can be a possible mechanism of those effects. In a CCA murine model (myr-AKT/Yap^{S127A}), silencing CNNM4 after tumoral development, via a liver-specific molecule, produces its reversion.

Conclusion: In conclusion, silencing CNNM4 is a potential therapeutic target in CCA whose effect could be mediated by iron-dependent cell death.

SAT-245

Exploiting RuvBL1 as a target to improve mTOR -driven hepatocarcinogenesis in mice

Alice Guida¹, Irene Simeone², Simone Polvani², Gabriele Dragoni², Elisabetta Ceni², Lucia Picariello², Andrea Galli², Tommaso Mello².
¹GenOMeC Doctorate, University of Siena, Siena, Italy, Siena, Italy,
²University of Florence, Department of Clinical and Experimental Biomedical Sciences "Mario Serio", Italy
Email: tommaso.mello@unifi.it

Background and aims: RuvBL1 belongs to the highly conserved ATPases associated with several cellular activities (AAA⁺) including DNA repair, telomerase complex assembly and mTOR pathway activity. It is deregulated in various human cancers and its expression correlates with a worse prognosis in HCC patients. We have

previously demonstrated that RuvBL1 haploinsufficiency impairs insulin signalling affecting the PI3K/Akt/mTOR pathway *in vivo*. Given the relevance of mTOR pathway hyperactivation in HCC, we hypothesized that RuvBL1 genetic targeting could reduce mTOR driven hepatocarcinogenesis in Pten^{hep-/-} mice.

Method: Pten^{hep-/-} and Ruvbl1^{hep±} mice were crossed to generate Pten^{hep-/-}Ruvbl1^{hep±} mice. The impact of RuvBL1 haploinsufficiency on NASH development was assessed by histology at 12 weeks of age. Metabolic and inflammatory markers were evaluated by qPCR and IHC. mTOR pathway was analysed by WB of liver lysates. PPARalpha transcriptional activity was evaluated by luciferase reporter assay. The identification of RuvBL1-protein interactions was achieved by MS proteomics analysis of RuvBL1 immunoprecipitation. The impact of RuvBL1 haploinsufficiency on HCC development was assessed by multiplicity evaluation of macroscopic tumours and by histological classification by Edmondson-Steiner grading system at 15 months of age.

Results: Oil red, Sirius red and F4/80 staining revealed a significant reduction of steatosis, fibrosis, and inflammation in Pten^{hep-/-}Ruvbl1^{hep±} compared to Pten^{hep-/-} mice. Similar mRNA expression of mTOR-driven lipogenic targets was found in the two mice models. However, expression of *Ppara* and its target CPT1 was increased in Pten^{hep-/-}Ruvbl1^{hep±}, indicating a lipid-lowering action mediated by PPARalpha in this mouse model. Moreover, promoter reporter experiments revealed that inhibition of RuvBL1 activity by CB-6644 increases PPARalpha transcriptional activity in AML-12 hepatocytic cell line. Next, MS proteomics analysis of RuvBL1-IP in murine AML-12 and Hepa1-6 cells revealed that RuvBL1 interacts with members of the lysosomal AMPK complex (V-ATPase, LAMTOR1, LAMTOR4, Rag C). Furthermore, p-AMPK and p-RAPTOR were increased in Pten^{hep-/-}Ruvbl1^{hep±} compared to Pten^{hep-/-} mice, suggesting a role of RuvBL1 at the interplay between mTOR and AMPK in hepatic lipid metabolism. Finally, Pten^{hep-/-}Ruvbl1^{hep±} mice aged to 15 months showed better survival than Pten^{hep-/-} which developed significantly more HCC and of higher grade. qPCR analysis showed a significant upregulation of key lipolytic genes, such as *Cpt1a*, *Acadl*, *Acadvl* and *Ppara*, in Pten^{hep-/-}Ruvbl1^{hep±} at 15 months of age.

Conclusion: RuvBL1 targeting reduces mTOR pathway hyperactivation hampering NASH-HCC progression in Pten^{hep-/-} mice, likely promoting the switch from mTOR-driven lipogenesis to AMPK-induced fatty acid catabolism.

SAT-246

Determination of human polyploid hepatocellular carcinoma by pathological image diagnosis utilizing artificial intelligence

Tomonori Matsumoto¹, Takanori Matsuura², Masatoshi Abe³, Masahiro Kido⁴, Hajime Nagahara⁵, Eiji Hara¹, Hirohiko Niioka⁶, Yoshihide Ueda². ¹Research Institute for Microbial Diseases, Osaka University, Department of Molecular Microbiology, Suita, Japan, ²Kobe University Graduate School of Medicine, Division of Gastroenterology, Department of Internal Medicine, Japan, ³Faculty of Medicine, Osaka University, Japan, ⁴Kobe University Graduate School of Medicine, Department of Surgery, Division of Hepato-Biliary-Pancreatic Surgery, Japan, ⁵Osaka University Institute for DataBility Science, Japan, ⁶Graduate School of Information Science and Technology, Osaka University, Department of Information and Physical Sciences, Japan
Email: tomomatsumoto@biken.osaka-u.ac.jp

Background and aims: Cancer genomic analysis has revealed that a subset of hepatocellular carcinomas (HCCs) are polyploid. Importantly, polyploidy in HCCs has been suggested to be associated with poor prognosis, and polyploidy may serve as a new prognostic marker for HCC. In our previous study, we established a method to assess ploidy in HCC by multicolored fluorescence in situ hybridization (FISH) for chromosomes in formalin-fixed paraffin-embedded (FFPE) sections and showed that polyploid HCC exhibited a worse prognosis after surgical resection than diploid HCC. However, in routine practice, it is difficult to evaluate chromosome duplications in

POSTER PRESENTATIONS

HCC by FISH, and a simpler method applicable to high-throughput testing is desired. In the present study, we aimed to establish a novel method for determining ploidy in HCC by developing an artificial intelligence (AI)-based pathological image model.

Method: Whole-slide images of hematoxylin and eosin (HE) staining were captured by a digital slide scanner and divided into small non-overlapping patches for analysis. The ploidy status of 49 HCCs that underwent hepatectomy at our institution between 2017 and 2021 was determined by multicolored FISH for chromosomes, and their HE images were used for training. EfficientNetB0, a convolutional neural network model of deep learning, to determine HCC ploidy was trained, and its usefulness was examined on images derived from 192 HCCs that were not used for training.

Results: We constructed a model to diagnose HCC ploidy, and its area under the receiver operating characteristic curve was 0.931 in cross-validation with training data. In the test dataset, the model identified 76 polyploid HCCs, accounting for 39.6% of cases. Consistent with our previous finding that macrotrabecular-massive (MTM) architectures were significantly more common in polyploid HCCs than diploid HCCs, the prevalence of MTM architecture was significantly higher ($p < 0.05$) in the polyploid HCCs determined by our model than their counterparts. Moreover, polyploid HCCs determined by our model had significantly higher serum alpha-fetoprotein levels, suggesting that this model can efficiently determine polyploid HCCs with aggressive features. Importantly, the polyploid HCCs showed a significantly poorer prognosis than their counterparts, indicating the possible utility of AI-based ploidy classification in the prediction of HCC prognosis.

Conclusion: An AI-based model diagnosing pathological images could determine HCC ploidy and predict a subset of HCC with poor prognosis. Classification of HCC ploidy utilizing AI-based pathological image diagnosis would be a useful new method for HCC practice.

SAT-247

Pediatric liver cancer: Hepatoblastoma and Neddylation post-translational modification

Leidy Estefanía Zapata-Pavas¹, Marina Serrano-Macia¹, Miguel Angel Merlos Rodrigo², Patricia Peña-San Felix¹, Claudia Gil-Pitarch¹, Naroa Goikoetxea¹, Hana Michalkova², Zbynek Heger², Alvaro del Rio³, Montserrat Domingo-Sàbat³, Laura Royo³, Jon Ander Barrenechea-Barrenechea¹, Maria Mercado-Gómez¹, Sofia Lachiondo-Ortega¹, Teresa Cardoso Delgado¹, Dimitris Xirodimas⁴, Jose Marin^{5,6}, Maite G Fernandez-Barrena^{6,7}, Matías A Avila^{6,7}, Carolina Armengol³, María Luz Martínez-Chantar^{1,6}. ¹Center for Cooperative Research in Biosciences (CIC bioGUNE), Basque Research and Technology Alliance (BRTA), Liver Disease Lab, Spain; ²Mendel University in Brno, Department of Chemistry and Biochemistry, Czech Republic; ³ Germans Trias i Pujol Research Institute (IGTP), Program for Predictive and Personalized Medicine of Cancer (PMPPC), Childhood Liver Oncology Group, Badalona, Spain; ⁴Univ. Montpellier, CRBM (Cell Biology Research Centre of Montpellier), CNRS, Montpellier, France; ⁵University of Salamanca, IBSAL, Experimental Hepatology and Drug Targeting (HEVEFARM), Salamanca, Spain; ⁶Carlos III National Health Institute, Centro de Investigación Biomédica en Red de Enfermedades Hepáticas y Digestivas (CIBERehd), Spain; ⁷University of Navarra, Hepatology Program, CIMA, Spain
Email: mlmartinez@cicbiogune.es

Background and aims: Hepatoblastoma (HB), although a rare disease, is the most common form of childhood primary liver cancer. Current therapeutic options are limited or inadequate and involve significant side effects; they include surgical resection with chemotherapeutic agents such as cisplatin or doxorubicin. Ongoing research has uncovered molecular, genetic, and epigenetic mechanisms that have expanded the understanding of HB, but it is an open field with many unknowns. The identification of neddylation, a post-translational modification regulated by NEDD8, widely involved in

several signalling pathways and in modulation of protein homeostasis, as a mechanism associated with the development of HB, has opened the doors to new therapeutic strategies. In this sense, the implications of this post-translational modification in the tumour context of HB and its modulation as a potential therapy was evaluated.

Method: A cohort of HB patients, preclinical animal model and in vitro model in tumour cells were used to characterise NEDDylation pathway in HB. Besides the modulation of NEDP1 levels using an in vitro approach was made to study cell proliferation, cell cycle, drug resistance, proteome homeostasis, and metabolic status. In vivo, the implications of NEDP1 overexpression in metastatic capability and its tumour suppressor capacity was evaluated.

Results: Transcriptomic analysis of HB patient samples has demonstrated modulation of the neddylation cycle, and NEDD8 levels correlate with the degree of tumour stratification. The preclinical models of HB, as well as the vitro models in tumour cells, shows an increase in NEDD8 and NAE1, related to an increase in global neddylation, in addition to a significant reduction of NEDP1, demonstrating the importance of this process in the development and progression of this pathology. Moreover, the silencing of NEDP1 in human hepatocytes results in a proliferative phenotype. In contrast, its overexpression in HB tumour lines (HepT1 and HepG2) results in the induction of apoptosis, modulation of migratory and proliferative capacity, metabolic reprogramming, sensitization to chemotherapeutic treatments, and regulation of cellular stress mechanisms and immune and inflammatory responses, with an important modulation of proteins such as LIN28. Similarly, its overexpression in patient-derived xenografts (PDX) from a distal metastasis showed modulation of proliferation and migration, in addition to the metabolic reprogramming like the observed in HB tumour lines. In vivo, in Ovo and ex Ovo experiments showed reduced tumorigenicity and decreased metastatic phenotype, and animal models of HB in mice in which NEDP1 overexpression has been carried out showed a reduction in proliferation and tumorigenesis at the histological level, with modulation of some key proteins like HOOK2.

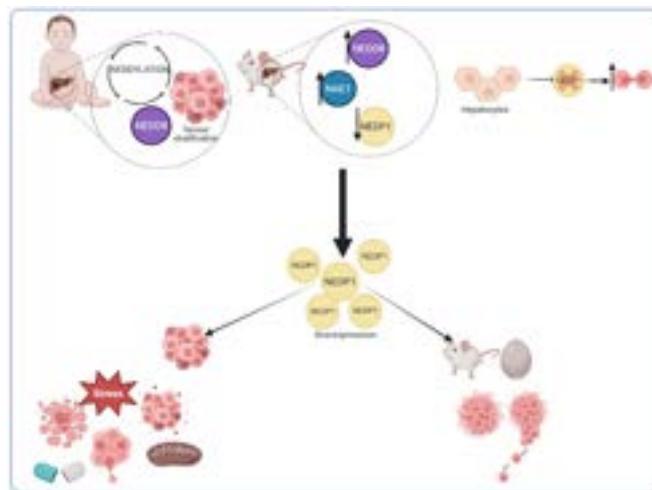


Figure:

Conclusion: Therefore, it is noteworthy that the effect observed with NEDP1 overexpression points to the importance of post-translational modifications in pathologies such as HB and highlights the relevance of neddylation, not only in the molecular characterization of HB, but also in the development of new specific treatments.

Made with BioRender.com

SAT-248

Chromosome engineering and CRISPR-Cas9 viability screening reveals increased metastatic capacity targetable by patient-specific synthetic lethality

Thorben Huth¹, Emely Dreher¹, Steffen Lemke², Sarah Fritzsche¹, Raisatun Sugiyanto¹, Darko Castven³, David Ibberson⁴, Carsten Sticht⁵, Eva Eiteneuer¹, Anna Jauch⁶, Stefan Pusch⁷, Thomas Albrecht¹, Benjamin Goepfert¹, Jens Marquardt³, Sven Nahnsen², Peter Schirmacher¹, Stephanie Roessler¹. ¹Institute of Pathology, University Hospital Heidelberg, Germany, ²Quantitative Biology Center (QBiC), University of Tübingen, Germany, ³Department of Medicine I, University Medical Center Schleswig Holstein, Germany, ⁴Deep Sequencing Core Facility, University of Heidelberg, Germany, ⁵NGS Core Facility, Medical Faculty Mannheim, Germany, ⁶Institute of Human Genetics, University of Heidelberg, Germany, ⁷Department of Neuropathology, University Hospital Heidelberg, Germany
Email: stephanie.roessler@med.uni-heidelberg.de

Background and aims: Chromosomal aberrations are a frequent event in a majority of tumor entities and a hallmark of cancer. In hepatocellular carcinoma (HCC), chromosome 8p (chr8p) loss of heterozygosity (chr8pLOH) can be found overserved predominantly and is correlated with poor overall patient survival. However, no single chr8p tumor suppressor gene reveals strong pro-tumorigenic effects and can account for the increased mortality alone. Given the extent and complexity of chr8pLOH, this suggests that co-suppression of multiple genes can concomitantly promote tumor growth.

Method: In this study, we use chromosomal engineering and CRISPR-Cas9 viability screens to investigate the effects of concurrent loss of multiple chr8p genes. Chromosomal deletions were introduced by a dual guide CRISPR-Cas9 approach. Single cell clones with chr8pLOH were obtained by FACS sorting. PCR, Sanger Sequencing, fluorescence in situ hybridization (FISH) and RNA sequencing (RNAseq) were used to validate effective chr8p deletions. Functional effects were analyzed by viability, proliferation, migration and invasion assays. Gene dependencies were investigated by genome-wide CRISPR-Cas9 screens in chr8pLOH clones and validated by RNAi-mediated knockdown.

Results: Chromosomal deletions were introduced into different HCC cell lines and stable single clones with chr8pLOH were obtained. PCR, FISH and sequencing confirmed loss of heterozygosity in single cell clones. Genome-wide mRNA abundance was significantly altered and gene set enrichment revealed deregulations in migration and tumor microenvironment. Metastasizing potential of chr8pLOH cells was further investigated in vitro and in vivo and goes in line with increased patient mortality. Subsequently, several metastasis suppressor genes were identified on chr8p in an RNAi migration screen. In addition, by performing a genome-wide knockout screen, we discovered and independently validated dependencies specific for chr8pLOH patients with decreased survival. These include novel synthetic lethality of the Nudix hydrolase NUDT17 in chr8pLOH cells but not in wildtype cells.

Conclusion: We developed a new approach and cell model to study large scale genomic aberrations and chr8pLOH in cancer. State-of-the-art genomic technologies were integrated to explain increased patient mortality by the loss of cooperating metastasis suppressors. Extending the view to patient treatment, we identified novel synthetic lethality as potential targets and therapeutic options in patients with chr8pLOH.

SAT-249

Expression and role of the metabotropic glutamate receptor type 3 in hepatocarcinoma

Isabel Méndez¹, Andy Hernández-Abrego¹, Ana Cristina García-Gaytán¹, Dalia De Ita-Pérez¹, Ericka de los Ríos-Arellano¹, Isaías Turrubiate¹, Emanuel Gámez², Mauricio Díaz-Muñoz¹. ¹UNAM Institute of Neurobiology, Querétaro, Mexico, ²Centro Médico Nacional de Occidente, Instituto Mexicano del Seguro Social, Mexico
Email: isabelcm@unam.mx

Background and aims: Glutamate acts on metabotropic glutamate receptors (mGluRs) to exert a variety of regulatory effects through the recruitment of second messengers. It has been demonstrated that mGluRs are expressed in various types of cancer cells and contribute to cancer development, such as increased proliferation and metastasis. mGluR type 3 (mGluR3) is a seven transmembrane Gi-protein coupled receptor that inhibits cAMP, and it could positively regulate the pro-inflammatory cytokine interleukin 6 via the transcription factor NF-kappa B. We aim to evaluate the expression of mGluR3 and the glutamate transporter xCT, which exports glutamate from the cell, in hepatocarcinoma (HCC) induced by DEN in rats and the role of the mGluR3 on survival through cAMP and NF-kappa B in the HCC-derived cell line HepG2.

Method: Male Wistar rats received weekly intraperitoneal injections of diethylnitrosamine (DEN- 50 mg/kg body weight) to induce the progressive pathologies fibrosis, cirrhosis, and HCC. Control rats received saline solution at the same intervals. Histopathological and biochemical analyses were achieved to corroborate the establishment of each pathology. Intrahepatic glutamate concentrations were evaluated using a commercial kit. Expression of mGluR3 and xCT mRNA was analyzed in tissue samples by RT-qPCR. Expression of mGluR3 protein was analyzed on cells (HepG2 and C9 normal hepatocytes cell line) by Western Blot and immunocytochemistry. The effect of the activation of mGluR3 was analyzed under the treatment with glutamate or the selective agonist LY354740, in the presence or the absence of the selective antagonist LY341495 in HepG2. Live and dead cells were quantified by tripan blue assay. cAMP generation and translocation of NF-kappa B to the nucleus were analyzed by immunocytochemistry. Activation of NF-kappa B was evaluated using the inhibitor BAY 11-7082.

Results: Overexpression of mGluR3 was observed according to the progression from normal condition to HCC in rats. This observation was corroborated in HepG2 compared to C9 normal hepatocytes. Both, intrahepatic glutamate and xCT expression increased in HCC. The activation of mGluR3 by glutamate and by the mGluR3 agonist inhibited intracellular cAMP induced by forskolin. Glutamate and the mGluR3 agonist increased live cells in a dose-dependent manner and did not affect cellular death. This effect over the live cells was reverted by the mGluR3 antagonist and by the NF-kappa B inhibitor. Cell death was increased in the presence of the mGluR3 antagonist and the NF-kappa B inhibitor.

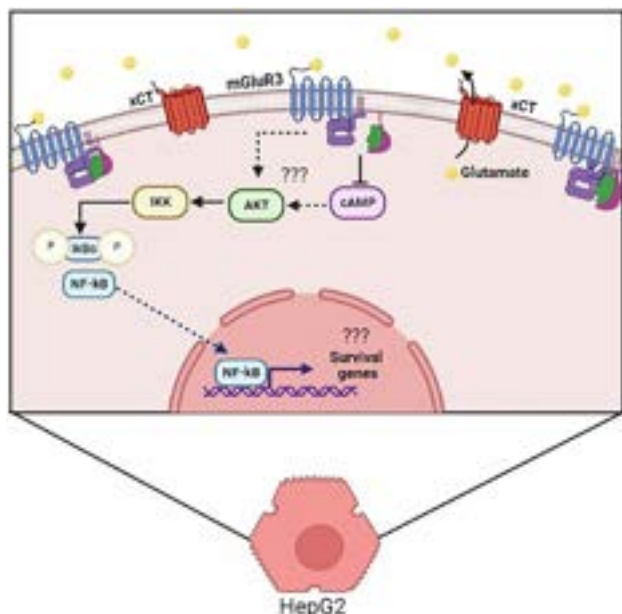


Figure: A suggested mechanism in which mGluR3 could contribute to hepatocarcinoma cell survival

Conclusion: Our data demonstrate that mGluR3 and the transporter xCT are overexpressed in HCC. Moreover, mGluR3 has a role in the survival of HCC cells by inhibiting cAMP and activating the NF-kappa B pathway. This study suggests that the overexpressed mGluR3 could be activated by the enhanced glutamate exported to the extracellular milieu by xCT and may contribute to the survival of HCC. As well, mGluR3 could serve as a possible biomarker and therapeutic target in this pathology.

This research was supported by DGAPA-PAPIIT, UNAM (IN206418 and N222821), and CONACyT (239250).

SAT-250

The rs72613567: TA polymorphism in hydroxysteroid 17-beta dehydrogenase 13 (HSD17B13) is associated with survival benefit after development of hepatocellular carcinoma

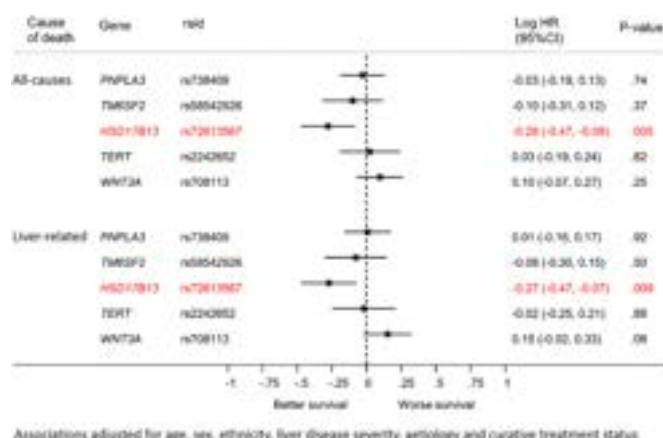
Hamish Innes¹, Marsha Morgan², Felix Stickel³, Jochen Hampe⁴, Stephan Buch⁴. ¹Glasgow Caledonian University, School of Health and Life Sciences, Glasgow, United Kingdom, ²University College London, UCL Institute for Liver and Digestive Health, London, United Kingdom, ³University Hospital of Zurich, Department of Gastroenterology and Hepatology, Zurich, Switzerland, ⁴University Hospital Dresden, TU Dresden, Medical Department 1, Dresden, Germany
Email: stephan.buch@uniklinikum-dresden.de

Background and aims: Genetic risk factors play an important role in determining the susceptibility to develop hepatocellular carcinoma (HCC) in people with chronic liver disease. It is unclear whether these same genetic risk factors influence survival following diagnosis. This study aimed to determine whether genetic polymorphisms influencing susceptibility to HCC are also associated with HCC prognosis.

Method: United Kingdom (UKB) Biobank participants diagnosed with HCC after study enrolment were included. The primary outcome event was all-cause mortality. Patients were followed from the date of HCC diagnosis to death or the registry completion date. Five HCC susceptibility polymorphisms were considered: rs738409 (PNPLA3), rs58542926 (TM6SF2); rs72613567 (HSD17B13); rs2242652 (TERT) and rs708113 (WNT3A). Non-HCC UKB participants (n = 467,673) served as controls. Cox regression was used to determine the independent association between these genetic loci and HCC mortality risk. All associations were adjusted for age, sex, ethnicity, aetiology and severity of the underlying liver disease and receipt of curative HCC treatment.

Results: The final sample included 439 participants (mean [±1SD] age 69.2 ± 6.9 years; men 77.5%; white British ancestry 84.3%); non-alcohol-related fatty liver disease (NAFLD) was the most common underlying liver disease (41%) followed by alcohol-related liver disease (33%) and chronic viral hepatitis (11%). Patients were followed for a median of 1.9 years; a total of 321 patients died. Of the 321 deaths, 295 (92%) were 'liver-related' deaths, of which 235 were attributed to HCC and 60 to liver-disease per se. The median time to death from all-causes was 1.30 years (95%CI: 0.89–1.59). Kaplan Meier survival estimates at 1, 3 and 5 years were 53.2%, 31.2%, and 22.6%, respectively. In multivariate analysis, rs72613567:TA (HSD17B13) was associated with a significant reduction in both overall mortality (aHR:0.75; 95%CI:0.63–0.92; p = 0.005) and liver-related mortality risk (aHR: 0.76; 95%CI: 0.63–0.93; p = 0.009); no other genetic associations with mortality risk were identified (Figure 1). Treatment of HCC with curative intent was also associated with a significant reduction in mortality risk (aHR: 0.25; 95%CI: 0.17–0.37; p < 0.001) while Baveno 3–4 staging was associated with an increased risk (aHR: 1.65; 95%CI:1.06–2.59; p = 0.03).

Figure 1. association between genetic variants and mortality risk.



Conclusion: The rs72613567 polymorphism in HSD17B13 is not only associated with a reduction in the risk of developing HCC but is associated with survival benefit in HCC once established. HSD17B13 might be a potential therapeutic target for HCC prevention and outcome.

SAT-251

Selective inhibition of human β-catenin DNA transactivation activity using splice switching oligonucleotides for an improved therapeutic window in treating hepatocellular carcinoma

Jin Hong¹, Vera Huang¹, Laxman Eltepu¹, Hua Tan¹, Vivek Rajwanshi¹, Aneerban Bhattacharya¹, Elen Rosler¹, Kang Hyunsoon¹, Min Luo¹, Saul Montero¹, John Cortez¹, Dana Cho¹, David Smith¹, Lawrence Blatt¹, Julian Symons¹, Leonid Beigelman¹. ¹Aligos Therapeutics, South San Francisco, United States
Email: jhong@aligos.com

Background and aims: Wnt/β-catenin plays a critical role in embryonic development, tissue homeostasis and repair after injury. Aberrations in this pathway are implicated in many human diseases including cancers. Dysregulation of the Wnt/β-catenin pathway may play a key role in the pathogenesis of HCC. Reducing β-catenin by siRNAs or ASOs in an HCC mouse model has shown significant inhibition of liver tumor growth. Due to the importance of Wnt/β-catenin in normal cellular function, many drugs targeting this pathway have failed due to toxicity. We designed splice switching oligonucleotides (SSO) targeting the DNA transactivation domain of β-catenin to reduce the downstream proteins responsible for HCC

development, while leaving intact the domains interacting with α -catenin and E-cadherin that are important for cell adhesion.

Method: The HepG2 Topflash cell line was used to assay the SSO inhibition of β -catenin transcriptional activity. Anti-proliferative assays with SSO were carried out in Huh-6, HepG2 and Hep3B cell lines using CellTiterGlow. SSO effects on different regions of the β -catenin transcript were analysed by qPCR or Western blot. Effects of SSO on downstream gene expression such as c-Myc, CCND1 and AXIN2 were analysed by qPCR. SSO in vivo efficacy (10×15 mg/kg or 10×30 mg/kg, SC, QOD) was carried out in a Hep3B-luc orthotopic mouse model with the positive control sorafenib (20×60 mg/kg, PO, QD).

Results: A lead SSO, ALG-135041 inhibited the transcriptional activity of β -catenin with an EC_{50} of 4.1 nM in the HepG2 TopFlash cell line. In the Huh-6 cell line, ALG-135041 reduced the 3' transcript while maintaining the 5' transcript. After a 72-hour treatment in Huh-6, ALG-135041 significantly reduced c-Myc, CCND1 and AXIN2 as measured by qPCR. Western blot with an N-terminal β -catenin antibody showed a truncated protein of ~81 kD in ALG-135041 treated Huh-6 cells. In three cell lines used in the orthotopic HCC mouse model, HepG2, Hep3B and Hep3B-Luc, the anti-proliferative EC_{50} values were 142, 86 and 119 nM respectively. In the Hep3B-luc orthotopic mouse model, ALG-135041 showed a dose response with the high dose group achieving tumor growth inhibition (TGI) of 66% by bioluminescence and 84% by tumor weight at the end of study, similar to the results of sorafenib group. There was no difference in body weight between the high dose of ALG-135041 and the vehicle group, while the sorafenib group lost significant body weight. When compared with representative β -catenin siRNAs or ASOs, ALG-135041 demonstrated a significantly better therapeutic window.

Conclusion: ALG-135041, a human β -catenin SSO, selectively inhibits DNA transactivation activity in the nucleus and showed a better therapeutic window than either siRNAs or ASOs. We therefore significantly improved the therapeutic window by precision targeting of only the disease-causing region of the multifunctional protein β -catenin.

SAT-252

Ductular reaction is mediated by CD24 and regulated by miR-122

Nofar Rosenberg¹, Matthias Van Haele², Maytal Gefen¹, Tomer Freemann¹, Tania Roskams², Rifaat Safadi^{2,3}, Hilken Marko⁴, Christoph Schramm⁴, Hilla Giladi¹, Mathias Heikenwalder⁵, Eithan Galun¹. ¹The Goldyne Savad Institute of Gene and Cell Therapy, Jerusalem, Israel, ²University of Leuven, Department of translational cell and tissue research, Leuven, Belgium, ³Hadassah Hebrew University Hospital, The Liver Institute, Israel, ⁴University Medical Center Hamburg-Eppendorf, Dept. of Medicine and Martin Zeitz Center for Rare Diseases, Germany, ⁵DFKZ, chronic Inflammation and Cancer, Ghana
Email: nofar.ros@gmail.com

Background and aims: Ductular Reaction (DR) is associated with chronic liver inflammations, liver fibrosis and presides liver cancer development. DR is characterized by cholangiocytes and hepatic progenitor cells (HPCs) proliferation. CD24, (a marker of HPC) is expressed on cholangiocytes in DR and is overexpressed in HCC and in combined-mixed HCC-Cholangiocarcinoma (CCA). CD24 is essential for self-renewal, proliferation, migration, invasion, and drug resistance of HCC and HCC-CCA tumors through activation of pSTAT3. However, the mechanism of DR is still unknown. We aimed to determine the molecular mechanism regulating DR.

Method: We analyzed bioinformatic data of clinical samples from human with chronic liver diseases as well as samples from mice with acute and chronic liver diseases. We performed transcriptomic investigations including single cell analysis. We have generated numerous genetically modified cell lines and we generated a miR-122 KO mice and we also used the CD24 KO mice model.

Results: Our bioinformatic analysis revealed that CD24 is a target gene of the liver-specific miR-122, which we have also proven by

numerous *in vitro* studies both for the human and mouse miR-122 and CD24. A significant negative correlation was found between CD24 and miR-122 in livers of four human clinical diseases manifesting DR, including CAH, PBC, NASH and PSC. In addition, we identified a strong negative correlation between CD24 and miR-122 in a set of human HCC samples. Similarly, we observed a negative correlation between miR-122 and CD24 in a mouse model of acute and chronic liver inflammation. Our *in-vitro* studies showed that over-expression of CD24 resulted with increased cell proliferation via pSTAT3 protein. *In vitro*, HCC cell proliferation was attenuated upon miR-122 supplementation only in cells with CD24 bearing an authentic miR-122 seed at its 3'-UTR but was not attenuated when the miR-122 seed was mutated. In miR-122 KO mice, CD24 expression increases significantly, and DR is enhanced.

Conclusion: DR is mediated by CD24 expression and regulated by miR-122.

SAT-253

Hepatitis B surface antigen impairs endoplasmic reticulum stress-related autophagic flux via down-regulation of LAMP2, thereby participating in hepatocarcinogenesis

Yaojie Liang¹, Stefan Schefczyk¹, Xufeng Luo^{1,2}, Lorraine Muungani¹, Baoju Wang³, Hui Deng³, Hideo Baba⁴, Mengji Lu⁵, Heiner Wedemeyer⁶, Hartmut Schmidt¹, Ruth Broering¹. ¹University of Duisburg-Essen, Dept of Gastroenterology, Hepatology and Transplant Medicine, Germany, ²The Affiliated Cancer Hospital of Zhengzhou University, Institute for Lymphoma Research, China, ³Huazhong University of Science and Technology, Union Hospital, Tongji Medical College, China, ⁴University Duisburg-Essen, Institute of Pathology, Germany, ⁵University Duisburg-Essen, Institute for Virology, Germany, ⁶Hannover Medical School, Dept. of Gastroenterology, Hepatology and Endocrinology, Germany
Email: ruth.broering@uni-due.de

Background and aims: Hepatitis B virus surface antigen (HBsAg) drives hepatocarcinogenesis. Factors and mechanisms being involved in this progression remain poorly defined, thus hindering the development of effective therapeutic strategies. Therefore, mechanisms involved in HBsAg-induced transformation of normal liver into hepatocellular carcinoma were explored.

Method: Hemizygous Tg (Alb1HBV)44Bri/J mice were investigated for this HBsAg-driven carcinogenic events by data mining, western blotting, immunohistochemical and immunocytochemical staining. Findings were verified in HBsAg-overexpressing Hepa1-6 cells and validated in human liver specimens.

Results: Gene set enrichment analysis identified significant signatures in HBsAg-transgenic mice correlating with endoplasmic reticulum (ER) stress, unfolded protein response (UPR), autophagy, and proliferation. These events were further investigated in 2-, 8- and 12-month-old HBsAg-transgenic mice. Increased BiP expression in HBsAg-transgenic mice indicated induction of UPR. Furthermore, in HBsAg-transgenic mice, autophagy was enhanced at the early stage (increased BECN1 and LC3B) and blocked at the late stage (increased p62). Finally, HBsAg changed lysosomal acidification by down-regulating LAMP2 expression. In patients, HBV-related HCC and adjacent tissue showed increased BiP, p62 and down-regulated LAMP2, compared to uninfected controls. *In vitro*, use of ER stress inhibitors reversed the HBsAg-related suppression of LAMP2. Furthermore, HBsAg promoted hepatocellular proliferation, indicated by I) Ki67, AFP and cleaved caspase 3 staining in paraffin-embedded HBsAg-transgenic mice liver sections and II) colony formation assay in HBsAg-expressing Hepa1-6 cells. Interestingly, ER stress inhibition in HBsAg-overexpressing Hepa1-6 cells suppressed HBsAg-mediated cell proliferation.

Conclusion: These findings revealed that HBsAg directly induces ER stress, impairs autophagy and promotes proliferation thereby driving hepatocarcinogenesis. Moreover, this study expanded the understanding of HBsAg-mediated intracellular events in carcinogenesis.

SAT-254

RuvBL1 is required for mitochondrial integrity and supports the metabolic reprogramming of HCC cells

Irene Simeone¹, Alice Guida^{1,2}, Simone Polvani¹, Elisabetta Ceni¹, Daniele Bani³, Patrizia Nardini³, Daniele Guasti³, Massimo Bonora⁴, Alice Santi¹, Andrea Galli¹, Tommaso Mello¹. ¹University of Florence, Experimental and Clinical Biomedical Sciences, Italy, ²University of Siena, GenOMeC Doctorate, Italy, ³University of Florence, Clinical and Experimental Medicine, Italy, ⁴University of Ferrara, Department of Medical Sciences, Italy
Email: tommaso.mello@unifi.it

Background and aims: RuvBL1 is a AAA+ ATPase involved in multiple cellular activities, including proliferation, chromatin remodeling, DNA repair, transcription/translation and mTOR pathway activity. High RuvBL1 expression in hepatocellular carcinoma (HCC) correlates with poor prognosis. We have previously shown that hepatic RuvBL1 haploinsufficiency impairs mTORC1 signaling thereby altering liver metabolism and glucose homeostasis, suggesting that RuvBL1 overexpression may support the metabolic rewiring of HCC. We therefore aimed at dissecting RuvBL1 role in HCC cell metabolism.

Method: Experiments were performed in human HCC cell lines (HepG2, Hep3B, Huh7), mouse HCC cell line (Hepa1-6) and mouse normal hepatocytes (AML-12 and freshly isolated hepatocytes). RuvBL1 was targeted either by RNAi or by inhibiting its ATPase activity with CB-6644. Metabolomics analysis was performed by untargeted GC/MS or by 13C-glucose and 13C-glutamine metabolic tracing. OXPHOS was evaluated by Seahorse analyzer. Mitochondria morphology and potential were evaluated by fluorescence microscopy/HCS and TEM. RuvBL1 localization was assessed via STED microscopy and immunogold labelling. RuvBL1 mitochondrial interactome was evaluated by co-immunoprecipitation coupled with MS. Correlative analysis in human HCC samples was performed on the TCGA_LIHC dataset.

Results: RuvBL1 silencing in Huh7 cells altered many mitochondrial metabolites central to glucose, TCA and aminoacid metabolism, and significantly associated with processes such as cancer metabolic reprogramming by pathway enrichment analysis. Metabolic tracing with 13C-glucose and 13C-glutamine in CB-6644 treated Huh7 revealed alterations in glycolysis and TCA. Targeting RuvBL1 by RNAi or by inhibition with CB-6644 significantly impaired mitochondrial respiration in normal hepatocytes and HCC cell lines. ATP production by OXPHOS and glycolysis was inhibited by CB-6644 treatment in a dose- and time-dependent manner. Interestingly, CB-6644 treatment increased mitochondrial membrane potential, as assessed by JC-1 and by TMRM staining in high content microscopy analysis, eventually disrupting mitochondria structure as shown by the reduced matrix density and disarranged cristae. By super-resolution microscopy and immunogold-TEM we were able to localize RuvBL1 within mitochondria. Gene ontology analysis of mitochondrial RuvBL1-interactome revealed that this ATPase impact on TCA, aminoacid and lipid metabolism, mito-ribosome assembly, and mitochondrial membrane organization. Analysis of human HCC samples in the TCGA-LIHC cohort revealed that high RuvBL1 expression was significantly associated with an enrichment of mitochondria-related GO terms.

Conclusion: Our data uncover a novel localization and function of RuvBL1 in mitochondria, suggesting that RuvBL1 overexpression is exploited in HCC to support mitochondria-related metabolic processes.

SAT-255

Combining non-selective beta-blockers with sorafenib in HCC: targeting the culprits of metastasis

Tasnim Mahmoud¹, Olfat Hammam², Mahmoud Khattab³, Aiman El-Khatib³, Yasmeen Attia¹. ¹Faculty of Pharmacy, The British University in Egypt, Department of Pharmacology and Biochemistry, Cairo, Egypt, ²Theodor Bilharz Research Institute, Department of Pathology, Egypt, ³Faculty of pharmacy, Cairo University, Department of Pharmacology and Toxicology, Cairo, Egypt
Email: Tasnim120764@bue.edu.eg

Background and aims: Hepatocellular carcinoma (HCC) is the most prevalent type of liver cancer and the fifth most common cancer worldwide. For unresectable HCC, sorafenib (SOR), an oral multi-tyrosine kinase inhibitor, is used as first-line therapy, however, acquired resistance towards SOR develops leading to treatment failure. The underlying mechanisms of SOR resistance are not clearly understood, yet strong evidence suggests a role of epithelial-to-mesenchymal transition (EMT), the main culprit of metastasis, in its development. Meanwhile, non-selective beta-blockers (NSBB) were shown to improve outcomes and responsiveness in HCC. The detailed mechanism remains elusive though. This study aims at deciphering whether using carvedilol (CAR), as a NSBB, can enhance HCC responsiveness to SOR. Further, it unravels the potential interception of CAR with EMT at the glycogen synthase kinase (GSK)- 3 beta/Wnt signaling.

Method: Male Sprague Dawley rats were injected intraperitoneally with diethyl nitrosamine (DEN) at a dose of 50 mg/kg, once a week. After a 16 -week period of DEN treatment, the rats underwent a one-week washout period followed by a 4 -week period of oral treatment with SOR at a dose of 30 mg/kg/day, CAR at a dose of 10 mg/kg/day, each alone and combined. By the end of week 20, the rats were sacrificed and livers were collected for further analyses which included histopathological examination, gene expression analysis of Axin- 1 by qRT-PCR along with estimating protein levels of GSK- 3 beta, snail- 1 and twist- 1 by ELISA. One-way ANOVA followed by Tukey Kramer's for multiple comparisons was used for statistical analysis. p values less than 0.05 were considered statistically significant.

Results: In hematoxylin and eosin (HandE)-stained sections, histopathological examination revealed fewer sheets of malignant cells with areas of necrosis and fewer cells showing high nucleocytoplasmic ratios in the SOR+CAR-treated group compared to SOR alone. The combination group also showed lower levels of the EMT markers, snail- 1 and twist- 1, as compared to the HCC group. The latter was also significantly lower with SOR+CAR than with SOR alone (Fig 1A). Axin- 1, the negative regulator of the Wnt signaling, was noticeably upregulated in the combination group compared to the positive control group. This was paralleled with an increase in GSK- 3 beta levels in the SOR+CAR group relative to both control and SOR groups (Fig 1B).

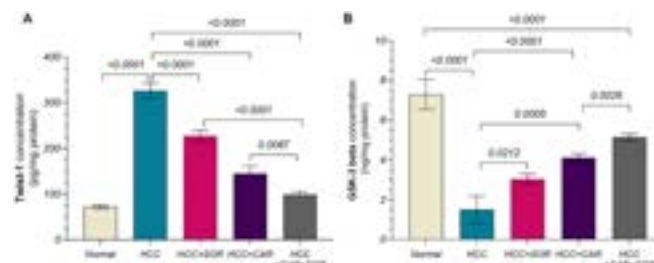


Figure: Protein levels of (A) Twist- 1 and (B) GSK- 3 beta in livers of normal, positive control (HCC), sorafenib (SOR)-treated, carvedilol (CAR)-treated, and SOR+CAR-treated groups, as estimated by ELISA.

Conclusion: Overall, the present findings demonstrated the ability of CAR to impede the EMT program in HCC enhancing SOR efficacy. These results might also suggest the potential inclusion in therapeutic regimens of HCC patients.

SAT-256

Investigation of novel hepatoblastoma chemosensitizers based on the inhibition of ABC pumps-mediated drug efflux

Candela Cives-Losada¹, Oscar Briz^{1,2}, Stefano Cairo³, Emilie Indersie⁴, Thomas Efferth⁵, María Luz Martínez-Chantar^{2,6}, Matías A Avila^{2,7}, Carolina Armengol^{2,8}, Elisa Lozano^{1,2}, Jose Marin^{1,2}, Rocio Ir Macias^{1,2}.
¹University of Salamanca, IBSAL, Spain, ²National Institute for the Study of Liver and Gastrointestinal Diseases (CIBERehd), Spain, ³Champions Oncology, United States, ⁴XenTech, France, ⁵Johannes Gutenberg University, Germany, ⁶Center for Cooperative Research in Biosciences (CIC bioGUNE), Spain, ⁷Cima-University of Navarra, Spain, ⁸Germans Trias i Pujol Health Sciences Research Institute (IGTP), Spain
Email: rociorm@usal.es

Background and aims: The poor prognosis of about one-third of patients with hepatoblastoma (HB) is mainly due to the refractoriness of this cancer to neoadjuvant chemotherapy, which is commonly based on cisplatin and doxorubicin. In previous studies, we have demonstrated that the high expression of drug export pumps belonging to the ABC superfamily of proteins, mainly MDR1, MRP1, and MRP2, plays a primary role in HB chemoresistance. The aim of this study was to search for non-toxic inhibitors of these transporters and to evaluate in vitro their ability to sensitize HB cells to antitumor chemotherapy.

Method: Cell lines with endogenous or chemically induced high expression of MDR1 (HepG2/DR) or MRP1/MRP2 (HB-282) were used. Gene expression was determined by RT-qPCR, Western blot, and immunofluorescence. ABC-mediated transport activity was determined by flow cytometry using fluorescent substrates and specific inhibitors. Known inhibitors of ABC pumps were used as controls. In silico analysis by molecular docking was performed to look for potential ABC inhibitors using homology models for these proteins and a library of 40,000 natural or semi-synthetic compounds. Potentially harmful compounds were discarded based on toxicity prediction using the online tool ProTox-II. Cell viability was determined by the MTT-formazan and sulforhodamine B assays. SynergyFinder 3.0 was used to assess drug combination synergy.

Results: Besides known MDR1 inhibitors (verapamil, elacridar, and tariquidar), 11 novel compounds, among 40 potential inhibitors studied, significantly reduced rhodamine-123 efflux from HepG2/DR cells. Among these with no cytotoxic effect, only CCL-40 was able to slightly increase the sensitivity of cells to doxorubicin. However, CCL-17 and CCL-24, both tyrosine kinase inhibitors, markedly enhanced the cytostatic effect of doxorubicin, which was due to a synergistic mechanism. Regarding MRP1 and MRP2, the molecular docking study identified 1,000 compounds with potential interaction with these pumps. Among them, the best eight compounds, based on low binding energy to both proteins, low predicted toxicity, and commercial availability, were further studied. The results revealed that two of them, CCL-45 and CCL-46, significantly reduced MRP1/MRP2-mediated calcein efflux in HB-282 cells. The chemosensitizing potency of CCL-45 was even stronger than the typical MRP1/MRP2 inhibitor MK-571.

Conclusion: Inhibition of ABC drug export pumps, such as MDR1, MRP1, and MRP2, by several non-toxic natural compounds and drugs commonly used in the clinic for other purposes, could be a helpful strategy to overcome the lack of response to chemotherapy in HB patients.

SAT-257

Dual effects of brown-fat activation limit hepatocellular carcinoma (HCC) progress in steatotic liver

Juan Gao^{1,2}. ¹Karolinska Institute, Sweden, ²Third Affiliated Hospital of Sun Yat-sen University, China
Email: gaoj59@mail2.sysu.edu.cn

Background and aims: Obesity, a metabolism abnormal disease with increasing incidence, also is a high-risk factor for various tumors. It is often associated with Non-alcoholic fatty liver disease (NAFLD), which could show steatosis, hepatitis, cirrhosis, and finally lead to cancer. Accumulating free fatty acids (FFAs) may contribute to cancerogenesis due to lipid metabolic disorders. Our previous studies suggested that cancer lipid metabolism confers antiangiogenic drug resistance (Iwamoto et al., 2018, Cell Metabolism 28, 104–117), and cold exposure suppresses tumor growth by brown fat activation alters global metabolism (Seki et al., 2022, Nature 608). We are interested in how the host metabolism reshapes the hepatocellular carcinoma (HCC) microenvironment and affects their response to drugs. We also gain insight into the potential mechanisms of the combination of metabolic stimulators and existing drug therapies.

Method: To establish metabolic abnormalities in animal models, adult male C57BL/6N mice were fed with high-fat diet (HFD) for more than 3 months to induce obesity and liver steatosis. Hepa1-6 hepatocarcinoma cells were implanted in the mice's liver under inhaling anaesthetization as the orthotopic HCC model. Approximately 1 week after tumor implantation, mice were randomly grouped and treated with different temperatures exposure for the next three weeks. 4 degree celsius (4 °C) environmental temperature as the cold exposure group, and 30 degree celsius (30 °C) environmental temperature as the control group. Glucose tolerance test (GTT) and insulin tolerance test (ITT) were performed during the treatment. Then mice were sacrificed, blood, liver with tumor and fat tissue were collected for histological and biochemistry analysis. Data presented as mean determinants ± SEM. Statistical computations were performed using the standard two-tailed Student t-test, * $p < 0.05$, ** $p < 0.01$, and *** $p < 0.001$ were considered statistically significant.

Results: The body weight of obese mice showed a decrease in the 4 °C group in the first week, with noticeable differences between the two groups after three weeks of treatment ($p < 0.001$, Figure A). Both GTT and ITT suggested host metabolic disorders were improved in the 4 °C group (AUC, $p < 0.05$). The tumor volumes of the orthotopically implanted HCC were limited in the 4 °C group than in the 30 °C group ($p < 0.001$, Figure B). Furthermore, qPCR indicated that metabolic-related genes were downregulated in the tumors of the 4 °C group, such as *cd36*, *fabp4*, *plin2* and *glut1* (both $p < 0.01$, Figure C). Besides, histopathology showed that the liver steatosis was relieved in the 4 °C group compared to the 30 °C group ($p < 0.05$). And both proliferation and metabolism of the tumor were limited in the 4 °C group, showed by IHC staining of KI67 and COX4 (both $p < 0.01$, Figure D).

Conclusion: The dual effect of activating brown-fat relieves liver steatosis and HCC progress in the steatotic liver. The combination of brown-fat activators and drug therapies may contribute to better outcomes in HCC patients with metabolic disorders.

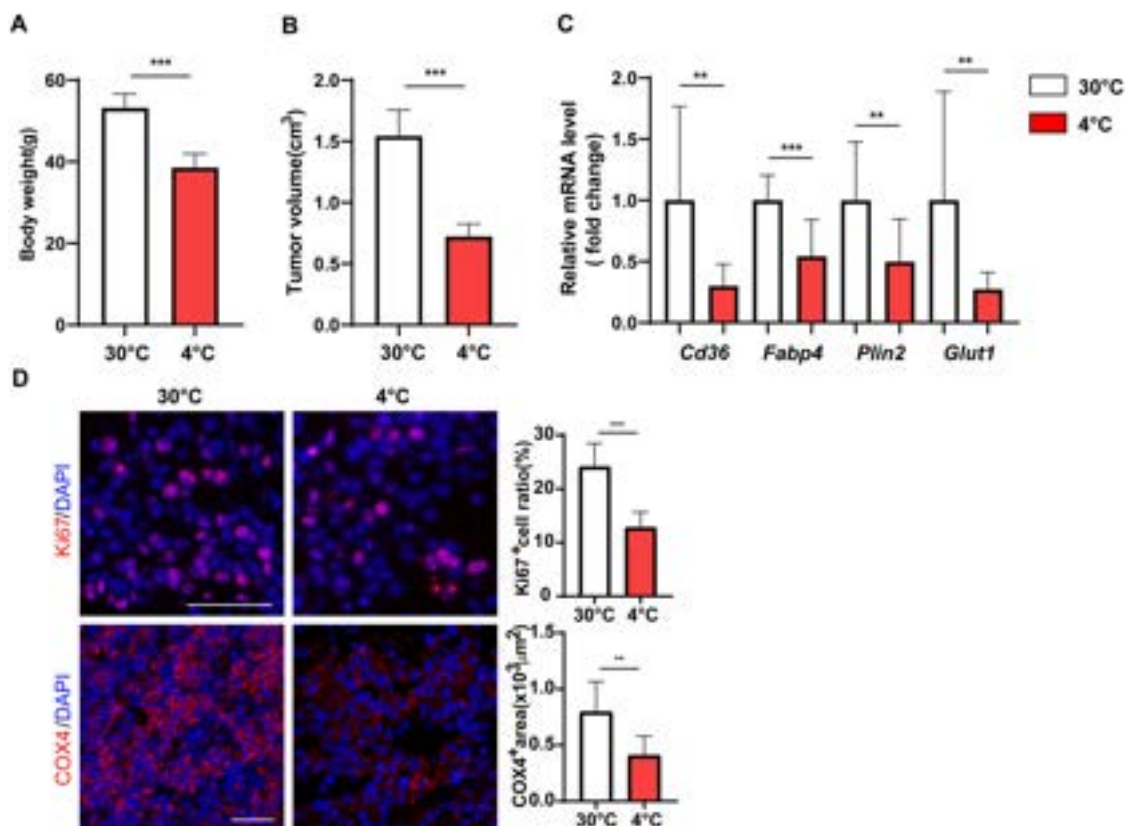


Figure: (abstract: FRI-257).

SAT-258

Development of new personalized therapies targeting VDAC1 in intrahepatic cholangiocarcinoma using patient-derived liver organoids

Silvia De Siervi¹, Stefano Conti Nibali¹, Stefania Mantovani², Barbara Oliviero², Mario Mondelli^{2,3}, Laura Giuseppina Di Pasqua³, Davide Ronchi⁴, Marco Gaetano Lolicato¹, Cristian Turato¹. ¹University of Pavia, Molecular Medicine, Pavia, Italy, ²Division of Clinical Immunology and Infectious Diseases, Fondazione IRCCS Policlinico San Matteo, Pavia, Italy, ³University of Pavia, Department of Internal Medicine and Therapeutics, Pavia, Italy, ⁴University of Pavia, Department of Electrical, Computer and Biomedical Engineering, Pavia, Italy
Email: cristianturato@gmail.com

Background and aims: Intrahepatic cholangiocarcinoma (iCCA) is characterized by a very poor outcome, and reliable biomarkers as well as new therapeutic strategies are urgently needed. Voltage Dependence Anion Selective Channel isoform 1 (VDAC1) has emerged as a prominent drug target because it plays a key role in the regulation of mitochondria-mediated cell death and survival signalling pathways. There have been several compounds developed, but none of them have been widely employed to treat patients due to promiscuity and side effects. The aim of this study was to test a new class of small molecules targeting VDAC1 to induce activation of the apoptotic pathway in iCCA patient-derived liver cells and organoids.

Method: We minced tumour and paired non-tumour samples, shortly digested in small cell clusters, and then seeded into Matrigel in order to develop organoids. Following immunofluorescence and qPCR analysis, we treated primary cell cultures and organoids with different concentrations of small molecules targeting VDAC1, detecting cell viability and ROS levels release, to verify the *in vitro* effects and the efficiency of these compounds on cells.

Results: We generated and characterized a biobank of human iCCA-derived organoids, analyzing the morphological characteristics and

performing a mathematical tool that allow to simulate tumour progression. We also examined the presence of specific CCA markers, such as CK19, CK7, EpCAM, E-Cadherin, Ki67. In addition, we highlighted the increased levels of VDAC1 expression in iCCA cells compared to non-tumor cells ($p < 0,005$). The impact of novel small compounds targeting VDAC1 was then investigated at different times points and concentrations, both in patient-derived cell cultures and organoids. In particular, we showed a significant decrease of viability in tumor cells and a modulation in ROS production.

Conclusion: We established and characterized a reliable *in vitro* iCCA model that allowed us to study the impact of small molecules targeting VDAC1 as a new personalized treatment.

SAT-259

Morphological architectures of patient-derived hepatocellular carcinoma organoids with GSK3-beta expression dependent variability according to lenvatinib resistance

Kyung Joo Cho¹, Jun Yong Park^{1,2,3,4}, Hye Won Lee^{1,3,4}, Hye Jung Park¹, Eun Kong Lee¹, Sang Hyun Seo^{1,2}, Jae Seung Lee^{1,3,4}, Beom Kyung Kim^{1,3,4}, Seung Up Kim^{1,3,4}, Do Young Kim^{1,3,4}, Sang Hoon Ahn^{1,3,4}. ¹Yonsei Liver Center, Severance Hospital, Seoul, Korea, Rep. of South, ²Brain Korea 21 PLUS Project for Medical Science, Yonsei University, Seoul, Korea, Rep. of South, ³Department of Internal Medicine, Yonsei University College of Medicine, Seoul, Korea, Rep. of South, ⁴Institute of Gastroenterology, Yonsei University College of Medicine, Seoul, Korea, Rep. of South
Email: drpjy@yuhs.ac

Background and aims: Organoid models using patient-derived cancer tissues has allowed a better understanding of human cancer as well as development of precision medicine. We evaluated the potential differential sensitivity of HCC organoids (HCOs) to lenvatinib and analyzed the relationship between the resistance group of lenvatinib and intracellular signaling pathways.

Method: Patient-derived tumor tissue was digested at 37 °C and mixed with Matrigel. After polymerization of Matrigel, medium was added and changed twice a week. To evaluate whether HCO exhibit different sensitivity to drugs, we tested its sensitivity and analyzed the sensitivity in HCO lines with the difference in gene expression.

Results: We successfully established HCO lines at a 76% success rate, presenting as two different morphological types: solid-type and mixed-type. Heterogeneous morphological features of HCOs exhibited differential gene expression and response to lenvatinib, showing highly expressed EGFR, GSK3-beta and FOXO3 with lower sensitivity to lenvatinib in solid type HCOs, compared to mixed type HCOs. To confirm the association of morphological classification with GSK3-beta activation and lenvatinib sensitivity, we generated a rHCO from re-biopsied tissue from a patient with advanced HCC progression after lenvatinib treatment and compared it with a HCO from first biopsied tissue. Specifically, the lenvatinib-resistant rHCO expressed much lower levels of the inactive form of GSK3-beta and higher levels of the active form of GSK3β compared with the original HCO, suggesting higher GSK3-beta activity and Ki-67 levels in resistant cells. Knockdown of GSK3-beta with selective GSK3-beta inhibitor and siRNA restores sensitivity to lenvatinib in association with GSK3-beta activity and morphological features.

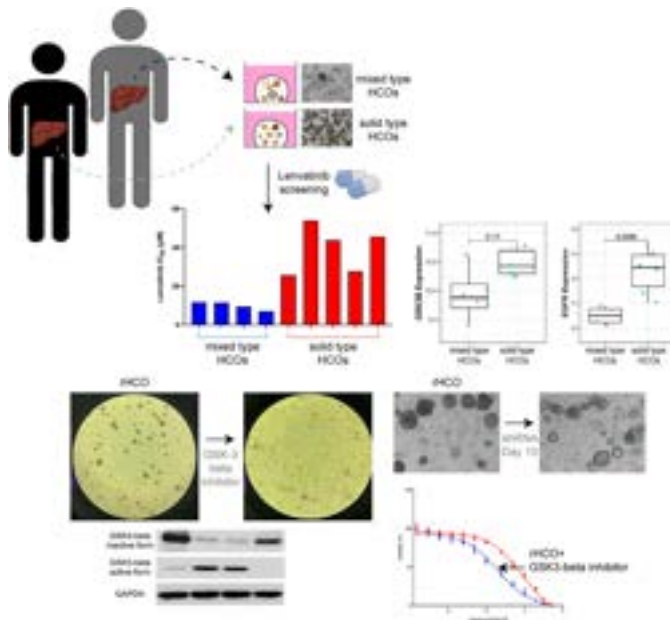


Figure:

Conclusion: Our work demonstrates the relationship between lenvatinib sensitivity and morphological features with GSK3-beta expression and identifies regulators of GSK3-beta activity as potential novel therapeutic agents for restoring lenvatinib sensitivity.

SAT-260

Immunomagnetic enrichment of hepatocyte-specific extracellular vesicles using magnetic beads and click chemistry

Sven Mentink¹, Richell Booiijink¹, Maureen Brusse¹, Ruchi Bansal¹.

¹University of Twente, Netherlands

Email: r.s.booiijink@utwente.nl

Background and aims: Extracellular vesicles (EVs) are cell-derived nano- and micro-sized vesicles that are abundantly present in body fluids emphasizing their potential utility in liquid biopsies. EVs have great potential as early hepatocellular carcinoma biomarkers since tumor-derived EVs are found at an early stage, and their inherent stability guarantees the integrity of biomolecular cargos. Unfortunately, conventional EV isolation techniques including ultracentrifugation and/or size exclusion chromatography are based

on EVs' density or size respectively, and are incapable of separating tumor-derived EVs from total EVs. Here, we present an unique approach of isolating hepatocellular derived EVs by immunomagnetic enrichment using surface antibodies, magnetic beads and click chemistry.

Method: We developed an EV enrichment system whereby magnetic beads (1–5 μm) were functionalized with tetrazine (Tz). Antibodies [EpCAM (epithelial-specific), CD9 (EV specific) and ASGPR1 (hepatocyte specific)] used to capture EVs was functionalized with trans-cyclooctene (TCO). EVs isolated from the conditioned medium obtained from serum-starved HepG2 cells were captured using antibody-TCO conjugate and the EV-antibody-TCO conjugate was incubated with the magnetic beads-Tz, creating a click reaction between the Tz and the TCO, leading to capture of the hepatocyte specific EVs to the magnetic beads. Magnetic beads were enriched using magnets; and EV release from the magnetic beads was achieved using 1,4-dithiothreitol (DTT, by cleavage of disulfide bonds incorporated during Tz conjugation). Characterization of efficiency of conjugation, click reaction and EV release was performed using flow cytometric analysis.

Results: To validate the efficiency of the EV isolation, EVs were fluorescently labelled with Calcein-AM prior to conjugation, and the EVs captured using magnetic beads were analyzed through a flow cytometer. We confirmed a successful enrichment of the EVs using magnetic beads. Similar results were obtained with EpCAM or ASGPR1 antibodies suggesting antibody-specific EV-capture can be achieved using different antibodies. Hepatocyte-specific EVs (bound to magnetic beads) were separated from other particles in suspension using magnetic enrichment. Finally, DTT treatment released the captured EVs from the magnetic beads for downstream analysis.

Conclusion: We confirm the successful immunomagnetic enrichment of specific hepatocyte-derived EVs by combining cell specific antibodies, magnetic beads and click chemistry. We present an attractive and unique approach for the isolation and analysis of cell-specific EVs. This approach can be extended to other cell types i.e., HSCs, endothelial cells, immune cells based on the availability of the antibodies. We believe this approach will pave the way to the identification of early circulating biomarkers for HCC.

SAT-261

Circular RNA hsa_circ_0062682 promotes oncogenesis in hepatocellular carcinoma and binds to YBX1

Rok Razpotnik¹, Hana Trček¹, Martin Zaplotnik², Blaž Trotovšek³, Mihajlo Djokić³, Miha Petrič³, Boštjan Plešnik³, Irena Plahuta⁴, Arpad Ivanecz⁴, Linda Cellner², Rado Janša², Petra Hudler⁵, Robert Vidmar⁶, Marko Fonovič⁶, Uršula Prosenc Zmrzljak⁷, Damjana Rozman¹, Tadeja Rezen¹. ¹University of Ljubljana, Faculty of Medicine, CFGBC, IBKMG, Slovenia, ²University Medical Centre Ljubljana, Department of Gastroenterology, Slovenia, ³University Medical Center Ljubljana, Department of Abdominal Surgery, Slovenia, ⁴University Medical Center Maribor, Department of Abdominal and General Surgery, Slovenia, ⁵University of Ljubljana, Faculty of Medicine, MCMB, IBKMG, Slovenia, ⁶Jozef Stefan Institute, Department of Biochemistry and Molecular and Structural Biology, Slovenia, ⁷BIA Separations CRO, Labena d.o.o, Slovenia

Email: tadeja.rezen@mf.uni-lj.si

Background and aims: Circular RNAs (circRNAs) have gained increasing interest in recent years and have been shown to play an important role in cancer. Although increased efforts have been made to identify their role and differential expression in cancer, the role of most dysregulated circRNAs is unknown, and their function in cancer pathogenesis remains to be assessed. Here, we report the characterization of a circRNA hsa_circ_0062682 with oncogenic properties in hepatocellular carcinoma (HCC) and evaluate its expression and diagnostic potential in HCC patients.

Method: We identified differentially expressed circRNAs in HCC tumors by reanalyzing published microarray datasets. We

POSTER PRESENTATIONS

investigated the oncogenic potential of circRNA hsa_circ_0062682 in cell lines using various functional cell-based assays, including proliferation, migration, invasion, and colony formation assays. We used microarrays to analyze systemic changes in the transcriptome after modulation of circRNA expression in HCC cell lines. In addition, biotinylated oligonucleotide pulldown coupled with mass spectrometry was used to identify binding partners and RNA immunoprecipitation to confirm binding partners. We analyzed circRNA expression in paired liver tumor and paratumor samples from the Slovenian HCC cohort with metabolism-associated and alcohol-related etiologies. We measured the presence of circRNA in plasma from the same patients by RT-qPCR and ddPCR to evaluate its diagnostic potential.

Results: By analyzing available microarray datasets, published at the time of analysis, we identified 32 upregulated and 6 downregulated circRNAs in HCC tumors. We overexpressed and knocked down the expression of hsa_circ_0062682 in various HCC cell lines and confirmed its oncogenic potential using several functional assays. By integrating pathway enrichment analysis and gene set enrichment analysis, we uncovered systemic changes triggered by perturbations of hsa_circ_0062682 expression and we identified enriched transcription factors (E2F1, Sp1, HIF-1 α , and NF κ B), known to be oncogenic regulators in HCC, as well as signaling pathways previously associated with HCC that could explain the observed phenotype. Using the proteomics approach, we uncovered protein binding partners of hsa_circ_0062682 and confirmed an interaction with YBX1, a known oncogene, by RNA immunoprecipitation. A cell type-specific role of hsa_circ_0062682 was detected based on differential sorafenib sensitivity, migratory ability and differential localization of the studied proteins in stably transduced cell lines. Interestingly, the expression of this circRNA was downregulated in our cohort, which has a metabolic and alcohol-associated etiology. In our opinion, this discrepancy could be due to different etiologies and molecular subtypes of the HCC cohorts used in the microarray datasets. Furthermore, we evaluated the diagnostic potential of hsa_circ_0062682 as a non-invasive biomarker in plasma by measuring its expression in plasma and comparing it with its expression in liver.

Conclusion: Our data suggest that hsa_circ_0062682 promotes oncogenesis in HCC, binds to YBX1, affects multiple signaling pathways involved in oncogenesis, and may act in a cell type specific context.

SAT-262

The mutated ENTPD6 as neoantigen in hepatocellular carcinoma

Dongbo Chen¹, Pu Chen¹, Hongsong Chen¹, ¹Peking University People's Hospital, Peking University Hepatology Institute, Beijing Key Laboratory of Hepatitis C and Immunotherapy for Liver Disease, Beijing International Cooperation Base for Science and Technology on NAFLD Diagnosis, China

Email: chen hongsong2999@163.com

Background and aims: Tumor neoantigens, new peptides generated by somatic mutations from tumor tissues but not normal tissues, have good tumor specificity and strong immunogenicity. Though Clinical trials testing neoantigen immunotherapy have yielded encouraging results in patients with hepatocellular carcinoma (HCC) worldwide, it's hard to know which neoantigens are dominant in determining the responsiveness to immunotherapy treatment. In this study, we used the Co-HA system, a single-plasmid system co-expressing patient HLA and antigen, to detect the immunogenicity of neoantigens and identify new dominant hepatocellular carcinoma (HCC) neoantigens.

Method: First, we enrolled 14 HCC patients for next-generation sequencing for variation calling and predicting potential neoantigens. Then, the specific cytotoxicity generated by this neoantigen was shown using the Co-HA system. Finally, potential HCC-dominant neoantigens were screened out by tetramer staining and validated by

the Co-HA system using methods including flow cytometry, ELISPOT, ELISA and sequencing.

Results: First, 2875 somatic mutations were identified in 14 HCC patients. The main base substitutions were C>T/G>A transitions, and the main mutational signatures were 4, 1 and 16. The high-frequency mutated genes included HMCN1, TTN and TP53. Then, 541 potential neoantigens were predicted. Moreover, 37 predicted neoantigens restricted by HLA-A*11:01, HLA-A*24:02 or HLA-A*02:01 were assayed by tetramer staining to screen out potential HCC-dominant neoantigens. Furthermore, the Co-HA system identified that the HLA-A*24:02-restricted epitope 5'-FYAFSCYYDL-3', produced by the mutated ectonucleoside triphosphate diphosphohydrolase 6 (ENTPD6) had strong immunogenicity in HCC. Finally, Huh-7 cells co-expressing HLA-A*24:02 and ENTPD6 neoantigen were selected as the target cells and implanted into the B-NDG-B2m^{tm1}Fcrn^{tm1}(mB2m)/Bcgen mouse model. When tumor size was approximately 150 \pm 50 mm³, they were treated with the neoantigen-specific T cells through intratumor injection every 2 days. After 3 times of treatment, the volume and weight of tumors with neoantigens were both smaller than those of WT type.

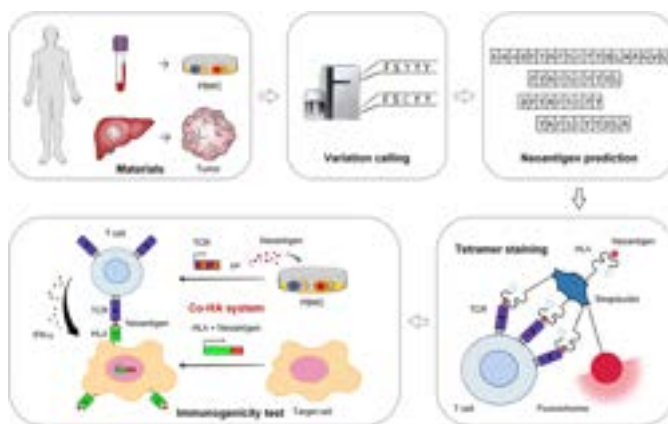


Figure:

Conclusion: The HLA-A*24:02-restricted epitope 5'-FYAFSCYYDL-3', produced by the mutated ENTPD6, was the dominant neoantigen with high immunogenicity in HCC.

SAT-263

Relevance of hypoxia-inducible factor 1 alpha in hepatocellular carcinoma: clinical and pre-clinical analysis

Tania Payo-Serafin^{1,2}, Paula Fernández-Palanca^{1,2}, Carolina Méndez-Blanco^{1,2}, Jennifer Martínez-Geijo^{1,2}, Beatriz San Miguel de Vega^{1,2}, Andrés García-Palomo³, Juan José Ortiz de Urbina⁴, Javier González-Gállego^{1,2}, María Jesús, Tuñón González^{1,2}, José Luis Mauriz^{1,2}. ¹Institute of biomedicine (IBIOMED), University of León, León, Spain, ²Centro de investigación biomédica en red de enfermedades hepáticas y digestivas (CIBERehd), Institute of Health Carlos III, Madrid, Spain, ³Service of Medical Oncology, Complejo Asistencial Universitario de León (CAULE), Hospital of León, León, Spain, ⁴Pharmacy Service, Complejo Asistencial Universitario de León (CAULE), Hospital of León, León, Spain
Email: jl.mauriz@unileon.es

Background and aims: Hepatocellular carcinoma (HCC), the main type of liver cancer, stands as one of the deadliest type of cancer with an increasing prevalence worldwide. Hypoxia plays a major role in tumorigenesis and in the development of chemotherapy-resistant tumor cells. The adaptive cell response to this condition is mainly mediated by the hypoxia-inducible factors 1 and 2 alpha (HIF-1alpha and HIF-2alpha, respectively), which triggers the activation of several cellular pathways contributing to cell survival and the loss of sensitivity to chemotherapy, and leading to tumor progression.

Therefore, our aim was to assess the role of HIF-1 α on HCC patients' outcome and tumor cell survival.

Method: We analyzed HIF-1 α gene expression and RNA-seq data in several HCC repositories such as The Cancer Genome Atlas (TCGA), the European Genome-Phenome Archive (EGA), Genotype-Tissue Expression (GTEx) and GSE14520. Data were obtained from UALCAN, Gene Expression Profiling Interactive Analysis (GEPIA) and Gene Expression Omnibus (GEO) databases. We performed a screening of HIF-1 α expression in eight different human HCC cell lines, employing CoCl₂ to simulate a cell response to hypoxia. Western blot and immunofluorescence with laser confocal imaging were used to analyze protein expression, while qRT-PCR was used to assess gene expression. Moreover, HIF-1 α gene knockdown was performed using siRNA transfection. MTT assay and nuclear Ki67 protein levels assessment were used to determine cell viability and proliferation, respectively. Image-iT Red Hypoxia Reagent was employed to monitor hypoxia in the 3D models of HCC. GraphPad Prism 8 software was used to conduct statistical analysis, considering significant differences when $p < 0.05$.

Results: HIF-1 α was found to be overexpressed in HCC tissues, being also associated with higher tumor grades and a poor survival rate in HCC patients. Huh-7 and PLC/PRF/5 cell lines showed a higher expression of HIF-1 α under hypoxia conditions. For this reason, these cell lines were selected to perform HIF-1 α gene silencing and to generate two spheroid models of HCC showing a physiological hypoxia. A decrease in viability and Ki67 protein levels was detected after gene knockdown, suggesting a pro-survival ability associated with HIF-1 α . Moreover, HIF-1 α -silenced cells showed higher levels of pro-apoptotic proteins under hypoxic conditions, revealing the potential effect of HIF-1 α in HCC cell survival through apoptosis evasion.

Conclusion: Altogether, these findings suggest that HIF-1 α expression and stabilization plays a key role in HCC progression and patients' outcome, leading to tumor cell survival through apoptosis evasion under a hypoxic environment, highlighting HIF-1 α activity blockage as a potential therapeutic strategy to restrain HCC progression.

SAT-264

Therapeutic targets associated with conserved subtypes of hepatocellular carcinoma

Ju-Seog Lee¹, Yun Seong Jeong¹, Sun Young Yim², Sung-Hwan Lee³, Sang Hee Kang². ¹The University of Texas MD Anderson Cancer Center, Systems Biology, Houston, United States, ²Korea University College of Medicine, Korea, Rep. of South, ³Cha University Bundang medical center, Korea, Rep. of South
Email: jlee@mdanderson.org

Background and aims: While many studies revealed clinically relevant conserved subtypes of hepatocellular carcinoma (HCC), their discovery is not translated to the clinic yet due to lack of associated therapeutic intervention for subtypes. We aim to examine consensus of discovered subtypes and uncover their clinical significance and to identify potential therapeutic targets for each subtype.

Method: We integrated 16 previously established transcriptomic signatures for HCC to uncover consensus subtypes. We also developed and validated a robust predictor of consensus subtype with 100 genes (PICS100). Informatics and statistics approaches were applied to find clinical relevant association of genomic features. Patient derived xenograft (PDX) models were used for testing hypothesis from analysis of transcriptomic data.

Results: Integrative analysis of genomic and proteomic data uncovered five subtypes of HCC with substantial difference in clinical outcomes. STM (Stem) is characterized by high stem cell features, vascular invasion, and poor prognosis. CIN (Chromosomal INstability) has moderate stem cell features but high genomic instability and low immune activity. High expression of IGF2 is another unique feature of

CIN subtype, suggesting that CIN subtype might have benefit of treatment targeting IGF2/IGFR pathway. IMH (IMMune High) is best characterized by its high TCR diversity and high baseline immune activity. BCM (Beta-Catenin with high Male predominance) is characterized by prominent beta-catenin activation, low miRNA expression, hypomethylation, and high sensitivity to sorafenib. Interestingly, subtype BCM had a significantly higher male-to-female ratio than the other subtypes. Another unique molecular characteristic of subtype D was miRNA downregulation. DLP (Differentiated and Low Proliferation) is differentiated with high HNF4A activity. We also identified potential serum biomarkers that can stratify patients into 5 subtypes. Our PICS100 predictor is available in the website (<https://kasaha1.shinyapps.io/pics100/>) with test data set for those who wish to run genomic predictor. Multistep analysis of genomic and proteomic data identified therapeutic targets for poorest prognostic STM subtype and their therapeutic potential was further validated in cell line and mouse models.

Conclusion: Newly discovered subtypes are associated with response to standard and experimental treatments and highly conserved in pre-clinical models such as cell lines and PDX tumors. Therefore, our study may provide a framework for selecting the most appropriate models for preclinical studies of new drugs and potentially for future clinical trials.

SAT-265

In vivo MRI characterization of pathological changes in liver microstructures

Xiaoyu Jiang¹, Manhal Izzy², Kay Washington², John Gore², Junzhong Xu². ¹Vanderbilt University Medical Center, Radiology, United States, ²Vanderbilt University Medical Center, United States
Email: xiaoyu.jiang@vumc.org

Background and aims: Cell volume, cell density, and their variations are fundamental concepts in liver pathology. Currently, cell volume and cell density measurements are possible via assessing liver biopsies, which are subject to sampling bias and may not reliably reflect the spatial heterogeneity in the liver as a whole. In vivo MRI cytometry may provide means to overcome this limitation. This study aims to 1) prove the feasibility of in vivo mapping of non-fat cell volume (or equivalent cell size) and cell density in the liver using clinical 3T scanners 2) histologically validate MRI measurements using human liver specimens.

Method: MRI cytometry combines measurements of water diffusion rates over different time scales corresponding to probing cellular microstructure over different distances. The range of sizes of most interest in liver tissues is from 5 μ m to 25 μ m (e.g., hepatocytes ~ 15–25 μ m, inflammatory cells ~ 5–10 μ m, cancer cells ~ 10–5 μ m). These correspond to diffusion times of order 5–70 ms which can be achieved using a combination of OGSE (oscillating gradient spin echo) and PGSE (pulsed gradient spin echo) measurements on clinical scanners. Microstructural properties are derived by fitting multi-b value-multi-diffusion time fat-suppressed diffusion-weighted MRI signals to a three-compartment (blood, intra and extracellular water) signal model. Details of the signal model and imaging protocol have been published previously. ex vivo validation: Microstructures of fixed human liver specimens, including normal liver tissues, cirrhosis, steatosis, hepatocellular carcinoma (HCC), cirrhotic regenerative nodules (CRN), and intrahepatic cholangiocarcinoma (iCCA), were quantified using MRI ex vivo and histology. in vivo feasibility: MRI cytometry was performed in a healthy subject and an HCC patient using a Phillips 3T scanner.

Results: For ex vivo experiments, MRI-based assessment of HCC and iCCA showed that tissues have significantly smaller cell volumes and higher cell densities than normal liver and CRN without steatosis. Cell sizes for fatty areas and CRN with steatosis are smaller than those for normal liver and CRN without steatosis (note that our MRI-derived cell sizes are converted from non-fat cell volumes). These

POSTER PRESENTATIONS

observations matched histological assessment of microstructures. For in vivo experiments, MRI cytometry demonstrated that the HCC tumor has decreased cell sizes and ~ 2 higher cell densities than the healthy subject.

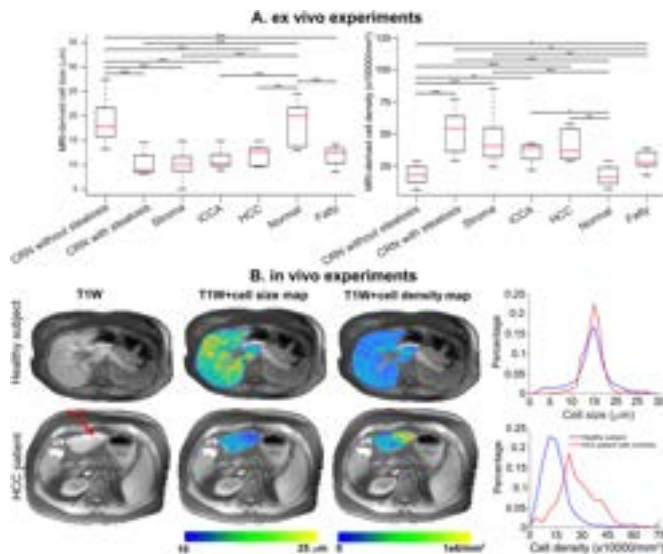


Figure: A. Box-and-whisker plots of MRI-derived cell sizes and cell densities for liver ROIs with different pathologies. For all the Box-and-whisker plots, the 25th–75th percentiles are blocked by the box, the red bands inside the box are the mean values, and the whiskers mark the SD. *P < 0.05, **P < 0.01, ***P < 0.001, and ****P < 0.0001 as measured by one-way analysis of variance (ANOVA) with Bonferroni correction. B. in vivo MR cell size and cell density imaging for a healthy subject and an HCC patient. The in-plane resolution is $4 \times 4 \text{ mm}^2$ and the slice thickness is 10 mm.

Conclusion: This study demonstrates that the novel MRI cytometry can characterize pathological changes in liver microstructures using clinical 3T scanners in <12 minutes. These findings provide a solid foundation for future investigation of the role of non-invasive evaluation of liver cellular characteristics in diagnosing liver disease aiming to further decrease the need for liver biopsy.

SAT-266

Prognostic and genomic portrait of hepatocellular carcinomas with bi-allelic inactivation of RB1 gene

Jihyun An¹, Bora Oh², Jin-Sung Ju², Ju Hyun Shim². ¹Hanyang University College of Medicine, Korea, Rep. of South, ²Asan Medical Center, Korea, Rep. of South
Email: starlit1@naver.com

Background and aims: Although RB1 gene loss have been correlated with progression of HCC, its molecular and pathogenic makeups are poorly defined. We comprehensively characterized a genomic subtype of HCC with true loss-of-function alteration of RB1.

Method: We performed integrative analysis of DNA and RNA sequencing data from 561 HCCs included in our hospital and TCGA projects. We classified the tumors according to the presence of RB1 bi-allelic inactivation (Bi) such as deep deletion and copy-loss/neutral loss-of-heterozygosity: RB1-Bi and RB1-nonBi groups. Their impacts on clinical and genomic features of HCC were investigated.

Results: Among the entire samples, 82 (14.6%) corresponded to the RB1-Bi group, with deep deletion in 58 and copy-loss or copy-neutral loss-of-heterozygosity in 24. RB1-Bi tumors were independently associated with poorer disease-free survival and overall survival after hepatectomy, irrespective of RB1 alteration type. poorly differentiated tumors were more frequently observed in the RB1-Bi group (48.8% vs. 34.6%, $P < 0.05$). The RB1-Bi group was enriched for cell cycle-regulated, replication stress, and DNA damage repair-associated genes, while downregulated for CD8+ T cell markers. RB1

alteration events occurring in the RB1-Bi group were mostly clonal, and completely arose before whole genome doubling that was more frequent in the subset.

Conclusion: Bi-allelic RB1 loss in the HCC confers worse prognosis through relevant functional and genomic aberrations. Tailored therapies for the disease that might be resistant to immunotherapy should be developed and tested.

SAT-267

Bacterial exosomes cargo vaccine with EpCAM aptamers for targeting hepatocellular carcinoma

Pushpa Yadav¹, Preedia Babu E¹, Nuno Viegas², Anupama Parasar¹, Riddhi Sharma¹, Gayatri Ramakrishna¹, Nirupma Trehanpati¹, Shiv Kumar Sarin³. ¹Institute of Liver and Biliary Sciences, Molecular and Cellular Medicine, New Delhi, India, ²Mantis Pharmaceuticals, Leiden, Netherlands, ³Institute of Liver and Biliary Sciences, Hepatology, New Delhi, India
Email: shivsarin@gmail.com

Background and aims: Hepatocellular carcinoma (HCC) is the fourth most cause of cancer-associated mortality and leads to approximately 700,000 deaths worldwide annually and is expected to increase over 1 million by 2030. HCC is a highly heterogeneous tumor with extensively proliferating and differentiating EpCAM or CD133 positive cancer stem cells. Despite existing chemo, radiation, and immune therapies for non-resectable tumours, 5-year survival rate is quite low with high recurrence rate. Therefore, our aim was to develop anti-EpCAM aptamer equipped bacterial outer membrane vesicles (OMVs) loaded with the chemotherapeutic drug, doxorubicin (DOX) as vaccine for specific targeting of cancer stem cells.

Method: We have designed EpCAM specific DNA (EP166 and SyL3C) and RNA-DNA hybrid aptamers and analysed their in vitro binding efficiency in HepG2, HuH7 cell lines as well as their spheroids and toxicity using MTT assay at 24, 48 and 72 hours of treatment. *Salmonella typhimurium* has the potential to kill tumor cells, therefore isolated and purified outer membrane vesicles (OMVs) were used to load DOX by incubating them together at an appropriate mass ratio for 4 hours at 37°C. As the aptamer cannot bind to the OMVs on its own, carbodiimide (EDC/NHS) coupling chemistry was applied for conjugating the carboxylic group of DSPE-PEG-COOH linker to the amine group of anti-EpCAM aptamer. The linker conjugated aptamer was then mixed with the bacterial exosomes cargo to develop anti-EpCAM aptamer equipped DOX loaded OMVs.

These novel OMVs were then used for testing in vivo efficacy in HepG2 cells derived subcutaneous xenograft model. Apt- conjugated DOX or DOX alone was used as control treatment.

Results: All the aptamers analysed for binding with HepG2 cells with flow cytometry showed maximum binding at 150 nM with SyL3C showing 47.3% binding (Fig1A).

In vivo experiments showed decreased tumor burden as compared to tumor control after treatment with DOX alone, Apt-DOX and Apt-DOX-OMVs (Average tumor volume: 448.26, 307.58, 168.29, 112.85 mm³) after 12 days of treatment. Apt-DOX conjugate also showed increased specific DOX toxicity and reduced tumor burden in comparison to DOX alone (Average tumor size: 4.8 g and 2.7 g respectively).

Conclusion: Apt-DOX-OMVs and Apt-DOX conjugate and are more efficient in specifically targeting cancer cells in comparison to DOX alone or tumor control.

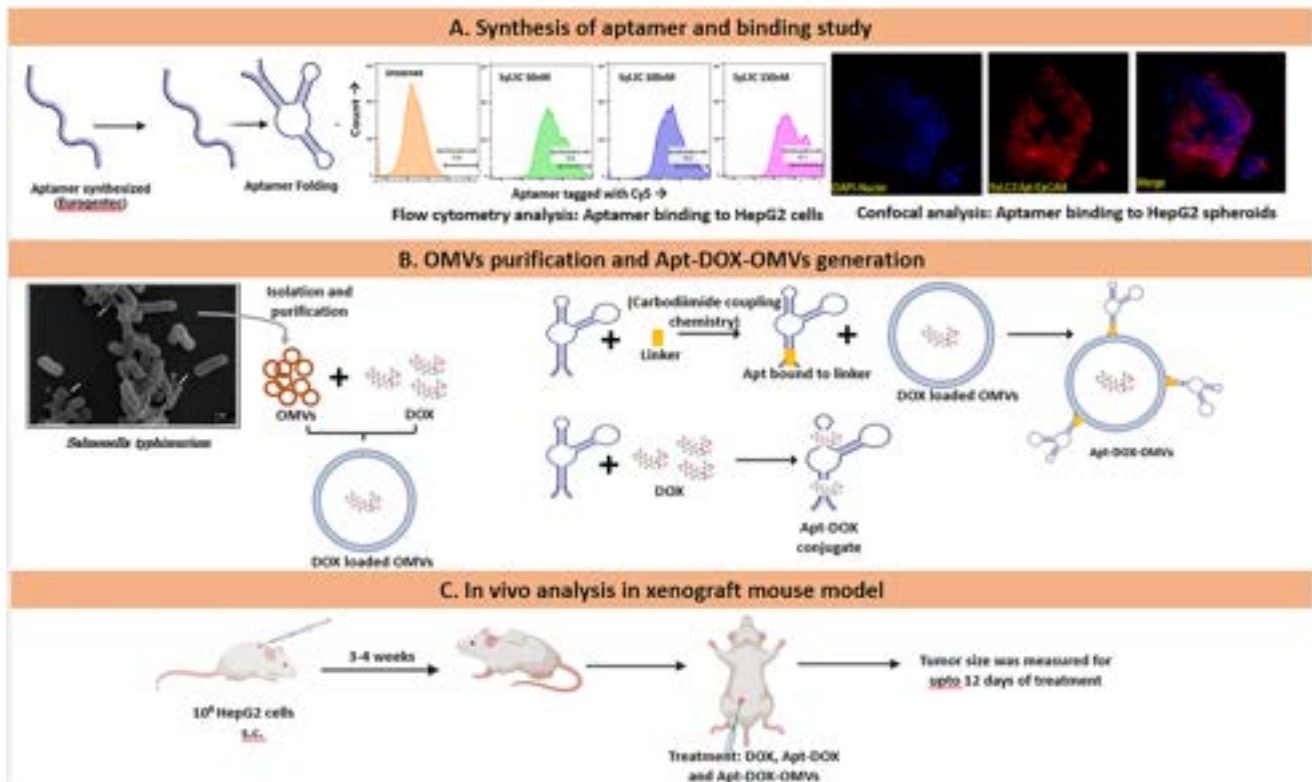


Figure: (abstract: SAT-267).

SAT-268

Poor sorafenib response in hepatocellular carcinoma patients is mediated by hypoxia-related 14-3-3 scaffolding proteins and induces a shift in tumor immune microenvironment

Jovana Castven¹, Diana Becker², Sophia Heinrich³, Carolin Zimpel¹, Darko Castven¹, Beate Straub², Peter Grimminger², Peter Galle², Arndt Weinmann², Jens Marquardt¹. ¹Universitätsklinikum Schleswig-Holstein, Campus Lübeck, Germany, ²Universitätsmedizin Mainz, Germany, ³Medizinische Hochschule Hannover, Germany
Email: hajdukjovana@gmail.com

Background and aims: Advanced stage of hepatocellular carcinoma (HCC) is frequently accompanied by poor response to the drug treatment or relapse quickly after initial remission. Therefore, identification of molecular drivers of poor response to sorafenib with large focus on novel prognostic markers associated with observed distinct tumor immune landscapes was our ultimate goal.

Method: From a cohort of 91 patients treated with sorafenib, we identified 17 HCC patients with particularly good or bad response. Integrative RNA sequencing and whole-exome sequencing analyses were performed to identify predictive markers of sorafenib resistance. *In vitro* validation of defined targets were performed in a model of sorafenib resistance, followed by subsequent functional and mechanistic validation.

Results: Patients with worst response (n = 7) were characterized by significantly shorter treatment duration and poor overall survival than good responders (n = 10). Molecular analyses revealed that acquisition of drug resistance observed in poor responder group was associated with upregulation of hypoxia-related targets from 14-3-3 scaffolding protein family. WST-1 viability assay displayed that hypoxia contributes to sorafenib resistance. Specific peptide inhibition of this protein family, in combination with sorafenib, showed synergistic effects and efficiently reduced cell proliferation and viability. Dual inhibition consequently reversed sorafenib resistance under both conditions, normoxia and hypoxia, with predominant

effects noticed in normoxia. Furthermore, a shift in immune-cell composition with predominant enrichment of M2-immunosuppressive macrophages in worst responders was observed.

Conclusion: Defining the actionable targets of resistance and their subsequent inhibition might greatly help delineate molecular alterations driving drug resistance. In our model, specific peptide inhibition of 14-3-3 scaffolding proteins, when combined with sorafenib, showed a positive correlation in reversing sorafenib resistance. Importantly, synergistic effects of this dual inhibition influenced sorafenib resistance in normoxic and hypoxic microenvironments, but with different potency. This highlights the significance of the tumor microenvironment in modulating the therapy response. Further, characterization of the immune microenvironment in different subgroups of patients could be of particular importance to depict treatment resistance and warrants further investigations.

SAT-269

RBCK1 promotes the stabilization of HBx by linear ubiquitination to drive the progression of HBV-associated hepatocellular carcinoma

Zheyu Dong¹, Peng Chen¹, Yuxin Zhou¹, Qiuyue Ye¹, Junling Chen¹, Jianzhong Cai^{1,2}, Yiyang Huang^{1,2,3}, Jiayue Yang^{1,2}, Yaoting Feng^{1,2}, Liangxing Chen^{1,2}, Libo Tang¹, Yongyin Li¹. ¹State Key Laboratory of Organ Failure Research, Guangdong Provincial Key Laboratory of Viral Hepatitis Research, Department of Infectious Diseases, Nanfang Hospital, Southern Medical University, Guangzhou, China, ²The First School of Clinical Medicine, Southern Medical University, Guangzhou, 510515, China, ³China
Email: yongyinli@foxmail.com

Background and aims: Linear ubiquitin chain assembly complex (LUBAC) has been reported to participate in cancer progression, but its role in hepatocellular carcinoma (HCC) remains unknown. This study aimed to investigate the functions and potential tumorigenic mechanisms of LUBAC components in HBV-associated HCC.

POSTER PRESENTATIONS

Method: The expression of LUBAC components (RBCK1, RNF31, and Sharpin) and Met1-linked ubiquitination (M1-Ubi) and their correlation with prognosis were detected. The biological functions of RBCK1 in HBV-associated HCC were investigated in vitro and in vivo. The regulation of RBCK1 on the HBx protein expression was analyzed by cycloheximide chase assays, coimmunoprecipitation, and ubiquitination assays.

Results: We found that the expression of LUBAC components and M1-Ubi was significantly upregulated in HCC and correlated with poor prognosis. Interestingly, subgroup analysis revealed that RBCK1, not RNF31 or Sharpin, was exclusively overexpressed in HBV-associated HCC compared to non-HBV-associated HCC. Upregulated RBCK1 expression was associated with larger tumor size, higher AFP level, and poor prognosis in HBV-associated HCC cohort. Functionally, RBCK1-knockdown suppressed cell growth and migration, and also inhibited the progression of xenografted tumors in HBV-associated HCC mouse model. Mechanistically, RBCK1 interacted with HBx to promote its stabilization by increasing M1-Ubi ubiquitination and reducing K48-linked ubiquitination. Furthermore, clinical analysis confirmed a positive correlation between RBCK1 and HBx, and the co-expression of which predicted poor prognosis for HCC patients.

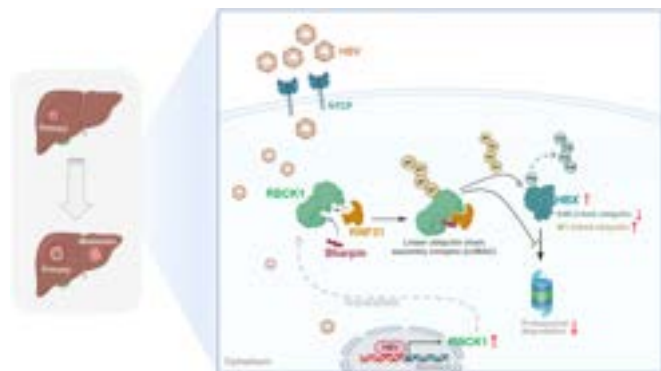


Figure:

Conclusion: RBCK1 is an oncogenic gene to promote tumor progression and may serve as a potential target for HBV-associated HCC.

SAT-270

Molecular determinants of period-specific recurrences in patients with surgically resected hepatocellular carcinoma

Jihyun An¹, Bora Oh², Jin-Sung Ju², Ju Hyun Shim². ¹Hanyang University College of Medicine, Korea, Rep. of South, ²Asan Medical Center, Korea, Rep. of South
Email: starlit1@naver.com

Background and aims: Postsurgical early-phase recurrence is associated with poorer clinical outcomes of patients with hepatocellular carcinoma (HCC). We hypothesized that the immune environments of the early- and late-recurrent HCCs differ, and investigated whether molecular changes differed according to the time of cancer recurrence by a cut-off of 5 years after resection.

Method: We included 253 patients who had HCCs initially without any gross vascular invasion or metastatic lesion, and received curative hepatectomy at the Asan Medical Center. RNA sequencing data and paraffin-embedded tissues derived from the resected tumors were available for all patients. The distributions of molecular subtypes as classified by Hoshida et al. and Boyault et al. were compared according to time of HCC recurrence using *MS.liverK*. For gene set enrichment and pathway analyses by GSEA v4.0.3, we used the gene sets in the Molecular Signatures Database (MSigDB) and the published literature. Immune phenotypes were classified based on previously defined immune and stromal classifiers.

Immunohistochemical staining were performed with antibody against PD-L1 using DAKO 22c3 assays.

Results: Among the entire 253 patients, 134 cases (53.0%) experienced recurrence episodes, with 109 and 25 within (early) and beyond 5 years (late) after resection, respectively. The proportions of the three mRNA expression-based HCC subclasses according to Hoshida et al. (termed S1, S2, and S3) were significantly different in the two recurrence groups: the S2 subclass was enriched in the early recurrence group, and S1 in the late recurrence group (S1, 24.8% vs. 52.0%; S2, 30.3% vs. 8.0%; and S3, 45.0% vs. 40.0%, $P < 0.05$). The G2 subtype of Boyault et al. was exclusively observed in the early recurrence cases (19.3% vs. 0%, $P < 0.05$). In terms of immune and stromal classification, the immune-desert types were more abundant in the former (50.5% vs. 32.0%) and the exhausted types in the latter (32.1% vs. 52.0%). These findings are in agreement with the disproportionate enrichment of PD-L1 determined by combined positive score in the late recurrence group (5.5% vs. 24.0%, $P < 0.05$). Gene set enrichment analyses revealed that most of the gene expression signatures associated with immune responses were down-regulated in the early-period recurrence group (all P s < 0.001).

Conclusion: We found that early-period recurrence events after resection are strongly associated with immune-silent HCCs and the scarcity of PD-L1 expression of the disease. Together with closer surveillance, adjuvant therapies should be tested in combination with immune system boosters in selective patients with such tumors.

SAT-271

Monitoring the local HCC immune landscape by fine needle aspiration

Gloryanne Aidoo-Micah^{1,2}, Stephanie Kucykowicz¹, Nathalie Schmidt¹, Amy Trinh³, Laura J Pallett¹, Daniel Brown Romero¹, Vishnu Naidu⁴, Rushabh Shah⁴, Upkar Gill⁵, Edward Green⁴, Tim Meyer^{2,3}, Mala Maini¹. ¹University College London, Institute of Immunity and Transplantation, London, United Kingdom, ²UCL, Cancer Institute, United Kingdom, ³Royal Free Hospital London, Oncology, London, United Kingdom, ⁴Royal Free London, Radiology, London, United Kingdom, ⁵Queen Mary University of London, United Kingdom
Email: m.maini@ucl.ac.uk

Background and aims: Accumulating data underscore the importance of harnessing local tissue-resident immunity in tumour immunotherapy. Sampling immune responses sequestered in tumours that cannot be sampled in blood could provide vital insights to improve immunotherapy. Diagnostic biopsies contain a mixture of immune cells from HCC and surrounding liver and their invasive nature precludes longitudinal monitoring. We postulated that fine needle aspirates (FNA) would provide a minimally invasive approach suitable for repetitive sampling of the tissue-resident HCC immune landscape.

Method: Patients with HCC undergoing systemic therapy with anti-PD-L1 and anti-VEGF consented to provide matched blood, FNA and biopsy samples for *ex vivo* multiparameter flow cytometric analysis of effector and regulatory immune populations.

Results: FNA reproducibly yielded viable leukocytes with all the major myeloid and lymphocyte populations detectable and an immune landscape distinct from blood. In the myeloid compartment, granulocytic myeloid suppressor cells (gMDSC/PMN-MDSC) were strikingly enriched in tumour FNA compared to blood, whereas dendritic cells were reduced. Amongst lymphocytes, FNA contained a significantly lower proportion of CD4 T cells and B cells than blood. Crucially FNA were able to detect tissue-resident T cells (T_{RM} , CD69⁺CD103⁺CD8 and CD69^{hi}CD4) and liver-resident NK cells (CXCR6⁺CD69⁺) in HCC that cannot be sampled in blood, albeit at lower frequencies than were detected in matched core biopsies. The majority of tumour CD8⁺ T_{RM} sampled by FNA or biopsy before immunotherapy expressed checkpoints like PD-1, Tim-3 and 2B4, accounting for significantly higher expression of these therapeutic

targets on the global CD8⁺T cells extracted from FNA or biopsies than from blood.

Conclusion: Blood sampling can grossly underestimate the expression of key immunotherapeutic targets including checkpoints on T cells and gMDSC that can be detected on populations sequestered within HCC, sampled by either FNA or biopsy. FNA have the capacity to comprehensively monitor the HCC immune landscape to enhance the selection and development of targeted immunotherapy.

SAT-272

Clinicopathological analysis of polyploidization in human hepatocellular carcinoma and the development of an evaluation methodology

Takanori Matsuura¹, Yoshihide Ueda¹, Yoshiyuki Harada¹, Kazuki Hayashi², Kisara Horisaka², Yoshihiko Yano¹, Shinichi So³, Masahiro Kido³, Takumi Fukumoto³, Yuza Kodama¹, Eiji Hara², Tomonori Matsumoto². ¹Kobe University Graduate School of Medicine, School of Medicine, Division of Gastroenterology, Department of Internal Medicine, Kobe, Japan, ²Research Institute for Microbial Diseases, Osaka University, Department of Molecular Microbiology, Osaka, Japan, ³Kobe University Graduate School of Medicine, School of Medicine, Department of Surgery, Division of Hepato-Biliary-Pancreatic Surgery, Kobe, Japan
Email: tomomatsumoto@biken.osaka-u.ac.jp

Background and aims: The cross-organ examination of cancer genomes has revealed that polyploidization, the acquisition of multiple sets of chromosomes, is a prevalent phenomenon in various neoplasms, including hepatocellular carcinoma (HCC). This suggests that polyploidization plays a significant role in carcinogenesis and tumor progression. However, the significance of polyploidization in HCC remains largely unknown. To address this, we aimed to establish a methodology for evaluating polyploidization in HCC using pathological specimens and to ascertain the clinicopathological characteristics of polyploid HCC.

Method: We performed multicolored fluorescence in situ hybridization (FISH) on paraffin-embedded, formalin-fixed pathology specimens from 56 HCC patients who underwent hepatectomy between 2017 and 2021 at our institution and determine the ploidy of HCC. Polyploid and diploid HCCs were compared to investigate the clinicopathological characteristics of polyploid HCC. We also explored a surrogate marker for polyploid HCC based on the transcriptome data of human hepatoma cell line Huh7 and verified its overexpression in polyploid HCC by immunostaining.

Results: Determination of tumor ploidy by FISH for three chromosomes revealed that 35.7% of HCCs (20/56 cases) were polyploid. There was no significant difference between polyploid and diploid HCCs in terms of tumor size and fibrosis of the non-tumor region. Notably, however, polyploid HCCs exhibited high serum alpha-fetoprotein levels ($p=0.026$), poor differentiation ($p=0.013$), and poor overall survival rates ($p=0.013$). Moreover, polyploid HCCs contained polyploid giant cancer cells within the tumor at a significantly higher frequency than diploid HCCs. Among some genes that were significantly highly expressed in polyploid Huh7 cells compared to their diploid counterparts, we identified that ubiquitin-conjugating enzymes 2C (UBE2C) was significantly overexpressed in human polyploid HCCs. The abundance of polyploid giant cancer cells and overexpression of UBE2C could efficiently indicate polyploid HCC and predict their poor prognosis in combination.

Conclusion: Polyploidy in HCC was associated with tumor aggressiveness and exhibited a poor prognosis compared to diploid HCC. The assessment of ploidy in HCC utilizing FFPE tissue samples may serve as a novel prognostic marker of HCC.

SAT-273

Epigenetic reprogramming synergizes with PD-1/PD-L1 inhibition for cell-targeted therapy in hepatocellular carcinoma

Caecilia Sukowati^{1,2}, Loraine Kay Cabral^{2,3}, Beatrice Anuso⁴, Claudio Tiribelli². ¹National Research and Innovation Agency of Indonesia, Eijkman Research Center for Molecular Biology, Indonesia, ²Fondazione Italiana Fegato ONLUS, Italy, ³University of Trieste, Doctoral School in Molecular Biomedicine, Italy, ⁴University of Trieste, Department of Life Science, Italy
Email: caecilia.sukowati@fegato.it

Background and aims: Hepatocellular carcinoma (HCC) is a heterogeneous cancer characterized with various cellular and molecular subtypes. HCC is one of the major causes of cancer-related mortality worldwide with poor prognosis and limited therapeutic options. This study aimed to investigate whether combination strategy between immunotherapy (against PD-L1) and epigenetic reprogramming (DNA demethylation inhibition) would be a potential therapy against heterogeneous HCC.

Method: This study used *in vivo* animal model and *in vitro* manipulations. To assess the dynamics of PD-1/PD-L1, hepatic samples were taken from HBV-transgenic mouse C57BL/6J-TG (ALB1HBV)44BRI/J with age: 3 (inflammation), 6 and 9 (dysplasia; pretumoral), and 12 (tumor) together with its wild type counterpart. DNA methylation status of the PD-L1 was checked using the methylation-specific polymerase chain reaction (MSP). PD-L1 RNA silencing was performed by siRNA in several human HCC cell lines consisting of S1/TGF β -Wnt subtype (HLE, HLF, and JHH6) and S2/progenitor subtype (HepG2 and Huh7). The combination therapy was performed in a co-culture system between HCC cells and immortalized lymphocytes, using a long-term treatment with non-toxic DNA methylation inhibitor 5-Azacytidine (5-AZA) and an antibody against PD-L1.

Results: In the mouse model, during the development of HCC, the gene expressions of both PD-L1 and its receptor PD-1, as well as Dnmt1 (DNA methylation marker) were significantly higher in HCC mouse compared to normal mouse ($p<0.01$). Analysis of PD-L1 methylation status by MSP showed that the methylation of PD-L1 DNA was significantly higher in HCC mice compared to normal mice ($p<0.001$). This implied double-targeting combining epigenetic and immunotherapy would be favorable. For *in vitro* data, the knockdown of PD-L1 gene was accompanied with that of DNMT1 gene, mostly noted in aggressive HCC cell lines. The reduction of PD-L1 was also followed by dysregulation of cancer stem marker EpCAM in all cell lines expressing this marker. By combination therapy in a co-culture system between HCC cells and lymphocytes, using a long-term treatment with non-toxic DNA methylation inhibitor 5-AZA and antibody against PD-L1, the growth of lymphocytes was limited by the PD-L1 antibody, and it was furtherly reduced in the presence of 5-AZA for up to 20% ($p<0.001$). For HCC cells, however, the PD-L1 antibody reduced the cells growth, but the addition of 5-AZA was not significant.

Conclusion: To conclude, we propose that a combination therapy between DNA methylation inhibition and PD-L1 blocking can be potential strategy for the treatment of heterogeneous HCCs.

SAT-274

Lysosomotropic PIP5K inhibitors sensitize hepatic cancer to reactive oxygen species by inhibiting proliferative and adaptive pathway

P.A. Shantanu¹, Sameer Panda¹, Bishal rajdev¹, Sai Balaji Andugulapati², N.P Syamprasad¹, Akash Kumar Mourya³, Ramakrishna Sistla², Savneet Kaur³, Vegi Naidu¹, Dinesh Mani Tripathi³. ¹National Institute of Pharmaceutical Education and Research, Guwahati, India, ²Medicinal Chemistry and Pharmacology Division, CSIR-Indian Institute of Chemical Technology (IICT), Hyderabad, Hyderabad, India, ³Institute of liver and biliary sciences, India
Email: dineshmanitripathi@gmail.com

Background and aims: The complex interplay between ROS-molecular signaling governs proliferation, adaptation, and death. To date, how cancer cells modulate PIP5K levels to control proliferative and adaptive signaling is not known.

Method: Firstly, we investigated the protein expression of PIP5K isoforms, Beclin-1 (autophagy marker), and Nrf2 (antioxidant master regulator) in 36 HCC patients and immortalized cells viz PRF5, SNU-387, Skhep-1 and HepG2. To understand ROS-mediated effect on PIP5K, autophagy, and antioxidants, HCC cells exposed to H₂O₂. Further, effect on cell viability, mitochondrial superoxide, lysosome turnover, expression of PIP5K isoforms, autophagy and antioxidant enzymes through MTT, MitoSOX, lysotracker was evaluated. The effect of PIP5K inhibition on the cancer cells sensitization was investigated with novel investigational molecules NG-TZ-17 and IITZ01 and finding was confirmed with standard PIP5K1A inhibitor ISA-2011B. Also, the Autophagy inhibition of NG-TZ-17 and IITZ01 was examined with respect to autophagy inhibitor Chloroquine and NRF2 inhibitor ML-385. In vivo GFP-HepG2 induced hepatic cancer model in SCID mice was developed for exploring therapeutic efficacy. In HCC Mice, 50 mg/kg NG-TZ-17 and IITZ01 and compared with 60 mg/kg Sorafenib administered orally for seven days.

Results: We observed a positive correlation between PIP5K isoforms, Beclin-1 and Nrf2 in hepatocellular carcinoma liver tissue and cell lines. Cytotoxicity and Protein expression showed a concentration-dependent starvation-induced proliferation, resisted cell death by increasing PIP5K isoforms, Nrf2, HO-1, and SOD2 levels. At cytotoxic concentration resulted in autophagic cell death as indicated by the decrease in PIP5K isoforms, Akt, Nrf2, HO-1, and SOD2 expression however an increase in SRC and Beclin-1 was observed. The inhibition of PIP5K with lysosomotropic NG-TZ-17, IITZ01, and ISA-2011B (standard) sensitized HCC cells showed proliferative, autophagy and Nrf2 pathway downregulation compared to HCC cells exposed to mild stress. We observed the PIP5K inhibitors (both) was superior to Chloroquine and ML385. In vivo we observed 50 mg/kg NG-TZ-17 (p < 0.001) and IITZ01 (p < 0.001) reduced the tumor burden in the HepG2-xenograft SCID mice model (p < 0.001 compared to tumor control). The treatment was equipotent to standard sorafenib 60 mg/kg (p < 0.001 vs tumor control).

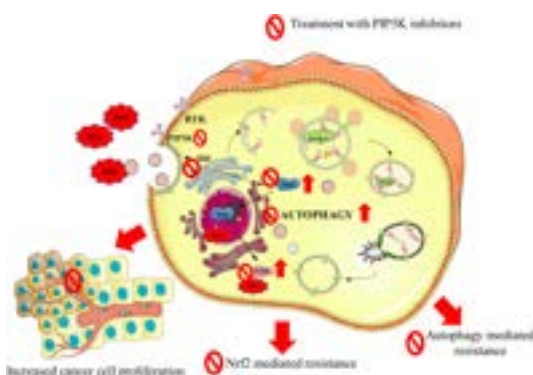


Figure:

Conclusion: HCC clinical and in vitro data showed that PIP5K isoforms involved switching of cancer cells from adaptive to proliferative state vice-versa in response to ROS levels. PIP5K inhibitors sensitized cancer cells to mild ROS. Thus, targeting PIP5K will overcome limitations of standard RTK, autophagy and Nrf2 inhibitors. This study also confers the therapeutic efficacy of novel PIP5K inhibitor viz NG-TZ-17 and IITZ01 in Hepatic cancer.

SAT-275

Functional and mechanistic role of lncRNA-A1 in cholangiocarcinoma

Alberto Tinahones¹, Joan Blázquez Vicens², Jorge Cañas³, Alba Capelo³, J.L. Lavin⁴, Maria Jesus Perugorria Montiel⁵, Maite García-Fernandez de Barrena⁶, Marcos Fernandez Fondevila³, Begoña Porteiro³, J. Lozano⁷, M. Coll⁸, Pau Sancho-Bru⁸, Ester Gonzalez-Sanchez⁹, Jesús Bañales⁵, Piotr Milkiewicz¹⁰, Malgorzata Milkiewicz¹⁰, Luis Bujanda⁵, Ma Avila⁶, Ana María Aransay¹¹, Ruben Nogueiras³, Juan Turnes¹², Beatriz Pelacho¹³, J. Amengual⁹, Isabel Fabregat⁹, Javier Vaquero⁹, Rodrigo Entrialgo¹⁴, Silve Vicent¹⁴, Ashwin Woodhoo³, Marta Varela-Rey³. ¹Center for Research in Molecular Medicine and Chronic Diseases (CiMUS), Gene Regulatory Control in Disease, A Coruña, Spain, ²Center for Research in Molecular Medicine and Chronic Diseases (CiMUS) Gene Regulatory Control in Disease, Spain, ³CiMUS-Centro Singular de Investigación en Medicina Molecular y Enfermedades Crónicas, Santiago de Compostela, Spain, ⁴Genomic Platform, CIC bioGUNE-Ciberehd, Spain, ⁵Department of Liver and Gastrointestinal Diseases, Biodonostia Health Research Institute-Donostia University Hospital, University of the Basque Country (UPV/EHU); National Institute for the Study of Liver and Gastrointestinal Diseases (CIBERehd), Spain, ⁶Hepatology Program, CIMA, University of Navarra. Instituto de Investigaciones Sanitarias de Navarra-IdiSNA. CIBERehd., Spain, ⁷Bioinformatics Platform, CIBERehd., Spain, ⁸Liver cell plasticity and tissue repair, Hospital Clinic Barcelona, IDIBAPS, CIBERehd, University of Barcelona. ⁹Hospital General Universitario Gregorio Marañón. CIBERehd., Spain, ¹⁰TGF-β and Cancer Group, Oncobell Program, Bellvitge Biomedical Research Institute (IDIBELL), Barcelona, Spain., Spain, ¹¹Translational Medicine Group, Pomeranian Medical University, Szczecin, Poland. Liver and Internal Medicine Unit, Medical University of Warsaw., Spain, ¹²Genomic Platform, CIC bioGUNE-Ciberehd., Spain, ¹³Servicio de Digestivo del Complejo Hospitalario Universitario de Pontevedra (CHUP), Spain, ¹⁴Department of Hematology and Cell Therapy (B.P., F.P.), Clínica Universidad de Navarra, Pamplona, Spain., Spain, ¹⁵University of Navarra, Centre for Applied Medical Research, Program in Solid Tumours, Pamplona, Spain., Spain
Email: martavarela.rey@usc.es

Background and aims: Cholangiocarcinoma (CCA) constitutes a cluster of highly heterogeneous biliary malignant tumors that can arise at any point of the biliary tree. The silent presentation of these tumors combined with their highly aggressive nature and refractoriness to chemotherapy contribute to their alarming mortality (2% of all cancer-related deaths worldwide yearly). Long non-coding RNAs (lncRNA) can interact with DNA, RNA and proteins to regulate global gene expression patterns. They are remarkably versatile regulators, influencing multiple biological processes and playing key roles in the pathogenesis of several disorders. Their function in cholangiocarcinoma development, however, remains largely unexplored. In this proposal, our main aim is to examine the biological function and mechanism of action of the lncRNA-A1.

Method: We have studied the expression of lncRNA-A1 in samples from patients with primary biliary cirrhosis (PBC) and primary sclerosing cholangitis (PSC), and in mice models of cholestasis, and several cholangiocarcinoma cell lines (CCA). Finally, we have performed functional analysis by *in vitro* targeting of lncRNA-A1.

Results: In key preliminary experiments, we have observed that lncRNA-A1 was significantly upregulated in liver samples from patients with primary biliary cirrhosis (PBC) and primary sclerosing

cholangitis (PSC), and that its expression was consistently elevated in three different mice models of cholestasis at different time points: bile duct ligation (BDL), mice fed with a cholic acid diet and MDR2-KO mice. Surprisingly, we did not observe any change in its expression in livers from NAFLD models or CCl₄ intoxicated mice, suggesting that the upregulation of this gene could be restricted to cholestatic liver injury. At cellular level, we observed that LncRNA-A₁ was upregulated specifically in the biliary tree from MDR2-KO mice, but was not significantly altered in hepatocytes, Kupffer, endothelial or hepatic stellate cells. Remarkably, LncRNA-A₁ was generally observed upregulated in CCA cells with KRAS or BRAF mutations (KKU-213, RBE, EGI-1, SK-ChA-1) or in EGF-treated human cholangiocytes (MMNK1), in comparison with CCA cells without KRAS or BRAF mutations (TFK-1, SG231) or with untreated MMNK1 cells. In addition, we found that LNCRNA-A₁ was consistently elevated in tumoral liver from three different animal models of CCA (SB1-Singeneic, AKT-NICD and AKT-YAP) in comparison with non-tumoral liver. Next, we performed *in vitro* targeting of LncRNA-A₁ and examined its effects in CCA cell lines and immortalized cholangiocytes (MMNK1). Silencing of this LncRNA induced cell death and reduced the expression of proliferative genes in CCA cell lines but not in MMNK1 cells.

Conclusion: Altogether these data suggest that hepatic upregulation of LncRNA-A₁ in liver could be involved in CCA survival, although the physiological and mechanistic relevance of this upregulation is still under further investigation.

SAT-276

Identification of hepatocyte-restricted antigens, epitopes, and T cell receptors to treat recurrent hepatocellular carcinoma after liver transplantation

Yannick Rakke¹, Dian Kortleve², Astrid Oostvogels², Robbie Luijten³, Monique de Beijer^{2,3}, Stijn De Man³, Michael Doukas⁴, Jan Ijzermans¹, Sonja Buschow³, Reno Debets², Dave Sprengers³. ¹Erasmus MC-Transplant Institute, University Medical Centre Rotterdam, Rotterdam, the Netherlands, Department of Surgery, Division of HPB and Transplant Surgery, Netherlands, ²Erasmus MC-Cancer Institute, University Medical Centre Rotterdam, Rotterdam, the Netherlands, Laboratory of Tumor Immunology, Department of Medical Oncology, Netherlands, ³Erasmus MC-Cancer Institute, University Medical Centre Rotterdam, Rotterdam, the Netherlands, Department of Gastroenterology and Hepatology, Netherlands, ⁴Erasmus MC-Cancer Institute, University Medical Centre Rotterdam, Rotterdam, the Netherlands, Department of Pathology, Netherlands
Email: y.rakke@erasmusmc.nl

Target antigens, epitopes, and T cell receptors are not disclosed due to patent filing.

Background and aims: HCC recurrence in the context of an HLA-mismatched donor liver provides the unique setting that liver antigens from HCC versus the liver allograft are presented by different alleles of Human Leukocyte Antigen (HLA). Here, we present the development of an adoptive therapy with T cell receptor (TCR)-engineered T cells directed against hepatocyte-restricted antigens (HRAs) presented by the recipient, but not donor HLA.

Method: We have applied an integrative approach of *in silico* antigen and epitope prediction, immunopeptidomics, and *in vitro* laboratory tools to stringently select and validate HRAs, their immunogenic epitopes, as well as corresponding TCRs.

Results: 58 presumed liver antigens retrieved from the human protein atlas were further evaluated for liver-restricted expression in 6 public RNA databases and 1 protein database (HIPED), short-listing 14 candidate HRAs. 3/14 HRAs did not show RNA expression in healthy tissues, except for liver, in another five tissue datasets (n = 1,709) and validated using qPCR. Two HRAs demonstrated RNA expression in >70% of HCC patients (n = 421). Immunopeptidomics of HCC-derived hepatocytes (n = 12), together with *in silico* predictions of immunogenicity, revealed 36 HLA-A2-restricted epitopes. These

epitopes were tested and ranked according to *in vitro* HLA-A2 binding ability. Epitope-specific T cells were enriched from healthy donors for 6 of these epitopes using an *in vitro* co-culture with autologous antigen presenting cells. Eleven TCRαβs directed against 4 HRA-derived epitopes were selected following epitope-MHC-directed fluorescence-activated sorting of T cells. Five TCRs were functionally expressed upon gene transfer into T cells and recognized their cognate peptide, of which 4 TCRs harboured a stringent safety profile according to amino acid scanning, and are expected to mediate no to negligible cross-reactivity.

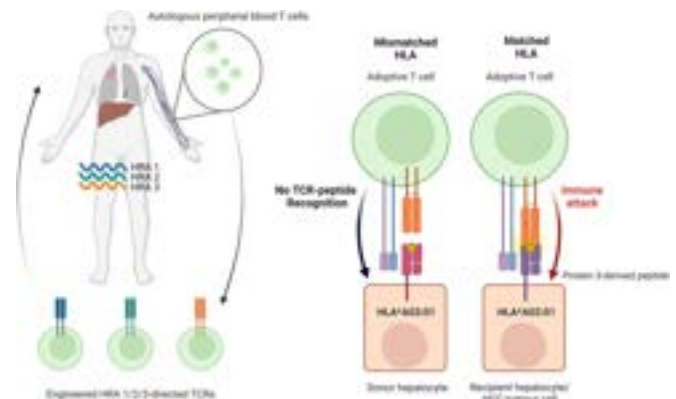


Figure: Concept of TCR-engineered T cells to exclusively target recipient-derived hepatocytes and hepatocellular carcinoma. In the current study, hepatocyte-restricted antigens (HRA) and their epitopes are identified following which HRA-specific T cell receptors (TCRs) are obtained with reactivity towards hepatocytes/HCC tumour cells but not to donor hepatocytes. These TCRs, when used to gene-engineer autologous, peripheral blood T cells, constitute a therapeutic to treat HCC recurrence after liver transplantation leaving the liver allograft unaffected.

Conclusion: We have identified HRAs, epitopes and corresponding TCRs, of which the lead TCRs will be further exploited for the treatment of recurrent HCC after liver transplantation with adoptive therapy of TCR-engineered T cells.

SAT-277

Characterization of the immune tumor microenvironment in HCC

Charlotte Hoffmann¹, Simon Peter¹, Valery Volk¹, Melanie Bathon¹, Tanja Reineke-Plaß¹, Nadine Schadt¹, Friedrich Feuerhake¹, Arndt Vogel¹, Anna Saborowski¹. ¹Medizinische Hochschule Hannover, Germany
Email: hoffmann.charlotte@mh-hannover.de

Background and aims: Current frontline therapy for hepatocellular carcinoma (HCC) is based on immune checkpoint inhibitors (ICIs) targeting the programmed cell death protein 1/-ligand 1 (PD-1/PD-L1) axis, but alternative ICIs are under preclinical and clinical investigation. A more granular understanding of the immune contexture of HCC will be critical to determine recurrent patterns of the HCC immune tumormicroenvironment (iTME) and identify potential biomarkers that may ultimately allow for a more stratified approach to using immunomodulatory cancer therapies. We employed multiplex immunohistochemistry (mIHC) to spatially resolve and clinically annotate the iTME in HCC in the context of the underlying etiologies.

Method: FFPE tissues from 95 resected and clinically annotated HCCs were selected, and attention was paid that both tumor- and surrounding non-tumoral liver tissue were represented on a single section. Using a mIHC platform (Phenoptics system, Akoya Bioscience) the sections were stained for the following markers: CD3, CD20, CD68, Perforin, PD-L1, TIM3, LAG3 and Arginase, and regions of interests for subsequent multispectral high-resolution image acquisition were placed i) within the tumor, ii) the margin (tumor invasive front) and iii) the adjacent non-tumoral liver. The

tissue samples were stratified according to the respective underlying diagnosis, ASH (n = 28), NASH (n = 40) and viral (HBV or HCV, n = 27). **Results:** No significant etiology-dependent differences were evident in immune cell densities detected by our marker panel across all tumor areas and adjacent liver. According to the intratumoral localization, CD3 and CD20 positive cells were lowest within the tumor compared to margin and surrounding liver. Quantitative assessment of immune checkpoint expression revealed a striking dominance of PD-L1 over LAG3 and TIM3 in tumoral and non-tumoral regions, with a comparatively pronounced relative contribution of TIM3 signals in the margin area. Total PD-L1 signal was increased in HCCs with viral etiology, compared to those arising in the ASH context, but not to NASH-related HCC. Clinical correlations are currently under investigation and will be presented.

Conclusion: The iTME of human HCCs exhibits not only spatial dependencies, but also segregates with the respective underlying etiology. Distinct marker expression in NASH vs. ASH argues in favor of a more differentiated view of “non-viral” subgroups of HCCs. In addition, we posit that instead of quantitative assessments of single markers, a deeper understanding of the spatially resolved and “etiologically” annotated iTME will be required to identify translationally relevant markers, especially in the context of immunotherapy clinical trials.

SAT-278

Nuclear translocation of YAP drives BMI1-associated hepatocarcinogenesis in hepatitis B virus infection

Xufeng Luo¹, Rui Zhang², Stefan Schefczyk³, Shi Liu⁴, Yaojie Liang³, Hideo Baba⁵, Christian M. Lange⁶, Heiner Wedemeyer⁷, Mengji Lu⁸, Ruth Broering³. ¹The Affiliated Cancer Hospital of Zhengzhou University and Henan Cancer Hospital, Institute for Lymphoma Research, China, ²Sun Yat-sen University, Dept. of Biliary-Pancreatic Surgery, China, ³University Duisburg-Essen, Dept. of Gastroenterology, Hepatology and Transplant Medicine, Germany, ⁴College of Life Sciences, Wuhan University, State Key Laboratory of Virology, China, ⁵University Duisburg-Essen, Institute of Pathology, Germany, ⁶LMU University Hospital Munich, Dept. of Internal Medicine II, Germany, ⁷Hannover Medical School, Dept. of Gastroenterology, Hepatology and Endocrinology, Germany, ⁸University Duisburg-Essen, Institute for Virology, Germany
Email: ruth.broering@uni-due.de

Background and aims: Hepatitis B virus (HBV) infection is a major cause of hepatocellular carcinoma (HCC) development and progression. The aim of this study was to mechanistically investigate the involvement of Hippo signalling in HBsAg-dependent neoplastic transformation.

Method: Liver tissue and hepatocytes from HBsAg-transgenic mice were examined for the Hippo cascade and proliferative events. Functional experiments in mouse hepatoma cells included knock-down, overexpression, luciferase reporter assays and chromatin immunoprecipitation. Results were validated in HBV-related HCC biopsies.

Results: Hepatic expression signatures in HBsAg-transgenic mice correlated with YAP responses, cell cycle control, DNA damage and spindle events. Polyploidy and aneuploidy occurred in HBsAg-transgenic hepatocytes. Suppression and inactivation of MST1/2 led to the loss of YAP phosphorylation and the induction of BMI1 expression *in vivo* and *in vitro*. Increased BMI1 directly mediated cell proliferation associated with decreased level of p16INKA4, p19ARF, p53 and Caspase 3 as well as increased Cyclin D1 and γ -H2AX expression. Chromatin immunoprecipitation and the analysis of mutated binding sites in DLR assays confirmed that the YAP/TEAD4 transcription factor complex bound and activated the Bmi1 promoter. In chronic hepatitis B patients, paired liver biopsies of non-tumour and tumour tissue indicated a correlation between YAP expression and the abundance of BMI1. In a proof-of-concept, treatment of

HBsAg-transgenic mice with YAP inhibitor verteporfin directly suppressed the BMI1-related cell cycle.

Conclusion: HBsAg-mediated inhibition of Hippo signalling pathway was shown to be responsible for BMI1-mediated cell proliferation by controlling cell cycle checkpoints. YAP and BMI1 might be important factors linking HBV infection and the development of proliferative hepatocellular carcinoma. HBV-associated proliferative HCC might be related to the HBsAg-YAP-BMI1 axis and offer a potential target for the development of new therapeutic approaches.

SAT-279

Nonresolving inflammation in liver cancer; differential regulation of miR-122 signaling by BMP6 and TGF β

Martha Paluschinski¹, Mihael Vucur¹, Philipp Lang², Tom Lüdde¹, Mirco Castoldi³. ¹University Hospital Düsseldorf, Gastroenterology, Hepatology and Infectious Diseases, Düsseldorf, Germany, ²University Hospital Düsseldorf, Institute for Molecular Medicine II, Düsseldorf, Germany, ³University Hospital Düsseldorf, Gastroenterology, Hepatology and Infectious Diseases, Düsseldorf, Germany
Email: mirco.castoldi@med.uni-duesseldorf.de

Background and aims: Persistent inflammation is known to promote and exacerbate malignancy. The identification of key inflammatory signaling pathways causing transition from acute to chronic liver injury and from dysplasia to hepatocellular carcinoma (HCC) could depict novel predictive biomarkers and targets to identify and treat patients with chronic liver inflammation. microRNAs (miRNAs) are sequence-specific inhibitors of gene expression, which control cellular processes, whereas cellular signals and pathological conditions alter miRNA expression. With the aim of identifying miRNAs and mRNAs associated with nonresolving inflammation, genome-wide miRNome and transcriptomic analyses were performed in the livers of animal models characterized by inflammation-driven liver cancer.

Method: Low density and Affymetrix arrays were used to identify miRNAs and mRNAs altered in animal model with inflammation-driven liver cancer. Expression of genes of interest was independently validated by qPCR in animal models and in cohort of HCC patients. Luciferase vectors carrying the promoter region of human or murine MIR122 were transfected into tumor cell lines or primary hepatocytes, and the activity of selected cytokines was evaluated.

Results: The liver enriched miR-122 was identified as the most significantly downregulated microRNA in the liver of animal models with inflammation-driven liver cancer. Compelling evidence indicate that miR-122 is required for maintaining hepatic functionality. However, it remains unclear whether the observed phenotype is the trigger or consequence of ongoing diseases. Through this study, analysis of *in-vitro* and *in-vivo* experimental models, identified that miR-122 transcription is tightly interlinked with inflammation. We discovered that Lymphocytic choriomeningitis virus (LCMV) induced acute hepatitis in wild-type mice correlated with decreased level of hepatic miR-122. We identified that miR-122 transcription is differentially modulated by the immunoregulatory cytokines TGF β and BMP6. We show that Smad4 is required for mediating TGF β activity.

Conclusion: Collectively, our study provides new insights into the molecular mechanisms that potentially lead to downregulation of miR-122 in liver disease. As a result, new regulatory networks linking inflammation to the modulation of miR-122 expression have been identified. We propose that metabolic overload of regulatory networks driving cytokine-mediated deregulation of miR-122 expression may contribute to the development of chronic liver disease. Model 1; positive feedback loop; In this model the role of miR-122 is to fine-tune HAMP transcription via inhibiting HJV and HFE translation. Model 2; negative feedback loop; In this model, the role of miR-122 down-regulation is to activate inflammatory response via release of miR-122 inhibitions on its target genes.

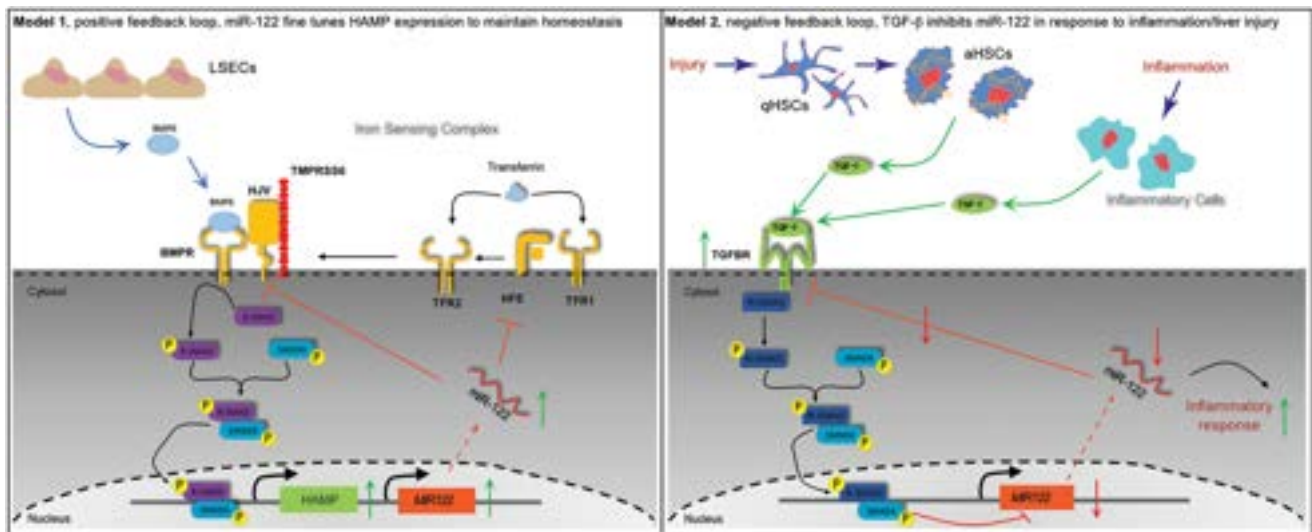


Figure: (abstract: SAT-279): Proposed models for regulatory networks up-stream to miR-122.

SAT-280

Genetic variant in the hepatic sterol transporter is associated with increased gallstone risk in obese patients and with higher odds of developing gallbladder cancer in general

Piotr Kalinowski¹, Joanna Ligocka², Łukasz Krupa³, Marc Dauer⁴, Krzysztof Jankowski⁵, Jolanta Gozdowska⁶, Beata Kruk⁷, Susanne N Weber⁸, Frank Lammert⁹, Marcin Krawczyk^{4,7}.

¹Department of General, Transplant and Liver Surgery, Medical University of Warsaw, Warsaw, Poland, ²Department of Gastroenterology and Internal Medicine, Medical University of Warsaw, Warsaw, Poland, ³Department of Gastroenterology and Hepatology with Internal Disease Unit, Medical Department, University of Rzeszów, Rzeszów, Poland, ⁴Saarland University Medical Center, Department of Medicine II, Germany, ⁵Department of Internal Medicine and Cardiology, Medical University of Warsaw, Warsaw, Poland, ⁶Department of Transplantation Medicine and Nephrology, Medical University of Warsaw, Warsaw, Poland, ⁷Laboratory of Metabolic Liver Diseases, Medical University of Warsaw, Warsaw, Poland, ⁸Department of Medicine II, Saarland University Medical Center, Department of Medicine II, Homburg, Germany, ⁹Hannover Medical School (MHH), Hannover, Germany
Email: marcin.krawczyk@uks.eu

Background and aims: Gallstone disease (GD) is one of the most common hepatobiliary conditions in Europe. In most cases gallstones remain asymptomatic. However, they might also cause complications like choledocholithiasis or gallbladder cancer in case of a long-lasting GD. Here, we analyse the common genetic risk modifier of GD (p. D19H variant in the sterol transporter ABCG8) in patients scheduled for bariatric surgery as well as in patients with gallbladder cancer and with recurrent common bile duct stones.

Method: Prospectively, we recruited three Polish cohorts of patients: 170 obese individuals scheduled for bariatric surgery (115 women, age range 19–65 years, 40 with GD), 65 patients with gallbladder cancer (49 women, age range 31–77 years), and 72 patients who underwent ERCP due to *de novo* stones that developed at least six months after cholecystectomy (49 females, age range 26–94 years). The control cohort comprised 172 gallstone-free adults. The ABCG8 p. D19H variant was genotyped in all cases and controls using TaqMan assays. In addition, we genotyped the c.711 (rs2109505) variant in the hepatic phospholipid transporter ABCB4 given the potential involvement of the ABCB4 locus in gallbladder cancer risk (Mhatre et al. *Lancet Oncol* 2017).

Results: Significantly more individuals carried at least one copy of the ABCG8 p.D19H risk allele among cases with either gallstones or gallbladder cancer (16.5%) as compared to controls (7.5%, $p = 0.016$). In particular, this variant was associated with an increased risk of developing gallbladder cancer (common OR 2.24, $p = 0.017$). It also increased the risk of GD in the obese scheduled for bariatric surgery (OR = 2.85, 95%CI 0.98–8.23, $p = 0.045$). On the other hand, it was not linked with *de novo* choledocholithiasis after cholecystectomy. We also did not find any significant link between the tested ABCB4 variant and the risk of gallbladder cancer either.

Conclusion: To the best of our knowledge, this is one of the first studies showing that the common ABCG8 risk variant increases the risk of gallbladder cancer in central Europeans. Moreover, this variant seems to increase the risk of gallstones in obese patients. Given the dismal prognosis of gallbladder cancer as well as the potential difficulties of treating symptomatic gallstones in obese patients, we reckon that carriers of this variant might profit from personalized diagnostic and therapeutic strategies to prevent both conditions.

SAT-281

CRISPR-engineered cholangiocarcinoma tumoroids generation from chemically-derived hepatic progenitor organoid for disease modelling

Michael Adisasmita^{1,2}, Hyomin Lee³, Myounghoi Kim^{1,2}, Hayoon Kim^{1,2}, Elsy Soraya Salas Silva^{1,2}, Ji Hyun Shin^{1,2}, Woonchang Hwang⁴, Junho Hur³, Dongho Choi^{1,2}. ¹Hanyang University College of Medicine, Surgery, Korea, Rep. of South, ²Research Institute of Regenerative Medicine and Stem Cells, Hanyang University, Korea, Rep. of South, ³Hanyang University College of Medicine, Genetics, Korea, Rep. of South, ⁴Hanyang University College of Medicine, Pre-Medicine, Korea, Rep. of South
Email: crane87@hanyang.ac.kr

Background and aims: Intrahepatic cholangiocarcinoma (iCC) is a deadly malignancy of the liver's biliary epithelial cells. This cancer has a high degree of heterogeneity, is extremely difficult to treat, and has a severely low survival rate. A vital discovery that significantly advances cancer research is the development of cancer organoid technique. These organoids can be derived from iCC patients' specimens but with very limited efficiency due to its insufficient sample cell size and quality. In addition, cancer organoids can be derived from normal adult stem cells edited by CRISPR technology to emulate the gene mutation that occurred during early carcinogenesis. **Method:** To generate the iCC tumoroid model, we transfected normal human chemically-derived hepatic progenitor cells (hCdHs) with

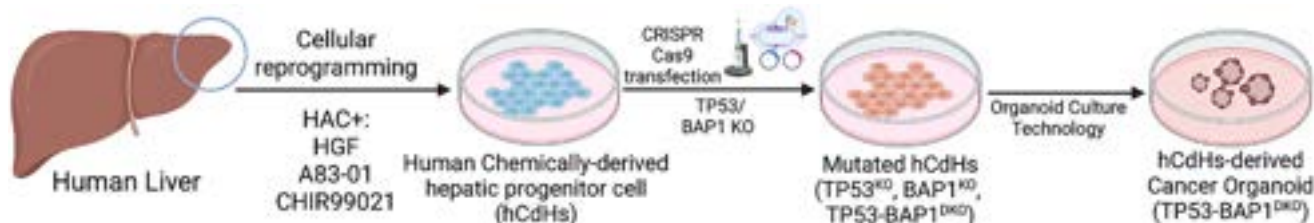


Figure: (abstract: SAT-281).

CRISPR-Cas9 plasmid and gRNA plasmids for TP53 and BAP1 by electroporation. Following the transfection, we generated tumoroids in matrigel dome from these mutated progenitor cells and performed various analyses of this tumoroids.

Results: To overcome the current limitation of the patient-derived cancer organoid, we successfully generated tumoroids from hCdHs that can be robustly expanded from a relatively small cell number. Then, we introduced the double knock-out mutation of TP53 and BAP1 genes, a well-established iCC cancer driver gene. These CRISPR-engineered hCdHs-derived cancer organoids showed comparable phenotypes with the iCC tumour malignant features. We observed pathological features of biliary adenocarcinoma on these tumoroids and confirmed the presence of mucus including mucin in the tumoroids lumen.

Conclusion: These results demonstrated the capability of our CRISPR-engineered hCdHs-derived cancer organoid as a powerful cancer disease modelling platform.

This research is funded by grants Korean Fund for Regenerative Medicine funded by Ministry of Science and ICT, and Ministry of Health and Welfare (21A0401L1). MA is supported by Hyundai Motor Chung Mong-Koo Global Scholarship.

SAT-282

Immunological impact of Axl/TGF-beta signaling in hepatocellular carcinoma

Gregor Ortmayr¹, Viola Hedrich², Patrick Starlinger³, Thomas Grünberger⁴, Doris Chen⁵, Wolfgang Mikulits². ¹Medical University of Vienna, Center for Cancer Research, Wien, Austria, ²Medical University of Vienna, Center for Cancer Research, Wien, Austria, ³Mayo Clinic Rochester, Department of Surgery, Division of Hepatobiliary and Pancreatic Surgery, Rochester, Minnesota, United States, ⁴Clinic Favoriten, Viennese Health Network, Department of Surgery, HPB Center, Vienna, Austria, ⁵University of Vienna, Max Perutz Labs, Department of Chromosome Biology, Center for Integrative Bioinformatics Vienna, Vienna, Austria

Email: gregor.ortmayr@gmail.com

Background and aims: A minority of hepatocellular carcinoma (HCC) patients is susceptible to conventional immune checkpoint blockade (ICB) as determined by immunological subtyping. The majority about 80% of HCC cases present an immunosuppressive or immune-excluded tumor microenvironment (TME). Interestingly, the class of immune-exhausted HCC, which is associated with poor response to ICB and prognosis, is also linked to “highly activated,” aberrant TGF-beta signaling. In HCC, the receptor tyrosine kinase Axl collaborates with TGF-beta by the phosphorylation of Smad3 at serine 213 in the linker region (Smad3L-Ser213) causing an aberrant, tumor-promoting TGF-beta signaling, which most likely also translates into the TME. As underlying mechanisms remain unclear, we aim to assess how Smad3L-Ser213-linked TGF-beta signatures shape an immunosuppressive TME.

Method: We used RNA-seq analysis and VENN relations of HCC models to identify targets of the Axl/TGF-beta signaling. Modulation of Axl/TGF-beta activity and analyses in publicly available data sets of HCC patients were employed to verify target expression.

Results: HCC cells showing aberrant TGF-beta signaling together with either proficiency or deficiency in Axl expression, the latter in the absence or presence of Axl reconstitution, were subjected to Gas6 and TGF-beta stimulation and subsequent RNA-seq analysis. Bioinformatics and VENN relations revealed uridine phosphorylases (UPP)1 as the most promising target since upregulation is associated with poor prognosis and immune evasion of HCC patients. Interference with Smad3L-Ser213 phosphorylation by inhibition of 14-3-3ζ or c-JNK confirmed UPP1 as a target of aberrant TGF-beta signaling. Genetic intervention with UPP1 reduced cell invasion and migration, while proliferation and survival of HCC cells remained unaffected. In line, cells exhibiting mesenchymal characteristics showed strong UPP1 expression.

Conclusion: We identified UPP1 as a target of Axl-driven, aberrant TGF-beta signaling in HCC cells. The link to immune escape and poor prognosis provides a clear rationale for further assessing its impact in reshaping the TME based on in vivo models and analyses in prospective HCC patient samples.

SAT-283

Intrahepatic cholangiocarcinoma developing in patients with metabolic syndrome is characterized by Osteopontin overexpression in the tumor stroma

Massimiliano Cadamuro^{1,2}, Samantha Sarcognato³, Riccardo Camerotto⁴, Noemi Girardi⁴, Alberto Lasagni¹, Giacomo Zanus^{5,6}, Umberto Cillo^{6,7}, Enrico Gringeri^{6,7}, Giovanni Morana⁸, Mario Strazzabosco⁹, Elena Campello^{1,2,10}, Paolo Simioni^{1,2,10}, Maria Guido^{2,3}, Luca Fabris^{1,4,9}. ¹Padua University-Hospital, General Internal Medicine Unit, Italy, ²University of Padua, Department of Medicine (DIMED), Italy, ³Azienda ULSS2 Marca Trevigiana, Department of Pathology, Italy, ⁴University of Padua, Department of Molecular Medicine (DMM), Italy, ⁵Azienda ULSS2 Marca Trevigiana, 4th Surgery Unit, Italy, ⁶University of Padua, Department of Surgery, Oncology and Gastroenterology (DISCOG), Italy, ⁷University of Padua, Hepatobiliary Surgery and Liver Transplantation Unit, Italy, ⁸Treviso Regional Hospital, Division of Radiology, Italy, ⁹Yale University, Digestive Disease Section, Liver Center, United States, ¹⁰University of Padua, Thrombotic and Haemorrhagic Disease Unit and Haemophilia Center, Department of Medicine (DIMED), Italy

Email: massimiliano.cadamuro@unipd.it

Background and aims: Metabolic syndrome (MetS) is a common condition closely associated with non-alcoholic fatty liver disease/non-alcoholic steatohepatitis (NAFLD/NASH). Recent meta-analyses show that MetS can be prodromal to intrahepatic cholangiocarcinoma (iCCA) development, a liver tumor with features of biliary differentiation characterized by dense extracellular matrix (ECM) deposition. Since ECM remodeling is a key event in the vascular complications of MetS, we aimed at evaluating whether MetS patients with iCCA present qualitative and quantitative changes in the ECM able to incite biliary tumorigenesis.

Method: Serial sections of liver tissue specimens of iCCA on a background of MetS (n = 22) and without MetS (non-MetS, n = 44), and relative peritumoral areas, were stained with Masson's Trichrome (histological staining for fibrosis) and with immunohistochemistry to highlight ductular reaction (DR) and hepatic

progenitor cells (keratin 7), and to depict the ECM proteins Osteopontin (OPN), Tenascin C (TnC) and Periostin (POSTN). Type and extent of DR, HPC, and fibrosis was evaluated by histological analysis, while extent of OPN; TnC and POSTN was assessed with computer-assisted morphometry. Patients were divided between the two cohorts based on biochemical and radiological data (CT scan for abdominal fat accumulation).

Results: In iCCAs with MetS patients undergoing surgical resection, we found a significant increased deposition of OPN, TnC, and POSTN compared to the matched peritumoral areas. Moreover, OPN deposition in MetS iCCAs was also significantly increased when compared to iCCA samples without MetS (non-MetS iCCAs). Using an *in vitro* approach, we have seen that OPN, TnC and POSTN treatment significantly stimulated cell motility and cancer stem cell-like phenotype in HuCCT-1.

Conclusion: In MetS iCCAs, fibrosis distribution and components differed quantitatively and qualitatively from non-MetS iCCAs. We therefore propose overexpression of OPN as a distinctive trait of MetS iCCA. Since OPN stimulate malignant properties of iCCA cells, it may provide an interesting predictive biomarker and a putative therapeutic target in MetS patients with iCCA.

SAT-284

Modelling hepatocellular carcinoma in precision-cut liver slices for therapeutic screening and as a precision medicine tool

Amy Collins^{1,2}, Jack Leslie^{1,2}, Daniel Geh^{1,2}, Erik Ramon Gil^{1,2}, Maja Laszczewska^{1,2}, Glyn Nelson³, Rainie Cameron¹, Kenny Dalgarno⁴, Helen Louise Reeves^{2,5}, Derek A Mann^{1,2}, Fiona Oakley^{1,2}. ¹Newcastle Fibrosis Research Group, Newcastle University, Newcastle upon Tyne, United Kingdom, ²The Newcastle University Centre for Cancer, Newcastle University, Newcastle upon Tyne, United Kingdom, ³Bioimaging Unit, Newcastle University, Newcastle upon Tyne, United Kingdom, ⁴School of Engineering, Newcastle University, Newcastle upon Tyne, United Kingdom, ⁵Translational and Clinical Research Institute, Newcastle University, Newcastle upon Tyne, United Kingdom

Email: a.l.collins1@newcastle.ac.uk

Background and aims: Liver cancer is one of the most common causes of cancer-related death worldwide, and hepatocellular carcinoma (HCC) accounts for approximately 90% of cases. Recent therapeutic advances extend overall survival by a few months, but only for a minority of patients. Realistic HCC models are necessary in order to bridge the gap between preclinical research and *in situ* human disease, and provide valuable insight into disease pathogenesis and drug discovery. Here we describe the development of two HCC models in precision-cut liver slices (PCLS): a murine precision-cut tumour slice (PCTS) model utilising the Hep-53.4 cell line, and a spheroid-engrafted human PCLS model.

Method: Hep-53.4 PCTSs were generated from orthotopic tumours 21 days after an intrahepatic injection of 1 million cells in C57BL/6 mice, and subsequently treated in the presence or absence of the receptor tyrosine kinase (RTK) inhibitors sorafenib or lenvatinib. An *ex vivo* human HCC model was developed by engrafting spheroids generated from HuH7 cells that express a secreted luciferase, onto human PCLSs. The spheroid-engrafted PCLS were then cultured in the presence or absence of the RTK inhibitors sorafenib, lenvatinib or regorafenib. Primary HCC cell lines derived from patient biopsies were expanded and lentiviral-transduced to express mCherry, and spheroids generated from these cells were also implanted onto human PCLSs. All tissue was cultured in a bioreactor system capable of maintaining the viability of the tissue for 7 days.

Results: Treatment of Hep-53.4 PCTSs with the RTK inhibitors sorafenib and lenvatinib results in decreased proliferation (Ki-67) and increased apoptosis (active caspase-3). Immunohistochemical characterisation of the PCTSs determined that they maintain a rich immune profile in culture, and treatment with anti-PD-1 immunotherapy results in significantly higher CD3 T-cell numbers, as well as

increased HCC apoptosis. In relation to the human spheroid-PCLS model, complete invasion of the spheroids into the PCLSs was confirmed via multiphoton imaging. Measurement of luciferase secreted following treatment with RTK inhibitors indicated a significant and dose-dependent reduction in cancer growth, whilst the PCLSs remained viable. Primary HCC spheroids implanted onto human PCLS also displayed complete engraftment and invasion into the tissue (Figure 1).

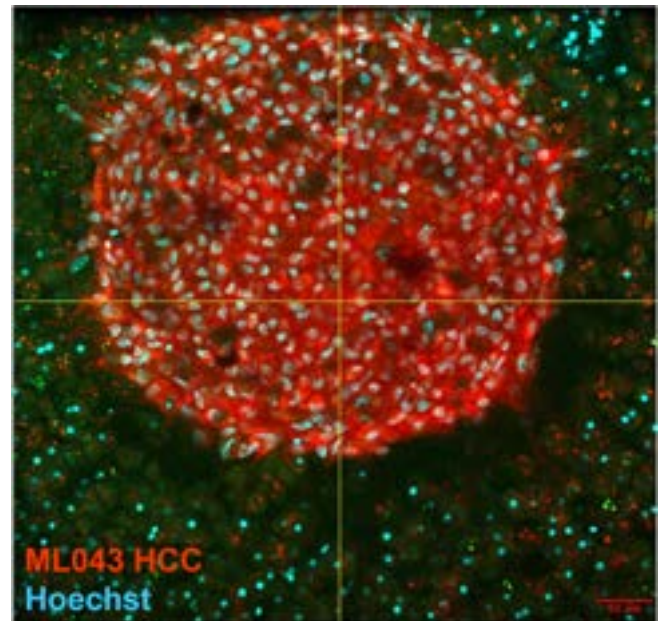


Figure:

Conclusion: The two models described potentially provide unique tools for discovery biology and precision medicine, where therapies can be tested on both PCTSs and patient-derived HCC cells in the context of the tumour microenvironment.

SAT-285

Investigation of optimization model for predicting ICI treatment efficacy on contrast-enhanced CT images of hepatocellular carcinoma using AI

Yasuhiko Nakao¹, Ryu Sasaki¹, Masanori Fukushima¹, Satoshi Miuma¹, Hisamitsu Miyaaki¹, Kazuhiko Nakao¹. ¹Nagasaki University Hospital, Gastroenterology and Hepatology, Nagasaki, Japan
Email: yasuo.nakao@nagasaki-u.ac.jp

Background and aims: The introduction of immune checkpoint inhibitors (ICIs) for unresectable hepatocellular carcinoma (HCC) is expected to improve prognosis. However, since the introduction of ICI, it has been found that there are individual differences in treatment efficacy, and studies have been reported to examine the factors associated with treatment failure based on the contrast effect of the hepatocellular phase of EOB-MRI prior to the introduction of ICI. ICI may improve the prognosis of patients. In this study, we developed an AI-based prediction model to predict treatment efficacy based on the characteristics of contrast-enhanced CT scan before ICI introduction, including hepatocellular carcinoma (HCC) and contrast effect of the background liver.

Method: We evaluated the efficacy of atezolizumab and bevacizumab in 43 patients at Nagasaki University Hospital from 2020 to November 2022 using mRECIST. 197 PD (9 patients), 271 PR (14 patients), 342 SD (20 patients) contrast CT images of liver cancer including the background liver were used as a learning dataset. ResNet18 as the Convolutional Neural Network (CNN) model and YOLOv7 as the You Only Look Once (YOLO) model was used to learn to predict the treatment effect. Precision-Recall curves were used to

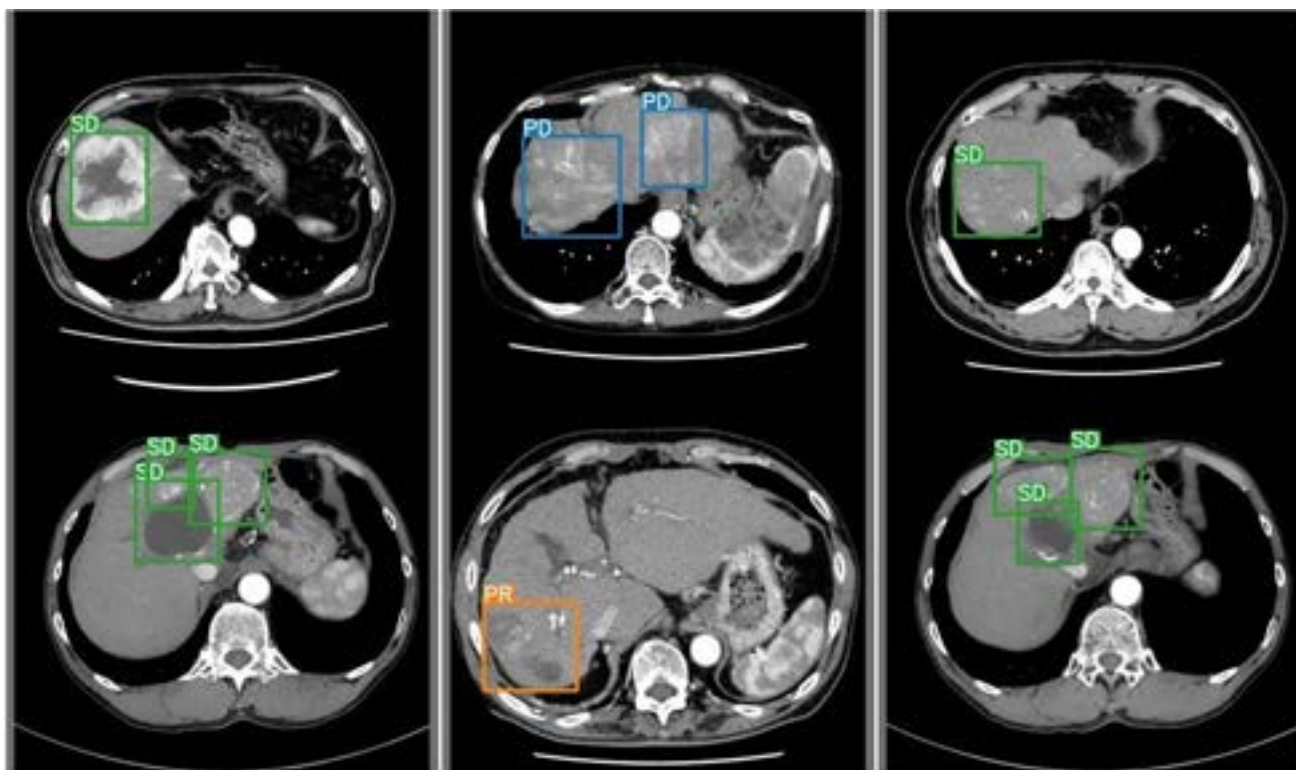


Figure: (abstract: SAT-285).

evaluate diagnostic performance, and class activation maps (CAM) were used to interpret the CNN models. The tSNE was used for feature analysis of the entire image.

Results: (1) The CNN model had a PD prediction sensitivity of 84%. Due to the interpretation of the model, the sites indicated by CAM did not correspond to the tumors. tSNE analysis showed that they were clustered for each case. Although the accuracy of prediction by the CNN model was high, it was expected to over-learn the CT image features of each case other than the tumor site. (2) In the analysis using the YOLO model, the AUC of the Precision-Recall curve for PD was 0.995. The prediction by the YOLO model is not only accurate but also has high clinical versatility because it can identify the point that led to the decision (Figure).

Conclusion: Since it is difficult to prepare a large amount of training data for a drug effect prediction model for tumors compared to a general tumor diagnosis model, a large-scale validation using a more efficient YOLO model is expected.

SAT-286

CD40 expression in liver cancer cells is upregulated by CD4⁺T cells through IFN-gamma and ERK 1/2 pathway

Norifumi Kawada¹, Hanh Ngo Vinh¹, Le Thi Thanh Thuy¹, Hieu Vu², Hai Hoang¹, Akihiro Tamori¹, Masaru Enomoto¹, Sawako Uchida-Kobayashi¹. ¹Osaka Metropolitan University, Japan, ²Hanoi Medical University, Viet Nam
Email: kawadanori@omu.ac.jp

Background and aims: Hepatocellular carcinoma (HCC) is one of the most common primary liver cancers which is a leading cause of cancer-related death worldwide. CD40 is a costimulatory receptor essential for the survival and activation of antigen-presenting cells while its functional role in cancer remains controversial. This study aimed to examine the biological role of CD40 in liver tumor progression.

Method: 168 hepatitis C virus (HCV) -infected patients including 47 HCC and 121 non-HCC were enrolled in this study. The level of soluble

(s) and membrane-bound (m) CD40 were examined in plasma and human liver tissues, respectively. Immunoblot and quantitative RT-PCR were performed to assess the expression of CD40 in five human HCC cell lines. The methylation index of the CD40 promoter region was examined. CD4⁺T cells isolated from the peripheral blood of healthy donors were stimulated to express CD40 ligand (CD40L). Human recombinant IFN-gamma was used to induce CD40 expression in HCC cells.

Results: The plasma level of sCD40 was increased significantly in HCC patients compared to non-HCC patients at baseline ($p = 0.0003$), end of HCV treatment ($p = 0.047$), sustained viral response ($p = 0.035$), end point (time of HCC occurrence, $p = 0.011$), and correlated with HCC accumulation. Immunohistochemistry revealed a dominant mCD40 expression in poorly differentiated HCC tissues compared with non-tumor areas. Consistent with the observations in human samples, CD40 was highly expressed in poorly differentiated HCC cells (SNU387, HLE, and HLF) while well-differentiated HCC cells (Huh7 and HepG2) showed no or weak signal. CD40 promoter region exhibited a low methylation index (all 5%) in SNU387, HLE, and HLF cells compared to a higher one (Huh7: 57.5%, HepG2: 27.5%) in the well-differentiated group. CD4⁺T cells isolated from healthy donors and activated by culturing on the anti-CD3-coated dish (5 microgram/ml) for 12 hours exhibited marked CD40L expression under flow cytometry analysis. The elevation of CD40 at both RNA and protein levels was noted in HLFs when cocultured with activated CD4⁺T cells compared to single-culture in both ratio- and time-dependent manners. Coculturing with unactivated TCD4⁺ cells that lack CD40L induces lower CD40 expression on HLF than with activated TCD4⁺ cells. Alternatively, this increase was partially canceled when a linkage between HLFs and CD4⁺T cells was disturbed by using a trans-well culture, denoting the involvement of their both direct and indirect interaction in CD40 expression in HLFs. RNA sequencing from HLF co-cultured with activated TCD4⁺ cells from healthy donors revealed top three upregulated pathways including interferon response, immune response, and Jak-Stat signaling compared with

single cultured HLF. We then stimulated HLFs with IFN-gamma (5 ng/ml) for 24 hours resulting in the phosphorylation of p65, Jak1 and ERK1/2 pathways, but not p38 nor Akt pathways, and the upregulation of CD40 at both mRNA and protein levels in HLFs. Jak1 inhibitor, CYT387 (2–16 micromolar), and ERK1/2 inhibitor, U0126 (5–80 micromolar), reduced CD40 expression in HLF cells under IFN-gamma stimulation.

Conclusion: CD40 expression in poorly differentiated HCC cells is possibly regulated by CD4⁺T cells and IFN-gamma. A high level of soluble CD40 in the plasma of HCV-SVR patients may indicate the risk of HCC development.

SAT-287

Potential biomarkers predicting ferroptosis sensitivity in hepatocellular carcinoma

Hyun Young Kim¹, Wan Seob Shim¹, Ga Hee Baek², Sang Kyum Kim², Keon Wook Kang¹. ¹Seoul National University, College of Pharmacy and Research Institute of Pharmaceutical Sciences, Seoul, Korea, Rep. of South, ²Chungnam National University Daedeok Campus, College of Pharmacy, Daejeon, Korea, Rep. of South
Email: kwkang@snu.ac.kr

Background and aims: Hepatocellular carcinoma (HCC) is one of the most common and aggressive forms of liver cancer characterized by high morbidity and mortality. Despite recent advances in understanding the mechanism underlying HCC progression, there are still limited treatment options in the clinical field. Ferroptosis, a typical form of regulated cell death induced by iron-mediated oxidative stress, has been proposed as a new strategy to treat HCC. Indeed, erastin-a ferroptosis inducer-has been shown to effectively inhibit

the growth of tumour cells in preclinical studies. Herein, we aim to suggest potential biomarker (s) of erastin sensitivity to HCC.

Method: Ferroptosis-inducing effects of erastin in various HCC cell lines were examined using C11 BOBIPYTM 581/591 dye, which is a lipid peroxidation sensor. HCC cells were treated with erastin in phenol-red free, serum-containing media. The integrated intensity of green fluorescence and confluency of the cells were calculated automatically in IncucyteTM Live-Cell Imaging System. For stable isotope tracing, HCC cells were incubated with cystine- and methionine-free media supplemented with 0.2 mM ³⁴S-methionine. Metabolites were analyzed by sample injection using an autosampler and separated by an AQUASIL C18 column. Protein and mRNA expressions were examined by Western blot and qPCR, respectively.

Results: The ferroptosis-inducing efficacy of erastin in nine HCC cell lines was cell-type dependent. Among these cell lines, HepG2, Huh7, and SKHep1 were selected for further experiments. Western blot and qPCR analyses revealed that expression of cancer stemness markers, enzymes for transsulfuration pathway and iron metabolism-related proteins were significantly correlated with erastin sensitivity. Next, stable isotope tracing confirmed that the activation of the transsulfuration pathway protects HCC cells from erastin-induced ferroptosis. Finally, the biomarkers listed above were validated by survival analysis using the Kaplan-Meier curve from public datasets.

Conclusion: Ferroptosis, an iron-dependent, reactive oxygen species-mediated cell death has been proposed as a promising strategy in treating HCC. To successfully clarify erastin-sensitive HCC, we propose several genes as predictive biomarkers related to cancer stemness, transsulfuration pathway and iron metabolism. Identifying these phenotypic signatures in HCC would help predict the efficacy of erastin-induced ferroptosis.

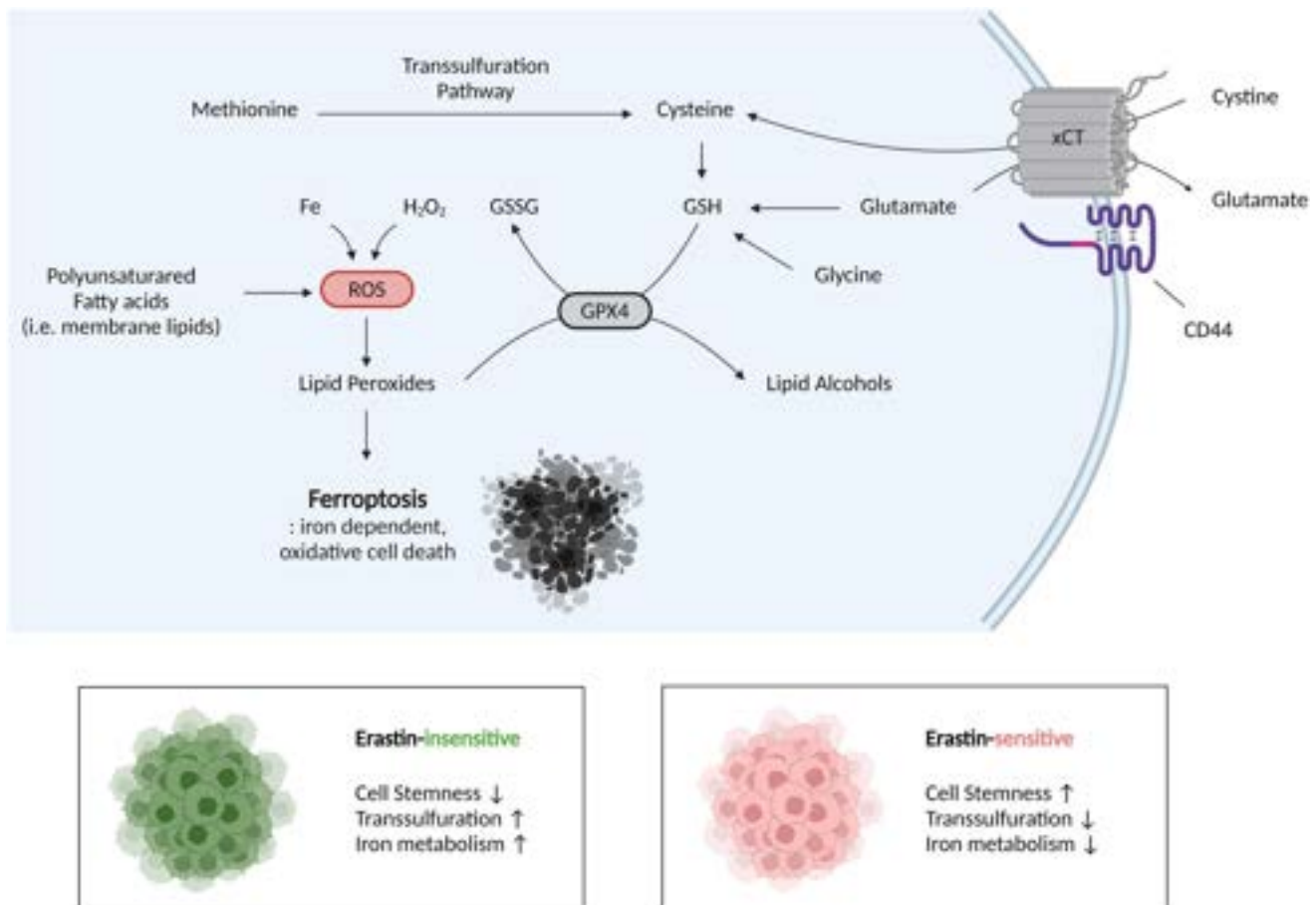


Figure: (abstract: SAT-287).

SAT-288

Genetic biomarkers for sorafenib response in patients with hepatocellular carcinoma

Giuseppa Augello¹, Mariamena Arbitrio², Lydia Giannitrapani³, Francesca Scionti², Domenico Ciliberto⁴, Nicoletta Staropoli⁴, Giuseppe Agapito⁵, Pierfrancesco Tassone⁴, Pierosandro Tagliaferri⁴, Maurizio Soresi³, Aurelio Seidita³, Marco Affronti³, Gaetano Bertino⁶, Maurizio Russello⁷, Francesca Di Gaudio³, Rosaria Ciriminna⁸, Francesca Spinnato⁹, Francesco Verderame⁹, Melchiorre Cervello¹.
¹Institute for Biomedical Research and Innovation, National Research Council (CNR), Palermo, Italy, ²Institute for Biomedical Research and Innovation, National Research Council (CNR), Catanzaro, Italy, ³Department of Health Promotion, Mother and Child Care, Internal Medicine and Medical Specialties, University of Palermo, Palermo, Italy, ⁴Medical and Translational Oncology Unit, AOU Mater Domini, Catanzaro, Italy, ⁵Department of Legal, Economic and Social Sciences, Magna Graecia University, Catanzaro, Italy, ⁶Hepatology Unit, AOU San Marco University of Catania, Catania, Italy, ⁷Liver Unit, ARNAS Garibaldi-Nesima, Catania, Italy, ⁸Istituto per lo Studio dei Materiali Nanostrutturati, National Research Council (CNR), Palermo, Italy, ⁹Oncology Unit, Villa Sofia-Cervello Hospital, Palermo, Italy
 Email: giuseppa.augello@irib.cnr.it

Background and aims: Sorafenib, a multitarget tyrosine kinase inhibitor (TKI) which exerts a strong antiangiogenic effect, is now one of the first-line treatments for patients with advanced hepatocellular carcinoma (HCC). Although sorafenib is well tolerated, a significant proportion of HCC patients do not respond to sorafenib treatment. It is increasingly necessary to find suitable biomarkers to predict interindividual response variability to sorafenib in HCC. Patient stratification based on genomic variations may help guide physicians in treatment selection.

Method: Thirty-four patients with advanced HCC, treated for the first time with sorafenib, were enrolled in our study. Patients came from 5 Sicilian hospital centers. Based on published data, five single nucleotide polymorphisms (SNPs) in angiogenesis-related genes, including rs2010963 (VEGF-A), rs4604006 (VEGF-C), rs12434438 (HIF-1 α), rs55633437 (ANGPT2) and rs2070744 (NOS3), were tested for in 34 HCC patients, of which 9 were responders and 25 were non-responders to sorafenib. Additionally, a subgroup of 23 patients was genotyped for 1,931 SNPs and 5 copy number variations (CNVs) using the DMET Plus microarray platform.

Results: Analyzing the SNPs associated with angiogenesis, we found that only in VEGF-A (rs2010963) was the frequency of the G allele and CG/GG genotypes, compared to CC genotype, significantly associated with response to sorafenib. However, when we examined the cumulative effects of selected angiogenesis-related SNPs, developing a genetic response score (GRS), a higher mean GRS was significantly associated with responders compared to non-responders when the sum of the five scores for the rs2010963, rs4604006, rs12434438, rs55633437, and rs2070744 variants was considered for each patient ($p=0.042$). The predictive performance of GRS was confirmed in vitro using HCC cells that displayed different responsiveness to sorafenib. ADME-related gene analysis allowed the identification of 10 predictive polymorphic variants in ADH1A (rs6811453), ADH6 (rs10008281), SULT1A2 (rs11401), CYP26A1 (rs7905939), DPYD (rs2297595 and rs1801265), FMO2 (rs2020863) and SLC22A14 (rs149738, rs171248 and rs183574) that were significantly associated with response to sorafenib. Pathway enrichment analysis (PEA) showed that the analyzed genes are associated in several key common biological pathways correlated to sorafenib and HCC.

Conclusion: We identified 15 SNPs associated with angiogenesis and ADME genes, inserted in key points of several biological pathways, as potential predictive biomarkers for response to sorafenib which could be considered as a proof of concept to be further validated in follow-up studies for the definition of a better treatment options to promote better outcomes in HCC patients.

SAT-289

Association between gadoteric acid-enhanced MR imaging, organic anion transporters, and farnesoid X receptor in benign focal liver lesions

Belle van Rosmalen^{1,2}, Michele Visentin³, Alicia Furumaya^{1,2}, Otto van Delden^{1,2}, Geert Kazemier^{4,5}, Thomas Van Gulik^{1,2}, Joanne Verheij^{1,2}, Bruno Stieger³. ¹Amsterdam Gastroenterology Endocrinology Metabolism, Netherlands, ²Amsterdam UMC, University of Amsterdam, Netherlands, ³University Hospital Zurich, Switzerland, ⁴Amsterdam UMC, location VUmc, Netherlands, ⁵Cancer Center Amsterdam, Netherlands
 Email: b.vanrosmalen@gmail.com

Background and aims: Organic anion uptake and efflux transporters (OATP1B1, OATP1B3, MRP2 and MRP3) are direct or indirect targets of the farnesoid X receptor (FXR) pathway, influencing homeostasis of lipids and bile acids. In benign liver tumours, FXR is not yet characterized. We investigated the expression of FXR and its targets in hepatocellular adenoma (HCA) and focal nodular hyperplasia (FNH) and its correlation with gadoteric acid (Gd-EOB-DTPA) MRI.

Method: Gd-EOB-DTPA MRI were assessed by an expert radiologist and correlated to mRNA expression levels of OATP1B1, OATP1B3, MRP2, MRP3, FXR and SHP in fresh surgical specimens of patients with FNH or HCA subtypes. Transporter expression was profiled with respect to the FXR pathway in the explorative part of this study, in search of novel molecular markers for HCA subclassification.

Results: Normal and tumour sample pairs of 43 HCA and 15 FNH were included. Of 58 patients, 48 had an Gd-EOB-DTPA MRI. FNH was detected with 100% sensitivity and 82% specificity. HCA was detected with 82% sensitivity and 100% specificity. Of patients who underwent Gd-EOB-DTPA MRI, 28/48 lesions were hypointense and 20/48 lesions were hyperintense. OATP1B3 was downregulated in 23 hypointense tumours, by approximately a 5-fold compared to normal surrounding liver tissue (2.77 ± 3.59 vs 12.9 ± 15.6 , $p < 0.001$). Hyperintense HCA showed upregulation in 5/6 patients. OATP1B1, OATP1B3 and MRP2 were significantly downregulated in HNF-1 α -mutated HCA (H-HCA). A significant positive correlation between FXR expression and activation and OATP1B3 expression level in HCA was found.

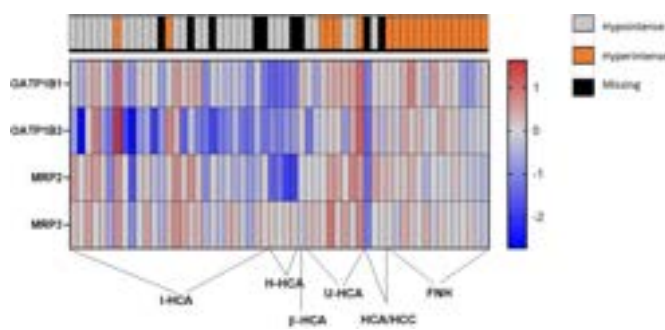


Figure:

Conclusion: A central role for OATP1B3 in Gd-EOB-DTPA uptake in HCA was confirmed. The MRI relative signal may reflect expression level of FXR and SHP. HNF1 α may be a regulator of SHP expression in vivo.

SAT-290

Comprehensive analysis of single-cell and bulk RNA sequencing data identifies antioxidant-1 as a novel immune biomarker associated with immune cell infiltration in hepatocellular carcinoma metastasis

Ruijia Liu¹, Xudong Yu¹, Zao Xiaobin¹, Xu Cao¹, Yong'an Ye^{1,2}.

¹Dongzhimen hospital, Beijing university of Chinese medicine, China,

²Beijing University of Chinese Medicine, Liver Diseases Academy of Traditional Chinese Medicine, Beijing, China

Email: yeyongan@vip.163.com

Background and aims: Copper is involved in cancer progression by affecting biological processes such as cell proliferation, invasion, metastasis, and angiogenesis. Antioxidant-1 (ATOX1) is aberrantly expressed as a copper chaperone protein in several cancers, but its function and mechanism in hepatocellular carcinoma (HCC) are unknown and were the purpose of this study.

Method: The expression, diagnostic, prognostic, clinical features, functional enrichment, and immune characteristics of ATOX1 in HCC were explored through R software using data from multiple

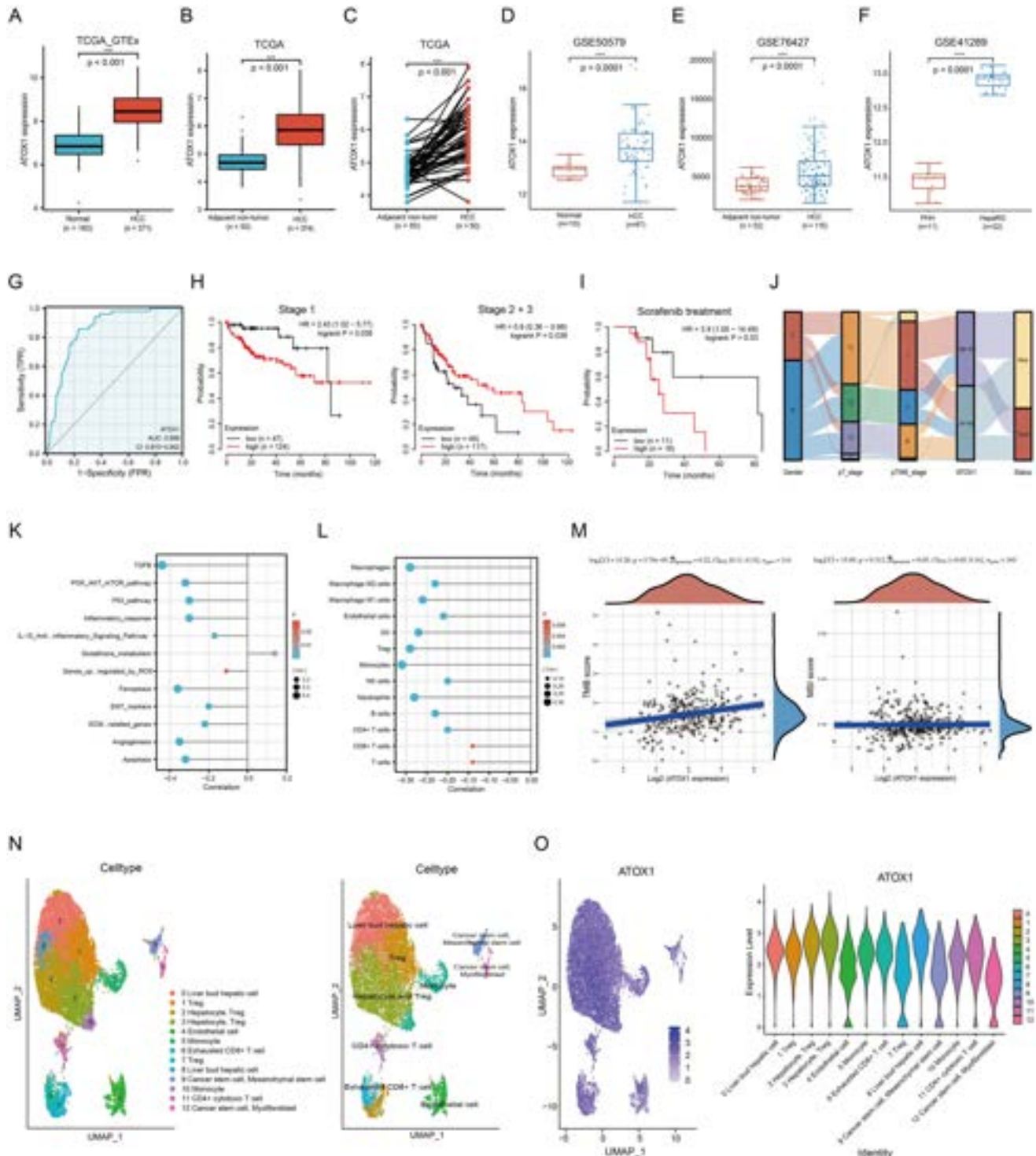


Figure: (abstract: SAT-290).

POSTER PRESENTATIONS

databases. ATOX1 expression in HCC cells and stromal cells was observed by single cell sequencing analysis.

Results: Compared with the non-tumor tissues, ATOX1 was significantly upregulated in HCC tissues. The GSE50579 and GSE76427 datasets validated this conclusion. And ATOX1 mRNA in HCC cells was also significantly higher than that in primary human hepatocytes. Meanwhile, ATOX1 expression had a certain accuracy for HCC diagnosis, and lower expression predicted better prognosis in the stage 1 and sorafenib treatment subgroups. Enrichment analysis showed that ATOX1 was markedly negatively associated with most cancer-related pathways, such as PI3K-AKT-mTOR, EMT, ECM, Angiogenesis, Apoptosis, Ferroptosis, Reactive oxygen species and Inflammatory response. ATOX1 was significantly negatively associated with immune cell infiltration (ICI) in the tumor microenvironment (TME), including macrophages, monocytes, endothelial cells, dendritic cells, neutrophils, B cells, T cells, CD4+ T cells, CD8+ T cells, regulatory T cells (Treg) and natural killer cells. And it was remarkably positively correlated with tumor mutational burden. Single-cell sequencing showed that ATOX1 was highly expressed on HCC cells and stromal cells, especially Treg, endothelial cells, monocytes, T cell subsets and hepatocytes.

Conclusion: Our results revealed that ATOX1 activity was closely associated with cellular redox status and might play an important role in HCC invasion and migration by regulating ICI in TME. In conclusion, ATOX1 might be a promising predictive biomarker for immunotherapy of HCC.

SAT-291

PD-L1 small molecule inhibitors and Paclitaxel orchestrating CD8+ cell cytotoxicity via tumor-associated macrophages: a personalized HCC immunotherapeutic approach

Israa Helal¹, Monica A. Kamal¹, Ahmed Ramadan², Tamer Elbaz², Mohamed Mahmoud Nabeel², Sally Elfishawi³, Hend Ibrahim Shousha², Ashraf Omar², Yasmine M. Mandour^{4,5}, Hend El Tayebi¹. ¹German University in Cairo, Clinical Pharmacology and Pharmacogenomics Research Group, Department of Pharmacology and Toxicology, Faculty of Pharmacy and Biotechnology, Cairo, Egypt, ²Cairo University, Endemic Medicine, Faculty of Medicine, Cairo, Egypt, ³National Cancer Institute, Cairo University, Clinical Pathology department, Egypt, ⁴School of Life and Medical Sciences, University of Hertfordshire Hosted by Global Academic Foundation, Cairo, Egypt, ⁵German University in Cairo, Department of Pharmaceutical Chemistry, Faculty of Pharmacy and Biotechnology, Cairo, Egypt
Email: hend.saber@guc.edu.eg

Background and aims: The numerous side effects of chemotherapy, such as paclitaxel, in Hepatocellular Carcinoma (HCC) have triggered the development of novel treatment approaches. Combining immunotherapy with chemotherapy has become one of the most prevalent treatment modalities recently. Since 2018, small molecule inhibitors (SMIs) as immune checkpoint inhibitors have received the spotlight in immunotherapy research due to their safety and low cost of production. Specifically, programmed cell death 1 and its ligand (PD-1/PD-L1) inhibitors have shown promising results on a myriad of cancers including HCC in clinical trials. In HCC tumor microenvironment (TME), tumor associated macrophages (TAMs) were found to be a major contributor in several molecular pathways involved in HCC progression. CCL5 protein was reported to be upregulated in TAMs and a key molecule in downstream signalling of several molecular pathways that lead to HCC progression along with regulating the activity of multiple immune cells as CD8+ cells. The aim of our study

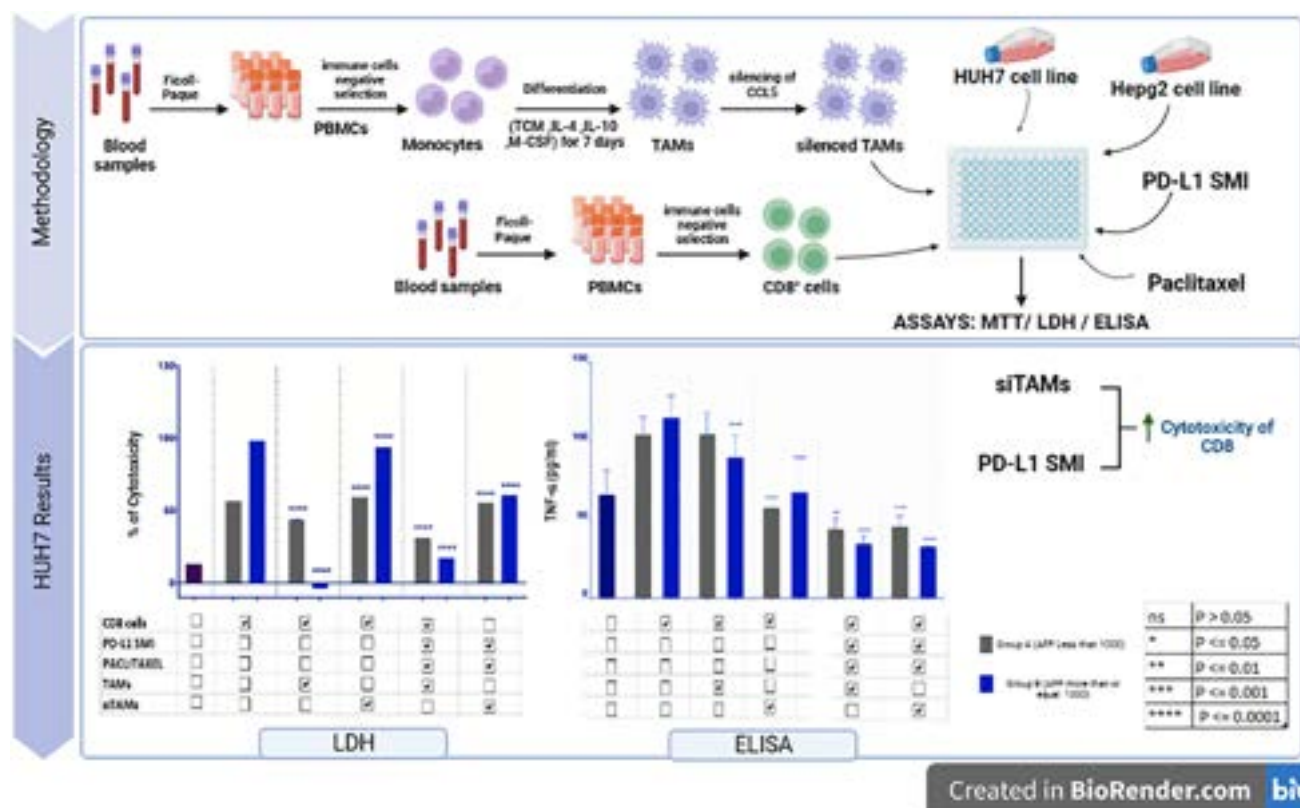


Figure: (abstract: SAT-291).

is investigating the synergistic effect of tuning TAMs by silencing CCL5 along with PD-L1 SMI on activating the anti-tumor response exerted by CD8⁺ cells in presence of paclitaxel as a combinational therapy approach. PD-L1 SMI used in this study is obtained through a virtual screening protocol, of commercial databases, that is reported by our group in a previous study.

Method: Monocytes were isolated from whole blood samples of 45 HCC patients (classified according to their alpha fetoprotein levels into two groups), differentiated into TAMs where finally CCL5 was silenced by siRNAs. Silenced TAMs (siTAMs) were co-cultured with CD8⁺ cells from HCC patients, HCC cell lines (Huh7 and HepG2 as a confirmatory cell line), PD-L1 SMI and paclitaxel. Cell cytotoxicity was performed to assess the effect of regulation of TAMs on CD8⁺ cytotoxicity after coculturing (LDH assay). Cell viability assays were performed to assess the effect of all conditions on HCC cell lines (MTT assay). Tumor Necrosis Factor alpha (TNF- α), a pro-inflammatory cytokine, was measured in tumor-cultured media (TCM) using Enzyme-linked immunosorbent assay.

Results: The presented data in the figure attached is showing the experiments done on Huh7 cells: CD8⁺ tumor cytotoxicity showed a significant increase upon CCL5 knockdown in TAMs in the coculture with and without the combined therapy. TNF- α expression significantly declined upon CCL5 knockdown in TAMs and addition of combined therapy. Cell viability of HCC cell lines declined consequent to the knockdown of CCL5 in TAMs, also with combined therapy. Consistent results were observed in HepG2 cells as confirmation.

Conclusion: Combining the PD-L1 SMI with the siTAMs showed a synergistic effect on the activity of CD8⁺ cells. Combinational approach is more effective than either alone. The development of PD-1/PD-L1 immune checkpoint SMI opens a new avenue for alternative treatment modalities with less immune related adverse events.

SAT-292

Intermittent fasting improves tumor-directed drug delivery by caveolar-mediated endocytosis

Svea Becker¹, Ilaria Biancacci², Diana Möckel², Qingbi Wang¹, Jan-Niklas May², Huan Su¹, Jeffrey Momoh², Lena Susanna Candels¹, Marie-Luise Berres¹, Fabian Kiessling², Maximilian Hatting¹, Twan Lammers², Christian Trautwein¹. ¹Medical Department III, Germany, ²Experimentelle Molekulare Bildgebung, Germany
Email: svbecker@ukaachen.de

Background and aims: Tumor cells rely on the Warburg effect to maintain their high proliferative activity, making them dependent on external glucose supply for cell metabolism and proliferation. Therefore, fasting may have health benefits to combat tumor growth. Furthermore, it can reduce toxicity and improve the efficacy of chemotherapy. This makes it a beneficial approach for cancers with limited systemic and local ablative therapies, such as hepatocellular carcinoma (HCC).

Method: The effects of intermittent (IF) fasting were investigated on tumor growth, development of the tumor microenvironment (TME) and tumor-targeted drug delivery in an intrahepatic murine hepatocellular carcinoma model and were subsequently subjected to IF for 24 days. Cy7-labeled liposomes were applied *i.v.* and their biodistribution and tumor accumulation was examined via combined micro-CT and fluorescence tomography (μ CT-FLT). These effects were validated using immunohistochemistry staining and fluorescence microscopy. *In vitro* studies were performed with the hepatoma cancer cell line Hep-55.1C to identify the effect of liposome uptake under fasting conditions on a cellular level. The cells were stimulated with forskolin and inhibitors of endocytic mechanisms. Uptake was then analysed by flow-cytometry and fluorescence microscopy.

Results: Analyses of MRI-scans demonstrated that IF decreased intrahepatic tumor growth compared to animals fed *ad libitum*. Fluorescence microscopy and two-photon laser microscopy images revealed significant changes in TME as evidenced by decreased

extracellular matrix e.g. collagen production, and increased angiogenesis e.g. lectin-perfused vessels. These changes contributed to increased tumor-directed liposome accumulation and uptake in IF treated animals.

In vitro, Hep-55.1C were stimulated to fast and liposome uptake was analysed via flow cytometry and immunofluorescence microscopy. Together, the *in vitro* data demonstrate that the fasting equivalent forskolin causes a significant increase in liposome uptake, which could be reversed specifically by nystatin inhibition. These results identified that the increase in liposome uptake in HCC cells is mediated by caveolar endocytosis.

Conclusion: Intermittent fasting improves tumor-directed targeting by modifying the TME, due to increased angiogenesis and decreased collagen abundance, and modifying intracellular mechanisms using a caveolar-mediated endocytosis-dependent mechanism. These influences make IF a promising approach when applied concomitantly to HCC targeted therapy.

Liver tumours Therapy

WEDNESDAY 21 TO SATURDAY 24 JUNE

TOP-067

A simple characterization of dynamic changes in circulating CD8⁺PD1⁺ lymphocytes early predicts response to atezolizumab-bevacizumab in hepatocellular carcinoma

Fabio Piscaglia^{1,2,3}, Fabrizia Suzzi^{1,4}, Francesco Tovoli^{1,2}, Mariangela Bruccoleri⁵, Mariarosaria Marseglia², Eleonora Alimenti⁵, Francesca Fornari^{3,6}, Massimo Iavarone⁵, Laura Gramantieri^{2,4}, Catia Giovannini^{1,4}. ¹University of Bologna, Department of Medical and Surgical Science, Italy; ²Division of Internal Medicine, Hepatobiliary and Immunoallergic Diseases, IRCCS Azienda Ospedaliero-Universitaria di Bologna, Italy; ³Centre for Applied Biomedical Research-CRBA, University of Bologna, Italy; ⁴Centre for Applied Biomedical Research-CRBA, University of Bologna, Italy; ⁵Fondazione IRCCS Cà Granda Ospedale Maggiore Policlinico di Milano. Division of Gastroenterology and Hepatology Milan, Italy; ⁶University of Bologna, Department for Life Quality Studies, Italy
Email: fabio.piscaglia@unibo.it.

Background and aims: Atezolizumab+bevacizumab improves survival of patients with advanced Hepatocarcinoma (HCC) in comparison to Sorafenib. No biomarker predicts responders from non-responders to atezolizumab+bevacizumab or patients who benefit from this combination instead of TKIs. To identify early on treatment predictive biomarkers, we investigated whether baseline and early on treatment variation of CD8⁺, PD1⁺, PD-L1⁺, CD8+PD1⁺, CD8+PDL1⁺ peripheral lymphocytes might offer a non-invasive, cheap and feasible assay.

Method: A prospective cohort of 31 patients treated with atezolizumab+bevacizumab and a control prospective cohort of 15 patients treated with sorafenib or lenvatinib were subjected to repeated blood tests, at baseline and during the course of treatments. At first imaging re-evaluation, 11 patients receiving atezolizumab+bevacizumab showed objective response, 13 stable disease, accounting for the responder group, while 7 patients displayed tumor progression, corresponding to primary non-response. Baseline and early on treatment variation of CD8⁺, PD1⁺, PD-L1⁺, CD8+PD1⁺, CD8+PDL1⁺ peripheral lymphocytes were tested by cytofluorimetric analysis and compared in responders and non-responders.

Results: Baseline CD8⁺ and CD8+PDL1⁺ peripheral lymphocytes were lower in responders versus non-responders (mean \pm SD CD8⁺: 68 \pm

POSTER PRESENTATIONS

30 vs 95 ± 5; T-test, $p < 0.0001$; mean ± SD CD8+PD-L1+: 77 ± 9.4 vs 82 ± 4.6; T-test: $p = 0.004$ respectively). Dynamic changes in CD8+PD1+ lymphocytes assessed at 3-weeks, before the second drug infusion, were the most informative test: 22 of 24 responders displayed a rise of CD8+PD1+ peripheral lymphocytes with a positive mean fold change of 4.63 (±5.5 SD). Conversely, 6 of 7 non-responders displayed a negative mean fold change of 0.89 (±0.84 SD) of CD8+PD1+ lymphocytes. These changes were restricted to patients treated with atezolizumab+bevacizumab, while they were not documented in TKI patients, irrespective of the response.

Conclusion: Early changes in circulating PD1+CD8+ lymphocytes predict the type of response to atezolizumab+bevacizumab and encourage evaluating this minimally invasive, cheap, easy and repeatable test in a larger cohort of patients to confirm its informativeness in this setting.

TOP-071

Impact of statin on the survival of patients with advanced hepatocellular carcinoma treated with sorafenib or lenvatinib

Hyo Jung Cho¹, Ji Eun Han¹, Jae Youn Cheong¹, Soon Sun Kim¹. ¹Ajou university school of medicine, Gastroenterology, Korea, Rep. of South Email: pilgrim8107@hanmail.net.

Background and aims: To overcome drug resistance to multityrosine kinase inhibitors (TKI) such as sorafenib and lenvatinib is major challenging issue for systemic treatment of hepatocellular carcinoma (HCC). Statin reduced the risk of developing HCC in patients with hepatitis B, C and diabetes mellitus and was also reported to potentiate anticancer effect of the TKIs. We aimed to verify the potential survival benefit of statin combined with the TKIs in patients with advanced HCC. Further, we investigated the impact of timing of statin administration, optimal statin type and dose on survival outcome of patients with HCC treated with the TKIs.

Method: Using large-scale data from 2010 to 2020 provided by National Health Insurance Service in Korea, we identified the effect of statin use on the patients with advanced HCC treated with the TKIs.

Statin user was defined as 28 cumulative defined daily dose (cDDD) ≥ 28 of filled statin prescriptions. After propensity score matching (PSM), 1,534 statin users were 1:4 matched with 6,136 non-users. Primary and secondary outcome were defined as overall survival (OS) and progression-free survival (PFS), respectively. Multivariate cox regression analyses were performed to identify the risk factors associated with survival outcome.

Results: Statin use improved both OS (Hazard ratio [HR] = 0.77, 95% Confidence interval [CI] = 0.72–0.82; $p < 0.0001$) and PFS (HR = 0.78, 95% CI = 0.74–0.84, $p < 0.0001$). Regarding the timing of statin use, continuous statin use without interruption from before TKI treatment (HR = 0.87, 95% CI = 0.80–0.95; $p = 0.0016$), post-TKI statin use (HR = 0.87, 95% CI = 0.80–0.95; $p < 0.0001$) significantly improved OS, while pre-TKIs statin use but stop after TKI prescription (HR = 1.33, 95% CI = 1.14–1.54; $p = 0.0002$) was independent risk factor of poor OS. Lipophilic statin use improved OS (HR = 0.75, 95% CI = 0.69–0.81, $p < 0.0001$) and PFS (HR = 0.74, 95% CI = 0.69–0.80, $p < 0.0001$). Hydrophilic statin use also improved OS (HR = 0.59, 95% CI = 0.53–0.66, $p < 0.0001$) and PFS (HR = 0.63, 95% CI = 0.57–0.69, $p < 0.0001$). 730 or higher cDDD of statin use was significantly associated with greater survival outcome.

Conclusion: In a nation-wide retrospective study, statin offered substantial survival benefit for overall death and tumor progression in dose and duration dependent manner, upon co-administration with the TKIs in patients with advanced HCC. Our study emphasizes the importance of continuous statin administration without interruption even after the TKI treatment.

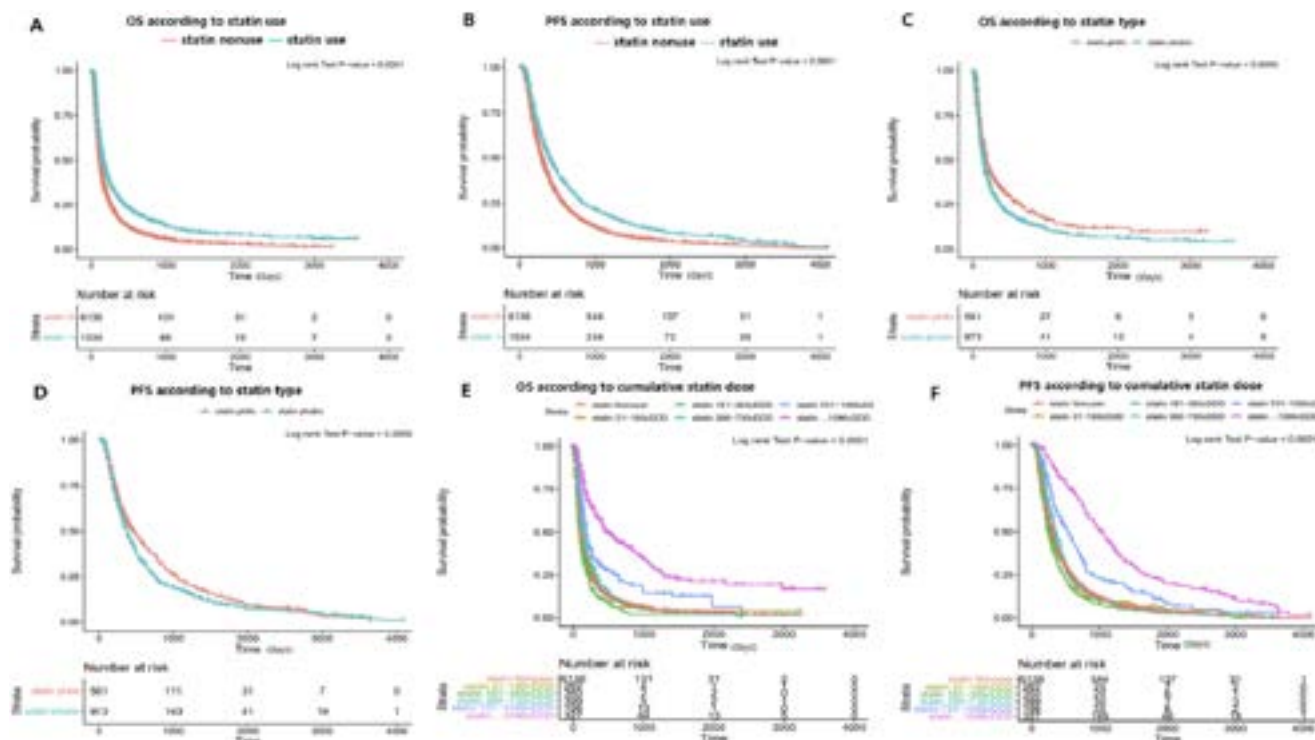


Figure: (abstract: TOP-071): Comparison of OS and PFS according to statin use, statin type and cumulative statin dose through Kaplan-Meier analysis in the entire PS-matched cohort

THURSDAY 22 JUNE

THU-113

Prediction for gastrointestinal bleeding in patients receiving atezolizumab and bevacizumab for hepatocellular carcinoma

Kanghee Park¹, Euichang Kim¹, Ji won Yang¹, Won-Mook Choi¹, Danbi Lee¹, Ju Hyun Shim¹, Kang Mo Kim¹, Young-Suk Lim¹, Han Chu Lee¹, Jonggi Choi¹. ¹Asan Medical Center, Korea, Rep. of South
Email: jkchoi0803@gmail.com.

Background and aims: The IMbrave 150 phase 3 trial did not include patients with a variceal bleeding history or a high-risk varix. Little is known regarding the actual risk of gastrointestinal bleeding (GIB) in hepatocellular carcinoma (HCC) patients receiving atezolizumab with bevacizumab (A/B). Therefore, we sought factors associated with GIB in these patients.

Method: We performed a retrospective analysis of 321 HCC patients who underwent endoscopy prior to A/B treatment at Asan Medical Center, Seoul, Republic of Korea between 2018 and 2022. GIB was defined as documented hematemesis, melena, or hematochezia, or performing endoscopic hemostasis between the start of A/B treatment and 3 months following the last dose of A/B treatment. Using multivariable logistic regression analysis, GIB-associated factors were sought. A prediction model was developed based on this multivariable analysis. Our model's performance was displayed as the area under the receiver operating curve (AUROC).

Results: The median age was 60.9 years, and 82.6% of the patients were male. At the time of A/B treatment, 29 (9.0%) and 292 (91.0%) patients were in BCLC stage of B and C, respectively. Of the 321 patients, 287 (89.4%) patients were classified as Child-Pugh class A. A total of 20 patients experienced GIB with a median onset of 3.0 months after the first dose of A/B. Cumulative incidence rates of GIB at 3, 6, 9, and 12 months were 3.2%, 7.3%, 8.0%, 9.6%, respectively. No patient died because of GIB. Variceal bleeding was the most common cause of GIB in 12 (60.0%) patients, followed by unknown origin of GIB (n = 6), and benign gastric ulcer (n = 2). Platelet count <100,000/mm³, prothrombin time (PT) with INR ≥1.3, portal vein invasion (PVI), and endoscopic variceal categorization ≥F2 were significantly associated with an increased risk of GIB in multivariable analysis. Risk scores were assigned to platelet <100,000 (1 point), PT INR ≥1.3 (1 point), PVI (1 point), and EV ≥F2 (3 points). Our prediction model had an AUROC of 0.839 (95% confidence interval: 0.765–0.914). Patients categorized as low (0–1 points), intermediate (2–3 points), and high-risk group (≥4 points) showed an estimated risk of GIB of 1–2%, 2–4%, and 5–11%, respectively, after receiving A/B treatment.

Factors	score	Applying the prediction model			
		Group	Range of estimated GIB risk	Score	Estimated GIB risk
Platelet <100,000	1	Low	1-2%	0	1.1%
Prothrombin time, INR ≥1.3	1			1	1.7%
Portal vein invasion	1	Intermediate	2-4%	2	2.5%
				3	3.6%
Esophageal varix ≥F2	3	High	5-11%	4	5.3%
				5	7.7%
				6	11.1%

Figure:

Conclusion: Factors associated with GIB after A/B treatment for HCC were lower platelet, prolonged PT, PVI, and EV ≥F2 by endoscopic findings. Our prediction model has a high predictive performance when estimating the real GIB risk following A/B treatment in patients with advanced HCC.

THU-114

Quality of life in patients with unresectable hepatocellular carcinoma treated with selective internal radiation therapy (SIRT) and nivolumab: a sub-analysis of the NASIR-HCC trial

Manuel de la Torre¹, Ana Matilla², Maria Varela³, Mercedes Iñarrairaegui¹, María Reig^{4,5}, José Luis Lledó^{5,6}, Juan Ignacio Arenas Ruiz-Tapiador⁷, Sara Lorente Perez⁸, Milagros Testillano⁹, Laura Marquez Perez¹⁰, Gemma Iserte⁴, Josep Maria Argemi^{1,5}, Carlos Gomez-Martin¹¹, Macarena Rodriguez-Fraile¹², Jose Ignacio Bilbao¹³, Ion Agirrezabal¹⁴, Bruno Sangro^{1,5}. ¹Clinica Universidad de Navarra, Liver Unit, Spain; ²Hospital universitario Gregorio Marañón, Liver unit and gastroenterology, Spain; ³Hospital Universitario Central de Asturias, Liver Unit, Spain; ⁴Hospital Clinic, Barcelona, Liver Oncology Unit, Liver Unit, ICMDM, Spain; ⁵Centro de Investigación Biomédica en Red de Enfermedades Hepáticas y Digestivas (CIBEREHD), Spain; ⁶Hospital universitario Ramón y Cajal, Liver unit and gastroenterology, Spain; ⁷Hospital Universitario Donostia, Liver unit and gastroenterology, Spain; ⁸Hospital Clinico Universitario Lozano Blesa, Liver Unit, Spain; ⁹Hospital universitario de Cruces, Spain; ¹⁰Hospital universitario Gregorio Marañón, Spain; ¹¹Hospital Universitario 12 de Octubre, Spain; ¹²Clinica Universidad de Navarra, Nuclear Medicine department, Spain; ¹³Clinica Universidad de Navarra, Interventional Radiologist service, Spain; ¹⁴Sirtex Medical Europe GmbH., Spain
Email: bsangro@unav.es.

Background and aims: Patient reported outcomes (PRO) are increasingly recognized as key end points in clinical trials in addition to safety and efficacy. The aim of this study was to assess health related quality of life (HRQoL) of patients with unresectable hepatocellular carcinoma (uHCC) during treatment with SIRT and the anti-programmed cell death-1 (PD1) agent nivolumab.

Method: NASIR-HCC is a single-arm, multicenter, phase 2 trial (NCT03380130) that recruited patients with uHCC free from distant metastasis but not good candidates for chemoembolization. Patients with large single tumors, multinodular disease or predominantly unilobar tumors with segmental or lobar portal vein invasion were treated with SIRT using SIR-Spheres resin microspheres followed 3 weeks later by 240 mg of nivolumab given every 2 weeks until 24 doses, disease progression or unacceptable toxicity. HRQoL was assessed as an exploratory end point using EQ-5D-3L, the 3-level version of EQ-5D, and the FACT-Hep questionnaires at baseline and at day 1 of every treatment cycle thereafter (every 6 weeks, approximately) and during follow-up. Analyses were performed of all patients with a valid baseline assessment and at least one other post-baseline assessment and were limited to the treatment period of 8 cycles. Thresholds for clinically meaningful change were prespecified based on published minimal important differences (MIDs). Time to deterioration (TTD) was evaluated for all HRQoL scores and was defined as the time from treatment initiation to the first date of a worsening meeting or exceeding the MID.

Results: 42 patients received SIRT and 10 patients with no baseline measurement or only one measurement were excluded from the analyses. PRO analysis population therefore included 32 patients. At most timepoints (62%) completion rates were above 70%, the expected threshold for meaningful interpretation, and in 98% it was above 60%. All FACT-Hep scores remained within the limits established by MIDs over the time frame analysed, with only a clinically meaningful decline in social well-being. A statistically significant decrease in scores that did not reach the MIDs was observed for physical well being, FACT-General total and FACT-Hep total scores. EQ5D utility index score showed a slight decline (mean change per cycle, -0.011, p < 0.05) while EQ5D VAS remained stable (mean change per cycle, -0.102, p = 0.778). The inclusion of age and ECOG as covariates for adjustment did not have a substantial impact on results. Median TTD in FACT-Hep Total Score was 5.5 months (95% CI 5.5-NR) while median TTD in HCS was not reached.

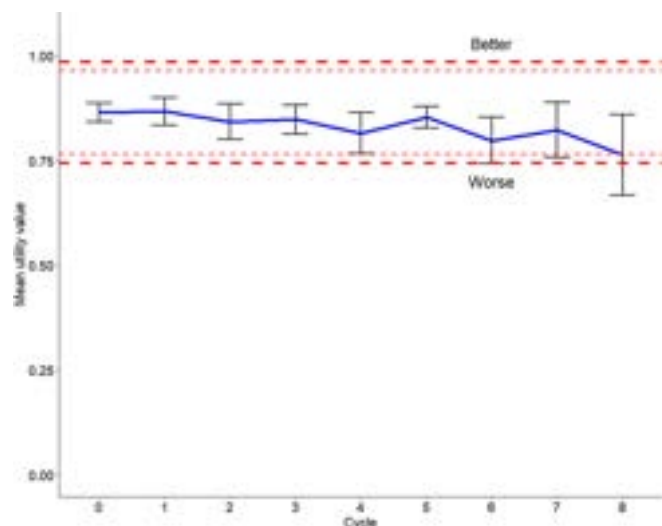


Figure 1: EQ5D VAS.

Conclusion: No clinically meaningful decline in HRQoL was observed in the vast majority of evaluable time points during treatment with nivolumab following SIRT. This combination does not compromise quality of life for this difficult-to-treat population of patients with uHCC.

THU-115

Impact of baseline liver function on overall survival (OS) and safety in patients (pts) with unresectable hepatocellular carcinoma (HCC) treated with first-line (1L) tislelizumab (TIS): results from the RATIONALE-301 study

Masatoshi Kudo¹, Arndt Vogel², Tim Meyer³, Frederic Boissier⁴, Songzi Li⁵, Ramil Abdrashitov⁶, Yaxi Chen⁷, Andrew X. Zhu^{8,9}, Shukui Qin¹⁰, Richard S. Finn¹¹. ¹Kindai University Faculty of Medicine, Department of Gastroenterology and Hepatology, Osaka, Japan; ²Hannover Medical School, Department of Gastroenterology, Hepatology and Endocrinology, Hannover, Germany; ³Royal Free Hospital NHS Trust and University College London, Academic Department of Oncology, London, United Kingdom; ⁴BeiGene Ltd., Ridgefield Park, Clinical Science, NJ, United States; ⁵BeiGene Ltd., Ridgefield Park, Biometrics, NJ, United States; ⁶BeiGene USA, Inc., Clinical Development, Fulton, MD, United States; ⁷BeiGene (Beijing) Co., Ltd., Clinical Development, Beijing, China; ⁸Jiahui Health, Jiahui International Cancer Center, Shanghai, China; ⁹Harvard Medical School, Massachusetts General Hospital, MA, United States; ¹⁰Cancer Center of General Hospital of Eastern Theater of PLA, Nanjing, China; ¹¹Geffen School of Medicine, University of California Los Angeles, Department of Medicine, Division of Hematology/Oncology, Los Angeles, CA, United States
Email: m-kudo@med.kindai.ac.jp.

Background and aims: TIS is a monoclonal antibody with high binding affinity to programmed cell death protein 1. The phase 3

RATIONALE-301 study (NCT03412773) demonstrated non-inferior OS with TIS versus sorafenib (SOR) (median [m] OS 15.9 vs 14.1 months [mo], respectively; HR: 0.85 [95% CI: 0.71, 1.02]) in 1L treatment of pts with unresectable HCC; OS superiority versus SOR was not met. As liver function is a known predictor of survival in pts with HCC, we evaluated baseline liver function and its impact on OS and safety in pts enrolled in RATIONALE-301.

Method: Systemic therapy-naïve adults with histologically confirmed HCC were randomized (1:1) to receive TIS (200 mg intravenously every 3 weeks) or SOR (400 mg orally twice daily) until disease progression, intolerable toxicity, or withdrawal. The primary end point was OS. In this exploratory analysis, OS and safety were assessed by Child-Pugh score (CPS; 5 vs 6) and albumin-bilirubin (ALBI) grade (1 vs 2).

Results: In pts randomized to TIS (n = 342), at baseline, 76.9% and 22.5% had a CPS of 5 and 6, respectively, and 74.9% and 23.7% had an ALBI grade of 1 and 2, respectively. In pts randomized to SOR (n = 332), 74.7% and 25.3% had a CPS of 5 and 6, respectively, and 68.1% and 29.5% had an ALBI grade 1 and 2, respectively. At data cutoff (July 11, 2022; minimum study follow-up 33 mo), mOS was similar in pts treated with TIS and SOR, and numerically longer in pts with CPS 5 vs 6, and ALBI grade 1 vs 2, regardless of treatment arm (Table). Incidence of any grade and grade ≥3 treatment-emergent adverse events (TEAEs) and treatment-related adverse events (TRAEs) were lower in pts treated with TIS versus SOR across CPS and ALBI grades (Table).

Conclusion: Survival was similar between arms, and TIS showed a favorable safety profile compared with SOR, regardless of CPS or ALBI grade, supporting the primary analysis. Pts with CPS 6 and ALBI grade 2 had poorer mOS than those with CPS 5 and ALBI grade 1, regardless of treatment arm, affirming that pts with better liver function have improved outcomes.

Table (abstract: THU-115).

	CPS 5		CPS 6		ALBI grade 1		ALBI grade 2	
Efficacy*	TIS (n = 263)	SOR (n = 248)	TIS (n = 77)	SOR (n = 84)	TIS (n = 256)	SOR (n = 226)	TIS (n = 81)	SOR (n = 98)
Median OS, mo (95 % CI)	19.5 (15.4, 23.5)	18.4 (14.5, 20.9)	8.7 (6.2, 12.3)	8.3 (5.6, 10.0)	19.9 (15.9, 24.2)	16.9 (13.7, 19.8)	9.5 (7.3, 10.8)	9.1 (6.2, 13.1)
Unstratified HR (95 % CI)	0.88 (0.71, 1.08)		0.73 (0.52, 1.03)		0.85 (0.69, 1.06)		0.83 (0.60, 1.14)	
Safety, n (%)†	TIS (n = 261)	SOR (n = 243)	TIS (n = 75)	SOR (n = 81)	TIS (n = 256)	SOR (n = 226)	TIS (n = 81)	SOR (n = 98)
TEAE any grade	251 (96.2)	243 (100)	72 (96.0)	81 (100)	244 (95.3)	226 (100)	80 (98.8)	98 (100)
TEAE grade ≥3	120 (46.0)	155 (63.8)	42 (56.0)	57 (70.4)	113 (44.1)	145 (64.2)	49 (60.5)	67 (68.4)
TRAE any grade	194 (74.3)	238 (97.9)	63 (84.0)	73 (90.1)	194 (75.8)	218 (96.5)	65 (80.2)	93 (94.9)
TRAE grade ≥3	56 (21.5)	131 (53.9)	18 (24.0)	42 (51.9)	46 (18.0)	121 (53.5)	29 (35.8)	52 (53.1)

*Efficacy analysis set;

†Safety analysis set.

THU-116

The ALBI grade refines prognostic prediction in advanced hepatocellular cancer and enables risk stratification for bleeding events following atezolizumab plus bevacizumab

Antonio D'Alessio^{1,2}, Claudia Fulgenzi^{1,3}, Bernhard Scheiner^{1,4}, James Korolewicz¹, Jaekyung Cheon⁵, Naoshi Nishida⁶, Celina Ang⁷, Thomas Marron⁷, Linda Wu⁷, Anwaar Saeed⁸, Brooke Wietharn⁹, Antonella Cammarota^{10,11}, Tiziana Pressiani¹², Matthias Pinter⁴, Lorenz Balcar⁴, Yi-Hsiang Huang¹³, Aman Mehan¹, Samuel Phen¹⁴, Caterina Vivaldi¹⁵, Francesca Salani^{15,16}, Gianluca Masi¹⁵, Dominik Bettinger¹⁷, Arndt Vogel¹⁸, Martin Schoenlein¹⁹, Johann von Felden²⁰, Kornelius Schulze²⁰, Henning Wege²⁰, Adel Samson²¹, Peter Galle²², Masatoshi Kudo⁶, Alessio Cortellini^{1,3}, Amit Singal¹⁴, Lorenza Rimassa^{10,12}, Rohini Sharma¹, Hong Jae Chon⁵, David J. Pinato^{1,2}. ¹Imperial College London, Department of Surgery and Cancer, London, United Kingdom; ²University of Piemonte Orientale, Department of Translational Medicine, Novara, Italy; ³Division of Medical Oncology, Policlinico Universitario Campus Bio-Medico, Rome, Italy; ⁴Division of Gastroenterology and Hepatology, Department of Internal Medicine III, Medical University of Vienna, Vienna, Austria, Austria; ⁵Medical Oncology, Department of Internal Medicine, CHA Bundang Medical Center, CHA University, Seongnam, Korea, Korea, Rep. of South; ⁶Department of Gastroenterology and Hepatology, Kindai University Faculty of Medicine, Osaka, Japan; ⁷Department of Medicine, Division of Hematology/Oncology, Tisch Cancer Institute, Mount Sinai Hospital, New York, NY, USA, United States; ⁸Division of Hematology/Oncology, Department of Medicine, University of Pittsburgh (UPMC), USA, United States; ⁹Department of Medicine, Division of Medical Oncology, Kansas University Cancer Center, Kansas City, Kansas, USA, United States; ¹⁰Department of Biomedical Sciences, Humanitas University, Via Rita Levi Montalcini 4, 20072 Pieve Emanuele, Milan, Italy; ¹¹Drug Development Unit, Sarah Cannon Research Institute UK, London, United Kingdom; ¹²Medical Oncology and Hematology Unit, IRCCS Humanitas Research Hospital, Rozzano (Milan), Italy; ¹³Division of Gastroenterology and Hepatology, Department of Medicine, Taipei Veterans General Hospital, Taipei, Taiwan; Institute of Clinical Medicine, National Yang Ming Chiao Tung University School of Medicine, Taipei, Taiwan; ¹⁴University of Texas Southwestern Medical Center, Dallas, Texas, USA, United States; ¹⁵Department of Translational Research and New Technologies in Medicine and Surgery, University of Pisa, Pisa, Italy; Unit of Medical Oncology 2, Azienda Ospedaliero-Universitaria Pisana, Pisa, Italy; ¹⁶Sant'Anna School of Advanced Studies, Pisa, Italy; ¹⁷Department of Medicine II (Gastroenterology, Hepatology, Endocrinology and Infectious Diseases), Freiburg University Medical Center, Faculty of Medicine, University of Freiburg, Freiburg, Germany; ¹⁸Hannover Medical School, Hannover, Germany; ¹⁹Department of Oncology, Hematology and Bone Marrow Transplantation with Section of Pneumology, University Medical Center Hamburg-Eppendorf, Hamburg, Germany; ²⁰Department of Gastroenterology and Hepatology, University Medical Center Hamburg-Eppendorf, Hamburg, Germany; ²¹Leeds Institute of Medical Research at St James's (LIMR), School of Medicine, Faculty of Medicine and Health, University of Leeds, St James's University Hospital, Leeds, United Kingdom; ²²University Medical Center Mainz, I. Dept. of Internal Medicine, Mainz, Germany
Email: david.pinato@imperial.ac.uk.

Background and aims: The combination of atezolizumab plus bevacizumab (A+B) is the current standard of care for Child-Pugh A (CP-A) unresectable or metastatic hepatocellular carcinoma (HCC) and is being evaluated in CP-B patients. Whilst highly effective, A+B can lead to potentially life-threatening adverse events (AEs), including bleeding. We investigated whether liver dysfunction as measured by the albumin-bilirubin (ALBI) grade is associated with survival and adverse events (AEs) following A+B.

Method: We performed a multi-centre, retrospective study on patients consecutively treated with A+B in 15 tertiary referral centres. Patients exposed to systemic treatments or Child-Pugh (CP) C liver function were excluded. We correlated baseline ALBI grade

with overall survival (OS) and progression-free survival (PFS) with the Kaplan-Meier method and we estimated predictors of survival with the Cox regression model. We assessed the predictive value for 6-months OS landmark with ROC curves. Association with treatment-related (tr)AEs was assessed with the χ^2 test.

Results: From the initial cohort of 433 patients, 368 were included in the analysis, mostly with underlying viral hepatitis (37.5% HBV, 24.2% HCV) and a diagnosis of cirrhosis (78.8%). 295 patients (80.2%) were in CP-A functional class and 73 (19.8%) CP-B. 163 patients (44.3%) were graded as ALBI 1, 192 (52.2%) ALBI 2, and 13 (3.5%) ALBI 3. After a median follow-up of 9.7 months (95% CI, 9.2–10.3), ALBI 1 patients did not reach a median OS (mOS), ALBI 2 achieved a mOS of 9.7 months (95% CI, 6.98–12.29) compared to 5.6 months of ALBI 3 (95% CI, 0.1–12.0, $p < 0.001$, Fig. 1). Similarly, ALBI grade was associated with improved mPFS: 8.1 months (95% CI, 6.0–10.2) for ALBI 1, 4.5 months (95% CI, 3.7–5.3) for ALBI 2, and 1.2 months (95% CI, 0.1–3.6) for ALBI 3 patients ($p < 0.001$). ALBI was independently associated with OS and PFS in multivariable models ($p < 0.001$) and outranked CP for 6-months OS prediction, with an area under the curve of 0.79 (95% CI, 0.73–0.85) for ALBI score and 0.71 (95% CI, 0.63–0.78) for CP score ($p = 0.013$). Whilst rates of bevacizumab-related gastrointestinal bleeding events of any grade were similar according to CP class (6.8% in CP-A vs 8.2% in CP-B, $p = 0.67$), pre-treatment ALBI was associated with a 3-fold increase in risk of bleeding (3.1% in ALBI 1 vs 10.2% in ALBI 2/3, $p = 0.008$). Neither ALBI grade nor CP score were associated with atezolizumab-related AEs. At treatment discontinuation ($n = 252$, 68.5%) all patients were either ALBI 2 or 3. ALBI score predicted for worse OS after discontinuing A+B, with ALBI 2 patients achieving a post-treatment mOS of 6.8 months (95% CI, 4.4–9.2) while ALBI 3 reached 1.6 months (95% CI, 0.6–2.7, $p < 0.001$).

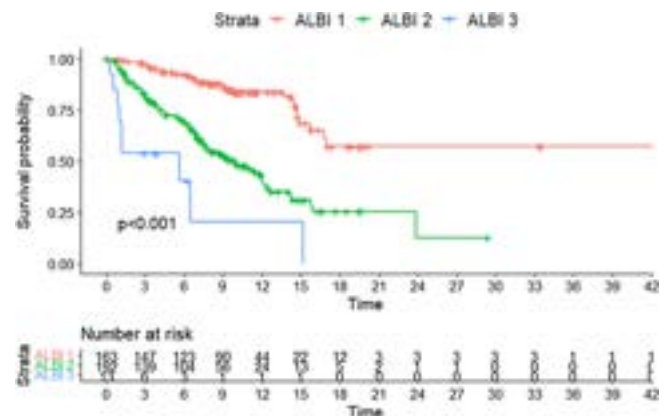


Figure:

Conclusion: ALBI grade identifies a subset of patients with higher probability of achieving an improved survival. Further studies should validate the role of ALBI as a predictor of bleeding events following A+B.

THU-117

Dipeptidyl-peptidase 4 inhibitors improve survival of patients with diabetes mellitus and hepatocellular carcinoma receiving immunotherapy

Dorothy Cheuk-Yan Yiu^{1,2}, Huapeng Lin^{1,2}, Terry Cheuk-Fung Yip^{1,2}, Mandy Sze-Man Lai^{1,2}, Vincent Wai-Sun Wong^{1,2}, Ken Liu³, Grace Lai-Hung Wong^{1,2}. ¹The Chinese University of Hong Kong, Medical Data Analytics Centre, Hong Kong; ²The Chinese University of Hong Kong, Department of Medicine and Therapeutics, Hong Kong; ³Royal Prince Alfred Hospital, AW Morrow Gastroenterology and Liver Centre, Sydney, Australia
Email: wonglaihung@cuhk.edu.hk.

Background and aims: Preclinical studies suggest that dipeptidyl-peptidase 4 inhibitors (DPP4i) improve anti-tumor immunity in

POSTER PRESENTATIONS

hepatocellular carcinoma (HCC). By enhancing intrahepatic inflammatory cell infiltration, DPP4i may enhance response to immunotherapy regimens. This study aimed to investigate the impact of dipeptidyl-peptidase 4 inhibitors (DPP4i) on survival of patients who had advanced HCC undergoing immunotherapy in a real-world setting.

Method: This was a multi-center retrospective cohort study in Hong Kong and Australia. All patients with advanced HCC who had received at least one dose of immunotherapy were identified. Clinical, biochemical and medication data were collected and analyzed. The primary outcome was overall survival. The analysis was performed using Cox proportional hazards models.

Results: Among 451 patients with advanced HCC on immunotherapy, the mean age was 62.3 ± 12.4 years old. The cohort was predominantly male ($n = 373$, 82.7%) and the main etiology of HCC was chronic viral hepatitis ($n = 331$, 78.1%). 169 (37.5%) patients had diabetes and of which, 38 (22.5%) were treated with DPP4i. In diabetic patients, DPP4i use was associated with better survival (hazard ratio [HR] = 0.60 [95% CI 0.38–0.95], $p = 0.029$) in univariate analysis. After adjusting for patient demographics (age, sex) and pathologic variables (HCC etiology, albumin-bilirubin [ALBI]-grade, alpha-fetoprotein, platelets, alanine aminotransferase), the survival advantage of DPP4i remained similar in patients with diabetes (HR = 0.57 [0.35–0.92], $p = 0.022$). Within 23 DPP4i users who died, 17 (73.9%) died of cancer, 1 (4.3%) died of sepsis and 1 (4.3%) died of pneumonia.

Table 1. Univariate and multivariable analyses on the association between dipeptidyl-peptidase 4 inhibitor use and overall survival in all patients and diabetes subgroup.

	No. of subjects	Univariate analysis		Multivariable model 1		Multivariable model 2	
		HR (95% CI)	p	Adjusted HR (95% CI)	p	Adjusted HR (95% CI)	p
DPP4i use in all patients	451	0.75 (0.49–1.14)	0.177	0.72 (0.47–1.12)	0.148	0.70 (0.44–1.09)	0.110
DPP4i use in diabetes subgroup	169	0.60 (0.38–0.95)	0.029	0.60 (0.37–0.95)	0.031	0.57 (0.35–0.92)	0.022

Multivariable model 1: adjusted for age, sex, HCC etiology (viral vs non-viral cause)

Multivariable model 2: adjusted for age, sex, HCC etiology, ALBI-grade, alpha-fetoprotein, platelet, alanine aminotransferase

CI = confidence interval, HR = hazard ratio, ALBI = Albumin-Bilirubin.

Figure:

Conclusion: The use of DPP4i is associated with improved survival in diabetic HCC patients receiving immunotherapy. The findings should be further validated in prospective studies with larger sample sizes.

THU-118

Application of deep learning auto-segmentation and unsupervised machine learning in developing a radiomic prognostic score to predict disease recurrence post radiofrequency ablation for hepatocellular carcinoma

Mathew Vithayathil¹, Akshayaa Vaidyanathan^{2,3}, Osman Ocal⁴, Matthias Fabritius⁴, Maciej Pech⁵, Thomas Berg⁶, Christian Loewe⁷, Heinz-Josef Klumpen⁸, Andrea Rockall¹, Henry Woodruff², Max Seidensticker⁴, Eric Aboagye¹, Jens Ricke⁴, Rohini Sharma¹.

¹Imperial College London, Department of Surgery and Cancer, United Kingdom; ²Maastricht University, The D-Lab, Maastricht, Netherlands;

³Radiomics, Luik, Belgium; ⁴Ludwig Maximilian University of Munich, Department of Radiology, München, Germany; ⁵Otto-von-Guericke-University Magdeburg, Department of Radiology and Nuclear Medicine, Magdeburg, Germany;

⁶Universitätsklinikum Leipzig, Klinik und Poliklinik für Gastroenterologie, Sektion Hepatologie, Leipzig, Germany; ⁷Medical University of Vienna, Section of Cardiovascular and Interventional Radiology, Department of Bioimaging and Image-Guided Therapy, Wien, Austria; ⁸University of Amsterdam, Department of Medical Oncology, Amsterdam University Medical Centers, Amsterdam, Netherlands

Email: mathew.vithayathil@doctors.org.uk.

Background and aims: Disease recurrence after radiofrequency ablation (RFA) for hepatocellular carcinoma (HCC) is 60–85% at five years. Radiological features within the HCC and background liver may predict risk of reoccurrence. Through using a combination of deep-learning (DL) and machine-learning (ML) we developed a radiomic

prognostic score to predict disease recurrence in patients undergoing RFA.

Methods: Patients undergoing RFA with or without sorafenib as part of the SORAMIC trial across 12 centers were included. An auto-segmentation tool for whole liver area was developed using DL on post-contrast hepatobiliary MRI sequences, and visually verified by experienced radiologists. Voxel resampling and intensity normalization was applied to segmented areas. 666 radiomic features were extracted using previously validated software (TexLAB 2.0). Least absolute shrinkage and selection operator (LASSO) Cox regression identified radiomic features and coefficients to construct the radiomic prognostic vector (RPV). RPV was evaluated for predicting time-to-recurrence (TTR) in Kaplan-Meier and Cox regression survival analysis.

Results: DL-derived auto-segmentation was applied to pretreatment MRIs in 79 patients undergoing RFA. Four radiomic features were identified from LASSO Cox regression to form the RPV score. Three RPV-associated clusters were identified using unsupervised k-means clustering. Kaplan-Meier survival analysis demonstrated these clusters correlated with low- (median TTR 54.3 months; 95% confidence interval [29.5–*]) medium- (median TTR 20.8 months; 95% CI [8.8–36.6]; log rank cf. low risk $p < 0.005$) and high- risk (median TTR 10.8 months; 95% CI [4.5–20.7]; $p < 0.005$) of HCC reoccurrence (Figure 1). In a multivariate Cox regression model including age, Barcelona Clinic Liver Cancer stage and adjuvant sorafenib, RPV was significant in predicting recurrence (Hazard ratio 3.08 [1.94–4.88]; $p = < 0.005$).

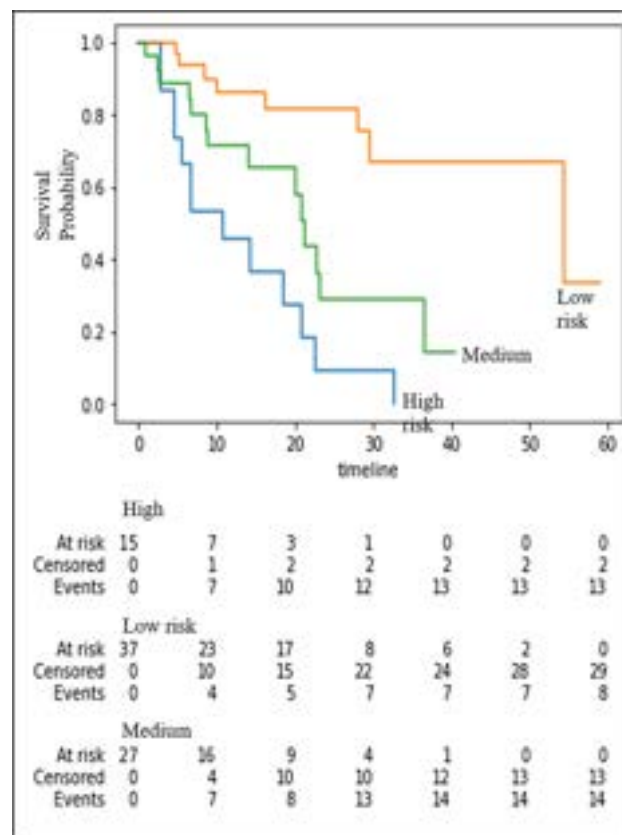


Figure: Kaplan-Meier curves for time-to-recurrence post radiofrequency ablation of HCC for clusters derived from k-means unsupervised learning for radiomic prognostic vectors

Conclusion: DL derived auto-segmentation in combination with pretreatment radiomic feature extraction from whole liver imaging can predict disease recurrence in HCC patients post RFA. Radiomic scores can be used to stratify high-risk patients for post treatment surveillance.

THU-119

Atezolizumab and bevacizumab for non-resectable or metastatic combined hepatocellular-cholangiocarcinoma: a multicentric retrospective study

Elia Gigante¹, Mohamed Bouattour², José Ursic Bedoya³, Helene Regnault⁴, Marianne Zioli⁵, Eric Assenat⁶, Valérie Paradis⁷, Julien Calderaro⁸, Nathalie Ganne-Carrié⁹, Karine Bouhier Leporrier¹⁰, Giuliana Amadeo⁴, Jean Charles Nault⁹.
¹Hôpital Robert Debré et Université Reims-Champagne-Ardenne, Service d'Hépatogastroentérologie et de Cancérologie digestive, Reims, France; ²Hôpital Beaujon AP-HP, Service d'Hépatologie, unité d'onco-hépatologie, Clichy, France; ³University Hospital Center Saint Eloi Hospital, service d'Hépatogastro-entérologie, Montpellier, France; ⁴Henri-Mondor University Hospital, Service d'Hépatologie, Créteil, France; ⁵Avicenne Hospital (AP-HP), département de Pathologie, Bobigny, France; ⁶University Hospital Center Saint Eloi Hospital, service d'oncologie médicale, Montpellier, France; ⁷Hôpital Beaujon AP-HP, département de Pathologie, Clichy, France; ⁸Henri-Mondor University Hospital, département de Pathologie, Créteil, France; ⁹Avicenne Hospital (AP-HP), Service d'Hépatologie, Bobigny, France; ¹⁰Chu Caen Normandie, Hépatogastro-entérologie et nutrition, Caen, France
 Email: elia.gigante@hotmail.it.

Background and aims: The efficacy of atezolizumab/bevacizumab (AB) had never been reported in patients with metastatic/unresectable combined hepatocellular carcinoma-cholangiocarcinoma (cHCC-CCA). Therefore, the purpose of our study is to describe the effects of atezolizumab/bevacizumab treatment in patients with advanced cHCC-CCA.

Method: We retrospectively included patients with a histological diagnosis of unresectable/metastatic cHCC-CCA and treated by AB (2020 to 2022) in 7 centers. Clinical, and radiological features were collected at the beginning of AB. We reported radiological response using RECIST criteria and overall survival and progression-free survival.

Results: Sixteen patients with cHCC-CCA were included and were predominantly male (75%) with advanced fibrosis/cirrhosis (69%). Nine patients received AB as a first-line systemic treatment, 5 as a second line, one as a third line and one as a fifth line. Severe digestive bleeding occurred in two patients. Among the 9 patients treated in first-line, four experienced radiological progression, three partial response and one had stable disease. Patients treated with AB in first line had a median overall survival of 13 months and a median progression-free survival of 3 months (Figure 1). Among the 7 patients receiving AB as a second line or more, 4 patients harbored a stable disease, two a partial response, and one a progressive disease.

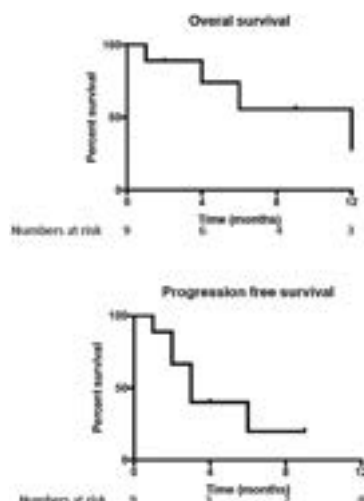


Figure: Overall survival and progression-free survival in patients treated by atezolizumab/bevacizumab as a first line systemic treatment

Overall survival and progression-free survival were represented using Kaplan-Meier curve with the number at risk under the X axis. The median overall survival was 13 months. The median progression-free survival was 3 months.

Conclusion: The combination of atezolizumab and bevacizumab showed signs of anti-tumor efficacy in patients with unresectable/metastatic cHCC-CCA.

THU-120

Fragility index of positive phase 2 and 3 randomized clinical trials of treatment of hepatocellular carcinoma (2002–2022)

Sabrina Sidali^{1,2}, Nanthara Sritharan³, Claudia Campani², Jules Grégory^{4,5}, Francois Durand⁶, Nathalie Ganne^{2,7,8}, Maxime Ronot^{4,9}, Vincent Lévy^{10,11}, Jean Charles Nault^{2,7,7,8}.
¹Université de Paris, Service d'Hépatologie, DMU DIGEST, Hôpital Beaujon, APHP Nord, Clichy, France; ²Centre de Recherche des Cordeliers, Sorbonne Université, Inserm, Université de Paris, team « Functional Genomics of Solid Tumors », Equipe labellisée Ligue Nationale Contre le Cancer, Labex Oncolimmunology, F-75006 Paris, France; ³Department of Clinical Research, Paris Seine Saint Denis Hospital, Sorbonne Paris University, Bobigny, France; ⁴Department of Radiology, FHU MOSAIC, Hôpital Beaujon APHP Nord, Clichy, France; ⁵Université de Paris, INSERM, UMR1153, Epidemiology and Biostatistics Sorbonne Paris Cité Center (CRESS), METHODS Team, Paris, France; ⁶Université de Paris, Service d'Hépatologie, DMU DIGEST, Hôpital Beaujon, APHP Nord, Clichy, France; ⁷Liver unit, Hôpital Avicenne, Hôpitaux Universitaires Paris-Seine-Saint-Denis, Assistance-Publique Hôpitaux de Paris, Bobigny, France; ⁸Unité de Formation et de Recherche Santé Médecine et Biologie Humaine, Université Sorbonne Paris nord, Bobigny, France; ⁹Université de Paris, INSERM U1149 "Centre de Recherche sur l'inflammation", CRI, Paris, France; ¹⁰Department of Clinical Research, Paris Seine Saint Denis Hospital, Sorbonne Paris University, AP HP, Bobigny, France; ¹¹ECSTRRA team, CRESS UMR 1153, Hôpital Saint-Louis, APHP, Paris, France
 Email: sidali.sabrina@gmail.com.

Background and aims: The fragility index (FI), i.e., the minimum number of best survivors reassigned to the control group required to revert the statistically significant result of a clinical trial to non-significant, has been developed as a metric to evaluate the robustness of randomized, controlled trials (RCTs). We aimed to assess the FI in the field of HCC.

Method: This is a retrospective analysis of phase 2 and 3 RCTs for the treatment of HCC published between 2002 and 2022. We included two-arm studies with 1:1 randomization and significant positive results for a primary time-to-event end point for the FI calculation, which involves the iterative addition of a best survivor (patients with the longest follow-up time, regardless of having an event or being censored) from the experimental group to the control group, until positive significance ($p < 0.05$, Log-rank test) is lost.

Results: We identified 51 phase 2 and 3 positive RCTs, of which 29 (57%) were eligible for fragility index calculation. After reconstruction of the Kaplan-Meier curves, 25/29 studies remained significant, among which the analysis was performed. The median (interquartile range (IQR)) FI was 5 (2–10) and Fragility Quotient (FQ) was 3% (1%–6%). Ten trials (40%) had a FI of 2 or less. FI was positively correlated to the blind assessment of the primary end point (median FI 9 with blind assessment versus 2 without, $p = 0.01$), the number of reported events in the control arm ($R_s = 0.45$, $p = 0.02$) and to impact factor ($R_s = 0.58$, $p = 0.003$), and negatively correlated to the p value ($R_s = -0.83$, $p < 0.0001$).

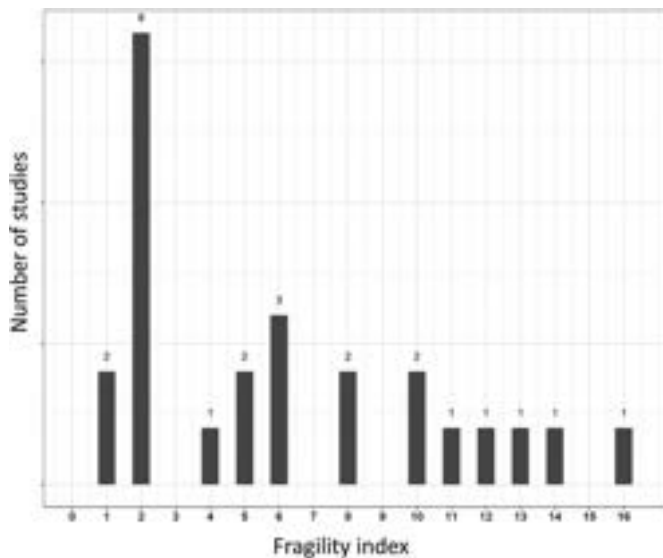


Figure: Distribution of Fragility index across studies (N = 25)

Conclusion: Several phases 2 and 3 RCTs in HCC have a low fragility index, underlying the limited robustness on the conclusion of their superiority over control treatments. The fragility index might provide an additional tool to assess the robustness of clinical trial data in HCC.

THU-121

Genomic characteristics of hepatocellular carcinoma patients with response to sorafenib

Sun Young Yim¹, Sang-Hee Kang¹, Young-Sun Lee¹, Yoonseok Lee¹, Ji-Hwan Lim¹, Tae Hyung Kim¹, Young Kul Jung¹, Yeon Seok Seo¹, Hyung Joon Yim¹, Jong Eun Yeon¹, Ju-Seog Lee², Ji Hoon Kim¹. ¹Korea University Hospital, Korea, Rep. of South; ²MD Anderson Cancer Center, United States
Email: kjhhepar@naver.com.

Background and aims: Sorafenib is a multiple receptor tyrosine kinase inhibitor which is the standard systemic therapy for advanced hepatocellular carcinoma (HCC). However, the objective response rate is low only reaching 10% and since there are other new 1st line treatment options such as lenvatinib and immune checkpoint inhibitors, biomarkers that may predict patients who will respond well to sorafenib is required. We implemented RNA sequencing (RNA-seq) in HCC tumors to identify potential biomarkers that would predict response to sorafenib and uncover underlying biological features associated with better response.

Method: A total of 33 patients who had undergone liver resection prior to sorafenib treatment were enrolled. Matched tumor/surrounding tumor tissues were obtained and RNA-seq was performed with the NextSeq500. Cluster analysis was performed and gene signature associated with sorafenib response was identified. The gene signature was validated in independent Sorafenib as Adjuvant Treatment in the Prevention Of Recurrence of Hepatocellular Carcinoma (STORM) cohort. Gene network analysis by Ingenuity Pathway Analysis (IPA) was performed to uncover activated pathways and key upstream regulators associated with response to sorafenib. The composition of infiltrated immune cells in tumors was also investigated by using the CIBERSORTx algorithm.

Results: The mean age was 58 ± 11 years with male predominance (81.8%), median child pugh score was 5 (range, 5–8) and 57.6% of the patients switched to second-line chemotherapy mostly due to HCC progression. The best response among 33 patients was complete response (CR) observed in 1 patient, partial response (PR) in two patients, stable disease (SD) in 12 patients while 18 patients showed disease progression. Gene signature (721 genes) associated with disease control (SD, PR, CR vs. no response) was derived using cluster analysis and was named as Korea University Sorafenib Response

(KUSOR) gene signature. When applied on STORM cohort, KUSOR gene signature was able to predict patients who do not recur on adjuvant setting of sorafenib treatment after HCC resection or ablation with sensitivity of 91% and specificity of 74%. Gene network analysis by IPA revealed that patients who showed disease control were characterized by IL-6 and IL-1 β activation. In contrast, MYC was more activated in HCC tumors showing no benefit of the treatment, suggesting that MYC may trigger resistance of HCC cells to sorafenib. In addition, regulatory T cells (Treg cells) and M2 macrophage fractions were significantly higher in poor response group while the fraction of activated NK cells and CD4 cells were substantially higher in disease control group.

Conclusion: Our study reveals that KUSOR gene signature was able to identify patients who would show disease control when treated with sorafenib. MYC promotes hepatocarcinogenesis in chronic liver disease and overexpression is associated with poor response. Furthermore, it can also be inferred that poor response to sorafenib could be related immune evasion through overexpression of Treg cells and M2 macrophages in tumor microenvironment. Our study is in accord with previous studies where patients with high MYC activation showed poor response to sorafenib indicating that combination therapy such as immune checkpoint blockade should be recommended for these patients.

THU-122

Efficacy and safety of atezolizumab and bevacizumab in the real-world treatment of Child Pugh B patients with advanced hepatocellular carcinoma

Leonardo Stella¹, Francesca Ponziani¹, Francesco Santopaolo¹, Clemence Hollande², Antonio Gasbarrini¹, Sabrina Sidali², Maurizio Pompili¹, Mohamed Bouattour². ¹IRCCS Policlinico Universitario Agostino Gemelli, Italy; ²APHP-Beaujon Hospital, France
Email: leonardo.dr.stella@gmail.com.

Background and aims: Immunotherapy has changed the prognosis and the treatment paradigm in patients with advanced HCC. Despite the lack of well-designed multicenter studies involving cirrhotic patients with reduced liver function, initial evidence suggests that treatment with atezolizumab plus bevacizumab can be safely administered in patients with Child Pugh B (CP-B) class.

Method: We conducted a 2-years multicenter retrospective study enrolling 132 patients with unresectable or metastatic HCC treated with atezolizumab plus bevacizumab as part of routine clinical care, after a multidisciplinary team evaluation. We evaluated the coprimary end points, more precisely overall survival (OS), progression-free survival (PFS, as assessed at an independent review facility according to Response Evaluation Criteria in Solid Tumors or RECIST 1.1), and decompensation-free survival (defined as “the length of time during and after the treatment, that a patient does not develop new cirrhosis complications”), in CP-B cirrhotic patients compared to CP-A patients. Then, safety has been analyzed as a secondary outcome in the same subgroups of patients.

Results: CP-B patients achieved a median OS of 6.2 months (95% CI 5.0–7.2), which was significantly worse than CP-A patients (HR 2.78, 95%CI 1.34–5.64; $p < 0.0001$). However, there wasn't any difference in PFS between CP-A and CP-B patients (HR 1.68, 95%CI 0.78–3.65, $p = 0.6$). Moreover, disease control rate (DCR) was 69% in CP-A patients and 57% in CP-B patients ($p > 0.5$). Median time to decompensation (TTD) was 7 months (95%CI 5.3–8.7) in CP-B patients, remarkably lower than in CP-A patients (HR 3.27, 95%CI 1.4–7.4, $p < 0.01$). Main predictors of death were performance status, serum platelet count, serum albumin, and signs of portal hypertension. Main predictors of liver decompensation were performance status, signs of portal hypertension, diabetes, and serious adverse events linked to cancer treatment. The only protective factor for death and liver decompensation was chronic treatment with non-selective beta-blockers.

Decompensation Risk - Child A vs Child B (all patients)

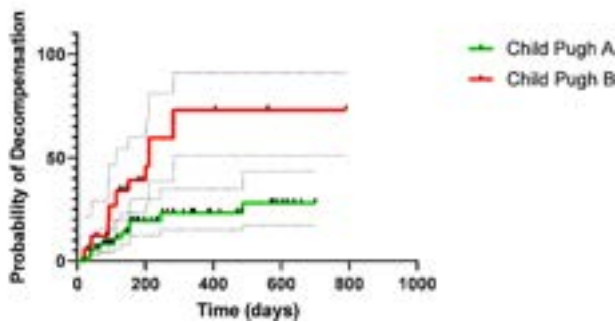


Figure 1: Decompensation risk in CP-A and CP-B patients treated with atezolizumab plus bevacizumab.

Conclusion: CP-B patients receiving treatment with atezolizumab plus bevacizumab showed a worse survival compared with CP-A patients, due to the competing effect of liver dysfunction over tumour progression. Response rates did not seem to differ according to the CP class. Thus, our data confirm that liver decompensation, rather than cancer progression, is the leading cause of death in CP-B patients.

THU-123

Transarterial chemoembolization and systemic treatment in patients with autoimmune liver disease-associated hepatocellular carcinoma: outcome and safety profile

Louisa Stern¹, Constantin Schmidt², Christian Casar³, Aurélie Walter⁴, J.P.H. Drenth⁵, Frederik Nevens⁶, Maria Papp⁷, Nikolaos Gatselis⁸, Kalliopi Zachou⁸, Matthias Pinter⁹, Bernhard Scheiner⁹, Arndt Vogel¹⁰, Martha M Kirstein¹¹, Fabian Finkelmeier¹², Arndt Weinmann¹³, Oliver Waidmann¹², Piotr Milkiewicz¹⁴, Douglas Thorburn¹⁵, Neil Halliday¹⁵, Ana Leo¹⁶, Samuel Huber², George Dalekos⁸, Ansgar W. Lohse², Henning Wege², Jean Charles Nault^{17,18}, Johann von Felden², Kornelius Schulze².

¹University Medical Center Hamburg-Eppendorf, Department of General, Visceral and Thoracic Surgery, Hamburg, Germany; ²University Medical Center Hamburg-Eppendorf, Department of Internal Medicine and Gastroenterology, Hamburg, Germany; ³University Medical Center Hamburg-Eppendorf, Bioinformatics Core, Hamburg, Germany; ⁴Hôpital Avicenne, Hôpitaux Universitaires Paris-Seine-Saint-Denis, Service d'Hépatologie, Bobigny, France; ⁵Radboud University Medical Center, Department Gastroenterology and Hepatology, Nijmegen, Netherlands; ⁶University Hospital KU Leuven, Department of Gastroenterology and Hepatology, Leuven, Belgium; ⁷University of Debrecen, Division of Gastroenterology, Department of Internal Medicine, Debrecen, Hungary; ⁸General University Hospital of Larissa, Department of Medicine and Research Laboratory of Internal Medicine, National Expertise Center of Greece in Autoimmune Liver Diseases, Larissa, Greece; ⁹Medical University of Vienna, Department of Internal Medicine III, Division of Gastroenterology and Hepatology, Vienna, Austria; ¹⁰Medical School Hannover, Department of Gastroenterology, Hepatology and Endocrinology, Hannover, Germany; ¹¹UKSH Lübeck, First Department of Medicine, Lübeck, Germany; ¹²University Hospital Frankfurt, Department of Gastroenterology, Hepatology and Endocrinology, Frankfurt, Germany; ¹³University Hospital Mainz, Department of Gastroenterology and Hepatology, Mainz, Germany; ¹⁴Liver and Internal Medicine Unit, Department of General, Transplant and Liver Surgery, Warsaw, Poland; ¹⁵Royal Free Hospital, 15Sheila Sherlock Liver Centre and UCL Institute for Liver and Digestive Health, London, United Kingdom; ¹⁶Humanitas University, Department of Biomedical Sciences, Italy; ¹⁷Université Paris Nord, Unité de Formation et de Recherche Santé Médecine et Biologie Humaine, Paris, France; ¹⁸Sorbonne Université, Centre de Recherche des Cordeliers, INSERM, Paris, France
Email: l.stern@uke.de.

Background and aims: Hepatocellular carcinoma (HCC) develops in patients with autoimmune liver disease (AILD) such as autoimmune hepatitis (AIH) and primary biliary cholangitis (PBC). Due to the low incidence of AILD, this subgroup is regularly underrepresented in HCC clinical trials. Data on treatment tolerability and prognosis in these rare liver patients is scarce. Hence, the aim of this study was to investigate, whether patients with HCC-AILD will equally benefit from systemic treatment with tyrosinkinase inhibitors (TKIs) or transarterial chemoembolization (TACE) and demonstrate a similar safety profile compared to patients with HCC due to viral, or non-/alcoholic liver disease.

Method: For this European retrospective study, conducted by the ERN Rare Liver, we initially enrolled 107 patients with HCC-AILD (55 × AIH, 52 × PBC) treated at 13 centers from 1996 to 2020. Of these, 72 remained for the final analysis (exclusions criteria: treatment other than TACE or TKIs, 38 × AIH, 34 × PBC). Propensity score matching 1:1 with a pool of 347 non-AILD associated HCC patients from Hamburg was conducted to adjust for differences in major clinical confounders between the two groups. Subsequently, comparative analyses of median overall survival (mOS) and treatment tolerability were performed, thereby applying a sequential analysis method for patients having undergone both TACE and systemic treatment.

Results: The final propensity-matched cohort included a total of 130 patients who were treated with TACE and 56 with systemic treatment. HCC-AILD patients demonstrated a comparable mOS for both TACE (19.5 months [10.1–28.3] vs 22.1 months [11.4–30.2], $p=0.9$) and systemic treatment with TKIs (15.4 months [5.3-na] vs 15.1 months [9.4–35], $p=0.5$). For TACE, adverse events (AE) occurred less frequently in HCC-AILD patients than in controls (e.g. post-TACE embolization syndrome) (≥ 1 AE: 34% vs 62%, $p=0.003$), whereas there was no significant change in rate of AEs for systemic treatment (≥ 1 AE: 68% vs 82%, $p=0.2$).

Conclusion: In conclusion, we present the first study, investigating the outcome and safety profile of rare liver patients with HCC-AILD treated with TACE or TKIs. Patients with HCC-AILD have similar mOS to both local and systemic treatment, and a more favorable tolerability compared to non-AILD associated HCC. Due to the exclusion of HCC-AILD patients in recent immunotherapy trials, systemic treatment with TKIs will continue to be the standard of care for HCC-AILD.

THU-124

Interim analysis of the ACTION trial: Cabozantinib for hepatocellular carcinoma patients who discontinued first line treatment other than sorafenib or due to sorafenib intolerance

Marco Sanduzzi Zamparelli^{1,2,3,4}, Sergio Muñoz Martínez^{1,2,3,4}, Mariona Calvo⁵, Maria Varela⁶, Neus Llarch^{1,2,3,4}, Gemma Iserre^{1,2,3}, Berta Laquente⁵, Andrés Castano-García⁶, José Luis Lledó⁷, Christie Perelló^{2,8,9}, Gemma Domenech¹⁰, Ezequiel Mauro^{1,2,3,4}, Maria Ángeles García-Criado^{1,4,11}, Carmen Ayuso^{1,4,11}, Angels Kateb¹², Jordi Rimola^{1,4,11}, Jordi Bruix^{1,2,3,4}, María Reig^{1,2,3,4}. ¹BCLC group. Fundació Clínica per a la Recerca Biomèdica-IDIBAPS, Barcelona, Spain; ²CIBERehd, Madrid, Spain; ³Liver Oncology Unit. Liver Unit, Hospital Clinic of Barcelona, Barcelona, Spain; ⁴University of Barcelona, Barcelona, Spain; ⁵Catalan Institute of Oncology, Hospital Duran i Reynals, Institut d'Investigació Biomèdica de Bellvitge (IDIBELL), Department of Oncology, L'Hospitalet de Llobregat, Spain; ⁶Hospital Universitario Central de Asturias, IUOPA, FINBA, University of Oviedo, Oviedo, Liver Unit, Gastroenterology Department, Oviedo, Spain; ⁷Hospital Universitario Ramón y Cajal, IRYCIS, CIBERehd, University of Alcalá, Madrid, Spain; ⁸Gastroenterology Department. Hepatology Unit, Hospital Universitario Puerta de Hierro, Madrid, Spain; ⁹IDIPHISA, Spain; ¹⁰Medical Statistics Core Facility, Fundació de Recerca Clínica Barcelona (FRCB)-IDIBAPS, Barcelona, Spain; ¹¹Radiology Department, Hospital Clínic of Barcelona, IDIBAPS, Barcelona, Spain; ¹²Fundació Clínica per a la Recerca Biomèdica-IDIBAPS, Barcelona, Spain
Email: mreig1@clinic.cat.

Background and aims: The landscape of hepatocellular carcinoma (HCC) changed in the last 5 years. Cabozantinib was approved for HCC, but the outcome of HCC patients who received cabozantinib as second-line due to sorafenib intolerance or after discontinuing first line treatment other than sorafenib, mostly come from retrospective analysis. This clinical trial evaluates the safety profile established by the rate of adverse events (AE), rate of related-AEs and rate of death in HCC patients who received cabozantinib in second-line.

Method: Phase II, open label and investigator initiated clinical trial (CT) including HCC patients intolerant to sorafenib or those who discontinued first-line treatment with lenvatinib or atezolizumab-bevacizumab. Cabozantinib was initiated at 60 mg every day, which was modified upon development of AE. Treatment continued until symptomatic tumor progression, unacceptable AEs, patient's decision or death. An interim analysis was planned when 14 patients had a minimum follow-up of 30 days, while the CT would have to be stopped because of futility if there were 8 or more patients with critical AEs according to investigators.

Results: At November 2022, 22 patients had been enrolled: 19 included, 11 on treatment and 8 discontinued cabozantinib. Four patients discontinued due to symptomatic progression, and the other 4 due to anorectal hemorrhage, intestinal ischemia, hand-foot skin reaction grade 3 and investigator decision, respectively. Twelve out of the 14 patients with >30 days follow-up (interim analysis) were sorafenib intolerant, 6 were BCLC-C and all had preserved liver function when starting cabozantinib. Eight patients developed 17 AE >grade 3, 11 of them were cabozantinib-related and 7 meet the definition of serious adverse events (SAE). Table 1 shows the 7 SAEs observed in 5 patients, among which 4 SAEs were cabozantinib-related and occurred in 3 patients.

Table 1: Severe adverse events

Subject PatientID	Sorafenib intolerance	AE description	Start date	End date	Grade (1-5) NCI CTCAE v5.0	Cabozantinib Relationship	Cabozantinib dose (mg)	Action taken (Cabozantinib)	Death
1	Dermatologic adverse event and fatigue	Hypokalemia	2020-09-09	2020-10-07	3	Related	60	Cabozantinib interrupted	Yes
		Gastrointestinal bleeding	2020-12-17	2020-12-22	3	Related	60	None	
2	Rectal ulcer	Ano-rectal Hemorrhage	2020-12-11	2020-12-29	3	Related	60	None	Yes
		Spontaneous bacterial peritonitis	2021-01-28	2021-02-10	3	Not Related	0	None	
3	Dermatologic adverse event	Intestinal ischemia	2021-01-16	2021-01-26	3 (SUSAR)*	Related	60	Cabozantinib interrupted	No
4	Dermatologic adverse event	Fever	2021-04-03	2021-04-09	1	Not related	0	None	No
5	Not reported	Acute cholecystitis	2021-02-04	2021-02-18	3	Not related	0	None	Yes

Table: (abstract: THU-124).

Conclusion: The Data and Safety Monitoring Board concluded that the ACTION trial could continue, since it did not met the safety futility criteria. The final analysis is expected on June 2023.

THU-125
Association of tumor response with survival in patients with unresectable hepatocellular carcinoma treated with first-line tislelizumab versus sorafenib: results from the RATIONALE-301 study
Tim Meyer¹, Richard S. Finn², Masatoshi Kudo³, Andrew X. Zhu^{4,5}, Songzi Li⁶, Yaxi Chen⁷, Frederic Boissier⁸, Ramil Abdrashitov⁹, Arndt Vogel¹⁰, Shukui Qin¹¹. ¹Royal Free Hospital NHS Trust and University College London, Academic Department of Oncology, London, United Kingdom; ²Geffen School of Medicine, University of California Los Angeles, Department of Medicine, Division of Hematology/Oncology, Los Angeles, CA, United States; ³Kindai University Faculty of Medicine, Department of Gastroenterology and Hepatology, Osaka, Japan; ⁴Jiahui Health, Jiahui International Cancer Center, Shanghai, China; ⁵Harvard Medical School, Massachusetts General Hospital, MA, United States; ⁶BeiGene Ltd., Ridgefield Park, Biometrics, NJ, United States; ⁷BeiGene (Beijing) Co., Ltd., Clinical Science, Beijing, China; ⁸BeiGene Ltd., Ridgefield Park, Clinical Science, NJ, United States; ⁹BeiGene USA, Inc., Clinical Development, Fulton, MD, United States; ¹⁰Hannover Medical School, Department of Gastroenterology, Hepatology and Endocrinology, Hannover, Germany; ¹¹Cancer Center of General Hospital of Eastern Theater of PLA, Nanjing, China
Email: t.meyer@ucl.ac.uk

Background and aims: Tislelizumab (TIS) is a monoclonal antibody with high affinity and binding specificity to programmed cell death protein 1. In RATIONALE-301 (NCT03412773) TIS was non-inferior to sorafenib (SOR) for overall survival (OS) as first-line treatment of patients (pts) with unresectable hepatocellular carcinoma (HCC); OS superiority vs SOR was not met. We evaluated the association of response with survival in pts from the RATIONALE-301 study.

Method: In this phase 3, open-label study, systemic therapy-naïve adult pts with histologically confirmed Barcelona Clinic Liver Cancer Stage B/C HCC were randomized (1:1) to receive TIS (200 mg intravenous every 3 weeks) or SOR (400 mg orally twice daily) until disease progression, intolerable toxicity, or withdrawal. The primary end point was OS; secondary efficacy end points included progression-free survival (PFS) and best overall response (BOR; per RECIST v1.1) by blinded independent review committee. We assessed OS and PFS according to BOR (complete response [CR] vs partial response [PR] vs stable disease [SD] vs progressive disease [PD]). Limitation of this analysis is related to its retrospective nature.

Results: Overall, 674 pts were randomized (TIS: n = 342; SOR: n = 332). At data cutoff (Jul 11, 2022), minimum study follow-up was 33 months. Pt characteristics were generally balanced at baseline in both arms. Survival outcomes across response categories are presented in the table. Response was associated with longer median OS and PFS for both arms. The OS rate at 24 months was higher in responders treated with TIS vs SOR (TIS; OS: 91.7%, 95% CI: 79.4, 96.8; SOR; OS: 72.2%, 95% CI: 45.6, 87.4).

Conclusion: Though there are limitations in the analysis, response achieved on treatment with TIS was associated with better survival vs SOR, in pts with unresectable HCC.

Table: (abstract: THU-125).

	Tislelizumab (n = 342)			Sorafenib (n = 332)			Hazard Ratio*	
	n (%)	mOS, mo (95% CI)	mPFS, mo (95% CI)	n (%)	mOS, mo (95% CI)	mPFS, mo (95% CI)	OS (95% CI)	PFS (95% CI)
Responders	49 (14.3)	NE (NE, NE)	38.2 (21.7, NE)	18 (5.4)	38.8 (21.9, NE)	15.9 (10.4, 32.4)	0.34 (0.14, 0.80)	0.38 (0.18, 0.79)
Non-responders	274 (80.1)	13.3 (11.0, 15.9)	2.1 (2.1, 2.1)	280 (84.3)	14.1 (13.1, 17.4)	2.5 (2.1, 4.1)	1.00 (0.83, 1.21)	1.43 (1.18, 1.73)
CR	10 (2.9)	NE	NE (28.2, NE)	1 (0.3)	NE	NE	NE	NE
PR	39 (11.4)	NE	29.5 (13.1, 45.0)	17 (5.1)	38.8 (19.0, NE)	13.3 (10.4, 19.0)	0.41 (0.17, 0.96)	0.50 (0.24, 1.04)
SD	94 (27.5)	24.0 (19.4, 29.3)	4.9 (4.2, 6.2)	139 (41.9)	19.1 (15.2, 21.7)	6.5 (6.2, 8.2)	0.73 (0.54, 1.00)	1.23 (0.88, 1.71)
PD	169 (49.4)	9.9 (8.6, 10.9)	2.0 (2.0, 2.1)	121 (36.4)	10.4 (7.6, 13.4)	2.1 (2.0, 2.1)	1.05 (0.81, 1.35)	1.13 (0.89, 1.42)

*Unstratified hazard ratio of tislelizumab vs sorafenib

CI, confidence interval; CR, complete response; NE, not estimable; mo, months; mOS, median overall survival; PD, progressive disease; mPFS, median progression-free survival; PR, partial response; SD, stable disease

THU-126

Effectiveness and safety of conversion surgery for patients with initially unresectable hepatocellular carcinoma using lenvatinib combined with TACE plus PD-1 inhibitors: a real-world study

Xingzhi Li¹, Xiaobo Wang¹, Tao Bai¹, Jie Chen¹, Zhihong Tang¹, Tao Wei¹, Shaolong Lu¹, Lequn Li¹, Feixiang Wu¹. ¹Guangxi Medical University Cancer Hospital, Department of Hepatobiliary Surgery, China Email: wufeixiang@gxmu.edu.cn

Background and aims: Conversion surgery for patients with initially unresectable hepatocellular carcinoma (uHCC) using lenvatinib combined with transcatheter arterial chemoembolization (TACE) plus programmed cell death protein-1 (PD-1) inhibitors (LTP) has been promising. However, the effectiveness and safety of conversion surgery for initially uHCC requires additional study. The purpose of this real-world, retrospective study was to compare the effectiveness and safety of conversion surgery for patients with initially uHCC managed with LTP to initial surgery in patients with resectable HCC.

Method: The data of 32 consecutive patients with initially uHCC receiving conversion surgery and 419 consecutive patients with resectable HCC receiving initial surgery from November, 2019, to September, 2022, were analyzed retrospectively. After propensity score matching (PSM) in a 1:2 ratio, 65 patients were selected. The major outcomes were safety of the operation, event-free survival (EFS), overall survival (OS), and clinicopathological factors.

Results: Compared to initial surgery, conversion surgery was safe. Before matching, the conversion surgery group had longer EFS (not reached vs 11.5 months, $p = 0.003$) and similar OS (not reached vs not reached, $p = 0.62$) compared with the initial surgery group. Similar results for EFS ($p = 0.005$) and OS ($p = 0.28$) were also obtained after matching. Multivariate analysis confirmed that conversion surgery was an independent prognostic factor of EFS. The conversion surgery group had significantly lower incidence of microvascular invasion (MVI) (3.1% vs 50.4%; $p < 0.001$), grade III/IV tumor differentiation (15.6% vs 45.8%; $p < 0.001$), and incomplete tumor capsule (12.5% vs 54.7%; $p < 0.001$). Before matching, patients with MVI-negative in the conversion surgery group had significantly longer EFS than those in the initial surgery group (not reached vs 14 months, $p = 0.008$). After matching, patients with MVI-negative in both groups had similar EFS ($p = 0.39$).

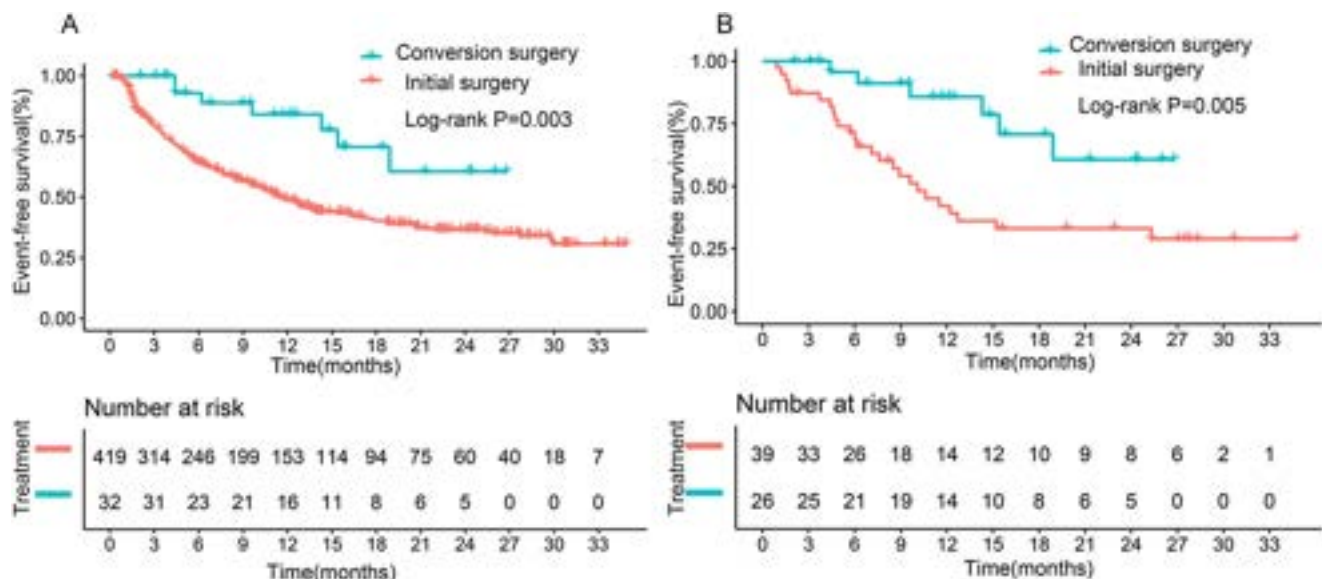


Figure: (abstract: THU-126).

Conclusion: Conversion surgery is effective and safe for patients with initially uHCC receiving LTP. Conversion therapy of LTP has the potential to reduce risk factors for postoperative recurrence, especially MVI, which may change surgical decision-making.

THU-128

Efficacy and tolerability of atezolizumab and bevacizumab in patients with hepatocellular carcinoma previously treated with systemic therapy: a global, observational study

Vincent Jörg¹, Bernhard Scheiner^{2,3}, Antonio D'Alessio², Claudia Fulgenzi², Martin Schoenlein⁴, Lorenz Kocheise¹, Ansgar W. Lohse¹, Samuel Huber¹, Henning Wege¹, Ahmed Kaseb⁵, Yinghong Wang⁶, Mahvish Muzaffar⁷, Yehia Abugabal⁸, Shadi Chamseddine⁸, Samuel Phen⁹, Jaekyung Cheon¹⁰, Pei-Chang Lee¹⁰, Lorenz Balcar³, Anja Krall¹¹, Celina Ang¹², Linda Wu¹², Anwaar Saeed¹³, Yi-Hsiang Huang¹⁴, Bertram Bengsch^{15,16}, Lorenza Rimassa^{17,18}, Arndt Weinmann¹⁹, Rudolf E. Stauber¹¹, James Korolewicz², Matthias Pinter³, Amit Singal⁹, Hong Jae Chon¹⁰, David J. Pinato^{2,20}, Kornelius Schulze¹, Johann von Felden²¹. ¹I. Department of Medicine, University Medical Center Hamburg-Eppendorf, Hamburg, Germany, Germany; ²Department of Surgery and Cancer, Imperial College London, United Kingdom, United Kingdom; ³Division of Gastroenterology and Hepatology, Department of Internal Medicine III, Medical University of Vienna, Austria, Austria; ⁴Department of Oncology, Hematology and Bone Marrow Transplantation with Section of Pneumology, University Medical Center Hamburg-Eppendorf, Hamburg, Germany, Germany; ⁵Department of Gastrointestinal Medical Oncology, MD Anderson Cancer Center, University of Texas, Houston, TX, USA, United States; ⁶Department of Gastroenterology, Hepatology and Nutrition, MD Anderson Cancer Center, University of Texas, Houston, TX, USA, United States; ⁷Division of Hematology and Oncology, East Carolina University, Greenville, NC, USA, United States; ⁸Department of Gastrointestinal Medical Oncology, MD Anderson Cancer Center, University of Texas, Houston, TX, USA, United States; ⁹Department of Internal Medicine, Southwestern Medical Center, University of Texas, USA, United States; ¹⁰Medical Oncology, Department of Internal Medicine, CHA Bundang Medical Center, CHA University, Seongnam, Republic of Korea., Korea, Rep. of South; ¹¹Department of Internal Medicine, Division of Gastroenterology and Hepatology, Medical University of Graz, Austria, Austria; ¹²Department of Medicine, Division of Hematology/Oncology, Tisch Cancer Institute, Mount Sinai Hospital, New York, NY, USA, United States; ¹³Division of Hematology/Oncology, Department of Medicine, University of Pittsburgh (UPMC), USA, United States; ¹⁴Institute of Clinical Medicine, National Yang Ming Chiao Tung University School of Medicine; Division of Gastroenterology and Hepatology, Taipei Veterans General Hospital, Taipei, Taiwan, Taiwan; ¹⁵Department of Medicine II (Gastroenterology, Hepatology, Endocrinology and Infectious Diseases), Freiburg University Medical Center, Faculty of Medicine, University of Freiburg, Freiburg, Germany, Germany; ¹⁶Partner Site Freiburg, German Cancer Consortium (DKTK), Heidelberg, Germany, Germany; ¹⁷Medical Oncology and Hematology Unit, Humanitas Cancer Center, IRCCS Humanitas Research Hospital, Milan, Italy, Italy; ¹⁸Department of Biomedical Sciences, Humanitas University, Pieve Emanuele (Milan), Italy, Italy; ¹⁹Department of Internal Medicine I, University Medical Centre of the Johannes Gutenberg University, Mainz, Germany, Germany; ²⁰Department of Translational Medicine, University of Piemonte Orientale, Novara, Italy, Italy; ²¹University Medical Center Hamburg-Eppendorf, I. Department of Medicine, Hamburg, Germany Email: v.joerg@uke.de

Background and aims: Since the introduction of the combination treatment of anti-PD-L1 antibody atezolizumab and anti-VEGF antibody bevacizumab (AB) median overall survival (OS) in hepatocellular carcinoma (HCC) has drastically improved. However, evidence on efficacy and safety of the novel treatment standard in patients with prior exposure to systemic treatment is scarce. Up to now, global positive phase 3 clinical trials for second line treatments

are limited to regorafenib, cabozantinib, and ramucirumab following sorafenib treatment. The aim of this global, multi-center, observational study was to evaluate efficacy and safety of AB in patients after previous systemic therapy.

Method: We screened our global, multi-center, prospectively maintained registry database for patients who received any systemic therapy before AB. Primary end point was OS, secondary end points were time-to-progression (TTP), progression-free survival (PFS), objective response rate (ORR), and safety (rate and severity of adverse events).

Results: Among 493 patients who received AB for unresectable HCC, 61 patients received prior systemic therapy and were included in this analysis. Median age of the study population was 66 years, with 91.8% males. Predominant risk factors for HCC were viral hepatitis (59%) and alcohol (23%). OS for AB was 16.2 (95% CI, 14.5–17.9) months, TTP and PFS were 4.1 (95% CI, 1.5–6.6) and 3.1 (95% CI, 1.1–5.1) months, respectively. ORR was 38.2% (7.3% with complete and 30.9% with partial response). Overall survival was not influenced by treatment line (2nd vs >2nd) or previous systemic treatment modality (tyrosin kinase inhibitors (TKI) vs. immune checkpoint inhibitors (ICI)). Treatment-related adverse events (trAE) of any grade according to CTCAE were documented in 42.6% of patients with only 13.1% of grade ≥3, incl. one death.

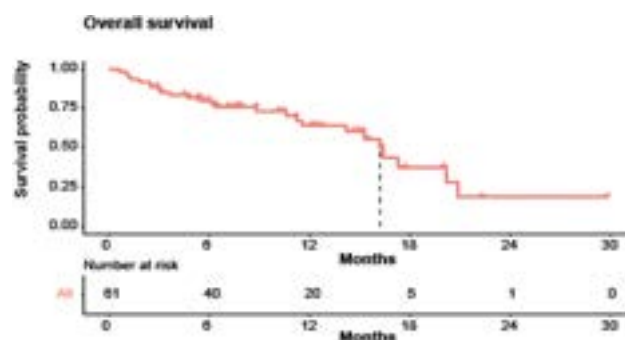


Figure:

Conclusion: In this observational study, AB emerges as a safe and effective treatment option in patients with HCC previously treated with other systemic agents.

THU-129

Survival outcomes of hepatocellular carcinoma after yttrium-90 selective internal radiation therapy in an Asian population stratified by tumour volume and distribution

Kaina Chen^{1,2}, Fiona Ni Ni Moe³, Aaron Kian Ti Tong⁴, David Chee Eng Ng⁴, Richard Hoau Gong Lo⁵, Apoorva Gogna⁵, Sean Xuexian Yan⁴, Sue Ping Thang⁴, Kelvin Siu Hoong Loke⁴, Karaddi Venkatanarasimha Nanda Kumar⁵, Hian Liang Huang⁴, Chow Wei Too⁵, Weng Yan Ng³, Marjorie Hoang², Pierce Chow^{2,6,7}. ¹Singapore General Hospital, Gastroenterology and Hepatology, Singapore, Singapore; ²Duke-NUS Medical School, Singapore, Singapore; ³National Cancer Centre Singapore, Singapore; ⁴Singapore General Hospital, Nuclear Medicine, Singapore, Singapore; ⁵Singapore General Hospital, Vascular and Interventional Radiology, Singapore; ⁶National Cancer Centre Singapore, Surgical Oncology, Singapore; ⁷Singapore General Hospital, Hepato-pancreato-biliary and Transplant Surgery, Singapore, Singapore Email: cknworkemail@gmail.com

Background and aims: Selective internal radiation therapy (SIRT) with yttrium-90 (Y90) has been approved by the U.S. Food and Drug Administration (FDA) for solitary hepatocellular carcinoma (HCC) up to 8 cm with preserved liver function. Y90 SIRT is also a widely used locoregional therapy for a wider range of unresectable locally advanced HCC given its favourable safety profile. Our study aims to evaluate the survival outcomes of HCC patients treated with SIRT Y90,

stratified by tumour volume and tumour distribution to improve prognostication.

Method: Included are patients at least 18 years old treated with resin microsphere Y90 SIRT for unresectable HCC between 1st January 2008 and 22nd May 2019 at National Cancer Centre Singapore (NCCS) \Singapore General Hospital (SGH) and had follow-up data. Patients with metastatic HCC, a second primary cancer, or lost to follow-up were excluded. The study cohort was divided into the following subgroups to improve prognostication: 1) within Milan (<Milan); 2) unilobar HCC beyond Milan within Up-To-7 (<UT7-u); 3) bilobar HCC beyond Milan within Up-To-7 (<UT7-b); 4) unilobar HCC beyond Up-To-7 (>UT7-u); 5) bilobar HCC beyond Up-To-7 (>UT7-b); 6) portal vein invasion (PVI) and Child-Pugh class A (PVI-CPA) and 7) PVI and Child-Pugh class B (PVI-CPB).

Results: Among 721 patients treated with Y90 SIRT within the study duration, 413 patients fulfilled inclusion/exclusion criteria. The median follow-up was 16.3 months. The median overall survival (mOS) of the whole cohort was 20.9 months (95% CI 18.2–24.0) and did not significantly differ with age or gender. In patients with HCC without PVI, survival differed significantly with performance status, liver function (Child-Pugh class, Albumin-Bilirubin grade), tumour size and distribution, whereas in patients with PVI, alpha-fetoprotein levels and extent of PVI were additional predictors of OS. Of note, patients with solitary HCC (25.3 months, 95% CI 20.4–37.0) and 2–5 tumours (25.7 months, 95% CI 20.2–31.1) had comparable mOS ($p = 0.323$). Solitary HCCs with an absorbed Y90 dose above 150Gy tend towards a better mOS (46.4 months, 95% CI 26.2–NE) versus mOS 22.7 months (95% CI 13.7–37) in those with ≤ 150 Gy ($p = 0.085$). Median OS of the subgroups is shown in the Figure. Seventy patients (70/413, 16.9%) received curative modalities after Y90 SIRT downstaged the disease with mOS of 79.7 months (95% CI 40.4–NE), versus those who did not receive subsequent curative treatments (mOS 17.1 months; 95% CI 13.5–20.4, $p < 0.001$), and this was observed among all the subgroups.

Conclusion: Treatment outcomes of Y90 SIRT are favourable for patients with unresectable intermediate-locally advanced HCC. Incorporating tumour distribution improved prognostication of intermediate HCC, whereas the Child-Pugh class can stratify HCC with PVI. Patients downstaged with Y90 SIRT who subsequently received curative therapy had significantly improved mOS.

THU-130

Salvage hepatectomy for recurrent hepatocellular carcinoma after radiofrequency ablation

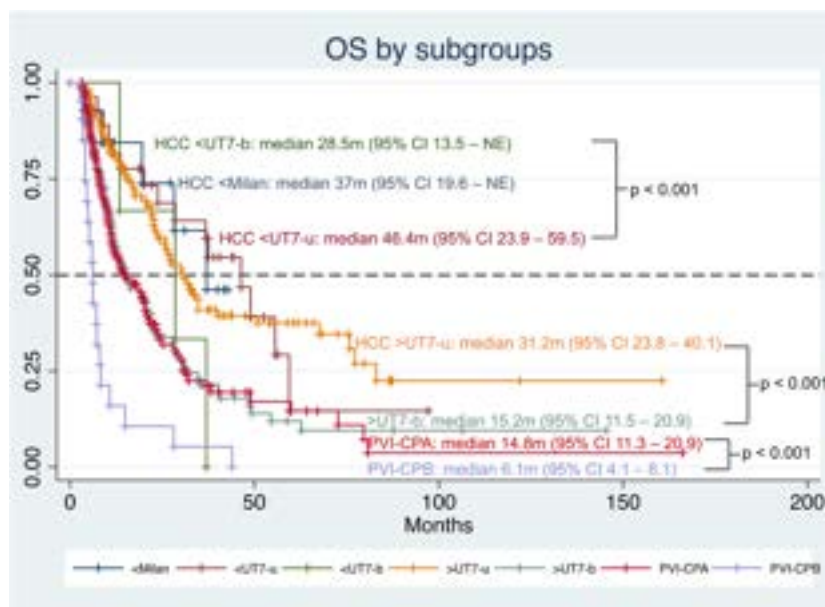
Jai Young Cho¹, Ho Seong Han¹, Hae Won Lee¹, Boram Lee¹, Yesong Park¹, MeeYoung Kang¹, Sook-Hyang Jeong², Jin-Wook Kim², Gwang Hyeon Choi². ¹Seoul National University Bundang Hospital, Surgery, Korea, Rep. of South; ²Seoul National University Bundang Hospital, Internal Medicine, Korea, Rep. of South
Email: jycho9@gmail.com

Background and aims: Radiofrequency ablation (RFA) is a widely used percutaneous local ablation technique for the treatment of hepatocellular carcinoma (HCC). Yet the optimal treatment for marginal recurrence after RFA is not established, and the role of salvage hepatectomy is still unclear.

Method: A retrospective analysis was performed on 60 patients who underwent salvage hepatectomy (SH) for recurrent HCC after RFA between January 2004 and August 2022 at a single tertiary referral center. Short-term and long-term outcomes were compared to a matched control group ($n = 60$) of patients who underwent primary hepatectomy (PH) as initial treatment during the same period.

Results: The two groups showed no statistically significant difference in operative extent, operation time, and intraoperative blood loss. Postoperative morbidity rates were similar, and there was no postoperative mortality in either group. After intention-to-treat analysis, recurrence rates were significantly higher in the SH group for both local recurrence (36 [60.0%] vs. 14 [23.3%], $p < 0.001$) and systemic recurrence (22 [36.7%] vs. 3 [5.0%], $p < 0.001$). The 1-, 3-, and 5-year DFS rates were significantly worse in the SH group compared to the PH group (83.1% vs. 94.5%, 46.9% vs. 70.4%, and 26.2% vs. 66.9%, respectively; $p < 0.001$). Cancer-related death showed higher incidence in the SH group (13 [21.7%] vs. 4 [6.7%], $p = 0.018$). However, the difference in 1-, 3-, and 5-year overall survival rates between the two groups was not statistically significant (93.0% vs. 98.1%, 81.9% vs. 95.8%, and 78.0% vs. 92.2%, respectively; $p = 0.091$).

Conclusion: Salvage hepatectomy is an acceptable treatment option for recurrence after RFA with short-term outcomes comparable to primary resection. However, treatment should be planned carefully, because recurrent HCC after RFA exhibits more aggressive behavior.



Subgroup	N	median OS	95% CI
<Milan	14	37 months	19.6 – NE
<UT7-u	28	46.4 months	23.9 – 59.5
Solitary	16	46.4 months	10.6 – NE
2-5 tumours	11	49.0 months	20.2 – NE
<UT7-b	3	28.5 months	13.5 – NE
>UT7-u	110	31.2 months	23.8 – 40.1
Solitary	56	27.6 months	22.6 – 34.8
2-5 tumours	16	30.4 months	20.2 – NE
>5 tumours	38	32.4 months	20.6 – 73
>UT7-b	104	15.2 months	11.5 – 20.9
PVI-CPA	133	14.8 months	11.3 – 20.9
Solitary	40	20.4 months	10.5 – 38.3
2-5 tumours	19	14.8 months	10.2 – 21.4
>5 tumours	71	13.3 months	9.5 – 24.0
PVI-CPB	21	6.1 months	4.1 – 8.1

Figure: Kaplan-Meier (KM) overall survival curves of HCC patients treated with Y90 SIRT, subgrouped based on Milan Criteria, Up-To-7 Criteria and tumour distribution. HCC with PVI was stratified with Child-Pugh class.

Figure: (abstract: THU-129).

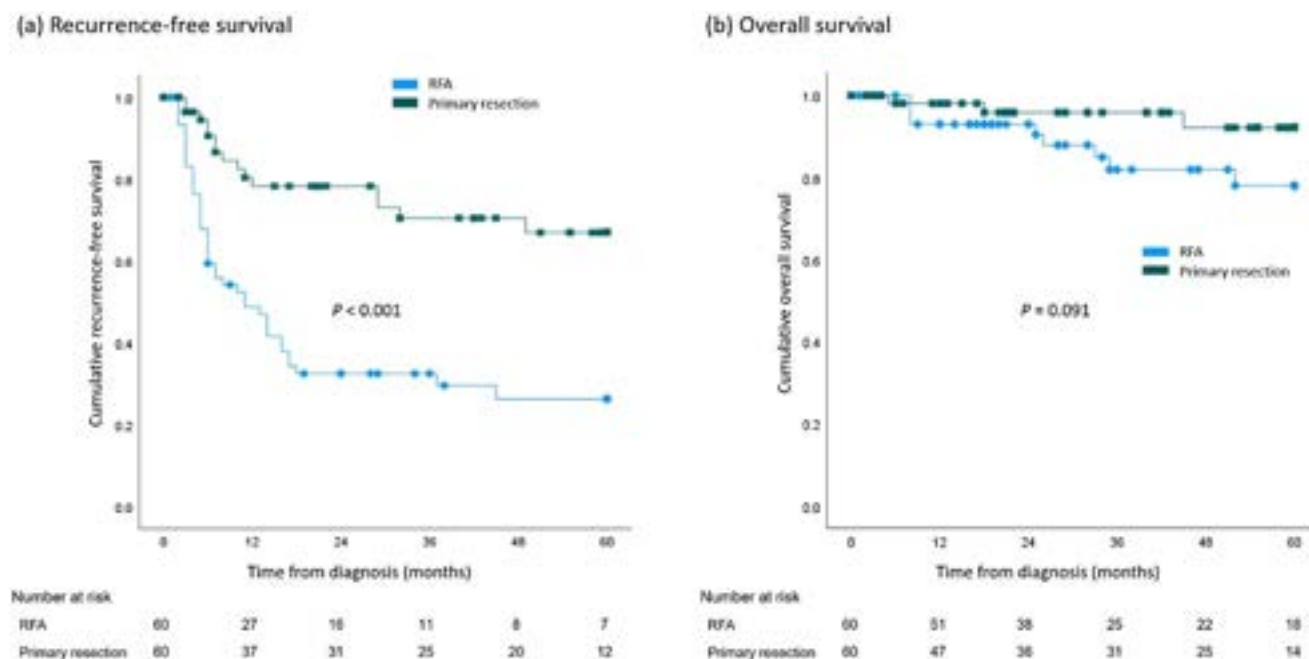


Figure: (abstract: THU-130).

THU-131

Incidence and risk factors of esophagogastric varices bleeding in patients with advanced hepatocellular carcinoma treated with lenvatinib

Massimo Iavarone¹, Eleonora Alimenti², Toshifumi Tada³, Shimose Shigeo⁴, Goki Suda⁵, Changhoon Yoo⁶, Caterina Soldà⁷, Fabio Piscaglia⁸, Andrea Casadei Gardini⁹, Fabio Marra¹⁰, Caterina Vivaldi^{11,12}, Fabio Conti¹³, Marta Schirripa¹⁴, Hideki Iwamoto⁴, Takuya Sho⁵, So Heun Leo⁶, Mario Domenico Rizzato¹⁵, Matteo Tonnini¹⁶, Margherita Rimini⁹, Claudia Campani¹⁰, Gianluca Masi^{11,12}, Francesco Foschi¹³, Mariangela Brucoleri¹, Takumi Kawaguchi⁴, Takashi Kumada¹⁷, Atsushi Hiraoka¹⁸, Masanori Atsukawa¹⁹, Shinya Fukunishi²⁰, Toru Ishikawa²¹, Kazuto Tajiri²², Hironori Ochi²³, Satoshi Yasuda²⁴, Hidenori Toyoda²⁴, Takeshi Hatanaka²⁵, Satoru Kakizaki²⁶, Kazuhito Kawata²⁷, Fujimasa Tada²⁸, Hideko Ohama¹⁸, Norio Itokawa¹⁹, Tomomi Okubo¹⁹, Taeang Arai¹⁹, Michitaka Imai²¹, Atsushi Naganuma²⁸, Giulia Tosetti¹, Pietro Lampertico^{1,29}.

¹Foundation IRCCS Ca' Granda Ospedale Maggiore Policlinico, Division of Gastroenterology and Hepatology, Milan, Italy; ²Department of Medical Sciences, University of Pavia, Italy; ³Japanese Red Cross Society Himeji Hospital, Internal Medicine, Japan; ⁴Kurume University School of Medicine, Division of Gastroenterology, Department of Medicine, Japan; ⁵Hokkaido University Graduate School of Medicine, Gastroenterology and Hepatology, Japan; ⁶Department of Oncology, Asan Medical Center, University of Ulsan College of Medicine, Seoul, Korea, Rep. of South; ⁷Medical Oncology 1, Veneto Institute of Oncology Iov-Irccs, Italy; ⁸Irccs Azienda Ospedaliero-Universitaria Di Bologna, Department of Medical and Surgical Sciences, Italy; ⁹Irccs-San Raffaele Hospital, Italy; ¹⁰University of Florence, Medicina Sperimentale e Clinica, Italy; ¹¹Department of Translational Research and New Technologies in Medicine, University of Pisa, Italy; ¹²Unit of Medical Oncology 2, Azienda Ospedaliero-Universitaria Pisana, Italy; ¹³Medicina Interna Di Faenza, Ausl Romagna, Italy; ¹⁴Medical Oncology Unit, Central Hospital of Belcolle, Viterbo, Department of Oncology and Hematology, Italy; ¹⁵Department of Surgical, Oncological, and Gastroenterological Sciences, University of Padua, Italy; ¹⁶Dept Medical and Surgical Sciences, University of Bologna, Italy; ¹⁷Gifu Kyoritsu University Department of Nursing, Japan; ¹⁸Gastroenterology Center, Ehime Prefectural Central

Hospital, Matsuyama, Japan; ¹⁹Division of Gastroenterology and Hepatology, Department of Internal Medicine, Nippon Medical School, Japan; ²⁰Osaka Medical College 2nd Department of Internal Medicine, Japan; ²¹Department of Gastroenterology, Saiseikai Niigata Hospital, Japan; ²²Toyama University, Gastroenterology, Japan; ²³Matsuyama Red-Cross Hospital Hepato-Biliary Center, Japan; ²⁴Department of Gastroenterology and Hepatology, Ogaki Municipal Hospital, Ogaki, Gifu, Japan; ²⁵Gunma Saiseikai Maebashi Hospital Department of Gastroenterology, Japan; ²⁶National Hospital Organization Takasaki General Medical Center Department of Clinical Research, Japan; ²⁷Hamamatsu University School of Medicine Hepatology Division, Department of Internal Medicine, Japan; ²⁸National Hospital Organization Takasaki General Medical Center, Gastroenterology, Japan; ²⁹CRC "A. M. and A. Migliavacca" Center for Liver Disease, Department of Pathophysiology and Transplantation, University of Milan, Jamaica Email: massimo.iavarone@gmail.com

Background and aims: Lenvatinib (LEN) is among the drugs used in the forefront treatment of patients with advanced hepatocellular carcinoma (HCC) and in the future it could be part of therapeutic combinations with immunotherapy. However, the presence of esophagogastric varices (EGV) and the risk of bleeding might either contraindicate or limit this therapeutic choice. Thus study aimed to assess prevalence, risk factors and clinical consequences of EGV in LEN-treated patients with HCC.

Method: Among 816 patients of a large international cohort of patients treated with LEN for HCC not eligible for other therapies, we selected those with an upper-gastrointestinal endoscopy (UGE) available in the 6 months before treatment starts. Primary end points were: prevalence and risk factors for EGV bleeding during LEN treatment; secondary end points were prevalence and risk factors for presence of high risk EGV at baseline.

Results: We enrolled 535 patients with baseline UGE [median age 72 years, 78% male, 63% viral aetiology, 89% Child-Pugh A, 16% neoplastic portal vein thrombosis (nPVT), 56% BCLC-C]. At baseline, 301 (56%) patients were EGV free. Among the 234 patients with EGV (44%), 206 had esophageal varices (EV), 16 gastric varices (GV) and 12 both; 70/234 (30%) were high-risk EGV (small EV with red signs, medium/large EV, any GV) at baseline and 59 of them were treated with primary prophylaxis (non-selective beta-blockers 25, endoscopic band

ligation 32 and both 2). Child-Pugh B (OR 2.11; 95% CI 1.18–3.77, $p = 0.01$), platelets $<150,000$ (OR 3.19; 95% CI 2.17–4.70, $p < 0.001$) and nPVT (OR 2.44; 95% CI 1.48–4.02, $p < 0.001$) independently predicted presence of EGV; while Child-Pugh B (OR 2.12; 95% CI 1.08–4.17, $p = 0.03$), platelets $<150,000$ (OR 2.47; 95% CI 1.35–4.50, $p = 0.003$) and nPVT (OR 2.54; 95% CI 1.40–4.61, $p = 0.002$) independently predicted high risk EGV. During LEN therapy, 17 patients bled from EGV (3 grade 2, 11 grade 3–4 and 3 grade 5); prevalence of EGV bleeding was 3% overall, 7% among patients with EGV and 17% among those with high-risk varices. Among the 234 patients with baseline EGV, the only independent predictor of bleeding was the presence of high-risk varices (HR 6.94; 95% CI 2.23–21.57, $p = 0.001$). Risk of EGV bleeding can be stratified according to Child-Pugh B, presence of nPVT and platelets $<150,000/\mu\text{L}$ into low (0/3 risk factors, 6-months cumulative incidence 0.77%), intermediate (1/3 risk factors, 6-months cumulative incidence 2.31%) and high (2/3 or 3/3 risk factors, 6-months cumulative incidence 7.40%).

Conclusion: In HCC patients treated with lenvatinib, the risk of EGV bleeding is low but it increases in patients with high-risk EGV at baseline. A risk stratification for high-risk EGV and bleeding can be applied for decision-making, according to liver reserve, platelet count and nPVT.

THU-132

Risk stratification for early recurrence after resection in patients with intermediate stage hepatocellular carcinoma

Han Ah Lee¹, Jeong-Ju Yoo², Minjong Lee¹, Ho Soo Chun¹, Hwi Young Kim¹, Tae Hun Kim¹, Yeon Seok Seo³, Dong Hyun Sinn⁴.
¹Ewha Womans University College of Medicine, Korea, Rep. of South;
²Soonchunhyang University Bucheon Hospital, Korea, Rep. of South;
³Korea University College of Medicine, Korea, Rep. of South;
⁴Sungkyunkwan University School of Medicine, Korea, Rep. of South
 Email: minjonglee2@naver.com

Background and aims: It is unclear which patients will benefit from resection at intermediate stage of hepatocellular carcinoma (HCC). We aimed to identify high-risk patients for early recurrence in patients resectable for intermediate-stage HCC.

Method: This multicenter, retrospective study involved 1,686 patients who underwent resection or transarterial chemoembolization (TACE) for intermediate-stage HCC (2008–2019). Multivariable Cox proportional analysis for identifying high-risk patients treated with resection was performed. A prediction model for 2-year recurrence-free survival (RFS) was developed in the training cohort and validated in the validation cohort. 2-year RFS in each risk group was compared to those treated with TACE after propensity-score matching.

Results: During median follow-up of 31.4 months, 2-year RFS was significantly higher in the resection group (28.5%, $n = 480$) than in the TACE group (71.5% $n = 1,206$) (adjusted hazard ratio [aHR] = 1.471, 95% CI = 1.199–1.803, $P < 0.001$). Higher alpha-fetoprotein (aHR = 0.202), ALBI grade (aHR = 0.709), tumor number (aHR = 0.404), and maximal tumor size (aHR = 0.323) were significant risk factors for 2-year RFS in patients with resection. The newly developed Surgery Risk score in BCLC-B (SR-B score) with four variables showed an area under the curve of 0.801 for 2-year RFS and was externally validated. Based on risk stratification by the SR-B score, low-risk patients had a significantly higher 2-year RFS (training: aHR = 5.834; validation: aHR = 5.675) than high-risk patients (all $P < 0.001$). In a propensity-score matched cohort, low-risk patients treated with resection had a significantly higher 2-year RFS than those with TACE (aHR = 3.891); high-risk patients had a comparable 2-year RFS than those with TACE (aHR = 0.816).

Conclusion: Resection may be beneficial to resectable patients with intermediate-stage HCC based on the SR-B score.

THU-133

Impact of radiological response and pattern of progression on overall survival in patients with hepatocellular carcinoma treated by atezolizumab-bevacizumab

Claudia Campani^{1,2,3}, Ariane Vallot⁴, Haroun Ghannouchi⁵, Manon Allaire^{6,7}, Manon Evain⁶, Philippe Sultanik⁶, Sabrina Sidali^{1,8}, Lorraine Blaise^{9,10}, Dominique Thabut^{6,11}, Nathalie Ganne^{1,9,10}, Mathilde Wagner⁴, Olivier Sutter⁵, Jean Charles Nault^{1,9,10}.
¹Centre de Recherche des Cordeliers, Sorbonne Université, Inserm, Université de Paris Cité, Team « Functional Genomics of Solid Tumors », Paris, France;
²Equipe labellisée Ligue Nationale Contre le Cancer, Labex OncoImmunology, Paris, France;
³Department of Experimental and Clinical Medicine, Internal Medicine and Hepatology Unit, University of Firenze, Florence, Italy;
⁴Service de Radiologie AP-HP Sorbonne Université, Hôpital Universitaire Pitié Salpêtrière, Paris, France;
⁵Unité de Radiologie Interventionnelle, Hôpital Avicenne, Hôpitaux Universitaires Paris-Seine-Saint-Denis, Assistance-Publique Hôpitaux de Paris, Bobigny, France;
⁶Service d'Hépatogastroentérologie, AP-HP Sorbonne Université, Hôpital Universitaire Pitié Salpêtrière, Paris, France;
⁷Centre de Recherche des Cordeliers, INSERM, Sorbonne Université, Université de Paris, Team Proliferation Stress and Liver Physiopathology, Paris, France;
⁸Assistance-Publique Hôpitaux de Paris, Hôpital Beaujon, Service d'Hépatologie, DMU DIGEST, Clichy, France;
⁹Liver Unit, Hôpital Avicenne, Hôpitaux Universitaires Paris-Seine-Saint-Denis, Assistance-Publique Hôpitaux de Paris, Bobigny, France;
¹⁰Unité de Formation et de Recherche Santé Médecine et Biologie Humaine, Université Paris Nord, Bobigny, France;
¹¹Sorbonne Université, INSERM, Centre de recherche Saint-Antoine (CRSA), Institute of Cardiometabolism and Nutrition (ICAN), Paris, France
 Email: naultjc@gmail.com

Background and aims: The combination of atezolizumab and bevacizumab (A-B) is the first-line treatment for patients with unresectable hepatocellular carcinoma (HCC). RECIST 1.1 are the validated criteria used to define the response to systemic therapy in oncology whereas mRECIST criteria have been proposed for the radiological evaluation of patients treated for HCC. Our study aims to assess the radiological response (rR) to A-B therapy using RECIST 1.1 and mRECIST criteria, to define the predictors of rR and radiological progression (rP) for each of the criteria, and the ability of these criteria and of the pattern of progression to predict overall survival (OS).

Method: HCC patients treated with A-B were retrospectively included in two centers between July 2020 and October 2022. A retrospective blinded central analysis was performed using contrast-enhanced liver imaging at 12w after the start of treatment by two radiologists in order to assess RECIST 1.1 and mRECIST response. Inter-reader agreement was analyzed using weighted kappa statistics and logistic regression was used to assess predictors of rR and rP. The association between the variables at the start of A-B treatment, rR, and OS were modelled in univariate and multivariate analysis using the Cox model. Differences in survival between the different categories of rR and according progression pattern were assessed using Kaplan-Meier curves and the log-rank test.

Results: A total of 125 patients were included, median age was 65y and 79% were male. Etiology included hepatitis B (23.2%) and C (39.2%), excessive alcohol consumption (35.2%) and/or NAFLD (25.6%). Cirrhosis was present in 73.6% of the patients including 80.4% Child-Pugh A; 69.6% of the patients were classified as BCLC C. The median OS of the population was 12.4 months (95%CI:9.43–15.37). At the first imaging assessment, according to RECIST 1.1 and mRECIST, 13.6% and 20.8% had response, 39.2% and 35.2% stable disease and 47.2% and 44% progression respectively. Interobserver agreement with weighted kappa values was substantial with both criteria (0.789 for RECIST 1.1 and 0.790 for mRECIST, $p < 0.001$). The presence of extrahepatic metastases (HR:4.22, CI95%:1.90–9.32, $p < 0.001$) was independently associated with a higher risk of rP in RECIST 1.1 in multivariate analysis. No significant predictors of response or

progression were identified using mRECIST criteria. OS was increased in patients with rR in RECIST1.1 (HR:0.38 CI95% 0.15–0.94, $p=0.04$) and mRECIST (HR:0.13 CI95%:0.04–0.40, $p=0.037$). Conversely, OS was shorter in patients who progressed in RECIST 1.1 (HR:2.67 CI95%:1.59–4.51, $p<0.001$) and mRECIST (HR:3.14 CI95%:1.85–5.32, $p<0.001$) compared to other. Patients classified as responders, regardless of the criteria used, had not reached median OS, which was 16.20 and 15.87 months with RECIST 1.1 and mRECIST criteria for patients classified as stable and 9.07 months for patients classified as progressors for both criteria ($p<0.001$). Among the patterns of progression on A-B, only the appearance of new metastatic lesions was associated with a worse OS (HR:1.93 CI95%:1.04–3.57, $p=0.036$)

Conclusion: RECIST 1.1 and mRECIST criteria similarly predict OS in A-B treated HCC patients with more patients identified as responders with mRECIST criteria. Presence of extrahepatic metastases at baseline was associated with a higher risk of radiological progression and the occurrence of new metastatic lesions at progression with a decreased survival.

THU-134

Feasibility of systemic anti-cancer therapy as an alternative to best supportive care in patients with advanced HCC and Child-Pugh B liver dysfunction

Claudia Fulgenzi^{1,2}, Antonio D'Alessio^{1,3}, Bernhard Scheiner^{1,4}, Naoshi Nishida⁵, Celina Ang⁶, Thomas Marron⁶, Linda Wu⁷, Anwaar Saeed⁸, Brooke Wietharn⁸, Antonella Cammarota^{3,9}, Tiziana Pressiani⁹, Matthias Pinter⁴, Rohini Sharma¹, Jaekyung Cheon¹⁰, Yi-Hsiang Huang¹¹, Pei-Chang Lee¹¹, Samuel Phen¹², Anuhya Gampa¹³, Anjana Pillai¹³, Andrea Napolitano¹⁴, Caterina Vivaldi¹⁵, Francesca Salani^{15,16}, Gianluca Masi¹⁵, Dominik Bettinger¹⁷, Robert Thimme¹⁸, Arndt Vogel¹⁸, Martin Schoenlein¹⁹, Kornelius Schulze²⁰, Johann von Felden²⁰, Henning Wege²⁰, Peter Galle²¹, Mario Pirisi²², Joong-Won Park²³, Masatoshi Kudo⁵, Lorenza Rimassa^{3,9}, Amit Singal¹², Alessio Cortellini^{1,2}, Hong Jae Chon¹⁰, Giorgia Ghittoni²⁴, Calogero Camma²⁵, Benedetta Stefanini²⁶, Franco Trevisani²⁶, Edoardo Giovanni Giannini²⁷, David J. Pinato^{1,22}.

¹Imperial College London, Hammersmith Campus, United Kingdom; ²Bio-Medico Campus University Hospital, Roma, Italy; ³Humanitas University, Italy; ⁴Medical University of Vienna, Wien, Austria; ⁵Kindai University Hospital, Osakasayama, Japan; ⁶Mount Sinai Medical Center, New York, United States; ⁷Mount Sinai Medical Center, New York, United States; ⁸The University of Kansas Cancer Center, Kansas City, United States; ⁹Humanitas Research Hospital, Cascina Perseghetto, Italy; ¹⁰CHA Bundang Medical Center, CHA University, Medical Oncology, Department of Internal Medicine, Seongnam-si, Korea, Rep. of South; ¹¹Taipei Veterans General Hospital, Taiwan; ¹²University of Texas Southwestern Medical School, Dallas, United States; ¹³UChicago Medicine, Chicago, United States; ¹⁴The Royal Marsden Hospital, United Kingdom; ¹⁵Pisan University Hospital Cisanello, Pisa, Italy; ¹⁶Scuola Superiore Sant'Anna, Pisa, Italy; ¹⁷University Medical Center Freiburg, Freiburg im Breisgau, Germany; ¹⁸Hannover Medical School, Hannover, Germany; ¹⁹University Medical Center Hamburg-Eppendorf, Department of Oncology, Hamburg, Germany; ²⁰University Medical Center Hamburg-Eppendorf, Department of Medicine, Hamburg, Germany; ²¹University medicine at the Johannes Gutenberg University in Mainz, Mainz, Germany; ²²University of Eastern Piedmont, Vercelli, Italy; ²³National Cancer Center, Goyang-si, Korea, Rep. of South; ²⁴Belcolle Hospital, Viterbo, Italy; ²⁵Università degli Studi di Palermo, Palermo, Italy; ²⁶Alma Mater Studiorum-Università di Bologna, Semeiotics Unit, Department of Medical and Surgical Sciences, Bologna, Italy; ²⁷University of Genoa, Genova, Italy

Email: c.fulgenzi@imperial.ac.uk

Background and aims: No randomized controlled trial evidence exists to support use of systemic therapy in patients with hepatocellular carcinoma (HCC) in the setting of liver dysfunction. Although selected patients with Child-Pugh (CP) B cirrhosis can likely be safely

treated with immunotherapy, whether systemic anti-cancer therapy (SACT) improves survival in this population is unclear. In this retrospective study, we described outcomes of CP-B patients treated with either sorafenib (Sor), nivolumab (Nivo) or atezolizumab plus bevacizumab (A+B) and compared them to best supportive care (BSC) in a propensity score weighted (PSW) analysis.

Method: From two international consortia, we selected CP-B patients receiving A+B ($n=72$), Nivo ($n=46$) or Sor ($n=114$) as first-line systemic therapy for advanced HCC between 2010 and 2022 and compared outcomes to a cohort of 159 patients receiving BSC in the same timeframe. SACT exposure was evaluated in relationship to OS using propensity score weighted (PSW) multivariate regression models.

Results: In the unmatched population ($n=392$), the 233 patients receiving active treatment for HCC had a longer mOS compared to the 159 receiving BSC (6.5 vs. 5.5 months, $p=0.011$).

Following PS matching for Barcelona Clinic Liver Cancer (BCLC) stage (A/B vs C), alpha-fetoprotein (AFP) (>400 vs ≤ 400 ng/ml), CP score (7/8 vs 9) and presence of main portal vein tumor thrombosis (PVTT), 114 couples were left, and receipt of SACT remained associated with improved mOS (7.7 vs 5.8 months, $p<0.001$).

PSW univariate regression analyses demonstrated a significant reduction in the risk of death in patients exposed to A+B (HR: 0.6, 95%CI: 0.4–0.8); Nivo (HR: 0.5, 95%CI:0.4–0.8) and Sor (HR: 0.6, 95%CI: 0.5–0.9, $p=0.001$). Better OS was observed in patients exposed to A+B (HR: 0.6, 95%CI: 0.4–0.8), Nivo (HR: 0.4, 95%CI:0.3–0.7) and Sor (HR: 0.7, 95%CI: 0.6–0.9, $p<0.001$) following adjustment for unbalanced prognostic traits in PSW-multivariate models.

Significantly inferior survival was observed in patients with AFP >400 ng/ml (HR: 1.9, 95%CI: 1.5–2.5); CP score of 9 (HR: 1.7, 95%CI: 1.2–2.4) and in the presence of PVTT (HR: 1.8, 95%CI: 1.4–2.4).

In the SACT-exposed group, incidence of treatment-related adverse events (trAEs) of all grades was 59%. trAEs rates were higher in A+B (69%) and Sor (67.5%) than Nivo (43.2%, $p<0.001$).

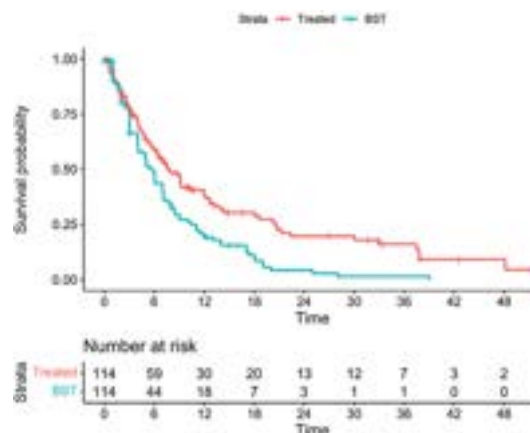


Figure: KM curves for OS in the PS matched population

Conclusion: Receipt of SACT was associated with a small but significant OS improvement in CP-B patients treated with SACT compared to BSC. PS-weighted OS estimates indicate extended survival times in patients with CP 7–8, AFP <400 ng/ml and no PVTT, identifying a patient sub-population where SACT may be delivered with higher clinical benefit. This retrospective study provides a benchmark for the survival extension potentially associated with SACT delivered in CP-B patients.

THU-135

Clinical profile and outcomes of hepatocellular carcinoma in primary Budd Chiari syndrome

Ankit Agarwal^{1,2}, Sagnik Biswas¹, Manas Vaishnav¹, Shekhar Swaroop¹, Rithvik Golla¹, Shubham Mehta¹, Shivanand Gamangatti², Subrata Acharya¹, Sashi Paul², Shalimar¹.
¹AIIMS Hospital, Gastroenterology and HNU, New Delhi, India; ²AIIMS Hospital, New Delhi, India
 Email: drshalimar@yahoo.com

Background and aims: There is scant literature on Budd-Chiari syndrome (BCS) in Hepatocellular carcinoma (HCC). Radiological interventions play an important role in the management of BCS and HCC. The feasibility and outcomes of interventions for the management of BCS and HCC in primary BCS-HCC are unclear. We aimed to assess the clinical presentations and outcomes of patients with primary BCS-HCC.

Method: All consecutive patients diagnosed with primary BCS-HCC evaluated between January 1987 and January 2023 were included in this retrospective analysis of a prospectively maintained database. The diagnosis was based on either imaging/liver biopsy with elevated alfa-fetoprotein (AFP). As a protocol, BCS was managed first with endovascular intervention followed by HCC therapy.

Results: Overall, 35/904 (3.8%) BCS patients evaluated had primary BCS-HCC. BCS-HCC patients, when compared to patients with BCS alone, were older (mean age: 32 vs 26 years, $P = 0.001$), with higher proportion of IVC block, cirrhosis and long-segment vascular obstruction. 18 had HCC at first presentation [prevalence 18/904 (1.99%) and 17 developed HCC (among 886) over a follow-up of 4601 person-years with an incidence of 0.36 (0.22–0.57) per 100 person-years. The median AFP levels in BCS-HCC group was 1310 ng/ml, with higher levels in patients with BCS-HCC at first presentation, compared to those who developed HCC at follow-up (13029 vs 500 ng/ml, $P = 0.01$). The BCLC presentation included A: 5 (14.28%), B: 17 (60.71%), C: 9 (25.71%) and D: 4 (11.4%). Of the 35 BCS-HCC, 26 (74.3%) underwent radiological interventions for BCS and 22 (62.8%) patients underwent treatment for HCC. Thirteen (37.1%) BCS-HCC patients were not treated for HCC: 7 (53.8%) in group at first presentation and 6 (46.2%) in the BCS-follow-up group. The interventions for HCC included transarterial chemoembolization in 18 (81.8%), oral TKI in 3 (13.6%) and TARE in 1 (4.5%) patient. The response at 1 month based on m-RECIST criteria was available in 15/

22 (68.2%). Of these 15, 5/15 (33.3%) showed complete response, 6/15 (40.0%) showed partial response, 4/15 (26.7%) had progressive disease. One patient died within 1 month of TACE. The median number of interventions for HCC were 1 (range, 1–5). The median survival among patients who did not undergo interventions for HCC, compared with those who did, was 3.5 years vs 3.1 months ($p = 0.0001$) (figure a). The median survival among those who underwent intervention as per BCLC stages A, B, C, D was 172 days, 1352 days, 240 days and 40 days, respectively (figure b).

Conclusion: Hepatocellular carcinoma is not uncommon in patients with BCS. Radiological interventions are feasible in select primary BCS-HCC patients and may improve outcomes.

THU-136

Surgical resection of hepatocellular carcinoma has high feasibility, safety and survival in non-cirrhotic liver: a prospective Spanish multicentre study

Marta Romero-Gutiérrez¹, Laura Monserrat Lopez Torres¹, Ana Matilla², Mariano Gómez³, Sonia Pascual⁴, Carlos Aracil⁵, Maria Teresa Ferrer Rios⁶, Mireia Miquel⁷, Laura Marquez², Vanesa Bernal Monterde⁸, Diana Horta⁹, Cristina Alarcón¹⁰, Maria Belen Piqueras Alcol¹¹, Jesús Manuel González¹², Cristina Fernández Marcos¹³, Ana Martin Algibez¹⁴, Julia Morillas¹⁵, Raquel Latorre Martínez¹⁶, Paloma Rendon¹⁷, Sonia Blanco¹⁸, Milagros Testillano¹⁹, Maria Luisa Gutierrez Garcia²⁰, Dalia Morales Arraez²¹, Inmaculada Chico²², Rafael Gómez Rodríguez¹.
¹Hospital Universitario de Toledo, Spain; ²Hospital General Universitario Gregorio Marañón, Madrid, Spain; ³Hospital Universitario de Getafe, Madrid, Spain; ⁴Hospital General Universitario de Alicante, Spain; ⁵Hospital Universitario Arnau de Vilanova, Lleida, Spain; ⁶Hospital Universitario Virgen del Rocío, Sevilla, Spain; ⁷Hospital Parc Taulí de Sabadell, Barcelona, Spain; ⁸Hospital Universitario Miguel Servet, Zaragoza, Spain; ⁹Hospital Universitario Mútua de Terrassa, Barcelona, Spain; ¹⁰Hospital General de Villalba, Madrid, Spain; ¹¹Hospital Universitario de Fuenlabrada, Madrid, Spain; ¹²Hospital Universitario de Salamanca, Spain; ¹³Hospital Universitario de Burgos, Spain; ¹⁴Hospital Universitario Doce de Octubre, Madrid, Spain; ¹⁵Hospital Virgen de la Luz, Cuenca, Spain; ¹⁶Hospital Universitario Son Llàtzer, Palma de Mallorca, Spain; ¹⁷Hospital Universitario Puerta del Mar, Cádiz, Spain; ¹⁸Hospital Universitario de Basurto, Bilbao, Spain; ¹⁹Hospital Universitario de Cruces, Vizcaya, Spain; ²⁰Hospital Universitario Fundación de Alcorcón, Madrid, Spain;

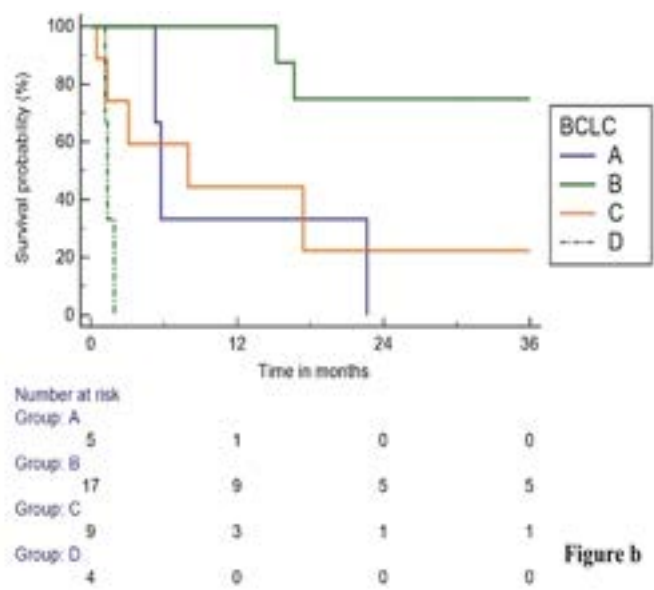
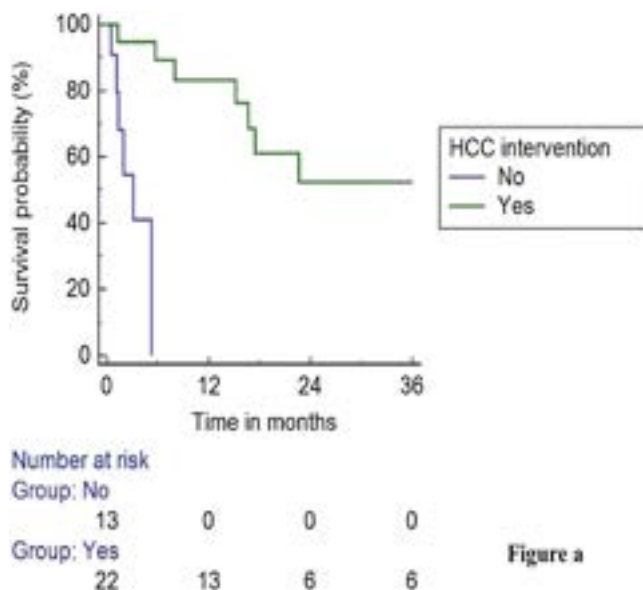


Figure: (abstract: THU-135): KM curves of BCS-HCC patients with (a) intervention and without intervention (log-rank $P < 0.001$) (b) as per BCLC stages (log-rank $P < 0.001$).

POSTER PRESENTATIONS

²¹Hospital Universitario de Canarias, Canarias, Spain; ²²Hospital Universitario Infanta Elena, Madrid, Spain
Email: m.romero.gutierrez@gmail.com

Background and aims: There are scarce data in the literature about liver resection of hepatocellular carcinoma (HCC) in non-cirrhotic patients.

Method: One hundred and forty-one non-cirrhotic patients with HCC diagnosed by histology were included in a Spanish multicenter prospective registry (23 centers, May 2018–October 2022). Surgical resection was performed in 90 patients (63.8%). Liver cirrhosis was excluded by histology. We analyzed the baseline characteristics, evolution and prognostic factors.

Results: Median age was 70.4 (range: 31–86) years. Eighty-three percent were male, 25.6% had other cancers, 2.2% had family history of HCC, 56.7% hypertension and 35.6% diabetes. Toxic habits: non-smoker 27.8%, non-alcohol 52.2%. Etiological study showed hepatopathy in 80%: NASH ± alcohol 26.7%, viral infection ± alcohol 25.5% (HCV 17.7%, HBV 7.8%), alcohol 14.6%, other 8.8% and unknown etiology 4.4%. Twenty percent had no underlying liver disease. Fibrosis stage was mild fibrosis (0–1) in 57.8%, stage 2 in 20%, 3 in 18.9% and unknown in 3.3%. aMAP score had 14.4% in the low-risk group. In 23.3% the diagnosis was made by follow-up ultrasonography, 56.7% was casual and 20% by symptoms. A single nodule was detected in 85.6%. The median size of main nodule was 49 (10–190) mm. Sixty percent had typical hallmark for HCC at least in some of the dynamic imaging explorations performed. Only 2.2% had vascular invasion and 1.1% extrahepatic spread. Median alpha-fetoprotein (AFP) level was 3.6 (range: 0.9–24868) ng/ml (21.1% >20 ng/ml). ECOG 0: 88.9%. The Barcelona Clinic Liver Cancer (BCLC) staging was 0 in 7.8%, A in 80%, B in 10%, C in 2.2%. Resection was anatomical in 85.7% (39.6% laparoscopy/46.1% laparotomy) and non-anatomical in 14.3% (1.1% laparoscopy/13.2% laparotomy), with Pringle maneuver in 46.2%. Surgical piece had: microvascular invasion 25.3%, satellitosis 7.7% and capsule 36.3%. Tumor differentiation: well 29%, moderate 61.1%, poor 4.4%, undifferentiated 1.1%, other histologic variants 4.4%. There were some complications in 15 patients (16.7%): 10 mild and 5 severe, with only 2 cases of perioperative mortality (2.2%). Median follow-up was 31 (range: 2–53) months. Recurrence was 19% at 1 year, 31% at 2 years, 35% at 3 years. AFP > 20 ng/ml was a predictor of relapse. Twenty nine percent received sequential therapy: 6.7% surgery, 2.2% TACE, 13.4% systemic therapy, 2.2% ablation, 4.4% other (1 liver transplantation). The global 1-, 2-, 3- and 4-years survival rate was 95.5%, 84%, 77% and 63.5% respectively. Deaths: 23.3% (71.4% due to liver related causes). BCLC staging, differentiation degree and microvascular invasion were predictors of survival.

Conclusion: This multicenter prospective study showed that surgical resection of non-cirrhotic HCC is an adequate therapeutic approach, with favorable results even in extensive tumors. Less than a third of patients received subsequent therapies. Perioperative morbidity and mortality were low.

THU-137

Real-world experience of atezolizumab plus bevacizumab combination treatment in high risk patients with advanced hepatocellular carcinoma

Sangyoun Hwang¹, Hyun Young Woo², Jeong Heo², Hyung Jun Kim¹, Young Joo Park², Kiyoun Yi², Yu Rim Lee³, Soo Young Park³, Byoung Kuk Jang⁴, Woo Jin Chung⁴, Won Young Tak³. ¹Dongnam Institute of Radiological and Medical Sciences, Korea, Rep. of South; ²Pusan National University Hospital, Korea, Rep. of South; ³Kyungpook National University Hospital, Korea, Rep. of South; ⁴Keimyung University Dongsan Hospital, Korea, Rep. of South
Email: jheo@pusan.ac.kr

Background and aims: Atezolizumab plus bevacizumab was established as the first line therapy for patients with advanced Hepatocellular carcinoma through phase 3 clinical trial.

However, real world data is lacking in patients who showed poor response to this combination regimen such as high risk patients.

Method: This is a multicenter retrospective study. Between January 2020 to April 2022, 215 patients treated for advanced HCC with atezolizumab plus bevacizumab (ATE+BEV) from four tertiary hospital was analyzed. High risk patients was defined as patients with Vp4 portal vein thrombus, bile duct invasion, or liver infiltration >50%. Tumor response was evaluated with the Response Evaluation Criteria in Solid Tumors (version 1.1.).

Results: Out of 215, 98 (45.6%) was high risk population. Child-Pugh class was A in 186 (86.5%) and B in 29 (13.5%). 128 (59.5%) received neoadjuvant or concomitant radiation treatment. In overall population, objective response rate (ORR) was 21.9% and disease control rate (DCR) was 73.9%. The median progression free survival (PFS) was 8.68 months (95% CI, 7.26–10.10) and median overall survival (OS) was 11.25 months (95% CI, 9.50–13.00). In high risk population, ORR and DCR were 23.5% and 67.3%. The median PFS was 7.32 months (95% CI, 4.78–9.87) and median OS was 10 months (95% CI, 8.19–11.82). Only OS was significantly shorter in high risk population. In total population, neutrophil to lymphocyte (NLR) was common factor associated with both PFS and OS in multivariate analysis. In high risk population, preemptive or concomitant radiation therapy was common factor associated with better PFS and OS in multivariate analysis. Baseline Child-Pugh score was only associated with OS. A total of 92 (42.8%) patients experienced any grade of adverse events (AEs). The most common AEs was proteinuria (14.8%). The rate of grade 3 or higher AE is higher in high risk population (24.5% vs. 11.3%).

Conclusion: ATE+BEV treatment showed consistent efficacy and tolerable safety event including patients with the high risk advanced HCC and Child-Pugh class B. Furthermore, radiation therapy could improve the PFS and OS in the high risk patients.

THU-138

Atezolizumab plus bevacizumab for patients with unresectable hepatocellular carcinoma and high hepatitis B viral load: focusing on hepatic safety and viral kinetics

San-Chi Chen¹, Hsiao-Hui Sophie Tsou², Teng-Yu Lee³, Hung-Wei Wang⁴, Yen-Hao Chen⁵, Tseng-En Wang⁶, Yung-Yeh Su², Shengshun Yang³, Chang-Fang Chiu⁴, Tsang-Wu Liu², Ann-Lii Cheng⁷, Li-Tzong Chen⁸, Chiun Hsu⁷. ¹Taipei Veterans General Hospital, Taiwan; ²National Health Research Institutes, Taiwan; ³Taichung Veterans General Hospital, Taiwan; ⁴China Medical University Hospital, Taiwan; ⁵Chang Gung Medical Foundation, Taiwan; ⁶Mackay Memorial Hospital, Taiwan; ⁷National Taiwan University Hospital, Taiwan; ⁸Kaohsiung Medical University Chung-Ho Memorial, Taiwan
Email: sunkist.chen37@gmail.com

Background and aims: The safety of immune checkpoint inhibitor therapy for hepatitis B (HBV)-related unresectable hepatocellular carcinoma (uHCC) with high viral load was not clear. This study, sponsored by Taiwan Cooperative Oncology Group (ClinicalTrials.gov: NCT04180072), aimed to clarify the liver-related adverse events (AE) of atezolizumab (atezo) plus bevacizumab (bev) for uHCC with high HBV viral load.

Method: Eligible patients were histologically proven uHCC, Child A liver function, HBV DNA >2000 IU/ml, and ≥ 1 measurable tumor by RECIST 1.1. Patients with VP4 portal vein invasion or tumors occupying >50% of liver volume were excluded. Atezo 1200 mg plus bev 15 mg/kg were given on day 1 every 3 weeks until tumor progression or occurrence of unacceptable toxicity. Anti-HBV nucleoside analogs were given prior to start of and during atezo + bev therapy. The primary end point was overall response rate (ORR) by RECIST v1.1. Secondary end points included ≥ grade 3 liver-related AE, HBV reactivation, and patient survival.

Results: Thirty patients were enrolled (mean age 58.6 years, M/F 29/1, macrovascular invasion 11, distant metastasis 11, median baseline HBV DNA 134,500 IU/ml (range 2010–1760000)). Seventeen patients achieved virological response (VR, defined as HBV DNA decrease to

<25 IU/ml). The median time to VR was 2.1 months and was not correlated with baseline viral load. No HBV seroconversion occurred. All-grade liver AE occurred to 13 patients and 6 of them considered immune-related (grade 3, 1 patient; grade 1–2, 5 patients). This grade 3 liver immune-related AE (hepatitis), along with grade 4 Stevens-Johnson syndrome, occurred after 2 cycles of atezo + bev therapy, and resolved after methylprednisolone treatment. No patients experienced HBV reactivation. Five partial responses and 15 stable diseases according to RECIST 1.1 were documented among 28 evaluable patients. One additional patient with documented partial response, after initial progressive disease, that lasted for about 8 months. As of December 31, 2022 (median follow-up 8.21 months, range 1.90–30.03), the median progression-free and overall survival was 6.28 months (95% CI 3.75–8.34) and 19.70 months (95% CI 7.79–NR).

Conclusion: Atezo + bev was generally safe and efficacious in uHCC patients with high HBV viral load (grant support T2219, MOHW112-TDU-B-221-124007).

THU-139

Portal-hypertension parameters are associated with survival and ascites occurrence in patients with hepatocellular carcinoma treated by external radiotherapy

Heloïse Giudicelli-Lett¹, Mickael Andraud¹, Mathilde Wagner¹, Rémi Bourdais², Jean-Marc Simon¹, Dominique Thabut¹, Manon Allaire¹. ¹Pitié Salpêtrière, France; ²ICSM 77, France
Email: heloise.giudicelli@gmail.com

Background and aims: Radiotherapy (RT) appears as a new treatment in the hepatocellular carcinoma (HCC) therapeutic arsenal but can expose to radiation induced liver disease that includes ascites occurrence. We aimed (i) to study the impact of PHT on RT outcome and (ii) to identify predictive factors of ascites occurrence as this could preclude the access to further HCC treatment.

Method: We conducted a retrospective monocentric study in which all cirrhotic patients who received either stereotactic ablation body radiation therapy (SABR) or conventionally fractionated radiotherapy (CFRT) for HCC between 2012 and 2022 were included. PHT was assessed on upper endoscopy and on imaging using the Portal hypertension score (PHT Score) based on the presence on imaging of ascites (0–3), varices (0–3), and spleen size (0–3). Threshold of 6 was chosen according AUROC analyze. Time-to-events data were estimated by Kaplan-Meier method with log-rank test, along with Cox-models.

Results: 60 patients were included (female 27%, median age 49 yrs, Child-Pugh class A 82%, cause of liver diseases alcohol/metabolic syndrome/hepatitis C in 56/40/32%). 40% and 15% presented history of ascites and acute variceal bleeding (AVB) respectively, 26% had large size esophageal varices (EV), median HTP score was 4 and 19% presented a HTP score ≥ 6 . All patients underwent appropriate prophylaxis for AVB when indicated (1 TIPS and 9 NSBB). 92% were BCLC-0/A, median tumor size was 30 mm. An infiltrative form and vascular invasion were present in 2% and 3% respectively. SABR was performed in 39 (48Gy/9 fractions) and CFTR in 21 patients (54Gy/29 fractions). The maximal PTV1 EQD2 (a/b = 10) and PTV1 volumes were 124Gy and 103cc (SABR) and 64Gy ($p < 0.001$) and 173cc ($p = 0.91$) (CFTR). Median EQD2 to uninvolved liver (a/b = 3) were 11Gy and 13Gy ($p = 0.41$) in the SABR and CFTR group respectively. Overall survival (OS) was 75%, 50% and recurrence free survival 54%, 22% at 1 and 3 years after RT, respectively. At six months, progressive disease according to RECIST1.1 was more frequent in patients treated by CFTR vs SABR (18% vs 7%, $p < 0.001$). In univariate but not in multivariate analysis, SABR (HR = 2.65, $p = 0.03$), albumin (HR = 1.00, $p = 0.05$), maximal PTV1 EQD2 (a/b = 10) (HR = 1.02, $p = 0.01$) and PTV1 volume (HR = 0.99, $p = 0.04$) were associated with mortality. In log rank analysis, HTP score ≥ 6 was associated with lower survival ($p = 0.07$). EV and platelets were not associated with OS in univariate analysis. OS was lower in SABR patients compared to CFTR ($p = 0.03$) and no

specific predictor of mortality was identified in Cox analysis. HTP score was similar between both group ($p = 0.68$). Compared to CFTR patients, SABR patients were significantly older (median age: 73 vs 49 yrs, $p < 0.001$) with more metabolic disease (51% vs 19%, $p = 0.02$). Ascites incidence after RT was 24%, 34%, and 38% at 6, 12, and 24 months, respectively. In univariate analysis, platelets count (HR = 1, $p = 0.08$), history of AVB (HR = 2.58, $p = 0.09$) and SABR tended (HR = 2.59, $p = 0.09$) to be associated with ascites but the only significant predictive factor was a HTP score ≥ 6 (HR = 4.25, $p = 0.007$) and this result was confirmed in log rank analysis ($p = 0.003$). Presence of large size EV was not associated with ascites occurrence ($p = 0.12$). Among 14 patients who developed ascites, 11 were treated with NSBBs.

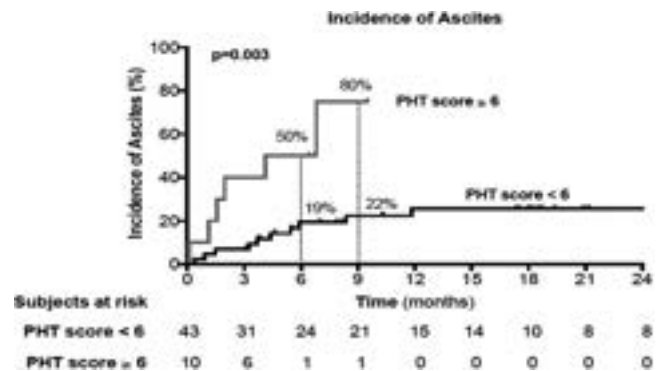


Figure:

Conclusion: This retrospective study suggests that RT should be avoided in patients with a HTP score ≥ 6 to prevent ascites occurrence that could preclude access to further HCC treatments.

THU-140

Outcomes between surgical resection and transarterial chemoembolization in patients with multifocal BCLC-A and Child-Pugh B

Ji won Yang¹, Won-Mook Choi¹, Danbi Lee¹, Ju Hyun Shim¹, Kang Mo Kim¹, Young-Suk Lim¹, Han Chu Lee¹, Jonggi Choi¹. ¹Liver Center, Asan Medical Center, University of Ulsan College of Medicine, Gastroenterology, Korea, Rep. of South
Email: jkchoi0803@gmail.com

Background and aims: 2022 version of the Barcelona Clinic Liver Cancer (BCLC) system does not recommend resection for multinodular hepatocellular carcinoma (HCC) within Milan criteria. Thus, transarterial chemoembolization (TACE) is regarded the preferred treatment option. In addition, no specific recommendation exists regarding patients with Child-Pugh (CP) class B and this multifocal BCLC stage A of HCC. Therefore, we aimed to compare the outcomes between surgical resection and TACE in patients with multinodular HCC and CP class B.

Method: We retrospectively analyzed 487 patients with multinodular treatment-naïve HCC within Milan criteria and CP class B who received either resection or TACE as an initial therapy at Asan Medical Center, Seoul, the Republic of Korea between 2013 and 2022. Overall survival (OS) was estimated using Kaplan-Meier method and comparison of the OS between resection and TACE was conducted by log-rank test. Propensity-score (PS) matching analysis was also used to minimize biases between the two groups. Cox proportional model was used to identify factors associated with a worse prognosis. Median follow-up period was 5.3 years.

Results: The median age was 68 years, and 85.0% of the patients were men. 72.5% of the patients had two lesions of HCC and the median size of the largest tumor was 2.0 cm. The 3-, 5-year survival rates were 96.2% and 90.0% in the resection group and 82.2% and 68.3% in the TACE group, respectively. Median OS was significantly longer in the resection group than the TACE group ($p < 0.01$). In multivariate

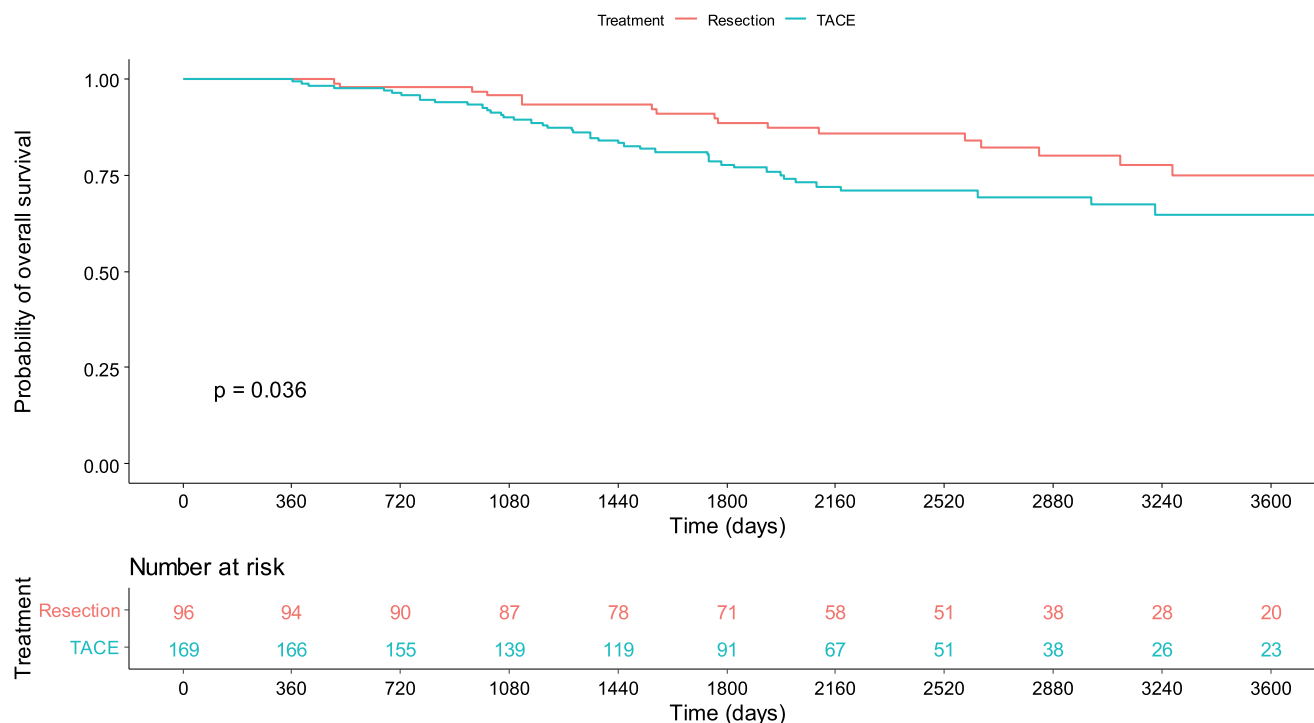


Figure: (abstract: THU-140): Kaplan-Meier curve for overall survival in the resection and TACE groups after applying propensity score matched analysis.

analysis, TACE (hazard ratio [HR]: 1.91, 95% confidence intervals [CIs]: 1.12–3.26, $p = 0.02$), age (HR: 1.05, 95% CIs: 1.03–1.07, $p < 0.01$), and tumor size (HR: 1.41, 95% CIs: 1.08–1.83, $p = 0.01$) were associated with a worse prognosis. PS matched analysis also demonstrated that the resection group had a significantly longer OS than the TACE group ($p = 0.036$).

Conclusion: In the present study, surgical resection showed a better OS than TACE in patients with multinodular HCC (within Milan criteria) and CP class B. Surgical resection can be considered as an effective treatment option in this category of patients.

THU-141

Downstaging hepatocellular carcinoma with checkpoint inhibitor therapy safely improves access to curative liver transplantation: a case series

Margaret Liu¹, Blanca Lizaola-Mayo¹, Channa Jayasekera¹, Amit Mathur², Nitin Katariya², Bashar Aqel¹, David Chascsa¹. ¹Mayo Clinic Arizona, Gastroenterology and Hepatology, Scottsdale, United States; ²Mayo Clinic Arizona, Transplant Surgery, United States
Email: liu.margaret@mayo.edu

Background and aims: Hepatocellular carcinoma (HCC) is the third most common cause of malignancy related mortality globally. Checkpoint inhibitor therapy (CPIT) has traditionally been used as a treatment modality in unresectable HCC, but recent advances have demonstrated the possibility of CPIT as an innovative method of downstaging patients with advanced HCC with the caveat that CPIT prior to transplantation has recognized risks including potentially irreversible graft rejection. The aim of this case series is to report the outcomes of patients at our center who received CPIT in an attempt to shrink the tumor volume of HCC to meet transplant criteria.

Method: A retrospective chart review with descriptive statistics was conducted for all patients at Mayo Clinic Arizona who were diagnosed with HCC who underwent downstaging of HCC with CPIT with the goal of meeting criteria for liver transplantation.

Results: We present 5 cases (mean age 59.4 [40.0–70.0], 100% men) at our center who received CPIT in an attempt to shrink the tumor

volume to within Milan criteria to allow candidacy for liver transplantation. All patients were approved and listed for liver transplantation; 3 patients ultimately received a transplant, 1 was delisted due to his exceptional response to therapy and preserved quality of life, and 1 was waitlisted. The etiologies of liver disease included alcohol ($n = 1$), non-alcoholic steatohepatitis ($n = 2$), hepatitis C ($n = 2$), and primary sclerosing cholangitis ($n = 1$). The average native MELD prior to listing was 13.4 (SD 10.5) with a range of 7–32. All patients received locoregional therapy, including bland or chemoembolization (40%), Y-90 (60%), and/or ablation (60%). Maximum AFP pre-transplant pre-CPIT ranged from 8 to 24 000 ng/ml, which decreased to 5.8–19.6 on CPIT. In addition to CPIT, 2 patients received sorafenib and 1 patient received lenvatinib. CPIT regimens included atezolizumab and bevacizumab (60%), ipilimumab and nivolumab (20%), and pembrolizumab (20%). The median length of time CPIT was held prior to transplant was 3 months, with a range of 2–10 months. Immunosuppression regimens were standard to our center except in 1 patient who received thymoglobulin for induction. There were no cases of rejection upon most recent follow-up, which ranged from 4 months to 2 years post-transplant.

Conclusion: The 5 cases at our center thus far have shown promising outcomes with CPIT as a downstaging tool in order to meet criteria for liver transplantation. The 3 cases who ultimately received a liver transplant demonstrated no evidence of rejection or recurrence up to 2 years post-transplant. Future studies are needed to further assess the outcomes of a larger sample size as well as evaluate areas of interest, such as optimal timing of CPIT discontinuation prior to transplant and to assess whether novel tumor biomarkers may provide insight into which patients will respond to this intervention.

Age (on initial presentation) and sex	Etiology of liver disease (native MELD)	Locoregional therapy	CPIT regimen	Other systemic therapy	Maximum AFP pre-transplant pre-CPIT; maximum AFP on CPIT (ng/mL)	Maximum total tumor diameter prior to CPIT; maximum tumor diameter prior to transplant listing (cm)	Explant residual tumor	Months CPIT was held prior to transplant	Induction immuno-suppression	Time from transplant to last follow up	Recurrence; rejection
61yoM	HCV (9)	Bland embolization (x4), microwave / ethanol ablation (x1)	Atezolizumab, bevacizumab	Lenvatinib	8; 5.8	11.2; 0	no	10	Standard: steroids, then tacrolimus, mycophenolate mofetil, prednisone taper	4 months	No; no
63yoM	NASH (32)	Y-90 (x2)	Nivolumab, ipilimumab	Sorafenib	24,000; 19.6	2.8; 0	no	2	Thymoglobulin, methyl-prednisolone	2 years	No; no
70yoM	NASH (7)	Chemo-embolization (x1), microwave ablation (x1)	Atezolizumab, bevacizumab	n/a	1,719.4; 14.9	14; 0	n/a	n/a	n/a	n/a	No; n/a
63yoM	HCV, EtOH (11)	Y-90 (x1), microwave ablation (x1)	Atezolizumab, bevacizumab	n/a	12; 6.8	17; 0	Multifocal HCC (moderately differentiated), negative margins, no lymphovascular invasion	3	Standard: steroids, then tacrolimus, mycophenolate mofetil, prednisone taper	4 months	No; no
40yoM	PSC (8)	Y-90 (x1), hepatectomy (for ex vivo tumor evaluation for targeted therapy)	pembrolizumab	Sorafenib	37.6; 16.3	5.3; 1.9	n/a	n/a (listed 3 months after discontinuation of CPIT)	n/a	n/a	No; n/a

Table: (abstract: THU-141): Patient demographics, treatment regimens, and outcomes.

THU-142

Clinical outcomes of surgical resection vs yttrium 90 radioembolization (Y90) in hepatocellular carcinoma (HCC) patients with macrovascular invasion (MVI)

Zhaozhen Zou¹, Brian Goh², Peng Chung Cheow², Alexander Chung², London Lucien Ooi², David Chee Eng Ng³, Richard Hoau Gong Lo⁴, Karaddi Venkatanarasimha Nanda Kumar⁴, Apoorva Gogna⁴, Chow Wei Too⁴, Farah Irani⁴, Sean Xuexian Yan³, Kelvin Siu Hoong Loke³, Sue Ping Thang³, Aaron Kian Ti Tong³, Hian Liang Huang³, Kaina Chen⁵, Fiona Ni Ni Moe⁶, Weng Yan Ng⁶, Siou Sze Chua⁶, Jade Shu Qi Goh⁶, Pierce Chow^{1,2}. ¹Duke-NUS Medical School, Singapore; ²Singapore General Hospital, Department of Hepatopancreatobiliary and Transplantation Surgery, Singapore; ³Singapore General Hospital, Department of Nuclear Medicine and Molecular Imaging, Singapore; ⁴Singapore General Hospital, Department of Vascular and Interventional Radiology, Singapore; ⁵Singapore General Hospital, Department of Gastroenterology, Singapore; ⁶National Cancer Centre Singapore, Singapore
Email: pierce.chow@duke-nus.edu.sg

Background and aims: Hepatocellular carcinoma (HCC) patients with macrovascular invasion (MVI) have poorer prognosis, and are more challenging to treat due to the increased likelihood of tumour progression and metastasis. The best treatment method for these patients remain unproven and controversial. In this study, we compared the overall survival (OS) and progression free survival

(PFS) of HCC patients with MVI treated with surgical resection or with Y90 radioembolization.

Method: The retrospective study included non-metastatic HCC patients with MVI who underwent Y90 radiotherapy or surgical resection at the National Cancer Centre Singapore and Singapore General Hospital between January 2000 and May 2019. The patients were stratified based on the degree of portal vein thrombosis (according to Cheng's classification) and compared using inverse probability of treatment weighting (IPTW) -adjusted Kaplan-Meier analysis.

Results: A total of 209 patients were included, with 68 patients undergoing surgical resection and 141 undergoing Y90. After IPTW, the population was well balanced. The OS and PFS of resection patients and Y90 patients were similar (OS: 15.686 vs 14.93, $p = 0.343$, PFS: 5.907 vs 3.38, $p = 0.132$). Length of hospital stay for Y90 patients was significantly shorter than the resection group (3.94 ± 1.27 vs 13.12 ± 11.55 days, $p = 0.003$). For type I PVTT patients, the IPTW-adjusted Kaplan Meier analysis showed significantly better OS for the Y90 group than the surgical resection group ($p = 0.046$), but PFS did not differ significantly between the two groups ($p = 0.248$). For type II PVTT, there was no significant difference between the two groups in either OS ($p = 0.243$) or PFS ($p = 0.193$).

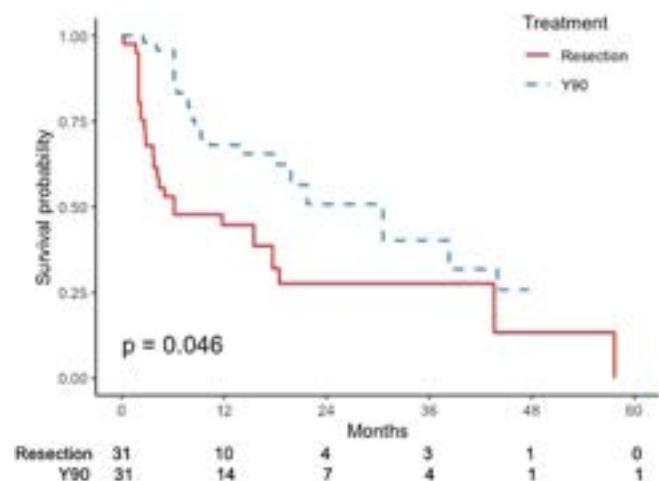


Figure 1: Kaplan-Meier analysis of overall survival in the Y90 group compared with the surgical resection group after IPTW

Conclusion: Compared with surgical resection, Y90 radiotherapy is associated with shorter hospital stay and significantly prolonged overall survival in HCC patients with PVTT and better OS in patients with Type I PVTT.

THU-143

Survival outcomes from Atezolizumab plus Bevacizumab versus Lenvatinib versus Sorafenib in Child Pugh B unresectable hepatocellular carcinoma patients

Margherita Rimini¹, Mara Persano², Toshifumi Tada³, Goki Suda⁴, Shimose Shigeo⁵, Masatoshi Kudo⁶, Jaekyung Cheon⁷, Fabian Finkelmeier⁸, Ho Yeong Lim⁹, José Presa¹⁰, Sara Lonardi¹¹, Fabio Piscaglia¹², Hong Jae Chon⁶, Gianluca Masi¹³, Mario Scartozzi², Stefano Cascinu¹, Andrea Casadei-Gardini¹, ¹Vita-Salute San Raffaele University, Italy; ²University Hospital of Cagliari, Italy; ³Japanese Red Cross Himeji Hospital, Japan; ⁴Graduate School of Medicine, Japan; ⁵Kurume University School of Medicine, Italy; ⁶Kindai University Faculty of Medicine, Japan; ⁷CHA Bundang Medical Center, Korea, Dem. People's Rep. of; ⁸University Hospital Frankfurt, Germany; ⁹Samsung Medical Center, Korea, Dem. People's Rep. of; ¹⁰Liver Unit-CHTMD, Portugal; ¹¹Veneto Institute of Oncology IOV-IRCCS, Italy; ¹²IRCCS Azienda Ospedaliero-Universitaria di Bologna, Italy; ¹³University Hospital of Pisa, Italy

Email: margherita.rimini@gmail.com

Background and aims: The best first line treatment for patients with advanced hepatocellular carcinoma (HCC) and Child-Pugh (CP) class B remains unknown. The aim of the present study was to perform a real-world analysis on a large sample of patients with unresectable HCC with CP B treated with atezolizumab plus bevacizumab Vs Lenvatinib.

Method: The study population included patients affected by advanced (BCLC-C) or intermediate (BCLC-B) HCC patients not suitable for locoregional therapies from both Western and Eastern world (Italy, Germany, Republic of Korea and Japan), who received atezolizumab plus bevacizumab or Lenvatinib as first line treatment. All the study population presented a CP class of B. The primary end point of the study was overall survival (OS) of CP B patients treated with Lenvatinib compared to atezolizumab plus bevacizumab. Survival curves were estimated using the product-limit method of Kaplan-Meier. The role of stratification factors was analyzed with log-rank tests. Finally, an interaction test was performed for the main baseline clinical characteristics.

Results: 217 CP B HCC patients were enrolled in the study: 65 (30%) received atezolizumab plus bevacizumab, and 152 (70%) received lenvatinib. The mOS for patients receiving Lenvatinib was 13.8

months (95% CI: 11.6–16.0), compared to 8.2 months (95% CI 6.3–10.2) for patients receiving atezolizumab plus bevacizumab as first line treatment (atezolizumab plus bevacizumab Vs Lenvatinib: HR 1.9, 95% CI 1.2–3.0, $p = 0.0050$). No statistically significant differences were highlighted in terms of mPFS. The multivariate analysis confirmed that patients receiving Lenvatinib as first line treatment has a significantly longer OS compared to patients receiving atezolizumab plus bevacizumab (HR 2.01; 95% CI 1.29–3.25, $p = 0.0023$). By evaluating the cohort of patients who received atezolizumab plus bevacizumab, we found that Child B patients with ECOG PS 0, or BCLC B stage or ALBI grade 1 were those who had benefit from the treatment thus showing survival outcomes no significantly different compared to those receiving Lenvatinib.

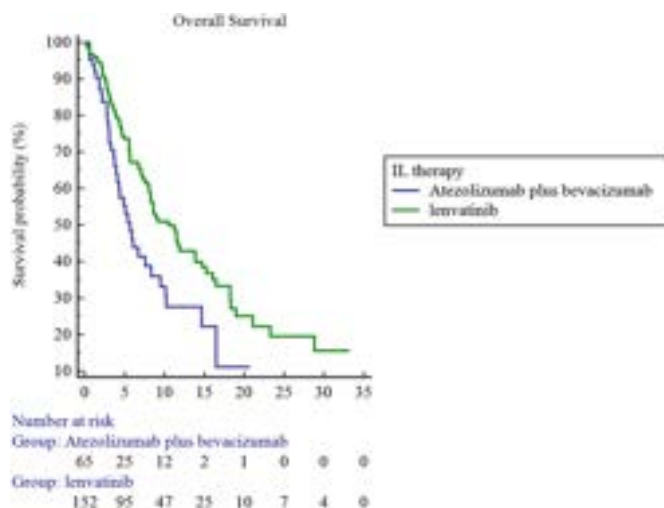


Figure:

Conclusion: The present study suggests for the first time a major benefit from Lenvatinib compared to atezolizumab plus bevacizumab in a large cohort of patients with CP B class HCC.

THU-144

Balancing efficacy and tolerability of first-line systemic therapies for advanced hepatocellular carcinoma: a network metanalysis

Ciro Celsa¹, Giuseppe Cabibbo¹, Gabriele Di Maria¹, Marco Vaccaro², Salvatore Battaglia³, Giacomo Emanuele Maria Rizzo¹, Roberta Ciccio¹, Alessandro Grova¹, Mauro Salvato¹, Paolo Giuffrida¹, Marco Giacchetto¹, Gabriele Rancatore¹, Maria Vittoria Grassini¹, Michela Antonucci⁴, Piera Morana¹, Marco Enea¹, Calogero Camma¹.

¹University of Palermo, Section of Gastroenterology and Hepatology, PROMISE Department, Italy; ²University of Palermo, Italy; ³University of Palermo, Dipartimento di Scienze Economiche, Aziendali e Statistiche, Italy; ⁴University of Palermo, Department of Biomedicine, Neurosciences and Advanced Diagnostics (BiND), Italy

Email: celsaciro@gmail.com

Background and aims: Atezolizumab plus Bevacizumab represents the current standard of care for first-line treatment of advanced HCC. However, direct comparison with other combination treatments including immune-checkpoint inhibitors (ICI) plus tyrosine-kinase inhibitors (TKIs) or anti-CTLA4 are lacking. The aim of this network meta-analysis (NMA) is to indirectly compare the efficacy and the safety of first-line systemic treatments.

Method: Literature search of MEDLINE, EMBASE and SCOPUS databases was conducted up to October, 2022. Phase 3 randomized controlled trials (RCTs) testing TKIs, including Sorafenib and Lenvatinib, or ICIs reporting overall survival (OS) and progression-free survival (PFS) were included. Individual survival data were extracted from OS and PFS curves to calculate restricted mean survival time (RMST). A Bayesian NMA was performed to compare treatments in terms of efficacy (15- and 30-month OS, 6-month PFS)

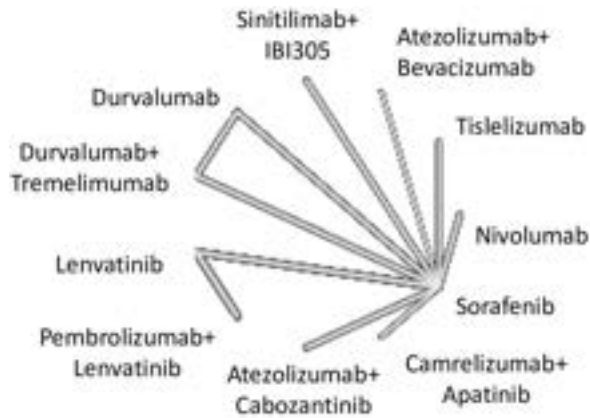


Figure: (abstract: THU-144).

and safety, represented by grade ≥ 3 (severe) adverse events (SAEs). The incremental safety-effectiveness ratio (ISER) as measure of net health benefit was calculated as the difference in probability of SAEs divided by difference in survival between the 2 most effective treatments.

Results: Nine RCTs enrolling 6600 patients were included. Atezolizumab+bevacizumab showed the highest probability (88%) of being the best in 30-month OS. Pembrolizumab+lenvatinib and Lenvatinib showed the highest probability (93% and 86%, respectively) of being the best in terms of PFS. ICI monotherapies were the most safe combination. At a willingness-to-risk threshold of 10% of SAEs for month-year gained, atezolizumab+bevacizumab was favored in 76% of cases, while at a threshold of 30% of SAEs for month-year gained, pembrolizumab+lenvatinib was favored in 72% of cases.

Conclusion: Atezolizumab plus Bevacizumab is the preferred option in unfit patients with high tumor burden, while Lenvatinib with or without Pembrolizumab could be preferred for fit patients with less advanced vascular tumor spread

THU-145

Sequential therapies after atezolizumab plus bevacizumab or lenvatinib first-line treatments

Mara Persano¹, Margherita Rimini², Toshifumi Tada³, Goki Suda⁴, Shimose Shigeo⁵, Masatoshi Kudo⁶, Jaekyung Cheon⁷, Fabian Finkelmeier⁸, José Presa⁹, Gianluca Masi¹⁰, Changhoon Yoo^{11,12}, Sara Lonardi¹², Fabio Piscaglia¹³, Massimo Iavarone¹⁴, Giuseppe Di Costanzo¹⁵, Fabio Marra¹⁶, Giuseppe Cabibbo¹⁷, Francesco Foschi¹⁸, Marianna Sileta¹⁹, Stefano Cascinu², Mario Scartozzi¹, Andrea Casadei Gardini². ¹Medical Oncology, University Hospital of Cagliari, Italy; ²Department of Oncology, Vita-Salute San Raffaele University, IRCCS San Raffaele Scientific Institute Hospital, Milan, Italy; ³Department of Internal Medicine, Japanese Red Cross Himeji Hospital, Himeji, Japan; ⁴Department of Gastroenterology and Hepatology, Graduate School of Medicine, Hokkaido University; North 15, West 7, Kita-ku, Sapporo, Hokkaido 060-8638, Japan; ⁵Division of Gastroenterology, Department of Medicine, Kurume University School of Medicine, Kurume, Fukuoka 830-0011, Japan; ⁶Department of Gastroenterology and Hepatology, Kindai University Faculty of Medicine, Higashi-osaka, Japan; ⁷Department of Medical Oncology, CHA Bundang Medical Center, CHA University School of Medicine, Seongnam, Korea, Rep. of South; ⁸Department of Internal Medicine 1, University Hospital Frankfurt, Goethe University, Frankfurt am Main, Germany; ⁹Liver Unit-CHTMD, Vila Real, Portugal; ¹⁰Unit of Medical Oncology 2, University Hospital of Pisa, Pisa, Italy; ¹¹Department of Oncology, ASAN Medical Center, University of Ulsan College of Medicine, 88, Olympic-ro 43-gil, Songpa-gu, Seoul 05505, Korea, Rep. of South; ¹²Oncology Unit 1, Veneto Institute of Oncology IOV-IRCCS, Padua, Italy; ¹³Division of Internal Medicine,

30-month overall survival		6-month progression-free survival	
Treatment	SUCRA	Treatment	SUCRA
Atezolizumab+Bevacizumab	0.883	Pembrolizumab+Lenvatinib	0.926
Camrelizumab+Apatinib	0.865	Lenvatinib	0.858
Pembrolizumab plus Lenvatinib	0.722	Camrelizumab+Apatinib	0.786
Durvalumab+Tremelimumab	0.626	Sinitilimab+IBI305	0.732
Nivolumab	0.506	Atezolizumab+Cabozantinib	0.695
Lenvatinib	0.466	Atezolizumab+Bevacizumab	0.538
Tislelizumab	0.352	Sorafenib	0.347
Durvalumab	0.342	Durvalumab+Tremelimumab	0.324
Atezolizumab+Cabozantinib	0.120	Nivolumab	0.153
Sorafenib	0.114	Durvalumab	0.107
-	-	Tislelizumab	0.070

Hepatobiliary and Immunoallergic diseases, IRCCS Azienda Ospedaliero-Universitaria di Bologna, via Albertoni 15 Bologna, Italy; ¹⁴Division of Gastroenterology and Hepatology, Fondazione IRCCS Ca' Granda Ospedale Maggiore Policlinico di Milano, Milan, Italy; ¹⁵Department of Hepatology, Naples, 80131, Italy; ¹⁶Dipartimento di Medicina Sperimentale e Clinica, Università di Firenze, Firenze, Italy; ¹⁷Section of Gastroenterology and Hepatology, Department of Health Promotion, Mother and Child Care, Internal Medicine and Medical Specialties, PROMISE, University of Palermo, 90127 Palermo, Italy; ¹⁸Department of Internal Medicine, Ospedale per gli Infermi di Faenza, Faenza, Italy; ¹⁹Division of Medical Oncology, Policlinico Universitario Campus Bio-Medico, Rome, Italy
Email: marapersano@alice.it

Background and aims: Today the most used first-line treatments in hepatocellular carcinoma (HCC) patients are lenvatinib (L) and atezolizumab plus bevacizumab (AB). All the data available about second-line therapies derive from trials conducted in patients who progressed to first-line sorafenib (S) therapy. The aim of this retrospective proof-of-concept study is to compare different second-line drugs for HCC patients progressed to first-line L or AB.

Method: The overall cohort included 2225 consecutive patients from 5 countries (Italy, Germany, Portugal, Japan, and Republic of Korea). A total of 1381 patients had progressed disease (PD) at first-line therapy. 917 patients were in L first-line arm, and 464 patients were in AB first-line arm.

Results: 49.6% of PD patients received second-line therapy without any statistical difference in OS between L first-line arm (20.6 months) and AB first-line arm [15.7 months; $p = 0.12$; hazard ratio (HR) = 0.80]. In L first-line arm, there was a statistical difference between second-line therapy subgroups [$p = 0.04$; S HR = 1; trans-arterial chemoembolization (TACE) HR = 0.65; immunotherapy (I) HR = 0.69; other therapies (O) HR = 0.85]. 40.1% of patients were treated with S achieving an OS of 15.8 months; 36.8% of patients underwent TACE with an OS of 24.7 months; 13.1% of patients were treated with I not reaching a median OS; 10.0% of patients received O with an OS of 20.8 months. Patients who underwent TACE had a significant longer OS than patients who received S ($p < 0.01$; HR = 0.64). In AB first-line arm, there was a statistical difference between second-line therapy subgroups [$p < 0.01$; S HR = 1; L HR = 0.50; cabozantinib (C) HR = 1.34; TACE HR = 0.39; O HR = 0.54]. 18.4% of patients were treated with S achieving an OS of 14.2 months; 36.0% of patients were treated with L with an OS of 17.0 months; 9.9% of patients received C achieving an OS of 12.4 months; 11.6% of patients underwent TACE with an OS of 15.9 months; 24.0% of patients received O not reaching a median OS. Patients who received L had a significant longer OS than patients treated with S ($p = 0.01$; HR = 0.45). Patients who underwent TACE had a significant longer OS than patients who received S ($p < 0.05$;

POSTER PRESENTATIONS

HR = 0.46). No other statistical differences were highlighted between the other subgroups and patients treated with S in both first-line arms.

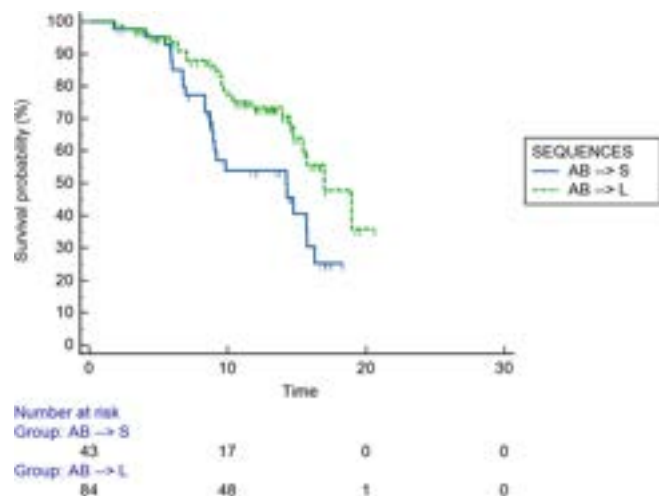


Figure:

Conclusion: The L-I and AB-L sequences are able to achieve the longest median survivals. For patients eligible for locoregional therapy after first-line systemic therapy, TACE has been shown to achieve longer survivals than second-line S in both first-line arms.

THU-146

Prognostic factors of intrahepatic cholangiocarcinoma after radical surgical resection

Keun Soo Ahn¹, Yong Hoon Kim¹, Tae-Seok Kim¹, Koo Jeong Kang¹.
¹Keimyung University Dong-San Hospital, Surgery, Daegu, Korea, Rep. of South
 Email: kjkang@dsmc.or.kr

Background and aims: Still it is not clear what status of intrahepatic cholangiocarcinoma shows a good prognosis after surgical resection. We evaluated prognostic factors of intrahepatic cholangiocarcinoma (iCCA) to suggest surgical indications.

Method: Between 2001 and 2020, surgical resection for iCCA was performed in 204 patients. We analyzed demographic factors perioperative results, and long-term prognostic factors.

Results: Mean age of patients was 66.1 ± 9.7 . The mass-forming type was most frequent (n = 124), followed by periductal infiltrating (n = 59) and intraductal growing (n = 21). The overall 5-year survival was 33.9%, and the disease-free survival rate was 23%. On univariate analysis, a mass size larger than 5 cm, high CEA level, portal vein invasion, perineural invasion, lymphovascular invasion, and lymph node metastasis were significantly poor prognostic factors. Patients with small less than 5 cm sized had a good prognosis (53.6% of 5-year overall survival). On multivariate analysis, the presence of lymph node metastasis was the only significant independent poor prognostic factor.

Conclusion: Present retrospective study showed that lymph node metastasis shows the only significant prognostic factor. Tumor size, number, and the level of the tumor markers affect survival, but these factors are not barriers to obtaining significantly better survival if it is resected radically.

THU-147

Sequential systemic treatment in patients with hepatocellular carcinoma: real-world data in the era of immune checkpoint inhibition

Jana Pauly¹, Cyrill Wehling^{1,2}, Christoph Springfield^{2,3}, Aurelie Tomczak^{2,4}, De-Hua Chang^{2,5}, Jakob Liermann^{2,6}, Clemens Kratochwil^{2,7}, Arianeb Mehrabi^{2,8}, Antje Brockschmidt^{2,9}, Thomas Longerich^{2,4}, Conrad Rauber^{1,2}, Jan Pfeifferberger^{1,2}, Patrick Michl^{1,2}, Michael Dill^{1,2,10}. ¹Department of Gastroenterology, Infectious Diseases, Intoxication, Heidelberg University Hospital, Heidelberg, Germany; ²Liver Cancer Center Heidelberg, Heidelberg, Germany; ³Medical Oncology, National Center for Tumor Diseases, Heidelberg, Germany; ⁴Institute of Pathology, Heidelberg University Hospital, Heidelberg, Germany; ⁵Department of Diagnostic and Interventional Radiology, Heidelberg University Hospital, Heidelberg, Germany; ⁶Department of Radiation Oncology, Heidelberg University Hospital, Heidelberg, Germany; ⁷Department of Nuclear Medicine, Heidelberg University Hospital, Heidelberg, Germany; ⁸Department of General, Visceral and Transplantation Surgery, Heidelberg University Hospital, Heidelberg, Germany; ⁹Clinical Cancer Registry, National Center for Tumor Diseases, Heidelberg, Germany; ¹⁰Experimental Hepatology, Inflammation and Cancer Research Group, German Cancer Research Center, Heidelberg, Germany
 Email: jana.pauly@med.uni-heidelberg.de

Background and aims: The approval of new systemic therapy (ST) agents for patients with advanced hepatocellular carcinoma (HCC) has increased therapeutic options and allows for sequential ST (SST). Approved agents have generally been tested only in first or second line. The introduction of Atezolizumab/Bevacizumab as novel first-line therapy further led to a shift in ST lines. Data is currently limited to assess how much patients benefit from additional treatment lines. Our aim was to investigate survival parameters using real-world data. **Method:** A total of 161 patients with advanced HCC who started ST for HCC at Heidelberg University Hospital between 02/2008 and 03/2022 were included into this retrospective study and follow-up data available until death or data cut-off (12/2022) were included into this retrospective study. To avoid bias, we compared a historical cohort of patients receiving sorafenib (SOR, n = 87) monotherapy with a modern cohort, once multiple systemic agents were available (SST, n = 74), receiving between one to six lines of treatment. Kaplan Meier estimates were performed for assessment of overall survival (OS). Univariate and multivariate cox regression was used to identify favourable survival parameters.

Results: The baseline characteristics between the two cohorts were mostly similar, except the SOR cohort containing significantly more cases of portal vein thrombosis (PVT) than the SST cohort (33% vs 19%, respectively). The SST cohort with up to 6 ST lines had a significant superior median OS (mOS) in comparison to the SOR cohort (8.5 months (SOR) vs 16.9 months (SST), $p < 0.0001$). Among the parameters identified to positively influence OS in the univariate analysis (ECOG ≤ 1 , Child Score ≤ 6 , ALBI score, PVT, AFP < 200 ng/ml, pre-treatment, combined loco-regional treatment (LRT) during or after ST), PVT, AFP, pre-treatment, and LRT remained significant in the multivariate analysis. Accordingly, combined ST and LRT had a significantly positive impact on mOS (8.6 months (ST) vs 25.9 months (ST and LRT), $p < 0.0001$) in all patients with ST. In the SST cohort, 31/74 patients (42%) received immune checkpoint inhibitors (ICI) either in combination (Atezolizumab/Bevacizumab, Ipilimumab/Nivolumab) or as monotherapy (Nivolumab, Pembrolizumab), of which 19 patients (61%) at 2nd line or higher. ICI-therapy, including given as second or higher line, had a significantly positive impact on mOS (9.1 months (non-ICI SST) vs 25.7 months (ICI SST), $p = 0.0002$).

Conclusion: A selection of patients with advanced HCC seem to profit from a combination of ST with LRT indicating a rationale for further investigation in a prospective trial. Patients treated with ICI, also when administered in advanced therapy lines, had a substantial longer OS.

THU-148

Comparison of clinical outcome between Nivolumab and Regorafenib as second-line systemic therapy after Sorafenib failure in patients with advanced hepatocellular carcinoma

Jae Seung Lee^{1,2,3}, Hong Jun Lee⁴, Hye Won Lee^{1,2,3}, Beom Kyung Kim^{1,2,3}, Seung Up Kim^{1,2,3}, Jun Yong Park^{1,2,3}, Sang Hoon Ahn^{1,2,3}, Do Young Kim^{1,2,3}. ¹Yonsei University College of Medicine, Department of Internal Medicine, Seoul, Korea, Rep. of South; ²Yonsei University College of Medicine, Institute of Gastroenterology, Seoul, Korea, Rep. of South; ³Severance Hospital, Yonsei Liver Center, Seoul, Korea, Rep. of South; ⁴Yonsei University College of Medicine, Seoul, Korea, Rep. of South
Email: dyk1025@yuhs.ac

Background and aims: Nivolumab and regorafenib are used as second-line therapies for patients with advanced hepatocellular carcinoma (HCC). We aimed to compare the effectiveness of nivolumab to regorafenib.

Method: We retrospectively reviewed HCC patients treated with nivolumab or regorafenib after sorafenib failure. Progression-free survival (PFS) and overall survival (OS) were analyzed. Inverse probability of treatment weighting (IPTW) using the propensity score (PS) was conducted to reduce treatment selection bias.

Results: Among the recruited 189 patients, 137 and 52 patients received regorafenib and nivolumab after sorafenib failure, respectively. Nivolumab users showed higher Child-Pugh B patients (42.3% vs. 24.1%) and shorter median sorafenib maintenance (2.2 vs. 3.5 months) compared to regorafenib users. Compared to regorafenib users, nivolumab users showed shorter median OS (4.2 vs. 7.4 months, $P=0.045$) and similar median PFS (1.8 vs. 2.7 months, $P=0.070$), respectively. However, median OS and PFS were not different between the two treatment groups after 1:1 PS matching yielded 34 pairs (log-rank $P=0.810$ and 0.810 , respectively), and after stabilized IPTW (log-rank $P=0.445$ and 0.878 , respectively). In addition, covariate-adjusted Cox regression analyses showed that the nivolumab (vs. regorafenib) use was not significantly associated with the PFS and OS after 1:1 PS matching and stabilized IPTW (all $P>0.05$).

Conclusion: Clinical outcomes in patients treated with nivolumab and regorafenib after sorafenib failure did not differ significantly.

THU-149

Efficacy of Atezolizumab/Bevacizumab combination therapy in BCLC-C cirrhotic patients with hepatocellular carcinoma according to the type of disease progression and liver disease severity

Spyridon Pantzios¹, antonia syriha¹, Dionysia Mandilara¹, Ioanna Stathopoulou¹, Georgia Barla¹, Petros Galanis¹, Nikolaos Ptohis², Ioannis Elefsiniotis¹. ¹General Oncology Hospital of Kifisia "Oi Agioi Anargyroi", Academic Department of Internal Medicine-Hepatogastroenterology Unit, National and Kapodistrian University of Athens, Kifisia, Greece; ²General Hospital of Athens G.Gennimatas, Department of Interventional Radiology, Athens, Greece
Email: spiros_pant@hotmail.com

Background and aims: Registrational study (IM BRAVE 150) mainly included hepatocellular carcinoma (HCC) patients at BCLC-C stage, irrespective of the type of progression to this stage, with well compensated liver disease (CPT-A stage). The aim of our study was to retrospectively evaluate, under real life conditions, the overall survival (OS) of patients with advanced HCC (BCLC-C stage), either initially presenting in the advanced stage or migrating from BCLC-A to BCLC-C stage within 2 years after curative LR or RFA, treated either with atezolizumab-bevacizumab (ATZ/BEV) combination or with TKIs sequentially (sorafenib as 1st line and cabozantinib as 2nd line treatment).

Method: Sixty four cirrhotic patients with advanced HCC (56 males, mean age 67y, 22 with diabetes, CPT-A = 45/B = 19, mean MELD/Na = 11, ALBI grade I = 20/grade II = 38, 28 with varices, 18 with extrahepatic metastasis, 24 with macrovascular invasion) who either initially presented on the BCLC-C stage and were treated with ATZ/BEV (group A, N = 23) or TKIs (group B, N = 15) or who migrated from BCLC-A to BCLC-C stage within 2 years after LR or RFA and were treated with ATZ/BEV (group C, N = 12) or TKIs (group D, N = 14) were evaluated.

Results: The four groups were comparable for all the baseline parameters evaluated (age $p=0.9$, gender $p=0.08$, platelets $p=0.246$, chronic liver disease etiology $p=0.408$, coexistence of diabetes $p=0.314$, presence of varices $p=0.066$, CPT stage $p=0.067$, ALBI grade $p=0.398$) except for CPT score ($p=0.012$) and MELD/Na score ($p=0.002$). As expected, median OS was significantly higher for group C patients (61 m) compared to group D (27 m), group A (11 m) and group B (8 m) patients ($p<0.001$). Moreover, post-recurrence

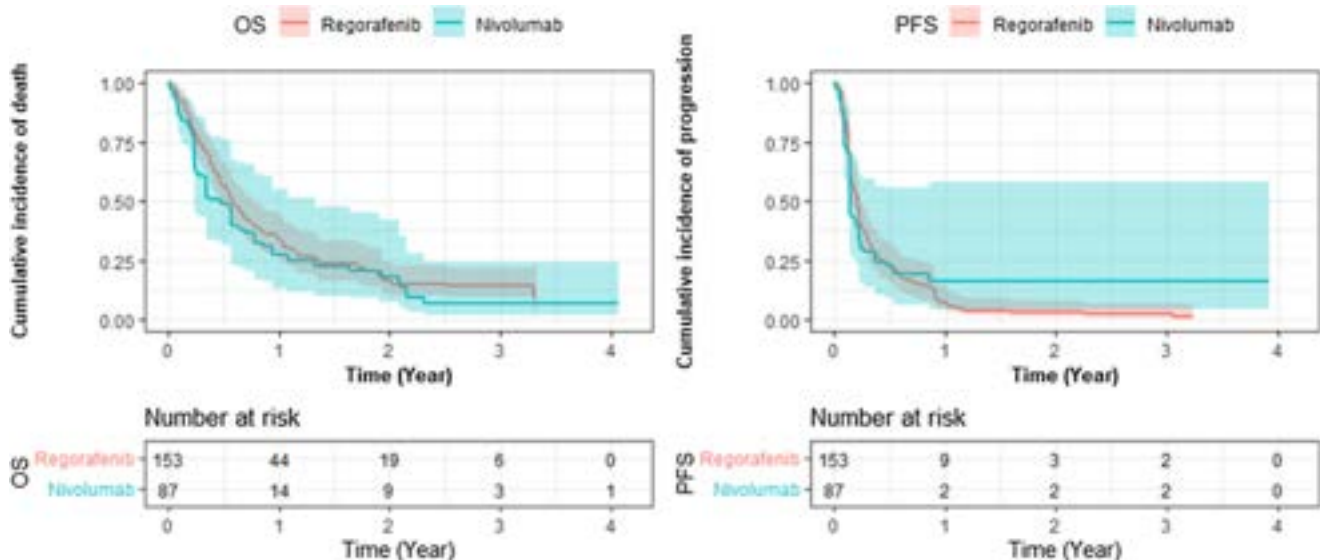
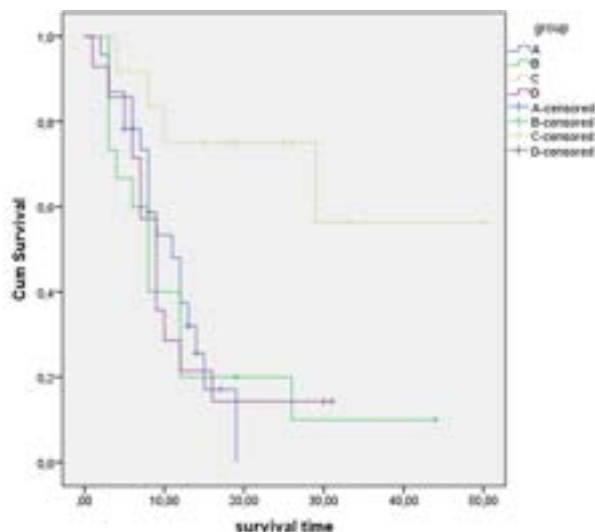


Figure: (abstract: THU-148): Kaplan-Meier curves of overall survival ($p=0.445$) and progression free survival ($p=0.878$) for regorafenib and nivolumab users using the stabilized inverse probability of treatment weighting.

POSTER PRESENTATIONS

survival for group C patients seems to be significantly higher compared to those of group D (9 m) patients ($p=0.007$) as well as for group A and B (figure). Using cox regression analysis, we observe that the OS of group A (HR=3.71, 1.20–11.46, $p=0.02$) was significantly worse than post-recurrence survival of group C, which was comparable to group D (HR = 3.14, 0.95–10.35 $p=0.06$), adjusted for CPT, ALBI and MELD/Na score (figure).



Variables	Hazard ratio	95% confidence interval	P-value
Child number	1.03	0.69 to 1.52	0.89
Meld-Na	1.13	0.98 to 1.31	0.09
ALBI	0.86	0.47 to 1.57	0.62
A vs. C	3.71	1.20 to 11.46	0.02
B vs. C	2.89	0.87 to 9.56	0.08
D vs. C	3.14	0.95 to 10.35	0.06

Figure: Survival of group A (blue), B (green), C (yellow) and D (purple) and cox regression analysis for survival after the beginning of systemic therapy comparing group C to the other groups and adjusted for CPT, ALBI and MELD/Na scores.

Conclusion: Median survival of ATZ/BEV or TKI-treated patients who were initially classified in BCLC-C stage is less than 12 m, irrespective of treatment schedule, as was post-recurrence survival of sequentially TKI-treated patients. ATZ/BEV therapy seems to benefit mainly BCLC-C patients who migrate from earlier stages after curative LR or RFA compared to patients initially presented in the advanced stage. Liver disease severity assessed using CPT and MELD/Na scores seems to drive the overall as well as post-recurrence survival.

THU-150

Changing treatment landscape associated with improved survival in patients with hepatocellular carcinoma: a nationwide, population-based study

Najib Ben Khaled¹, Bernhard Mörtl², Dominik Beier³, Alexander Philipp¹, Andreas Teufel⁴, Ilja Kubisch⁵, Daniel Schwade⁶, Andreas Geier⁷, Florian P. Reiter⁷, Christian M. Lange¹, Julia Mayerle¹, Karin Berger², Enrico de Toni¹, Stefan Munker¹. ¹University Hospital, Ludwig Maximilian University of Munich, Department of Medicine II, Germany; ²University Hospital, Ludwig Maximilian University of Munich, Department of Medicine III and Comprehensive Cancer Center (CCC Munich LMU), Germany; ³InGef-Institute for Applied Health Research Berlin GmbH, Germany; ⁴University Medical Center Mannheim, Medical Faculty Mannheim, Heidelberg University,

Department of Medicine II, Germany; ⁵Klinikum Chemnitz, Department of Internal Medicine II, Gastroenterology, Hepatology, Endocrinology, Metabolic Disorders, Oncology, Germany; ⁶Technical University Munich, Germany; ⁷University Hospital Würzburg, Division of Hepatology, Department of Medicine II, Germany
Email: najib.benkhaled@med.uni-muenchen.de

Background and aims: The treatment of hepatocellular carcinoma (HCC) is undergoing a historic transformation with the availability of several new systemic therapies. The impact of this changing landscape on patient outcomes has not yet been studied in a German cohort in a nationwide, real-world setting.

Method: This observational, retrospective study is based on a claims data base including anonymized, longitudinal data of around 8.8 million persons (InGef database). A sample of four million persons representative for the German population was drawn. We assessed the implementation and impact of systemic therapies for patients with HCC in nationwide clinical routine in three parts: First, we describe patient characteristics, drug treatments, and associated costs in a large, representative cohort of patients with HCC between 2015 and 2020. Second, we examine the association between drug availability and outcomes comparing survival of HCC patients by date of initiation of systemic therapy. Third, we explore the impact of treatment sequencing based on lenvatinib or sorafenib in the first line setting after the approval of lenvatinib in 2018.

Results: We identified a total of 5586 individuals with a diagnosis of HCC in the study period. Statistically significant developments included an increase in mean age and proportion of patients receiving systemic therapies, and a decrease in chronic hepatitis C virus infection. To investigate the association between systemic therapy availability and survival, we identified patients with HCC started on first line systemic therapy in the study period and grouped them according to time of treatment initiation, defining the cut-off date of the two groups as the approval of lenvatinib into period A (01/2015–07/2018, $n=255$) and period B (08/2018–12/2020, $n=205$). Baseline characteristics among patients in both periods were similar. Median overall survival (mOS) in the whole cohort was 5.5 months (95% confidence interval (CI) : 4.8–6.9). In period B, a superior mOS of 6.5 months (95% CI : 4.9–8.9) was identified as compared to period A with an mOS of 5.3 months (95% CI : 4.5–6.3) ($p=0.046$). Multivariate Cox's regression analysis to adjust for confounders revealed that treatment initiation in period B was an independent, statistically significant factor for a longer survival (period B vs period A hazard ratio 0.77, 95% CI : 0.61–0.96, $p=0.0196$). When comparing first line treatment options, lenvatinib showed a significantly longer OS as compared to sorafenib. Median OS with lenvatinib was 9.7 months ($n=103$, 95% CI : 6.3–18.4) versus 4.8 months with sorafenib ($n=102$, 95% CI : 4.0–7.1, $p=0.008$). Patients treated with lenvatinib were younger and had a lower proportion of metastatic disease.

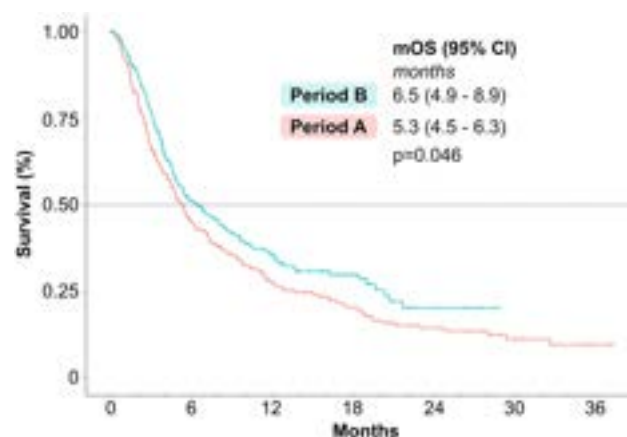


Figure:

Conclusion: The introduction of multiple new treatment options resulted in survival improvements of patients with HCC in Germany.

THU-151

Efficacy and tolerability of stereotactic body radiation therapy in patients with hepatocellular carcinoma: a retrospective cohort study

Dorothy Liu¹, Jennifer Tan², Marcus Robertson¹. ¹Monash Health, Gastroenterology, Clayton, Australia; ²Peter MacCallum Cancer Centre, Radiation Oncology, Bentleigh East, Australia
Email: dorothyliu22@gmail.com

Background and aims: Hepatocellular carcinoma (HCC) is a leading cause of cancer-related mortality worldwide. There is emerging evidence for the role of stereotactic body radiation therapy (SBRT) as an alternative locoregional therapy in the management of HCC, with high rates of local control and low rates of significant toxicity reported. A multicentre retrospective cohort series was conducted to evaluate the efficacy and safety of SBRT for the treatment of HCC.

Method: A retrospective analysis of a prospective database including adult patients that underwent treatment for HCC with SBRT between July 2012 and September 2021 in Melbourne, Australia, was performed. The primary outcome was local tumour control and secondary outcomes included progression-free survival, overall survival and adverse events (AEs).

Results: 60 patients were included with a median follow-up of 16 months (IQR 7–23). Cirrhosis was documented in 37 (62%) patients with the most common underlying aetiology being alcohol (49%), and a median baseline Child-Pugh grade of A and albumin-bilirubin (ALBI) score of –2.35 (IQR –2.65–2.15). Forty-seven patients had received prior alternative HCC therapies. A total of 81 lesions were

treated (median size 40.5 mm, IQR 30–59 mm) with a median biologically effective dose (BED₁₀) of 86 Gy. The most common reported AE was fatigue. AEs of at least grade 2 severity were reported in 19% of patients. One patient died from radiotherapy induced liver disease 3 months following SBRT. Local control was 76% and 41% at 1 and 2 years, respectively. Progression free survival and overall survival at 1 year were 40% and 75%, respectively. Progression free survival and overall survival at 1 and 2 years were 16% and 42%, respectively.

Conclusion: SBRT can provide durable local control of HCC in the short term with low rates of significant AEs, however disease progression remains common. Thus, larger prospective studies are required to establish the role of SBRT in combination with other therapies in the management of HCC.

THU-153

Prognostic impact of metastatic site in patients receiving first-line sorafenib therapy for advanced hepatocellular carcinoma

Luca Lelasi^{1,2}, Francesco Tovoli^{1,2}, Matteo Tonnini^{1,2}, Bernardo Stefanini^{1,2}, Raffaella Tortora³, Giulia Magini⁴, Rodolfo Sacco^{5,6}, Tiziana Pressiani⁷, Franco Trevisani^{2,8}, Fabio Piscaglia^{1,2}, Alessandro Granito^{1,2}. ¹IRCCS Azienda Ospedaliero-Universitaria di Bologna, Division of Internal Medicine, Hepatobiliary and Immunoallergic Diseases, Bologna, Italy; ²University of Bologna, Department of Medical and Surgical Sciences, Bologna, Italy; ³Cardarelli Hospital, Liver Unit, Department of Transplantation, Naples, Italy; ⁴Papa Giovanni XXIII Hospital, Department of Gastroenterology and Transplant Hepatology, Bergamo, Italy; ⁵Azienda Ospedaliero-Universitaria Pisana,

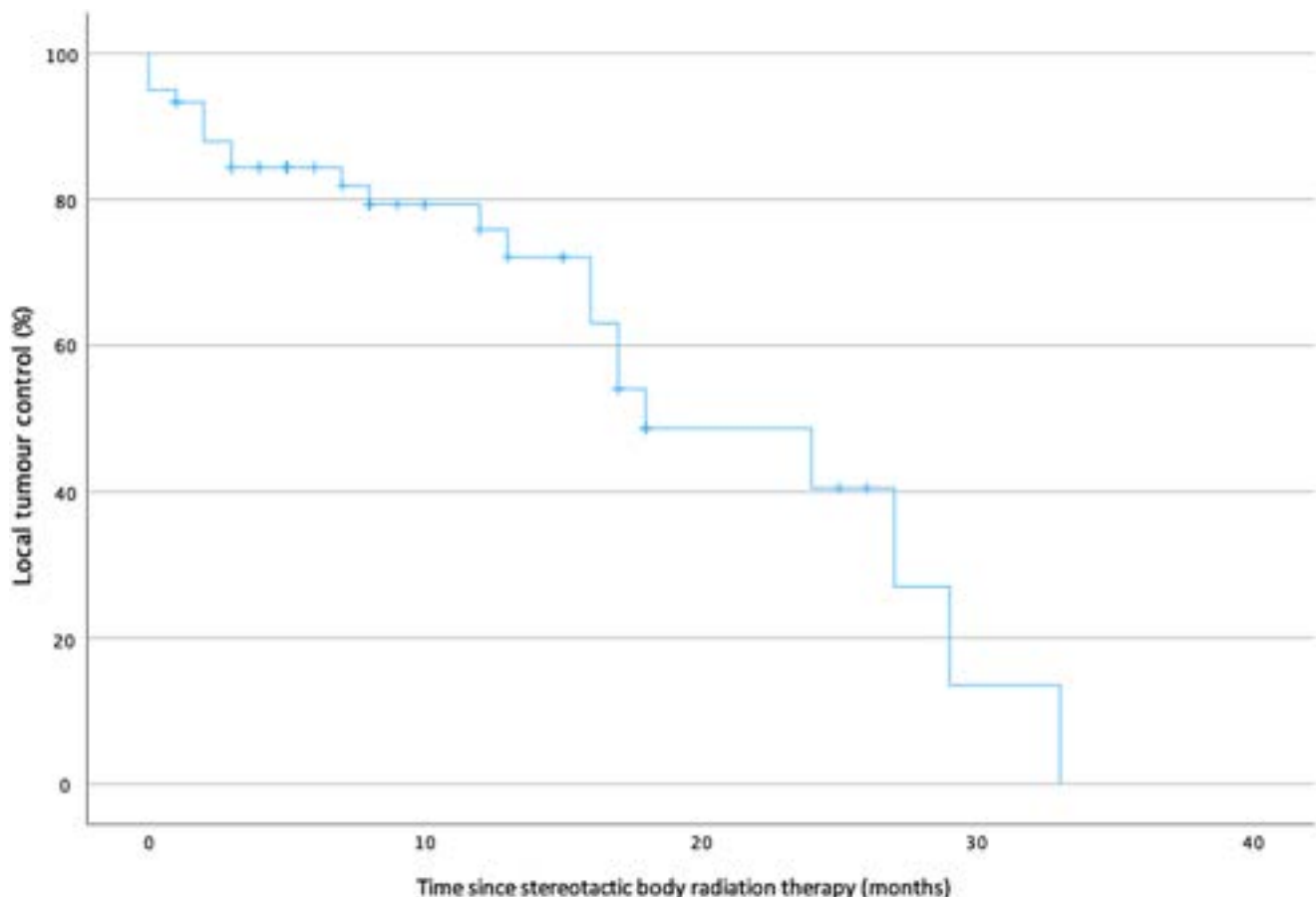


Figure: (abstract: THU-151): Local tumour control following stereotactic body radiation therapy

POSTER PRESENTATIONS

Gastroenterology Unit, Pisa, Italy; ⁶Foggia University Hospital, Gastroenterology and Digestive Endoscopy Unit, Foggia, Italy; ⁷IRCCS Humanitas Research Hospital, Humanitas Cancer Center, Rozzano, Italy; ⁸IRCCS Azienda Ospedaliero-Universitaria di Bologna, Semeiotica Medica, Bologna, Italy
Email: luca.ielasi.kr@gmail.com

Background and aims: Extrahepatic spread is a well-known negative prognostic factor in patients with advanced hepatocellular carcinoma (HCC). The prognostic role of different metastatic sites and their response rate to systemic treatment is still being debated.

Method: We considered 237 metastatic HCC patients treated with sorafenib as first-line therapy in five different Italian centers from 2010 to 2020.

Results: The most common metastatic sites were lymph nodes, lungs, bone and adrenal glands. In survival analysis, the presence of dissemination to lymph nodes (OS 7.1 vs 10.2 months; $p = 0.007$) and lungs (OS 5.9 vs 40 10.2 months; $p < 0.001$) were significantly related to worse survival rates compared with all other sites. In the subgroup analysis of patients with only a single metastatic site, this prognostic effect remained statistically significant. Palliative radiation therapy on bone metastases significantly prolonged survival in this cohort of patients (OS 19.4 vs 6.5 months; $p < 0.001$). Furthermore, patients with lymph node and lung metastases had worse disease control rates (39.4% and 30.5%, respectively) and shorter radiological progression-free survival (3.4 and 3.1 months, respectively).

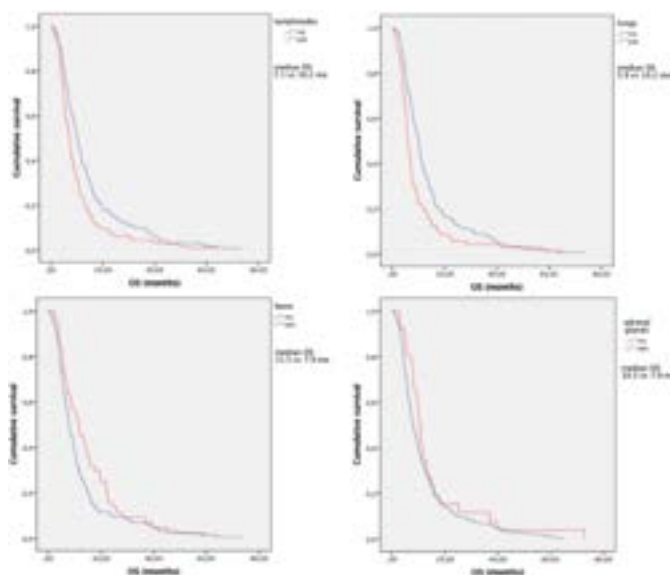


Figure:

Conclusion: In conclusion, some sites of extrahepatic spread of HCC have a prognostic impact on survival in patients treated with sorafenib; in particular, lymph node and lung metastases have worse prognosis and treatment response rate.

THU-154

Improved identification of good candidates for the treatment of intermediate/advanced hepatocellular carcinoma by Yttrium-90 transarterial radioembolization

Carole Vitellius¹, Severine Poulard¹, Julien Fontana¹, Ines Oreistein¹, Pacome Fosse¹, Anita Paisant¹, Laurent Vervueren¹, Frédéric Oberti¹, Christophe Aubé¹, Franck Lauceille¹, Jerome Boursier¹. ¹Angers University Hospital, France
Email: jeboursier@chu-angers.fr

Background and aims: Yttrium-90 transarterial radioembolization (TARE) is a treatment for intermediate/advanced hepatocellular carcinoma (HCC), but its position in the therapeutic arsenal

remains poorly defined. We aimed to validate the prognostic score for HCC treated with TARE recently proposed by Spreafico, and to improve prediction by considering also pre-operative dosimetry.

Method: Eighty-six patients with HCC treated by TARE in our center were included. The preisional tumoral dose of 90Yttrium was calculated using images acquired during the work-up. The Spreafico prognostic score was calculated as previously described and delineated three patients groups with “favorable,” “intermediate,” and “dismal” prognosis (PMID 29331342). The main study outcome was overall survival (OS) and the secondary outcome was progression-free survival (PFS).

Results: Fifty-three patients (62%) were treated with 90Yttrium-glass-microspheres (Therasphere®), and 33 patients (38%) were treated with 90Yttrium-resin-microspheres (Sirsphere®). Sixty-nine patients died during the follow-up. Median OS was 12.0 months (95% CI: 9.0–15.0), and median PFS was 5.0 months (95% CI: 3.5–6.5). OS was 15, 10, and 4 months in the three prognostic groups defined by the Spreafico score ($p < 0.001$, Figure A). Independent predictors of OS were the presence of cirrhosis, an optimal preisional tumoral dose, and the ALBI grade. The CODAG score, developed as the sum of points attributed to these three independent predictors, identified three patient groups: good (0–1 point), intermediate (2 points) and poor (3–4 points) candidates. The CODAG score better discriminated the prognosis with median OS in the three groups being respectively 32, 11, and 4 months ($p < 0.001$, Figure B). Median PFS was respectively 8, 5, and 3 months in the three CODAG groups ($p < 0.001$). The preisional and the received tumoral doses were very well correlated ($R_s = 0.814$, $p < 0.001$).

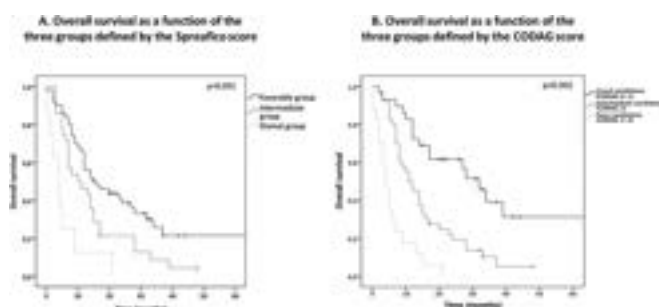


Figure:

Conclusion: The CODAG score improves the identification of good candidates for the treatment of intermediate/advanced hepatocellular carcinoma with transarterial radioembolization.

THU-155

Clinical impact of relative dose intensity over the first four weeks in cabozantinib therapy for unresectable hepatocellular carcinoma

Kaoru Tsuchiya¹, Tsubasa Nobusawa¹, Yutaka Yasui¹, Taisei Keitoku¹, Nobuharu Tamaki¹, Hiroyuki Nakanishi¹, Masayuki Kurosaki¹, Namiki Izumi¹. ¹Musashino Red Cross Hospital, Department of Gastroenterology and Hepatology, Tokyo, Japan
Email: tsuchiyaakaoru3@gmail.com

Background and aims: Cabozantinib (CAB) has been used as 2nd or later-line worldwide in patients with unresectable hepatocellular carcinoma (u-HCC). In the phase III study of CAB (CELESTIAL study), the initial dose of CAB was 60 mg/day, while in the phase III study of the combination of atezolizumab plus CAB (COSMIC312 study), the initial dose of CAB was 40 mg/day. Recently the standard first-line therapy for u-HCC is atezolizumab plus bevacizumab or durvalumab plus tremelimumab. We investigated the clinical impact of relative dose intensity over the first four weeks (4W-RDI) in CAB therapy for u-HCC.

Method: A total of 43 u-HCC patients who received CAB between Jan 2021 and Dec 2022 at our institution was included. Tumor

assessments in accordance with RECIST ver1.1 were performed using dynamic CT or MRI within 4–8 weeks and every 8–10 weeks thereafter. The 4W-RDI was calculated as the cumulative dose in the initial 4 weeks divided by the standard dose (60 mg/day), and we evaluated its association with overall survival (OS) and progression-free survival (PFS).

Results: The median age was 74 (24–87) years, and 33 patients were male. Sixteen patients had HBV (n = 7) or HCV (n = 9) infection, and 30 patients were Child-Pugh A. BCLC stage A/B/C were 0/14/29 patients, and 38 patients (88%) were previously treated with atezolizumab plus bevacizumab. CAB was administered as 2nd or 3rd-line in 25 and 4th or later-line in 18 patients. The median follow-up duration was 6.8 months, and the median duration of CAB was 2.7 months. The initial dose of CAB was 60 mg (n = 14), 40 mg (n = 13), and 20 mg/day or less (n = 16). The median PFS and OS were 4.1 and 16.2 months. The objective response rate (ORR) and disease control rate (DCR) was 12.1% and 84.8%. The median 4W-RDI was 33%, and there was no significant difference in PFS and OS between 4W-RDI <40% (n = 27) and ≥40% (n = 16) (3.1 vs. 4.4 months, p = 0.25 and 19.0 vs. 10.2 months, p = 0.78). Adverse events due to CAB were observed in all patients, requiring dose reduction in 35 patients (81%) and interruption of CAB in 32 patients (74%). The rate of molecular targeted therapies after CAB was 62.5%. In a multivariate analysis, the pretreatment ALBI score (HR 7.57, 95% CI 2.09–27.5, P = 0.002) was the only significant factor associated with OS. The 4W-RDI of CAB and treatment -line (CAB as 4–6 line) were not associated with OS. The median OS of the patients who received atezolizumab plus bevacizumab before CAB was 19.1 months.

Conclusion: Maintaining a high 4W-RDI of CAB was not associated with OS and PFS in real-world practice. Prior atezolizumab plus bevacizumab would contribute to prolonged survival in CAB therapy for u-HCC.

THU-156

Tolerability of first line systemic therapy in elderly patients with advanced hepatocellular carcinoma

Giulia Francesca Manfredi^{1,2}, Davide Di Benedetto^{1,2}, Antonio Acquaviva³, Francesca Baorda^{1,2}, Carla De Benedittis², Chiara Gerevini^{1,2}, Cristina Rigamonti^{1,2}, Michela Burlone², Mario Pirisi^{1,2}. ¹Università degli Studi del Piemonte Orientale, Department of Translational Medicine, Novara, Italy; ²AOU Maggiore della Carità, Division of Internal Medicine, Novara, Italy; ³PO Sant'Andrea, Division of Internal Medicine, Vercelli, Italy
Email: gf.manfredi01@gmail.com

Background and aims: Hepatocellular carcinoma (HCC) accounts for 90% of primary liver cancer. The average age of HCC development is 70, with aging being a known risk factor. Elderly patients should not be excluded from systemic therapy based upon age alone and all available treatments can be recommended for them.

Method: We considered 126 patients affected by advanced HCC, treated with first line systemic therapy. Four patients were excluded from the final analysis due to lack of follow-up (FU) information, 6 patients on atezolizumab/bevacizumab therapy were excluded for less than 3 months of FU at the time of data collection. We studied patients' overall survival (OS), time to progression (TTP) represented as therapy duration and adverse events (AE) secondary to two systemic therapies, namely sorafenib (SB) and lenvatinib (LB).

Results: Patients were predominantly men (80.3%); 84.6% of them suffered from cirrhosis, which the most frequent etiology was hepatitis C (44.4%). Thirty-nine percent of patients carried steatosis and metabolic syndrome. Median age at diagnosis of HCC was 72 [27–88], median age at systemic therapy start was 73 [28–88]. Patients older than 65 years represented the 80.2% of our cohort, over 70 were the 42.2%, while over 80 were 19.8% of the total. The median alpha-fetoprotein value before initiation of therapy was 45 [1.2–83000]. Twenty-six patients were treated with LB and median age at therapy start was 76, 90 patients were treated with SB, median age at therapy

start was 72.5 (p = 0.04). Median systemic therapy duration was 11 months in patients treated with LB, 4 months in patients treated with SB (p < 0.05). Median OS was 18.8 months in SB group and 52.7 months in LB group (p < 0.05). No difference was observed in therapy duration considering age >80 years (p = 0.97). No difference was observed in term of OS considering patients younger or older than 80 years (p = 0.72). Most reported AE were fatigue, anorexia and diarrhea, with the latter more common in patients younger than 80 years (p < 0.05). Regarding diarrhea, only 4 patients over 80 (17.4%) had a Common Terminology Criteria for Adverse Events grade >1. Patients over 80 years did not require a dose reduction more than younger ones (p = 0.97). Considering the reason for discontinuing therapy, no difference was observed between patients older than or younger than 80 years of age (p = 0.70).

Conclusion: Our study demonstrates how elderly patients could be treated safely with the same intensity as younger ones. AE didn't represent a crucial factor for discontinuing therapy in elderly. It is essential to know how to manage AE in a timely way, educating the patient to recognize them. Knowing that the epidemiology of HCC will increasingly affect elderly patients, the choice of treatment based on the comorbidity and characteristics of the subject will be decisive, but age alone should not represent a limitation at the beginning of systemic therapy.

THU-157

Incidence and risk factors of post-transarterial chemoembolization complications in patients with hepatocellular carcinoma: a single center retrospective cohort analysis in a large tertiary hospital

Melissa April Pajinag¹, Stephanie Ventura¹, Jose Guillain Cataluña², Nathaniel Paragas³, Dennis Villanueva³. ¹St. Luke's Medical Center Quezon City, Department of Medicine, Quezon City, Philippines; ²St. Luke's Medical Center Quezon City, Institute of Liver and Digestive Diseases, Quezon City, Philippines; ³St. Luke's Medical Center Quezon City, Section of Interventional Radiology, Institute of Radiology, Quezon City, Philippines
Email: melissa_pajinag@yahoo.com

Background and aims: Transarterial chemoembolization (TACE) is used most often for the treatment of large unresectable hepatocellular carcinoma (HCC) that are not amenable to other treatments or as a bridging therapy prior to liver transplantation. This procedure is generally well tolerated with an incidence of major complications post-TACE described as 2–7% with a risk of mortality estimated at 1%. Complications contribute to the prognosis of patients which can be associated with several other risk factors. Once these risk factors are identified, clinicians can carefully select, stratify, and prepare patients for TACE. At present, there is a lack of analysis of the risk factors of complications after TACE of patients with HCC. This study investigated the incidence and risk factors in developing infection, acute kidney injury (AKI), and acute liver decompensation in patients with HCC receiving TACE.

Method: A retrospective cohort study of all adult patients with HCC who have undergone TACE from January 2013 to October 2022 was conducted. Incidence and risk factors developing post-TACE complications were analyzed. Univariate and multivariate analyses were performed to identify factors predictive of infection, AKI, and acute liver decompensation.

Results: Out of the total of 318 patients who underwent TACE, 220 TACE sessions were included. Of these, major complications occurred in 56 cases with an incidence rate of 25.45%. Majority were managed as post-embolization syndrome (43.2%), while 11.8% had infections, 9.1% had acute liver decompensation, and 4.5% had AKI. Total of 4 mortalities were seen with a mortality rate of 1.8%. Larger tumor size (OR 0.19, CI 0.05–0.69, p = 0.03) was identified as a risk factor for the development of infection. While older age was a significant risk factor for developing both AKI (OR 1.09, CI 1.00–1.18, p = 0.10) and acute liver decompensation (OR 1.08, CI 1.02–1.14, p = 0.02). Barcelona

POSTER PRESENTATIONS

Clinic Liver Cancer (BCLC) stage B was also a risk factor in developing AKI (OR 0.08, CI 0.01–0.95, $p = 0.09$). Over-all multivariate analysis of the major complications showed that older age (OR 1.06, CI 1.02–1.11, $p = 0.01$), larger tumor size (OR 0.34, CI 0.13–0.90, $p = 0.07$), multinodular tumor (OR 5.64, CI 1.17–27.18, $p = 0.07$) and longer prothrombin time (OR 1.50, CI 1.16–1.95, $p = 0.01$) were independent risk factors of over-all major complications post-TACE.

Variable	Adjusted OR (90% CI)	p value
Age (years)	1.06 (1.02–1.11)	0.012
Tumor size (cm)	0.34 (0.13–0.90)	0.070
Tumor classification	5.64 (1.17–27.18)	0.070
Baseline prothrombin time (sec)	1.50 (1.16–1.95)	0.011

Figure:

Conclusion: Majority of complications post-TACE consist of minor post-embolization syndrome. The incidence of major complications was notably high at 25% with a mortality rate of 1.8%. Older age poses risk of developing AKI, and acute liver decompensation. Larger tumor size poses risk for infection while BCLC Stage B in developing acute liver decompensation. Risk factors in developing major complications include older age, larger tumor size, multinodular tumor, and longer prothrombin time.

NAFLD Clinical aspects except therapy

WEDNESDAY 21 TO SATURDAY 24 JUNE

TOP-079

Risk of bacterial infections in non-alcoholic fatty liver disease: a nationwide population-based cohort study

Axel Wester¹, Ying Shang¹, Linnea Widman¹, Fahim Ebrahimi¹, Jonas Ludvigsson¹, Hannes Hagström¹. ¹Karolinska Institutet, Sweden
E-mail: axel.wester@ki.se

Background and aims: Previous literature suggests an association between non-alcoholic fatty liver disease (NAFLD) and bacterial infections. We aimed to determine the rate and risk of severe bacterial infections in NAFLD compared to the general population.

Method: In this population-based cohort study, we used national registers to identify all patients diagnosed with NAFLD in Sweden between 1987 and 2020 ($n = 14,869$). The patients were matched at the date of diagnosis with up to ten controls from the general population for age, sex, and municipality ($n = 137,145$). Cox regression was used to estimate hazard ratios (HR) for infections in patients with NAFLD compared to the controls. Cumulative incidences were calculated while accounting for competing risks (non-infection death and liver transplantation).

Results: Severe bacterial infections leading to death or hospitalization occurred in 1990 (13.4 %) patients with NAFLD and 9899 (7.2 %) controls during 94,852 and 1,083,713 person-years of follow-up, respectively. The rate of severe bacterial infections per 1000 person-years was higher in patients with NAFLD (21.0, 95 % CI 20.1–21.9) than controls (9.1, 95 % CI 9.0–9.3) irrespective of comorbidities, including components related to the metabolic syndrome (fully adjusted HR 1.9, 95 % CI 1.8–2.0). The result was similar when additionally including cirrhosis as a time-varying covariate in the model (HR 1.8, 95 % CI 1.7–1.9). Moreover, patients with NAFLD had a higher rate of infections of any severity (fully adjusted HR 1.5, 95 % CI 1.4–1.5) and infection-related mortality (fully adjusted HR 1.8, 95 % CI 1.6–2.2) compared to controls. The ten-year cumulative incidence of severe

bacterial infections was 16.6 % (95 % CI 15.8–17.4) in NAFLD and 8.0 % (95 % CI 7.8–8.2) in controls.

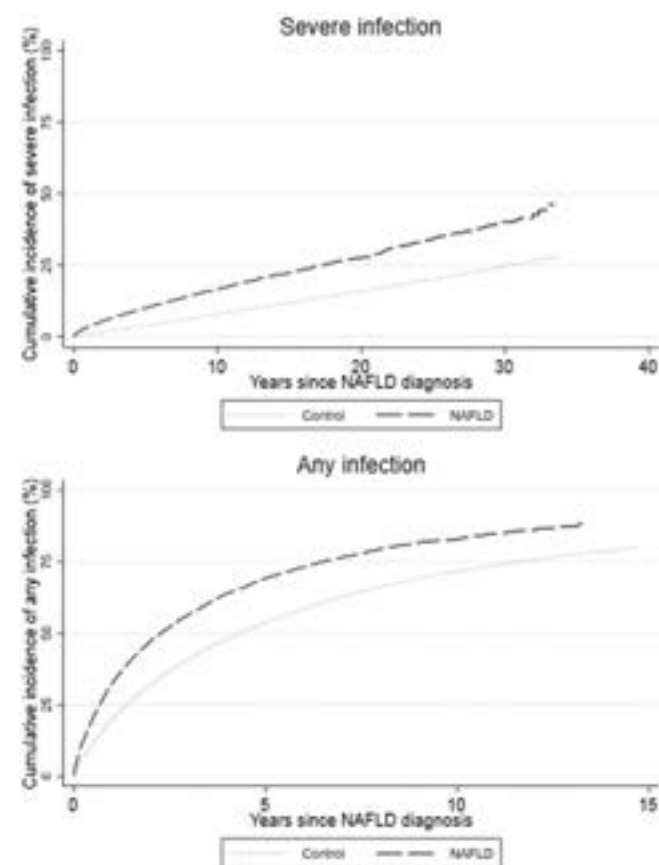


Figure:

Conclusion: NAFLD was associated with incident severe bacterial infections, infections of any severity, and infection-related mortality, independently of components associated with the metabolic syndrome. Increased clinical vigilance of bacterial infections in NAFLD may diminish the risk of premature death.

TOP-081

The growing global burden of non-alcoholic fatty liver disease (NAFLD) among teenagers

Zobair Younossi^{1,2,3}, James Paik^{1,2,4}, Shira Zelber-Sagi⁵, Jeffrey Lazarus⁶, Dipam Shah^{1,7}, Leyla Deavila^{1,2}, Huong Pham¹, Pegah Golabi^{1,2,3,8}, Janus Ong⁹, Saleh Alqahtani¹⁰, Linda Henry^{1,2,3,8}.
¹Inova Health System, Betty and Guy Beatty Center for Integrated Research, Falls Church, United States; ²Inova Health System, Inova Medicine, Falls Church, United States; ³The Global NASH Council, Washington, United States; ⁴The Global NASH Council, Washington, United States; ⁵University of Haifa, School of Public Health, Haifa, Israel; ⁶University of Barcelona, Barcelona Institute for Global Health (ISGlobal), Barcelona, Spain; ⁷Inova Fairfax Medical Campus, Center for Liver Disease, Department of Medicine, Falls Church, United States; ⁸Inova Fairfax Medical Campus, Center for Liver Disease, Department of Medicine, Falls Church, United States; ⁹University of the Philippines, College of Medicine, Manila, Philippines; ¹⁰King Faisal Specialist Hospital and Research Center, Riyadh, Saudi Arabia
E-mail: zobair.younossi@inova.org

Background and aim: NAFLD affects all age groups and all countries. Our aim was to assess NAFLD-related prevalence and liver mortality among teenagers (10–19 years) using the Global Burden of Disease (GBD) dataset.

Method: We analyzed data from 21 GBD regions and countries. GBD modelled NAFLD prevalence based on population-based studies that report NAFLD (ultrasound or imaging). NAFLD-related liver mortality rates (cirrhosis and liver cancer) per 100,000 are reported. The socio-demographic index (SDI) was used as a summary measure as it quantifies each country's rank in the socio-economic development spectrum. Countries are divided into 5 equal groups (quantile) according to their SDI scores. Time trends were assessed by annual percent change (APC) calculated by using Joinpoint regression model.

Results: In 2019, the highest NAFLD prevalence among teenagers was observed in the North Africa and the Middle East region (5.71%), led by Egypt (8.68%), Qatar (8.04%) and Saudi Arabia (7.53%). In this group, the second highest prevalence was observed in Latin America (2.81%), led by Mexico (3.01%) and El Salvador (2.94%). This was followed by Southern Sub-Saharan Africa (2.76%), led by Swaziland (3.17%) and South Africa (3.04%), and East Asia (2.63%), led by Taiwan (3.27%) and China (2.63%). Across SDI quantiles, the prevalence was highest in the middle SDI quintile (2.96%) while the prevalence was lowest in the low SDI quintile (1.70%) groups. In contrast, the liver-death rate (per 100,000) was lowest in the high SDI quintile (0.009) and highest in the low SDI quintile (0.041) groups. From 1990 to 2019, the global NAFLD prevalence increased from 1.84% (19.37 million prevalent cases) to 2.31% (29.16 million prevalent cases) with an APC of +0.80% [95% confidence interval, 0.78%–0.82%] (Figure). In contrast, during the same period, NAFLD-related liver deaths among teenagers remained low and unchanged (400 to 404 cases). From 2010 to 2019, the highest increase in NAFLD prevalence among teenagers was seen in the low-middle SDI quintile (APC = +1.04% [0.95%–1.14%]), followed by those in low SDI quintile (APC = +0.74% [1.09%–1.28%]) and high SDI quintile (APC = +0.25% [0.17%–0.33%]).

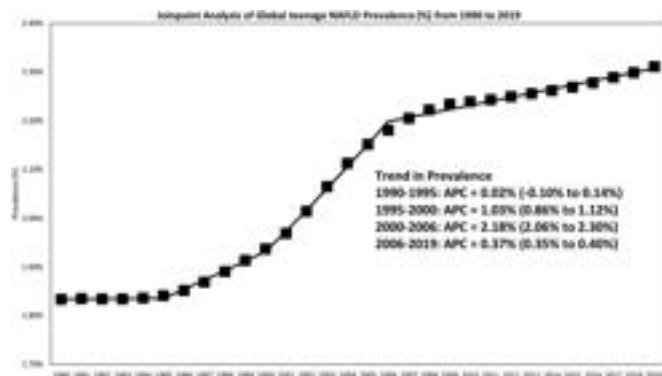


Figure: Joinpoint Analysis of the Global prevalence (%) of NAFLD Among Teenagers

Conclusion: The global prevalence of NAFLD among teenagers is increasing. Although death rates are low, it is expected that the growing prevalence of NAFLD among young populations will drive future liver mortality. Regional and global policies should address NAFLD as an important non-communicable disease.

TOP-082

Identification of a new gene signature that accurately predicts the risk of hepatic decompensation in non-alcoholic fatty liver disease

Maria Jimenez Ramos¹, Timothy Kendall¹, Jessica Minnier^{2,3}, Lucia Bandiera^{4,5}, Filippo Menolascina^{4,5}, Jonathan Fallowfield¹.
¹University of Edinburgh, Centre for Inflammation Research, Edinburgh, United Kingdom; ²Oregon Health and Sciences University, OHSU-PSU School of Public Health, Portland, United States; ³Oregon Health and Sciences University, Knight Cancer Institute Biostatistics Shared Resource, Portland, United States; ⁴Edinburgh University, Institute for Bioengineering, Edinburgh, United Kingdom; ⁵University of Edinburgh, Centre for Engineering Biology, Edinburgh, United Kingdom
 E-mail: jonathan.fallowfield@ed.ac.uk

Background and aims: The global burden of non-alcoholic fatty liver disease (NAFLD) continues to rise, magnifying the unmet need for tools to enable patient stratification and prognostication. The use of molecular features to predict patient outcomes is unexplored. Using SteatoSITE (<https://steatosite.com/>), a national-level resource containing integrated time-stamped pathological, transcriptomic and clinical outcome data from NAFLD patients, we aimed to identify genes associated with a higher risk of hepatic decompensation events in patients with advanced fibrotic NAFLD.

Method: Hepatic bulk RNA-sequencing data from needle biopsies showing NASH-CRN stage F3/F4 fibrosis (n = 226) was compared with samples showing stage F0/F1 fibrosis (n = 295). We performed differential gene expression analysis to identify genes with potential to predict a composite outcome of hepatic decompensation events. Ten runs of the 10-fold cross-validated LASSO-penalised Cox regression was used for feature reduction and subsequent development of a model to subdivide patients into high- and low-risk prognostic groups. We evaluated both groups with Kaplan-Meier (K-M) curves and log-rank test. A time-dependent receiver operating characteristic (ROC) curve was used to evaluate the model predictive ability.

Results: Advanced fibrosis stages (F3/F4) were predictive of subsequent decompensation (p < 0.0001). We identified 1127 dysregulated genes when comparing F3/F4 and F0/F1 patients. When performing the LASSO Cox regression model with these differentially expressed genes, 15 were associated with decompensation events, some of which could translate to circulating biomarkers based on initial analysis using the TexSEC (Translation of tissue gene expression to secretome) tool. Furthermore, there are biologically plausible links to hepatic decompensation for several of the 15-gene panel such as DPEP1 (implicated in acute kidney injury), CXCL1 (a potential biomarker for acute-on-chronic liver failure), CLEC4M (a pathogen-recognition receptor involved in peripheral immune surveillance in liver) and CTGF (a multiorgan fibrogenic master switch and tractable therapeutic target). The generated risk scores were positively associated with decompensation events and the K-M curves delineate clear prognostic separation into high-risk and low-risk groups (p < 0.0001). The measured performance by areas under the ROC curve (AUROCs) were 0.86, 0.81 and 0.83 for 1, 3 and 5 years, respectively.

Conclusion: We have identified a 15-gene signature that predicts the risk of decompensation in patients with advanced NAFLD. Further validation is required in a suitable NAFLD cohort with integrated pathology, transcriptomics and clinical outcomes. This data provides new insights into the pathobiology of NAFLD and sheds light on new potential biomarkers and therapeutic targets.

TOP-088

Altered gut barrier integrity as a mediator of host-microbiome interactions in diabetic patients with advanced Non-alcoholic fatty liver disease

Roberta Forlano¹, Laura Martinez-Gili¹, Jesus Miguens Blanco¹, Charlotte Skinner¹, Mark Thursz¹, Julian Marchesi¹, Benjamin H. Mullish¹, Pinelopi Manousou¹. ¹Imperial college london, Liver unit, Department of Metabolism, Digestion and Reproduction, London, United Kingdom
 E-mail: r.forlano@imperial.ac.uk

Background and aims: Aberration of the complex crosstalk between the intestine and the liver, so-called the "gut-liver axis," has been to be a contributory factor in the development and progression of liver disease in patients with Non-alcoholic fatty liver disease (NAFLD).

Method: Consecutive patients with T2DM were screened for liver disease by bloods, ultrasound and liver stiffness measurements (LSM). Elevated LSM was defined as LSM ≥ 8.1 kPa. Microbiota composition was analysed in stools by 16S rRNA gene sequencing, while metabolites were measured by liquid chromatography-mass spectrometry. Microbiome signatures were analysed in the whole

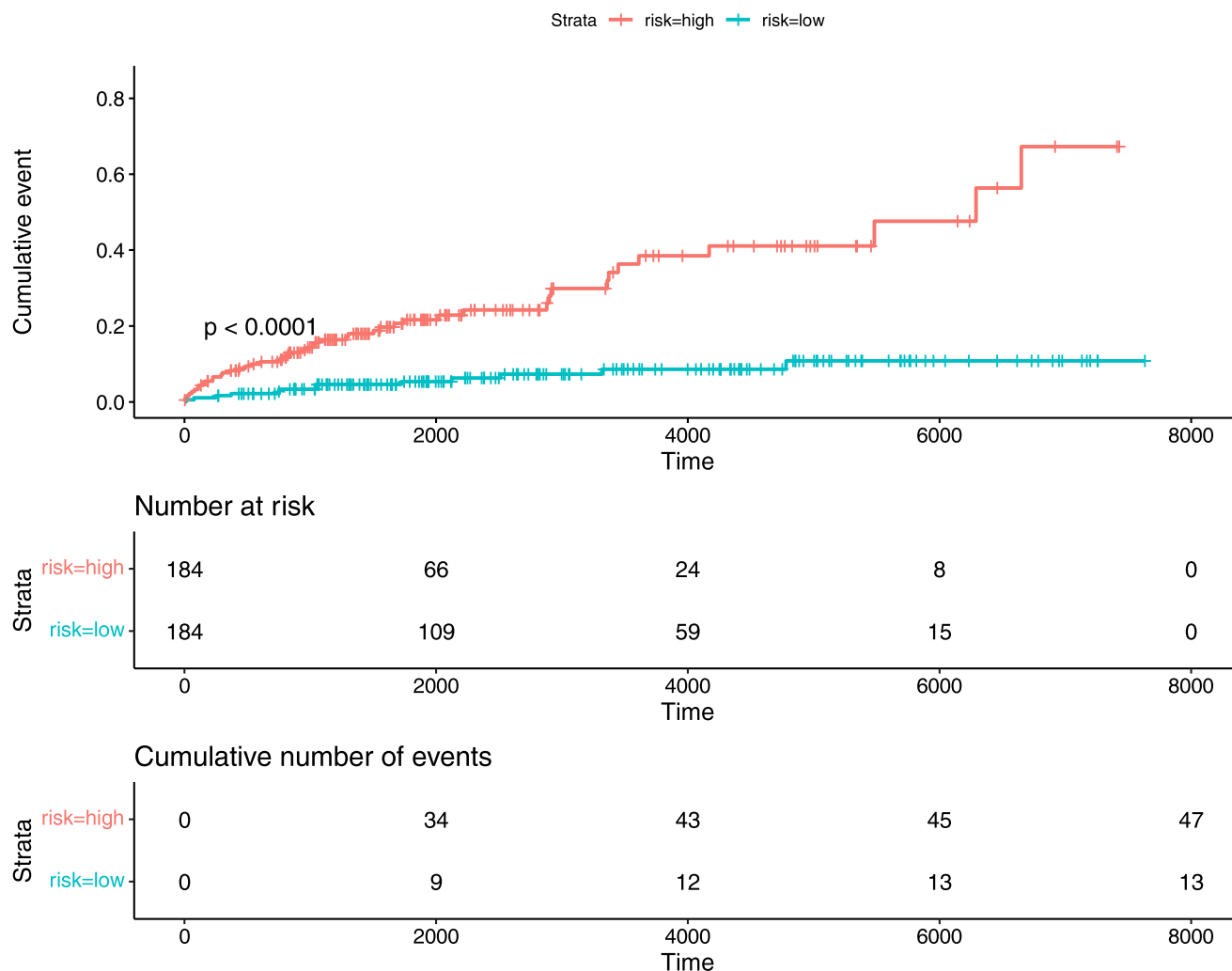


Figure: (abstract: TOP-082).

population (unmatched), as well as in subsets matched for metabolic factors (NAFLD vs non-NAFLD and elevated vs normal LSM). An in-vitro model of gut permeability was set up using monolayers of Madin-Darby canine kidney cells. Permeability was estimated by trans-epithelial electric resistance (TEER) on epithelial volt/ohm meter. Faecal water was derived by stool samples, while E. faecalis spent medium and phosphate-buffered saline were used as positive and negative controls.

Results: Overall, stools from 89 patients were analysed: 17 (17%) had normal liver, 54 (55%) NAFLD and normal LSM and 17 (17%) NAFLD and elevated LSM. Only three ASV were different across unmatched groups: Anaeroplasmata and Escherichia/Shigella ASV were higher, and Butyricococcus ASV lower in those with normal liver (Fig. 1A). In the matched groups, Butyricococcus ASV was significantly higher in those with NAFLD vs non NAFLD (Fig. 1B). Among those with NAFLD, Butyricococcus ASV was significantly higher in those with normal LSM vs those with elevated LSM (Figure 1C). Overall, 12 stool samples were used for the gut permeability. Faecal water from patients with NAFLD and elevated LSM ($n = 4$) caused the greatest drop in the TEER vs those with normal liver ($n = 5$), suggesting a leaky monolayer (Fig. 1D). Clinically, TEER correlated inversely with BMI ($p = 0.029$) and waist ($p = 0.019$) and positively with LSM ($p = 0.009$) and AST ($p = 0.036$). Faecal valerate was significantly lower in those with elevated LSM, compared to normal liver (0.28 vs 0.47 mmol/l, $p = 0.007$) (Fig. 1E).

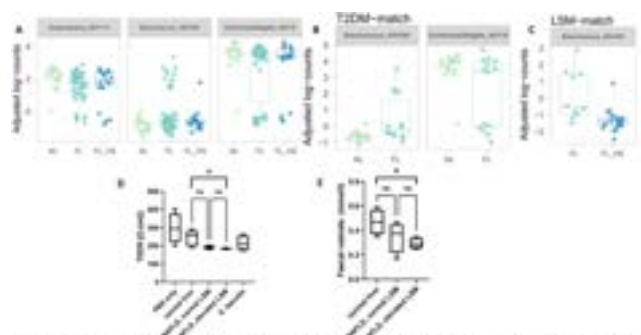


Figure 1: A) Microbiome signatures in the whole population (unmatched analysis). B) Microbiome signatures in NAFLD vs non-NAFLD (matched subset). C) Microbiome signatures in elevated LSM vs normal LSM (matched subset). D) Permeability measurements using TEER. E) Faecal valerate in stool samples from study groups. Abbreviations: NAFLD: Non-alcoholic fatty liver disease; LSM: liver stiffness measurement; NL: normal liver; N: NAFLD with normal LSM; EL: NAFLD with elevated LSM; TEER: Trans-epithelial electric resistance.

Conclusion: In patients with NAFLD, a greater abundance of butyrate-producing bacteria in patients with NAFLD may represent an adaptive response to depleted pectin-degrading bacteria. In those with advanced liver disease, such adaptation may fail and translate into leakier gut and lower production of short-chain fatty acids. Restoring butyrate-producing bacteria could represent a valuable target to treat the disease.

THURSDAY 22 JUNE

THU-410

Systematic screening for NAFLD-related advanced fibrosis in high-risk population in diabetology using transient elastography: a prospective study

Amélie Rajot¹, Bruno Vergès², Sarah Beland-Bonenfant², Valerie Hervieu³, Dominique Delaunay¹, Marianne Maynard^{4,5}, Samy Hadjadj⁶, Jérémy Thureau⁶, Jean-Michel Petit², Sybil Charrière⁷, Philippe Moulin⁷, Massimo Levrero^{4,5}, Bérénice Ségrestin¹, Emmanuel Disse¹, Bertrand Cariou⁶, Cyrielle Caussy^{1,8,9}. ¹Hospices Civils de Lyon, Endocrinology Diabetes and Nutrition, France; ²Dijon University Hospital, Endocrinology, Diabetes and Metabolic Disorders, Dijon, France; ³Hospices Civils de Lyon, Biopathology of Tumours, Bon, France; ⁴Hospices Civils de Lyon, Hepatology, Lyon, France; ⁵Centre de Recherche sur le Cancer de Lyon, Unité 1052, Lyon, France; ⁶l'institut du thorax, Nantes, France; ⁷Hospices Civils de Lyon, Endocrinology, Diabetes and Nutrition, Bron, France; ⁸Université Claude Bernard Lyon 1, France; ⁹INSERM, CarMen Laboratory, Pierre-Bénite, France
E-mail: cyrielle.caussy@chu-lyon.fr

Background and aims: The systematic screening for non-alcoholic fatty liver disease (NAFLD)-related advanced fibrosis (AF) is currently recommended in high-risk population such as patients with type 2 diabetes (T2D) and/or obesity. However, there are limited prospective data from patients enrolled and systematically assessed using transient elastography (TE) in diabetology. Therefore, we aimed to examine the utility of non-invasive tests (NITs) and the prevalence of AF in a prospectively recruited population in diabetology.

Method: This is a multicenter prospective study (NAFLD-Care: NCT04435054), including patients with T2D and/or obesity and NAFLD, age between 40–80 years old and BMI <40 kg/m², enrolled in a systematic screening for NAFLD-related AF in four diabetology departments in France from October 2020 to November 2022. All patients underwent a standardized research visit with fasting labs including Fibrotest® and liver assessment by TE using a FibroScan®. All other causes of liver disease were systematically excluded. The presence of AF was determined after assessment in hepatology by either histological fibrosis stage ≥F3 or overt imaging diagnosis of cirrhosis or concordant TE ≥8 kPa and Fibrotest® ≥F3 according to EASL guidelines.

Results: Of 487 patients screened, 461 met eligibility. The mean age and BMI were 59.5 years (± 9.8) and 32.7 kg/m² (± 4.1), 46% were female, 75.5% had obesity, 87.4% had T2D, 72.2% were treated for dyslipidemia and 67.9% had hypertension. Among them, 55.5% had a FIB-4 <1.3 and the proportion of participants with TE ≥8 kPa and TE ≥12 kPa was 18.0% and 4.8%, respectively. The presence of AF was ruled out in 71.4% (n = 329) participants based upon concordant TE <8 kPa and Fibrotest® <F3 in diabetology. Among participants assessed in hepatology, 82 participants had a determined status of AF including 27 with a confirmed diagnosis of advanced fibrosis and 54 had an undetermined status of AF due to discordant NITs and no liver biopsy results. The prevalence of AF was 6.6% (27/407) among participants with a determined status of AF. A higher BMI was significantly associated with increased odds of AF, OR: 1.114 (95% CI: 1.01–1.24, p = 0.040) adjusted for age and sex. FIB-4 <1.3 had a high negative predictive value (NPV) of 98%. Among participants with AF, 15% (n = 4) had a false negative FIB-4 <1.3. These participants were significantly younger compared to those with AF and FIB-4 >1.3: mean age 51 (± 6.6) vs 66.1 (± 7.9), p = 0.004. An age below 60 years was significantly associated with false negative FIB-4, p < 0.001.

Conclusion: The estimated prevalence of AF in this multi-center prospective study in high-risk population was 6.6%. FIB-4 <1.3 had a very high NPV to rule out AF but significantly misclassified patients younger than 60 years. Further analysis, in a larger population will help refine the prevalence of AF and the optimal screening strategy in diabetology.

THU-411

Low-quality muscle mass predicts fibrosis progression in a prospective biopsy-proven non-alcoholic fatty liver disease cohort

Sae Kyung Joo¹, Yong Jin Jung¹, Won Kim¹. ¹Seoul National University Seoul Metropolitan Government Boramae Medical Center, Internal Medicine, Seoul, Korea, Rep. of South
E-mail: wonshiri@yahoo.com

Background and aims: Muscle quality rather than muscle mass has been suggested to play a pivotal role in the deterioration of non-alcoholic fatty liver disease (NAFLD). The muscle quality map developed for computed tomography (CT) images can separately assess normal-quality muscle mass, low-quality muscle mass, and intermuscular adipose tissue. We evaluated the predictive role of each skeletal muscle mass compartment by muscle quality in fibrosis progression up to advanced fibrosis in a NAFLD cohort.

Method: This prospective community-based cohort study included 326 participants who underwent liver biopsy and CT at baseline, with serial vibration-controlled transient elastography (VCTE) every 1 or 2 years. Fibrosis progression was defined as either an increase in liver stiffness measurement (LSM) more than 20% compared to baseline for patients with advanced fibrosis (≥F3) or an LSM more than 9.6 kPa for patients with fibrosis stage 0 to 2. Axial muscles of the third lumbar vertebra level CT image were analyzed with DeepCatch software. Skeletal muscle areas (SMAs) were categorized by pre-determined Hounsfield Unit (HU) thresholds as normal-attenuation muscle area (NAMA; +30 to +150 HU), low-attenuation muscle area (LAMA; -29 to +29 HU), and intermuscular adipose tissue (IMAT; -190 to -30 HU). SMAs were normalized by height to obtain the skeletal muscle index (SMI). Cox proportional hazards analysis was performed to determine risk factors for fibrosis progression, and cumulative incidence rates of fibrosis progression was estimated with Cox regression survival curves.

Results: The median time interval between the first and last VCTE was 44 months (IQR, 31–61 months). Baseline histological fibrosis severity was associated with increasing SMI_{LAMA} (p < 0.001) and decreasing SMI_{NAMA} (p = 0.011). In a multivariable analysis, SMI_{LAMA} and PNPLA3 rs738409 C > G were independently associated with fibrosis progression (HR, 1.05; 95% CI, 1.00–1.11; and HR, 2.24; 95% CI, 1.51–3.33, respectively). After full adjustment of confounders, risk of fibrosis progression increased with increasing SMI_{LAMA} quartiles (HR, 1.45; 95% CI, 1.13–1.87). SMI_{IMAT} also showed an increased dose-dependent risk of progression (HR, 1.37; 95% CI, 1.06–1.77), while SMI_{NAMA} did not (HR, 1.05; 95% CI, 0.78–1.42).

Conclusion: Increased low quality muscle mass, but not decreased normal-quality muscle mass, predicts fibrosis progression in patients with biopsy-proven NAFLD. Evaluation of the severity of myosteatosis may help select subjects requiring closer monitoring and early intervention to alleviate fibrosis progression.

THU-412

Natural history and long-term outcomes of the Newcastle non-alcoholic fatty liver disease cohort

Jenny Gallacher^{1,2}, Chris Day¹, Stuart McPherson^{1,2}, Quentin Anstee^{1,2}. ¹Translational and Clinical Research Institute, Faculty of Medical Sciences, Newcastle University, Newcastle upon Tyne, United Kingdom; ²Liver Unit, Newcastle NIHR Biomedical Research Centre, Newcastle upon Tyne Hospitals Foundation Trust, Newcastle upon Tyne, United Kingdom
E-mail: jennifer.gallacher@nhs.net

Background and aims: NAFLD is a leading cause of chronic liver disease worldwide, affecting >25% of the adult population. Yet, there remains uncertainty regarding disease natural history and long-term outcomes given the competing risks associated with the metabolic syndrome. The Newcastle NAFLD cohort is one of the longest established prospectively recruited, histologically characterised

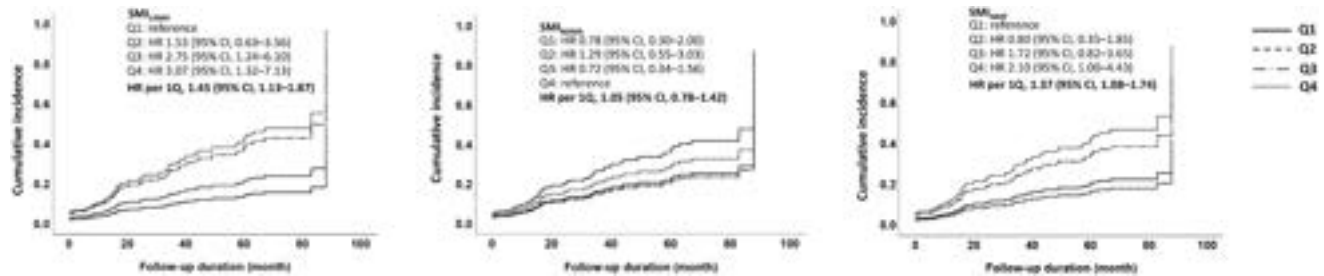


Figure: (abstract: THU-411): Cumulative incidence of fibrosis progression after adjusted for confounders, according to muscle mass compared by muscle quality.

single-centre patient cohorts. The aim of this study was assess incident comorbidities, and long-term outcomes/mortality in this cohort and seek predictors of adverse outcomes.

Method: Participants with biopsy proven NAFLD with a minimum of 12 months follow-up were recruited from the Newcastle Hospitals between 1990–2018. Data was collected at clinical events and outcomes of interest included co-morbidities, disease progression and adverse liver events such as HCC, liver transplantation and death. Outcomes were explored using Kaplan Meier log-rank test and Cox regression analysis. All cases were censored prior to the COVID19 pandemic to avoid this as a potential confounder.

Results: 605 patients (57% male; age 52 ± 13 years; 47.5% T2DM; BMI 34.7 ± 5.6 kg/m²) were included with a mean follow-up time of 11.8 ± 7.3 years. 116 (19.2%) had cirrhosis at baseline, with 50 (10.2%) cases progressing to cirrhosis during follow-up (mean time to cirrhosis diagnosis 10.0 ± 7.0 years). Incidence of metabolic co-morbidities (T2DM, HTN and MetS) increased over follow-up. 24 (4.0%) participants were diagnosed with HCC and 10 patients received a liver transplant. 112 patients (18.5%) died (mean age at death 64 ± 13 years and mean time to death 10.1 ± 6.0 years). Liver disease was the most common cause of death (28.6%), followed by cardiovascular disease (20.5%) and extra-hepatic malignancy (20.5%). Factors associated with all-cause mortality included fibrosis stage at baseline (aHR 8.31, 95% CI 4.31–16.01), T2DM (aHR 1.98, 95% CI 1.25–3.14), IHD (aHR 2.31, 95% CI 1.27–4.20) and “high risk” FIB-4 (aHR 10.02, 95% CI 6.14–16.35).

Conclusion: Liver related mortality was found to be the most common cause of death in a large, single centre cohort of NAFLD patients from the U.K. Factors which predicted adverse outcomes included T2DM, IHD, baseline fibrosis stage and “high risk” FIB-4 scores.

THU-413

Deep dive analysis into the screening failure reasons: combined data from multiple therapeutic clinical trials including more than 5000 patients (in collaboration with NAIL-NIT consortium)

Jörn Schattenberg¹, Julie Dubourg², Mazen Noureddin³, Naim Alkhouri⁴, Vlad Ratzu⁵, Michael Charlton⁶, Sophie Jeannin Megnier⁷, Stephen Harrison⁷. ¹Metabolic Liver Research Program, University Medical Center of the Johannes Gutenberg-University, Mainz, Germany, Germany; ²Summit Clinical Research, San Antonio, United States; ³Houston Methodist Hospital, Houston, United States; ⁴Arizona Liver Health, Chandler, United States; ⁵Institute for Cardiometabolism and Nutrition, France; ⁶UChicago Medicine, Chicago, United States; ⁷University of Oxford, United Kingdom E-mail: jdubourg@summitclinicalresearch.com

Background and aims: High screen failure (SF) rates in clinical trials for non-alcoholic steatohepatitis (NASH) are a major challenge and pose a high burden for patients, study centers and sponsors. We aimed to describe the main reasons for SF across multiple studies and compare the characteristics of patients meeting the liver biopsy eligibility criteria versus those who failed.

Method: We combined screening data from 7 ongoing non-cirrhotic NASH phase 2 trials. The percentage of patients failing to meet potential eligibility were assessed using common thresholds for non-invasive tests (NITs). Predictors of NASH, non-alcoholic fatty liver disease activity score (NAS) ≥ 4 and at least fibrosis stage 2, were examined using logistic regression and excluding patients with cirrhosis.

Results: 4808 patients with laboratory results were included. Among them: 1169 (24%) had AST ≤ 20 IU/L, 248 (5%) had platelets < 150 G/L, 189 (4%) had glycated hemoglobin (HbA1c) $> 9.5\%$, 185 (4%) had eGFR < 60 ml/min, 172 (4%) had total bilirubin > 1.3 mg/dL, and 37 (1%) had AST and/or ALT > 200 U/L. 2389 patients underwent a magnetic resonance imaging estimated proton density fat fraction (MRI-PDFF).

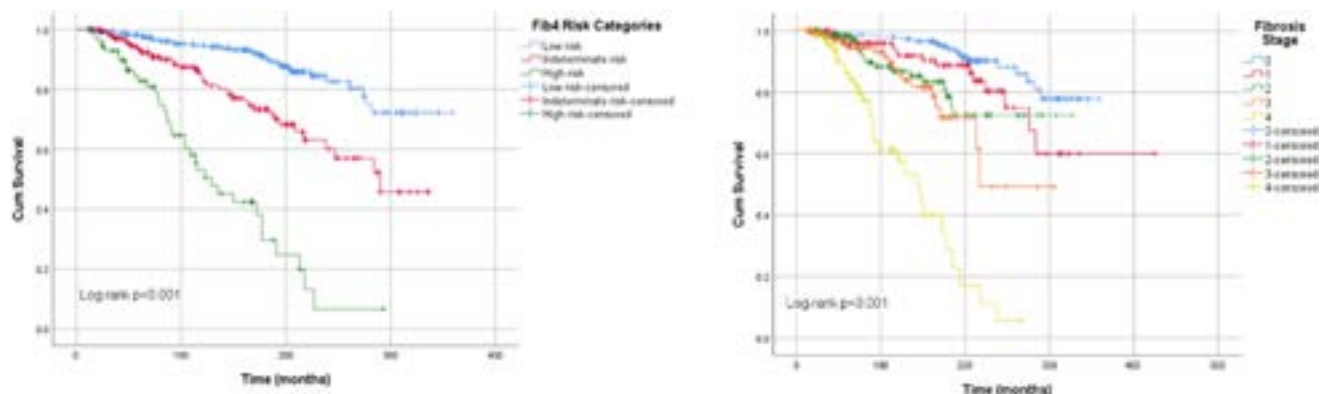


Figure: (abstract: THU-412): Kaplan Meier survival curves exploring the survival of patients across the different risk categories of FIB-4 and different fibrosis stages at baseline.

382 (16%) of them had a liver fat content (LFC) <8%. 2259 patients underwent a biopsy of which 924 (41%) had no NASH with 910 (98%) of those failing the histology criteria for the absence of ballooning. Among the patients with NASH, 135 (10%) had a NAS <4. Among the 2259 patients with biopsy, 1355 (60%) did not meet the common biopsy eligibility criteria (NASH + NAS \geq 4 + Fibrosis 2 or 3), including 104 (5%) patients with cirrhosis. The patients meeting biopsy eligibility criteria were older with higher HbA1c, liver enzymes, FIB-4 and FAST levels (Table). Among 166 patients with AST <20 IU/L at screening and having undergone a liver biopsy, 147 (89%) did not meet the eligibility criteria.

	Biopsy Fail N = 1251	NASH-NAS \geq 4 Fibrosis 2 or 3 N = 904	p value
	Mean (SD) or %		
Demographics			
Age, years	53.2 (12.1)	55.0 (11.1)	<0.01
Female	56 %	62 %	0.01
Hispanic	47%	42%	0.03
Liver Enzymes			
AST, IU/L	34 (19)	50 (29)	<0.01
ALT, IU/L	47 (29)	64 (37)	<0.01
AST/ALT	0.79 (0.27)	0.83 (0.37)	<0.01
GGT, IU/L	51 (55)	74 (72)	<0.01
Other Labs			
HbA1c, %	6.2 (1.0)	6.6 (1.1)	<0.01
LDL, mg/dL	106 (39)	99 (37)	<0.01
Triglyceride, mg/dL	160 (86)	166 (82)	0.14
Platelets, G/L	260 (65)	248 (63)	<0.01
Transient Elastography			
Liver Stiffness Measurement, kPa	11.9 (5.7)	13.7 (6.5)	<0.01
Controlled Attenuation Parameter, dB/m	344 (40)	345 (37)	0.52
MRI-PDFF			
LFC, %	18.5 (7.7)	18.0 (7.0)	0.25
Scores			
FIB-4	1.09 (0.57)	1.47 (0.69)	<0.01
FAST	0.48 (0.22)	0.62 (0.20)	<0.01

Figure:

Conclusion: Simple biological or imaging biomarkers such as aminotransferases and elastography were found to be significantly different between patients who screen failed or not based on liver biopsy. Low AST values (<20 IU/L) suggest the absence of at-risk NASH and could help avoid unnecessary biopsies.

THU-414

Causes of death by fibrosis stage in 959 biopsy-proven NAFLD patients

Ying Shang¹, Camilla Akbari¹, Maja Dodd¹, Patrik Nasr^{1,2}, Johan Vessby³, Fredrik Rorsman³, Stergios Kechagias², Per Stal¹, Mattias Ekstedt², Hannes Hagström¹. ¹Department of Medicine, Huddinge, Karolinska Institutet, Stockholm, Sweden; ²Department of Gastroenterology and Hepatology and Department of Health, Medicine, and Caring Sciences, Linköping University, Linköping, Sweden; ³Dept of Gastroenterology and Hepatology, Uppsala University Hospital, SE-751 85 Uppsala, Sweden
E-mail: ying.shang@ki.se

Background and aims: Causes of death in patients with non-alcoholic fatty liver disease (NAFLD) may differ based on the fibrosis stage at diagnosis. Our aim was to assess the distribution of different causes of death by fibrosis stage in patients with biopsy-proven NAFLD.

Method: We conducted a retrospective cohort of 959 biopsy-proven patients with NAFLD enrolled from three university hospitals in Sweden between 1974 and 2020. Causes of death were classified by

ICD codes from the Swedish Causes of Death Register until the end of 2021. Liver-related deaths were defined as hepatocellular carcinoma, cirrhosis, decompensated cirrhosis, or liver failure.

Results: Among 959 patients (mean age at biopsy 49.5 years, 61.7% male), 335 (34.9%) died during a median follow-up of 17.9 years (IQR 8.0–28.5). Mean age at death was 74.6 years and 52.7% were male. Of these, 75 (33.8%) patients in F0, 120 (32.4%) in F1, 69 (32.7%) in F2, 45 (45%) in F3, and 26 (47.3%) in F4 died. Liver-related mortality was the leading cause of death for patients with F4 (53.9%), followed by extrahepatic cancer (15.4%) and respiratory diseases (11.5%) (Figure). In non-cirrhotic patients with NAFLD (F0–F3), liver-related mortality increased with the severity of fibrosis stage (6.8% in F0, 10.8% in F1, 14.5% in F2, 17.8% in F3). However, these patients' death attributable to cardiovascular diseases and extrahepatic cancers were more common than death in liver-related causes.

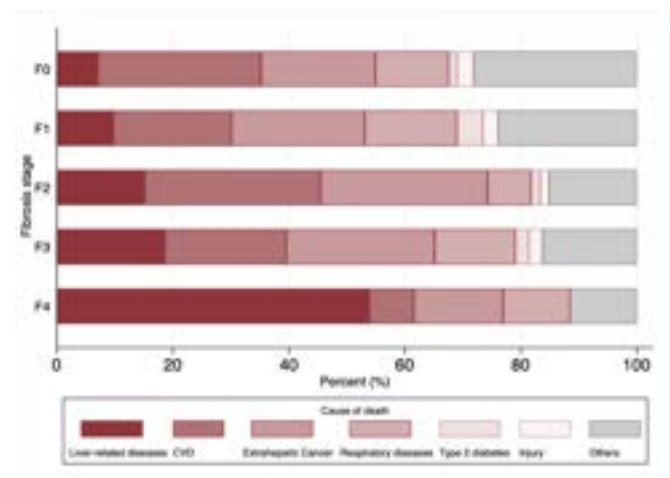


Figure: Proportions of causes of death by fibrosis stage

Conclusion: In patients with NAFLD and cirrhosis at diagnosis, liver disease is the most common cause of death. In patients with no or non-cirrhotic fibrosis, cardiovascular and extrahepatic cancer death were more common than liver-related death. Different management strategies and goals according to fibrosis stage at time of diagnosis can be implemented in patient counselling to improve prognosis.

THU-415

Glucose and lipid metabolism alterations after an oral lipid meal in patients with non-alcoholic fatty liver disease carrying the PNPLA3 rs738409 polymorphism

Chiara Rosso¹, Fabrizia Carli², Francesca Saba¹, Gian Paolo Caviglia¹, Samantha Pezzica², Patrizia Infelise², Angelo Armandi¹, Marta Guariglia¹, Daphne D'Amato¹, Maria Lorena Abate¹, Antonella Olivero¹, Nuria Pérez Diaz del Campo¹, Gabriele Castelnovo¹, Federico Salomone³, Giorgio Maria Saracco¹, Roberto Gambino¹, Elisabetta Bugianesi¹, Amalia Gastaldelli². ¹University of Turin, Department of Medical Sciences, Italy; ²Institute of Clinical Physiology, CNR, Pisa, Cardiometabolic Risk Unit, Italy; ³Azienda Sanitaria Provinciale di Catania, U.O.C. of Gastroenterology, Italy
E-mail: chiara.rosso@unito.it

Background and aims: In subjects with non-alcoholic fatty liver disease (NAFLD), hepatic fat accumulation is the result of insulin resistance (IR) and the impairment of hepatic glucose and lipid metabolism. In addition, the rs738409 C > G patatin-like phospholipase domain-containing 3 (PNPLA3) polymorphism is one of the main predisposing factors for the onset and progression of NAFLD and hepatic fibrosis. Here, we aimed to assess if PNPLA3 rs738409 polymorphism may affect both glucose and lipid metabolism in a

POSTER PRESENTATIONS

group of non-diabetic subjects with biopsy-proven NAFLD who underwent an oral lipid meal coupled with tracers.

Method: We have studied glucose and lipid metabolism after a lipid load (200 ml dairy cream and egg yolk) in 20 subjects with biopsy proven NAFLD (18 male; median age 41 years, range: 23–57) and 9 healthy controls (CT). Tracers (6, 6-²H₂-glucose and 2H₅-glycerol) were infused for 120 min before meal, and 240 min after lipid load to evaluate glucose metabolism (endogenous glucose production [EGP] and glucose clearance[GluClear]) and lipolysis. Throughout the test, we measured glucose, insulin (INS), free fatty acids (FFAs) composition, triglyceride (TG) and cholesterol profile. IR components were derived from tracers as follow: hepatic IR (Hep-IR = EGP × INS), adipose tissue IR (Lipo-IR = lipolysis × INS or AT-IR = FFAs × INS). Genotyping was performed by allelic discrimination assay. The mean value of the area under the curve (mAUC) was calculated for each variable.

Results: Prevalence of PNPLA3 rs738409 G minor allele was 75% (15/20) in NAFLD patients and 44% (4/9) in CT (p = 0.116). During fasting EGP, lipolysis and GC were similar in both groups even if NAFLD subjects were more insulin resistant than CT (Hep-IR: 88 vs. 52, p = 0.004; Lipo-IR 24 vs. 13, p = 0.011; AT-IR: 5.1 vs. 4.4, p = 0.043). When we compared NAFLD patients carrying the PNPLA3 G risk allele with those carrying the CC genotype, we showed no differences in fasting EGP, lipolysis, GC and IR components. Conversely, during lipid load, lipolysis was more suppressed in subjects who carried the PNPLA3 CC genotype and in CT. Moreover, lipid meal reduced GluClear with respect to baseline in CC and CG but not in GG carriers. Cholesterol profile did not change during meal in CT vs. NAFLD. Conversely, in all subjects FFAs and TG concentrations increased during the last hour (180–240 min) and TG levels were slightly higher in NAFLD subjects who carried the PNPLA3 CC genotype compared to those carrying the G minor allele, reflecting TG retention in the hepatocytes.

Conclusion: NAFLD patients carrying the PNPLA3 rs738409 G minor allele show an altered lipid but not glucose metabolism after an oral lipid meal. The implications of these results should be further explored.

Funded by Horizon2020 under grant agreement no.634413, EPoS

THU-416

Patatin-like phospholipase domain-containing 3 (PNPLA3) risk allele increases rate of progression to end-stage liver disease outcomes and decreases survival rate over time irrespective of degree of fibrosis

Javier Armissen¹, Jenny Blau², Nellie Fernando³, Monika Hun⁴, Mitra Rauschecker², Linda Wernevik⁵, Ola Fjellstrom⁵, Dirk Paul⁶, Björn Carlsson⁵, Nils Svengård⁴. ¹AstraZeneca, Early Development, Cardiovascular, Renal and Metabolism, BioPharmaceuticals, RandD, Cambridge, United Kingdom; ²AstraZeneca, Early Development, Cardiovascular, Renal and Metabolism, BioPharmaceuticals, RandD, United States; ³AstraZeneca, AI and Advanced Analytics, Data Science and Artificial Intelligence, RandD, Cambridge, United Kingdom; ⁴AstraZeneca, AI and Advanced Analytics, Data Science and Artificial Intelligence, RandD, Sweden; ⁵AstraZeneca, Early Development, Cardiovascular, Renal and Metabolism, BioPharmaceuticals, RandD, Sweden; ⁶AstraZeneca, Centre for Genomics Research, Discovery Sciences, RandD, United Kingdom
E-mail: javier.armisengarrido@astrazeneca.com

Background and aims: Non-alcoholic fatty liver disease (NAFLD) is the most common cause of chronic liver disease. Progression to Non-alcoholic steatohepatitis (NASH), can lead to cirrhosis, hepatocellular carcinoma (HCC), end-stage liver disease and death. The severity of hepatic fibrosis is the most important predictor of liver-related mortality. Among known risk factors increasing the risk of progression are genetic factors. The strongest genetic risk factor is a single-nucleotide polymorphism (rs738409) in the PNPLA3 gene I148M. The 148M allele has been associated with increased hepatic triglyceride accumulation, liver injury and fibrosis. The aim of the study was to

evaluate the characteristics and progression rates to outcomes among homozygous PNPLA3 148MM risk allele carriers as compared to heterozygous carriers (PNPLA3 148IM) and non-risk allele carriers (PNPLA3 148II) utilizing the well-characterized longitudinal biopsy-confirmed NashBio cohort.

Method: A Cox proportional hazards model was used to determine the effect of the PNPLA3 risk allele (148MM) on liver outcomes including cirrhosis, HCC and transplant as compared with 148IM and 148II. Survival analysis was performed with adjustments for confounders including age, BMI, gender, T2DM, and fibrosis stage, censored at study drop out or death.

Results: The NashBio cohort (n = 1508 evaluable patients, median age 48) included biopsy-confirmed NAFL or NASH (n = 117 526 271 for Fibrosis stage = 0–1, 2–3, 4 respectively) and PNPLA3 genotypes (n = 133 509 866 PNPLA3 148MM, IM, and II, respectively) with longitudinal electronic health record follow-up over a median of 49 months (range 0–23 years). PNPLA3 148MM had a more rapid progression to end-stage liver disease outcomes when compared to 148IM and 148II individuals with a hazard ratio = 1.6 (95% CI 1.01–2.56; p = 0.05). Predicted survival analyses highlighted nearly a two-fold increase in liver events in PNPLA3 148MM over 148II at 20 years (22% vs 12%, respectively; p = 0.0079). Even after stratification of patients according to fibrosis severity, PNPLA3 148MM patients had an increased risk of liver related events compared to PNPLA3 148II patients.

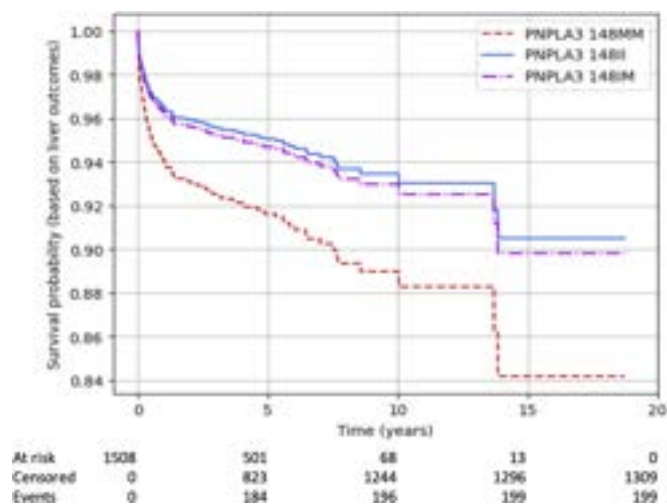


Figure:

Conclusion: Biopsy-confirmed NASH homozygous PNPLA3 148MM risk allele carriers progress to liver-related outcomes significantly faster than PNPLA3 148II and 148IM carriers, adjusted for age, gender, BMI, diabetes status, and fibrosis stage.

THU-417

A risk prediction model for hepatocellular carcinoma for non-alcoholic fatty liver disease without cirrhosis

Gi-Ae Kim¹, Yewan Park¹, Jui Jung², Jaehil Kim³, Han Chu Lee⁴. ¹Kyung Hee University Hospital, Kyung Hee University, Department of Internal Medicine, Seoul, Korea, Rep. of South; ²Korea University, Department of Biostatistics, Korea, Rep. of South; ³Asan Medical Center, University of Ulsan College of Medicine, Health Screening and Promotion Center, Korea, Rep. of South; ⁴Asan Medical Center, University of Ulsan College of Medicine, Department of Gastroenterology, Korea, Rep. of South
E-mail: hch@amc.seoul.kr

Background and aims: Non-alcoholic fatty liver disease (NAFLD) is becoming a leading cause of hepatocellular carcinoma (HCC) and burden of NAFLD-related HCC is on the rise. We aimed to develop and validate an HCC risk prediction model for NAFLD patients without cirrhosis using clinical factors widely available.

Method: A nationwide cohort of non-cirrhotic NAFLD patients in Korea were recruited to develop a risk prediction model and its internal validation (n = 409,088, derivation cohort). A model using a simplified point system was developed by Cox proportional hazard model and k-fold cross-validation assessed the accuracy, discrimination, and calibration of the model. The model was externally validated using a hospital cohort recruited from Asan Medical Center (n = 8721, external validation cohort).

Results: The 10-year cumulative HCC incidence rates were 0.21% and 0.20% in the derivation and external validation cohorts. In the derivation cohort, an 11-point HCC risk prediction model for non-cirrhotic NAFLD was developed, using six independent risk factors of age, sex, diabetes, obesity, serum alanine aminotransferase level, and gamma-glutamyl transferase level (c-index 0.75). The average area under receiver operating curves (AUROCs) of the model was 0.72 at 5-year and 0.75 at 10-year. In the external validation cohort, the c-index of the model was 0.82 and the AUROCs were 0.79 [95% confidence interval (CI), 0.59–0.95] at 5-year and 0.84 (95% CI, 0.73–0.94) at 10-year. The calibration was satisfactory. Risk stratification categorized patients into minimal (0–1), low (2–6), and moderate (≥ 7) risk groups.

Conclusion: A novel HCC risk prediction model targeting non-cirrhotic NAFLD patients was developed and validated with a fair prediction performance. The model is expected to serve as a simple and reliable tool to assess HCC risk.

THU-418

Histological classifications versus liver-related events: results from the multicentric, European, hepatic outcomes and survival fatty liver registry (HOTSURFR) study

Vlad Ratziu¹, Javier Ampuero², Jerome Boursier³, Stergios Kechagias⁴, Salvatore Petta⁵, Hannes Hagström⁶, Jörn Schattenberg⁷, Lisa Belin⁸, Stacy Cyrille⁸, Frederic Charlotte⁸, Leila Kara⁹, Pierre Bedossa¹⁰.

¹Sorbonne Université, France; ²Hospital Universitario Virgen del Rocío de Sevilla, Spain; ³University Hospital of Angers, France; ⁴Linköping University, Sweden; ⁵Università degli Studi di Palermo, Italy; ⁶Karolinska University Hospital, Sweden; ⁷Mainz Universität, Germany; ⁸Assistance Publique Hôpitaux de Paris, France; ⁹ICAN, France; ¹⁰Liverpat, France
E-mail: vlad.ratziu@inserm.fr

Background and aims: NASH trials assume that histological classifications predict hepatic events. We evaluated the diagnostic performance of the new European EPOS staging and SAF grading systems.

Method: Pts from 7 European centers biopsied <2011 for suspected NAFLD and with long-term follow-up were scored by the NASHCRN and the EPOS 7 tier (1 minimal fibrosis, 2: portal/periportal fibrosis, 3: early bridging, 4: advanced bridging, 5 early cirrhosis, 6 advanced cirrhosis) fibrosis staging systems by a central pathologist. Activity was scored by NAS and SAF grading. Hepatic morbidity (HMM) was a composite of liver-related death, occurrence of cirrhosis, cirrhosis decompensation events. Overall mortality, primary liver cancer (PLC), cardiovascular events (CVE) and extrahepatic malignancies (EHM) were recorded. Median follow-up was calculated by reverse Kaplan-Meier. Incidence rates were compared using log-rank test and univariate and multivariate Cox proportional hazard models were used to estimate hazard ratios (HR) for each outcome.

Results: 711 patients were included: 63% males, mean age 52 yrs, BMI 30.1 kg/m², diabetes 36%, arterial hypertension 59%, dyslipidemia 54%, daily alcohol 0–5 g: 84%, 5–20/30 g: 13%, moderate (20/30–50) g: 3%, active smokers 19%. NASH CRN stages were: F0:45%, F1:24%, F2:11%, F3:14%, F4:6%. EPOS stages were: 0:48%, 1:20%, 2:11.5%, 3:6.5%, 4:4%, 5:6%, 6:4%.

Median follow-up was 11.12 yrs (0.1–20). 84 pts died (11.8%), 92 pts developed HMM (12.9%), 32 PLC (4.5%), 72 CVE (10.1%) and 80 EHM (11.3%). The 5 and 10 yr incidence of HMM was 4.8% 95% CI [3.2–6.4] and 12.7% 95% CI [10–15], and that of all-cause death 2.9% 95% CI [1.6–4.1] and 9.3% 95% CI [7–11.5]. In multivariable analysis, age, diabetes,

arterial hypertension and moderate alcohol consumption were associated with an increased risk of HMM.

After adjustment for clinical variables and NAS, fibrosis stage was associated with HMM: HRs for NASH CRN: stage 1: 3.06; stage2: 11.04; stage3: 21.1; stage 4: 21.2 vs stage 0. For EPOS: stage 1: 2.3; stage 2: 8.3; stage 3: 19.8; stage 4: 18.1; stage5+6: 21.7 vs stage 0. Both staging systems had similar calibration and discrimination Harrell's C index was 0.84 and AUROCs for cumulative incidence of HMM at 5 yrs was 0.83 and at 10 yrs 0.86. Both were significantly associated with overall survival, PLC, CVE and EHM. Histological activity by SAF was associated with HMM starting grade 2 (p < 0.001). Steatohepatitis stage 2–4 (but not 0–1) by EPOS and cirrhosis (5–6 by EPOS) were significantly associated with HMM. Only cirrhosis was associated with CVE. Baseline FIB4 risk strata were significantly associated with HMM, overall survival, PLC, cardiovascular events but not EHM.

Conclusion: This large multicentric cohort demonstrated the prognostic value of the EPOS classification. Fibrosis starting stage 1 (NASH CRN) or stage 2 (EPOS) and activity grade predicted hepatic events. (supported by a grant from Gilead Sciences)

THU-419

GL0034 (Utregrlutide), a novel, long acting, glucagon-like peptide 1 receptor agonist (GLP-1 RA), results of a phase 1 study in healthy individuals

Rajamannar Thennati¹, Vinod Burade¹, Muthukumaran Natarajan¹, Pradeep Shahi¹, Ravishankara Nagaraja¹, Satish Panchal^{1,1}, Sudeep Agrawal¹, Bernard Jandrain², Thierry Duvauchelle³, Richard E. Pratley⁴, Bernard Thorens⁵, Tina Vilsbøll⁶. ¹Sun Pharmaceutical Industries Ltd, High Impact Innovations-Sustainable Health Solutions (HISHS), Vadodra, India; ²Academic Hospital of Liège, Clinical Pharmacology Unit, ATC Co, Nutrition and Metabolic Disorders, Liège, Belgium; ³Phaster1, Paris, France; ⁴AdventHealth Translational Research Institute, Orlando, United States; ⁵University of Lausanne, Center for Integrative Genomics, Lausanne, Switzerland; ⁶University of Copenhagen, Clinical Research, Steno Diabetes Center, Copenhagen, Denmark

E-mail: rajamannar.thennati@sunpharma.com

Background and aims: GL0034 (GL) is a potent glucagon-like peptide 1 receptor agonist under development for the treatment of metabolic disorders and NAFLD/NASH. In *in-vivo* preclinical studies GL attenuates NAFLD/NASH-relevant pathways of steatosis, liver injury and inflammation. Here, we present NAFLD/NASH relevant pharmacodynamic (PD) and safety results of a multiple ascending dose phase 1 study in healthy individuals.

Method: A randomized, double-blind, placebo (PBO)-controlled study was conducted to evaluate the safety, tolerability and PD of multiple ascending doses of GL. Healthy individuals (N = 12) with BMI 18 to 28 kg/m² were randomized (9:3) to subcutaneous GL or PBO. Individuals received weekly dose of GL for a total period of eight weeks. First, they received doses of 450 mcg over two weeks, then 900 mcg over the next two weeks and finally 1520 mcg over four weeks. Biomarker measurements included, body weight, glycated haemoglobin A1c (HbA1c), liver enzymes (alanine transaminase (ALT), aspartate aminotransferase (AST), gamma-glutamyl transferase (GGT)) and lipid profiles (triglycerides (TG), total cholesterol (TC), high-density lipoprotein (HDL) and low-density lipoprotein (LDL)).

Results: GL was generally well tolerated and related adverse effects were mainly gastrointestinal with dose-dependent nausea, vomiting and decreased appetite however adverse events became less frequent over time despite increased dosing. Clinically meaningful changes in the body weight, HbA1c and lipid profile were observed when compared to baseline (Table). HDL increase at EOS (Table) and trends towards lower ALT, AST and GGT were observed vs PBO (Table).

POSTER PRESENTATIONS

Table:

Treatment Groups	GL0034, 450 mcg × 2, 900 mcg × 2, 1520 mcg × 4 (n = 8)			Placebo (n = 3)		
	BL		Change from BL	BL		Change from BL
	D1	D51/52 [§]	EOS (D78)	D1	D51/52 [§]	EOS (D78)
Biomarkers						
Body Weight (kg)	71.8 ± 8.1	-7.7 ± 1.9***	-6.4 ± 2.1***	76.0 ± 3.4	1.7 ± 1.0***	2.6 ± 0.8***
ALT (U/L)	25.1 ± 10.2	-7.4 ± 10.3	-1.0 ± 9.4	22.7 ± 6.7	14.3 ± 9.5*	10.3 ± 1.2
AST (U/L)	27.6 ± 6.5	-4.0 ± 7.5	-1.1 ± 6.7	25.0 ± 1.0	4.3 ± 5.0	2.7 ± 3.2
GGT (U/L)	14.9 ± 6.0	-3.4 ± 3.5*	-1.0 ± 2.7	15.7 ± 2.1	0.3 ± 2.9	3.3 ± 2.1
TG (mg/dL)	93.4 ± 26.7	-21.0 ± 27.5	-11.0 ± 55.3	145.3 ± 88.2	-33.0 ± 34.0	4.0 ± 49.5
TC (mg/dL)	165.8 ± 39.8	-29.1 ± 23.3**	-5.8 ± 12.6	177.7 ± 6.4	20.7 ± 16.0	29.3 ± 9.5*
LDL (mg/dL)	107.3 ± 32.1	-24.0 ± 24.3	-19.5 ± 35.8	123.7 ± 11.0	25.7 ± 9.3**	24.0 ± 6.2**
HDL (mg/dL)	49.9 ± 9.1	-6.1 ± 5.3**	2.9 ± 3.1	41.0 ± 8.9	7.0 ± 4.0*	6.7 ± 1.53*
% HbA1c	5.11 ± 0.3	-	-0.25 ± 0.2**	5.37 ± 0.3	-	-0.13 ± 0.25

One-way ANOVA followed by Bonferroni's post-test respectively. * p < 0.05, **p < 0.01, ***p < 0.001, vs respective Day 1 Levels; §-Day 52 for Body weight data; Day 51 for all other parameters, EOS: End of Study.

Conclusion: GL0034, a potent, long-acting GLP-1RA, was safe, well tolerated and with improved liver function in healthy individuals. The observed PD effects suggest potential therapeutic benefits in NAFLD/NASH patients.

THU-420

Association between consumption of ultra-processed foods and non-alcoholic fatty liver disease in the Framingham heart study

Natalie Sun¹, Vanessa Xanthakis^{2,3}, Jiantao Ma⁴, Michelle Long^{5,6}, Maura Walker^{2,3,7}. ¹Boston Medical Center, Boston, United States; ²Boston University Chobanian and Avedisian School of Medicine, Preventive Medicine and Epidemiology, Boston, United States; ³Framingham Heart Study, United States; ⁴Friedman School of Nutrition Science and Policy, Tufts University, Nutritional Epidemiology, Boston, United States; ⁵Novo Nordisk A/S, Clinical Drug Development, Medicine and Science, Denmark; ⁶Boston University Chobanian and Avedisian

School of Medicine, Medicine, United States; ⁷Sargent college of health and rehabilitation sciences nutrition program, Nutrition Programs, Boston, United States
E-mail: nataliesuneras@gmail.com

Background and aims: Ultra-processed food (UPF) intake is associated with cardiovascular disease, poor metabolic health, and mortality. Consumption of UPFs and prevalent non-alcoholic fatty liver disease (NAFLD) have increased in parallel over recent years, but little is known about the association between the two. We performed a cross-sectional, retrospective, observational study to examine the relationship between consumption of UPFs and presence of liver steatosis and fibrosis in Framingham Heart Study (FHS) participants. **Method:** We evaluated FHS participants from the 2016–2019 exam cycle who completed vibration-controlled transient elastography and had valid dietary data (n = 2507, mean age 55 years, 55.6% female). Participants with missing covariate data and excessive alcohol use were excluded from the analysis. Diet was assessed via the self-administered semi-quantitative Harvard food frequency questionnaire and was categorized by level of food processing via the NOVA (not an abbreviation) system, which groups food items by level of industrial processing. We used multivariable-adjusted logistic regression models to evaluate the association of energy-adjusted UPF intake (per 1 standard deviation unit and by quintile) with imaging-defined hepatic steatosis (Controlled Attenuation Parameter [CAP] ≥ 290 dB/m), fibrosis (Liver Stiffness Measurement [LSM] ≥ 8.2 kPa), and hepatic steatosis with fibrosis (CAP ≥ 290 dB/m and LSM ≥ 8.2 kPa); separate models for each outcome. Our primary model adjusted for age, sex, smoking, alcohol intake, physical activity and intake of remaining NOVA levels. Additional models adjusted for diet quality index or body mass index (BMI).

Results: Prevalence of hepatic steatosis, fibrosis, and steatosis with fibrosis was 29.72%, 9.77% and 5.42%, respectively. We observed a statistically significant positive association of UPF consumption with presence of hepatic steatosis (OR 1.33 [95% CI 1.21, 1.46] per SD-increase, i.e. 2.3 servings/day), fibrosis (OR 1.15 [1.01, 1.31]) and hepatic steatosis with fibrosis (OR 1.24 [1.06, 1.47]; Table). Associations were similar when accounting for an index of diet quality (Table). When accounting for BMI, the association between UPF consumption and hepatic steatosis remained significant (OR 1.13

Table. Association of ultra-processed food intake with hepatic steatosis, hepatic fibrosis, and hepatic steatosis with fibrosis

	UPF (Continuous) [†] n=2507 OR (95% CI)	Q1 n=501 OR (95% CI)	Q2 n=502 OR (95% CI)	Q3 n=501 OR (95% CI)	Q4 n=502 OR (95% CI)	Q5 n=501 OR (95% CI)
Hepatic steatosis (CAP ≥ 290 dB/m)[‡]						
Model 1	1.33 (1.21, 1.46) *	Ref	1.27 (0.92, 1.75)	1.54 (1.12, 2.12) *	1.88 (1.37, 2.59) *	2.51 (1.82, 3.46) *
Model 2	1.28 (1.17, 1.41) *	Ref	1.24 (0.91, 1.70)	1.44 (1.05, 1.96) *	1.71 (1.26, 2.34) *	2.17 (1.56, 2.98) *
Model 3	1.13 (1.01, 1.27) *	Ref	1.15 (0.79, 1.67)	1.23 (0.84, 1.78)	1.34 (0.92, 1.94)	1.52 (1.04, 2.23) *
Hepatic fibrosis (LSM ≥ 8.2 kPa)[‡]		Ref				
Model 1	1.15 (1.01, 1.31) *	Ref	1.09 (0.70, 1.71)	1.10 (0.70, 1.73)	0.87 (0.54, 1.40)	1.47 (0.94, 2.31)
Model 2	1.13 (1.00, 1.29) *	Ref	1.09 (0.70, 1.70)	1.08 (0.69, 1.68)	0.84 (0.53, 1.35)	1.40 (0.90, 2.18)
Model 3	1.00 (0.87, 1.16)	Ref	1.01 (0.64, 1.61)	0.94 (0.58, 1.50)	0.65 (0.39, 1.07)	1.00 (0.62, 1.60)
Hepatic steatosis with fibrosis (LSM ≥ 8.2 kPa & CAP ≥ 290 dB/m)[‡]		Ref				
Model 1	1.24 (1.06, 1.47) *	Ref	1.05 (0.56, 1.97)	1.07 (0.57, 2.01)	1.12 (0.60, 2.10)	1.68 (0.912, 3.09)
Model 2	1.23 (1.05, 1.45) *	Ref	1.04 (0.55, 1.95)	1.04 (0.56, 1.95)	1.09 (0.59, 2.02)	1.59 (0.88, 2.02)
Model 3	0.96 (0.79, 1.18)	Ref	0.92 (0.46, 1.86)	0.75 (0.37, 1.52)	0.63 (0.31, 1.27)	0.80 (0.40, 1.60)

LSM was log-transformed to normalize the distribution

Multivariable Logistic Regression Models:

Model 1: Adjusted for age, sex, smoking, alcohol, physical activity, NOVA1, NOVA2, NOVA3

Model 2: Adjusted for age, sex, smoking, alcohol, physical activity, 2015 Healthy Eating Index

Model 3: Adjusted for age, sex, smoking, alcohol, physical activity, NOVA1, NOVA2, NOVA3, BMI

Abbreviations: Q: quintile; CAP: controlled attenuation parameter; LSM: liver stiffness measurement; BMI: Body mass index; UPF: ultra-processed foods; note: NOVA is not an abbreviation

*Indicates statistical significance (p < 0.05)

[†]Continuous by 1-standard deviation unit (2.3 UPF servings)

[‡]Binary

Figure: (abstract: THU-420).

[1.01, 1.27]); however, associations were attenuated for hepatic fibrosis (OR 1.00 [0.87, 1.16]), and for steatosis with fibrosis (OR 0.96 [0.79, 1.18]).

Conclusion: In our community-based sample, we observed associations of UPF consumption with hepatic steatosis. Additional longitudinal studies are needed to determine if UPF consumption contributes to progression of NAFLD and if BMI serves as an intermediate factor in the relationship between the two. Our findings suggest that the consumption of UPFs may be a modifiable risk factor for NAFLD.

THU-421

Presence and severity of esophageal varices drives portal hypertension-related complications in compensated advanced non-alcoholic fatty liver disease

Grazia Pennisi¹, Marco Enea¹, Mauro Viganò², Filippo Schepis³, Victor de Ledinghen⁴, Annalisa Berzigotti⁵, Vincent Wai-Sun Wong⁶, Anna Ludovica Fracanzani⁷, Giada Sebastiani⁸, Manuel Romero Gomez⁹, Elisabetta Bugianesi¹⁰, Gianluca Svegliati-Baroni¹¹, Fabio Marra¹², Alessio Aghemo^{13,14}, Luca Valenti^{15,16}, Vincenzo Calvaruso¹, Antonio Colecchia³, Gabriele Di Maria¹, Claudia La Mantia¹, Huapeng Lin⁶, Yuly Mendoza⁵, Nicola Pugliese¹⁴, Federico Ravaioli^{3,17}, Carmen Lara-Romero⁹, Dario Saltini³, Antonio Craxi¹, Vito Di Marco¹, Calogero Camma¹, Salvatore Petta¹. ¹Sezione di Gastroenterologia e Epatologia, Dipartimento di Promozione della Salute, Materno-Infantile, di Medicina Interna e Specialistica di Eccellenza "G. D'Alessandro," University of Palermo, Italy, Italy; ²Hepatology Unit, Ospedale San Giuseppe, University of Milan, Milan, Italy, Italy; ³Division of Gastroenterology, Azienda Ospedaliero-Universitaria di Modena and University of Modena and Reggio Emilia, Modena, Italy, Italy; ⁴Centre d'Investigation de la Fibrose Hépatique, INSERM U1053, Hôpital Haut-Lévêque, Bordeaux University Hospital, Pessac, France, Italy; ⁵Department of Visceral Surgery and Medicine, Inselspital, Bern University Hospital, University of Bern, Switzerland, Italy; ⁶Department of Medicine and Therapeutics, The Chinese University of Hong Kong, Hong Kong, Italy; ⁷Department of Pathophysiology and Transplantation, Ca' Granda IRCCS Foundation, Policlinico Hospital, University of Milan, Italy, Italy; ⁸Division of Gastroenterology and Hepatology, McGill University Health Centre, Montreal QC, Canada, Canada; ⁹Hospital Universitario Virgen del Rocío, Instituto de biomedicina de Sevilla, Universidad de Sevilla, Ciberehd, Spain; ¹⁰Division of Gastroenterology, Department of Medical Sciences, University of Torino, Torino, Italy, Italy; ¹¹Liver Injury and Transplant Unit, Università Politecnica delle Marche, 60121 Ancona, Italy, Italy; ¹²Dipartimento di Medicina Sperimentale e Clinica, University of Florence, Italy; Research Center DENOTHE, University of Florence, Italy, Italy; ¹³Department of Biomedical Sciences, Humanitas University, 20090 Pieve Emanuele, Italy, Italy; ¹⁴Division of Internal Medicine and Hepatology, Department of Gastroenterology, IRCCS Humanitas Research Hospital, 20089 Rozzano, Italy, Italy; ¹⁵Department of Pathophysiology and Transplantation, Università degli Studi di Milano, Milan, Italy, Italy; ¹⁶Translational Medicine, Department of Transfusion Medicine, Fondazione IRCCS Ca' Granda Ospedale Maggiore Policlinico IRCCS, Milan, Italy, Italy; ¹⁷IRCCS Azienda Ospedaliero-Universitaria di Bologna, Bologna, Italy, Italy
E-mail: graziapennisi901@gmail.com

Background and aims: We aimed to evaluate the impact of esophageal varices (EV) and their changes during follow-up on the risk of developing liver events in patients with compensated advanced chronic liver disease (cACLD) due to NAFLD. We also assessed diagnostic accuracy of non-invasive scores for predicting the development of liver events and for identifying patients at low risk of high-risk EV.

Method: We assessed 629 patients with NAFLD-related cACLD who had baseline and follow-up esophagogastroduodenoscopy (EGD), and clinical follow-up to record decompensation, portal vein thrombosis (PVT) and hepatocellular carcinoma.

Results: Small and large EV were observed at baseline in 30% and 15.9% of patients, respectively. The 4-year rate of EV development from absence at baseline, and of progression from small to large EV were 16.3% and 22.4%, respectively. Presence of diabetes and $\geq 5\%$ increase in BMI were associated with worsening of EV status. At multivariate Cox regression analysis, small (HR 2.24, 95%CI. 1.47–3.41) and large (HR 3.86, 95%CI. 2.34–6.39) EV were independently associated with decompensation. When considering EV status and EV trajectories, baseline and/or follow-up small EV (HR 2.65, 95%CI. 1.39–5.05), and baseline and/or follow-up large EV (HR 4.90, 95%CI. 2.49–9.63) were independently associated with decompensation as compared to baseline and/or follow-up absence of EV. Presence of small (HR 2.8 (95%CI.1.16–6.74) and large (HR 5.29, 95%CI. 1.96–14.2) EV were also independently associated with PVT occurrence.

Conclusion: In NAFLD-related cACLD, the presence, severity and evolution of EV well stratify the risk of developing decompensation and PVT.

THU-422

PNPLA3 GG genotype is associated with higher incidence of cirrhosis and liver-related events among patients with non-alcoholic fatty liver disease

Karn Wijarnpreecha^{1,2}, Fang Li³, Anna Lok², Vincent Chen².

¹University of Arizona College of Medicine-Phoenix, Internal Medicine, United States; ²University of Michigan Health System, United States;

³The University of Texas Health Science Center at Houston, United States
E-mail: dr.karn.wi@gmail.com

Background and aims: Non-alcoholic fatty liver disease (NAFLD) can develop in persons without obesity. PNPLA3 genetic variant is associated with NAFLD, cirrhosis, and hepatocellular carcinoma (HCC) but its association with non-liver outcomes is unknown. We investigated the association between PNPLA3 genetic variants and mortality and risk of liver and non-liver outcomes among NAFLD patients with and without obesity.

Method: We conducted a retrospective cohort study of NAFLD patients with PNPLA3 data available. NAFLD was defined via imaging, transient elastography, or biopsy without other liver diseases. We excluded patients with baseline cirrhosis or cancer, underweight, bariatric surgery, or missing data on body mass index (BMI). The primary outcome is the association between PNPLA3-rs738409 genotype and incident (hazard ratio [HR] and 95% confidence interval [CI]) cirrhosis, liver-related events (LREs) (ascites, variceal bleeding, hepatic encephalopathy, or HCC), cardiovascular disease (CVD), diabetes (DM), cancers, and mortality among obese and non-obese NAFLD patients without prevalent outcomes. The multivariable model was adjusted for age, sex, and genetic principal components 1–10 to account for race/ethnicity. Analyses of the total population were also adjusted for body mass index category.

Results: A total of 3039 patients with NAFLD: 259 lean, 652 overweight, and 2128 obese, followed for a median of 54.7 months and total follow-up of 15311 person-years were studied. 84.1% were Caucasian, 6.4% African American, and 3.3% Asian. PNPLA3 genotype was CC, CG, and GG in 52.7%, 38.1%, and 9.2% of patients overall; 43.2%, 38.0%, and 8.7% of obese patients; and 51.4%, 38.3%, and 10.3% of lean/overweight patients ($p > 0.05$). NAFLD patients with PNPLA3 GG but not those with CG genotype had higher incidence of cirrhosis compared to patients with CC genotype. PNPLA3 GG was significantly associated with LREs in obese but not in non-obese NAFLD. PNPLA3 genetic variants were not associated with all-cause mortality or incidence of CVD, DM, or cancer.

Conclusion: Among patients with NAFLD, PNPLA3 GG but not CG genotype was associated with higher incidence of cirrhosis in non-obese and obese patients and with LREs in obese patients. Clinical trials of NAFLD treatment should stratify for PNPLA3 genotype.

POSTER PRESENTATIONS

Table (abstract: THU-422).

	Mortality		Cirrhosis		LREs		CVD		DM		Cancer	
	HR (95% CI)	p value	HR (95% CI)	p value	HR (95% CI)	p value	HR (95% CI)	p value	HR (95% CI)	p value	HR (95% CI)	p value
PNPLA3 CC (Reference)												
Total population (n = 3689)												
PNPLA3 CG (n = 1423)	0.97 (0.56–1.68)	0.90	1.07 (0.67–1.69)	0.78	1.05 (0.68–1.62)	0.81	1.06 (0.80–1.39)	0.69	0.74 (0.54–1.00)	0.051	0.90 (0.70–1.14)	0.38
PNPLA3 GG (n = 369)	1.09 (0.45–2.66)	0.85	2.23 (1.25–4.00)	0.007	1.87 (1.04–3.34)	0.04	0.94 (0.58–1.53)	0.81	0.85 (0.55–1.35)	0.51	0.93 (0.62–1.39)	0.73
Non-obese subjects (n = 911)												
PNPLA3 CG (n = 349)	0.36 (0.10–1.34)	0.13	0.66 (0.16–2.82)	0.58	0.44 (0.11–1.76)	0.24	1.21 (0.69–2.10)	0.50	0.57 (0.27–1.22)	0.15	1.12 (0.72–1.73)	0.61
PNPLA3 GG (n = 94)	Unstable model	0.99	3.22 (1.17–8.85)	0.02	2.04 (0.66–6.24)	0.21	0.33 (0.07–1.47)	0.15	0.78 (0.28–2.13)	0.62	1.11 (0.58–2.12)	0.75
Obese subjects (n = 2778)												
PNPLA3 CG (n = 1074)	0.36 (0.10–1.34)	0.13	2.92 (1.02–8.37)	0.046	2.92 (1.02–8.37)	0.04	0.99 (0.71–1.39)	0.98	0.80 (0.57–1.11)	0.17	0.78 (0.57–1.05)	0.10
PNPLA3 GG (n = 275)	Unstable model	0.99	6.26 (1.81–21.65)	0.004	6.26 (1.81–21.65)	0.004	1.11 (0.66–1.88)	0.69	0.92 (0.55–1.52)	0.74	0.81 (0.49–1.35)	0.43

THU-423

Long-term prognosis of patients with non-alcoholic fatty liver disease: a retrospective cohort study to understand the impact of surrogate disease end points on long-term outcomes in South Korea

Sungwon Chung¹, Min Kyung Park¹, Xiao Zhang², Tongtog Wang², Thomas Jemielita², Gail Fernandes², Samuel Engel², Heejoon Jang^{1,3}, Yun Bin Lee¹, Eun Ju Cho¹, Jeonghoon Lee¹, Su Jong Yu¹, Jung-Hwan Yoon¹, Yoon Jun Kim¹. ¹Seoul National University College of Medicine, Department of Internal Medicine and Liver Research Institute, Korea, Rep. of South; ²Mereck and Co., Inc., Rahway, NJ, United States; ³Seoul Metropolitan Government Seoul National University Boramae Medical Center, Department of Internal Medicine, Korea, Rep. of South E-mail: yoonjun@snu.ac.kr

Background and aims: Prognosis of NAFLD can be difficult to predict without liver biopsy. Previous studies have been focused on assessing the prognostic performance of non-invasive fibrosis scoring systems ascertained at NAFLD diagnosis (baseline). The aim of this study was to examine whether adding time-varying variables for these scores improves prediction of long-term outcomes in NAFLD patients.

Method: This is a retrospective cohort study of 2290 NAFLD patients diagnosed at the Seoul National University Hospital between January 2001 and December 2016. Primary outcomes were overall mortality, composite liver-related outcomes (liver transplant, cirrhosis, hepatocellular carcinoma), and composite cardiovascular outcomes (myocardial infarction, ischemic stroke, heart failure, peripheral artery disease). Multivariable Cox regression models with baseline and time-varying values of the fibrosis scoring systems including fibrosis-4 index (FIB-4) (high risk for advanced fibrosis: >2.67; intermediate risk: 1.30–2.67; low risk<1.30) and NAFLD fibrosis score (NFS) (high-risk: >0.676; intermediate risk: –1.455–0.676; low

risk: <–1.455) were fit to the data separately, to assess the association between baseline/current value of these scores at the visit and the primary outcomes.

Results: The median follow-up was 10.4 years. During follow-up, 217 deaths, 132 liver-related outcomes, and 320 cardiovascular events occurred. In the multivariable Cox regression models with baseline score considered, higher baseline NFS (high- versus low-risk group) was associated with higher risk of mortality (adjusted hazard ratio (aHR) = 2.72, 95% Confidence Interval (CI): 1.38–5.37), liver-related outcomes (aHR = 3.49, 95%CI: 1.21–10.07), and cardiovascular events (aHR = 1.12, 95%CI: 0.59–2.12). Similar findings were observed for the association of baseline FIB-4 (high- versus low- risk group) with mortality (aHR = 2.56, 95%CI: 1.48–4.42), liver-related outcomes (aHR = 11.38, 95%CI: 6.04–21.45), and cardiovascular events (aHR = 1.10, 95%CI: 0.62–1.95). In models with time-varying scores considered, stronger association was observed. For NFS, higher current value (high- versus low-risk group) was associated with higher risk of mortality (aHR = 2.89, 95%CI: 1.59–5.26), liver-related outcomes (aHR = 6.36, 95%CI: 2.52–16.09), and cardiovascular events (aHR = 1.18, 95%CI: 0.66–2.10). For FIB-4, higher current value (high- versus low-risk group) was associated with higher mortality (aHR = 2.81, 95%CI: 1.66–4.76), liver-related outcomes (aHR = 14.55, 95%CI: 7.47–28.34), and cardiovascular events (aHR = 1.24, 95%CI: 0.71–2.19).

Conclusion: Current values of FIB-4 and NFS were associated with long-term outcomes. In addition to the baseline measurement, a routine monitoring on these scores is important in predicting prognosis of NAFLD patients.

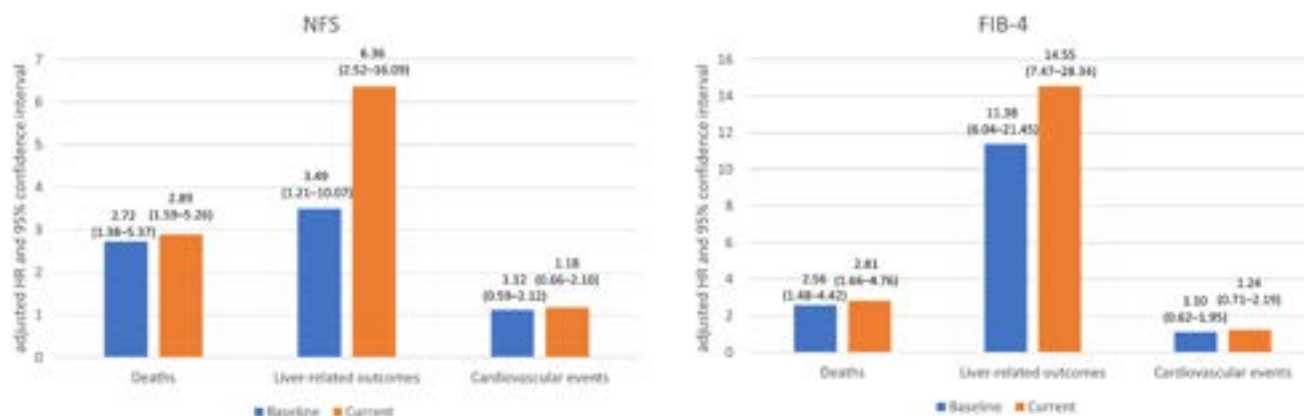


Figure: (abstract: THU-423): Adjusted hazard ratios (aHRs) for primary outcomes comparing high- versus low-risk (for advance fibrosis) group in non-alcoholic fatty liver disease (NAFLD) patients, by scoring system and model (multivariable Cox regression model with baseline measurement considered versus multivariable Cox regression model with current value)

THU-424

Prevalence of extrahepatic manifestations in non-alcoholic fatty liver disease in lean individuals compared to non-lean individuals

Majd Aboona¹, Claire Faulkner¹, Pooja Rangan², Vincent Chen³, Cheng Han Ng⁴, Fang Li⁵, Karn Wijarnprecha^{6,7}. ¹The university of arizona college of medicine-phoenix, Phoenix, United States; ²The university of arizona college of medicine-phoenix, division of clinical data analytics and decision support, Phoenix, United States; ³University of michigan health system, division of gastroenterology and hepatology, department of internal medicine, Ann arbor, United States; ⁴Yong loo lin school of medicine, Singapore, Singapore; ⁵The university of texas health science center at houston, school of biomedical informatics, Houston, United States; ⁶The university of arizona college of medicine-phoenix, Department of medicine, Division of gastroenterology and hepatology, Phoenix, United States; ⁷Banner-university medical center phoenix, Department of internal medicine, Division of gastroenterology and hepatology, Phoenix, United States
E-mail: aboona@arizona.edu

Background and aims: Non-alcoholic Fatty Liver Disease (NAFLD) has increased in prevalence worldwide in recent years. Data from multi-center study regarding NAFLD in lean individuals are lacking and whether they have higher prevalence of cardiovascular disease (CVD), cirrhosis, and extrahepatic manifestations than non-lean patients with NAFLD still inconclusive. Thus, we conducted a multi-center study to estimate the prevalence of cirrhosis and extrahepatic manifestations among NAFLD.

Method: A multi-state health system based study was conducted on NAFLD patients seen at the Banner Health System, from 2012 to 2022 using ICD Code. Patients with other causes of liver disease, alcohol-related diseases, underweight, baseline decompensated cirrhosis, cancer, prior bariatric surgery, or missing data on race, BMI, aspartate and alanine aminotransferase, and platelet were excluded. Patients were defined as lean, overweight, class obesity I, and class obesity II-III. The primary outcomes are the prevalence of cirrhosis, CVD, diabetes mellitus (DM), and chronic kidney disease (CKD) among lean versus non-lean patients. We performed a multivariate logistic regression analysis to determine the risk of disease prevalence adjusted for multiple confounders.

Results: Of the 51 452 patients in the cohort, 9.60 % were lean, 23.73 % were overweight, 28.97 % were obese class I, and 37.70 % were obese class II-III. The median age was 52 years with 63.33 % White, 27.96 % Hispanic, 3.45 % Black, 2.31 % Native American/Alaskan, and 0.97 % Asian/Pacific Islander. Prevalence of DM was 25.54 % in lean and 40.06 % in non-lean individuals. In the multivariate analysis, patients who were overweight, obese class I, or obese class II-III patients had lower prevalence peripheral vascular disease, coronary artery disease, cerebrovascular disease, and any CVD compared with lean patients

(Figure). Moreover, patients with obesity class II-III had significant higher prevalence of cirrhosis and CKD than lean persons.

Conclusion: In this large cohort of patients with NAFLD, lean persons with NAFLD had higher prevalence of CVD than non-lean persons despite lower prevalence of DM. Intervention to optimize CVD risk is warranted in lean patients with NAFLD.

THU-425

De novo lipogenesis discriminates advanced hepatic fibrosis after an oral glucose load in non-obese subjects with non-alcoholic fatty liver disease

Chiara Rosso¹, Fabrizia Carli², Angelo Armandi¹, Samantha Pezzica², Patrizia Infelise², Francesca Saba¹, Gian Paolo Caviglia¹, Marta Guariglia¹, Nuria Pérez Diaz del Campo¹, Gabriele Castelnovo¹, Amina Abdulle¹, Maria Lorena Abate¹, Federico Salomone³, Antonella Olivero¹, Giorgio Maria Saracco¹, Roberto Gambino¹, Amalia Gastaldelli², Elisabetta Bugianesi¹. ¹University of Turin, Department of Medical Sciences, Italy; ²Institute of Clinical Physiology, CNR, Pisa, Cardiometabolic Risk Unit, Italy; ³Azienda Sanitaria Provinciale di Catania, U.O.C. of Gastroenterology, Italy
E-mail: chiara.rosso@unito.it

Background and aims: Elevated free fatty acid (FFA) flux and hepatic triglycerides (TG) accumulation are prominent features in subjects with non-alcoholic fatty liver disease (NAFLD). De novo lipogenesis (DNL) is up to 3-fold higher in NAFLD compared to healthy controls. Under DNL stimulation, the production of saturated FFAs is increased and leads to oxidative stress, inflammation thus enhancing hepatic fibrogenesis. Here, we used a marker of DNL (DNLi) to evaluate its relationship with hepatic fibrosis in a group of non-diabetic subjects with biopsy-proven NAFLD who underwent an oral glucose load.

Method: We have studied glucose and lipid metabolism during fasting in 45 non-diabetic subjects with biopsy proven NAFLD (35 male; median age 41 years, range: 23–57). Among them, 25 patients underwent a double tracers oral glucose tolerance test (dtOGTT). Tracers (6, 6-2H₂-glucose and 2H₅-glycerol) were used to assess glucose (endogenous glucose production and glucose clearance [GlucClear]) and lipid metabolism (lipolysis). Throughout the study we measured glucose, insulin (INS), free fatty acids (FFAs) composition, triglyceride (TG), oxidized low density lipoprotein (ox-LDL) and cholesterol profile. DNLi was derived as the ratio palmitic/linoleic acid. The area under the curve (AUC) was calculated for each variable.

Results: Overall, fasting DNLi was associated with BMI ($r = 0.31$, $p = 0.04$), TG levels ($r = 0.29$, $p = 0.05$) and FFAs levels ($r = 0.36$, $p = 0.002$). Among FFAs, DNLi significantly correlated with MUFA and SFA concentration ($r = 0.38$, $p = 0.012$ and $r = 0.54$, $p < 0.001$, respectively). Concerning liver histology, fasting DNLi correlated with the degree of hepatic steatosis ($r = 0.34$, $p = 0.027$) and showed a stepwise

Table (abstract: THU-424).

BMI category	Any CVD		Coronary artery disease		Peripheral artery disease		Cerebrovascular accident		Congestive heart failure		Cirrhosis		CKD stage ≥ 3		Type II DM	
	OR (95 % CI) ^a	p value	OR (95 % CI)	p value	OR (95 % CI)	p value	OR (95 % CI)	p value	OR (95 % CI)	p value	OR (95 % CI)	p value	OR (95 % CI)	p value	OR (95 % CI) ^b	p value
Lean	Referent		Referent		Referent		Referent		Referent		Referent		Referent		Referent	
Overweight	0.73 (0.67–0.80)	<0.001	0.77 (0.70–0.85)	<0.001	0.75 (0.68–0.84)	<0.001	0.72 (0.64–0.82)	<0.001	0.65 (0.57–0.73)	<0.001	1.07 (0.86–1.32)	0.558	0.98 (0.87–1.11)	0.732	1.31 (1.21–1.43)	<0.001
Obesity class I	0.73 (0.66–0.80)	<0.001	0.82 (0.74–0.90)	<0.001	0.67 (0.60–0.75)	<0.001	0.67 (0.59–0.76)	<0.001	0.722 (0.64–0.81)	<0.001	1.07 (0.87–1.33)	0.502	1.09 (0.96–1.23)	0.17	1.81 (1.67–1.97)	<0.001
Obesity class II-III	0.78 (0.71–0.85)	<0.001	0.84 (0.76–0.92)	<0.001	0.60 (0.54–0.68)	<0.001	0.57 (0.50–0.64)	<0.001	0.98 (0.88–1.10)	0.768	1.25 (1.02–1.54)	0.032	1.16 (1.03–1.31)	0.014	2.84 (2.62–3.08)	<0.001

Abbreviations: CI, confidence interval; OR, odds ratio.

^aOR adjusted for age, sex, race, smoking status, hypertension, dyslipidemia, DM, and aspirin and statin use.

^bFor Type II DM, OR was adjusted with the same confounders excluding DM.

POSTER PRESENTATIONS

increased from F0/F1 to F2 to F3/F4 (median values from 1.06 to 1.13 to 1.31, respectively). Throughout the OGTT, the AUC-DNLi inversely correlated with AUC-GluClear ($r = -0.45$, $p = 0.05$). During the first 60 min of OGTT, TG levels increased by 8% in subjects with F3-F4 compared to those with F0-F2 ($p = 0.09$) despite elevated insulin levels, suggesting a significant contribution of DNLi. Accordingly, the AUC-DNLi significantly correlated with AUC-INS, AUC-TG and with the AUC-LDLox ($r = 0.47$, $p = 0.044$; $r = 0.43$, $p = 0.05$; $r = 0.44$, $p = 0.05$, respectively) underlying the contribution of oxidative stress in promoting hepatic fibrogenesis

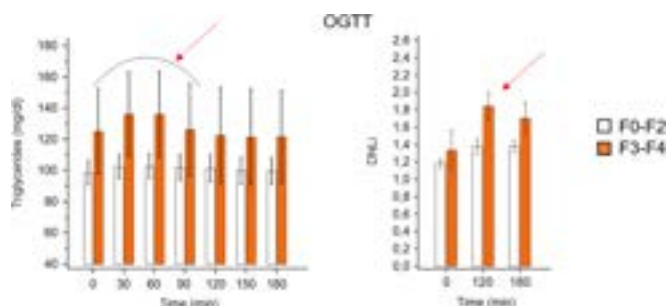


Figure:

Conclusion: Oral glucose load is associated with changes in DNLi and hepatic triglyceride synthesis contributing to liver fibrogenesis in patients with NAFLD.

Funded by Horizon2020 under grant agreement no.634413, EPoS

THU-426

A social media listening study of patients' experiences toward NAFLD (LISTEN-NAFLD)

Jeffrey Lazarus^{1,2}, William Alazawi³, Ron Basuroy⁴, Laurent Castera⁵, Dmitrii Estulin⁶, Yiannoula Koulla⁷, Preethy Prasad⁴, Manuel Romero Gomez^{8,9}, Vincent Wai-Sun Wong¹⁰, Jörn Schattenberg¹¹. ¹Barcelona Institute for Global Health (ISGlobal), Barcelona, Spain; ²CUNY Graduate School of Public Health and Health Policy (CUNY SPH), New York, United States; ³Barts Liver Centre, Blizard Institute, Queen Mary University London, United Kingdom; ⁴Novo Nordisk, Copenhagen, Denmark; ⁵Hospital Beaujon AP-HP, Paris, France; ⁶Novo Nordisk, Zurich, Switzerland; ⁷European Liver Patient's Association, Cyprus; ⁸Digestive Diseases Department and Ciberehd, Virgen del Rocio University Hospital, Seville, Spain; ⁹Institute of Biomedicine of Sevilla (HUVR/CSIC/US), University of Seville, Spain; ¹⁰The Chinese University of Hong Kong, Hong Kong; ¹¹Metabolic Liver Research Program, Department of Medicine, University Medical Center Mainz, Germany
E-mail: Jeffrey.Lazarus@isglobal.org

Background and aims: Patients increasingly use social media to share and access health-related information and experiences. Social listening is a mixed-method approach that identifies and assesses what is being said about a topic on social media platforms. This study used social listening to gain patient-centric insights into NAFLD, a liver disease with increasing prevalence and healthcare system burden.

Method: Data from blogs, forums, and social media platforms including Twitter, Facebook, and YouTube were collected using pre-defined keywords through licensed aggregator tools for 8 countries (Brazil, China, France, Germany, Japan, South Korea, Spain, UK), from Nov 2020 to Nov 2022. Manual and automated algorithms were used to filter the dataset, and thematic analysis was used to summarise country-specific data.

Results: Country-specific random samples of data (~10 000 posts for all countries) were manually reviewed to identify a total of 1600 relevant posts for in-depth analysis (balanced for country representation). Patient journey posts ($n = 1479$) were mainly about ongoing disease management (72%, 1061/1479), diagnosis and tests (50%, 734/

1479), and causes and risk factors (36% 534/1479). Dietary changes (55%, 588/1061), exercise (39%, 417/1061) and weight loss methods (25%, 268/1061) were the most frequently discussed management techniques. The key diagnostic tests mentioned were ultrasound (31%, 170/553), blood tests (24%, 130/553) and liver function tests (16%, 91/553). Unhealthy diet (39%, 208/534), overweight/obesity (32%, 169/534) and harmful effects of medication (12%, 65/534) were perceived as the key causes leading to the condition. 12% (192/1600) discussed the impact of the disease on quality of life. Emotional analysis (84%, 1338/1600) revealed patients were worried (20%, 266/1338) and frustrated (19%, 252/1338) about their condition, but they were also hopeful (14%, 186/1338) and determined (20%, 273/1338) to improve their health. In 19% (311/1600) of conversations, an unmet need was highlighted, especially the need to access knowledgeable HCPs (16%, 51/311), driven by European countries. Other needs were better education (25%, 79/311) and management options (13%, 40/311), driven by Asian countries.

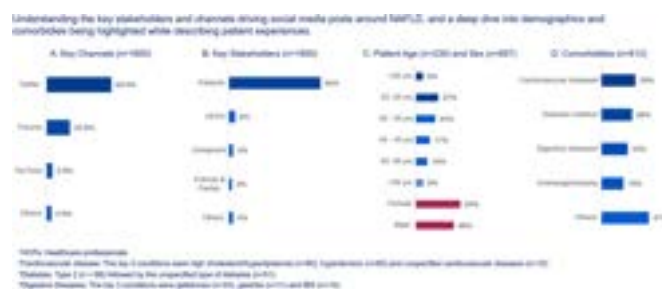


Figure:

Conclusion: This social media listening study highlights the experiences of people living with NAFLD, including perceived challenges, coping strategies and unmet needs. Insights from social media can help us improve communication and patient care through education and support.

THU-427

Genetic risk factors for NAFLD and clinically significant fibrosis in persons living with HIV

Eduardo Vilar Gomez¹, Samer Gawrieh¹, Tiebing Liang¹, Jordan Lake², Susanna Naggie³, Tinsay Woreta⁴, Jennifer Price⁵, Richard Sterling⁶, Sonya Heath⁷, Holly King¹, Laura Wilson⁸, James Tonascia⁹, Meena Bansal¹⁰, Kathleen Corey¹¹, Rohit Loomba¹², Mark S. Sulowski¹³, Naga Chalasani¹. ¹Indiana University School of Medicine, Indianapolis, United States; ²UTHealth Houston (The University of Texas Health Science Center at Houston), Houston, United States; ³Duke Clinical Research Institute, Durham, United States; ⁴Johns Hopkins Hospital, Baltimore, United States; ⁵University of California San Francisco Parnassus Campus, San Francisco, United States; ⁶Virginia Commonwealth University, Richmond, United States; ⁷University of Alabama at Birmingham, Birmingham, United States; ⁸Johns Hopkins Bloomberg School of Public Health, Baltimore, United States; ⁹Johns Hopkins University, Baltimore, United States; ¹⁰Icahn School of Medicine at Mount Sinai, New York, United States; ¹¹Harvard Medical School, Boston, United States; ¹²Medical Center, San Diego, United States; ¹³The Johns Hopkins Hospital, Baltimore, United States
E-mail: nchalasa@iu.edu

Background and aims: The role of genetic risk variants in modulating the risk and severity of NAFLD has been extensively studied in general populations but not in persons with HIV (PWH) with NAFLD (HIV-NAFLD). We investigated the associations between candidate gene variants and risk of HIV-NAFLD and clinically significant fibrosis (CSF) in PWH.

Method: PWH prospectively enrolled in US multicenter studies underwent detailed phenotyping including VCTE for controlled attenuation parameter (CAP) and liver stiffness measurement (LSM). Participants with history of excessive alcohol use or other

Figure: (abstract: THU-427): Association of genetic variants with NAFLD or CSF. Results based on logistic univariate and multivariable^a analysis.

	NAFLD				CSF			
	Univariate		Multivariable ^a		Univariate		Multivariable ^a	
	OR (95% CI)	P value	OR (95% CI)	P value	OR (95% CI)	P value	OR (95% CI)	P value
PNPLA3 rs738409	1.7 (1.2–2.3)	<0.01	1.7 (1.2–2.5)	<0.01	1.8 (1.1–3.0)	0.02	1.9 (1.01–3.5)	0.04
TM6SF2 rs58542926	1.5 (0.8–3.1)	0.22	2.1 (1.0–4.6)	0.04	0.3 (0.05–2.6)	0.30	-	-
HSD17B13 rs72613567	1.1 (0.8–1.7)	0.51	-	-	0.7 (0.3–1.6)	0.37	-	-
MBOAT7 rs641738	1.1 (0.8–1.5)	0.58	-	-	2.7 (1.6–4.6)	<0.01	2.8 (1.6–5.1)	<0.01
HFEC282Y rs1800562	1.9 (0.8–4.5)	0.13	-	-	1.1 (0.2–4.8)	0.92	-	-
ADH1B rs1229984	0.8 (0.4–1.8)	0.67	-	-	0.9 (0.2–3.7)	0.90	-	-
GCKR rs1260326	1.4 (1.1–1.9)	0.01	1.5 (1.03–2.1)	0.03	1.1 (0.6–1.9)	0.69	-	-
FKBP5 rs3800373	0.7 (0.5–0.9)	0.04	0.8 (0.6–0.9)	0.05	0.5 (0.3–0.9)	0.02	0.6 (0.3–0.9)	0.04

^aCovariate-adjusted analysis included age, sex, race/ethnicity, diabetes, and hypertension. All genetic variants were simultaneously included in the multivariable analysis.

liver diseases were excluded. CAP was assessed on a continuous scale and ≥ 285 dB/m to define steatosis. LSM was assessed on a continuous scale and ≥ 9.7 kPa to define CSF. The PNPLA3 rs738409, TM6SF2 rs58542926, HSD17B13 rs72613567, MBOAT7-TMC4 rs641738, HFEC282Y rs1800562, ADH1B rs1229984, GCKR rs1260326, FKBP5 rs3800373 were genotyped by TaqMan assay. Associations between CAP and LSM and genetic variants were analyzed with linear and logistic regression models.

Results: 396 participants were evaluated: age 50 years, male 74%, White 28%, Black 44%, Hispanic 24%, BMI 30 kg/m², 41% with NAFLD and 8% with CSF. PWH and NAFLD, compared to those without NAFLD, more frequently were White and Hispanic, had hypertension, diabetes, and higher BMI, waist circumference, triglycerides, ALT, and CD4+ cells, higher frequency of PNPLA3 GG (15% vs 4%), GCKR TT (16% vs 8%), and lower frequency of FKBP5 AC/CC (55% vs 67%) ($p < 0.05$ for all). Other HIV-related factors such as duration and level of HIV were not significantly different between the two groups. Variants in PNPLA3, TM6SF2, MBOAT7-TMC4, and GCKR were independently associated with higher whereas FKBP5 with lower odds of NAFLD (Table). PWH with CSF vs those without CSF had higher frequency of PNPLA3 GG (22% vs 7%) and MBOAT7-TMC4 TT (41% vs 11%), and lower frequency of FKBP5 AC/CC (44% vs 62%) ($p < 0.05$ for all). PWH and CSF vs those without CSF had higher frequency of metabolic condition but not HIV-related factors. On multivariable analysis, variants in PNPLA3, and MBOAT7-TMC4 were associated with higher whereas FKBP5 with lower odds of CSF (Table).

Association of genetic variants with NAFLD or CSF. Results based on logistic univariate and multivariable^a analysis.

Conclusion: Several genetic variants influence risk of NAFLD and CSF in PWH. A novel variant in FKBP5 was protective against NAFLD and clinically significant fibrosis in PWH. Genetic and metabolic but not HIV viral factors are key modifiers of HIV-NAFLD disease risk and severity.

THU-428

Digital pathology with artificial intelligence analyses provides deeper insights into lifestyle intervention-induced fibrosis regression in NASH

Haiyang Yuan¹, Yayun Ren², Yangyang Li³, Xinlei Wang², Sui-Dan Chen³, Xiao-Zhi Jin¹, Fa-Ling Wu¹, Xiao-Yan Pan⁴, Wen-Yue Liu⁴, Xiaodong Wang⁵, Ming-Hua Zheng^{1,5}. ¹the First Affiliated Hospital of Wenzhou Medical University, MAFLD Research Center, Department of Hepatology, China; ²HistoIndex Pte Ltd, Singapore; ³the First Affiliated Hospital of Wenzhou Medical University, Department of Pathology, China; ⁴the First Affiliated Hospital of Wenzhou Medical University, Department of Endocrinology, China; ⁵Key Laboratory of Diagnosis and Treatment for the Development of Chronic Liver Disease in Zhejiang Province, China
E-mail: zhengmh@wmu.edu.cn

Background and aims: Lifestyle intervention is the basic treatment for non-alcoholic steatohepatitis (NASH) and liver fibrosis is a crucial determinant of clinical outcome in this condition. The second harmonic generation/two-photon excitation fluorescence (SHG/TPEF) microscopy with artificial intelligence analyses can provide automated quantitative assessment of fibrosis features on a continuous scale, called qFibrosis. We used this approach to gain insight into the impact of lifestyle intervention intensity on fibrosis in NASH.

Method: Unstained sections from 72 liver biopsies (paired: baseline and end-of-treatment) from 36 NASH patients who received routine lifestyle intervention (RLI, n = 24) or strengthen lifestyle intervention (SLI, n = 12) were examined. Fibrosis regression was determined by pathological reading. Liver fibrosis (qFibrosis) were quantified by SHG/TPEF microscopy. Collagen parameters were quantified from the five regions, including portal tract (PT), peri-PT, Zone 2, central vein (CV) and peri-CV, which were identified from the SHG/TPEF images.

Results: 21% (5/24) and 50% (6/12) of patients had fibrosis regression for RLI group and SLI group, respectively. 50% of patients had fibrosis no change for both RLI and SLI groups. Numerical analysis showed that fibrosis progression tended to no change or regression in NASH patients after lifestyle interventions, and this phenomenon was more pronounced in the SLI group. Among the patients with fibrosis regression, compared with the RLI group, the fibrosis index of SLI group was reduced more ($p < 0.001$) in the PT, peri-CV and CV regions, but increased more ($p < 0.001$) in zone 2 region. In patients with no change in the fibrosis outcome of conventional pathology, we found a more significant regression in zone 2 region in the SLI group than the RLI group.

Table: Average relative difference of parameters in different regions between RLI group and SLI group in regression patients and no change patients.

Region	Regression patients		p value	No change patients		
	RLI (n = 5)	SLI (n = 6)		RLI (n = 12)	SLI (n = 6)	p value
PT	73%	-32%	<0.001	30%	31%	0.452
Peri-PT	13%	-4%	0.053	-31%	1%	<0.001
Zone 2	-17%	18%	<0.001	-14%	-30%	<0.001
Peri-CV	97%	-81%	<0.001	65%	99%	<0.001
CV	84%	-78%	<0.001	92%	79%	0.063

Conclusion: With enhanced lifestyle intervention, we can see a more pronounced regression of fibrosis, mainly in the portal and central vein segments for the regression patients. Digital pathology provides new insights into lifestyle intervention-induced fibrosis regression, which are not captured by current staging systems.

THU-429

Societal costs and labor market affiliation of histologically confirmed non-alcoholic steatohepatitis-a Danish register-based study

Jan Håkon Rudolphsen¹, Lise Lotte Gluud², Henning Grønbaek^{3,4}, Majken Jensen⁵, Mogens Vyberg^{6,7}, Jens Olsen¹, Peter Bo Poulsen⁸, Nanna Hovelsø⁹, Nikolaj Gregersen⁹, Anne Bloch Thomsen⁹, Peter Jepsen^{3,4}. ¹Incentive, Holte, Denmark; ²Copenhagen University Hospital Hvidovre, Gastro Unit, Copenhagen, Denmark; ³Aarhus University Hospital, Department of Hepatology and Gastroenterology, Denmark; ⁴University of Aarhus, Department of Clinical Medicine, Aarhus, Denmark; ⁵University of Copenhagen, Department of Public Health, Section of Epidemiology, Copenhagen, Denmark; ⁶Aalborg University Campus Copenhagen, Department of Clinical Medicine, Aalborg, Denmark; ⁷Copenhagen University Hvidovre, Department of Pathology, Copenhagen, Denmark; ⁸Pfizer Denmark Aps, Health and Value, Ballerup, Denmark; ⁹Pfizer Denmark Aps, Medical Affairs, Ballerup, Denmark
E-mail: peterbo.poulsen@pfizer.com

Background and aims: Non-alcoholic steatohepatitis (NASH) is associated with increased risk of cirrhosis, hepatocellular carcinoma, cardiovascular diseases and type 2 diabetes. Evidence on the burden of disease of NASH is limited. This population-based register study examines the healthcare costs, use of healthcare services, labor market affiliation and survival of NASH patients compared to individuals without liver disease.

Method: Patients with biopsy-confirmed NASH and corresponding hospital-diagnosed liver disease from 1997 to 2021 were identified in the Danish National Pathology Register and the Danish National Patient Register. Patients were matched 1:5 with liver disease-free comparators. Outcomes were costs associated with healthcare services, contacts with hospital care, use of home care services, production loss measured by wage differences (NASH patients vs. comparators), incidence of long-term sick leave, weeks of unemployment, early retirement, and survival. All outcomes were estimated based on data from national Danish registers. Patients were followed for 16 years-five years before and 11 years after diagnosis. Excess costs of NASH were calculated as the difference in mean costs for the NASH group and the comparators.

Results: 1039 NASH patients were identified (total population in Denmark (2021): 5 840 000). In the year leading up to diagnosis, a NASH patient generated €6318 in excess costs of healthcare services on average, and total costs in that year were 4.1 times higher than for the average comparator. Within a 10-year window, starting a year before diagnosis, the corresponding excess costs of NASH was €41 998 (2.9 times higher than the comparators) and with 4.4-fold (95% CI 3.18–6.06) higher hazard of early retirement. The NASH patients had significantly lower income than comparators from five year before start of study until nine years after diagnosis (t-test, $p < 0.05$), and 2.4-fold (95% CI 1.80–3.25) higher mortality hazard than comparators.

Conclusion: There are substantial excess societal costs associated with NASH. Patients exit the labour market earlier and have higher mortality than their comparators without liver disease.

THU-430

Prevalence and mortality of non-alcoholic fatty liver disease (NAFLD) in non-diabetics, pre-diabetics, and diabetics in the United States

James Paik^{1,1,2}, Ameeta Kumar³, Reem Al-Shabeeb³, Katherine Eberly³, Nagashree Gundu Rao^{2,4}, Zobair Younossi^{1,2,3}. ¹Inova Health System, Betty and Guy Beatty Center for Integrated Research, Falls Church, United States; ²Inova Health System, Inova Medicine, Falls Church, United States; ³Inova Fairfax Medical Campus, Center for Liver Disease, Department of Medicine, Falls Church, United States; ⁴Inova Health System, Division of Endocrinology, Inova Medicine Services, Falls Church, United States
E-mail: zobair.younossi@inova.org

Background and aims: Type 2 diabetes (T2D) with NAFLD is associated with adverse outcomes. Lacking is knowledge on the prevalence and outcomes of NAFLD among pre-diabetics (Pre-D) and non-diabetics (ND) which we have assessed here.

Method: NHANES III and mortality data (thru 2019) via National death index were used. NAFLD was defined by ultrasound, absence of other liver diseases, and excess alcohol use. Pre-D was defined as fasting glucose of 100–125 mg/dL or HbA1c level of 5.7%–6.4% without T2D. ND was defined as not having T2D or Pre-D. Metabolically healthy (MH) was defined if all following criteria were absent: waist circumference of ≥ 102 cm (men) or ≥ 88 cm (women); blood pressure (BP) $\geq 130/85$ mm Hg or using BP-lowering

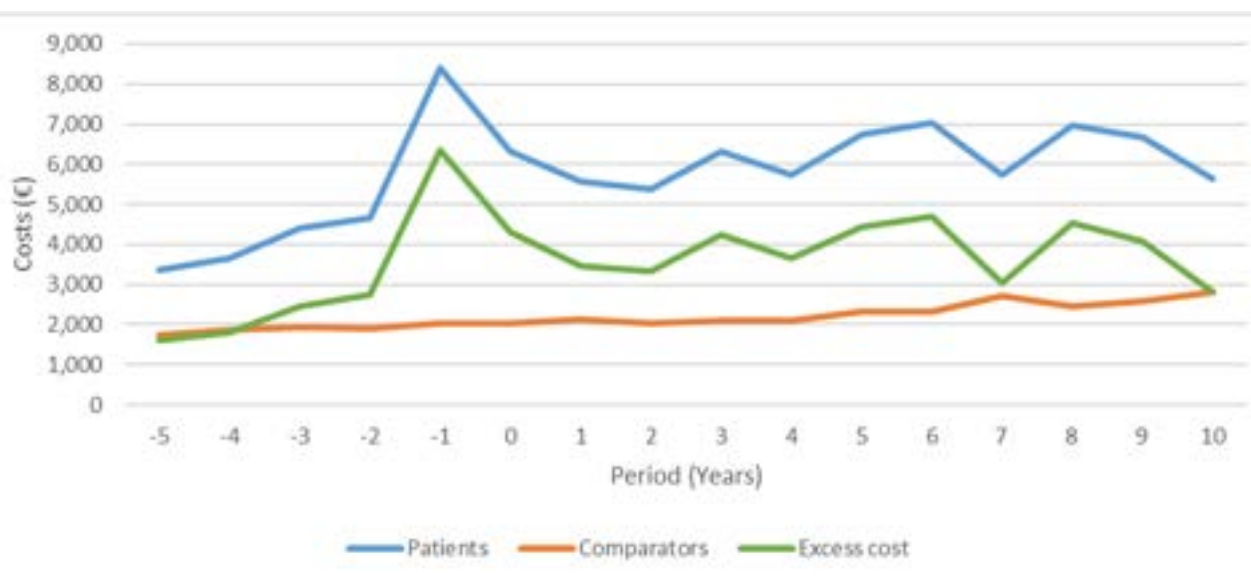


Figure: (abstract: THU-429): Annual total costs healthcare services (hospital care, primary care, prescription medication and home care) for NASH patients and a matched group of liver disease-free comparators. Period 0 start at date of diagnosis; period length was one year. Excess costs are the difference in costs between NASH patients and the comparators

Table: (abstract: THU-430): Factors Associated with Mortality Among NAFLD subjects, Stratified by Diabetes group

	ND with MH HR (95% CI)	ND without MH HR (95% CI)	Prediabetics HR (95% CI)	T2D HR (95% CI)
Hypertension	NA	1.38 (0.90–2.13)	1.44 (1.08–1.90)	1.40 (0.82–2.37)
High C-reactive protein	NA	1.49 (0.54–4.12)	3.42 (1.23–9.51)	2.05 (1.23–3.39)
Cardiovascular Diseases	NA	2.10 (1.35–3.26)	2.13 (1.17–3.87)	2.04 (1.38–3.03)
High FIB4 ≥ 2.67	NA	1.76 (0.93–3.35)	2.80 (0.91–8.60)	1.58 (1.08–2.30)
Chronic Kidney Diseases	NA	1.39 (0.79–2.42)	2.68 (2.00–3.60)	1.91 (1.22–2.98)
Sarcopenia	NA	1.24 (0.73–2.10)	1.53 (1.15–2.03)	1.04 (0.72–1.48)
Aged 20–39	Reference	Reference	Reference	Reference
Aged 40–59	16.29 (2.67–99.37)	3.21 (1.78–5.79)	3.08 (1.39–6.82)	4.50 (1.80–11.26)
Aged 60–74	858.91 (99.05–7448.05)	19.33 (9.93–37.63)	14.7 (6.62–32.66)	16.55 (7.20–38.06)
Male	7.05 (2.29–21.71)	1.62 (1.17–2.24)	1.14 (0.83–1.55)	1.03 (0.75–1.41)
Non-Hispanic White	0.38 (0.12–1.22)	1.44 (0.91–2.28)	1.43 (1.02–2.01)	1.96 (1.29–2.96)
Low income	0.35 (0.07–1.69)	1.42 (1.00–2.02)	1.28 (0.91–1.81)	1.73 (1.22–2.45)
Active smoker	18.06 (3.78–86.36)	2.03 (1.43–2.88)	1.55 (1.09–2.19)	1.84 (1.08–3.13)

Models were adjusted for age, sex, race, income, education, smoking, physical activity, healthy eating.
Bold p < .05

medication; triglyceride ≥ 150 mg/dL or using lipid-lowering medication; cholesterol level of <40 mg/dL (men) or <50 mg/dL (women); homeostasis model assessment of insulin resistance score ≥ 2.5 ; C-reactive protein level of >2 mg/L. Cause-specific competing risk mortality analyses were performed.

Results: Among 11 231 adults (mean age 43.4 years; 43.9% male; 18.9% NAFLD; 6.9% T2D; 25.2% Pre-D; 44.3% ND without MH; and 23.6% ND with MH). Age-standardized NAFLD prevalence among T2D, Pre-D, ND without MH and ND with MH were 40.9%, 23.8%, 19.2% and 5.1%. During mean follow-up of 24.6 years, 3982 died. Age-standardized mortality was higher in NAFLD than in non-NAFLD (32.7% vs. 28.7%, $p < .001$). Among NAFLD subjects, the highest age-standardized mortality was T2D (43.9%), then Pre-D (34.9%), ND without MH (29.9%), and ND with MH (22.0%) (pairwise p values < .04 vs. ND with MH). Multivariable cox models showed that compared to NAFLD without T2D or Pred-D but with metabolic health, NAFLD with T2D had the highest risk of all-cause and cardiac-specific mortality { [HR] = 4.79 [95% CI: 2.23–10.24] and HR = 17.41 [3.27–92.6]}], followed by NAFLD with Pre-D { (HR = 2.93 [1.43–6.01] and HR = 9.21 [1.78–47.77])} and then NAFLD without T2D or Pred-D and without metabolic health { (HR = 2.60 [1.27–5.31] and HR = 5.81 [1.07–31.69])}. Independent predictors of mortality varied by groups (Table).

Conclusion: Presence of T2D or Pre-D increased the prevalence and adverse outcomes of subjects with NAFLD.

THU-431

Genetic and metabolic characteristics of lean non-alcoholic fatty liver disease in Asian

Huiyul Park¹, Eileen Yoon², Sang Bong Ahn³, Hye-Lin Kim⁴, Jun-Hyuk Lee⁵, Mimi Kim⁶, Chul-min Lee⁶, Bo-Kyeong Kang⁶, Joo Hyun Sohn², Jihyun An², Joo Hyun Oh³, Hyo Young Lee⁷, Hyunwoo Oh⁷, Jang Han Jung⁸, Dae Won Jun², Eun Chul Jang⁹.

¹Myoungji Hospital, Hanyang University College of Medicine, Department of Family Medicine, Korea, Rep. of South; ²Hanyang University, College of Medicine, Department of Internal Medicine, Korea, Rep. of South; ³Nowon Eulji Medical Center, Eulji University School of Medicine, Department of Internal Medicine, Korea, Rep. of South; ⁴Sahmyook University, College of Pharmacy, Korea, Rep. of South; ⁵Nowon Eulji Medical Center, Eulji University School of Medicine, Department of Family Medicine, Korea, Rep. of South; ⁶Hanyang University, College of Medicine, Department of Radiology, Korea, Rep. of South; ⁷Uijeongbu Eulji Medical Center, Eulji University College of

Medicine, Department of Internal Medicine, Korea, Rep. of South; ⁸Dongtan Sacred Heart Hospital of Hallym University Medical Center, Department of Internal Medicine, Korea, Rep. of South; ⁹Soonchunhyang University College of medicine, Department of Occupational and Environmental Medicine, Korea, Rep. of South
E-mail: noshin@hanyang.ac.kr

Background and aims: The pathophysiology of lean non-alcoholic fatty liver disease (NAFLD) remains unclear and is associated to have more diverse pathogenic mechanisms than obese NAFLD. We aimed to investigate the characteristics of genetic- or metabolic-associated lean NAFLD in a community-based cohort.

Method: A total of 10 345 health check-up participants enrolled. Lean individuals were categorized according to the body mass index cut-off of 23 kg/m². Single nucleotide polymorphism was analyzed using Genotyping Arrays. Anthropometric measurements of waist circumference, total fat mass, and lean mass were included.

Results: The prevalence of lean NAFLD was 21.6% among total NAFLD subjects, and proportion of lean NAFLD was 18.5% in lean subjects (<23 kg/m²). Prevalence of metabolic syndrome and diabetes among lean NAFLD was 12.4% and 10.4%, respectively. Around 20.1% of lean NAFLD seems to be associated with metabolic-associated. Homozygous minor allele (GG) of PNPLA3 (rs738409) and heterozygous minor allele (CT, TT) of TM6SF2 (rs58542926) associated with lean NAFLD. However, the prevalence of fatty liver was not associated with the genetic variants of MBOAT7 (rs641738), HSD17B13 (rs72613567), MARC1 (rs2642438), or AGXT2 (rs2291702) in lean individuals. Around 32.1% of lean NAFLD seems to be associated with PNPLA3 or TM6SF2 genetic variation. Multivariable risk factor analysis showed that the metabolic risk factors, genetic risk variants, and waist circumference were independent risk factor for lean NAFLD.

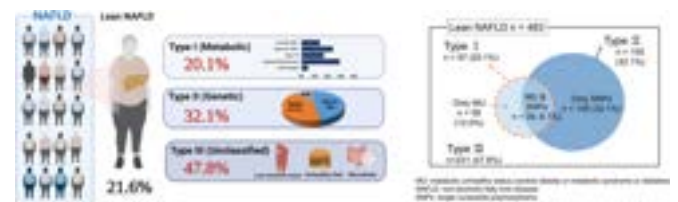


Figure 1: Schematic diagram for the proportion of metabolic, genetic, and unspecified lean non-alcoholic fatty liver disease (NAFLD).
Figure:

Conclusion: Further studies on risk factors beyond central obesity, metabolic syndrome, and genetic risk factors are needed to understanding the pathogenesis of lean NAFLD.

THU-432

PNPLA3 protein levels are increased in liver and decreased in adipose tissue from patients with obesity-associated non-alcoholic steatohepatitis

Helena Castañé^{1,2}, Andrea Jiménez Franco^{1,2}, Cristian Martínez Navidad², Cristina Placed¹, Jordi Camps Andreu³, Jorge Joven Maried³. ¹Universitat Rovira i Virgili, Unitat de Recerca Biomèdica, Reus, Spain; ²Fundació IISPV, Unitat de Recerca Biomèdica, Reus, Spain; ³Hospital Universitari Sant Joan, Unitat de Recerca Biomèdica, Reus, Spain
E-mail: helenacastanev@gmail.com

Background and aims: Non-alcoholic fatty liver disease (NAFLD) is the most prevalent form of chronic liver disease, affecting 25% of the population. It can progress to non-alcoholic steatohepatitis (NASH), a severe condition characterized by fibrosis, that can lead to cirrhosis, and even liver cancer, requiring a liver transplant. Accurate diagnosis of NAFLD/NASH progression requires a liver biopsy, and there is currently no effective drug treatment. PNPLA3 (patatin-like phospholipase domain-containing 3), an enzyme involved in lipid metabolism, is one of the protein genes linked to NAFLD. The expression of PNPLA3 is associated with NAFLD, and its accumulation leads to larger lipid droplets, a hallmark of NASH steatosis. Finding new targets to halt NAFLD progression is crucial, and PNPLA3 may be a promising candidate, however its role is unknown in other tissues. This study aimed to compare PNPLA3 protein levels in different tissues from patients with and without NASH, including liver, subcutaneous adipose tissue (SAT), and visceral adipose tissue (VAT). **Method:** Samples included liver, SAT, and VAT from n = 98 patients with morbid obesity candidates to receive bariatric surgery. During the procedure, tissue biopsies were performed, from which we performed histological analyses, protein extraction and subsequent western blot to explore PNPLA3 protein levels. Semi-targeted lipidomics was performed to quantify the concentration of triglycerides and glycerophospholipids.

Results: We found significative differences in PNPLA3 protein levels in the liver samples of NASH patients compared to those without NASH (Figure A). Also, patients with NASH showed a more prominent expression around the fibrotic areas (Figure B; a: fibrosis, b: PNPLA3 protein shown by immunohistochemistry). Lipid content was significantly higher in the hepatic tissue from patients with NASH (Figure C), triglycerides were significantly increased, meanwhile glycerophospholipids were significantly decreased. Adipose tissue levels of PNPLA3 protein were not significantly different between the studied groups (Figure D), nor the distribution among the tissue (Figure E; a: fibrosis shown by Masson's Trichrome, b: PNPLA3 immunohistochemistry in adipose tissue). On the other side, lipid content in VAT was significantly different between NASH and non-NASH patients, meanwhile in SAT there were no differences in total lipid content between NASH and non-NASH patients (Figure D).

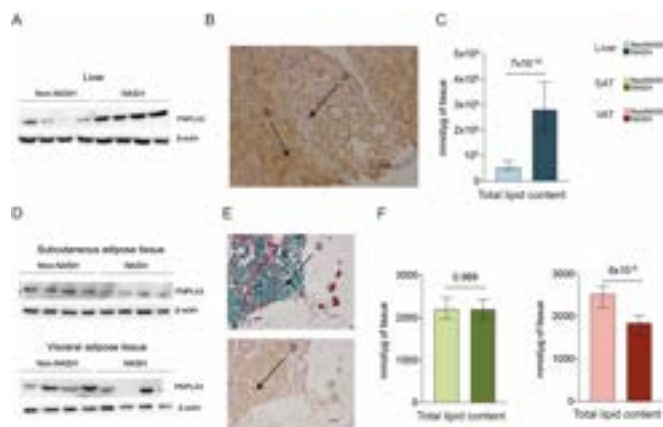


Figure:

Conclusion: PNPLA3 protein levels were significantly increased in the hepatic tissue of patients with NASH and was present in higher quantities around areas of fibrosis. This was correlated with an increased total lipid content. In contrast, no significant differences in PNPLA3 protein levels or localization were observed in adipose tissue between NASH and non-NASH patients, however lipid content in VAT was significantly decreased in NASH patients.

THU-433

Impact of PNPLA3 polymorphism on non-alcoholic fatty liver disease in Japan: a multicenter cohort study

Yuya Seko¹, Kanji Yamaguchi¹, Toshihide Shima², Michihiro Iwaki³, Hirokazu Takahashi⁴, Miwa Kawanaka⁵, Saiyu Tanaka⁶, Yasuhide Mitsumoto², Masato Yoneda³, Atsushi Nakajima³, Ola Fjellstrom⁷, Jenny Blau⁸, Björn Carlsson⁷, Takeshi Okanoue², Yoshito Itoh¹. ¹Kyoto Prefectural University of Medicine, Department of Gastroenterology and Hepatology, Japan; ²Saiseikai Suita Hospital, Japan; ³Yokohama City University Graduate School of Medicine, Japan; ⁴Saga University Hospital, Japan; ⁵Kawasaki Medical School, Japan; ⁶Nara City Hospital, Japan; ⁷BioPharmaceuticals RandD, AstraZeneca, Sweden; ⁸BioPharmaceuticals RandD, AstraZeneca, United States
E-mail: yuyaseko@koto.kpu-m.ac.jp

Background and aims: PNPLA3 rs738409 has been associated with an increased risk of liver-related events in patients with non-alcoholic fatty liver disease (NAFLD). In this study, we investigated the epidemiology of NAFLD and the impact of PNPLA3 on prognosis in Japan.

Method: A longitudinal multicenter cohort study, the JAGUAR study, includes 1550 patients with biopsy-proven NAFLD in Japan. We performed genetic testing and evaluated outcomes from this cohort. Liver-related events were defined as hepatocellular carcinoma (HCC) and decompensated liver cirrhosis events.

Results: During follow-up (median [range], 7.1 [1.0–24.0] years), 80 patients developed HCC, 104 developed liver-related events, and 59 died of any cause. The 5-year rate of liver-related events for each single-nucleotide polymorphism was 0.5% for CC, 3.8% for CG, and 5.8% for GG. Liver-related deaths were most common (n = 28); only 3 deaths were due to cardiovascular disease. Multivariate analysis identified carriage of PNPLA3 CG/GG (hazard ratio [HR] 16.04, p = 0.006) and FIB-4 index >2.67 (HR 10.70, p < 0.01) as predictors of liver-related event development. No HCC or liver-related death was found among patients with PNPLA3 CC. There was a significantly increased risk of HCC, liver-related events, and mortality for CG/GG versus CC, but no difference between the CG and GG genotypes.

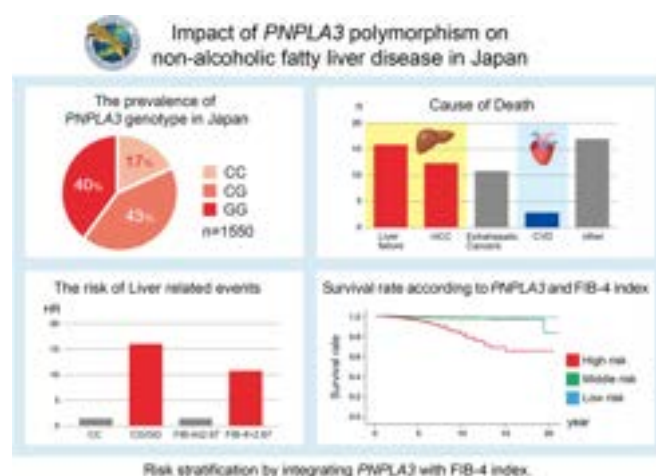


Figure:

Conclusion: In Japanese individuals, the main cause of death from NAFLD is liver-related death. The increased risks of liver-related events incurred by PNPLA3 CG and GG are comparable and

significantly different from the low risk identified with CC. Risk stratification for NAFLD in Japan is best accomplished by integrating PNPLA3 with the FIB-4 index.

THU-434

Pilot results for a multidisciplinary community metabolic liver clinic

Theresa Hydes^{1,2}, Cyril Sieberhagen², Mike Merrimen³, Louise Millard³, David Riley¹, Daniel Cuthbertson^{1,2}. ¹University of Liverpool, United Kingdom; ²Liverpool University NHS Hospitals Foundation Trust, United Kingdom; ³Millbrook Medical Centre, United Kingdom
E-mail: therasa@doctors.org.uk

Background and aims: Non-alcoholic fatty liver disease (NAFLD) affects over 1 in 4 people in the UK, with an increased prevalence in areas of deprivation. Most patients with NAFLD do not have significant liver fibrosis and are best managed in the community. Thorough screening and optimisation of cardiometabolic disease is vital, as metabolic disease increases the risk of liver fibrosis and hepatocellular carcinoma, and NAFLD is associated with increased risk of diabetes, chronic kidney disease and cardiovascular disease. We aimed to pilot a community metabolic liver clinic in an area of high deprivation to examine feasibility, burden of undetected disease and the potential for meaningful intervention (lifestyle/pharmacological).

Method: Four pilot clinics ran in a large primary care centre in the Northwest of England October-November 2022. Adults who had type 2 diabetes or a body mass index >25 (without a prior diagnosis of cirrhosis or another cause of chronic liver disease), were invited via text message to book a clinic appointment and attend for bloods. The clinic proforma was designed by a multidisciplinary team (general practitioners/hepatologists/diabetologists/patients) informed by national guidelines, consisting of an assessment (history/anthropometrics/fibroscan/review of bloods) and management section (education/lifestyle/pharmacological). Personalised written feedback using traffic light systems and lifestyle recommendations were integrated into the proforma which was uploaded to the primary care electronic medical records and shared with each patient. Any complex cases were reviewed in a virtual multi-disciplinary team meeting.

Results: Of 24 patients booked in, 19 attended (79.2%). The clinic took 30 minutes including administration time. There was a high burden of known underlying cardiometabolic disease (table 1). In total 73.7% of individuals had a controlled attenuation parameter score >275 dB/m and 31.6% of individuals had a fibroscan score of ≥ 8 kPa at which point a full liver screen was requested and referral to secondary care was made. The clinic generated the following outputs: (i) Lifestyle intervention: brief alcohol intervention 15.8%; smoking cessation advice 5.3%, referral to community lifestyle hub (free pass to leisure centre/weight management class) offered and accepted by patient 26.3%; (ii) Onward referral: diabetes secondary care clinic 5.3%, hepatology secondary care clinic 31.6%, health care assistant clinic for management of newly diagnosed hypertension 15.8%, or poorly controlled hypertension 42.1%, enhanced weight management services 10.5%; (iii) Pharmacological intervention: escalation of glucose-lowering therapy 57.9%; statin initiation or dose titration 10.5%. Written feedback from patients identified that all patients thought the clinic was useful, 100% said the clinic and written information helped them better understand their results and health conditions and 93% said the clinic and written information would prompt lifestyle changes.

Demographics	
Age (yrs.), median (range)	67 (58-85)
Gender (male), %	42.1
Highest two deciles nationally for multiple deprivation, %	78.9
Audit C score (alcohol) ≥ 8 , %	15.8
Metabolic disease	
Body mass index > 25kg/m ² , %	78.9
Body mass index > 30kg/m ² , %	63.2
Waist circumference men > 102cm, women > 88cm, %	94.4
Known diagnosis diabetes, %	94.7
HbA1c ≥ 48 mmol/mol, %	72.2
Known diagnosis of hypertension, %	73.7
Triglycerides ≥ 150 mg/dl, %	47.4
Cardiovascular morbidity	
Acute coronary syndrome/peripheral vascular disease/stroke, %	47.4
QRS/QTc ≥ 10 , or prior acute coronary syndrome, %	94.7
Known chronic kidney disease, %	10.5
Urine albumin creatinine ratio ≥ 3 mg/mol, %	26.3

Figure: Table 1. Baseline status of participants

Conclusion: A thorough cardiometabolic assessment for patients with, and at risk of NAFLD, can be performed within 30 minutes in a primary care setting and generates high levels of intervention which is likely to impact future clinical outcomes. A combined form for medical assessment and personalised feedback of individual risk and management is associated with high levels of patient satisfaction.

THU-435

Influence of chronotype and adherence to the mediterranean diet on the risk of liver fibrosis in patients with non-alcoholic fatty liver disease

Gabriele Castelnovo¹, Gian Paolo Caviglia¹, Chiara Rosso¹, Nuria Pérez Díaz del Campo¹, Angelo Armandi^{1,2}, Marta Guariglia¹, Amina Abdulle¹, Daphne D'Amato¹, Kamela Gjini¹, Irene Poggiolini¹, Antonella Olivero¹, Maria Lorena Abate¹, Giorgio Maria Saracco^{1,3}, Elisabetta Bugianesi^{1,3}. ¹University of Turin, Department of Medical Sciences, Turin, Italy; ²University Medical Center of the Johannes Gutenberg-University, I. Department of Medicine, Mainz, Germany; ³Città della Salute e della Scienza-Molinette Hospital, Gastroenterology Unit, Turin, Italy
E-mail: gabriele.castelnovo@unito.it

Background and aims: Late chronotype, i.e. an individual's aptitude to perform daily activities late in the day, has been associated with low adherence to the mediterranean diet (MedDiet) and metabolic syndrome. The aim of this work was to investigate the potential association between chronotype and adherence to MedDiet with the risk of significant ($F \geq 2$) and severe ($F \geq 3$) liver fibrosis in individuals with non-alcoholic fatty liver disease (NAFLD).

Method: A total of 156 patients with a diagnosis of NAFLD by ultrasound were consecutively enrolled. All patients underwent liver stiffness measurement (FibroScan® 530). $F \geq 2$ and $F \geq 3$ were defined by liver stiffness values ≥ 7.1 kPa and ≥ 8.8 kPa, respectively. The chronotype (MSFsc) was defined by the Munich Chronotype Questionnaire (MCTQ) as the mid-sleep on free days (MSF) corrected for sleep debt on working days, and was expressed as h:min. To carry out the analyses, we defined early, intermediate and late chronotype by splitting the MSFsc into tertiles, evaluating the effect of tertile one versus tertile two + three. In addition, mid-sleep on workdays (MSW) was recorded. The adherence to the MedDiet was assessed by the mediterranean diet score (MDS).

Results: Median age was 52 (43-62) years; 60.8 % of participants were male. Median body mass index (BMI) was 29.5 (26-32.5) kg/m². The principal comorbidities were type-2 diabetes mellitus (T2DM) (n = 38; 24.3 %), arterial hypertension (n = 79; 50.6 %), dyslipidemia (n = 99; 63.4 %), obstructive sleep apnea (OSAS) (n = 8; 5.1%) and depression (n = 7; 4.4 %). Overall, 22 (13.9 %) patients had $F \geq 2$, while 15 (9.5 %) had $F \geq 3$. Most subjects (67.9 %) had intermediate or

late chronotype and showed higher MSF ($p < 0.001$) and MSW ($p < 0.001$) compared to those with early chronotype. Remarkably, at logistic regression analysis adjusted for MDS, sex, age, BMI, T2DM, OSAS, arterial hypertension, dyslipidemia, and depression, only intermediate+late chronotype (OR = 6.8, 95% CI 1.3–35.3, $p = 0.022$), MDS (OR = 0.7, 95% CI 0.5–0.9, $p = 0.025$) and T2DM (OR = 6.4, 95% CI 1.9–20.9, $p = 0.002$) resulted significantly and independently associated to $F \geq 2$. Similarly, in a logistic regression model adjusted for the same variables, only intermediate + late chronotype (OR = 20.4, 95% CI 1.4–282.9, $p = 0.024$), MDS (OR = 0.6, 95% CI 0.4–0.9, $p = 0.015$) and T2DM (OR = 20.2, 95% CI 3.9–102.4, $p < 0.001$) resulted significantly and independently associated to $F \geq 3$.

Conclusion: We observed that intermediate/late chronotype and low adherence to MedDiet were associated with both significant and severe liver fibrosis in patients with NAFLD. Future research is needed to better understand the multidisciplinary management of this complex disease.

Italian Ministry for Education, University and Research (MIUR) under the programme “Dipartimenti di Eccellenza 2018–2022” Project code D15D18000410001.

THU-436

Relationship of hepcidin levels to metabolic factors, anthropometric indicators of adiposity and disease severity in NAFLD patients

Claudia Cravo¹, Cristiane Villela-Nogueira¹, Ana Carolina Cardoso¹, Fernanda Calçado¹, Guilherme Rezende¹, Frederico Campos Ferreira², Joao Marcello de Araujo Neto¹, Jorge Eduardo Pinto^{1,2}, Henrique Sergio Coelho^{1,3}, Renata Perez^{1,4}, Nathalie Leite¹.

¹Universidade Federal do Rio de Janeiro, Brazil; ²Hospital Universitário Pedro Ernesto-UERJ, Brazil; ³Hospital São Lucas/Rede DASA, Brazil; ⁴D’Or Institute for Research and Education (IDOR), Rio de Janeiro, Brazil
E-mail: nathaliecleite@gmail.com

Background and aims: Non-alcoholic fatty liver disease (NAFLD) affects approximately 25% of the world’s western population. Both iron and lipid metabolism seem to play a role in NAFLD pathogenesis. We aimed to investigate the association between hepcidin levels, ferritin levels and iron overload with body composition indices, metabolic risk factors and the presence of NASH with significant fibrosis ($F \geq 2$).

Method: It was a cross-sectional study in a cohort of patients with NAFLD in the outpatient clinic of our tertiary-care University Hospital. All participants gave written informed consent, and the local Ethics Committee had previously approved the study protocol. Inclusion criteria were patients aged between 18 and 70 years, with an ultrasound diagnosis of NAFLD who agreed to undergo percutaneous liver biopsy. Exclusion criteria were NAFLD patients with other etiologies of chronic liver disease, acute or chronic inflammatory diseases, chronic anemia, kidney disease, hemochromatosis, patients using parenteral iron and those with malignant neoplasms. All patients were evaluated by a standard protocol that included anthropometric indices, clinical and laboratory data. Percutaneous liver biopsy was analyzed by an experienced hepatopathologist. Steatohepatitis was defined by NASH-CRN system and iron was graded according to the Scheuer’s classification. A multivariate logistic regression analysis was carried on to investigate if hepcidin levels, ferritin levels and iron overload were independently associated with active NASH (NAS ≥ 4) and significant fibrosis ($F \geq 2$).

Results: 162 patients were included (73% female (F), age 54 ± 9 y); 78% had type 2 diabetes (T2DM), 66% were obese. Both hepcidin and ferritin levels varied according to gender (F:18.9 vs M: 31.8 $p = 0.001$; F:131 vs M:280 $p < 0.001$) and to different anthropometric indicators of adiposity. Higher hepcidin and ferritin levels were found in participants with elevated neck circumference and body adiposity index, whereas lower levels of both iron regulators were found in those with the highest values of visceral adiposity index (VAI). T2DM was the only metabolic risk factor significantly associated with lower

hepcidin levels (20.1 vs. 34.3; $p = 0.007$). On liver biopsy, 24% had NASH (NAS ≥ 4) and significant fibrosis ($F \geq 2$); 19% had siderosis. Patients with NASH with $F \geq 2$ were less likely to have obesity (51% vs. 71%; $p = 0.025$) but had higher baseline levels of HbA1c (7.6 vs. 6.6; $p = 0.018$) and liver enzymes (AST: 31 vs. 25; $p = 0.031$; ALT 51 vs. 41; $p = 0.05$; GGT 62 vs. 46; $p = 0.001$). Regarding iron parameters, those patients with NASH and $F \geq 2$ had significant lower hepcidin levels (18.7 vs 25.4; $p = 0.039$). On multivariate logistic regression, hepcidin levels were independently associated with NASH with $F \geq 2$ (OR: 0.975; 95% CI: 0.955–0.996. $p = 0.020$) in models hierarchically-adjusted for ferritin levels, iron overload on liver biopsy, age, gender, BMI, diagnosis of arterial hypertension or type 2 diabetes, liver enzymes and parameters of lipid profile and glycemic control.

Conclusion: Our results suggest an association of active and progressing NASH with lower hepcidin levels. There is no association between NAFLD severity with other iron laboratory and histologic parameters. Lower levels of hepcidin are also found in participants with T2DM and those with the highest values of VAI, which, through the mechanisms of insulin resistance and ectopic fat deposition, play an important role in the NAFLD development and progression.

THU-437

Impairment of health-related quality of life among people with type 2 diabetes and advanced fibrosis

Maurice Michel¹, Michelle Doll¹, Angelo Armandi¹, Christian Labenz¹, Peter Galle¹, Jörn Schattenberg¹. ¹Metabolic Liver Research Program, I. Department of Medicine, University Medical Center Mainz, Mainz, Germany

E-mail: maurice.michel@unimedizin-mainz.de

Background and aims: People living with type 2 diabetes mellitus (T2DM) show a high prevalence of non-alcoholic fatty liver disease (NAFLD) and hepatic fibrosis. Their health-related quality of life (HRQL) is affected by multiple in part overlapping factors and aggravated by metabolic comorbidities and fibrosis stage. However, the association of advanced fibrosis (AF) and HRQL in people with T2DM in secondary care remains poorly established. Therefore, the aim of this prospective study was to investigate the effect of AF on the HRQL in people with T2DM.

Method: A total of 149 individuals with T2DM treated at a secondary care diabetes outpatient clinic within the German disease management program (DMP) were included in the final analysis. Vibration-controlled transient elastography (VCTE) was used to non-invasively define hepatic steatosis (HS) and AF. A controlled attenuation parameter (CAP) of ≥ 275 dB/m and a liver stiffness measurement (LSM) of ≥ 12 kPa were used to define HS and AF, respectively. The EQ-5D-3L questionnaire was used to assess HRQL. This questionnaire contains five dimensions, and a visual analogue scale (VAS). Using country-specific value sets, an index value (time trade-off, TTO), that summarises overall HRQL, was obtained. Uni- and multivariable linear regression models were used to identify independent clinical predictors of impaired HRQL (VAS, TTO).

Results: The majority of this cohort was male (63.1%) and the median age was 67 (IQR 59; 71). The prevalence of HS and AF was 77.9% ($n = 116$) and 12.8% ($n = 29$), respectively. The majority of these individuals were identified to have NAFLD ($n = 104$, 89.7%). The mean VAS and TTO index scores in the entire cohort were 71.9 ± 18.4 and 0.85 ± 0.21 , respectively. People with T2DM and HS (TTO: 0.92 ± 0.13 vs. 0.83 ± 0.22 , $p = 0.037$) and/or AF (VAS: 74.8 ± 16.4 vs. 59.9 ± 21.3 , $p < 0.001$; TTO: 0.88 ± 0.17 vs. 0.71 ± 0.29 , $p = 0.001$) had an overall lower HRQL in comparison to those without HS and/or AF. The most strongly affected dimensions were mobility ($p = 0.001$), usual activities ($p = 0.032$) and pain/discomfort ($p = 0.027$) in people with T2DM and AF (Figure 1). Obesity (VAS: beta -0.247 , $p = 0.005$; TTO: beta -0.225 , $p = 0.012$), AF (VAS: beta -0.222 , $p = 0.011$; TTO: beta -0.171 , $p = 0.049$) and age (VAS: beta -0.171 , $p = 0.046$) remained independent predictors of a poor HRQL. In turn, T2DM-related comorbidities and HS did not remain predictive of an impaired HRQL.

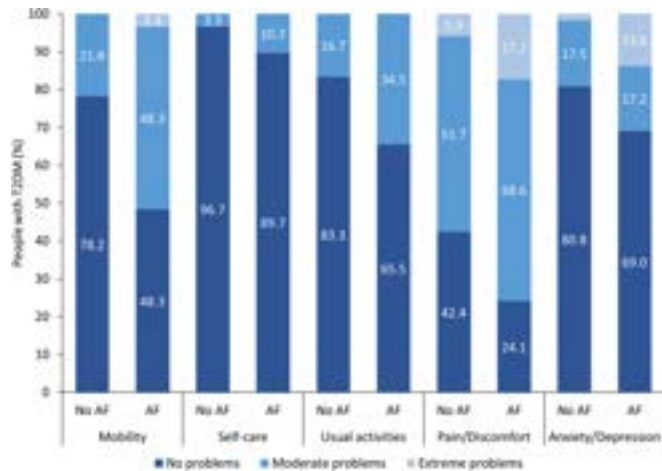


Figure: Distribution (%) of the EQ-5D-3L dimensions in people with T2DM and without advanced fibrosis (no AF) or with advanced fibrosis (AF)

Conclusion: Obesity and AF negatively affect the HRQL in patients with NAFLD and T2DM in secondary care. Interventions aiming at weight reduction may improve patient-reported and liver-related outcomes in people with T2DM.

THU-438

The impact of glycemic control on progressive forms of non-alcoholic fatty liver disease: combined data from multiple clinical trials including more than 5000 patients (in collaboration with NAIL-NIT consortium)

Mazen Nouredin¹, Julie Dubourg², Jörn Schattenberg³, Michael Charlton⁴, Stephen Harrison⁵, Naim Alkhouri⁶, Sophie Jeannin Megnien⁷, Vlad Ratziu⁸. ¹Houston Methodist Hospital, Houston, United States; ²Summit Clinical Research, San Antonio, United States; ³University Medicine at the Johannes Gutenberg University in Mainz, Mainz, Germany; ⁴UChicago Medicine, Chicago, United States; ⁵University of Oxford, United Kingdom; ⁶Arizona Liver Health, Chandler, United States; ⁷Summit Clinical Research, United States; ⁸Institute for Cardiometabolism and Nutrition, France
E-mail: jdubourg@summitclinicalresearch.com

Background and aims: Type 2 diabetes mellitus (T2DM) is a well-known risk factor for non-alcoholic steatohepatitis (NASH) and liver fibrosis but whether glycemic control is an important predictor is not well known. Glycated hemoglobin (HbA1c), a measure of glycemic control has been identified as an independent risk factor of cardiovascular outcomes, independent of T2DM status. We aimed to describe patients' characteristics and liver histology across different groups of HbA1c level.

Method: We combined screening data from 6 ongoing biopsy-proven therapeutic NASH trials (>5000 patients). Patients were classified into 4 groups according to their HbA1c. At-risk NASH was defined as NASH with a non-alcoholic fatty liver disease activity score of at least 4 and a fibrosis stage of 2 (F2) or 3 (F3). The descriptive analyses were repeated in a subset of patients with recorded T2DM status. Patients with HbA1c $\geq 6.5\%$ were reclassified as having undiagnosed T2DM. Univariate linear and logistic regressions were performed.

Results: 2177 patients with liver histology and HbA1c data were included. The liver histology results and patients' characteristics in each group are shown in the Table. The proportion of NASH and at-risk NASH patients increased with each HbA1c group ($p < 0.01$). Lipid parameters (LDL and triglycerides) were associated with HbA1c level. A subset of 913 T2DM patients with recorded status of T2DM were stratified based on HbA1c levels: Group 1, HbA1c $< 6.5\%$ ($n = 119$, 13%); Group 2, HbA1c 6.6–7.4% ($N = 429$, 47%), Group 3, HbA1c $\geq 7.5\%$ ($N = 356$, 39%). The proportion of NASH increased with higher HbA1c values: 62%, 70% and 74% in groups 1, 2 and 3, respectively ($p = 0.01$). The proportion of at risk-NASH was significantly higher in T2DM

patients with higher HbA1c: 46%, 50% and 56% in groups 1, 2 and 3, respectively ($p = 0.02$).

	HbA1c <5.7 N = 552	HbA1c [5.7–6.5] N = 785	HbA1c [6.5–7.5] N = 458	HbA1c ≥ 7.5 N = 382
	n (%) or mean (SD)			
NASH	267 (48%)	408 (52%)	322 (70%)	287 (75%)
NAS	3.8 (1.6)	3.9 (1.6)	4.3 (1.6)	4.5 (1.6)
Fibrosis Stage				
0–1	296 (54%)	385 (49%)	176 (38%)	125 (33%)
2–3	233 (42%)	371 (47%)	254 (56%)	235 (61%)
4	23 (4%)	29 (4%)	28 (6%)	22 (6%)
At-risk NASH	172 (31%)	281 (36%)	213 (47%)	203 (53%)
Age, years	50 (13)	55 (11)	57 (11)	56 (11)
AST, IU/L	41 (26)	40 (23)	42 (25)	43 (27)
ALT, IU/L	57 (37)	53 (33)	54 (31)	54 (32)
GGT, IU/L	59 (60)	56 (53)	69 (78)	70 (73)
LDL, mg/dL	110 (41)	107 (36)	94 (36)	96 (36)
Triglyceride, mg/dL	144 (69)	156 (73)	169 (77)	192 (121)
Liver Stiffness	13.4 (5.7)	12.9 (7.1)	13.4 (6.9)	13.6 (5.9)
Measurement-transient elastography, kPa				
Liver fat content, %	18 (8)	18 (7)	18 (7)	17 (7)
FIB-4	1.2 (0.7)	1.2 (0.6)	1.4 (0.6)	1.4 (0.7)

Conclusion: HbA1c level as a surrogate of glycemic control appears to be an independent risk factor of NASH and at-risk NASH, in diabetic patients. Additional studies are needed to further confirm the independent association of HbA1c with NASH severity.

THU-439

Glycated hemoglobin as an independent predictor of hepatocyte ballooning in non-alcoholic steatohepatitis: combined data from multiple clinical trials including more than 5000 patients (in collaboration with NAIL-NIT consortium)

Stephen Harrison¹, Julie Dubourg², Sophie Jeannin Megnien², Jörn Schattenberg³, Vlad Ratziu⁴, Michael Charlton⁵, Naim Alkhouri⁶, Mazen Nouredin⁷. ¹University of Oxford, United Kingdom; ²Summit Clinical Research, United States; ³University Medical Center Mainz, Germany; ⁴Institute for Cardiometabolism and Nutrition, France; ⁵UChicago Medicine, Chicago, United States; ⁶Arizona Liver Health, Chandler, United States; ⁷Houston Methodist Hospital, Houston, United States
E-mail: jdubourg@summitclinicalresearch.com

Background and aims: One of the major challenges in non-alcoholic steatohepatitis (NASH) drug development is liver histology, serving both as primary end point for conditional approval and as eligibility criteria. The failure to meet the histologic criteria is a major contributor of the high screen failure rate in non-cirrhotic NASH trials. There is a high inter- and intra-reader variability for all histologic features, though the hepatocyte ballooning remains the highest hurdle. We aimed to describe the main reasons for histologic failure across multiple phase 2 trials and to explore the predictors of hepatocyte ballooning.

Method: We combined screening data from 6 ongoing non-cirrhotic NASH phase 2 trials. We detailed the histologic features for NASH and fibrosis (table). Predictors of hepatocyte ballooning were examined using logistic regression in a subset of patients with at least stage 2 fibrosis, a non-alcoholic fatty liver disease activity score (NAS) of at least 3 and at least 1 point in inflammation and 1 point in steatosis (table). This subset was aimed to reduce the biases for the presence or

POSTER PRESENTATIONS

absence of hepatocyte ballooning in a population susceptible of having more severe NASH.

Fibrosis Stage	Histologic results			All N = 2259
	F0-F1 N = 1020	F2- F3 N = 1135	F4 N = 104	
No NASH				
1 histologic feature missing	739 (72%)	159 (14%)	26 (25%)	924 (41%)
No ballooning	607 (82%)	148 (93%)	20 (77%)	775 (84%)
No inflammation	4 (1%)	3 (2%)	0	7 (0.5%)
No steatosis	0	3 (2%)	3 (11.5%)	6 (0.5%)
≥2 histologic features missing	128 (17%)	5 (3%)	3 (11.5%)	136 (15%)
NASH	281 (28%)	976 (86%)	78 (75%)	1335 (59%)
NAS 3	49 (17%)	72 (7%)	14 (18%)	135 (10%)
NAS 4-5	176 (63%)	515 (53%)	44 (56%)	735 (55%)
NAS 6-8	56 (20%)	389 (40%)	20 (26%)	465 (35%)
Predictors of Ballooning	No ballooning (n = 115)	Ballooning (n = 1054)	p value (Univariate)	
Age, years	52 (11)	55 (11)	<0.01	
Female	55%	64%	0.06	
Hispanic	37%	42%	0.31	
AST, IU/L	39 (15)	49 (29)	<0.01	
ALT, IU/L	56 (27)	63 (36)	0.04	
GGT, IU/L	66 (101)	75 (75)	0.25	
HbA1c, %	6.2 (1.0)	6.6 (6.6)	<0.01	
LDL, mg/dL	110 (40)	100 (36)	<0.01	
Triglyceride, mg/dL	166 (108)	163 (82)	0.79	

Figure:

Results: 2259 patients with liver biopsy were included. The absence of hepatocyte ballooning was the main reason for not meeting NASH criteria across all stages of fibrosis. In a specified analysis subset, patients with hepatocyte ballooning were older, had higher levels of AST, ALT, and glycated hemoglobin (HbA1c). After adjustment for fibrosis, inflammation, and steatosis stages, only HbA1c remained significantly different between the groups. For every 1% increase in HbA1c, the adjusted odds of hepatocyte ballooning increased by 1.54 (95% confidence interval: 1.20–1.99).

Conclusion: In this large cohort of centrally read biopsies, HbA1c has been observed as an independent predictor of hepatocyte ballooning, regardless of other histologic features. Further studies are warranted to confirm these results.

THU-440

Liver fibrosis is associated with cardiovascular disease burden amongst patients with non-alcoholic steatohepatitis: the unCoVer-NASH longitudinal cohort study

Kathleen Corey¹, Anurag Mehta², Kamal Kant Mangla³, Abhishek Shankar Chandramouli⁴, Ahsan Shoaib Patel³, Sharat Varma³, Elisabetta Bugianesi⁵. ¹MGH Fatty Liver Program, Massachusetts General Hospital, United States; ²VCU Health Pauley Heart Center, United States; ³Novo Nordisk A/S, Denmark; ⁴NovoNordisk Service Center India Pvt Ltd, India; ⁵Department of Medical Sciences, University of Torino, Italy
E-mail: kknm@novonordisk.com

Background and aims: Cardiovascular (CV) disease (CVD) burden in patients with non-alcoholic steatohepatitis (NASH) is incompletely understood. The unCoVer-NASH longitudinal cohort study assessed baseline CVD burden and subsequent CV events in patients with NASH stratified by Fibrosis-4 Index (FIB-4) using real-world de-identified US healthcare data from a federated network (TriNetX).

Method: Patients were identified using the International Classification of Diseases code (ICD-10-CM) for NASH from October

2015-June 2022 and required ≥1 FIB-4 measurement (s) calculated from data obtained 180 days prior to, or 30 days after, NASH diagnosis (index date) and ≥12 months of data prior to index date (baseline period). FIB-4 score categories were low (<1.3), intermediate (1.30–2.67) and high (≥2.67). Exclusion criteria included baseline evidence of cirrhosis, viral hepatitis, human immunodeficiency virus, liver-related complications and alcohol use disorder. Data analysed were baseline characteristics, CVD prevalence and risk of CV events (s) in follow-up (index date to end of enrolment, death or study end) amongst patients with no history of respective CV event (s) during baseline. For CV risk, cumulative incidence was plotted, incidence rate (IR) was presented per 100 person-years (PY) and hazard ratios (HR) were calculated using Cox proportional hazard models (crude and adjusted for CV risk factors [age, sex, type 2 diabetes (T2D), chronic kidney disease, obesity, hyperlipidaemia, hypertension]).

Results: Of 717 patients included, those with high FIB-4 (N = 102) vs intermediate (N = 201) and low (N = 414) were older (60 vs 57 and 44 years), less likely to have obesity (38% vs 45% and 54%), more likely to have T2D (50% vs 45% and 36%) and be female (71% vs 54% and 57%). The most prevalent CVD phenotypes in all FIB-4 groups (high, intermediate and low FIB-4, respectively) were ischaemic heart disease (18%, 17%, 11%), cerebrovascular disease (16%, 7%, 8%) and heart failure (10%, 9%, 6%). Cumulative incidence of any CV event increased with FIB-4 score (Figure). IRs for any CV event were 24.6, 17.2 and 10.4 per 100 PY for high, intermediate and low FIB-4, respectively. HRs (95% confidence interval) for high and intermediate vs low FIB-4 were 3.43 (2.21, 5.31); p < 0.0001 and 1.53 (1.02, 2.29); p = 0.04 and remained significant for high vs low FIB-4 after adjustment for CV risk factors, similar to results for individual CV events.

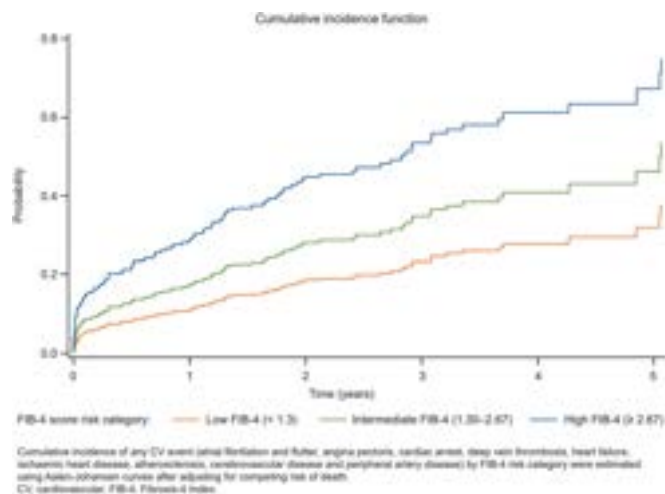


Figure:

Conclusion: CVD prevalence and incidence in patients with NASH was associated with baseline FIB-4 score, indicating higher CV burden as fibrosis worsens. CV risk with high vs low FIB-4 was significantly higher even after adjusting for CV risk factors. Patients with intermediate FIB-4 had an increased incidence of CV event (s) relative to those with low FIB-4 and should be monitored and managed; further research around CV risk in this group may be needed.

THU-441

Low rates of fibrosis scoring in the primary care records of 5987 people living with type 2 diabetes

James Hallimond Brindley¹, Kushala Abeysekera^{2,3}, Ann Archer², Gillian Hood¹, John Moore¹, Michael James¹, Matthew Hickman², William Alazawi¹. ¹Blizard Institute, Queen Mary University of London, Barts Liver Centre, London, United Kingdom; ²Bristol Medical School, University of Bristol, Population Health Sciences, Bristol, United Kingdom; ³University Hospitals Bristol and Weston NHS Foundation Trust, Bristol, UK, Liver Medicine, Bristol, United Kingdom
E-mail: halbrindley@gmail.com

Background and aims: Type 2 diabetes (T2D) is an independent risk factor for non-alcoholic fatty liver disease (NAFLD) development, progression to fibrosis and end-stage liver disease. EASL guidelines recommend looking for NAFLD in all people with T2D and calculating surrogate markers of fibrosis for all people with NAFLD. PRELUDE-1 (Trial ID: ISRCTN14585543) is a study evaluating the feasibility and acceptability of adding fibrosis-4 (FIB-4) scoring to the annual T2D review and direct access to community or secondary care transient elastography assessment for individuals with FIB-4 ≥ 1.3 . We sought to determine the extent of liver fibrosis scoring in primary care prior to commencing the study.

Method: We performed an anonymised retrospective data capture of all adults with T2D registered at seven primary care practices in England who were enrolled in PRELUDE-1. Practices were invited to join the study with key inclusion criteria: practice size >4000 and 85% completion of T2D annual review. Patient-level data included selected SNOMED CT codes for demographics, pathology (including alanine transaminase (ALT), aspartate aminotransferase (AST), platelet count and Fib-4 score) and diagnostic data.

Results: Across the initial 7 primary care sites (4 in Bristol and 3 in London), there were a total of 5987 individuals with type 2 diabetes. 47% were female with mean age 60.9 years, 45% of South Asian ethnicity, 32% White, 16% Black and 7% other. NAFLD and NASH were coded for 491 (8.2%) and 12 (0.2%) people with T2D respectively. 65% (n = 3862) of the cohort had a coded ALT result in their primary care record; male mean 35.9 IU/L and female mean 25.5 IU/L. 42% (n = 2535) of the cohort had a platelet count reported, mean value $256 \times 10^9/L$. 31% (n = 184) had AST values recorded; male mean 39.0 IU/L and female mean 30.9 IU/L. Only 26 individuals (0.4%) had a FIB-4 score coded in their primary care records. The complete dataset from the enrolled seven sites will be presented.

Conclusion: Despite current EASL guidance and increasing primary care physician awareness of NAFLD, few people with T2D have a coded diagnosis of NAFLD or surrogate markers of fibrosis despite recognition as an at risk population. New ways of working are needed to raise awareness and recognition of people with T2D and liver disease in primary care.

THU-442

A machine learning-based classification of adult-onset diabetes identifies patients at risk for liver-related complications

Lukas Otero Sanchez¹, Clara-Yongxiang Zhan², Carolina Gomes Da Silveira Cauduro³, Laurent Crenier³, Hassane Njimi⁴, Gael Englebert², Antonella Putignano², Antonia Lepida², Delphine Degre², Nathalie Boon², Thierry Gustot², Pierre Deltenre⁵, Astrid Marot⁶, Jacques Deviere², Christophe Moreno², Miriam Cnop³, Eric Trépo². ¹Erasme Hospital, Brussels, Department of Gastroenterology, Hepatopancreatology and digestive Oncology, Brussels, Belgium; ²Erasme Hospital, Department of Gastroenterology, Hepatopancreatology and digestive Oncology, Brussels, Belgium; ³Erasme Hospital, Endocrinology, Belgium; ⁴Université Libre de Bruxelles, Statistics, Belgium; ⁵Clinique Saint-Luc, Gastroenterology, Bouge, Belgium; ⁶Université Catholique de Louvain, Yvoir, Gastroenterology, Belgium
E-mail: lukas.otero.sanchez@ulb.be

Background and aims: Diabetes mellitus is a major risk factor for fatty liver disease development and progression. A novel machine learning method identified five clusters of patients with diabetes, with different characteristics and risk of diabetic complications using six clinical and biological variables. We evaluated whether this new classification could identify individuals with an increased risk of liver-related complications.

Method: We used a prospective cohort of patients with a diagnosis of type 1 or type 2 diabetes without evidence of advanced fibrosis at baseline recruited between 2000 and 2020. We assessed the risk of each diabetic cluster of developing liver-related complications, using competing risk analyses.

Results: We included 1068 patients, of whom 162 (15.2%) were determined to be in the severe autoimmune diabetes (SAID) subgroup, 266 (24.9%) were severe insulin-deficient diabetes (SIDD), 95 (8.9%) were severe insulin-resistant diabetes (SIRD), 359 (33.6%) were mild obesity-related diabetes (MOD), and 186 (17.4%) were in the mild age-related diabetes (MARD) subgroup. In multi-variable analysis, patients in the SIRD cluster and those with excessive alcohol consumption at baseline had the highest risk for liver-related events. The SIRD cluster, excessive alcohol consumption, and hypertension were independently associated with clinically significant fibrosis. Using a simplified classification, patients assigned to severe and mild insulin-resistant groups had a 3- and 2-fold greater risk, respectively, of developing significant fibrosis compared to the insulin-deficient group.

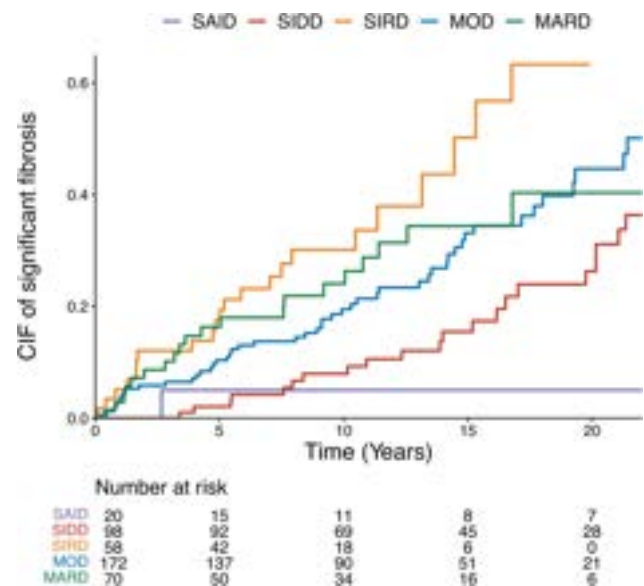


Figure: Time to clinically significant fibrosis by cluster

Conclusion: A novel clustering classification adequately stratifies the risk of liver-related events and liver fibrosis in a diabetes population. Our results also underline the impact of the severity of insulin resistance and alcohol consumption as key prognostic risk factors for liver-related complications.

CIF, cumulative incidence function; SAID, Severe autoimmune diabetes; SIDD, Severe insulin-deficient diabetes; SIRD, Severe insulin-resistant diabetes; MOD, Mild obesity-related diabetes; MARD, Mild age-related diabetes

THU-443

NAFLD prevalence in the elderly declines with age and is associated with increased frailty, reduced physical function and social disadvantage status: results from the ASPREE study

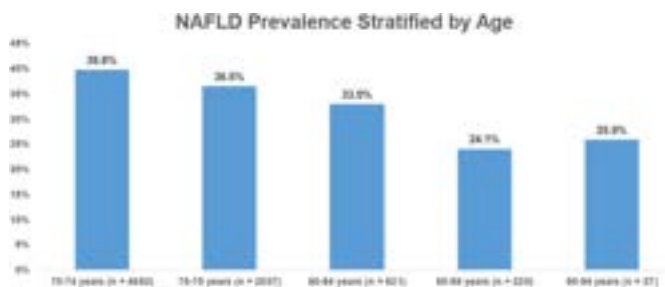
Daniel Clayton-Chubb^{1,2,3}, Ammar Majeed^{1,3}, John Lubel^{1,3}, Robyn Woods⁴, Alex Hodge^{2,5}, Hans Schneider⁶, John McNeil⁷, William Kemp^{1,3}, Stuart Roberts^{1,3}. ¹The Alfred, Gastroenterology, Melbourne, Australia; ²Eastern Health, Gastroenterology, Box Hill, Australia; ³Monash University-Central Clinical School, Medicine, Melbourne, Australia; ⁴Monash University, School of Public Health and Preventive Medicine, Australia; ⁵Monash University-Eastern Health Clinical School, Box Hill, Australia; ⁶The Alfred, Pathology, Melbourne, Australia; ⁷Monash University, School of Public Health and Preventive Medicine, Australia

E-mail: chubb.daniel@gmail.com

Background and aims: Several global data suggest that Non-Alcoholic Fatty Liver Disease (NAFLD) prevalence increases with age. However, the Rotterdam study showed decreasing prevalence of NAFLD with increasing age among older adults. To further explore NAFLD in older persons we evaluated the prevalence of NAFLD in a large group of older Australians (who were sufficiently healthy to be enrolled in a primary prevention clinical trial). We also aimed to determine factors associated with NAFLD in this group including markers of frailty and social disadvantage.

Method: We included participants involved in the ASPREE (ASpirin in Reducing Events in the Elderly) randomised-controlled trial that enrolled 16 703 community-dwelling Australian participants aged 70 years or older without independence-limiting physical disability, dementia, or cardiovascular disease. Detailed anthropometric, biochemical, and questionnaire data were collected at baseline. We calculated the Fatty Liver Index (FLI), a composite score based on gamma-glutamyl transferase, triglycerides, abdominal circumference, and BMI. Using a score ≥ 60 to define NAFLD, we identified NAFLD prevalence as well as associations via logistic regression analysis.

Results: Data from 7757 (mean age 75.0 ± 4.21 years, 47.1% male) participants were analysed. We excluded 8946 participants for not meeting standard NAFLD inclusion criteria or delayed/missing data. The overall prevalence of NAFLD was 37.7% and this decreased with age (Figure 1) ($p < 0.001$). In logistic regression analysis of NAFLD (FLI ≥ 60 , $n = 2314$) vs no-NAFLD (FLI < 30 , $n = 1755$), age (OR 0.93; 95% CI 0.91–0.94; $p < 0.001$), male gender (OR 2.69; 95% CI 2.34–3.09; $p < 0.001$), diabetes (OR 4.19; 95% CI 3.25–5.39; $p < 0.001$), chronic kidney disease (OR 1.51; 95% CI 1.28–1.77), and hypertension (OR 1.75; 95% CI 1.50–2.05; $p < 0.001$) were all significantly associated with NAFLD. Additionally, multiple markers of frailty and social disadvantage were significantly associated with NAFLD, including low gait speed (OR 1.62, 95% CI 1.27–2.07; $p < 0.001$) and worsening frailty using the Fried Frailty Index (OR 1.29; 95% CI 1.10–1.51; $p = 0.002$ for pre-frail participants; OR 2.08; 95% CI 1.19–3.62; $p = 0.01$ for frail participants). Completing more than 12 years of education (OR 0.72; 95% CI 0.63–0.83; $p < 0.001$) and being in the top half of an Australian composite measure of advantage and disadvantage (IRSAD) (OR 0.80; 95% CI 0.70–0.92; $p = 0.002$) appeared to be protective.



Conclusion: Similar to the Rotterdam study we found a decreasing prevalence of NAFLD with increasing age. In addition, our study shows important novel associations between NAFLD in older persons and worsening physical function and frailty, as well as an inverse association between NAFLD and markers of social advantage.

THU-444

Ascites is the most frequent decompensating event in stable and strictly compensated NAFLD with advanced fibrosis

Zouhir Gadi^{1,2}, Luisa Vonghia^{2,3}, Jolien Derdeyn³, Toon Steinhäuser³, Thomas Vanwolleghem^{2,3}, Sven Francque^{2,3}, Wilhelmus Kwanten^{2,3}. ¹Antwerp University Hospital, Department of Gastroenterology and Hepatology, Edegem, Belgium; ²University of Antwerp, Laboratory of Experimental Medicine and Paediatrics (LEMP), Antwerpen, Belgium; ³Antwerp University Hospital, Gastroenterology and Hepatology, Edegem, Belgium

E-mail: jolien.derdeyn@uza.be

Background and aims: The natural history of advanced fibrosis in non-alcoholic fatty liver disease (NAFLD) might behave differently compared to other CLD. We aim to describe the natural history of stable and strictly compensated NAFLD patients with advanced fibrosis.

Method: Patients at the Antwerp University Hospital diagnosed between 03/2006 and 11/2021 with a biopsy proven NAFLD and fibrosis F3 or F4 were retrospectively collected. Available clinical follow-up time needed to be ≥ 12 months after the histological confirmation of advanced fibrosis. Only strictly and stable compensated patients were included, defined as baseline Child Pugh score ≤ 7 , the absence of prior hepatic decompensation, or development thereof within 12 m after biopsy. Hepatic decompensation was defined as variceal bleed (VB), overt hepatic encephalopathy (HE) or ascites needing large volume paracentesis (LVP). The following clinically relevant events were collected as well: hepatocellular carcinoma (HCC) or death.

Results: 100 out of 185 patients met the inclusion criteria (56 F3; 44 F4), with a mean follow-up time of 264 (56–864) weeks. First decompensation events were noted in 16 (16%) patients during follow-up distributed as LVP/HE/VB with $n = 11/6/4$ patients respectively (figure 1), 5 patients experienced >1 event. Mean time to first decompensation was respectively 258/195/155 weeks. Compared to patients without decompensation, decompensated patients had at baseline (i.e. at time of biopsy) significantly higher age (64.8 ± 8.6 vs. 58.1 ± 10.3 year; $p = 0.016$), lower platelet count (159 ± 53 vs. 213 ± 80 $10^9/L$; $p = 0.011$), higher serum GGT (225 ± 155 vs. 126 ± 128 U/L; $p = 0.013$), lower serum Na (137.87 ± 2.36 vs. 140.07 ± 2.53 mmol/L; $p = 0.002$), higher Na-MELD (9.88 ± 2.42 vs. 7.85 ± 2.81 ; $p = 0.008$), higher predicted Hepatic Venous Pressure Gradient (HVPG-3P model) (11.56 ± 1.75 vs. 10.01 ± 2.69 mmHg; $p = 0.029$). HVPG (measured in 66/100) was insignificantly higher (9.95 ± 5.33 vs. 7.45 ± 3.64 mmHg; $p = 0.106$). Decompensated patients were more frequently on non-selective beta-blockers at baseline (8/16). Interestingly, 5/16 (31.3%) patients with decompensation had F3 fibrosis and 7/15 (46.7%) had a HVPG < 10 mmHg. 4 cases developed HCC with a mean follow-up time of 211 (29–473) weeks and 15 deaths (3 liver-related) were noted with a mean follow-up time of 221 (75–733) weeks. Of these cases 1/4 and 8/15 experienced prior decompensation.

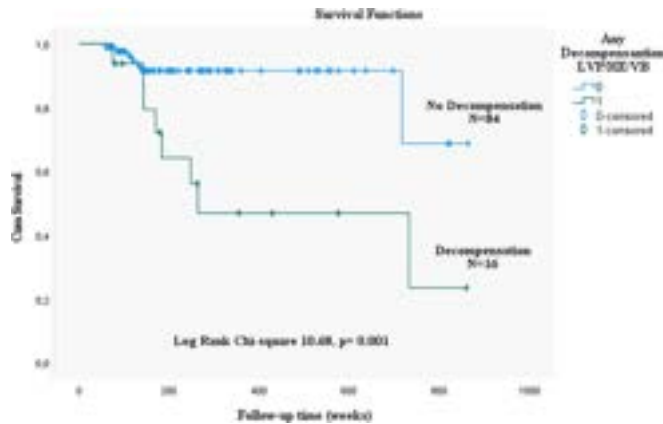


Figure: Kaplan-Meier survival curve patients with and without decompensation after at least 1 year follow-up (p = 0.001, log-rank test)

Conclusion: In this large single centre cohort of NAFLD patients with advanced fibrosis and strictly compensated disease with a mean follow-up of >5 years, roughly 1/6 patients developed a first decompensating event. Ascites needing LVP was the most frequent decompensation event. Age, sodium, platelets and GGT and use of NSBB at baseline were associated with decompensation. About a 1/3 of patients with decompensation had F3 fibrosis and about 1/2 a baseline HVPG of <10 mmHg.

THU-445

The impact of *Clostridium difficile* on mortality and outcomes in patients with NAFLD vs. NASH

Ankoor Patel¹, Gaurav Pathak², Alexander Chen¹, Carlos Minacapelli², Carolyn Catalano², Vinod Rustgi². ¹Rutgers-Robert Wood Johnson Medical School, Medicine, New Brunswick, United States, ²Robert Wood Johnson Medical School, Dept of Gastroenterology and Hepatology, New Brunswick, United States
E-mail: ahp60@rwjms.rutgers.edu

Background and aims: *Clostridium difficile* (*C. Diff*) infection (CDI) is the most common cause of infectious nosocomial diarrhea among adults in developed countries. The rate of CDI has increased over the last few decades and is associated with significant mortality and morbidity. NAFLD is the most common chronic liver disease due to the increasing prevalence of obesity and other metabolic diseases. Several studies show a correlation between NAFLD and bacterial infections; however, outcomes in patients with NAFLD/NASH and CDI are limited. Using the National Inpatient Sample (NIS), our study evaluated outcomes, including mortality and complications, length of stay (LOS), and costs among patients with NAFLD/NASH and CDI.

Method: We performed a retrospective cohort study using the National Inpatient Sample (NIS) from 2015 to 2017. Patients with *C. Difficile* infection, NAFLD, and NASH were identified using ICD-10 codes. Patients with diagnoses of both NAFLD and NASH were excluded. Primary outcomes included mortality, length of stay, total hospitalization costs. Secondary outcomes included AKI, pneumonia, respiratory failure, ventilatory dependence, acute pulmonary embolism, intestinal perforation, peritonitis, toxic megacolon, acute liver failure, liver failure, liver cancer. Multivariate logistic regression analysis was used to compare the two groups.

Results: A total of 761 175 patients with CDI were included and 11 335 (1.49%) had NAFLD and 4365 (0.57%) had NASH. The NASH cohort had a higher degree of comorbidities (CCI mean, CDI and NASH, CDI only, CDI and NAFLD, 6.33 vs 5.12 vs 3.40; p < 0.001). Patients hospitalized for CDI with NASH had an increased risk of mortality compared to those with NAFLD and those without NASH or NAFLD (CDI and NASH vs CDI and NAFLD vs CDI only, 7.11% vs 2.61% vs 6.36%). Patients with CDI and NASH were at increased risk for liver related complications, including liver failure and liver cancer, acute kidney injury, and septic shock (p < 0.001) compared to patients with CDI only.

Conclusion: Patients with NASH have a higher rate of mortality, AKI, septic shock, and liver-related complications following CDI.

Figure: Table 1. (abstract: THU-445): Outcomes of CDI in Patients with NASH, NAFLD, and without NAFLD/NASH.

Summary Statistics for CDI Patients Overall & By NAFLD/NASH Status (N=10,710)							
Study Measure	Total Sample (n = 10,710)	CDI-NAFLD Only (n = 745, 47%)	CDI-NASH (n = 4,365)	CDI-NAFLD+NASH (n = 11,335)	Number of Tests	NAFLD vs NASH P-Value	NAFLD vs CDI P-Value
DEMOGRAPHICS							
Age (Mean ± SD)	66.07 (17.88)	66.25 (17.87)	61.03 (17.47)	55.18 (16.70)	77	p < 0.001	p < 0.001
Sex, n (%)					13	p < 0.001	p < 0.001
Female	51,703 (47.82)	33,043 (44.38)	14,402 (33.00)	49,007 (43.13)			
Male	55,407 (51.18)	41,457 (55.62)	29,238 (66.99)	60,028 (52.87)			
CCI					77	p < 0.001	p < 0.001
CCI - Overweight (BMI ≥ 25, n (%))	1,018 (9.42)	519 (6.97)	85 (1.93)	1,102 (9.70)	13	p < 0.001	p < 0.001
CCI - Obese (BMI ≥ 30, n (%))	1,184 (10.99)	599 (8.05)	100 (2.29)	1,284 (11.28)	13	p < 0.001	p < 0.001
CCI - Morbidly Obese (BMI ≥ 35, n (%))	1,844 (17.23)	939 (12.73)	171 (3.90)	1,920 (16.93)	13	p < 0.001	p < 0.001
CCI - Morbidly Morbidly Obese (BMI ≥ 40, n (%))	1,483 (13.85)	747 (10.16)	124 (2.84)	1,444 (12.70)	13	p < 0.001	p < 0.001
CCI - Morbidly Obese w/ Hypertension, n (%)	1,045 (9.75)	533 (7.26)	89 (2.00)	1,045 (9.28)	13	p < 0.001	p < 0.001
CCI Total Score (Mean ± SD)	5.10 (4.43)	5.12 (4.44)	6.33 (4.48)	5.40 (4.47)	77	p < 0.001	p < 0.001
PRIMARY OUTCOMES							
Mortality/Primary Events, n (%)	4,790 (44.72)	4,779 (64.13)	300 (6.87)	1,000 (8.82)	13	p < 0.001	p < 0.001
Length of Stay (Mean ± SD)	10.08 (10.84)	10.05 (10.84)	9.48 (9.71)	8.49 (10.49)	77	p < 0.001	p < 0.001
Total Charges (Mean ± SD)	\$87,138.82 (\$103,778.77)	\$88,117.70 (\$104,341.34)	\$70,305.13 (\$84,113.70)	\$78,175.30 (\$103,778.77)	77	p < 0.001	p < 0.001
SECONDARY OUTCOMES/OUTCOMES OF INTEREST							
Acute Kidney Injury, n (%)	1,150 (10.73)	1,170 (15.71)	1,000 (22.91)	1,150 (10.15)	13	p < 0.001	p < 0.001
Respiratory Failure, n (%)	487 (4.53)	487 (6.53)	100 (2.29)	487 (4.29)	13	p < 0.001	p < 0.001
Septic Shock, n (%)	1,400 (12.97)	1,400 (18.93)	1,000 (22.91)	1,400 (12.32)	13	p < 0.001	p < 0.001
Septic Shock, n (%)	1,150 (10.73)	1,150 (15.71)	1,000 (22.91)	1,150 (10.15)	13	p < 0.001	p < 0.001
Intestinal Perforation, n (%)	1,000 (9.33)	1,000 (13.57)	100 (2.29)	1,000 (8.82)	13	p < 0.001	p < 0.001
Peritonitis, n (%)	1,150 (10.73)	1,150 (15.71)	1,000 (22.91)	1,150 (10.15)	13	p < 0.001	p < 0.001
Acute Liver Failure, n (%)	1,000 (9.33)	1,000 (13.57)	100 (2.29)	1,000 (8.82)	13	p < 0.001	p < 0.001
Chronic Liver Failure, n (%)	1,150 (10.73)	1,150 (15.71)	1,000 (22.91)	1,150 (10.15)	13	p < 0.001	p < 0.001
Acute Kidney Injury, n (%)	1,150 (10.73)	1,150 (15.71)	1,000 (22.91)	1,150 (10.15)	13	p < 0.001	p < 0.001
Respiratory Failure, n (%)	487 (4.53)	487 (6.53)	100 (2.29)	487 (4.29)	13	p < 0.001	p < 0.001
Septic Shock, n (%)	1,400 (12.97)	1,400 (18.93)	1,000 (22.91)	1,400 (12.32)	13	p < 0.001	p < 0.001
Septic Shock, n (%)	1,150 (10.73)	1,150 (15.71)	1,000 (22.91)	1,150 (10.15)	13	p < 0.001	p < 0.001
Intestinal Perforation, n (%)	1,000 (9.33)	1,000 (13.57)	100 (2.29)	1,000 (8.82)	13	p < 0.001	p < 0.001
Peritonitis, n (%)	1,150 (10.73)	1,150 (15.71)	1,000 (22.91)	1,150 (10.15)	13	p < 0.001	p < 0.001
Acute Liver Failure, n (%)	1,000 (9.33)	1,000 (13.57)	100 (2.29)	1,000 (8.82)	13	p < 0.001	p < 0.001
Chronic Liver Failure, n (%)	1,150 (10.73)	1,150 (15.71)	1,000 (22.91)	1,150 (10.15)	13	p < 0.001	p < 0.001

POSTER PRESENTATIONS

THU-446

Poor performance at five times sit-to-stand test, but not at handgrip test, is related to significant liver fibrosis and correlates with major cardiovascular events in non-alcoholic fatty liver disease patients

Giordano Sigon¹, Roberta Forlano¹, Benjamin H. Mullish¹, Jian Huang¹, Michael Yee², Robert D. Goldin³, Mark Thursz¹, Pinelopi Manousou¹.
¹Liver Unit/Division of Digestive Diseases, Department of Metabolism, Digestion and Reproduction, Faculty of Medicine, Imperial College London, London, United Kingdom, United Kingdom; ²Section of Endocrinology and Metabolic Medicine, St Mary's Hospital, Imperial College NHS Trust, London, United Kingdom, London, United Kingdom; ³Department of Cellular Pathology, Faculty of Medicine, Imperial College London, London, United Kingdom, London, United Kingdom
 E-mail: gio.sigon@virgilio.it

Background and aims: Non-alcoholic fatty liver disease (NAFLD) causes both liver and cardiovascular morbidity and mortality. While many studies suggest worse clinical outcomes for sarcopenic patients with cirrhosis, few data are available on sarcopenia in NAFLD patients with early liver disease. Our aim is to assess sarcopenia against fibrosis stage and clinical outcomes in patients with NAFLD.

Method: We consecutively enrolled NAFLD patients followed up in the specialist clinic at Imperial College Healthcare NHS Trust, London, UK. NAFLD was diagnosed either clinically or based on histology. We collected anthropometric, biochemical parameters, medical history and cardiovascular risk factors. For the evaluation of sarcopenia, we performed bioimpedance analysis (BIA), 5 times sit-to-stand test (5TST) and handgrip strength test (HST). As suggested in literature, poor performances were considered 5TST >15 sec, and HST <27 kg for males or <16 kg for females. Patients who were not able to perform the 5TST were included in the 5TST >15 sec category. Major cardiovascular events (MACE) were defined as acute coronary syndrome, transient ischemic attack and stroke. Significant fibrosis was defined as liver stiffness measurement (LSM) >8 kPa, while cirrhosis as a combination of clinical parameters (LSM, bloods and imaging) or on histology.

Results: Overall, 130 NAFLD patients were included, with median age 58 [50–67] years and BMI 29.9 [26.8–34.6] kg/m². 86 (67%) were males, 101 (79%) had type 2 diabetes mellitus and 73 (57%) hypertension. BIA and handgrip measurement were available in the whole cohort, while 5TST only in 70 patients (54%). As per BIA, absolute fat mass was 28 [20–40] kg (34 [26–34] %), while muscle mass was 54 [47–65] kg (62 [56–70] %). Furthermore, 22 of 130 (17%) were below the HST cutoff, while 19 out of 70 (28%) had a 5TST >15 sec. Poor HST was associated with lower muscle mass measured with BIA. In terms of severity of liver disease, 51 (41%) showed LSM >8 kPa, while 7 (5%) had cirrhosis. Previous history of MACE was positive in 19 (15%) patients.

On multivariate analysis, 5TST >15sec was significantly associated with LSM >8 kPa (OR 6.7, 95%CI: 1.1–39.9, p = 0.04). Moreover, while no association was found at multivariate analysis between MACE and HST, 5TST >15 was significantly related to history of MACE (OR 5.4, 95%CI: 1.1–26.3, p = 0.04).

	Odds ratio	95% confidence interval	p value
Age	1.1	0.9–1.2	0.52
Male gender	1.2	0.2–9.1	0.83
Type 2 diabetes mellitus	5.8	0.5–60.3	0.14
Statin	3.1	0.5–20.6	0.24
Cirrhosis	3.4	0.4–30.3	0.24
5TST >15	5.4	1.1–26.3	0.04

5TST: five times sit-to-stand test.

Figure: Logistic regression for history of major cardiovascular event

Conclusion: Poor performance at 5TST was associated both with significant liver fibrosis and MACE. In contrast, HST was not related with MACE. The 5TST could be integrated into the cardiovascular risk stratification of NAFLD patients.

THU-447

The national audit of non-alcoholic fatty liver disease (NAFLD) identifies variations and shortfalls in delivery of care in the UK

Wenhao Li¹, David Sheridan², Stuart Mcpherson³, William Alazawi¹.
¹Barts Liver Centre, Blizard Institute, Queen Mary University of London, London, United Kingdom; ²University Hospitals Plymouth NHS Trust, United Kingdom; ³The Newcastle upon Tyne Hospitals NHS Foundation Trust, United Kingdom
 E-mail: wenhao.li@doctors.org.uk

Background and aims: Non-alcoholic fatty liver disease (NAFLD) is a major cause of liver-related morbidity and mortality. The British Association for the Study of the Liver (BASL) and British Society of Gastroenterology (BSG) NAFLD Special Interest Group (SIG) recently published Quality Standards for NAFLD management which includes auditable key performance indicators (KPIs) of good clinical care. This national audit, endorsed by BASL and BSG, aimed to benchmark the care in UK hospitals for people with NAFLD against these KPIs and compared practice in 2012/9 with 2022.

Method: An electronic survey was designed by BASL/BSG NAFLD SIG and published and distributed via BASL and BSG webpages, mailing lists and twitter accounts. Participating hospitals collected retrospective data from all new NAFLD patients reviewed in outpatient clinic in the month of March 2019 and March 2022.

Results: Data relating to KPIs from 776 NAFLD patients (374 in 2019, 402 in 2022) in 34 hospitals covering all four UK countries were collected (Table 1). Mean age of audited population was 52.7 years, 55.2% were male and 63.4% were of White ethnicity. 85.3% of services reported established local liver disease assessment pathways, yet only 27.9% of patients with suspected NAFLD had non-invasive fibrosis assessment documented at point of referral to secondary care. In secondary care, non-invasive tests were used or liver biopsy was conducted in 79.1% of patients. 34.6% of patients without non-invasive fibrosis assessment at point of referral to secondary care had low-risk of advanced fibrosis (low Fib4 or NAFLD Fibrosis score, Fibroscan <8 kPa). There was considerable variation in the assessment cardiometabolic risk factors including obesity (73.2%), type 2 diabetes [T2DM] (33.0%), hypertension (19.3%) and smoking (54.9%). Giving appropriate diet and lifestyle advice to address cardiometabolic risk was poorly performed. Only 9.1% of NAFLD patients at increased cardiovascular risk (T2DM and/or QRISK-3 >10%) were advised statin treatment in line with NICE guidelines. Significant improvements in several KPIs were identified between 2019–2022: non-invasive fibrosis assessment at referral increased 20.8% to 35.1% (p < 0.0001), statin recommendations increased from 4.3% to 12.5% (p = 0.012) and providing patient information material regarding NAFLD increased from 11.6% to 24.5% (p < 0.001).

Conclusion: This national audit of NAFLD management in the UK has identified significant variation and areas for improvement, particularly in fibrosis risk assessment prior to secondary care referral and management of associated cardiometabolic risk factors. Improvements from 2019 to 2022 gives cause for optimism but further work is needed to drive changes in service delivery and patient care.

References

- McPherson S. *et al.* Lancet Gastroenterol. Hepatol. 7, 755–769 (2022).

THU-448

Non-alcoholic fatty liver disease mediates the effect of obesity on arterial hypertension

Carlos Pirola¹, Silvia Sookoian². ¹Consejo Nacional de Investigaciones Científicas y Técnicas (CONICET), Systems Biology of Complex Diseases. Centro de Altos Estudios en Ciencias Humanas y de la Salud (CAECIHS), Universidad Abierta Interamericana, Ciudad Autónoma de Buenos Aires, Argentina; ²Consejo Nacional de Investigaciones Científicas y Técnicas (CONICET), Clinical and Molecular Hepatology. Centro de Altos Estudios en Ciencias Humanas y de la Salud (CAECIHS), Universidad Abierta Interamericana, Argentina
E-mail: cpirola@gmail.com

Background and aims: Non-alcoholic fatty liver disease (NAFLD) is highly prevalent among subjects with metabolic syndrome. Obesity, as estimated by body mass index (BMI) is a modifiable risk factor for both NAFLD and cardiovascular disease (CVD), including arterial hypertension (HTN). Herein, we explored to which extent NAFLD mediates the association between obesity and arterial hypertension.

Method: A two-step approach was used. First, we included cross-sectional data (1392 adults aged 29.4 ± 5.1 years) from the Bogalusa Heart Study (BHS) that was designed to assess the early natural history of CVD in a cohort of young adults in a semirural community. NAFLD was assessed using the fatty liver index (FLI). Liver fibrosis was estimated using the NAFLD fibrosis score. To replicate the findings, we included data from the National Health and Nutrition Examination Survey (2017–2018 cycle, NHANES). NAFLD was defined by the controlled attenuation parameter (CAP >268 dB/m) obtained via transient elastography (non-NAFLD = 1876; NAFLD = 1483). Liver fibrosis was defined based on stiffness measurements (n = 3359 subjects). Variables were log-transformed as they showed non-normal distribution according to Q-Q plots. Causal mediation analyses were performed using generalized structural models (GSEM) to examine the causal role of liver steatosis and fibrosis in the relation between obesity and hypertension. Results were adjusted for relevant demographic, anthropometric, clinical, and biochemical variables including age, sex, ethnics, and impaired fasting glucose, or type 2 diabetes.

Results: In the BHS, HTN was associated with NAFLD (OR: 1.70, 95% CI: 1.23–2.35, p: 1.1E-3) and BMI (OR: 1.06, 95% CI: 1.02–1.09, p: 2.4E-3) after adjusting for relevant confounders. Significant effects were also found for systolic (SBP) and diastolic (DBP) blood pressure, and heart rate (HR). These findings were replicated in NHANES survey. Specifically, HTN was associated with NAFLD (OR: 1.39, 95% CI: 1.01–1.92) and BMI (OR: 6.43, 95% CI: 2.80–14.8).

In the BHS, causal mediation analysis showed that significant indirect effects of BMI on HTN, SBP, DBP, and HR through FLI gradation explain up to 88%, 91%, 93%, and 100% of the total effect, respectively. In NHANES, these indirect effects also explain a significant proportion of the total effects (HTN = 51%, SBP = 60.4%, HR = 100%, and pulse pressure = 88%). Liver fibrosis mediated the effect of BMI on SBP (52%).

Conclusion: NAFLD mediates a substantial proportion of the effect of obesity on the presence of arterial hypertension. This conclusion has important clinical implications in both NAFLD and hypertension management.

THU-449

Nutritional behavior and food pattern are sex-specific with higher salt intake and consumption of ultra-processed foods in a large cohort of NAFLD patients

Monika Rau¹, Julia Jerzynski¹, Bianca Heller¹, Florian P. Reiter¹, Hans Benno Leicht¹, Ina Bergheim², Peter Heuschmann³, Andreas Geier¹. ¹University Hospital Würzburg, Department of Internal Medicine II, Germany; ²University of Vienna, Department of Nutritional Sciences, Molecular Nutritional Science, Austria; ³University of Würzburg, Institute of Clinical Epidemiology and Biometry, Germany
E-mail: rau_m@ukw.de

Background and aims: Non-alcoholic fatty liver disease (NAFLD) is the leading cause of chronic liver disease. “Western” dietary patterns with high salt content and ultra-processed foods (UPF) are generally linked to hepatic inflammation in NAFLD, but scarce information exists on its particular impact on NAFLD disease stage. Aim of this study is to analyze food pattern and specific nutritional behavior in NAFLD patients as a first step in specific nutritional intervention.

Method: Prospectively, 310 clinically characterized NAFLD patients were included (04/21–11/22) in this single center study at a tertiary hospital. All patients completed a nutrition questionnaire based on FFQ (DEGS¹) including 53 food groups for the calculation of dietary sodium consumption/day (DSC). UPF consumption was classified by NOVA food classification. Nutritional behavior was assessed by questionnaires such as SINU-Salt², the the Intuitive Eating Scale-2³ and the Adult Eating Behaviour Questionnaire⁴.

Results: Slightly more women (57%) than men (43%) were included in this study with an average age of 52.7 for men and 52.3 for women. Men had significantly higher consumption of UPF (708 ± 464 kcal/d) compared to women (478 kcal/d ± 554), but women had higher meal frequency per day. Higher UPF consumption was associated with higher DSC. Mean daily salt intake in the study cohort was 7 g/d. Men had higher DSC (8.3 g/d vs 6.1 g/d in women) and had different behavior with significantly lower salt awareness in everyday life. Furthermore, men had different nutritional behavior with lower agreement to slowness in eating and satiety responsiveness but higher consent to eating for physical rather than emotional reasons. Nutritional behavior with high responsiveness on hunger and satiety cues (as a positive feedback signal) was linked to milder disease phenotype with lower ALT, AST, gGT, Ferritin, and lower DSC in this cohort. NAFLD patients with higher DSC (>5 g/d) had a significantly higher serum ALT, GGT and ferritin compared to low DSC (<5 g/d) (ALT: 165 vs.130U/L; p = 0,001). Patients with high DSC (>5 g/d) had higher weight and more steatosis by CAP (153.2 vs. 116.7 dB/m; p = <0,001) compared to low DSC.

Conclusion: Consumption of ultra-processed food, daily salt intake and nutritional behavior is sex-specific in a large cohort of NAFLD patients. High daily salt intake is linked to higher liver enzymes and more pronounced liver steatosis. The findings of this study represent the basis for a prospective interventional trial.

References

- Haftenberger M, Heuer T, Heidemann C, et al. Relative validation of a food frequency questionnaire for national health and nutrition monitoring. *Nutrition journal* 2010;9:36. doi: 10.1186/1475-2891-9-36 [published Online First: 2010/09/16]
- Iaccarino Idelson P, D'Elia L, Cairella G, et al. Salt and Health: Survey on Knowledge and Salt Intake Related Behaviour in Italy. *Nutrients* 2020;12 (2) doi: 10.3390/nu12020279 [published Online First: 2020/01/25]
- Tylka TL, Kroon Van Diest AM. The Intuitive Eating Scale-2: item refinement and psychometric evaluation with college women and men. *Journal of counseling psychology* 2013;60 (1):137–53. doi: 10.1037/a0030893
- Hunot C, Fildes A, Croker H, et al. Appetitive traits and relationships with BMI in adults: Development of the Adult Eating Behaviour Questionnaire. *Appetite* 2016;105:356–63. doi: 10.1016/j.appet.2016.05.024 [published Online First: 20160520]

THU-450

Prevalence of dysmetabolic iron overload syndrome in non-alcoholic fatty liver disease

Noel Ravindranayagam¹, Monique Fernandez¹, Karl Vaz¹, Julie Lokan², Andrew Grigg³, Marie Sinclair^{1,4}. ¹Austin Health, Victorian Liver Transplant Unit, Heidelberg, Australia; ²Austin Health, Department of Anatomical Pathology, Heidelberg, Australia; ³Austin Health, Department of Haematology, Heidelberg, Australia; ⁴University of Melbourne, Melbourne, Australia
Email: noel.ravindranayagam@austin.org.au

Background and aims: Dysmetabolic iron overload syndrome (DIOS) is defined by histologic iron overload in the context of insulin-

resistance. Its occurrence with Non-alcoholic fatty liver disease (NAFLD) has been reported to be associated with more severe fibrosis. Little data is available regarding the prevalence of DIOS in those with NAFLD. This study aimed to evaluate the prevalence of histologic hepatic iron overload in adults with biopsy-proven NAFLD, and to determine the correlation between serum ferritin and hepatic iron overload.

Method: This single center, retrospective study included adult patients (≥ 18 years old) with biopsy-proven NAFLD between 01/01/2010–31/12/2019. The electronic medical record was used to assess detailed data on patient demographics, biochemistry, and clinical parameters. NAFLD is defined as $\geq 5\%$ steatosis in the absence of any co-factors for liver disease. For the purpose of this study, DIOS is defined by histological evidence of iron deposits on Perl's stain in the presence of any component of the metabolic syndrome (hypertension, type 2 diabetes mellitus, dyslipidemia).

Results: In total 224 patients were included in this study, with mean age 52.3 years and the majority female (64.7%). Forty-one (19.2%) patients had evidence of histologic iron overload, $n=39$ (17.4%) fulfilling diagnosis for DIOS. Those with DIOS were more likely to be male (56.4% vs 30.8%, $p=0.002$), leaner (body mass index [BMI] 34.9 vs 38.0 kg/m², $p=0.01$) and had higher serum ferritin (329 vs 94 micrograms/L, $p<0.001$) and transferrin saturation (29.7% vs 21.5%, $p<0.001$). Ferritin >1000 micrograms/L (odds ratio [OR] 7.60, 95% confidence interval [CI] 1.26–45.86, $p=0.027$) and transferrin saturation as continuous variables (OR 1.06, 95% CI 1.01–1.11, $p=0.017$) were independent predictors for histological iron overload after adjusting for age, gender, and BMI on multivariate logistic regression analysis. There was a statistically significant but weak correlation between serum ferritin and hepatocellular iron content (Spearman's rho = 0.378, 95% CI 0.213–0.523, $p<0.001$) and reticuloendothelial cell compartment iron content (Spearman's rho = 0.341, 95% CI 0.172–0.491, $p<0.001$). DIOS was not an independent predictor for fibrosis on multivariable linear regression analysis or F3–4 fibrosis on logistic regression analysis.

Conclusion: Prevalence of DIOS is nearly 20% in those with biopsy-proven NAFLD. While higher levels of ferritin and transferrin saturation were associated with DIOS, most patients with DIOS had ferritin <500 micrograms/L and transferrin saturation $<45\%$, limiting the ability of these parameters to predict DIOS. Hepatic iron overload did not predict presence of advanced fibrosis/cirrhosis in this cohort.

THU-451

Effect of PNPLA3 (rs738409 C > G) and TM6SF2 (rs58542926 C > T) polymorphisms on the prognosis of non-alcoholic fatty liver disease (NAFLD) in patients with type-2 Diabetes Mellitus

Natália Lavrado¹, Claudia Regina Cardoso¹, Natalia Wajbrot², Paulo Henrique França³, Gil Salles¹, Nathalie Leite², Cristiane Villela-Nogueira¹. ¹Federal University of Rio de Janeiro, School of Medicine, Internal Medicine Division, Rio de Janeiro, Brazil; ²Federal University of Rio de Janeiro, Hepatology Division, Brazil; ³Universidade de Joinville, Brazil
E-mail: crisvillelanog@gmail.com

Background and aims: The impact of the association of genetic polymorphisms in the progression of liver disease in patients with type-2 Diabetes Mellitus (T2DM) and NAFLD is still under debate. We aimed to evaluate the effect of PNPLA3 and TM6SF2 alleles in the prognosis of liver and extrahepatic outcomes in a cohort of T2DM patients with NAFLD.

Method: T2DM individuals with NAFLD had the PNPLA3 (rs738409 C > G) and TM6SF2 (rs58542926 C > T) genotypes determined. Each polymorphism was categorized into two groups considering the presence of at least one or none risk allele. We evaluated the impact of harbouring at least one risk allele (G or T) from each polymorphism regarding the occurrence of the following outcomes: cirrhosis, esophageal or gastric varices, hepatocellular carcinoma, major cardiovascular events (MACE), extrahepatic cancer and death.

Multivariate analysis evaluated the associations between PNPLA3 and TM6SF2 alleles and the outcomes. Several hierarchical models were built to assess the association, independently of confounding factors: model (1) only polymorphism (PNPLA3 or TM6SF2) as the main covariate, (2) model 1 plus age and gender, (3) model 2 plus hypertension, dyslipidaemia, use of insulin, smoking history, alcohol consumption, body mass index, glycated haemoglobin and gamma-glutamyl transpeptidase. Results were presented as odds ratios with their 95% confidence intervals, and a 2-tailed p value <0.05 was regarded as significant.

Results: 407 T2DM with NAFLD (mean age 62 ± 10 years, 67% women) were followed for 66 ± 19 months. Frequencies of the genotypes' categories were: PNPLA3 CC 44.2% and CG+GG 55.8%; TM6SF2 CC 87.5% and CT+TT 12.5%. Forty-seven (11.5%) patients had cirrhosis and esophageal or gastric varices were found in 16 (3.9%) patients. Hepatocellular carcinoma was diagnosed prospectively in 7 (1.7%) patients. Regarding extrahepatic outcomes, 43 (10.6%) patients had extrahepatic cancer, and MACE occurred in 103 (25.3%) patients. Sixty-four (15.7%) participants died during follow-up, the leading causes being cardiovascular (42.2%) and infection (32.8%). Having at least one G allele of PNPLA3 independently increased the risk of developing cirrhosis (OR 12.33/95% CI 3.58–42.38; $p<0.001$) and esophageal or gastric varices (OR 13.24/95% CI 1.49–117.52; $p=0.02$), and decreased the risk of having extrahepatic cancer (OR 0.41/95% CI 0.18–0.90; $p=0.02$). There was no association between the G allele of PNPLA3 and hepatocellular carcinoma, MACE or death. Regarding the T allele of TM6SF2, none of the analyses showed results with statistical significance.

Conclusion: T2DM NAFLD patients harbouring at least one minor allele of PNPLA3 rs738409 polymorphism have a worse prognosis regarding liver disease and should be followed carefully due to the higher odds of disease progression.

THU-452

Interferon gamma-induced protein 10 levels increase across the spectrum of liver disease and are associated with insulin resistant components in subjects with non-alcoholic fatty liver disease

Marta Guariglia¹, Chiara Rosso¹, Fabrizia Carli², Gian Paolo Caviglia¹, Angelo Armandi^{1,3}, Eleonora Dileo¹, Nuria Pérez Diaz del Campo¹, Gabriele Castelnovo¹, Maria Lorena Abate¹, Antonella Olivero¹, Daphne D'Amato¹, Amina Abdulle¹, Irene Poggiolini¹, Davide Ribaldone^{1,4}, Giorgio Maria Saracco^{1,4}, Amalia Gastaldelli², Elisabetta Bugianesi^{1,4}. ¹University of Turin, Department of medical science, Turin, Italy; ²Institute of Clinical Physiology, CNR, Cardiometabolic Risk Unit, Pisa, Italy; ³University medical center of the Johannes Gutenberg-University, I.Department of medicine, Mainz, Germany; ⁴Città della salute e della scienza- Molinette Hospital, Gastroenterology Unit, Turin, Italy
E-mail: marta.guariglia@unito.it

Background and aims: The most important determinant of the progression of non-alcoholic fatty liver disease (NAFLD) to non-alcoholic steatohepatitis (NASH) and fibrosis is insulin resistance (IR). Interferon gamma-induced protein 10 (IP-10), a proinflammatory chemokine, plays a crucial role in inflammatory diseases but its interaction with IR in the setting of NAFLD is not clear.

Method: We analysed data from 200 patients with biopsy proven NAFLD (M/F 121/79; mean age 47 ± 12). A subgroup of 46 non-diabetic NAFLD subjects underwent tracers studies (6, 6 -D2-glucose and [2H5] glycerol). Tracers enrichment was determined by GC-MS and data were used to calculate hepatic (Hep)-IR and adipose tissue (AT)-IR components. Serum IP-10 levels were assessed by Bio-Plex (BioRad Laboratories).

Results: Overall, 81/200 (40.5%) patients had $F \geq 2$ and 151/200 (75.5%) had NASH. The prevalence of type 2 diabetes was 27.5% and 47.5% of the patients were obese. IP-10 levels significantly increased across lean to overweight to obese subjects ($p=0.009$), showed a stepwise

increase according to the stages of hepatic fibrosis ($p = 0.006$) and were significantly higher in patients with NASH compared to those with NAFL (457 pg/ml vs 383 pg/ml, $p = 0.039$). Moreover, IP-10 levels were increased in diabetic compared to non-diabetic patients (491 pg/ml vs 393 pg/ml, $p = 0.021$) and showed a significant correlation with HOMA-IR ($r = 0.30$, $p = 0.006$). In the subgroup of non-obese, non-diabetic NAFLD patients who underwent tracers' studies, IP-10 levels showed a significant correlation with both Hep-IR and AT-IR ($r = 0.32$, $p = 0.030$ and $r = 0.33$, $p = 0.049$, respectively). At multivariate analysis, IP-10 was independently associated to the degree of hepatic fibrosis ($r_p = 0.3$, $p = 0.05$).

Conclusion: IP-10 may be involved in the complex pathogenesis of NAFLD. Further studies are needed to demonstrate its causality in determining liver damage.

This research has been supported by the Italian MIUR under the programme "Dipartimenti di Eccellenza 2018–2022," n. D15D18000410001 and by EU/EFPIA-IMI2 under g.a. no.777377, LITMUS

THU-453

Stigma in NAFLD and NASH: a global survey of patients and providers

Zobair Younossi^{1,2,3}, Yusuf Yilmaz^{4,5}, Jian-Gao Fan⁶, Vincent Wai-Sun Wong⁷, Mohamed El Kassas⁸, Shira Zelber-Sagi⁹, Alina Allen¹⁰, Mary Rinella¹¹, Ashwani Singal¹², Stuart C. Gordon¹³, Michael Fuchs¹⁴, Wayne Eskridge¹⁵, Naim Alkhouri¹⁶, Khalid Alswat¹⁷, Hirokazu Takahashi¹⁸, Takumi Kawaguchi¹⁹, Jane Ranagan²⁰, Ming-Hua Zheng²¹, Ajay Kumar Duseja²², Patrizia Burra²³, Carrieri Patrizia²⁴, Marco Arrese²⁵, Achim Kautz²⁶, Janus Ong²⁷, Laurent Castera²⁸, Sven Francque²⁹, Marcelo Kugelmas³⁰, Yuichiro Eguchi³¹, Sombat Treeprasertsuk³², Marlen Ivon Castellanos Fernández³³, Manuel Romero Gomez³⁴, Philip N. Newsome³⁵, Kenneth Cusi³⁶, Rohit Loomba³⁷, Jörn Schattgenberg^{38,39}, Ming-Lung Yu⁴⁰, Moises Diago⁴¹, Lynn Gerber³, Brian Lam^{2,3}, Lisa Fornaresio⁴², Fatema Nader⁴³, Linda Henry^{1,2,43}, Andrei Racila^{2,3,43}, Pegah Golabi³, Maria Stepanova^{1,3,43}, Saleh Alqahtani^{43,44}, Jeffrey Lazarus⁴⁵. ¹Inova Health System, Medicine Service Line, United States; ²Inova Health System, Department of Medicine, Center for Liver Diseases, United States; ³Beatty Liver and Obesity Research Program, Inova Health System, United States; ⁴Liver Disease Research Center, Department of Medicine, College of Medicine, King Saud University, Turkey; ⁵Recep Tayyip Erdogan University, Department of Gastroenterology, Turkey; ⁶Xinhua Hospital, Shanghai Jiao Tong University School of Medicine, China; ⁷The Chinese Institute of Hong Kong, Department of Medicine and Therapeutics, Hong Kong; ⁸Cairo University, Endemic Medicine and Hepatogastroenterology Department, Egypt; ⁹Tel Aviv University, School of Public Health, Israel; ¹⁰Mayo Clinic, Department of Hepatology and Gastroenterology, United States; ¹¹University of Chicago, College of Medicine, United States; ¹²University of South Dakota and Avera Transplant Institute, United States; ¹³Henry Ford Hospital, Department of Medicine, United States; ¹⁴Veteran's Administration Medical Center, Department of Medicine, United States; ¹⁵Fatty Liver Foundation, United States; ¹⁶Arizona Liver Transplant Center, United States; ¹⁷King Saud University College of Medicine, Liver Research Unit, Saudi Arabia; ¹⁸Department of Hepatology, Diabetes, Metabolism and Endocrinology at Saga Medical School, Japan; ¹⁹Kurume University, Division of Gastroenterology, Department of Medicine, Japan; ²⁰Chronic Liver Disease Foundation, United States; ²¹Chinese Academy of Medical Sciences and Peking Union Medical College, China; ²²Postgraduate Institute of Medical Education and Research, Department of Hepatology, India; ²³Padua University, Division of Gastroenterology and Hepatology, Italy; ²⁴Aix Marseille Univ, INSERM, IRD, SESSTIM, Sciences Économiques and Sociales de la Santé et Traitement de l'Information Médicale, Marseille, France, France; ²⁵Pontificia Universidad Católica de Chile, Chile; ²⁶Kautz5 gUG, Germany; ²⁷University of the Philippines, College of Medicine, Philippines; ²⁸Hopital Beaujon, Assistance Publique-Hôpitaux de Paris, University of Paris, France; ²⁹Antwerp University Hospital,

Belgium; ³⁰South Denver Gastroenterology, United States; ³¹Saga University, Department of Hepatology, Liver Center, Japan; ³²Chulalongkorn University, Division of Gastroenterology, Thailand; ³³Instituto Nacional de Gastroenterología, La Habana, Cuba, Cuba; ³⁴Institute of Biomedicine of Seville (HUVR/CSIC/US), Spain; ³⁵University of Birmingham, United Kingdom; ³⁶University of Florida, College of Medicine- Department of Endocrinology, United States; ³⁷UC San Diego Medical Center, San Diego, CA, USA, United States; ³⁸Metabolic Liver Research Program, Germany; ³⁹University Medical Center of the Johannes Gutenberg-University, Germany; ⁴⁰Kaohsiung Medical University Hospital, Kaohsiung Medical University, Taiwan; ⁴¹Hospital Univ. Gral de Valencia, Spain; ⁴²Johns Hopkins University, Department of Cardiac Surgery, United States; ⁴³Center for Outcomes Research in Liver Disease, United States; ⁴⁴King Faisal Specialist Hospital and Research Center, Saudi Arabia; ⁴⁵Barcelona Institute for Global Health, Spain E-mail: zobair.younossi@inova.org

Background and aims: Patients with fatty liver disease may experience stigmatization due to the disease or associated comorbidities. Aim: To understand stigma among NAFLD patients and providers.

Method: Members of the Global NASH Council created two surveys about experiences and attitudes toward NAFLD and related terms: a 68-item patient and a 41-item provider survey.

Results: The surveys were completed by 475 NAFLD patients [12 countries; 58% USA, 20% Middle East/North Africa (MENA), 20% East Asia (EA)] and 555 providers [63% GI/hepatologists, 14 countries; 28% USA, 44% MENA, 25% EA]. Of all patients, 71% ever disclosed having NAFLD/NASH to family/friends; the most used words were "fatty liver" and "NAFLD or NASH" (35–54%), while "metabolic disease" or "MAFLD" were rarely used (never by 83–88%). There were 46% who reported experiencing stigma or discrimination (at least sometimes) due to obesity/overweight vs. 17% due to NAFLD (Figure). The greatest social-emotional burden among NAFLD patients was feeling partially to blame for their liver disease (69% agree) and others believing that they do not eat properly (58% agree). Providers believed that lack of patient motivation (70%) and training in effective communication (62%) were the biggest obstacles to weight loss discussions. Furthermore, provider discomfort was related to perceived patients' lack of willpower for lifestyle changes and taking care of their diabetes (45–49% providers; 13–17% USA vs. 64–70% MENA, 31–67% EA). Regarding how various diagnostic terms are perceived by patients, there were no substantial differences between "NAFLD," "fatty liver disease (FLD)," "NASH," or "MAFLD": the most popular response was being neither comfortable nor uncomfortable with either term (47%–57%), with some greater discomfort with FLD among U.S. patients (45% uncomfortable). Among providers, 42% (49% USA, 43% MENA, 32% EA) believed that the term "fatty" in the name is stigmatizing, while 38% believed that the term "non-alcoholic" is stigmatizing, more commonly in MENA (47%). Also, 38% of the providers reported the term "FLD" as being stigmatizing (47% USA, 40% MENA, 24% EA). Finally, 54% of the providers (GI/hep 58% vs. 42% other specialties; 46% USA, 59% MENA, 51% EA) believe that a name change may reduce stigma.

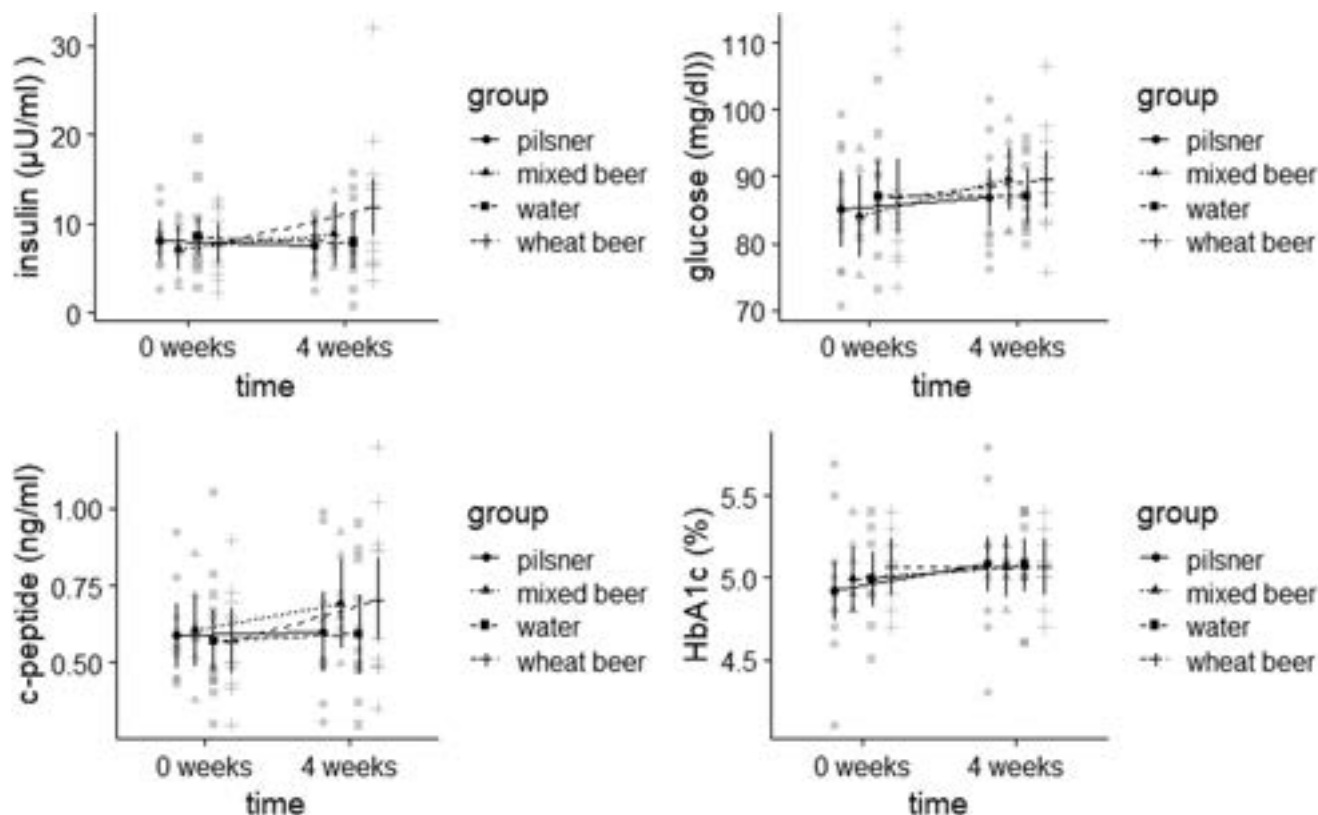


Figure: (abstract: THU-454).

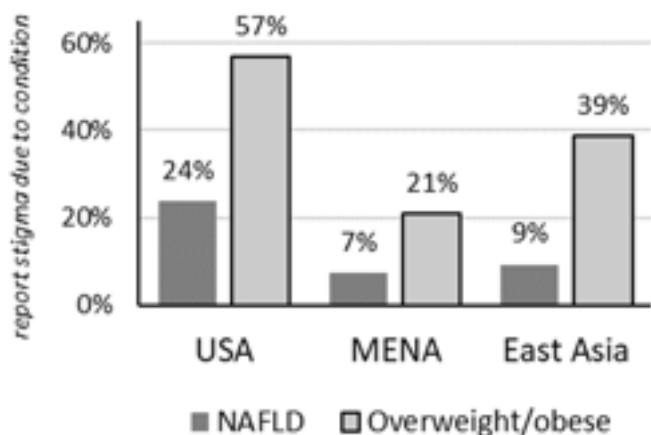


Figure:

Conclusion: Perception of NAFLD stigma varies according to patients, providers, geographic location and sub-specialty. NAFLD patients reported the term obesity to be more stigmatizing than NAFLD.

THU-454

Effects of a one-month consumption of different non-alcoholic beers on metabolic and liver health in young men

Henriette Kreimeyer¹, Svenja Sydor¹, Lara Kaiser¹, Gagatay Toskal¹, Anja Figge¹, Jan Best¹, Josef Pospiech¹, Oliver Götze¹, Jan-Peter Sowa¹, Mustafa Özcürümez¹, Ali Canbay¹, Lars Bechmann¹, Paul Manka¹.

¹Universitätsklinikum Knappschafts-Krankenhaus Bochum Langendreer, Germany

E-mail: henriette.kreimeyer@gmail.com

Background and aims: The amount of alcohol that can be consumed healthily without causing harm is currently under discussion.

Recently, the gender-specific limit for daily alcohol consumption has been further reduced. Non-alcoholic alternatives to regular beer are often promoted. However, data on the effects of non-alcoholic beer on liver health are lacking. We investigated the influence of different non-alcoholic beer beverages [Pilsner (PI), wheat beer (WB), lemon-lime flavored drink/mixed drink (MD), and water (WA) as control] on fatty degeneration and liver damage and effects on glucose and lipid metabolism.

Method: In this monocentric, randomized, multi-arm study, 48 healthy young men were evaluated for serum markers of liver injury, glucose, and lipid metabolism. In addition, liver status was assessed by transient elastography, including measurement of the controlled attenuation parameter (CAP). Blood samples were collected at the beginning and end of a four-week period, during which the subjects were required to consume two 330 ml bottles of each beverage daily.

Results: Deterioration of glucose metabolism markers was observed in all groups compared to controls. Insulin and c-peptide increased significantly in the WB group, while fasting glucose increased in the MB group, and HbA1c increased in the PI group. Triglyceride levels increased in the MB and WB groups and decreased in the WA and PI groups, but not significantly. HDL showed a significant increase in the WA group. Liver enzymes showed a substantial increase in the MB group, while transient elastography results showed no differences. M30, an apoptosis marker, showed a significant decrease in liver damage in the WA and PI groups.

Conclusion: Four weeks of alcohol-free beverage consumption altered several serum parameters associated with glucose, liver, and lipid metabolism in this cohort of healthy young men. In addition, consumption of mixed beer was associated with more significant liver inflammation.

THU-455

Cognitive impairment is frequent in obesity and not restricted to persons with biopsy-proven NAFLD

Charlotte Wernberg¹, Lea Ladegaard Grønkjær², Birgitte Jacobsen², Vineesh Indira Chandran³, Jonas Graversen³, Aleksander Krag⁴, Karin Weissenborn⁵, Hendrik Vilstrup⁶, Mette Munk Lauridsen².

¹University Hospital of Southern Denmark, Gastroenterology and Hepatology, Esbjerg, Denmark; ²University Hospital of Southern Denmark, Gastroenterology and Hepatology, Esbjerg V, Denmark;

³University of Southern Denmark, Department of Molecular Biology, Odense, Denmark; ⁴FLASH Liver Research Centre University Hospital Odense, Gastroenterology and Hepatology, Odense, Denmark;

⁵Medizinische Hochschule Hannover, Neurologische Klinik, Germany;

⁶Aarhus University Hospital, Hepatology and Gastroneterology, Denmark

E-mail: mettelauridsen@gmail.com

Background and aims: Non-alcoholic fatty liver disease (NAFLD) may be associated with cognitive dysfunction due to metabolic and micro-ischemic encephalopathy. We aimed to identify the prevalence of cognitive impairment in an obese cohort, assess the association to biopsy-proven NAFLD, and describe the nature of the impairment.

Method: Liver biopsy and basic cognitive testing with Continuous Reaction Time test (CRT), Portosystemic Encephalopathy-Syndrome test (PSE), and Stroop EncephalApp were performed in all. A representative sub-group further underwent Repeatable Battery for the Assessment of Neuropsychological Status (RBANS). 'Cognitive impairment' was defined as ≥ 2 abnormal basic cognitive tests or abnormal RBANS.

Results: We included 180 persons with BMI >35 kg/m, 72 % women, age 46 ± 12 years, 54 % had NAFLD, and 24 % had steatohepatitis. Eight percent were impaired as defined by CRT, PSE, and Stroop, and 41 % by RBANS. Executive functions and memory were the most affected domains. Male gender, the use of 2 or more psychoactive medications, and low LDL were risk factors (table). There was no correlation to BMI, NAFLD severity, or other metabolic co-morbidities. The few with advanced liver fibrosis performed worse in PSE.

Conclusion: Cognitive impairment was frequent in our obese cohort; not associated with NAFLD severity; and differed from hepatic encephalopathy by severely impacting immediate and late memory.

Fibrosis was associated with poor performance in PSE, which might reflect a pre-cirrhosis hepatic encephalopathy.

THU-456

Non-alcoholic fatty liver disease and the longitudinal risks of clinical outcomes: a meta-analysis

Kai En Chan¹, Elden Yen Hng Ong¹, Charlotte Chung Hui Ong¹, Christen En Ya Ong¹, Benjamin Wei Feng Koh¹, Ansel Tang¹, Margaret Teng^{1,2}, Wen Hui Lim¹, Darren Jun Hao Tan¹, Daniel Huang^{1,2}, Mohammad Shadab Siddiqui³, Mazen Nouredin⁴, Arun Sanyal³, Cheng Han Ng¹, Mark Muthiah^{1,2}. ¹Yong Loo Lin School of Medicine, National University of Singapore, Singapore; ²National University Health System, Gastroenterology and Hepatology, Singapore; ³Division of Gastroenterology, Department of Internal Medicine, Virginia Commonwealth University, United States; ⁴Houston Research Institute, United States

E-mail: margaret.tenglp@gmail.com

Background and aims: Non-alcoholic fatty liver disease (NAFLD) is the fastest growing cause of chronic liver disease globally. Beyond hepatic complications, NAFLD is associated with extra-hepatic disorders such as cardiometabolic diseases, oncological disorders, and other clinical conditions that pose adverse health effects. This study aims to provide an updated meta-analysis on the umbrella of incident clinical complications associated with NAFLD and the effects when stratified by gender and severity of NAFLD.

Method: Medline and Embase databases were searched from inception to 13 November 2022. Search terms included but were not limited to "non-alcoholic fatty liver disease" and "longitudinal outcomes." The DerSimonian and Laird random effects model was used to pool reported effect sizes assessing the longitudinal risks of clinical outcomes associated with NAFLD. Subgroup analyses stratified by NAFLD diagnostic modality, gender, weight class and NAFLD severity were conducted to explore possible heterogeneity.

Results: 129 articles were included in this study. A pooled analysis of 44 articles and 6 151 043 individuals found that NAFLD patients had a greater risk of cardiovascular outcomes ($n = 44$, HR: 1.43, 95%CI: 1.27–1.60, $p < 0.01$, $I^2 = 97.50\%$) compared to non-NAFLD individuals. In the assessment of incident metabolic disorders, NAFLD patients were found to have a significantly greater risk of incident hypertension (n

Figure: (abstract: THU-455): Regression analysis of the association between impaired cognition and possible predictor variables

Variables	OR	95 % CI	p value	OR	95 % CI	p value
Sex (Male)	3.46	1.61–7.44	0.002	3.67	1.32–10.27	0.013
Age (years)	1.00	0.97–1.03	0.93	0.96	0.93–1.00	0.051
Education (years)	0.84	0.72–0.96	0.013	0.86	0.72–1.02	0.077
Steatohepatitis, NASH (Yes)	1.13	0.48–2.64	0.778			
Severe fibrosis, F3–4 (Yes)	2.99	0.80–11.2	0.100	2.95	0.60–14.3	0.181
Ammonia ion ($\mu\text{mol/L}$)	1.05	1.00–1.11	0.069			
CRP (mg/L)	0.98	0.93–1.04	0.55			
AST (U/L)	1.00	0.70–1.01	0.39			
Type 2-diabetes (Yes)	1.31	0.57–2.99	0.528			
HOMA-IR (mmol/mol)	1.00	0.96–1.04	0.97			
Lipid-lowering drugs (Yes)	0.83	0.34–1.99	0.684			
Triglycerides (mmol/L)	0.65	0.38–1.09	0.11			
LDL cholesterol (mmol/L)	0.58	0.39–0.86	0.007	0.59	0.37–0.96	0.035
HDL cholesterol (mmol/L)	0.81	0.21–3.15	0.76			
Sleep Apnoea (Yes)	1.98	0.89–4.44	0.096			
Hypertension (Yes)	1.31	0.62–2.74	0.48			
>2 types of psychoactive meds	1.94	0.62–6.07	0.25	5.24	1.34–20.4	0.017
Major depression inventory	1.01	0.97–1.04	0.67			

HOMA-IR, homeostatic model assessment for insulin resistance; AST, aspartate aminotransferase; LDL, low-density lipoprotein; HDL, high-density lipoprotein cholesterol; CRP, c-reactive protein; psychoactive medication are antidepressants, antipsychotics, morphine or analogues.

POSTER PRESENTATIONS

= 9, HR: 1.75, 95%CI: 1.46–2.08, $p < 0.01$, $I^2 = 74.00\%$), diabetes ($n = 37$, HR: 2.56, 95%CI: 2.10–3.13, $p < 0.01$, $I^2 = 98.90\%$), pre-diabetes ($n = 4$, HR: 1.69, 95%CI: 1.22–2.35, $p < 0.01$, $I^2 = 54.80\%$), chronic kidney disease ($n = 14$, HR: 1.38, 95%CI: 1.27–1.50, $p < 0.01$, $I^2 = 80.20\%$) and metabolic syndrome ($n = 5$, HR: 2.57, 95%CI: 1.13–5.85, $p = 0.02$, $I^2 = 96.10\%$). By subgroup analysis, NAFLD patients with advanced liver disease were also found to have a significantly higher risk ($p = 0.02$) of incident diabetes than those with less severe NAFLD in comparison to non-NAFLD individuals. There was a positive relationship ($n = 15$, HR: 1.54, 95%CI: 1.35–1.76, $p < 0.01$, $I^2 = 97.30\%$) between NAFLD and incident cancers when compared to a non-NAFLD cohort. NAFLD was also found to be associated with a significantly greater risk of liver-related outcomes ($n = 14$, HR: 3.92, 95%CI: 2.05–7.49, $p < 0.01$, $I^2 = 98.50\%$) and gallstone formation ($n = 2$, HR: 1.24, 95%CI: 1.16–1.32, $p < 0.01$, $I^2 = 0.00\%$) when compared to non-NAFLD. No statistical association was found between NAFLD and the risk of incident reflux esophagitis and dementia.

Conclusion: This meta-analysis provides a necessary update on the longitudinal risks of clinical outcomes associated with NAFLD. While this study suggests that NAFLD is associated with an increased risk of disease outcomes and extra-hepatic complications, further research is required to understand the pathophysiology linking NAFLD with development of extra-hepatic disorders.

THU-457

Metabolic dysfunction-associated fatty liver disease is associated with increased risk of extrahepatic malignancies: a nationwide cohort study

Min Kyung Park¹, Hye-Sung Moon², Sungwon Chung¹, Sungho Won^{2,3}, Yun Bin Lee¹, Eun Ju Cho¹, Jeong-Hoon Lee¹, Su Jong Yu¹, Jung-Hwan Yoon¹, Yoon Jun Kim¹. ¹Seoul National University College of Medicine, Department of Internal Medicine and Liver Research Institute, Korea, Rep. of South; ²RexSoft Inc., Korea, Rep. of South; ³Seoul National University, Department of Public Health Sciences, Graduate School of Public Health, Korea, Rep. of South
E-mail: yoonjun@snu.ac.kr

Background and aims: Metabolic dysfunction-associated fatty liver disease (MAFLD), a new definition encompassing the entire liver disease associated with metabolic disorders, has been recently proposed. We aimed to analyze the long-term outcome of MAFLD by focusing on extrahepatic malignancy.

Method: We analyzed data from the National Health Insurance Service of Korea that includes 7 454 412 participants who participated health screening program in 2009. MAFLD was defined by an international expert consensus statement previously proposed. Participants were further categorized into four groups followed by the MAFLD definition; non-MAFLD, DM-MAFLD, overweight/obese-MAFLD, and lean-MAFLD. The primary outcome was the development of any primary extrahepatic malignancy. The Cox proportional hazard model was used, including adjustment for competing risks.

Results: Of the study subjects, 2 500 080 (33.5%) had MAFLD. During the median follow-up of 10.3 years (interquartile range, 10.1–10.6), 447 880 patients (6.0%) were diagnosed with primary extrahepatic malignancy. The MAFLD group had a higher overall risk of extrahepatic malignancy than non-MAFLD group (adjusted subdistribution hazard ratio [aSHR] = 1.02; 95% confidence interval [CI] = 1.02–1.03; $P < .001$). The DM-MAFLD group showed a significantly higher risk of extrahepatic malignancy compared to the non-MAFLD group (aSHR = 1.13; 95% CI = 1.11–1.14; $P < .001$). Furthermore, the lean-MAFLD group also showed a 1.12-fold higher risk of extrahepatic malignancy than the non-MAFLD group (aSHR = 1.12; 95% CI = 1.10–1.14; $P < .001$). However, the overweight/obese-MAFLD group showed no significant overall risk of extrahepatic malignancy compared to the non-MAFLD group (aSHR = 1.00; 95% CI = 0.99–1.00; $P = 0.42$). Sensitivity analysis after excluding underlying liver disease, the MAFLD group maintained a significantly higher extrahepatic

malignancy than the non-MAFLD group (aSHR = 1.02; 95% CI = 1.02–1.03; $P < .001$).

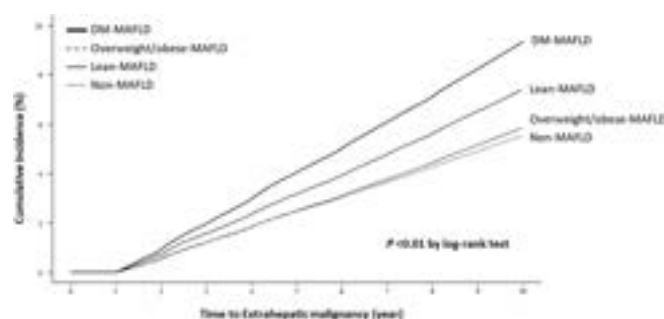


Figure:

Conclusion: MAFLD is associated with developing extrahepatic malignancy, while MAFLD caused by overweight or obese demonstrated no association with developing extrahepatic malignancy. Categorizing MAFLD subgroup according to the positive definition criteria representing the phenotypes of metabolic disorders could help the stratification of the risk of extrahepatic malignancy in MAFLD.

THU-458

Non-alcoholic fatty liver disease (NAFLD) is associated with an increased risk of type 2 diabetes mellitus

Sven H. Loosen¹, Tom Lüdde¹, Christoph Roderburg¹. ¹University Hospital Düsseldorf, Medical Faculty of Heinrich Heine University Düsseldorf, Clinic for Gastroenterology, Hepatology and Infectious Diseases, Düsseldorf, Germany
E-mail: christoph.roderburg@med.uni-duesseldorf.de

Background and aims: Non-alcoholic fatty liver disease (NAFLD) has become the most common liver disease worldwide and represents the leading cause of liver-related morbidity and mortality. Its all cause mortality is often driven by co-existing metabolic disease such as type 2 diabetes mellitus (T2DM), which share many pathophysiological characteristics. The risk of developing T2DM among NAFLD patients in Germany is only poorly described. Here, we evaluated the risk of T2DM development in a large cohort of primary care patients in Germany

Method: A cohort of 17 245 NAFLD patients and a propensity score matched cohort of equal size were identified from the Disease Analyzer database (IQVIA) between 2005 and 2020. The incidence of T2DM was evaluated as a function of NAFLD during a five years study period using Cox-regression models.

Results: Within 5 years of the index date, 18.8% and 11.7% of individuals with and without NAFLD were diagnosed with T2DM ($p < 0.001$, Figure 1). Regression analysis revealed a Hazard Ratio (HR) of 1.77 (95%CI: 1.68–1.88) for the development of T2DM among NAFLD patients. Subgroup analyses confirmed this association for all age groups (18–50, 51–60, 61–70, and >70 years), male and female patients, as well as normal weight (BMI <25 kg/m²), overweighted (BMI 25–30 kg/m²) and obese (BMI >30 kg/m²) patients.

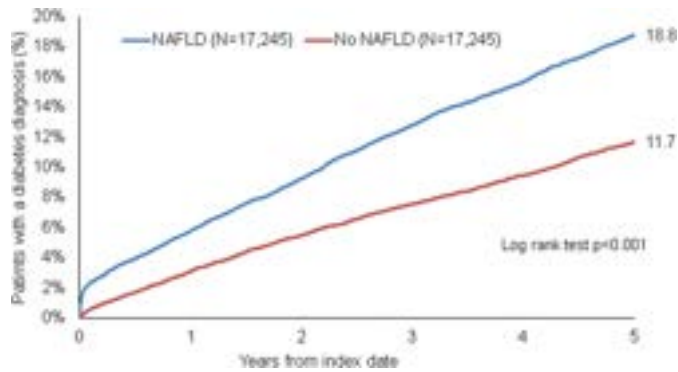


Figure: Kaplan-Meier curves estimating the time to diagnosis of T2DM in patients with and without NAFLD.

Conclusion: Our data revealed a significantly increased incidence of T2DM among NAFLD patients in Germany. Given the dramatically increasing global relevance of NAFLD, we believe that prevention and regular screening programs for T2DM in NAFLD patients could help to reduce its high mortality and morbidity in the future.

NAFLD: Non-alcoholic fatty liver disease, T2DM: Type 2 diabetes mellitus

THU-459

Metabolic dysfunction associated fatty liver disease and the risk of hepatocellular carcinoma

Byeong Geun Song¹, Aryoung Kim¹, Sung Chul Choi², Myungji Goh¹, Wonseok Kang¹, Geum-Yon Gwak¹, Yong-Han Paik¹, Moon Seok Choi¹, Joon Hyeok Lee¹, Seung Woon Paik¹, Dong Hyun Sinn¹. ¹Samsung Medical Center, Sungkyunkwan University School of Medicine, Department of Medicine, Korea, Rep. of South, ²Samsung Medical Center, Sungkyunkwan University School of Medicine, Center for Health Promotion, Korea, Rep. of South
E-mail: sinndhn@hanmail.net

Background and aims: The metabolic dysfunction-associated fatty liver disease (MAFLD) is a new inclusive term proposed to replace non-alcoholic fatty liver disease (NAFLD). We analysed whether hepatocellular carcinoma (HCC) risk differs by MAFLD or NAFLD status in large asymptomatic adults.

Method: Total of 73 691 adults were followed-up for the development of HCC. NAFLD was diagnosed among participants without other liver disease (n = 65 992).

Results: Participants with MAFLD showed higher incidence of HCC compared with those without MAFLD (0.37 and 0.24 per 1000 person-years, p = 0.006). However, MAFLD was not an independent factor associated with HCC in multivariable analysis [hazard ratio (HR), 1.21; 95% confidence interval (CI), 0.92–1.60]. When stratified according to presence of other liver diseases, MAFLD was not associated with HCC in participants with other liver diseases. In participants without other liver disease, both MAFLD (adjusted HR, 1.84; 95% CI, 1.09–3.11) and NAFLD (adjusted HR, 1.71; 95% CI, 1.01–2.90) was independent factor associated with HCC. When stratified according to NAFLD and MAFLD status, there was no HCC development among NAFLD only participants, but these NAFLD only group comprised 3.4%, and majority with hepatic steatosis fulfilled both NAFLD and MAFLD criteria.

Conclusion: MAFLD could be diagnosed for broader population including participants with other liver diseases, however, MAFLD demonstrated no association with HCC in participants with other liver diseases. The risk of HCC was very low for NAFLD only participants but made up a very small percentage. These findings do not support change in nomenclature from NAFLD to MAFLD.

THU-460

Assessing treatment outcomes in an AIH/NAFLD overlap cohort

Eleanor Belilos¹, Jessica Strzepka¹, Shiriam Jakate¹, Costica Aloman¹, Nancy S Reau¹. ¹Rush University Medical Center, United States
E-mail: eleanor_a_belilos@rush.edu

Background and aims: Overlap between autoimmune hepatitis (AIH) and non-alcoholic fatty liver disease (NAFLD) has become increasingly common in recent years as NAFLD has emerged as the main cause of liver disease worldwide. AIH treatment includes steroids, which have adverse metabolic effects that can worsen NAFLD. No specific treatment guidelines are available to mitigate these effects or redefine treatment goals in the AIH/NAFLD overlap population. Previous data from our study cohort found that AIH/NAFLD overlap patients have lower rates of biochemical remission but have similar clinical outcomes, despite a treatment course that is less likely to adhere to AIH standard of care per AASLD guidelines. This new study aims to expand our understanding of this unique patient cohort by validating previous findings with a larger sample size as well as examining additional outcomes such as time to completion of steroid treatment, Fibrosis-4 (FIB4), and AST to Platelet Ratio Index (APRI) at additional defined time points (three months, one year, two years, and three years).

Method: This was a single-center, retrospective descriptive study examining biopsy proven AIH and AIH/NAFLD patients (2009–2019). Baseline and follow-up clinical and biochemical parameters, FIB-4, APRI and clinical outcomes (if off steroids, all-cause mortality, need for liver transplantation, or decompensated cirrhosis) at three months, one year, two years, and three years were recorded and compared using appropriate statistical testing for continuous (t-tests) and categorical variables (Chi-square, Fisher's exact).

Results: A total of 123 patients (44.7% AIH/NAFLD and 55.3% AIH) were included. AIH patients had higher AST and ALT, FIB4, and APRI at baseline, but also greater improvement from baseline in transaminase levels at all time points (p < 0.001). AIH/NAFLD patients were more likely to be in biochemical remission (defined as normalization of AST and ALT) at three months (p = 0.007), but less likely at one year (p < 0.001), and three years (p = 0.011). Although AIH/NAFLD patients less frequently received AIH standard of care treatment (p < 0.001), those who did were then less likely to be off steroids (p = 0.011) at one year. No significant differences were seen in FIB4, APRI, all-cause mortality, need for liver transplantation, or incidence of decompensated cirrhosis at all future time points (three months, one year, two years, three years).

		AIH	AIH/NAFLD	p value
Biochemical Remission, 3 months (%)	No	30 (46.2%)	37 (71.2)	0.007*
	Yes	35 (53.8)	15 (28.8)	
Biochemical Remission, 1 year (%)	No	8 (13.3)	25 (46.3)	<0.001*
	Yes	52 (86.7)	29 (53.7)	
Biochemical Remission, 2 years (%)	No	6 (12.0)	13 (27.1)	0.059
	Yes	44 (88.0)	35 (72.9)	
Biochemical Remission, 3 years (%)	No	4 (9.3)	14 (31.1)	0.011*
	Yes	39 (90.7)	31 (68.9)	
Off steroids, 3 months (%)	No	49 (84.5)	30 (85.7)	0.872
	Yes	9 (15.5)	5 (14.3)	
Off steroids, 1 year (%)	No	17 (31.5)	20 (58.8)	0.011*
	Yes	37 (68.5)	14 (41.2)	
Off steroids, 2 years (%)	No	9 (20.0)	12 (37.5)	0.089
	Yes	36 (80.0)	20 (62.5)	
Off steroids, 3 years (%)	No	7 (18.4)	10 (31.2)	0.212
	Yes	31 (81.6)	22 (68.8)	

Figure:

Conclusion: The results of this study support that while AIH/NAFLD patients have lower initial biochemical activity than those with AIH alone, biochemical response to treatment appears to be lower. Given that similar clinical outcomes were observed, this may indicate that AIH/NAFLD overlap may benefit from an alternative remission definition as well as unique treatment guidelines.

THU-461

Metabolic associated fatty liver disease: different impact of the three defining criteria on the hepatic and cardiovascular complications

Rosa Lombardi^{1,2}, Jaqueline Currà², Annalisa Cespiati^{1,2}, Andrea Dalbeni^{3,4}, Floriana Santomenna², Lucia Colavolpe², Francesca Alletto², Giovanna Oberti², Felice Cinque², Daniel Smith², Erika Fatta¹, Cristina Bertelli¹, Paola Dongiovanni¹, David Sacerdoti^{3,4}, Silvia Fargion², Anna Ludovica Fracanzani^{1,2}. ¹Unit of Medicine and Metabolic Disease, Fondazione IRCCS Ca' Granda Ospedale Maggiore Policlinico of Milan, Milan, Italy, Italy; ²Department of Pathophysiology and Transplantation, University of Milan, Milan, Italy, Italy; ³Division of General Medicine C, Department of Medicine, University and Azienda Ospedaliera Universitaria Integrata Verona, Verona, Italy, Italy; ⁴Liver Unit, Department of Medicine, University and Azienda Ospedaliera Universitaria Integrata of Verona, Verona, Italy, Italy
E-mail: rosallombardi@hotmail.it

Background and aims: Metabolic associated fatty liver disease (MAFLD) is defined by the presence of hepatic steatosis and one criteria among: (1) body mass index (BMI) >25 kg/m²; (2) type 2 diabetes (DM); (3) metabolic dysregulation in lean subjects (BMI <25). MAFLD exposes to hepatic and cardiovascular (CV) disease. Aim: to evaluate the different impact of each of the three features of MAFLD on the hepatic and CV disease.

Method: 688 subjects (69% males, mean age 53 ± 12 ys) were classified as MAFLD and enrolled in two Italian liver units. Liver disease was evaluated by ultrasound (US) to detect and grade hepatic steatosis and by Fibroscan to diagnose advanced fibrosis (≥F3) (liver stiffness measurement, LSM >8.2 kPa). CV disease was evaluated by carotid Doppler US and radiofrequency (carotid plaques; carotid stiffness as pulse wave velocity (PWV)).

Results: Eighty% of patients had BMI >25 without other metabolic alterations (obese, group 1), 2% had DM without other metabolic alterations (group 2), 13% had BMI >25+DM (group 3) and 5% had BMI <25 with metabolic dysregulation (lean, group 4). Because of the small number of pure DM, we considered group 2 and 3 together (BMI >25+DM, group 2a). By comparing group 1 and 4, obese and lean patients had the same severity of liver (severe steatosis 16% vs 12%, p = 0.63; advanced fibrosis 8% vs 3%, p = 0.49) and CV disease (plaques 30% vs 44%, p = 0.129; increases EAT 27% vs 33%, p = 0.53; PWV 7.8 ± 1.9 vs 7.9 ± 1.9 m/s, p = 0.77). When comparing patients with BMI >25+DM with simple obese or lean, an increased prevalence of severe steatosis was evident in this group vs the other two (30% vs 16%, p = 0.006; 30% vs 12%, p = 0.06) and ≥F3 (31% vs 8%, p < 0.001; 31% vs 3%, p = 0.001). As for CV disease, a higher prevalence of increased EAT (40%, p = 0.02), carotid plaques (61% vs 30%, p < 0.001) and increased PWV values (8.7 ± 2 m/s vs 7.8 ± 1.9, p < 0.001) was seen in group BMI >25+DM compared only to pure obese, with superimposable results compared to lean subjects. In multivariate analysis (adjusted for age, sex, smoking and statins use), BMI >25+DM remained an independent risk factor for severe steatosis (OR 2.4, CI 95 1.5–4.1), ≥F3 (OR 3.6, CI 95 1.9–6.6) and carotid plaques (OR 1.8, CI 95 1.1–3.0).

Conclusion: Among all features of MAFLD, lean subjects with metabolic dysregulation present the same hepatic and cardiovascular alterations of obese subjects without DM and even the same CV alterations of patients with coexistence of obesity and DM. As expected, the coexistence of obesity and DM seems to play the major role in the onset of hepatic and CV damage. This stresses on the need of a careful screening for complications and metabolic alterations in MAFLD patients, even if lean.

THU-462

Histological and biopsychosocial predictors of quality of life in Spanish and UK cohorts of patients with non-alcoholic fatty liver disease

Jesús Funuyet-Salas¹, Agustín Martín-Rodríguez¹, María Angeles Pérez-San-Gregorio¹, Luke Vale^{2,3,4}, Tomos Robinson^{2,4}, Quentin Anstee^{5,6}, Manuel Romero Gomez⁷, on behalf of the LITMUS consortium investigators. ¹Department of Personality, Assessment, and Psychological Treatment, Faculty of Psychology, University of Seville, Seville, Spain, Spain; ²Health Economics Group, Population Health Sciences Institute, Faculty of Medical Sciences, Newcastle University, Newcastle upon Tyne, UK, United Kingdom; ³National Institute for Health Research (NIHR) Newcastle In vitro Diagnostics Co-operative, Newcastle upon Tyne, UK, United Kingdom; ⁴NIHR Applied Research Collaboration North East and North Cumbria, Newcastle University, Newcastle upon Tyne, UK, United Kingdom; ⁵Translational and Clinical Research Institute, Faculty of Medical Sciences, Newcastle University, Newcastle upon Tyne, UK and Newcastle NIHR Biomedical Research Centre, Newcastle upon Tyne Hospitals NHS Trust, Newcastle upon Tyne, UK, United Kingdom; ⁶Newcastle NIHR Biomedical Research Centre, Newcastle upon Tyne Hospitals NHS Trust, Newcastle upon Tyne, UK, United Kingdom; ⁷UCM Digestive Diseases and Ciberehd, Virgen del Rocío University Hospital, Institute of Biomedicine of Seville, University of Seville, Seville, Spain, Spain
E-mail: jfunuyet1@us.es

Background and aims: It is unclear what biopsychosocial factors affect the impact of non-alcoholic fatty liver disease (NAFLD) on quality of life (QoL), and if these factors are equally important between different nationalities. We sought to: 1) Compare QoL of NAFLD patients based on place of origin and liver severity; and 2) Identify which variables predict QoL in Spanish and UK patient cohorts.

Method: The total sample of 737 biopsy-proven NAFLD patients was evaluated using CLDQ-NAFLD. Five groups (G₁, n = 513, Spain; G₂, n = 224, UK; G₃, n = 370, none/mild fibrosis; G₄, n = 286, moderate fibrosis; G₅, n = 81, severe fibrosis) were formed and a 2 × 3 factorial ANOVA (Snedecor's F) was performed to analyse the influence of place of origin and liver severity on QoL. A logistic regression was used to determine the effects of NASH, fibrosis, body mass index (BMI), gender, age, education and employment status on QoL in both patient cohorts separately. Cohen's d was used as an index of effect size.

Results: The strongest evidence of differences (medium effect size) were that, regardless of fibrosis stage, UK participants (G₂) were more worried (p < 0.001, d = 0.53) than Spanish participants (G₁). Regardless of place of origin, participants with severe fibrosis (G₅) were more fatigued (p < 0.001, d = 0.54), had more systemic symptoms (p < 0.001, d = 0.50), more worry (p < 0.001, d = 0.51), and lower QoL (p < 0.001, d = 0.64) than those with none/mild fibrosis (G₃). In addition, for Spanish participants, QoL reduced as fibrosis (OR = 0.29, 95% CI = 0.16–0.51, p < 0.001) and BMI (OR = 0.92, 95% CI = 0.87–0.97, p = 0.002) increased. Lower QoL was also independently associated with female gender (OR = 0.30, 95% CI = 0.18–0.50, p < 0.001). For UK participants, QoL reduced as BMI (OR = 0.94, 95% CI = 0.89–1.00, p = 0.047) increased. Lower QoL was also associated with female gender (OR = 0.45, 95% CI = 0.22–0.91, p = 0.028), non-active employment status (OR = 0.34, 95% CI = 0.15–0.74, p = 0.007) and younger age (OR = 1.06, 95% CI = 1.03–1.10, p < 0.001).

Conclusion: QoL was mainly lower in UK than Spanish participants, and they had more worry about the liver disease. Higher fibrosis stage predicted lower QoL, mainly in the Spanish cohort. Female gender and higher BMI contributed to the impact on QoL in both cohorts and

should be considered in future multinational intervention studies in NAFLD.

THU-463

Clinical features of non-obese NAFLD: analysis of health check-up cohort

Shunsuke Sato¹, Hidehiko Kawai², Rifa Omu³, Yuji Kita³, Yuji Ikeda³, Sho Sato³, Ayato Murata³, Yuji Shimada³, Takuya Genda³. ¹Juntendo University Shizuoka Hospital, Gastroenterology and Hepatology, Shizuoka, Japan; ²Fuji Town Medical Center, Shizuoka, Japan; ³Juntendo University Shizuoka Hospital, Gastroenterology and Hepatology, Shizuoka, Japan
E-mail: syusato@juntendo.ac.jp

Background and aims: Non-alcoholic fatty liver disease (NAFLD) is commonly associated with obesity, but it is increasingly being recognized in non-obese individuals, particularly in Asia. We aimed to clarify the frequency and clinical features of non-obese NAFLD using a health check-up cohort.

Method: A total of 1046 subjects underwent a quantitative evaluation of liver steatosis (attenuation: ATT) and fibrosis (shear wave elastography: SWE) using ARIETTA 850SE (Fujifilm Healthcare) in 2020. Among them, 7 with obvious chronic liver disease and 22 who consumed >60 g alcohol/day were excluded. Finally, 1017 subjects were enrolled. Non-obese was defined as BMI <25 kg/m². Based on previous studies, cut of values for steatosis were S1 (0.62), S2 (0.67), and S3 (0.73), and NAFLD was defined as ≥0.62 dB/cm/MHz. In addition, cut of values for fibrosis were F1 (1.26), F2 (1.51), and F3 (1.63), and NAFLD with fibrosis was defined as ATT ≥0.62 dB/cm/MHz and SWE ≥1.26 KPa.

Results: The overall prevalence of NAFLD was 36.9%, while those for obese and non-obese subjects were 59.6% and 29.1%, respectively. Despite having a relatively normal BMI, most non-obese NAFLD versus normal liver subjects had a large waist circumference (80.0% vs. 9.9%) and dyslipidemia (59.5% vs. 42.1%). Logistic regression analysis revealed that dyslipidemia (OR = 1.898), ALT level (OR = 1.045), and GGT level (OR = 0.994), and platelet count (OR = 1.037) were significantly associated with liver steatosis. Dyslipidemia was present in 36.7% of the non-obese NAFLD subjects. Many obese NAFLD subjects showed abnormal liver function test (S1, 18.2%; S2 26.4%; S3 48.3%; P = 0.001), whereas most non-obese NAFLD subjects did not (S1, 6.1%; S2, 5.5%; S3, 10.4%; P = 0.241). Among the 220 non-obese NAFLD subjects, 62 (28.1%) presented liver fibrosis (F1, 20.5%; F2, 4.1%; F3, 2.5%) and a large waist circumference (22.6% vs. 10.1%), hypertension (38.7% vs. 25.9%), and diabetes (12.9 vs. 2.5%) versus those without fibrosis. Logistic regression analysis revealed that male sex (OR = 2.328), diabetes (OR = 3.928), and AST level (OR = 1.051) were significantly associated with fibrosis. The non-obese NAFLD subjects with diabetes had a high prevalence of liver fibrosis (52.5% vs. 28.4%). A high FIB-4 index (>1.30) was observed in many obese NAFLD subjects with fibrosis (F1, 26.2%; S2, 16.7%; S3, 55.6%; P = 0.002), but non-obese NAFLD subjects (F1, 33.3%; F2 22.2%; F3 28.6%; P = 0.267).

Conclusion: NAFLD was present in 29.1% of non-obese subjects and fibrosis was present in 28.1% of non-obese NAFLD subjects. Non-obese NAFLD was significantly associated with metabolic disorders. Our study findings suggest that the liver function test and FIB-4 index may be less useful in non-obese NAFLD.

THU-464

Sarcopenia is an independent risk factor for non-alcoholic fatty liver disease regardless of fat mass in men: 1:1 propensity score matching analysis

Jun-Hyuk Lee¹, Yu-Jin Kwon², Da-Hye Son^{2,3}, Eileen Yoon⁴, Sang Bong Ahn⁵, Dae Won Jun⁴. ¹Nowon Eulji Medical Center, Eulji University School of Medicine, Family medicine, Seoul, Korea, Rep. of South; ²Yongin Severance Hospital, Yonsei university college of medicine, Family medicine, Yongin-si, Korea, Rep. of South; ³Gangnam Severance Hospital, Yonsei university college of medicine, Family medicine, Seoul, Korea, Rep. of South; ⁴Hanyang university college of medicine, Internal medicine, Seoul, Korea, Rep. of South; ⁵Nowon Eulji Medical Center, Eulji University School of Medicine, Internal medicine, Seoul, Korea, Rep. of South
E-mail: dr486@eulji.ac.kr

Background and aims: Although sarcopenia is positively related to non-alcoholic fatty liver disease (NAFLD), it is unclear whether patients with sarcopenia is still at higher risk of NAFLD than normal people under the same fat mass. This study aimed to evaluate the association of low skeletal muscle mass index (LSMI) and NAFLD in Korean adults using 1:1 propensity score matching.

Method: Data from 2008–2010 Korean National Health and Nutrition Examination Survey was analyzed. Propensity score matching was applied using logistic regression with covariates including age, height-adjusted waist circumference, height-adjusted body fat mass, height-adjusted bone mass, total energy intake, physical activity, drinking status, and smoking status. LSMI was defined as height-adjusted skeletal muscle mass <7.0 kg/m² in men and <5.4 kg/m² in women using dual-energy X-ray absorptiometry. NAFLD was defined as NAFLD-liver fat score >−0.640. A total of 3098 adults (497 men with LSMI, 497 men without LSMI, 1052 women with LSMI, and 1052 women without LSMI) included in the study. Logistic regression analysis was performed to estimate odds ratio (OR) with confidence interval (CI) for NAFLD of people with LSMI compared with those without LSMI, separately in men and women.

Results: After propensity score matching, there were no differences in the mean values of age, height-adjusted waist circumference, height-adjusted body fat mass, height-adjusted bone mass, and total energy intake as well as the proportion of regular exerciser, current drinker, and current smokers between LSMI group and non-LSMI group in both men and women, unlike before propensity score matching. The prevalence rate of NAFLD was 33.5% in men and 20.4% in women, respectively. Men with LSMI had higher OR with 95% CI for NAFLD compared with men without LSMI (OR = 1.50; 95% CI: 1.13–1.98, p = 0.005) indicating that the average effect of the LSMI is to increase risk of NAFLD. There was no significant difference in OR with

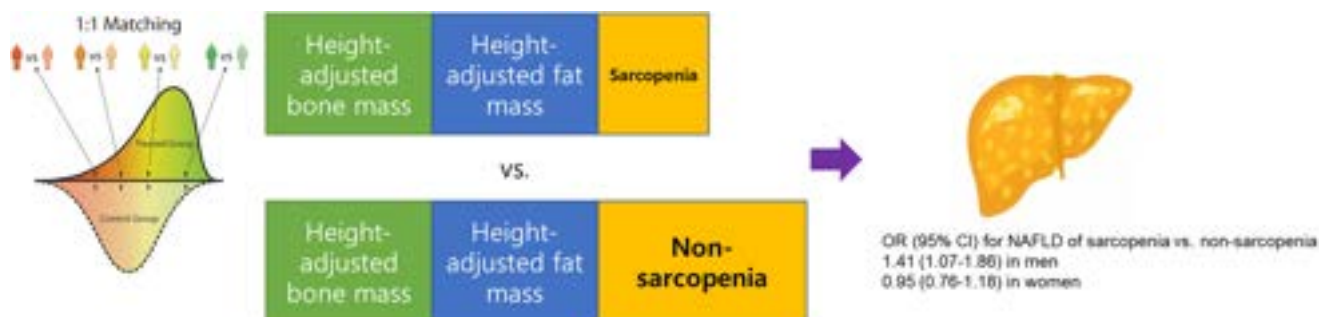


Figure: (abstract: THU-464).

POSTER PRESENTATIONS

95% CI for NAFLD between women with LSMI and those without LSMI (OR = 1.04; 95% CI: 0.84–1.30, $p = 0.721$).

Conclusion: LSMI was significantly related to NAFLD in men, not in women. This suggests that risk assessment for NAFLD may differ by gender, and such an assessment is particularly warranted for men with low muscle mass regardless of fat mass.

THU-465

Serum uric acid levels and prognosis of patients with non-alcoholic fatty liver disease

Su Lin^{1,1}, Yang Xinyi¹, Jiaofeng Huang¹, Chi Yujing¹. ¹The first affiliated hospital, Fujian medical university, China
E-mail: smer5129@fjmu.edu.cn

Background and aims: Uric acid (UA) is closely associated with non-alcoholic fatty liver disease (NAFLD). Previous studies have shown a significant association between hyperuricaemia and the development of NAFLD. However, it is unclear whether UA plays a predictive role in NAFLD prognosis. This study aimed to explore the relationship

between UA levels and mortality in NAFLD patients without severe renal disease.

Method: Data were obtained from the Third National Health and Nutrition Examination Survey (NHANES). The survey was performed in 1988–1994 and all individuals were followed up until December 2015 for survival status. A Kaplan-Meier survival curve was plotted to illustrate mortality between cohorts. X-tile was used to determine the best UA cut-off value to discriminate between survival and death. Time-dependent Cox regression was used to estimate the hazard ratio (HR) and 95% confidence interval (CI) for mortality. Propensity score matching (PSM) was applied to match age and sex, to balance the baseline characteristics between the two study groups.

Results: Overall, 2493 individuals with NAFLD and estimated glomerular filtration rate (eGFR) >60 ml/min/1.73 m² were included in this study. The mean age was 44.21 ± 15.03 years and 56.56% were male patients. The median follow-up period was 26.58 years. During this period, 849 (34.06%) deaths were recorded. The mean UA level was 325.63 ± 86.60 in the death group, which was significantly higher than that of the survival group (304.86 ± 84.17, $p < 0.001$). According

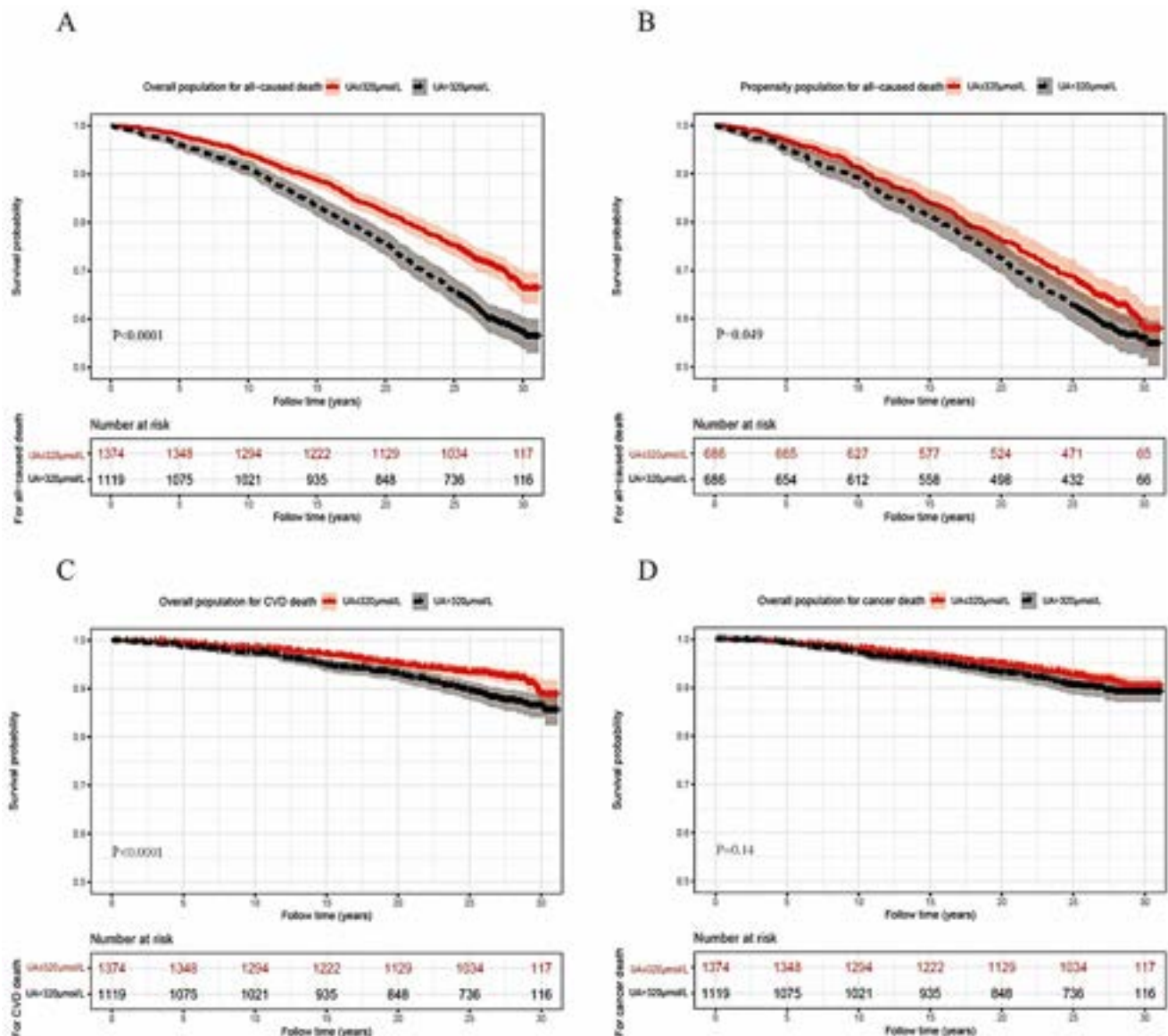


Figure 1: (abstract: THU-465): (A) Kaplan-Meier curve for overall death before PSM. (B) Kaplan-Meier curve for overall death after PSM. (C) Kaplan-Meier curve for cardiovascular-related death. (D) Kaplan-Meier curve for cancer-related death.

to the UA level, participants were classified into high-UA group (UA>320 $\mu\text{mol/L}$) and low-UA group ($\leq 320 \mu\text{mol/L}$). There were 1119 (44.89%) participants had a UA level >320 $\mu\text{mol/L}$. The high-UA group had a higher BMI level than the low-UA group. The death rate was 39.86% in high-UA group (>320 $\mu\text{mol/L}$), compared to 29.33% in low-UA group ($\leq 320 \mu\text{mol/L}$) ($p < 0.001$). Compared with low-UA group, patients in high-UA group tend to have more severe metabolic dysfunction. The survival probability between the two UA groups is illustrated as a Kaplan-Meier curve in Figure 1, indicating the association between baseline high UA levels and risk of death ($p < 0.001$). However, by the adjustment for the metabolic profiles, the effect of UA level on long-term outcome was no longer significant (All with a p value >0.05). Time-independent Cox regression also showed that UA level was not an independent risk factor for mortality in NAFLD patients without decreased eGFR ($>60 \text{ ml/min/1.73 m}^2$) ($p > 0.05$). After matching age and sex by using the propensity score matching method, UA remained not independently associated with death in NAFLD patients ($p > 0.05$). Similar results were found for cardiovascular-related and cancer-related deaths, showing the association between UA level and the risk of cause-specific death was dependent on metabolic confounders.

Conclusion: Although UA is closely related to NAFLD, UA levels are not independently associated with the long-term survival of patients

with NAFLD without decreased eGFR. Metabolic disorders may play a mediating role in the relationship between UA level and NAFLD outcome.

THU-466

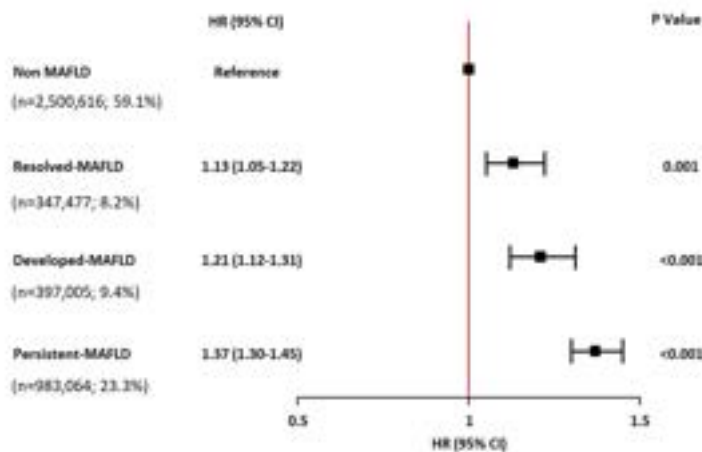
The risk of liver-related long term outcomes is altered by dynamic changes in metabolic dysfunction-associated fatty liver disease status: a nationwide cohort study

Min Kyung Park¹, Hye-Sung Moon², Sungwon Chung¹, Sungho Won^{2,3}, Yun Bin Lee¹, Eun Ju Cho¹, Jeong-Hoon Lee¹, Su Jong Yu¹, Jung-Hwan Yoon¹, Yoon Jun Kim¹. ¹Seoul National University College of Medicine, Department of Internal Medicine and Liver Research Institute, Korea, Rep. of South; ²RexSoft Inc., Korea, Rep. of South; ³Seoul National University, Department of Public Health Sciences, Graduate School of Public Health, Korea, Rep. of South
E-mail: yoonjun@snu.ac.kr

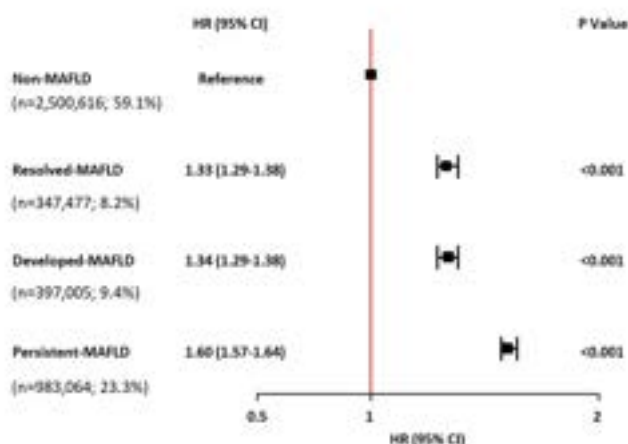
Background and aims: Metabolic dysfunction-associated fatty liver disease (MAFLD) status, defined by hepatic steatosis with metabolic dysfunction, could be dynamic changes by treatment such as lifestyle modification. We aimed to evaluate the association between the risk of MALFD long-term outcomes and changes in MAFLD status.

Method: We analyzed data from 4 228 162 participants who participated in health screening programs both in 2009 and 2013

A. Liver-related outcomes



B. Cardiovascular outcomes



C. Extrahepatic malignancy outcomes

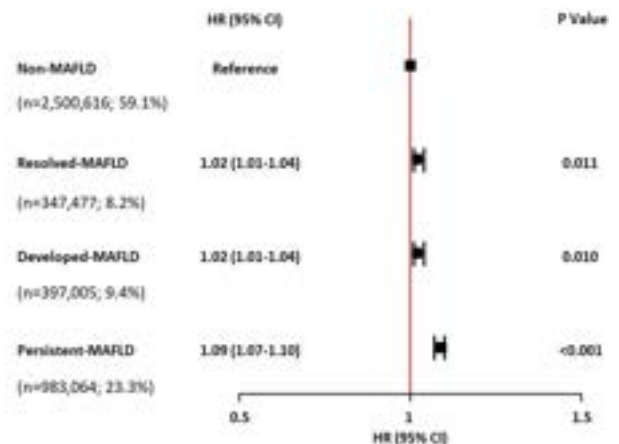


Figure: (abstract: THU-466).

POSTER PRESENTATIONS

using nationwide claims data from the National Health Insurance Service of South Korea. Participants were divided into four groups based on changes in MAFLD status from 2009 to 2013; non-MAFLD, resolved-MAFLD, developed-MAFLD, and persistent-MAFLD. The primary outcome was the incidence of liver-related complications, and the secondary outcomes were the incidence of cardiovascular complications and primary extrahepatic malignancy.

Results: During the median follow-up of 6.4 years (interquartile range, 6.1–6.6 years), 7828 patients (0.2%) developed liver-related complications. The persistent-MAFLD group had significant higher risk of liver-related complication compared to non-MAFLD group (adjusted hazard ratio [aHR] = 1.37; 95% confidence interval [CI] = 1.30–1.45; $P < .001$; Figure 1A), followed by the developed-MAFLD group (aHR = 1.21; 95% CI = 1.12–1.31; $P < .001$; Figure 1A) and resolved-MAFLD group (aHR = 1.13; 95% CI = 1.05–1.22; $P < .001$; Figure 1A). Interestingly, the recovered MAFLD group showed a significantly lower risk of liver-related outcomes compared to the persistent MAFLD group (aHR = 0.82; 95% CI = 0.76–0.89; $P < .001$). The risk of cardiovascular complications and the risk of primary extrahepatic malignancy were also higher in the persistent-MAFLD than non-MAFLD group (aHR = 1.60; 95% CI = 1.57–1.64; $P < .001$; Figure 1B, aHR = 1.09; 95% CI = 1.07–1.10; $P < .001$; Figure 1C, respectively). On the sensitivity analysis after excluding underlying liver disease, the persistent MAFLD group maintained a significantly higher risk of liver-related complication than the non-MAFLD group (aHR = 1.37; 95% CI = 1.29–1.46; $P < .001$).

Conclusion: Patients with persistent MAFLD status showed a higher risk of liver-related complications than non-MAFLD patients. Patients with newly developed MAFLD also had a higher risk of liver-related complications than patients who never experienced the MAFLD, while resolved MAFLD status could ameliorate the risk of liver-related complications.

THU-467

Dietary patterns associated with metabolic associated fatty liver disease protection

Simon Schophaus¹, Kate Townsend Creasy², Jan Clusmann¹, Alexander Koch¹, Christian Trautwein¹, Kai Markus Schneider¹, Carolin Victoria Schneider¹. ¹RWTH Aachen University, Medizinische Klinik III, Aachen, Germany; ²University of Pennsylvania, Philadelphia, United States

E-mail: cheimes@ukaachen.de

Background and aims: Metabolic-associated fatty liver disease (MAFLD) is characterised by lipid droplet accumulation in the hepatocytes and affects approximately 20–30% of the general population. High caloric western style diet is a well-established risk factor for MAFLD. However, there is little data that the consumption of specific nutrients might help prevent MAFLD development in the general population.

Method: We analyzed the UK Biobank (ID 71300) dataset and selected our study population based on the availability of nutritional assessment (five questionnaires). We excluded patients with liver diseases diagnosed before the food questionnaires. We investigated the association between nutrients calculated from food questionnaires and MAFLD development during the 11-year follow-up (ICD code and 39 000 MRI images of the liver) in the first nutrient-wide association study–“Nutri-WAS.” All analyses are corrected for age, sex, BMI, Townsend index for socioeconomic status, kcal, alcohol, protein intake, fat intake, carbohydrate intake, and for multiple testing.

Results: Data from >210 000 participants demonstrate despite confirming known associations (e.g., Vitamin E or Fructose) that among 50 tested nutrients, manganese showed the strongest protection from liver fat on MRI (Figure 1A). We demonstrate that increased dietary manganese intake was associated with a lower prevalence of MAFLD. Each standard deviation (SD) manganese increase intake reduced the association of MAFLD ICD-10 diagnosis (K76.0) by 14.9% ($p < 0.0001$) and a reduced MRI diagnosis of MAFLD

by 17.2% ($p < 0.0001$). In addition, there was a significant effect of manganese on metabolomics data, which were available in >49 000 individuals (Figure 1B) and showed an association with reduced VLDL secretion.

Conclusion: Our study showed that increased dietary manganese intake may be beneficial for preventing MAFLD. Randomized clinical trials are needed to confirm the beneficial effects of manganese for MAFLD prevention.

Multivariable Nutrient wide association study for liver fat >5% on MRI.

Manhattan plot of adjusted log₁₀ (P values) for all nutrients (n = 50) comparing liver fat >5% on MRI per SD increase for each nutrient adjusted for age, sex, body mass index, kcal/day, alcohol/day, fat/day, carbohydrates/day, protein/day, and Townsend socioeconomic status index. Highlighted are associations results with P values <10^{−7}.

Associations of metabolic biomarkers with manganese intake among >49 000 participants

Hazard ratios (with 95% confidence intervals) are presented per 1-SD higher metabolic biomarker on the natural log scale, stratified by age, sex, body mass index, alcohol consumption/day, fat/day, carbohydrates/day, protein/day, and Townsend socioeconomic status index.

*False discovery rate-controlled $p < 0.01$. DHA, docosahexaenoic acid; FA, fatty acids; Faw3, omega-3 fatty acids; Faw6, omega-6 fatty acids; HDL-D, high-density lipoprotein particle diameter; LA, linoleic acid; LDL, low-density lipoproteins; LDL-D, low-density lipoprotein particle diameter; LP, lipoprotein; MUFA, monounsaturated fatty acids; PUFA, polyunsaturated fatty acids; SFA, saturated fatty acids; VLDL-D, very low-density lipoprotein particle diameter; (original code by Diego J Aguilar-Ramirez).

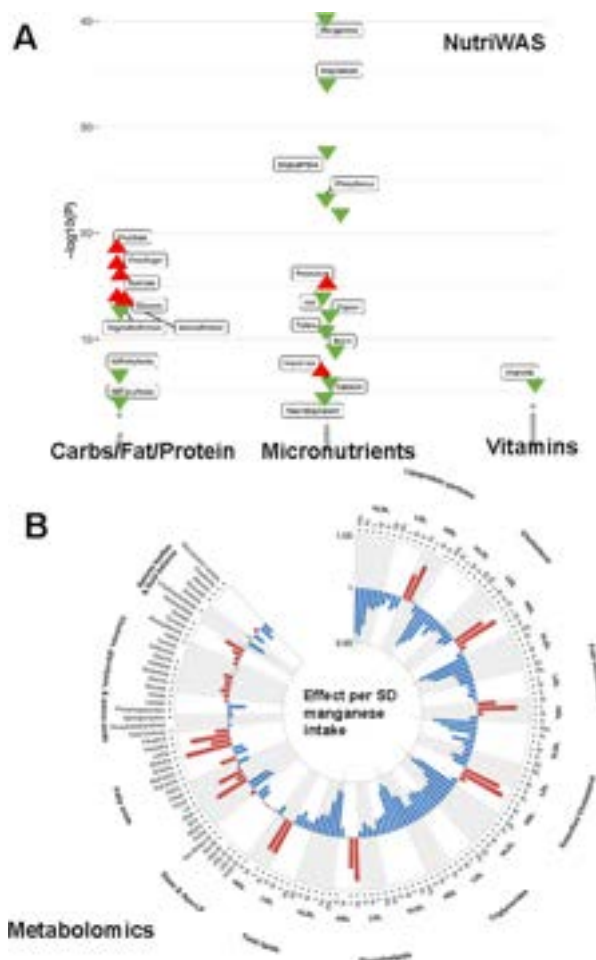


Figure:

THU-468

Rheological properties of bile in patients with non-alcoholic steatohepatitis with and without obesity

Olena Barabanchyk¹, Iryna Biriuchenko², Volodymyr Bulda¹.
¹Educational and Scientific Centre "Institute of Biology and Medicine" of Taras Shevchenko National University of Kyiv, Internal Medicine, Kyiv, Ukraine; ²Bogomolets National Medical University, Internal Medicine, Ukraine
 E-mail: alenabarabanchyk@gmail.com

Background and aims: Studies have shown that changes in the synthesis and composition of bile acids can potentiate hepatotoxicity through anti-inflammatory mechanisms, membrane damage or cytotoxicity, leading to severe liver fibrosis [1, 2]. Our aim was to assess the changes in bile acids (BA) profile in patients with non-alcoholic steatohepatitis (NASH) with and without obesity compared to healthy controls.

Method: Three study arms were formed: 1st arm-NASH with obesity, 2nd arm-NASH without obesity, 3rd arm-healthy controls. Although liver biopsy is the gold standard for the NASH diagnosis, the vast majority of patients refrained from biopsy. So the diagnosis of NASH was established based on the following criteria: 1) non-alcoholic aetiology (less than 20 g ethanol per day), 2) detection of steatosis by ultrasound imaging, 3) exclusion of other liver diseases. The obesity was considered if BMI was 30 or higher. The bile was obtained after intubation of the duodenum under the ultrasound control. The spectrum of BA and bile properties were assessed using photo-calorimetry. To evaluate the colloidal stability of the bile the cholate-cholesterol ratio (CCR), the ratio of taurochenodeoxycholic acid (TCDCA) and taurodeoxycholic acid (TDCA) to taurocholic acid (TCA) and the ratio of glycochenodeoxycholic acid (GCDCA) and glycodeoxycholic acid (GDCA) to glycocholic acid (GCA) were calculated.

Results: 67 adult patients (21–55 years, males 26 (38.8%)) were included into the study. Of these, 29 patients were allocated to the 1st arm, 23 patients to the 2nd arm, and 15 healthy controls to the 3rd one. The groups were statistically comparable in age and sex. The bile of healthy patients predominantly consisted of BA conjugated with glycine. The level of tauroconjugates varied between 15–20% of the total amount of BA. Free trihydroxycholanolic and dihydroxycholanolic BA were presented in approximately the same concentrations. The analysis of BA in patients of the 1 and 2 study groups showed the following: levels of cholic acid (CA) were much increased in patients of the 1 arm, but slightly decreased in case of NASH only. Deoxycholic acid (DCA) was increased both in groups 1 and 2. The levels of TCA were decreased in patients of the 1 arm, but slightly increased in the 2 arm, and the levels of GCA were decreased in both groups compared to the 3 group. Free bile cholesterol which was increased in arms 1 and 2. Cholate-cholesterol ratio (CCR) was significantly decreased in patients with NASH (1 and 2 arms) comparing to the group 3 ($p < 0.001$). But the ratios of TCDCA + TDCA to TCA and GCDCA + GDCA to GCA were decreased only in the 1st group ($p < 0.05$).

Parameters	1 arm mg/%	2 arm mg/%	3 arm mg/%	p
CA	39.65 ± 1.4	7.4 ± 0.8	16.7 ± 1.1	$p < 0.05$
DCA	48.45 ± 1.9	35.3 ± 8.2	21.5 ± 1.07	$p < 0.05$
GCA	238.7 ± 4.3	183.5 ± 2.3	347.6 ± 3.9	$p < 0.05$
TDCA	62.7 ± 2.1	172.3 ± 1.7	115.8 ± 2.5	$p < 0.05$
Free bile cholesterol	141.3 ± 2.6	98.28 ± 2.20	83.26 ± 2.5	$p < 0.001$

Figure:

Conclusion: Our data suggest that changes of rheological properties of bile in patients with NASH especially in association with obesity

may possibly lead to the increased lithogenicity of bile thus enhancing the risks of gallstones formation.

THU-469

Risk factors for significant fibrosis in non-obese Asian patients with NAFLD

Jae Yoon Jeong¹, Ju-Yeon Cho², Jung Hee Kim³, Yong Kyun Cho⁴, Byung Ik Kim⁴, Won Sohn⁴. ¹National Medical Center, Korea, Rep. of South; ²Chosun University Hospital, Korea, Rep. of South; ³Hallym University Dongtan Sacred Heart Hospital, Korea, Rep. of South; ⁴Kangbuk Samsung Hospital, Sungkyunkwan University School of Medicine, Korea, Rep. of South
 E-mail: hand0827@naver.com

Background and aims: It is unclear which risk factors are associated with hepatic fibrosis in non-obese patients with non-alcoholic fatty liver disease (NAFLD). This study aimed to investigate the risk factors for significant liver fibrosis in non-obese Asian patients with NAFLD including body mass index (BMI).

Method: A cross-sectional study was conducted using nationally representative samples from the Korean National Health and Nutrition Examination Survey 2012–2019. A total of 1200 Korean patients with NAFLD and BMI <25 kg/m² were enrolled in the study. NAFLD was defined as hepatic steatosis index ≥ 36 . Liver fibrosis was assessed using Fibrosis-4 (FIB-4) index. The significant liver fibrosis was defined as FIB-4 index was more than 1.3. We classified into lean NAFLD (BMI <25 kg/m²) and overweight NAFLD (BMI 23–25 kg/m²). Univariable and multivariable logistic regression analyses were done to assess the risk factors including lean and overweight for significant liver fibrosis in patients with NAFLD.

Results: The mean age was 51 years and 47% ($n = 560$) was male sex. The proportion of significant fibrosis was 14% ($n = 169$). They consisted of 20% ($n = 236$) of lean NAFLD and 80% ($n = 964$) of overweight NAFLD. There was no difference in age and sex between two groups. However, the prevalence of hypertension and visceral obesity were higher in overweight NAFLD than in lean NAFLD (all $p < 0.05$). A univariable analysis indicated that overweight NAFLD was associated with significant fibrosis compared to lean NAFLD (odds ratio [OR] 1.86 with 95% confidence interval [CI]: 1.15–3.00, $p = 0.012$). However, a multivariable analysis showed that there was no difference in significant difference between two groups (OR 1.37 with 95% CI: 0.82–2.30, $p = 0.231$). On the other hand, significant fibrosis was associated with other metabolic factors in the multivariable analysis: visceral obesity (OR 2.12 with 95% CI: 1.45–3.09, $p < 0.001$), diabetes mellitus (OR 3.19 with 95% CI: 2.17–4.68, $p < 0.001$), and hypertension (OR 2.91 with 95% CI: 2.01–4.22, $p < 0.001$).

Conclusion: BMI is not a risk factor for significant fibrosis in non-obese Asian patients with NAFLD. However, metabolic factors such as visceral obesity, diabetes, and hypertension are associated with liver fibrosis in non-obese Asian patients with NAFLD.

THU-470

Impact of PNPLA3 rs738409 single nucleotide polymorphism and carbohydrate intake for the personalized management of patients with non-alcoholic fatty liver disease

Nuria Pérez Díaz del Campo¹, Eleonora Dileo¹, Gabriele Castelnovo¹, Chiara Rosso¹, Gian Paolo Caviglia¹, Daphne D'Amato¹, Amina Abdulle¹, Marta Guariglia¹, Angelo Armandi^{1,2}, Kamela Gjini¹, Irene Poggolini¹, Antonella Olivero¹, Maria Lorena Abate¹, Giorgio Maria Saracco^{1,3}, Elisabetta Bugianesi^{1,3}. ¹University of Turin, Department of Medical Sciences, Turin, Italy; ²University Medical Center of the Johannes Gutenberg-University, I. Department of Medicine, Mainz, Germany; ³Città della Salute e della Scienza-Molinette Hospital, Gastroenterology Unit, Turin, Italy
 E-mail: nuria.perezdzdelcampo@unito.it

Background and aims: The Patatin-like phospholipase domain-containing 3 (PNPLA3) rs738409 single nucleotide polymorphism (SNP) is one of the major genetic determinant of non-alcoholic fatty

POSTER PRESENTATIONS

liver disease (NAFLD) and is strongly regulated by changes in energy balance and dietary factors. We aimed to investigate the association between the *PNPLA3* rs738409 SNP, nutrient intake and NAFLD severity.

Method: *PNPLA3*-rs738409 SNP was genotyped in 181 patients with NAFLD who completed the EPIC Food Frequency Questionnaire. Liver steatosis was evaluated by Controlled Attenuation Parameter (CAP) (Fibroscan®530, Echosens). According to the established cut-off, a CAP value ≥ 300 dB/m was used to identify severe steatosis (S3). An independent group of 47 biopsy-proven NAFLD subjects was used as validation cohort.

Results: Overall, median age was 53 years (range 44–62) and 60.2 % of patients were male. Most subjects (56.3 %) had S3 and showed increased liver stiffness ($p < 0.001$), AST ($p = 0.003$) and ALT levels ($p < 0.001$) compared to those with CAP < 300 dB/m. At logistic regression analyses we found that the interaction between carbohydrates intake and the carriers of the *PNPLA3* G risk allele was significantly associated with S3 ($p = 0.001$). The same result was confirmed in the validation cohort, where the interaction between high carbohydrate intake (48%) and *PNPLA3* SNP was significantly associated with steatosis $\geq 33\%$ ($p = 0.017$) and with advanced fibrosis ($\geq F3$) ($p = 0.058$).

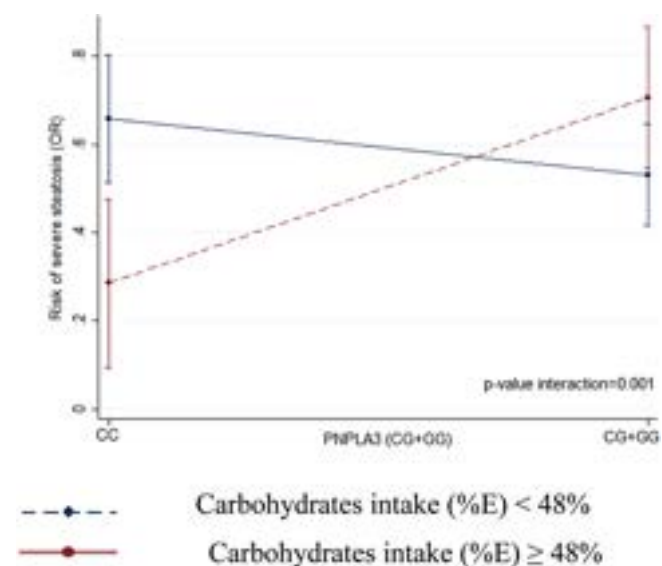


Figure: Impact of the *PNPLA3* rs738409 polymorphism on carbohydrates intake on the risk for severe steatosis (CAP ≥ 300 dB/m). The model was adjusted by sex, age, energy intake, protein intake, fat intake and diabetes.

Conclusion: The intake of greater than or equal to 48 % carbohydrate in NAFLD patients carriers of the CG/GG allele of *PNPLA3* rs738409 may increase the risk of significant steatosis.

This work has received support from EU/EFPIA/IM2 Joint Undertaking (LITMUS grant no. 777377) and Italian Ministry for Education,

University and Research (MIUR) under the programme “Dipartimenti di Eccellenza 2018–2022” n. D15D18000410001.

THU-471

Diabetes mellitus (DM) is the strongest risk factor of significant inflammation or fibrosis in chronic hepatitis B (CHB) combined with non-alcoholic fatty liver disease (NAFLD)

Jie Li¹, Fajuan Rui¹, Brian Nguyen², Chuanwu Zhu³, Yuanwang Qiu⁴, Weimao Ding⁵, Qi Zheng⁶, Qing-Lei Zeng⁷, Zebao He⁸, Junping Shi⁹, Chao Wu¹, Mindie Nguyen². ¹Department of Infectious Diseases, Nanjing Drum Tower Hospital, The Affiliated Hospital of Nanjing University Medical School, Nanjing, Jiangsu, China, China; ²Division of Gastroenterology and Hepatology, Stanford University Medical Center, Palo Alto, CA, USA, United States; ³Department of Infectious Diseases, The Affiliated Infectious Diseases Hospital of Soochow University, Suzhou, Jiangsu, China, China; ⁴Department of Infectious Diseases, The Fifth People's Hospital of Wuxi, Wuxi, Jiangsu, China, China; ⁵Department of Hepatology, Hua'an No. 4 People's Hospital, Hua'an, Jiangsu, China, China; ⁶Department of Hepatology, Hepatology Research Institute, the First Affiliated Hospital, Fujian Medical University, Fuzhou, China, China; ⁷Department of Infectious Diseases, The First Affiliated Hospital of Zhengzhou University, Zhengzhou, Henan, China, China; ⁸Department of Infectious Diseases, Taizhou Enze Medical Center (Group) Enze Hospital, Taizhou, Zhejiang, China, China; ⁹Department of Infectious Diseases, The Affiliated Hospital of Hangzhou Normal University, Hangzhou, Zhejiang, China, China
E-mail: mindiehn@stanford.edu

Background and aims: Chronic hepatitis B (CHB) patients and non-alcoholic fatty liver disease (NAFLD) frequently co-exist, but the association of diabetes mellitus (DM) with hepatic inflammation and fibrosis is not well characterized. The aim of this study is to investigate the association of DM with significant hepatic inflammation and/or fibrosis in CHB patients combined with NAFLD.

Method: We enrolled CHB patients with concurrent NAFLD who underwent liver biopsy from eight medical centers of China between April 2004 and October 2020. Univariable and multivariable logistic regression analyses were conducted to explore the association of DM with significant inflammation (grade [G] 2–4) and fibrosis (stage [S] 2–4).

Results: A total of 869 CHB patients with NAFLD with available liver histology data were included in study analysis (mean age 40.6 ± 10.4 years old, 79.9% male), with 71 (8.2%) having DM. The mean body mass index was 24.9 ± 3.3 kg/m² and the mean HBV-DNA was 5.3 ± 2.0 log₁₀ IU/ml. About half (380 patients, 46.3%) were HBeAg-positive, and 5.9% (42 patients) were on antiviral therapy. Moderate and severe FLD (grade 2–3) was present in 206 patients (24.3%). The majority (529 patients, 60.9%) had significant inflammation (G2–4), and about half (431, 49.6%) had significant fibrosis (F2–4). Compared with non-DM patients, DM patients more likely had significant inflammation (76.1% vs 59.7%, $P = 0.02$) or significant fibrosis (76.1% vs 47.3%, $P < 0.001$). On multivariable logistic analysis adjusting for DM, hepatic steatosis, age, sex, BMI, HBV DNA, and HBeAg, DM was independently associated with significant inflammation (OR: 3.38; 95% CI: 1.46–7.86; $P = 0.005$) and significant fibrosis (OR: 4.49; 95% CI: 2.08–9.72; $P < 0.001$) (Table).

Table: Factors associated with hepatic inflammation or fibrosis in hepatitis B patients

	Univariate analysis		Multivariate analysis	
	OR (95% CI)	P value	OR (95% CI)	P value
Inflammation Grade ≥ 2				
Diabetes Mellitus (%)	2.15 (1.224–3.774)	0.008	3.38 (1.455–7.858)	0.005
Steatosis (%)				
Grade 0–1	Referent	0.168	Referent	0.708
Grade 2–3	1.26 (0.908–1.737)		1.08 (0.711–1.652)	
Age (years)	1.00 (0.991–1.017)	0.57	1.01 (0.992–1.029)	0.266
Sex (%)	0.93 (0.663–1.308)	0.681	1.13 (0.729–1.743)	0.589
Body mass index (kg/m ²)	1.03 (0.989–1.082)	0.144	1.03 (0.975–1.090)	0.278
HBV DNA (Log ₁₀ IU/ml)	1.14 (1.056–1.225)	0.001	1.09 (0.971–1.217)	0.148
HBeAg positive (%)	1.68 (1.265–2.229)	<0.001	1.81 (1.131–2.899)	0.013
Fibrosis Stage ≥ 2				
Diabetes Mellitus (%)	3.55 (2.021–6.226)	<0.001	4.49 (2.079–9.717)	<0.001
Steatosis (%)				
Grade 0–1	Referent	0.732	Referent	0.949
Grade 2–3	0.95 (0.693–1.294)		0.99 (0.657–1.482)	
Age (years)	1.01 (1.001–1.027)	0.032	1.02 (1.002–1.039)	0.031
Sex (%)	0.86 (0.620–1.20)	0.381	1.02 (0.668–1.567)	0.917
Body mass index (kg/m ²)	0.99 (0.950–1.037)	0.736	0.98 (0.928–1.033)	0.434
HBV DNA (Log ₁₀ IU/ml)	0.99 (0.925–1.065)	0.83	0.85 (0.764–0.954)	0.005
HBeAg positive (%)	1.33 (1.010–1.747)	0.042	2.53 (1.578–4.042)	<0.001

Figure:

Conclusion: CHB patients with DM was more than 3 times more likely to have significant hepatic inflammation and more than 4 times more likely to have significant fibrosis compared to non-DM patients, independent of the presence of hepatitis steatosis, other metabolic (body mass index), viral and demographic factors. DM should be considered as part of the algorithm for CHB management.

THU-472

PNPLA3 I148M polymorphism does not promote liver disease progression in severe alpha1-antitrypsin deficiency

Ines Volkert¹, Malin Fromme¹, Huan Su², Nurdan Gueldiken¹, Mohamed Ramadan Mohamed¹, Cecilia Lindhauer¹, Pavel Strnad³, Christian Trautwein². ¹RWTH Aachen University hospital, Medical department III, Aachen, Germany; ²RWTH Aachen University hospital, Medical department III, Aachen, Germany; ³RWTH Aachen University hospital, Medical department III, Aachen, Germany
E-mail: ivolkert@ukaachen.de

Background and aims: Alpha-1 antitrypsin (AAT) deficiency (AATD) is one of the most common genetic disorders. A homozygous PiZ mutation in the AAT gene (called PiZZ genotype) is the predominant cause of severe AATD and predisposes to lung and liver damage. Non-alcoholic fatty liver disease (NAFLD) comprises a disease spectrum ranging from steatosis to cirrhosis, inflammation and hepatocellular carcinoma (HCC). The most established genetic risk factor for NAFLD is the patatin-like phospholipase domain containing protein 3 (PNPLA3) I148M that promotes disease progression. This polymorphism is characterized by a substitution of isoleucine to methionine at position 148 (I148M). The aim of the study was to evaluate the interaction between the PNPLA3 and the PiZ variants.

Method: Mice carrying the human PiZ variant and the PNPLA3 I148M polymorphism were generated (PiZ/PNPLA3I148M), characterized at the age of 8 and 52 weeks and compared to WT, PiZ and PNPLA3I148M controls. The mice were subjected to a Western-style Diet (WSD) for 24 weeks to assess the effects on NASH progression. The presence of PNPLA3 I148M polymorphism was evaluated in peripheral blood-derived DNA from 478 Pi*ZZ subjects participating in the European AATD registry.

Results: At weeks 8 and 52, PiZ mice showed higher transaminases than WT and PNPLA3I148M animals, but no difference to PiZ/

PNPLA3I148M group was seen. At 52 weeks of age, the PiZ and PiZ/PNPLA3I148M mice showed significantly stronger fibrosis than WT and PNPLA3I148M mice, but no difference between both PiZ subgroups was seen. After WSD, no changes in the liver physiology nor fibrogenesis or inflammatory parameters were noted. Neither PiZ expression nor accumulation was altered by the presence of PNPLA3I148M or through WSD feeding.

In the analyzed Pi*ZZ subjects, PNPLA3 I148M variant was found at the expected Mendelian ratio. The carriers displayed significantly increased GLDH values and more often had elevated ALT and bilirubin levels. However, there was no difference in transient elastography-based liver fibrosis and steatosis measurements.

Conclusion: Our results demonstrate that the presence of the PNPLA3 I148M polymorphism does not play a major role in progression of AATD-associated liver disease in mouse and humans.

THU-473

Frailty in metabolic dysfunction-associated fatty liver disease is related to the presence of diabetes and the severity of liver fibrosis

Alexis Goffaux¹, Guillaume Henin^{1,2}, Audrey Loumaye³, Géraldine Dahlqvist², Nicolas Lanthier^{1,2}. ¹Université catholique de Louvain, Laboratory of Hepato-Gastroenterology, Institut de Recherche Expérimentale et Clinique, Brussels, Belgium; ²Cliniques universitaires Saint-Luc (UCLouvain), Service d'Hépatogastroentérologie, Bruxelles, Belgium; ³Cliniques universitaires Saint-Luc (UCLouvain), Service d'Endocrinologie et de nutrition, Brussels, Belgium
E-mail: nicolas.lanthier@saintluc.uclouvain.be

Background and aims: Frailty is very common in end-stage liver disease, regardless of disease etiology, and has a significant impact on clinical outcome and quality of life, due to impaired skeletal muscle function, quality and quantity. However, there are few data available on the relationship between liver and skeletal muscle, especially in patients with earlier disease stages. Our aims are to evaluate the prevalence of frailty in a prospective cohort of patients with metabolic-dysfunction associated fatty liver disease (MAFLD) according to its severity.

Method: Patients with MAFLD were recruited in a prospective single-center cohort study. Epidemiological, clinical, biological and anthropometric data were collected. All patients underwent a non-invasive assessment for frailty screening, including a dominant hand grip strength test, a balance test, and the time required to do five times sit to stand to calculate the liver frailty index (LFI). The severity of MAFLD was assessed by the fatty liver index (FLI), fibrosis 4 (FIB-4) index, and by transient elastography (elasticity and controlled attenuation parameter).

Results: 92 patients with MAFLD were recruited, including 44 men (47.8 %) and 44 patients with type 2 diabetes (47.8 %). Mean age was 55 years (19–78), mean BMI was 32.7 kg/m² (23.9–47.5) and mean HOMA-IR was 7.6 (0.5–30.1). Regarding the severity of MAFLD, the mean elasticity was 6.45 KPa (3.1–35) and the mean FIB-4 score was 1.33 (0.31–5.61). The mean FLI was 85.1 (28–100) and the mean controlled attenuation parameter (CAP) was 332.3 dB/m (207–400). Regarding frailty parameters, the mean dominant grip strength was 31 kg (8–62), the mean time to do five chair stands was 8.2 seconds (4.25–24.25), the mean balance test score was 9.9 seconds (2.1–10) and the mean LFI was 2.98 (1.13–4.71). 51 patients had an LFI score <3 (robust group, 56 %), 36 had a score between 3 and 4.5 (pre-frail group, 39.6 %), and 4 had a score greater than 4.5 (frail group, 4.4 %). No correlation was observed between the degree of steatosis (assessed by the FLI or CAP values) and frailty. In contrast, a significant increase in the level of frailty is observed in patients with type 2 diabetes (p=0.03) and with a high liver elasticity compatible with an F4 stage (mean LFI: 3.7 vs 2.9, p=0.0078) (Figure), independent of age. Frailty is also significantly higher according to the FIB-4 index with a mean LFI of 3.72 in case of FIB-4 >2.67 vs 2.8 in case of FIB-4 <1.3 (p=0.042) (Figure).

POSTER PRESENTATIONS

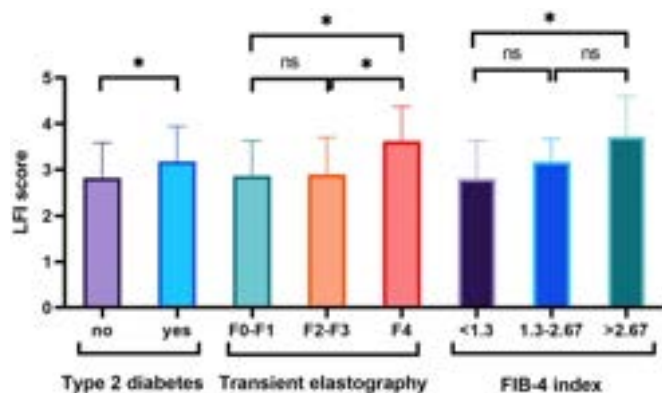


Figure:

Conclusion: 44% of MAFLD patients already have a frail or pre-frail status regardless of age. This reduction of strength is associated with the presence of diabetes and the severity of MAFLD in terms of fibrosis. Further research is needed to determine the cause of this frailty and its potential impact on liver disease severity and prognosis.

THU-474

Significant fibrosis is a risk factor for worse health perception and impaired mental health in people living with HIV

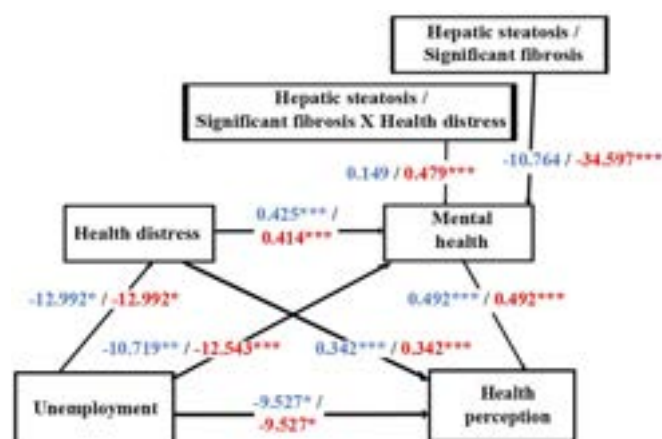
Jesús Funuyet-Salas¹, Maurice Michel^{2,3}, María Angeles Pérez-San-Gregorio¹, Agustín Martín-Rodríguez¹, Manuel Romero Gomez⁴, Peter Galle², Martin Sprinzl², Jörn Schattenberg^{2,3}. ¹Department of Personality, Assessment, and Psychological Treatment, Faculty of Psychology, University of Seville, Seville, Spain, Spain; ²I. Department of Medicine, University Medical Center Mainz, Mainz, Germany, Germany; ³Metabolic Liver Research Program, I. Department of Medicine, University Medical Center Mainz, Mainz, Germany; Germany; ⁴Digestive diseases unit, Virgen del Rocío University Hospital. SeLiver group at Institute of Biomedicine of Seville (IBIS). University of Seville, Spain, Spain
E-mail: jfunuyet1@us.es

Background and aims: Significant fibrosis has been shown to be a critical factor for the biopsychosocial profile of patients with chronic liver disease. However, the role of significant fibrosis in models predicting health perception and mental health in people living with human immunodeficiency virus (PLWH) remains unknown. We aimed to evaluate 1) if health distress and mental health mediated the relationship between unemployment and health perception, 2) if social functioning mediated the relationship between lower education and mental health, and 3) if hepatic steatosis or fibrosis exerted a moderating effect in both relationships.

Method: Two hundred and seven PLWH (147 male and 60 female, mean age 51 ± 12) were evaluated using the MOS-HIV instrument, which assesses ten dimensions of quality of life. Vibration-controlled transient elastography was used to assess hepatic steatosis and significant fibrosis by measuring the controlled attenuation parameter (≥ 275 dB/m) and liver stiffness measurement (≥ 8.2 kPa), respectively. Mediation and moderated mediation models were estimated using the SPSS PROCESS macro v3.5. Bootstrapping was used to test the indirect effects estimated, considered significant when the confidence interval (CI) at 95% did not include 0.

Results: Health distress and mental health mediated the association between unemployment and health perception (effect = -3.00 , CI = -6.07 to -0.13). Social functioning mediated the association between lower education and mental health (effect = 4.37 , CI = 1.31 to 7.82). Significant fibrosis exerted a moderating effect on both relationships (health perception, beta = 0.48 , $p = 0.001$; mental health, beta = 0.48 , $p = 0.001$), but hepatic steatosis did not (Figure). The indirect conditional effects of unemployment and lower education on health perception and mental health, respectively, were higher in

patients with significant fibrosis than in those who did not have significant fibrosis.



Moderator: Hepatic steatosis

Moderator: Liver fibrosis

Figure:

Conclusion: Unemployment was related to health distress and poorer mental health, which in turn predicted worse self-perceived health in PLWH. Lower education was linked to lower social functioning, which predicted poorer mental health. Specifically, PLWH with significant fibrosis were more vulnerable to the negative effects of unemployment and lower education on health perception and mental health. Our results confirmed liver fibrosis as a risk factor to be considered in future multidisciplinary interventions in PLWH.

THU-475

Caloric input is inadequate in predicting the presence of liver steatosis and fibrosis in a population adhering to a screening program for metabolic syndrome

Lucia Brodosi^{1,2}, Michele Stecchi¹, Valentino Osti^{1,3}, Valeria Guarneri¹, Michela Genovese¹, Francesca Marchignoli², Dorina Mita¹, Maximiliano Zioutas², Maria Letizia Petroni^{1,2}, Loris Pironi^{1,2}. ¹University of Bologna, Department of Medical and Surgical Sciences, Italy; ²IRCCS AOUBO, Clinical Nutrition and Metabolism Unit, Italy; ³Azienda USL di Bologna, Department of Public Health, Italy
E-mail: lucia.brodosi2@unibo.it

Background and aims: Non-Alcoholic Fatty Liver Disease (NAFLD) is the liver manifestation of metabolic syndrome (MetS) and can progress to steatohepatitis (NASH). Scores could be calculated to predict the risk of NAFLD and liver fibrosis (LF) in a non-invasive way. The most used ones are Fibrosis-4 (FIB-4), NAFLD Fibrosis Score (NFS), Fatty Liver Index (FLI) and FibroScan[®] (FAST). In addition, FibroScan[®] allows evaluating steatosis through Controlled Attenuation Parameter (CAP) and LF. An essential link between NASH and MetS is obesity, resulting from a chronic positive caloric balance due to a caloric input (CI) greater than caloric output (CO). Precise CI assessment represents a challenge in clinical practice and usually requires a 1-to-1 inpatient visit with a dietitian; we previously developed Quanto Mangio Veramente (QMV), a questionnaire that easily allows estimating the daily CI. This work aimed to evaluate a possible link between CI, FibroScan results, and non-invasive steatosis and fibrosis scores.

Method: from 2020 to 2022, we screened patients for MetS according to National Cholesterol Education Program criteria. For each patient, weight, Body Mass Index (BMI), and Basal Metabolic Rate (BMR) were collected. We also administered QMV and performed Fibroscan[®]. FIB-4, NFS, FLI, FAST and Caloric Surplus (CS, obtained from CI-BMR) were

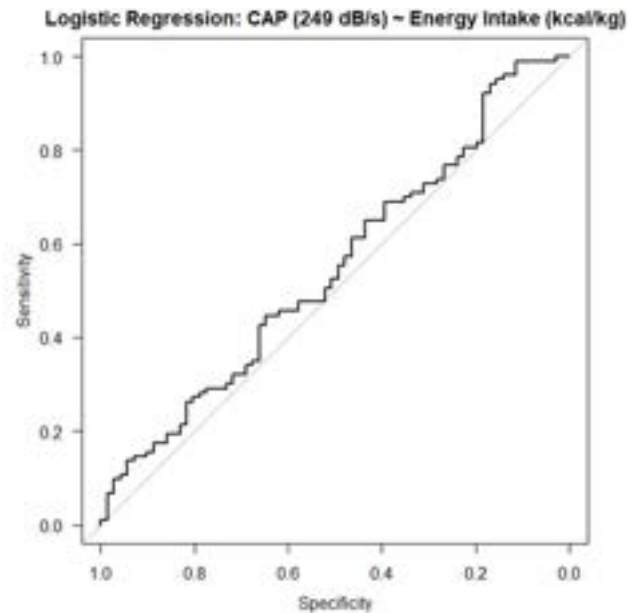
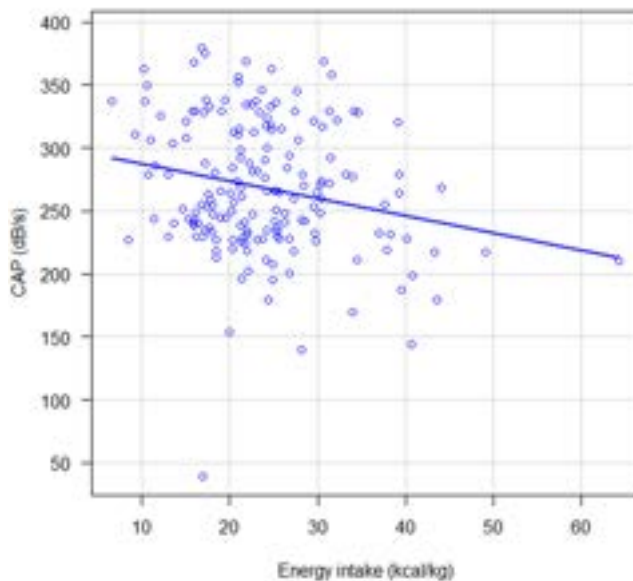


Figure: (abstract: THU-475).

calculated for each patient. For Statistics: median \pm IQR, and AUROCs are reported with a 95% confidence interval.

Results: 189 consecutive non-cirrhotic patients were included in the study, 80 with and 99 without MetS. CI and CS, even when normalized by weight or BMI, did not correlate to any of the criteria for MetS, nor to FAST, FIB-4, FLI and NFS, and they did not differ significantly after grouping by MetS diagnosis. We observed a weak inverse correlation between CAP and CI normalized by weight or BMI, by -21.8% ($p < 0.01$) and -18.3% ($p < 0.05$), respectively, suggesting that people with a higher steatosis degree ingested fewer calories (kcal/kg). The same degree of inverse correlation was present after grouping by MetS diagnosis in the group with the syndrome ($p < 0.01$). When considering a cut-off of 249 dB/s for liver steatosis diagnosis, CI and its normalizations did not translate into mathematically appropriate regression models and AUROCs; the same results were obtained after grouping by liver steatosis categories according to CAP.

Conclusion: Our work does not support using QMV to predict NAFLD or LF in healthy and MetS subjects. We hypothesize that adaptive mechanisms, due to weight history, could play a role in disrupting the caloric balance. In addition, QMV did not allow the evaluation of diet quality. Moreover, physical activity levels were not considered. Our study highlights the need for more accurate tools to assess the relationship between the quality and content of the diet and NAFLD parameters.

THU-476

Disparities in the in-hospital mortality among patients with non-alcoholic fatty liver disease admitted with acute myocardial infarction: a nationwide analysis

Umar Hayat¹, Saba Afroz², Muhammad Farhan³, Atif Nasrullah⁴, Naeem Ijaz⁴, Faisal Kamal⁵, Tariq Ahmad⁶. ¹Geisinger Wyoming Valley Medical Center, Internal medicine, division of Gastroenterology, Wilkes-Barre, United States; ²Geisinger Wyoming Valley Medical Center, Internal medicine, Wilkes-Barre, United States; ³United Regional, Wichita Falls, United States; ⁴The Wright Center for Community Health, Internal medicine, Scranton, United States; ⁵Thomas Jefferson University Hospitals, Internal medicine, division of Gastroenterology, Philadelphia, United States; ⁶Geisinger Wyoming Valley Medical Center, Internal medicine, division of Cardiology, Wilkes-Barre, United States
E-mail: umarhayat216@gmail.com

Background and aims: Non-alcoholic fatty liver disease (NAFLD) is associated with an increased risk for cardiovascular disease (CVD). Indeed, cardiovascular disease is considered the most common cause of death among NAFLD patients. However, few studies have reported the association between CVD and NAFLD. Therefore, our study aims to assess the association between NAFLD and acute myocardial infarction (AMI) and disparities in in-hospital mortality due to AMI among NAFLD patients by age, gender, and race in the USA.

Method: Hospitalizations with a primary diagnosis of AMI with a concurrent diagnosis of NAFLD were identified in the National Inpatient Sample database (2016–2019) using ICD-10-CM codes. The prevalence and trends over four years were calculated among different sociodemographic groups (Table 1). We stratified the patients into two age groups (>50 years and <50 years). A univariate regression model was used to determine mortality outcomes due to AMI among NAFLD patients by age, gender, and race. A multivariate regression analysis was performed to determine NAFLD as an independent predictor of mortality among patients who had AMI after adjusting for potential confounding factors (sociodemographic and clinical variables).

Results: A total of 5450 patients were admitted to the hospital with AMI and were identified to have a concurrent diagnosis of NAFLD. Among them, 5.11% (279) died in the hospital. Males with NAFLD admitted to the hospital due to AMI were more likely to die than females [OR 1.58, 95% CI 1.25–1.91, $p < 0.001$]. Also, patients >50 had higher odds of dying due to AMI if they had NAFLD compared to those <50 [OR 4.29, 95% CI 2.94–6.27, $p < 0.001$]. Compared with the white population, black patients [OR 0.79, 95% CI 0.54–1.15, $p < 0.001$], Hispanics [OR 1.21, 95% CI 0.85–1.74, $p < 0.001$], Asian and Pacific Islanders [OR 0.95, 95% CI 0.45–2.03, $p < 0.001$], and Native Americans [OR 0.58, 95% CI 0.08–4.17, $p < 0.001$] are less likely to die due to AMI if they have NAFLD. The NAFLD patients had higher odds of dying if admitted to the hospital with AMI [OR 1.96, 95% CI 1.74–2.21, $p < 0.001$] (Table 1).

Variables	AMI without NAFLD (n = 24212420)	AMI with NAFLD (n = 5450)	p value
Baseline Patient and Hospital Characteristics			
Age (%)	>50 yrs 15959913 (65.90) <50 yrs 8257626 (34.09)	>50 yrs 4487 (82%) <50 yrs 964 (18%)	p < 0.001
Female (%)	13940284 (57.57)	1150 (49.3)	p < 0.001
Race (%)			
White	15787986 (67.30)	3709 (68.05)	p = 0.04
Hospital Type (%)			
Urban	2192821 (9.05)	292 (2.0)	p < 0.001
Teaching	16670307 (68.83)	3956 (72.6)	p < 0.001
b) Logistic regression for AMI mortality (Unadjusted)			
	Odds Ratio	95% CI	p value
Sex			
Female (reference)	-	-	-
Male	1.58	1.25–1.91	p < 0.001
Age			
<50 (reference)	-	-	-
>50	4.29	2.94–6.27	p < 0.001
Race			
White (reference)	-	-	-
Black	0.79	0.54–1.15	p < 0.001
Hispanic	1.21	0.85–1.74	p < 0.001
Asian and Pacific Islanders	0.95	0.45–2.03	p < 0.001
Native Americans	0.58	0.08–4.17	p < 0.001
NAFLD and AMI (Adjusted)	1.96	1.74–2.21	p < 0.001

Figure:

Conclusion: Elderly white male patients with NAFLD are more likely to die if admitted to the hospital due to AMI. Moreover, NAFLD was found to be an independent predictor of death among patients who had AMI.

THU-550

Differential risk of 23 specific incident cancers and cancer-related mortality in patients with metabolic dysfunction-associated fatty liver disease: a population-based cohort study with 9.7 million Korean subjects

Goh Eun Chung¹, Su Jong Yu², Jeong-Ju Yoo³, Yuri Cho⁴, Kyu-na Lee⁵, Dong Wook Shin⁶, Yoon Jun Kim², Jung-Hwan Yoon², Kyungdo Han⁷, Eun Ju Cho². ¹Seoul National University Hospital Healthcare System Gangnam Center, Korea, Rep. of South; ²Seoul National University College of Medicine, Korea, Rep. of South; ³Soonchunhyang University Bucheon Hospital, Korea, Rep. of South; ⁴National Cancer Center, Korea, Rep. of South; ⁵Catholic University of Korea, Korea, Rep. of South; ⁶Samsung Medical Center, Sungkyunkwan University School of Medicine, Korea, Rep. of South; ⁷Soongsil University, Korea, Rep. of South
E-mail: creatioex@gmail.com

Background and aims: Although an association between metabolic dysfunction-associated fatty liver disease (MAFLD) and cardiovascular disease or overall mortality has been reported, it is unclear whether MAFLD predicts cancer incidence and mortality. We aimed to investigate the differential risk of all- and specific-cancer incidence and mortality according to MAFLD subgroups categorized by additional etiologies of liver disease.

Method: Using the Korean National Health Insurance Service database, we stratified the participants into three groups: 1) single-etiology MAFLD (S-MAFLD), or MAFLD of pure metabolic origin; 2) mixed-etiology MAFLD (M-MAFLD), or MAFLD with additional etiological factor (s) (i.e., concomitant liver diseases and/or heavy alcohol consumption); and 3) non-MAFLD. Hepatic steatosis and

fibrosis were defined using the fatty liver index and the BARD score, respectively.

Results: Among the 9 718 182 participants, the prevalence of S-MAFLD and M-MAFLD was 29.2% and 6.7%, respectively. Compared with non-MAFLD, the risk for all-cancer incidence and mortality was slightly higher among patients with S-MAFLD (incidence, adjusted hazard ratio [aHR] = 1.03; 95% confidence interval [CI]: 1.02–1.04; mortality, aHR = 1.06; 95% CI: 1.04–1.08) and markedly higher among patients with M-MAFLD (incidence, aHR = 1.31; 95% CI: 1.29–1.32; mortality, aHR = 1.45; 95% CI: 1.42–1.48, respectively). The M-MAFLD with fibrosis group (BARD score ≥ 2) showed the highest risk of all-cancer incidence (aHR = 1.38, 95% CI = 1.36–1.39), followed by the M-MAFLD without fibrosis group (aHR = 1.09, 95% CI = 1.06–1.11). Similar trends were observed for cancer-related mortality.

Conclusion: MAFLD criteria by additional etiology identified a subgroup of people with poor cancer-related outcomes. These criteria may help identify high-risk groups for cancer.

THU-551

The rising burden of non-alcoholic fatty liver disease (NAFLD) related HCC: is time running out to contain this silent epidemic?

Saima Ajaz¹, James Lok¹, Paul Ross², Riham Soliman¹, Maria Guerra Veloz¹, Abid Suddle¹, Kosh Agarwal¹. ¹King's College Hospital, Institute of Liver studies, London, United Kingdom; ²Guy's and St Thomas' NHS Foundation Trust, United Kingdom
E-mail: saima.ajaz@nhs.net

Background and aims: Non-alcoholic fatty liver disease (NAFLD) is the most common cause of chronic liver disease due to the exponential increase in obesity and metabolic syndrome. Given this upward trajectory, as well as improvements in viral hepatitis management, NAFLD is predicted to become the leading aetiology of hepatocellular carcinoma (HCC) over the coming years. However, its true oncogenic burden in developed countries remains unclear. The aim of this project was to analyse the prevalence of NAFLD in HCC patients discussed in the HCC multidisciplinary meetings (MDM) at King's College Hospital (KCH).

Method: Data was obtained from patients discussed in the HCC MDM at KCH from 2013 to 2019. A total of 400 patients with a definitive diagnosis of HCC (as per standard radiological and/or histological criteria) were reviewed. The etiologies were grouped as NAFLD, chronic viral hepatitis (Hepatitis B Virus, HBV; Hepatitis C virus, HCV), treated viral hepatitis with co-existent NAFLD, and all other causes. Outcome was measured in terms of the all-cause mortality.

Results: We analysed data from 400 HCC patients. The underlying etiologies were as follows: NAFLD only (n = 116; 29 %), treated HCV with co-existent NAFLD (n = 60; 15 %), chronic HCV without NAFLD (n = 75; 18.5 %), chronic HBV (n = 52; 13 %) and all other etiologies (n = 97; 24.2 %). NAFLD was a contributing factor in 44% of cases (n = 176). The NAFLD patients having HCC had 78 % all-cause mortality and those with treated Chronic Hepatitis C with NAFLD had 83 % all-cause mortality over the follow-up period.

Conclusion: The data suggests that in a tertiary hepatology center in the United Kingdom, NAFLD was the most common underlying cause for HCC. The mortality was high and especially in HCV treated patients with NAFLD. This highlights the importance of early diagnosis and management of NAFLD to reduce the impending burden of NAFLD-related HCC.

THU-552

Comparison of non-alcoholic steatohepatitis severity between Hispanics and non-Hispanics: combined data from multiple therapeutic clinical trials including more than 5000 patients (in collaboration with NAIL-NIT consortium)

Sophie Jeannin Megnien¹, Julie Dubourg¹, Jörn Schattenberg², Vlad Ratziu³, Stephen Harrison⁴, Mazen Nouredin⁵, Naim Alkhoury⁶, Michael Charlton⁷. ¹Summit Clinical Research, United States; ²University medicine at the Johannes Gutenberg University in Mainz, Mainz, Germany; ³Institute for Cardiometabolism and Nutrition, France; ⁴University of Oxford, United Kingdom; ⁵Houston Methodist Hospital, Houston, United States; ⁶Arizona Liver Health, Chandler, United States; ⁷UChicago Medicine, Chicago, United States
E-mail: jdubourg@summitclinicalresearch.com

Background and aims: Hispanic ethnicity has been associated with a higher risk of non-alcoholic steatohepatitis (NASH) with advanced fibrosis. We aimed to describe the demographic, metabolic and histological characteristics, between Hispanics and non-Hispanics, to further delineate the level of disease severity in this group.

Method: We combined screening data from 6 ongoing biopsy-proven therapeutic NASH trials (>5000 patients). Patients were categorized according to their ethnicity. At-risk NASH was defined as NASH with a non-alcoholic fatty liver disease activity score (NAS) of at least 4 and a fibrosis stage of 2 or 3. Screen failure rates were compared between the 2 groups before and after liver biopsy. We performed descriptive statistics, logistic, and linear regressions to compare the 2 groups.

Screening			
	Hispanic N = 2213 n (%) or mean (SD)	Non- Hispanic N = 2579 n (%) or mean (SD)	p value
Age, years	52 (12)	56 (11)	<0.01
Glycated hemoglobin (HbA1c), %	6.6 (1.5)	6.5 (1.3)	<0.01
Proportion of HbA1c ≥ 6.5%	42%	39%	0.04
Proportion of HbA1c >9.5%	5%	3%	<0.01
AST, IU/L	37 (27)	37 (28)	0.97
ALT, IU/L	50 (39)	48 (35)	0.03
GGT, IU/L	61 (73)	65 (83)	0.13
LDL, mg/dL	102 (38)	102 (38)	0.57
Triglyceride, mg/dL	167 (137)	168 (103)	0.73
Liver Biopsy time point			
	Hispanic N = 980 n (%) or mean (SD)	Non- Hispanic N = 1223 n (%) or mean (SD)	p value
NASH	561 (57%)	750 (61%)	0.06
Fibrosis Stage			
0-1	482 (49%)	505 (41%)	<0.01
2-3	454 (46%)	660 (54%)	
4	44 (4%)	59 (5%)	
At-risk NASH	370 (38%)	516 (42%)	0.04
Age, years	52 (12)	56 (11)	<0.01
Glycated hemoglobin (HbA1c), %	6.4 (1.1)	6.4 (1.0)	0.41
Proportion of HbA1c ≥ 6.5%	376 (39%)	458 (39%)	0.86
AST, IU/L	40 (24)	42 (25)	0.18
ALT, IU/L	55 (34)	54 (33)	0.22
GGT, IU/L	58 (58)	65 (72)	0.01
LDL, mg/dL	103 (38)	103 (38)	0.93
Triglyceride, mg/dL	159 (90)	164 (79)	0.24
Liver Stiffness Measurement- transient elastography, kPa	13.1 (6.9)	13.3 (6.2)	0.59
Liver fat content, %	18 (7)	18 (8)	0.14

Figure:

Results: 4792 patients with ethnicity data were included and 2203 had liver histology data. At screening, 2213 (46%) were Hispanic. Among Hispanic 1233 (56%) screen failed before biopsy compared to 1356 (53%) in non-Hispanic. The table shows the differences in

characteristics between groups. At screening Hispanics were younger and had a higher glycated hemoglobin (HbA1c) with a higher proportion of patients with HbA1c >9.5% (considered a screen failure reason in many trials). This difference in HbA1c did not persist in patients who underwent liver biopsy. After adjustment for age, GGT and FIB-4, the non-Hispanic group had more advanced fibrosis (p = 0.02).

Conclusion: Hispanics had less advanced fibrosis compared to non-Hispanics. Enrichment with Hispanic patients in non-cirrhotic NASH clinical trials might not help improve the screen failure rate due to liver histology. Further studies including genotyping are important to further investigate the importance of minority groups in clinical trials of NASH.

THU-553

Study of an association of the serum iron markers, hepatic iron deposition and severity of non-alcoholic fatty liver disease: a single-centered prospective study

Shubham Jain¹, Saurabh Bansal¹, Pankaj Nawghare¹, Anuraag Jena¹, Sanjay Chandnani¹, Pravin Rathi¹. ¹Topiwala National Medical College, Mumbai, Gastroenterology, Mumbai, India
E-mail: dr.shubhamjazz@gmail.com

Background and aims: Non-alcoholic fatty liver disease (NAFLD) is commonly associated with elevated serum ferritin (SF) levels, seen in almost 30% of patients. However, whether this raised serum ferritin is a marker of hepatic inflammation or hepatic iron overload is still debatable. Recent studies have incorporated levels of serum ferritin (SF) to assess the progression of NASH and liver fibrosis. Moreover, the probable relationship between SF, Hepatocellular iron deposition, and stages of NAFLD disease is a pleasing surprise but not fully understood. Therefore we aimed to study the association of hepatic iron deposition in patients with histologically proven NAFLD and the role of serum ferritin as a predictor of the severity of NAFLD.

Method: We prospectively evaluated 103 outpatients with biopsy-proven NAFLD from our tertiary care centre over 2 years. Standard histological and clinical criteria were used for the diagnosis of NAFLD. Complete serum iron profile, hepatic, and metabolic parameters were collected at the time of liver biopsy. Hyperferritinemia was defined when serum ferritin levels were more than 150 ng/ml. Significant fibrosis was defined as F2 fibrosis on histopathology/>8 kpa on transient elastography. Iron deposition in hepatocytes was assessed with staining and graded.

Results: Out of 103 included patients, 60 patients had steatohepatitis (NASH). Among those, 36 (60%) patients had elevated SF levels and iron staining was positive in 18 (30%) patients. however, there was no significant association found between serum hyperferritinemia and the presence of NASH (p = 0.68). Although NASH patients had no significant elevated ferritin levels but hepatic iron deposition was seen significantly higher in NASH vs non-NASH patients (18/60, 30% vs 4/43, 9%, p = 0.014). A total of 64 (62.1%) patients had hyperferritinemia, whereas hepatic iron stain was positive in 22 (21.3%) patients. The association of hyperferritinemia was significant in the early stages of fibrosis F0-F2 (p value- 0.04) whereas advanced stages of fibrosis F3-F4 were noted to have significantly decreased ferritin levels (p = 0.045). The stainable hepatic iron deposition has no significant association with the progression of liver fibrosis as seen in Pre-cirrhotic stage (F0-F2) 11/48, 22.9% vs cirrhotic stage (F3-F4) 11/55, 20%, p value- 0.81

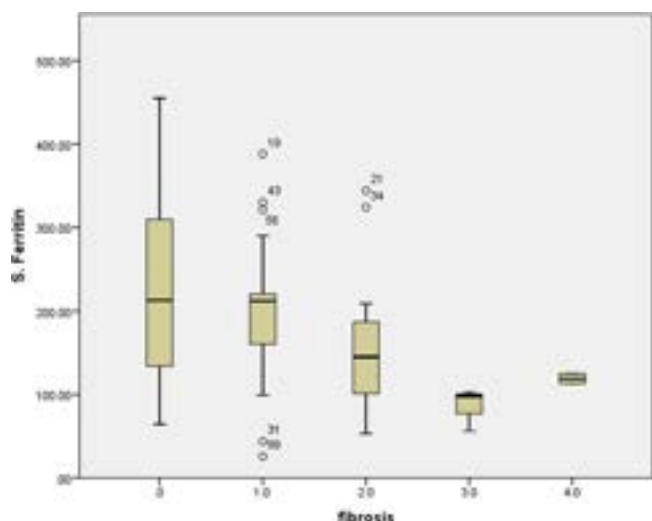


Figure: Relationship between Serum ferritin level (ng/ml) and stages of hepatic fibrosis

Conclusion: Hyperferritinemia is seen in almost two third of NAFLD patients but most of the cases are not associated with hepatic iron deposition and progression of fibrosis. Stainable hepatic iron is more significantly associated with the presence of steatohepatitis (NASH) and less likely to correlate with advanced fibrosis. We conclude that there is no association between hyperferritinemia with hepatic iron deposition and the severity of disease in NAFLD patients. In addition serum ferritin levels can be supplemented as the non-invasive diagnostic panel in individual NAFLD patients.

THU-554

The importance of regular screening for HCC in non-alcoholic steatohepatitis/non-alcoholic fatty liver disease

Taisei Keitoku¹, Nobuharu Tamaki¹, Masayuki Kurosaki¹, Naoki Uchihara¹, Keito Suzuki¹, Yuki Tanaka¹, Haruka Miyamoto¹, Michiko Yamada¹, Shun Ishido¹, Hiroaki Matsumoto¹, Tsubasa Nobusawa¹, Mayu Higuchi¹, Kenta Takaura¹, Shohei Tanaka¹, Chiaki Maeyashiki¹, Yutaka Yasui¹, Yuka Takahashi¹, Kaoru Tsuchiya¹, Hiroyuki Nakanishi¹, Daniel Huang², Namiki Izumi¹. ¹Musashino Red Cross Hospital, Gastroenterology and Hepatology, Tokyo, Japan; ²National University of Singapore, Singapore, Singapore
E-mail: kurosakim@gmail.com

Background and aims: Although it is necessary to detect HCC at an early stage by appropriate screening, a strategy for screening has not yet been established. Therefore, we decided to investigate the importance of regular screening in patients with NASH/NAFLD.

Method: We studied 317 NASH/NAFLD patients diagnosed with first-episode liver cancer at Musashino Red Cross Hospital and National University of Singapore. We investigated whether these patients had regular imaging screening (AUS/CT/MRI) at least once every 6 months prior to the diagnosis of HCC. The primary outcome was the whether or not curative treatment (curative treatment is defined as RFA or surgery in Barcelona clinic liver cancer (BCLC) Stage0 or A patients) was performed. Survival rates in the patients with or without screening were compared as secondary outcomes.

Results: There were 233 patients without screening and 84 with screening. Patient background without/with screening: age (mean \pm standard deviation) was 74 (\pm 11) vs 72 (\pm 11) years and BMI (mean \pm SD) was 24.7 (\pm 4.6) vs 26.0 (\pm 4.4). The number of patients with cirrhosis were 106 (45.5%) vs 57 (67.9%). Among cirrhosis cases, Child-Pugh Class A/B/C: 67.6% vs 75.0%/25.5% vs 22.7%/6.9% vs 2.3% (p = 0.5). BCLC Stage 0/A was 10.4% vs 44.6%/48.7% vs 39.8% (p < 0.001). Cases with screening were significantly to receive curative treatment (34.8% vs. 64.3%, p < 0.001). The 1-, 3-, and 5-year survival rates of the patients without/with screening were 72.5% vs 92.1% /

55.1% vs 80.7%/48.0% vs 66.3% (p < 0.001), indicating a significantly lower survival rate in patients without screening.

Conclusion: Routine screening for NASH/NAFLD can detect early HCC and provide curative therapeutic intervention.

THU-555

Long-term clinical outcomes of adults with metabolic dysfunction-associated fatty liver disease: a single-centre prospective cohort study with baseline liver biopsy

Wah Loong Chan¹, Shi-En Chong¹, Felicia Chang¹, Kee Huat Chuah¹, Nik Raihan Nik Mustapha², Sanjiv Mahadeva¹, Wah-Kheong Chan¹. ¹Universiti Malaya, Gastroenterology and Hepatology Unit, Department of Medicine, Faculty of Medicine, Kuala Lumpur, Malaysia; ²Hospital Sultanah Bahiyah, Department of Pathology, Alor Setar, Malaysia
E-mail: wljack90@gmail.com

Background and aims: There are limited data on the long-term clinical outcomes of adults with metabolic dysfunction-associated fatty liver disease (MAFLD), especially in Asian population. The primary objective of this study was to provide long-term clinical outcome data of adult patients with MAFLD in Malaysia.

Method: This is a single-centre prospective study of a well-characterized cohort of biopsy-proven MAFLD patients. The patients were followed every 6–12 months for cardiovascular events, liver-related events, malignancy, and mortality. The incidence of clinical outcomes and mortality were compared between patients with and without steatohepatitis and between patients with and without advanced liver fibrosis. Advanced liver fibrosis was defined as histological fibrosis stages 3 or 4. Steatohepatitis was defined as histological presence of steatosis, lobular inflammation, and hepatocyte ballooning (\geq grade 1 each). The comparison between groups was performed using Kaplan-Meier curve and log rank test. Significant was assumed when p was < 0.05.

Results: The data for 202 patients were analyzed (median age 55.0 years old, 47.5% male, 88.6% obese, 71.3% diabetes mellitus, 76.7% steatohepatitis, 27.2% advanced liver fibrosis). The median follow-up interval was 7 years (range 1–9 years). The rates of cardiovascular events, malignancy, liver-related events, and mortality was 2.49, 0.69, 0.43, and 0.60 per 100 person-years of follow-up, respectively. Liver-related events were only seen in patient with advanced liver fibrosis at 9.1% vs 0% in patient without advanced liver fibrosis (p = 0.001). Advanced liver fibrosis was not associated with cardiovascular events, malignancy, or mortality. NASH was not associated with cardiovascular events, malignancy, liver-related events, or mortality.

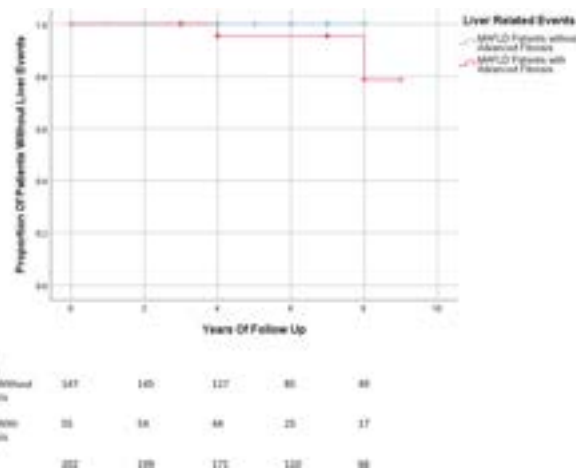


Figure:

Conclusion: The overall liver-related event rate in MAFLD patients is low, but it is significantly higher among patients with advanced liver fibrosis. Cardiovascular disease is the leading cause of mortality in MAFLD patients.

THU-556

Serum vitamin D is strongly associated with liver steatosis but not with liver and spleen stiffness assessed by transient elastography in patients at risk

Gediz Dogay Us^{1,2}, Ozgur Koc^{1,3}, Francesco Innocenti⁴, İhsan Nuri Akpınar⁵, Ger Koek^{1,3}. ¹Maastricht University, School of Nutrition and Translational Research in Metabolism, Maastricht, Netherlands; ²Pax Clinic, Department of Gastroenterology, Istanbul, Turkey; ³Maastricht University Medical Center, Division of gastroenterology and hepatology, Maastricht, Netherlands; ⁴Maastricht University, Department of Methodology and Statistics, CAPHRI Care and Public Health Research Institute, Maastricht, Netherlands; ⁵Pax Clinic, Department of Radiology, Istanbul, Turkey
E-mail: dogaygediz@gmail.com

Background and aims: Vitamin D exerts a significant role in liver-related pathologies by interacting at multiple steps in development of liver steatosis, steatohepatitis, and liver fibrosis, as well as several related extrahepatic manifestations. Its insufficiency not only associates with obesity and metabolic syndrome but also has been shown to have a causative relationship with the severity and incidence of liver steatosis. However, the association between vitamin D insufficiency (VDI) and the stiffness of liver and spleen is not as well-defined. Therefore, we investigated the relationship between VDI and liver steatosis, liver stiffness (LS) and spleen stiffness (SS) assessed by transient elastography (TE).

Method: We recruited 395 participants for a single-centered prospective study in an outpatient clinic during a one-year period (between 01/2022 and 01/2023). All participants were older than 18 and presented at least with one component of the metabolic syndrome. Body weight, height, and waist circumference (WC) were measured, and body mass index (BMI) was calculated. Vitamin D status was measured as serum 25 (OH)D level and <30 ng/ml was considered as VDI. Liver steatosis by Controlled attenuation parameter (CAP), liver stiffness and spleen stiffness were assessed using a TE device (FibroScan®; Echosens, Paris, France). Multivariable linear regression analyses were used to investigate the association of vitamin D with CAP, LS and SS, adjusting for the following potential confounders: age, sex, WC, BMI, diabetes, hypertension, dyslipidemia, and metabolic syndrome.

Results: VDI was present in 33.4% of the participants. Vitamin D was negatively associated with CAP, with an unadjusted effect on CAP of -0.657 (95% CI: -0.921, -0.392). After adjusting for age, sex, BMI, waist circumference, diabetes, hypertension, dyslipidemia and metabolic syndrome, the association remained statistically significant but the effect of Vitamin D on CAP reduced to -0.342 (95% CI: -0.523, -0.160). There was a very weak and non-statistically significant association between Vitamin D and liver stiffness (-0.01, 95% CI: -0.02, 0.001) and spleen stiffness (-0.046, 95% CI: -0.110, 0.018), which vanishes when controlling for age, BMI, WC, sex, diabetes, hypertension, dyslipidaemia, and metabolic syndrome (-0.004, 95% CI: -0.014, 0.006 and -0.005, 95% CI: -0.071, 0.061, consecutively).

Conclusion: VDI is a predictor of the severity of liver steatosis independently from obesity and all components of metabolic syndrome, however liver and spleen stiffness does not show a significant association with it. Further studies demonstrating the impact of vitamin D in liver-related outcomes are warranted.

THU-557

Hepatic steatosis in people with HIV is associated with lower BMI and more liver fibrosis compared to metabolic dysfunction-associated fatty liver disease

Florian Santomenna¹, Rosa Lombardi^{1,2}, Felice Cinque^{1,3}, Jaqueline Currà¹, Dana Kablawi⁴, Annalisa Cespiati^{1,2}, Luca Marchesi¹, Erika Fatta², Cristina Bertelli², Giovanna Oberti², Wesal Elgretli³, Bertrand Lebouche⁴, Marc Deschenes⁴, Thierry Fosind Tadjou⁴, Giada Sebastiani^{3,4}, Anna Ludovica Fracanzani^{1,2}. ¹Department of Pathophysiology and Transplantation, University of Milan, Milan, Italy, Italy; ²Unit of Medicine and Metabolic Disease, Fondazione IRCCS Ca' Granda Ospedale Maggiore Policlinico of Milan, Milan, Italy, Italy; ³Division of Experimental Medicine, McGill University, Montreal QC, Canada; ⁴Chronic Viral Illness Service, McGill University Health Centre, Montreal QC, Canada
E-mail: rosallombardi@hotmail.it

Background and aims: People with HIV (PWH) are at risk of hepatic steatosis (HS) possibly evolving to hepatic fibrosis. The pathogenesis of HS in these patients is complex, including HIV-related inflammation, frequent metabolic comorbidities and lifelong exposure to antiretroviral therapy. Recently, a new concept of metabolic dysfunction-associated fatty liver disease (MAFLD) has emerged, defined the presence of HS associated with at least one metabolic alteration. There are limited data whether HIV-associated HS differs in clinical presentation from metabolic dysfunction-associated fatty liver disease (MAFLD). We aimed at comparing severity of metabolic and hepatic dysfunction between PWH with HS and MAFLD patients.

Method: In this international case-control study, 212 consecutive HIV mono-infected patients with HS at McGill University in Montreal were compared to a sex and age matched MAFLD control group at Policlinico Hospital in Milan. Fibroscan with controlled attenuation parameter (CAP) was used to define HS (CAP ≥248 dB/m), severe HS (CAP > 280 dB/m), and significant liver fibrosis (liver stiffness measurement >7.0 kPa). Serum fibrosis biomarkers APRI, FIB-4 and Fibroscan-AST (FAST) score were also computed.

Results: PWH presented lower median BMI (28[25-31] vs 29[27-32] Kg/m², p = 0.002) and lower prevalence of obesity (26% vs 44%, p < 0.001) compared to MAFLD patients, along with a lower prevalence of hypertension (21% vs 38%, p < 0.001). The prevalence of dyslipidemia (41% vs 26%, p < 0.001) and statin prescription (23% vs 11%, p = 0.003), as well as of high triglycerides (26% vs 9%, p < 0.001) and low HDL cholesterol (34% vs 15%, p < 0.001), was higher among PWH compared to MAFLD patients. No difference in cardiovascular events and diabetes prevalence was observed between the two groups. As for liver disease, PWH had a lower prevalence of severe HS (54% vs 74% p < 0.001) but higher prevalence of significant liver fibrosis (15 vs 7%, p = 0.03) by Fibroscan, as well as higher serum fibrosis biomarkers APRI, FIB-4 and FAST score, compared to MAFLD patients.

Conclusion: Despite having lower BMI, PWH seem to have a more severe hepatic and atherogenic presentation of HS than MAFLD patients. Screening and follow-up for HS and especially for liver fibrosis in PWH is recommended, even if lean.

THU-558

Impact of visceral adiposity for coronary artery calcification progression in patients with metabolic dysfunction-associated fatty liver disease; multicenter cohort study

Min Kyu Kang¹, KyeWhon Kim², Jung Eun Song³, Jung Gil Park¹. ¹College of Medicine, Yeungnam University, Internal Medicine, Korea, Rep. of South; ²Yeungnam University Hospital, Korea, Rep. of South; ³School of Medicine, Daegu Catholic University, Korea, Rep. of South
E-mail: gsnrs@naver.com

Background and aims: Metabolic dysfunction-associated fatty liver disease (MAFLD) as well as non-alcoholic fatty liver disease (NAFLD) is associated with coronary artery calcification (CAC) progression. Although body composition parameters are emerging as novel

POSTER PRESENTATIONS

prognostic factors for NAFLD, the clinical significance of those on CAC progression in patients with MAFLD is lacking. We investigated the impact of body composition parameters on the CAC progression in patients with MAFLD.

Method: A cross-sectional analysis of retrospective cohort study was conducted at two health promotion centers, including 457 MAFLD patients who performed ultrasound and abdominal and cardiac CT. Fatty liver was defined using ultrasound and presence of CAC as a CAC score >0 was defined using cardiac CT. The CAC progression was classified by Greenland methods (0, 1 to 100, 101 to 300, and >300) Using cross-sectional CT images of 3rd lumbar vertebra, sarcopenia, visceral adiposity, and myosteotosis were defined.

Results: Median age was 57 years (interquartile range: 52.0–63.0) and 364 (79.6 %) were male. The presence of CAC was 44.6% and the CAC progression groups were identified by 253 (26.3%) in 1 to 100 group, 42 (9.2%) in 101 to 300 group, and 42 (9.2%) in >300 group, respectively. The visceral adiposity progression was correlated with the CAC progression ($p < 0.001$). In the multivariate analysis, visceral adiposity (odds ratio, 1.79; 95% confidence interval; 1.14–2.83, $p = 0.011$) was significant risk factors for presence of CAC, independent of pre-existing prognostic factors.

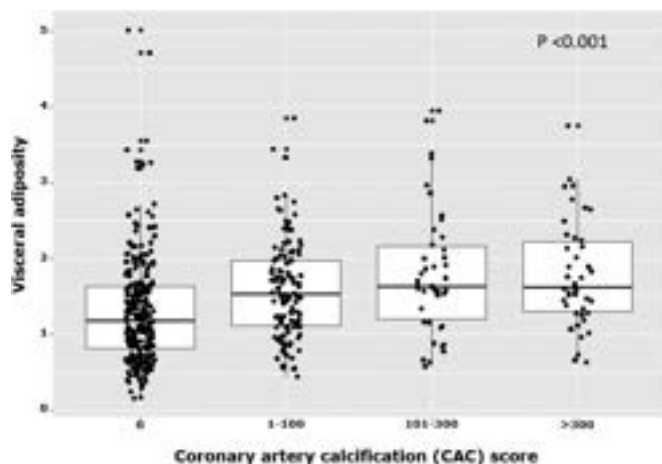


Figure:

Conclusion: Visceral adiposity is associated with an CAC progression in patients with MAFLD, independent of traditional risk factors.

THU-559

Evaluation of Google search trends for liver diseases in Europe

Andreas Teufel¹, Timo Itzel¹, Anca Zimmermann², Dan Dumitrascu³, Elisabetta Bugianesi⁴, Luca Valenti⁵, Laurent Castera⁶, Maria Patrizia Carrieri⁷, Javier Crespo⁸, Manuel Romero Gomez⁹, Robert Flisiak¹⁰, Marcin Krawczyk¹¹, Matthias Ebert¹², Jeffrey Lazarus¹³, Frank Tacke¹⁴. ¹Heidelberg University, Division of Hepatology, Department of Medicine II, Medical Faculty Mannheim, Mannheim, Germany; ²Clinic of Worms, Medical Clinic 2, Dept. of Diabetology and Endocrinology, Worms, Germany; ³University of Medicine and Pharmacy, 42nd Department of Internal Medicine, "Iuliu Hatieganu", Cluj-Napoca, Romania; ⁴University of Turin, Department of Medical Sciences, Division of Gastroenterology and Hepatology, A.O. Città della Salute e della Scienza di Torino, Turin, Italy; ⁵Università Degli Studi di Milano, Department of Pathophysiology and Transplantation, Milano, Italy; ⁶Université de Paris, UMR1149 (CRI), Inserm, Paris, France and Service d'Hépatologie, AP-HP, Hôpital Beaujon, Clichy, France; ⁷Aix Marseille Univ, Inserm, IRD, SESSTIM, Sciences Economiques and Sociales de la Santé et Traitement de l'Information Médicale, ISSPAM, Marseille, Germany; ⁸Hospital Universitario Marqués de Valdecilla, Gastroenterology and Hepatology, Santander, Spain; ⁹University of

Seville, Virgen del Rocío University Hospital, Institute of Biomedicine of Seville, Sevilla, Spain; ¹⁰Uniwersytecki Szpital Kliniczny w Białymstoku, Klinika Chorób Zakaźnych i Hepatologii UMB, Białystok, Poland;

¹¹Saarland University, Department of Medicine II, Saarland University Medical Center, Homburg, Germany, ¹²Heidelberg University, Department of Medicine II, Mannheim, Germany, ¹³University of Barcelona, Barcelona Institute for Global Health (ISGlobal), Hospital Clínic, Barcelona, Spain; ¹⁴Charité-Universitätsmedizin Berlin, Department of Hepatology and Gastroenterology, Campus Virchow-Klinikum and Campus Charité Mitte, Berlin, Germany
E-mail: andreas.teufel@medma.uni-heidelberg.de

Background and aims: Chronic liver diseases belong to the most common diseases worldwide and are associated with increased morbidity and mortality. Although every fourth adult might be affected by non-alcoholic fatty liver disease (NAFLD), awareness of this condition is low amongst the general public, health care professionals and policy makers. However, meaningful knowledge transfer is essential for raising awareness and improving prevention and treatment of liver disease. Thus, investigating the use of internet search engines might offer valuable insights on how knowledge transfer has evolved and which liver-related issues are currently searched.

Method: We investigated Google search trends by measuring the number of hits relating to liver diseases between 2004 and 2021 in seven languages and European countries but also worldwide. All analyses were performed in R using the R Google trends package gtrendsR.

Results: We found that interest in NAFLD has generally increased over time, but that interest in non-alcoholic steatohepatitis (NASH)-the most severe form of NAFLD-has decreased. Interest in viral hepatitis C has decreased, whereas the number of queries regarding viral hepatitis B have been stable but dominated by interest in vaccination for it. Recent medical developments (in viral hepatitis) did not lead to a noticeable change in overall search behavior. Users preferred searching using their native language and less complex medical terms and acronyms (e.g., fatty liver instead of NAFLD).

Conclusion: In the last two decades, public Google search trends have followed the general changes in hepatology. Searches are dominated by non-healthcare professionals and generally avoid complex and specific medical terms. Awareness and communication strategies around NAFLD should consider these preferences when addressing the general public.

THU-560

Salivary analytical device (SAD) a good tool for monitoring the metabolic status of patients with fatty liver disease

Gaia Sinatti¹, Silvano Junior Santini¹, Giovanni Brienza¹, Marco Lampieri¹, Giovanna Fracassi¹, Clara Balsano¹. ¹University of L'Aquila, Department of Life, Health and Environmental Sciences (MESVA), L'Aquila, Italy
E-mail: gaia.sinatti@graduate.univaq.it

Background and aims: Physical inactivity and sedentary lifestyle have contributed worldwide to the epidemic spread of obesity and non-alcohol related fatty liver disease (NAFLD), the most common cause of chronic liver disease. Besides leading to increased morbidity and mortality due to the possible evolution of the disease into non-alcohol related steatohepatitis (NASH) and/or into advanced fibrosis, NAFLD is also associated with cardiovascular disease (CVD). Monitoring NAFLD patients at risk of developing complications by using a more effective health technology would allow the implementation of preventive health strategies and follow-up programs that would bring considerable benefits to the individual and reduce the burden of this disease on the health care system. Saliva has hundreds of components that can serve as biomarkers of both physiological and pathological status. The purpose of this study was to develop a device, with multiple integrated sensors, that could use saliva to monitor patients with dysmetabolism and derive reliable

NAFLD Diagnostics and non-invasive assessment

WEDNESDAY 21 TO SATURDAY 24 JUNE

TOP-074

Significant dose-dependent reduction in liver stiffness using transient elastography in a phase 3 randomized placebo-controlled trial of obeticholic acid over 48 months in patients with pre-cirrhotic fibrosis due to non-alcoholic steatohepatitis

Rohit Loomba¹, Quentin Anstee², Stephen Harrison³, Naim Alkhouri⁴, Mary Rinella⁵, Thomas Capozza⁶, Christopher Gasink⁶, Amarita Randhawa⁶. ¹NAFLD Research Center, University of California, San Diego, La Jolla, United States; ²Translational and Clinical Research Institute, Faculty of Medical Sciences, Newcastle University, Framlington Place, Newcastle upon Tyne, United Kingdom; ³Pinnacle Clinical Research Center, San Antonio, United States; ⁴Arizona Liver Health, Chandler, United States; ⁵University of Chicago, Pritzker School of Medicine, Chicago, United States; ⁶Intercept Pharmaceuticals Inc, Morristown, United States

Email: thomas.capozza@interceptpharma.com

Background and aims: Transient elastography (TE) may reduce the need for liver biopsies to diagnose and monitor progression of pre-cirrhotic liver fibrosis due to non-alcoholic steatohepatitis (NASH). Interim analyses of the ongoing phase 3 REGENERATE trial showed that obeticholic acid (OCA) significantly improved hepatic fibrosis vs placebo in patients with NASH as assessed by histologic analysis of liver biopsies using individual readers or a consensus panel. Secondary study objectives included non-invasive assessment of the antifibrotic effect of OCA vs placebo. Here, we describe the effect of OCA vs placebo on TE liver stiffness measurement (LSM) over 48 months in patients with pre-cirrhotic fibrosis due to NASH in the REGENERATE study.

Method: TE (FibroScan) was performed every 6 months at study sites where it was available. LSM was analyzed in the intent-to-treat (ITT) population, which included all randomized patients with baseline fibrosis stage 2 or 3 (histologic staging) who received at least 1 dose of placebo, OCA 10 mg, or OCA 25 mg and who had a post-baseline measurement. Fibrosis staging was determined by a consensus method for histologic analysis using NASH Clinical Research Network scoring criteria.

Results: In the ITT population (N = 2187), mean (standard deviation) baseline LSM across cohorts was similar (placebo, 12.2 [6.7] kilopascal [kPa]; OCA 10 mg, 12.1 [6.2] kPa; OCA 25 mg, 11.7 [6.4] kPa). Mean LSM in OCA-treated patients decreased relative to those in the placebo group as early as month 6 (about 50% had $\geq 20\%$ reduction from baseline) and was sustained through month 48 in the OCA 25 mg group (Figure 1A). At month 18, LSM reductions were observed in both OCA groups whereas LSM in the placebo group worsened (OCA 10 mg vs placebo, $p = 0.0006$; OCA 25 mg vs placebo, $p = 0.0015$; Figure 1B). At month 48, there was a dose-dependent reduction of LSM, with OCA 25 mg achieving a -2.32 kPa least-squares mean change from baseline ($p = 0.0172$ vs placebo). In a responder analysis, LSM reductions occurred even in OCA-treated patients whose histologic fibrosis was assessed as unchanged at month 18 by central pathologists (Figure 1C).

Conclusion: Treatment with 48 months of OCA provided a dose-dependent and cumulative benefit in liver stiffness vs placebo in patients with pre-cirrhotic liver fibrosis due to NASH. These findings support the regulatory primary end point of histologic improvement in hepatic fibrosis in the REGENERATE study, which was demonstrated by 2 biopsy-reading methodologies.

detections comparable with blood values to allow and improve telematic control of the patient.

Method: In this study, a small cohort of thirty patients was enrolled. We evaluated and compared each value of lipid profile (total cholesterol, High Density Lipoprotein HDL, triglycerides) and glucose, detected in blood samples, with those identified in saliva samples by using commercial enzymatic kit assay. Besides that, hematological parameters were measured in saliva samples by a lab on chip to validate a prototype of device, with multiple integrated sensors, created in collaboration with electronic engineers and called SAD, Salivary Analytical Device. (Figure)

Results: we obtained a good degree of correlation between blood determinations and salivary values of total cholesterol ($r = 0.65$, $p = 0.04$), HDL ($r = 0.73$, $p = 0.04$), triglycerides ($r = 0.84$, $p = 0.02$) and glucose ($r = 0.98$, $p = 0.003$) both using commercial kits. Moreover, SAD prototype displayed an excellent reliability for salivary parameters evaluation and dosing.

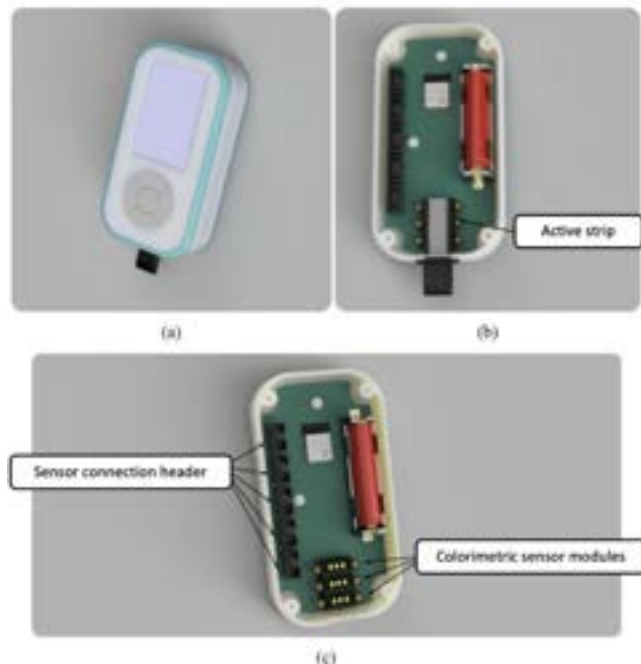


Figure: SAD, Salivary Analytical Device render. a) general view of the device prototype, b) housing arrangement of a commercial strip, c) arrangement of sensor connection header and connector colorimetric sensor modules.

Conclusion: Although our results need to be validated on a larger cohort of patients, our preliminary data confirm that our device SAD can be a good tool for monitoring total cholesterol, HDL, triglycerides, and glucose levels in saliva samples. Offering the possibility of monitoring multiple biochemical parameters with a non-invasive device, in a simple and fast way, capable of analyzing metabolic parameters in a few drops of saliva, is desirable, and would unequivocally implement the performance and reliability of remote telemonitoring.

Figure: Validation of the AGA Clinical Pathway for NAFLD (A) and an alternate pathway using ELF (B) with MRE as the reference standard in patients with type 2 Diabetes Mellitus

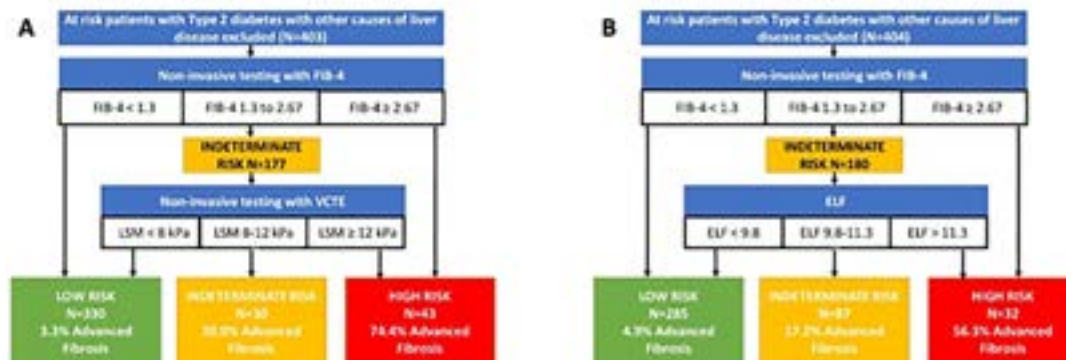


Figure: (abstract: TOP-075).

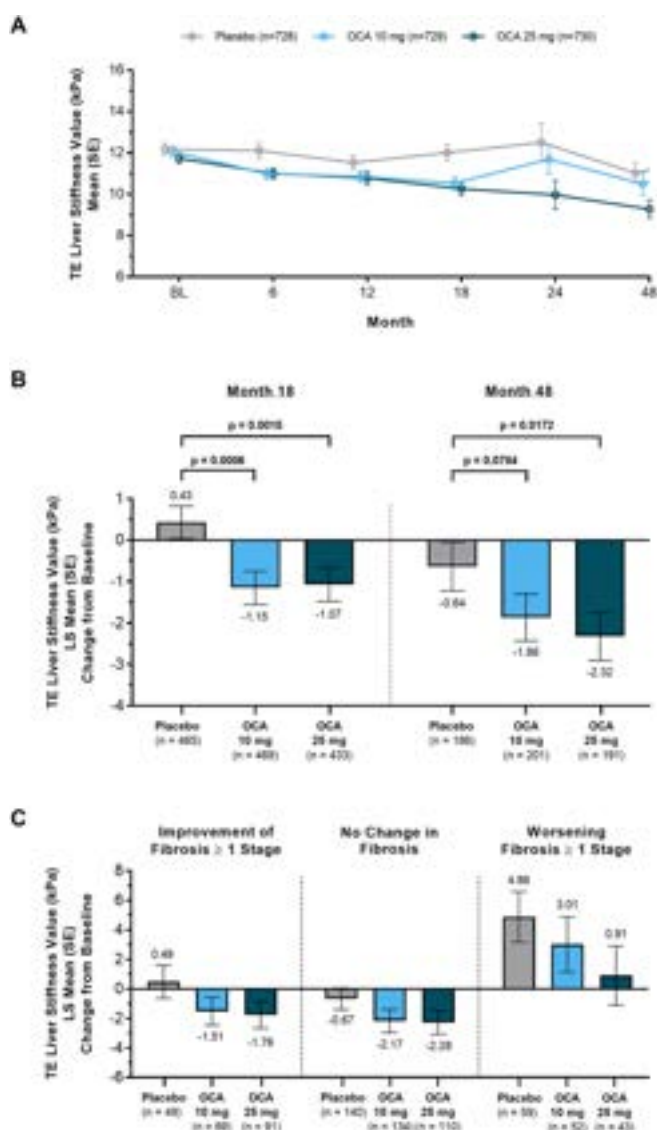


Figure: Change in transient elastography liver stiffness measurement (LSM) in patients with pre-cirrhotic liver fibrosis due to non-alcoholic steatohepatitis treated with obeticholic acid (OCA) vs placebo. (A) LSM

from baseline (BL) to month 48. (B) Comparison of LSM at months 18 and 48. (C) Change from BL in LSM at month 18 by fibrosis responder status.

Abbreviations: kPa, kilopascal; LS, least squares.

TOP-075

Validation and expansion of the American gastroenterological association clinical care pathway for non-alcoholic fatty liver disease in a prospective cohort of patients with type 2 diabetes

Veeral Ajmera¹, Kaleb Tesfai¹, Scarlett Lopez¹, Vanessa Cervantes¹, Egbert Madamba¹, Ricki Bettencourt¹, Lisa Richards¹, Rohit Loomba¹.

¹UCSD NAFLD Research Center, United States

Email: v1ajmera@ucsd.edu

Background and aims: A multidisciplinary task force commissioned by the American Gastroenterological Association (AGA) recently developed a clinical care pathway with guidance on screening high-risk populations including those with type 2 diabetes (T2DM). We aimed to validate the pathway in a prospectively recruited cohort of patients with T2DM and evaluate the diagnostic performance of an alternate pathway with enhanced liver fibrosis (ELF) testing.

Method: This prospective study enrolled adults age ≥50 years with T2DM recruited from primary care or endocrinology clinics. Participants underwent a standardized clinical research visit with magnetic resonance imaging proton-density-fat-fraction (MRI-PDFF), magnetic resonance elastography (MRE), vibration-controlled transient elastography (VCTE) and controlled attenuation parameter (CAP) and ELF testing. The primary outcome was the diagnostic performance of the AGA clinical pathway and an alternate pathway with ELF for advanced fibrosis using MRE ≥3.63 kPa as the reference.

Results: 417 patients (36% men) with T2DM with FIB-4 and MRE data were included. The mean (± SD) age and BMI were 65 (± 8) years and 30 (± 5) kg/m², respectively. The prevalence of NAFLD (MRI-PDFF ≥5% after exclusion of other liver diseases) was 64% and 12% had advanced fibrosis (MRE ≥3.63 kPa). FIB-4 values of <1.3, 1.3–2.67 and ≥2.67 were present in 208 (50%), 183 (44%), and 26 (6%) of patients respectively. VCTE values <8 kPa, 8–12 kPa and ≥12 kPa were present in 309 (77%), 58 (14%), and 36 (9%) of patients respectively. ELF scores of <9.8, 9.8–11.3 and >11.3 were present in 236 (58%), 146 (36%) and 22 (6%) patients respectively. Applying the AGA pathway (N = 403), 202 patients were low risk by FIB-4 and 128 additional patients had VCTE <8 kPa and were classified as low risk. The false negative rate was 3.3% and 18% would qualify for specialty referral (Figure 1A). Applying the alternate pathway with ELF (N = 404), 200 patients were low risk by FIB-4 and 85 additional patients had low ELF and were low

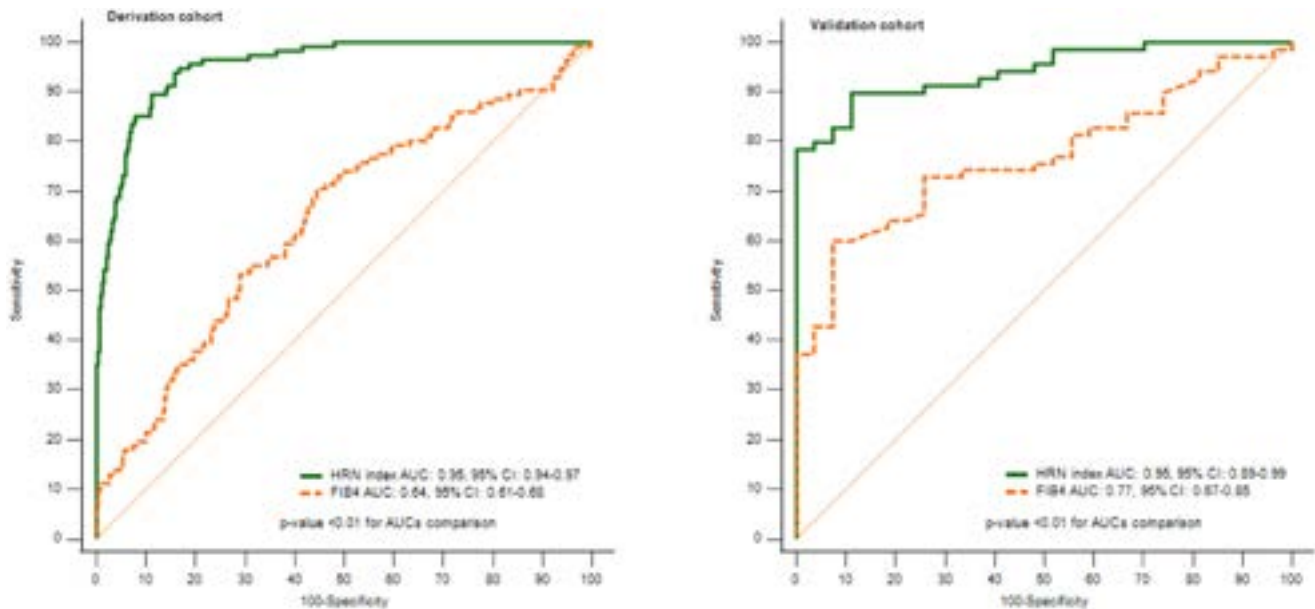


Figure: (abstract: TOP-080).

risk. The false negative rate was 4.8% and 29% would qualify specialty referral (Figure 1B).

Conclusion: Validation of the AGA clinical pathway in a well-phenotyped, prospectively recruited cohort with T2DM revealed a low false negative rate, 3.3% and identified 82% of patients as low-risk. An alternative pathway with FIB-4 + ELF, which does not require VCTE prior to specialty referral, had a low false negative rate and similar performance and may serve as a viable alternative for primary care and endocrinology clinics without access to VCTE.

TOP-080

A validated tool consisting of bedside variables predicts high-risk NASH (HRN) in individuals with type 2 diabetes

Eduardo Vilar Gomez¹, Deven Parmar², Niharika Samala¹, Raj Vuppalanchi¹, Samer Gawrieh¹, Oscar Cummings¹, Stephen Harrison³, Rohit Loomba⁴, Naga Chalasani¹. ¹Indiana University School of Medicine, Indianapolis, United States; ²Zydus Therapeutics Inc, United States; ³Pinnacle Clinical Research, San Antonio, United States; ⁴Medical Center, San Diego, United States
Email: nchalasa@iu.edu

Background and aims: FIB4 is currently recommended to screen patients with NAFLD at increased risk of clinically significant fibrosis (CSF). However, rigorous data are lacking to support screening of CSF via FIB4 in patients with type 2 diabetes (T2D). We developed and externally validated a model to predict the presence of high-risk NASH (HRN) in patients with T2D and compared its performance against FIB4.

Method: 807 T2D participants with vibration-controlled transient elastography (VCTE) in the US population-based National Health and Nutrition Examination Survey (NHANES, 2017–2018) constituted the derivation cohort. 97 T2D screened for a phase 2 clinical trial (NCT05011305) comprised the validation cohort. HRN, defined as NAS ≥ 4 and fibrosis stage ≥ 2 , was assessed using a FibroScan-AST (FAST) score threshold of ≥ 0.35 obtained from VCTE and aspartate aminotransferase (AST). Diabetes was defined by HbA1c levels $\geq 6.5\%$ or fasting plasma glucose of ≥ 126 mg/dl or current use of glucose-lowering medications. Logistic regression models were used for variable selection and model development in the derivation cohort. The area under the ROC curve (AUC) was computed to determine the diagnostic performance of the final predictive model and Fib-4 and select different thresholds for discriminating participants with HRN.

Results In the derivation cohort, the prevalence of HRN was 15%. The bias-corrected AUC and Akaike Information Criterion (AIC) of a model (Diabetes-HRN index) comprising of variables independently associated with HRN (log-transformed values of ALT, GGT, and BMI along with AST/ULN-to-platelet ratio, HDL-C, and age) were 0.95 (95% CI 0.93–0.97) and 309.6, respectively. A score threshold of >15.82 , selected by Youden's index, correctly identified a total of 717 (89%) out of 805 participants, with a sensitivity of 90%, specificity of 89%, NPV of 98%, and PPV of 57%. In the validation cohort, the Diabetes-HRN index yielded an AUC of 0.95 (95% CI: 0.89–0.99), and a score threshold of >15.82 correctly classified a total of 81 (84%) out of 97 participants, with NPV of 74% and PPV of 87%. The Diabetes-HRN index outperformed Fib-4 in predicting HRN in the derivation (AUC: 0.64, 95% CI: 0.61–0.67) and validation (AUC: 0.77, 95% CI: 0.67–0.84) cohorts. The DeLong test p values for comparing AUCs between HRN Diabetes and FIB4 was <0.01 (Figure). In a separate analysis consisting of 1237 T2D participants in NHANES 2011–2012 and 2013–2014, our Diabetes-HRN index, after adjusting for age, gender, race/ethnicity, history of CVD and cancer, and smoking status, was significantly associated with overall mortality [HR: 1.6 (95% CI: 1.04–2.3), $P = 0.03$]. **Conclusion:** A newly developed and validated Diabetes-HRN index based on 6 bedside variables accurately identifies diabetic patients at high risk of fibrotic NASH. This model significantly outperforms FIB4.

TOP-083

Utility of serum phosphatidylethanol in differentiating NAFLD from alcohol-associated liver disease among individuals with overweight and obesity: the San Diego liver study

Monica Tincopa¹, Ricki Bettencourt¹, Maral Amangurbanova¹, Christian Butcher¹, Christie Hernandez¹, Egbert Madamba¹, Seema Singh¹, Lisa Richards¹, Veeral Ajmera¹, Rohit Loomba¹. ¹UCSD, United States
Email: mtincopa@health.ucsd.edu

Background and aims: Differentiating non-alcoholic fatty liver disease (NAFLD) from alcohol-associated liver disease (ALD) can be challenging in individuals with overweight and obesity. There are limited prospective data from cohorts of individuals with overweight or obesity who have been systematically assessed for hepatic steatosis. This study aimed to evaluate the prevalence of NAFLD and ALD among individuals with overweight and obesity and to

POSTER PRESENTATIONS

determine the clinical utility of serum phosphatidylethanol (PEth) in differentiating NAFLD from ALD.

Method: This prospective study enrolled adults aged 40–75 with overweight (BMI ≥ 25 – <30 kg/m²) and obesity (BMI ≥ 30). Participants completed a research visit with vibration controlled transient elastography (VCTE) with controlled attenuation parameter, MRI proton-density-fat-fraction (MRI-PDFF) and MR elastography (MRE). Alcohol use was assessed with Alcohol-Use-Disorder-Identification-Test (AUDIT)-C, Skinner Lifetime Drinking History and serum PEth. NAFLD was defined as MRI-PDFF $\geq 5\%$ and AUDIT-C <4 for males and <3 for females with exclusion of other liver diseases and consistent with AASLD Practice Guidance. ALD was defined as MRI-PDFF $\geq 5\%$ with self-reported measures consistent with alcohol use disorder. Advanced fibrosis was defined using established liver-stiffness cut-points on MRE.

Results: The cohort included 278 consecutive individuals, median age 54 years, 46% males, 41% Latinos, median BMI 31 kg/m² with 29.5% having diabetes. The prevalence of NAFLD was 68.7% and ALD 11.2%. Median hepatic fat-content by MRI-PDFF was 13.2% in NAFLD versus (vs.) 11% in ALD. Median MRE liver stiffness measures were 2.2 kPa in NAFLD vs. 2.1 kPa in ALD. The prevalence of advanced fibrosis by MRE was 11.5% in NAFLD vs. 12.9% with ALD. PEth >20 –40 ng/ml, >40 –60 ng/ml and >60 ng/ml was detected in 4.3%, 2.1% and 5.4% of NAFLD patients. Serum PEth correlated with MRE liver stiffness measures in NAFLD (r_s 0.20, p 0.01). A PEth cut-point of <17 ng/ml yielded an AUC of 0.82 with a negative predictive value of 96% to distinguish those with NAFLD from those with ALD (Figure 1).

Figure 1. Clinical Utility of PEth in Differentiating NAFLD from ALD

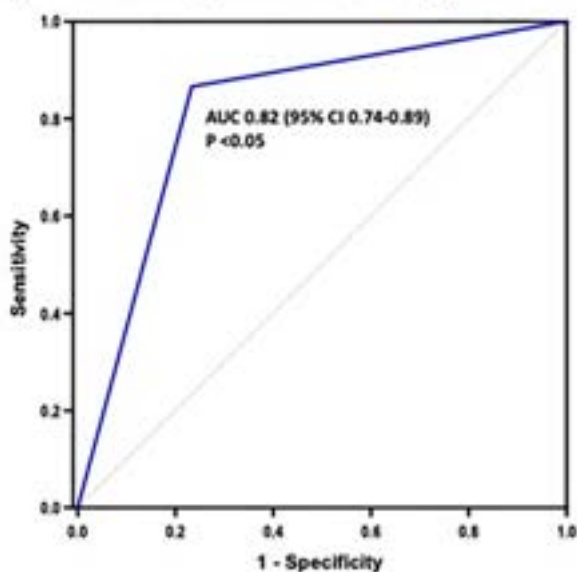


Figure:

Conclusion: Among a well characterized prospective cohort of individuals with overweight and obesity, the prevalence of NAFLD was 69% and ALD 11%. The prevalence of advanced fibrosis was 10%. Serum PEth is associated with increased liver stiffness in NAFLD, raising concern for synergistic effects of even low amounts of alcohol on disease progression in NAFLD. A PEth of <20 ng/ml may serve as a simple serum-based tool to differentiate those with NAFLD from those with ALD in patients with overlapping risk factors. These data have important implications for clinical practice and trials.

TOP-085

Long-term liver-related outcomes in 1,260 patients with non-cirrhotic NAFLD

Camilla Akbari¹, Maja Dodd¹, Xiao Zhang², Tongtong Wang², Thomas Jemielita², Gail Fernandes², Samuel Engel², Patrik Nasr^{1,3}, Johan Vessby⁴, Fredrik Rorsman⁴, Stergios Kechagias³, Per Stal¹, Mattias Ekstedt³, Hannes Hagström¹, Ying Shang¹. ¹Department of Medicine, Huddinge, Karolinska Institutet, Stockholm, Sweden; ²Merck and Co., Inc., Rahway, NJ, USA, United States; ³Department of Gastroenterology and Hepatology and Department of Health, Medicine, and Caring Sciences, Linköping University, Linköping, Sweden; ⁴Dept of Gastroenterology and Hepatology, Uppsala University Hospital, SE-751 85 Uppsala, Sweden
Email: ying.shang@ki.se

Background and aims: Non-alcoholic fatty liver disease (NAFLD) can progress to cirrhosis, decompensated cirrhosis and hepatocellular carcinoma (HCC). Previous studies on the prognosis of NAFLD have been limited to less than 1000 patients, have few hard outcomes and frequently short follow-up time or low granularity. Here, we aimed to investigate the long-term prognosis of a large cohort of patients with NAFLD regarding the risk of liver-related outcomes.

Method: We conducted a retrospective cohort study with data from three Swedish university hospitals. Patients were diagnosed with NAFLD through biopsy, vibration-controlled transient elastography (VCTE) or as a clinical diagnosis between 1974–2020 and followed up until 2020. We excluded patients with cirrhosis at baseline. Each NAFLD patient was matched on age, sex and municipality with up to ten reference individuals, identified from the Swedish Total Population Register. Liver-related outcomes were defined as clinically recorded diagnoses of cirrhosis, decompensated cirrhosis, HCC or liver-related death, or ascertained through linkage to Swedish national registers. The risk of liver-related outcomes was estimated by Cox regression, and Harrell's C-statistic was performed to assess model discrimination.

Results: 1,260 non-cirrhotic NAFLD patients and 12,529 matched controls were included. The median age at inclusion was 52 years (IQR: 39–60) and 748 (59.4%) were men. 904 (71.8%) patients were diagnosed through biopsy, 118 (9.4%) through VCTE and 238 (18.9%) through a clinical diagnosis. During follow-up, 339 outcomes occurred in the NAFLD group (IR = 5.9/1000 PY), and 597 in the reference individuals (IR = 1.0/1000 PY). NAFLD was associated with a higher rate of liver-related outcomes (hazard ratio: 6.6; 95% CI 5.2–8.5). The cumulative incidence of liver-related outcomes was highly associated with the stage of fibrosis at diagnosis after considering competing risks (Figure). Around 40% of patients with F3 developed a liver-related outcome after 20 years. In the biopsy subcohort, patients with F3 and NASH had a higher overall mortality than patients with F3 without NASH, mainly from extrahepatic cancers, but there was no difference in the cumulative risk for liver-related outcomes. In patients with biopsy-diagnosed NAFLD, the predictive ability of FIB-4 showed a similar C-statistic as compared to biopsy for prediction of liver-related outcomes at 5 years (0.713 for FIB-4 vs 0.701 for biopsy) and at 10 years (0.728 vs 0.734). In the full cohort, C-statistic reflecting FIB-4's prediction of liver-related outcomes at 5 years and 10 years were 0.724 and 0.730, respectively.

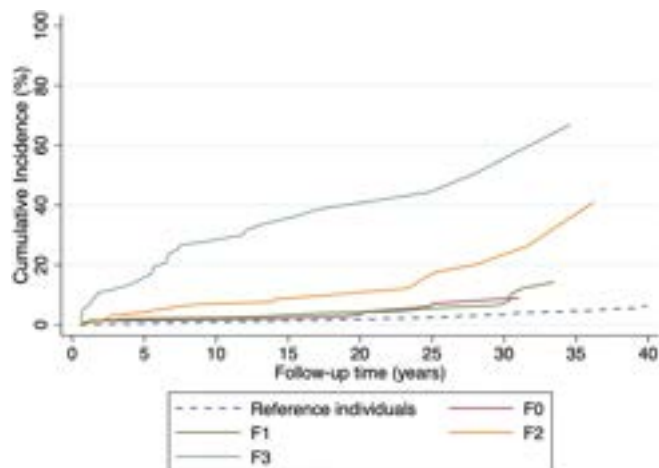


Figure: Cumulative incidence of liver-related outcomes stratified on fibrosis stage and compared against reference individuals from the general population.

Conclusion: The cumulative incidence of liver-related outcomes was considerable in this large cohort of patients with NAFLD and fibrosis stage 2–3. We found some indication of a more severe prognosis in those with F3 and NASH. Prognostic information from biopsy was comparable to FIB-4, although both modalities had modest discriminative ability. New prediction models are needed in NAFLD.

SATURDAY 24 JUNE

SAT-393

Early aminotransferase improvement in the phase 2b NATIVE study is predictive of response pattern of liver histology as well as hepatic and cardiometabolic health markers at the end of treatment in patients with non-cirrhotic NASH

Quentin Anstee¹, Philippe Huot-Marchand², Lucile Dzen², Jean-Louis Junien², Pierre Broqua², Sven Francque³, Manal Abdelmalek⁴, Michael Cooreman², Stephen Harrison⁵.
¹Newcastle University, United Kingdom; ²Inventiva, Research and Development, Daix, France; ³Antwerp University Hospital, Edegem, Belgium; ⁴Mayo Clinic, Rochester, United States; ⁵University of Oxford, United Kingdom

Email: michaelcooreman@msn.com

Background and aims: There is a need to identify non-invasive tests (NITs) that provide an early prediction of evolving histological response/non-response to therapy. Lanifibranor has shown efficacy on liver histology and metabolic-immune markers of NASH. We evaluated the correlation of ALT and AST response at treatment week (TW) 4 with subsequent histological response and change in cardiometabolic health (CMH) in lanifibranor treated patients at TW24 in the ph2b NATIVE trial.

Method: NATIVE evaluated lanifibranor 800 and 1200 mg/d versus placebo in patients with non-cirrhotic NASH over 24 weeks. We assessed the early kinetics of liver biochemistry improvements for AST and ALT at TW4, and their abilities for predicting histological non-response at TW24 for 'NASH resolution with no worsening of fibrosis' (E1) and 'improvement of fibrosis with no worsening of NASH' (E2), mainly using the Negative Predictive Value (NPV) but including also Sensitivity (Sens), Specificity (Spec) and Negative Likelihood Ratio (NLR) at TW4. Analyses were performed on data available for transaminases at TW4 and histological response at TW24 (N = 142 pooled lanifibranor treated patients) individually for each NIT. Based on the results, we then analyzed the correlation of early ALT and AST improvement at TW4 and response of CMH markers at TW24.

Results: For E1, an ALT reduction $\geq 15\%$ from baseline value to TW4 showed Sens 0.90 (95%CI 0.83–0.98), Spec 0.22 (0.13–0.31) for histological response. Reductions $< 15\%$ were observed in 21.5% of non-responders versus 9.5% of responders, giving a NPV of 0.74 (0.56–0.92) and NLR 0.44. AST reduction $\geq 15\%$ was less sensitive but more specific: Sens 0.60 (0.48–0.72), Spec 0.47 (0.36–0.58), reductions $< 15\%$ gave a NPV 0.60 (0.48–0.72), NLR 0.85. For E2, biochemical changes performed less well as predictive markers. Reductions $\geq 15\%$ showed Sens 0.82 (0.72–0.92), Spec 0.15 (0.08–0.23) and Sens 0.54 (0.41–0.67), Spec 0.42 (0.31–0.52) for ALT and AST respectively. ALT and AST decrease at TW4 correlated with improvement in markers of glucose and lipid metabolism, adiponectin, GGT at TW24, with a correlation more pronounced for ALT than AST.

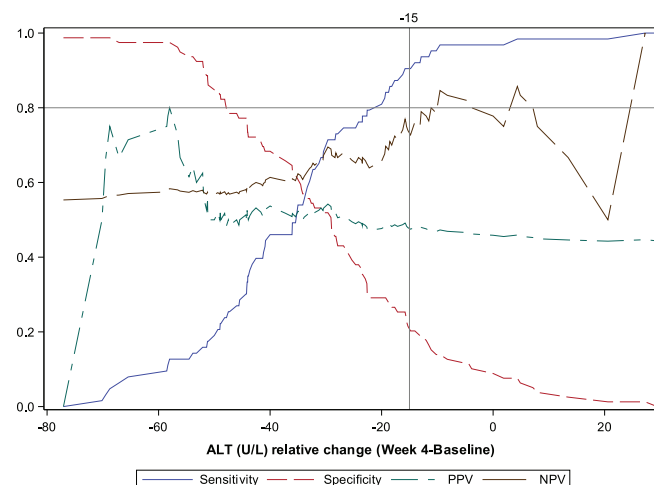


Figure: NASH resolution without worsening of fibrosis.

Conclusion: Considering detection of NASH resolution, absence of a $\geq 15\%$ reduction from baseline in ALT at TW4 in the NATIVE study was a simple, effective tool to predict non-response to lanifibranor at TW24. Early decrease in ALT or AST correlated with improvement of non-invasive hepatic and CMH biomarkers at TW24.

SAT-394

Novel artificial intelligence-assisted digital pathology quantitative image analysis predicts the occurrence of liver-related clinical events in the multicentric, European, hepatic outcomes and survival fatty liver registry (HOTSURFR) study

Li Chen¹, Louis Petitjean¹, Javier Ampuero², Jerome Boursier³, Stergios Kechagias⁴, Salvatore Petta⁵, Hannes Hagström⁶, Jörn Schattenberg⁷, Frederic Charlotte⁸, Leila Kara⁹, Pierre Bedossa¹⁰, Mathieu Petitjean¹, Vlad Ratzu¹¹.
¹PharmaNest, United States; ²Hospital Universitario Virgen del Rocío de Sevilla, Spain; ³CHU Angers, France; ⁴Linköping University, Sweden; ⁵Università degli Studi di Palermo, Italy; ⁶Karolinska University Hospital, Sweden; ⁷Mainz Universität, Germany; ⁸Assistance Publique Hôpitaux de Paris, France; ⁹ICAN, France; ¹⁰Liverpat, France; ¹¹Sorbonne Université, France

Email: vlad.ratzu@inserm.fr

Background and aims: Artificial intelligence-assisted digital pathology provides an automated, operator independent, sensitive and quantitative assessment of histological changes with the ability to identify patterns of fibrosis progression or regression. However, its value for predicting clinical events is unknown. We have previously shown that quantitative traits in collagen fiber parameters can be used to build fibrosis scores that are correlated with the semiquantitative histological NASH CRN stages. We aimed to determine if quantitative fibrosis scores from baseline liver biopsies are correlated with incident liver-related events (LRE) in a large, multicentric, European cohort with long-term follow-up.

POSTER PRESENTATIONS

Method: 304 patients (pts) from 6 European centers with liver biopsy performed for suspected NAFLD before 2011 and clinical follow-up, were retrospectively analyzed. LRE were defined as occurrence of cirrhosis, cirrhosis decompensation events or hepatocellular carcinoma. Formalin-fixed, paraffin-embedded biopsies where stained with collagen stains (Masson Trichrome or Picro Sirius Red) and digitized at 40X. Histology was read centrally (NASH CRN classification). Quantitative image analysis extracted 315 single-fiber quantitative traits (qFTs) to assess fibrosis composition, morphometric and architectural histological phenotypes. The qFTs that exhibited a significant (>50%) mean change between pts with or without events were identified, normalized and combined in a Liver Event Predictive Score (LEPS). A quantitative fibrosis severity score, Ph-FCS, ranging from 1 to 10, previously optimized to model the F0-F4 fibrosis progression, and derived from a selection of the same 315 qFTs was also assessed.

Results: Mean age was 53.5 yrs, 56% were males, mean BMI 30.6 kg/m², 39% had diabetes and 62% arterial hypertension. The proportion of histological fibrosis stages were: 0/1/2/3/4, 53%/17%/8%/14%/8%, respectively. Median follow-up was 11.4 yrs (IQR 4.7). 52 pts (17%) had at least one LRE. Mean (sd) LEPS was 1.88 (0.67) in pts with LRE vs 2.68 (0.78) in pts without LRE ($p < 0.001$). Using a cut-off value of 2.9, LEPS had a sensitivity of 71% and specificity of 68% for the prediction of LRE. When the cut-off value was changed by $\pm 5\%$ the sensitivity and specificity varied within a -11% to $+6.5\%$ range. Ph-FCS demonstrated a similar performance as LEPS (sensitivity = 79%, specificity = 62%) for a cut-off value of 4. There was a strong correlation between LEPS and Ph-FCS ($r = 0.77$, $p < 0.001$), confirming that fibrosis severity is a major predictor of clinical events.

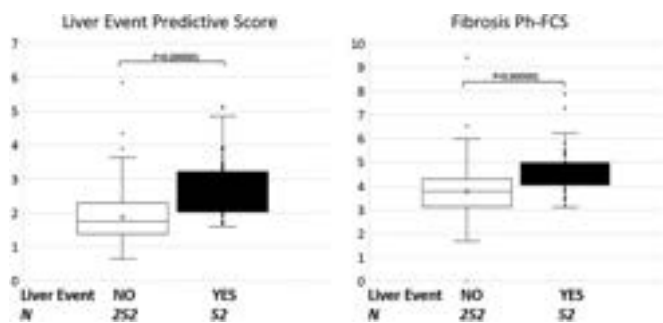


Figure:

Conclusion: Quantitative image analysis by digital pathology performed on stained liver slides provides continuous scores that identify NAFLD patients at risk of incident clinical outcomes. Further validation on additional cases is ongoing, aiming to provide better histological surrogates for therapeutic trials.

SAT-395

Risk-stratification of patients with non-alcoholic fatty liver disease (NAFLD) in primary care: lessons from the Calgary NAFLD pathway

Abdel-Aziz Shaheen¹, Elizabeth Baguley¹, Wendy Schaufert², Mark G Swain¹. ¹University of Calgary, Canada; ²Alberta Health Services, Canada

Email: az.shaheen@ucalgary.ca

Background and aims: The Calgary non-alcoholic fatty liver disease (NAFLD) pathway (CNP) is the largest primary care-based NAFLD pathway in North America. We aimed to evaluate the performance of different risk-stratification modalities among CNP patients according to their baseline liver enzymes and metabolic syndrome risk factors.

Method: The CNP uses validated shearwave elastography (SWE) assessment as the primary tool of risk-stratification for patients with a history of fatty liver or 'at-risk' of metabolic syndrome since March 2017. In the CNP, 'at-risk' of advanced fibrosis patients with SWE ≥ 8.0 kPa or inconclusive results are referred to hepatology. Since only

an ALT assessment was mandatory at baseline, some patients did not have all baseline serum fibrosis-4 variables (FIB-4). We compared the performance of both SWE ≥ 7.0 and 8.0 kPa, and FIB-4 ≥ 1.3 , according to sex, age, rural residence, body mass index (≥ 35), normal ALT (25 U/L for women and 30 U/L for men), and presence of Type 2 diabetes mellitus (DM).

Results: A total of 12,122 patients completed SWE assessment with a confirmed NAFLD diagnosis in the CNP between March 2017 and June 2022. Baseline FIB-4 was available in 8,590 patients (70.9%). Among those patients with available FIB-4, 2,643 (33.8%) had FIB-4 ≥ 1.3 , 402 (4.8%) had an inconclusive SWE, 1,042 (11.9%) SWE ≥ 7.0 kPa, and 762 (8.9%) SWE ≥ 8.0 kPa. The performance of different modalities among different cohorts is presented in Table 1. Patients with normal baseline ALT levels had FIB-4 ≥ 1.3 ($p = 0.61$) and SWE ≥ 8.0 kPa ($p = 0.09$) similar to patients with elevated ALT. While SWE ≥ 7.0 and 8.0 kPa were significantly higher among patients with a BMI ≥ 35 , these patients had lower advanced fibrosis confirmed by liver biopsy ($n = 232$ patients) compared to patients with BMI < 35 ($p < 0.001$). Patients with DM had significantly higher rates of FIB-4 ≥ 1.3 and SWE ≥ 7.0 and 8.0 kPa, Table 1.

Table: Comparison of FIB-4 1.3 and SWE 7.0 and 8.0 kPa among different demographic and clinical characteristics.

	Female cohort N = 4,538 (52.9%)	Age ≥ 50 yrs cohort N = 5,284 (61.5%)	BMI ≥ 35 N = 2,085 (30.2%)	Normal ALT N = 2,585 (30.1%)	Elevated ALT N = 6,005 (69.9%)	DM N = 2,922 (34.2%)
Modality cut-off						
FIB-4 ≥ 1.3	1,289 (28.4%)	2,350 (44.5%)	579 (27.8%)	785 (30.4%)	1,858 (30.9%)	1,081 (37.0%)
SWE ≥ 7.0 kPa	540 (11.9%)	781 (14.8%)	387 (18.6%)	275 (10.6%)	749 (12.5%)	554 (19.0%)
SWE ≥ 8.0 kPa	404 (9.0%)	596 (11.4%)	287 (13.9%)	208 (8.1%)	554 (9.3%)	448 (15.5%)

Conclusion: In this primary care-based cohort to risk-stratify NAFLD patients for advanced fibrosis, patients with normal ALT had similar risk of elevated liver stiffness compared to those with elevated ALT. Priority of risk-stratification should be given to patients with DM.

SAT-396

Thrombospondin-2 as a new biomarker for at risk NASH and advanced fibrosis in a large multicentric European cohort

Vlad Ratzu¹, Rambabu Surabattula², Elisabetta Bugianesi³, Jörn Schattenberg², Maharajah Ponnaiah⁴, Chiara Rosso³, Angelo Armandi³, Sudha Myneni², Raluca Pais⁴, Leila Kara⁴, Detlef Schuppan². ¹Sorbonne Université, Paris, France; ²Mainz Universität, Germany; ³University of Torino, Italy; ⁴ICAN, France
Email: vlad.ratzu@inserm.fr

Background and aims: New biomarkers with strong biological rationale are needed for identifying patients with progressive or advanced NASH in clinical practice and for selection in therapeutic trials. Liver transcriptomic data from NAFLD patients identified thrombospondin-2 (TSP2), a matricellular glycoprotein that mediates cell-matrix interactions and collagen fibrillogenesis, as strongly induced in patients with NASH and those with advanced fibrosis. We tested the diagnostic performance of Tsp2, I7 (a matricellular and metabolic marker) and CD163 (a macrophage marker) in a large, multicentric European cohort.

Method: Retrospective study of patients with NAFLD, available liver biopsy and frozen serum collected within 3 months of the biopsy. TSP2 and I7 were measured by validated proprietary ELISAs, and CD163 was determined by commercial ELISA (R&D). FIB4 was calculated. Liver biopsies were graded and staged according to the NASH CRN histological classification. Histological outcomes were at-risk NASH (steatohepatitis with NAS ≥ 4 and fibrosis stage 2-4) and

advanced fibrosis (stages 3–4). We developed combinatorial scores (with clinical variables and/or multi-biomarkers) for NASH and advanced fibrosis using multivariate logistic regression controlling for centers, age, BMI, and gender. Training and validation sets were defined using a machine learning algorithm which randomly split 80% and 20% of the total cohort, for 100 iterations, followed by averaging of the AUROC predictions.

Results: 481 patients were included from Turin (219), Paris (173) and Mainz (89): mean age 51.4 years (s.d. 12.7), 61% males, Mean BMI 30.6 kg/m² (s.d. 5.6), 44% with type 2 diabetes, 53% with arterial hypertension, mean ALT 66 (s.d. 55), mean GGT 113 (s.d. 162). There were no significant differences between the three centers. The proportion of at risk NASH was 45.5%, of advanced fibrosis 30%. Median TSP2 was 55.9 ng/ml [IQR 48.6], median I7: 86 ng/ml [IQR 114], median CD163: 531 [IQR 278], FIB4 1.13 [IQR 0.87]. AUROCs for at-risk NASH were TSP2: 0.823; I7: 0.757; CD163: 0.733 and FIB4: 0.726. AUROCs for advanced fibrosis were TSP2: 0.817; I7: 0.678; CD163: 0.761 and FIB4: 0.726. Combining TSP2 with clinical and biological variables (AST, platelets, albumin, GGT) achieved an AUROC of 0.872 for at risk NASH (Se 0.77, Spe 0.85) and 0.822 for advanced fibrosis (Se 0.72, Spe 0.83) (combined with age and platelets). The addition of I7 and C163 to the TSP2-clinical biological score only marginally improved diagnostic performance: AUROCs 0.884 and 0.829 for at-risk NASH and advanced fibrosis, respectively.

Conclusion: Serum levels of TSP2, a molecule with high biological rationale, have a strong discriminative performance for at-risk NASH and advanced fibrosis, especially when combined with simple clinical and biological variables. TSP2 should be prioritized as a strong biomarker candidate in patients with NAFLD.

SAT-397

Predicting severe liver outcomes in NAFLD using repeated measurements of biomarkers—a cohort study in 1,260 patients

Ying Shang¹, Camilla Akbari¹, Maja Dodd¹, Xiao Zhang², Tongtong Wang², Thomas Jemielita², Gail Fernandes², Samuel Engel², Patrik Nasr^{1,3}, Johan Vessby⁴, Fredrik Rorsman⁴, Stergios Kechagias³, Per Stal¹, Mattias Ekstedt³, Hannes Hagström¹. ¹Karolinska Institutet, Department of Medicine, Huddinge, Sweden; ²Merck and Co., Inc., Rahway, NJ, USA, United States; ³Department of Gastroenterology and Hepatology and Department of Health, Medicine, and Caring Sciences, Linköping University, Linköping, Sweden; ⁴Dept of Gastroenterology and Hepatology, Uppsala University Hospital, SE-751 85 Uppsala, Sweden
Email: ying.shang@ki.se

Background and aims: Non-invasive biomarkers measured at a single timepoint have prognostic information for development of severe liver disease (SLD) in patients with non-alcoholic fatty liver disease (NAFLD), but these biomarkers may change over time and the predictive capacity of changes in biomarkers has yet to be determined. Herein, we aimed to assess if the change in biomarkers could predict SLD in patients with NAFLD better than the same biomarkers measured at a single timepoint.

Method: We used a retrospective cohort of 1,260 patients with non-cirrhotic NAFLD (among which 904 [71.7%] had biopsy-proven NAFLD) from three university hospitals in Sweden between 1974 and 2019. Medical charts were reviewed, and biomarkers were measured at baseline and at follow-up visits. Severe liver disease outcomes including cirrhosis, decompensated cirrhosis, hepatocellular carcinoma, liver failure, liver transplantation or MELD score over 15 were determined through medical charts or linkage to national registers until the end of 2020. We used multivariable Cox regression to determine baseline risk factors and biomarkers associated with SLD. We quantified the associations between the trajectory of biomarkers (including current value and slope) with risk of SLD using a joint modeling approach.

Results: The median age at NAFLD diagnosis was 52 years (IQR: 39–60) and 59% were male. During a median follow-up of 12.2 years, 111 (8.8%) patients developed SLD. Higher aspartate aminotransferase (AST), higher Fibrosis-4 score (FIB-4), and lower platelets at baseline were independently associated with a higher SLD risk after adjusting for metabolic factors and fibrosis stage. The average of log-transformed (log) FIB-4 increased steadily over time whereas the average of platelets count and log (AST) remained roughly constant. The multivariable joint modeling showed that higher current value of FIB-4 (HR 2.96, 95% CI 2.08–4.26), AST (HR 2.48, 95% CI 1.85–3.34) and lower platelets (HR 0.99, 95% CI 0.99–1.00) was associated with increased risk of SLD, whereas the rate of change in these biomarkers had no significant association to the risk of SLD (Table).

Table: The association between repeated values of the AST, platelets, FIB-4 and the event of SLD from joint modeling

Current value of biomarker level*	HR [#]	95% confidence interval	p value
log (AST), $\mu\text{kat/L}$	2.96	2.08–4.26	<0.001
Platelets, $10^9/\text{L}$	0.99	0.99–1.00	<0.001
log (FIB4)	2.48	1.85–3.34	<0.001
Instantaneous slope of temporal pattern**			
log (AST)-slope	0.37	0.11–1.58	0.188
log (AST)-value, $\mu\text{kat/L}$	3.43	2.38–5.06	<0.001
Platelets-slope	1.00	0.98–1.02	0.618
Platelets-value, $10^9/\text{L}$	0.99	0.99–1.00	0.002
log (FIB4)-slope	1.40	0.38–5.39	0.591
log (FIB4)-value	2.60	1.84–3.84	<0.001

*The basic joint model, which combines a linear mixed submodel of biomarkers and a survival submodel of time to SLD.

[#]HR includes the baseline covariates: age, sex, type 2 diabetes, hyperlipidemia, body mass index, fibrosis stage.

**The slope of the marker is modeled and added to the basic joint model.

Conclusion: In addition to the baseline measurement of the non-invasive biomarkers such as FIB-4, AST, and platelets taken at NAFLD diagnosis, monitoring their value over time is important as the current value of them is closely associated with the risk of future SLD. The rate of change may not affect the prognosis to severe liver disease.

SAT-398

Improvements in liver fibroinflammation (as assessed by corrected T1 [cT1]) with HTD1801 (berberine ursodeoxycholate) treatment in patients with non-alcoholic steatohepatitis and type 2 diabetes mellitus

Stephen Harrison¹, Nadege Gunn², Guy Neff³, Abbey Flyer⁴, Alexander Liberman⁵, Leigh MacConell⁵. ¹Pinnacle Clinical Research, United States; ²Impact Research Institute, United States; ³Covenant Metabolic Specialists, United States; ⁴Pacific Northwest Statistical Consulting, United States; ⁵HighTide Therapeutics USA, LLC, United States

Email: sharrison@pinnacleclinicalresearch.com

Background and aims: HTD1801 is a new molecular entity consisting of an ionic salt of berberine and ursodeoxycholic acid with a unique microstructure which has been shown to significantly reduce liver fat content (LFC) as determined by MRI-PDFF in an 18-Week, placebo-controlled Phase 2 study in patients with non-alcoholic steatohepatitis (NASH) and Type 2 Diabetes (T2DM) (NCT03656744). cT1 is an MRI-based quantitative metric for assessing liver inflammation and fibrosis. Previous studies have reported that cT1 improvements are moderately correlated with histologic improvements in NAS and fibrosis and cT1 levels are associated with clinical outcomes (liver and CVD) in patients with NASH. The purpose of this post-hoc analysis

POSTER PRESENTATIONS

was to evaluate the effects of HTD1801 on cT1 in patients with NASH and T2DM.

Method: One hundred patients were randomized and treated with HTD1801 1000 mg BID (n = 34), HTD1801 500 mg BID (n = 33), or placebo (n = 33) for 18 weeks. MRI data was collected prospectively for evaluation of the primary end point (proton density fat fraction), and cT1 was evaluated after the completion of the study for subjects who had been randomized to HTD1801 1000 mg BID or placebo. p values (nominal) were obtained from an ANCOVA model with treatment group as a fixed effect, and baseline ALT and baseline cT1 as covariates. Values are Mean (SD) unless otherwise specified.

Results: On average at baseline, patients were 56 (11) years, 72% female, 91% White, 38% Hispanic or Latino, with an HbA1c of 7.1% (1.0). At baseline, subjects had significantly elevated LFC by MRI-PDFF [19.3% (6.5)] and fibroinflammation by cT1 (942.1 [91.5] ms and 937.5 [97.7] ms for HTD1801 1000 mg BID and placebo, respectively). As shown in Figure 1, after 18 weeks of treatment there was a significant reduction in cT1 with HTD1801 compared to placebo (-60.9 [75.9] ms vs -14.7 [68.9] ms, $p < 0.05$). Similarly, a significant reduction was observed in ALT, a marker of liver function, in the HTD1801 1000 mg BID group compared to placebo (-19 [27.2] U/L vs -3 [19.2] U/L, $p < 0.01$). At Week 18, a larger proportion of subjects receiving HTD1801 compared to placebo (39% vs 16%, respectively) experienced at least an 80 ms reduction in cT1, which has been correlated with a 2-point reduction in the NAS.

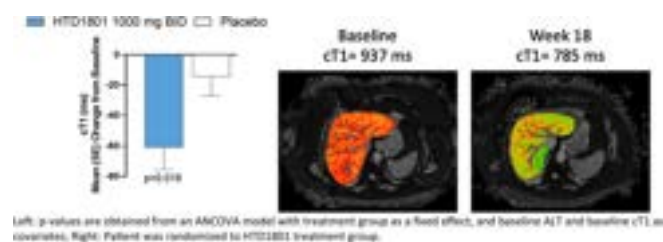


Figure: Subjects Receiving HTD1801 Had Significant Reduction in Fibroinflammatory Disease as Assessed by cT1

Conclusion: These data provide further evidence that HTD1801 may improve measures of disease activity in patients with NASH and T2DM and warrant further investigation. A Phase 2b study is currently ongoing to evaluate the histologic effects of HTD1801 in patients with NASH and confirm the findings of this evaluation (NCT05623189).

SAT-399

Prevalence of NAFLD and advanced fibrosis in Stockholm, Sweden

Emilie Toresson Grip^{1,2}, Helena Skräder¹, Ying Shang², Oskar Ström^{1,2}, Hannes Hagström^{2,3}. ¹Quantify Research AB, Stockholm, Sweden; ²Karolinska Institutet, Department of Medicine, Huddinge, Stockholm, Sweden; ³Karolinska University Hospital, Clinical Epidemiology Division, Department of Medicine Solna, Stockholm, Sweden

Email: emilie.toresson-grip@quantifyresearch.com

Background and aims: Estimates of prevalence of NAFLD in Sweden are lacking, despite globally unique register data. Use of invasive or costly diagnostics such as histology or imaging are scarce in primary care, leading to underdiagnosis of NAFLD, and subsequently under-reporting of NAFLD in registers. Therefore, non-invasive measures of NAFLD, such as the commonly used Hepatic Steatosis Index (HSI), can be used to estimate the prevalence of probable NAFLD in broad populations. Here, we used data from the HERALD (Health outcomes and risk assessment in chronic liver disease) cohort to estimate prevalence of NAFLD in primary or secondary care settings in Stockholm, using data from national health registries and regional electronic health records.

Method: All patients with any liver-related tests taken in Stockholm during 2015–2020 were included (n = 715,161). The HSI was

calculated using the latest available information on AST, ALT and BMI during 2015–2020, in either primary or secondary care. A cut-off of ≥ 36 was used to define patients with probable NAFLD. Patients with alcohol-related diseases or other liver diseases than NAFLD since 2001 were excluded. The FIB-4 score was calculated using a cut-off of ≥ 1.3 (age < 65) and ≥ 2.0 (age ≥ 65) to define intermediate or high-risk (≥ 2.67) of advanced fibrosis among all patients with NAFLD.

Results: In total 341,305 patients with assessable HSI were included, of which 45% (n = 151,939) had probable NAFLD. Among the patients with probable NAFLD, 25% had T2DM, median age was 57 years, and 56% were females. In addition, 23% of patients with probable NAFLD had an intermediate (15%) or high risk (8%) of advanced fibrosis, but only 1.7% had a NAFLD/NASH diagnosis code (ICD-10 K76.0/K75.8) recorded in primary or secondary care, despite allowing for a 19-year look back period for such diagnoses. Of patients with a recorded NAFLD diagnosis, 88% had high HSI, and 32% had intermediate or high risk of advanced fibrosis. Among the patients without a recorded NAFLD diagnosis, the corresponding fractions were 44% for high HSI and 31% for intermediate or high risk for advanced fibrosis.

Conclusion: This study provides an up-to-date estimate of NAFLD prevalence in a unique, unselected heterogeneous population of individuals in Stockholm. The results support previous indications that there are many undiagnosed patients with NAFLD. Advanced fibrosis may be equally common in patients with and without a recorded diagnosis of NAFLD, highlighting needs for further improvement of identification of at-risk patients.

SAT-400

Accuracy of 100 Hz transient elastography-based spleen stiffness for the identification of advanced fibrosis in biopsy-proven non-alcoholic fatty liver disease

Angelo Armandi^{1,2}, Antonio Liguori^{3,4}, Talal Merizian², Merle Marie Werner², Maurice Michel², Christian Labenz², Carmen Lara Romero², María Del Barrio Azaceta^{5,6}, Belen Pino⁵, Beate Straub⁷, Manuel Romero Gomez^{5,8}, Luca Miele^{3,4}, Jörn Schattenberg². ¹Division of Gastroenterology and Hepatology, Department of Medical Sciences, University of Turin, Turin, Italy; ²Metabolic Liver Disease Research Program, I. Department of Medicine, University Medical Center of the Johannes Gutenberg-University, Mainz, Germany; ³DiSMC-Department of Scienze Mediche e Chirurgiche, Fondazione Policlinico Gemelli IRCCS, Rome, Italy; ⁴Department of Medicina e Chirurgia Traslationale, Università Cattolica Del Sacro Cuore, Rome, Italy; ⁵Digestive Diseases Unit, Hospital Universitario Virgen del Rocío, SeLiver Group, Institute of Biomedicine of Sevilla (HUVR/CSIC/US), Department of Medicine, University of Seville, Seville, Spain; ⁶Gastroenterology and Hepatology Department, Clinical and Translational Research in Digestive Diseases, Valdecilla Research Institute (IDIVAL), Marqués de Valdecilla University Hospital, Santander, Spain; ⁷Institute of Pathology, University Medical Center of the Johannes Gutenberg-University Mainz, 55131 Mainz, Germany; ⁸Centro de Investigación Biomédica en Red de Enfermedades Hepáticas y Digestivas (CIBEREHD), Madrid, Spain
Email: angelo.armandi@unito.it

Background and aims: The non-invasive identification of advanced fibrosis in Non-Alcoholic Fatty Liver Disease (NAFLD) represents an unmet need. In NAFLD, the liver-spleen axis may be affected by the chronic, low-grade splanchnic inflammation, leading to spleen tissue congestion even in the absence of portal hypertension. We aimed to explore the accuracy of spleen stiffness measurement (SSM) as a non-invasive tool to detect advanced fibrosis in individuals with biopsy-proven NAFLD.

Method: Retrospective cohort study of 167 patients with biopsy-proven NAFLD analyzed from 3 centers (Mainz, Rome, Seville). Liver stiffness measurement (LSM) and SSM were collected within 6 months from the index liver biopsy, using the Fibroscan 630 Expert. For SSM, the 100 Hz spleen-specific probe was employed. Patients

Model	AUC	Se (%)	Sp (%)	PPV (%)	NPV (%)	DeLong p
Mainz cohort (n = 50)						
SSM - FIB-4	0.92	82.1	94.1	95.8	76.2	0.69 (with SSM-LSM)
SSM - LSM	0.94	89.3	88.2	92.6	83.3	0.13 (with LSM-FIB-4)
LSM - FIB-4	0.88	92.9	70.6	83.9	85.7	0.39 (with SSM-FIB-4)
Rome/Seville cohort (n = 117)						
SSM - FIB-4	0.84	78.0	80.0	75.0	83.1	0.43 (with SSM-LSM)
SSM - LSM	0.87	82.0	80.6	75.9	85.7	0.41 (with LSM-FIB-4)
LSM - FIB-4	0.85	90.0	70.1	69.2	90.4	0.82 (with SSM-FIB-4)

Table 1. Area Under the Curve (AUC) of the predictive models for the identification of advanced fibrosis. FIB-4: Fibrosis-4 score; LSM: liver stiffness measurement; SSM: spleen stiffness measurement.

Figure: (abstract: SAT-400).

with a history or presence of decompensation were excluded. Advanced fibrosis was defined by histological stages F3 and F4.

Results: Median age was 58 [50–64] years and 50.3% were male. Obesity and type 2 diabetes (T2D) were present in 63.5% and 59% of cases. A total of 83 (49.7%) cases had advanced fibrosis on liver histology. Median LSM was 10.2 [7.0–17.7] kPa and median Fibrosis-4 (FIB-4) score was 1.6 [1.08–2.79]. Median SSM was 30.5 [20.0–45.1] kPa, showing a stepwise increase across fibrosis stages, with higher values in advanced fibrosis, when compared to F0–F2 stages (median 38.4 [32.0–59.3] kPa versus 21.8 [16.4–30.6] kPa, $p < 0.000001$). Overall, SSM correlated with longitudinal spleen size ($r = 0.63$, $p < 0.001$) and inversely with platelet count ($r = 0.44$, $p < 0.001$), and was associated with advanced fibrosis after adjusting for age, sex, Body Mass Index, T2D and transaminases (OR 1.08 [95% CI 1.04–1.13], $p < 0.0001$). In the whole cohort, SSM had AUC of 0.85 for advanced fibrosis (Se 93.6%, Sp 61.9%, PPV 65.2%, NPV 91.2%), which was similar to that of LSM (AUC 0.87, DeLong p for SSM 0.475), and FIB-4 (AUC 0.80, DeLong p for SSM 0.228). In the Mainz cohort (derivation cohort), a model combining LSM and SSM reached the best accuracy for advanced fibrosis (AUC 0.94), when compared to the other models (Table 1). In the combined Rome and Seville cases (validation cohort), the same model reached an AUC of 0.87. In the derivation cohort, the cut-off of 24.6 kPa was identified by the lowest negative likelihood ratio for ruling out advanced fibrosis (Se 92.8%, Sp 58.9%, PPV 79.4%, NPV 90.9%). In the validation cohort, the consecutive use of SSM could identify F3–F4 patients that would have been ruled out by other non-invasive tests ($n = 12$ FIB-4 < 1.3 ; $n = 5$ LSM < 8 kPa).

Conclusion: SSM displays a progressive increase across fibrosis stages and is associated with advanced fibrosis. In this cohort with high prevalence of advanced fibrosis, the accuracy of SSM is comparable to LSM and FIB-4. The combined use of LSM and SSM in the NAFLD diagnostic algorithm may improve liver disease staging and risk stratification.

Boehringer-Ingelheim sponsored the study.

SAT-401

Performance of non-invasive tests as exclusion criteria for cirrhosis in trials targeting at-risk non-alcoholic steatohepatitis: combined data from multiple trials including more than 5,000 patients (in collaboration with NAIL-NIT consortium)

Naim Alkhouri¹, Julie Dubourg², Stephen Harrison³, Mazen Nouredin⁴, Michael Charlton⁵, Vlad Ratziu⁶,

Sophie Jeannin Megnier⁷, Jörn Schattenberg⁷. ¹Arizona Liver Health, Chandler, United States; ²Summit Clinical Research, San Antonio, United States; ³University of Oxford, United Kingdom; ⁴Houston Methodist Hospital, Houston, United States; ⁵UChicago Medicine, Chicago, United States; ⁶Institute for Cardiometabolism and Nutrition, France; ⁷University medicine at the Johannes Gutenberg University in Mainz, Mainz, Germany

Email: jdubourg@summitclinicalresearch.com

Background and aims: Non-alcoholic steatohepatitis (NASH) cirrhosis is a distinct group of patients which is usually excluded from NASH with F2–F3 clinical trials for reasons related to safety and efficacy assessments. We aimed to assess non-invasive tests (NITs) including Fibrosis-4 score (FIB-4), vibration-controlled transient elastography (VCTE) and FibroScan-based score Agile 4 to distinguish this group of patients.

Method: We combined screening data from 6 ongoing non-cirrhotic NASH clinical trials (>5,000 patients). Liver histology data were assessed centrally, and cirrhosis was defined as a fibrosis stage of 4 with or without NASH. Diabetes status required by the Agile 4 formula was defined using glycated hemoglobin (HbA1c). Area under the receiver operating characteristic (AUROC) analysis was used to determine the diagnostic accuracy of each test to rule-in cirrhosis. Considering the low prevalence of cirrhosis in NASH with fibrosis stage (F) 2 or 3 trials, we presented the positive likelihood ratio (LR+) as it is independent of the prevalence of cirrhosis, rather than the positive predictive value. We calculated the pre- and post-test probability of cirrhosis to express the clinical utility of each score.

Results: 1,104 patients with histology results were included, with a fibrosis prevalence of: 94 (9%) for F0, 231 (21%) for F1, 294 (27%) for F2, 440 (40%) for F3, and 45 (4%) for F4. AUROC for FIB-4, VCTE and Agile 4 are shown in the Figure. The LR+ of the published Agile 4 rule-in cut-off (≥ 0.57) was 9.25. This reflects a post-test probability of cirrhosis of 30% compared to a pretest probability of 4%. Among the 1,104 patients included in this analysis, 39 (3.5%) had Agile 4 ≥ 0.57 with 28 of those having no cirrhosis. The LR+ of the published FIB-4 rule-in cut-off (≥ 3.48) was 1.81. This reflects a post-test probability of cirrhosis of 7% compared to a pretest probability of 4%. Among the 1,104 patients included in this analysis, 12 (1%) had a FIB-4 ≥ 3.48 , with only 1 of those having cirrhosis and 13 having no cirrhosis. The LR+ of the published VCTE rule-in cut-off (≥ 20) was 4.56. This reflects a post-test probability of cirrhosis of 16% compared to a pretest

probability of 4%. Among the 1,104 patients included in this analysis, 117 (11%) had a VCTE ≥ 20 , with 98 of those having no cirrhosis but mainly F2 and F3.

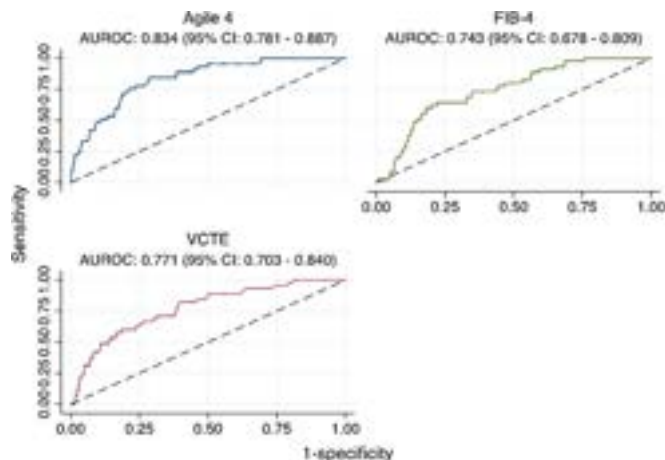


Figure:

Conclusion: In comparison to FIB-4 and VCTE, Agile 4 is the best test to be used as exclusion criteria for cirrhosis in NASH F2-F3 clinical trials.

SAT-402

FIB-4 predicts the risk of hepatocellular carcinoma in patients with type 2 diabetes: a longitudinal multicentre study

Vincent Mallet^{1,2}, Mathis Collier³, Nathanael Beeker³, Lucia Parlati^{1,2,4}, Stanislas Pol^{2,3}, Emmanuel Tsochatzis⁵. ¹AP-HP, Centre, Groupe Hospitalier Cochin Port Royal, DMU Cancérologie et spécialités médico-chirurgicales, Service d'Hépatologie, Paris, France; ²Université Paris Cité, F-75006, Paris, France; ³AP-HP, Centre, Groupe Hospitalier Cochin Port Royal, DMU PRIME, Unité de Recherche Clinique, Paris, France; ⁴Institut Cochin, Université Paris Cité, CNRS, INSERM, F-75014 Paris, France; ⁵UCL Institute for Liver and Digestive Health, Royal Free Hospital and UCL, London, United Kingdom
Email: e.tsochatzis@ucl.ac.uk

Background and aims: Patients with type-2 diabetes (T2D) are at risk for NAFLD and hepatocellular cancer (HCC). FIB-4 is recommended to delineate liver fibrosis in patients with NAFLD. We evaluated the performances of FIB-4 and the FIB-4 variation to predict HCC risk in patients with T2D.

Method: The data source was the Assistance Publique—Hôpitaux de Paris (AP-HP) Clinical Data Warehouse, that contains all clinical and biological data for acute inpatient/day case hospital admissions; post-acute care; and outpatient visits to 36 Greater Paris university hospitals. We selected, among all patients discharged from the AP-HP between August 1, 2017 and March 9, 2022, those with T2D mellitus (ICD-10: E11; n = 144,378). We excluded patients with an extra-hepatic cause of thrombopenia; those without synchronous serum transaminase and/or platelet measurement; and those without any FIB-4 measurement >3 months before censoring. We assessed the ability of a random FIB-4 and of FIB-4 variations to predict hepatocellular cancer (HCC) risk using the c-Index metric. The primary outcome was development of HCC and secondary outcome was liver disease progression to decompensated cirrhosis or HCC. Models were trained with two-third of the dataset and validated in the other third.

Results: 69,225 patients were included, mean age 66.7 years, 57.1% males. The average (standard deviation) number of FIB-4 measurements per patient was 9.3 (14.4), with a total of 643,755 FIB-4 measurements. 408 (0.6%) patients were diagnosed with HCC over 378,734 person-years, corresponding to a median follow-up of 2 years per patients. FIB-4 was associated with HCC risk in Cox

univariate [HR 1.668 (1.602–1.738)] and multivariate [aHR 1.52 (1.453–1.59)] analyses in the training set, and yielded concordant predictions in the validation set [c-index 0.804 (0.761–0.847) and 0.83 (0.789–0.871), respectively]. Adding absolute or relative FIB-4 variations, or FIB-4 slope over ≥ 3 previous FIB-4 measures, to a single, random FIB-4 measure, did not increase the prognostic value. Results were similar in nonparametric machine learning random forest survival models. The areas under the ROC curve (95% CI) of a single, random, FIB-4 measurement to predict 12- and 24-months HCC risk were 0.823 (0.797–0.849) and 0.829 (0.806–0.851). The FIB4 cut-offs for 90% sensitivities were 1.21 and 1.245, respectively. The cut-offs for 90% specificities were 3.075 and 2.954, respectively. Similar results were obtained for the risk of liver disease progression.

Figure: Performance of a single, random, measure of FIB-4 to predict 2-year HCC risk, by strata.

FIB-4 Threshold	Sensitivity	Specificity
Strata = men		
1.045	95.2%	32.6%
1.245	90.3%	44.2%
3.118	54.3%	90%
4.291	40.2%	95%
AUC	0.81 [0.782–0.837]	
Strata = women		
1.094	95.7%	44%
1.21	91%	50.9%
2.742	63.9%	90%
3.761	51%	95%
AUC	0.862 [0.82–0.904]	
Strata = alcohol use disorders		
1.596	95.6%	46.1%
2.111	90.2%	61%
5.798	40%	90%
Inf	0.0%	100.0%
AUC	0.822 [0.782–0.862]	
Strata = no alcohol use disorders		
1.045	95.1%	36.9%
1.183	90.2%	45.4%
2.832	51%	90%
3.834	37.9%	95%
AUC	0.798 [0.77–0.826]	

Strata = liver risk factors

Conclusion: FIB-4 predicts the risk of HCC in patients with T2D. These data support its use as a liver health check measure in this patients' group.

SAT-403

FIB-4 as a screening tool for significant liver fibrosis in a cohort of overweight subjects involved in a weight loss program conducted in a primary care setting

Charlotte Costentin¹, Odile Fabre², Remy Legrand², Sébastien Bailly¹. ¹Centre Hospitalier Universitaire de Grenoble, La Tronche, France; ²Franchise Groupe Ethique and Santé-Siège social, Aubagne, France
Email: charlotte.costentin.pro@gmail.com

Background and aims: International societies have issued guidelines supporting systematic screening for liver fibrosis in the primary care setting whenever a risk factor for chronic liver disease is identified. FIB-4 has been selected as the first line tool of choice to stratify patients according to the risk of advanced fibrosis and need for additional liver assessment (FIB-4 > 1.3). The objective of this study was to assess prevalence and characteristics of patients at risk for advanced fibrosis in a cohort of obese and overweight subjects involved in a weight loss program conducted in a primary care setting.

Method: It is a multicenter prospective cohort study including obese and overweight subjects participating in a weight loss program after referral by their physician and conducted in 110 centers distributed across France. Patient characteristics, anthropometrics and biological

		FINAL FIB4 class		
		[0-1.3] N=4274	[1.3-2.67] N=1380	>2.67 N=81
INITIAL FIB4 CLASS	[0-1.3] N=4468	89.2% N=3987 Δ Weight = -11.8 [-16.2; -8.3] Δ BMI = -4.3 [-5.9; -3.1] Δ Waist C = -13 [-17; -9]	10.6% N=475 Δ Weight = -11.7 [-15.7; -8.5] Δ BMI = -4.2 [-5.7; -3.1] Δ Waist C = -13 [-17; -9]	0.1% N=6 Δ Weight = -10.8 [-15.7; -8.5] Δ BMI = -3.7 [-4.4; -2.8] Δ Waist C = -9 [-12; -7]
	[1.3-2.67] N=1202	23.6% N=284 Δ Weight = -10.6 [-14.1; -7.4] Δ BMI = -3.8 [-5.2; -2.8] Δ Waist C = -12.5 [-17; -8]	73.2% N=880 Δ Weight = -10.4 [-14.4; -7.2] Δ BMI = -3.8 [-5.2; -2.7] Δ Waist C = -12 [-16; -8]	3.2% N=38 Δ Weight = -11.9 [-5; -8.2] Δ BMI = -4 [-5.3; -3.1] Δ Waist C = -12 [-16; -9]
	>2.67 N=65	4.6% N=3 Δ Weight = -12.5 [-13.8; -7.7] Δ BMI = -4.1 [-4.4; -2.9] Δ Waist C = -15 [-17; -12]	38.5% N=25 Δ Weight = -12.7 [-15.2; -8.3] Δ BMI = -4.6 [-5.3; -2.7] Δ Waist C = -12 [-19; -9]	56.9% N=37 Δ Weight = -10.9 [-17.3; -5.5] Δ BMI = -3.7 [-5.5; -1.9] Δ Waist C = -11.5 [-17.5; -7]

Figure: (abstract: SAT-403).

data were collected in each center by using a single electronic medical record.

Results: From 63 744 adult participants in the RNPC® program, 27 643 had baseline FIB4 data and were included in the subsequent analysis: predominantly women (78.3%), median age of 54 years [IQR 44; 63], median initial body mass index (BMI) was of 32.6 [IQR 29.2; 36.4] kg/m² (70% with BMI ≥30), median initial waist circumference (WC) 107 cm [IQR 97; 117]. Fatty Liver Index (FLI) was available in 12 454 participants, in which steatosis defined by Fatty Liver Index FLI>60 was present in 8 452 subjects (66%). FIB4 at baseline was <1.3 in 22 353 participants (80.9%), and >2.67 in 264 (1%). When moving from the lower risk category (FIB4<1.3) to the intermediate (1.3–2.67) and the higher risk (FIB4>2.67), the population was enriched in male gender (from 19.1, to 32% and 47.3% respectively), waist circumference increased (from 106 to 110 and 116 cm) as well as rates of metabolic comorbidities such as of sleep apnea (from 14.9 to 26.9% and 37.7%), diabetes (from 36.8 to 39.7 and 40.2%), arterial hypertension from 40 to 58.2% and 66.7%) (p <0.01). When available, rates of FLI>60 increased from 65.5 to 69.9% and 77.5%. Diagnosed non-alcoholic fatty liver disease was more prevalent in the higher risk category compared to the lowest (22.3% vs 5.3%; p <0.01). After 5 [3–7] months into the program, all anthropometric parameters improved: median WC decreased from 108.6 to 95.6 cm, fat mass decreased from 40.9% to 37%, muscle mass increased from 29.7% to 30.7% (; p <0.001). A follow-up FIB-4 value was available in 5 735 participants. Among participants from the low-risk category at baseline, 481 (10.6%) changed classes, but only 6 (0.1%) moving to the higher-risk category. Among participants from the high-risk category at baseline, 28 (43%) changed classes, 3 (4.6%) moving to the lower risk-category (Figure 1). In the population with FIB-4 > 1.3 eligible for additional liver assessment, results of specialized second line fibrosis testing were not recorded.

Conclusion: In a cohort of overweight and obese patients from the primary care setting, prevalence of patients at risk for advanced fibrosis according to initial FIB-4 >1.3 was 19.1%. Higher-risk participants (FIB-4 >2.67, 1%) displayed higher rates of metabolic comorbidities. General practitioners and nutrition professionals are important assets to implement the two-steps algorithm to screen for advanced fibrosis in patients at risk. Efforts should be made to improve the care pathway to the second line non-invasive fibrosis tests.

SAT-404

Soluble TREM2 and PRO-C3 as efficacy of intervention markers in NASH

Charlotte Wernberg^{1,2}, Vineesh Indira Chandran³, Mette Lauridsen², Maria Kløjgaard Skyttø³, Camilla Dalby Hansen¹, Johanne Kragh Hansen¹, Lea Ladegaard Grønkjær², Birgitte Jacobsen², Tina Di Caterino³, Sönke Detlefsen², Maja Thiele¹, Alejandro Mayorca Guiliani⁴, Diana Leeming⁴, Morten Karsdal⁴, Ida Villesen¹, Jonas Graversen³, Aleksander Krag¹. ¹Fibrosis, Fatty liver and Steatohepatitis Research Center Odense (FLASH), Denmark; ²Institute for Regional Health Research, University of Southern Denmark, Denmark; ³Clinical Institute, University of Southern Denmark, Department of Molecular Medicine, University of Southern Denmark, Odense, Denmark; ⁴Nordic Bioscience Biomarkers and Research A/S, Denmark

Email: charlotte.wilhelmina.wernberg@rsyd.dk

Background and aims: Patients with obesity and type 2 diabetes have a high risk of developing non-alcoholic steatohepatitis. Diet and weight loss are currently the mainstay of treatment in most patients with non-alcoholic fatty liver disease (NAFLD) and some drugs are approved for the use in NAFLD, but multiple drugs are at advanced stages of clinical testing. There is consequently an unmet medical need for non-invasive tests that can help clinicians assess treatment response. Our aim was to explore the ability of NITs to reflect a change of at least one stage in histologic NAFLD Activity Score (NAS).

Method: A longitudinal study of 173 patients with type 2 diabetes or severe obesity, suspected of NAFLD, and ≥6 months follow-up including dual liver biopsies and blood samples. We measured soluble TREM2, collagen formation markers (III, IV, VI, VIII, XVIII) using ELISA assays PRO-C3, PRO-C4, PRO-C6, PRO-C8, and PRO-C18L (Nordic Bioscience), FAST-score using Fibroscan (Echosens), and calculated HOMA-IR. We calculated Fibrosis-4 (FIB-4) and NAFLD Fibrosis Score (NFS). Patients were stratified into three outcome groups according to NAS change between baseline and end of study: worsened ≥1 NAS stage, no change in NAS, and improved ≥1 NAS stage.

Results: The mean age was 52 years (± 12), 38% were males, 70% had low fibrosis (F0-F1), and 23% had NASH (n = 39) at baseline. Outcome groups were balanced regarding age, BMI, triglycerides, and fibrosis grades; but participants that improved had the highest HOMA-IR of 7.7 (p = 0.002) and a higher prevalence of NASH (p < 0.001). Several NITs were significantly reduced in patients who improved NAS at follow-up, and there was an overall dose-response between outcome groups (worsened (n = 22), no change (n = 50), improved (n = 101)):

POSTER PRESENTATIONS

sTREM2 ($p < 0.001$), PRO-C3 ($p < 0.01$), HOMA-IR ($p < 0.001$), and FAST-score ($p < 0.001$). On the other hand, levels of PRO-C18L were downregulated in patients that worsened in NAS ($p < 0.01$). Seventy percent of patients that improved had a change in inflammation and/or ballooning. In multivariable analysis, sTREM2 combined with PRO-C3 predicted NAS improvement well (AUROC 0.75) with an OR for every unit decrease respectively of 1.05 (95% CI 1.02–1.09) and 1.13 (95% CI 1.05–1.21) ($p < 0.01$). HOMA-IR also performed well (AUROC 0.76), but even better in combination with sTREM2 (AUROC 0.79). FIB-4 and NFS did not (AUROC < 0.60 , OR < 1.05 $p > 0.5$). The Fibroscan yielded non-valid measurements in 16%, at either one or both visits, making it less ideal for monitoring.

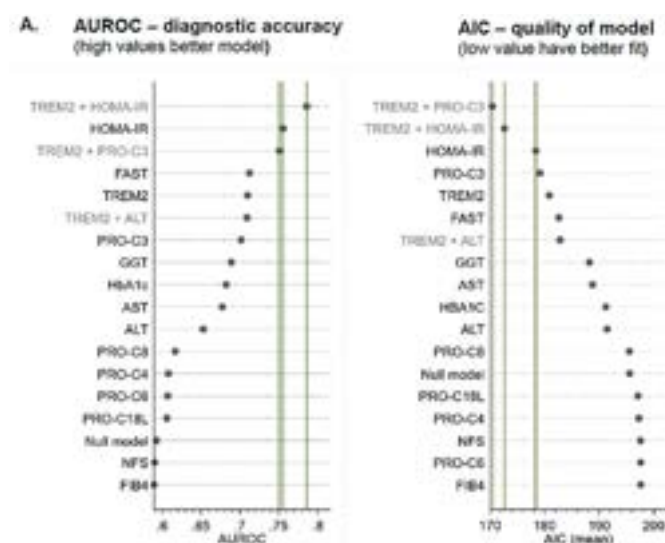


Figure: Figure legend. Logistic regression analysis to assess the probability of NAS improvement ≥ 1 stage (=1), as opposed to no improvement (no-change and worsened = 0). We include each NITs' units change from baseline in models as a difference. A. Dot plot shows area under the receiver operation characteristic curve (AUROC) diagnostic accuracy and Akaike information Criterion (AIC) estimator of prediction error and, thereby, the relative quality of statistical models for a given set of data for all models (green vertical lines mark the best models).

Conclusion: sTREM2 and PRO-C3 in combination reflect NAS improvement and should be further explored as surrogate markers for efficacy of interventions. Divergently, FIB-4 and NFS showed low accuracy for monitoring histological response in this cohort.

SAT-405

Dynamic changes in liver stiffness assessed by transient elastography as a prognostic factor in NAFLD patients with prediabetes and type 2 diabetes

Elias Maleh¹, Claudia Regina Cardoso¹, Gil Salles¹, Ana Carolina Cardoso¹, Lorrane Santos¹, Henrique Sérgio Coelho¹, Cristiane Villela-Nogueira¹, Nathalie Leite¹. ¹Federal University of Rio de Janeiro, Brazil
Email: nathaliecleite@gmail.com

Background and aims: Baseline liver stiffness measure (LSM) associates with a higher risk of liver events (LEs) and mortality in NAFLD patients. We aimed to assess the prognostic value of dynamic changes of LSM for predicting survival and the occurrence of liver (LEs) and cardiovascular events (CVEs) in prediabetes (PreDM) type 2 diabetes (T2DM) NAFLD patients.

Method: NAFLD adults with PreDM or T2DM with two consecutive reliable LSMs by TE were included. Clinical, biochemical and elastography data (Fibroscan Touch 502, Fr) were collected at baseline. Follow-up LSM was recorded accordingly. Dynamic changes in LSM (Δ LSM) were categorized as improvement (LSM reduction of $\geq 25\%$ from baseline) and impairment (LSM increase of

$\geq 25\%$ from baseline). During follow-up, LEs (ascites, encephalopathy, variceal bleeding, HCC) and CVEs (myocardial infarction, new-onset heart failure, any myocardial revascularization, stroke, any aortic or lower limb revascularization, any amputation above the ankle) were recorded. The follow-up period was from the baseline LSM to the last clinical visit or the outcome. Multivariate cox analysis evaluated the associations between Δ LSM (as continuous and categorized variables) and the occurrence of LEs, CVEs events or mortality.

Results: 301 patients were included (68% female, age 59 ± 10 y): 19% had PreDM and 81% T2DM.

At the first TE examination, 12% had LSM > 15 kPa [median 6.9 kPa (5.1–10.1)]. Overall, 26% experienced Δ LSM improvement [median 32.7 (22.3–42.2)], and 25% had Δ LSM impairment [median 29.6 (14.6–56.2)] on a 38 (27–55) months interval. During an observation period of 76 (65–86) months (1878 person-years), there were 31 deaths, 24 CVEs and 20 LEs. Cumulative incidences by Kaplan Meier showed a higher incidence of CVEs in those with Δ LSM impairment. (log-rank test: $p = 0.007$), but not for LEs or mortality (log-rank test: $p = 0.449$ and $p = 0.581$, respectively). On multivariate Cox analysis, continuous and categorized Δ LSM were independently associated with CVEs adjusted for age, gender, BMI, diabetes, arterial hypertension, smoking, previous cardiovascular event, statin use, HbA1c levels and baseline LSM. (Δ LSM for each 1% increase HR:1.009; 95% CI, 1.003–1.015; $p = 0.004/\Delta$ LSM 25% impairment HR:3.026; 95% CI, 1.298–7.051; $p = 0.01$). For LEs, adjusting for the same potential risk factors, only continuous and categorized baseline LSM were the independently associated variables (baseline LSM for each 1 kPa increase HR:1.115; 95% CI, 1.073–1.158; $p < 0.001$ /baseline LSM > 15 kPa HR:15.927; 95% CI, 5.686–44.61; $p < 0.001$).

Conclusion: Dynamic changes in LSM, more specifically an increase of $\geq 25\%$ from baseline LSM, can predict adverse CVEs in NAFLD individuals with either prediabetes or type 2 diabetes. In contrast, only baseline LSM is associated with a higher risk of LEs or death. LSM impairment does not seem to be an additional risk of liver events or overall mortality in this population.

SAT-406

Fibrosis-4 score and liver stiffness measurement by vibration-controlled transient elastography predict risk of liver-related events in non-alcoholic fatty liver disease

Esteban Urias¹, Tianyu Qiu², Michael Song³, Tanvi Goyal³, Jing Hong Loo⁴, Yu Jun Wong⁴, Vincent Chen³. ¹Michigan Medicine, Department of Internal Medicine, Ann Arbor, United States; ²Changi General Hospital, Department of Gastroenterology and Hepatology, Singapore; ³Michigan Medicine, Department of Gastroenterology and Hepatology, United States; ⁴Yong Loo Lin School of Medicine, National University of Singapore, Singapore
Email: uesteban@med.umich.edu

Background and aims: Both the Fibrosis-4 (FIB-4) score and liver stiffness measurement (LSM) by vibration-controlled transient elastography (VCTE) are non-invasive tests used to classify risk of adverse events in patients with non-alcoholic fatty liver disease (NAFLD). Current practice guidelines recommend a sequential approach to risk stratification in NAFLD with FIB-4 followed by VCTE. However, whether LSM more accurately predicts risk of liver-related events (LREs) than FIB-4 or outweighs FIB-4 is not known. We sought to determine combined effects of FIB-4 and LSM to predict LREs in NAFLD.

Method: This was a retrospective study of consecutive patients with NAFLD undergoing VCTE and serum testing within 12 months of VCTE at the University of Michigan Health System (USA) and Changi General Hospital (Singapore) from 2015 to 2022. NAFLD was defined by hepatic steatosis without alternative chronic liver diseases or excess alcohol intake. The index date was the date of VCTE. The primary outcome was LREs defined as decompensation or hepatocellular carcinoma. The primary predictors were FIB-4 score, stratified

		LSM						
		< 8 kPa		8 - 12 kPa		> 12 kPa		
		Cumulative Incidence	LRE/total patients	Cumulative Incidence	LRE/total patients	Cumulative Incidence	LRE/total patients	p value
FIB-4	< 1.3	-	0/684	-	0/151	-	0/90	-
	1.3 - 2.67	-	0/263	5.21 (0.63 - 18.82)	2/118	13.17 (4.28 - 30.73)	5/120	0.0061
	> 2.67	18.78 (2.27 - 67.58)	2/33	18.71 (2.27 - 67.58)	2/35	62.44 (34.95 - 102.98)	15/78	0.071
	p value	<0.0001		0.021		<0.0001		

Figure: (abstract: SAT-406).

by low (<1.3), intermediate (1.3–2.67), and high (>2.67); and LSM, stratified by low (<8 kPa), intermediate (8–12 kPa), high (>12 kPa).

Results: We included 1,572 patients meeting inclusion criteria. Median age was 53 years, 54% were male, 57% were White, and 32% were Asian. FIB-4 scores were low, intermediate, and high in 59%, 32%, and 9% of patients, and LSM was low, intermediate, and high in 62%, 19%, and 18%, respectively. Median follow-up was 38 months with 4,969 person-years of follow-up in total. There were no LREs in patients with FIB-4 <1.3 regardless of LSM and no LREs in patients with FIB-4 <2.67 and LSM <8 kPa in 3,321 person-years of follow-up (Figure). Within each FIB-4 category, higher LSM was associated with higher incidence rate of LREs, and similarly within each LSM category, higher FIB-4 was associated with increased risk of LREs. For example, for FIB 1.3–2.67, the incidence rate was 5.2 and 13.2 per 1,000 person-years for LSM 8–12 kPa and >12 kPa, respectively. For FIB-4 >2.67, the incidence rate was 18.7 and 62.4 events per 1,000 person-years for LSM ≤ 12 and >12 kPa, respectively.

Conclusion: FIB-4 and LSM in combination more accurately predict risk of LREs in NAFLD than either alone. However, no LREs occurred in patients with FIB-4 <1.3 regardless of LSM, supporting existing guidelines to not obtain VCTE in this patient population.

SAT-407

A stepwise screening approach using non-invasive tests to identify phenotypic non-alcoholic steatohepatitis (NASH) patients with fibrosis for clinical trials

Naim Alkhouri¹, Rohit Loomba², Mazen Nouredin³, Eric Lawitz⁴, Kris Kowdley⁵, Hiba Graham⁶, Erin Quirk⁶, Diana Chung⁶. ¹Arizona Liver Health, Tucson, United States; ²University of California San Diego, NAFLD Research Center, La Jolla, United States; ³Houston Research Institute, Houston, United States; ⁴Texas Liver Institute, University of Texas, San Antonio, United States; ⁵Liver Institute Northwest, Seattle, United States; ⁶Terns Pharmaceuticals, Foster City, United States
Email: dchung@ternspharma.com

Background and aims: Non-invasive tests (NITs) have become essential to diagnose and stage non-alcoholic steatohepatitis (NASH). Biopsy-based screen failure (SF) rates are high in NASH trials, which lead to increased cost and extended enrollment durations. LIFT and AVIATION were double-blind, placebo-controlled studies in adults with non-cirrhotic NASH evaluating TERN-101, a potent, nonsteroidal farnesoid X receptor (FXR) agonist with enhanced liver distribution, and TERN-201, a highly specific vascular adhesion protein-1 (VAP-1) inhibitor, respectively. A stepwise NIT screening approach was implemented to recruit similar study populations in both trials: patients with presumed NASH and a high degree of liver fat and fibro-inflammation, reflecting F2 and F3 fibrosis.

Method: Screening and baseline characteristics from the phase 2a LIFT and phase 1b AVIATION studies were combined. In screening step 1, both trials required age ≥18, BMI ≥25 kg/m², ALT above the median central laboratory normal range, vibration controlled transient elastography (VCTE) of 7.5 (LIFT) and 6.5 (AVIATION) to 21 kPa, and controlled attenuation parameter (CAP) of 280 (AVIATION) and 300 (LIFT) dB/m within 3 months of screening. Neither trial required liver

biopsy. Potential subjects remaining eligible after the step 1 screening underwent MRI to assess liver fat content eligibility ≥10% by proton density fat fraction (PDFF) for LIFT or corrected T1 (cT1) >800 msec for AVIATION. Common SF reasons were tabulated, and multiparametric MRI SF rates were calculated.

Results: 567 (446 in LIFT; 121 in AVIATION) patients were screened and 153 (101 in LIFT; 52 in AVIATION) were randomized; overall SF rate was 73%. Recruitment durations were 6 and 3 months for LIFT and AVIATION, respectively. Of the 567 patients, 181 (32%) met step 1 eligibility criteria, with a SF rate of 68%. The most common reason for SF was not meeting the ALT enrollment eligibility threshold value. Of the 181 patients, 155 (86%) met either MRI-PDFF in LIFT or cT1 criteria in AVIATION, resulting in a step 2 MRI SF rate of 14% (26/183; 2 patients not treated for other reasons post step 2). Per baseline characteristics, each study enrolled a population with VCTE ranging from 4.4 to 19.6 kPa, CAP 261 to 400 dB/m, PDFF 6.0 to 48.2% and cT1 721.0 to 1461.0 msec.

Conclusion: A stepwise screening approach first using clinical assessments, laboratory tests and VCTE with CAP allowed for screening of patients that were more likely to meet the MRI eligibility criteria. As a result, this reduced the number of MRI assessments that were required which reduced costs and the need for patients to be scheduled for a separate imaging visit. These NIT-guided studies recruited efficiently and enrolled subjects likely to have presumed NASH. These biomarkers may be used in combination with medical history to identify phenotypic at-risk NASH patients in a non-invasive fashion to enable clinical trials of experimental NASH therapies.

SAT-408

Machine learning with routine laboratory tests and clinical features performs similar to current NAFLD clinical pathways

Devon Y. Chang¹, Emily Truong², Ju Dong Yang³, Naim Alkhouri⁴, Stephen Harrison⁵, Mazen Nouredin⁶, Arnold O. Beckman High School, United States; ²Cedars Sinai Medical Center, United States; ³Cedars-Sinai, United States; ⁴Arizona Liver Health, United States; ⁵Pinnacle Clinical Research, United States; ⁶Houston Liver Institute, United States
Email: mazen.nouredin@cshs.org

Background and aims: AGA's NAFLD Clinical Care Pathway (Kanwal, et al. Gastro 2021) screens patients with risk factors for NAFLD with Fibrosis-4 index (FIB-4) to determine risk (low, indeterminate, or high) for clinically significant liver fibrosis. Indeterminate patients subsequently undergo FibroScan® to further stratify risk for clinically significant liver fibrosis. In this study, we assessed the performance of established machine learning (ML) models (Chang et al, Hepatology 2022) versus sequential testing with FIB-4 followed by FibroScan® (STFF) in predicting the risk of clinically significant liver fibrosis.

Method: We implemented ML models including logistic regression (LR), random forests (RF), and artificial neural network (ANN) to predict risk of significant fibrosis (defined by histological stage of fibrosis ≥F3) using 17 routine demographic, clinical, and laboratory features in 1223 NAFLD patients at multiple US centers. These patients had ≥1 risk factors for NAFLD, including ≥2 metabolic risk factors, type 2 diabetes mellitus, steatosis on any imaging modality,

POSTER PRESENTATIONS

	Correctly Classified (CC) Measurement (%)	Percentage of Indeterminate-Risk Patients (%)
Logistic Regression	63.96 [61.12, 66.8]	8.2 [7.14, 9.26]
Random Forests	67.47 [64.67, 70.27]	14.16 [12.47, 15.86]
ANN	63.06 [60.35, 65.78]	10.41 [8, 12.82]
FIB-4 + FibroScan	70.53 [66.51, 74.55]	11.51 [10.13, 12.89]

Figure: (abstract: SAT-408).

or elevated aminotransferases, and underwent liver biopsy, FibroScan®, and labs within a 6-month period. 29.52% of these 1223 patients had significant fibrosis, according to liver biopsy results. Patients with low, indeterminate, and high risk for significant liver fibrosis were predicted using the ML models and STFF according to the NAFLD Clinical Care Pathway. We used 80% of the cohort to train and 20% to test the ML models. Finally, we used the correctly classified (CC) measurement, defined as (true negative for rule-out cutoff + true positive for rule-in cutoff)/total, to compare the performances of the ML models to STFF. We also used the percentage of indeterminate-risk patients to compare the abilities of the ML models to separate the positive and negative classes to that of STFF.

Results: The performances of the ML models and STFF are shown in Table 1. LR had a CC of 63.96% (confidence interval, or CI: 61.12%–66.8%) and a percentage of indeterminate-risk patients of 8.2% (CI: 7.14%–9.26%). RF had a CC of 67.47% (CI: 64.67%–70.27%) and a percentage of indeterminate-risk patients of 14.16% (CI: 12.47%–15.86%). ANN had a CC of 63.06% (CI: 60.35%–65.78%) and a percentage of indeterminate-risk patients of 10.41% (CI: 8%–12.82%). STFF had a CC of 70.53% (CI: 66.51%–74.55%) and a percentage of indeterminate-risk patients of 11.51% (CI: 10.13%–12.89%). Overall, there was no statistically significant difference when comparing the CCs of LR and RF to that of STFF. While there was no statistically significant difference in percentage of indeterminate-risk patients when comparing RF or ANN to STFF, LR had a statistically significantly lower percentage of indeterminate-risk patients compared to STFF.

Conclusion: There was no statistically significant difference in the performances of LR, RF, and STFF in the prediction of risk of clinically significant liver fibrosis. LR better separated the positive and negative classes compared to STFF. ML may replace STFF in the NAFLD Clinical Care Pathway to predict the risk of clinically significant liver fibrosis.

SAT-409

Validation of elastography criteria and cACLD risk model for diagnosis of compensated advanced chronic liver disease (cACLD) in NAFLD patients

Antonio Liguori^{1,2}, Mirko Zoncapè^{2,3}, Roshni Patel², Davide Roccarina², Nicholas Viceconti¹, Lucrezia Petrucci¹, Laura Iogna Prat², Francesca D'Ambrosio¹, Giuseppe Marrone¹, Marco Biolato¹, Anna Mantovani^{2,3}, Jennifer-Louise Clancy², Atul Goyale², Antonio Gasbarrini¹, Antonio Grieco¹, Luca Miele¹, Emmanuel Tsochatzis². ¹Department of Translational Medicine and Surgery, Fondazione Policlinico Universitario Agostino Gemelli IRCCS, Università Cattolica del Sacro Cuore, Rome, Italy; ²University College London (UCL) Institute for Liver and Digestive Health, Royal Free Hospital and UCL, London, UK, United Kingdom; ³Liver Unit, Division of General Medicine C, Department of Internal Medicine, University and Azienda Ospedaliera Universitaria Integrata of Verona, Verona, Italy Email: lig.antonio91@gmail.com

Background and aims: Fibroscan is a well-established NIT for the diagnosis of advanced fibrosis (F_{≥3}) in patients with NAFLD, recently defined as compensated advanced chronic liver disease (cACLD). EASL Guidelines¹ proposed 8 and 12 kPa, respectively, as rule-out and rule-in cut-offs for cACLD. Patients with Fibroscan measurement between 8 and 12 fall in a grey zone where further investigations are recommended. We recently proposed the cACLD Risk Score to further stratify this population. The main aim of this study was to test the diagnostic performance of the main NITs in two European cohorts of patients with histological diagnosis of NAFLD. Secondly, we assessed the performance of the cACLD risk score to further stratify patients in the Fibroscan's grey zone.

Method: This is a retrospective observational study. We enrolled consecutive patients with histological diagnosis of NAFLD/NASH from

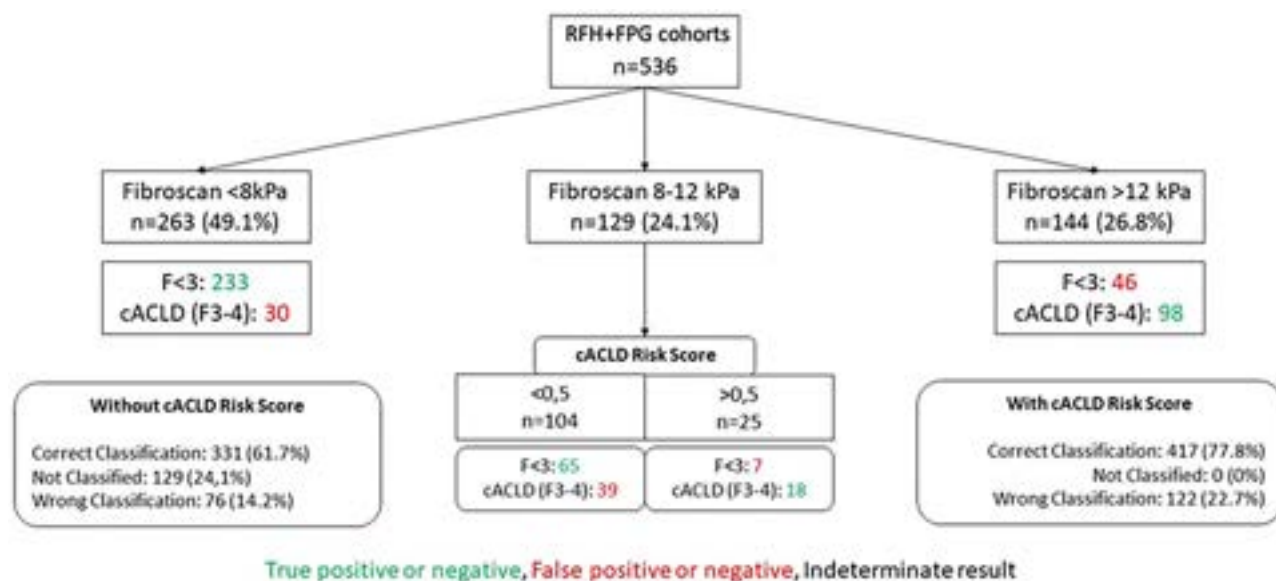


Figure: (abstract: SAT-409).

January 2014 to December 2021 at two tertiary liver units in UK (Royal Free Hospital, London-RFH) and Italy (Fondazione Policlinico Universitario A. Gemelli IRCCS, Rome-FPG). We excluded patients who did not perform at least one of these NITs at time of biopsy (± 6 months): FIB4, NAFLD Fibrosis score (NFS), Fibroscan, APRI, AGILE3+, cACLD Risk Score. We performed a ROC analysis to explore the diagnostic performance of NITs for cACLD ($F > 2$). Secondly, in patients with intermediate Fibroscan results (between 8 and 12 kPa), we tested the diagnostic performance of cACLD Risk Score, considering the originally proposed cutoff of 0, 5.

Results: We included 536 patients; 201 were female, median age was 53 years, and 44% had diabetes. Fibroscan and AGILE3+ score had the best diagnostic performances for cACLD with an AUROC of 0.81 and 0.83 respectively. EASL criteria showed a high sensitivity and high specificity for 8 kPa and 12 kPa Fibroscan's cutoffs, respectively (Sens 84.3%; Spec 86.6%), a wrong classification rate of 14.2%. 129 patients (24.1%) fell in the grey zone (between 8 and 12 kPa). Diagnostic performance of cACLD Risk Score in Fibroscan's grey zone was suboptimal (AUROC: 0.682). The use of Fibroscan+cACLD Risk Score vs Fibroscan alone showed a better overall accuracy (77.8% vs 61.7%) and a slight worsening of overall wrong classification rate (22.7% vs 14.2%) mainly due to a higher number of false negatives than false positives. Among patients with intermediate Fibroscan (8–12 kPa), cACLD risk score correctly classify 64.4% of patients with a PPV of 72.0% and NPV of 62.5%.

Conclusion: Our results suggest that cACLD Risk Score should be used in patients with indeterminate Fibroscan results to further stratify their risk of cACLD. The use of cACLD Risk Score improve the performance in identifying patients with cACLD (high PPV) although its false negative rate could lead to missed diagnosis (suboptimal NPV). Patients with intermediate fibroscan and low cACLD risk score should be still considered for further investigation (liver biopsy).

SAT-410

Predictors of liver stiffness changes in consecutive cohorts of patients with non-alcoholic fatty liver disease and longitudinal follow-up

Mirko Zoncapè^{1,2}, Antonio Liguori^{1,3}, Serena Pelusi⁴, Cristiana Bianco⁴, Roshni Patel¹, Davide Roccarina¹, Laura Iogna Prat¹, Anna Mantovani^{1,2}, Jennifer-Louise Clancy¹, Atul Goyale¹, Luca Valenti⁴, Emmanuel Tsochatzis¹. ¹Royal Free Hospital, University College London (UCL) Institute for Liver and Digestive Health, London, United Kingdom; ²Azienda Ospedaliera Universitaria Integrata Verona, Liver Unit, Division of General Medicine C, Department of Internal Medicine, Verona, Italy; ³Università Cattolica del Sacro Cuore, 3Department of Translational Medicine and Surgery, Fondazione Policlinico Universitario Agostino Gemelli IRCCS, Roma, Italy; ⁴Policlinico of Milan, Department of Pathophysiology and Transplantation and Translational Medicine, Department of Transfusion Medicine and Hematology, Milano, Italy
Email: mirko.zonky@yahoo.it

Background and aims: The serial use of non-invasive fibrosis tests can refine prognosis in patients with non-alcoholic fatty liver disease (NAFLD) and evaluate the progression or improvement of liver fibrosis. We evaluated predictors of improvement or worsening of liver stiffness measurements (LSM) in well characterized cohorts of patients with NAFLD from London (UK) and Milan (Italy).

Method: We included two consecutive cohorts of 405 patients with at least two outpatient visits between 2014 and 2022. The minimum time interval between baseline and follow-up LSM was >6 months. LSM worsening was defined as an increase of >20% kPa if the baseline LSM was ≥ 5 kPa, or a follow-up LSM >6 kPa if the baseline LSM was <5 kPa. An LSM improvement was defined as an LSM decrease of >20% kPa (if the baseline LSM was >6 kPa). A significant change in weight was defined as a >5% reduction or increase at follow-up, while a

Variable	Multivariate for LSM worsening		Multivariate for LSM improvement	
	OR (95% CI)	p-value	OR (95% CI)	p-value
Age	-	-	1.02 (0.99 – 1.0)	0.16
Weight change, %	-	-	0.93 (0.87 – 0.99)	0.03
BMI	-	-	1.00 (0.95 – 1.07)	0.77
DM	-	-	1.92 (0.81 – 4.55)	0.13
Follow up time	1.01 (0.98 – 1.02)	0.48	1.00 (0.99 – 1.02)	0.60
AST/ALT ratio at baseline	1.01 (0.98 – 2.24)	0.28	-	-
Total cholesterol change, %	0.98 (0.95 – 0.99)	<0.05	-	-
AST change, %	0.98 (0.96 – 0.99)	0.04	1.02 (1.01 – 1.04)	0.03
ALT change, %	1.02 (1.01 – 1.03)	0.02	0.98 (0.98 – 0.99)	0.02
HbA1c change, %	1.03 (1.01 – 1.06)	0.03	0.97 (0.95 – 1.00)	0.06
Difference between expected and actual FIB-4 at follow up	1.39 (0.28 – 6.94)	0.68	0.49 (0.21 – 1.20)	0.12

Figure: Multivariate analysis for Fibroscan LSM increase and for LSM decrease. Numbers in bold represent statistical significance. Legend: ALT, alanine amino-transferase; AST, aspartate aminotransferase; BMI, body mass index; DM, type II diabetes mellitus; FIB-4, fibrosis-4 index; HbA1c, glycated hemoglobin.

POSTER PRESENTATIONS

significant change in glycated hemoglobin (HbA1c) was defined as a >10% reduction or increase. The variation between the true and expected FIB-4 index (based on the patient's age at the follow-up visit, but using the blood tests performed at the first visit) was calculated. A significant improvement or worsening in FIB-4 was defined as a >20% variation between the actual and "expected" FIB-4.

Results: Of the 405 patients, 282 (70%) were males; mean age was 54 ± 11 years. The median time from the first visits was 20.3 (13.9–28.7) months. 128 and 54 patients had an LSM >8 kPa and LSM >12 kPa at follow-up, respectively. 77 patients (19.3%) had an LSM improvement, while 67 (16.8%) had an LSM worsening; 256 patients (63.9%) maintained a stable value. In patients with an LSM improvement, 22 had an improvement, 12 had worsening, while 37 had stable FIB-4. In patients with an LSM worsening, 10 had an improvement, 20 had worsening, while 33 had a stable FIB-4. In multiple logistic regression analysis, LSM worsening was independently associated with an increase in ALT and in HbA1c levels (OR 1.02 and 1.03 respectively), but also with a reduction in total cholesterol and AST levels (OR 0.98 for both). LSM improvement was independently associated with weight and ALT reduction (OR 0.93 and 0.98 respectively), but also with an increased AST level (OR 1.02).

Conclusion: More than 35% of patients with NAFLD have significant changes in their LSM measurements over a period of 20 months, with worsening or improvement at similar rates. Improvement in weight is independently associated with significant improvement in LSM measurements. On the converse, worsening in metabolic comorbidities, particularly glycemic control, could be associated with significant worsening in LSM, further supporting a multidisciplinary model of care.

Disclosure: All authors declare no conflict of interest. This work received no public or private funds.

SAT-411

Association of non-high-density lipoprotein cholesterol trajectories with the development of non-alcoholic fatty liver disease

Jun-Hyuk Lee¹, Jiyeon Kim², Jung Oh Kim², Yu-Jin Kwon³, Eileen Yoon⁴, Dae Won Jun⁴, Sang Bong Ahn¹. ¹Nowon Eulji Medical Center, Eulji University School of Medicine, Internal Medicine, Seoul, Korea, Rep. of South; ²Institute of genetic epidemiology, Basgenbio Co., Ltd., Korea, Rep. of South; ³Yongin Severance Hospital, Yonsei university college of medicine, Family medicine, Yongin-si, Korea, Rep. of South; ⁴Hanyang university college of medicine, Internal medicine, Seoul, Korea, Rep. of South
Email: noshin@hanyang.ac.kr

Background and aims: Dyslipidemia including non-high-density lipoprotein (non-HDL) cholesterol can induce hepatic insulin resistance, which contributes to the incidence of non-alcoholic fatty liver disease (NAFLD). To date, the effect of longitudinal trends in non-HDL cholesterol on NAFLD development is unknown. This study aimed to

verify relationship between non-HDL cholesterol trajectories and incident NAFLD and identify genetic differences contributing to the development of NAFLD between non-HDL cholesterol trajectory groups.

Method: From a total of 10,030 participants aged 40–69 years who participated in the Korean Genome and Epidemiology Study, we analyzed data from 2203 adults without NAFLD at baseline who consecutively participated in the first, second, and third follow-up surveys. During the 6-year exposure periods (from baseline to third follow-up periods), participants were classified into increasing non-HDL cholesterol trajectory group (n=934) and stable group (n=1269). NAFLD was defined as NAFLD-liver fat score >–0.640. Multiple Cox proportional hazard regression analysis was performed to estimate the hazard ratio (HR) and 95% confidence interval (CI) for incident NAFLD of increasing group compared with stable group. For genome-wide association study (GWAS), we applied the interaction polygenic risk scores (PRS) to clarify effects of single-nucleotide polymorphisms (SNPs) on NAFLD phenotypes. For case-control comparison, we set control group by randomly selecting 2203 samples from total participants in the KoGES and calculate interaction PRSs using same difference of effect sizes.

Results: During the median 7.8-year of event accrual period, 666 (30.2%) newly developed NAFLD cases were collected. Incidence rate per 2 years of NAFLD was ranged from 5.03 to 11.14. Kaplan-Meier curves showed significant higher cumulative incidence rate of NAFLD in increasing group than in stable group (log-rank test $p < 0.001$). Compared with stable group, the adjusted HR (95% CI) for incident NAFLD of increasing non-HDL cholesterol group was 1.54 (1.32–1.80, $p < 0.001$). Linear mixed model revealed that increasing group had consistently and significantly higher NAFLD-liver fat score than stable group during the follow-up periods except the baseline. On GWAS, no significant SNPs were identified. PRS was highest in increasing group, followed by stable group and control group.

Conclusion: A trend in increasing non-HDL cholesterol was positively related to incident NAFLD. Results from GWAS suggested that lifestyle (diet) or external environmental factors have a greater effect size of factors involved in NAFLD progression risk than genetic factors. Intensive lifestyle modification could be an effective prevention strategy for NAFLD for people with elevated non-HDL cholesterol.

SAT-412

A gut-mycobiome-derived signature predicts advanced fibrosis in people with diabetes

Daniel Huang^{1,2}, Tae Gyu Oh³, Megan Hill⁴, Ricki Bettencourt², Egbert Madamba², Harris Siddiqi², Maral Amangurbanova², Michael Downs³, Ronald Evans³, Jack Gilbert⁴, Rohit Loomba^{2,5}. ¹National University of Singapore, Yong Loo Lin School of Medicine, Department of Medicine, Singapore; ²University of California, San Diego, NAFLD Research Center, Division of Gastroenterology and Hepatology, United States; ³Salk Institute for Biological Studies, Gene Expression

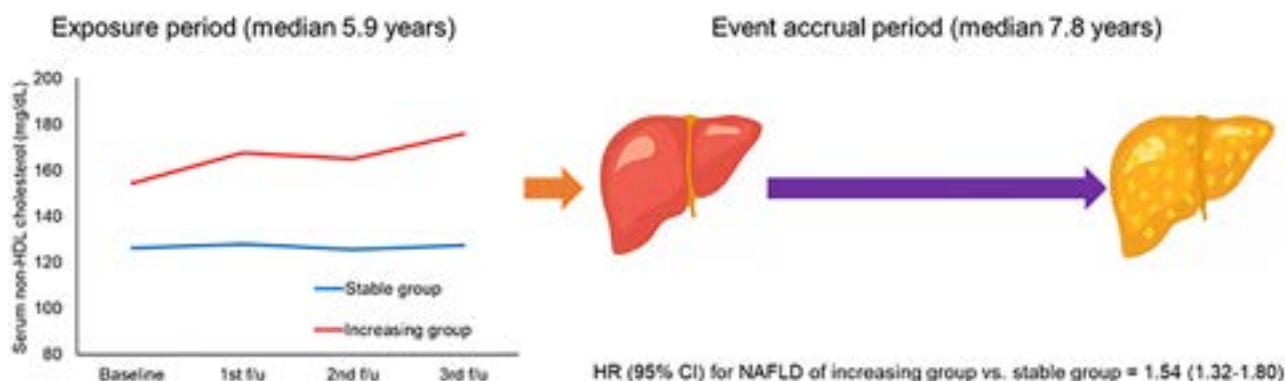


Figure:

Laboratory, United States; ⁴University of California, San Diego, Department of Pediatrics and Scripps Institution of Oceanography, United States; ⁵University of California San Diego, Division of Epidemiology, Department of Family Medicine and Public Health, United States
Email: roloomba@health.ucsd.edu

Background and aims: One in seven older adults with type 2 diabetes mellitus (T2DM) have advanced liver fibrosis (stage 3–4) due to non-alcoholic fatty liver disease (NAFLD). T2DM is associated with dysbiosis of the gut mycobiome, and emerging data suggest that the gut mycobiome may influence the progression of NAFLD to advanced fibrosis and cirrhosis. However, it is unknown if a stool mycobiome signature can be utilized as a non-invasive test for advanced fibrosis in individuals with T2DM.

Method: This prospective study enrolled participants with T2DM aged ≥ 50 years from primary care or endocrine clinics. Participants underwent MRI-proton density fat fraction, magnetic resonance elastography (MRE), vibration-controlled transient elastography (VCTE) and controlled-attenuation parameter. The presence of advanced fibrosis was defined by the presence of concordant findings between MRE and VCTE (MRE ≥ 3.63 kPa and VCTE ≥ 12 kPa). We performed fungal internal transcribed spacer (ITS) 2 sequencing using stool samples from 186 participants (64% female). A random forest machine learning algorithm and differential abundance analysis were utilized to identify signatures to identify advanced fibrosis.

Results: The mean (SD) age and body mass index (BMI) were 65.3 (8.19) years and 31.8 (6.31) kg/m², respectively. The composition of the mycobiome was substantially different in participants with NAFLD and advanced fibrosis, compared to those without advanced fibrosis. Notably, there was an increase in *Candida albicans* (p value = 8.6E-34), *Kazachstania humilis* (p value = 2.6E-03), and *Penicillium concentricum* (p value = 2.4E-16), and a decrease in *Saccharomyces cerevisiae* (p value = 3.7E-07), *Aspergillus versicolor* (p value = 2.1E-04), and *Fusarium fujikuroi* (p value = 2.8E-05). A unique stool mycobiome signature in combination with BMI was able to accurately distinguish the presence of advanced fibrosis (AUC 0.89, CI = 0.87–0.91) (Figure 1) and displayed consistent findings in an ethnically and geographically distinct cohort.

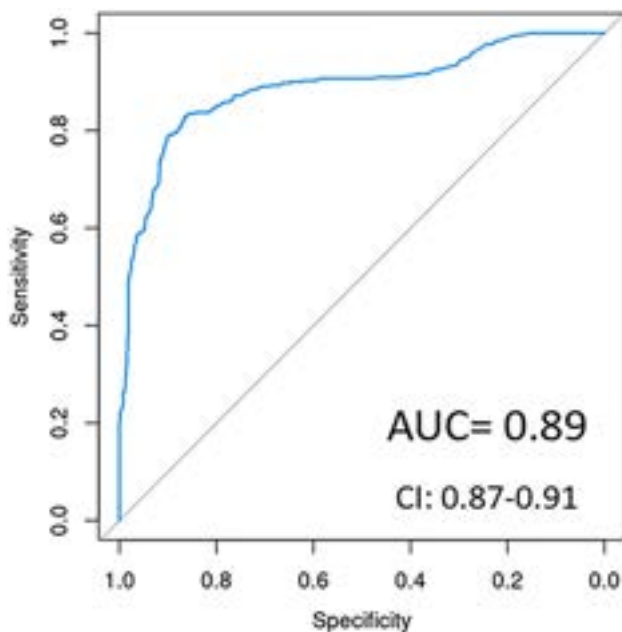


Figure: Diagnostic accuracy of the gut-mycobiome-derived signature in identifying advanced fibrosis.

Conclusion: These findings demonstrate that a core set of gut mycobiome species may be useful as a non-invasive diagnostic test for advanced fibrosis in participants with T2DM.

SAT-413

Diagnostic and prognostic performance of the SAFE score in non-alcoholic fatty liver disease

Guanlin Li^{1,2}, Huapeng Lin^{1,2}, Pimsiri Sripongpun^{3,4}, Yan Liang^{1,2}, Xinrong Zhang^{1,2}, Vincent Wai-Sun Wong^{1,2}, Grace Lai-Hung Wong^{1,2}, W. Ray Kim³, Terry Cheuk-Fung Yip^{2,5}. ¹The Chinese University of Hong Kong, Department of Medicine and Therapeutics, Hong Kong; ²The Chinese University of Hong Kong, Institute of Digestive Disease, Hong Kong; ³Stanford University, Department of Medicine, United States; ⁴Prince of Songkla University, Division of Internal Medicine, Thailand; ⁵The Chinese University of Hong Kong, Department of Medicine and Therapeutics, Hong Kong
Email: tcfyip@cuhk.edu.hk

Background and aims: The steatosis-associated fibrosis estimator (SAFE) was developed for detection of significant (\geq stage 2) fibrosis (SF) in patients with non-alcoholic fatty liver disease (NAFLD) for non-hepatologists (Hepatology 2023;77 (1):256–267). We validate the performance of the SAFE score in comparison to other non-invasive tests to diagnose SF, and to assess their performance in predicting liver-related complications in NAFLD patients in Hong Kong.

Method: This is a retrospective cohort study involving two datasets. The first cohort, prospectively recruited between 2006 and 2021, consisted of adult patients who underwent liver biopsy at Prince of Wales Hospital. The second cohort composed of territory-wide adults with NAFLD (ICD-9-CM code 571.8) first diagnosed from January 2000 to July 2021, retrieved from the Clinical Data Analysis and Reporting System (CDARS) under the management of the Hospital Authority, Hong Kong. Diagnostic and prognostic performance characteristics of the SAFE, FIB-4, NAFLD Fibrosis Score (NFS) and AST-plate ratio index (APRI) were compared. Liver stiffness data by transient elastography were also available in the biopsy cohort.

Results: Four hundred and seventy patients of the biopsy cohort and 4603 patients of the territory-wide cohort were included. In the primary analysis detecting SF, liver stiffness had the highest AUROC (0.844), followed by SAFE score (0.773), FIB-4 (0.746), NFS (0.737) and APRI (0.697). Results were similar for the detection of fibrosing NASH and advanced fibrosis (Figure, *p < 0.05 compared to SAFE). Based on cut-off values of SAFE score (0 and 100 points), 854 (18.6%), 1596 (34.6%) and 2153 (46.8%) were in the low-, intermediate- and high-risk groups, respectively. Six (0.7%), 15 (0.9%) and 59 (2.7%) developed liver-related events in these three groups from territory-wide cohort. Among diabetic patients who had liver-related events at 10 years, using the high cut-off, SAFE score could predict 90.7% of patients accurately, compared to 80.6% for FIB-4 and 66.8% for APRI. In subgroup analyses of NAFLD patients with and without type 2 diabetes, SAFE score had consistently good performance in detecting SF and liver-related events.

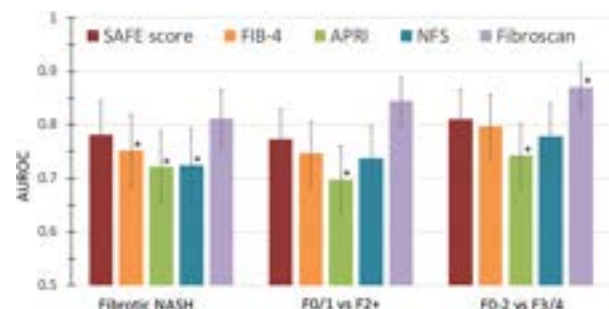


Figure: Comparison of area under the receiver-operating characteristics curves (AUROC) of non-invasive tests in patients with biopsy-proven NAFLD.

POSTER PRESENTATIONS

Conclusion: The SAFE score has good overall accuracy in diagnosing SF and predicting liver-related events in NAFLD patients. It has similar performance in patients with and without diabetes and is therefore well-suited for initial assessment of a broad spectrum of NAFLD patients to assess liver fibrosis and future risk of liver-related complications.

SAT-414

Standardized non-invasive screening for non-alcoholic fatty liver disease in people with type 2 diabetes identifies a substantial number of individuals with advanced liver disease

Naomi Lange^{1,2}, Jonas Schropp¹, Martin Hilpert³, Andreas Melmer³, Markus Laimer³, Christoph Stettler³, Annalisa Berzigotti¹, Jean-François Dufour⁴. ¹Department of Visceral Surgery and Medicine, Inselspital, Bern University Hospital, University of Bern, Bern, Switzerland; ²Graduate School for Health Sciences, University of Bern, Switzerland; ³Department of Diabetes, Endocrinology, Nutritional Medicine and Metabolism, Inselspital, Bern University Hospital and University of Bern, Bern, Switzerland; ⁴Centre des Maladies Digestives Lausanne, Lausanne, Switzerland
Email: naomi.lange@insel.ch

Background and aims: International guidelines recommend screening for advanced non-alcoholic fatty liver disease (NAFLD) in high-risk populations using validated, non-invasive tests. We implemented an algorithm to systematically screen and refer people with type 2 diabetes (T2DM), based on the simultaneous use of fibrosis-4 (FIB4) score and vibration controlled transient elastography (VCTE). Our objective was to assess feasibility, and evaluate the prevalence of clinically suspected and histologically assessed liver disease in referred patients.

Method: We included adult people with T2DM from a tertiary care diabetes outpatient clinic. Hepatology referral was recommended to patients who 1.) presented with a high FIB4 and/or VCTE, or 2.) intermediate values of both FIB4 and VCTE using previously validated cut-offs (FIB4: low <1.30, intermediate 1.30–2.67, high >2.67; VCTE [kPa]: low <7.9, intermediate 7.9–9.6, high >9.6). Clinical suspicion of advanced liver disease was defined as indication for the performance of liver biopsy, clinical diagnosis of cirrhosis, and detection of hepatocellular carcinoma (HCC), and significant liver disease was defined as liver disease warranting follow-up. Histological fibrosis

was staged according to NASH-Clinical Research Network (CRN) criteria.

Results: Of 840 eligible individuals, 276 (32.9%) were included. Valid screening test results were obtained in 95.7% of participants (1.8% and 2.5% invalid results of FIB4 and VCTE, respectively). Among 261 participants evaluated for hepatology referral, mean age was 60.7 years, 28% were female and prevalence of steatosis assessed by controlled attenuation parameter (CAP) was 76.6%. 16.9% of participants (n=44) were recommended for hepatology referral due to elevated screening tests and 43 did undergo hepatology work-up (Fig. 1). Referred patients were older (64.4 vs. 59.9 years, p=0.021), and had higher body mass index (33.6 vs. 31.5 kg/m², p=0.047), CAP (330 vs. 288 dB/m, p=0.001) and HbA1c (7.6 vs. 7.1%, p=0.014). Overall, 90.7% (n=39) of referred patients were clinically diagnosed with advanced (n=24) or significant (n=15) liver disease. 75% of cases without identifiable or only mild liver disease in work-up were referred due to high FIB4 in combination with low VCTE. The most common liver-related diagnosis was NAFLD in 60.5% (n=26) of cases, followed by metabolic liver disease (MAFLD) with dual etiology due to alcohol-related and viral liver disease in 20.9% (n=9) of cases.

Conclusion: Implementation of an algorithm to screen people with T2DM for liver disease using a combination of FIB4 and VCTE was feasible and identified a large number of clinically relevant liver disease cases in a tertiary care setting. Our data suggest a high prevalence of MAFLD with dual etiology in this population, highlighting the necessity of offering screening to high-risk T2DM populations beyond the suspicion of NAFLD.

SAT-415

Patients with risk factors for liver diseases associated with hepatic steatosis constitute the target population for liver fibrosis assessment in primary care

Rosario Hernández¹, Jordi Hoyo¹, Marta Carol^{2,3,4,5}, Ruth Nadal^{2,3,4}, Adria Juanola^{2,3,4}, Anna Soria^{2,3,4}, Ana Belen Rubio Garcia^{2,3,4}, Marta Cervera^{2,3,4}, Martina Perez^{2,3,4}, Matilde Fuentes⁶, Guillem Pera⁷, Sara Martinez^{2,3,4}, Carla Chacon⁷, Maria Sanchez⁸, Aura Capdevila⁶, Marife Alvarez⁹, Jordi Gratacos^{2,3,4}, Pere Torán⁷, Isabel Graupera^{2,3,4}, Elisa Pose^{2,3,4}, Alba Martínez-Escudé⁷, Pere Ginès^{2,3,3,4,5}, Llorenç Caballeria⁷, Núria Fabrellas^{2,3,5}. ¹Institut

Clinical algorithm findings (n)

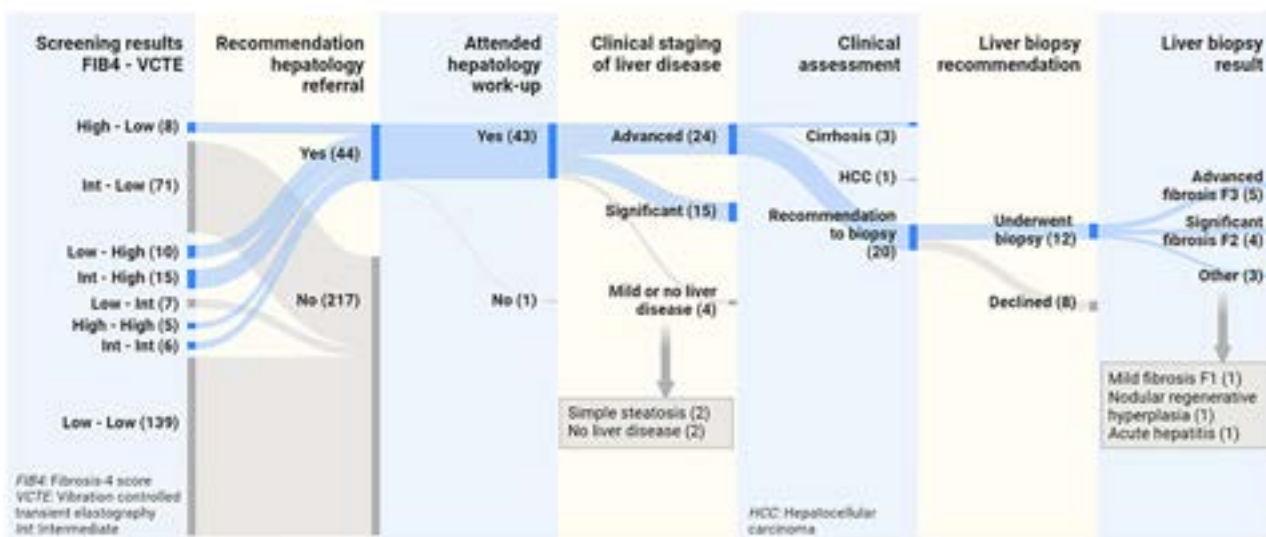


Figure: (abstract: SAT-414): Findings of a clinical referral algorithm in people with T2DM based on the simultaneous use of FIB4 (low <1.30, intermediate 1.30–2.67, high >2.67) and VCTE (low <7.9, intermediate 7.9–9.6, high >9.6 [kPa]).

Catala de la Salut (ICS). BCN. Ambit d'Atencio Primaria, Barcelona, Spain; ²Institut D'Investigacions Biomèdiques August Pi I Sunyer (IDIBAPS), Barcelona, Spain; ³Centro de Investigación En Red de Enfermedades Hepáticas Y Digestivas (Ciberehd), Barcelona, Spain; ⁴Liver Unit Hospital Clínic, University of Barcelona, Barcelona, Catalonia, Spain; ⁵Faculty of Medicine and Health Sciences, University of Barcelona, Barcelona, Spain; ⁶Centre d'atenció primària Bordeta-Magòria, Barcelona, Spain; ⁷Unitat de Suport a la Recerca Metropolitana Nord, Fundació Institut Universitari per a la recerca a l'Atenció Primària de Salut Jordi Gol i Gurina (IDIAPJGol), Metropolitana Nord, IDIAP Jordi Gol, ICS Institut Català de la Salut, Barcelona, Spain; ⁸Centre d'Atenció Primària Vila de Gràcia-Cibeles, Barcelona, Spain; ⁹Centre d'Atenció Primària Numància, Barcelona, Spain
Email: nfabrellas@ub.edu

Background and aims: Primary care is the ideal setting for early identification of subjects with liver fibrosis before cirrhosis or liver cancer occurs. Early diagnosis is critical to undertake personalized effective therapeutic interventions to stop disease progression and prevent liver-related mortality. However, the target population for liver fibrosis assessment in primary care is not well defined. The objective of this study was to investigate the characteristics of target population for liver fibrosis assessment, particularly the relationship between risk factors of liver fibrosis and presence of steatosis.

Method: Prospective cohort of 5760 subjects without known liver disease randomly selected from primary care. Fibrosis was estimated by liver stiffness (LS) with transient elastography. A LS ≥ 9.2 kPa was considered suggestive of liver fibrosis, as reported by previous studies in population-based cohorts. Hepatic steatosis was estimated with fatty liver index (FLI). A FLI ≥ 60 was considered suggestive of moderate/severe hepatic steatosis. Risk factors of fibrosis were metabolic syndrome and its components, obesity, type2DM, or risk alcohol consumption.

Results: Out of the 5760 subjects included, 3,614 (63%) had at least one risk factor of liver fibrosis. Among subjects with risk factors, the prevalence of LS ≥ 9.2 kPa was higher compared to that of subjects without risk factors (4.7% vs 0.3%, $p < 0.001$). We then assessed the prevalence of LS ≥ 9.2 kPa in patients with risk factors categorized according to presence/absence of associated hepatic steatosis (FLI ≥ 60). Interestingly, prevalence of LS ≥ 9.2 kPa was higher among subjects with risk factors and steatosis compared to that of subjects with risk factors without steatosis (7.5% vs 0.6%, respectively; $p < 0.01$). Remarkably, the vast majority of subjects with LS ≥ 9.2 kPa belonged to the subgroup of subjects with risk factors and associated steatosis (162 of 178, 91%). By contrast, only a small fraction of subjects with LS ≥ 9.2 kPa had risk factors and increased FIB-4 (> 2.67) (23 out of 178, 13%). In subjects with risk factors, FLI had higher accuracy in the diagnosis of LS ≥ 9.2 kPa compared to FIB-4 (AUROC: 0.83 vs 0.62, respectively).

Conclusion: In primary care, the target population for evaluation of liver fibrosis should consist of subjects with risk factors for liver fibrosis and associated hepatic steatosis. In subjects without risk factors or with risk factors but without steatosis, the prevalence of increased LS is very low and does not seem to justify the assessment of liver fibrosis. In subjects with risk factors, FLI is more accurate than FIB-4 to predict individuals with high likelihood of liver fibrosis.

SAT-416

Performance of non-invasive fibrosis tests for long-term liver and heart outcomes in Europeans with metabolic risk factors from the UK Biobank

Federica Tavaglione^{1,2}, Antonio De Vincentis^{2,3}, Oveis Jamialahmadi⁴, Raffaele Antonelli Incalzi^{2,5}, Antonio Picardi^{2,6}, Stefano Romeo^{7,8,9}, Umberto Vespasiani Gentilucci^{2,6}. ¹Fondazione Policlinico Universitario Campus Bio-Medico, Clinical Medicine and Hepatology Unit, Rome, Italy; ²Università Campus Bio-Medico di Roma, Department of Medicine and Surgery, Rome, Italy; ³Fondazione Policlinico

Universitario Campus Bio-Medico, Internal Medicine Unit, Rome, Italy; ⁴University of Gothenburg, Department of Molecular and Clinical Medicine, Sahlgrenska Academy, Gothenburg, Sweden; ⁵Fondazione Policlinico Universitario Campus Bio-Medico, Internal Medicine Unit, Rome, Italy; ⁶Fondazione Policlinico Universitario Campus Bio-Medico, Clinical Medicine and Hepatology Unit, Rome, Italy; ⁷University of Gothenburg, Department of Molecular and Clinical Medicine, Sahlgrenska Academy, Gothenburg, Sweden; ⁸Sahlgrenska University Hospital, Cardiology Department, Gothenburg, Sweden; ⁹University Magna Graecia, Clinical Nutrition Unit, Department of Medical and Surgical Sciences, Catanzaro, Italy
Email: fede.tavaglione@gmail.com

Background and aims: Non-alcoholic fatty liver disease (NAFLD) is the leading cause of chronic liver disease in Western countries. NAFLD is associated with both liver-related and extrahepatic complications, including cardiovascular disease (CVD). Non-invasive tests (NITs) for advanced fibrosis are increasingly used to identify individuals with NAFLD who are at risk for liver-related complications. Their performance for extrahepatic complications has been recently tested in tertiary care settings and found to be limited. Herein, we investigated the performance of NITs for predicting long-term liver and heart outcomes in individuals with dysmetabolism from the large prospective UK Biobank.

Method: To assess the performance of NITs for liver and heart outcomes, we selected 305,745 Europeans with overweight/obesity and/or type 2 diabetes, without any liver disease at baseline, and 194,236 Europeans with overweight/obesity and/or type 2 diabetes, without chronic viral hepatitis and CVD at baseline, respectively. Then, we estimated the performance of NITs for predicting incident severe liver disease (SLD: cirrhosis, decompensated liver disease, hepatocellular carcinoma, liver transplantation) or incident CVD (angina, myocardial infarction, stroke, transient ischemic attack) by Cox proportional hazards models. Follow-up length was calculated from the date of baseline assessment visit up to the first date of target outcome diagnosis, the date of death, or the date of end of follow-up at the assessment center (July 1st, 2022), whichever occurred first. The following NITs were tested: fibrosis-4 index (FIB-4), NAFLD fibrosis score (NFS), fibrotic NASH index (FNI), AST to platelet ratio index (APRI), BARD.

Results: After a median follow-up of 9 years, FNI was the best score for predicting liver outcomes (area under the curve [AUC] 0.77, $p < 0.05$ vs all the other NITs). After a median follow-up of 13 years, NFS was the best score for predicting heart outcomes (AUC 0.60, $p < 0.05$ vs all the other NITs). All NITs showed a worse and limited performance for heart outcomes compared with that for liver outcomes.

Score	SLD (N = 305,745)		CVD (N = 194,236)	
	AUC	P value	AUC	P value
FIB4	0.75 (0.73–0.77)	0.03	0.59 (0.59–0.60)	<0.001
NFS	0.72 (0.70–0.74)	<0.001	0.60 (0.60–0.61)	reference
FNI	0.77 (0.75–0.79)	reference	0.59 (0.58–0.60)	0.003
APRI	0.75 (0.73–0.77)	0.01	0.53 (0.53–0.54)	<0.001
BARD	0.62 (0.61–0.64)	<0.001	0.55 (0.54–0.55)	<0.001

Conclusion: NITs showed a satisfactory performance for predicting liver outcomes, but a rather limited performance for predicting heart outcomes in individuals with dysmetabolism from the general population.

SAT-417

Impact of age as a confounding factor on non-invasive blood-based tests for the evaluation of non-alcoholic fatty liver disease: comparing NIS2+™ to established tests

Quentin Anstee^{1,2}, Jeremy Magnanensi³, Yacine Hajji³, Alexandra Caron³, Zouher Majd³, Christian Rosenquist³, Dean Hum³, Bart Staels⁴, Margery A. Connelly⁵, Rohit Loomba⁶, Stephen Harrison^{7,8}, Vlad Ratziu⁹, Arun Sanyal¹⁰. ¹Translational and Clinical Research Institute, Faculty of Medical Sciences, Newcastle University, Newcastle upon Tyne, United Kingdom; ²Newcastle NIHR Biomedical Research Centre, Newcastle upon Tyne Hospitals NHS Foundation Trust, Freeman Hospital, Newcastle upon Tyne, United Kingdom; ³GENFIT S.A., Loos, France; ⁴Univ. Lille, INSERM, CHU Lille, Institut Pasteur de Lille, U1011-EGID, Lille, France; ⁵Labcorp, Morrisville, United States; ⁶NAFLD Research Center, Division of Gastroenterology, Department of Medicine, University of California at San Diego, La Jolla, United States; ⁷Summit Clinical Research, San Antonio, United States; ⁸Radcliffe Department of Medicine, University of Oxford, Oxford, United Kingdom; ⁹Sorbonne Université, Institute for Cardiometabolism and Nutrition, Hôpital Pitié-Salpêtrière, Paris, France; ¹⁰Division of Gastroenterology, Hepatology and Nutrition, Virginia Commonwealth University School of Medicine, Richmond, United States
Email: jeremy.magnanensi@genfit.com

Background and aims: Non-alcoholic steatohepatitis (NASH) is the more progressive form of non-alcoholic fatty liver disease (NAFLD), the leading cause of chronic liver disease. Timely diagnosis of specific conditions associated with higher risk of liver-related/all-cause mortality, such as “at-risk NASH” (NASH with a NAFLD activity score [NAS] ≥ 4 and a fibrosis stage [F] ≥ 2) or advanced fibrosis (F ≥ 3), is critical and different non-invasive tests (NITs) have been developed for these purposes. NAFLD affects patients of all ages, therefore, NITs

should perform consistently across age groups to simplify large-scale use in clinical practice. This work investigated the effect of age on several well-established NITs including NIS2+™ and compared it to a histological reference standard.

Method: An analysis cohort (N=2108; ≤ 45 years [n=496], 46–55 years [n=569], 56–64 years [n=625], and ≥ 65 years [n=418]) containing all patients with liver biopsies and data for NIS2+™, aspartate aminotransferase-to-platelet ratio index (APRI), NAFLD fibrosis score (NFS), Fibrosis-4 (FIB-4), and Enhanced Liver Fibrosis (ELF) was selected among those screened for the phase 3 RESOLVE-IT clinical trial (NCT02704403). To avoid potential confounding effects and allow for a robust analysis of the age impact on NITs, a well-balanced cohort (N=800, n=200 per age group) was obtained by applying a propensity score matching algorithm to the analysis cohort. Baseline values of biomarkers and NITs were compared across age groups using one-way ANOVA, and age impact on NITs distribution was compared to the effect of histology (F, NAS) using 3-way type-2 ANOVA and associated effect sizes. Using derived Youden cutoffs, the impact of age on NITs’ clinical performance (sensitivity, specificity) for the diagnosis of targeted condition was analysed.

Results: NIS2+™ and APRI were not impacted by age ($p = 0.70$ and $p = 0.91$, resp.), while the means of NFS, FIB-4, and ELF increased significantly with age ($p < 0.0001$), driven notably by decreasing ALT (NFS, FIB-4) and increasing hyaluronic acid (ELF) concentrations ($p < 0.0001$). Age had a higher effect size for FIB-4, NFS, and ELF than liver fibrosis, the hypothesized main driver of these NITs. The age impact on FIB-4, NFS and ELF led to a decrease in specificity (FIB-4: 0.91–0.34; NFS: 0.81–0.23; ELF: 0.86–0.42) and an increase in sensitivity (FIB-4: 0.26–0.89; NFS: 0.49–0.92; ELF: 0.49–0.93) for the detection of F ≥ 3 across the different age groups. While not being impacted by age, NIS2+™ was the only NIT for which both F stage and

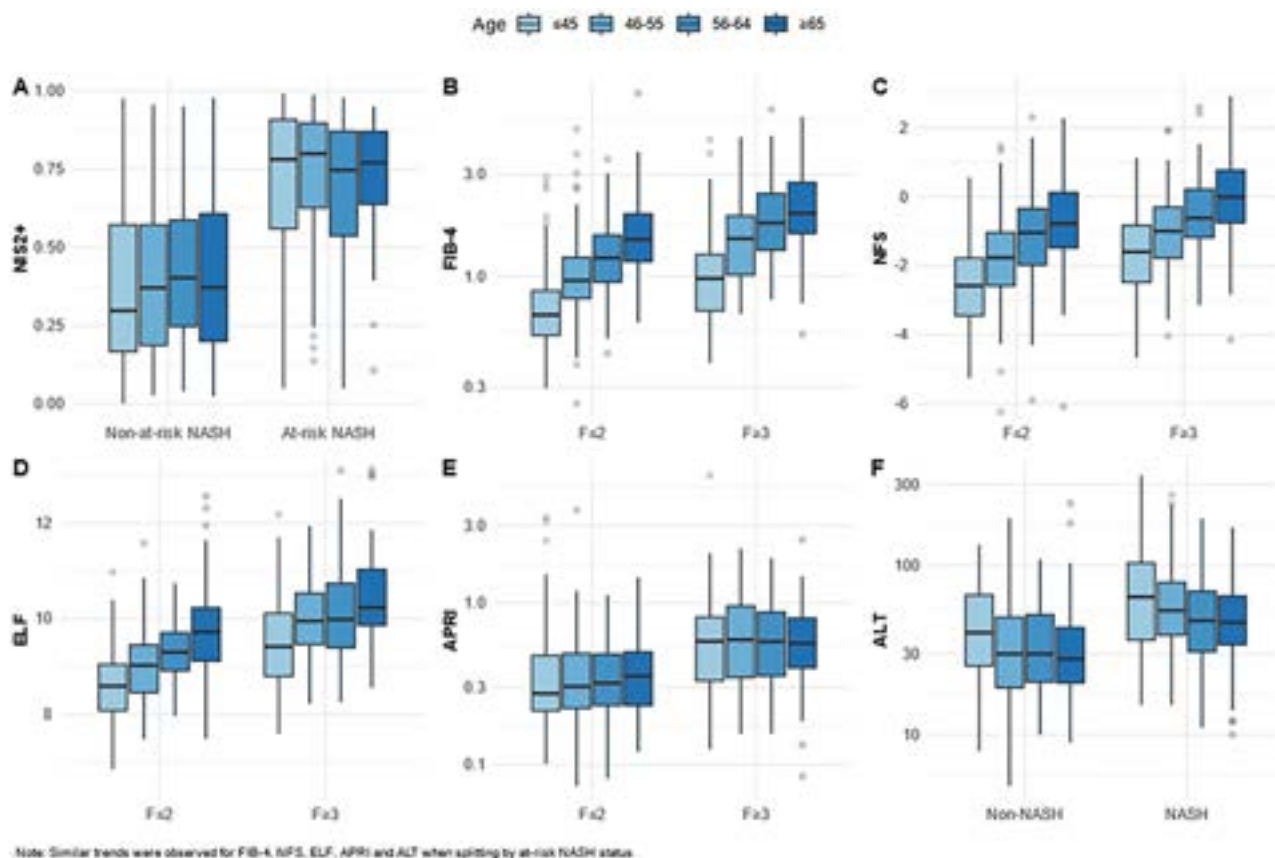


Figure: (abstract: SAT-417).

NAS score had medium to large effect sizes (partial omega squared = 0.16 and 0.12, resp.), confirming its adequacy for the detection of at-risk NASH as a composite end point.

Conclusion: FIB-4, NFS and ELF were impacted by age, therefore consideration should be given to adopting age-adapted cutoffs. NIS2 +TM was not impacted by age, demonstrating robust assay performance for ruling in/out at-risk NASH with fixed medical decision points.

SAT-418

Cost effectiveness analysis of screening for advanced hepatic fibrosis in patients with various 'at-risk population' in guidelines

Hye-Lin Kim¹, Huiyul Park², Hyo Young Lee³, Eileen Yoon⁴, Mimi Kim⁵, Sang Bong Ahn⁶, Chul-min Lee⁵, Bo-Kyeong Kang⁵, Joo Hyun Sohn⁴, Jihyun An⁴, Joo Hyun Oh⁶, Dae Won Jun⁴, Eun Chul Jang⁷. ¹Sahmyook University, College of Pharmacy, Korea, Rep. of South; ²Myoungji Hospital, Hanyang University College of Medicine, Department of Family Medicine, Korea, Rep. of South; ³Uijeongbu Eulji Medical Center, Eulji University College of Medicine, Department of Internal Medicine, Korea, Rep. of South; ⁴Hanyang University, College of Medicine, Department of Internal Medicine, Korea, Rep. of South; ⁵Hanyang University, College of Medicine, Department of Radiology, Korea, Rep. of South; ⁶Nowon Eulji Medical Center, Eulji University School of Medicine, Department of Internal Medicine, Korea, Rep. of South; ⁷Soonchunhyang University College of medicine, Department of Occupational and Environmental Medicine, Korea, Rep. of South
Email: noshin@hanyang.ac.kr

Background and aims: Current guidelines for non-alcoholic fatty liver disease (NAFLD) recommend that the screening test for hepatic fibrosis should be performed to at-risk group for hepatic fibrosis. This study aimed to evaluate the cost-effectiveness of screening strategy using sequential combination of FIB-4 followed by transient elastography for advanced hepatic fibrosis in various at-risk populations.

Method: We built a combined model of decision tree model and Markov model to compare expected costs and quality-adjusted life-years (QALYs) between 'screening' and 'no screening' groups from healthcare system perspective. At-risk group was mainly defined as the group of individuals with any of the following risk factors: fatty liver, two or more metabolic abnormalities (three or more in the European Association for the Study of the Liver (EASL)), diabetes mellitus, and abnormal liver function test based on American Gastroenterological Association (AGA) guideline. Patients with pre-diabetes or obesity in American Association for the Study of Liver Diseases (AASLD) and overweight in EASL were additionally added in at-risk group, respectively. Fibrosis distribution of at-risk group was based on real world data from 8,545 health check-up examiners who underwent magnetic resonance elastography. Patients who diagnosed as advanced fibrosis in screening group were applied with intensive life-style intervention (ILI). The model included not only liver disease-related health states, but also cardiovascular disease (CVD) and extrahepatic cancer states that could be affected by NAFLD. Incremental cost-effectiveness ratio (ICER) was calculated for 20-year horizon and evaluated by applying the definition of 'at-risk' population to various guidelines.

Results: The cost-effectiveness analysis showed that screening group had \$253 incremental costs and additional 0.0191 QALY per patient compared to no screening group in at-risk population. Through the base-case analysis ICER was \$13,234/QALY. The result indicated that screening was cost-effective based on the implicit ICER threshold of \$25,000/QALY in Korea. Sequential algorithm based on FIB-4 and transient elastography was more cost-effective considering the effects of ILI on cardiovascular and other malignancy in the 'at-risk group'. In addition to the at-risk group defined by AGA guideline, the screening algorithm with ILI was also cost-effective in the at-risk group definition suggested by other guidelines (\$14,211/QALY in EASL, \$13,986/QALY in AASLD). Even when replacing medical costs in

other countries, they were cost-effective because they were below the ICER threshold (\$44,860/QALY in the US and \$6147 in Japan).

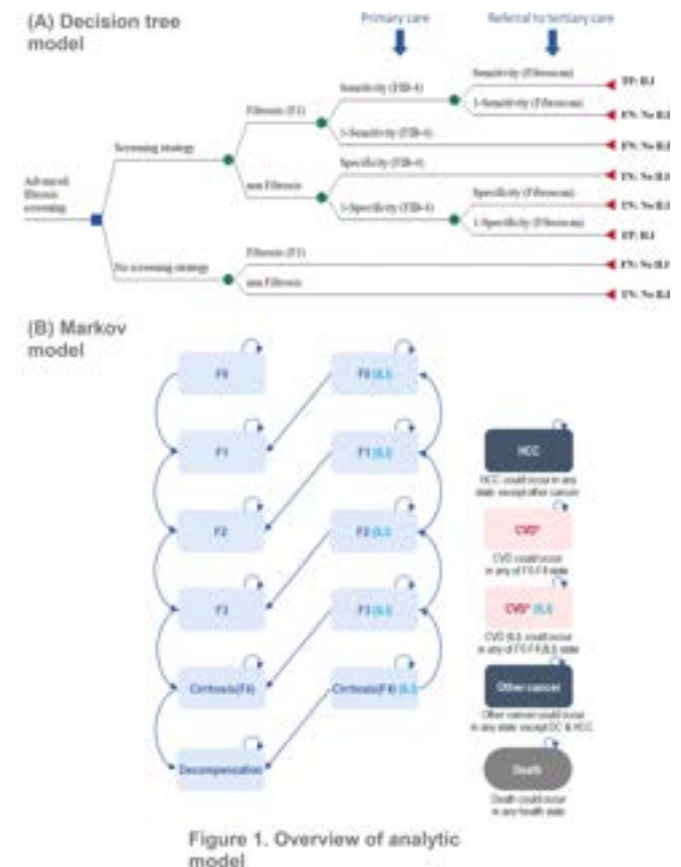


Figure:

Conclusion: Screening for advanced hepatic fibrosis using FIB-4 in patients with at-risk population would be cost-effective when applying definitions in most of all guidelines about at-risk populations.

SAT-419

Which screening of advanced liver fibrosis in NAFLD?

Paul Cales¹, Clémence M Canivet², Lannes Adrien², Frédéric Oberti², Isabelle Fouchard², Charlotte Costentin³, Victor de Lédighen⁴, Jerome Boursier². ¹Angers University Hospital, Angers, France; ²Angers University Hospital, France; ³Grenoble University Hospital, France; ⁴Bordeaux University Hospital, France
Email: paul.cales@univ-angers.fr

Background and aims: The EASL and AGA guidelines recommend screening advanced fibrosis in patients at risk of NAFLD using sequential tests. Our aim was to compare and improve these algorithms.

Method: 1051 NAFLD patients were divided in derivation (n = 637) and validation (n = 414) sets. The outcome was advanced fibrosis (Kleiner F3+F4). The main descriptors were sensitivity, accuracy, indeterminate rate, liver stiffness measurement (LSM by Fibroscan) recourse and direct costs. The recommended algorithms were evaluated according to cut-offs either original or adapted to derivation set. In the EASL algorithm, we included either the agreement between LSM and Fibrotest (FT) or FibroMeter (FM), or the FM+LSM (EFM) combination. A new 3-steps Fibs algorithm used first FIB9 (using 9 usual liver blood markers), then FIB11 (adding 2 specialized blood markers) and finally FIB-12 (adding LSM). These new FIB tests were obtained by multi-targeting (PMID: 29619423) improved by machine learning in the derivation set.

POSTER PRESENTATIONS

Results: They are given in the validation set. AUROC were, FIB4: 0.757, FT: 0.766, FM: 0.850, LSM: 0.852, FIB9: 0.863, FIB11: 0.880, EFM: 0.894, FIB12: 0.912 ($p < 0.001$). 1/The recommended algorithms with original cut-offs had the same fair sensitivity (70.3%) but the AGA algorithm had a significantly higher indeterminate rate and cost. The indeterminate rate of EASL algorithm was, FT: 13.5%, FM: 7.5% ($p < 0.001$). 2/Optimized EASL or AGA algorithms by adapted cut-offs improved sensitivity and accuracy vs original algorithms at the expense of increased indeterminate rate and cost. 3/The modified EFM-EASL algorithm significantly reduced the indeterminate rate (5.3%, $p < 0.001$) and cost vs optimized algorithms. The new Fibs algorithm improved all outcomes (Figure), e.g. sensitivity: 82.1% vs AGA: 77.2% or EASL: 74.5% ($p = 0.052$), indeterminate rate: 3.1% vs AGA: 16.4% or EASL: 9.7% ($p < 0.001$), LSM recourse: 15.5% vs AGA: 66.9% or EASL: 49.0% ($p < 0.001$) and mean cost: 57€ vs AGA: 188€, EASL: 134€ ($p < 0.001$).



Figure:

Conclusion: The characteristics of the recommended algorithms show significant differences depending on their type or the patented blood test included. Their sensitivity, indeterminate rate and cost are perfectible. The modified EFM-EASL algorithm, improved by test combination, is immediately applicable. The new Fibs algorithm significantly improved all characteristics including greatly reduced indeterminate rate, LSM recourse (promoting ubiquitous applicability) and cost.

SAT-420

Glomerular hyperfiltration: a new marker of fibrosis severity in non-cirrhotic non-alcoholic fatty liver disease

Andrea Dalbeni^{1,2}, Marta Garbin^{1,2}, Mirko Zoncapè^{1,2,3}, Sara Sara Romeo^{1,2}, Filippo Cattazzo^{1,2}, Anna Anna Mantovani^{1,2,3}, Annalisa Cespiati⁴, Alessandro Mantovani⁵, Anna Ludovica Fracanzani⁴, Emmanuel Tsochatzis³, David Sacerdoti², Rosa Lombardi^{3,4}. ¹General Medicine C, University and Azienda Ospedaliera Integrata of Verona, Department of Medicine, Italy; ²Liver Unit, University and Azienda Ospedaliera Integrata of Verona, Department of Medicine, Italy; ³Royal Free Hospital and UCL, UCL Institute for Liver and Digestive Health, United Kingdom; ⁴Unit of Internal Medicine and Metabolic Disease; Granda IRCCS Foundation, Policlinico Hospital, University of Milan, Department of Pathophysiology and Transplantation, Italy; ⁵Endocrinology Unit, University and Azienda Ospedaliera Integrata of Verona, Department of Medicine, Italy
Email: marta.garbin@studenti.univr.it

Background and aims: Non-alcoholic fatty liver disease (NAFLD), mainly in its advanced form with hepatic fibrosis, represents a risk factor for the development of cardiovascular (CV) disease and chronic kidney failure, the latter early expressed by glomerular hyperfiltration (GH). GH shares the same CV and metabolic risk factors with NAFLD, and their association has been already evaluated in adults with metabolic syndrome. However, association between GH and NAFLD fibrosis has not been investigated yet.

Method: 772 patients (mean age 47.3 ± 8.9 (range 40–65 ys), 67.1% male) with non-cirrhotic NAFLD diagnosed by abdominal ultrasound were enrolled at three hepatology centers (Verona, Milan and London). Hepatic fibrosis was diagnosed by Fibroscan (echoSense) by a liver stiffness measurement (LSM) ≥ 7.2 kPa. Glomerular filtration rate (GFR) was estimated using 2012CKD-EPI formula and GH was defined by $GFR \geq 110$ ml/min, whereas normal filtration (nGFR) by $GFR 60$ – 110 ml/min. Anthropometric and biochemical data, as well as medical history and current therapy were recorded at enrollment.

Results: In the whole cohort, 152 (20%) belonged to the GH group. Compared to the nGFR, the GH group presented younger age (38.4 ± 8.3 vs 49.5 ± 7.7 years, $p < 0.001$), higher prevalence of severe steatosis (39.9% vs 27.1%, $p = 0.03$) and higher LSM values (8.04 ± 6.15 kPa vs 7.47 ± 6.12 kPa, $p = 0.023$). In multivariate analysis adjusted for age, sex, type 2 diabetes, hypertension and obesity, age (OR 0.83, CI 95% 0.77–0.89) and LSM (OR 6.6, CI 95% 2.2–19.9) were independent risk factors for GH. LSM remained independently associated with GH even when considered diagnostic for fibrosis (LSM > 7.2 kPa) (OR 1.83, CI 95% 1.10–3.03). These association were maintained even adjusting for diuretic and ACE/ARBs therapy.

Conclusion: GH is associated with hepatic fibrosis by LSM independently of other metabolic alterations. Therefore, GH could be considered an early marker of liver fibrosis in non-cirrhotic NAFLD patients and calculation of a simple index as GFR could suggest the need for a Fibroscan assessment in NAFLD patient even in primary care.

SAT-421

NIS2+™ as a screening tool for optimizing patient selection in non-alcoholic steatohepatitis therapeutic trials

Vlad Ratzu¹, Stephen Harrison^{2,3}, Yacine Hajji⁴, Jeremy Magnanensi⁴, Stéphanie Petit⁵, Zouher Majd⁵, Christian Rosenquist⁵, Dean Hum⁵, Bart Staels⁶, Quentin Anstee^{7,8}, Arun Sanyal⁹. ¹Sorbonne Université, Institute for Cardiometabolism and Nutrition, Hôpital Pitié-Salpêtrière, Paris, France; ²Summit Clinical Research, San Antonio, TX, United States; ³Radcliffe Department of Medicine, University of Oxford, Oxford, United Kingdom; ⁴GENFIT, Loos, France; ⁵GENFIT, Loos, France; ⁶Université de Lille, INSERM, CHU Lille, Institut Pasteur de Lille, Lille, France; ⁷Translational and Clinical Research Institute, Faculty of Medical Sciences, Newcastle University, Newcastle upon Tyne, United Kingdom; ⁸Newcastle NIHR Biomedical Research Centre, Newcastle upon Tyne Hospitals NHS Foundation Trust, Freeman Hospital, Newcastle upon Tyne, United Kingdom; ⁹Division of Gastroenterology, Hepatology and Nutrition, Virginia Commonwealth University School of Medicine, Richmond, VA, United States
Email: yacine.hajji@genfit.com

Background and aims: In clinical trials of non-cirrhotic patients with at-risk NASH (NAS ≥ 4 ; F ≥ 2), the screen failure rate of liver biopsy (LB) is unacceptably high. Standard non-invasive fibrosis tests aimed at detecting advanced fibrosis are not optimal to identify at-risk NASH. NIS2+™ is an improved version of the blood-based NIS4® biomarker, designed to identify at-risk NASH. We assessed the potential of NIS2+™ for optimized biopsy referral in therapeutic trials targeting at-risk NASH.

Method: Among >5000 patients who were screened in the RESOLVE-IT Phase 3 trial (NCT02704403), 1929 patients were selected with non-historical LB, available NIS2+ and FIB4 results and less than 3 months between LB and serum samples. This cohort was representative of the overall screening population and was used to perform a simulation to compare the actual screening performance observed in the RESOLVE-IT trial (based on clinical judgment of the investigators and standard local practices) with two simulated pathways using NIS2+™ alone, and FIB4-NIS2+™ sequentially. The number of patients needed to screen, the LB failure rate, and the screening cost (based on average costs of RESOLVE-IT in US sites) were assessed for a range of cutoff values of 0–0.8 for NIS2+™; and 0–2.0 for FIB4.

Performances were estimated for the inclusion of 1000 patients as confirmed by liver biopsy.

Results: The RESOLVE-IT screening process (RSP) cost \$15 million per 1000 included patients, with a LB failure rate of 60.3% and 3220 patients needed to screen. Using, NIS2+™ for screening with a cost-optimized cutoff of 0.53, reduced the LB failure rate to 39%, saving 884 unnecessary biopsies (~58%) with a \$2.3 million cost reduction (~16%) for only 812 (+25%) additional patients to be screened, corresponding to a NNT (number needed to be tested) of 4. For this cost-optimized cutoff, the sensitivity of NIS2+™ would have been 80%, specificity 66%, NPV 83% and PPV 61%. Compared to NIS2+™ alone, neither FIB4 alone nor FIB4-NIS2+™ would have reduced cost of inclusion or LB failure rates without considerably increasing the number of screenings. Unlike FIB4, NIS2+™ did not alter the demographic profile of patients included, in particular for important stratification parameters such as diabetes, histological activity or advanced fibrosis.

Conclusion: In therapeutic trials of non-cirrhotic at-risk NASH, the NIS2+™ blood-based biomarker would substantially optimize the referral pathway for liver biopsy by reducing unnecessary liver biopsies and overall costs thus greatly improving a major aspect of feasibility of NASH clinical trials.

SAT-422

Abdominal adiposity and insulin resistance are the main predictors of CAP values in individuals with metabolic dysfunction: the liver-bible cohort

Cristiana Bianco¹, Serena Pelusi¹, Sara Margarita¹, Francesco Malvestiti², Giulia Periti¹, Jessica Rondena¹, Melissa Tomasi¹, Rossana Carpani¹, Matteo Vidali³, Ferruccio Ceriotti³, Daniele Prati¹, Luca Valenti^{1,2}. ¹Fondazione IRCCS Ca' Granda Ospedale Ospedale Maggiore Policlinico di Milano, Precision Medicine-Department of Transfusion Medicine, Italy; ²Università degli Studi di Milano, Department of Pathophysiology and Transplantation, Italy; ³Fondazione IRCCS Ca' Granda Ospedale Maggiore Policlinico di Milano, Clinical Pathology Unit, Italy
Email: biancocristiana.md@gmail.com

Background and aims: Evaluation of controlled attenuation parameter (CAP) during vibration controlled transient elastography (VTCE) permits the non-invasive estimation of hepatic fat content and the presence of fatty liver disease (FLD), a key driver of liver disease. Aim of the study was to examine the independent determinants and clinical predictors of CAP values in a cohort of apparently healthy individuals at high risk of FLD due to metabolic dysfunction.

Method: We considered 1230 consecutive blood donors (Liver-Bible cohort up to June 2022) with ≥3 features of metabolic dysfunction (overweight/obesity, hyperglycemia, hypertension, low HDL/high triglycerides), who underwent cardiometabolic evaluation from June 2019 to June 2022. CAP was measured by VTCE with Fibroscan. CAP determinants and predictors were identified by backward stepwise analysis and introduced in generalized linear models.

Results: Among participants, 210 (17.1%) were females, mean age was 53.8 ± 6.4 yrs, BMI 28.6 ± 3.2 Kg/m², 600 (48.8%) had steatosis (CAP ≥275 dB/m) and 27 (2.2%) had liver stiffness measurement (LSM) ≥8 kPa. CAP values correlated with higher LSM ($p < 10^{-22}$). At multivariable analysis, independent determinants of CAP values were fasting insulin and abdominal circumference (AC; $p < 10^{-7}$ for both), together with body mass index (BMI; $p < 10^{-4}$), age, diabetes, triglycerides, ferritin, and lower HDL and thyroid stimulating hormone (TSH; $p < 0.05$ for all). AC was also an independent determinant of CAP ≥275 dB/m ($p < 10^{-5}$), with insulin and diabetes, BMI, and lower HDL and TSH ($p < 0.05$ for all). In a subgroup of 592 participants for whom the information was available, we observed an independent association between higher fT3 levels, correlating with higher TSH, and CAP values (estimate 11.78 ± 3.92, $p = 0.0027$), independently of TSH levels and of levothyroxine treatment. A

clinical score based on age, BMI, AC, HDL, HbA1c and ALT predicted CAP ≥275 dB/m with moderate accuracy (AUROC = 0.73), which was better than that of ALT alone and fatty liver index (AUROC = 0.61/0.70 respectively).

Figure: Independent determinants of CAP values in the LIVER-BIBLE-2022 cohort.

	Overall Liver-Bible-2022 cohort (n = 1,230)			Subgroup with fT3/T4 determination (n = 592)		
	Estimate	SE	p value ^a	Estimate	SE	p value ^a
Age, years	0.59	0.17	0.0005	0.53	0.24	0.0258
Sex, F	0.81	1.60	0.6118	2.19	2.45	0.3699
BMI, Kg/m ²	2.23	0.55	4.80 × 10⁻⁵	1.83	0.80	0.0220
AC, cm	1.06	0.20	1.11 × 10⁻⁷	1.11	0.29	0.0001
Glucose, mg/dL	0.14	0.07	0.06	0.24	0.11	0.0332
Insulin, mIU/L	0.68	0.12	1.31 × 10⁻⁸	0.46	0.17	0.0073
T2D, yes	10.31	4.46	0.0209	14.80	6.88	0.0315
HDL-C, mg/dL	-0.28	0.11	0.0153	-0.27	0.17	0.1063
TG, mg/dL	0.03	0.01	0.0375	0.01	0.02	0.7178
Ferritin, log ng/ml	3.60	1.27	0.0045	1.55	1.79	0.3871
TSH, mU/L	-1.57	0.74	0.0324	2.38	1.64	0.1456
fT3, ng/L				11.87	3.93	0.0025

^aAt GLM, adjusted for ethnicity, Levothyroxine replacement therapy and reported variables (identified at backward stepwise analysis, not shown). AC: abdominal circumference; BMI: body mass index; F: female; fT3: free triiodothyronine; HDL-C: high-density lipoprotein cholesterol; SE: standard error; T2D: type 2 diabetes; TG: triglycerides; TSH: thyroid stimulating hormone.

Conclusion: The severity of insulin resistance and abdominal adiposity were the main independent determinants of CAP in individuals with metabolic dysfunction and may improve the risk stratification of FLD at an early stage of development. CAP values were modulated by hypophysis-thyroid-axis activity.

SAT-423

A cost-effective non-invasive serum test for diagnosing NASH-cirrhosis (NC-3) in high-risk metabolic syndrome and/or type 2 diabetes patients

Shira Shaham-Niv¹, Eldad Kepten¹, Boris Sarvin¹, Avishai Gavish¹, Claudia Filozof², Tomer Shlomi^{1,3}. ¹MetaSight Diagnostics, Rehovot, Israel; ²Labcorp Drug Development, Israel; ³Technion, Department of Computer Science and Biology, Haifa, Israel
Email: shira.s@metasightdx.com

Background and aims: Liver cirrhosis is majorly underdiagnosed and with an estimated prevalence of 6% among T2D patients; hence, ~70% of cirrhosis cases are only incidentally found. However, currently high-risk T2D and metabolic syndrome patients are typically not screened for NASH-cirrhosis as part of common general practice. Here, we develop a robust non-invasive test (NIT) for NASH-cirrhosis based on cost-effective metabolomics and lipidomics, amenable for screening asymptomatic high-risk patients.

Method: Serum samples from ~500,000 subjects (>50 years old) were collected as part of standard clinical routine by a central Israeli HMO between July 2021 and January 2023, within the ongoing Israeli multi-OMICS Serum Screening (IMOSS-500 K) study. De-identified electronic health records (EHR) were used to identify ~60,000 samples from patients diagnosed with NAFLD, among which 183 were diagnosed with cirrhosis within ±6 months from serum collection. Cirrhosis cases were identified based on ICD-9 and were individually validated by a health specialist (based on biopsy, imaging and/or clinical assessment data). Patients with matching age, gender, and metabolic syndrome features (n = 183) were selected as controls. All samples were analyzed with high-throughput liquid-

POSTER PRESENTATIONS

chromatography mass-spectrometry (LC-MS) based metabolomics and lipidomics. Logistic regression was used to identify a serum molecular signature of NASH-cirrhosis patients.

Results: We identified a novel metabolic signature of NASH-cirrhosis (NC-3) based on 3 serum metabolites and lipids (all of which could be readily associated with liver physiology). In a standard cross-validation test, NC-3 showed high diagnostic performance of liver cirrhosis, with an AUROC of 0.81; versus slightly lower AUROC of 0.78 by FIB-4. However, focusing on patients with intermediate FIB-4 levels (<2.67 and >1.3; cases = 66, controls = 87), the performance of NC-3 remains similarly high (AUROC = 0.81), markedly outperforming FIB-4 (AUROC = 0.68). Accordingly, focusing on matched T2D controls NC-3 shows high diagnostic performance for patients with intermediate FIB-4 levels (NC-3 AUROC = 0.81, compared to FIB-4 AUROC = 0.69, cases = 42 and controls = 45). Importantly, NC-3 performs similarly well when focusing strictly on patients without any sign of NASH-cirrhosis, having diagnosis confirmation within 1 to 6 months after serum collection (NC-3 AUROC = 0.85, compared to FIB-4 AUROC = 0.73).

Conclusion: NC-3 is a novel non-invasive method for the identification of patients with NASH-cirrhosis. The data suggests higher accuracy in FIB-4 indeterminate zone and in asymptomatic metabolic syndrome or T2D patients. The cost-efficiency of the metabolomics method would enable screening large at-risk populations, reducing the current high rates of NASH-cirrhosis under-diagnosis.

SAT-424

Comparison between EASL and AGA algorithms for hepatology referral in 1572 outpatients with type 2 diabetes and suspected NAFLD seen in a diabetes clinic

Laurent Castéra¹, Tiphaine Vidal-Trecan², Tania Khoury³, Jean-Baptiste Julia², Jean-Pierre Riveline⁴, Valérie Paradis⁵, Dominique Valla¹, Jean-François Gautier⁴. ¹Beaujon hospital, Université Paris Cité, Hepatology, Clichy, France; ²Lariboisière hospital, Diabetology, Paris, France; ³Beaujon hospital, Hepatology, Clichy, France; ⁴Lariboisière hospital, Université Paris Cité, Diabetology, France; ⁵Beaujon hospital, Université Paris Cité, pathology, clichy, France
Email: laurent.castera@bjn.aphp.fr

Background and aims: Recently, two algorithms screening patients at risk for NAFLD and advanced fibrosis to decide if a referral to a hepatologist is needed have been proposed by EASL (J Hepatol 2021) and AGA (Kanwal Gastroenterology 2021). Screening of patients with type 2 diabetes (T2D), who are the most at risk of advanced fibrosis, is

an unmet need. We aimed to compare the performance of these two algorithms in term of hepatology referral in a large cohort of T2D outpatients seen in a diabetes clinic.

Method: 1572 T2D outpatients seen in our diabetes clinic between October 2019 and February 2022, were systematically screened for NAFLD (steatosis and/or elevated ALT) and underwent FIB-4 and liver stiffness measurement (LSM) by vibration-controlled transient elastography (VCTE). Excessive alcohol consumption and viral hepatitis B and C were excluded. According to EASL algorithm, patients with FIB-4 ≥ 1.3 should undergo VCTE and those with LSM ≥ 8 kPa should be referred to a hepatologist. According to AGA algorithm, patients with FIB-4 >2.67 or with FIB-4 between 1.3 and 2.67 and LSM ≥ 8 kPa should be referred to a hepatologist.

Results: The characteristics of the 1572 patients were as follows: male 60%; median age 61 years; BMI 29 kg/m²; waist circumference 103 cm; HbA1c 7.6%; AST 28 IU/L; ALT 28 IU/L. A liver biopsy (LB) was performed in 163 patients (advanced fibrosis 30%). Comparison of the two algorithms is shown in the Figure. According to EASL, 186 (12%) should be referred to a hepatologist (LSM ≥ 8 kPa). The 1386 remaining patients were considered at low risk. According to AGA, 227 patients (15%) should be referred (132 at high risk (FIB-4 >2.67 or LSM >12 kPa) and 95 at intermediate risk). The 1345 remaining patients were considered at low risk. Among the 163 patients with LB, the rate of false positive was higher than that of false negative and similar between algorithms (38%, and 15%, respectively).

Conclusion: EASL and AGA algorithms performed similarly allowing to identify 12 to 15% of intermediate-high risk T2D patients, who should be referred to a hepatologist. These numbers are higher than reported in the general population, highlighting the urgent need for screening these patients.

SAT-425

Non-Alcoholic Steatohepatitis impacts on visceral adipose tissue proteomic signature

Cristian Martínez Navidad¹, Cristina Placed², Helena Castañé¹, Andrea Jiménez Franco², Jordi Camps³, Jorge Joven³. ¹Fundació IISPV, Unitat de Recerca Biomèdica, Reus, Spain; ²Universitat Rovira i Virgili, Unitat de Recerca Biomèdica, Reus, Spain; ³Hospital Universitari San Joan de Reus, Unitat de Recerca Biomèdica, Reus, Spain
Email: cristian.marnav@gmail.com

Background and aims: Obesity is a major global health concern due to its growing prevalence and associated diseases, leading to reduce the quality and life expectancy of those affected. Non-alcoholic

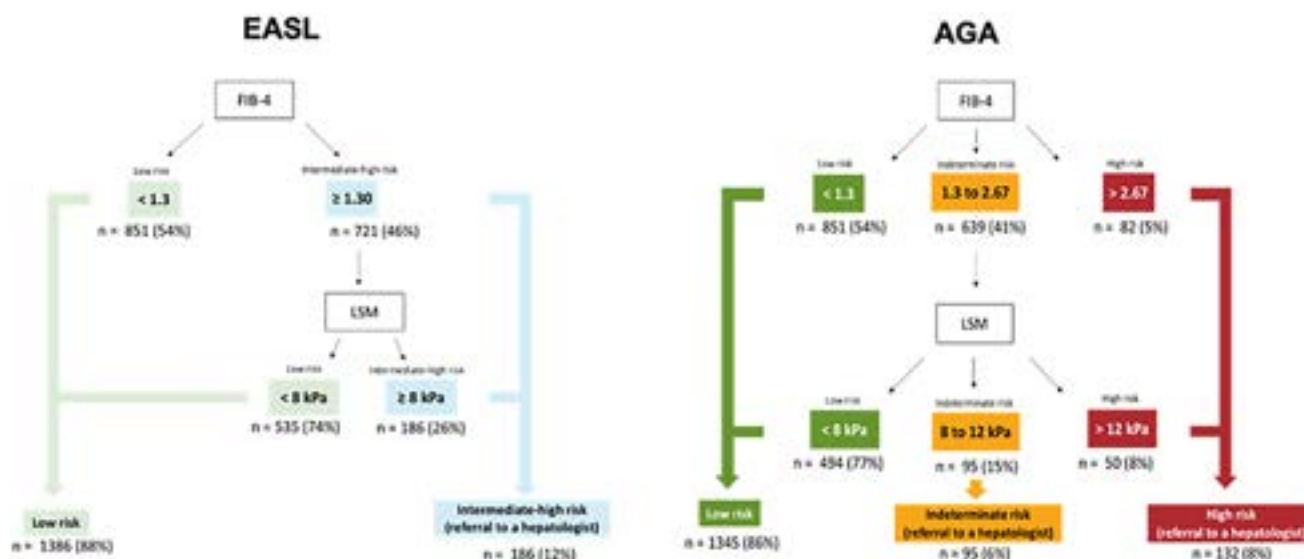


Figure: (abstract: SAT-424): Comparison of AGA and EASL algorithms in 1572 T2D outpatients

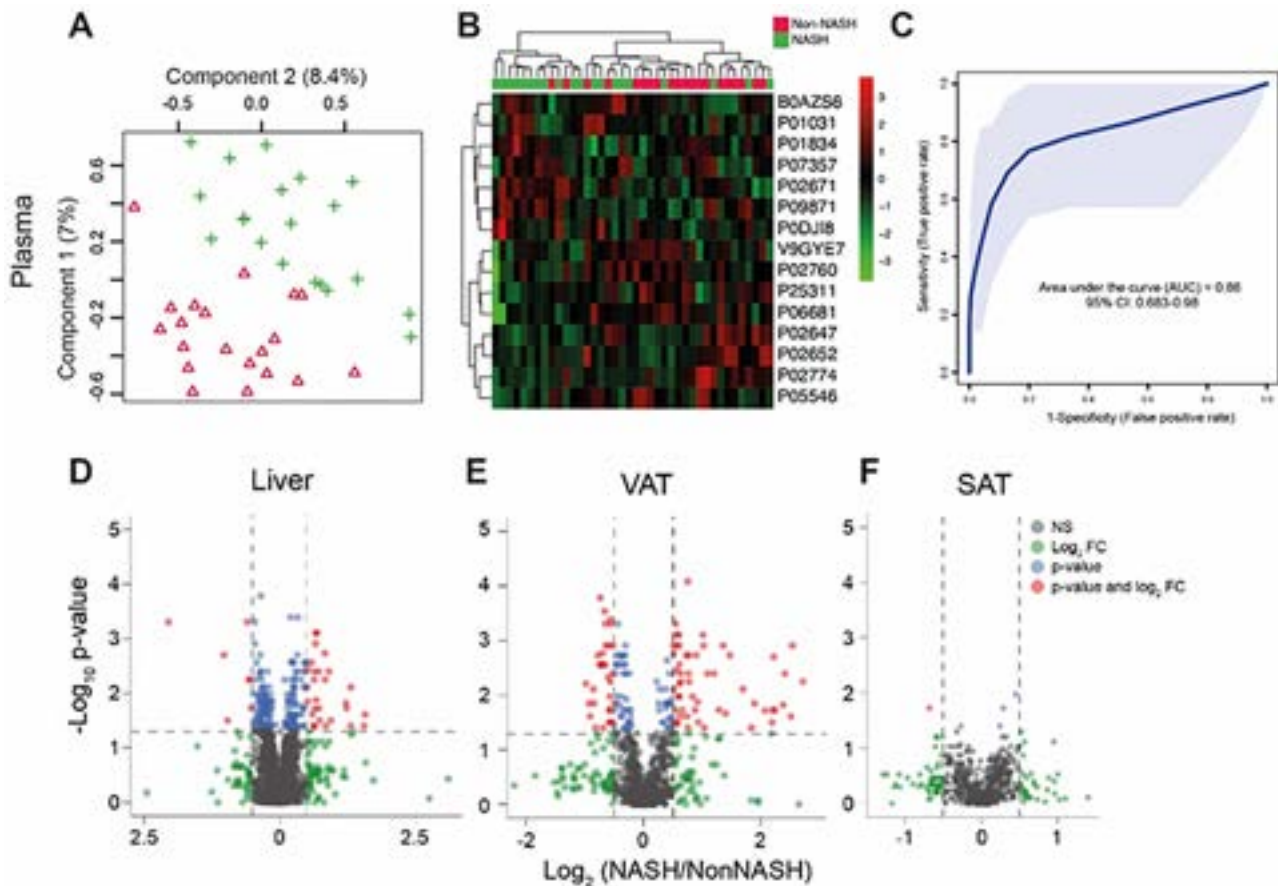


Figure: (abstract: SAT-425).

steatohepatitis (NASH), a form of non-alcoholic fatty liver disease (NAFLD), is commonly linked to obesity and manifests as liver damage and inflammation, caused by the fat accumulation. The diagnosis of NASH is challenging due to its silent and non-specific symptoms, often going undetected until late stages of the disease. Proteomics allows us to examine the mechanisms involved in these biological successes. The objective is to investigate the differences in protein profiles of plasma, liver and adipose tissue between NASH and non-NASH patients using proteomic analysis, with the goal for identifying a biological marker for earlier NASH diagnosis.

Method: To carry out the analyses, plasma samples were collected from patients undergoing bariatric surgery (n=40), including patients with NASH (n=20) and patients without NASH (n=20). Additionally, biopsies of a portion of these (n=18) were obtained to perform a proteomic analysis of visceral adipose tissue, subcutaneous adipose tissue and liver to determine possible biomarkers that would differentiate patients with NASH (n=9) from patients without it (n=9).

Results: Multivariate analysis revealed differences in plasma proteomic profiles between NASH and non-NASH groups. A PCA showed highlight P09871 to be significantly reduced and P25311 and V9GYE7 significantly increased in NASH patients. PLSDA (A) and heat map (B) analyses provide a separation with almost no overlap between both groups of patients. These results suggest that the difference on the plasma proteomic profile has diagnostic capacity (C). As for the liver (D), multivariate analysis revealed a significantly increasing on P1640 and K7EIV0 and a decreasing of A0A087X1G1 between both groups. These suggest that the liver proteomic profiles also have diagnostic potential. In addition to the impact on plasma and liver, a signature has also been observed in visceral adipose tissue (E), characterized by

increasing of P12814 and decreasing P53007. In subcutaneous adipose tissue (F), no NASH proteomic signature is observed.

Conclusion: Patients with NASH present significant differences in the proteome of plasma, liver and visceral adipose tissue compared to patients without the pathology. In the liver, there is an increase in proteins associated with cell growth and inflammation, and a decrease in mitochondrial respiration. In visceral adipose tissue, proteins linked to mitochondrial metabolism decrease and those related to the cytoskeleton increase. However, no proteomic signature is observed in subcutaneous adipose tissue.

SAT-426

AI-enabled virtual hematoxylin and eosin and Masson's trichrome staining for non-alcoholic fatty liver disease activity scoring from single unstained slide

Carson McNeil¹, Pok Fai Wong¹, Niranjana Sridhar¹, Yang Wang¹, Charles Santori¹, Cheng Hsun Wu¹, Andrew Homyk¹, Michael Gutierrez¹, Ali Behrooz¹, Dina Tiniakos², Alastair Burt^{2,3}, Rish Pai⁴, Kamilla Tekiel¹, Po-Hsuan Cameron Chen⁵, Sudha Rao¹, Debra Hanks¹, Shamira Sridharan¹, Eduardo Bruno Martins⁶, Star Seyedkazemi⁶, Laurent Fischer⁶, Charlie Kim¹, Peter Cimermancic¹. ¹Verily Life Sciences, United States; ²Newcastle University, United Kingdom; ³The University of Adelaide, Adelaide, Australia; ⁴Mayo Clinic, Scottsdale, United States; ⁵Google, Mountain View, United States; ⁶Allergan, United States
Email: cpeter@verily.com

Background and aims: Pathologists' interpretation of disease activity using hematoxylin-and-eosin (HandE) and Masson's trichrome (MT) stained slides from liver biopsies is the current gold standard for monitoring response in non-alcoholic steatohepatitis

POSTER PRESENTATIONS

(NASH) clinical trials. However, staining and scoring variability, and limited tissue availability have created challenges in NASH clinical trials that impact efficiency, cost, and end point assessment. Our aim was to develop a virtual staining approach that relies on digitization and computational prediction of HandE and MT from a single unstained tissue section. This approach reduces the need for chemical staining and the amount of tissue used.

Method: We present a novel digital pathology platform that digitizes information in unstained tissue sections and then uses machine learning to perform virtual staining. The tissue is digitized using autofluorescence (AF) imaging of unstained tissue at hundreds of excitation-emission wavelength pairs using a hyperspectral microscope developed at Verily. The virtual staining step utilizes recent advances in computer vision and deep learning. Importantly, the platform is non-destructive, with the tissue samples remaining unstained and available for other analyses. To develop the virtual staining module, paired AF and stained images of the same tissue sections were collected by imaging 200 unstained liver biopsies from the completed Phase 2b CENTAUR trial, followed by HandE or MT staining and scanning. The virtual stains were evaluated on an independent test set of 45 cases using a reader study with 3 adjudicator hepatopathologists (co-authors of this abstract), as follows: (a) all cases were presented to each pathologist in a randomized order and blinded to the stain modality (real or virtual); (b) consensus scores based on NASH Clinical Research Network (NASH CRN) system were generated via in-person adjudication; (c) the accuracy of virtual stains was measured by computing linearly-weighted Kappa values between adjudicated NASH CRN scores on real versus virtual stains. Additionally, 9 hepatopathologists (not authors) scored the same set of chemically stained cases to measure inter-observer variation on real stains. We define success of virtual staining by real versus virtual kappa values being non-inferior to those from inter-observer variation on real stains.

Results: In the blinded and randomized adjudication reader study, concordance (linearly-weighted kappa) of NASH-CRN scores derived from virtual stains versus real stains were 0.86 (95% CI [0.74, 0.96]), 0.33 (95% CI [0.06, 0.57]), 0.76 (95% CI [0.61, 0.88]), and 0.55 (95% CI [0.35, 0.70]) for steatosis, lobular inflammation, ballooning, and Ishak fibrosis stage, respectively. The Kappa values for inter-observer variability were 0.57 (95% CI [0.49, 0.65]), 0.28 (95% CI [0.17, 0.40]), 0.31 (95% CI [0.22, 0.40]), and 0.50 (95% CI [0.39, 0.61]), respectively.

Conclusion: The virtual staining platform generates HandE and MT images equivalent to chemical stains as demonstrated by the equivalence of hepatopathologist NASH-CRN scoring of liver biopsies. This demonstrates the high potential for improving efficiency and maintaining consistency of histopathologic end point assessment.

Furthermore, the tissue-sparing stain-free system conserves tissue for downstream analyses.

SAT-427

Practical diagnosis of cirrhosis by liver specialists in non-alcoholic fatty liver disease using currently available non-invasive fibrosis tests

Jerome Boursier¹, Marine Roux¹, Charlotte Costentin², Julien Chaigneau¹, Céline Fournier-Poizat³, Aldo Trylesinski⁴, Clémence M Canivet¹, Sophie Michalak⁵, Brigitte Le Bail⁶, Valérie Paradis⁷, Pierre Bedossa⁸, Nathalie Sturm², Victor de Lédinghen⁶, Philip N Newsome⁹. ¹Angers University, France; ²Grenoble University Hospital, France; ³Echosens, France; ⁴Advanz Pharma, United Kingdom; ⁵Angers University Hospital, France; ⁶Bordeaux University Hospital, France; ⁷APHP Beaujon, France; ⁸Liverpat, France; ⁹Birmingham University, United Kingdom
Email: jeboursier@chu-angers.fr

Background and aims: Unlike for advanced liver fibrosis, the practical rules for the early non-invasive diagnosis of cirrhosis in NAFLD remain not well defined. We aimed to develop and validate an accurate diagnosis of cirrhosis in NAFLD using the best non-invasive tests currently available to liver specialists.

Method: Patients with NAFLD and liver biopsy from four independent cohorts were allocated to derivation and validation sets according to a phase 3 TRIPOD design. All patients had six non-invasive fibrosis tests utilizing different modalities (elastography, blood tests) and dedicated to different diagnostic targets (advanced liver fibrosis, cirrhosis): FIB4, FibroMeter^{V3G}, CirrhoMeter^{V3G}, Fibroscan, Agile3+, and Agile4. Cirrhosis was defined as fibrosis stage F4 according to the NASH CRN staging.

Results: 1,568 patients were included (872 in the derivation set, 696 in the validation set). Median age was 57.6 years, 59.1% of the patients were male, median biopsy length was 25 mm, and the prevalence of cirrhosis was 12.1%. AUROC for cirrhosis were: 0.816 ± 0.016 (FIB4), 0.820 ± 0.016 (FibroMeter^{V3G}), 0.812 ± 0.017 (CirrhoMeter^{V3G}), 0.870 ± 0.013 (VCTE), 0.893 ± 0.011 (Agile3+), and 0.893 ± 0.012 (Agile 4). However, despite this good to very good global accuracy, fibrosis tests showed an imbalance with a much better accuracy to rule out cirrhosis than to rule-in the diagnosis. A stepwise algorithm, using first the Agile3+/Agile4 elastography-based tests and then the FibroMeter^{V3G}/CirrhoMeter^{V3G} specialized blood tests, was developed in the derivation set. This algorithm applied fibrosis tests in the same order as recommended by the 2021 EASL guidelines and provided stratification in four groups, the last of which being enriched in cirrhosis (71% prevalence in the validation set). We also derived a risk prediction chart to allow estimation of the individual

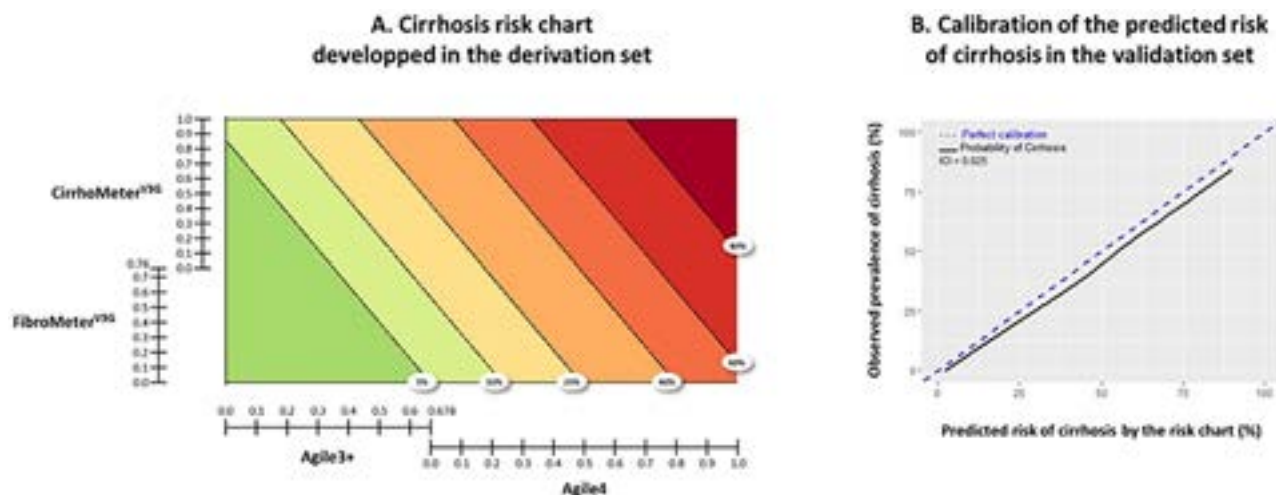


Figure: (abstract: SAT-427).

probability of cirrhosis (Figure). In the validation set, calibration of the predicted risk was excellent: the integrated calibration index was 0.025, and mean difference with perfect prediction was only -2.9% (extremes: -5%; -2%). Quantitative morphometric analysis confirmed that both approaches (sequential algorithm, risk prediction chart) stratified patients into subgroups with significantly different amounts of liver fibrosis.

Conclusion: The new tools we developed improve the personalized non-invasive diagnosis of cirrhosis in NAFLD patients.

SAT-428

Associations of genetic risk panel with enhanced liver fibrosis scores among patients with non-alcoholic fatty liver disease

Zobair Younossi^{1,2,3}, James M Estep³, Sean Felix³, Elena Younossi³, Nagashree Gundu Rao³, Leyla Deavila³, Huong Pham³, Rebecca Cable³, Jillian Price³, Andrei Racila³, Maria Stepanova^{3,4}.

¹Inova Health System, Medicine Service Line, United States; ²Inova Health System, Department of Medicine, Center for Liver Diseases, United States; ³Beatty Liver and Obesity Research Program, Inova Health System, United States; ⁴Center for Outcomes Research in Liver Disease, United States

Email: zobair.younossi@inova.org

Background and aims: Genetic risk factors have been linked to advanced histologic stage of fibrosis among patients with NAFLD. It is unknown if these genetic risk factors are also associated with non-invasive biomarkers such as enhanced Liver Fibrosis (ELF) and FIB-4. Our aim was to assess the associations of select SNPs with the risk of having elevated ELF and FIB-4 in NAFLD.

Method: After informed consent, clinical data, serum and whole blood were collected from patients with NAFLD. In addition to standard laboratory test (liver enzymes, platelet count, to calculate FIB-4), ELF score was measured (ADVIA Centaur, Siemens Healthineers). Genomic DNA was extracted from the whole blood [QIAamp DNA Blood Mini Kit (Qiagen)] and used for determination of minor allele frequency for genomic loci rs641738 (MBOAT7), rs58542926 (TM6SF2), rs738409 (PNPLA3), rs62305723 (HSD1713B) using CFX96 (BioRad). Individual alleles were evaluated for the association with elevated (≥ 9.8) and high (≥ 11.3) ELF, elevated FIB-4 (> 2.67) in NAFLD.

Results: There were 953 NAFLD patients included: 57 ± 14 years, 57% male, BMI 34.0 ± 9.1 , 33% type 2 diabetes. Of those, 83% had low ELF (< 9.8), 14.5% had elevated ELF (9.8–11.2) and 2.5% had high ELF (≥ 11.3). Furthermore, 6.9% had elevated FIB-4 score (> 2.67). Of the studied four SNPs, only PNPLA3-rs738409 (51% CC, 42% CG, 7% GG) was significantly ($p < 0.05$) associated with elevated and high ELF scores: elevated ELF 12% in CC vs. 19% in CG/GG, high ELF 0.7% in CC vs. 4.1% in CG/GG (both $p < 0.01$). In multivariate analysis adjusted for age, sex, BMI and type 2 diabetes, having PNPLA3-rs738409 CG/GG genotype was independently associated with increased risk of elevated and high ELF: odds ratio (OR) = 1.87 (1.25–2.78) for elevated ELF, OR = 5.82 (1.67–20.30) for high ELF (both $p < 0.01$). Similarly, only PNPLA3-rs738409 CG/GG was associated with elevated FIB-4: 5.1% in CC vs. 8.0% in CG vs. 13.7% in GG ($p = 0.05$). In multivariate analysis, having PNPLA3-rs738409 CG/GG genotype was independently associated with a higher risk of elevated FIB-4: odds ratio (OR) = 2.10 (1.13–3.90) ($p = 0.019$).

Conclusion: The well-known SNP in the PNPLA3 gene linked to advanced histologic fibrosis is also associated with elevated/high ELF

and FIB-4 scores in NAFLD. These data validate the association of non-invasive biomarkers with the genetic risks in NAFLD.

SAT-429

Morphometric analysis of sonic hedgehog in non-alcoholic fatty liver steatohepatitis patients by MorphoQuant: a potential biomarker of disease severity

Cindy Serdjebi¹, Bastien Lepoivre¹, Florine Chandes¹, Linda Willis², Julé Yvon¹. ¹Biocellvia, Marseille, France; ²Histologix Ltd, United Kingdom

Email: cindy.serdjebi@biocellvia.com

Background and aims: Sonic hedgehog (Shh) is an important pathway activated in non-alcoholic fatty liver diseases and its expression is known to increase along with the severity of non-alcoholic steatohepatitis (NASH). In addition, computer-assisted morphometry previously demonstrated that Shh expression was associated with ballooning degeneration score as well as fibrosis grading. Yet, the use of this immune-histo-chemistry (IHC) has long been ignored in the current general practice and/or in clinical trials. In this study, we have developed and a fully automated morphometry software to detect and quantify Shh expression and investigated the interest of measuring the area of active injury in patients' liver biopsies.

Method: Liver biopsies were scored by a blinded expert pathologist according to the NASH CRN for steatosis, inflammation, ballooning and fibrosis. Shh labeling was developed using SG vector as chromogen. MorphoQuant, a fully automated and deterministic artificial intelligence, based on morphometry and expert system-completely independent from pathologist's annotations, was developed to specifically detect Shh and areas of active liver injury from whole slide images. As an edge effect was seen on a significant number of labeled slides, a 150- μ m safety margin was automatically removed from all biopsy fragments before analysis. The quantitative data of Shh expression and areas of active injuries were thus compared to the pathologist's reading and correlations were calculated using the Spearman correlation test for fibrosis, steatosis, lobular and portal inflammation, Mallory-Denk bodies, interface hepatitis, NAS and NASH status.

Results: A total of 271 slides were processed for quantitative image analysis by MorphoQuant. Results are presented in Table 1. Shh was expressed in all patients, 5.49 % in average, ranging from 0.046 to 44.88 % while active injury area ranged from 0 to 82.06 % with a mean at 5.239 %. Both Shh and active injury area were higher in NASH than in non-NASH patients (6.428 vs 3.270; 6.632 vs 1.943, respectively; p values < 0.0001 for both). Shh was significantly associated with fibrosis, ballooning, lobular inflammation, interface hepatitis, Mallory-Denk bodies, NAS and NASH status. Active injury area also correlated with the same items, though the strength of the correlation was systematically higher for all the compared items.

Conclusion: The current study demonstrates the utility of Shh IHC to discriminate NAFLD from NASH patients. Active injury always correlated more with the histopathological reading than Shh, identifying this new readout as a potential biomarker for disease activity.

SAT-430

Burden of non-alcoholic fatty liver disease and usefulness of non-invasive tests to identify advanced liver disease in patients with type 2 diabetes mellitus: interim analysis of an Italian prospective multicentre study

Gian Paolo Caviglia¹, Angelo Armandi^{1,2}, Roberta D'Ambrosio^{3,4}, Pietro Lampertico^{3,4}, Cristiana Bianco⁵, Luca Valenti⁵, Carlo Ciccioli⁶, Grazia Pennisi⁶, Salvatore Petta⁶, Lucia Brodosi^{7,8}, Maria Letizia Petroni^{7,8}, Francesca Marchignoli^{7,8}, Loris Pironi^{7,8}, Alessandra Sagripanti⁹, Maria Eva Argenziano⁹, Gianluca Svegliati-Baroni⁹, Elisabetta Bugianesi¹. ¹University of Turin,

Table 1.(abstract: SAT-429): Spearman correlations between Shh-related readouts and pathologist's score

Feature from the NASH CRN	Shh (%)		Active injury area	
	Spearman correlation rate r (CI95 interval)	p	Spearman correlation rate r (CI95 interval)	p
Fibrosis	0.4111 (0.2901 - 0.5192)	<0.0001	0.5292 (0.4226 - 0.6214)	<0.0001
Steatosis	0.1193 (-0.02005 - 0.2541)	0.0839	0.1222 (-0.01706 - 0.2569)	0.0764
Ballooning	0.427 (0.3047 - 0.5332)	<0.0001	0.5329 (0.4254 - 0.6256)	<0.0001
Lobular inflammation	0.2997 (0.1676 - 0.4211)	<0.0001	0.4130 (0.2906 - 0.5220)	<0.0001
Portal inflammation	0.06690 (-0.07278 - 0.2040)	0.335	0.08778 (-0.05186 - 0.2241)	0.2041
Interface hepatitis	0.1526 (0.01384 - 0.2855)	0.0267	0.1782 (0.04018 - 0.3095)	0.0095
Mallory-Denk bodies	0.2826 (0.1495 - 0.4057)	<0.0001	0.3430 (0.2142 - 0.4600)	<0.0001
NAFLD Activity Score	0.3964 (0.2724 - 0.5075)	<0.0001	0.4953 (0.3826 - 0.5934)	<0.0001
NASH status	0.3160 (0.1851 - 0.4359)	<0.0001	0.3996 (0.02759 - 0.5102)	<0.0001

Medical Sciences, Turin, Italy; ²Johannes Gutenberg University Mainz, Department of Internal Medicine I, Germany; ³Foundation IRCCS Ca' Granda Ospedale Maggiore Policlinico, Division of Gastroenterology and Hepatology, Milan, Italy; ⁴CRC "A. M. and A. Migliavacca" Center for Liver Disease, Department of Pathophysiology and Transplantation, Milan, Italy; ⁵Foundation IRCCS Ca' Granda Ospedale Maggiore Policlinico, Department of Transfusion Medicine and Haematology, Milan, Italy; ⁶University of Palermo, Section of Gastroenterology and Hepatology, Dipartimento Di Promozione Della Salute, Materno Infantile, Medicina Interna e Specialistica Di Eccellenza (PROMISE), Italy; ⁷University of Bologna, Department of Medical and Surgical Sciences, Italy; ⁸IRCCS Azienda Ospedaliero-Universitaria di Bologna, Italy; ⁹Polytechnic University of Marche, Liver Disease and Transplant Unit, Ancona, Italy Email: elisabetta.bugianesi@unito.it

Background and aims: Non-alcoholic fatty liver disease (NAFLD) is closely associated with type 2 diabetes mellitus (T2DM). However, systematic data on the epidemiology and severity of NAFLD in T2DM are scarce and mostly relying on data from gastroenterological referral centers.

In a cohort of diabetic patients consecutively referred by Diabetes Units, we aimed to assess a) the prevalence of NAFLD and the prevalence of advanced liver fibrosis and compensated advanced chronic liver disease (cACLD) and b) to investigate the efficacy of a model of care based on the sequential use of non-invasive tests (NITs) and vibration controlled transient elastography (VCTE) for the identification of patients at risk of advanced liver disease.

Method: From April 2021 to August 2022, a total of 461 consecutive patients with T2DM attending 6 different diabetes referral centers were prospectively enrolled. Liver stiffness (LS) was assessed by VCTE and liver steatosis by controlled attenuation parameter (CAP). Liver steatosis was defined according to CAP values ≥ 275 dB/m. AVTCE cut-off value of 8.0 kPa was used to rule out advanced liver fibrosis, while cACLD was defined according to liver stiffness (LS) values ≥ 10.0 kPa. The following NITs were calculated: AST-to-platelets ratio (APRI), Fibrosis-4 (FIB-4), and NAFLD fibrosis score (NFS). The cut-offs adopted to rule-out advanced liver disease were 0.5 for APRI, 1.3 for FIB-4, and -1.455 for NFS.

Results: Overall 413 out of 461 patients underwent VCTE + CAP. Patients' median age was 58 (52–63) years and 241 (58.4%) of them were males; 288 (69.7%) patients were obese (BMI >30 kg/m²) and 245 (59.3%) had arterial hypertension. Elevated liver enzymes (ALT and/or AST and/or γ GT) were found in 116 (28.1%) patients. Liver steatosis by CAP was detected in 257 (62.2%) patients, among them 57 (22.2%) had a LS ≥ 8 kPa, while 36 (14.1%) had a LS ≥ 10 kPa. In our cohort of T2DM patients, the sequential use of NITs followed by VCTE would have resulted in the highest hepatologist referral rate for NFS

(20.0%), followed by FIB-4 (11.9%) and APRI (5.5%). The lowest probability of missing advanced liver fibrosis was observed for NFS (5.8% of patients with NFS <-1.455 and LS ≥ 8.0 kPa) in spite of the highest VCTE referral rate (71.1% vs 32.6% for FIB-4 and 9.7% for APRI, respectively). On the contrary, screening by FIB-4 could spare a substantial number of VCTE (Table 1).

Figure:

NITs	VCTE referral rate	Hepatologist referral rate (LS ≥ 8.0 kPa)	False negative (LS ≥ 8.0 kPa)
APRI ≥ 0.5	9.7%	5.5%	16.9%
FIB-4 ≥ 1.3	32.6%	11.9%	10.6%
NFS ≥ -1.455	71.1%	20.0%	5.8%

Conclusion: In patients with T2DM and NAFLD, the prevalence of advanced liver fibrosis by VTCE is approximately 22%, while cACLD can be found in 14% of subjects. In Diabetes Units, pre-screening by NFS or FIB-4 is the most convenient referral approach to hepatologists for the identification of T2DM patients at risk of advanced liver fibrosis by VTCE.

This research was supported by Gilead Sciences, Inc (study ID: IN-IT-989–5790).

SAT-431

LIVERFAST GP+, first-line screening tool in at-risk MAFLD patients outperforms the standard-of-care (SOC) FIB-4

Ronald Quiambao¹, Paul Hermabessière², Adele Delamarre³, Imtiaz Alam^{4,5}, Juan Manuel Minoz Perez⁶, John Lee⁷, Mona Munteanu¹, Victor de Lédighen⁸. ¹Fibronostics, Medical Affairs, United States; ²CHU Bordeaux, Hepatology Department, United States; ³CHU Bordeaux, France; ⁴Austin Hepatitis Center, United States; ⁵Dell Medical School, United States; ⁶Fibronostics, IT, United States; ⁷Fibronostics, IT, Singapore; ⁸CHU Bordeaux, Hepatology, France Email: mona_munteanu@hotmail.com

Background and aims: LIVERFAST GP+ (GP+) is a AI-based blood test conceived for the screening of MAFLD at risk subjects. GP+ combines common blood biomarkers (lipid panel, liver enzymes, glucose and bilirubin) with patient's anthropometrics. Recently, GP+ has been validated to predict the short-term severe outcomes in those patients infected with SARS-CoV-2 virus and liver fibrosis. (Hepatology-Suppl2022). The primary aims of this retrospective analysis was: 1/ to construct and validate a new MAFLD screening test, GP+, noninferior to the SOC reference, FIB-4, for bridging fibrosis (F3F4 stages), and 2/with less drawbacks related to age-adapted cutoffs.

Method: N = 580 MAFLD patients prospectively included with liver biopsy and concomitant GP+ and FIB-4 were randomly assigned in

two subsets. GP+ was trained to identify the presumed MAFLD clinical stages: N0 no-fibrosis/steatosis, N1 steatosis only, N2 fibrosis non-bridging, N3 fibrosis bridging with reference the liver biopsy and using AUROCs (95%CI).

Results: Characteristics: 56% males, median age 59.5yo, BMI 31.5, ALT 55IU/l. The AUROCs for F3F4, for GP+ and FIB-4 in the subsets 1 and 2 were, respectively: 0.806 (0.737–0.841) vs. 0.807 (0.630–0.756, $p = \text{NS}$) and 0.759 (0.701–0.808) vs. 0.757 (0.698–0.805, $p = \text{NS}$) in the subset 2. FIB4 underperformed in males aged ≥ 65 yo for identifying F3F4 stages in both subsets 1 and 2: 0.586 (0.451–0.695, $p = \text{NS}$ vs. hazard and $p = 0.02$ vs GP+).

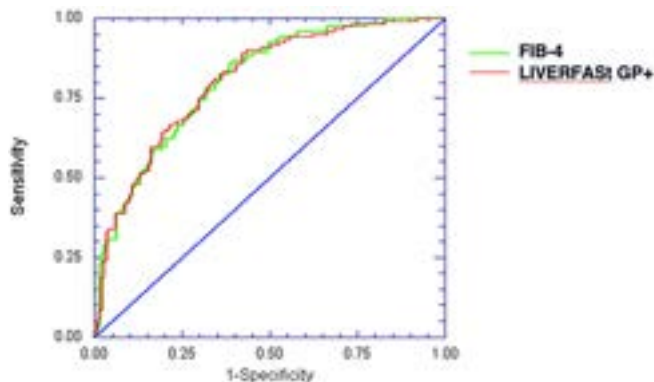


Figure: AUROCs (95%CI) for bridging fibrosis in the subset 1 of FIB-4 and LIVERFAST GP+

Conclusion: In a MAFLD cohort LIVERFAST GP+, compared to FIB-4, demonstrated several advantages to identify MAFLD from steatosis to bridging fibrosis without grey zone and no drawbacks related to age and male gender.

SAT-432

Velacur ACE outperforms CAP for liver fat quantification using MRI PDFF as the gold standard

Rohit Loomba¹, Alnoor Ramji², Tarek Hassanein³, Emily Peng⁴, Caitlin Schneider⁵, Michael Curry⁶. ¹University of California San Diego,

La Jolla, United States; ²The University of British Columbia, Vancouver, Canada; ³Southern California Research Center, United States; ⁴Vancouver Coastal Health (VCH), Vancouver, Canada; ⁵Sonic Incytes Medical Corp., Vancouver, Canada; ⁶Beth Israel Deaconess Medical Center, Boston, United States
Email: caitlin@sonicincytes.com

Background and aims: With the global rise of non-alcoholic fatty liver disease (NAFLD) and the potential new therapeutics, it is imperative to accurately measure the amount of fat in the liver. Although Magnetic Resonance Imaging Proton Density Fat Fraction (MRI PDFF) has become the gold standard in non-invasive liver fat assessment, two point of care methods are presented here in comparison to MRI PDFF; Velacur's Attenuation Coefficient Estimation (ACE) and FibroScan's Controlled Attenuation Parameter (CAP).

Method: Velacur ACE was compared to CAP in patients with clinically proven NAFLD or non-alcoholic steatohepatitis (NASH). The study was completed at five sites in the US and Canada. All patients received a contemporaneous magnetic resonance imaging proton density fat fraction (MRI PDFF) scan. Using the MRI PDFF cut offs of 5%, 15%, and 20%, the AUROC and 95% confidence intervals were computed for both ACE and CAP, allowing for the optimal cutoff for this set of patients. DeLong's test was used to compare the AUC's. The overall correlation coefficient and correlation for BMI categories for both ACE and CAP to MRI PDFF was calculated.

Results: A total of 164 patients were enrolled into this study. Of these, 132 had complete data sets. The average MRI PDFF for all patients was $13.8 \pm 8.7\%$, with the average for ACE and Cap being $310. \pm 54 \text{ dB/m}$ and $304. \pm 60 \text{ dB/m}$ respectively. There were 21, 56, 26 and 29 patients in the $\leq 5\%$, 5–15%, 15–20% and $>20\%$ groups respectively. Using the MRI PDFF cut offs of $\leq 5\%$, $\leq 15\%$, and $\leq 20\%$, ACE was able to separate the patients with AUROC [95% confidence interval] of 0.816 [0.715, 0.907], 0.878 [0.823, 0.940] and 0.902 [0.846, 0.945] respectively. CAP has AUC's of 0.859 [0.766, 0.919], 0.820 [0.731, 0.891] and 0.797 [0.700, 0.864]. DeLong's test showed that the AUC of ACE and CAP were statistically different for separation patients with $>20\%$ fat. The correlation coefficient (r) between ACE and PDFF was 0.69, while r for CAP and PDFF was 0.59. When separating the patients into $<27 \text{ kg/m}^2$, $27\text{--}33 \text{ kg/m}^2$, and $\geq 33 \text{ kg/m}^2$, the correlation coefficients were 0.71, 0.68, and 0.68 for ACE, and 0.60, 0.58, and 0.59 for CAP respectively.

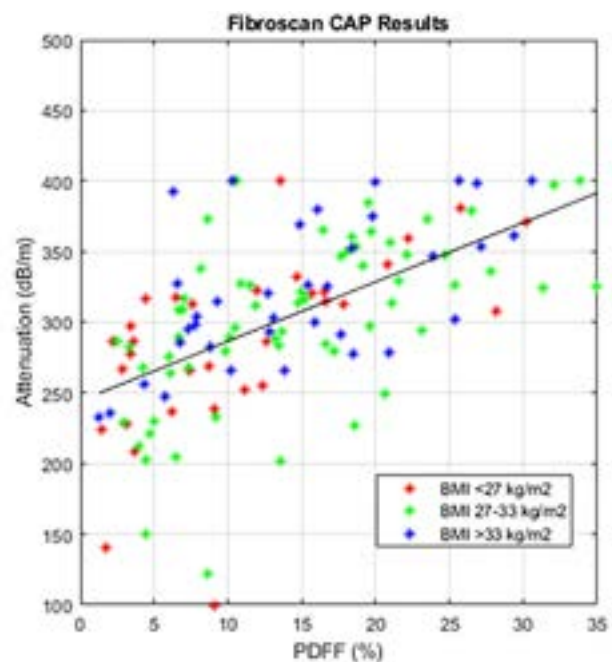
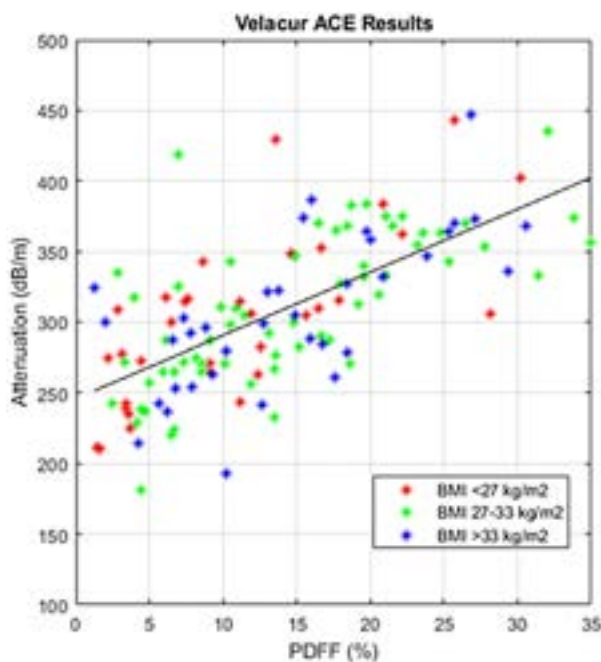


Figure: (abstract: SAT-432).

POSTER PRESENTATIONS

When examining the graph, colored by BMI category, there were 5 patients with CAP of 390 dB/m or more but MRI PDFF $\leq 20\%$ indicating a possible overestimation by CAP. Of these, 60% were in the highest BMI category.

Conclusion: At each fat percentage, Velacur ACE shows a numerically higher AUC than FibroScan CAP and was statistically different for patients with the highest measures of liver fat.

The correlation coefficients between ACE and MRI PDFF were greater than that of CAP, in all patients and in each BMI category.

Velacur ACE was shown to be a superior point-of-care method for measuring liver fat in patients with NAFLD and NASH.

SAT-433

Assessing the role of organokines as biomarkers for diagnosing non-alcohol related liver disease

Andrea Jiménez Franco¹, Cristian Martínez Navidad², Cristina Placed¹, Helena Castañé², Jordi Camps³, Jorge Joven³. ¹Universitat Rovira i Virgili, Unitat de Recerca Biomèdica, Reus, Spain; ²Fundació IISPV, Unitat de Recerca Biomèdica, Reus, Spain; ³Hospital Universitari Sant Joan de Reus, Unitat de Recerca Biomèdica, Reus, Spain
Email: andreafranco99@gmail.com

Background and aims: Non-alcoholic Fatty Liver Disease (NAFLD) and obesity are widespread global health issues. NAFLD starts as simple fat buildup in the liver and can progress to non-alcoholic

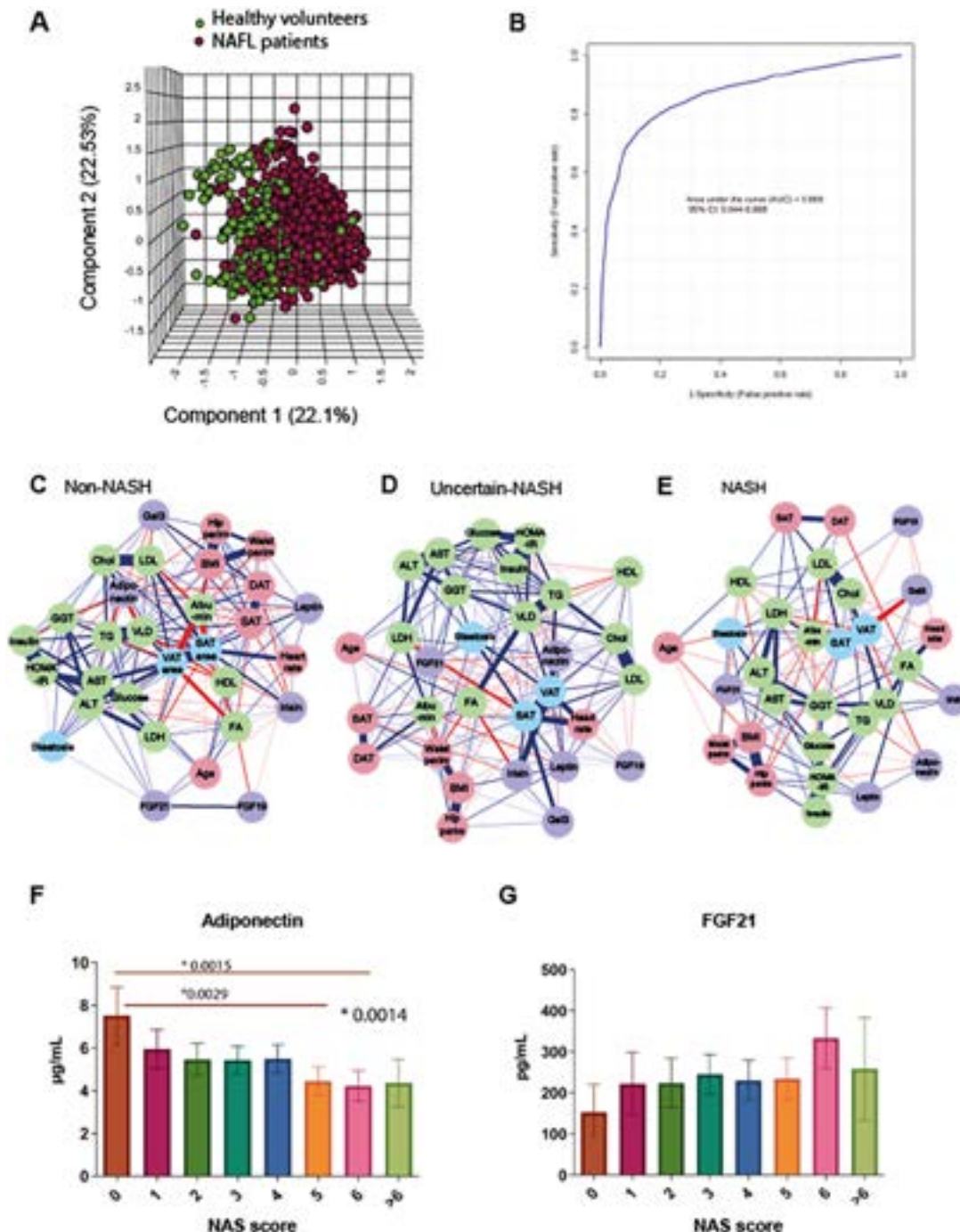


Figure: (abstract: SAT-433).

steatohepatitis (NASH), a more severe stage that involves inflammation and tissue damage. The gold standard for diagnosing NAFLD/NASH progression is liver biopsy. As the disease progresses, the body regulates metabolic and physiological changes in organs through cytokines or organokines, but the intricacy of this inter-tissue communication remains unclear. This study aims to measure the concentration of six organokines in plasma and evaluate their role in the progression of obesity-related NAFLD.

Method: Plasma samples from 1068 NAFLD patients with obesity and different stages and 414 healthy volunteers were analyzed using sandwich Enzyme-Linked Immunosorbent Assay (ELISA) to determine the concentration of Adiponectin, Leptin, Irisin, Galectin2, Fibroblast growth factor 19 (FGF19), and Fibroblast growth factor 21 (FGF21).

Results: We identified significant differences in the organokines profile between healthy volunteers and patients with obesity-related NAFLD (Figure A). Combining the six organokines produced an Area under the Curve (AUC) of 0.860 in the Receiver Operating Characteristics (ROC) curve, suggesting their potential as a diagnostic biomarker (Figure B). Correlation network showed different associations between clinical variables and organokines on the different stages of NAFLD (Figure C, D, and E). Adiponectin and FGF21 demonstrated the ability to differentiate between NASH, uncertain NASH, and non-NASH groups (Figure F and G). Although Adiponectin and FGF21 showed significant differences in classifying patients based on liver histology, they were not strong enough as fibrosis biomarkers.

Conclusion: Significant differences were found between healthy volunteers and NAFL patients regarding the analyzed organokines' profile. However, only Adiponectin and FGF21 were found to be associated with NAFLD progression. Organokines' concentration was not significantly related to hepatic histological features.

SAT-434

Evaluating the prevalence of liver fibrosis in children with non-alcoholic fatty liver disease using transient elastography, Dutch Fibrokids cohort

Jalina Rooseboom¹, Laura Draijer¹, Malika Chegary², Marc Benninga¹, Bart Koot¹. ¹Amsterdam University Medical Centre, Pediatric Gastroenterology, Amsterdam, Netherlands; ²OLVG Hospital, General Pediatrics, Netherlands
Email: j.b.rooseboom@amsterdamumc.nl

Background and aims: Major international guidelines currently recommend screening for non-alcoholic fatty liver disease (NAFLD) in children with obesity, but the method for screening is not forthright due to insufficient evidence. This study evaluates the screening for advanced NAFLD guided by alanine aminotransferase (ALT) based screening algorithm and identifies additional risk factors for probable significant fibrosis.

Method: A prospective cohort study in children (8–18 years) with obesity or overweight with at least one metabolic risk factor visiting our University Clinic after referral from local obesity outpatient clinics. Referral was based on the three ALT thresholds defined in the NASPGHAN 2017 Clinical Practice Guideline. Additionally, a fourth group of children with obesity and normal ALT was analysed. Transient elastography (Fibroscan) was used to detect probable significant fibrosis with a cut-off of 7.4 kPa.

Results: Our cohort consisted of 322 children, 64% male. Median age 13 years [11.00, 15.75], BMI z-score 3.5 (0.63). The prevalence of probable significant fibrosis differed significantly from 1.9% in the normal ALT group and 16.3%, 18.6% and 41.2% in three elevated ALT groups ($p < 0.001$). (Figure 1). Lasso regression for variable selection with subsequent logistic regression showed that fibrosis was correlated with male gender (OR = 2.98) higher age (OR = 1.39), ALT > 80 IU/L (OR = 15.66), higher BMI z-score (OR = 3.20) and presence of acanthosis nigricans (OR = 5.67).

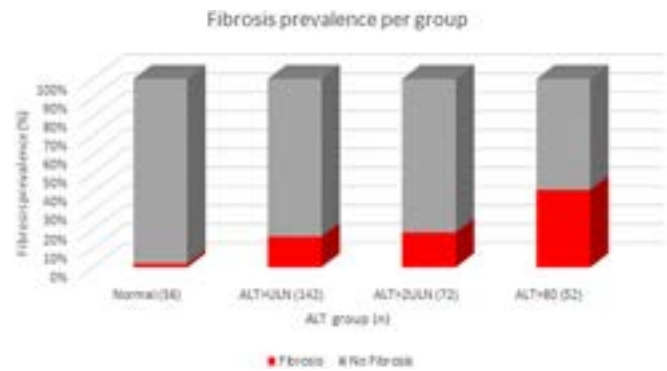


Figure:

Conclusion: ALT is a strong predictor of probable significant fibrosis in screening population of children with obesity and overweight, supporting its use as a primary screening test. Fibrosis evaluation for children with obesity with ALT > 80 IU/L seems warranted. In children with lower elevated ALT levels this needs further evaluation balancing risk, benefits and costs. Gender, age, BMI and presence of acanthosis nigricans could be taken into account in this consideration.

SAT-436

The impact of projected increases in obesity prevalence on incident liver disease in the UK: insights from bayesian-network modelling

Tom Waddell^{1,2}, Ana Namburete³, Paul Duckworth¹, Daniel Cuthbertson⁴, Celeste McCracken⁵, John Michael Brady². ¹The University of Oxford, Department of Engineering Science, Oxford, United Kingdom; ²Perspectum Ltd, United Kingdom; ³The University of Oxford, Department of Computer Science, Oxford, United Kingdom; ⁴University of Liverpool, United Kingdom; ⁵The University of Oxford, United Kingdom
Email: tom.waddell@perspectum.com

Background and aims: Obesity is a complex multi-system disease and a growing public health challenge. Recent projections estimate that 71% of adults living in England will be overweight or obese by 2040, with the percentage of people living with obesity (37%) surpassing that of those of a 'healthy weight'. Obesity is associated with non-alcoholic fatty liver disease and non-alcoholic steatohepatitis (NASH) and a complex set of variables that interact in myriad ways. We use Bayesian-network (BN) analysis applied to a large UK-based cohort, specifically magnetic resonance imaging (MRI) derived measures of liver steatosis and fibroinflammation, both to explore likely projected increases in obesity prevalence and to illustrate the power of BN methods to address such complexity.

Method: Proton density fat fraction (PDFF) and corrected T1 (cT1) were obtained from 27,002 UK Biobank cases (application 9914). These were combined with additional participant data to construct a BN. Each directed edge is supported by medical literature, making it a "semantic" BN. BNs explicitly model conditional dependencies as a directed acyclic graph, where network variables denote biomarkers and the directed edges connecting such variables the direction of causality. The probabilities of being normal weight, overweight, obese, and severely obese in this dataset were then fixed to 2040 projections (29%, 27%, 37% and 7%, respectively), and conditional probability queries explored the resultant changes in the probability of liver steatosis and NASH (defined by PDFF > 10% and cT1 > 800 ms).

Results: The rate of obesity in the study population was substantially lower than the UK population estimate (16% vs 29%). Fixing the variable 'Obesity' to 2040 projections resulted in an 8% (2160 participants), 5% (1350) and 3% (800) increase in the probability of severe steatosis (PDFF > 10%), moderate steatosis (PDFF 5.6–10%) and NASH, respectively. We observed a 2% (470 participants) and 6% (1620 participants) increase in the probability of elevated blood glucose (HbA1c > 42 mmol/mol) and hypertension, respectively.

POSTER PRESENTATIONS

Furthermore, when fixing the value of 'Obesity' to projected obesity estimates in areas of low socioeconomic status (46%), we observed an additional 1440 and 550 participants with severe steatosis and NASH, respectively, above our previous estimates for the entire UK population. Such increases equate to an additional £~7.5 million in direct NASH-related costs within our population of 27,002 participants, only <1% of the entire UK population.

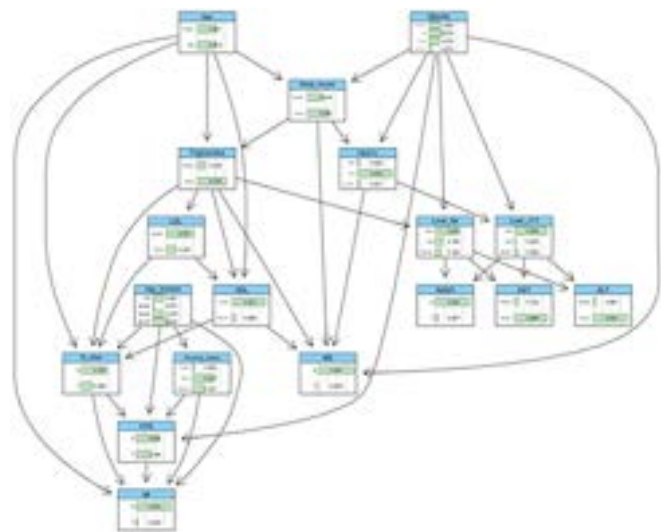


Figure: Bayesian-network structure (here the probabilities of 'Obesity' have been fixed to 2040 projections). Waist circum = waist circumference; LDL = low density lipoprotein; HDL = high density lipoprotein; H_chol = high cholesterol; HTN = hypertension; MI = myocardial infarction; MS = metabolic syndrome.

Conclusion: BN analysis models the complexity of liver disease and, in this case, illustrates a 'best case scenario' of the impact of projected increases in obesity on liver disease. This disproportionately impacts areas of low socio-economic status, and the cost associated with increasing rates of NASH.

SAT-437

The prevalence and predictors of non-alcoholic fatty liver disease by vibration controlled transient elastography among lean adults in the United States

Ifrah Fatima¹, Mohamed Ahmed¹, Wael Mohamed¹, Alisa Likhitsup².

¹University of Missouri- Kansas City School of Medicine, United States;

²Saint Luke's Hospital System, United States

Email: ifrahfatima@umkc.edu

Background and aims: Non-Alcoholic Fatty Liver Disease (NAFLD) affects about 25–30% of individuals worldwide. About 16.7% of all NAFLD individuals are lean. This study aims to identify the prevalence and predictors of NAFLD among lean United States (US) adults.

Method: Lean adults ≥ 18 years of age from the National Health and Nutrition Examination Survey (NHANES) 2017–2018 with BMI <25 in Asians and <30 in other races were included. NAFLD was identified according to the controlled attenuation parameter (CAP) score ≥ 248 dB/m. Viral hepatitis, significant alcohol use history (>1 drink/day in women, >2 drinks/day in men) were excluded. The sample weights were utilized according to the complex survey analysis guidance. Characteristics were compared using Fisher's exact test/Chi-square and Student's t-test/Mann-Whitney test. Odds ratios and 95% confidence interval were calculated for the association between chronic medical conditions and DS use adjusted for confounding variables. Two-sided $p < 0.05$ were considered statistically significant. Statistical analyses were conducted using STATA/SE version 16.1 (StataCorp, College Station, TX)

Results: A total of 2629 observations representing an underlying population of 123,341,002 were included. 40% of lean adults had

NAFLD identified by Vibration-controlled Transient Elastography (VCTE) (CAP score ≥ 248 dB/m). The mean age in the NAFLD group was 54.1 ± 0.50 versus 42.4 ± 0.85 years in the non-NAFLD group. Predictors associated with NAFLD were older age (aOR 1.91; 95% CI 1.4–2.6 for age 40–59 and 2.22; 95% CI 1.59–3.11 for age ≥ 60), male (aOR 1.47; 95% CI 1.04–2.06), non-Hispanic Asian (aOR 1.85; 95% CI 1.26–2.70), Mexican or other Hispanic (aOR 1.41; 95% CI 1.02–1.96), BMI 25–29.9 (aOR 3.13; 95% CI 2.33–4.21) but not education level, marital status, or the presence or absence of hypertension, diabetes, prediabetes, dyslipidemia or cardiovascular disorders. Hemoglobin A1C and triglyceride levels were associated with NAFLD among lean US adults with aOR 1.54; 95% CI 1.25–2.91, and 1.006; 95% CI 1.004–1.009, respectively.

Conclusion: 40% of lean US adults have NAFLD based on VCTE evaluation. Age ≥ 40 years, male, non-Hispanic Asian or Mexican/other Hispanic, BMI 25–29.9, HbA1C, and triglyceride levels were predictors for NAFLD among lean US adults.

SAT-438

Utility of SomaSignal™ panels for drug response and monitoring disease progression in patients with advanced fibrosis due to non-alcoholic steatohepatitis

Kris Kowdley¹, Kaiyi Zhu², Jun Xu², Jason Melehan², Lisa Boyette², Timothy R. Watkins², Sharlene Lim², Vlad Malkov², Andrew Billin², Mazen Nouredin³, Rohit Loomba⁴. ¹Liver Institute Northwest, Seattle, United States; ²Gilead Sciences, Inc., United States; ³Houston Research Institute, United States; ⁴NAFLD Research Center, Division of Gastroenterology and Hepatology, Medicine, United States
Email: roloomba@health.ucsd.edu

Background and aims: Non-alcoholic steatohepatitis (NASH) is characterized by liver steatosis, inflammation, and hepatocellular ballooning and may lead to progressive fibrosis and cirrhosis. Changes in NASH activity score (NAS) and fibrosis stage by histology are commonly used to assess treatment response in clinical trials. However, liver biopsy is subject to sampling variability, invasive, and expensive; thus reliable non-invasive tests to measure treatment response are needed. SomaSignal™ NASH scores provide a predictive probability and binary classification of the presence of the individual histological components of liver biopsy (Fibrosis, Inflammation, Steatosis, Ballooning). Our study aimed to apply composite serum biomarker panels, SomaSignal™ scores, to evaluate hepatic steatosis, lobular inflammation, hepatocyte ballooning and liver fibrosis in a randomized, placebo-controlled, phase 2b NASH clinical study.

Method: A total of 198 patients with bridging fibrosis or compensated cirrhosis (F3–F4) due to NASH were randomized to placebo, cilofexor (CLO) 30 mg or firsocostat (FIR) 20 mg alone, or two-drug combination groups. Fibrosis stage and NAS were staged according to NASH CRN. Serum proteome was analyzed in 166 subjects with paired baseline (BL) and Week 48 (W48) samples via SomaScan® (SomaLogic, Boulder, CO). Associations of SomaSignal™ scores with NAS components and fibrosis stage were assessed by Jonckheere's trend test, and the binary classification results were evaluated by Fisher's exact test. The changes in SomaSignal™ NASH scores at W48 from BL (on the logit scale) among the treatment groups were compared by a linear model adjusting for age, gender, diabetes, and baseline cirrhosis status.

Results: NASH SomaSignal™ scores showed strong correlation with histologic features ($p < 0.001$), and the binary classification prediction results were largely consistent with biopsy histology (AUC >0.72; $p < 0.005$). At W48, combination therapy significantly reduced all SomaSignal™ scores compared to placebo (all $p < 0.05$). FIR monotherapy significantly reduced the SomaSignal™ fibrosis and hepatocyte ballooning scores but not the other SomaSignal™ scores; CLO monotherapy numerically reduced the SomaSignal™ score (Figure). Through W48, 15 of 67 NASH patients had reduced (reduction ≥ 1) fibrosis stage by biopsy in the combo cohort. Compared to patients without histological improvement, NASH patients with improved

Table 1. Odds Ratios and 95% CI of predictors associated with NAFLD among lean U.S. Adults

Characteristics	Unadjusted OR (95% CI)	p-value	Adjusted ^a OR (95% CI)	p-value
Age				
18-39	Reference		Reference	
40-59	3.43 (2.55 – 4.60)	<0.0005	1.91 (1.40 – 2.60)	<0.0005
≥ 60	4.22 (3.23 – 5.52)	<0.0005	2.22 (1.59 – 3.11)	<0.0005
Gender				
Female	Reference		Reference	
Male	1.52 (1.16 – 1.96)	0.004	1.47 (1.04 – 2.06)	0.03
Race				
NH White	Reference		Reference	
NH Black	0.59 (0.43 – 0.82)	0.03	0.65 (0.50 – 0.85)	0.004
NH Asian	0.96 (0.70 – 1.33)	0.82	1.85 (1.26 – 2.70)	0.004
Mexican /Other Hispanic	1.46 (1.13 – 1.88)	0.007	1.41 (1.02 – 1.96)	0.04
Others	1.76 (0.98 – 3.16)	0.06	1.36 (0.73 – 2.53)	0.31
BMI				
<18.5	0.49 (0.16 – 1.55)	0.17	0.64 (0.14 – 3.05)	0.61
18.5 – 24.4	Reference		Reference	
25 – 29.9	3.82 (3.11 – 4.69)	<0.0005	3.13 (2.33 – 4.21)	<0.0005
Marital status				
Married	Reference		Reference	
Widowed	0.97 (0.59 – 1.58)	0.90	0.66 (0.34 – 1.11)	0.11
Divorced	0.74 (0.43 – 1.26)	0.25	0.72 (0.37 – 1.34)	0.28
Separate	0.88 (0.47 – 1.63)	0.67	1.33 (0.51 – 3.45)	0.53
Never married	0.28 (0.21 – 0.38)	<0.0005	0.68 (0.42 – 1.10)	0.11
Living with partner	0.48 (0.31 – 0.74)	0.001	0.74 (0.50 – 1.09)	0.12
Education				
Less than high school	Reference		Reference	
High school graduate	0.70 (0.53 – 0.92)	0.015	0.96 (0.76 – 1.21)	0.39
Some college or AA degree	0.74 (0.53 – 1.03)	0.07	1.19 (0.86 – 1.65)	0.85
College graduate or higher	0.65 (0.47 – 0.90)	0.014	0.89 (0.62 – 1.27)	0.31
Chronic medical Conditions				
None	0.43 (0.35 – 0.53)	<0.0005	0.89 (0.59 – 1.35)	0.57
Hypertension	2.63 (1.99 – 3.49)	<0.0005	0.88 (0.73 – 1.07)	0.18
Diabetes or Prediabetes	2.97 (2.12 – 4.15)	<0.0005	0.98 (0.78 – 1.24)	0.87
Dyslipidemia	2.20 (1.66 – 2.92)	<0.0005	1.18 (0.86 – 1.61)	0.28
*Cardiovascular disorders	2.39 (1.80 – 3.15)	<0.0005	1.03 (0.77 – 1.39)	0.24
HbA1C	2.48 (2.09 – 2.93)	<0.0005	1.54 (1.25 – 1.91)	0.001
Total Cholesterol	1.006 (1.003 – 1.000)	0.001	1.00 (0.99 – 1.004)	0.89
Triglyceride	1.01 (1.009 – 1.01)	<0.0005	1.006 (1.004 – 1.009)	<0.0005
HDL	0.97 (0.97 – 0.98)	<0.0005	1.004 (0.99 – 1.02)	0.99
^a Adjusted for age, gender, race, BMI, marital status, education level, chronic medical conditions, total cholesterol, triglyceride, and HDL level.				
*Includes heart failure, coronary heart disease, angina, heart attack, stroke				

Figure: (abstract: SAT-437).

POSTER PRESENTATIONS

The least square means with the 95% confidence interval (CI) of the predicted NASH SomaSignal score changes at W48 from BL (A. Fibrosis B. Lobular inflammation C. Hepatocyte ballooning D. Steatosis) are shown for each treatment arm. Statistical significance of each treatment arm against placebo is annotated as follows: “****” for $P < 0.001$, “***” for $P < 0.01$, “**” for $P < 0.05$, “ns” for $P > 0.05$.

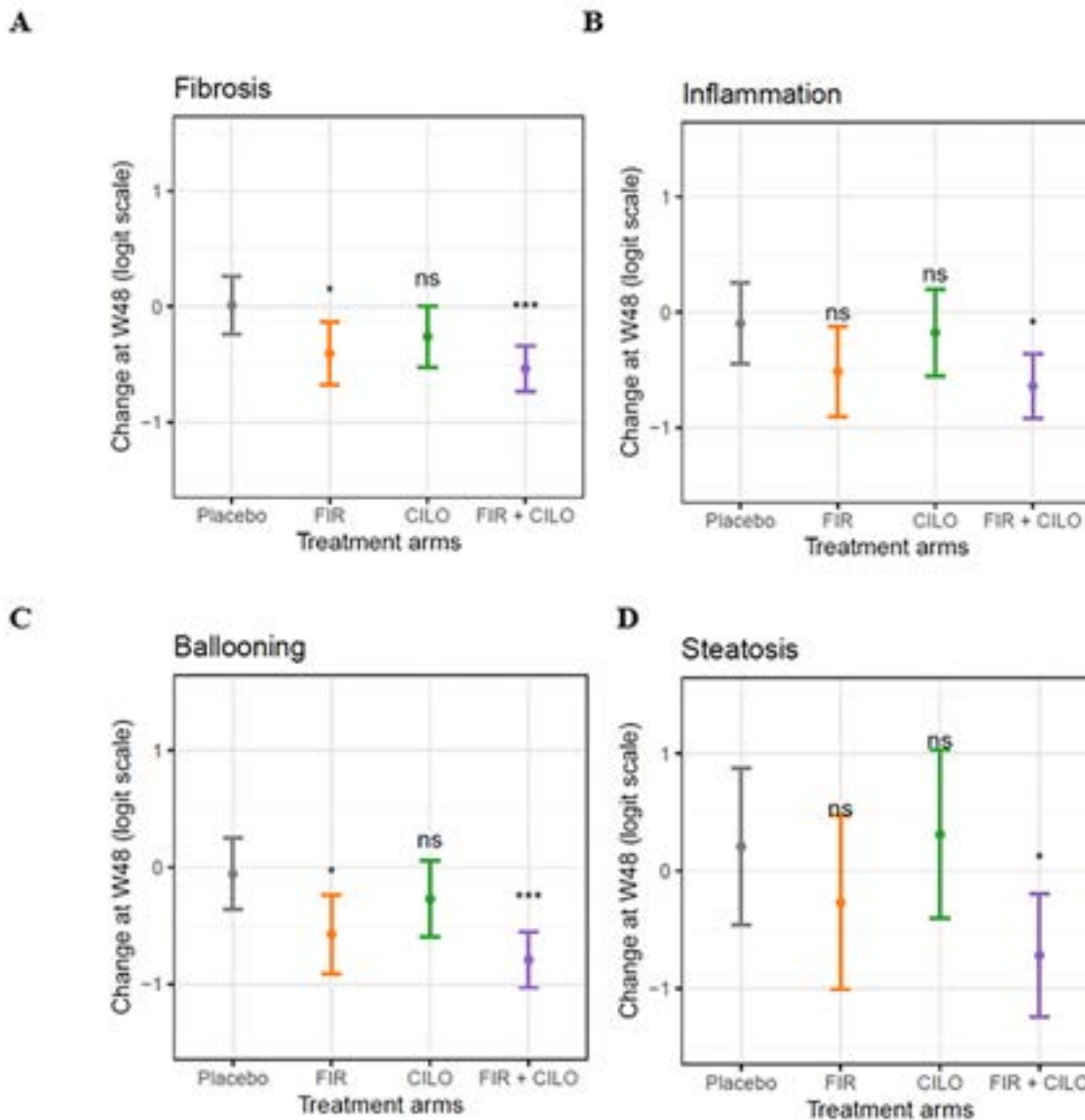


Figure: (abstract: SAT-438): Combination Therapy with Cilofexor and Firsocostat Reduced SomaSignal™ NASH Scores Compared to Placebo

fibrosis stage had greater reductions in the SomaSignal™ fibrosis scores (Wilcoxon test $p < 0.05$). The AUROC for the SomaSignal™ fibrosis score to predict histological improvement was 0.67 (95% CI: 0.52–0.82).

Conclusion: The proteomic SomaSignal™ NASH scores including measures of hepatic steatosis, lobular inflammation, hepatocyte ballooning and liver fibrosis showed significant correlations with NASH CRN fibrosis stage and NAS components. Greater reductions of SomaSignal™ fibrosis and NAS scores were observed in the combo treatment group, consistent with the observed histological changes. We propose that SomaSignal platform may be useful to assess treatment responses in NASH trials.

SAT-439

Wearable technology utilizing an electrical impedance tomography (EIT) system for hepatic steatosis quantification and the role in ambulatory monitoring

Lung Yi Loey Mak¹, James H.W. Li^{2,3}, Adrien Touboul³, Fedi Zouari³, Pak-To Cheung³, Eddie Wong^{1,3}, Iris Y. Zhou⁴, Ellie Wei¹, Man-Fung Yuen¹, Russell Chan³, Wai-Kay Seto¹. ¹The University of Hong Kong, School of Clinical Medicine, Hong Kong; ²The Hong Kong University of Science and Technology, Hong Kong; ³Gense Technologies Ltd, Hong Kong; ⁴Massachusetts General Hospital and Harvard Medical School, Radiology, Massachusetts, United States
Email: wkseto@hku.hk

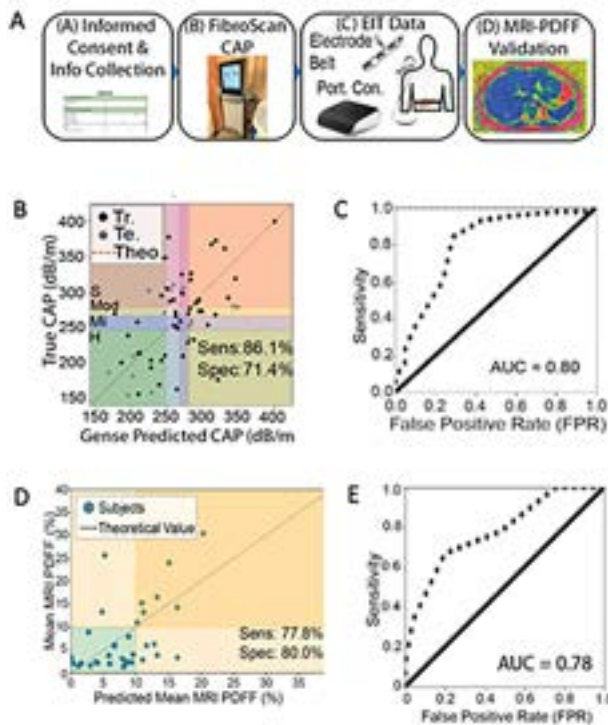
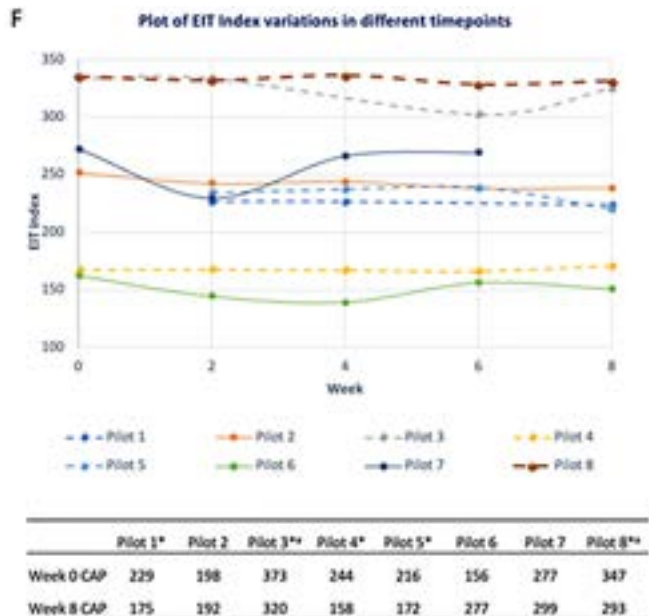


Figure: (abstract: SAT-439).

Background and aims: The current effective treatment for patients with non-alcoholic fatty liver disease (NAFLD) is achieving weight loss through lifestyle modifications. We developed a wearable device using the electrical impedance tomography (EIT) technology to quantify hepatic steatosis (part 1). In this pilot study, we then explored the role of ambulatory monitoring of hepatic steatosis using the EIT system (part 2).

Method: In part 1, 21 healthy controls and 43 patients with known NAFLD were recruited for cross-sectional evaluation by vibration controlled transient elastography (VCTE), which can measure hepatic steatosis by controlled attenuation parameter (CAP). The EIT examination was performed after VCTE with a 16-electrode belt worn on the waist connected to a portable non-ionizing non-invasive system, which is designed for use without the need of trained operators. A random subgroup of subjects with NAFLD ($n = 27$) also underwent magnetic resonance imaging proton density fat fraction (MRI-PDFF) to further validate the accuracy of the wearable EIT system (Figure A). In part 2, 8 subjects (2 with NAFLD, 6 healthy controls) were recruited and underwent EIT scan at baseline and every 2 weeks. VCTE was performed at baseline and week 8 for CAP values. Significant CAP reduction was defined as ≥ 40 dB/m decline from baseline.

Results: Part 1: The predicted CAP by EIT system achieved area under the receiver-operating characteristic curve (AUROC) of 0.799 (Figures B and C), with 86.1% sensitivity and 71.4% specificity. The predicted MRI-PDFF score by EIT system achieved AUROC of 0.782 (Figures D and E), with 77.8% sensitivity and 80% specificity. Part 2: All 8 subjects underwent ambulatory monitoring using the EIT system at a frequency of ≥ 3 times over the 8-week observation period, confirming feasibility of this approach. 5/8 (62.5%) subjects, including the 2 subjects with known NAFLD, achieved significant CAP reduction (Figure F). EIT and CAP values at baseline and week 8 yielded 8 pairs of values, with 14/16 (87.5%) concordance in categorizing liver fat quantity. Most subjects agreed the wearable was easy to use (87.5%), confident to self-administer at home (75%), and accept the need to use on a long-term basis (62.5%). No subjects experience intractable discomfort.



*Subjects with significant CAP reduction at week 8 (defined as ≥ 40 dB/m); corresponding to dashed lines in the graph

* Known NAFLD

Conclusion: The novel portable EIT system can predict VCTE-derived CAP and MRI-PDFF, allowing a safe, well-tolerated and low-cost ambulatory alternative for hepatic steatosis quantification.

SAT-440

Head-to-head comparison of Agile 3+, LSM-VCTE, NFS, and FIB-4 scores for detecting advanced fibrosis in patients with type 2 diabetes seen in diabetes clinic

Laurent Castéra¹, Tiphaine Vidal-Trecan², Tania Khoury³, Jean-Baptiste Julla², Valérie Paradis⁴, Jean-Pierre Riveline⁵, Dominique Valla¹, Jean-François Gautier⁵. ¹Beaujon hospital, Université Paris Cité, Hepatology, Clichy, France; ²Lariboisiere hospital, Diabetology, Paris, France; ³Beaujon hospital, Hepatology, Clichy, France; ⁴Beaujon hospital, Université Paris Cité, Pathology, Clichy, France; ⁵Lariboisiere hospital, Université Paris Cité, Diabetology, Paris, France
Email: laurent.castera@bjn.aphp.fr

Background and aims: Among patients with type 2 diabetes (T2D), prevalence of NAFLD and advanced fibrosis is high. Identification of these patients is a priority as advanced fibrosis is the main prognostic factor associated with liver outcomes and overall mortality. Non-invasive tests (NITs) based on vibration-controlled transient elastography (VCTE), including Agile 3+, LSM (liver stiffness measurement), and serum-based scores such as FIB-4, and NAFLD fibrosis score (NFS) have been proposed recently for this purpose. Data comparing the performance of these tests in patients with T2D are lacking. The aim of this study was to compare head-to-head, the performance of Agile 3+, LSM, FIB-4 and NFS, for detecting advanced fibrosis in a large cohort of T2D patients with suspected NAFLD.

Method: Among 1620 T2D outpatients seen in a diabetes clinic between June 2019 and February 2022 screened for NAFLD (steatosis and or elevated ALT) who had VCTE, 174 underwent a liver biopsy (LB). Agile 3+, FIB-4, and NFS scores were calculated according to published formula and cutoffs used were those published for Agile 3+ (<0.351 , ≥ 0.679) as well as those recommended by guidelines for NFS (<-1.455 , >0.676), FIB-4 (<1.3 , >2.67) and LSM (<8 , ≥ 12 kPa)). Comparison of performance was done by comparing AUROCs using the DeLong's test for paired data, and percentage of correctly

POSTER PRESENTATIONS

classified patients (true positive and true negative) taking liver biopsy as a reference.

Results: 163 patients had all data available for head-to-head comparison. Their characteristics were as follows: male 58%; median age 59 years; BMI 32 kg/m²; waist circumference 108 cm; HbA1c 7.7%; AST 35 IU/L; ALT 47 IU/L; advanced fibrosis 30%. Performances of scores are shown in the Table. LSM and Agile 3+ had similar accuracy (AUROCs 0.87 vs. 0.85, $p=0.43$) but LSM outperformed FIB-4 (0.87 vs. 0.75; $p=0.009$) and NFS (0.87 vs. 0.66; $p<0.0001$). The grey zone (patients between the two cutoffs) was higher for NFS than for Agile 3+, LSM and FIB-4. LSM and Agile 3+ had a higher rate of correctly classified patients than NFS and FIB-4

Table: Comparison of performance of Agile 3+, NFS, FIB-4 and LSM in 163 T2D patients with liver biopsy

Scores	AUROC (95% CI)	P value*	Cut-offs	Se	Sp	PPV	NPV	Grey Zone	Correctly classified
Agile 3+	0.85 (0.79– 0.91)	0.43	<0.351 ≥0.679	0.94 0.69	0.47 0.87	0.69	0.95	35%	54%
NFS	0.66 (0.56– 0.75)	<10–4	<-1.455 >0.676	0.82 0.33	0.30 0.90	0.59	0.79	57%	31%
FIB-4	0.75 (0.66– 0.83)	0.009	<1.3 >2.67	0.69 0.20	0.63 0.98	0.83	0.83	39%	50%
LSM	0.87 (0.82– 0.93)	ref	<8 KPa ≥12 KPa	0.96 0.51	0.60 0.92	0.74	0.97	36%	57%

*Performance comparisons of NITs with respect to histologic results using De Long's test for paired data.

Conclusion: LSM and Agile 3+ score outperformed FIB-4 and NFS for identifying advanced fibrosis in T2D patients with suspected NAFLD.

SAT-441

Screening for advanced fibrosis due to NAFLD in patients with type 2 diabetes in a retina scanning facility

Andrea Lindfors^{1,2}, Rickard Strandberg¹, Hannes Hagström^{1,2}.

¹Karolinska Institutet, Department of Medicine, Huddinge, Sweden;

²Karolinska University Hospital, Division of Hepatology, Department of Upper GI Diseases, Stockholm, Sweden

Email: andrea.lindfors@ki.se

Background and aims: Non-alcoholic fatty liver disease (NAFLD) is prevalent in patients with type 2 diabetes (T2D), and international guidelines suggest specific screening for advanced fibrosis. However, how this should be implemented is less clear. Here, we evaluated the feasibility of offering patients with T2D that attended a retina scanning facility as part of their routine care to also undergo vibration-controlled transient elastography (VCTE) to detect NAFLD and advanced fibrosis.

Method: Patients with T2D who attended retina scanning at a single facility between 2020 and 2022 were asked for participation. Patients were assessed for clinical characteristics and underwent VCTE after a two-hour fasting period. NAFLD and advanced fibrosis were defined as controlled attenuation parameter (CAP) values of ≥280 dB/m and ≥12 kPa, respectively. Patients with liver stiffness ≥8 kPa were referred to the Karolinska University Hospital for a liver evaluation, a second VCTE examination and offered standard clinical care.

Results: 1102 eligible patients were asked for participation, of which 818 (74%) were included. The mean age was 65 years (SD 9.6) and 62% were men. 51% had a CAP value of 280 dB/m or more, indicating NAFLD, and 137 (17%) had a liver stiffness above or equal to 8 kPa, with 45 (6%) having values suggestive of advanced fibrosis (≥12 kPa). Of those with values above or equal to 8 kPa, 93/137 patients (68%) have so far accepted and been referred for a liver evaluation, while 28 (20%) were lost to follow-up and 16 (12%) are waiting for a follow-up.

At repeat VCTE measurement, 41/93 persons (44%) had a normal VCTE (<8 kPa), and 29 (31%) had values between 8 and 11.9 kPa, while advanced fibrosis was found in 23/93 persons (25%).

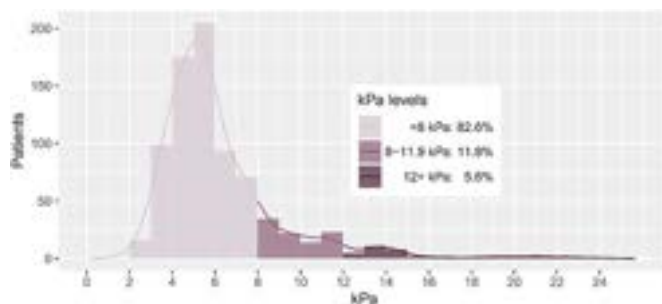


Figure: Distribution of liver stiffness in included patients with type 2 diabetes.

Conclusion: Offering patients with T2D opportunistic screening with VCTE at the time of routine retina scanning is accepted by a high proportion. NAFLD and advanced fibrosis are common in this population, however false-positive findings are also frequent and risks of overdiagnosis needs to be considered if implementing this in routine clinical care.

SAT-442

MRI-PDFF captures the whole spectrum of lipid composition beyond traditional histological evaluation of macrosteatosis

David Marti-Aguado^{1,2}, María Pilar Ballester^{1,2}, Victor Merino², Salvador Benlloch³, Ana Crespo³, Elena Coello⁴, Victoria Aguilera Sancho^{4,5}, Cristina Montón², Mercedes De La Torre Sanchez⁶, Moises Diago⁶, Matias Fernandez-Paton⁷, Amadeo Ten-Esteve⁷, Alba Sánchez-Martín⁸, Clara Alfaro-Cervello^{8,9,10}, Judith Pérez¹¹, Monica Bauza¹¹, Victor Puglia¹², Alexandre Perez Girbes^{7,13}, Desamparados Escudero-García^{1,2,10}, Luis Marti-Bonmati^{7,13}. ¹INCLIVA Institut d'Investigació Sanitària, Hepatology Department, Valencia, Spain; ²Hospital Clínic Universitari, Hepatology Department, València, Spain; ³Hospital Arnau de Vilanova, Hepatology Department, València, Spain; ⁴La Fe University and Polytechnic Hospital, Hepatology Department, València, Spain; ⁵Institut d'Investigació Sanitària La Fe de València, València, Spain; ⁶Consortium General University Hospital of Valencia, Hepatology Department, Valencia, Spain; ⁷Institut d'Investigació Sanitària La Fe de València, Radiology, València, Spain; ⁸Hospital Clínic Universitari, Pathology Department, València, Spain; ⁹INCLIVA Institut d'Investigació Sanitària, Valencia, Spain; ¹⁰University of Valencia, València, Spain; ¹¹La Fe University and Polytechnic Hospital, Pathology Department, València, Spain; ¹²Hospital Arnau de Vilanova, Pathology department, València, Spain; ¹³La Fe University and Polytechnic Hospital, Radiology, València, Spain
Email: davidmmaa@gmail.com

Background and aims: The histologic evaluation of hepatic steatosis is based on the percentage of hepatocytes with macrovesicular steatosis, ignoring the lipid composition. MRI-PDFF is the most accurate non-invasive method for detecting hepatic steatosis. We aimed to evaluate the influence of lipid droplets composition in PDFF values.

Method: Prospective, multicenter study including chronic liver disease patients with paired liver biopsy and MRI between 2017–2022. MR examination included the MECSE sequence to measure PDFF after automatic whole-liver segmentation. Histologic samples were evaluated with conventional microscope and digital image analysis (Ventana iScan HT). Slides were stained with HandE for semiquantitative scoring of steatosis according to NAS-CRN system (S0–3 macrosteatosis grade and presence/absence of microsteatosis) and IHQ adipophilin for digital pathology assessment. Lipid droplets were categorized as large macrovesicular steatosis (≥80 μm²), small

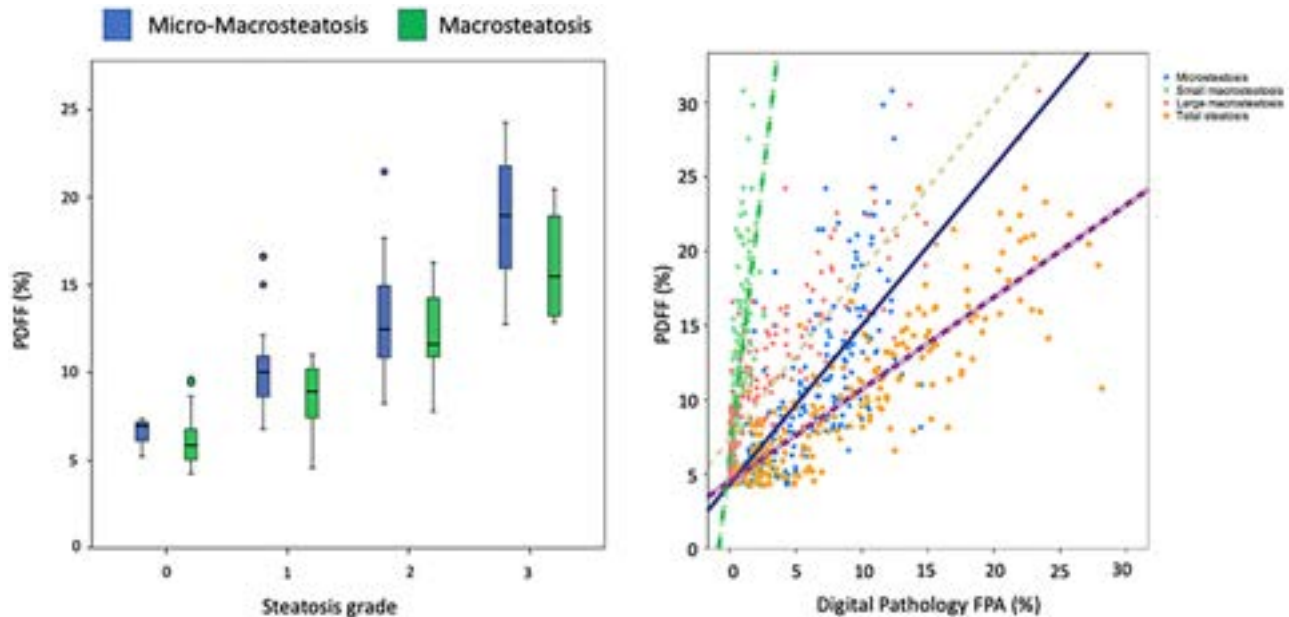


Figure: (abstract: SAT-442).

macrovesicular ($<80 \mu\text{m}^2$) and microsteatosis (non-droplet positive adipophilin). Fat proportionate areas (FPA) and number of lipid droplets were measured with digital pathology. Total FPA was calculated as: large-droplet FPA + small-droplet FPA + microsteatosis FPA. Total lipid droplets were calculated as: number of large-droplets + small-droplets macrovesicular steatosis.

Results: There were 206 patients (57% women; 55 ± 12 years) with mean PDFF of $11.9 \pm 4.9\%$. Main liver disease aetiology was fatty liver (61% NAFLD, 6% ALD), followed by autoimmune diseases (22%) and viral hepatitis (6%). Histologic steatosis distribution included 37% S0, 23% S1, 19% S2, 21% S3. The strength of PDFF-FPA correlation increased with lipid droplet size as follows: $r = 0.74$ for microsteatosis, $r = 0.78$ for small-droplet macrovesicular, $r = 0.84$ for large-droplet macrovesicular; being higher ($r = 0.88$) for total FPA. The correlation between PDFF and number of lipid droplets also increased as follows: $r = 0.70$ for small-droplet macrovesicular, $r = 0.85$ for large-droplet macrovesicular; being higher ($r = 0.87$) for total lipid droplets. In all steatosis grades (S0-S3) PDFF values were higher if microsteatosis was present (Figure 1). Overall, mean PDFF was 10.8% if microsteatosis was absent vs. 14.3% if microsteatosis was present ($p < 0.01$).

Conclusion: Pathologists grading system of steatosis should consider lipid droplet composition, unifying macro and microsteatosis assessment, as MRI-PDFF correlates with the whole spectrum of hepatic steatosis.

SAT-443

Two steps algorithm for the diagnosis of advanced liver fibrosis in general population. Real-life data

Ana Pérez¹, Marta Hernández Conde¹, Christie Perelló¹, Diana Karen Tapia Calderón², Elba Llop¹, Francisco A. Bernabeu-Andreu¹, Javier Vega¹, Marta López-Gómez¹, Natalia Fernández Puga¹, Javier Abad Guerra¹, Carlos Fernández-Carrillo¹, José Luis Martínez Porras¹, María Traperó¹, Enrique Fraga¹, José Luis Calleja Panero¹. ¹Hospital Universitario Puerta de Hierro, Spain; ²Guadalajara, Guadalajara, Mexico

Email: ana.perez.gs96@gmail.com

Background and aims: Chronic liver disease is an increasingly prevalent entity. Additionally, due to its silent evolution, it is an underdiagnosed disease.

Method: In this cohort study, Fibrosis-4 index (FIB4) was performed on all patients between 18 and 65 years old from area 6 of Madrid Community with a request for glycated hemoglobin in the routine analysis of primary care. We suggested the request of a transient elastography (TE) by the primary care physician in patients with $\text{FIB4} \geq 1.3$ in a medium time of 1 month. If TE was $>8 \text{ kPa}$, patient was referred to the Hepatology consultation. According to medical indication, a complete study was performed on those patients.

Results: Between April and September 2022, 1,635 patients were included (1,155 patients – 70.6% – with low-risk FIB4, 439 – 26.9% – with indeterminate FIB4 and 41 – 2.5% – with high-risk FIB4). Of the 480 patients (29.4%) with $\text{FIB4} \geq 1.3$, TE was requested for 400 patients (83.3%). Of which, 376 TE (94%) were performed. The reasons for not performing TE were: not attending the appointment (22 patients), technical limitations due to obesity (2 patients). The data of the first 166 patients with TE were analyzed. The baseline characteristics are detailed in Table 1. The prevalence of significant fibrosis ($\text{TE} > 8 \text{ kPa}$) was 15.5% in the indeterminate FIB4 group and 55.6% in the high-risk FIB4 group ($p < 0.01$). In addition, the prevalence of advanced fibrosis ($> 9.6 \text{ kPa}$) was significantly higher in the high-risk FIB4 group in relation to the indeterminate FIB4 group (50 vs. 10.3%; $p < 0.01$).

Figure:

Baseline Characteristics (n = 383)	Results
Sex (male), n (%)	107 (73.8)
Age (years), mean (SD)	58 (6.4)
TE (F0–1, F2, F3, F4), %	80.3/5.3/5.9/8.6
TE (Kpa), medium (P25; P75)	5.8 (4.4;7.8)
Hypertension, n (%)	72 (50)
Type II Diabetes Mellitus (DM2), n (%)	42 (29.2)
Dyslipidemia, n (%)	71 (49.3)
Cardiovascular disease, n (%)	17 (11.8)
Mass corporal index (kg/m ²), mean (SD)	29.7 (5.3)
Overweight, n (%)	25 (46.2)
Obesity, n (%)	30 (38.5)
Ceruloplasmin (mg/dl), mean (SD)	24.9 (4.2)
Cholesterol- HDL (mg/dl), mean (SD)	50.5 (16.7)
Cholesterol-LDL (mg/dl), mean (SD)	98.6 (34.8)
Triglycerides (mg/dl), medium (P25; P75)	124 (90; 186)
Hemoglobin (g/dl), mean (SD)	15.4 (1.4)
Platelets (10E3/microL), mean (SD)	202.5 (51.2)
Albumin (g/dL), mean (SD)	4.5 (0.3)
Glucose (mg/dl), mean (SD)	109 (37.9)
Glycohemoglobin (%), mean (SD)	6 (1.2)
Bilirubin (mg/dl), mean (SD)	0.8 (0.4)
ALT (U/L), mean (SD)	69.8 (46.5)
AST (U/L), mean (SD)	54.9 (37)
ALP (U/L), mean (SD)	84.3 (34.1)
GGT (U/L), medium (P25; P75)	47 (30;93)

Conclusion: The sequential FIB4-TE algorithm is an adequate initial tool for the screening of liver fibrosis. However, only 15.5% of patients with indeterminate FIB4 had significant fibrosis. To improve the cost-effectiveness of screening, it is necessary to increase the diagnostic yield of elastography, probably by adding a second serological test in that group of patients before performing TE.

SAT-444

Imaging and biomarker thresholds to accurately diagnose NASH cirrhosis in a 180 patient biopsy confirmed cohort

Rohit Loomba¹, Mazen Noureddin², Rebecca Taub³, Naim Alkhouri⁴, Kris Kowdley⁵, Greg Everson⁶, Stephen Harrison^{7,8}. ¹UCSD, United States; ²CSHS, United States; ³Madrigal Pharmaceuticals, United States; ⁴AZ Liver, United States; ⁵Liver institute NW, United States; ⁶HepQuant, United States; ⁷Oxford, United States; ⁸Pinnacle Research, United States
Email: rebeccataub@yahoo.com

Background and aims: MAESTRO-NAFLD-1 (NCT04197479) is a 52-week study that includes an open label active resmetirom treatment arm in 180 patients with well-compensated Child-Pugh A NASH cirrhosis, treated for 52 weeks with daily oral 80 mg resmetirom. A goal of the study was characterization of non-invasive baseline measures to diagnose and stage NASH cirrhosis.

Method: Eligibility required at least 3 metabolic risk factors (metabolic syndrome), and NASH cirrhosis diagnosed on liver biopsy or according to accepted criteria. A series of non-invasive biomarkers and imaging procedures at baseline and during the study was used to help define criteria to diagnose NASH cirrhosis non-invasively including FibroScan, MRE, MRI-PDFF, ELF and other laboratory parameters. A subset of patients had HepQuant analyses conducted to measure their hepatic functional capacity and estimate shunting.

Results: 180 patients with well-compensated CP-A NASH cirrhosis were enrolled, most with history of diagnosis by liver biopsy, 70% confirmed F4 on biopsy score reports. Demographics included mean age 61.5 (9.3 (SD)), female 62%, BMI 35.5 (7.5), diabetes 69%, hypertension 79%, dyslipidemia >70%, ASCVD score 15.2%, hypothyroid 23%, statin use 51%, MRE 5.5 kPa (2.1), FibroScan VCTE 25.6 kPa (15.4), CAP 322 dB/m (56), MRI-PDFF 8.1% (5), ELF 10.7 (1.1), FIB-4 2.3 (median) mean 2.8 (1.6), platelets 143 (median), mean 159 (65). Based on literature guidelines, thresholds were assessed for prediction of NASH cirrhosis; approximately 89% met criterion of FibroScan

≥15 kPa and at least one additional test (Table, "MRE/Plts/ELF"). About half of the 10% of patients excluded by these tests had confirmed F4 on biopsy. The threshold, FIB-4 ≥3.25, was not independent of low platelet criteria and was not a useful index for this CP-A population. Statin use was associated with reduced AST (AST, mean 42 (28) (no statin) vs 35 (16) (statin)) and FIB-4 in this population. Highly significant correlations with increasing FIB-4 (rho = 0.7), reduced platelet count (rho = -0.4), and other markers of cirrhosis progression were observed in the subpopulation of patients as a function of reduced liver function as determined by HepQuant. NASH resolution without worsening of fibrosis.

	Met Criterion	Confirmed by additional criteria	Did not meet criterion	Did not meet criterion but met other criteria	Total meeting any cirrhosis criteria
FibroScan (FS) ≥15 kPa	79%	94% (MRE/Plts/ELF)	21%	10% (MRE/Plts/ELF)	89%
FibroScan ≥20 kPa	53%		47%		
MRE ≥4.2, and/or platelets <140 K, and/or ELF ≥10.25 (MRE/Plts/ELF)	87%	87% (FS ≥15)	13%	5% (FS ≥15)	92%
MRE ≥4.2	74%		26%		
ELF ≥10.25	66%		34%		
Platelets <140 K	49%		51%		
FIB-4 ≥3.25	32%		68%		

Conclusion: NASH cirrhosis may be predicted using imaging and biomarker tests in the absence of liver biopsy. Patients with metabolic syndrome and a history consistent with NASH and VCTE of kPa ≥15 could be screened with other tests (ELF, MRE, platelet level) to determine a likelihood of NASH cirrhosis.

SAT-445

Assessment of hepatic fibrosis screening in primary care using the FIB-4 score, followed in second line by an ELF (Enhanced liver Fibrosis) test

Denis Ouzan^{1,2}, Guillaume Penaranda³, Jlael Malik⁴, Corneille Jeremie⁵. ¹Institut Arnault Tzanck, France; ²RHECCA, France; ³BIOGROUP ALPHABIO-Laboratoire Européen, France; ⁴BIOGROUP BIOESTEREL-Laboratoire Mandelieu-Passero, France; ⁵BIOGROUP BIOESTEREL-Laboratoire Mougins-L'espérance, France
Email: denis.ouzan@wanadoo.fr

Background and aims: Screening for liver fibrosis in the general population is a public health issue. We have shown in a previous study (1) that FIB-4, a simple score combining age, ALT, AST, and platelet, can detect liver fibrosis in general practice and identify a possible cause of liver disease. The FIB-4 thresholds usually used are: low risk if <1.30, intermediate risk between 1.3 and 2.67, and high risk if ≥2.67. The objective of our work was to evaluate the screening of hepatic fibrosis in general practice using the FIB-4 score, followed in second line if ≥1.3 by an ELF test.

Method: The FIB-4 score was performed prospectively from March to September 2022 in all consecutive patients seen by 17 general practitioners (GP), outside the emergency. When the FIB-4 was ≥1.3, it was defined as positive and confirmatory ELF test was systematically performed. The positive FIB-4 test was confirmed when the second line ELF test was ≥9.8 (indicating an advanced fibrosis).

Results: Among the 3427 patients included, 869 (25%) had a positive FIB4 score, which was confirmed by the ELF test in 509 (59%) of cases. 35% of them were older than 65 years. Among the 869 FIB-4 positive patients, 784 (90%) were at intermediate risk (FIB-4 between 1.3 and 2.67) and 85 (10%) at high risk of fibrosis (FIB-4 ≥2.67). FIB-4 positivity was significantly linked to age over 65 years, ASAT >N and

platelets levels $<150\,000$ $p < 0.001$. Confirmation by ELF was observed among 80% of the patients with high risk of fibrosis, and among 51% of the patients with intermediate risk of fibrosis ($p < .0001$). Clinical information was obtained in 680 out of 869 (78%) of the FIB-4 positive patients. The confirmation by ELF test was significantly higher in patient with patients over 65 years (83 vs 57%, $p < .0001$), in patients with FIB-4 ≥ 2.67 (80 vs 56%, $p < .0001$), BMI >25 (47 vs 37%, $p = 0.0121$), and in those with a diabetes (24 vs 14%, $p = 0.0010$), but not in those with excessive alcohol consumption (15 vs 14%, $p = 0.9283$). Only 8% of the patients were known to have a liver disease. In the patients without known liver disease (92%), the GP define a cause in 28% of cases: Nash 67%, Alcohol 23%, NASH+ Alcohol 9%, other 5% and requires an specialized advice in one third of cases.

Conclusion: Liver fibrosis was suspected by FIB4 score in 25% of patients who consulted a GP. The percentage of confirmation by the second line ELF test was significantly higher in patients with a FIB4 ≥ 2.67 and in those with a risk factor of liver disease overweight or diabetes, who need to be confirmed in priority. For FIB-4 positive patients without known liver disease, the FIB-4 allow the GP to recognize a liver disease in nearly one third of cases, mainly NASH.

Reference

1. Ouzan D *et al.* Prospective screening for significant liver fibrosis by FIB-4 in primary care patients without known liver disease. *Eur J Gastroenterol Hepatol* 2021;33:986–991.

SAT-446

Fully automated approach of machine learning combined with deep learning to forecast the coronary artery disease in patients with non-alcoholic fatty liver disease

Antonio Cirella¹, Gaia Sinatti¹, Angelica Bracci¹, Laura Evangelista¹, Pierangela Bruno², Silvano Junior Santini¹, Gianluigi Greco², Antonella Guzzo², Francesco Calimeri², Ernesto di Cesare¹, Clara Balsano¹. ¹Università degli studi di L'Aquila, Italy; ²Università della Calabria, Italy

Email: cirella.nt@gmail.com

Background and aims: Non-alcoholic fatty liver disease (NAFLD) has become the most prevalent liver disease worldwide, affecting a quarter of world's population. Growing evidence indicates that in these patients, the presence of NAFLD increases the risks cardiovascular disease (CVD) and morbidity and mortality. CVD represent the principal outcome greater than the progression of liver disease. Coronary arteries disease (CAD) is detected by Coronary CT, moreover CT is used also for the determination liver steatosis. The aim of our study was to implement ML/DL models to analyse CT images integrated with clinical parameters, in order to develop a comprehensive prognostic stratification model to forecast, in NAFLD patients, the onset of CAD.

Method: Our retrospective study analyzed clinical data and CT images of 401 patients (217 males and 184 females), who underwent coronary CT between 2017 and 2021. Images were acquired by cardio-synchronous technique. Hounsfield Unit (HU), Agatston score, Fib-4 score were used to measure radiodensity, calcium score (CS) and the degree of fibrosis, respectively. In order to perform disease classification, we used a combination of Machine Learning (ML) and Deep Learning (DL) algorithms. In particular, the algorithms are first trained on clinical data and CT images, respectively, and then the obtained models are properly combined. We performed an ablation study to identify the most appropriate methods, resulting in Densely Connected Convolutional Networks (Densenet-169) and K-nearest neighbors (KNN).

Results: In order to show the viability of our approach, we first test the ML algorithm on the task of binary classification using clinical data of 84 patients and, then, the DL algorithms using CT images. The results reveal that our combined approach is able to predict absent and severe CAD with a mean accuracy of 94% in NAFLD and healthy patients. Furthermore, we tested ML and DL algorithms in the task of multi classification using only clinical data of 401 patients. Our

algorithms were able to distinguish patients in 5 classes from healthy patients to patients affected by NAFLD and CVD, with a mean accuracy of 87% and a mean specificity of 86% for ML and a mean accuracy of 77% and a mean specificity of 76% for DL. To improve the performance of these prediction models, we are integrating them with DL algorithms for liver CT images for all the patients.

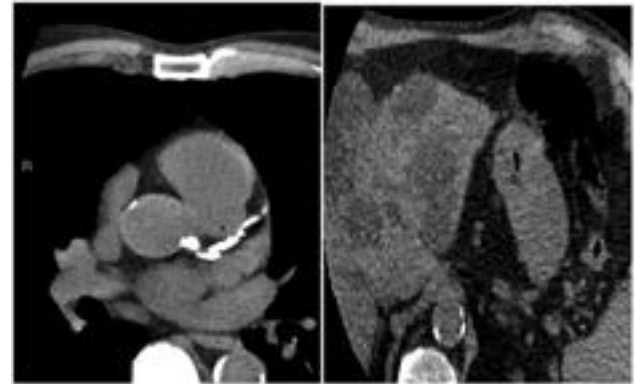


Figure:

Conclusion: Our integrated ML/DL approach could be used in practice to flag NAFLD patients at high risk of CVD.

SAT-447

Low risk FIB-4 results in patients under 50 years accurately risk assessed patients for adverse liver outcomes over a follow-up of up to 35 years

Jenny Gallacher^{1,2}, Stuart Mcpherson^{1,2}, Quentin Anstee^{1,2}.

¹Translational and Clinical Research Institute, Faculty of Medical Sciences, Newcastle University, Newcastle upon Tyne, United Kingdom;

²Liver Unit, Newcastle NIHR Biomedical Research Centre, Newcastle upon Tyne Hospitals Foundation Trust, Newcastle upon Tyne, United Kingdom

Email: jennifer.gallacher@nhs.net

Background and aims: Non-invasive tests of fibrosis such as the FIB-4 score are routinely used by clinicians to assess patients with NAFLD and guide management. Current EASL and AASLD guidelines suggest those who fall into the “low risk” category (FIB-4 <1.30) can be managed in a primary care setting, with advice to repeat these tests every 2 years. This practice has been widely adopted as a way to cost effectively screen for advanced fibrosis, from an ever-growing number of patients with NAFLD, given the components of FIB-4 are routinely clinically available and the high negative predictive value of the score. However, there are few long-term studies which explore the outcomes of those deemed “low risk.” This study aims to review outcomes of interest including incident HCC, liver transplantation and mortality in “low risk” patients aged <50 yrs over a period of up to 35 years.

Method: Participants with biopsy proven NAFLD were prospectively recruited from the Newcastle Hospitals, U.K., between 1990 and 2018 with a minimum of 12 months follow-up. Data was collected at clinical events and outcomes explored including survival analysis with Kaplan Meier log-rank tests.

Results: 158 participants were included with a mean follow-up of 14.3 ± 7.2 years (1–35.4 years). 74.1% were male, mean age 37 ± 9 and BMI 34.3 ± 5.6 kg/m². T2DM was present in 24.7% (39), HTN 24.8% (34) and MetS 63.8% (74). The prevalence of these co-morbidities increased over the course of the follow-up to 55.3% (84) T2DM, 51.0% (76) HTN and 87.1% (81) MetS. Five patients died, with cardiovascular disease, the most common cause (60%). Mean time to death was 11.7 ± 7.2 years. No liver related deaths, incident HCC or liver transplantation were observed in the cohort. Survival of this cohort was compared to a larger cohort of patients aged <50 years from the same centre, recruited during the same time frame but including all FIB-4

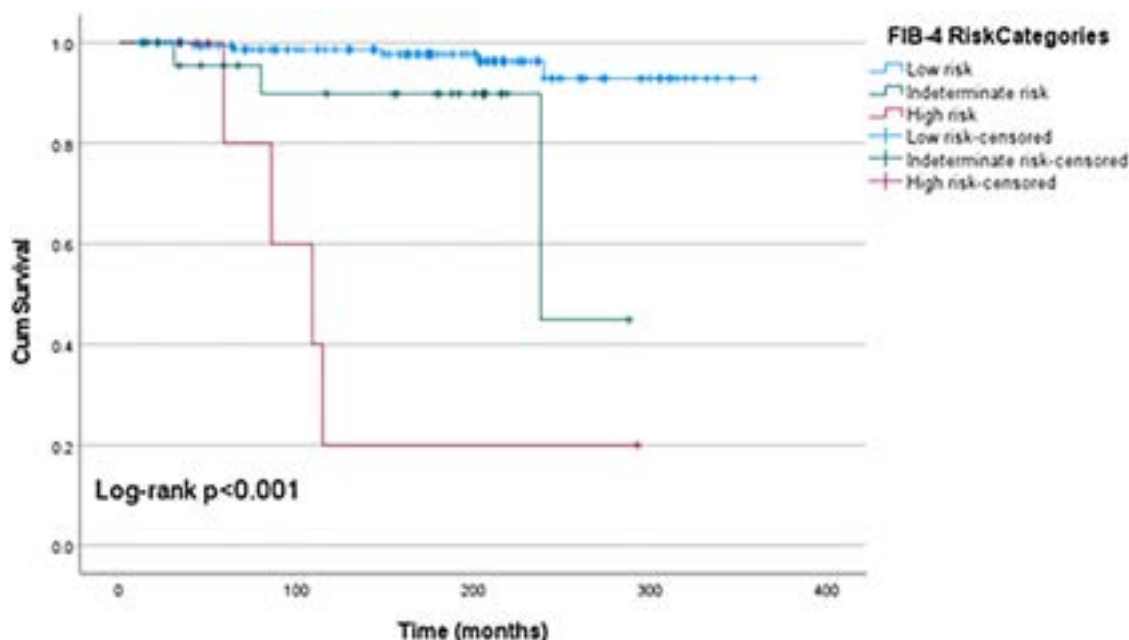


Figure: (abstract: SAT-447): Kaplan Meier survival curves of patients <50 years stratified by FIB-4 risk categories.

risk strata (n = 191). Significant differences in survival were observed, $p < 0.001$. 80% of FIB4 “high risk” patients were dead at 10 years, and 55% of “indeterminate risk” cases were dead by 20 years. In contrast, the majority (93%) of “low risk” individuals were still alive at up to 35 years follow-up.

Conclusion: These results require further independent validation in large prospective cohorts but indicate that patients under 50 years of age with low-risk FIB-4 are unlikely to experience liver-related hard clinical outcomes over an extended follow-up period.

SAT-448

Serum levels of type IV collagen 7S can predict liver-related mortality and events as well as advanced fibrosis: a multi-center study

Hiroshi Ishiba¹, Yoshio Sumida², Yoshihiro Kamada³, Hideki Fujii⁴, Michihiro Iwaki⁵, Hideki Hayashi⁶, Hidenori Toyoda⁷, Satoshi Oeda⁸, Hideyuki Hyogo⁹, Miwa Kawanaka¹⁰, Asahiro Morishita¹¹, Kensuke Munekage¹², Kazuhito Kawata¹³, Tsubasa Tsutsumi¹⁴, Koji Sawada¹⁵, Tatsuji Maeshiro¹⁶, Hiroshi Tobita¹⁷, Yuichi Yoshida¹⁸, Masafumi Naito¹⁸, Shingo Araraki^{16,16}, Takumi Kawaguchi¹⁴, Hidenao Noritake¹⁹, Masafumi Ono²⁰, Tsutomu Masaki²⁰, Satoshi Yasuda²¹, Eiichi Tomita²², Masato Yoneda²³, Akihiro Tokushige²⁴, Hirokazu Takahashi²⁵, Shinichiro Ueda¹⁶, Atsushi Nakajima²³, Takeshi Okanoue²⁶. ¹Osaka general hospital of West Japan railway compnay, Japan; ²Aichi Medical University, Division of Hepatology and Pancreatology, Department of Internal Medicine, Japan; ³Osaka University, Department of Advanced Metabolic Hepatology, Japan; ⁴Osaka Metropolitan University, Departments of Premier Preventive Medicine and Hepatology, Japan; ⁵Yokohama City University Graduate School of Medicine, Division of Gastroenterology and Hepatology, Japan; ⁶Gifu Municipal Hospital, Department of Gastroenterology and Hepatology, Japan; ⁷Ogaki Municipal Hospital, Department of Gastroenterology, Japan; ⁸Saga University, Department of Laboratory Medicine, Japan; ⁹Hyogo life care clinic, Japan; ¹⁰Kawasaki Medical School, Department of General Internal Medicine2, Japan; ¹¹Kagawa University, Department of Gastroenterology and Neurology, Japan; ¹²Kochi Medical School, Department of Gastroenterology and Hepatology, Japan; ¹³Hamamatsu University School of Medicine, Hepatology Division, Department of Internal Medicine II, Japan;

¹⁴Kurume University School of Medicine, Japan; ¹⁵Asahikawa Medical University, Japan; ¹⁶University of the Ryukyus, Japan; ¹⁷Shimane University Hospital, Japan; ¹⁸Suita Municipal Hospital, Japan; ¹⁹Hamamatsu University School of Medicine, Japan; ²⁰Kagawa University, Japan; ²¹Ogaki Municipal Hospital, Japan; ²²Gifu Municipal Hospital, Japan; ²³Yokohama City University Graduate School of Medicine, Japan; ²⁴Kagoshima University Graduate School of Medical and Dental Sciences, Japan; ²⁵Saga University, Japan; ²⁶Saiseikai Suita Hospital, Japan
Email: sumida19701106@yahoo.co.jp

Background and aims: Type IV collagen 7S (COL4-7S) is one of the simple non-invasive tests for detecting liver fibrosis. However, it was not clarified whether COL4-7S can detect the advanced fibrosis (stage 3/4) and predict the prognosis of non-alcoholic fatty liver disease (NAFLD). In this study, we estimated the clinical efficacy of COL4-7S for detection of advanced fibrosis and prognosis of NAFLD.

Method: The total of 881 Japanese patients with biopsy-prove NAFLD from 1994 to 2020 were enrolled. Serum levels of COL4-7S were determined by the method of radioimmunoassay. Two cutoff points were set on specificity 90% and sensitivity 90% by ROC analysis of COL4-7S for detecting advanced fibrosis. This clinical utility was validated by the 10-fold cross validation. Patients were assigned to three groups on the settled cutoff points. Cox regression analysis were performed to estimate the predictive capacity of COL4-7S for liver-related mortality (LRM) and events (LREs).

Results: The median follow-up period were 4.3 years. 31 patients developed liver-related events and 9 patients died by LREs. The AUROC of COL4-7S was 0.847. The low and high cutoff points were set on 4.8 and 6.8 ng/ml, respectively. The adjusted hazard ratio (aHR) of the high-risk group by COL4-7S for LRM was 46.22 ($p < 0.01$), while aHR of advanced fibrosis was 1.38 ($p = 0.683$). The aHR for LREs of the intermediate and high-risk by COL4-7S were 5.94 ($p < 0.01$) and 27.17 ($p < 0.01$). The aHR of advanced fibrosis by liver biopsy was 1.61 ($p = 0.248$). In the same fibrosis stage, the incidence of LRM/LREs was more frequent with a higher risk stratification.

Conclusion: Serum levels of COL4-7S has good diagnostic accuracy for predicting advanced fibrosis and can accurately predict LRM and LREs. COL4-7S help physicians estimate both fibrosis stage and patient prognosis in clinical practice.

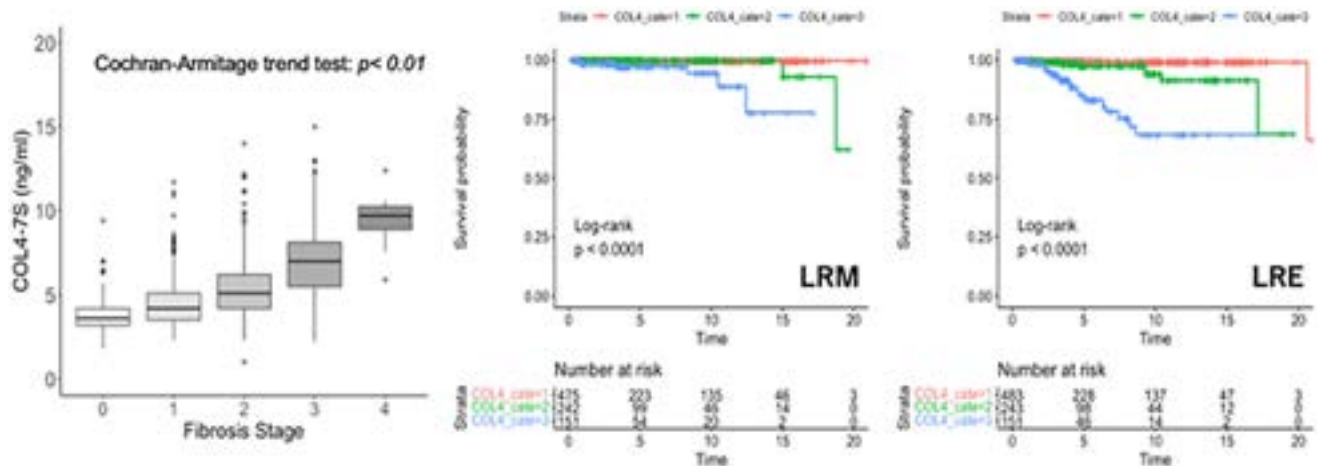


Figure: (abstract: SAT-448).

SAT-449

The genetic background of NAFLD patients markedly affects their metabolomic and lipidomic signatures

Lina Jegodzinski¹, Ashok Rout², Friedhelm Sayk¹, Franziska Schmelter³, Bandik Föh⁴, Henrike Dobbermann¹, Monika Herr¹, Sebastian Meyhöfer^{1,5}, Svenja Meyhöfer^{1,5}, Monika Rau⁶, Susanne N Weber⁷, Marcin Krawczyk⁷, Andreas Geier⁶, Ulrich Gunther², Jens Marquardt¹. ¹University Hospital Schleswig-Holstein, Lübeck, Department of Medicine I, Lübeck, Germany; ²University of Lübeck, Institute of Chemistry and Metabolomics, Lübeck, Germany; ³University Hospital Schleswig-Holstein and University of Lübeck, Institute of Nutritional Medicine, Lübeck, Germany; ⁴Gemeinschaftspraxis im Gesellenhaus, Lübeck, Germany; ⁵University of Lübeck, Institute for Endocrinology and Diabetes, Lübeck, Germany; ⁶University Hospital Würzburg, Department of Medicine II, Würzburg, Bayern, Germany; ⁷University Hospital Saarland, Department of Medicine II, Homburg, Germany
Email: lina.jegodzinski@uksh.de

Background and aims: Non-alcoholic fatty liver disease (NAFLD) encompasses a heterogeneous spectrum of patients with different clinical and molecular characteristics. Pathophysiologically, obesity, diabetes and the metabolic syndrome are major exogenous determinants for metabolic liver diseases. In recent years, several common genetic variants have been identified with significant impact on NAFLD development and progression. Herein, the *patatin*-like phospholipase domain-containing 3 (*PNPLA3*) p.I148M was identified as a major genetic risk factor for NAFLD. While its impact on clinical progression is well established, metabolomic and lipidomic profile of *PNPLA3* variants are not fully understood.

Method: In this bi-centric study, a total of 256 NAFLD patients were recruited. Chronic and acute liver disease other than NAFLD were excluded in all patients. Genotyping of the *PNPLA3* p.I148M polymorphism was performed using TaqMan assays. Proteo-metabolomics of patient sera was performed by NMR spectroscopy, covering a range of ca. 30 metabolites as well as 100 lipoprotein and glycoprotein parameters.

Results: Homozygous *PNPLA3* p.I148MM variant was present in 42 patients (16.4%), whereas 90 patients (35.2%) carried the p.I148IM genotype. We were able to show clear differences in analysed serum metabolites as well as in lipoprotein subtype profiles between patients with different *PNPLA3* genotypes. For example, there was a significantly higher proportion of LDL triglyceride and VLDL cholesterol subfractions in serum of patients carrying the p.I148MM genotype. Additionally, we observed differences in the amino acid status of the patients, especially in the levels of phenylalanine, tyrosine and glutamine.

Conclusion: The *PNPLA3* p.I148M polymorphism has a profound impact on metabolomic and lipidomic profile of NAFLD patients. Results might contribute to our understanding how the variant affects progression in NAFLD patients. A detailed characterization of key molecules could provide a useful tool for the identification of patients at risk in the future.

SAT-450

Prevalence of diagnosed advanced liver fibrosis in high-risk population with metabolic-dysfunction associated fatty liver disease screened in diabetology using transient elastography

Adrien Aubin¹, Marianne Maynard^{2,3}, Bérénice Ségrestin¹, Yasmina Chouik², Laurent Milot⁴, Valerie Hervieu⁵, Fabien Zoulim^{2,3}, Emmanuel Disse^{1,6}, Massimo Levvero^{2,3}, Cyrielle Caussy^{1,6}. ¹Hospices Civils de Lyon, Endocrinology, Diabetes and Nutrition, Pierre Bénite, France; ²Hospices Civils de Lyon, Hepatology, Lyon, France; ³Centre de Recherche sur le Cancer de Lyon, INSERM 1052, Lyon, France; ⁴Hospices Civils de Lyon, Radiology, Lyon, France; ⁵Hospices Civils de Lyon, Pathology, Lyon, France; ⁶Université Lyon 1, CarMen Laboratory, Pierre-Bénite, France
Email: cyrielle.caussy@chu-lyon.fr

Background and aims: The systematic screening for advanced fibrosis (AF) is recommended in high-risk population such as patients with type 2 diabetes (T2D) and/or obesity and metabolic dysfunction-associated fatty liver disease (MAFLD). However, there are limited data regarding clinical care pathways using liver assessment by transient elastography (TE) performed in diabetology. Therefore, we aimed at assessing the prevalence of diagnosed AF in patients with MAFLD screened for the presence of AF in diabetology prior to hepatology referral.

Method: This is a cross-sectional study including consecutive adult patients with T2D and/or obesity and MAFLD who underwent a liver assessment by TE using a Fibroscan® performed at the Department of Endocrinology, Diabetes and Nutrition, Lyon South Hospital at Hospices Civils de Lyon, France between January 2020 and October 2022. Pseudonymized clinical data, fasting labs including a Fibrotest® and TE reports were systematically extracted from medical electronic records and informed consents were obtained. The presence of suspected AF was defined by a reliable TE ≥ 8 kPa. The confirmed presence of AF was recorded according to assessment in hepatology defined as composite end point including either histological fibrosis stage ≥ F3 or overt imaging diagnosis of cirrhosis on magnetic resonance imaging (MRI) or concordant TE ≥ 8 kPa and Fibrotest® ≥ F3 according to EASL guidelines. Patients with discordant TE and Fibrotest® without histological assessment that underwent a

POSTER PRESENTATIONS

third line magnetic resonance elastography <3.62 kPa were considered as patients without AF in the analysis.

Results: The study included 727 patients with DT2 and/or obesity and MAFLD. The mean age was 54.3 years (\pm SD 13.6) and the BMI 37.2 kg/m² (\pm 7.9). 50.3% were female, 36.6% had a BMI \geq 40 kg/m², 69.9% had T2D. Sixty-one patients (8.4%) had an unreliable TE. Among the 666 patients with reliable TE, the prevalence of suspected AF with TE \geq 8 kPa was 28.4% (n = 189) and 10.2% (n = 68) had a TE \geq 12 kPa. In the whole population, the prevalence of confirmed AF was 7.4% (n = 54) including 24 patients with histological stage \geq F3, 23 with concordant TE and Fibrotest® for stage \geq F3, and 7 with a diagnosis of cirrhosis by MRI. In this population, 18.8% (n = 137) had an undetermined stage of fibrosis. Severe obesity BMI \geq 40 kg/m² was significantly associated with increased odds of undetermined stage of fibrosis (OR 3.4; 95%CI: 2.27–5.09; p < 0.001) in a multivariable model adjusted for age and sex and remained significant even when excluding individuals with unreliable TE (OR 4.4; 95%CI: 2.65–7.40; p < 0.001).

Conclusion: In high-risk individuals with MAFLD consecutively enrolled in a screening for AF in diabetology using TE, the prevalence of diagnosed AF was 7.4%. Severe obesity was significantly associated with undetermined status of AF highlighting the need to optimize the screening strategy in these individuals.

SAT-451

Serological biomarkers of extracellular matrix related disease activity are elevated in patients at risk of NASH with significant liver stiffness

Thomas Møller^{1,2}, David Provenghi³, Peder Frederiksen¹, Heidi Guthrie³, Morten Karsdal¹, Marcus Hompesch³, Diana Leeming¹. ¹Nordic Bioscience A/S, Denmark; ²University of Copenhagen, Department of Biomedical Sciences, Denmark; ³ProSciento, Inc, United States
Email: twm@nordicbio.com

Background and aims: In non-alcoholic steatohepatitis (NASH), inflammation of the hepatic tissue leads to an increased formation and deposition of extracellular matrix proteins, such as collagens. Over time accumulation of collagens causes hepatic fibrosis, which is associated with increased liver stiffness (LS). Type III, IV, and VI collagen formation may be assessed non-invasively using PRO-C3, PRO-C4, and PRO-C6 assessing the pro-peptide of type III and VI collagen, and the 7S domain of type IV collagen. We aimed to investigate how PRO-C3, PRO-C4, and PRO-C6 may identify patients with increased liver stiffness measure (LSM), in patients identified as at risk of NASH, due to obesity and presence of type 2 diabetes (T2D).

Method: 958 patients from the NASH-PASS study, were identified as at risk of NASH due to being obese and presence of T2D, whom all had LSM using vibration-controlled transient elastography (VCTE) by Fibroscan. Blood samples were collected at the time of LSM. PRO-C3 and PRO-C6 were assessed using fully validated competitive immunoassays, and PRO-C4 was assessed using a fully validated automated competitive chemiluminescent immunoassay. Between groups comparisons of biomarker levels were performed using Mann-Whitney or Kruskal-Wallis test.

Results: The median (Q1, Q3) age and BMI of the 958 included patients were 56.4 (48.3, 63.7) years and 35.1 (31.7, 38.9) kg/m², respectively, and 473 patients had T2D. 22% of the patients had significant LS (VCTE $>$ 8 kPa). While weak Spearman correlation between LS and our biomarkers was observed, the levels of PRO-C3, PRO-C4, and PRO-C6 were significantly elevated in patients with significant LS, compared to those without (VCTE $<$ 8 kPa), (p < 0.0001, p < 0.05, and p < 0.0001), (AUROC = 0.672, 0.546, and 0.623).

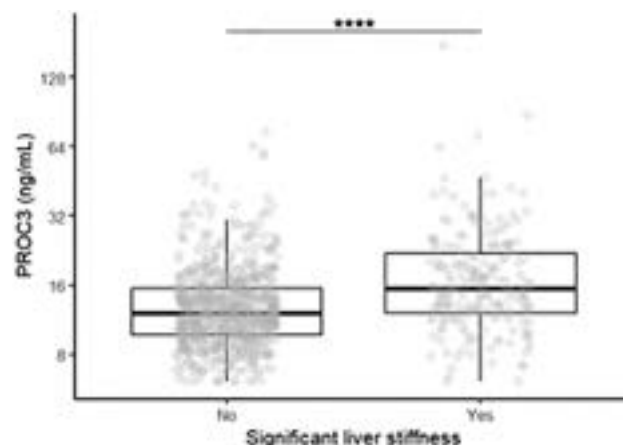


Figure:

Conclusion: This study did not find strong correlation between LS and the PRO-C3, PRO-C4, and PRO-C6 biomarkers. This was expected as such biomarkers are related to ECM related disease activity rather than status of LS. However, patients with increased LSM (VCTE $>$ 8 kPa) had significantly increased disease activity assessed as the formation of type III, IV, and VI collagens, compared to patients without (VCTE $<$ 8 kPa).

SAT-452

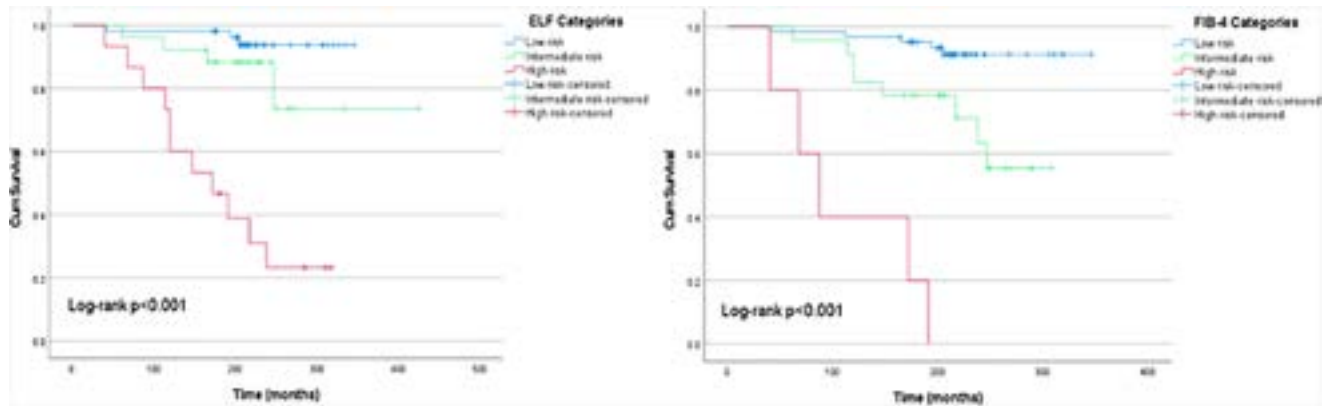
Prognostic value of the Enhanced Liver Fibrosis (ELF) test to predict long-term outcomes in a NAFLD cohort with up to 35 years follow-up

Jenny Gallacher^{1,2}, Stuart Mcpherson^{1,2}, Quentin Anstee^{1,2}. ¹Translational and Clinical Research Institute, Faculty of Medical Sciences, Newcastle University, Newcastle upon Tyne, United Kingdom; ²Liver Unit, Newcastle NIHR Biomedical Research Centre, Newcastle upon Tyne Hospitals Foundation Trust, Newcastle upon Tyne, United Kingdom
Email: jennifer.gallacher@nhs.net

Background and aims: There are emerging data that non-invasive tests (NIT) can predict long-term clinical outcomes and mortality however the majority of studies are of short duration. ELF is an established biomarker panel, developed to detect advanced fibrosis (\geq F3). Fifteen years after the original publication demonstrating the performance of ELF as a *diagnostic* biomarker in NAFLD¹, we report the long-term follow-up of the same cohort of patients and assess the performance of ELF in comparison to FIB-4 as *prognostic* biomarkers for predicting liver-related and all-cause mortality.

Method: Patients recruited at a UK tertiary centre in the original NAFLD-ELF study¹ were followed until 2020 to explore outcomes of interest including progression to cirrhosis, incident HCC and mortality. Cox regression analysis was performed to explore the prognostic ability of ELF and FIB-4 to predict mortality.

Results: 95 patients were included (mean follow-up 17.9 \pm 5.3 years [3.3–35.4 years]; 62% male; mean age at baseline 47 \pm 13 years). Using cut-offs to group patients as “low,” “intermediate” and “high” risk (ELF = $<$ 9.80, 9.80–11.1, $>$ 11.1. FIB-4 = $<$ 1.30, 1.30–2.67, $>$ 2.67) the distribution of ELF results in the cohort were 56.8% (54) low, 27.4% (26) intermediate and 15.8% (15) high at baseline. FIB-4 results were similar with 68.9% (62), 25.6% (23) and 5.6% (5) respectively. 17.9% (17) of patients had advanced fibrosis (F3–4) at baseline, with 11.6% (11) being classed as cirrhotic. ELF performed well at identifying presence of advanced fibrosis (AUROC 0.954, 95% CI 0.91–1.00; FIB-4 AUROC 0.824, 95% CI 0.72–0.93). The number of patients with cirrhosis by the end of the study increased to 24.1% (21), 8.4% (8) developed HCC and 18.9% (18) died. Liver-related death was the most common cause (44.5%), followed by extrahepatic malignancy (16.7%) and cardiovascular disease (11.1%). Hazard ratios for all-cause mortality were generated using the risk categories above and



adjusted for age. Patients in the “high risk” categories had an increased association with all-cause mortality compared to those “low risk”: ELF aHR 9.05, 95% CI 2.35–34.88, $p=0.001$, FIB-4 aHR 16.04, 95% CI 3.46–74.33, $p<0.001$. 10 year survival rates were 98%, 92% and 60% in those with low, intermediate, and high ELF results.

Conclusion: Consistent with the recognised link between fibrosis stage and outcomes, ELF and FIB-4 exhibited prognostic value for prediction of mortality in patients with NAFLD. These NITs offer clinically utility for both the diagnostic and prognostic contexts of use in NAFLD.

Reference

1. Guha IN, Parkes J, Roderick P, Chattopadhyay D, Cross R, Harris S, *et al.* Non-invasive markers of fibrosis in non-alcoholic fatty liver disease: Validating the European Liver Fibrosis Panel and exploring simple markers. *Hepatology*. 2008;47(2):455–60.

SAT-453

Utilization of fibroscan-AST scoring system to risk-stratify non-alcoholic steatohepatitis patients for clinical trials and novel therapies

Phillip Leff^{1,2}, Prido Polanco¹, Rida Nadeem¹, Aria Raman¹, Gagana Ameneni¹, Shray Patel¹, Rayan Ahmed¹, Anushka Kadharia¹, Naim Alkhouri¹. ¹Arizona Liver Health, United States; ²Creighton University, United States
Email: phillipleff@creighton.edu

Background and aims: The Fibroscan-AST (FAST) score is a non-invasive test that utilizes liver elastography with a complex formula to determine a patient’s risk of progressive Non-Alcoholic Fatty Liver Disease (NAFLD). Multiple studies have validated the FAST score at predicting the patient’s risk of progressing to Non-Alcoholic Steatohepatitis (NASH) more accurately than other non-invasive tests (NIT) i.e. NAS, FIB4, and the APRI score. The aim of this study was to determine if the FAST score would be an effective NIT to stratify high risk patients to receive medical therapies for NASH in conjunction with the AGA guideline for hepatology referrals for NAFLD.

Method: This was a retrospective chart review, in the setting of an outpatient hepatology clinic. Patients 18 years and older who presented to the outpatient clinic that underwent liver elastography, with a complete metabolic panel were included. Patients that did not undergo liver elastography were excluded from the study. NAFLD fibrosis score was calculated using: $FAST = \frac{\exp(-1.65 + 1.07 \times \ln(LSM) + 2.66 \times 10^{-8} \times CAP^3 - 63.3 \times AST^{-1})}{1 + \exp(-1.65 + 1.07 \times \ln(LSM) + 2.66 \times 10^{-8} \times CAP^3 - 63.3 \times AST^{-1})}$. AGA guidelines were followed, patients were initially screened using Fib-4, Fib-4 > 1.6 underwent elastography. Fib-4 was calculated using $Fib-4 = \text{age} \times AST / PLT \times ALT$. Elastography cut-off was kPa ≥ 8 . In addition to this protocol, patients with kPa ≥ 8 were selected for FAST scoring.

Results: Our cohort included 925 patients. 593 were female (64.11%), 499 were Caucasian (53.95%), 25 were African American (2.70%), 19 were Asian (2.05%), 6 were Native American (0.65%), 172 were other (18.59%), and 172 declined to answer (18.59%). 377 (40.76%) patients were non-Hispanic, 192 (20.76%) were Hispanic, and 356 (38.49%) were unknown/declined to answer. 350 (37.84%) had diabetes mellitus, 288 (31.14%) had dyslipidaemia, and 420 (45.41%) had hypertension. The average FAST score was 0.45. 263 had a FAST score ≥ 0.67 (28.43%). 662 (71.57%) were <0.67 . 492 patients had Fib-4 ≥ 1.3 , of those 492 patients 367 had a kPa ≥ 8 . Out of those 367 patients, 207 patients had a FAST score ≥ 0.67 .

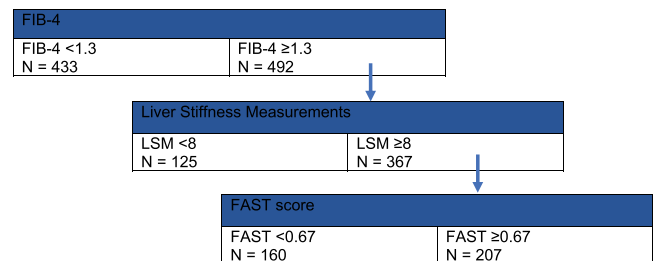


Figure:

Conclusion: With the advent of new therapies currently in clinical trials awaiting approval for commercial use, there is need for a standardized method of risk stratifying patients to receive these limited therapeutics. The FAST score with a cut-off of ≥ 0.67 had a high specificity and PPV compared to biopsy. This notion implies patients with high FAST scores have a high risk of f2 or greater fibrosis. The decision to start new/limited medication should be reserved for the highest-risk patients, the results of this study conclude patients should follow the AGA guidelines but could consider adding a FAST score to screen for patients that would be the most at need for pharmaceutical therapy.

SAT-454

A screening strategy of hidden compensated advanced chronic liver disease in diabetic outpatients using sequential and automatic fibrosis-4 and enhanced liver fibrosis scores

Clara Amiama Roig¹, Miriam Romero¹, María Sanz de Pedro², Alexa Pamela Benítez Valderrama³, Cristina Suárez Ferrer¹, Carlota Siljeström Berenguer¹, Mariana Serres Gómez², Carmen Amor¹, Irene Gonzalez Diaz¹, Noemi González Pérez de Villar³, Antonio Buño Soto², Antonio Oliveira Martín¹. ¹La Paz University Hospital, Gastroenterology and Hepatology Department, Madrid, Spain; ²La Paz University Hospital, Laboratory Medicine Department, Madrid, Spain; ³La Paz University Hospital, Endocrinology Department, Madrid, Spain
Email: camiamaroig2@gmail.com

Background and aims: The high prevalence of metabolic liver disease (MAFLD) requires efficient screening and referral strategies. Probably a high number of patients are suffering unknown advanced chronic compensated liver disease (cACLD). The usual non-invasive tests have low positive predictive value, so that the referral of patients based exclusively on one of them is an inefficient overload for our offices. Objective: to efficiently establish the prevalence of unknown cACLD in a cohort of patients with type 2 diabetes.

Method: Ongoing prospective study. In the Diabetes analytical requests the Laboratory determined, automatically and without specific medical request, both FIB4, and ELF in those with FIB4 >1.3 (>2 in >65 years). In agreement with Endocrinology and with the Ethics Committee approval, the Laboratory generated a referral to Hepatology in those with FIB4 >1.3/2. According to Baveno VII, cACLD was considered absent if Fibroscan <10 kPa and cACLD if >15 kPa. Between 10–15 kPa (suggestive of cACLD) we considered cACLD when ≥12 kPa (Papatheodoridis. J Hepatol 2020). ELF cut-off for cACLD was >9.8. Exclusion criteria were age <35/>80 years, already diagnosed MAFLD or other liver diseases, patient refusal and severe comorbidities (advanced cancer, degenerative diseases...). Normally distributed quantitative variables were described using the mean; otherwise, the median was calculated. Diagnostic performance of ELF was assessed with receiver operating characteristic curves (AUROC).

Results: Between March and November 2022 FIB4 was performed in 1958 patients, 491 (25.1%) with FIB4 >1.3/2. Of these, only 43 (8.8%) were already diagnosed with cACLD (MAFLD 19), being excluded along with 130 other patients (comorbidities, refusal, etc). Of the remaining patients, we have hitherto studied 121 (Table). Twenty-five patients (20.6%) had unknown cACLD. The AUROC for ELF >9.8 was 0.82 (S 95%, E 51%, NPV 97.5%, PPV 32%). The sequential use of FIB4 and ELF would have missed only 1 patient with cACLD and 1 out of 3 referred patients would have cACLD.

Conclusion: the prevalence of unknown cACLD is high in Diabetes outpatient clinic. The sequential use of FIB4 and ELF is very effective in its detection. Its automated determination would be very efficient avoiding unnecessary referrals.

SAT-455

Diagnostic efficacy of Mac-2 binding protein glycosylation isomer for predicting liver fibrosis in patients with metabolic associated fatty liver disease: multicenter cohort study

Dae Won Jun¹, Se Young Jang², Ki Tae Yoon³, Young Youn Cho⁴, Hoon Gil Jo⁵, Yang-Hyun Baek⁶, Sang Yi Moon⁶, Aejeong Jo⁷. ¹Hanyang University College of Medicine, Department of Internal Medicine, Korea, Rep. of South; ²Kyungpook National University Hospital, Department of Internal Medicine, Korea, Rep. of South; ³Pusan National University Hospital, Department of Internal Medicine, Korea, Rep. of South; ⁴Chung-Ang University Hospital, Department of Internal Medicine, Korea, Rep. of South; ⁵Wonkwang University College of Medicine and Hospital, Department of Internal Medicine, Korea, Rep. of South; ⁶Dong-A University College of Medicine, Department of Internal Medicine, Korea, Rep. of South; ⁷Andong National University, Department of Information Statistics, Korea, Rep. of South
Email: gongori1004@gmail.com

Background and aims: The definition of metabolic associated fatty liver disease (MAFLD) has newly been proposed. We aimed to investigate the efficacy of Mac-2 binding protein glycosylation isomer (M2BPGi), non-invasive fibrosis marker, for discriminating significant and advanced fibrosis, and cirrhosis, respectively according to MAFLD and NAFLD definitions.

Method: Serum M2BPGi levels were collected and analyzed from 2,177 patients among 6 tertiary hospitals between April 2020 and May 2021. Liver fibrosis was graded by transient elastography. Diagnostic efficacy of serum M2BPGi and other serum based liver fibrosis markers [AST to platelet index (APRI), fibrosis index based on four factors (FIB-4), and NAFLD fibrosis score (NFS)] was evaluated using area under the ROC curve (AUC) and Delong's test.

Results: There were 1,379 patients and 1,194 patients by the MAFLD and NAFLD definition, respectively. The AUC values of M2BPGi were 0.682, 0.715, and 0.834 for predicting fibrosis (F) >1, F >2, and F >3, respectively in NAFLD group. The AUC values of M2BPGi were 0.68, 0.711, and 0.814 for predicting F >1, F >2, and F >3, respectively in MAFLD group. The AUC values of M2BPGi for predicting severity of fibrosis were greater than those of serum based liver fibrosis markers. The diagnostic efficacies of M2BPGi predicting significant and advanced fibrosis, and cirrhosis in NAFLD and MAFLD patients, respectively, were not statistically different according to Delong's test (p value; 0.94, 0.90, 0.60, respectively).

Figure: Table 1: (abstract: SAT-454): Baseline patients' characteristics.

Sex		Age	BMI (kg/m ²)	GPT (U/L)	GOT (U/L)	Fibroscan (kPa)	CAP (dB/m)	Diabetes Comorbidities		Treatment	
Women	Men										
43(35.5%)	78(64.5%)	67.3±3.7	29.7±5.3	34.1±18.2	35.3±16.8	9.8±9.3	274±67	Nephropathy	31 (25.6%)	Metformin	68 (56.2%)
								Neuropathy	13 (10.7%)	SGLT2 inhibitors	50 (41.3%)
								Peripheral Arterial Disease	10 (8.3%)	DPP4 inhibitors	29 (23.9%)
								Stroke	11 (9.1%)	GLP1 Agonists	30 (24.7%)
								Coronary Syndrome	26 (21.5%)	Insulin	59 (48.7%)

(BMI: Body Mass Index, GPT: Glutamic-pyruvic transaminase, GOT: glutamic-oxaloacetic transaminase, SGLT: Sodium-glucose cotransporter-2, DPP4: Dipeptidyl peptidase-4, GLP1: Glucagon-like peptide 1).

Conclusion: M2BPGi showed better diagnostic efficacy for diagnosing the severity of liver fibrosis in MAFLD patients, as well as in NAFLD patients, comparing with other liver fibrosis markers.

SAT-456

Shortcomings of “FIB-4 First” strategy in screening for non-alcoholic fatty liver disease (NAFLD) patients at risk for disease progression in a real life setting: will we be detracting therapeutic opportunities from patients?

Simone Cappelli¹, Antonio Salvati¹, Giovanni Petralli², Laura De Rosa³, Gabriele Ricco¹, Lidia Surace¹, Piero Colombatto¹, Barbara Coco¹, Veronica Romagnoli¹, Filippo Oliveri¹, Ferruccio Bonino⁴, Maurizia Brunetto^{1,4}, ¹Hepatology Unit, Pisa University Hospital, Italy; ²Department of surgical, Medical, Molecular and Critical Area Pathology, University of Pisa, Italy; ³Department of Information engineering and computer Science, University of Trento, Italy; ⁴Biostructure and bio-imaging institute of National research council of Italy, Italy
Email: brunettomaurizia@gmail.com

Background and aims: The Fibrosis 4 score (FIB-4) is a non-invasive scoring system derived from Age, Aspartate aminotransferase (AST), Alanine aminotransferase (ALT) and Platelets (PLTs), that has been recently promoted in AASLD guidelines as a tool in the Primary Care setting to screen for clinically significant fibrosis (CSF) in NAFLD patients (pts); A value ≥ 1.30 identifies pts at a higher risk for progressive liver disease that need a hepatologist referral for Liver Stiffness Measurement (LSM).

In this retrospective study, we evaluated the overall performance of the score among different clinical sub-groups.

Method: 367 NAFLD pts between 35 and 65 years (yrs) (M : F = 213 : 154; 51.7 yrs \pm 7.5) followed at the Hepatology Unit in Pisa from January 2017 to October 2022 underwent clinical evaluation including: AST, ALT, GGT, ALP, blood count, p.glucose, insulin, HbA1c, lipid profile, body mass index (BMI), waist circumference (WC) and LS by transient elastography (TE, Fibroscan®).

Results: 262 pts (71.3%) had FIB-4 <1.30 (M : F = 149 : 113, 50.5 yrs \pm 7.6), among them 34 (13%) had a TE >8 kPa, of which 18 (7% of the total) even higher than 9.7 kPa, indicative of CSF. Compared to the general population, in this group of pts where the FIB-4 score failed in identify CSF we found a statistically significant higher prevalence of Obesity, Type 2 Diabetes Mellitus (T2DM), and T2DM along with Obesity, with a Risk Ratio of 2.3 (CI 95%, 1.1–4.9, $p = 0.026$), 4.4 (CI 95%, 2–9.6, $p < 0.0001$) and 5.5 (CI 95%, 2.3–12.8, $p < 0.0001$), respectively. Given an overall prevalence of TE >8 kPa of 21.1%, the FIB-4 held a negative predictive value (NPV) of 88.5% in non diabetic and lean/overweight pts, 78.3% in diabetic pts, 75.6% in obese pts, while the performance of the score dropped to a NPV of 65.4% in obese and diabetic pts.

Negative Predictive value (NPV) of FIB-4 among clinical sub groups of the cohort (%)

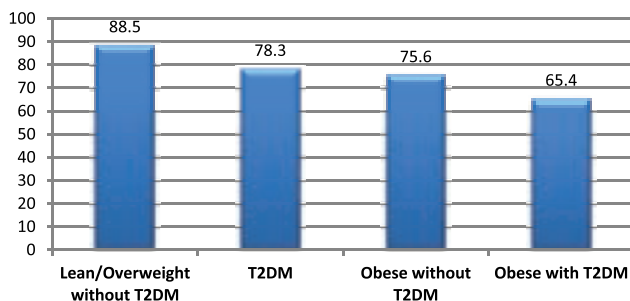


Figure:

Conclusion: These data show that the categories of patients where the proposed “FIB-4 first” strategy has a worse screening performance are also the one that could benefit more from a specialist referral for the inclusion in a lifestyle change program, a tailoring of their

therapy, or even bariatric surgery. These findings should guide the physician not to rely on the FIB-4 score alone when screening NAFLD patients, but rather on a more comprehensive evaluation of the patients clinical characteristics and comorbidities.

SAT-457

Analysis of correlation and predictive ability of oral glucose tolerance tests with insulin assays for liver stiffness measurement in non-cirrhotic overweight and obese patients

Valentino Osti^{1,2}, Michele Stecchi², Michela Genovese², Lucia Brodosi^{2,3}, ¹Azienda USL di Bologna, Department of Public Health, Bologna, Italy; ²University of Bologna, Department of Medical and Surgical Sciences, Bologna, Italy; ³IRCCS Azienda Ospedaliero-Universitaria di Bologna, Department of Digestive, Liver and Endocrine-Metabolic Diseases, Bologna, Italy
Email: valentino.osti@ausl.bologna.it

Background and aims: Non-Alcoholic and Metabolic Associated Fatty Liver Disease (NAFLD/MAFLD) is the leading cause of steatohepatitis and end-stage liver disease. Aberrations of glucose metabolism, such as insulin-resistance, Impaired Glucose Tolerance (IGT), Impaired Fasting Glucose (IFG) or Type 2 Diabetes Mellitus (T2DM), and obesity are described as the main metabolic diseases related to NAFLD; to the best of our knowledge, there's no evidence of a quantitative relationship between the post-prandial glucoinsulinemic response in obese patients and Liver Stiffness Measurement (LSM). As an audit in our third level nutrition center in Italy, we investigated the potential of data extraction from Oral Glucose Tolerance Tests (OGTTs) with insulin assay in predicting liver stiffness measured with an elastography.

Method: We analyzed data from 267 non cirrhotic patients with obesity or morbid overweight (Body Mass Index, BMI ≥ 27 kg/m²) who underwent both a 75 g OGTT with insulin assay at 0', 60' and 120', and a liver elastography (FibroScan) within a 12 week window. The analysis was performed with R, and we excluded subjects who reported significant alcohol consumption (>1 IU/day women, >2 IU/day men), and those who lost weight or underwent metabolic or weight pharmacotherapy in that time window. After data collection, total insulin and glucose (0'-120') were calculated with the trapezoidal rule, including baseline determinations. Data are reported as median \pm IQR (Interquartile Range), hypothesis testing was lead with a 1% alpha error, and 95% confidence intervals are identified as [CI95].

Results: We evaluated several linear regression models derived from the analysis of the OGTTs. Considering the most practical and efficient model, FIB4 and fasting insulin are necessary, and it has a 33% [20.2–44.1] correlation coefficient, and a median difference of 0.52 ± 0.25 kPa, between estimated and measured LSM. When compared to the measured LSM as a reference, the model predicts subjects with significant liver stiffness (LSM ≥ 8.0 kPa) with a 4% [1–20.4] sensibility and a 98.4% [95.5–99.7] specificity. Post-prandial insulin-resistance MATSUDA index displays a high diagnostic accuracy for an LSM ≥ 8.0 kPa, as expressed by an AUC of 0.7 [0.598–0.802], with a Youden's best cut-off of 1.82 associated to a 76.4% specificity and a 63% sensibility. When considering the subgroup of patients with NAFLD (as by Controlled Attenuation Parameter, CAP ≥ 249 dB/s), the model predicts subjects with LSM ≥ 7.0 kPa with a 16% [4.5–36.1] sensibility and a 100% [92.8–100] specificity.

POSTER PRESENTATIONS

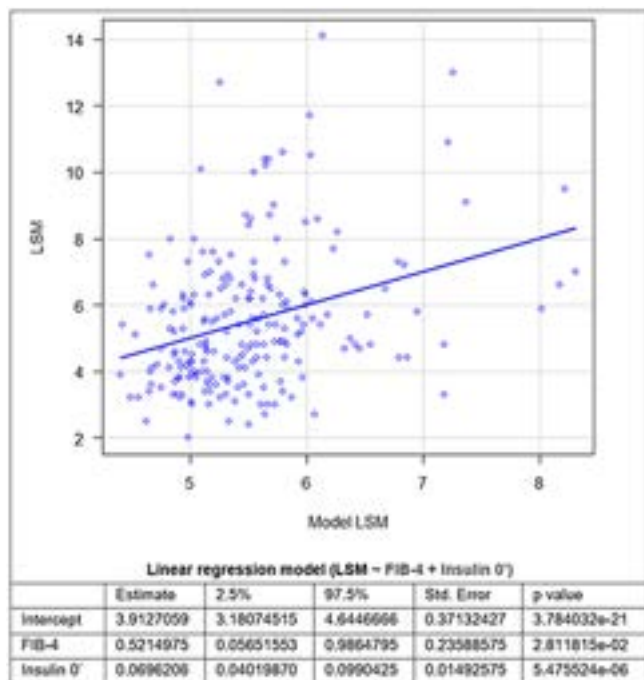


Figure:

Conclusion: Our results support the relationship between fasting and post-prandial insulin levels and liver stiffness in subjects with obesity and morbid overweight. The key strength of our work lies in the innovation of finding a formula that could potentially help rule out significant liver stiffness, strongly linked to fibrosis and advanced liver disease. The main limitations of this work are the relatively small sample size and the possible interaction between hypolipidemic agents and glucose homeostasis. The most practical model to predict liver stiffness in dysmetabolic subjects needs a single blood test with liver enzymes, blood count and fasting insulin, but further studies are needed to either verify our formula or to create more accurate

algorithms to screen patients with obesity at risk for advanced metabolic liver disease.

SAT-458

Lower ALT levels are associated with increased all-cause and cardiovascular mortality in patients with NAFLD in the United States population

Bo Feng¹, Zheng Jiarui². ¹Peking University Hepatology Institute, Peking University People's Hospital, Beijing, China; ²Peking University Hepatology Institute, Peking University People's Hospital, Beijing, China
Email: fengbo@pkuph.edu.cn

Background and aims: The serum alanine aminotransferase (ALT) level is often considered as a marker to evaluate the activity of liver disease and the severity of liver injury. In this study, we aimed to investigate the association between ALT levels and all-cause and cause-specific mortality in non-alcoholic fatty liver disease (NAFLD) patients.

Method: National Health and Nutrition Examination Survey (NHANES)-III from 1988 to 1994 and NHANES-III related mortality data from 2019 were used. NAFLD was defined as hepatic steatosis diagnosed by ultrasound, without other liver diseases. ALT levels were categorized into four groups according to different recommended upper limit of normal in men and women: <0.5 upper limit of normal (ULN), 0.5–1 ULN, 1–2 ULN, ≥2 ULN. The hazard ratios (HRs) for all-cause mortality and cause-specific mortality were analyzed with Cox proportional hazard model.

Results: Multivariate logistic regression analysis demonstrated odds ratio of NAFLD correlated positively with increasing serum ALT levels. In patients with NAFLD, all-cause mortality and cardiovascular mortality are the highest when ALT<0.5ULN, yet cancer-related mortality is the highest when ALT ≥2ULN. The same results could be found in both men and women. Univariate analysis showed that severe NAFLD with normal ALT level had the highest all-cause and cause-specific mortality, but the difference was not statistically significant after adjustment for age and multivariate factors.

Conclusion: The risk of NAFLD was positively correlated with ALT level, but all-cause and cardiovascular mortality were the highest when ALT<0.5ULN. Regardless of the severity of NAFLD, normal or

TABLE 1. Association of ALT level, cardiovascular disease, cancer-related and others-related mortality stratified by the presence/absence of NAFLD.

	Total population		No NAFLD		NAFLD	
	HR (95% CI)	P value	HR (95%CI)	P value	HR (95%CI)	P value
ALT level						
Cardiovascular						
<0.5ULN	1		1		1	
0.5-1ULN	0.74 (0.65-0.85)	<0.001	0.82 (0.68-0.97)	0.022	0.66 (0.52-0.82)	<0.001
1-2ULN	0.63 (0.50-0.79)	<0.001	0.78 (0.56-1.09)	0.149	0.55 (0.39-0.78)	<0.001
≥2ULN	0.63 (0.35-1.12)	0.113	0.70 (0.26-1.86)	0.469	0.68 (0.31-1.50)	0.342
Cancer						
<0.5ULN	1		1		1	
0.5-1ULN	0.74 (0.64-0.86)	<0.001	0.70 (0.58-0.84)	<0.001	0.85 (0.66-1.11)	0.230
1-2ULN	0.67 (0.52-0.86)	0.002	0.61 (0.42-0.88)	0.009	0.77 (0.54-1.12)	0.171
≥2ULN	1.11 (0.67-1.86)	0.682	0.86 (0.35-2.11)	0.738	1.39 (0.70-2.75)	0.346
Others						
<0.5ULN	1		1		1	
0.5-1ULN	0.89 (0.80-0.99)	0.029	0.92 (0.81-1.05)	0.227	0.80 (0.67-0.95)	0.011
1-2ULN	0.98 (0.83-1.16)	0.809	1.25 (0.98-1.60)	0.074	0.73 (0.57-0.93)	0.012
≥2ULN	0.75 (0.51-1.09)	0.131	0.69 (0.33-1.45)	0.331	0.53 (0.32-0.89)	0.015

Note: The multivariate model was adjusted for age, sex, race/ethnicity, body mass index, waist circumference, AST, Alb, TG, TC, HDL, smoking status, diabetes, hypertension, and sedentary lifestyle.

Others: chronic lower respiratory diseases, accidents (unintentional injuries), cerebrovascular diseases, Alzheimer's diseases, diabetes mellitus, influenza and pneumonia, nephritis, nephrotic syndrome and nephrosis and all other causes (residual).

Abbreviations: CI, confidence interval; HR, hazard ratio; NAFLD, nonalcoholic fatty liver disease.

Figure: (abstract: SAT-458).

lower ALT levels are associated with higher mortality than elevated ALT levels. Clinicians should be aware of not only high ALT, indicating liver injury, but also low ALT associated with higher risk of death.

SAT-459

ABDA score: a non-invasive model to identify subjects with fibrotic non-alcoholic steatohepatitis in the community

Shalimar¹, Abhinav Anand¹, Sagnik Biswas¹, Manas Vaishnav¹, Nikhil Tandon². ¹All India Institute of Medical Sciences, New Delhi, Gastroenterology and Human Nutrition, Delhi, India; ²All India Institute of Medical Sciences, New Delhi, Endocrinology, Delhi, India
Email: drshalimar@yahoo.com

Background and aims: Non-alcoholic fatty liver disease (NAFLD) and steatohepatitis (NASH) are prevalent in the community, especially among those with metabolic syndrome. Patients with fibrotic NASH are at increased risk of liver-related-events. Currently available non-invasive tests have not been utilized for screening for fibrotic NASH among the community. We aimed to develop a screening tool for fibrotic NASH among community members.

Method: We included two large cohorts aimed at assessing cardiovascular disease among community members. Fibrotic NASH was defined using FibroScan-AST (FAST) score of ≥ 0.67 that identifies $\geq F2$ fibrosis and NAFLD activity score ≥ 4 with a specificity of 90%. Metabolic parameters, biochemical tests, and anthropometry were used to develop a multivariate model.

Results: The derivation cohort (n = 1660) included a population with median age 45 years, 42.5% males, metabolic syndrome in 66%, and 2.7% (n = 45) with fibrotic NASH. Multivariate analysis identified 4 significant variables (Age, BMI, Diabetes and ALT levels) used to derive the ABDA score. The score had high diagnostic accuracy (area under receiver-operating characteristic curve, AUROC 0.952) with adequate internal validity (Figure). ABDA score ≥ -3.52 identified fibrotic NASH in the derivation cohort with a sensitivity and specificity of 88.9% and 88.3%. The score was validated in a second cohort (n = 357) that included 21 patients (5.9%) with fibrotic NASH, where it demonstrated a high AUROC (0.948), sensitivity (81%) and specificity (89.3%).

Conclusion: ABDA score utilizes four easily available parameters to identify fibrotic NASH with high accuracy in the community.

SAT-460

Evaluation of serum biomarkers for the diagnosis of non-alcoholic fatty liver disease in the general population: a cross-sectional Spanish population-based study

Jesús Rivera^{1,2,3}, Paula Iruzubietta⁴, Alba Jiménez-Masip¹, Ramiro Manzano^{1,2}, Elba Llop⁵, Christie Perelló⁵, Marta Hernández Conde⁵, María Teresa Arias Loste⁴, María Del Barrio Azaceta⁴, Desamparados Escudero-García⁶, Miguel Serra⁶, Juan M Pericas^{1,2}, José Luis Calleja Panero⁵, Javier Crespo⁴. ¹Vall d'Hebron Hospital Universitari, Liver Unit, Spain; ²Vall d'Hebron Institut of Research (VHIR), Spain; ³Universitat Autònoma de Barcelona, Bellaterra, Barcelona, Spain; ⁴Hospital Universitario Marqués de Valdecilla, Spain; ⁵Hospital Universitario Puerta de Hierro, Spain; ⁶Hospital Clínico de Valencia, Spain
Email: jesusriveraest@gmail.com

Background and aims: Non-alcoholic fatty liver disease (NAFLD) is a highly prevalent entity that relies on non-invasive tests (NITs) for disease detection and stratification. Serological NITs for steatosis are useful tools for the initial assessment of NAFLD, whereas validation studies in different populations are needed. The study aimed to evaluate the diagnostic accuracy of serological NITs in the general population from Spain and to investigate the correlation between these tests and the controlled attenuation parameter (CAP) of transient elastography (TE).

Method: Multicentric, cross-sectional study based on a representative cohort of the general adult population in Spain (PREVHEP-ETHON) with TE and CAP data. We excluded subjects with suspected viral hepatitis or excessive alcohol consumption (≥ 15 units/day). The reference test was the TE-CAP and a value ≥ 275 dB/m was considered diagnostic of NAFLD. A liver stiffness ≥ 8 kPa was considered suggestive of significant fibrosis. We evaluated the diagnostic ability of Fatty Liver Index (FLI), Fatty Liver Disease (FLD) index, Hepatic Steatosis Index (HSI), Lipid Accumulation Product (LAP) index, NAFLD index, Visceral Adiposity Index (VAI), and Zhejiang University (ZJU) index. The area under the curve (AUC) and the predictive values (PV) for NAFLD applying the foreknown cut-offs were calculated in the overall cohort and specifically in obese patients (body mass index ≥ 30 kg/m²). In addition, we assessed the concordance to confirm or exclude NAFLD using Cohen's Kappa index (k) and the correlation between the different indices and TE-CAP using Pearson's linear test (r).

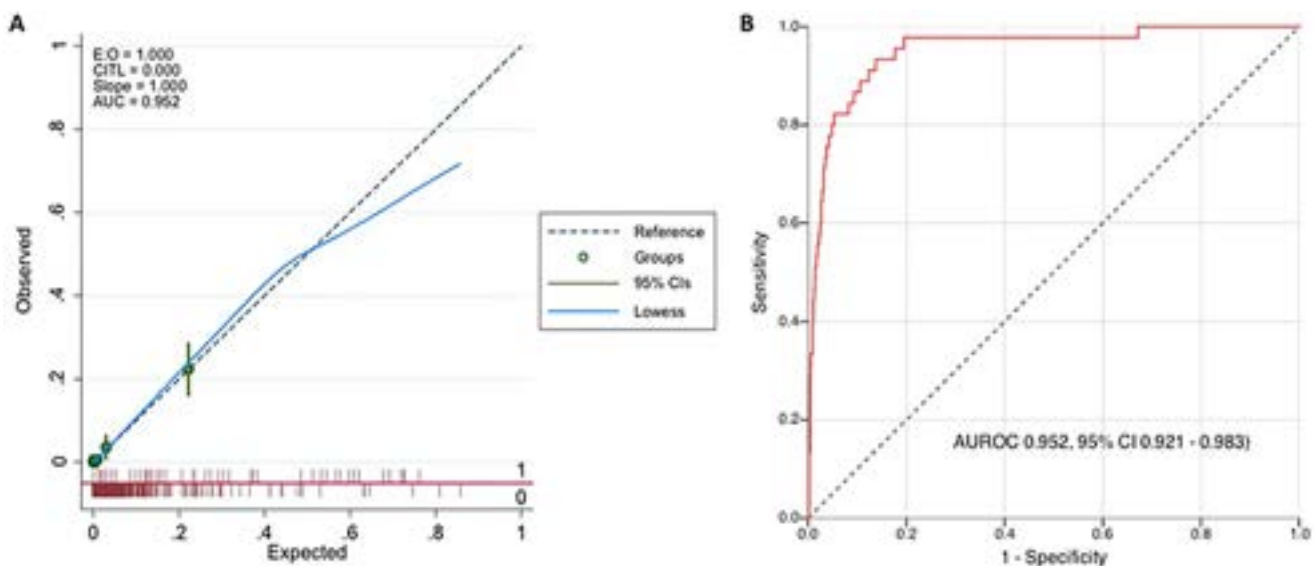


Figure: (abstract: SAT-459): (A) Hosmer Lemeshow calibration plot, with Loess smoothing, for the prediction model in the overall derivation cohort showing satisfactory fit. EO: expected/observed ratio; CITL: calibration-in-the-large; AUC: area under the curve; Loess (B) Receiver operating characteristic (ROC) curve for the ABD score in predicting fibrotic non-alcoholic steatohepatitis (NASH) in the derivation cohort.

POSTER PRESENTATIONS

Results: We included 9637 patients, 4268 (44.2%) of whom had TE-CAP data. The estimated prevalence of NAFLD was 33.0%. NAFLD subjects were predominantly male (54.8 vs 37.5%; $p < 0.001$), had a higher median age (55 (47–64) vs 48 (42–57) years; $p < 0.001$), and a higher metabolic burden than those without NAFLD ($p < 0.001$ for all metabolic diseases). Overall, serological NITs showed an adequate diagnostic ability (AUC > 0.70), showing FLI the highest diagnostic accuracy (AUC 0.81; 95%CI 0.79–0.82), a NPV of 89.6% and a PPV of 63.2% for FLI 30 and 60, respectively. Besides, FLI had a proper concordance ($k = 0.45$) and linear correlation ($r = 0.55$) with TE-CAP. In obese individuals, the diagnostic accuracy of serological NITs decreased significantly, presenting FLI an AUC of 0.72 (95%CI 0.69–0.76), and an AUC < 0.70 for the rest of the indices. Finally, when tested for significant fibrosis evaluation, FLI showed the highest AUC (0.72–95%CI 0.67–0.76-) of the studied NITs.

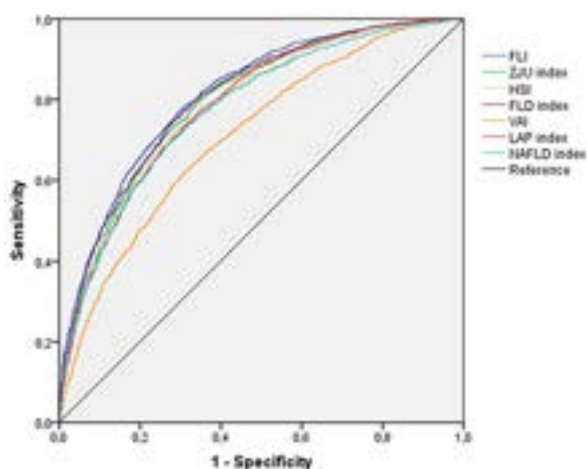


Figure: ROC curves of the serologic indices for NAFLD detection in the general population from Spain.

Conclusion: The serological indices of steatosis, particularly FLI, represent a valid option for NAFLD approaches in the general Spanish population. Further data are needed in high-risk populations, such as people living with obesity, along with histologically-back tested and cost-effectiveness studies to define the best diagnostic strategy for NAFLD at the population level.

SAT-461

MorphoQuant, the first fully-automated morphometric software for the assessment of liver biopsy, identified significant differences between non-alcoholic fatty liver disease and steatohepatitis biopsies

Cindy Serdjebi¹, Bastien Lepoivre², Florine Chandes², Linda Willis³, Julé Yvon². ¹Biocellvia, Marseille, France; ²Biocellvia, Marseille, France; ³Histologix Ltd, United Kingdom
Email: cindy.serdjebi@biocellvia.com

Background and aims: Non-alcoholic steatohepatitis (NASH) is the most severe form of fatty liver diseases, and no treatment has been approved so far. Among the reasons for this lack of valid pharmacological treatment, the subjectivity and variability in the pathology reading has been identified as a confounding factor, probably weakening the ability to assess a treatment effect. We have developed the first fully-automated user-independent morphometric software (MorphoQuant) allowing the assessment of liver biopsies and investigated its performance.

Method: 271 liver biopsies were collected and analyzed. Patients were scored by a blinded expert pathologist according to the NASH CRN for steatosis, inflammation, ballooning and fibrosis using hematoxylin-eosin (HandE) and Masson's trichrome stained slides. MorphoQuant, a fully automated and deterministic artificial intelligence, based on morphometry and expert system-completely independent from pathologist's annotations, was developed to assess NASH features. For digital quantification, slides were stained with HandE (inflammation area, and number of foci), picosirius red (PSR) alone or combined with CK19 (steatosis, vesicle size, total

Table(abstract: SAT-461): Comparison of MorphoQuant readouts in non-NASH versus NASH biopsies

MorphoQuant Readout	Non-NASH biopsies* (mean; min-max; n)	NASH biopsies** (mean; min-max; n)	Mann-Whitney p-value
Steatosis S (%)	7.89 (0.81 - 23.55; 74)	10.24 (1.186 - 28.23; 175)	0.0001
Steatosis T (%)	8.609 (1.044 - 1.358; 74)	11.28 (1.358 - 30.13; 175)	<0.0001
Vesicle area (μm^2)	119.9 (34.93 - 273.5; 73)	137.1 (43.23 - 422.2; 175)	0.002
Inflammation area (mm^2)	4.784 (0 - 13.96; 68)	8.094 (0.035 - 25.70; 164)	<0.0001
Number of foci (mm^2)	19.81 (0 - 58.34; 68)	28.99 (0.447 - 78.5; 164)	<0.0001
CD68 (%)	2.943 (1.885 - 5.031; 42)	2.955 (1.586 - 5.118; 61)	0.4291
hCLS (n/ mm^2)	0.1441 (0 - 0.909; 42)	0.4180 (0 - 3.771; 61)	<0.0001
Shh (‰)	3.270 (0.046 - 18.35; 63)	6.428 (0.06 - 44.88; 149)	<0.0001
Ballooned/injured area (‰)	1.943 (0 - 14.15; 63)	6.632 (0 - 82.06; 149)	<0.0001
Collagen S (%)	7.470 (1.917 - 20.22; 74)	7.195 (1.246 - 19.96; 174)	0.2195
Collagen T (%)	8.918 (2.671 - 24.44; 74)	8.909 (1.580 - 22.34; 174)	0.4887
Periductular collagen (%)	3.098 (0.508 - 8.441; 40)	4.774 (0.5230 - 13.84; 53)	0.0029
Perisinudoisal collagen (%)	3.134 (0.8860 - 8.031; 75)	2.444 (0.4790 - 5.857; 174)	<0.0001
Perivascular collagen (%)	2.969 (0.465 - 12.86; 75)	3.179 (0.181 - 11.60; 174)	0.2372
Septal collagen (%)	0.6122 (0.0780 - 4.919; 75)	0.8740 (0.0270 - 3.469; 174)	0.0001
CK19 (%)	0.1438 (0.002 - 0.4890; 40)	0.2049 (0.003 - 0.970; 52)	0.02

* NAFLD Activity Score (NAS) < 5

** NAS ≥ 5

bold italic: significant

hCLS: hepatic crown-like structures

collagen, periductular, perisinusoidal, perivascular and septal collagens), labelled with CD68 (CD68 and hepatic crown-like structures) or with Sonic hedgehog (Shh and ballooning/injury), and digitized as whole slide images. MorphoQuant readouts of NASH (NAS ≥ 5) and non-NASH (NAS < 5) biopsies were compared using a Mann-Whitney test.

Results: A total of 929 slides were processed for histology and digitized for quantitative image analysis by MorphoQuant. Steatosis and size of lipid vesicles were significantly higher in NASH patients. The inflammation area, the number of foci and of hepatic crown-like structures were also higher in NASH patients, while CD68 expression did not increase. Ballooning, as investigated through the expression of Shh and injury area, were also shown to be significantly higher in NASH patients. Regarding collagen, collagen proportionate area and perivascular collagen was equivalent in both NASH and non-NASH patients, while perisinusoidal collagen was lower in NASH patients. Periductular and septal collagen were more important in NASH patients, along with CK19 expression.

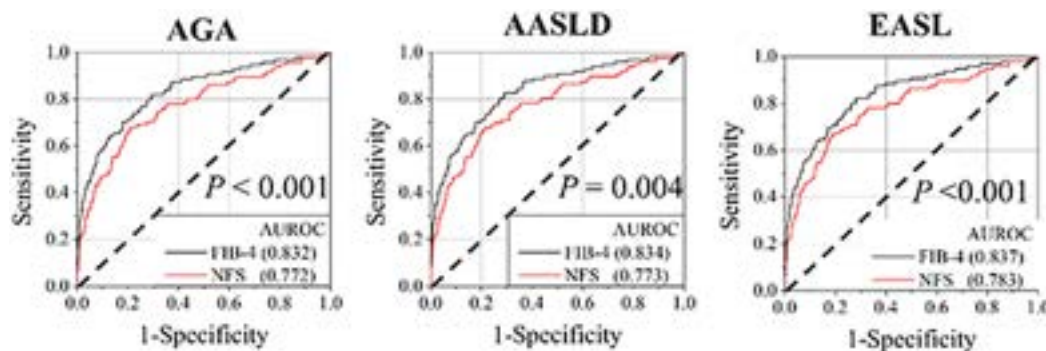
Conclusion: The current study demonstrates that MorphoQuant is a powerful image analysis tool, using current and original histological methods. In addition, this study highlights that a reliable digital pathology software can be developed independently from pathologist's annotations.

SAT-462

Diagnostic performance of fibrosis-4 index and NAFLD fibrosis score in at-risk group from low prevalence population

Huiyul Park¹, Mimi Kim², Sang Bong Ahn³, Hyo Young Lee⁴, Jun-Hyuk Lee⁵, Eileen Yoon⁶, Chul-min Lee², Bo-Kyeong Kang², Joo Hyun Sohn¹, Jihyun An⁶, Joo Hyun Oh³, Hye-Lin Kim⁷, Hyunwoo Oh⁴, Jang Han Jung⁸, Dae Won Jun⁶, Eun Chul Jang⁹.
¹Myoungji Hospital, Hanyang University College of Medicine, Korea, Rep. of South; ²Hanyang University, College of Medicine, Department of Radiology, Korea, Rep. of South; ³Nowon Eulji Medical Center, Eulji University School of Medicine, Korea, Rep. of South; ⁴Uijeongbu Eulji Medical Center, Eulji University College of Medicine, Department of Internal Medicine, Korea, Rep. of South; ⁵Nowon Eulji Medical Center, Eulji University School of Medicine, Department of Family Medicine, Korea, Rep. of South; ⁶Hanyang University, College of Medicine, Department of Internal Medicine, Korea, Rep. of South; ⁷Sahmyook University, College of Pharmacy, Korea, Rep. of South; ⁸Dongtan Sacred Heart Hospital of Hallym University Medical Center, Korea, Rep. of South; ⁹Soonchunhyang University College of Medicine, Korea, Rep. of South
 Email: noshin@hanyang.ac.kr

Background and aims: A non-invasive screening test for hepatic fibrosis is recommended in at-risk group (those with fatty liver, elevated liver enzymes, diabetes, and ≥ 2 metabolic risk factors). The performances of fibrosis-4 index (FIB-4) and non-alcoholic fatty liver disease (NAFLD) fibrosis score (NFS) have not been evaluated in at-risk group. We aimed to evaluate the diagnostic performance of FIB-4



Populations	Risk factors				
	Fatty liver	Diabetes	Abnormal liver enzyme	Metabolic risk factors	Obesity
At risk group in AGA	o	o	o	o (≥ 2)	x
At risk group in AASLD	o	o (Prediabetes)	o	o (≥ 2)	o
At risk group in EASL	o	o	o	o (≥ 3) or CVD	o (Overweight)

Figure 1. Receiver operating characteristic (ROC) curves for diagnosis of advanced fibrosis by FIB-4 or NFS in at-risk group in various guidelines.

The definition of at-risk group according to different guidelines was summarized at table.

P-value when ROC curve by FIB-4 was compared with ROC curve by NFS in at-risk population

Abbreviation: AASLD, American Association for the Study of Liver Diseases; AGA, American Gastroenterological Association; AUROC, area under receiver operating characteristic; CVD, cardiovascular disease; EASL, European Association for the Study of Liver; LFT, liver function test; NFS, NALFD, non-alcoholic fatty liver disease; NAFLD fibrosis score; FIB-4, fibrosis-4 index.

Figure: (abstract: SAT-462).

POSTER PRESENTATIONS

and NFS in at-risk group with advanced hepatic fibrosis in a population with low prevalence of hepatic fibrosis.

Method: This retrospective, cross-sectional study included 8,545 participants who underwent magnetic resonance elastography (MRE) at 13 nationwide health-promotion centers during a routine health check-up. The area under the receiver-operating characteristic (AUROC) curves of FIB-4 and NFS were compared using DeLong's test.

Results: Overall, 67.4% of individuals in health check-up cohort without the risk of viral or alcoholic hepatitis was at-risk group. At-risk group and those with NAFLD had comparable rates of significant and advanced (9.2% vs. 8.9% and 2.8% vs. 2.3%, respectively) hepatic fibrosis; furthermore, the AUROCs of FIB-4 (0.832 vs. 0.826, respectively; $p=0.873$) and NFS (0.772 vs. 0.803, respectively; $p=0.457$) in advanced hepatic fibrosis were similar them. However, the AUROC (0.772 vs 0.832, respectively; $p<0.001$) and sensitivity (61.7% vs 71.6%, respectively) in the at-risk group were lower for NFS than those for FIB-4. This feature was consistently observed, regardless of the kinds of guidelines such as American Gastroenterological Association (AGA) (0.832 in FIB-4 vs. 0.772 in NFS, $p<0.001$), American Association for the Study of Liver Diseases (AASLD) (0.834 in FIB-4 vs. 0.773 in NFS, $p=0.004$), and European Association for the Study of Liver (EASL) (0.837 in FIB-4 vs. 0.783 in NFS, $p<0.001$).

Conclusion: The diagnostic performance of FIB-4 in at-risk group in a low-prevalence population is comparable to that in individuals with NAFLD. However, the diagnostic performance and sensitivity of NFS in at-risk group were low.

SAT-463

A diagnostic non-invasive model for liver advanced fibrosis and cirrhosis in chronic hepatitis B (CHB) concurrent with non-alcoholic fatty liver disease (NAFLD) based on machine learning (ML)

Jie Li¹, Yayun Xu², Fajuan Rui¹, Xiaorong Tian³, Qi Xue⁴, Qi Zheng⁵, Qing-Lei Zeng⁶, Zebao He⁷, Jian Wang¹, Weimao Ding⁸, Chuanwu Zhu⁹, Yuanwang Qiu¹⁰, Yunliang Chen³, Junqing Fan³, Junping Shi¹¹, Chao Wu¹. ¹Nanjing Drum Tower Hospital, The Affiliated Hospital of Nanjing University Medical School, Nanjing, Jiangsu, China, China; ²Shandong Provincial Hospital, Shandong University, Ji'nan, Shandong, China; ³School of Computer Science, China University of Geosciences, Wuhan, China; ⁴Shandong Provincial Hospital Affiliated to Shandong First Medical University, Ji'nan, Shandong, China; ⁵Hepatology Research Institute, the First Affiliated Hospital, Fujian Medical University, Fuzhou, China; ⁶The First Affiliated Hospital of Zhengzhou University, Zhengzhou, Henan, China; ⁷Taizhou Enze Medical Center (Group) Enze Hospital, Taizhou, Zhejiang, China; ⁸Huai'an No. 4 People's Hospital, Huai'an, Jiangsu, China; ⁹The Affiliated Infectious Diseases Hospital of Soochow University, Suzhou, Jiangsu, China; ¹⁰The Fifth People's Hospital

of Wuxi, Wuxi, Jiangsu, China; ¹¹The Affiliated Hospital of Hangzhou Normal University, Hangzhou, Zhejiang, China
Email: lijie@sina.com

Background and aims: As NAFLD is prevalent globally, the concurrence of chronic hepatitis B (CHB) with non-alcoholic fatty liver disease (NAFLD) is increasing. But there are still lack of non-invasive models to accurately evaluate liver advanced fibrosis and cirrhosis in those patients. This study aimed to establish a novel diagnostic model for liver advanced fibrosis and cirrhosis in CHB patients concurrent with NAFLD based on machine learning (ML).

Method: This study consecutive enrolled CHB patients concurrent with NAFLD underwent liver biopsy and laboratory examination from six medical centers of China between April 2004 and September 2021 as training cohort and patients from other three medical centers of China between April 2004 and October 2020 as independent external validation cohort. We implemented ML models including gaussian naive bayes (GNB) and logistic regression (LR) to predict advanced fibrosis ($S \geq 3$) and cirrhosis ($S = 4$). Pearson correlation coefficient was used to explore the correlation between 29 clinical features and fibrosis grade. The features with the absolute value >0.2 of Pearson correlation coefficient were included in the diagnostic model. To avoid overfitting, 5-fold cross validations were used in the ML models building process. Model performance was compared to fibrosis index based on the four factors (FIB-4), activated partial thromboplastin time (APRI), and NAFLD Fibrosis Score (NFS) in patients of CHB concurrent with NAFLD.

Results: A total of 1427 CHB patients with NAFLD underwent liver biopsy were enrolled, with a average age of 38 (32–47) years (1093 males and 334 females). 298 cases (20.9%) have advanced fibrosis ($S \geq 3$), and 118 cases (8.3%) have cirrhosis ($S = 4$). Prothrombin time (PT) was positively associated with advanced fibrosis and cirrhosis, and albumin (ALB), platelet (PLT) were negatively associated with advanced fibrosis and cirrhosis. GNB model had the best performance, and its AUC for the diagnosis of advanced fibrosis and cirrhosis were 0.770 (0.714–0.827), 0.844 (0.795–0.893) in training cohort, and 0.716 (0.669–0.762), 0.812 (0.772–0.853) in validation cohort, which was significantly better than that of FIB-4, APRI and NFS (all $P < 0.05$).

Conclusion: GNB model performed better overall than FIB-4, APRI, and NFS. ML could be an effective tool for identifying clinically liver fibrosis and cirrhosis in CHB patients concurrent with NAFLD.

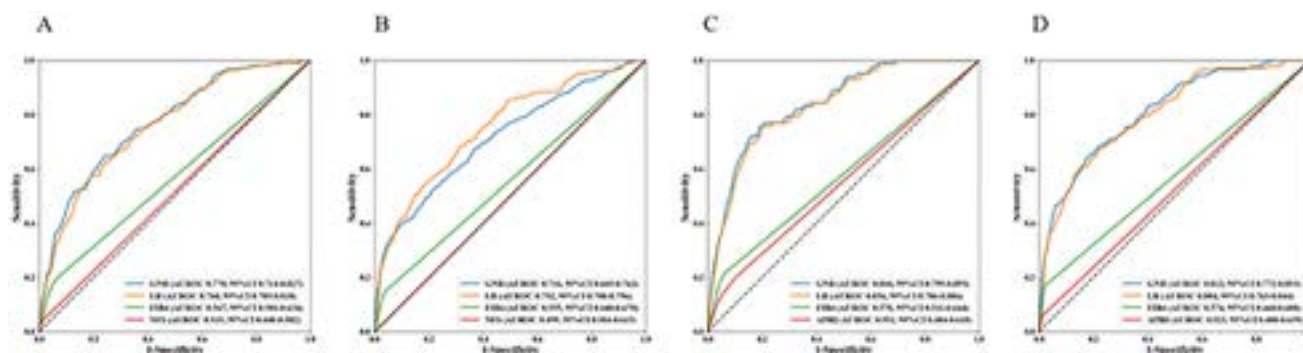


Figure: (abstract: SAT-463): AUC of machine learning models for fibrosis grade in training cohort and validation cohort: A. Advanced fibrosis ($\geq S3$) in training cohort; B. Advanced fibrosis ($\geq S3$) in validation cohort; C. Cirrhosis ($S = 4$) in training cohort; D. Cirrhosis ($S = 4$) in validation cohort.

SAT-464

Effect of diabetes mellitus and fatty liver on hepatic fibrosis

Byung Ik Kim¹, Yong Kyun Cho¹, Jung Hee Kim², Ju-Yeon Cho³, Jae Yoon Jeong⁴, Won Sohn¹. ¹Kangbuk Samsung Hospital, Sungkyunkwan University School of Medicine, Korea, Rep. of South; ²Hallym University Dongtan Sacred Heart Hospital, Korea, Rep. of South; ³Chosun University Hospital, Korea, Rep. of South; ⁴National Medical Center, Korea, Rep. of South
Email: hand0827@naver.com

Background and aims: Diabetes mellitus is associated with fatty liver and hepatic fibrosis. However, it is unclear whether there is a risk of hepatic fibrosis in diabetes without fatty liver or no diabetes with fatty liver. This study aimed to investigate the risk factors for significant fibrosis in patients according to the presence of diabetes and fatty liver.

Method: A cross-sectional study was conducted based on a cohort from a health examination program which included magnetic resonance elastography (MRE). We classified four groups according to diabetes mellitus and fatty liver: Group 1, no diabetes without fatty liver; Group 2, no diabetes with fatty liver; Group 3, diabetes without fatty liver; Group 4, diabetes with fatty liver. Fatty liver was evaluated by ultrasonography. Significant fibrosis was defined as liver stiffness measurement (LSM) ≥ 2.97 kPa on MRE. We evaluated the difference in significant fibrosis by four groups and analyzed the risk factors for significant fibrosis after adjusting for confounding factors.

Results: A total of 1,899 subjects were included. The number of Group 1, Group 2, Group 3, and Group 4 was 902 (47%), 796 (42%), 47 (3%), and 154 (8%), respectively. Mean values of LSM in Group 1, 2, 3, and 4 were 2.34 ± 0.31 kPa, 2.42 ± 0.37 kPa, 2.49 ± 0.51 kPa, and 2.66 ± 0.70 kPa, respectively ($p < 0.001$). There was a significant difference in significant fibrosis (≥ 2.97 kPa) between four groups: 2.3%, 3.6%, 6.4%, and 19.5% in Group 1, 2, 3, and 4, respectively ($p < 0.001$). The multivariable-adjusted hazard ratios (aHR) with 95% confidence intervals (CI) for significant fibrosis comparing Group 4, Group 3, and Group 2 to Group 1 were 4.35 (2.14–8.85), 2.43 (0.65–9.12), and 0.96 (0.50–1.85), respectively ($p < 0.001$, $p = 0.197$, and $p = 0.907$).

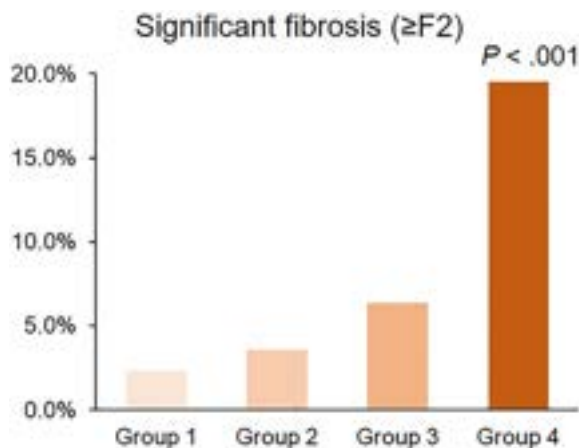


Figure:

Conclusion: The risk of significant fibrosis is high in patients with diabetes and fatty liver rather than those who have one of each. Although all patients with fatty liver have the risk of hepatic fibrosis, it is needed to assess and manage hepatic fibrosis in patients accompanied by diabetes in particular.

SAT-465

High performance of serological indexes in the non-invasive assessment of liver steatosis

Beatriz Pillado Pérez¹, Carlota Siljestrom Berenguer¹, Luis Eduardo Pariente Zorrilla¹, Marta Abadia¹, Gloria Ruiz-Fernandez¹, Joaquin Poza¹, Eva Marín¹, Carmen Amor¹, Clara Amiana Roig¹, Irene Gonzalez Diaz¹, Miriam Romero¹, Araceli García-Sánchez¹, Maria Dolores Martin-Arranz¹, Antonio Olveira Martin¹. ¹Hospital La Paz, Spain
Email: beapillado@gmail.com

Background and aims: steatosis biomarkers are well validated by clinical guidelines but are not used frequently in daily practice. They are mainly used for epidemiological studies or in situations in which other techniques such as ultrasound or controlled attenuation parameter (CAP) are not available. Their real diagnostic value is limited because most studies compare them with ultrasound, CAP or magnetic resonance imaging (MRI) and not with liver biopsy which is still currently the gold standard. We aimed to determine diagnostic value and limitations of steatosis biomarkers using liver biopsy as reference.

Method: we performed a prospective study that included all patients undergoing hepatic biopsy. Clinical, anthropometric, laboratory, ultrasonographic and CAP (EchoSens' Fibroscan 502 Touch) were measured on the same day before the liver biopsy. Hepatic Steatosis Index (HSI: sex, body mass index [BMI], alanine aminotransferase [ALT], aspartate aminotransferase [AST], diabetes), Fatty Liver Index (FLI: BMI, waist circumference, gamma-glutamyl transferase [GGT], triglycerides) and TyG (triglycerides, glucose) were calculated. Biopsies were performed percutaneously using Tru-cut 16/18G needles. Exclusion criteria were biopsy length < 1.5 cm or < 11 portal tracts, focal lesions, acute hepatitis. Steatosis was diagnosed if liver fat content $> 5\%$ on biopsy. Receiver operating characteristic (ROC) curves were performed to calculate the performance of the three steatosis biomarkers and CAP.

Results: 245 patients were included between March/20 and October/22. The majority of patients were male (59.8%), and the mean age was 54 years. Mean BMI was 27.4 kg/m². With regard to liver histology, 42% of patients did not have steatosis, mild steatosis (6–33%) was detected in 23% and moderate (33–66%) or severe steatosis ($> 66\%$) in the remaining 35%. Liver fibrosis was not present in 48.4% of patients, mild fibrosis (F1/F2) was detected in 33.9% and advanced fibrosis (F2/F4) was seen in 17.7%. According to the aetiology, 44% of patients had Metabolic-associated Fatty Liver Disease, 18.5% autoimmune diseases, 2.4% genetic diseases, 1.6% alcoholic diseases, 22% normal biopsies and 11.5% other findings. Figure 1 summarises results.

Figure:

	Optimal cut-off value	Sens (%)	Spec (%)	PPV (%)	NPV (%)	AUC	CI 95%
N = 245							
CAP (dB/m)	254	78	78	81.1	74.6	0.83	0.78–0.88
FLI	60.2	74.8	75.9	78.5	71.9	0.81	0.76–0.87
TyG	4.42	91	58	72	84.4	0.81	0.75–0.86
HSI	41.8	60.9	73.2	73	61.2	0.72	0.66–0.79

Sens: sensitivity, spec: specificity, PPV: positive predictive value, NPC: negative predictive value, AUC: area under the curve, CI: confidence interval, CAP: Coefficient Attenuated Parameter, FLI: Fatty Liver Index, TyG: triglycerides, glucose, HSI: Hepatic Steatosis Index.

Conclusion: steatosis biomarkers FLI and TyG are an excellent tool for the non-invasive diagnosis of steatosis

POSTER PRESENTATIONS

SAT-466

Fibrosis-4 and M2BPGi combination screening algorithm for screening advanced hepatic fibrosis in diabetes is cost-effective

Mimi Kim¹, Dae Won Jun¹, Hye-Lin Kim², Eileen Yoon¹, Se Young Jang³, Ki Tae Yoon⁴, Young Youn Cho⁵, Hoon Gil Jo⁶, Yang-Hyun Baek⁷, Sang Yi Moon⁷, Aejeong Jo¹. ¹Hanyang University, College of Medicine, Korea, Rep. of South; ²Sahmyook University, College of Pharmacy, Korea, Rep. of South; ³Kyungpook National University, Kyungpook National University Hospital, Daegu, South Korea, Korea, Rep. of South; ⁴Pusan National University, Korea, Rep. of South; ⁵Chung-Ang University Hospital, Seoul, Korea, Korea, Rep. of South; ⁶Wonkwang University College of Medicine and Hospital, Korea, Rep. of South; ⁷Department of Internal Medicine, Dong-A University College of Medicine, Busan, South Korea, Korea, Rep. of South
Email: noshin@hanyang.ac.kr

Background and aims: The advanced hepatic fibrosis screening strategy using FIB-4-based non-invasive tests (NITs) in diabetes has been shown low sensitivity and specificity, so it is recommended to perform transient elastography (TE) or MR elastography (MRE) first, or combination with NITs. However, TE or MRE is often not available to primary care physicians (PCPs), and screening algorithm in which PCPs first use NITs followed by further evaluation at a tertiary hospital may increase the rates of unnecessary referrals. This study aimed to find out whether the FIB-4 and M2BPGi combination screening algorithm reduces unnecessary referral rates and is cost-effective for diabetic patients in PCPs settings.

Method: We constructed a combined model of the decision tree model and Markov model to compare expected costs and quality-adjusted life-years (QALYs) between 'screening' and 'no screening' groups from healthcare system perspectives. CVD and extrahepatic malignancy conditions potentially related to diabetes and hepatic fibrosis were also included in the model. Patients diagnosed with advanced fibrosis in the screening group were given intensive lifestyle intervention (ILI). Screening strategies compared in our model were (1) M2BPGi, (2) Fibrosis-4 (FIB4), (3) NAFLD fibrosis score (NFS), (4) AST to platelet ratio index (ARPI) (5) FIB4+M2BPGi (6) NFS+M2BPGi (7) ARPI+M2BPGi. The prevalence of advanced fibrosis (7.9%) and diagnostic performance of each screening strategy were obtained from cohort data of 9,850 health check-up examiners from 13 health examination centers, and 809 diabetes patients from six tertiary hospitals, respectively. The incremental cost-effectiveness

ratio (ICER) was calculated for 20-year horizon. We conducted various sensitivity analyses for varying input values and assumptions. **Results:** In the base-case analysis, the estimated ICERs for all the screening strategies were shown below \$25,000/QALY which is regarded as an implicit ICER threshold in Korea. FIB-4 with M2BPGi combination screening was not only cost-effective but also was shown to have a lower false positive rate than others, which led to decreasing referral rate to a tertiary hospital. This tendency was more pronounced when the MRE, which has a more precise performance than the TE, was used in the second step. The unnecessary referral rate was 45.4%-46.3% in the single algorithm of M2BPGi and FIB-4, but it decreased to 23.0% in their combination.

Conclusion: The FIB-4 and M2BPGi combination screening algorithm reduces 23.3% unnecessary referral rate compared to FIB-4 screening and is cost-effective for diabetic patients in PCPs setting.

SAT-467

Performance of non-invasive markers in evaluating presence and severity of liver fibrosis in non-alcoholic fatty liver disease: results from a multi-ethnic Asian cohort of biopsy-proven non-alcoholic fatty liver disease patients

En Ying Tan¹, Sin Hui Melissa Chua¹, Eunice Tan¹, Daniel Huang¹, Jonathan Lee¹, Margaret Teng¹, Nur Halisah Binte Jumat¹, Yock Young Dan¹, Mark Muthiah¹. ¹National University Hospital (NUH)-Singapore, Department of Gastroenterology and Hepatology, Singapore, Singapore
Email: tanenying@hotmail.com

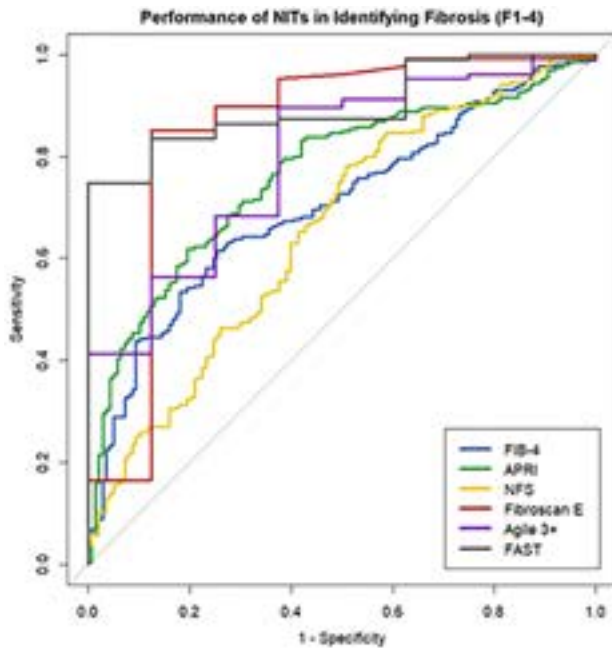
Background and aims: Non-alcoholic fatty liver disease (NAFLD) is the most common liver disease worldwide. It is an umbrella term for a spectrum of disease including hepatic steatosis, non-alcoholic steatohepatitis, fibrosis and cirrhosis. Evaluation for presence and degree of fibrosis is essential in prognostication, determining treatment plans and monitoring response to therapy. Historically, liver biopsy has been the gold standard for achieving this. However, significant shortcomings such as procedural complications, poor patient acceptance, cost and availability issues, sampling error and intra/inter-observer variability have driven development and adoption of non-invasive tests. We aim to evaluate the performance of various NITs in evaluating fibrosis in a multi-ethnic Asian cohort of biopsy-proven NAFLD patients.

Table 1. Base-case analyses by screening strategy (compared to 'No screening')

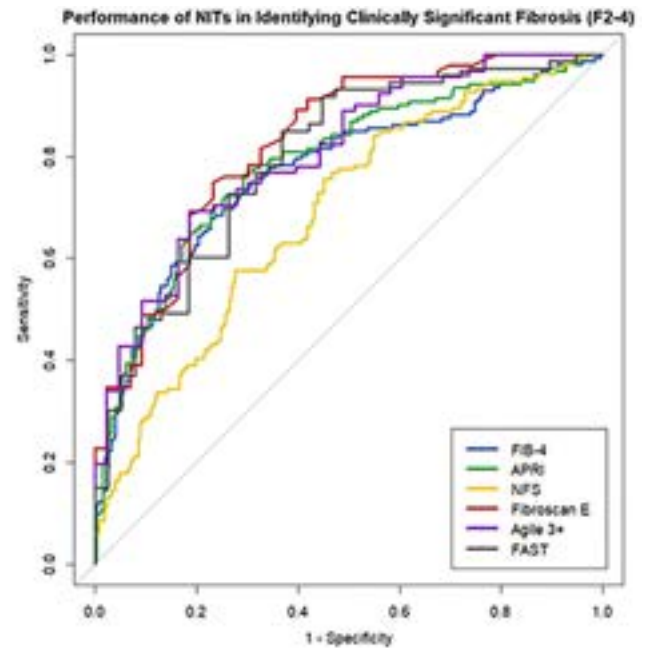
Strategy	Sensitivity	Specificity	ICER (\$/QALY)	TP	FP	TN	FN	Refer rate	Unnecessary referral proportion
Followed by MRE (Sensitivity 88%; Specificity 90%)									
M2BPGi, 0.8	73.1%	54.1%	12,648	5.1%	4.2%	87.9%	2.8%	9.3%	45.4%
FIB4, 1.3	85.3%	44.3%	11,142	5.9%	5.1%	87.0%	2.0%	11.1%	46.3%
NFS, -1.455	84.4%	27.3%	12,463	5.9%	6.7%	85.4%	2.0%	12.6%	53.3%
ARPI, 0.5	69.5%	78.5%	9,261	4.8%	2.0%	90.1%	3.1%	6.8%	29.0%
FIB-4+M2BPGi	57.5%	87.0%	11,079	4.0%	1.2%	90.9%	3.9%	5.2%	23.0%
NFS+M2BPGi	74.7%	68.8%	11,629	5.2%	2.9%	89.2%	2.7%	8.1%	35.6%
ARPI+M2BPGi	68.2%	63.1%	12,375	4.7%	3.4%	88.7%	3.2%	8.1%	41.7%
Followed by TE (Sensitivity 85%; Specificity 75%)									
M2BPGi, 0.8	73.1%	54.1%	11,607	4.9%	10.6%	81.5%	3.0%	15.5%	68.3%
FIB4, 1.3	85.3%	44.3%	10,349	5.7%	12.8%	79.3%	2.2%	18.6%	69.1%
NFS, -1.455	84.4%	27.3%	11,232	5.7%	16.7%	75.4%	2.2%	22.4%	74.7%
ARPI, 0.5	69.5%	78.5%	8,957	4.7%	4.9%	87.1%	3.2%	9.6%	51.4%
FIB-4+M2BPGi	57.5%	87.0%	10,706	3.9%	3.0%	89.1%	4.0%	6.9%	43.6%
NFS+M2BPGi	74.7%	68.8%	10,979	5.0%	7.2%	84.9%	2.9%	12.2%	58.8%
ARPI+M2BPGi	68.2%	63.1%	11,478	4.6%	8.5%	83.6%	3.3%	13.1%	64.9%

ARPI, aspartate aminotransferase to platelet ratio; FIB-4, fibrosis-4; FN, false negative; FP, false positive; ICER, incremental cost-effectiveness ratio; MRE, MR elastography; NFS, NAFLD fibrosis score; TE, transient elastography; TN, true negative; TP, true positive; QALY, quality-adjusted life-year

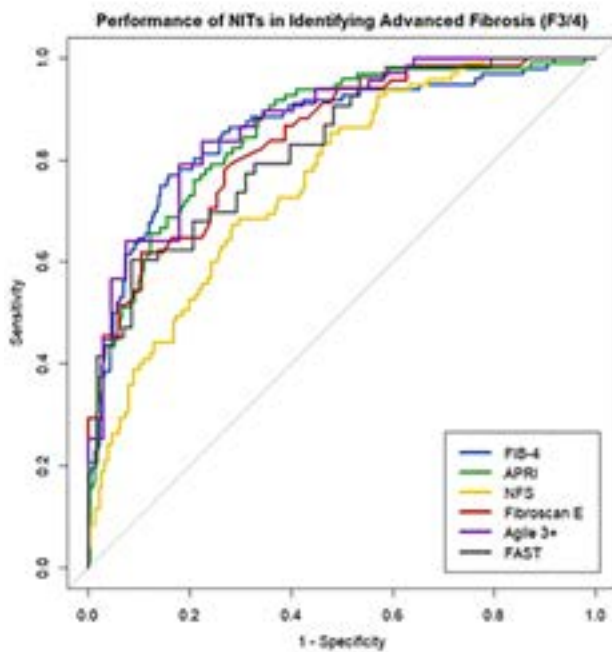
Figure: (abstract: SAT-466).



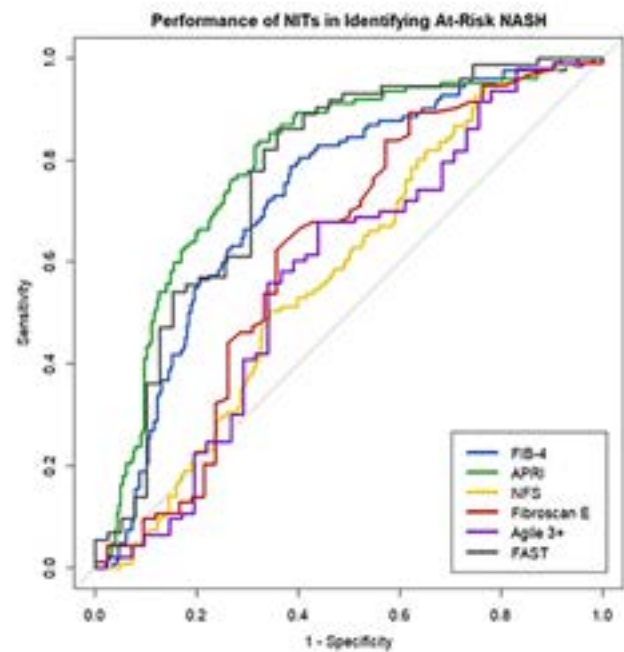
AUCs	
FIB-4	0.702 (0.651 - 0.754)
APRI	0.763 (0.716 - 0.811)
NFS	0.655 (0.598 - 0.712)
VCTE	0.852 (0.655 - 1.000)
Agile 3+	0.798 (0.642 - 0.954)
FAST	0.898 (0.823 - 0.974)



AUCs	
FIB-4	0.769 (0.719 - 0.819)
APRI	0.785 (0.737 - 0.832)
NFS	0.688 (0.635 - 0.741)
VCTE	0.827 (0.752 - 0.902)
Agile 3+	0.805 (0.729 - 0.882)
FAST	0.797 (0.709 - 0.885)



AUCs	
FIB-4	0.860 (0.814 - 0.906)
APRI	0.858 (0.816 - 0.900)
NFS	0.760 (0.708 - 0.812)
VCTE	0.841 (0.776 - 0.905)
Agile 3+	0.872 (0.814 - 0.930)
FAST	0.828 (0.753 - 0.902)



AUCs	
FIB-4	0.727 (0.674 - 0.779)
APRI	0.793 (0.746 - 0.840)
NFS	0.578 (0.531 - 0.635)
VCTE	0.624 (0.511 - 0.737)
Agile 3+	0.581 (0.466 - 0.695)
FAST	0.770 (0.823 - 0.974)

Figure: (abstract: SAT-467).

POSTER PRESENTATIONS

Method: Patients with biopsy-proven NAFLD were enrolled from National University Health System, Singapore to undergo various non-invasive tests. Patients with any other causes for their liver disease were excluded. Fibrosis-4 index (FIB-4), AST to Platelet Ratio Index (APRI), NAFLD Fibrosis Score (NFS), BMI AST/ALT ratio and Diabetes score (BARD), as well as vibration-controlled transient elastography (VCTE), AGILE 3+ and FibroScan-AST score were evaluated for performance in assessment for fibrosis. These NITs were evaluated for performance in identifying clinically significant (F2–4) or advanced (F3–4) fibrosis and “at-risk NASH,” a commonly used cutoff for recruitment into clinical trials.

Results: 399 multi-ethnic Asian patients with biopsy-proven NAFLD were recruited to undergo non-invasive tests from 2014 to 2021. Area under receiver-operator-characteristics (AUC) values for identifying clinically significant fibrosis for FIB-4, APRI, NFS, VCTE, AGILE 3+ and FAST were 0.769, 0.785, 0.688, 0.827, 0.806 and 0.797 respectively. AUC values for identifying advanced fibrosis were 0.860, 0.858, 0.760, 0.841, 0.872 and 0.828. AUC values for identifying at-risk NASH were 0.727, 0.793, 0.578, 0.624, 0.581 and 0.770. BARD performed poorly across all analyses, with AUCs of 0.435 to 0.569. Analysis on subgroups with different histological score of steatosis revealed that FIB-4, APRI and NFS performed worse with increasing steatosis, while the performance of VCTE appeared better preserved across grades of steatosis.

Conclusion: VCTE, FIB-4 and APRI performed significantly better than NFS and BARD in identifying clinically significant and advanced fibrosis. VCTE performed well in identifying fibrosis of all severities but performed poorer in identifying at-risk NASH. APRI and FAST were superior to all other indices in prediction of at-risk NASH. FAST and AGILE 3+ scores did not otherwise show benefit over VCTE alone. Composite scores performed worse with more severe steatosis, suggesting VCTE may be the preferred NIT in such cases.

SAT-468

Impact of obesity on transient elastography accuracy among patients with non-alcoholic fatty liver disease

María Del Barrio Azaceta¹, Paula Iruzubieta¹, Rebeca Sigüenza², Carolina Jiménez-González¹, Luis Ibañez³, Laura Izquierdo-Sánchez⁴, Jesús Rivera⁵, Javier Abad Guerra⁶, Javier Ampuero⁷, Isabel Graupera⁸, Carmelo García-Monzón⁹, Judith Gómez-Camarero¹⁰, Rosa M Morillas¹¹, Vanesa Bernal Monterde¹², Rosa Martín-Mateos¹³,

Patricia Aspichueta¹⁴, Mercedes De La Torre Sanchez¹⁵, Salvador Benlloch¹⁶, Juan Turnes¹⁷, María Teresa Arias Loste¹, Manuel Romero Gomez⁷, José Luis Calleja Panero⁶, Juan M Pericàs⁵, Rafael Bañares³, Jesús M. Bañales⁴, Rocío Aller², Javier Crespo¹.

¹Gastroenterology and Hepatology Department, Clinical and Translational Research in Digestive Diseases, Valdecilla Research Institute (IDIVAL), Marqués de Valdecilla University Hospital, Santander, Spain; ²Servicio de Aparato Digestivo, Hospital Clínico Universitario de Valladolid, CiberINFEC, Universidad de Valladolid, Valladolid, Spain; ³Servicio de Gastroenterología y Hepatología, Hospital Universitario Gregorio Marañón-Instituto de Investigación Sanitaria Gregorio Marañón (IISGM), Universidad Complutense de Madrid, Madrid, Spain; ⁴Departamento de Enfermedades Hepáticas y Gastrointestinales, Instituto de Investigación Sanitaria Biodonostia-Hospital Universitario Donostia, Universidad del País Vasco (UPV/EHU), San Sebastián, Spain; ⁵Unidad de Hepatología, Hospital Universitario Vall d'Hebron-Instituto de Investigación Vall d'Hebron (VHIR), Universidad Autónoma de Barcelona, Barcelona, Spain; ⁶Servicio de Aparato Digestivo, Unidad de Hepatología, Hospital Universitario Puerta de Hierro-IDIPHSA, Madrid, Spain; ⁷Digestive Diseases Unit, Hospital Universitario Virgen del Rocío, SeLiver Group, Institute of Biomedicine of Sevilla (HUVR/CSIC/US), Department of Medicine, University of Seville, Seville, Spain; ⁸Unidad de Hepatología, Hospital Clinic-Instituto de Investigaciones Biomédicas August Pi i Sunyer (IDIBAPS), Universidad de Barcelona, Barcelona, Spain; ⁹Unidad de Investigación, Hospital Universitario Santa Cristina-Instituto de Investigación Sanitaria del Hospital Universitario de La Princesa, Madrid, Spain; ¹⁰Unidad de Hepatología, Servicio de Aparato Digestivo, Hospital Universitario de Burgos, Burgos, Spain; ¹¹Servicio de Aparato Digestivo, Hospital Universitario Germans Trias i Pujol, Badalona, Barcelona, Spain; ¹²Departamento de Gastroenterología y Hepatología, Hospital Miguel Servet, Zaragoza, Spain; ¹³Departamento de Gastroenterología y Hepatología, Hospital Universitario Ramón y Cajal, Instituto Ramón y Cajal de Investigación Sanitaria (IRYCIS), Madrid, Spain; ¹⁴Departamento de Fisiología, Universidad del País Vasco UPV/EHU, Instituto de Investigación Sanitaria Biocruces Bizkaia, Vizcaya, Spain; ¹⁵Unidad de hepatología, Consorcio Hospital General Universitario de Valencia, Valencia, Spain; ¹⁶Hospital Universitari i Politècnic La Fe, Valencia, Spain; ¹⁷Servicio de Digestivo, Hospital Universitario de Pontevedra, Pontevedra, Spain
Email: javiercrespo1991@gmail.com

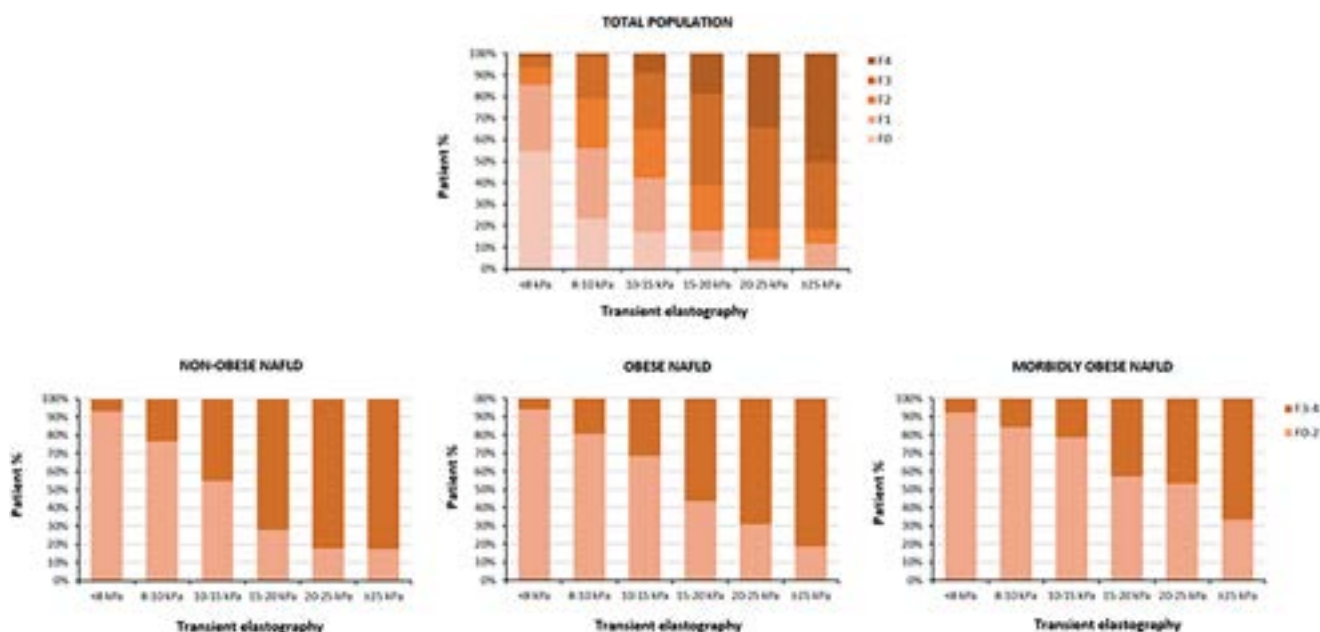


Figure: (abstract: SAT-468).

Background and aims: Liver stiffness measurement by transient elastography (TE) is the most widely used and validated non-invasive method for the assessment of liver fibrosis in non-alcoholic fatty liver disease (NAFLD). However, the presence of obesity can affect the result of TE. Our aim was to evaluate the impact of obesity in the diagnostic performance of TE for NAFLD patients in specialized care centres.

Method: Multicentre and cross-sectional study with biopsy-proven NAFLD patients from the national HEPAMet registry. Inclusion criteria: Non-surgical liver biopsy and valid TE measure, with less than 6 months of difference from the biopsy. Exclusion criteria: Hepatocellular carcinoma, liver transplantation, portal thrombosis and use of beta-blockers.

Results: A total of 1,124 NAFLD patients were included (mean age 55.7 ± 11.0 years, 47% diabetic, 65.7% obese, 11.9% morbid obese). Advanced fibrosis (F3-F4) was present in 32.8% of patients. The 8 kPa cut-off point for advanced fibrosis had a sensitivity, specificity, PPV, and NPV of 94.6%, 39.6%, 43.3%, and 93.7%, respectively. The figure shows the distribution of fibrosis stages among different TE ranges in the overall cohort and according to the presence of obesity/morbid obesity. TE values of 10–15 kPa overestimates advanced fibrosis with more frequency among obese patients than non-obese (68.5% vs. 54.3%; $p = 0.03$). Obesity and controlled attenuation parameter (CAP) were associated with overestimation of advanced fibrosis by TE. The areas under the curve for diagnosis of advanced fibrosis in non-obese, obese, and morbidly obese patients were 0.84 ± 0.02 , 0.80 ± 0.02 and 0.76 ± 0.04 , respectively. Among patients with a TE ≥ 15 (n = 273), 33 patients had gastroscopy, of whom 12 (36.4%) presented oesophageal varices and/or portal hypertensive gastropathy. Of these 12 patients, 2 (16.7%) had F2 and both were obese.

Conclusion: In NAFLD patients, obesity may overestimate the value of TE and decrease its accuracy to detect advanced fibrosis. However, TE would predict liver-related outcomes better than liver biopsy.

SAT-469

A sequential use of transient elastography followed by Agile 3+ score significantly improves the screening of advanced fibrosis in patients with NAFLD with or without severe obesity

Adrien Aubin¹, Marianne Maynard^{2,3}, Bérénice Ségréstin¹, Yasmina Chouik², Laurent Milot⁴, Valerie Hervieu⁵, Fabien Zoulim^{2,3}, Emmanuel Disse¹, Massimo Leviero^{2,3}, Cyrielle Caussy^{1,6}. ¹Hospices Civils de Lyon, Endocrinology Diabetes and Nutrition, Pierre-Bénite, France; ²Hospices Civils de Lyon, Hepatology, France; ³Centre de Recherche sur le Cancer de Lyon, INSERM-1052, Lyon, France; ⁴Hospices Civils de Lyon, Radiology, Lyon, France; ⁵Hospices Civils de Lyon, Service d'Anatomie Pathologique, Lyon, France; ⁶Université Lyon 1, Médecine School, Pierre-Bénite, France
Email: cyrielle.caussy@chu-lyon.fr

Background and aims: The Agile 3+ (A3+) score has been proposed to reduce the false positive (FP) rate for the diagnosis of advanced fibrosis (AF) in non-alcoholic fatty liver disease (NAFLD). There are limited data on A3+ diagnostic performance applied in its clinical context of use. Therefore, we aimed at comparing the diagnostic performance of A3+ and vibration controlled transient elastography (VCTE) in patients with NAFLD with or without severe obesity and screened for liver fibrosis.

Method: This cross-sectional study included adult patients with NAFLD followed at the Lyon Hepatology Institute consecutively presented at a monthly multidisciplinary board for suspected fibrotic NASH between March 2020 and December 2022. Other causes of liver diseases were systematically excluded. Pseudonymized clinical data, fasting labs and non-invasive tests (NITs) including Fibrotest®, VCTE, magnetic resonance elastography (MRE) and liver biopsy reports were systematically extracted from medical electronic record. The presence of AF was determined by a composite end point: histological fibrosis stage $\geq F3$ or overt imaging diagnosis of cirrhosis by MRE or concordant VCTE and Fibrotest® for $\geq F3$ according to EASL

guidelines. Patients with uncertain stage of fibrosis due to discordant NITs and no histological results were excluded from the analysis.

Results: The study included 368 patients with NAFLD, mean (\pm SD) age was $57.2 (\pm 12.3)$ years and BMI $34.5 (\pm 7.1)$ kg/m², 21.5% (n = 79) had severe obesity (BMI ≥ 40 kg/m²). The overall prevalence of AF was 38.9% (n = 143) and was significantly lower in patients with BMI ≥ 40 : 22.8% versus 43.2% in patients with BMI < 40 , $p = 0.001$. The FP rate of VCTE ≥ 8 kPa was significantly higher in severe obesity compared to non-severe obesity: 38.1% vs 18.3%, $p < 0.001$. Overall, the area under the ROC (AUROC) of A3+ for the detection of AF was significantly higher: 0.85 (95%CI: 0.81–0.89) compared to VCTE: 0.80 (95%CI: 0.75–0.84), $p < 0.01$ with an indeterminate rate of 20.6%. A sequential use of VCTE, followed by A3+ for VCTE ≥ 8 kPa significantly increased the AUROC: 0.87 (0.83–0.90), $p < 0.001$ with a high specificity: 88.7% and lower indeterminate rate 16.8%. These results were observed in patients with and without severe obesity (Table).

AUROC (95% CI)	AUROC (95%CI)	Sensitivity (%)	Specificity (%)	Indeterminate (%)
Overall				
VCTE cut-off 8kPa	0, 80 (0, 75–0, 84)	97, 2	62, 7	NA
A3+ cut-offs 0, 45/0, 68	0, 85 (0, 81–0, 89)	88, 1	85, 6	20, 6
Sequential VCTE/A3+	0, 87 (0, 83–0, 90)	88, 2	88, 7	16, 8
BMI < 40 kg/m ²				
VCTE	0, 82 (0, 82–0, 91)	97, 2	62, 7	NA
A3+	0, 87 (0, 77–0, 86)	88, 4	88, 8	20, 2
Sequential VCTE/A3+	0, 89 (0, 85–0, 92)	88, 5	91, 7	16, 2
BMI ≥ 40 kg/m ²				
VCTE	0, 75 (0, 69–0, 87)	100	49, 2	NA
A3+	0, 80 (0, 69–0, 89)	85, 7	76, 6	22, 8
Sequential VCTE/A3+	0, 81 (0, 71–0, 89)	85, 7	80, 0	18, 9

Conclusion: A sequential use of VCTE followed by Agile 3+ score significantly improves the detection of AF in patients with or without severe obesity.

SAT-470

Cost-effectiveness of screening for advanced hepatic fibrosis by non-invasive test in general population

Bo-Kyeong Kang¹, Mimi Kim¹, Hye-Lin Kim², Huiyul Park³, Eileen Yoon¹, Jun-Hyuk Lee⁴, Joo Hyun Oh⁴, Chul-min Lee¹, Joo Hyun Sohn¹, Jihyun An¹, Hyo Young Lee⁵, Hyunwoo Oh⁵, Jang Han Jung⁶, Dae Won Jun¹, Eun Chul Jang⁷. ¹Hanyang University, College of Medicine, Korea, Rep. of South; ²Sahmyook University, College of Pharmacy, Korea, Rep. of South; ³Myoungji Hospital, Hanyang University College of Medicine, Korea, Rep. of South; ⁴Nowon Eulji Medical Center, Eulji University School of Medicine, Korea, Rep. of South; ⁵Uijeongbu Eulji Medical Center, Eulji University College of Medicine, Korea, Rep. of South; ⁶Dongtan Sacred Heart Hospital of Hallym University Medical Center, Korea, Rep. of South; ⁷Soonchunhyang University College of medicine, Korea, Rep. of South
Email: noshin@hanyang.ac.kr

Background and aims: The prevalence of advanced fibrosis in the general population of Koreans is significant at 2.2%, and diagnosis of advanced fibrosis is important for the prognosis of patients. However, the diagnostic performance of non-invasive tests [Fibrosis-4 (FIB4), and NAFLD fibrosis score (NFS)] differs according to age in the general population, and there is insufficient evidence for screening for advanced fibrosis in the general population. This study aimed to evaluate the cost effectiveness of screening strategy using sequential combination of non-invasive test followed by transient elastography (TE) for advanced hepatic fibrosis in the general population, as well as evaluating whether there is an optimal age for effective screening.

Method: We constructed a combined model of decision tree model and Markov model to compare expected costs and quality-adjusted life-years (QALYs) between 'screening' and 'no screening' groups from healthcare system perspectives. CVD and extrahepatic malignancy conditions that potentially lead to advanced hepatic fibrosis were also

POSTER PRESENTATIONS

included in the model. Patients diagnosed with advanced fibrosis in the screening group were given intensive lifestyle intervention (ILI), and the failure rate of ILI was assumed to be 60%. According to the age of the population (30 s to 70 s), the prevalence of advanced fibrosis was applied as 1.2% to 6.9%. The sensitivity/specificity of test was applied as 37.5% to 81.8%/44.0% to 96.7% in FIB4 and 16.7% to 73.5%/62.3% to 96.3% in NFS based on a data from 9850 health check-up examiners who underwent magnetic resonance elastography. Other input parameters applied to the model were obtained from literature review. Incremental cost-effectiveness ratio (ICER) was calculated for 20-year horizon. We conducted various sensitivity analyses for varying input values, including the screening starting age.

Results: In the base-case analysis, the estimated ICERs (for FIB4 and NFS) were \$28,609 and \$27,963 per QALY, which exceeded the \$25,000 which is regarded as an implicit ICER threshold in Korea. However, considering the effects of CVD and extrahepatic cancer, the ICERs were decreased under the threshold, which indicates screening is cost-effective. In the subgroup analysis for screening starting age, the ICER of the age group over 40 years old was calculated below the cost-effective threshold. In the various sensitivity analyses, the most influential parameters on cost-effectiveness were the ILI failure rate and effect of CVD and extrahepatic cancer.

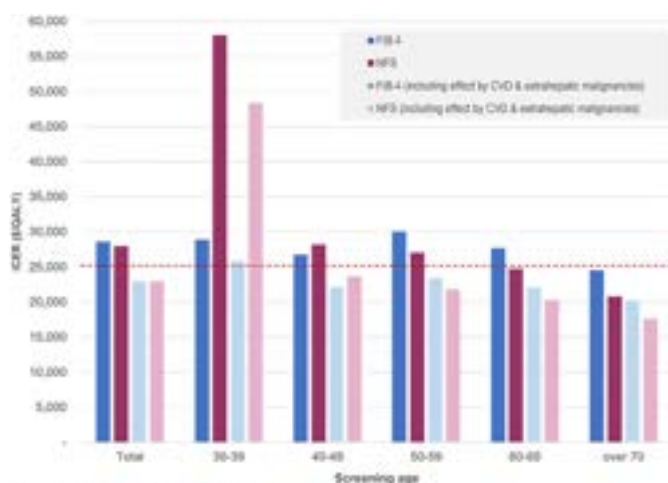


Figure 1. Estimated ICERs by screening starting age.

CVD, cardiovascular disease; FIB-4, fibrosis-4 score; ICER, incremental cost-effectiveness ratio; NFS, NAFLD fibrosis score; QALY, quality-adjusted life year

Figure:

Conclusion: Screening using non-invasive tests followed by TE in the general population is not cost-effective, but, it could be cost-effective, considering not only the liver-related condition but the effects of CVD and extrahepatic malignancies aged over 40.

SAT-471

Using elevated plasma alanine transaminase to screen for non-alcoholic fatty liver disease in overweight and obese individuals from the Danish general population

Elias Rashu¹, Mikkel Werge¹, Mira Thing¹, Liv Hetland¹, Puria Nabilou¹, Anders Junker¹, Anne-Sofie Houlberg Jensen¹, Børge Nordestgaard², Stefan Stender³, Lise Lotte Gluud¹. ¹Gastro Unit, Copenhagen University Hospital Hvidovre, Denmark, Denmark;

²Department of Clinical Biochemistry, Copenhagen University Hospital-Herlev and Gentofte, Denmark; ³Department of Clinical Biochemistry, Rigshospitalet, Copenhagen, Denmark

Email: elias.badal.rashu@regionh.dk

Background and aims: Affecting up to 30% of the general population, non-alcoholic fatty liver disease (NAFLD) is one of the leading causes of liver disease. The disorder covers a broad clinical spectrum ranging from hepatic steatosis through non-alcoholic steatohepatitis (NASH) to fibrosis and cirrhosis. A major unresolved issue is whether (and if

so: how) to screen for NAFLD in the general population. We tested the hypothesis that elevated plasma alanine transaminase (ALT) can be used as a screening tool for NAFLD in overweight and obese individuals from the Danish general population.

Method: This study screened adults in the Copenhagen General Population Study (CGPS), a population-based cohort of the Danish general population. Individuals with a body mass index (BMI) above 25 kg/m² and elevated plasma ALT at baseline (>71 U/L for men and >51 U/L for women) were invited to a hepatological evaluation, including a detailed medical history, extensive blood tests, and fibroscan. Individuals with clinical sign of NASH, evidence of fibrosis on fibroscan or elevated fibrosis-4 score (FIB-4), were offered further clinical assessment with a liver biopsy. Those who fulfilled the inclusion criteria for FLINC, an ongoing prospective NASH-cohort were included in this study. We aim to follow the participants from FLINC for >5 years.

Results: Of 997 individuals invited from the CGPS, 344 were enrolled (51.5% male, mean age: 60.6 years, mean BMI: 30.9 kg/m²). A total of 204 individuals (59.3%) were diagnosed with simple steatosis, whereas 61 (17.8%) had no sign of liver disease, and 15 were diagnosed with alcohol-related liver disease. A total of 53 (15.4%) had clinical signs of NASH fibrosis on fibroscan. Of these, 20 underwent liver biopsy, which identified various degrees of NASH fibrosis, that is, 5 with F0, 5 with F1, 3 with F2, and 7 with F3. In addition, 6 participants were diagnosed with advanced fibrosis and cirrhosis by biopsy due to alcohol-related liver disease (3 with F3 and 3 with F4). Finally, two serious incidental findings of cancer (premalign colon cancer and multiple myeloma), and one case of previously undiagnosed hepatitis C and autoimmune hepatitis were identified.

Figure: Characteristics and findings in the examined individuals.

N	344
Age (years)	60.6
Male	177 (51.5)
BMI (kg/m ²)	30.9
Type 2 diabetes	86 (25)
ALT (U/L)	43.4
Fibroscan median (kPa)	5.9
CAP value (dB/m)	293
Steatosis on Fibroscan (CAP > 260 dB/m)	204 (59.3)
NASH fibrosis on Fibroscan, (kPa>8 kPa)	53 (15.4)
-Biopsy available in n = 20 out of the 53 with NASH fibrosis on Fibroscan	
-F0	5 (25)
-F1	5 (25)
-F2	3 (15)
-F3	7 (35)
-F4	0 (0)
No liver disease	61 (17.8)
Advanced alcohol-related liver disease fibrosis/cirrhosis*	7 (2.0)
Hepatitis C	1 (0.3)
Autoimmune hepatitis	1 (0.3)
Cancer	2 (0.6)

Values are number and (%) or means. *F3 (n = 3) or F4 (n = 3) on histology.

Conclusion: Screening individuals from the Danish general population with BMI>25 kg/m² and elevated ALT identified approximately 15% with NASH fibrosis on fibroscan and FIB-4 score.

SAT-472

Analysis of the diagnostic accuracy of the non-invasive fibrosis indices NFS, HFS, and FIB-4 in the staging of advanced fibrosis in patients with metabolic fatty liver: meta-analysis of comparative studies

Carmen Lara Romero^{1,2}, Jia-Xu Liang¹, Javier Ampuero^{1,2}, Javier Castell³, Isabel Fernández-Lizaranzu⁴, Manuel Romero Gomez^{1,2}. ¹Hospital Universitario Virgen del Rocío, Department of Digestive and Liver Diseases, Sevilla, Spain; ²Institute of Biomedicine of Seville, Sevilla, Spain; ³Hospital Universitario Virgen del Rocío, Department of Radiology, Spain; ⁴Institute of Biomedicine of Seville, Interdisciplinary physics group, Spain
Email: carmenlararomero@gmail.com

Background and aims: Advanced fibrosis is related to a greater number of liver-related outcomes in patients with Metabolic Associated Fatty Liver Disease. Several non-invasive tests (NITs) have been developed to evaluate liver fibrosis in these patients to minimize the number of liver biopsies. We have performed a metanalysis to evaluate the diagnostic performance of the following NITS: Fibrosis-4 (FIB-4) NAFLD Fibrosis Score (NFS) and Hepamet Fibrosis Score (HFS).

Method: We have analyzed 4 databases until December 2022. Data has been taken from original studies showing data about the diagnostic accuracy of FIB-4, NFS and HFS, using standard cut-offs of biopsy-proven MAFLD patients. We extracted data according to the lower cut-off, higher cut-off and double cut-off methods. We included data of true positives, true negatives, false negatives and false positives patients. ROC curves were estimated using a random effects model.

Results: We included 7 studies with 5143 patients with MAFLD biopsy-proven patients. In the FIB-4 group, for the lower cut-off: $S = 0.76[0.67-0.84]$, $E = 0.65[0.49-0.78]$; for the upper cut-off (2.67): $(S:0.34[0.28-0.40]$, $E:0.96[0.92-0.98]$). In the NFS group, for the lower cut-off (-1.455) : $(S:0.80[0.71-0.87]$, $E = 0.48[0.34-0.62]$); for the upper cut-off (0.675): $(S:0.37[0.28-0.47]$, $E = 0.94[0.87-0.97]$). In the HFS group, for the lower cut-off (0.12): $(S: 0.78[0.70-0.84]$, $E: 0.66[0.49-0.80]$); for the upper cut-off (0.47): $(S: 0.43[0.38-0.49]$, $E: 0.92[0.87-0.95]$). ROC curves for FIB-4, HFS, NFS to predict advanced fibrosis ($\geq F3$) were 0.80 [0.76-0.83], 0.78[0.74-0.81], 0.73 [0.69-0.77], respectively. With the double cut-off method, we found a lower prevalence of indeterminate values for HFS (27% [20%-34%]).

Conclusion: In our metanalysis, HFS and FIB-4 showed higher diagnostic accuracy than NFS to identify advanced fibrosis in MAFLD patients, while HFS showed a lower rate of patients in the grey zone (indeterminate values).

SAT-473

Correlation between serial Fibrosis-4 scores and liver stiffness measurements in patients with low-risk non-alcoholic fatty liver disease

Tanvi Goyal¹, Jing Hong Loo², Michael Song¹, Tianyu Qiu³, Esteban Urias¹, Yu Jun Wong³, Vincent Chen¹, Karn Wijarnpreecha⁴. ¹Michigan Medicine, Internal Medicine, Ann Arbor, United States; ²National University of Sinapor, Yong Loo Lin School of Medicine, Singapore; ³Changi General Hospital, Singapore; ⁴Unviersity of Arizona, United States
Email: tagoyal@med.umich.edu

Background and aims: In patients with non-alcoholic fatty liver disease (NAFLD) at baseline low risk, major professional societies recommend risk stratification using non-invasive tests such as Fibrosis-4 (FIB4) score in lieu of liver stiffness measurement (LSM) by vibration-controlled transient elastography (VCTE). However, there are limited data on how changes in FIB4 and LSM correlate, and on whether meaningful changes in LSM can occur without changes in FIB4. Here, we evaluated associations between changes in FIB4 and LSM in NAFLD patients with serial VCTE studies.

Methods: This was a retrospective study of consecutive patients at Michigan Medicine in the United States with NAFLD who had at least two VCTE studies, spaced at least two years apart. We excluded patients with baseline LSM ≥ 20 kPa. The primary predictors were change between follow-up FIB4 (FIB4-2) and initial FIB4 (FIB4-1), which we call delta-FIB4. The primary outcome was a $\geq 25\%$ increase in the second LSM (LSM-2) relative to baseline (LSM-1). The secondary outcome, which was applied to only patients with LSM-1 < 8 kPa, was disease progression defined as a $\geq 25\%$ increase in LSM-2 vs. LSM-1 and new advanced fibrosis (LSM-2 ≥ 8 kPa).

Results: We included 311 patients. Median age was 54 years, 53% were male, and 84% were white. Median follow-up time between VCTEs was 38.6 months. On follow-up, 30% of patients had a $\geq 25\%$ increase in LSM, 24% had a $\geq 25\%$ decrease, and 46% had a $< 25\%$ change. 15% of low-risk NAFLD patients developed incident advanced fibrosis (LSM-2 ≥ 8 kPa and $\geq 25\%$ increase vs. LSM-1). Delta-FIB4 correlated strongly with delta-LSM: $r = 0.31$ ($p < 0.0001$). Among patients with $\geq 25\%$ increase in LSM, FIB4 did not change over time (delta-FIB4 = 0.15, $p = 0.025$ for difference from 0). In contrast, among patients with no LSM change or with LSM decrease, FIB4 did not change (delta-FIB4 = 0.02, $p = 0.61$ for difference from 0). Similarly, among patients with baseline LSM < 8 kPa and disease progression, FIB4 increased over time with delta-FIB4 = 0.31 ($p = 0.044$ for difference from 0), but there was no change in FIB4 in those with baseline LSM < 8 kPa and without disease progression (delta-FIB4 = 0.04, $p = 0.31$).

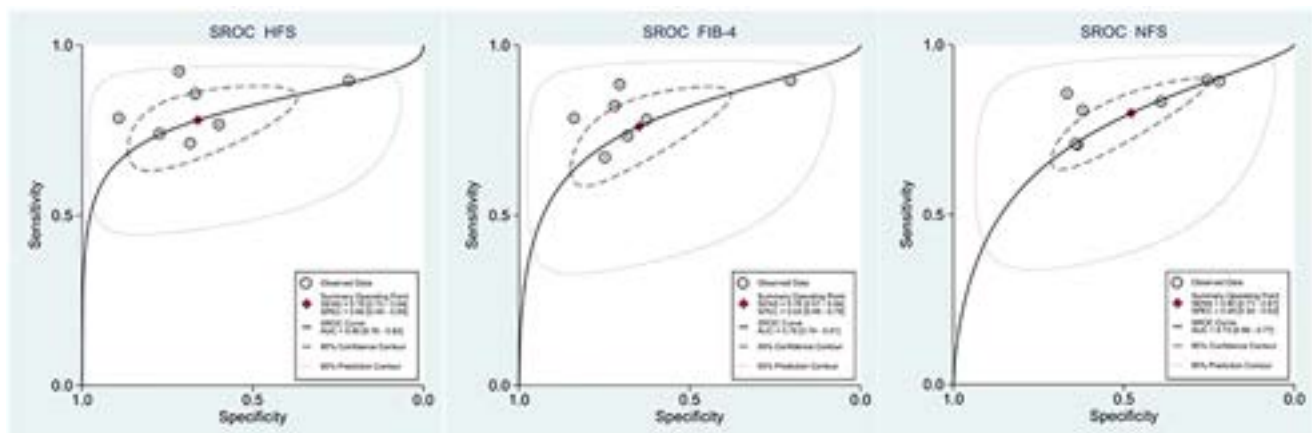


Figure: (abstract: SAT-472): Summary Receiving Operator Curves of the different non-invasive tests: FIB-4, NFS and HFS.

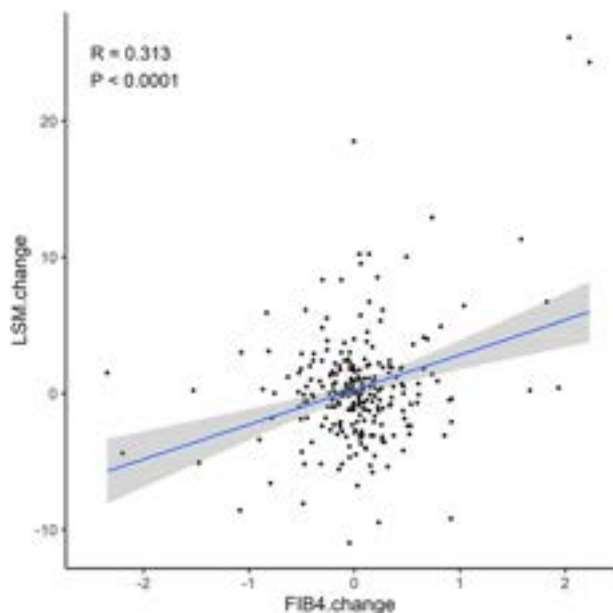


Figure:

Conclusion: Among patients with NAFLD and serial VCTEs, changes in FIB4 correlate strongly with changes in LSM. These findings support current guidelines to obtain serial serum non-invasive tests in patients with low-risk NAFLD.

SAT-474

AGILE 3+ and AGILE 4 scores for the diagnosis of advanced fibrosis and cirrhosis in patients with non-alcoholic fatty liver disease

Kamela Gjini¹, Angelo Armandi^{1,2}, Gian Paolo Caviglia¹, Chiara Rosso¹, Daphne D'Amato¹, Amina Abdulle¹, Gabriele Castelnovo¹, Nuria Pérez Diaz del Campo¹, Marta Guariglia¹, Elisabetta Bugianesi¹.
¹Division of Gastroenterology and Hepatology, University of Turin, Italy;
²Metabolic Liver Disease Research Program, University Medical Center of the Johannes Gutenberg-University of Mainz, Germany
 Email: kamelagjini@gmail.com

Background and aims: non-invasive assessment of advanced fibrosis in Non-Alcoholic Fatty Liver Disease (NAFLD) is crucial for the identification of patients at greatest risk of progression. Among non-invasive tests, AGILE3+ and AGILE 4 have been recently proposed, combining liver stiffness measurement (LSM) by vibration-controlled transient elastography (FibroScan) with clinical-biochemical variables. We aimed to assess the accuracy of AGILE 3+ and AGILE 4 for the identification of advanced (F3-F4) and cirrhosis (F4), respectively, against LSM in individuals with biopsy-proven NAFLD.

Method: we retrospectively included 315 biopsy proven-NAFLD patients. No clinical, radiological or biochemical signs of cirrhosis were present at inclusion. Clinical-biochemical data and LSM were collected at time of the biopsy.

Results: median age was 48 (IQR 38–47) years, 62% of patients were male. Median LSM was 7.5 kPa (IQR 5.8–10.1). Advanced fibrosis was present in 28%, cirrhosis in 10% and NASH in 28% of cases. Eighty subjects had type 2 diabetes. At Area Under the Curve (AUC) analysis, LSM had a value of 0.807 (Se 70%, Sp 80%) for advanced fibrosis and 0.877 for cirrhosis (Se 88%, Sp 76%). AGILE 3+ had AUC of 0.77 for advanced fibrosis (cut-off by Youden Index 0.30, Se 68%, Sp78%), while AGILE 4 had AUROC 0.78 for cirrhosis (cut-off by Youden Index 0.11, Se 55%, Sp 89%). Comparison of AUC showed that AGILE 3+ was similar to LSM for identifying advanced fibrosis (DeLong p = 0.254). Similarly, AUC comparison between AGILE 4 and LSM for cirrhosis was not different (DeLong p = 0.739).

Conclusion: when compared to LSM, AGILE3+ and AGILE 4 had similar accuracy for the detection of advanced fibrosis and cirrhosis in NAFLD patients. This research has been supported by the Italian

Ministry for Education, University and Research (MIUR) “Dipartimenti di Eccellenza 2018–2022” Project code D15D18000410001.

SAT-475

Diagnostic performance of NAFLD fibrosis score in lean NAFLD

Huiyul Park¹, Eileen Yoon², Sang Bong Ahn³, Hye-Lin Kim⁴, Jun-Hyuk Lee⁵, Mimi Kim⁶, Chul-min Lee⁶, Bo-Kyeong Kang⁶, Joo Hyun Sohn⁷, Jihyun An², Joo Hyun Oh³, Hyo Young Lee⁷, Hyunwoo Oh⁷, Jang Han Jung⁸, Dae Won Jun², Eun Chul Jang⁹.
¹Myoungji Hospital, Hanyang University College of Medicine, Department of Family Medicine, Korea, Rep. of South; ²Hanyang University, College of Medicine, Department of Internal Medicine, Korea, Rep. of South; ³Nowon Eulji Medical Center, Eulji University School of Medicine, Department of Internal Medicine, Korea, Rep. of South; ⁴Sahmyook University, College of Pharmacy, Korea, Rep. of South; ⁵Nowon Eulji Medical Center, Eulji University School of Medicine, Department of Family Medicine, Korea, Rep. of South; ⁶Hanyang University, College of Medicine, Department of Radiology, Korea, Rep. of South; ⁷Uijeongbu Eulji Medical Center, Eulji University College of Medicine, Department of Internal Medicine, Korea, Rep. of South; ⁸Dongtan Sacred Heart Hospital of Hallym University Medical Center, Department of Internal Medicine, Korea, Rep. of South; ⁹Soonchunhyang University College of medicine, Department of Occupational and Environmental Medicine, Korea, Rep. of South
 Email: noshin@hanyang.ac.kr

Background and aims: Diagnostic performance of fibrosis-4 index (FIB-4) and non-alcoholic fatty liver disease (NAFLD) fibrosis score (NFS) for advanced fibrosis in lean patients with NAFLD is limited. We aimed to evaluate the diagnostic performance and current cut-offs of FIB-4 and NFS in individuals with NAFLD.

Method: This multicenter, retrospective, cross-sectional study analyzed 1,501 patients with biopsy-proven NAFLD. The difference in diagnostic performance of FIB-4 and NFS between lean (body mass index (BMI) <23 kg/m²) and non-lean (BMI ≥23 kg/m²), and their sensitivity and specificity at the current cut-off value were also evaluated.

Results: Diagnostic performance and area under the receiver operating characteristic curves (AUROCs) of FIB-4 and NFS were comparable between the lean and non-lean groups. The AUROC of FIB-4 and NFS were not different in the lean group (0.807 vs. 0.790). The sensitivity and specificity of the current FIB-4 cut-off values did not change. But, the sensitivity of the current NFS cut-off values was lower in the lean group than in the non-lean group (54.4% vs. 72.7%). The NFS sensitivity decreased with the BMI quartiles. The FIB-4 sensitivity and specificity did not change according to BMI quartiles.

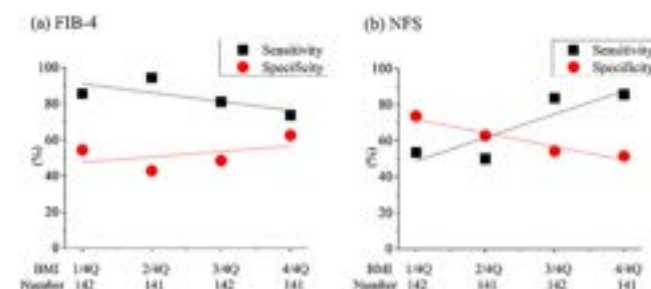


Figure 1. Sensitivity (black squares) and specificity (red circles) trend of FIB-4 (a) and NFS (b) for diagnosing patients with advanced hepatic fibrosis by using their lower cut-off values according to BMI quartiles.
 Abbreviation: BMI, body mass index; FIB-4, fibrosis-4 index; NFS, NAFLD fibrosis score.

Figure:

Conclusion: The overall diagnostic performance (AUROC) of FIB-4 and NFS in diagnosing advanced fibrosis did not differ between the lean and non-lean groups. However, the sensitivity of NFS at the current cut-off value decreased in lean individuals. FIB-4 at the current cut-off value would be a better screening parameter of advanced NAFLD fibrosis in lean individuals.

SAT-476

Fatty liver score: a novel fatty liver index based on magnetic resonance imaging-proton density fat fraction

Chul-min Lee¹, Bo-Kyeong Kang¹, Mimi Kim¹, Eileen Yoon², Sang Bong Ahn³, Jun-Hyuk Lee⁴, Joo Hyun Oh³, Joo Hyun Sohn⁵, Ji Hyun An⁵, Dae Won Jun⁵. ¹Hanyang University, College of Medicine, Department of Radiology, Korea, Rep. of South; ²Hanyang University, College of Medicine, Department of Internal Medicine, Korea, Rep. of South; ³Nowon Eulji Medical Center, Eulji University School of Medicine, Department of Internal Medicine, Korea, Rep. of South; ⁴Nowon Eulji Medical Center, Eulji University School of Medicine, Department of Family Medicine, Korea, Rep. of South; ⁵Hanyang University College of Medicine, Department of Internal Medicine, Korea, Rep. of South
Email: noshin@hanyang.ac.kr

Background and aims: We aimed to develop a simple and intuitive model with high accuracy for predicting hepatic steatosis based on the gold standard method.

Method: We collected retrospective data from 2,111 participants who underwent magnetic resonance imaging-proton density fat fraction (MRI-PDFF) at six referral centers in three countries (Korea, Japan, and the United States). The full cohort was randomly assigned to a training cohort and a validation cohort at a ratio of 7:3. Variables were selected via multivariate logistic analysis, and additional linearity was confirmed using the smoothing spine method. Finally, a model maintaining a reasonable area under the receiver operating characteristics (AUROC) with minimum variables was presented; it compared diagnostic performance with the pre-existing model.

Results: We developed new Fatty liver score (FLS) was using male sex, age, diabetes mellitus, alanine aminotransferase, triglyceride, and body mass index. FLS showed good diagnostic performance for predicting fatty liver with an AUC of 0.841 in the training cohort. The AUC of the FLS in the validation cohort was 0.848, higher than Fatty liver index (FLI) (0.796, $p = 0.014$), and similar to Hepatic steatosis index (HSI) (0.810, $p = 0.058$) for predicting fatty liver. The best cut-off for FLS was 3.0, with a sensitivity of 80.0% and specificity of 71.6%.



Figure:

Conclusion: A new simplified prediction model, FLS, showed good diagnostic performance for predicting fatty liver with high sensitivity in large cohorts from multinational and multicenter studies using MRI-PDFF as the reference standard.

SAT-477

The role of M2BPGi in screening for advanced hepatic fibrosis in diabetic patients

Mimi Kim¹, Hye-Lin Kim², Eileen Yoon¹, Se Young Jung³, Ki Tae Yoon⁴, Young Youn Cho⁵, Hoon Gil Jo⁶, Yang-Hyun Baek⁷, Sang Yi Moon⁸, Dae Won Jun¹, Aejeong Jo¹. ¹Hanyang University, College of Medicine, Korea, Rep. of South; ²Sahmyook University, College of Pharmacy, Korea, Rep. of South; ³Kyungpook National University, Kyungpook National University Hospital, Daegu, South Korea, Korea, Rep. of South; ⁴Pusan National University, Korea, Rep. of South; ⁵Chung-Ang University Hospital, Seoul, Korea, Korea, Rep. of South; ⁶Wonkwang University

College of Medicine and Hospital, Korea, Rep. of South; ⁷Dong-A University College of Medicine, Busan, South Korea, Korea, Rep. of South; ⁸Dong-A University College of Medicine, Busan, South Korea, Korea, Rep. of South
Email: noshin@hanyang.ac.kr

Background and aims: There is a lack of algorithms that can identify and predict advanced hepatic fibrosis in diabetic patients, despite much evidence of a high rate of hepatic fibrosis in subjects with diabetes. The purpose of this study is to determine whether Mac-2-binding protein glycan isomer (M2BPGi) and other non-invasive test (NIT) and their combinations can help to exclude advanced hepatic fibrosis in diabetic clinics.

Method: 2,177 patients visiting the endocrinology clinic of six tertiary hospitals and performing M2BPGi and transient elastography (TE) between April 2020 and May 2021 were included. Of them, only patients with diabetes were included. FIB-4 and NAFLD fibrosis score (NFS) were calculated for all subjects and evaluated the diagnostic performance of single or combined tests for advanced fibrosis. Advanced fibrosis was defined by TE ≥ 8.0 kPa.

Results: Of them, 641 diabetic patients with mean age, of 58.5 ± 12.6 years were included. Diagnostic performance of predicting advanced hepatic fibrosis was highest in FIB4 (the area under the receiver operating characteristics curve [AUROC] = 0.756), followed by M2BPGi and NFS (AUROC = 0.702 and 0.690, respectively). The multivariate regression analysis revealed that M2BPGi was an independent risk factor for advanced liver fibrosis (odds ratio (OR): 1.33, $p < 0.001$). M2BPGi at a cut-off of 0.6 showed a similar diagnostic performance to the low cut-off of other NITs (sensitivity: 85.4% in M2BPGi vs. 84.4–85.3% in other NITs; specificity: 34.8% in M2BPGi vs. 27.3–44.3% in other NITs). The sequential combination of FIB4 followed by M2BPGi showed the sensitivity, specificity, positive predictive value, and negative predictive value of 94.4%, 19.1%, 38.5%, and 86.5%, respectively.

Conclusion: A combination of M2BPGi and APRI can help to exclude advanced hepatic fibrosis in diabetic patients. Through the two-step pathway, diabetic patients with advanced fibrosis could be referred to liver specialists.

SAT-478

One-step diagnosis: detection and stratification of incidental hepatic steatosis by multiparametric abdominal ultrasound

Irene Gonzalez Diaz¹, Carlota Siljestrom Berenguer¹, Luis Eduardo Pariente Zorrilla¹, Marta Abadia¹, Eva Marín², Gloria Ruiz-Fernandez¹, Joaquin Poza¹, Clara Amiana Roig¹, Carmen Amor¹, Maria Dolores Martin-Arranz¹, Antonio Oliveira Martin¹. ¹Hospital la Paz, Gastroenterology and Hepatology Service, Spain; ²Hospital la Paz, Spain
Email: irenegonzalezdiaz@gmail.com

Background and aims: The high prevalence of hepatic steatosis requires an efficient screening and stratification strategy. Non-invasive tests have low positive predictive value, and the referral of patients based exclusively on one of them is an excessive, inefficient overload for Liver Clinics. Within this broad population, a specific subgroup is incidental hepatic steatosis (IncHS) or hepatic steatosis not previously suspected on imaging tests, in which the risk of advanced liver fibrosis strategy is unknown (AASLD Guidelines 2018). Our aim was to determine the prevalence of IncHS, its characteristics, and the most efficient referral strategy of these patients from an Ultrasound Unit.

Method: Longitudinal and prospective study between November 2021 and June 2022. Consecutive patients presenting for abdominal ultrasound (Aplio i800, Canon) with criteria of hepatic steatosis: 1) Liver hyperechogenicity with respect to renal cortex plus at least one of the following: Posterior beam attenuation, portal or hepatic veins blurring, gallbladder wall blurring or 2) Attenuation Imaging (ATI) ≥ 0.63 dB/cm/MHz. Steatosis not previously diagnosed and not suspected based on the ultrasound request was considered

POSTER PRESENTATIONS

incidental. Patients with a previous diagnosis of steatosis, liver disease, or any reason for suspecting a liver disease according to the ultrasound request were excluded. Simultaneously, shear-wave elastography (2D-SWE) was performed, with a risk of advanced fibrosis if ≥ 7 kPa. In the same ultrasound room, the FIB-4 index was calculated according to available results (<1 year).

Results: 1724 patients were included in the study period. 762 (44.2%) showed steatosis, of which 198 (26%; 95%CI: 23–29.2) were considered incidental: mean age 58 years, women 56.5%, liver test alteration 25%. Factors associated with steatosis were: metabolic dysfunction 48% (obesity 77.9%, diabetes 13%, hypertension/dyslipidaemia 45.5%), alcohol 6.5%, steatogenic medication 0.5%. The most frequent reasons for ultrasound requests were biliopancreatic (31%) and abdominal pain (19.6%). In the 198 with IncHS, the mean elastography value was 4.7 ± 1.5 kPa, 87 (44%) had FIB-4 >1.3 and 17 (8.6%) 2D-SWE ≥ 7 kPa. Only 11/198 patients (5.6%; 95%CI: 3.1–9.7) had FIB-4 >2.67 and 2D-SWE ≥ 7 kPa, and were referred primarily to the Liver Clinic; the remaining 187 (94.4%) followed their standard pathway.

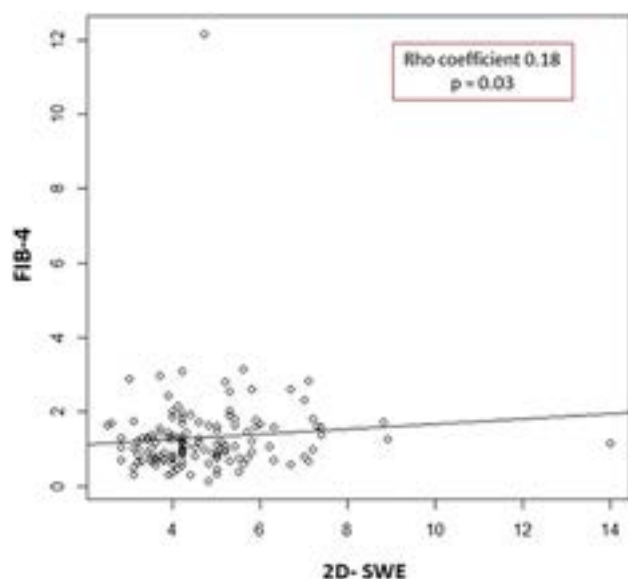


Figure 1: Linear regression model between 2D-SWE and FIB-4

Conclusion: Incidental hepatic steatosis is frequent in a Gastroenterology Ultrasound Unit. As expected, the prevalence of risk of advanced fibrosis is low. Multiparametric ultrasound allows for a one-step diagnosis, and stratification, avoiding unnecessary referrals.

SAT-479

High performance of new multiparametric ultrasound in the non-invasive assessment of liver disease

Gloria Ruiz-Fernandez¹, Marta Abadia², Miriam Romero¹, Cristina Suárez¹, Joaquín Poza¹, Eva Marín¹, Clara Amiana Roig¹, Carmen Amor¹, Irene Gonzalez Diaz¹, Carlota Siljeström Berenguer¹, Beatriz Pillado Pérez¹, Luis Eduardo Pariente Zorrilla¹, María Dolores Martín-Arranz¹, Antonio Oliveira Martín¹. ¹Hospital La Paz, Gastroenterology, Spain; ²Hospital La Paz, Spain
Email: gloria.ruizf@gmail.com

Background and aims: Liver diseases affect millions of people worldwide. There is an increasing interest in accessible, reliable tools in the non-invasive assessment of liver disease. We assessed the performance of new Attenuation Imaging and Shear-Wave elastography multiparametric ultrasound tools for the diagnosis of steatosis and advanced fibrosis.

Method: Adult patients consecutively programmed for liver biopsy were prospectively included between February 2020–November

2022. On the same day of percutaneous liver biopsy and prior to it, we conducted the following procedures: transient elastography (TE) and controlled-attenuation parameter (CAP): Fibroscan 502 Touch, EchoSens, France; and bidimensional shear-wave (2D-SWE) and Attenuation Imaging (ATI): Aplio i800, Canon, Japan. We excluded patients with acute liver disease, biopsy <11 portal tracts, and contraindication for liver biopsy. 16–18G Tru-cut needle was used under ultrasound guidance. Metabolic-associated fatty liver disease (MAFLD) was staged according to non-alcoholic steatohepatitis Clinical Research Network scoring (NASH CRN). Chronic hepatitis was classified according to METAVIR. Normally distributed quantitative variables were described using the mean. Diagnostic performances for steatosis (fatty content $>5\%$) and advanced fibrosis (F3–F4) were assessed with receiver operating characteristic curves.

Results: A total of 249 patients were included, the mean age was 51 years, 60% were female, the mean BMI was 27.4 kg/m^2 , and the mean GPT was 70 U/L . The mean biopsy length was 25 mm, 15 portal tracts. The distribution of final diagnosis after biopsy was as follows: MAFLD ($n = 115$, 46%) of which steatohepatitis 68 (60%), AIH ($n = 32$, 13%), CBP ($n = 10$, 4%), others or minimal changes ($n = 92$, 37%). Fibrosis grades were: F0 123 (49%), F1/F2 82 (33%), F3/F4 44 (17, 7%). Considering the liver biopsy as reference variable, for steatosis the performances were: CAP 0.83, ATI 0.91. For advanced fibrosis (F3/F4), the performances were: TE 0.93, 2D-SWE 0.95. In the subgroup of MAFLD, the performances for advanced fibrosis were: TE 0.89, 2D-SWE 0.95 (table 1)

Table: ATI and CAP accuracy for $>5\%$ steatosis detection. ET, 2D-SWE accuracy for advanced fibrosis detection in the total group and in the MAFLD subgroup.

N = 249	AUROC	95% CI; p	Best cut-off	Sensitivity (%)	Specificity (%)	Accuracy (%)
$>5\%$ Steatosis						
CAP (dB/m)	0.83	0.78–0.88; 0.0001	254	78	78	78
ATI (dB/cm/MHz)	0.91	0.87–0.95; 0.0001	0.62	82.7	90.2	86.1
F3/F4 Fibrosis						
TE (kPa)	0.93	0.90–0.97; 0.0001	7.75	90.9	82.7	84, 1
2D-SWE (kPa)	0.95	0.91–0.99; 0.0001	7.15	93.2	92.6	92, 7
F3/F4 Fibrosis MAFLD (N = 115)						
TE (kPa)	0.89	0.82–0.96; 0.0001	8.1	80	80	80
2D-SWE (kPa)	0.95	0.91–1; 0.0001	7.1	96	92	92.9

AUROC: area under the receiver operating characteristic curve; CI: confidence interval; CAP: controlled-attenuation parameter; ATI: attenuation imaging; TE: transient elastography; 2D-SWE: bidimensional shear wave elastometry; MAFLD: metabolic-associated fatty liver disease.

Conclusion: Bidimensional shear-wave and Attenuation Imaging technologies using multiparametric ultrasound are very reliable tools in the non-invasive assessment of liver disease, including MAFLD.

SAT-480

Inclusion of the fatty liver-associated variants in the clinical workup of patients: results of an eight years' experience in a tertiary referral center with genotyping facility

Susanne N Weber¹, Mathias Straub¹, Frank Lammert², Marcin Krawczyk^{1,3}. ¹Department of Medicine II, Saarland University Medical Center, Homburg, Germany; ²Hannover Medical School (MHH), Hannover, Germany; ³Laboratory of Metabolic Liver Diseases, Medical University of Warsaw, Warsaw, Poland
Email: marcin.krawczyk@uks.eu

Background and aims: Genetic testing has become increasingly available in clinical practice. In our center we have introduced the genotyping of fatty liver-associated variants in the clinical work-up of patients with chronic liver diseases in 2013. Here, we present the genotyping results of patients treated in our department up to the year 2021.

Method: In total, we analysed 462 patients with fatty liver phenotypes who were referred by the physicians working in our department for genetic testing of the two common fatty liver-associated variants, namely *PNPLA3* p.I148M and *MBOAT7* p.E17G. In addition to our panel, we genotyped the newly detected *MTARC1* rs2642438 variant that was recently shown to have protective effects on liver status (Fairfield et al. *Hepatol Commun* 2022). Genotyping procedures were performed using allelic discrimination assays. Liver steatosis and fibrosis were quantified non-invasively using controlled attenuation parameter (CAP) and liver stiffness measurement (LSM) by transient elastography.

Results: The results of genotyping procedures were provided to the admitting physicians within an average time of 24 days from blood sampling. The minor allele frequencies (MAF) of the *PNPLA3*, *MBOAT7* and *MTARC1* variants were 25.2%, 40.8%, and 21.5%, respectively, and did not significantly differ from reference data available for Europeans. Among the three tested variants, the *PNPLA3* p.I148M genotype correlated with increased serum ALT, AST as well as serum transferrin (all $p < 0.01$) and iron concentrations ($p = 0.02$) in carriers of the homozygous [MM] genotype. These patients also presented with significantly ($p < 0.01$) higher CAP values (299 ± 62 dB/m) as compared to carriers of the common allele (267 ± 74 dB/m), but we did not find any major effect of this variant on LSM ($p = 0.09$). The only correlation for *MBOAT7* p.E17G was found with increased levels of leukocytes ($p = 0.02$), but not with liver phenotypes (all $p > 0.05$). Finally, we did not find any relevant associations between the *MTARC1* variant and liver steatosis, fibrosis markers or other patient characteristics.

Conclusion: Our data underscore the central role of *PNPLA3* p.I148M variant in the fatty liver phenotype. Routine genotyping of this variant in clinical practice can be rapidly performed and might help to identify at-risk patients with worse liver status.

SAT-481

Performance of novel collagen turnover biomarkers in relation to FIB-4 to detect advanced fibrosis in NAFLD

Hannes Hegmar¹, Thomas Möller², Patrik Nasr³, Johan Vessby⁴, Stergios Kechagias³, Nils Nyhlin⁵, Hanns-Ulrich Marschall⁶, Åsa Danielsson Borssén⁷, Morten Karsdal², Diana Leeming², Mattias Ekstedt³, Hannes Hagström¹. ¹Karolinska Institutet/Karolinska University Hospital, Department of Medicine, Huddinge, Sweden; ²Nordic Bioscience Biomarkers and Research A/S, Denmark; ³Department of Health, Medicine and Caring Sciences, Linköping University, Sweden; ⁴Department of Medical Sciences, Gastroenterology Research Group, Uppsala University, Sweden; ⁵School of Medical Sciences, Örebro University, Sweden; ⁶Department of Molecular and Clinical Medicine, University of Gothenburg, Sweden; ⁷Department of Public Health and Clinical Medicine, Umeå University, Sweden
Email: hhegmar@gmail.com

Background and aims: Cleavage products from different types of collagens that reflect the formation, and degradation, of fibrosis are

potential novel biomarkers to detect advanced fibrosis in patients with non-alcoholic fatty liver disease (NAFLD). Here, we investigated the diagnostic performance of PRO-C3, PRO-C6, C4M, PRO-C18L, ADAPT, a score based on PRO-C3 and clinical parameters, and FIB-4 to diagnose advanced fibrosis, based on liver biopsy or liver stiffness measurement (LSM) by vibration-controlled transient elastography (VCTE).

Method: Serum from 299 patients with NAFLD from six Swedish university hospitals were analyzed with an ELISA-based method for PRO-C3, PRO-C6, C4M and PRO-C18L. LSM by VCTE was performed at inclusion, and when clinically motivated, a liver biopsy was performed ($n = 134$). Blood samples were collected at the time of the LSM. FIB-4 and ADAPT scores were calculated. Advanced fibrosis was defined as fibrosis stage 3–4 on liver biopsy, or an LSM ≥ 15 kPa in patients without biopsy data. The area under the receiver operating characteristic curve (AUROC) were calculated for all biomarkers to evaluate their ability to diagnose advanced fibrosis.

Results: Advanced fibrosis was found in 48 (14.6%) patients. These were older than patients without advanced fibrosis (64.5 years vs 55 years, $p < 0.001$) and more commonly had type 2 diabetes (75% vs 43%, $p < 0.001$). When investigating the diagnostic performance of advanced fibrosis, PRO-C3 had an AUROC of 0.73 (95% Confidence Interval [CI] = 0.65–0.80), PRO-C6 0.56 (95%CI = 0.48–0.64), C4M 0.57 (95%CI = 0.48–0.66), and PRO-C18L 0.46 (95%CI = 0.38–0.54). The ADAPT score had the highest AUROC for diagnosis of advanced fibrosis (0.85 (95%CI = 0.79–0.90)). However, ADAPT was not significantly better than the FIB-4 score (AUROC 0.83, 95%CI = 0.78–0.89, $p = 0.54$) (Figure). None of the biomarkers could accurately diagnose presence of NASH.

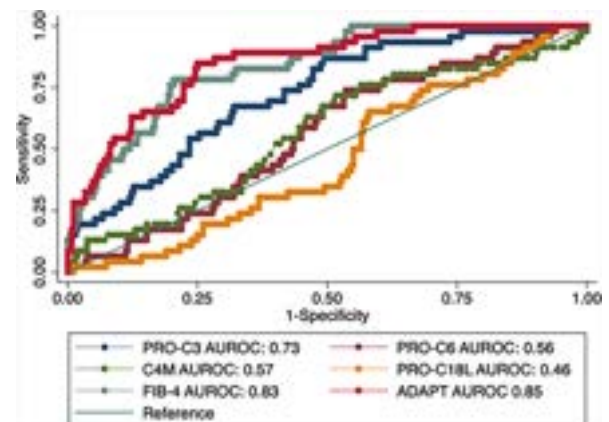


Figure:

Conclusion: Among the evaluated novel biomarkers in this cohort, PRO-C3 had a good diagnostic performance, which improved when implemented in the score ADAPT. FIB-4 and ADAPT had an excellent performance in detecting advanced fibrosis. These results suggests that FIB-4 remains a favorable biomarker to, as a first-line test, predict presence of advanced fibrosis in patients with NAFLD.

SAT-482

Evaluating the role of novel magnetic resonance imaging-based biomarkers in non-invasive assessment of hepatic fibrosis and activity in non-alcoholic fatty liver disease

En Ying Tan¹, Sin Hui Melissa Chua¹, Eunice Tan¹, Daniel Huang¹, Jonathan Lee¹, Margaret Teng¹, Nur Halisah Binte Jumat¹, Yock Young Dan¹, Mark Muthiah¹. ¹National University Hospital (NUH)-Singapore, Department of Gastroenterology and Hepatology, Singapore, Singapore
Email: tanenying@hotmail.com

Background and aims: Non-alcoholic fatty liver disease (NAFLD) encompasses a spectrum of disease including hepatic steatosis, non-alcoholic steatohepatitis, fibrosis and cirrhosis. It is the most common

POSTER PRESENTATIONS

liver disease worldwide. Identification of those with significant fibrosis and disease activity is the cornerstone of risk stratification of NAFLD patients and preventing progression to irreversible liver disease. Liver biopsy is considered the gold standard for diagnosis and assessment of NAFLD, but drawbacks such as procedural risks, sampling error, cost, poor acceptability and limited availability highlight the need for robust non-invasive tests (NITs). We aimed to evaluate the performance of LiverMultiScan (LMS) and Body Composition Profiling (BCP). We also aimed to correlate BCP to disease activity to generate novel associations in the disease.

Method: Patients at the National University Health System, Singapore who had NAFLD and underwent liver biopsy were recruited to undergo LMS and BCP. All patients were extensively evaluated for alternative causes of liver disease and results were negative. LMS cT1 and various BCP indices were evaluated for their performance in assessment of fibrosis and activity.

Results: 106 multi-ethnic Asian patients with biopsy-proven NAFLD were recruited from 2020 to 2022 to undergo the two scans. PDFF had AUCs of 0.979 for any steatosis, 0.867 for S2–3 steatosis and 0.906 for S3 steatosis. AUC values for cT1 were 0.702, 0.740, 0.702 and 0.714 for identifying NAFLD Activity Score (NAS) of at least 5, SAF activity score of at least 3, NASH and at-risk NASH respectively. cT1 appeared to perform well for the above metrics regardless of grade of steatosis. AUCs improved when combining cT1 with some NITs (PDFF, Fib-4, APRI) via logistic regression modelling, but this did not reach statistical significance. In particular, cT1 with APRI achieved the highest AUC of 0.824. Logistic regression models including all BCP indices achieved much higher performance compared to individual indices, with AUCs of 0.803, 0.846, 0.846 and 0.780 for at-risk NASH, advanced fibrosis, NAS ≥ 5 and SAF ≥ 3 . BCP indices relating to visceral adiposity had the largest AUCs for predicting fibrosis, activity and steatosis. HOMA-IR score is correlated to visceral adipose tissue index (VATi). On multiple linear regression, VAT ratio (VATr) and HOMA-IR both independently correlate with stage of fibrosis, while VATr correlates independently with activity.

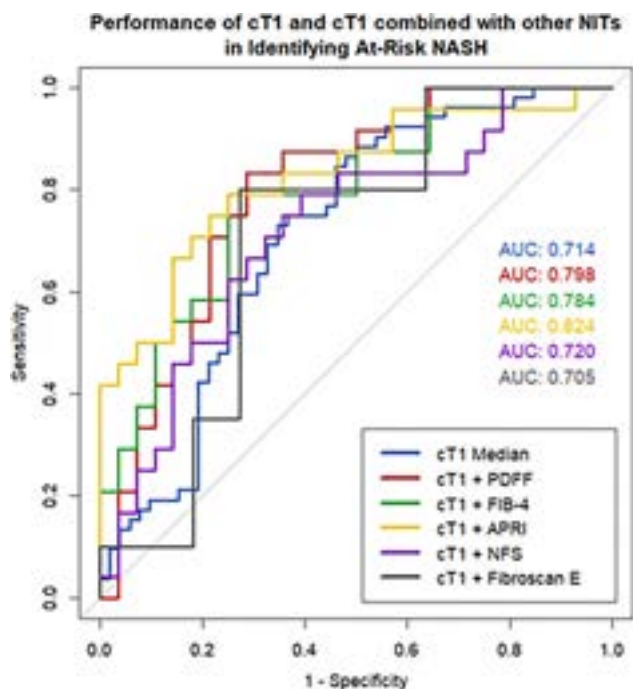


Figure:

Conclusion: Quantitative MRI-based biomarkers from both LMS and BCP scans were able to identify patients with more advanced or more aggressive NAFLD. There may be a role for novel predictive models that combine multiple biomarkers to enhance diagnostic

performance. BCP has a role in investigating the mechanisms linking NAFLD, visceral adiposity and insulin resistance.

SAT-483

Developing a risk stratification tool for advanced NAFLD fibrosis using routinely measured clinical variables in a diabetes clinic annual review

Hamish Miller^{1,2}, Santo Colosimo^{2,3}, Wenhao Li¹, Jeremy Cobbold⁴, William Alazawi¹, David Harman⁵, Guruprasad Aithal⁶, Pinelopi Manousou⁷, Richard Parker⁸, Philip N Newsome⁹, David Sheridan¹⁰, Kalpana Devalia¹¹, John Loy¹¹, Jeremy Tomlinson².

¹Barts Liver Centre, Blizard Institute, Queen Mary University London, United Kingdom; ²University of Oxford, OCDEM, United Kingdom;

³School of Nutrition Science, University of Milan, Italy; ⁴John Radcliffe Hospital, United Kingdom; ⁵Royal Berkshire Hospital NHS Foundation Trust, United Kingdom; ⁶The University of Nottingham, United Kingdom;

⁷Imperial College London, United Kingdom; ⁸Leeds Teaching Hospitals NHS Trust, United Kingdom; ⁹University of Birmingham, United Kingdom; ¹⁰University Hospitals Plymouth NHS Trust, United Kingdom;

¹¹Department of Bariatric Surgery, Homerton University Hospital, United Kingdom

Email: hamish.miller@nhs.net

Background and aims: Despite increasing evidence demonstrating a strong relationship between poor glycaemic control and NAFLD severity, routine assessment to diagnose and stage NAFLD is not included in national UK guidance in the management of type 2 diabetes (T2D). As a consequence, liver chemistry and platelet counts (critical components of many non-invasive risk scoring systems, including NAFLD Fibrosis Score and Fib-4) are often not measured. We therefore assessed whether age and HbA1c alone could be used to rule out advanced fibrosis in people with T2D.

Method: Data from 324 patients (181 male) with and without T2D from 4 different UK secondary care cohorts were retrospectively analysed. These cohorts comprised patients recruited to a urinary biomarker study (TrUSt NAFLD: Translating the potential of the urinary steroid metabolome to diagnose and stage NAFLD) and its pilot phase in Oxford, the DRWF (Diabetes Research and Wellness Foundation) NAFLD study and a bariatric study in London. All subjects had liver biopsy proven and staged NAFLD and had available HbA1c and Fib-4 data. Data were collected within 12-months of the liver biopsy.

Results: 141/324 (44%) participants had T2D, and advanced fibrosis (F3-F4) was identified in 58% of biopsies. After adjustment for both age and BMI, HbA1c positively correlated with the degree of fibrosis on liver biopsy ($R = 0.479$, $R^2 = 0.229$, $p = 0.023$). A binomial logistic regression model was developed that included the following variables; Fibrosis (absent/mild vs severe) as the dependent variable, HbA1c and age as independent variables. The model demonstrated a significant relationship of HbA1c and age with the severity of fibrosis on liver biopsy (AUROC = 0.77, $p < 0.001$, C.I.95% [0.71–0.82]). There was no correlation between the severity of fibrosis and BMI. The performance of this model to identify advanced fibrosis was similar to that of the established non-invasive risk stratification score, Fib-4 (AUROC = 0.81, $p < 0.001$, C.I.95% [0.75–0.86]).

Conclusion: A regression model based on HbA1c and age is similar to Fib-4 in predicting the risk of advanced fibrosis in a population of subjects with and without T2D attending a secondary care metabolic hepatology clinic. Whilst there is a need for validation in an independent cohort, use of simple non-invasive tests to exclude significant disease and focus attention on those at increased risk is desirable. More work is needed to consider the impact of HbA1c and age on risk of fibrosis in clinical care models.

SAT-484

Diagnostic performance of non-invasive fibrosis markers in patients with immune-mediated disease and hepatic steatosis

María Del Barrio Azaceta¹, Paula Iruzubieta¹, Juan Carlos Rodríguez Duque¹, Carolina Jiménez-González¹, Marta Hernández Conde², Coral Rivas¹, Álvaro Santos-Laso¹, Laura Rasines¹, Lorena Cayon¹, Ana Álvarez Cancelo¹, Sara Arias-Sánchez¹, Andrea Fernández-Rodríguez¹, Christie Perelló², María Teresa Arias Loste¹, José Luis Calleja Panero², Javier Crespo¹.
¹Gastroenterology and Hepatology Department, Clinical and Translational Research in Digestive Diseases, Valdecilla Research Institute (IDIVAL), Marqués de Valdecilla University Hospital, Santander, Spain; ²Servicio de Aparato Digestivo, Unidad de Hepatología, Hospital Universitario Puerta de Hierro-IDIPHSA, Madrid, Spain
 Email: javiercrespo1991@gmail.com

Background and aims: High prevalence of non-alcoholic fatty liver disease (NAFLD) has been evidenced in patients with immune-mediated diseases (IMID), regardless of classical metabolic factors. However, the performance of non-invasive fibrosis tests in these patients is unknown. Our aim was to assess the accuracy of non-invasive tests in identifying advanced fibrosis (AdF) among patients with NAFLD and IMID.

Method: Multicentre, cross-sectional study that included patients with IMID (inflammatory bowel disease, psoriasis, hidradenitis suppurativa, and/or spondyloarthritis) who attended to two university hospitals (Santander and Madrid) between March 2018 and December 2019. Liver stiffness was obtained using FibroScan (FS) and the following tests were calculated: NAFLD Fibrosis Score (NFS), Fibrosis Index-4 (FIB-4), AST to Platelet Ratio Index (APRI), Hepamet Fibrosis Score (HFS). Fatty liver was defined as CAP ≥ 248 dB/m. The sensitivity, specificity, positive (PPV) and negative (NPV) predictive value of the tests were calculated considering the liver histological result as reference in patients with liver biopsy.

Results: Among the 1,535 patients with valid FS, fatty liver without other causes of liver disease was detected in 668 (43.5%) (mean age 54 ± 11.5 years; 57% men; 41.2% obese; 12.1% diabetics). A FS ≥ 8 kPa was detected in 20.2% of patients, while a FS ≥ 12 kPa was evidenced in 5.5% of patients. Risk of AdF measured by NFS, FIB-4, APRI, and HFS was obtained in 1.7%, 4.9%, 0.5%, and 0.5% of patients, respectively. Liver biopsy was proposed to all patients with FS ≥ 8 kPa and/or increased ALT values (n = 217), accepting a total of 85 patients (mean age 55.3 ± 8.8 years; 49.4% men; 76.5% obese; 28.0% diabetics; 18.8% with advanced fibrosis). The table shows the diagnostic accuracy for AdF of each of non-invasive test.

Conclusion: APRI, FIB-4, and FS are the most useful screening tools for the detection of AdF among patients with NAFLD and IMID.

SAT-485

The liver worsens in non-alcoholic fatty liver disease patients as diabetes mellitus worsens and lasts longer

Zühal İstemihan¹, Fatih Bektaş², Ali Emre Bardak³, Cansu Kızıldaş³, Gamze Kemeç³, Ziya İmanov¹, Volkan Senkal¹, Kanan Nuriyev¹, Aynure Rüstemzade¹, Sezen Genç¹, Hülya Hacışahinoğulları², Kubilay Karşıdağ², Bilger Çavuş¹, Aslı Çifcibaşı Örmeci¹, Filiz Akyuz¹, Kadir Demir¹, Fatih Besisik¹, Sabahattin Kaymakoglu¹. ¹Istanbul University, Istanbul Faculty of Medicine, Department of Internal Medicine, Division of Gastroenterohepatology, Istanbul, Turkey; ²Istanbul University, Istanbul Faculty of Medicine, Department of Internal Medicine, Division of Endocrinology and Metabolic Diseases, Istanbul, Turkey; ³Istanbul University, Istanbul Faculty of Medicine, Department of Internal Medicine, Istanbul, Turkey
 Email: kaymakoglus@hotmail.com

Background and aims: Type 2 diabetes mellitus (T2DM) is a major driver of non-alcoholic fatty liver disease (NAFLD). It was aimed to investigate the frequency of NAFLD with non-invasive tests and the factors affecting liver fibrosis in type 1 diabetes mellitus (T1DM) and T2DM patients.

Method: We prospectively evaluated the frequency of NAFLD and liver fibrosis with biomarkers based on blood tests and FibroScan® in adult (≥ 18 years) patients with T1DM and T2DM who were followed up from the diabetes mellitus (DM) outpatient clinic in a tertiary center. ≥ 8 kPa was accepted as significant fibrosis (F2), and ≥ 9.6 kPa was accepted as advanced fibrosis (F3-F4) in FibroScan® measurements. The cut-off value of the CAP score was accepted as 274 dB/m in FibroScan® measurements. Fibrosis and steatosis was compared with FibroScan® and with scores based on blood tests.

Results: A total of 520 diabetic patients (55.6% female, 82.1% T2DM) who follow-up consecutively were included in our study. The mean age of the patients was 56.28 ± 14.78 years, DM duration was 13.27 ± 8.96 years, body mass index (BMI) was 28.63 ± 6.06 kg/m², waist circumference was 101.38 ± 14.27 cm, hip circumference was 107.76 ± 12.87 cm. Liver stiffness measurements (LSM) and CAP scores with serum scores of the study group are summarized in Fig. The frequency of NAFLD was higher in patients with T2DM than in patients with T1DM (48.7%, 12.9%, respectively, $p = 0.01$). When fibrosis scores were compared with non-invasive fibrosis markers of patients with T1DM and T2DM, fibrosis values in patients with T2DM were found to be significantly higher in all kinds of non-invasive biomarkers ($p = 0.001$). When the factors affecting fibrosis are investigated; age, BMI, waist/hip ratio, and DM duration were found to be significantly correlated with fibrosis. The incidence of significant fibrosis was higher in patients with T2DM compared to T1DM (29%, 5%, respectively, $p = 0.01$). Advanced fibrosis rate was found to be higher in patients with T2DM than in T1DM (20%, 5%, respectively, $p < 0.05$). Microvascular complications of diabetes mellitus were observed more frequently in the presence of significant fibrosis ($p = 0.03$). The mean CAP score in patients with and without microvascular complications was 267.24 ± 56.74 , 256.51 ± 58.13 dB/m ($p < 0.05$), and in patients with and without macrovascular

	AUC (IC 95%)		Sensitivity (IC95%)	Specificity (IC95%)	PPV (IC95%)	NPV (IC95%)		Sensitivity (IC95%)	Specificity (IC95%)	PPV (IC95%)	NPV (IC95%)
NFS	0,67 (0,49-0,85)	NFS (cut point -1,455)	81,2 (57,0-93,41)	49,3 (37,8-60,8)	27,1 (16,6-41,0)	91,9 (78,7-97,2)	NFS (cut point 0,675)	18,7 (6,6-41,0)	95,6 (88,0-98,5)	50,0 (18,8-81,2)	83,5 (73,8-90,1)
FIB-4	0,73 (0,57-0,89)	FIB-4 (cut point 1,3)	81,2 (57,0-93,4)	63,8 (52,0-74,3)	34,2 (21,2-50,1)	93,6 (82,8-97,8)	FIB-4 (cut point 2,67)	18,7 (6,6-41,0)	95,6 (88,0-98,5)	50,0 (18,8-81,2)	83,5 (73,8-90,1)
APRI	0,83 (0,71-0,94)	APRI (cut point 0,5)	81,2 (56,7-93,4)	72,5 (60,9-81,6)	40,6 (25,5-57,7)	94,3 (84,6-98,1)	APRI (cut point 1,5)	12,5 (3,5-36,0)	100 (94,7-100)	100 (14,2-100)	83,1 (73,7-89,7)
HFS	0,81 (0,69-0,93)	HFS (cut point 0,12)	55,6 (26,7-81,1)	77,8 (63,7-87,5)	33,3 (15,2-58,3)	89,7 (76,4-95,9)	HFS (cut point 0,47)	11,1 (2,0-43,5)	91,1 (79,3-96,5)	20,0 (1,6-62,4)	83,7 (71,0-91,5)
FibroScan	0,81 (0,67-0,94)	FibroScan (cut point 8kPa)	100 (80,6-100)	24,6 (16,0-36,0)	23,5 (15-34,9)	100 (81,6-100)	FibroScan (cut point 12kPa)	68,7 (44,4-85,8)	79,7 (68,8-87,5)	44,0 (26,7-62,9)	91,7 (81,9-96,4)

Figure: (abstract: SAT-484).

POSTER PRESENTATIONS

complications, the mean CAP score was 266.44 ± 54.01 , 260.9 ± 58.78 dB/m ($p < 0.05$), respectively. While LSM was most significantly correlated with FIB4 and NAFLD fibrosis scores ($p < 0.01$, $r = 0.518$; $p < 0.01$, $r = 0.361$, respectively), CAP score was correlated with fatty liver index and hepatic steatosis index ($p < 0.01$, $r = 0.6$; $p < 0.01$, $r = 0.583$, respectively).

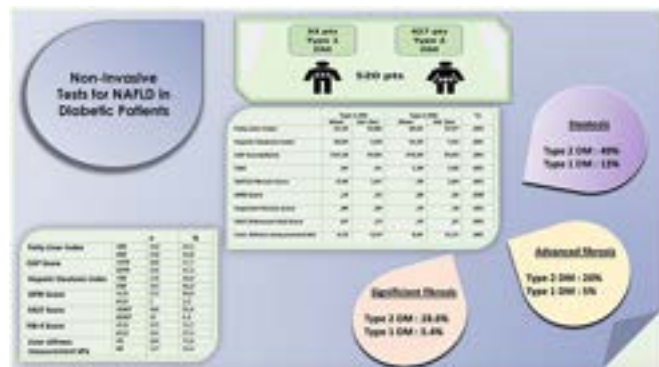


Figure:

Conclusion: NAFLD was detected more frequently in patients with T2DM than in T1DM. BMI, waist/hip ratio, age, duration of DM and complications of DM were found to be the main factors affecting liver fibrosis in T2DM. Microvascular and macrovascular complications of DM are significantly more common in diabetic patients with NAFLD.

SAT-486

Implementing a clinical care algorithm for screening of liver fibrosis in specialist diabetes care

Muna Tajudin^{1,2}, Johan Hoffstedt¹, Hannes Hagström^{1,2}, Sophia Rössner¹. ¹Karolinska Institutet, Department of Medicine, Huddinge, Sweden; ²Karolinska University Hospital, Department of Upper GI Diseases, Sweden
Email: muna.tajudin.2@ki.se

Background and aims: Non-alcoholic fatty liver disease (NAFLD) is the most common chronic liver disease, affecting approximately one third of the global adult population. Patients with type 2 diabetes (T2D) constitute a risk group for presence and severity of NAFLD. Yet, there are few published examples of collaborations between endocrinologists and hepatologists in caring for patients with T2D and NAFLD. Here, we describe preliminary results and patient characteristics from a novel pathway for screening of liver fibrosis in routine specialist diabetes care at a tertiary care hospital.

Method: Patients with T2D seen at the Endocrinology department at Karolinska University Hospital, Stockholm, Sweden, during a structured intervention for T2D between October 2016 and December 2022 were eligible for inclusion. These were patients with complicated T2D referred for a comprehensive assessment. Subjects with excessive alcohol consumption, viral hepatitis or other chronic liver diseases were excluded. Liver stiffness measurement (LSM) and Controlled attenuation parameter (CAP) was obtained utilizing vibration-controlled transient elastography (VCTE). A LSM cut-off to exclude advanced fibrosis was set to 8 kPa.

Results: A total of 167 patients with a valid LSM were included. The median age was 59 years and 39% were women. The mean LSM was 8.3 (SD 6.4) kPa, and the median CAP was 317 dB/m. In total, 32% had LSM ≥ 8 kPa; 19% had LSM ≥ 10 kPa; and 11% had LSM ≥ 15 kPa. NAFLD defined as CAP ≥ 280 dB/m was present in 94 (66%) patients. Baseline characteristics stratified on a LSM measurement of 8 kPa are presented in Table 1.

Variable	All patients (N = 167)	LSM <8 kPa (N = 113)	LSM ≥ 8 kPa (N = 54)	p value	Missing data, n
Age (years)	59 (50–67)	59 (49–66)	60 (52–68)	0.36	0
Sex (female, %)	65 (38.9%)	45 (39.8%)	20 (37.0%)	0.73	0
CAP (dB/m)	317 (263–364)	297 (258–345)	344 (292–384)	0.003	24
Hypertension	115 (68.9%)	75 (66.4%)	40 (74.1%)	0.048	2
BMI (kg/m ²)	30.0 (27.4–34.3)	29.2 (26.5–32.4)	32.0 (29.1–37.1)	<0.001	5
HbA1c (mmol/mol)	68 (59–81)	67 (59–81)	70 (59–80)	1.00	4
Glucose (mmol/L)	9.40 (7.6–11.5)	9.2 (7.1–12.1)	9.8 (8.0–11.4)	0.32	44
Creatinine (μmol/L)	73 (60–90)	73 (61–90)	69 (55–91)	0.44	6
Low-density lipoprotein (mmol/L)	2.30 (1.60–3.10)	2.34 (1.80–3.12)	2.30 (1.40–2.90)	0.27	30
Platelet count (10 ⁹ /L)	251 (207–318)	248 (212–321)	251 (189–312)	0.53	9
Non-smoker	71 (42.5%)	51 (45.1%)	20 (37.0%)	0.040	3
Former smoker	78 (46.7%)	54 (47.8%)	24 (44.4%)		
Current smoker	15 (9.0%)	8 (7.1%)	7 (13.0%)		
Excessive alcohol consumption	57 (34.1%)	37 (32.7%)	20 (37.0%)	0.22	10

Figure:

Data are presented as median (IQR) for continuous measures, and n (%) for categorical measures.

Conclusion: The prevalence of NAFLD and elevated LSM, indicative of advanced fibrosis, in this cohort of patients with advanced T2D was high. Cap values, BMI, hypertension and smoking might be potentially interesting parameters to further identify patients with elevated LSM. Based on these results, a clinical care algorithm is now being introduced in our hospital, offering patients with advanced T2D a VCTE measurement and hepatological evaluations in those with values ≥ 8 kPa. We hope to spread this model to other hospitals in Sweden through local collaborations between hepatology and endocrinology services.

SAT-487

The use of non-invasive tests compared with histological fibrosis stage in predicting liver-related events in metabolic dysfunction-associated fatty liver disease

Wah Loong Chan¹, Shi-En Chong¹, Felicia Chang¹, Kee Huat Chuah¹, Nik Raihan Nik Mustapha², Sanjiv Mahadeva¹, Wah-Kheong Chan¹. ¹Universiti Malaya, Gastroenterology and Hepatology Unit, Department of Medicine, Faculty of Medicine, Kuala Lumpur, Malaysia; ²Hospital Sultanah Bahiyah, Department of Pathology, Alor Setar, Malaysia
Email: wljack90@gmail.com

Background and aims: To study the use of non-invasive tests (NITs) compared with histological fibrosis stage in predicting liver-related events in adults with metabolic-dysfunction-associated fatty liver disease (MAFLD).

Method: This is a single-centre prospective study of a well-characterized cohort of biopsy-proven MAFLD patients who were followed for liver-related events. The patients were followed every 6–12 months for cardiovascular events, liver-related events, malignancy, and mortality. The performance of NITs was evaluated using area under receiver operating characteristic curve (AUROC).

Results: The data for 202 patients were analyzed (median age 55.0 years old, male 47.5%, steatohepatitis 76.7%, advanced liver fibrosis 27.3%). The median follow-up interval was 7 years (range 1–9 years). Seven liver-related events (ascites, n = 1; hepatocellular carcinoma, n = 1; variceal bleeding, n = 1; gastroesophageal varices, n = 4) occurred in 2.5% (5/202) of patients. LSM and histological fibrosis stage were good predictors of liver-related events with AUROC of 0.88 and 0.89, respectively, while NFS was fair with AUROC of 0.78. FIB-4 and APRI performed poorly with AUROC of 0.63 and 0.56, respectively. The optimal cut-off for each of the NITs (based on Youden index), and its sensitivity, specificity, positive predictive value (PPV), and negative predictive value (NPV) for liver-related events are shown in Table 1.

Using the 10 kPa cut-off, the sensitivity, specificity, PPV and NPV of LSM for liver-related events were 100%, 65.5%, 6.7% and 100%, respectively. Using the 15 kPa cut-off, the corresponding values were 60%, 84.3%, 8.8% and 98.8%, respectively.

Table 1 The optimal cut-off for each of the noninvasive tests (based on Youden index), and its sensitivity, specificity, positive predictive value, and negative predictive value for liver-related events

	Histological fibrosis stage	LSM	APRI	FIB-4	NAFLD fibrosis score (NFS)
AUROC	0.89 (0.81-0.96)	0.88 (0.79-0.96)	0.56 (0.26-0.83)	0.63 (0.36-0.87)	0.78 (0.66-0.91)
Optimal Cut-off	F3	11.1 kPa	0.81	0.89	-0.930
Sensitivity	100%	100%	40%	100%	100%
Specificity	75%	70%	80%	36%	62%
PPV	9%	6%	9%	4%	6%
NPV	100%	100%	98%	100%	100%

LSM, liver stiffness measurement; APRI, aspartate aminotransferase to platelet ratio index; FIB-4, fibrosis-4 index; NAFLD, nonalcoholic fatty liver disease; AUROC, area under the receiver operating characteristic curve; 95% CI, 95% confidence interval; PPV, positive predictive value; NPV, negative predictive value

Figure:

Conclusion: LSM, but not simple blood-based fibrosis scores, appeared to be as good as histological fibrosis stage in predicting liver-related events in MAFLD patients.

SAT-488

LIVERFAS[®] GP+ (GP+), a non-invasive blood testing for NAFLD staging, improves risk stratification of patients with indeterminate FIB-4 results

Naim Alkhour¹, Anita Kohli¹, Phillip Leff¹, Rida Nadeem¹, Mona Munteanu². ¹Arizona Liver Health, United States; ²Fibronostics, United States

Email: mona_munteanu@hotmail.com

Background and aims: GP+, an AI-based blood test, was validated against liver biopsy (LB) to identify the presumed NAFLD clinical stages. GP+ clinical variables are: total bilirubin, liver enzymes, glucose and lipid panel. The aim was to assess retrospectively the GP+ performance and concordance rate (CR) as second step after FIB-4 for the assessment of advanced fibrosis (F3-F4) in NAFLD patients.

Method: Patients included from a tertiary hepatology clinic had LB-proven NAFLD and concomitant FIB-4, GP+ and liver stiffness measurement (LSM). AUC (SE) and C-statistics were used to assess the accuracy of each no-invasive test (NIT) against LB.

Results: 176 patients were included [mean (se) age 57.2 (0.8) years, BMI 37.7 (0.6)kg/m², ALT 52 (3)U/L, diabetes 47.4%]. AUC (SE) for F3-F4 for FIB-4, GP+ and LSM, respectively, were 0.76 (0.04), 0.69 (0.04), 0.76 (0.04), all p values = ns. 27 patients had FIB-4 ≥ 2.67; the LB CRs for F3-F4 and all NITs were 68%; LB CRs for F3-F4 with LSM and GP+, respectively, were higher (68% each) than with FIB-4 (58%). In 64 patients FIB-4 ranged 1.30–2.67; LB stage was F1-F2 in 34 and F3-F4 in 26. For F1-F2, LB CR with GP+ was 60%, significantly higher than with LSM (28%, p < 0.001). For F3-F4, LB CRs with LSM and GP+ were similar (43%). 85 patients had FIB-4 < 1.3; LB CR with FIB-4 for ruling out F3-F4 was 17%; LB CR with GP+ for F1-F2 staging was 71%, higher than with LSM (31%).

Conclusion: GP+ is readily available and can be used to identify F3-F4 as a second step in patients with indeterminate FIB-4.

SAT-489

Assessing the feasibility of AI-based Hamaguchi score estimation for NAFLD diagnosis using ultrasound images

Alessia Visintin¹, Mauro Giuffrè^{2,3}, Francesca Dottor², Christian Francescut², Flora Masutti¹, Lisa Rebuzzi², Marco Sartori², Massimiliano Loddo², Caterina Zoratti², Simone Kresevic⁴, Silvia Palmisano^{2,3,5}, Saveria Lory Croce^{1,2,3}. ¹Azienda Sanitaria Universitaria Giuliano Isontina (ASUGI), Clinica Patologie del Fegato, Trieste, Italy; ²Università degli Studi di Trieste, Dipartimento di Scienze Mediche, Trieste, Italy; ³Fondazione Italiana Fegato Onlus, Trieste, Italy; ⁴Prodigys, Trieste, Italy; ⁵Azienda Sanitaria Universitaria Giuliano Isontina (ASUGI), Clinica Chirurgica, Trieste, Italy
Email: gff.mauro@gmail.com

Background and aims: NAFLD is a liver disease caused by fat accumulation and ranges from simple steatosis to NASH with increasing liver damage. 25% of the world population has NAFLD and is projected to rise to 33.5% by 2030. Ultrasound B-mode imaging is the preferred diagnostic method but has limitations. This study aims to improve diagnosis using ML and DL algorithms to estimate scores for US images using the Hamaguchi Score and provide a new approach for automatic analysis.

Method: The study evaluated 220 patients with NAFLD who underwent US assessment at Trieste University Hospital. The clinical and radiological data were analyzed to create the study dataset, divided into 3 datasets (Hepatorenal, Diaphragm, Vessel) based on the visibility of liver and renal parenchyma, intrahepatic vessels, and the diaphragm. The Hamaguchi score was assigned to each dataset by 4 physicians, and pre-processing was applied to locate the US cone containing the info. The study proposed a framework for automatic estimation of Hamaguchi score based on semiautomatic analysis of US images using 3 sub-score related algorithms. The liver brightness score was calculated using clustering and K-means, while diaphragm and vessel scores were evaluated using 2 CNNs with transfer learning. To prevent overfitting, data augmentation was used to balance the datasets. Ten CNNs were implemented with transfer learning (VGG-16 and VGG-19) and the best performing network was selected. The development was implemented using Python and Tensorflow/Keras libraries.

Results: A predictive model for liver brightness contrast score was developed and had a 90.5% classification accuracy using sub-scores labeled by physicians. For misclassified cases, the maximum error was one point. The best models for diaphragm deep attenuation and vessel blurring sub-scores based on their performance on the validation dataset. For diaphragm deep attenuation: accuracy 83.25%, loss 0.48, AUC 0.93, precision 83%. Whereas for vessel blurring: accuracy 84.05%, loss 0.44, AUC 0.89, precision 89%.

The algorithm for diaphragm deep attenuation showed an accuracy of 81.8% with misclassified scores under- or over-estimated by one point. The vessel blurring sub-score model had an accuracy of 86.4% on the test dataset, maintaining its performance from training and validation.

Conclusion: This study aimed to assess the possibility of estimating Hamaguchi's score for NAFLD diagnosis using advanced image analysis. The results showed that AI-based methods can estimate the three sub-scores that determine the score with high classification accuracy. These results suggest that such decision support systems could support liver disease diagnosis in the future and reduce intra- and inter-operator assessment error. However, the study had limitations such as a moderate sample size and a retrospective nature that limited the possibility of building a balanced dataset. Further studies with larger samples and clinically balanced datasets are needed to confirm and improve these preliminary results. An automatic tool for ROI selection could also enhance the presented approach.

SAT-490

Metabolic and adipocytokine disorders as a background cause of the progression of non-alcoholic steatohepatitis in obese patients depending on comorbidity with chronic obstructive pulmonary disease

Olha Hryniuk¹, Oksana Khukhlina¹, Olha Mandryk¹, Ivanna Rachynska¹. ¹Bukovinian State Medical University, Department of Internal Medicine, Clinical Pharmacology and Occupational Diseases, Chernivtsi, Ukraine
Email: olha.hryniuk@bsmu.edu.ua

Background and aims: The aim of the research was to analyze changes in glycemia, blood lipid profile and their endocrine (insulin, leptin, adiponectin) regulation during the isolated and combined course of non-alcoholic steatohepatitis (NASH) and chronic obstructive pulmonary disease (COPD) against the background of obesity.

Method: The study involved 160 patients: 35 patients with NASH and obesity of the 1st stage (1 group), 90 patients with NASH, obesity of the 1st stage and COPD 2–3 B, C, D (group 2) and 35 patients with COPD 2–3 B, C, D (group 3). The control group (CG) consisted of 30 practically healthy persons. The state of carbohydrate metabolism was determined by performing the glucose tolerance test using the glucose oxidase method, fasting insulin (DRG System) by the enzyme-linked immunosorbent assay (ELISA). The degree of insulin resistance (IR) was determined by the body mass index, waist circumference/hip circumference; the HOMA-IR index was calculated using the HOMA Calculator Version 2.2 Diabetes Trials Unit University of Oxford (United Kingdom). Blood lipid spectrum was studied by total lipid content (TL), total cholesterol (TC), triacylglycerols (TG), and high-density lipoprotein (HDL) and low-density (LDL) using diagnostic standard sets of "Simko Ltd" (Ukraine). Hormonal regulation of lipid metabolism was determined by blood leptin, adiponectin (DRG System) by ELISA.

Results: The fasting glycemia index in patients of the 1st and 2nd groups was slightly increased by 10.9% and 14.3% ($p_{1-2} < 0.05$) compared to the CG. Analysis of the postprandial glycemia in patients of the 1st and 2nd groups showed a significant increase glucose level by 18.6% and 34.4% respectively ($p_{1-2} < 0.05$) in comparison to data CG. In patients with an isolated course of COPD improbable changes ($p_3 > 0.05$) were observed. The fasting insulin study revealed probable hyperinsulinemia and HOMA IR index increases which were 2.4 and 2.9 times higher in patients of the 1st and 2nd groups comparing to CG ($p_{1-2} < 0.05$). In patients of the 3rd group insulin content and HOMA-IR index were higher than the score in CG by 1.6 times ($p_3 > 0.05$). Blood total lipid concentration in the 3 groups were higher by 29.5%, 39.8% and 14.9% ($p_{1-3} < 0.05$) respectively and blood content of TC increases by 36.3%, 45.7% and 14.9% ($p_{1-3} < 0.05$) respectively in comparison to CG. A probable increase the TG blood concentration (1.9 and 2.2 times respectively, $p_{1-2} < 0.05$) was registered in the 1st and 2nd groups, while in the 3rd group in 1.6 times increase ($p_3 < 0.05$). A significant increase in the atherogenic index was established in patients of the 1st group by 2.3 times, but in the 2nd group the indicator was lower than in CG by 1.2 times ($p_{1-2} < 0.05$), in patients of the 3rd group-changes were not improbable ($p_3 > 0.05$). Serum leptin level in the 1st group exceeded the scale of CG by 4.7 times, and in the 2nd group-by 5.4 times ($p_{1-2} < 0.05$). Plasma adiponectin level of patients of the 1st and 2nd groups were 1.7 and 2.4 times lower than the indicator of CG ($p_{1-2} < 0.05$). In the 3rd group there were no probable changes in indicators ($p_3 < 0.05$).

Conclusion: The metabolic prerequisites to the progression of NASH in comorbidities with obesity are deepened under the conditions of COPD, which is an additional powerful inducing factor of the lipid distress syndrome and carbohydrate disorders with a likely higher increase in the blood of TG, TC, LDL-C, HDL-C level, atherogenicity index, the degree of IR accompanied by hyperleptinemia, adiponectin deficiency.

SAT-491

The role of M2BPGi for screening of advanced hepatic fibrosis in elderly patients

Hoon Gil Jo¹, Dae Won JUN², Eileen Yoon², Mimi Kim², Hye-Lin Kim³, Eun Young Cho¹, Se Young Jang⁴, Young Youn Cho⁵, Ki Tae yoon⁶, Yang-Hyun Baek⁷, Sang Yi Moon⁷, Aejeong Jo². ¹Wonkwang University College of Medicine and Hospital, Korea, Rep. of South; ²Hanyang University, College of Medicine, Korea, Rep. of South; ³Sahmyook University, College of Pharmacy, Korea, Rep. of South; ⁴Kyungpook National University, Kyungpook National University Hospital, Daegu, South Korea, Korea, Rep. of South; ⁵Chung-Ang University Hospital, Seoul, Korea, Korea, Rep. of South; ⁶Pusan National University, Korea, Rep. of South; ⁷Department of Internal Medicine, Dong-A University College of Medicine, Busan, South Korea, Korea, Rep. of South
Email: noshin@hanyang.ac.kr

Background and aims: Non-invasive fibrosis markers such as Fibrosis-4 (FIB-4) or NAFLD Fibrosis Score (NFS) are simple and powerful tools to rule out progressive fibrosis in middle age. However, it is known that FIB-4 and NFS showed very low specificity in the elderly. The purpose of this study is to determine if Mac-2 binding protein glycan isomer (M2BPGi) and non-invasive test (NIT) and their combination could be helpful in diagnosing advanced liver fibrosis in elderly patients aged ≥ 65 years.

Method: Of the 2,177 patients who visited the gastroenterology department of six tertiary general hospitals and performed M2BPGi and transient elastography test (TE), 521 elderly patients aged 65 years or older were finally analyzed. FIB-4 and NFS were calculated for all subjects. Progressive fibrosis was defined as a TE ≥ 8.0 kPa.

Results: A total of 521 elderly patients were included, with an average age of 74.1 ± 5.3 years. Based on the FIB-4 cut-off 2.0, the sensitivity and specificity for screening advanced hepatic fibrosis were 90.4% and 45.2%. When the M2BPGi cut-off was set as 0.8, the sensitivity and specificity in the elderly patients were 83.9% and 38.8%, respectively. The sequential combination of FIB-4 and M2BPGi showed 77.1%, 62.1%, 54.0%, and 82.5% of sensitivity, specificity, positive predictive value, and negative predictive value, respectively. In the case of using the sequential combination of FIB-4 and M2BPGi, the unnecessary referral rate for transient elastography examination in elderly patients was reduced by 24.7% compared to the case of using FIB-4 alone.

Conclusion: The sequential combination of FIB-4 followed by M2BPGi may reduce unnecessary referral rates and decrease consequently further investigations in elderly patients with mild fibrosis.

SAT-492

Development of a novel non-invasive test for prediction of liver fibrosis in patients with clinically severe obesity defined by a BMI over 50 kg/m²

Maximilian Joseph Brol¹, Uta Drebber², Xiaojie Yu², Robert Schierwagen¹, Sabine Klein¹, Andreas Plamper³, Margarete Odenthal², Wenyi Gu¹, Frank Erhard Uschner¹, Karl-Peter Rheinwald³, Jonel Trebicka^{1,4}. ¹University Hospital Münster, Department of Internal Medicine B, Münster, Germany; ²University Hospital of Cologne, Department of Pathology, Cologne, Germany; ³St. Franziskus-Hospital, Department of Bariatric, Metabolic, and Plastic Surgery, Cologne, Germany; ⁴European Foundation for the Study of Chronic Liver Failure-EF Clif, Barcelona, Spain
Email: maximilian.brol@ukmuenster.de

Background and aims: Liver fibrosis is the major driver in chronic liver disease progression. Especially in non-alcoholic fatty liver disease (NAFLD) awareness of liver fibrosis is key for patient stratification and follow-up planning. Non-invasive tests (NIT) for liver fibrosis perform poor in patients with obesity and to date no NIT was validated in the rapidly growing cohort of patients with clinically severe obesity, namely a body mass index (BMI) over 50 kg/m².

Method: This prospective, single-center cohort study included 95 patients who were referred to bariatric surgery. Liver biopsies were acquired during surgery. Liver fibrosis was histopathologically determined according to Kleiner. AST-to-platelet ratio index (APRI), Fibrosis-4 score (FIB-4), NAFLD fibrosis score (NFS) and BMI, AST/ALT-ratio and diabetes score (BARD) with classic and optimized thresholds, determined by maximal Youden-Index were performed. Accuracy, sensitivity, specificity, negative predictive value (NPV) and positive predictive value (PPV) were calculated for each NIT. Multiple regression analysis of clinical variables were used to identify predictive factors in our cohort.

Results: Commonly used NITs showed poor prediction of liver fibrosis in our cohort, with maximum AUROC of .70. Multiple linear regression and ANOVA analyses identified five variables (presence of dyslipidemia, presence of diabetes, serum levels of ALT, AST and creatinine) significantly predicting fibrosis. This resulted in the Severely-Obese-Score (SOS) with an AUROC of .79. Sensitivity was 0.4 for APRI, 0.49 for FIB-4, 0.73 for NFS, 0.64 for BARD and 0.74 for SOS. Specificity was 0.93 for APRI, 0.71 for FIB-4, 0.57 for NFS, 0.43 for BARD and 0.79 for SOS. Accuracy in predicting fibrosis for commonly used NITs ranged between 48–71%. Our score had the best accuracy (75% correctly classified patients) and best NPV for prediction of any degree of fibrosis.

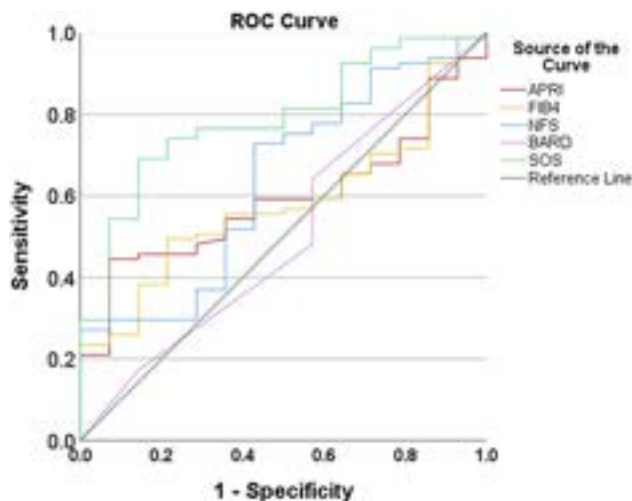


Figure:

Conclusion: Performance of established NITs is weak in patients with clinically severe obesity and a BMI over 50 kg/m². The here presented score is a useful tool this setting. Prospective evaluation of our score should be performed in further studies.

SAT-493

Detecting early improvements in a NAFLD patient population during diet-induced weight loss

Pietro Torre¹, Luigi Schiavo¹, Mario Masarone¹, Benedetta Maria Motta¹, Federica Belladonna¹, Marco Aquino¹, Marcello Persico¹. ¹University of Salerno, Department of Medicine, Surgery and Dentistry, "Scuola Medica Salernitana", Italy
Email: pietro.torre90@gmail.com

Background and aims: Weight loss is the cornerstone in the treatment of NAFLD and was found associated with a histological improvement proportional to its extent. However, it is a difficult goal to achieve and maintain. Moreover, the precise link between weight changes and NAFLD is not fully understood. The aim of this study is to describe the possible positive influences of a nutritionist-guided low-glycemic index diet on anthropometric parameters, Transient Elastography (TE), Controlled Attenuation Parameter (CAP, with the SmartExam software), and blood chemistry in overweight or obese

NAFLD patients. The genetic correlation with TE/CAP measurements was also taken into account.

Method: 69/106 patients who were attending our Hepatology Unit, with NAFLD, aged ≥ 18 , and with a BMI ≥ 25 accepted to start the nutritionist-guided diet. Baseline anthropometric data, TE/CAP, and blood test results were recorded. Single nucleotide polymorphisms in NAFLD risk genes were analyzed and genetic risk score (GRS) was calculated. Control visits were scheduled after 1 and 3 months. TE/CAP was performed during each visit, and after 3 months blood tests were repeated.

Results: 57/69 patients (82.61%) attended at least one of the control visits. A significant difference from baseline was observed at both 1-month and 3-month visit in weight (-4.26 kg [-4.78%] $p < 0.0001$, and -7.67 kg [-8.43%] $p < 0.0001$), BMI (-1.55 Kg/m², $p < 0.0001$, and -2.75 Kg/m², $p < 0.0001$), and CAP (-27.67 dB/m, $p = 0.0062$, and -42 dB/m, $p = 0.0182$). Changes in CAP were proportional to the extent of weight loss, whereas mean liver stiffness remained almost unchanged. Baseline CAP was proportional to GRS; high GRS patients presented a higher decrease in TE/CAP values after 3 months of diet. After 3 months of diet, significant differences in glycemia and triglycerides were observed; AST, ALT, total cholesterol and HDL cholesterol also improved.

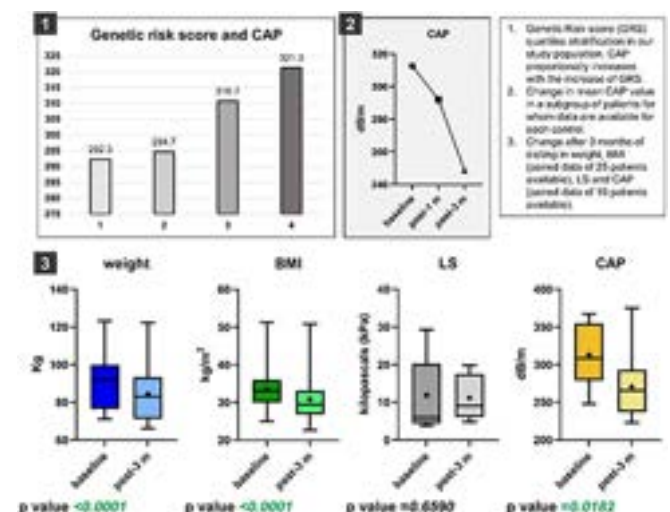


Figure:

Conclusion: In our NAFLD population, after diet-induced weight loss, an improvement in metabolic parameters was observed. The early reduction of CAP could increase patient awareness of the ongoing improvements. Genetics could influence the reduction of steatosis during weight loss.

SAT-494

Echocardiography-based markers for subclinical cardiac dysfunction in patients with non-alcoholic fatty liver disease and significant fibrosis with preserved ejection fraction: preliminary data from a prospective monocentric Italian cohort

Angelo Armandi^{1,2}, Daphne D'Amato¹, Alessandro Andreis³, Matteo Bellettini³, Gian Paolo Caviglia¹, Gabriele Castelnovo¹, Irene Poggiolini¹, Chiara Rosso¹, Nuria Pérez Diaz del Campo¹, Amina Abdulle¹, Kamela Gjini¹, Davide Ribaldone¹, Gaetano De Ferrari³, Giorgio Maria Saracco¹, Davide Castagno³, Elisabetta Bugianesi¹. ¹Division of Gastroenterology and Hepatology, Department of Medical Sciences, University of Turin, Turin, Italy; ²Metabolic Liver Disease Research Program, I. Department of Internal Medicine, University Medical Center of the Johannes Gutenberg University of Mainz, Mainz, Germany; ³Division of Cardiology,

POSTER PRESENTATIONS

Cardiovascular and Thoracic Department, Città della Salute e della Scienza di Torino Hospital, Department of Medical Sciences, University of Turin, Italy
Email: daphne.damato@gmail.com

Background and aims: Individuals with Non-Alcoholic Fatty Liver Disease (NAFLD) have abnormal myocardial energy metabolism and reduced coronary functional capacity, even in the absence of risk factors for cardiovascular disease (CVD), potentially associated with cardiac fibrosis and heart failure (HF). We aimed to evaluate diastolic and systolic function in NAFLD patients and significant fibrosis with preserved ejection fraction (EF).

Method: We prospectively included patients with ultrasound-diagnosed NAFLD undergoing screening echocardiography *per protocol*, in the absence of overt CVD or HF. Echocardiography was performed according to European Society of Cardiovascular Imaging guidelines, including speckle tracking analysis with left ventricular global longitudinal strain (GLS) measurement for accurate quantification of systolic function (Philips, Andover, US). Diastolic dysfunction with increased filling pressures was defined as a mitral E/E' ratio >9. Liver fibrosis was assessed by non-invasive tests and transient elastography (TE, Fibroscan F530); significant liver fibrosis (SLF) was defined by either FIB-4 score >1.3 or liver stiffness (LS) >7 kPa. Clinical and biochemical parameters, as well as TE and echocardiography, were collected within one month from NAFLD diagnosis.

Results: A total of 95 patients were included. Median age was 53.0 [IQR 44.5–62.5] years and 44.6% was male. Type 2 diabetes mellitus (T2DM) and obesity were present in 21.1% and 43.3% of the cohort, while 46.2% had arterial hypertension. Median FIB-4 was 0.97 [IQR 0.67–1.24]. SLF, diastolic and systolic dysfunction were found in 20%, 17% and 18.3% of the total. Higher FIB-4 levels were found in both diastolic and systolic dysfunction ($p = 0.003$ and $p = 0.001$). SLF was associated with diastolic dysfunction (OR 6.8 [95%CI 1.8–25.5], $p = 0.004$), showing an Area Under the Curve of 0.76 (Se 76.9%, Sp 72.2%, PPV 33.3%, NPV 94.5%) (Figure 1). In a multiple stepwise logistic regression model including T2D, obesity, arterial hypertension, dyslipidemia, male sex and SLF, both SLF and T2D were significantly and independently associated with diastolic dysfunction (aOR of SLF 6.2 [95%CI 1.5–25.1, $p = 0.011$). In the same regression model for systolic dysfunction, only T2D showed a significant association (aOR 4.6 [95%CI 1.3–16.8], $p = 0.021$).

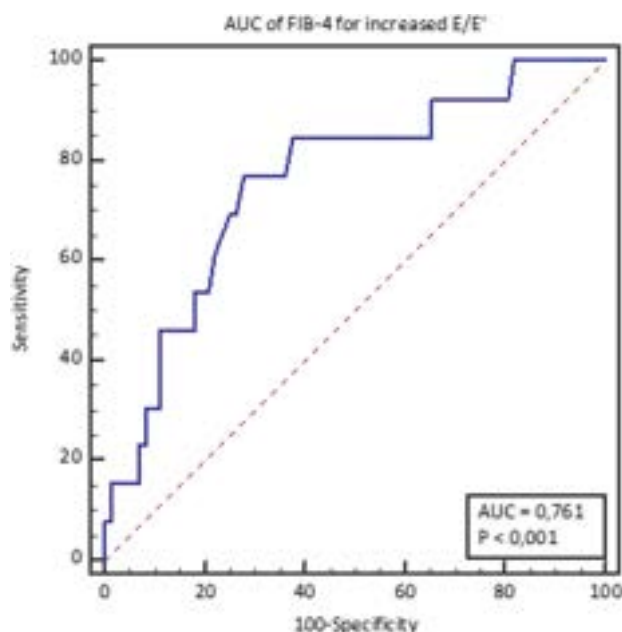


Figure: Discriminative capacity of liver fibrosis for diastolic dysfunction, area under the curve (sensitivity 76.6%, specificity 72.2%, positive predictive value 33.3%, negative predictive value 94.5%).

Conclusion: In NAFLD patients with preserved EF, significant liver fibrosis by FIB-4 and TE correlate with markers of diastolic dysfunction and lower GLS systolic values. T2DM is the strongest factor associated with diastolic dysfunction in this population. Screening echocardiography may be recommended in this population. The research has been supported by the Italian Ministry for Education, University and Research (MIUR) under the programme “Dipartimenti di Eccellenza 2018–2022” Project code D15D18000410001.

SAT-495

Comparison of performance of non-invasive indices in assessing degree of steatosis in non-alcoholic fatty liver disease

En Ying Tan¹, Sin Hui Melissa Chua¹, Eunice Tan¹, Daniel Huang¹, Jonathan Lee¹, Margaret Teng¹, Nur Halisah Binte Jumat¹, Yock Young Dan¹, Mark Muthiah¹. ¹National University Hospital (NUH)-Singapore, Department of Gastroenterology and Hepatology, Singapore, Singapore
Email: tanenying@hotmail.com

Background and aims: Non-alcoholic fatty liver disease (NAFLD) is the most prevalent chronic liver disease worldwide, of which the earliest manifestation is simple hepatic steatosis. Most of the patients with NAFLD have hepatic steatosis, without the presence of steatohepatitis or fibrosis. Liver biopsy is the gold standard for assessment of steatosis, but is associated with significant cost, risks and limited availability, and is not feasible in a disease for which identification in large swathes of the population is key. To identify NAFLD in population cohorts, it is essential to evaluate non-invasive tests (NITs) that are easily performed in primary care. We aim to evaluate the performance of various NITs in predicting presence and severity of hepatic steatosis, comparing to histology as the reference standard.

Method: Patients with biopsy-proven NAFLD were enrolled from National University Health System, Singapore to undergo various non-invasive tests. Patients who also had other causes for liver disease were excluded. Hepatic steatosis index (HSI), visceral adiposity index (VAI), NAFLD liver fat score (NLFS), triglyceride-glucose index (TGI), fatty liver index (FLI) and FibroScan Controlled Attenuation Parameter (CAP) were evaluated for performance in assessment for steatosis.

Results: 399 multi-ethnic Asian patients with biopsy-proven NAFLD were recruited from 2014 to 2021. AUC values for identifying steatosis (S1–3) for HSI, FLI, NLFS, TGI, VAI and FibroScan CAP were 0.792, 0.720, 0.905, 0.714, 0.823 and 0.957 respectively. Optimal cut offs for diagnosis of hepatic steatosis were HSI 38.2, FLI 124.8, NLFS –0.818, TGI 8.45, VAI 1.33 and CAP 254 kPa.

Respective AUC values for identifying S2–3 steatosis for the above-mentioned tests were 0.647, 0.592, 0.736, 0.664, 0.671 and 0.677. Respective AUC values for identifying S3 steatosis were 0.581, 0.585, 0.703, 0.613, 0.668 and 0.616. All indices performed better at identifying steatosis than at distinguishing severity of steatosis. In particular, FibroScan CAP was excellent in identifying steatosis. NLFS had significantly better performance than several other composite scores, especially in diagnosing steatosis.

Conclusion: Our findings suggest NLFS to be a potential NIT for identifying steatosis in population cohorts, given its favourable performance as well as cost and accessibility. As with other NITs, it may be less robust in distinguishing severity of steatosis. FibroScan CAP remains a good option, particularly in places with access to them at the primary care level.

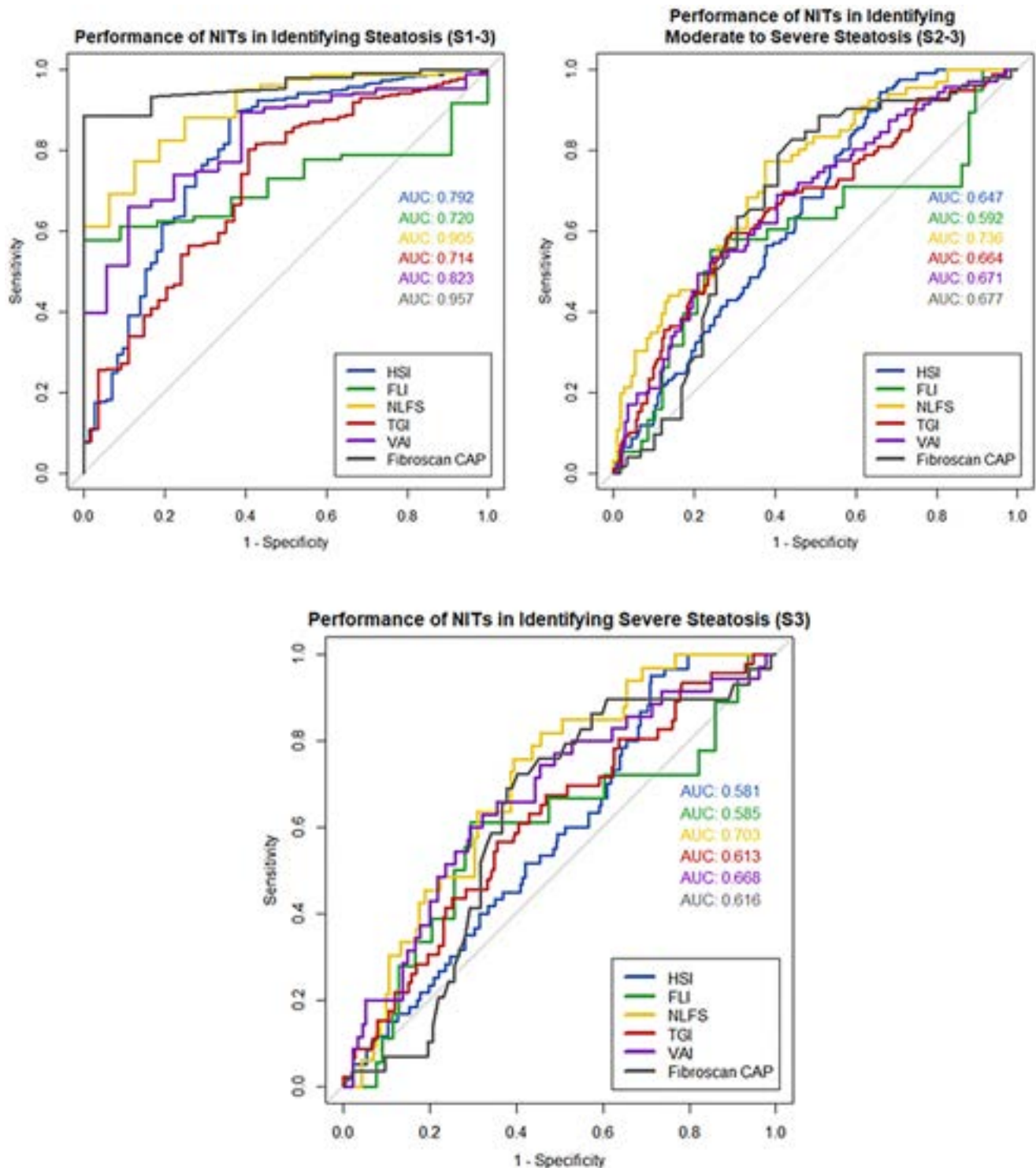


Figure: (abstract: SAT-495).

SAT-496

Evaluation of the performance of a novel single-nuclei digital pathology method for the continuous quantification of steatosis and inflammation in liver biopsies and its correlation with NASH-CRN scores in patients with NASH

Louis Petitjean¹, Li Chen¹, Dmitri Fedorov², Aras Mattis³, Mojgan Hosseini⁴, Mathieu Petitjean¹, Arun Sanyal⁵, Cynthia Behling⁴.
¹PharmaNest, Inc, Princeton, United States; ²ViQi Inc, Santa Barbara,

United States; ³University of California San Francisco, San Francisco, United States; ⁴University of California San Diego, La Jolla, United States; ⁵Virginia Commonwealth University, Division of Gastroenterology, Hepatology and Nutrition, Richmond, United States
 Email: mathieu.petitjean@pharmanest.com

Background and aims: The quantification of HandE liver biopsy with Digital Pathology methods based on annotation provided by pathologists (steatosis, inflammation) result in continuous scores of

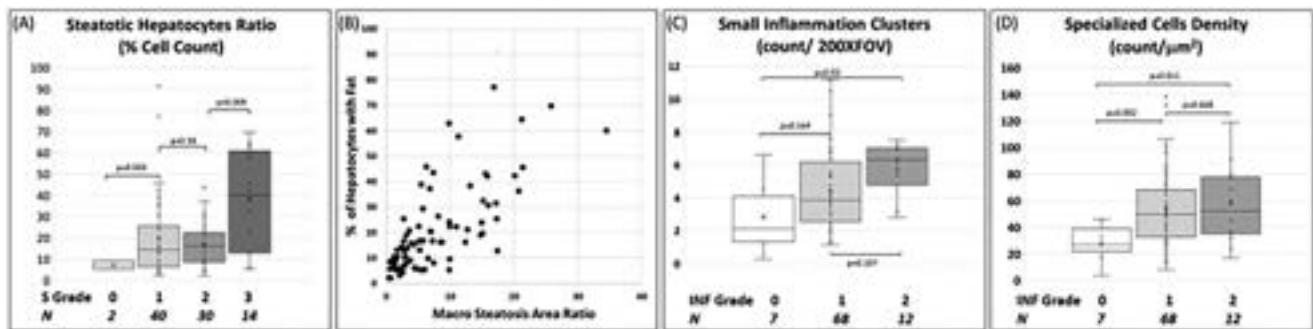


Figure: (abstract: SAT-496).

moderate performances. Here, we report results of a new AI-assisted single-nuclei quantification approach that benefits from (a) training received from pathologists on highly consensual features (cell types) and (b) generates mathematically defined outcomes. This approach address limitations of current histological current nomenclatures and methods (doi:10.1002/hep.32475)

Method: This retrospective cohort included 87 patients with NASH diagnosed by histologic assessment of liver biopsy with lobular inflammation grades of 0 (N=7), 1 (68), and 2 (12), and steatosis grades of 0 (N=2), 1 (40), 2 (30) and 3 (14). Quantitative image analysis of 20X Digital pathology images of HandE stained sections was performed to identify cell nuclei (~20 k per biopsy) and quantify their morphometric and local surroundings in 86 parameters. A subset of 13 images (~260 K nuclei) was used to develop a machine learning (ML) model using 3.0 K annotations (respectively 3.0 K, 3.3 K, 3.7 K, 1.7 K, 3.0 K) for steatotic hepatocytes, normal hepatocytes, inflammatory cells (all kinds), liver specialized cells (all kinds), and “debris” (cells in apoptosis or distorted). Once classified, a cell tissue panel was calculated to account for cell densities (count/mm²) and relative cell count %. Macro-steatosis Area Ratio was calculated. Clusters of inflammatory cells were identified using “closest neighbor” method and the morphometric features of these clusters was used to classify them into small (<5000 μm²), medium and large clusters which are then quantified by several continuous and normalized parameters (biopsy area ratio, count per mm² or 200XFOV).

Results: The cell classification accuracy (error) of the ML model ranged from 14.6% (24.3%) for specialized cells to 77.7% (26.9%) for inflammatory cells. The steatotic hepatocytes count ratio (Fig. A, 0.008<p values<0.38) exhibited similar trends reported previously using ML from pathologists’ annotations and correlates well with Area Ratio (Fig. B, R²=0.5226). The count of small inflammation clusters (Fig. C, 0.107<p values<0.034) moderately corresponds to the histological grades, which is attributed to the histological definition of inflammatory clusters and their assessment. The inflammatory cell density detects the presence of inflammation with good performance (Fig. D).

Conclusion: Quantitative digital pathology can automatically generate tissues panels from HandE stained sections. While the scores extracted from these tissues panels moderately correspond to NASH-CRN histological stages, they present the benefit of being quantitative and translational, and not sensitive to liver tissue variation due to swelling, fat invasion, or various artifacts.

SAT-497

Development of ultra-sensitivity enzyme linked immunosorbent assay for hepatitis delta virus antibody detection

Nomin Ariungerel^{1,2}, Ulziigerel Yanjinkham¹, Saruul Enkhjargal^{1,2}, Naranjargal Dashdorj², Odgerel Oidovsambu³. ¹School of engineering and applied sciences, Department of chemical and biological engineering, Ulaanbaatar, Mongolia; ²Liver center, Ulaanbaatar, Mongolia; ³National University of Mongolia, Department of Chemical and Biological Engineering, Ulaanbaatar, Mongolia
Email: a.nomin@onomfoundation.org

Background and aims: The prevalence of hepatitis delta virus (HDV) is unequally distributed in the world. In most countries, the infection rate is very low, but some countries, especially Mongolia has a disproportionally high prevalence of HDV infection. Therefore, the introduction of sophisticated diagnostic assays for detection of HDV infection is less attractive for most companies, and diversity of commercially available kits are very limited. Also, we have found that most ELISA diagnostic kits for anti-HDV IgG detection have single origin in China and their quality issues should be accounted. In this study, we have developed an ultra-sensitive ELISA assay using self-assembled monolayer method, which applies covalent attachment of sHDAG on the plate surface in more organized manner that produces much better results than the conventional physical absorption method in terms of sensitivity and specificity.

Method: Recombinant His-tagged sHDAG protein (23 kDa) was produced in E. Coli and purified by Ni-NTA metal-affinity chromatography. First, the surface of the polystyrene plate was functionalized by treating with 1% sodium hydroxide for binding of 2% 3-(aminopropyl)triethoxysilane (APTES). Then 10 ug/ml HDV-Ag proteins were cross-linked with N-ethyl-N’-3-dimethylaminopropyl carbodiimide/N-hydroxysuccinimide (EDC/NHS) agents. Then 100 ul of activated proteins were immobilized on the functionalized surface via the crosslinking agents in a self-assembled monolayer. Finally, 100 ul of 5% BSA (bovine serum albumin), healthy human serum and 3% skim milk were used by blocking plates and prevent unspecific binding. For the analysis of sensitivity and specificity, 2 groups (positive and negative) of a total of 131 samples were used. The positive group consisted of samples from 46 patients, who were previously identified as HDV-RNA positive and HBsAg positive. The negative group consisted of samples from 85 people, who were previously identified as healthy by showing HBsAg negative and anti-HCV negative. The optimal conditions for the new ELISA tests were established using checkerboard dilutions of the secondary antibody and serum. Main parameters of the optimal ELISA assay were found as follows: Serum dilution scale 1:100, Secondary Ab dilution scale 1:80000, incubation time 15 min at 37°C, color development time 3 min, and total test duration 30 min. For comparison analysis of sensitivity, the commercially available Wantai anti-HDV IgG kit was used.

Results: Our results showed that our in-house developed ELISA assay has a specificity of 98.8%, a sensitivity of 100%, and an agreement of

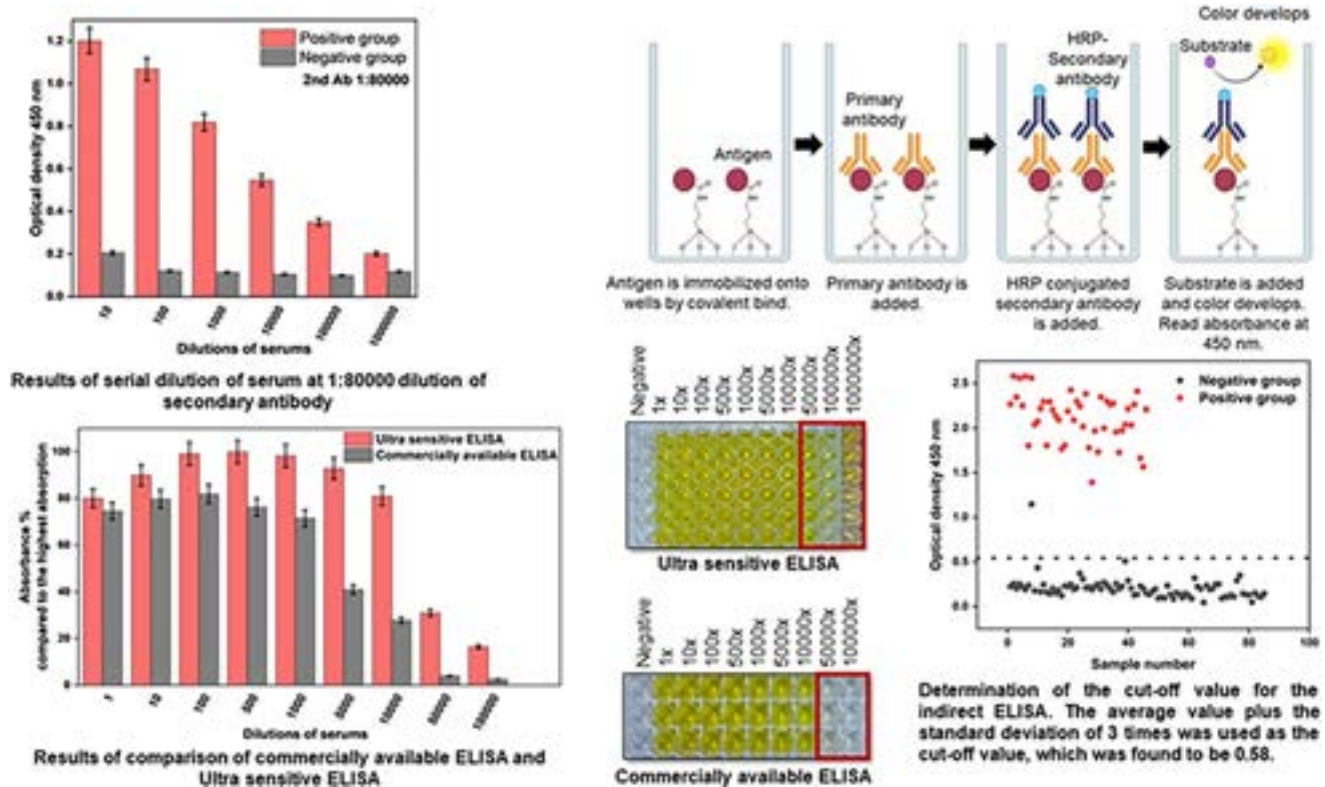


Figure: (abstract: SAT-497).

99.2% respectively. Ultra-sensitivity of the assay was confirmed by the detection of 1:1000000 times diluted serum while the commercially available kit was only able to detect up to 1:50 000 times diluted serum. The total testing process could be done in 30 min, which is 3 times shorter than the commercial testing kit. All these superior results indicate that the self-assembled monolayer method has principally advantageous in terms of design and method.

Conclusion: The ELISA assay developed by self-assembled monolayer method has very high sensitivity and this technology should be introduced to the HDV-diagnostic field.

SAT-498

Biomarkers of hepatocyte basement membrane turnover reflect disease activity in patients with early-stage non-alcoholic fatty liver disease

Ida Lønsmann^{1,2}, Jane I. Grove^{3,4,5}, Asma Haider⁶, Philip Kaye⁶, Morten Karsdal², Diana Leeming², Guruprasad Aithal^{3,4,5}, ¹University of Southern Denmark, Department of Clinical Research, Odense, Denmark; ²Nordic Bioscience, Hepatic Research, Herlev, Denmark; ³University of Nottingham, MRC/EPSRC Nottingham Molecular Pathology Node, Nottingham, United Kingdom; ⁴Nottingham University Hospitals NHS trust and University of Nottingham, NIHR Nottingham Biomedical Research Centre, Nottingham, United Kingdom; ⁵University of Nottingham, Nottingham Digestive Diseases Centre, Translational Medical Sciences, School of Medicine, Nottingham, United Kingdom; ⁶Nottingham University Hospitals NHS Trust, Department of Pathology, Nottingham, United Kingdom
Email: llc@nordicbio.com

Background and aims: Halting progressive liver disease necessitate novel non-invasive methods to identify and monitor patients in need of early intervention. Investigating the pathophysiology of early liver injury might help to identify unique biomarkers. Early liver injury is characterized by recomposition of the hepatocyte basement membrane (BM) of the extracellular matrix. Thus, we quantified

biomarkers targeting two distinct neo-epitopes of the major BM collagen, type IV collagen (PRO-C4 and C4M), in patients spanning the non-alcoholic fatty liver disease (NAFLD) spectrum.

Method: We evaluated BM biomarkers in a cross-sectional study with 97 patients with NAFLD confirmed on histology. Serological levels of PRO-C4 and C4M were quantified using validated competitive enzyme-linked immunosorbent assays (ELISAs). Using the fatty liver inhibition of progression (FLIP) algorithm, we stratified data into two groups: non-alcoholic fatty liver (NAFL) and non-alcoholic steatohepatitis (NASH). Biomarker levels in the two groups were stratified by the NAFLD activity score (NAS). In both groups, biomarker measurements were analyzed in relation to histological scorings of steatosis, inflammation, ballooning, and fibrosis.

Results: The included patients had a body mass index (BMI) of 30.9 ± 5.6 kg/m², age of 53 ± 13 years and a NAS range of 1–8. Upon stratification by FLIP, the NASH patients had higher platelets, ALT, and AST levels than the NAFL group. Both PRO-C4 ($p = 0.0125$) and C4M ($p = 0.003$) increased with increasing NAS solely within the NAFL group. Furthermore, both markers were significantly associated with lobular inflammation ($p = 0.020$ and $p = 0.048$) and steatosis ($p = 0.004$ and $p = 0.015$) in patients with NAFL.

Conclusion: This study found that BM turnover is associated with liver injury in patients with NAFL but not those with NASH. These findings support BM turnover as a clinical feature in early disease development.

SAT-499

Development of loop-mediated isothermal amplification assay for detection of hepatitis delta virus

Saruul Enkhjargal¹, Nomin Ariungerel¹, Naranjargal Dashdorj², Naranbaatar Dashdorj³, Odgerel Oidovsambuu⁴. ¹National university of Mongolia, Department of Chemical and Biological Engineering, School of Engineering and Applied Sciences, Ulaanbaatar, Mongolia; ²Liver center, Ulaanbaatar, Mongolia; ³Onom foundation, Ulaanbaatar, Mongolia; ⁴National University of Mongolia, Department of Chemical and Biological Engineering, Ulaanbaatar, Mongolia
Email: srl@onomfoundation.org

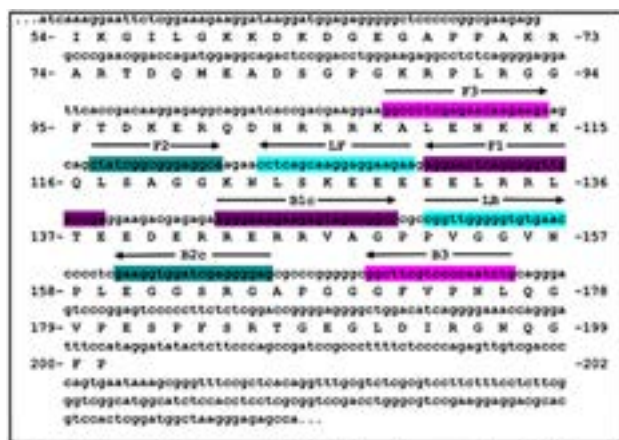
Background and aims: Infection of hepatitis delta virus (HDV) is one of the leading factors for liver disease-related mortality in some countries. For these countries, it is crucial to implement a suitable strategy to eliminate the endemicity of HDV using of sophisticated technologies. Correct diagnostic approaches and management, which enable early detection of HDV infection play a key role in effective elimination. However, HDV-infected people know their infection at a very late time when cirrhosis already developed to a serious stage. Therefore, some countries including Mongolia have initiated a mass screening campaign for the detection of hepatitis viral infection in the entire population, and currently, some apparent improvements were observed in the national viral hepatitis status. Loop-mediated isothermal amplification (LAMP) could be one of the possible options for the detection of active HDV infection in Mongolia, especially since this method might be very useful outside of big cities. LAMP-PCR does not require special equipment like an expensive real-time PCR cyclers, and its simple, fast-processing characteristic is very attractive.

The aim of this study was to develop and characterize a LAMP-PCR assay for the detection of HDV-RNA (HDV-LAMP assay).

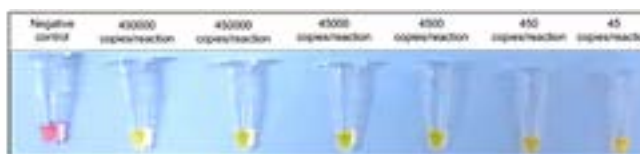
Method: Different primer sets were designed using NEB-online tools on a high homology region of HDV genomic sequence. In this study, commercially available WarmStart Colorimetric and Fluorescent LAMP 2X Master Mix (DNA and RNA) kits from NEB were used. For RNA extraction, Viral RNA isolation kit from Bioactiva Diagnostica was used. Serum samples from 13 HDV-infected patients and 15 healthy people (a total of 28 people) were used for this study. Serially diluted recombinant construct containing HDV genomic sequence were used for the analysis of the limit of detection (LOD). Both colorimetric and fluorescent assays were done for all 23 samples in different protocols to adjust the optimal condition. The amplified products were confirmed by gel electrophoresis and dissociation curve analysis. The overall HDV-LAMP assay was characterized by its sensitivity, specificity, optimal reaction temperature, and time-point of detection.

Results: We tested 5 different primer sets and the best primer set was identified by judging the rate of false positive results. The optimal reaction temperature for the best setting was found as 68°C. Our result indicated that LOD of HDV-LAMP assay is 4.5 copies/reaction, which can be considered a very sensitive assay. The optimal time-point of detection was 50–60 min for colorimetric and 40–50 min for fluorescent assays. Exceeded incubation time increases the probability of false positive results. Our pilot results showed that HDV-LAMP assay has a sensitivity of 100% and a specificity of 94.4%.

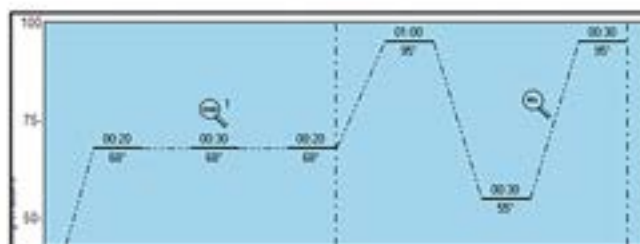
Conclusion: Our study concludes that the currently developed HDV-LAMP assay is a rapid, easy-to-use, and highly sensitive diagnostic assay for detecting HDV-RNA in blood samples. The assay can be



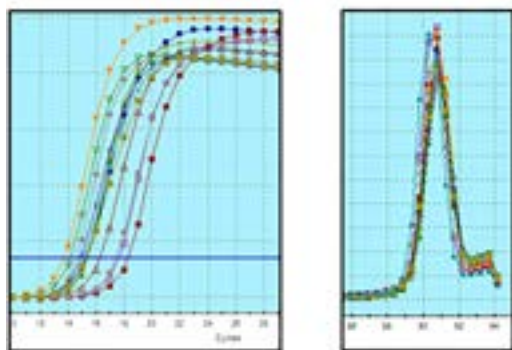
A. Best primer set shown on the high homology region of HDV genomic sequence



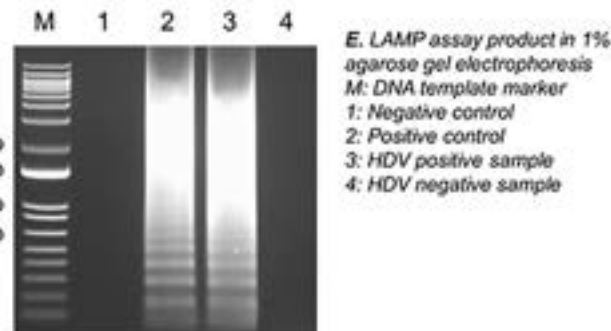
B. Colorimetric HDV-LAMP assay results of HDV standard serial dilution; pink indicates no infection, yellow indicates HDV infection



C. Suitable thermal settings of fluorescent HDV-LAMP assay



D. The amplification curve and dissociation curve of the fluorescent HDV-LAMP assay



E. LAMP assay product in 1% agarose gel electrophoresis
M: DNA template marker
1: Negative control
2: Positive control
3: HDV positive sample
4: HDV negative sample

Figure: (abstract: SAT-499).

broadly utilized in places without real-time PCR equipment and the testing cost will be cheaper. In further, analytical sensitivity and specificity should be determined using a bigger number of patient samples.

SAT-500

Incorporating artificial intelligence in portable infrared thermal imaging for the diagnosis and staging of non-alcoholic fatty liver disease

Yana Davidov¹, Rafael Brzezinski², Monika Kaufmann³, Mariya Likhter¹, Oranit Cohen-ezra¹, Yair Zimmer⁴, Orit Pappo³, Jonathan Leor^{5,6}, Ziv Ben-Ari^{1,2}, Oshrit Hoffer⁴. ¹Sheba Medical Center, Liver Diseases Center, Israel; ²Tel Aviv University, Sackler School of Medicine, Israel; ³Sheba Medical Center, Institute of Pathology, Israel; ⁴School of Electrical Engineering, Afeka Tel Aviv Academic College of Engineering, Tel Aviv, Israel, Israel; ⁵Sheba Medical Center, Tamman Cardiovascular Research Institute, Leviev Heart Center, Israel; ⁶Tel Aviv University, Neufeld Cardiac Research Institute, Israel
Email: y.davidov@gmail.com

Background and aims: Non-alcoholic fatty liver disease (NAFLD) is the most prevalent chronic liver disease worldwide. NAFLD comprises a spectrum of progressive liver pathologies, ranging from simple steatosis to non-alcoholic steatohepatitis (NASH). NASH can progress to advanced liver fibrosis stage, liver failure and liver cancer. Liver biopsy is currently the gold standard for staging NAFLD. In our NAFLD mouse model, thermal imaging combined with advanced image processing and machine learning analysis, the derived algorithm demonstrated a 100% detection rate and classified all mice correctly according to their disease status.

Method: This is a prospective study of 46 patients; all underwent a liver biopsy. Liver thermal imaging using a commercially available portable infrared camera was obtained on the same day the liver biopsy was scheduled. We developed an image processing algorithm that measures relative spatial thermal variation across the skin covering the liver. Thermal parameters including temperature variance, homogeneity levels and other textural features were fed as input to a t-SNE dimensionality reduction algorithm followed by k-means clustering. Patients were diagnosed with NAFLD and stratified according to the NAFLD activity score (NAS) and the fibrosis stage using the Metavir score).

Results: Twenty-one out of 46 patients (median age 54 years (ranges, 19–75); 61% males) were diagnosed with NAFLD, of them NAS >4 was detected in 7 (33%). Using thermal imaging processing, the accuracy to detect patients with NAS >4 was AUC = 0.74, (specificity and sensitivity 56% and 81%). For differentiating advanced fibrosis (F3–4) from early fibrosis stage F0–F2, thermal imaging accuracy was AUC 0.87, with specificity and sensitivity 77% and 88%, respectively.

Conclusion: Non-invasive thermal advanced imaging combined with machine learning-based analysis may improve our ability to diagnose and classify patients with NAFLD.

SAT-501

Metabolic profile reflects stages of fibrosis in patients with non-alcoholic fatty liver disease

Roberta Forlano¹, Nila Jambulingam¹, Benjamin Preston¹, Benjamin H. Mullish¹, Greta Portone¹, Yama Baheer¹, Michael Yee², Robert D. Goldin³, Mark Thursz¹, Pinelopi Manousou¹. ¹Imperial college london, Liver unit/Division of Digestive Diseases, Department of Metabolism, Digestion and Reproduction, United Kingdom; ²Imperial college NHS Trust, Section of Endocrinology and Metabolic Medicine, United Kingdom; ³Imperial college london, Department of Cellular Pathology, United Kingdom
Email: r.forlano@imperial.ac.uk

Background and aims: Non-alcoholic fatty liver disease (NAFLD) is a leading cause of chronic liver disease worldwide, with fibrosis stage being the main predictor for clinical outcomes. Here, we present the metabolic profile of NAFLD patients with regards to fibrosis progression.

Method: We included all consecutive new referrals for NAFLD services between 2011 and 2019. Demographic, anthropometric, clinical features and non-invasive markers of fibrosis were recorded at baseline and at follow-up. Significant and advanced fibrosis were defined using Liver Stiffness Measurement (LSM) as LSM ≥ 8.1 kPa and LSM ≥ 12.1 kPa respectively. Cirrhosis was diagnosed either histologically or clinically. Fast progressors of fibrosis were defined as those with delta stiffness ≥ 1.03 kPa/year (25% upper quartile of delta stiffness distribution). Targeted and untargeted metabolic profiles were analysed on fasting serum samples using Proton nuclear magnetic resonance (1H NMR).

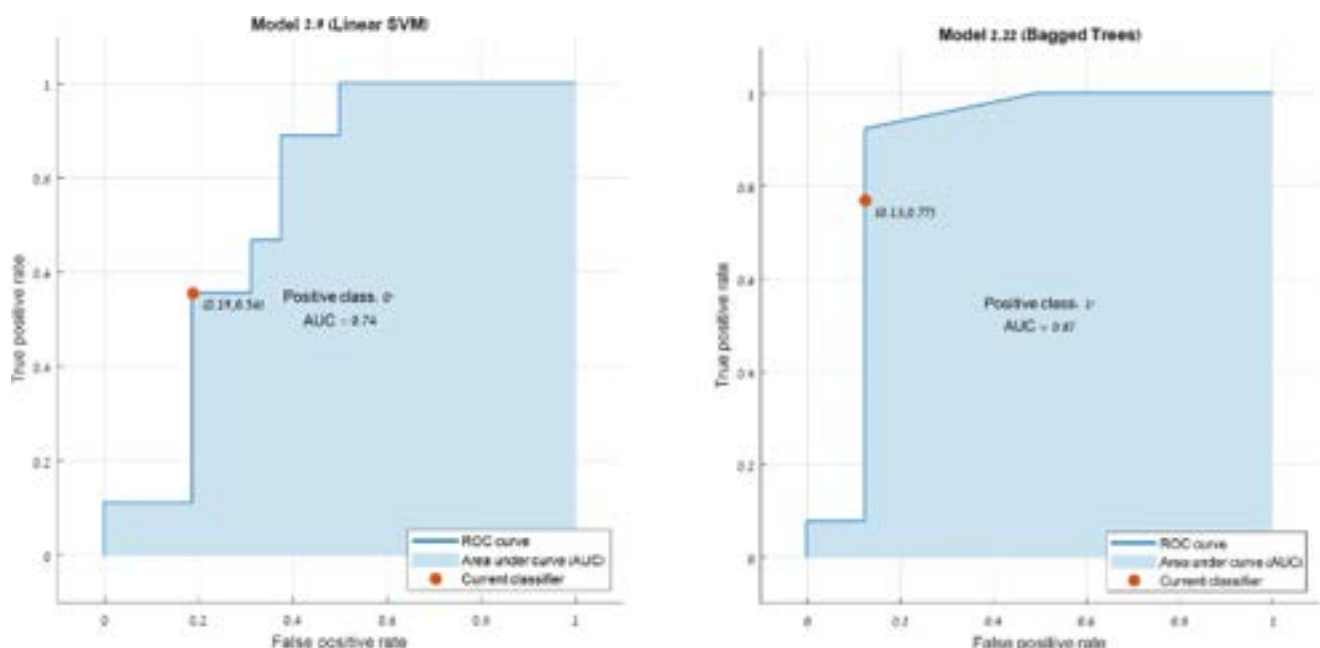
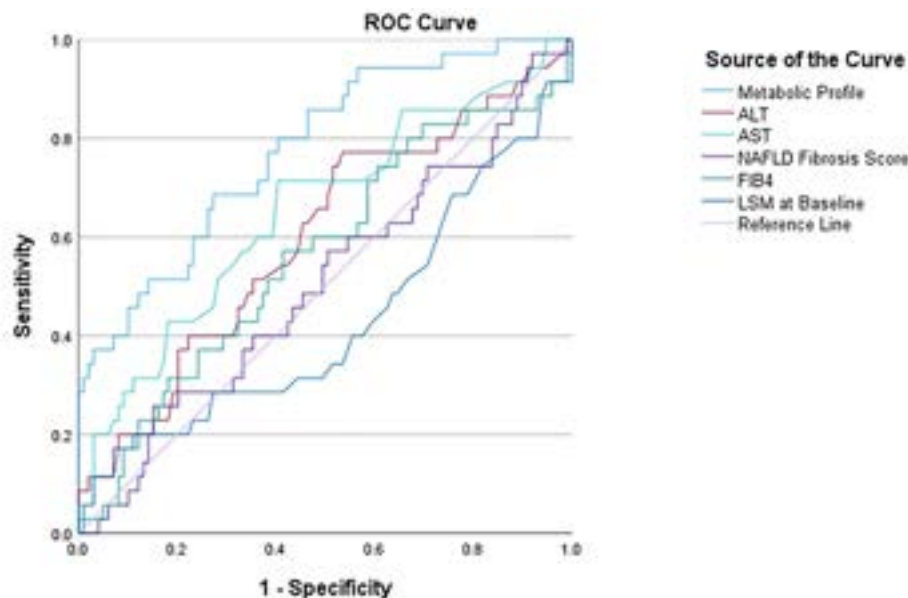


Figure: (abstract: SAT-500).



Metabolic profile formula: $30.485 \cdot H2TG \text{ (mg/dl)} + 0.706 \cdot H4A1 \text{ (mg/dl)} + 1.586 \cdot H4PL \text{ (mg/dl)} + 1.989 \cdot H4A2 \text{ (mg/dl)} + 0.063 \cdot V4FC \text{ (mg/dl)} + 0.719 \cdot IDTG \text{ (mg/dl)} + 12.94 \cdot VLFC \text{ (mg/dl)} + 0.103 \cdot V3CH \text{ (mg/dl)} + 42.376 \cdot Proline \text{ (mmol/l)} + 3.18 \cdot IDAB \text{ (mg/dl)} + 0.284 \cdot VLAB \text{ (mg/dl)} + 44.243 \cdot V3PL \text{ (mg/dl)} + 0.532 \cdot VLPL \text{ (mg/dl)} + 0.319 \cdot H2A2 \text{ (mg/dl)} + 0.339$

Figure 1: Diagnostic performance of metabolic profile for predicting fibrosis progression compared to ALT, AST, NAFLD fibrosis score, FIB-4 and LSM.

Abbreviations: ALT, alanine aminotransferase; AST, aspartate aminotransferase; LSM: liver stiffness measurement

Figure: (abstract: SAT-501).

Results: 189 patients were included in the study, 111 (58.7%) underwent liver biopsy. Overall, 11.1% patients were diagnosed with cirrhosis, while 23.8% were classified as fast progressors. A combination of metabolites and lipoproteins (formula in Figure 1) could identify the fast fibrosis progressors (AUROC 0.788, 95% CI: 0.703–0.874, $p < 0.001$) and performed better than non-invasive markers: ALT (AUROC 0.59, 95%CI: 0.48–0.71, $p = 0.08$), AST (AUROC 0.65, 95% CI: 0.52–0.76, $p = 0.006$), FIB-4 (AUROC 0.5, 95%CI: 0.39–0.61, $p = 0.9$), NAFLD fibrosis score (AUROC 0.56, 95%CI: 0.44–0.67, $p = 0.26$) and LSM at baseline (AUROC 0.43, 95% CI: 0.31–0.55, $p = 0.2$) (Figure 1).

Conclusion: Specific metabolic profile predicts fibrosis progression in patients with non-alcoholic fatty liver disease. Algorithms combining metabolites and lipids could be integrated in the risk-stratification of these patients.

SAT-502

Diagnostic performance of magnetic resonance imaging, vibration-controlled transient elastography and controlled attenuation parameter in predicting steatohepatitis in NAFLD patients

Sun Young Yim¹, Hyung Sun Yim¹, Jong Su Kim¹, Yeon Seok Seo¹.

¹Korea University Hospital, Korea, Rep. of South

Email: drseo@korea.ac.kr

Background and aims: Non-alcoholic fatty liver disease (NAFLD) ranges from benign non-alcoholic fatty liver to non-alcoholic steatohepatitis (NASH) where NASH includes progressive fibrosis. Liver biopsy is the gold standard method for the diagnosis of NASH and although there are no reliable non-invasive means of differentiating NAFLD from NASH, non-invasive models that correlate with

individual histologic parameters have been developed. The aim of the current study was to examine the diagnostic accuracy of magnetic resonance imaging (MRI) and transient elastography (TE) in classifying fibrosis while MRI-derived proton density fat fraction (PDFF) and controlled attenuation parameter (CAP) in classifying degree of steatosis.

Method: We retrospectively reviewed database of 213 patients who had undergone liver MRI and TE from November 2018 to February 2022 and cross-sectional analysis was performed in 113 patients who had undergone both imaging study and liver biopsy. A systematic NAFLD activity score (NAS) was scored using NASH Clinical Research Network. The Area Under the Receiver Operating Characteristics (AUROCs), sensitivity, and specificity of MRI and TE were analyzed according to degree of steatosis and fibrosis. Further analysis was performed to observe if combination of imaging analysis could detect presence of NASH using linear regression analysis.

Results: Out of 113 patients, 78 patients (69%) were male and mean body mass index was $29.3 \pm 4.8 \text{ kg/m}^2$. The proportion of patients with probable NASH (NAS 3, 4) and definite NASH (NAS ≥ 5) were 40.7% and 23%, respectively. The correlation between MRI-PDFF and CAP was moderate ($r = 0.57$, $P < 0.001$). The AUROCs of MRI-PDFF and CAP were 0.905 (CI 0.856–0.964, $P < 0.001$) and 0.739 (CI 0.644–0.835, $P < 0.001$), respectively in detecting advanced steatosis (score ≥ 3 , steatosis $> 33\%$). MRI-PDFF provided significantly more reliable fat content measurement than did CAP for every degree of steatosis. The AUROC values for MRI-PDFF and TE were 0.936 vs 0.563 for steatosis grade ≥ 1 and 0.922 vs 0.92 for steatosis grade ≥ 2 ($p = 0.005$ and $P < 0.001$, respectively). In predicting degree of liver fibrosis, the correlation between MRE and TE was also moderate (r

=0.631, $P < 0.001$). The predictive efficacy between MRE and TE did not differ in predicting any degree of liver fibrosis. Since there is no imaging modality that can exactly predict degree of NASH, next we analyzed whether the diagnostic ability of combined modalities improved. The predictive efficacy significantly increased when MRI-PDFF was added to MRE alone (AUROC; 0.869 vs 0.619, $P < 0.001$) in identifying both definite NASH (NAS ≥ 5) and probable NASH (NAS 3–4) (AUROC; 0.823 vs 0.602, $P < 0.001$) but not for the combination of TE and CAP. In multivariate analysis, there was significant correlation between MRE and degree of hepatocyte ballooning in addition to degree of fibrosis (both, $P < 0.001$).

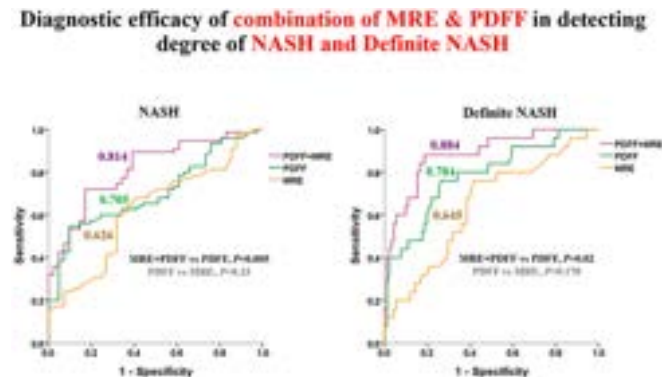


Figure:

Conclusion: MRI-PDFF have higher diagnostic performance in non-invasive detection of liver steatosis than TE but no significant difference was observed in identifying degree of liver fibrosis. Combination of MRE and MRI-PDFF enabled detection of NASH in NAFLD patients with high diagnostic efficacy. Our result presents the possibility of non-invasive method in predicting NASH and could possibly reduce the need for liver biopsy following further validation in a larger cohort.

SAT-503

SAFE score yielded a better performance than FIB-4 and NFS in predicting significant fibrosis among Asian NAFLD patients

Pimsiri Sripongpun^{1,2}, Sombat Treeprasertsuk³, Phunchai Charatcharoenwitthaya⁴, Apichat Kaewdech¹, Naichaya Chamroonkul¹, Wah-Kheong Chan⁵, Cheng Han Ng⁶, Mark Muthiah⁶, Yock-Young Dan⁶, W. Ray Kim². ¹Prince of Songkla University, Internal Medicine, Thailand; ²Stanford University School of Medicine, Gastroenterology and Hepatology, United States; ³Chulalongkorn University, Thailand; ⁴Siriraj Hospital Mahidol University, Thailand; ⁵University of Malaya, Malaysia; ⁶National University of Singapore, Singapore
Email: pim072@hotmail.com

Background and aims: In patients with non-alcoholic fatty liver disease (NAFLD), having fibrosis stage 2 or higher (significant fibrosis; SF) is independently associated with an increased overall mortality. Recently, the Steatosis-Associated Fibrosis Estimator (SAFE) score has been developed as a non-invasive tool to screen for SF among NAFLD patients in primary care (Hepatology 2022, DOI: 10.1002/hep.32545). We aimed to externally validate and compare SAFE with FIB-4 and NFS in Asian population with NAFLD.

Method: Biopsy-proven NAFLD patients' data from 6 centres in 3 Southeast Asian countries (Thailand, Malaysia, and Singapore) were collected (N=889). Using liver biopsy as the gold standard, liver fibrosis stage was graded using NASH CRN criteria. Patients with incomplete data on variables used to calculate SAFE, FIB-4, and NFS were excluded. The performance of SAFE, FIB-4, and NFS were evaluated using areas under the receiver operating characteristics curve (AUROC), sensitivities (Sn) and specificities (Sp) in diagnosing F \geq 2.

Results: A total of 640 patients were included in the analysis, SF was presented in 176 patients (27.5%). As expected, the median age, aspartate and alanine aminotransferase, alkaline phosphatase, serum globulin levels were higher in patients with SF than in those without SF, whereas the serum albumin and platelet levels were lower. Among 3 non-invasive biomarkers, SAFE, FIB-4, and NFS yielded AUROCs (95%CI) of 0.744 (0.700–0.788), 0.731 (0.687–0.775), 0.658 (0.612–0.704), respectively ($p = 0.31$ for SAFE vs FIB-4, and $p < 0.001$ for SAFE vs NFS). At the given low cutoffs for detecting SF (SAFE $<$ 0, FIB-4 $<$ 0.81, NFS $<$ 2.45), SAFE showed the highest Sn of 89.77%, significantly better than FIB-4 (Sn 80.11%, $p < 0.001$) and NFS (Sn 80.11%, $p = 0.001$). At the high cutoffs (SAFE \geq 100, FIB-4 \geq 1.81, NFS \geq 0.03), the Sp of SAFE, FIB-4, and NFS for detecting SF were 71.77%, 89.22%, and 89.44%, respectively. The proportion of patients categorized by low and high cutoffs of each score are shown in the Figure.

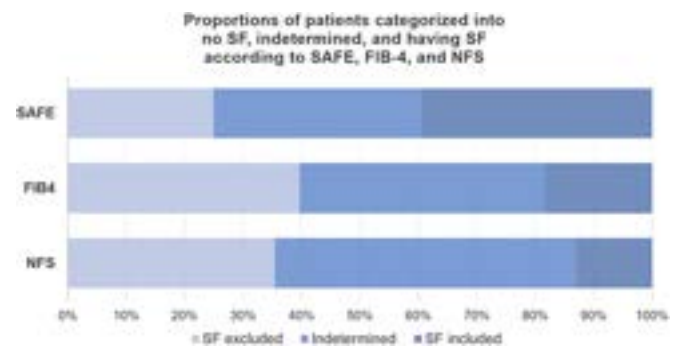


Figure:

Conclusion: SAFE showed the highest AUROC compared to FIB-4 and NFS in the diagnosis of SF in NAFLD patients. SAFE also had a better sensitivity in detecting SF than FIB-4 and NFS. Based on these data, we should emphasize the utility of SAFE score as a non-invasive screening tool for identifying NAFLD patients at a low risk for SF in primary care setting.

SAT-504

A descriptive analysis of transient elastography results and metabolic co-morbidities in people living with HIV mono-infection in an urban clinic in the UK

Claire Mullender^{1,2}, Rhiannon Owen¹, Manik Kohli^{1,2}, Irfaan Maan³, Laura Jane Waters², Sarah Pett^{1,2,4}, Alejandro Arenas-Pinto^{1,4}, Indrajit Ghosh², Stuart Flanagan², Richard Gilson^{1,2}. ¹Institute for Global Health, University College London, London, United Kingdom; ²Central and North West London NHS Foundation Trust, Department of Sexual Health and HIV, United Kingdom; ³Institute for Global Health, University College London, Faculty of Population Health Sciences, London, United Kingdom; ⁴University College London, Medical Research Council Clinical Trials Unit, Institute of Clinical Trials and Methodology, United Kingdom
Email: r.gilson@ucl.ac.uk

Background and aims: Liver-related morbidity remains high among people living with HIV (PLWH) despite advances in the management of viral hepatitis. Fatty liver disease (FLD) will likely become the leading cause of liver disease in PLWH, who are impacted disproportionately by comorbidities that contribute to the metabolic syndrome (MetS)-obesity, dyslipidaemia, hypertension and insulin resistance. The utility of transient elastography (TE) in PLWH with viral hepatitis co-infection is established, but its use in assessing FLD in PLWH is not well described. To better understand the burden of FLD in PLWH we reviewed results of TE with Controlled Attenuation Parameter (CAP) scores in PLWH with unexplained transaminitis.

Method: We undertook a retrospective review of all PLWH mono-infection with unexplained transaminitis (alanine transaminase (ALT) above 35 IU/L for men and 25 IU/L for women) who had a TE/CAP (by FibroScan®) at our central London clinic between 1/2017–3/

POSTER PRESENTATIONS

2022. FLD and fibrosis were defined as a CAP score >238 dB/m and a liver stiffness measurement of >7.1 kPa respectively. Logistic regression analyses and χ^2 test for trends were performed to assess factors associated with FLD including demographics, HIV-specific variables (antiretroviral medications, CD4+ T-cell count, HIV viral load (VL)), alcohol use, and MetS comorbidities. The definition for MetS included use of diagnostic parameters collected as part of routine care for PLWH (HBA1c, lipids, blood pressure, Body Mass Index (BMI)); or medication history for treatment for any of the above.

Results: 408 PLWH were included: median age 51 years (IQR 45–57), 87% male, 68% of White ethnicity, 99% on ART, 93% undetectable HIV VL and median CD4+ T-cell count 610 cells/mm³. 70% (263/379) had a BMI >25 Kg/m² and 45% had ≥2 metabolic comorbidities. Median ALT was 54 IU/L (IQR 37–75). A valid CAP score was available for 385/408 (94%). 65% (249/385) had FLD, of whom 80% (201/249) were moderate-to-severe (S2/S3, CAP >260 dB/m). Fibrosis was identified in 14% (57/408). There was no association between HIV-specific variables and FLD. Male gender, dyslipidaemia, type 2 diabetes mellitus and BMI were significantly associated with FLD (all $p < 0.05$). An increasing number of metabolic comorbidities was associated with increasing odds of FLD ($p < 0.001$) and fibrosis ($p < 0.001$) compared with individuals with no MetS comorbidities. In a multivariable model including age, gender and significant MetS comorbidities, BMI >25 Kg/m² (aOR 6.2 95% CI 3.6–10.6) and dyslipidaemia (aOR 2.4 95% CI 1.4–4.2) remained significantly associated with FLD.

Conclusion: We identified a high prevalence of FLD in our cohort of PLWH with well controlled HIV and low grade transaminitis using TE with CAP. TE/CAP should be more widely applied in screening guidelines to identify FLD in PLWH, especially those with markers of metabolic syndrome and identified as overweight or obese.

SAT-505

Liver stiffness measurements with a new point-of-care device, hepatoscope, using two-dimensional transient elastography showed both very good reproducibility and correlation to fibroscan

Victor de Lédighen^{1,2}, Dan Dutartre³, Françoise Manon², Joëlle Abiven², Anne-Laure de Araujo², Rhizlane Houmadi², Julie Dupuy², Juliette Foucher², Joel Gay⁴, Claude Cohen-Bacrie⁴.

¹INSERM U1312, BRIC, Bordeaux University, Bordeaux, France;

²Bordeaux University Hospital, Hepatology unit, Pessac, France; ³Inria Bordeaux Sud-Ouest, Bordeaux, France; ⁴E-Scopics, Saint-Cannat, France

Email: joel.gay@e-scopics.com

Background and aims: Liver stiffness measurement (LSM) by ultrasound-based transient elastography (TE) is recommended in risk stratification algorithms for patients with or at risk of non-alcoholic fatty liver disease (NAFLD). Fibroscan® (FS) is widely used today in hepatology practice and provides a 1D-measurement of shear wave speed. Large-scale screening of NAFLD-NASH could benefit from an available and affordable tool in primary care that would provide point-of-care reproducible and reliable LSM. Our goal was to assess the reproducibility of LSM on a new ultrasound point-of-care device, Hepatoscope™, with TE using 2D-measurements of shear wave speed (2DTE) under ultrasound guidance, and to compare 2DTE LSM with FS and blood tests.

Method: 96 adult patients referred to routine outpatient hepatology consultation for CLD, including LSM with FS, were enrolled in this prospective single centre study (NCT04782050). Four Hepatoscope liver exams were performed by 1 expert and 1 novice operator, to assess the intra-operator and inter-operator reproducibility of LSM. Stiffness values were computed in real time within a region of interest positioned within the liver image. Each exam consisted of a prospective record of 15 consecutive stiffness values with their quality indicator (QI) above 85%. Operators were blinded to any median value for each series of 15 values. LSM was estimated using

the median of an incremented number of several stiffness values selected using different QI thresholds. Data were analysed with R to determine the Hepatoscope LSM, reproducibility intraclass correlation coefficients (ICC), and the r^2 correlation of LSM by experts with other non-invasive tests.

Results: Intra-operator reproducibility of the median of 15 values (LSM_{Med15}) was very good (ICC = 0.85; 95%CI [0.77–0.89]), excellent for experts (ICC = 0.90; 95%CI [0.85–0.93]), and good for novices (ICC = 0.76; 95%CI [0.66–0.83]). Inter-operator reproducibility was very good (ICC = 0.83; 95%CI [0.78–0.88]). With stiffness values having a QI ≥90%, very good intra- and inter-operator reproducibility could be achieved from only 4 values (LSM_{Med4}) (ICC = 0.86; 95%CI [0.78–0.91] and ICC = 0.85; 95%CI [0.80–0.89], respectively). Intra-operator reproducibility for experts and novices was very good (ICC = 0.89; 95%CI [0.85–0.93] and ICC = 0.81; 95%CI [0.73–0.87], respectively). When considering Hepatoscope LSM exams with an IQR/Median <30% (similar to FS routine use), the correlation between LSM performed with Hepatoscope and FS devices was good: $r^2 = 0.79$ with LSM_{Med4}, $r^2 = 0.79$ with LSM_{Med15}. Correlation coefficients (r^2) between LSM from Hepatoscope and FS to conventional liver fibrosis blood tests is presented in Table 1.

Table 1:

r^2 coef.	FIB-4	APRI	NAFLD Fibrosis Score
FS LSM	0.12	0.27	0.16
LSM _{Med4}	0.19	0.63	0.05
LSM _{Med15}	0.22	0.61	0.08

Conclusion: LSM can be performed with the new point-of-care device Hepatoscope and 2DTE modality by experts and novices. Using a QI of at least 90%, Hepatoscope LSM could be defined as the median of only 4 values, possibly leading to exam time savings. LSM measured with Hepatoscope showed good correlation with FS. These results are very encouraging regarding the use of Hepatoscope 2DTE and LSM at the point of care for large scale screening purposes. Future comparative studies against liver histopathology should allow the validation of existing LSM cutoff values for a specific screening and triage of patients at risk of fibrotic NASH.

SAT-506

Are non-invasive tests of fibrosis effective in patients with metabolic associated fatty liver disease? Comparative study between liver biopsy and non-invasive scores or fibroscan

Annalisa Cespiati^{1,2}, Rosa Lombardi^{1,2}, Sofia Carvalhana³, Daniel Smith², Cristina Bertelli¹, Giuseppina Pisano¹, Helena Cortez-Pinto³, Anna Ludovica Fracanzani^{1,2}. ¹Unit of Medicine and Metabolic Disease, Fondazione IRCCS Cà Granda Ospedale Maggiore Policlinico, Milan, Italy; ²Department of Pathophysiology and Transplantation, University of Milan, Italy; ³Departamento de Gastroenterologia, Centro Hospitalar Universitário Lisboa Norte, Departamento de Dietética e Nutrição, Lisbon, Centro Hospitalar Universitário Lisboa Norte Portugal, Portugal
Email: annalisa.cespiati@unimi.it

Background and aims: Metabolic dysfunction-associated fatty liver disease (MAFLD) is characterized by liver steatosis and at least one metabolic comorbidity. Due to limitations of liver biopsy, non-invasive tests of fibrosis (NITs) (FIB4 and NFS) and liver stiffness measurement (LSM) by Fibroscan are used to diagnose fibrosis. Aims 1) to evaluate the diagnostic accuracy of NITs and LSM in MAFLD 2) to evaluate their performance specifically in diabetic and obese subjects 3) to identify new thresholds for scores NITs and LSM in MAFLD.

Method: We enrolled 164 biopsy-proven MAFLD (mean age 56 ± 12 ys, 62% males) in Milan and Lisbon. Clinical, laboratory and Fibroscan data were collected within 6 months from biopsy. FIB-4 < 1.3, NFS <–

1.455 and LSM<8 kPa ruled out advanced fibrosis ($\geq F3$), FIB-4 > 3.25, NFS>0.675 and LSM \geq 8 kPa suggested advanced fibrosis.

Results: Prevalence of fibrosis $\geq F3$ was 24% at histology. FIB4 and NFS ruled out advanced fibrosis in 49% and 44% of cases, diagnosed it in 7% and 8% and had indeterminate values in 43% and 49% of cases, respectively. LSM \geq 8 kPa in 62% of subjects. All NITs showed a lower accuracy for both identification (AUROCs FIB-4 0.62; NFS 0.57; LSM 0.72) and exclusion (AUROCs FIB-4 0.65; NFS 0.68; LSM 0.72) of advanced fibrosis at biopsy compared to those for non-alcoholic fatty liver disease (NAFLD). The 59% of the cohort was obese, 47% diabetic. For ruling-in advanced fibrosis, FIB-4 and LSM performed worst in diabetic vs non-diabetic (AUROCs FIB-4 0.58 vs 0.69 $p < 0.001$; LSM 0.66 vs 0.71 $p < 0.001$) and in obese vs non-obese MAFLD (AUROCs FIB-4 0.59 vs 0.65 $p < 0.001$; LSM 0.68 vs 0.75 $p < 0.001$). NFS accuracy did not significantly differ between diabetic and non-diabetic (AUROCs 0.58 vs 0.50 $p = 0.06$), whereas it seemed to perform better in obese vs non-obese (AUROCs 0.58 vs 0.55 $p = 0.01$). For the exclusion of fibrosis, all NITs and LSM performed worst in diabetic vs non-diabetic (AUROCs FIB-4 0.59 vs 0.67 $p = 0.001$; NFS 0.58 vs 0.63 $p = 0.003$; LSM 0.68 vs 0.69 $p = 0.06$) and in obese vs non-obese (AUROCs FIB-4 0.66 vs 0.69 $p = 0.002$; NFS 0.65 vs 0.70 $p = 0.003$; LSM 0.68 vs 0.74 $p < 0.001$). The Youden indexes of current cut-offs for FIB4 and NFS were <0.5 for both ruling in and ruling out advanced fibrosis, whereas new thresholds as FIB-4 > 1.63/NFS > 1.09 and FIB-4 < 1.22/NFS < 1.23 had the best Youden indexes. As for Fibroscan, LSM > 10.4 kPa seemed to better identify MAFLD patients with advanced fibrosis, whereas a cut-off of 8.4 kPa to exclude it.

Conclusion: In MAFLD, both FIB4 and NFS and Fibroscan performed worse compared to NAFLD, with the latter having the higher accuracy. The presence of diabetes and obesity impairs the performance of score and LSM. In MAFLD lower cut-off of both FIB-4 and NFS are warranted, whereas no change seems to be needed for LSM. Nevertheless, more accurate NITs should be developed specifically for MAFLD.

SAT-507

A biomarker of fibrosis resolution, CTX-III, increases after bariatric surgery in early NAFLD patients with histological liver improvements

Ida Lønsmann^{1,2}, Julie Steen Pedersen³, Morten Karsdal¹, Judith Ertle⁴, Corinna Schoelch⁵, Diana Leeming¹, Flemming Bendtsen³. ¹Nordic Bioscience, Hepatic Research, Herlev, Denmark; ²University of Southern Denmark, Department of Clinical Research, Odense, Denmark; ³Hvidovre Hospital, Gastrounit, Hvidovre, Denmark; ⁴Boehringer Ingelheim International GmbH, Ingelheim am Rhein, Germany; ⁵Boehringer Ingelheim Pharma GmbH and Co. KG, Biberach, Germany
Email: llc@nordicbio.com

Background and aims: The formation of fibrotic bands is characterized by an increase in extracellular matrix components such as collagens. Over time, collagens become inter- and intramolecularly cross-linked. Thus, serological detection of cross-linked collagens resulting from collagen degradation may non-invasively detect fibrosis resolution. Here, we investigated a neo-epitope marker of cross-linked type III collagen resolution (CTX-III) mediated by matrix metalloproteinases. We aimed to investigate whether changes could be observed in CTX-III levels in patients with early-stage non-alcoholic fatty liver disease (NAFLD) with observed improvements in liver histology induced by weight loss after bariatric surgery.

Method: Blood samples and liver biopsies were collected from 70 patients on the day of bariatric surgery. Additional blood samples were taken at three, six, and twelve months past surgery and forty patients had an additional liver biopsy at twelve months follow-up. CTX-III was measured using a fully validated sandwich chemiluminescence immunoassay and levels were analyzed using a linear mixed-effect analysis on log-transformed data.

Results: 61% of the included 70 patients were females and mean age and mean BMI were 44 years and 42 kg/m², respectively. Patients had a median NAFLD activity score of 3 and mild-to-moderate fibrosis F0 (3%), F1 (86%), and F2 (11%). In general, CTX-III increased in patients after bariatric surgery ($p < 0.0001$). The most significant rise was observed from baseline to three-months follow-up ($p < 0.001$).

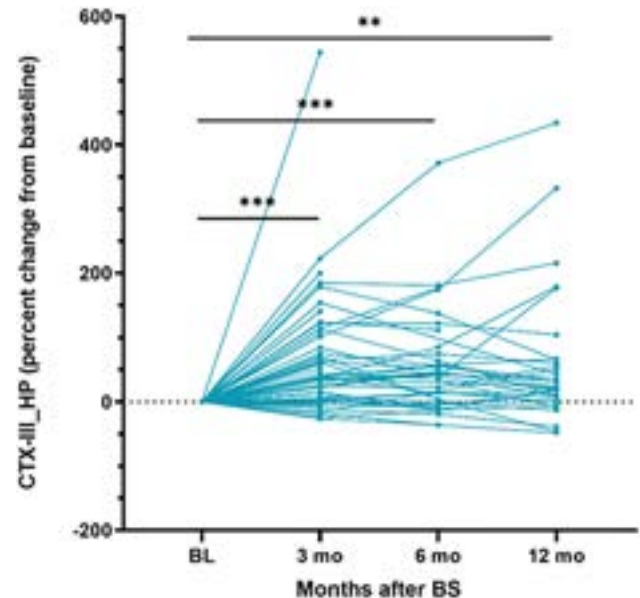


Figure:

Conclusion: This study indicates that CTX-III may be a biomarker of fibrosis resolution in patients with NAFLD undergoing bariatric surgery.

SAT-508

Free light chains: novel serum biomarkers for NASH stratification, an update

Antonio Liguori^{1,2}, Umberto Basile^{1,3}, Francesca D'Ambrosio^{1,3}, Cecilia Napodano^{1,3}, Lidia Tomasello^{1,2}, Fabrizio Mancuso^{1,2}, Giuseppe Marrone², Marco Biolato^{1,2}, Gianludovico Rapaccini¹, Antonio Gasbarrini^{1,2}, Antonio Grieco^{1,2}, Luca Miele^{1,2}. ¹Università Cattolica del Sacro Cuore, Italy; ²Policlinico Universitario A. Gemelli, scienze mediche e chirurgiche, Italy; ³Policlinico Universitario A. Gemelli, Scienze di laboratorio e infettivologiche, Italy
Email: luca.miele@policlinicogemelli.it

Background and aims: NAFLD is the most common chronic liver disease with a worldwide prevalence of 25%. It encompasses a wide spectrum of diseases, including non-alcoholic steatohepatitis (NASH) characterized by hepatocyte ballooning, lobular inflammation and progressive fibrosis. For these reasons, one of the most important NASH features is the overexpression of pro-inflammatory biomarkers (IL1-beta, IL6, TNF-alfa). Polyclonal free light chains (FLCs) λ and κ reflect B cell activation and high serum levels of FLCs are observed in a variety of inflammatory conditions. The aim of this study is to evaluate the potential role of FLC as biomarker of inflammation and fibrosis in NAFLD/NASH patients.

Method: We enrolled 254 patients with metabolic liver disease at Liver Outpatient clinic at Policlinico A. Gemelli: 89 with NAFLD, 88 with NASH and 77 with compensated liver cirrhosis. Diagnosis of NASH was histologically assessed. Medical and pharmacological anamnesis, anthropometric measurements and laboratory tests (included FLC λ and κ) were obtained for all patients.

Results: Both serum κ and λ FLCs were significantly higher in patients with cirrhosis than in patients with NAFLD or NASH (113.45 vs 31.76 mg/L $p < 0.01$). No significant difference in λ and κ FLCs levels were observed between NASH and NAFLD patients (respectively

POSTER PRESENTATIONS

31.423 vs 32.134 mg/L $p=0.2$). Among patients who undergone biopsy, λ FLCs tended to increase gradually with lobular inflammation severity ($p=0.03$). Both k and λ FLCs increased proportionally with fibrosis stages ($p<0.01$). Finally, total FLCs were significantly higher in patients with a diagnosis of compensated cirrhosis compared with patients with advanced fibrosis (F3–F4) and no fibrosis ($p<0.01$).

Conclusion: We assessed that FLCs serum levels are significantly higher in patients with advanced fibrosis and cirrhosis being strictly related to the severity of the inflammatory process. FLCs might be considered useful tools in monitoring the inflammatory status of patients with NAFLD.

SAT-509

Non-alcoholic fatty liver disease made easy for diabetologists: the automated fibrosis-4 index

Mona Ismail^{1,2}, Lameya Alsheekh², Murtaga Makki², Jaber Alelyani², Zahra Hassan², Zahra Alhadhiah³, Hind Al-Faddagh², Nazih Alkhatam³, Reem Alarqan^{1,3}, Yasir Elamin^{1,3}, Alanoud Alanazi^{1,3}. ¹Imam Abdulrahman Bin Faisal University, College of Medicine, Dammam, Saudi Arabia; ²King Fahad Hospital of the University, Division of Gastroenterology, Department of Internal Medicine, Al Khobar, Saudi Arabia; ³King Fahad University Hospital, Endocrinology Division, Internal Medicine, Al Khobar, Saudi Arabia
Email: monai4@hotmail.com

Background and aim: Non-alcoholic fatty liver disease (NAFLD) commonly causes chronic liver disease (CLD), has a global prevalence of 24%, and can progress to cirrhosis and hepatocellular carcinoma. Patients with type 2 diabetes mellitus have a high prevalence of NAFLD (55%), and diabetes is a strong predictor for developing non-alcoholic steatohepatitis (NASH), the severe form of NAFLD, and progressing to bridging fibrosis and cirrhosis in these patients. Recently, the American Diabetes Association recommended screening patients with type 2 diabetes for NASH and advanced fibrosis. Thus, this study aims to evaluate the role of automated Fibrosis-4 (FIB-4) Index calculations in electronic medical records (EMR) in assisting diabetologists in identifying advanced fibrosis in diabetic patients.

Method: In this prospective study, patients with type 2 diabetes attending the diabetes clinic at a tertiary university hospital and unaware of having NAFLD were recruited. We incorporated automated FIB-4 calculations into the EMRs (QuadraMed®, TX, USA). Clinical and demographical data collected were age, sex, body mass index, complete blood count, liver and renal function, body mass index, insulin resistance, presence of comorbidities, dyslipidemia, ischemic heart disease, and medications used. We used logistic regression to identify predictors of advanced fibrosis. Patients with a high FIB-4 index of ≥ 1.3 and ≤ 65 years or ≥ 2.0 and ≥ 65 years were considered advanced fibrosis and referred to the Hepatology clinic. Patients with a FIB-4 index of <1.3 and <65 years or <2 and <65 years will continue to follow-up with their diabetologist and have a repeat FIB-4 calculation after 3–5 years.

Results: A total of 318 patients were included, and advanced fibrosis was seen in 9.7% of patients with type 2 diabetes. The mean age was 54.8 ± 13.3 years. The majority were females (54.7%), Saudi nationals (89.9%), obese (57.2%), and with HbA1C ≥ 7 (67.6%). On univariate analysis, advanced fibrosis by FIB-4 index was significantly associated with older age (OR = 1.07, 95% CI 1.02–1.11, $p=0.002$), elevated bilirubin (OR = 3.19, 95% CI 1.62–6.30, $p=0.001$), elevated GGT (OR = 2.48, 95% CI 1.60–3.84, $p<0.001$), and elevated INR (OR = 9.43, 95% CI 1.76–50.39, $p=0.009$).

Conclusion: Advanced fibrosis is a significant health issue in diabetic patients with NAFLD. Advanced fibrosis diagnosed by FIB-4 is associated with older age and a worse laboratory profile. Incorporating automated FIB-4 calculation into EMRs created an easy-to-follow clinical care pathway for diabetologists to quickly identify patients with advanced fibrosis as recommended by the

American Diabetes Association and facilitate their early referral to specialists for further management.

SAT-510

Establishment and validation of a diagnostic model for liver inflammation in chronic hepatitis B (CHB) patients concurrent with non-alcoholic fatty liver disease (NAFLD) based on machine learning (ML)

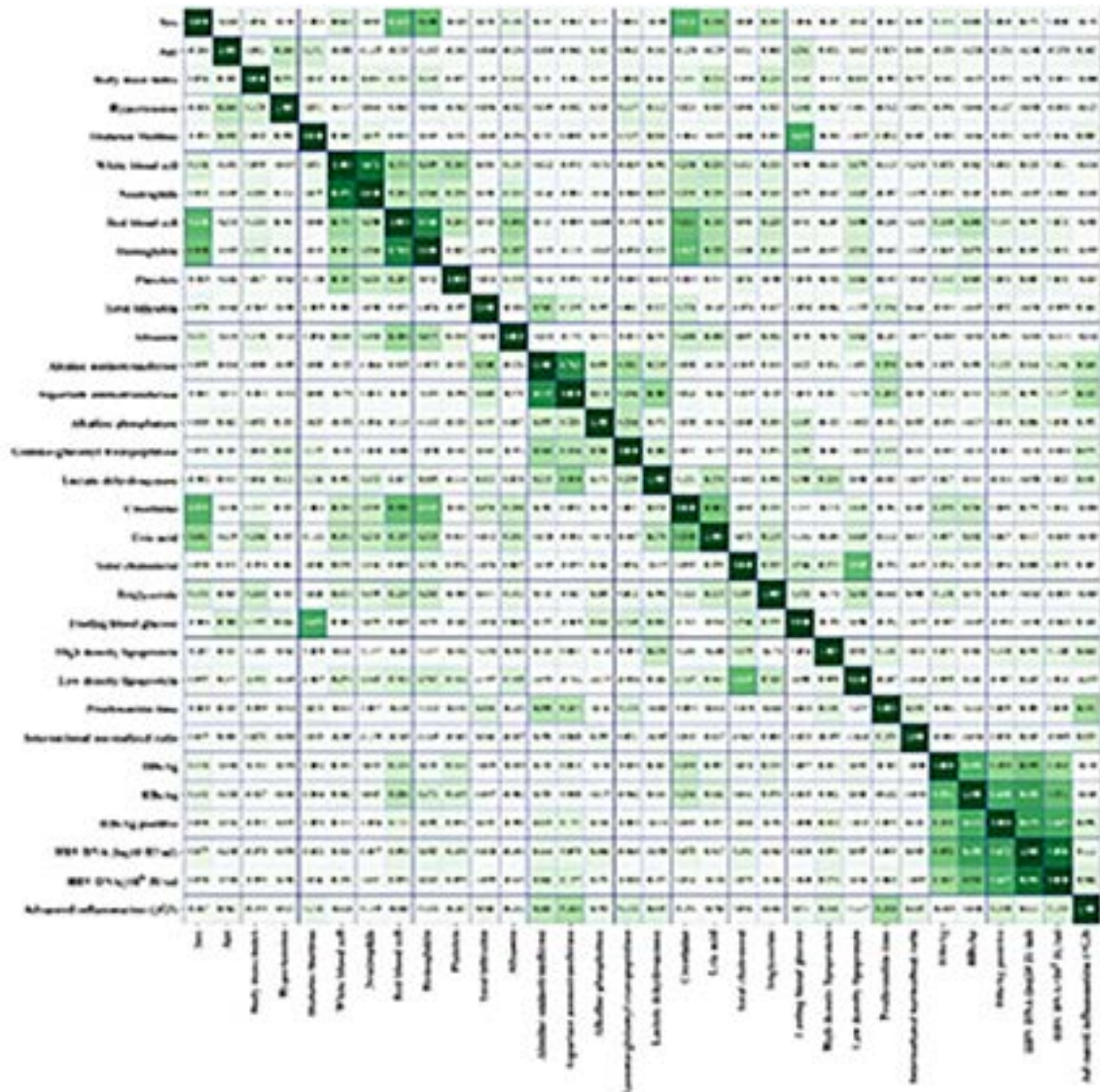
Jie Li¹, Qi Xue², Fajuan Rui¹, Xiaorong Tian³, Yayun Xu⁴, Qi Zheng⁵, Qing-Lei Zeng⁶, Zebao He⁷, Jian Wang¹, Weimao Ding⁸, Chuanwu Zhu⁹, Yuanwang Qiu¹⁰, Yunliang Chen³, Junqing Fan³, Junping Shi¹¹, Chao Wu¹. ¹Department of Infectious Diseases, Nanjing Drum Tower Hospital, The Affiliated Hospital of Nanjing University Medical School, China; ²Department of Infectious Disease, Shandong Provincial Hospital Affiliated to Shandong First Medical University, China; ³School of Computer Science, China University of Geosciences, China; ⁴Shandong Provincial Hospital, Shandong University, China; ⁵Hepatology Research Institute, the First Affiliated Hospital of Fujian Medical University, China; ⁶The First Affiliated Hospital of Zhengzhou University, China; ⁷Department of Infectious Diseases, Taizhou Hospital of Zhejiang Province affiliated to Wenzhou Medical University, China; ⁸Department of Hepatology, Huai'an No. 4 People's Hospital, China; ⁹Department of Infectious Diseases, The Affiliated Infectious Diseases Hospital of Soochow University, China; ¹⁰Department of Infectious Diseases, The Fifth People's Hospital of Wuxi, China; ¹¹Department of Infectious Diseases, The Affiliated Hospital of Hangzhou Normal University, China
Email: lijier@sina.com

Background and aims: Chronic hepatitis B (CHB) patients concurrent with non-alcoholic fatty liver disease (NAFLD) are common, but there are still lack of non-invasive models to evaluate liver inflammation. We aimed to build a diagnosis model for liver inflammation in those patients.

Method: This study consecutive enrolled CHB patients concurrent with NAFLD underwent liver biopsy and laboratory examination from eight medical centers of China between April 2004 and October 2020 as training cohort and patients from Tianjin Municipal Infectious Disease Hospital between January 2016 and September 2021 as independent external validation cohort. Inflammation grade 3–4 were predicted using ML models (logistic regression (LR), random forest (RF), decision tree classifier (DCT), gaussian naive bayes (GNB), and K nearest neighbor (KNN)). Features with Pearson correlation coefficients >0.2 were included in the diagnostic model. To avoid overfitting, 5-fold cross validations were used in the ML models building process.

Results: A total of 1340 CHB patients with NAFLD underwent liver biopsy included in the final analysis, with an average age of 38 (32–47) years (1032 males and 308 females). 216 cases (16.12%) were inflammation grade 3–4. Prothrombin time (PT), Aspartate transaminase (AST), alanine transaminase (ALT) were positively associated with inflammation grade 3–4, and albumin (ALB), platelet (PLT) were negatively associated with inflammation grade 3–4. LR model had the best performance, and its AUC for the diagnosis of inflammation grade 3–4 were 0.863 (0.810–0.916) in training cohort, and 0.890 (0.864–0.917) in validation cohort.

Conclusion: LR model performed the best overall performance in predicting inflammation. ML could be an effective tool for identifying clinically liver inflammation in CHB patients concurrent with NAFLD.

Inflammation grade ≥ 3

Inflammation grade ≥ 3	Accuracy	Area under the ROC Curve	Sensitivity	Specificity	Positive Predictive Value	Negative Predictive Value
Inflammation grade ≥ 3 in the training cohort						
LR	0.831 (0.773-0.889)	0.863 (0.810-0.916)	0.879	0.257	0.854	0.248
RF	0.825 (0.766-0.884)	0.848 (0.792-0.903)	0.858	0.371	0.868	0.296
DTC	0.757 (0.691-0.824)	0.657 (0.583-0.730)	0.857	0.482	0.844	0.510
GNB	0.819 (0.759-0.878)	0.854 (0.799-0.909)	0.922	0.104	0.823	0.169
KNN	0.796 (0.734-0.859)	0.726 (0.657-0.795)	0.897	0.283	0.830	0.421
Inflammation grade ≥ 3 in the validation cohort						
LR	0.900 (0.875-0.925)	0.890 (0.864-0.917)	0.966	0.690	0.966	0.694
RF	0.896 (0.871-0.922)	0.867 (0.838-0.895)	0.955	0.798	0.976	0.671
DTC	0.807 (0.774-0.841)	0.705 (0.666-0.743)	0.955	0.867	0.968	0.821
GNB	0.907 (0.882-0.931)	0.882 (0.855-0.909)	0.976	0.578	0.958	0.711
KNN	0.866 (0.837-0.895)	0.747 (0.711-0.784)	0.972	0.723	0.958	0.801

Figure: (abstract: SAT-510).

SAT-511

Economic modelling of clinical management options of unexplained hyperferritinaemia in the adult general population: a proposed new model of care

John Olynyk^{1,2,3}, Mukesh Nasa¹, Khurshid Alam⁴, ¹Fiona Stanley Hospital, Murdoch, Australia; ²Edith Cowan University Joondalup Campus, Joondalup, Australia; ³Curtin University, Medicine, Bentley, Australia; ⁴Murdoch University, Murdoch, Australia
Email: john.olynyk@health.wa.gov.au

Background and aims: Unexplained hyperferritinaemia in the absence of iron overload or HFE haemochromatosis is common, especially in association with non-alcoholic fatty liver disease, and of no direct clinical significance. We modelled the discharge of unexplained hyperferritinaemia individuals from care either following diagnosis or after magnetic resonance FerriSmart (MR) measurement of hepatic iron concentration to exclude iron overload (Intervention MR model) compared to the standard of care, involving varying degrees of clinician review, ferritin testing and phlebotomy therapy which all become more likely as ferritin levels rise (comparator model). We hypothesise that the intervention model is more cost-efficient than the comparator model.

Method: A cost-minimization analysis was undertaken from the Australian health system perspective using Medicare and industry-provided costs. Costs of the intervention and comparator models were determined over a 5-year period for unexplained hyperferritinaemia individuals with elevated serum ferritin levels of 620–999 ug/L or ≥1000 ug/L.

Results: For the intervention model, the year 1 and 5-year average costs per individual for the 620–999 ug/L and ≥1000 ug/L groups were AU\$464.83 and AU\$92.97 and AU\$784.70 and AU\$156.94, respectively. For the comparator model, the year 1 and 5-year average costs per individual for the 620–999 ug/L and ≥1000 ug/L groups were AU\$298.74 and AU\$312.38 and AU\$745.84 and AU\$560.89, respectively. The intervention model was most cost-efficient after the first year.

Figure: Cost comparisons (per patient per year) of the group receiving MR intervention followed by discharge from care for no proven clinically significant iron overload compared with standard of care (SOC) in which there is continued management of UH individuals.

Ferritin group (mg/L)	Intervention MR Model		Comparator SOC Model	
	620–999	≥1000	620–999	≥1000
Cost (\$/patient/year)				
Year 1	464.83	784.70	307.99	745.84
Year 2	0	0	367.30	598.60
Year 3	0	0	330.57	538.74
Year 4	0	0	297.51	484.87
Year 5	0	0	267.76	436.38
Average over 5 years	92.97	156.94	314.23	560.89

Modelling based on algorithms described in methods and assuming a 10% loss each year for follow-up in years 2–5 in the SOC group.

Conclusion: It is more cost-efficient to discharge unexplained hyperferritinaemia individuals, with or without MR measurement, compared with the standard of care.

SAT-512

A systematic review and meta-analysis of the prevalence and cross-sectional severity of South Asian patients with non-alcoholic fatty liver disease

Michael James¹, Naheeda Rahman¹, Melanie Smuk¹, Georgia Black², William Alazawi¹, ¹Blizard Institute, Centre for Immunobiology, United Kingdom; ²Wolfson Institute of Population Health, United Kingdom
Email: mikejames5289@gmail.com

Background and aims: Patients of South Asian (SA) ethnicity represent a distinct cohort in non-alcoholic fatty liver disease (NAFLD), with an aggressive phenotype, embodying a growing proportion of the patients referred to hepatology services. We performed a systematic review and meta-analysis to assess overall prevalence and cross-sectional severity of NAFLD in SA patients.

Method: PubMed, Embase, Ovid and Cochrane databases were searched from January 2002–November 2022. We included observational/cross-sectional studies and clinical trials, in English, involving adults (age >18 years) of SA ethnicity (defined as Indian, Pakistani, Bangladeshi, Sri Lankan). All contained data on prevalence of NAFLD in the general or diabetic population, diagnosed by ultrasound (US) or biopsy. Data on severity were collected, measured by AST:ALT ratio, fibrosis score F0–F4 on biopsy or steatosis grade S1–S3 on US. Abstracts were screened for relevance and then full-text review undertaken by two reviewers. Random effects meta-analyses were performed. Quality of included studies was assessed using The National Institutes of Health quality assessment tool.

Results: We identified 3175 articles from the literature search and included 43 eligible studies with a total of 24419 individuals, average mean age of 47 (95% confidence interval (CI) 43.9–50.1). 32 studies were based on Indian populations, 6 Sri Lankan, 3 Pakistani and 2 Bangladeshi. 33 studies had data on prevalence of NAFLD in general and in diabetic populations, with 22 using US as the sole method of diagnosis. AST:ALT ratio, FIB4 and vibration-controlled transient elastography were utilized in 4 studies. The pooled prevalence of NAFLD in the general population was 47% (CI 34–60%). In people with diabetes, this increased to 66% (CI 55–77%). 34 studies reported on severity, 17 with biopsy, with 12 having a breakdown of fibrosis scores. Of these, 216/1278 had clinically significant fibrosis (≥F3). The pooled proportion of patients who had ≥F3 on biopsy was 12.67% (CI 6.74–18.6) (figure). In terms of risk stratification, only 8/17 liver histology studies reported non-invasive assessment prior to biopsy (all US) and none reported on the use of a formal diagnostic assessment pathway. The proportion of patients biopsied with clinically significant fibrosis is higher than reports from multiethnic cohorts in Britain (7.7%, 1) and in the United States (4.28%, 2).

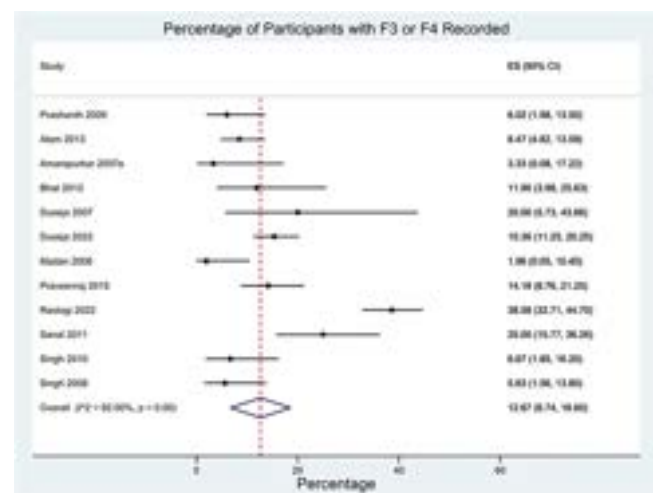


Figure:

Conclusion: The pooled prevalence of NAFLD in general and diabetic South Asian populations is higher than reported in previous systematic reviews. More work is needed to understand the epidemiology and natural history of NAFLD and the mechanisms that underlie the more aggressive disease phenotype in South Asian populations.

References

1. Srivastava A, Gailer R, Tanwar S, Trembling P, Parkes J, Rodger A *et al*. Prospective evaluation of a primary care referral pathway for patients with non-alcoholic fatty liver disease. *J Hep*. 2019; 71: 371–378.
2. Harrison S, Gawreih S, Roberts K, Lisanti CJ, Schwoppe RB, Cebe KM *et al*. Prospective evaluation of the prevalence of non-alcoholic fatty liver disease and steatohepatitis in a large middle-aged US cohort. *J Hep*. 2021; 75 (2): 284–291.

SAT-513

Serum glycochenodeoxycholic acid-3-sulfate can discriminate non-alcoholic steatohepatitis from steatosis

Barbora Nováková^{1,2}, Kateřina Žížalová², Vaclav Smid¹, Karel Dvorak^{3,4}, Aleš Kuběna², Libor Vitek^{2,3}, Martin Lenicek⁵, Radan Bruha³. ¹First Faculty of Medicine, Charles University and General University Hospital in Prague, 4th Department of Internal Medicine-Department of Hepatogastroenterology, Prague 2, Czech Republic; ²First Faculty of Medicine, Charles University and General University Hospital in Prague, Institute of Medical Biochemistry and Laboratory Diagnostics, Prague 2, Czech Republic; ³First Faculty of Medicine, Charles University and General University Hospital in Prague, 4th Department of Internal Medicine-Department of Hepatogastroenterology, Prague 2, Czech Republic; ⁴Regional Hospital Liberec, Liberec, Czech Republic; ⁵First

Faculty of Medicine, Charles University and General University Hospital in Prague, Institute of Medical Biochemistry and Laboratory Diagnostics, Prague 2, Czech Republic
Email: cizkova.barbora@gmail.com

Background and aims: Currently, liver biopsy is the only way to differentiate between non-alcoholic steatohepatitis (NASH) and steatosis (NAFL). Although the role of bile acids (BA) as a potential surrogate marker of NASH has already been investigated, the role of sulfated BA has not been tested yet. Therefore, our objective was to determine whether BA, including their 3-sulfates, can distinguish NASH from NAFL.

Method: We compared fasting serum concentrations of 22 individual BA and 23 BA 3-sulfates between the groups in an exploratory patient cohort (NASH n = 24, NAFL n = 18, healthy controls (CTRL) n = 15). The Kruskal-Wallis ANOVA with the appropriate post hoc test was used to compare BA concentrations between the groups. Two potential markers, glycochenodeoxycholic acid-3-sulfate (GCDCA-3S) and glyoursodeoxycholic acid-3-sulfate (GUDCA-3S) were further analysed in the biopsy-proven validation cohort (NASH n = 43, NAFL n = 21). Furthermore, we tested their ability to discriminate NASH using the ROC curve and a general linear model that contained potential confounders (liver fibrosis or cirrhosis, age, sex, BMI).

Results: Patients with NASH had significantly higher concentrations of GCDCA-3S compared to NAFL and CTRL (medians [μmol/L]: exploratory cohort NASH 0.306, NAFL 0.127, CTRL 0.105, p (NASH×NAFL)=0.030, p (NASH×CTRL)=0.008; validation cohort NASH 0.200, NAFL 0.049, p <0.0001). Furthermore, in the validation cohort, GCDCA-3S could distinguish NASH with 90% specificity and 60% sensitivity (AUROC=0.785). The ability of GCDCA-3S to

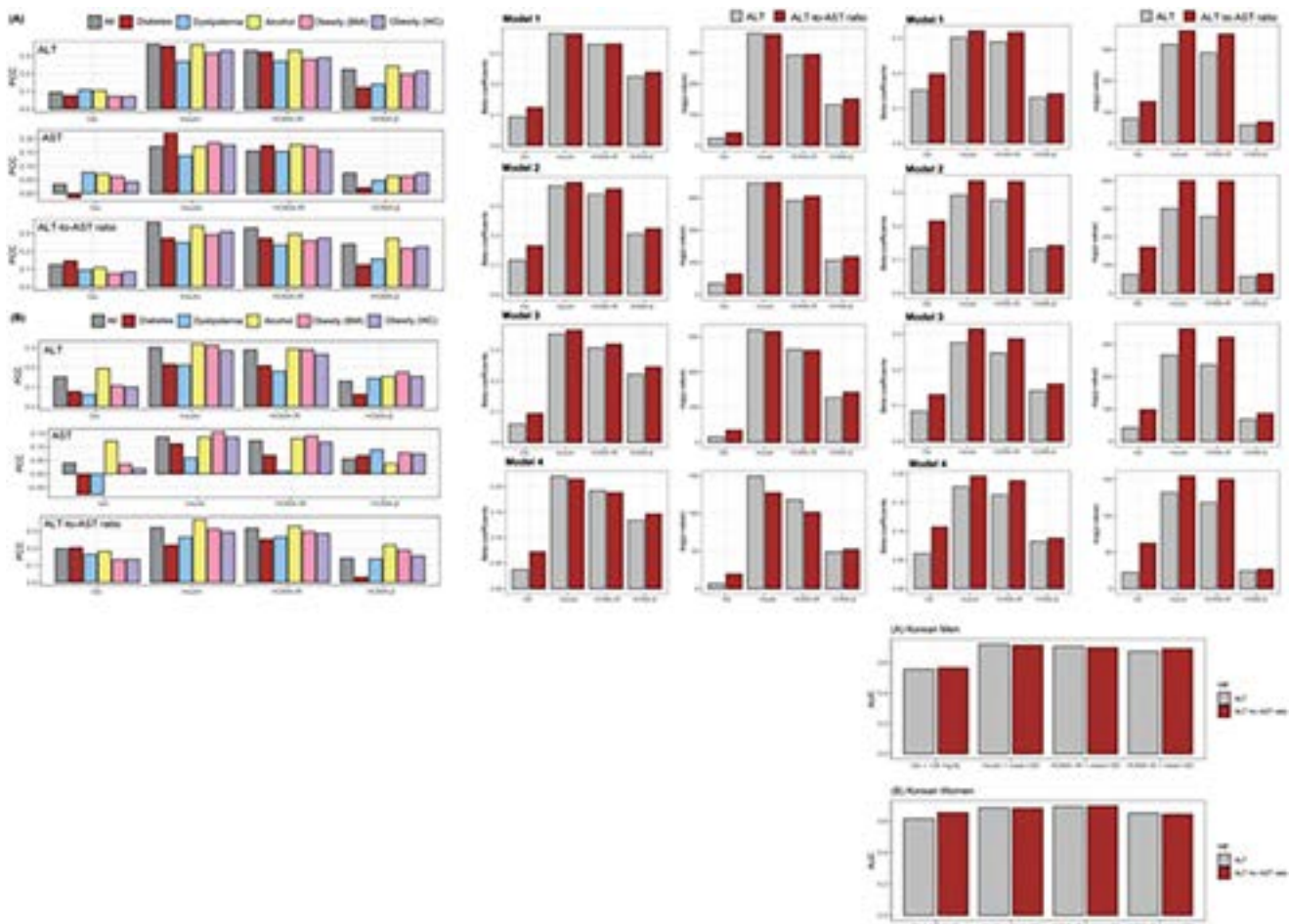


Figure: (abstract: SAT-514).

POSTER PRESENTATIONS

discriminate between NASH/NAFL remained significant in the linear model that contained the presence of moderate to severe fibrosis or cirrhosis ($p=0.006$). Fibrosis/cirrhosis was the only significant confounder in the model ($p=0.028$). Concentrations of another candidate, GUDCA-3S, were significantly elevated in NASH in the exploratory cohort; however, this was not confirmed in the validation cohort.

Conclusion: Serum GUDCA-3S concentration appears to distinguish NASH from NAFL.

SAT-514

ALT/AST ratio: the useful predictive marker for insulin resistance

Han Seul Ki^{1,2}, Moon Young Kim^{1,2}, Taesic Lee^{3,4}. ¹Yonsei University Wonju College of Medicine, Department of Internal Medicine, Division of Gastroenterology and Hepatology, Wonju-si, Korea, Rep. of South; ²Wonju Severance Christian Hospital, Regenerative Medicine Research Center, Wonju-si, Korea, Rep. of South; ³Yonsei University Wonju College of Medicine, Division of Data Mining and Computational Biology, Wonju-si, Korea, Rep. of South; ⁴Yonsei University Wonju College of Medicine, Department of Family medicine, Wonju-si, Korea, Rep. of South
Email: drkimmy@yonsei.ac.kr

Background and aims: Insulin resistance (IR) is common pathophysiology in type 2 diabetes mellitus, cardiovascular disease, and non-alcoholic fatty liver disease. As increased to the prevalence of these diseases, screening the risk for IR becomes important to prevent disease progression. To predict insulin resistance in the general population, regardless of comorbidity, we analyzed the health examination data using ALT/AST ratio for analysis.

Method: 2015, 2019, and 2020 Korea National Health and Nutrition Examination Survey (KNHANES) were analyzed to validate our hypothesis. For the evaluation of insulin resistance, the following four indices were implemented: fasting serum glucose (Glc) and insulin; Homeostatic Model Assessment for Insulin Resistance (HOMA-IR) and β cell function (HOMA- β). Pearson correlation coefficient (PCC) was implemented to evaluate the degree of association of liver profiles with indices for IR. Linear or logistic regression (LiR or LR) was implemented to identify the association of liver profiles with IR value or status, respectively. Classification performance was evaluated based on the area under curve of Receiver Operating Characteristic (AUC).

Results: Based on PCC, serum ALT in Korean men and women was positively related to four IR indices, including Glc, insulin, HOMA-IR (Homeostatic Model Assessment for Insulin Resistance), and HOMA- β . These positive relationships remained after selecting subjects diagnosed with diabetes or dyslipidemia, alcohol consumption, or subjects having general obesity or abdominal obesity. ALT/AST ratio was also robustly correlated with the four IR indices. In the multivariate LiR, when comparing ALT levels, ALT/AST ratio in Korean men exhibited better predictive performance for Glc and HOMA- β , besides, that in Korean women provided improved outcomes for all IR indices. Based on the prediction for the binary form of IR status, the ALT/AST ratio in Korean men and women could well predict HOMA- β and HOMA-IR, compared to the sole ALT level, respectively.

Conclusion: In the analysis that includes a large community-based population, ALT/AST ratio is a useful predictive marker compared with HOMA-IR. A simple, precise marker that is represented to ALT/AST could be a practical method to screen insulin resistance in the general population regardless of DM, alcohol intake, and gender.

SAT-515

Validation of Baveno VII criteria in NAFLD patients according to body mass index

María Del Barrio Azaceta¹, Carmen Lara Romero², Paula Iruzubieta¹, Andrea Cornejo², María del Carmen Rico², María Teresa Arias Loste¹, Javier Crespo¹, Manuel Romero Gomez^{2,3}. ¹Gastroenterology and Hepatology Department, Clinical and Translational Research in Digestive Diseases, Valdecilla Research Institute (IDIVAL), Marqués de Valdecilla University Hospital, Santander, Spain; ²Digestive Diseases Unit, Hospital Universitario Virgen del Rocío, SeLiver Group, Institute of Biomedicine of Sevilla (HUVIR/CSIC/US), Department of Medicine, University of Sevilla, Sevilla, Spain, Spain; ³Centro de Investigación Biomédica en Red de Enfermedades Hepáticas y Digestivas (CIBEREHD), Madrid, Spain
Email: mromerogomez@us.es

Background and aims: In Baveno VII consensus, new criteria have been defined to try to identify the presence of clinically significant portal hypertension (CSPH). "The rule of 5 (R5)" establishes liver stiffness values in combination with the platelet count, to predict the presence of CSPH. However, in obese patients with Metabolic associated fatty liver disease (MAFLD) these criteria have not been validated.

Method: Bicentric cross-sectional study of 131 patients with MAFLD diagnosed by biopsy ($n=41$; 31.3%) or clinical criteria ($n=90$; 68.7%) and who had a transient elastography (TE) with significant fibrosis (≥ 8 kPa). CSPH was defined as the presence of esophageal varices or gastropathy, hepatic decompensation, collaterals, or ascites. The R5 Baveno VII inclusion criteria were used: A) $ET \geq 25$ kPa; B) $20 \text{ kPa} < ET < 25 \text{ kPa}$ and $< 150,000$ platelets; C) $15 \text{ kPa} > ET < 20 \text{ kPa}$ and $< 110,000$ platelets; exclusion criteria: $ET < 10 \text{ kPa}$ or $10 \text{ kPa} < ET < 20 \text{ kPa}$ and $> 150,000$ platelets.

Results: Ninety-one patients had obesity (BMI > 30). In patients with MAFLD, the R5 had an overall sensitivity (Sen) of 68.08%, specificity (Spe) 51.19%, PPV 58.18% and NPV 90.38%. Sensitivity and PPV were lower in obese MAFLD patients (BMI $> 30 \text{ kg/m}^2$): (S: 63.3% E: 55.7%; PPV 51.4%; NPV: 90.38%), compared to those with BMI ≤ 30 (S: 76.5%; E: 56.52% and PPV: 72.2%; NPV: 86.7%); $p < 0.05$. The probability of classification in the grey area was 17/91 (18.7%) in obese patients compared to 7/40 (17.5%) in BMI $< 30 \text{ kg/m}^2$ ($p = \text{ns}$); presenting CSPH 10/24 (41.6%) and being absent in 14/24 (58.3%). Figure. In the univariate and multivariate (LR) analysis, the only independent predictor variable to predict the failure was age with $\text{Exp} = 5.050 - 0.76 \times \text{Age (year)}$.



Figure:

Conclusion: Predictive criteria proposed by Baveno VII for CSPH are less accurate in obese patients with MAFLD and should be corrected for age.

SAT-516

A real world experience utilising the FAST score to identify patients with NASH fibrosis

Gres Karim¹, Dewan Giri¹, Brooke Wyatt², Ilan Weisberg³, Amreen Dinani^{2,4}. ¹Mount Sinai Beth Israel, United States; ²Icahn School of Medicine at Mount Sinai, United States; ³New York Presbyterian-Brooklyn Methodist Hospital, United States; ⁴Duke Health, Gastroenterology and Hepatology, United States
Email: gres.karim@mountsinai.org

Background and aims: The need to develop simple and non-invasive methods to diagnose non-alcoholic steatohepatitis (NASH) and fibrosis is one of the tasks the NAFLD community recognizes as important and necessary. Several non-invasive tests (NITs) have been studied and validated with moderate predictive capability to accurately rule out advanced fibrosis. The FibroScan-AST (FAST) score is a NIT that uses a combination of the liver stiffness measurement (LSM) and controlled attenuation parameter (CAP) from vibration controlled transient elastography (VCTE), and aspartate aminotransferase (AST) to identify patients with 'fibrotic NASH', defined as NASH with significant liver fibrosis (stage 2 fibrosis or higher [$>F2$]). The aim of this study was to test the performance of the FAST score to accurately identify NASH + $>F2$ in a cohort of patients with a histological diagnosis of NASH, using a cutoff of >0.35 as a rule in factor. The cut off of 0.65 was not tested in this study as it has been proposed to identify those with $>F3$ fibrosis (advanced fibrosis). We compared the performance of the FAST score to LSM $>8kPa$ and Fibrosis-4 Index (FIB-4) >1.3 (both cut-off for $>F2$) and attempted to identify risk factors to develop a model for improving diagnostic accuracy.

Method: Patients with a histological diagnosis of NASH were identified from 2020 to 2021. Demographic information, laboratory data, and VCTE data was collected. FAST score and FIB-4 were calculated. Univariate and backwards entry multivariate logistic regression analysis were performed to identify additional risk factors to diagnose NASH + $>F2$. Discrimination and overall accuracy (c-statistic) was assessed using area under receiver operating characteristic (AUROC) curves.

Results: Using a rule in cutoff of >0.35 , the FAST score performed with a sensitivity, specificity, NPV, and PPV of 96.4%, 36.8%, 77.7%, 81.8%, respectively. Independent logistic regressions within this sample showed age (OR = 0.05, CI: 1.0–1.07, $p = 0.05$) and a FAST >0.35 (OR = 15.75, CI: 2.9–85.48, $p = 0.001$) to be associated with correctly identifying NASH + $>F2$ based on histological evidence. Although the FAST score >0.35 performed with the highest accuracy (81.3%), it performed with the lowest c-statistic (0.70, CI: 0.55–0.84) when compared to LSM $>8kPa$ (0.72, CI: 0.59–0.85) and FIB-4 >1.3 (0.73, CI: 0.59–0.87). Our proposed FAST + Age model outperformed the others with a sensitivity of 94.6%, specificity of 42.1%, PPV of 82.7%, NPV of 96.4% and c-statistic of 0.78 (CI: 0.64–0.92).

NASH diagnostic Criteria/tests	Sensitivity	Specificity	PPV	NPV	Overall Accuracy	C statistic	C statistic Confidence Interval
FAST ≥ 0.35	96.4%	36.8%	81.8%	77.7%	81.3%	0.70	(0.55, 0.84)
FIB-4 ≥ 1.3	64.3%	68.4%	86%	40%	65.0%	0.73	(0.59, 0.87)
LSM $\geq 8kPa$	75%	52.6%	82.4%	41.6%	69.0%	0.72	(0.59, 0.85)
FAST ≥ 0.35 + Age	94.6%	42.1%	82.7%	96.4%	81.3%	0.78	(0.64, 0.92)

Conclusion: A FAST score with a cutoff of >0.35 as a rule in factor performed reasonably well (AUROC: 0.70, and 0.78 when age was incorporated into the model) in detecting NASH + $>F2$ fibrosis in the real world. The FAST score + Age performed superiorly to LSM and FIB-4 in detecting individuals with NASH + $>F2$.

SAT-517

The sequential use of liver stiffness measurement and direct biomarkers of fibrosis is able to identify patients with severe non-alcoholic steatohepatitis

Filippo Gabrielli^{1,2}, Simonetta Lugari³, Alessia Cavicchioni³, Amedeo Lonardo³, Cristina Feliciani³, Antonia Rudilosso³, Chiara Pacchioni⁴, Carla Greco⁴, Chiara Valenti⁴, Luigi Valerio⁴, Mario Bondi⁴, Daniele Santi⁴, Giorgia Spaggiari⁵, Stefano Ballestri⁶, Tommaso Trenti⁵, Valentina Pecoraro⁵, Manuela Simoni⁴, Pietro Andreone², Fabio Nascimbeni³. ¹Università degli studi di Bologna, Medical and surgical sciences, Bologna, Italy; ²University of Modena and Reggio Emilia, Department of Medical and Surgical Sciences Maternal-Childish and Adult, Modena, Italy; ³Azienda Ospedaliero-Universitaria di Modena, Internal Medicine, Modena, Italy; ⁴Azienda Ospedaliero-Universitaria di Modena, Endocrinology, Modena, Italy; ⁵Azienda Ospedaliero-Universitaria di Modena, Corelab, Modena, Italy; ⁶Pavullo Hospital, Internal Medicine, Pavullo Nel Frignano, Italy
Email: judeslash1@gmail.com

Background and aims: The identification of patients with severe non-alcoholic steatohepatitis (NASH), who are at greater risk of progression to cirrhosis, and who most deserve targeted interventions and recruitment in clinical trials, is a major priority. Several non-invasive tests (NITs) have been developed to detect patients at risk of severe NASH and to reduce the use of liver biopsy. We conducted a prospective single-centre study aimed at evaluating the diagnostic performance of different NITs in the identification of biopsy-confirmed severe NASH. Moreover, we explored if the sequential use of NITs was able to improve their diagnostic accuracy. **Method:** 56 consecutive patients (73.2% men; age 52 [22–69] years) performed liver biopsy for the suspicion of severe NASH, defined as the presence of NASH, NAFLD activity score ≥ 4 and fibrosis stage $\geq F3$. Simple wet NITs [aspartate aminotransferase (AST), alanine aminotransferase (ALT), albumin, platelet count, AST/ALT ratio (AAR) and AST to platelet ratio index (APRI)], complex wet NITs, [BARD score, Fibrosis-4 index (FIB-4), NAFLD fibrosis score (NFS), Forns Index and Hepamet fibrosis score (HFS)], direct biomarkers of fibrosis [collagen IV (CIV), laminin (LM), cholyglycine (CG), hyaluronic acid (HA) and procollagen type III amino-terminal peptide (PIIIP)], measurement of liver stiffness (LS) with Fibroscan[®], and AGILE 3+ and AGILE 4 scores, were all evaluated at the time of liver biopsy. The area under the receiver operating characteristic curve (AUROC) for the identification of severe NASH of each single NIT was calculated. Finally, we evaluated the diagnostic accuracy of the sequential use of the NITs yielding the best diagnostic performance at AUROC analysis.

Results: Severe NASH was present in 12 (21.4%) patients. Simple wet NITs were not able to significantly detect severe NASH (AUROCs ranging from 0.46, $p = 0.68$ for albumin to 0.67, $p = 0.08$ for GOT, platelet and AAR). Among complex wet NITs, only BARD was able to significantly detect severe NASH (AUROC 0.77, $p = 0.004$), while FIB-4, NFS, Forns Index and HFS were not (AUROCs ranging from 0.45, $p = 0.71$ for Forns Index to 0.65, $p = 0.12$ for NFS). All direct biomarkers of fibrosis significantly detected severe NASH, with PIIIP (AUROC 0.81, $p = 0.001$) and CIV (AUROC 0.80, $p = 0.002$) showing the best diagnostic performance. NITs based on LS with Fibroscan[®] also significantly detected severe NASH, however AGILE 3+ (AUROC 0.71, $p = 0.03$) and AGILE 4 (AUROC 0.70, $p = 0.04$) scores did not improve the diagnostic performance of LS alone (AUROC 0.76, $p = 0.007$). The sequential use of LS (cut-off 8.5 kPa) and PIIIP (cut-off 22 ng/ml) or CIV (cut-off 16.5 ng/ml) had a diagnostic accuracy of 85.7% and 91.1%, respectively.

Conclusion: The sequential use of LS and direct biomarkers of fibrosis, such as PIIIP and CIV, may be a promising approach to non-invasively identify patients with severe NASH.

SAT-518

The clinical significance of transient elastography and cap in the diagnosis and surveillance of non-alcoholic fatty liver disease

Eleni Gigi¹, Despoina Vasileiou¹, Theodoros Michailidis¹. ¹Aristotle's University of Thessaloniki, Hepatology Dep of 2nd Internal Medicine, Greece

Email: elengigi@auth.gr

Background and aims: Non-alcoholic fatty liver disease (NAFLD) is characterized nowadays as the most common liver disease with a prevalence of 25–30% in the general population. While in most cases it has a benign course, a significant percentage of patients progress to non-alcoholic steatohepatitis (NASH), which is characterized by inflammation of the hepatocytes, and then a percentage of them end up with cirrhosis, with an increased risk of developing HCC. The gold standard method for the diagnosis of NAFLD is liver biopsy, but due to the fact that it is an invasive method accompanied by complications, there has been an attempt in recent years to use new non-invasive diagnostic methods such as transient elastography. The purpose of this thesis is to clarify whether transient elastography is a reliable method for the diagnosis and monitoring of NAFLD.

Method: In this context, a cross sectional study was carried out at the Hepatology Department of General Hospital of Thessaloniki "Ippokratio." 81 participants with different liver diseases underwent transient elastography, upper abdomen ultrasound and laboratory blood tests.

Results: The results of the study showed that the participants had an average CAP value of 254 dB/m, which corresponds to stage 1 steatosis, but 18, 52% showed a high risk of disease progression based on the FAST score. In addition, it was shown that the results of the transient elastography were strongly related to the results of the ultrasound with a Spearman rank correlation coefficient = 0.589 and a p value <0.001. It was also found that BMI, SGPT, fasting glucose, uric acid and triglycerides were significantly associated with CAP with p values <0.001, 0.004 and 0.002, 0.036 and 0.041 respectively. Regarding severe NAFLD only BMI appeared to have a strong correlation with a p value = 0.006. However, in the multivariate analysis only the first three variables showed a significant correlation and so they were used to form a multivariate model: CAP_{new} = 27, 249 + 4, 723xBMI + 0, 26x SGPT + 0, 536xFasting glucose.

Conclusion: Transient elastography is a reliable diagnostic tool for the management of NAFLD, however, it has weaknesses in terms of confounding factors that affect its results and reduce its diagnostic accuracy.

NAFLD Experimental and pathophysiology

WEDNESDAY 21 TO SATURDAY 24 JUNE

TOP-084

Caspase 8 reverses progression of NASH after hepatocyte-specific JNK deletion

Ines Volkert¹, Julia Piche¹, Christian Trautwein¹. ¹RWTH Aachen University hospital, Medical department III, Aachen, Germany
Email: ivolkert@ukaachen.de

Background and aims: Non-alcoholic fatty liver disease (NAFLD) is the most common chronic liver disorder in the Western world. Despite intensive research the mechanisms that may lead to progression towards end-stage cirrhosis and hepatocellular carcinoma (HCC) remain unclear. c-Jun N-terminal kinases (JNKs) are known to play a significant role in liver physiology and disease pathogenesis. In the present study, we aimed to investigate the

mechanisms of liver damage after hepatocyte-specific Jnk1 and Jnk2 deletion in an experimental NASH model.

Method: NASH was induced by feeding animals a Western-style diet (WSD) to compare disease development between wild-type (WT) and mice with a hepatocyte-specific deletion of Jnk1 and Jnk2 (JNK1/2^{Δhepa}). After pathway analysis, JNK1/2^{Δhepa}/caspase8^{Δhepa} animals were generated.

Results: WSD of JNK1/2^{Δhepa} mice caused significantly increased transaminases, enhanced fibrogenesis and strongly increased inflammation, as evidenced by infiltration of immune cells and liver cytokines and chemokines, compared to WT mice. A gene set pathway analysis revealed distinct pathways, which are activated among WSD in JNK1/2^{Δhepa} livers. Besides inflammatory signals, we specially found a strong increase of apoptotic pathways, which was further confirmed by TUNEL and Cleaved Caspase 3 staining. Hence, JNK1/2^{Δhepa}/caspase8^{Δhepa} animals were fed with a WSD. Triple ko animals showed significantly decreased liver transaminases and inflammation. Moreover, fibrogenesis and cell death were completely rescued. Interestingly, pathway analysis showed that most genes that were upregulated in JNK1/2^{Δhepa} mice, were reversed after additional caspase 8 knockdown. Thus, an additional knockout of Caspase 8 achieved a complete reversal of the severe phenotype.

Conclusion: Our results demonstrate that hepatocyte-specific deletion of Jnk1 and Jnk2 triggers a strong oxidative stress response leading to increased NASH progression associated with apoptotic cell death. Interestingly additional hepatocyte-specific caspase 8 deletion completely rescued the phenotype. Hence, caspase 8 seems a promising hepatocyte-specific therapeutic target during NASH progression.

TOP-086

Novel role of macrophage Foxo1-mediated YAP-Notch axis in NASH progression

Dongwei Xu^{1,2}, Xiaoye Qu^{1,2}, Tao Yang¹, Xiao Wang¹, Michael Ke¹, Jun Li³, Longfeng Jiang³, Qiang Xia², Douglas Farmer¹, Bibo Ke¹. ¹The Dumont-UCLA Transplant Center, Division of Liver and Pancreas Transplantation, Surgery, Los Angeles, United States, ²Renji Hospital, Shanghai Jiaotong University School of Medicine, Liver Surgery, Shanghai, China, ³The First Affiliated Hospital, Nanjing Medical University, Infectious Diseases, Nanjing, China
Email: bke@mednet.ucla.edu

Background and aims: Innate immune activation is critical in initiating and amplifying hepatic inflammation in NASH progression. However, the mechanisms of immunoregulatory molecules in recognizing lipogenic, fibrotic, and inflammatory signals remain unclear.

Method: A mouse model of a high-fat diet (HFD)-induced NASH was used in the myeloid-specific Foxo1, YAP, or Notch1 knockout or double knockout mice. Liver injury, lipid accumulation, fibrogenic genes, and immune regulatory molecules were assessed *in vivo* and *in vitro*.

Results: HFD-induced oxidative stress activates Foxo1, YAP, and Notch1 signaling in hepatic macrophages. Macrophage Foxo1 deficiency (Foxo1^{M-KO}) ameliorates hepatic inflammation, steatosis, and fibrosis in HFD-challenged livers, accompanied by reduced STING, TBK1, and NF-κB activation in HFD-challenged livers. However, disruption of Foxo1 and YAP double knockout (Foxo1/YAP^{M-DKO}) or Foxo1 and Notch1 double knockout (Foxo1/Notch1^{M-DKO}) enhances STING function and exacerbates HFD-induced liver injury. Interestingly, Foxo1^{M-KO} markedly reduces TGF-β1 release from palmitic acid (PA)-stimulated Kupffer cells, and decreases Col1α1, CCL2, and Timp1 but increases MMP1 expression in primary hepatic stellate cells (HSCs) after co-culture with Kupffer cells. Notably, the PA challenge in Kupffer cells augments LIMD1 and LATS1 co-localization and interaction, which induces YAP nuclear translocation. Foxo1^{M-KO} activates PGC-1α and enhances nuclear YAP activity. Disruption of YAP in Foxo1^{M-KO} macrophages increases ROS

production in hepatocytes after co-culture exposed to PA challenge. Moreover, YAP deletion in Foxo1^{M-KO} macrophages reduces mitochondrial transcription factor A (TFAM) and mitochondrial DNA (mtDNA) expression but augments intracellular lipid levels in PA-stimulated hepatocytes after co-culture. Using chromatin immunoprecipitation (ChIP) coupled with massively parallel sequencing (ChIP-Seq) and *in situ* RNA hybridization approaches, we find that NICD co-localizes with YAP and targets *Mb21d1* (cGAS) and modulates STING function leading to impeding NASH development. **Conclusion:** Macrophage Foxo1-mediated YAP-Notch1 axis controls NASH progression via regulating cGAS-STING immune activation and mitochondrial biogenesis. YAP is a novel coactivator of NICD, and the YAP-NICD interaction is crucial for inhibiting STING function in NASH progression.

TOP-089

NAFLD is a night-time disease driven by nocturnal hepatic, adipose, and skeletal muscle insulin resistance

Thomas Marjot^{1,2,3}, Sarah White^{1,3}, Elspeth Johnson¹, Felix Westcott¹, Kate Gralton¹, Riccardo Pofi¹, David Dearlove¹, David Ray^{1,3}, Leanne Hodson^{1,3}, Jeremy Tomlinson^{1,3}. ¹Oxford Centre for Diabetes, Endocrinology and Metabolism, Churchill Hospital, University of Oxford, Oxford, United Kingdom, ²Oxford Liver Unit, Translational Gastroenterology Unit, Nuffield Department of Medicine, University of Oxford, Oxford, United Kingdom, ³NIHR Oxford Biomedical Research Centre, Oxford University Hospitals NHS Foundation Trust, Oxford, United Kingdom

Email: thomas.marjot@ndm.ox.ac.uk

Background and aims: Rodent models show that hepatic lipid and glucose metabolism are under tight circadian control yet there are no clinical studies exploring diurnal patterns in functional processes governing intrahepatic lipid accumulation. We have characterised these metabolic pathways during day and night in patients with NAFLD before and after weight loss as well as matched controls.

Method: 11 NAFLD patients and 11 controls underwent detailed metabolic phenotyping during the day (07:00 AM-13:00 PM) and at night (19:00 PM-01:00 AM) under standardised fasting conditions. Investigations included a 2-step hyperinsulinaemic euglycaemic clamp, stable isotope assessments of glucose utilization, and paired biopsies of adipose and skeletal muscle tissue. Identical day and night-time investigations were performed in patients with NAFLD after a 12-week weight loss program.

Results: In NAFLD patients, glucose utilization (M/I value) was lower at night compared to day during both low- (12.1 ± 4.8 vs. 23.2 ± 3.7 mg/kg/min per uU/ml; $p = 0.046$) and high-dose insulin infusions (13.5 ± 2.3 vs. 20.6 ± 3.6 mg/kg/min per uU/ml; $p = 0.042$) indicative of night-time hepatic and skeletal muscle insulin resistance respectively (Fig. 1A). Isotopically measured glucose disposal (Gd) was also lower at night compared to day (18.6 ± 2.0 vs. 27.3 ± 2.7 μ mol/kg/min; $p < 0.001$) (Fig. 1B) as was total body glucose oxidation assessed by ¹³CO₂ detection in breath (1.57 ± 0.1 vs. 1.72 ± 0.1 mmol/min/kg; $p = 0.03$). In contrast, control participants had no diurnal differences in M/I values, glucose disposal, or glucose oxidation. Patients with NAFLD also had markedly elevated plasma non-esterified fatty acids (NEFA) at night compared to day during basal (384 ± 58 vs. 299 ± 461 mmol/L; $p = 0.001$) and low-dose insulin phases of the clamp (234 ± 74 vs. 173 ± 49 mmol/L; $p = 0.006$) (Fig. 1C). These data are consistent with night-time adipose insulin resistance which positively correlated with degree of hepatic steatosis measured by controlled attenuation parameter (CAP) ($r = 0.806$; $p = 0.005$). Self-reported food diaries demonstrated that NAFLD patients consumed 48% of their mean daily calories during a single evening meal which may compound their night-time metabolic dysfunction. 9/11 (81%) NAFLD patients completed the lifestyle intervention achieving 6% weight loss and a 19% CAP reduction. Whilst there were global improvements in insulin sensitivity and adipose function, diurnal differences in M/I values ($p = 0.02$) and circulating NEFA levels ($p = 0.008$) persisted with continued metabolic dysfunction at night. Across all groups, there were no significant differences in calory intake, physical activity, and sleep quality in the week preceding day and night-time investigations suggesting that observed metabolic changes were related to time-of-day rather than external lifestyle factors. Proteomic analysis of adipose and skeletal muscle tissue will now help establish a mechanistic basis for this diurnal variability in metabolic phenotype.

Conclusion: Night-time metabolic dysfunction may represent a unique risk factor for NAFLD with multiple contributory pathogenic pathways augmented at night compared to day. These findings will help establish the optimal window for energy intake in patients with NAFLD and guide the best time-of-day to deliver medications currently in development.

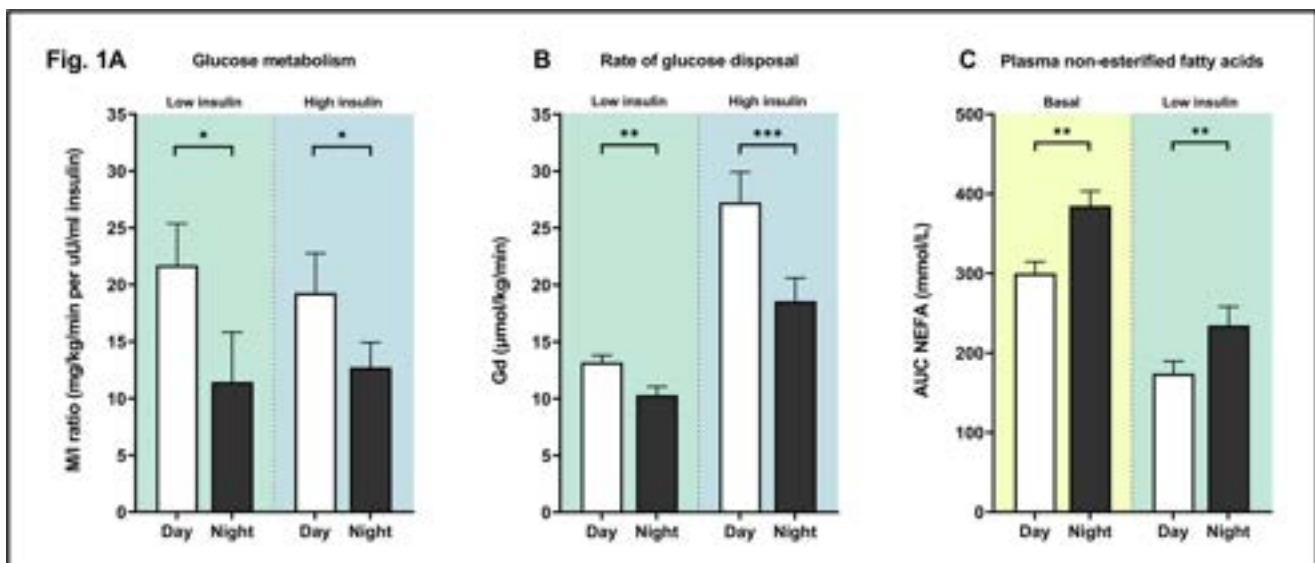


Figure: (abstract: TOP-089).

TOP-090

Single-cell RNA sequencing in DIAMOND mice reveals differentially regulated pathways specifically associated with the transition from simple steatosis towards NASH

Rocío Gallego-Durán^{1,2}, Douglas Maya^{1,2}, Ignacio Benedicto³, José María Herranz^{2,4}, Lucía López-Bermudo^{5,6}, Elena Vázquez-Ogando⁷, Rocío Montero-Vallejo^{1,2}, M^a José Robles-Frias⁸, Blanca Escudero-López^{5,6}, Antonio Cárdenas-García^{5,6}, Ana Quintas⁹, Elena Blázquez-López^{2,7}, Francisco Javier Cubero^{2,3}, Javier Vaquero^{2,7}, Yulia Nevzorova³, Maite G Fernandez-Barrena^{2,4}, Matías A Avila^{2,4}, Jordi Gracia-Sancho², Rafael Bañares^{2,7}, Franz Martin-Bermudo^{5,6}, Manuel Romero Gomez^{1,2}, Javier Ampuero^{1,2}. ¹UCM Digestive Diseases, Hospital Universitario Virgen del Rocío; SeLiver Group, Instituto de Biomedicina de Sevilla (HIVR/CSIC/US), Departamento de Medicina Universidad de Sevilla, Sevilla, Spain, ²CIBEREHD- Centro de Investigación Biomédica en Red de Enfermedades Hepáticas y Digestivas, Spain, ³Departamento de Inmunología, Oftalmología y ORL, Facultad de Medicina, Universidad Complutense de Madrid, Madrid, Spain, ⁴Program of Hepatology, Centre of Applied Medical Research (CIMA), University of Navarra, Spain, ⁵Centro Andaluz de Biología Molecular y Medicina Regenerativa-CABIMER, Universidad Pablo de Olavide, Universidad de Sevilla, Consejo Superior de Investigaciones Científicas (CSIC), Spain, ⁶CIBERDEM- Centro de Investigación Biomédica en Red de Diabetes y Enfermedades Metabólicas Asociadas, Spain, ⁷HepatoGastro Lab, Servicio de Ap. Digestivo del HGU Gregorio Marañón, Instituto de Investigación Sanitaria Gregorio Marañón, Spain, ⁸Pathology Department, Hospital Universitario Virgen del Rocío, Spain, ⁹Centro Nacional de Investigaciones Cardiovasculares (CNIC), Spain
Email: jampuero-ibis@us.es

Background and aims: DIAMONDTM mice have been validated as preclinical model mirroring the metabolic and histological features of human NASH without significant fibrosis. The main aim was to employ single-cell RNAseq (scRNAseq) technology in this preclinical model to unveil the differential changes specifically associated with the progression from simple steatosis to NASH.

Method: We performed scRNAseq on parenchymal and non-parenchymal cells (NPCs) isolated from 8 DIAMONDTM mice fed high-fat high-fructose diet (HF-HFD) vs. controls at 19 and 32 weeks. For cell isolation purposes, livers were perfused and divided into two different fractions, one for hepatocytes and the other for the evaluation of NPCs. Briefly, hepatic tissue was dissociated,

centrifuged, purified, sorted by FACS and prepared to single-cell sequencing analysis using 10x Genomics. Several ingenuity pathway analyses (IPA) tools were used to find altered pathways, upstream regulators and toxic molecules specifically associated to NASH transition ($\Delta_{33w-19w}$ activation z-score >|2|). Mitochondrial gene presence filtering was tested with several cut-offs selecting the most appropriate one for the experiment and validating its effect in clustering and differential expression. Clustering was carried out using the Seurat package in R with different resolutions to find the most adequate one for the experiment and validating the biological existence of the cluster using published markers and human protein atlas. Cell type annotation was generated using celldex package and validated using published and human protein atlas cell type markers to rename liver specific populations. The similarity with human NASH progression was measured using a robust NASH signature from previously published data. Mice livers were stained for haematoxylin-eosin and Masson's trichrome, SAF Score and fibrosis were calculated by a pathologist blinded to the provenance of samples.

Results: Histopathological analysis following SAF Score showed NASH exclusively at 32 w despite significant inflammation at 19w of diet. Mild fibrosis was observed in all animals fed HF-HFD. We obtained a total of 70637 hepatocytes and 151132 NPCs, and identified six clusters of hepatocytes at week 19 and five at week 32 (see figure). NPCs clustering identified 21 clusters at week 19 and 24 at week 32, and 12 out of 21 and 10 out of 24 were assigned as known cell types respectively. Preliminary IPA analysis on hepatocytes reinforced the idea that the presence of NASH is associated with mitochondrial dysfunction (Mitochondrial dysfunction $\Delta_{z-score} = 3.78$; Oxidative phosphorylation $\Delta_{z-score} = -5$; Sirtuin signalling pathway $\Delta_{z-score} = 5.74$). Interestingly, we observed a significant downregulation of several pathways linked to caspase-dependent apoptosis (Apoptosis of hepatocytes $\Delta_{z-score} = -2.178$; Cell death of hepatocytes $\Delta_{z-score} = -2.662$) despite a much higher presence of ballooned hepatocytes in NASH tissue together with an activation of a pathway related to caspase-independent apoptosis (Granzyme A signalling $\Delta_{z-score} = 3.74$).

Conclusion: A single-cell model to analyse the transition towards NASH independently of fibrosis stage using DIAMONDTM mice has been established. Preliminary results link mitochondrial dysfunction in hepatocytes to NASH and ballooning, and highlight some noteworthy deregulations in pathways mediating apoptosis.

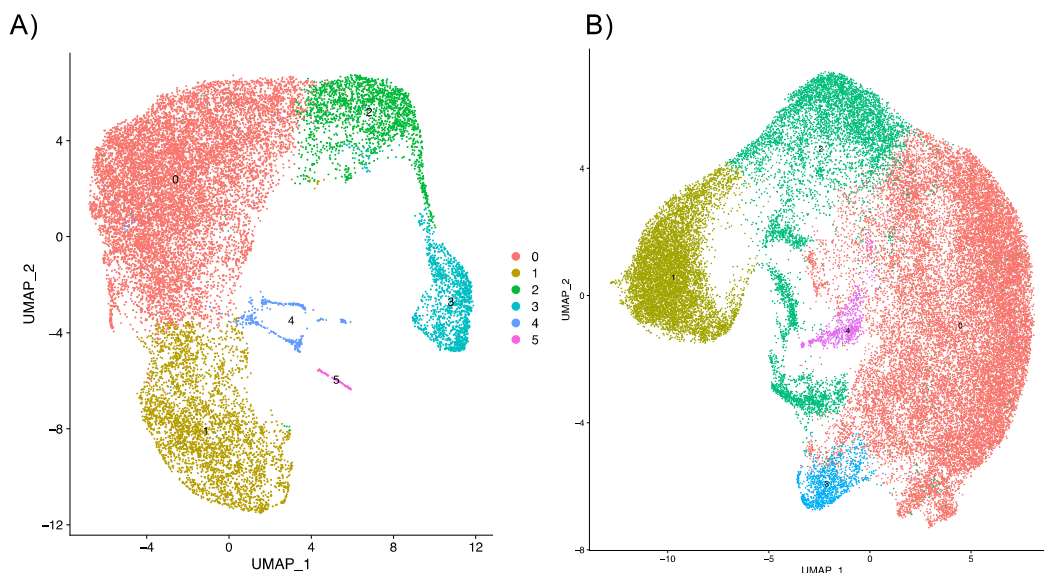


Figure: (abstract: TOP-090): UMAP results from parenchymal cells isolated from livers at 19w (a) and 32w (b) of diet.

WEDNESDAY 21 JUNE

WED-393

A functional interaction between hepatic estrogen receptor- α and PNPLA3 p.I148M inherited variant drives fatty liver disease susceptibility in women

Alessandro Cherubini¹, Mahnoosh Ostadreza¹, Oveis Jamialahmadi², Serena Pelusi¹, Eniada Rrapaj¹, Elia Casirati³, Giulia Passignani¹, Guido Alessandro Baselli¹, Luisa Ronzoni¹, Sara Della Torre⁴, Paola Dongiovanni⁵, Daniele Prati¹, Stefano Romeo⁶, Luca Valenti^{1,7}.
¹Fondazione IRCCS Ca' Granda Ospedale Maggiore Policlinico, Transfusion Medicine, Milano, Italy, ²Gothenburg University, Department of Molecular and Clinical Medicine, Gothenburg, Sweden, ³University of Milan, Pathophysiology and Transplantation, Milano, Italy, ⁴University of Milan, Department of Pharmaceutical Sciences, Italy, ⁵Fondazione IRCCS Ca' Granda Ospedale Maggiore Policlinico, General Medicine and Metabolic Diseases, Milano, Italy, ⁶University of Gothenburg, Department of Molecular and Clinical Medicine, Sweden, ⁷University of Milan, Pathophysiology and Transplantation, Italy
 Email: alessandro.cherubini@policlinico.mi.it

Background and aims: Fatty liver disease (FLD) related to metabolic dysfunction and excessive alcohol affects almost one third of the global population and is a leading cause of liver related mortality. The PNPLA3 p.I148M variant accounts for the largest fraction of FLD heritability. Although women are protected during the reproductive age, especially after menopause some are susceptible to FLD, but this sexual dimorphism is neglected in clinical studies. Aim was to examine the PNPLA3 p.I148M*female sex interaction in FLD development, and to investigate the underlying mechanism.

Method: The female sex*PNPLA3 p.I148M interaction on FLD was tested in the Liver Biopsy (n = 1861), severe FLD case-control (n = 4374), Liver-Bible-2021 (n = 817) and UK Biobank (n = 347,127) cohorts. PNPLA3 expression was determined in transcriptomic cohort (n = 107). HepG2 cells were used for estrogen receptor (ER) modulation and fatty acid treatment, and to generate PNPLA3-ER element (ERE) knock-out clones.

Results: In all cohorts we observed an interaction between female sex and PNPLA3 p.I148M, but not other FLD genetic risk variants, in determining FLD development and progression, with a larger effect in postmenopausal women (p < 0.05). Higher hepatic PNPLA3 mRNA expression was independently associated with the p.I148M variant and female sex (p = 0.002 and p = 0.007, respectively). At chromatin immunoprecipitation, ER α agonists induced the ER binding to a specific ERE at a PNPLA3 enhancer site, enhancing its transcriptional activity at luciferase assays. PNPLA3 mRNA and protein expression was upregulated via direct ER α agonists, leading to intracellular fat accumulation in p.I148M homozygous HepG2 cells, but not in wild-type hepatocytes. Genetic deletion of the PNPLA3-ERE by Crispr/Cas9 editing in HepG2 abolished the ER α -induced PNPLA3 and intracellular lipid accumulation in response to fatty acids.

Conclusion: We identified a driver of FLD acceleration occurring in a subset of women with metabolic dysfunction at menopause, highlighting at the same time a therapeutic target of particular relevance.

WED-395

Brain-derived neurotrophic factor knock-out mice develop non-alcoholic steatohepatitis

Mayuko Shimizu¹, Masami Kojima^{2,3}, Shingo Suzuki⁴, Misaki Miyata², Toshiyuki Mizui³, Koichi Tsuneyama¹. ¹Tokushima University, Pathology and Laboratory Medicine, Japan, ²Kanazawa Institute of Technology, Applied Bioscience, Japan, ³National Institute of Advanced Industrial Science and Technology, Biomedical Research Inst, Japan, ⁴Kagawa University, Anatomy and Neurobiology, Japan
 Email: masamikojima@neptune.kanazawa-it.ac.jp

Background and aims: Brain-derived neurotrophic factor (BDNF), which is originally discovered as a growth factor that promotes neuronal survival, differentiation, and synaptic plasticity in the brain, is associated with the development of brain diseases. The aim of the present study was to investigate the role of BDNF in peripheral disease in life stages from adulthood to advanced age.

Method: Male BDNF knock-out mice (BDNF^{-/-}) and controls (BDNF^{+/+}) were fed with a normal diet in group housing. At 10 months of age, whole body organs were histopathologically analysed. Histological findings from the liver were scored using the non-alcoholic steatohepatitis (NASH) Clinical Research Network Scoring System. RNA-seq and gene ontology analysis were performed on the liver of animals. In addition, to ensure the implication of reduced BDNF expression, the histological study was performed in the liver of proBDNF knock-in (BDNF^{+/pro}) mice, genetically engineered mouse line in which precursor BDNF is inefficiently converted into the matured form of BDNF.

Results: BDNF^{-/-} mice developed symptoms of NASH: zone 3 steatosis, lobular inflammation, ballooning hepatocytes, and fibrosis, while no histological lesions were seen in the heart, kidney, intestine, lung, pancreas and spleen. Obesity and higher serum levels of glucose and insulin—major pathologic features in human NASH—were dramatic. Dying adipocytes were surrounded by macrophages in visceral fat, suggesting that chronic inflammation occurred in adipose tissue. RNA-seq studies of the liver revealed that the most significantly enriched term includes the fatty acid metabolic process and modulation of neutrophils aggregation, pathologies that well characterize NASH. The results of gene ontology analysis were experimentally verified using the liver tissues of BDNF^{-/-} mice and immunostaining with myeloperoxidase, a marker for activated neutrophils, indicating the infiltration of neutrophils in the liver of mutant animals. Gene expression analysis by RNA-seq also suggests that the BDNF^{-/-} mice are under oxidative stress, as indicated by alterations in the expression of cytochrome P450 family and reduction of glutathione S-transferase p, an antioxidant enzyme (Figure). Lastly, histopathologic phenotypes of NASH were observed in BDNF^{+/pro} mice as well.

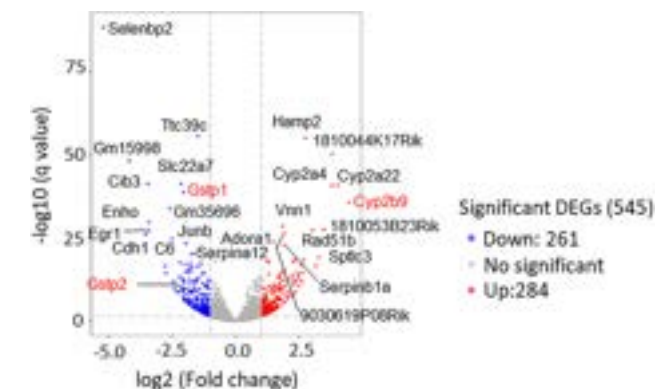


Figure:

Conclusion: This is the first report demonstrating that reduced BDNF expression induces the critical pathogenic mechanism leading to the development of the full spectrum of NASH. Our study thus describes a new model animal of the brain-liver connection.

WED-396

The PNPLA3 p.I148M risk variant was fixed in Neanderthals and segregates neutrally in humans

Andreas Geier¹, Jonas Trost¹, Ke Wang², Marcin Krawczyk³, Stephan Schiffels⁴. ¹University Hospital Würzburg, Division of

POSTER PRESENTATIONS

Hepatology, Department of Internal Medicine II, Würzburg, Germany, ²Max Planck Institute of Geoanthropology, Department of Archaeogenetics, Jena, Germany, ³Saarland University Hospital, Department of Medicine II, Homburg/Saar, Germany, ⁴Max-Planck-Institute for Evolutionary Anthropology, Department for Archaeogenetics, Leipzig, Germany
Email: geier_a2@ukw.de

Background and aims: The liver is the central organ in the human body responsible for carbohydrate and lipid metabolism and plays a key role in fat storage under conditions of overnutrition. Fat deposition is modulated by environmental factors and genetic predisposition. GWAS studies identified PNPLA3 p.I148M as a common variant that increases risk of developing non-alcoholic fatty liver. The association of this variant to harmful phenotypes including end-stage liver disease suggests a potential effect on fitness and hence a potential role of natural selection. To understand its past trajectory throughout human evolution, we turn to archaeogenetic data spanning the last 50,000 years.

Method: 6444 published ancient (modern humans, Neanderthal, Denisovan) and 3943 published present-day genomes were used for analysis after extracting genotype calls for PNPLA3 p.I148M (rs738409). The deeper evolutionary context was explored using reference genome sequences of current primates. To quantify changes through time, two regression analyses were performed: logistic regression based on presence/absence of the risk allele in ancient and modern individuals from different continents; linear regression based on allele frequencies by grouping individuals according to geography and age. To compare these changes with expected changes due to neutral factors such as genetic drift, we compiled a reference dataset of 1000 randomly selected SNPs for genome wide analysis, and performed the exact same logistic and linear regressions.

Results: The ancestral (reference) allele is fixed among all great apes (Chimpanzee, Bonobo, Gorilla, Orangutan). In contrast, on the human lineage, all available Neanderthal (n = 5) and Denisovan individuals (n = 3 including a Neanderthal/Denisovan hybrid) exclusively carry the risk (derived) allele, suggesting fixation of the allele in the ancestor of all archaic humans (Figure). In contrast, present-day humans exhibit a wide range of minor allele frequency ranging from 8% in Kenya up to 72% in Peru. Over the last 15,000 years, distributions of ancestral and derived alleles roughly match the present day distribution, including a high frequency in the Americas even in the earliest samples from 10,000BP. On all continents, the observed frequency change of PNPLA3 variant were within the expected distribution as estimated from the neutral reference SNP set. Similarly, in a logistic regression along latitude again compared to the randomly selected reference SNP set, and finally a multivariate logistic regression against both time and latitude, the observed changes were within the expected variation, consistent with absence of natural selection.

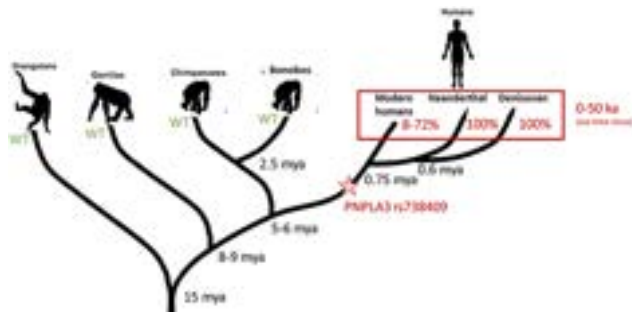


Figure: Presence of PNPLA3 rs738409 ancestral (Wildtype; WT) and derived alleles in the great ape lineage family tree.

Conclusion: Archaic human individuals exclusively carried a fixed PNPLA3 risk allele, whereas allele frequencies in modern human

populations range from very low in Africa to more than 50% in Mesoamerica. Our observation might underscore the advantage of fat storage in cold climate and particularly for Neanderthal under ice age conditions. The negative genome-wide analysis without signals of natural selection during modern human history does not support the thrifty gene hypothesis in case of PNPLA3 p.I148M polymorphism where other mechanisms like gene drift may contribute to present day allele distribution.

WED-397

Role of TGR5 in fat-to-liver communication during NAFLD

André L. Simão¹, Diogo Fernandes¹, Daniela Silva¹, Margarida Silva¹, Marta B. Afonso¹, André A. Santos¹, Mariana Moura Henriques¹, Carolina Santos Palma¹, Ainhwa Lapitz², Laura Izquierdo-Sánchez², Pedro Miguel Rodrigues², Alessia Perino³, Bruno Costa-Silva⁴, Cecília M. P. Rodrigues¹, Helena Cortez-Pinto^{5,6}, María Luz Martínez-Chantar⁷, Kristina Schoonjans³, Jesus Maria Banales^{2,8}, Rui E. Castro¹. ¹Research Institute for Medicines (iMed.Ulisboa), Faculty of Pharmacy, Universidade de Lisboa, Portugal, ²Department of Liver and Gastrointestinal Diseases, Biodonostia Health Research Institute, Donostia University Hospital, University of the Basque Country (UPV/EHU), San Sebastian, Spain, ³Institute of Bioengineering, Faculty of Life Sciences, Ecole Polytechnique Fédérale de Lausanne, Lausanne, Switzerland, ⁴Champalimaud Centre for the Unknown, Champalimaud Foundation, Lisbon, Portugal, ⁵Departamento de Gastrenterologia, Centro Hospitalar Universitário Lisboa Norte, Lisbon, Portugal, ⁶Clínica Universitária de Gastrenterologia, Faculdade de Medicina, Universidade de Lisboa, Portugal, ⁷Liver Disease Lab, Center for Cooperative Research in Biosciences (CIC bioGUNE), Basque Research and Technology Alliance, Derio, Spain, ⁸Department of Biochemistry and Genetics, School of Sciences, University of Navarra, Pamplona, Spain
Email: adlsimao@ff.ulisboa.pt

Background and aims: Non-alcoholic fatty liver disease (NAFLD) is characterized by intracellular lipid accumulation in the liver and associates with pathogenic changes in additional metabolic tissues, particularly the adipose tissue (AT). In parallel, increasing evidence supports a functional role for extracellular vesicles (EVs) in inter-organ crosstalk during NAFLD progression. Finally, activation of Takeda G-protein coupled bile acid receptor 5 (TGR5) ameliorates NAFLD in experimental mouse models. Here, we aimed to elucidate whether modulation of TGR5 activity in adipocytes affects the content of its secreted EVs and in turn alters hepatocyte function, in vitro. In parallel, we evaluated the role of AT TGR5 in a mouse model of NAFLD.

Method: AT-derived EVs were isolated from adipocytes exposed to LPS and then incubated with unstimulated hepatocytes. Alternatively, EVs were isolated from adipocytes after silencing of TGR5 or upon exposure to different TGR5 agonists and then incubated with hepatocytes stimulated with LPS. AT-derived EVs were isolated by polymer-based precipitation and characterized by nanoparticle tracking analysis. AT-specific TGR5 KO mice and respective littermate controls were fed a high-fat diet (HFD) for 14 weeks. Gene and protein expression levels were analyzed by qRT-PCR and immunoblotting, respectively.

Results: Results showed that AT TGR5 plays a key role in the metabolic response of mice to high-calorie intake. In particular, AT-specific TGR5 KO mice fed an HFD displayed significantly increased body weight, compared to littermate controls, starting at 9 weeks of feeding. EVs released from LPS-stimulated adipocytes triggered an inflammatory response in hepatocytes, as seen by the increased mRNA expression of different pro-inflammatory cytokines, resulting in enhanced cell death. Interestingly, incubation of unstimulated hepatocytes with EVs from TGR5-silenced adipocytes similarly increased the expression of pro-inflammatory cytokines, while also promoting lipogenesis. Compared to unstimulated cells, incubation of adipocytes with different TGR5 agonists activated critical intracellular signalling mediators and led to decreased EV release. Of note,

EVs released from TGR5-activated adipocytes reduced the inflammatory response of hepatocytes stimulated with LPS.

Conclusion: Overall, our results suggest that EVs from TGR5-activated adipocytes contain anti-inflammatory molecules capable of exerting a functional role within hepatocytes, with in vivo data underscoring the role of TGR5 in ameliorating obesity and inter-organ lipid accumulation. A better characterization of TGR5-dependent fat-to-liver signalling will unravel the prospective therapeutic potential of TGR5 agonists for metabolic diseases (HR17-00601, Fat2LiverTGR5; PTDC/MED-PAT/31882/2017, EXPL/MED-OUT/1317/2021 and SNSF 31003A_125487).

WED-398

Hepatic lipid flux, and not lipid amount, damages the liver during starvation-induced steatosis

Macarena Pozo-Morales¹, Ansa Cobham², Cielo Centola², Nicolas Rohner², Sumeet Singh¹. ¹UNIVERSITÉ LIBRE DE BRUXELLES (ULB), IRIBHM, Anderlecht, Belgium, ²Stowers Institute for Medical Research, United States
Email: sumeet.pal.singh@ulb.be

Background and aims: During starvation, animals utilize the liver as lipid storage organ. For instance, patients suffering from anorexia nervosa, overnight fasted mice and starved zebrafish larvae have been reported to develop fatty liver. Like other cases of non-alcoholic fatty liver diseases (NAFLD), starvation-induced hepatic steatosis is related to liver damage. But it is not clear if the organ damage is due to the accumulation of lipid droplets in hepatocytes or their utilization as an energy source. Also, it remains unknown if the resolution of lipid droplets is beneficial to the animal. Here, we use the zebrafish model system to investigate the impact of lipid amount and lipid flux on liver damage. Further, we study how cavefish, a model of starvation resistance, protects its liver from atrophy during starvation.

Method: Our previous work in the zebrafish model system had shown that starvation-induced hepatic steatosis is regulated by calcium signaling (Pozo-Morales et al, *Hepatology*, 2022; doi: 10.1002/hep.32663). In line with our findings, in this study we manipulated lipid droplet flux by altering calcium flux. We increased calcium oscillations in the liver by mobilization of endo-lysosomal calcium stores, using TPC2 agonist. In contrast, we utilized a genetically encoded calcium chelator to reduce the turnover of lipid droplets.

Further, to understand how animals with enhanced starvation resistance deal with hepatic steatosis and liver damage, we investigated the starvation response in Mexican cavefish, *Astyanax mexicanus*. Here, we labeled hepatic lipid droplets using Nile Red staining and performed comparative analysis between surface and cavefish.

Results: In zebrafish, increase of calcium flux using TPC2 agonist efficiently reduced lipid droplets in the liver. However, the resolution of steatosis enhanced macrophage infiltration, hepatocyte phagocytosis and starvation-induced mortality. Thus, suggesting that fatty liver helps with starvation resistance.

On the other hand, buffering cytoplasmic calcium reduced the turnover of lipid droplets, increasing hepatic steatosis in later stages of starvation. The reduced lipid turnover led to reduced liver inflammation and increased the lifespan of starved animals, thereby suggesting that hepatic lipid flux damages the liver.

In the cavefish model, we found that, surprisingly, cavefish do not accumulate lipid droplets in the liver upon starvation and are protected from liver damage. In contrast, surface fish accumulate lipid droplets in the liver during starvation and display liver atrophy. Using transcriptome analysis, we identify the long-chain fatty acid importer, SLC27A2, as one of the gene responsible for hepatic steatosis during starvation. Zebrafish and surface fish, but not cavefish, upregulate the expression of slc27a2a in the liver upon starvation. Pharmacological inhibition of SLC27A2 inhibits lipid accumulation in the starved zebrafish liver.

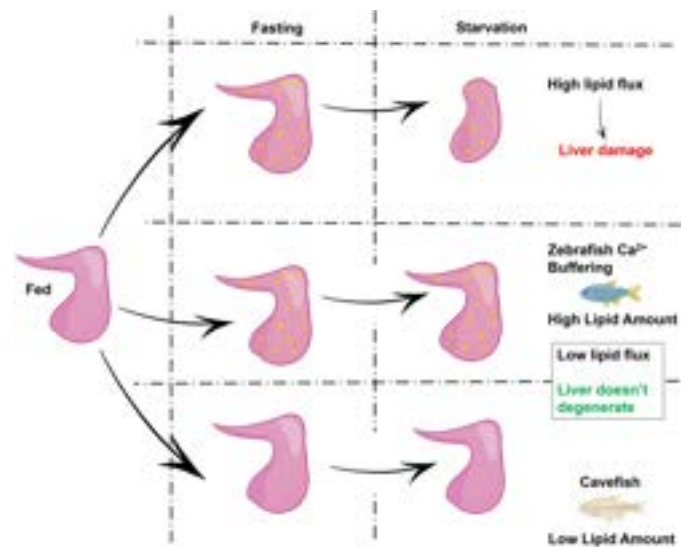


Figure:

Conclusion: Our study demonstrates that the turnover of lipid droplets in hepatocytes during starvation is detrimental to liver health and identifies a protective mechanism in cavefish against liver atrophy.

WED-399

Targeting Apolipoprotein J restores autophagy and improves metabolic-associated fatty liver disease and diabetic nephropathy

Wang Hsin-Tzu¹, Duan Shuangdi², Qin Nong², Pi Jiayi², Sun Pei², Sun Hung-Yu¹. ¹National Cheng Kung University, Taiwan, ²Hunan University, China
Email: s5893149@gmail.com

Background and aims: Metabolic disorders affect 20–25% of adult population globally and have become a heavy burden on society. Targeting hepatic lipid deposition represents a therapeutic strategy against metabolic syndromes. In this investigation, Apolipoprotein J (ApoJ) was identified as a potential target of aberrant lipid accumulation to relieve metabolic-associated fatty liver disease (MAFLD) and diabetic nephropathy (DN).

Method: The diet-induced MAFLD, streptozotocin-induced type-II diabetes (T2DM), and genetically diabetic db/db mice were administered intravenously with ApoJ antagonist peptide (10 mg/kg/3 days) or intraperitoneally with liraglutide (200 µg/kg/day) for 8 weeks. The tissue pathology was examined by histochemical staining. The glucose and insulin tolerance test was performed to address insulin sensitivity.

Results: We first demonstrated that targeting ApoJ reactivates autophagy and lysosomal activity and prevents intracellular lipid deposition. Next, a peptide with a K_d of 2.54 µM was applied to antagonize ApoJ and restore mTOR-FWB7 E3 ligase interaction to promote proteasomal degradation of mTOR. Administration of ApoJ antagonist peptide improved hepatic pathology, serum lipid and glucose homeostasis, and insulin sensitivity in mice with MAFLD or T2DM. In addition, the peptide reactivated TFEB, restored autophagy, and prevented accumulation of lipid and reactive oxygen species of renal tubular, thus reversed renal injury and fibrosis in mouse models of DN.

Conclusion: The findings demonstrated ApoJ would be a therapeutic target for intracellular lipid deposition and a proof-of-concept ApoJ antagonist peptide was proposed as a novel strategy against metabolic syndromes.

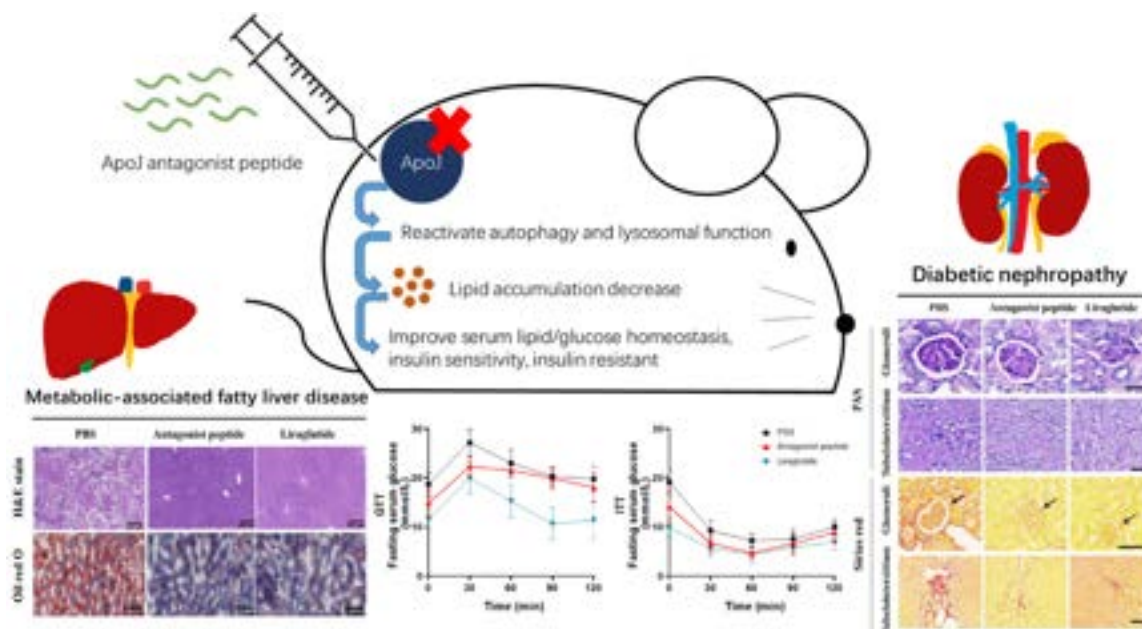


Figure: (abstract: WED-399).

WED-400

mTORC1 response to glucose via dihydroxyacetone phosphate is regulated by MAT1A. Role in NAFLD

María de los Reyes Luque Urbano^{1,2}, Jon Bilbao¹, David Fernández Ramos^{1,3}, Fernando Lopitz Otsoa¹, Virginia Gutiérrez de Juan¹, Ganeko Bernardo-Seisdedos^{1,4}, Luis Manuel Cervera Seco⁵, Urko M Marigorta⁵, Lucía Barbier Torres⁶, Shelly C. Lu⁶, Oscar Millet^{1,3,4}, José M. Mato^{1,3}. ¹CIC bioGUNE-Centro de Investigación Cooperativa en Biociencias, Precision Medicine and Metabolism Laboratory, Derio, Spain, ²Atlas Molecular Pharma, Spain, ³CIBERehd, Instituto de Salud Carlos III, Spain, ⁴Atlas Molecular Pharma, Spain, ⁵CIC bioGUNE-Centro de Investigación Cooperativa en Biociencias, Integrative Genomics Laboratory, Derio, Spain, ⁶Karsh Division of Gastroenterology and Hepatology, Department of Medicine, Cedars-Sinai Medical Center, Los Angeles, CA., United States
Email: director@cicbiogune.es

Background and aims: Deletion in mice of MAT1A, the main enzyme responsible for the hepatic synthesis of S-adenosylmethionine (SAME), leads to the spontaneous development of liver steatosis and its progression to NASH, fibrosis, and hepatocellular carcinoma. Because it is not yet fully understood how MAT1A loss induces hepatic fat accumulation, we studied how MAT1A-deficient mouse hepatocytes respond to glucose challenge.

Method: Murine primary hepatocytes were isolated by liver perfusion from wild-type (WT) and MAT1A knockout (-KO) mice. After plating, hepatocytes were serum starved overnight and incubated with ¹³C- glucose (25 mM, 3 hours). Protein and mRNA expression of glycolysis, pentose phosphate pathway (PPP), AMPK and mTOR pathways were studied by western blot and qPCR. Metabolites content was measured by NMR.

Results: Here we show that glucose sensing by mTORC1 is impaired in MAT1A-KO hepatocytes exposed to high glucose, as evidenced by inhibition of phosphorylation of mTORC1 and its downstream substrate S6K1, leading to reduced synthesis of phosphatidylcholine via the CDP-choline pathway, impaired VLDL export, and accumulation of intracellular lipids. We found that the concentration of dihydroxyacetone phosphate (DHAP), a glycolytic intermediate and activator of mTORC1, is reduced 8-fold in MAT1A-KO hepatocytes exposed to 25 mM glucose compared with WT hepatocytes. We also found that mRNA content of aldolase B (ALDOB), the enzyme that catalyzes the reversible conversion of fructose 1, 6-bisphosphate to

DHAP and glyceraldehyde 3-phosphate (G3P), was reduced in MAT1A-KO hepatocytes. To neutralize this reduction in glucose flux between the upper and lower glycolysis, MAT1A-KO hepatocytes increased the expression of glucose-6-phosphate dehydrogenase (G6PD), the rate-limiting step of the PPP, and transketolase (TKT), the enzyme that channels excess sugar phosphates in the PPP to lower glycolysis at the G3P level. These alterations were prevented by the addition of SAME to the culture medium. Consistent with the redirection of glucose flux through the PPP, we found that at high glucose AMPK and its target enzyme acetyl-CoA carboxylase 1, the rate limiting step in fatty acid synthesis, were hypophosphorylated in MAT1A-KO hepatocytes leading to increased lipogenesis.

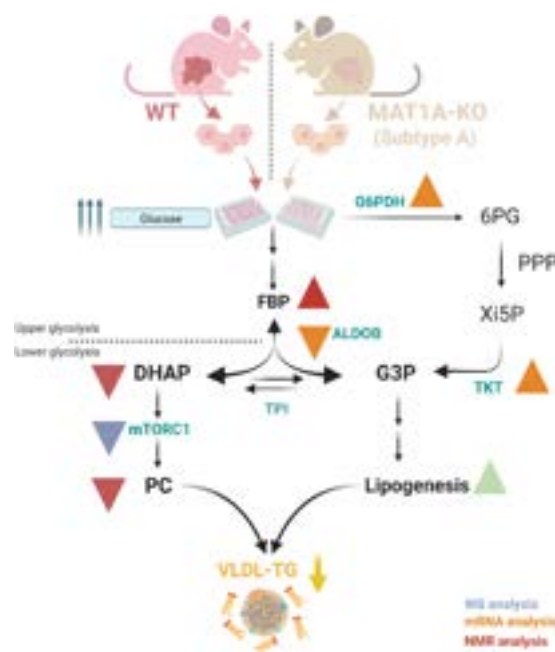


Figure:

Conclusion: The present findings, together with the observation that MAT1A expression is often reduced in NASH patients and our

previous finding demonstrating that NAFLD patients displaying a serum lipidomic signature similar to MAT1A-KO mice (subtype A) have lower VLDL secretion rate and serum VLDL levels than patients with a different lipidomic profile, suggest that DHAP-mediated mTORC1 response to glucose is impaired in NAFLD patients with subtype A. These results suggest that increasing hepatic DHAP content may be a therapeutic target in NAFLD patients with subtype A.

WED-401

Development of a target engagement biomarker for HSD17B13: preclinical pharmacodynamic studies of small molecule inhibition of HSD17B13 by INI-822

Cindy McReynolds¹, Michael Carleton¹, Chuhan Chung¹, Heather Hsu¹
.¹Inpharm, RandD, Bellevue, United States
Email: hhsu@inpharm.com

Background and aims: Polymorphisms rendering the lipid droplet-located protein HSD17B13 enzymatically inactive protect against NASH, cirrhosis, and liver cancer. Analysis of human liver tissue demonstrated increased hepatic phosphatidylcholines in individuals with inactive HSD17B13 (Luukkonen 2020 JCI). INI-822, a selective small molecule inhibitor of HSD17B13, was used to test for lipidomic changes consistent with humans carrying the inactive HSD17B13 gene.

Method: INI-822 was dosed orally once daily in multiple rat models of liver injury including Zucker rats (3 weeks dosing, n = 4/group) on an atherogenic diet and CDAA-HFD and Sprague-Dawley rats (2 weeks dosing, n = 8/group). Changes in liver transaminase levels, circulating and hepatic phospholipids (GC/MS, LC/MS) and hydroxylated lipid substrates (LC/MS) were measured. Statistical significance was evaluated by ANOVA followed by a Bonferroni multiple comparison test. All parameters presented have a p < 0.05. The ED50 was calculated by a nonlinear 4 parameter fit.

Results: INI-822 treatment of Zucker obese rats led to a decrease in ALT in all models. INI-822 treatment in Zucker rats led to increased hepatic phosphatidylcholines seen in both diets but to a greater degree in rats on the CDAA-HFD. In contrast, plasma levels of phosphatidylcholines were decreased in animals treated with INI-822 on the CDAA-HFD. There was an increase in plasma levels of esterified hydroxy-lipid HSD17B13 substrates while these same substrates were decreased in free fatty acid form. This was seen on both diets but was more pronounced on the atherogenic diet. There was a dose-dependent increase in a panel of hydroxy-lipid HSD17B13 substrates with a mean ED50 of 5.6 ± 2.4 mg/kg. The change in these endogenous hydroxy-lipids was as great as 5.9-fold for 15-HETE under these conditions. There was also a dose-dependent decrease in the keto-lipid HSD17B13 product, 9-oxoODE, with an ED50 also of 5.6 mg/kg ($r^2 = 0.5215$).

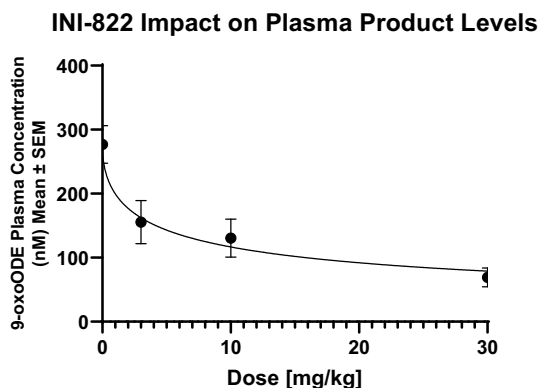


Figure:

Conclusion: HSD17B13 inhibition with INI-822 decreased liver transaminases and led to increased hepatic phosphatidylcholine

content in multiple preclinical models. Inhibition of HSD17B13 resulted in increases in plasma levels of hydroxy-lipid HSD17B13 substrates, particularly in the esterified form. These changes in hydroxy-lipid substrates indicate their use as potential target engagement biomarkers and suggest that INI-822 phenocopies the human protective allele of HSD17B13.

WED-402

Modelling the biological mechanisms of a PNPLA3 polymorphism in a 3D human liver spheroid for NASH progression and drug efficacy

Francisco Verdeguez¹, Radina Kostadinova¹, Philipp Vonschallen¹, Jesus Glaus¹, Thomas Hofstetter¹, Simon Ströbel¹.¹InSphero, Liver Discovery, Switzerland
Email: francisco.verdeguez@insphero.com

Background and aims: Non-alcoholic steatohepatitis (NASH) is a progressive severe disease characterized by lipid accumulation, inflammation and fibrosis in the liver. Single nucleotide polymorphisms (SNPs) at specific loci have revealed differential propensity to develop NASH. Among them, "GG" rs738409 located in PNPLA3 results in the I148M amino acid change. PNPLA3 is a triacylglycerol lipase localized in lipid droplets but its function in the context of NASH is not fully understood and yet represents an interesting therapeutic target. The aim of this study was to investigate the effect of PNPLA3 (I148M) mutant on the development of NASH hallmarks in a 3D human liver *in-vitro* culture model.

Method: We generated a human *in-vitro* liver spheroid model by co-culturing primary human hepatocytes, Kupffer cells, endothelial cells and hepatic stellate cells obtained from human donors. Hepatocytes were obtained from either the major allele for PNPLA3 or PNPLA3 (I148M) variant. Spheroids were incubated with either physiological or steatotic and proinflammatory media conditions to assess the influence of PNPLA3 in NASH hallmarks by performing biochemical, imaging and transcriptomics analysis.

Results: We show that steatotic and proinflammatory conditions lead to increased intracellular triglycerides levels and secretion of inflammatory markers IL-6, MIP-1 α , TNF- α , IL-10, MCP-1 and IL-8 and increased secretion of procollagen peptides I and III. These results show a recapitulation of the hallmarks of NASH. PNPLA3 (I148M) genotype in liver spheroids resulted in an increased levels of steatosis and fibrosis measured by triglyceride content and collagen secretion compared to the major allele. In line with these results, transcriptomics analysis show that both *de-novo* lipogenesis and fibrotic pathways are elevated in the PNPLA3 (I148M) donors compared to major allele. These results are in agreement with the expected phenotypic propensity to develop NASH in the human population carrying the PNPLA3 (I148M) variant.

Finally, small molecules Firsocostat, Selonsertib and ALK5i lead to a decrease levels of triglycerides and inflammatory markers and collagen secretion compared to NASH, and the response was exacerbated in PNPLA3 (I148M) variants.

Conclusion: In summary we show a spheroid model that recapitulates NASH hallmarks and differential drug responses to specific SNPs relevant for NASH.

WED-403

Perivascular macrophages contribute to adipose tissue angiogenesis in patients with advanced non-alcoholic fatty liver disease

Celia Martinez-Sanchez^{1,2}, Octavi Bassegoda³, Hilmar Berger⁴, Xènia Almodovar¹, Laia Aguilar³, Yilliam Fundora³, Ainitze Ibarzabal³, Ana de Hollanda³, Pep Vidal³, Anna Soria³, Irina Luzko³, Alex Guillamon¹, Frank Tacke⁴, Pau Sancho-Bru¹, Pere Ginès^{1,2,3}, Isabel Graupera^{1,3}, Mar Coll¹.¹Institut d'Investigacions Biomèdiques August Pi i Sunyer (IDIBAPS), Spain, ²Centro de Investigación Biomédica en Red de Enfermedades Hepáticas y Digestivas (CIBEREHD), Spain,

POSTER PRESENTATIONS

³Hospital Clínic de Barcelona, Spain, ⁴Charité Universitätsmedizin Berlin, Germany
Email: cmartinezs@recerca.clinic.cat

Background and aims: In non-alcoholic fatty liver disease (NAFLD) macrophages infiltrating the adipose (ATMs) acquire a pro-inflammatory phenotype and contribute to liver damage. However the heterogeneity of ATM populations and its relationship along disease progressions is still unknown. The aim of the present study is to unveil the main ATMs' subsets with a significant role in NAFLD patients.

Method: Single cell RNA sequencing from sorted myeloid cells (CD14+) was performed from the adipose tissue of obese patients without NAFLD (n = 2); NAFLD patients with mild hepatic fibrosis (n = 2) and NAFLD patients with advanced fibrosis (n = 2). We integrated our single cell data with those of previously reported single cell data from obese adipose tissue (Hildreth et al. 2021). Validation of scRNAseq findings by gene expression and immunohistological analysis was performed in adipose tissue of a larger cohort of NAFLD patients without fibrosis (n = 24) and with advanced fibrosis (n = 12). Moreover, we performed an adipose tissue clearing technique to have a 3D volumetric image of the entire tissue. Finally we isolated ATMs and collected their secretome to evaluate the secretion of angiokines by ELISA.

Results: scRNAseq analysis of myeloid cells clustered into 10 different sub-types according to their transcriptome signature. Interestingly perivascular macrophages (PVMs) subset was found significantly enriched in patients with advanced fibrosis. The increase of PVMs was confirmed by gene expression of several key PVMs markers including *RNASE1*, *LYVE1*; *MAF*; *CSF1R* and by IHC using the surface marker FOLR2 (p = 0.006) in the adipose tissue of the NAFLD cohort. The functional analysis revealed, among others, the role of PVMs on local endothelial cell proliferation. Moreover integration of our ATMs' scRNA seq with adipose tissue scRNAseq confirmed the interaction between PVMs and adipose tissue endothelial cells in the VEGF signaling pathway. By assessing the gene expression of the angiogenic markers: *NRP1*; *EGFL7* and *CXCL12* (p = 0.004; p = 0.037 and p = 0.04, respectively) and protein expression of CD31 and VWF (p = 0.023 and p = 0.001), we confirmed the presence of increased angiogenesis in the adipose tissue in patients with advanced fibrosis. Furthermore, we found a positive correlation between angiogenesis and PVMs (r = 0.51, p = 0.04). Finally, using the clearing technique we found that the angiokine EGFL7 co-localize with PVMs. Moreover, we found that PVMs from patients with advanced fibrosis had higher EGFL7 secretion compared to PVMs from patients without hepatic fibrosis (p = 0.042).

Conclusion: We report an increased abundance of PVMs' subset in the adipose tissue at advanced stages of NAFLD which might contribute to local angiogenesis. The correlation between PVMs and adipose tissue angiogenesis in advanced NAFLD suggests that this subset of ATM could promote liver disease progression.

WED-404

The E2F2-miR34a-5p axis is involved in the biliary metabolism dysregulation in NASH

Maider Apodaka-Biguri¹, Francisco Gonzalez-Romero¹, André L. Simão², Daniela Mestre Congregado¹, Igor Aurrekoetxea^{1,3}, Beatriz Gómez Santos¹, Igotz Delgado¹, Xabier Buque^{1,3}, Ane Nieva-Zuluaga¹, Mikel Ruiz de Gauna¹, Idoia Fernández-Puertas¹, Ainhoa Iglesias⁴, Ana María Aransay^{5,6}, Juanjo Lozano^{5,7}, Cesar Augusto Martín^{8,9}, Irantzu Bernalles¹⁰, Pedro Miguel Rodrigues^{5,11}, Jesus Maria Banales^{5,11,12}, Ana Zubiaga⁴, Rui E. Castro², Patricia Aspichueta^{1,3,5}. ¹Department of Physiology University of the Basque Country UPV/EHU, Faculty of Medicine and Nursing, Leioa, Spain, ²Research Institute for Medicines, Faculty of

Pharmacy, Universidade de Lisboa, Lisbon, Portugal, ³Biocruces Bizkaia Health Research Institute, Cruces University Hospital, Barakaldo, Spain, ⁴Department of Genetic, Physical Anthropology and Animal Physiology, Faculty of Science and Technology, University of Basque Country UPV/EHU, Leioa, Spain, ⁵National Institute for the Study of Liver and Gastrointestinal Diseases (CIBERehd, Carlos III Health Institute), Madrid, Spain, ⁶Genome analysis platform, Center for Cooperative Research in Biosciences (CIC bioGUNE), Derio, Spain, ⁷Bioinformatic Platform, Clinic Hospital, Barcelona, Spain, ⁸Department of Molecular Biophysics, Biofisika Institute (University of Basque Country and Consejo Superior de Investigaciones Científicas (UPV/EHU, CSIC)), Leioa, Spain, ⁹Department of Biochemistry and Molecular Biology, University of the Basque Country (UPV/EHU), Leioa, Spain, ¹⁰SGIKER, University of Basque Country UPV/EHU, Leioa, Spain, ¹¹Department of Liver and Gastrointestinal Diseases, Biodonostia Health Research Institute, Donostia University Hospital, University of the Basque Country UPV/EHU, San Sebastian, Spain, ¹²IKERBASQUE, Basque Foundation for Science, Bilbao, Spain
Email: patricia.aspichueta@ehu.eus

Background and aims: Accumulation of toxic bile acids together with lipotoxic lipids promote non-alcoholic steatohepatitis (NASH) progression. E2F2 transcription factor is upregulated in metabolic associated fatty liver disease (MAFLD). A connection between E2F2 and miRNAs has been described in several pathologies but not in liver disease. Our aims were 1) to identify if liver E2F2 regulates biliary metabolism in NASH-progression 2) to investigate the implication of liver E2F2 in bile acid induced liver damage.

Method: Progressive NASH was induced in *E2f2*^{-/-} and WT mice by injection of diethylnitrosamine (DEN) and feeding a high-fat diet (HFD) for 6 months or by a Choline-deficient HFD (ChD-HFD) for 6 months. Chow diet-fed (CD) 3 month-old mice were also used. E2F2 was overexpressed in liver using adeno-associated viruses serotype 8 (AAV8). Biliary duct ligation (BDL) was included as a cholestasis model. miRNA sequencing was performed in mouse livers. Metabolic fluxes, lipid content, transcriptome analysis and gene expression were analyzed.

Results: *E2f2*^{-/-} mice were protected from NASH in DEN-HFD and ChD-HFD models. The expression of *Chpt1*, involved in phosphatidylcholine (PC) synthesis, *Abcg5* and *Abcg8*, regulators of cholesterol (CL) secretion in bile, and *Cyp7a1* and *Bsep*, involved in bile acid metabolism, was increased in DEN-HFD *E2f2*^{-/-} and ChD-HFD *E2f2*^{-/-} compared with corresponding WTs. Analysis of metabolic fluxes showed that in DEN-HFD *E2f2*^{-/-} mice the increased synthesis of PC and CL did not induce their storage in liver, suggesting an increased efflux into bile. Moreover, hepatic bile acid content was lower in ChD-HFD *E2f2*^{-/-} mice when compared with their controls. miRNA sequencing and validation by qPCR showed that in DEN-HFD *E2f2*^{-/-} mice, resistant to MAFLD-progression, miR34a-5p, miR155-5p and miR146a-5p were downregulated. miR34a-5p was the only miRNA found decreased in CD-fed *E2f2*^{-/-} mice, and increased when E2F2 was overexpressed in liver. The same profile was observed in *E2f2*^{-/-} ChD-HFD mice, showing lower miR34a-5p levels when compared with corresponding WTs. A crosschecked analysis between upregulated genes in DEN-HFD *E2f2*^{-/-} mice and miR34a-5p predicted targets, according to miRWalk software, showed that analyzed genes involved in synthesis and secretion of bile and biliary lipid genes were among them. *E2f2*^{-/-} mice were also protected from BDL-induced cholestasis, a model in which E2F2 and miR34a-5p are upregulated. This protection was lost when primary hepatocytes of *E2f2*^{-/-} mice were treated with bile acids and miR34a-5p mimic.

Conclusion: E2F2 regulates miR34a-5p expression in liver disease. Its deficiency promotes the generation and efflux of bile acids and biliary lipids, protecting the liver against their accumulation in NASH and cholestasis.

WED-405

The PNPLA3 I148M variant initiates metabolic reprogramming in macrophages

Emmanuel Dauda Dixon¹, Thierry Claudel¹, Jakob-Wendelin Genger², Ci Zhu³, Sarah Stadlmayr⁴, Erika Paolini⁵, Alexander D Nardo¹, Veronika Mlitz¹, Claudia Fuchs¹, Andreas Bergthaler², Christine Radtke⁴, Paola Dongiovanni⁵, Wilfried Ellmeier³, Michael Trauner¹. ¹Medical University of Vienna, Hans Popper Laboratory of Molecular Hepatology, Division of Gastroenterology and Hepatology, Department of Internal Medicine III, Wien, Austria, ²CeMM Forschungszentrum für Molekulare Medizin GmbH, Center for Pathophysiology, Infectiology and Immunology, Wien, Austria, ³Medical University of Vienna, Institute of Immunology, Austria, ⁴Medical University of Vienna, Department of Plastic, Reconstructive and Aesthetic Surgery, Austria, ⁵Fondazione IRCCS Cà Granda Ospedale Maggiore Policlinico; Department of Pharmacological and Biomolecular Sciences, Università degli Studi di Milano, Italy
Email: michael.trauner@meduniwien.ac.at

Background and aims: Progressive non-alcoholic fatty liver disease is increasingly becoming a global health problem associated with underlying genetic polymorphism, the rs738409; C > G in patatin-like phospholipase domain-containing protein 3 (PNPLA3). Inflammation is the main driver for advanced liver injury, and we previously established that PNPLA3 I148M (148M^{oe}) macrophage is pro-inflammatory. Since the metabolic state of macrophage determines its pro-inflammatory phenotype, we were interested in whether the

PNPLA3 I148M affects mitochondrial function and thereby alters metabolic function.

Method: To explore mitochondrial and metabolic function in a macrophage cell line, we established a THP-1 stable cell line overexpressing the PNPLA3 wildtype and I148M isoforms. Gel-shift, gene expression analysis, metabolomics, and extracellular flux analysis were conducted. Reactive oxygen species (ROS) was measured by flow cytometry using MitoSOX assay.

Results: In 148M^{oe} M1 macrophages, glycolytic genes like *GLUT1*, *HK1*, *LDHA*, and *HIF-alpha* were significantly increased compared to the WT^{oe}. The 148M^{oe} M1 macrophage had reduced basal (−29%) and maximum (−48%) mitochondrial respiration, as well as downregulation of *CPT1-alpha* (−63%), compared to the WT^{oe}. In agreement, the metabolic fluxes like Itaconate, succinate, fumarate, FAD, and NAD were reduced significantly in the 148M^{oe} macrophage, suggesting reduced oxidative phosphorylation. In line with the extracellular flux analysis, the 148M^{oe}, compared to the WT^{oe}, has reduced mitochondrial ROS-positive cells (−15%). Significantly downregulated *MCU* and *IP3R* suggest that impaired Ca²⁺ signaling may, at least in part, be responsible for the reduced ROS in 148M^{oe} macrophages. Despite high ROS levels in the WT^{oe}, their mitochondrial function remained intact, suggesting that potential protective mechanisms are in place. The expression levels of *SOD2*, *SOD3*, and *TXNRD1*, *TXNRD2* were significantly upregulated in the WT^{oe} compared to 148M^{oe}. In addition, glutathione biosynthesis and metabolism were reduced in the 148M^{oe} compared to the WT^{oe}. In line, genes associated with mitochondrial function like *PGC1-alpha*, *NRF1/2*, *mt-ND1*, *16sRNA*,

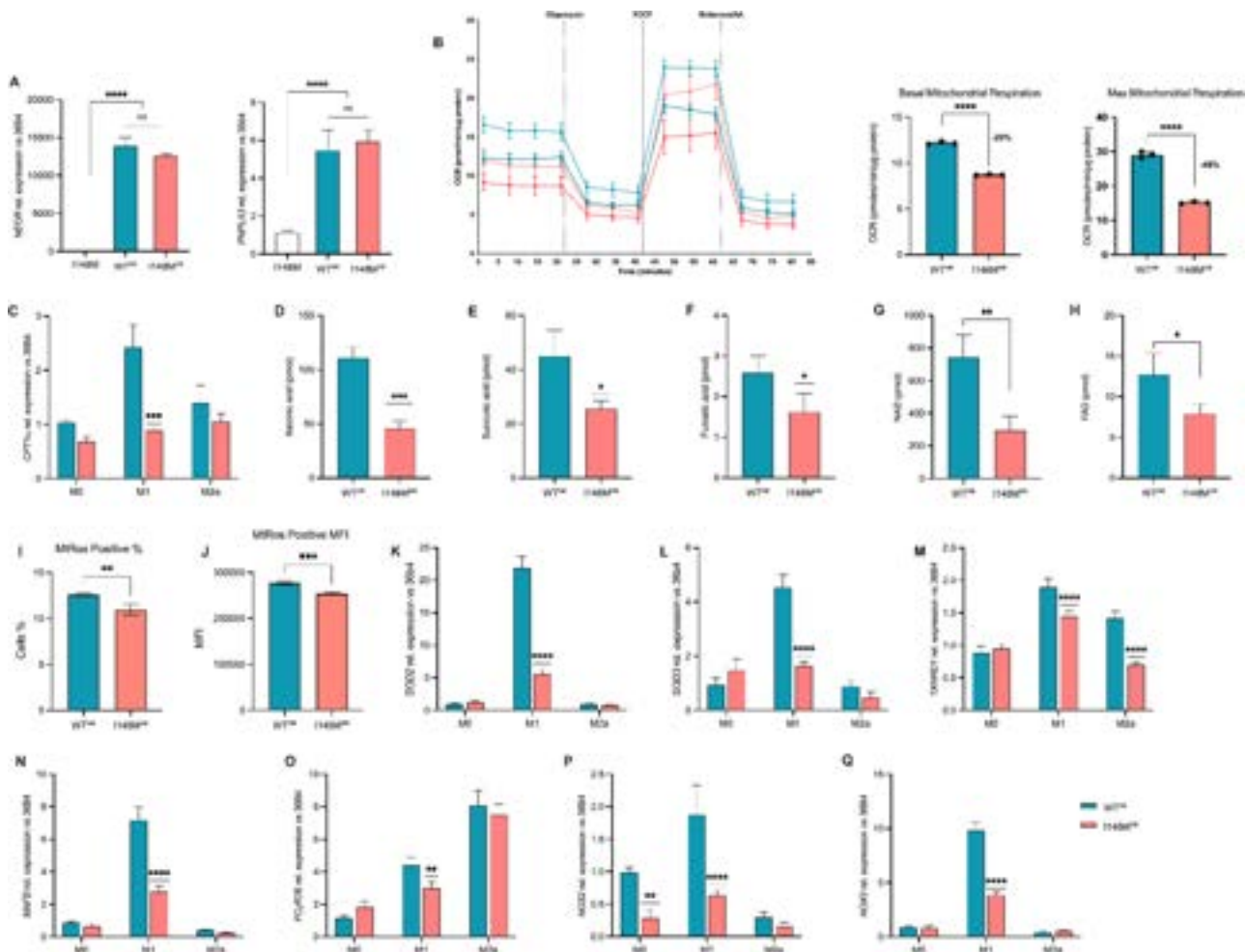


Figure: (abstract: WED-405).

POSTER PRESENTATIONS

LC3A, and *LC3B* were markedly reduced in the 148M^{oe}. WT^{oe} macrophages had a higher number of mitochondria, as reflected by significantly upregulated *mt-ND1* and *16sRNA* compared to the 148M^{oe}. Interestingly, *MAFB* (−57%), which controls phagocytosis through the opsonic phagocytic receptor, *FCγR2B* (−30%), was significantly reduced in the 148M^{oe} macrophage. Likewise, *NOS2* and *NOX2*, the two components of the phagolysosome, were reduced, respectively, by 61% and 55% in the 148M^{oe} macrophages. In addition, Itaconate, a macrophage-induced metabolite that acts as an antimicrobial effector, was reduced by 59% in 148M^{oe} macrophage. **Conclusion:** Our findings show that the PNPLA3 148M^{oe} reprograms macrophage metabolism away from mitochondrial respiration. Reduction of mitochondrial ROS, *NOS2*, *NOX2*, *MAFB* and *FCγR2B* coupled with reduction of itaconate in the 148M^{oe} may lower their phagocytotic and antimicrobial activities.

WED-406

Toll-like receptor 5 signalling mediates pro-inflammatory and fibrogenic responses in non-alcoholic steatohepatitis (NASH)

Wenhao Li¹, Patricia Garrido¹, Iris Gines Mir¹, Kathryn Waller¹, Anja Versteeg-de Jong¹, James Hallimond Brindley¹, Waleed Khan¹, Gillian Hood¹, James Boot², Chaz Mein², Kalpana Devalia³, John Loy³, William Alazawi¹. ¹Barts Liver Centre, Blizard Institute, London, United Kingdom, ²Genome Centre, Queen Mary University of London, London, United Kingdom, ³Homerton University Hospital NHS Foundation Trust, United Kingdom
Email: wenhao.li@doctors.org.uk

Background and aims: Non-alcoholic steatohepatitis (NASH) is a common, progressive inflammatory liver condition with no approved therapies. Hepatocyte lipotoxicity results in inflammation, immune (T cell) infiltration and stellate cell activation leading to fibrosis. Hepatic Toll-like receptors (TLR) sense gut-derived inflammatory signals such as lipopolysaccharide (via TLR4) and flagellin (TLR5) and may represent therapeutic targets in NASH. Flagellin and TLR5 have been implicated in murine NASH models and here we test the hypothesis that this pathway plays a pathogenic role in human disease.

Method: Plasma TLR5 binding capacity and flagellin, stool *Flic* gene load (shotgun metagenomics sequencing) and hepatic *TLR5* gene expression were measured in samples from 139 patients and 24 controls recruited from outpatient clinics and elective bariatric surgery. Lipotoxicity was modelled in vitro using oleic (1 mM) and palmitic (0.5 mM) acid in human hepatocyte-like (HepG2) and stellate (LX2) cells.

Results: Compared to controls, plasma TLR5-binding capacity was increased in advanced NASH fibrosis but not earlier stages of disease (TLR4-binding increased at all disease stages) as was flagellin concentration (538.3v 745.8 pg/ml, $p = 0.004$) which normalised in samples taken median 83 days following bariatric surgery ($n = 20$, $p = 0.005$). Stool *Flic* gene expression and hepatic *TLR5* (but not *TLR2* or *TLR4*) expression were increased in NASH, along with markers of intestinal permeability (FABP2, D-lactate). In vitro, TLR5 inhibition attenuated toxic lipid-mediated IL8 protein expression (all $p < 0.001$, vs control) in HepG2. TLR5 inhibition also attenuated both flagellin- and toxic lipid-induced IL8 production in LX2 cells by 1.9-fold ($p = 0.019$) and 2.1-fold ($p = 0.032$) respectively. Although neither flagellin nor toxic lipids directly induced pro-collagen 1a1 production in LX2 cells, lipid-injured HepG2-conditioned media induced 3.2-fold increase in pro-collagen 1a1 production compared to control ($p = 0.0015$). TLR5 inhibition in HepG2 cells prior to media transfer led to a reduction in LX2 pro-collagen 1a1 production ($p = 0.030$). Similarly, lipid-injured HepG2-conditioned media induced Th1 differentiation of naïve T cells from healthy donors in a TLR5-dependent manner ($p < 0.001$).

Conclusion: TLR5 signalling is activated in human NASH, reverses following bariatric surgery and is associated with mechanisms of

lipid-mediated inflammation and stellate cell activation. This pathway has potential as a novel therapeutic target in NASH.

WED-407

Characterization of extracellular vesicles derived from human precision-cut liver slices in non-alcoholic fatty liver disease

Yana Geng¹, Ke Luo¹, Janine Stam^{1,2}, Dorenda Oosterhuij¹, Alan Gorter¹, Marius van den Heuvel³, Rossella Crescitelli⁴, Vincent de Meijer⁵, Justina Wolters¹, Peter Olinga¹. ¹University of Groningen, Department of Pharmaceutical Technology and Biopharmacy, Netherlands, ²University of Groningen, Department of Analytical Biochemistry, Netherlands, ³University Medical Center Groningen, Department of Pathology and Medical Biology, Netherlands, ⁴University of Gothenburg, Sahlgrenska Center for Cancer Research and Wallenberg Centre for Molecular and Translational Medicine, Sweden, ⁵University Medical Center Groningen, Department of Surgery, Netherlands
Email: p.olinga@rug.nl

Background and aims: Extracellular vesicles (EVs) are membranous and cell-derived vesicles that contain multiple biomolecules which reflect the cellular state. In non-alcoholic fatty liver disease (NAFLD), EVs show great potential in helping understand the pathogenesis of the disease and be used as biomarkers. However, so far, there is no information available on liver tissue-derived EVs in the context of NAFLD. Therefore, in this study, we aim to characterize tissue-derived EVs from an *ex vivo* model of human precision-cut liver slices (PCLS). **Method:** EVs were isolated from human PCLS, prepared from either healthy livers (patients undergoing partial hepatectomy or organ donation) or non-alcoholic steatohepatitis (NASH) cirrhotic livers (liver explants from transplantations). PCLS were incubated for 48 hours in a normal medium (WEGG: Williams' Medium E with GlutaMAX medium supplemented with 11 mM glucose and 10 µg/ml gentamycin) or a modified medium to mimic the pathophysiological condition of NAFLD (GFIP: WEGG supplemented with 25 mM glucose, 5 mM fructose, 1 nM insulin, 0.24 mM palmitic acid, 0.48 mM oleic acid). The PCLS-derived EVs were isolated by differential ultracentrifugation and further characterized by transmission electron microscopy (TEM), western-blot, nanoparticle tracking analysis and mass spectrometry.

Results: The transmission electron microscopy pictures showed the presence of particles with typical EV elements, with sizes between 50 and 250 nm. We confirmed by western blot typical markers of EVs: CD81, CD9 and Rab7 and the absence of cytochrome-c indicating high purity of the EV pellet. NASH PCLS produced a higher amount of EVs compared to healthy PCLS ($p < 0.05$), although there was no significant difference regarding the size of EVs. Using mass spectrometry we identified 2636 proteins both in NASH PCLS-derived EVs and healthy PCLS-derived EVs. There are 151 proteins significantly up-regulated, and 142 proteins significantly down-regulated in EVs derived from NASH PCLS compared to EVs derived from healthy PCLS (FDR < 0.05). GO molecular function analysis showed that those significantly changed proteins were largely enriched for protein/lipid binding functions. By employing the EV proteins as ligands and using a manually curated ligand-receptor database-Cellinker, we found 150 cognate-binding partners that were significantly different in NASH PCLS-derived EVs. The up-regulated cognate-binding partners showed potential in modulating metabolic status (via inhibin β E (INHBE)), promoting fibrosis (via latent transforming growth factor β binding protein 1 (LTBP1), integrin subunit β 5 (ITGB5)) and inducing inflammation (via C-X-C motif chemokine 12 (CXCL12)). Furthermore, we found that epithelial cell adhesion molecule (EPCAM) and integrin subunit α 3 (ITGA3) enriched in our EVs are positively and increasingly associated with the progression of NAFLD, which showed the potential of liver-derived EVs as biomarkers for NAFLD.

Conclusion: In this study, we characterized the EVs derived from healthy and NASH human PCLS with the characterization of their protein compositions. The different protein cargos in EVs from NASH

versus healthy PCLS may assist future studies on identifying liver-specific EVs, understanding the pathogenesis of NAFLD and NAFLD-associated complications, as well as in finding specific EV biomarkers for NAFLD.

WED-408

E2F2-promoted DNA damage in NASH worsens the metabolic scenario

Beatriz Gómez Santos¹, Idoia Fernández-Puertas¹, Paul Gomez-Jauregui¹, Nerea Muñoz-Llanes¹, Natalia Sainz-Ramírez¹, Ane Nieva-Zuluaga¹, Mikel Ruiz de Gauna¹, Maider Apodaka-Biguri¹, Francisco González-Romero¹, Igotz Delgado¹, Igor Aurrekoetxea^{1,2}, Lorena Mosteiro González², Gaizka Errazti Olarteoetxea², Sonia Gaztambide², Luis A Castaño González², Luis Bujanda^{3,4}, Jesus Maria Banales^{3,4,5}, Xabier Buque¹, Ana Zubiaga⁶, Patricia Aspichueta^{1,2,4}, ¹Faculty of Medicine and Nursing, University of the Basque Country (UPV/EHU), Department of Physiology, Spain, ²Biocruces Bizkaia Health Research Institute, Spain, ³Biodonostia Health Research Institute-Donostia University Hospital, University of the Basque Country (UPV/EHU), Spain, ⁴Centro de Investigación Biomédica en Red de Enfermedades Hepáticas y Digestivas (CIBERehd), Spain, ⁵Ikerbasque, Basque Foundation for Science, Spain, ⁶Faculty of Science and Technology, University of Basque Country (UPV/EHU), Department of Genetics, Physical Anthropology and Animal Physiology, Spain
Email: patricia.aspichueta@ehu.es

Background and aims: Lipotoxicity is associated to non-alcoholic steatohepatitis (NASH) and generates stress and toxic species that activate the DNA damage response (DDR). This response is associated with the progression of the disease, characterized by the overexpression of the E2F transcription factors. The aims here were to: 1) Identify the role of DNA damage in the metabolic dysregulation of NASH; 2) Investigate the involvement of E2F2.

Method: A cohort of obese patients with liver biopsy classified as NASH or no-NASH was used to analyze hepatic levels of pH2AX (DNA damage marker) and E2F2, hepatic and serum parameters and the activity of hepatic mitochondrial complexes. E2F2 knockout mice (E2F2^{-/-}) and their controls, injected with diethylnitrosamine (DEN) (DNA damage-inducing agent) and fed a high-fat diet (DEN-HFD) for 10 weeks or a choline-deficient diet HFD (CD-HFD) for 6 months were used to induce progressive liver disease. Primary cultures of hepatocytes were used to induce DNA damage by DEN or palmitic acid (PA).

Results: NASH patients showed higher levels of pH2AX than no-NASH patients, which correlated positively with parameters of worse metabolic status. In addition, those NASH patients with higher DNA damage had increased hepatic triglyceride (TG) and diglyceride (DG) levels, and higher mitochondrial complex IV activity, without showing higher levels of ketone bodies, suggesting higher ROS-generating activity but inefficient fatty acid oxidation (FAO). These results were reproduced in mouse models of NASH, suggesting that DNA damage participates in the metabolic rewiring inhibiting FAO in a condition of lipid-overload. Precisely, levels of the FAO regulator E2F2 correlated positively with pH2AX just in NASH patients. Furthermore, E2F2^{-/-} mice were protected from the DNA damage induced by DEN and lipotoxic diets. The in-vitro studies corroborated that E2F2^{-/-} hepatocytes were protected from PA-induced DNA damage and the associated rewiring in lipid metabolism. In concordance, overexpressing E2f2 in hepatocytes led to increased DNA damage when treated with PA or DEN. When classifying NASH patients in a subset of high E2F2 and high pH2AX-hepatic protein levels, these patients showed increased alteration of glucose metabolism, liver accumulation of lipids, markers of atherogenesis and FGF21 secretion compared to NASH patients with lower levels of both proteins. This subset of NASH patients with high E2F2 and high pH2AX levels were younger, suggesting that this subpopulation has an accelerated disease progression.

Conclusion: DNA damage dysregulates lipid metabolism affecting the progression of NASH in an E2F2-dependent mechanism. Lack of E2F2 protects against lipotoxicity-induced DNA damage, while its overexpression exacerbates it. Thus, targeting E2F2 might be valuable to reduce the DDR associated to NASH and its metabolic complications.

WED-409

Uncovering a novel potential target in non-alcoholic fatty liver disease

Stine Marie Praestholm¹, Jorge Correia¹, Jorge Ruas¹, ¹Karolinska Institutet, Physiology and pharmacology, Stockholm, Sweden
Email: jorge.ruas@ki.se

Background and aims: Non-alcoholic fatty liver disease (NAFLD) is the most common chronic liver disease in the world affecting 25% of the adult population. The global prevalence of NAFLD is expected to increase in consistence with the increase in type 2 diabetes and obesity, which are well-known risk factors for NAFLD. We have identified a zinc finger protein of previously unknown function (TRAIN) and discovered that it operates as a regulator of inflammation, extracellular matrix remodeling, and fibrogenesis. In this project we investigate the function of TRAIN in NAFLD/non-alcoholic steatohepatitis (NASH) and evaluate its potential as a novel therapeutic target.

Method: We are using genetic and viral approaches to modulate TRAIN expression in mice and in cell cultures in combination with NAFLD/NASH/liver injury inducing treatments to investigate the role of TRAIN in liver disease. Specifically, we have generated whole-body and hepatocyte-specific TRAIN knockout (KO) mice and are using adenovirus (Ad) and adeno-associated virus (AAV) delivery systems to acutely induce, repress or KO TRAIN expression. These mice are then challenged in different models of NAFLD/NASH/liver injury including feeding mice on a western diet, methionine-choline deficient (MCD) diet or through CCl4 injections. Hepatocyte and hepatic stellate cell lines as well as mouse and human primary hepatocytes are treated with NAFLD-associated stimuli to investigate the NAFLD-driven pathways regulating TRAIN expression. Lastly, we are using GST pull-down followed by mass spectrometry to investigate the molecular function of TRAIN.

Results: TRAIN expression is elevated in liver disease in both human patients and in various mouse models. Importantly, we have found that increasing liver TRAIN expression, within pathophysiological levels, is sufficient to drive NASH-like metabolic, morphological, histological, and hepatic transcriptional characteristics. This includes TRAIN-induced expression of a panel of genes associated with immune response, extracellular tissue remodeling and fibrosis. Interestingly, TRAIN gene ablation in hepatocytes ameliorates glucose homeostasis and energy expenditure in NASH-diet fed mice. In cell cultures, NAFLD-associated conditions including oxidative stress, lipid accumulation as well as TGFβ1, IL-6 and IFNγ activated pathways drive TRAIN expression in both hepatocytes and in hepatic stellate cells. Moreover, we have found that TRAIN associates with RNA binding proteins and binds a specific set of RNAs.

Conclusion: TRAIN is a novel regulator of inflammation involved in some of the key molecular and cellular events of NAFLD/NASH development and progression. Research in this project could form the foundation for finding a new class of pharmacological therapies for NAFLD/NASH and potentially other liver inflammatory diseases, such as alcoholic hepatitis.

WED-410

miR-22 inhibition as glp1 agonist orthogonal mechanism for nash and nash treatment

Riccardo Panella¹, Sakari Kauppinen¹, Simone Tomasini¹, Henrik B. Hansen², Michael Feigh². ¹Aalborg University, Center for RNA Medicine, Clinical Medicine, Copenhagen SV, Denmark, ²Gubra, Hørsholm, Denmark
Email: riccardop@dcm.aau.dk

Background and aims: MicroRNA-22 (miR-22) orchestrates multiple pro-lipogenic and adipogenesis programs through both direct and indirect signaling mechanisms. Genetic ablation of miR-22 has been demonstrated to suppress these programs resulting in stimulated energy expenditure and brown adipose tissue activation. Collectively, this supports the relevance of miR-22 inhibition in the treatment of obesity and associated disease complications, notably non-alcoholic steatohepatitis (NASH). The present study aimed to characterize locked nucleic acid (LNA) oligonucleotide-based therapy targeting miR-22 in preclinical models of obesity and NASH.

Method: The LNA-based anti-miR-22 oligo was designed using a mix-mer strategy targeting the seed region of hsa-miR-22-3p, evolutionary conserved between mouse and human. Female C57BL/6 mice were made diet-induced obese by feeding a high-fat diet (60 kcal% fat) for 24 weeks (DIO mice). DIO mice (n = 5–8 per group) received (SC) vehicle, scrambled LNA (10 mg/kg) or LNA anti-miR-22 (10 mg/kg) once weekly throughout the feeding period. Other female C57BL/6 mice were fed the Gubra-Amylin-NASH (GAN) diet high in fat, fructose and cholesterol for 38 weeks prior to study start (GAN DIO-NASH mice). Only GAN DIO-NASH mice with liver biopsy-confirmed NASH (NAFLD Activity Score, NAS ≥ 5) and fibrosis (stage ≥ 1) were included and stratified into treatment groups based on quantitative fibrosis histology. GAN DIO-NASH mice (n = 14–16 per group) were administered (SC) vehicle, scrambled LNA (SCR, 10 mg/kg) or LNA anti-miR-22 (10 mg/kg) once weekly for 24 weeks. Vehicle-dosed chow-fed mice (n = 10) served as normal controls. Histopathological pre-to-post individual assessment of NAS and fibrosis stage was performed in GAN DIO-NASH mice. In both studies, terminal end points included body weight and quantitative liver histology.

Results: Vehicle and SCR-dosed DIO mice showed similar robust and progressive weight gain over the course of the study. In contrast, LNA anti-miR-22 treatment completely prevented development of obesity and steatosis in DIO mice. Food intake in DIO mice was unaffected by treatments. LNA anti-miR-22 reduced body weight in GAN DIO-NASH mice while also reducing NAS, driven by significant improvements in steatosis and lobular inflammation scores. The benefits on liver histology in GAN DIO-NASH mice were further supported by reduced quantitative histological markers of steatosis (% area of lipids, % lipid-laden hepatocytes) and inflammation (galectin-3).

Conclusion: We have developed a locked nucleic acid (LNA) oligonucleotide efficiently inhibiting miR-22 function. LNA anti-miR-22 treatment effectively prevents development of obesity and improves liver disease hallmarks in clinical translational mouse models of obesity and NASH without affecting food consumption, supporting further development of LNA anti-miR-22 for obesity and obesity-related liver complications.

WED-411

Biomarkers identifying hepatic inflammation in non-alcoholic fatty liver disease (NAFLD)

Mikkel Werge¹, Annabelle Hoegl², Marie Louise Therkelsen², Mads Grønberg², Gianluca Mazzoni², Lea Mørch Harder², Henning Hvid², Elias Rashu¹, Mira Thing¹, Liv Hetland¹, Anders Junker¹, Reza Serizawa³, Mogens Vyberg^{3,4}, Elisabeth Galsgaard², Lise Lotte Gluud^{1,5}. ¹Copenhagen University Hospital Hvidovre, Gastro Unit, Hvidovre, Denmark, ²Novo Nordisk A/S, Research and Early Development, Maaloev, Denmark, ³Copenhagen University Hospital Hvidovre, Pathology, Hvidovre, Denmark, ⁴Aalborg University Copenhagen, Center for RNA Medicine, Copenhagen SV, Denmark, ⁵University of Copenhagen, Clinical Medicine, Copenhagen N, Denmark
Email: edg@novonordisk.com

Background and aims: Hallmarks of non-alcoholic steatohepatitis (NASH) are steatosis, lobular inflammation and hepatocyte ballooning driving fibrosis and progression to cirrhosis, end-stage liver disease and hepatocellular carcinoma. The aim of the study was to identify plasma proteins as non-invasive biomarkers of hepatic inflammation in NAFLD patients.

Method: LC-SM based plasma proteomics was conducted on 77 healthy controls and 198 NAFLD patients (F0 = 42, F1 = 55, F2 = 45, F3 = 26, F4 = 30) in the Fatty Liver Disease in Nordic Countries (FLINC) cohort. A combination of differential expression analyses and machine learning (SVM) was used to identify novel biomarker candidates. Immunohistochemistry of pan-leucocyte marker CD45 in formalin-fixed paraffin-embedded (FFPE) liver biopsies determined overall hepatic inflammatory. CD45 proportionate area for 148 NAFLD and 14 controls were calculated by digital image analysis. Gene expression of candidate biomarkers was assessed from bulk transcriptomics in the same FFPE liver biopsies from 118 NAFLD patients and 12 controls.

Results: Analysis of the LC-MS dataset identified a 4-protein panel that were able to identify NAFLD patients and controls in 93% and 93% of cases, respectively: Aldolase B (ALDOB), paraoxonase 3 (PON3), a disintegrin and metalloproteinase with thrombospondin motifs like 2 (ADAMTSL2), and cathepsin D (CSTD). CD45 proportionate area was 2.08% and 3.11% (median) in controls and NAFLD patients, respectively. Differential expression analysis of plasma proteomics identified 6 upregulated proteins in non-cirrhotic NAFLD patients with

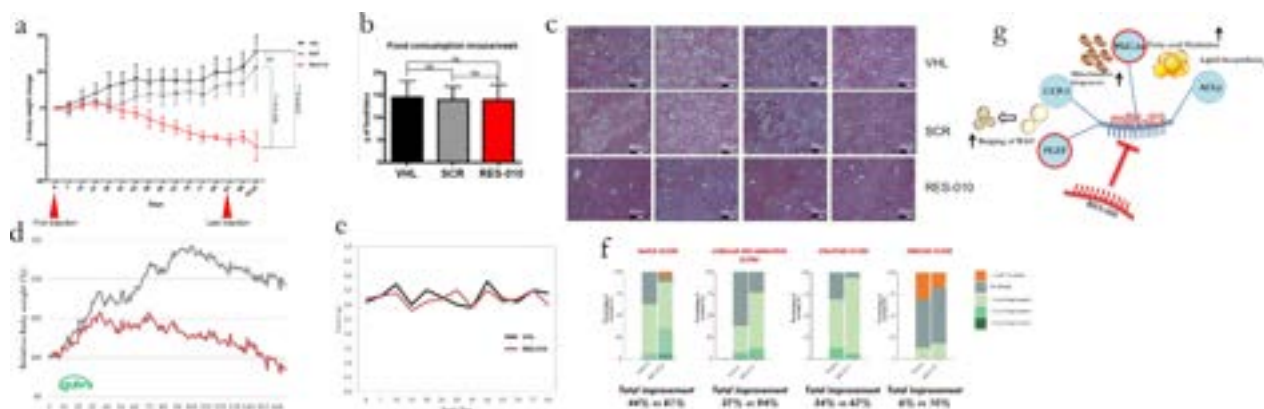


Figure: (abstract: WED-410).

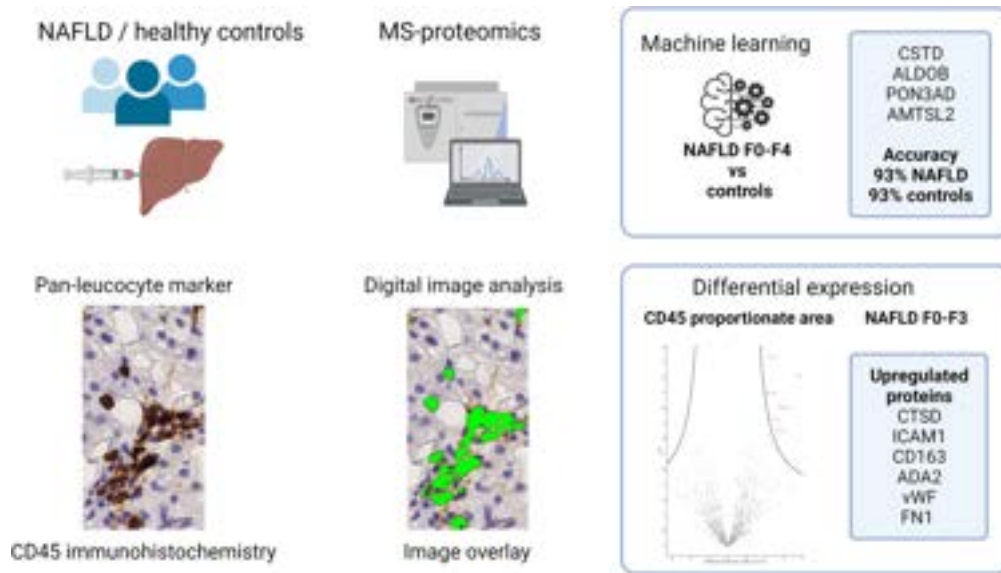


Figure: (abstract: WED-411).

increased hepatic CD45 proportionate area [High >3.5 (n = 60) % vs Low <2.5% (n = 49)]; Intracellular adhesion molecule 1 (ICAM1) mediating leukocyte endothelial transmigration), adenosine deaminase 1 (ADA2) expressed predominantly in macrophages), CD163 marker of monocyte/macrophage lineage, von Willebrand factor (vWF) increased with adverse changes to the endothelium, fibronectin 1 (FN1) a fibroblast-derived glycoprotein present both in plasma and extracellular matrix, and cathepsin D (CSTD) an endolysosomal protease linked to deregulated metabolism and inflammation in NAFLD. Interestingly, only CSTD was upregulated in non-cirrhotic NAFLD patients with biopsy-confirmed lobular inflammation. Hepatic gene expression of ICAM1, ADA2, CD163, and vWF was, moreover, positively associated with CD45 proportionate area when assessed by bulk transcriptomics ($p=0.0002$, $p=1.06 \times 10^{-7}$, $p=0.0008$, and $p=0.001$, respectively). In contrast, hepatic CSTD and FN1 gene expression did not correlate with CD45 area fraction. Increased plasma levels of CSTD, ICAM1, ADA2, CD163, and vWF, but not FN1, were associated with fibrosis.

Conclusion: We identified 6 plasma proteins as potential biomarkers of overall hepatic inflammation in non-cirrhotic NAFLD patients. High levels of hepatic inflammation were associated with fibrosis and characterized by endothelial activation and increased monocyte/macrophage cell infiltration.

WED-412

Peroxisome proliferator-activated receptor alpha and estrogen related receptor alpha ligand combinations ameliorate non-alcoholic fatty liver disease

Milton Antwi^{1,2,3,4}, Sander Lefere^{2,4}, Lisa Koorneef¹, Anneleen Heldens^{2,4}, Louis Onghena^{2,4}, Anja Geerts^{2,4}, Lindsey Devisscher^{2,3}, Karolien De Bosscher¹. ¹Translational Nuclear Receptor Research lab, VIB-Ugent Center for Medical Biotechnology, Ugent Department of Biomolecular Medicine, Gent, Belgium, ²Liver Research Center Ghent, Ghent University, Ghent University Hospital, Gent, Belgium, ³Gut-Liver Immunopharmacology unit, Ghent University, Department for Basic and Applied Medical Sciences, Gent, Belgium, ⁴Hepatology Research Unit, Department Internal Medicine and Pediatrics, Liver Research Center, Ghent University, Gent, Belgium
Email: milton.antwi@vib-ugent.be

Background and aims: As a result of the increasing prevalence of obesity, non-alcoholic fatty liver disease (NAFLD) has become the most common liver disease worldwide. Left untreated, NAFLD can progress to non-alcoholic steatohepatitis (NASH), cirrhosis and

primary liver cancer. There is currently no approved pharmacotherapy available for NAFLD. Two nuclear receptor candidates, peroxisome proliferator-activated receptor (PPAR) alpha and estrogen-related receptor (ERR) alpha independent findings have been linked as a therapeutic target against NAFLD. Additionally, literature findings support a close functional interconnection between both receptors. We therefore studied whether pharmacological modulation of PPARalpha and ERRalpha in tandem can inhibit NAFLD progression.

Method: The *in situ* protein expression and localization of PPARalpha and ERRalpha in healthy control, NAFLD, and NASH patients from Ghent University Hospital were studied by confocal microscopy. To evaluate a potential nuclear receptor crosstalk, serum-starved human hepatoma (HEPG2) cells were treated with PPARalpha agonist Pemaifibrate (5 μ M) and ERRalpha inverse agonist compound C29 (5 μ M). Using a diabetic background streptozotocin (STZ)-western diet (WD) mouse model, male mice were fed a western diet from 4 to 12 weeks of age, and treated with Pemaifibrate (0.1 mg/kg) and C29 (10 mg/kg) from weeks 6 to 12 via daily oral gavage. Clinical features, blood parameters, histology and gene expression of the liver were evaluated.

Results: Total PPARalpha protein expression decreased in NAFLD patients and further diminished in NASH patients ($p=0.042$). Conversely, ERRalpha protein expression was not significantly affected in both NAFLD and NASH patients. PPARalpha protein expression outside the nucleus of the hepatocytes decreased in NASH patients ($p=0.0293$). ERRalpha protein expression was localized more outside the nucleus similarly in healthy, NAFLD and NASH patients. Both nuclear receptors overlapped to a greater extent in healthy controls compared to NASH patients ($p=0.046$). In vitro, PPARalpha and ERRalpha ligand combination increased the expression of genes involved in lipid metabolism. In vivo, mice treated with the ligand combination showed improved steatosis, inflammation, NAFLD activity score ($p < 0.0001$) and fibrosis ($p=0.042$), and fewer and smaller liver tumours compared to untreated or single treated mice. The ligand combination decreased blood serum triglyceride level ($p=0.0042$), and improved gene expression of markers involved in glucose and lipid metabolism.

Conclusion: These findings support that dual nuclear receptor targeting by increasing PPARalpha and diminishing ERRalpha activity may represent a viable novel strategy against NAFLD.

WED-413

PNPLA3, MBOAT7 and TM6SF2 modify mitochondrial dynamics in NAFLD patients: dissecting the role of cell-free circulating mtDNA and copy number

Miriam Longo¹, Erika Paolini¹, Marica Meroni¹, Michela Ripolone¹, Laura Napoli¹, Giada Tria¹, Marco Maggioni¹, Maurizio Moggio¹, Anna Ludovica Fracanzani¹, Paola Dongiovanni¹. ¹Fondazione IRCCS Cà Granda Ospedale Maggiore Policlinico, Milan, Italy, Italy
Email: paola.dongiovanni@policlinico.mi.it

Background and aims: Mitochondrial (mt) dysfunction is a hallmark of progressive NAFLD. MtDNA copy number (mtDNA-CN) and cell-free circulating mtDNA (ccf-mtDNA), which reflect mt-mass and mt-dysfunction, respectively, are gaining attention for NAFLD non-invasive assessment. We demonstrated that *PNPLA3*, *MBOAT7* and *TM6SF2* deficiency in HepG2 cells increased mt-mass, mtDNA-CN and ccf-mtDNA. To assess the genetic contribution on mt-dynamics, mtDNA-CN and ccf-mtDNA in 1) primary mouse hepatocytes silenced for *PNPLA3/MBOAT7/TM6SF2* genes; 2) Discovery (n = 28) and Validation (n = 773) cohorts, including biopsied NAFLD patients, stratified according to number of risk variants (NRV = 3).

Method: Mt-morphology was assessed by TEM. mtDNA-CN was measured in the entire Validation cohort (n = 773), while ccf-mtDNA in a subgroup (n = 300) with available serum samples. mtDNA-CN and mt-related genes were evaluated in liver biopsies.

Results: Primary mouse hepatocytes challenged with fat overload or *PNPLA3/TM6SF2/MBOAT7* co-silencing lowered mt-fusion paralleled by higher mt-fission and ccf-mtDNA release, suggesting that lipid accumulation and genetics may independently unbalance mt-dynamics. In the Discovery cohort, NRV = 3 patients showed the highest mtDNA-CN compared to those with 1-2 or no variants. At TEM, NRV = 3 carriers increased mt-mass and presented an elevated pattern of mt-morphological alterations (swollen shapes, double membranes rupture). In the Validation cohort, mtDNA-CN associated with the NAFLD histological spectrum and NRV = 3 at multivariate analyses, supporting that both NAFLD severity and genetics may modulate mt-dynamics. In liver biopsies, mtDNA-CN was higher in NRV = 3 patients together with reduction of mt-fusion and activation of mt-fission, resembling what observed in hepatocytes. Ccf-mtDNA was augmented in NRV = 3 patients with low-moderate/severe NAFLD, thereby sustaining that this effect was amenable to the 3 at-risk polymorphisms. ROC curves showed that mtDNA-CN discriminated NAFLD subjects vs controls (AUC: 0.71), while ccf-mtDNA was highly predictive of NAFLD-HCC vs NALFD (AUC: 0.79).

Conclusion: mtDNA-CN and ccf-mtDNA may have pathological and predictive significance in NAFLD patients at high-risk, especially in those genetically-predisposed.

WED-414

NAT10-mediated N4-acetylcytidine of hepatic lipogenesis-associated mRNA contributes to maternal high-fat diet-induced non-alcoholic fatty liver disease in juvenile offspring

Qianren Zhang¹, Tianyi Ren¹, Jiangao Fan¹. ¹Xinhua Hospital Affiliated to Shanghai Jiao Tong University School of Medicine, China
Email: fanjiangao@xinhuaamed.com.cn

Background and aims: Growing evidence have shown that early life exposure to maternal high fat diet (HFD) during pregnancy and lactation increases the risk of non-alcoholic fatty liver disease (NAFLD) in juvenile offspring, which is regulated by epigenetic machinery. As a novel epi-transcriptomic modification, N4-acetylcytidine (ac4C) could enhance the expression of target gene by increasing mRNA stability and translation efficiency. The aim of this study was to explore the involvement of ac4C and its writer protein N-acetyltransferase 10 (NAT10) in maternal HFD-induced NAFLD.

Method: 6-week-old female C57BL/6J mice were fed either chow diet or HFD for 6 weeks before fertilization and kept on the same diet throughout gestation and lactation. At weaning, morphological and biochemical indicators of pups were analyzed. Hepatic NAT10

expression and ac4C abundance were also assessed. Hepatocyte-specific *Nat10* knockout (*Nat10*^{HKO}) mice were generated by intercrossing *Nat10*^{fl/fl} mice with Alb-Cre mice. Chow-fed male *Nat10*^{HKO} mice were mated with chow-fed or HFD-fed (6-week feeding before fertilization, maintained respective diets during gestation and lactation) female *Nat10*^{fl/fl} mice to generate *Nat10*^{HKO} and *Nat10*^{fl/fl} littermates which could be subdivided into 4 groups: chow *Nat10*^{fl/fl}, chow *Nat10*^{HKO}, HFD *Nat10*^{fl/fl} and HFD *Nat10*^{HKO}. All pups were sacrificed at weaning to assess body weight, liver histopathology and lipid metabolism. Transcriptomic-wide mapping of ac4C modification was performed on mRNA samples isolated from primary hepatocytes of pups, with the aid of RNA-seq and acetylated RNA immunoprecipitation sequencing (acRIP-seq).

Results: C57BL/6J offspring of HFD dams weighed more at weaning, exhibited higher hepatic triglyceride levels, had more hepatic lipid accumulation, expressed significantly higher NAT10, and presented markedly improved ac4C abundance in hepatocyte mRNAs, when compared with pups of chow C57BL/6J dams. Similarly, pups of the HFD *Nat10*^{fl/fl} group exhibited more lipid droplets and triglyceride contents in livers than offspring from the chow *Nat10*^{fl/fl} group. However, genetic ablation of *Nat10* in offspring hepatocytes markedly ameliorated hepatic steatosis induced by maternal HFD. Moreover, expression of lipogenesis-associated proteins, including SREBP-1c, phosphorylated ACC and FASN were also inhibited in HFD *Nat10*^{HKO} pups when compared with HFD *Nat10*^{fl/fl} pups. RNA-seq and acRIP-seq results showed that *Nat10* deletion led to significantly reduced ac4C abundance in *Srebp1c*, *Acc* and *Fasn*, which was in line with suppressed transcriptional expressions and reduced half-lives of these mRNAs.

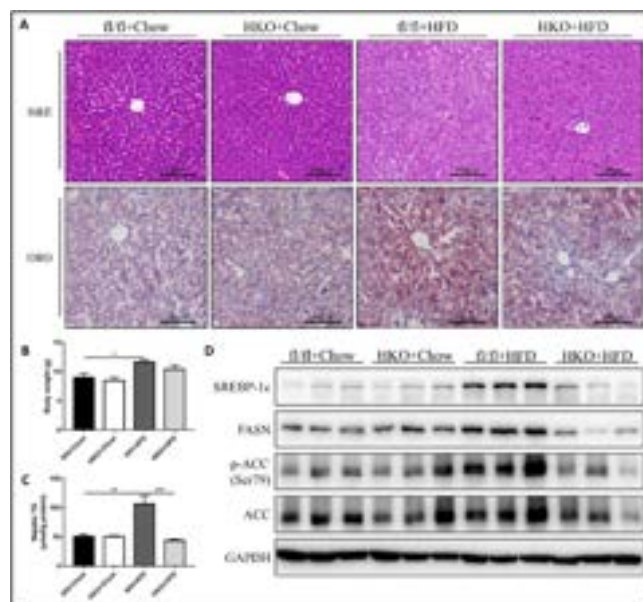


Figure:

Conclusion: NAT10-mediated ac4C modification on mRNAs of lipogenic genes played an important in maternal HFD induced offspring NAFLD, which serves as a potential therapeutic target.

WED-415

Type I NKT cells are involved in exacerbation of steatohepatitis in aged mice

Kazuyoshi Kon¹, Kumiko Arai¹, Akira Uchiyama¹, Hiroo Fukada¹, Toshifumi Sato¹, Shunhei Yamashina¹, Kenichi Ikejima¹. ¹Juntendo University School of Medicine, Department of Gastroenterology, Japan
Email: kazukon@juntendo.ac.jp

Background and aims: The pathogenesis of non-alcoholic steatohepatitis (NASH) is still unclear. Aging is an independent risk factor for

exacerbation of NASH; however, the underlying mechanism is not well understood. NKT cells are classified into type I (iNKT cells) and type II NKT cells, and exhibit different interrelationships depending on disease. Therefore, our aim in this study was to investigate the role of type I and type II NKT cells in age-related exacerbation of steatohepatitis using aged mice and NKT knockout (KO) mice.

Method: Wild-type C57Bl/6 mice, type I NKT cell KO mice ($V\alpha 14$ KO), and type I + type II NKT cell KO mice (CD1dKO) aged 8 weeks (young) and 55 weeks (elder) mice were fed a high-fat/high-cholesterol diet (HFHC) or a control diet for 8 weeks. Expression of mRNA in liver tissue was quantified by RT-PCR. Liver fibrosis was visualized with Sirius Red staining.

Results: Whereas HFHC-fed wild young mice developed only trivial hepatic steatosis with slight elevation of serum ALT levels to 54 ± 11 IU/L, HFHC-fed wild elder mice showed severe macrovesicular steatohepatitis and the serum ALT level reached to 406 ± 46 IU/L. Serum ALT levels in young mice were unchanged in $V\alpha 14$ KO and significantly decreased to 41 ± 5 IU/L in CD1dKO compared to wild mice. In contrast, serum ALT levels of both $V\alpha 14$ KO and CD1dKO mice significantly decreased compared to the elder wild mice to 268 ± 45 IU/L and 159 ± 23 IU/L, respectively. HFHC increased the expression of TNF α /TLR4 mRNA in the liver tissue, and the expression was approximately twice as high in HFHC-fed elder mice as in HFHC-young mice. HFHC-induced upregulation of TNF α and TLR4 was significantly suppressed by $V\alpha 14$ KO/CD1dKO in both young and elder mice. Although the expression of PPAR α mRNA in elder mice was not significantly changed by HFHC in wild mice, it was significantly enhanced in both $V\alpha 14$ KO/CD1dKO mice fed HFHC. Sirius Red staining showed pericentral fibrosis in HFHC-aged mice, while $V\alpha 14$ KO/CD1dKO did not induce fibrosis. Expression of TGF β mRNA was enhanced only in HFHC-fed elder mice, and was significantly suppressed in both $V\alpha 14$ KO/CD1dKO.

Conclusion: These findings demonstrated that the type I NKT cells became more dominant for the induction of inflammatory cytokines in elder mice and causes the exacerbation of steatohepatitis and development of fibrosis. It was concluded that the activation of type I NKT cells plays a key role in the exacerbation of steatohepatitis with aging.

WED-416

Single-cell transcriptomics depicts metabolism reprogramming and immune landscape of bariatric surgery intervened non-alcoholic fatty liver

Shuai Chen¹, Xiurong Cai², Liming Tang¹, Adrien Guillot³, Frank Tacke³, Hanyang Liu^{1,3}. ¹Nanjing medical university, Changzhou medical center, China, ²Charité Universitätsmedizin Berlin, Department of hematology, oncology and tumor immunology (CVK), Germany, ³Charité Universitätsmedizin Berlin, Department of hepatology and gastroenterology (CVK), Germany
Email: hanyang.liu@charite.de

Background and aims: Non-alcoholic fatty liver disease (NAFLD) is one of the most common chronic liver diseases worldwide, composed of metabolic dysfunction, steatosis, inflammation and fibrosis. Importantly, non-alcoholic fatty liver (NAFL) caused by the elevated hepatic lipid deposition acts as not only the consequence of obesity, but also the early stage of the NAFLD. It has been reported that morbidly obese patients represent more than 90% of patients with NAFLD. Till now, no effective resolutions have been approved to effectively prevent the disease progression. Current evidence suggests that the weight loss has been considered as a potential treatment for NAFLD by remising hepatic steatosis, inflammation and fibrosis. Weight loss approaches include lifestyle alterations (mainly diet management), metabolic medicine and bariatric surgery (BS). Recently, BS is considered as a novel disease-modifying therapy for NAFLD, according to clinical studies. Despite physiological alterations, underlying mechanisms of cellular crosstalk and microenvironment remain indeterminate.

Method: In this study, we gathered open bulk RNA-seq datasets from patient's cohorts. Gene alterations of metabolism, inflammation and carcinogenesis were compared according to liver-derived transcriptomic data from post-surgery and diet managed patients. Furthermore, we established mouse BS models (including sleeve gastrectomy and by-pass surgery). As the ongoing work, we perform the single-cell transcriptomic analysis on liver tissues from mouse models [healthy, high-fat diet (HFD) + regression, HFD + sham surgery and HFD + BS mice]. Furthermore, we will identify metabolism reprogramming and immune landscape according to cell clustering, cellular interactions and functional enrichment analysis. To reveal the metabolism-related immune modulation, the metabolism-immune association and key factor will be demonstrated.

Results: We demonstrated that the post-BS livers show more improvements of metabolism-, inflammation- and carcinogenesis-related markers, compared to the diet management. In addition, differences were disclosed in immune cell infiltration (especially macrophage populations) in post-BS patients' livers. Accordingly, we speculate that the immune modulation in post-surgery livers might contribute to metabolic improvement, exerting superior effectiveness than the diet management. On this basis, we will be able to reveal the metabolism reprogramming and immune modulation, aiming to characterize metabolism-inflammation interactions and key molecules in BS intervened NAFLs.

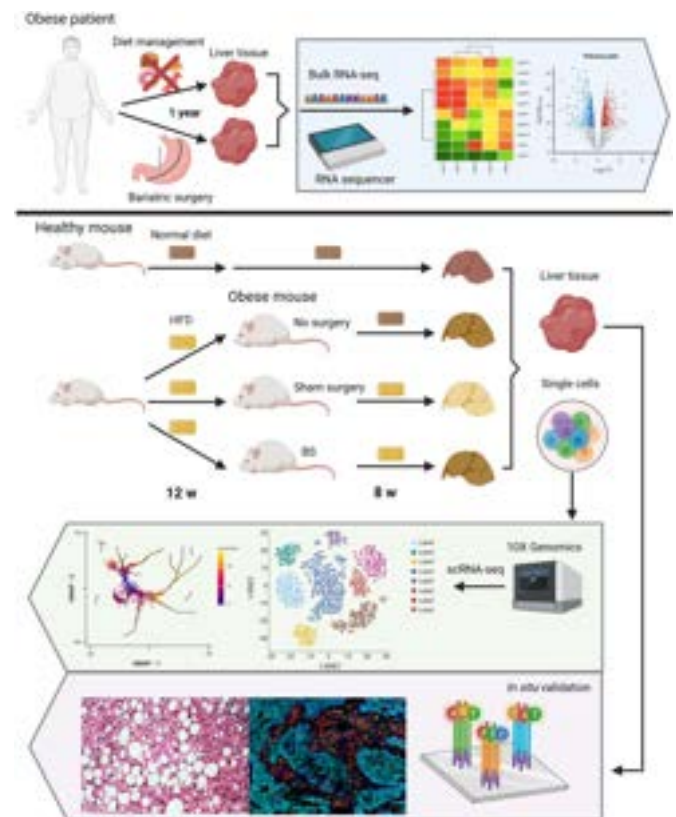


Figure:

Conclusion: This study determined superior functions of BS on metabolism improvement and NAFL attenuation, compared to the diet management. Furthermore, this study will disclose novel mechanisms and clinical potentials of the BS intervenes non-alcoholic fatty liver.

WED-417

Efficacy and reproducibility of AI-assisted Gubra Histopathological Objective Scoring Technique (GHOST) in preclinical rodent models of NASH

Susanne Pors¹, Jacob Nøhr-Meldgaard¹, Denise Oró¹, Casper G Salinas¹, Henrik B. Hansen¹, Michael Feigh¹. ¹Gubra, Hørsholm, Denmark
Email: sup@gubra.dk

Background and aims: Drug efficacy studies in animal models of non-alcoholic steatohepatitis (NASH) typically include histopathological end points. While the clinical-derived NAFLD Activity Scoring (NAS) and Fibrosis Staging system, outlined by Kleiner et al., is largely reproducible in preclinical models of NASH, manual histopathological scoring systems are prone to inter- and intra-observer variability which can influence robustness and reproducibility of study results. To enable objective and unbiased histopathological assessment in liver biopsies from mouse models of NASH, we developed Gubra Histopathological Objective Scoring Technique (GHOST), an automated deep learning-based digital imaging analysis pipeline for the NAS and fibrosis staging system.

Method: Liver biopsies were obtained from two rodent models of NASH, i.e. the GAN diet-induced obese (GAN DIO-NASH) mouse and choline-deficient L-amino acid defined high fat diet (CDAA-HFD) rat model, respectively. Age-matched chow-fed mice and rats served as normal controls. Automated GHOST deep learning computational analysis of NAS and fibrosis scores was performed on hematoxylin-eosin (HE) and picosirius red (PSR) stained sections, respectively. Also, the GHOST module was extended to enable automated analysis of fibrosis severity in CDAA-HFD rats using the Ishak scoring system. All GHOST data were validated against manual scoring by an expert histopathologist. Quantitative morphometrics were derived from the scoring variables, expressed as density of hepatocytes with lipid droplets, number of inflammatory foci, as well as fractional area of fibrosis.

Results: GHOST accurately and reproducibly detected central veins and portal areas in liver biopsy sections from GAN DIO-NASH mice and CDAA-HFD rats, enabling segmentation of zones relevant for clinical histopathological scoring. In HE stained sections, hepatocytes, inflammatory cells, and ballooned hepatocytes were identified. Inflammatory foci were considered as clusters of ≥ 4 inflammatory cells. NAS was computed and validated using a test set of 338 mouse liver biopsies with a Cohen's Kappa value of 0.72 between the AI and manual scoring of NAS. PSR-stained collagen fibers were localized in the sinusoidal and periportal space by GHOST, reproducibly identifying collagen forming bridges and branch points. From these segmentations, Kleiner fibrosis stage was computed and validated using a test set of 537 mouse liver biopsies, achieving a Cohen's Kappa value of 0.84 between AI and manual scores. For Ishak fibrosis scores, PSR stained sections were divided into smaller images that was classified using convolutional neural network (CNN) analysis. The output of the CNN model was used in a machine learning algorithm (random forest) to predict fibrosis stage and a Cohen's Kappa value of 0.82 was achieved with a test-set of $n = 86$ liver biopsies from CDAA-HFD rats.

Conclusion: In conclusion, we confirm high concordance between GHOST-automated and expert histopathologist manual scores in industry-standard rodent models of NASH, including the GAN DIO-NASH mouse and CDAA-HFD rat. Using GHOST for automated assessment of NAS and fibrosis scores provides fast, accurate and reproducible histopathological scoring, thus being instrumental for the assessment of test drug effects in preclinical models of NASH.

WED-418

The PNPLA3 I148M variant aggravates inflammation through dysfunctional LXR and PPAR gamma signalling in macrophages

Emmanuel Dauda Dixon¹, Thierry Claudel¹, Jakob-Wendelin Genger², Ci Zhu³, Erika Paolini⁴, Alexander D Nardo¹, Sarah Stadlmayr⁵, Veronika Mlitz¹, Claudia Fuchs¹, Christine Radtke⁵, Andreas Berghthaler⁶, Paola Dongiovanni⁴, Wilfried Ellmeier³, Michael Trauner¹. ¹Medical University of Vienna, Hans Popper Laboratory of Molecular Hepatolog, Division of Gastroenterology and Hepatology, Internal Medicine III, Wien, Austria, ²Medical University of Vienna, Austria; Center for Pathophysiology, Infectiology and Immunology, Wien, Austria, ³Medical University of Vienna, Institute of Immunology, Vienna, Austria, ⁴Fondazione IRCCS Cà Granda Ospedale Maggiore Policlinico; Department of Pharmacological and Biomolecular Sciences, Università degli Studi di Milano, Italy, ⁵Medical University of Vienna, Department of Plastic, Reconstructive and Aesthetic Surgery, Vienna, Austria, ⁶CeMM Forschungszentrum für Molekulare Medizin GmbH, Center for Pathophysiology, Infectiology and Immunology, Wien, Austria
Email: michael.trauner@meduniwien.ac.at

Background and aims: Several studies have associated the single nucleotide polymorphism (rs738409; C > G) in patatin-like phospholipase domain-containing protein 3 (PNPLA3) with the development and progression of non-alcoholic fatty liver disease. Most functional studies focused on the role of PNPLA3 I148M in hepatocytes and hepatic stellate cells, but its role in inflammation has not yet been addressed. Here, we explored the impact of the PNPLA3 I148M variant on macrophage immunometabolism.

Method: We isolated monocytes from the human peripheral blood of volunteers carrying the PNPLA3 I148M variant and conducted flow cytometry analysis. We established a THP-1 stable cell line over-expressing the PNPLA3 wildtype and I148M isoforms to enable mechanistic dissection. Gel-shift, gene expression analysis, cytokine array analysis, lipidomic, and cholesterol efflux assay were conducted.

Results: Unstimulated monocytes from PNPLA3 I148M patients showed increased levels of CD16 marker and expressed higher *CCL2*, *IL-8*, *TNF α* , and *IL-1 β* compared to the WT patients. To unravel the molecular mechanisms, we generated stable THP-1 cells over-expressing the PNPLA3 WT and I148M. The transfected cells, THP-1 WT^{oe} (+387%) and I148M^{oe} (+428%) showed significantly increased levels of the *PNPLA3* mRNA transcript compared to the untransfected cells. In M0 and M1 macrophage, the proinflammatory cytokines *IL-1 β* (M0, +481%; M1, +446%), *IL-6* (M1, +24%) and the LPS receptor *TLR4* (M0, +86%; M1, +24.5%) were significantly induced in the I148M^{oe} compared to WT^{oe}. Conversely, in M2 macrophages, the anti-inflammatory cytokine *IL-10* was reduced (-83.7%) in the I148M^{oe} compared to the WT^{oe}. Accordingly, I148M^{oe} conditioned medium inhibited SCGB adipocyte differentiation because *PPAR gamma*, *FABP4*, and *GLUT4* were significantly reduced while inducing adipocyte inflammation. Gel-shift analysis revealed reduced LXR binding activity. LXR-alpha gene expression in the I148M^{oe} M1 macrophages was reduced significantly, leading to the downregulation of cholesterol efflux machinery, *ABCA1* (-36.7%), and *ABCG1* (-32%). Furthermore, LXR agonist T0901317 treatment in the I148M^{oe} M1 macrophages restored LXR signalling and cholesterol efflux at the gene level and improved inflammation (*IL-6*, -25%), indicating impaired LXR signalling in macrophages carrying the PNPLA3 I148M variant. Similarly, the PNPLA3 I148M^{oe} showed impaired PPAR gamma and GR alpha signalling due to abnormal phosphorylation mediated by CDK5.

Conclusion: Our results suggest that the PNPLA3 I148M variant aggravates inflammation in macrophages, at least in part, due to impaired LXR and PPAR gamma signalling. These findings could enhance our understanding of the metabolic role of PNPLA3 in immunometabolism, which may lead to the development of novel therapeutic strategies.

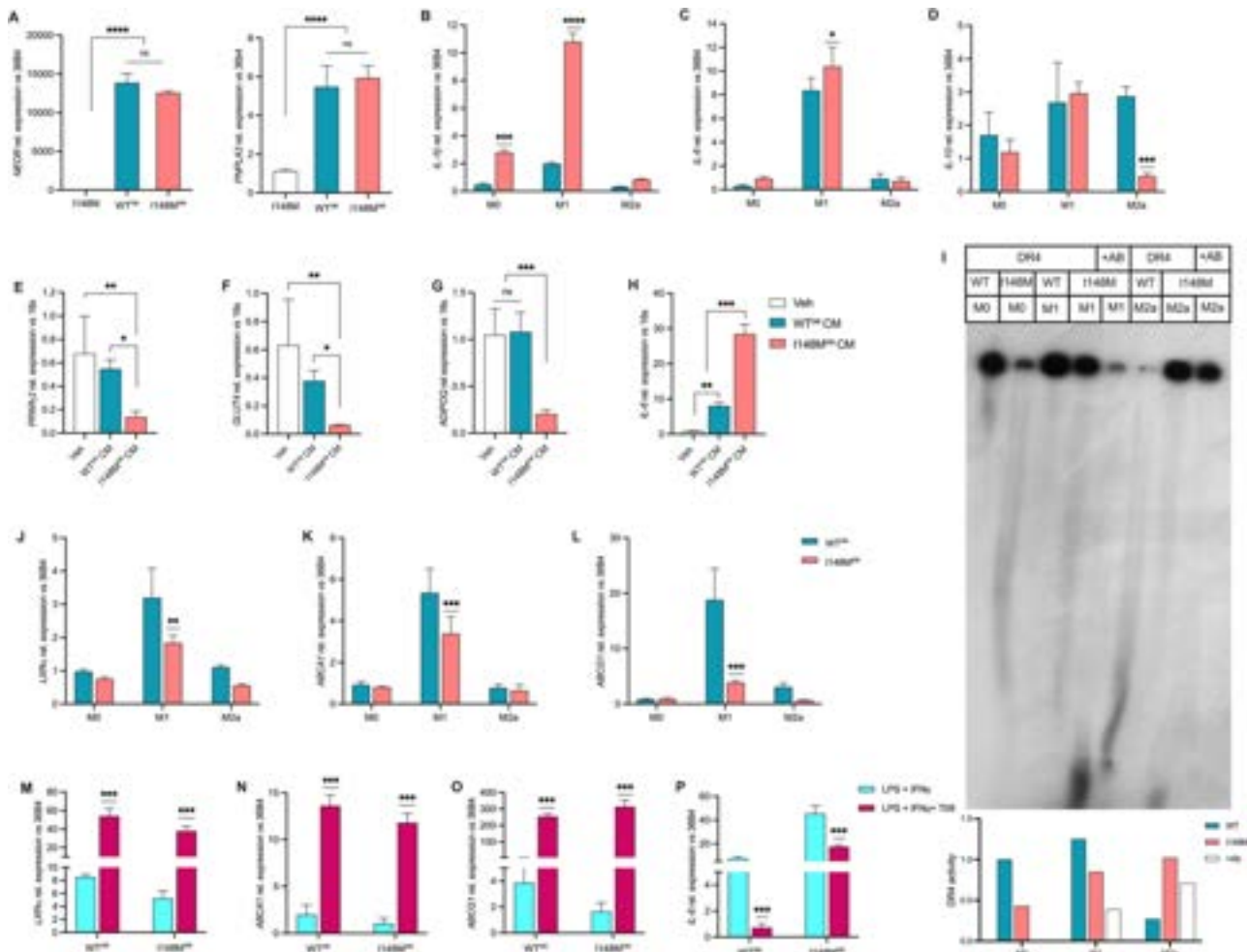


Figure: (abstract: WED-418).

WED-419

The disturbance of intracellular chloride induces the development and progression of non-alcoholic fatty liver disease

Jiaxing Zhu¹, Hai Jin¹, Xingyue Yang¹, Li Zhang¹, Liming Zheng¹, Hui Wang¹, Shun Yao¹, Yanxia Hu¹, Guorong Wen¹, Jiaxing An¹, Xuemei Liu¹, Biguang Tuo¹. ¹Affiliated Hospital of Zunyi Medical University, Gastroenterology, China
Email: tuobiguang@aliyun.com

Background and aims: Non-alcoholic fatty liver disease (NAFLD) has become the most common chronic liver disease worldwide. The advanced stage of NAFLD, non-alcoholic steatohepatitis (NASH), has been recognized as a leading cause of end-stage liver diseases. Although many clinical and experimental studies have been performed, the mechanisms of NAFLD remain to be elucidated. Chloride is a physiologically important anion. Changes in intracellular chloride concentration affect diverse cellular functions. Here we demonstrate that the disturbance of intracellular chloride induces the development and progression of NAFLD.

Method: Hepatocyte-specific transgene mice for chloride channels, ANO1, CLIC1, CLCN2, and SLC26A6, were generated by Cyagen Biosciences Inc. High-fat diet (HFD)-induced simple NAFLD and high-fat high-cholesterol (HFHC) diet-induced NASH models in mice were established. Intracellular chloride was measured with chloride assay kit. Intracellular lipid deposition was examined with oil red O staining assay and triglyceride level measurement.

Results: The hepatocyte-specific ANO1, CLIC1, CLCN2, and SLC26A6 overexpression mice all spontaneously developed liver steatosis at

the age of 6 months and marked features of NASH, liver steatosis, ballooning, and inflammation accompanied by liver fibrosis at the age of 12 months, whereas the wild type control mice had no liver steatosis and NASH at the same age. These transgene mice also displayed higher fasting blood glucose, insulin, HOMA-IR (homeostasis model assessment of insulin resistance) levels, less glucose tolerant and insulin sensitive at the age of 6 and 12 months compared to control littermates. The results from intracellular chloride assay in the liver tissues revealed that the intracellular chloride content in ANO1, CLIC1, and SLC26A6 overexpression mice was higher than that in control mice, but intracellular chloride content in CLCN3 overexpression mice was lower than that in control mice. In primary hepatocytes, LO2 cells and HepG2 cell, low chloride (58 mM) and high chloride (158 mM) mediums, which induced the decrease and increase of intracellular chloride respectively, markedly enhanced palmitate-induced intracellular lipid deposition in comparison with normal chloride (118 mM) medium. Further studies showed that 4, 4'-diisothiocyano-2, 2'-stilbenedisulfonic acid disodium salt, a chloride channel blocker, markedly inhibited the incidence of HFD-induced simple NAFLD and HFHC diet-induced NASH and attenuated HFD-induced simple NAFLD and HFHC diet-induced NASH in mice.

The liver and its histology of SLC26A6 overexpression mice

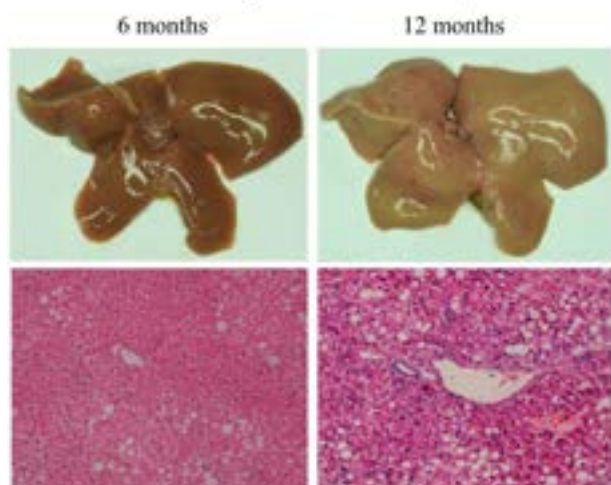


Figure:

Conclusion: These data demonstrated that the disturbance of intracellular chloride plays a key role in the pathogenesis of NALFD and targeting chloride disturbance may be a promising therapeutic target for the treatment of NAFLD and NASH. But the detailed mechanisms of chloride action need further investigation.

WED-420

Mice lacking Cyclophilin B, but not Cyclophilin A, are significantly protected from the development of major features of NAFLD/NASH in a diet and chemical-induced model

Winston Stauffer¹, Daren Ure², Robert Foster², Philippe Gallay¹.

¹Scripps Research, United States, ²Hepion Pharmaceuticals, Canada

Email: wstauffer@scripps.edu

Background and aims: The large percentage of the population affected by NAFLD/NASH is in need of new effective treatments developed from drugs previously shown to be effective in animal models that replicate human disease. In mice, repeated administration of the potent hepatotoxin carbon tetrachloride (CCl₄), together with the “western diet” (WD) of high-fat, high-sugar, and high-cholesterol chow and high-sugar solution, reproduces many prominent features of human NAFLD/NASH, including high NAFLD Activity Scores and liver fibrosis. We previously reported that the pan-cyclophilin inhibitor drug CRV431 (reconfilstat) decreased NASH in mice under the western-diet/CCl₄ model. Reconfilstat inhibits several cyclophilin isoforms, among which cyclophilin A (CypA) and B (CypB) are most abundant. Here, we report evidence that *Ppib*^{-/-} mice lacking CypB, an endoplasmic reticulum (ER) chaperone, develop significantly reduced features of NASH in this model, relative both to wild-type (WT) mice, and to other knockout mice lacking CypA.

Method: 10-week-old male *Ppib*^{-/-} mice, together with *Ppia*^{-/-} and WT C57/BL/6J control mice, were administered 0.2 uL/g CCl₄ intraperitoneally twice weekly. While some groups continued on normal chow and water, other groups received *ad libitum* WD chow containing 21.1% fat, 41% sucrose, and 1.25% cholesterol by weight, together with high-sugar solution (23.1 g/L fructose and 18.9 g/L glucose) instead of water. After 20 weeks, mice (n = 10 per group) were sacrificed at 30 weeks old. Body and liver weight were recorded and livers were fixed for histological analysis. Sections of livers stained with HandE were assigned NAFLD Activity Scores (NAS) based on inflammation, steatosis, and hepatocyte ballooning. Liver sections were also stained with Sirius Red for examination of collagen fibrosis. Unpaired Student's t-tests were conducted with GraphPad Prism.

Results: Naïve *Ppib*^{-/-} mice were smaller than WT but neither exhibited liver fibrosis or steatosis. In both CCl₄-only and CCl₄+WD conditions, *Ppib*^{-/-} mice exhibited liver fibrosis that was reduced by more than 40% and 72%, respectively, compared to WT counterparts,

(p < 0.001). Additionally, in the CCl₄+WD condition, WT livers exhibited a NAS over 7, indicative of NASH, while *Ppib*^{-/-} livers were not significantly changed (p > 0.05) from naïve conditions. *Ppia*^{-/-} mice under CCl₄-only and CCl₄+WD conditions did not significantly differ from their respective WT controls in either liver fibrosis or NAS. **Conclusion:** Cyclophilin inhibition is a promising and novel avenue of treatment for diet-induced NAFLD/NASH. In this study, mice without CypB, but not mice without CypA, were significantly protected from the development of the characteristic features of NASH. Further investigation is necessary to determine whether the specific role of CypB in the ER secretory pathway is of significance to its effect on NASH development.

WED-421

Growth differentiation factor 15 in plasma and liver is associated with hepatic oxidative stress in non-alcoholic fatty liver disease

Mikkel Werge¹, Josephine Grandt¹, Mira Thing¹, Liv Hetland¹, Elias Rashedi¹, Anne-Sofie Houlberg Jensen¹, Anders Junker¹, Martin Richter¹, Søren Møller², Flemming Bendtsen¹, Lea Mørch Harder³, Gianluca Mazzoni³, Birgitte Viuff⁴, Henning Hvid⁴, Sebastian Jørgensen⁵, Kristian Bendtsen⁶, Jonas Kildegaard⁶, Mogens Vyberg⁷, Reza Serizawa⁷, Elisabeth Galsgaard⁶, Nicolai J Wewer Albrechtsen⁸, Lise Lotte Gluud¹.

¹Copenhagen University Hospital Hvidovre, Gastro Unit, Denmark,

²Copenhagen University Hospital Hvidovre, Department of Clinical Physiology and Nuclear Medicine, Denmark, ³Novo Nordisk, Global Research Technologies, Denmark, ⁴Novo Nordisk, Global Drug Discovery, Denmark, ⁵Novo Nordisk, Bio Innovation Hub, United States, ⁶Novo Nordisk, Global Translation, Denmark, ⁷Copenhagen University Hospital Hvidovre, Department of Pathology, Denmark, ⁸Faculty of Health and Medical Sciences, University of Copenhagen, NNF Center for Protein Research, Denmark

Email: mikkel.parsberg.werge@regionh.dk

Background and aims: Growth Differentiation Factor 15 (GDF15) is a stress-inducible protein with known centrally mediated effects, including regulation of food intake and food preference, weight loss, emesis and delayed gastric emptying. We investigated the association of GDF15 with non-alcoholic fatty liver disease (NAFLD) based on a discovery (n = 30; healthy controls, NAFLD and cirrhosis (F4 fibrosis)) and a validation cohort (n = 276; healthy controls and NAFLD with F0 to F4 fibrosis).

Method: Plasma GDF15 was measured by enzyme-linked immunosorbent assays (ELISA) and a proteomics platform (SomaScan). Hepatic GDF15 mRNA expression was determined by in-situ hybridisation in liver samples from 33 patients with NAFLD and by bulk RNA-sequencing in samples from 12 healthy controls and 118 NAFLD patients with F0 to F4 fibrosis. Liver sections were immunostained for p62 as a marker of oxidative stress, and the percentage of positive p62 staining (area fraction) was calculated by digital image analysis.

Results: Plasma GDF15 was increased in patients with NAFLD and in patients with cirrhosis (p < 0.0001) compared to controls and was associated with increasing fibrosis stage (p < 0.0001) but not steatosis (p = 0.67). Patients with advanced fibrosis (F2–F4) had the highest levels of GDF15; the area under the ROC curve for diagnosing advanced fibrosis (F2–F4) was 0.83 (95% CI: 0.76–0.91). The association of advanced fibrosis with plasma GDF15 remained after adjustment for age, sex, BMI and type 2 diabetes in multivariate logistic regression.

GDF15 plasma levels were obtained at 1-year and 2-year follow-up for 71 NAFLD patients and showed an increase (14%, 95% CI: 3–27, p = 0.01) at 2-year follow-up. However, those patients treated with a glucagon like peptide-1 receptor agonist (GLP-1-RA) at baseline had an estimated treatment effect on GDF15 levels of –28% (p = 0.01). Hepatic GDF15 mRNA was observed to be mainly expressed in a subset of hepatocytes throughout the parenchymal area in the liver, including steatotic hepatocytes. Expression was also observed in

some cholangiocytes and in a small subset of non-parenchymal cells, with high expression in fibrotic areas.

Hepatic GDF15 was increased in NAFLD patients ($p = 0.007$) compared to controls, but there was no association with liver fibrosis ($p = 0.93$). Among NAFLD patients, GDF15 expression was highest in patients with non-alcoholic steatohepatitis (NASH, $p = 0.01$).

GDF15 levels in plasma and liver were found to be correlated to the p62 area fraction ($\beta = 0.12$, $p = 0.006$; $\beta = 0.49$, $p < 0.0001$, respectively).

Conclusion: Plasma GDF15 was highest in patients with advanced fibrosis, while the hepatic expression of GDF15 mRNA was highest in patients with NASH. Both plasma and hepatic GDF15 are associated with the degree of oxidative stress in the liver. Further research is necessary to understand the molecular connection between GDF15 expression and oxidative stress in the NASH liver.

WED-422

Decoding hepatocyte transcriptional responses in murine non-alcoholic steatohepatitis using single-nucleus RNA-sequencing

Juliet Luft¹, Mulugeta Seneshaw², Faridoddin Mirshahi², Eleni Papachristoforou¹, Huiping Zhou^{3,4}, Arun Sanyal², Prakash Ramachandran¹. ¹University of Edinburgh, Centre for Inflammation Research, United Kingdom, ²Virginia Commonwealth University, Department of Internal Medicine, United States, ³Virginia Commonwealth University, Department of Microbiology and Immunology, United States, ⁴Central Virginia VA Health Care System, United States

Email: jlluft@ed.ac.uk

Background and aims: Single cell transcriptomics has transformed our understanding of liver non-parenchymal cell (NPC) heterogeneity in non-alcoholic steatohepatitis (NASH). Despite hepatocytes being the primary target of NASH-related injury, it remains unknown how NASH impacts the hepatocyte transcriptome at single-cell resolution, how these effects differ across the zones of the liver lobule and how hepatocyte injury regulates NPC activation to drive the fibroinflammatory cascade. Consequently, we utilised single-nucleus RNA-seq (snRNAseq) to interrogate changes in hepatocyte transcription in the diet-induced animal model of non-alcoholic fatty liver disease (DIAMOND) model of murine NASH.

Method: NASH was induced in B6/129 mice by treatment Western diet for 40 weeks (DIAMOND model). Age matched mice fed with standard chow were used as controls. SnRNAseq was performed on liver nuclei of NASH ($n = 2$) or healthy controls ($n = 2$) using the 10X Genomics Chromium platform. A total of 17,511 single nuclei passed quality control. Computational analysis was performed in R.

Results: DIAMOND mice developed NASH with advanced bridging fibrosis. Unsupervised clustering and annotation enabled atlasing of all major liver cell lineages (Figure A), identifying subpopulations of NASH-associated *Trem2*+*Cd9*+ macrophages and *Pdgfra*+*Col1a1*+ myofibroblasts, key NPC populations which regulate liver inflammation and fibrosis. Focusing on hepatocytes, NASH resulted in global transcriptional changes with significant increases in genes associated with cytokine signaling and apoptosis. Trajectory inference was performed using Slingshot to reconstruct the spatially defined periportal-pericentral axis of hepatocyte zonation, defining zone-specific NASH responses. Ligand-receptor analysis using CellChat, showed that NASH resulted in an increase in both the number and strength of predicted cell-cell interactions between hepatocytes and NPCs (Figure B). Specifically, hepatocytes from NASH livers signaled to mesenchymal, endothelial and immune cells via families of ligands including Angiopoietin-Like Proteins, Platelet derived Growth Factors, Complement and Ephrins. Ligand expression also varied zonally across the liver lobule, with Neuregulins and Junctional Adhesion Molecules upregulated in the periportal hepatocytes of NASH livers, and Fibroblast Growth Factors in the pericentral.

Conclusion: Using snRNAseq in a tractable pre-clinical model, we have defined the transcriptional responses of hepatocytes in NASH, identifying zone-specific injury responses and modelling cross-talk between injured hepatocytes and NPCs which drive liver inflammation and fibrosis. This work provides a molecular framework for future interventional studies aimed at targeting hepatocyte-NPC interactions as a therapeutic strategy for NASH.

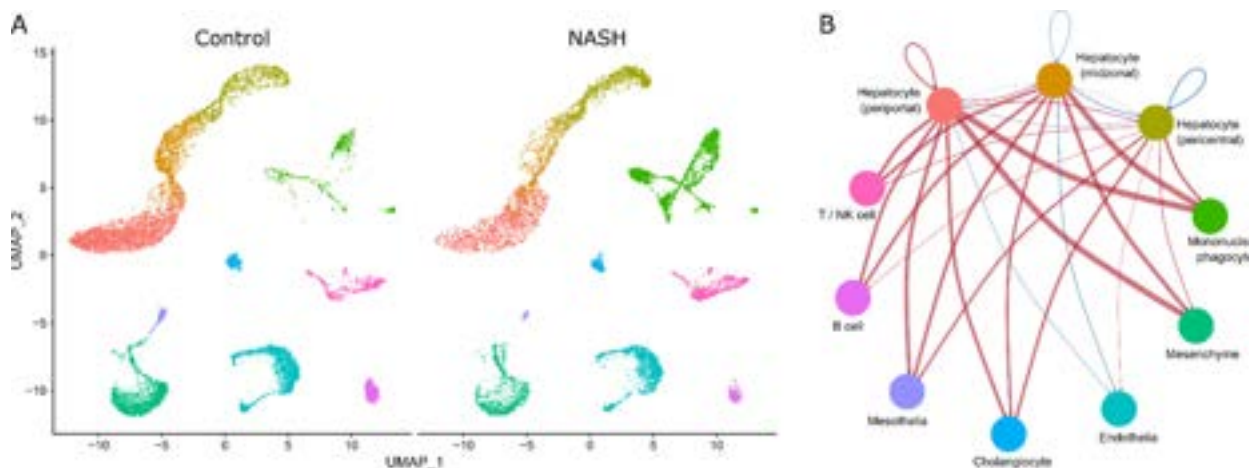
WED-423

Hepatic inactivation of the epigenetic regulators Suv420h1-h2 mitigates NAFLD development and progression in mice

Alessia Pagani¹, Valeria Furiosi¹, Mariateresa Pettinato¹, Letizia Bavuso Volpe¹, Sandro Altamura², Antonella Nai^{1,3}, Davide Gabellini⁴, Simona Pedrotti⁴, Laura Silvestri^{1,3}. ¹IRCCS Ospedale San Raffaele, Regulation of Iron Metabolism Unit- Division of Genetics and Cell Biology, Milan, Italy, ²University of Heidelberg and Molecular Medicine Partnership Unit (MMPU), Department of Pediatric Hematology, Oncology and Immunology, Heidelberg, Germany, ³Università Vita-Salute San Raffaele, Milan, Italy, ⁴IRCCS Ospedale San Raffaele, Gene Expression and Muscular Distrophy Unit, Division of Genetics and Cell Biology, Milan, Italy

Email: pagani.alessia@hsr.it

Background and aims: The molecular mechanisms involved in the development and progression of NAFLD to NASH are still under investigation, and their identification represent an unmet clinical



(A): UMAP of cell lineages, coloured as in B. (B): Differential strength of outgoing hepatocyte ligand-receptor interactions. Red = increase, blue = decrease.

Figure: (abstract: WED-422).

POSTER PRESENTATIONS

need. Several factors contribute to NAFLD development, including deregulated iron metabolism. Notably, a genomic region encompassing the histone methyltransferase *Suv420h* has been associated to iron-dependent liver steatosis in mice. Thus we hypothesize that liver *Suv420h*, by modulating the crosstalk between lipid- and iron metabolism, may play a role in NAFLD-NASH.

Method: we generated mice lacking both *Suv420h1* in the liver and *Suv420h2* in whole body (dKO). Eight week-old male mice were fed a NAFLD-NASH-inducing diet (FPC diet) or a normal diet for 16 weeks. Body weight was monitored weekly. At termination, histological, biochemical and gene expression analysis was performed for phenotypic characterization.

Results: dKO mice showed no developmental defects and perinatal lethality, and their body weight was comparable to control mice. FPC diet induced mild obesity and hepatomegaly in control mice, whereas dKO animals were protected. Inactivation of *Suv420h* in hepatocytes counteracted hepatocyte ballooning, reduced lipid droplet formation, monocyte recruitment and inflammation, and collagen deposition. Hypertrophy of subcutaneous and visceral adipose tissues was mitigated by *Suv420h* deletion, and decreased lipid droplet numbers and size were observed in brown adipose tissues. RNAseq was performed on total liver: dKO mice showed enrichment of PPARα-dependent genes and reduced SMAD3-dependent genes, suggesting a protective gene signature. Since deregulated iron metabolism contributes to NAFLD-NASH, we analyzed iron-related genes in control and dKO mice. In normal diet, expression of *Tfr1*, *ferroportin*, *Bmp6*, BMP-SMAD target genes and the iron-regulatory hormone *hepcidin* were comparable between genotypes. However, in FPC-treated control mice *hepcidin* was downregulated in a BMP-SMAD independent way, and *Tfr1* upregulated, suggesting liver iron deficiency. On the contrary, in FPC-treated dKO mice *hepcidin* and *Tfr1* expression remained unchanged.

Conclusion: *Suv420h1/h2* deletion in hepatocyte counteracts NAFLD-NASH in mice. *Hepcidin* expression, decreased by FPC in control mice, remains unchanged in dKO animals, suggesting a protective effect in counteracting body iron accumulation. Further studies are needed to dissect the signaling pathway modulated by *Suv420h1/h2* in hepatocytes. However, these methyltransferases can be considered a promising therapeutic target for NAFLD treatment and NASH prevention.

WED-424

Peculiar monocyte bioenergetic profile in non-alcoholic steatohepatitis (NASH)

Moris Sangineto¹, Martina Ciarnelli¹, Antonino Romano¹, Rosanna Villani¹, Gaetano Serviddio¹. ¹University of Foggia, Department of Medical and Surgical Sciences-Liver Unit, Italy
Email: moris.sangineto@unifg.it

Background and aims: In Non-alcoholic steatohepatitis (NASH), several pathogenetic mechanisms have been described, although treatment options remain elusive. Beyond the “multiple hit hypothesis” it seems that different triggers converge to the activation of innate immunity, which in turn orchestrates inflammation in NASH. Kupffer cells are activated by pathogen- and damage-associated molecular patterns (PAMPs and DAMPs), with the consequent recruitment of circulating monocyte-derived macrophages which perpetuate inflammation. Recent studies shed light on the promising field of immunometabolism, although very little is known about immunometabolic alterations in chronic diseases such as NASH. This is relevant as the modulation of immune cell bioenergetics may extinguish inflammatory processes, suggesting immune cell metabolism as a potential therapeutic target. Here we aimed to investigate the immunometabolic alterations in patient monocytes in the NASH.

Method: Circulating monocytes from 20 NASH patients (histologically determined) and 10 healthy controls were isolated in order to dissect cellular bioenergetics by using a Seahorse analyser (Agilent). To do this, glycolysis and mitochondrial respiration were studied by quantifying extracellular acidification rate (ECAR) and oxygen consumption rate (OCR), respectively. In a second step, Wild-type (C57BL/6) mice were fed with high-fat and high-cholesterol diet (HF-HC) for 6 weeks in order to induce steatohepatitis. During the last 3 weeks mice were intraperitoneally treated with Dimethyl malonate (DMM) (160 mg/kg) every second day, while vehicle (PBS) injection served as control. DMM is a succinate dehydrogenase (SDH) inhibitor with demonstrated immunomodulating effects in macrophages. Biochemical and histological alterations were assessed.

Results: Interestingly, the examination of bioenergetic profile of NASH monocytes, showed a considerable increase of both glycolysis and mitochondrial respiration (MR) compared to controls. In particular, MR in NASH patients was characterized by increase of

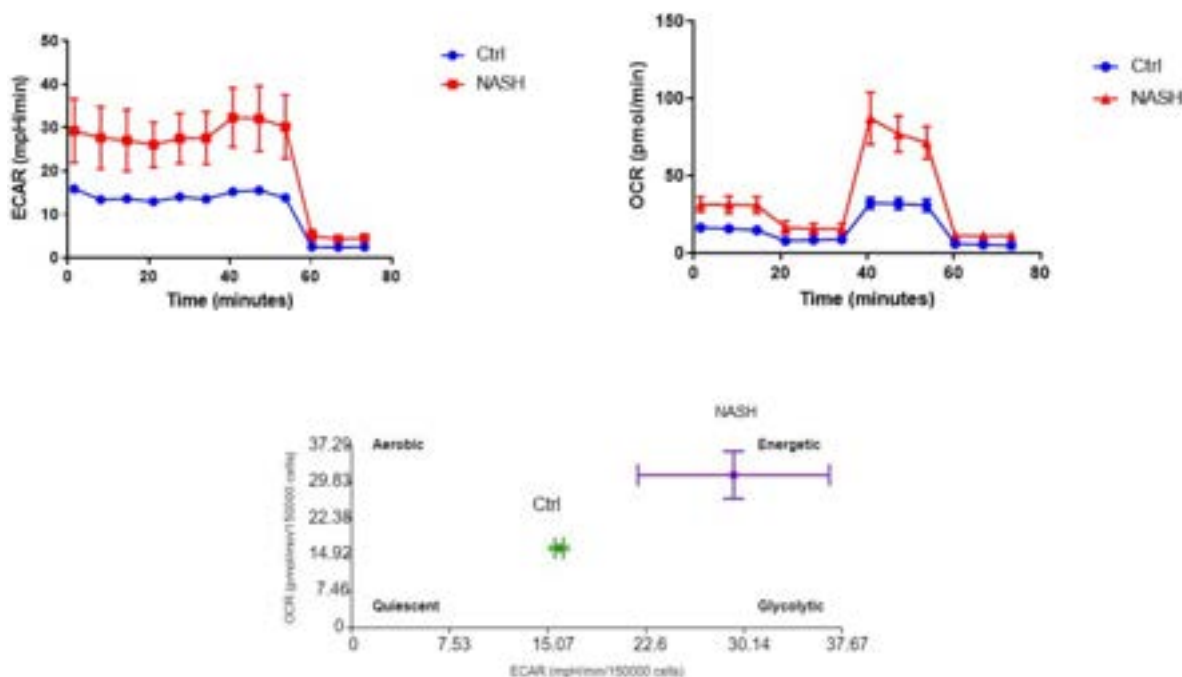


Figure: (abstract: WED-424).

basal and maximal respiration, although a part of this respiration was dissipated by proton leak and not finalized to the ATP production. Moreover, we found that NASH monocytes presented a higher respiratory chain (RC) complex I enzymatic activity and higher mRNA expression of several RC subunits and mitochondrial biogenesis markers such as TFAM and PGC-1 α . Taken together these results underline that monocytes in NASH exhibit an aberrant bioenergetic profile characterized by high glycolysis and high MR levels with mitochondrial dysfunction. Therefore, in order to analyse the potential effects of targeting immunometabolism, HFHC-fed mice were treated with DMM. In fact, DMM is a malonate derivative and a known immunometabolic modulator in macrophages. Interestingly, DMM treated mice improved in terms of liver injury, steatosis and inflammation as indicated by serum ALT levels, hepatic fat, number of inflammatory foci and expression of inflammatory cytokines (e.g., IFN- γ and IL-1 β).

Conclusion: Immunometabolism candidates as a novel therapeutic target in NASH.

WED-425

Co-stimulatory signals mediated by inducible T-cell co-stimulator (ICOS) influence the hepatic expansion auto-aggressive CD8⁺T-cells in non-alcoholic steatohepatitis (NASH)

Cristina Vecchio¹, Alessia Provera¹, Laila lavanya Gadipudi¹, Ramavath Naresh Naik^{1,2}, Renzo Boldorini¹, Nausicaa Clemente¹, Luca C.igliotti¹, Elena Boggio¹, Umberto Dianzani¹, Emanuele Albano¹, Salvatore Sutti¹. ¹University of East Piedmont, Dept. of Health Sciences, Italy, ²Washington University in St. Louis, Dept. of pediatrics, endocrinology and diabetes, United States
Email: cristina.vecchio@uniupo.it

Background and aims: Recent evidence indicated that cytotoxic CD8⁺ T-lymphocytes play important role in the progression of non-alcoholic steatohepatitis (NASH) toward fibrosis. The Inducible T-cell Co-Stimulator (ICOS) present on T lymphocytes and its ligand ICOSL (B7h) expressed on myeloid cells are member of the B7/CD28 family and play multiple roles in immunity by regulating T-cell activation/survival. From the observation that ICOS-expressing CD8⁺ T-cells are important in driving liver healing following acute injury, we have here investigated the possible involvement of ICOS-ICOSL dyad in modulating T-cells functions during NASH evolution.

Method: ICOS and ICOSL were investigated in experimental model of NASH based on mice feeding with choline/methionine deficient (MCD) or a cholesterol-enriched Western (WD) diets.

Results: Liver CD8⁺ T cells expressing ICOS expanded in animal models of NASH in parallel with an up-regulation of ICOSL in CD11b^{high}/F4-80⁺ monocytes/macrophages (MoMFs). Mice deficient for ICOS receiving the MCD diet for 6 weeks had milder steatohepatitis. This effect was confirmed in mice fed with the WD diet for 24 weeks that also showed reduced hepatic fibrosis. The characterization of ICOS⁺/CD8⁺ T-cells in WD-fed mice showed that they featured C-X-C motif chemokine receptor 6 (CXCR6) and programmed cell death protein-1 (PD-1) previously associated with the capacity of killing hepatocytes. Conversely, ICOSL⁺ MoMFs expressed CD9, and the triggering receptor expressed on myeloid cells-2 (TREM-2) that characterize NASH-associated macrophages (NAMs). ICOS deficiency strongly reduced CD8⁺ T-cell expansion and prevented PD-1 upregulation. Such effect also associated with a lowering in the expression of CD122, the β -chain component of both IL-2 and IL-15 receptors responsible for CD8⁺ T-cell proliferation and survival.

Conclusion: Altogether these data indicate that ICOS signals are critical for the expansion auto-aggressive CD8⁺ T cells in NASH and suggest a possible interaction between these lymphocytes and NAMs, thus indicating ICOS/ICOSL dyad as a possible target for therapeutic interventions.

WED-426

Uncovering the role of ISOC1 in non-alcoholic fatty liver disease

Fabrice Marger¹, Etienne Delangre¹, Tiffany Schaefer¹, Francesco Negro^{1,2}, Sophie Clément-Leboubé², Michelangelo Foti¹, Nicolas Goossens^{1,2}. ¹University of Geneva, Geneva, Switzerland, ²Hôpitaux Universitaires de Genève (HUG), Genève, Switzerland
Email: nicolas.goossens@hcuge.ch

Background and aims: Non-alcoholic fatty liver disease (NAFLD) is a complex disease with heterogeneous hepatic molecular pathways and gene expression alterations. Innovative strategies to identify novel molecular targets of NAFLD are urgently needed to help drive therapeutic discovery. Using a large scale computational approach we identified Isochorismatase Domain Containing 1 (ISOC1) gene deregulation as a novel molecular target in NAFLD and we aimed to validate its role *in vitro* and in an animal model of NAFLD.

Method: We generated a consensus human NAFLD liver gene expression signature (NAFLD-sig) using whole-genome meta-analysis of multiple available datasets. Comparison of NAFLD-sig with over one million perturbation gene signatures in the CMap database resulted in the identification of ISOC1 downregulation as the most closely associated signature with human NAFLD in both early and late stages. Knockdown (KD) of ISOC1 was performed through siRNA-mediated KD and CRISPR/Cas9-mediated knockout in human hepatocyte (Huh7) and hepatic stellate (LX2) cell lines. The effects of ISOC1 KD were also evaluated in a mouse model using hepatotropic AAV8 encoding for shRNA directed against ISOC1 in C57BL/6 mice following a 19-day Methionine/Choline Deficient (MCD) diet.

Results: To identify the NAFLD-sig we identified 14 publicly available datasets comparing 300 subjects at different stages of NAFLD. We combined these datasets using gene expression meta-analysis and found that the ISOC1 downregulation gene expression signature most closely approximated the NAFLD-sig at all stages of NAFLD. We next proceeded to validate the association between ISOC1 deregulation and NAFLD *in vitro*. CRISPR/Cas9-mediated knockout of ISOC1 in Huh7 cells was associated with a significant increase in lipid droplet size, number and total area. Expression of key genes involved in lipid metabolism and transport were deregulated (CPT1A, ACAT2, MTTP, all $p < 0.05$). In hepatic stellate cells, ISOC1 knockout and KD was associated with increase of fibrogenic genes (COL1A1, MMP2, TGFBR1, all $p < 0.05$) expression. Microarray analysis of ISOC1 KD in LX2 cells showed induction of pathways associated with hepatic stellate cell activation and collagen deposition. In the murine model of NAFLD, a 19-day MCD diet was associated with a reduction of the hepatic gene expression of ISOC1 and development of steatosis but no fibrosis due to the relatively short duration. Preliminary analysis showed that ISOC1 KD was associated with increased serum ALT levels and increased hepatic lobular inflammation.

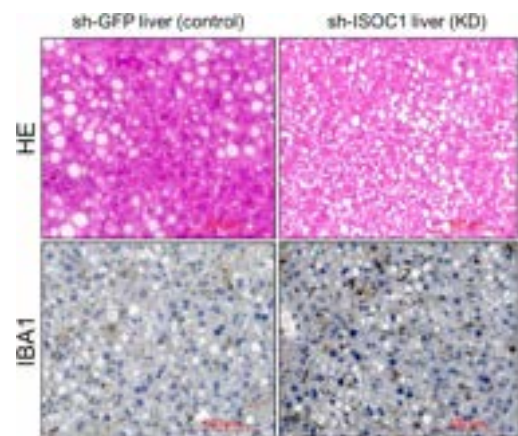


Figure: ISOC1 KD in MCD mice is associated with increased inflammatory infiltrates characterized by increased infiltration of IBA1 positive macrophages.

POSTER PRESENTATIONS

Conclusion: Our study provides novel insights into the role of the ISOC1 gene in the development of NAFLD. Using a large-scale computational approach, we identified ISOC1 downregulation as the most closely associated gene expression signature with human NAFLD in both early and late stages. Our *in vitro* and animal model results validate ISOC1 as a novel molecular target in NAFLD however, further studies are necessary to fully understand the mechanisms and potential consequences of ISOC1 modulation in NAFLD.

WED-427

APB-R3, a novel long-acting IL-18 binding protein, inhibits IL-18 activity, and thereby ameliorates NASH progress with reduced liver fibrosis

Eun-Bi Song¹, Jin Joo Park², Mi-Hyun Park², Young Saeng Jang³, Kyungsun Lee², Jaekyu Han², Susan Chi², Moo Young Song², Seung Goo Kang^{2,3}, Sang-Hoon Cha², Yong-Hyun Han¹. ¹Laboratory of Pathology and Physiology, College of Pharmacy, Kangwon National University, Korea, Rep. of South, ²AprilBio Co., Ltd., Korea, Rep. of South, ³Division of Biomedical Convergence, College of Biomedical Science, Kangwon National University, Korea, Rep. of South
Email: yhhhan1015@kangwon.ac.kr

Background and aims: Non-alcoholic steatohepatitis (NASH) is chronic inflammatory diseases in the liver, which leads to progression from simple steatosis to cirrhosis. Despite recent advances in understanding the pathogenesis of NASH, there are no clinically approved drugs to relieve NASH-induced fibrosis. Interestingly, IL-18, one proinflammatory cytokines that belong to IL-1 subfamily, had been known to be a strong inducer of hepatic fibrosis. Knowing that IL-18BP is a negative feedback controller of IL-18 in a physiological condition, we, herein, developed the long-acting IL-18BP, referred to APB-R3, via recombinantly fused to an anti-albumin Fab, and accessed the therapeutical effect of APB-R3 in rodent NASH models.

Method: We employed two experimental NASH models including STAM and fructose, palmitic acid, and cholesterol-containing (FPC) diet. STAM mice were intraperitoneally injected with 10 mg/kg dose of APB-R3 from 6 to 12 weeks of age. For diet-induced NASH model, FPC diet were fed for 19 weeks. To evaluate combination therapy, APB-R3 and Liraglutide (GLP-1R agonist) were administered independently or combinedly from 11 to 19 weeks of feeding period.

Results: APB-R3 significantly lowered NASH injury markers such as plasma ALT and hepatic triglyceride levels in STAM model. In particular, we found that APB-R3 strongly ameliorated STAM-induced hepatic fibrosis. In the FPC diet-fed NASH model, APB-R3 prevented development of NASH and reduced plasma ALT, inflammatory foci and IFN γ . Similarly, fibrotic changes such as collagen deposition and mRNA expression of pro-fibrotic genes were largely attenuated by administration of APB-R3. Importantly, the combination treatment with both APB-R3 and Liraglutide completely inhibited NASH progression.

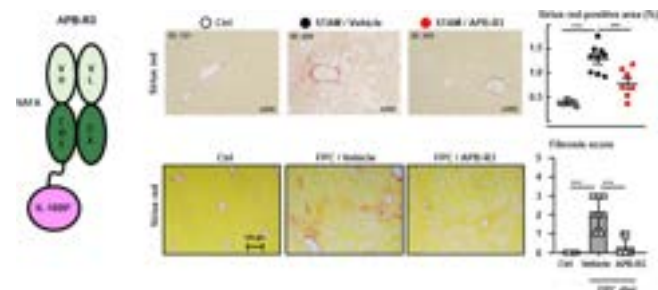


Figure:

Conclusion: APB-R3 treatment exhibits significant reduction of hepatic injury and fibrosis in mice NASH models, and our results emphasize the marked value of APB-R3 as a novel therapeutic arsenal in treating NASH especially when combined with anti-steatotic agents.

WED-428

In vitro investigation of the role of adipocyte-derived exosomes in the development of non-alcoholic steatohepatitis

Robim M Rodrigues¹, Berta Vazquez Olivet², Alexandra Gatzios², Matthias Rombaut², Vera Rogiers², Joost Boeckmans², Joery De Kock², Tamara Vanhaecke². ¹Faculty of Medicine and Pharmacy-Free University of Brussels (VUB), In vitro Toxicology and Dermato-cosmetology, Brussels, Belgium, ²Faculty of Medicine and Pharmacy-Free University of Brussels (VUB), In vitro Toxicology and Dermato-cosmetology, Belgium

Email: robim.marcelino.rodrigues@vub.be

Background and aims: Non-alcoholic fatty liver disease (NAFLD) is associated with visceral obesity. Adipocyte atrophy and accompanying inflammation of the adipose tissue (AT) lead to the secretion of a plethora of factors that once taken up by the liver, exacerbate the development of non-alcoholic steatohepatitis (NASH). Yet, the exact mechanisms behind the interplay between AT and the liver is not fully understood. In this study, we investigate the potential steatogenic and inflammatory effects that adipocyte-derived exosomes might have on the liver using multipotent stem cell-based *in vitro* models.

Method: Human adipose-derived stromal cells (hATSc) were isolated from liposuction material after ethical approval and informed consent of the patients. Upon expansion, the cells were differentiated towards adipocyte-like cells (hATSc-adipo). To mimic the micro-environment of AT in NASH patients, these cells were then exposed for 24 h to a cocktail of multiple NASH-specific factors. The latter were identified from transcriptomics datasets of AT samples of patients with histologically proven NASH and also mimic hyperglycemic and hypertriglyceridemic blood levels of obese patients. Upon a recovery wash-out period of 24 h, exosomes were isolated from the cell supernatants of hATSc-adipo cultures. The steatogenic and inflammatory effects of the isolated exosomes were evaluated using human skin-derived precursors (hSKP) differentiated towards hepatic cells (hSKP-HPC).

Results: Compared to control conditions, the expression of proinflammatory leptin (*LEP*, 1.5 fold) was upregulated in hATSc-adipo cells exposed to the NASH cocktail, whereas the expression of anti-inflammatory adiponectin was downregulated (*ADIPOQ*, -4.0 fold). Furthermore, an upregulation of interleukin beta (*IL1B*, 1.5 fold), tumour necrosis factor alfa (*TNFA*, 1.5 fold), interleukin 6 (*IL6*, 62 fold) and the chemokines C-X-C motif chemokine 5 (*CXCL5*, 1510 fold) and C-C motif chemokine ligand 2 (*CCL2*, 243 fold) was observed in the triggered hATSc-adipo cells. These results suggest that hATSc-adipo cells exposed to a NASH-specific cocktail respond in a similar way as inflamed adipose tissue. Of note, the expression of the exosomal marker human exosome component 9 (*EXOSC9*) remained constant. The exosomes isolated from the cell supernatants of the hATSc-adipo cells exposed to the cocktail or vehicle control conditions had a diameter of 101 nm (91% mode) and 117 nm (82% mode), respectively. Exposure of hSKP-HPC to these exosomes released by the triggered hATSc-adipo cells, induced stearoyl-CoA desaturase-1 (*SCD1*, 1.6 fold) and fatty acid synthase (*FASN*, 1.2 fold), which both play a role in *de novo* lipogenesis. Contrarily, perilipin 2 (*PLIN2*), which promotes the formation of lipid droplets and *CD36* that play a role in fatty acids uptake, were 1.5 and 6.3 fold downregulated, respectively. Strikingly, the expression of proinflammatory cytokines *IL6*, *IL1A*, *CCL2* and *CXCL5* was highly upregulated (2.9, 3.7, 3.3 and 46.3 fold, respectively).

Conclusion: Our data show that adipocyte-like cells derived from human hATSc can mimic cellular responses specific to inflamed AT during NASH. The exosomes secreted by these cells induce the expression of steatogenic and inflammatory markers in an established hepatic *in vitro* system. This study shows the value of human-based *in vitro* cell systems in the investigation of complex pathophysiological processes, such as the interplay between AT and the liver during NASH.

WED-429

A novel HIF2A mutation causes dyslipidemia and promotes hepatic lipid accumulation

Feiqiong Gao¹, Qigu Yao¹, Jiaqi Zhu¹, Wenyi Chen¹, Xudong Feng¹, Bing Feng¹, Jiong Yu¹, Hongcui Cao¹. ¹The First Affiliated Hospital, Zhejiang University School of Medicine, China
Email: hccao@zju.edu.cn

Background and aims: Hypoxia-inducible factor -2α (HIF-2 α) is a transcription factor responsible for regulating genes related to angiogenesis and metabolism. Mutations in the oxygen-dependent domain (ODD) of HIF-2 α have been reported in association with erythrocytosis and tumors. This study aims to explore the effect of a previously unreported mutation c.C2473T (p.R825S) in the C-terminal transactivation domain (CTAD) of HIF-2 α that we detected in tissue of patients with liver disease.

Method: We sequenced liver samples obtained during partial liver resection or liver transplantation performed for clinical indications such as hepatocellular carcinoma and liver failure. In tandem, we constructed cell lines and a transgenic mouse model bearing the corresponding identified mutation in HIF-2 α from which we extracted primary hepatocytes. We evaluated lipid accumulation in these cells and liver tissue from the mouse model using Oil Red O staining; serum, intrahepatic, and intracellular lipid levels from the same model were measured by biochemical detection kit. Lipidomics was used to assess the lipid metabolism of mouse liver.

Results: Herein, we found a mutation in the CTAD of HIF-2 α (c. C2473T; p.R825S) in 5 of 356 liver samples obtained from patients with hepatopathy and dyslipidemia. We also found that introduction of this mutation into the transgenic mouse model led to an increase in triglyceride levels, lipid droplet accumulation in the liver of the mutant mice and in their extracted primary hepatocytes, and increased transcription of genes related to hepatic fatty acid transport and synthesis in the mutant compared to the control groups. In mutant mice and cells, the protein levels of nuclear HIF-2 α and its

target gene perilipin-2 (PLIN2) were also elevated. Decreased autophagy was observed in mutant groups.

Conclusion: We identify a mutation in HIF-2 α and find that patients with it are more likely to have dyslipidemia. The HIF-2 α ^{R825S} mutation elevates blood fatty levels and leads to non-alcoholic fatty liver disease (NAFLD). Identification of the subset of patients with HIF-2 α ^{R825S} mutation may help to cure patients with surgery and developed targeted personalized therapeutics.

WED-430

Adipose tissue macrophage dysfunction and depletion are associated with a breach of vascular integrity in non-alcoholic steatohepatitis

Markus Boesch¹, Andreas Lindhorst², Rita Furtado Feio de Azevedo¹, Paola Brescia³, Alessandra Silvestri³, Matthias Lannoo⁴, Ellen Deleus⁴, Joris Jaekers⁴, Halit Topal⁴, Baki Topal⁴, Marie Wallays¹, Lena Smets¹, Lukas Van Melkebeke^{1,4}, Tania Roskams⁵, Pierre Bedossa⁶, Jef Verbeek^{1,4}, Sven Francque^{7,8}, Alejandro Sifrim¹, Thierry Voet¹, Maria Rescigno^{3,9}, Martin Gericke², Hannelie Korf¹, Schalk van der Merwe^{1,4}. ¹KU Leuven, Belgium, ²Leipzig University, Germany, ³IRCCS Humanitas Research Hospital, Italy, ⁴UZ Leuven, Belgium, ⁵KU Leuven and University Hospitals Leuven, Belgium, ⁶Liverpat, France, ⁷Antwerp University Hospital, Belgium, ⁸University of Antwerp, Belgium, ⁹Humanitas University, Italy
Email: markus.boesch@kuleuven.be

Background and aims: Non-alcoholic fatty liver disease (NAFLD) is reaching epidemic proportions, fueled by the obesity pandemic. In NAFLD, monocytes infiltrate visceral adipose tissue that promote local and hepatic inflammation. It however remains unclear what drives inflammation and how the immune landscape in adipose tissue differs across the NAFLD severity spectrum. We aimed to assimilate the adipose tissue macrophage (ATM) heterogeneity in a NAFLD cohort.

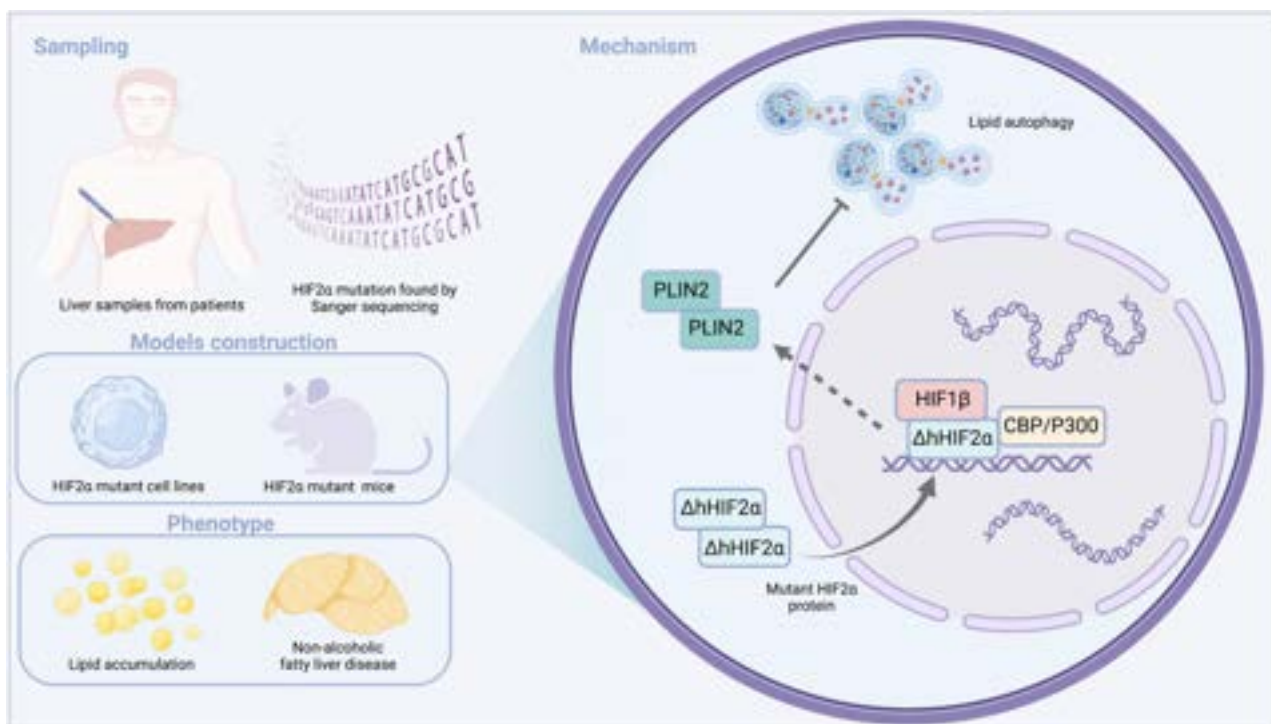


Figure: (abstract: WED-429).

POSTER PRESENTATIONS

Method: Visceral adipose tissue macrophages from obese patients stratified into NAFLD phenotypes underwent single-cell RNA sequencing. Adipose tissue vascular integrity and breaching was assessed via immunohistological staining on paraffin embedded human adipose tissue sections of plasmalemma vesicle-associated protein 1 (PV1) and albumin, respectively.

Results: We discovered multiple ATM populations, including resident vasculature-associated macrophages (ResVAMs) and distinct metabolically active macrophages (MMacs). Using trajectory analysis, we show that ResVAMs and MMacS replenish from a common transitional macrophage subtype (TransMac) and localize around the vasculature, where they interact with endothelial cells. Across the NAFLD severity spectrum, the adipose tissue MMac subset is progressively depleted and not effectively replenished by TransMac precursors. This coincided with an adipose tissue vasculature breach characterized by albumin extravasation into the perivascular tissue.

Conclusion: NAFLD-related macrophage depletion and dysfunction coincides with a loss of adipose tissue vascular integrity providing a strong plausible mechanism by which tissue inflammation is perpetuated in adipose tissue and downstream in the liver.

WED-431

Circadian sleep-wake rhythms in non-alcoholic fatty liver disease

Sofia Roth^{1,2}, Andrijana Bogdanovic¹, Talitha Hildebrandt¹, Anne Geng¹, Emilio Flint³, Michael Strumberger⁴, Martin Meyer⁵, Markus Heim^{1,6}, Christian Cajochen⁵, Christine Bernsmeier^{1,6}.

¹Department of Biomedicine, University of Basel, Switzerland, ²University Centre for Gastrointestinal and Liver Diseases, Basel, Switzerland, ³Department of Biomedicine, University of Basel, Switzerland, ⁴Centre for Chronobiology, Psychiatric Hospital of the University of Basel, Basel, Switzerland, ⁵Centre for Chronobiology, Psychiatric Hospital of the University of Basel, Switzerland, ⁶University Centre for Gastrointestinal and Liver Diseases, Switzerland

Email: sofia.roth@unibas.ch

Background and aims: Non-alcoholic fatty liver disease (NAFLD) has a multifactorial pathogenesis including dietary, environmental and genetic factors. Previous mouse models and data from sleep questionnaires suggested circadian misalignment might influence liver homeostasis and development of NAFLD. In this study, we aimed to objectively assess the sleep-wake rhythm in patients with NAFLD and healthy controls (HC) using actigraphy.

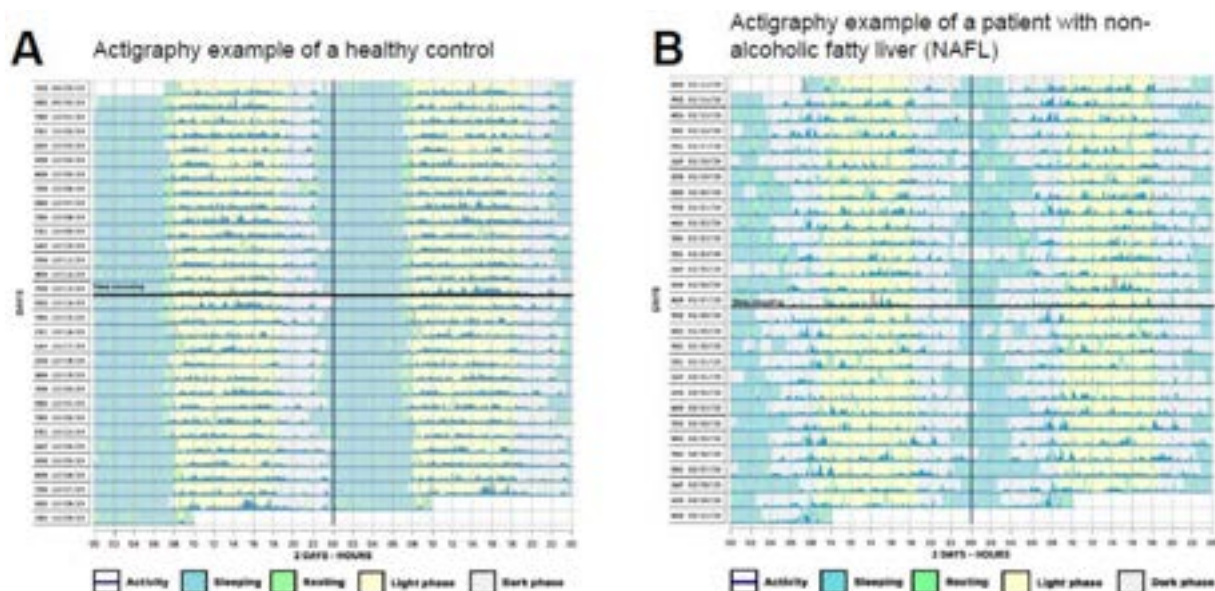


Figure A: (abstract: WED-431).

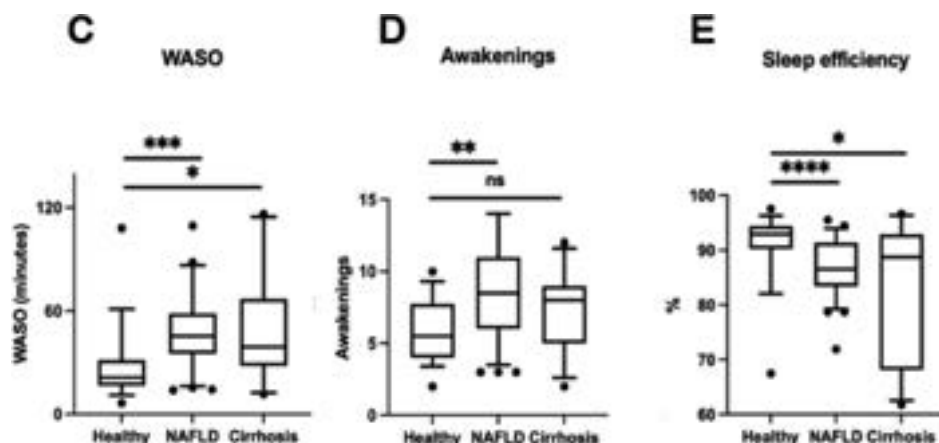


Figure B: (abstract: WED-431).

Method: We included 62 subjects: patients with NAFLD (non-alcoholic fatty liver (NAFL, n=11), non-alcoholic steatohepatitis (NASH, n=16), NASH with cirrhosis (n=8)), patients with cirrhosis of other origin (n=11) and HC (n=16). Sleep-wake rhythm was assessed by actigraphy (ActTrust, Condor) 24/7 for 4 weeks. Additionally, metabolic, laboratory data and subjective sleep parameters were assessed at baseline and week 4. After 2 weeks a single standardised sleep hygiene counselling was performed.

Results: Actigraphy analysis revealed NAFLD patients had more fragmented sleep with more nocturnal awakenings per night (NAFLD vs. HC 8.5 vs. 5.5, $p=0.003$) and longer wakefulness after sleep onset (WASO; NAFLD vs. HC, 45.4 min vs. 21.3 min, $p=0.0004$) compared with HC, while sleep duration was comparable. Sleep efficiency was lower in NAFLD and cirrhosis patients compared with HC (NAFLD vs. HC 86.5% vs. 92.8%, $p=0.0008$; cirrhosis vs. HC 88.7% vs. 92.8%, $p=0.03$). A single session of sleep hygiene counselling did not change sleep and laboratory parameter, nor subjective sleep quality ($p>0.05$).

Conclusion: Using an objective method, NAFLD patients had more fragmented nocturnal sleep with increased awakenings and reduced sleep efficiency compared with HC. A single session of sleep hygiene education was not successful in improving objective or subjective sleep parameters.

WED-432

A novel ALK5 inhibitor (TLR-X) attenuates steatosis and fibrosis in non-alcoholic steatohepatitis in vivo

Marit ten Hove¹, Ruchi Bansal¹. ¹University of Twente, Enschede, Netherlands

Email: m.m.tenhove@utwente.nl

Background and aims: Non-alcoholic steatohepatitis (NASH) represents a major health burden worldwide with no FDA-approved therapies available. Transforming growth factor-beta 1 (TGF- β 1) is significantly upregulated in human NASH. Through Smad signaling, TGF- β 1 promotes NASH by inducing lipid accumulation in

hepatocytes and contributing to hepatocyte death, and activating hepatic stellate cells (HSCs). TGF- β receptor 1 (ALK5) is an attractive target for intervention in canonical TGF- β 1 signaling due to its druggability, centrality, and specificity in the pathway. Silencing this pathway is expected to attenuate hepatic steatosis and fibrosis. In this study, we investigated the novel, highly selective, and orally administrable ALK5 inhibitor (TLR-X) for the treatment of NASH.

Method: Based on promising in vitro results, we investigated the effects of orally administered TLR-X in a NASH mouse model. C57BL/6J mice (8-weeks old) were fed western-diet (WD) containing 21.1% fat, 41% sucrose and 1.25% cholesterol by weight supplemented with high sugar solution (23.1 g/L d-fructose and 18.9 g/L d-glucose), combined with increasing low weekly doses (0.05–0.2 ml/kg) of carbon tetrachloride (CCl₄) for 12 weeks. In the last three weeks, TLR-X (30 mg/kg) was orally administered twice daily. Blood, liver and different organs were collected for subsequent analysis.

Results: We observed a significant decrease in plasma cholesterol levels in TLR-X-treated WD/CCl₄ mice (n=7) compared to vehicle-treated mice (n=7). Oil-red-O staining showed a significant decrease in intrahepatic fat accumulation in TLR-X-treated mice. Additionally, the expression of genes involved in de novo synthesis of fatty acids (FASN, SCD1 and ACACA) was significantly decreased in the TLR-X-treated group compared to the vehicle-treated group. We further assessed the effect of TLR-X on fibrosis and observed that total hydroxyproline content, collagen-I immunostaining and profibrotic gene expression (TGFB1, PDGFRB and ACTA2) were significantly decreased in the TLR-X treated group compared to the vehicle group. Overall, these results indicate the attenuation of hepatic steatosis and fibrosis by TLR-X.

Conclusion: Our results demonstrate that inhibition of the canonical TGF β signaling using TLR-X represents a potential therapeutic approach for the treatment of NASH, by attenuating steatosis and fibrosis, with possible clinical implications.

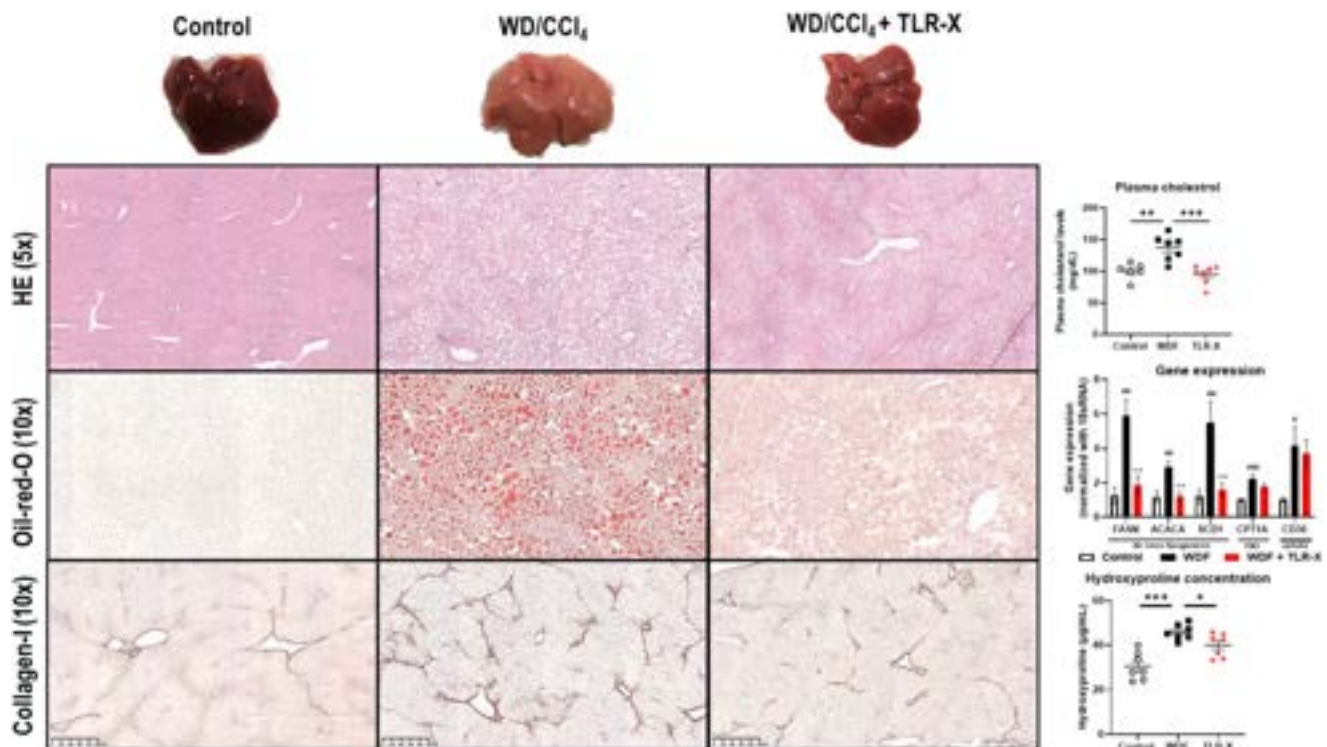


Figure: (abstract: WED-432).

WED-433

Gamma-muricholic acid inhibits steatosis-dependent peroxidative impairment to attenuates non-alcoholic steatohepatitis by activation of FXR/SHP/LXR α /FASN signaling

Yang Xie¹, Rui-Xu Yang¹, Feng Shen², Jiangao Fan¹, Qin Pan^{1,3}. ¹Xinhua Hospital Affiliated To Shanghai Jiaotong University School of Medicine, Department of Gastroenterology, Shanghai, China, ²Xinhua Hospital Affiliated To Shanghai Jiaotong University School of Medicine, Endoscopy center, Shanghai, ³Shanghai University of Medicine and Health Sciences Affiliated Zhoupu Hospital, Research center, Shanghai, China
Email: pan_qin@yeah.net

Background and aims: Non-alcoholic steatohepatitis (NASH) reflects the key step from non-alcoholic fatty liver to hepatic fibrosis/cirrhosis and hepatocellular carcinoma depending on steatosis-induced oxidative stress. γ -muricholic acid (γ -MCA) with effect of lipogenic inactivation by farnesoid X receptor (FXR) agonizing plays potential role against liver steatosis and then peroxidative impairments.

Method: Except for the normal controls, experimental NASH was established in mice by 16-week high-fat high-cholesterol (HFHC) diet, with (NASH+10 mg/kg γ -MCA, NASH+100 mg/kg γ -MCA groups) or without simultaneous γ -MCA exposure (NASH, NASH+vehicle groups). Both oil red O staining and triglyceride (TG) analysis revealed the impact of γ -MCA on hepatic steatosis. Liver concentrations of malondialdehyde (MDA) and 4-hydroxynonenal (4-HNE) exhibited steatosis-dependent lipid peroxidation. Peroxidative injury and related hepatocyte apoptosis were further investigated by transference levels and terminal deoxynucleotidyl transferase nick end labeling (TUNEL) assay, respectively. NAFLD activity score (NAS) finally exhibited the outcome of γ -MCA treatment. Mechanically, effect of γ -MCA on FXR and downstream signalling of small heterodimer partner (SHP)/liver X receptor α (LXR α)/fatty acid synthase (FASN) was investigated *in vivo* and *in vitro*.

Results: γ -MCA agonized FXR to upregulate the SHP expression of hepatocytes. An increase in SHP attenuated the TG-dominated hepatic steatosis induced *in vivo* by HFHC diet, and *in vitro* by free fatty acids, on the basis of LXR α and FASN inhibition. In contrast, FXR knockdown abrogated the γ -MCA-dependent lipogenic inactivation. When compared to their excessive production in HFHC diet-induced rodent NASH, products of lipid peroxidation (MDA, 4-HNE) exhibited significant reduction upon γ -MCA treatment. Moreover, the decreased levels of serum ALT and AST demonstrated an improvement in peroxidative injury of hepatocytes. By TUNEL assay, injurious amelioration protected the γ -MCA-treated mice against hepatic apoptosis. The abolishment of apoptosis resultantly prevented lobular inflammation, which downregulated the incidence of NASH by lowering NAS (NASH group vs NASH+100 mg/kg γ -MCA group: 5.75 ± 0.590 vs 1.375 ± 0.420 , $p < 0.05$).

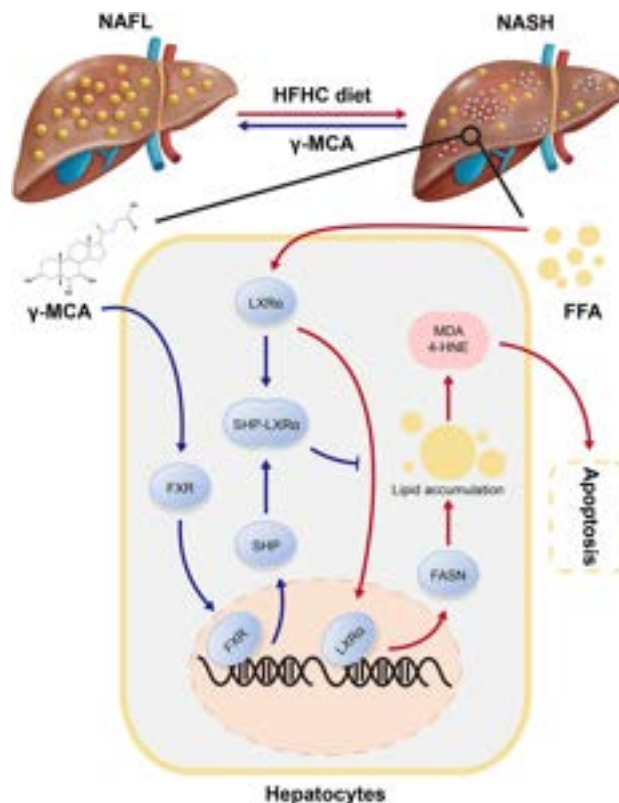


Figure:

Conclusion: γ -MCA inactivates lipogenesis to ameliorate hepatic steatosis by targeting FXR/SHP/LXR α /FASN signalling. Mitigation of steatosis-based peroxidative injury results in the NASH attenuation.

WED-434

Statins regulate PNPLA3 through a mechanism that requires SREBF2 in human liver cells

Osman Ahmed^{1,2}, Vladimir S Shavva¹, Wanmin Dai¹, Laura Tarnawski¹, Stephen Malin¹, Anders Franco-Cereceda³, Per Eriksson¹, Hanna Björck¹, Peder Olofsson¹. ¹Karolinska institutet and Karolinska University Hospital, Department of Medicine Solna, Stockholm, Sweden, ²University of Khartoum, Department of Biochemistry, Khartoum, Sudan, ³Karolinska institute and Karolinska University Hospital, Department of Molecular Medicine and Surgery, Stockholm, Sweden
Email: osman.ahmed@ki.se

Background and aims: Genetic variation within the patatin-like phospholipase domain containing 3 (PNPLA3) gene is associated with both susceptibility to NAFLD and response to statin treatment in NAFLD patients. Here, we studied the association between statin treatment and hepatic expression of PNPLA3 from liver biopsies of patients without any known liver diseases.

Method: Liver biopsies were collected from 261 patients undergoing open-heart surgery. Patients were stratified by 1) Statins versus non-statin users in all cohort 2) by presence of the metabolic syndrome among non-statin users 3) Statins versus non-statin users among patients with metabolic syndrome only. In this cohort, 81 patients were treated with statins and 144 were not while 36 patients did not fulfil the inclusion criteria. Among the 144 non statins users 26 patients fulfilled the criteria of metabolic syndrome defined by the International Diabetes Federation. Liver gene expression and genotypes data in addition to plasma proteomic and lipoprotein profile were analyzed. Using atorvastatin, we validated the data from the human liver cohorts using *in vitro* models of HepG2 and hepatic stellate cells (HSC) LX2.

Results: Among non-statin users, mRNA levels of NAFLD- and lipogenesis-associated genes (*PNPLA3*, *ACACA*, *SCD-1* and *ACLY*) were significantly different between patients that did and did not fulfill criteria for the metabolic syndrome. Moreover, patients with metabolic syndrome and on statin therapy have higher fasting glucose, insulin and HbA1c levels in plasma compared to non-statin-treated metabolic syndrome patients. In addition, the mRNA levels of *PNPLA3*, *ACACA* and *ACLY* in liver were higher in patients with metabolic syndrome and on statin therapy than in non-statin-treated metabolic syndrome patients. Exposure of HepG2 hepatocyte-like cells and LX2 stellate-like cells, respectively, to atorvastatin *in vitro* significantly increased mRNA levels of *SREBF2*, *HMGCR*, *PCSK9*, *LDLR* and *PNPLA3* when compared to vehicle-treated cells. Knock-down of *SREBF2* in HepG2 hepatocyte-like cells and LX2 hepatic stellate-like cells, respectively, abolished this effect and significantly reduced levels of these mRNAs both in cultures exposed to vehicle- and to atorvastatin.

Conclusion: Both statin treatment and the metabolic syndrome itself are associated with upregulation of lipogenesis-associated genes and *PNPLA3* mRNA levels in the human liver. *SREBF2* is essential for the regulation of *PNPLA3* by atorvastatin in hepatocyte-like cells and hepatic stellate-like cells. Our study suggests that statins exaggerate hyperglycemic features in patients that fulfilled criteria for metabolic syndrome which may be a consequence of transcriptionally induced hepatic lipogenesis.

WED-435

Deletion of mixed lineage kinase domain like pseudokinase aggravate chronic alcohol induced liver injury via increasing apoptosis

Hyo Young Lee¹, Dae Won Jun², Eileen Yoon², Huiyul Park³, Sang Bong Ahn⁴, Mimi Kim², Chul-min Lee², Bo-Kyeong Kang², Joo Hyun Sohn², Jihyun An², Hyunwoo Oh¹, Jang Han Jung⁵, Joo Hyun Oh⁴, Eun Chul Jang⁶, Young Eun Chon⁷. ¹Uijeongbu Eulji Medical Center, Eulji University College of Medicine, Korea, Rep. of South, ²Hanyang University, College of Medicine, Korea, Rep. of South, ³Myoungji Hospital, Hanyang University College of Medicine, Korea, Rep. of South, ⁴Nowon Eulji Medical Center, Eulji University School of Medicine, Korea, Rep. of South, ⁵Dongtan Sacred Heart Hospital of Hallym University Medical Center, Korea, Rep. of South, ⁶Soonchunhyang University College of medicine, Korea, Rep. of South, ⁷CHA Bundang Medical Center, Korea, Rep. of South
Email: noshin@hanyang.ac.kr

Background and aims: The mixed lineage kinase domain like pseudokinase (MLKL) is known to play a protective role in non-alcoholic fatty liver disease (NAFLD) via inhibition of necroptosis pathway. However, the role of MLKL in alcoholic liver disease (ALD) is not yet clear.

Method: C57BL/6N wild-type (WT) and MLKL-knockout (KO) mice (8–10 weeks old) were randomly divided into eight groups. To establish ALD model of different durations ethanol (EtOH) was fed to WT and MLKL KO for 10 days, 4 weeks and 8 weeks. The control group was fed with Lieber-DeCarli control diet for 8 weeks. Mortality, degree of hepatic inflammation, and steatosis were compared among the groups. Bulk mRNA transcriptome analysis was performed. Abundance of transcript and gene expressions were calculated based on read count or Transcript by Million (TPM) value.

Results: Survival rate of MLKL KO mice compared to WT was similar until 4 weeks, but the survival of MLKL KO mice significantly decreased after 8 weeks in ALD model. There was no difference in degree of inflammation, steatosis, and NAS scores between EtOH fed MLKL KO and EtOH fed WT mice at 10 days. However, at 4 weeks and 8 weeks, the degree of hepatic steatosis, NAS and inflammation were increased in MLKL KO mice. RNA transcriptome data showed that fatty acid synthesis, and lipogenesis, mitochondria, and apoptosis related pathways were upregulated in EtOH fed MLKL KO mice compared to EtOH fed WT mice. Although hepatocyte apoptosis

(BAX/BCL2 ratio, caspase-3, and TUNEL staining) increased after EtOH intake; however, apoptosis was more significantly increased in EtOH fed MLKL KO mice compared to the WT group. At the same time, hepatic cFLIP was decreased in EtOH fed MLKL KO mice compared to the WT group.

Conclusion: MLKL deletion did not prevent chronic alcohol-induced liver damage independently of necroptosis and exacerbated hepatic steatosis by increasing hepatocyte apoptosis.

WED-436

Validation and utility of artificial intelligence-based zonal annotations as an additional assessment tool for the histopathologic review of fibrosis in non-alcoholic steatohepatitis patients

Gwyneth Soon¹, Aileen Wee², Wei Qiang Leow³, Elaine Chng⁴, Dean Tai⁴, Yayun Ren⁴, Feng Liu⁵, Lai Wei⁶, Arun Sanyal⁷. ¹National University Hospital, Department of Pathology, Singapore, ²Yong Loo Lin School of Medicine, National University of Singapore, Department of Pathology, Singapore, ³Singapore General Hospital, Singapore and Duke-NUS Medical School, Department of Anatomical Pathology, Singapore, ⁴HistoIndex Pte Ltd, Singapore, ⁵Peking University Hepatology Institute, Peking University People's Hospital, China, ⁶Hepatopancreatobiliary Center, Beijing Tsinghua Changgung Hospital, China, ⁷Stravitz-Sanyal Institute of Liver Disease and Metabolic Health, VCU School of Medicine, United States

Email: gwyneth_st_soon@nuhs.edu.sg

Background and aims: Inter-observer variability for categorical scores of liver fibrosis among pathologists ranges from fair to moderate weighted kappa. Artificial intelligence (AI) and advances in digitised whole-slide imaging (WSI) have facilitated the use of AI-assistive tools in pathology to improve histopathologic interpretation. Second harmonic generation/two-photon excitation fluorescence (SHG/TPEF) microscopy with qFibrosis staging and continuous values as AI-assistive tools has been shown to help standardize pathologist assessment, contributing to higher overall intra- and inter-rater agreements. With the additional provision of AI-based zonal annotations, we aim to explore whether there will be further improvements on the overall inter-pathologist agreement on fibrosis assessment.

Method: Unstained sections of liver biopsies from 50 untreated NASH patients (F0–F4) were evaluated. Fibrosis was quantitated using SHG/TPEF microscopy (qFibrosis). Unassisted reads comprised digitized HandE and Masson trichrome-stained images uploaded to a WSI platform. Level I assisted reads included additional SHG images with qFibrosis outputs. Level II assisted reads further included zonal annotations. The zonal annotations serve to highlight the portal tract (PT), central vein (CV), peri-PT, peri-CV and perisinusoidal regions. To evaluate performance for assisted and unassisted reads, three pathologists with 5 to 40 years' experience interpreted images in 2 sessions: a) Unassisted versus Assisted level I, b) Unassisted versus Assisted level II. Each session consisted of 4 reads, starting with the unassisted read followed by sample randomization before proceeding to the assisted read. This was repeated after a 3–4-week washout period.

Results: When assisted by the level I AI tool, the concordance rate between pathologists improved to near-perfect agreement, with 0.82 linear weighted kappa, as compared to 0.72 for the unassisted review. Mean overall percentage agreement (PA) between pathologists improved from 89.38% to 92.93% ($p = 0.032$). Mean linear weighted kappa for intra-observer agreement was also higher, achieving 0.91 kappa compared to 0.79 for unassisted reads. When compared with the assistive level I tool, the concordance between pathologists with assistive level II tools showed marginal improvement from 0.82 to 0.84. The overall PA increased slightly from 92.9% to 93.8% ($p = 0.473$).

POSTER PRESENTATIONS

Zonal annotations and the impact of AI-assistive tools on intra- and inter-rater agreements.

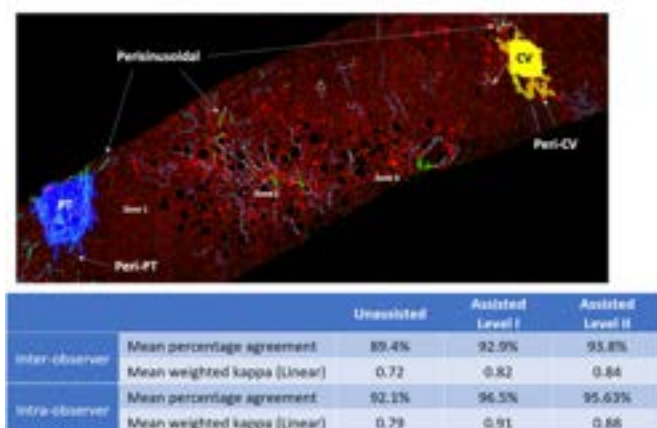


Figure:

Conclusion: qFibrosis as an AI-assistive tool can improve inter-pathologist weighted kappa to near-perfect (close to 93%) agreement. Additional AI-based zonal annotations provide negligible improvement in inter-pathologist weighted kappa.

WED-437

Anti-inflammatory and anti-fibrotic effects by simultaneous activation of glucagon, GIP, and GLP-1 of efocipegtrutide (HM15211) in thioacetamide-induced mouse model of liver injury and fibrosis

Jung Kuk Kim¹, Yohan Kim¹, Jong Suk Lee¹, Hyunjo Kwon¹, Eun Jin Park¹, Jeong A Kim¹, Sung Min Bae¹, Dae Jin Kim¹, Sang Hyun Lee¹, In Young Choi¹. ¹Hanmi Pharm.Co., Ltd., Korea, Rep. of South

Email: iychoi@hanmi.co.kr

Background and aims: Despite of increase in number of fibrosis due to NASH which becomes a major cause of liver-related outcomes, no approved drug is available. Recently, potential benefit of incretins

such as glucagon (GCG), GIP and GLP-1 beyond metabolism has been proposed especially in inflammation and fibrosis. Thus, to optimally implement these incretins, efocipegtrutide, a long-acting GCG/GIP/GLP-1 triple agonist, was developed. Here, we evaluated and compared the therapeutic effects of efocipegtrutide with available incretin drugs in TAA (thioacetamide)-induced liver injury and fibrosis mouse.

Method: TAA was intraperitoneally injected to mouse for 12 weeks to induce liver injury and fibrosis, and efocipegtrutide was administered during last 10 weeks, and semaglutide as well as tirzepatide were included as comparative controls. At end of treatment, hepatic hydroxyproline content was measured and the liver tissues were subjected to HandE and Sirius red staining followed by histological grading. qPCR and ELISA were performed to evaluate relevant hepatic and blood bio-markers.

Results: Efocipegtrutide treatment was associated with significant reduction of hepatic hydroxyproline content (231.9 nmol/g vs. 350.4 nmol/g for TAA, vehicle; $p < 0.001$) while that of semaglutide (322.5 nmol/g) or tirzepatide (322.1 nmol/g) had minor effects. Similarly, treatment of efocipegtrutide (0.83%, $p < 0.001$), significantly reduced Sirius red positive area (vs. 5.75% for TAA, vehicle), unlike neither semaglutide (4.93%) nor tirzepatide (3.61%). To further confirm the potential benefit of efocipegtrutide, histological grading was conducted by using Sirius red and HandE staining, in which efocipegtrutide (1.29, 1.00 vs. 3.00, 3.00 for TAA, vehicle) exhibited greater reduction effects on both fibrosis and portal inflammation score compared to semaglutide (2.14, 2.71) or tirzepatide (2.00, 2.57). Consistent with such histologic analysis, expression of hepatic marker genes for fibrosis and inflammation were significantly/numerically reduced only in efocipegtrutide group. Significant reduction in blood TIMP-1 level was also observed.

Conclusion: Efocipegtrutide effectively improved liver inflammation and fibrosis in TAA mice. Notably, greater improvement effect over semaglutide and tirzepatide highlights the potential benefit of simultaneous use of GCG, GIP, and GLP-1. Thus, efocipegtrutide could be a novel therapeutic option for fibrosis due to NASH. Human study is ongoing to assess the clinical relevance of these findings.

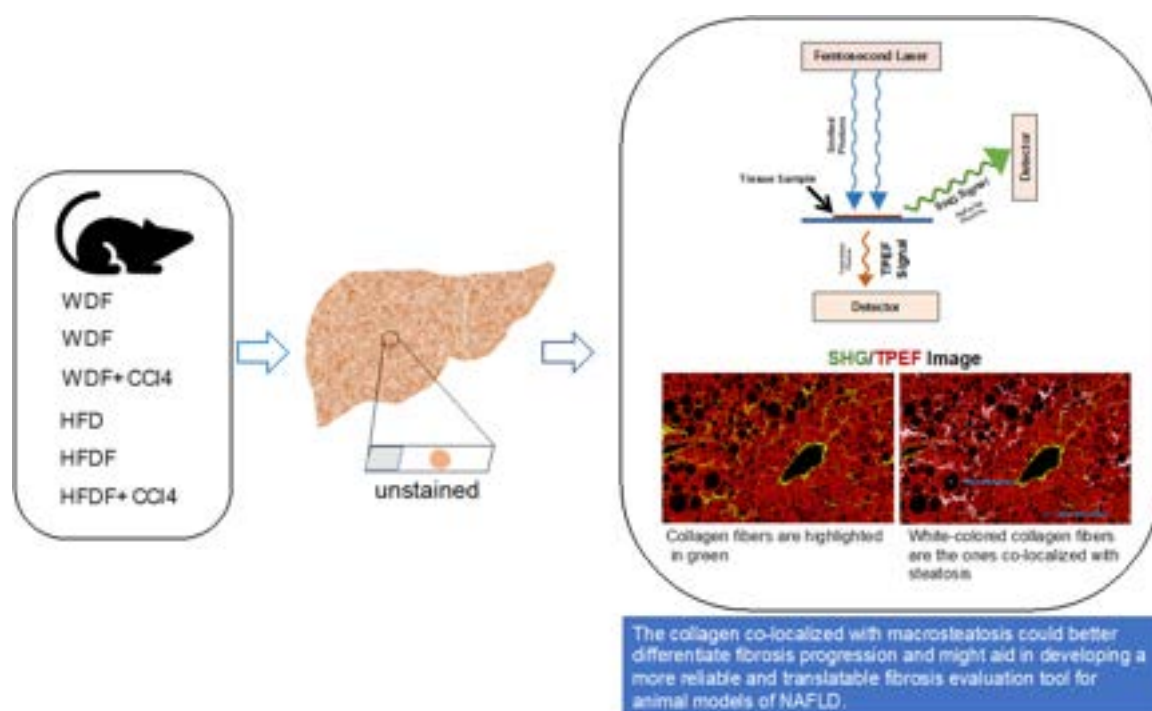


Figure: (abstract: WED-438).

WED-438

Collagen co-localized with macrovesicular steatosis better differentiates fibrosis progression in non-alcoholic fatty liver disease mouse models

XiaoXiao Wang¹, Rui Jin¹, Xiaohe Li¹, Qiang Yang², Xiao Teng³, Fangfang Liu⁴, Nan Wu¹, Huiying Rao¹, Feng Liu¹. ¹Peking University People's Hospital, Peking University Hepatology Institute, Beijing Key Laboratory of Hepatitis C and Immunotherapy for Liver Diseases, Beijing International Cooperation Base for Science and Technology on NAFLD Diagnosis, Beijing, China, ²Hangzhou Choutu Technology Co, China, ³HistoIndex Pte Ltd, Singapore, ⁴Peking University People's Hospital, China
Email: liu1116m@sina.com

Background and aims: Non-alcoholic fatty liver disease (NAFLD) is a global commonly occurring liver disease. However, its exact pathogenesis is not fully understood. The purpose of this study was to quantitatively evaluate the progression of steatosis and fibrosis by examining their distribution, morphology, and co-localization in NAFLD animal models.

Method: Six mouse NAFLD groups were established: (1) western diet (WD) group; (2) WD with fructose in drinking water (WDF) group; (3) WDF + carbon tetrachloride (CCl₄) group, WDF plus intraperitoneal injection of CCl₄; (4) high-fat diet (HFD) group, (5) HFD with fructose (HFDF) group; and (6) HFDF + CCl₄ group, HFDF plus intraperitoneal injection of CCl₄. Liver tissue specimens from NAFLD model mice were collected at different time points. All the tissues were serially sectioned for histological staining and Second-harmonic generation (SHG)/two-photon excitation fluorescence imaging

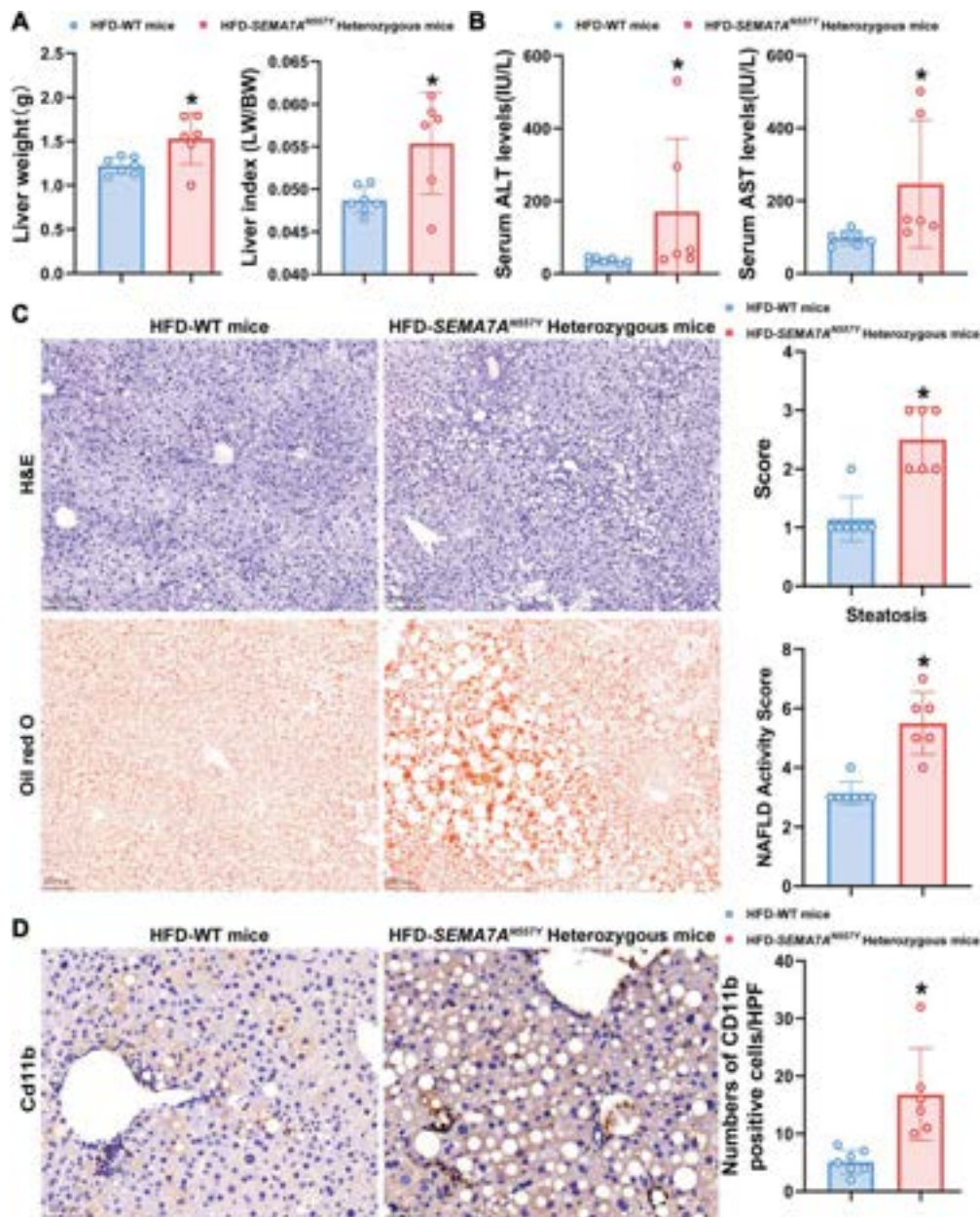


Figure: (abstract: WED-439) The *Sema7a*^{N557Y} heterozygous mutation aggravates liver injury, steatosis and inflammation in NAFLD induced by high-fat diet in mice. Liver weights and the liver/body weight ratios. HFD-WT (n = 7), HFD-*Sema7a*^{N557Y} (n = 6). (B) Serum ALT and AST levels. (C) HandE and oil red O-stained liver histology. Scale bar, 100 μ m. NAFLD activity score is shown. (D) Representative images of IHC staining of Cd11b and their quantitative assessments of randomly selected microscopic fields. Scale bar, 50 μ m. Data are presented as mean \pm SD. **p* < 0.05 versus the HFD-WT mice. The data were analyzed with Student's t test.

POSTER PRESENTATIONS

(TPEF) imaging. The progression of steatosis and fibrosis was analyzed using SHG/TPEF quantitative parameters with respect to the NASH CRN scoring system.

Results: qSteatosis showed a good correlation with steatosis grade (R: 0.823–0.953, $P < 0.05$) and demonstrated high performance (AUC: 0.617–1) in six mouse models. Based on their high correlation with histological scoring, qFibrosis containing four shared parameters (#LongStrPS, #ThinStrPS, #ThinStrPSAgg, and #LongStrPSDis) were selected to create a linear model that could accurately identify differences among fibrosis stages (AUC: 0.725–1). qFibrosis co-localized with macrosteatosis generally correlated better with histological scoring and had a higher AUC in six animal models (AUC: 0.846–1).

Conclusion: Quantitative assessment using SHG/TPEF technology can be used to monitor different types of steatosis and fibrosis progression in NAFLD models. The collagen co-localized with macrosteatosis could better differentiate fibrosis progression and might aid in developing a more reliable and translatable fibrosis evaluation tool for animal models of NAFLD.

WED-439

A heterozygous N559Y mutation in Semaphorin 7A promotes non-alcoholic fatty liver disease progression through induction of hepatic ROS production and inflammation

Yao Tong¹, Xiaoxun Zhang¹, Nan Zhao¹, Jin Chai¹. ¹*the First Affiliated Hospital (Southwest Hospital) of Third Military Medical University (Army Medical University), China*
Email: jin.chai@cldcsw.org

Background and aims: Non-alcoholic fatty liver disease (NAFLD) is a serious liver disease of worldwide concern, which can lead to cirrhosis and hepatocellular cancer. Notably, genetic factors play an important role in the pathogenesis of NAFLD. Semaphorin 7A (SEMA7A), as a membrane-bound protein, contributes to axon growth, T cell activation, and other biological processes. In this study, we examined mechanism of SEMA7A^{N559Y} heterozygous mutation aggravating non-alcoholic fatty liver disease.

Method: We generated *Sema7a*^{N559Y} (equal to human SEMA7A^{N559Y}) heterozygous mutated mice to investigate the role of SEMA7A^{N559Y} mutation in the progression of NAFLD. 8-week-old wild type mice and *Sema7a*^{N559Y} heterozygous mutated mice were fed with high-fat diet (HFD) for 8 weeks. All mice were sacrificed and their serum and liver tissue were collected and analyzed. HandE staining, Oil Red O staining, and immunohistochemistry (IHC) of Cd11b protein were performed to evaluate liver steatosis and inflammation. Western blot analysis was used to measure the expression of lipid metabolism and cell pyroptosis-related proteins. NOX, CAT, and MDA content were measured as oxidative stress markers in liver tissue. Expression of Il-1 β , Il-18, Il-6, Tnf- α , Ccl2 and Cd11b was determined in total liver by real-time qPCR.

Results: In our previous study, SEMA7A^{N559Y} heterozygous mutation was identified in NAFLD patients. HFD-*Sema7a*^{N559Y} mice had higher liver weight, liver index, serum ALT and AST levels than that of HFD-WT mice. Liver histologic analyses revealed that the *Sema7a*^{N559Y} variant markedly increased liver steatosis and inflammation. Further studies indicated that *Sema7a*^{N559Y} mutation can significantly increased the proteins expression of lipid metabolism and ROS levels by enhancing PI3 K/AKT signaling. In addition, *Sema7a*^{N559Y}

mutation markedly activate the ROS/NLRP3 pathway and cause liver inflammatory response.

Conclusion: In conclusion, our research demonstrates that SEMA7A^{N559Y} heterozygous variant may be a new genetic determinant of NAFLD and promotes liver injury by inducing hepatocytes pyroptosis and liver inflammation.

WED-440

Endothelial and platelet-derived microvesicles as a biomarker of cardiovascular risk in patients with metabolic dysfunction-associated fatty liver disease (MAFLD)

Sheila Gato Zambrano¹, Rocio Munoz Hernandez¹, Rocio Montero-Vallejo¹, María del Carmen Rico¹, Vanessa García Fernández¹, Angela Rojas Alvarez-Ossorio¹, Antonio Gil-Gomez¹, Javier Gallego¹, Rocio Gallego-Durán¹, Douglas Maya Miles¹, Javier Ampuero¹, Manuel Romero Gomez¹.
¹*Servicio de Aparato Digestivo, Hospital Universitario Virgen del Rocío; SeLiver Group, Instituto de Biomedicina de Sevilla (HUVR/CSIC/US), Departamento de Medicina Universidad de Sevilla; CIBEREHD, Sevilla, Spain*
Email: mromerogomez@us.es

Background and aims: MAFLD is associated with cardiovascular risk (CVR), but it is not clear if it contributes independently to the development of this disease. Early detection of endothelial dysfunction and CVR reduces premature morbidity and mortality. Endothelial dysfunction is associated with increased plasma levels of endothelial (EMVs) and platelet-derived microvesicles (PMVs). The objective of the study was to evaluate the levels of EMVs and PMVs in MAFLD patients and their relationship with CVR.

Method: 97 MAFLD biopsy-proven patients were included and classified according to the SAF-score as steatosis (SS) or steatohepatitis (NASH). We assessed the presence of subclinical atherosclerosis using the ankle-brachial index (ABI) and the atherosclerotic cardiovascular disease risk index (ASCVD). We quantified PMVs (AV+CD31+CD41+), EMVs (AV+CD31+CD41+) and activated EMVs (AV+CD62e+) in heparin-plasma samples by flow cytometry.

Results: Baseline patients characteristics are represented in Table 1. We did not observe differences in the proportion of patients with pathological ABI and ASCVD between the different MAFLD groups. In contrast, PMVs (AV+CD41+) are increased in patients with NASH vs. SS ($p = 0.02$) (Fig 1a), although platelet levels are similar. In addition, patients with lobular inflammation present higher levels of PMVs (AV+CD31+CD41+) compare to those without inflammation ($p = 0.029$, Fig1b); on the other hand, there were no differences according to the degree of ballooning. Moreover, levels of activated EMVs (AV+CD62e+) are increased in MAFLD and hypertension (AHT) patients vs. those without AHT ($p = 0.037$) (Fig 1c), in the same way, are increased in patients with ASCVD $> 10\%$ ($n = 16$) vs. those with ACSVP $< 10\%$ ($n = 17$) (365.7 ± 104.3 vs. 649.7 ± 158.6 ; $p = 0.045$). Finally, according to the severity of liver disease and the presence of atherosclerosis (depending on ABI and ASCVD), we did not observe differences in the levels of EMVs or PMVs.

Conclusion: PMVs levels are associated with disease and lobular inflammation, suggesting the presence of endothelial damage. Activated EMVs increase in patients with hypertension, suggesting that the impact of MAFLD on endothelial activation and, therefore, on vascular structure, may depend on the coexistence of other CVR factors such as hypertension.

Table 1. Biochemical and anthropometric characteristics of patients. Quantitative data are expressed as $\bar{x} \pm SD$. Qualitative data are expressed as n, %.

	SS (n=23)	NASH (n=74)	p value
Age (years)	50.04 \pm 13.22	58.28 \pm 10.28	0.002
Sex (n, % male)	16 (69.6%)	34 (45.9%)	ns
BMI (kg/m ²)	31.48 \pm 5.14	34.78 \pm 7.21	0.04
AHT (n, %)	9 (39.1%)	54 (73%)	0.005
T2DM (n, %)	11 (47.8%)	42 (57.5%)	ns
Hypercholesterolemia (n, %)	12 (52.2%)	36 (48.6%)	ns
Hypertriglyceridemia (n, %)	8 (34.8%)	32 (43.2%)	ns
AST (UI/L)	31.61 \pm 14.53	53.73 \pm 34.07	<0.001
ALT (UI/L)	38.91 \pm 20.92	63.18 \pm 44	0.012
GGT (UI/L)	63.7 \pm 55.34	109.07 \pm 126.7	ns
Platelets (10 ⁹ /L)	208.13 \pm 64.31	217.29 \pm 63.4	ns
Bilirubin (mg/dL)	0.87 \pm 1.13	0.55 \pm 0.33	ns
HOMA-IR	3.52 \pm 1.85	6.77 \pm 4.85	<0.001
TC (mg/dL)	179.43 \pm 52.17	187.59 \pm 41.37	ns
LDL (mg/dL)	105.63 \pm 41.64	107.38 \pm 37.75	ns
HDL (mg/dL)	45.39 \pm 17.42	47.68 \pm 12.79	ns
Fibrosis (grado)	1.04 \pm 1.26	1.8 \pm 1.38	0.021
Cirrhosis (n, %)	1 (4.3%)	7 (9.5%)	ns
Pathological ABI (n, %)	8 (42.1%)	24 (35.8%)	ns
ASCVD>10% (n, %)	8 (66.7%)	35 (63.6%)	ns

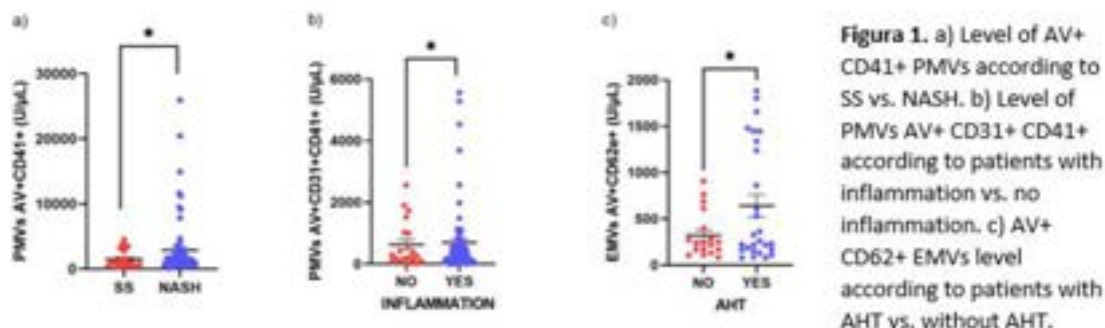


Figure: (abstract: WED-440)

WED-441

A novel orally available type IV autotaxin inhibitor, IOA-289, ameliorates steatosis and fibrosis in a preclinical model of non-alcoholic steatohepatitis

Marit ten Hove¹, Giusy Di Conza², Karolina Niewola², Marcel Deken², Lars van der Veen², Ruchi Bansal¹. ¹University of Twente, Netherlands, ²iOnctura SA, Genève, Switzerland
Email: m.m.tenhove@utwente.nl

Background and aims: Non-alcoholic steatohepatitis (NASH) represents a major health burden worldwide with no FDA-approved therapies available. Lysophosphatidic acid (LPA), produced by autotaxin (ATX), is correlated with the progression of NASH, and regulates lipid homeostasis, and induces liver inflammation and fibrosis. Hepatic ATX knockdown in a high-fat diet mouse model showed protection against NASH by decreasing hepatic steatosis, inflammation, and fibrosis. Recently, we have shown that inhibiting ATX using a type-IV inhibitor (that occupy the tunnel and the pocket of ATX) possess better potential in ameliorating NASH than a type-I inhibitor (that targets the catalytic site and the pocket of ATX). In this study, we aim to further investigate the therapeutic effects of a novel and orally available type IV ATX inhibitor, IOA-289, for the treatment of NASH.

Method: First, we examined the expression of ATX and LPA receptors in different liver pathologies. Thereafter, we tested the efficacy of IOA-289 in vitro employing disease-specific stimulated hepatic cell types

to recapitulate different processes of NASH. Based on promising in vitro results, we investigated the effects of orally administered IOA-289 in a NASH mouse model. C57BL/6J mice were fed western-diet (WD) containing 21.1% fat, 41% sucrose and 1.25% cholesterol supplemented with high sugar solution (23.1 g/L d-fructose and 18.9 g/L d-glucose), combined with increasing low weekly doses (0.05–0.2 ml/kg) of carbon tetrachloride (CCl₄) for 12 weeks. In the last six weeks, IOA-289 (30 mg/kg) or PF-8380 (a type-I ATX inhibitor, 30 mg/kg) was orally administered twice daily. Blood, liver, and different organs were collected for subsequent analysis.

Results: In our NASH mouse model, Oil-red-O staining showed a significant decrease in intrahepatic fat accumulation in IOA-289-treated mice (n = 7) and PF-8380-treated mice (n = 7) compared to vehicle-treated mice (n = 7). Additionally, the expression of genes involved in de novo synthesis of fatty acids (FASN, SCD1 and ACACA) were significantly decreased in the ATX inhibitor-treated groups compared to the vehicle-treated group. We further assessed the effect of both ATX inhibitors on fibrosis and observed that total hydroxyproline content, collagen-I immunostaining and profibrotic gene expression (TGFB1, PDGFRB and ACTA2) were significantly attenuated only in the IOA-289 treated group, but not in the PF-8380 treated group, compared to the vehicle group. Overall, these results indicate the amelioration of hepatic steatosis and fibrosis by IOA-289.

Conclusion: Our results demonstrate that inhibition of the LPA-ATX pathway, particularly using a type IV inhibitor, represents a potential

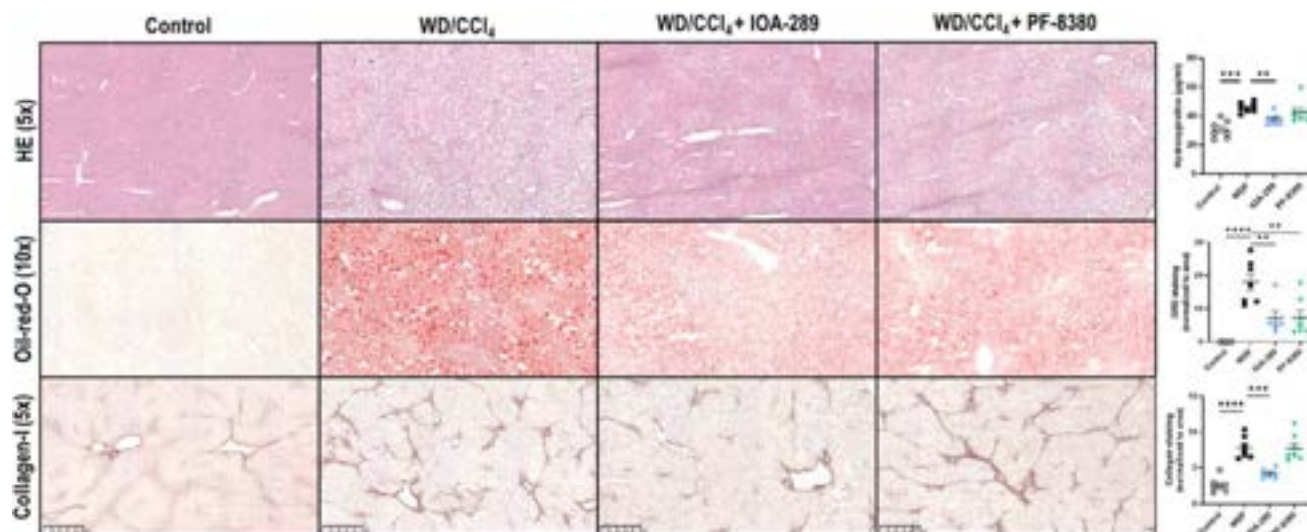


Figure: (abstract: WED-441).

therapeutic target in NASH, by attenuating steatosis and fibrosis, with possible clinical implications.

WED-442

Cannabidiolic acid (CBDA) regulates energy homeostasis and protects against non-alcoholic fatty liver disease (NAFLD) in mice

Albert Giral¹, Battsetseg Batchuluun^{2,3}, Robin Willows¹, Steve Lassueur¹, Christian Chabert¹, Dongdong Wang^{2,3}, Emily Day^{2,3}, Marisa Morrow^{2,3}, Evelyn Tsakiridis^{2,3}, Russta Fayazi^{2,3}, Sonia Rehal^{2,3}, James Lally^{2,3}, Eris Desjardins^{2,3}, Jaya Gautam^{2,3}, Carles Canto¹, Olivier Ciclet¹, Martine Naranjo Pinta¹, Denis Barron¹, Philippe Delerive⁴, Gregory Steinberg^{2,3,5}, Marine Kraus¹, Matthew Sanders¹. ¹Nestlé Institute of Health Sciences, Nestlé Research, Société des Produits Nestlé S.A., Lausanne, Switzerland, ²Centre for Metabolism, Obesity and Diabetes Research, McMaster University, Hamilton, Canada, ³Division of Endocrinology and Metabolism, Department of Medicine, McMaster University, Hamilton, Canada, ⁴Nestlé Health Sciences, Société des Produits Nestlé S.A., Switzerland, ⁵Department of Biochemistry and Biomedical Sciences, McMaster University, Hamilton, Canada
Email: albert.giral¹@rd.nestle.com

Background and aims: There has been growing interest in the potential health benefits of cannabinoids found in Cannabis Sativa for several years, however, their therapeutic potential for non-alcoholic fatty liver disease (NAFLD) remains largely unexplored. The aim of this study was to evaluate whether the main cannabinoid found in Cannabis Sativa, cannabidiolic acid (CBDA), could improve NAFLD in a mouse model.

Method: We examined the effect of CBDA on de novo lipogenesis (DNL) in mouse primary hepatocytes and in mice after a 4-day treatment with CBDA (10 mg/kg or 30 mg/kg, oral gavage). NAFLD was induced in C57BL/6J male mice by placing them at thermoneutrality (29°C) and feeding them a NASH diet (40% fat, 20% fructose, 0.02% cholesterol) for 16 weeks. After the onset of obesity and NAFLD, mice were treated daily with either CBDA (10 mg/kg or 30 mg/kg, oral gavage) or a vehicle for an additional 9 weeks. Insulin tolerance and glucose tolerance tests were performed at week 7 and 8 after the beginning of treatment, respectively. The impact of CBDA on liver triglycerides and lipid droplet area were quantified. NASH status was assessed by a blinded pathologist (NAFLD activity score) and liver fibrosis was quantified by picro-Sirius red staining area. Liver gene expression was assessed by RNA-seq. Primary human hepatic stellate cells (hHSC) were pre-treated with CBDA (1 h) and stimulated with TGFβ (48 h) and alpha-SMA1 levels and pro-collagen secretion in the

media were measured. The effects of CBDA on cellular respiration in cells were evaluated using the Seahorse analyzer (Agilent) and the effects of CBDA on mitochondrial respiration in isolated mouse liver mitochondria were evaluated using the Oroboros (Oroboros Instruments).

Results: CBDA inhibited hepatic DNL in mouse primary hepatocytes and in vivo. CBDA treatment in a NAFLD mouse model successfully improved glucose tolerance and insulin sensitivity without significant changes in body weight. CBDA stimulated whole-body fat oxidation and significantly reduced hepatic steatosis. CBDA promoted NASH resolution and significantly decreased liver fibrosis. Liver gene expression analyses revealed a stimulation of pathways linked to lipid oxidation and a decrease in pathways associated with inflammation and fibrosis in response to CBDA treatment. In agreement, CBDA blunted TGFβ-induced activation of primary human HSCs and procollagen secretion, which was associated with DNL inhibition. Mechanistically, CBDA activates AMP-activated protein kinase (AMPK) in vitro and acutely stimulates cellular and mitochondrial respiration. These effects extended to several cannabinoid acid derivatives and were not observed in their respective neutral derivatives (e.g., cannabidiol, CBD).

Conclusion: This study demonstrates that CBDA inhibits hepatic DNL and improves several features of NAFLD, concomitantly with an improvement in glucose tolerance and insulin sensitivity. Additionally, for the first time, we show that CBDA and other cannabinoid acids increase mitochondrial respiration. These data provide evidence for a novel mechanism of action for the cannabinoid acids that could be exploited for the treatment of NAFLD and other metabolic diseases.

WED-443

Quantification of vessel and bile duct parameters using Second Harmonic Generation in patients with NAFLD across fibrosis stages

Jörn Schattenberg¹, Yayun Ren², Dean Tai², Elaine Chng², Maurice Michel³, Christian Labenz³, Beate Straub⁴. ¹Metabolic Liver Research Center, University Medical Center of the Johannes Gutenberg-University, Germany, ²HistoIndex Pte Ltd, Singapore, ³University Medical Center of the Johannes Gutenberg-University, Department of Medicine, Germany, ⁴University Medical Center of the Johannes Gutenberg-University, Department of Pathology, Germany
Email: joern.schattenberg¹@unimedizin-mainz.de

Background and aims: Liver histology defines the pathophysiological alterations occurring in patients with NAFLD while they

POSTER PRESENTATIONS

single agents or in combination in biopsy-confirmed GAN DIO-NASH mice (n=16/group) for 12 weeks. Histological analyses were performed at baseline and end of treatment to assess steatosis, inflammation, and fibrosis on stained biopsies. Liver biopsies were also assessed by stain-free artificial intelligence (AI)-based digital pathology (HistoIndex®) using second harmonic generation and two photon emission.

Results: The NAFLD Activity Score (NAS) was improved to a greater extent by combination treatment with 19%, 25%, and 43% of mice showing ≥ 2 -pt NAS improvement from baseline in the Low, Med, and High combination arms, respectively. Quantitative liver histomorphometry on stained biopsies showed the combination treatment had greater anti-steatotic activity, including reduced liver lipids, fewer hepatocytes containing lipid droplets, and reduced lipid droplet size. Analyses by HistoIndex indicated that the combination treatment significantly lowered fibrosis colocalized with macrosteatotic vesicles and reduced the progression of fibrosis colocalized with microsteatotic vesicles. The perisinusoidal area showed significant reduction of fibrosis in the Med and High combination arms.

Conclusion: Treatment with the THR-beta agonist TERN-501 in combination with the FXR agonist TERN-101 led to greater NAS and fibrosis improvements from baseline compared with single agent treatments, likely driven by increased anti-steatotic activity. These data suggest that combining the robust anti-steatotic effects of a selective THR-beta agonist with an FXR agonist may provide a superior therapeutic benefit for NASH over either agent alone. The use of AI-digital pathology can provide granularity in NASH drug development during the preclinical phase, which may be translated to current use in NASH clinical trials.

WED-446

Unravelling the role of iron-catalysed ferroptotic cell death in non-alcoholic steatohepatitis

Cédric Peleman^{1,2}, Ine Koeken³, Geraldine Veeckmans³, Astrid Van den Branden³, Emily Van San^{3,4,5}, Behrouz Hassannia^{3,4,5}, Luc Van Nassauw⁶, Els Goeman⁶, Ann Driessen^{7,8}, Lieve Vits¹, Annelies Van Eyck^{1,9}, Wilhelmus Kwanten^{1,2}, Luisa Vonghia^{1,2}, Joris De Man¹, Benedicte De Winter^{1,2}, Christophe Van Steenkiste^{1,2}, Tom Vanden Berghe^{3,4,5}, Sven Francque^{1,2}. ¹University of Antwerp, Laboratory of Experimental Medicine and Pediatrics, Infla-Med Centre of Excellence, Belgium, ²Antwerp University Hospital, Department of Gastroenterology and Hepatology, Belgium, ³University of Antwerp, Laboratory of Pathophysiology, Belgium, ⁴Ghent University, Department of Biomedical Molecular Biology, Belgium, ⁵VIB-UGent Center for Inflammation Research, Belgium, ⁶University of Antwerp, Department of ASTARC, Faculty of Medicine and Health Sciences, Belgium, ⁷Antwerp University Hospital, Department of Pathology, Belgium, ⁸University of Antwerp, Centre for Oncological Research, Belgium, ⁹Antwerp University Hospital, Department of Pediatrics, Belgium
Email: cedric.peleman@uantwerpen.be

Background and aims: Hepatocyte cell damage and cell death are hallmarks of non-alcoholic steatohepatitis (NASH). Cell death inhibition might constitute a therapeutic option for NASH, but the dominant subtype of hepatocyte cell death in NASH remains to be elucidated. Accumulating evidence points towards ferroptosis as an important driver in NASH pathogenesis. Ferroptosis is a type of regulated necrotic cell death executed by iron-catalysed peroxidation of polyunsaturated fatty acids (PUFA) in membrane phospholipids. In the present study we examined the determinants of increased ferroptosis sensitivity of hepatocytes *in vitro* and the effects of ferroptosis inhibition on NASH *in vivo* in a murine dietary model.

Method: *In vitro*, we studied the sensitivity of HepG2 cell line to undergo ferroptosis after exposure to a NASH environment, i.e. oleic and palmitic acid (non-PUFA), hyperglycemia, hyperinsulinemia and cytokines. Finally, lipidomics assessed membrane phospholipid composition of HepG2 cells to elucidate determinants of ferroptosis sensitivity. *In vivo*, in C57BL/6J mice fed the choline-deficient L-

amino acid defined high-fat diet (CDAHFD) for 4 weeks, the ferroptosis markers malondialdehyde (MDA) and 4-hydroxynonenal (4HNE) were assessed. The effect of ferroptosis inhibition by the third-generation ferrostatin analogue UAMC-3203 was tested in mice fed CDAHFD or standard diet (SD) on serum liver enzymes, hepatomegaly, liver fat and histology.

Results: *In vitro*, steatotic HepG2 cells displayed higher sensitivity towards ferroptosis inducer ML162, as evidenced by lower EC50 values for cell death with Sytox Green assay. Mechanistically, excess non-PUFA fatty acids increased PUFA incorporation in membrane phosphatidylglycerol in HepG2 cells, making them more vulnerable towards ferroptosis. *In vivo*, murine livers displayed NASH with increased hepatic MDA levels and panlobularly increased 4HNE staining on immunohistochemistry, compared to controls displaying normal liver histology. Simultaneous (preventive) treatment with UAMC-3203 for 4 weeks reduced hepatic MDA ($p < 0.01$ treatment effect, Fig 1A), hepatomegaly ($p < 0.001$, Fig 1B) and alanine transaminase levels ($p < 0.01$, Fig 1C) in CDAHFD, compared to vehicle. Likewise, therapeutic administration of UAMC-3203 during the last 2 out of 4 weeks of diet reduced MDA ($p < 0.05$) and alanine transaminase levels ($p < 0.01$), while attenuating macrovesicular steatosis and immune cell infiltration, compared to vehicle.

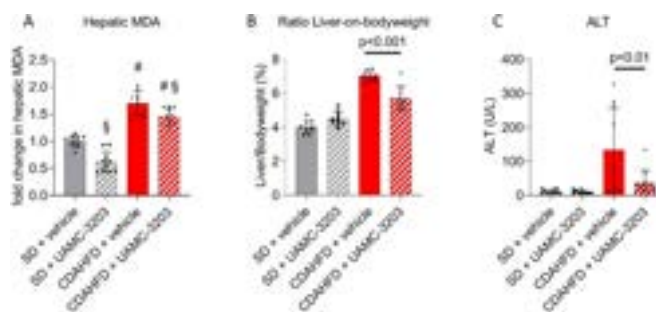


Figure:

Conclusion: Ferroptotic cell death is present in murine NASH livers, while its inhibition reduces systemic liver enzymes and attenuates hepatic lipid accumulation and immune cell infiltration. Mechanistically, non-PUFA fatty acids increased the vulnerability of hepatocytes to ferroptosis. Our findings imply that ferroptosis is a detrimental factor in NASH and thus may constitute a new therapeutic target.

WED-447

Antagonism of C-C motif chemokine receptor 2 (CCR2) using a novel *in silico* designed peptide attenuates macrophage infiltration and non-alcoholic steatohepatitis *in vivo*

Eline Geervliet^{1,2}, Ralf Weiskirchen², Ruchi Bansal¹. ¹University of Twente, Medical cell biophysics, Enschede, Netherlands, ²RWTH Aachen, Institute of Molecular Pathobiochemistry, Experimental Gene Therapy and Clinical Chemistry, Aachen, Germany
Email: ekgeervliet@gmail.com

Background and aims: Non-alcoholic steatohepatitis (NASH) represents a major health burden worldwide. Upon injury, C-C motif chemokine ligand 2 (CCL2) secreted by hepatocytes, hepatic stellate cells, and Kupffer cells trigger the recruitment of C-C motif chemokine receptor 2 (CCR2) expressing circulating monocytes that significantly contribute to the macrophage compartment of the liver and liver inflammation that further progresses to liver fibrosis, cirrhosis and/or hepatocellular carcinoma. CCR2 antagonism by Cenicriviroc (CVC), a small molecule CCR2/CCR5 dual inhibitor, showed reduction in macrophage/monocyte recruitment *in vitro* and *in vivo* in acute and chronic mouse models. Despite promising results in the phase 2b (Centaur) trial, CVC failed in phase 3 (Aurora) trial due to the lack of efficacy possibly because of poor pharmacokinetic profile and lack of specificity. Using *in silico* modelling

approach, we have designed an antagonizing peptide against CCR2 to inhibit monocyte recruitment and liver inflammation. Our previous data has shown that AP2 significantly attenuated CCL2-induced macrophage/monocyte infiltration *in vitro* and *in vivo* in an acute carbon tetrachloride (CCl₄)-induced liver injury mouse model. Here, in this study, we investigate the effects of AP2 in a chronic NASH mouse model.

Method: We established a NASH mouse model by feeding mice with western diet (21.1% fat, 41% sucrose and 1.25% cholesterol) supplemented with high sugar solution (23.1 g/L d-fructose and 18.9 g/L d-glucose), combined with low weekly doses of CCl₄ for 12 weeks. After 8 weeks, mice were treated intraperitoneally with 1 µmol/kg AP2 or CVC (2x per day) for 4 weeks. To assess intrahepatic monocyte infiltration *in vivo*, liver tissues were mechanically dissociated using Tissue Grinder, and cell population characterized by CD11b and F4/80 expression levels were analyzed using flow cytometry. Effects of AP2 and CVC on disease pathogenesis (steatosis, inflammation and fibrosis) were assessed using immunohistochemistry, RNA-sequencing, and plasma analysis.

Results: Flow cytometric analysis revealed a decrease in intrahepatic monocytes-derived macrophages in AP2 and CVC treated mice. Immunohistochemical analysis evidenced decreased steatosis (oil-red-O), inflammation (F4/80) and fibrosis (Collagen-I) in AP2 (and CVC) treated mice. AP2 and CVC treatment significantly inhibited the total plasma levels of AST, ALT, cholesterol and triglycerides. RNA sequencing analysis showed an improved NASH specific gene expression profiles in AP2 and CVC treated animals. CVC-treated mice showed reduced body weight on treatment and higher mortality compared with AP2.

Conclusion: Our CCR2 antagonizing peptide successfully inhibited intrahepatic monocyte/macrophage infiltration and ameliorated liver disease progression *in vivo*, in a chronic NASH mouse model.

WED-448

Longitudinal ultrasound imaging assessment of murine liver fibrosis in a high fat, fructose, cholesterol (FFC) model and its response to therapy

Heather Holmes¹, Caroline Sussman¹, Qianqian Guo¹, Juan Rojas², Ryan Gessner², Tomasz Czernuszewicz², Matthew Urban¹, Samar Ibrahim¹, Michael Romero¹. ¹Mayo Clinic College of Medicine and Science, United States, ²PerkinElmer, Inc., United States
Email: ryan.gessner@perkinelmer.com

Background and aims: Ultrasound and shear wave elastography (SWE) can be used to non-invasively monitor liver disease phenotypes, such as steatosis and fibrosis, and are clinically widespread. These imaging technologies have recently been adapted for small animal use in a robotic *in vivo* imaging system capable of automated scanning (Vega®, PerkinElmer). Our goal was to evaluate the feasibility of using this device to monitor response to therapy in the high fat, fructose, and cholesterol (FFC) model, a highly translatable preclinical model of obesity and metabolic disease. Non-invasive imaging of FFC mice is of particular interest (as opposed to invasive/terminal studies) due to intra-group phenotypic variability, extended time required to instantiate the model, and associated costs for these mice. This work represents a feasibility study aimed to use a robotic ultrasound scanner to monitor a cohort of mice over time developing diet-induced fibrosis of the liver, and then attempt to detect differences between un-treated and treated mice responding to a therapy.

Method: Two-month-old male C57Bl6 mice (N = 22) were used for this study and imaged at 32 weeks. Mice were split into four groups: (a) standard chow without treatment, (b) standard chow with treatment, (c) FFC diet without treatment, and (d) FFC diet with treatment. N = 8 mice were placed on standard chow, and N = 14 were

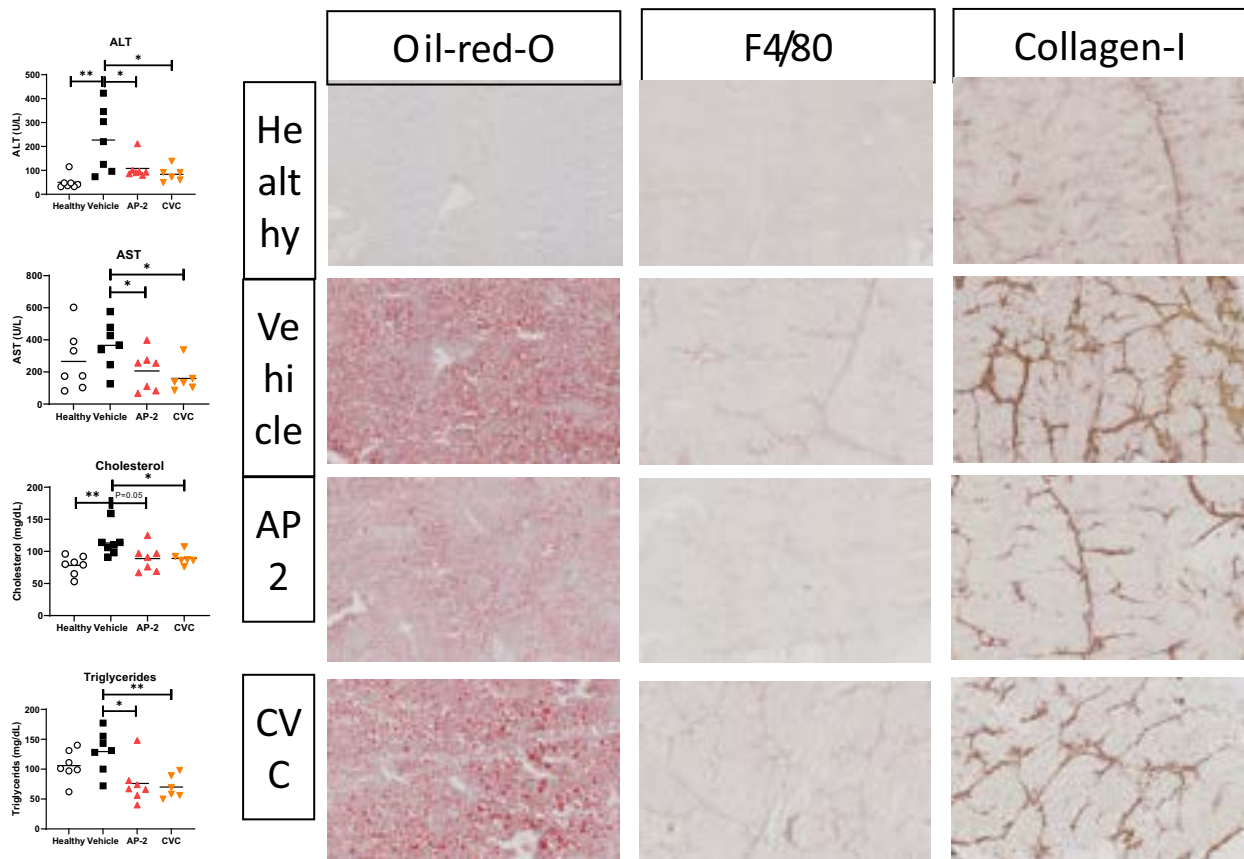


Figure: (abstract: WED-447).

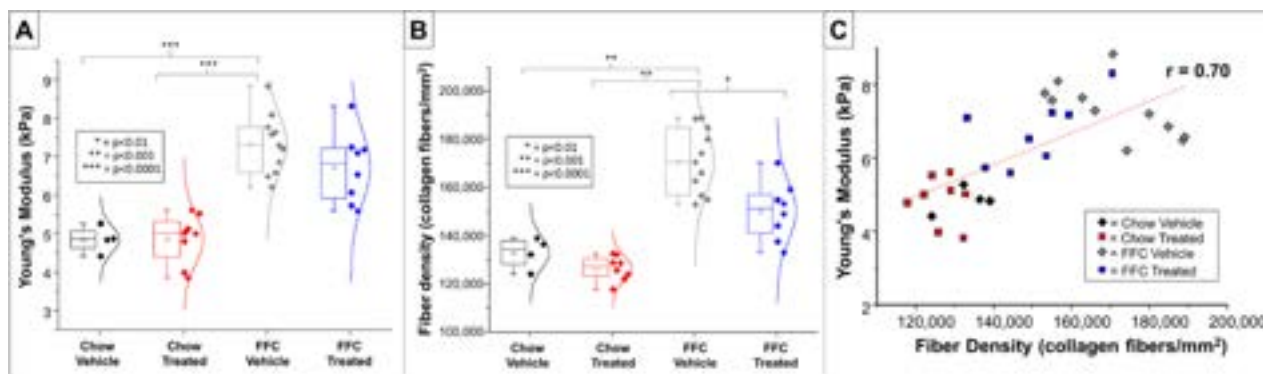


Figure: (abstract: WED-448) **A:** Non-invasive *in vivo* ultrasound SWE measures of tissue stiffness as a biomarker of liver fibrosis. **B:** *Ex vivo* validation of collagen fiber density after final timepoint via CT-FIRE. **C:** Correlation between *in vivo* ultrasound and *ex vivo* CT-FIRE measures of liver fibrosis pooled across all groups. Pearson's *r* correlation was 0.7 between the *in vivo* and *ex vivo* measurement approaches.

placed on FFC diet (AIN-76A, TestDiet, St Louis, MO); both diet groups were split evenly between treated and untreated. The treatment was delivered intraperitoneally at 10 mg/kg body weight/dose, 3 times a week for the last 4 weeks of the study. Imaging consisted of 3D B-mode for liver localization, and targeted SWE captures for liver stiffness measurements. For comparison, collagen fiber density, width, length, and straightness were determined by Sirius red staining and automated fiber detection and quantification using CT-FIRE software.

Results: Young's modulus (YM), a measure of tissue stiffness known to correlate with liver fibrosis, was significantly increased in the FFC diet group when compared to the chow controls ($p < 0.001$). FFC animals in the treatment group exhibited a slight, but nonsignificant, decrease in YM compared to the untreated FFC animals. There was no significant difference in liver stiffness between the treated and untreated mice in the standard chow group. Similarly, fiber density was significantly increased in FFC diet vs chow controls and lower in the FFC treatment group vs FFC vehicle controls ($p < 0.01$). Overall, collagen fiber density positively correlated with YM ($r = 0.70$). Collagen fibers were narrower and longer with FFC diet than chow controls, and with greater fiber curvature in the FFC treatment group vs no treatment.

Conclusion: These studies demonstrate the potential of the automated robotic ultrasound system to provide insights into the progression (and regression) of liver fibrosis in NASH models non-invasively. Future work will investigate improvements to sensitivity and specificity of the technique.

WED-449

Inhibition of CCAT/enhancer-binding protein beta-serpinB3 axis by 1-piperidin propionic acid: a new targeted therapy for non-alcoholic steatohepatitis

Francesca Protopapa¹, Gianmarco Villano², Erica Novo¹, Cristian Turato³, Santina Quarta², Mariagrazia Ruvoletto², Alessandra Biasiolo², Monica Chinellato², Andrea Martini⁴, Elisabetta Trevellin², Marnie Granzotto², Stefania Cannito¹, Laura Cendron², Maria Guido², Maurizio Parola¹, Roberto Vettor², Patrizia Pontisso². ¹University of Torino, Italy, ²University of Padova, Italy, ³University of Pavia, Italy, ⁴Azienda Ospedaliera Padova, Italy
Email: erica.novo@unito.it

Background and aims: Non-Alcoholic Fatty Liver Disease (NAFLD) is becoming the major cause of chronic liver disease worldwide, with a 25% prevalence in the general population and a higher prevalence in obese and type II diabetes patients. NAFLD includes a spectrum of liver diseases ranging from simple hepatic steatosis to non-alcoholic steatohepatitis (NASH). The serine protease inhibitor SerpinB3 has been proposed as a novel hepatokine able to modulate liver inflammation, fibrosis as well as insulin resistance during NASH

development. In the present study we have tested a specific SerpinB3 inhibitor, 1-Piperidin Propionic Acid (1-PPA), in *in vivo* and *in vitro* models of NASH as a novel targeted therapeutic strategy for NASH.

Method: *In vivo* pre-clinical models: histological parameters and gene expression of pro-fibrotic and pro-inflammatory markers were analyzed in the liver of both SerpinB3-transgenic (TG) fed on either MCD or CDAA diets to induce experimental NASH; in some experiments, SerpinB3 TG mice, starting from the second month, were injected with 1-PPA (70 ng/g). *In vitro* models: expression of pro-fibrotic and pro-inflammatory genes was assessed in THP1 and LX2 cell lines exposed to human recombinant SerpinB3 (hrSB3, 200 ng/ml) alone or with 1-PPA (100 ng/ml). The expression of CCAAT Enhancer Binding Protein Beta (CEBP-beta), a SerpinB3 transcription factor, also involved in metabolic disorders and inflammatory response, was analyzed in the mentioned cell lines with or without 1-PPA as well as in mouse livers in relation to SerpinB3 expression.

Results: Treatment with 1-PPA of TG/SB3 mice fed on CDAA or MCD diet led to a significant reduction of liver fibrosis and inflammatory infiltrate as compared to control mice fed on the same diets, as showed by Sirius Red staining, immunohistochemistry for F4/80 and analysis of transcript levels of major fibrotic and inflammatory mediators. *In vitro* experiments showed that in LX2 cells, pre-treatment with 1-PPA led to a significant reduction of SB3-dependent chemotaxis as well as of transcript levels of Col1A1, alpha-SMA, TGF-beta1. Moreover, 1-PPA treatment also reduced transcript levels of pro-inflammatory mediators, including IL-1beta, CCL-2 and TNF-alpha in THP1 cells exposed to hrSB3. Moreover, the inhibitory mechanism exerted by 1-PPA is likely to also act by affecting a peculiar C/EBP-beta/SerpinB3 axis, in which C/EBP-beta transcription factor was found to up-regulate SB3 but at the same time to be elicited by this serpin.

Conclusion: C/EBP-beta-SerpinB3 axis could have a role in the development of NASH. The SerpinB3 inhibitor 1-PPA is effective in down-regulating inflammatory and fibrogenic responses both *in vitro* and in NASH murine models, suggesting that this molecule has the potential markedly to reduce NASH progression.

WED-450

Senescence sensitizes hepatocytes for fatty acid-induced cytotoxicity by compromising the mitochondrial function

Lilli Rausch¹, Pavitra Kumar¹, Felix Heymann¹, Mohsin Hassan¹, Akosua Boakye Yiadom¹, Fausto Andreola², Frank Tacke¹, Cornelius Engelmann^{1,2,3}, ¹Charité—Universitätsmedizin Berlin, Department of Hepatology and Gastroenterology, Berlin, Germany, ²University College London, Institute for Liver and Digestive Health, London, United Kingdom, ³Berlin Institute of Health (BIH), Berlin, Germany
Email: cornelius.engelmann@charite.de

Background and aims: Senescence is an irreversible cell cycle arrest caused by cellular stressors leading to a senescent phenotype that includes elevated p53, p21, and γ H2A.X expression and cytokine release. Steatotic liver has increased hepatocellular senescence and in pre-clinical models, senolysis reduces the senescent phenotype and fat content in the liver. As the molecular link (s) between cellular senescence and fat accumulation remain unclear, in the present study we explore the cause or consequences of hepatocyte steatosis and senescence. We hypothesize that senescent hepatocytes are susceptible to steatosis and lipotoxicity and senolysis could provide therapeutic cues against the free fatty acid (FFA)-induced cytotoxicity.

Method: Primary hepatocytes were isolated from C57BL/6J mice and cultured overnight. Cells were sensitized for 24 hours with pre-optimized dosages of senescence inducers H_2O_2 (250 μ M) (via oxidative stress) and Nutlin 3a (10 μ M) (via p53 stabilization) and subsequently incubated with 0.3 mM oleic acid (OA, unsaturated fatty acid), palmitic acid (PA, saturated fatty acid), or their 1:1 mixture (MIX) for further 24 hours. For the rescue experiment, steatotic and senescent cells were treated with senolytics, dasatinib and quercetin D+Q for 24 hours. Neutral lipid accumulation in cells was measured by Oil Red O staining (ORO) and senescence markers (p53, p21 and γ H2A.X) were measured by immunofluorescence. Mitochondrial function was assessed by XFe Seahorse analyser with 10 mM glucose, 2 mM pyruvate, and 1 mM glutamine as substrates.

Results: FFA treatment increased lipid accumulation in mice hepatocytes, OA and MIX by 4-fold, and PA by 3-fold ($p < 0.02$). Additionally, 24 h OA treatment resulted in the upregulation of senescent markers (p53, γ H2A.X, and p21) whilst MIX caused primarily a p53 and γ H2A.X elevation. PA downregulated senescence makers but acted toxic to the cells. In senescent cells (H_2O_2 or Nutlin

3a-treated), OA further increased lipids accumulation along with increased p53 and γ H2A.X levels (Figure 1A) when compared to non-senescent OA-treated cells and to MIX or PA treated cells. Senescent cells showed lower cellular respiration (glycolysis and oxidative phosphorylation), that was further compromised after fatty acid treatment. Senolysis (D+Q) rescued the cellular respiration (glycolysis and oxidative phosphorylation) significantly in both steatotic and senescent hepatocytes (Figure 1B).

Conclusion: Free fatty acids induce senescent phenotype in murine hepatocytes. Senescent hepatocytes are prone to steatosis. Senolysis could rescue the cytotoxic effects of free fatty acids-induced senescence via elevating cellular respiration.

WED-451

Ageing rates and oxidative stress in patients with non-alcoholic fatty liver disease and profound insulin resistance

Olena Kolesnikova¹, Anastasiia Radchenko¹, Vilena Chupina², ¹L.T. Malaya Therapy National Institute of the National Academy of Medical Sciences of Ukraine, Department of Study of Aging Processes and Prevention of Metabolic-Associated Diseases, Kharkiv, Ukraine, ²Kharkiv National Medical University, Kharkiv, Ukraine
Email: anastasha.radchenko@gmail.com

Background and aims: Redox imbalance can be both a cause and a consequence of many metabolic pathologies, including non-alcoholic fatty liver disease (NAFLD) and insulin resistance (IR). Data regarding ageing rates and redox markers in NAFLD patients based on the IR level is limited. The aim of our study was to evaluate the parameters of oxidative stress (OS) and ageing rates in patients with NAFLD and IR of various severity.

Method: Our study included 82 patients with NAFLD with a mean age of 48.5 [41.0;57.0] years (62.5% women) and comparison group of 62 patients without NAFLD with a mean age of 49.0 [38.4;54.9] years (64.6% women). Patients were divided into subgroups according to IR index (HOMA-IR): patients without IR ($n = 22$ and $n = 28$ with/without NAFLD accordingly), with IR less than 3 times the upper limit of normal (ULN) ($n = 32$ and $n = 34$) and with IR 3 times higher than ULN ($n = 28$, present only in NAFLD group). Markers of OS included content of total hydroperoxides (THP) and total antioxidant activity (TAA), measured using colorimetric method. Ageing rates were estimated based on the difference between biological age calculated

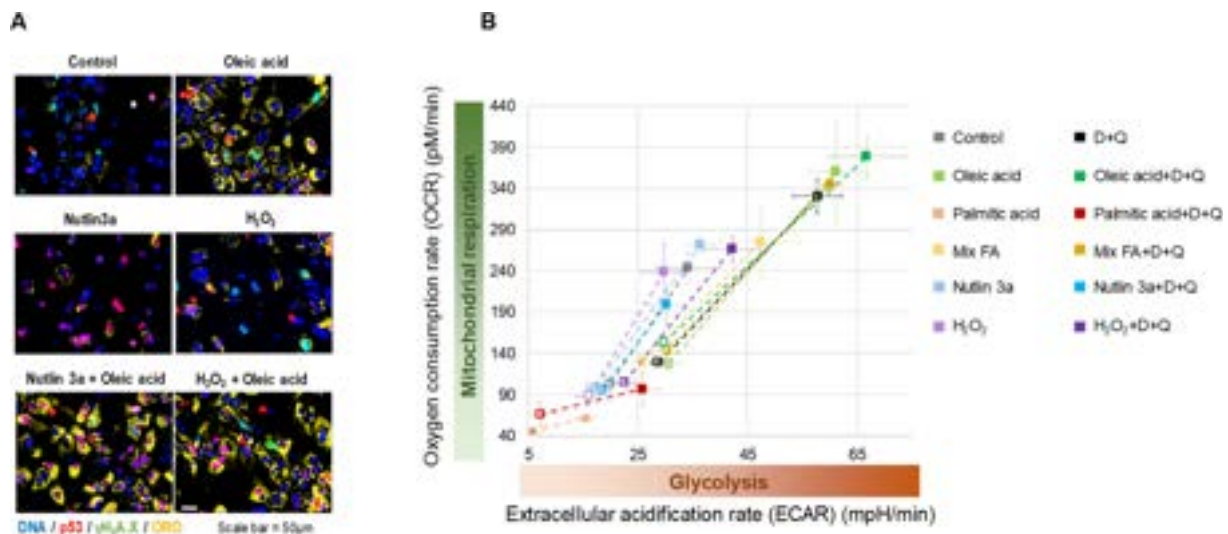


Figure 1. Effect of senescence on free fatty acid-induced cytotoxicity **A)** senescence markers and lipid accumulation **B)** cell energy phenotype measured by XFe Seahorse analyser

Figure: (abstract: WED-450).

POSTER PRESENTATIONS

according to the M. Levine et al. (2018) and calendar age for each patient.

Results: Analysis of studied parameters in patients with NAFLD and IR 3 times higher UNL revealed significant higher levels of glucose, alkaline phosphatase and THP compared to NAFLD patients with IR less than 3 UNL ($p=0,015$, $p=0,014$ and $p=0,004$) and NAFLD patients without IR ($p=0,004$, $p=0,036$ and $p=0,046$). No such differences were observed between NAFLD patients without IR and with IR less than 3 UNL. In addition, NAFLD patients with IR 3 times higher UNL had higher ageing rates compared with NAFLD patients without IR. Such data indicate the appearance of impaired glucose tolerance, pronounced increase in the activity of oxidative processes and, as a result, noticeable increase in the rate of aging in NAFLD patients with profound IR only. No differences were found between patients without IR with versus without NAFLD, but patients with IR less than 3 times UNL without NAFLD had lower levels of THP than patients with similar IR level without NAFLD ($p=0,010$). In patients without NAFLD higher THP levels were observed in the absence of IR ($p=0,027$). Available data indicate that insulin suppresses, while elevated glucose levels increase lipid peroxidation. So hyperinsulinemia in patients without NAFLD with mild IR and normal glucose levels may be the reason for lower THP levels. In patients with NAFLD IR is probably not the cause but rather a consequence of redox disturbances, so higher IR levels are accompanied by higher THP levels.

Conclusion: NAFLD patients with IR 3 times UNL had higher ageing rates compared with NAFLD patients with lower IR level or without it, probably due to higher levels of THP. IR emergence in NAFLD patients most likely mediated by the increased OS. The data obtained can be useful for the prevention of accelerated aging rates in patients with NAFLD.

WED-452

The potential role of Omentin-1 in metabolic associated fatty liver disease (MAFLD): evidence from translational studies

Noel Salvoza^{1,2,3}, Pablo J Giraudi¹, Silvia Gazzin⁴, Deborah Bonazza⁵, Silvia Palmisano⁶, Claudio Tiribelli^{1,4}, Natalia Rosso¹. ¹Fondazione Italiana Fegato Onlus, Metabolic Liver Disease Unit, Basovizza, Italy, ²University of Trieste, PhD Program in Molecular Biomedicine, Trieste, Italy, ³Philippine Council for Health Research and Development, DOST, Taguig, Philippines, ⁴Fondazione Italiana Fegato Onlus, Brain-Liver Unit "Rita Moretti," Basovizza, Italy, ⁵Cattinara Hospital, Surgical Pathology Unit, Trieste, Italy, ⁶Cattinara Hospital, Department of Medical, Surgical and Health Sciences, Trieste, Italy
Email: noel.salvoza@fegato.it

Background and aims: Obesity, characterized by excessive visceral adipose tissue (VAT) is tightly associated with MAFLD. The pathogenesis of MAFLD is complex but recent studies reveal that the adipose tissue-liver axis plays a key role in MAFLD development. We investigated the potential role of omentin-1, a novel adipokine expressed by VAT, in MAFLD pathogenesis.

Method: *In silico* analysis of differentially expressed genes in VAT from obese patients with and without MASH, showed that omentin-1 might play a significant role. For *in vivo* clinical validation, omentin-1 mRNA expression and plasma protein levels were measured in lean controls and obese patients with biopsy-proven MAFLD. mRNA and protein levels of omentin-1 in VAT of juvenile mice MAFLD model have also been assessed. For *in vitro* and *ex vivo* studies, we assessed the effects of omentin-1 in the MAFLD-related mechanisms such as steatosis, inflammation, and oxidative stress. Finally, the effects of D-glucose and insulin on VAT omentin-1 were also analyzed *ex vivo*.

Results: The obese groups showed significantly lower VAT mRNA expression and plasma levels of omentin-1 as compared to the lean

group (all p values <0.05). Interestingly, within the MASH group, fibrosis does not affect omentin-1 expression. Likewise, VAT of mice fed with high-fat diet, showing histological signs of MASH showed decreased omentin-1 mRNA ($p=0.012$) and protein expression ($p=0.038$) as compared to their control diet counterpart. *In vitro*, the addition of omentin-1 on fat-loaded (FFA) human hepatocytes showed no effect on steatosis but significantly decreased TNF- α levels (mRNA and protein), reduction in ER stress markers (*BiP* and *Chop*), and enhanced superoxide dismutase (SOD) antioxidant activity (all p values <0.05 vs. FFA). The same results were obtained using *ex vivo* VAT explants from obese patients upon omentin-1 supplementation (all p values <0.05 vs. control). In addition, omentin-1 reduced nuclear factor kappa B (*NF- κ B*) mRNA expression in both *in vitro* (p value <0.01 vs. FFA) and *ex vivo* (p value <0.01 vs. control) studies. In VAT explants, D-glucose and insulin significantly reduced omentin-1 mRNA expression and protein levels (all p values <0.05 vs. control).

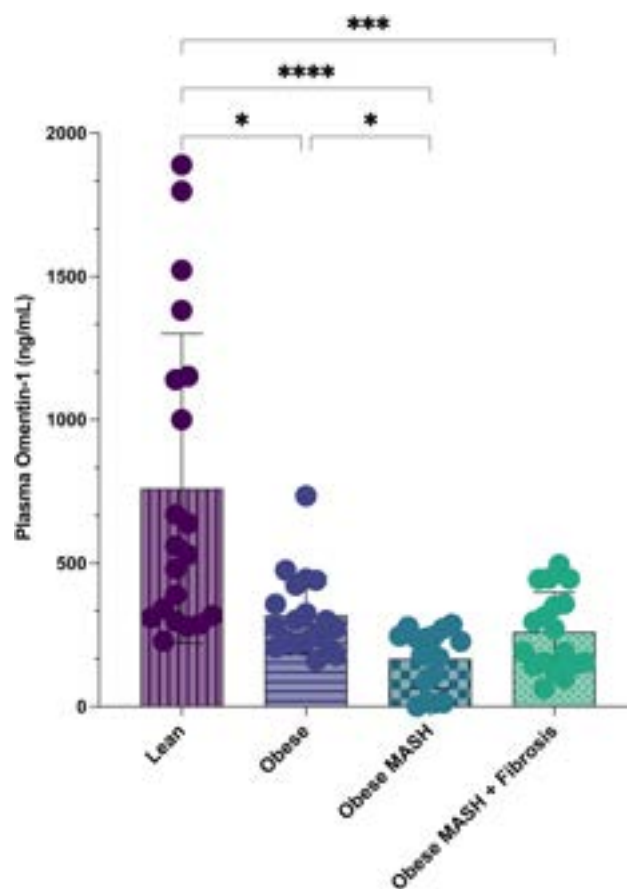


Figure: Human plasma omentin-1 levels in obese groups and lean controls. Values presented in the boxplots are the means \pm SD of individual patients. Group comparison by Kruskal-Wallis and post hoc Dunn's test. * $p < 0.05$, ** $p < 0.01$, *** $p < 0.001$, **** $p < 0.0001$.

Conclusion: Taken together, our findings suggest that reduced levels of omentin-1 contribute to MAFLD development. Omentin-1 supplementation reduces inflammation and oxidative stress probably via inhibiting the *NF- κ B* pathway, and might also play a role in the regulation of glucose and insulin. Further studies are needed for omentin-1 to be considered as a therapeutic target and/or biomarker.

WED-453

Two-dimensional versus one-dimensional transient elastography: benefits of ultrasound imaging-based processing for liver stiffness measurements

Adrien Besson¹, Baptiste Hériard-Dubreuil¹, Victor de Lédighen^{2,3}, Dan Dutartre⁴, Françoise Manon², Joëlle Abiven², Anne-Laure de Araujo², Rhizlane Houmadi², Julie Dupuy², Juliette Foucher², Joel Gay¹, Claude Cohen-Bacrie¹. ¹E-Scopics, Saint-Cannat, France, ²Bordeaux University Hospital, Hepatology Unit, Pessac, France, ³INSERM U1312, BRIC, Bordeaux University, Bordeaux, France, ⁴Inria Bordeaux Sud-Ouest, Bordeaux, France
Email: adrien.besson@e-scopics.com

Background and aims: Fibroscan® (FS) Transient Elastography (TE) performs liver stiffness measurements (LSM) using a measure of the velocity of a shear wave generated by a 50 Hz single element probe mechanical vibration. It relies on a high pulse repetition frequency capture of the one-dimensional (1D) ultrasound (US) signal of that same probe. A new point of care ultrafast US imaging device (POCUS), Hepatoscope™, has been used to compute maps of shear wave velocities generated by a 50 Hz mechanical vibration of a US imaging probe. That same POCUS device provides conventional US imaging of the liver to help positioning the 2DTE map. We hypothesized that 2D processing of shear wave speed in tissue using 2DTE would somehow overcome an intrinsic limitation of 1D TE, where shear wave propagation speed can only be measured in the direction of the single element piston as opposed to a measurement that follows the direction of the shear wave propagation. The aim of this work was to assess the benefits of 2DTE against 1D TE methods, as available on the FS device, and as processed from US per-channel raw-data collected with Hepatoscope on patients with chronic liver diseases.

Method: 96 adult patients referred to a routine hepatology consultation for chronic liver disease, including a FS exam, were enrolled in this prospective single centre study (NCT04782050). Four Hepatoscope consecutive liver exams were added to routine care, performed by 2 operators (1 expert and 1 novice). US per-channel raw-data corresponding to at least three 2DTE stiffness values by Hepatoscope were recorded for each exam. Hepatoscope LSM computed as the median of 3 stiffness values obtained from both 1D (LSM_{1D}) and 2D (LSM_{2D}) processing of these data were compared to FS LSM. The intra- and inter-operator reproducibility of LSM_{1D} and LSM_{2D} were also assessed.

Results: LSM_{2D} showed a significant improvement over LSM_{1D} of the intra-operator reproducibility for experts (ICC_{2D} = 0.84; 95% CI [0.73, 0.91] vs ICC_{1D} = 0.53; 95% CI [0.33, 0.68]), and of the inter-operator reproducibility (ICC_{2D} = 0.74; 95% CI [0.60, 0.84] vs ICC_{1D} = 0.59; 95% CI [0.43, 0.72]). Figure 1 illustrates the ability of 2DTE to better track the shear wave and measure its speed in its propagation direction, thus eliminating measurement bias.

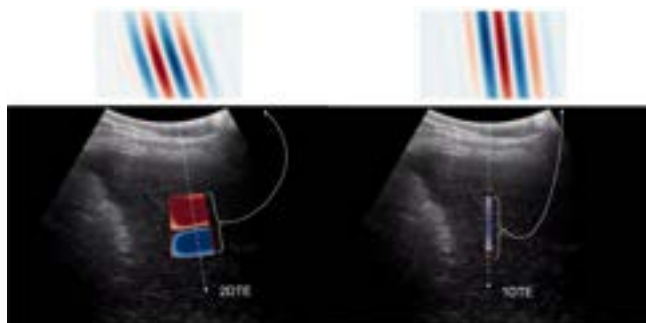


Figure 1: From left to right, Shear-Wave Propagation overlaid on B-Mode image as seen with 2DTE (leftmost image) and 1D TE (rightmost image). As the direction of propagation is not aligned with the analysis direction, 1D TE overestimates the shear-wave velocity.

Figure:

Linear regression analysis between LSM_{1D} and LSM_{2D} obtained by experts showed a slope of 0.95 and an intercept of 2.05 ($p = 10^{-19}$, $r =$

0.72), demonstrating an overestimation of LSM_{1D} as compared to LSM_{2D} in the range [0 kPa, 40 kPa]. This was confirmed by linear regression analysis between LSM_{1D} (resp. LSM_{2D}) and FS LSM which exhibited a slope of 1.18 (resp. 1.04) and an intercept of 1.97 (resp. 1.39) ($p = 10^{-13}$ (resp. $p = 10^{-20}$), $r = 0.63$ (resp. $r = 0.72$)).

Conclusion: 2D processing of US data to measure the shear wave velocity along the direction of shear wave propagation, has demonstrated its ability to eliminate over-estimation bias of LSM. In addition, the estimation of liver stiffness in 2D has led to an increased intra- and inter-operator reproducibility, even considering LSM performed by novices. These results are encouraging as they support a broader use of 2DTE LSM, as available on the Hepatoscope POCUS device, as a less user-dependent method for widespread screening programs of liver fibrosis.

WED-454

Zebrafish larvae as a model system to characterize effects of metabolic, drug and genetic perturbations on liver fat accumulation

Endrina Mujica¹, Hanqing Zhang¹, Anastasia Emmanouilidou¹, Amin Allalou², Marcel den Hoed¹. ¹The Beijer Laboratory and Department of Immunology, Genetics and Pathology; Uppsala University and SciLifeLab, Uppsala, Sweden, ²Department of Information Technology; Division of visual information and interaction; Uppsala University and SciLifeLab, Uppsala, Sweden
Email: endrina.mujica@igp.uu.se

Background and aims: Non-alcoholic fatty liver disease (NAFLD) has a complex pathology that includes a spectrum of liver insults. No FDA-approved pharmacological treatment is currently available. The aim of this study is to validate a zebrafish model system for systematic genetic and drug screens for liver fat using CRISPR/Cas9, fluorescence imaging, and deep learning-based image analysis.

Method: To validate the model system, we first compared liver fat in larvae fed 3x more than sibling controls ($n = 721$). In overfed larvae, we subsequently examined the effect of i) 4% extra dietary cholesterol; and/or ii) 3% glucose added to the water ($n = 574$). Next, we examined the effect of treating metabolically challenged larvae with 0, 10 or 25 μ M rosiglitazone ($n = 865$). Finally, we targeted the zebrafish orthologues of *MTARC1* ($n = 383$) and *GPAM* ($n = 307$) using CRISPR/Cas9, in fertilized eggs from parents with transgenically expressed, fluorescently labeled hepatocytes (*Tg (Ifabp10a:EGFP)*). Larvae from all experiments were phenotyped at 10 or 11 days post fertilization. Before imaging, lipids were stained by incubation with a fluorescent dye (monodansylpentane) that labels neutral lipids. Next, optical sections of the liver were acquired using fluorescence microscopy. Liver size and the number of lipid droplets in the liver were automatically segmented and quantified using deep learning-based image analysis pipelines.

Results: Overfeeding resulted in more liver fat ($\beta \pm SE$ 0.49 \pm 0.10 SD units, $p = 6.5 \times 10^{-7}$). In overfed larvae, both cholesterol (0.61 \pm 0.10) and glucose (1.35 \pm 0.10) challenges resulted in more liver fat, in a non-additive manner (-1.29 ± 0.14). In overfed larvae challenged with extra cholesterol and glucose, treatment with 10 or 25 μ M rosiglitazone protected from liver fat accumulation (-0.25 ± 0.09 , $p = 5.8 \times 10^{-3}$). Finally, mutations in zebrafish orthologues of *MTARC1* and *GPAM* resulted in less liver fat compared with controls (-0.28 ± 0.14 and -0.56 ± 0.24). These findings are directionally consistent with effects of loss-of-function mutations identified in humans and are in line with these genes being the culprits in loci recently identified by genome-wide association studies for NAFLD.

Conclusion: Image-based screens in zebrafish larvae can be used to systematically characterize genes and drugs for a role in the development of NAFLD and prioritize the most promising candidates for further in-depth characterization and drug development.

WED-455

Cyclophilin inhibition with rencofilstat shifts the liver transcriptome and lipidome in preclinical models toward resolution of non-alcoholic steatohepatitis

Daren Ure^{1,2}, Winston Stauffer³, Bhavesh Variya^{1,2}, Lacey Haddon^{1,2}, Patrick Mayo^{1,2}, Philippe Gallay³, Robert Foster^{1,2}. ¹Hepion Pharmaceuticals, United States, ²Hepion Research, Canada, ³Scripps Research Institute, United States
Email: dure@hepionpharma.com

Background and aims: Cyclophilins are a multi-isoform class of enzymes that regulate the structure and function of proteins across a wide cross-section of the human proteome and have been shown to contribute to many disease processes. Rencofilstat is a potent inhibitor of several cyclophilin isoforms and has demonstrated antifibrotic, anti-inflammatory, and other therapeutic activities in liver disease models, supporting its current evaluation in Phase 2 clinical trials for non-alcoholic steatohepatitis (NASH). The aim of the present investigations was to characterize rencofilstat's effects on the liver transcriptome and lipidome in three liver disease models to better delineate its modes of action.

Method: Three liver disease studies were conducted: 1) DIAMOND mouse model of NASH; 2) western diet plus carbon tetrachloride mouse model of NASH/fibrosis; 3) thioacetamide-induced liver fibrosis in rats (Physiogenex, France). Rencofilstat was administered in all studies. Elafibranor (ELF) and obeticholic acid (OCA) were additionally administered in the DIAMOND mouse study. Liver steatosis, inflammation, and fibrosis were measured histologically. RNA sequencing and mass spectrometry-based lipidome analysis (OWL, Spain) was performed on liver samples from all three studies.

Results: Rencofilstat decreased liver fibrosis in all three experimental models by 50–80% as measured by percentage Sirius red. RNA sequencing showed that rencofilstat altered the expression of 500–1500 genes in diseased livers which was approximately one-third the number of differentially expressed genes (DEGs) from ELF-treated or OCA-treated mice. A range of 74–81% of the rencofilstat DEGs overlapped with ELF or OCA DEGs. KEGG pathway mapping and network hub gene prediction similarly showed extensive overlap among the three drugs. Furthermore, all three treatments significantly attenuated KEGG pathways that were activated in vehicle-treated animals and in human NASH. Lipidomic analyses revealed that rencofilstat altered 4–19% of the liver lipid species across the three models, which was similar to OCA but less than ELF. Rencofilstat effects included reductions in saturated triglycerides, lysophospholipids, and sphingolipids, and especially the shorter-chain species of these lipids. The lipids decreased by rencofilstat were typically increased in vehicle animals and correlated with percentage-area Sirius red staining.

Conclusion: Despite no known mechanisms of transcriptional regulation, rencofilstat positively changed gene expression networks similarly to FXR and PPAR agonists. Rencofilstat also altered liver lipid signatures consistent with attenuation of lipotoxic processes. These findings suggest that cyclophilins contribute to many pathophysiologic processes and blocking their modulatory actions with rencofilstat shifts the liver transcriptome and lipidome towards NASH resolution.

WED-456

Tyrosol reduces steatosis, fibrosis and inflammation in a murine model of NASH by modulating the immune hepatic phenotype

Daniela Gabbia¹, Katia Sayat², Martina Colognesi¹, Ilaria Zanotto¹, Francesco Paolo Russo², Sara De Martin¹. ¹University of Padova, Dept. of Pharmaceutical and Pharmacological Sciences, Italy, ²University of Padova, Department of Surgery, Oncology and Gastroenterology, Italy
Email: sara.demartin@unipd.it

Background and aims: Besides its metabolic and detoxifying activity, the liver is an immunological organ where innate and adaptive immune cells are in close contact with blood-borne and gut-

derived pathogens. Recent evidence indicates that NASH patients display a dysregulation of the hepatic immune landscape, mainly due to the increased influx of myeloid-derived monocytes and monocyte-derived cells. Such changes fuel uncontrolled inflammation and cooperate with hepatocytes, hepatic stellate cells (HSCs) and liver sinusoidal endothelial cells in disease progression. Phenolic compounds of natural origin including tyrosol are known to mitigate hepatic fibrosis through the regulation of NADPH oxidases (NOXs), whose exaggerated expression has been related to increased ROS-induced oxidative stress. This study aims at unravelling whether and how tyrosol modulates the hepatic recruitment of immune cells in a murine model of NASH.

Method: The murine model of NASH was obtained by feeding male C57BL6 mice with a high fructose-high fat diet for 14 weeks, combined to the IP administration of CCl₄ (0.05 mg/kg) in the last 4 weeks. Starting from week 4, tyrosol was administered daily by oral gavage (10 mg/kg). Behavioral and motor tests, e.g. grid, rotarod and open field test, were performed to assess signs of extrahepatic manifestations of NASH, e.g. sarcopenia and mood disorders. Inflammation, fibrosis, and steatosis were evaluated by liver histology by means of HandE, Masson's trichrome, and Oil Red O staining, respectively. NOX1 and αSMA expression was assessed by means of IHC. The presence of immune cells (CD4⁺, CD8⁺ lymphocytes, Tregs, M1- and M2- macrophages) in the liver was assessed by means of flow cytometry.

Results: Tyrosol attenuated fatigue and anxious behavior in NASH mice, restoring performances similar to those of healthy animals. Furthermore, tyrosol reduced steatosis, fibrosis and αSMA expression, that were significantly lower than those of NASH untreated animals ($p < 0.01$). Accordingly, tyrosol-treated NASH mice had less inflammatory foci in the liver than untreated ones ($p < 0.05$), a decreased expression of NOX1 ($p < 0.05$), suggesting a reduction of hepatic inflammation and oxidative stress. This was confirmed by the significant reduction in proinflammatory M1-type macrophages ($p < 0.05$), CD4⁺ ($p < 0.05$) and T helper effector lymphocytes ($p < 0.05$), and the significant increase of Treg cells ($p < 0.05$) observed in tyrosol-treated mice, with respect to untreated ones.

Conclusion: In a mouse model of NASH, tyrosol modulates the different populations of immune cells in the liver, counteracting steatosis, fibrosis, oxidative stress and inflammation, all hallmarks of this complex liver disease.

WED-457

Biomarkers of endothelial dysfunction in patients with non-alcoholic fatty liver disease (NAFLD)

Rocío Montero-Vallejo¹, Rocío Gallego-Durán¹, Douglas Maya¹, Sheila Gato Zambrano¹, Vanessa García Fernández¹, Rocio Munoz Hernandez¹, Antonio Gil-Gomez¹, Angela Rojas Alvarez-Ossorio², Maite G Fernandez-Barrena³, José María Herranz³, Virginia Hernandez-Gea⁴, Genís Campreciós⁴, Aina Anton⁴, María del Carmen Rico², Franz Martin-Bermudo⁵, Manuel Romero Gomez², Javier Ampuero². ¹Servicio de Aparato Digestivo, Hospital Universitario Virgen del Rocío; SeLiver Group, Instituto de Biomedicina de Sevilla (HUVR/CSIC/US), Departamento de Medicina Universidad de Sevilla; CIBEREHD Sevilla, Sevilla, Spain, ²Servicio de Aparato Digestivo, Hospital Universitario Virgen del Rocío; SeLiver Group, Instituto de Biomedicina de Sevilla (HUVR/CSIC/US), Departamento de Medicina Universidad de Sevilla; CIBEREHD, Sevilla, Spain, ³Programa de Hepatología. CIMA. Universidad de Navarra. CIBEREHD., Pamplona, Spain, ⁴Unidad de Hemodinámica Hepática. Servicio de Hepatología, Hospital Clinic, Universidad de Barcelona, IDIBAPS, CIBEREHD, Barcelona, Spain, ⁵Centro Andaluz de Biología Molecular y Medicina Regenerativa (CABIMER), Sevilla, Spain
Email: jampuero-ibis@us.es

Background and aims: The main aim was to identify endothelial dysfunction biomarkers in serum and hepatic tissue in biopsy-proven NAFLD patients.

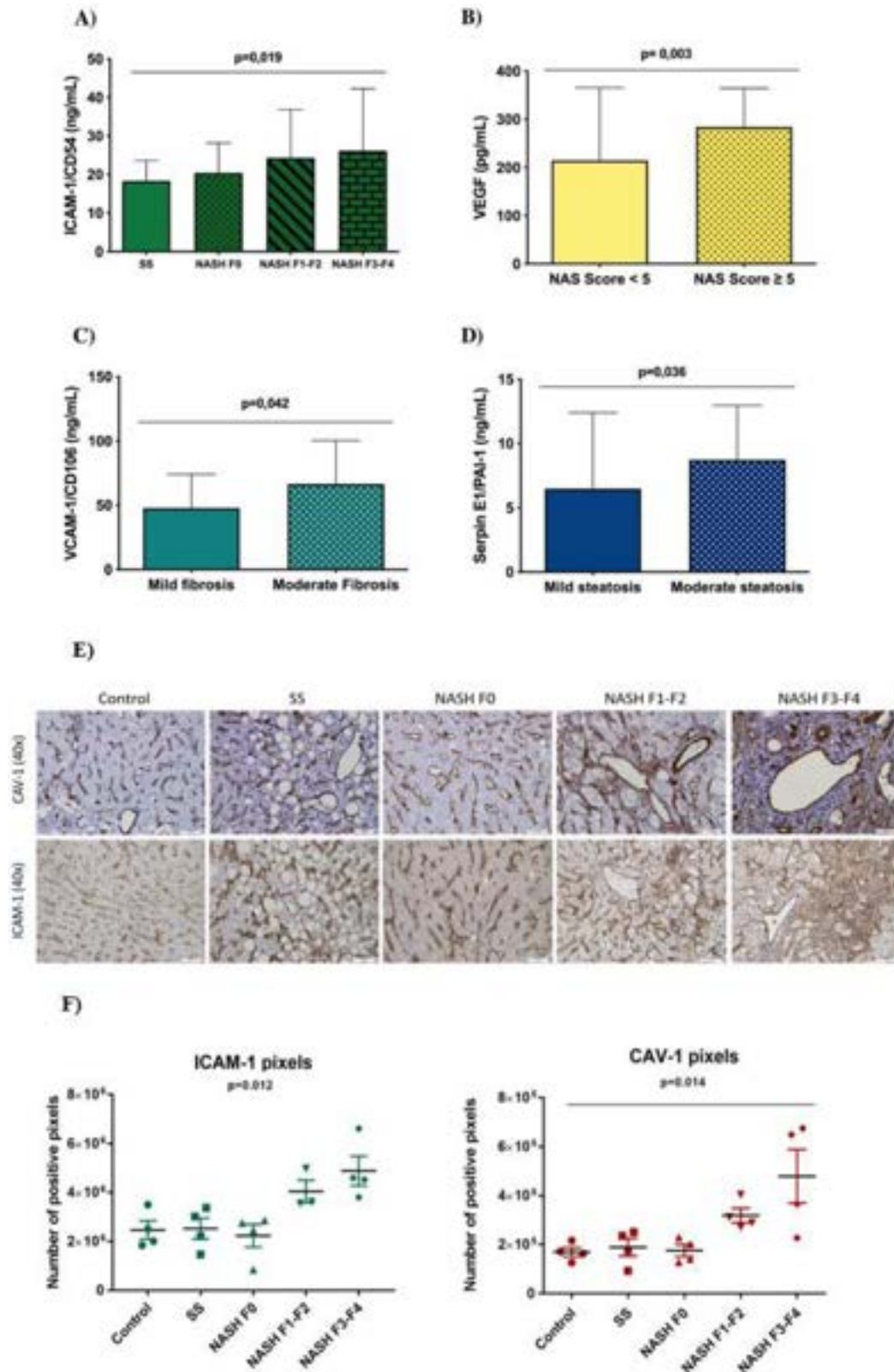


Fig 1. (abstract: WED-457) A) Circulating levels of ICAM-1/CD54 in biopsy-proven NAFLD patients (steatosis simple (SS), nash without fibrosis (NASH F0), nash with fibrosis F1/F2 (NASH F1-F2) and NASH with moderate fibrosis (F3-F4). B) VEGF expression in NAFLD patients with respect to NAS Score. C) VCAM-1/CD106 serum levels related to the levels of fibrosis in the disease. D) Circulating levels of Serpin E1/PAI-1 in NAFLD patients correlated to with steatosis levels. E) Immunohistochemistry of endothelial dysfunction markers CAV-1 and ICAM-1, of the different stages of patients biopsied for NAFLD suspected. F) Quantification of positive pixels of immunohistochemical images for ICAM-1 and CAV-1 antibodies with ImageJ.

Method: Forty patients were included with different stages of the disease (steatosis simple group (n = 7), NASH F0 group (n = 11), NASH F1-F2 group (n = 10) and NASH F3-F4 group (n = 12)). ELISA techniques were performed for the selected endothelial dysfunction markers (ICAM-1/CD54, VCAM-1/CD106, VEGF, Serpin E1/PAI-1 and ADAM12). The following outcomes were analysed: mild/moderate steatosis, mild/moderate fibrosis and NAS score. Due to relevant analyses results, subsequent validation of ELISA in ICAM included a total of 120 patients recruited. In addition, immunohistochemistry of hepatic sections was performed in 20 patients with different stages of the disease following the same groups as described below together with a control group (n = 4 patients/group) for caveoline-1 (CAV-1), angiotensinogen (AG) and intercellular adhesion molecule 1 (ICAM-1). Cardiovascular events were also recorded and Castelli index was calculated.

Results: Mean age was 60 ± 9 , of them, 52.5% (21/40) were women. Circulating levels of ICAM-1 were associated with liver fibrosis (SS: 18.35 ± 5.26 vs. NASH-F0 20.48 ± 7.79 vs. F1-F2 24.38 ± 12.34 vs. F3-F4 26.21 ± 16.05 ng/ml, $p = 0.019$; n = 120; Figure 1A). Moreover, ICAM positively correlated with the NAS Score (r: 0, 413; $p < 0.001$). Circulating levels of VCAM-1 were associated with the presence of significant fibrosis (F0-F1 47.9 ± 26.2 vs. F2-F4 66.5 ± 33.9 ng/ml; $p = 0.042$; n = 40; Figure 1C); and a positive correlation was found between VCAM and ICAM (r: 0.523; $p = 0.001$). VEGF circulating levels were increased in patients with NAS Score > 5 : 284.05 ± 80.8 vs. 214.4 ± 151.4 pg/ml; $p = 0.03$; n = 40; Figure 1B). Circulating levels of Serpin E1 increased with the degree of hepatic steatosis (mild steatosis 6.49 ± 5.9 vs. moderate/severe steatosis 8.73 ± 4.2 ng/ml; $p = 0.036$; n = 40; Figure 1D), and correlated with the Castelli index (r: 0.368; $p = 0.023$). No significant differences in circulating ADAM12 were found in this study. Moreover, the hepatic expression of CAV-1 and ICAM-1 were found to be increased following the hepatic injury, and no significant differences in angiotensin were found (Fig 1E and 1F). Finally, a correlation with liver fibrosis was observed in both ICAM-1 (r = 0.706; n = 19; $p = 0.001$) and CAV-1 (r = 0.681; n = 20; $p = 0.001$).

Conclusion: Markers of endothelial dysfunction are related to the main histopathological features of NAFLD, such as fibrosis, hepatic steatosis or NASH, both at the circulating and the hepatic level in NAFLD patients.

WED-458

Increasing gut microbiota produced secondary bile acids to protect against non-alcoholic steatohepatitis

Justine Gillard^{1,2}, Martin Roumain³, Corinne Picalausa¹, Morgane Thibaut², Giulio G. Muccioli³, Anne Tailleux⁴, Bart Staels⁴, Laure Bindels², Isabelle Leclercq¹. ¹Université catholique de Louvain, Laboratory of Hepato-Gastroenterology, Belgium, ²Université catholique de Louvain, Metabolism and Nutrition Research Group, Belgium, ³Université catholique de Louvain, Bioanalysis and Pharmacology of Bioactive Lipids, Belgium, ⁴University of Lille, Inserm, CHU Lille, Institut Pasteur de Lille, U1011-EGID, France
Email: justine.gillard@uclouvain.be

Background and aims: Bile acids (BAs) regulate immunometabolic pathways impaired in NASH by activating BA-receptors, such as FXR and TGR5. Hence, BAs are attractive candidates for therapeutic development. An imbalance between primary BAs (reflecting hepatic synthesis) and secondary BAs (reflecting transformation by gut microbes) is a recurrent feature in NASH. We previously reported that secondary BAs were low in mice with NASH. Here, we aimed at restoring the balance between primary and secondary BAs by (1) a dietary supplementation with deoxycholic acid (DCA), a secondary BA, or (2) a probiotic approach to enhance endogenous production of secondary BAs by gut bacteria. We evaluated the effects of both approaches on the composition and signaling of BAs and on NASH progression.

Method: We used high fat diet (HFD)-fed *foz/foz* mice as a model of NASH whose BA pool is depleted in secondary BAs. They received (1)

a HFD containing DCA or a plain HFD or (2) an oral suspension of *C. scindens*, a gut bacterium supporting the conversion of primary BAs to secondary BAs, or vehicle for 12 weeks.

Results: Supplementation of the HFD with DCA increased total BAs, total secondary BAs and DCA concentrations in *foz/foz* mice, shifting the BA pool towards a more TGR5- and FXR-agonistic pool. Notably, DCA elevated the TGR5 activation capacity of the portal blood. The restoration of BA signaling by DCA supplementation significantly lowered body weight gain, fasting glycemia and insulinemia and protected from NASH (Figure). Indeed, DCA reduced steatosis, macrophage infiltration and ballooning. Hence, only 15% of treated mice still presented NASH, while 100% of untreated mice met the criteria for NASH diagnosis. We next aimed at increasing endogenous DCA production by targeting the gut microbiota with a probiotic approach. We confirmed by a functional assay that *C. scindens* transforms primary BAs to secondary BAs. However, *C. scindens* administration to *foz/foz* mice did not change the endogenous production of secondary BAs, the portal BAs pool and the activation of BA-receptors FXR and TGR5. Coherently, it had no significant effect on liver and metabolic phenotype (Figure), despite a massive increase of the fecal load of *C. scindens* and its survival in the gut of treated mice.

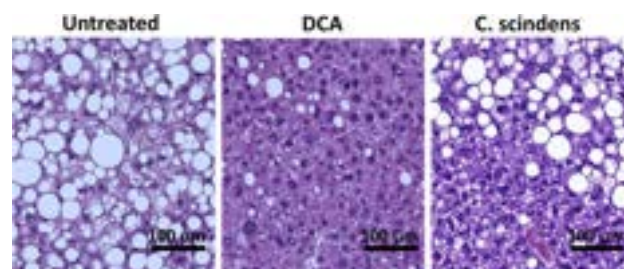


Figure:

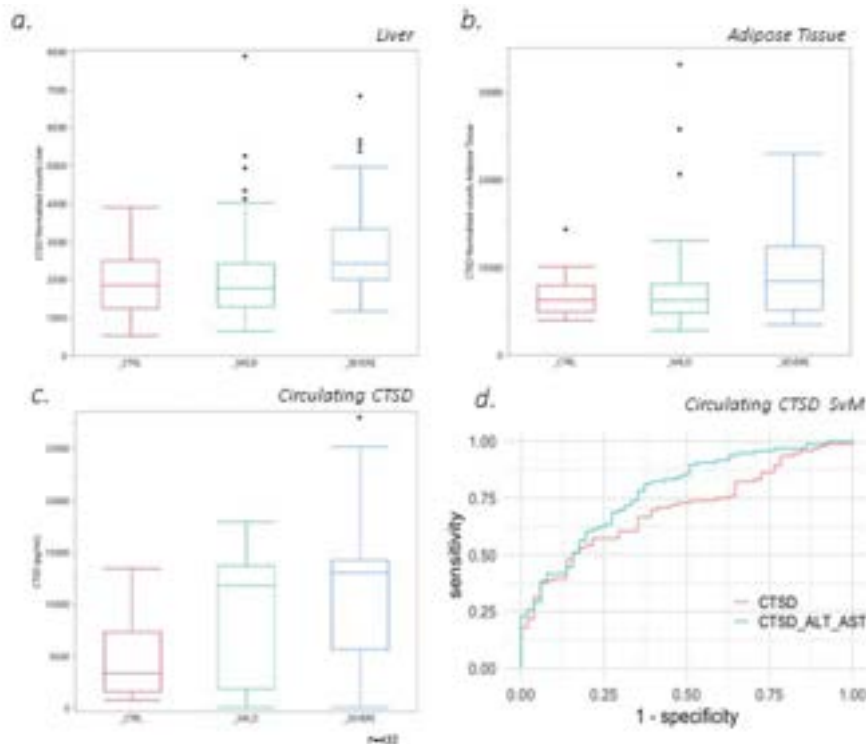
Conclusion: The administration of *C. scindens* did not enhance the endogenous production of secondary BAs. A too low dose and frequency of administration, a too low biological effect of *C. scindens* on a complex microbial community or a high hepatic reconversion of secondary BAs to primary BAs are possible explanations for the lack of impact of *C. scindens* on the BA pool of a mouse model with a complex gut microbiota. Nevertheless, we demonstrated that the restoration of the balance between primary and secondary BAs by a dietary supplementation with the secondary BA DCA protected from NASH and associated dysmetabolic features.

WED-459

Combined hepatic and adipose tissue transcriptomics highlights circulating NASH biomarkers

Marica Meroni¹, Emilia Rita De Caro¹, Federica Chiappori², Miriam Longo¹, Erika Paolini¹, Ettore Mosca², Ivan Merelli², Rosa Lombardi¹, Sara Badiali¹, Marco Maggioni¹, Alessandro Orro², Alessandra Mezzelani², Luca Valenti³, Anna Ludovica Fracanzani^{1,3}, Paola Dongiovanni¹. ¹Fondazione IRCCS Cà Granda Ospedale Maggiore Policlinico, Milan, Italy; General Medicine and Metabolic Diseases; Milan, Italy, ²Institute for Biomedical Technologies, National Research Council (ITB-CNR), Segrate, Italy, ³University of Milan, Department of Pathophysiology and Transplantation, Milan, Italy
Email: paola.dongiovanni@policlinico.mi.it

Background and aims: Obesity represents the main contributor to non-alcoholic fatty liver disease (NAFLD) and adipose tissue is strongly interlaced with the liver in the disease pathogenesis and progression. Previous studies were restricted to investigate the hepatic transcriptome across the entire spectrum of NAFLD, whereas the transcriptomic changes which occur in white adipose tissue (WAT) in relation to liver damage have been poorly investigated. Therefore, we aimed to compare hepatic and adipose tissue



Serum cathepsin D (CTSD) as possible biomarker to detect severe NAFLD. CTSD expression is stratified according to the severity of NAFLD in both liver (A) and adipose tissue (B). Boxes span from 25th to 75th percentile, while whiskers indicate the 10th and 90th percentile. Normal liver (CTRL) is plotted in red, mild in green, while Severe NAFLD in blue. CTSD serum concentration was evaluated in n=432 patients (Liver Clinic cohort) (C). $p < 0.05$ at one-way ANOVA. ROC curves describe the accuracy of circulating CTSD (pg/mL) in foreseeing severe NAFLD from mild NAFLD (SvM) (D), obtained considering CTSD alone, or in a generalized linear model with transaminases (ALT and AST).

Figure: (abstract: WED-459).

transcriptome in NAFLD patients with the purpose to identify shared biomarkers useful for the diagnosis of advanced liver damage.

Method: We performed high-throughput RNA-sequencing in 167 hepatic samples from obese patients and in a subset of 79 matched adipose tissues. Patients were subdivided in normal liver, mild and severe NAFLD according to histology. Circulating cathepsin D (CTSD) was assessed by ELISA.

Results: We identified a specific transcriptomic signature that may discriminate patients with severe NAFLD and isolated steatosis, including 424 deregulated genes in liver and 209 in adipose tissue. According to pathway and network analyses, inflammation, ECM remodeling and mitochondrial dysfunction were upregulated whereas oxidative phosphorylation was downregulated in both tissues. We highlighted 13 genes commonly deregulated in both tissues and among them, CTSD showed the most robust diagnostic accuracy in discriminating mild and severe NAFLD. In 52 obese subjects and in a validation cohort of 432 histologically-characterized NAFLD patients, serum CTSD progressively increased from normal liver to severe NAFLD and it was associated with steatosis, necroinflammation, fibrosis, steatohepatitis (NASH) and NAS>5. The area under the curve (AUC) weighted for transaminases to foresee severe NAFLD versus mild and normal liver was 0.78 and 0.87, respectively.

Conclusion: CTSD may be a possible biomarker of severe NAFLD since its hepatic/adipose tissue expression as well as circulating levels correlated with liver damage thus allowing to discriminate advanced disease.

WED-460

Thermoacoustic assessment of fatty liver disease-an early clinical feasibility study

Jang Hwan Cho¹, Michael Thornton¹, Jing Gao², Colby Adamson², Idan Steinberg¹. ¹ENDRA Life Sciences inc, ANN ARBOR, United States, ²Rocky Vista University, Ultrasound Research medical center, Ivins, United States

Email: thornto@gmail.com

Background and aims: Thermoacoustics (TA) is a non-invasive, non-ionizing, molecular-sensitive imaging technology based on the absorption of radio frequency waves combined with low-cost ultrasound. Unlike purely ultrasonic approaches (such as backscatter and attenuation) that are sensitive to changes in the speed of sound, and tissue density, that may be confounded by fibrosis, TA signals are similar to Magnetic Resonance Proton Density Fat Fraction (MRI-PDFF) as they both represent stoichiometric mixing of adipose and lean tissue and thus provide a high diagnostic value. The Thermo-Acoustic Enhanced Ultrasound (TAEUS) Fatty Liver Imaging Probe (FLIP) is a hand-held, point-of-care system that quantitatively assesses liver fat content. This work describes an early clinical feasibility study with TAEUS-FLIP and a comparison to MRI-PDFF for demonstrating the potential of TA for assessing fatty liver disease.

Method: 16 subjects with suspected Non-Alcoholic Fatty Liver Disease (NAFLD) were scanned at Rocky Vista University, Ultrasound Research medical center, USA. For each subject, after fasting for 6–8 hours, an anatomic B-mode ultrasound scan was obtained by a trained sonographer to determine the locations of the

POSTER PRESENTATIONS

liver capsule and overlying tissue (muscle, fat, and skin), followed by up to 10 consecutive FLIP scans over a 5–8 minute procedure. MRI-PDFF measurements were obtained to assess liver fat fraction. The median value of their individual FLIP scans was used to avoid outlier acquisitions. 3 subjects were excluded from the analysis based on FLIP measurements that were not concordant with the study subject's muscle thickness obtained by B-mode ultrasound. Linear regression and unpaired t-test were used to compare the estimated FLIP metric with liver fat fraction as measured by MR-PDFF. In a 2nd study, a trained user of the FLIP system performed 12 separate exams, each consisting of 6–8 measurements per exam, to determine intra-operator variability.

Results: Figure 1 shows the median FLIP metric for each subject compared to MRI-PDFF. The two methods are strongly correlated, with a Pearson correlation coefficient of $r = 0.79$. Linear regression reveals that the FLIP metric of only 3 out of 13 subjects falls out of the 95% confidence interval, indicating a clear relation between the FLIP-derived measurements and MRI-PDFF values, with 85% of the subjects staged the same by both. To assess the FLIP method's ability to discriminate early stages of NAFLD (S0 and S1) from later stages (S2 and S3), an unpaired t-test was performed on the FLIP metric with $p < 0.02$. In a second study involving 12 FLIP procedures, intra-operator variability was 9.4% (S.D. 4.5%).

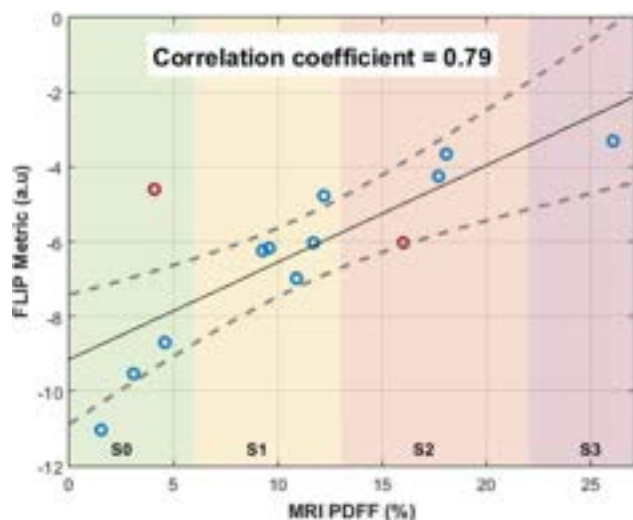


Figure:

Conclusion: This early feasibility liver fat fraction study compares TAEUS-FLIP to MRI-PDFF. It provides insight into the potential of TA methods to assess liver fat content, similar to MRI-PDFF, at the point of care, at a fraction of the cost.

WED-461

BMP-SMAD pathway upregulation in hepatocytes delays NAFLD-NASH development

Laura Silvestri^{1,2}, Mariateresa Pettinato³, Valeria Furiosi³, Letizia Bavuso Volpe³, Shuling Guo⁴, Antonella Nai^{2,3}, Alessia Pagani³.
¹IRCCS Ospedale San Raffaele, Regulation of Iron Metabolism Unit, Division of Genetics and Cell Biology, Milan, Italy, ²Università Vita-Salute San Raffaele, Italy, ³IRCCS Ospedale San Raffaele, Regulation of Iron Metabolism Unit, Division of Genetics and Cell Biology, Italy, ⁴Ionis Pharmaceutical, United States
 Email: silvestri.laura@hsr.it

Background and aims: Non-alcoholic Fatty Liver Disease (NAFLD) is characterized by liver fat accumulation and insulin resistance, and may progress to steatohepatitis (NASH), cirrhosis and hepatocellular carcinoma. Currently, the molecular players involved in its progression are poorly defined and no specific therapies are available. Lipid and iron metabolisms are interconnected since excess iron in

hepatocytes favors NAFLD. Iron homeostasis is regulated by the hepatic hormone hepcidin, whose expression is increased by iron-mediated BMP-SMAD activation, and downregulated by the BMP-SMAD inhibitor TMPRSS6. *Tmprss6*-KO mice show attenuated hepatosteatosis and insulin resistance in high-fat diet, independently of body iron, suggesting a role for the BMP-SMAD pathway/hepcidin in lipid and glucose metabolisms. To deeply define the mechanism, we re-evaluated liver differentially expressed genes from *Tmprss6*-KO and control mice, demonstrating that increased BMP-SMAD/hepcidin upregulates *Ppara* and its target genes. Since *Ppara* activation improves NAFLD-NASH, we hypothesize that *Tmprss6* targeting might be a potential therapeutic approach to this disorder.

Method: Wild-type male mice were kept a NAFLD-NASH-inducing diet (FPC) for 18 weeks. Antisense oligonucleotides (ASOs) against *Tmprss6* (*Tmprss6*-ASO) or control-ASO were injected biweekly for 6 weeks, when hepatosteatosis was established. Histological and gene expression analysis was performed for phenotypic characterization.

Results: Liver *Tmprss6* is downregulated and BMP-SMAD target genes (*hepcidin/Id1*) increased as expected. *Tmprss6*-ASO treatment counteracts FPC-induced hepatomegaly, improves hepatosteatosis and ameliorates lipid metabolisms, decreasing the expression of genes involved in lipid, storage and *de novo* lipogenesis. *Tmprss6*-ASO treatment improves FPC-induced liver mitochondrial dysfunction, decreases the expression of pro-inflammatory cytokines and oxidative stress. In addition, *Tmprss6* targeting prevents collagen deposition and fibrosis.

Conclusion: *Tmprss6* downregulation, by activating the hepatocyte BMP-SMAD pathway, counteracts NASH development. Although the molecular mechanisms are still under investigation, our approach could be considered highly translatable to patients since TMPRSS6-ASOs are currently in Phase 2 clinical trials for iron-loaded diseases due to impaired erythropoiesis. Our study highlights a new therapeutic application of this drug, worth to be tested in NAFLD-NASH patients.

WED-462

Hepatocyte depletion of ERK5 impairs the response to lipotoxic oxidative stress resulting in defective insulin receptor signaling

Alessio Menconi¹, Giovanni Di Maira¹, Giulia Lori¹, Benedetta Piombanti¹, Claudia Campani¹, Maria Letizia Taddei¹, Salvatore Petta², Rosaria Pipitone², Stefania Grimaudo², Armando Curto^{1,3}, Elisabetta Rovida¹, Fabio Marra¹.
¹University of Florence, Italy, ²University of Palermo, Italy, ³Careggi, DMSC, Firenze, Italy
 Email: fabio.marra@unifi.it

Background and aims: Insulin resistance is an early event in non-alcoholic fatty liver disease (NAFLD), but the molecular mechanisms underlying the reduced response to insulin are still elusive. The mitogen-activated protein kinase ERK5 has been implicated in the development of hepatic fibrosis and cancer. Aim of this study was to investigate the role of ERK5 in the regulation of hepatocyte sensitivity to insulin.

Method: A murine hepatocyte cell line (MMH) was silenced using lentiviral vectors encoding shRNA for the ERK5 gene. Mitochondrial depolarization was assayed using the TMRE staining protocol. OXPHOS was measured by Seahorse. Mice with hepatocyte-specific deletion of ERK5 (*ERK5 Δ Hep*) were fed with a high-fat diet (HFD) for 16 weeks. For Glucose and insulin tolerance tests were conducted injecting 1 g/kg BW glucose or 0.8 U/kg BW insulin, respectively, i.p.

Results: MMH stably silenced for ERK5 showed reduced Akt activation following insulin stimulation. When ERK5-silenced cells were exposed to palmitic acid and then stimulated with insulin, Akt activation was abrogated, and expression of the insulin receptor (IR) reduced. Additionally, ERK5 silencing induced phosphorylation and activation of JNK, resulting in phosphorylation of IRS-1 on inhibitory residues (S307). In parallel, an increase of mitochondrial ROS generation was observed in ERK5-depleted MMH. ERK5 is known

to induce a NRF2-dependent anti-oxidative stress response. Expression of the NRF2-target genes HMOX1 and NQO1 was reduced in ERK5-silenced MMH. Treatment with NAC, a free-radical scavenger, prevented the downregulation of the IR and the increase in IRS1 phosphorylation on S307. Measurement of the mitochondrial membrane potential indicated a strong depolarization in ERK5-silenced cells, together with an impairment of mitochondrial OXPHOS, associated with up-regulated expression of PGC-1 α and TRIB3, a negative regulator of insulin signalling through inhibition of Akt. ERK5 Δ Hep mice exhibited impaired glucose tolerance and reduced insulin sensitivity. Hepatocyte depletion of ERK5 in vivo was also associated with reduced expression of IR, and increased expression of PGC-1 α and TRIB3.

Conclusion: We have elucidated a new role of ERK5 in maintaining hepatocyte insulin sensitivity, via an antioxidant response involving IRS-1, PGC-1 α , and TRIB3, and converging on Akt activation.

WED-463

Hepatic Apolipoprotein J facilitates metabolic disease progression by promoting mTOR-mediated suppression of autophagy

Duan Shuangdi¹, Qin Nong¹, Pi Jiayi¹, Wang Hsin-Tzu², Sun Hung-Yu².
¹Human University, China, ²National Cheng Kung University, Taiwan
Email: s5893149@gmail.com

Background and aims: Ectopic lipid accumulation increases vulnerability of the liver to promote liver injury and metabolic syndromes (MetS). Previously, our group had showed that Apolipoprotein J (ApoJ), a Golgi-resident molecular chaperone, participated in pathogen- and nutrient-induced aberrant lipid accumulation. Herein, we demonstrated that ApoJ modulates mTOR-TFEB-autophagy axis to facilitate development of MetS, e.g. metabolic-associated fatty liver disease (MAFLD) and diabetic nephropathy (DN).

Method: The ApoJ-mTOR interaction was identified and validated by differential proteomic approach and co-immunoprecipitation assay. The function of ApoJ on mTOR-TFEB-autophagy axis and intracellular lipid deposition was evaluated using in vitro and in vivo gain- or loss-of-function experiments. The autophagic flux was addressed GFP-RFP-tagged LC3 construct and live image analysis.

Results: mTOR was demonstrated as a novel client protein for ApoJ chaperone. ApoJ interacted with mTOR kinase domain and prevented proteasomal degradation of mTOR by competing with FBW7 E3 ubiquitin ligase through its R324 residue. Persistent mTOR activation impeded autophagy and lysosomal function and disturbed hepatic lipid homeostasis, which promoted MAFLD progression. Notably, accumulation of ApoJ in proximal tubule was found in mouse models of diabetic kidney disease. Pathologically, ApoJ interfered TFEB-autophagy axis by increasing mTOR-TFEB interaction, leading to lipid and ROS accumulation and promote epithelial-mesenchymal transition of proximal tubular cells. By using liver- and kidney-specific ApoJ knockout mice, hepatocyte-derived ApoJ was identified to coordinate with renal ApoJ to accelerate the development of DN.

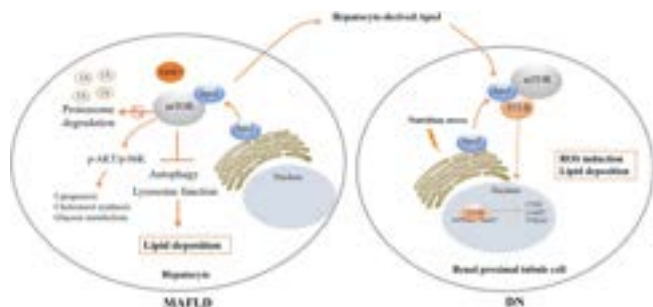


Figure:

Conclusion: The present study highlighted the pathological role of hepatic ApoJ in lipid homeostasis and suggested ApoJ as a therapeutic target for MetS.

WED-464

Bridging the gap-how human microphysiological systems improve the translatability of NASH drug discovery

Ovidiu Novac¹, Raul Silva¹, Tomasz Kostrzewski¹. ¹CN Bio, Milton, United Kingdom
Email: Ovidiu.Novac@cn-bio.com

Background and aims: Non-alcoholic fatty liver disease (NAFLD) is one of the most prominent forms of chronic liver disease worldwide, reflecting the epidemic of global obesity. Those with progressive variant of NAFLD, non-alcoholic steatohepatitis (NASH), are at significantly greater risk of multisystem morbidity and mortality. Traditionally, preclinical trials are mainly based on 2D and in vivo animal models but have failed constantly to predict human drug efficacy as they lack translatability and inadequately recreate the complexity and multifaceted nature of this human disease. Building more predictive, human-relevant models is crucial to successfully bringing efficient anti-NASH therapies to the market. Microphysiological systems (MPS) recapitulate key aspects of human organs' phenotype and architecture. MPS models are currently undergoing rigorous validation studies so that in the future they may be fully adopted as standard preclinical assessment tools.

Method: Our in vitro NASH model uses a triple culture consisting of primary human hepatocytes, Kupffer and hepatic stellate cells, which are cultured together in 3D microtissue structures in a perfused MPS. The microtissues are cultured in medium containing free fatty acids for at least 2 weeks to induce a NASH-like phenotype.

Results: The PhysioMimix™ NASH model captures all key aspects of the human disease: intracellular hepatic fat accumulation, inflammation (secreted cytokines and chemokines such as IL-6, IL-8 and TNF α) and fibrosis (extracellular matrix components and profibrotic markers such fibronectin, and TIMP-1). Recently we validated our advanced MPS NASH model using two anti-NASH compounds, Obeticholic acid and Elafibranor. Both compounds matched clinical findings by significantly reducing inflammatory and fibrosis markers. Here, we further expand the validation of our NASH model by measuring the effects of two more anti-NASH compounds that are currently in late-stage NASH/NAFLD clinical trials. Selonsertib showed no antifibrotic or anti-inflammatory effects in our MPS NASH model at clinically relevant dosage, matching results from phase III STELLAR trials, despite reduced fibrosis and inflammation being detected in alternative 3D spheroid models. Aramchol showed a significant reduction in fibrosis (matching data from ARMOR Phase III study) and proved to be safe at highest tested concentration without altering liver microtissues' functionality.

Conclusion: Overall, we demonstrate how this NASH liver MPS provides translatable insights into drug efficacy for NASH therapeutics and brings a promising, sensitive alternative for pre-clinical NASH screening to help fast-track decision making and access to the market.

WED-465

Human skin stem cell-derived hepatic cells with genetic predisposition for liver fat accumulation mimic susceptibility to develop metabolic dysfunction-associated fatty liver disease

Alexandra Gatzios¹, Robim M Rodrigues¹, Joery De Kock¹, Matthias Rombaut¹, Dinja De Win¹, Vera Rogiers¹, Joost Boeckmans¹, Tamara Vanhaecke¹. ¹Vrije Universiteit Brussel, In vitro Toxicology and Dermato-cosmetology, Brussels, Belgium
Email: alexandra.gatzios@vub.be

Background and aims: Recently, a polygenic risk score was developed to predict hepatic fat content (PRS-HFC) based on single nucleotide polymorphisms (SNPs) in four genes, namely patatin-like phospholipase domain-containing protein 3 (PNPLA3) rs738409 C > G, transmembrane 6 superfamily member 2 (TM6SF2) rs58542926 C > T, glucokinase regulator (GCKR) rs1260326 C > T and membrane bound O-acyltransferase domain-containing 7 (MBOAT7) rs641738 C

POSTER PRESENTATIONS

>T. Here, we aim to investigate the impact of the PRS-HFC on the metabolic effects induced by triggers related to metabolic dysfunction-associated fatty liver disease (MAFLD), employing human skin-derived precursors (hSKP) differentiated towards hepatic cells (hSKP-HPC).

Method: The PRS-HFC was determined for 79 hSKP cell lines established from different donors and they were classified in three risk categories (R1, R2 and R3). Five cell lines were selected per category and differentiated towards hSKP-HPCs. The cultures were incrementally exposed for 24 hours to environmental MAFLD triggers, including fatty acids/fructose (condition 1) + ethanol (condition 2) + lipopolysaccharide (LPS)/tumor necrosis factor alpha (TNF α) (condition 3). The neutral lipid load was quantified and the expression of genes related to inflammation, oxidative stress, and lipid processing and synthesis was measured.

Results: Minor allele frequencies of 0.31, 0.04, 0.38 and 0.41 were found for *PNPLA3*, *TM6SF2*, *GCKR* and *MBOAT7*, respectively, which is in line with frequencies reported for the general population. The triggers from condition 3 induced the neutral lipid load significantly in all risk categories. Yet, R3 hSKP-HPC cultures exhibited a 1.5- to 2-fold higher lipid load in every test condition compared to R1 and R2 cultures. In addition, in condition 3, the induction of interleukin 6 (*IL6*) was approximately twice as high in R3 cultures (77-fold) compared to the other categories (R1 29-fold and R2 55-fold), whereas C-C motif chemokine ligand 2 (*CCL2*) was increased equally (approximately 15-fold) over all three categories. *Glutathione peroxidase 7* (*GPX7*), a marker of oxidative stress, was 1.3-fold higher in both R2 and R3 cultures compared to R1 hSKP-HPC cultures. In all test conditions, R3 donors appeared to have impaired mitochondrial beta oxidation, as indicated by a 2.5-fold lower expression of very long-chain acyl-coenzyme A dehydrogenase (*ACADVL*). Furthermore, *PNPLA3* levels were at least 2-fold lower in R3 hSKP-HPC cultures for all tested conditions compared to both R1 and R2, suggesting deficient lipase activity in these donors.

Conclusion: With increasing PRS-HFC, hSKP-HPC cultures exhibit greater susceptibility to MAFLD-inducing triggers and therefore could represent a human- and disease-relevant *in vitro* model to investigate the impact of genetic predisposition in the pathogenesis of MAFLD.

WED-466

The pan-PPAR agonist Lanifibranor improves increased portal pressure, endothelial dysfunction and liver histology in a rat model of early NAFLD

Shivani Chotkoe¹, Yao Liu¹, Guillaume Wettstein², Jean Louis Junien², Luisa Vonghia^{1,3}, Hannah Ceuleers¹, Joris De Man¹, Benedicte De Winter^{1,3}, Wilhelmus Kwanten^{1,3}, Sven Francque^{1,3}.

¹University of Antwerp, Laboratory of experimental medicine and pediatrics, Antwerp, Belgium, ²Inventiva, Daix, France, ³Antwerp university hospital, Gastroenterology and hepatology, Edegem, Belgium
Email: shivani.chotkoe@uantwerpen.be

Background and aims: An increased intrahepatic vascular resistance, related to endothelial dysfunction in early stages of non-alcoholic fatty liver disease (NAFLD), can potentially contribute to disease progression. The pan-peroxisome proliferator-activated receptor agonist Lanifibranor has demonstrated beneficial effects on liver histology in NAFLD patients, and in preclinical models of cirrhosis and portal hypertension. We studied the effects of Lanifibranor on the functional intrahepatic vascular alterations and on the histological features in early NAFLD in a preventive set-up in rats.

Method: Male Wistar rats (n = 8 per group) were fed a methionine-choline-deficient diet (MCD) or control diet (CD) for 4 weeks and received simultaneously vehicle or 100 mg/kg Lanifibranor daily via oral gavage QD. *In vivo* haemodynamics and blood pressures of the carotid artery, portal vein and inferior caval vein were measured, followed by *in situ ex vivo* liver perfusion in the same animal to assess

baseline transhepatic pressure gradient (THPG) at different flows (10–50 ml/min). Dose-response curves were generated with vasoconstrictors endothelin-1 (ET-1), methoxamine (Mx), and vasodilator acetylcholine (ACh) after Mx preconditioning. Histological staining was performed on liver tissue for examination using the steatosis-activity-fibrosis score and particle analysis for % steatosis quantification.

Results: In vehicle-treated animals, livers of MCD rats showed severe, grade 3 steatosis, without inflammation or fibrosis, compared to normal livers in CD rats. Moreover, MCD rats showed a significantly increased portal pressure *in vivo* compared to CD rats (5.64 ± 0.63 vs. 3.52 ± 0.24 mmHg, $p < 0.0001$), and THPG *ex vivo* was increased as well at every perfusion flow velocity (e.g., at 30 ml/min: 8.78 ± 0.35 vs. 6.73 ± 0.28 mmHg) with $p < 0.001$. Furthermore, the MCD rats were significantly hyperreactive to ET-1 and Mx, and hyporeactive to ACh compared to their CD counterparts. Treatment with Lanifibranor induced no changes in *in vivo* and *ex vivo* THPG measurements in CD rats, but completely normalized the portal pressure *in vivo* (from 5.64 ± 0.63 to 3.08 ± 0.28 mmHg, $p < 0.0001$) and THPG *ex vivo* at all flows (e.g., at 30 ml/min: from 8.78 ± 0.35 to 6.31 ± 0.15 mmHg, $p < 0.001$) in MCD rats. Lanifibranor improved the hyperreactivity to Mx and the hyporeactivity to ACh in MCD rats. Histology confirmed that Lanifibranor also improved steatosis with a $19.7 \pm 4.8\%$ ($p = 0.0001$) decrease of steatosis in MCD rats compared to vehicle.

Conclusion: Lanifibranor substantially reduces the increased portal pressure and related functional intrahepatic vascular alterations associated with early NAFLD, and it improves liver histology as well. These data support the role of intrahepatic vascular alterations in the development of NAFLD and NAFLD-related portal hypertension, and the potential of Lanifibranor as treatment for NAFLD.

WED-467

A new nuclear-erythroid-2-related factor 2 activator for the treatment of non-alcoholic steatohepatitis: evidence of metabolic and anti-fibroinflammatory effects in human precision cut liver slices

Adel Hammoutene^{1,2}, Samira Laouirem¹, Nathalie Colnot³, Miguel Albuquerque³, Angélique Brzustowski¹, Dominique Valla¹, Nicolas Provost², Philippe Delerive², Valérie Paradis^{1,3}. ¹Université Paris Cité, Inserm, Centre de recherche sur l'inflammation, F-75018 Paris, France, France, ²Cardiovascular and Metabolic Diseases Research, Institut de Recherches Servier, Suresnes, France, France, ³Département de Pathologie, Hôpital Beaujon, Assistance Publique-Hôpitaux de Paris, Clichy, France, France

Email: amsadel@hotmail.com

Background and aims: Oxidative stress triggers non-alcoholic steatohepatitis (NASH) and fibrosis. Previous animal studies demonstrated that the transcription factor NRF2, the master regulator of anti-oxidant response, protects against NASH and fibrosis. S217879, a next generation NRF2 activator has been shown to trigger NASH resolution and to reduce established fibrosis in rodents. Our aim was to evaluate the therapeutic potential of S217879 in NASH using the relevant experimental 3D model of human precision cut liver slices (PCLS), and to compare its effects to those of a reference molecule, Elafibranor (PPAR α /delta agonist).

Method: We treated PCLS from ten patients with various stages of metabolic-associated fatty liver disease (MAFLD, from simple steatosis to advanced NASH with cirrhosis) with S217879 (3 μ M) or Elafibranor (10 μ M) for two days. Safety and efficacy profile including impact on steatosis, liver injury, inflammation and fibrosis were assessed. Mechanisms involved in NASH pathophysiology, namely anti-oxidative stress response, autophagy and endoplasmic reticulum-stress, were also evaluated.

Results: Neither Elafibranor nor S217879 had toxic effects on human PCLS with MAFLD. PPAR α /delta target genes (*PDK4* and *FGF21*) and NRF2 target genes (*NQO1* and *HMOX1*) were strongly upregulated in PCLS in response to Elafibranor and S217879, respectively ($p <$

0.05). Compared to untreated PCLS, Elafibranor and S217879-treated slices displayed lower triglycerides and reduced inflammation (*IL-1 β* , *IL-6*, *CCL2*) ($p < 0.05$). Additional inflammatory markers (*CCL5*, *STING*, *ICAM-1*, *VCAM-1*) were downregulated by S217879 ($p < 0.05$). S217879 but not Elafibranor lowered DNA damages (p-H2A.X, *RAD51*, *XRCC1*) and apoptosis (cleaved Caspase-3), and inhibited fibrogenesis markers expression (α -SMA, *COL1A1*, *COL1A2*) ($p < 0.05$). Such effects were mediated through an improvement of lipid metabolism, activated anti-oxidant response and enhanced autophagic flux, without effect on endoplasmic reticulum-stress.



Figure:

Conclusion: This study highlights the therapeutic potential of a new NRF2 activator for NASH using patient-derived PCLS, and is a step towards the use of NRF2 activating strategies in clinical trials.

WED-468

The NRF2/b-TrCP axis: new therapeutic target in non-alcoholic steatohepatitis (NASH)

Raquel Fernández Ginés¹, Ana Isabel Rojo¹, José Antonio Encinar², Pilar López-Larrubia¹, Patricia Rada¹, Angela Martínez Valverde¹, Antonio Cuadrado¹. ¹Instituto de Investigaciones Biomédicas "Alberto Sols". IIBm (CSIC-UAM), Madrid, Spain, ²Universidad Miguel Hernández de Elche, Elche, Spain

Email: rfgines@iib.uam.es

Background and aims: Transcription factor NRF2 (nuclear factor erythroid 2-related factor 2) has been proposed recently as a promising target to treat non-alcoholic steatohepatitis (NASH). However, the most widely analysed NRF2 activators, acting on its main repressor, KEAP1, elicit many off-targets effects. As an alternative, we have described the first disrupter of the interaction between NRF2 and another NRF2 repressor, beta-TrCP, that we call PHAR.

Method: We evaluated the activity of this compound in the main cell types of the liver parenchyma: immortalized hepatocytes, hepatic resident macrophages (Kupffer cells) and hepatic stellate cells. Also, we tested the selective exposure to PHAR and NRF2 activation in liver through pharmacokinetics analysis in mice. Finally, we further analyzed the effect of this compound in the STAM model of progressive liver damage by Magnetic resonance imaging (NMR), measuring the fat/water ratio, and histochemistry of oil red (fat) and Sirius red (fibrosis), and correlated inflammatory and metabolic parameters with NRF2 activation.

Results: This compound activated NRF2 in the three main liver cell types. In hepatic resident macrophages (Kupffer cells) from wild type mice but not in Nrf2 knock-out mice, the compound protected against LPS-mediated inflammation. Moreover, PHAR protected against TGF-beta-induced fibrosis in stellate LX-2 cells. Importantly, mice that developed NASH in the STAM mouse model and were then submitted to chronic treatment with this compound for 2 weeks exhibited a significant protection against the fat accumulation, inflammation and fibrosis.



Figure:

Conclusion: These findings report an innovative mechanism to activate NRF2 that could be used as an alternative to conventional anti-inflammatory therapies and to protect the liver from NASH and fibrosis.

WED-469

Quantitative ultrasound for liver steatosis assessment: benefits of measurements over a large two-dimensional region of interest on the performance of image-brightness-based parameters

Baptiste Hériard-Dubreuil¹, Adrien Besson¹, Victor de Lédinghen^{2,3}, Dan Dutartre⁴, Françoise Manon², Joëlle Abiven², Anne-Laure de Araujo², Rhizlane Houmadi², Julie Dupuy², Juliette Foucher², Joel Gay⁵, Claude Cohen-Bacrie⁵. ¹E-Scopics, Ultrasound RandD, Saint-Cannat, France, ²Bordeaux University Hospital, Hepatology Unit, Pessac, France, ³INSERM U1312, BRIC, Bordeaux University, Bordeaux, France, ⁴Inria Bordeaux Sud-Ouest, Bordeaux, France, ⁵E-Scopics, Saint-Cannat, France

Email: baptiste.heriard-dubreuil@e-scopics.com

Background and aims: Ultrasound (US) imaging is recommended as the first line non-invasive modality to screen for significant steatosis, using qualitative assessment of liver US brightness. Quantitative brightness-derived parameters, US attenuation (UA) and backscatter coefficient (BSC), are known to be related to liver steatosis as US propagation properties of tissues correlate with fat content. Fibroscan® (FS) uses US signals captured with a 1D single element probe to measure UA, called Controlled Attenuation Parameter (CAP). The CAP measurement workflow requires a continuous acquisition and accumulation of independent values of UA over time so as to sample a large area of the liver with the 1D-single beam interrogation. This may lead to long screening times. We studied the benefits of a large region of interest (ROI) for the computation of UA and BSC based on US data collected with a new ultrafast point of care device, Hepatoscope™.

Method: 60 adult patients referred to routine hepatology consultation for chronic liver disease, including a FS exam, were enrolled in this prospective study (NCT04782050). Four Hepatoscope consecutive liver exams were added to routine care, performed by 2 operators (1 expert and 1 novice), during which 10 consecutive sets of US per-channel raw-data were collected. UA and BSC values, alongside individual quality indicators, were computed using three different sizes of ROI (small, medium and large). Medians of BSC and UA available values with sufficient quality were considered. Data were analysed to determine the intra- and inter-operator reproducibility and the r^2 correlation with FS new CAP.

Results: As show in the figure, the overall inter-operator reproducibility of medians of UA and BSC increased significantly with the size of ROI, starting from good and very good for small ROIs ($ICC_{UA} = 0.72$ and $ICC_{BSC} = 0.80$) and reaching excellent for large ROIs ($ICC_{UA} = 0.92$ and $ICC_{BSC} = 0.93$). The same trend was observed for intra-operator repeatability, reaching excellent for both experts ($ICC_{UA} = 0.93$ and $ICC_{BSC} = 0.94$) and novices ($ICC_{UA} = 0.91$ and $ICC_{BSC} = 0.93$). The

POSTER PRESENTATIONS

correlation between UA and BSC medians obtained with large ROIs and FS new CAP was good: $r^2_{UA} = 0.60$ and $r^2_{BSC} = 0.64$. The use of large ROIs improved the robustness of brightness-derived parameters estimation such that only one single UA and BSC value was sufficient to yield very good inter-operator reproducibility ($ICC_{UA} = 0.84$ and $ICC_{BSC} = 0.87$), very good and excellent intra-operator repeatability for both experts ($ICC_{UA} = 0.86$ and $ICC_{BSC} = 0.93$) and novices ($ICC_{UA} = 0.84$ and $ICC_{BSC} = 0.90$), and still showed good correlation with FS new CAP: $r^2_{UA} = 0.54$ and $r^2_{BSC} = 0.62$.

		Small ROI	Medium ROI	Large ROI
Inter-operator Reproducibility	ICC_{exp} [CI 95%]	0.72 [0.56-0.83]	0.81 [0.68-0.88]	0.92 [0.85-0.96]
	ICC_{nov} [CI 95%]	0.60 [0.49-0.68]	0.84 [0.73-0.91]	0.93 [0.88-0.97]
Intra-operator Reproducibility (experts)	ICC_{exp} [CI 95%]	0.77 [0.61-0.87]	0.82 [0.69-0.90]	0.93 [0.88-0.97]
	ICC_{nov} [CI 95%]	0.83 [0.71-0.90]	0.89 [0.79-0.94]	0.94 [0.88-0.97]
Intra-operator Reproducibility (novices)	ICC_{exp} [CI 95%]	0.79 [0.64-0.88]	0.89 [0.79-0.94]	0.91 [0.77-0.96]
	ICC_{nov} [CI 95%]	0.86 [0.78-0.93]	0.91 [0.83-0.96]	0.93 [0.84-0.97]
Correlation with new CAP (r^2)	r^2_{UA}	0.48	0.51	0.6
	r^2_{BSC}	0.57	0.59	0.64
Failure rate		8% (5 patients)	10% (6 patients)	22% (13 patients)
		Good (0.70-0.8)	Very good (0.80-0.9)	Excellent (0.90-1)

Figure:

Conclusion: UA and BSC measurements could be performed with the ultraportable point-of-care device Hepatoscope with very good intra- and inter-operator reproducibility. The performance of such measurements was directly linked to the size of the considered ROI, i.e., the volume of liver tissue that is being investigated. We found that using only one snapshot with a large ROI to estimate UA and BSC yielded excellent results, allowing low screening times for liver steatosis assessment. Future comparative studies with MRI-PDFF and histological scores will allow better assessment of the use of large ROIs UA and BSC estimation for steatosis staging.

WED-470

PNPLA3 I148M substitution exacerbate NAFLD under a long-term high fat diet

Huan Su¹, Madhuri Haque¹, Svea Becker¹, Karolina Edlund², Julia Duda², Qingbi Wang¹, Johanna Reißing¹, Hanns-Ulrich Marschall³, Lena Susanna Candels¹, Mohamed Ramadan Mohamed¹, Wilhelm Sjöland³, Till Strowig⁴, Jörg Rahnenführer², Jan G. Hengstler², Maximilian Hatting¹, Christian Trautwein¹. ¹University Hospital RWTH Aachen, Aachen, Germany, ²Technical University Dortmund, Dortmund, Germany, ³Gothenburg University, Gothenburg, Sweden, ⁴Helmholtz Centre for Infection Research, Braunschweig, Germany
Email: hsu@ukaachen.de

Background and aims: Initiation and progression of non-alcoholic fatty liver disease (NAFLD) is dependent on different genetic risk factors. Here, PNPLA3 I148M mutation of the phospholipase patatin-like phospholipid domain containing protein 3 (PNPLA3) is associated with severe disease progression. However, the role of PNPLA3 in chronic liver disease was not completely understood. Our aim is to investigate how PNPLA3 I148M mutation influences initiation and progression of chronic metabolic liver disease under high fat diet (HFD).

Method: Mice bearing wild-type *Pnpla3* (*Pnpla3*^{WT}), or the human polymorphism PNPLA3 I148M (*Pnpla3*^{I148M}) were subjected to a HFD for 24 and 52 weeks. The HFD contains 40 kcal% fat, 20 kcal% fructose and 2% cholesterol diet. The mice were set to fast for 3 hours before sacrifice. A detailed analysis was performed including the basic phenotype, inflammation, proliferation, cell death, fibrosis progression, microbiota as well bile acid (BA) metabolism.

Results: *Pnpla3*^{I148M} animals gained more body weight compared to *Pnpla3*^{WT} animals after the 17 weeks' time-point under HFD. After 24

weeks HFD liver injury marker AST/ALT were increased in I148M mice with 24 weeks HFD, in line with increased cell death and proliferation. *Pnpla3*^{I148M} mice had more immune cells infiltration in the liver compared to *Pnpla3*^{WT} animals only after 52 weeks HFD feeding. Moreover, *Pnpla3*^{I148M} mice fed with HFD for 52 weeks have stronger fibrosis and hepatic stellate cells activation as well as increased ductular proliferation and higher BA stool levels. Bacterial dysbiosis during HFD feeding were influenced by HFD feeding (36%) and the PNPLA3 I148M genotype (12%). RNA-sequencing analysis of liver tissue defined a *Pnpla3*^{I148M} specific expression pattern, which defines Kupffer cell and monocytes-derived macrophages as significant drivers of disease progression in *Pnpla3*^{I148M} animals.

Conclusion: The PNPLA3 I148M knockin model only develops a severe NASH liver phenotype after long-term feeding leading to obesity. Here significant differences were found compared to *Pnpla3*^{WT} animals showing that *Pnpla3*^{I148M} animals develop a specific phenotype triggered by bacterial dysbiosis and higher BA levels associated with a stronger Kupffer cell- and monocytes-derived inflammatory response leading to stronger fibrosis progression.

WED-471

A novel autophagy inducer attenuated non-alcoholic steatohepatitis by regulating the adenylylate cyclase 6 in hepatocytes

Hyun Jin Jung¹, Ming Li Jin¹, Ju-hee Kang¹, Jung Ho Hwang¹, Min Woo Kim¹, Sumin Hur², Sun Kyoung Kim³, Sung-Won Song³, Jung Ju Kim³, Hwan Mook Kim¹, Jae Hyun Kim⁴, Ki Tak Nam², Gyoonee Han⁴, Kwang Won Jeong¹, Seung Hyun Oh¹, Se Yong Park⁵. ¹College of Pharmacy, Gachon University, Korea, Rep. of South, ²Yonsei University College of Medicine, Korea, Rep. of South, ³Autophagy Sciences, Korea, Rep. of South, ⁴Yonsei University, Korea, Rep. of South, ⁵Seoul National University, College of veterinary medicine, Seoul, Korea, Rep. of South
Email: eyeball@hanmail.net

Background and aims: Autophagy is a critical process that regulates cellular metabolic homeostasis and was recently shown to be associated with non-alcoholic steatohepatitis (NASH). However, although NASH is one of the most prevalent diseases, approved pharmaceutical treatments are lacking. Here, we report that the therapeutic effects of an autophagy inducer (A4368) on NASH involve adenylylate cyclase 6 (AC6) regulation.

Method: A4368 was selected as an autophagy inducer from a focused library, and its effects were evaluated *in vitro* and *in vivo*. *In vitro* assays (kinase and enzyme-linked immunosorbent assays and immunoblotting) revealed that A4368 induced hepatic autophagy and decreased lipid accumulation and inflammatory and fibrogenic responses via AC6 regulation. Three different types of mouse models were used to investigate the therapeutic effects of A4368. NASH was induced by feeding mice a choline-deficient high-fat diet or western diet, and a Stelic animal model was developed.

Results: A4368 increased autophagic flux in hepatocytes but not in hepatic stellate cells or macrophages. It induced autophagy by directly binding to and inhibiting AC6, which resulted in accelerated clearance of lipid droplets in hepatocytes. A4368 significantly alleviated several parameters associated with NASH, including histological features in mouse models of NASH induced by three different types of high-fat diets.

Conclusion: In summary, the novel autophagy inducer A4368 could be a new therapeutic agent for NASH.

WED-472

Effect of vitamin D receptor signaling on endoplasmic reticulum stress in non-alcohol related steatohepatitis: exploring potential autophagy dependence

Basma Alaa¹, Olfat Hammam², Aiman El-Khatib³, Yasmeen Attia¹. ¹The British University in Egypt-BUE, Department of pharmacology, Cairo, Egypt, ²Theodor Bilharz research institute, Department of pathology, Giza, Egypt, ³Faculty Of Pharmacy Cairo University, Department of pharmacology and toxicology, Cairo, Egypt
Email: Basma.alaa@bue.edu.eg

Background and aims: Protecting the liver against cellular stress upon exposure to either exogenous or endogenous insults is a pivotal process governed by various processes among which is the endoplasmic reticulum (ER) protein folding in addition to autophagy induction, conserving cell homeostasis and fine-tuning apoptotic responses. A growing body of evidence suggests a correlation between ER stress and autophagy towards preserving the homeostatic immune response in the liver. The modulation of ER stress via autophagy induction has gained much traction recently, however, its role in a non-alcohol related steatohepatitis (NASH) context was little explored. Interestingly, vitamin D3 impact on either ER stress or autophagy was underscored in multiple pathological settings. This study, therefore, sought to unravel the potential impact of calcitriol (CAL), the active form of vitamin D3, on the modulation of ER stress in an experimental NASH model, providing insights on the likely autophagy dependence.

Method: Male C57BL/6 mice were kept on a dietary high-fat diet (HFD) to induce NASH and were allocated to the following 4 groups: (I) Normal group that was fed a balanced diet, (II) Positive control group (HFD) that was kept on a HFD, (III) CAL-treated group that received CAL at a dose of 5 ng/gm/day, i.p., twice per week, and (IV) CAL+HCQ-treated group that received CAL and the autophagy inhibitor, hydroxychloroquine (HCQ) at a daily dose of 60 mg/kg/day, p.o. Treatment started after 8 weeks of induction for a duration of 4 weeks. By the end of the experiment, livers were collected for histopathological examination, determining NASH score, and further analyses. Vitamin D receptor (VDR) gene expression levels were determined using qRT-PCR. Hepatic levels of inositol-requiring enzyme-1a (IRE1a) and caspase-3 were determined using ELISA for the assessment of ER stress and apoptosis, respectively. Statistical analysis was performed using one-way ANOVA followed by Tukey Kramer's post hoc test. Significance was considered at p values less than 0.05.

Results: Our findings demonstrated NASH amelioration and near-normal hepatic architecture with regard to hepatocytes, sinusoids, and portal tract arrangement in the livers of CAL-treated group. A reduction in NASH score with CAL treatment compared to the HFD group was also evident. This was coupled by an upregulation in hepatic VDR expression with CAL compared to the HFD untreated group. Regarding ER stress, IRE1a protein levels surged in the HFD group compared to normal, an effect that was curtailed by CAL treatment. Intriguingly, autophagy inhibition using HCQ reversed CAL effect on IRE1a, implying a likely autophagy dependency (Fig. 1). The increased hepatic levels of the apoptotic marker, caspase-3, observed in the HFD group were curbed by CAL treatment. Likewise, the latter effect was reversed when HCQ was given in combination.

Conclusion: The current study, therefore, suggests a potential autophagy-dependent impact of CAL on ER stress in NASH.

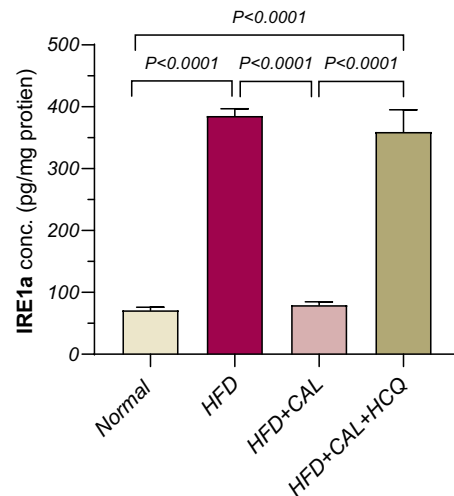


Figure: Effect of CAL on IRE1a protein levels in normal, HFD, CAL-treated, and CAL+HCQ-treated groups, as determined by ELISA. Statistical analysis was performed using One-way ANOVA followed by Tukey Kramer post hoc test for multiple comparisons. Data are presented as means \pm SD.

WED-473

Improvement of liver fibrosis by a novel long acting Glucagon/GLP-1/GIP triple agonist, efocipegtrutide (HM15211) in carbon tetrachloride-induced mouse model of liver injury and fibrosis

Jong Suk Lee¹, Yohan Kim¹, Jung Kuk Kim¹, Hyunjo Kwon¹, Eun Jin Park¹, Jeong A Kim¹, Sang Hyun Park¹, Sung Min Bae¹, Sang Hyun Lee¹, In Young Choi¹. ¹Hanmi Pharm.Co., Ltd., Korea, Rep. of South
Email: iychoi@hanmi.co.kr

Background and aims: Fibrosis is the pathologic result of chronic inflammation due to NASH, which can progress to liver cirrhosis, and causes liver-related complications. However, no drug has been approved to date. Thus, to provide a novel therapeutic option with more predictable therapeutic benefits, a novel long-acting Glucagon/GLP-1/GIP triple agonist, efocipegtrutide, was developed and its efficacy has been extensively evaluated in various animal models of NASH and/or fibrosis such as MCD, AMLN, CDAHFD, and TAA mice. To generalize its potential therapeutic benefits, anti-fibrotic effect of efocipegtrutide was further evaluated in carbon tetrachloride (CCl₄)-induced fibrosis mouse, one of the well-established models of liver fibrosis.

Method: To induce liver fibrosis, 20% CCl₄ was 3 times/week intraperitoneally injected to C57BL/6 male mouse for 10 weeks and efocipegtrutide was administrated during the last 6 weeks. To evaluate the therapeutic effect of efocipegtrutide on fibrosis, hepatic pro-collagen 1 alpha 1 contents, hydroxyproline contents (HP) and Sirius red staining area were measured. Additionally, blood surrogate markers and hepatic fibrosis related gene expression level were analyzed.

Results: CCl₄ mice showed various liver fibrosis profiles. However, treatment of efocipegtrutide effectively improved these fibrosis profiles such as hepatic pro-collagen 1 alpha 1 contents (0.89 μ g/g vs. 1.22 μ g/g for CCl₄, vehicle; p < 0.05), hydroxyproline contents (348.6 nmol/g vs. 430.5 nmol/g for CCl₄, vehicle; p < 0.001) and sirius red positive area (2.46% vs. 4.81% for CCl₄, vehicle; p < 0.001). Also, meaningful reduction of hepatic fibrosis marker genes expression (collagen 1 alpha 1, collagen 3 alpha 1 and alpha-smooth muscle actin) were observed in efocipegtrutide-treated group. Furthermore, blood surrogate biomarkers of fibrosis and inflammation (TIMP-1, PIINP and TNF-alpha) were markedly improved by efocipegtrutide treatment.

POSTER PRESENTATIONS

Conclusion: Efocipegrutide effectively improved liver fibrosis in CCL₄-induced fibrosis mice. These results are consistent with previous study results in various NASH/fibrosis animal models, in which further reinforcing the robust anti-fibrotic effect of efocipegrutide via simultaneous action of GCG, GLP, and GLP-1. Human study is ongoing to assess the clinical relevance of these findings.

WED-474

A translational rat model to study metabolic associated fatty liver disease with fibrosis and portal hypertension

Aurora Barberá¹, Imma Raurell^{1,2}, María Martínez-Gómez¹, Mar Gil¹, Juan Manuel Pericàs^{1,2}, Joan Genesca^{1,2}, María Martell^{1,2}. ¹Liver Diseases, Vall d'Hebron Institut de Recerca (VHIR), Liver Unit, Hospital Universitari Vall d'Hebron (HUVH), Vall d'Hebron Barcelona Hospital Campus; Universitat Autònoma de Barcelona (UAB), Barcelona, Spain, ²Centro de Investigación Biomédica en Red de Enfermedades Hepáticas y Digestivas (CIBERehd), Madrid, Spain
Email: maria.martell@vhir.org

Background and aims: The use of animal models is crucial to understand the underlying mechanisms in the onset and progression of metabolic associated fatty liver disease (MAFLD) and to develop novel therapeutic strategies. Moreover, the concept of MAFLD is not as restrictive as NAFLD and other potential causes of liver damage can coexist with metabolically-induced fatty liver and steatohepatitis (NAFLD), being alcohol consumption the most frequent liver injury in Southern European countries (MAFLD-OH). Although several animal models have been used in the field, there is an ongoing challenge to identify those models that best mimic human pathology to allow good translation of the obtained results into the clinics. We aimed to

develop a dietary rat model that reproduces the full MAFLD phenotype observed in human disease, including features of the metabolic syndrome, steatohepatitis with liver fibrosis and portal hypertension.

Method: For model development, male Sprague-Dawley rats were fed 16 weeks with control diet (CD), high-fat high-cholesterol diet with glucose/fructose beverage (HFHC/GF) or the same diet plus 1–3% ethanol added to the GF drink (HFHC/GF-OH). Liver biopsies were performed on some individuals at 12 weeks to evaluate fibrosis. By the end of week 16, liver hemodynamics, histology and metabolic parameters were characterized.

Results: Sirius Red staining revealed that the rats from HFHC/GF and HFHC/GF-OH groups developed perisinusoidal fibrosis by week 12. The HFHC/GF and HFHC/GF-OH livers also showed severe steatosis and inflammatory infiltrates. The diet intervention did not induce significant increments in body weight at any time point. However, the liver to body weight ratio increased significantly more in the HFHC groups compared with the CD at 16 weeks. Portal pressure (PP) significantly increased in both HFHC/GF and HFHC/GF-OH groups compared to CD group (13.29 and 12.16 mmHg vs 8.74 mmHg, respectively). No significant differences in PP were found between HFHC groups. HFHC diet was associated with significant increases in fasting blood concentrations of AST, ALT, cholesterol, alkaline phosphatase, creatine kinase and albumin.

Conclusion: This translational animal model could become a suitable model for basic research of advanced stages of MAFLD and also for drug testing in this pathology.

Funded by Instituto de Salud Carlos III [PI18/00947, PI21/00691].

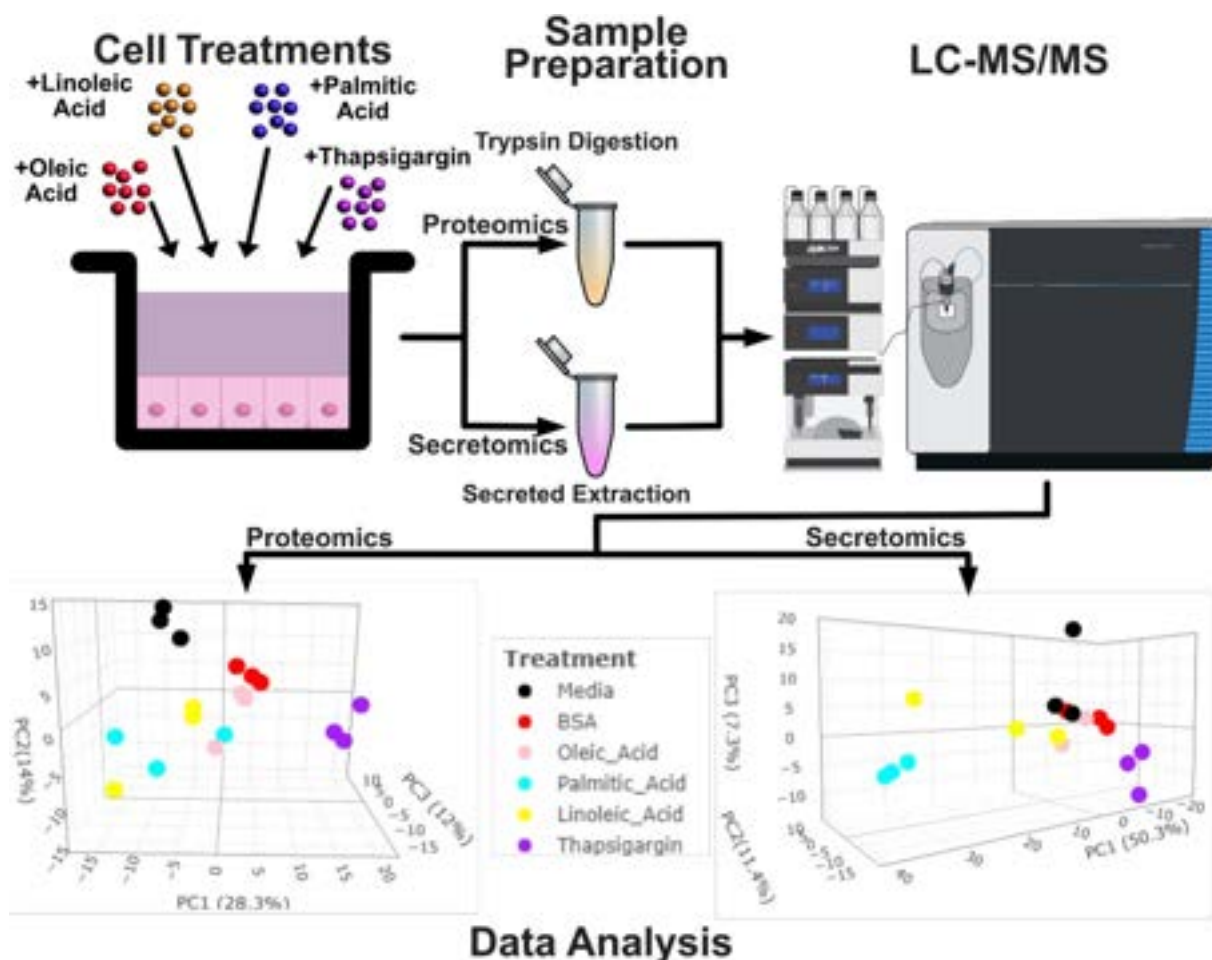


Figure: (abstract: WED-475).

WED-475

Secretomics identifies IGFBP1 as a stress signaling marker in human models for NAFLD

Ruth Walker¹, Maria Emilia Dueñas¹, Jeremy Palmer², Jose Luis Marin-Rubio¹, Quentin Anstee^{2,3}, Matthias Trost¹, Olivier Govaere^{3,4}. ¹Newcastle University, Biosciences Institute, Faculty of Medical Sciences, Newcastle Upon Tyne, United Kingdom, ²Newcastle University, Translational and Clinical Research Institute, Faculty of Medical Sciences, Newcastle Upon Tyne, United Kingdom, ³Newcastle upon Tyne Hospitals NHS Trust, Newcastle NIHR Biomedical Research Centre, Biomedical Research Building, Newcastle Upon Tyne, United Kingdom, ⁴KU Leuven, Translational Cell and Tissue Research lab, Department of Imaging and Pathology, Leuven, Belgium
Email: r.h.walker2@newcastle.ac.uk

Background and aims: Lipid accumulation is a key part of the pathogenesis of non-alcoholic fatty liver disease (NAFLD) and has recently been associated with endoplasmic reticulum (ER) stress. *In vitro* lipid loading is often used as an experimental model for NAFLD, though an understanding of the metabolic changes and lipotoxicity is still lacking. This work explored the proteomic and secretomic differences induced by ER stress or lipid accumulation in cell models by using mass spectrometry (MS)-based approaches to gain an insight into the mechanism underlying NAFLD.

Method: Primary human hepatocyte cells were treated with saturated and unsaturated fatty acids including linoleic (LA), oleic (OA), and palmitic acid (PA) at 400 μ M, or with the ER stress inducer thapsigargin (1 mM) for 24 hours. Secreted proteins in the culture media were isolated 3 hours before collection. Treated samples were screened by Matrix-assisted laser desorption/ionization-time-of-flight mass spectrometry (MALDI-TOF MS) to determine differences in the phenotypic profiles of metabolites and high molecular weight biomolecules, and proteins were identified by data-independent acquisition on an Orbitrap Fusion Lumos Tribrid MS (LC-MS/MS).

Results: Distinctive metabolite profiles were established for each condition by MALDI-TOF MS, allowing multiplexing and identification of biomarkers. LA and PA, especially, induced a comprehensive switch in metabolites, while substantial protein changes were observed upon PA and ER-stress treatment. LC-MS/MS proteomics analysis of the primary cells identified 170 differentially expressed proteins in the LA condition, 8 in the OA, 225 in the PA, and 966 in the ER-stress condition. Changes in the expression of NAFLD-relevant markers as p62 or GDF15 proved to be dependent on the treatment condition. Interestingly, ER-stress induction showed an increase in metabolic-related proteins, including perilipin-2 and glucokinase. A strong increase in Insulin-like growth factor-binding protein 1 (IGFBP1) expression was observed in LA, PA, and ER-stress treatments. The secretomic phenotype of primary human hepatocytes differed drastically depending on the underlying lipid or ER-stress challenge. The analysis characterized 21 differentially expressed proteins upon LA treatment, only 1 with OA, 1789 with PA, and 77 upon ER stress induction, when compared to their respective controls. The release of perilipin-2 was observed in each lipid treatment condition. PA and ER-stress treatments had an intersection of 42 proteins, many relating to metabolic processes such as retinol or steroid metabolism, with IGFBP1 being the top marker in both comparisons.

Conclusion: This study identified commonalities but also distinct different secretomic and proteomic profiles of stress mediators in NAFLD.

WED-476

Serum exosomal mir-4668-5p in Non-alcoholic Fatty liver Disease (NAFLD) patients with significant liver fibrosis

Jong Eun Yeon¹, Young-Sun Lee¹, Eunjung Ko¹, Yoonseok Lee¹, Sun Young Yim², Young Kul Jung³, Ji Hoon Kim¹, Yeon Seok Seo², Hyung Joon Yim³. ¹Korea University Medical College Guro Hospital, Internal Medicine, Seoul, Korea, Rep. of South, ²Korea University Medical College Anam Hospital, Korea, Rep. of South, ³Korea University Medical College Ansan Hospital, Korea, Rep. of South
Email: jeyyeon@hotmail.com

Background and aims: In worldwide, fatty liver disease in non-significant amount of alcoholic drinker (Non-alcoholic fatty liver disease (NAFLD)) are on the rise as obesity and diabetes increase. Among the histologic changes, degree of liver fibrosis is the most important factor for predicting long term outcomes. Although liver biopsy is the gold standard for diagnosis, serious complication and variability of sampling and interpretation made it difficulties in routine clinical practice. Aim of our study is to explore the clinical significance of serum exosomal miRNA in liver fibro-genesis of NAFLD patients.

Method: 47 biopsy-proven NAFLD patients were included. Exosome was isolated from serum samples and serum exosomal miRNA was analyzed with GeneChip miRNA 4.0 array (Affymetrix, U.S.A.). Also, we analyzed the expression of miRNA in liver tissues of the same patient who had been tested for serum exosomal miRNA. To define the role of miRNA in liver fibrogenesis, human hepatic stellate cell was transfected with miRNA of interests. Serum and liver samples from mice feed with high fat high fructose (HFHF) diet for 24 weeks were analyzed for comparison with human.

Results: NAFLD patients with advance fibrosis group (Gr1) were older, having more metabolic syndrome, lower platelet counts, prolonged PT INR compared to that of non-significant fibrosis group (Gr2). A total of 86 serum exosomal miRNA were significantly changed between Gr.1 and Gr.2, Of which 42- and 44-miRNA showed significantly higher or lower expression in Gr.1 compared to Gr.2. Of them, MiR4668-5p was selected because of it were one of the highest altered miRNA in Gr.1 compare to Gr.2. When human hepatic stellate cell (LX2 cell) was transfected with 4668-5p mimics or inhibitors, mRNA of TGF- β , α -SMA and collagen1A1 expression were significantly elevated and reduced after each transfection. In mice feed with HFHF diets, mRNAs involved in lipid uptake, transport, and oxidation were altered. TGF-b1 and a-SMA and col1A1 expression were altered in HFHF group.

Conclusion: Serum exosomal miRNAs were significantly altered in NAFLD patients with advanced fibrosis. Among them, serum exosomal miRNA-4668-5p has significant role in liver fibrosis. Although additional researches are required, serum exosomal miRNA may have a diagnostic value or therapeutic target of liver fibrosis in NAFLD patients.

WED-505

Rilpivirine as an anti-inflammatory agent in non-alcoholic fatty liver disease: evidence from human hepatocytes, hepatic stellate cells and blood cells

Isabel Fuster-Martínez^{1,2}, Ángela B. Moragrega^{1,2}, Aleksandra Gruevska^{1,2}, Ana Benedicto^{1,2}, Joan Tosca³, Cristina Montón³, Elena Muñoz⁴, Dimitri Dorcarrato⁴, Juan V. Esplugues^{1,2,5}, Nadezda Apostolova^{1,2,5}, Ana Blas-García^{2,5,6}. ¹University of Valencia, Department of Pharmacology, Valencia, Spain, ²FISABIO-University Hospital Dr. Peset, Valencia, Spain, ³Hospital Clínic Universitari de Valencia, Department of Digestive Medicine, Valencia, Spain, ⁴Hospital Clínic Universitari de València, Department of Surgery, Liver, Biliary, and Pancreatic Unit, Biomedical Research Institute INCLIVA, Valencia, Spain, ⁵Biomedical Research Networking Center in Hepatic and Digestive Diseases (CIBERehd), Spain, ⁶University of Valencia, Department of Physiology, Valencia, Spain
Email: ana.blas@uv.es

POSTER PRESENTATIONS

Background and aims: Drug repurposing is emerging as an attractive approach to identify compounds with potential applications in non-alcoholic fatty liver disease (NAFLD). Rilpivirine (RPV), an antiretroviral used to treat HIV infection, has been described as an anti-fibrotic, anti-inflammatory and anti-steatotic drug in several *in vivo* studies. We aimed to characterize the mechanisms underlying its anti-inflammatory effects, focusing on its specific actions on blood and hepatic cells.

Method: The effects of RPV were evaluated both *in vitro* (human hepatic cell lines, primary hepatic stellate cells -HSC- and monocyte-derived macrophages -MDM-, both from healthy donors) and *ex vivo* (peripheral blood mononuclear cells -PBMC- isolated from patients with chronic liver disease). To reproduce NAFLD conditions, cells were incubated for different periods of time with RPV in the absence or presence of fatty acids and/or pro-inflammatory (LPS) or fibrogenic cytokines (TGF beta) in the medium. The molecular routes involved were studied using transcriptomic analysis and standard molecular biology techniques (RT-PCR, Western Blot and ELISA).

Results: RPV reduced the phosphorylation and the nuclear translocation of p65, as well as its pro-inflammatory target genes *IL1B*, *IL18*, *CASP1*, *TNFA* and *CXCL8* in fatty acid-overloaded hepatocytes. Similar effects were observed in activated HSC and LPS-treated MDM, in which RPV also inhibited the NLRP3-inflammasome pathway, decreasing NLRP3 protein expression, Caspase-1 activation and *IL1B* gene expression. RNA sequencing transcriptomic analysis and gene set enrichment analysis in activated HSC demonstrated that RPV downregulated GO processes associated with response to cellular stress, including the positive regulation of stress-activated MAPK cascade. In line with these results, analysis of stress-activated protein

kinases by Western Blot showed a clear inhibition of the JNK-mediated pathway induced by this drug in these cells as well as in FA-overloaded hepatocytes and MDM. RPV also significantly decreased the synthesis and release of the chemoattractant CCL2 in HSC and MDM, downregulating leukocyte chemotaxis and migration. Finally, *ex vivo* experiments with PBMC demonstrated that RPV exerted an anti-inflammatory effect by enhancing the expression of STAT3-mediated pathways and downregulating the activation of STAT1 and its target genes.

Conclusion: The antiretroviral drug RPV exerts anti-inflammatory actions on injured hepatocytes, activated HSC, macrophages and PBMC. The findings point to a beneficial role of RPV in NAFLD.

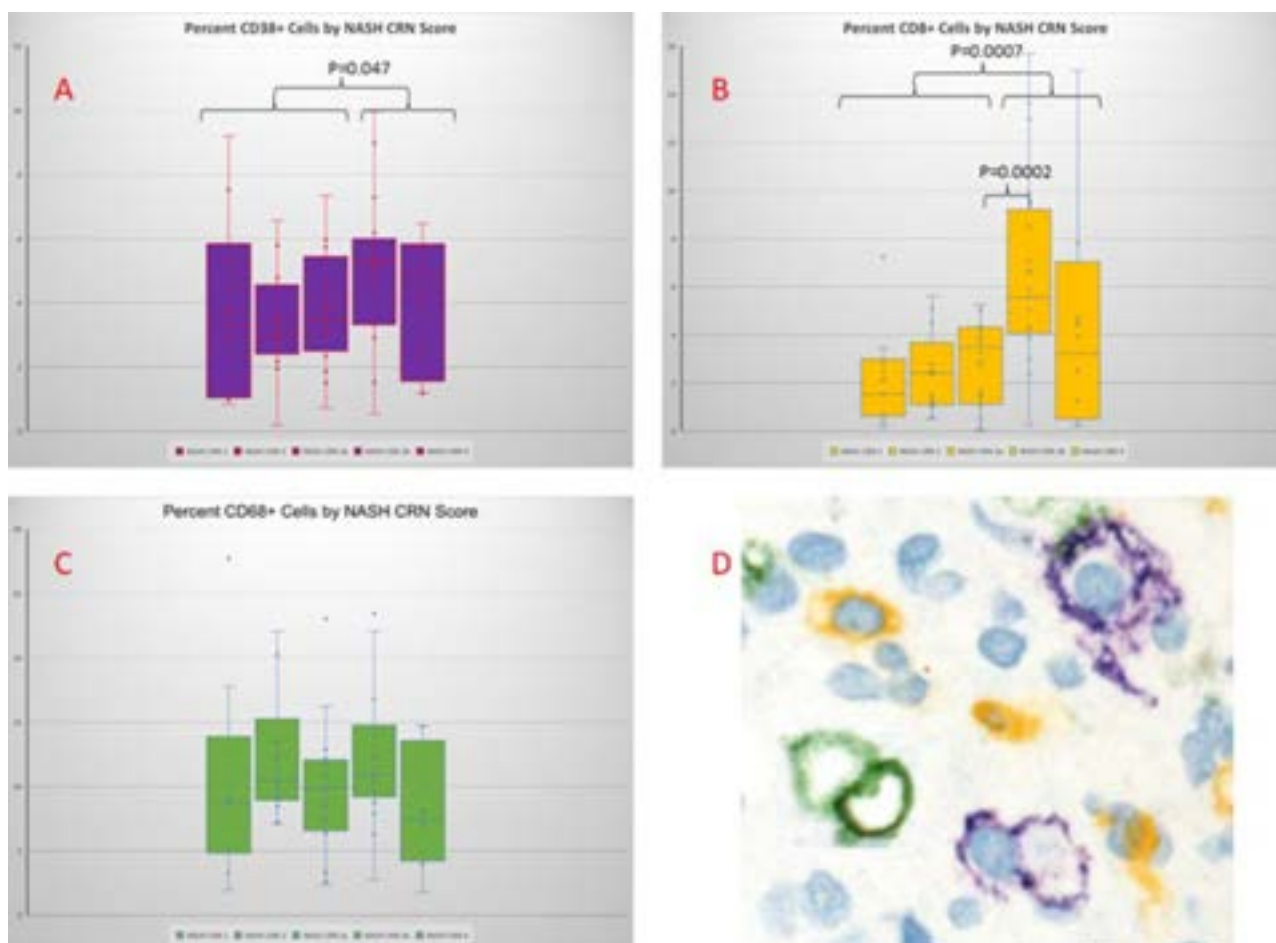
WED-506

Characterization of portal inflammation and hepatic fibrosis in non-alcoholic fatty liver disease

Annie Masters¹, James M Estep^{1,2}, Lakshmi Alaparthy³, Gary Brattbauer³, Aybike Bireddinc^{1,2}, Fanny Monge³, Cassandra Sharp³, Daisong Tan⁴, Hala Abdelaal³, Zachary Goodman³, Zobair Younossi^{1,2,3}. ¹George Mason University, School of Systems Biology, United States, ²Inova Health System, Beatty Liver and Obesity Research Program, Department of Medicine, United States, ³Inova Health System, Center for Liver Disease, Department of Medicine, United States, ⁴Inova Health System, Center for Liver Disease, Department of Medicine, Falls Church, United States

Email: zobair.younossi@inova.org

Background and aims: The relationship between inflammation and the progression of hepatic fibrosis in the context of non-alcoholic



fatty liver disease (NAFLD) has not been formally characterized. The aim of this pilot study is to histologically quantify lymphocytic effector cells and Kupffer cell/macrophage populations in the liver biopsies of NAFLD patients with various stages of fibrosis.

Method: Liver needle biopsy slides from patients with NAFLD and a range of NASH CRN scores (N=65) were immunohistochemically stained on a Discovery Ultra (Roche) in multiplex CD8 (Yellow; cytotoxic T-cells), CD68 (Green; Kupffer cells/macrophages), and CD38 (Purple; plasma cells). Stained biopsies were scanned using an Aperio AT2 (Leica Microsystems) and analyzed using HALO's Multiplex IHC module. Cells were segmented using a combination of the nuclear/cytoplasmic staining and each cell is individually measured for nuclear/or cytoplasmic Frequency of stained cell types by NASH CRN score was assessed by descriptive statistics and Mann-Whitney analysis.

Results: Of the biopsies analyzed in this pilot study (N=65), 10 subjects were categorized as NASH CRN stage 1, 14 stage 2, 33 stage 3 which was split into 3a (mild bridging, N=16) and 3b (marked bridging, N=17) inspired by the Ishak scoring system, and 8 were stage 4. The relative frequency of effector lymphocytes increased with NASH CRN stage ($p=0.03$). Pairwise analysis revealed a significant increase in cytotoxic T-cells between NASH CRN stages 3a and 3b ($p=0.0002$), as well as an overall increase in both plasma cells and cytotoxic T-cells when comparing stages 3b and above to stages 1 through 3a ($p=0.047$, and $p=0.0007$, respectively) (Figure).

Conclusion: Progression to advanced fibrosis in NAFLD is characterized by an increase in effector B and T cell types. In this pilot study, our method has been effectively used to objectively quantify inflammatory cell types as they relate to hepatic fibrosis in NAFLD patients. This quantification method can be used in future studies to assess the contribution region specific immune cell infiltration to the progression of fibrosis in NASH.

WED-507

b-Klotho deficiency in hepatic stellate cells (HSCs) prompts inflammation, oxidative stress and a pro-fibrotic phenotype

Giada Tria¹, Erika Paolini¹, Miriam Longo¹, Nadia Panera², Roberto Piciotti¹, Anna Alisi², Marica Meroni¹, Paola Dongiovanni¹.

¹Fondazione IRCCS Cà Granda Ospedale Maggiore Policlinico, Milan, Italy; ²General Medicine and Metabolic Diseases; Milan, Italy, ²Bambino Gesù Children's Hospital-IRCCS, Research Unit of Molecular Genetics of Complex Phenotypes, Italy

Email: paola.dongiovanni@policlinico.mi.it

Background and aims: β -Klotho (*KLB*) gene encodes the hepatic co-receptor of fibroblast growth factor receptor 4 (FGFR4). We previously reported that the rs17618244 G > A *KLB* gene variant dampened *KLB* hepatic and plasma levels, leading to inflammation, ballooning and fibrosis both in pediatric and adult patients with non-alcoholic fatty liver disease (NAFLD). Hepatic stellate cells (HSCs) are directly involved in the fibrotic processes, playing a crucial role in the switching to severe forms of NAFLD. Aim of this study was to generate a cell line of hepatic stellate cells (HSCs), responsible for hepatic fibrosis, which are deleted for *KLB*, and to investigate the impact of its deficiency on their pro-fibrotic phenotype, inflammation and oxidative stress.

Method: We stably silenced *KLB* gene in LX2 cells (referred to as HSCs *KLB*^{-/-}) by Crispr-Cas9 technology. Then, markers of activation, cellular stress, inflammation and proliferation have been investigated.

Results: *KLB* mRNA and protein levels were reduced in HSC *KLB*^{-/-} cells ($p < 0.05$). Markers of activation (i.e., α SMA, COL1A1/3A1/4A1, TGF β , PDGFR β) were increased in *KLB*^{-/-} cells at both gene and protein levels. Accordingly, retinol synthesis (RALDH) and the expression of *BAMBI* were reduced ($p < 0.05$), suggesting a more pro-fibrotic phenotype. Moreover, *KLB* deletion strongly induced oxidative stress, enhancing ROS/reactive nitrite species (RNS) and aldehyde derivative concentrations (MDA) ($p < 0.05$). These events triggered the release of pro-inflammatory cytokines (TNF α , IL1 β and IL6) into the

KLB^{-/-} cultured media. Finally, *KLB* shortage leads to reduced ATP synthesis and higher lactate release, which may be suggestive of enhanced glycolytic rate and of a trend towards a pro-cancerous microenvironment. In keeping with these findings, *KLB*^{-/-} cells also showed an elevated proliferative rate, more rapid wound healing repair and higher invasiveness compared to wild-type counterpart ($p < 0.05$).

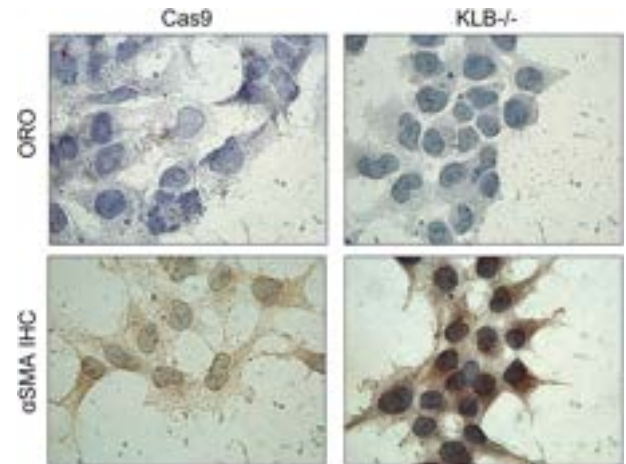


Figure: Oil Red O (ORO) staining (upper panel) and α SMA IHC (lower panel) on LX2 control (Cas9 positive) and silenced for *KLB* gene in 1000x magnification.

Conclusion: We generated, for the first time, a stable knock-out of *KLB* in HSCs. Our preliminary results outlined that *KLB* deficiency induced an enhanced pro-fibrotic phenotype with increased proliferation, inflammation and oxidative stress, thus possibly explaining the association between the rs17618244 *KLB* at-risk variant and more severe forms of liver damage. Altogether, these observations pointed *KLB* a novel target to prevent severe NAFLD.

WED-508

A functional investigation of NASH-associated gene polymorphisms in human liver tissue

Amy Shepherd¹, Jack Leslie¹, Fiona Oakley¹, Derek Mann¹, Jelena Mann¹. ¹Biosciences Institute, Newcastle Fibrosis Research Group, 4th Floor, William Leech Building, Biosciences Institute, Newcastle University, Medical School, Newcastle upon Tyne, United Kingdom
Email: jelena.mann@newcastle.ac.uk

Background and aims: Development of NAFLD has a multifactorial etiology that includes a strong genetic component. A number of single nucleotide polymorphisms (snps) have been identified within genes involved in regulation of hepatic fat metabolism; these snps have been shown in population studies to be associated with differential long-term disease outcome. We have established precision cut liver slices (PCLS) that maintain the architectural integrity, functionality and metabolic activities of the tissue over an extended period, which for the first time allows in vitro modelling of liver disease using genotypically diverse human donor tissue.

Method: PCLS were generated from 44 liver donors and tissue genotyped using the primers for: MBOAT7 rs641738 C > T, GCKR rs1260326 (P446L) and PNPLA3 rs738409 C > G (I148M). PCLS were exposed to profibrogenic stimuli or to lipid loading to examine the effect of the snps on induction of fibrosis, lipid accumulation and inflammation in the human liver tissue. PCLS media was sampled longitudinally and assayed for Collagen1a1 and IL6 while tissue harvested at the end of experiments was assayed for triglyceride content and stained with Picrosirius Red to measure fibrosis induction.

Results: Presence of MBOAT7 rs641738 C > T, GCKR rs1260326 (P446L) and PNPLA3 rs738409 C > G (I148M) snps on one or both

POSTER PRESENTATIONS

alleles caused an increase in triglyceride accumulation in the lipid loaded donor tissue, which was in some patients associated with increase in inflammatory markers but not always associated with increase in fibrogenesis. For some snps, the increase in donor age or gender had an effect on triglyceride accumulation in PCLS.

Conclusion: Human PCLS modelling of liver fibrosis and lipid loading has, for the first time, provided experimental evidence of the effect that MBOAT7 rs641738 C>T, GCKR rs1260326 (P446L) and PNPLA3 rs738409 C>G (I148M) snps exert on liver tissue responses to profibrogenic and lipid mediated stimuli. This provides new mechanistic insights into disease processes and provides an unrivalled platform for study of genotype and phenotype in aged tissue.

WED-509

Effect of housing temperature on non-alcoholic fatty liver disease development in C57BL/6N mice

Olga Horakova¹, Gabriella Sistilli¹, Veronika Kalendova¹, Tomas Cajka², Carolin Lackner³, Martin Rossmeisl¹. ¹Institute of Physiology of the Czech Academy of Sciences, Laboratory of Adipose Tissue Biology, Prague, Czech Republic, ²Institute of Physiology of the Czech Academy of Sciences, Laboratory of Translational Metabolism, Prague, Czech Republic, ³Medical University of Graz, Institute of Pathology, Graz, Austria
Email: olga.horakova@fgu.cas.cz

Background and aims: Non-alcoholic fatty liver disease (NAFLD) is associated with obesity and metabolic syndrome. NAFLD can progress to more severe stages, such as steatohepatitis. Recently, thermoneutral housing (TN) was found to promote human-like NAFLD in high-fat diet (HFD)-fed C57BL/6J mice, characterized by obesity and increased pro-inflammatory liver responses. Given the known differences in the development of steatohepatitis between substrains of C57BL/6 mice, we aimed to determine how TN affects NAFLD pathogenesis in another frequently used substrain, i.e. C57BL/6N.

Method: Male C57BL/6N mice were fed standard diet or HFD (lipids ~60 energy%) for 24 weeks starting at 11 weeks of age. Mice were housed in either standard (22°C) or TN (30°C) environment. At week 21, tail blood was collected from overnight fasted mice to measure glycemia and plasma levels of metabolites and hormones. Metabolipidomic profiling of liver samples (~20 mg) was performed using an untargeted workflow combining lipidome, metabolome and exposome (LIMeX) and partial least squares discriminant analysis (PLS-DA). Histopathologic analysis of hepatic steatosis, inflammation and fibrosis was also performed.

Results: Weight gain and hepatic steatosis were increased in HFD-fed mice, regardless of ambient temperature. No difference was observed in histological scores of liver inflammation and fibrosis, which were generally low and did not correspond to increased tissue expression of inflammatory and tissue remodeling markers in HFD-fed mice, showing only marginal increase due to TN. Although the results of liver metabolipidomic profiling in HFD-fed mice supported the involvement of autophagy-related metabolites in HFD-induced NAFLD, they did not reveal a substantial effect of TN. Conversely, in standard-diet-fed mice, TN increased weight gain, overall adiposity, adipocyte hypertrophy, hepatic steatosis, and NAFLD activity score. This was accompanied by increased de novo lipogenesis and marked changes in the hepatic metabolome characterized by a complex decrease of various phospholipid species and metabolites involved in the urea cycle and oxidative stress defense.

Conclusion: In conclusion, TN appears to exacerbate NAFLD phenotype depending on C57BL/6 substrain and diet.

WED-510

Preclinical characterization of HPG7233, a potent, liver-target and highly selective thyroid hormone receptor beta agonist for non-alcoholic steatohepatitis

Michael Xu¹, Shijia Chen¹, Fang Guo¹, Que Liu¹, Yongheng Liu¹, Cheng Mo¹, Yihong Peng¹, Yating Xiong¹, Peibin Zhai¹, Pan Zhang¹, Xinpeng Zhao¹, Xin Zhou¹, Xin-Jie Chu¹. ¹Hepagene, Shanghai, China
Email: michael.xu@hepagene.com

Background and aims: Non-alcoholic fatty liver disease (NAFLD) is rapidly becoming the most common chronic liver disease worldwide, with an approximate prevalence of 20–30% in western countries. An estimated 20–25% of these patients will further progress to non-alcoholic steatohepatitis (NASH), marked by steatosis, inflammation and hepatocyte ballooning with or without fibrosis. HPG7233 is a novel liver-targeted and highly selective small molecule thyroid hormone receptor beta (THR-beta) agonist aimed at serum and liver lipid metabolism. Here we report favorable pharmacology and pharmacokinetic profiles of HPG7233 for NAFLD and NASH treatment.

Method: In vitro binding assay: The binding assay of THR alpha and THR beta in vitro is determined by coactivator peptide to the receptors. In vivo pharmacokinetic study: Both selected and control compounds are evaluated in Sprague-Dawley rats at 3 mg/kg and in beagle dog at 10 mg/kg for single dose of oral administration. In vivo efficacy study: Liver index, serological markers and NAFLD activity score (NAS) in the efficacy study are evaluated in a HFD-CCl4 NASH model at 5 mg/kg.

Results: HPG7233 shows a superior liver targeting profile in vivo. L/P (liver/plasma) exposure ratio is about 20 in animals, meanwhile, the relative beta/alpha binding selectivity in vitro is about 7-fold normalized to T3, offering enhanced liver-targeting property and potentially less off-target effects. In model animals, compared to the NASH control, HPG7233 induced a pronounced reduction in hepatic fat and serum lipid levels, especially in hepatic triglyceride (TG) levels. Furthermore, HPG7233 significantly reduced ballooning and steatosis, thus significantly lowered NAS score ($p < 0.001$).

Conclusion: HPG7233 demonstrated high selectivity and potency, great liver-enrichment and liver/plasma exposure profile in rodent and non-rodent animals, significant reduction of liver index and serological markers level, and significant reduction of NAS score in NASH model. These results provide strong evidence to support continuing efforts in HPG7233 development for NAFLD and NASH treatment.

WED-511

Plasma short chain fatty acids are associated with non-alcoholic fatty liver disease and fibrosis severity

Mira Thing¹, Mikkel Werge¹, Liv Hetland¹, Elias Rashu¹, Puria Nabilou¹, Anders Junker¹, Elisabeth Galsgaard², Nina Kimer¹, Johnny Laupsa-Borge³, Adrian McCann³, Lise Lotte Gluud¹. ¹Copenhagen University Hospital Hvidovre, Gastro Unit, Medical section, Hvidovre, Denmark, ²Novo Nordisk A/S, Research and Early Development, Målev, Denmark, ³Bevital AS, Bergen, Norway
Email: mira.thing@regionh.dk

Background and aims: Non-alcoholic fatty liver disease (NAFLD) and progression to non-alcoholic steatohepatitis and cirrhosis have been linked to microbiome-derived metabolites, including short-chain fatty acids (SCFAs). Acetate, propionate, and butyrate have been described as beneficial and anti-inflammatory in studies measuring fecal levels, yet the role of circulating levels of SCFAs in the pathophysiology of NAFLD and NASH remains unclear. This exploratory study investigated circulating levels of SCFAs in NAFLD patients with fibrosis scores ranging from F0 to F4.

Method: 100 patients with histologically verified NAFLD (49 with F2–F4 fibrosis and 51 with F0–F1 fibrosis) and 50 healthy controls were included from the Fatty Liver Disease in Nordic Countries (FLINC) prospective cohort. Using fasting blood samples, we measured

plasma concentrations of eight SCFAs by gas chromatography-tandem mass spectrometry (GC-MS/MS). Data were analysed by logistic regression models adjusted for age and sex.

Results: The mean BMI in healthy controls and patients with NAFLD was 23.6 (SD 2.67) and 34.7 (SD 6.73) kg/m², respectively. Plasma concentrations of formate ($p = 0.004$), propionate ($p = 0.02$), valerate ($p = 0.02$), and alpha methyl-butyrate ($p = 0.01$) were increased, while acetate was decreased ($p = 0.0001$) in NAFLD patients compared with healthy controls. Among NAFLD patients, plasma concentrations of propionate ($p = 0.02$), butyrate ($p = 0.03$), valerate ($p = 0.03$), and alpha methyl-butyrate ($p = 0.02$) were increased in patients with significant fibrosis (F2-F4). See figure 1 for odds ratios and 95% CI.

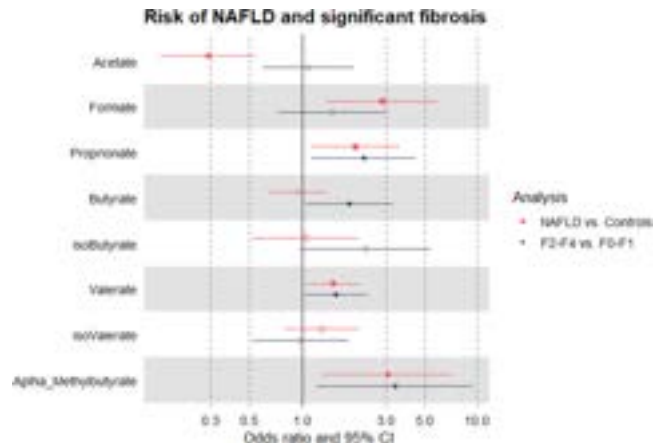


Figure 1. Odds Ratio and 95% CI of having NAFLD and significant fibrosis. SCFA values were log₂-transformed in the analysis. Empty squares or circles indicates non-significant results.

Conclusion: SCFAs differed between patients with NAFLD and healthy controls and between patients with significant and non-significant fibrosis. In particular, we found higher plasma concentrations of propionate, valerate, and alpha methyl-butyrate in patients with NAFLD and increased fibrosis severity. The implications of our observations are yet unknown and warrant further investigation.

WED-512

Artificial neural networks predict via label-free imaging analysis cellular injury in a human steatohepatitis model

Julian Weihs¹, Milad Rezvani^{1,2,3,4}. ¹Charité Campus Virchow Clinic, Department of Pediatrics, Division of Gastroenterology, Nephrology and Metabolic Medicine, Berlin, Germany, ²Berlin Institute of Health, Clinician Scientist Program, Berlin, Germany, ³Berlin Institute of Health, Center for Regenerative Therapies, Berlin, Germany, ⁴Cincinnati Children's Hospital Medical Center, Division of Gastroenterology, Hepatology and Nutrition, Cincinnati, United States
Email: milad.rezvani@charite.de

Background and aims: Drug screenings on human cellular injury models can be time-consuming and are often limited to detecting specific protein markers. An unbiased imaging algorithm that utilizes high-throughput microscopy of unprocessed cells to predict cellular injury would expand the capabilities of such screens. Artificial neural networks (ANNs) in imaging analysis have become a powerful tool for identifying phenotypic nuances at scale. We hypothesized that ANN-guided, label-free brightfield imaging analysis could predict hepatocellular injury. For proof of principle, we established a screening pipeline involving a non-alcoholic fatty liver disease (NAFLD) model with hepatocytes from human pluripotent stem cells (iHeps) exposed to different grades of subcellular injury.

Method: We modeled different severities of NAFLD-related subcellular injuries by exposing iHeps to free fatty acids or combining the same with extrahepatic signaling molecules relevant to NAFLD

(Resistin, Myostatin; "augmented injury"). To model steatohepatitis (a more advanced form of NAFLD), we co-cultured iHeps with human peripheral blood mononuclear cells (PBMCs) using a transwell system. We experimentally evaluated injury severity by measuring hallmarks of NAFLD, namely steatosis, mitochondrial function (assessed by mitochondrial membrane potential), and endoplasmic reticulum (ER) stress. Using unstained brightfield images of the monoculture conditions, we trained ANNs to distinguish cells from different hepatocyte injuries and let them define respective "injury scores." The trained ANNs then computed injury scores for cells from wells that were left out during the training process and were projected to score iHeps in the steatohepatitis condition that was not used to train the model.

Results: Our results demonstrate that in all injury conditions, iHeps displayed similar levels of steatosis and a significantly increased ER stress response upon exposure to free fatty acids. The augmented injury compromised mitochondrial function. The steatohepatitis condition exacerbated mitochondrial dysfunction further. The ANNs could identify all injury conditions from untreated cells with extremely high accuracy ($p < 0.001$). Of note, the ANNs could also distinguish cells from the different injury conditions, scoring cells of the augmented NAFLD model with higher injury scores than cells that underwent basic free fatty acid injury ($p < 0.01$). The projection of ANN to the steatohepatitis conditions revealed higher injury scores, which was consistent with our experimental data. The injury scores correlated highly with mitochondrial dysfunction ($R = -0.45$, $p = 3.3 \times 10^{-6}$). Thereby, ANNs predicted subcellular stress responses upon varying degrees of cellular injury.

Conclusion: Here, we describe how ANN-based image analysis allows label-free prediction of cellular injury in a human NAFLD model. ANNs could distinguish conditions ranging from steatosis to subcellular toxicity and returned injury scores that we could correlate with impaired mitochondrial function. In sum, combining human liver disease models and ANNs can identify cellular stress or its relief, enabling large-scale drug screenings to identify novel treatments for liver diseases quickly.

WED-513

IFI16 expression and its genotype variant are associated with NAFLD progression

Doyoon Kim^{1,2}, Masaud Shah¹, JungMo Kim³, Yang-Hyun Baek⁴, Jin Sook Jeong⁵, Sangyoung Han⁶, Yong Sun Lee⁷, Gaeul Park⁸, Yeon-Su Lee⁸, Hyun Goo Woo^{1,2,3}. ¹Ajou University School of Medicine, Physiology, Korea, Rep. of South, ²Ajou University, Biomedical Science, Graduate School, Korea, Rep. of South, ³Ajou University, Ajou Translational Omics Center (ATOC), Research Institute for Innovative Medicine, Korea, Rep. of South, ⁴Dong-A University College of Medicine, Liver Center, Internal Medicine, Korea, Rep. of South, ⁵Dong-A University Medical Center, Pathology, Korea, Rep. of South, ⁶On Hospital, Liver Center, Korea, Rep. of South, ⁷National Cancer Center, Department of Cancer Biomedical Science, Graduate School of Cancer Science and Policy, Korea, Rep. of South, ⁸National Cancer Center, Division of Rare Cancer, Research Institute, Korea, Rep. of South
Email: hg@ajou.ac.kr

Background and aims: Non-alcoholic fatty liver disease (NAFLD) is a broad and continuous spectrum of liver diseases ranging from fatty liver to steatohepatitis. The study is aimed to obtain an integrative insight into genomic and transcriptomic alterations during NAFLD progression.

Method: We performed RNA-Seq profiling ($n = 146$) and whole exome sequencing (WES) from the biopsied tissues of NAFLD patients ($n = 132$).

Results: We identified three transcriptomic subtypes of NAFLD (G1-G3), demonstrating their associations with distinct pathologic features and genetic variations. In particular, single nucleotide variations (SNVs) of IFI16 (rs6940) were closely associated with its transcriptional levels and the molecular subtypes. This finding could

POSTER PRESENTATIONS

be validated using the blood samples of the pair-matched patients (n = 94), indicating the clinical utility of the rs6940 in predicting NAFLD progression. In addition, cell type analysis revealed that *IFI16* expression is largely due to increased macrophage infiltration during the molecular progression of NAFLD. We also report that structural conformation by the *al* alteration of *IFI16* rs69450 enhances its DNA binding affinity, which may aggravate subsequent inflammatory responses.

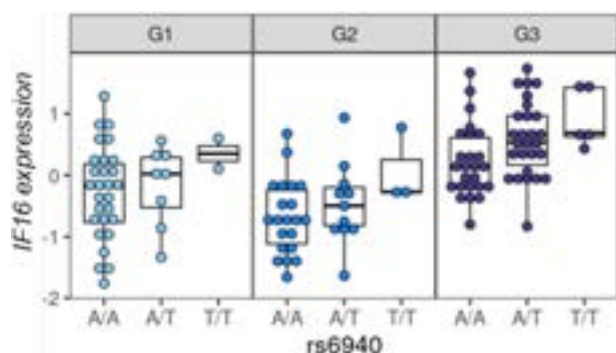


Figure:

Conclusion: We suggest that *IFI16* polymorphism and expression levels are associated with the aggressive progression of NAFLD through macrophage activation.

WED-514

Knockdown of a novel target gene enhances liver regeneration and attenuates chronic liver damage related liver fibrosis

Shainan Hora¹, Rong Gao¹, Viktoriia Iakovleva¹, Yong-An Lee¹, Amanpreet Kaur¹, Agnes Bee Leng Ong¹, Torsten Wuestefeld¹.

¹Genome Institute of Singapore, Singapore

Email: Shainan_Hora@gis.a-star.edu.sg

Background and aims: Non-alcoholic fatty liver disease (NAFLD), characterised by excessive fat accumulation and coupled with rising incidence of acute and chronic liver disease, remains a healthcare burden. A distinct phenomenon seen in NAFLD patients is the aberrant regenerative capacity that limits liver re-compensation. Our unbiased genome wide *in-vivo* functional genetic screen aims at identifying novel regulators of NAFLD to reverse this end-stage liver disease and to contribute towards hepatic regenerative therapy.

Method: A genome-wide mouse shRNA library (shERWOOD-UltramiR) was cloned into transposon-based doxycycline (Dox)-inducible vector, divided into 32 pools and delivered into C57BL/6 mice liver using hydrodynamic-tail vein (HDTV) injections. Mice were fed western diet and fructose-supplemented water for 8 weeks followed by induction of shRNA-expression by Dox administration and continued diet feeding for additional 16 weeks. Animal livers were harvested, primary NGS analysis performed, and abundance of each shRNA determined using differential expression analysis method. Top candidate genes were selected based on several stringent criteria, validated *in-vitro* and re-injected into fumarylacetoacetate hydrolase (FAH) knockout animals to test for liver repopulation and liver regeneration after partial hepatectomy. Additionally, mouse model of chronic liver disease, Non-Alcoholic Steatohepatitis (NASH), was employed to test for pathological findings, such as fibrosis score as well as other associated microscopic markers such as oval cell hyperplasia, inflammation and necrosis, among others.

Results: We have identified several shRNAs that confer a negative or positive effect on the regenerative capacity of hepatocytes when subjected to a detrimental environment such as a high fat diet. Among the many top scoring genes, knockdown of a novel gene, Target Gene 1 accelerated cell migration and proliferation, followed by enhanced clonal expansion using FAH knockout mouse model. Furthermore, increased liver regeneration and a significant reduction

in fibrosis score was observed compared to control animals, confirming an attenuation of NASH related liver fibrosis.

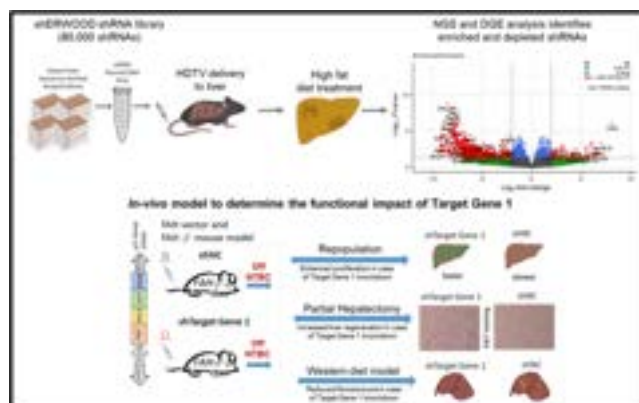


Figure:

Conclusion: Knockdown of a novel gene about which very little is known except that is a protein coding gene and enables RNA binding activity accelerates liver repopulation, regeneration and attenuates chronic liver damage related fibrosis.

WED-515

Translational characterization of the temporal dynamics of metabolic dysfunctions in liver, adipose tissue and the gut during diet-induced NASH development in *Ldlr*^{-/-} Leiden mice

Eveline Gart¹, Wim van Duyvenvoorde¹, Jessica Snabel¹, Christa de Ruyter¹, Joline Attema¹, Martien P. M. Caspers^{2,3}, Serene Lek⁴, Bertie Joan van Heuven⁵, Arjen Speksnijder⁵, Martin Giera⁶, Aswin L. Menke¹, Kanita Salic¹, Kendra Bence⁷, Gregory Tesz⁷, Jaap Keijer⁸, Robert Kleemann¹, Martine C. Morrison¹.

¹TNO, Metabolic Health Research, Netherlands, ²TNO, Microbiology and Systems Biology, Netherlands, ³The Netherlands Organization for Applied Scientific Research (TNO), Department of Microbiology and Systems Biology, Leiden, Netherlands, ⁴Clinnovate Health, United Kingdom, ⁵Naturalis, Netherlands, ⁶LUMC, Center for Proteomics and Metabolomics, Netherlands, ⁷Pfizer, Development and Medical, Internal Medicine Research Unit, United States, ⁸Wageningen University, Human and Animal Physiology, Netherlands

Email: eveline.gart@tno.nl

Background and aims: NAFLD progression, from steatosis to inflammation and fibrosis, results from an interplay of intra- and extrahepatic mechanisms. Disease drivers likely include signals from white adipose tissue (WAT) and gut. However, the temporal dynamics of disease development remain poorly understood.

Method: High-fat-diet (HFD)-fed *Ldlr*^{-/-} Leiden mice were compared to chow-fed controls. At t=0, 8, 16, 28 and 38w mice were euthanized, and liver, WAT depots and gut were analyzed biochemically, histologically and by lipidomics and transcriptomics together with circulating factors to investigate the sequence of pathogenic events and organ cross-talk during NAFLD development.

Results: HFD-induced obesity was associated with an increase in visceral fat mass, plasma lipids and hyperinsulinemia at 8 weeks, along with an increase in liver steatosis and circulating biomarkers indicative of liver damage (ALT, AST, CK18-M30, TIMP1). Liver steatosis was mainly attributable to increased triacylglycerols and to a lesser extent free-fatty acids, cholesteryl esters and diacylglycerols. In parallel, regulators involved in lipid catabolism (e.g., ACOX1) were deactivated and in lipid synthesis (e.g., SREBF1) activated by HFD. Subsequently, hepatocyte hypertrophy, oxidative stress (4-HNE) and hepatic inflammation developed. Hepatic collagen accumulated at t=16w and became particularly prominent after 28–38 weeks. Epididymal WAT adipocytes were maximally hypertrophic from t=8w, which coincided with inflammation development in this depot.

Mesenteric and subcutaneous WAT hypertrophy developed slower and did not appear to reach a maximum within the period studied, with minimal inflammation. In the gut, HFD significantly increased permeability, induced a major shift in microbiota composition (ileum and colon) from t=8w and associated with circulating gut-derived metabolite changes (short-chain fatty acids and bile acids).

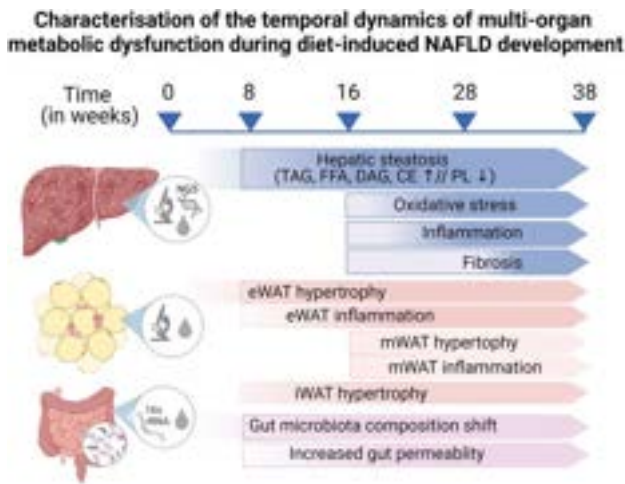


Figure:

Conclusion: Ldlr^{-/-}.Leiden mice on a HFD develop obesity, dyslipidemia and insulin resistance, essentially as observed in obese NASH patients. We demonstrate that marked epididymal-WAT inflammation, and gut permeability and dysbiosis precede the development of NAFLD stressing the importance of a multiple-organ approach in the prevention and treatment of NAFLD.

WED-516

Novel bariatric surgery models in mice-differential effects on body weight loss and fatty liver disease

Louis Onghena^{1,2,3}, Anneleen Heldens^{2,3}, Milton Antwi^{2,3,4}, Hans Van Vlierberghe^{2,3}, Xavier Verhelst^{2,3}, Lindsey Devisscher^{2,4}, Yves Van Nieuwenhove¹, Anja Geerts^{2,3}, Sander Lefere^{2,3}. ¹Ghent University Hospital, Department for Human Repair and Structure, Department of Gastrointestinal Surgery, Ghent, Belgium, ²Ghent University Hospital, Liver Research Center Ghent, Ghent University, Ghent, Belgium, ³Ghent University Hospital, Department of Internal Medicine and Paediatrics, Hepatology Research Unit, Ghent, Belgium, ⁴Ghent University, Department for Basic and Applied Medical Sciences, Gut-Liver Immunopharmacology unit, Ghent, Belgium
Email: Louis.onghena@ugent.be

Background and aims: Bariatric surgery (BS) is an effective treatment for obesity and associated comorbidities, including non-alcoholic fatty liver disease (NAFLD). In recent years, the number of available bariatric procedures has increased, yet their outcome and mechanisms of action have not been compared in detail. We performed vertical sleeve gastrectomy (VSG) and plication (VSP), Roux-en-Y gastric bypass (RYGB), and one-anastomosis gastric bypass (OAGB) with three different biliary limb lengths (25% = Omega₁, 50% = Omega₂, 75% = Omega₃) for comparison, as the latter are gaining in popularity.

Method: Mice were fed a Western diet (WD) for 12 weeks, followed by surgery, and subsequent sacrifice at week 20. Six different types of BS were performed and compared with each other, with a sham and a control group (WD, no surgery). Weight loss, NAFLD severity, fat cell hypertrophy, and intestinal remodeling were evaluated by histology and biochemistry. Intestinal and hepatic inflammation and bacterial translocation were measured. Statistical differences between group mean values were assessed by one-way ANOVA tests with Tukey post-hoc test.

Results: Notably, the Omega₃ procedure resulted in 100% mortality after just three weeks due to severe malnutrition and rapid weight

loss. Relative weight loss differed significantly ($p < 0.0001$) amongst the groups (sham +12.71%, VSG -9.18%, VSP +6.05%, RYGB -33.52%, Omega₁ -22.47%, and Omega₂ = -24.03%, Figure 1). Average food intake was significantly lower in VSG and VSP compared to RYGB ($p < 0.05$), Omega₁ ($p < 0.01$), and Omega₂ ($p < 0.001$). In RYGB, Omega₁, and Omega₂, relative visceral adipose tissue weight was significantly lower compared to the sham mice ($p < 0.0001$). Fat cell diameter and area were significantly decreased ($p < 0.0001$) in all BS groups compared to sham mice and differed significantly amongst each other as well. RYGB, Omega₁, and Omega₂ significantly attenuated the elevated serum ALT levels and liver triglyceride content ($p < 0.01$). Histologically, sham-operated mice had developed severe liver steatosis and moderate inflammation after 20 weeks of WD feeding, which was attenuated by BS, especially by Omega₁ ($p < 0.05$), and Omega₂ ($p < 0.01$). Bacterial translocation in the liver was observed in RYGB, Omega₁, and Omega₂ ($p < 0.001$). Signs of intestinal inflammation were detected in the terminal ileum, but not jejunum, in mice that underwent Omega₂ ($p < 0.01$). The jejunal tunica muscularis was thicker after RYGB, Omega₁, and Omega₂ ($p < 0.0001$).

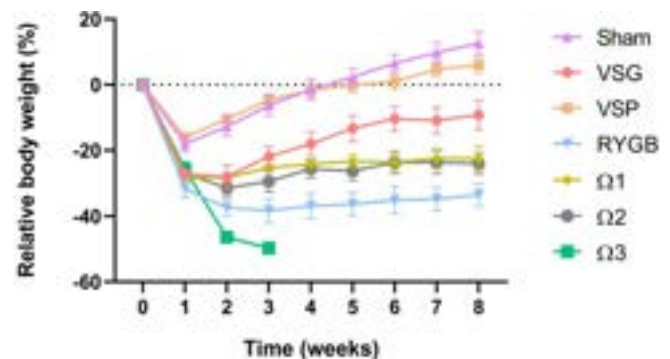


Figure:

Conclusion: BS procedures in mice, especially RYGB, Omega₁, and Omega₂, improved histological NAFLD. However, the observed bacterial translocation in these models requires further investigation regarding long-term effects. Our models open up the field of research into the mechanisms of action of BS on hepatic and intestinal physiopathology, and on how the gut and the liver interact following surgery.

WED-517

The effect of cholesterol and its metabolites on human pluripotent stem cell-derived hepatic stellate cells

Ingrid Wilhelmsen^{1,2}, Kristina Kõmurcu³, Aleksandra Aizenshtadt¹, James Thorne⁴, Steven Wilson^{1,3}, Hanne Røberg-Larsen³, Stefan Krauss^{1,2}. ¹University of Oslo, Institute of Basic Medical Sciences, Hybrid Technology Hub, Oslo, Norway, ²Oslo University Hospital, Institute of Clinical Medicine, Department of Immunology, Oslo, Norway, ³University of Oslo, Department of Chemistry, Oslo, Norway, ⁴University of Leeds, School of Food Science and Nutrition, Leeds, United Kingdom
Email: ingrid.wilhelmsen@medisin.uio.no

Background and aims: Non-alcoholic fatty liver disease (NAFLD) is a major health concern that encompasses a range of diseases initiated by the accumulation of excessive lipids in the liver. The progression of NAFLD eventually leads to fibrotic scarring in which hepatic stellate cells (HSCs) play a crucial role. In the homeostatic liver, HSCs exhibit a quiescent phenotype. However, upon liver injury such as NAFLD, HSCs transdifferentiate to an activated phenotype and become the main drivers towards hepatic fibrosis. It is known that NAFLD is associated with elevated levels of cholesterol and cholesterol derivatives such as the oxysterols 25-hydroxycholesterol (25-HC) or 26-hydroxycholesterol (26-HC), regulating the key NAFLD modulator liver x-receptor (LXR). Increased levels of oxysterols were detected in

POSTER PRESENTATIONS

supernatant medium samples from *in vitro* steatosis models based on liver organoids comprising predominantly liver parenchymal cells. As the role of cholesterol and its metabolites on HSCs and in particular the HSC activation status is unknown, we aimed to investigate the effect of cholesterol and oxysterols on HSCs.

Method: HSCs were differentiated from three human pluripotent stem cell (PSC) lines (H1, WTC-11 and WTSli013-A). At the end of the differentiation protocol, the PSC-derived HSCs were treated with cholesterol, 25-HC or 26-HC both alone and in combination with the potent pro-fibrotic inducer TGF- β 1 for 48 hours. Changes in HSC phenotype were assessed by RT-qPCR and imaging of intracellular vitamin A storage.

Results: PSC-derived HSCs displayed an increase in LXR target gene *ABCA1* expression upon treatment with both cholesterol and oxysterols, confirming successful stimulation of the intended pathway. The fibrosis-associated gene *ACTA2* was downregulated in HSCs in the presence of 25-HC and 26-HC. Expression of *CCL2*, encoding a chemokine crucial for monocyte recruitment, was reduced after treatment with 26-HC. Yet, the presence of cholesterol, 25-HC and 26-HC had no effect on the response of the HSCs to TGF- β 1, which was evident by increased expression of *ACTA2*, *COL1 α 1* and *CCL2*. These results connect HSCs to existing literature that implicates oxysterols in the attenuation of early-stage NAFLD; however, without affecting more advanced NAFLD as modeled by pro-fibrotic stimulation with TGF- β 1.

Conclusion: Collectively, the results implicate cholesterol metabolites 25-HC and 26-HC as modulators of the HSC activation status and suggest that PSC-derived HSCs can be suitable for *in vitro* models of NAFLD.

WED-518

Opposite correlations between hepatic β -oxidation activity and triglyceride levels in male and female rats after a high-fat diet supplemented with liquid fructose

Roger Bentanachs^{1,2}, Laia Blanco¹, Maria Montesinos¹, Aleix Sala-Vila³, Iolanda Lázaro³, Juan Carlos Laguna^{1,2,4}, Núria Roglans^{1,2,4}, Marta Alegret^{1,2,4}. ¹University of Barcelona, School of Pharmacy and Food Sciences, Pharmacology, Toxicology and Therapeutic Chemistry, Spain, ²Institute of Biomedicine of the University of Barcelona, Spain, ³Hospital del Mar Medical Research Institute (IMIM), Cardiovascular Risk and Nutrition, Spain, ⁴CIBER de Fisiopatología de la Obesidad y Nutrición, Instituto de Salud Carlos III, Spain

Email: alegret@ub.edu

Background and aims: We previously reported that the administration of a high-fat diet supplemented with 10% w/v fructose in drinking water (HFHFr diet) results in hypertriglyceridemia and a moderate increase in hepatic triacylglycerol (TAG) levels in males, while females showed less hypertriglyceridemia but more than doubled their liver TAG content. Moreover, hepatic β -oxidation activity was reduced in female rats, whereas males showed a significant increase (Bentanachs et al. 8th MetNet International Annual Meeting). Our aim is to study the mechanisms involved in the sexual dimorphic response to this diet.

Method: Two-month-old male (n = 16) and female (n = 16) Sprague Dawley rats were randomly assigned to two groups (n = 8 in each) and fed ad libitum for 3 months. The control groups were fed regular chow diet (2018 Teklad Global, 18% of provided calories as fat), whereas the high-fat-high-fructose groups (HFHFr) were fed an HFD (Teklad Custom Diet TD180456, 46.9% of energy as fat, of which 21% w/w was cocoa butter) and had free access to a 10% w/v fructose solution as the drinking beverage. Total liver TAG was determined by a colorimetric method, and then hepatic TAG were isolated by solid-phase extraction and fatty acid methyl esters from this fraction were determined by gas chromatography. Hepatic diacylglycerols (DAG) and ceramides (Cer) were determined by liquid chromatography-tandem mass spectrometry. β -oxidation activity was determined by

the method of Lazarow (Methods Enzymol. 1981, 72, 315). Correlation analysis between plasma/hepatic TAG and β -oxidation activity was performed using GraphPad prism software (v. 9.0.0).

Results: The fatty acid composition of the hepatic TAG in male rats was significantly altered by the HFHFr diet, with significant increases of several saturated (C14:0, C16:0, C:18:0) and monounsaturated fatty acids (C16:1 n-7, C18:1 n9). The opposite was observed for many polyunsaturated fatty acids (C18:2 n-6, C20:4 n-6, C20:5 n-3). Several DAG species were increased by the diet (DAG-C16:0, DAG-C18:0, DAG-C18:1 and DAG-C18:0/18:2). No significant changes were observed for ceramide levels in the livers of male rats. These changes in lipid species were qualitatively similar to those observed in female rats in response to the same diet (Velázquez et al., Mol. Nutr. Food Res 2022, 2101115). However, correlation analysis showed striking differences: liver β -oxidation activity in females inversely correlated with plasma TAG levels (Spearman's r = -0.60, p = 0.022) and total hepatic TAG levels (Spearman's r = -0.64, p = 0.012); in male rats, liver β -oxidation activity correlated with both plasma (Pearson's r = 0.78, p = 0.0007) and hepatic TAG (Spearman's r = 0.66, p = 0.08).

Conclusion: The sexual dimorphism observed in rats in response to a HFHFr diet cannot be explained by qualitative changes in the liver lipidome. Only in female rats, the decrease in liver β -oxidation activity significantly contributes to increase the hepatic and plasma TAG, whereas in males these correlations are direct. This work was supported by grants PID2020-112870RB-I00, funded by MCIN/AEI/10.13039/501100011033 and 2021SGR-00345.

WED-519

Prophylactic and therapeutic hepatoprotective effects of lanifibranor in the CDAA-HFD mouse model of advanced NASH with progressive fibrosis

Jacob Nøhr-Meldgaard¹, Ditte Denker Thorbek¹, Denise Oró¹, Henrik B. Hansen¹, Michael Feigh¹. ¹Gubra, Hørsholm, Denmark
Email: jnm@gubra.dk

Background and aims: The pan peroxisome proliferator-activated receptor (PPAR- $\alpha/\delta/\gamma$) agonist has recently been reported to improve liver histological outcomes in patients with non-alcoholic steatohepatitis (NASH) and fibrosis (NATIVE study; Francque et al, NEJM, 2021). Lanifibranor is currently in phase-3 clinical trial (NATIV3) for the treatment of NASH. The present study aimed to evaluate prophylactic vs. therapeutic lanifibranor intervention in the non-obese choline-deficient L-amino-acid defined high-fat diet (CDAA-HFD) mouse model of advanced NASH with progressive fibrosis.

Method: C57BL/6J mice were fed chow or CDAA-HFD (45 kcal% fat, 0.1% methionine, 1% cholesterol, 28 kcal% fructose) for 3 or 6 weeks prior to treatment start (i.e. before or after onset of fibrosis, respectively). Animals were randomized into treatment groups based on body weight. A baseline group (n = 12) was terminated at study start (3 and 6 weeks). CDAA-HFD fed mice (n = 12 per group) received treatment (PO) with vehicle or lanifibranor (30 mg/kg) for 8 or 9 weeks. Chow-fed mice (n = 8) served as normal controls. Terminal end points included plasma biomarkers metalloproteinase inhibitor 1 (TIMP-1) and amino terminal peptide of type III procollagen (PIIINP), liver biochemistry, NAFLD Activity Score (NAS), fibrosis stage and quantitative liver histology.

Results: Prophylactic and therapeutic lanifibranor interventions reduced body weight, liver weight and concomitantly reduced levels of liver triglycerides and total cholesterol content. Furthermore, prophylactic and therapeutic lanifibranor intervention significantly improved NAS, mainly driven by reduced steatosis and lobular inflammation scores. These effects were supported by quantitative liver histology, demonstrating reduced levels of liver fat accumulation (%-area of lipids, number of lipid-laden hepatocytes) and inflammation (%-area of galectin-3, number of inflammatory foci). Prophylactic treatment with lanifibranor improved fibrosis stage, while no effect on fibrosis stage was observed with therapeutic

treatment. In contrast, both interventions equally reduced liver hydroxyproline concentrations and quantitative levels of fibrosis (% area of PSR). Moreover, a decrease in plasma levels of metalloproteinase inhibitor 1 (TIMP-1) and amino terminal peptide of type III procollagen (PIIINP) were reduced in the prophylactic setting, which further supports the anti-fibrotic effect of lanifibranor in the current model.

Conclusion: The beneficial effects of early and late lanifibranor intervention in the non-obese CDAA-HFD mouse model are in good agreement with clinical trial outcomes in NASH patients, thus highlighting the suitability of the CDAA-HFD mouse model for profiling novel drug therapies targeting advanced NASH with progressive fibrosis.

WED-520

Light cytokine-deficiency effects in immune cells subpopulations in a murine non alcohol-related steatohepatitis model

María Aguilar Ballester¹, Elena Jiménez-Martí^{1,2}, Gema Hurtado-Genovés¹, Alida Taberner-Cortés¹, Ángela Vinué¹, Andrea Herrero-Cervera¹, Sergio Martínez-Hervás^{1,3}, Herminia González-Navarro^{1,2}. ¹Health Research Institute INCLIVA, Valencia, Spain, ²University of Valencia, Department of Biochemistry and Molecular Biology, Faculty of Medicine, València, Spain, ³University of Valencia, Department of Medicine, Faculty of Medicine, València, Spain Email: herminia.gonzalez@uv.es

Background and aims: Hepatic inflammation is known to increase fibrosis in non-alcoholic fatty liver disease (NAFLD) as well as in the transition to non-alcohol-related steatohepatitis (NASH) and hepatocellular carcinoma (HCC). Specifically, several studies have pointed to a key role for natural killer T (NKT) cell sublinages in this progression. In our previous studies, Light cytokine-deficient mice provoked a decreased expression of the master transcription factor for NKT differentiation, PLZF. In the present study, we investigated the role of LIGHT at determining NKT cell differentiation subsets in the context of NAFLD.

Method: Both Wt and Light-deficient mice were fed a control or a high fat high cholesterol diet (HFHC) for 16 weeks. At the end of the study mice were analysed for NAFLD development, using hepatic triglyceride content and NAS score, and for hepatic fibrosis using collagen content in Masson trichromic-stained cross-sections. Inflammatory status, including NKT cell determination, was evaluated by analysing circulating and hepatic leucocyte subpopulations by flow cytometry.

Results: Compared with control diet-fed mice, all mice fed with HFHC diet displayed increased hepatic collagen content and NAS score, although collagen was significantly lower in Light-deficient mice. Hepatic leukocyte determinations demonstrated significantly reduced anti-inflammatory F4/80+CD206+ macrophages in HFHC diet-fed mice, compared with control diet-treated mice regardless of their genotype. Notably, NKT17 subpopulation was significantly increased in Wt mice fed the HFHC diet compared with Wt mice fed control diet, but this increase was not observed in HFHC diet fed Light-deficient mice compared with their control diet-fed mice counterparts.

Conclusion: Our results suggest that Light-deficiency in HFHC diet fed mice reduces hepatic NKT17 subpopulation content and suggest a possible role of Light in NKT subpopulation differentiation in the context of NAFLD.

Funding: PI19-00169, PI22-00062.

WED-521

Evaluation of genetic risk score of a dysmetabolic and obese population of southern Italy

Benedetta Maria Motta¹, Mario Masarone², Pietro Torre², Pietro Calabrese², Marco Aquino², Federica Belladonna², Vincenzo Pilone², Marcello Persico². ¹University of Salerno, Department of Medicine, Surgery and Dentistry, "Scuola Medica Salernitana", Italy, ²University of Salerno, Dipartimento di Medicina, Chirurgia e Odontoiatria "Scuola Medica Salernitana", Baronissi, Italy Email: bmotta@unisa.it

Background and aims: Non-alcoholic fatty liver disease (NAFLD) is the leading cause of liver diseases, ranging from simple steatosis to non-alcoholic steatohepatitis, and the susceptibility to develop NAFLD is highly variable and influenced by environmental and genetic factors. The gold standard for diagnosis and staging of NAFLD is liver biopsy, however, it is an invasive procedure, subject to sampling errors and inter-observer variability. Several non-invasive methods aim at diagnosing hepatic steatosis and predicting significant/advanced fibrosis. GWAS studies identified genetic risk factors, and genetic risk scores (GRS) were developed for risk stratification. NAFLD susceptibility is associated with four genetic variants: *PNPLA3* rs738409, *TM6SF2* rs58542926, rs641738 close to *MBOAT7* locus, *GCKR* rs1260326. Our aim was to evaluate how these variants are distributed in an obese and dysmetabolic population of Southern Italy and how our polygenic risk score (PRS) correlates with liver steatosis and biochemical phenotypes.

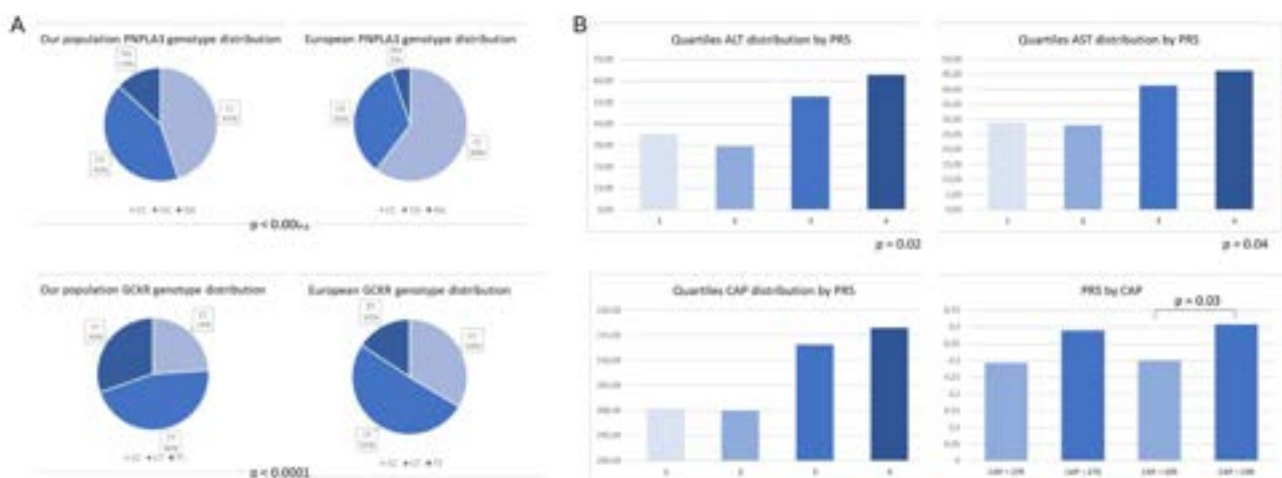


Figure 1. Characterization of dysmetabolic and obese population. A) PNPLA3 and GSKR variants distribution. Chi-Square test. B) Biochemical parameters stratified by GRS. One-way ANOVA test.

Figure: (abstract: WED-521).

POSTER PRESENTATIONS

Method: We enrolled 205 patients attending our Hepatology Clinic and Surgery department, which were genotyped for rs738409, rs58542926, rs641738, rs1260326 by TaqMan 5'-nuclease assays. We calculated a weighted PRS by multiplying the effect size (beta-coefficient) on steatosis by respective risk alleles and summing the products. Anthropometric data, FibroScan measurements, and blood test results were collected.

Results: In our population, we observed a higher MAF of PNPLA3 and GCKR variants compared to the ones reported in European population of 1000Genomes Project ($p < 0.0001$). The rs738409 G allele frequency is 34.1% vs. 23%. The rs1260326 T allele frequency is 53.2% vs. 41%. In a sub-cohort of 98 patients, we recorded Fibroscan parameters and biochemical data and evaluated the effect of the 4 variants together by PRS. PRS increased proportionally with ALT levels ($p = 0.02$), AST ($p = 0.04$), total cholesterol, triglycerides, and CAP ($p = \text{N.S.}$). PRS is higher in subjects with a CAP value of 275 dB/m, considered a cut-off for moderate/severe steatosis in general population; moreover, considering a CAP value >295 dB/m PRS is significantly higher in these subjects ($p = 0.03$).

Conclusion: This study shows that in our population, PNPLA3 and GCKR risk alleles frequency are higher, and that the polygenic risk score correlates with biochemical and Fibroscan parameters, identifying the most dysmetabolic subjects.

WED-522

Characterizing the histologic implications of resmetirom-induced liver volume reduction using artificial intelligence-powered digital pathology

Pratik Mistry¹, Adam Stanford-Moore¹, Robert Egger¹, Jonathan Glickman¹, Brian Baker¹, Nidhi Chandra¹, Dinkar Juyal¹, Archit Khosla¹, Michael Drage¹, Murray Resnick¹, Katy Wack¹, Jim Hennen², Rohit Loomba³, Stephen Harrison⁴, Rebecca Taub², Janani Iyer¹. ¹PathAI, Boston, United States, ²Madrigal Pharmaceuticals, Conshohocken, United States, ³UC San Diego School of Medicine, San Diego, United States, ⁴Pinnacle Clinical Research, San Antonio, United States

Email: janani.iyer@pathai.com

Background and aims: In non-alcoholic steatohepatitis (NASH) clinical trials, liver biopsies are evaluated for histologic evidence of NASH/fibrosis at screening and drug effect at study completion. An emerging hypothesis suggests drug-induced fat and/or liver volume (LV) reduction may complicate histologic interpretation and thus impact trial outcomes. Here, we train artificial intelligence (AI) models to characterize cell types present in NASH and identify morphologic correlates of LV reduction in biopsies from the Phase 2 trial of resmetirom for treatment of NASH.

Method: An AI cell classification model was trained using annotations provided by hepatopathologists on whole slide images (WSIs) of NASH HandE tissue sections from trials and diagnostic samples. Model performance accuracy was confirmed via agreement between model predictions for each cell type and consensus across five pathologists. This model and previously developed tissue segmentation models were deployed on WSIs from 101 patients enrolled in the Phase 2 trial of resmetirom for treatment of NASH (NCT02912260). Extracted quantitative proportion, count, and density features were correlated with MRI-derived LV measurements using Pearson's r .

Results: AI quantification revealed a statistically significant increase in overall cell density in resmetirom- versus placebo-treated patients ($p = 0.037$), where increasing cell density was directly associated with decreasing LV (A). Moreover, change in the count proportion of hepatocytes exhibiting steatosis was positively associated with LV change (LVC), while the count proportion of normal hepatocytes was negatively associated with LVC (B). By contrast, changes in the abundance and density of immune cells in the portal tract versus lobule had little to no correlation with LVC (D). AI quantification of fibrosis subcategories revealed that adjusting for the presence of

steatosis affected quantification of perisinusoidal and periportal fibrosis specifically, with greater drug-induced changes observed in these fibrosis subcategories relative to others (median change from baseline in proportionate area of F1 + F2 fibrosis = 27% versus 13% with versus without adjustment, respectively).

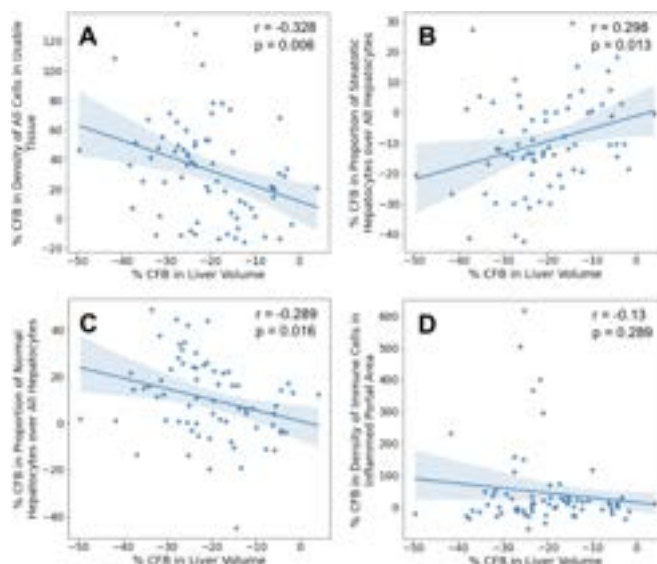


Figure: Percent CFB in LV is associated with overall cell density (A), steatosis (B), and normal hepatocytes (C), but not immune cell density (D) in resmetirom-treated patients.

Conclusion: These results suggest LVC is reflected in the abundance and densities of steatotic and normal hepatocytes, consistent with a model in which disintegration of large triglyceride-filled vesicles results in macroscopic LV reduction. These findings motivate further investigation into the morphologic biomarkers of LVC in NASH clinical trials and how these changes should be adjusted for when evaluating drug effect, particularly in fibrosis.

WED-523

Unraveling the individual contributions of the PPAR isotypes to the pan-PPAR agonist Lanifibranor-induced improvements of the vascular alterations and liver histology in a rat model of early NAFLD

Shivani Chotkoe¹, Yao Liu¹, Guillaume Wettstein², Jean Louis Junien², Luisa Vonghia^{1,3}, Hannah Ceuleers¹, Joris De Man¹, Benedicte De Winter^{1,3}, Wilhelmus Kwanten^{1,3}, Sven Francque^{1,3}.

¹University of Antwerp, Laboratory of experimental medicine and pediatrics, Antwerpen, Belgium, ²Inventiva, Daix, France, ³Antwerp university hospital, Gastroenterology and hepatology, Edegem, Belgium
Email: shivani.chotkoe@uantwerpen.be

Background and aims: The pan-peroxisome proliferator-activated receptor agonist Lanifibranor completely normalized the intrahepatic vascular resistance (IHVR), the related endothelial dysfunction, and liver histology in a rat model of early NAFLD. We studied the underlying mechanism by exploring the mono-PPAR agonists Fenofibrate (PPAR-alpha agonist), GW501516 (PPAR-delta agonist) and Rosiglitazone (PPAR-gamma agonist) using a rat model of early NAFLD.

Method: Male Wistar rats ($n = 8$ per group) were fed a methionine-choline-deficient diet (MCD) or control diet (CD) for 4 weeks simultaneously with either vehicle, 30 mg/kg Fenofibrate, 10 mg/kg GW501516, or 5 mg/kg Rosiglitazone treatment via oral gavage daily QD. *In vivo* blood pressure of portal vein was measured, followed by *in situ* *ex vivo* liver perfusion in the same animal to assess baseline transhepatic pressure gradient (THPG) at different flows (10–50 ml/min). Liver histology staining was performed using the steatosis-activity-fibrosis score and for morphometric steatosis quantification.

Results: In vehicle-treated animals, livers of MCD rats showed severe, grade 3 steatosis, without inflammation or fibrosis, compared to normal livers in CD rats. MCD rats showed a significantly increased portal pressure *in vivo* compared to CD rats (5.64 ± 0.63 vs. 3.52 ± 0.24 mmHg, $p < 0.0001$) and THPG *ex vivo* was increased at every perfusion flow velocity (e.g., at 30 ml/min: 8.78 ± 0.35 vs. 6.73 ± 0.28 mmHg) with $p < 0.001$. Fenofibrate, GW501516 and Rosiglitazone significantly decreased portal pressure *in vivo* (from 5.64 ± 0.63 to 4.37 ± 0.20 ; 4.34 ± 0.16 ; 4.43 ± 0.27 mmHg, respectively) with $p < 0.0001$ in MCD rats. THPG *ex vivo* was significantly decreased by Fenofibrate (e.g., at 30 ml/min: from 8.78 ± 0.35 to 6.63 ± 0.41 mmHg) with $p < 0.001$, by GW501516 (e.g., at 30 ml/min: from 8.78 ± 0.35 to 7.61 ± 0.34 mmHg) with $p < 0.01$, and by Rosiglitazone (e.g., at 30 ml/min: from 8.78 ± 0.35 to 7.95 ± 0.28 mmHg) with $p = 0.043$. Histology showed that Lanifibranor caused amelioration of steatosis in MCD rats with $19.7 \pm 4.8\%$ ($p = 0.0001$) decrease in steatosis, whereas Fenofibrate improved the degree of steatosis in MCD rats comparable to CD rats. GW501516 only weakly decreased steatosis with $11.72 \pm 5.28\%$. Rosiglitazone caused only minimal histological improvement of steatosis (decrease of $7.15 \pm 6.73\%$) in MCD rats.

Conclusion: The mono-PPAR agonists reduce the increased portal pressure and related functional vascular intrahepatic alterations associated with early NAFLD. However, with Lanifibranor all improvements in vascular function were more pronounced than with each specific agonist. Together with the impact on histology, these data suggest that there is an additive effect of combined PPAR agonism compared to mono-agonism leading to an improvement of the vascular alterations in early NAFLD.

WED-524

GTX-011 improves fibrosis and hepatic stellate cells phenotype in human precision cut liver slices

Maria Andres-Rozas¹, Zoe Boyer-Diaz¹, Eugenia Ruiz-Canovas², Sergi Guixé-Muntet³, Peio Aristu¹, Juanjo Lozano³, Raul Pasto³, Noemi Garcia-Delgado², Jaume Mercader², Jaime Bosch^{3,4}, Jordi Gracia-Sancho^{1,3,4} ¹Barcelona Liver Bioservices, Spain, ²GAT Therapeutics, Spain, ³IDIBAPS-Hospital Clinic Barcelona-CIBEREHD, Liver Vascular Biology Lab, Spain, ⁴Inselspital-University of Bern, Switzerland
Email: jgracia@recherche.clinic.cat

Background and aims: GTX-011 is a first-in-class drug with anti-inflammatory and anti-fibrotic properties mediated by the inhibition of the TGF β pathway. Previously, we demonstrated its beneficial effects on portal hypertension and hepatic fibrosis in a preclinical model of non-alcoholic steatohepatitis (NASH) by means of hepatic stellate cells (HSC) de-activation and endothelial cells re-differentiation. The aim of this study was to assess the effects of GTX-011m, the active metabolite of GTX-011, in Precision-Cut Liver Slices (PCLS) from human liver tissues, a 3D *ex vivo* model that preserves the structure and cellular composition of the liver, constituting an intermediate step between pre-clinical and clinical research.

Method: PCLS were obtained from human hepatic resections and individually cultured with GTX-011m (1–10 μ M) or vehicle (DMSO 0.1%) for 24 hours. Changes in gene expression were evaluated by RNAseq ($n = 6$ /group). Furthermore, gene deconvolution analysis was performed, combining our bulk RNAseq with previously published single-cell data, in order to better understand the changes in the phenotype of each liver cell type in response to treatment.

Results: PCLS treated with GTX-011m 1 μ M and 10 μ M revealed a total of 723 and 866 differentially expressed genes ($p < 0.05$, $f.c. > 1.5$), respectively, of which 345 were commonly modified in both concentrations. Transcriptomic analysis manifested that treatment with GTX-011m promoted HSC de-activation and inhibition of pro-fibrogenic pathways. Specifically, HSC activation and proliferation markers alpha-smooth muscle actin (α -sma) and desmin were down-regulated, together with higher expression of remodelling

extracellular matrix enzymes (matrix metalloproteinases 1, 3, 10 and 14), and lower expression of their inhibitors (tissue metalloproteinase inhibitors 3 and 4). Lastly, a reduction in collagens expression (col6a6 col14a1) was observed. On the other hand, gene deconvolution analysis confirmed the effects of GTX-011m on HSC, decreasing their cell population and promoting their de-activation compared to vehicle, with no effects on other cell types proportion (see Figure). These effects were associated with the activation of apoptotic pathways defined by the up-regulation of tumor necrosis factor-related apoptosis-inducing ligand (TRAIL), fas, fas-ligand, caspases 3, 8, 9 and 10 and BAX/BAK, as well as reduction of HSC activation markers (SRF-box transcription factor 9 (sox9) and desmin).

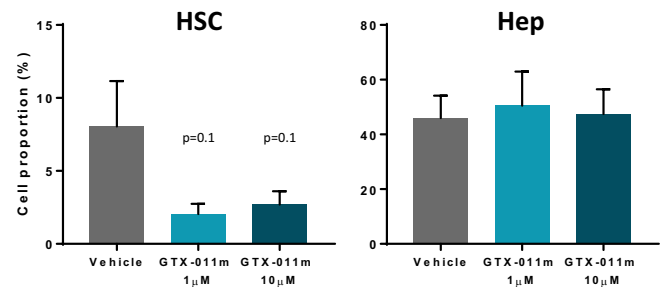


Figure:

Conclusion: This study shows for the first time the antifibrotic effects of GTX-011 in human liver tissue, confirming our previous results obtained in a preclinical model of NASH and encouraging its clinical evaluation as a possible new treatment for this disease.

WED-525

Beneficial effect of extravirgin olive oil on hepatic fatty acid accumulation and fibrogenesis: oleocanthalic acid as a promising compound for the treatment of NAFLD and NASH

Martina Colognesi¹, Ilaria Zanutto¹, Daniela Gabbia¹, Yahima Frion-Herrera¹, Maria Carrara¹, Alice Rossi¹, Maria Digiacomo², Doretta Cuffaro², Marco Macchia², Sara De Martin¹ ¹University of Padova, Department of Pharmaceutical and Pharmacological Sciences, Padova, Italy, ²University of Pisa, Department of Pharmacy, Pisa, Italy
Email: sara.demartin@unipd.it

Background and aims: Extravirgin olive oil (EVOO) is one of the major components of the Mediterranean diet, and its consumption has been correlated with beneficial effects on human health. EVOO gained a renewed interest for its ability to influence pathways involved in inflammation and oxidative stress. Recent preclinical studies stressed the importance of the EVOO phenolic oleocanthal (OC) in the modulation of these processes, and further established its possible role as an antifibrotic agent by counteracting NADPH oxidases upregulation, and reducing the expression of proinflammatory cytokines and metalloproteinases. Recently, the mono-oxidized derivative of OC oleocanthalic acid (Oca) was isolated from aged EVOO, but its biological activities are still controversial. In the light of these considerations, we evaluated Oca direct effect on lipid accumulation and fibrogenesis in 2D and 3D *in vitro* models of NASH.

Method: In this study, Oca modulation of fatty acid (FA) uptake was assessed in different *in vitro* models. Firstly, HepG2 cells were treated for 24 hours with a mixture of palmitic and oleic acid (PA/OA 1: 1, 0.1 mM) to obtain a 2D *in vitro* model of steatosis. The same cells were cocultured with LX-2 cells and M0 macrophages and treated with PA/OA, to obtain 3D spheroids simulating NASH-like microenvironment. Both models underwent a 24 h treatment with different concentrations of Oca (0.5 μ M, 1 μ M, 2 μ M, and 5 μ M), and intracellular neutral lipids were stained with Bodipy or Nile red stain. Subsequently, Oca modulation of lipid accumulation was evaluated in cocultures of HepG2 treated with PA/OA for 24 hours and THP-1-derived M1 proinflammatory macrophages, simulating the NASH-like

POSTER PRESENTATIONS

microenvironment. Lastly, the antifibrotic effect of OcA was evaluated in two different *in vitro* models, i.e., in LX2 cells activated either by a 24 hours treatment with TGF-beta1 (2 ng/ml) or by cocultures with HepG2 and THP-1 derived M0 macrophages. To assess OcA effect on fibrogenesis, the intracellular expression of alphaSMA, a well-known marker of LX2 activation, was evaluated by immunocytochemistry coupled to confocal microscopy.

Results: OcA-treated HepG2 cells incubated with the PA/OA mix reported a significant, dose-dependent, reduction of FAs uptake after treatment compared to control. In accordance with these results, OcA reduced the FAs overload in the coculture of HepG2 and M1-like macrophages compared PA/OA-treated cells ($p < 0.0001$), and in the 3D spheroids coculture of HepG2 and LX2 cells treated for 24 hours with PA/OA mix ($p < 0.01$), providing evidences of its positive effect on the intracellular accumulation of lipids. Concerning fibrogenesis modulation, LX2 activation was significantly decreased after 24 hours of OcA treatment ($p < 0.0001$), in both fibrogenesis models.

Conclusion: This study provides preliminary *in vitro* evidence of the beneficial effect of OcA on NASH onset, since it significantly reduced the accumulation of FAs and prevent HSC activation in a panel of *in vitro* models of NASH, acting on the two main mechanisms involved in NASH development.

WED-526

Novel image analysis and immunohistochemistry advances to accompany pathologist driven non-alcoholic fatty liver disease diagnosis

Maroua Tliba¹, Manon Motte¹, Christophe Sattonnet², Viviana Lamberti¹, Elena Baranova¹, Marie G rus-Durand¹, Renaud Burrer¹, Amanda Finan¹. ¹Cerba Research, France, ²Diag, France
Email: afinan@cerbaresearch.com

Background and aims: The prevalence of non-alcoholic fatty liver disease (NAFLD) is roughly 30% worldwide, a percentage that has rapidly increased over the past decade. There exist two types of NAFLD, non-alcoholic fatty liver (NAFL) and non-alcoholic steatohepatitis (NASH). Both subtypes are associated with lipid accumulation in the liver, the latter being more severe with inflammatory cell infiltration, fibrosis and subsequent hepatocyte damage and impaired organ function. The current gold standard for NAFLD diagnosis is liver biopsies evaluated by experienced pathologists who assign scores for several features (fibrosis, steatosis, inflammation

and ballooning). However, documented inter-pathologist variability in scoring and the semi-quantitative nature of the scoring system itself highlight the need for new methods to ensure the unbiased, consistent assessment of disease. Cerba Research has developed tools that could be implemented to solve the variability in NAFLD diagnosis.

Method: A digital pathology approach involving 30 NASH needle core biopsies stained with hematoxylin and eosin (HandE) and Masson's Trichrome was developed. A pathologist evaluated the classic diagnostic parameters on these matched stains for each liver sample to serve as the gold standard. The imaging team of Cerba Research developed in parallel an application on Visiopharm® software to quantify fibrosis and steatosis on Masson's Trichrome stained slides with help from the pathologist's annotations. Supplementary chromogenic multiplex immunohistochemistry panels were also developed at Cerba Research to assist in the analysis of the liver contexture.

Results: The development of the Masson's Trichrome application and the correlation with the pathologist will be presented. The evolution of an HandE application using Deep Learning will also be shown. Two multiplex panels were designed. The first includes CD45 for inflammation analysis, CD138 as a plasma cells marker, and adipophilin that allows for visualization of lipid droplets associated with metabolic dysregulation in the hepatocytes. The second panel allows for the detection of cytokeratin 8 and 18, the loss of which allows for a facilitated identification of ballooned hepatocytes that may increase the accuracy of distinguishing NASH from NAFL. Example images and quantification of the markers will be presented.

Conclusion: The approaches presented could provide a toolbox for clinical pathologists to aid in a more accurate and quantifiable classification of NAFLD as either NAFL or NASH.

WED-527

Evaluating the hepatic efficacy and cardiometabolic profile of PNPLA3, TM6SF2, and other therapeutic targets for NALFD: a drug-target Mendelian randomization analysis

Daniel Rosoff¹, Lucas Mavromatis¹, Andrew Bell¹, Ali Hamandi¹, Lauren Park¹, Jeeseun Jung¹, Josephin Wagner¹, David Ray², Falk Lohoff¹. ¹National Institutes of Health, National Institute on Alcohol Abuse and Alcoholism, Bethesda, United States, ²University of Oxford, Oxford Centre for Diabetes, Endocrinology and Metabolism, Oxford, United Kingdom
Email: daniel.rosoff@linacre.ox.ac.uk

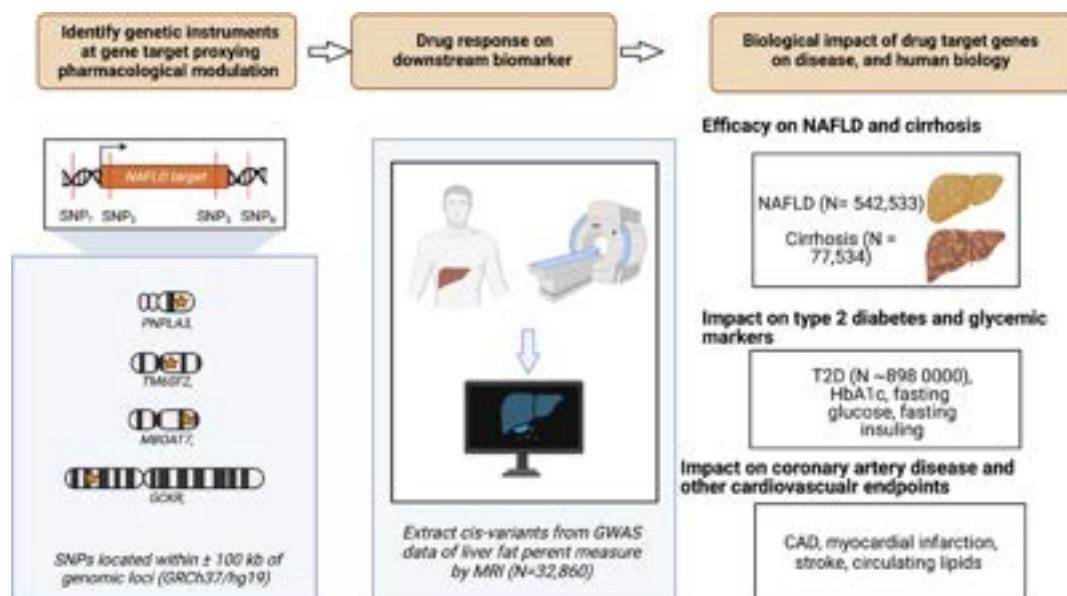


Figure: (abstract: WED-527).

Background and aims: While Non-alcoholic fatty liver disease (NAFLD) is the most prevalent cause of end-stage liver disease worldwide, including cirrhosis, and has been linked with increased risk for type 2 diabetes (T2D) and cardiovascular disease (CVD), there are currently no approved therapies. Previous studies have shown that NAFLD heredity is derived primarily from genes involved in hepatic lipid metabolism, i.e., *PNPLA3*, *TM6SF2*, *GCKR*, and *MBOAT7*, targeting these genes may be an important approach for developing NAFLD therapeutics. However, whether lowering liver fat via these targets impacts T2D, and CVDs remains unknown.

Method: Here, we used drug-target Mendelian randomization (MR) and data from large genome-wide association studies to investigate whether genetic variants within these genes that mimic the pharmacological reduction liver fat content (measured via magnetic resonance imaging) impact NAFLD, T2D, CVDs.

Results: Variants corresponding to a hepatic fat content reduction via these genes were each associated with a lower risk of NAFLD: *PNPLA3* OR = 0.30, P value = 2.03×10^{-42} ; *TM6SF2* OR = 0.52, P value = 5.47×10^{-7} ; and *GCKR* OR = 0.18, P value = 5.98×10^{-6} . Reduced liver fat content via *PNPLA3*, *TM6SF2* variants were also associated with reduced cirrhosis risk (e.g., *PNPLA3* OR = 0.18, P value = 3.13×10^{-17}). Genetically-proxied *PNPLA3* inhibition was also protective against the risk for T2D (OR = 0.844, P value = 4.28×10^{-8}). *PNPLA3* variants were linked with a slight increased risk for CVDs (e.g., coronary artery disease (CAD) OR = 1.11, P value = 2.52×10^{-7}). *PNPLA3* associations were robust to sensitivity analyses using *PNPLA3* instruments comprised of only the I148M variant and additional *PNPLA3* instruments derived from circulating alanine aminotransferase levels. MR estimates were broadly consistent across complementary MR methods, which strengthens causal inference.

Conclusion: These findings extend existing literature highlighting these genes as therapeutic targets for NAFLD, suggest protective effects for T2D, and replicate previous studies linking liver fat and cardiometabolic diseases, including the impact of *PNPLA3* variants on heart disease.

WED-528

High-fat diet exacerbates lipopolysaccharide-induced liver injury in obese KK-Ay mice

Satoshi Sakuma¹, Kazuyoshi Kon², Akira Uchiyama¹, Hiroo Fukada¹, Toshifumi Sato¹, Shunhei Yamashina¹, Kenichi Ikejima¹. ¹Juntendo University School of Medicine, Department of Gastroenterology, Japan, ²Juntendo University School of Medicine, Department of Gastroenterology, Tokyo, Japan
Email: kazukon@juntendo.ac.jp

Background and aims: Cytokine storm is the primary event for fatal multiple organ damage during systemic infections such as sepsis. Although obesity is an etiological risk factor for cytokine storm, the mechanisms underlying the exacerbation remains unclear. Therefore, the aim of this study was to investigate the role of obesity and high-fat diet (HFD) load in exacerbation of cytokine storm and liver damage following lipopolysaccharide (LPS) challenge using obese diabetic KK-Ay mice.

Method: Male KK-Ay mice were fed a diet containing high-fat (HFD; D12492, Research Diets, Inc.) or control (D12450J) for 4 weeks. Wild C57BL6/J mice (BL6) was used as a control strain. Mice were sacrificed at 1–24 hr after intraperitoneal injection of LPS 5 mg/kg BW or saline. Serum AST and ALT levels were determined by an enzymatic method. Hepatic expression levels of cytokine mRNA were measured by RT-PCR. Apoptotic cell death in the liver specimen was detected by TUNEL staining.

Results: Following HFD feeding for 4 weeks, BL6 controls and KK-Ay mice gained body weight nearly 15% and 40% over basal values, respectively. KK-Ay mice fed an HFD showed prominent hepatic steatosis after HFD feeding, whereas BL6 mice developed trivial steatosis even after HFD feeding. Indeed, liver weight increased greatly in HFD-fed KK-Ay from 2.44 ± 0.08 g to 3.41 ± 0.11 g, whereas

the values only increased from 0.77 ± 0.05 g to 0.91 ± 0.02 g in BL6 fed an HFD. After a single intraperitoneal injection of LPS of 5 mg/kg, all BL6 mice fed a control diet survived for 24 hr, indicating that this dose was sublethal. HFD-fed BL6 died within 24 hr after injection of LPS nearly 20%, which was not statistically significant. In sharp contrast, the mortality rate 24 hr after LPS injection reached 86% in HFD-fed KK-Ay mice, which was significantly higher than 16% of control diet-fed KK-Ay mice given LPS ($p = 0.029$). Serum AST and ALT levels 12 h after LPS in HFD-fed KK-Ay mice increased to 492 ± 112 IU/L and 673 ± 191 IU/L, which were obviously higher than those in HFD-fed BL6 reaching 247 ± 35 IU/L and 193 ± 58 IU/L, respectively. Indeed, HFD-fed KK-Ay mice showed marked apoptotic cell expression after LPS administration. Further, hepatic expression levels of TNF α mRNA 1 hr after LPS challenge were almost doubled in HFD-fed KK-Ay mice as compared to control diet-fed KK-Ay mice. Moreover, the induction levels of inflammasome-associated IL1 β mRNA in the liver was also significantly higher in HFD-fed KK-Ay mice 1–3 h after LPS than those in control diet-fed KK-Ay mice.

Conclusion: These findings clearly indicate that KK-Ay mice, which develop obesity and severe fatty liver following HFD-feeding, are obviously vulnerable to LPS, showing higher mortality and severer liver injury. The underlying mechanisms most likely involve sensitization of hepatic macrophages and inflammasome-related reactions against LPS, as well as increased sensitivity to proapoptotic cell death in hepatocytes. It is therefore concluded that metabolic dysfunction-associated fatty liver appears to be an important risk factor of exacerbation in multiple organ failure including severe liver damage under condition of cytokine storm.

WED-529

Exploring transcriptome profiles to combat non-alcoholic fatty liver disease

Eva Kocar¹, Tadeja Rezen¹, Pablo J Giraudi², Silvia Palmisano^{2,3,4}, Claudio Tiribelli², Natalia Rosso², Damjana Rozman¹. ¹Faculty of Medicine, Institute of biochemistry and molecular genetics, Centre for functional genomics and bio-chips, Ljubljana, Slovenia, ²Fondazione Italiana Fegato Onlus, Area Science Park Basovizza, Trieste, Italy, ³University of Trieste, Department of Medical, Surgical and Health Sciences, Trieste, Italy, ⁴Cattinara Hospital, Surgical Clinic Unit, Trieste, Italy
Email: damjana.rozman@mf.uni-lj.si

Background and aims: The incidence of non-alcoholic fatty liver disease (NAFLD) is increasing, making it the most common chronic liver disease in industrialized countries, with no evidence of decline. People with advanced stages of NAFLD are at high risk of developing other comorbidities. The biochemical mechanisms and signaling pathways that classify a particular stage of NAFLD and anticipate disease development remain to be determined. We applied transcriptome analysis and statistical modeling to the histologically identified fibrosis stages of NAFLD to find novel target genes that could better indicate the particular stage of NAFLD.

Method: Sixty liver samples were obtained by biopsy from an Italian population of morbidly obese individuals who had undergone bariatric surgery (discovery cohort). The stages of NAFLD fibrosis, ranging from S0 to S4, were determined histologically based on the Kleiner classification system. RNA was isolated from the preserved liver samples, but because of its low quality, expression profiling was performed using Affymetrix microarrays. Statistical analysis was performed using Transcriptome Analysis Console (TAC) software to identify genes that differ in expression. Enrichment analysis of KEGG and Reactome pathways was performed using Enricher and G:profiler tools. Several differentially expressed genes from the discovery cohort were selected for validation in another group of NAFLD patients (78 patients, validation cohort), along with a subset of genes recently published by others (PMID: 33268509; PMID: 35654907). Correlation of gene expression with fibrosis stage in a discovery

POSTER PRESENTATIONS

cohort of patients was performed in Orange. Patients' medical data and clinical parameters were also included in the statistical analysis.

Results: Several known and unknown gene candidates with $FDR \leq 0.05$ were differentially expressed when comparing different fibrosis stages in the discovery cohort of patients, including *ITGBL1*, *ANKRD29*, *PTGDS*, and *LUM*. Differential expression of some genes was successfully validated by RT-qPCR in a discovery and a validation cohort of patients. In addition, source of variation analysis revealed the influence of several clinical parameters on gene expression in a discovery cohort of patients. Interestingly, BMI, fatty acids, and age had a greater impact on gene expression than fibrosis stage itself. The latter may be one of the reasons for the low number of differentially expressed genes. Correlation of gene expression with fibrosis stage in a discovery cohort of patients showed *ITGBL1* as the best candidate gene with a positive correlation of +0.66. Reactome and KEGG enrichment analysis revealed significant changes ($FDR \leq 0.05$) in metabolic pathways comparing early stages (S0, S1) and later fibrosis stages (S3/S4) in a discovery cohort of patients.

Conclusion: Our study revealed several differentially expressed candidate genes that could differentiate between different fibrosis stages and thus contribute to better patient stratification and appropriate treatment. Genes that can be observed in serum samples by their transcripts or proteins (e.g. *ITGBL1*, *LUM*) are particularly relevant as potential blood biomarkers.

WED-530

Effects of HSD17B13-targeting siRNA-R0737072 on Liver Fibrosis and Steatosis in a mouse model of NASH

Li Ming Gan¹, Shuquan Zheng², Junshi Liang², Di Li², Hongyan Zhang², Zicai Liang², Shan Gao². ¹Ribocure Pharmaceuticals AB, Sweden, ²Ribo Life Science Co., Ltd, China
Email: ganlm@ribolia.com

Background and aims: HSD17B13 has been reported to correlate with NASH development. A siRNA targeting HSD17B13 (R0737072) is designed, GalNAc conjugated, and demonstrated good activity both in cell lines and mouse livers. The purpose of this study was to evaluate the potential therapeutic effects of R0737072 on liver steatosis and fibrosis in a mouse model of human non-alcoholic steatohepatitis (NASH).

Method: A NASH mouse model was induced by western diet and a fructose drinking protocol. After a period of 56 days' dietary challenge, a single dose of R0737072 was administrated subcutaneously into the NASH mice, and liver tissues were analyzed at D15, D29, and the end of the study (D43), with regard to HSD mRNA expression, as well as degree of hepatic fibrosis and steatosis, using Picro Sirius Red and hematoxylin staining, respectively.

Results: 1. Single dose of R0737072 resulted in robust and durable knockdown of HSD17B13 mRNA in NASH mice. Compared with the PBS group, the inhibitory rates of R0737072 on HSD17B13 mRNA expression were maintained at 98.53%, 89.85%, and 74.20% on D15, D29, and D43, respectively (Figure 1E). 2. R0737072 resulted in improvement of liver steatosis and fibrosis in the NASH mouse model. Following the dietary challenge, the NASH mouse model displayed signs of liver steatosis and fibrosis over time, which peaked at D15 and plateaued thereafter. At the end of the experiment on D43 post administration, a clearer reduction of damage of both fibrosis and steatosis was seen. Single sc dose of R0737072 resulted in significantly improved fibrosis IPP score at D15 and D43 compared to placebo. (Figure 1A-D and F).

Conclusion: R0737072 demonstrated durable and potent inhibitory effects on HSD17B13 mRNA expression, and is capable of halting worsening of steatosis and fibrosis in a mouse model of NASH.

WED-531

Discovery biomarker to optimize obeticholic acid treatment for non-alcoholic fatty liver disease

Eileen Yoon¹, Dae Won Jun¹, Huiyul Park², Sang Bong Ahn³, Hyo Young Lee⁴, Hyunwoo Oh⁴, Joo Hyun Oh³, Joo Hyun Sohn¹, Jihyun An¹, Jang Han Jung⁵, Eun Chul Jang⁶, Sung Eun Kim⁷. ¹Hanyang University, College of Medicine, Korea, Rep. of South, ²Myoungji Hospital, Hanyang University College of Medicine, Korea, Rep. of South, ³Nowon Eulji Medical Center, Eulji University School of Medicine, Korea, Rep. of South, ⁴Uijeongbu Eulji Medical Center, Eulji University College of Medicine, Korea, Rep. of South, ⁵Dongtan Sacred Heart Hospital of Hallym University Medical Center, Korea, Rep. of South, ⁶Soonchunhyang

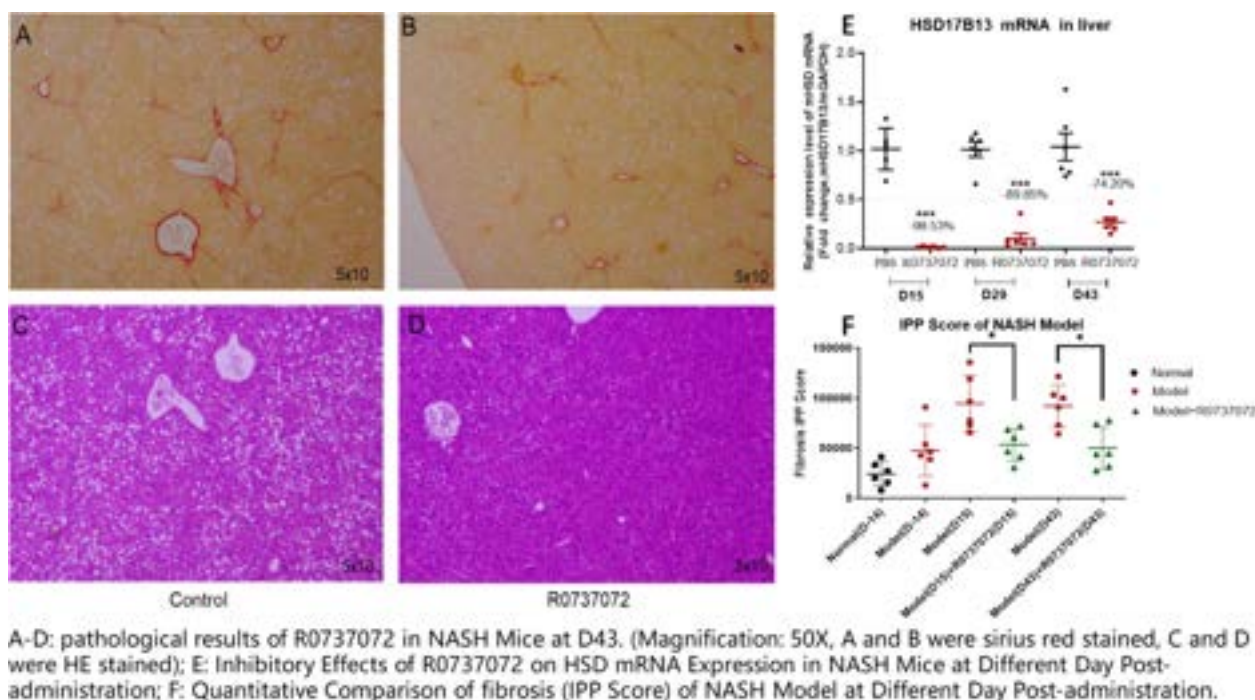


Figure: (abstract: WED-530).

University College of medicine, Korea, Rep. of South, ⁷Hallym University Sacred Heart Hospital, Hallym University College of Medicine, Korea, Rep. of South
Email: noshin@hanyang.ac.kr

Background and aims: Though obeticholic acid (OCA) is a promising drug for non-alcoholic fatty liver disease (NAFLD), the response rate of OCA is limited. This study aimed to develop a biomarker to optimize OCA treatment for NAFLD.

Method: C57BL/6N mice males were fed on a western diet for 24 weeks. Pre-study liver biopsy performed at 12 weeks, and stratified according to disease severity. Next, the mice were administered with OCA (5 mg/kg/day) or vehicle for additional eight weeks. Hepatic transcriptome, metabolome and intestinal microbiome analyses compared according to OCA treatment responder and non-responder using pre-study and end of study samples. LX-2 cells transfected with short-interfering RNA against CYP7B1 (siCYP7B1) and/or treated with OCA to evaluate the role of CYP7B1 in NAFLD.

Results: Resolution rate of steatohepatitis in the OCA and vehicle groups were 36.8% and 0%, respectively. The hepatic transcriptome and bile acid metabolite profile analyses revealed that the alternative bile acid synthesis pathway (Cyp7b1 and muricholic acid) in the OCA-responder group were upregulated compared with those in the OCA-non-responder group. Intestinal microbiome analysis also revealed that the abundances of *Bacteroidaceae*, *Parabacteroides*, and *Bacteroides*, which were positively correlated with the alternative bile acid synthesis pathway, were higher in the OCA-responder group than in the non-responder group. Pre-study hepatic mRNA levels of Cyp8b1 (classic pathway) were downregulated in the OCA-responder group. The OCA response rate increased up to 80% in cases with a hepatic Cyp7b1/Cyp8b1 ratio ≥ 5.0 . CYP7B1 expression was regulated by glucose concentration, and anti-fibrotic effect of OCA showed CYP7B1 dependent manner.

Conclusion: The upregulated alternative bile acid synthesis pathway or high hepatic CYP7B1 can be a potential biomarker for predicting OCA response.

WED-532

Unravelling an autophagy-dependent role of vitamin D in preserving gut integrity in experimental NASH

Andrew Hakeem¹, Basma Alaa¹, Olfat Hammam², Mahmoud Khattab³, Aiman El-Khatib³, Yasmeen Attia¹. ¹Faculty of Pharmacy, The British University in Egypt, Department of Pharmacology, Cairo, Egypt, ²Theodor Bilharz Research Institute, Department of Pathology, Egypt, ³Faculty of Pharmacy, Cairo University, Department of Pharmacology and Toxicology, Cairo, Egypt
Email: andrew.hakeem@bue.edu.eg

Background and aims: The widespread prevalence of non-alcoholic fatty liver disease (NAFLD) exacts a heavy toll on global economy posing an unmet medical need. Clinical data suggest a putative role for gut barrier integrity as a critical determinant of NAFLD progression towards non-alcoholic steatohepatitis (NASH) in a large subset of patients. Calcitriol (CAL), a vitamin D receptor (VDR) agonist, was previously shown to restore intestinal homeostasis under various pathological contexts. However, its effect on gut barrier integrity and the possible molecular underpinnings mediating its gut-protective effects in a NASH setting is little explored. Induced autophagy was previously linked to barrier maintenance in response to intestinal insults. VDR signaling has been shown to promote the activation of autophagy directly and indirectly. The current study was therefore set out to investigate the potential impact of CAL in modulating intestinal tight junction protein expression in NASH and whether these effects could potentially be mediated in an autophagy-dependent manner.

Method: A dietary NASH model was adopted in the current study using male C57BL/6 mice that were divided into four groups: (1) Normal standard chow-fed group; (2) high-fat diet (HFD)-fed NASH group; (3) CAL group, which received CAL (5 ng/gm/day, i.p., twice

weekly); and (4) CAL+HQ group, which received CAL and the autophagy inhibitor hydroxychloroquine (HQ; 60 mg/kg/day, p.o., daily). Treatments were initiated at week 12 and mice were sacrificed at the end of week 16. Hepatic and ileal tissues were harvested and preserved in 10% formalin for histopathological analysis. Tight junction proteins, claudin-1 and occludin, were estimated in ileal sections using immunohistochemistry to assess barrier integrity.

Results: Hematoxylin and eosin (H&E)-stained liver sections of HFD-fed mice showed macro- and microvesicular steatosis, hepatocyte ballooning, and increased portal lymphocytic infiltrates, insults reminiscent of NASH that were mitigated upon treatment with CAL. Meanwhile, H&E-stained ileal sections of NASH mice revealed atrophic mucosa with moderate inflammatory cells infiltration as well as partial loss of goblet cells. These histological derangements were ameliorated in CAL-treated mice with ileal sections showing preserved villous architecture, near normal goblet cells, and mild infiltration in mucosal and submucosal villous cores. Addition of HQ largely abolished CAL mediated improvement primarily manifesting in inflammatory cells infiltration. Furthermore, treatment with CAL resulted in surged ileal immunoreactivity to tight junction protein claudin-1 which was partially negated in the CAL+HQ treated group (Fig. 1). On the other hand, occludin showed augmented expression in NASH ileums which further increased upon treatment with CAL but did not significantly alter with HQ addition.

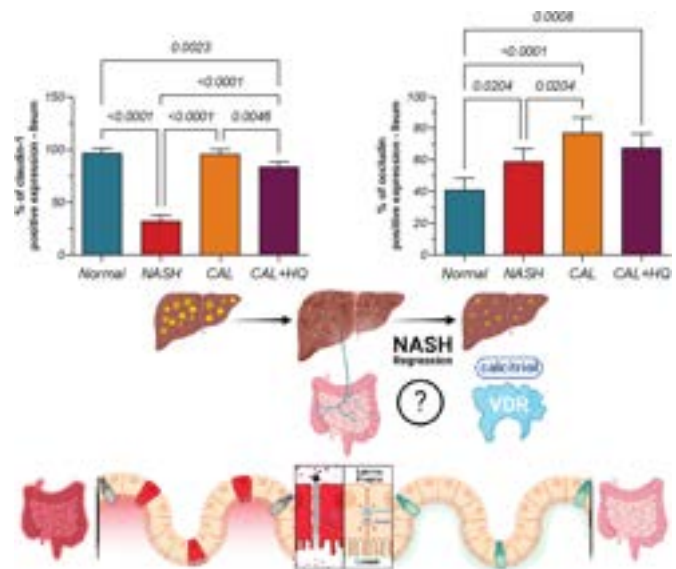


Figure: Immunohistochemical analysis against tight junction proteins, claudin-1 and occludin, in ileal sections of mice belonging to different treatment groups presented as means \pm S.D. of the percentages of cytoplasmic and membranous expression. Statistical significance was inferred at $p < 0.05$ using one-way ANOVA followed by Tukey's *post hoc* test.

Conclusion: The current study findings suggest that CAL confers gut-protective effects in NASH. These effects were mediated, at least in part, by modulating different tight junction proteins expression that is autophagy dependent.

WED-533

Selective modulation of mitochondrial complex I ameliorates steatosis and hepatic inflammation in MCD-diet fed rats

Laura Giuseppina Di Pasqua¹, Oriana Bosco¹, Marta Cagna¹, Peng Sun², Stefan Günther Kauschke², Mariapia Vairetti¹, Anna Cleta Croce³, Andrea Ferrigno¹. ¹University of Pavia, Department of Internal Medicine and Therapeutics, Pavia, Italy, ²Boehringer Ingelheim Pharma GmbH and Co. KG, Department of CardioMetabolic Diseases Research, Germany, ³Institute of Molecular Genetics-Italian National Research Council (CNR), Pavia, Italy
Email: lauragiuseppina.dipasqua01@universitadipavia.it

POSTER PRESENTATIONS

Background and aims: NAFLD is one of the most common liver diseases worldwide. Inflammation and ROS production play a key role in the pathology progression. ROS scavengers are currently employed to sustain natural antioxidant defense, however no specific pharmacological target has been identified yet. Recently, it has been demonstrated that metformin targets mitochondrial complex I, making it a new interesting target. NAFLD is strictly related with mitochondrial dysfunction: lipid accumulation increases beta-oxidation, causing an overproduction of reducing equivalents and ROS. Aim of this work was to investigate if the selective modulation of mitochondrial complex I, the main ROS producer in mitochondria, could play a role in decreasing hepatic lipid accumulation and NAFLD progression.

Method: male Wistar rats fed by a Methionine and Choline deficient (MCD) diet or Control diet for 6 weeks were orally administered, starting from the fourth week with complex I modulator (CIM, Boehringer Ingelheim) 10 mg/Kg/day or vehicle for 3 weeks. Lipid peroxidation and ROS were assayed by TBARS and DCHF-DA methods. ATP content and NAD (P)H bound/free ratio were measured. Hepatic Nitrate and Nitrite concentration was established and total lipid content was measured using Nile Red dye. The area of lipid droplets and the rate of inflammatory cells infiltration was calculated on HandE stained liver sections.

Results: TBARS increased in MCD-treated rats compared with Control rats, without changes after CIM administration. MCD groups showed a ROS content increase, but a significant reduction in CIM-treated Controls was detected, compared with vehicle-treated Controls. ATP content decreased in CIM-treated controls, but no significant differences were appreciated in MCD treated groups. The same trend was observed for NAD (P)H bound/free ratio. Nitrate and Nitrite were reduced in CIM-treated MCD rats compared with vehicle-treated MCD rats. Total lipid content was significantly reduced in CIM-treated MCD rats compared with vehicle-treated MCD rats. A significant decrease in lipid droplet areas was observed in MCD rats treated with CIM, compared with untreated MCD rats. A significant reduction in inflammatory cell infiltration was observed in MCD rats

treated with CIM. Lastly, a significant reduction in AST and ALT was observed in CIM-treated control rats, compared with untreated control rats.

Conclusion: our work demonstrated that the complex I modulator administration could be a promising strategy in the reduction of lipid accumulation and inflammatory process in our model of steatosis. At the best of our knowledge, although further investigation is needed to clarify the mechanisms underlying this process, this is the first attempt to demonstrate a possible role of complex I modulator in reducing lipid accumulation and NAFLD progression in a model of benign steatosis.

WED-534

Inhibition of NLRP3 inflammasome activation by MK571, a multidrug resistance-associated protein (MRP) inhibitor

Oh Seung Seok¹, Jeongwoo Park¹, Keon Wook Kang¹. ¹Seoul Nat.

University, Korea, Rep. of South

Email: kwkang@snu.ac.kr

Background and aims: The NLR family pyrin domain containing 3 (NLRP3) inflammasome is an intracellular multiprotein complex involved in the production of mature interleukin 1-beta (IL-1 β), and has been known to induce metabolic inflammation such as non-alcoholic steatohepatitis (NASH). Multidrug resistance-associated protein 4 and 5 (MRP4 and MRP5, also known as Abcc4 and Abcc5) functionally control intracellular levels of glutathione and cAMP via regulating their efflux amounts. Here, we tried to reveal the role of MRP4 and MRP5 in NLRP3 inflammasome activation during liver injury.

Method: To assess the function of MRP4 and MRP5, MK571, a selective inhibitor of MRP transporter family, was used. Protein and mRNA expression of MRP family was assessed in primary hepatocytes, kupffer cells, hepatic stellates cells and bone marrow-derived macrophages (BMDMs). For determining *in vivo* protective effect of MK571 on NLRP3 inflammasome-mediated liver injury, LPS/galactosamine-induced fulminant hepatitis model was used.

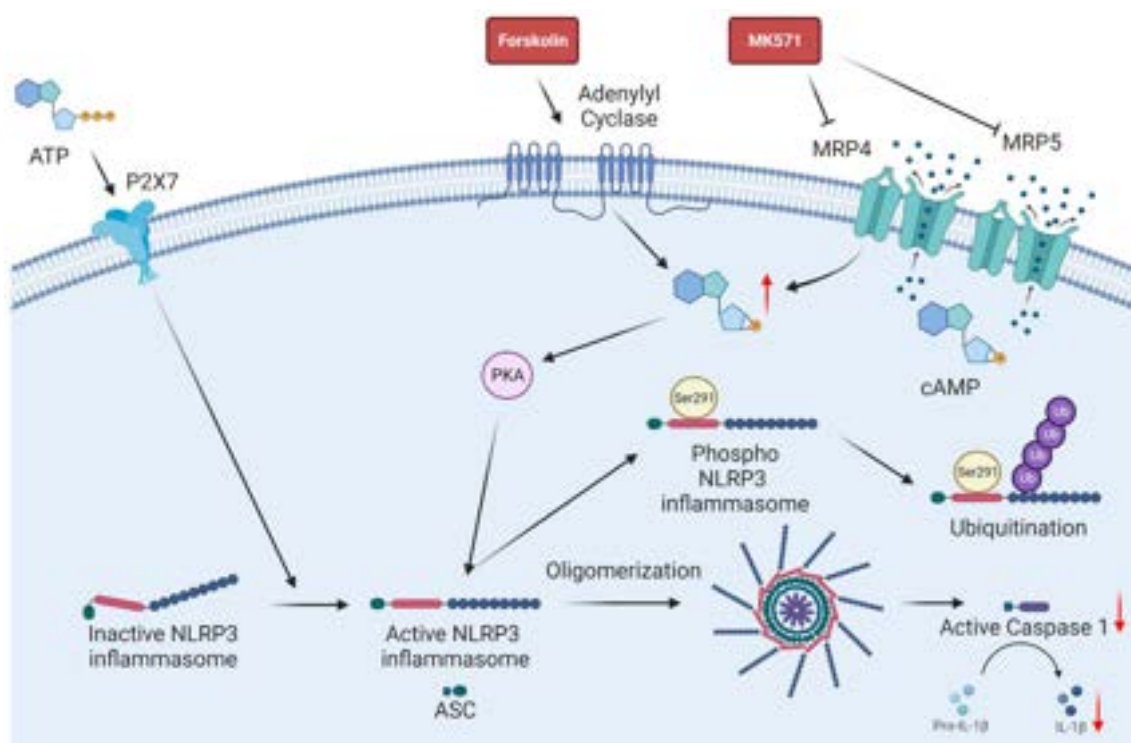


Figure: (abstract: WED-534).

Results: Protein levels of MRP4 were increased in kupffer cells from acetaminophen-injected mice. cAMP accumulation by MK571-mediated MRP4/5 inhibition concentration-dependently suppressed NLRP3 inflammasome via either transcriptional control of nuclear factor- κ B or ubiquitination of NLRP3 protein. In lipopolysaccharide/D-galactosamine-induced acute hepatitis mouse model, oral administration of MK571 suppressed the increases in several inflammatory marker proteins and serum IL-1 β .

Conclusion: These findings indicate that the MRP4 and 5 as energy-dependent transporters for the cyclic nucleotide, are involved in the regulation of NLRP3 inflammasome during liver injury.

WED-535

A formulation of palmitoylethanolamide and phenolic compounds improves NAFLD-associated hepatic lipid dysmetabolism and oxidative stress in obese mice

Stefania Melini¹, Claudio Pirozzi¹, Adriano Lama¹, Filomena Del Piano², Federica Comella¹, Nicola Opallo¹, Chiara Annunziata¹, Giuseppina Mattace Raso¹, Rosaria Meli¹.

¹University of Naples Federico II, Pharmacy, Italy, ²University of Naples Federico II, Department of Veterinary Medicine and Animal Production, Italy

Email: stefania.melini@unina.it

Background and aims: Gluco- and lipotoxicity, as well as insulin resistance, play a key role in the development of NAFLD associated with metabolic disorders characterizing obesity (Petersen et al. 2017). The excess of free fatty acids (FFA) facilitates the generation of lipotoxic metabolites contributing to the development of hepatic oxidative stress and inflammation (Hong et al 2021) which leads to insulin resistance and glucose intolerance (Tangvarasittichai et al. 2015). The N-acyl ethanolamine palmitoylethanolamide (PEA) and some phenolic compounds from olive leaves, such as rutin and hydroxytyrosol (HT), have shown different metabolic, anti-inflammatory and antioxidant effects (Annunziata et al. 2020, Pirozzi et al. 2016, Li et al 2022). This study evaluates the possible beneficial activity of a formulation containing PEA co-micronized with rutin and associated with HT in counteracting hepatic damage and metabolic alterations occurring in a mouse model of high-fat diet (HFD)-induced obesity.

Method: Male C57BL/6J mice were divided into 3 groups: a control group receiving standard chow diet; mice fed with HFD for 19 weeks; a HFD group administered NORM3 (PEA 10 mg/kg/die-Rutin 2 mg/kg/die, HT 0, 5 mg/kg/die *per os*) from week 12 up to week 19. Biochemical and molecular analysis were performed by ELISA assay and Western blot and Real-Time PCR analysis, respectively.

Results: The treatment with NORM3 reduced body weight and fat mass of obese mice compared with untreated HFD group. The protective effect of NORM3 was confirmed by the decrease of serum hepatic and metabolic parameters, (i.e. transaminases, triglycerides, and cholesterol). Moreover, NORM3 improved glucose homeostasis altered by HFD reducing fasting glycaemia and gluconeogenesis process, as shown by PTT. Consistently, NORM3 induced the activation of PI3K/AKT pathway, leading to the restoration of insulin signaling. AKT can also activate glycogen synthase kinase (GSK3 β), which may promote the activity of antioxidant mediators. NORM3 demonstrated a significant antioxidant effect reducing the production of ROS and malondialdehyde levels as well as increasing the hepatic transcription of nuclear factor erythroid (NRF2) and its downstream antioxidant genes. We also demonstrated the effect of NORM3 on the hepatic inflammation induced by lipid overnutrition. NORM3 treatment reduced the protein expression of NF κ B as well as the transcription of *Il1b* and *Ccl2*. Finally, since FFA accumulation is another hallmark in NAFLD and obesity, we investigated the effect of NORM3 on hepatic lipid dysmetabolism induced by HFD. The administration of NORM3 counteracted lipogenesis, reducing the hepatic mRNAs of fatty acid synthase (*Fasn*) and increasing PPAR- α , as a key upstream target of fatty acid oxidation.

Conclusion: Taken together, our findings identify NORM3 as a potential hepatoprotective approach in dampening the hepatic dysmetabolism and associated oxidative stress in NAFLD and obesity.

WED-536

Deletion of no-sensitive guanylyl cyclase protects from metabolic obesity but not from fibrosis in murine non-alcoholic fatty liver disease

Muhammad Ashfaq-Khan¹, Jan-Luca Wasser¹, Andreas Friebe¹.

¹Universität Würzburg, Germany

Email: m.ashfaq_biotech@yahoo.com

Background and aims: Non-alcoholic fatty liver disease (NAFLD) comprises bland steatosis that progresses to its more aggressive form, non-alcoholic steatohepatitis (NASH), which can finally develop into hepatocellular carcinoma in a subset of patients. The underlying mechanisms and the endogenous drivers of the development of NAFLD/NASH have not yet been fully elucidated. Recently, a stimulator of NO-sensitive guanylyl cyclase (NO-GC), the receptor for the signaling molecule nitric oxide (NO), was shown to inhibit fibrosis, inflammation and steatosis in rodent models of NASH. In our current study, we have characterized the role of NO-GC in an experimental model of NAFLD/NASH.

Method: 8–10-week old male mice carrying a global deletion of NO-GC and their wildtype siblings (C57BL/6J background) were fed a Western diet (21% fat, 0.2% cholesterol and 42 g/l fructose) for 16 weeks. Thereafter, mice were sacrificed, and liver tissues were fixed in paraformaldehyde for histological analysis.

Results: NO-GC knock mice had significantly lowered liver ($p = 0.0048$) and body weights ($p = 0.00019$) compared to wildtype control. In addition, epididymal, mesenteric and inguinal fat was strongly decreased in NO-GC KO mice compared to controls. Moreover, Western diet-fed wildtype mice showed highly elevated blood glucose levels in the intra-peritoneal glucose tolerance test after 120 min (341 ± 104 mg/dl) whereas levels in NO-GC KO were normal (156 ± 25 mg/dl). In line with this, steatosis was not observed in the livers of NO-GC KO mice whereas wildtype livers showed a steatosis score of 3 ($\geq 66\%$). Despite the lack of peripheral and hepatic obesity in the NO-GC KO mice, the extent of fibrosis was similar in both genotypes.

Conclusion: Deletion of NO-GC protects from peripheral and hepatic obesity but not from fibrosis upon feeding a Western diet. Our results indicate that hepatic fibrosis may result from Western diet independent of the development of steatosis.

WED-537

Empagliflozin improves non-alcoholic fatty liver disease in a new translational mice model even without impact on weight loss

Katharina Luise Hupa-Breier¹, Janine Dywicky¹, Björn Hartleben¹, Noyan Fatih¹, Heiner Wedemeyer¹, Matthias Hardtke-Wolenski^{1,2}, Elmar Jaeckel^{1,3}. ¹Hannover Medical School, Germany, ²University Duisburg-Essen, Germany, ³University of Toronto, Canada

Email: hupa.katharina@mh-hannover.de

Background and aims: Non-alcoholic steatohepatitis (NASH) is currently one of the most common causes of chronic liver disease with the metabolic syndrome as the main risk factor. However, current mice models only partial represent the human phenotype of the metabolic syndrome. Beside weight loss and lifestyle intervention, treatment options are very rare. Due to their insulin-independent mechanism leading to weight loss and improvement of hyperglycemia, SGLT-2 inhibitors seem to be a promising therapy in the field of NAFLD. The aim of this study was to investigate the effect of SGLT-2 inhibitor empagliflozin in a new dietary mice model for NAFLD with a polygenetic background for the metabolic syndrome.

Method: TALLYHO/JngJ (TH) mice received 16 weeks of high-fat/high-carbohydrate (HF-HC) diet with a surplus of cholesterol. After 12 weeks of HF-HC, mice were additionally treated with empagliflozin (Fig.1).

Results: After 16 weeks of HF-HC treatment, TH mice developed obesity, hyperglycemia and histological proven NAFLD (median NAS = 5). Treatment with empagliflozin led to a significant improvement of hyperglycemia, but had interestingly no effect on body weight in this mice model. Nevertheless, empagliflozin significantly improved both histological onset of NAFLD (median NAS = 3, $p = 0.0312$) and fibrosis ($p = 0.0017$). Detailed analysis demonstrated that empagliflozin significantly decreased intrahepatic B ($p < 0.0001$) and T cells ($p = 0.0031$) and in particular diminished proinflammatory CD8⁺ ($p = 0.0028$) as well as CD4⁺ ($p = 0.0051$) cells. In addition, empagliflozin attenuated intrahepatic infiltration of proinflammatory macrophages ($p = 0.039$). Furthermore, empagliflozin revealed anti-inflammatory potential by gene-downregulation of TNF and nitric oxide synthase and improvement of catalase and superoxiddismutase (SOD), which are both involved in oxidative stress.

Conclusion: This is the first study testing empagliflozin in a new mouse model for NAFLD with a polygenetic background for the metabolic syndrome. Most important, empagliflozin improves the histological outcome of NAFLD even without any impact on weight loss and thereby reveals anti-inflammatory potentials. As these results might have important impact on the treatment of NAFLD, further studies are needed for confirmation.

WED-538

The effects of lipopolysaccharides on inducing non-alcoholic fatty liver disease in human precision-cut liver slices

Mei Li¹, Ke Luo¹, Vincent de Meijer², Anika Nagelkerke¹, Peter Olinga¹, Yana Geng¹. ¹University of Groningen, Netherlands, ²University Medical Center Groningen, Netherlands
Email: yana.geng@rug.nl

Background and aims: Non-alcoholic fatty liver disease (NAFLD) is one of the most common chronic liver diseases, ranging from simple non-alcoholic fatty liver (NAFL) to non-alcoholic steatohepatitis (NASH), which may ultimately progress to cirrhosis, and eventually hepatocellular carcinoma (HCC). Pre-clinical studies suggested that lipopolysaccharides (LPS) from the gut microbiota contribute to the pathogenesis of NAFLD. However, the interplay between LPS and human NAFLD remains less clear. In our lab, we successfully developed an *ex vivo* NAFLD model from NAFL to fibrosis in precision-cut liver slices (PCLS). In this study, we aimed to assess the effects of LPS on NAFLD-PCLS in terms of inflammation, fibrosis and oncogenic signaling which would provide a potential model to investigate the relationship between LPS and human NAFLD.

Method: PCLS used in this study were derived from leftover liver material after transplant procedures. They were cultured in GF1PO (William's E Medium supplemented with Glucose (36 mM), Fructose (5 mM), Insulin (1 nM), Palmitic acid (0.24 mM) and Oleic acid (0.48 mM)) to mimic the NAFLD conditions, or WEGG (William's E Medium supplemented with Glucose (25 mM)) as control for 96 h. To investigate the effects of LPS stimulation, PCLS were treated with 100 ng/ml LPS in both WEGG and GF1PO medium. After incubation, PCLS were collected to assess viability and fat accumulation by measuring ATP levels and triglyceride (TG) content. Liver inflammation, fibrosis, cell proliferation and angiogenesis were evaluated by RT-qPCR to indicate the development of NAFLD and oncogenic signaling.

Results: PCLS remained viable for up to 96 h of incubation whilst being treated with LPS. TG content was increased significantly in GF1PO compared with WEGG group ($p < 0.0001$), but LPS had no significant influence on fat accumulation. mRNA expression of the inflammatory biomarkers *IL6*, *IL1 β* was upregulated by LPS in GF1PO or WEGG, whereas *TNF α* only showed a trend towards upregulation. *COL1a1*, *ACTA2* and *TIMP-1* showed an increasing trend as well, suggesting the contribution of LPS to fibrogenesis. To evaluate the early onset of HCC, we measured gene expressions related to cell proliferation and angiogenesis. The upregulation in proliferation biomarkers (*MKI67*, *PCNA*) only occurred under the incubation of

GF1PO, regardless of whether LPS was present, suggesting that LPS may have no effect on hepatocyte proliferation in PCLS. *CD34* and *VEGFA* expression showed a similar trend as was seen for cell proliferation, with LPS having a moderate impact on angiogenesis.

Conclusion: LPS mainly caused the development of liver inflammation, and may trigger fibrogenesis. Cell proliferation and angiogenesis were induced in non-alcoholic fatty liver disease in PCLS, with LPS having limited effect. This *ex vivo* model of human PCLS could be used to investigate the interplay between LPS and NASH, with inflammation and fibrosis being the primary factors affected.

WED-539

Oral antibiotic treatment protects mice against the development of diet-induced non-alcoholic fatty liver disease but not against diet-induced intestinal barrier dysfunction

Annette Brandt¹, Katja Csarman¹, Angelica Hernández-Arriaga², Anja Baumann¹, Raphaela Staltner¹, Amélia Camarinha-Silva², Ina Bergheim¹. ¹University of Vienna, Austria, ²University of Hohenheim, Germany
Email: ina.bergheim@univie.ac.at

Background and aims: Alterations in intestinal barrier function and an elevated translocation of bacterial endotoxin and induction of toll-like receptor 4 (TLR4)-dependent signaling cascades in the liver are discussed as major factors in development of non-alcoholic fatty liver disease (NAFLD). To date, molecular mechanisms underlying these alterations are not yet fully understood. Here the effects of an oral treatment with an antibiotic mixture on intestinal barrier function in a model of diet-induced NAFLD was assessed.

Method: For 7 weeks, male C57BL/6J mice were pair-fed either a liquid standard diet (control, C) or a liquid high-fat and high-fructose diet (FFr) \pm an antibiotic mixture (ampicillin, vancomycin, metronidazole, gentamycin, AB). Markers of liver damage and intestinal barrier function were examined and intestinal microbiota composition was determined. Moreover, everted gut tissue sacs from naïve male C57BL/6J mice were treated with fructose \pm antibiotics or \pm the inducible NO synthase (iNOS) inhibitor aminoguanidine *ex vivo*.

Results: The addition of AB to the diet almost completely abolished the development of NAFLD, e.g. macrovesicular steatosis and inflammatory alterations, being associated with a significantly lower Tlr4 mRNA expression in liver tissue and suppression of subsequent signaling cascades. In contrast, intestinal permeability was similarly significantly elevated in both FFr diet fed groups compared to the respective controls, while tight junction proteins in small intestinal tissue were significantly lower in both FFr-groups compared to C-fed mice. Furthermore, NOx levels were also similarly higher in both FFr-fed groups than in C-fed groups. Moreover, AB treatment had no effect on fructose-induced permeability in everted gut tissue sac, while the iNOS inhibitor aminoguanidine affected the development of intestinal permeability *ex vivo*.

Conclusion: Taken together, our results indicate that antibiotic treatment protects mice against the development of diet-induced NAFLD, but this is not primarily associated with an improvement in gut barrier function. Funded in parts by JPI HDHL-INTIMIC/FFG.

WED-540

MicroRNA as novel biomarker for disease severity evaluation and therapeutic target in NAFLD

Yoonseok Lee^{1,2}, Young-Sun Lee¹, Ji Hoon Kim¹, Eunho Choi¹, Tae Hyung Kim¹, Sun Young Yim¹, Young Kul Jung¹, Yeon Seok Seo¹, Jong Eun Yeon¹, Kwan Soo Byun¹. ¹Korea University College of Medicine, Department of Internal Medicine, Seoul, Korea, Rep. of South
Email: lys810@hanmail.net

Background and aims: Non-alcoholic fatty liver disease (NAFLD) is chronic and progressive liver disease with high prevalence of 30% of the general population. As global prevalence of NAFLD is increasing, it has become a major public health problem and major cause of chronic liver disease. Non-alcoholic steatohepatitis (NASH) with

hepatic fibrosis has poor prognosis compared with non-alcoholic fatty liver (NAFL) or NASH without hepatic fibrosis. Micro RNA (miR) is a non-coding RNA with about 20 nucleotides, and it can bind to the target mRNA, resulting in epigenetic reprogramming. Recently, many studies found that miRNA could be used as therapeutic targets and novel biomarkers for diagnosis and evaluation of severity in various diseases including NAFLD.

Method: Circulating miRNAs were analysed in sera from 24 patients with biopsy-proven NAFLD using small RNA sequencing. We treated palmitic acid to various cell lines to induce lipotoxicity, and checked miRNA4449 expression in supernatant and cells. We identified merlin, an important inhibitory regulator of YAP-TAZ signaling, as the target of miR-4449 by TargetScan (targetscan.org). We confirmed in human liver tissue whether the expression level of merlin changes depending on the presence of fibrosis, and tested the interaction with miR-4449 *in vivo*.

Results: Among 24 NAFLD patients, 15 patients were NAFL or NASH without fibrosis, whereas 9 patients were NASH with fibrosis. 31 miRNAs showed significant difference in expression level between two groups and miR-4449 was the most prominent among miRNAs that showed higher expression level in NASH with fibrosis compared to NAFL or NASH without fibrosis. Expression of miR-4449 increased in most supernatant and pellets from various cell lines when lipotoxicity was induced (Figure 1.). Therefore, hepatocytes are major source of miR-4449 during lipotoxicity and miR-4449 can be excreted to extracellular milieu. mRNA sequencing and quantitative PCR were performed on human liver tissue. Three patients were simple steatosis or NASH without fibrosis and three patients were NASH with fibrosis. Merlin showed significantly decreased in group of NASH with fibrosis (Figure 2.). When miR-4449 mimics and inhibitors were treated to Hep 3B cell lines, miR4449 mimic suppress merlin expression, whereas miR-4449 inhibitor increase expression of merlin (Figure 3.).

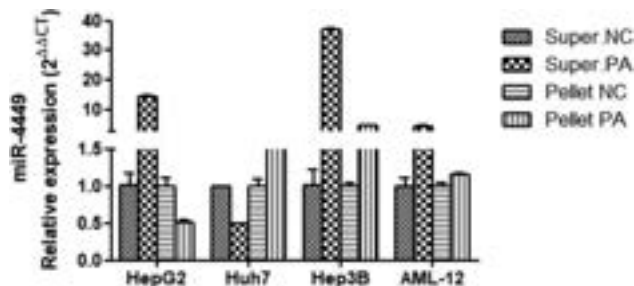


Figure 1:

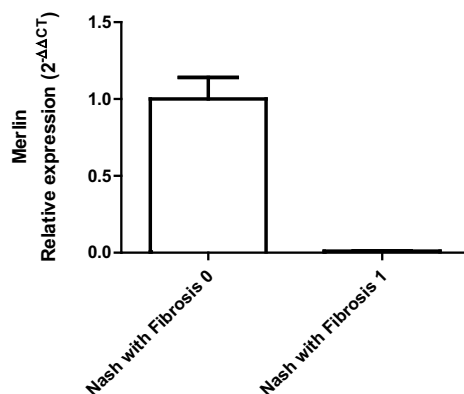


Figure 2:

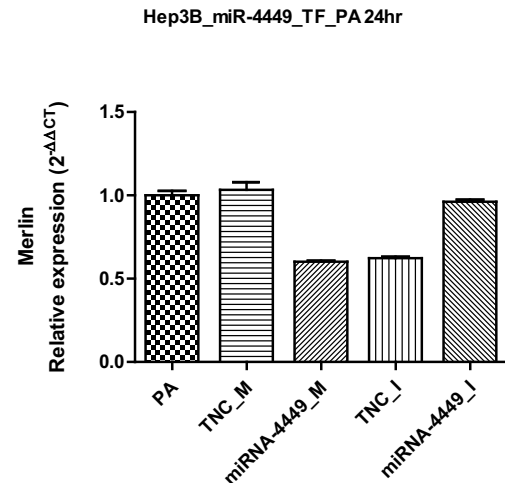


Figure 3:

Conclusion: miR-4449 might be used for novel therapeutic target of NASH-fibrosis.

WED-541

The role of chronic ER stress and calcium signalling in NASH associated carcinogenesis

Muhammad Umair Latif¹, Sercan Mercan¹, Ivan Bogeski², Volker Ellenrieder¹. ¹University Medical Center Goettingen, Department of Gastroenterology and Gastrointestinal Oncology, Goettingen, Germany, ²University Medical center Goettingen, Molecular Physiology, Institute of Cardiovascular Physiology, Goettingen, Germany
Email: umair.latif@med.uni-goettingen.de

Background and aims: The worldwide incidence of non-alcoholic fatty liver disease (NAFLD) continues to increase rapidly. It has become one of the most prevalent causes of progressive liver inflammation and a significant number of patients are at risk of developing cirrhosis and hepatocellular carcinoma (HCC). A better understanding of the processes leading to the development and progression of NASH and subsequent cancer development is essential to develop preventive strategies. We aim to investigate the role of ER-stress-induced NFATc1 activation in NASH associated carcinogenesis and define the underlying oncogenic mechanisms.

Method: We will perform comprehensive biochemical, molecular and functional analysis using *in-vitro* and *in-vivo* models, to scrutinize the impact of CRAC-NFATc1 activation in HCC. This study will certainly contribute to a better understanding of NASH-associated carcinogenesis and help to establish new strategies to prevent disease acceleration.

Results: NFATc1 is aberrantly activated in human NAFLD and advanced HCC. High NFATc1 activation correlates with the extent of liver damage and NASH incidence. We have demonstrated an important function of the Ca²⁺-responsive NFATc1 signaling and transcription pathway in mediating chronic ER-stress responses and subsequent manifestation of NASH. In numerous cancers, NFATc1 orchestrates cell adaptation mechanisms and converts stress signals into gene signatures involved in tumor initiation and progression.

Conclusion: Persistent ER-stress leads to increased Ca²⁺-dependent NFATc1 activation in hepatocytes *via* activation of Ca²⁺-release-activated Ca²⁺ channels (CRAC). We propose that CRAC-NFATc1 activation drives NASH-associated HCC development and formation of a tumor permissive immune microenvironment *via* transcriptional regulation of oncogenic gene signatures and interfering with CRAC-NFATc1 signaling has potential to prevent NASH acceleration and tumor formation.

WED-542

A N-acyl ethanolamines mixture counteracts hepatic dysmetabolism induced in high-fat diet-fed obese mice

Claudio Pirozzi¹, Stefania Melini¹, Nicola Opallo¹, Adriano Lama², Filomena Del Piano³, Federica Comella¹, Giuseppina Mattace Raso¹, Rosaria Meli⁴. ¹University of Naples Federico II, Pharmacy, Naples, Italy, ²University of Naples Federico II, Pharmacy, Naples, Italy, ³University of Naples Federico II, Veterinary Medicine and Animal Production, Naples, Italy, ⁴University of Naples Federico II, Pharmacy, Naples, Italy
Email: claudio.pirozzi@unina.it

Background and aims: Obesity is a multisystem disease characterized by the increased risk of many co-morbidities including hyperlipidemia, hyperglycemia, diabetes, metabolic syndrome and Non-Alcoholic Fatty Liver Disease (NAFLD) (Perumpail et al. 2017; James et al. 2008). NAFLD is the hepatic manifestation of metabolic syndrome due to the fat accumulation leading to hepatocyte death, inflammation, and fibrosis (Sharma et al. 2021). Several studies have shown metabolic and anti-inflammatory effects of specific N-acyl ethanolamine (NAE)s such as palmitoylethanolamide (PEA) and oleoylethanolamide (OEA) (Annunziata et al. 2022; Annunziata et al. 2020; Lama et al. 2020). The aim of this study is to evaluate the possible beneficial effects of a patented derivative of olive oil, consisting in a mixture of NAEs, named Olaliamid® (OLA) on hepatic glucose e lipid dysmetabolism induced by high-fat diet (HFD) in obese mice.

Method: Male C57BL/6J mice were randomly divided into 3 groups: control group (STD) receiving standard chow diet; mice fed with HFD for 19 weeks (HFD); HFD group treated with OLA (OEA, PEA, and LEA in the same ratio as that of the fatty acids naturally found in the oil) from week 12 to week 19. Body weight of all groups were monitored throughout the experimental period. Oral glucose tolerance test (OGTT) was performed at the 7th week of treatment and then the animals were sacrificed and livers were collected for the following molecular determinations.

Results: First, we found that OLA markedly reduced body weight and fat mass, measured by impedenziometric analysis. During OGTT, OLA treatment reduced hyperglycemia due to lipid overnutrition at different time point, suggesting an improvement of tissue insulin sensitivity. Consistently, OLA restored HFD-altered insulin signaling pathway in the liver of obese mice, inducing the phosphorylation of insulin receptor and the activation of PI3K/AKT pathway. Notably, we demonstrated that OLA treatment counteracted the alterations of hepatic lipid homeostasis by HFD, normalizing the phosphorylation of AMPK, and the protein expression of carnitine palmitoyltransferase (CPT)1, a rate-limiting enzyme of fatty acid oxidation. OLA also reduced the mRNA expression of a key marker of steatosis, such as cluster of differentiation (CD)36, and different genes involved in the regulation of lipid metabolism (i.e. peroxisome proliferator-activated receptor gamma, its coactivator PGC1alpha, fatty acid synthase, and SREBP1). Finally, regarding the strict relationship between insulin resistance and hepatic inflammation in obesity, we showed an anti-inflammatory effect of OLA in reducing the expression of different pro-inflammatory cytokines and enzyme, altered in HFD-fed obese mice.

Conclusion: Taken together, our results indicate a therapeutic potential of OLA in counteracting and limiting the hepatic glucose and lipotoxicity and the metabolic impairment associated with obesity and its co-morbidities.

WED-543

Preclinical efficacy and clinical translatability of resmetirom in the GAN diet-induced obese and biopsy-confirmed mouse model of NASH

Michael Feigh¹, Jacob Nøhr-Meldgaard¹, Susanne Pors¹, Henrik B. Hansen¹. ¹Gubra, Hørsholm, Denmark
Email: mfe@gubra.dk

Background and aims: Resmetirom, a selective THR- β agonist, has in a recent phase-3 clinical trial (MAESTRO-NASH) in NASH patients

with liver fibrosis, demonstrated significantly higher rate of NASH resolution and improvement in fibrosis stage as compared to placebo. The present study aimed to (i) evaluate the metabolic, biochemical and histopathological effects of resmetirom treatment in the Gubra-Amylin NASH (GAN) diet-induced obese (DIO) mouse model of fibrosing NASH; and (ii) compare primary histopathological end point analysis to the MAESTRO-NASH trial.

Method: Male C57BL/6 mice were fed the GAN diet high in fat, fructose and cholesterol for 38 weeks prior to study start. A liver biopsy was sampled 4 weeks prior to study start. Only animals with biopsy-confirmed NAFLD Activity Score (NAS ≥ 5) and fibrosis stage $\geq F1$ were included and stratified into treatment groups. Mice were administered (PO, QD) vehicle (n = 16) or resmetirom (3 mg/kg, n = 15) for 12 weeks. Vehicle-dosed chow-fed C57BL/6J mice (n = 10) served as normal controls. Histopathological pre-to-post individual assessment of NAS and fibrosis stage was performed and evaluated against primary end points applied in the corresponding MAESTRO-NASH trial (resolution of NASH with no worsening of liver fibrosis; ≥ 1 -stage fibrosis improvement without worsening of NASH). Other terminal end points in GAN DIO-NASH mice included quantitative liver histology, blood and liver biochemistry.

Results: Resmetirom was weight-neutral, improved hepatomegaly, plasma alanine transaminase and plasma/liver lipid levels compared to vehicle-dosed GAN DIO-NASH mice. The efficacy of resmetirom on primary clinical end points in GAN DIO-NASH mice was comparable to corresponding clinical phase-3 trial outcomes. Accordingly, resmetirom treatment demonstrated ≥ 2 point significant improvement in NAS and 1-point significant improvement in Fibrosis Stage. The benefits on liver histology were further supported by reduced quantitative histological markers of steatosis (% area of lipids, % lipid-laden hepatocytes, lipid droplet density and size) and fibrosis (% area of PSR).

Conclusion: Resmetirom treatment improved metabolic, biochemical and liver histological markers of steatosis and fibrosis in biopsy-confirmed GAN DIO-NASH mice. Therapeutic efficacy of resmetirom on primary clinical histopathological end points were recapitulated in GAN DIO-NASH mice. These findings further validate clinical translatability of the GAN DIO-NASH mouse model, highlighting its utility in preclinical drug development.

WED-544

Loss of gut barrier integrity in non-alcoholic fatty liver disease is associated with severe vibriosis

Punnag Saha^{1,2}, Dipro Bose¹, Subhajit Roy¹, Anna Mae Diehl³, Saurabh Chatterjee⁴. ¹University of California, United States, ²University of California Irvine, Environmental and Occupational Health, Irvine, United States, ³Duke University, Medicine, United States, ⁴University of California, Medicine, United States
Email: saurabhc@hs.uci.edu

Background and aims: Non-alcoholic Fatty Liver Disease (NAFLD) is now considered as a pandemic and is a huge public health challenge. Rising obesity and type 2 Diabetes incidences have led a spurt of NAFLD cases worldwide with 25% of cases progressing to an inflammatory phenotype also termed as non-alcoholic steatohepatitis. Parallely, climate change stressors, global warming and sea level rise has led to increase in cases of non-cholera vibriosis in coastal areas across the globe. Vibriosis often has poor outcomes in patients with underlying chronic liver disease. *Vibrio Vulnificus* and *Vibrio Parahaemolyticus* are mostly responsible for the vibriosis cases. We tested the hypothesis that underlying NAFLD can have severe inflammatory surge in patients with poor outcomes and sepsis-like symptoms.

Method: We used a murine model (C57BL/6J mice) of NAFLD that were fed with high fructose-high cholesterol diet for 12 weeks. We used a clinical strain of *Vibrio Vulnificus* (VV) to induce vibriosis. Mice were euthanized and gut and liver pathology were evaluated.

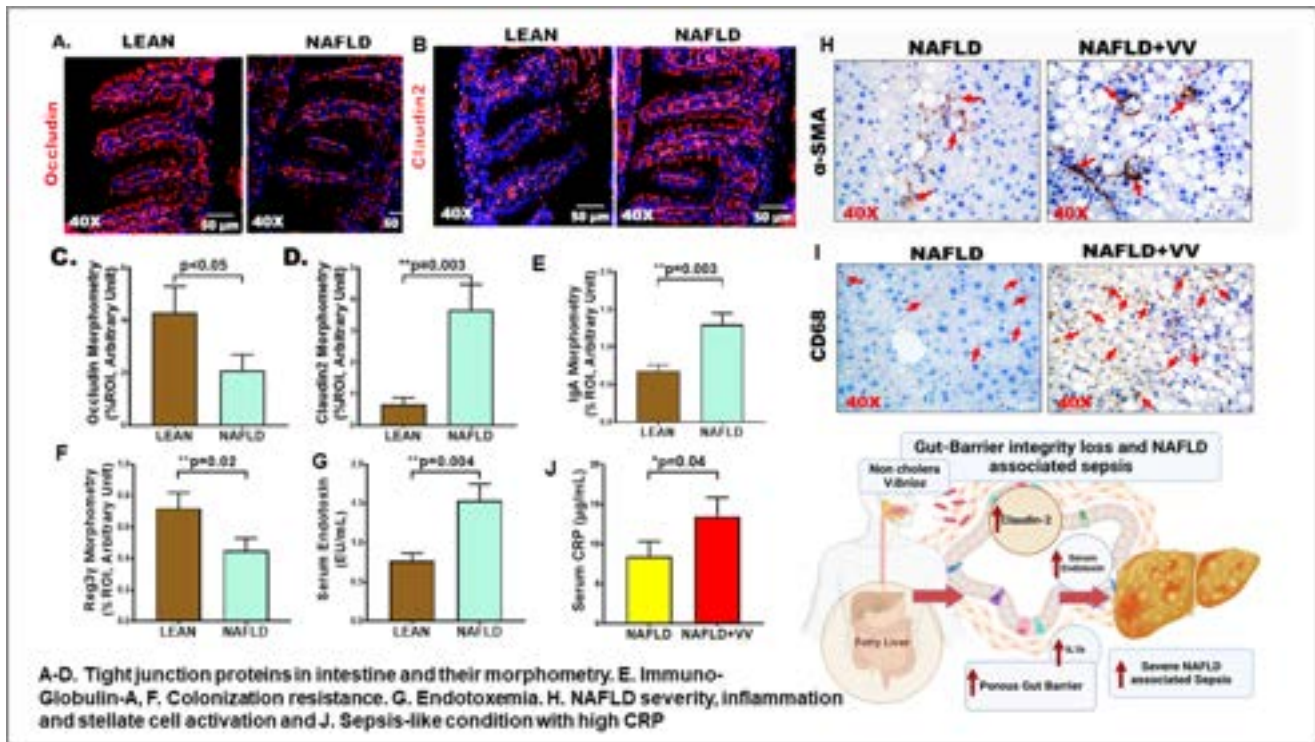


Figure: (abstract: WED-544).

Results: Results showed that NAFLD mice had an increased loss of gut barrier integrity with significantly higher levels of claudin-2 and a concomitant decrease in Occludin, both crucial proteins for maintaining tight junctions. Serum endotoxin and IL1β levels were significantly increased in mice with NAFLD when compared to lean controls. Mice with NAFLD had an elevated IgA and decreased levels of Reg3γ, a colonization resistance marker associated with gut barrier integrity. NAFLD mice also had higher intestinal permeability when assessed by FITC-dextran. NAFLD mice challenged with 10^8 CFU of *Vibrio Vulnificus* had significantly higher levels of Kupffer cell activation (CD68) and parallel higher stellate cell activation (increased α-SMA) when compared to control mice infected with VV. Histopathology showed severe leukocyte infiltration and necrosis in liver lobules in NAFLD mice infected with VV when compared to matched controls. Serum CRP levels were significantly higher in NAFLD+VV group when compared to controls suggesting septicemia and liver damage.

Conclusion: In conclusion we show a novel outcome of Non-cholera Vibriosis in NAFLD that is primarily associated with increased gut-barrier integrity loss and provides a Vibriosis risk assessment of patients with NAFLD.

WED-545

A guinea pig model of pediatric non-alcoholic steatohepatitis

Kamilla Pedersen¹, Jens Lykkesfeldt¹, Pernille Tveden-Nyborg¹.

¹University of Copenhagen, Department of Veterinary and Animal Sciences, Frederiksberg C, Denmark

Email: ptn@sund.ku.dk

Background and aims: Paediatric non-alcoholic fatty liver disease (NAFLD) affects 5–10% of children/adolescents; progressing to non-alcoholic steatohepatitis (NASH) in 25–50% of cases. Importantly, pediatric NASH differs from NASH in adults, e.g. displaying increased histological variation and disease severity, and leads to significant liver damage. However, studies in children are scarce and translational animal models few, leaving putative disease characteristics and

associated mechanisms largely undisclosed. Driven by an adverse diet and life-style that promotes inflammation and a state of oxidative stress, NASH progression may be exacerbated by a low vitamin C (VitC) intake. In addition, low VitC levels have been linked to several lifestyle-associated co-morbidities in humans, including NAFLD. The aim of this study was to explore a juvenile guinea pig model of NASH and investigate if a poor VitC status affects disease progression.

Method: Sixty-two male, one to two weeks old guinea pigs were block-randomized based on weight into four diet groups receiving either: Control High-VitC (n = 16), Control Low-VitC (n = 16), High-Fat High-VitC (n = 15), or High-Fat Low-VitC (n = 15). High-VitC diets contained 1500 mg VitC/kg feed while Low-VitC diets contained 50 mg VitC/kg feed.

Results: Irrespective of VitC deficiency, a high-fat diet promoted advanced NASH and reduced hepatic health, based on the calculated NAS index (median = 6; $p < 0.0001$) and elevated alanine aminotransferase levels ($p < 0.001$) compared to controls. Comparing histopathological findings to previous studies in adult guinea pigs on the high-fat diet (n = 28), the juvenile NASH guinea pigs (high-fat diet, n = 30) displayed decreased steatosis but increased inflammation score ($p < 0.0001$ and $p < 0.05$, respectively). The median fibrosis score was grade 2 for both juvenile and adult NASH guinea pigs, but contrary to adults, the degree of steatosis did not correlate with fibrosis grade in the juvenile NASH guinea pigs. A low intake of VitC increased plasma cholesterol in high-fat fed guinea pigs ($p < 0.05$) and also appeared to increase inflammation.

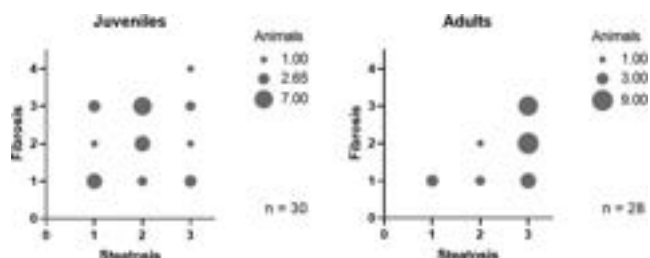


Figure:

Conclusion: NASH in young guinea pigs differed from the adult form, mimicking disease severity and histopathology of pediatric NASH, hereby supporting the guinea pig as a disease model with a high translational potential for pediatric NASH. Though our findings indicate a role of VitC in disease progression, specific links between VitC, deficiency and disease-associated mechanisms will require further investigations.

WED-546

Pemafibrate abrogates lipid liver accretion in a dietary model of fatty liver in rat

Roger Bentanachs^{1,2}, Laia Blanco¹, Maria Montesinos¹, Marta Alegret^{1,2,3}, Núria Roglans^{1,2,3}, Juan Carlos Laguna^{1,2,3}.
¹University of Barcelona, School of Pharmacy and Food Science, Pharmacology, Toxicology and Therapeutic Chemistry, Spain, ²Institute of Biomedicine of the University of Barcelona, Spain, ³CIBER de Fisiopatología de la Obesidad y Nutrición, Instituto de Salud Carlos III, Spain
 Email: jclagunae@ub.edu

Background and aims: Nowadays, there is not an approved drug therapy for the prevention/treatment of NAFLD. From a repurposing perspective, we aimed to investigate the effect of pemafibrate, mirabegron, and their combination in a dietary model of NAFLD, the high-fat high-fructose fed rat (HFHFr) (Velázquez et al., Mol. Nutr. Food Res 2022, 2101115).

Method: Female Sprague-Dawley rats were randomly distributed into 5 groups (n=8): (1) control (CT; standard rodent chow); (2) high-fat diet with 10% w/v fructose in drinking water (HFHFr); (3) HFHFr plus pemafibrate at 1 mg/Kg/day (PmA); (4) HFHFr plus mirabegron at 10 mg/Kg/day (MBG); (5) HFHFr plus pemafibrate and mirabegron at 0.5 and 5 mg/Kg/day, respectively (P+M). Rats were fed the HFHFr diet for three months, while groups 3, 4, and 5 received high fat diet supplemented with the corresponding drug for the last month. Plasma and hepatic triglycerides (TG) and cholesterol (Cho) and carnitinepalmitoyl transferase 1 (*cpt1*) and acyl-CoA (*aco*) gene expression in hepatic tissue were determined.

Results: As shown in the table, neither dietary nor drug-treatment interventions modified the total amount of ingested calories and final body weight, although HFHFr rats and those receiving pemafibrate (PmA and P+M groups) showed an increase in the ratio of liver/body weight. Only pemafibrate-treated rats (PmA and P+M groups) had significant reductions in liver lipids (both TG and Cho). No drug intervention reduced the hypertriglyceridemia associated to the HFHFr diet. Gene expression of liver *cpt1* and *aco*, which are directly involved in mitochondrial and peroxisomal fatty acid beta-oxidation, respectively, were markedly increased in pemafibrate-treated rats (PmA and P+M groups). Mirabegron administrated did not significantly modified any of the studied parameters.

Table:

	CT	HFHFr	PmA	MBG	P+M
AUC Kcal liquid/ cage/90 days	0	7280 ± 1768	7821 ± 1068	7323 ± 1374	7180 ± 920
AUC Kcal solid/ cage/90 days	6868 ± 198	4919 ± 1580 [#]	4530 ± 389	4951 ± 353	4958 ± 692
AUC total Kcal/ cage/90 days	6868 ± 198	12199 ± 263 ^{###}	12351 ± 892	12274 ± 1159	12147 ± 436
Final body weight (g)	248 ± 13	257 ± 21	268 ± 14	260 ± 13	273 ± 6
% liver/body weight	3.1 ± 0.2	3.7 ± 0.4 [#]	5.6 ± 0.5 ^{***}	3.6 ± 0.5	5.1 ± 0.5 ^{***}
TG liver (mg/g prot)	47 ± 11	129 ± 69 ^{###}	62 ± 15 [*]	129 ± 70	50 ± 13 [*]
Cho liver (mg/g prot)	36 ± 4	43 ± 8	32 ± 6 ^{***}	34 ± 8	29 ± 3 ^{***}
TG blood (mg/dl)	101 ± 21	138 ± 29 [#]	182 ± 38	149 ± 31	148 ± 30
<i>cpt1</i> mRNA (a.u)	100 ± 56	104 ± 62	362 ± 186 ^{**}	137 ± 84	300 ± 81 ^{**}
<i>aco</i> mRNA (a.u)	100 ± 30	97 ± 9	761 ± 322 ^{***}	107 ± 13	633 ± 185 ^{***}

[#]p > 0.05, ^{###}p > 0.001 vs CT; ^{*}p > 0.05, ^{**}p > 0.01; ^{***}p > 0.001.

Conclusion: In our dietary model of NAFLD in rat, only pemafibrate treatment was able to restore liver lipids (TG and Cho) to CT values. These changes were associated to liver hypertrophy and increased expression of liver markers of fatty acid beta-oxidation, pointing to a peroxisome proliferator activated receptor alpha-activation related effect. At this moment, we are searching possible molecular mechanisms involved in the lack of hypotriglyceridemic effect of pemafibrate. This work was supported by grants PID2020-112870RB-I00, funded by MCIN/AEI/10.13039/501100011033 and 2021SGR-00345.

WED-547

The overexpression of TM6SF2 and/or MBOAT7 wild-type genes restores the mitochondrial lifecycle and activity in an in vitro NAFLD model

Erika Paolini¹, Miriam Longo¹, Marica Meroni¹, Giada Tria¹, Roberto Picciotti¹, Massimiliano Ruscica², Anna Ludovica Fracanzani¹, Paola Dongiovanni¹. ¹Fondazione IRCCS Ca' Granda Ospedale Maggiore Policlinico, Milan, Italy, ²University of Milan, Italy
 Email: paola.dongiovanni@policlinico.mi.it

Background and aims: Mitochondrial dysfunction is a key player in the transition from NASH up to HCC. The knock-out (KO) of *MBOAT7* and/or *TM6SF2* hampers the mitochondrial dynamics in HepG2 cells resulting in an enrichment of misshapen and failed mitochondria. The overexpression of *MBOAT7* and/or *TM6SF2* wild-type genes in KO models through lentiviral vectors decreases the number of damaged-globular mitochondria, while increases the normo-shaped ones. In the attempt to deepen the impact of *PNPLA3/MBOAT7/TM6SF2* loss-of-function mutations on mitochondrial aberrances, we investigated the mitochondrial lifecycle and activity in KO cells overexpressed for the wild-type forms of *MBOAT7* and/or *TM6SF2*.

Method: Mitochondrial lifecycle and activity were assessed through RT-PCR, Western Blot, Seahorse assay and immunohistochemistry.

Results: The overexpression of *MBOAT7*, *TM6SF2* or both decreased PGC1α levels, the master regulator of mitobiogenesis, which was activated in KO cells in response to fusion-fission unbalance, boosted the expression of Mfn1, Mfn2 (mitochondrial outer membranes proteins involved in fusion) and OPA1 (inner mitochondrial membranes fusion protein) whereas decreased FIS1 and DRP1 (fission proteins) levels, thus re-establishing the mitochondrial turnover. Consistently, the mitophagy pathways (PINK/PARKIN/BNIP3/BNIP3-L/LC3/phospho-UBIQUITIN) increased after the *MBOAT7* and/or *TM6SF2* overexpression, prompting the disruption of damaged mitochondria. The balance of mitochondrial biogenesis is essential for organelles' homeostasis and activity. Indeed, the overexpressed models augmented the COX-I/SDHA ratio, COX-III, and citrate synthase activity alongside the oxygen consumption rate, thus

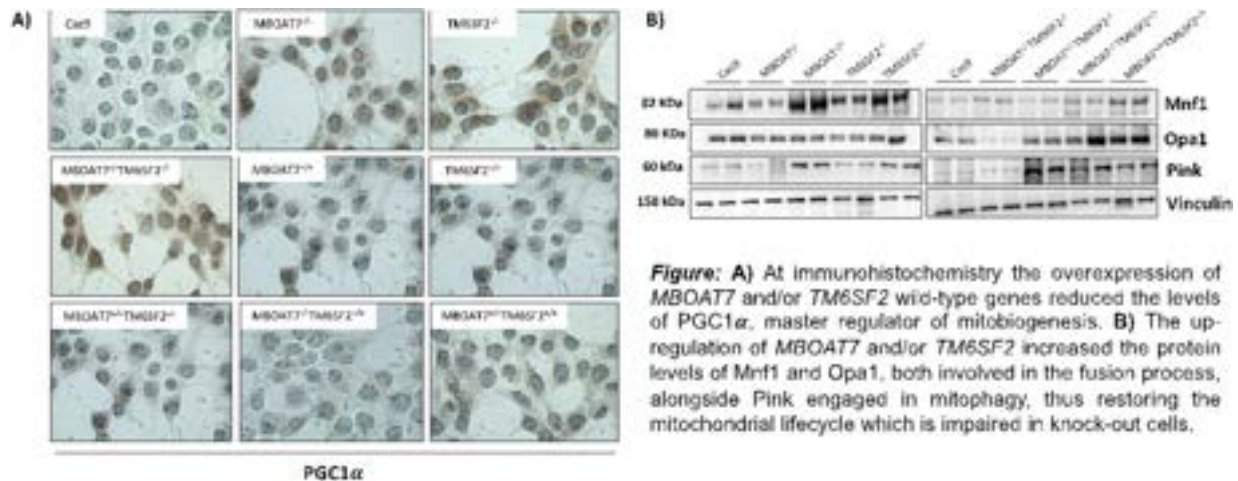


Figure: (abstract: WED-547).

recovering the OXPHOS capacity and Krebs cycle which were impaired in KO cells. Finally, lactate levels decreased after the upregulation of *MBOAT7* and/or *TM6SF2* wild-type genes together with the glycolytic extracellular acidification rate, thereby inhibiting the switch to anaerobic glycolysis which was promoted in KO cells to trigger tumorigenesis.

Conclusion: Genetics impacts on mitochondrial maladaptation during NAFLD and the overexpression of *MBOAT7* and/or *TM6SF2* wild-type genes in KO HepG2 cells re-balances the mitochondrial lifecycle and turnover, thus ensuring the organelles' function and possibly reversing hepatocellular damage.

WED-548

Development of a 2D nonalcohol-related steatohepatitis (NASH) model

Esther Arnaiz Gonzalez¹, Tahmid Choudhury¹, Ana Miar¹, Kenny Moore¹, Yuan-Yu Lin², Tess Lu², Quin Wills¹. ¹Ochre Bio, Oxford, United Kingdom, ²Ochre Bio, Taipei, Taiwan
Email: estherarnaiz@ochre-bio.com

Background and aims: One of the metabolic functions of the liver is to store excess energy (from sugars or fats) as lipid droplets. However, over time accumulation of lipids within hepatocytes can trigger pathological complications including immune activation and fibrosis resulting in nonalcohol-related steatohepatitis (NASH). Due to the silent nature of liver disease, diagnosis is usually performed at late stages (fibrosis and cirrhosis), when the only option for the patient is a transplant. Currently, there are no clinical therapies for NASH, and the research strategies for NASH often rely on complex 3D models such as spheroids, specific microfluidic devices or precision cut slices (PCLS), which are not suitable for the high throughput screening of new therapeutic targets. To overcome this limitation, we have developed an in vitro 2D NASH model using human primary cells, which maintains hepatic function, responds to dietary overload and fibrotic inducers in ways that resemble the stages of NASH and is modifiable with siRNA or drug intervention.

Method: Primary human hepatocytes are cultured alongside growth arrested 3T3-J2 mouse fibroblasts, human stellate cells and human peripheral blood mononuclear cell-derived monocytes. After cell adhesion, the media is changed to either lean or fat inducing co-culture media. Fibrosis induction is initiated on day 7 and the cells can be maintained to day 12, or longer if desired.

Results: Using LPS to demonstrate immunological function of the co-culture, we observe an increase in IL6 and MCP1. This can also be observed using our nutritional overload conditions which results in heavily lipid loaded hepatocytes and an inflammatory signature. Upon stimulation of the cultures with fibrosis inducers (PDGFbb and

TGFb) fibrotic markers were significantly upregulated and secreted, resulting in hepatocytes coated in collagen and known biomarkers of NASH (e.g. TIMP1) being released. These effects were diminished using an inhibitor of TGFb signaling and phenocopy those from more complex models such as PCLS.

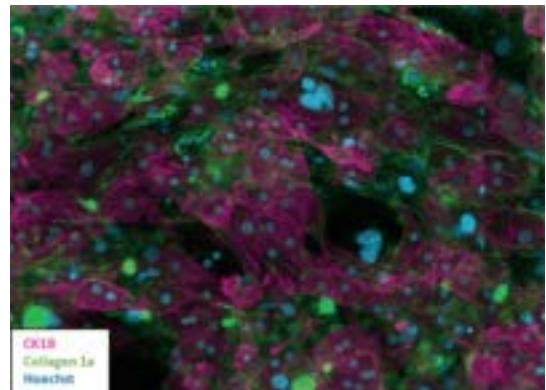


Figure:

Conclusion: Our 2D primary cell NASH model provides a useful tool to study different stages of the disease and to easily screen for both new targets and therapies.

WED-549

Programmed cell death 1 genetic variant and liver damage in non-alcoholic fatty liver disease

Alrazia Pennisi¹, Rosaria Maria Pipitone¹, Francesco Malvestiti², Oveis Jamialahmadi³, Paola Dongiovanni², Giorgio Bertolazzi⁴, Jussi Pihlajamäki⁵, Hannele Yki-Järvinen⁶, Umberto Vespasiani Gentilucci⁷, Federica Tavaglione⁷, Samantha Maurotti⁸, Cristiana Bianco⁹, Gabriele Di Maria⁹, Marco Enea¹⁰, Anna Ludovica Fracanzani⁹, Vesa Kärjä⁵, Giulia Lupo¹, Ville Männistö⁵, Marica Meroni¹¹, Roberto Piciotti¹¹, Sami Qadri⁶, Rossella Zito¹⁰, Antonio Craxi¹, Vito Di Marco¹, Calogero Camma¹, Claudio Tripodo⁴, Luca Valenti², Stefano Romeo³, Salvatore Petta¹, Stefania Grimaudo¹. ¹Policlinico Paolo Giaccone Palermo, Section of Gastroenterology and Hepatology, Italy, ²Department of Pathophysiology and Transplantation, Università degli Studi di Milano, Milan, Italy, Italy, ³Department of Molecular and Clinical Medicine, Sahlgrenska Academy, University of Gothenburg, Gothenburg, Sweden, Sweden, ⁴Tumor Immunology Unit, University of Palermo School of Medicine, Palermo, Italy, Italy, ⁵Department of Clinical Nutrition, Institute of Public Health

POSTER PRESENTATIONS

and Clinical Nutrition, University of Eastern Finland, Kuopio, Finland, Finland, ⁶Department of Medicine, University of Helsinki and Helsinki University Central Hospital, Helsinki, Finland, Finland, ⁷Clinical Medicine and Hepatology Unit, Department of Internal Medicine and Geriatrics, Campus Bio-Medico University, Rome, Italy, Italy, ⁸Nutrition Unit, Department of Medical and Surgical Sciences, Magna Graecia University Catanzaro, Italy, Italy, ⁹Precision Medicine, Department of Transfusion Medicine and Hematology, Fondazione IRCCS Cà Granda Pad Marangoni, Milan, Italy, Italy, ¹⁰Department of Health Promotion Sciences Maternal and Infant Care, Internal Medicine and Medical Specialties, PROMISE, University of Palermo, Palermo, Italy, Italy, ¹¹General Medicine and Metabolic Diseases, Fondazione IRCCS Ca' Granda Ospedale Maggiore Policlinico, Milan, Italy, Italy
Email: graziaipennisi901@gmail.com

Background and aims: Programmed cell death 1/programmed cell death-ligand 1 (PD-1/PDL-1) axis has been reported to modulate liver inflammation and progression to hepatocellular carcinoma (HCC) in patients with non-alcoholic fatty liver disease (NAFLD). Here, we examined whether the *PDCD1* variation associates with NAFLD severity in individuals with liver biopsy.

Method: We examined the impact of *PDCD1* gene variants on HCC, as robust severe liver disease phenotype in UK Biobank participants. The strongest genetic association with the rs13023138 G > C variation was subsequently tested for association with liver damage in 2,889 individuals who underwent liver biopsy for suspected non-alcoholic steatohepatitis (NASH). Hepatic transcriptome was examined by RNASeq in a subset of NAFLD individuals (n = 121). Transcriptomic and deconvolution analyses were performed to identify biological pathways modulated by the risk allele.

Results: The rs13023138 C > G showed the most robust association with HCC in UK Biobank ($p = 5.28E-4$, $OR = 1.32$, 95% $CI [1.1, 1.5]$). In the liver biopsy cohort, rs13023138 G allele was independently associated with severe steatosis ($OR 1.17$, 95% $CI 1.02-1.34$; $p = 0.01$), NASH ($OR 1.22$, 95% $CI 1.09-1.37$; $p < 0.001$) and advanced fibrosis ($OR 1.26$, 95% $CI 1.06-1.50$; $p = 0.07$). At deconvolution analysis, rs13023138 G > C allele was linked to higher hepatic representation of M1 macrophages, paralleled by upregulation of pathways related to inflammation and higher expression of CXCR6.

Conclusion: The *PDCD1* rs13023138 G allele was associated with HCC development in general population and with liver disease severity in patients at high risk of NASH.

WED-550

Obeticholic acid administration increases hepatic eNOS levels counteracting lipid accumulation and fibrosis in a diet-induced ob/ob mouse model of NASH

Marta Cagna¹, Giuseppina Palladini^{1,2}, Anna Cleta Croce³, Massimiliano Cadamuro⁴, Luca Fabris^{4,5}, Luciano Adorini⁶, Andrea Ferrigno¹, Mariapia Vairetti¹, Laura Giuseppina Di Pasqua¹.
¹University of Pavia, Department of Internal Medicine and Therapeutics, Pavia, Italy, ²Fondazione IRCCS Policlinico San Matteo, Pavia, Pavia, Italy, ³Institute of Molecular Genetics-Italian National Research Council (CNR), Italy, ⁴University of Padua, Department of Molecular Medicine (DMM), Italy, ⁵Yale University, Department of Internal Medicine, Liver Center and Section of Digestive Diseases, United States, ⁶Intercept Pharmaceuticals, San Diego, United States
Email: lauragiuseppina.dipasqua01@universitadipavia.it

Background and aims: This study evaluated endothelial nitric oxide synthase (eNOS) as a potential Farnesoid X receptor (FXR)-mediated mechanism in the treatment of non-alcoholic steatohepatitis (NASH). We previously reported that Obeticholic acid (OCA), a potent FXR agonist, restores RECK, an inverse modulator of metalloproteases, involved in fibrogenic processes (1). Recently, hepatic eNOS, a key regulator of liver vascular tone, was found strongly associated with the progression of NAFLD to NASH. Here, the effect of OCA was evaluated on hepatic eNOS content, lipid accumulation and fibrosis in a diet-induced ob/ob mouse model of NASH.

Method: Lep ob/ob (ob/ob) NASH mice fed the high fat (HF) diet (AMLN-diet; D09100301, with trans-fat, cholesterol and fructose) or control diet were used. After 9 weeks on diet, mice were treated with OCA dosed via dietary admixture 0.05% (30 mg/kg/d) or HF diet for 12 weeks. Liver weight, serum transaminase, bilirubin, cholesterol as well as hepatic eNOS and histological analysis of lipid droplets and fibrosis (by Sirius Red) were quantified. Type I procollagen carboxy-terminal propeptides (PICP) and type I procollagen aminoterminal propeptides (PINP), type I collagen synthesis markers, were also quantified; an increase in PICP/PINP ratio represents abnormal deposition of type I collagen (2).

Results: Histological results showed an accumulation of large lipid droplets in HF diet mice and the positive role of OCA treatment by reducing the number and diameter of lipid droplets. The same trend occurred for collagen deposition as documented by Sirius red and PICP/PINP ratio. A marked increase in eNOS was observed in livers from HF diet mice treated with OCA when compared with HF diet group. An inverse correlation was found comparing liver eNOS versus lipid droplets number ($p < 0.05$) and diameter ($p < 0.059$) as well as fibrosis by Sirius Red staining ($p < 0.01$). OCA treatment restored liver weight, serum bilirubin and cholesterol levels compared with HF-treated mice. No changes in serum transaminase were found.

Conclusion: In conclusion, OCA confers liver protection in a NASH model as shown by reduced hepatic lipid accumulation and fibrosis as well as serum bilirubin and cholesterol. This study also shows increased hepatic eNOS levels following OCA treatment associated with reduced lipid accumulation and fibrosis. Our data support the emerging role of eNOS as a key regulator and important target of NAFLD progression to NASH.

References

- Ferrigno et al., *PLoS One*. 2020;15 (9):e0238543
- Chen P et al., *Eur J Pharmacol* 2011; 658 (2-3):168-74.

WED-551

Cholesterol-free ketogenic diet feeding improves experimental non-alcoholic fatty liver disease (NAFLD)

Alessia Provera¹, Ramavath Naresh Naik^{1,2}, Laila Iavanya Gadipudi¹, Cristina Vecchio¹, Marina Caputo¹, Alessandro Antonioli¹, Simone Reano¹, Nicoletta Filigheddu¹, Marcello Manfredi³, Luca Simone Coccolin⁴, Ilario Ferrocino⁴, Emanuele Albano¹, Flavia Prodam^{1,5}, Salvatore Sutti¹.
¹University of East Piedmont, Dept. of Health Sciences, Italy, ²Washington University in St- Louis, Dept. of Pediatrics, Endocrinology, and Diabetes, United States, ³University of East Piedmont, Dept. of Translational Medicine, Italy, ⁴University of Turin, Dept. of Agricultural, Forestry and Food Science, Italy, ⁵University of East Piedmont, SCDU Endocrinology, Italy
Email: alessia.provera@uniupo.it

Background and aims: Non-alcoholic fatty liver disease (NAFLD) is now recognized as the most common liver disease worldwide. Despite continuous advances in the understanding of the disease pathogenesis and identifying therapeutic targets, up to now, there is not an approved therapy for NAFLD. Lifestyle changes, including diet, are, so far, the most effective interventions in NAFLD, even though there is not a definitive agreement on the most suitable dietary regimen. In recent years, low carbohydrates ketogenic diets (KDs) have been increasingly used for weight loss. However, the efficacy of KDs in improving NAFLD is controversial due to contradictory data obtained in animal experiments. In this study, we investigated the capacity of a cholesterol-free KD to improve NAFLD in mice.

Method: NAFLD was induced in C57BL/6 mice by feeding with a cholesterol-enriched Western Diet (WD) for up to 16 weeks, followed by switching animals to KD or standard diet (SD) for additional eight weeks.

Results: We observed that KD administration increased by three folds ketone bodies production and significantly reduced liver weights. Moreover, liver proteomic analysis and functional tests evidenced an improved glucose and lipid metabolism along with insulin resistance

in KD fed mice. These metabolic effects were associated with an amelioration in transaminase release and in the histological severity of steatosis and necro-inflammation. Mice receiving KD also showed a lowering in the hepatic expression of pro-inflammatory/pro-fibrogenic markers such as CCL2, IL-12, CD11b, α 1-procollagen, TGF- β 1, osteopontin and galectin-3, which were accompanied by a significant reduction in hepatic monocyte-derived macrophage infiltration and collagen fibres deposition as assessed by the Sirius-red staining. The improvement in liver damage and fibrosis likely relies on the capacity of KD of improving NAFLD associated dysbiosis leading to a recovery in gut bacterial flora similar to that of healthy mice.

Conclusion: Altogether, these results indicate that a cholesterol-free ketogenic diet is effective in improving metabolic derangements and steatohepatitis, and it might represent a potential therapeutic strategy for NAFLD.

WED-552

Metabolic effects of n-3 fatty acids administered as Calanus oil to transgenic mice lacking functional peroxisome proliferator-activated receptor alpha

Martin Rossmeisl¹, Veronika Kalendova¹, Olga Horakova¹. ¹*Institute of Physiology of the Czech Academy of Sciences, Laboratory of Adipose Tissue Biology, Prague 4, Czech Republic*
Email: martin.rossmeisl@fgu.cas.cz

Background and aims: Polyunsaturated fatty acids of n-3 series, specifically eicosapentaenoic acid (EPA) and docosahexaenoic acid (DHA), exert hypolipidemic and anti-inflammatory effects. They act as endogenous ligands of the transcription factor peroxisome proliferator-activated receptor alpha (PPARalpha), which primarily regulates genes involved in lipid metabolism in the liver. We aimed to determine to what extent the metabolic effects of Calanus oil, an alternative source of EPA and DHA bound to wax esters, depend on the presence of functional PPARalpha.

Method: Twelve-week-old male T29S1/SvImJ mice, including wild-type (WT) and PPARalpha-deficient (KO) mice, were either maintained on a low-fat standard chow or given a high-fat corn oil-based diet (cHF; 32% lipids by weight) for 8 weeks (n = 8). To supplement EPA and DHA, 15% of dietary lipids in the cHF diet was replaced by Calanus oil (cHF+CO diet; 6 mg EPA+DHA/g diet). Tissue lipid content quantification, gene expression analysis (quantitative PCR) and metabolomic profiling (LC-MS) were performed in liver samples. Glucose production and its suppression by insulin were evaluated in cultured hepatocytes isolated from different groups of mice. One-way ANOVA was used to determine statistical significance (p < 0.05 was considered significant).

Results: Administration of cHF increased liver fat accumulation in WT mice by 2.6-fold, whereas in KO mice by 6.9-fold, resulting in a 3-fold higher liver fat content in KO animals (cHF; WT, 82 \pm 4 vs. KO, 256 \pm 13 mg/g tissue). As expected, cHF-fed KO mice showed reduced expression of genes involved in beta-oxidation, as well as lower levels of acylcarnitines and coenzyme Q levels, as detected by metabolomic analysis. Interestingly, administration of cHF+CO was associated with a reduction in hepatic steatosis in the KO group, whereas it had no effect on liver fat content in WT mice (cHF+CO; WT, 84 \pm 8 vs. KO, 174 \pm 13 mg/g tissue). Altered composition of various triacylglycerol and phospholipid species was found in cHF+CO-fed mice compared to their cHF-fed counterparts, but regardless of genotype. Furthermore, hepatocytes isolated from KO (but not WT) mice fed cHF showed impaired glucagon-stimulated glucose production and its suppression by insulin, a phenotype that was not restored in hepatocytes isolated from KO animals fed cHF+CO.

Conclusion: Chronic administration of Calanus oil can alter the liver lipid profile independently of the presence of functional PPARalpha. However, its beneficial effects on hepatic steatosis can only occur under conditions of greatly increased lipid accumulation in the liver, probably due to some indirect mechanisms induced by Calanus oil outside the liver.

WED-553

Semaglutide has beneficial effects on non-alcoholic steatohepatitis in Ldlr^{-/-}.Leiden mice

José A. Inia^{1,2,3}, Geurt Stokman³, Martine C. Morrison³, Nicole Worms³, Lars Verschuren⁴, Martien P. M. Caspers^{4,5}, Aswin L. Menke³, Mathieu Petitjean⁶, Louis Petitjean⁶, Li Chen⁶, J. Wouter Jukema^{1,2,7}, Hans Princen³, Anita M. van den Hoek³. ¹*Leiden University Medical Center (LUMC), Cardiology, Leiden, Netherlands*, ²*Leiden University Medical Center (LUMC), Einthoven Laboratory for Experimental Vascular Medicine, Leiden, Netherlands*, ³*TNO, Metabolic Health Research, Leiden, Netherlands*, ⁴*TNO, Microbiology and Systems Biology, Leiden, Netherlands*, ⁵*The Netherlands Organization for Applied Scientific Research (TNO), Department of Microbiology and Systems Biology, Leiden, Netherlands*, ⁶*PharmaNest, Princeton, United States*, ⁷*Netherlands Heart Institute, Utrecht, Netherlands*
Email: jose.inia@tno.nl

Background and aims: Semaglutide, a glucagon-like peptide-1 receptor agonist, is an antidiabetic medication that has recently been approved for treatment of obesity as well. Semaglutide is also postulated to be a promising candidate for treatment of non-alcoholic steatohepatitis (NASH). Here, we evaluated the effects of semaglutide in a translational diet-induced model with advanced NASH and fibrosis.

Method: Ldlr^{-/-}.Leiden mice received a fast food diet (FFD) for 25 weeks, followed by another 12 weeks on FFD with daily subcutaneously injections of semaglutide or vehicle (control). Plasma parameters were evaluated, livers and hearts were examined and hepatic transcriptome analysis was performed.

Results: In the liver, semaglutide significantly reduced macrovesicular steatosis (-74%, p < 0.001), inflammation (-73%, p < 0.001) and completely abolished microvesicular steatosis (-100%, p < 0.001). Histological and biochemical assessment of hepatic fibrosis showed no significant effects of semaglutide. However, digital pathology revealed significant improvements in the degree of collagen fiber reticulation (-12%, p < 0.001). Semaglutide did not affect atherosclerosis relative to controls. Additionally, we compared the transcriptome profile of FFD-fed Ldlr^{-/-}.Leiden mice with a human gene set that differentiates human NASH patients with severe fibrosis from those with mild fibrosis. In FFD-fed Ldlr^{-/-}.Leiden control mice, this gene set was upregulated as well, while semaglutide predominantly reversed this gene expression.

Conclusion: Using a translational model with advanced NASH, we demonstrated that semaglutide is a promising candidate with particular potential for treatment of hepatic steatosis and inflammation, while for reversal of advanced fibrosis, combinations with other NASH agents may be necessary.

WED-554

Utilization of multicellular liver-on-chip to study non-alcohol-related fatty liver disease

Victoria Palasantzas¹, Isabel Tamargo², Gwen Weijer², Alfredo Rios-Ocampo³, Sebo Withoff², Johan Jonker³, Jing Fu¹. ¹*University Medical Centre Groningen, Department of Genetics and Pediatrics, Netherlands*, ²*University Medical Centre Groningen, Department of Genetics, Netherlands*, ³*University Medical Centre Groningen, Department of Pediatrics, Netherlands*
Email: v.e.j.palasantzas@umcg.nl

Background and aims: Non-alcoholic fatty liver disease (NAFLD) is the most prevalent liver disease, affecting nearly one-third of the global population. To study NAFLD, current experimental models e.g., animals and 2D cell cultures, pose various limitations including species-specific differences and lack of complexity. Here, I employ the innovative, human-based organ-on-chip system to overcome these limitations and explore lifestyle -based NAFLD interventions. Overcoming the limitations of current liver model systems with the liver-on-chip, I aim to study the effect of medicinal-implied nutrients ('nutriceuticals') to prevent or reverse NAFLD and the underlying molecular mechanism.

POSTER PRESENTATIONS

Method: We have recently established a hepatocyte-on-chip model utilizing healthy control-derived human induced pluripotent stem cells (hiPSCs) and a human hepatocyte cell line in our lab. Here, I present data on the development and characterization of a NAFLD-on-chip. Characterization of the NAFLD-on-chip includes steatohepatitis readouts e.g. lipid accumulation and detection of very-low-density lipoprotein and inflammatory cytokine excretion.

Results: Preliminary data reveals that the hepatocyte-on-a-chip models available in our lab exhibit important features of normal human hepatocyte physiology (e.g. expression of transport proteins and albumin production) and features often not observed in 'static' cell culturing models (e.g. lipoprotein excretion). Additionally, we identified the conditions to induce NAFLD in vitro for our further studies on nutraceuticals.

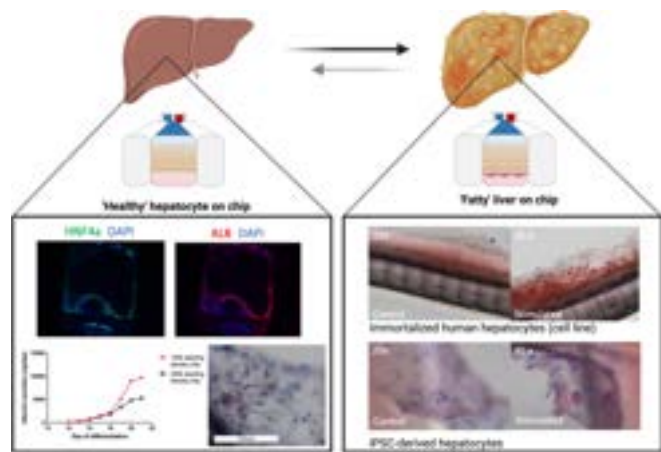


Figure:

Conclusion: We provide the first indications for the liver-on-chip model as a physiologically relevant model for complex diseases like NAFLD and how to study such a disease in our platform. Future perspectives include adding liver resident macrophages ('Kupffer cells') to recapitulate the inflammatory cross-talk present in NAFLD. Ultimately, we aim to use this model to assess NAFLD therapeutics as well as assess the impact of patient specific mutations on NAFLD.

WED-555

Improvement of NAFLD by Totum-448: effects in the liver, adipose tissue and gut in western-diet fed hamsters

Vivien Chavanelle¹, Yolanda Otero¹, Marie Vallier¹, Doriane Ripoché¹, Cédric Langhi¹, Florian Le Joubioux¹, Thierry Maugard², Valerie Hervieu³, Sébastien Peltier¹, Pascal Sirvent¹, Clement Besqueut-Rougerie¹, Gael Ennequin⁴. ¹Valbiotis, France, ²LIENSs, France, ³Hospices Civils de Lyon, France, ⁴Clermont Auvergne University, AME2P, Clermont-Ferrand, France
Email: vivien.chavanelle@valbiotis.com

Background and aims: The concerning rise in NAFLD prevalence worldwide urgently calls for therapeutic solutions. We have previously demonstrated the beneficial effects of Totum-448 (T448), a novel patented polyphenol-rich combination of 5 plant extracts and choline, on liver steatosis, inflammation, and fibrosis in a diet-induced hamster model of NAFLD. This new work sheds some light on the action of T448 on the liver-gut-adipose tissue axis to unveil some of the mechanisms that could be involved in the preventive effects of the product on NAFLD progression.

Method: Male golden Syrian hamsters were fed a western-diet (WD, high fat, mostly saturated, high cholesterol, N = 12), or a WD supplemented with T448 5% w/w (WD-T448, n = 12) for 12 weeks. A group of hamsters was fed a normal diet (ND, N = 6) and used as control. Body weight and composition (MRI) was monitored all throughout the study. NAFLD-associated features were assessed by

RT-PCR or through biochemical and histological biomarkers in serum, liver, adipose tissue pads, ileum, colon, and caecal content.

Results: Despite slightly higher body weight and fat mass, T448-supplemented hamsters displayed improved circulating lipid profile (lower triglycerides, TG, total cholesterol, TC, free fatty acids, FFA and phospholipids, PL). Liver weight was significantly reduced by T448 supplementation as well as hepatic lipid content (TG, TC, FFA, and PL). This improvement of steatosis was confirmed by histological analyses of Oil-Red-O-stained sections and was associated with concomitant reduction of hepatic expression of inflammatory and fibrotic gene markers. Interestingly, consistent with the slight increase in total fat mass, the weights of epididymal, perirenal, inguinal, and mesenteric fat pads were higher in T448-supplemented animals. In caecal content, T448 elicited a reduction of lipopolysaccharides (LPS) levels and subsequent serum LPS, which was associated with down-regulated inflammatory gene markers in the ileum. Additionally, faecal TC was found elevated in T448 supplemented hamsters.

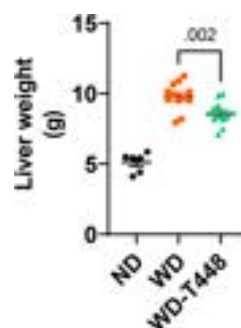


Figure:

Conclusion: This new work confirms the effects of T448 in improving circulating lipids and liver steatosis, inflammation, and fibrosis, some major hallmarks of NAFLD progression, in WD-fed hamsters. The reduction of ectopic fat accumulation in the liver was accompanied by an increased fat storage capacity in the different adipose tissue pads and LPS levels were reduced, both in caecal content and serum, suggesting improved metabolic endotoxemia.

NAFLD Therapy

WEDNESDAY 21 TO SATURDAY 24 JUNE

TOP-076

A deep exploration of bridging fibrosis evolution and individual septa parameters in NASH using quantitative second harmonic generation imaging reveals fibrosis changes in natural history and treatment-induced not seen with conventional histology

Elaine Chng¹, Nikolai Naoumov², David E Kleiner³, Dominique Brees⁴, Chandra Saravanan⁵, Yayun Ren⁶, Dean Tai⁷, Arun Sanyal^{8,9}.

¹Histoindex Pte. Ltd., Singapore; ²London, United Kingdom; ³National Cancer Institute, 2Post-Mortem Section, Laboratory of Pathology, Bethesda, MD, United States; ⁴Novartis Pharma AG, Basel, Switzerland; ⁵Novartis Pharma AG, Novartis Institute of Biomedical Research, MA, United States; ⁶HistoIndex Pte. Ltd, Singapore; ⁷Histoindex Pte Ltd, Singapore; ⁸Stravitz-Sanyal Institute of Liver Disease and Metabolic Health, United States; ⁹Virginia Commonwealth University School of Medicine, Richmond, United States
Email: elaine.chng@histoindex.com

Background and aims: Non-alcoholic steatohepatitis (NASH) with bridging fibrosis (stage F3) is a critical stage in the evolution of fatty

liver disease, which can progress to cirrhosis or reverse to milder disease with better prognosis. Second harmonic generation/two photon excitation fluorescence (SHG/TPEF) microscopy of unstained liver sections with artificial intelligence (AI) provides sensitive and reproducible quantitation of liver fibrosis. Using this novel approach, the present study aims to gain in-depth understanding of changes in liver fibrosis and individual septa parameters over time in a homogenous, well-characterised group of patients with NASH F3 fibrosis stage.

Method: Paired liver biopsies from 57 patients [placebo, n = 17] or tropifexor (TXR) [n = 40], all with bridging fibrosis (F3 stage) according to the CRN scoring system at baseline (BL), who participated in the FLIGHT-FXR clinical trial (NCT02855164), were included in this study. Unstained liver sections from BL and end-of-treatment (EOT) were examined using SHG/TPEF microscopy. Changes in liver fibrosis overall and in five different zones of liver lobules were quantitatively assessed by qFibrosis-a cumulative index based on measuring 184 collagen features on a continuous scale. Radar maps were developed as a novel approach for assessing fibrosis changes in liver lobules. In addition, septa morphology-progressive or regressive septa and 12 individual septa parameters were analysed at BL and EOT biopsies.

Results: SHG revealed fibrosis progression or regression (BL to EOT) in 14/17 (82%) of patients receiving placebo, in contrast the CRN scoring where changes were detected in 6/17 (35%) patients while the majority 11/17 (65%) were adjudged as "no change." Radar maps of qFibrosis readouts illustrated fibrosis dynamics in 5 areas of liver lobule (Figure A). Quantitation of 12 septa parameters objectively demonstrated significant differences between regressive and progressive septa (Figure B). Regressive changes in individual septa parameters (BL and EOT) were significantly greater in the TXR-treated patients, than in the placebo group, in particular-septa area, septa width, fiber interactions and aggregated septa, which were present both in the "no change" and the "regression" subgroups, as defined by the CRN scoring. qFibrosis readouts at BL were able to predict the outcomes-fibrosis regression vs non-progression.

Conclusion: SHG/TPEF microscopy with AI provides greater granularity and precision in assessing fibrosis dynamics in NASH patients with bridging fibrosis and reveal worsening or improvement undetectable by conventional microscopy, enhancing the understanding of pathogenesis and treatment response. These results

support the use of digital approaches for quantitative fibrosis assessment, in the natural history and treatment of NASH and other liver diseases.

TOP-077

Safety, tolerability, and preliminary efficacy of ascending doses of Human Allogeneic Liver-derived Progenitor Cells (HepaStem®) in patients with cirrhotic and pre-cirrhotic non-alcoholic steatohepatitis (NASH)

Sven Francque¹, Christophe Moreno², Faouzi Saliba³, Victor Vargas⁴, Luis Ibañez⁵, German Soriano⁶, Jordan Genov⁷, Krum Katzarov⁸, Ewa Janczewska⁹, Elena Laura Iliescu¹⁰, Anja Geerts¹¹, Noelia Gordillo¹², Yelena Vainilovich¹², Mustapha Najimi¹², Virginie Barthel¹², Frederic Lin¹², Etienne Sokal^{12,13}. ¹Antwerp University Hospital, UZA, Division of Gastroenterology and Hepatology, Edegem, Belgium; ²CUB Hôpital Erasme, Université Libre de Bruxelles, Department of Gastroenterology, Hepatopancreatology and Digestive Oncology, Brussels, Belgium; ³Paul Brousse Hospital, France; ⁴Hospital Vall d'Hebron, Universitat Autònoma, Barcelona, Spain; ⁵Hospital General Universitario Gregorio Marañón, Spain; ⁶Hospital de la Santa Creu i Sant Pau, Spain; ⁷University Multiprofile Hospital for Active Treatment "Tsaritsa Yoana-ISUL", Bulgaria; ⁸Multiprofile hospital for active treatment (MHAT), Bulgaria; ⁹ID Clinic, Poland; ¹⁰Fundeni Clinical Institute, Bucharest, Romania; ¹¹UZ Gent, Belgium; ¹²Cellaion, Belgium; ¹³University Hospital Saint-Luc, Belgium

Email: etienne.sokal@cellaion.com

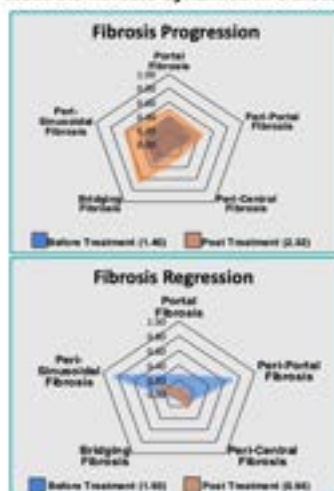
Background and aims: Inflammation plays a major role in the progression of non-alcoholic steatohepatitis (NASH). As previously demonstrated, Human Allogeneic Liver-derived Progenitor Cells (HepaStem®) have immunomodulatory effects and the capacity to modulate liver tissue inflammation. No anti-NASH treatments have been approved yet.

Method: In the HEP201 (PANASH) study, adult patients from 6 European countries with either F3 or F4 NASH (SAF fibrosis score) received a single or 3 repeated weekly infusions of either 0.5 or 1.0 × 10⁶ cells of HepaStem/kg body weight and were followed up for 6 months post infusion. No formal statistical analyses were performed as the number of patients was small.

Results: Twenty-three patients were included: mean age 56.5y, 14 T2D; 18 obese, 5 overweight; 11 had F3 and 12 F4, all compensated

SHG assessment of liver fibrosis changes in patients with NASH F3 stage

A) Radar maps of qFibrosis readouts illustrate fibrosis dynamics in 5 areas



B) Comparison of individual parameters in Regressive septa vs Progressive septa

No.	Septa parameters	Progressive septa N = 43, mean	Regressive septa N=50, mean	p value
1	Septa Area	234638.21	27002.33	<0.001
2	Cellular/acellular	0.75	0.56	0.082
3	Cellular/Collagen	1.27	0.93	0.169
4	Septa length	947.27	543.95	<0.001
5	Septa width	167.45	40.88	<0.001
6	Intersection Septa	2475.00	262.00	<0.001
7	Number Thick Fiber Septa	64.00	5.00	<0.001
8	Number Thin Fiber Septa	3016.00	344.50	<0.001
9	Thick/Thin Septa ratio	0.02	0.02	0.420
10	Aggregated Septa	80490.42	8730.77	<0.001
11	Distributed collagen within septa	2218.02	407.71	<0.001
12	Aggregated/Distributed collagen within septa	36.09	26.11	0.228

Figure: (abstract: WED-076).

POSTER PRESENTATIONS

except for 2 early decompensated (total bilirubin >2 mg/dL). Safety. Up to 3 infusions at the highest dose were safe and well tolerated. No death or dose-limiting toxicity was detected. No adverse event (AE) led to study discontinuation. The majority (91.7%) of the AEs were non-serious and considered not study drug-related. Of the 4 serious AEs, 2 were considered by the Investigator as possibly related: a mild ischaemic stroke (in a context of pre-existing hypertension, T2D and carotid plaques) and a resected dysplastic liver nodule (which was present before study participation). Both events resolved without sequelae. Most coagulation parameters did not change, except for some transient increase in D-dimers 24 h after infusion. Plasminogen activator inhibitor-1 levels tended to slightly decrease 24 hours after infusion. Three patients (13.0%) developed de novo anti-HLA Class I or II donor-specific antibodies transiently on D28 and/or M3. Efficacy. Serum levels of ALT and AST, which were mildly elevated at baseline, tended to normalize by M6, particularly in F3 patients. Bilirubin, as well as triglyceride levels, gradually decreased over time, particularly in patients with higher values at baseline. Adiponectin levels were increased in most patients (70%) on D28. No change was noted in glycaemic or anthropometric parameters. MELD score, which was low at baseline, further decreased slightly by M6. Serum levels of inflammatory parameters (CRP, IFN-gamma, and TNF-alpha), which were low at baseline, did not change over a period of 6 months, except

for IL-6 which tended to decrease by D28, particularly in patients with higher levels at baseline. Regarding fibrosis, APRI and FIB-4 scores tended to decrease by M6, particularly in F3 patients. No decompensation of cirrhosis was reported.

Conclusion: This first dose-finding, safety, and preliminary efficacy study of HepaStem in adult NASH patients with F3 or cirrhosis confirmed previous safety findings. Preliminary indicators of efficacy on liver health, metabolic and inflammation markers support further study of HepaStem's potential to prevent progression towards cirrhosis and decompensation.

TOP-091

Non-invasive tests of liver injury, inflammation and fibrosis are improved by efruxifermin and correlate with histological improvements in F2-F3 NASH patients: secondary analysis of Ph2b HARMONY study

Jörn Schattenberg¹, Juan P Frias², Guy Neff³, Gary Abrams⁴, Kathryn Jean Lucas⁵, William Sanchez⁶, Sudhanshu Gogia⁷, Muhammad Y Sheikh⁸, Cynthia Behling⁹, Pierre Bedossa¹⁰, Lan Shao¹¹, Erica Fong¹², Brittany de Temple¹², Reshma Shringarpure¹², Doreen Chan¹², Erik Tillman¹², Tim Rolph¹², Andrew Cheng¹², Kitty Yale¹², Stephen Harrison¹³. ¹Johannes

Table: Analysis of Non-invasive Markers by Treatment Group at 24 Weeks

Parameter (Unit) Category LS Mean (SE) unless otherwise noted	Placebo	EFX 28 mg	EFX 50 mg
LFC (%), MRI-PDFF	N=42	N=38	N=35
Relative (%) Change from Baseline at week 24	-6.0 (4.01)	-51.6 (4.31)	-63.7 (4.42)
p-value vs. placebo	---	<0.001	<0.001
Pro-C3 (ng/mL)	N=40	N=37	N=35
Absolute Change from Baseline at week 24	0.1 (0.70)	-5.1 (0.74)	-5.2 (0.74)
p-value vs. placebo	---	<0.001	<0.001
ELF Score	N=41	N=37	N=32
Absolute Change from Baseline at week 24	0.1 (0.10)	-0.6 (0.10)	-0.7 (0.11)
p-value vs. placebo	---	<0.001	<0.001
NIS4 Score	N=39	N=35	N=31
Absolute Change from Baseline at week 24	0.0 (0.03)	-0.3 (0.04)	-0.3 (0.04)
p-value vs. placebo	---	<0.001	<0.001
Liver Stiffness, FibroScan (VCTE)	N=42	N=38	N=36
Relative (%) Change from Baseline at week 24	-0.4 (5.82)	-15.4 (6.19)	-24.7 (6.37)
p-value vs. placebo	---	0.064	0.004
FAST Score	N=39	N=37	N=34
Mean (SD) Change from Baseline at week 24	-0.05 (0.19)	-0.31 (0.22)	-0.46 (0.14)
p-value vs. placebo	---	<0.0001	<0.0001
Normalization of LFC, in patients with >5% LFC at baseline¹	N=41	N=38	N=35
Proportion of patients, n (%)	0	13 (34%)	18 (51%)
Odds Ratio of NASH Resolution (without worsening of fibrosis) [95% CI], EFX-treated ²	---	4.6 [1.5, 14.2] **	
Normalization of ALT in patients >ULN at baseline³	N=22	N=18	N=20
Proportion of patients, n (%)	3 (14%)	13 (72%)	17 (85%)
Odds Ratio of NASH Resolution (without worsening of fibrosis) [95%CI], EFX-treated ⁴	---	+inf [2.9, +inf] **	

¹LFC normalization defined as >5% LFC at baseline, ≤5% LFC at Week 24
²Two EFX-treated patients analyzed for LFC normalization did not have week 24 biopsies available
³ALT normalization defined as >1x ULN at baseline, ≤ULN at Week 24 with ≥15% decrease
⁴One EFX-treated patient analyzed for LFC normalization did not have week 24 biopsies available
**p<0.01; inf = infinity (100% of EFX-treated patients achieving NASH resolution also normalized ALT)
LFC=liver fat content; Pro-C3=N-terminal type III collagen propeptide; ELF=Enhanced Liver Fibrosis;
VCTE=vibration-controlled transient elastography; FAST=FibroScan-AST; ULN=upper limit of normal.
The LS Means, SEs, and p-values are from a mixed-model repeated-measures (MMRM) with baseline as a covariate and controlling for stratification factors for comparisons between the EFX arms and the Placebo arm for Pro-C3 and ELF. FAST p-values are from one-way ANOVA, Dunnett's multiple comparisons test. Baseline is the last non missing measurement prior to the first dose of study drug.

(abstract: TOP-091).

Gutenberg University of Mainz, Germany; ²Velocity Clinical Research, United States; ³Covenant Metabolic Specialists, United States; ⁴Prisma Health, United States; ⁵Lucas Research, United States; ⁶Floridian Clinical Research, United States; ⁷TDDCTX, United States; ⁸Fresno Clinical Research, United States; ⁹Pacific Rim Pathology, United States; ¹⁰LiverPat, France; ¹¹Labcorp, United States; ¹²Akero Therapeutics, United States; ¹³Pinnacle Clinical Research, United States
Email: reshma@akerotx.com

Background and aims: Non-invasive tests (NITs) to predict histological improvement in clinical trials are of great unmet need. Efruxifermin (EFX), a long-acting Fc-FGF21 fusion protein decreased liver fat content and markers of liver injury, inflammation fibrosis, as well as improved metabolic health of NASH patients with F1-F3 fibrosis or compensated cirrhosis.^{1, 2} These observations were confirmed in the phase 2b HARMONY study.³ The current analysis evaluated the responses of NITs to EFX treatment for 24 weeks, and potential association with observed resolution of histopathology.

Method: Changes in NITs were explored across 115 patients randomized within the ongoing, randomized, placebo-controlled phase 2b HARMONY study evaluating EFX 28 and 50 mg once-weekly for 96 weeks, with primary end point evaluation at 24 weeks.³ NITs were analyzed for correlation with histological improvements, based on evaluation at week 24 of fibrosis improvement without NASH worsening; NASH resolution without fibrosis worsening; and both fibrosis improvement and NASH resolution.

Results: Both EFX treatment groups met all key histological end points³ at week 24. In parallel, Pro-C3, enhanced liver fibrosis (ELF) score, NIS4, and liver stiffness by transient elastography were significantly reduced in the treated groups (Table 1). The composite imaging and serum biomarker test, FibroScan-AST (FAST), indicated a significantly smaller proportion of patients at moderate or high risk of disease progression after treatment. High rates (>50% with 50 mg EFX) of normalization for LFC ($\leq 5\%$ LFC) or serum ALT, appeared to underlie the substantial resolution of steatohepatitis (>60%, placebo adjusted).

Conclusion: Consistent with observed histological benefits, EFX significantly improved circulating and imaging-based biomarkers of liver injury, inflammation and fibrosis compared to placebo. In a substantial proportion of patients, EFX treatment for 24 weeks was associated with normalization of liver fat and serum ALT, which appeared to underlie improvements in NASH histopathology. Thus, changes in NITs with EFX therapy can be extrapolated to predict improvement in liver histology, enabling non-invasive monitoring of EFX response among patients with moderate-to-advanced fibrosis and NASH.

References

1. Harrison S, et al. 2021 *Nature Medicine*. 27; p. 1262.
2. Harrison S et al. 2023. *JHEP Reports* 5; p. 1.
3. The Liver Meeting AASLD (2022).

FRIDAY 23 JUNE

FRI-466

Efficacy and safety of LPCN 1144 in hypogonadal and eugonadal subjects for the treatment of non-alcoholic steatohepatitis (NASH) with fibrosis

Benjamin Bruno¹, Josh Weavil¹, Jonathan Ogle¹, Kongnara Papankorn¹, Anthony DelConte^{1,2}, Nachaippan Chidambaram¹, Mahesh Patel¹, Somaya Albhaisi³, Arun Sanyal³. ¹Lipocine Inc, Salt Lake City, United States; ²Saint Joseph's University, Department of Food, Pharma, and Healthcare, Philadelphia, United States; ³Virginia Commonwealth University, Division of Gastroenterology, Hepatology and Nutrition, Richmond, United States
Email: bjb@lipocine.com

Background and aims: NASH is the fastest growing chronic liver disease and can progress to cirrhosis, hepatocellular carcinoma, and

death. Recently, data from the Phase 2 clinical trial LiFT support LPCN 1144, an oral prodrug of testosterone (T), as a novel therapeutic treatment for patients with NASH. Although there is a high prevalence of low T in NASH, not all patients present with this diagnosis. Thus, the aim of the current analysis was to examine the efficacy and safety of LPCN 1144 in hypogonadal and eugonadal subjects of the LiFT trial.

Method: In LiFT, biopsy-confirmed NASH (F1-F3) males were randomized 1:1:1 to three arms for 36 weeks; 1) Treatment A (n = 18): oral LPCN 1144 twice daily (BID), 2) Treatment B (n = 19): oral LPCN 1144 with d-alpha tocopherol BID, and 3) oral matching placebo (n = 19) BID. Due to similar positive outcomes in LiFT, the two LPCN 1144 treatment arms were pooled (n = 37) to examine the impact of baseline gonadal status on the safety and efficacy of LPCN 1144 treatment in men with NASH. Subjects were stratified into hypogonadal (HYPO), defined as subjects with at least two baseline T measurements <300 ng/dl or a documented history of hypogonadism, and eugonadal (EU) groups.

Results: Within the pooled treatment arms, 41% (15/37) were eugonadal and 59% (22/37) were hypogonadal. Baseline characteristics were similar between EU and HYPO, with the exception of a lower basal T and higher basal BMI and whole-body fat mass in HYPO. When stratified by gonadal status at baseline, the positive effects of LPCN 1144 therapy were not significantly different between EU and HYPO for MRI-PDFF (-8.5 vs -7.8%), total NAS (-2.1 vs -2.3), proportion of patients with NASH resolution without worsening of fibrosis (50% vs 61%), ALT (-15.7% vs -12.0%), AST (-15.2% vs -11.7%) or whole-body fat mass (-3.9% vs -5.6%), respectively. The number of participants with treatment emergent adverse events (TEAEs) were similar between EU (11/15), HYPO (16/22), and placebo (15/19). TEAEs of interest (diarrhea, nausea, vomiting, pruritis, benign prostatic hyperplasia, increased prostate-specific antigen, new or worsening hypertension, and peripheral edema) were less frequent in the EU subjects (2) than HYPO (7) and placebo (8) subjects.

Conclusion: The efficacy and safety of LPCN 1144 therapy for treatment of NASH in male patients is independent of basal gonadal status. These data suggest that oral LPCN 1144 treatment is a safe and effective therapy for the male NASH population which is comprised of both hypogonadal and eugonadal patients. The observed benefit to risk profile warrants further investigation of LPCN 1144 in a larger trial with a longer duration.

FRI-467

Incidence and risk of dyslipidemia and hyperglycemia in a phase 3 study of obeticholic acid for the treatment of non-alcoholic steatohepatitis

Manal Abdelmalek¹, Thomas Capozza², Pamela Davis², Amarita Randhawa², Sangeeta Sawhney². ¹Mayo Clinic, Gastroenterology and Hepatology, Rochester, United States; ²Intercept Pharmaceuticals Inc, Morristown, United States
Email: sangeeta.sawhney@interceptpharma.com

Background and aims: Non-alcoholic steatohepatitis (NASH) is associated with increased cardiovascular (CV) risk due to atherogenic dyslipidemia and insulin resistance. Therapies for NASH should have a well-characterized profile showing they do not increase CV risk. We aimed to characterize changes in lipid and glycemic markers and the incidence of dyslipidemia and hyperglycemia in the REGENERATE trial of obeticholic acid (OCA) for NASH (NCT02548351).

Method: The incidence of dyslipidemia and hyperglycemia was determined using standard Medical Dictionary for Regulatory Activities queries and laboratory tests for lipid and glycemic markers in the safety population (all randomized patients [pts] receiving ≥ 1 dose of placebo, OCA 10 mg, or OCA 25 mg).

Results: In this population, 976/2477 (39.4%) pts had exposures >4 years (median, 39 months). At baseline (BL), 496/825 (60.1%), 489/825 (59.3%), and 511/827 (61.8%) pts in the placebo, OCA 10 mg, and OCA 25 mg groups had low-density lipoprotein (LDL) ≥ 100 mg/dL;

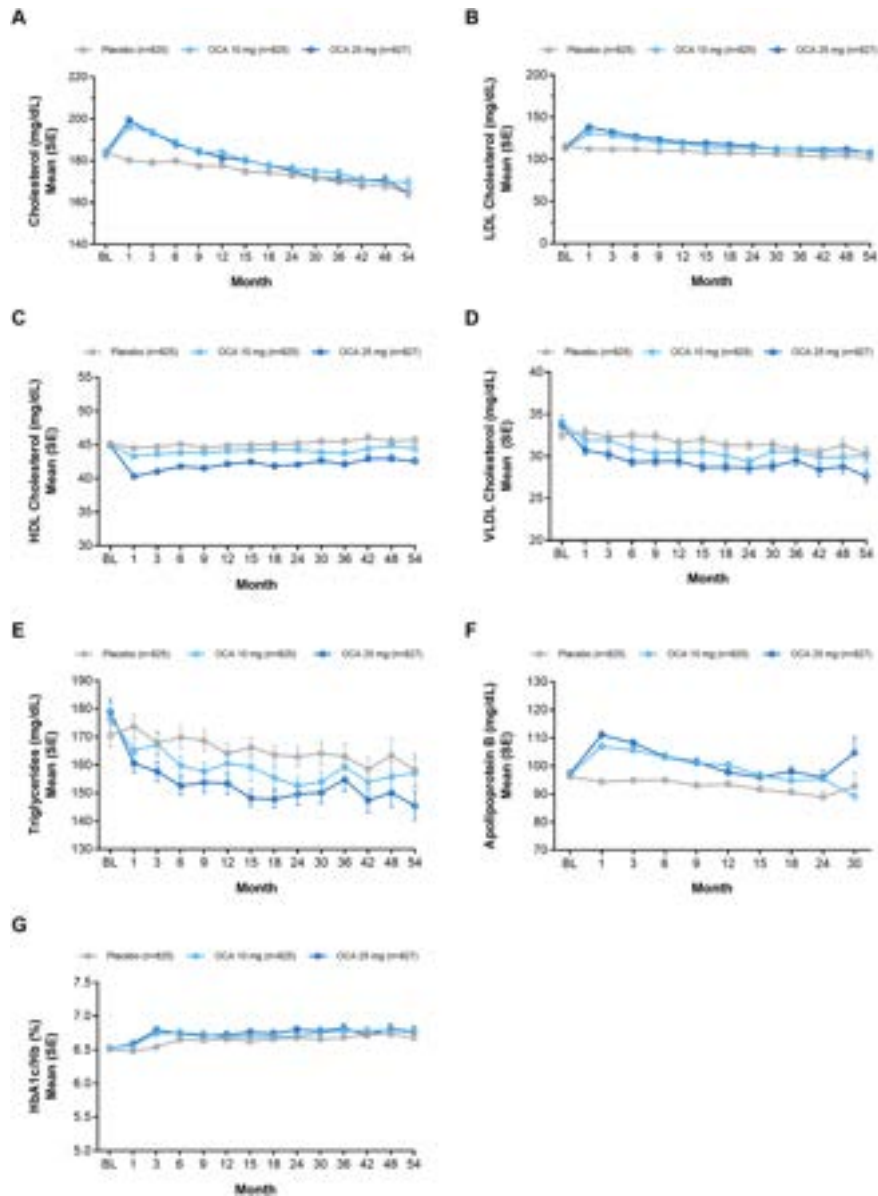


Figure: (abstract: FRI-467) Mean concentrations of (A) total cholesterol, (B) low-density lipoprotein (LDL), (C) high-density lipoprotein (HDL), (D) very low-density lipoprotein (VLDL), (E) triglycerides, (F) apolipoprotein B, and (G) hemoglobin A1c (HbA1c) over time.

450 (54.5%), 436 (52.8%), and 452 (54.7%) were on lipid-lowering drugs; and 470 (57.0%), 476 (57.7%), and 479 (57.9%) had diabetes, respectively. Most dyslipidemia and hyperglycemia events were mild/moderate; <0.5% of pts discontinued treatment due to these events. Dyslipidemia AEs were reported in 193 (23.4%), 354 (42.9%), and 390 (47.2%) pts who received placebo, OCA 10 mg, or OCA 25 mg, respectively. No serious adverse events (SAEs) were reported. In the OCA groups, mean LDL increased from BL to month 1 (M1) but returned to near BL by M18 with no difference from placebo through M54 (Figure 1B). This reduction occurred regardless of statin use. The incidence of hyperglycemia was similar in the placebo (190 [23.0%]), OCA 10 mg (223 [27.0%]), and OCA 25 mg (201 [24.3%]) groups. Hyperglycemia SAEs occurred in 2 (0.2%), 5 (0.6%), and 11 (1.3%) pts,

respectively, and were mostly related to hospitalization for glycemic control in pts with type 2 diabetes (1, 3, and 9 pts, respectively). There was an early transient increase in mean hemoglobin A1c (HbA1c) from BL (6.52%) to M3 (6.77%) in the OCA groups. After M9, HbA1c levels did not differ between placebo and OCA groups (Figure 1G).

Conclusion: OCA 25 mg is associated with an early transient increase in LDL, which returned to BL independent of the addition of a statin. After an early increase in HbA1c, there was no evidence of increased hyperglycemia risk with long-term treatment. These results suggest transient changes in lipids and glycemic markers can be managed per guidelines in pts with pre-cirrhotic liver fibrosis due to NASH.

Abbreviations: BL, baseline; OCA, obeticholic acid.

FRI-468

Prospective, multi-center, open-label, randomized, omega-3-acid ethyl ester-controlled trial to assess the impact of the pemafibrate on liver function in hypertriglyceridemia patients with non-alcoholic fatty liver disease (Portrait study)

Yoshio Sumida¹, Masashi Yoneda¹, Kiyooki Itoh¹, Yukiomi Nakade¹, Satoshi Kimoto¹, Kazumasa Sakamoto¹, Hidenori Toyoda². ¹Aichi Medical University, Japan; ²Ogaki Municipal Hospital, Japan
Email: sumida@koto.kpu-m.ac.jp

Background and aims: Hypertriglyceridemia is a frequent complication of non-alcoholic fatty liver disease (NAFLD), but its treatment has not been established. We conducted a multicenter, randomized, open-label study of pemafibrate versus omega-3 fatty acid ethyl esters (PORTRAIT study: jRCTs041200011) in patients with hypertriglyceridemia and NAFLD to compare their effects on liver function.

Methods: Patients with hypertriglyceridemia and NAFLD who provided written consent to participate in the study were randomly assigned to receive pemafibrate 0.2 mg/day or the omega-3 fatty acid ethyl esters 2 g/day for 24 weeks. The primary end point was the change in ALT from baseline to week 24, and the secondary end points were the change in liver function-related markers, lipid profiles, HbA1c, and liver fibrosis markers. This study was approved by a Certified Review Board (CRB4200004).

Results: A total of 199 patients were enrolled, among which 80 were eligible, and 39 were assigned to the pemafibrate group and 41 to the omega-3 fatty acid ethyl esters group. The mean change in ALT (U/L) at 24 weeks was -19.7 and 6.8 in the pemafibrate group and omega-3 fatty acid ethyl esters group, respectively, where the difference between the groups was significant (-26.5 U/L, 95% confidence interval -42.3 to -10.7 U/L, $p = 0.001$). The adjusted mean TG, non-HDL-C, γ -GTP, ALP, M2BPGi in the secondary end points were significantly lower and the adjusted mean HDL-C was significantly higher in the pemafibrate group compared with the omega-3 fatty

acid ethyl esters group. There were no cases of discontinuation due to adverse drug reactions in either group with no safety concerns.

Conclusion: Pemafibrate is recommended over omega-3 fatty acid ethyl esters for lipid management and treatment of NAFLD in patients with hypertriglyceridemia and NAFLD. This study demonstrated the short-term efficacy and safety of pemafibrate. Further large-scale and long-term studies, including evaluation of liver histology, are expected in the future.

FRI-469

Prevalence of, and effect of semaglutide on, features of non-alcoholic steatohepatitis in patients with obesity with and without type 2 diabetes: analysis of data from two randomised placebo-controlled trials using SomaSignal tests

Jörn Schattenberg¹, Henning Grønbaek², Iris Kliers³, Steen Ladelund³, Michelle Long³, Sune Boris Nygård³, Arun Sanyal⁴, Melanie Davies^{5,6}. ¹Metabolic Liver Research Program, University Medical Center Mainz, Mainz, Germany; ²Department of Hepatology and Gastroenterology, Aarhus University Hospital, Aarhus, Denmark; ³Novo Nordisk, Søborg, Denmark; ⁴Division of Gastroenterology, Hepatology and Nutrition, Virginia Commonwealth University School of Medicine, VA, USA, United States; ⁵Diabetes Research Centre, University of Leicester, Leicester, United Kingdom; ⁶NIHR Leicester Biomedical Research Centre, Leicester, United Kingdom
Email: joern.schattenberg@unimedizin-mainz.de

Background and aims: Novel, non-invasive biomarkers to grade and stage non-alcoholic fatty liver disease (NAFLD) and its progressed form, non-alcoholic steatohepatitis (NASH), are urgently needed. A targeted proteomics signature derived from patients with histologically-defined NASH has been developed collaboratively with the NASH Clinical Research Network (SomaSignal tests) to relate to the presence and severity of NASH components and changes over time. In this analysis, SomaSignal tests were applied to proteomics data

Figure: Odds ratios for presence of NASH components at the end of the study for semaglutide (s.c.) vs placebo in STEP 1 (top panels) and STEP 2 (bottom panels) based on SomaSignal prediction probabilities (left) and binary classification (right)

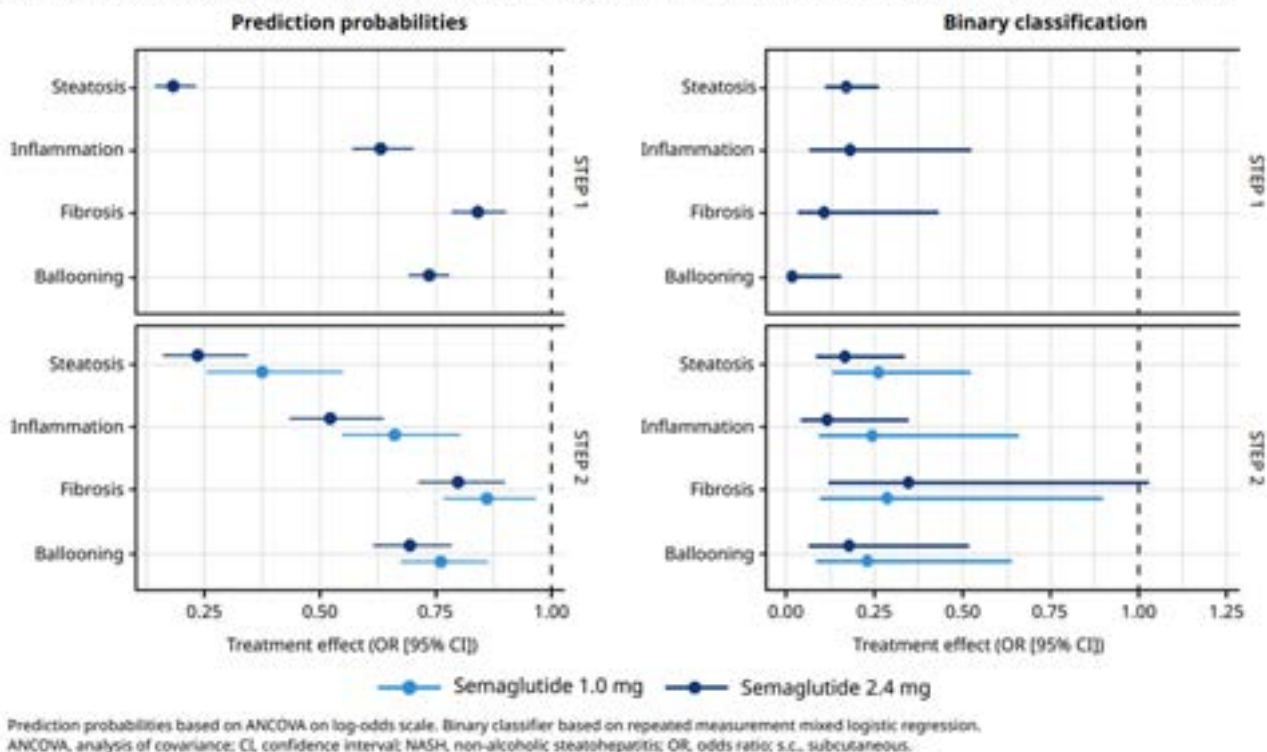


Figure: (abstract: FRI-469).

POSTER PRESENTATIONS

generated from two weight-loss trials in order to characterise the prevalence of NASH components at baseline and investigate the effect of semaglutide.

Method: STEP 1 (NCT03548935) and STEP 2 (NCT03552757) were phase 3a, randomised, placebo-controlled trials of once-weekly subcutaneous semaglutide (2.4 mg in STEP 1; 1.0 mg and 2.4 mg in STEP 2) vs placebo for weight reduction in adults with overweight/obesity without (STEP 1) or with (STEP 2) type 2 diabetes (T2D). Patients received treatment for 68 weeks. Prediction probabilities (PP) for NASH components at baseline were derived using SomaSignal models. The efficacy of semaglutide vs placebo was analysed as presence or absence of NASH components using a binary classifier derived from the PP (PP ≥ 0.5) at the end of the trial (EOT) and as odds ratios at EOT based on PPs directly. The SomaSignal categories included: steatosis grade 1–3 vs 0; lobular inflammation grade 2–3 vs 0–1; hepatocyte ballooning grade 1–2 vs 0; and fibrosis stage 2–4 vs 0–1. Based on the SomaSignal classifiers, patients were characterised into NAFLD stages: NAFL if steatosis was present but with no other NASH components; indeterminate if some, but not all, NASH components or fibrosis were present; and NASH if steatosis, inflammation and ballooning (with or without fibrosis) were present.

Results: Proteomics data were available for 1307/1961 and 643/1210 randomised patients in STEP 1 and 2; these patients were representative of the full study populations in each trial. At baseline, steatosis was present in 43% of patients in STEP 1, and the prevalence of the other components was 5% or less. In STEP 2, steatosis was present in 72% of patients, 15% had NASH and 12% had NASH with fibrosis. The odds of having each NASH component were significantly lower at EOT for patients who received semaglutide vs placebo, with a dose-dependency trend in STEP 2, using both PP and binary classification (Figure). Further, semaglutide was associated with significantly lower odds of having a more severe NAFLD stage after treatment vs placebo.

Conclusion: Steatosis is highly prevalent in people with overweight/obesity, with NASH likely present in 15% of patients with overweight/obesity and T2D (STEP 2). Semaglutide had a favourable effect on NASH components in the current analysis in populations with overweight/obesity, with and without T2D, as measured by SomaSignal models.

FRI-470

HPG1860 in patients with NASH: a phase II double-blind, placebo-controlled, dose-ranging study

Naim Alkhour¹, Yongheng Liu², Nian Liang², Peibin Zhai², Sandra Wu², Xin Zhou², Michael Xu², Que Liu², Stephen Harrison³.

¹Liver Health II LLC dba Arizona Liver Health, Chandler, United States;

²Hepagene, Shanghai, China; ³Pinnacle Clinical Research-PLLC, Austin, United States

Email: stephenharrison87@gmail.com

Background and aims: HPG1860 is an oral non-steroidal, next generation farnesoid X receptor (FXR) agonist with selective liver distribution under investigation for treatment of non-alcoholic steatohepatitis (NASH). A phase I study of HPG1860 in healthy subjects demonstrated a benign safety profile and strong target engagement. Therefore, we aimed to evaluate safety, tolerability and efficacy of HPG1860 in patients with non-cirrhotic NASH.

Method: In this double-blind, placebo-controlled, dose ranging phase IIa RISE study (NCT05338034), patients with non-cirrhotic NASH, diagnosed by historical liver biopsy or met following criteria: liver stiffness ≥ 8.0 kPa and controlled attenuation parameter >300 dB/m or T2DM patients with elevated ALT and BMI ≥ 27 kg/m², were randomized in a 1:1:1:1 ratio to receive HPG1860 3 mg (n = 22), 5 mg (n = 21), 8 mg (n = 22) or placebo (n = 22) orally once daily for 12 weeks. All patients were required to have liver fat content (LFC) $\geq 10\%$ at screening based on magnetic resonance imaging proton density fat fraction (MRI-PDFF). The primary end point of this study was safety and tolerability. The key secondary efficacy end point of

this study was the change from baseline in relative LFC measured by MRI-PDFF at week 12.

Results: Between November 2021 and May 2022, 87 patients with either liver biopsy proven NASH or phenotypic diagnosis of NASH were enrolled and included for intent-to-treat analysis.

The most common ($\geq 10\%$) adverse events were pruritus, nausea, fatigue, headache and dizziness. Treatment-related pruritus occurred in 9.1%, 9.5%, 27.3% of patients in the 3, 5, 8 mg and only 1 patient in 3 mg cohort withdrew from the study due to grade 2 pruritus. No significant change in LDL cholesterol (LDL-C) was observed in the 3 mg, 5 mg and 8 mg HPG1860 cohorts as compared to placebo. Mean LFC at baseline was 20.11%, 19.74%, 14.83% and 19.29% in placebo, 3 mg, 5 mg and 8 mg cohort, respectively. At week 12, mean relative change of LFC in placebo, 3 mg, 5 mg and 8 mg cohort was 0.68%, -20.15% (p = 0.004 vs placebo), -7.08% (p = 0.965 vs placebo), and -38.64% (p < 0.001 vs placebo) respectively. 25.0% patients in 3 mg cohort, and 63.2% patients in 8 mg cohort achieved $\geq 30\%$ relative LFC reduction at week 12. For patients with ALT $>ULN$ at baseline, mean ALT in placebo, 3 mg, 5 mg and 8 mg cohort was 70, 62, 62 and 72 U/L, respectively. At week 12, mean ALT percentage change from baseline in placebo, 3 mg, 5 mg and 8 mg cohort was 32.6%, -7.0% , -7.6% and -22.5% respectively, indicating dose-dependent reduction of ALT in HPG1860 treated patients.

Conclusion: HPG1860 was safe and well tolerated. LFC significantly reduced with 3 mg and 8 mg cohorts over 12 weeks in patients with NASH. HPG1860 demonstrated a differentiated pruritus and LDL-C profile, providing favorable risk-benefit data to support further clinical development by assessing histological biopsy end points in patients with NASH.

FRI-471

The effects of a structured dietetics intervention in patients with non-alcoholic fatty liver disease

Dominic Crocombe^{1,2}, Antonio Liguori^{1,2}, Mirko Zoncapè^{1,2}, Jennifer-Louise Clancy^{1,2}, Atul Goyale^{1,2}, Davide Roccarina^{1,2}, Anna Mantovani^{1,2}, Laura Iogna Prat^{1,2}, Roshni Patel^{1,2}, Emmanuel Tsochatzis^{1,2}, ¹Royal Free London NHS Foundation Trust, Sheila Sherlock Liver Centre, London, United Kingdom; ²University College London, Institute of Liver and Digestive Health, London, United Kingdom

Email: dominic.crocombe@nhs.net

Background and aims: Diet and lifestyle modification to aid weight loss remains the cornerstone of NAFLD management. Since 2014, selected patients attending a multi-disciplinary NAFLD clinic have been referred to a specialist dietitian. They either receive a single appointment (SA) with follow-up after 3 months and as required thereafter, or a comprehensive, structured package of care (POC) consisting of 4 sessions within 6 months. Our aim was to assess whether this dietetic POC is associated with more favourable outcomes.

Method: In this retrospective service evaluation, we reviewed the outcomes (changes in weight and liver stiffness) of patients in 3 groups: those who had completed $\geq 3/4$ sessions in the dietetic POC, those who had completed a SA, and those who had not seen a specialist dietitian (controls). In the POC and SA groups, weight was recorded from the first dietetic appointment (baseline), final dietetic appointment (intervention end), and at 18 months from baseline (long term). For controls, weight at baseline, 6 months, and 18 months was recorded. Fibroscan (TE) results before and after intervention were recorded. Significant improvement in TE was considered $\geq 20\%$ reduction if baseline ≥ 6 kPa; significant worsening was considered $\geq 20\%$ increase if baseline ≥ 5 kPa, or a change to ≥ 6 kPa if baseline <5 kPa.

Results: 381 patients were included: 89 POC, 49 SA, and 243 controls. Mean weight changes from baseline to intervention end were -2.9 kg (-2.8%) for POC, -1 kg (-0.9%) for SA, and -1.3 kg (-1.2%) for controls (Figure 1a). Patients who received the POC lost significantly more

weight (both kg and %) than controls (Tukey post-hoc test, $p = 0.02$). There was also a significant difference between POC and controls in weight change of $\geq 5\%$ (X^2 , $p = 0.017$) but not $\geq 7\%$ or $\geq 10\%$. There was no significant difference in weight loss between POC and SA, or SA and controls. At multivariate logistic analysis, the POC was associated with $\geq 5\%$ weight loss (OR 2.15, $p < 0.01$) independent of time interval, age, sex, and metabolic comorbidities. At long term (mean 18 months) follow-up, all groups achieved further weight loss (-3.4% SOC, -2.3% SA, -2.3% controls, Figure 1b) but there was no longer a significant difference in weight change from baseline between groups. Regarding liver stiffness, the mean interval between Fibroscans was 24 months. Overall, 28.1% patients had a significant improvement and 22.7% had a significant worsening. There was no significant difference in changes of TE between groups. Overall, $\geq 5\%$ weight loss after 6 or 18 months was associated with a significant improvement in TE (X^2 , $p < 0.01$).

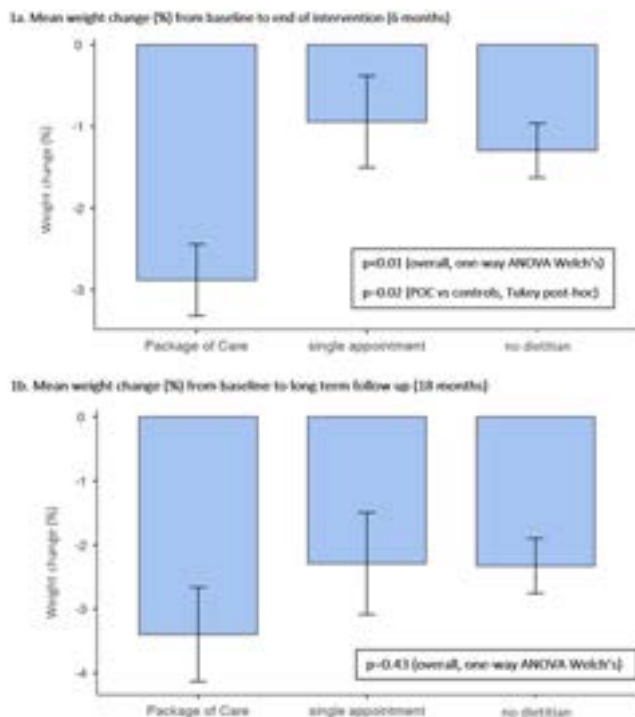


Figure:

Conclusion: A structured dietetics POC consisting of 3 or 4 sessions over 6 months was associated with greater rate of $\geq 5\%$ weight loss than controls, and the effect was maintained beyond the end of the intervention. $\geq 5\%$ weight loss after 6 or 18 months was associated with significant improvement in liver stiffness.

FRI-472

Resmetirom improves the lipid/lipoprotein profile in patients with non-alcoholic fatty liver disease

Naim Alkhour¹, Rebecca Taub², Guy Neff³, Kathryn Jean Lucas⁴, Dominic Labriola², Sam Moussa⁵, Mustafa Bashir⁶, Stephen Harrison^{7,8}. ¹Arizona Liver Health, Tucson, United States; ²Madrigal Pharmaceuticals, Conshohocken, United States; ³Covenant Metabolic Specialists, Sarasota, United States; ⁴Lucas Research, Morehead City, United States; ⁵University of Arizona for Medical Sciences, Tucson, United States; ⁶Duke University Medical Center, Durham, United States; ⁷University of Oxford, Oxford, United Kingdom; ⁸Pinnacle Clinical Research, San Antonio, United States
Email: nalkhour@azliver.com

Background and aims: Patients with non-alcoholic fatty liver disease (NAFLD)/non-alcoholic steatohepatitis (NASH) have an increased risk of cardiovascular disease (CVD). Resmetirom is an oral liver-targeted thyroid hormone receptor-beta selective agonist in clinical development for treatment of NASH. In addition to significantly reducing hepatic fat, data from Phase 2/3 clinical trials have consistently demonstrated that resmetirom significantly reduces low-density lipoprotein cholesterol (LDL-C), apolipoprotein B (apoB), and triglyceride (TG) levels in patients with NAFLD/NASH. Here we report data from the Phase 3 MAESTRO-NAFLD-1 trial on the effect of resmetirom treatment on additional components of the lipid/lipoprotein profile. **Method:** MAESTRO-NAFLD-1 (NCT04197479) was a Phase 3 trial to evaluate the safety and tolerability of resmetirom over 52 weeks of treatment in adults with NAFLD (presumed NASH) diagnosed via non-invasive tests. Patients were randomized 1:1:1 to 3 double-blind arms (resmetirom 100 mg, resmetirom 80 mg, or placebo administered once daily) or an open-label arm (resmetirom 100 mg administered once daily). Lipid, lipoprotein, and lipid particle levels were measured at baseline, Week 24, and Week 48.

Results: At Week 24, remnant-like particle cholesterol (RLP-C), very low-density lipoprotein cholesterol (VLDL-C), and VLDL and chylomicron TG levels were significantly reduced from baseline in all resmetirom groups compared with placebo ($p < 0.05$ vs placebo for all); these significant reductions were maintained at Week 48 (TABLE). In addition, lipoprotein (a) (Lp(a)) and apolipoprotein CIII (apoCIII) levels were significantly reduced from baseline with

TABLE. Percent change from baseline in lipid, lipoprotein, and lipid particle levels at Week 48.				
	LSM %CFB (SE)			
	Resmetirom 100mg OL	Resmetirom 100mg DB	Resmetirom 80mg DB	Placebo DB
RLP-C, mg/dL	-8.7 (3.6) ^a	-6.1 (3.1) ^a	-0.8 (3.0) ^a	12.4 (3.0)
VLDL-C, mg/dL	-11.2 (5.9) ^a	-7.6 (5.0) ^a	0.7 (5.0) ^b	19.0 (4.9)
VLDL and chylomicron TG, mg/dL	-16.3 (4.3) ^a	-14.4 (3.7) ^a	-10.5 (3.7) ^a	7.1 (3.6)
Lp(a), nmol/L (among patients with baseline Lp(a) >10 nmol/L)	-18.7 (3.5)	-33.6 (4.0) ^a	-24.0 (4.1) ^a	-4.4 (4.1)
ApoCIII, mg/dL	-13.6 (3.1) ^a	-14.4 (2.6) ^a	-9.7 (2.6) ^a	7.7 (2.6)
LDL particles, nmol/L	-21.0 (2.3) ^a	-15.6 (2.0) ^a	-15.1 (2.0) ^a	-2.1 (1.9)
Small LDL particles, nmol/L	-24.5 (2.7) ^a	-18.3 (2.3) ^a	-18.7 (2.4) ^a	-6.7 (2.3)
VLDL and chylomicron particles, nmol/L	-6.7 (5.8) ^a	-7.2 (5.0) ^a	1.8 (5.0) ^a	22.6 (4.9)

^a $p < 0.0001$ vs placebo; ^b $p < 0.001$ vs placebo.
ApoCIII, apolipoprotein CIII; CFB, change from baseline; DB, double-blind; LDL, low-density lipoprotein; Lp(a), lipoprotein (a); LSM, least squares mean; OL, open-label; RLP-C, remnant-like protein cholesterol; SE, standard error; TG, triglyceride; VLDL-C, very low-density lipoprotein cholesterol.

Figure: (abstract: FRI-472).

POSTER PRESENTATIONS

resmetirom 100 mg and 80 mg versus placebo at Week 24 ($p < 0.0001$ vs placebo for all); the significant reductions in lipoproteins were maintained at Week 48 with continued resmetirom treatment. Atherogenic lipoprotein particles, including LDL, small LDL, and VLDL and chylomicron, were also significantly reduced from baseline in the resmetirom groups compared with placebo at Week 24 ($p < 0.05$ vs placebo for all) with these significant reductions maintained at Week 48.

Conclusion: In addition to significantly reducing hepatic fat, resmetirom significantly improved the overall lipid/lipoprotein profile in adults with NAFLD/NASH. Both resmetirom 100 mg and 80 mg significantly reduced atherogenic lipids/lipoproteins, including RLP-C, VLDL-C, Lp (a), and apoCIII, at Week 24. Furthermore, improvements in the lipid/lipoprotein profile were maintained throughout the entire treatment period of MAESTRO-NAFLD-1. As CVD is the most common cause of mortality in patients with NASH, the effect of potential therapies on cardiovascular risk factors, including elevated atherogenic lipids/lipoproteins, is important to consider.

FRI-473

Different class effects of oral hypoglycemic agents on non-alcoholic fatty liver disease regression and clinical outcomes: a nationwide cohort study

Heejoon Jang¹, Yeonjin Kim², Donghyeon Lee¹, Sae Kyung Joo¹, Bo Kyung Koo¹, Yong Jin Jung¹, Woojoo Lee², Won Kim¹. ¹Seoul Metropolitan Government Seoul National University Boramae Medical Center, Internal Medicine, Seoul, Korea, Rep. of South; ²Graduate School of Public Health, Seoul National University, Public Health Sciences, Seoul, Korea, Rep. of South
Email: wonshiri@yahoo.com

Background and aims: Sodium-glucose cotransporter 2 (SGLT2) inhibitors, thiazolidinediones, and dipeptidyl peptidase-4 (DPP-4) inhibitors are known to improve non-alcoholic fatty liver disease (NAFLD). We aimed to determine which drug is most effective for NAFLD in patients with type 2 diabetes mellitus (T2DM) in real-world settings.

Method: Based on the National Health Information Database covering over 50 million South Koreans, patients with NAFLD and T2DM who use SGLT2 inhibitors, thiazolidinediones, DPP-4 inhibitors, or sulfonylureas in combination with metformin for more than 80% of 90 consecutive days were included. Inverse probability of treatment weighting was used to adjust differences in baseline characteristics between the groups. NAFLD regression assessed by the fatty liver index was the primary outcome. Severe NAFLD was the secondary outcome, defined as a composite of liver-related hospitalization, liver-related mortality, or hepatocellular carcinoma (HCC). All-cause mortality and liver transplantation were considered competing risks.

Results: A total of 103,228 patients were followed for a median of 878 days, and 4,960 patients experienced NAFLD regression. Compared with sulfonylureas, SGLT2 inhibitors (adjusted subdistribution hazard ratio [aSHR] 2.15, 1.88–2.47), thiazolidinediones (aSHR 1.74, 1.47–2.06), and DPP-4 inhibitors (aSHR 1.58, 1.45–1.72) were associated with higher NAFLD regression. SGLT2 inhibitors were significantly associated with higher NAFLD regression than either thiazolidinediones (aSHR 1.38, 1.12–1.71) or DPP-4 inhibitors (aSHR 1.38, 1.24–1.54), whereas thiazolidinediones did not show a significant difference from DPP-4 inhibitors (aSHR 1.11, 0.95–1.29). SGLT2 inhibitors were not significantly associated with a lower incidence of severe NAFLD compared to thiazolidinediones (aSHR 1.06, 0.39–2.88) or DPP-4 inhibitors (aSHR 0.85, 0.40–1.79).

Regression of NAFLD

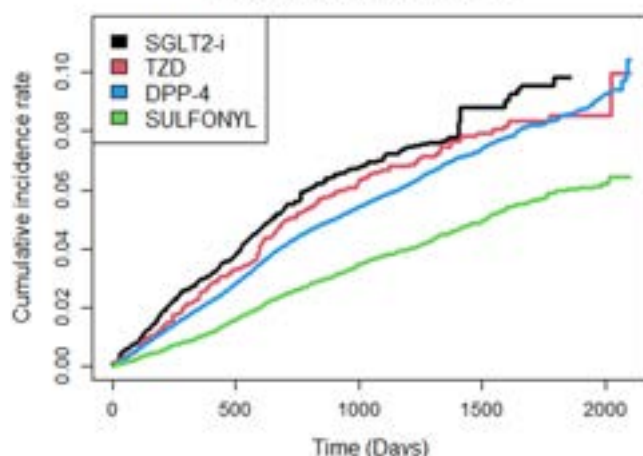


Figure:

Conclusion: NAFLD patients with T2DM may be preferred to use SGLT2 inhibitors as an oral hypoglycemic agent in terms of regression of NAFLD.

FRI-474

SGLT2 inhibitors improve hepatic fibrosis assessed by Fibroscan in NAFLD patients with type 2 diabetes: a five-year follow-up study

Rosa Lombardi^{1,2}, Alessandro Mantovani³, Annalisa Cespiati^{1,2}, Gabriele Maffi², Elena Del Zanna², Paolo Francione², Felice Cinque², Rosanna Villani⁴, Nicola Passigato³, Emanuela Orsi⁵, Valeria Grancini⁵, Giuseppina Pisano¹, Claudio Maffei⁶, Daniela Bignamini¹, Gaetano Serviddio⁴, Giovanni Targher³, Silvia Fargion², Anna Ludovica Fracanzani^{1,2}. ¹Unit of Medicine and Metabolic Disease, Fondazione IRCCS Ca' Granda Ospedale Maggiore Policlinico of Milan, Milan, Italy; ²Department of Pathophysiology and Transplantation, University of Milan, Milan, Italy; ³Division of Endocrinology, Diabetes and Metabolism, Department of Medicine, University and Azienda Ospedaliera Universitaria Integrata of Verona, Verona, Italy; ⁴Centro C.U.R.E. Dept. of Medical and Surgical Sciences, University of Foggia, Foggia, Italy; ⁵Endocrinology and Diabetes Unit, Fondazione IRCCS Ca' Granda Ospedale Maggiore Policlinico of Milan, Milan, Italy; ⁶Pediatric Diabetes and Metabolic Disorders Unit, Department of Surgical Sciences, Dentistry, and Pediatrics, and Gynaecology, University Hospital of Verona, Verona, Italy
Email: rosallombardi@hotmail.it

Background and aims: Subjects with non-alcoholic fatty liver disease (NAFLD) and type 2 diabetes mellitus (T2DM) present high progression of liver disease to fibrosis, which is the main determinant of long-term adverse outcomes. Data are accumulating on the benefits of sodium glucose cotransporter 2 inhibitors (SGLT-2i) on hepatic fibrosis mainly in pharmacologic or retrospective studies, to prospectively evaluate change in metabolic alterations and hepatic disease in patients with NAFLD and T2DM and predisposing factors.

Method: 237 patients with NAFLD (mean age 67 ± 9 years, 54% male) were enrolled at the diabetology outpatient clinics and re-evaluated after 5 years. Information about diabetic control, metabolic comorbidities and medications were collected at baseline and follow-up. Additionally, NAFLD was assessed by liver ultrasonography, whereas LSM was detected by Fibroscan® at baseline and after 5 years.

Results: During follow-up no change in the prevalence of metabolic alterations except for hypertension (81% vs 73%, $p < 0.001$) was observed, whereas an increase in LSM values (6.0 ± 2.8 vs 5.8 ± 2.7 kPa, $p = 0.02$) was registered, despite stability of diabetic control. In particular, LSM worsened in 133 (56%) subjects, with 92 (39%) having a worsening of $>10\%$ from baseline and 20 (8%) of at least 1 fibrosis stage at Fibroscan from baseline. Moreover, a higher

prescription of SGLT2i was seen (21% vs 6%, $p < 0.001$). Compared with those with no worsening of LSM, patients with worsening of LSM had a higher prevalence of increase in BMI during follow-up (45% vs 32%, $p = 0.06$). In multivariate analysis, after adjustment for age, sex, liver enzymes and HbA1c, the use of SGLT2-inhibitors at follow-up (adjusted-hazard ratio 0.34, 95% CI 0.13–0.91) was associated with a reduced risk of worsening of LSM by Fibroscan, even if considered >10% from baseline. However, this association was markedly attenuated after further adjusting for change in BMI over time.

Conclusion: Despite a high prevalence of fibrosis progression in NAFLD subjects with T2DM, we showed a potential effect of SGLT2-inhibitors in reducing the risk of worsening of liver stiffness, possibly also mediated by weight loss. Therefore, our data suggest that using this category of antidiabetic drug in NAFLD patients may prevent progression of fibrosis, especially if weight control is obtained in these patients.

FRI-475

Semaglutide improves non-alcoholic steatohepatitis: a 10-year retrospective study

Parth Shah¹, Megan White¹, Alex Sievert², Alexander Conway³, Adam Kneepkens², Gregory Sayuk^{1,4}, Mauricio Lisker-Melman^{1,4}, Jill Elwing^{1,4}. ¹Washington University School of Medicine Department of Gastroenterology, St. Louis, United States; ²Washington University School of Medicine, Internal Medicine, St. Louis, United States; ³Washington University School of Medicine, St. Louis, United States; ⁴St. Louis VA Medical Center-John Cochran Division, St. Louis, United States
Email: parth@wustl.edu

Background and aims: The glucagon-like peptide-1 receptor agonist semaglutide (SEMA) has been studied in patients with non-alcoholic steatohepatitis (NASH) due to the potential benefit from weight loss on liver inflammation. Preclinical studies suggest that the NASH improvement may be independent of weight loss. We aim to assess the impact of SEMA on objective NASH measures independent of weight loss.

Method: This retrospective study evaluated 1236 patients with type II diabetes and included 420 patients that were on SEMA for at least 12 months between 2011 and 2022. Exclusion criteria were chronic liver disease other than NASH, decompensated cirrhosis, any malignancy, and bariatric surgery. Primary end points were clinically significant improvements in AST or ALT (defined as mean difference >6.3 U/L and >10.6 U/L respectively based on Ng et al. *Hepatology* 2022). Statistical analysis included Student's t-test/ANOVA, Wilcoxon signed-rank test/Friedman test as appropriate, and binary logistic regression.

Results: Within 420 patients (median 71 years old, 94% male, 79% Caucasian), the median duration of SEMA was 22.5 months and 80% received 1 mg/week. Ninety-nine percent of patients had diabetes and 87% had a body mass index (BMI) ≥ 30 . BMI improved by a mean (SD) of 1.9 points (2.8), weight by 13.3 pounds (19.1), AST by 4.1 U/L (11.5), and ALT by 5.3 U/L (14.2). In 28% and 22% of patients, AST and ALT respectively, had a clinically significant improvement. The NASH scores (NFS, FIB4, and APRI), improved after SEMA ($p < 0.001$). No statistically significant differences in AST or ALT improvement were found when patients were stratified by BMI prior to SEMA (BMI <25; ≥ 25 to <30; ≥ 30 to <35; ≥ 35 to <40; ≥ 40). No statistically significant differences were found in AST or ALT improvement when stratified by percentage of weight loss after SEMA (no weight loss; 0–5%; 5–10%; >10%). On logistic regression analysis (Table 1), duration of SEMA and pre-SEMA APRI score increased odds of clinically significant improvements of AST and ALT.

Figure: Table 1. Logistic regression analysis on SEMA with clinically significant improvement.

	Clinically significant AST improvement		Clinically significant ALT improvement	
	Univariate	Multivariate	Univariate	Multivariate
Months of treatment	OR 1.03 $p = 0.002^*$	OR 1.06 $p < 0.001^*$	OR 1.02 $p = 0.08$	OR 1.03 $p = 0.02^*$
Compensated cirrhosis	OR 2.7 $p = 0.03^*$	OR 1.2 $p = 0.75$	OR 3.9 $p = 0.003^*$	OR 2.2 $p = 0.14$
APRI score 0.5 to 1.5 prior to treatment	OR 4.3 $p < 0.001^*$	OR 4.4 $p < 0.001^*$	OR 5.3 $p < 0.001^*$	OR 4.8 $p < 0.001^*$
Change in BMI after treatment	OR 0.95 $p = 0.16$	–	OR 0.92 $p = 0.05$	–
Weight loss after treatment	OR 0.99 $p = 0.23$	–	OR 0.99 $p = 0.08$	–

OR = odds ratio.

*statistically significant $p < 0.05$.

Conclusion: SEMA treatment was associated with beneficial effects on biochemical NASH measures, including transaminases and NASH scores in a diabetic population. Higher odds of positive SEMA effects were observed with longer treatment duration and were independent of weight loss.

FRI-476

Resmetirom helps regulate thyroid hormone levels within the liver in patients with non-alcoholic fatty liver disease

Stephen Harrison^{1,2}, Rebecca Taub³, Guy Neff⁴, Mustafa Bashir⁵, Dominic Labriola³, Sam Moussa⁶, Naim Alkhouri⁷, Kathryn Jean Lucas⁸. ¹University of Oxford, Oxford, United Kingdom; ²Pinnacle Clinical Research, San Antonio, United States; ³Madrigal Pharmaceuticals, Conshohocken, United States; ⁴Covenant Metabolic Specialists, Sarasota, United States; ⁵Duke University Medical Center, Durham, United States; ⁶University of Arizona for Medical Sciences, Tucson, United States; ⁷Arizona Liver Health, Tucson, United States; ⁸Lucas Research, Morehead City, United States
Email: stephenharrison87@gmail.com

Background and aims: Thyroid hormone receptor (THR)-beta is responsible for regulating critical metabolic pathways in the liver. In patients with non-alcoholic fatty liver disease (NAFLD)/non-alcoholic steatohepatitis (NASH), THR-beta signaling within the liver is diminished. The lipotoxicity that occurs in NASH induces intrahepatic hypothyroidism resulting in reduced conversion of prohormone T4 to active hormone T3 (in favor of increased conversion of T4 to the inactive metabolite reverse T3 [RT3]). Exogenous thyroxine treatment does not improve intrahepatic hypothyroidism in patients with NAFLD/NASH. Resmetirom, an oral liver-targeted THR-beta selective agonist in clinical development for treatment of NASH, aims to address this underlying pathophysiology in NAFLD/NASH. Here we report data from the Phase 3 MAESTRO-NAFLD-1 trial on the effect of 52 weeks of resmetirom treatment on thyroid hormone levels.

Method: MAESTRO-NAFLD-1 (NCT04197479) was a Phase 3 trial to evaluate the safety of resmetirom treatment over 52 weeks in adults with NAFLD (presumed NASH) who were diagnosed using non-invasive tests. Patients were randomized 1:1:1 to 3 double-blind arms (resmetirom 100 mg, resmetirom 80 mg, or placebo administered once daily) or an open-label arm (resmetirom 100 mg administered once daily). Thyroid hormone levels (thyroid-stimulating hormone [TSH], free T3 [FT3], free T4 [FT4], and RT3) were evaluated at baseline and Week 52 in the overall trial population, thyroxine-treated population, and euthyroid population.

TABLE. Change from baseline in thyroid hormone levels at Week 52.				
	Resmetirom 100mg OL	Resmetirom 100mg DB	Resmetirom 80mg DB	Placebo DB
Overall population				
TSH, mIU/L				
Baseline mean (SD)	2.3 (1.8)	2.3 (1.9)	2.0 (1.1)	2.2 (1.1)
Week 52 LSM %CFB (SE)	0.2 (0.3)	-0.4 (0.2)	-0.4 (0.2)	-0.3 (0.2)
FT3, ng/L				
Baseline mean (SD)	2.8 (0.5)	2.9 (0.4)	2.9 (0.5)	3.0 (0.4)
Week 52 LSM CFB (SE)	-0.2 (0.0)	-0.1 (0.0)	-0.0 (0.0)	-0.1 (0.0)
FT4, ng/dL				
Baseline mean (SD)	1.2 (0.2)	1.1 (0.2)	1.1 (0.2)	1.1 (0.2)
Week 52 LSM %CFB (SE)	-16.1 (1.8) ^a	-14.9 (1.5) ^a	-9.6 (1.4) ^a	1.2 (1.4)
RT3, ng/dL				
Baseline mean (SD)	18.1 (5.5)	16.3 (4.6)	17.8 (5.1)	16.8 (4.6)
Week 52 LSM CFB (SE)	-3.3 (0.4) ^a	-3.2 (0.3) ^a	-2.7 (0.3) ^a	0.7 (0.3)
Thyroxine-treated population				
TSH, mIU/L				
Baseline mean (SD)	2.4 (2.3)	3.0 (4.4)	1.6 (1.2)	2.2 (1.6)
Week 52 LSM %CFB (SE)	0.4 (1.2)	-0.6 (1.5)	-0.9 (1.5)	-0.6 (1.5)
FT3, ng/L				
Baseline mean (SD)	2.7 (0.6)	2.6 (0.4)	2.9 (0.7)	2.7 (0.4)
Week 52 LSM CFB (SE)	-0.1 (0.1)	-0.0 (0.1)	0.0 (0.1)	-0.0 (0.1)
FT4, ng/dL				
Baseline mean (SD)	1.3 (0.2)	1.1 (0.2)	1.3 (0.3)	1.2 (0.2)
Week 52 LSM %CFB (SE)	-14.8 (3.0) ^a	-19.2 (3.8) ^a	-6.4 (3.9) ^c	3.8 (3.9)
RT3, ng/dL				
Baseline mean (SD)	20.1 (5.3)	18.1 (6.8)	19.6 (5.6)	18.6 (5.5)
Week 52 LSM CFB (SE)	-3.9 (0.8) ^a	-4.9 (1.0) ^a	-3.8 (1.0) ^b	0.6 (1.0)
Euthyroid population				
TSH, mIU/L				
Baseline mean (SD)	2.2 (1.3)	2.2 (1.3)	2.0 (1.1)	2.2 (1.0)
Week 52 LSM %CFB (SE)	-0.2 (0.1)	-0.3 (0.1)	-0.3 (0.1)	-0.3 (0.1)
FT3, ng/L				
Baseline mean (SD)	3.0 (0.4)	3.0 (0.4)	2.9 (0.4)	3.0 (0.4)
Week 52 LSM CFB (SE)	-0.1 (0.1)	-0.1 (0.0)	-0.1 (0.0)	-0.1 (0.0)
FT4, ng/dL				
Baseline mean (SD)	1.1 (0.2)	1.1 (0.2)	1.1 (0.2)	1.1 (0.2)
Week 52 LSM %CFB (SE)	-18.9 (2.2) ^a	-14.3 (1.6) ^a	-9.9 (1.6) ^a	1.1 (1.6)
RT3, ng/dL				
Baseline mean (SD)	16.5 (5.1)	16.1 (4.2)	17.5 (4.9)	16.5 (4.4)
Week 52 LSM CFB (SE)	-3.5 (0.5) ^a	-2.9 (0.3) ^a	-2.5 (0.3) ^a	0.9 (0.3)

^a p < 0.0001 vs placebo; ^b p < 0.001 vs placebo; ^c p < 0.05 vs placebo.

CFB, change from baseline; DB, double-blind; FT3, free T3; FT4, free T4; LSM, least squares mean; OL, open-label; RT3, reverse T3; SD, standard deviation; SE, standard error; TSH, thyroid-stimulating hormone.

Table: (abstract: FRI-476)

Results: At baseline, patients on thyroxine treatment had elevated RT3 levels relative to euthyroid patients (TABLE). At Week 52, no significant change from baseline was noted in TSH or FT3 levels in the overall population of any resmetirom group compared with placebo. In contrast, RT3 and FT4 levels were significantly reduced from baseline at Week 52 in the resmetirom groups when compared with placebo in the overall population ($p < 0.0001$ vs placebo). The FT3/RT3 ratio was also significantly improved in all resmetirom groups at Week 52 compared with placebo ($p < 0.0001$ vs placebo). Similar effects as reported for TSH, FT3, RT3, and FT4 in the overall population were observed with resmetirom treatment in the thyroxine-treated and euthyroid populations.

Conclusion: Resmetirom treatment significantly reduced RT3 and FT4 levels from baseline relative to placebo treatment at Week 52 in the overall population as well as among the thyroxine-treated and euthyroid populations of MAESTRO-NAFLD-1. These results are consistent with increased conversion of T4 to T3 and decreased conversion of T4 to RT3 in the resmetirom groups. Overall, these data indicate resmetirom treatment restores thyroid hormone signaling within the liver in patients with NAFLD/NASH.

FRI-505

CVI-301, a potent and selective thyroid hormone receptor beta full agonist, demonstrates profound total cholesterol and LDL-cholesterol reductions in a hyperlipidemic mouse efficacy model

Jingwen Liu^{1,2}, Zhenyu Wang¹, Gang Liu³. ¹CVI Pharmaceuticals Shanghai Limited, Shanghai, China; ²CVI Pharmaceuticals US, Inc, Mountain View, United States; ³Shanghai Haoyuan Chemexpress Co., Ltd., China

Email: jingwen.liu@cvishanghai.com

Background and aims: Non-alcoholic steatohepatitis (NASH) is a severe form of non-alcoholic fatty liver disease and a leading cause of liver related mortality. While there are no FDA-approved treatments for NASH, selective thyroid hormone receptor beta (THR- β) agonism is emerging as a promising therapy for NASH. Selective THR- β agonist, Resmetirom (MGL-3196), has shown strong efficacy in improving hepatic lipid metabolism without THR- α mediated cardiac side effects in NASH patients. Applying a new screening method that combines computer assisted THR- β docking modeling and LDL receptor promoter reporter assay with rational new chemical synthesis, we have discovered a series of novel compounds including CVI-301 that are able to activate hepatic THR- β in single-digit nmol concentrations. Here we investigated the potency and selectivity of

CVI-301 in biochemical assays and assessed its *in vivo* efficacy in a hyperlipidemic mouse efficacy model.

Method: Potency and selectivity of CVI-301 in activation of THR were determined by cell based nuclear receptor protein-protein interaction assays using full-length human THR- β or THR- α with Triiodothyronine (T3) and MGL-3196 as reference compounds. Mice fed a diet containing high fat and high cholesterol for 4 weeks received vehicle (n = 9), MGL-3196 (5 mg/kg, n = 8) or CVI-301 (1 mg/kg, n = 8) for 14 days by intraperitoneal injection once a day. Serum total cholesterol (TC) and LDL-cholesterol (LDL-C) were measured at baseline and Day 15. Terminal liver and heart samples were collected for gene expression analysis by quantitative RT-PCR.

Results: CVI-301 activates THR- β with 100% T3 maximal activity at 4.5 nM EC₅₀ and 20.1-fold β -selectivity, which is more potent and β -selective than MGL-3196 (THR- β EC₅₀ = 4071 nM; β -selectivity = 3.2). In hyperlipidemic mice after two-week treatment, TC and LDL-C were significantly reduced to 56.9% and 49% of vehicle control (p < 0.0001), respectively by CVI-301 at 1 mg/kg dose, that were comparable to effects of 5 mg/kg MGL-3196 which lowered TC and LDL-C to 57.3% and 46% of vehicle control, respectively. Hepatic mRNA levels of THR- β direct target genes malic enzyme 1 (Me1) and deiodinase 1 (Dio1) were increased to 7.8-fold (p < 0.0001) and 3.3-fold (p < 0.0001) of vehicle control by CVI-301 treatment and to 5.1-fold (p < 0.05) and 2.7-fold (p < 0.0001) of vehicle control by MGL-3196 treatment. Furthermore, mRNA levels of THR- α regulated genes Myh6, Atp2a2 and Me1 in heart tissues remained unchanged in animals treated with CVI-301 or MGL-3196.

Conclusion: CVI-301 is a potent and highly selective THR- β full agonist *in vitro* and *in vivo*. These preclinical data warrant further investigation of CVI-301 as a potential treatment for NASH.

FRI-506

Effects of a novel tetra-specific drug (OGB21502) in the obese mice model of liver disease

Jihye Kim¹, Nakho Chang¹, Yunki Kim¹, Jaehyun Lee¹, Minsun Kim¹, Junyeob Lee¹, Jeonghwa Lee¹, DaeSeong Im¹, Sungjin Park¹. ¹Onogene biotechnology, Korea, Rep. of South
Email: sungjin.park@onogene.com

Background and aims: Non-alcoholic steatohepatitis (NASH) is a complex disease resulting from chronic liver injury associated with obesity and type 2 diabetes. In this study, we hypothesized that simultaneous regulation of multiple mechanisms within the NASH microenvironment could provide a holistic cure for the disease.

OGB21502 is a novel tetra-specific drug developed using the multi-specific UniStac[®] platform, which targets GLP-1 (glucagon-like peptide 1), GCG (glucagon), FGF21 (fibroblast growth factor 21), and IL-1RA (interleukin-1 receptor antagonist) receptors. The aim of this study is to evaluate the metabolic and histopathological effects of OGB21502 in the GAN (Gubra-Amylin NASH) diet-induced obese (DIO) mouse model.

Method: Male C57BL/6 mice were divided into two groups and subjected to a normal diet or a GAN diet, high in saturated fat (40%), fructose (22%), and cholesterol (2%) for 38 weeks. In the remaining 8 weeks, the mice were administered either OGB21502 or reference drugs (Fc-FGF21, obeticholic acid and semaglutide). The mice were sacrificed, followed by determination of blood ALT, cholesterol, and liver weight.

Results: In GAN-DIO mice, OGB21502 treatment resulted in reduction in liver weight, ALT and cholesterol levels compared to reference drugs. Histological analysis further demonstrated a significant improvement in hepatic inflammation and steatosis as indicated by reduced NAFLD activity score (NAS). Notably, OGB21502 led to a remarkable improvement in levels of fasting blood glucose, insulin, and HOMA-IR.

Conclusion: OGB21502 treatment improved glucose level, insulin resistance, liver damage, as well as cholesterol accumulation in the GAN-DIO mice. OGB21502 treatment might also be effective in controlling glucose metabolism by targeting liver, compared to reference therapeutics. The results suggest that OGB21502 may be a promising multi-specific therapeutic option for the treatment of NASH.

FRI-507

Treatment monitoring with the Agile 3+ score in patients with non-alcoholic steatohepatitis: analysis of data from a randomised placebo-controlled trial of semaglutide

Laurent Castéra¹, Céline Fournier-Poizat², Julie Fouquier², Mette Kjaer³, Niels Krarup³, Véronique Miette², Sune Boris Nygård³, Ahsan Shueb Patel³, Laurent Sandrin², Jörn Schattenberg⁴.

¹Department of Hepatology, Beaujon Hospital, Université Paris Cité, Clichy, France; ²Echosens, Paris, France; ³Novo Nordisk, Søborg, Denmark; ⁴Metabolic Liver Research Program, University Medical Center Mainz, Mainz, Germany

Email: laurent.castera@bjn.aphp.fr

Background and aims: There is an unmet need to evaluate non-invasive biomarkers for monitoring and predicting change in fibrosis

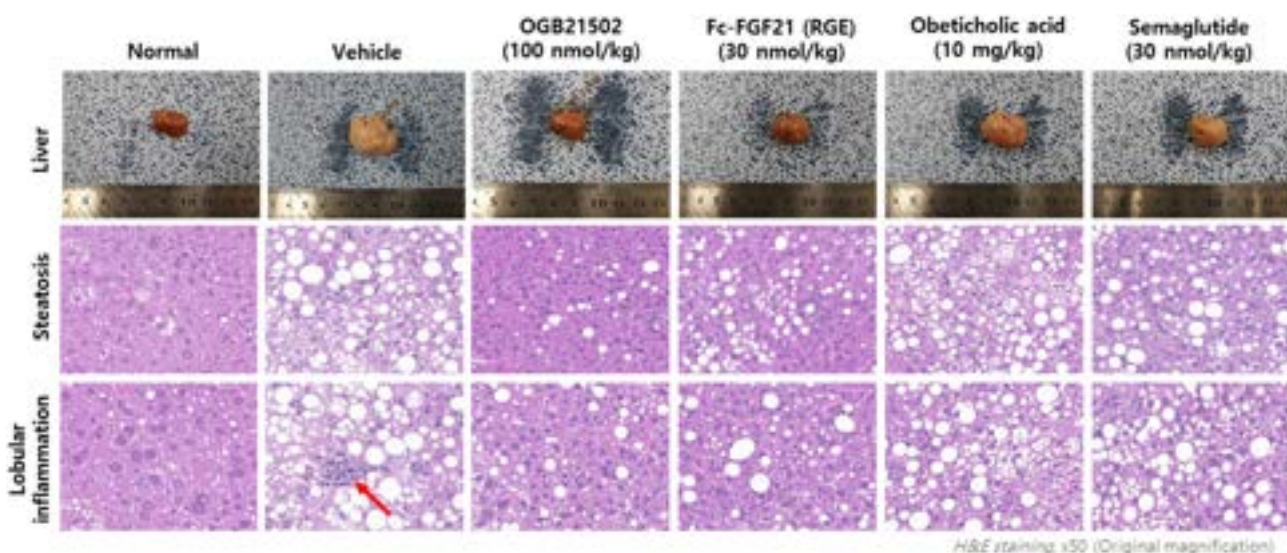


Figure: (abstract: FRI-506).

POSTER PRESENTATIONS

in patients with non-alcoholic steatohepatitis (NASH) who are receiving treatment. Several biomarkers have been validated for grading and staging in NASH, including the Agile 3+ score, which can identify advanced fibrosis in non-alcoholic fatty liver disease. Agile 3+ was applied to patients enrolled in a clinical trial of semaglutide to investigate the score's ability to monitor treatment effect and to predict change in fibrosis stage.

Method: Data were from a phase 2b study in which patients with NASH and fibrosis stage 1–3 were randomised to 72 weeks' treatment with subcutaneous semaglutide 0.1, 0.2 or 0.4 mg, or placebo, once daily (NCT02970942). For this analysis, Agile 3+ scores were calculated at baseline and weeks 28, 52 and 72 using liver stiffness measurements (LSM) from vibration-controlled transient elastography (VCTE) (where available), alanine- and aspartate aminotransferase levels, platelet count, age, sex and diabetes status. A mixed model for repeated measures was used to assess treatment effect on Agile 3+ (missing values were not imputed) during the on-treatment period. Change from baseline in Agile 3+ at weeks 28, 52 and 72 and its association with histological fibrosis improvement at week 72 in the 0.4 mg semaglutide and placebo arms was examined using logistic regression with an interaction effect between relative change in Agile 3+ and treatment. Odds ratios (OR) for improvement in fibrosis of ≥ 1 stage at week 72 associated with a 0.5-fold change in Agile 3+ at each time point were calculated.

Results: The numbers of patients with Agile 3+ data at baseline and weeks 28, 52 and 72 were 208, 210, 209 and 203, respectively. Mean baseline Agile 3+ (standard deviation) was 0.50 (0.28), 0.61 (0.27) and 0.55 (0.30) for semaglutide 0.1, 0.2 and 0.4 mg, respectively, and 0.46 (0.30) for placebo. Agile 3+ was significantly reduced with semaglutide 0.4 mg vs placebo at weeks 28 (estimated treatment ratio 0.64 [95% confidence interval (CI) 0.48; 0.87]; $p = 0.004$), 52 (0.63 [0.48; 0.83]; $p = 0.001$) and 72 (0.59 [0.41; 0.85]; $p = 0.005$) (Figure). In the placebo group, associations between a decrease in Agile 3+ at weeks 28 and 52 and improvement in fibrosis at week 72 were significant (OR [95% CI] 4.10 [1.50; 11.19]; $p = 0.006$ and 3.71 [1.28; 10.75]; $p = 0.016$, respectively). A similar trend was seen in the semaglutide 0.4 mg group, but this did not reach significance. For changes in Agile 3+ at week 72, the trend did not reach significance for either the placebo or semaglutide groups. Although this analysis is limited by the number of study participants, the results indicate that changes in Agile 3+ as early as week 28 may be predictive of histological changes at week 72.

Figure: Geometric mean plot of ratio to baseline in Agile 3+ by treatment arm.

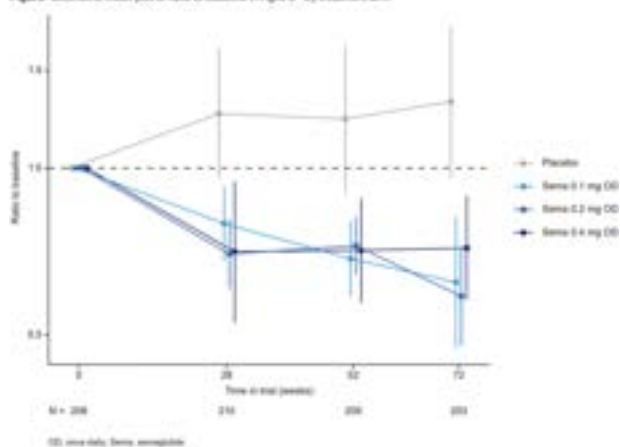


Figure:

Conclusion: Semaglutide demonstrated a significant treatment effect on Agile 3+, with change in Agile 3+ partially predicting histological outcomes, irrespective of treatment allocation. A decrease in Agile 3+ was associated with an improvement in histological fibrosis.

FRI-508

Impact of oral semaglutide on liver pathology and glucose metabolism in patients with non-alcoholic fatty liver disease complicated by type 2 diabetes mellitus

Tadamichi Kawano¹, Masanori Atsukawa¹, Tomomi Okubo¹, Taeang Arai¹, Norio Itokawa¹, Akihito Tsubota², Tsunekazu Oikawa³, Toru Ishikawa⁴, Toshifumi Tada⁵, Hiroshi Abe⁶, Keizo Kato⁶, Joji Tani⁷, Asahiro Morishita⁷, Kentaro Matsuura⁸, Katsuhiko Iwakiri¹. ¹Nippon Medical School, Division of Gastroenterology and Hepatology, Tokyo, Japan; ²The Jikei University School of Medicine, Core Research Facilities for Basic Science, Tokyo, Japan; ³The Jikei University of Medicine, Division of Gastroenterology and Hepatology, Tokyo, Japan; ⁴Saiseikai Niigata Hospital, Department of Hepatology, Niigata, Japan; ⁵Japanese Red Cross Society Himeji Hospital, Department of Gastroenterology, Himeji, Japan; ⁶Shinmatsudo Central General Hospital, Division of Gastroenterology and Hepatology, Chiba, Japan; ⁷Kagawa University, Department of Gastroenterology, Kagawa, Japan; ⁸Nagoya City University Graduate School of Medical Sciences, Department of Gastroenterology and Metabolism, Nagoya, Japan
Email: k-tadamichi@nms.ac.jp

Background and aims: This study aimed to clarify the efficacy and safety of oral semaglutide in patients with non-alcoholic fatty liver disease (NAFLD) complicated by type 2 diabetes mellitus (T2DM).

Method: Eighty-seven patients with NAFLD who received oral semaglutide for T2DM were included in the analysis. Oral semaglutide was initiated at a dose of 3 mg once daily, and the dose was sequentially increased to 7 mg at 4 weeks and 14 mg at 8 weeks, all the while monitoring for any adverse events. Of the 87 patients, 51 could be verified at 24 weeks of treatment.

Results: Significant decreases in body weight, BMI, liver-related biochemistry (AST, ALT, and γ -GTP), plasma glucose, and HbA1c were found at 12 weeks, compared to the baseline values. These significant reductions were maintained at 24 weeks. As for changes in fasting lipids, LDL-cholesterol (112 mg/dL to 102 mg/dL, $p < 0.01$) and triglyceride (156 mg/dL to 119 mg/dL, $p < 0.01$) levels significantly decreased at 24 weeks. The median CAP values significantly decreased from 322 dB/m at baseline to 300 dB/m at week 24 ($p < 0.05$). Changes in body weight were correlated with those in CAP ($r = 0.57$, $p < 0.01$). In terms of changes in liver fibrosis markers, the platelet counts significantly increased from baseline to 24 weeks ($232 \times 10^3/\mu\text{L}$ to $242 \times 10^3/\mu\text{L}$, $p < 0.01$), while the FIB-4 index (1.22 to 1.00, $p < 0.001$) and type IV collagen 7 s (4.1 ng/mL to 3.5 ng/mL, $p < 0.001$) significantly decreased. LSM values showed no significant changes from baseline to 24 weeks of the treatment. The 23 patients who switched from DPP-4 inhibitors also showed favorable effects in weight reduction, glycemic control, and liver transaminases. No grade 3 or higher adverse events were observed during the observation period. Grade 1–2 adverse events were mostly gastrointestinal disorders including nausea. Two patients were discontinued due to semaglutide-related adverse events, both due to nausea.

Conclusion: In patients with NAFLD complicated by T2DM, oral semaglutide may improve hepatic steatosis/inflammation and serum lipid metabolism as well as improve glucose metabolism and decrease body weight.

FRI-509

Lessons for the setting of an international integrated research platform to conduct adaptive trials in non-alcoholic steatohepatitis: results of the EU-PEARL project

Juan M Pericàs^{1,2,3,4}, Elena de Sena¹, Frank Tacke⁵, Quentin Anstee⁶, Nicholas Di Prospero⁷, Mette Kjaer⁸, Peter Mesenbrink⁹, Franz Koenig¹⁰, Joan Genescà^{1,2,4}, Vlad Ratzu¹¹, Sergio Muñoz Martínez¹. ¹VHIR-Vall d'Hebron Institut de Recerca, Liver Unit, Barcelona, Spain; ²Vall d'Hebron University Hospital, Internal Medicine Department, Barcelona, Spain; ³Universitat Autònoma de Barcelona, Bellaterra, Spain; ⁴Centros de Investigación Biomédica en Red en Enfermedades Hepáticas y Digestivas (CIBERehd), Spain; ⁵Charité-Universitätsmedizin Berlin, Department of Hepatology and Gastroenterology, Berlin, Germany; ⁶Translational and Clinical Research Institute, Faculty of Medical Sciences, Newcastle University, Newcastle Upon Tyne, United Kingdom; ⁷Janssen Research and Development, Raritan, New Jersey, United States; ⁸Novo Nordisk A/S, Bagsvaerd, Denmark; ⁹Novartis Pharmaceuticals Corporation, East Hanover, New Jersey, United States; ¹⁰Medical University of Vienna, Vienna, Austria; ¹¹Pitié-Salpêtrière Hospital, Department of Hepatology, Paris, France Email: juanmanuel.pericas@vallhebron.cat

Background and aims: Traditional designs, methodological and operational features of clinical trials in non-alcoholic steatohepatitis (NASH) have several shortcomings and no drugs have been approved for almost two decades. The EU Patient-centric clinical trial pLatforms (EU-PEARL) project (IMI2-853966) aims at developing the necessary tools to deploy integrated research platforms (IRP) to conduct adaptive-design trials in various diseases, including NASH. IRP consist of trial master protocols (MP) and supporting research resources (e.g., clinical and data networks, labs, governance, and legal and regulatory aspects) that represent a unique opportunity to accelerate drug development while lowering overall costs and creating a more patient-centric environment. Here, we describe the lessons from EU-PEARL regarding how the current NASH pipeline, stakeholders, operational and funding barriers and opportunities are at play in the setting of a European-based or global NASH platform trial in the years to come.

Method: Through interactions with regulatory agencies, academics, experts on methodology, patients and their representatives, and pharmaceutical industry and biotech, we have designed a NASH Phase IIb/III MP for non-cirrhotic patients. Amongst other elements, simulations were conducted to assess whether a Bayesian approach is suitable and cost-efficient for a NASH IRP rather than a more traditional frequentist approach. We held meetings with the US Food and Drug administration (FDA) and European Medicines Agency (EMA), and two external advisory boards with key opinion leaders (KOLs) in the field of NASH from both academia and industry. The specific features of participating sites and clinical research organizations and labs was discussed and agreed upon. Moreover, a reach-out survey was conducted to ask NASH investigators about their knowledge on MP and their interest in joining a future NASH IRP.

Results: Building and operationalizing an IRP comes with different challenges and possibilities (Pericàs et al, J Hepatol 2022). Consulted KOLs in the NASH field as well as patients and regulators agree that MP are a promising tool to enhance drug development in a more patient-centric manner. Simulations suggested that for a Bayesian approach to prove superior to a frequentist approach the scope of the IRP would need a global clinical network and moderate-high recruiting rates (Laurin-Meyer et al, PLoS One 2023). However, due to the current situation of the NASH pipeline, it is unlikely that the first platform trial in NASH is funded by the industry in the short term, whereas an international IRP has largely demanding requirements in terms of operationalization and costs. The most likely sponsor institution for the NASH IRP is a large academic hospital, with potential support from non-profit organizations. Compared to other therapeutic areas, the involvement of the patient community in the design of clinical trials in NASH is low in Europe.

Conclusion: "Proof-of-platform" for NASH should be provided before escalating the scope of the IRP and therefore the most likely scenario is the set-up of a few countries platform first, mostly based on non-invasive end points, and public or mixed funding in order to validate the operational, statistical and regulatory tools developed within EU-PEARL before fully deploying a global NASH IRP.

FRI-510

The influence of probiotics on biologic and imagistic alterations in non-alcoholic steato-hepatitis

Elena Laura Iliescu^{1,2}, Adriana Mercan-Stanciu¹, Letitia Toma^{1,2}, Mircea Istrate^{1,2}, Razvan Rababoc^{1,2}, Radu Dumitru², Cristian Mugur Grasu². ¹Fundeni Clinical Institute, Internal Medicine, Bucharest, Romania; ²"Carol Davila" University of Medicine and Pharmacy, Bucharest, Romania Email: laura_ate@yahoo.com

Background and aims: Non-alcoholic fatty liver disease (NAFLD) is one of the most common causes of chronic liver disease, with rising prevalence. By perpetuating a systemic inflammation, NAFLD is an independent cardiovascular risk factor. Furthermore, modulation of gut microbiota appears to have systemic anti-inflammatory effects than can prove beneficial in NAFLD. This study aims to determine the impact of a combination of probiotics (Bifidobacterium longum BB536®) fructooligosaccharides (Actilight) and B complex vitamins on steato-hepatitis (SH), gut inflammation and liver steatosis.

Method: We performed a prospective trial which included 148 consecutive patients with newly diagnosed SH, evaluated in our clinic between January 2021- September 2022. Patients with other causes of liver disease, uncontrolled diabetes or active infection were excluded. All patients received study medication as per the producer's recommendations (1 dose daily) for three months and were advised accordingly for life-style changes. Patients were monitored before and after therapy by serum alanine aminotransferase (ALT), aspartate aminotransferase (AST), gamma- glutamyl transpeptidase (GGT), fecal calprotectin, Fibroscan (for fibrosis) and controlled attenuation parameter (CAP) (for steatosis). In diabetic patients we also evaluated basal glycemia and glycosylated hemoglobin levels (HbA1c).

Results: The study included 95 non-diabetic and 53 diabetic patients. The mean age in the study group was 45.36 ± 14.28 years, with 58.1% female. Before treatment patients presented high levels of ALT and AST, with normal or mildly increased GGT. 28 patients (18.9%) had normal values of serum calprotectin. After therapy, we noticed a significant decrease in AST, ALT, fecal calprotectin levels, mean liver stiffness and CAP values (Table 1). In diabetic patients, we noted a decrease in glycemia (92.5 mg/dL versus 113 mg/dL, p=0.03) and in HbA1c (5.7% versus 6.2%, p=0.09). Regression of liver fibrosis was observed by the changes in distribution: F1: 28 versus 45 patients, F2: 71 versus 95 patients, F3: 49 versus 8 patients. For steatosis the distribution changes were: S1: 31 versus 67 patients, S2: 86 versus 81 patients. S3: 31 patients versus none.

Figure: Table Evolution of biologic and imagistic parameters

	Before therapy	After therapy	p value
ALT (U/L)	75.24 ± 24.13	36.29 ± 10.24	<0.01
AST (U/L)	62.57 ± 31.72	29.13 ± 15.81	<0.01
GGT (U/L)	46.23 ± 19.18	38.12 ± 11.08	=0.8
Fecal calprotectin (µg/mg)	129.35 ± 83.61	58.91 ± 24.17	=0.02
Liver stiffness (KPa)	7.33 ± 3.46	6.18 ± 1.15	=0.03
CAP (dB/m)	290.64 ± 40.82	244.93 ± 18.85	=0.02

Conclusion: Probiotic formulas may contribute to a decrease in liver inflammation, steatosis and fibrosis associated with NAFLD, by their modulating the inflammatory response triggered by gut dysbiosis. Considering the low risks associated with these therapies, we consider them useful future tools in the treatment of NAFLD.

FRI-511

Efficacy of pemafibrate in patients with non-alcoholic fatty liver disease complicated by dyslipidemia: a single-arm prospective study

Hiroki Ono¹, Masanori Atsukawa¹, Kaori Koyano¹, Yuta Hasegawa¹, Tadamiichi Kawano¹, Tomohide Tanabe², Yuji Yoshida³, Tomomi Okubo³, Taeang Arai¹, Korenobi Hayama³, Norio Itokawa¹, Katsuhiko Iwakiri¹. ¹Nippon Medical School Hospital, Gastroenterology and Hepatology, Bunkyo-ku, Tokyo, Japan; ²Nippon Medical School Musashi Kosugi Hospital, Gastroenterology, Kawasaki, Japan; ³Nippon Medical School Chiba Hokusoh Hospital, Gastroenterology, Inzai, Japan
Email: h-ono00@nms.ac.jp

Background and aims: Patients with non-alcoholic fatty liver disease (NAFLD) are often complicated by dyslipidemia. In some patients, dyslipidemia is known to lead to the development of liver fibrosis. Pemafibrate, a novel selective peroxisome proliferator-activated receptor modulator (SPPARM α) is an agent approved in Japan for the treatment of hypertriglyceridemia. Previous clinical studies have shown that pemafibrate not only reduced TG level but also improved serum liver enzymes among patients with dyslipidemia. The aim of this study is to evaluate the long-term effect of pemafibrate in patients with NAFLD complicated by dyslipidemia in real world setting.

Method: Ninety-one NAFLD patients with dyslipidemia were treated with pemafibrate; lipid metabolism and liver-related factors were analyzed during 48 weeks.

Results: Significant decreases in triglyceride (198 mg/dL to 121 mg/dL, $p < 0.001$), total cholesterol (223 mg/dL to 205 mg/dL, $p < 0.001$), and a significant increase in HDL cholesterol (47 mg/dL to 50 mg/dL, $p < 0.001$) were found at 12 weeks, compared with the baseline values without body weight loss. These significant changes were maintained throughout 48 weeks, and LDL cholesterol (137 mg/dL to 131 mg/dL, $p < 0.05$) was significantly decreased at 48 weeks, compared with the baseline. Liver-related factors such as AST (36 U/L to 33 U/L at week 48, $p < 0.01$), ALT (52 U/L to 34 U/L, $p < 0.001$), γ -GTP (56 U/L to 32 U/L, $p < 0.001$), and ALP (118 U/L to 59 U/L, $p < 0.001$) also showed significant reductions from baseline throughout the 48 weeks. A significant reduction of HOMA-IR was observed (4.34 at baseline to 3.89 at week 48, $p < 0.05$) in the insulin-resistant group (HOMA-IR ≥ 2.5). As for changes in liver fat and fibrosis, CAP values did not change significantly throughout 48 weeks ($p = 0.42$), and the median levels of the WFA+M2BP, type IV collagen 7 s, and NFS significantly decreased from 0.94 C.O.I., 4.3 ng/ml, and -1.183 at baseline to 0.65 C.O.I., 3.8 ng/ml, and -1.655 at week 48, respectively. Focusing on changes in platelets and albumin, both significantly increase from baseline to week 48, and notably platelets and albumin showed marked increase in patients with low platelets ($< 192 \times 10^3/\mu\text{L}$ at baseline) ($165 \times 10^3/\mu\text{L}$ to $193 \times 10^3/\mu\text{L}$; $p < 0.001$) and low albumin levels (≤ 4.0 g/dL at baseline) (3.9 g/dL to 4.2 g/dL; $p < 0.01$). In all 38 patients for whom LSM could be measured, LSM did not show significant decreases. LSM significantly decreased in high-risk groups for liver fibrosis including 20 patients with ≥ 6.5 kPa at baseline (9.4 kPa at baseline to 8.8 kPa at week 48; $p < 0.05$).

Conclusion: Pemafibrate therapy for 48 weeks may improve not only lipid metabolism but also hepatic inflammation and fibrosis without body weight loss. Improvement of insulin resistance by pemafibrate may contribute to improvement of liver-related factors.

FRI-512

Characterization of the patterns of resolution of histopathology after efruxifermin treatment of patients with NASH fibrosis (F2/3) for 24 weeks

Cynthia Behling¹, Pierre Bedossa², Lan Shao³, Erica Fong⁴, Brittany de Temple⁴, Doreen Chan⁴, Reshma Shringarpure⁴, Erik Tillman⁴, Tim Rolph⁴, Andrew Cheng⁴, Kitty Yale⁴, Stephen Harrison⁵. ¹University of California, San Diego, United States;

²LiverPat, France; ³Labcorp, United States; ⁴Akero Therapeutics, United States; ⁵Pinnacle Clinical Research, United States
Email: reshma@akerotx.com

Background and aims: Liver biopsy remains the regulatory standard for diagnosis and monitoring of NASH. Treatment with EFX for 16 weeks (Phase 2a, BALANCED)^{1,2} or 24 weeks (Phase 2b, HARMONY)³ was associated with rapid improvements in liver histology including regression of fibrosis and resolution of NASH. The rapid improvements in the Ph 2a study prompted a post-hoc qualitative evaluation of histopathology which revealed evidence of regression of fibrotic structures and extent of collagen deposition across not only subjects who had a categorical improvement of ≥ 1 stage but also those who had not.⁴ The aim of this analysis was to further characterize these changes in biopsies from the Ph 2b study by qualitative and alternative quantitative analyses.

Method: HARMONY is an ongoing, randomized, placebo-controlled trial evaluating EFX 28 and 50 mg once weekly for 96 weeks, with a completed primary end point evaluation at 24 weeks.³ Evaluation of histologic end points in the primary efficacy analysis was based on the NASH CRN scoring system, with all biopsies reviewed by consensus between two pathologists blinded to treatment and sampling sequence, without being paired. Additional post hoc evaluations are ongoing to assess effects of EFX on histopathology based on the steatosis-activity-fibrosis (SAF) score and other metrics.

Results: Of 128 patients randomized in HARMONY, 113 had baseline and Week 24 biopsies. Histologic end points, based on NASH CRN to quantitate primary efficacy, and a post hoc analyses based on the SAF score are provided in the Table below. Additional exploratory histological analyses are ongoing.

Conclusion: EFX treatment for only 24 weeks improved liver histopathology, with reversal of fibrosis and reductions in steatosis, ballooning, and inflammation as assessed by multiple measures in addition to the regulatory end point definitions. EFX 50 mg demonstrated striking rates of ballooning resolution, associated with improved NAS, SAF-Activity and total SAF scores. Resolution of histopathology was mirrored by normalization of non-invasive biomarkers of NASH disease activity (ALT, AST) and fibrogenesis (Pro-C3) in the majority ($> 60\%$) of treated patients.³ Evaluation of qualitative patterns of regression of NASH and fibrosis with EFX may be useful in understanding the breadth of response across the NASH population and assessing the potential for further improvements with longer-term treatment.

References

1. Harrison S. 2021 *Nature Medicine*. 27; p. 1262.
2. Harrison S. 2023. *JHEP Reports* 5; p. 1.
3. Harrison S. The Liver Meeting (AASLD 2022).
4. Behling C. The Liver Meeting (AASLD 2021).

FRI-513

Fat versus lean tissue loss in short term versus long term weight loss: a dynamic effect with implications for NASH trials

Lars Johansson^{1,1}, Magnus Sundbom², Edvin Johansson¹, Joel Kullberg¹. ¹Antaros Medical, Molndal, Sweden; ²Uppsala University Hospital, Department of Surgery, Uppsala, Sweden
Email: lars.johansson@antarosmedical.com

Background and aims: Weight loss via diet interventions, bariatric surgery and pharmacological interventions have been shown to improve non-alcoholic fatty liver disease (NAFLD) and non-alcoholic steatohepatitis (NASH). It has been reported in several clinical trials that substantial loss of lean tissue may occur secondary to weight loss. Early phase clinical trials of novel treatments based on weight loss for NASH are usually short term 8–16 weeks with a single point readout of adipose tissue and lean tissue volumes based on DEXA or MRI. Little is however known about the short-term effects of weight loss versus long term effects on the change in fat mass versus lean tissue mass. The purpose of this study was therefore to investigate the

Table 1. Proportion of Patients Achieving the Specified Histologic Endpoints

Endpoint	Placebo N = 41	EFX 28 mg N = 38	EFX 50 mg N = 34
Primary and Secondary Endpoints (NASH CRN)			
Fibrosis improvement without worsening of NASH ^a	8 (19.5%)	15 (39.5%)*	14 (41.2%)*
NASH resolution without worsening of fibrosis ^b	6 (14.6%)	18 (47.4%)**	26 (76.5%***)
NASH Resolution without worsening of fibrosis plus a ≥ 2 -point reduction in overall NAS score ^{c, nt}	3 (7.3%)	18 (47.3%)	25 (73.5%)
Fibrosis improvement and resolution of NASH	2 (4.9%)	11 (28.9%)**	14 (41.2%***)
Improvement in NAS by ≥ 2 without worsening of fibrosis ^{nt}	8 (19.5%)	27 (71.1%)	28 (82.4%)
Resolution of ballooning ^{d, nt}	10 (24.4%)	20 (52.6%)	29 (85.3%)
Post-hoc analyses (Steatosis-Activity-Fibrosis or SAF score)^e			
Improvement in SAF-A by ≥ 2 ^{f, nt}	4 (9.8%)	17 (44.7%)	24 (70.6%)
Improvement in total SAF by ≥ 2 ^{nt}	9 (22%)	30 (78.9%)	30 (88.2%)

*p<0.05 ; **p<0.01; ***p<0.001 versus placebo [Cochran-Mantel-Haenszel (CMH) test]; nt = post-hoc analysis not tested for significance.

^a Consistent with FDA published guidance, no worsening of NASH is defined as no increase in any one or more of steatosis, inflammation or ballooning score; ^b Consistent with FDA published guidance, NASH resolution is defined as a ballooning score of 0 and a lobular inflammation score of 0 or 1, with any score (0 to 3) for steatosis; ^c In contrast to FDA published guidance that permits any steatosis score (0 to 3) for a patient to achieve NASH resolution, this endpoint requires that a patient must achieve a ≥ 2 -point reduction in overall NAS score, in addition to a ballooning score of 0 and lobular inflammation score of 0 or 1, to be deemed a NASH resolution responder; ^d Defined as ballooning score ≥ 1 at baseline and 0 at Week 24; ^e SAF scores were derived from NASH CRN scores in consultation with pathologists ^f SAF-A: Activity component of the SAF score defined as the sum of ballooning and lobular inflammation scores.

Table: (abstract: FRI-512)

dynamic effects on adipose and lean tissue loss during substantial weight loss.

Method: 7 obese subjects with a BMI of 43.7 kg/m² (range 38–48) undergoing Roux-and-Y bariatric surgery were investigated with whole body MRI assessing adipose tissue depots at baseline and 1-, 6- and 12-months post-surgery. Total Adipose Tissue (TAT) mass was investigated. The relative contribution of different tissue compartments to the total weight loss calculated at each timepoint with the assumption that 1 L of adipose tissue have a weight of 0.9 kg.

Results: The total weight and TAT weight, and the relative contributions to the total weight loss are shown in the figure.

Conclusion: The relative contribution of weight loss from adipose versus lean tissue changed over time, with more lean tissue being lost early on in weight loss and more adipose tissue being lost during prolonged weight loss. Non-adipose tissue loss constitutes 37% of the total body weight loss at 1 month while only 20.5% after 12 months. This could possibly be attributed to more excessive amount of water being lost in early weight loss while the negative energy balance over time will turn into loss of excessive adipose tissue. This finding has

implications for investigations of body composition changes in short term NASH trials where weight loss is induced. Hence, one should be cautious when drawing conclusions on induction of sarcopenia from short-term weight loss data.

FRI-514

Efficacy of digital health-supported lifestyle modification on patients with non-alcoholic fatty liver disease: a systematic review and meta-analysis

Joo Hyun Oh¹, Yewan Park², Myungji Goh³, Sang Bong Ahn¹, Wonseok Kang³, Dong Hyun Sinn³, Geum-Yon Gwak³, Yong-Han Paik³, Joon Hyeok Lee³, Moon Seok Choi³, Seung Woon Paik³. ¹Eulji Medical Center, Korea, Rep. of South; ²Kyung Hee University Hospital, Korea, Rep. of South; ³Samsung Medical Center, Korea, Rep. of South
Email: drms.choi@samsung.com

Background and aims: The current recommendation for patients with non-alcoholic fatty liver disease (NAFLD) is to achieve and

Months	Baseline	1	6	12
Weight (kg) (SD)	122 (±13)	110 (±12)	93 (±11)	80 (±11)
TAT (l) (SD)	66.9 (±9.0)	58.5 (±9.0)	41.9 (±9.0)	29.8 (±9.0)
TAT(kg)	60.2	52.7	37.7	26.8
Total Fat loss as % of total weight loss (mean)		63	77.6	79.6
Total non-fat loss as % of total weight (mean)		37	22.4	20.5
%Fat mass of total body mass (mean)	43.4	47.9	40.5	33.5

Figure: (abstract: FRI-513).

POSTER PRESENTATIONS

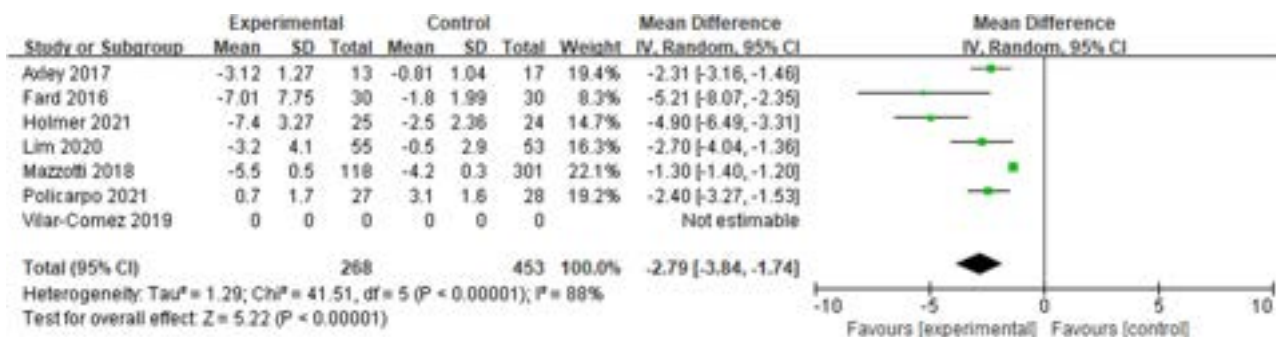


Figure: (abstract: FRI-514).

maintain weight reduction via counseling and calorie restriction. However, adherence to lifestyle modification is insufficient due to financial and time constraints. We investigated whether digital health-supported lifestyle change help patients with NAFLD lose weight and reduce hepatic inflammation.

Method: Relevant studies were selected from MEDLINE, EMBASE, and Cochrane Central Register of Controlled Trials until September 28th, 2022. The search terms included NAFLD, digital health, and telemedicine. The primary outcome is change in body weight and secondary outcome is change in alanine aminotransferase (ALT) and aspartate aminotransferase (AST). Random effect method was performed for pooling the data.

Results: Seven studies (six randomized controlled trials and one prospective study) comprising 1,245 patients with NAFLD were analyzed. The mean reduction in body weight was greater for patients whose lifestyle modification were supported by digital health (weighted mean difference (WMD): -2.79 kg, 95% confidence interval (CI) -3.84 , -1.74). Digital health-supported lifestyle modification was associated with greater reductions in ALT and AST compare to conventional treatment (WMD: -12.85 , 95% CI -22.82 , -2.88 and WMD: -8.57 , 95% CI -12.23 , -4.92 , respectively). Lifestyle change assisted by digital health substantially reduced triglycerides levels (WMD: -12.30 , 95% CI -19.96 , -4.64) but had no significant effect on insulin resistance assessed by homeostatic model assessment for insulin resistance (WMD: -3.88 , 95% CI -9.55 , 1.79).

Conclusion: Digital health-supported lifestyle modification is effective in body weight, ALT, AST, and triglycerides reduction, indicating that NAFLD patients may benefit from digital health technology.

FRI-515

A novel prescription digital therapeutic for the treatment of non-alcohol related fatty liver disease: feasibility study

Naim Alkhouri¹, Katherine Edwards², Mark Berman², Erin Rudolf², Heather Finn², Heidi Dusky², Nicole Guthrie², Rafael Escandon³, Angie Coste¹, Jesus Topete¹, Mazen Nouredin⁴. ¹Arizona Liver Health, Fatty Liver Program, Chandler, United States; ²Better Therapeutics, San Francisco, United States; ³DGBI Consulting, LLC, Bainbridge Island, United States; ⁴Houston Liver Institute, Houston Research Institute, Houston Methodist Hospital, Houston, United States
 Email: kate@betttertx.com

Background and aims: Non-alcoholic fatty liver disease (NAFLD) is a global public health crisis growing in parallel with the obesity and diabetes pandemics. Behavioral modification including weight loss, improving dietary quality, and increasing physical activity have been proven to have favorable effects on slowing or reversing the progression of liver steatosis and fibrosis; however, behavior change is difficult to facilitate in clinical practice and health systems are poorly equipped to scale behavioral interventions needed to address the enormous population with NAFLD. The aim of this feasibility study was to explore the safety, efficacy, and usability of a novel prescription digital therapeutic (PDT) platform, in individuals with NAFLD or non-alcoholic steatohepatitis (NASH).

Method: This single arm study was conducted at two affiliated specialty hepatology clinics. The PDT was created by Better Therapeutics using a novel form of cognitive behavioral therapy (CBT) intended to treat cardiometabolic disease. Participants accessed the PDT on their smartphone for up to 90 days. The intervention was delivered without requiring additional participation from clinic providers. Laboratory assessments, FibroScan and magnetic resonance imaging proton density fat fraction (MRI-PDFF) imaging were conducted at baseline and post-intervention. Percent change in steatosis was measured by MRI-PDFF in participants with elevated baseline liver fat (PDF $\geq 10\%$).

Results: The study enrolled 22 participants. At baseline, the mean age was 48 years, 77% were female, 50% Hispanic, and 46% had type 2 diabetes. The mean baseline fat fraction on MRI-PDFF was 19%. After 90 days of exposure to the PDT, the mean relative reduction in MRI-PDFF was -16% ($p = 0.011$) in the primary ITT population. ALT was reduced by an average of -17 IU/L ($p = 0.002$) (Fig). FibroScan Controlled Attenuation Parameter (CAP) Score was reduced (-19 dB/m, $p = 0.021$) and was accompanied by an average relative reduction of -20% in the FAST score ($p = 0.011$). Participants achieved an average weight loss of -3% ($p = 0.008$) of total body weight, following a pattern of gradual and consistent weight loss without any signs of a plateau or peak. No serious adverse events nor any device related adverse events were reported. Participants reported an improvement in their health-related quality of life (assessed via CDC HRQOL-4) with an average improvement of 2.2 Healthy Days per month added ($p = 0.500$) and a high degree of satisfaction with the treatment (mean Net Promoter Score of +75).

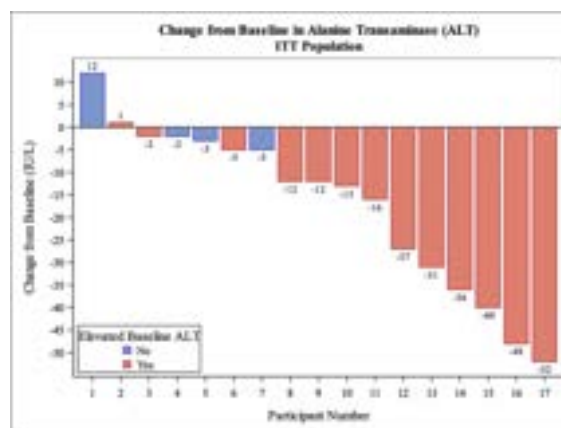


Figure:

Conclusion: Clinically meaningful improvements in liver health were observed in multiple end points after 90 days of digitally-delivered CBT without any adverse device effects. Weight data suggests that further liver health improvements may be possible with further PDT use beyond 90 days. The totality of safety, efficacy and usability data

collected strengthen the hypothesis that a PDT could be an important and scalable clinical tool for the treatment of NAFLD and NASH.

FRI-516

Incidence and median times to onset and resolution of pruritus adverse events in a phase 3 study of obeticholic acid in patients with non-alcoholic steatohepatitis

Zobair Younossi¹, Leighland Feinman², Amarita Randhawa², Rina Leyva², Maria Stepanova³, Sangeeta Sawhney². ¹Beatty Liver and Obesity Research Program, Center for Liver Diseases, Inova Medicine, Falls Church, United States; ²Intercept Pharmaceuticals Inc, Morristown, United States; ³Center for Outcomes Research in Liver Diseases, Washington DC, United States
Email: sangeeta.sawhney@interceptpharma.com

Background and aims: Non-alcoholic steatohepatitis (NASH) is associated with pruritus in real-world practice. In the REGENERATE study (NCT02548351) of obeticholic acid (OCA) for pre-cirrhotic liver fibrosis due to NASH, pruritus was the most common treatment-emergent adverse event, and its frequency was dose dependent. We report the incidence, times to onset and resolution, and management of pruritus adverse events (AEs) in an expanded safety population.

Method: Pruritus symptoms were monitored every 3 to 6 months. Pruritus was managed with drug holiday, reduced dosing frequency, discontinuation, or use of antipruritic therapies. The incidence of pruritus AEs was determined using Medical Dictionary for Regulatory Activities queries in the safety population of the REGENERATE study, which included all randomized pts who received at least 1 dose of placebo, OCA 10 mg, or OCA 25 mg.

Results: In this population (N=2477), 976 pts were exposed >4 years (median 39 months) to study drug. Pruritus was the most common AE and the most common reason for study drug discontinuation; about half of discontinuations due to pruritus were mandated. Pruritus AEs were dose dependent and predominantly mild/moderate (Table). Most pruritus AEs did not require any intervention regardless of treatment arm. Drug holiday was the most frequent management, with most pts having a single interruption. Antihistamines were the most common concomitant therapy for grade 1 or 2 pruritus, followed by bile acid sequestrants and corticosteroids. In the placebo, OCA 10 mg, and OCA 25 mg arms, median time to onset of the first pruritus event was 191, 100, and 44 days, respectively. The impact of treatment-emergent pruritus on patient-reported outcomes is being analyzed.

Table: Pruritus AEs in patients with pre-cirrhotic liver fibrosis due to non-alcoholic steatohepatitis in the REGENERATE study

	Placebo (n = 825)	OCA 10 mg (n = 825)	OCA 25 mg (n = 827)
Patients with treatment-emergent pruritus, n (%)	221 (26.8)	289 (35.0)	476 (57.6)
Severity, n (%)			
Mild	161 (19.5)	180 (21.8)	181 (21.9)
Moderate	57 (6.9)	99 (12.0)	238 (28.8)
Severe	3 (0.4)	10 (1.2)	57 (6.9)
Not related to study drug, n (%)	56 (6.8)	58 (7.0)	39 (4.7)
Study drug management for pruritus (all grades) per protocol, n (%)			
No dose change	204 (24.7)	257 (31.2)	366 (44.3)
Interruption	17 (2.1)	34 (4.1)	133 (16.1)
Withdrawal	8 (1.0)	14 (1.7)	100 (12.1)
Time to event for first pruritus AE, median (Q1, Q3), days			
Time to onset	191 (69, 478)	100 (23, 372)	44 (15, 158.5)
Time to resolution	53 (17, 174)	60 (23, 154)	50 (19, 148)

Abbreviations: AE, adverse event; Q1, quartile 1; Q3, quartile 3.

Conclusion: The first pruritus AE associated with OCA generally occurred within the first 3 months of therapy, was mild/moderate, and was manageable with a single drug holiday or addition of antipruritic therapy.

FRI-517

Correlation between severity of hepatic steatosis and markers of cardiometabolic health, and effect of lanifibranor therapy in patients with non-cirrhotic NASH

Michael Cooreman¹, Sven Francque², Philippe Huot-Marchand¹, Lucile Dzen¹, Martine Baudin¹, Jean-Louis Junien¹, Pierre Broqua¹, Manal Abdelmalek³. ¹Inventiva Pharma, Research and Development, Daix, France; ²University Hospital Antwerp, Belgium; ³Mayo Clinic, United States
Email: michaelcooreman@msn.com

Background and aims: Lanifibranor has shown efficacy on 'histological NASH resolution and improvement of fibrosis' and on markers of cardiometabolic health (CMH) in the NATIVE phase 2b study. Hepatic steatosis is a known cardiovascular risk factor and the NAFLD-associated atherogenic lipid profile is considered a pathophysiological link. We therefore evaluated the correlation between steatosis and CMH markers at baseline (BL) and between steatosis reduction with lanifibranor and improvement of CMH markers.

Method: NATIVE evaluated lanifibranor 800 and 1200 mg/d versus placebo in 247 patients with non-cirrhotic NASH for a treatment duration of 24 weeks. Markers of CMH [adiponectin (ADP), insulin resistance (HOMA-IR), HbA1c, fasting triglycerides, HDL-c, apolipoproteins, blood pressure (BP)], liver tests and steatosis by histological NASH-CRN/SAF grading and Continuous Attenuation Parameter™ (CAP™ on Fibroscan®) were evaluated at BL and at end of treatment (EOT). Correlations between BL steatosis (histological and CAP™) and CMH markers were assessed for all randomized patients; correlations between changes at EOT were assessed in the pooled lanifibranor arms. BL CAP™ was considered quantitatively and categorized (≤ 302 and >302 dB.m⁻¹); changes in CAP™ at EOT were expressed as continuous variables or categorical (relative change $<-10\%$, $10-20\%$, $>+10\%$).

Results: BL CAP™ values correlates with BL HOMA-IR (Spearman $p = 0.008$), HbA1c, triglycerides, and inversely with HDL-c and Apo-A1; mean triglycerides were 1.72 and 2.04 mmol/L, and mean HDL-c values were 1.30 and 1.18 mmol/L for CAP™ ≤ 302 and >302 dB.m⁻¹, resp ($p = 0.012$ and 0.007 , resp). BL CAP™ values also correlated with diastolic BP and ALT and AST. At EOT, improvement of HOMA-IR was seen independent of the degree of steatosis reduction; HbA1c lowering was correlated with improvement of the histological grade ($p < 0.001$) and with change in CAP™ (Spearman $p = 0.05$); triglyceride decreases correlated with changes in CAP™: -30 , -13 and -2% from BL for $<-10\%$, $10-20\%$, and $>+10\%$ relative CAP™ change, resp.; HDL-c increase correlated with histological steatosis improvement ($p = 0.006$). BL ADP did not differ with severity of steatosis (grading and CAP™), but steatosis improvement was correlated with pronounced increases in ADP at EOT: fold-increase ADP from BL was 3.1, 3.9, 5.3 and 6.0 for no change, 1, 2 and 3 points reduction of steatosis grade, resp ($p < 0.001$), and correlated similarly with continuous CAP™ value changes (Spearman $p = 0.002$).

Conclusion: Markers of cardiometabolic health are related with the severity of hepatic steatosis in patients with NASH. Improvement of steatosis with Lanifibranor therapy is significantly correlated with a robust ADP response and with an improvement of lipid and glycemic profile, supporting the concept that steatosis improvement with lanifibranor could translate in improved long-term cardiovascular outcomes.

FRI-518

Hepatic fat and liver volume reductions-impact on non-alcoholic steatohepatitis trials and potential solutions using concomitant fibrosis with ballooning with fibrosis

Jörn Schattenberg¹, Yayun Ren², Dean Tai², Elaine Chng², Stephen Harrison³. ¹Metabolic Liver Research Center, Department of Medicine, Mainz, Germany; ²HistoIndex Pte Ltd, Singapore; ³Pinnacle Research, San Antonio, United States
Email: elaine.chng@histoindex.com

Background and aims: Experimental treatment of non-alcoholic steatohepatitis (NASH) leads to reduction of hepatic fat and liver volume (LV) as assessed by Magnetic Resonance Imaging-Proton Density Fat Fraction (MRI-PDFF). The impact of hepatic fat and LV reduction on histological fibrosis interpretation using the CRN system remains unexplored. We propose analyzing the concomitant changes of qFibrosis (qF) with qSteatosis (qS) and qBallooning (qB) in zonal regions to evaluate the impact of hepatic fat and LV reduction on fibrosis changes.

Method: NASH patients were included from two phase 2b studies: 24-week study of Aldafermin (NCT02443116) and 36-week study of Resmetirom (NCT02912260). Steatosis correction (SC) was done by subtracting the steatosis area as detected by qS from total tissue area followed by an analysis of zonal fibrosis in the respective zones 1, 2, and 3. Concomitant fibrosis with drug-induced steatosis and ballooning changes were evaluated by co-localization of qF changes around qS and qB, respectively.

Results: qF continuous measures on the phase 2 Aldafermin study revealed 54% fibrosis regression in the treated group versus 19% in placebo group ($p=0.007$). With SC, zonal qF assessment showed trends of dose-dependent fibrosis reduction in portal, periportal ($p=0.02$) and zone 2 regions. In the Resmetirom study where the treated group had markedly reduced LV, LV correction was applied and there was a greater reduction in concomitant fibrosis, as well as significant zonal steatosis reduction across all zones (Figure 1A, 1B). In contrast, the impact of LV is negligible on concomitant qB/qF. Further qB analysis revealed an association between 1-stage fibrosis improvement with a decrease in qB area from baseline to end-of-treatment (Figure 1C). Using cut-off of -30.46% , the performance for predicting 1-point reduction was 50% sensitivity, 58% specificity with 39% negative predictive value and 68% positive predictive value.

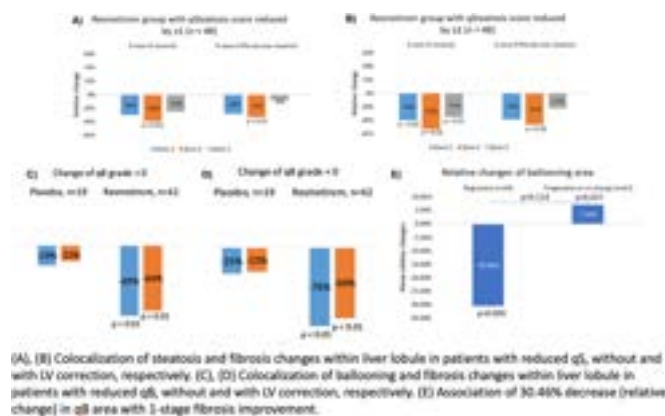


Figure:

Conclusion: Results from this proof-of-concept analysis highlights the impact of hepatic fat reduction on fibrosis regression in NASH. The impact of SC and LV correction is great on the concomitant fibrosis around steatosis, but minimal on the concomitant fibrosis around ballooning. Therefore, concomitant analyses with digital pathology can augment the interpretation of the mechanism of action of drugs in NASH as well as allow for a better understanding of the impact these drugs have on histopathology and should be considered in future trials. Validation with clinical outcomes is ongoing.

FRI-519

Effectiveness of prebiotic treatment in patients with non-alcoholic fatty liver disease (NAFLD)-a randomized trial

Yaakov Maor^{1,2}, Naama Reshef^{3,4}, Uri Gophna⁵, Fred Konikoff^{6,7}, Hilla Knobler^{2,3}. ¹Kaplan Medical Center, Institute of Gastroenterology and Hepatology, Rehovot, Israel; ²The Hebrew University, Hadassah School of Medicine, Jerusalem, Israel; ³Kaplan Medical Center, Institute of Diabetes and Metabolism, Rehovot, Israel; ⁴The Hebrew University, Faculty of Agriculture, Food and Environment, School of Nutritional Sciences, Rehovot, Israel; ⁵Tel-Aviv University, Faculty of Life Sciences, Department of Molecular Microbiology and Biotechnology, Tel-Aviv, Israel; ⁶Tel-Aviv University, Sackler School of Medicine, Tel-Aviv, Israel; ⁷Sapir Medical Center, Institute of Gastroenterology and Hepatology, Kfar Sava, Israel
Email: halishy@netvision.net.il

Background and aims: Several observations show that fecal microbial species of patients with NAFLD differ from that of healthy population. Recent studies explored pathways linking altered composition of gut microbiota with the pathogenesis of NAFLD. Prebiotics are dietary fibers that manipulate gut microbiota to a more favorable profile. The aim of the study was to explore the effectiveness of prebiotic supplementation in liver fat reduction and on the composition of the fecal microbiome.

Method: 19 patients with NAFLD were randomized to receive either 16 gr/day Inulin Type Fructans (ITF) (Inulin/OFS75/25) prebiotic or ($n=9$) placebo-maltodextrin ($n=10$) for 12 weeks. Patients were instructed to maintain their usual diet and physical activity to ensure stable weight throughout the study. Liver fat content was measured by magnetic resonance spectroscopy (MRS). Fecal microbiome was analyzed by 16S ribosomal DNA sequencing. We collected detailed anthropometric, metabolic, liver-related and inflammatory mediators from all participants.

Results: Baseline and end-of-study liver fat content did not change significantly in the prebiotic ($22.1\pm 12.7\%$ and $19.8\pm 11.7\%$) and in the placebo group ($15.2\pm 8.6\%$ and $12.5\pm 9.4\%$). Fecal samples from patients who received the prebiotic had higher proportions of Bifidobacterium, while there was no change in the concentration of Bifidobacterium species in the placebo group (Figure). We observed an increase in FGF-19 levels in the prebiotic group, compared with the placebo group, this however, did not reach a meaningful difference. Bifidobacterium negatively correlated with the difference in FGF-19: $R=-0.88$, $p=0.03$. Body weight and body composition remained stable in both groups.

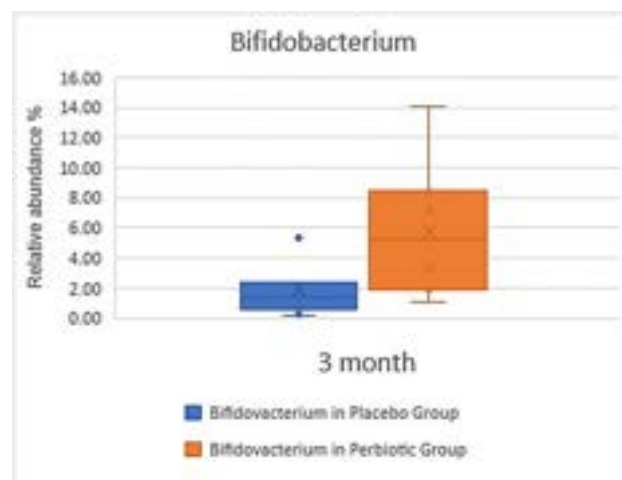


Figure:

Conclusion: Prebiotic treatment enriched fecal microbiota with Bifidobacterium compared with placebo, this did not result in

reduction of liver fat content. Weight loss may still have a pivotal role in NAFLD management.

FRI-520

B-cell activating factor in non-alcoholic steatohepatitis

Iris Gines Mir¹, Raju Kumar¹, Patricia Garrido¹, Wenhao Li¹, Hamish Miller¹, Hajar Saihi¹, Gillian Hood¹, William Alazawi¹. ¹Barts Liver Centre, Blizard Institute, Queen Mary University of London, Immunobiology, London, United Kingdom
Email: i.g.mir@qmul.ac.uk

Background and aims: Non-alcoholic fatty liver disease (NAFLD) is one of the most prevalent causes of liver disease worldwide. In a subset of patients, hepatic fat is associated with liver cell injury and inflammation; non-alcoholic steatohepatitis (NASH) and fibrosis. While NASH is the likely driver of disease, the extent of liver fibrosis is more predictive of liver-related clinical events, but the mechanisms that link metabolic dysfunction, inflammation and fibrosis in NASH are poorly understood. B cell-activating factor (BAFF) is a pro-inflammatory adipokine with 3 known receptors (BAFF-R, BCMA and TACI). It is associated with impaired insulin sensitivity, liver steatosis and inflammation in mice and serum BAFF is higher in human NASH patients compared to simple steatosis. In this study we test the hypothesis that BAFF signalling is associated with fibrosis in blood and liver tissue from people living with NAFLD.

Method: Concentration of BAFF in sera from 106 people with biopsy-proven NAFLD and NASH was measured using ELISA. The RNA and protein expression of BAFF and its receptors in liver tissue were evaluated using RT-PCR (GAPDH housekeeping gene), Western blot and immunofluorescence assays in liver biopsy tissue from patients with NASH and in hepatocyte-like cells and stellate-like cells, using B-cells as positive control.

Results: BAFF concentrations were higher in patients with NASH F3-4 compared to those with NASH F0 1118.06 pg/ml vs 1333.39 pg/ml, $p = 0.03$ (figure) with an association of BAFF concentration with age, fibrosis grade and BMI, but no association, with ballooning or inflammation nor with, ethnicity or type 2 diabetes. BCMA, BAFF-R and TACI mRNA were detectable in liver tissue, and this was recapitulated at the protein level, but TACI was not detected by either Western blot or immunofluorescence. BCMA relative gene expression was higher in patients with NASH F3 (no F4 patients in this analysis) compared to NASH F0-2 (4.5-fold, $p = 0.05$). In hepatocyte-like cells (HepG2) and stellate-like cells (LX-2), BAFF, BCMA and BAFF-R but not TACI were detected at RNA and protein levels. Treatment with a toxic combination of oleic acid and palmitic acid (1 mM and 0.5 mM) resulted in an up regulation of BAFF-R in LX-2 cells (1.7-fold, $p = 0.02$).

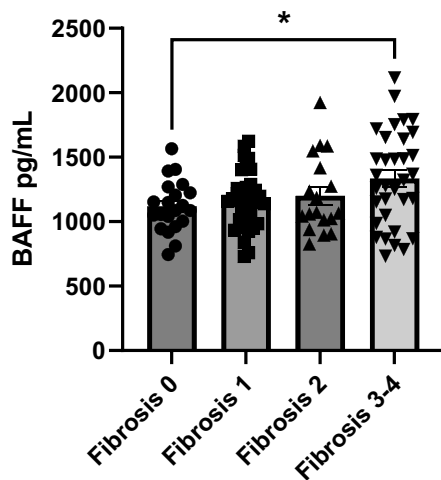


Figure:

Conclusion: BAFF is increased in patients with advance liver fibrosis. BAFF-R, BCMA, TACI and BAFF itself are detected in human liver. BAFF-R, BCMA and BAFF are detected in hepatocyte-like and stellate-like cells.

FRI-521

SNP-630, a novel compound with multiple mechanisms, reverses liver inflammation and fibrosis in preclinical model and NASH phase 2 clinical trial

Hsin-Tien Ho¹, Shin-Wei Chen^{1,2}, Yu-Lueng Shih³, Tien-Yu Huang³, Wen-Hui Fang⁴, Jung-Chun Lin³, Te-Yu Lin⁵, Chang-Hsien Liu⁶, Chih-Weim Hsiang⁶, Kai-Min Chu¹, Cheng-Huei Hsiong¹, Yung-En Wu¹, Jia-Yu Hao¹, Guan-Ju Chen¹, Yi-Hsuan Lin¹, Yoa-Pu Hu^{7,8}. ¹Sinew Pharma Inc., Taipei, Taiwan; ²Sinew Pharma Inc., Taipei City; ³Division of Gastroenterology, Tri-Service General Hospital, National Defense Medical Center, Taipei, Taiwan; ⁴Department of Family Medicine, Tri-Service General Hospital, National Defense Medical Center, Taipei, Taiwan; ⁵Division of Infectious, Tri-Service General Hospital, National Defense Medical Center, Taipei, Taiwan; ⁶Department of Radiology, Tri-Service General Hospital, National Defense Medical Center, Taipei, Taiwan; ⁷National Defense Medical Center, School of Pharmacy, Taiwan; ⁸Taipei Medical University, Taiwan
Email: cwei207@gmail.com

Background and aims: Non-alcoholic steatohepatitis (NASH) is a metabolic liver disease characterized by hepatic lipid accumulation, chronic inflammation and fibrosis. Recent studies have been underlined the pathogenesis of NASH and the complex interplay between them will be essential for the developing therapies that can effectively against the multiple hits that lead to the disease. SNP-630 is a prospective novel synthetic molecule inhibits NASH processing by multiple mechanisms of action. In *in vitro* hepatocytes and hepatic stellate cells co-culture system, we elucidated that SNP-630 significantly decreases fibrosis markers expression with multiple mechanisms of action such as hepatic de novo lipogenesis (DNL) pathway inhibition and inflammation. Most importantly, we are already seeing improvement in both *in vivo* mouse model and the NASH patients clinically treated with SNP-630 and its active metabolites SNP-612.

Method: [*in vitro* model] HepG2 and LX2 were seeded in the same plate considering a ratio of 5:1 respectively. After 24 hours, cells were exposed to 750 μ M of palmitic acid combined with SNP-630 for 24 hrs, then cells and supernatants were harvested for analysis. [*in vivo* model] Male C57BL/6 mice were fed with a high fat diet (HFD) for 21 weeks. In week 21, the HFD-induced NASH mice continued to receive a HFD along with SNP-630 or its metabolites SNP-612 by oral gavage once daily for more 6–10 weeks. [phase2 clinical trial] SNP-612 tolerability, safety, and efficacy in 35 NASH patients were evaluated. The primary and secondary end points were the change in serum alanine aminotransferase (ALT), liver inflammation, steatosis and fibrosis at week 12 of administration

Results: NASH regression led to significant changes at haematological, histological, whole-liver transcriptional, and single-cell levels. In *in vitro* HepG2-LX2 co-culture model, the expression level of triacylglycerol synthesis enzyme (*DGAT1*), inflammation related cytokines (*IL1b*, *IL6*, and *CCL2*), and fibrosis-related markers (*ACTA2*, *COL1A1*, and *TIMP1*) were significantly decreased in SNP630-treatment. Also, in HFD-induced NASH mice, SNP-630 or SNP-612 treatment significantly decreased serum ALT, hepatic steatosis (triglyceride), inflammation (*Ccl2*), and fibrosis (*Col1A1* and *Timp1*). In the clinical trial, patients treated with the active metabolites, SNP-612, demonstrated a significant change in ALT at week 12 compared to baseline values, with no severe adverse events observed. In addition, SNP-612 demonstrated antifibrotic potential, including a significant decrease in fibrogenesis-related biomarkers (ie, CCL4 and CCL5). Moreover, FibroScan measurements indicated the efficacy of SNP-612 to ameliorate liver fibrosis in subgroup analysis.

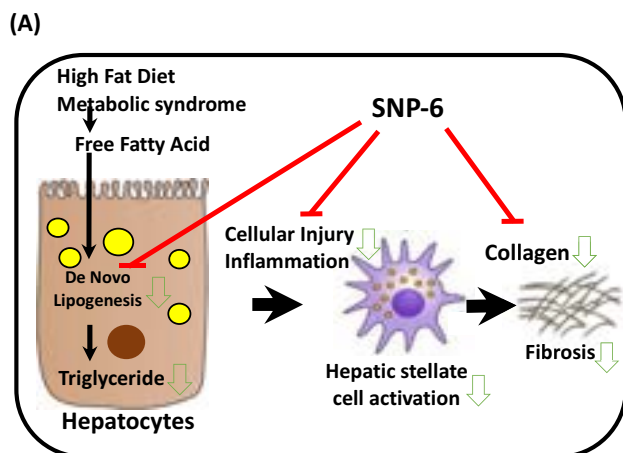
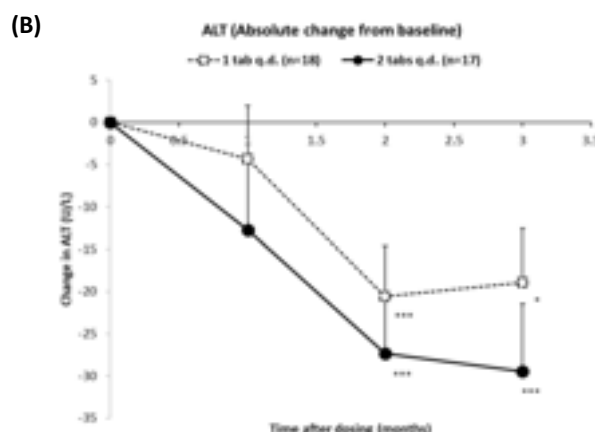


Figure A. The mechanism of SNP-630 and its active metabolites.

Figure B. SNP-612 achieves the primary endpoint of an improvement in ALT after 12-weeks treatment in the mITT population.



- Primary endpoint was met:** ALT at week 12 were both significant reduced from baseline in the two dosage groups.
- ALT improvements were also observed in all subgroups:** Subgroup analysis were performed based on PNPLA3 genotype, sex, age, BMI, MRI-PDFF, T2DM, and dose of SNP-612.

Figure: (abstract: FRI-521).

Conclusion: These preclinical and phase 2 clinical data demonstrated that SNP-630 and its metabolites can suppress NASH fibrosis through DNL inhibition and inflammation.

FRI-522

Serological biomarkers PRO-C3 and PRO-C6 reveal the anti-fibrotic and pro-metabolic effects of MSDC-0602 K, an insulin sensitizer, in non-alcoholic steatohepatitis patients during the EMMINENCE phase IIb study

Alejandro Mayorca Guiliani¹, Peder Frederiksen¹, Morten Karsdal¹, Diana Leeming¹, Jerry Colca². ¹Nordic Bioscience, Biomarkers and Research, Herlev, Denmark; ²Cirius Therapeutics, Kalamazoo, United States

Email: amg@nordicbio.com

Background and aims: MSDC-0602K is a second-generation insulin sensitizer designed to inhibit the mitochondrial carrier (MPC) without direct activation of the transcription factor PPAR γ . The EMMINENCE trial evaluated efficacy and safety of MSDC-0602K in patients with non-alcoholic steatohepatitis (NASH). As previously published, MSDC-0602K missed statistical significance on the pre-specified primary analysis of liver histology, but led to significant reductions in glucose, glycated Hb and liver enzymes. Notably edema, the principle PPAR γ agonist-associated side effect, was not higher than placebo and there were more dropouts in the placebo than in the active arms. Here, we assessed the serological extracellular matrix biomarkers PRO-C3, PRO-C4 and PRO-C6, which serve as surrogates of fibroblast activity, pericellular fibrosis formation and the pro-fibrotic and proinflammatory fragment endotrophin.

Method: In the EMMINENCE study (NCT02784444), 392 NASH patients were randomized to placebo (PL), 62.5 mg, 125 mg or a 250 mg daily dose of MSDC-0602K for 12 months. The primary efficacy end point was defined as an improvement of ≥ 2 points in NAS score, with ≥ 1 decrease in either ballooning or inflammation and no increase in fibrosis at 12mo based on randomized readings of only completing subjects. Liver biopsy was performed at baseline (BL) and at 12mo. Plasma samples were collected at BL, 6mo and 12mo to measure PRO-C3, PRO-C4 and PRO-C6 and analyzed statistically at the end of the study.

Results: PRO-C3 levels increased along with fibrosis stage at baseline ($p=0.0021$). 125 and 250 mg doses of MSDC-0602K significantly reduced PRO-C3 at 6mo and 12mo ($p=0.003-0.03$; PL: -3%, MSDC-0602K: -6 to -11% at 12mo). MSDC-0602K significantly reduced PRO-C6 at 12mo for all three doses ($p=0.026-0.047$, PL: +3%, MSDC-0602K: -2.5 to -3.5% at 12mo) compared to PL (See figure below). Furthermore, our data suggested the presence of a F3/4 patient responder subgroup, characterized by lower levels of PRO-C3 at baseline.

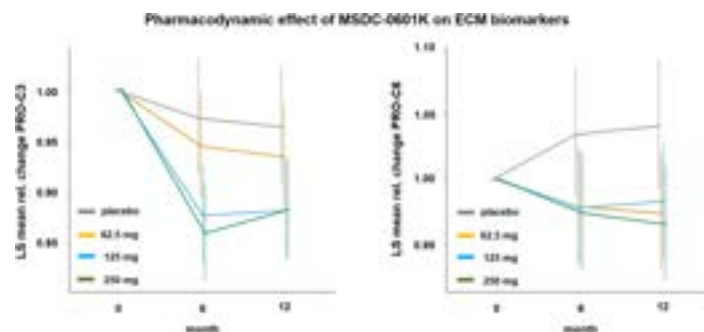


Figure:

Conclusion: MSDC-0602K reduced both PRO-C3 and PRO-C6 levels, indicating an anti-fibrotic and pro-metabolic effect. Furthermore, the biomarkers identified a subgroup of patients with lower baseline PRO-C3 and a F3-F4 diagnosis at BL that had a high likelihood of improvement in fibrosis. Our findings suggest that measuring ECM neo-epitope biomarkers may aid in understanding the pharmacodynamic effects of MSDC-0602K as well as support future exploration of MSDC-0602K in patients with NASH.

FRI-523

Similar weight loss with semaglutide regardless of diabetes and cardiometabolic parameters in individuals with non-alcoholic fatty liver disease

Matthew Armstrong¹, Takeshi Okanoue², Mads Sundby Palle³, Anne-Sophie Sejlind³, Mohamed Tawfik³, Michael Roden⁴. ¹Liver Unit, Queen Elizabeth University Hospital Birmingham, UK, National Institute for Health Research, Birmingham Biomedical Research Centre at University Hospitals Birmingham NHS Foundation Trust, Birmingham, United Kingdom; ²Department of Gastroenterology and Hepatology, Saiseikai Suita Hospital, Osaka, Japan; ³Novo Nordisk A/S, Søborg, Denmark; ⁴Division of Endocrinology and Diabetology, Medical Faculty, Heinrich-Heine University and University Hospital, Düsseldorf, Germany; Institute of Clinical Diabetology, German Diabetes Center, Leibniz Center for Diabetes Research, München-Neuherberg, Germany Email: asji@novonordisk.com

Background and aims: In the absence of any globally approved pharmacotherapy, current guidelines recommend lifestyle modification and weight loss in people with obesity and non-alcoholic fatty liver disease (NAFLD), including non-alcoholic steatohepatitis (NASH). Semaglutide, a glucagon-like peptide (GLP)-1 analogue indicated for management of body weight and type 2 diabetes (T2D), is under investigation in NASH. However, T2D seems to reduce GLP-1 analogue-mediated weight loss in people with overweight/obesity. We evaluated the impact of T2D and other cardiometabolic parameters on weight loss in randomised controlled trials of subcutaneous semaglutide in NAFLD including NASH.

Method: Data were taken from adults in NCT03357380 (NAFLD; semaglutide 0.4 mg or placebo once daily [OD] for 72 weeks), NCT02970942 (NASH and fibrosis stage [F] 1–3; semaglutide 0.1, 0.2 or 0.4 mg or placebo OD for 72 weeks) and NCT03987451 (NASH, F4 and compensated liver cirrhosis; semaglutide 2.4 mg or placebo once weekly [OW] for 48 weeks). This *post-hoc* analysis pooled data for semaglutide (0.4 mg OD and 2.4 mg OW) and placebo, with weight changes grouped by baseline T2D status (previously diagnosed or glycated haemoglobin [HbA_{1c}] ≥6.5%, pre-T2D [HbA_{1c} ≥5.7–<6.5%] or no T2D [HbA_{1c} <5.7%]). Mean on-treatment changes from baseline to 1 year were used to derive estimated treatment differences (ETDs) and 95% confidence intervals for semaglutide vs placebo. Impact of cardiometabolic factors including baseline fasting lipids, plasma glucose, diabetes duration and Homeostatic Model Assessment for Insulin Resistance (HOMA-IR) were assessed.

Results: Of the 300 participants included, 209 (70%) had T2D, 51 (17%) pre-T2D and 40 (13%) non-T2D. ETDs ranged from -9.8 kg in the pre-T2D group to -11.6 kg in the non-T2D group; there was no significant difference between the non-T2D vs pre-T2D, pre-T2D vs T2D and non-T2D vs T2D groups in terms of weight change (Table). Weight change was not influenced by known diabetes duration, or baseline HOMA-IR or glucose and lipid levels.

Table:

	Semaglutide		Placebo			
	n	Weight change (kg)	n	Weight change (kg)	ETD (95% CI) (kg)	P value vs non-T2D
						P value vs pre-T2D
Overall	163	-11.1	137	-0.7	-10.4 (-11.9; -8.9)	-
T2D	117	-11.1	92	-0.8	-10.2 (-12.0; -8.5)	0.57
Pre-T2D	25	-9.8	26	0.0	-9.8 (-13.4; -6.3)	0.54
Non-T2D	21	-12.7	19	-1.1	-11.6 (-15.7; -7.4)	-

CI, confidence interval; ETD, estimated treatment difference; T2D, type 2 diabetes.

Conclusion: Individuals with NAFLD including NASH treated with semaglutide had similar weight loss, and parameters of insulin resistance, and glucose and lipid metabolism, regardless of T2D

status. Unlike previously reported differences in weight change in people with and without T2D, the presence of T2D did not influence efficacious weight loss with semaglutide; however, alternative explanations, such as hepatic steatosis, cannot be ruled out.

FRI-524

Safety and efficacy of oral semaglutide in overweight diabetic patients with non-alcoholic fatty liver disease: an interim analysis

Arun Valsan¹, Gauri Unnithan², Arathi Venu², Nipun Verma³, Muhammed Shafi Pa², Arjun Santhosh², Ajeet K L⁴, Narmadha Mp², Harish Kumar¹, Nimitha K Mohan⁵, Priya Nair¹, Shine Sadasivan¹, Sudhindran S¹, Manjima Nair¹, Arunima Sumith², Gouripriya Ls², Suja Kumari S⁴, Vaishnavy S Vinod¹, Anoop Koshy¹. ¹Amrita Institute of Medical Sciences, Kochi, India; ²Amrita School of Pharmacy, India; ³Post Graduate Institute of Medical Education and Research, Chandigarh, Chandigarh, India; ⁴Amrita College of Nursing, India; ⁵Aster Medcity, Kochi, India

Email: drarunvalsan@gmail.com

Background and aims: Currently there are no approved therapies for non-alcoholic fatty liver disease. Many drugs are in varying stages of approval for application in NAFLD. Semaglutide (Rybelsus) is a first-of-its-kind orally active glucagon-like peptide-1 (GLP-1) analogue that has recently been approved by US FDA for treatment of diabetes mellitus. Injectable semaglutide has proven to be efficacious in fibrosis reduction in a recently concluded phase 2 trial.

Method: This is a single-centre, single-arm, open-labelled study of oral semaglutide in a tertiary care hospital in southern India. Patients with co-existent liver disease (significant alcohol, viral hepatitis, autoimmune hepatitis etc) were excluded. All patients were administered lifestyle modification with advice for calorie restricted diet and gradually intensifying aerobic exercise regimen, culminating in 45 minutes aerobic exercise for at least 5 days per week. The compliance to dietary and exercise regimen was ensured by weekly telephonic interview by trained allied health personnel. The subjects were initiated on a 3 mg dose for one week, followed by a teleconsultation to assess tolerability. From week 2, all subjects who tolerated the drug were administered 7 mg drug on an empty stomach. The patients were followed up for 24 weeks.

Results: A total of 59 overweight (BMI>23.5 kg/m²), diabetic patients with imaging evidence of NAFLD were recruited to the study; however, 9 patients were excluded from final analysis [Laparoscopic sleeve gastrectomy (n=2), drug non-compliance (n=2), drug intolerance (n=5)]. The mean age of study population was 50.4, with predominant males (62%), mean BMI-33.7 kg/m² and mean duration of diabetes of 7.8 years were included. The associated comorbidities were systemic hypertension (26%), hypothyroidism (18%), dyslipidemia (64%), coronary heart disease (10%). At the start of the study, percentage of patients on insulin (34%), metformin (74%), saroglitazar (14%), statins/fibrates (42%), vitamin E (5%). After 24 weeks of semaglutide therapy, there was significant reduction in LSM, CAP, FIB-4, ALT, cholesterol, LDL, HDL (p < 0.005, each). The LSM and CAP improvements were consistently significant in 3 BMI strata (25–30, 30–35, >35 Kg/m²) (p < 0.016, each). (Fig. 1).

Conclusion: Oral Semaglutide was safe and efficacious and well tolerated in overweight diabetic patients with NAFLD in this interim analysis at 24 weeks. There was a significant reduction in BMI, ALT, liver stiffness, CAP and lipid profile. There were no significant treatment-emergent adverse events. There is a need of randomized placebo-controlled trials to further explore its role in diabetes-associated NAFLD.

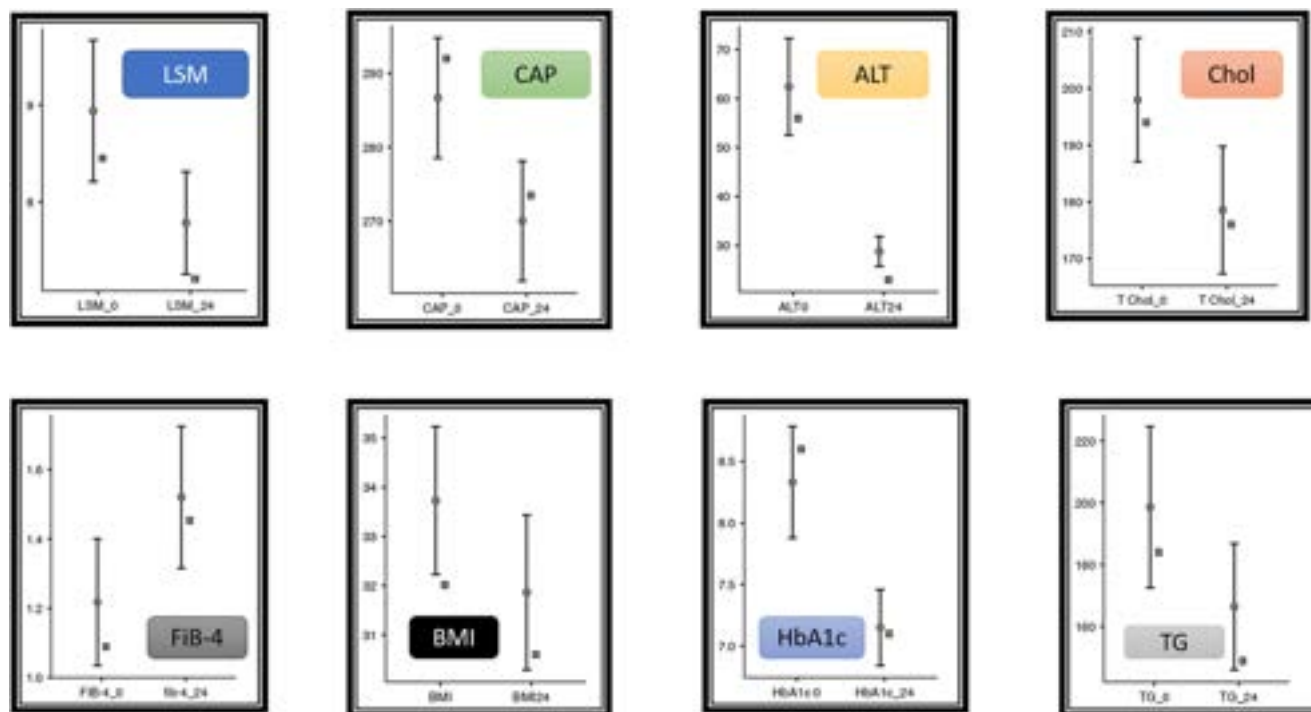


Figure: (abstract: FRI-524) The median change in clinic-laboratory parameters

FRI-525

The effects of a novel online app (Noom Weight) on weight loss and liver biomarkers in patients with NAFLD: a single arm proof-of-concept study

Naim Alkhouri¹, Jesus Topete¹, Meaghan McCallum², Kelly Blessing², Mazen Nouredin³, Angie Coste¹, Anita Kohli¹. ¹Arizona Liver Health, Phoenix, United States; ²Noom, United States; ³Houston Research Institute, United States
Email: naim.alkhouri@gmail.com

Background and aims: Weight loss through lifestyle modifications remains the mainstay for NAFLD treatment; however, implementing effective lifestyle interventions in clinical practice has been challenging due to time and cost constraints. Having a comprehensive approach to weight loss in patients with NAFLD that can be scaled and provided at low cost is a key unmet need. The objective of this study is to assess the effects of a mobile weight management program on weight loss and liver health biomarkers in adults with obesity and NAFLD.

Method: Adults with obesity (BMI 30 to 49.9 kg/m² inclusive) and evidence of NAFLD based on Fibroscan CAP ≥ 274 dB/m were included. Patients were given access to the Noom Weight program for 16 weeks (midpoint) and then were followed for an additional 8 weeks (week 24 or end point). Measurements completed at baseline, midpoint, and end point included: weight/BMI, Fibroscan, routine labs (Complete Metabolic Panel and CBC), and the exploratory biomarker cyokeratin 18 fragment (CK18f). All tests of significance were performed at $\alpha = 0.05$, two sided.

Results: 40 subjects were enrolled and 82.5% (33/40) completed the study. The mean age was 55.9 years (range 29–79) with a mean BMI of 38 kg/m² (30.5–49.8) and a mean baseline CAP score of 331.9 dB/m² (276–396) and a mean LSM of 7.54 kPa (4.9–13.3). The average change in body weight from baseline was a 4.0% reduction and 32.4% (11/34) achieved total body weight reduction by 5% or more. There was a significant reduction in the CAP score by end point of 21.35 dB/m (p = 0.024). The ALT decreased by 10 U/L or more in 27.3% (9/33). There was moderate correlation between BMI decrease and reduction in the CAP score (R = 0.533). There was no change in the LSM at the

end point, and 62% (21) of subjects achieved >5% drop in CK18f. The change in CK18f correlated weakly (R = 0.215) with BMI drop but more strongly with Fibroscan CAP score (R = 0.468) and LSM (R = 0.764).

Conclusion: The Noom Weight program had beneficial effects in patients with obesity and NAFLD, including significant reduction in the CAP score and one third of patients achieving 5% or more reduction in their weight. Steatosis of the liver was affected by weight loss as a result of engagement with the Noom Weight program. Fibrosis was not significantly affected by the Noom Weight program in the timeframe of the study. Fibrosis may require a longer timeframe for changes to be measured.

FRI-526

The effect of standard of care lifestyle advice by a hepatologist in a routine clinical practice on steatosis and fibrosis development among NAFLD patients

Leen Heyens^{1,2,3}, Wouter Robaey^{1,3}, Mathieu Struyve³, Gert Stockmans³, Sven Francque^{4,5}, Geert Robaey¹. ¹Hasselt University, Faculty of Life Sciences and Medicine, Hasselt, Belgium; ²Maastricht University, NUTRIM, Maastricht, Netherlands; ³Hospital Oost-Limburg, Gastro-enterology, Genk, Belgium; ⁴University of Antwerp, Gastro-enterology and Hepatology, Antwerpen, Belgium; ⁵Antwerp University Hospital, Gastro-enterology and Hepatology, Edegem, Belgium
Email: leen.heyens@uhasselt.be

Background and aims: Non-alcoholic fatty liver disease (NAFLD) has become the most frequent cause of chronic liver disease. The leading cause of NAFLD has been defined as a behavioural phenotype comprising low physical activity and an obesogenic diet. The primary therapeutic advice is lifestyle changes leading to weight loss. Previous studies indicated that a weight reduction of 5% or more could induce regression of steatosis or fibrosis. However, hepatologists only have time during consultations to give a short outline of the optimal lifestyle. As no data is available on the outcome of this routine practice, we evaluated the effect of this lifestyle advice on steatosis and fibrosis development among NAFLD patients.

Method: Data were collected retrospectively using the electronic patient files of NAFLD patients in whom a baseline and a follow-up FibroScan® measurement (for assessment of steatosis by CAP™ and of liver stiffness (LSM) as a surrogate for fibrosis) were performed between November 2019 and 2022 at Ziekenhuis Oost-Limburg, Genk, Belgium. At the start, patients received Mediterranean diet related-advice, tips on improving exercise, and an information brochure concerning NAFLD from the hepatologist. Clinically meaningful weight loss was defined as a loss of at least 1 kg.

Results: Of the 218 NAFLD patients evaluated, 130 (59.6%) were excluded due to the usage of semaglutide, not fasting, IQR/MED>30%, or bariatric surgery. In total, 88 (40.4%) patients were included, of whom 53 (60.2%) were men and 38 (43.2%) had type 2 diabetes mellitus (T2DM). The mean age, median BMI, and mean waist circumference were 54 ± 13 years, 31.0 (28.4 – 34.9) kg/m^2 and 105.2 ± 12.7 cm, respectively. On average, there were 186 (124 – 280) days between the measurements. The median weight loss between measurements was -1.2 (-4.1 ; 1.4) kg. The decrease in LSM and CAP™ were -1.2 (-3.1 ; 0.3) kPa and -7.0 (-50.5 ; 8.8) dB/m, respectively. Within this group, 47 (53.4%) had clinically meaningful weight loss, while 41 (46.6%) did not lose any weight or gained weight. The group with weight loss developed a significantly ($p < 0.001$) lower CAP™ compared to baseline values, but there was no significant change in LSM during the same time period. Furthermore, within the weight loss group, there were no differences in magnitude of weight loss or CAP™ when stratified based on sex, age categories (≤ 50 years vs. > 50 years), or having T2DM or not ($p > 0.05$).

Conclusion: To the best of our knowledge, this is the first study to assess the effect of routine lifestyle advice by a hepatologist on body weight, steatosis, and fibrosis, measured by FibroScan®. The lifestyle advice leads to a weight reduction of at least -1 kg in almost half of NAFLD patients and a significant reduction in steatosis over six months in those patients. However, the recommended reduction in body weight (at least 5%) is not reached. Other measures to support the advice on lifestyle change given by the hepatologist are hence necessary to improve efficacy.

FRI-527

Comparison of efficacy between liraglutide and phentermine/topiramate in obese patients with non-alcoholic fatty liver disease

Young Eun Chon¹, Kwan Sik Lee¹, Yeonjung Ha¹, Joo Ho Lee¹. ¹CHA Bundang Medical Center, CHA University, Korea, Rep. of South
Email: nachivysoo@chamc.co.kr

Background and aims: Anti-obesity drugs are known to improve hepatic inflammation in patients with non-alcoholic fatty liver disease (NAFLD). We aimed to compare the effect of liraglutide and phentermine/topiramate in obese NAFLD patients.

Method: We retrospectively enrolled 65 obese NAFLD patients without type 2 diabetes mellitus (liraglutide group [$n = 30$], phentermine/topiramate group [$n = 35$]) who were treated with liraglutide or phentermine/topiramate for 12 months. Changes in laboratory data, body weight, degree of steatosis and fibrosis were compared between two groups. Steatosis was assessed using the fatty liver index, NAFLD liver fat score, and controlled attenuation parameter (CAP). Fibrosis was assessed using fibrosis index based on four factors (FIB4) and liver stiffness.

Results: The mean body weight (80.3 ± 12.3 kg) and body mass index (29.4 ± 3.2) were similar between two groups. After 12 month of treatment, phentermine/topiramate group showed significantly greater effect in weight loss than liraglutide group (-8.4 ± 0.6 vs. -6.3 ± 0.4 kg, $p = 0.003$). Both group showed similar effect showing significant steatosis reduction (phentermine/topiramate vs. liraglutide; Δ fatty liver index: -8.9 ± 2.3 vs. -8.4 ± 1.7 , $p = 0.449$; Δ NAFLD liver fat score: -0.5 ± 0.2 vs. -0.4 ± 0.2 , $p = 0.835$; Δ CAP: -9.2 ± 6.9 vs. -8.3 ± 4.6 dB/m², $p = 0.129$). Fibrosis improvement was noted in both

groups (Δ liver stiffness, -2.2 ± 1.0 vs. -1.8 ± 0.9 , $p = 0.052$; Δ FIB-4 index: -0.10 ± 0.10 vs. -0.11 ± 0.13 , $p = 0.860$).

Conclusion: Liraglutide or phentermine/topiramate treatment significantly ameliorated liver steatosis and inflammation, but either treatment showed minimal effect on fibrosis improvement.

FRI-528

Development of physiologically based pharmacokinetic model to predict liver exposure of SRT-015, a next-generation inhibitor of apoptosis signal-regulating kinase 1

Artur Plonowski¹, Daniel Burge¹, Kathleen Elias¹, Neil D. McDonnell¹.
¹Seal Rock Therapeutics, Inc., United States
Email: aplonowski@sealrocktx.com

Background and aims: SRT-015 is a novel, clinical-stage, small molecule inhibitor of Apoptosis Signal-regulating Kinase 1 (ASK1) in development for liver diseases, including alcoholic hepatitis (AH), acute-on-chronic liver failure (ACLF), and non-alcoholic steatohepatitis (NASH). In all preclinical species evaluated, SRT-015 is preferentially distributed to liver, with liver/plasma ratio ranging 10–60x. We aimed to develop a physiologically based pharmacokinetic (PBPK) model to non-invasively estimate liver exposure of SRT-015 in humans

Method: GastroPlus software (Simulation Plus, Lancaster, CA) was used first to build and validate PBPK models for SRT-015 PK in mouse, rat, and non-human primates to explain the observed plasma concentrations vs. time profiles following intravenous (IV) and oral administration. The model was further expanded with the addition of efficacious liver and plasma concentrations of SRT-015 determined in preclinical models of NASH (DIO-NASH model, Gubra), AH/ACLF and acetaminophen overdose toxicity. Knowledge gained during preclinical PBPK modeling was then applied to build a human PBPK model for SRT-015 and predict First-in-Human (FIH) exposure following oral administration. Actual plasma exposure of SRT-015 from the FIH study (NCT04887038) was then used to refine the human PBPK model and predict human liver exposure of SRT-015. The established model was also used to simulate human plasma and liver exposure after IV administration of SRT-015.

Results: The preclinical PBPK model was highly predictive of human SRT-015 plasma exposure with all observed values of C_{max} and AUC from FIH study falling within the predicted ranges across all dose levels (40, 80, 160, 320, and 640 mg; po) administered to healthy participants. After further refinement, the C_{max} and AUC values predicted by the model correlated well with the observed values ($r^2 = 0.89$ and $r^2 = 0.99$, respectively). The clinical PBPK model of orally administered SRT-015 predicted a robust exposure of SRT-015 within the liver, with dose-proportional increase of C_{max} between 40 and 320 mg, and less-than-proportional increase between 320 and 640 mg. Importantly, the predicted hepatic C_{max} values were well above the efficacious exposure levels observed in preclinical efficacy models. Additionally, the model predicts efficacious exposure with IV formulated, continuous infusion SRT-015.

Conclusion: We have established a highly predictive PBPK model of SRT-015 exposure in human liver. The model indicates efficacious exposure in the liver with all oral doses tested in the phase 1 clinical trial in healthy participants and will help in the dose selection for Phase 2 trials. The model also indicates the feasibility to attain efficacious exposure via IV infusion, which could be a preferred administration route in ACLF patients with impaired consciousness or otherwise unable to swallow an oral drug.

FRI-529

Barriers for regular exercise in people with non-alcoholic fatty liver disease

Kedar Deshpande¹, Ken Nosaka¹, Oyekoya Ayonrinde², John Olynky¹, Marcelle Scagliotta², Wendy Lam², Huirong Ma², Crystal Connelly².

¹Edith Cowan University, School of Medical and Health Sciences, Australia; ²Fiona Stanley Hospital, Gastroenterology and Hepatology, Australia

Email: kdeshpan@our.ecu.edu.au

Background and aims: Performing regular exercises is an important alternative or adjunct to pharmacotherapy for treating non-alcoholic fatty liver disease (NAFLD). While many people with NAFLD do not perform adequate physical activity and exercise, it is important to understand barriers for them to achieve an effective exercise routine. We therefore aimed to examine associations between patients' knowledge of exercise as treatment of NAFLD, their self-perceived barriers to exercise, and their stages in NAFLD.

Method: Patients with NAFLD attending an outpatient hepatology clinic were recruited. They were assessed for the severity of hepatic steatosis using controlled attenuation parameter (CAP) and fibrosis by transient elastography (TE). An online questionnaire was administered to them to ask their self-reported exercise patterns, barriers to exercise, and knowledge regarding effectiveness of different types of exercise for NAFLD. We sought associations between the questionnaire responses and liver characteristics.

Results: Forty-seven patients (29 females) with a mean age of 57.6 ± 11.7 years and body mass index (BMI) of 33.7 ± 6.3 completed the questionnaire. The mean CAP and liver stiffness measurement (LSM) values by TE were 336.2 ± 44.5 dB/m and 13.2 ± 12.6 kPa, respectively. Although the majority of patients ($n = 42$, 89%) considered NAFLD to be a serious health concern, 72% ($n = 34$) of them did not achieve recommended exercise levels of ≥ 150 minutes of moderate-intensity physical activity per week, and 64% ($n = 30$) were unsure about the role of exercise in NAFLD treatment. The most common barriers to exercise reported were health problems (64%), lack of time (36%), and lack of enjoyment in exercising (26%). There were no significant associations between CAP, LSM and exercise questionnaire responses.

Conclusion: The majority of patients were unaware of the role of exercise as a potential treatment for NAFLD and were not achieving recommended exercise levels. Inadequate time to exercise, physical and mental health problems, and lack of enjoyment in exercise were the major barriers for them to exercise. Future randomised exercise trials and behavioural research for NAFLD should focus on individualised and sustainable exercise programs to improve patients' long-term adherence to exercise to reduce the burden of NAFLD.

FRI-530

A randomized controlled trial of kalmegh supplementation on non-alcoholic fatty liver disease

Sanket Nandekar¹, Sunil Kumar¹, Devesh Yadav², Binay Sen³, Pournima Gadgil⁴. ¹Institute of medical sciences, Banaras hindu university, Department of community medicine, Varanasi, India;

²Institute of medical sciences, Banaras hindu university, Department of gastroenterology, Varanasi, India; ³Institute of medical sciences, Banaras hindu university, Department of dravyaguna, Varanasi, India; ⁴Apex institute of ayurvedic medicine and hospital, Department of prasuti tantra, Mirzapur, India

Email: snktmv@bhu.ac.in

Background and aims: Non-alcoholic fatty liver disease (NAFLD) is the most common liver disease worldwide (prevalence 20–30%). Kalmegh (Botanical name: *Andrographis paniculata* nees, Family: Acanthaceae) is an exceptional herb from classical Indian literature having comprehensive action over liver. Our aim was to assess the safety, effectiveness and cost of treatment for kalmegh supplementation in NAFLD using modern day investigations and standard procedures of randomized controlled trial.

Method: We have enrolled 91 patients of age group 18–60 years from Gastroenterology OPD of tertiary care hospital in northern India. Written and informed consent was obtained and patients were randomized to group A and group B. Patients in group A ($n = 49$) were given kalmegh capsules and group B ($n = 42$) were given placebo capsules, each having dose of 1600 mg per day. Standard lifestyle modification and dietary intervention were advised in both the groups. Patients were followed up for the period of 90 days at 30 days interval for 3 subsequent visits. Anthropometric measurements along with blood and radiological investigation were performed during each follow-up.

Ethical approval was obtained from institutional ethical committee- ECR/526/Inst/UP/2014/RR-20.

CTRI (clinical trial registry India) registration no. CTRI/2021/10/037692.

Results: Patients in both the groups has shown significant improvement in anthropometric parameters with $p < 0.05$ at all the follow-ups. In group A, serum low density lipoprotein (Sr. LDL), LDL/HDL ratio and serum triglyceride reduced significantly ($p < 0.05$) at all the subsequent follow-ups while in group B reduction was non-significant at most of the follow-up except some. Similarly in group A aspartate aminotransferase (AST) and alanine aminotransferase (ALT) reduced significantly ($p < 0.05$) at all the subsequent follow-ups while in group B reduction was non-significant in some follow-ups. In group A, liver stiffness reduced significantly ($p < 0.05$) when compared with group B.

Cost of treatment of NAFLD for 1 month with modern medicine was Rs 1394 and with kalmegh it is Rs 82.

Figure: Showing improvement in clinical and biochemical parameters in both groups at different follow-ups

Parameter	Group	Initial Vs 1 st follow up		Initial Vs 2 nd follow-up		Initial Vs 3 rd follow up	
		Change in percentage (%)	p	Change in percentage (%)	p	Change in percentage (%)	p
Serum	A	22.32 (–)	0.000	24.22 (–)	0.001	26.63 (–)	0.016
Triglycerides	B	16.39 (–)	0.000	19.81 (–)	0.000	23.92 (–)	0.015
Serum LDL	A	6.57 (–)	0.004	13.80 (–)	0.000	13.45 (–)	0.022
	B	6.65 (–)	0.046	2.45 (–)	0.977	9.67 (–)	0.821
LDL/HDL ratio	A	5.03 (–)	0.072	15.35 (–)	0.001	10.70 (–)	0.144
	B	5.67 (–)	0.121	3.05 (–)	0.577	2.09 (–)	0.839
AST	A	14.88 (–)	0.000	26.99 (–)	0.001	21.53 (–)	0.009
	B	9.65 (–)	0.045	17.96 (–)	0.008	18.55 (–)	0.094
ALT	A	14.23 (–)	0.004	22.06 (–)	0.002	27.40 (–)	0.026
	B	11.37 (–)	0.045	22.22 (–)	0.011	19.24 (–)	0.069
Fibroscan (Kpa)	A	19.47 (–)	0.047	20.18 (–)	0.046	35.41 (–)	0.043
	B	6.20 (–)	1.000	14.97 (–)	0.482	1.05 (+)	0.285

Note: (–) reduced; (+) increased.

Conclusion: Study shows that patients taking kalmegh supplementation has shown more significant improvement in lipid profile, liver enzymes and liver stiffness when compared with patients taking placebo. No patient in both the group has shown any adverse reaction or progress of the disease pathogenesis. This supports the safety and effectiveness of kalmegh in NAFLD and also, we can conclude that treatment of NAFLD with kalmegh is 17 times more economical than that of modern medicine.

FRIDAY 23 JUNE

Non-invasive assessment of liver disease except NAFLD

FRI-477

Dynamics of liver stiffness measurements provide incremental prognostic information in advanced chronic liver disease

David JM Bauer^{1,2,3}, Zhenwei Yang⁴, Fiona Köck¹, Laurenz Fritz¹, Benedikt Hofer^{1,2,5}, Lorenz Balcar^{1,2}, Lukas Hartl^{1,2}, Mathias Jachs^{1,2}, Katharina Stopfer¹, Theresa Bucsis^{1,2}, Benedikt Simbrunner^{1,2,5}, Bernhard Scheiner^{1,2}, Michael Trauner¹, Mattias Mandorfer^{1,2}, Thomas Reiberger^{1,2,5}, Georg Semmler^{1,2}. ¹Medical University of Vienna; Division of Gastroenterology and Hepatology, Department of Internal Medicine III, Wien, Austria; ²Medical University of Vienna, Vienna Hepatic Hemodynamic Lab, Division of Gastroenterology and Hepatology, Vienna, Austria; ³Klinik Ottakring-Wiener

Gesundheitsverbund, 4. Medical Division with Gastroenterology, Hepatology, Endoscopy, Wien, Austria; ⁴Erasmus University Medical Center, Department of Biostatistics, Netherlands; ⁵Medical University of Vienna, Christian-Doppler Laboratory for Portal Hypertension and Liver Fibrosis, Wien, Austria
Email: thomas.reiberger@meduniwien.ac.at.

Background and aims: Liver stiffness measurements (LSM) allow for non-invasive assessment of the severity of chronic liver disease and identification of advanced chronic liver disease (ACLD). Yet, the clinical relevance of dynamics in LSM within ACLD are unclear. This study examines the significance of LSM dynamics as a marker of liver disease regression or progression, and as a predictor of hepatic decompensation and liver-related mortality.

Method: Patients with chronic liver disease who underwent ≥ 2 reliable LSM, least 6 months apart, were retrospectively included. At baseline (BL), participants were divided into three groups: non-ACLD with BL-LSM < 10 kPa, and compensated ACLD (cACLD) with BL-LSM ≥ 10 kPa. Joint modelling (combining a linear mixed effects model with a cause-specific proportional hazard model) was used to assess the association of longitudinal changes in LSM with hepatic decompensation and liver-related mortality.

Results: 2123 patients (67% non-ACLD, 33% cACLD) were followed for a median of 65 months, during which 4 (0.3%) non-ACLD and 72

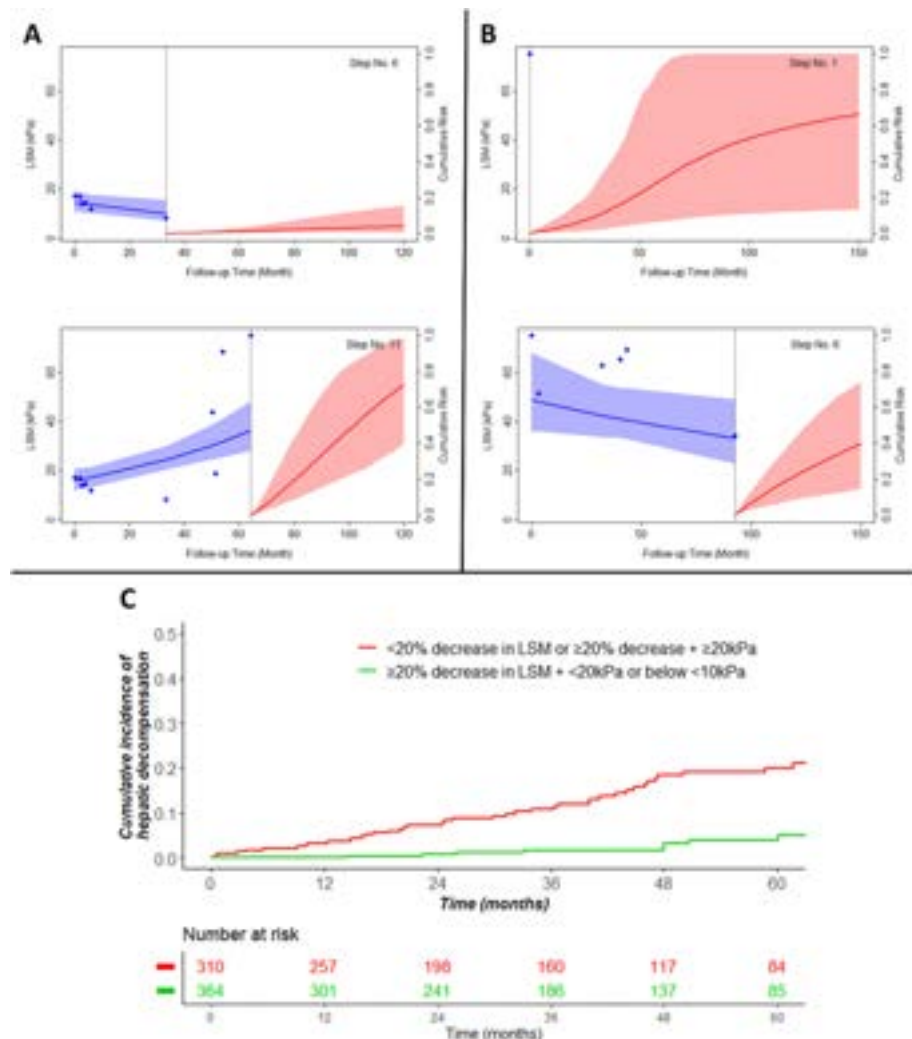


Figure: (abstract: FRI-477) Updated risk prediction of the longitudinal LSM model for (A) increasing LSM and (B) decreasing LSM (LSM values and a regression line in blue on the left side, cumulative risk of hepatic decompensation in red on the right side), and (C) Kaplan Meier curve for hepatic decompensation in cACLD patients according to the BAVENO cutoff for a clinically significant LSM decrease.

POSTER PRESENTATIONS

(9.9%) cACLD patients developed hepatic decompensation, while 2 (0.1%) and 41 (5.9%) died of liver-related causes. In cACLD patients, doubling of LSM at any point was linked to a significantly higher risk of hepatic decompensation (adjusted hazard ratio (aHR) per log-increase: 4.33 [95%CI: 2.74–7.06], $p < 0.001$) and liver-related death (aHR: 4.00 [95%CI: 2.47–6.87], $p < 0.001$), indicating a ~50% change in risk for every 20% change in LSM over time, in a model adjusted for age, platelet count, MELD, and albumin. Results were robust and numerically similar in subgroup analyses of hepatitis C patients, and in a model adjusted for etiological cure as a time-dependent covariable.

The accuracy of LSM dynamics (ROC: 0.847) for predicting hepatic decompensation within 2 years was higher than was superior to a single BL-LSM (0.805), and dynamics in platelet count (0.754), MELD (0.722) or albumin (0.559).

The definition of a clinically significant LSM-decrease suggested by the BAVENO VII consensus, i.e., a 20% decrease in LSM to a value < 20 kPa or < 10 kPa was validated to identify patients with a significantly reduced risk of hepatic decompensation (HR: 0.18, 95% CI: 0.09–0.37, $p < 0.001$).

Conclusion: Repeated longitudinal measurements of LSM facilitate an individualized and continuously updated risk prediction for hepatic decompensation and liver-related mortality. Importantly, the prognostic value of dynamics in LSM was superior to those of other established prognostic markers.

FRI-478

Liver stiffness measurement Baveno VII rule of 5 and risk of hepatocellular carcinoma after HCV eradication in patients with cirrhosis

Binu John¹, Yangyang Deng², David Kaplan³, Janice Jou⁴, Tamar Taddei⁵, Paul Martin⁶, Dustin Bastaich², Hann-Hsiang Chao⁷, Bassam Dahman². ¹Miami VA Health System and University of Miami, Gastroenterology and Hepatology, Miami, United States; ²Virginia Commonwealth University, United States; ³University of Pennsylvania, United States; ⁴Portland Va and Oregon Health Sciences University, United States; ⁵VA Connecticut Health System and Yale University, United States; ⁶University of Miami, United States; ⁷VA Richmond Health Care, United States

Email: binu.john@gmail.com.

Background and aims: Liver stiffness (LSM) using the Baveno VII “Rule of 5” cut-offs can reliably predict risk of hepatic decompensation. Patients with cirrhosis secondary to chronic hepatitis C (HCV)

are at risk for hepatocellular carcinoma (HCC) despite sustained virological response (SVR). We examined if post-SVR LSM using the Baveno VII “Rule of 5” cut-offs can be used for risk stratification to predict the annual risk of HCC.

Method: This was a retrospective cohort study of 1,605 participants from the VOCAL cohort, with HCV cirrhosis and SVR. Patients were followed from the time of post-SVR LSM until diagnosis of HCC, death, or 03/01/2022 in the VOCAL cohort for a total follow-up of 4444.06 person-years.

Results: The annual risk of HCC was 1.43% among participants with post SVR LSM < 10 KPa, 2.52% in those with LSM 10–14.9 KPa (adjusted Hazard Ratio [aHR] vs. baseline 1.83, 95% CI 1.06–3.18, $p = 0.03$), 2.15% for LSM 15–19.9 KPa (aHR 1.56, 95% CI 0.76–3.21, $p = 0.22$), 3.43% among LSM 20–24.9 KPa (aHR 2.51, 95% CI 1.24–5.07, $p = 0.01$), and 4.14% in LSM ≥ 25 KPa (aHR 3.20, 95% CI 1.84–5.56, $p < 0.0001$).

When post SVR Fib-4 was used, the annual risk of HCC was 1.47% in participants with post-SVR Fib-4 < 1.45 (baseline) and similar at 1.82% in those with Fib-4 1.45–3.25 (aHR 1.29, 95% CI 0.68–2.43, $p = 0.44$), but elevated at 3.96% (aHR 2.91, 95% CI 1.47–5.75 $p = 0.002$) in participants with Fib-4 ≥ 3.25 .

Conclusion: Increase in LSM using the Baveno VII criteria “rule of 5” on liver elastography predicts higher rates of HCC in HCV cirrhosis after SVR at multiple cut-off levels, compared to dichotomous risk stratification by Fib-4, and offers a single test to predict risk of hepatic decompensation and HCC.

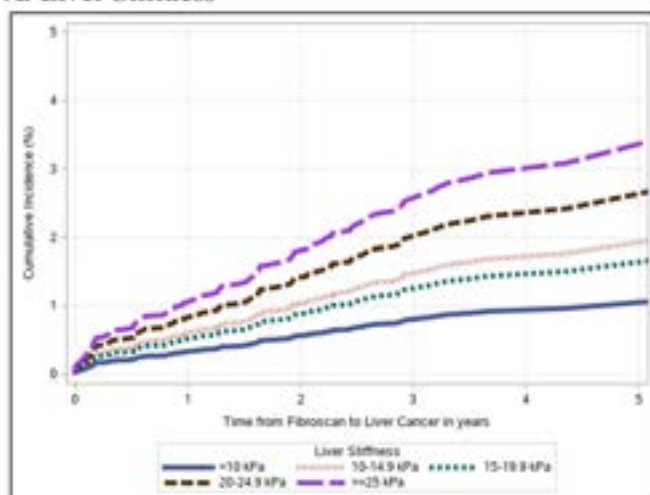
FRI-479

Liver stiffness can monitor disease severity and changes predict decompensation in alcohol-related liver disease

Katrine Thorhauge^{1,2}, Georg Semmler³, Stine Johansen^{1,2}, Katrine Prier Lindvig^{1,2}, Maria Kjærgaard^{1,2}, Nikolaj Torp^{1,2}, Johanne Kragh Hansen^{1,2}, Camilla Dalby Hansen^{1,2}, Peter Andersen^{1,2}, Mads Israelsen^{1,2}, Jonel Trebicka⁴, Thomas Reiberger³, Maja Thiele^{1,2}, Aleksander Krag^{1,2}. ¹Fibrosis, fatty liver and steatohepatitis Research Center Odense (FLASH), Department of gastroenterology and hepatology, Odense University Hospital, Odense, Denmark; ²Institute of Clinical Research, Faculty of Health Sciences, University of Southern Denmark, Odense, Denmark; ³Division of Gastroenterology and Hepatology, Department of Internal Medicine Iii, Medical University of Vienna, Vienna, Austria; ⁴Münster University Hospital, WWU, Department of Internal Medicine B, Münster, Germany

Email: katrine.holtz.thorhauge@rsyd.dk.

A. Liver Stiffness



B. FIB-4

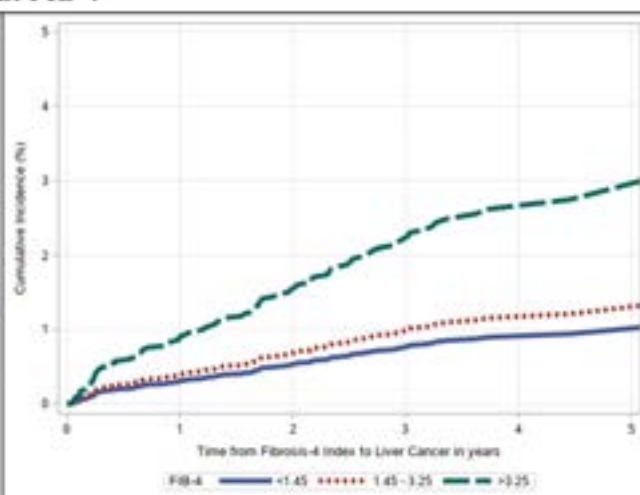


Figure: (abstract: FRI-478) Cumulative incidence frequency for adjusted hazard ratio of liver cancer by liver stiffness and FIB-4, among patients with HCV cirrhosis after SVR

Background and aims: More than 75 million people worldwide are at-risk of alcohol-related liver disease (ALD). Transient elastography (TE) is an established diagnostic and prognostic tool, but is not yet validated for disease monitoring in compensated advanced chronic liver disease (cACLD). We aimed to evaluate the value of TE for disease monitoring in ALD, as suggested by Baveno VII.

Method: Two cohorts of compensated ALD patients with long-term outcome evaluation were included. Based on repeated TE, we evaluated the risk of decompensation in cACLD (TE ≥ 10 kPa) stratified for changes in disease severity and compared to patients without cACLD (TE < 10 kPa). According to the rule-of-five (e.g. TE: 10–15–20–25 kPa), we defined disease progression as an increase of ≥ 5.0 kPa, while disease regression was defined as a repeated TE < 10 kPa or a repeated TE < 20 kPa with an associated decrease of $\geq 20\%$. We calculated subdistribution hazard ratios (SHR) from competing risk analysis with death prior to decompensation as a competing event. Moreover, we report the 3-year decompensation-free survival for the full cohort.

Results: We included 537 patients (n = 440 Odense, n = 97 Vienna) with a median age of 57 years (IQR: 49–63) and baseline TE of 8.2 kPa (IQR: 5.0–21.6). 371 patients (69%) had a repeated TE after a median of 25 months (IQR: 18–38) and were followed for additionally 37 months (IQR: 25–61) during which 41 decompensated (11%) and 55 died (15%). In cACLD patients with repeated TE (n = 125/371) 10% progressed (progressors), 43% regressed (regressors), while 14% had stable non-severe disease (TE < 25 kPa) and 33% had stable severe disease (TE ≥ 25 kPa). We found an increased risk of decompensation for patients with cACLD vs. without cACLD (SHR = 17.5, CI: 7.1–43.0, $P < 0.01$). Moreover, progressors (SHR = 3.6, CI: 1.2–11.1, $P = 0.03$) and patients with stable severe disease (SHR = 3.9, CI: 1.6–9.1, $P < 0.01$) had a significant higher risk of decompensation than regressors (figure). 13% of patients without cACLD at baseline progressed to cACLD (n = 33/246) associated with a higher risk of decompensation, but not statistically significant (SHR = 4.6, CI: 0.8–26.0, $P = 0.08$). The overall 3-year decompensation-free survival was 69% in patients with cACLD at baseline (CI: 0.62–0.75) and 97% in patients without cACLD at baseline (CI: 0.95–0.99).

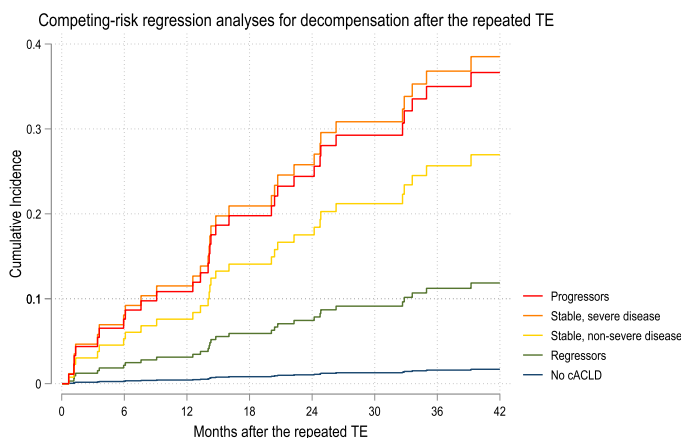


Figure:

Conclusion: Repeated TE is useful for monitoring disease severity in cACLD as defined by Baveno VII, and changes in TE accurately predicts decompensation in patients with ALD.

FRI-480

Transient elastography efficiently detects severe fibrosis in patients with chronic hepatitis D

Dominique Roulot¹, Segolene Brichler², Layese Richard³, Nathalie Ganne-Carrié¹, Christiane Stern⁴, Veronique Loustaud-Ratti⁵, Martial Gouton⁶, Françoise Roudot-Thoraval⁵, Victor de Lédinghen⁷. ¹AP-HP, hôpital

Avicenne, Liver Unit, Université Sorbonne Paris Nord, Bobigny, France; ²AP-HP, hôpital Avicenne, Laboratoire de microbiologie clinique, Université Sorbonne Paris Nord, Bobigny, France; ³AP-HP, hôpital Henri Mondor, Unité de recherche clinique, Université Paris-Est, Créteil, France; ⁴AP-HP, hôpital Beaujon, Liver Unit, Clichy, France; ⁵CHU Limoges, hôpital Dupuytren, Liver Unit, Limoges, France; ⁶AP-HP, hôpital Avicenne, Liver Unit, France; ⁷CHU Bordeaux, Hôpital Haut Leveque, Liver Unit, Bordeaux Pessac, France
Email: dominique.roulot@aphp.fr.

Background and aims: Hepatitis D virus infection (HDV) is associated with accelerated progression of liver disease to cirrhosis. Identifying severe fibrosis in chronic HDV-infected patients requiring urgent treatment is crucial. Non-invasive transient elastography (TE) has transformed the management of chronic hepatitis B and C virus infection. In patients with chronic hepatitis D, liver biopsy remains the gold standard procedure for fibrosis staging. The aim of this study was to evaluate the performance of TE (FibroScan) for the diagnosis of liver fibrosis in HDV-infected patients.

Method: TE was evaluated in HDV RNA-positive patients with liver biopsy (LB) included in a national cohort. LB and laboratory parameters were performed within 6 months from TE. Hepatic fibrosis was assessed using the Metavir stages (F0–F4). TE diagnostic performance in identifying cirrhosis (F4), severe fibrosis (F3) and significant fibrosis (F2) was compared to that of non-invasive fibrosis tests, such as the aspartate aminotransferase to platelet ratio index (APRI), the fibrosis-4 score (FIB-4) and the Delta-4 fibrosis score (D4FS). Area under receiver operator characteristics (AUROC) and Youden indexes were used to establish new cut-offs values.

Results: Data from 192 HDV-infected patients with valid TE measurements were analyzed (66% males, median age 35 [29–43] yrs, median BMI 24.0 [21.6–27.3] kg/m²). The prevalence of histologic fibrosis stages was 22.6% for F0/F1, 25.5% for F2, 8.4% for F3 and 33.5% for F4. TE demonstrated excellent diagnostic accuracy for the detection of cirrhosis with an AUROC of 0.87, compared with that of APRI (0.72), FIB-4 (0.75) and D4FS (0.84) ($p = 0.002$). TE was also superior for the detection of severe fibrosis (AUROC of 0.84, compared to 0.70 for APRI and 0.74 for FIB-4 ($p = 0.002$)). TE performance was not better, however, for the detection of significant fibrosis (AUROC of 0.78 compared to 0.73 for APRI and 0.70 for FIB-4). At the optimized cut-off value of 11 kPa for determining cirrhosis, TE showed a sensitivity of 79%, a specificity of 80%, a predictive positive value (PPV) of 67% and a negative predictive value (NPV) of 88%; 80% of the patients being correctly classified. At the optimized cut-off value of 9 kPa for determining severe fibrosis, TE had a sensitivity of 81%, a specificity of 72%, a PPV of 77% and a NPV of 77%, with 77% of correctly classified patients.

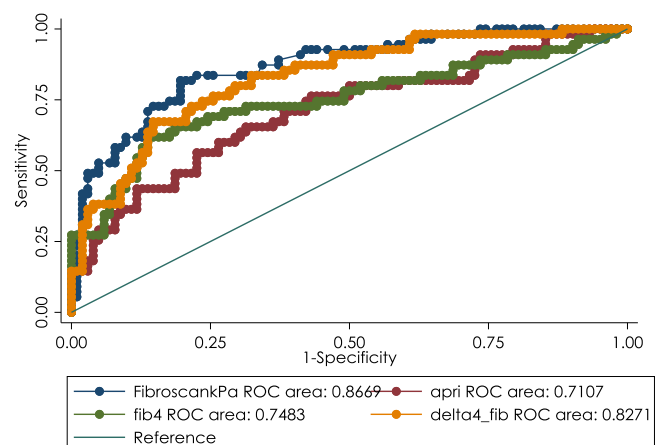


Figure: AUROC for Diagnosis of HDV cirrhosis.

Conclusion: In summary, based on these data from a large real-life cohort, TE has a good diagnostic performance for determining severe

POSTER PRESENTATIONS

fibrosis and cirrhosis in patients with chronic HDV infection at baseline.

The high probability of severe fibrosis or cirrhosis in patients with LSM >9 kPa necessitates rapid appropriate treatment. In case of LSM <9 kPa, a liver biopsy is recommended. Additional studies will evaluate the potential superior diagnostic performance of combining TE with biomarkers.

FRI-481

Screening for hepatic fibrosis in primary care by FIB-4 score, followed in second line by the ELF (enhanced liver fibrosis) test: what are the best thresholds?

Denis Ouzan^{1,2}, Guillaume Peneranda^{3,4}, Malik Jlaiei⁵, Jeremie Corneille⁶, ¹Institut Arnault Tzanck, SAINT LAURENT DU Var, France; ²RHECCA, France; ³AlphaBio, Marseille, France; ⁴BIOGROUP ALPHABIO-Laboratoire Européen, France; ⁵BIOGROUP BIOESTEREL-Laboratoire Mandelieu-Passero, France; ⁶BIOGROUP BIOESTEREL-Laboratoire Mougins-L'espérance, France
Email: denis.ouzan@wanadoo.fr.

Background and aims: Screening for liver fibrosis in the general population is a public health issue. We have shown in a previous study that FIB-4 (1), can detect liver fibrosis in general practice and identify a possible cause of liver disease. But the optimal FIB-4 threshold remains to be specified. The FIB-4 thresholds usually used are: low risk if <1.30, intermediate risk between 1.3 and 2.67, and high risk if ≥2.67. Only one study (2) has proposed an age-dependent FIB-4 threshold: FIB-4 ≥1.3 for subjects younger than 65 years and ≥2 for those older than 65 years. The objective of our work was to explore different FIB-4 thresholds and in particular the threshold of >2 for all patients, which is much simpler and independent of age, by performing a second-line ELF (Enhanced Liver Fibrosis) score, after screening for liver fibrosis by FIB-4 in general practice.

Method: The FIB-4 score was performed prospectively from March to September 2022 in all consecutive patients seen by 17, outside the emergency. When the FIB-4 was ≥1.3, it was defined as positive, and a confirmatory ELF test was systematically performed. The positive FIB-4 test was confirmed when the second line ELF test was ≥9.8 (indicating an advanced fibrosis).

Results: The results are reported in the table below. Among the 3427 patients seen in general practice, 869 (25%) had a positive FIB4 score, which was confirmed by the ELF test in 59% (n = 509) of cases. 35% of them were older than 65 years. Confirmation was significantly more frequent in subjects over 65 years of age compared to those under 65 years of age: 67% vs 36%, p < .0001. For an age-dependent FIB-4 threshold (>1.3 (<65 yrs.)/≥2 (>65 yrs.) which concerned 55% of the FIB-4 positive subjects (n = 481), 56% were confirmed by the ELF test (n = 271). For the FIB-4 threshold of 2, regardless of age which concerned 33% of the FIB-4 positive subjects (n = 284), 74% of the FIB-4 ≥2 subjects were confirmed by ELF testing versus 51% of those with a FIB-4 score <2 (Relative Risk (IC95) 1.88 (1.52, 2.32) p < 0.001). 80% of the subjects in the high risk zone of fibrosis (FIB-4 ≥2.67) were confirmed by ELF test. The percentage of subjects in the intermediate fibrosis risk decreases from 90% for a FIB-4 between 1.3 and 2.67, to 45% for a FIB-4 between 1.3/2 and 2.67, and to 23% for a FIB-4 between 2 and 2.67.

Figure: FIB4 confirmation by ELF according to FIB4 thresholds

FIB-4 Threshold	N (%)	ELF ≥ 9.8	% confirmation by ELF test in subjects < FIB-4 threshold
FIB-4 > 1.3	869 (100%)	509 (59%)	NA
FIB-4 > 1.3/2	481 (55%)	271 (74%)	61%
FIB-4 ≥ 2	284 (33%)	210 (74%)	51%
FIB-4 ≥ 2.67	85 (10%)	68 (80%)	56%

Conclusion: ELF testing performed in the second line had significantly confirmed proven fibrosis in subjects with FIB-4 ≥ 2. The high

percentage of confirmation when the FIB-4 is ≥ 2.67 confirms the high fibrosis risk of this area. A threshold of 2 retains a high percentage of confirmation while reducing the size of the intermediate risk zone for fibrosis and may allow more effective screening for liver fibrosis in primary care.

References

- Ouzan D *et al.* Prospective screening for significant liver fibrosis by FIB-4 in primary care patients without known liver disease. *Eur J Gastroenterol Hepatol* 2021;33:986–991.
- McPherson S. *et al.* Age as a Confounding Factor for the Diagnosis of Advanced NAFLD fibrosis. *Am J Gastroenterol* 2017;112:740–51.

FRI-482

Validation of cut-off values proposed by the society of radiologists in ultrasound liver elastography for diagnosis of compensated advanced chronic liver disease using 2D shear wave elastography

Ji Hun Kang¹, Yeri Lee¹, Young Seo Cho¹, Yongsoo Kim¹, Nam Hee Kim². ¹Hanyang University College of Medicine, Hanyang University Guri Hospital, Radiology, Guri, Korea, Rep. of South; ²Sungkyunkwan University School of Medicine, Kangbuk Samsung Hospital, Division of Gastroenterology, Department of Internal Medicine, Korea, Rep. of South
Email: jihunkang@hanyang.ac.kr

Background and aims: The Society of Radiologists in Ultrasound Liver Elastography proposed dual cut-off values of <9 and >13 kPa to rule out and rule in compensated advanced chronic liver disease (cACLD) using acoustic radiation force impulse techniques. However, the diagnostic performance of this recommendation has not been extensively validated. Therefore, this study aimed to validate the cut-off values for the diagnosis of cACLD using 2D shear wave elastography (SWE).

Method: From the database of liver stiffness (LS) measurement in a single center using an Supersonic Aixplorer ultrasound between 2018 and 2021, we included patients who performed esophagogastroduodenoscopy or liver biopsy within 1 year of their LS measurement. We selected the first examination in cases of multiple LS measurements and excluded unreliable LS measurement. cACLD was defined as varices shown on EGD or severe fibrosis or cirrhosis on liver biopsy, according to the Baveno VII consensus.

Results: In total, 1440 patients (mean age 58 ± 12 years, 61% males) were included and cACLD was confirmed in 717 (50%) patients. The cohort consisted of patients with chronic hepatitis B (n = 563, 39%), chronic hepatitis C (n = 92, 6%), alcohol-related liver disease (n = 475, 33%), non-alcoholic fatty liver disease (n = 151, 11%), and other etiologies (n = 159, 11%). Overall, 688 (48%) and 548 (38%) patients had LS <9 and >13 kPa, respectively. Using cut-off values of <9 and >13 kPa, the sensitivity and specificity for ruling-out and ruling-in cACLD were 84% and 92%, respectively. However, a more optimal dual cut-off of <7 and >12 kPa was found to have 92% sensitivity and 90% specificity for ruling-out and ruling-in cACLD (AUROC = 0.89; 95% CI = 0.87–0.91; p < 0.001).

Conclusion: Our study suggests that a dual cut-off of <7 and >12 kPa, as measured by 2D SWE, is more optimal for ruling-out and ruling-in cACLD than the previously proposed cut-off values.

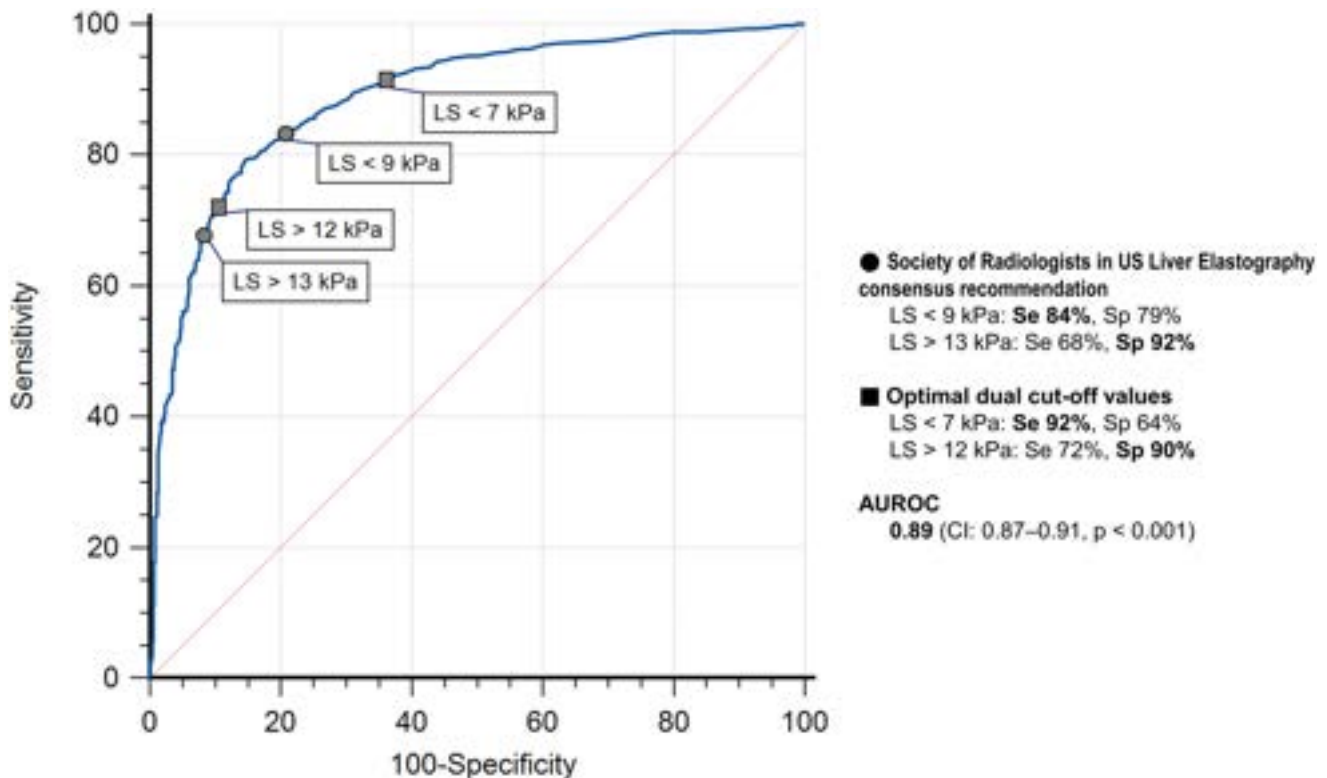


Figure: (abstract: FRI-482).

FRI-483

Hospital discharge after percutaneous liver biopsy-less is more?

Isabel Garrido¹, Rosa Coelho¹, Guilherme Macedo¹. ¹Centro Hospitalar Universitário de São João, Gastroenterology Department, Portugal
Email: isabelmng@hotmail.com

Background and aims: Liver biopsy is a technique frequently performed in clinical practice. However, the recommended surveillance period after the procedure is not established in the guidelines. The primary objective of this study was to assess the safety of hospital discharge 2 hours after a percutaneous liver biopsy. The secondary objectives were to assess the degree of patient satisfaction with early hospital discharge and to report the incidence of complications.

Method: Prospective monocentric study which included all patients who underwent percutaneous liver biopsy between December 2020 and November 2022. Individuals were discharged 2 hours after the procedure according to a protocol that was implemented in our institution. The ethical approval for this study was obtained from the Ethics Committee.

Results: A total of 200 patients were included, the majority male (52.0%), with a median age of 52 years old (IQR 40–60). There were 191 (95.5%) outpatients and 9 (4.5%) inpatients. Most procedures were made under conscious sedation with midazolam (97.0%) or under anesthesia with propofol (1.0%). A total of 88 (44.0%) US-guided biopsies were performed with the Tru-cut needle (16G or 18G) and 112 (56.0%) after US site marking with the Menghini needle. Two-needle passes were required in 33 (16.5%) cases, three-needle passes in 8 (4.0%) cases and four-needle passes in 1 (0.5%) case. In addition to a biopsy of the liver parenchyma, 6 (3.0%) patients also underwent a biopsy directed to a liver lesion/nodule. Forty-two (21.0%) individuals had complications at the time of or within 2 hours of the procedure (abdominal pain $n=29$, pain radiating to the shoulder $n=11$, headache $n=2$). Most complications (90.4%) occurred in the first hour after the liver biopsy. Thirty-five (17.5%) patients required analgesia. Only 5 (2.5%) patients were kept under observation for 4 hours due to abdominal/shoulder pain. On the phone call made by

the nurse, carried out 4 hours after the procedure, 28 (14.0%) patients reported abdominal/shoulder pain, 2 (1.0%) patients reported nausea and 1 (0.5%) patient reported headache. Only 5 of these individuals underwent analgesic therapy and all of them reported symptomatic improvement. In addition, 2 (1.0%) patients contacted the on-call physician for shoulder pain (4 days after the procedure) and nausea (3 days after the procedure). There were no serious complications and no patient required admission. The majority of individuals reported being satisfied (21.6%) or very satisfied (77.8%) and felt safe (98.9%) with this protocol.

Conclusion: This is one of the first prospective studies worldwide to prove that patients requiring percutaneous liver biopsy can be safely discharged after a short recovery time. In fact, major complications after liver biopsy are rare and manifest early. In addition, patients showed a preference for early hospital discharge and felt safe with this protocol.

FRI-484

Non-invasive assessment of adult bilirubin based on multispectral reconstruction technology and a smartphone platform

WenQian Geng¹, Zhiyuan Sun², Wanyu Li¹. ¹The first hospital of Jilin University, Department of hepatobiliary and pancreatic Medicine, Changchun, China; ²Chinese academy of sciences, Changchun institute of optics, fine mechanics and physics, Changchun, China
Email: liwanyu@jlu.edu.cn

Background and aims: Jaundice refers to yellow coloration of the skin and sclera caused by increased levels of serum bilirubin, which is an important indicator of liver function. The aim of this study is to evaluate jaundice in a meticulous, non-invasive and intelligent way by using multispectral reconstruction technology on the platform of smartphone.

Method: A total of 351 patients with normal or elevated total serum bilirubin (TSB) were selected. Non-invasive detection equipment was set up, and scleral images were obtained without an external light

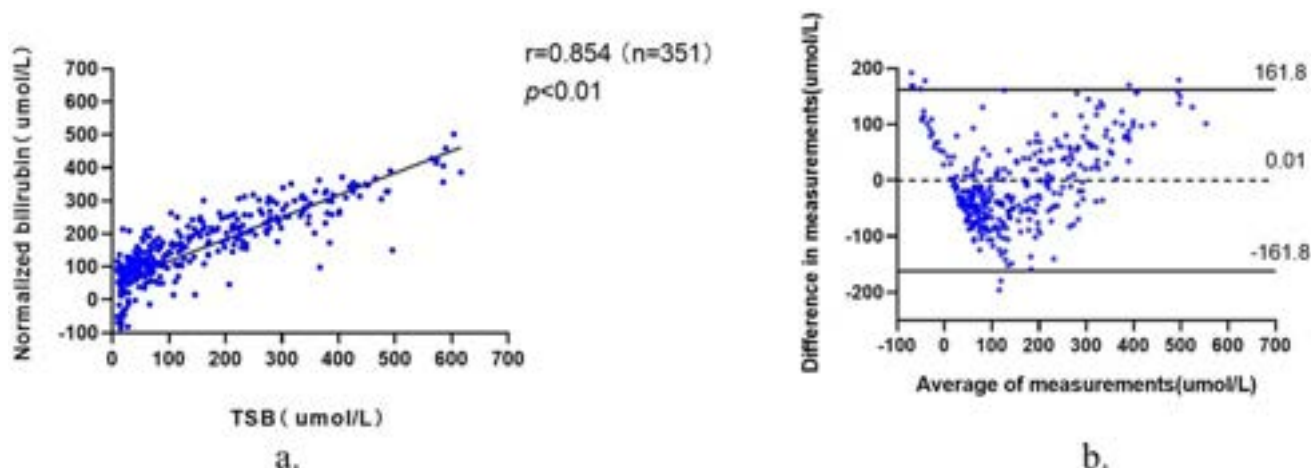


Figure: (abstract: FRI-484): **a.** Correlation between total serum bilirubin (TSB) and normalized bilirubin: $r=0.854$, $p<0.01$. TSB: Total serum bilirubin. **b.** Bland-Altman plot of TSB versus normalized bilirubin. The mean difference is zero and 97.4% of the values were within the 95% limits of agreement, i.e., ± 161.8 umol/L.

source in the room. After the scleral image was extracted, the RGB image of the sclera was reconstructed into a multispectral image to obtain the quantized bilirubin level, namely, the normalized bilirubin value.

Results: The linear correlation coefficient between the normalized bilirubin value and TSB was 0.854 (Fig. a). The Bland-Altman consistency test indicated that 97.4% of the values were within the 95% limits of agreement (LOA) (Fig. b). There were no significant differences in the normalized bilirubin values of the sclera at different orientations in the same patient. There was a high correlation between normalized bilirubin and TSB in different groups of sex, age, bilirubin grade, disease spectrum and bilirubin elevation type. The area under the receiver operating characteristic (ROC) curve was 0.90, the sensitivity was 75.0%, and the specificity was 92.0%.

Conclusion: The non-invasive bilirubin detection method we proposed has high accuracy, sensitivity and universality. Compared

with the “gold standard” of bilirubin detection, this non-invasive detection method is cost-effective, easy to perform, and can reduce the discomfort of patients, suitable for long-term monitoring of bilirubin.

FRI-485

Diagnosis and treatment of patients with suspected mucinous cystic neoplasms according to the EASL-guidelines: a retrospective cohort study

Alicia Furumaya^{1,2}, Hannah Schulz^{1,2}, Joanne Verheij^{1,2}, Bart Takkenberg^{1,2}, Marc Besselink^{1,2}, Geert Kazemier^{3,4}, Joris Erdmann^{1,2}, Otto van Delden^{1,2}. ¹Amsterdam Umc, University of Amsterdam, Netherlands, ²Amsterdam Gastroenterology Endocrinology Metabolism, Netherlands, ³Amsterdam Umc, Vrije Universiteit Amsterdam, Netherlands; ⁴Cancer Center Amsterdam, Netherlands<Please check the city names are missing.> Email: a.furumaya@amsterdamumc.nl

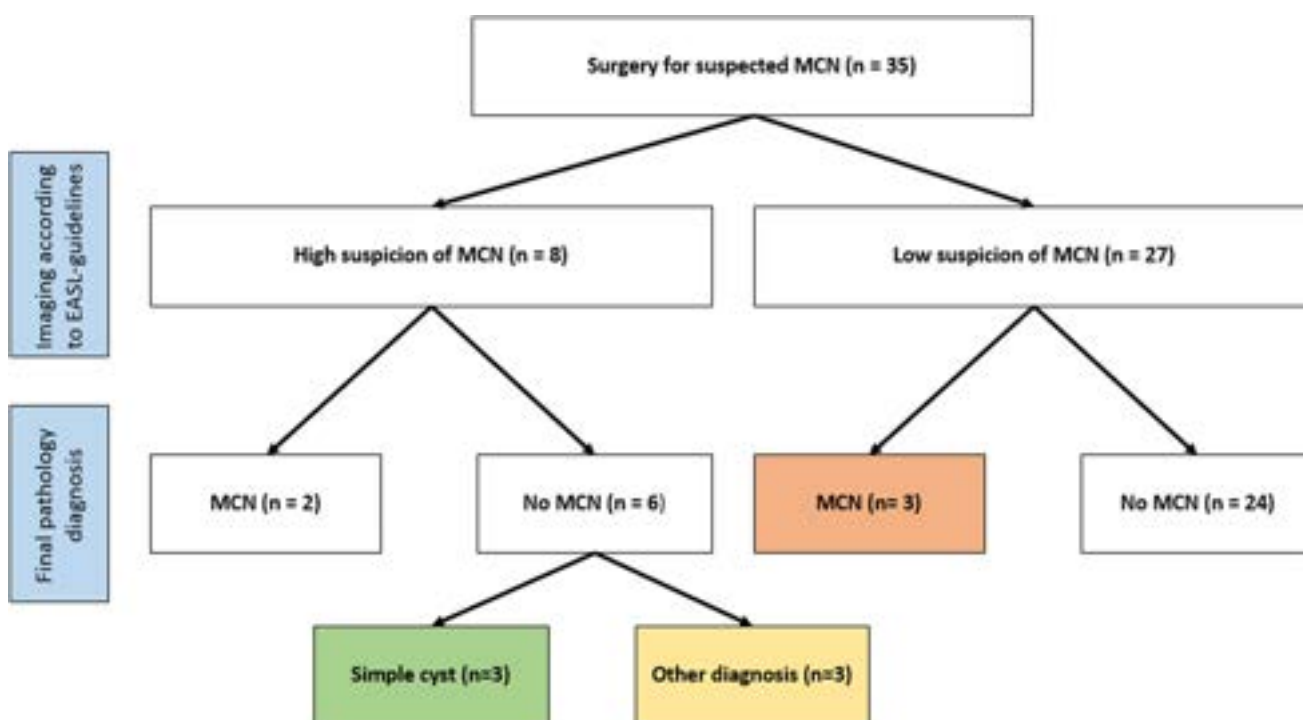


Figure: (abstract: FRI-485).

Background and aims: Mucinous cystic neoplasms (MCNs) are a rare subset of hepatic cysts with a low malignant potential. The recent European Association for the Study of the Liver (EASL) guidelines provide guidance on the imaging features and surgical management of MCNs, yet are hampered by a lack of studies adhering to the revised World Health Organization (WHO) criteria. Therefore, the current study attempted to validate the new 2022 EASL-guidelines in a retrospective cohort study of patients who underwent surgery for suspected MCN.

Method: Patients undergoing surgery for suspected MCN in a single center between 2010 and 2020 were included. Imaging features were assessed according to the EASL guidelines and were compared to final pathological diagnoses, according to the WHO criteria. Surgical outcomes were compared between deroofing and complete (minor or major) resection.

Results: In total, 35 patients were included. In three patients, there were no worrisome imaging features, yet final pathological diagnosis showed MCN. Contrarily, three patients with worrisome imaging features had simple cysts and another three patients with worrisome imaging features had an alternative diagnosis. The sensitivity of the EASL-guidelines for the diagnosis of MCN was 40% (95%CI: 5.3–85%) and the specificity was 80% (95% CI: 61–92%). More recurrences occurred after deroofing (n = 4/15) compared to complete, minor resection (n = 0/17, p = 0.038).

Conclusion: In conclusion, although the new EASL-guidelines provide some guidance, they could not reliably distinguish MCN from other cysts in our series. Thus, we should be careful in selecting surgical strategies based on these criteria.

FRI-486

Use of magnetic resonance elastography for accurate staging of liver fibrosis in children with autoimmune hepatitis

Wojciech Janczyk¹, Jędrzej Sarnecki², Piotr Pawliszak², Paulina Opyrchal², Kamil Janowski³, Diana Kamińska³, Małgorzata Woźniak³, Wiesława Grajkowska⁴, Maciej Pronicki⁴, Elżbieta Jurkiewicz², Piotr Socha³. ¹Children's Memorial Health Institute, Gastroenterology, Hepatology, Feeding Disorders and Pediatrics, Warsaw, Poland; ²Children's Memorial Health Institute, Radiology, Poland; ³Children's Memorial Health Institute, Gastroenterology, Hepatology, Feeding Disorders and Pediatrics, Poland; ⁴Children's Memorial Health Institute, Pathology, Poland
Email: w.janczyk@ipczd.pl

Background and aims: Autoimmune hepatitis (AIH) may present as hepatitis, chronic or acute liver failure. Liver fibrosis may progress to cirrhosis. Pharmacological treatment is aimed to preserve liver function and induce remission. Magnetic resonance elastography (MRE) has been already applied in many chronic liver diseases for non-invasive assessment of liver fibrosis. Previously we showed an excellent diagnostic accuracy of transient elastography in assessment of advanced liver fibrosis in children with AIH. Now we aimed to evaluate the usefulness of MRE in relation to liver biopsy and selected laboratory markers of liver function in the large pediatric AIH cohort.

Method: We included 48 children (26 females) with mean age of 13.9 yrs with established AIH and 16 healthy children aged 14.4 yrs as controls. All patients with AIH underwent liver biopsy and MRE to assess liver fibrosis. Liver biopsy was performed for monitoring purposes. Histology was described semiquantitatively based on modified scoring system by Ischak. Statistical analysis was performed to assess correlation between liver fibrosis on histology, MRE and selected lab tests. The area under the curve (AUC) for the ROC and its 95% CI were calculated to determine diagnostic accuracy of MRE in estimating mild fibrosis vs advanced fibrosis. The AUC were calculated by using the logistic procedure in MedCalc v. 20.215

Results: Our patients with AIH presented with increased liver fibrosis on MRE 3 kPa (2.4; 3.8) [median (lower; upper quartile)] and various grade of fibrosis according to histological score. Fibrosis on MRE was

significantly higher in AIH than in healthy control group 2.3 kPa (2.2; 2.6); p = 0.002 using Mann-Whitney U test.

For diagnosis of advanced fibrosis (>=F4) MRE showed very good diagnostic accuracy (AUROC 0.88) and even better for >F5 (AUROC 0.9). Optimal cut-off point for >F5 was 3.65 kPa with high sensitivity and specificity (see Figure below).

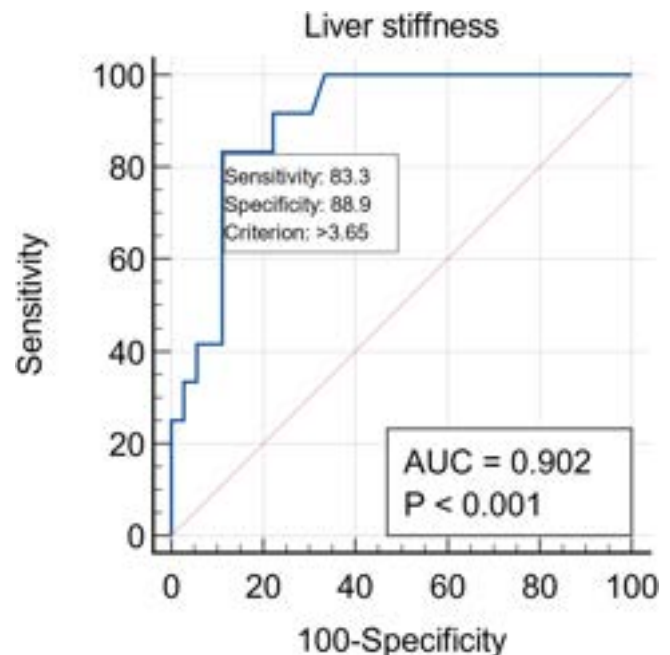


Figure:

Conclusion: MRE was highly accurate to discriminate between mild and advanced fibrosis when compared to liver biopsy. MRE can be used in children with autoimmune hepatitis for assessment of liver fibrosis and especially to pick up those patients with advanced fibrosis.

FRI-487

Fibrosis-4 index is associated with cardiovascular risk in people living with HIV

Giulia Morsica¹, Costanza Bertoni^{1,2}, Daniele Ceccarelli¹, Laura Galli¹, Hamid Hasson¹, Alessia Siribelli^{1,2}, Riccardo Lolatto¹, Antonella Castagna^{1,2}, Caterina Uberti-Foppa^{1,2}. ¹San Raffaele, Scientific Institute, Dept. of Infectious Diseases, Milan, Italy; ²Vita Salute, University, Milan, Italy
Email: morsica.giulia@hsr.it

Background and aims: The severity of liver fibrosis dictates the risk of cardiovascular complications. We investigated the association between Fib4 and the cardiovascular risk (CVR) in patients living with HIV (PLWH) and the diagnostic performance of fibrosis4 (Fib4) index as non-invasive marker of liver fibrosis (NILF).

Method: CVR and Fib4 were calculated in 5235 PLWH using the atherosclerotic cardiovascular disease (ASCVD) score categorized as <7.5 = low risk, 7.5–20 = intermediate risk, >20 = high risk. LF by fibroscan was categorized according to manufacturer's cutoff: F0-F1 = <7 KPa; F2 = 7–9 KPa; F3-F4 >9 KPa). The diagnostic performance of Fib4 was assessed in 855 PLWH with paired fibroscan as gold standard for LF. The area-under-the-curve (AUC) and the cut-off values of Fib4, compared to LF classification (F0-F1 vs F2 and F2 vs F3-F4), were determined by the logistic regression and the receiver operating characteristics (ROC) curves.

Results: The AUC-ROC identified a Fib4 threshold of 1.30 for F2 vs F0-F1 and 2.35 for F3-F4 vs F2 (Fig. 1). Of 5235 PLWH, 3167 had Fib-4 < 1.30 (group1) 1551 had Fib4 >1.30<2.35 (group2) and 517 had Fib4

POSTER PRESENTATIONS

>2.35 (group3). PLWH in group1 were younger, median age 47 years (yr) compared with group2 and 3 (median age 57 and 57 yr, respectively) $P < 0.0001$. PLWH in group2 and 3 had a longer duration of ART, median 17.9 and 18.5 yr, respectively, vs 10 yr in group1 with higher rate of detectable HIV-RNA (>50 copies/ml in 10% of group2 and 13% of group3) compared to group1 (7%) lower CD4, median 547 and 662 cells/mm³, respectively, vs 733 cells/mm³ in group1. HBV and HCV were present in 5.0% and 16% of group1, in 7% and 31% of group2 and 10% and 50% of group3, respectively, $P < 0.001$; PLWH with a Fib4 >1.30–2.35 compared to those with a Fib4 ≤1.30 had a risk of intermediate ASCVD of 2.89 (95%CI: 2.52–3.32) and a risk of high ASCVD of 6.26 (95%CI: 4.91–7.99). PLWH with a Fib4 >2.35 compared to those with a Fib4 >1.30–2.35 had a risk of intermediate ASCVD of 1.44 (95%CI: 1.26–1.66) and a risk of a high ASCVD of 2.72 (95%CI: 2.98–3.23).

Figure 1. FIB-4 values according to stiffness categories (Panel A); ROC curves predict FIB-4 thresholds in predict F1 vs F0/F1 stiffness categories (Panel B) and F3 vs F2 vs F3-F4 stiffness categories (Panel C).

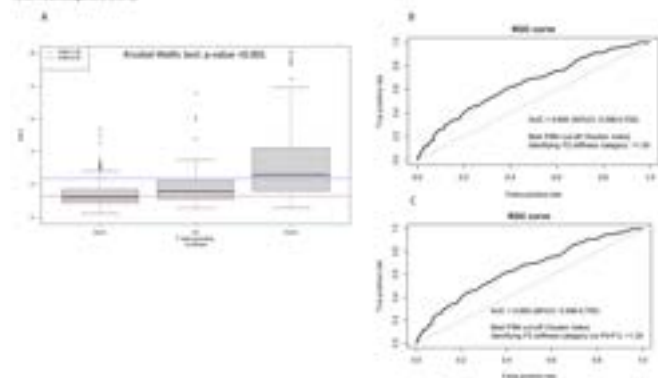


Figure:

Conclusion: We identified a Fib4 thresholds distinguishing F0-F1 vs F2 vs F3-F4 stiffness categories in PLWH. We found the correlation of Fib4 with CVR assessed by ASCVD in a large sample size of PLWH.

FRI-488

Diagnostic accuracy of magnetic resonance elastography, transient elastography and predictive scores in cystic fibrosis related liver steatosis and fibrosis

Ana Piñar Gutiérrez¹, Carmen Lara Romero¹, Silvia García Rey¹, María C. Roque-Cuellar¹, Javier Castell¹, Ángeles Pizarro Moreno¹, Esther Quintana Gallego¹, Pedro Pablo García-Luna¹, Manuel Romero Gomez¹. ¹Virgen del Rocío University Hospital, Sevilla, Spain

Email: mromerogomez@us.es

Background and aims: Cystic fibrosis-related liver disease is a complication whose definition, etiopathogenesis, diagnostic criteria and associated factors are not well known. In this entity, liver biopsy has been shown to be inconsistent, so other diagnostic tools should be sought. In addition, it is still unclear whether liver steatosis is part of its varied clinical presentation or a separate entity. Aims were to determine the prevalence of steatosis and liver fibrosis in a cohort of adult patients performing imaging-derived proton density fat fraction (PDFF) and magnetic resonance elastography (MRE) respectively; the usefulness of non-invasive liver tests (NITs) and transient elastography (TE) in the diagnosis of this entity; as well as factors related to a higher prevalence of both entities.

Method: Cross-sectional study. Adult patients cared for in a Cystic Fibrosis Unit were included. Liver assessment was performed by TE, NITs (APRI, FIB4, HSI, NFS), PDFF and MRE. To evaluate the specificity and sensitivity of TE and NITs compared to PDFF and MRE as gold-standards, ROC curves were performed. A univariate analysis was performed to search for factors associated with both entities.

Results: N = 84. Age = 32.5 (24.75–41) years. Women = 35 (41.7%). Exocrine pancreatic insufficiency = 55 (65.5%); endocrine pancreatic

insufficiency = 39 (46.4%); malnutrition = 7 (8.3%). 20.2% presented with liver steatosis in PDFF; 23.8% in TE. 10.7% presented with liver fibrosis in MRE; 10.7% in TE. The ROC curves of diagnostic accuracy of TE compared to PDFF and MRE are shown in Figure 1. None of the NITs performed had a statistically significant diagnostic accuracy. In univariate analysis, malnutrition (95% CI 0.165 (0.033–0.829); $p = 0.029$) and elevated alkaline phosphatase levels (95% CI 1.013 (1.003–1.029); $p = 0.015$) were related to liver steatosis; and age (95% CI 0.906 (0.824–0.996); $p = 0.042$), endocrine pancreatic insufficiency (95% CI 11.355 (1.351–95.459); $p = 0.025$), elevated GOT (95% CI 6.7 (1.487–30.189); $p = 0.013$), GPT (CI 95% 4.665 (1.079–20.086); $p = 0.039$), total bilirubin (CI 95%; 29.583 (5.14–170.277); $p < 0.001$) and alkaline phosphatase (CI 95% 1.025 (1.008–1.042) $p = 0.005$) levels, thrombocytopenia (95% CI 21.143 (1.697–263.427); $p = 0.018$) and vitamin A (95% CI 0.915 (0.848–0.987); $p = 0.022$) and E (95% CI 0.997 (0.995–1); $p = 0.03$) deficiency were related to liver fibrosis.

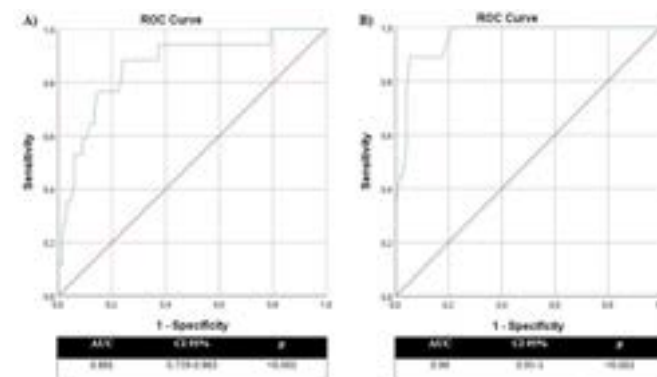


Figure 2. ROC curves of transient elastography for the diagnosis of hepatic steatosis (A) and hepatic fibrosis (B) compared to MRE.

Figure:

Conclusion: One fifth of the patients presented liver steatosis and one tenth liver fibrosis. The diagnostic accuracy of TE may be comparable to that of PDFF and MRE, which is less accessible. The factors associated with both entities were mainly related to poor nutritional status and biochemical parameters related with liver dysfunction.

FRI-489

Negative and positive predictive values of utilizing a two-stage approach to non-invasive fibrosis testing in patients with hepatitis C virus infection

Rachel Epstein^{1,2}, Benjamin Buzze³, Laura F. White⁴, Jordan J. Feld⁵, Laurent Castera⁶, Richard Sterling⁷, Benjamin Linas¹, Lynn Taylor⁸.

¹Boston University Chobanian and Avedisian School of Medicine, Medicine, Section of Infectious Diseases, United States; ²Boston University Chobanian and Avedisian School of Medicine, Pediatrics, Section of Infectious Diseases, United States; ³Boston Medical Center, Infectious Diseases, United States; ⁴Boston University School of Public Health, Biostatistics, United States; ⁵University of Toronto, Toronto Centre for Liver Disease, Toronto, Canada; ⁶Hopital Beaujon, Assistance Publique-Hôpitaux de Paris, University of Paris, Hepatology, France; ⁷Virginia Commonwealth University, Internal Medicine, Division of Gastroenterology, Hepatology and Nutrition, United States; ⁸University of Rhode Island, United States

Email: rachel.epstein@bmc.org

Background and aims: Non-invasive liver disease staging methods have supplanted liver biopsy for clinical care of most individuals with hepatitis C virus (HCV). Few data exist to compare test accuracy when using a two-test approach of an initial screening serum-based test followed by a second test with higher specificity. This study aims to estimate sensitivity, specificity, negative and positive predictive values (NPV and PPV) for detecting cirrhosis when using tests in combination.

Table: (abstract: FRI-489).

Test	Single Test				Staged two-test approach: Indicated test + TE for F2/F3 Only				Two-tests for all approach: Indicated test + TE for all			
	Sensitivity	Specificity	NPV	PPV	Sensitivity	Specificity	NPV	PPV	Sensitivity	Specificity	NPV	PPV
APRI	68.6%	79.4%	98.3%	14.3%	95.8%	81.6%	99.8%	18.6%	95.8%	81.2%	99.8%	18.2%
FIB-4	60.8%	90.1%	98.2%	27.2%	93.1%	89.3%	99.7%	27.6%	94.8%	88.7%	99.8%	26.8%
FibroTest	85.7%	71.3%	99.0%	12.3%	98.1%	72.9%	99.9%	13.6%	98.1%	72.6%	99.9%	13.5%
TE	86.7%	91.9%	99.4%	51.3%	-	-	-	-	-	-	-	-

NPV and PPV calculated using a prevalence of cirrhosis that reflects US population with chronic HCV accessing care at federally qualified health centers: 44.8% F0, 25.5% F1, 21% F2, 4.5% F3, 4.2% F4.

Method: We performed secondary data analysis on clinical trial and retrospective data from collaborators and the literature for patients with HCV with or without HIV co-infection for four major fibrosis staging methods: Fibrosis-4 (FIB-4; N = 579), AST-to-platelet ratio index (APRI; N = 580), FibroTest (N = 101), and Transient Elastography (TE; N = 282). We used a stochastic, individual-based microsimulation model (HEP-CE) to predict Metavir fibrosis stage using independent probabilities from each staging test based on this data, using liver biopsy as gold standard for true Metavir fibrosis stage. We compared two strategies: each serum test in combination with TE only for those with intermediate (F2/F3) results on the first test (staged approach) or each test in combination with TE for all individuals (two tests for all), and selected the maximum result from the two tests. We then calculated sensitivity, specificity, NPV and PPV of correctly identifying cirrhosis (F4), using Metavir fibrosis stage prevalence of a US national federally qualified health center cohort with chronic HCV.

Results: With the calculated population prevalence of cirrhosis of 4.2%, individual test NPVs for cirrhosis ranged from 98.2% for FIB-4 to 99.4% with TE (Table). PPV ranged from 12.3% (FibroTest) to 51.3% (TE). Sensitivity of detecting cirrhosis improved from 60.8–86.7% with individual tests to 93.1–98.1% with two-test approaches. However, combining serum testing strategies with TE resulted in only slightly higher NPV (range: 99.7% for FIB-4 to 99.9% for FibroTest) and PPV (range: 13.5% with FibroTest to 27.6% with FIB-4) for correctly staging F4 than serum testing alone. NPV and PPV changed minimally between using a second testing method for all vs. only for those with intermediate stages (F2/F3) on the first test.

Conclusion: We demonstrate that with low prevalence of cirrhosis, combining results from a serum staging test plus TE minimally improves NPV for detecting cirrhosis over using a serum test alone, and performing TE in all yields limited clinical benefit over the staged approach. These data can help inform clinicians practicing in various settings with different availability of testing and also decision modelers to estimate clinical and cost-effectiveness of fibrosis staging methods.

FRI-490

Repeatability of liver stiffness measurement by vibration-controlled transient elastography and controlled attenuation parameter in patients with cirrhosis

Rohit Loomba¹, Jaclyn Bergstrom¹, Maral Amangurbanova¹, Christie Hernandez¹, Egbert Madamba¹, Claude Sirlin¹, Daniel Huang¹. ¹University of California San Diego, United States
Email: daniel_huang@nus.edu.sg

Background and aims: The regulatory qualification of non-invasive tests (NITs) for liver fibrosis severity assessment is a major unmet need for drug development and clinical care in cirrhosis. Ultrasound-based methods such as vibration-controlled transient elastography (VCTE) evaluate liver stiffness measurement (LSM) and controlled attenuation parameter (CAP) as a marker for fibrosis severity and steatosis, respectively. Repeated use of VCTE has the potential to assess disease response and progression. However, this potential application has been limited by a paucity of repeatability data in the

patient population at risk. The aim of this prospective study from the San Diego Cirrhosis Registry was to address this knowledge gap and contribute to the evidentiary basis needed for the qualification of ultrasound-based methods in various contexts of use in clinical trials and practice.

Method: A prospective cohort of adults with suspected or established cirrhosis underwent two FibroScan examinations (Fibroscan Expert 630, Echosens, France) on the same day performed by the same experienced operator. LSM by VCTE and CAP measurements were reported and analyzed in units of kPa and dB/m, respectively. The primary end point was the same-day/same-operator repeatability coefficient (RC), which represents the value under which the difference between repeated measurements should fall with a 95% probability. Secondary outcomes include the intra-class correlation coefficient (ICC) which represents the proportion of total variation explained by between-patient differences rather than measurement variation, and the within-case coefficient of variation (wCV), which represents the ratio of within-patient variation to overall measurement values.

Results: Repeat scans were available on 24 participants (mean age of 61 years, 58% were women, mean body mass index (BMI) was 30.4 kg/m²). The percentage of cases due to non-alcoholic steatohepatitis (NASH), alcohol, hepatitis C virus, and hepatitis B virus were 67%, 13%, 17%, and 4%, respectively. RC was 7.4 kPa for LSM by VCTE and 82.1 dB/m for CAP, meaning that any change greater than those values has a 95% probability to reflect true change rather than measurement error. ICC was excellent for LSM (.96) and fair for CAP (.74), while wCV indicates that the within-patient variation is close to the overall measurement values for LSM and CAP (Table 1).

Table: Repeatability, intra-class correlation, and within-case coefficients for LSM by VCTE and CAP

	Mean (SD)	Repeatability Coefficient (RC)	Intra-class Correlation ICC (95% CI)	Within-case Coefficient of Variation (wCV)
LSM by VCTE (kPa)	19.9 (13.1)	7.4	.96 (.91–.98)	13.1%
CAP (dB/m)	262.5 (54.7)	82.1	.74 (.50–.88)	11.6%

Conclusion: LSM and CAP measurement by FibroScan XXX model, demonstrated good repeatability within patients with cirrhosis. These repeatability estimates are likely to inform ultrasound-based NIT qualification by defining the values that are expected to reflect a true change in the context of clinical trials or clinical care.

FRI-491

Pattern of transient elastography in Egyptian people living with HIV: predictors of hepatic steatosis and fibrosis

Naeema El Garhy¹, Lamiaa Al sehem¹, Reham Awad Awad Ibrahim¹, Mariam I. Abdelraouf¹, Ammar Hatem¹, Aya M. Al-shari¹, Haidi Karam-Allah², Engy Alkhatib¹, Rahma Mohamed¹, Gamal Esmat¹, Ahmed Cordie¹. ¹Kasr Alainy, Egypt; ²Assuit University, Egypt

Email: naemaelgarhy92@gmail.com

Background and aims: Liver related disease contributes to 13–18% of all-cause mortality in people living with HIV (PLWHIV). Transient elastography (TE) has been validated as a non-invasive tool for assessment of liver fibrosis stage. By means of controlled attenuation parameter (CAP), TE proved to be a useful screening tool for steatosis (HS) in patients at high-risk for NAFLD. TE use in HIV mono-infected patients has not yet been validated as in patients with other liver diseases. The aim of this study was to analyze the TE data in an Egyptian cohort of PLWHIV, and determine the predictors of fibrosis and HS in them.

Method: This cross-sectional study was conducted on PLWHIV in Kasr Alainy Viral Hepatitis Centre between July-December 2022. Focused clinical interview was performed including smoking, alcohol use, hepatitis C or B (HCV or HBV) co-infection, hypertension, dyslipidaemia or diabetes mellitus (DM) and any co-morbidity suggestive of metabolic syndrome. Body mass index (BMI) was calculated, and patients were examined for signs of liver disease. Active HCV or HBV co-infection was excluded. Patients who previously received HCV treatment and achieved SVR were included in this cohort. Testing was done for liver enzymes, glycated haemoglobin (HbA1c), lipogram, HIV RNA and CD4 count. After fasting, a good quality TE was performed. Results of fibrosis were considered significant if liver stiffness (LS) >7.1 and significant HS if CAP >238 dB/m.

Results: A total of 145 patients were included; 83.4% were males, 36.25 ± 10.2 years was the mean age, 45.5% were smokers, 15.9% reported occasional alcohol intake, 13.8% had previous HCV, and 46.2% were obese. The median ALT and AST were 22 and 25, respectively. Mean HbA1c was 5.59 ± 0.7 and undetected HIV viral load in 58.6%. As indicated by TE, 11.7% had significant fibrosis, F4 in 1.4%, 32.4% had HS, significant HS in 24.8%, and 8.3% had both HS and fibrosis. HbA1c and higher cholesterol were predictors of fibrosis (OR: 7.02 and 1.04, respectively). Meanwhile, obesity and older age were predictors of HS (OR: 3.41, and 1.07, respectively).

Items	Hepatic fibrosis				Hepatic steatosis			
	P value	OR	95% CI Lower level	95% CI Upper level	P value	OR	95% CI Lower level	95% CI Upper level
Age	0.25	1.04	0.97	1.11	0.01*	1.07	1.02	1.12
Sex	0.08	0.08	0.00	1.39	0.27	1.87	0.61	5.72
HCV	0.14	3.67	0.66	20.32	0.68	0.76	0.21	2.79
DM	0.89	0.86	0.09	8.53	0.88	0.88	0.17	4.54
Hypertension	0.31	4.08	0.27	62.59	0.71	0.62	0.05	7.65
Obesity	0.48	0.58	0.13	2.61	0.01*	3.41	1.31	8.89
HIV RNA	0.42	1.88	0.41	8.67	0.67	0.81	0.32	2.08
CD4 count	0.35	0.99	0.99	1.00	0.82	1.00	0.99	1.00
Triglyceride	0.23	1.01	0.995	1.02	0.26	1.00	0.99	1.01
Cholesterol	0.03*	1.04	1.00	1.08	0.55	0.99	0.98	1.01
HDL	0.94	0.99	0.92	1.08	0.74	0.99	0.95	1.04
HbA1c	0.02*	7.02	1.33	36.96	0.28	1.52	0.71	3.24

Conclusion: In this first Egyptian report on PLWHIV, older age, DM, dyslipidemia, and obesity were predictors of significant fibrosis and hepatic steatosis.

FRI-492

Enhanced detection of cirrhosis and risk of advanced fibrosis with dynamic breath analysis

Giuseppe Ferrandino¹, Antonio Murgia¹, Iris Banda¹, Yusuf Ahmed¹, Menisha Manhota¹, Kelly Sweeney¹, Louise Nicholson-Scott¹, Lucinda McConville¹, Federico Ricciardi¹, Olga Gandelman¹, Max Allsworth¹, Billy Boyle¹, Agnieszka Smolinska^{1,2}, Carmen Alexandra Ginesta Frings^{3,4}, Jorge Contreras⁴, Claudia Del Carmen Asenjo Lobos⁵, Víctor Gabrielli Rivera³, Viviana Barrientos Parra³, Nataly Clavo Morales³, Angela Novoa Arce⁴, Amy Riviotta⁵, Melissa Javiera Jerez Pardo⁶, Luis Arnaldo Mendez Alcama^{3,4}. ¹Owlstone Medical, United Kingdom; ²Department of Pharmacology and Toxicology, School for Nutrition and Translational Research in Metabolism (NUTRIM), Maastricht University Medical Center, Netherlands; ³Hospital Padre Hurtado, Chile; ⁴Clinica Alemana, Gastroenterología, Chile; ⁵Instituto de Ciencias e Innovación en Medicina (ICIM), Las Condes, Chile; ⁶University of the Americas, Chile
Email: giuseppe.ferrandino@owlstone.co.uk

Background and aims: Recent calls for action and a keynote statement on EU health policy highlighted the clinical need for chronic liver disease detection before decompensation to reduce the associated burden and premature mortality. Chronic liver diseases alter the systemic bioavailability of xenobiotics undergoing phase 1 metabolism. Limonene, one of these xenobiotics, is partially excreted unchanged in the breath, where it can be non-invasively measured to assess alterations associated with chronic liver diseases. With an unprecedented study design, dynamic limonene breath analysis was evaluated for classification performance for cirrhosis, and correlations with risk of liver fibrosis and disease severity.

Method: A total of 30 subjects with cirrhosis [21 female (f), 9 males (m)] [10 non-alcoholic fatty liver disease (NAFLD), 1 alcoholic, 1 viral hepatitis, 7 autoimmune hepatitis, 11 other] [Child-Pugh: 23 A, 5 B, 2 NAs] and 29 controls without liver diseases [17 f, 12 m], were enrolled with random recruitment, and orally administered 100 mg limonene after an overnight fasting. Breath samples were collected before, and 20, 40, 60, 90, and 120 minutes after ingestion using the ReCIVA® breath sampler. Absolute limonene quantification was obtained by gas chromatography mass spectrometry. Blood tests were administered to all the subjects within 6 months from breath sampling. Logistic regression with cross-validation was used to estimate Area Under the Curve (AUC) for each timepoint. Correlation of breath limonene with risk of fibrosis and disease severity was evaluated using canonical correlation analysis (CCA).

Results: Subjects with cirrhosis with a Median (M) age of 59 years (y) and IQR (54.3–66.8 y) showed significant difference in age compared to controls (M = 43 y, IQR = 38–57y) (p value <0.01). All tested timepoints, showed higher levels of breath limonene in subjects with cirrhosis compared to controls (p <0.01). At baseline limonene discriminated subjects with cirrhosis from controls with an AUC (SD) of 0.87 (0.11). Limonene administration induced a spike on breath of >100 folds with a peak (Cmax) after 20 or 40 minutes (Tmax) in more than 90% of the subjects. AUCs (sd) at post administration timepoints were respectively: 0.89 (0.10); 0.93 (0.06) (Fig. 1A); 0.91 (0.08); 0.92 (0.07); 0.94 (0.06).

In subjects with cirrhosis, breath limonene levels at Cmax showed a collective correlation with liver fibrosis risk estimated with FIB4 and APRI, and disease severity estimated with MELD score [R² = 0.76, p = 3e-5] (Fig. 1B). No correlations were observed in the control group.

Conclusion: The dynamic limonene breath analysis demonstrates excellent performance to discriminate cirrhosis. It may also serve to identify fibrosis and have a prognostic role in patients with liver disease. This premise should be evaluated with/against Fibroscan in patients with various stages and etiologies.

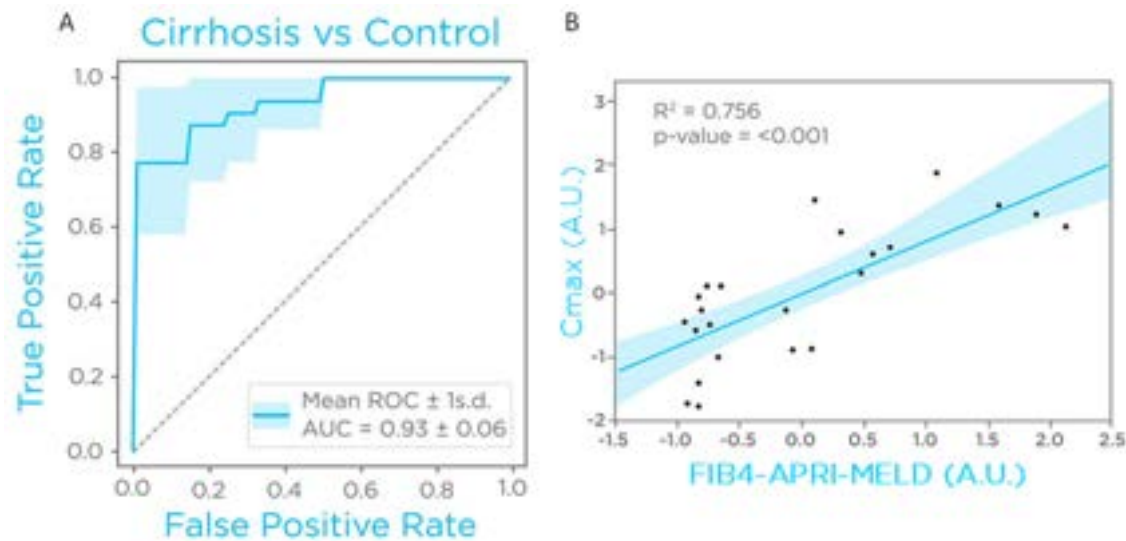


Figure:

FRI-493

Safety and signal intensity of a novel liver-specific MRI contrast agent, Orvigance® (manganese chloride tetrahydrate), in adult subjects with mild, moderate, or severe hepatic impairment

Nadilka Hettiarachchige¹, Andreas Norlin¹, Hanna Persson Hedman¹, Eric Lawitz², ¹Ascelia Pharma AB, Sweden; ²The Texas Liver Institute, United States

Email: nadilka.h@ascelia.com

Background and aims: Orvigance is a novel oral magnetic resonance imaging (MRI) contrast agent developed for visualization of focal liver lesions. In this study, we investigated safety and change in MRI signal intensity (SI) in the liver over time after a single dose of Orvigance in adult subjects with hepatic impairment.

Method: Subjects with mild (n = 9), moderate (n = 6) or severe (n = 7) hepatic impairment as defined by the Child-Pugh score and matched controls with normal hepatic function (n = 13) were given a single dose of Orvigance. Safety was evaluated until 72 hours post-dose. Absolute change in liver SI was assessed pre-dose and at 1, 4, 8 and 24 hours post-dose.

Results: 10 (28.6%) of the 35 subjects reported adverse events. All adverse events were gastrointestinal disorders of mild to moderate severity, with no differences across stages of hepatic impairment. No safety findings were observed for ECG, vital signs or laboratory parameters. Mean liver SI enhancement peaked at 4 hours post-dose and was 53.2, 31.7 and 26.3 compared to pre-dose levels in subjects with mild, moderate and severe hepatic impairment, respectively. Corresponding SI enhancement for subjects with normal hepatic function was 79.0.

Conclusion: Orvigance was safe and well tolerated in subjects with varying degrees of hepatic impairment. Consistently with previous studies, highest liver SI enhancement was observed at 4 hours after administration independently of hepatic impairment severity. A consistent reduction in liver SI enhancement was observed with increasing severity of hepatic impairment.

The safety profile suggests that Orvigance can be used in patients with any degree of hepatic impairment.

FRI-494

Soluble CD163 as a biomarker of liver fibrosis in liver transplant recipients

Emilie Høegholm Ernst Lauridsen¹, Rasmus Hvidbjerg Gantzel¹, Allan Rasmussen², Henning Grønbaek¹, Susanne Dam Nielsen³, Gerda Villadsen¹, ¹Aarhus University Hospital, Department of Hepatology and Gastroenterology, Aarhus, Denmark; ²Copenhagen University, Department of Surgical Gastroenterology, Copenhagen, Denmark; ³Copenhagen University, Department of Infectious Diseases, Copenhagen, Denmark

Email: emllur@rm.dk

Background and aims: Soluble CD163 (sCD163) is a marker of liver inflammation and fibrosis in acute and chronic inflammatory liver diseases. However, it remains unknown whether the plasma sCD163 level reflects liver fibrosis in patients following liver transplantation. This study aims to investigate the associations between the non-invasive inflammation and fibrosis marker plasma sCD163, the FIB-4 score, and liver stiffness (FibroScan) in liver transplant recipients.

Method: This project is a sub-study of the Danish Comorbidity in Liver Transplant Recipients (DACOLT) study and consists of 110 liver transplant recipients recruited from Aarhus University Hospital. FibroScan stiffness is considered as the non-invasive golden standard for liver fibrosis.

Results: The included patients had a median age of 51 years (range: 21–76), 51 (46.4%) patients were male and the median time from transplantation to inclusion was 6 years (range: 0.4–31). Autoimmune diseases were the most common causes of transplantation with primary sclerosing cholangitis as the predominant etiology (26%). The median sCD163 was 2.64 mg/L (IQR: 2.02–3.54) and 19 patients (17%) had sCD163 levels above the normal range (>3.86 mg/L). The patients with a liver stiffness >8 kPa (n = 16) had significantly higher sCD163 than patients with a liver stiffness <8 kPa (3.84 mg/L (IQR: 3.13–5.01) vs. 2.57 mg/L (IQR: 1.95–3.06), p < 0.001). We observed a significant correlation between sCD163 and liver stiffness (rho = 0.38, p < 0.001). Patients with a FIB4 score >1.45 (n = 51) had higher median sCD163 than patients with a FIB4 score <1.45 (2.86 mg/L (IQR: 2.23–3.77) vs. 2.48 mg/L (IQR: 1.99–3.14), p = 0.07). However, there was no correlation between sCD163 and the FIB-4 score. In addition, we observed no correlation between the FIB-4 score and FibroScan liver stiffness (rho = 0.13, p = 0.20).

Conclusion: In liver transplant recipients, plasma sCD163 correlated with liver stiffness but not with the FIB-4 score. There was no correlation between the FIB-4 score and liver stiffness, questioning

POSTER PRESENTATIONS

the FIB-4 score as a marker of liver fibrosis in liver transplant recipients. In contrast, our data suggest that sCD163 is a clinically relevant biomarker for detection of liver fibrosis in liver transplant recipients.

FRI-495

Does methotrexate therapy harm the liver in psoriatic patients?

Isabel Bessa¹, Ana Correia-Sá², Letícia Marques Leite¹, Hugo Oliveira³, Margarida Gonçalves^{3,4}, Arsénio Santos^{1,5}, Armando Carvalho^{1,5}, Adelia Simão^{1,5}. ¹Centro Hospitalar e Universitário de Coimbra, Internal Medicine, Coimbra, Portugal; ²Centro Hospitalar e Universitário de Coimbra, Internal Medicine, Coimbra, Portugal; ³Centro Hospitalar e Universitário de Coimbra, Dermatology, Coimbra, Portugal; ⁴University of Coimbra, Faculty of Medicine, Dermatology, Coimbra, Portugal; ⁵University of Coimbra, Faculty of Medicine, Internal Medicine, Coimbra, Portugal
Email: aspcarvalho@gmail.com

Background and aims: Psoriasis is associated with a greater risk of hepatic damage, including steatosis and fibrosis. A popular and crucial medication for the treatment of psoriasis is methotrexate (MTX), that is known to cause transaminasemia, but it isn't clear yet how this affects liver fibrosis or steatosis. Patients with psoriasis who also suffer from obesity, diabetes or metabolic syndrome have a greater risk of developing liver fibrosis, and there is evidence that MTX can act synergistically, contributing to the liver damage in these patients. Transient elastography (TE) and controlled attenuation parameter (CAP) are non-invasive methods to assess liver fibrosis and steatosis, respectively. The aim of our study is to assess if psoriatic patients treated with MTX have higher degrees of fibrosis and steatosis than those not treated with MTX.

Method: A case-control prospective study was undertaken on 85 patients (45 males, 40 females) with psoriasis, 65 of them treated (study group) and 20 not treated with MTX (control group). Epidemiological and clinical data were collected, and TE and CAP (Fibroscan) were performed on all patients. Data were analysed using the SPSS Statistics* platform.

Results: Both groups appear to be similar, with no statistically significant difference regarding sex, BMI, duration of disease, other comorbidities (dyslipidaemia, type 2 diabetes mellitus and hypertension), and alcohol consumption, but with a significant difference in mean age (60 years for treated patients and 52 years for those not treated with MTX). The mean elasticity in treated patients was 7.38 (+/- 5.60) kPa and in the control group was 5.97 (+/- 3.03) kPa ($p = 0.160$). The mean CAP was 270.66 (+/- 70.14) dB/m in treated patients and 250.85 dB/m (+/- 64.70) dB/m in non-treated ($p = 0.170$). We did not find a statistically significant correlation between the duration of the disease, or the cumulative MTX dose (less or more than 2 g) and the grade of steatosis or the stage of fibrosis. There was a statistically significant difference concerning steatosis in obese versus non-obese patients ($p = 0.012$)-including those treated with MTX ($p = 0.001$)-but not for fibrosis. There was no statistically significant difference for fibrosis or steatosis in the presence versus absence of type 2 diabetes mellitus, dyslipidaemia, or alcohol consumption in our psoriatic patients.

Conclusion: In our psoriatic patients, MTX has no significant effect in the stage of fibrosis or grade of steatosis. Obesity has a significant correlation with steatosis, but not with fibrosis, independently of MTX therapy. Type 2 diabetes mellitus and dyslipidaemia and alcohol consumption have no correlation with fibrosis or steatosis in all the patients. Studies with more patients and follow-up are needed to better clarify the impact of MTX therapy in the liver of psoriatic patients.

FRI-496

Performance of the scores diagnosis of autoimmune hepatitis in Moroccan patients

Sara Chbourk¹, Mohamed Borahma¹, Imane Benelbarhdadi¹, Fatima Zahrae Ajana¹. ¹Mohamed V university, Ibn Sina hospital, department of gastroenterology C, Rabat, Morocco
Email: docteurchbourk@gmail.com

Background and aims: Autoimmune hepatitis (AIH) is a chronic liver disease whose diagnosis use diagnostic scores that were established by the international autoimmune hepatitis group in 1993 with a revision in 1999. Since 2008, a simplified score is more commonly used taking into account 4 histo-biological parameters. The aim of this study is to compare the performance of these 2 scores in the diagnosis of autoimmune hepatitis in the Moroccan population.

Method: In this mono-center retrospective study, the 2 diagnostic scores were used in 31 patients followed for autoimmune hepatitis and in 32 patients followed for other chronic liver diseases (porto-sinusoidal vascular disease = 16, non-alcoholic fatty liver disease = 13, primary sclerosing cholangitis = 3). The sensitivity and specificity of each score were calculated using Jamovi software.

Results: The mean age in our study was 42 years with extremes between 15 and 74 years, a clear female predominance was noted with a sex ratio of 0.14. Using the simplified autoimmune hepatitis score, the sensitivity and specificity for the detection of probable autoimmune hepatitis (scores ≥ 6) were 45% and 100%, with a positive and negative predictive value of 100% and 65%, respectively. For the diagnosis of definite AIH (scores ≥ 7), the sensitivity and specificity were 6.45% and 100%, with a positive and negative predictive value of 100% and 52%, respectively. On the other hand using the Revised International Autoimmune Hepatitis Group Scoring System the sensitivity and specificity for the detection of probable autoimmune hepatitis were 96% and 62% respectively with a positive predictive value of 71% and a negative predictive value of 95%.

Conclusion: Our statistical study shows that both scores are efficient tools for the diagnosis of AIH, the simplified score which is a practical and easily applied in the clinical setting presents a better specificity while the Revised International Autoimmune Hepatitis Group Scoring System is more sensitive for the detection of autoimmune hepatitis.

FRI-497

Assessment of international normalized ratio to albumin ratio in predicting mortality in decompensated liver disease at a resource limited medical centre

Marium Fatima Waqar¹, Madiha Qadir¹, Zeeshan Junejo¹, Syed Masroor Ahmed¹, Shabnam Naveed¹. ¹Jinnah Postgraduate Medical Centre, Medical unit III, ward 7, Karachi, Pakistan
Email: mariumwaqar5@gmail.com

Background and aims: Decompensated liver disease (DCLD) has a high mortality and morbidity irrespective of its etiology. It is characterized by reduced liver reserves resulting in reduced synthesis of albumin and deranged international normalized ratio (INR). Prothrombin time- INR and serum albumin both reflect the functional capacity of the liver. Abnormalities in their levels can frequently lead to a poor prognosis in liver cirrhosis.

Our study aims to evaluate Prothrombin time- INR and serum albumin ratio (PTAR) as a prognostic score for predicting 30 day mortality and its association with Model for End Stage Liver Disease Sodium (MELD Na) in patients with DCLD presenting at tertiary care hospital in a resource limited country.

Method: This prospective study was conducted at a medical unit of a tertiary care centre Jinnah Postgraduate Medical Centre. The baseline characteristics and laboratory parameters were recorded. The Child-Turcotte-Pugh (CTP) and the MELD Na scores were calculated to assess the severity of liver disease. The PTAR was calculated as INR divided by serum albumin in g/dl of the enrolled patients.

Data was stored and analyzed using IBM-SPSS version 25.0. Receiver operating characteristic curve (ROC) analysis was performed on PTAR and Meld Na scores to identify the cutoff of these parameters. The sensitivity and specificity were also estimated using ROC curve. After obtaining cutoff value for PTAR using ROC, all quantitative and qualitative parameters were assessed using Mann Whitney U test and Fisher's exact test. The p value less than 0.05 was considered statistically significant.

Results: Out of a total 307 DCLD patients enrolled, male patients outnumbered female patients, 54.7% (n = 168) versus 45.3% (n = 139). The median age of the patients was 54 (45–61) years. Total number of deceased patients was 61 (19.9%). The ROC curve analysis showed the area under the curve for PTAR was 58%, with 95% confidence interval I (0.51–0.66) and for Meld Na score it was 65% with 95% confidence interval (0.58–0.72). Both were found statistically significant with p < 0.05. The cutoff value of PTAR suggested by the ROC curve was 0.25 for mortality. The sensitivity and specificity for PTAR was 95.1% and 3.7%. Upon further analysis, ROC curve showed that as the sensitivity increases, the value of 1-specificity also increase and the cut off value of PTAR for mortality decreases.

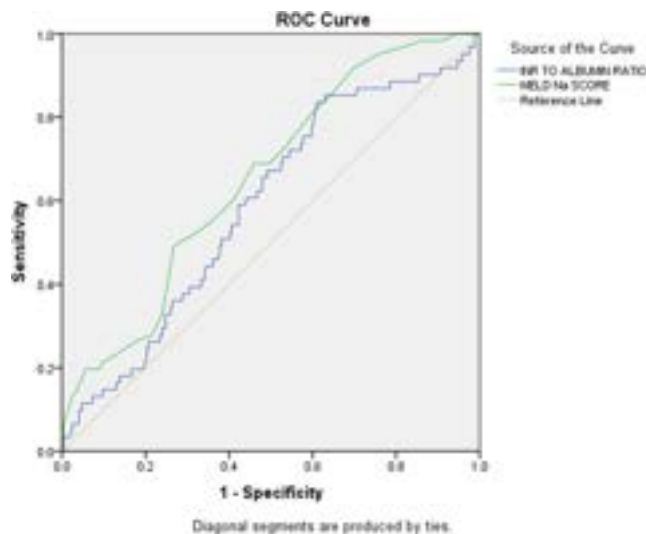


Figure:

Conclusion: In our study PTAR showed significant positive correlation with MELD Na and high sensitivity in predicting mortality of DCLD patients. The PTAR is easily calculated through commonly available laboratory investigations. It can serve as a prognostic tool and can facilitate health care professionals to make early decisions regarding admission of these patients into high dependency units in a resource constraint medical centre. However, multicentric studies at larger scale need to be conducted to validate the results.

FRI-498

Moving toward a more perfect liver function test: the next generation of HepQuant tests

Michael McRae¹, Steve Helmke², Greg Everson². ¹Custom Diagnostic Solutions, LLC, United States; ²HepQuant, LLC, United States
Email: michaelpmcrae@gmail.com

Background and aims: The HepQuant SHUNT Test (V1.0) uses stable isotopes of cholate administered both intravenously (13C-CA) and orally (d4-CA) to quantify liver function and physiology. The Test has been used in over 26 clinical trials and studies, encompassing a broad range of etiologies and stages of liver disease, where it has compared favorably to other liver diagnostic tests. However, the Test is sensitive to variability in the timing of collection of the 5-minute blood sample and difficulty in maintaining intravenous access. The aim of this study was to enhance the Test and its performance by simplifying the

sampling procedure and shortening the time of testing. Herein we evaluate two new versions of the Test: V1.1 and V2.0.

Method: In V1.0, the volume of distribution (Vd) is calculated from In-linear regression of 5- and 20-minute 13C-CA concentrations versus time. V1.1 estimates Vd based on body weight and height (Lemmens et al. 2006), eliminating the requirement for the 5-minute blood sample. V2.0 is based on our published compartmental analysis (McRae et al. 2022) and further simplifies sampling requirements to 2 timepoints at 20 and 60 minutes. To compare reproducibility, coefficients of variation (CV) and intraclass correlation coefficients (ICC) with one-sided test for lower acceptable limit of 0.7 were analyzed in a study of 16 controls, 16 NASH patients, and 16 HCV patients, each with 3 replicate tests conducted on 3 separate days (Burton et al. 2021). We assessed differences in areas under the receiver operator characteristic curve (AUROC) for predicting large esophageal varices (LEVs) in hepatitis C (HCV) subjects from the HALT-C study (N = 217) (Everson et al. 2012) by the DeLong method. Test outputs include a Disease Severity Index (DSI) and portal-systemic shunting (SHUNT%).

Results: For the measurement of DSI, V1.1 and V2.0 demonstrated similar ICCs but improved CVs relative to the V1.0 method. For the measurement of SHUNT%, the V1.1 and V2.0 test versions demonstrated improved reproducibility based on both ICC and CV%. Diagnostic performance based on AUROCs for V1.1 and V2.0 was equivalent to V1.0 in most cases and improved in V1.1 for SHUNT%.

Figure:

Test Parameter and Method	Reproducibility (N = 48 Control, NASH, HCV)			Diagnostic performance of in the prediction of LEVs (N = 217)	
	CV (%)	ICC	p value	AUROC	p value
Disease Severity Index (DSI)					
V1.0	11.17%	0.94	<0.001	0.81 (0.72–0.89)	-
V1.1	8.48%	0.95	<0.001	0.82 (0.71–0.89)	0.5795
V2.0	8.98%	0.94	<0.001	0.84 (0.77–0.90)	0.1218
Portal-systemic Shunt (SHUNT%)					
V1.0	15.11%	0.73	0.3209	0.80 (0.66–0.88)	-
V1.1	11.88%	0.85	<0.001	0.83 (0.74–0.90)	0.0321
V2.0	12.57%	0.84	0.0012	0.83 (0.73–0.90)	0.1019

Conclusion: The next generation of HepQuant SHUNT tests V1.1 and V2.0 simplify the test administration by eliminating the 5-minute sample (V1.1), reducing the total samples required to 2 (V2.0), and shortening the time from 90 minutes to 60 minutes (V2.0). These improvements should enhance operator performance, resource utilization, and patient acceptance of the HepQuant testing procedure, allowing for greater utilization of HepQuant for measuring liver function and physiology.

FRI-499

Liver elastography is a useful technique to assess the severity of liver congestion in patients with Budd-Chiari syndrome

Marcos Andres Thompson¹, Oana Nicoara-Farcu¹, Ernest Belmonte¹, Maria Angeles García-Criado¹, Anna Darnell¹, Valeria Perez¹, Lara Orts¹, Pamela Vizcarra¹, M Àngels Falgà¹, Joana Codina Jane¹, Fanny Turon¹, Anna Baiges¹, Pol Olivas¹, Marta Magaz¹, Giuseppe Grassi¹, Sarah Shalaby¹, Virginia Hernandez-Gea¹, Juan Carlos Garcia Pagan¹. ¹Hospital Clinic Barcelona, Hepatic Hemodynamic Laboratory, Liver Unit, Hospital Clinic, Barcelona, Spain
Email: thompsonmarcos86@gmail.com

Background and aims: In Budd-Chiari syndrome (BCS), hepatic congestion is the main cause of portal hypertension development. Liver congestion is a recognized cause of increase in liver stiffness (LS). Recent publications suggest that LS could be useful in assessing on congestion and the response to treatment in BCS. Our study aimed

POSTER PRESENTATIONS

to assess this issue and the LSM as a tool to assess on BCS follow-up in a large cohort of BCS patients.

Method: Observational retrospective study including patients with BCS with at least 2 LS measurements (LSM) by Fibroscan® (Echosens, Paris, France). LSM were performed at different stages of the disease: clinical stability or instability under medical and/or interventional radiological treatment (IR: TIPS or hepatic vein stent-HVS).

Results: We included 51 patients with BCS. 15 patients were clinically stable while on anticoagulation treatment (ACO) and remained compensated throughout the whole follow-up (median of 2 years; 4 months–11 years). These patients had 82 LSMs (median 4/patient; range 2–11) with 79 LSMs (96%) of these <25 kPa; the remaining 3 LSMs (in 2 patients) were between 25–30 kPa. Twelve patients had LSMs while decompensated. Once under ACO, only one of those achieved compensation with: LSM pre-ACO-64 kPa; 32 kPa at 3 months and 20 kPa at 6 months of ACO. The 11 patients that remained decompensated had 80 LSMs (median 8/patient; range 3–12); median follow-up of 8 months (2 months–13 years); 76 (95%) LSMs were >25 kPa with 67 (84%) being >30 kPa.

IR was performed in 29 decompensate patients (28 TIPS and 1 angioplasty/HVS). LSM pre and post IR were available in 10 patients. Median LSM pre-IR: 59 kPa (IQR 45.1–75) decreasing to 33.6 kPa (IQR 26.75–41.5) at 24 h; to 25 kPa (IQR 21.8–29.4) at 1 month; 22 kPa (IQR 21–24) at 3 months; and 23.6 kPa (IQR 22–25) at 6–12 months post IR. 18 IR treated patients had 105 LSMs while clinically stable (13 patients throughout the whole follow-up and 5 during long periods of clinical stability between periods of IR dysfunction) (median 5 LSMs/patient, range 2–13) during a median follow-up of 3.5 years (2 months–12 years). 101 LSMs (96%) were <25 kPa and 4 between 25 and 30 kPa which decreased <25 kPa when repeated. 16 patients had 97 LSMs while presenting IR dysfunction (median 6/patient; range 2–14); 84 were >30 kPa and 13 between 25–30 kPa, all above 25 kPa.

Conclusion: In patients with BCS, LSM values <25 kPa suggest an adequate hepatic decongestion under medical or IR treatment. LSM values >30 kPa are highly suggestive of persistent hepatic congestion due to medical treatment inefficacy or TIPS/stent dysfunction. Values between 25–30 kPa represent a grey zone and if possible, should be repeated shortly during follow-up to assess whether there is a LSM increase/decrease.

FRI-500

Fibrosis-4 score less than 2.67 and normal gamma-glutamyl transferase levels are associated with high negative predictive value for high-risk of liver stiffness in patients with primary biliary cholangitis

Alan Bonder¹, Vilas Patwardhan¹, Joanna MacEwan², Anran Shao Shao², Leona Bessonova³, Erik Ness³, Tracy Mayne³, Darren Wheeler³, Radhika Nair³, Jing Li³, Shari Orbach³. ¹Division of Gastroenterology, Beth Israel Deaconess Medical Center, Boston, United States; ²Genesis Research, Hoboken, United States; ³Intercept Pharmaceuticals Inc, Morristown, United States
Email: erik.ness@interceptpharma.com

Background and aims: Transient elastography (TE), an imaging test for liver stiffness and fibrosis, is a non-invasive alternative to liver biopsy that is predictive of liver outcomes in individuals living with primary biliary cholangitis (PBC). Here, we assess the sensitivity, specificity, positive predictive value (PPV), and negative predictive value (NPV) of biochemical markers and commonly used composite liver fibrosis scores versus liver stiffness measured by TE in people living with PBC.

Method: Liver biochemistries, commonly used fibrosis scores, and TE stiffness measurements were obtained from electronic health records of people living with PBC followed at Beth Israel Deaconess Medical Center through October 2022. The agreement between liver biochemistries/fibrosis scores and liver stiffness (TE >10 kPa) was evaluated by sensitivity, specificity, PPV, and NPV. Normal limits for

biochemistries and commonly used thresholds for fibrosis scores were assessed.

Results: Data were analyzed from 74 patients (mean 54 years of age, 96% female). Mean ALP was $1.6 \times \text{ULN}$ (± 1.2 ; ULN = 120 U/L) and mean total bilirubin was $0.6 \times \text{ULN}$ (± 0.3 ; ULN = 1 mg/dL). The PPV of liver biochemistries and composite fibrosis scores ranged from 22% to 69%; the NPV for all individual labs and composite labs was >75% (Table).

Table: Agreement between liver biomarkers/composite fibrosis scores and liver stiffness assessed by transient elastography (TE) in patients with primary biliary cholangitis

	Threshold	TE Data Pairs ^a n	Sensitivity	Specificity	PPV ^b	NPV ^c
Albumin	≤4 g/dL	85	0.409	0.937	0.692	0.819
Gamma glutamyl transferase	≥40 U/L	51	0.900	0.390	0.265	0.941
Immunoglobulin G	≥1600 mg/dL	48	0.154	0.943	0.500	0.750
Immunoglobulin M	≥250 mg/dL	50	0.846	0.622	0.440	0.920
Alkaline phosphatase	≥120 U/L	109	0.846	0.374	0.297	0.886
Total bilirubin	≥1 mg/dL	109	0.192	0.952	0.556	0.790
Aspartate transaminase	Female, ≥30 U/L Male, ≥35 U/L	109	0.731	0.566	0.346	0.870
Alanine transaminase	≥40 U/L	109	0.385	0.735	0.313	0.792
Platelet count	≤150 × 10 ³ /L	106	0.083	0.915	0.222	0.773
FIB-4 score ^d	≥2.67	106	0.208	0.927	0.455	0.800
APRI score ^e	≥0.5	106	0.458	0.768	0.367	0.829

^aTE scores and liver biomarkers/fibrosis scores assessed within ± 60 days of each other.

^bProbability of a positive TE test (liver stiffness ≥10 kPa).

^cProbability of a negative TE test (liver stiffness ≤10 kPa).

^dComposite of age, AST, ALT, and platelet count.

^eRatio of AST as a multiple of ULN to platelet count.

Conclusion: These findings indicate that these readily available liver biochemistries and commonly used fibrosis scores are excellent predictors of a low-risk liver stiffness value (TE <10 kPa) in people living with PBC. When TE testing is not available, healthcare providers can use standard liver biochemistries to further assess overall liver health.

FRI-501

Suitability of Fibroscan, APRI and FIB-4 indexes compared with liver biopsy in the evaluation of liver fibrosis: a single-centre retrospective study

Benjamin Polo Lorduy¹, Alvaro Yagüe¹, Andres Castañeda¹, Rocio Calvo Hernandez¹, Juan Carlos Porres Cubero¹. ¹Hospital Universitario Fundación Jiménez Díaz, Spain
Email: bpolo@fjd.es

Background and aims: The prognosis and management of liver diseases largely depend on the amount and progression of liver fibrosis and the possibility of developing cirrhosis. Liver biopsy has traditionally been considered the gold standard for the diagnosis of cirrhosis and staging of fibrosis. However, it is an invasive and inaccurate technique with many drawbacks. In order to overcome the limitations of liver biopsy, a number of non-invasive markers have been developed over the past decade for the evaluation of liver fibrosis. The aim of this study is to evaluate the ability of FibroScan, APRI and FIB-4 indexes to predict liver fibrosis using liver biopsy as the reference standard.

Method: The case records of 204 patients who underwent liver biopsy from March 2019 until November 2022 were retrospectively reviewed. Those patients who had undergone FibroScan measurements and blood samples simultaneously or with a maximum difference of one month from liver biopsy were included in the study,

with a final number of 188 patients. Liver fibrosis stage was determined using the METAVIR system.

Results: 188 patients with a mean age of 51.8 ± 13.3 years were examined, being women the majority of them (72.9%). FibroScan liver stiffness results ranged from 4.50 to 8.30 kPa (median: 5.9 kPa), while serological marker values ranged from 0.85 to 2.01 (median: 1.34) for FIB-4 and from 0.36 to 1.11 (median: 0.54) for APRI. In liver biopsy, 81.4% of the patients presented F0-1, while mild fibrosis ($F \geq 2$) was found in the remaining 18.6%. For the detection of $F \geq 2$, FibroScan showed a sensitivity of 77% and a specificity of 80% with a positive predictive value of 47% and a negative predictive value of 94%. Its degree of concordance with the biopsy was moderate (kappa index: 0.45). Regarding FIB4 and APRI, both showed high sensitivity (91% for FIB4 and 86% for APRI) and low specificity (63% for FIB4 and 50% for APRI), with a kappa index of 0.35 and 0.20, respectively.

Variable	Media \pm DT Mediana (Q1, Q3)	Rango	FibroScan	
			Biopsia	
Edad	51.8 ± 13.3	(20.0, 81.0)	F0-1	122
CAP	242 ± 70.5	(1.17, 400)	F2-4	31
FibroScan	$5.90 (4.50, 8.30)$	(2.50, 45.0)	F0-1	8
% ESTEATOSIS	$0.00 (0.00, 15.0)$	(0.00, 95.0)	F2-4	27
FIB 4	$1.34 (0.85, 2.01)$	(0.29, 9.36)	FIB4	
APRI	$0.54 (0.36, 1.11)$	(0.13, 18.1)	Biopsia	
			F0-1	97
			F2-4	56
			APRI	
			F0-1	76
			F2-4	77

Figure:

Conclusion: FIB-4 and APRI indexes had an acceptable ability to detect the presence or absence of mild fibrosis; this capacity is due for their high negative predictive values. However, the weak degree of agreement and the lack of specificity shown by these non-invasive methods indicates that liver biopsy is still necessary for the diagnosis of liver fibrosis stage. In the other hand, FibroScan is more accurate and comparable to liver biopsy with a moderate degree of agreement, but it also needs a specific device and a trained health practitioner that might not be available in some cases.

FRI-502

Hepatobiliary manifestations in pediatric COVID-19

Tetiana Stoieva¹, Olga Dzhagiashvili¹, Vira Dovzhyk². ¹Odessa National Medical University, Department of Pediatrics №2, Odessa, Ukraine;

²Odessa National Medical University, Faculty of Medicine №1, Odessa, Ukraine

Email: olga.dzhagiashvili@onmedu.edu.ua

Background and aims: Mechanisms of digestive damage in COVID-2019 are important. Possible factors include virus-induced influence, systemic inflammation, hypoxia, hypovolemia, drug-induced hepatotoxicity, etc. The aim of this study is analysing the digestive system and hepatobiliary tract in children who had COVID-19.

Method: We examined 27 children aged 11 to 16 who had COVID-19 and signs of digestive damage.

Results: The mean age of the examined patients was (13.8 ± 1.6) years, with no gender differences. It was found that $(71.4 \pm 8.7)\%$ children had a history of functional disorders: the cyclic vomiting syndrome- $(4.8 \pm 4.1)\%$, the overlap syndrome- $(19.0 \pm 7.5)\%$, functional disorders of the gallbladder and sphincter of Oddi- $(47.6 \pm 9.6)\%$. Gastroesophageal reflux disease- $(28.5 \pm 8.7)\%$ and chronic gastroduodenitis- $(14.3 \pm 6.7)\%$ occurred among organic diseases. The infection was manifested by an increase in temperature from subfebrile $(37.0 \pm 9.3)\%$ to febrile $(63.0 \pm 9.3)\%$ with a severe disease course and such respiratory symptoms as dry cough, nasal congestion, rhinorrhea, hyperemia of the posterior pharyngeal wall. Gastrointestinal symptoms in children with a history of digestive diseases appeared on the 2nd-3rd days, in other children a little later by the 4-5th and were characterized by the following symptoms:

abdominal pain- $(70.4 \pm 8.8)\%$, nausea- $(40.7 \pm 9.5)\%$, vomiting- $(25.9 \pm 8.4)\%$, diarrhea- $(33.3 \pm 9.1)\%$. Along with gastrointestinal symptoms, some children $(22.2 \pm 8.0)\%$ had changes in taste and eating behavior. Hepatobiliary symptoms were as follows: heaviness in the right hypochondrium $(51.9 \pm 9.6)\%$, bitter taste in the mouth $(29.6 \pm 8.8)\%$, stool acholia $(40.7 \pm 9.5)\%$, which were accompanied by dyspeptic disorders. The laboratory data revealed: a slight increase of transaminases $(25.9 \pm 8.4)\%$, an increase in alkaline phosphatase $(7.4 \pm 5.0)\%$, the presence of neutral fat in the coprogram $(18.5 \pm 7.5)\%$ of children. Ultrasound revealed enlarged gallbladder $(37.0 \pm 9.3)\%$, thickening of its wall $(22.2 \pm 8.0)\%$, a moderate enlargement of the liver $(14.8 \pm 6.8)\%$, microliths and gallbladder sludge $(29.6 \pm 8.8)\%$. Gastrointestinal manifestations proceeded 10-32 days. A dynamic ultrasound revealed progression of gallbladder sludge in $(18.5 \pm 7.5)\%$ children, which required administration of ursodeoxycholic acid preparations.

Conclusion: Among the digestive disorders, the hepatobiliary pathology often occurs in children with COVID-19. Liver damage takes place because of several mechanisms combination, and is characterized mainly by signs of cholestasis. Treatment should include hepatoprotectors and choleretic therapy along with antiviral therapy.

Nurses and Allied Health Professionals

WEDNESDAY 21 TO SATURDAY 24 JUNE

TOP-054

Health-related quality of life in a population at-risk of NAFLD or ArLD

Helle Lindholm Schnefeld¹, Katrine Prier Lindvig^{1,2}, Anita Arslanow³, Isabel Graupera³, Maria Kjærgaard^{1,2}, Katrine Thorhauge^{1,2}, Johanne Kragh Hansen^{1,2}, Camilla Dalby Hansen^{1,2}, Stine Johansen^{1,2}, Mads Israelsen^{1,2}, Peter Andersen¹, Nikolaj Torp^{1,2}, Katrine Bech¹, Sönke Detlefsen^{2,4}, Núria Fabrellas³, Pere Ginès³, Aleksander Krag^{1,5}, Maja Thiele^{1,2}. ¹Centre for Liver Research, Department of Gastroenterology and Hepatology, Odense University Hospital, Odense C, Denmark; ²Department of Clinical Research, University of Southern Denmark, Odense C, Denmark; ³Liver Unit, Hospital Clinic of Barcelona, Barcelona, Spain; ⁴Department of Pathology, Odense University Hospital, Odense C, Denmark; ⁵Department of Clinical Research, University of Southern Denmark, Odense C, Denmark
Email: helle.lindholm.hansen@rsyd.dk

Background and aims: Patients with decompensated cirrhosis exhibit poor health-related quality of life (HRQoL). However, little is known about HRQoL in people at risk of non-alcoholic fatty liver disease (NAFLD) and alcohol-related liver disease (ArLD). Stigmatization, physical symptoms, and increased morbidity may impair HRQoL. We aimed to investigate the correlation between HRQoL and alcohol overuse, metabolic syndrome (MetS), obesity, and type 2 diabetes (T2D), in a population screened for liver fibrosis, and whether fibrosis stage correlated with HRQoL in a liver-biopsied subgroup.

Method: We screened individuals from the general population and individuals at-risk of liver fibrosis with no established diagnosis of chronic liver disease, using transient elastography. We referred those with liver stiffness ≥ 8 kPa for a biopsy to stage fibrosis. We assessed HRQoL by the Short-Form-36 questionnaire (SF36; range 0-100), consisting of eight domains; physical health, limitations due to physical health, emotional well-being, limitations due to emotional problems, energy, social functioning, pain, and general health. We compared HRQoL based on: alcohol overuse, MetS, obesity, and T2D

POSTER PRESENTATIONS

to those with no risk factors. We performed multivariable regression on age, gender, risk factors, predisposing illnesses, and social economic parameters.

Results: The cohort consisted of 6,444 individuals, with a median age of 57 (IQR 52–63), 52% female. The prevalence of behavioral risk factors for fibrosis was 1,852 (29%) alcohol overuse, 2,551 (40%) obesity, 621 (10%) T2D, and 3456 (54%) MetS. 2,850 participants had two or more risk factors, 2,000 only had one risk factor and 1,594 had no risk factors. We performed biopsies on 203 individuals with elevated liver stiffness (165 Kleiner fibrosis stage F0–F2, 38 F3–F4). Obesity was the strongest predictor of poor HRQoL overall. Individuals with obesity reported lower physical health and energy, whilst having more pain than other groups. Individuals with alcohol overuse or obesity had lower emotional and social well-being. Individuals with MetS reported the highest HRQoL overall, only surpassed by the group with no risks. We found no significant differences in HRQoL between groups with fibrosis or cirrhosis on any of the domains. Obesity was the only risk factor significantly negatively associated with all eight domains after multivariable regression e.g. general health -4.78 (95%CI -6.02 to -3.54). Alcohol overuse was more negatively associated in domains concerning emotional and social well-being, compared to no risks, emotional -4.25 (95%CI -5.31 to -3.19) vs. no risks (.01 95%CI -1.38 to 1.40).

Conclusion: Individuals with obesity report lower HRQoL than any other group at risk of liver fibrosis. This is independent of the fibrosis stage and the presence of other risk factors. Alcohol overuse correlates with lower emotional and social well-being.

WEDNESDAY 21 JUNE

WED-477

Effectiveness of vaccine education on vaccine awareness and vaccine uptake in patients with cirrhosis of liver of a tertiary care center in South India

K L Ajee¹, Arun Valsan², A Athira¹, Devika Menon¹, S Devika¹, Aswin Shaji¹, K T Moly³, Priya Nair². ¹Amrita College of Nursing, Foundations of Nursing, Ernakulam, India; ²Amrita Hospital, Kochi, Gastroenterology, Kochi, India; ³Amrita College of Nursing, Principal, Ernakulam, India
Email: capt.ajee@gmail.com

Background and aims: Patients with cirrhosis of the liver are prone to bacterial or viral infections that can lead to increased morbidity and mortality. Many of these infections are vaccine preventable and the Centers for Disease Control (CDC) currently recommends vaccination for all susceptible chronic liver disease patients. It is observed that vaccination status of patients with liver disease is poor and currently there are no guidelines available in India for vaccination of patients with cirrhosis. Hence, we aimed to study the effectiveness of vaccine education on vaccine awareness and vaccine uptake in patients with cirrhosis of liver.

Method: A pilot study was undertaken among 100 adult patients with cirrhosis of liver who were vaccine naive except for Covid-19 from October 2022 to Dec 2022. We used one group pre-test post-test design with a total enumerative sampling technique. A validated questionnaire with a Cronbach's alpha of 0.81 was used to measure the level of vaccination awareness. The awareness questionnaire had twenty closed ended questions with maximum score of 60. The awareness level was categorized as lack of awareness (≤ 15), low level awareness (16–30), medium-level awareness (31–45) and high-level awareness (>45). After collecting information on vaccination status and state of awareness of adult vaccination from the eligible sample presenting at outpatient services using a direct interview technique, information about adult vaccination was given one-on-one basis by a trained nurse. After 7 days, a post-test (interview) was done to assess awareness, thereafter within 45 days after the first interaction, the

immunization record was reviewed. Statistical analysis was done with SPSS 29.0. The study was approved by the institutional ethics committee ECASM-AIMS-2022-158 dated 11 October 2022.

Results: The mean age of the study population was 60 years with predominantly males (81%). All were vaccinated against Covid-19. About 65% had comorbidities like Diabetes (34%) and hypertension (31%). Seventy-six percentage of patients had low-level awareness about vaccination. After the vaccine education module was administered, post-test interview revealed significant ($p < 0.00$) improvement in level of awareness from low to high (97%). Also, this led to significant vaccine uptake within day 45. The uptake of vaccination status improved from non-vaccinated to vaccinated in hepatitis B (95%), hepatitis A (76%), influenza (49%) and pneumococcal (40%). This is of significance considering the fact that nearly half (49%) of them were diagnosed to have cirrhosis with a median diagnosis time of 3 years. About 5% of patients did not take hepatitis B vaccine due to increased bilirubin or CRP level by their treating physician's advice. The most important reason for lesser vaccine uptake of hepatitis A, influenza and pneumococcal vaccine was cost (88%), lack of insurance coverage for preventive vaccinations (61%), accessibility (42%), lack of care-giver support (32%), fear or anxiety related to vaccination (18%).

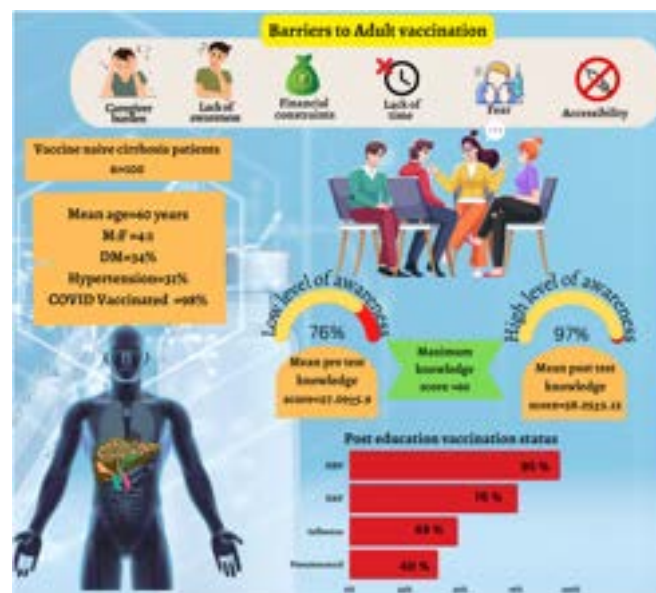


Figure:

Conclusion: Despite robust literature to support administration of vaccines in cirrhosis, the level of vaccine awareness and uptake is low in India. A structured nurse-led awareness campaign led to significant increase in vaccine knowledge and uptake. The lack of insurance coverage low awareness was the prime reasons for low vaccination status in our cohort.

WED-478

Better strategies are needed to increase engagement of patients with cirrhosis with allied health and community services

Elizabeth Powell¹, Katherine Stuart¹, Simon Finnigan¹, Jan Hinson², Christina Bernardes³, Gunter Hartel³, Patricia Valery³. ¹Princess Alexandra Hospital, Woolloongabba, Australia; ²Australian Catholic University, Brisbane Campus, Banyo, Australia; ³QIMR Berghofer Medical Research Institute, Herston, Australia
Email: patricia.valery@qimrberghofer.edu.au

Background and aims: Psychosocial care needs are not routinely attended to during outpatient hepatology management, and relatively little is known about the category and effectiveness of support services accessed by patients with cirrhosis. We quantified the type

and self-reported use of community and allied health services and whether patients were satisfied with the support received.

Method: Adults attending hepatology/gastroenterology clinics with a diagnosis of cirrhosis were enrolled in the CirCare study (n = 562). Health service use for support with their liver disease was assessed via interview and via linkage to the Australian Medicare Benefits Schedule (MBS). Patient needs were assessed using the Supportive Needs Assessment tool for Cirrhosis (SNAC),¹ and clinical data obtained from medical records.

Results: Although most patients (85.9%) used at least one community or allied health service for support with their liver disease, many patients reported requiring additional help with psychosocial (67.4%), lifestyle (34.3%) or practical needs (21.9%) that were not met by available services, or patients did not access services. In the 12 months prior to recruitment, a multidisciplinary care plan or case conference was accessed by 48% of patients and 56.2% self-reported the use of a GP for support with liver disease. The allied health clinician most commonly accessed by patients was a dietician (45.9%). Only a minority of patients reported accessing an exercise physiologist (4.4%) or physiotherapist (11.6%). Despite the high prevalence of ongoing psychosocial needs, there was relatively limited use of mental health and social work services. Only 14.1% of patients self-reported the use of a psychologist, confirmed by a low prevalence of use of mental health services (17.7%) in the linked MBS data. When comparing patients' psychosocial needs with use of and satisfaction with self-reported consultation with relevant psychosocial health professionals, overall, 483 patients (85.9%) reported at least one psychosocial need. As displayed in Figure and out of 562 patients, the need for additional help with at least one area of psychosocial challenge was reported by 125 (22.2%) patients who reported accessing relevant services and 254 (45.2%) patients who did not access relevant services. All psychosocial needs were met for 104 patients (18.5%), and 16 (2.9% of 562) patients reported accessing relevant services.

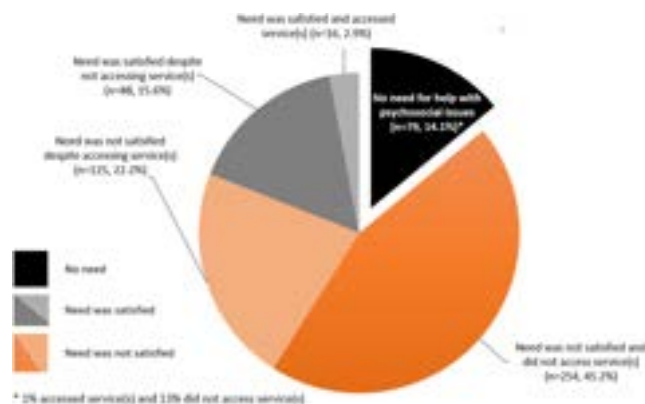


Figure: Need for help with psychosocial issues and self-reported consultation with a psychologist, psychiatrist, social worker or mental health team professionals and patient's satisfaction with care

Conclusion: Better strategies to increase engagement of patients with cirrhosis who have unmet complex physical and psychosocial needs with allied health and community services are needed.

Reference

1. Valery PC, et al. *Patient Prefer Adherence* 2020;14:599–611.

WED-479

Who's testing whom? Healthcare professional and patient knowledge of hepatitis delta virus and appropriate testing in an East Midlands hospital

Rachel Ryder¹, Kathryn Jack¹, William Irving². ¹Nottingham University Hospitals NHS Trust, Research and Innovation, Nottingham, United Kingdom; ²University of Nottingham, Clinical Virology, Nottingham, United Kingdom

Email: rachel.ryder2@nuh.nhs.uk

Background and aims: The World Health Organisation (WHO) aims to eliminate viral hepatitis as a public health threat by 2030. This includes Hepatitis Delta virus (HDV), a satellite virus which infects approximately 5–6% of HBV patients. Little is known about the true prevalence of HDV in the United Kingdom; testing and follow-up vary from region to region. This proof of concept study provides a snapshot of the acceptability and approaches to HDV testing of healthcare professionals and knowledge of HDV among HBV patients in a large teaching hospital in the East Midlands.

Method: The attitudes of healthcare professionals towards the acceptability of HDV testing were surveyed utilizing the eight constructs of the "Theoretical Framework of Acceptability" (Sekhon et al, 2017; 2022). Over a four month period, 39 hepatology healthcare professionals (31 doctors, 8 nurses) were recruited by opportunistic and snowball sampling, via UK and European specialist groups. Each participant completed an anonymous online survey, with questions including knowledge of National Institute for Health and Care Excellence (NICE) and European Association for the Study of the Liver (EASL) guidelines on HDV testing, acceptability of testing, barriers and facilitators to testing and long-term patient follow-up. 70 HBV surface antigen positive patients were recruited from routine clinics and were surveyed by telephone, answering questions about their primary language, knowledge of HDV and their own HDV testing status. Medical records were used to provide retrospective data on their HDV testing status.

Results: The results showed that in healthcare professionals there was a communication failure between professional bodies producing testing guidelines (NICE/EASL) and clinicians as to which patients should be tested for HDV. Only 66.6% of clinicians surveyed were able to correctly cite EASL testing guidelines, and only 53.8% were able to correctly cite NICE guidelines on appropriate HDV testing. However, there was a high level of belief that HDV testing was an acceptable intervention to perform against all eight of Sekhon et al's constructs, with 97.5% of clinicians surveyed stating that HDV testing was either completely acceptable, or acceptable to them. There was a similar communication failure between clinicians and patients in explaining what HDV is, how it may affect HBV patients and why HDV testing is important, with 77.1% on HBV patients stating that they were unaware of HDV and that it had never been discussed by their healthcare professional. In contrast, 95.7% of HBV patients sampled had been tested for HDV, indicating that testing was being performed, but communication to patients was lacking. The data also showed a huge diversity of patient backgrounds within the cohort, reflecting the linguistic and cultural challenge faced by clinicians when treating HBV patients and provides some explanation for this communication failure.

Conclusion: This study shows that HDV testing is acceptable to healthcare professionals, but that many clinicians lack familiarity with recommendations laid down in clinical guidelines. Similarly in patients surveyed, a lack of knowledge and communication from healthcare professionals left them uncertain as to the nature of HDV and their own HDV testing status. A diversity of patient languages and cultures may be one cause of this, but communication need to be sharpened if the WHO objective of eliminating viral hepatitis as a public health threat by 2030 is to be met.

WED-480

First hepatitis C mass-testing in a category A prison in the United Kingdom

Alison West¹, Harriet Deverell¹, Ambrose Brown², Lisa Noble³, Suzanne Ingram³, Tara McKevitt³, Lee Christensen², Nicholas Easom^{1,4}. ¹Hull University Teaching Hospitals NHS Trust, Department of Infection, Cottingham, United Kingdom; ²Hepatitis C Trust, United Kingdom; ³Spectrum Community Health CIC, HMP Full Sutton, United Kingdom; ⁴University of Hull, Hull York Medical School, Hull, United Kingdom
Email: nicholas.easom@nhs.net

Background and aims: As part of ongoing efforts to eliminate Hepatitis C in England and Wales, we undertook mass-testing of the inmates of HMP Full Sutton, a Category A prison in the East Riding of Yorkshire, UK. Micro-elimination in prisons through a combination of Hepatitis Intensive Test and Treat (HITT) events and high-uptake reception testing is an important arm of the elimination programme. However this had not previously been attempted in a Category A prison.

Method: A multiprofessional team was assembled comprising staff from the Humber and North Yorkshire Operational Delivery Network (ODN), The Hepatitis C Trust, Full Sutton prison healthcare staff, NHS England, and Spectrum Community Health. Regular planning meetings were established to coordinate between services. Prison peer-mentors were trained leading up to the event, who disseminated information to other prisoners. Two teams, each consisting of an ODN nurse, prison healthcare lead nurse, Spectrum member and a prison officer, offered testing throughout the prison across two days. Oral hepatitis C virus (HCV) antibody swabs were used to screen for HCV antibodies, sero-positive individuals received follow-up HCV RNA testing with results available same-day. HCV RNA-positive individuals were offered treatment with pangenotypic oral antiviral therapy.

Results: In total, 584 prisoners were offered HCV testing and 514 (88%) accepted a test, in addition to 161 prison staff, 15 prisoners and 1 staff member were HCV antibody positive. On HCV RNA testing, 3 prisoners were positive and 0 staff members. All three HCV RNA-positive individuals commenced oral antiviral therapy within one week of the test results.

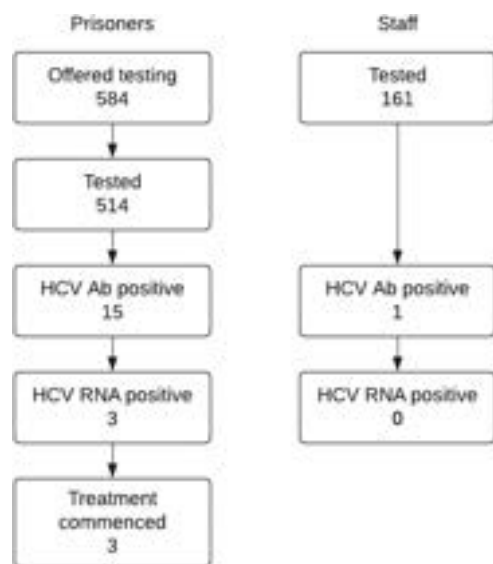


Figure:

Conclusion: Although the micro-elimination target of 95% testing uptake was not met, it was possible to test a high proportion of the prison population through a coordinated, multi-professional approach. Reasons for declining testing were related to concerns

about the potential for DNA sampling or a belief that the individual did not want or deserve to be treated for this infection. Despite this, high uptake was achieved by early engagement with the prison population through peer-mentors, active participation of prison officers, and the existing good relationship between prison healthcare staff and inmates. Learning has been disseminated to other ODNs for use in future Category A prison testing events.

WED-481

A prospective study to assess medication adherence to systemic therapy among patients with hepatocellular carcinoma

Suja Kumari¹, Ajee Kurunjiapadath Lakshmanan², Arun Valsan³, Nipun Verma⁴, Priya Nair⁵, Shine Sadasivan⁵, K Pavithran⁵, S Sudhindran⁵, Merin Babu^{6,7}, Vaishnavy S Vinod⁵, S Krishnapriya⁵, Manjima P Nair⁵, Ms Arunima⁸. ¹Amrita College of Nursing, Foundations of Nursing, Kochi, India; ²Amrita College of Nursing, Foundations of Nursing, India; ³Amrita Institute of Medical Sciences, Dept of Gastroenterology, Kochi, India; ⁴Postgraduate Institute of Medical Education and Research, Hepatology, India; ⁵Amrita Institute of Medical Sciences, Dept of Gastroenterology, India; ⁶Amrita Institute of Medical Sciences, Dept Of Oncology, India; ⁷Amrita Hospital, Kochi, Medical Oncology, Kochi, India; ⁸Amrita School of Pharmacy, India
Email: arunvalsan@aims.amrita.edu

Background and aims: Hepatocellular carcinoma (HCC) represent fifth most common malignancy and the third leading cause of death due to cancer worldwide. Recent data suggest that orally administered systemic therapy (ST) can improve quality of life and survival amongst patients with advanced HCC. Real-world adherence and tolerance to ST are currently unknown outside the clinical trial settings. This study aimed to assess medication adherence, perceived barriers to adherence, and reasons for non-compliance among patients with advanced hepatocellular carcinoma.

Method: A prospective observational study was conducted among advanced hepatocellular carcinoma patients receiving systemic therapy with either lenvatinib or sorafenib. The institutional ethics committee approved the study (ECASM-AIMS-2022-111, 01 July 2022). Patients' socio-demographic and clinic-laboratory data were recorded. A modified Morisky medication adherence tool with a reliability of 0.94 was used to measure adherence to the medication, and perceived barriers to compliance with medication were assessed by a self-structured tool with a reliability of 0.86.

Results: Of the 150 patients interviewed, 118 (79%) were males with a mean age of 65 ± 5 years, with the predominant aetiology of cirrhosis being alcohol (78%) and NASH (22%). Twenty-two patients (14.6%) had permanently discontinued the drug, whereas 73 (49%) patients discontinued the drug temporarily, with a mean drug intake of 2.5 months. The study population was divided into three adherence groups based on the Morisky scale: high (n = 66), moderate (n = 18), and low (n = 66). The mean adherence score was 5.44. There was significant association between non-adherence and body mass index, potassium level, albumin and cost of medications. The common reasons cited for non-adherence were fear of side effects (98%), forgetfulness (90%), perceived worsening of the clinical condition (45%), lack of accessibility to health information (21.3%), and lack of social support (14.6%) and Lenvatinib therapy (31%).



Figure:

Conclusion: According to the study's findings, several perceived obstacles, including side effects, cost concerns, and a lack of motivation and support, deter patients from taking their medications as prescribed. Our findings highlight the necessity of modifying the perceived barriers and enhancing adherence in a population at risk by implementing prompt interventions.

WED-482

Advanced practice nurses' scope of practice in liver care: evaluation of two different Swiss settings

Patrizia Kuenzler^{1,2,3}, Barbara Schoop², David Semela¹, Beat Müllhaupt⁴, Andreas E Kremer⁴, Sonja Beckmann^{3,5}. ¹Cantonal Hospital St.Gallen, Division of Gastroenterology and Hepatology, St. Gallen, Switzerland; ²Cantonal Hospital St.Gallen, Departement of Nursing, St. Gallen, Switzerland; ³University of Basel, Institute of Nursing Science, Basel, Switzerland; ⁴University Hospital Zurich, Department of Gastroenterology and Hepatology, Zürich, Switzerland; ⁵University Hospital Zurich, Center of Clinical Nursing Science, Zürich, Switzerland
Email: patrizia.kuenzler-heule@kssg.ch

Background and aims: Advanced Practice Nurses (APN) have an increasing role in Switzerland to meet the needs of patients with liver diseases and their caregivers related to their physical, psychosocial and practical problems. Although holding a master or PhD, their scope of practice is limited as e.g., by law, nurses are not allowed to prescribe or perform interventions (e.g., paracentesis). In Switzerland, two APNs at the Cantonal Hospital St.Gallen (KSSG) and University Hospital Zurich (USZ) provide in- and outpatient care within a liver transplant setting. Their roles were developed and implemented independently, depending on the clinical context and patients' needs. The APN at the KSSG provides outpatient therapies (HCV/HCC), counsels inpatients and performs, for example, hepatic encephalopathy (HE) assessments. The USZ implemented the APN role with a dedicated focus on case management in complex inpatient situations. We aimed to describe and compare the APNs' scope of practice.

Method: The APNs prospectively collected data from August-December 2022. The dataset included: patient data (e.g., characteristics, diagnosis, transplant status), process variables (e.g., type of contact, referral, setting), assessment (e.g., clinical, psychosocial, behavior) and interventions (e.g., counseling, self-management support, coordination of care). Data were descriptively analyzed on organizational level.

Results: Both APNs provided 294 consultations in 123 patients. KSSG: The APN performed 168 consultations in 80 patients, mainly in the outpatient setting (68%). Patients' mean age was 59 years, 20% had HCC, 66% had liver cirrhosis with a mean MELD score of 12.6, 9% were pre-, and 9% post-transplant. USZ: The APN performed 126

consultations in 45 patients, mainly in the inpatient setting (80%). Patients' mean age was 57 years, 11% had HCC, 93% had liver cirrhosis with a mean MELD score of 18.5, 17% were pre-, and 9% post-transplant. **Scope of practice:** Both APNs equally supported patients in symptom management (36% vs 32%) and provided education (24% vs 29%, Figure). At the KSSG, the APN interventions mostly addressed patients alone (73%) with self-management support (50%), psychosocial care (40%), decision-making (32%), outpatient medical treatment (24%), and HE assessment (18%). At the USZ, the APN interventions mostly addressed patients (65%) or caregivers alone (20%) with care coordination (44%), discharge planning (33%) and advanced care planning (22%).

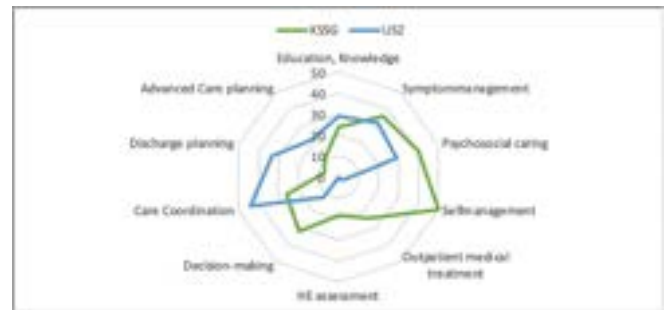


Figure: APN's scope of practice at the KSSG (green) and USZ (blue) in percentages

Conclusion: Our results highlight the diverse scope of APN activity in relation to their main clinical context (in- or outpatient setting), thereby reflecting the divergent patient needs along the care continuum. Other clinics may use our findings to develop APN roles according to their specific context and available resources.

WED-483

Value based healthcare: patient perception of the liver cancer advanced practice nurse care at the Barcelona clinic liver cancer

Neus Llarch^{1,2,3,4}, Eva Palou⁵, Jessica Farre⁵, Gemma Iserte^{1,2,3}, Núria Granel^{1,6}, Marta Campos Gomez^{1,2}, Joan Escarabill⁵, María Reig^{1,2,4,7}. ¹BCLC group, Fundació Clínica per a la Recerca Biomèdica-IDIBAPS., Barcelona, Spain; ²CIBERhd, Madrid, Spain; ³Liver Oncology Unit, Institut de Malalties Digestives i Metabòliques, Hospital Clínic de Barcelona, Barcelona, Spain; ⁴University of Barcelona (UB), Barcelona, Spain; ⁵Patient Experience Unit, Hospital Clínic de Barcelona, Barcelona, Spain; ⁶Institut de Malalties Digestives i Metabòliques, Hospital Clínic de Barcelona, Barcelona, Spain; ⁷Liver Oncology Unit, Liver Unit, Hospital Clínic de Barcelona, Barcelona, Spain
Email: mreig1@clinic.cat

Background and aims: Management of hepatocellular carcinoma (HCC) was traditionally based on the treatment's safety and efficacy. However, patient experience, which is the third pillar of the quality of Health Care was less evaluated. This study assesses the patient valued-health care areas and experience of the liver cancer patients in the outpatient clinic at the BCLC. The interview was based on the patients' experience with the Advanced Practice Nurse (APN) program at BCLC.

Method: Liver cancer patients included in APN-led-educational programs were recruited and were purposefully selected based on gender, age and disease stage. Individual interviews were conducted between September and October 2020. From September to October, a qualitative study through interview techniques were carried out. The interviews, which lasted on average 22.4 minutes, (Range 13–50) were audio-recorded and transcribed verbatim and analyzed by MAXQDA software. Patients were divided into two groups according to their knowledge of the APN program (with and without knowledge).

Results: Twenty-one interviews were performed. From the transcription analysis, 306 considerations were obtained which were

POSTER PRESENTATIONS

grouped into 34 categories and 8 meta-categories (Figure 1). Although 'Nurses' duties and 'humanely' were the main themes in all patients, other different topics were in the top-third category in each group: 'Expectations' in patients without knowledge and 'emotions' in patients who were already familiar with the APN program. Under 'emotions' some patients mentioned that nurses bring peace of mind, reassurance, others nervousness, fear and some patients commented that they felt alone during admission. Regarding 'expectations', the patients mentioned that what they expected from the nurses is to be treated well and professionalism, which was the case. Surprisingly, punctuality (4% and 5% in patients with and without previous contact with BCLC-APN; respectively) and administrative support (6% in both groups) were less mentioned than the nurses expected.



Figure:

Conclusion: In qualitative studies results are not generalizable to all patients. Their needs/priorities can be interpreted as areas of the BCLC-APN program which need to be covered or the reflection of patients' needs according to their knowledge of the program. These results are the rationale for developing a Value Based-APN program which includes the patients' perceptions.

WED-484

Hepatitis C education and training for community pharmacists in Ireland

Miriam Coghlan¹, Nessa Quinn¹, Declan Bradley², James Kee², Jennifer McCartan², Clare Fitzell³, Aiden McCormick⁴, Bernard Carr¹, Gail Melanophy¹. ¹St. James's Hospital, Pharmacy Department, Dublin, Ireland; ²Health Service Executive, Primary Care Reimbursement Service, Ireland; ³Irish Pharmacy Union, Ireland; ⁴National Hepatitis C Treatment Programme, Ireland
Email: coghlanm@tcd.ie

Background and aims: The availability of highly effective direct acting antivirals (DAAs) has made the elimination of Hepatitis C (HCV) a realistic goal. Simplified and devolved models of HCV care are needed to reach patients most in need of treatment. In 2019, the National Hepatitis C Treatment programme (NHCTP) in Ireland initiated a pilot programme for treatment in the community by general practitioners (GPs). DAAs prescribed could then be dispensed via a patient's local community pharmacy. Community pharmacists are well positioned to participate in the HCV treatment process. To provide community pharmacists with the right tools to enable them to successfully participate in the HCV treatment process we needed to devolve the knowledge gained in the hospital setting in an innovative and accessible way.

Method: An online training module was developed by a hospital HCV specialist pharmacist in collaboration with the NHCTP, the Irish

Pharmacy Union (IPU) and the Primary Care Reimbursement Service (PCRS). This module was hosted on the IPU website. The online module delivery was complimented by a virtual question and answer session between community pharmacists and the above stakeholders prior to patients initiating treatment. Module evaluation and feedback was captured electronically at the end of the online module. Rates of uptake and completion of the module were captured. Data on the number of patients started on HCV treatment via the community pathway was obtained from the PCRS.

Results: Since initiation of the pilot in July 2019, 110 pharmacists working across 87 pharmacies have completed the community pharmacist training module. Treatment has been commenced by 98 patients to date in the community setting. Among pharmacists who completed the online training module, 99% agreed that the training made them more competent in the area of Hepatitis C patient care with 99% agreeing that they will use the knowledge they gained to develop new workplace practices or services. Participants identified that the training increased their confidence in engaging and working with GPs and hospital-based colleagues to treat patients with HCV infection in their communities.

Conclusion: The online module has facilitated the involvement of community pharmacists in the processes of medication reconciliation, drug-drug interaction review, dispensing new medication and adherence counselling as related to DAAs in a patient's local community setting. The online module has allowed specialist HCV pharmacists to disseminate knowledge and learnings to community pharmacists in a standardised way. This training model has also supported greater inter-professional working among GPs and pharmacists across primary and secondary care settings.

WED-485

Quality improvement project: improving early identification of liver disease in diabetic patients in a district general hospital with opportunistic FibroScan®

Amy Thatcher¹, Catherine Mitchell², Vijay Grover². ¹Hillingdon Hospital, United Kingdom; ²The Hillingdon Hospital, United Kingdom
Email: amy.thatcher@nhs.net

Background and aims: The vast majority of liver disease is preventable, early detection is imperative to manage the disease and prevent complications. Despite diabetes being well recognised as a risk factor for fatty liver disease, diabetic patients are not routinely screened for liver fibrosis. The aim of this quality improvement project (QI) is to improve early identification of liver disease in patients with diabetes in both in and out patient district general hospital setting using FibroScan.

Method: Inpatients admitted to hospital and out-patients attending the diabetic clinic with type 1 and 2 diabetes were offered a FibroScan by the Hepatology Clinical Nurse Specialist (CNS). Patients were provided with information prior to the FibroScan and those who consented were scanned. If the FibroScan was suggestive of liver fibrosis (>8 kPa), the Hepatology CNS provided health promotion, requested a non-invasive liver screen and booked appropriate follow-up. The Hepatology CNS collected data on patients Alanine Transaminase (ALT), Liver Stiffness Measurement (LSM), Controlled Attenuation Parameter (CAP), Body Mass Index (BMI) and Metabolic Risk Factors (MRF) (Hypertension and Dyslipidaemia). Patients were excluded if they were known to have liver fibrosis, acute hepatitis, alcohol excess (>14 units per week) or raised inflammatory markers.

Results: 40 patients were offered a FibroScan, 21 outpatients and 9 inpatients, 10 outpatients declined. 30 patients accepted a FibroScan, of which 14 had Type 1 Diabetes Mellitus (T1DM) (age range 26–65) and 16 Type 2 Diabetes Mellitus (T2DM) (age range 30–86). 14% of T1DM had fibrosis with 7% CAP score of >Steatosis grade 1 (S1). 78% BMI >25, 35% had one or more MRF with an average ALT of 19. 56% with T2DM had fibrosis with 50% CAP score of >S1, 62% BMI >25, 81% one or more MRF with an average ALT of 29. 19% of T2DM had newly diagnosed cirrhosis.

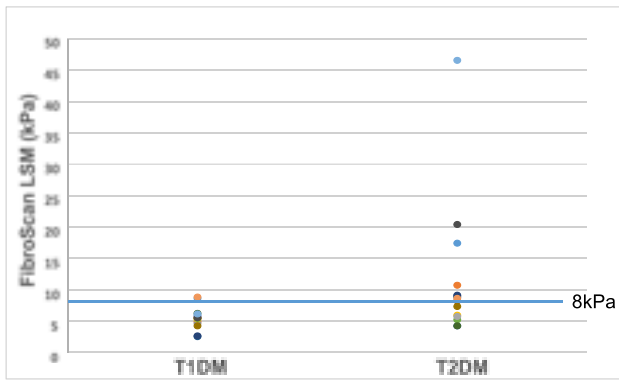


Figure:

Conclusion: This opportunistic screening QI project identified a significant number of T2DM patients with previously undiagnosed liver fibrosis, with majority having unremarkable liver enzymes. This has demonstrated the importance for this cohort of patients to be screened for liver fibrosis to prevent the complications of advanced liver disease.

WED-486

Changes in frailty as a predictor of readmission risk in patients with liver cirrhosis. Preliminary results

Martina Perez^{1,2}, Marta Cervera^{2,3}, Marta Carol^{2,3}, Ana Belén Rubio², Ruth Nadal³, Jordi Gratacos^{1,3}, Anna Soria^{1,3}, Anita Arslanow³, Adria Juanola^{1,3}, Elisa Pose^{1,2,3}, Isabel Graupera^{1,2,3}, Pere Ginès^{1,2,3}, Núria Fabrellas^{2,3}. ¹Liver Unit, Hospital Clínic de Barcelona, Spain; ²University of Barcelona, Spain; ³Institut d'Investigacions Biomèdiques August Pi i Sunyer (IDIBAPS), Spain
Email: maperezgu@clinic.cat

Background and aims: In addition to the complications of cirrhosis, the decompensated phase of the disease is characterized by the presence of sarcopenia, physical deterioration and/or malnutrition, all of which are associated with the concept of frailty. Recent studies have shown that frailty is a poor prognostic factor in patients with liver cirrhosis. Elevated frailty is also associated with an increase in unplanned hospitalizations, regardless of the severity of liver disease. The most frequently used tool to assess frailty is the Liver Frailty Index (LFI), designed specifically for patients with cirrhosis. Most published studies have assessed frailty at a single point; however, decompensated cirrhosis is a dynamic disease and patients' status can vary over a short period of time. The evolution of LFI changes in this population could be of interest as a tool to predict disease prognosis. The aim of this study is to investigate the relationship between changes in frailty and disease progression in patients with decompensated cirrhosis after hospital discharge.

Method: Prospective observational study in patients with decompensated cirrhosis who had been discharged after admission for a complication of cirrhosis. Frailty was measured by LFI at two points: at hospital discharge and at 7 days, and correlated with hospital readmissions within 28 days after inclusion. The cohort was divided into two groups, patients who had been readmitted within 28 days after inclusion and those who had not. The delta value of the LFI was calculated (taking into account the baseline and day 7 values) and the patients were classified into two groups, those who had improved and those who had remained the same or worsened.

Results: A total of 52 patients have been included so far, 38 of whom have completed a follow-up of 28 days. The baseline characteristics of the cohort are: mean age 62 years, mean 7 days of admission, 52% of the patients were alcoholic, and the most frequent complication was ascites, present in 63% of the patients. Considering a 28-day period, 8 patients were readmitted and 30 were not. The association between the readmission group and the LFI delta value was calculated. Of the group of patients who were readmitted, 5 patients (62% of the total of

this group) had worsened LFI and 3 (38%) had improved LFI. Of the group of patients who were not readmitted, 11 (37%) had worse LFI and 19 (63%) had better LFI.

Conclusion: Although the N of this study does not allow affirmation, the analysis provides crucial evidence to suggest that the delta value of the LFI may be a useful tool to predict the risk of readmission in patients with decompensated cirrhosis. Another added value of these data lies in demonstrating the importance of improving frailty status in this population.

WED-487

Mental health, quality of life, and stigmatization in Danish patients with liver disease

Nadja Østberg¹, Birgitte Jacobsen¹, Mette Lauridsen¹, Lea Ladegaard Grønkjær¹. ¹University Hospital of Southern Denmark, Department of Gastroenterology and Hepatology, 6700 Esbjerg, Denmark
Email: ns_@live.dk

Background and aims: Understanding the patient perspective is pivotal in the achievement of concordance with care and treatment. However, the mental health of patients with liver diseases is often overlooked when assessing their overall health and planning liver care, although the presence of mental health disorders are associated with poor patient outcomes, including symptom progression, increased hospitalization burden, and mortality. Thus, the aim of this study was to assess anxiety, depression, hopelessness, quality of life, and the perception of stigmatization in a large cohort of patients with chronic liver disease of different aetiologies and severity, as well as to identify predictors associated with mental health disorders.

Method: A total of 340 patients completed a survey assessing mental health using the Beck Anxiety Inventory, the Beck Hopelessness Scale, and the Major Depression Inventory. Quality of life was measured with the Chronic Liver Disease Questionnaire and the European Quality-of-Life visual analogue scale. To assess stigmatization, eight validated questions from the Danish nationwide survey of patient experiences were used. Predictors associated with anxiety, hopelessness, and depression were analysed using univariable and multivariable logistic regression analyses.

Results: Fifteen percent of the patients had moderate or severe anxiety, 3% had moderate or pronounced hopelessness, and 8% had moderate or severe depression. The prevalence of all three was highest in patients with cirrhosis and was associated with a low quality of life. More patients with cirrhosis had experienced stigmatization compared to patients with liver disease without cirrhosis, and more than one third of the patients, regardless of aetiology and severity, refrained from telling others about their liver disease.

Conclusion: Mental health disorders were present and associated with low quality of life in patients with liver disease and worst in patients with fully developed cirrhosis. In addition, patients experienced stigmatization. Our results emphasize the need for increased focus on mental health problems, development of intervention studies to explore the effect of therapy on quality of life and disease outcomes, and awareness on preventing discrimination and stigmatization of patients with liver disease.

WED-488

Clinical interdisciplinary development of a home-based enteral nutrition initiation and refeeding monitoring model of care for patients with chronic liver disease

Erin Russell¹, Suong Le^{2,3,4}, Patricia Anderson², Anita Figredo⁵, Sheree Phillips¹, Sally Bell^{2,4}, Thomas Worland². ¹Monash Health, Nutrition and Dietetics Department, Australia; ²Monash Health, Gastroenterology Department, Australia; ³Monash Digital Therapeutics and Innovation Laboratory (MoTILa), Australia; ⁴Monash University, School of Clinical Sciences, Australia; ⁵Monash Health, Hospital in the home, Australia
Email: russell.lee@hotmail.com

Background and aims: Malnutrition and sarcopenia are prevalent in 20 to 70% of adults with chronic liver disease (CLD) and are independently associated with increased mortality. Enteral nutrition (EN) can promote muscle mass restoration and improve objective liver function markers including Child-Pugh score. Malnourished CLD patients, and those with alcohol abuse, are at risk of refeeding syndrome on commencing EN. Inpatient capacity for EN initiation and monitoring was reduced during the COVID-19 pandemic. We developed an interdisciplinary home-based model of care to safely commence EN and monitor for complications in CLD patients.

Method: Monash Health is the second largest Australian tertiary healthcare network. Between February and June 2022, an interdisciplinary team of dietitians, gastroenterologists, general physicians, pharmacists, and nurses developed a home-based model of care. The protocol was derived from existing internal protocols and international guidelines for enteral feeding and refeeding management. Key elements include initiating, progressing, monitoring, escalation and ceasing enteral nutrition.

Results: We created an organisation-wide framework for supportive and collaborative patient care between multiple hospital departments (Hepatology, Hospital in the Home [HITH] and Dietetics). Our protocol includes roles and responsibilities, escalation pathways, instructions for initiating enteral feeding, precautions for refeeding management and a checklist for HITH nurses. Training for monitoring of these patients was completed at regular intervals to optimise stakeholder engagement. Communication pathways were developed to streamline inter-disciplinary collaboration. Our measures of success for this model of care include preventing hospital admissions, adverse events (including severe electrolyte requiring IV replacement or tube displacement), patient tolerance, weight restoration and improvement in Child-Pugh score. Two CLD patients successfully completed the feeding program without requiring inpatient admission. There was one tube dislodgement and one IV electrolyte replacement, successfully managed as outpatients.

Conclusion: We have developed and piloted a new model of care for home-based EN initiation program within a large tertiary healthcare network. This provided safe and effective EN therapy to a vulnerable group without requiring hospitalisation. The safety, efficacy, acceptability, and cost effectiveness of this model of care compared to traditional inpatient management will be evaluated as part of our feasibility study.

WED-489

Hepatology nursing consultation in a tertiary hospital without liver transplantation: initial experience

Alia Martín¹, Sandra Borrego¹, Sandra Díez¹, Irene Latras¹, Isabel González¹, Víctor Blázquez¹, Carolina Broco¹, Verónica Patiño¹, Raísa Quiñones¹, Rubén Díez¹, Francisco Jorquera¹, Pilar Moreno¹, Yolanda Méndez¹. ¹University Hospital of León, León, Spain
Email: amartiniz@saludcastillayleon.es

Background and aims: Patients with chronic liver disease require continuous monitoring in order to detect complications or decompensations of their pathology. It is in this context that hepatology units, and therefore their patients, benefit from having an advanced practice nurse. The proposal was to set up a nursing practice to carry

out intermediate follow-ups of patients with compensated chronic liver disease who are being followed up according to specific protocols for each disease. The objective was to analyse the activity of the hepatology nursing practice at the beginning of its activity in a tertiary care centre without liver transplantation.

Method: We retrospectively analysed the activity data of the nursing consultation at Complejo Asistencial Universitario de León from 1st January 2022 to 28th November 2022. The patient's express approval was required for referral to this care modality.

Results: Data from 211 patients assessed in the nursing consultation were analysed. Mean age was 63 years (SD 13.1) and 60% of patients were male. 98.6% (208/211) of the appointments were scheduled and 77.3% were on-site (163/211). After the nursing consultation it was necessary to consult a hepatologist on 13 occasions (6.2%). The main reasons for consultation were: control of B-blockers 49 (23.2%), follow-up of HBV infection (without previous liver disease) 41 (19.4%), chronic liver disease due to HCV 28 (13.3%), alcohol 22 (10.4%) and MAFLD 10 (4.7%) and follow-up of PBC without liver disease 17 (8.1%). The nurse performed a total of 299 interventions in the consultation. She provided advice on diet, exercise and lifestyle modification guidelines 134 times, adjusted medication 74 times, gave test results to 145 patients and referred 5 patients to the doctor's office. During the consultation the following tests were requested: blood tests in 176 patients, serology in 9, abdominal ultrasound in 110, MRI in 4, Fibroscan in 19 and gastroscopy in one patient. Thirty-four patients (16.1%) did not have any tests ordered.

Conclusion: The consultation of a hepatology nurse allows efficient follow-up of the patient with chronic liver disease, emerging as a key figure in bringing the hepatology unit closer to the patient.

WED-490

Development of a web-based mobile health application (ReLiver-N App) for patient activation, self-efficacy, and quality of life in patients with liver cirrhosis

Ferya Celik¹, Hicran Bektas¹. ¹Akdeniz University, Internal Medicine Nursing, Turkey
Email: feryacelik@gmail.com

Background and aims: Liver cirrhosis is an important health problem that increases morbidity and mortality. Utilizing accessible and sustainable mobile health applications could help provide patient education and enhance activation. When the level of patient activation gets higher, patients' self-efficacy and quality of life get higher. Achieving this can be contributed to hepatic rehabilitation. To develop a web-based mobile health application (ReLiver-N App) led by a nurse for patient activation, self-efficacy, and quality of life support in patients with liver cirrhosis.

Method: This study was the first stage of our randomized controlled trial registered in clinical trials (ClinicalTrials.gov Identifier: NCT05658393). The development process included creating the content and designing the ReLiver-N App. We developed the ReLiver-N App-based ADDIE which is an instructional design framework and created its contents of it. After preparing the content, 10 experts evaluated the quality of the contents through "Evaluation of the Written Materials Appropriateness," and "Teaching Materials Evaluation Form." We evaluated the readability of the contents through Atesman Readability Formula. After that, we conducted a feasibility test with three patients to assess the usability of the ReLiver-N App. The patients evaluated ReLiver-N App through the "System Usability Scale" and "Rate Us" tabs.

Results: Our content included patient education information about liver cirrhosis and patient activity tasks and measurement questionnaires. Patient education information topics included "healthy lifestyle, let's learn about liver cirrhosis, complications of liver cirrhosis, diagnosis, and treatment methods." Patient activity tasks are divided into two groups, "daily activity tasks," and "weekly activity tasks." Daily activity tasks included "weight measurement, edema evaluation, fluid balance, bleeding check, and taking

medications." Weekly activity tasks included "taking blood pressure, heart rate, and body temperature." Patients can access the contents at this website "https://kcsiroz.com/." The score obtained from the experts was high (20.20 ± 3.01). The high score indicated that the readability level of the ReLiver-N App was easy. In line with expert opinions, the content of the ReLiver-N App was found to be reliable (Cronbach's alpha score: 0.83). According to the experts' opinions, we also did some changes to the content. The score obtained from the patients was 67 points. This score indicated the usability of the ReLiver-N App was acceptable. The patients rated the ReLiver-N App three out of five points.

Conclusion: We created a reliable web-based mobile health application for free. We estimate that the ReLiver-N App could help patients with liver cirrhosis to enhance their patient activation level, self-efficacy, and quality of life, and have healthier life at their homes.

WED-491

Analysis of health-related quality of life in the liver transplant patient conducted more than 10 years ago, statewide study

Sara Román Serrano¹, Fernando García Pérez¹. ¹Spanish Federation of Liver Patients and Transplants (FNETH), Spain
Email: innovacion.social@fneth.org

Background and aims: To determine the health-related quality of life of patients who have undergone liver transplantation more than 10 years ago.

Method: Quantitative pilot study, in the form of an online survey, which was distributed through the website and social networks of the Spanish Federation of Liver Patients and Transplants (FNETH), and with the dissemination of our federated associations distributed throughout the national territory, after approval of the questionnaire by the Spanish Society of Liver Transplantation (SETH). To determine the health-related quality of life of patients who underwent liver transplantation more than 10 years ago. 1.0 questionnaire was used as the basis for the cross-cultural adaptation of the specific quality of life questionnaire for chronic liver diseases for use in the Spanish population. Statistical analysis of the data was performed with the Statistical Package for Social Sciences program (SPSS, version 28.0).

Results: The survey was open between 1 January 2021 and 31 October 2021, receiving a total of 114 surveys, of which 68 were finally valid for analysis. Socio-demographic characteristics: 58.8% of the participants were men and 41.2% were women, the age of the participants ranged from 27 to 79 years, and the average age was 58 years. The study showed a wide national demographic variety in terms of the place of origin of the participants. Immunosuppressant: 88.2% of respondents said they had all the information they needed to know about their immunosuppressant treatment, while 11.8% said they did not. Mainly the information about all aspects related to immunosuppressant is given by the doctor in 86.8%, in 7.4% of the cases the information has been provided by the nursing staff and it is striking that 5.9% say that they have to find out this information themselves. Psychological aspects: It is worth noting the low percentage of people who have received psychological help at some point (26.5%), compared to a large majority of participants who have never sought this type of support (73.5%). 82.3% of respondents consider psychological help to be quite or very important for the recovery of a transplant patient effect of the Covid-19 health crisis on health-related quality of life: These data are quite relevant since, without knowing the reasons for this, 35.3% of the total sample in the survey do not consider psychological support to be necessary to help them improve a psychological state which they claim to have been notably affected by the pandemic. It should be noted that of the 50 people who said they had never received psychological support, there were five participants who did feel they needed such support after the start of the pandemic.

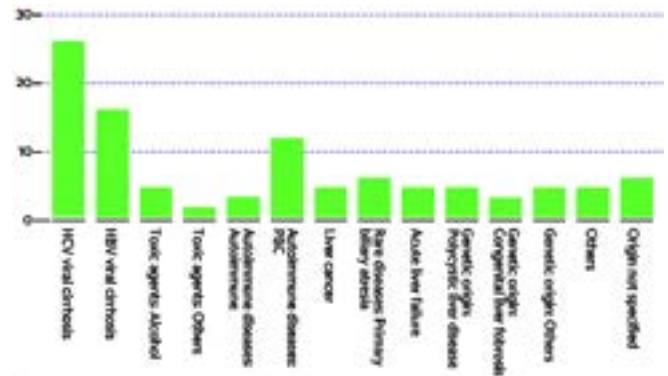


Figure: Causes of transplant

Conclusion: There is a need to provide more training and information to patients by healthcare staff on immunosuppressive treatments. It could be promoted with this type of professionals in order to resolve these doubts and acquire all the necessary information on immunosuppressive treatments. The fact that people who have been receiving treatment for more than 10 years now say that they lack information and knowledge about it has made us realize that this is an area that needs to be covered and improved. COVID-19 has increase in the number of people who have needed psychological support. However, we have seen that the majority of participants do not end up seeing a psychological professional.

WED-492

Fellowship for hepatology nurses-a new exchange program at Karolinska university hospital

Pia Loqvist¹. ¹Karolinska university Hospital, Dept Of Upper Intestinal Diseases, Stockholm, Sweden
Email: pia.loqvist@regionstockholm.se

Background and aims: When patient transferred from other Swedish hospitals, nurses have noticed a variance regarding nursing care, especially in patients with diagnosis and conditions leading to hospitalization at Karolinska University Hospital. To give the patients with chronic liver diseases the most optimal, equal care and sense of security regardless of treating hospital, it is important that all have the same knowledge and follow the same guidelines. One way of reaching this goal is by well-planned and organized Fellowship programs. As Karolinska University Hospital is accredited as a Cancer Comprehensive Center it follows a responsibility to share our specific knowledge in nursing care of the hepatology patient. The aim with a Fellowship program is to encourage national and international network together with competence exchange with the purpose to give all patient equal nursing care regardless of treating hospital.

Method: The planned Fellowship program includes a two week period at the Hepatology clinic at Karolinska University Hospital. The period will be based on an individual planning with focus of the Fellows experiences and medical interests. Mandatory elements such as follow the livertransplant coordinator, follow the patient through specific treatments like SIRT and TACE, and get an idea in how our excellent Dieticians works will be included. The participant will during those two weeks get an opportunity to receive increased practical and theoretical knowledge regarding nursing care and medical treatment.

Results: The planned Fellowship program includes a two week period at the Hepatology clinic at Karolinska University Hospital. The period will be based on an individual planning with focus of the Fellows experiences and medical interests. Mandatory elements such as follow the livertransplant coordinator, follow the patient through specific treatments like SIRT and TACE, and get an idea in how our excellent Dieticians works will be included. The participant will during those two weeks get an opportunity to receive increased

POSTER PRESENTATIONS

practical and theoretical knowledge regarding nursing care and medical treatment.

Conclusion: Increased awareness through Fellowship for nurses in hepatology in combination with sharing expertise and networking should potentially lead to equal nursing care for the patient suffering of liver diseases.

Public Health Except viral hepatitis

WEDNESDAY 21 TO SATURDAY 24 JUNE

TOP-094

Global, regional, and national burdens of cirrhosis in children and adolescents aged under 19 years from 1990 to 2019: a systematic analysis based on the global burden of disease study 2019

Chi Zhang¹, Yiqi Liu¹, Hong Zhao¹, Gui-Qiang Wang¹. ¹Peking University First Hospital, Department of Infectious Disease, Center for Liver Disease, China

Email: john131212@126.com

Background and aims: Cirrhosis and other chronic liver diseases (collectively referred to as cirrhosis) were the leading cause of morbidity and mortality in adults, but data on the burden and trends were sparse in children and adolescents. We aimed to assess the trends in 204 countries and territories over the past 30 years in children and adolescents aged 0–19 years

Method: Data on cirrhosis was collected by the Global Burden of Disease (GBD) 2019 database from 1990 to 2019. We reported on the number, rates, and average annual percentage changes (AAPCs) of incidence and disability-adjusted life-years (DALYs) of cirrhosis at global, regional, and national level. Joinpoint regressions were used to calculate the AAPC of cirrhosis.

Results: Globally, the incident numbers of cirrhosis in children and adolescents increased from 204767 in 1990 to 241364 in 2019, an increase of 17.9%, with an AAPC 0.13 (0.10 to 0.16). Substantial change in incidence of cirrhosis in 1996, 2006, 2009, and 2017. Prevalence (AAPC = -2.27 [-2.39 to -2.15]), mortality (AAPC = -1.68 [-1.86 to -1.5]), and DALYs rate (AAPC = -1.72 [-1.88 to -1.56]) of cirrhosis have decreased significantly. Cirrhosis incident rates varied between sex and age groups. Rates of cirrhosis caused by alcohol use (AAPC = 1 [0.8 to 1.1]; incidence cases increased most obvious 48%), hepatitis C (AAPC = 0.4 [0.4 to 0.5]), NAFLD (AAPC = 0.5 [0.3 to 0.6]) have been increasing, while only hepatitis B (-0.3 [-0.4 to -0.2]) decreasing. Incidence cases of cirrhosis were increased in low (101.6%) and low-middle sociodemographic index (SDI 21.1%) areas, while decreasing in middle and above SDI areas. At the regional level, the largest increases count was observed in Sub-Saharan Africa.

Conclusion: Global incidence rate of cirrhosis has been increasing, while the DALYs rate has been decreasing in children and adolescents. Morbidity of cirrhosis caused by hepatitis B declined, while hepatitis C, NAFLD, and alcohol use increased. We appealed for that in low SDI regions and countries, promoting the widespread vaccination of hepatitis B vaccine and reducing HCV infection were prominent; in middle and high SDI regions and countries, reducing cirrhosis caused by NAFLD and alcohol use were urgent.

TOP-095

A systematic review of interventions for alcohol use disorder in patients with cirrhosis or alcohol-related hepatitis

Christopher Oldroyd^{1,2}, Olivia Greenham¹, Graham Martin³, Michael Allison^{1,2}, Caitlin Notley⁴. ¹Liver Unit, Cambridge University Hospitals NHS Foundation Trust, Cambridge, United Kingdom; ²NIHR Biomedical Research Centre, Cambridge University Hospitals NHS Foundation Trust, Cambridge, United Kingdom; ³THIS Institute, University of Cambridge, Cambridge, United Kingdom; ⁴Faculty of Medicine and Health Sciences, Norwich Medical School, University of East Anglia, Norwich, United Kingdom
Email: christopher.oldroyd@nhs.net

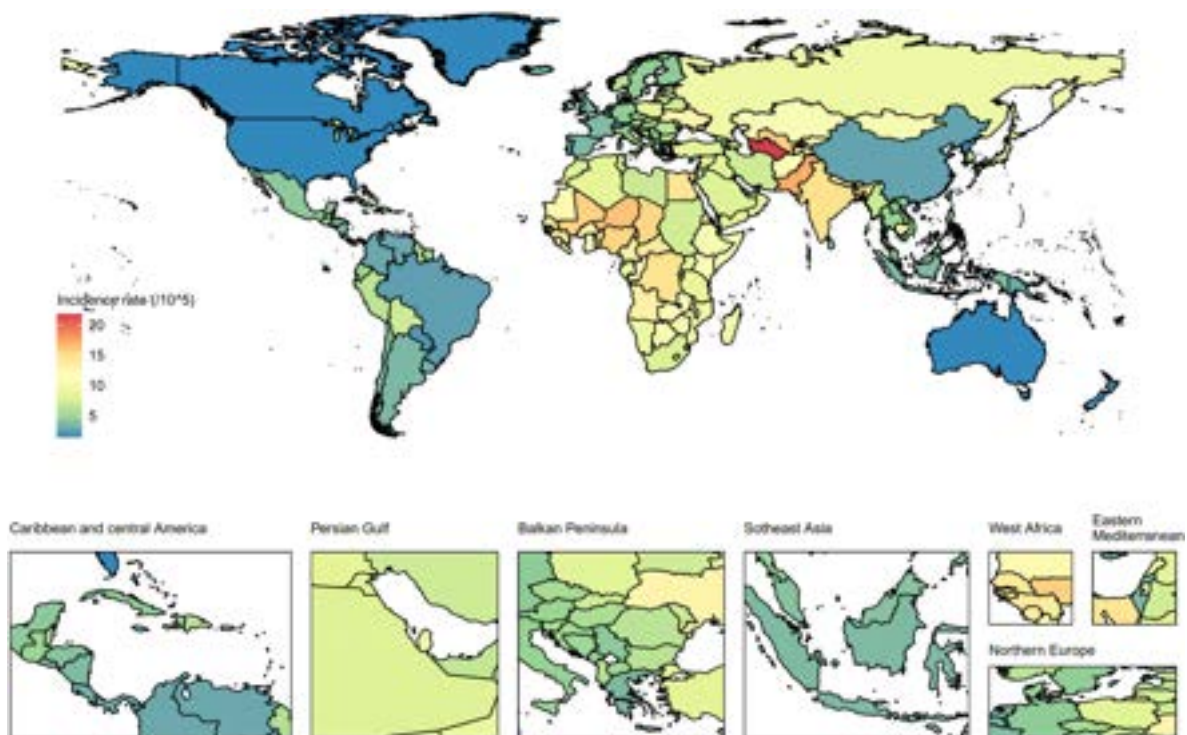


Figure: (abstract: TOP-094) The incidence rate of cirrhosis in children and adolescents at countries and regions level in 2019

Background and aims: Continued alcohol use is the most important factor in determining the prognosis of patients with alcohol-related cirrhosis and alcohol-related hepatitis. Previous systematic reviews of interventions for alcohol use disorder (AUD) have not been specifically targeted at patients with cirrhosis or alcohol related hepatitis. This review addresses this evidence gap.

Method: We followed the PRISMA guidelines for systematic reviews. Five databases were searched (MEDLINE, Web of Science, Embase, CINAHL and PSYCinfo) between inception of the database until November 2022. We included randomised trials and cohort studies which assessed the impact of an intervention to reduce alcohol intake with and without an active comparator. Only studies which included data specific to patients with cirrhosis or alcohol related hepatitis were included. We present a narrative synthesis of the results.

Results: 23 studies were included in the final analysis. The study population was dominated by two, large, retrospective, database-derived cohorts which included 101,745 patients with cirrhosis. The remaining 21 studies included 2574 patients, including 7 randomised controlled trials (RCTs) with 293 patients (Table 1). The most frequently assessed intervention was attendance at addiction therapy or alcohol rehabilitation (7 studies). Other interventions were pharmacological (baclofen, acamprosate, naltrexone, faecal transplant), psychological (motivational therapy, educational sessions) and attendance at specialist clinics. Two studies looked generically at the impact of any intervention for AUD. One retrospective cohort examined the impact of using low alcohol drinks. Studies variably reported outcomes related to liver disease (decompensation of cirrhosis, mortality and hospital admissions (n = 6)), alcohol use only (n = 10) or both outcome categories (n = 6). All of the studies which recorded alcohol outcomes reported that the intervention was beneficial in reducing intake or preventing relapse. In studies with control groups which reported on mortality, addiction treatment, attendance at outpatient clinics and (in a large database derived cohort) any AUD treatment had a statistically significant beneficial effect ($p < 0.05$). Three studies with control groups examined readmissions with only one finding a statistically significant reduction, this being associated with addiction therapy. Seven studies looked at new episodes of hepatic decompensation or change in MELD score. Of these, five of the interventions were found to have a statistically significant beneficial effect.

Figure: RCTs in the review

Reference	Country	Age (Mean or Median)	Males	n	Intervention	Outcomes	Follow-up
Sussman 2005	USA	44	75%	25	Educational sessions	Alcohol only	3 months
Addolorato 2007	Italy	56	64%	84	Baclofen	Alcohol only	90 days
Bajaj 2021	USA	65	100%	20	Faecal Transplant	Alcohol and Liver Disease	6 months
DeMartini 2018	USA	50.8	73%	15	Text message-based alcohol intervention	Alcohol only	8 weeks
Proeschold-Bell 2020	USA	54.9	71.3%	58	Alcohol Treatment	Alcohol only	12 months
Weinrieb 2011	USA	49.2	84%	91	Motivational Therapy	Alcohol only	24 months

Conclusion: Interventions for alcohol use disorder can be effective in improving clinical outcomes of patients with cirrhosis and alcohol related hepatitis. The evidence base is dominated by large database derived cohorts and the interventions are not well defined, indicating the need for further research in this area.

TOP-098

Socioeconomic disparities and survival in patients with primary liver cancer by subtype: a french population-based study

Thi Thu Nga Nguyen^{1,2}, Olivier DeJardin³, Jean Baptiste Nousbaum^{4,5}, Anne-Marie Bouvier⁶, Joséphine Gardy³, Guy Launoy³, Veronique Bouvier^{3,7}, Isabelle Ollivier-Hourmand². ¹Normandie University UNICAEN, France; ²Caen University Hospital, Hepatogastroenterology, Caen, France; ³ANTICIPE U1086 INSERM-UCN, Normandie University UNICAEN, Caen, France; ⁴Brest University Hospital, Hepatogastroenterology, Brest, France; ⁵Registry of Digestif Cancers of Finistère, EA 7479 SPURBO, Université de Bretagne Occidentale, Brest, France; ⁶Registry of Digestif Cancers, INSERM UMR 1231, UFR Santé de Bourgogne, Dijon, France; ⁷Registry of Digestif Cancers of Calvados, Caen, France
Email: nguyen.nga@live.com

Background and aims: Hepatocellular carcinoma (HCC) and intra-hepatic cholangiocarcinoma (iCCA) are the two most common histological subtypes of primary liver cancer (PLC). These two subtypes are recorded under distinct topological codes by the French Network of Cancer Registries (FRANCIM). There is no solid study evaluating distinctly prognosis of these two cancers as well as the influence of socioeconomic inequalities. We aim to assess the influence of socioeconomic disparities on net survival in patients with HCC and iCCA using population-based data.

Method: All patients diagnosed between 2013 and 2015, recorded under the topological code C22.0 (HCC) and C22.1 (iCCA) by the French Network of Cancer Registries FRANCIM were included with a follow-up until Juin 2018. Social environment was assessed by the European Deprivation Index (EDI). Flexible parametric analyses with multidimensional penalized splines were used to model excess mortality hazard and estimate the effect of EDI on net survival.

Results: A total of 6528 patients were included comprising 5271 patients diagnosed with HCC and 1257 with iCCA. Median age was 69.67 years in HCC patients and 72.42 years in iCCA patients. Male gender was predominant in both cancers (85% in HCC and 60% in iCCA). Net survival was higher in HCC patients than those with iCCA at any time of follow-up, regardless of sex (5-year survival: 19.07%, 19.84%, 10.67% and 9.58% in HCC men, HCC women, iCCA men and iCCA women, respectively). Net survival was significantly shorter in HCC men and iCCA women living in a more deprived environment compared to those living in a less deprived one. Excess mortality hazard was up to 14% higher and 20% higher among HCC men and iCCA women living in the most deprived areas compared to the least deprived ones, respectively (HR = 1.14, CI95% 1.139–1.142 in HCC men and HR = 1.209, CI95% 1.207–1.212 in iCCA women). EDI had no significant effect on net survival in HCC women nor in iCCA men.

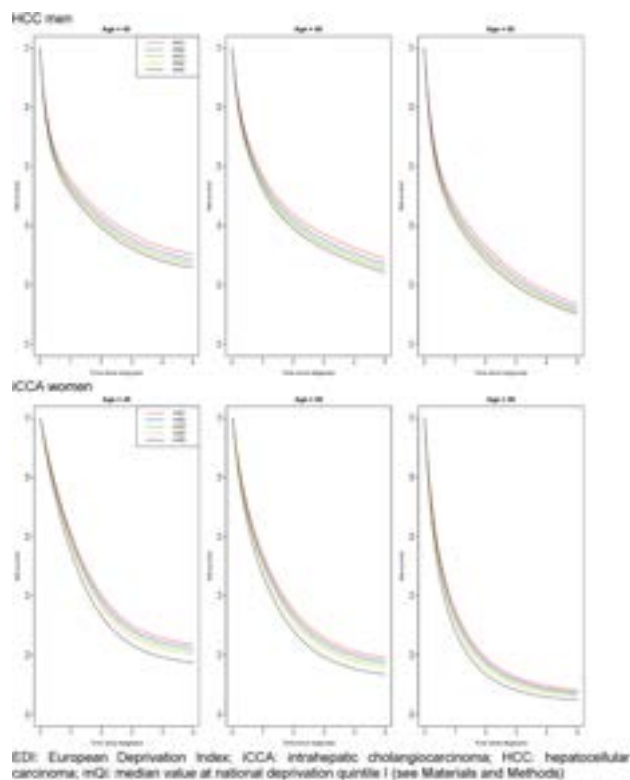


Figure: Net survival over time since diagnosis by level of deprivation for each cancer site and sex for which EDI effect was significant, predicted by selected model for 40-, 60- and 80- year-old.

Conclusion: In conclusion, our study provides an original and distinct survival analysis in HCC and ICCA patients, showing a higher mortality in ICCA. It also highlights a social gradient in survival which differs according to sex and cancer site. Our findings suggest the implementation of targeted actions especially among men at risk of HCC living in disadvantaged environment.

TOP-099

Higher ultra-processed food intake positively associated with non-alcoholic fatty liver disease in both adolescents and adults

Longgang Zhao¹, Xinyuan Zhang², Chun-Han Lo³, Euridice Martinez⁴, Fang Fang Zhang⁵, Xuehong Zhang^{2,6,7}. ¹University of South Carolina, Columbia, United States; ²Brigham and Women's Hospital, Boston, United States; ³Kirk Kerkorian School of Medicine at UNLV, Las Vegas, United States; ⁴University of São Paulo, Brazil; ⁵The Gerald J. and Dorothy R. Friedman School of Nutrition Science and Policy, Boston, United States; ⁶Harvard Medical School, United States; ⁷Harvard T.H. Chan School of Public Health, United States
Email: poxue@channing.harvard.edu

Background and aims: The influence of consumption of ultra-processed foods (UPF) on non-alcoholic fatty liver diseases (NAFLD) remains poorly understood. Related evidence for adult NAFLD is limited and no study has yet evaluated NAFLD in adolescence.

Method: We conducted a study among 806 adolescents and 2,734 adults who participated in the National Health and Nutrition Examination Survey (2017–2018). UPF intake was estimated using the dietary data collected by two 24-hour dietary recalls. NAFLD was defined by transient elastography in the absence of other causes of chronic liver disease. Logistic regression was used to estimate the multivariable odds ratio (OR) and 95% confidence intervals (CI) for associations between UPF consumption and NAFLD with survey weight adjustments.

Results: The mean consumption of UPF was 810 grams/day for adolescents and 823 grams/day for adults. A total of 12.4% (n = 111) among adolescents and 35.6% of the participants (n = 1,053) among

adults had NAFLD. Higher UPF intake was associated with higher odds of NAFLD in both adolescents (OR_{Quintile 5 vs Quintile 1} = 2.34, 95% CI = 1.01–5.41, P_{trend} = 0.15) and adults (OR_{Quintile 5 vs Quintile 1} = 1.78, 95% CI = 1.04–3.03, P_{trend} = 0.002). In adults, about 68% and 71% of the association between UPF intake and NAFLD was mediated by BMI and waist circumference (all P values < 0.001), respectively. We also found higher UPF intake was positively associated with serum levels of albumin and C-reactive protein in adults. Results were similar for adolescents though not statistically significant.

Conclusion: Higher UPF intake was associated with higher odds of having NAFLD among both adolescents and adults. These associations are largely mediated by elevated body fatness. Further prospective studies are needed to confirm our findings. If confirmed, reducing UPF intake might help prevent NAFLD in both adolescents and adults.

SATURDAY 24 JUNE

SAT-114

An explainable artificial intelligence model for prediction of high-risk non-alcoholic steatohepatitis

Basile Njei¹, Eri Osta², Nelvis Njei³, Joseph Lim¹. ¹Yale University, United States; ²The University of Texas Health Science Center at San Antonio, United States; ³Centers for Medicare and Medicaid Services, United States
Email: basile.njei@yale.edu

Background and aims: High-risk Non-alcoholic Steatohepatitis (NASH) is defined by non-alcoholic fatty liver disease (NAFLD) activity score ≥ 4 and fibrosis stage ≥ 2 on liver biopsy. The FibroScan-AST (FAST) score, calculated using liver stiffness measurement and controlled attenuation parameter values from FibroScan and aspartate aminotransferase levels, is a validated algorithm to identify individuals with high-risk NASH. However, liver biopsy and FibroScan are not always available in resource-limited settings. Early identification of high-risk NASH can offer patients access to novel therapeutic options and potentially decrease the risk of progression to cirrhosis. We used explainable artificial intelligence (XAI) to develop an algorithm integrating demographic, clinical, and laboratory data for predicting high-risk NASH.

Method: Data were derived from the National Health and Nutrition Examination Surveys (NHANES) 2017–March 2020. We used FAST score ≥ 0.35 , to identify individuals with high-risk NASH. Three machine learning models, extreme gradient boosting (XGBoost), random forest (RF), and logistic regression (LR), were used to establish the prediction. The training set contained 50% of included patients. The optimized model was then validated by the independent holdout test set, on the remaining 50%. We illustrated the clinical feature's importance and provided visualized interpretation using SHapley Additive exPlanations (SHAP) and local interpretable model-agnostic explanations (LIME). To identify high-risk NASH subphenotypes, an unsupervised distance-based clustering method was used.

Results: There was a total of 5281 subjects meeting the inclusion criteria. The mean age was 53 (range 18–80 years), and 2602 (49%) were women. Subjects with high-risk NASH comprised 6.5% and 7.5% of training and test set, respectively. Figure 1 shows the areas under our models' receiver operating characteristic curve (AUC) for predicting high-risk NASH. The optimized XGBoost model demonstrated a superior ability to predict high-risk NASH vs. FIB-4, BARD, and NAFLD fibrosis scores (AUC of 0.97 vs. 0.75, 0.81 and 0.72, respectively, all $p < 0.001$). To explain the high performance of the XGBoost model, we found that the top 5 predictors of high-risk NASH were ALT, AST, waist circumference, BMI, and glycohemoglobin. Using cluster analysis, 4 novel subphenotypes of high-risk NASH were identified: (1) women with low ALT; (2) young patients with low waist circumference; (3) Mexican Americans and Non-Hispanic Black

Americans with high platelets; and (4) patients with prediabetes/diabetes and low ALT.

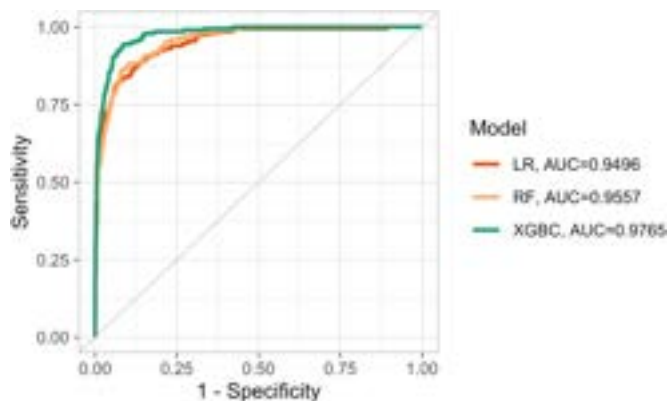


Figure 1: Areas under the receiver operating characteristic curve (AUC) plot of our models for predicting high-risk NASH

Conclusion: We used an XAI approach to develop a clinically applicable model that outperforms commonly used clinical risk indices and could increase the identification of high-risk NASH patients in resource-limited settings.

SAT-115

Healthcare resource use and costs among patients with primary sclerosing cholangitis in Sweden-a retrospective population-based cohort study

Annika Bergquist^{1,2}, Nandita Kachru³, Martina Aldvén⁴, Oskar Ström⁴, Douglas Knutsson⁵, Emilie Toresson Grip^{2,4}, Hannes Hagström^{1,2}. ¹Department of Medicine, Huddinge, Karolinska Institutet, Stockholm, Sweden; ²Division of Hepatology, Department of Upper GI Diseases, Karolinska University Hospital, Stockholm, Sweden; ³Gilead Sciences Inc., Foster City, United States; ⁴Quantify Research AB, Sweden; ⁵Quantify Research AB, Sweden
Email: Nandita.Kachru@gilead.com

Background and aims: Primary sclerosing cholangitis (PSC) is a rare, chronic, cholestatic liver disease characterized by biliary inflammation and fibrosis of both small and large bile ducts, that can potentially lead to cholestasis and cirrhosis. This study characterized the baseline comorbidities, healthcare resource utilization (HRU) and costs among PSC patients in Sweden.

Method: Using the Swedish National Patient Register which captures all hospitalizations and outpatient hospital visits, PSC patients (≥ 18 years) were identified via ICD-10 codes from 01/01/2002 to 12/31/2020 using diagnosis of PSC (K83.0A) and/or combination of cholangitis (K83.0) and inflammatory bowel disease (IBD) (K50 or K51). Those with prior diagnosis of biliary atresia, cystic fibrosis, human immunodeficiency virus or primary biliary cholangitis were excluded. First date of PSC diagnosis within this period defined the index date. Patients were required to have ≥ 360 days look-back (baseline) period and ≥ 30 days of follow-up. Incident patients (with no PSC diagnosis 1 year prior to index date) were followed from the index date to death, emigration, or end of study. Annualized mean all-cause HRU and costs, reported as 2021 Euros, were calculated during the baseline and follow-up period.

Results: After applying inclusion/exclusion criteria, 4,819 PSC patients were included in the study. Of these, 4,213 (mean age 48.4 years, 56.8% male) were identified as incident. During the follow-up period (mean 6.7 years; range 0.1–19.0; 28,283 person-years), 935 (22%) patients died. PSC patients reported liver complications during baseline (4.6% had compensated or decompensated cirrhosis, 4.7% had hepatobiliary or pancreatic malignancy and 1.0% had been transplanted). 73% patients had IBD and 16.4% showed use of ursodeoxycholic acid. The mean length of inpatient stay, number of

hospitalizations and outpatient visits were found to significantly increase from baseline to follow-up period (5.1 ± 12.9 vs. 15.5 ± 43.1 , 0.9 ± 1.7 vs. 1.8 ± 3.8 , 4.9 ± 7.5 vs. 6.6 ± 9.6 respectively; $p < 0.0001$). Similarly, total all-cause healthcare costs reported a significant increase by 117% (from € 9424.4 to € 20,487.2; $p < 0.0001$), hospitalization costs were the primary driver (Figure).

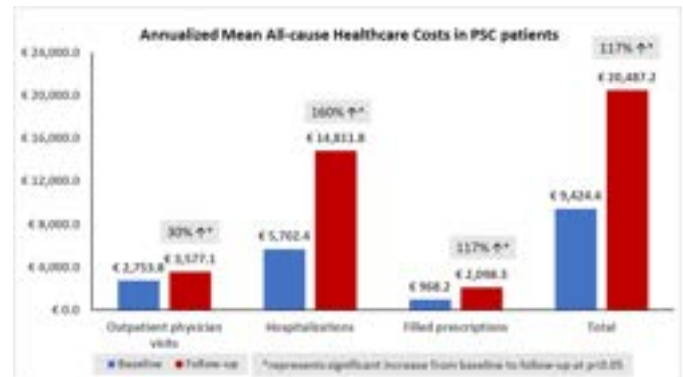


Figure:

Conclusion: Although PSC is considered a rare disease, the impact on HRU and costs are reported to be substantial. Early identification and effective therapies are needed to reduce the risk of disease progression and subsequent healthcare costs.

SAT-116

Health economics of the enhanced liver fibrosis test in the detection of advanced liver fibrosis in patients with non-alcoholic fatty liver disease in the UK

Zobair Younossi^{1,2,3}, Maria Stepanova⁴, James Paik^{2,3}, Fatema Nader⁴, Linda Henry⁴, Richard Pollock⁵. ¹Inova Health System, Medicine Service Line, United States; ²Beatty Liver and Obesity Research Program, Inova Health System, United States; ³Inova Health System, Department of Medicine, Center for Liver Diseases, United States; ⁴Center for Outcomes Research in Liver Disease, United States; ⁵Covalence Research Ltd, Harpenden, United Kingdom
Email: zobair.younossi@inova.org

Background and aims: The enhanced liver fibrosis (ELF) test is a non-invasive blood test to assess the risk of advanced fibrosis in patients with non-alcoholic fatty liver disease (NAFLD). The aim of the present study was to evaluate the cost-effectiveness of a diagnostic pathway including the Fibrosis-4 (FIB-4) index plus ELF for patients with an indeterminate FIB-4 index (1.30–2.67), compared versus FIB-4 alone, FIB-4 plus Transient Elastography (TE), and standard of care (SoC), in the detection of advanced fibrosis in patients with NAFLD from the perspective of a UK healthcare payer.

Method: A cost-utility model was developed with two modules: a diagnostic pathway module which distributes patients between true and false positive and negative diagnoses of advanced fibrosis, and then a long-term extrapolation based on a Markov model. The performance of the FIB-4/ELF, FIB-4/TE and FIB-4 alone pathways was based on published literature. UK standard of care was based on Srivastava et al. (J Hepatol 2019). The long-term Markov model captured transitions through fibrosis stages, cirrhosis, decompensated cirrhosis, hepatocellular carcinoma, liver transplant, and death. UK-specific cost data were obtained from the literature and utility values were derived from patients with NAFLD using EQ5D or equivalent instrument. Future cost and effectiveness outcomes were discounted at 3.5% per annum and the long-term model was run over a 20-year time horizon.

Results: The decision tree reported that, with FIB-4/ELF, 5.6% of patients with NAFLD had a false positive diagnosis of advanced fibrosis versus 6.0% with FIB-4/TE, 22.1% with FIB-4 alone, and 29.8% with SoC. The model showed that the costs of a FIB-4/ELF pathway

POSTER PRESENTATIONS

would be the lowest of the four options; the higher initial cost of the FIB-4/ELF diagnostic pathway was more than offset by a reduction in resource utilisation arising from false positive diagnoses. The long-term extrapolation showed that FIB-4/ELF would be dominant versus SoC, reducing costs while increasing quality-adjusted life-years gained.

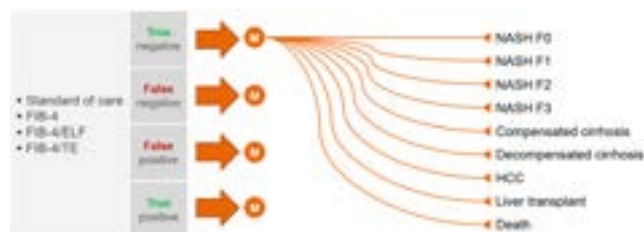


Figure:

Conclusion: A pathway combining FIB-4/ELF to detect advanced fibrosis in patients with NALFD in the UK would be cost saving relative to SoC, FIB-4/TE and FIB-4 alone. FIB-4/ELF would also dominate SoC over a 20-year extrapolation and would therefore be considered a cost-effective use of UK healthcare resources.

SAT-117

Influence of the COVID-19 pandemic on liver cancer-related mortality in the United States

Zhu Zhan¹, Dan Shi², Chengchen Zhang³, Yujing Shi¹, Na Wu¹, Hong-Gang Ren¹, Hong Ren¹. ¹Key Laboratory of Molecular Biology for Infectious Diseases (Ministry of Education), Institute for Viral Hepatitis, Department of Infectious Diseases, the Second Affiliated Hospital of Chongqing Medical University, China; ²Department of Nutrition and Food Hygiene, School of Public Health, Chongqing Medical University, China; ³Center of Clinical Research, Shanghai Children's Medical Center Affiliated with Shanghai Jiaotong University School of Medicine, China Email: renhong0531@cqmu.edu.cn

Background and aims: The COVID-19 pandemic has caused a diverse and extensive impact on the public health system. This study attempted to examine the influence of the pandemic on liver cancer (LC)-related mortality in the United States (U.S.).

Method: We reviewed data from the National Vital Statistics System from the Center for Disease Control and Prevention Wide-Ranging Online Data for Epidemiologic Research (CDC WONDER) platform and ICD-10 codes, and screened for LC-related deaths. We also analyzed the actual event versus estimated mortality rate for 2020–2021, according to the patterns from 2010 to 2019 using joinpoint and prediction modelling analysis.

Results: We identified 322,698 LC-related deaths in the U.S. from 2010 to 2022. Hepatocellular carcinoma (HCC) and intrahepatic cholangiocarcinoma (ICC) are the most prominent LC types, accounting for 61% and 38% of all cases, respectively. The HCC age-standardized mortality rate (ASMR, per 100,000) revealed an overall upward trend from 2010 to 2019, with a mean annual percentage change (APC) of 3.7%. However, the HCC ASMR remained unchanged in 2020, and showed a sharp increase since January 2021, with a peak in December 2021, compared to the levels predicted from pre-pandemic trend (ASMR of 4.36 vs. 4.35 in 2020, 6.45 vs. 4.48 in 2021). This delayed rise in mortality during the COVID-19 pandemic was also found in ICC and other LC types. Although the older population (≥ 65 years) contributed to over half of the deaths among people with LC, the younger population (25–44 years) revealed the highest APC for HCC (11.6%) and ICC (6.4%) during the COVID-19 pandemic. In addition, female, American Indian/Alaska Native (AI/AN), Asian, and Pacific Islanders (API) were more susceptible to the COVID-19 pandemic, compared to their counterparts.

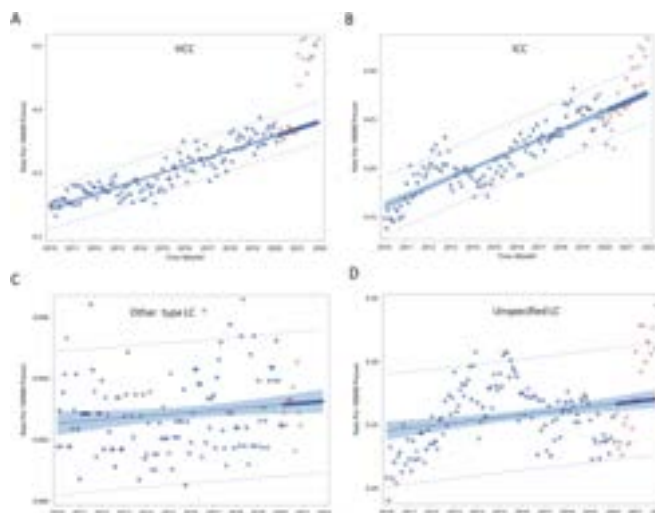


Figure:

Conclusion: We observed a delayed rise in LC-related mortality during the COVID-19 pandemic, and young, female, AI/AN, and API populations were most at risk.

SAT-118

Acceptability and feasibility of a multimodal early detection pilot study for liver disease in high risk groups: "Alright My Liver?"

Ann Archer^{1,2}, Sally Tilden¹, Tom May^{2,3}, Jo Kesten^{2,3,4}, Jane Gitahi¹, Lucy Yardley^{2,3,4,5,6}, Matthew Hickman^{2,3}, Kushala Abeysekera^{1,2}, Fiona Gordon¹. ¹University Hospitals Bristol and Weston NHS Foundation Trust, Bristol, UK, Liver Medicine, Bristol, United Kingdom; ²Bristol Medical School, University of Bristol, Bristol, UK, Population Health Science, Bristol, United Kingdom; ³University of Bristol, NIHR Health Protection Research Unit (HPRU) in Behavioural Science and Evaluation, Bristol, United Kingdom; ⁴University Hospitals Bristol and Weston NHS Foundation Trust, UK, NIHR Applied Research Collaboration West (NIHR ARC West), Bristol, United Kingdom; ⁵University of Bristol, School of Psychological Science, Bristol, United Kingdom; ⁶University of Bristol, Centre for Academic Primary Care, Bristol, United Kingdom Email: ann.archer@uhbw.nhs.uk

Background and aims: 75% of people with cirrhosis are diagnosed during an emergency admission to hospital, at which point mortality is 1 in 6. Cirrhosis prevalence is <1% in the general population, making a targeted approach to case finding desirable. In 2022, NHS England funded the Bristol and Severn hepatitis C operational delivery network to broaden its existing outreach work as part of the "Piloting Community Liver Health Checks" scheme. The aim of this study is to report disease detection and acceptability outcomes of the "Alright My Liver?" service, developed in collaboration with service users, to screen and detect advanced liver fibrosis from alcohol, viral hepatitis and metabolic syndrome in those deemed high risk.

Method: Liver health screening events were co-located with existing services that serve vulnerable and high risk groups. These included drug and alcohol services, primary care services in areas with a high index of deprivation and with Caafi Health, an organization providing health outreach to black and ethnic minority communities in the region. A health history, transient elastography (TE) using FibroScan® and capillary blood borne virus testing if indicated were collected. All patients received personalized advice including brief alcohol reduction interventions and cessation service signposting if indicated. To encompass multiple aetiologies of liver disease, commissioners advocated a liver stiffness measurement (LSM) by TE of ≥ 11.5 kPa for advanced fibrosis, 8.5–11.4 kPa for moderate fibrosis and <8 kPa normal. Clients identified with advanced fibrosis were booked directly into hepatology clinic with an offer of funded transport and telephone reminders. Semi-structured interviews were conducted with service

users and providers to which the agile co-production and evaluation (ACE) framework is being applied to optimize the service.

Results: 622 people were assessed at outreach events between July and Dec 2022. Median age 46 years (IQR 16), median BMI 26.1 kg/m² (IQR 7.1 kg/m²), 49% female (n = 308/622). 18.9% (n = 118/622) had experienced homelessness. The population screened had an ethnicity case of mix of 40% white British/12% Black African/4% South Asian. Median LSM 5.1 kPa (IQR 2.7 kPa), median IQR/M 17% (IQR 13%). Inpatient and outpatient addiction settings were highest yield, with 14% (n = 6/43) and 9.5% (n = 10/135) respectively of clients identified as having advanced fibrosis. Five patients were identified as having active hepatitis C infection, of whom four have now started treatment. One case of chronic hepatitis B infection was identified. Attendance rate at hepatology clinic appointment was 78% (n = 18/23) and attendance rate for ultrasound was 85% (n = 32/37). Semi-structured interviews with service users returned overwhelmingly positive feedback, suggesting that the service is acceptable to its target group.

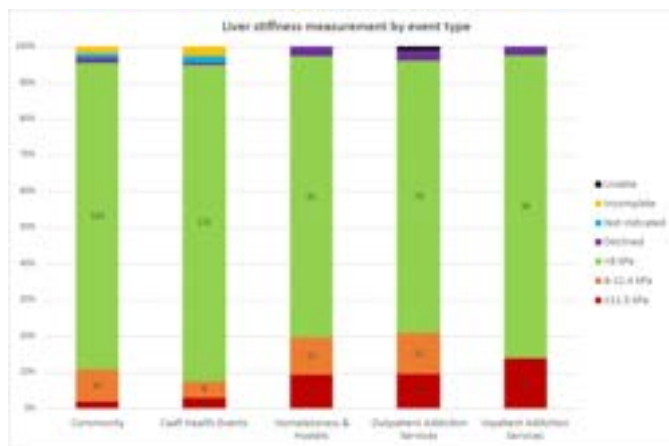


Figure:

Conclusion: Early detection of advanced fibrosis in high risk groups within the community setting is achievable and acceptable to patients. The drug and alcohol services setting provides the highest yield for advanced fibrosis. Longer term follow-up will clarify how well patients engage with liver services and treatment to impact clinical outcomes.

SAT-119

Lifestyle-related population-attributable risk for non-alcoholic fatty liver disease in adolescents and youth

Vanessa Garcia-Larsen¹, Hani Tamim², Saad Alghamdi³, Mohammad Ali Shagrani⁴, Faisal Abaalkhail⁵, Walled Alhamoudil⁶, Faisal Sanai⁷, Saleh Alqahtani^{8,9}. ¹Bloomberg School of Public Health, The Johns Hopkins University, International Health, United States; ²Alfaisal University, College of Medicine, Saudi Arabia; ³King Faisal Specialist Hospital and Research Centre, Liver and Small Bowel Transplant and Hepatology Surgical, Riyadh, Saudi Arabia; ⁴King Faisal Specialist Hospital and Research Centre, Liver and Small Bowel Transplant and Hepatology Surgical Department, Saudi Arabia; ⁵King Faisal Specialist Hospital and Research Centre, Department of Medicine, Gastroenterology Section, Saudi Arabia; ⁶King Faisal Specialist Hospital and Research Centre, Liver and Small Bowel Transplant and Hepatology Surgical, Saudi Arabia; ⁷King Abdulaziz Medical City, Gastroenterology Unit, Department of Medicine, Jeddah, Saudi Arabia; ⁸King Faisal Specialist Hospital and Research Centre, Liver Transplant Centre, Saudi Arabia; ⁹Johns Hopkins University, Division of Gastroenterology and Hepatology, Baltimore, United States
Email: vgla@jhu.edu

Background and aims: Non-alcoholic fatty liver disease (NAFLD) affects an estimated 15–25% of the adult population worldwide.

Obesity and metabolic syndrome are among the most important risk factors for the disease, but evidence in children and youth has been less examined. This study aimed to quantify the population-attributable risk (PAR) for NAFLD due to lifestyle-related factors in youth.

Method: We included data from the 2017–2018 U.S. National Health and Nutrition Examination Survey (NHANES) cycle on youth aged 12 to <21 years who underwent vibration-controlled transient elastography with controlled attenuation parameter (CAP). Liver steatosis (NAFLD) was defined as a CAP score of ≥ 248 dB/m. PAR (%), i.e., the prevalence of NAFLD attributed to each factor under study, was investigated for exposures previously shown to be independently associated with liver steatosis in adolescents, namely body mass index (BMI), systolic blood pressure, waist-to-height ratio (WHR), and the homeostatic model assessment for insulin resistance (HOMA-IR). The Dietary Approaches to Stop Hypertension (DASH; higher scores = higher adherence) and the Alternative Healthy Eating Index (AHEI; 0 = low adherence, 110 = highest adherence) were also included as measures of diet quality, a domain seldom studied in relation to NAFLD in this age group. Survey-weighted, z-transformed PARs were calculated (adjusting for age, sex, ethnicity, BMI [when applicable], total energy intake, household income, and education) by comparing an unhealthier vs. healthier scenario for each factor (namely, having a BMI ≥ 30 vs. a BMI <25; having a BMI ≥ 25 <30 vs. a BMI <25; no physical activity vs. practicing physical activity for at least 60 minutes during the week/vigorous recreational activities during the week; highest vs. lowest quartile of WHR; highest vs. lowest quartile of HOMA-IR; and lowest vs. highest quartile of diet quality adherence).

Results: A total of 972 participants (mean age 15.7 ± 2.4 ; male 51.0%) with complete data were included in this study. The prevalence of liver steatosis was 28.3%. The adjusted risks of liver steatosis attributable to overweight and obesity were 3.3% (95% confidence interval [CI]: 2.1, 4.7) and 10.1% (CI: 7.9, 12.4), respectively. The PAR associated with NAFLD was 7.2% for higher systolic blood pressure (CI: 3.9, 10.6), and 4.4% for lower DASH adherence (CI: 0.2, 8.5). The risks attributable to a higher WHR, lack of physical activity and low AHEI adherence were not statistically significant.

Conclusion: NAFLD in adolescents and youth from the U.S. is highly prevalent. Obesity, overweight, systolic blood pressure, and diet quality are important contributors to the disease among youth. As the DASH diet has a recognized benefit in the control of overweight and hypertension, improving its adherence during adolescence may contribute to reducing the burden of NAFLD.

SAT-120

COVID-19 and excess mortality of patients with liver cancer in France, January 2020–September 2022

Stylianos Tzedakis^{1,2,3}, Ortal Yzhaky Shapira¹, Michael Schwarzwinger⁴, Sandrine Katsahian⁵, Andrea Lazzati⁶, Anthony Dohan⁷, Romain Coriat⁸, Philippe Sogni⁹, Stanislas Pol⁹, David Fuks¹⁰, Vincent Mallet⁹. ¹Hôpital Cochin, AP-HP Centre, Groupe Hospitalier Cochin Port Royal, DMU Cancérologie et spécialités médico-chirurgicales, Service de chirurgie hépatobiliaire, digestive et endocrinienne, Paris, France; ²Université Paris Cité, F-75006, Paris, France; ³INSERM, UMR 1138, Centre de Recherche des Cordeliers, Centre Inria de Paris, Équipe HeKA, France; ⁴CHU Bordeaux, Service de soutien méthodologique et d'innovation en prévention, 33000 Bordeaux, France; ⁵Université de Bordeaux, Inserm UMR 1219-Bordeaux Population Health, 33000 Bordeaux, France; ⁶AP-HP, Hôpital Européen Georges-Pompidou, Service d'Épidémiologie et de Biostatistiques, Paris, France; ⁷Centre intercommunal de Créteil (CHIC), Service de chirurgie générale, digestive et de l'obésité, Université Paris-Est Créteil (UPEC), Créteil, France; ⁸AP-HP, Centre, Groupe Hospitalier Cochin Port Royal, DMU Imagina, Service de Radiologie, Paris, France; ⁹AP-HP, Centre, Groupe Hospitalier Cochin Port Royal, DMU Cancérologie et spécialités médico-chirurgicales, Service de gastroentérologie, d'endoscopie et d'oncologie digestive, Paris, France; ¹⁰AP-HP, Centre, Groupe Hospitalier Cochin Port Royal, DMU

POSTER PRESENTATIONS

Cancérologie et Spécialités Médico-Chirurgicales, Service d'Hépatologie, Paris, France, France; ¹⁰AP-HP Centre, Groupe Hospitalier Cochin Port Royal, DMU Cancérologie et spécialités médico-chirurgicales, Service de chirurgie hépatobiliaire, digestive et endocrinienne, Paris, France, France Email: stylianos.tzedakis@aphp.fr

Background and aims: Meta-analyses showed that the Coronavirus Disease 2019 (COVID-19) pandemic reduced cancer screening and treatment. However, most studies were inconclusive for primary liver cancer.

Method: We analyzed the French, nationwide, cohort of all newly recorded adult inpatients with primary liver cancer between January 1, 2018, and September 30, 2022. The primary exposure was the period of first diagnosis: Pre-pandemic (January 1, 2018 to December 31, 2019), COVID-19 Pandemic (January 1, 2020 to June 30, 2021), and COVID-19 Post-pandemic (July 1, 2021, to September 30, 2022) periods. The outcomes were access to a curative treatment (defined as liver resection, liver transplantation and/or percutaneous ablation) and mortality. Independent associations were analyzed in multivariate logistic and Cox models.

Results: Out of 51,572 patients [median (IQR) age, 71 (63.0; 78.0) years; 74% men], 13,873 (27%) had a curative treatment. The incidence of primary liver cancer [median (IQR), 907 (857; 946) new cases per trimester] remained stable ($p=0.08$). Compared with [Pre-pandemic] patients, and adjusted for age, sex, malnutrition, cancer stage, decompensated cirrhosis, severe comorbidities, and deprivation, the odds ratios (95% CI) for access to a curative treatment were 0.90 (0.86–0.95, $p<0.001$) and 0.69 (0.66–0.73, $p<0.001$) for [Pandemic] and [Post-pandemic] patients, respectively. Probabilities of 6-month survival for [Pandemic] and [Post-pandemic] patients were 60.3% (59.5–61.1; $p=0.91$) and 55.5% (54.5–56.5; $p<0.001$), respectively. The corresponding adjusted hazard ratios for mortality were 1.02 (0.99–1.05; $p=0.2$) and 1.22 (1.18–1.26; $p<0.001$), respectively. The results remained stable in a 1:1 propensity-matched sample of 28,232 [Pre-pandemic] and [Post-pandemic] patients.

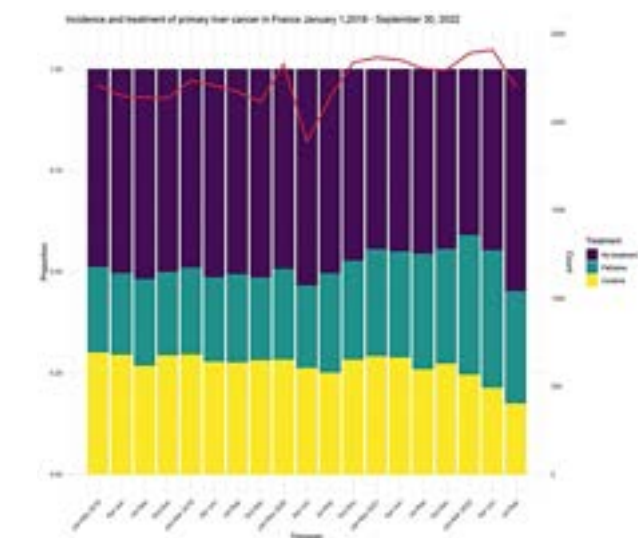


Figure:

Conclusion: COVID-19 crisis decreased access to curative treatment for primary liver cancer. The risk of dying without a curative treatment was highest in the [Post-pandemic] period.

SAT-121

Identify, screen and treat via electronic pathway (I-STEP): an innovative approach to wait list management for general liver hospital outpatient referrals

Eliza Flanagan^{1,2}, Stephen Pianko^{1,2}, Julianne Grant¹, Edward Saxby¹, Sally Bell^{1,2}, Suong Le^{1,2}. ¹Monash Medical Centre, Gastroenterology, Clayton, Australia; ²Monash University Clayton Campus, Department of Medicine, Clayton, Australia Email: elizaflanagan2@gmail.com

Background and aims: Wait times for hospital specialist outpatient clinics are long, with patients often triaged incorrectly due to incomplete clinical information. We developed a multifaceted intervention to semi-automatically prioritise patients with untreated hepatitis C virus (HCV) and/or advanced liver disease, awaiting an initial liver appointment at Monash Health (MH), an Australian tertiary hospital network.

Method: Our novel triage intervention consisted of 1) semi-automated electronic re-triage of patients based on new pathology results, 2) reflexive HCV polymerase chain reaction (PCR) testing in those with positive antibodies, and 3) a liver care guide (LCG) to augment patient uptake.

We excluded patients who were deceased, non-residents (due to additional costs), and those without mobile phone numbers. Eligible patients received a short message service (SMS) that explained the initiative (with a website link for further information) and were invited to participate by completing a blood test. The LCG conducted a follow-up phone call to answer questions. Our pathology panel included a full blood count, urea, electrolytes and creatinine, liver function tests, international normalised ratio, HCV antibody testing, and if positive, reflexive PCR testing. An AST to Platelet Ratio Index (APRI) and Fibrosis-4 (FIB4) score was auto-calculated. Patients with an APRI ≥ 1 , FIB4 ≥ 3.25 , or positive HCV PCR were flagged and re-triaged for urgent review.

Results: In May 2022, MH had 1026 adult patients on the waitlist for an initial liver clinic appointment. 20 patients were excluded due to no mobile phone ($n=9$), non-residents ($n=6$) and deceased ($n=5$). The median historical waitlist time for eligible patients was 283 days (IQR 183–450.25). The median age was 51 years (IQR: 40–61) and 527 (52.29%) were male. 690 patients (68.59%) responded 'Yes' to the SMS; 387 (56.09%) required a prompting call from the LCG before responding. 51 patients (5.07%) responded 'No', and 265 patients (26.34%) did not respond. 490 patients (71.01%) completed pathology testing and 40 (8.16%) were re-triaged based on APRI/FIB4/HCV PCR results (table 1). 26/40 of the re-triaged patients underwent a fibroscan with a median stiffness of 15.4 kilopascals (IQR 7.5–26.55). Sub analysis of 120 patients demonstrated increased engagement through implementation of the LCG. Over a two-week period, 60 patients received a text followed by phone call, whilst the other 60 only received a SMS. There was a higher uptake of pathology testing in those who had LCG and SMS compared to those who received SMS only (42 (70%) vs 27 (45%), p value 0.03).

Table 1:

RETRIAGED	
APRI ≥ 1 only	14
APRI ≥ 1 + FIB4 ≥ 3.25	14
APRI ≥ 1 + HCV PCR+ve	1
APRI ≥ 1 + HCV PCR+ve + FIB4 ≥ 3.25	2
FIB4 ≥ 3.25 only	7
HCV PCR+ve only	2
Total	40

Conclusion: We successfully piloted a novel semi-automated method for identifying patients with advanced liver disease and/or active HCV awaiting a general liver clinic appointment. There were high levels of engagement with this approach augmented by the LCG,

which may be scaled to other clinics or repeated longitudinally to screen for and proactively manage high risk liver patients.

SAT-122

Socio-economic disparities drive the prevalence of non-alcoholic fatty liver disease (NAFLD) among teenagers in the United States

Zobair Younossi^{1,2,3}, James Paik^{1,2,4}, Shira Zelber-Sagi⁵, Jeffrey Lazarus⁶, Pegah Golabi^{1,2,7,8,9}, Leyla Deavila⁹, Jillian Price⁹, Janus Ong¹⁰, Saleh Alqahtani¹¹, Linda Henry^{1,2,3,8}. ¹Inova Health System, Betty and Guy Beatty Center for Integrated Research, Falls Church, United States; ²Inova Health System, Inova Medicine, Falls Church, United States; ³The Global NASH Council, Washington, United States; ⁴The Global NASH Council, Falls Church, United States; ⁵University of Haifa, School of Public Health, Haifa, Israel; ⁶University of Barcelona, Barcelona Institute for Global Health (ISGlobal), Barcelona, Spain; ⁷The Global NASH Council, Washington, United States; ⁸Inova Fairfax Medical Campus, Center for Liver Disease, Department of Medicine, Falls Church, United States; ⁹Inova Health System, Beatty Liver and Obesity Research Program, Inova Medicine, Falls Church, United States; ¹⁰University of the Philippines, College of Medicine, Manila, Philippines; ¹¹King Faisal Specialist Hospital and Research Center, Riyadh, Saudi Arabia
Email: zobair.younossi@inova.org

Background and aims: Socio-economic factors and obesity have driven NAFLD to become the most common cause of liver disease among adults. Given the increasing rate of obesity in younger population, we assessed the prevalence of NAFLD among teenagers.

Method: National Health and Nutrition Examination Survey (2017–2018) data was used. NAFLD and Significant Fibrosis (SF) were defined by transient elastography (TE) as controlled attenuation parameter (CAP) of ≥ 285 dB/m and stiffness of > 8.0 kPa without other causes of liver disease. Obesity was defined as age-sex-specific body mass index (BMI) $\geq 95^{\text{th}}$ percentile. Central obesity was defined by age-sex-specific waist circumference. Low-income household was defined as household income $\leq 138\%$ federal poverty level. Low household education was defined as the head of the household without college education.

Results: 712 teenagers (age 13–18) were included [mean age 15.3 ± 1.6 ; 53.0% male; 50.0% white, 13.9% Black, 16.4% Mexican American, 6.9% Hispanic and 5.2% Asian; 22.2% obesity; 45.8% central obesity; 1.0% diabetes]. The prevalence of NAFLD and SF were 11.5% (95% confidence interval [CI]: 8.2–14.8%) and 2.8% (0.8–4.9%), respectively. There were disparities according to sex, race/ethnicity, household income and education. The prevalence of NAFLD was higher among teenage boys (13.7% vs. 9.1%); Mexican Americans (21.9% vs. 7.1% whites); living in low income (17.1% vs. 8.6%) and low education (14.0% vs. 4.4%) households (all p values < 0.03). The prevalence of NAFLD was higher in those with obesity (according to BMI 42.2% vs. 2.9% and waist circumference 24.3% vs. 1.1%). SF was more common in Black Americans (7.2% vs. 1.9% white); those with low household education (2.8% vs. 0.5%); and those with obesity (7.1% vs. 1.3%). After adjustment for demographic factors, living in a low-income (odds ratio [OR] = 2.05, 95% CI: 1.16–3.62) and low education (OR = 3.14, 1.40–7.04) households were associated with a higher risk of NAFLD. However, the addition of obesity to the model made this risk no

longer significant. On the other hand, low household education remained a significant predictor of SF (OR = 4.67, 2.15–10.15) even after adjustment for demographics and obesity.

Conclusion: NAFLD and SF were found to be more common among teenagers living in low income/education households. Targeting obesity prevention interventions to such settings should become an important aspect of all policies that address the burden of fatty liver disease.

SAT-123

Non-alcoholic fatty liver disease prevalence has increased in Australia, particularly amongst women

Karl Vaz^{1,2}, William Kemp^{1,2}, Ammar Majeed^{1,2}, John Lubel^{1,2}, Dianna Magliano³, Kristen Glenister⁴, Lisa Bourke⁴, David Simmons^{4,5}, Stuart Roberts^{1,2}. ¹Alfred Health, Gastroenterology and Hepatology, Melbourne, Australia; ²Monash University, Central Clinical School, Australia; ³Baker Heart and Diabetes Institute, Diabetes and Population Health, Australia; ⁴University of Melbourne, Department of Rural Health, Australia; ⁵Western Sydney University, Macarthur Clinical School, Australia
Email: karlpvaz@hotmail.com

Background and aims: Non-alcoholic fatty liver disease (NAFLD) is the most prevalent liver condition globally. Despite Australia having one of the highest rates of obesity worldwide, epidemiological data on NAFLD is scant. The aim of this study was to evaluate the change in age- and sex-standardised prevalence of NAFLD in regional Australia over a 15-year period and explore the underlying factors associated with differences over time.

Method: Repeat cross-sectional studies with equivalent methodology conducted in regional Victoria, Australia between 2001 and 2003 and 2016–2018 (CrossRoads I and II [CR-1 and CR-2] respectively). Households were randomly selected from residential address lists from local government organisations, with a single adult member of each household randomly selected to undertake a clinic sub-study. Detailed information collected included baseline demographics, anthropometric, and health-related clinical and laboratory data including alcohol use. NAFLD was defined by Fatty Liver Index (FLI) ≥ 60 in absence of excess alcohol consumption and viral hepatitis.

Results: In total, 1048 and 747 participants enrolled into CR-1 and CR-2, respectively, with sufficient data evaluable for FLI in $n = 1040$ (99%) and $n = 721$ (97%), respectively. Crude and age-/sex-standardized prevalence for NAFLD significantly increased from 32.7% and 32.4% (95% confidence interval [CI] 29.5–35.4) to 38.8% and 35.4% (95% CI 31.3–39.5) ($p = 0.09$ and $p < 0.01$), respectively, over the 15-year study period (Figure 1). Crude and age-standardized NAFLD prevalence remained stable for men (crude: 41.7% to 43.3%, $p = 0.66$; standardized: 38.2% [95% CI 33.9–42.4] to 38.4% [95% CI 31.9–44.8], $p = 0.52$) but significantly rose for women (crude: 25.5% to 35.1%, $p = 0.01$; standardized: 27.2% [95% CI 23.1–31.4] to 33.0% [95% CI 28.0–38.1], $p < 0.01$) (Figure 1). There was also a rise in prevalence of obesity (crude: 27.8% to 35.5%, $p < 0.01$; standardized: 29.9% [95% CI 27.1–32.7] to 33.5% [95% CI 29.4–37.6], $p < 0.01$), elevated waist circumference (crude: 48.2% to 60.1%, $p < 0.01$; standardized: 50.3% [47.3–53.4] to 54.8% [50.9–58.7], $p < 0.01$) and consumption of takeaway food one or

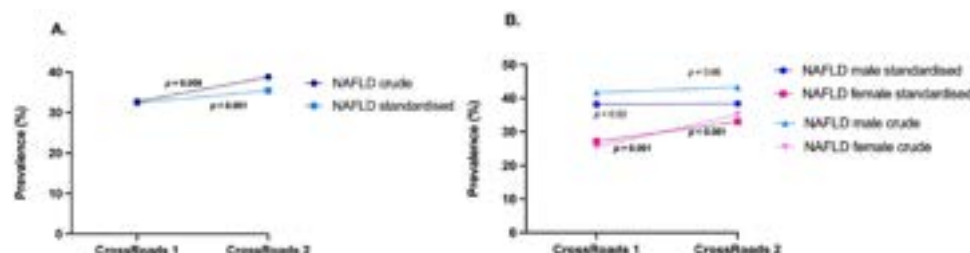


Figure: (abstract: SAT-123) Changes in NAFLD prevalence; A-entire cohort; B-according to gender

POSTER PRESENTATIONS

more times per week (crude: 26.1% to 30.7%, $p = 0.04$; standardized: 24.6% [95% CI 22.1–27.2] to 39.1% [34.9–43.3], $p < 0.01$).

Conclusion: Prevalence of NAFLD has risen significantly over a 15-year period in a regional part of Australia, paralleling rising obesity prevalence and most significantly in women. Public health programs to curb this trend are urgently required.

SAT-124

Multiple vitamin co-exposure and mortality risk in metabolic dysfunction-associated fatty liver disease

Wang Zilong¹, Linxiang Huang¹, Xiaoxiao Wang¹, Rui Jin¹, Baiyi Liu¹, Feng Liu¹, Huiying Rao². ¹Peking University People's Hospital, Peking University Hepatology Institute, China; ²Peking University People's Hospital, China

Email: rao.huiying@163.com

Background and aims: Metabolic-associated fatty liver disease (MAFLD) has emerged as a growing health burden worldwide. Existing studies have explored the associations between individual vitamin effects and disease progression in patients with NAFLD, and controversial findings were obtained. However, the effect of multiple vitamin co-exposure on MAFLD has not been fully elucidated. This study aims to elucidate the associations of multiple circulating vitamin co-exposure with mortality risks in MAFLD.

Method: The National Health and Nutrition Examination Survey (NHANES) III from 1988 to 1994 and NHANES III-linked mortality data through 2019 were used. MAFLD was defined as ultrasonically diagnosed hepatic steatosis in combination with metabolic dysfunction. We prospectively evaluated the concentrations of four kinds of

vitamins (A, C, D, and E) in serum with mortality risk among U.S. adults. An unsupervised K-means clustering was used to cluster the participants into several vitamin co-exposure patterns. The logistical and cox proportional hazard model were used for statistical analysis.

Results: Three co-exposure patterns were generated based on the vitamins (A, C, D, and E), as follows: low-level exposure (cluster 1), vitamin D exposure (cluster 2), and vitamin A/C/E exposure (cluster 3) (Figure A, B). Compared with those in cluster 1, participants in cluster 2 and 3 had a lower risk of MAFLD ($p < 0.01$). In MAFLD patients, participants in cluster 2 have lower all-cause mortality risks, with hazard ratios (95% confidence intervals [CIs]) of 0.73 (0.58, 0.92), while cluster 3 was not associated with a decreased risk of all-cause mortality, with hazard ratios (95% confidence intervals [CIs]) of 0.87 (0.70, 1.09). Going one step further, we then performed a specific analysis for the 4 kinds of vitamins. Vitamin A and D at moderate levels have lower all-cause mortality risks, with hazard ratios (95% confidence intervals [CIs]) of 0.63 (0.47, 0.83) and 0.63 (0.48, 0.81). Vitamin D at moderate levels has lower cardiovascular mortality risks, with hazard ratios (95% confidence intervals [CIs]) of 0.52 (0.31, 0.87) (Figure C). Furthermore, a J-shaped nonlinear exposure-response relationship was observed between all studied vitamins and all-cause mortality risk (except for vitamin D) (Figure D).

Conclusion: Our findings indicated that high levels of circulating vitamin D levels have a lower risk of illness and death in MAFLD. Thus, the detection of Vitamin D levels may have a prognostic value in MAFLD patients.

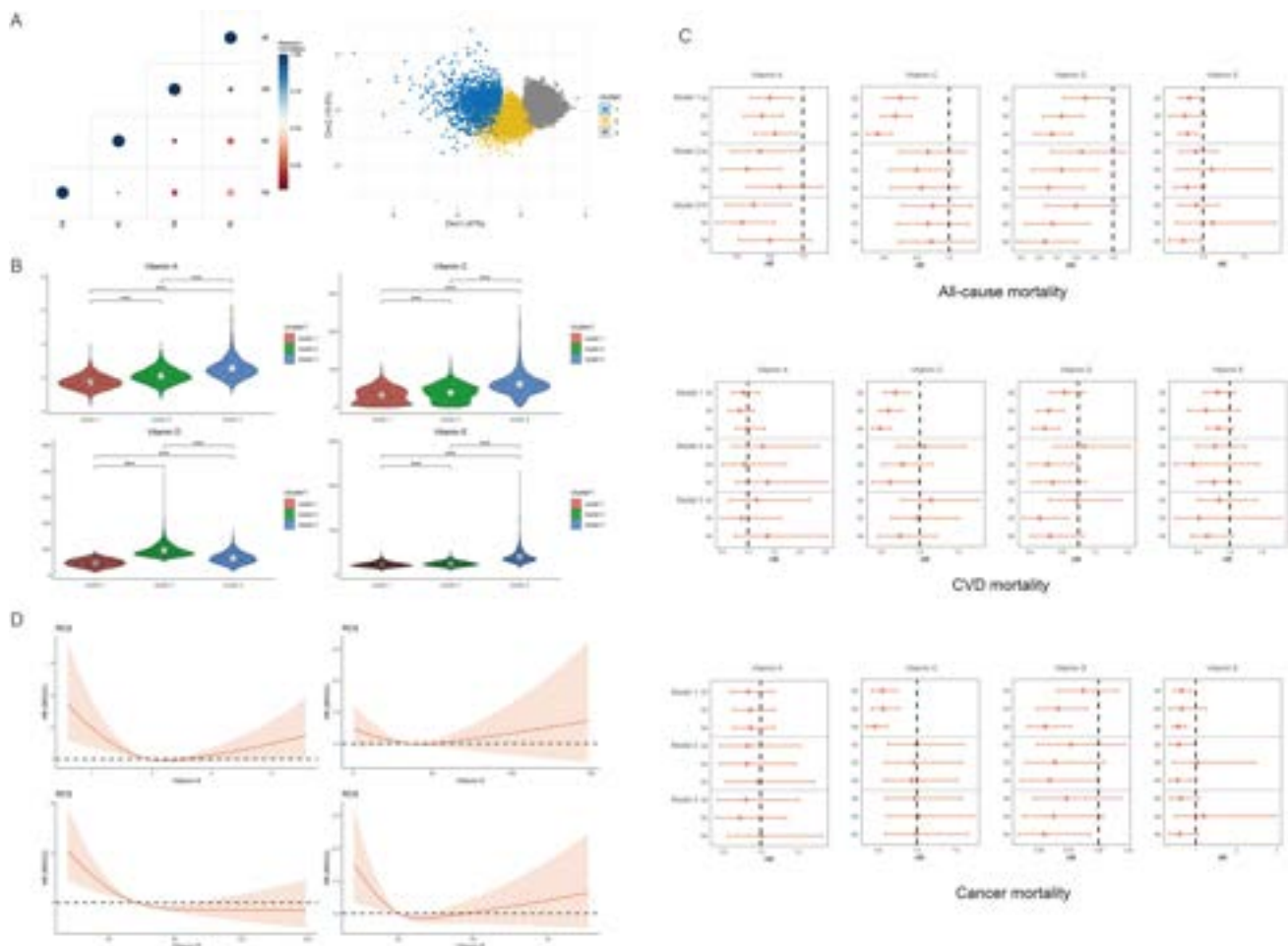


Figure: (abstract: SAT-124).

SAT-125

Prevalence and predictors of clinically significant pruritus in patients with non-alcoholic fatty liver disease (NAFLD): data from the global NASH registry™ (GNR™)

Zobair Younossi^{1,2}, Yusuf Yilmaz^{3,4}, Ming-Lung Yu⁵, Vasily Isakov⁶, Marlen Ivon Castellanos Fernández⁷, Vincent Wai-Sun Wong⁸, Yuichiro Eguchi⁹, Nahum Méndez-Sánchez¹⁰, Ajay Kumar Duseja¹¹, Jacob George¹², Elisabetta Bugianesi¹³, Ashwani Singal¹⁴, Saeed Sadiq Hamid¹⁵, Jian-Gao Fan¹⁶, Khalid Alswat¹⁷, George Papatheodoridis¹⁸, Mohamed El Kassas¹⁹, Wah-Kheong Chan²⁰, Stuart C Gordon²¹, Manuel Romero Gomez²², Stuart Roberts²³, Brian Lam^{2,24}, Issah Younossi²⁵, Andrei Racila^{1,2,24,25}, Linda Henry^{1,24,25}, Saleh Alqahtani^{2,25}, Maria Stepanova^{2,24,25}. ¹Inova Health System, Medicine Service Line, Falls Church, United States; ²Inova Health System, Department of Medicine, Center for Liver Diseases, Falls Church, United States; ³Institute of Gastroenterology, Marmara University, Liver Research Unit, Istanbul, Turkey; ⁴School of Medicine, Recep Tayyip Erdogan University, Department of Gastroenterology, Rize, Turkey; ⁵Kaohsiung Medical University Hospital, Kaohsiung Medical University, National Sun Yatsen University, Kaohsiung, Taiwan; ⁶Federal Research Center of Nutrition, Biotechnology and Food Safety, Department of Gastroenterology and Hepatology, Moscow, Russian Federation; ⁷University of Medical Sciences Havana, Institute of Gastroenterology, Havana, Cuba; ⁸The Chinese Institute of Hong Kong, Department of Medicine and Therapeutics, Hong Kong, Hong Kong; ⁹Locomedical Medical Cooperation, Locomedical General Institute, Ogi, Sage, Japan; ¹⁰National Autonomous University of Mexico, Liver Research Unit, Medica Sur Clinic and Foundation, Mexico City, Mexico; ¹¹Postgraduate Institute of Medical Education and Research, Department of Hepatology, Chandigarh, India; ¹²Westmead Institute for Medical Research, Westmead Hospital and University of Sydney, Storr Liver Centre, Sydney, Australia; ¹³University of Torino, Division of Gastroenterology, Department of Medical Sciences, Torino, Italy; ¹⁴University of South Dakota and Avera Transplant Institute, Sioux City, United States; ¹⁵Aga Khan University, Department of Medicine, Karachi, Pakistan; ¹⁶Xinhua Hospital, Shanghai Jiao Tong University School of Medicine, Department of Gastroenterology, Shanghai, China; ¹⁷King Saud University College of Medicine, Liver Disease Research Center, Department of Medicine, Saudi Arabia; ¹⁸National and Kapodistrian University of Athens, Athens, Greece; ¹⁹Helwan University, Endemic Medicine Department, Faculty of Medicine, Cairo, Egypt; ²⁰University of Malaysia, Gastroenterology and Hepatology Unit, Department of Medicine, Faculty of Medicine, Kuala Lumpur, Malaysia; ²¹Henry Ford Hospital, Department of Hepatology and Gastroenterology, Detroit, United States; ²²Virgen del Rocio University Hospital, Institute of Biomedicine of Seville, Digestive Diseases Department- Ciberehd, Seville, Spain; ²³The Alfred, Department of Hepatology and Gastroenterology, Melbourne, Australia; ²⁴Beatty Liver and Obesity Research Program, Inova Health System, Falls Church, United States; ²⁵Center for Outcomes Research in Liver Disease, Washington DC, United States

Email: zobair.younossi@inova.org

Background and aims: Pruritus is an important but under-appreciated symptom of chronic liver diseases. We assessed factors associated with pruritus among patients with NAFLD.

Method: Patients with NAFLD seen in real-world clinical practices were prospectively enrolled in the Global NAFLD/NASH Registry (GNR)™. Clinical parameters and patient reported outcomes (PROs; FACIT-F, CLDQ-NASH, WPAI) were collected. Clinically significant pruritus was defined as score ≤ 4 in the respective item of CLDQ-NASH (range 1–7; lower score indicates more severe pruritus).

Results: We included 4203 NAFLD subjects from 17 countries: age 52 ± 13 years, 48% male, 48% employed, 23% advanced fibrosis and 14% cirrhosis (by biopsy or non-invasive FIB-4), 44% type 2 diabetes (T2D), 21% history of depression and 45% clinically overt fatigue. Furthermore, 78% of those with a biopsy had NASH. The prevalence of clinically significant pruritus among NAFLD was 28%. The highest

prevalence of significant pruritus was in patients enrolled in Middle East/North Africa and Latin America (36–39%), the lowest in South Asia (7%). NAFLD patients with pruritus were less commonly employed (42% vs. 51%), more commonly female (61% vs. 49%) and obese (69% vs 63%). Also, they more commonly had T2D (51% vs 41%), advanced fibrosis (27% vs. 22%), anxiety (47% vs. 31%), depression (30% vs 18%), fatigue (58% vs. 40%), abdominal pain (37% vs. 20%), and sleep apnea (27% vs 21%) (all $p < 0.01$) than those without pruritus, despite similar age ($p > 0.05$). NAFLD patients with pruritus experienced significantly lower PRO scores (FACIT-F, CLDQ-NASH, and WPAI) ranging from –4% to –19% of a PRO score range (all $p < 0.0001$). All CLDQ-NASH domain scores were lower in NAFLD patients with pruritus as compared to those without (Figure). In multivariate analysis adjusted for the regions of enrollment, independent predictors of an increased risk of pruritus included female sex, T2D, depression, clinically overt fatigue, abdominal pain, and the lack of regular (≥ 3 /times week; ≥ 30 min/time) exercise (odds ratios range 1.30 to 1.96, all $p < 0.01$). Among patients with 1-year follow-up, lower pruritus scores and higher prevalence of clinically significant pruritus were still observed in patients who had experienced pruritus at baseline: mean pruritus score increased from 3.1 to 4.6 in those with baseline pruritus vs. decreased from 6.4 to 6.0 in those without baseline pruritus while the prevalence of clinically significant pruritus at 1-year follow-up was 52% vs 19%, respectively (all $p < 0.0001$).

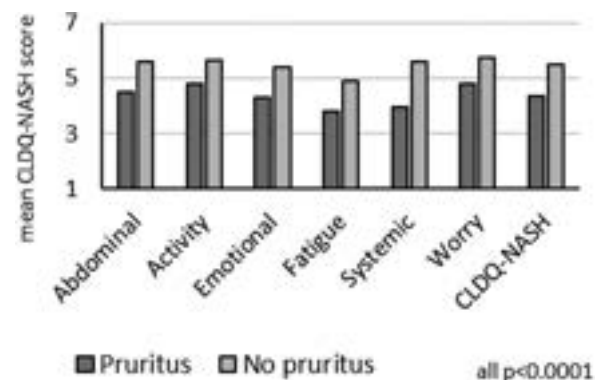


Figure:

Conclusion: Pruritus is a common and persistent symptom among patients with NAFLD, especially those with T2D and female subjects. Presence of pruritus negatively affects all PRO scores and is impacted by non-hepatic comorbidities.

SAT-126

Relationships between education and non-alcoholic fatty liver disease

Florian Koutny¹, Bernhard Paulweber², Elmar Aigner², Christian Datz³, Sophie Gensluckner², Andreas Maieron¹, Stefano Novati⁴, Bernhard Iglseder⁵, Patrik Langthaler⁶, Vanessa Frey⁶, Eugen Trinka⁶, Bernhard Wernly³. ¹University Hospital St. Pölten, Department for Gastroenterology, Hepatology and Rheumatology, Sankt Pölten, Austria; ²Gemeinnützige Salzburger Landeskliniken Betriebsges.mbH, First Department of Medicine, Salzburg, Austria; ³Gerneral Hospital Oberndorf, Teaching Hospital of the Paracelsus Medical University, Department of Internal Medicine, Austria; ⁴Bolzano Regional Hospital, Gastroenterology, Italy; ⁵Christian-Doppler-Klinik, Department of Geriatric Medicine, Austria; ⁶Christian-Doppler-Klinik, Department of Neurology, Austria

Email: bernhard.wernly@pmu.ac.at

Background and aims: Low socioeconomic status (SES) is associated with associated with adverse health outcomes, including metabolic syndrome and NAFLD. However, it has remained enigmatic whether the association of NAFLD with SES is independent of age, sex and

POSTER PRESENTATIONS

metabolic syndrome. Therefore, the aim of this study was to investigate an independent relationship between NAFLD and degree of education as measured by the International Standard Classification of Education (ISCED) as a surrogate marker for SES.

Method: This study evaluated 8,315 participants from the Paracelsus 10,000 study. Anthropomorphic, clinical and laboratory parameters were collected from all participating subjects. To assess the association between NAFLD and ISCED, multivariable logistic regression models and multivariable linear regression were calculated. The primary end points were an increased fatty liver index (FLI) score (≥ 30) as a surrogate marker for NAFLD and liver fibrosis as indicated by an elevated fibrosis-4 index (FIB-4) score (≥ 1.3) as a surrogate marker. In a subgroup analysis of 789 participants the end point NAFLD was specified by liver stiffness measurement data. Trichotomized ISCED categories (low, middle and high) were chosen as an independent fixed variable with a lower ISCED as the reference category. MetS was defined according to the National Cholesterol Education Program (NCEP) Adult Treatment Panel III.

Results: Participants with a high education level had a significantly lower odds ratio (FLI score ≥ 30 , odds ratio 0.41, 95% CI 0.34–0.50, $p < 0.01$) for liver steatosis compared to those in the low-ISCED group independent of age, sex, MetS and alcohol consumption (g/d). Univariate linear regression analysis showed that liver fibrosis defined by the FIB-4 Score was also associated with a lower ISCED. Further subgroup analysis has shown that participants in the high-ISCED group exhibited lower rates of liver stiffness compared to those in the low-ISCED group ($r: -1.73 [-3.06 \text{ to } -0.40]$; $p < 0.01$). The same applied for patients in the intermediate-ISCED group compared to participants with the lowest education levels ($r: -1.44 [-2.66 \text{ to } -0.22]$; $p < 0.01$). Significance of the linear regression coefficient remained after forcing sex, age MetS and daily alcohol consumption into the system.

Conclusion: Results of our study suggests that a low ISCED is associated with a higher risk for liver steatosis and fibrosis. These liver parenchymal damages have a significant impact on morbidity and may even lead to hepatocellular carcinoma. Thus, the outcome of the current study is of importance in clinical practice and highlights the need for considering socioeconomic factors in the prevention and management of NAFLD. We therefore advocate prevention strategies tailored to socioeconomic groups. Further studies are needed to evaluate the impact of socioeconomic interventions on NAFLD.

SAT-127

A pilot study to improve the uptake of hepatocellular carcinoma surveillance

Maria Qurashi¹, Nina Stafford², Laith Al-Rubaiy², Shahid Khan¹, Rohini Sharma¹. ¹Imperial College London, United Kingdom; ²London North West University NHS Trust, United Kingdom
Email: maria.qurashi09@imperial.ac.uk

Background and aims: Ninety percent of HCC cases arise on a background of liver cirrhosis (1). EASL and other international guidelines recommend six-monthly ultrasound surveillance for patients with cirrhosis, advanced fibrosis or high risk hepatitis B (2). Surveillance for HCC has been shown to lead to earlier diagnosis and improved survival (3). However, surveillance uptake is less than 25% internationally; a US study suggests the most common reason for this is a failure to order surveillance in those who are eligible (4). We aimed to improve surveillance uptake by implementing an automated system to issue reminders to healthcare professionals about which patients were due surveillance imaging.

Method: We created a database of patients at three district general hospitals in London who are regularly seen in specialist hepatology clinics and eligible for HCC surveillance. We implemented an automated “call-recall” system which notified clinicians about which of their patients required surveillance imaging booking.

Results: 243 patients eligible for surveillance were included. Baseline characteristics were: 69% male; median age 58 years; 60% alcohol related liver disease (ArLD), 26% viral hepatitis, 10% NAFLD.

In July 2022, prior to the automated recall system being activated, 19% (45 patients) were up-to-date with their HCC surveillance. The automated “call-recall” system was initiated in August 2022. Two months later (September 2022), 38% (93 patients) were up-to-date with their HCC surveillance.

Conclusion: HCC surveillance uptake is low. An automated “call-recall” system aims to flag to clinicians when individual patients need surveillance imaging. In a pilot study, this system doubled HCC surveillance attendance in three district general hospitals in London. Further work will look at the long-term efficacy of an automated recall system on surveillance rates, HCC diagnosis and clinically relevant outcomes, as well as exploring patient-related barriers to HCC surveillance.

References

1. Yang JD, Kim WR, Coelho R *et al.* Cirrhosis is present in most patients with hepatitis B and hepatocellular carcinoma. *Clin. Gastroenterol. Hepatol.* 9 (1), 64–70 (2011).
2. European Association for the Study of the Liver. Electronic address: easloffice@easloffice.eu, European Association for the Study of the Liver, Galle PR, *et al.* EASL Clinical Practice Guidelines: Management of hepatocellular carcinoma. *J Hepatol* 2018;69:182–236. doi:10.1016/j.jhep.2018.03.019
3. Singal AG, Zhang E, Narasimman M, *et al.* [1] surveillance improves early detection, curative treatment receipt, and survival in patients with cirrhosis: A meta-analysis. *J Hepatol* 2022;77:128–39. doi:10.1016/j.jhep.2022.01.023
4. Singal AG, Yopp AC, Gupta S, *et al.* Failure rates in the hepatocellular carcinoma surveillance process. *Cancer Prev Res (Phila)* 2012;5:1124–30. doi:10.1158/1940-6207.CAPR-12-0046

SAT-128

Non-alcoholic fatty liver disease awareness, misperception, and their association with healthcare access in Korean general population: a nationally representative survey

Jun-Hyuk Lee¹, Eileen Yoon², Dae Won Jun², Sang Bong Ahn³, Joo Hyun Oh³, Hyunwoo Oh⁴, Hyo Young Lee⁴, Jihyun An², Joo Hyun Sohn², Eun Chul Jang⁵. ¹Nowon Eulji Medical Center, Eulji University School of Medicine, Family Medicine, Seoul, Korea, Rep. of South; ²Hanyang university college of medicine, Internal medicine, Seoul, Korea, Rep. of South; ³Nowon Eulji Medical Center, Eulji University School of Medicine, Internal Medicine, Seoul, Korea, Rep. of South; ⁴Uijeongbu Eulji Medical Center, Eulji University College of Medicine, Korea, Rep. of South; ⁵Soonchunhyang University College of medicine, Korea, Rep. of South
Email: noshin@hanyang.ac.kr

Background and aims: Non-alcoholic fatty liver disease (NAFLD) is the most common chronic liver disease in Korea. Health check-up examinations are extensively conducted in Korea, almost all adults (esp. >40 years) receive health examinations, but systematic management of NAFLD is not effective. This study conducted to investigate the hurdles of the NAFLD treatment cascade through a nationwide survey in Korea.

Method: This cross-sectional study was conducted using an online survey. A total of 1,000 panels was finally selected according to distribution of sex, age group, and residential area in Korean adult. The survey consisted of a 3-domain and 18-item questionnaires. Content validity of questionnaire was measured by a total of 14 experts including medical doctors, nutritionists, and a methodologist who did not participate in the development of the questionnaire. Content validity index (CVI) for each item was rated above 0.80.

Results: A total of 27.2% responded that they had never heard of NAFLD terminology. Approximately half of responders (60.2%) heard of NAFLD through media (TV, newspaper, and radio), only 24.8% of people had heard of NAFLD through medical staff. A total 42.9% of the respondents recognized that liver cirrhosis, and hepatocellular carcinoma can be developed in NAFLD. Only 25.7% of the respondents

recognized that angina pectoris, myocardial infarction, ischemic stroke associated with NAFLD. Only 40.2% who diagnosed with NAFLD visited clinic for the further evaluation and management of NAFLD. The most common reason for not visiting the medical facility after diagnosis of NAFLD was 'I could manage the disease on my own' (50.6%), followed by 'never been told from my physician that I need disease management' (32.9%). The most common response by gender was 'lack of time to visit the hospital' in men (84.6%) and 'I could manage the disease on my own' in women (45.0%). Most 20s-40s thought they could manage the disease on my own, and fatty liver was not regarded as a serious disease' in 50s-60s.

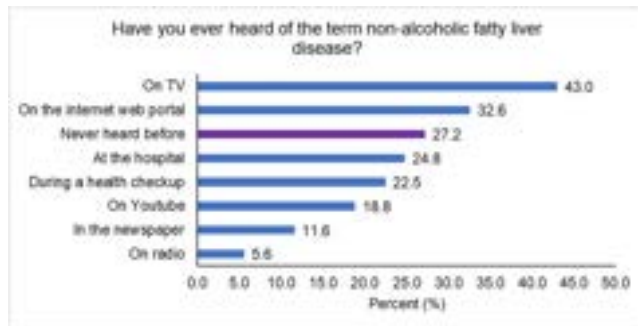


Figure:

Conclusion: Only 40% visited the clinic after diagnosis with NAFLD. Reasons for not visiting the clinic after diagnosis of NAFLD differed significantly according to gender and age.

SAT-129

Sub-optimal global public health policies and strategies to combat hepatocellular carcinoma

Luis Antonio Diaz^{1,2}, Blanca Norero¹, Oscar Corsi¹, Gustavo Ayares¹, Francisco Idalsoaga¹, Sergio García³, Valeria Vázquez⁴, Lucas Lacalle⁵, Mariana Lazo⁶, Catterina Ferreccio⁷, Manuel Mendizabal⁸, Federico Piñero⁸, Edmundo Martínez⁹, Ifeora Ijeoma¹⁰, Alexandre Louvet¹¹, Salvatore Piano¹², Helena Cortez-Pinto¹³, Vincent Wai-Sun Wong¹⁴, Anand Kulkarni¹⁵, Thomas Cotter¹⁶, Mayur Brahmanian¹⁷, Juan Pablo roblero¹⁸, Melisa Dirchwolf¹⁹, Florencia Pollarsky²⁰, Jacob George²¹, Rudolf E. Stauber²², Sven Francque²³, Patricia Guerra²⁴, Claudia Oliveira²⁵, Roberta Araujo²⁶, Mario Álvares-da-Silva²⁷, Nkegoum Blaise²⁸, Juan G Abalde²⁹, Ming-Hua Zheng³⁰, Luis Toro³¹, Juan Carlos Restrepo³², Wagner Ramirez³³, Ivica Grigorević³⁴, Mirtha Infante³⁵, Charles Mbendi³⁶, Enrique Carrera³⁷, Mohamed El Kassas³⁸, Abdelmajeed Mahmoud³⁹, Yonas Gedamu Tesfaye⁴⁰, Sewale Anagaw Tadesse⁴¹, Tiruwork Fekadu Akalu⁴², Hailemichael Desalegn⁴³, Manon Allaire⁴⁴, Carrieri Patrizia⁴⁵, Jörn Schattenberg⁴⁶, Joan Aguyire⁴⁷, Eileen Akonobe Micah⁴⁸, Kenneth Tachi⁴⁹, Katherine Emilia Maldonado Cardona⁵⁰, Abel Sanchez⁵⁰, Marco Sánchez⁵¹, Einar S. Björnsson⁵², Massimo Iavarone⁵³, Ryuichi Okamoto⁵⁴, Fatuma Some⁵⁵, Mohammad Fadel Hellani⁵⁶, Veronica Enith Prado Gonzalez⁵⁷, Norberto Carlos Chávez-Tapia⁵⁸, Nahum Méndez-Sánchez⁵⁸, Sheila Constância Mabote Mucumbi⁵⁹, Rose Ashinedu Ugiagbe⁶⁰, Kolawole Akande⁶¹, Chinenye Nwoko⁶², Uchenna Simon Ezenkwa⁶³, Ifeoma Joy Okoye⁶⁴, Saeed Sadiq Hamid⁶⁵, Julissa Lombardo Quezada⁶⁶, Marcos Giralá⁶⁷, P. Martin Padilla⁶⁸, Javier Diaz-Ferrer⁶⁹, Martin Tagle⁷⁰, Michał Kukla⁷¹, Emuobor Odeghe⁷², Rasheed mumini wemimo⁷³, Daniela Reis⁷⁴, Sergei Mozgovoi⁷⁵, Mona Ismail⁷⁶, Tomas Koller⁷⁷, Wendy Spearman⁷⁸, Moawia Elhassan⁷⁹, Per Stal⁸⁰, Swaleh Pazi⁸¹, Anthony Ocanit⁸², Steven Masson⁸³, Winston Dunn⁸⁴, Patrick S. Kamath⁸⁵, Ashwani Singal⁸⁶, Jose Debes⁸⁷, María Reig⁸⁸, Rohit Loomba⁸⁹, Ramon Bataller⁹⁰, Jeffrey Lazarus^{91,92}, Marco Arrese¹, Juan Pablo Arab^{1,93,94,94}. ¹Departamento de Gastroenterología, Escuela

de Medicina, Pontificia Universidad Católica de Chile, Santiago, Chile, Chile; ²Observatorio Multicéntrico de Enfermedades Gastrointestinales (OMEGA), Santiago, Chile, Chile; ³Escuela de Medicina, Pontificia Universidad Católica de Chile, Santiago, Chile, Chile; ⁴Escuela de Medicina, Instituto Tecnológico de Monterrey, Monterrey, México, Mexico; ⁵Departamento de Ciencias de la Salud, Facultad de Medicina, Pontificia Universidad Católica de Chile, Santiago, Chile, Chile; ⁶Department of Community Health and Prevention and Urban Health Collaborative, Dornsife School of Public Health, Drexel University, Philadelphia, Pennsylvania, United States; ⁷Public Health Department, School of Medicine, Pontificia Universidad Católica de Chile, Santiago, Chile. Advanced Center for Chronic Diseases, ACCDis, Santiago, Chile, Chile; ⁸Hepatology and Liver Transplant Unit, Hospital Universitario Austral, Buenos Aires, Argentina, Argentina; ⁹Servicio de Gastroenterología, Hospital Dr. Sótero del Río, Santiago, Chile, Chile; ¹⁰Microbiology Unit, Department of Medical Laboratory Sciences, College of Medicine, University of Nigeria Nsukka Enugu Campus, Nsukka, Nigeria, Nigeria; ¹¹Hôpital Claude Huriez, Services des Maladies de l'Appareil Digestif, CHRU Lille, and Unité INSERM 995, Lille, France, France; ¹²Unit of Internal Medicine and Hepatology (UIMH), Department of Medicine – DIMED, University of Padua, Padova, PD, Italy, Italy; ¹³Clínica Universitária de Gastroenterologia, Laboratório de Nutrição, Faculdade de Medicina, Universidade de Lisboa, Portugal, Portugal; ¹⁴Department of Medicine and Therapeutics, Chinese University of Hong Kong, Hong Kong Special Administrative Region, China, China; ¹⁵Department of Hepatology, Asian Institute of Gastroenterology, Hyderabad, India. ¹⁶Department of Hepatology, Asian Institute of Gastroenterology, Hyderabad, India; ¹⁷Division of Digestive and Liver Diseases, UT Southwestern Medical Center, Dallas, Texas, USA, United States; ¹⁸Univeristy of Calgary, Cumming School of Medicine, Calgary, Alberta, Canada, Canada; ¹⁹Sección Gastroenterología, Hospital Clínico Universidad de Chile, Escuela de Medicina Universidad de Chile, Santiago, Chile, Chile; ²⁰Unidad de Hígado, Hospital Privado de Rosario, Rosario, Argentina, Argentina; ²¹Sección Hepatología, Hospital de Gastroenterología Dr. Carlos Bonorino Udaondo, Buenos Aires, Argentina, Argentina; ²²Storr Liver Centre, Westmead Millennium Institute, Westmead Hospital and University of Sydney, Sydney, Australia, Australia; ²³Department of Internal Medicine, Medical University of Graz, Graz, Austria, Austria; ²⁴Department of Gastroenterology and Hepatology, Antwerp University Hospital, Edegem, Belgium, Belgium; ²⁵Instituto de Gastroenterología Boliviano-Japonés, Cochabamba, Bolivia, Bolivia; ²⁶Department of Gastroenterology, University of Sao Paulo School of Medicine, Sao Paulo, Brazil, Brazil; ²⁷Gastroenterology Division, Ribeirão Preto Medical School, University of São Paulo, Ribeirão Preto, SP, Brazil, Brazil; ²⁸Hospital de Clínicas de Porto Alegre, Porto Alegre, Brazil, Brazil; ²⁹Centre Hospitalier Universitaire, Cameroon, Cameroon; ³⁰Division of Gastroenterology, Liver Unit, University of Alberta, Edmonton, Canada, Canada; ³¹MAFLD Research Center, Department of Hepatology, the First Affiliated Hospital of Wenzhou Medical University, China, China; ³²Hepatology and Liver Transplant Unit, Hospitales de San Vicente Fundación de Medellín y Rionegro, Colombia, Colombia; ³³Unidad de Hepatología del Hospital Pablo Tobon Uribe, Grupo de Gastrohepatología de la Universidad de Antioquia, Medellín, Colombia, Colombia; ³⁴Clínica Equilibrium, San José, Costa Rica, Costa Rica; ³⁵University of Zagreb School of Medicine, University Hospital Dubrava, Croatia, Croatia; ³⁶Universidad de Ciencias Médicas de La Habana, Havana, Cuba, Cuba; ³⁷Department of Internal Medicine, University of Kinshasa, Kinshasa, Democratic Republic of the Congo., Congo, Dem. Republic of (formerly known as Zaire); ³⁸Servicio de Gastroenterología-Hepatología, Hospital Eugenio Espejo, Universidad San Francisco de Quito, Quito, Ecuador, Ecuador; ³⁹Endemic Medicine Department, Faculty of Medicine, Helwan University, Cairo, Egypt, Egypt; ⁴⁰Tropical Medicine and Gastroenterology Department, Aswan University, Aswan, Egypt, Egypt; ⁴¹University of Gondar, Gondar, Ethiopia, Ethiopia; ⁴²Bahir Dar University, Bahir Dar, Ethiopia, Ethiopia; ⁴³Delt-Yemariamwerk Hospital, Dire Dawa, Ethiopia, Ethiopia; ⁴⁴St. Paul's Hospital Millennium Medical College, Addis Ababa, Ethiopia, Ethiopia; ⁴⁵Centre de Recherche sur l'Inflammation, Faculté de Médecine

POSTER PRESENTATIONS

Xavier Bichat, Paris, France, France; ⁴⁵Aix-Marseille University, Inserm, Institut de recherche pour le développement, Sciences Economiques et Sociales de la Santé et Traitement de l'Information Médicale (SESSTIM), ISSPAM, Marseille, France, France; ⁴⁶Metabolic Liver Research Program, Department of Medicine I, University Medical Centre, Johannes Gutenberg University Mainz, Germany, Germany; ⁴⁷Tamale Teaching Hospital, Tamale, Ghana, Ghana; ⁴⁸Komfo Anokye Teaching Hospital, Kumasi, Ghana, Ghana; ⁴⁹Korle-Bu Teaching Hospital, Accra, Ghana, Ghana; ⁵⁰Gastroenterología Endoscopia Digestiva, Hospital Roosevelt, Ciudad de Guatemala, Guatemala, Guatemala; ⁵¹Hospital Escuela Universitario, Tegucigalpa, Honduras, Honduras; ⁵²Department of Gastroenterology, Landspítali University Hospital Reykjavík, University of Iceland, Reykjavík, Iceland, Iceland; ⁵³Foundation IRCCS Ca' Granda Ospedale Maggiore Policlinico, Division of Gastroenterology and Hepatology, Milan, Italy, Italy; ⁵⁴Department of Gastroenterology and Hepatology, Tokyo Medical Dental University, 1-5-45 Yushima, Bunkyo-ku, Tokyo, Japan, Japan; ⁵⁵Department of Medicine, School of Medicine, College of Health Sciences, Moi University, Eldoret, Kenya, Kenya; ⁵⁶Lebanese university, Beirut, Lebanon, Lebanon; ⁵⁷Centre Hospitalier de Luxembourg, Luxembourg, Luxembourg; ⁵⁸Liver Research Unit, Medica Sur Clinic and Foundation, Faculty of Medicine, National Autonomous University of Mexico, Mexico City, 14050, Mexico, Mexico; ⁵⁹Hospital Central de Maputo, Maputo, Mozambique, Mozambique; ⁶⁰Department of Medicine, University of Benin, University of Benin Teaching Hospital, Benin City, Nigeria, Nigeria; ⁶¹College of Medicine, University of Ibadan, Ibadan, Oyo, Nigeria, Nigeria; ⁶²Lagoon Hospitals, Lagos, Nigeria, Nigeria; ⁶³Federal Medical Centre, Azare, Bauchi State, Nigeria, Nigeria; ⁶⁴Department of Radiology, University of Nigeria Teaching Hospital, Ituku-Ozalla, Enugu State, Nigeria, Nigeria; ⁶⁵Department of Medicine, The Aga Khan University, Karachi, Pakistan, Pakistan; ⁶⁶Hospital Punta Pacífica, Ciudad de Panamá, Panamá, Panamá; ⁶⁷Departamento de Gastroenterología, Hospital de Clínicas, Universidad Nacional de

Asunción, Asuncion, Paraguay, Paraguay; ⁶⁸Unidad de Trasplante Hepático, Hospital Nacional Guillermo Almenara, Lima, Peru, Peru; ⁶⁹Hospital Nacional Edgardo Rebagliati Martins-Es up Salud, Lima, Peru, Peru; ⁷⁰Clinica Anglo Americana, Lima, Peru, Peru; ⁷¹Department of Internal Medicine and Geriatrics, Faculty of Medicine, Jagiellonian University Medical College, Cracow, Poland, Poland; ⁷²Lagos University Teaching Hospital, Lagos, Nigeria; ⁷³Federal Medical Center, Birnin Kudu, Jigawa State, Nigeria; ⁷⁴Hospital de Egas Moniz-Centro Hospitalar de Lisboa Ocidental, Lisboa, Portugal; ⁷⁵Omsk State Medical University, Omsk, Russian Federation; ⁷⁶King Fahd Hospital of the University, Al-khobar, Saudi Arabia; ⁷⁷College of Medicine, Imam Abdulrahman bin Faisal University, Saudi Arabia; ⁷⁸Subdivision of Hepatology and Gastroenterology, 5th Department of Internal Medicine, Comenius University Faculty of Medicine, University Hospital Bratislava, Slovakia; ⁷⁹104Division of Hepatology, Department of Medicine, Faculty of Health Sciences, University of Cape Town, Cape Town, South Africa; ⁸⁰Oncology Department, National Cancer Institute, University of Gezira, Wad Madani, Sudan; ⁸¹Department of Gastroenterology and Hepatology, Karolinska University Hospital, Karolinska Institutet, Stockholm, Sweden; ⁸²Muhimbili National Hospital, Dar es-Salam, Tanzania; ⁸³Kiruddu National Referral Hospital, Uganda; ⁸⁴Faculty of Medical Sciences, Newcastle University Medical School, Framlington Place, United Kingdom; ⁸⁵University of Kansas Medical Center, KS, USA, United States; ⁸⁶Division of Gastroenterology and Hepatology, Mayo Clinic, Minnesota, United States; ⁸⁷Department of Medicine, University of South Dakota Sanford School of Medicine, Division of Transplant Hepatology, Avera Transplant Institute, Sioux Falls, SD, United States, United States; ⁸⁸Department of Medicine, Division of Gastroenterology and Division of Infectious Diseases, University of Minnesota, Minnesota, United States; ⁸⁹Barcelona Clinic Liver Cancer group, Liver Unit, IDIBAPS, Hospital Clínic, University of Barcelona, Barcelona, Spain; ⁹⁰NAFLD Research Center, Division of Gastroenterology, Department of Medicine, University of California at San Diego, California, United States; ⁹¹Liver Unit,

Public health policies and strategies for Hepatocellular carcinoma (HCC) worldwide

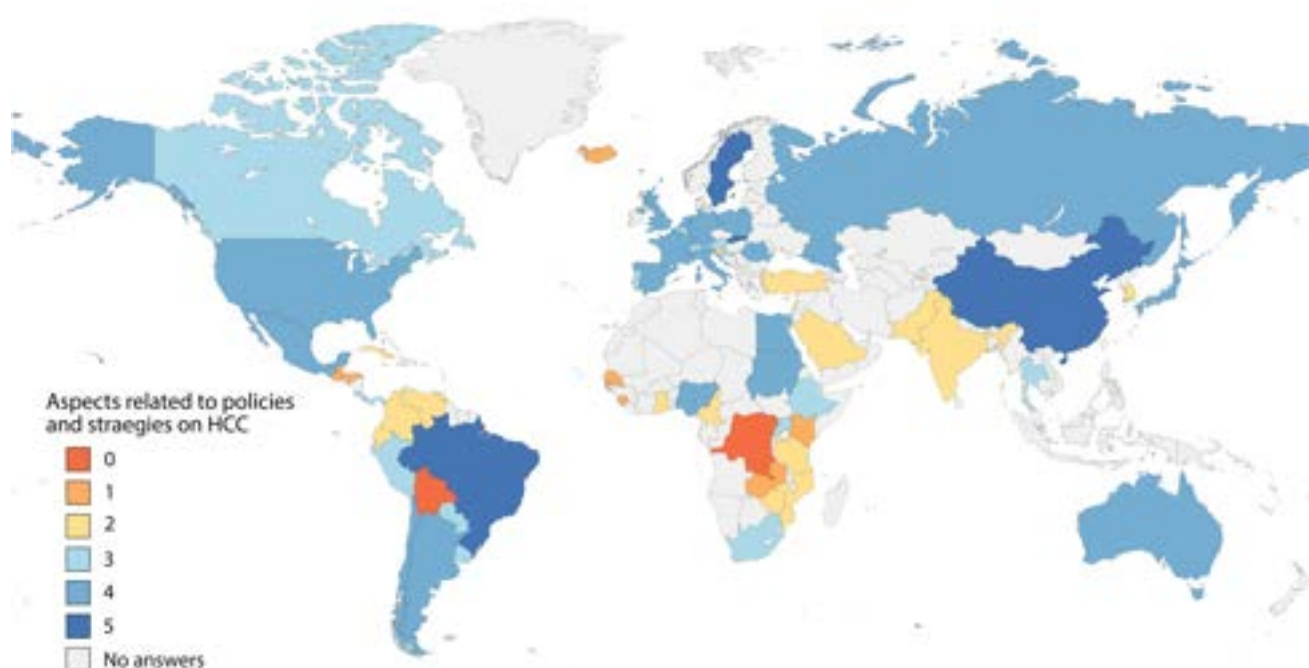


Figure: (abstract: SAT-129) Policies, strategies, and treatments for hepatocellular carcinoma (HCC) in 66 countries. The data reflects the existence of a national cancer plan, existence of a specific national plan/strategy on HCC, a national or subnational disease registry including HCC, a national clinical guideline on HCC, and availability of liver transplantation.

Hospital Clinic, Barcelona, Spain; ⁹¹CUNY Graduate School of Public Health and Health Policy (CUNY SPH), New York, NY, USA, United States; ⁹²Barcelona Institute for Global Health (ISGlobal), Hospital Clinic, University of Barcelona, Barcelona, Spain, Spain; ⁹³Division of Gastroenterology, Department of Medicine, Schulich School of Medicine, Western University and London Health Sciences Centre, London, Ontario, Canada, Canada; ⁹⁴ON BEHALF OF THE OMEGA COLLABORATORS, Santiago, Chile
Email: jparab@gmail.com

Background and aims: Hepatocellular carcinoma (HCC) is the third most common cause of cancer-related deaths worldwide. The aims of the study were to explore HCC-related population-wide public health policies (PHP) in terms of prevention, treatments availability, epidemiological surveillance, and awareness campaigns worldwide. **Method:** We conducted a 43-item survey about HCC: policies and civil society (18 questions), clinical guidelines (5 questions), epidemiology (7 questions), and care management (13 questions). We invited 249 gastroenterologists, hepatologists, oncologists, surgeons, radiation therapists, and public health experts from 74 countries/territories. The survey was administered using an electronic form between May 14, 2022, and January 24, 2023. Data were collected in a spreadsheet, revised by two independent reviewers, and verified with governmental institutions, regulatory agencies, scientific societies, and scientific publications.

Results: We obtained 132 responses from 66 countries/territories (Africa N = 16, the Americas N = 18, Asia N = 10, Europe N = 21, and Oceania N = 1). A total of 46 (69.7%) countries had a written national cancer strategy or action plan (including solid and haematological neoplasms). However, only 5 (7.6%) had a specific written national strategy or action plan on HCC (Figure). Thirty-two (48.5%) countries had national clinical practice guidelines on HCC, mainly focused on prevention (84.4%), screening (93.8%), diagnosis (93.8%), treatment (93.8%), and palliative care (68.8%). Fifty-four (81.8%) countries had a national disease registry that included HCC. Several providers are involved in management of HCC: oncologists (83.3%), gastroenterologists (75.8%), hepatologists (74.2%), surgeons (60.6%), and palliative medicine specialists (33.3%). The most common strategies for staging of HCC were Barcelona Clinic Liver Cancer (BCLC) (85%) and TNM classification (10%). The survey reflects important differences in the availability of treatments, including surgery (98.4%), tyrosine kinase inhibitors (95.1%), chemoembolization (85.2%), radiofrequency or alcohol ablation (82%), immunotherapy plus anti-VEGF (82%), liver transplant (74.2%), stereotactic body radiation therapy (42.6%), and radioembolization (36.4%).

Conclusion: Existence of PHP on HCC is insufficient worldwide. The most common strategy for staging is BCLC, but there are important differences on treatment availability across countries, especially regarding curative therapies.

SAT-130

Exploring attitudes towards non-invasive liver fibrosis tests in secondary care pathways: comparing national surveys between 2014 and 2021

Kushala Abeysekera^{1,2}, Ankur Srivastava³, Ian Rowe⁴, Helen Jarvis⁵, Stephen Ryder⁶, Andrew Yeoman⁷, John Dillon⁸, William Rosenberg⁹. ¹University of Bristol, United Kingdom; ²University Hospitals Bristol and Weston NHS Foundation Trust, Department of Liver Medicine, United Kingdom; ³North Bristol NHS Trust, United Kingdom; ⁴University of Leeds, United Kingdom; ⁵University of Newcastle, United Kingdom; ⁶University of Nottingham, United Kingdom; ⁷Anuerin Bevan University Health Board, United Kingdom; ⁸University of Dundee, United Kingdom; ⁹University College London, United Kingdom
Email: k.abeysekera@bristol.ac.uk

Background and aims: Increasing availability of non-invasive liver tests (NITs) has created the opportunity to apply them to improving early detection and risk stratification of advanced liver disease. This study aimed to determine changes in attitudes and practices of

secondary care specialists involved in managing liver disease in the UK, focusing primarily on attitudes to fibrosis assessment and the use of NITs. Secondary aims included exploring knowledge of NITs, use of designated early detection and risk stratification pathways, and barriers to implementing NITs in practice.

Method: Specialists managing patients with liver disease were invited to complete web-based surveys between 1st Oct 2014 to 1st Oct 2015 (Survey 1), and again between 1st Nov and 24th Dec 2021 (Survey 2) in the UK via the British Society of Gastroenterology, the British Association for the Study of the Liver, and using Twitter®. The second survey was closed early due to national clinical pressures from the COVID19 Omicron wave.

Results: Two hundred and fifteen healthcare professionals (HCPs) completed Survey 1 (49.5% hepatologists). The repeat survey was completed by 112 HCPs (64.3% hepatologists). Respondents represented 71 acute services in Survey 1 compared to 60 in 2021. Between the surveys the proportion of HCPs performing fibrosis assessment in all or nearly all cases rose by almost two-thirds from 45.1% to 74.1% ($\chi^2 = 25.01$; $p < 0.0001$). The proportion of respondents who considered FIB-4 to be useful in fibrosis assessment doubled from 40.7% ($n = 87/215$) 83.0% ($n = 93/112$; $\chi^2 = 53.93$; $p < 0.0001$). In 2014 87.0% ($n = 187/215$) considered transient elastography useful for fibrosis assessment, rising to almost all respondents (95.5%; $n = 107/112$; $\chi^2 = 5.96$, $p = 0.148$). Enhanced Liver Fibrosis (ELF) test was more favourably viewed amongst respondents for fibrosis assessment, increasing from 25.3% ($n = 54/215$) to 43.7% ($n = 49/112$; $\chi^2 = 11.85$; $p = 0.0006$) usage in 2021. A further 49.1% of respondents considered ELF useful but did not use it in their practice in 2021. Of the acute services represented by respondents, 46.5% ($n = 33/71$) respondents in acute services reported the use of NITs in clinical pathways, rising to 70.0% ($n = 42/60$) in Survey 2 ($\chi^2 = 7.35$; $p = 0.007$). Availability of tests has increased but is not universal. The proportion reporting availability as a barrier to uptake has fallen from 57.2% of responses in Survey 1 to 38.4% in 2021 ($\chi^2 = 11.01$; $p = 0.0009$).

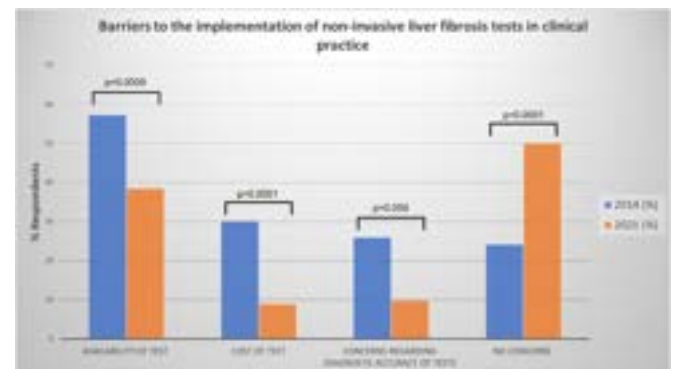


Figure:

Conclusion: Between 2014 and 2021, there has been a substantial increase in the use of NITs for fibrosis assessment accompanied by their use in clinical pathways to guide the management of people at risk or with liver disease. Poor access to NITs remains the predominant barrier. There is a pressing need for a simple, coordinated national strategy for testing individuals at risk of cirrhosis in primary care to ensure that cases can be identified and provided with prompt specialist care.

POSTER PRESENTATIONS

SAT-131

Evidence of significant alcohol-associated mortality in a large population cohort in Uganda

Cori Campbell¹, Joseph Mugisha², Elizabeth Waddilove³, Ronald Makanga², Tingyan Wang¹, Beatrice Kimono², Florence Nambaziira Muzaale², Philippa Matthews³, Eleanor Barnes¹.

¹University of Oxford, Nuffield Department of Medicine, United Kingdom; ²Medical Research Council/Uganda Virus Research Institute/London School of Hygiene and Tropical Medicine (MRC/UVRI/LSHTM) Uganda Research Unit, Entebbe, Uganda, Uganda; ³The Francis Crick Institute, 1 Midland Way, London, UK, United Kingdom
Email: cori.campbell@ndm.ox.ac.uk

Background and aims: Liver function tests (LFTs) can be used as prognostic biomarkers of all-cause mortality, however few investigations have been undertaken in African populations despite a high burden of liver disease in these settings. Previous analysis of the General Population Cohort (GPC) in Uganda suggested high prevalence of alcohol-related liver disease, HIV infection, HBV and associated primary liver cancer. We aimed to investigate how LFTs associated with risk of all-cause mortality in the GPC.

Method: The prospective GPC was established in 1989 in Kalungu District in rural south-western Uganda. In the 22nd survey round (years 2010/11), selected participants underwent measurement of biophysical and blood parameters to investigate disease risk factors and outcomes. Outcomes were ascertained via presentation to health clinic. Descriptive statistics were used to summarise parameters and compare correlations between LFTs, blood lipids (including low density lipoprotein, LDL), AST:ALT ratio (values >2 indicate alcoholic hepatitis), Haemoglobin A1C (HbA1c). We investigated characteristics/biomarkers associated with hazards of death via Cox proportional hazards modelling.

Results: In 7896 individuals with median age 30 years (IQR 17–46), 43.8% were male (n = 3455). Minorities of individuals had confirmed chronic hepatitis B virus (HBV) (n = 216, 2.7%) or human immunodeficiency virus (HIV) (n = 582, 7.4%) infections throughout follow-up. Over 6.30 mean years (SD 3.26) of follow-up, 629 (7.8%) individuals died from any cause. Risk factors for all-cause mortality included increasing age, male sex, HIV positivity (Figure 1). Nearly a quarter (23.3%, n = 147) of participants who died had an AST:ALT value >2, as compared to 9.8% (n = 710) of individuals who survived. A one-unit increase in AST:ALT ratio was associated with 17% higher hazards of death, and a 10 unit increase in gamma-glutamyl transferase (GGT) with a 1% increase in hazards. Other cardiometabolic factors associated with death included HbA1c and LDL.

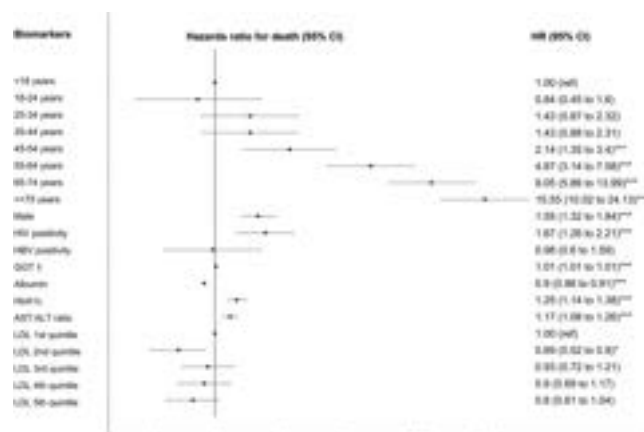


Figure: Forest plot for factors associated with all-cause mortality in Ugandan General Population Cohort (GPC). † Per 10-unit increase in GGT

Conclusion: Understanding of liver disease in the WHO Africa region must urgently improve. Using AST:ALT ratio cutoff (established in Western populations) suggests an association of alcoholic hepatitis with mortality, which is substantiated by elevated GGT. Clinical and public health programmes should be informed by data suggesting high alcohol consumption is a significant contributor to mortality.

SAT-132

Detection of potential subjects at risk of liver fibrosis in general population in Spain

María Del Barrio Azaceta¹, Paula Iruzubieta¹, Armando Raúl Guerra Ruiz¹, Marta Alonso-Peña¹, María Teresa Arias Loste¹, Aitor Odriozola¹, Ángela Antón¹, Sara Alonso¹, Bernardo Alio Lavin², Javier Crespo¹. ¹Gastroenterology and Hepatology Department, Marqués de Valdecilla University Hospital, Clinical and Translational Digestive Research Group, IDIVAL, Santander, Spain, Spain; ²Análisis Clínicos y Bioquímica. Hospital Universitario Marqués de Valdecilla, Santander, Spain
Email: javiercrespo1991@gmail.com

Background and aims: A two-step assessment with fibrosis index-4 (FIB-4) and transient elastography has been established as an appropriate screening strategy for liver fibrosis in >50 years old with metabolic risk factors. However, a screening program needs to guarantee the greatest accessibility for the population at risk. Our aim was to determine the prevalence of high risk of advance fibrosis (AdF) by FIB-4 in the general population and, therefore, subjects susceptible to undergo a second fibrosis assessment.

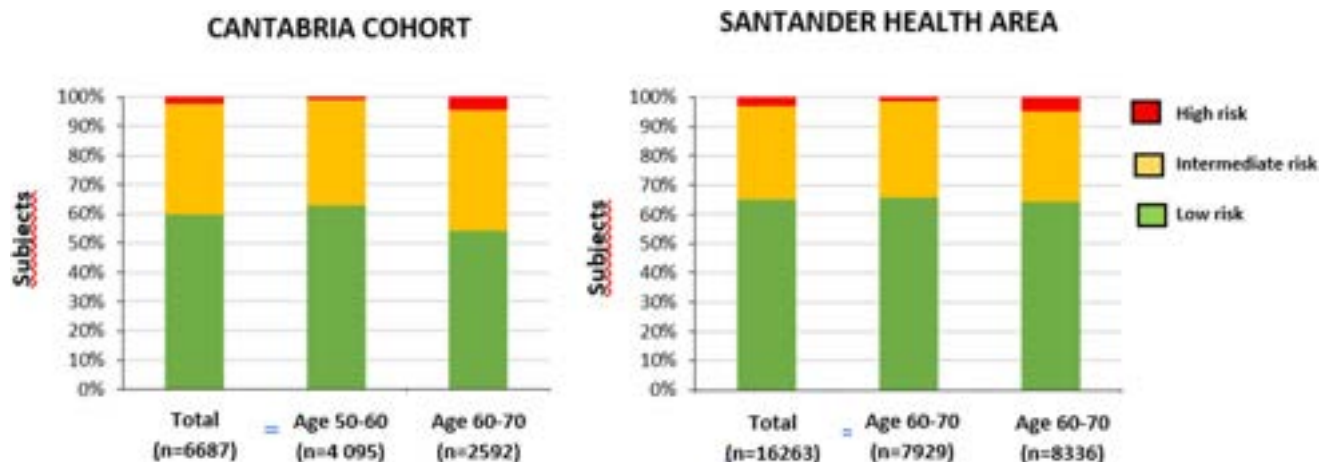


Figure: (abstract: SAT-132).

Method: Cross-sectional study in Spain based on general population that included subjects aged 50–70 from: A) Cantabria Cohort (volunteers and random sampling of the entire population of Cantabria –585,222 inhabitants–) enrolled from October 2021 to April 2022; B) Santander health area (315,000 inhabitants) who had an analysis from Primary Care between August–October 2021. The risk of AdF was determined using FIB-4: low risk (FIB-4 <1.3/<2.0 in >65 years), intermediate risk (1.3–2.67/2.0–2.67 in >65 years) and high risk (>2.67).

Results: From Cantabria cohort, 6,687 subjects were included (mean age 58.7 ± 5.8 ; 41.0% men; 23.6% obese). 2,545 subjects (38.1%) had an intermediate risk, and 155 subjects (2.3%) had a high risk. No differences were found in the prevalence of high risk of AdF between obese and non-obese subjects (2.0% vs. 2.3%; $p = 0.4$). FIB-4 could be calculated in 16,263 of the subjects in the Santander health area (mean age 60.4 ± 6.0 ; 41.7% men). Intermediate risk was observed in 5,185 cases (31.9%) and high risk in 498 (3.1%), similar to the general population cohort (Fig).

Conclusion: In a health area of 315,000 inhabitants, a two-step fibrosis screening strategy in subjects aged 50–70 years, without considering metabolic factors, would entail the application of a second test in approximately 1500 subjects/month and, therefore, this implies that approximately 150 subjects/month need to be referred to a specialized consultation; which is a number of patients that can be assumed by the Hepatology unit service of a tertiary referral hospital.

SAT-133

Comparison of the opt in vs opt out policy and its impact on the donation rate of liver transplantation in the Colombian healthcare system

Andres Gomez Aldana^{1,2}, Diana Carolina Gomez³. ¹Fundación Santa Fe de Bogota, Bogota, Colombia; ²McMaster University, Canada; ³Sanitas EPS, Colombia

Email: andresgomezmd@hotmail.com

Background and aims: The organ donation process around the world is supported by two systems denominated opt-in (the patient agrees to be a donor) and opt-out (it is presumed that the person consents to the donation unless they have registered their contrary decision); This last policy was pursuing to bolster donations rate. Given the lack of potential donors and our low donor rate (8 per million inhabitants), Colombia promulgated some laws (823 in 2015 and 714 in 2016), seeking to expand the legal presumption of donation of anatomical components for transplant purposes or other therapeutic uses, designing a legal framework to increase the donation rate to all those people who had not expressed the refusal to do so while alive.

Method: This is a retrospective study comparing two years before and two years after the establishment of this new law in terms of the number of liver transplants.

Results: The absolute number of organ donations in Colombia (This organ donation and distribution in 6 different geographical regions across the country), was assessed during the period of 2015–2016. Therefore, this time will be known as the opt-in period. Moreover, the period 2017–2018 was covered during the opt-out policy period. Overall, the national donation rate increases reach up to 11.6%.

Otherwise, the refusal rate of family members, before and after the enacted legislation, shows a decrease of 61%, which suggests a favorable outcome. Moreover, the liver transplant rate during the opt-in period (2015–2016), showed a slight increase in the number of transplants, reaching 3.44% in the absolute number. By contrast, during the period 2017–2018, a decrease of 17% is observed in the number of transplants compared.

Conclusion: In summary, the new legislation switching to the "opt-out" policy has been a favorable strategy for transplants of different solid organs. Unfortunately, the liver transplant rate has shown an unfavorable trend with this intervention, which would make it necessary to carry out more studies to identify which other causes are inducing this negative impact on this population. Otherwise, there is still more research required to assess the impact of COVID-19 on this policy.

SAT-134

Global burden of common cancers attributable to metabolic risks from 1990 to 2019

Qing-Qing Xing¹, Jing-Mao Li², Chen Chen Zhi-Jian¹, Xiaoyun Lin¹, You You Yan-Ying³, Mei-Zhu Hong⁴, Shangeng Weng⁵, Jin-Shui Pan¹.

¹First Affiliated Hospital of Fujian Medical University, Department of Hepatology, Fuzhou, China; ²Xiamen University, Department of Statistics, School of Economics, Xiamen, China; ³First Affiliated Hospital of Fujian Medical University, Department of Hepatology, Fuzhou, China; ⁴Mengchao Hepatobiliary Hospital of Fujian Medical University, Department of Traditional Chinese Medicine, Fuzhou, China; ⁵First Affiliated Hospital of Fujian Medical University, Hepatopancreatobiliary Surgery Department, Fuzhou, China

Email: 363111396@qq.com

Background and aims: Non-alcoholic fatty liver disease (NAFLD) is usually accompanied by metabolic syndrome, which is associated with increased risk of cancer. To inform a tailored cancer screen in patients at higher risks, we estimated the global burden of cancer attributable to metabolic risks.

Method: Data of common metabolism-related neoplasms (MRNs) were derived from the Global Burden of Disease (GBD) 2019 database. Age-standardized, disability-adjusted life year (DALY) rates and death rates of patients with MRNs were extracted from the GBD 2019 database and stratified by metabolic risk, sex, age, and level of socio-demographic index (SDI). The annual percentage changes of age-standardized DALYs and death rates were calculated.

Results: Metabolic risks, consisting high body-mass index and fasting plasma glucose, contributed substantially to the burden of neoplasms, including colorectal cancer (CRC), tracheal, bronchus, and lung cancer (TBLC), etc. Globally, in 2019, there was an estimated age-standardized DALYs rate (ASDR) of 234.0 (95% CI 124.0–376.0) per 100,000 person-years for neoplasms attributable to metabolic risks. ASDRs of MRNs were higher for CRC, TBLC, men, patients aged ≥ 50 years, and patients with high or high-middle SDI.

Conclusion: These findings further underpin the correlation between NAFLD and intrahepatic and extrahepatic cancers and highlight the possibility of tailored cancer screening for the NAFLD population at higher risks.

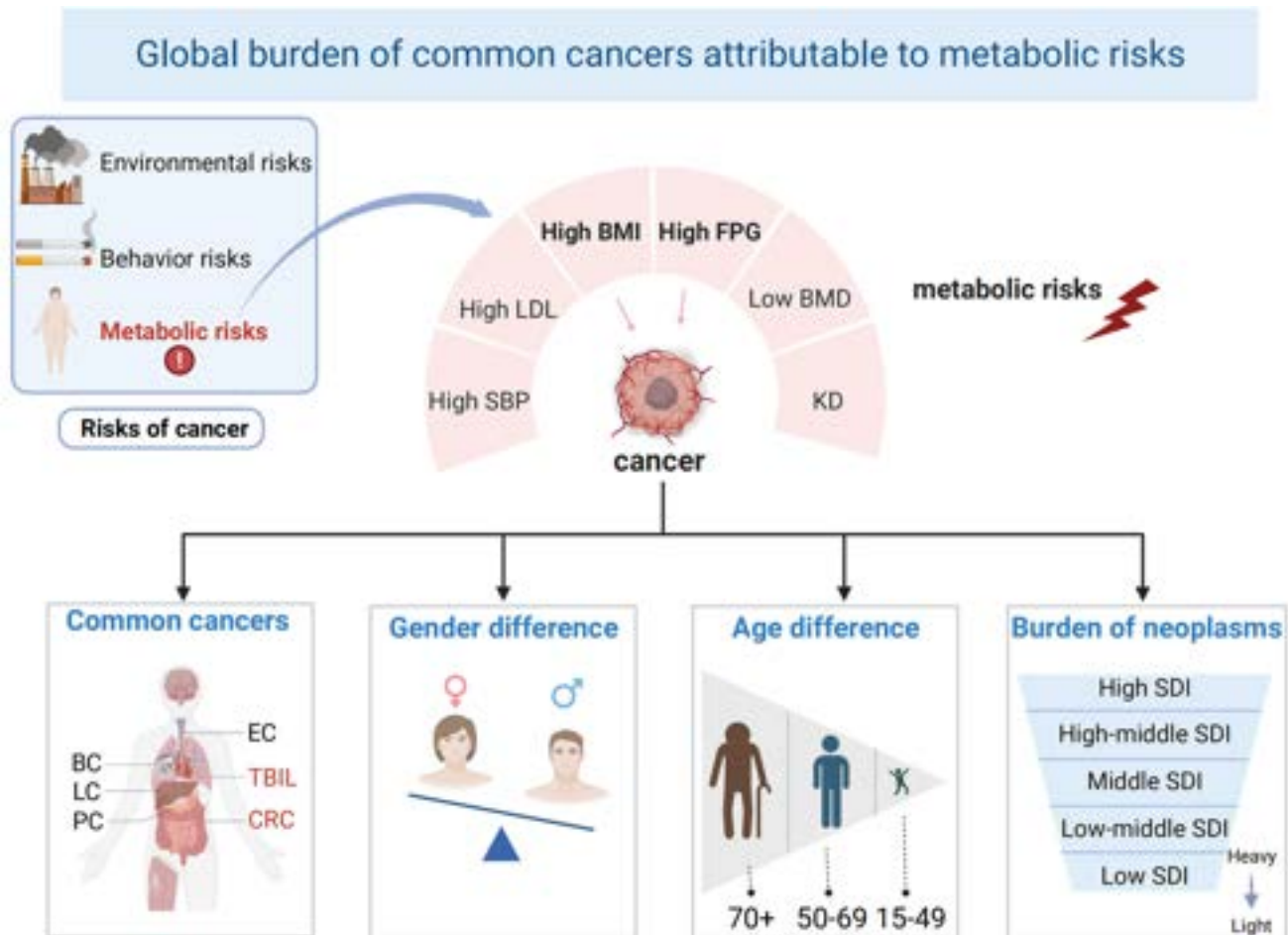


Figure: (abstract: SAT-134).

SAT-135

Impact of coronavirus disease pandemic on hospitalizations due to chronic liver disease in Belgrade, Serbia

Ivana Pantic¹, Nina Rajovic², Sofija Lugonja³, Svetlana Miltenovic⁴, Tamara Milovanovic^{1,5}. ¹Clinic of gastroenterology and hepatology, University clinical center of Serbia, Belgrade, Serbia; ²Institute for medical statistics and informatics, Faculty of medicine, University of Belgrade, Belgrade, Serbia; ³General hospital "Djordje Joanovic", Serbia; ⁴Institute of public health of Belgrade, Serbia; ⁵Faculty of medicine, University of Belgrade, Serbia
Email: tamara.alempijevic@med.bg.ac.rs

Background and aims: The consequences of severe and worldwide health-care disruption as a result of coronavirus disease (COVID-19) pandemic still have to be dealt with. Besides the decreased availability of health-care services during the lockdown, it is also hypothesized that patients detained themselves from seeking help. Additionally, an increase in alcohol consumption during that period is well documented. The aforementioned mechanisms contributed to higher morbidity and mortality of patients suffering from all chronic diseases-including the chronic diseases of the liver. The aim of our study was to evaluate whether there are any differences in hospital admissions due to chronic liver disease (CLD) and outcomes during the pandemic in Belgrade, Serbia, compared to the previous years.

Method: Hospital admissions due to alcohol-related, viral, autoimmune, and overlapping liver disease were identified using primary and secondary discharge diagnosis codes, based on the 10th revision of the International Statistical Classification of Diseases and Related Health Problems. All hospitalization reports (including re-hospitalizations) which included adult subjects on the territory of Belgrade,

between 2016 and 2021, and contained pre-defined principal discharge codes were selected. We compared the period of pandemic (2020 and 2021) with previous years (2016–2019).

Results: A total of 6789 hospitalizations due to CLD were noted during the study period. The mean age of patients was 52.5 ± 15.9 years, and majority were male (65.5%). Median hospital stay of the patients was 4 days (25th–75th percentile: 1–12). Number of hospitalizations due to CLD per year from 2016 to 2021 was as follows: 1395 (20.5%), 1259 (18.5%), 1268 (18.7%), 1533 (22.6%), 800 (11.8%), and 534 (7.9%), respectively. Average number hospitalizations per year before COVID-19 pandemic was 1364 ± 129, while during COVID-19 pandemic, average number of hospitalizations per year was 667 ± 188 ($p=0.005$). During COVID-19 pandemic hospitalized patients were more often female ($p<0.001$), younger ($p=0.006$), and more often had autoimmune liver disease than patients admitted due to CLD before COVID-19 pandemic ($p<0.001$). During COVID-19 pandemic, shorter hospital stay (4 days vs. 1 day; $p<0.001$) was reported, while mortality rate increased (7.6% vs. 8.8%; $p=0.048$) compared to patients admitted for CLD before COVID-19 pandemic. Before COVID-19 pandemic, patients with alcohol-related/overlapping liver disease had the highest mortality rate (15.1%; $p<0.001$). During COVID-19 pandemic, mortality rate for alcohol-related/overlapping liver disease increased to 21.2% ($p<0.001$). In both groups (before and after COVID-19 pandemic), male ($p<0.001$) and older ($p<0.001$) patients were at increased risk for overall mortality ($p<0.001$ and $p<0.001$, respectively).

Conclusion: During COVID-19 pandemic less hospital admissions due to CLD was noted. Overall length of stay was shorter, overall mortality increased, while a significant increase in mortality was

noted in hospitalizations due to alcohol-related/overlapping liver disease. During the pandemic, hospitalized patients were younger and more often female, and patients were more commonly admitted due to autoimmune liver disease.

SAT-136

SIRIUS project: sensing probe exploring liver fibrosis in Slovakia

Lubomir Skladany¹, Daniel Jan Havaj¹, Svetlana Adamcova Selcanova¹, Janka Vnencakova¹, Natalia Bystrianska¹, Daniela Žilinčanová¹, Karolina Sulejova¹, Beata Skvarkova¹, Marek Rac², Sylvia Dražilová³, Martin Janičko³, Peter Jarcuska³, Tomáš Koller⁴. ¹F. D. Roosevelt University Hospital in Banská Bystrica, Slovakia; ²Faculty Hospital Nitra, Nitra, Slovakia; ³Louis Pasteur University Hospital Kosice, Slovakia; ⁴Faculty of Medicine (University of Comenius), Bratislava, Slovakia
Email: lubomir.skladany@gmail.com

Background and aims: In Slovakia, liver cirrhosis is the most prevalent of all the countries in the world and, it is the number-one cause of death in young adults (25–45 y/o). One of the responses on the side of the professional liver community was the launch of country-wide screening project SIRIUS. SIRIUS Project was aimed primarily at detecting liver fibrosis in general population and to try to find its associations with the most common risk factors for chronic liver diseases. This is the first interim analysis, aimed at the prevalence of liver fibrosis as detected by transient elastography (TE) with the threshold for increased stiffness as proposed by the LiverScreen project.

Method: In this community-outreach project, SIRIUS teams composed of physicians, nurses, volunteers and liver patient organization members travelled to pre-selected sociomes of six types from cities to remote villages and roma communities in all the regions of the country and recorded: brief medical history, demography, anthropometry, capillary blood chemistry, TE and, in a subset of participants gut microbiome samples. Liver stiffness was considered increased if the result of standardized TE (FibroScan[®]) measurement was above 8 kPa. We included only consenting adult community dwellers without known (ICD registered) liver disease apart from trivial NAFLD, and without active/unstable/life-threatening extrahepatic comorbidity. In the case TE, or laboratory parameters suggested liver disease, recall policy was two-pronged: 1) patients were offered on-site consultation by a physician from the liver unit and they were issued 2) Green Card with SIRIUS personal identifier serving as a passport for the subsequent in-depth examination in the respective regional liver outpatient clinic. In the case local show-up exceeded the capacity of SIRIUS day, unserved interested persons were issued Orange Card with SIRIUS personal identifier allowing for the SIRIUS exam in the future. SIRIUS has been granted Institutional Ethics committee approval and NCT registration number.

Results: Between August 23, 2022 and January 31, 2023, SIRIUS team visited nineteen sites and completed the data collection in 1 663 adult participants. Issued were 560 Green Cards and 332 Orange Cards, respectively. We detected liver stiffness >8 kPa in 243 participants (15%).

Conclusion: In this country-wide endeavour, the prevalence of increased liver stiffness was considerably higher than in other regions of Europe. Before we claim the prevalence is concordant with staggering prevalence of end-stage liver disease in Slovakia, we have to exclude self-selection bias by continuing enrollment until tsunami of interest to be screened levels off.

SAT-137

Anti-hepatitis B surface antigen negativity can be a risk factor for SARS-CoV-2 infection in SARS-CoV-2 vaccinated healthcare workers

Tomohide Kurahashi, Atsuishi Hosui¹, Naoki Hiramatsu¹. ¹Osaka-Rosai Hospital, Department of Gastroenterology and Hepatology, Sakai, Japan
Email: tkurahashi@osakah.johas.go.jp

Background and aims: Severe acute respiratory syndrome coronavirus 2 (SARS-CoV-2) infection has raged around the world. It is important for health care institutions providing SARS-CoV-2 medical care to understand the risk factors of infection among health care workers. Vaccination has been used as an effective method for health care workers fighting SARS-CoV-2, however, nevertheless, infection can often occur after vaccination. In this study, we investigated the factors involved in SARS-CoV-2 infection in health care workers after vaccination.

Method: We registered 1133 healthcare workers (826 women, 307 men) who received first SARS-CoV-2 vaccination between February and April 2021 in our hospital. The BNT162b2 vaccines (Pfizer/BioNTech) were inoculated three times according to the pharmaceutical reference. Self-reported questionnaires and medical checkup were used to collect medical histories and demographic characteristics. The alinity SARS-CoV-2 IgG II quant (Abbott) quantitative IgG spike protein serology assay were examined in a group of participants who have passed 1, 4, 6 months after the second vaccination and 1 month after the third vaccination of the BNT162b vaccine. Lower antibody (Ab) titers were defined under median at each time step. The risk factors of SARS-CoV-2 infection to persons who received vaccination three times were analyzed. The log-rank test was used as the analysis method.

Results: The mean observation period was 16.1 ± 2.0 months (mean ± standard deviation) after first vaccination. The median titers at 1, 4, 6 months after the second vaccination were 9293 U/ml (interquartile range [IQR], 5840–14392 U/ml), 1658 U/ml (IQR, 999–2676) and 832 U/ml (IQR, 523–1300), respectively. The median titers at 1 month after the third vaccination was 13780 U/ml (IQR, 9085–22722). SARS-CoV-2 infected 40.1% of the enrolled healthcare workers during the observation period. In univariate analysis, the risk factors for SARS-CoV-2 infection were hepatitis B surface antibody (HBsAb) negative ($p = 0.011$, OR = 1.613) and high γ GTP ($p = 1.768$, OR = 0.032) participants. The participants with underlying disease was marginally significant ($p = 0.072$, OR = 1.407). No significant association was found between SARS-CoV-2 infection and Ab titer at the time of our measurement. Multivariate analysis showed that HBsAb negative was the only significant factor for SARS-CoV-2 infection ($p = 0.021$, OR = 1.595). The 1-year cumulative infection rates of SARS-CoV-2 infection in HBsAb negative and positive people were 5.2% and 3.7%, respectively ($p = 0.007$). Next, 238 participants who had previously vaccinated against hepatitis B in this cohort were examined in order to investigate the relationship in detail between HBsAb status and SARS-CoV-2 infection. Of these participants, 129 were responders who acquired HBsAb from the vaccine and 109 were vaccine refractory (non-responders). HBV vaccine non-responders were more susceptible to SARS-CoV-2 infection compared to responders (non-responders 4.6% vs responders 0.8%, $p = 0.042$, OR = 1.51).

Conclusion: HBsAb negativity can become a factor indicating susceptibility to SARS-CoV-2 infection. Recently, three segments in the hepatitis B protein have been reported to have antigenic properties that can induce protective effect against SARS-CoV-2 infection (Haddad-Boubaker et al. BMC Bioinformatics, 2021). Our results can suggest a protective effect of HBsAb against SARS-CoV-2 infection clinically.

Public Health Viral hepatitis

WEDNESDAY 21 TO SATURDAY 24 JUNE

TOP-096

Trends in hepatitis B and hepatitis C related hepatocellular carcinoma, 2015 to 2030

Devin Razavi-Shearer¹, Sarah Blach¹, Ivane Gamkrelidze¹, Kathryn Razavi-Shearer¹, Alexis Voeller¹, Homie Razavi¹. ¹Center for Disease Analysis Foundation, Lafayette, United States
Email: dravishearer@cdafound.org

Background and aims: Hepatocellular carcinoma (HCC) secondary to hepatitis B (HBV) and/or hepatitis C (HCV) virus infection is an important cause of morbidity and mortality. We aimed to estimate the change in incident HCC cases from 2015 through 2030 under the current HBV and HCV treatment paradigms.

Method: To estimate the number of HCC cases attributed to HBV or HCV, first the annual number of incident liver cancers cases was collected (by country for all available years) from national cancer registries. If registry data were unavailable, estimates from local hospitals or clinics were collected and extrapolated to the country level in consultation with local experts. Next, incident liver cancer cases were adjusted for type (HCC), etiology (HBV or HCV) and underreporting (if indicated by local experts). Proportions used to adjust for type, etiology, and underreporting were retrieved from published literature, local databases, or expert input.

In parallel, country-specific models for HBV (PRoGrEsS Model) and HCV (Bright Model) were developed using epidemiological data and expert input. These estimated the natural history (from 1950 to 2050) of HBV or HCV disease and future burden, including HCC. After calibration, model calculated incident HCC cases were validated against reported cases, where available.

Finally, the modeled numbers of HBV- or HCV-related incident HCC cases from 2015 to 2030 were retrieved by country. If country-specific data were not available, regional averages were used. Country data were summed, by disease, to estimate the global number of incident HBV- or HCV-related HCC. Finally, the number of viral hepatitis-related HCC cases was calculated by summing HBV-related and HCV-related cases. Incidence rates were calculated per 100,000 population (adults 18+).

Results: At the country level, the incidence of viral hepatitis-related HCC in 2022 was generally correlated with viral hepatitis prevalence in the same year. Given current prophylaxes and treatment trends,

the global number of incident viral hepatitis-related HCC cases would increase from 860,000 (16.9 per 100,000) in 2015 to 1.08 million (17.5 per 100,000) by 2030. HCV-related incident HCC cases would increase 3% (from 210,000 in 2015 to 216,000 in 2030), while the incidence rate would decrease 15% (from 4.1 to 3.5 per 100,000). Meanwhile, HBV-related incident HCC would increase (33% for cases, 10% for rate), from 652,000 (12.8 per 100,000) in 2015 to 864,000 (14.0 per 100,000) by 2030. Due to the changing trends by disease area, the proportion of viral hepatitis-related HCC cases attributed to HBV would increase from 76% in 2015 to 80% in 2030.

Conclusion: HBV-related HCC was the major driver of increasing trends in incident HCC cases. Prevention and treatment of HBV and HCV should be pursued not only for the elimination of viral hepatitis, but also as a strategy for cancer prevention.

TOP-097

Engagement of patients with viral hepatitis diagnosed by opt-out universal emergency department testing

Amy Teague¹, Jingwei Zeng², Tanzina Haque², Douglas Macdonald^{1,3}, Kathleen Bryce^{1,4}. ¹Department of Hepatology, Royal Free London NHS Foundation Trust, London, United Kingdom; ²Department of Virology, Royal Free London NHS Foundation Trust, London, United Kingdom; ³Institute of Liver and Digestive Health, University College London, London, United Kingdom; ⁴Institute for Global Health, University College London, London, United Kingdom

Email: kathleenbryce@doctors.org.uk

Background and aims: We report on the engagement and assessment outcomes of adults diagnosed with viral hepatitis through a recently implemented universal opt-out blood-borne virus testing program across two emergency departments (ED) in London.

Method: Opt-out blood-borne virus (BBV) testing (HCV Ab, HBsAg and HIV) commenced for all adults attending ED at the Royal Free London NHS Trust from 15th April 2022. Reflex testing of HCV RNA and HBV DNA were performed in positive HCV Ab and HBsAg samples. Patient engagement was nurse-led and managed by a bespoke patient management system from which data was extracted to 24th January 2023. Patients were initially contacted by phone and then by letter if this was unsuccessful after two separate attempts. All patients contacted were offered assessment in a hospital outpatient setting.

Results: A total of 52 new hepatitis C and 195 new hepatitis B diagnoses were made during the study period. The subsequent engagement and treatment cascade is shown in Table 1. The proportion of those not under care that have since been assessed are the same for both groups (56%) but the non-attendance rate of

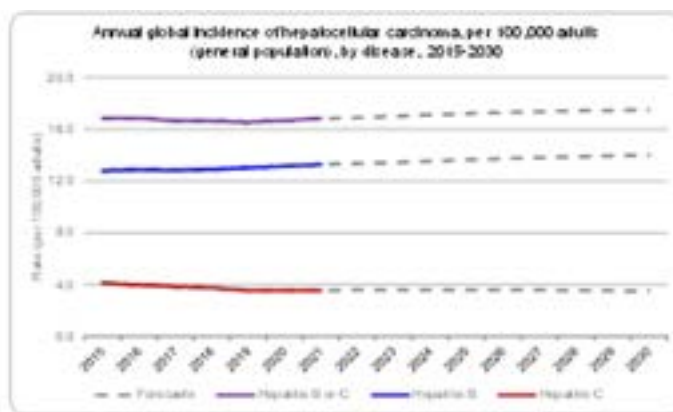
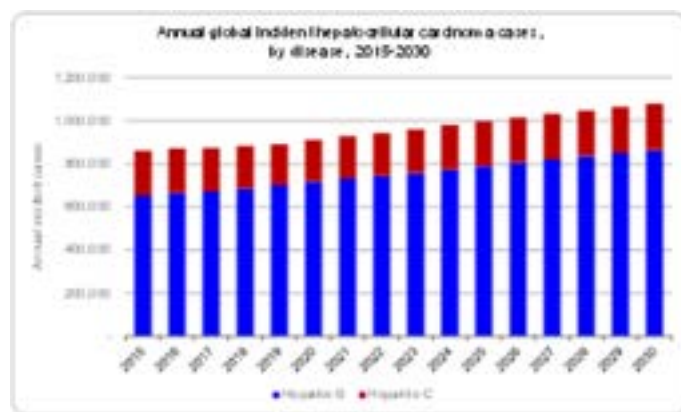


Figure: (abstract: TOP-096).

patients after successful contact was higher in those with hepatitis B than those with hepatitis C (21% vs 9%). 13% of those with hepatitis B spoke English as a first language compared with 65% of those with hepatitis C ($p < 0.0001$, Fisher's exact test). Of those assessed in clinic with hepatitis B, 15.8% had an HBV DNA >2000 and 13.9% had F2 or greater fibrosis. 14% ($n = 16$) have been commenced on nucleotide therapy. 2 new HCC diagnoses were made at baseline imaging. Of those assessed with hepatitis C, 22% had F3 or greater fibrosis and 62.5% ($n = 20$) had been commenced on treatment by the censor date. A further 5 patients with hepatitis C who were not contactable or disengaged after assessment have been successfully engaged and treated by a mobile Find-and-Treat service.

Conclusion: We have shown that opt-out ED BBV testing is feasible at scale and can identify large numbers of new cases of viral hepatitis, particularly hepatitis B. However, subsequent engagement presents challenges which differ between hepatitis B and C cohorts. In implementation of opt-out ED testing appropriate resource allocation to subsequent engagement, assessment and treatment is essential if patients are to benefit from diagnosis.

Table 1:

	HCV RNA+	HBsAg+
Total tests	54509	54398
Total positives (% of all tests)	64 (0.117%)	253 (0.465%)
– New diagnoses (% of all positives)	52 (81%)	195 (77%)
– Lost to follow-up (% of all positives)	8 (13%)	32 (13%)
– Already under follow-up (% of all positives)	4 (6%)	26 (10%)
Total requiring assessment (% of all positives)	57 (89%)	204 (81%)
– Contacted (% of total requiring assessment)	42 (74%)	177 (87%)
– Attended (% of all appointments booked before censor date)	32 (89%)	115 (76%)
Commenced on treatment (% of all attended)	20 (62.5%)	16 (13.9%)

FRIDAY 23 JUNE

FRI-113

Estimating the economic value allocation of the social surplus generated by the utilization of second-generation direct-acting antivirals for hepatitis C in the United States, 2015–2019

Louis Garrison^{1,2}, Boshen Jiao^{1,3}, Zizi Elsis^{1,2}, Alon Yehoshua⁴, Roy Koruth⁴, Bruce Kreter⁴, Jens Grueger^{2,5}. ¹University of Washington, United States; ²VeriTech Corporation, Mercer Island, United States; ³Harvard School of Public Health, United States; ⁴Gilead Sciences, Inc., United States; ⁵Boston Consulting Group, United States
Email: jens.grueger@t-online.de

Background and aims: While the rising costs for innovative medicines are discussed widely, they are rarely put in context of the total social surplus that is generated for health systems and society. Between 2014 and 2019, several innovative direct-acting antiviral therapies (DAAs) were introduced with the potential to cure patients with hepatitis C (HCV). They generate surplus in the form of the value of the health gains for patients as well as the cost-savings for health systems. As an incentive for innovation, manufacturers of patent-protected medicines are rewarded with a share of this social surplus in the form of the revenues that they accrue over the life cycle of a product—from initial launch through eventual patent expiry and perhaps beyond. This analysis focuses on the U.S. during this period and addresses the question: what share of the aggregate economic value generated by DAA utilization from 2015 to 2019 was allocated to manufacturers versus the rest of society?

Method: This analysis took a national healthcare system perspective. We projected the impact of DAAs on health outcomes and costs compared with the counterfactual scenario using the pre-DAA standard of care (SOC). Analyses are based on CDAF-Polaris database on the utilization of HCV treatments from 2011 to 2019. Projections

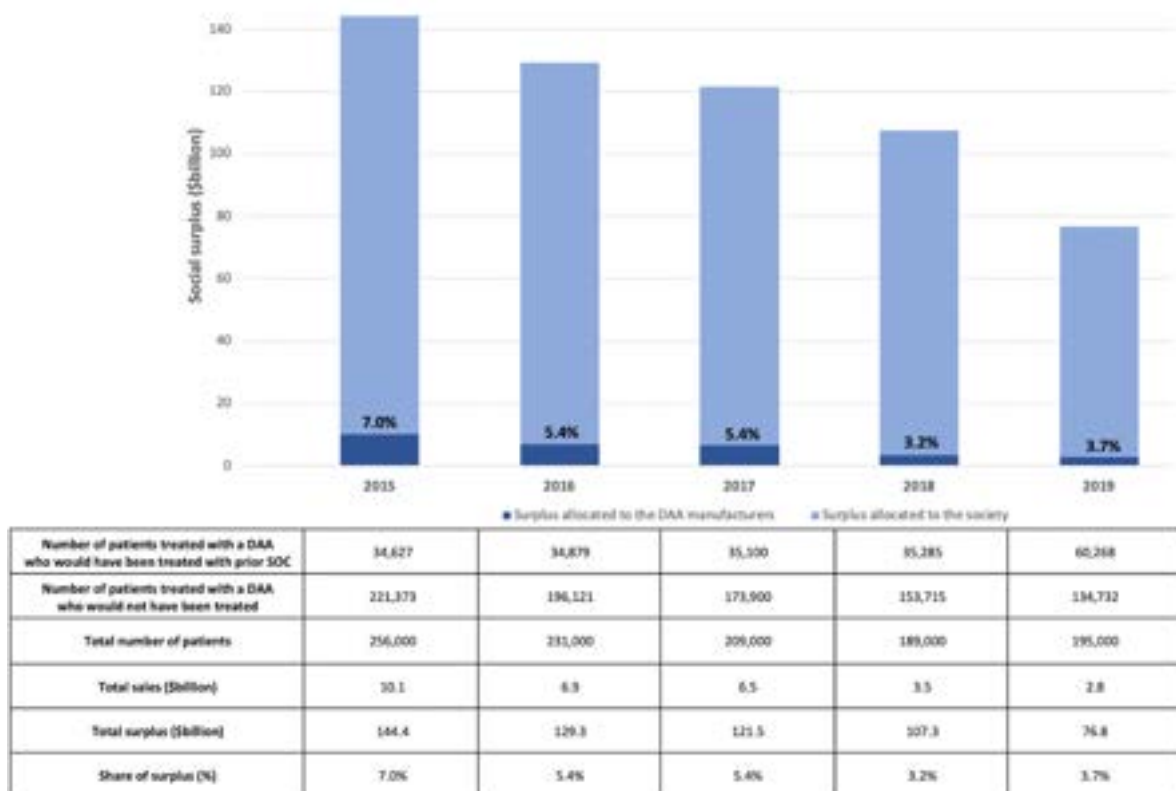


Figure: (abstract: FRI-113).

POSTER PRESENTATIONS

of the expected patient lifetime quality-adjusted life-years (QALYs) gained and expected patient lifetime medical costs avoided were made using a standard HCV disease progression model of DAA treatment versus the prior SOC as well as versus no treatment. The underlying model has nine health states based on degree of fibrosis and cirrhosis as well as hepatocellular cancer and liver transplantation. The model generated estimates of expected lifetime discounted QALYs and non-DAA costs for a typical (55-year-old) HCV patient. The counterfactual was constructed by extrapolating treatment rates from the period 2008–2011 prior to the adoption of DAAs. Annual QALY gains were valued at \$114 k (2× per-capita U.S. GDP in 2015\$). All outcomes and costs were discounted at 3%. Estimates for manufacturer revenues for DAAs were based on IQVIA sales data in 2015\$.

Results: Of the estimated 1,080,000 patients who received DAAs in 2015–19, the estimated share who would not have been treated (pre-DAA) is 81.5%. They are projected, on average, to gain 4.4 QALYs and save \$104,400 in lifetime costs while those who would have been treated gain 1.7 QALYs and save \$41,500 in lifetime costs. In the aggregate, those who would not have been treated generate the larger social surplus of \$531.8 billion, vs. \$47.4 billion for those who would have been treated.

Conclusion: The uptake of DAAs in the US from 2015 to 2019 generated substantial aggregate social surplus, valued at \$579.3 billion. Manufacturers had \$29.9 billion in sales (2015\$) in this period, implying that they were allocated 5.2% of the economic value generated for these cohorts.

FRI-114

Late diagnosis of hepatitis C in Quebec, Canada, 1990–2018: a population-based study

Ana Maria Passos-Castilho^{1,2}, Donald Murphy³, Karine Blouin⁴, Marina B. Klein⁵, Julie Bruneau⁶, Andrea Benedetti⁷, Jeff Kwong⁸, Beate Sander^{9,10}, Naveed Janjua¹¹, Christina Greenaway^{1,2,12}, ¹Lady Davis Institute, Jewish General Hospital, Centre for Clinical Epidemiology, Canada; ²McGill University, Department of Medicine, Canada; ³Institut National de Santé Publique du Québec, Laboratoire de Santé Publique du Québec, Canada; ⁴Institut National de Santé Publique du Québec, Unité sur les Infections Transmissibles Sexuellement et par le Sang, Canada; ⁵Research Institute of the McGill University Health Center, Canada; ⁶Research Center, Centre Hospitalier de l'Université de Montréal, Canada; ⁷School of Population and Global Health, McGill University, Department of Epidemiology, Biostatistics and Occupational Health, Canada; ⁸Dalla Lana School of Public Health, University of Toronto, Canada; ⁹Toronto General Hospital Research Institute, University Health Network, Canada; ¹⁰Institute of Health Policy, Management and Evaluation, University of Toronto, Canada; ¹¹BC Centre for Disease Control, Canada; ¹²Division of Infectious Diseases, Jewish General Hospital, Canada

Email: anampassos@gmail.com

Background and aims: Timely diagnosis and treatment of all individuals infected with HCV is needed to prevent poor outcomes such as decompensated cirrhosis (DC), hepatocellular carcinoma (HCC), and liver-related deaths. We estimated annual rates and predictors of late HCV diagnosis in Quebec, Canada.

Method: A population-based cohort of all reported HCV cases in Quebec (1990–2018) were linked to several health administrative databases including the landed immigrant database (1980–2018). People who inject drugs (PWID) and liver related outcomes (DC/HCC) were defined using published algorithms. Missing data were addressed with multiple imputation by chained equations. Late diagnosis was defined as the occurrence of DC or HCC any time before up until 2 years after HCV diagnosis. Annual crude rates of late diagnosis per 100 HCV diagnoses were estimated until 2016 to avoid truncation bias. Rate ratios (RR), yearly percent change, and 95% confidence intervals (CI) were estimated using Poisson regression. Predictors of late diagnosis were analyzed using multiple logistic

regression adjusting for demographics, social/material deprivation and comorbidities. Results are shown as adjusted odds ratio (aOR), 95% CI, and p value.

Results: Among 40,667 individuals diagnosed with HCV from 1990 to 2016, 67% were male, with a mean age of 44.2 years (standard deviation 14.9); 56% were born in 1945–1965, 46% were PWID, and 13% immigrants. Overall, 17% of all HCV diagnoses were late, with an increase of 4.5%/year (95% CI, 2.2–6.7, $p < 0.001$) between 1998 and 2004, 9.0%/year (7.3–10.7, $p < 0.001$) between 2005 and 2012, and then with a decrease of –9.3%/year (–15.5–3.1, $p = 0.001$) between 2013 and 2016. The rate of late diagnosis/100 HCV cases was higher among immigrants compared to non-immigrants (20.9 vs. 16.3; RR 1.28, 95% CI 1.18–1.40, $p < 0.001$) with highest rates among those from Sub-Saharan Africa (25.8; 1.58, 1.22–2.04, $p = 0.001$). Overall predictors of higher risk of late diagnosis in adjusted analysis included alcohol use disorder (aOR 1.40, 95% CI 1.32–1.47, $p < 0.001$), being born <1945 compared to >1965 (1.38, 1.29–1.47, $p < 0.001$), social deprivation (1.12, 1.03–1.23, $p = 0.012$), male sex (1.11, 1.07–1.14, $p < 0.001$), and immigrant status (1.10, 1.05–1.16, $p < 0.001$). Factors associated with a lower risk of late diagnosis included PWID status (0.78, 0.75–0.81, $p < 0.001$), mental health diagnosis (0.93, 0.89–0.96, $p < 0.001$), being born in 1945–1965 compared to >1965 (0.94, 0.90–0.98, $p = 0.007$), and rural residence (0.95, 0.92–0.99, $p < 0.008$). Among immigrants, those from Sub-Saharan Africa compared to High Income regions (1.40, 1.03–1.92, $p = 0.034$) and women (1.10, 1.01–1.19, $p = 0.023$) were at higher risk of late diagnosis.

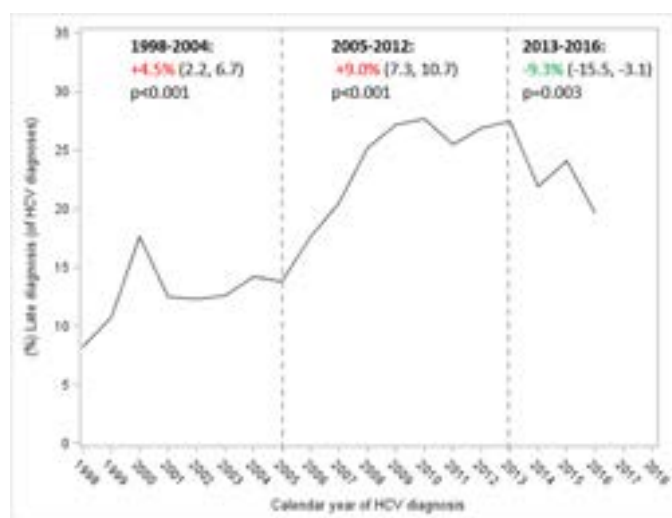


Figure: Prevalence of late diagnosis of hepatitis C in Quebec, Canada, 1990–2018 (yearly change in rate of late diagnosis shown per period as percent with 95% confidence interval and p value).

Conclusion: Older individuals, those with comorbidities, alcohol use disorder, and immigrants should be targeted for HCV screening and treatment to prevent liver-related sequelae.

FRI-115

An international coalition to eliminate hepatitis B virus (ICE-HBV) survey confirms inadequate HBV/HDV screening and diagnosis diminishing elimination targets in resource limited settings

Daryl Lau¹, Anna Kramvis², Camila Picchio³, Kathy Jackson⁴, Alice Lee⁵, Gail Matthews⁶, Jess Howell⁷, Carla Coffin⁸, Maud Lemoine⁹, Peter Revill¹⁰, Mark Sonderup^{11,12}, Fatou Fall¹³, Vonthanak Saphonn¹⁴, Margaret Hellard¹⁵, David Anderson¹⁶, Wendy Spearman¹¹, Massimo Levrero¹⁷, Capucine Penicaud¹⁸, Manal Hamdy El-Sayed¹⁹. ¹Liver Center, Department of Medicine, Beth Israel Deaconess Medical Center, Harvard Medical School, Boston, United States; ²Hepatitis Virus Diversity Research Unit, Department of Internal Medicine, University of the Witwatersrand, South Africa; ³Barcelona Institute for Global Health (ISGlobal), Hospital Clínic, University of Barcelona, Spain; ⁴Section of Molecular Microbiology, Doherty Institute, Australia; ⁵World Gastroenterology Organization, Australia; ⁶The Kirby Institute, University of New South Wales, Australia; ⁷Department of Gastroenterology, Burnet Institute, Australia; ⁸Cumming School of Medicine, University of Calgary, Canada; ⁹Division of Digestive Diseases, Department of Metabolism, Digestion, and Reproduction, Imperial College London, United Kingdom; ¹⁰Department of Microbiology and Immunology, Doherty Institute, Australia; ¹¹Faculty of Health Sciences, University of Cape Town, South Africa; ¹²University of Cape Town Faculty of Health Sciences, Division of Hepatology, Cape Town, South Africa; ¹³Dakar University Hospital, Senegal; ¹⁴University of Health Sciences (UHS), Cambodia; ¹⁵Burnet Institute, Australia; ¹⁶Global Health Diagnostics Laboratory, Burnet Institute, Australia; ¹⁷Université Claude Bernard Lyon, Hospital de la Croix-Rousse, France; ¹⁸The Hepatitis Fund, Switzerland; ¹⁹Department of Pediatrics, Ain Shams University, Egypt Email: dlau@bidmc.harvard.edu

Background and aims: The availability of diagnostic tools and technologies in resource limited settings (RLS) is critical to achieve the WHO 2030 goal to eliminate hepatitis B virus (HBV) as a public health challenge. HBV/hepatitis Delta virus (HDV) coinfection is associated with rapid liver disease progression and is under-diagnosed. Our objective was to assess the perceived priorities for

HBV elimination among healthcare providers and to evaluate the availability of diagnostic tests for HBV and HDV in RLS.

Method: Between Jan-Dec 2022, ICE-HBV launched a global online survey in three languages (English, French, Spanish) to better understand the challenges in delivering HBV care in RLS. The survey had 53 items addressing the priorities to reach the goal for HBV elimination, and the accessibility to diagnostic tests and therapies.

Results: Among the 178 health care worker (HCWs) survey respondents, specialists made up 50%; hepatologists (33%), gastroenterologists (6.9%), and infectious disease physicians (12.2%). The majority of the respondents worked in sub-Saharan Africa (sSA) (37%), South/South East Asia (SEA) (22%), and Europe (EU) (15%). Increasing HBV screening, diagnosis, and optimizing strategies to prevent mother-to-child-transmission (MTCT) were considered the highest priorities in achieving HBV elimination by 80% of responders. Universal HBV screening of pregnant women at antenatal visit were only routinely practiced in 59% of sSA and 66% of SEA settings. HBsAg ELISA testing was reported to be available in all regions, but in only 45% of sSA settings. Unlike HBsAg ELISA, HBsAg rapid diagnostic tests (RDT) were accessible in >90% of sSA regions. Similarly, HBV-DNA quantification with PCR were available in >80% of SEA and EU regions but only in 54% of sSA settings. More than 55% of all responders strongly agreed that an affordable point-of-care (POC) HBV DNA test is necessary in their locations if HBV DNA is in the treatment algorithm. HDV serological (36%) and molecular (34%) testing were the least frequently available diagnostic tests and were particularly low in sSA (Figure). Only 20% of all the respondents reported routine screening for anti-HDV among HBsAg-positive persons and the rates were even lower in sSA (3%) and SEA (12%). HDV-RNA PCR testing was least available in sSA (13%), SEA (20%), and South America (30%). Seventy-one (45%) of respondents reported inadequate training and resources available to HCWs for hepatitis B management in their settings.

Conclusion: Increased HBV screening and optimizing strategies to prevent MTCT were considered the highest priorities in achieving the WHO 2030 goal for HBV elimination. sSA has high HBV prevalence

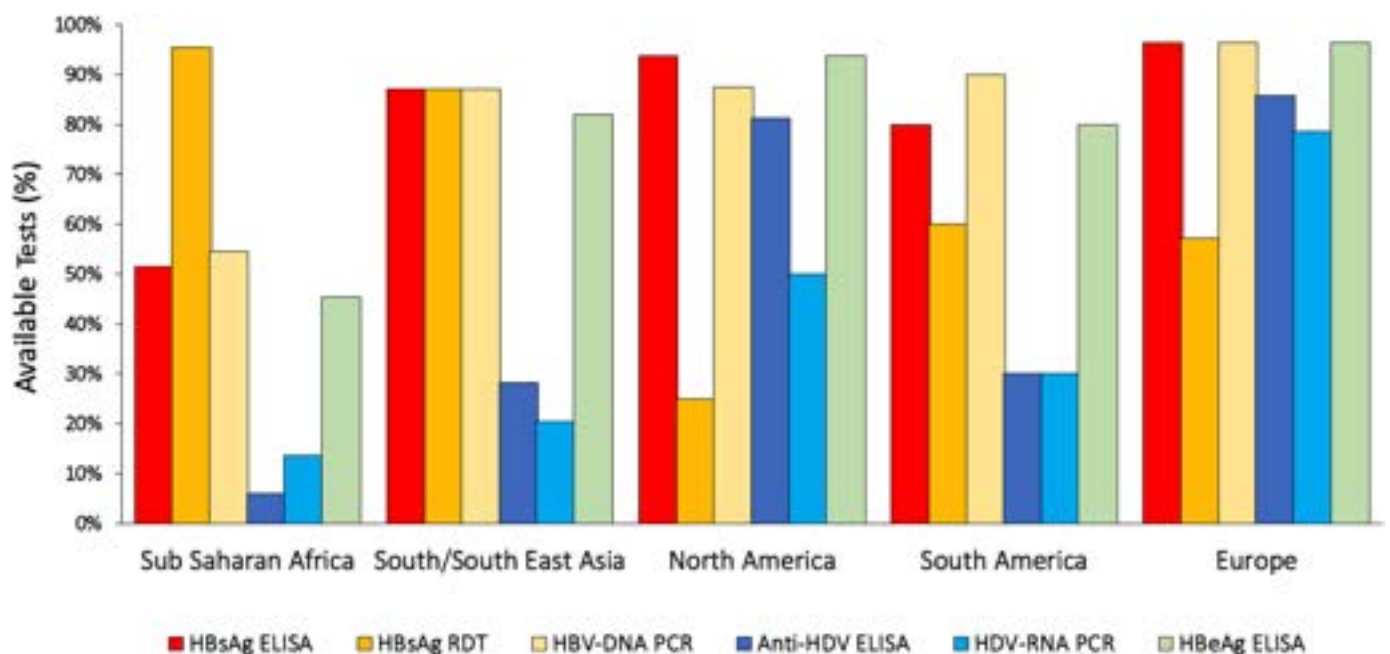


Figure: (abstract: FRI-115): Reported available HBV and HDV diagnostic tools in resource limited settings by regions.

POSTER PRESENTATIONS

but least access to essential HBV screening assays. While effective HDV therapies are becoming available, RLS are not equipped to appropriately screen and diagnose HBV/HDV coinfection, particularly in regions where HDV infection is prevalent. Improved HBV and HDV screening strategies, resources to increase antenatal HBV screening of pregnant women and training for HCWs are urgently needed in RLS to accelerate progress towards the WHO elimination targets.

FRI-116

Population adjusted prevalence of hepatitis delta virus in 21 countries and territories

Devin Razavi-Shearer¹, Kathryn Razavi-Shearer¹, Homie Razavi¹.

¹Center for Disease Analysis Foundation, Lafayette, United States

Email: dravishearercdafound.org

Background and aims: The hepatitis delta virus (HDV), a satellite RNA virus, requires the hepatitis B virus (HBV) for assembly and propagation. Individuals co-infected with HDV progress to advanced liver disease at a faster rate than HBV mono-infected. Recent studies have estimated the global prevalence of anti-HDV among the HBV-infected population at 5–15%. This study aimed to better understand HDV prevalence at the population level in 21 countries and territories.

Method: A comprehensive literature review was conducted for anti-HDV and HDV-RNA-positive prevalence for all countries/territories. Virtual meetings were held with experts from each setting to discuss the literature search findings, collect unpublished data/reports, and weight data for patient segments and regional heterogeneity to estimate the adjusted prevalence in the HBV-infected population. The findings were then combined with The Polaris Observatory HBV data to estimate the overall anti-HDV and HDV-RNA prevalence in each country/territory at the population level.

Results: After adjusting for geographical distribution, disease stage and special populations, the anti-HDV prevalence among the HBsAg+ population changed from the literature estimate in all but three countries. The highest anti-HDV prevalence was in Israel at

6.8% (Table 1). However, once adjusted for HBV+ population and HDV-RNA+, China had the highest absolute number of HDV-RNA+ cases.

Conclusion: We found significantly lower HDV prevalence than previously reported as prior meta-analyses primary focused on studies conducted in groups/regions that have a higher probability of being positive. When available data were weighted appropriately, the anti-HDV prevalence decreased by >50% in many countries. The implementation of reflex testing would result in more accurate estimates while allowing earlier linkage to care for HDV-RNA+ individuals. The burden of reflex testing would be limited as it would only screen HBV+ cases. Cost effectiveness studies of reflex testing will be needed in East Asia where the hepatitis B prevalence is high and HDV prevalence is relatively low.

FRI-117

Prevalence and incidence of delta hepatitis in HIV-HBV coinfecting patients in the Dat'AIDS cohort

Dulce Alfaite¹, Pierre Pradat², Isabelle Poizot Martin³, Eric Billaud⁴, David Rey⁵, Christine Jacomet⁶, Alain Makinson^{7,8,9}, Laurent Cotte¹.

¹Hospices Civils de Lyon, Service des Maladies Infectieuses-Hôpital de La Croix Rousse, France; ²Hospices Civils de Lyon, Centre de Recherche Clinique-Hôpital de La Croix Rousse, France; ³Assistance Publique des Hôpitaux de Marseille, Service des Maladies Infectieuses-Hôpital Sainte Marguerite, France; ⁴Centre Hospitalier Universitaire de Nantes, Service des Maladies Infectieuses, Nantes, France; ⁵Hôpitaux Universitaires de Strasbourg, Trait d'Union, Strasbourg, France; ⁶Centre Hospitalier Universitaire de Clermont Ferrand, Clermont Ferrand, France; ⁷Centre Hospitalier Universitaire de Montpellier, Service des Maladies Infectieuses, Montpellier, France; ⁸INSERM, U1175, Montpellier, France; ⁹Université de Montpellier, Montpellier, France

Email: dulce.alfaite@chu-lyon.fr

Background and aims: The epidemiology of delta hepatitis (HDV) remains largely unknown and there is to date no large multicentric study of its incidence at a country level. We report HDV prevalence,

Table 1. Prevalence of HDV among the HBV+ Population in 21 countries/territories

Country/Territory	2020 HBsAg+	Literature % anti-HDV+	Adjusted % anti-HDV+	% RNA +	Adjusted RNA+ HDV Prevalence	Adjusted RNA+ HDV Cases
Brazil	1,057,700	3.2%	1.7%	75.3%	1.3%	13,600
Canada	223,200	1.6%	4.4%	64.8%	2.9%	6,400
China, Mainland	83,083,000	1.2%	1.2%	66.6%	0.8%	664,000
Colombia	329,000	5.2%	1.0%	69.9%	0.7%	2,300
England	361,900	2.9%	1.0%	50.0%	0.5%	1,800
France	308,400	1.8%	3.5%	75.0%	2.6%	8,100
Germany	226,900	5.5%	3.0%	60.0%	1.8%	4,100
Hong Kong	347,200	0.2%	0.2%	60.0%	0.1%	300
Israel	134,400	6.5%	6.8%	60.0%	4.1%	5,500
Italy	315,100	8.3%	4.2%	60.5%	2.5%	8,000
Japan	562,000	8.5%	0.5%	40.8%	0.2%	1,100
Korea, Republic of	1,409,400	0.3%	0.3%	54.0%	0.2%	2,300
Mexico	122,200	2.4%	0.2%	69.9%	0.2%	200
Portugal	116,600	12.6%	1.5%	72.9%	1.0%	1,200
Romania	622,100	23.1%	2.9%	80.0%	2.3%	14,400
Saudi Arabia	560,500	8.6%	4.0%	60.0%	2.4%	13,400
Spain	249,400	5.2%	2.3%	72.9%	1.7%	4,200
Sweden	30,000	3.8%	2.0%	75.0%	1.7%	500
Taiwan	963,400	3.3%	0.9%	60.0%	0.5%	5,200
Turkey	2,001,100	2.8%	2.8%	68.0%	1.9%	38,100
USA	1,834,600	6.0%	3.0%	66.0%	2.0%	36,300

Figure: (abstract: FRI-116).

incidence and risk factors in a large cohort of people living with HIV (PLWH).

Method: A retrospective analysis was performed in the DataIDS cohort, a nationwide cohort representing roughly half of PLWH in care in France. Demographics, HBV, HDV and HCV serology and individual risk factors were collected. HDV prevalence was determined in patients with chronic hepatitis B infection (CHB) and a known HDV serology result. HDV incidence was determined in patients with at least one consecutive serology following a first negative one.

Results: HBV serology was available in 62473 of 74550 PLWH (83.8%), among whom 3737 had CHB (6.0%). HDV serology was available in 2406 patients with CHB (64.4%), of whom 376 had a positive HDV serology (HDV prevalence rate 15.6%). Among HIV-HBV coinfecting patients, HDV prevalence rate reached 56.5% in IV drug users (IVDU), 38.2% in patients from Eastern Europe and 42.4% in patients coinfecting with HCV. Among HDV-infected patients, blood contact was reported more frequently in patients born outside Africa than in patients from Africa (70.8% vs 10.0%, $p < 0.001$). In a multivariable analysis, male gender (OR 1.5, $p = 0.02$), HIV risk factor IVDU (OR 7.0, $p < 0.001$) or heterosexual sex (OR 1.8, $p = 0.02$), country of origin in Eastern Europe (OR 3.2, $p = 0.002$) or in Africa (OR 2.8, $p < 0.001$) and HCV coinfection (OR 2.9, $p < 0.001$) were positively associated with HDV infection. Conversely, age at HBV diagnosis (OR 0.96/year, $p < 0.001$) and duration of HBV infection (OR 0.84/year, $p < 0.001$) were negatively associated with HDV infection. HDV serology was positive at first determination in 349 patients (prevalent HDV 92.8%) while 27 patients acquired HDV during follow-up (incident HDV 7.2%). Repeated HDV serology results were available in 1827 patients for a

total follow-up of 21006 patient-years (PY). HDV incidence rate was 0.12/100 PY (95%CI 0.08–0.18)–see Figure. For incident HDV infections, the median time separating HBV and HDV diagnoses was 11.4 years and these patients had similar demographics and characteristics than patients with prevalent HDV apart from older age at HDV diagnosis (48.0 years vs 37.3 years, $p < 0.001$).

Conclusion: HDV coinfection is common in HIV-HBV coinfecting patients in France. Most HDV infections are prevalent infections, but some incident infections occurred during follow-up indicating that HDV transmission is still present in this population. Patients born in Africa or in Eastern Europe, IVDU and HBV-HCV coinfecting patients are high-risk populations for HDV infection and should be targeted for systematic screening.

FRI-118

Patients with persistently abnormal liver biochemistry are under-investigated and can be rapidly identified using a novel case-finding database

Almuthana Mohamed¹, Christina Owen¹, Sarah Gormley¹, Waqas Khan¹, Emma Wesley¹, Timothy Jobson¹. ¹Musgrove Park Hospital, Somerset NHS Foundation Trust, Gastroenterology, Taunton, United Kingdom

Email: almuthana700@gmail.com

Background and aims: Chronic liver disease (CLD) continues to increase in prevalence. However, it remains underdiagnosed, with many patients missing opportunities for treatment. Guidelines state that patients with persistently abnormal liver chemistry should have a non-invasive liver screen (NILS) to identify potentially treatable causes of CLD. Unfortunately, in practice, these guidelines are often

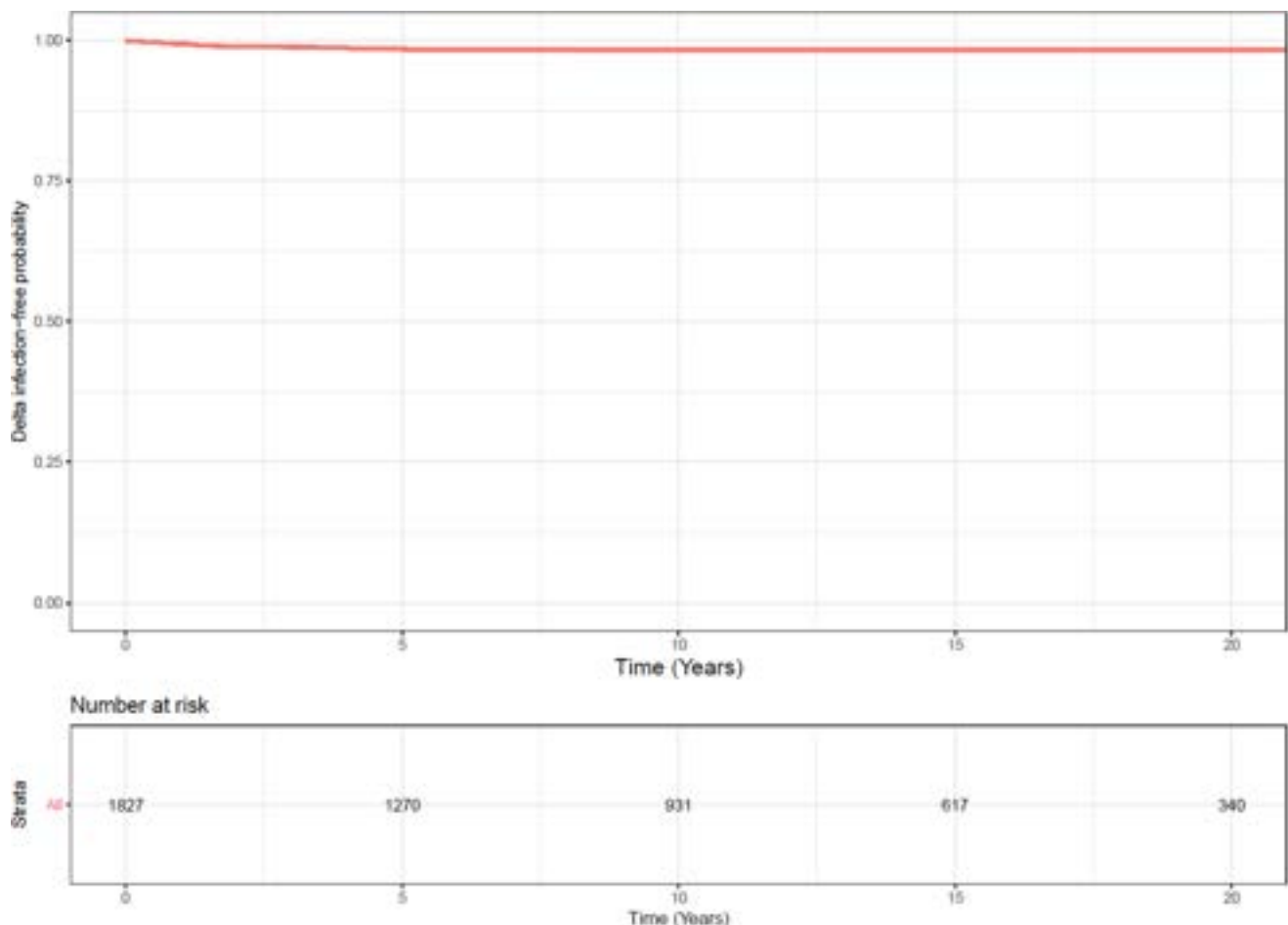


Figure: (abstract: FRI-117).

POSTER PRESENTATIONS

not followed. We have developed a novel case-finding database in Somerset, UK, currently with data on 560,000 individuals. We used this system to identify patients with persistently abnormal liver chemistry and quantify the completeness of subsequent investigation.

Method: Using data up to 31/12/2020, the case finding database was configured to identify patients between the ages of 30 and 75 with persistently abnormal liver chemistry (last ALT >40 IU/L and abnormal for at least the preceding 90 days). Within that cohort we further risk stratified to identify those with more concerning results (ALT >80; ALP >90; ALP >130; both ALT >80 and ALP >130). The number of patients in each group with a complete 'basic' NILS (defined as viral hepatitis B, C; autoimmune screen; ferritin; AST) was determined. The screen was considered complete if these tests were found within a six-month period (based on ferritin date as the commonest test). A sample of cases was reviewed manually to confirm the accuracy of the results. We also assessed which age cohorts were more likely to have persistently abnormal liver chemistry and if there was any difference in age and likelihood of having had the 'basic' NILS.

Results: 8224 males and 2537 females were identified as having persistently elevated liver biochemistry. Only 11% of males and 16% of females had a complete 'basic' NILS using our definition. 5% of men and 6% of women were deceased, with no difference in the investigation rate. Persistently abnormal LFTs were most likely to be identified in the age 50–59 cohort for both men and women. There was no significant difference in the likelihood of having a NILS when different age groups were compared. In the higher risk group (abnormal tests at least 90 days, last ALT >80, last ALP >130), there were a total of 547 patients identified, of whom 442 had never had a NILS (81%). The slight trend towards improved investigation in higher-risk groups was not statistically significant (Figure 1).

Conclusion: Our data confirm that patients with persistently abnormal liver chemistry are frequently not investigated, with a high likelihood of missed opportunities for treatment. Our novel case-finding database can rapidly identify in seconds nearly 9000 individuals who may benefit from further investigation. Furthermore, the system can be used to easily risk stratify these patients for more targeted interventions. Further work is needed to implement processes to identify those needing specialist treatment.

FRI-119

Care cascade for children with hepatitis C virus exposure in the United States and implications of early ribonucleic acid testing

Megan Curtis^{1,2,3,4}, Benjamin Buzze⁵, Benjamin Linas^{4,5}, Andrea Ciaranello^{1,3}, Rachel Epstein^{4,5}. ¹Massachusetts General Hospital, Boston, United States; ²Brigham and Women's Hospital, United States; ³Harvard Medical School, Boston, United States; ⁴Boston University School of Medicine, United States; ⁵Boston Medical Center, United States

Email: meg.rose.curtis@gmail.com

Background and aims: An estimated 3.26 million children and adolescents are living with hepatitis C virus (HCV) globally. The World Health Organization (WHO) recommends simplification of HCV care pathways to overcome low rates of detection and linkage among children with HCV. The United States (US) Centers for Disease Control and Prevention (CDC) has proposed simplified draft recommendations for ribonucleic acid (RNA) testing at ≥2–6 months for infants who are perinatally exposed to HCV. Current US guidelines for perinatally exposed infants recommend antibody testing at age 18 months. However, this approach is associated with high rates of loss to follow-up. Our objective was to characterize infant HCV testing patterns, linkage to care, and possible impact of the CDC draft recommendations.

Method: From TriNetX, a network of electronic health record data with approximately 90 million individuals from US healthcare organizations, we identified a cohort of children born 2010–2020 with an International Classification of Diseases (ICD) code for exposure to viral hepatitis (Z20.5). We defined presumed HCV exposure by excluding children with only hepatitis B virus testing. We calculated the number of children with any testing, complete testing, HCV infection, and HCV treatment. Testing was considered complete if one of the following criteria were met: negative antibody test at any age, positive antibody test at 18 months or greater followed by at least 1 RNA test, two positive RNA tests, or two negative RNA tests.

Results: Our cohort included 8517 children with presumed HCV exposure. Of those, 3899 (46%) had any HCV testing: 2041 (52%) had antibody testing, 980 (25%) had RNA testing, and 878 (23%) had both. Among those with complete testing, 125 (4%) children were identified with HCV infection, of whom 9 (7%) were linked to treatment. Of those with incomplete testing, 51 children had one positive RNA test

Figure1: Patients with abnormal liver chemistry

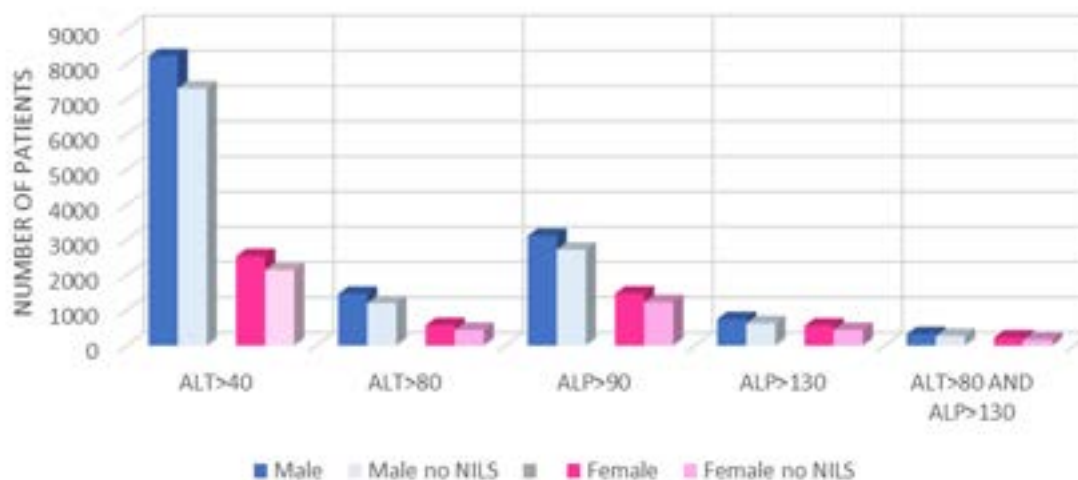


Figure: (abstract: FRI-118).

with no follow-up testing. These children would have been identified for early linkage by CDC draft recommendations but were lost to follow-up under current guidelines for antibody testing at 18 months.

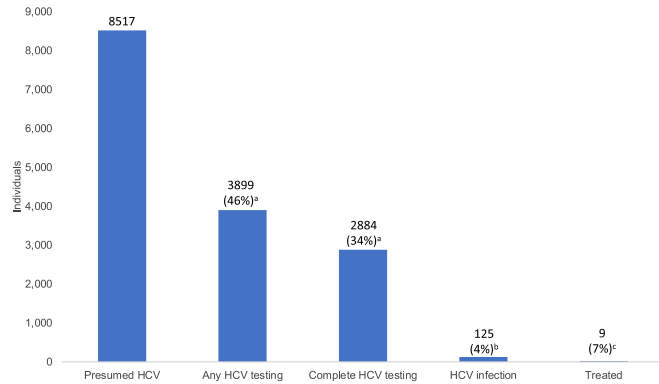


Figure: Current testing and treatment rates for children with presumed HCV exposure in the United States.
Percentage of total with HCV exposure.
Percentage of those with complete HCV testing.
Percentage of those with HCV infection.

Conclusion: Fewer than half of children identified with ICD codes for presumed HCV exposure in this cohort were tested, and very few children with HCV were treated. This analysis shows that some physicians are already offering early HCV RNA testing in exposed infants, and that this could capture more cases when compared to waiting until 18 months to complete antibody testing per current guidelines. The CDC's draft recommendation for RNA testing could improve identification of perinatal HCV and advance efforts towards HCV elimination in alignment with WHO goals.

FRI-120

Opt-out testing for hepatitis B and C infections in adults attending the emergency department of a London Hospital

Jingwei Zeng^{1,2}, Douglas Macdonald³, Russell Durkin⁴, Dianne Irish¹, Jennifer Hart¹, Tanzina Haque¹. ¹Royal Free Hospital, Department of

Virology, London, United Kingdom; ²Royal Free London NHS Foundation Trust, Department of Virology, London, United Kingdom; ³Royal Free Hospital, Department of Hepatology, London, United Kingdom; ⁴Royal Free Hospital, Emergency Department, London, United Kingdom
Email: thaque@nhs.net

Background and aims: The National Health Service in England commissioned opt-out testing in all London emergency departments (ED) to allow early identification and management of hepatitis B (HBV) and hepatitis C virus (HCV) infection in patients unaware of their HBV or HCV status. This retrospective study evaluates the effectiveness of this new ED hepatitis virus screening programme at the Royal Free Hospital in northwest London.

Method: All adults over the age of 16 undergoing blood tests in the ED at the Royal Free Hospital were tested for HBV surface antigen (HBsAg) and anti-HCV IgG antibody unless they opted out. A streamlined screening protocol was developed with input from ED, Virology and Hepatology departments to ensure follow-up of patients with positive results. Data was collected from the 12th of April 2022 to the 22nd of August 2022.

Results: Of 11,215 patients tested for HCV, 164 patients were found to be anti-HCV IgG positive (Table 1), giving a seroprevalence rate of 1.46%. 69% of HCV seropositive patients were male and 31% were female (Odds ratio (OR) 2.54; 95% confidence interval (CI) 1.82–3.54). 52 of the HCV IgG positive patients did not have previous HCV serology results on our system. In total, 23 of the HCV IgG positive patients were HCV RNA positive (RNA seroprevalence 0.2%), and 17 of those were new diagnoses of HCV viraemia. The most common HCV genotype was genotype 1a (39%), followed by genotype 3a (30%) and genotype 1b (13%); genotypes 4a and 4v constituted 4% each. At the time of this study, 14 patients (82%) with new diagnosis of HCV were contacted by the Hepatology team; median time to the first recorded attempted contact was 4 days (range 2 to 43 days) and 5 patients have been started on treatment. For HBV screening, 82 out of 11,192 patients tested were found to be HBsAg positive (prevalence 0.73%; male 55% and female 45%; OR 1.38; 95% CI 0.89–2.13), including one patient who presented acutely with a positive HBV core IgM. 39 of the HBsAg positive patients were previously unknown to us; of these, 9 had an HBV viral load of >2000 IU/ml, including 3 patients with

	Anti-HCV IgG	HCV RNA	HBsAg	HBeAg	Anti-HBe IgG	HBV DNA	Anti-HDV Antibody
Patients	11, 215	161	11, 192	82	82	40	39
Tested							
Positive	164	23	82	4	78	37	1
Sex							
Male	113	15	45	3	42	18	0
Female	51	8	37	1	36	19	1
Age							
16-35	11	3	10	0	10	4	0
36-55	61	9	34	1	33	19	0

Table: (abstract: FRI-120).

POSTER PRESENTATIONS

positive HBV e antigen (HBeAg) and one patient with hepatitis D virus (HDV) co-infection (Table 1). 38 (97%) of these new patients were contacted by the Hepatology team during the study period.

Conclusion: Opt-out screening of HBV and HCV in ED is effective at detecting previously unknown cases of infection and helps to identify patients who needed a link to care. HCV RNA prevalence was lower in our study at 0.21%, compared with RNA prevalence of 0.93% in a similar study conducted at our hospital in 2015 (Cieply et al., 2019), despite a similar HCV IgG seroprevalence (1.46% vs 1.63%).

FRI-121

Estimation of prevalence of chronic HCV infection in EU/EEA countries using multiparameter evidence synthesis

Ilias Gountas¹, Christos Thomadakis¹, Erika Duffell², Konstantinos Gountas¹, Benjamin Bluemel², Thomas Seyler³, Filippo Pericoli³, Dominique Van Beckhoven⁴, Els Plettingckx⁴, Thomas Vanwolleghem^{5,6}, Tonka Varleva⁷, Diana Nonkovic⁸, Mirjana Lana Kosanovic Licina⁹, Tatjana Nemeth-Blazic¹⁰, Fani Theophanous¹¹, Peer Brehm Christensen¹², Susan Cowan¹³, Kristi Rüütel¹⁴, Cécile Brouard¹⁵, Ruth Zimmermann¹⁶, Sandra Dudareva¹⁶, Georgia Nikolopoulou¹⁷, Zsuzsanna Molnár¹⁸, Emese Kozma¹⁸, Magnús Gottfredsson^{19,20}, Niamh Murphy²¹, Renate Putnina²², Ligita Jancoriene²³, Carole Devaux²⁴, Tanya Melillo²⁵, Marc van der Valk²⁶, Eline Op de Coul²⁷, Hilde Klovstad²⁸, Robert Neil Whittaker²⁸, Małgorzata Stepień²⁹, Magda Rosinka²⁹, Odette Popovici³⁰, Maria Avdicova³¹, Jana Kerlik³¹, Mojca Maticic³², Asuncion Diaz³³, Julia del Amo³⁴, Georgios Nikolopoulos¹, ¹University of Cyprus, Medical School, Cyprus;

²European Centre for Disease Prevention and Control, Sweden;

³European Monitoring Centre for Drugs and Drug Addiction, Portugal;

⁴Sciensano, Department of Epidemiology and Public Health, Belgium;

⁵University of Antwerp, Viral Hepatitis Research Group, Laboratory of

Experimental Medicine and Pediatrics, Belgium; ⁶University Hospital

Antwerp, Department of Gastroenterology and Hepatology, Belgium;

⁷Medical University, Pleven, Bulgaria; ⁸Teaching Institute of Public

Health Split and Dalmatia County, University of Split, Department of

Health Studies, Croatia; ⁹Andrija Stampar Teaching Institute of Public

Health, Communicable Disease Epidemiology Department, Croatia;

¹⁰Croatian Institute of Public Health, Croatia; ¹¹Ministry of Health,

Cyprus, Cyprus; ¹²Odense University Hospital, Department of Infectious

Disease, Denmark; ¹³Statens Serum Institut, Department of Infectious

Disease Epidemiology and Prevention, Denmark; ¹⁴National Institute of

Health Development, Estonia, Infectious Diseases and Drug Monitoring

Department, Estonia; ¹⁵Santé Publique France, Infectious Diseases

Direction, HIV, Hepatitis B/C, STI Unit, France; ¹⁶Robert Koch Institute,

Germany; ¹⁷Hellenic National Public Health Association, Greece;

¹⁸National Public Health Center, Hungary, Hungary; ¹⁹University of

Iceland, Faculty of Medicine, School of Health Sciences, Iceland;

²⁰Landsþítali University Hospital, Iceland; ²¹Health Protection

Surveillance Centre, Ireland, Ireland; ²²Center for Disease Control and

Prevention, Latvia, Latvia; ²³Vilnius University, Clinic of Infectious

Diseases and Dermatovenereology, Institute of Clinical Medicine, Medical

Faculty, Lithuania; ²⁴Luxembourg Institute of Health, Department of

Infection and Immunity, Luxembourg; ²⁵Ministry for Health, Health

Promotion and Disease Prevention, Malta, Department for Health

Regulation, Malta; ²⁶University of Amsterdam, Department of Infectious

Diseases, Amsterdam Infection and Immunity Institute (AlandII),

Amsterdam UMC, Netherlands; ²⁷National Institute for Public Health

and the Environment (RIVM), Netherlands; ²⁸Norwegian Institute of

Public Health, Section for Respiratory, Blood-Borne and Sexually

Transmitted Infections, Department of Infection Control and Vaccines,

Norway; ²⁹National Institute of Public Health NIH-National Research

Institute, Poland, Department of Infectious Diseases Epidemiology and

Surveillance, Poland; ³⁰National Institute of Public Health Romania,

National Centre for Surveillance and Control of Communicable Diseases,

Romania; ³¹Regional Authority of Public Health Banská Bystrica,

Slovakia, Slovakia; ³²University of Ljubljana, Clinic for Infectious

Diseases, University Medical Centre Ljubljana and Faculty of Medicine, Slovenia; ³³National Centre of Epidemiology, Carlos III Health Institute, CIBER in Infectious Diseases (CIBERINFEC), Spain; ³⁴Ministry of Health, Spain, Division for HIV, STI, Viral Hepatitis and Tuberculosis Control, Spain

Email: nikolopoulos.georgios@ucy.ac.cy

Background and aims: In Europe, hepatitis C virus (HCV) infection affects both the general population and specific groups, including people who inject drugs (PWID). Although countries have HCV prevalence estimates in the general population and/or specific population groups, those alone cannot be directly used to obtain a national estimate. Our aim was to estimate the national prevalence of chronic HCV infection (CHCV) and the contribution of injection drug use in the European Union (EU)/European Economic Area (EEA) countries in 2019.

Method: Multi-parameter evidence synthesis (MPES) is an approach that combines simultaneous information to derive an overall estimate. MPES was applied to each country to obtain national estimates. The overall CHCV prevalence (π) in the population was defined as: $\pi = \pi_{\text{rec}}\rho_{\text{rec}} + \pi_{\text{ex}}\rho_{\text{ex}} + \pi_{\text{non}}\rho_{\text{non}}$. The parameters π_{rec} , π_{ex} and π_{non} represent CHCV prevalence among recent PWID (injecting behavior in the last 12 months), ex-PWID, and non-PWID, respectively, while the parameters ρ_{rec} , ρ_{ex} and ρ_{non} represent the proportion of recent, ex-PWID, and non-PWID in the overall population. π_{rec} was provided by the ECDC (European Centre for Disease Prevention and Control) hepatitis national focal points (NFP), the EMCDDA (European Monitoring Centre for Drugs and Drug Addiction) databases or the published literature. CHCV prevalence among ever PWID was needed to indirectly calculate π_{ex} and was obtained through the EMCDDA databases or the NFP. π_{non} was obtained from an ECDC review or by the NFPs. A multi-state Markov model was used to estimate the number of recent and ex-PWID. Adjustment for treatment with direct-acting antivirals (DAAs) was made when appropriate. The national estimates were combined to obtain regional estimates. NFPs from 26 EU/EEA countries provided feedback.

Results: The overall CHCV (HCV RNA positive) prevalence in EU/EEA countries at the end of 2019 was 0.54% (95% credible interval-CrI: 0.50%, 0.59%). The highest and lowest CHCV prevalence were observed in the East (0.89%; 95% CrI: 0.82%, 0.96%) and the West (0.26%; 95% CrI: 0.20%, 0.35%) of EU/EEA. On country level, the Netherlands (0.04%), Slovenia (0.07%), and Iceland (0.1%) had the lowest CHCV prevalence. The highest CHCV prevalence was estimated in Romania (2.26%) and Estonia (1.71%). Still, the majority of the EU/EEA countries have a CHCV prevalence in 2019 of less than 1%. The model estimates that 37.6% (95% CrI: 35.1%, 40.3%) of the 2019 CHCV prevalence in EU/EEA countries is associated with injection drug use.

Conclusion: The overall CHCV prevalence among EU/EEA is relatively low but substantial part of the HCV burden is due to injection drug use. Countries in the east of the EU have the highest CHCV prevalence. Further efforts to monitor, prevent, and control CHCV, especially in this region and among PWID, are needed.

FRI-122

One step closer to the goal: mobile InfoHep centre offering detection, protection, prevention and treatment/linkage-to care services in Croatian penalty institutions

Tatjana Reic¹, Magda Pletikosa Pavić², Diana Nonkovic², Ana Visić¹, Anna Mrzljak³. ¹Croatian Society for the Liver Diseases "Hepatos", Croatia; ²Teaching Institute for Public Health Split-Dalmatia County, Croatia; ³University Hospital Center Zagreb, Croatia
Email: tatjana@hepatos.hr

Background and aims: In Croatia, during the COVID-19 pandemic, activities related to the prevention, testing, and treatment of viral hepatitis in penalty institutions were significantly limited. Given the high HCV prevalence in incarcerated settings, screening and planning further treatments is highly important. Aiming to provide linkage-to-

care services, NGO Hepatos implemented an HCV pilot project within Croatian penalty institutions.

Method: Hepatos has been providing services within the penalty system since 2009 as the only organization in the Western Balkans with a FibroScan® device as part of the Mobile InfoHep Center (MIHC) clinic. In cooperation with the Croatian Gastroenterological Society and Public Health Institute Split-Dalmatia County, an 18-month (Jun 2021–Dec 2022) project was implemented offering services to the 7 Croatian penalty institutions. Services included: screening, HCV and/or HIV testing, on-spot liver examination by FibroScan®, consultation, and referral of HCV+ prisoners to local specialists for the diagnostic workup necessary for the DAA approval by the Croatian Health Insurance Fund. The Ministry of Justice of the Republic of Croatia granted consent for the project.

Results: Linkage-to-care services were offered to 368 prisoners (287 male and 81 female). The response rate was 85%, with 313 prisoners (251 male and 62 female). Personal issues were the main reasons for the drop-out. 847 MIHC services included 313 hepatitis counseling, 130 HCV and 69 HIV testing, 299 on-site liver exams by FibroScan®, and 36 referrals to further diagnostic workup. In total, 2.2% of prisoners reported previous/current HCV infection. Out of the tested, 19 (14.6%) prisoners were HCV positive, and all were HIV negative. The mean liver stiffness measurement (LMS) and controlled attenuation parameter (CAP) were 6.15 ± 3.97 kPa and 264.99 ± 57.1 dB/m. Most prisoners (55.9%) had no fibrosis, whereas stage F1 to F4 was detected in 24.7%, 12%, 5%, and 2.3% of prisoners, respectively. FibroScan® was performed in 17 out of 19 HCV+ prisoners. Among HCV+ prisoners, fibrosis stage distribution (F1–F4) was 35.3%, 29.4%, 17.6%, and 11.8%, respectively. The LMS was significantly higher in HCV+ than in HCV- prisoners (10.97 ± 11.07 kPa vs. 6.27 ± 3.41 kPa, $p = 0.001$), whereas CAP did not differ. All HCV+ prisoners and HCV- prisoners ($n = 17$) with advanced fibrosis were referred to liver specialists.

Conclusion: The referral of prisoners to treating physicians represents a humble but vital contribution to the WHO's goal of HCV elimination. NGOs, medical experts and governmental bodies included in multi stakeholder's approach, through the Force of Four services (detection, protection, prevention, and treatment) within penalty institutions, may add one step closer. This linkage-to-care model brings change to HCV+ prisoners as it ensures that no one is left behind on our road to HCV elimination.

FRI-123

Late presentation of chronic hepatitis C for care in Georgia: data from the national hepatitis C elimination program, 2016–2021

Tengiz Tsertsvadze^{1,2}, Nikoloz Chkhartishvili¹, Shaun Shadaker³, Akaki Abutidze^{1,2}, Lali Sharvadze^{2,4}, Amiran Gamkrelidze⁵, Irina Tskhomelidze⁶, Senad Handanagic³, Tamar Gabunia⁷. ¹Infectious Diseases, AIDS and Clinical Immunology Research Center, Georgia; ²Ivane Javakishvili Tbilisi State University, Georgia; ³Centers for Disease Control and Prevention, Division of Viral Hepatitis, National Center for HIV, Hepatitis, STD and TB Prevention, Atlanta, United States; ⁴Hepatology Clinic HEPA, Georgia; ⁵National Center for Disease Control and Public Health, Georgia; ⁶The Task Force for Global Health, Georgia; ⁷Ministry of IDPs from the Occupied Territories, Labour, Health and Social Affairs of Georgia, Georgia

Email: tt@aidscenter.ge

Background and aims: Timely diagnosis and treatment of hepatitis C reduces liver-related morbidity and mortality as well as prevents onward transmission of the virus. We aimed to assess trends in late presentation for hepatitis C care in Georgia since the launch of the national hepatitis C elimination program.

Method: Data were extracted from the national hepatitis C elimination program database. Analysis included treatment-naïve persons with chronic hepatitis C enrolling in the elimination program during January 1, 2016 to December 31, 2021. Late presentation was defined as significant fibrosis assessed by either FIB-4 score >3.25 or transient elastography >9.5 kPa. Trends were assessed using Kendall Tau-B test. Comparisons between population characteristics for patients with and without late presentation were tested using Pearson's Chi-square test.

Results: Among 72,187 persons who enrolled in the elimination program during the study period, 55,822 (77.3%) were men and 41,057 (56.9%) were in the age category of 40–59 years. A total of 19,842 (27.5%) met criteria for late presentation. The rate of late presentation declined from 30.6% in 2016 to 24.3% in 2020 and then increased to 29.0% in 2021 (p for trend <0.0001). Rates of late presentation increased with age, from a low of 2.7% in those aged 18–29 years to a high of 50.2% among people aged ≥ 60 years ($p < 0.0001$). Women had a higher percentage of late presentation 28.8% vs. 27.1%, $p < 0.0001$. Women were the only population sub-group with no statistically significant changes in late presentation over the study period (from 29.9% in 2016 to 31.2% in 2021, p for trend = 0.41). Higher percentages of late presentation were observed among: alcohol consumers (32.2% vs. 23.1%, $p < 0.0001$), people with BMI ≥ 25 (29.8% vs. 19.4%, $p < 0.0001$), and those with diabetes mellitus (48.1%

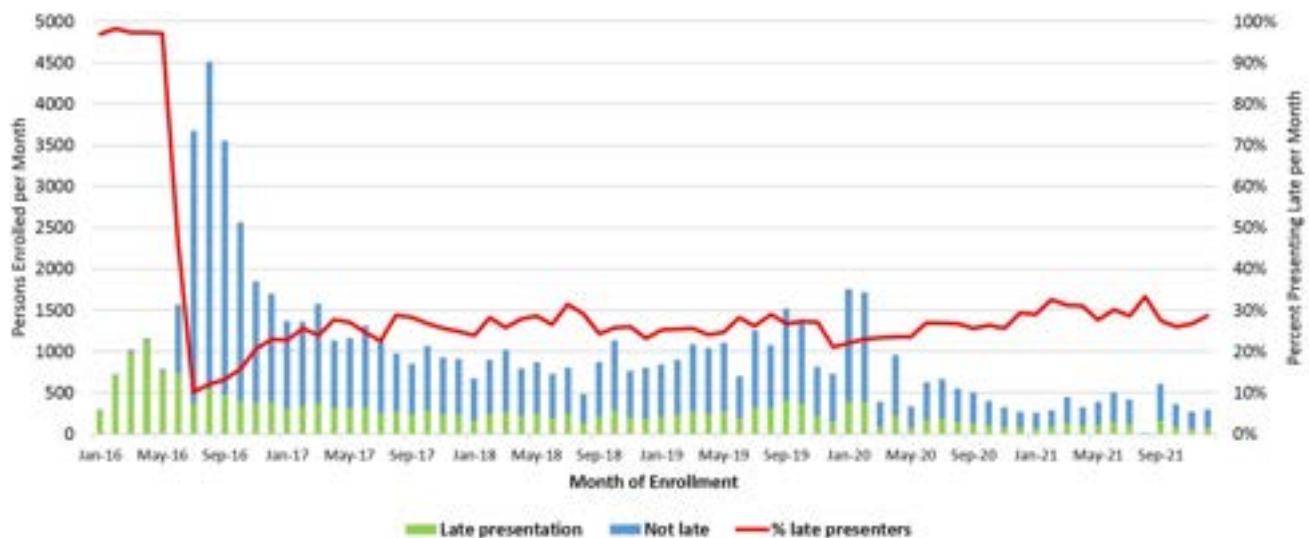


Figure: (abstract: FRI-123): Trends in late presentation by month of enrolment, Jan 2016–Dec 2021.

POSTER PRESENTATIONS

vs. 24.7%, $p < 0.0001$). Incarcerated persons had a lower percentage of late presentation (18.0% vs. 27.0%, $p < 0.0001$). No statistically significant differences were found among those reactive for hepatitis B surface antigen (24.5% vs. 25.7%, $p = 0.28$).

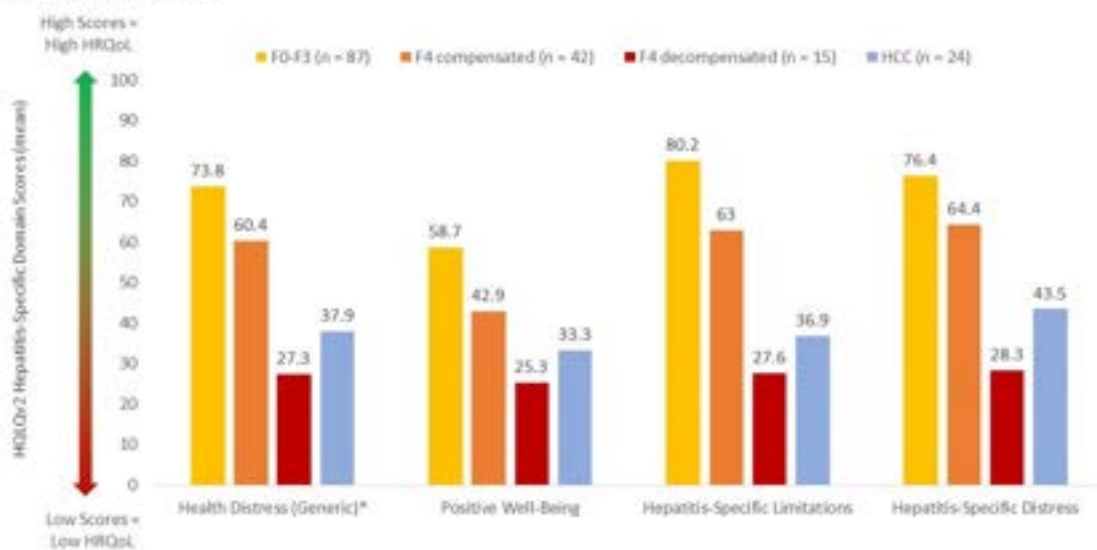
Conclusion: Despite statistically significant changes in percentages among sub-groups and trend over time, late presentation for hepatitis C care remains a significant problem emphasizing a need for improving testing and linkage to care. Targeted interventions among women, older people, alcohol consumers and those with metabolic disorders can reduce late presentation.

FRI-124

The impact of hepatitis D virus infection on health-related quality of life and fatigue in patients untreated for HDV: descriptive results from a cross-sectional study across Italy, Germany, Spain and the US

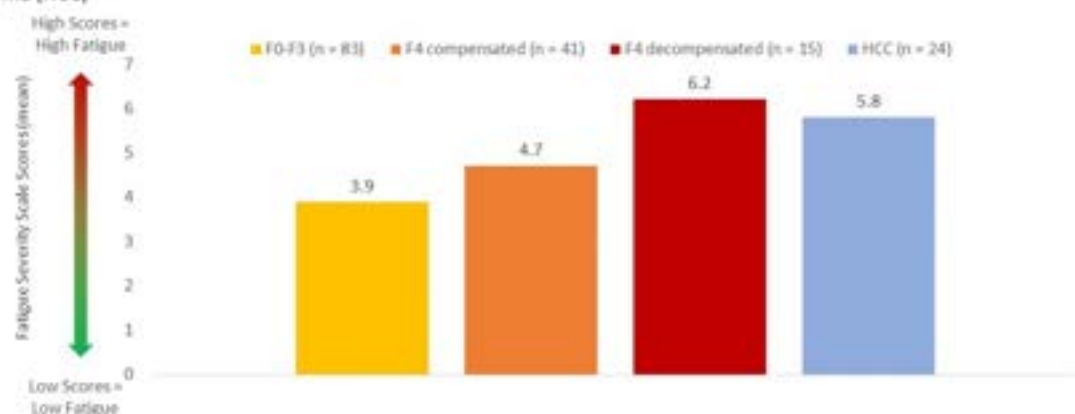
Pietro Lampertico^{1,2}, Robert G. Gish³, Nancy S. Reau⁴, Heiner Wedemeyer⁵, Maria Buti⁶, Ankita Kaushik⁷, Laura Mirams⁸, Hilary Ellis⁸, Teresa Taylor-Whiteley⁸, Alon Yehoshua⁷. ¹Foundation IRCCS Ca' Granda Ospedale Maggiore Policlinico, Division of Gastroenterology and Hepatology, Milan, Italy; ²CRC "A. M. and A. Migliavacca" Center for Liver Disease, Department of Pathophysiology and Transplantation, Milan, Italy; ³Hepatitis B Foundation, Doylestown,

A: Mean HQLQv2 scores in patients with F0-F3, F4 compensated, F4 decompensated fibrosis and in patients with hepatocellular carcinoma (HCC)



*Due to missing data the overall sample size for HQLQv2 Health Distress domain was n = 166.

B: Mean FSS scores in patients with F0-F3, F4 compensated, F4 decompensated fibrosis and in patients with hepatocellular carcinoma (HCC)



Due to missing data the overall sample size for the FSS was n = 163

HQLQv2: Hepatitis Quality of Life Questionnaire Version 2

FSS: Fatigue Severity Scale

HCC: Hepatocellular carcinoma

Figure: (abstract: FRI-124).

United States; ⁴Rush Medical College, Department of Internal Medicine, Division of Digestive Diseases and Nutrition, Chicago, United States; ⁵Hannover Medical School, Department of Gastroenterology, Hepatology, and Endocrinology, Hannover, Germany; ⁶Hospital Universitario Valle Hebrón and Ciber-ehd del Instituto Carlos III, Liver Unit, Barcelona, Spain; ⁷Gilead Sciences, California, United States; ⁸Adelphi Real World, Macclesfield, United Kingdom
Email: laura.mirams@adelphiigroup.com

Background and aims: Hepatitis D virus (HDV) is associated with accelerated progression to advanced liver disease compared to mono-infection with hepatitis B (Fattovich, et al. 2000). Poorer overall prognosis may result in reduced health-related quality of life (HRQoL) relative to the general population and other hepatitis infections (Buti et al., 2021), however there is limited evidence regarding the effect of HDV on HRQoL. This study aimed to understand the impact of HDV infection at various stages of fibrosis by investigating HRQoL among untreated patients living with chronic HDV.

Method: A cross-sectional survey including the Hepatitis Quality of Life Questionnaire (HQLQv2) and the Fatigue Severity Scale (FSS) was completed by adults with a physician confirmed diagnosis of chronic HDV infection in Italy, Germany, Spain, and the US between July–November 2022. Patients who were heavily immunocompromised, received interferon (IFN)/peg-IFN in the past six months, were diagnosed with human immunodeficiency virus or hepatitis C, or had received an organ transplant were not included. Patients receiving any licensed HDV treatment were also excluded for this analysis.

Results: Descriptive results from a group of 168 patients (74% male, mean age = 52.8) who were not receiving treatment indicated for HDV are presented. This group included patients across all fibrosis stages, F0–F3 (52%), F4 compensated (F4C, 25%), F4 decompensated (F4D, 9%) and 24 (14%) patients with concomitant hepatocellular carcinoma (HCC). The majority of patients (81%) had been diagnosed with HDV between 0 and 5 years. HQLQv2 scores were lowest in patients with F4C and F4D cirrhosis across all domains (Figure 1), suggesting that HRQoL worsens as the disease progresses. All HDV patients regardless of fibrosis stage suffered from fatigue, which was severe in F4C (4.7), F4D (6.2), and HCC (5.8) patients, as defined by a mean FSS score of ≥ 4 (Rossi et al. 2017) and also seemed to have worsened with higher disease severity.

Conclusion: This study demonstrates that HRQoL and fatigue scores were detrimentally impacted by HDV regardless of fibrosis stage, but the impact is greater in later stages and in those with a concomitant HCC diagnosis. Newer treatment interventions which slow down disease progression could be considered to lower the impact of HDV on HRQoL and fatigue.

FRI-125

The impact of Covid-19 on hepatocellular carcinoma screening in British Columbia

Makuza Jean Damascene^{1,2}, Stanley Wong³, Mawuena Binka⁴, Maryam Darvishian⁵, Dahn Jeong^{1,6}, Prince Adu⁶, Georgine Cua², Amanda Yu³, Hector Velasquez^{1,2}, Maria Alvarez⁷, Sofia Bartlett³, Eric Yoshida⁸, Alnoor Ramji⁸, Mel Krajden³, Naveed Janjua^{1,3,9}. ¹The University of British Columbia, School of Population and Public Health, Vancouver, Canada; ²BC Centre for Disease Control, Clinical Prevention Services, Vancouver, Canada; ³BC Centre for Disease Control, Clinical Prevention Services, Vancouver, Canada; ⁴BC Centre for Disease Control, Clinical Prevention Services, Vancouver, Canada; ⁵BC Cancer Research Centre, Vancouver, Canada; ⁶BC Centre for Disease Control, Vancouver, Canada; ⁷BC Centre for Disease Control, Vancouver, Canada; ⁸The University of British Columbia, Division of Gastroenterology, Vancouver, Canada; ⁹St. Paul's Hospital, Centre for Health Evaluation and Outcome Sciences, Vancouver, Canada
Email: makorofr@gmail.com

Background and aims: Hepatocellular carcinoma (HCC) has the second highest incidence among all cancers in Canada. Individuals with HCV who have cirrhosis should be screened twice yearly for HCC

in Canada. Coronavirus disease 2019 (COVID-19) has disrupted many health services globally since 2020, including HCC screening among eligible individuals. We assessed the impact of the COVID-19 pandemic on HCC screening using surveillance data from the BC-Hepatitis Testing cohort (BC-HTC).

Method: We performed a retrospective cohort study using data from the BC-HTC, which includes about 1.7 million individuals tested for HCV or HIV or reported as a case of HCV, HIV, or HBV from January 1990 to December 31, 2015. Our primary outcome was HCC screening among individuals with HCV and cirrhosis according to Canadian guidelines. In our dataset, HCC screening was flagged by the first HCC-related medical screening following the initial cirrhosis diagnosis with liver or abdomen ultrasound and CT scan if the ultrasound is unclear among individuals with HCV. We summarized the number of individuals screened each month between March 2018 and December 2020. We included interruption on March 2020 when the BC government implemented COVID-19 restriction measures. We conducted interrupted time-series (ITS) analysis using a segmented linear regression model to assess the impact of COVID-19 and included first-order auto-correlation terms to control for data correlation.

Results: Overall, 7809 HCC screenings were performed among 1641 individuals living with HCV and cirrhosis. Among these screenings, 6168 (78.98%) were conducted from March 2018 to December 31, 2020 and 1,476 (23.84%) during the COVID-19 period (March 2020–December 2020). During the study period, the average monthly number of individuals screened was 181. Number of individuals screened dropped to 138 in March 2020 and 54 in April 2020 (72% drop from April 2019), the lowest point during pandemic, then started to recover with 129 screening in May 2020. The ITS also showed an immediate decline in March 2020 and a sharp decline in April 2020, with some recovery afterward. The decline was not shown in individuals non-treated for HCV and those under 45 years of age.

Conclusion: There was a sharp decline in the number of individuals with HCV with cirrhosis screened for HCC immediately after implementing public health measures, with recovery later in 2020.

FRI-126

HCV screening automation at hospitals level based on extrahepatic manifestations and risk profile. Preliminary results from the Hospitals without_C programme (hospitales sin C)

Antonio Garcia Herola¹, Sonia Pascual^{2,3}, Rubén Cuesta⁴, Mármol Aguilar Carlos Josué⁵, Ana Bejarano⁶, Antonio Diaz Sanchez⁷, Marina Eliana Millan Lorenzo⁸, Marinela Mendez⁹, Raquel Domínguez-Hernández¹⁰. ¹Hospital Marina Baixa de Villajoyosa (Alicante), Digestive Medicine Section, Spain; ²Hospital General Universitario de Alicante, Hepatic Unit, Gastroenterology Service, Spain; ³Center for Biomedical Research in Liver and Digestive Diseases Network (CIBERehd), Alicante, Spain; ⁴Hospital de Sagunto (Valencia), Digestive Diseases Section. Service of Internal Medicine, Spain; ⁵Hospital Sant Joan de Deu de Manresa, Service of Digestive Medicine, Spain; ⁶Hospital Juan Ramón Jiménez (Huelva), Service of Digestive Medicine, Spain; ⁷Hospital Universitario del Sureste, Arganda del Rey (Madrid), Digestive Diseases Section, Spain; ⁸Hospital Sierrallana, Torrelavega (Cantabria), Digestive Service, Spain; ⁹Gilead Sciences SLU, Madrid, Spain, Medical Department, Spain; ¹⁰Pharmacoeconomics and Outcomes Research Iberia (PORIB), Spain
Email: rdominguez@porib.com

Background and aims: Hepatitis C virus (HCV) infection is associated with risk factors and highly prevalent extrahepatic manifestations, whose identification could help to find HCV-infected patients. The objective of Hospitals without_C program is to raise awareness of hepatitis C in different hospital services, set protocol for HCV screening, and protocol automation in these settings.

Method: The Hospitals without_C program consisted of training sessions to healthcare professionals to promote education on the

POSTER PRESENTATIONS

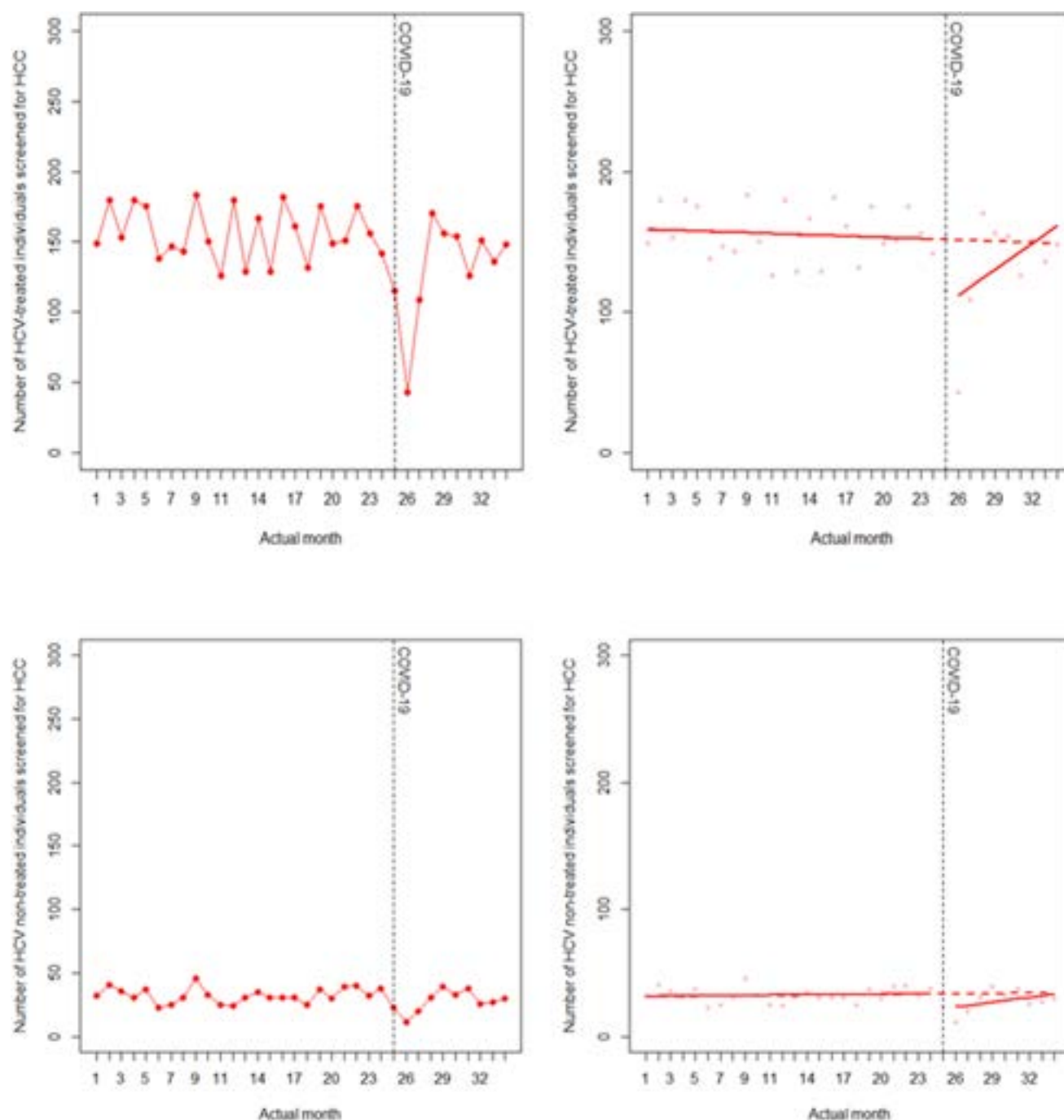


Figure: (abstract: FRI-125): Evolution of monthly HCC screening among individuals living with HCV with cirrhosis treated and non-treated for HCV in BC from March 2018 to December 2020 (left: observed plot, right: model plot).

relevance of hepatitis C diagnosis in different hospital services. The selection of services was carried out considering those treating patients with extrahepatic manifestations related to HCV and where a high number of anti-HCV serologies are requested. The services in which the sessions were held included Psychiatry, Emergency, Internal Medicine, Gynaecology/Obstetrician, and Haematology, among others. The training sessions were conducted by hepatologists, infectious diseases specialists, internal medicine specialists and microbiologists. After the sessions, a follow-up was carried out every 6–12 months to collect information about the number of: i) updated protocols to introduce HCV screening in each service; ii) protocols automated; iii) patients' identification and referral, including those of

new diagnosis or lost to follow-up i.e. diagnosed but untreated patients (DBU); iv) implementation of an alert between Microbiology lab and HCV specialist to notify RNA-HCV positive cases.

Results: 54 hospitals participated until Oct 2022, with 207 training sessions conducted in different services; with an average of 3.8 sessions per hospital and a maximum value of 12 sessions. After the sessions, almost half of the services (101 services, 49%) had an updated, but non-automated protocol, whereas 26 services (12.5%) of 9 hospitals had an updated and automated protocol. After the sessions, 246 HCV patients were identified. HCV-positive viremia alerts to HCV-specialist allowed patient journey simplification,

allowing direct linkage to care for disease management, helping to avoid loss to follow-up of DBU patients through the care cascade.

Conclusion: Hospitals without C program has proven to be a key strategy for raising awareness of the infection among professionals in different hospital services managing patients with HCV-associated extrahepatic manifestations. Moreover, the program favours the setup, updating and automation of protocols to find HCV patients of new diagnose and lost to follow-up in the health system.

FRI-127

Policy and implementation needs for hepatitis B birth dose in the WHO African region: a survey of national program managers

Henry Njuguna¹, Lindsey Hiebert¹, Neil Gupta¹, John Ward¹. ¹Coalition for Global Hepatitis Elimination, Decatur, United States
Email: hnjuguna@taskforce.org

Background and aims: Two thirds of the 1.5 M new chronic hepatitis B virus (HBV) infections globally occur in Africa. Most new infections are preventable with HepB vaccination beginning with a timely birth dose (BD) for new-borns. However less than one in five new-borns in Africa receive timely HepB BD vaccination. Due to COVID 19 pandemic, Gavi, the Vaccine Alliance, paused plans to support HepB BD implementation. To understand the status of HepB BD vaccination in Africa, CGHE conducted a survey with three objectives: assess development of national policies, the impact of COVID-19 pandemic, and operational challenges and resource needs for introduction or scale-up of HepB BD vaccination.

Method: CGHE developed an electronic 23-question survey. Respondents were solicited via targeted emails among Expanded Program on Immunization (EPI) managers and hepatitis focal persons in 36 countries in WHO Africa region.

Results: From October 11, 2022, to January 10, 2023, one respondent from each of 24 countries participated in the survey. Of countries represented, 21 (88%) were eligible for Gavi support, 13 (54%) had no policies for HepB BD vaccination, 9 (38%) and 2 (8%) had policies for universal or targeted HepB BD vaccination, respectively. Of 13 countries without policies for HepB BD vaccination, 7 (54%) National Immunization and Technical Advisory Groups (NITAGs) had recommended routine HepB BD vaccination, 4 (31%) NITAGs were considering a recommendation and 2 (15%) were not. Respondents from only 3 (23%) countries reported their NITAGs focus on COVID-19 vaccination impacted their country's introduction plans for HepB BD vaccination. In contrast, respondents from 19 (79%) of 24 countries reported that immediate availability of Gavi funds was of high (n = 16) or moderate (n = 3) importance in decisions to introduce or scale-up HepB BD vaccination; 18 (75%) reported that Gavi's funding would increase their priority for HepB BD introduction or scale-up. The most frequently reported challenges for HepB BD introduction or scale-up were out-of-facility births (n = 17), training health care workers (n = 16), and political and civil society awareness (n = 16). The most frequent recommendations for the priorities for Gavi funding included health care worker training (n = 23), HepB BD demand creation (n = 19) and vaccination of neonates born outside health facilities (n = 19).

Conclusion: Many countries in Africa are planning or beginning introduction or scale-up of HepB BD vaccination. Compared to the resource demands for pandemic response, the lack of Gavi support is the major factor influencing national decisions to implement HepB vaccination of newborns. Unpausing GAVI's support for HepB BD is urgently needed to substantially increase coverage of this critical

intervention to eliminate mother to child transmission of HBV in Africa.

FRI-128

Influence of language barrier and cultural differences in hepatitis B disease knowledge in the chinese community of Barcelona

Anna Pocurull¹, Laura Tapias¹, Tao Wang¹, Maria Jose Moreta¹, Anna Miralpeix¹, Cristina Collazos¹, Sabela Lens¹, Zoe Mariño¹, Xavier Forns¹. ¹Liver Unit, Hospital Clínic de Barcelona, University of Barcelona, IDIBAPS and CIBEREHD, Barcelona, Spain
Email: apocurull@gmail.com

Background and aims: Hepatitis B is prevalent in patients of Asian origin. Due to language barriers and cultural differences, it is not always straightforward to evaluate disease knowledge in the liver clinics. We aimed to assess the current awareness on HBV infection and its mechanisms of transmission in HBV-infected Chinese patients and their household contacts.

Table 1: Differences in knowledge on the mechanisms of HBV transmission between Chinese and non Chinese patients.

Patients	All patients N = 182	Chinese N = 85	Non Chinese N = 97	P
Spanish understanding				<0.01
No	26 (14%)	25 (29%)	1 (1%)	
Limited	47 (26%)	43 (51%)	4 (4%)	
Good	109 (60%)	17 (20%)	92 (95%)	
Knowledge on horizontal transmission				0.045
No	12 (6%)	9 (10%)	3 (3%)	
Yes	170 (94%)	76 (90%)	94 (97%)	
Knowledge on sexual transmission				0.054
No	14 (8%)	10 (11%)	4 (4%)	
Yes	168 (92%)	75 (88%)	93 (96%)	
Knowledge on vertical transmission				<0.01
No	36 (20%)	5 (6%)	31 (32%)	
Yes	146 (80%)	80 (94%)	66 (68%)	
Prevention measures (horizontal transmission)				<0.01
No	31 (17%)	6 (7%)	25 (26%)	
Yes	148 (83%)	76 (93%)	72 (74%)	
No answer	3 (1%)	3 (4%)	0	
Prevention measures (sexual transmission)				0.138
No	73 (40%)	29 (34%)	44 (45%)	
Yes	108 (60%)	55 (66%)	53 (55%)	
No answer	1 (1%)	1 (1%)	0	

Method: HBV-infected Chinese patients and their household contacts were interviewed by a nurse (Chinese or native) about their knowledge on hepatitis B transmission mechanisms, use of preventive measures and vaccination status. Non-Chinese HBV-infected patients were defined as a control group.

Results: A total of 182 patients and 398 relatives/household contacts participated in the study. Eighty-five (48%) patients and 240 (60%) of household contacts were from China. Language barrier was documented in 80% of Chinese patients and 44% of their household contacts. Knowledge on horizontal and sexual HBV transmission was high (90%) in both groups of patients. However, Chinese patients were significantly more aware of vertical transmission (94% vs 68%, p < 0.01) and were more forewarned in the use of horizontal transmission measures (93% vs 74%; p < 0.01). No differences in preventive sexual measures were detected. Chinese household contacts were

POSTER PRESENTATIONS

less knowledgeable on horizontal and sexual HBV transmission compared to controls (86% vs 96% for horizontal; 81% vs 95% for sexual, $p < 0.01$). However, Chinese household contacts used preventive measures more frequently than controls (79% vs 65% for horizontal transmission, $p < 0.01$). Differences in vaccination coverage between Chinese (78%) and control (86%) household contacts did not reach statistical significance.

Conclusion: Despite relevant language barriers, Chinese HBV-infected patients are well informed on the mechanisms of HBV transmission, particularly on the vertical route. Cultural differences may explain a higher use of preventive measures among the Chinese population. HBV vaccination of household contacts should be reinforced in both groups of individuals.

FRI-129

Health outcomes of hepatitis C direct-acting antivirals: beyond real life sustained viral response data

Carmen Alonso Martín¹, Irene Peñas Herrero¹, Carolina Almohalla Alvarez¹, Félix García Pajares¹, Nieves Martín Sobrino², Laura Isusi Lomas², Albero Rodríguez Palomo², Gloria Sánchez Antolín¹. ¹Hospital Universitario Rio Hortega, Valladolid, Spain; ²Dirección Técnica de Farmacia, Gerencia Regional de Salud, Consejería Sanidad, Spain
Email: calonsoma@saludcastillayleon.es

Background and aims: Hepatitis C (HCV) infection was the leading cause of liver transplantation worldwide, causing significant mortality associated with end-stage liver disease. The appearance in 2015 of HCV direct-acting antivirals (DAAs) for the treatment of Hepatitis C with an efficacy close to 100% has changed the natural history of hepatitis C. Its economic impact conditioned the prioritization of its use, initially in more severe patients. Health results of DAA treatment have been described, such as reducing the liver transplant waiting list, but there are no studies on the impact of DAAs on the activity of health systems. The aim of our study is to find out if new DAA-based treatments for hepatitis C have had an impact on the outcomes of a healthcare system. We analyzed the evolution of hospital discharges of patients with a primary diagnosis of hepatitis C, hospital discharges for hepatocellular carcinoma, and hospital discharges for other causes with an additional diagnosis of hepatitis C.

Method: The number of hospital discharges from 2012 to 2020 was analyzed, selecting patients with hepatitis C as primary or secondary diagnosis. The information of the admitted patients was obtained from the minimum basic set of hospital discharge data. We also analyzed the average number of discharges due to hepatocellular carcinoma or bile duct neoplasm in the same period and compared the average number of discharges for the period 2012–2015 with the average for 2016–2020.

Results: Hospital discharges associated with HCV infection decreased progressively from 2015 to 2022. The average number of discharges in the period 2012–2015 was significantly higher than that of 2016–2020 for patients admitted for any reason with a diagnosis of hepatitis C associated (2327.5 vs. 1505.2, $p < 0.005$). The mean number of discharges due to hepatocarcinoma and cholangiocarcinoma was also significantly higher in the first period (95.5 vs. 72.8, $p < 0.05$). The % variation of hospital discharges compared to 2012 was –32.74% in 2015, –40.93% in 2016, –44.84 in 2017, –55.52% in 2018, –53.38 in 2019 and –61.57% in 2020. The average age ranged from 54 years old in the 2012–2015 period to 57 in the 2016–2020 period.

Conclusion: The introduction of direct-acting antivirals (DAAs) for the treatment of chronic hepatitis C infection (HCC) has led to a significant decrease in the number of hospital discharges for hepatitis

C-related diseases. The variation in hospital discharges since 2012 represents a drop of up to 60% in 2020. A progressive decrease in the number of discharges due to hepatocellular carcinoma and other causes with an additional diagnosis of HCV was also demonstrated. Most of the hospital discharges of patients with HCV due to other causes were classified in ICD10 group 9: diseases of the digestive system, followed by group 1: infectious and parasitic diseases, and group 2: neoplasms. Our study demonstrates the efficacy of DAAs on health outcomes.

FRI-130

Low HBV treatment uptake among Rwandan people with HIV and HCV co-infections: a cohort study from 2016 to 2019

Makuzi Jean Damascene^{1,2,3}, Dahn Jeong^{1,3}, Phymar Soe³, Prince Adu¹, Mawuena Binka¹, Hector Velasquez^{1,3}, Marie Paul Nisingizwe³, Albert Tuyishime², Caren Rose⁴, Alnoor Ramji⁵, Naveed Janjua^{1,3,6}. ¹BC Centre for Disease Control, Clinical Prevention Services, Vancouver, Canada; ²Rwanda Biomedical Center (RBC), IHDPC, Kigali, Rwanda; ³The University of British Columbia, School of Population and Public Health, Vancouver, Canada; ⁴BC Centre for Disease Control, Vancouver, Canada; ⁵The University of British Columbia, Division of Gastroenterology, Vancouver, Canada; ⁶St. Paul's Hospital, Centre for Health Evaluation and Outcome Sciences, Vancouver, Canada
Email: makorofr@gmail.com

Background and aims: Treatment of chronic hepatitis B virus (HBV) infection is associated with prevention of complications such as cirrhosis, hepatocellular carcinoma, and overall improved survival. In Sub-Saharan Africa, data on HBV treatment uptake is limited overall and among people living with HIV. We assessed the HBV treatment uptake and associated factors among people diagnosed with HBV mono-infection, HBV/HCV co-infection, and HBV/HIV co-infection in Rwanda during 2016–2019.

Method: We used data from the District Health Information System 2, which included data on 915,800 individuals screened for HBV in Rwanda, from January 2016 to December 2019. Individuals were included if they were >2 years old, had information on HBV treatment eligibility criteria according to Rwanda's national HBV prevention and treatment guidelines: HIV co-infection, HBV DNA $\geq 20,000$ copies/ml, cirrhosis, abnormal ALT on 3 consecutive tests, and aspartate aminotransferase to platelet ratio index (APRI)-score ≥ 1.5 . HBV treatment uptake is the study primary outcome defined as the proportion of individuals who received HBV treatment among those who met the HBV treatment eligibility criteria. We estimated the proportions of treatment uptake, and assessed factors associated with HBV treatment uptake to account for confounders through multivariable logistic regression.

Results: Among 22,570 individuals with HBV infection, 3,750 (1,986 with HBV mono-infection, 1,764 with co-infection HBV/HIV, 14 with co-infected HBV/HCV, and 5 with HBV/HCV/HIV triple infection) were eligible for HBV treatment during the study period. The majority were males ($n = 1,972$, 52.6%), between 35 and 54 years old ($n = 1,545$, 48.5%, median age = 41 years). Among all individuals, 246 with HBV mono-infection (12.3%) and 31 (1.8%) with HIV/HBV co-infection, had cirrhosis. Among 1,332 people with data on HBV DNA, 1,076 (80.8%) had $\geq 20,000$ copies of HBV DNA per ml. Among 1,521 people with data on ALT, 562 (36.9%) had ≥ 45 IU per ml. Among 1,215 with information on APRI scores, 175 (14.4%) had ≥ 1.5 . During the study period, 2,584 (68.9%) individuals started HBV treatment. People with HBV mono-infection had a greater proportion of treatment uptake compared to those with HBV/HIV co-infection [1,601 (80.6%) vs. 983

(55.7%). In the multivariable model, HIV coinfection (adjusted odd ratio [aOR]: 0.46; 95%CI: 0.32–0.66), and living in provinces other than Kigali city: East (aOR: 0.11; 95%CI: 0.04–0.28), North (aOR: 0.17; 95%CI: 0.06–0.47), West (aOR: 0.15; 95%CI: 0.06–0.37), and South (aOR: 0.29; 95%CI: 0.11–0.74) were associated with a lower likelihood

of HBV treatment uptake. Follow-up at provincial and referral hospitals (aOR: 6.09; 95% CI: 2.50–14.83) compared to follow-up at district hospitals, and having health insurance for public and private employees compared to having community-based health insurance

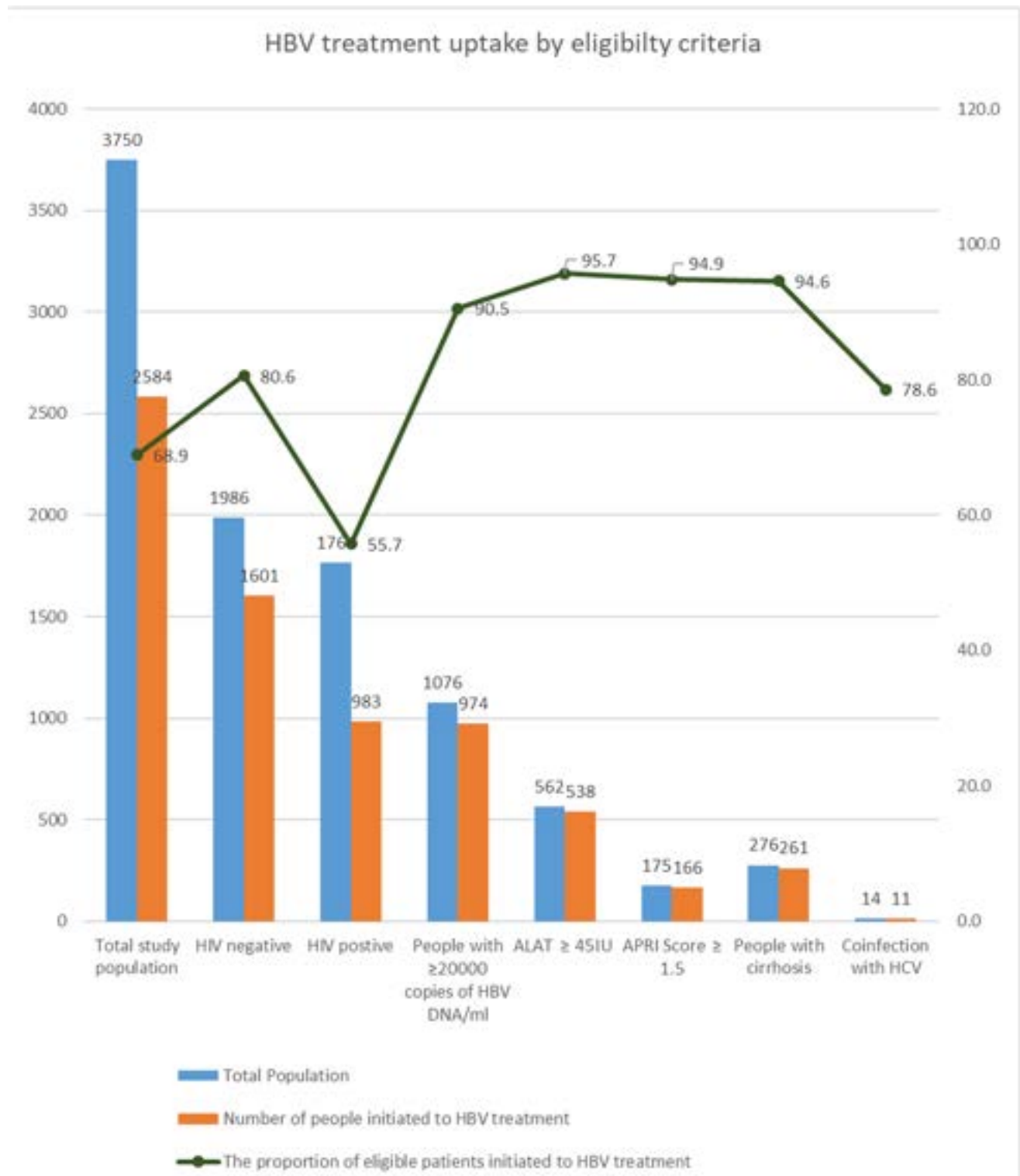


Figure: (abstract: FRI-130).

POSTER PRESENTATIONS

(aOR: 2.53; 95%CI: 1.03–6.26) were associated with higher treatment uptake.

Conclusion: This study found that during the study period, the treatment initiation was low overall, especially among people with HBV/HIV and HBV/HCV co-infections. These findings highlight the need for scale-up of HBV care and treatment, especially in people with HIV and HCV co-infection.

FRI-131

Prevalence of chronic hepatitis C on the Swiss organ transplantation list from 2009 to 2019

Philip Bruggmann^{1,2}, Simone Temperli³, Luis Falcato¹, Franz Immer³.

¹Arud Centre for Addiction Medicine, Internal Medicine, Zurich, Switzerland; ²Institute of Primary Care, University and University Hospital of Zurich, Zurich, Switzerland; ³Swisstransplant, Bern, Switzerland

Email: p.bruggmann@arud.ch

Background and aims: The prevalence of chronic hepatitis C (CHC) is high on the organ transplant waiting list compared to the general population. This is mainly due to HCV-induced liver damage and increased risk of infection by hemodialysis in patients with advanced renal failure. Since 2013, HCV can be cured, and sequelae prevented by timely therapy with directly acting antivirals (DAA's). The aim of this study is to analyze the time trends of the number of HCV-RNA positive patients (RNA+) on the organ transplantation waiting list in Switzerland from 2009 to 2019 and examine the effects of DAA's.

Method: The study is a retrospective secondary analysis of aggregated data on the subsample of RNA+ on the Swiss organ transplantation list. The yearly numbers of listed patients, grouped by requested organ (liver, kidney, any organ), and of delisted patients, grouped by reason (transplanted, deceased) were analyzed. Besides descriptive and visual evaluation of the respective time series, linear regression models ($y = \text{constant} + b \cdot x$) were calculated, using above variables as dependent (y), and the transformed calendar years (2010 = 0; increment = 1) as predictor (x). Parameter estimate, significance, and model fit were assessed.

Results: In 2009, there were 36 RNA+ on the total, 33 on the liver and 3 on the kidney waiting list. For the total and the liver list this number peaked in 2013 with 50 resp. 42 patients, while the peak on the kidney list was in 2012 with 6 patients. In 2019 there were 9, 8 resp 1 RNA+ on the total, liver resp kidney list. In 2009 27 RNA+ were transplanted, 4 died. The number of transplants peaked in 2012 with 28 patients, the number of deaths in 2012 with 8 deaths. In 2019 6 RNA+ were transplanted and none died. Inear regression showed significant yearly decreases in cases waiting for any organ ($b = .41$, $p = 0.002$), liver ($b = -3.6$, $p = 0.001$) and kidney ($b = -0.5$, $p = 0.041$), and decrease for transplantation ($b = -2.3$, $p = 0.001$) and death ($b = -0.8$, $p = 0.001$) as delisting reasons.

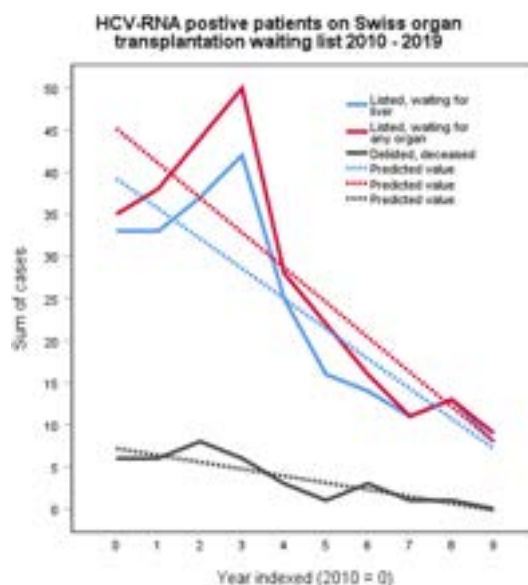


Figure:

Conclusion: Since the introduction of DAAs, few more patients with CHC died on the organ transplant waiting list and the number of individuals with CHC decreased significantly. However, in 2019, 6 years after the first availability of DAAs, CHC patients were still listed for organ transplantation. Every single one of these cases should be considered a failure of the care system, in a country with such a high standard of healthcare as Switzerland.

FRI-132

The impact of removing all hepatitis B virus (HBV) testing and treatment restrictions

Homie Razavi¹, Erkin Musabaev², Shakhlo Sadirova³, Kathryn Razavi-Shearer¹, Shokhista Bakieva², Krestina Brigida².

¹Center for Disease Analysis Foundation, Lafayette, United States;

²Research Institute of Virology, Tashkent, Uzbekistan; ³Center For Disease Analysis Foundation, Tashkent, Uzbekistan

Email: hrazavi@cdafound.org

Background and aims: Simplifying HBV testing and treatment guidelines has been a topic of debate with proponents arguing for a higher linkage to care and opponents arguing for potential over-treatment.

Method: In 2020, 62,975 individuals visiting polyclinics in Tashkent, Uzbekistan were tested for HBV using rapid tests with 30,727 tested before the COVID-19 shut-down, and the remaining tested post-COVID. All positive individuals were tested with HIV and creatinine rapid tests in an adjoining room. Pre-COVID, they were referred to specialists at the Virology Institute and post-COVID to trained General Practitioners (GPs) in the same polyclinic.

Results: 1,509 individuals were newly diagnosed. The cascade of care is shown below with 29% of all diagnosed cases initiating treatment in our program and the private sector. A survey of those who did not seek treatment found that 42% did not know HBV infection can lead to cancer. A separate analysis of GPs prescription and treatment initiation found treatment initiation rates between 12%-84% of their patients even though all GPs received the same training.

Conclusion: Our study suggests that significant difficulties remain even if all testing and treatment barriers are removed due to a very low level of awareness of HBV and the corresponding disease burden in the general population. It also highlights the importance of

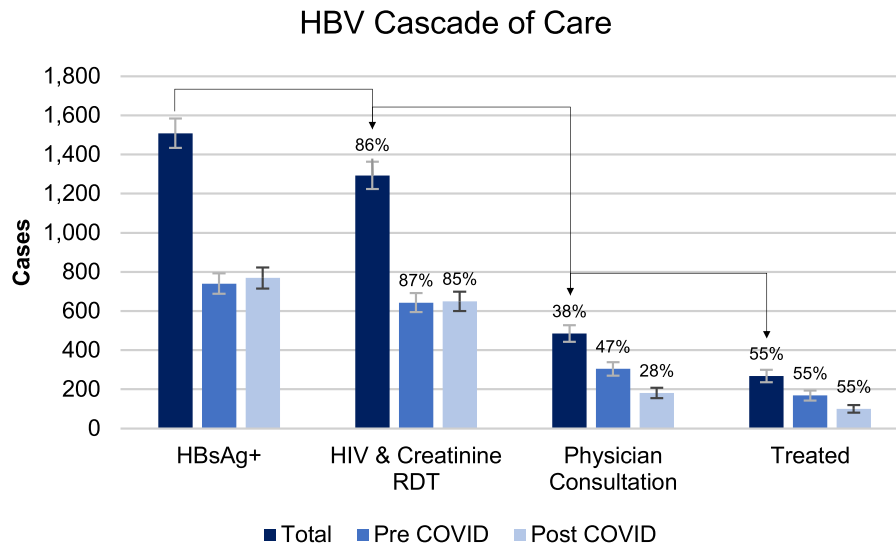


Figure: (abstract: FRI-132).

training and retraining GPs as they are typically the first medical experts who explain the implications of the positive HBV test. Finally, the private sector cannot be ignored as it accounted for 38% of all treated patients.

FRI-133

Spontaneous clearance of hepatitis C virus infection in the country of Georgia, 2015–2021

George Kamkamidze¹, Maia Butsashvili¹, Davit Baliashvili², Shaun Shadaker³, Maia Kajaia¹, Mamuka Zakalashvili⁴, Tengiz Tsertsvadze⁵, Lali Sharvadze⁶, Maia Tsreteli⁷, Senad Handanagic³. ¹Health Research Union and Clinic NeoLab, Tbilisi, Georgia; ²The Task Force for Global Health, Georgia; ³Centers for Disease Control and Prevention, United States; ⁴Medical Center Mrcheveli, Georgia; ⁵Infectious Diseases, AIDS and Clinical Immunology Research Center, Georgia; ⁶Clinic Hepa, Georgia; ⁷National Center for Disease Control and Public Health Georgia, Georgia
Email: georgekamkamidze@gmail.com

Background and aims: The majority of hepatitis C virus (HCV) infections persist, while approximately 15–30% of infections clear spontaneously and do not progress to chronic hepatitis C. Epidemiological, viral, and host factors have been associated with HCV clearance in previous studies, showing that a strong virus-specific host immune response favors viral clearance. Female sex, younger age at infection, lower HCV RNA levels, co-infection with hepatitis B virus, and specific polymorphisms of IL28 gene were positively associated with spontaneous clearance, while alcohol consumption showed a negative correlation. The aim of our study was to evaluate HCV spontaneous clearance among persons tested for HCV infection within the national HCV elimination program in the country of Georgia and association with sex, age, and the specific population subgroups.

Method: Spontaneous clearance was defined as a reactive HCV-antibody test followed by no detection of HCV RNA or core antigen, with no HCV treatment history. Data were extracted from Georgia's screening registry and HCV elimination program database, which contain all hepatitis C testing and treatment data nationally. Chi-square tests and logistic regression were used for statistical analysis of the data.

Results: Data for 137,981 persons tested for HCV infection during 2015–2021 were analysed. Overall, 20.7% of persons tested for viremia had spontaneously cleared the virus. Spontaneous clearance of HCV infection increased each year during 2015–2021 (table).

Overall spontaneous clearance was higher among women than men (27.1% vs. 18.5%, respectively; prevalence ratio [PR] = 1.47 and 95% confidence interval [CI] = 1.43–1.49). Clearance was lowest among those aged 40–49 years (17.9%) and highest among children aged <18 years (58.2%). Compared to the general population, lower spontaneous clearance was documented for people living with HIV infection (PR = 0.50; 95% CI: 0.32–0.79) and persons in penitentiary settings (PR = 0.57; 95% CI: 0.38–0.59).

Year	Anti-HCV positive N	Tested for HCV		HCV spontaneous Clearance N (%)	Prevalence Ratio (PR)	PR 95% CI
		RNA or Core Antigen N (%)	Antigen N (%)			
2021	8098	5460 (67.4)	1712 (31.4)	Reference	Reference	
2020	10755	8070 (75.0)	2445 (30.3)	0.97	0.92–1.02	
2019	21210	17533 (82.7)	4489 (25.6)	0.82	0.78–0.86	
2018	23697	20103 (84.8)	4724 (23.5)	0.75	0.72–0.79	
2017	29619	23022 (77.7)	4143 (18.0)	0.57	0.55–0.60	
2016	25432	22726 (89.4)	3924 (17.3)	0.55	0.52–0.58	
2015	19170	18125 (94.5)	2419 (13.3)	0.43	0.40–0.45	

Figure: Spontaneous clearance of HCV by year, Georgia.

Conclusion: Substantial increases in HCV spontaneous clearance over time may be considered as an indirect outcome of a positive impact of the HCV elimination program on the structure of HCV infections in the population of Georgia. Updated estimates of HCV clearance are important for the strategic planning of further activities towards HCV elimination.

FRI-134

Automation of hepatitis C screening through electronic health record algorithm

Vitor Magno Pereira¹, Madalena Pestana¹, Elisa Xavier², Luís Jasmins¹, Nuno Ladeira¹, Ana Reis³, Nancy Faria³, José Bruno Freitas², Nuno Canhoto², Alba Carrodegua⁴, Diogo Medina⁴. ¹Hospital Dr. Nélito Mendonça, Gastroenterology and Hepatology, Funchal, Portugal; ²Hospital Dr. Nélito Mendonça, Funchal, Portugal; ³Hospital dos Marmeleiros, Funchal, Portugal; ⁴Gilead Sciences Inc, Madrid, Spain
Email: magnovitorp@gmail.com

Background and aims: The high proportion of people living with hepatitis B and C who are undiagnosed is a key finding of ECDC recent

POSTER PRESENTATIONS

report on the elimination of viral hepatitis. World Health's Organization (WHO) 2030 goals for the elimination of viral hepatitis are still therefore unreachable by many of these countries. In January 2020, we embraced the mission to achieve these goals through the implementation of a universal program for Hepatitis C virus screening (HCV), a systemic policy defended by all players in our region.

Method: The initiative consists of an opportunistic HCV screening with HCV antibody in patients aged 18–70, without prior records of HCV antibody or HCV RNA, who required blood work for any purpose across all public health facilities (primary care, emergency department, hospital clinics and wards).

Electronic health record (EHR) algorithms were developed in order to determine eligibility and oral opt-out consent was obtained. Whenever a positive antibody test is found, a reflex confirmatory test is automatically generated on the same sample.

Results: From January 2020 until December 2022, we screened 32418 patients (average of 900 tests/month) and found 155 positive antibody (0.47%) and 51 viremic patients (0.16%). Linkage to care was achieved at 94% of viremic patients. Usage of intravenous drugs and other patients' social issues are the major barriers in complying with healthcare. An analysis of fibrosis staging at screening using non-invasive scores was performed for all viremic patients. Fibrosis-4 (FIB-4) Index for Liver Fibrosis was calculated with the following Results: 20 patients low risk (FIB-4 <1.3), 13 patients indeterminate risk (FIB-4 1.3–2.67) and 16 patients high risk (FIB-4 >2.67).

For patients with SVR available (15), there were no treatment failures (SVR of 100%).

Conclusion: This automated screening strategy permitted the diagnosis of 51 previously undiagnosed HCV viremic patients, including a third with advanced liver fibrosis. The authors report a global HCV antibody prevalence of 0.47% and 0.16% HCV RNA in this general screening population. This kind of strategy is an important measure to ensure a reduction in the significant number of undiagnosed patients with chronic viral hepatitis.

FRI-135

Hepatitis C seroconversion rates among individuals with repeated testing-Georgia, 2017–2021

Davit Baliashvili¹, Shaun Shadaker², Nathan Furukawa²,

Maia Tsereteli³, Vladimer Getia³, Paige A. Armstrong²,

Senad Handanagic². ¹The Task Force for Global Health, Georgia;

²Centers for Disease Control and Prevention, United States; ³National

Center for Disease Control and Public Health, Georgia

Email: dato.baliashvili@gmail.com

Background and aims: As Georgia moves closer to achieving hepatitis C virus (HCV) elimination, demonstrating the program's impact on the ongoing transmission of hepatitis C becomes a priority. One way to monitor reduction in incidence is to observe temporal trends of seroconversion and new viremic cases among repeatedly tested persons. Using nationwide programmatic data, we aimed to estimate annual rates of seroconversion and new viremic infections among persons repeatedly tested in Georgia.

Method: We used data from 2017 to 2021 and identified a subset of adults with at least two anti-HCV tests ≥ 14 days apart and nonreactive results for the first anti-HCV test. Seroconversion was defined as nonreactive anti-HCV test followed by a reactive. The seroconversion rate was calculated by dividing number of seroconversions by total person-time within the given calendar year and expressed per 100,000 person-years (PY). Person-time was calculated as the number of days from the first anti-HCV test to either the last nonreactive test (for consistently nonreactive individuals) or the first reactive test (for individuals who seroconverted). We estimated the seroconversion rate by year and sex. Among those with seroconversion, we identified persons with subsequent HCV RNA or HCV core antigen testing and calculated the rate of new viremic infection with the same methodology as above. Rate ratios and 95% confidence intervals (CI) were calculated to compare rates between different years.

Results: We identified 942,030 individuals with more than one anti-HCV test with an initial nonreactive result. After a median follow-up time of 654 days (IQR: 334–1012), 13,022 (1.4%) individuals seroconverted. The seroconversion rate per 100,000 PY decreased

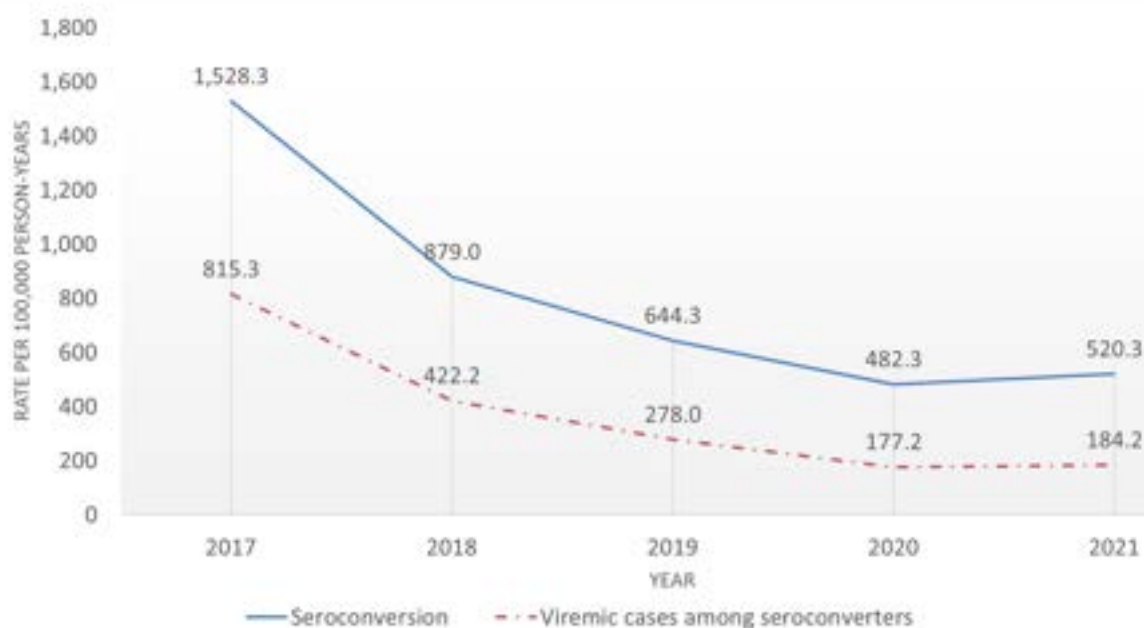


Figure: (abstract: FRI-135): Rate of new hepatitis C cases per 100,000 person-years among repeat testers- Georgia, 2017–2021.

by 66% over five years, from 1,528 in 2017 to 520 in 2021 (rate ratio = 0.34, 95% CI: 0.32, 0.37). Incidence was lowest in 2020 (482 per 100,000 PY), followed by an increase in 2021. Overall, the seroconversion rate was more than twice as high among males than females, but rate of decrease was similar in both sexes. Among those with seroconversion, 10,159 (78%) were tested for viremia, and 5,824 (57%) were detectable. The annual rate of new viremic cases per 100,000 PY decreased by 77%, from 815 in 2017 to 184 in 2021 (rate ratio = 0.23, 95%CI: 0.20, 0.25) (figure).

Conclusion: The seroconversion rate in Georgia decreased approximately three-fold during 2017–2021. A slight reversal of the trend in 2021 could be explained by the potential negative impact of the COVID-19 pandemic on preventive programs and infection prevention and control practices. During a similar period (2015–2021), prevalence of hepatitis C decreased by 67% in Georgia, suggesting use of seroconversion rates may provide a valuable tool for monitoring progress towards elimination. Continued progress toward elimination will require further scale-up of both treatment and preventive programs.

FRI-136

Characterization of recent HCV infections and re-infections among the high-risk population from Georgia using global hepatitis outbreak and surveillance technology

Adam Kotorashvili¹, Amiran Gamkrelidze², Tamar Gabunia², Nato Kotaria², Maia Tsereteli², Ana Papkauri², Ketevan Galdavadze², Maia Alkhazashvili², Paata Imnadze², Tinatin Kuchuloria^{3,4}, Lilia Ganova-Raeva⁵, Sumathi Ramachandran⁵, Shaun Shadaker⁵, Saleem Kamili⁵, Paige A. Armstrong⁵, Yuri Khudyakov⁵. ¹National Center for Disease Control and Public Health, Genome Center, Tbilisi, Georgia; ²National Center for Disease Control and Public Health, Tbilisi, Georgia; ³The Task Force for Global Health, United States; ⁴The Task Force for Global Health, Tbilisi, Georgia; ⁵Centers for Disease Control and Prevention, Atlanta, United States
Email: adam.kotorashvili@gmail.com

Background and aims: Global Hepatitis Outbreak and Surveillance Technology (GHOST), developed at the Centers for Disease Control and Prevention, is a novel technology that identifies any transmission links among individuals infected with hepatitis C virus (HCV), generating a user-friendly graphic display. The National Center for Disease Control and Public Health (NCDC) of Georgia became the first international GHOST-implemented regional center outside of the United States. Using the GHOST bioinformatics platform, the goal of the study was to gain insight into the HCV variability and any potential transmission networks in recently seroconverted and reinfected persons who inject drugs (PWID) in selected harm reduction (HR) centers of Georgia.

Method: GHOST uses next-generation deep sequencing of Hyper Variable Region 1 (HVR1) of the HCV. Genotypes of the HCV strains were determined by HVR1 sequence data analysis. Two HR sites in the cities of Tbilisi and Zugdidi were selected for participation. Samples were collected from HR beneficiaries with documented reinfection or seroconversion. All participants provided written informed consent to participate in the study and completed a questionnaire on the relevant epidemiologic information. All specimen processing and molecular testing laboratory methods were executed according to the respective Standard Operating Procedures developed and approved by the Division of Viral Hepatitis Laboratory (CDC Atlanta, GA)

Results: Overall, 131 PWID were recruited to participate, including 55 (42%) in Tbilisi and 76 (58%) in Zugdidi. Among the 131 participants observed between June 2021–May 2022, 12 (9%) had HCV reinfection and 119 (91%) seroconverted during the observation period. In the 6 months prior to the study, 109 participants (83%) reported injecting drugs and 4 (3%) reported needle sharing. Among participants experiencing reinfection, 1 (8%) received a blood transfusion, and 11 (92%) had an invasive medical procedure; none were incarcerated.

Among participants with new infection, 23 (19%) received a blood transfusion, 58 (49%) had invasive medical procedures more than 1 year prior, and 8 (7%) were incarcerated prior to seroconversion. HCV recombinant genotype 2k/1b was predominant (n = 22, 36%), followed by 1b genotype (n = 18, 29%), 3a (n = 11, 18%), 2c (n = 5, 8%), 1a (n = 3, 5%) and 2a (n = 1, 2%). Using the GHOST transmission detection module, two transmission clusters consisting of 3 and 6 individuals reinfected with HCV genotypes 2c and 1b were identified in Tbilisi. No linkage among the individuals from Zugdidi was found. The Tbilisi participant carried mixed HCV genotype infection (clade with 6 individuals). Additionally, we found two mixed infections, one in Tbilisi and one in Zugdidi, indicating a high rate of exposure.

Conclusion: This is the molecular epidemiological report among the high-risk PWID population of Georgia using GHOST. The detected transmission clusters and mixed genotype infections indicate a high rate of exposure in these communities. GHOST can be utilized for surveillance for early intervention on networks as well as successfully applied to other infectious diseases including hepatitis B virus, hepatitis A virus and HIV-coinfection.

FRI-137

Zero-HCV before end stage renal disease (ESRD): a collaborative “treat-all” approach to eliminate HCV in chronic kidney disease population in Taiwan

Tsung-Hui Hu¹, Shiou-Shiang Chen², Chen-Yang Hsu³, Wei-Wen Su⁴, Sam Li-Sheng Chen⁵, Chih-Chao Yang⁶, Yen-Po Yeh², Hsiu-Hsi Chen⁷. ¹Kaohsiung Chang Gung Memorial Hospital, and Chang Gung University College of Medicine, Kaohsiung, Taiwan, Taiwan; ²Changhua County Public Health Bureau, Changhua, Taiwan, Taiwan; ³Institute of Epidemiology and Preventive Medicine, College of Public Health, National Taiwan University, Taipei, Taiwan, Taiwan; ⁴Changhua Christian Hospital, Changhua, Taiwan, Taiwan; ⁵School of Oral Hygiene, College of Oral Medicine, Taipei Medical University, Taipei, Taiwan, Taiwan; ⁶Changhua Hospital, Ministry of Health and Welfare, Changhua, Taiwan, Taiwan; ⁷Graduate Institute of Epidemiology and Preventive Medicine, College of Public Health, National Taiwan University, Taipei, Taiwan, Taiwan
Email: yeh.leego@gmail.com

Background and aims: The Changhua integrated program to stop HCV infection (CHIPS-C) adopted a multidisciplinary care approach since 2019. The elimination of HCV among dialysis population has been successfully completed in Changhua in 2019¹. To ensure the quality of achievement, we move forward to the HCV elimination in Chronic Kidney Disease (CKD) population to prevent new infection and disease burden in dialysis units from new participants.

Method: Changhua county has conducted Chronic Kidney Disease (CKD) program (including early CKD, stage 1–3a; and pre-ESRD stage 3b, 4, 5 and proteinuria) since 2006. For a better containment of HCV among the well-recognized high-risk population of CKD, a systematic approach by integrating health administrative, health care facilities from primary to medical center guided by CHIPS-C was utilized since 2019. HCV screening and treatment were implemented and evaluated. The achievement rate of HCV care chain-related indicators, and treatment rate were analyzed. The end of follow-up was Dec 31, 2022.

Results: Following the initiation of CHIPS-C for pre-ESRD cohort in Changhua in 2019, there were total 9,155 subjects included. By excluding those who were unable to enter the program such as deaths, aging, and mobility, the screening targets total 8,933 people. The HCV antibody screening rate reached 94.45% (8,438 people), with HCV antibody positive rate of 7.44% (628 people), HCV RNA virus checking rate of 91.7% (576 people), detectable HCV RNA rate of 63.0% (363 people), eligible treatment rate was 98.6% (358 people), and final treatment rate was 91.1% (326 people). Furthermore, there have been total 71,949 CKD subjects initially included. The HCV antibody screening rate reached 81.4% (58,536 people), with HCV antibody positive rate of 6.6% (3,883 people), HCV RNA virus checking rate of 83.1% (3,226 people), detectable HCV RNA rate of 59.4% (1,916

POSTER PRESENTATIONS

people), and final treatment rate was 89.2% (1,710 people). We further evaluate the impact of treatment of CKD cohort on the dialysis unit. There have been 1683 new participant of dialysis since 2019 in Changhua County. The positivity rate of HCV RNA was 50% at the end of 2019; 28.6% at the end of 2020; 7.7% at end of 2021, and 0% at June of 2022.

Conclusion: After implementation of the CKD program, the percentage of people who were with active hepatitis C (viremic) upon entry into dialysis units gradually decreased. Zero HCV before ESRD could serve as a surveillance surrogate indicator to monitor the progress of HCV elimination in CKD.

FRI-138

Low coverage of hepatitis D virus testing in individuals with HIV and HBV in the Netherlands: a retrospective, cross-sectional and longitudinal study

Anders Boyd¹, Colette Smit¹, Annemiek Van der Eijk², Hans Zaaier³, Bart Rijnders², Berend van Welzen⁴, Marc Classen⁵, Katalin Pogany⁶, Theodora de Vries-Sluijs², Eline Op de Coul⁷, Marc van der Valk¹.

¹Stichting Hiv Monitoring, Netherlands; ²Erasmus MC University Medical Center, Netherlands; ³Amsterdam University Medical Centers, Netherlands; ⁴University Medical Center Utrecht, Netherlands;

⁵Rijnstate Ziekenhuis, Netherlands; ⁶Maastricht Hospital, Netherlands;

⁷National Institute for Public Health and the Environment (RIVM), Netherlands

Email: a.c.boyd@amsterdamumc.nl

Background and aims: European guidance recommends that all individuals with hepatitis B virus (HBV) be tested for hepatitis D virus (HDV). Little is known on the extent of and reasons for HDV testing in individuals with HIV and HBV during routine practice. We aimed to assess the changes in HDV testing in 2000 to 2021 in individuals with HIV and HBV infection in care in the Netherlands, both overall and according to key population. We also intended to understand the determinants of those who ever received an HDV test.

Method: Data from the ATHENA cohort of people with HIV who were ever hepatitis B surface antigen positive, aged ≥ 18 years or older, and attended any of the 24 HIV treatment centers in the Netherlands between 2000 and 2021 were assessed. We estimated the percent of included individuals ever tested for HDV (i.e., documented anti-HDV antibody or HDV RNA test) across calendar years. Determinants for ever being tested by the end of follow-up were assessed using relative risk (RR) regression using a Poisson regression model with robust variance estimation.

Results: Of the 1668 included individuals with HIV and HBV, only 212 (12.7%) had a documented HDV test. The percentage of individuals tested for HDV increased from 5.0% (95% confidence interval [CI] = 3.4–7.3) in 2000 to 14.0% (95%CI = 12.1–16.2) in 2021. In 2021, the percentage tested for HDV was 13.0% (95%CI = 10.7–15.7) in men who have sex with men, 23.5% (95%CI = 9.1–48.6) in persons who inject drugs, and 15.6% (95%CI = 12.2–19.8) in heterosexual/others. In multivariable analysis, ever having an HDV test was associated with ever having detectable HBV DNA viral load during follow-up (adjusted RR = 3.61, 2.39–5.46, $p < 0.001$), ever presenting with elevated alanine aminotransferase (ALT) levels (adjusted RR = 1.48, 95%CI = 1.14–1.93, $p = 0.003$), advanced fibrosis/cirrhosis (versus no fibrosis/cirrhosis, adjusted RR = 1.78, 95%CI = 1.35–2.34, $p = 0.001$), and being overweight/obese (versus normal/underweight, adjusted RR = 1.44, 95%CI = 1.11–1.87, $p = 0.006$). The percentage of individuals with HIV and HBV who tested positive for HDV remained relatively stable over calendar year: 15.4% ($n = 4/26$; 95%CI = 5.9–34.6) in 2000 and 7.2% ($n = 11/152$; 95%CI = 4.1–12.6) in 2021.

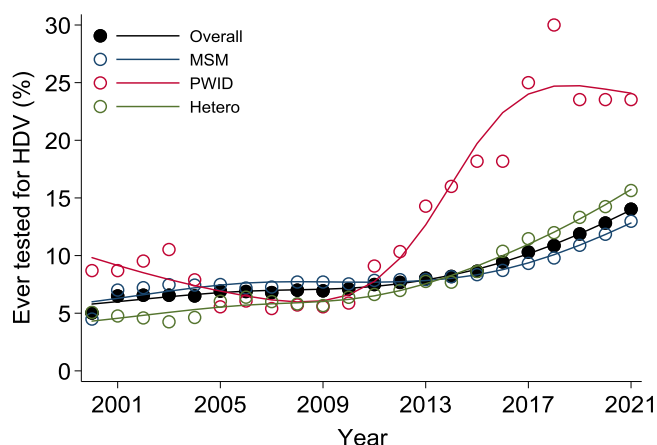


Figure: Hepatitis D virus testing in individuals with HIV and hepatitis B virus in the Netherlands.

Conclusion: HDV testing coverage in the Netherlands is low for individuals with HIV and HBV. Although testing was more common in those with advanced liver disease, a considerable proportion at risk of HDV still needs HDV testing in the Netherlands.

FRI-139

Retrospective study of hepatitis C virus antibodies and active viral replication in at-risk population with dual diagnosis in a Spanish university hospital

Cristina del Rio-Cubilledo¹, Aitana Carla Morano Vázquez², Denise Monserrat Arroyo Jarrin³, Miriam Soriano García³, Henar las Heras Miralles¹, Jose Manuel Olivares Díez⁴, Luis Enrique Morano Amado⁵. ¹South Galicia Health Research Institute, South Galicia Biomedical Foundation, Vigo, Spain; ²Preventive Medicine Service, Gregorio Marañón University Hospital, Madrid, Spain; ³Psychiatry Service, Álvaro Cunqueiro University Hospital, Vigo, Spain; ⁴Psychiatry Service, Vigo Health Area, Álvaro Cunqueiro University Hospital, Vigo, Spain; ⁵Infectious Disease Unit, Álvaro Cunqueiro University Hospital, Vigo, Spain

Email: cristina.delrio@iisgaliciasur.es

Background and aims: In 2019, WHO estimated the prevalence of chronic HCV about 58 million globally, however only 21% were diagnosed and 9.4 million were treated with direct-acting antivirals. In Spain the prevalence of antibodies was 0.85% and the active infection 0.22% in general population between 2017 and 2018. HCV can cause hepatocellular carcinoma and cirrhosis. Among at-risk groups, HCV and other Blood-Borne Viruses (BBV) are very common in people with dual diagnosis (DD), whose infection complicates due to alcohol and substance abuse. People with DD should be screened for BBV as a standard health assessment. Screening in the psychiatric unit of a hospital showed that 9% of patients were VHC positive. Other study showed that testing all psychiatric patients is cost-effective and helps to wipe out HCV. However, people with DD have been under-recognized as a priority group for HCV screening, and studies in patients with DD are few. We aimed to analyse the prevalence of HCV in DD patients at our Psychiatry Unit.

Method: We did a retrospective study of 1631 patients admitted in the Psychiatry Unit at Álvaro Cunqueiro University Hospital between 2019 and 2021 to identify patients with DD to detect the presence of HCV antibodies (anti-HCV) and HCV ribonucleic acid (RNA). We searched for HCV-untreated patients with active viral replication (AVR), HCV-treated patients with sustained virologic response (SVR), spontaneous viral clearance (SVC), HCV-uninfected and HCV-unknown. The selected covariates were age, sex and other BBV.

Results: 291 patients had DD, 186 were male, 105 female and their age average was 41 years. 22.3% of patients had alcohol abuse, 44.7% single drug abuse and 33% several substance abuses. 249 (85.6%) were tested for HCV antibodies. anti-HCV were confirmed in 62

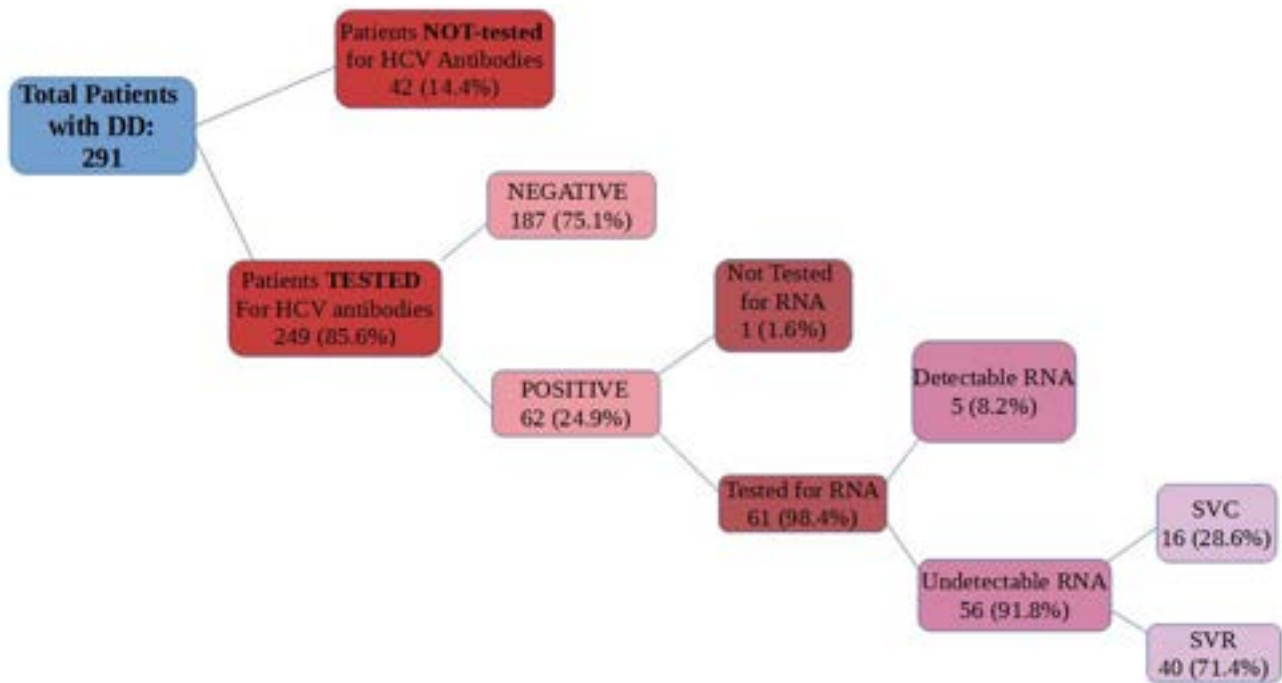


Figure: (abstract: FRI-139): Percentages of patients with DD who had HCV antibodies, RNA detectable or undetectable and patients who received treatment or who reached SVC.

(24.9%) patients. Among these, 56 (91.8%) showed undetectable RNA, of which only 40 (71.4%) received treatment with SVR and the rest reached SVC. 1.6% were not tested for RNA replication and 5 (8.2%) had AVR and did not follow any treatment. Finally, 69 (23.7%) had also other BBV.

Conclusion: The prevalence of anti-HCV in our Psychiatry Unit was 29.3 times higher than in general population in Spain. Our results highlight the need to address the high prevalence of HCV in people with DD. The Health System should provide an effective screening method to identify patients with HCV at at-risk populations and

develop a system to test all patients admitted in psychiatry units in hospitals.

FRI-140

Acceptance and feasibility of hepatitis C screening by assisted self-testing in high-risk and general population: a randomized clinical trial

Federica Benitez Zafra¹, Felicitas Diaz-Flores², Francisco Javier Perez-Hernandez³, Paula Haridian Quintana Diaz¹, Fabiola Perez Gonzalez¹, Maria Jesus Medina Alonso⁴, María Cristina Reygosa Castro¹, Dalia Morales Arraez¹,

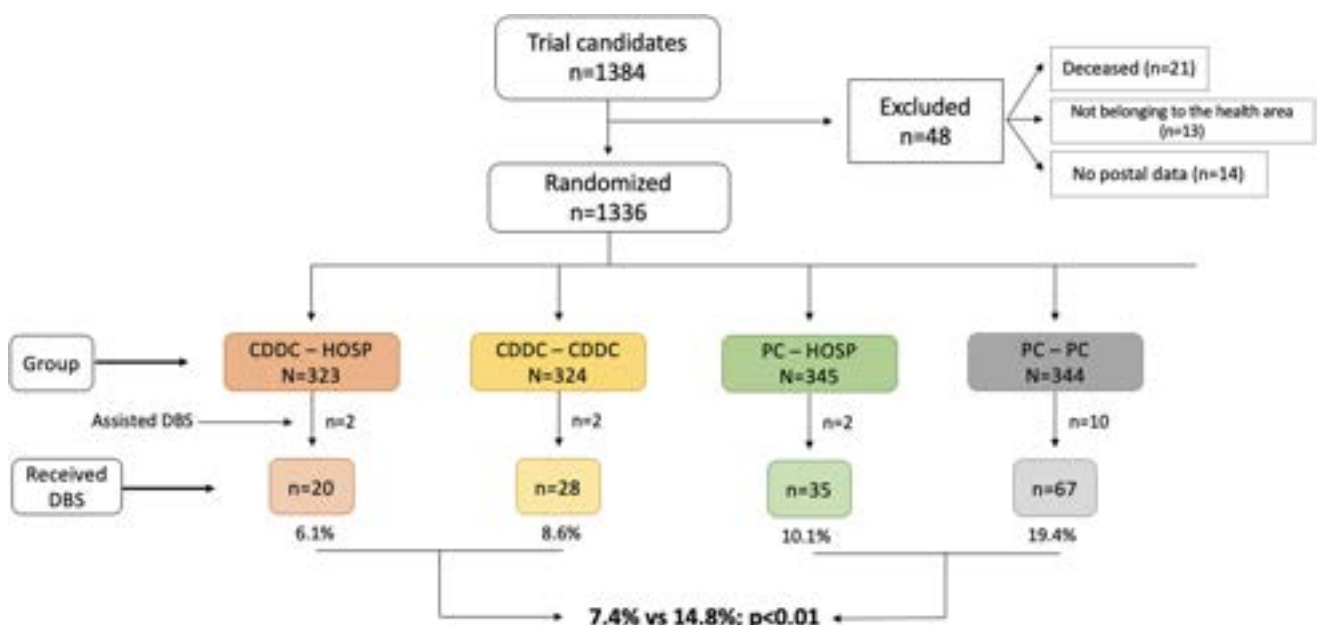


Figure: (abstract: FRI-140).

POSTER PRESENTATIONS

Maria del Carmen Plasencia Alvarez³, Victor Perez Perez⁴, Manuel Hernández Guerra¹, ¹Servicio de Aparato Digestivo, Hospital Universitario de Canarias, Tenerife, Spain; ²Laboratorio Central, Hospital Universitario de Canarias, Tenerife, Spain; ³Servicio de Medicina Familiar y Comunitaria de la Zona Norte de Tenerife, La Laguna, Spain; ⁴Unidad de atención a las drogodependencias, Spain
Email: federicabenitezafra@gmail.com

Background and aims: Strategies for the micro-elimination of hepatitis C virus (HCV) have been implemented, including integrated decentralized diagnostic programs at centers for drug dependence care (CDDC) using the dried blood spot test (DBS). However, many subjects at high-risk of having HCV infection were discharged or lost from follow-up from CDDC before these actions were taken. This study aims to evaluate the effectiveness (acceptance and feasibility) of an HCV screening strategy using home-based self-testing with DBS in patients that missed HCV screening at CDDC and compare it with general population.

Method: Patients who were attended and discharged or lost to follow-up by the CDDC between 2013 and 2017 and subjects from a primary care (PC; general population) cohort were identified and offered to participate by sending the self-testing kit. Deceased subjects, those not belonging to the health area, and those with no postal data were excluded. They were randomized (clinicaltrials.gov NCT05146609) into two groups in each population, according to whether they were offered assistance to perform the test in the hospital, CDDC, or PC center. The sample return rate of the test and the feasibility of processing DBS samples and obtaining ARN results were evaluated. Characteristics associated with sample return were analyzed using logistic regression.

Results: Overall, 1336 subjects (67.7% males, 48.8 ± 0.3 years) were included and the figure shows acceptance rates in each group. The home-based screening was lower in high-risk population compared to general population (7.4% vs 14.8%; $p < 0.01$). Subjects that returned de sample were older (51.0 ± 14.3 vs 43.7 ± 14 years; $p = 0.04$), had longer drug use duration (25.8 ± 15.1 vs 19.0 ± 13.5 years, $p = 0.001$), daily drug consumption (9.3 vs 5.0%, $p = 0.04$), a previous HCV positive test (19.5 vs 6.8%, $p = 0.08$), previous digestive system specialist's appointment (15.6 vs 5.9%, $p = 0.001$) and absence of psychiatric doctor's appointment (19 vs 6.3%, $p = 0.004$). Having a previous HCV positive test was the only predictive factor associated with a high rate of returning the sample (OR 6.6, CI95% 2.1–20.7; $p = 0.001$). All returned samples, except 2 DBS, were valid and negative for viremia.

Conclusion: This retrieval home-based self-testing screening strategy is feasible, but has a low acceptance rate in the high-risk population, especially among those unaware of the disease. More effective targeted strategies must be sought to achieve 2030 WHO goals.

FRI-141

Cost-effectiveness analysis of a new paradigm to simplify testing, monitoring and treatment of hepatitis C virus in the United States

Douglas T. Dieterich¹, Nancy S. Reau², Aijaz Ahmed³, Rob Blissett⁴, Adam Igloi-Nagy⁴, Alon Yehoshua⁵, ¹Institute for Liver Medicine, Mount Sinai Health System, United States; ²Rush University Medical Center, Department of Hepatology, Chicago, United States; ³Stanford University School of Medicine, Division of Gastroenterology and Hepatology, Stanford, United States; ⁴Maple Health Group, LLC, New York, United States; ⁵Gilead Sciences, Inc, United States
Email: douglas.dieterich@mountsinai.org

Background and aims: The current treatment pathway for hepatitis C virus (HCV) patients in the United States (US) includes a range of tests and appointments that delay treatment and cause substantial loss to follow-up. Our analysis aimed to assess the cost-effectiveness of simplifying the testing and treatment of HCV patients from the US payer perspective.

Method: A series of linked Markov models were developed to estimate the health outcomes and cost differences of simplifying the treatment pathway for HCV patients in the US. The analysis compared three scenarios, one based on the latest treatment guidelines ("status quo" [SQ]), one based on real-world practice as informed by expert opinion ("real-world scenario" [RW]) and a hypothetical scenario with a simplified pathway ("new paradigm" [NP]). The scenarios differed in testing and treatment process steps and time needed to complete each step. Patients in the new paradigm initiated treatment earlier and with fewer tests and appointments required, resulting in a shorter overall process time and less resource use. The model considered the US HCV population, stratified by subpopulations (general population, incarcerated, people who inject drugs, men who have sex with men). Model inputs included direct costs (health state, testing, treatment), treatment effectiveness expressed as sustained virologic response at 12 weeks (SVR12) and health state utilities. Outcomes included the incremental cost per quality-adjusted life year (QALY) and per life year (LY) of introducing the new paradigm compared to the SQ and RW scenarios. Advanced liver disease outcomes (compensated and decompensated cirrhosis, hepatocellular carcinoma, liver transplant, and extrahepatic mortality) were also compared between each scenario. Costs and health effects were discounted at 3.0% over a lifetime horizon.

Results: In the base case analysis with all subpopulations considered, the new paradigm resulted in incremental costs of −\$19,751 (vs. SQ) and −\$16,448 (vs. RW). The new paradigm was associated with incremental QALYs of 0.42 and 0.70 compared to the SQ and RW scenarios, respectively, and therefore was a dominant strategy compared to both. In addition, the new paradigm was associated with a 60.4% and 58.2% reduction in total advanced liver disease outcomes, compared to the SQ and RW scenarios, respectively. Sensitivity and scenario analyses confirmed the robustness of the model; key drivers included health state utilities and treatment effectiveness inputs.

Table: Summary Model Results

	Status Quo	Real-World Scenario	New Paradigm
Cumulative outcomes, discounted			
LYs per person	13.31	12.97	13.66
QALYs per person	10.81	10.53	11.23
Cumulative costs, discounted			
Total costs per person (\$)	65,461	62,158	45,710
Cost effectiveness ratios-New Paradigm vs. Status Quo			
Incremental cost per QALY (\$)	DOMINANT		
Net mean benefit @ 100,000 WTP (\$)	61,660		
Cost effectiveness ratios-New Paradigm vs. Real-World Scenario			
Incremental cost per QALY (\$)	DOMINANT		
Net mean benefit @ 100,000 WTP (\$)	85,884		

HCV: hepatitis C virus; **QALY:** quality adjusted life year; **LY:** life year; **WTP:** willingness to pay.

Conclusion: This analysis demonstrated that simplifying the testing and treatment of HCV patients in the US may be a cost-effective strategy that would allow a quicker path to successful treatment and reduce the number of patients lost to follow-up.

FRI-142

Consider schistosomiasis screening in hepatitis B patients from endemic regions: a hepatic comorbidity that should not be neglected

Oriane Palaprat¹, Marie Gladys Robert¹, Marie-Pierre Brenier-Pinchart¹, Justine Barthemon², Hélène Fricker Hidalgo², Cécile Garnaud¹, Hervé Pelloux¹, Marie-Noëlle Hilleret², ¹Grenoble Alpes University Hospital,

Year	2012	2013	2014	2015	2016	2017	2018	2019	2020	2021	2022
Number of positive patients	294	144	91	109	88	113	49	24	102	71	51
- Born in schistosomiasis endemic areas	103 (35%)	59 (41%)	40 (44%)	49 (45%)	42 (48%)	65 (58%)	30 (61%)	13 (54%)	73 (72%)	54 (76%)	34 (67%)
o With serological screening for schistosomiasis	10 (10%)	5 (8%)	5 (13%)	7 (14%)	7 (17%)	8 (12%)	8 (27%)	6 (46%)	44 (60%)	31 (57%)	24 (71%)
o With positive serology for schistosomiasis	2	2	1	0	6	4	5	4	24	14	9

Figure: (abstract: FRI-142): Evolution of serological screening requests for schistosomiasis in patients with HBV in the hepato-gastroenterology department of the Grenoble Alpes University Hospital.

Parasitology-Mycology Laboratory, Grenoble, France; ²Grenoble Alpes University Hospital, Hepatology-Gastroenterology Department, Grenoble, France
Email: mrobert2@chu-grenoble.fr

Background and aims: Highly endemic countries for hepatitis B virus (HBV), particularly sub-Saharan Africa, are also endemic regions for schistosomiasis, a parasitic infection affecting more than 200 million people worldwide and caused by helminths of the genus *Schistosoma*. HBV-schistosomiasis co-infection is therefore common in these regions and can lead to cumulative chronic liver disease and especially to portal hypertension. Thus, it is recommended to screen all migrants from sub-Saharan Africa for both HBs antigen (HBsAg), and anti-*Schistosoma* antibodies. The aim of this study was to evaluate the effectiveness of this serological screening for schistosomiasis following the diagnosis of hepatitis B in our center.

Method: This single-center retrospective study investigated the records of all patients with a positive HBsAg from January 1, 2012 to November 30, 2022 in the hepato-gastro-enterology department of the Grenoble Alpes University Hospital. The availability of a serological screening for schistosomiasis by ELISA, rapid diagnostic test and/or western blot was examined for patients originating from Africa.

Results: Over the past 10 years, of the 1136 HBsAg-positive patients in our center, 562 (49.5%) were from schistosomiasis-endemic areas. However, serological screening for schistosomiasis was available for only 155 (27.6%) of these patients. In addition, 71 (45.8%) of the schistosomiasis serology performed in patients born in endemic areas were positive by at least one technique. Review of hepatic events related to schistosomiasis is currently ongoing among this population.

Conclusion: Although the prevalence of hepatitis B-schistosomiasis co-infection is significant in the population followed in hepato-gastroenterology for hepatitis B in France, screening for schistosomiasis remains insufficiently solicited. It is therefore essential to emphasize the potential impact this parasitic infection may have on the clinical outcomes of these patients and to remind the importance of screening at-risk patients and treating them if necessary.

FRI-143

Micro-elimination of Hepatitis C virus infection in mountainous and remote areas of Taiwan-a multi-center collaborative care model

Ching-Chu Lo¹, Wei-Yi Lei², Ying-Che Huang³, Jow-Jyh Hwang⁴, Chen-Yu Lo⁵, Ming-Jong Bair⁶, Chia-Yen Dai⁷, Ming-Lung Yu⁸, Chien-Hung Lin⁹, Hsu-sheng Cheng⁹, Yee-Tam Liao⁹, Mei-Tsu Chen⁹, Po-Cheng Liang¹⁰. ¹Division of Gastroenterology and Hepatology,

Department of Internal Medicine, St. Martin De Porres Hospital, Chiayi, Taiwan, Chung-Jen junior College of Nursing, Health Sciences and Management, Chiayi, Taiwan, Internal Medicine, Chiayi, Taiwan; ²Hualien Tzu Chi Hospital, Buddhist Tzu Chi Medical Foundation, and Tzu Chi University, Hualien, Taiwan, Taiwan; ³Taipei Veterans General Hospital Yuli Branch, Taipei, Taiwan, Taiwan; ⁴St. Martin De Porres Hospital, Chiayi, Taiwan, Chung-Jen junior College of Nursing, Health Sciences and Management, Chiayi, Taiwan, Taiwan; ⁵Eberly College of Science, Department of Biology, Schreyer Honors College, Pennsylvania State University, Taiwan; ⁶Taitung Mackay Memorial Hospital, Taitung, Taiwan, Department of Medicine, Mackay Medical College, New Taipei, Taiwan, Taiwan; ⁷Hepatobiliary Division, Department of Internal Medicine, Kaohsiung Medical University Hospital, Kaohsiung Medical University, Kaohsiung, Taiwan, Taiwan; ⁸School of Medicine, College of Medicine and Center of Excellence for Metabolic Associated Fatty Liver Disease, National Sun Yat-sen University, Kaohsiung, Taiwan, Taiwan; ⁹St. Martin De Porres Hospital, Chiayi, Taiwan, Taiwan; ¹⁰Kaohsiung Medical University Hospital; Hepatitis Research Center, College of Medicine and Center for Liquid Biopsy and Cohort Research, Kaohsiung, Taiwan, Taiwan
Email: fish6069@gmail.com

Background and aims: Taiwan has several hepatitis C virus (HCV) hyper-endemic areas. We aimed to evaluate the effectiveness and safety of a collaborative HCV care system with an outreach decentralized strategy among the resource-constrained Mountainous/remote areas of Taiwan

Method: The pilot study was conducted in four high HCV-endemic townships in the rural/remote areas of Taoyuan, Alishan, Zhuoxi and Xiulin. Registered residents who worked or lived in the four areas and were aged 30 to 75 years were invited to participate in this program. Multidisciplinary HCV care teams provided outreach decentralized services of anti-HCV screening, link-to-diagnosis, and link-to-treatment with direct-acting antiviral agents (DAA). The primary end point was sustained virological response (SVR).

Results: Of 8,291 registered residents who were invited as the target population, 7,807 (94.2%) subjects received anti-HCV screening, with the average anti-HCV prevalence rate of 14.2% (1108/7807) (range among four areas: 11.8%–16.7%). The rate of link-to-diagnosis was 94.4% (1046/1108) of anti-HCV-positive subjects (range: 90.9%–100%) with an average HCV viremic rate of 55.1% (576/1046) (range: 50.0%–64.3%). The link-to-treat rate was 94.4% (544/576) in HCV-viremic subjects (range from 92.7%–97.2%). Overall, 523 (96.1%) patients achieved an SVR (range: 94.7%–97.6%). Eventually, the overall effectiveness was 80.7% (range: 74.6%–93.1%) (Table 1). The presence of hepatocellular carcinoma at baseline was the only factor associated with DAA failure. The DAA regimens were well-tolerated.

POSTER PRESENTATIONS

Table: (abstract: FRI-143): HCV care cascade of HCV micro-elimination program in Mountainous/remote areas of Taiwan

	(A) Subjects receiving screening, n (%)	Anti-HCV seropositive n (%)	(B) Link-to-care n (%)	HCV RNA seropositive n (%)	(C) DAA treatment n (%)	(D) SVR12 n (%)	(E) Effectiveness
Taoyuan District	1092	1092 (100%)	129 (11.8%)	129 (100%)	72 (55.8%)	70 (97.2%)	93.1%
Alishan Township	2600	2511 (96.6%)	319 (12.7%)	311 (97.5%)	200 (64.3%)	192 (96.0%)	86.6%
Zhuoxi Township	1982	1833 (92.5%)	264 (14.4%)	246 (93.2%)	123 (50.0%)	114 (92.7%)	75.7%
Xiulin Township	2617	2371 (90.6%)	396 (16.7%)	360 (90.9%)	181 (50.3%)	168 (92.8%)	74.6%
Total	8291	7807 (94.2%)	1108 (14.2%)	1046 (94.4%)	576 (55.1%)	544 (94.4%)	80.7%

(E) = (A) × (B) × (C) × (D).

Conclusion: The outreach decentralized community-based care system with DAA therapy was highly effective and safe in the achievement of HCV micro-elimination in the resource-constrained rural and remote regions, which could help us to tackle the disparity.

FRI-144

Impact of the anti-HDV reflex testing on the reduction of hepatitis D burden in Spain

Maria Buti^{1,2}, Raquel Domínguez-Hernández³, Adriana Palom^{1,2}, Ariadna Rando-Segura^{2,4}, Mar Riveiro Barciela^{1,2}, Rafael Esteban^{1,2}, Francisco Rodríguez-Frías^{2,4}, Miguel Ángel Casado³. ¹Liver Unit, Hospital Universitari Vall d'Hebron, Barcelona, Spain, Spain; ²Centro de investigación biomédica en red de enfermedades hepáticas y digestivas, Instituto de Salud Carlos III, Madrid, Spain, Spain; ³Pharmacoeconomics and Outcomes Research Iberia (PORIB), Madrid, Spain, Spain; ⁴Microbiology Department, Clinical Laboratories, Hospital Universitari Vall d'Hebron, Barcelona, Spain, Spain
Email: mariabutiferret@gmail.com

Background and aims: Chronic hepatitis D (CHD) is the most severe form of chronic viral hepatitis due to rapid progression to liver cirrhosis and hepatocellular carcinoma. Early diagnosis and treatment could be able to stop the disease progression if suppression of viral replication is achieved. The aim of this study is to evaluate the impact of performing anti-HDV reflex testing in all HBsAg-positive subjects, on the burden of CHD in Spain in the coming years.

Method: A decision tree was designed to simulate the CHD care cascade from screening to treatment within a temporal horizon of 8 years. Two scenarios were compared: the current screening scenario (7.64% of HBsAg-positive patients tested for anti-HDV), and a reflex test screening scenario (100% of HBsAg-positive patients tested). The study target was the adult Spanish population (18–80 years). The estimated prevalence of HBsAg was 0.22% and of anti-HDV between 7.7%–9.6% of those HBsAg-positive. HDV-RNA was detectable in 60–73% of cases. It was assumed that 66% of viraemic patients would receive pegIFN with a 10% of long-term response. The incidence of complications and hepatic mortality were estimated based on the results of a cohort of patients previously followed for more than 8 years.

Results: The implementation of anti-HDV reflex testing in the HBsAg-positive Spanish population (total 78,965 subjects) would increase the diagnosis of 5,498 positive anti-HDV cases compared to the current scenario, of which 3,225 would be viraemic (Fig 1a). The cost for each anti-HDV+ diagnosed case would be €129. Considering that when using reflex testing, 2,128 more patients would receive treatment and 213 would achieve undetectable HDV-RNA levels, in the median time of the analysis, liver complications would be reduced between 7%–31% (Fig 1b). The prevention of these liver complications would estimatedly save around 40 M euros.

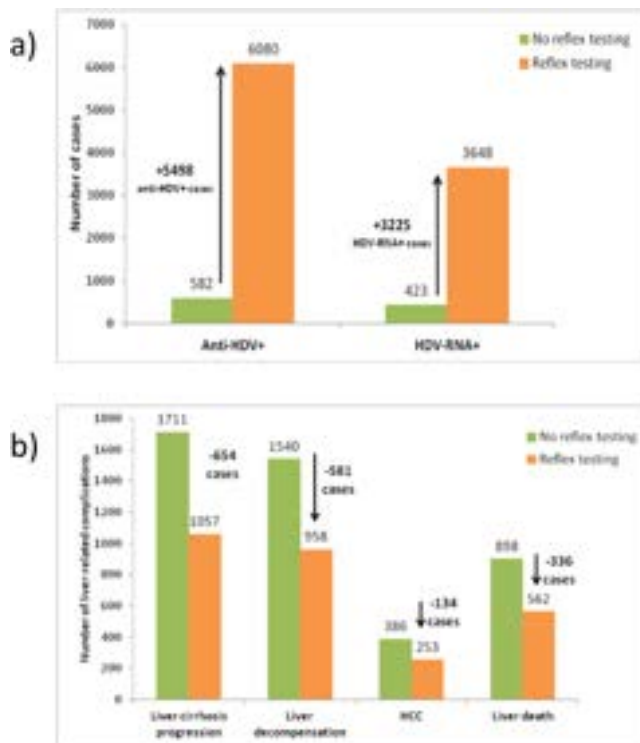


Figure:

Conclusion: In Spain, the use of anti-HDV reflex testing would increase more than 9 times the diagnoses of CHD, reducing the clinical and economic burden of the disease in the next 8 years.

FRI-145

Final results of a hepatitis C micro-elimination campaign in a highly endemic, well-defined demographic area of peri-urban Karachi, Pakistan

Saeed Sadiq Hamid¹, Aliya Hasnain¹, Sultan Salahuddin¹, Wasiuddin Shah¹, Taj Muhammad¹. ¹Aga Khan University, Medicine, Pakistan
Email: saeed.hamid@aku.edu

Background and aims: Pakistan has one of the highest burden of HCV with a nationwide prevalence of 6% with recognized “hot spots” where prevalence and liver disease related mortality is reported to be much higher. The aim of this study was to achieve highest possible HCV elimination in an endemic district by implementing and scaling

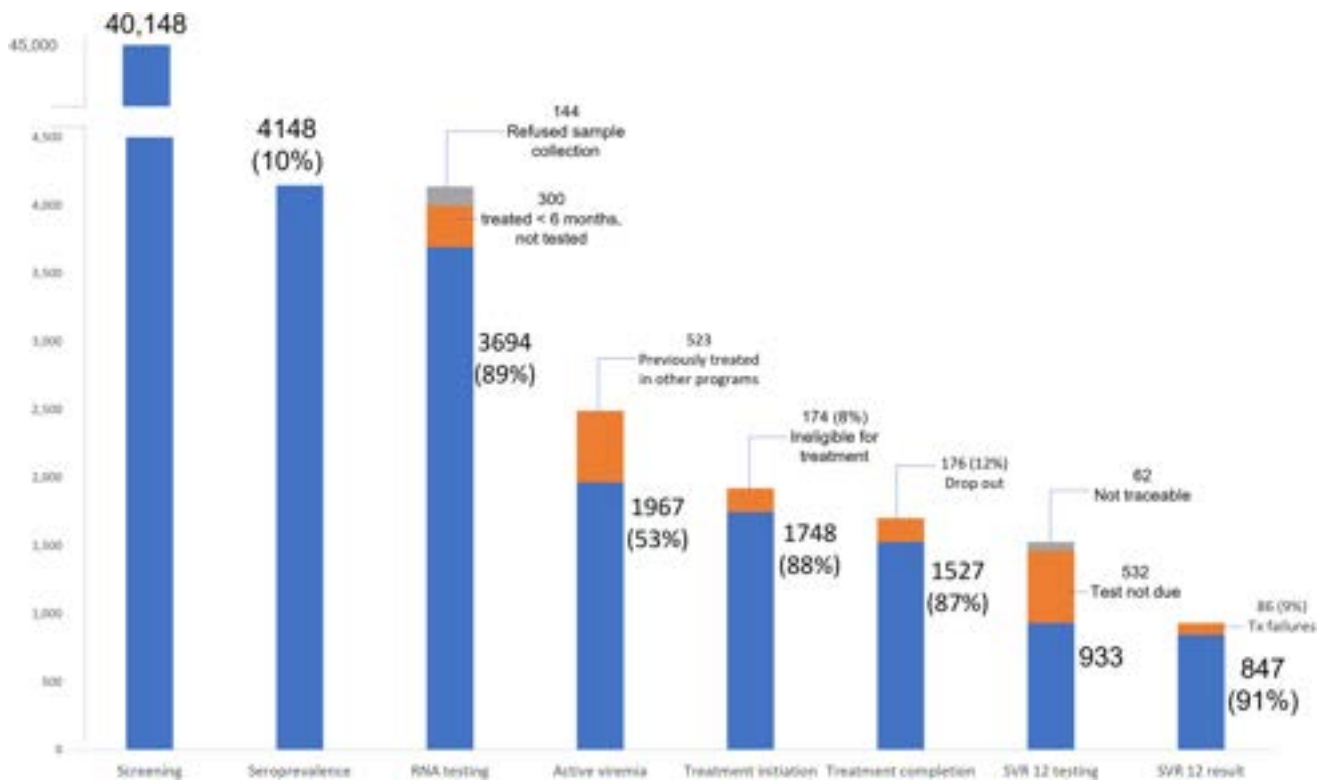


Figure: (abstract: FRI-145): Cascade of Care for Elimination.

up a highly simplified, community based, low-cost test-and-treat model.

Method: This study targeted 40,000 individuals over 12 years of age, across selected Union Councils (UCs) of Malir district, Karachi, based on known sero-prevalence in previous studies. After a concentrated campaign of public awareness, a two-step test and treat campaign was started through door-to-door visits guided by community mapping. First, a finger-stick rapid-diagnostic test (RDT) was used to screen for HCV. In those screened positive, reflex testing was done for confirmation of infection using GeneXpert, or HCV core antigen, and blood tests to calculate APRI and FIB-4. On the 2nd visit, individuals with confirmed infection were started on Sofosbuvir plus daclatasvir, for 12 or 24 weeks based on APRI and/or FIB-4 scores, after clinical evaluation by a physician. Follow-up visits were done on monthly basis to deliver medication. RNA testing was done 12 weeks after last dose to assess sustained viral response (SVR). A cohort of individuals previously screened negative was selected for re-screening to identify incidence of HCV infection in this population.

Results: Of the 40,148 individuals screened, 4,148 (10%) were positive (mean age 48.37 ± 14.46 years with 69% females). Average seroprevalence in males and females was 10% and 12% respectively. 3,694 individuals underwent HCV RNA testing of which 53% (1,967/3,694) had active viremia. 89% (1,748/1,967) of these patients started treatment of which currently 1,527 have completed treatment, with a dropout rate of 12% (176/1,693). Sustained virologic response (SVR) was achieved in 91%. Incidence of infection in the population re-screened was found to be 0.6% (6/1,008), with 2/6 viremic cases.

Conclusion: This study demonstrates feasibility of a highly simplified HCV-micro elimination program, using a low-cost community-based model which can be scaled up and implemented in diverse resource-limited settings

FRI-146

Evaluation of hepatitis B core-related antigen rapid test (HBcrAg-RDT) to identify HBV-infected women eligible for peripartum antiviral prophylaxis in resource-limited countries

Jeanne Perpétue Vincent¹, Olivier Segéral², Amariane Kone³, Laurence Borand⁴, Jean-Pierre Adoukara⁵, Dramane Kania³, Abdoul Tiendrebeogo⁶, Adeline Pivert⁷, Saren Sovan⁴, Jee-Seon Yang⁴, Gauthier Delvallez⁴, Françoise Lunel Fabiani⁷, Yasuhito Tanaka⁸, Yusuke Shimakawa¹. ¹Institut Pasteur, France; ²French Agency for Research on AIDS, Viral Hepatitis and Emerging Infectious Diseases (ANRS-MIE), Cambodia; ³Centre Muraz, Burkina Faso; ⁴Institut Pasteur du Cambodge, Cambodia; ⁵Hôpital de Tokombéré, Cameroon; ⁶Agence de Médecine Préventive (AMP), Burkina Faso; ⁷University Hospital of Angers, France; ⁸Kumamoto University, Japan
Email: yusuke.shimakawa@pasteur.fr

Background and aims: Prevention of mother-to-child transmission (PMTCT) of hepatitis B virus (HBV) is a key intervention to globally eliminate HBV as a public health issue. WHO currently recommends universal infant hepatitis B vaccination starting immediately after birth and peripartum antiviral prophylaxis to HBV-infected pregnant women having high HBV DNA levels ($\geq 200,000$ IU/ml). However, access to HBV DNA test is severely limited for pregnant women living in resource-limited countries. To enable decentralization of HBV PMTCT to antenatal care services at peripheral health facilities, we recently developed an immunochromatographic rapid test for hepatitis B core-related antigen (HBcrAg). We evaluated its diagnostic performance to identify HBV-infected women with high viral loads ($\geq 200,000$ IU/ml) using real-time PCR as reference in three countries with high HBV prevalence: Cambodia, Cameroon, and Burkina Faso.

Method: We evaluated the performance of HBcrAg-RDT: i) retrospectively using stored sera obtained from pregnant women positive for hepatitis B surface antigen (HBsAg) who participated in two large cohorts in Cambodia (ANRS 12345 TA PROHM) and Cameroon (ANRS 12303); and ii) prospectively using capillary blood collected by finger prick from mothers of infants in Burkina Faso (NéoVac study).

POSTER PRESENTATIONS

Results: In Cambodia, a total of 1194 HBsAg-positive pregnant women were tested and 367 had HBV DNA levels $\geq 200,000$ IU/ml. The sensitivity and specificity (95% CI) were 93.7% (90.7–96.0) and 95.2% (93.5–96.5), respectively. In Cameroon, of 502 HBsAg-positive pregnant women 88 had high viral load $\geq 200,000$ IU/ml. The sensitivity and specificity were 89.8% (81.5–95.2) and 91.7% (88.6–94.2), respectively. In Burkina Faso, a total of 1338 women participated, of whom 115 (8.6%) were positive for HBsAg and 14 had high viral load $\geq 200,000$ IU/ml. The sensitivity was 85.7% (57.2–98.2) and the specificity was 96.7% (90.6–99.3). In 1223 HBsAg-negative women, none were tested positive for HBcrAg-RDT.

Conclusion: HBcrAg-RDT may be a useful alternative to identify pregnant women eligible for peripartum antiviral prophylaxis at decentralized settings in resource-limited context.

FRI-147

Implementing hepatitis C self-testing (HCVST) among the general population in Georgia: preliminary results

Ketevan Stvilia¹, Maia Tsereteli², Ketevan Galdavazde², Senad Handanagic³, Shaun Shadaker³, Niklas Luhmann⁴, Irinka Tskhomelidze⁵, Antons Mozalevskis⁴, Sonjelle Shilton⁶, Tamar Gabunia^{7,8}, ¹National Center for Disease Control and Public Health, Georgia; ²National Center for Disease Control and Public Health, Georgia; ³Centers for Disease Control, United States; ⁴WHO Headquarters, Testing, Prevention and Populations Team, Global HIV, Hepatitis and Sexually Transmitted Infections Programmes, Swaziland; ⁵The Task Force for Global Health, Georgia; ⁶FIND, Operational and Implementation Research Unit, Swaziland; ⁷Ministry of Internally Displaced Persons from Occupied Territories, Labour, Health and Social Affairs, Deputy Minister, Georgia; ⁸National Center for Disease Control and Public Health, Acting Director General, Georgia
Email: stviliak@gmail.com

Background and aims: The 2015 hepatitis C virus (HCV) serosurvey estimated that more than half (57.3%) of all anti-HCV positive persons were males aged 30–59 years in Georgia. Innovative testing strategies to reach this group—such as HCV self-testing (HCVST)—are important to reach elimination. HCVST is recommended by the World Health Organization as a safe, acceptable, and feasible approach. Despite this, some questions remain about uptake and linkage to treatment following HCVST in different settings and populations. Thus, we evaluated both the uptake of HCVST and linkage to care for a secondary distribution model of HCVST among males aged 30–59 in Tbilisi, Georgia.

Method: This is an observational implementation study of a model of secondary distribution of HCVST among men aged 30–59 years recruited through female household members attending cancer screening clinics in Tbilisi, Georgia. Women who were amenable to recruiting their male household members were provided with HCVST kits to take home. After HCVST, male participants were able to register on an online platform to self-report their test results and complete an online survey to provide their demographic data, knowledge of HCV, HCV risk factors, and their experience with self-testing. Participants received a monetary incentive (about 3 USD) for completing the survey. Survey data will be linked with the national Hepatitis C Elimination Program database to assess linkage-to-care and treatment initiation among the anti-HCV positive participants.

Results: During June 9, 2022–January 1, 2023, a total of 1040 female participants were enrolled in the study (refusal rate 29%). A total of 541 male partners self-tested and shared their test results. Seven (1.3%) participants reported a reactive anti-HCV test result; all were more than age 43 years. Of those completing the online survey ($n = 533$), most said they would self-test again ($n = 421$, 78.9%); 455 (85.4%) felt they were able to correctly self-test and interpret the test result, and 15 (2.8%) said the self-tests did not work. Most participants reported self-testing independently ($n = 288$, 60.0%) or receiving assistance from a friend or household member ($n = 177$,

36.9%). The remaining participants were assisted by the study team ($n = 7$) or found information online ($n = 4$).

Conclusion: Preliminary results from this study show that more than half of women who received HCVST kits at the cancer screening sites were able to recruit male partners/household members into the HCV self-testing study. Implementation of this test distribution model was limited because of low internet literacy among the target population, thus additional options should be developed for reporting the HCV self-testing results. Engaging female household members may be instrumental in reaching important, highly burdened segments of the population who are unlikely to access traditional testing strategies.

FRI-148

Retrospective study of hepatitis C virus antibodies and active viral replication in patients with severe mental illness in a Spanish university hospital

Cristina del Rio-Cubilledo¹, Aitana Carla Morano Vázquez², Denise Monserrat Arroyo Jarrin³, Miriam Soriano García³, Henar las Heras Miralles¹, Jose Manuel Olivares Díez⁴, Luis Enrique Morano Amado⁵, ¹South Galicia Health Research Institute, South Galicia Biomedical Foundation, Vigo, Spain; ²Preventive Medicine Service, Gregorio Marañón University Hospital, Madrid, Spain; ³Psychiatry Service, Álvaro Cunqueiro University Hospital, Vigo, Spain; ⁴Psychiatry Service, Vigo Health Area, Álvaro Cunqueiro University Hospital, Vigo, Spain; ⁵Infectious Disease Unit, Álvaro Cunqueiro University Hospital, Vigo, Spain
Email: cristina.delrio@iisgaliciasur.es

Background and aims: In 2019, WHO estimated the prevalence of chronic HCV about 58 million globally, however only 21% were diagnosed and 9.4 million were treated with direct-acting antivirals (DAA). In Spain the prevalence of antibodies was 0.85% and the active infection was 0.22% in general population. HCV can cause hepatocellular carcinoma and cirrhosis. Among at-risk groups, HCV and other Blood-Borne Viruses (BBV) are very common in people with severe mental illness (SMI). People with SMI should be screened for BBV as a standard health assessment. Screening in the psychiatric unit of a hospital showed that 9% of patients were HCV positive. Other study showed that testing all psychiatric patients is cost-effective and should help to wipe out HCV. However, people with SMI have been under-recognized as a priority group for HCV screening.

Method: We did a retrospective study of 1631 patients admitted in the Psychiatry Unit at Álvaro Cunqueiro University Hospital (Vigo, Spain) between 2019 and 2021 to detect patients with HCV antibodies, HCV-untreated patients with active RNA replication, HCV-treated patients with sustained virologic response (SVR), HCV spontaneous viral clearance, HCV-uninfected and HCV-unknown. The selected covariates were age, sex, psychiatric diagnosis and other BBV.

Results: From 1631 patients with age average of 46 years, 785 were male and 846 female. 1097 (67.3%) were tested for antibodies. Antibodies were confirmed in 102 (9.3%) patients. Among these patients 93 (93.0%) showed undetectable RNA replication, of which only 64 (68.8%) have followed a treatment with SVR and the rest reached spontaneous viral clearance (SVC). 2% were not tested for RNA replication and 7 (7.0%) had active replication and did not follow any treatment. Among patients with positive antibodies, 26.5% had schizophrenia and 18.6% other psychotic disorder, followed by patients with personality disorder (15.7%), bipolar disorder (7.8%), depressive disorder (5.9%), adaptive disorders (3.9%) and 21.6% had other disorders.

Conclusion: The prevalence of HCV in our Psychiatry Unit was 10.9 times higher than in general population. Our results highlight the need to address the issue of higher prevalence of HCV in people with severe mental illness. The Health System should provide an effective screening method to identify patients with HCV at at-risk

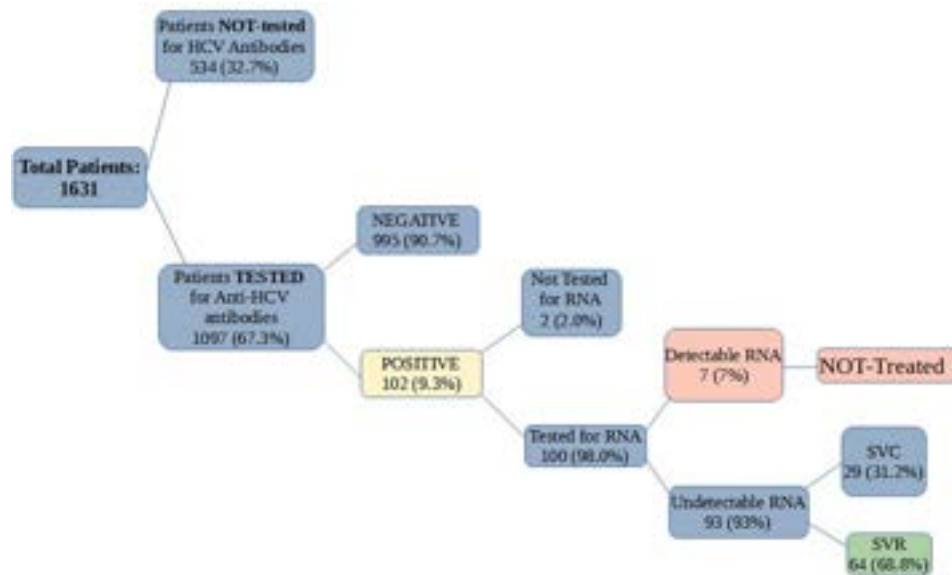


Figure: (abstract: FRI-148): Percentages of patients with HCV antibodies, RNA detectable or undetectable and patients who took treatment or reached SVC.

populations and develop a system to test all patients admitted in psychiatric units in hospitals.

FRI-149

Tailored message intervention by nudge theory increases the number of the viral hepatitis screening for Japanese workers and consultation behavior of positive patients -Consideration of 1.7 million general check-up participants

Masaaki Korenaga¹, Chieko Ooe², Keiko Kamimura², Tatsuya Ide³, Tatsuya Kanto⁴. ¹Hepatitis Information Center, The Research Center for Hepatitis and Immunology, National Center for Global Health and Medicine, Ichikawa Chiba, Japan; ²Japan Health Insurance Association, Japan; ³Kurume University, Japan; ⁴Hepatitis Information Center, The Research Center for Hepatitis and Immunology, National Center for Global Health and Medicine, Japan
Email: dmkkorenaga@hospk.ncgm.go.jp

Background and aims: Although the overall number of hepatitis B virus (HBV) and hepatitis C virus (HCV) carriers in Japan has decreased, actions against hepatitis at work sites in Japan have not yet been fully implemented. In Japan Health Insurance Association (JHIA), which is belonged to more than 40 million Japanese who are working in Medium and Small Sized Companies, the attendance rates of hepatitis screening were less than 2% even the cost of only €6. The aim of this study was to investigate the effectiveness of a tailored message intervention using nudge theory promoted the numbers of viral hepatitis screening and how many of those found to be positive patients have been followed up with examinations and hospital treatment.

Method: More than 1.7 million Japanese workers at Fukuoka branch of the JHIA who wish to get annual general checkup from 2017 to 2020 received client reminders by using nudge theory for an optional hepatitis virus screening. For control subjects, we enrolled general checkup applicants with typical message condition in 2016. The main outcome measure was attendance rates in HBV and HCV screening which were examined HBs antigen (HBsAg) and Anti-HCV antibody (HCVAb), respectively. In addition, 6 months after the checkup, we analyzed how many workers who were positive for HCVAb visited to physicians by medical prescription system.

Results: There was a significant difference in viral hepatitis screening attendance rates between the client reminders by using nudge theory (n = 109,003 6.5%) and the control (n = 4,791 1.2%; p < 0.001). One

thousand four workers (0.94%) were positive of HBsAg (n = 631, 0.58%) and HCVAb (n = 373, 0.38%), respectively. The positive rate of HCVAb in the 50 s (0.60%) were higher than those in 60 s (0.49%). One hundred eighty-five with HCVAb positive (50%) were confirmed to visit specialists within 6 months after the screening. Seventy (38%) were treated with IFN-free direct-acting antivirals and three males (1.6%) in 60 s were detected hepatocellular carcinoma.

Conclusion: There were still many positive patients with viral hepatitis at work sites. A simply modifying the client reminders using nudge theory could increase the viral hepatitis screening rates. Promoting hepatitis virus screening for workers at general checkup can rescue hepatitis virus carriers who are unaware of their infection and require to therapy for viral elimination and liver cancer.

FRI-150

Metabolic-associated fatty liver disease in socio-economic vulnerable population with chronic hepatitis B and C

Speranta Iacob^{1,2}, Razvan Iacob^{1,2}, Mihaela Ghioca^{1,2}, Cristian Gheorghe^{1,2}, Liana Gheorghe^{1,2}. ¹Carol Davila University of Medicine and Pharmacy, Gastroenterology, București, Romania; ²Fundeni Clinical Institute, București, Romania
Email: msiaacob@gmail.com

Background and aims: Viral hepatitis and metabolic-associated fatty liver disease (MAFLD) are the two leading causes of chronic liver disease in Romania. We are currently conducting a screening project in vulnerable population intended to provide preventive medical services, screening, diagnosis and linkage to care for patients detected with chronic HBV and HCV infection. The aim of our study was to investigate the presence of MAFLD in patients detected with viral hepatitis B and C in the screening project.

Method: 724 patients with B and C viral hepatitis detected at screening, staged and treated during 1 year period (September 2021–2022) in Fundeni Clinical Institute, were also screened for MAFLD using ultrasound, Fibroscan with CAP, FINDERISC (Finnish diabetes risk) score and AUDIT-C score.

Results: There were 61.5% of patients with HBV infection and 38.5% with chronic hepatitis C. Associated MAFLD was encountered in 55.8% of patients. The following statistical significant differences were encountered in HCV vs HBV infections: older age, higher prevalence of diabetes mellitus, higher liver stiffness values, higher percentage of cardiovascular and psychiatric disorders (p values < 0.05), but had

POSTER PRESENTATIONS

similar nonsignificant differences regarding BMI values, liver steatosis evaluated by CAP and chronic alcohol consumption. Liver stiffness values were not influenced by the presence of severe steatosis. Grade III liver steatosis evaluated by CAP was significantly higher in patients with higher BMI values and excessive alcohol drinking evaluated by AUDIT-C score ≥ 3 . FINDRISC score was significantly higher in female patients with HCV infection and correlated well with BMI values. Moderate FINDRISC score to develop diabetes mellitus in the next 10 years was associated with higher AST, ALT, triglycerides and BMI values. A higher FINDRISC and AUDIT scores were not associated with higher liver stiffness measurement. **Conclusion:** MAFLD is highly prevalent in patients with chronic hepatitis B and C in Romania, being associated with high BMI and AUDIT-C scores. Liver stiffness measurement was not influenced by the presence of MAFLD, but was significantly higher in HCV chronic hepatitis patients.

FR-151

Strategies to eliminate hepatitis C virus infection in the Americas

Luis Antonio Diaz^{1,2}, Sergio García³, Rayan Khan⁴, Gustavo Ayares⁵, Javier Uribe Monasterio⁶, Francisco Idalsoaga⁵, Eduardo Fuentes^{2,6}, María Paz Medel⁷, Carolina Ramirez⁸, Mariana Lazo^{9,10}, Catterina Ferreccio^{11,12}, Manuel Mendizabal¹³, Melisa Dirchwolf¹⁴, Patricia Guerra¹⁵, Claudia Oliveira¹⁶, Mário Pessoa¹⁶, Mario Álvares-da-Silva¹⁷, Giada Sebastiani¹⁸, Mayur Brahmanian¹⁹, Alnoor Ramji²⁰, Mina Niaz²¹, Hin Hln Ko²², Jordan J. Feld²³, Juan Carlos Restrepo²⁴, Wagner Ramirez²⁵, Omar Alfaro²⁶, Marlen Castellanos-Fernández²⁷, Enrique Carrera²⁸, Jose Roberto Aguirre²⁹, Katherine Emilia Maldonado Cardona³⁰, Abel Sanchez³¹, Marco Sánchez³², Maria Teresa Andara³³, Graciela Castro-Narro^{34,35,36}, Norberto Carlos Chávez-Tapia³⁶, Nahum Méndez-Sánchez³⁶, Enrique Adames³⁷, Julissa Lombardo³⁸, Marcos Giral³⁹, Elías Morán³⁹, P. Martin Padilla⁴⁰, Javier Diaz-Ferrer⁴¹, Martin Tagle⁴², Victoria Mainardi⁴³, Nélia Hernandez⁴⁴, Edmundo Martinez⁴⁵, Edilmar Alvarado-Tapias⁴⁶, Leon Robert⁴⁷, Maria Hernandez-Tejero⁴⁸, Mauricio Garcia Saenz De Sicilia⁴⁹, Wei Zhang⁵⁰, Jasmohan S. Bajaj⁵¹, Elliot Tapper^{52,53}, Manhal Izzy⁵⁴, Robert G. Gish⁵⁵, Bashar Attar⁵⁶, Thomas Cotter⁵⁷, Patrick S. Kamath⁴⁸, Ashwani Singal⁵⁸, Ramon Bataller⁵⁹, Gabriel Mezzano⁶⁰, Alejandro Soza^{61,62}, Jeffrey Lazarus^{63,64}, Marco Arrese^{61,62}, Juan Pablo Arab^{61,62,65}.

¹Departamento de Gastroenterología, Escuela de Medicina, Pontificia Universidad Católica de Chile, Chile; ²Observatorio Multicéntrico de Enfermedades Gastrointestinales (OMEGA), Chile; ³Escuela de Medicina, Pontificia Universidad Católica de Chile, Chile; ⁴Division of Gastroenterology, Department of Medicine, Schulich School of Medicine, Western University and London Health Sciences Centre, London, Canada; ⁵Departamento de Gastroenterología, Escuela de Medicina, Pontificia Universidad Católica de Chile, Chile; ⁶Departamento de Ciencias de la Salud, Facultad de Medicina, Pontificia Universidad Católica de Chile, Chile; ⁷Departamento de Medicina Familiar, Escuela de Medicina, Pontificia Universidad Católica de Chile, Chile; ⁸Department of Anesthesiology, London Health Sciences Centre, Western University, Canada; ⁹Department of Community Health and Prevention and Urban Health Collaborative, Dornsife School of Public Health, Drexel University, Philadelphia, United States; ¹⁰Division of General Internal Medicine, Johns Hopkins University School of Medicine, Baltimore, United States; ¹¹Public Health Department, School of Medicine, Pontificia Universidad Católica de Chile, Chile; ¹²Advanced Center for Chronic Diseases, ACCDis, Chile; ¹³Hepatology and Liver Transplant Unit, Hospital Universitario Austral, Buenos Aires, Argentina; ¹⁴Unidad de Hígado, Hospital Privado de Rosario, Rosario, Argentina; ¹⁵Instituto de Gastroenterología Boliviano-Japonés, Cochabamba, Bolivia; ¹⁶Division of Gastroenterology and Hepatology, University of Sao Paulo School of Medicine, Sao Paulo, Brazil; ¹⁷Hospital de Clínicas de Porto Alegre, Porto Alegre, Brazil; ¹⁸Department of Medicine, McGill University Health Centre, Montreal, Quebec, Canada; ¹⁹University of Calgary, Cumming School of Medicine,

Calgary, Alberta, Canada; ²⁰University of British Columbia, Vancouver, British Columbia, Canada; ²¹Department of Gastroenterology and Hepatology, University of Saskatchewan, Saskatoon, Saskatchewan, Canada; ²²Division of Gastroenterology, St Paul's Hospital, University of British Columbia, Vancouver, British Columbia, Canada; ²³Toronto Center for Liver Disease, Toronto General Hospital, Toronto, Canada; ²⁴Unidad de Hepatología del Hospital Pablo Tobon Uribe, Grupo de Gastrohepatología de la Universidad de Antioquia, Medellín, Colombia; ²⁵Clínica Equilibrium, San José, Costa Rica; ²⁶Hospital San Carlos, Ciudad Quesada, Costa Rica; ²⁷Department of Research and Teaching, Institute of Gastroenterology, University of Medical Sciences of Havana, Havana City, Cuba; ²⁸Hospital Eugenio Espejo, Quito, Ecuador; ²⁹Instituto Salvadoreño del Seguro Social, San Salvador, El Salvador; ³⁰Gastroenterología Endoscopia Digestiva, Hospital Roosevelt, Ciudad de Guatemala, Guatemala; ³¹Gastroenterología Endoscopia Digestiva, Hospital Roosevelt, Ciudad de Guatemala, Guatemala; ³²Hospital Escuela Universitario, Tegucigalpa, Honduras; ³³Instituto Hondureño de Seguridad Social, Tegucigalpa, Honduras; ³⁴Department of Gastroenterology, Instituto Nacional de Ciencias Médicas y Nutrición "Salvador Zubirán," Mexico City, Mexico; ³⁵Asociación Latinoamericana para el Estudio del Hígado (ALEH), Mexico; ³⁶Medica Sur Clinic and Foundation, Mexico City, Mexico; ³⁷Hospital Santo Tomas, Ciudad de Panamá, Panamá; ³⁸Hospital Punta Pacífica, Ciudad de Panamá, Panamá; ³⁹Departamento de Gastroenterología, Hospital de Clínicas, Universidad Nacional de Asunción, Asunción, Paraguay; ⁴⁰Unidad de Trasplante Hepático, Hospital Nacional Guillermo Almenara, Lima, Peru; ⁴¹Hospital Nacional Edgardo Rebagliati Martins-Es up Salud, Lima, Peru; ⁴²Clínica Anglo Americana, Lima, Peru; ⁴³Hepatology and Liver Transplant Unit, Hospital Central de las Fuerzas Armadas, Montevideo, Uruguay; ⁴⁴Clínica de Gastroenterología, Hospital de Clínicas, Facultad de Medicina, Universidad de la República Uruguay, Montevideo, Uruguay; ⁴⁵Servicio de Gastroenterología, Hospital Dr. Sótero del Río, Santiago, Chile; ⁴⁶Hospital de la Santa Creu i Sant Pau, Barcelona, Spain; ⁴⁷Instituto Médico La Floresta, Caracas, Venezuela; ⁴⁸Division of Gastroenterology and Hepatology, Mayo Clinic, Rochester, MN, United States; ⁴⁹Division of Gastroenterology and Hepatology, University of Arkansas for Medical Sciences, United States; ⁵⁰Gastroenterology Unit, Massachusetts General Hospital, Boston, MA, United States; ⁵¹Virginia Commonwealth University and Central Virginia Veterans Health Care System, Richmond, Virginia, United States; ⁵²Division of Gastroenterology and Hepatology, University of Michigan, Ann Arbor, Michigan, United States; ⁵³Gastroenterology Section, Veterans Affairs Ann Arbor Healthcare System, Ann Arbor, Michigan, United States; ⁵⁴Division of Gastroenterology, Hepatology, and Nutrition, Department of Medicine, Vanderbilt University Medical Center, Nashville, Tennessee, United States; ⁵⁵Hepatitis B Foundation, Doylestown, United States; ⁵⁶Division of Gastroenterology and Hepatology, Cook County Health, and Hospital Systems, Chicago, Illinois, United States; ⁵⁷Division of Digestive and Liver Diseases, UT Southwestern Medical Center, Dallas, Texas, USA, United States; ⁵⁸Department of Medicine, University of South Dakota Sanford School of Medicine, Division of Transplant Hepatology, Avera Transplant Institute, Sioux Falls, SD, United States; ⁵⁹Liver Unit, Hospital Clinic, Barcelona, Spain, Spain; ⁶⁰Gastroenterología-Hepatología, Hospital del Salvador. Universidad de Chile, Santiago, Chile; ⁶¹Departamento de Gastroenterología, Escuela de Medicina, Pontificia Universidad Católica de Chile, Santiago, Chile; ⁶²Observatorio Multicéntrico de Enfermedades Gastrointestinales (OMEGA), Santiago, Chile; ⁶³CUNY Graduate School of Public Health and Health Policy (CUNY SPH), New York, NY, United States; ⁶⁴Barcelona Institute for Global Health (ISGlobal), Hospital Clinic, University of Barcelona, Barcelona, Spain; ⁶⁵Division of Gastroenterology, Department of Medicine, Schulich School of Medicine, Western University and London Health Sciences Centre, London, Ontario, Canada
Email: jparab@gmail.com

Background and aims: Although the WHO strategy has the goal to eliminate the hepatitis C virus (HCV) as a public health threat by 2030, the existence of national strategies is variable worldwide. We

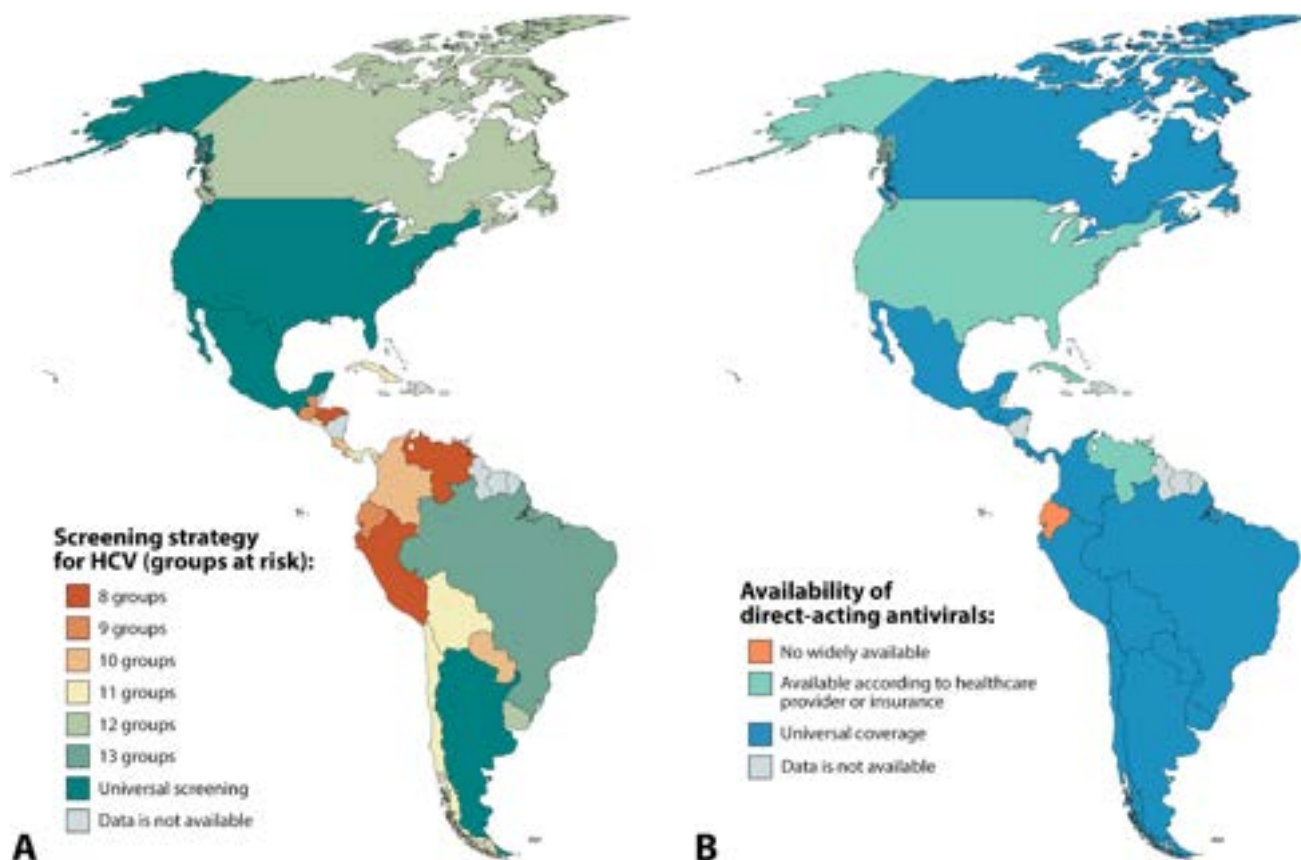


Figure: (abstract: FRI-151): Screening strategies (A) and availability of direct-acting antiviral treatments (B) among 19 countries in the Americas. The potential groups for screen were solid organ transplantation, haematological transplantation, chronic kidney disease, haemodialysis, human immunodeficiency virus infection, cirrhosis (any aetiology), hepatocellular carcinoma, bleeding disorders who have received a transfusion of blood products, sexually transmitted infections, injectable drug users, serious mental health disorders, migrants from countries with a high prevalence of HCV, pregnant women, and people of a certain age (e.g., baby boomers).

aimed to assess the establishment of different policies and strategies to eliminate HCV in the Americas.

Method: We conducted a 23-item survey about HCV infection among gastroenterologists and hepatologists in the Americas. Questions were classified into four categories: policies and civil society (1 question), diagnosis (6 questions), care management (14 questions), and monitoring systems (2 questions). The survey was administered using an electronic form between November 7, 2022– January 8, 2023. Data were collected in a spreadsheet, revised by two independent reviewers, and compared with governmental institutions, regulatory agencies, scientific societies, and scientific publications.

Results: We obtained 47 responses from 19 out of 21 countries targeted (Argentina, Bolivia, Brazil, Canada, Chile, Colombia, Costa Rica, Cuba, Ecuador, El Salvador, Guatemala, Honduras, Mexico, Panama, Paraguay, Peru, United States, Uruguay, and Venezuela). Fifteen (78.9%) countries have adopted a national strategic plan to eliminate HCV. Three (15.8%) countries have universal screening for HCV infection (Figure 1A). HCV was more commonly diagnosed in older cirrhotic patients (57.8%), followed by young patients who inject drugs (21.1%), and men who have sex with men (21.1%). After a positive HCV serological test, 10 (52.6%) countries perform reflex testing to confirm HCV diagnosis using the same sample. However, only 7 (36.8%) countries have an alert system for the requesting physician. Twelve (63.2%) countries have a direct referral system for specialized care of HCV positive cases. There is universal access to direct-acting antivirals (DAAs) in 15 (78.9%) countries (Figure 1B). Seven (36.8%) countries have generic DAAs available. Only 3 (15.8%)

countries perform a retrospective search for HCV positive cases that could have been lost to follow-up.

Conclusion: Although most countries have adopted a national strategic plan to eliminate HCV, there are several issues and barriers to elimination in the Americas.

FRI-152

Qualitative interviews to assess the impact of chronic hepatitis delta virus infection on health-related quality of life in untreated patients from the US, Italy, Spain, and Germany

Pietro Lampertico^{1,2}, Robert G. Gish³, Nancy S. Reau⁴, Heiner Wedemeyer⁵, Maria Buti⁶, Hannah Elwick⁷, Nicola Williamson⁷, Aishwarya Chohan⁷, Margaret Guy⁷, Rowena Jones⁷, Ankita Kaushik⁸, Alon Yehoshua⁸. ¹Foundation IRCCS Ca' Granda Ospedale Maggiore Policlinico, Division of Gastroenterology and Hepatology, Milan, Italy, Italy; ²CRC "A. M. and A. Migliavacca" Center for Liver Disease, Department of Pathophysiology and Transplantation, University of Milan, Milan, Italy, Italy; ³Hepatitis B Foundation, Doylestown, PA, United States; ⁴Department of Internal Medicine, Division of Digestive Diseases and Nutrition, Rush Medical College, Chicago, United States; ⁵Department of Gastroenterology, Hepatology, and Endocrinology, Hannover Medical School, Hannover, Germany; ⁶Liver Unit, Hospital Universitario Valle Hebrón and Ciber-ehd del Instituto Carlos III, Barcelona, Spain; ⁷Patient-Centred Outcomes, Adelphi Values, Bollington, United Kingdom; ⁸Gilead Sciences, California, United States

Email: pietro.lampertico@unimi.it

POSTER PRESENTATIONS

Background and aims: Hepatitis delta virus (HDV) is the most severe form of viral hepatitis, which often results in accelerated progression to cirrhosis and poor prognosis, impacting patients' health-related quality of life (HRQoL). Patient-Reported Outcome (PRO) instruments can capture the patient perspective and provide additional insights beyond surrogate markers such as viral load and alanine aminotransferase changes. The US Food and Drug Administration's guidance states that PRO instruments should have sufficient evidence of content validity in the target population prior to use. This study aimed to explore the experience of patients living with chronic HDV and evaluate the content validity of the Hepatitis Quality of Life Questionnaire (HQLQ) and the Fatigue Severity Scale (FSS) for use in HDV.

Method: Semi-structured concept elicitation and cognitive debriefing qualitative interviews were conducted with patients in the US, Germany, Italy, and Spain with a clinician-confirmed diagnosis of chronic HDV. Patients were eligible to participate if they were not treated with interferon at the time of the study or in the previous six months. Patients diagnosed with Hepatitis C or had experienced an acute episode of liver disease in the previous six months were excluded. Participants described their experience living with HDV and then completed two instruments using a think-aloud technique to assess understanding, comprehension, and relevance of items, instructions, response scales, and recall period. Interviews were conducted in the native language of each country, and official translations of instruments were used. Thematic and framework analyses of verbatim interview transcripts were performed.

Results: The study sample (n = 32) included participants with a range of liver fibrosis stages from F0-F3 or F4 compensated, and two participants diagnosed with hepatocellular carcinoma. The majority of participants were aged over 55, and 63% of the sample were female. Fatigue, loss of appetite, pain over liver, nausea, and fever were the most frequently reported symptoms. Participants reported that HDV impacted their emotional wellbeing (low mood, anxiety), physical functioning (inability to exercise, difficulty walking), social functioning (including stigma), and work (difficulty meeting job responsibilities). By this approach, participants demonstrated good understanding of HQLQ and FSS items, instructions, response scales and recall periods, and concepts assessed in the instruments were considered relevant to HDV by most participants.

Table 1. Participant clinical and demographic characteristics

Clinical and demographic characteristics of sample, n (%)	Total (n=32)
Liver fibrosis stage	
F0-F1	17 (53)
F2	5 (16)
F3	3 (9)
F4 compensated	7 (22)
F4 decompensated	0 (0)
HCC diagnosis status	
Diagnosed	2 (6)
Not diagnosed	30 (94)
HBV treatment status	
Untreated	2 (6)
Previously treated	11 (34)
Currently treated	19 (60)
HDV treatment status	
Untreated	14 (44)
Previously treated	18 (56)
Currently treated	0 (0)
Age	
18-30 years	3 (10)
31-55 years	11 (34)
>55 years	18 (56)
Sex	
Male	12 (37)
Female	20 (63)

Conclusion: Findings contribute to the understanding of the patient experience of HDV and support the content validity of the HQLQ and FSS as outcome assessments for use in HDV. Further research to examine the psychometric validity of the PRO instruments and support their use as clinical trial end points is recommended.

FRI-153

Microbiological analysis of acute hepatitis of unknown aetiology in children in Spain

Ana Avellon Calvo^{1,2}, Milagros Munoz-Chimeno¹, Carmen Varela³, Maria Guerrero³, Marina Peñuelas³, Lucia Morago¹, Nazaret Sanchez¹, Monica Gonzalez⁴, David Tarrago⁵, Juan Emilio Echevarria⁵, Maria Dolores Fernandez⁵, Raquel Escudero⁶, Francisco Pozo⁷, Sarai Varona⁸, Victoria Hernando³, Asuncion Diaz³. ¹National Centre for Microbiology, Hepatitis Unit, Spain; ²Instituto de Salud Carlos III, Hepatitis Unit, Spain; ³National Centre for Epidemiology, Spain; ⁴National Centre for Microbiology, Central Laboratory, Spain; ⁵National Centre for Microbiology, Viral Detection Unit, Spain; ⁶National Centre for Microbiology, Bacteriology, Spain; ⁷National Centre for Microbiology, Respiratory Viruses, Spain; ⁸Instituto de Salud Carlos III, Bioinformatics Unit, Spain

Email: aavellon@isciii.es

Background and aims: On 2022 5th April, United Kingdom notified to WHO an alert of severe acute hepatitis in children. Since then to the end of 2022 Spain has detected 61 cases with 3 deaths. Microbiological analysis, complementary to that performed at the hospitals, has been performed at the National Centre for Microbiology in 42 cases.

The aim of this report is to describe the microbiological analysis performed at the National Centre for Microbiology in 42 cases, including the metagenomic analysis.

Method: Samples (serum, total blood, faeces, urine and nasopharyngeal swab) were studied through PCRs of: herpes simplex viruses, virus varicella-zoster, cytomegalovirus, Epstein-Barr virus, herpes 6, 7 and 8, enterovirus, parvovirus B19, adenovirus, hepatitis A and E, norovirus and leptospira. Massive sequencing was performed in most of the cases with a metagenomic approach.

Results: Among serum and total blood samples, 11/42 (26.2%) cases were positive to herpes and 3/42 (7.1%) positive to enterovirus. Adenovirus were detected in 18/42 (42.8%) of the cases, obtaining 2 complete genomes. Adeno-associated viruses were detected by metagenomics in 8/42 (19.0%) cases. Some other viruses were detected as: CoVNL63, Coronavirus HKU1, Sapporovirus, Respirovirus and Parechovirus.

Conclusion: Obtained results parallels those reported in other European countries in where adenoviruses and adeno-associated viruses were the most common viruses detected. However, the aetiology of the hepatitis cases remains unclear, as more case and control studies are needed to define the exact role of each microorganism.

FRI-154

Emergency department contribution to hepatitis C elimination through opportunistic screening in Cascais, Portugal

Inês Vaz Pinto¹, Catarina Esteves Santos¹, Mafalda Guimarães¹, Rita Vale Rodrigues¹, Vanda Castro¹, Alba Carrodegua², Diogo Medina². ¹Hospital de Cascais Dr. José de Almeida, Alcubideche, Portugal; ²Gilead Sciences, Lda, FOCUS Program, Lisboa, Portugal
Email: diogomedina@gmail.com

Background and aims: Advancing screening and linkage to care practices is necessary to eliminate hepatitis C in Portugal toward WHO goals for 2030. We aimed to ascertain whether screening of patients seeking urgent care could effectively complement existing targeted screening policies.

Method: We implemented opportunistic screening in the emergency department from September 2018 to September 2021 (36 months), using existing infrastructure and staff, aided by electronic health

record system automations to identify screening eligibility and request serologies. Patients aged 18–64 were eligible upon verbal consent IF they had no recorded tests in the previous year AND required blood work. Follow-up or discharge were provided regardless of test results. Case managers contacted positive patients to ensure linkage to care.

Results: We screened 88.9% (n = 38,357) of eligible patients, finding 1.49% (n = 571) HCV antibody seroprevalence, 0.56% (n = 215) HCV RNA prevalence, and 26.5% (n = 57) unknown infection. Most were Portuguese (74%), male (61%), with an average age of 51.3 (19–65). Injected drug use and heterosexual transmission accounted for 75% and 25% of known modes of transmission. 1a (44%) and 3 (32%) were the most found genotypes. We linked 80.7% (n = 46) of patients to care post-diagnosis. Of 38 patients subject to real-time elastography or serum biomarkers for liver stiffness measurement at our hospital, 31% presented with either advanced fibrosis (F3) or cirrhosis (F4).

Conclusion: Our project led to a significant increase in the number of patients diagnosed at our hospital. Changes in testing stigma were also apparent, with high patient and provider adherence to screening. Opportunistic blood-borne virus screening approaches in emergency departments are feasible and effective.

FRI-155

Implementation of anti-HDV reflex testing among HBsAg-positive in a tertiary center in South Italy

Valentina Cossiga¹, Annachiara De Conte¹, Stefano Brusa², Eduardo Molinari², Francesco Maria Cutolo¹, Luisa Ranieri¹, Raffaele Lieto¹, Enza Zaccchia², Maria Rosaria Attanasio¹, Fortunato Mazzitelli¹, Maria Guarino¹, Giuseppe Portella², Filomena Morisco¹. ¹Department of Clinical Medicine and Surgery, Diseases of the Liver and Biliary System Unit, University of Naples “Federico II”, Naples, Italy, Italy; ²Department of Translational Medical Science, University of Naples “Federico II”, 80131 Naples, Italy, Italy
Email: valentina.cossiga@gmail.com

Background and aims: In Italy, the prevalence of HDV infection in HBsAg carriers is about 9.9% (6.4% in Italian natives and 26.4% in immigrants) [1]. However, the actual prevalence is probably underestimated because the anti-HDV test is not performed routinely in all HBsAg carriers. The HDV causes a rapidly progressive liver disease and as new antiviral therapies are coming, it is fundamental to know the exact HDV prevalence. The aim of this study was to describe the impact of the introduction of anti-HDV reflex test in all HBsAg-positive subjects at AOU Federico II and to compare the results before and after its implementation.

Method: From April 2021 to December 2022, reflex test for the detection of total HDV antibodies was performed in all HBsAg positive subjects observed at AOU Federico II. Demographic, clinical and laboratory data were collected. Liver fibrosis was evaluated with FIB-4. Sera were evaluated with ADVIA Centaur HBsAgII Qualitative, Liaison Murex HBsAg Quantitative and Liaison Murex Total Anti-HDV Qualitative.

Results: Before reflex testing, anti-HDV had been tested in 16.4% (84/512) of HBsAg positive subjects, while after its implementation, 100% (423/423) of HBsAg positive patients was tested for anti-HDV. The anti-HDV positive prevalence was higher before the introduction of reflex test (16% vs 12%), but the absolute number of anti-HDV positive patients increased (14 vs 51). Of 423 HBsAg carriers, 51 (12%) resulted positive for total anti-HDV. The majority of them (90.2%) were Italian natives and only 5 (9.8%) of them were immigrants. Twenty-four (47%) were males with a median age of 62.2 years, not different from anti-HDV negative subjects. Twenty (39.2%) patients were already aware of HBV/HDV coinfection. HDV-RNA was performed in 37 (72.5%) subjects and resulted detectable in 22 (59.4%) of them, with a median HDV-RNA level of 84.300 [25th–75th percentiles: 1.685–547.796] IU/ml. Twenty (39.2%) anti-HDV positive subjects had advanced liver fibrosis.

Conclusion: Our data showed that the implementation of anti-HDV reflex test increased the number of diagnosis of HDV infection and revealed the real prevalence of HDV prevalence (higher than expected). Moreover, the HDV-RNA is performed only in a part of the anti-HDV positive subjects. In this setting, due to the forthcoming approval of specific anti-HDV drugs, a reflex test for HDV-RNA should be implemented to identify viremic patients needing antiviral treatment.

FRI-156

Effectiveness of a direct care action strategy at the drug addiction center (test and treat in point of care) for the detection and treatment of hepatitis C in drug users on opioid agonist substitution therapy

Adrià Rodríguez^{1,2}, Inés Sáenz de Miera^{1,2}, Maria Assumpció Sendra³, Patricia Méndez³, María Ángeles Roch⁴, Montserrat Vargas¹, Silvia Montoliu^{1,2}, Albert Pardo^{1,2}, Joan Colom⁵, Juan Carles Quer Boniquet^{1,2}. ¹Joan XXIII University Hospital of Tarragona, Gastroenterology, Spain; ²Pere Virgili Health Research Institute, Tarragona, Spain; ³Tarragona Drug Addiction Center, GIPPS, Spain; ⁴Joan XXIII University Hospital of Tarragona, Pharmacy, Spain; ⁵Catalonia Public Health Agency (ASPCAT), Program PCAVIHV, Sub-Directorate General of Drug Dependences, Spain
Email: senisamier@yahoo.com

Background and aims: Drug users are a vulnerable group with difficulty accessing the diagnosis and treatment of chronic infection by the hepatitis C virus (CHC); for this reason, targeted micro-elimination strategies are being developed to act specifically in this group, with the aim to facilitate their access to treatment. This study aims to evaluate the effectiveness of an onsite strategy at the drug addiction center (DAC) (test and treat in point of care) to characterize, treat and cure patients with CHC undergoing opioid agonist substitution therapy (OAT) in their usual environment.

Method: Using one-step virological detection, patients with positive viremia were assessed at the DAC's office by a hepatologist, a pharmacist, and DAC professionals. During the same visit, baseline clinical, laboratory and elastographic characteristics were determined, as well as potential drug interactions, before starting direct-acting antivirals (DAA). Therapy began on the same day of the visit and was fully facilitated by the DAC, where adherence control was carried out. Sustained viral response (SVR) was evaluated at week 12 post-treatment (SVR12). We present descriptive data of 48 patients visited and treated at the DAC in the periods of January-March 2020 and November 2020-December 2022.

Results: 91.2% of the patients were men with a mean age of 48 years. 96% were caucasian; 83% were Spanish. 90% were treatment-naïve, and genotype 1a was the most frequent (50%). Most were F0-1 (73%) and only 3 (6%) were F4. 35 received treatment for 8 weeks with Glecaprevir/Pibrentasvir and 13 for 12 weeks with Sofosbuvir/Velpatasvir. In the pre-interaction study, only 3 patients required modifications to their usual treatment. In total, 8 patients had side effects (4 mild and 4 moderate) without requiring treatment modifications. The adherence of patients who have already completed treatment (48) has been excellent in 90%. The response of 45 patients is evaluated (2 are completing treatment and 1 died before being evaluated): At the end of treatment: 43 (96%) had responded and in 2 (4%) the response is unknown due to loss of follow-up. At week 12 post-treatment: 40 patients (89%) had achieved SVR12, 1 presented criteria for treatment failure and in 4 (9%) this was unknown due to loss of follow-up. The maintenance of the response one year post-treatment has been evaluated in 43 patients: 25 (58%) maintain SVR, 4 (9%) present criteria for reinfection (3 of them have already been retreated), while in 14 (33%) the response is unknown due to loss of follow-up.

Conclusion: A high adherence to treatment was observed applying the test and treat in point of care strategy. The efficacy of the novel

POSTER PRESENTATIONS

strategy was significantly higher than those described for this group of patients with the usual strategies (*standard of care*). Only one case of virological failure has been observed, however, the loss of follow-up after completing the treatment makes it difficult to obtain efficacy comparable to the general population. The study also found a significant rate of reinfection at one year of follow-up. Most reinfected patients have already been retreated. The center-based action strategy was found to be superior to usual strategies for treating this difficult-to-treat population.

FRI-157

Comparison of HCVRNA results using plasma separation card with gold standard veni-puncture

Huma Qureshi¹, Hassan Mahmood², Syeda Zahida Sarwar³, Khalid Mahmood⁴. ¹Ministry of National Health Services, Regulations and Coordination, Pakistan, Pakistan; ²Integral Global, Pakistan; ³Independent Consultant, Lahore, Pakistan; ⁴Punjab Health Department, Lahore, Pakistan
Email: drhumapmrc@gmail.com

Background and aims: Drawing a venous sample for HCVRNA testing requires an expert. The transportation of this sample and its storage also requires special care and refrigeration especially in the low middle income countries. The plasma separation card is a solution for all these issues where whole blood collected from a finger stick is placed onto the card and is transported without separating or refrigerating it. HCV RNA is extracted from it at the laboratory. To compare the ease of extraction and results HCVRNA using Plasma Separation Card with Gold standard venous blood collected in a gel tube.

Method: A total of 350 anti HCV reactive persons underwent reflex blood collection for HCVRNA. From each individual 5 ml of venous blood was collected in a gel tube and stored for HCVRNA testing. From the other hand, using a finger stick, 140 microliters of whole blood were collected in the capillary tube and poured over the marked point of the plasma separation card (PSC). The gel tube and the PSC were transported to the main laboratory for RT PCR, where plasma was separated from the gel tubes and was run for HCVRNA testing (both qualitative and quantitative assays). From the plasma separation card, one punch of spot was removed and placed in the virus extracting solution and tested for HCVRNA using standard steps (both qualitative and quantitative assays). The two tests were run simultaneously for comparison. A correlation factor of 50 was applied to the PSC viral quantification and then compared with the quantitative HCVRNA levels obtained from the venous samples.

Results: A total of 352 anti HCV reactive cases underwent venous blood sampling and the finger stick blood collection on PSC. Both samples were run for HCVRNA at the laboratory. There were 54% males and majority were anti HCV reactive between 21 and 50 years. HCVRNA testing was done in 84% cases before starting the treatment while in others it was done after completion of the treatment. Preference for finger stick blood collection was seen in patients and technicians. Time taken in venous collection was much less than that in the finger stick. Gold standard venous sample collected in gel tube detected virus in 144 samples while finger stick blood collected on PSC detected HCVRNA in 153 cases. The sensitivity of the PSC was 93.8% with 91.3% specificity. The positive predictive value was 88.2% and negative predictive value was 95.5%. Overall, a good correlation of $r = 0.63$ was seen between HCVRNA extracted from venous sample vs PSC.

Conclusion: Plasma separation card for blood collection, transportation, storage and extraction of HCVRNA was found to be user friendly when compared with the venous blood collection. The HCVRNA extracted from the PSC correlated well with the venous sample suggesting its wider use especially in difficult to reach populations and areas.

FRI-158

Patients with hepatitis B and D are more often linked to medical care than patients with hepatitis C

Elena Vargas Accarino¹, Anna Feliu-Prius¹, Adriana Palom¹, Ariadna Rando-Segura², Ana Barreira¹, Joan Martinez-Camprecios¹, Judit Vico-Romero¹, Juan Carlos Ruiz-Cobo¹, Jordi Llaneras¹, Mar Riveiro Barciela¹, Francisco Rodríguez-Frías², Rafael Esteban¹, Maria Buti¹. ¹Vall d'Hebron University Hospital, Liver Unit, Spain; ²Vall d'Hebron University Hospital, Microbiology Department, Spain
Email: mbuti@vhebron.net

Background and aims: The WHO established the goal to decrease hepatitis B and C associated mortality to less than 6 cases/100.000 people for 2030. To achieve this goal, it is important to identify and link to care patients with viral hepatitis. The objective of this study was to retrieve hepatitis B, C and D lost to follow-up patients and to deepen the reasons why they were not linked to care. This study was performed in the Spanish public health system.

Method: Retrospective and prospective search in the microbiology database of the northern area of Barcelona (450.000 inhabitants) of patients with hepatitis C (HCV-RNA+), hepatitis B (HBsAg+) and hepatitis D (anti-HDV+). Patient medical records were reviewed to identify lost to follow-up patients. Candidates to contact were telephoned a maximum of 5 times to offer them a medical visit.

Results: A total of 3407 patients were screened between January 2019 and June 2022. Among them, 1540 (45%) were HBsAg+, 53 (2%) anti-HDV+, and 1.814 (53%) HCV-RNA+. 498 (31%) from the HBsAg+ patients were not linked to care, 14 (26%) from the anti-HDV patients and 1018 (56%) from the HCV-RNA+; being hepatitis D patients significantly more linked to care than hepatitis C patients ($p < 0.0001$). After the telephone calls, 226 (46%) from the 498 HBsAg+ patients not linked to care, 12 (85%) from the 14 anti-HDV+ (2 of which HDV-RNA+) and 54 (5.3%) from the 1.018 HCV-RNA+ were finally linked; being HCV-RNA+ patients significantly less linked to care ($p < 0.0001$). Patients with hepatitis C had significantly more advanced age or comorbidities (703 (23%)), compared to patients with hepatitis B or D (17 (1%) and 1 (2%)) ($p < 0.0001$). Of the total number of patients, 670 (20%) could not be contacted due to missing personal data.

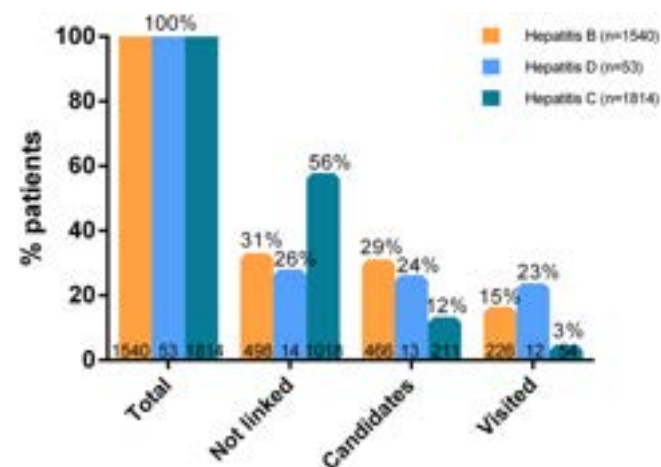


Figure:

Conclusion: From the patients not linked to care, 46% (226) from the HBsAg+, 85% (12) from the anti-HDV+ and 5.3% (54) from the HCV-RNA+ were finally linked. In total, 292 (19%) patients have been linked to care, suggesting this is an effective strategy. Patients with hepatitis D are more linked and predisposed to be linked to care than patients with hepatitis C. The biggest challenge of this strategy has been the lack of contact details.

FRI-159

The impact of hepatitis B and C serologies on the outcomes of non-liver solid organ transplantation

Maria Stepanova^{1,2,3}, Reem Al Shabeeb⁴, Katherine Eberly⁵, Janus Ong⁶, Saleh Alqahtani⁷, Zobair Younossi^{1,5}. ¹Inova Health System, Inova Medicine Services, Falls Church, United States; ²Beatty Liver and Obesity Research Program, Inova Health System, United States; ³Center for Outcomes Research in Liver Disease, United States; ⁴Inova Fairfax Hospital, Center for Liver Disease, Inova Medicine, United States; ⁵Inova Fairfax Hospital, Department of Medicine, Center for Liver Diseases, United States; ⁶College of Medicine, University of the Philippines, Manila, Philippines; ⁷Johns Hopkins University, Division of Gastroenterology and Hepatology, Baltimore, United States
Email: zobair.younossi@inova.org

Background and aims: Viral hepatitis B (HBV) and C (HCV) could negatively affect the outcomes of non-liver solid organ transplantation. Our aim was to assess post-transplant survival in patients with HBV and HCV serologies who received a non-liver solid organ transplants.

Method: We used Scientific Registry of Transplant Recipients (SRTR) 2006–2021 to collect data for all patients ≥18 years of age who received a lung, heart, or kidney single organ transplant in the U.S. History of hepatitis C virus (HCV) infection was determined as positive HCV Ab, and history of hepatitis B (HBV) infection was determined as positive HBsAg.

Results: We included a total 348,024 non-liver solid organ transplant recipients (N = 30,872 lung: mean age 57 ± 13 years, 60% male, 4% re-transplants, 15% type 2 diabetes (T2D); N = 36,990 heart: age 54 ± 13 years, 74% male, 3% re-transplants, 26% T2D; N = 280,162 kidney: age 52 ± 14 years, 61% male, 12% re-transplants, 30% T2D). The prevalence of pre-transplant HBsAg was 1.3% in lung, 1.5% in heart, and 1.7% in kidney transplant recipients. The HCV Ab was positive in 2.2%, 2.2%, and 5.0% in lung, heart, and kidney transplants; respectively. The post-transplant 1- and 5-year survival of patients with vs. without HBsAg was not different in all solid organ transplants (all p > 0.05). Similarly, there was no difference in post-transplant survival between lung transplant recipients with vs. without anti-HCV: 42% vs. 43% at 5 years, 69% vs. 69% at 10 years (all p > 0.05). In contrast, heart transplant recipients with HCV Ab (+) had higher crude post-transplant mortality: 27% vs. 21% at 5 years, 50% vs. 38% at 10 years (all p < 0.01). Similarly, there was higher post-transplant mortality in kidney transplant recipients with HCV Ab (+): 6% vs. 3% at 1 year, 21% vs. 13% at 5 years, 47% vs. 31% at 10 years (all p < 0.0001). In multivariate analysis controlling for confounders, the association of HCV Ab (+) with higher post-kidney transplant mortality remained significant: adjusted hazard ratio (aHR) (95% CI) = 1.13 (1.09–1.17), p < 0.0001. There was no association of viral hepatitis with the risk of graft failure in solid organ transplants (p > 0.05) except for the association of HBsAg with the risk of kidney graft loss (cumulative 4.3% vs. 3.1%, p < 0.01).

Conclusion: In most cases, presence of HBV and HCV serologies are not associated with adverse post-transplant outcomes in non-liver solid organ transplantation. However, kidney transplant recipients with HCV Ab (+) seem to have an increased risk for post-transplant mortality.

FRI-160

Development of a rapid workflow for detecting HCV RNA from whole blood

Matthew Pauly¹, Sabrina Torres¹, Tonya Hayden¹, Lilia Ganova-Raeva¹, Saleem Kamili¹. ¹Centers for Disease Control and Prevention, United States
Email: omx4@cdc.gov

Background and aims: Chronic hepatitis C virus (HCV) infection is a leading cause of cirrhosis, hepatocellular carcinoma, and other liver complications. Effective treatments are available, yet only 20% of the estimated 58 million global HCV infections have been diagnosed.

Accurate and timely diagnosis of HCV infection is important for linking people with HCV infections to care and stopping virus spread. Most diagnostic tests for HCV are expensive and performed in a laboratory, which limits their effectiveness in some at-risk populations. Diagnostic tests for HCV infection that are compatible with point-of-care use could greatly improve access to testing.

Method: We developed a workflow for the extraction, amplification, and detection of HCV RNA from whole blood samples that uses simple and inexpensive equipment. First, a brief spin in a mini-centrifuge removes blood cells from a small volume of whole blood. Cell-free blood is mixed with a lysis solution containing paramagnetic solid phase reversible immobilization (SPRI) beads capable of binding nucleic acids. The beads are washed once, and then the bound nucleic acids are eluted. The eluted nucleic acids are added to an HCV-specific reverse-transcription loop-mediated isothermal amplification (RT-LAMP) reaction. Positive amplification is detected using either measured fluorescence or lateral-flow test strips.

Results: The workflow for HCV RNA detection from whole blood takes 45 minutes from sample preparation to result and the reagents can cost less than 5.00 USD per sample. The 95% limit of detection by probit analysis is 2.8 log₁₀ (IU/ml) (95% CI 2.5–3.4) for HCV RNA in whole blood, which would permit detection of approximately 98% of global HCV infections. This workflow can detect HCV genotypes 1–6. This workflow detected 75/80 (94%) samples from a panel of whole blood spiked with diverse HCV RNA-positive plasma samples. Each of the samples from this panel that were not detected contained HCV RNA levels below 3.0 log₁₀ (IU/ml). Simplifying the procedure to include a magnetic wand in place of precision pipettes for processing the paramagnetic SPRI beads during the nucleic acid extraction steps allowed for similar HCV RNA detection results.

Conclusion: We have developed a rapid, sensitive, and inexpensive workflow for the detection of HCV RNA from small volumes of whole blood. With additional procedural simplifications, this workflow may form the basis for a point-of-care test for the detection of HCV RNA from clinical samples.

FRI-161

Hepatitis D infection in a HBsAg cohorts referred from specialist liver clinics vs. reflex community referred patients in South East London

Ivana Carey¹, James Lok¹, Maria Guerra Veloz¹, Christiana Moigboi¹, Geoffrey Dusheiko¹, Kosh Agarwal¹. ¹King's College Hospital, Institute of Liver Studies, London, United Kingdom
Email: ivana.kraslova@kcl.ac.uk

Background and aims: Chronic hepatitis delta (HDV) represents the most severe form of chronic viral hepatitis with accelerated rates of advanced liver fibrosis and hepatocellular carcinoma, compared to those infected with hepatitis B alone, and for this reason early diagnosis is critical despite the lack of curative therapies. It is estimated that 5% of HBV infected patients are co-infected with hepatitis D virus (HDV). The true prevalence is not known, as HBsAg positive patients are not universally screened for the presence of anti-HDV antibodies, and the data may be skewed in cohorts referred for chronic liver disease. We aimed to compare the seroprevalence of anti-HDV antibodies and HDV RNA status in two referral settings: a specialist viral hepatitis laboratory ('liver specialist cohort') where testing for anti-HDV antibodies all newly diagnosed HBsAg positive patients is universally applied vs. a community laboratory ('community reflex cohort') where reflex testing of all HBsAg positive patients was similarly applied.

Methods: All new HBsAg-positive patients seen in a tertiary hospital liver clinic-'liver specialist cohort 2021' (n = 238) between 1.1.2021–31.12.2021 were tested for the presence of anti-HDV (ETI-AB-DELTA-K-2 by DiaSorin) and all anti-HDV-positive samples were tested by a pan-genotypic in-house HDV RNA assay (LLQD = 640 IU/ml). Testing in a second cohort of newly diagnosed HBsAg-positive patients in the liver clinic ('liver specialist cohort 2022')-was repeated between

POSTER PRESENTATIONS

1.1.2022–31.12.2022 (n = 322). For comparison of the prevalence of hepatitis D infection, samples from 214 HBsAg-positive patients referred from a community laboratory-‘community reflex cohort’- (i. e. a cohort identified in GP practice and non-liver clinics/wards) between 1.1.2022–31.12.2022 had a sample sent for reflex testing in liver specialist laboratory for anti-HDV antibodies and similarly all anti-HDV-positive samples were tested for HDV RNA.

Results: In 2021, out of 238 newly referred liver clinic referred HBsAg positive patients-‘liver specialist cohort 2021’ (tested in a specialist laboratory) 17 (7%) were anti-HDV- positive; 9 (3.8%) had detectable HDV RNA. In 2022, out of 322 newly diagnosed HBsAg positive patients (‘liver specialist cohort 2022’) similarly tested 23 (7%) patients were anti-HDV positive and 12 (3.7%) of these patients had detectable HDV RNA. In contrast, out of 214 HBsAg-positive patients (35 newly diagnosed) tested from the community laboratory referral cohort (‘community reflex cohort’) only 5 (2.3%) were anti-HDV-positive and only one (0.5%) was HDV RNA positive. All newly diagnosed HBsAg-positive patients tested in a community laboratory including 1 (2.8%) anti-HDV positive patient (1 was HDV RNA positive) were linked into care in liver clinics.

Conclusion: The seroprevalence of anti-HDV was lower in HBsAg-positive patients tested in community referral laboratory setting than in newly diagnosed HBsAg-positive patients diagnosed in a specialist liver setting (2.3% vs. 7%). Similarly, there was a higher proportion of HDV RNA- positive patients in the ‘liver specialist’ cohorts vs. ‘community reflex cohort’. Reflex testing in both settings facilitated linkage to specialist care for HDV RNA positive patients.

FRI-162

Screening, confirmation, and treatment rates of hepatitis C virus infections in patients undergoing surgery in a single tertiary academic centre

Jae Seung Lee^{1,2,3}, Hye Won Lee^{1,2,3}, Beom Kyung Kim^{1,2,3}, Jun Yong Park^{1,2,3}, Do Young Kim^{1,2,3}, Sang Hoon Ahn^{1,2,3}, Seung Up Kim^{1,2,3}. ¹Yonsei University College of Medicine, Department of Internal Medicine, Seoul, Korea, Rep. of South; ²Yonsei University College of Medicine, Institute of Gastroenterology, Seoul, Korea, Rep. of South; ³Severance Hospital, Yonsei Liver Center, Seoul, Korea, Rep. of South
Email: ksukorea@yuhs.ac

Background and aims: A lack of awareness compromises appropriate consideration of hepatitis C virus (HCV) infections in patients undergoing surgery. We evaluated the status of HCV screening, confirmation, and treatment in patients undergoing surgery.

Method: Patients who underwent surgery in a tertiary academic center between 2019 and 2021 were eligible for this retrospective study. The testing and positivity rates for anti-HCV antibodies and HCV RNA were analyzed.

Results: Among 96,894 patients (40,121 males, 41.4%) who underwent surgery under general anaesthesia, 83,920 (86.6%) were tested for anti-HCV antibodies before surgery. Of these patients, 576 (0.7%)

were positive for anti-HCV antibodies and had significantly higher rates of diabetes mellitus (32.6% vs. 18.5%), hypertension (50.5% vs. 28.6%), liver cirrhosis (13.2% vs. 1.7%), and unfavourable laboratory test results compared with those who were negative (all p < 0.05). The HCV RNA status was assessed in 215 (37.3%) of the anti-HCV antibody-positive patients, and the rate of HCV RNA positivity was 20.5% (n = 44 of 215). Of these 44 patients, 42 (95.5%) were referred for treatment, and all 29 treatable patients were successfully treated with direct-acting antiviral therapy. The HCV RNA positivity rate was significantly higher in the hepatobiliary and transplant surgery department (76.6%) than in other surgical departments (25.0–33.5%).

Conclusion: A significant number of preoperative anti-HCV antibody-positive patients did not receive appropriate HCV management. An automated alert system may be required.

FRI-163

Impact of hepatitis B family screening, counselling and education program on active case detection: a step towards elimination through preventive hepatology clinic in India

Ajeet Singh Bhadoria¹, Gaurika Saxena¹, Abhishek Sadasivan¹, Rohit Gupta². ¹All India Institute of Medical Sciences Sciences Rishikesh, Preventive Hepatology, Rishikesh, India; ²All India Institute of Medical Sciences Rishikesh, Gastroenterology, Rishikesh, India
Email: ajeetsinghbhadoria@gmail.com

Background and aims: Finding the missing millions is the biggest challenge towards elimination by 2030. Recent studies have documented intrafamilial transmission including vertical transmission as the most common mode of transmission for Hepatitis B virus (HBV) infection. Thus, we targeted maximum yield in case detection via counselling and screening of first degree relatives of Hepatitis B infected patients and their spouse for hepatitis B infection through preventive hepatology clinic in India

Method: A multi-level public health approach was utilized to implement Hepatitis B family screening, counselling and education program to persuade first degree relatives (parents, siblings, and children) and spouse of HBV infected patients for HBV screening. The enrolled and counselled relatives got themselves tested, either at our institute’s virology laboratory or from any recognized laboratory in the country as per their convenience. A 3 tier counselling and education by Gastroenterologist, Public Health Specialist and Resident was adopted for screening for 3 HBV markers:-HBsAg, Anti-HBc (total), and Anti-HBs. Necessary actions were taken as per the lab results i.e. vaccination, further investigations for treatment eligibility. The information and education material was also distributed to the relatives, consisting of literature on natural history of hepatitis B infection, available diagnostic and screening tests.

Results: A total of 463 family members were approached from 93 index cases of chronic hepatitis B (CHB) infection (age 33.1 ± 12.3 years, 72.8% males). A total of 40.3% of CHB patients were HBeAg +ve. Median HBV DNA levels was 29.8 (IQR 0.8–5312 × 10³) IU/ml. We have successfully screened 221 contacts out of 463 relatives which include

Table: (abstract: FRI-162): HCV RNA status and treatment of HCV RNA-positive patients according to preoperative anti-HCV antibody status.

Population	Tested for anti-HCV antibodies (patients)	Tested for HCV RNA status in anti-HCV antibody-positive patients	Treated patients positive for HCV RNA
All	83,920 of 96,894 (86.6)	215 of 576 (37.3)	29 of 42 (69.0)
Surgery department			
Hepatobiliary and transplantation	5,154 of 6,886 (74.8)	72 of 94 (76.6)	13 of 17 (76.5)
Other GS, paediatric*, and OBGY	31,729 of 37,932 (83.6)	34 of 121 (28.1)	4 of 8 (50.0)
CS, NS, and OS	26,031 of 29,484 (88.3)	74 of 221 (33.5)	10 of 14 (71.4)
Others [†]	21,006 of 22,592 (93.0)	35 of 140 (25.0)	2 of 5 (40.0)

Variables are expressed as “number of number (%)”

*Surgery in adult patients (age ≥19 years) performed by paediatric surgeons.

[†]Ear, neck, and throat surgery, oral and maxillofacial surgery, plastic surgery, urology, ophthalmology, and dermatology.

Abbreviations: HCV, hepatitis C virus; GS, general surgery; OBGY, obstetrics and gynaecology; CS, cardiothoracic surgery; NS, neurosurgery; OS, orthopaedic surgery.



Figure: (abstract: FRI-163): Patient Information Brochure.

parents, siblings, children and spouse. The efficacy of HBSCE program was 47.7% (221/463). HBsAg was found positive in one fourth (24.2%) of contacts and Anti- HBe was positive in about two third (31.2%) of contacts. The overall infection rate (either HBsAg+ or any antibody positive with no history of immunization) was 42.1%. Past Exposure Rate (HBsAg -ve with Anti-HBc (Total) +ve, or Anti-HBs +ve, with no history of vaccination) was seen in 15.7%. Out of 128 uninfected individuals, 32 were already vaccinated, and 61 (47.6%) were vaccinated after the counselling. Prevalence of HBV infection was significantly higher among mothers (51.1%) as compared to other family members (28.1%) (OR 3.2, 95%CI 2.3–4.6) supporting vertical transmission.

Conclusion: Familial clustering of HBV infection was seen. Opportunistic screening and multilevel counselling of family members was an effective strategy for active case finding. Younger

index cases, with two out of every four mothers being infected strongly suggest vertical transmission as the most common mode of infection. This data suggests family screening as important additional strategy to eliminate hepatitis B by 2030 via test and treat approach.

FRI-164

HCV elimination in persons living with HIV (PLWH): the NoCo (No-Coinfection) study of the ICONA network

Antonella d'Arminio Monforte¹, Alessandro Tavelli¹, Roberto Rossotti², Roberta Gagliardini³, Annalisa Saracino⁴, Sergio Lo Caputo⁵, Matteo Sala⁶, Eugenia Quiros-Roldan⁷, Cristina Mussini⁸, Enrico Girardi⁹, Andrea Antinori³, Massimo Puoti^{2,10}. ¹Icona Foundation, Milan, Italy; ²ASST Grande

POSTER PRESENTATIONS

Ospedale Metropolitano Niguarda, Infectious Diseases Unit, Milan, Italy;
³National Institute for Infectious Diseases Lazzaro Spallanzani IRCCS, Clinical and Research Infectious Diseases Department, Rome, Italy;
⁴University of Bari, University Hospital Policlinico, Clinic of Infectious Diseases, Department of Biomedical Sciences and Human Oncology, Bari, Italy;
⁵University of Foggia, Department of Clinical and Surgical Sciences, Foggia, Italy;
⁶ASST Santi Paolo e Carlo, University of Milan, Unit of Infectious and Tropical Diseases, Milan, Italy;
⁷University of Brescia, ASST Spedali Civili di Brescia, Department of Clinical and Experimental Sciences, Unit of Infectious and Tropical Diseases, Brescia, Italy;
⁸University of Modena and Reggio Emilia, AOU of Modena, Clinic of Infectious Diseases, Modena, Italy;
⁹National Institute for Infectious Diseases Lazzaro Spallanzani IRCCS, Scientific Direction, Rome, Italy;
¹⁰University of Milano-Bicocca, Milan, Italy
 Email: antonella.darminio@unimi.it

Background and aims: PLWH are often HCV coinfectd and undergo more frequently to progressive disease. Early diagnosis and treatment are essential to eliminate HCV in this population. No-Co is a prospective cohort study on PLWH aimed to estimate: prevalence of past and active HCV infection in PLWH in care in 2017–2022, the incidence of HCV re-infections and HCV seroconversions and DAA-uptake and response.

Method: No-Co study included PLWH screened for HCV from Sept-2017 to Oct-2022, independently of their HCV status, belonging to centers of the Italian ICONA network. Prevalence of HCV infection (HCVAb+) and active HCV infection (HCV-RNA+) were evaluated at baseline. Incidence of HCV seroconversions, in those HCVAb-at baseline, and of HCV re-infections (in those HCVAb+/HCV-RNA-who turned to HCV-RNA+) were evaluated and predictors identified by Poisson regression models. Standard survival methods (Kaplan-Meier curves and Cox models) used to estimate the probability and predictors of DAA-start from first HCV screening in the study, for

those HCV-RNA +. Logistic regression models have been used to investigate predictors of SVR12.

Results: 4,569/16,743 (27.3%) were HCVAb + at baseline. HCVAb + were older (median 54 vs 46 yrs), more frequently Italian (94% vs 78%), and with higher CD4/mmC (median 644 vs 598). In a median follow-up of 1.6 years, 42/4,890 seroconverted, with KM probability of 0.5% (95%CI 0.3–0.7) at 1 year. No factors were associated with seroconversion. 1,732/4,569 (37.9%) were HCV-RNA –; in a median follow-up of 1.3 years, 38 turned to HCV-RNA +; 10 relapsed, 28 were re-infections), KM probability of HCV reinfection at 1 year was 1.3% (95%CI 0.7–2.3). Younger age was the only factor independently associated to higher incidence of re-infection (aIRR 1.67, 95%CI 1.05–2.64). 1,374/1,732 HCV-RNA + PLWH had a follow-up, 1,184 (86.2%) started DAA, the KM probability of DAA uptake at 1-year was 79.5% (95%CI 77.3–81.7). Independent predictor of reduced access to DAA was CD4<200/mmC (aHR 0.59, 95%CI 0.43–0.80), HIV-RNA >50 copies/ml (aHR 0.72, 95%CI 0.57–0.91) and being IDU (aHR 0.72, 95%CI 0.60–0.87). SVR12 was obtained in 95.5%, CD4<200/mmC were associated with lower probability of SVR12 (aHR 0.18, 95%CI 0.06–0.52). Globally, the cascade of care of HCV indicates that 86.2% of HCV-RNA + were treated, of these 77, 2% reached 12 weeks follow-up after DAA, and 95.5% of these obtained SVR12, resulting in 63.6% of SVR among HCV-RNA + (Figure 1A–B). Finally, the yearly prevalence of active HCV infection decrease from 41.7% in 2017 to 11.7% in 2022 ($p < 0.001$, Figure 1C).

Conclusion: Only 12% of PLWH in this cohort are still viremic. Prevalence of active HCV infection decreased over time in PLWH, both because of DAA treatment and relatively low rate of new infection or reinfections. Access to DAA was lower in IDU and in those with uncontrolled HIV infection. Low CD4 counts were independent predictors of non-response.

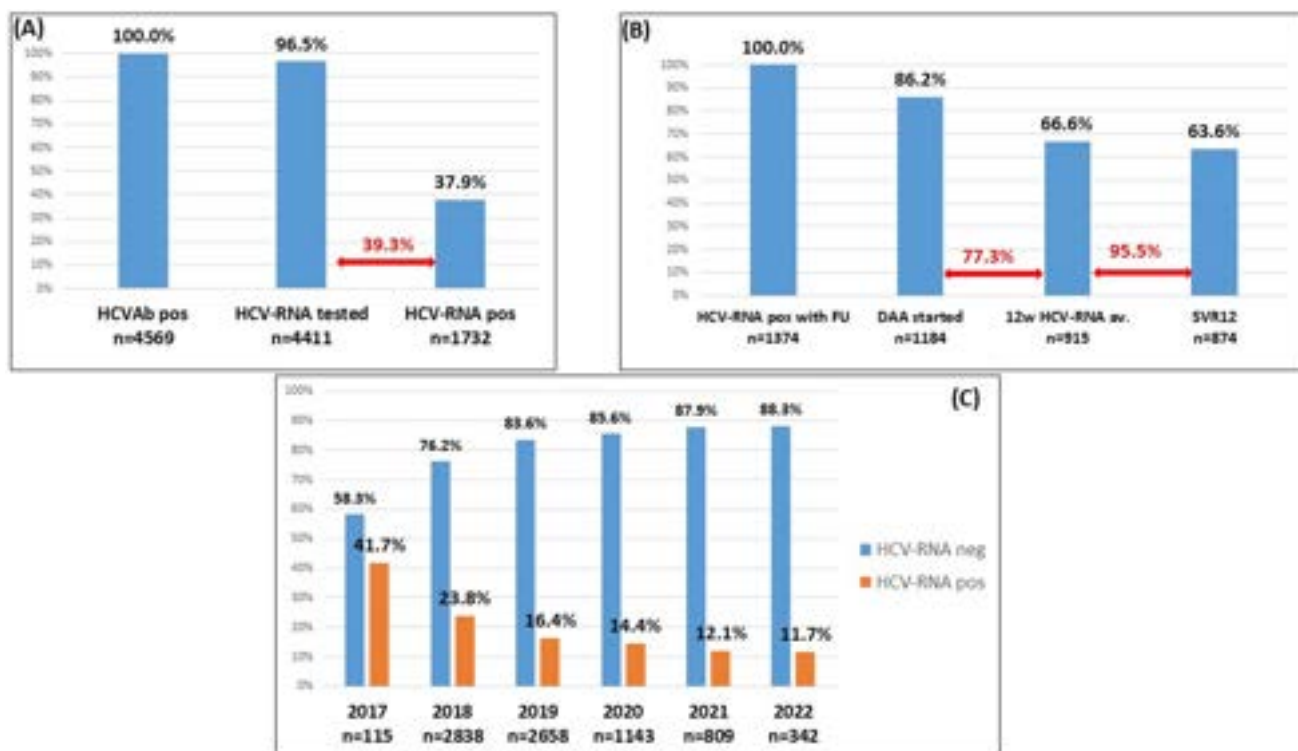


Figure: (abstract: FRI-164): HCV Cascade of Care in NoCo study (A–B) and proportion of HCV-RNA viremic subjects according to calendar year of test (C).

FRI-165

A modelling study of the impact of scaling up of HCV case finding and treatment for people who inject drugs in English region of Bristol and Severn

Zoe Ward¹, Hannah Fraser¹, Adam Trickey¹, Jo Kesten¹, Andy Gibson², Leila Reid³, Fiona Gordon⁴, Alec Miners⁵, Jack Williams⁶, Matthew Hickman¹, Graham Foster⁷, Monica Desai⁸, Sema Mandal⁸, Laura Coughlan⁸, Ruth Simmons⁸, Ross Harris⁸, Peter Vickerman¹.

¹University of Bristol, United Kingdom; ²University of West of England, United Kingdom; ³HepC Trust, United Kingdom; ⁴University Hospitals Bristol and Weston Trust, United Kingdom; ⁵Source Health Economics, United Kingdom; ⁶London School of Hygiene and Tropical Medicine, United Kingdom; ⁷Queen Mary University of London, United Kingdom; ⁸United Kingdom Health Security Agency, United Kingdom
Email: zoe.ward@bristol.ac.uk

Background and aims: People who inject drugs (PWID) are the main risk group affected by Hepatitis C (HCV) in the UK. The National Health Service in England (NHSE) aims to eliminate HCV as a public health threat by 2025, ahead of the WHO target of 2030. Scaling up HCV testing and treatment among PWID will be critical for reaching this elimination goal. This entails decreasing the incidence of HCV among PWID by 80% compared to 2015 levels or <2 per 100 person years (py) by 2025. We assess whether existing strategies are sufficient for reaching these elimination goals.

Method: A dynamic HCV transmission model among PWID, including incarceration and drug treatment centres (DTC), was used to project the impact of existing prevention, testing and treatment services in the Bristol and Severn region (defined by NHSE Operational Delivery Networks responsible for delivering HCV treatment). The model includes the pathway from testing to treatment in prison, DTC and other settings. Detailed data from NHSE HCV treatment database and HCV testing sentinel surveillance database and a yearly bio-behavioural survey among PWID were used to parameterise and calibrate the model using Approximate Bayesian Computation. Model outputs were used to project HCV chronic prevalence, incidence and number of treatments over time and determine whether existing testing and treatment strategies will reach the elimination goals by 2025 or 2030.

Results: Data suggests that 178, 72 and 270 treatments were undertaken in DTC, prison and other settings over 2015–2019 in Bristol and Severn, with the time from diagnosis to treatment decreasing from >1 year to <3 months in all settings. Our model projects that this treatment scale-up resulted in prevalence decreasing by median of 51% (47.9–58.6%) and incidence decreasing by 48.4% (44.6–56.2%) by start of 2020. If testing and treatment continued at the same rates from 2020, then chronic prevalence will decrease by 84.1% (79.8–91.1%) from 31.9% in 2015 to 5.0% by 2030 and incidence will decrease by 83.1% (78.1–90.6%) from 9.4 (8.0–11.4) to 1.5 per 100 py (0.8–2.3). In total, 2083 (1882–2217) treatments would be used over 2015–2030 (PWID population~5300). By 2025, incidence will decrease by 70.9% (65.9–79.9%) to 2.7 per 100 py (1.8–3.6) following 1722 (1536–1861) treatments.

Conclusion: Our modelling suggests the scale-up of HCV testing and treatment among PWID in Bristol and Severn will reach the WHO targets for HCV elimination between 2025 and 2030.

FRI-166

Treatment start resilience but testing decrement in a coordinated statewide HCV treatment program during COVID: lessons learned and future steps

Yvonne Lynch-Hill¹, Christina Leblanc¹, Barbara Goodall¹, Lisa Barrett².

¹Nova Scotia Health Authority, Infectious Diseases, Halifax, Canada; ²Dalhousie University, Infectious Diseases, Halifax, Canada
Email: lisabarrett@me.com

Background and aims: The SARS-CoV-2 pandemic was associated with marked decreases in access to lab based blood borne pathogen testing, including HCV molecular diagnostics. While new diagnoses

may have decreased, it was unclear if all other parts of the HCV care cascade engagement would also decrease during each year of the pandemic. Our goal was to describe engagement in care across the care cascade before and during the SARS-CoV-2 pandemic in a statewide coordinated virtual HCV care program.

Method: Nova Scotia is a Canadian province with approximately 1,000,000 population. From 2017 to 2022, the majority of HCV care was initiated through in a province wide program which converted to a fully virtual, nurse delegated program in July 2020 with the advent of the pandemic. We measured the number of referrals, care engagements, treatment starts, documented SVRs (sustained virologic responses), and treatment failures annually from 2019 (considered pre-pandemic) until December 2022.

Results: HCV program referrals decreased approximately 30% in 2020/21 (187, 183) compared to 2019 (264) and 2022 (220). However, initial virtual visits to establish care were stable across 2019 (69), 2020 (85), and 2021 (67), and increase to 114 in 2022. 158 people initiated treatment in 2019, compared with 135 in 2020, 115 in 2021 and 93 in 2022. SVR was status was known in 111 people in 2019, compared to 104 people in 2020, 75 in 2021, and 21 in 2022. Treatment failure or reinfection was stable over all years.

Conclusion: New HCV infection estimation was limited during the pandemic, given the lack of point of care and lab-based HCV testing in the province. However, conversion to a virtual platform, centralized referral and treatment, as well as expert delegated nurse role was associated with equivalent engagement in care but slightly decreased treatment initiation. Building HCV care resilience through virtual and delegated collaborative prescriber programs should be considered in future pandemic preparedness planning and blood borne pathogen management.

FRI-167

Who is missing? Analysis of the 2021 Georgian seroprevalence survey to identify the population left to be screened for hepatitis C

Sophia Surguladze¹, Davit Baliashvili¹, Shaun Shadaker², Tamar Gabunia³, Maia Tsereteli⁴, Paige A. Armstrong², Senad Handanagic².

¹The Task Force for Global Health, Georgia; ²Centers for Disease Control and Prevention, United States; ³Ministry of Labour, Health and Social Affairs of Georgia, Tbilisi, Georgia, Georgia; ⁴National Center for Disease Control and Public Health, Georgia
Email: sophiesurguladze@gmail.com

Background and aims: Georgia has made great progress towards hepatitis C virus (HCV) elimination since starting their elimination program in 2015; a 2021 serosurvey showed a 67% decrease in prevalence of current HCV infection. As a part of the program, people are screened at multiple different sites, the most common being mandatory inpatient screening at hospitals. However, low awareness of infection status and loss to follow-up after reactive HCV antibody or detected HCV RNA or HCV core antigen remains a challenge. This study used data from the 2021 survey to identify sub-groups of adults with low HCV screening and status awareness, highlighting gaps in the HCV elimination program and groups least served by the HCV elimination program.

Method: The 2021 serosurvey used a stratified, multi-stage cluster design with systematic sampling. Participants were interviewed and tested for anti-HCV. The weighted proportions with 95% confidence intervals (CI) for ever been screened for hepatitis C were calculated and stratified by demographic and behavioral variables to assess screening coverage in different groups. To assess awareness of anti-HCV status, weighted proportions of anti-HCV reactive persons who reported ever being screened positive were also calculated.

Results: Overall, 42.1% (95% CI: 39.6%–44.7%) of participants reported ever being screened for anti-HCV. This proportion was similar in men and women at 35.5% (95% CI: 32.7%–38.4%) and 39.9% (95% CI: 37.2%–42.5%) respectively. Reported screening was lowest in those aged >60 years (27.8% [95% CI: 25.3%–30.6%]) and the highest in the 30–39 year age group (49.9% [45.3%–54.5%]).

POSTER PRESENTATIONS

Among anti-HCV-reactive persons overall, 75.6% (95% CI: 68.2%–81.7%) knew their screening status. This proportion was 56.4% (95% CI: 47.9%–64.5%) for anti-HCV-reactive men and 38.8% (95% CI: 29.2%–49.3%) for anti-HCV-reactive women. Among those who were reactive, the proportion aware of their status was lowest in the 18–29 year age group (34.7% [95% CI: 8.5%–75.4%]) and highest in those aged 40–49 years (63.3% [95% CI: 50.1%–74.7%]). In terms of risk groups, awareness of anti-HCV reactivity was 61.4% (95% CI: 42.0%–77.7%) in previously incarcerated individuals, 62.2% (95% CI: 46.8–75.5%) in reported injection drug users, and 63.7% (95% CI: 47.1%–77.6%) in those reporting having ever received a blood transfusion.

Conclusion: Our analysis identified sub-groups in Georgia with low HCV screening and status awareness. The youngest and oldest participants had the lowest reported screening. Targeted interventions to improve HCV screening are needed in these sub-groups. Awareness of anti-HCV reactivity was lowest in the 18–29 year age group, and was higher in risk groups compared to the general population; improved follow-up for people with positive screening results is needed to ensure they are notified of their status.

FRI-168

Are primary healthcare facilities ready to provide hepatitis delta services in Mongolia: service availability and readiness assessment findings

Azzaya Oktyabri¹, Badmaa Otgonbayar², Enkhjargal Altangerel².

¹Mongolian National University of Medical Sciences, Mongolia;

²Anagaakh Ukhaany Mergejiltuudiin Academy, Mongolia

Email: mdnzula@gmail.com

Background and aims: Primary health care (PHC) facilities are the frontline service providers responsible for provision of the essential services to the population. Some portions of the clinical management for hepatitis patients are provided at PHC facilities within the National Liver Programme, especially for HBV and HCV related services. However, information on HDV service provision at PHC is uncertain. Therefore, we aimed to explore what services are available and how are they ready for HDV patients at the PHC level.

Method: WHO developed a tool for service availability and readiness assessment (SARA) was used, which comprised a set of indicators to define whether a health facility meets the required conditions for providing basic and specific services. The cross-sectional study examined randomly selected 79 PHC facilities from urban (82.3%) and rural (17.7%) areas. The assessment questionnaire was modified to the country context with focus on hepatitis and immunization services. Immunization service assessment was included to explore the possibility of applying temperature-controlled daily injections of Bulevertide for HDV patients. Collected data was analyzed using SPSS 21.0 to define the indicators of availability and readiness.

Results: Overall PHC basic service readiness score was 62.1%. Almost all (96.2%) of the facilities conduct rapid testing for HBV, with 70.83% have ready stock of the test strips. They do not provide HDV rapid testing. 45.83% of the facilities managed to train the staff for hepatitis management within the last two years. There is no unified registry system for HDV patients, and 44.3% of the facilities maintain the monitoring of the diagnosed patients, through referral to secondary hospitals and counseling on disease management. The immunization service readiness was assessed by exploring the presence of the routine vaccines, cold chain equipment, and trained staff and guidelines. All PHC facilities provide immunization services in both urban and rural areas. Overall readiness for immunization services was 86.87%, which included trained staff (80.38%), required equipment (99.79%); and supplies (69.11%).

Conclusion: The study revealed that the availability and readiness of basic PHC services is considerably good within the facilities. The service provision at PHC for HBV and HCV, obliged by the National Liver Programme, is well maintained at both urban and rural places. The screening and testing for HDV are not delivered at all PHC facilities. The availability of HDV specific treatment is none. The

required condition and readiness for immunization is built up well, therefore, it could be used for daily injectable treatment (Bulevertide) for hepatitis D patients at PHC facilities. The good level of availability and readiness for basic and hepatitis (B and C) services could serve as a good foundation for future introduction of HDV related services at PHC facilities in both urban and rural places.

FRI-169

Cascade of care among people with an HBV notification in New South Wales, Australia, including diagnosis, specialist assessment, and treatment uptake

Syed Hassan Bin Usman Shah^{1,2}, Heather Valerio¹, Behzad Hajarizadeh¹, Maryam Alavi¹, Gail Matthews¹, Gregory Dore¹.

¹The Kirby Institute, UNSW, Viral Hepatitis Clinical Research Program, Sydney, Australia; ²The Kirby Institute, UNSW, Viral Hepatitis Clinical Research Program, Sydney, Australia

Email: hbinusman@kirby.unsw.edu.au

Background and aims: Hepatitis B virus (HBV) care cascade characterisation is important for monitoring progress towards HBV elimination. This study evaluated the care cascade and factors associated with HBV DNA testing and treatment uptake during 2010–2018 in New South Wales, Australia.

Method: HBV testing, specialist consultation, and treatment care cascade were determined through linkage of HBV diagnoses/notifications (generally serological, 1993–2017) to Medicare and pharmaceutical benefits schemes (2010–2018), hospital admissions (2001–2018), and mortality (1993–2018) databases. Timely HBV testing was defined as DNA testing at or within four weeks of HBV notification. Multivariate cox proportional-hazards regression analyses were performed to evaluate factors associated with HBV DNA testing and antiviral treatment.

Results: Among 15,202 people with an HBV notification, 10,368 (68%) were tested for HBV DNA, of whom 5366 (52%) received timely testing. A total of 10,794 (71%) consulted a specialist post-HBV notification, and 3,166 (21%) initiated HBV treatment. HBV DNA testing was more likely among those ≥ 45 years old at HBV notification (adjusted Hazard Ratio [aHR] 1.13, 95%CI: 1.07, 1.18), those with a history of hepatocellular carcinoma (HCC) (aHR 1.25, 95%CI: 1.02, 1.53) and notified in the later period (2014–17) (aHR 1.46, 95%CI: 1.40, 1.52), and less likely among females (aHR 0.96, 95%CI: 0.92, 0.99), those with a history of alcohol use disorder (AUD) (aHR 0.77, 95%CI: 0.66, 0.89), and those coinfectd (HBV/HCV; aHR 0.62, 95%CI: 0.54, 0.69, HBV/HIV; aHR 0.75, 95%CI: 0.58, 0.98). Higher likelihood of HBV treatment was associated with age ≥ 45 years (aHR 1.40, 95%CI: 1.27, 1.53), a history of decompensated cirrhosis (aHR 2.08, 95%CI: 1.62, 2.66), a history of HCC (aHR 2.89, 95%CI: 2.28, 3.64), HBV/HIV coinfection (aHR 3.71, 95%CI: 2.93, 4.68) and HBV notification in the later period (2014–17) (aHR 1.61, 95%CI: 1.49, 1.73). HBV treatment was less likely among females (aHR 0.68, 95%CI: 0.63, 0.73), people of Indigenous ethnicity (aHR 0.58, 95%CI: 0.42, 0.80), and those with a history of AUD (aHR 0.77, 95%CI: 0.60, 0.98).

Conclusion: Most people with an HBV notification got HBV DNA testing and consulted a specialist. Of those tested, about half received timely HBV DNA testing, higher in the later period. Treatment coverage has increased, but may be sub-optimal among some sub-populations, including Indigenous Australians and those with AUD.

FRI-170

Reimplementation of a revamped cost-effective national elimination strategy is the only way Brazil moves towards eliminating HCV

Alexis Voeller¹, Devin Razavi-Shearer¹, Ivane Gamkrelidze¹, Homie Razavi¹. ¹Center for Disease Analysis Foundation, United States
Email: avoeller@cdafound.org

Background and aims: In 2018, Brazil developed the Hepatitis C Elimination Plan, a national strategy to achieve HCV elimination, but in 2019 the intervention was discontinued by the national

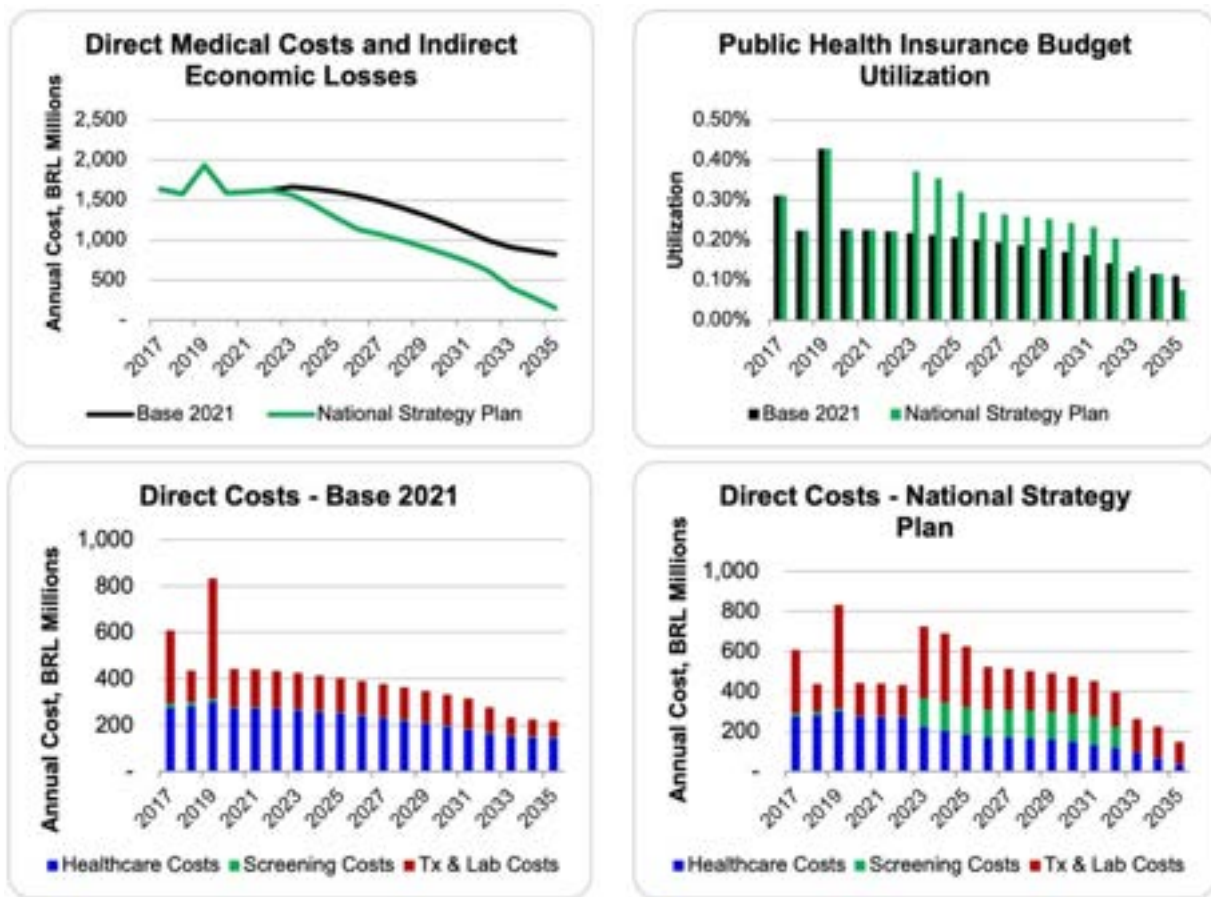


Figure: (abstract: FRI-170).

government. The goal of this analysis was to evaluate the impact of this policy change.

Method: A Markov mathematical model was used to quantify the HCV disease and economic burden under three scenarios: National Elimination (developed in 2018); 2021 base (reflecting empirical data through 2021) and National Elimination Reimplementation (empirical data through 2021; elimination assumptions after 2021). This work built on a previously published model for Brazil that was updated using publicly available data for treatment and diagnosis. The base case was compared to the 2018 elimination plan to evaluate which WHO elimination targets would be met and whether this type of strategy still proved cost-effective given the current HCV burden.

Results: Under the original National Elimination Strategy, Brazil would have seen a 53% decrease in HCV-related mortality and a 51% decrease in HCV-related liver cancer. Considering empirical data through 2021, the 2021 base could result in an additional 207,000 HCV infections by 2030 along with an excess 12,600 liver-related deaths, 1,700 incident HCC cases and 1,340 incident decompensated cirrhosis cases, relative to the original national strategy. Reimplementing the national strategy from 2022 forward would only achieve the absolute, treatment and incidence targets. To reimplement the national strategy beginning in 2022, Brazil would need to undertake up-front direct costs peaking at 724 million BRL for the scaling up of screening, diagnosis, and treatment to meet all elimination targets. These costs would drop to 146 million BRL annually within 10 years to combat HCV. Annual indirect economic losses would decrease dramatically within a similar timeframe from 1,184 million BRL to nearly 3 million BRL as a result of a reimplemented strategy. The cost per DALY averted from 2017 to 2035 with an elimination strategy is estimated to be 5,263 BRL, which

is significantly lower than the GNI per capita of 28,757 BRL demonstrating the high cost-effectiveness of disease intervention.

Conclusion: If Brazil wants to move forward to HCV elimination by 2030, a form of the national strategy program needs to be reinstated. If the previous Hepatitis C Elimination Plan is reused, WHO elimination targets will not be met by 2030 due to significant loss of time. For the country to continue combating HCV, it needs to increase screening, diagnosis, and treatment of patients – soon. Model outputs demonstrate that Brazil is not currently on track to eliminate viral hepatitis C by 2030 without utilizing a revamped intervention.

FRI-171

The evaluation of people suspected of sexually transmitted diseases requires tools for the comprehensive diagnosis of viral hepatitis and HIV

Joaquín Cabezas^{1,2}, Eva Torres-Sangiao^{3,4}, Susana Llerena^{1,2}, Carmen Ribes^{1,2}, Carlos Gutierrez^{1,2}, Sara Alonso^{1,2}, Víctor Echavarría^{1,2}, Ángela Antón^{1,2}, Andrea González^{1,2}, María Eliece Cano³, Jorge Calvo³, Javier Crespo^{1,2}. ¹Marqués de Valdecilla University Hospital, Gastroenterology and Hepatology Department, Santander, Spain; ²Research Institute Valdecilla-IDIVAL, Santander, Spain; ³Marqués de Valdecilla University Hospital, Microbiology Department, Santander, Spain; ⁴Clinic University Hospital Of Santiago de Compostela, Microbiology Department, Santiago de Compostela, Spain

Email: joweycabezas@gmail.com

Background and aims: The prevalence of viral hepatitis is higher in patients with a sexually transmitted disease (STD). The World Health

POSTER PRESENTATIONS

Organization recommends ruling out the existence of a secondary STD and/or concomitant viral hepatitis in all people with a suspected STD. Objective: To evaluate the simultaneous diagnosis of viral hepatitis in subjects suspected of having an STD.

Method: Review of STD studies (syphilis, *Trichomonas vaginalis*, *Chlamydia trachomatis*, *Mycoplasma genitalum*, and *Neisseria gonorrhoeae*) to assess the performance of diagnostic tests for hepatitis B, hepatitis C, and HIV in the three months before or after the index sample for STD diagnosis. The results available between April 2019 and September 2022 from the Microbiology Department of our center were evaluated.

Results: We found 157,185 serology determinations against syphilis and/or exudates against STD. Of the 49,664 serologies for the study of syphilis, anti-HCV serology was determined in 62.2% of the cases; in 1092 subjects with syphilis, an anti-HCV prevalence of 2.3% was detected; 3 viremic, 12 with sustained viral response and 8 spontaneous clearance. HBsAg was requested in 82.4%, detecting 20 positive cases (0.8% prevalence in patients with anti-treponemal antibodies). Finally, the presence of anti-HIV was evaluated in 89.3% of the requests for syphilis, being positive in 150 cases (prevalence = 5.8%; 72 new cases and 78 already known). The determination of HBsAg and anti-HCV and anti-HIV antibodies in subjects with other STD were respectively: 1) *Trichomonas vaginalis* (27,924 samples): 1.6% of the cases had a study for HBsAg, detecting 2 positives; 1% study for HCV (1 positive) and 1.6% study for HIV (2 positive). 2) *Chlamydia trachomatis* (6,018 samples): 2.2%, 2.3% and 2.7% had an HBV, HCV and HIV study, respectively; detecting 2 anti-HCV positive subjects and 4 anti-HIV positive subjects. 3) *Mycoplasma genitalum* (4,879 samples): 1.9%, 2.1% and 2.5% had an HBV, HCV and HIV study respectively, detecting 2 positive anti-HCV and 4 positive anti-HIV. 4) *Neisseria gonorrhoeae* (5,978): 2.2%, 2.3% and 2.7% had an HBV, HCV and HIV study respectively, detecting 3 anti-HCV positive subjects and 4 anti-HIV positive subjects.

Conclusion: In subjects with suspected syphilis there is an under-diagnosis of viral hepatitis, higher for HCV than for HBV (60% vs 80%). The reflex diagnosis of HIV, although not optimal, is clearly better (90%). The absence of a diagnostic study aimed at ruling out a concomitant infection by viral hepatitis is the rule in the rest of the STD. These results highlight the need to implement tools for the complete and comprehensive diagnosis of viral hepatitis in subjects with suspected sexually transmitted diseases.

FRI-172

The impact of hepatitis C and socio-demographic variables on Health-related quality of life among patients in Pakistan

Siwaporn Niyomsri¹, Josephine Walker¹, Ejaz Alam², Ambreen Arif², Muhammad Asim³, Basil Ather³, Mishal Azam⁴, Auj Chaudhry⁴, Asad Chaudhry⁴, Naheed Choudhry⁵, Graham Foster⁵, Saeed Sadiq Hamid⁶, Aliya Hasnain⁶, Polychronis Kemos⁵, Pir Zarak Khan³, Aaron G. Lim¹, Saad Niaz³, Noor Saba⁶, Sultan Sallahuddin⁶, Muhammad Nabeel Shafqat⁴, Huma Qureshi², Wasiuddin Shah⁶, Peter Vickerman¹. ¹Bristol Medical School, Population Health Sciences, United Kingdom; ²Doctors Plaza, Karachi, Pakistan; ³Dow University of Health Sciences (DUHS), Karachi, Pakistan; ⁴The Liver Clinic, Gujranwala, Pakistan; ⁵Queen Mary University of London, United Kingdom; ⁶Aga Khan University, Karachi, Pakistan
Email: josephine.walker@bristol.ac.uk

Background and aims: Pakistan has a high burden of hepatitis C virus. We assessed health-related quality of life (HRQoL) among the general population screened for hepatitis C virus in Pakistan, and identified key socio-demographic factors associated with HRQoL

Method: We conducted a case-control study to measure HRQoL among patients screened for HCV in four community and clinic-based settings in Karachi and Gujranwala, Pakistan. Cases were those diagnosed with chronic hepatitis C (CHC) and controls were negative for HCV antibodies (HCV Ab-negative). Patients diagnosed with CHC were initiated on treatment for 12 weeks, or 24 weeks if APRI and Fib-

4 scores suggested liver cirrhosis. At the point of screening, prior to HCV antibody status being reported to the patient, HRQoL was assessed using the EuroQol EQ-5D-3L survey tool and Visual Analogue Scale from 0 to 100 (VAS). EQ-5D-3L scores were converted to HRQoL weights between 0 and 1 based on a value set from the United Kingdom general population as no value set is available for Pakistan. Beta regression analyses were performed to identify associations between HCV status or cirrhosis status (defined by treatment duration for those who started treatment) and HRQoL, controlling for patient socio-demographic characteristics (age, gender, employment status, rural/urban location, ethnicity, education level, and city). Model selection was performed using a stepwise algorithm to define the best linear predictor according to Akaike Information Criterion (AIC).

Results: The study included a total of 4,402 participants, with a median age of 36.2 (inter-quartile range: 27.1, 47.6) years and 59.6% males. Of these, 836 individuals were identified as having CHC (HCV RNA positive). The average HRQoL and VAS of CHC patients were 0.855 (95%CI: 0.842–0.867) and 68.5 (95%CI: 67.5–69.4), lower than for HCV Ab-negative controls (0.937, 95%CI: 0.932–0.939 and 80.7, 95%CI: 80.3–81.2, $p < 0.001$, respectively). Among all patients, the best fit model included city, employment, age, gender, and HCV status. Having CHC was significantly associated with lower HRQoL ($B = -0.236$, $p < 0.001$), as was being unemployed ($B = -0.296$, $p < 0.001$), living in Gujranwala ($B = -0.552$, $p < 0.001$), older age ($B = -0.011$, $p < 0.001$), or being female ($B = -0.327$, $p < 0.001$). Among CHC patients, older age ($B = -0.017$, $p < 0.001$), living in Gujranwala ($B = -0.368$, $p < 0.001$), and being female ($B = -0.230$, $p = 0.05$) were significantly associated with lower HRQoL. Having cirrhosis (defined by being on longer treatment regimen) was not significantly associated with HRQoL.

Conclusion: HRQoL was worse among individuals with chronic Hepatitis C infection or if they had older age, female gender, were unemployed or came from study sites based in Gujranwala. The study findings suggests that the high burden of HCV in Pakistan is associated with reduced HRQoL and emphasizes the need for health promotion, diagnosis and treatment for Hepatitis C patients.

FRI-173

Hepatitis C screening program in Lithuania: first results and scenarios for virus elimination

Limas Kupcinskas¹, Egle Ciupkeviciene², Alexis Voeller³, Gediminas Urbonas⁴, Ligita Jancoriene⁵, Valentina Liakina^{6,7}, Danute Speiciene⁶, Viaceslavas Zaksas⁸, Marcelo Naveira³, Sarah Blach³, Janina Petkeviciene². ¹Lithuanian University of Health Sciences, Department of Gastroenterology and Institute for Digestive Research, Kaunas, Lithuania; ²Lithuanian University of Health Sciences, Health Research Institute, Kaunas, Lithuania; ³Centre for Disease Analysis Foundation, Lafayette, United States; ⁴Lithuanian University of Health Sciences, Department of Family Medicine, Kaunas, Lithuania; ⁵Vilnius University, Clinic of Infectious Diseases and Dermatovenerology, Vilnius, Lithuania; ⁶Vilnius University, Clinic of Gastroenterology, Nephrourology and Surgery, Vilnius, Lithuania; ⁷Vilnius Gediminas Technical University, Department of Chemistry and Bioengineering, Vilnius, Lithuania; ⁸National Health Insurance Fund under the Ministry of Health, Vilnius, Lithuania
Email: l.kupcinskas@gmail.com

Background and aims: In 2016, WHO announced a plan to eliminate viral hepatitis C as a public health threat by 2030. To achieve this goal, it is important to detect hidden infections by launching national screening programs. In 2022, Lithuanian health authorities decided to pay general practitioners (GPs) a special fee for a service of promoting and performing serological tests for hepatitis C virus (HCV) antibodies: 1) for the population born in 1945–1994 (once per life) and 2) for people who inject drugs (PWID) or are HIV-infected (annual HCV testing). Such an initiative is the first in Central and Eastern Europe. This study aimed to evaluate the first results of the

HCV screening program and develop different scenarios to achieve WHO targets.

Method: Patients were invited to participate in the HCV screening by GPs during the visits. Screening included a serum blood test for the presence of HCV antibodies. Patients who tested positive were referred to a gastroenterologist or infectious disease doctor. HCV RNA testing was used to identify the current infection. If the test result was positive, the doctor prescribed direct-acting antiviral (DAA) therapy. Information about screened and treated patients was obtained from the database of the National Health Insurance Fund. The Markov disease progression model elaborated by the CDA Foundation was used to assess HCV elimination progress in Lithuania. The data from the 2022 screening and previously published data were used as inputs. Three scenarios were developed: the 'Base' scenario-return to pre-screening program level in 2023 and 2 scenarios with different extents of treatment.

Results: At the beginning of 2022, about 1.8 million people born in 1945–1994 lived in Lithuania. Between May 5 and December 31 458980 people (59.5% women) were tested for HCV antibodies. Positive test results were found in 7494 (1.6%) people. Seroprevalence of HCV antibodies was higher among men than women, 2.0% and 1.4%, respectively. In the risk group, 4681 PWID and HIV-infected people were screened, of whom 32.8% were seropositive. Viremia was detected in 58.2% of patients. In 2022, 1586 patients were treated with DAA. If the number of tested patients remains the same as in the last three months in 2022, HCV antibody testing will be completed in 2023/2024. Scenario 1: if the same number of patients are treated as before the screening, the WHO targets will not be reached. Scenario 2: treating 70% of infected patients (13000 in 2023/2024) will meet most but not all WHO targets. Scenario 3: by treating all infected patients by 2030, the WHO target will be met by saving 150 lives and preventing 90 new cases of decompensated cirrhosis and 120 cases of hepatocellular carcinoma.

Conclusion: In the Lithuanian screening program, HCV antibody testing by GPs is active; however, the number of patients treated needs to be increased to reach the WHO targets.

FRI-174

Challenges and strategies to improve linkage to care and treatment for hepatitis C in pregnancy: perspectives from a global community of practice

Neil Gupta¹, Lindsey Hiebert¹, Martina Badell^{2,3}, Megan Buresh^{4,5}, Catherine Chappell^{6,7}, Manal Hamdy El-Sayed⁸, Saeed Sadiq Hamid⁹, Ravi Jhaveri^{10,11,12}, Ali Judd¹³, Tatyana Kushner^{11,14}, Mona Prasad^{7,15}, Jennifer Price^{11,16,17}, John Ward¹⁸. ¹Coalition for Global Hepatitis Elimination, The Task Force for Global Health, United States; ²Emory University School of Medicine, Department of Gynecology and Obstetrics, Atlanta, United States; ³Society of Maternal Fetal Medicine, United States; ⁴Johns Hopkins University School of Medicine, Division of Addiction Medicine, Baltimore, United States; ⁵American Society of Addiction Medicine, United States; ⁶University of Pittsburgh, Department of Obstetrics, Gynecology, and Reproductive Sciences, United States; ⁷American College of Obstetrics and Gynecology, United States; ⁸Ain-Shams University, Pediatric Department, Cairo, Egypt; ⁹The Aga Khan University, Department of Medicine, Karachi, Pakistan; ¹⁰Northwestern University Feinberg School of Medicine, Department of Pediatrics, Chicago, United States; ¹¹AASLD/IDSA HCV Guidelines Panel, United States; ¹²AASLD Viral Hepatitis Elimination Task Force, United States; ¹³University College London, MRC Clinical Trials Unit, United States; ¹⁴Icahn School of Medicine at Mount Sinai, Division of Liver Diseases, United States; ¹⁵OhioHealth, System Chief of Obstetrics, Columbus, United States; ¹⁶University of California San Francisco, Division of Gastroenterology and Hepatology, San Francisco, United States; ¹⁷AASLD Hepatitis C Special Interest Group, United States; ¹⁸Coalition for Global Hepatitis Elimination, The Task Force for Global Health, Decatur, United States
Email: ngupta-consultant@taskforce.org

Background and aims: Approximately 15 million women of reproductive age are estimated to have chronic hepatitis C virus (HCV) infection worldwide, and an increasing number are diagnosed during pregnancy. Treatment is not currently recommended during pregnancy or breastfeeding due to a lack of safety data. Routine clinical practice is to refer pregnant individuals for treatment after pregnancy and breastfeeding; however, successful linkage to care is extremely limited. The Coalition for Global Hepatitis Elimination established a Community of Practice (CoP) to share existing programmatic experiences and identify best practices for linkage and treatment for pregnant individuals.

Method: A virtual CoP was advertised to interested clinicians, public health professionals, researchers, and advocates, via website posting, social media, professional societies, and targeted outreach. From November 2022 to January 2023, two 90-minute online sessions were conducted, consisting of expert presentations, panel discussions, and first-hand accounts from affected persons. CoP members were polled at the conclusion of each session.

Results: In total, 378 participants from 43 countries attended the CoP sessions, representing all six WHO regions. Most participants self-identified in the fields of public health (33%), primary care (family medicine, obstetrics, pediatrics, or other healthcare provider) (24%), or specialties (hepatology or infectious diseases) (23%). The most frequent challenges for linkage and treatment in pregnancy reported by participants were lack of safety data for HCV treatment in pregnancy (55%), lack of guidelines or recommendations (48%), lack of provider understanding of treatment options (40%), inadequate insurance coverage or payment restrictions (35%), high cost or unavailability of HCV medications (32%), and other patient-side socioeconomic barriers (28%) (n=96 respondents). The most frequent recommendations to improve linkage to care and treatment were co-location of perinatal and HCV treatment services (76%), training of antenatal care providers in HCV treatment (68%), integration of harm reduction or opiate use disorder services (67%), outreach programs (59%), patient navigators (58%), patient communication materials (54%), and guidance from professional societies (48%) (n=85). More participants believed that referral during pregnancy (75%) or HCV treatment during pregnancy (71%) were optimal strategies compared to immediate post-partum treatment (42%), treatment after delivery and breastfeeding (38%), or referral immediately after delivery (35%).

Conclusion: Through a CoP, specific challenges for HCV linkage and treatment for pregnant individuals were identified, and actionable strategies were defined to improve linkage and treatment. Adequate safety data for antenatal administration of direct-acting antivirals, evidence-based operational guidance, and innovative clinical models to increase linkage and treatment for pregnant individuals are urgently needed in order to achieve HCV elimination goals.

FRI-175

New and easy strategy for mass screening for hepatitis C in leisure spaces

Sonia Albertos Rubio^{1,2,3}, Rafael Esteban⁴, Joan Colom⁵, Maria Buti⁴. ¹Hospital Residència Sant Camil, Division of Gastroenterology and Hepatology, Barcelona, Spain; ²Hospital Residència Sant Camil, Barcelona, Spain; ³Hospital Residència Sant Camil, Spain; ⁴Vall d'Hebron University Hospital, Barcelona, Spain; ⁵Agència de Salut Pública de Catalunya ASPCAT, Barcelona, Spain
Email: sonia.albertos@gmail.com

Background and aims: Spain is one of the high income countries on the track for hepatitis C elimination. The prevalence of active hepatitis C in the general population is 0.22% but is higher in vulnerable group. Data from Men who have Sex with Men (MSM) in Catalonia has been established at 0.75%¹. The aim of the study is the HCV screening of the population at street level in leisure events of the LGTB+ collective, using a new screening strategy in leisure spaces. Saludes, V. *et al*. Community-based screening of hepatitis C with a one-step RNA

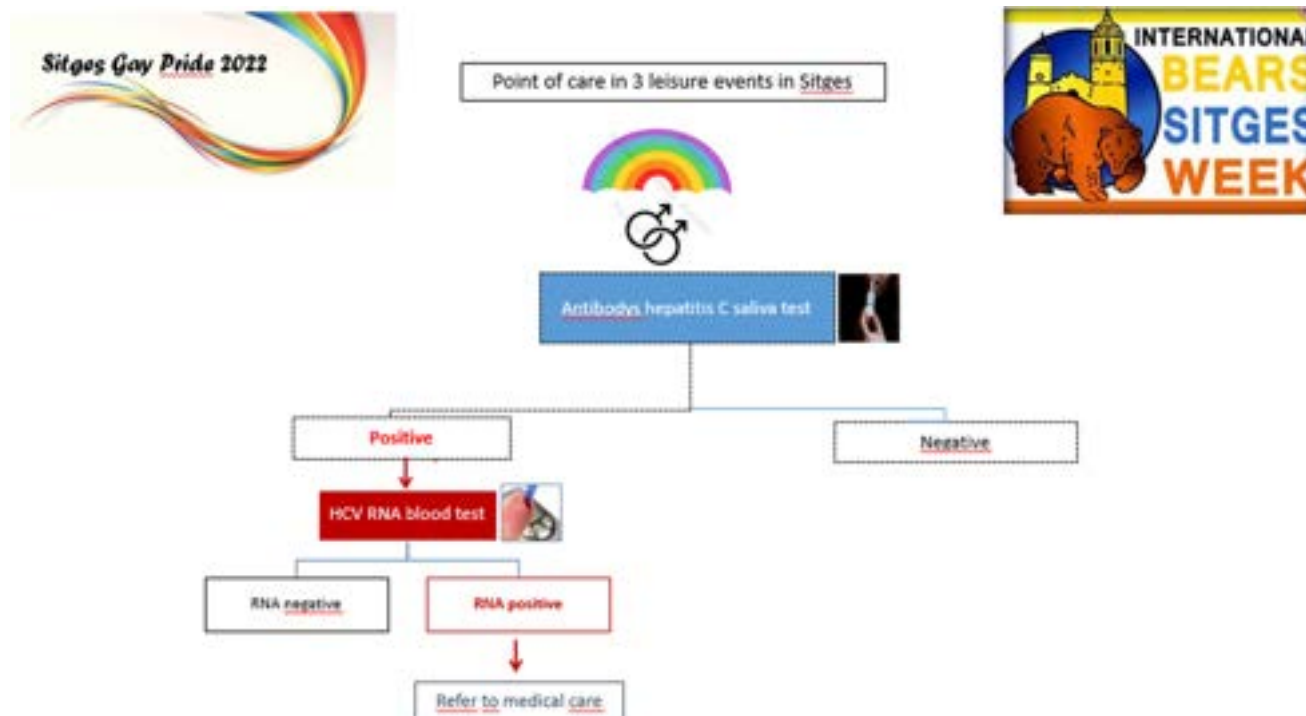


Figure: (abstract: FRI-175).

detection algorithm from dried-blood spots: Analysis of key populations in Barcelona, Spain. *J. Viral Hepat.* 25, 236–244 (2018).

Method: We designed a new method of mass screening for hepatitis C in adults, in 3 festive events of the LGBTI+ community in Sitges (Catalonia), in 2022. The participants were cared for in tents located in leisure spaces where an antibody saliva test was performed –ORAQUICK®– and, if positive, a second HCV RNA test was offered –Xpert HCV Fingerstick®. The baseline demographic value, prior knowledge of having or having had hepatitis C, self-perception of sexual transmission disease risk (visual scale from 0 to 10), risk practices identification test (RPIT) and informed consent were collected (8 items). The project was supported by a scholarship Gilead and Spanish Society of Hepatology, local authorities and the Colors Sitges LGBTI+ association.

Results: We tested 1249 adults, 1197 (96%) identified as MSM. Median age of 44 years (35–54), and 49 different nationalities (24.3% Spanish). The tests were performed in 33 hours (an average of 39 tests/hour). There were only 4 positive tests (3 from the MSM collective), all of them with undetectable RNA. Of the MSM group, 13% did not know their previous hepatitis C status, expressed self-perception of sexual transmission disease risk of 3 out of 10 and an average TISPR of 1.4 out of 8.

Conclusion: We present an efficient and well-accepted hepatitis C screening strategy at the community level, allowing rapid screening of large groups. Although the majority was MSM population exposed to STDs, we have only found a 0.32% HCV serological prevalence and no viremic. This strategy should be explored in other high-risk groups, with difficult access to medical care, such as parenteral drug addicts or homeless people.

FRI-176

Burden of hepatitis C in pregnant women and children in the United States

Paul Wasuwanich¹, Joshua So¹, Tony Wen², Robert Egberman², Wikrom Karnsakul³. ¹University of Florida College of Medicine,

Gainesville, United States; ²University of Florida College of Medicine, Division of Maternal-Fetal Medicine, Department of Obstetrics and Gynecology, Gainesville, United States; ³The Johns Hopkins University School of Medicine, Division of Pediatric Gastroenterology, Hepatology, and Nutrition, Department of Pediatrics, Baltimore, United States
Email: p.wasuwanich@ufl.edu

Background and aims: Cases of hepatitis C virus (HCV) infection are increasing every year in the United States, and while injection drug use remains the largest contributor to HCV transmission, another major route is vertical transmission. We aim to elucidate and extrapolate the financial and health burden of vertically transmitted hepatitis C in pregnant women and children with hepatitis C.

Method: We utilized the 2010–2019 National Inpatient Sample, a nationwide database of hospitalizations in the United States. We identified hepatitis C-related hospitalizations in pregnant women and children using ICD-9 and ICD-10 diagnosis codes. We extracted demographic, financial, and clinical data including all-cause mortality, length of stay, co-infections, and pregnancy outcomes. Financial calculations are inflation adjusted to 2020 and reported in USD. Trends were analyzed by Poisson regression and frequencies by chi-squared test, with significance defined as $p < 0.05$.

Results: We identified a total of 174,430 pregnancies and 134,574 deliveries between 2010 and 2019 that involved hepatitis C. Between 2010–2019, there is an increasing trend of hospitalizations of pregnant women with hepatitis C (incidence rate ratio = 1.14; 95% CI = 1.13–1.16; $p < 0.001$). Maternal deaths were rare ($< 0.1\%$) and similar to the non-hepatitis C pregnancy cohort ($p = 0.147$). However, the length of hospitalization was longer in the hepatitis C pregnancy cohort, 3 days versus 2 days ($p < 0.001$). Additionally, preterm delivery was more common in pregnant women with hepatitis C, 19.1% versus 10.2% ($p < 0.001$). Post-term deliveries were less common in pregnant women with hepatitis C, 8.7% versus 13.2%, ($p < 0.001$). Rates of stillbirths were similar in hepatitis C and non-hepatitis C pregnant cohorts ($p = 0.253$). HIV co-infection was also more common in the pregnant women with hepatitis C, 0.9% versus 0.1% ($p < 0.001$). Additionally, Caesarian deliveries were more frequent in the hepatitis C pregnancy cohort, 19.5% versus

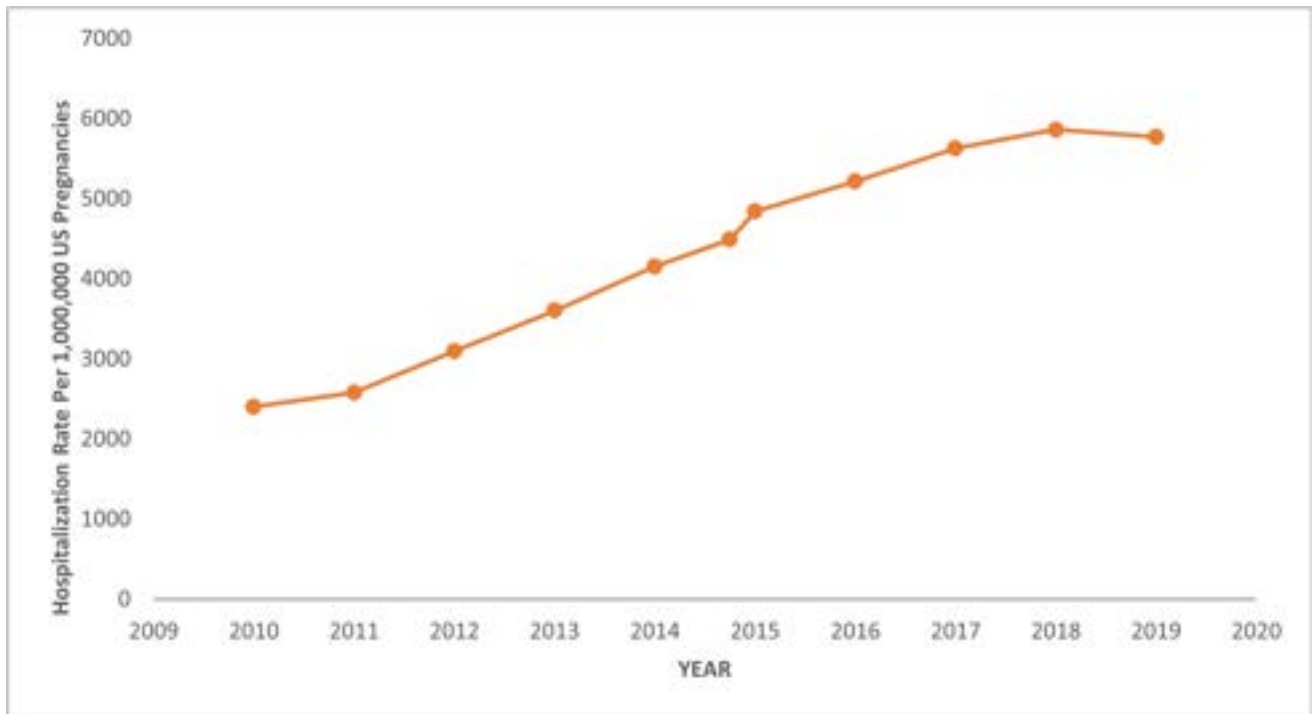


Figure: (abstract: FRI-176): Hepatitis C-related hospitalizations of pregnant women in the United States, 2010–2019.

16.8% ($p < 0.001$). Among the children (≤ 18 years) with hepatitis C, 4.1% developed non-alcoholic cirrhosis. In 2019, there was a financial burden of \$30,414 in excess cost in infants who have hepatitis C per hospitalization. However, for the pregnant women, hospitalization costs were similar between the hepatitis C and non-hepatitis C populations.

Conclusion: Hepatitis C-related hospitalizations in the pregnancy population are increasing yearly and so are the health burdens of the disease, on both the pregnant women and the infants/children. While the financial burden was not obvious the pregnant women, there is a clear cost burden is on the infants with hepatitis C.

FRI-177

Micro-elimination of chronic hepatitis C virus in patients with psychiatric disorders: a multidisciplinary strategy in the outpatient mental health center

Inés Sáenz de Miera^{1,2}, Joel López^{1,2}, Maite Royo^{2,3}, Isabel Plo^{2,4}, Adrià Rodríguez^{1,2}, Silvia Montoliu^{1,2}, Albert Pardo^{1,2}, Joaquín Ruiz^{2,3}, Juan Carles Quer Boniquet^{1,2}. ¹Joan XXIII University Hospital of Tarragona, Gastroenterology, Spain; ²Pere Virgili Health Research Institute, Tarragona, Spain; ³Pere Mata Institute, Mental Health Center for Adults, Tarragona, Spain; ⁴Joan XXIII University Hospital of Tarragona, Pharmacy, Spain
Email: senisamier@yahoo.com

Background and aims: The psychiatric population is considered a vulnerable group with difficulties in accessing diagnostic services and treatment for chronic hepatitis C virus (HCV) (CHC). The seroprevalence of the disease in the psychiatric population is not well known and ranges from 4 to 17%. Data on seroprevalence in Spain are scarce. A multidisciplinary care strategy has been implemented for screening, diagnosis, and treatment of CHC in patients with psychiatric pathology treated in the outpatient mental health center for adults (MHCA) in Tarragona, where the studied and treated population does not move from their usual care environment. The aims of the study are to evaluate the prevalence of CHC in this population and to assess the efficiency of the established circuit for its diagnosis and treatment.

Method: Prospective observational study. Preliminary data are presented with a analysed period of 9 months (January-September 2022). Rapid screening is offered with determination of antibodies for HCV (Ab-HCV) in saliva (OraQuick HCV). In positive cases, viral load of HCV (RNA-HCV) is performed. In cases with proven infection, a study of interactions (Pharmacy-Psychiatry) and prescription of treatment is carried out. The clinical visit, elastography, and initiation of treatment are performed on the same day. The medication is provided to patients at the MHCA, where adherence to treatment is monitored.

Results: Screening was offered to 610 individuals, 349 accepted inclusion (57.2%). 50% are men, median age 47 years; 39% with psychotic disorder, 13% bipolar disorder; 32% with a history of risk factor. Ab-HCV was detected in 9 cases (seroprevalence 2.6%): 7 men, median age 54 years; 8 of them with a history of drug use. Of the 9 cases, 3 had positive RNA-HCV (prevalence 0.85%); 2 of them with criteria for non-response to a previous treatment with Interferon-Ribavirin. 2 have received 12 weeks of treatment with Sofosbuvir-Velpatasvir, with good adherence. They did not require significant modifications of their usual psychiatric therapy and achieved SVR. The third is pending initiation. Of the remaining 6 seropositive cases, 5 had previously been treated and it is confirmed that they maintain SVR; the remaining one, does not have a risk factor and meets criteria for spontaneous resolution. 4 of the seropositive cases in blood had a negative saliva test result.

Conclusion: The inclusion rate of patients in the screening program has been acceptable, nevertheless, measures have been taken to improve recruitment. The seroprevalence of HCV detected in the sample analysed is higher than that described for the general population. Most of the seropositives had already been diagnosed and treated previously. The saliva test is reliable, so the false negative results obtained imply a need to improve the collection technique to avoid underdiagnosis. The treated cases have maintained excellent adherence and have required few modifications to their psychiatric therapy. These results suggest that a management strategy in the patient's environment can be effective.

FRI-178

Simple treatment eligibility score for chronic HBV infection at peripheral health facilities in sub-Saharan Africa

Nicolas Minier¹, Asgeir Johannessen^{2,3}, Alice Guingané⁴, Gilles Wandeler⁵, Michael Vinikoor^{6,7}, Jantjie Taljaard⁸, Alexander Stockdale^{9,10}, Wendy Spearman¹¹, Mark Sonderup¹¹, Roger Sombie¹², Edford Sinkala⁶, Moussa Seydi¹³, Nicholas Riches¹⁴, Edith Okeke¹⁵, Gibril Ndow^{16,17}, Adri Ramirez Mena⁵, Philippa Matthews^{18,19,20}, Tongai Gibson Maponga²¹, Hailemichael Desalegn^{2,22}, Fatou Fall²³, Monique Andersson^{18,21}, Maud Lemoine¹⁶, Yusuke Shimakawa¹. ¹Institut Pasteur Paris, Emerging Disease Epidemiology, Paris, France; ²Vestfold Hospital, Department of Infectious Diseases, Tønsberg, Norway; ³University of Oslo, Institute of Clinical Medicine, Oslo, Norway; ⁴Bogodogo University Hospital Center, Hepato-Gastroenterology Department, Ouagadougou, Burkina Faso; ⁵University of Bern, Institute of Social and Preventive Medicine, Bern, Switzerland; ⁶University of Zambia, Department of Internal Medicine, Lusaka, Zambia; ⁷University of Alabama at Birmingham, Birmingham, United States; ⁸Tygerberg Hospital and Stellenbosch University, Division of Infectious Diseases, Department of Medicine, Stellenbosch, South Africa; ⁹Institute of Infection, Veterinary and Ecological Sciences, University of Liverpool, Department of Clinical Infection, Microbiology and Immunology, Liverpool, United Kingdom; ¹⁰Malawi-Liverpool-Wellcome Trust Clinical Research Programme, Blantyre, Malawi; ¹¹Faculty of Health Sciences, University of Cape Town, Division of Hepatology, Department of Medicine, Cape Town, South Africa; ¹²Yalgado Ouédraogo University Hospital Center, Hepato-Gastroenterology Department, Ouagadougou, Burkina Faso; ¹³Centre Régional de Recherche et de Formation, Centre Hospitalier National Universitaire de Fann, Service de Maladies Infectieuses et Tropicales, Dakar, Senegal; ¹⁴Liverpool School of Tropical Medicine, Department of Clinical Sciences, Liverpool, United Kingdom; ¹⁵Faculty of Medical Sciences, University of Jos, Jos, Nigeria; ¹⁶Imperial College London, Department of Metabolism, Digestion and Reproduction, United Kingdom; ¹⁷London School of Hygiene and Tropical Medicine, MRC Unit The Gambia, Banjul, Gambia; ¹⁸University of Oxford, Nuffield Department of Medicine, Oxford, United Kingdom; ¹⁹The Francis Crick Institute, HBV Genomics for Elimination Laboratory, London, United Kingdom; ²⁰University College, London Hospitals, London, United Kingdom; ²¹Stellenbosch University Faculty of Medicine and Health Sciences, Division of Medical Virology, Cape Town, South Africa; ²²St. Paul's Hospital Millennium Medical College, Medical Department, Addis Ababa, Ethiopia; ²³Hopital Principal de Dakar, Department of Hepatology and Gastroenterology, Dakar, Senegal
Email: yusuke.shimakawa@pasteur.fr

Background and aims: To eliminate hepatitis B virus (HBV) infection in resource-limited settings, it is essential to decentralize HBV care services to peripheral health facilities. However, at these facilities, access to recommended diagnostic tools to assess eligibility for antiviral therapy (AVT), particularly quantitative HBV DNA tests and transient elastography, is severely limited. Through a multi-regional collaboration in sub-Saharan Africa (SSA), we developed and evaluated a simple scoring system, using tests available at peripheral health facilities, to identify eligibility for AVT in people with HBV.

Method: Through HEPSANET (Hepatitis B in Africa Collaborative Network), we conducted a site survey to define the availability of biomarkers potentially useful for HBV management at different levels of health facilities. Then, using the HEPSANET dataset, the largest cross-sectional database of people with chronic HBV in SSA, we divided the sample into derivation and validation sets. We used data from those with a known HBV DNA levels, elastography score, and treatment eligibility status according to the EASL 2017 criteria, which was used as a reference. Using the derivation set, we identified a combination of variables available at peripheral health facilities that can best identify people eligible for AVT through a stepwise logistic regression. With the validation set, we estimated the sensitivity and specificity of the simplified score to identify people eligible for AVT.

Results: The survey of 11 sites found that on average, transaminases (AST, ALT) and platelet counts were available at the district hospital level, hepatitis B e antigen (HBeAg) and near point-of-care HBV DNA test (Xpert) at regional/provincial hospital level, and transient elastography and conventional quantitative HBV DNA tests were only available at national reference centers. Liver decompensation (jaundice, ascites, encephalopathy, etc) was diagnosed clinically at all levels. We proceeded to create a scoring tool for use at district level. The analysis included 2928 treatment naïve individuals with HBV-mono from seven SSA countries, of which 398 (13.6%) were eligible for AVT according to EASL guidelines. AST, ALT, and platelet count remained in the multivariable stepwise regression model and the following scoring system was developed: platelet counts (10⁹/L), <100 (+2), 100–149 (+1), ≥150 (±0); AST (IU/L), <40 (±0), 40–79 (+1), ≥80 (+2); and ALT (IU/L), <40 (±0), 40–79 (+1), ≥80 (+2). Using a cut-off of ≥2, the score had a sensitivity of 79% and specificity of 87% to identify treatment-eligible individuals in the validation dataset.

Conclusion: We found that a low cost combination of platelet counts, AST and ALT levels-tests available even at low level health facilities-can identify the majority of people with HBV in need of AVT in SSA. This suggests that even in the absence of upgrades in laboratory/radiology, decentralization of clinical staging for people with HBV people may be realized in resource-limited settings.

FRI-179

A nationwide study on the core indicators related to elimination of viral hepatitis B and C in Korea

Chang Hun Lee¹, Gwang Hyeon Choi², Hwa Young Choi³, Sojung Han⁴, Young Eun Chon⁵, Young Chang⁶, Eun Sun Jang⁷, Kyung-ah Kim⁷, Do Young Kim⁸, Hyung Joon Yim⁹, Hye-Lin Kim¹⁰, Sook-Hyang Jeong², In Hee Kim¹. ¹Research Institute of Clinical Medicine of Jeonbuk National University-Biomedical Research Institute of Jeonbuk National University Hospital, Jeonju, Korea, Rep. of South; ²Seoul National University Bundang Hospital, Seoul National University College of Medicine, Internal Medicine, Seongnam-si, Korea, Rep. of South; ³Cancer Control and Population Health, Graduate School of Cancer Science and Policy, National Cancer Center, Goyang-si, Korea, Rep. of South; ⁴UiJeongbu Eulji Medical Center, Eulji University School of Medicine, Euijeongbu, Korea, Rep. of South; ⁵CHA Bundang Medical Center, CHA University, Internal Medicine, Seongnam-si, Korea, Rep. of South; ⁶Institute for Digestive Research, Digestive Disease Center, Soonchunhyang University College of Medicine, Internal Medicine, Seoul, Korea, Rep. of South; ⁷Inje University Ilsan Paik Hospital, Internal Medicine, Goyang-si, Korea, Rep. of South; ⁸Yonsei University College of Medicine, Severance Hospital, Seoul, Korea, Rep. of South; ⁹Korea University Ansan Hospital, Korea University College of Medicine, Ansan-si, Korea, Rep. of South; ¹⁰College of Pharmacy, Sahmyook University, Seoul, Korea, Rep. of South
Email: ihkimmd@jbnu.ac.kr

Background and aims: The World Health Organization (WHO) recognizes viral hepatitis as a global public health problem and proposed the elimination of viral hepatitis as a goal to be achieved by 2030. In June 2021, WHO published an interim guideline that sets impact and programmatic targets for country validation of viral hepatitis elimination. We aimed to calculate core indicators for country validation of viral hepatitis elimination in Korea.

Method: The incidence, linkage-to-care rate, treatment rate, and mortality rate related to hepatitis B and C in Korea were analyzed using the health insurance claims data provided by the Korean National Health Insurance Service (NHIS), infectious disease surveillance data from Korea Centers for Disease Control and Prevention Agency, and cause-of-death data from Statistics Korea.

Results: The incidence of acute hepatitis B in Korea was 0.71 per 100,000 patients, and the linkage-to-care rate of hepatitis B was only about 39.1%. Among those who need hepatitis B treatment, the treatment rate was 67.3%, which did not reach the WHO program index of 80%. Regarding liver-specific mortality, the annual liver-related mortality rate is as high as 18.1 per 100,000 people, and liver

Figure 1. Cascade of care of hepatitis B and C in Korea. (A) Hepatitis B (B) Hepatitis C

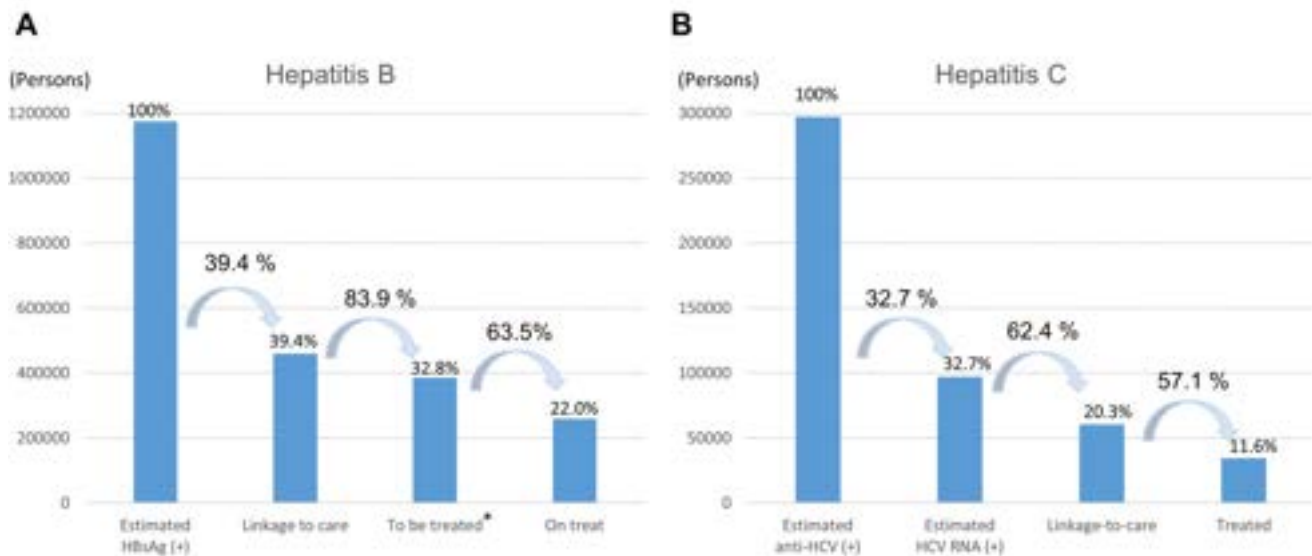


Figure: (abstract: FRI-179).

cancer accounted for the leading cause of death at about 54%. In Korea, the annual incidence of hepatitis C remains high at 11.0 per 100,000 people, whereas the hepatitis C linkage-to-care rate and the treatment rate are low (61.3% and 57.1%, respectively). Regarding the liver-specific mortality rate, the annual liver-related mortality rate for hepatitis C is 1.92 per 100,000 people.

Conclusion: A considerable number of core indicators of country validation for viral hepatitis elimination in Korea have not yet met the certification criteria. It is required to continuously monitor the certification criteria for viral hepatitis elimination in Korea and develop a comprehensive national viral hepatitis elimination strategy.

FRI-180

Hepatitis C seroprevalence screening and linkage to care of unknown infected patients admitted to a tertiary care emergency department: on the road to achieve the WHO 2030 virus elimination target

Roberta Lasco¹, Marco Tizzani¹, Rosa Claudia Stasio¹, Elisabetta Bretto¹, Yulia Troshina^{1,2}, Anna Castiglione³, Fabrizia Pittaluga⁴, Rossana Cavallo⁴, Fulvio Morello⁵, Giorgio Maria Saracco^{1,2}, Enrico Lupia^{2,5}, Alessia Ciancio^{1,2}. ¹S.C. Gastroenterology U, AOU Città della Salute e della Scienza, Turin, Italy; ²Department of Medical Sciences, University of Turin, Italy; ³Clinical Epidemiology, Città della Salute e della Scienza, Turin, Italy; ⁴S.C. Microbiology and Virology, AOU Città della Salute e della Scienza, Turin, Italy; ⁵Department of Emergency Medicine, AOU Città della Salute e della Scienza, Turin, Italy

Email: marco.tizzani91@gmail.com

Background and aims: direct-acting antivirals (DAAs), with their proven effectiveness, allowed WHO to define the elimination of the Hepatitis C virus (HCV) as a health-related global goal by 2030. Hence, worldwide screening campaigns were developed to detect unknown infections. The current study aims to determine the prevalence and characteristics associated with positive HCV serology in patients admitted to an academic tertiary care emergency department to increase diagnosis, define predictors of linkage to care (LTC) and properly achieve anti-viral treatment.

Method: a prospective screening was conducted between November 2021 and October 2022, in patients attending the Emergency Room

(E.R.) of the Molinette Hospital of Turin. Individuals with reactive HCV-Ab test were informed and, if the infection was unknown, HCV RNA testing was proposed. HCV-Ab production was investigated with ELISA method and HCV RNA was performed by RT-PCR testing. Patients were then interviewed to assess LTC and administer DAAs therapy.

Results: among 57715 patients attending the E.R. in study period, 5418 participated to the HCV screening. On a total of 5418 screened patients (51.1% Male/48.9% Female), we identified 188 (3.47%) HCV-Ab reactive patients. The positivity rate was higher in males than in females (4.6 vs 2.3%, $p < 0.001$), in over 50 years old than under 50 years old patients (4.4 vs 1.5%, $p < 0.001$), in patients with severe triage tags than in those with moderate tags (3.0% vs 4.2%, $p \text{ value} = 0.014$) and in patients admitted to hospital than home discharged patients (14.9% vs 8.5%, $p = 0.008$). Of the 188 HCV-Ab reactive patients, 53 (28.19%) were not aware of the Ab-positivity and 33 (17.6%) resulted HCV-RNA positive. Between the HCV-RNA positive patients, 17 (51.5%) had a new diagnosis of ongoing infection and 16 (41%) agreed to be treated with DAAs. Of these, 100% reached a viral sustained virological response (SVR).

Conclusion: the prevalence of HCV infection in the population recruited in the E.R. is greater than in general population (3.5% vs. 1%). HCV screening in the E.R. could be an effective way of identifying ongoing unknown infections and achieve the WHO 2030 elimination targets. Currently, the screening is still ongoing. A case control study has been designed to explore HCV risk factor and determinants to LTC.

FRI-181

D-Mongolia: new strategy for hepatitis B, D and C screening and linkage to care in Mongolians living in Spain

Adriana Palom^{1,2}, Edurne Almandoz³, Antonio Madejón^{2,4}, Ariadna Rando-Segura^{2,5}, Ylenia Pérez Castaño⁶, Judit Vico-Romero¹, Naranbaatar Battulga¹, Mar Riveiro Barciela^{1,2}, Jordi Gómez-Prat⁷, Juan Ignacio Arenas^{2,3}, Francisco Javier Garcia-Samaniego Rey^{2,4}, Maria Buti^{1,2}. ¹Liver Unit, Hospital Universitari Vall d'Hebron, Barcelona, Spain, Spain; ²Centro de Investigación Biomédica en Red en Enfermedades Hepáticas y Digestivas, Instituto de Salud Carlos III, Madrid, Spain, Spain; ³Gastrointestinal Unit, Hospital Universitario Donostia, Instituto de Investigación Biodonostia, San Sebastian, Spain, Spain; ⁴Liver Unit, Hospital Universitario La Paz, IdiPAZ, Madrid, Spain,

POSTER PRESENTATIONS

Spain; ⁵Microbiology Department, Clinical Laboratories, Hospital Universitari Vall d'Hebron, Barcelona, Spain, Spain; ⁶Digestology Unit, Hospital Bidasoa de Hondarribia, Instituto de Investigación Biodonostia, San Sebastián, Spain, Spain; ⁷Community and Public Health Department (ESPIC), International Health Unit, Drassanes-Hospital Universitari Vall d'Hebron, Barcelona, Spain, Spain
Email: mariabutiferret@gmail.com

Background and aims: Mongolia is one of the countries with the highest prevalence of viral hepatitis (B, C and D) in the world. One third of Mongolia's population lives outside the country. In Spain, there are 853 Mongolians registered on the census, mostly distributed between Barcelona, San Sebastián and Madrid. The reported prevalence of viral hepatitis in Spain is 0.22% for HBsAg, 0.85% for anti-HCV and 0.22% for HCV-RNA. The aims of this study were to screen Mongolians living in Spain for viral hepatitis B, D and C, describe their characteristics and in positive cases, offer them the possibility to be linked to care.

Method: Mongolian adults residing in Spain were contacted by a community worker to attend a community program consisting of an educational activity (audiovisual information on viral hepatitis), an epidemiological questionnaire (knowledge of the disease, risk factors...) and a point-of-care rapid test for hepatitis B and C. In positive cases, a dried blood spot test was performed to determine HBV-DNA, HCV-RNA and anti-HDV, and a blood test that included serological and virological parameters. The positive cases were linked to care during the same screening.

Results: From a total of 709 Mongolians residing in Barcelona, San Sebastián and Madrid, 290 were invited to the community program and 216 (75%) subjects carried out the educational activity and were tested. One-hundred-thirty-five were women (62.5%), mean age 41.1 ± 11.6 years, 73 (34%) subjects had one or more viral hepatitis risk factor, and 46 (21%) reported being already vaccinated against HBV. The rest were unaware of their vaccination status. Among them, 14 (6.5%) were anti-HCV+, 2 had detectable HCV-RNA (0.9%); 9 were HBsAg+ (4.2%) and 8 with detectable HBV-DNA (3.7%). From those HBsAg+, 2 had hepatitis B/D co-infection (0.9%), both with undetectable HDV-RNA. Peripheral blood serology confirmed the

results of the rapid test in all cases. However, the virological dried blood tests showed lower virological values than the peripheral blood ones. Among the 23 diagnosed patients, 15 (65%) were unaware of their diagnosis. All of them are currently linked to care.

Conclusion: The community program was feasible, widely accepted, and allowed linkage to care of 23 subjects, 65% of whom were unaware of the infection. The prevalence of viral hepatitis was higher than that described in the Spanish population. Among the screened participants, the prevalence of hepatitis B was higher than active hepatitis C, and an important number of adults were not aware of being vaccinated against HBV. In the future, hepatitis B vaccination needs to be included in these community programs.

This project has been funded by Gilead Sciences (GLD21/00139).

FRI-182

Improving blood borne virus screening in immigration removal centres in the UK

Katie Abraham¹, Nichola Royal¹, Arran Ludlow-Rhodes¹, Louise Missen². ¹Practice Plus Group Ltd, United Kingdom; ²Gilead Sciences Ltd, United Kingdom

Email: katie.abraham@practiceplusgroup.com

Background and aims: There are currently 7 Immigration Removal Centres (IRC) in the UK with 24,497 individuals being detained in 2021. Prevalence of blood borne viruses (BBVs) in IRCs is poorly understood, but residents in UK foreign national prisons have been shown to have significantly higher hepatitis B virus (HBV) and human immunodeficiency virus (HIV) prevalence compared to the general prison population. As a result of this, IRCs are potentially important sites to test for these BBVs and hepatitis C (HCV). Barriers to BBV testing include fast turnover of patients and hesitancy to treat due to risk of deportation. The aim of this pilot project is to assess and overcome potential barriers to implementation of BBV screening and linkage to care in IRCs.

Method: As part of National Health Service England plans to eliminate HCV in England by 2025, Practice Plus Group (PPG) and Gilead Sciences formed a partnership in May 2019 with the aim to optimise hepatitis C virus (HCV) testing and treatment in their secure

Number of BBV tests completed across two IRCs

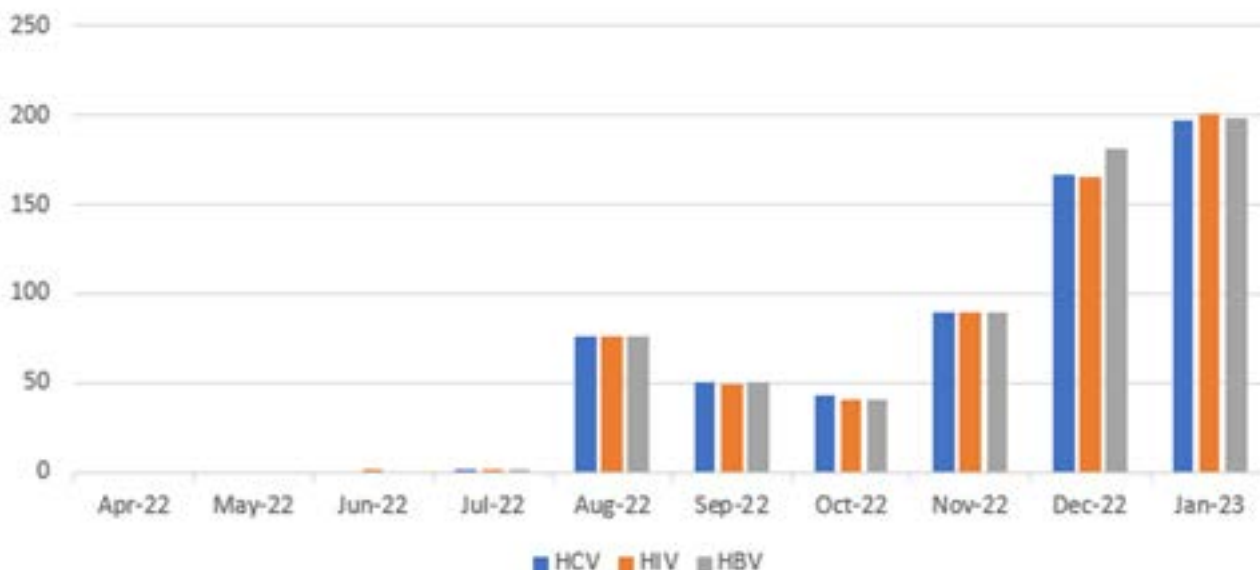


Figure: (abstract: FRI-182).

settings. A pilot project was developed at two London based IRCs where healthcare is provided by PPG. PPG regional BBV Lead Nurses and a Gilead Medical Scientist worked with the IRC and BBV stakeholders to optimise test and treat pathways for new IRC admissions. An important step was to gain agreement that every effort would be made to delay the transfer of residents if diagnosed, an issue that has previously been a barrier to screening. All IRC staff were trained in offering and administering point of care (PoC) BBV testing and regular review meetings were implemented to discuss progress and targets.

Results: The number of residents offered and tested increased rapidly from the start of the pilot in August 2022 with the majority of those tested being screened for all three BBVs (see Figure). Across both IRCs between April 2022 and December 2022, 18 HCV antibody positive cases, 14 hepatitis B surface antigen (HbSAg) positive cases and 9 HIV RNA positive cases were identified. The prevalence of HCV antibody, HbSAg and HIV RNA positivity was 2.9%, 2.2% and 1.4% respectively. Updated data on referral to treatment and treatment initiation for these cases will be available at the conference.

Conclusion: This pilot highlights the importance of ensuring that HBV, HCV, and HIV are all included in screening in IRC populations. Data from this project demonstrates that the BBV prevalence is significantly different to that of other UK secure settings and indicates the need for a multi-agency approach.

FRI-183

Exploring the impacts of the COVID-19 pandemic on access to HCV-related care and support: findings from a survey of people with lived experience of incarceration and/or substance use in British Columbia, Canada

Terri Buller-Taylor¹, Georgine Cua², Dahn Jeong^{3,4}, Naveed Janjua^{1,4,5}, Mawuena Binka^{1,4}. ¹British Columbia Centre for Disease Control, Vancouver, Canada; ²University of British Columbia, Canada; ³British Columbia Centre for Disease Control, Canada; ⁴School of Population and Public Health, University of British Columbia, Vancouver, Canada; ⁵Centre for Health Outcomes and Evaluation, St Paul's Hospital, Vancouver, Canada
Email: terri.buller-taylor@bccdc.ca

Background and aims: Understanding the size and scope of the impact of the COVID-19 pandemic and associated control measures on access to hepatitis C (HCV)-related services among marginalized groups is important for planning and resource allocation now, and during future pandemics. To address existing knowledge gaps, we surveyed people with lived experience of incarceration and/or substance use in British Columbia (BC) about barriers to accessing HCV-related care during the COVID-19 pandemic and preferred potential solutions.

Method: Between August and November 2022, people previously diagnosed with HCV were recruited through selected BC recovery houses (e.g., posters, e-mails to directors) who often serve people with histories of incarceration or substance use. The online survey included questions on the impact of the COVID-19 pandemic on access to HCV-related services. Participants were characterized overall, and then grouped by whether or not they received HCV-related (i) medical services, or (ii) support services (not mutually exclusive). Data on changes in services, the barriers experienced, and preferred solutions to these barriers were collected and analyzed.

Results: A total of 149 people participated in the survey: 56.4% male; 40.3% Indigenous, 39.6% White; and 30.2% 35–44 or 28.9% 45–54 years old. Participants were socially disadvantaged, including 95.3% people who use drugs, 87.2% experiencing food insecurity, 87.2% under-housed, 71.1% with a history of incarceration, 65.1% unemployed, and 38.3% with a disability. Among people who

received HCV-related medical (n = 95) and support services (n = 91), 59.3% and 76.2% reported a worsening in access to these services during the pandemic, respectively. Many reported at least one cancelled/postponed HCV medical (38.9%) or support service (74.7%) appointment. COVID-19-specific barriers at HCV testing/treatment facilities included COVID-19 control measures (28.4%) and concern about getting COVID-19 (29.5%). Top selected solutions to improving access to HCV-related services included increased peer worker funding/support (77.2%), same-day diagnosis and treatment initiation (71.1%), and no tax return requirement for treatment coverage (67.1%).

Conclusion: Survey findings suggest that the COVID-19 pandemic exacerbated existing barriers to HCV medical and support services for economically and socially marginalized individuals. Addressing respondents' preferred solutions will be vital to improving ongoing access to HCV care and for mitigating barriers in future pandemics.

FRI-184

Tenofovir prophylaxis during pregnancy for the elimination of mother-to-child transmission of hepatitis B virus: a cost-effectiveness analysis

Chawisar Janekrongtham¹, Wirichada Pan-ngum², Kittiyod Poovorawan³, Pisit Tangkijvanich⁴. ¹Department of Disease Control, Thailand Ministry of Public Health, Thailand; ²Department of Tropical Hygiene, Faculty of Tropical Medicine, Mahidol University, Thailand; ³Department of Clinical Tropical Medicine, Faculty of Tropical Medicine, Mahidol University, Thailand; ⁴Faculty of Medicine, Chulalongkorn University, Bangkok, Thailand
Email: pisittkvn@yahoo.com

Background and aims: Despite implementing hepatitis B immunoglobulin (HBIG) and vaccination, Tenofovir Disoproxil Fumarate (TDF) has been added for HBeAg-positive mothers during pregnancy to reduce HBV-DNA at birth. To optimize national strategies in Thailand, we assessed the effectiveness of TDF in preventing maternal to child transmission and conducted cost-effectiveness of different TDF-based strategies.

Method: We retrospectively reviewed medical records of mother and infant pairs whose mothers have HBeAg-positive and received TDF in preventing maternal to child transmission of viral hepatitis B according to Thai national guidelines during 2018–2020. Based on the available data of transmission rate, we also applied a decision tree to estimate the cost-effectiveness of different TDF-based strategies to eligible mothers. These included [1] HBIG for all HBV-exposed infants ("HBIG for all") [2] HBIG for only infants of HBeAg-positive mothers ("HBIG for e-positive") and [3] without HBIG to infants ("HBIG-free") The incremental cost-effectiveness ratio (ICER) between the different strategies and baseline intervention without TDF was calculated. The one-way sensitivity analysis was used to adjust prevalence of HBeAg-positive mothers, cost of HBIG, cost of TDF, and transmission rate.

Results: Of 223 infants enrolled, 212 (95.0%) received HBIG while 11 (5.0%) did not. None (0%, 95%CI = [0, 1.69]) of the infants had chronic HBV infection (Figure). The most cost-saving intervention was "HBIG-free" followed by "HBIG for e-positive." The one-way sensitivity demonstrated that the results were reasonably robust to changes. The cost-effectiveness was greater with a higher HBeAg prevalence. The HBIG-free strategy remained best at transmission rates of 0–1.4%, meeting the additional target for eliminations.

Conclusion: The study is the first cost-effectiveness analysis to provide evidence supporting HBIG-free strategy in the era of antivirals. This approach should be considered for preventing maternal to child transmission in resource-constrained settings, particularly in countries with high HBeAg prevalence.

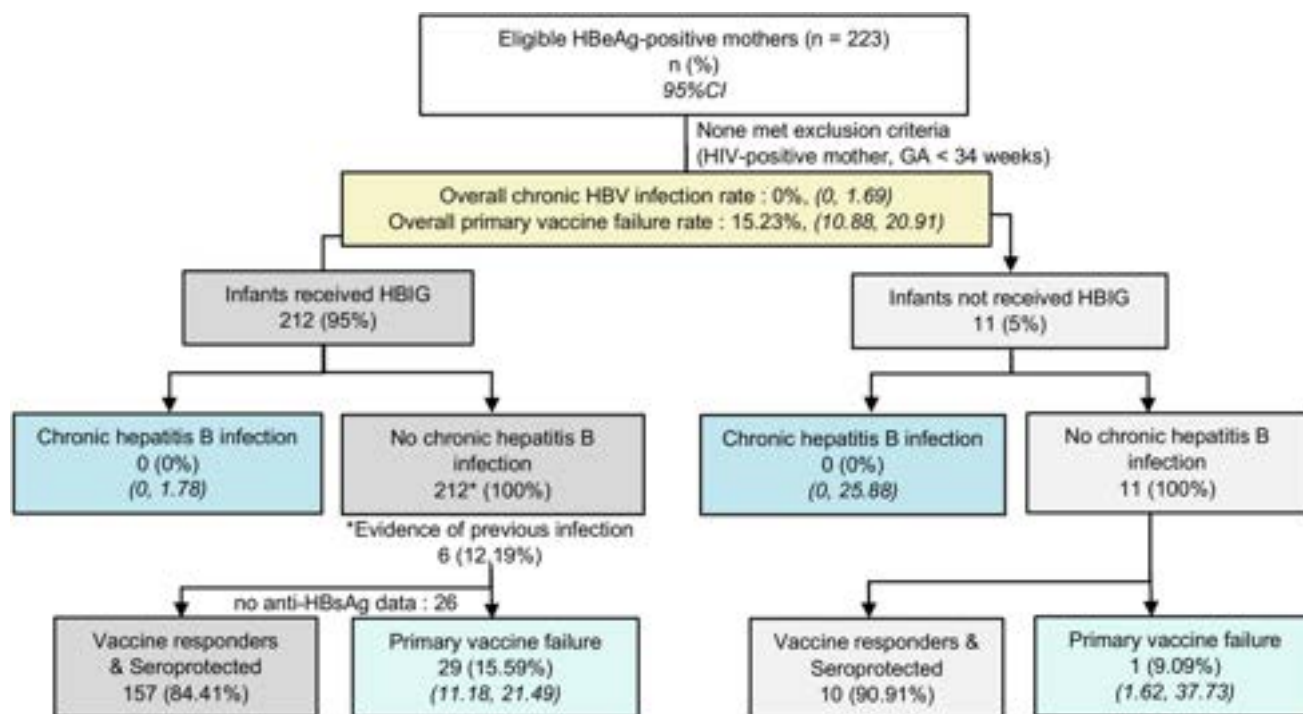


Figure: (abstract: FRI-184): Infant outcomes stratified by HBIG exposure.

FRI-185

A territory-wide opportunistic, hospital-based HCV screening in the general population from northern Italy: the 1969–1989 birth-cohort

Roberta D'Ambrosio¹, Sara Piccinelli², Benedetta Beccalli³, Angiola Spinetti⁴, Massimo Puoti⁵, Stefano Fagioli⁶, Carlo Federico Magni⁷, Silvana Castaldi⁸, Giulia Bombardieri⁹, Claudio Farina⁹, Sabrina Buoro³, Alessandro Amorosi³, Danilo Cereda³, Matteo Corradin³, Pietro Lampertico^{1,10}. ¹Foundation IRCCS Ca' Granda Ospedale Maggiore Policlinico, Department of Gastroenterology and Hepatology, Milan, Italy; ²University of Milan, Department of Biomedical Sciences for Health, Milan, Italy; ³DG Welfare Lombardy Region, Milan, Italy; ⁴ASST Ospedali Civili, Division of Infectious and Tropical Disease, Department of Clinical and Experimental Sciences, Brescia, Italy; ⁵ASST GOM Niguarda Milan and University of Milan Bicocca, Milan, Italy; ⁶ASST Papa Giovanni XXIII, Gastroenterology Hepatology and Transplantation Division, Bergamo, Italy; ⁷ASST Fatebenefratelli Sacco, First Division of Infectious Diseases, Milan, Italy; ⁸Foundation IRCCS Ca' Granda Ospedale Maggiore Policlinico, Quality Department, Milan, Italy; ⁹ASST Papa Giovanni XXIII, Microbiology and Virology Laboratory, Bergamo, Italy; ¹⁰CRC "A. M. and A. Migliavacca" Center for Liver Disease, Department of Pathophysiology and Transplantation, University of Milan, Italy
Email: roberta.dambrosio@policlinico.mi.it

Background and aims: The World Health Organization (WHO) goal of Hepatitis C Virus (HCV) elimination by 2030 rose awareness about the need of screening plans, worldwide. In Italy, it has been estimated that graduated screening starting from people born between 1969 and 1989 might be the most-effective strategy. Aim of this study was to perform a territory-wide opportunistic HCV screening study in the general population born between 1969 and 1989 and attending hospitals and outpatient blood collection centers in Lombardy region, Northern Italy.

Method: This is a prospective multicenter territory-wide opportunistic HCV screening study supported by the Regional Government of Lombardy, Italy. Between June 2022 and December 2022, all subjects born between 1969 and 1989 and hospitalized or accessing

outpatient blood collection centers in Lombardy were offered for-free anti-HCV and HCV-RNA tests. Patients with known anti-HCV positivity and/or previous anti-HCV treatment were excluded. Demographic features were uploaded into a regional web-based platform.

Results: 120,193 individuals underwent HCV screening in 76 screening centers in Lombardy. Their mean age was 44 ± 6 years, 65.2% were females, 83.7% were tested at outpatient blood collection centers. Anti-HCV tested positive in 604 (0.50%) subjects: mean age $47 (\pm 5)$, 51.1% females. HCV seroprevalence was higher in males than in females (0.71% vs. 0.39%; $p < 0.0001$), in elderly ($p < 0.00001$) and in in- vs. out-patients ($p = 0.0007$). HCV-RNA was detectable in 125 out of 441 (28.3%) anti-HCV positive subjects with available HCV-RNA. Patients with active HCV infection were 46 ± 6 years-old, mostly males (56.8%) and screened in wards or DH/DS services ($p < 0.00001$). Overall, the prevalence of active HCV infection in the overall population was 0.10%, and differed according to age-groups ($p = 0.001$), being higher in elderly.

Conclusion: The prevalence of active HCV infection in the general population born between 1969 and 1989 hospitalized or referred for blood testing in Northern Italy was low. However, since this prevalence was higher in older individuals, the extension of such opportunistic screening programs to lower birth-cohorts could be considered.

FRI-186

Cascade of care and HCV treatment of inner city populations engaged in care through community pop-up clinics (CPCs)

Brian Conway^{1,2}, Shawn Sharma¹, Shana Yi¹, Giorgia Toniato¹, David Truong¹, Rossita Yung¹. ¹Vancouver Infectious Diseases Centre, Vancouver, Canada; ²Simon Fraser University, Burnaby, Canada
Email: brian.conway@vidc.ca

Background and aims: Elimination of HCV infection as a public health concern by the end of this decade will require a concerted effort in all target populations, including vulnerable inner-city populations, many of whom are actively using drugs and are facing other issues more pressing than HCV infection. Several strategies

have been proposed to identify HCV-infected inner-city residents, engage them in care, provide them with antiviral therapy, establish conditions to maximize the likelihood of completion of treatment and cure of HCV infection. We have evaluated a novel approach of Community Pop-Up Clinics (CPCs) to achieve this goal within the inner city of Vancouver, Canada.

Method: CPC events are held weekly at various locations (mainly single room occupancy housing projects) interacting with up to 30 residents/half-day event. Point of care antibody testing for HCV is provided in the context of an offer of engagement of multidisciplinary care to address medical, social, psychologic and addiction-related concerns in a co-located manner. For those found to carry HCV antibodies, viremia is assessed by accessing the provincial database for prior results or on-site phlebotomy if required. All viremic individuals are offered HCV treatment in the context of other interventions, with medications administered at the place of residence or pharmacy as most appropriate. Daily/weekly dispensing is available as required. The end points of this analysis are the number of viremic individuals identified per event, the time from engagement to treatment initiation, and the outcome of HCV therapy.

Results: From 01/21–12/22 (24 months), we conducted 80 CPCs and evaluated 1420 individuals. 477 individuals (33.6%) were found to carry HCV antibodies. Of these, 331 individuals (69.4%) were found to be viremic, a mean of 4.1/event. Engagement in HCV therapy has been secured in 289 cases (87%). 247 (85%) individuals have started treatment and 41 remain in the pre-treatment phase, and 1 died of an overdose in the pre-treatment phase. The median time from CPC attendance to HCV treatment initiation was 6 weeks. Of 247, 233 have completed treatment, 9 are currently on treatment, 3 patients did not complete treatment, 2 died of an overdose while on treatment and 1 has been lost to follow-up. Of 233 subjects who have completed treatment, 205 are confirmed as cured (SVR 4/12), 25 are awaiting SVR 4, 2 have documented virologic relapse and 1 has been reinfect, a rate of 0.31/100 person-years. Of participants in whom an outcome of treatment has been ascertained, the cure rate is 97.2% (205/211).

Conclusion: Our program is very cost-effective, identifying over 4 individuals requiring HCV therapy per half-day event. The vast majority initiate treatment within weeks and complete it successfully, with a LTFU rate below 5%. Cure rates match or exceed those reported in clinical trials. Taken together, the data we present validates the development of multidisciplinary programs such as ours to eliminate HCV infection in vulnerable inner city populations.

FRI-187

Incidence of hepatitis C virus antibody seroconversion among people who inject drugs in Tbilisi, Georgia

Tengiz Tsertsvadze^{1,2}, Nikoloz Chkhartishvili¹, Akaki Abutidze^{1,2}, Marine Gogia³, Ketevan Shermadini¹, Francisco Averhoff⁴. ¹Infectious Diseases, AIDS and Clinical Immunology Research Center, Georgia; ²Ivane Javakhishvili Tbilisi State University, Georgia; ³Georgian Harm Reduction Network, Georgia; ⁴Department of Family and Preventive Medicine, Emory University School of Medicine, United States
Email: tt@aidcenter.ge

Background and aims: One of the priority directions of Georgian hepatitis C virus (HCV) elimination program is the prevention of HCV transmission among people who inject drugs (PWID). Furthermore, hepatitis C incidence among PWID is one of the key indicators set by the World Health Organization (WHO) for validating the elimination of hepatitis C, with a target of ≤ 2 cases per 100 person-years (PY). We established Georgian PWID cohort study to estimate incidence of HCV antibody (anti-HCV) seroconversion.

Method: This prospective observational cohort study enrolled PWIDs in the capital city of Tbilisi in 2017–2019. Participants were recruited using incentivized chain-referral sampling, with maximum of 5 peers recruited by each participant. The outcome of interest was anti-HCV seroconversion. Incidence was calculated as number of new anti-HCV

seroconversions divided by the number of total person-years of follow-up (PYFU). Crude estimates were adjusted using post-stratification weights. Factors associated with seroconversion were evaluated in Cox proportional hazards regression model.

Results: Study enrolled 1,744 PWID; among them, 563 (32.3%) were positive for anti-HCV+ at baseline and were excluded from follow-up. Among remaining 1,181 anti-HCV- PWID, 929 (78.7%) returned for at least one visit. Overall, 929 participants were followed for the mean of 11.7 months, contributing to the total of 906 PYFU. During the follow-up, 7 (0.8%) persons seroconverted, corresponding to an incidence rate of 0.77 (95% CI: 0.31–1.59) new infections per 100 PYFU. After adjusting for post-stratification weights, the incidence increased to 0.87 (95% CI: 0.43–1.74) new infections per 100 PYFU. In regression analysis, the only factor significantly associated with seroconversion was a history of sharing injection equipment (Hazard ratio: 50.51, 95% CI: 2.46–611.58, $p = 0.01$).

Conclusion: Our study suggests that the incidence of hepatitis C seroconversion among PWID is below the target set by the WHO. However, PWID remain at risk of contracting the virus, primarily through unsafe injection practices. Further scaling-up harm reduction services is needed to reach the elimination of hepatitis C.

FRI-188

Survey to evaluate the implementation of the recommendations on the comprehensive diagnosis of viral hepatitis in a single extraction: where are we?

Joaquín Cabezas^{1,2}, Antonio Aguilera³, Marina Berenguer⁴, María Buti^{5,6}, María Eliece Cano⁷, Xavier Forns⁸, Federico García García⁹, Francisco Javier García-Samaniego Rey¹⁰, Manuel Hernández-Guerra¹¹, Francisco Jorquera Plaza¹², Jeffrey Lazarus^{13,14}, Sabela Lens¹⁵, Elisa Martró^{16,17}, Juan Pineda¹⁸, Martín Prieto¹⁹, Francisco Rodríguez-Frías²⁰, Manuel Rodríguez²¹, Miguel Serra²², Juan Turnes²³, Araceli Casado Gómez²⁴, Raquel Domínguez-Hernández²⁴, Nerea Tejado Alsua²⁴, Miguel Ángel Casado²⁴, José Luis Calleja Panero²⁵, Javier Crespo^{1,2}. ¹University Hospital Marqués de Valdecilla, Gastroenterology and Hepatology Department, Santander, Spain; ²Research Institute Valdecilla-IDIVAL, Santander, Spain; ³Hospital Clínico Universitario de Santiago de Compostela, Servicio de Microbiología, Santiago de Compostela, Spain; ⁴Hospital Universitario y Politécnico La Fe, Unidad de Hepatología y Trasplante Hepático y Ciberehd, Valencia, Spain; ⁵Hospital Universitario Valle Hebrón, Servicio de Hepatología, Barcelona, Spain; ⁶CIBEREHD del Instituto Carlos III, Barcelona, Spain; ⁷University Hospital Marqués de Valdecilla, Microbiology Department, Santander, Spain; ⁸Hospital Clinic, Servicio de Hepatología, Barcelona, Spain; ⁹Servicio de Microbiología, Hospital Universitario Clínico San Cecilio, Instituto de Investigación IBS, Granada, Spain; ¹⁰Unidad de Hepatología, Hospital Universitario La Paz. CIBEREHD. IdiPAZ, Madrid, Spain; ¹¹Servicio de Aparato Digestivo, Hospital Universitario de Canarias, Tenerife, Spain; ¹²Servicio de Aparato Digestivo, Complejo Asistencial Universitario de León, León, Spain; ¹³Barcelona Institute of Global Health (ISGlobal), Hospital Clínic, Barcelona, Spain; ¹⁴Facultad de Medicina, Universidad de Barcelona, Barcelona, Spain; ¹⁵Servicio de Hepatología, Hospital Clínic. Universidad de Barcelona. IDIBAPS. CIBEREHD, Barcelona, Spain; ¹⁶Servicio de Microbiología, Laboratori Clínic Metropolitana Nord (LCMN), Hospital Universitari Germans Trias i Pujol, Institut d'Investigació Germans Trias i Pujol (IGTP), Badalona, Spain; ¹⁷Consorcio de Investigación Biomédica en Red de Epidemiología y Salud Pública (CIBERESP), Instituto de Salud Carlos III, Madrid, Spain; ¹⁸Grupo Virología Clínica e ITS, Hospital Universitario de Valme, Ciber de Enfermedades Infecciosas CIBERINFEC, Sevilla, Spain; ¹⁹Unidad de Hepatología y Trasplante Hepático, Hospital Universitario y Politécnico La Fe, Valencia, Spain; ²⁰Servicios de Microbiología y Bioquímica, Laboratorios Clínicos, Hospital Universitario Vall d'Hebron, CIBEREHD. Instituto de Investigación Vall d'Hebron (VHIR), Barcelona, Spain; ²¹Ección de Hepatología, Servicio de Digestivo, Hospital Universitario Central de Asturias, Instituto de Investigación Sanitaria del Principado de Asturias (ISPA), Oviedo, Spain; ²²Universidad de Valencia, Valencia,

POSTER PRESENTATIONS

Spain; ²³Servicio de Digestivo, Hospital Universitario de Pontevedra, Pontevedra, Spain; ²⁴Pharmacoeconomics and Outcomes Research Iberia (PORIB), Madrid, Spain; ²⁵Servicio de Gastroenterología y Hepatología, Hospital Universitario Puerta de Hierro. Instituto de Investigación Puerta de Hierro Majadahonda (IDIPHIM), Madrid, Spain
Email: joweycabesas@gmail.com

Background and aims: The SEPD (Spanish Association for Digestive Diseases), AEEH (Spanish Association for the Study of the Liver), SEIMC (Spanish Society of Infectious Diseases and Clinical Microbiology), SEIMC-GEHEP (Work-group for Viral Hepatitis) and AEHVE (Spanish Viral Hepatitis Elimination Alliance) agreed on a document at the beginning of 2022 to carry out a comprehensive diagnosis of viral hepatitis (B, C and D): a positive result in serology to detect viral hepatitis (HBV, HCV and HDV), as well as HIV, would trigger the analysis of the rest of the virus, including the viral load when necessary, from the same blood sample. This process would increase the diagnosis rate and it would reduce the time to be evaluated. Aim: To evaluate the situation in Spain regarding the comprehensive diagnosis of viral hepatitis in a single blood draw.

Method: A panel of experts prepared a structured survey disseminated through the Google Forms platform to all Spanish hospitals, public or private with teaching accreditation, with 200 beds or more. The survey was sent on 20th Oct 2022 and the reception of the results closed on 1st Dec. 2022.

Results: Of the 130 hospitals with inclusion criteria, 48 responded (37% response rate, 34 centers >500 beds). All centers have tools for the determination of HBV surface antigen, anti-HCV and HIV serology. 92% have a PCR technique for HBV/HCV. Only 67% of the centers have capacity for the determination of anti-HDV, and this drops to 31% for the detection of HDV-RNA; 88%, who do not have this technique, outsource it. The availability of Point-of-Care (POC) tests is low (21% of centers), GenXpert HCV (38%) and dry blood spot (38%) being the most frequent. Most of the POCs (90%) are supervised by Microbiologists and are always included in the clinical records. Reflex-test diagnosis is performed simultaneously in 88% of centers for HCV, 62% for HBV, 50% for HDV, and only 41% for HBV-HDV. Although 90% of centers believe that HBV and HCV serology should be performed on HIV-positive patients in the same sample, it is only

done on 18% of HBsAg-positive and/or anti-HCV-positive subjects. When there is an active infection, any communication strategy is used in 38/48 (79%) of the hospitals (38 hospitals for HCV, 18 for HBV and 10 for HDV). The automated appointment arrangement is only available in 19% of the centers. Only 44.2% of the respondents believe that the determinations to reach a definitive diagnosis must be made with a single blood sample.

Conclusion: Although most hospitals have the procedures to carry out a comprehensive diagnosis of viral hepatitis in a single analytical sample, this is used in less than 50% of cases for HBV/HDV. Alerts to maintain continuity of care are widely available for hepatitis C, but they need to be increased for HBV and HDV. Likewise, it is necessary to implement the devices for decentralized diagnosis.

FRI-189

Occult hepatitis B virus infection among blood donors in northwestern Greece

Maria Leontari¹, Fotios Fousekis¹, Gerasimos Baltayiannis¹, Dimitrios Christodoulou¹, Peter Karayiannis². ¹Department of Gastroenterology and Hepatology, University Hospital of Ioannina, Ioannina, Greece, Greece; ²Medical School, University of Nicosia, Cyprus, Greece
Email: fotisfous@gmail.com

Background and aims: Occult hepatitis B virus (HBV) infection (OBI) is characterized by the presence of HBV-DNA in blood or tissues in individuals with undetectable serum HBsAg. This study aimed to assess the prevalence and characteristics of (OBI) in Northwestern Greece.

Method: Serum samples from 702 blood donors were prospectively collected at University Hospital of Ioannina between February 2018 to September 2022 and were investigated for presence of HBV markers. The Abbott Architect HBsAg and HBcAb HB Qualitative II kit were used for detection of HBsAg and anti-HBc respectively. Serum from patients who were HBsAg (-)/anti-HBc (+) was further tested by polymerase chain reaction (PCR) for the detection of HBV-DNA. In cases of OBI, sequencing and mutation analysis of the HBV pre-S/S gene were performed.

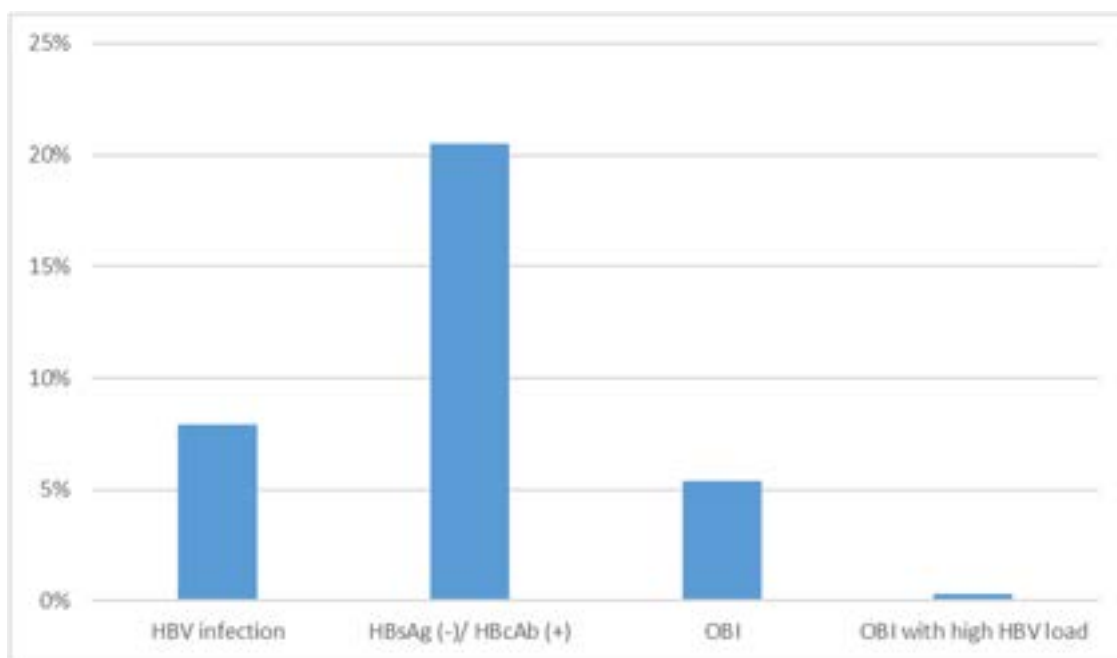


Figure: (abstract: FRI-189): Prevalence of HBV infection, occult HBV infection (OBI) and OBI with high HBV-DNA levels in blood donors.

Results: Screening revealed 56 cases (7.9%) with HBV infection (HBsAg positive) and 144 cases (20.5%) of past HBV infection [(HBsAg (-)/anti-HBc (+)], while 38 cases of OBI were identified. In 36 out of 38 cases, the HBV DNA load was <225 IU/ml. One patient with OBI had HIV co-infection. Furthermore, there were two cases with OBI and high HBV-DNA levels (>200,000 IU/ml). Sequencing demonstrated S- and pre-S mutations in 4 cases of OBI, including both OBI cases with high HBV-DNA levels.

Conclusion: High prevalence of HBV infection and OBI was detected in a region with a high proportion of immigrants from endemic countries. In addition, S gene mutations were associated with cases of OBI with high HBV-DNA levels.

FRI-190

Hepatitis E virus seroprevalence in immunosuppressed patients in Belgium: a prospective study

Marie Philippart¹, Michael Peeters², Hubert Piessevaux¹, Maria Badii³, Sarah Bailly⁴, Xavier Poiré⁴, Nada Kanaan⁵, Arnaud Devresse⁵, Benoit Kabamba⁶, Géraldine Dahlqvist¹. ¹Cliniques Universitaires Saint Luc, Service d'Hépatogastroentérologie, Bruxelles, Belgium; ²Sciensano, Viral Disease Department, Bruxelles, Belgium; ³Cliniques Universitaires Saint Luc, Service de cardiologie, Bruxelles, Belgium; ⁴Cliniques Universitaires Saint Luc, Service d'hématologie, Bruxelles, Belgium; ⁵Cliniques Universitaires Saint Luc, Service de néphrologie, Bruxelles, Belgium; ⁶Cliniques Universitaires Saint Luc, Laboratoire de microbiologie médicale, Bruxelles, Belgium
Email: marie.philippart01@gmail.com

Background and aims: Hepatitis E virus (HEV) is the commonest cause of acute viral hepatitis in Western countries. In immunocompromised patients, chronic HEV have been described, leading in certain cases to cirrhosis, decompensation and death or liver transplantation.

The aim of the study is to determine the prevalence of HEV infections in the immunosuppressed population followed in a single tertiary center in Belgium.

Method: From May 2022 to April 2023, we are prospectively screening for HEV (IgG, IgM and PCR) all patients transplanted from a solid organ (SOT) as well as patients suffering from a lymphoma or followed in the hematology department for a bone marrow transplantation under immunosuppression from at least three months.

We compared the data from our immunosuppressed patients to the data collected from national serum banks in Belgium in 2014 by Ho et al., representing the general seroprevalence in Belgian population. Chi² test or Fisher exact test were performed to compare the groups.

Results: We present here an intermediate analysis after 8 months of screening. Among 570 patients, 240 were followed for a kidney transplantation (KT), 139 for a heart transplantation (HT), 163 for a liver transplantation (LT), and 55 for haematological disease (HD). The median age was 61. The sex ratio F/M was 1/2. The mean IgG HEV seroprevalence was 9.29% in our population, 8.1% in KT, 13% in HT, 14.8% in LT and 0% in HD. A positive HEV PCR was found in 6 patients, 5 in the KT group and one followed for HD and genotype 3c was identified in all of them. There is a significant difference between the HEV IgG seroprevalence in Belgian population in 2014 (5.8%) and our population ($p = 0.001$). In subgroup analysis, there is a significant difference between the Belgian population and the patients followed for LT ($p = 0.0006$) and HT ($p = 0.0114$). There is also a significant difference between the different SOT groups and the patients followed for haematological diseases (LT vs HD: $p = 0.0026$; HT vs HD: $p = 0.0068$; KT vs HD: $p = 0.03$).

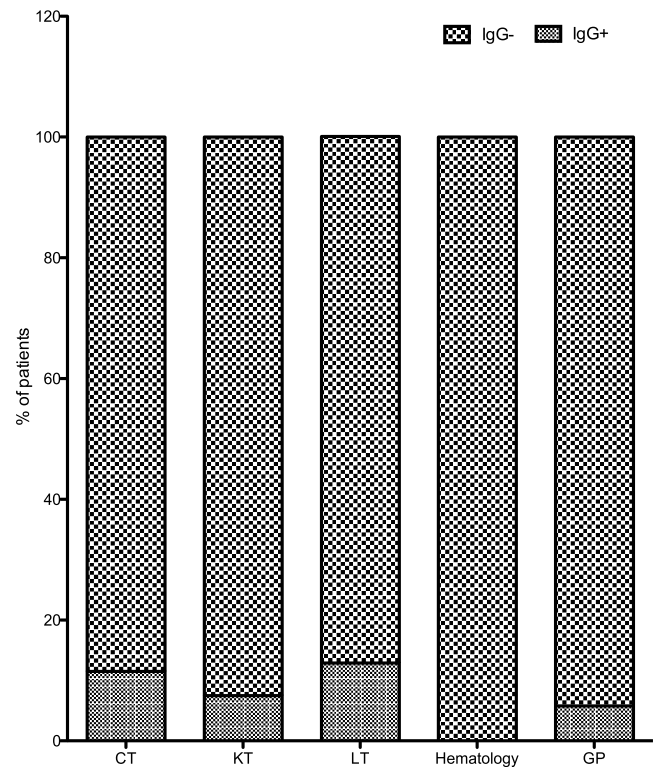


Figure:

Conclusion: The seroprevalence between our group of immunosuppressed patients and the Belgian population is significantly higher. Subgroup analysis showed a significantly higher seroprevalence in HT and LT patients but does not translate into an actual chronic infection rate. KT is a risk factor for the occurrence of chronic HEV compared to other SOT groups. The seroprevalence is however not significantly different in this group compared to the general population. More data are awaiting to draw conclusions on the importance of systematic screening in these immunosuppressed populations.

This study is supported by a Gilead fellowship grant.

FRI-191

What is the most effective strategy to identify HBV-infected pregnant women eligible for antiviral prophylaxis in Burkina Faso? A modelling study on different testing strategies

Andréa Gosset¹, Yusuke Shimakawa², Alice N. Guingané³, Abdoul Tiendrebeogo⁴, Maria Patrizia Carrieri¹, Tim Hallett⁵, Shevanthi Nayagam^{5,6}, Sylvie Boyer¹. ¹Aix Marseille University, INSERM, IRD, SESSTIM, Sciences Economiques et Sociales de la Santé and Traitement de l'Information Médicale, ISSPAM, 13005 Marseille, France, France; ²Unité d'Epidémiologie des Maladies Emergentes, Institut Pasteur, 75015 Paris, France, France; ³Hepatogastroenterology Department, Bogodogo University Hospital Center, Ouagadougou, Burkina Faso, Burkina Faso; ⁴Epidémiologie des Maladies Evitables par la Vaccination, Agence de Médecine Préventive (AMP), Ouagadougou BP 638, Burkina Faso, Burkina Faso; ⁵MRC Centre for Global Infectious Disease Analysis, School of Public Health, Imperial College London, London, United Kingdom, United Kingdom; ⁶Department of Surgery and Cancer, Imperial College London, London, United Kingdom, United Kingdom
Email: andrea.gosset@inserm.fr

Background and aims: To prevent mother-to-child transmission of hepatitis B (HBV), WHO recommends tenofovir (TDF) prophylaxis in high-risk pregnant women from the 28th week of pregnancy until at least birth, in addition to 3–4 doses of hepatitis B vaccination (HepB3) in all infants, including a timely birth dose (HepB-BD). TDF

POSTER PRESENTATIONS

Scenarios	Total number of new chronic infections	Total number of new chronic infections due to MTCT	Number of new chronic infections averted	Number of new chronic infections due to MTCT averted	Total number of pregnancies under antiviral treatment
0. HepB-BD + HepB3	84,091	29,976	-	-	0
1. TDF if high viral load + HepB-BD + HepB3	80,539	26,871	3,552 (-4.2%)	3,105 (-10.4%)	10,567
2. TDF if HBeAg+ + HepB-BD + HepB3	81,536	27,742	2,555 (-3.0%)	2,234 (-7.5%)	17,729
3. TDF if HBcrAg+ + HepB-BD + HepB3	80,350	26,706	3,741 (-4.4%)	3,270 (-15.6%)	40,573
4. TDF if HBsAg+ + HepB-BD + HepB3	78,743	25,313	5,348 (-6.4%)	4,663 (-10.9%)	263,779

Figure: (abstract: FRI-191): Total number of new chronic infections and number of pregnancies under antiviral treatment over the period 2021–2030 according to the different scenarios.

prophylaxis is recommended for HBV-infected pregnant women with an HBV DNA $\geq 5.3 \log_{10}$ IU/ml or those positive for hepatitis B e antigen (HBeAg) in settings without access to HBV DNA quantification. However, HBV DNA testing is not widely available at antenatal care in Burkina Faso (BF) and rapid diagnostic tests (RDTs) to detect HBeAg lack sensitivity. Therefore, alternative strategies could be to use hepatitis B core-related antigen (HBcrAg) RDT (data from The Gambia: 100% sensitivity and 87% specificity to detect HBV DNA $\geq 5.3 \log_{10}$ IU/ml) or to treat all pregnant women positive for hepatitis B surface antigen (HBsAg) without any additional tests. This study assessed the impact of different testing strategies to identify HBV-infected pregnant women who should receive TDF prophylaxis in BF. **Method:** We analysed five intervention strategies and used a deterministic model specified by age, sex, and type of transmission to estimate the effectiveness of each strategy over the period 2021–2030 in BF. The baseline strategy was the current policy-HepB-BD in addition of HepB3. The four other strategies additionally considered screening pregnant women for HBsAg using a RDT, and providing TDF prophylaxis to HBsAg-positive women if they had: i) HBV DNA $\geq 5.3 \log_{10}$ IU/ml, ii) positive HBeAg using RDT, iii) positive HBcrAg using RDT, or iv) without additional test. HepB-BD was introduced in 2022 in BF. We introduced TDF prophylaxis in 2023 in the model. We considered a linear scale up of HepB-BD, HBsAg screening and TDF prophylaxis to achieve 90% over 5 years. We estimated the costs of each strategy using a health system perspective.

Results: In 2021–2030, the total number of pregnancies requiring TDF treatment would be 10,567 in the HBV-DNA strategy, 17,729 in the HBeAg strategy, 40,573 in the HBcrAg strategy (including a higher number of women with low HBV-DNA treated unlike the first strategy), and 263,779 in the treat all strategy. In the baseline scenario, we estimated 84,091 new chronic infections including

29,976 infections due to MTCT in 2021–2030. Compared to the baseline scenario, the addition of TDF prophylaxis would allow to avert 3,552 new chronic infections (–4.2%) in the first strategy, 2,555 (–3.0%) in the second strategy, 3,741 (–4.4%) in the third strategy, 5,348 (–6.4%) in the fourth strategy.

Conclusion: The treat all strategy might be most effective, however the effects of treating all HBsAg-positive women are unknown and will drastically increase treatment needs in pregnant women and costs. The cost-effective analysis is ongoing and results will be presented at the conference.

FRI-192

Results from a community-based intervention to increase viral hepatitis screening among at-risk African migrants in Catalonia, Spain (2020–2022)

Camila Picchio¹, Daniel K. Nomah², Ariadna Rando-Segura³, Sabela Lens^{4,5}, Xavier Fornas^{4,5}, Sergio Rodríguez-Tajes^{4,5}, Lena van Selm¹, Delfina Boudou¹, Francisco Javier Pamplona Portero⁶, Carmen López Núñez⁷, Francisco Rodríguez-Frías³, Maria Buti^{5,8}, Jeffrey Lazarus^{1,9}. ¹Barcelona Institute for Global Health (ISGlobal), Hospital Clínic, University of Barcelona, Barcelona, Spain; ²Center for Epidemiological Studies on Sexually Transmitted Infections and HIV/AIDS in Catalonia (CEEISCAT), Department of Health, Generalitat of Catalonia, Badalona, Spain; ³Liver Pathology Unit, Biochemistry and Microbiology Service, Hospital Universitari Vall d'Hebron, Barcelona, Spain; ⁴Liver Unit, Hospital Clínic, IDIBAPS, University of Barcelona, Barcelona, Spain; ⁵CIBER Hepatic and Digestive Diseases (CIBERehd), Instituto Carlos III, Madrid, Spain; ⁶Department of Digestive Diseases, Hospital de Santa Caterina, Salt, Girona, Spain; ⁷Department of Digestive

Diseases, Hospital Dr Josep Trueta, Girona, Spain;⁸Liver Unit, Hospital Universitari Vall d'Hebron, Barcelona, Spain;⁹CUNY Graduate School of Public Health and Health Policy, New York, New York, United States
Email: camila.picchio@isglobal.org

Background and aims: Africans in Europe migrating from high-endemic hepatitis B and C virus (HBV and HCV) areas may not know their disease status due to unreliable testing and vaccination in their home countries and underutilization of the host country health services. In Catalonia, Spain, universal health coverage grants migrants access to health services, which offers an entry point into the health system. We aimed to use point-of-care testing in community settings to identify and link to care or vaccinate West African migrants in the greater Barcelona area, Spain.

Method: Between November 2020 and December 2022, viral hepatitis testing was offered to 636 people. Testing in community settings used an HBV surface antigen (HBsAg) rapid lateral flow test (DETERMINE® HBsAg 2) followed by whole blood sample collection using a plasma separation card (Roche Diagnostics), which analyzed HBV-DNA and anti-hepatitis D virus (HDV) among those HBsAg+ and anti-HBV core antigen (anti-HBc) among those HBsAg-. Anti-HCV testing with the OraQuick® was incorporated in June 2022. HBsAg+ participants were immediately referred to a collaborating tertiary hospital for full assessment.

Results: 622 participants were included for analysis (mean age 42 [SD 10]). They were primarily from Ghana (81%) and Senegal (16%), were male (63%), and 17% (n = 104) arrived to Spain ≤5 years ago. Most participants had never been tested for HBV nor HCV (70%), while 15% were unsure if they had been. HBsAg+ prevalence was 10% (n = 62) and no one was anti-HCV+. Of those HBsAg+, 50% (n = 31) had detectable HBV-DNA and one person was anti-HDV+. Of those who were HBsAg- (n = 560), 38% (n = 216) were anti-HBc+. The remaining, if not previously vaccinated (n = 292), were offered the first dose of the HBV vaccination *in situ* during the second visit (191 returned for results), of which, 85% (n = 164) accepted. Overall, 76% (n = 49) of those who were HBsAg+ had a first documented visit with a collaborating tertiary hospital; three preferred to visit their own physicians. The mean number of days between testing and linkage to care was 26 (SD 10.5). Successful linkage to care was documented in 65% of all participants.

Conclusion: This community-based viral hepatitis screening program provides an effective model for identifying and providing care to migrant populations at high risk of HBV infection who may otherwise not engage in care. Nearly half of all participants had evidence of past or current HBV virus, highlighting the importance of targeted interventions for this population.

FRI-193

Innovation linkage model to re-engage lost-to-follow-up individuals in the national hepatitis C elimination program in Georgia

Tamar Gabunia¹, Maia Tsereteli², Vladimer Getia², Sophia Surguladze³, Irina Tskhomelidze³, Shaun Shadaker⁴.
¹Georgian Ministry of IDPs from the Occupied Territories, Labour, Health, and Social Affairs, Tbilisi, Georgia; ²National Center for Disease Control and Public Health Georgia; Tbilisi, Georgia; ³The Task Force for Global Health, Tbilisi, Georgia; ⁴Centers for Disease Control and Prevention, Atlanta, United States
Email: tgabunia@moh.gov.ge

Background and aims: The National Hepatitis C Elimination Program has made notable progress in Georgia. However, in the setting of COVID-19 related restrictions, the number of individuals registering in the treatment program has declined over time. As of September 30, 2022, 72.5% (n = 2.1 million) of the adult population of Georgia had been screened for hepatitis C virus (HCV) antibodies, but among 146,518 antibody-reactive adults, 20,464 (14%) had not completed a viremia test. During 2019, the National Center for Disease Control and Public Health of Georgia piloted a project to link to care those

individuals who screened reactive for anti-HCV but had not completed a viremia test. The initial pilot was successful, and the model was scaled up across Georgia.

Method: All anti-HCV reactive adults (aged ≥18 years) who did not have a record of viremia testing in the national HCV electronic database 3 months from the date of an anti-HCV reactive result, and who were not registered in the HIV/AIDS treatment program or with a correctional facility, were eligible for follow-up. Using the phone number listed in the database, individuals were contacted by phone or home visit by patient navigators (trained epidemiologists and primary health care physicians) and referred to HCV care and treatment. If the first attempt was unsuccessful, one repeat attempt was made to contact the individual. Incentives were provided to navigators for each patient who was successfully linked to care, defined as presenting for viremia testing.

Results: As of December 2022, 18,063 phone numbers were identified for 20,464 anti-HCV reactive persons who did not complete a viremia test; patient navigators attempted to reach 18,063 (100%) with phone numbers in the database; 12,794 (70.8%) were reached. The remaining 5,269 did not answer, had an incorrect phone number, moved, or emigrated. Of those contacted, 2,349 (18.4%) presented for viremia testing, and 1,722 (73.3%) had HCV RNA or HCV core antigen detected. Overall, 620 (36.0%) persons with chronic HCV infection were enrolled in the hepatitis C treatment program as a result of this effort.

Conclusion: Program-wide implementation of the piloted model showed that this activity can be scaled up and is effective for re-engaging people in care. The main challenge in Georgia remains linkage to care, which is essential to meet hepatitis C elimination goals. Innovative approaches are necessary to reinforce linkage to care. This is especially important during the COVID-19 pandemic when there is an increased need for programs that can re-engage people in hepatitis C care.

FRI-194

Hepatocellular carcinoma associated with chronic hepatitis C: a case for an annual mortality and morbidity review

Neil McInnes¹, Peter Davies¹, Lynn Lavery², Stephen Barclay³, Erica Peters¹.
¹Queen Elizabeth University Hospital, Infectious Diseases, Glasgow, United Kingdom; ²Hunter Street Health Centre, Community Blood Borne Viruses, United Kingdom; ³Glasgow Royal Infirmary, Gastroenterology Department, Glasgow, United Kingdom
Email: neil.mcinnies4@nhs.scot

Background and aims: The concept of a *late diagnosis and mortality meeting* is well established in HIV services for clinical governance, and to disseminate wider learning to the clinical community. In Scotland, there is no equivalent for Hepatitis C (HCV) despite a significant associated morbidity and mortality, and similar "missed diagnosis opportunities." This cohort study aims to reflect on those with HCV and Hepatocellular carcinoma (HCC), to identify missed opportunities for earlier diagnosis with a view to wider clinical learning.

Method: From the Scottish HCV registry, 40 patients with both an HCV and subsequent HCC diagnosis between 2011 and 2021 were extracted. Demographics, risk factors for chronic liver disease (CLD), dates of HCC and HCV diagnosis, and circumstances of HCV diagnosis were extracted from the registry and electronic patient records. Date of peak-alanine aminotransferase (ALT) and first abnormal ALT (>50 U/L) prior to Hep-C diagnosis were recorded. Prior healthcare exposure to addiction liaison (via EMIS®) or hospitalisation was recorded.

Results: Of forty patients identified, 85% were male with a median age of 59 years. 23 (58%) patients had a raised ALT, on at least one occasion, >1 year prior to a Hep-C diagnosis, with a median time from first deranged ALT to HCV diagnosis of 2.5 years (IQR 6 years) and a median peak ALT of 112 U/L. The most common indication for HCV testing was deranged liver function and, at diagnosis, 7 (18%) patients

POSTER PRESENTATIONS

had developed HCC, with a further 7 presenting with decompensated liver disease. 24 (60%) had co-existing risk factors for CLD e.g. alcohol excess or Hepatitis-B. Ten (25%) had a pre-diagnostic inpatient stay and 3 (8%) pre-diagnostic Addictions input.

Conclusion: Abnormal biochemistry prior to a HCV diagnosis, often for many years, is a common finding. Where other CLD risk factors are present, HCV testing may be overlooked. Highlighting episodes of missed opportunities for HCV diagnosis in a timely manner to clinical teams involved in previous care episodes, using established clinical governance models, may reduce the risk of future similar missed diagnoses. Review of local data may lead to a consideration of reflex HCV testing in all patients with abnormal LFTs, or similar responses, to support early HCV diagnosis; not only to reduce liver related mortality but to support HCV elimination.

FRI-195

Prevalence of hepatitis B and C viral infections among transgenders and men who have sex with men in Pakistan

Hassan Mahmood¹, Quaid Saeed², Francisco Averhoff³, Huma Qureshi⁴. ¹Integral Global (IG), Pakistan; ²Islamabad Healthcare Regulatory Authority, Islamabad, Pakistan; ³Abbott Diagnostics, United States; ⁴Ministry of National Health Services, Regulations and Coordination, Pakistan, Pakistan
Email: hassanmahmood1@hotmail.com

Background and aims: In Pakistan, Transgenders (TGs) and Men who Have Sex with Men (MSM) are marginalized communities at high risk of sexually and parenterally transmitted infectious diseases. The prevalence of hepatitis B virus (HBV) and hepatitis C virus (HCV) infection in these populations has not been well described, and access to care and treatment is lacking.

To estimate the prevalence of HBV and HCV infection among TGs and MSM in two cities in Pakistan, Lahore and Larkana. To assess the effectiveness of screening and referral for treatment among those who screen positive for HBV and HCV, and response to treatment

Method: During 2020–2022 community health workers identified and recruited a total of 2241 TGs and MSM for testing by who prequalified rapid test for hepatitis B surface antigen (HBsAg) and antibody to HCV (anti-HCV) in the community. All participants who tested positive for HBsAg were referred to their respective public sector provincial hepatitis control program for further testing and care. For those who tested positive for anti-HCV, a “One Stop Shop” model was established where the local Community Based Organizations (CBOs) who were already providing free HIV care services to these communities were equipped and trained to provide HCV care and treatment services. Those who tested positive for anti-HCV and were referred to the CBO, were tested for HCV viremia (RNA) using GeneXpert machines. All the HCV RNA positive patients had additional testing including a complete blood count (CBC) and testing for aspartate aminotransferase (AST) to calculate their AST to platelet ratio index (APRI) score, to estimate degree of liver fibrosis. HCV cases were provided at the same visit free of cost oral medications (Sofosbuvir and Daclatasvir) to treat their HCV infection. All testing was done on the same day as the visit, and the results were available on the same day of treatment initiation.

Results: A total of 201/2241 (9%) tested positive for anti-HCV, and 69/2241 (3.1%) tested positive for HBsAg. All participants who tested HBsAg+ were referred to the provincial hepatitis control program for additional care. The 201 who tested anti-HCV+ were referred to CBOs for additional testing and care under One Stop Shop model. Of those, 161 (80%) were tested for HCV RNA, of which 99 (62%) tested positive for HCV RNA. Of these 87 (88%) initiated treatment and 77/87 (89%) completed treatment; all were tested for cure (sustained virologic response; SVR), of which 72 (94%) were HCV RNA negative (cured).

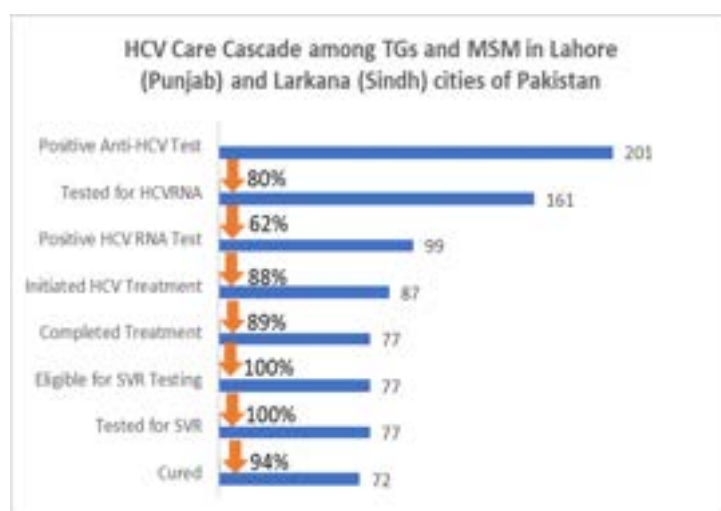


Figure:

Conclusion: Outreach to marginalized populations with same day testing and referral for HBV and HCV is feasible and effective in Pakistan. Partnering with CBOs was key to the success in this pilot project in reaching “key” populations with limited access to health services and achieving high rates of linkage to care and adherence with treatment for HCV and referral for HBV care and treatment.

FRI-196

Multidisciplinary approaches to increase hepatitis C screening rates in a New York City primary care clinic

Carolina Villarreal¹, Silpa Yarra¹, Gres Karim¹, Jake Debroff¹, Einat Kadar¹, Anna Mageras², Rebecca Roediger², Ilan Weisberg³. ¹Mount Sinai Beth Israel, Internal Medicine, United States; ²Icahn School of Medicine at Mount Sinai, New York, United States; ³NewYork-Presbyterian Brooklyn Methodist Hospital, United States
Email: carolina.villarreal@mountsinai.org

Background and aims: Hepatitis C virus (HCV) infection is a common cause of cirrhosis, hepatocellular carcinoma, and liver-related mortality, but also remains to be one of the leading indications for liver transplantation. In New York City (NYC), two out of five residents with HCV remain undiagnosed. In 2020, the Centers for Disease Control and Prevention (CDC) and the United States Preventive Services Task Force (USPSTF) expanded previous guidelines to recommend universal HCV screening among adults 18 and over. Baseline data of screening rates in 2021 at an NYC primary care clinic were 14%, well below the NYC Department of Health screening goal of 42%. Our study aimed to investigate the causes of low screening rates and promote physician knowledge and behaviors to increase overall screening rates to 20% in 6 months.

Method: Using the Plan-Do-Study-Act (PDSA) quality improvement methodology, an interdisciplinary team including hepatologists, internists, and a viral hepatitis program manager was created to investigate baseline HCV screening rates in an NYC primary care clinic. In January 2022, a campaign was initiated for HCV screening with four initiatives including: patient-facing signage in the clinic, a best practice alert (BPA) for HCV screening via electronic medical record system (EMR), weekly printed lists of eligible patients for screening for each primary care physician (PCP), and an oral educational presentation to providers. Baseline physician knowledge regarding HCV screening guidelines was assessed using a survey composed of six knowledge-based and PCP-level barrier questions as shown in Figure 1 immediately before and six weeks after the educational session to assess for retention of knowledge.

Results: A total of 45 internal medicine physicians were initially provided a survey to assess baseline knowledge regarding HCV screening criteria. Six weeks after an educational session to promote

New York City Primary Care Clinic

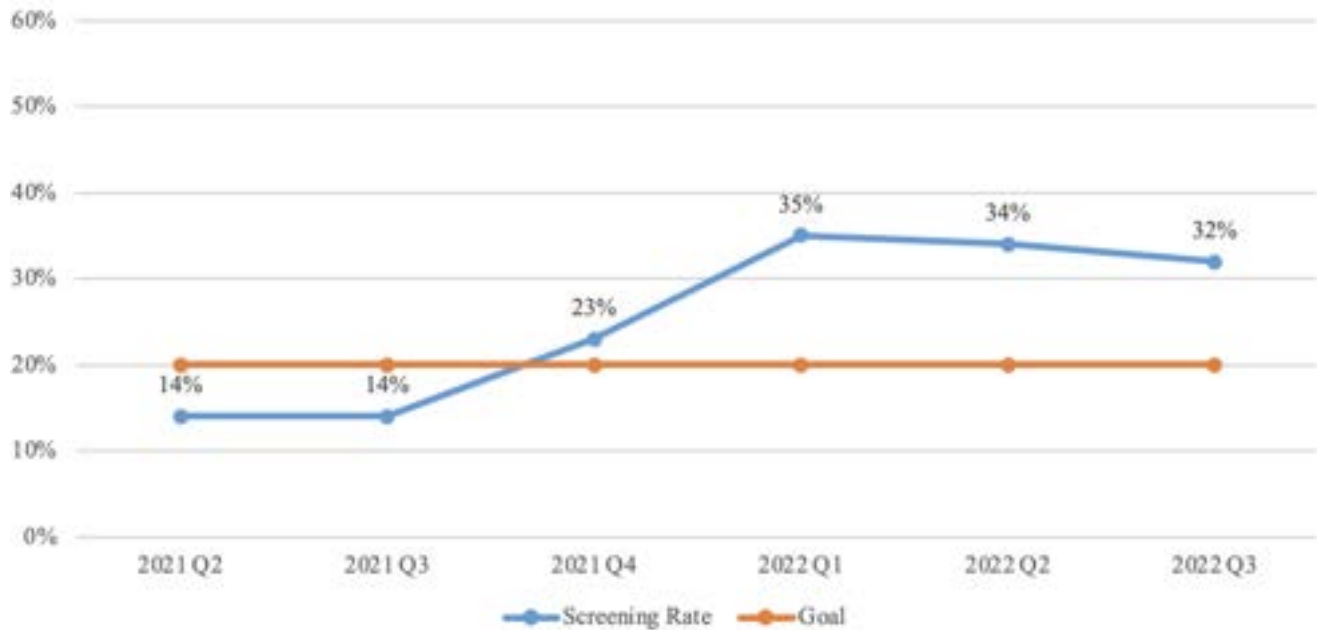


Figure: (abstract: FRI-196): HCV new screening rate.

HCV screening rates, 21 physicians responded (46%) to a follow-up survey to assess retention of knowledge. Respondent knowledge slightly increased after the educational session (80% of correct answers before the lecture vs. 81% after). However, our multi-initiative approach successfully resulted in an increase in HCV screening rates from 14% to 35% in the first quarter of 2022 and 32% by the third quarter of 2022, exceeding the study goal of 20%.

Conclusion: Given that there was a minimal difference in retained knowledge based on pre and post-surveys, we attribute the overall increased HCV screening rates from 14% to 35% to our other initiatives which include utilization of the automated BPA within the EMR and weekly reminders as printed lists for each PCP to increase awareness of HCV screening for timely detection and prompt referral for treatment of newly diagnosed HCV

FRI-197

Effectiveness of birth-dose vaccine in preventing mother-to-child transmission of hepatitis B virus in Ethiopia

Mebrihit Arefaine¹, Asgeir Johannessen², Tilahun Teklehaymanot¹, Andargachew Mulu³, Dawit Hailu³, Adane Mihret³, Mahlet Osman³,

Dareskedar Teshay³, Nega Berhe^{4,5}. ¹Addis Ababa University, Ethiopia; ²Vestfold Hospital Trust, Norway; ³Armauer Hansen Research Institute, Ethiopia; ⁴Aklilu Lemma Institute of Pathobiology, Addis Ababa University, Infectious Disease, Addis Ababa, Ethiopia; ⁵Oslo University Hospital-Ullevål, Regional Centre for Imported and Tropical Diseases, Oslo, Norway

Email: johannessen.asgeir@gmail.com

Background and aims: Studies from Asia have shown that mother-to-child transmission (MTCT) is a major transmission route of the hepatitis B virus (HBV). Administration of a monovalent HBV vaccine within 24 hours of birth (viz birth-dose vaccine), followed by completion of the vaccine series, is 85–95% effective in the prevention of MTCT. In Africa, studies from the 1980s suggested that vertical transmission of HBV was less common than in Asia, which led to a reluctant attitude towards birth-dose vaccination in many African countries. This study aimed to determine the effectiveness of the birth-dose vaccine in preventing MTCT of HBV in Ethiopia.

Method: Hepatitis B surface antigen (HBsAg) positive pregnant women who attended the delivery wards at five public hospitals in

Table: (abstract: FRI-197): Factors associated with mother-to-child transmission of hepatitis B virus, Ethiopia.

	Infant HBsAg at 9 months		Unadjusted			Adjusted		
	HBsAg + N (%)	HBsAg – N (%)	OR	95% CI	P	OR	95% CI	P
Birth-dose vaccine								
Yes	5 (35.7)	134 (83.8)	1	2.9–29.9	<0.001	1	3.5–90.4	<0.001
No	9 (64.3)	26 (16.2)	9.3			17.8		
Maternal HBeAg status								
Neg	6 (42.9)	141 (88.1)	1	3.1–31.7	<0.001	N.S.		
Pos	8 (57.1)	19 (11.9)	9.9					
Maternal viral load (IU/ml)								
<200 000	8 (57.1)	154 (96.2)	1	5.1–73.2	<0.001	1	2.0–135.7	0.010
>200 000	6 (42.9)	6 (3.8)	19.3			16.3		

POSTER PRESENTATIONS

Addis Ababa from January 2019 to May 2021 were included in a prospective, observational study. Maternal hepatitis B e-antigen (HBeAg) status, HBV DNA viral load, and demographic information was collected at birth. HBV birth-dose vaccine was recommended to all study participants, but was not part of the national policy, thus not all infants received it. All infants, however, received three doses of pentavalent HBV vaccine at 6, 10, and 14 weeks of age as part of the national immunization program. The infants were followed up and tested for HBsAg using an ELISA assay at 9 months of age; a positive HBsAg at 9 months was taken as evidence of MTCT. Logistic regression analysis was used to identify factors associated with MTCT of HBV.

Results: Of 12,318 pregnant women screened, 369 (3.0%) were HBsAg positive and 300 were included in this study. The current analysis included 174 infants who had a follow-up evaluation at 9 months of age. Five of 139 (3.6%) infants who received birth-dose vaccine were HBsAg positive at 9 months of age, compared to 9 of 35 (25.7%) who did not receive birth-dose vaccine ($p < 0.001$). Transmission of HBV occurred both in HBeAg positive and negative mothers, and in mothers with high ($>200\,000$ IU/ml) and moderate/low ($<200\,000$ IU/ml) viral load at birth. In multivariable logistic regression analysis, high maternal viral load and the absence of birth-dose vaccine were significantly associated with MTCT of HBV (Table 1).

Conclusion: Administration of birth-dose vaccine significantly reduced the risk of MTCT of HBV. Improved coverage of birth-dose vaccine will be needed to control the HBV epidemic in Africa.

FRI-198

Complete and maintained elimination of hepatitis C in patients in methadone substitution program

Esther Rodríguez Candelaria¹, Ana Laserna Ramos², Silvia Acosta-López¹, Pilar Díaz Ruiz³, Magdalena Lara⁴, Teresa De la Rosa Vilar², Luz Goretti Santiago Gutiérrez², Francisco Andrés Pérez Hernández¹. ¹Hospital Universitario Nuestra Señora de La Candelaria, Aparato Digestivo, Spain; ²San Miguel Adicciones, Spain; ³Hospital Universitario Nuestra Señora de La Candelaria, Farmacia, Spain; ⁴Hospital Universitario Nuestra Señora de La Candelaria, Microbiología, Spain
Email: estherrg65@gmail.com

Background and aims: To achieve WHO goals on hepatitis C (HCV) plans are necessary in populations with high prevalence and low adherence like users of centers for addiction treatment (CAT). We designed a Fast Track protocol demonstrating high cure rates ($>90\%$). A meta-analysis estimates the incidence of reinfection in these patients in 6%. Main objective: evaluate effectiveness of our protocol to achieve HCV elimination in Santa Cruz San Miguel CAT (CATSC). Secondary aims: know prevalence, results of treatment, rate of reinfections and incidental new cases.

Method: All CATSC users of Opioid Substitution Therapy (OST) were included. We analyzed with descriptive statistical prevalence of HCV before and after the elimination program, number of patients treated and cured. Patients cured more than a year ago were included for reinfection screening. CATSC new patients, included after the programme initiation, were also analyzed for new incidental cases.

Results: We include the 231 users of OST of CATSC. At the beginning we knew the HCV status in 72%. Among this patients, HCV prevalence was 42.5%; of negative RNA patients 43% were after treatment. These positive HCV patients weren't under treatment. After the implementation of screening program at CATSC we found out HCV diagnostic situation in 95.4%. Prevalence of viremic patients was 41% (55); prevalent genotypes were 1a (42%) and 3a (28%), 37.5% had advanced fibrosis or cirrhosis. None with negative serology before the study had been infected later. 50 patients (91%) were treated; one didn't receive treatment due to terminal illness. Virological cure was achieved in 49 (98%), the other abandoned treatment. In 2022 a new HCV screening was carried out in these users: 85% adhered. Only 3 were viremic: one wasn't treated due to severe comorbidity and the other two refused treatment. 49 patients received antivirals more than a year ago, reinfection screening was done in 46 (94%): 100% negative. After the study, 46 new OST users were admitted at CATSC: in 44 patients (95.6%) HCV status was known. 6 patients were RNA positive and 5 of them were treated.

Conclusion: Among the OST users of the CATSC, we achieve the WHO objective of eliminating hepatitis C with 97% of patients diagnosed and 90% treated with a cure rate of 98%. The elimination has been maintained after one year with 0 reinfections and 0 new infections. Screening and linkage to care of new patients is necessary to maintain these results.

FRI-199

Hepatitis delta virus infection in Turkey: A meta analysis of prevalence

Mehlika Toy¹, Begüm Güler Şentürk², Kayra Somay², Genco Gencdal³, Cihan Yurdaydin³. ¹Stanford University School of Medicine, Palo Alto, USA, Department of Surgery, United States; ²Koç University, School of Medicine, Department of Internal Medicine, Turkey; ³Koç University, School of Medicine, Department of Gastroenterology and Hepatology, Turkey
Email: gencogencdal@yahoo.co.uk

Background and aims: Turkey is a region that has a high burden of hepatitis delta virus (HDV) infection, and is considered an endemic country for the virus, occurring in large proportions of HBsAg-positive individuals. To provide a current and updated HDV prevalence, the authors performed a meta-analysis of prevalence to estimate country and region-specific prevalence of HDV infection in Turkey.

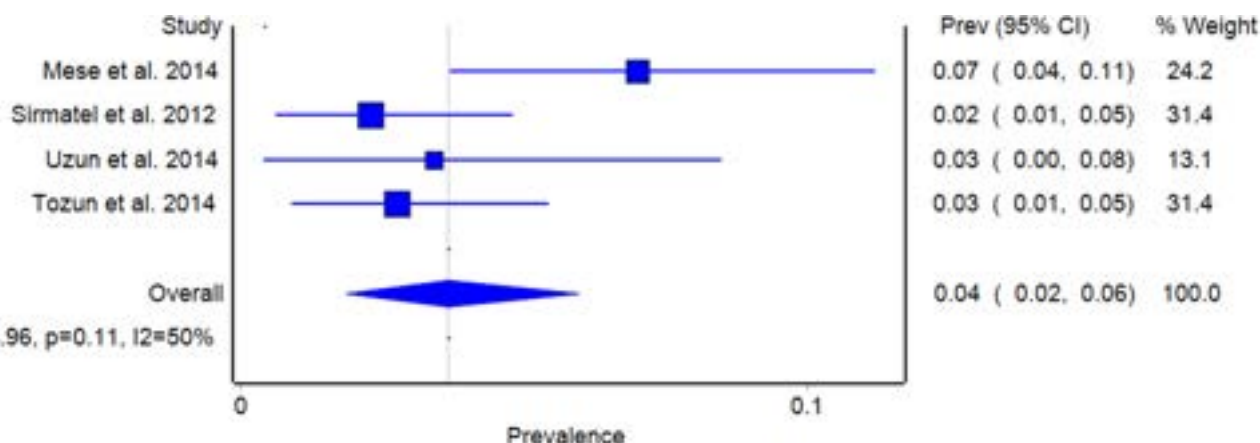


Figure: (abstract: FRI-199): Forrest plot of blood donor studies.

Method: A total of 462 studies with original data on the prevalence of HDV in Turkey and published between 2006 and 2022 were identified through a search of electronic databases, by reviewing citations, and by contacting authors. After a systematic assessment, the authors included 43 studies, divided into blood donor studies, outpatient clinic studies that comprised of asymptomatic and only non-cirrhotic chronic hepatitis B, and inpatient clinic studies that comprised of cirrhotic patients. Turkey was divided into three regions: West-, Central-, and Southeast Turkey. MetaXL software was used to calculate the prevalence.

Results: Using a quality effects model, we estimated that the prevalence for blood donors, outpatient clinic patients, and inpatient clinic patients was 3.65% (CI: 1.88–5.95), 4.41% (CI: 3.02–6.04), and 23% (CI: 5.2–47), respectively. The prevalence for West-, Central-, and Southeast Turkey was 3.28% (CI: 2.37–4.33), 2.09% (CI: 1.31–3.05), and 7.79% (CI: 4.33–12.12), respectively.

Conclusion: The findings of this study suggests that Turkey is still an endemic country for delta hepatitis, with regional differences. The public health efforts should be focused accordingly.

FRI-200

Sofosbuvir/Velpatasvir (S/V) for the treatment of HCV infection among vulnerable inner-city residents: extending the results of clinical trial part 2

Brian Conway^{1,2}, Rossitta Yung¹, David Truong¹, Shawn Sharma¹, Shana Yi¹, Giorgia Toniato¹. ¹*Vancouver Infectious Diseases Centre, Vancouver, Canada;* ²*Simon Fraser University, Burnaby, Canada*
Email: brian.conway@vidc.ca

Background and aims: The combination of Sofosbuvir/Velpatasvir (S/V) is approved for the treatment of chronic HCV infection. In registrational trials, cure rates of 95% or more were achieved when administered as one pill once a day for a period of 12 weeks regardless of genotype or disease stage. To achieve HCV elimination by 2030, there is a need to develop and evaluate systems of care in populations that are more challenging to engage in care than those enrolled in clinical trials. With this in mind, we evaluated the safety and efficacy of S/V in a prospective study of HCV-infected inner-city residents enriched for risk behaviors for non-adherence to therapy, including problematic drug use and unstable housing.

Method: Through dedicated outreach events, including regular community pop-up clinics (CPCs), we identified HCV-infected patients who were not currently engaged in health care and who were eligible to receive government-funded antiviral treatment for HCV infection. We offered them the opportunity to enroll in a multidisciplinary program of care to address medical, psychological, social, and addiction-related needs, and provide S/V therapy in this context, with daily or weekly supervision of adherence as appropriate. The end point of this preliminary analysis is the achievement of cue (SVR4/12) in those who initiated therapy.

Results: In this ongoing study, we have, to date, identified and started treatment in 203 eligible subjects. We note median age 46 years, 28.8% female, 49.5 and 42.3% GT1 and 3, 13.6% cirrhotic, 99.0% active drug users, 10.2% co-infected with HIV and over 80% unstably housed. The median time from CPC attendance to HCV treatment initiation is 6 weeks. Of 203, 178 have completed treatment, 21 are currently on treatment, 2 died of overdose, 2 discontinued prematurely. Of 178 subjects who have completed treatment, 155 are confirmed as cured (SVR 12), 2 achieved SVR4 (awaiting SVR12), 12 are awaiting SVR4, 4 (2.2%) have a documented virologic relapse and 5 (2.1%) have been lost to follow-up. In the context of an opioid crisis with 6 documented deaths/day in the province of British Columbia, we have observed x deaths in the treated study population from time of initial identification at CPC events to the present (median follow-up 30 weeks. Of participants in whom a final outcome can be ascertained, the cure rate is 97.5% (157/161).

Conclusion: Among inner city residents living with HCV infection, most of whom are active fentanyl users and unstably housed, the administration of S/V in the context of a robust program of engagement in care has led to HCV cure rates that exceed those achieved in clinical trials, with minimal opioid-related morbidity and loss to follow-up within our system of care. The data we present validate the development of multidisciplinary programs as an important tool for HCV elimination in this vulnerable population.

FRI-201

Screening for hepatitis C virus using rapid diagnostic test (RDT) coupled with mammography in women aged from 50 to 74 years in Montpellier (France). (Mamm'OC NCT05067374)

Magdalena Meszaros¹, Severine Coursier¹, Nicolas Nagot¹, Lionel Moulis¹, Patrice Taourel¹, Emma Pages¹, Nathalie Fabre Demard^{2,3}, Muriel Trentini⁴, Georges-Philippe Pageaux¹, Hélène Donnadieu-Rigole¹. ¹*Hospital Center University De Montpellier, Montpellier, France;* ²*Clinique du Millénaire, Montpellier, France;* ³*IMACAM-Radiologie, Sénologie, Centre Victor Hugo, Montpellier, France;* ⁴*Clinique Beau Soleil, Montpellier, France*

Email: m-meszaros@chu-montpellier.fr

Background and aims: The seroprevalence of hepatitis C virus (HCV) in the general French population is less than 1%; nevertheless, according to estimations, more than 75,000 people living in France are unaware of their seropositivity. In order to achieve the goal of elimination of hepatitis C by 2025 in France targeted screening of high-risk population is essential to identify asymptomatic carriers prior to development of advanced chronic liver disease. The most common risk factors associated with HCV infection are injection drug use, blood transfusions prior to 1992 and parenteral contamination. It was estimated that the seroprevalence of hepatitis C among women over 60 is higher than that among men of the same age. Organized breast cancer screening was introduced in France in 2004 and more than 70% of women aged from 50 to 74 are participating. We hypothesized that some women between 50 and 74 years may have previously undergone invasive surgical or obstetrical procedures and/or other at risk behaviours associated with HCV infection and may be unaware of their HCV status. Thus, screening for hepatitis C coupled with mammography may represent an efficient HCV micro-elimination strategy. The objective of the study was to assess acceptability rate to breast cancer screening coupled with hepatitis C testing using rapid diagnostic test (RDT) among women aged from 50 to 74 years old. Secondary objective was seroprevalence of HCV in this population.

Method: All women between 50 and 75 years participating in the national organized systematic breast cancer screening were prospectively enrolled in the study after signing informed consent. Adherence to HCV screening as well as data regarding HCV care cascade was recorded.

Results: Among 1430 women prospectively enrolled between March 2022–January 2023, 1173 accepted the two coupled exams (acceptability rate: 82%). The three main reasons for refusal were: recent HCV testing (51%), not feeling at risk of HCV (17%), and anxiety due to HCV testing (12%). The median age of the participants was 61.28 (±7.08) years; 44% were employed and 44% were retired. Among the participants, 86% had never had a blood transfusion, but 83% reported other risk factors such surgery or invasive procedure prior to 1992. Eight (0.68%) participants had a positive HCV RDT. One (0, 08%) participant was HCV RNA-positive and was treated and cured (SVR 100%) during the study period.

Conclusion: The acceptability of HCV screening using RDT coupled with mammography is high. Seroprevalence of hepatitis C in women aged from 50 to 74 years is low, similar to that of the general population.

FRI-202

Hepatitis B, C and D infections among nine high-risk populations in Burkina Faso, West Africa

Armel Moumouni Sanou¹, Aurélie Sausy², Abdoul Kader Ilboudo³, Mohamed Aly Belem⁴, Armel Poda⁵, Zékiba Tarnagda³, Judith Huebschen². ¹Institut de Recherche en Sciences de la Santé (IRSS), Equipe VIH, Hépatites Virales et autres IST, Bobo-Dioulasso, Burkina Faso; ²Luxembourg Institute of Health, Department of Infection and Immunity, Luxembourg; ³Institut de Recherche en Sciences de la Santé, National Influenza Reference Laboratory, Unité des Maladies à Potentiel Epidémique, Maladies Emergentes et Zoonoses, Ouagadougou, Burkina Faso; ⁴Centre Hospitalier Régional de Fada-Ngourma, Laboratoire d'analyses biomédicales, Burkina Faso; ⁵Université Nazi Boni (UNB), Institut Supérieur Des Sciences de la Santé (INSSA), Bobo-Dioulasso, Burkina Faso
Email: armelbf@gmail.com

Background and aims: Certain population groups have an increased risk for hepatitis B and C virus (HBV and HCV) infections due to their profession and/or behaviour. Thus, they constitute potential reservoirs for the spread of these infections to the general population. Despite this, comprehensive studies, including screening for most viral markers in many different risk groups are lacking in Africa. In this study, we investigated viral markers of HBV, HCV and hepatitis D virus (HDV) infections among nine high-risk populations in order to propose interventions for a better control of these infections.

Method: A cross-sectional study was carried out in the two main cities of Burkina Faso, Ouagadougou and Bobo-Dioulasso, and one village (Fandjora). The study population included sex workers (SW), men who have sex with men (MSM), prisoners (P), health care workers (HCW), lorry drivers (LD), illegal gold miners (IGM), hairdressers (H), haemodialysis patients (HD) and human immunodeficiency virus (HIV) patients. From each participant, socio-demographic data and blood were collected by well-trained personal. All serum samples were screened for viral markers of HBV, HCV and HDV infections using serological and molecular tests. Data analysis was performed using STATA SE version 14.0 software (Texas, USA).

Results: A total of 1373 participants were enrolled. HBsAg seroprevalence was 13.5%, ranging from 9.9% in SW to 25.9% in MSM, and anti-HBc seroprevalence was 75.5%. Among HBsAg positive samples, HBeAg, anti-HBe antibodies, and HBV DNA were detected in 18.3%, 79.4%, and 30.1%, respectively. Total anti-HDV antibodies were detectable in 4 (2.1%) samples and HDV RNA in 3 (75.0%). A vaccination profile (isolated anti-HBs) was found in 7.0%. Being male was significantly associated with HBsAg (aOR: 1.6) and anti-HBc (aOR: 1.8) positivity. HD (aOR: 2.13) and SW (aOR: 2.6) had a higher risk of HBsAg positivity than all other groups. Anti-HCV prevalence was 8.5%, ranging from 5.3% in H to 12.4% in HD. HCV RNA was detected in 13.7% of anti-HCV positive samples. The odds of being HCV positive were nearly five times higher in participants with no education (aOR: 4.7) compared to those with other education levels, while it was low in participants between 35 and 49 years of age (aOR: 0.5). Active HBV/HCV coinfection was found in 4 (0.3%) cases. Dual exposure to HBV and HCV was confirmed in 93 (9.0%) cases, and prior exposure to all three hepatitis viruses was detected in one (0.07%) case.

Conclusion: The results show much higher prevalences of HBV and HCV infections than in the general population. They underline the need of targeted programs comprising awareness, screening and treatment for these high-risk groups to support the 2030 hepatitis elimination goals.

FRI-203

Factors associated with HCV reinfection among treated people who inject drugs in the HCV elimination program in Georgia

Lasha Gulbiani¹, Maia Butsashvili¹, George Kamkamidze¹, Davit Baliashvili², Senad Handanagic³, Shaun Shadaker³, Sonjelle Shilton⁴, Maia Japaridze⁴, Paige A. Armstrong³. ¹Health

Research Union, Tbilisi, Georgia; ²The Task Force for Global Health, Tbilisi, Georgia; ³Centers for Disease Control and Prevention, Division of Viral Hepatitis National Center for HIV, Hepatitis, STD and TB Prevention, Atlanta, United States; ⁴FIND, the Global Alliance for Diagnostics, Geneva, Switzerland
Email: lashagulbiani7@gmail.com

Background and aims: During 2015, Georgia launched a hepatitis C elimination program providing free hepatitis C virus (HCV) testing, and treatment at no cost with direct-acting antivirals (DAAs) to all Georgian citizens with chronic HCV infection. People who inject drugs (PWID) are one of the target groups for the program due to high prevalence of HCV infection and risk of reinfection as a result of ongoing injecting. This study aimed to understand the risk factors for HCV reinfection among PWID treated and cured through the HCV elimination program.

Method: A case-control study was conducted among beneficiaries of harm reduction center services in four cities in Georgia (Tbilisi, Telavi, Batumi and Kutaisi). Eligible for inclusion were adults age ≥ 18 years who achieved sustained viral response (SVR) after hepatitis C treatment with DAAs. Cases were defined as persons with a detectable HCV RNA test result ≥ 1 year after achieving SVR; controls were defined as persons with an undetectable HCV RNA test result ≥ 1 year after achieving SVR. Frequent drug use was defined as injecting drugs every day or several times a week or month during the last 12 months. The ratio of cases to controls was 1:3. Socio-demographic and behavioral data were collected by interviewer-administered (face-to-face) questionnaire. Binary logistic regression was performed to understand the independent predictors of detectable HCV RNA after achieving SVR.

Results: A total of 287 PWID were included; 74 cases and 213 controls. The majority of respondents were male (98.6%), Georgian (97.9%), married (77.7%), and >45 years (66.2%). The proportion of PWID who first injected drugs at age ≤ 18 years was higher among HCV reinfected participants (37.0% vs 21.6%, $p < 0.05$). Sharing injection paraphernalia was twice as common among cases (33.8% vs 14.6%, $p < 0.01$), and 74.0% of cases and 53.3% of controls were injecting drugs frequently during the last 12 months ($p < 0.01$). Reinfected individuals were more likely to have injected drugs in the last month (79.5% vs 65.4%, $p < 0.05$). In multivariable analysis, sharing injection paraphernalia was the only independent predictor of HCV reinfection (odds ratio = 2.63; 95% confidence interval: 1.13–6.25).

Conclusion: To prevent HCV reinfection among PWID, preventive and educational activities should be scaled up focusing on the use of single-use injection paraphernalia together with expanding access to free syringes through needle and syringe programs.

FRI-204

HCV screening before endoscopy in hepatogastroenterology outpatient clinic: results of DEPISTC-ENDO study

André-Jean Remy¹, Serge Bellon², Mathias Vidon³, Ryad Smadhi⁴, Jacques Bottlander⁵, Armand Garioud⁶. ¹Perpignan Hospital, Hepatology, Perpignan, France; ²Avignon Hospital, Hepatology, Avignon, France; ³CHIC, Hepatology, Creteil, France; ⁴Creil Hospital, Hepatology, Creil, France; ⁵Colmar Hospital, Hepatology, Colmar, France; ⁶Villeneuve Saint Georges Hospital, Hepatology, Villeneuve Saint Georges, France
Email: andre.remy@ch-perpignan.fr

Background and aims: Systematic screening for hepatitis C once in a lifetime is recommended but not validated by the health authorities. Screening before digestive endoscopy has become routine since 2020 with the mandatory performance of a COVID PCR before endoscopy under general anesthesia. Two Spanish studies in 2019 had demonstrated the feasibility and acceptability of screening (by blotter and by TROD) for hepatitis C before digestive endoscopy. An older French study had shown its acceptability during the pre-anesthesia consultation. Screening focused on subjects over 40 years of age would seem to be more efficient, as the prevalence of hepatitis C

increases with age. Our aim was to propose HCV screening serology to patients undergoing digestive endoscopy with general anesthesia, to determine if HCV screening from 40 years of age before endoscopy is feasible and accepted, and to evaluate if the prevalence after 40 years of age is higher than in the general population.

Method: Minimal-risk interventional research study; proposal to all patients, men and women, aged over 40 years and having an indication for digestive endoscopy, to undergo HCV serological screening at the time of the gastroenterology consultation prior to the examination. There was no control group. Patients known to have positive HCV serology or negative HCV serology less than one year old and patients already hospitalized were excluded. Study proceeds as follows: 1/inclusion of patient with the provision of an information leaflet and signature of a consent form 2/prescription of HCV serology by the hepato-gastroenterologist during the pre-endoscopy consultation 3/serology performed on site or in a local laboratory 4/possible catch-up of serologies in outpatient hospitalization if serology not done. The objective is to evaluate the feasibility and acceptability of the screening, not the conditions of its realization, which have been adapted to the conditions and habits of each participating center. 5/ Patients with a positive HCV serology will be offered a C viral load and management according to good practice recommendations. Expected results are an acceptability higher than 95% and a prevalence higher than the prevalence in the general population (0.86%).

Results: As of December 31st, 2022, 314 patients were included; 56% men 44% women; average age 56 years (40–90). Screening colonoscopy for 40%, other colonoscopy 40%, gastroscopy for 42% and other exams for 5%; 63% patients had other blood tests, 78% HBV serology. HCV serology was done for 97% with 7,2% positive results (22 patients). Risk factors were drug use in 61%, transfusion history for 22% and endemic country for 17%; average age was 65 years (49–

85), 90% men, liver elastometry 8,5 Kpa; 9 patients patients had positive HCV viral load (2,9%) and will be treated. More detailed results on a larger number of patients will be presented at the congress.

Conclusion: The feasibility and acceptability of hepatitis C screening before digestive endoscopy is demonstrated. The prevalence seems to be higher than in the general population.

FRI-205

Progress in hepatitis C screening as part of the hepatitis C elimination program in Georgia

Vladimer Getia¹, Tamar Gabunia², Maia Tsereteli¹, Ekaterine Adamia², Davit Baliashvili³, Irina Tskhomelidze³, Sophia Surguladze³, Shaun Shadaker⁴, Senad Handanagic⁴. ¹National Center for Disease Control and Public Health Georgia, Tbilisi, Georgia; ²Georgian Ministry of IDPs, Labour, Health and Social Affairs, Tbilisi, Georgia; ³The Task Force for Global Health, Tbilisi, Georgia; ⁴Centers for Disease Control and Prevention, Division of Viral Hepatitis, Atlanta, United States
Email: kh.getia@ncdc.ge

Background and aims: The country of Georgia, with a population of 3.7 million and an estimated 150,000 adults with current hepatitis C virus (HCV) infection, initiated a national hepatitis C elimination program in April 2015. One aim of the program is to identify 90% of adults infected with HCV by providing hepatitis C screening (anti-HCV) to all citizens free of charge. Screening increased overall since the start of the program but declined sharply in 2020 due to the Covid-19 pandemic. Screening started increasing gradually after pandemic restrictions started to lift, but more needs to be done to reach elimination goals. The aim of this analysis is to describe coverage in hepatitis C testing by age and sex as part of the HCV elimination program.

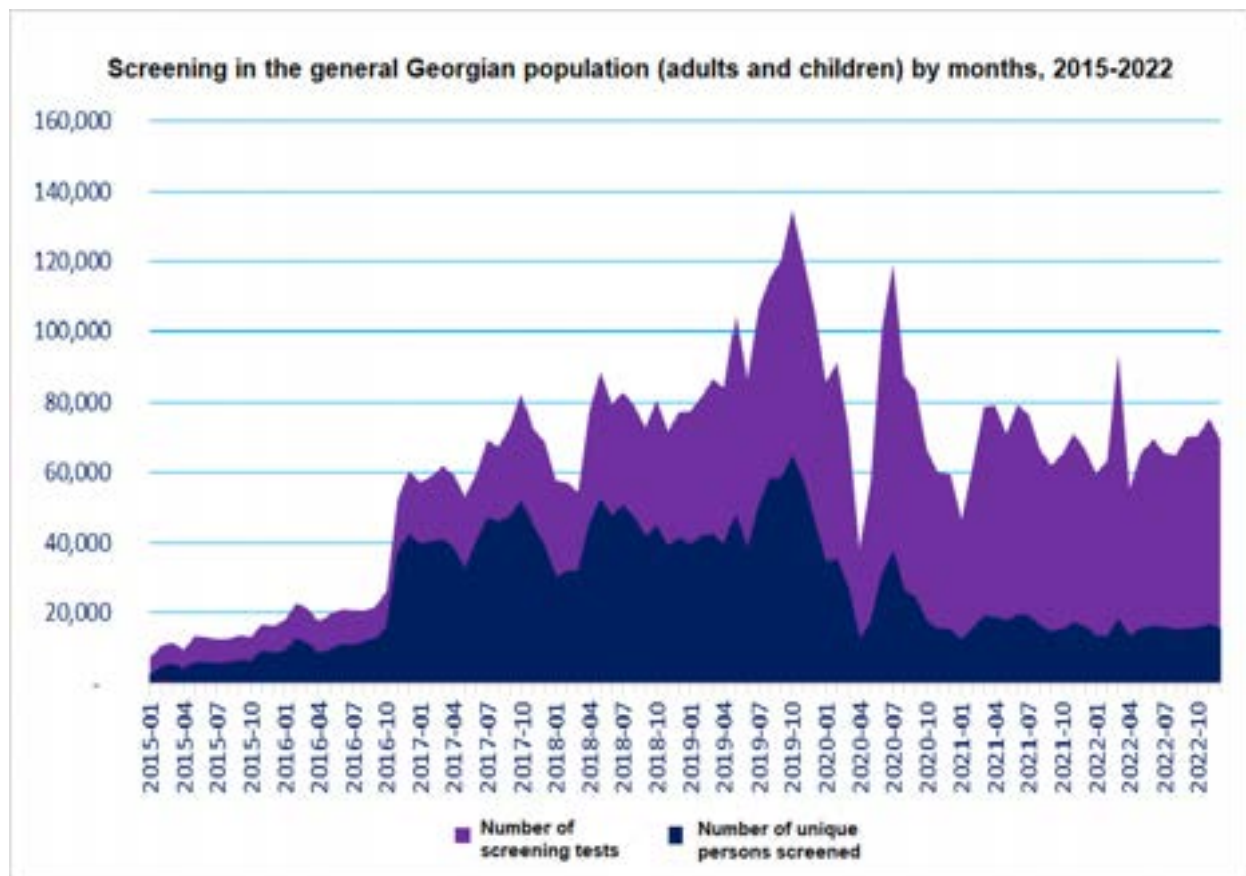


Figure: (abstract: FRI-205).

POSTER PRESENTATIONS

Method: This analysis utilized Georgia's national screening registry data from 2015 to 2022. This information system collects data from the elimination program utilizing patients' national IDs to monitor and evaluate program performance and surveillance. Required use of the national ID during screening causes duplication in the registry; for this analysis, we calculated unique persons screened. The 2014 general population census data were used to calculate screening coverage at the population level. This analysis excluded those screened anonymously at harm reduction sites; screened individuals who died between 2015 and 2022 were included.

Results: As of December 2022, 2,335,540 Georgian adults have been screened for hepatitis C, corresponding to 83% of the adult population. Screening coverage is similar for men and women at 82% and 84%, respectively. Among men, screening rates are above 70% in all age groups, the highest of which is among those aged 18–29 years at 84% and those aged ≥60 years at 86%. The lowest screening coverage in males is among those aged 40–49 years at 71%. In the general female population screening coverage is also above 70% in all age groups; it is highest among those aged ≥60 years at 95% and lowest among those aged 18–29 years at 70%.

Conclusion: Over 80% of the adult population in Georgia has been screened for hepatitis C. However, the remaining infected individuals still need to be identified. Innovative approaches to increase screening in the general population are needed to reach elimination goals.

FRI-206

New hepatitis C diagnoses in 2022. Who and where. Referral efficiency

Cristina Suárez Montesdeoca¹, Paula Moreno Martín¹, Magdalena Lara², Ruth Suarez Darias¹, Antonio González Rodríguez¹, Francisco Andrés Pérez Hernández¹. ¹Hospital Universitario Nuestra Señora de Candelaria, Digestive Department, Spain; ²Hospital Universitario Nuestra Señora de Candelaria, Microbiology Department, Spain
Email: cris.sua.mon@gmail.com

Background and aims: We have previously communicated our hepatitis C (HCV) elimination programme developed in several phases: 1) Treatment of known patients or new patients referred to our clinics. 2) Screening and treatment of patients in Primary Care (PC) and in Drug Dependency Care Units (DCU) or Prison. 3) Recovery of patients diagnosed from microbiology registers. But to complete the elimination we must also access new HCV diagnoses. 1. To describe the origin and characteristics of the new hepatitis C diagnoses. 2. To assess the efficiency of referral of these patients to hepatitis consultations (CH).

Method: A list of patients with positive RNA for HCV from January 1st to November 30th of 2022 was requested from the Microbiology Service. The clinical and laboratory history of these patients was reviewed.

Results: 148 patients were HCV RNA positive. There were 77 (52%) new diagnoses, 21 females and 56 males. However, in 23 (29%) patients a previous positive serological history was identified but the diagnosis had not been completed. The diagnosis had been made: in 40 (52%) in PC, in 16 (21%) digestive consultations in the context of study because of hypertransaminasemia; the rest were widely distributed: nephrology (2), psychiatry (2), paediatrics (2), emergency unit (2), medical oncology (2), endocrinology (1), pneumology (1), orthopaedics (1), DCU (2), intensive care unit (1). From the epidemiological background, it should be noted that in 27 (35%) patients there was a history of parenteral drug use; only in 3 (4.7%) the origin was attributed to post-transfusion, although 3 other patients had remote surgeries and did not know whether or not they had been transfused. 1 patient attributed the origin to accidental injection and in 5 (7.8%) patients there was a multiple history of sexually transmitted diseases. In 19 (24.7%) patients no epidemiological history was recorded in the clinical history. In 57 (74%) patients

there had been appropriate referral to CH and they were already on treatment or had been treated at the time of analysis.

Conclusion: Despite a large and prolonged HCV elimination plan, new diagnoses are still occurring in 2022. Some of these patients are not newly infected: they either have a previous positive serological result or an epidemiological history suggestive of remote infection. The population with a history of injecting drug use remains the main source. The majority of new HCV diagnoses occur in primary care or in digestive consultations due to hypertransaminasemia, although in up to a third of cases the diagnosis occurs in other contexts.

FRI-207

Hepatitis C screening and elimination strategy: implementation of the FOCUS program in Almería, Spain

Anny Camelo Castillo¹, Manuel Rodríguez Maresca¹, Teresa Cabezas Fernandez¹, Teresa Maria Jordan Madrid¹, Antonio Duarte Carazo¹, Alba Carrodegua², Diogo Medina³, José Luis Vega Sáenz¹, Marta Casado¹. ¹Torrecedenas University Hospital, Spain; ²Gilead Sciences-Madrid, Spain, Spain; ³Gilead Sciences –Lisboa, Portugal, Portugal
Email: mm.casado.m@gmail.com

Background and aims: Spain may be one of the first countries to achieve the World Health Organization's goal of eliminating viral hepatitis C by 2030. A serosurvey by the Ministry of Health 2017–2018 estimated a 0.22% hepatitis C virus (HCV) active infection prevalence among the general Spanish population, with 29.4% unknown infections. Increasing HCV screening is key. Emergency Departments (ED) often act as safety nets due to health equity issues for key populations affected by viral hepatitis, as they often lack optimal links with their primary care providers. We aimed to evaluate HCV screening efficacy in the ED of Torrecedenas University Hospital, in Almería, Spain.

Method: We implemented opportunistic HCV screening in the ED (FOCUS Program), using existing infrastructure and staff. Patients ages 18 to 69 were eligible for testing if they did not have a known diagnosis or test performed in the previous year and required blood tests at the current ED visit. We used the LIAISON®X- Diasorin assay for HCV antibodies (anti-HCV) and the Roche Cobas® 6800 for viral RNA (HCV RNA) in the same specimen. Appropriate follow-up or discharge was given regardless of test results. We contacted positive patients to ensure linkage to care.

Results: We screened 9,384 patients from August 2021 to December 2022, finding 159 (1.69%) anti-HCV positive patients (average age of 56, 76% male) and 38 (0.40%) HCV RNA positive patients (82% males). We identified risk exposures in 64% of viremic patients' records. Injected drug use (36%), HIV or HBV coinfection (36%), a history of incarceration (14%), and origin from countries with medium or high HCV prevalence (11%) were the top and only recorded risk exposures of the guidelines' 11 criteria. 93% of viremic patients had previously visited ED, and as of reporting, 16 patients have started antiviral treatment.

Conclusion: Undocumented HCV infection among our population is twice that estimated in the Spanish population. Hepatitis C screening in EDs is an effective strategy and should be considered in more hospitals.

FRI-208

Low prevalence found in HCV micro-elimination program among HIV-negative MSM and TW in a community center in Spain

Àngel Rivero Calaf^{1,2,3}, Felix Pérez Tejera¹, Albet Dalmau-Bueno¹, Pep Coll Verd^{2,3,4}, Jose Miguel Cabrera Guarín^{1,2,3}, Mariusz Lucejko^{1,2,3}, Joan Reguant Guitart^{1,3}, Javier Fernandez Pérez^{1,3}, Jorge Calderon Torres^{1,3}, Jaime Romero Rodriguez^{1,3}, Federico Caballero^{1,3}, Giovanni Marazzi¹, Carlos Oro¹, Daniel Jacobs¹, Horacio Vicoso¹, Lisandro Moises Enrique¹, Hector Taboada Gonzalez¹, Jorge Saz Berges¹, Ferran Pujol Roca¹, Michael Meulbroek¹,

Roger Paredes Deirós^{2,3,4}. ¹BCN Checkpoint-Projetxe dels NOMS HISPANOSIDA, Spain; ²Fundació Lluita Contra les Infeccions, Badalona, Spain; ³Hospital Germans Trias i Pujol, Infectious Diseases Unit, Badalona, Spain; ⁴IrsiCaixa AIDS Research Institute, Spain
Email: angel.rivero.calaf@outlook.com

Background and aims: Since 2000, multiple HCV outbreaks have been reported in Men who have Sex with Men and Transgender Women (MSM/TW) living with HIV, but to a much lesser extent in their HIV-negative peers. New developments (U=U, PrEP implementation and extension of ChemSex) may have contributed to fueling the transmission chain. A community center with experience of early HIV detection, linkage to care and treatment might be able to create a model with Point-of-Care (PoC) HCV detection in this understudied population. The study aims to determine the prevalence of acute and chronic HCV infection in HIV-negative MSM/TW community and to assess associated risk factors.

Method: All clients who entered the center for routine HIV testing, PrEP and non-PrEP users, were offered to be screened for HCV. A PoC serology test (Abbott® Bioline™ HCV) was performed. Positive results were immediately confirmed by a PoC PCR test (Xpert® HCV VL Fingerstick). Additionally, clients with a negative serology and pre-defined criteria (e.g. ChemSex, fisting, recent HIV diagnosis) were offered the PCR test to detect a potential acute infection. All confirmed cases were referred to start treatment rapidly. Sexual behavior and drug use were assessed with questionnaires.

Results: Between 23 August 2021 and 19 December 2022 a total of 8,570 MSM/TW were included (27.9% PrEP users). A total of 11 HCV active infections were found (3 among PrEP users), HCV prevalence 0.13% (IC95%: 0.07%-0.23%). From 43 (0.53%) users with previously known HCV infection 3 (7.0%) were reinfections. Also, 23 (0.53%) serologic scars were found in people without previously known HCV history. From 921 (10.7%) participants with negative serology who complied criteria for PCR testing 1 (0.11%) acute infection was uncovered. Percentage of HCV transmission risk factors during last 6 months are reported in Table 1, highlighting “Slamming,” OR 20.1 (IC95%: 4.6–88.6) and “Anal penetration with someone who practices slamming,” OR 8.5 (IC95%: 2.4–30.7).

Table:

Risk Factor over last 6 months	HCV+	HCV–
Alcohol	27,3%	31,4%
Cocaine	36,4%	28,5%
GHB	36,4%	19,4%
Ketamine	0,0%	7,1%
MDMA	9,1%	21,0%
Marijuana	9,1%	11,4%
Mephedrone	18,2%	11,0%
Amphetamines	0,0%	6,5%
Methamphetamine	27,3%	12,2%
Sildenafil/Tadalafil	0,0%	4,3%
Popper (Amyl Nitrite)	0,0%	13,4%
Sharing sniffing roll for drug consume	63,6%	61,2%
Sharing Needles	0,0%	0,8%
Infection by Venereal	18,2%	29,1%
Lymphogranuloma, syphilis or genital herpes (12 months)		
Practice of fisting	27,3%	20,9%
Anal penetration with someone who practices slamming	36,4%	6,3%
Receptive anal sex with occasional partners	45,5%	62,4%
Group sex without condom	54,5%	32,7%
Group Sex with Chemsex involved	54,5%	34,4%
Slamming	27,3%	1,8%
Tattoos or Piercings	27,3%	15,9%
Sharing sexual toys for anal sex.	0,0%	20,1%

Conclusion: Results show a low prevalence of HCV in HIV-negative MSM/TW. This study produced criteria that allow a follow-up phase of targeted screening to establish effective HCV testing and treat strategies. Community centers play an important role in detecting cases not linked to the health system or subpopulations with difficulties in accessing the public system.

FRI-209

Late presentation for hepatitis C treatment; prevalence and risk factors in the Swiss hepatitis C cohort

Nathalie Brunner¹, Thomas Grischott², Philip Bruggmann¹. ¹Arud Centres for Addiction Medicine, Switzerland; ²University Hospital Zurich, University of Zurich, Institute of Primary Care, Switzerland
Email: nbrunner@gmx.ch

Background and aims: Patients with ‘late presentation’ (LP) of chronic hepatitis C infection (HCV) have already developed advanced or late-stage liver disease before entering specialised care and direct-acting antiviral (DAA) treatment. Even after successful treatment of HCV, the risk of morbidity and premature death remains elevated in this population of LP, leading to an unnecessary burden of disease. HCV LP should therefore be considered a healthcare system failure, primarily in high-income economies. This study aimed to assess the prevalence of LP within the prospective observational Swiss hepatitis C cohort (SCCS) since the introduction of DAAs, and evaluate demographics, clinical and behavioural factors as determinants of LP.

Method: Treatment-naïve participants of SCCS who received DAA treatment between 2014 and 2022 were included. LP was specified as the presence of advanced or late-stage liver disease at the treatment initiation. Demographic (age, gender, origin, education), clinical (e.g., psychiatric treatment, HIV status), and behaviour (e.g., substance use, history of alcohol) data were summarised for the whole study population and compared between the LP and non-LP strata. LP prevalence was calculated over time. LASSO regression was used in a stacked multiply imputed dataset to identify potential risk factors for LP, and odds ratios were calculated by refitting logistic regression models to the same multiply imputed data.

Results: Of the total SCCS population at the end of 2022 (n = 5829), 1258 patients (21.6%) matched the inclusion criteria. The LP prevalence decreased from mid-2015 and stabilised at 46.3% (n = 583) by the end of the study period. Among the assessed factors, male gender, higher age, and a history of alcohol drinking were associated with a higher risk of LP.

Conclusion: A startling percentage of patients with LP was found in the SCCS compared to similar studies. A particular limiting selection bias must be acknowledged, as SCCS recruits mainly in tertiary treatment centres, representing more severe cases. Regardless, LP prevalence remains higher than anticipated, considering the period of availability of DAAs. As the appearance of LP is directly linked to the disease burden, LP must be included as a mandatory parameter in surveillance response systems of viral hepatitis elimination programs.

FRI-210

Characterizing individuals who remain to be screened and those lost to follow-up from Georgia’s HCV elimination program

Sophia Surguladze¹, Davit Baliashvili¹, Irina Tskhomelidze¹, Tamar Gabunia², Vladimer Getia³, Maia Tsreteli³, Paige A. Armstrong⁴, Senad Handanagic⁴, Shaun Shadaker⁴. ¹The Task Force for Global Health, Georgia; ²Ministry of Labour, Health and Social Affairs of Georgia, Tbilisi, Georgia, Georgia; ³National Center for Disease Control and Public Health, Georgia; ⁴Centers for Disease Control and Prevention, United States
Email: sophiesurguladze@gmail.com

Background and aims: Georgia initiated a National Hepatitis C Virus (HCV) Elimination program in 2015, aiming to diagnose 90% of those infected with HCV and treat 95% of those diagnosed. Individuals are tested for HCV antibodies (anti-HCV) and those reactive are tested for

POSTER PRESENTATIONS

viremia (HCV RNA or core antigen). By 2023, 83.4% of adults were screened, 86.3% of those anti-HCV reactive were tested for viremia, and 84.7% of those with current infection initiated treatment. This study aims to characterize those left to screen, anti-HCV-reactive individuals with no viremia testing, and currently infected persons who have not initiated treatment.

Method: This study used nationwide hepatitis C screening and treatment databases. The unscreened population was estimated by comparing the number of screened adults with 2021 adult population data from the Georgian National Statistics Office. Individuals without viremia testing and treatment were identified by linking screening and treatment databases using the Georgian unique 11-digit personal ID; children were included in these analyses. Persons with documented death dates in vital statistics and those screened anonymously at harm reduction sites (n = 150, 288) were excluded.

Results: As of April 2022, there were an estimated 848,100 adults (around 30% of the total adult population) to be screened, 21,597 anti-HCV reactive persons to be tested for viremia, and 14,435 persons with current HCV infection to be treated.

The majority of those not screened were male (51.1%); among unscreened males, the highest percentage were aged 60–69 years (20.2%) and the lowest were aged >80 years (4.8%). Among unscreened females, a plurality were aged 50–59 years (20.4%) and the lowest percentage were aged 18–29 years (6.6%). The majority of 21,597 anti-HCV-reactive persons without viremia testing were male (66.7%). A plurality of both males and females not tested were aged 40–49 years (28.5% and 17.4% respectively); the lowest percentage in males were aged >80 years (1.9%) and in females aged <18 years (4.0%). Loss to follow-up before viremia testing was more common among those screened in blood banks (38.2%) and prisons (36.0%) compared to other screening settings.

Among 14,435 persons with untreated HCV infection, 73.4% were male. Most individuals not initiating treatment were among those aged 40–49 years for males (30.6%) and 70–79 years for females (19.1%). The percentage of individuals with current HCV infection who had not initiated treatment was highest in those screened in hospital inpatient settings (34.5%).

Conclusion: Georgia has made substantial progress towards elimination, but loss-to-follow-up remains a challenge. While screening and testing in certain settings may be prone to loss-to-follow-up, retention in care should be ensured, especially in settings such as prisons. Innovative approaches to beneficiary retention are needed to reach elimination.

FRI-211

Cantabria on the way to HCV elimination. Differential prevalence of hepatitis C in Cantabria: @CohorteCantabria vs ETHON cohort

Joaquín Cabezas^{1,2}, Marta Alonso-Peña², Susana Llerena¹, Paula Iruzubieta^{1,2}, Antonio Cuadrado^{1,2}, María Eliece Cano³, Carlos Fernández-Carrillo^{4,5}, José Luis Calleja Panero^{4,5}, Javier Crespo^{1,2}. ¹University Hospital Marques de Valdecilla, Gastroenterology and Hepatology Department, Santander, Spain; ²Valdecilla Research Institute-IDIVAL, Santander, Spain; ³University Hospital Marques de Valdecilla, Microbiology Department, Santander, Spain; ⁴University Hospital Puerta de Hierro, Gastroenterology and Hepatology Department, Madrid, Spain; ⁵Research Institute Puerta de Hierro Majadahonda-IDIPHIM, Madrid, Spain
Email: joweycabezas@gmail.com

Background and aims: The overall prevalence of anti-HCV in the ETOHN cohort (EC; general population of Cantabria) in 2016 was 1.1%, with a prevalence of viremia of 0.34%. It is likely that the universal treatment of patients with HCV hepatitis in recent years has brought us closer to its elimination in our region.

Aims: 1) To determine the prevalence of seropositivity and chronic HCV infection and to analyze the associated factors in the Cantabria Cohort (CC, CohorteCantabria) in the year 2022. 2) To determine the incidence of new cases of hepatitis C and analyze the associated factors. 3) To compare these results with those obtained in the EC (year 2016).

Method: 1) CC: Cross-sectional study in the general population participating in the CC project, which includes volunteers and random sampling of the entire population of Cantabria between 40 and 70 years old. In the blood sample at baseline, HCV antibody (anti-HCV) detection was carried out and, in positive cases, automatic viraemia quantification was performed. The volunteers included in this cohort between March 2021 and March 2022 were analyzed. 2) EC: Population-based cross-sectional epidemiological study, carried out during the years 2015–2016, exclusively including the population of the Santander node. 3) Analysis of the set of all viremic subjects in Cantabria in the same period.

Results: CC: 11,094 subjects were included (4,355 from 40 to 49 years; 3,823 from 50 to 59 years and 2,916 from 60 to 69 years), 38% male. Anti-HCV was detected in 102 cases (0.9% prevalence). Excluding 10 cases pending definitive study, positive HCV-RNA was detected only in 7 cases (0.06% prevalence). The remaining anti-HCV positive subjects are divided into 18 cases with spontaneous clearance and 77 cases with SVR. The total incidence of viremic patients of the entire population of Cantabria (585,000 subjects) in this period was calculated (112 cases, 19 cases/100,000 inhabitants/year), of which 65 (58%) were previously known, accordingly the incidence rate of new cases was 10 cases/100,000 inhabitants/year. When we compare these results with those obtained in the EC (previously published, doi: 10.1111/jvh.13238) we observed a lower prevalence (1.1% vs 0.9%, $p < 0.001$) and a great decrease in the viraemia rate among seropositives in CC (34% vs 6%, $p < 0.0001$). The CC showed 11.8% (1310) of volunteers with elevated transaminases levels, compared to 17.8% of the population analyzed in the EC.

Conclusion: The current prevalence (2022) of anti-HCV was slightly lower than that reported previously (2016) in the same population; In addition, and as the most outstanding fact of the study, the prevalence of viraemia was less than 10% of the seropositives. This fact, associated with an incidence of 10 new-cases/100,000 inhab./year, places Cantabria close to the goals set by the WHO for the definition of HCV elimination in a certain geographical region.

FRI-212

Risk of developing cancer-comparison of HBV, HCV and smoking

Homie Razavi¹, Devin Razavi-Shearer¹, Sarah Blach¹, Kathryn Razavi-Shearer¹, Alexis Voeller¹, Ivane Gamkrelidze¹, Chris Estes¹. ¹Center for Disease Analysis Foundation, Lafayette, United States

Email: hrazavi@cdafound.org

Background and aims: Hepatitis B and C viruses (HBV and HCV) are oncoviruses, but the risk of developing cancer is often stated in an annual rate which is difficult to interpret by patients and healthcare workers. The objective of this work was to quantify the risk of cancer from viral hepatitis as compared to a known cancer-causing agent-smoking.

Method: A literature search was conducted to find longitudinal studies that reported the adjusted hazard ratio and odd ratio of developing hepatocellular carcinoma (HCC) among HBV/HCV infected individuals and cancer among active smokers.

Results: Fourteen studies were found, and the results are shown below. Adjusted hazard ratio of developing HCC for individuals infected with HBV or HCV was comparable to the risk of developing cancer for someone who is an active smoker. The odds ratio of developing HCC from HBV/HCV infection was 4–8 times higher than someone who actively smokes one pack of cigarette per day.

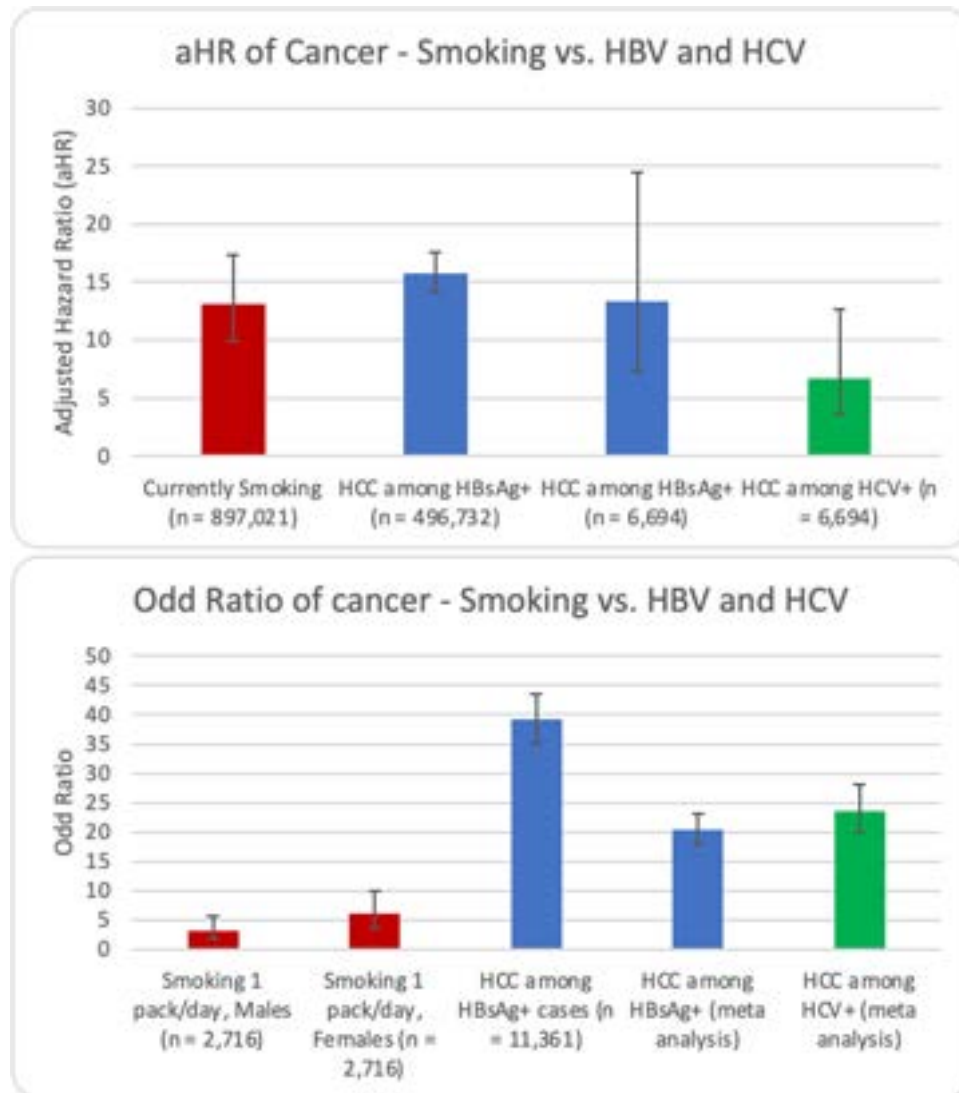


Figure: (abstract: FRI-212).

Conclusion: HBV/HCV infections are highly oncogenic and infected individuals have a similar or significantly higher risk of developing cancer than an active smoker or someone who smokes one pack of cigarette per day.

FRI-213

Pandemic preparedness and viral hepatitis-Global survey of hepatitis program managers and healthcare providers

Nida Ali¹, John Ward¹, Neil Gupta¹, Lindsey Hiebert¹. ¹*Coalition for Global Hepatitis Elimination-Task Force for Global Health, Decatur, United States*

Email: nida.ali4883@gmail.com

Background and aims: At the advent of COVID-19 pandemic, hepatitis programs testing, and clinical care resources were repurposed for pandemic response before the direct investments for pandemic were operationalized. The Coalition for Global Hepatitis Elimination (CGHE) conducted a survey of hepatitis program managers (PMs) and hepatitis healthcare providers (HCPs) to assess 1) the contribution of viral hepatitis care and treatment infrastructure to pandemic response and 2) potential opportunities for leveraging the pandemic response capacity for delivery of viral hepatitis care.

Method: A web-based survey was designed in RedCAP in English for PMs and HCPs with a separate set of questions for each. The study

team sent targeted solicitations via email to professional societies and CGHE networks, alongside promotions over CGHE website and social media.

Results: In all, 79 HCPs and 21 PMs responded to the survey from 46 countries across regions of the Americas (53%), Africa (26%), Eastern Mediterranean (13%), Europe (7%) and Western Pacific (1%). In some cases, the full requested information was not completed by the respondents, hence the denominators for assessment of some variables differ (particularly for multivariate questions). More than 80% (17/21) of PMs provided direct support to the pandemic response. 73% (58/78) of HCPs provided clinical care to COVID-19 patients and 20% (16/78) are still providing care to COVID-19 patients in addition to hepatitis. 63% (49/78) of HCPs reported that space in their hepatitis clinics was re-purposed for COVID-19 patients. 66% (14/21) of PMs and 71% (56/79) of HCPs reported that PCR platforms for hepatitis testing were repurposed for COVID-19 testing during pandemic. As reported by PMs, there was an increase in PCR testing capacity at national reference laboratories (48%, 10/21), provincial public laboratories (43%, 9/21) and private laboratories (43%, 9/21). 50% (8/16) of PMs and 66% (49/74) of HCPs reported that PCR equipment acquired for COVID-19 is now also being used for hepatitis testing. 67% (10/15) of PMs reported that PCR testing shifted from manual to automated at labs. Almost all (99%, 78/79 HCPs reported

POSTER PRESENTATIONS

that COVID-19 PCR turnaround time is faster than that for hepatitis B and C. Regarding teleconsultation, 72% (51/71) HCPs reported that teleconsultation was not in use before pandemic, 59% (38/64) reported that teleconsultation was introduced during pandemic and 37% (26/71) of HCPs reported that the use of teleconsultation increased during the pandemic. 42% (33/78) HCPs in the survey prefer in-person consultation, 5% (4/78) telemedicine and 53% (41/78) prefer mix of both approaches.

Conclusion: PMs and HCPs from a diverse set of countries reported that the resources of hepatitis testing and care were repurposed for the pandemic response, demonstrating the utility of robust hepatitis testing and treatment programs for health system resilience and epidemic response. Data suggests that COVID-19 response continues to require the use of care staff and clinic space previously used for delivery of hepatitis services. Respondents reported the expansion of COVID-19 testing services that are now being utilized for hepatitis testing. This reflects how investments in pandemic response have the potential to bolster hepatitis programs.

FRI-214

New tools reaching hepatitis C elimination: automatic hepatitis C virus detection in presurgical evaluations

Pablo Miles Wolfe García¹, Marina Eliana Millan Lorenzo¹, Marta González¹, Eduardo López Fernández¹, Carlos Rodríguez¹, Rafael Godino Vazquez¹, Rafael Ruíz Zorrilla¹, Laura García Alles¹, Jose Luis Fernández Forcelledo¹, Roya Taheri¹, Pablo Palomares Rivas¹, Rosa Ortiz De Diego¹. ¹Hospital Sierrallana, Torrelavega-Cantabria, Spain
Email: marinamillan@gmail.com

Background and aims: Hepatitis C virus (HCV) eradication is one of the many goals the WHO has set for 2030. Nevertheless, despite the efforts from the administration, scientific societies and the health care workers, it is still a defying feat. Our strategy for increasing HCV detection focuses on screening every single patient scheduled for a surgical procedure, taking advantage of the blood work extraction during their presurgical evaluation.

Method: We've included patients between 39 and 70 years old (age group with higher HCV prevalence). HCV antibodies (anti-HCV) were automatically added to their blood work requests by the anesthesiologists in the presurgical appointment. Prior to this, the patients are given an informative brochure where VHC is explained and verbal consent is requested, and if it is given, an additional blood sample is extracted for this specific matter. If anti-VHC antibodies come back positive, viral load is automatically added to the blood work. Both results are posteriorly sent to the Hepatology Unit, where the patients are given an appointment in order to perform a thorough physical examination, abdominal ultrasound, transient liver elastography (TLE) and broaden their blood analyses. If no counter-indication is found, antiviral therapy is initiated, which is provided by the Hospital's pharmacy.

Results: 1697 presurgical evaluations were carried out between February and March, 2022. No patients declined the serology extraction. Mean patient age was 56 years old, 52% of them were men. Our strategy entailed an increase by 23.5% in HCV serologies during this period ($p < 0.001$). We detected 17 anti-HCV positive patients, two of which presented a positive viral load, which represent a prevalence of 0.11%. Both patients were provided with a single-act HCV appointment in our unit. One patient presented a low VHC load, thus a second blood sample was extracted, resulting in a negative viral count; the patient was never treated for VHC. The second patient was a 61-year-old male who was unaware of his diagnosis. The patient presented a history of altered liver function tests and moderate alcohol consumption. In 2016, an Anti-HCV test

was requested, which was positive, but no viral load was performed and the patient did not return to the follow-up consultation. While at our single-act HCV appointment, severe steatosis and liver fibrosis grade 2 were detected on ultrasound and TLE. Treatment with Sofosbuvir/Velpatasvir was initiated for 12 weeks, pending verification of sustained viral response.

Conclusion: These results demonstrate that the automation of the HCV serology testing in all patients who require blood work extractions, regardless of the reason and the medical unit that requests it, significantly increases the diagnosis of HCV.

Rare liver diseases (including paediatric and genetic)

WEDNESDAY 21 TO SATURDAY 24 JUNE

TOP-055

Clinical features of portal hypertension and their prognostic implication in patients with Wilson's disease

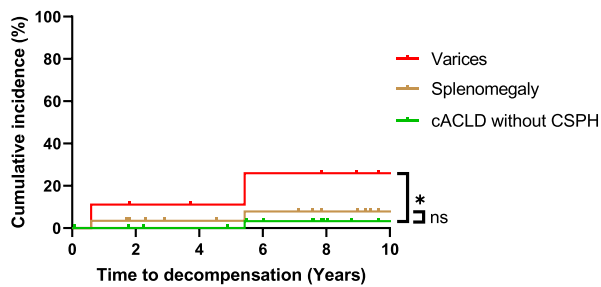
Lukas Burghart^{1,2}, Oleksander Petrenko¹, Peter Ferenci¹, Michael Trauner¹, Mattias Mandorfer¹, Michael Gschwantler², Thomas Reiberger¹, Albert Stättermayer¹. ¹Medical University of Vienna, Gastroenterology and Hepatology, Vienna, Austria; ²Klinik Ottakring-Wiener Gesundheitsverbund, Gastroenterology and Hepatology, Wien, Austria
Email: burghartlukas@gmail.com

Background and aims: Wilson's disease (WD) is a rare inheritable liver disease mediated by hepatic copper overload. Natural history studies indicate half of all WD patients will ultimately progress to advanced chronic liver disease (ACLD). Consequently, portal hypertension (PH) may develop, which in turn drives hepatic decompensation and impairs transplant-free survival (TFS). We therefore assessed (i) the prevalence and incidence of CSPH in the Vienna WD cohort, and (ii) evaluated the impact of CSPH on hepatic decompensation and TFS.

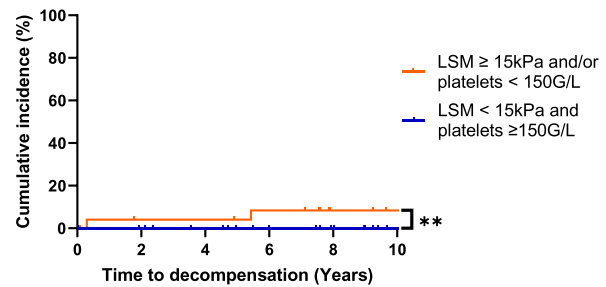
Method: Patients with verified WD diagnosis (Leipzig score ≥ 4), attending regular clinical visits at the Vienna General Hospital between Q1/2005-Q4/2021, were included in this retrospective study. Clinical information including CSPH-specific features and complications was recorded from individual medical records.

Results: Among 140 WD patients (mean age: 41.8 years, 50% women) 50 (35.7%) showed features of CSPH at diagnosis: 14 (10.0%) had gastroesophageal varices (GEV), 41 (29.3%) splenomegaly, 20 (14.3%) ascites, 19 (13.6%) hepatic encephalopathy (HE) and 3 (2.1%) experienced acute variceal bleeding. Only 10 (20.0%) WD patients with CSPH received NSBB, and only 1 (2.0%) was treated by TIPS. During a median follow-up of 9.2 years, 8 (5.7%) WD patients died with 3 deaths attributable to CSPH-related complications. GEV were associated with an increased 5-year (5Y) risk of decompensation (11.1%) (A) and an impaired 5Y-TFS (71.4%), whereas the occurrence of HE or ascites was associated with a profound decrease in 5Y-TFS to 42.1% and 35.0%, respectively (C). Patients with compensated ACLD (cACLD) had a comparable 5Y-TFS (96.0%) to non-ACLD patients (100%), which was contrasted by the steep decline of 5Y-TFS (42.3%) in patients with decompensated ACLD (dACLD). Importantly, the combination of liver stiffness < 15 kPa and platelets ≥ 150 G/L indicated excellent prognosis (5Y decompensation rate: 0%, 5Y-TFS of 97.7%),

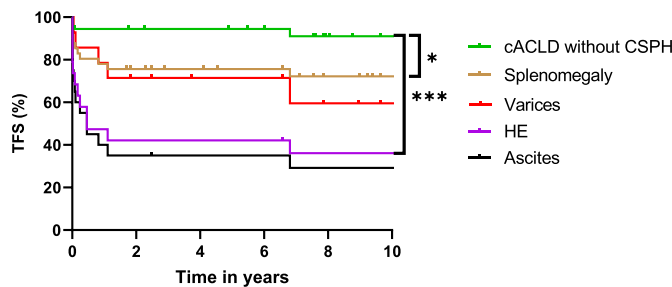
(A) C.I. of dACLD in WD with features of CSPH



(B) C.I. of dACLD according to LSM-PLT risk stratification



(C) TFS in WD with features of CSPH



(D) TFS according to LSM-PLT risk stratification

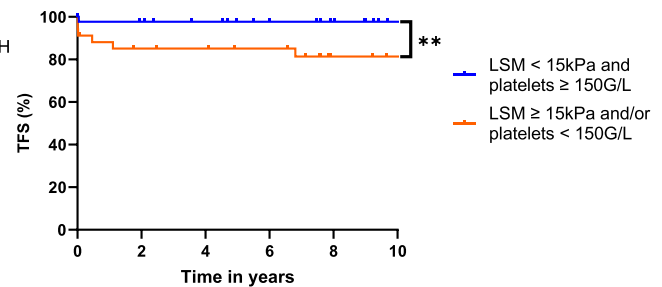


Figure: (abstract: TOP-055).

while patients with either liver stiffness ≥ 15 kPa or platelets < 150 G/L showed a 5Y decompensation rate of 4.0% and a 5Y-TFS of 85.1% (B) (D).

Conclusion: WD patients often develop CSPH with the presence of GEV indicating a significant risk for hepatic decompensation. WD patients with ascites and/or HE show a dismal prognosis with impaired survival without liver transplantation. Hence, regular CSPH screening-as by the non-invasive markers liver stiffness ≥ 15 kPa or platelets < 150 G/L-is warranted in patients with WD.

TOP-056

Modeling Alagille syndrome in vitro using complex induced pluripotent stem cell-derived human liver organoids

Marie-Agnès M'Callum¹, Silvia Selleri¹, Toan Pham¹, Alexandre Archambault-Marsan¹, Kristen Vieira Lomasney¹, Massimiliano Paganelli¹. ¹CHU Sainte-Justine, Université de Montréal, Liver Tissue Engineering and Cell Therapy, Montreal, Canada
Email: m.paganelli@umontreal.ca

Background and aims: Alagille syndrome (ALGS) is an autosomal dominant hereditary multisystemic disease. In the liver, ALGS is characterized by bile duct paucity, cholestasis, fibrosis, as well as other heterogeneous clinical manifestations. The genes involved (JAG1, NOTCH2) belong to the Notch signalling pathway. No direct genotype-phenotype correlation has been established. The aim of the study was to develop a representative human model of ALGS to better understand the pathophysiology of the disease.

Method: We developed a new 3D in vitro model of ALGS by generating liver organoids from human induced pluripotent stem cells (iPSC). Two iPSCs clones with mutations in exon 23 of JAG1 were obtained with CRISPR/Cas9: clone A2 had a large deletion, whereas clone B3 presented a single base substitution. We generated hepatic (HPC), mesenchymal (MPC) and endothelial (EPC) progenitor cells from JAG1-mutated iPSC clones and from isogenic control and used them to create the liver organoids. We previously showed that, within

the organoids, these cells interact to become hepatocytes, cholangiocytes/biliary epithelial cells, stellate and sinusoidal cells, and form ductal plate and bile ducts (Raggi et al. Stem Cell Reports 2022). In order to determine which progenitor cell type is more predominant to obtain the disease phenotype, we generated generate hybrid organoids mixing different progenitor cell types obtained from the mutated clones and the control. We studied the impact of the mutations on the different liver cell types, and assessed the ductal plate, bile duct formation and fibrogenesis in the organoids.

Results: HPCs from the two clones with different JAG1 mutations showed different gene expression profiles representing the heterogeneity of ALGS: expression of hepatic markers and Notch pathway targets was strongly decreased in HPCs-A2 compared to HPC-B3 or HPC from control iPSC. Moreover, HPCs-A2 and -B3 showed a strong expression of YAP1, which attests to a dedifferentiation of HPCs. Nevertheless, a strong expression of cytokeratin genes was observed in mutated HPCs compared to healthy cells, which is commonly observed in fibrosis and cholestasis. Organoids from the two mutated clones lacked biliary structures compared to healthy organoids (Figure 1), reproducing the phenotype of ALGS. Mutated organoids from both clones showed an overexpression of inflammatory markers and increased fibrosis, as well as a loss of bile duct-associated markers, compared to control organoids. Among the 18 hybrid organoid conditions generated, only organoids with healthy HPCs were able to form proper biliary structures, attesting that mutation in HPCs (i.e., bipotent hepatic progenitors), hepatocytes and biliary epithelial cells drives the disease phenotype.

Conclusion: We were able to generate a representative human developmental model of Alagille syndrome using complex liver organoids derived from iPSC. These organoids recreate the hepatic niche and reproduce the histological phenotype of Alagille syndrome, which makes them an ideal model to study the pathophysiology of the disease and discover new therapeutic targets.

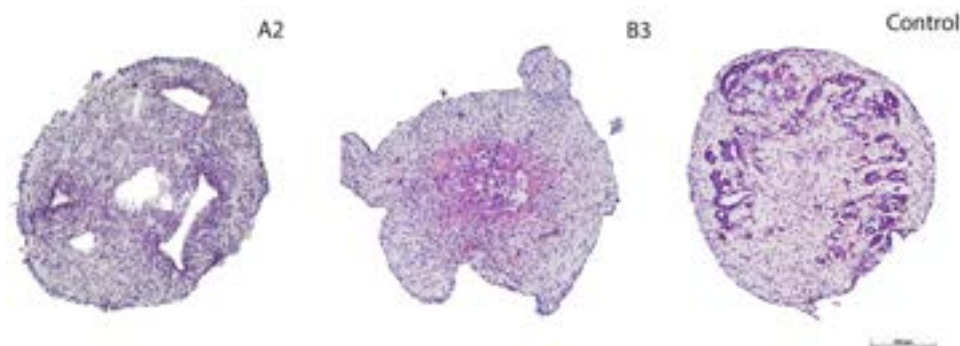


Figure: (abstract: TOP-056): Histological appearance of human liver organoids generated from JAG1-mutated iPSC (A2 and B3) showing bile duct paucity, increased fibrosis and cell death. In comparison, organoids from control iPSC show ductal plate structures with branching immature and mature bile ducts (HandE staining, representative images, scale bar 200 μ m).

TOP-057

Long-term efficacy and safety of odevixibat in patients with progressive familial intrahepatic cholestasis: results with 96 weeks or more of treatment

Richard Thompson¹, Ozlem Durmaz², Tassos Grammatikopoulos^{1,3}, Angelo Di Giorgio⁴, Quanhong Ni⁵, Philip Stein⁵, Christine Clemson⁵, Ekkehard Sturm⁶, ¹Institute of Liver Studies, King's College London, United Kingdom; ²Istanbul University, Istanbul Faculty of Medicine, Istanbul, Turkey; ³Paediatric Liver, GI, and Nutrition Centre and MowatLabs, King's College Hospital NHS Trust, United Kingdom; ⁴Paediatric Hepatology, Gastroenterology, and Transplantation, ASST Papa Giovanni XXIII, Italy; ⁵Albireo Pharma, Inc., Boston, United States; ⁶Paediatric Gastroenterology and Hepatology, University Children's Hospital Tübingen, Germany
Email: richard.j.thompson@kcl.ac.uk

Background and aims: Patients with progressive familial intrahepatic cholestasis (PFIC) may present with elevated serum bile acids (sBAs), intractable pruritus, impaired hepatic function, and growth deficits. The phase 3 studies in patients with PFIC that evaluated odevixibat, an ileal bile acid transporter inhibitor, are called PEDFIC 1 and PEDFIC 2. Using pooled data from these studies, we describe key outcomes in a subgroup of patients treated with odevixibat for ≥ 96 weeks.

Method: PEDFIC 1 was a 24-week, randomised, placebo-controlled study in children with PFIC1 and PFIC2. PEDFIC 2 is an ongoing 72-week open-label extension study that enrolled patients from PEDFIC 1 or new patients of any age with any type of PFIC. Following 72 weeks of treatment in PEDFIC 2, there is an optional extension period,

with visits every 16 weeks. Patients could have reached 96 weeks of odevixibat treatment in various ways, including by receiving 24 weeks of active treatment in PEDFIC 1 plus 72 weeks of treatment in PEDFIC 2 or by receiving 96 weeks of open-label treatment in PEDFIC 2 and its optional extension. This pooled analysis spans from patients' first dose of odevixibat to a cut-off date of 31 January 2022. The following outcomes were evaluated in patients with ≥ 96 weeks' odevixibat exposure and an sBA measurement at week 96: sBAs, scratching scores, hepatic parameters, growth, and safety. Scratching scores range from 0 to 4, with higher scores indicating worse symptoms. Pruritus data were collected through week 72 of PEDFIC 2. **Results:** Of the 111 patients in the pooled population (69 of whom continue on treatment at data cut-off), 36 had ≥ 96 weeks' odevixibat exposure and an sBA measurement at week 96. Among these 36 (50% female), 36% had PFIC1, 61% had PFIC2, and 3% had MYO5B deficiency. At baseline, patients had elevated mean sBA, transaminase, and total bilirubin levels, moderate-to-severe pruritus, and impaired growth (Table). After 96 weeks of odevixibat treatment, there were significant reductions in mean sBAs, transaminase levels, and scratching scores and improvements in growth; only minimal changes in bilirubin levels were observed (Table). All 36 patients (100%) had treatment-emergent adverse events (TEAEs); most were mild or moderate in severity. Serious TEAEs were recorded in 6 of 36 patients, but none were drug related.

Conclusion: Odevixibat treatment for ≥ 96 weeks was associated with improvements in sBAs, pruritus, transaminase levels, and growth. Odevixibat was generally well tolerated.

Table: (abstract: TOP-057).

Outcomes in Patients With PFIC Treated With Odevixibat for ≥ 96 Weeks

Outcome	Baseline		Week 96		p value ^a
	n	Mean (SE)	n	Mean (SE)	
Serum bile acids, μ mol/L	36	288 (22)	36	118 (20)	< 0.001
Scratching score	36	2.8 (0.1)	17	0.9 (0.2) ^b	< 0.001
ALT, U/L	36	102 (23)	32	38 (7)	0.022
AST, U/L	36	88 (10)	32	49 (5)	0.001
Total bilirubin, μ mol/L	36	56 (13)	32	50 (17)	0.713
Height Z score	36	-1.5 (0.3)	36	-0.9 (0.2)	< 0.001
Weight Z score	36	-0.9 (0.3)	36	-0.2 (0.2)	< 0.001

^ap values are based on 1-sample t test for changes from baseline to the week 96 visit window. ^bThe average of daily scratching scores from weeks 85–96 are reported. ALT, alanine aminotransferase; AST, aspartate aminotransferase; PFIC, progressive familial intrahepatic cholestasis.

TOP-058

Metabolomic profiles facilitate differential diagnosis of porto-sinusoidal vascular disorder versus liver cirrhosis

Georg Semmler^{1,2}, Oleksandr Petrenko^{1,2,3,4,5}, Behrang Mozayani⁶, Lorenz Balcar^{1,2}, Benedikt Simbrunner^{1,2,5}, Philipp Schwabl^{1,2,3,4}, Lukas Hartl^{1,2}, Mathias Jachs^{1,2}, Kerstin Zinöber^{1,2,5}, Katharina Lampichler⁷, Michael Trauner¹, Juan Sánchez-Avila⁸, Nara Marella⁸, J. Thomas Hannich⁸, Mattias Mandorfer^{1,2}, Thomas Reiberger^{1,2,3,4}, Bernhard Scheiner^{1,2,9}. ¹Medical University of Vienna, Division of Gastroenterology and Hepatology, Department of Internal Medicine III, Austria; ²Medical University of Vienna, Vienna Hepatic Hemodynamic Lab, Division of Gastroenterology and Hepatology, Department of Internal Medicine III, Austria; ³CeMM Research Center for Molecular Medicine of the Austrian Academy of Sciences, Austria; ⁴Ludwig Boltzmann Institute for Rare and Undiagnosed Diseases (LBI-RUD), Austria; ⁵Medical University of Vienna, Christian Doppler Laboratory for Portal Hypertension and Liver Fibrosis, Austria; ⁶Medical University of Vienna, Department of Pathology, Austria; ⁷Medical University of Vienna, Department of Biomedical Imaging and Image-Guided Therapy, Austria; ⁸CeMM Research Center for Molecular Medicine of the Austrian Academy of Sciences, CeMM Molecular Discovery Platform Metabolomics, Austria; ⁹Imperial College London, Department of Surgery and Cancer, United Kingdom

Email: thomas.reiberger@meduniwien.ac.at

Background and aims: Porto-sinusoidal vascular disorder (PSVD) is a rare vascular liver disease characterized by specific histological findings in the absence of liver cirrhosis (LC). Diagnosis and differentiation from LC remains challenging and importantly requires invasive liver biopsy. The aim of this study was to investigate metabolomic signatures of patients with PSVD, liver cirrhosis (LC) and healthy volunteers (HV) in regards to facilitating diagnosis and identifying metabolites involved in pathogenesis.

Method: We analyzed 20 serum samples from patients with histologically verified PSVD and LC as well as HV (Figure A). Participants were matched by age and gender (all three groups) as well as by BMI, MELD and current/previous hepatic decompensation (PSVD and LC). Following extraction, serum concentrations of lipids, hydrophilic metabolites and free-fatty acids were measured by LC-MS. Metabolites with $\geq 20\%$ missing entries were excluded. Data were analyzed in R environment (tidyverse, rstatix). Missing values were imputed using k-nearest neighbors algorithm. Concentrations of each run were log₂-normalized, scaled by Pareto technique and merged (POMA package). Partial least squares-discriminant analysis (PLS-DA) was performed for data exploration. Differential metabolites (PSVD vs LC vs HV) were identified using pairwise Limma contrasts and the Wilcoxon test. The diagnostic/discriminative value of metabolites was evaluated with MetaboAnalystR.

Results: From 539 identified metabolites, n = 208 (38.6%) were excluded, and n = 74 (13.7%) were complemented with imputation. PLS-DA discriminated LC and HV with component #1, however, PSVD

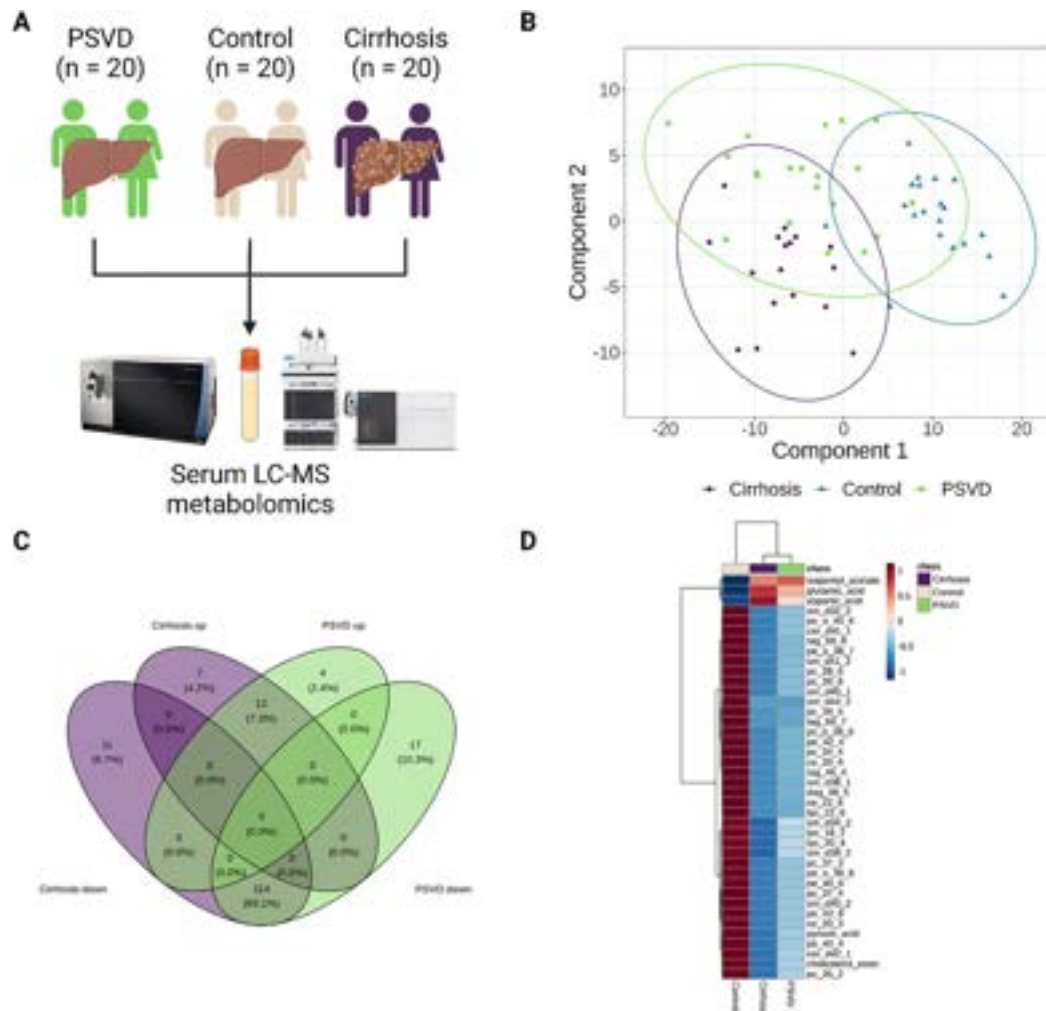


Figure: (abstract: TOP-058).

POSTER PRESENTATIONS

patients were partly present in both clusters (Figure B). Pyruvic acid, glutamine, triacylglycerols and isovaleric acid were key metabolites of the first component, while phosphatidylethanolamine and cholesteryl icosatetraenoate contributed to PSVD discrimination (component #2). We identified 165 differential metabolites in LC and PSVD versus HV ($p_{\text{adj}} \leq 0.01$, Figure C), of which $n = 39$ (23.6%) were unique to the respective groups. The metabolites that contributed to most of the dataset variation were mainly down-regulated in PSVD and even further in LC (Figure D). When analyzing single differential metabolites, 1-palmitoleyl-2-eicosaenoic acid identified PSVD vs HV (mean AUROC = 0.958), while tyrosine (AUROC = 0.859) and adipic acid (AUROC = 0.821) were among the best-performing discriminators between PSVD and LC.

Conclusion: High-throughput metabolomics identified common and unique metabolic profiles in PSVD and LC. Independent validation of the metabolomic signatures is required. If confirmed, mechanistic studies should investigate the underlying molecular mechanisms to gain insights into PSVD pathophysiology.

THURSDAY 22 JUNE

THU-249

Inhibition of the renal apical sodium-dependent bile acid transporter prevents cholemic nephropathy

Ahmed Ghallab^{1,2}, Daniela González¹, Ellen Strängberg³, Ute Hofmann⁴, Maiju Myllys¹, Reham Hassan^{1,2}, Tom Lüdde⁵, Peter Akerblad³, Jan Mattsson³, Hanns-Ulrich Marschall⁶, Paul Dawson⁷, Guido Stirnimann⁸, Peter Boor⁹, Karolina Edlund¹, Michael Trauner¹⁰, Erik Lindström³, Jan G. Hengstler¹. ¹Department of

Toxicology, Leibniz Research Centre for Working Environment and Human Factors, Technical University Dortmund, Germany; ²Department of Forensic Medicine and Toxicology, Faculty of Veterinary Medicine, South Valley University, Egypt; ³Albireo Pharma, Inc., Boston, MA, United States; ⁴Dr. Margarete Fischer-Bosch Institute of Clinical Pharmacology and University of Tübingen, Germany; ⁵Department of Gastroenterology, Hepatology and Infectious Diseases, University Hospital Duesseldorf, Medical Faculty at Heinrich-Heine-University, Dusseldorf, Germany; ⁶Department of Molecular and Clinical Medicine/Wallenberg Laboratory, Sahlgrenska Academy, University of Gothenburg, Gothenburg, Sweden; ⁷Division of Pediatric Gastroenterology, Hepatology, and Nutrition, Emory University School of Medicine, United States; ⁸University Clinic for Visceral Surgery and Medicine, Inselspital University Hospital and University of Bern, Bern, Switzerland; ⁹Institute of Pathology and Department of Nephrology, University Hospital RWTH Aachen, Germany; ¹⁰Hans Popper Laboratory of Molecular Hepatology, Division of Gastroenterology and Hepatology, Department of Internal Medicine III, Medical University of Vienna, Austria
Email: ghallab@ifado.de

Background and aims: Cholemic nephropathy (CN) is a severe complication of several liver diseases. Since no specific treatment is currently available, we revisited the pathophysiology and tested the therapeutic strategy of inhibiting renal bile acid (BA) uptake.

Method: Cholestasis was induced by bile duct ligation (BDL) in mice. Bile flux in kidneys and livers was visualized by intravital imaging, supported by matrix-assisted laser desorption/ionization-mass spectrometry imaging (MALDI-MSI) and liquid chromatography-tandem mass spectrometry (LC-MS/MS). AS0369, a selective and orally systemically available inhibitor of the apical sodium-dependent bile acid transporter (ASBT) was developed, and its renal and hepatic effects were tested by RNA sequencing, histological, serum, and urine

Renal apical sodium-dependent bile acid transporter inhibition by AS0369 in cholemic nephropathy

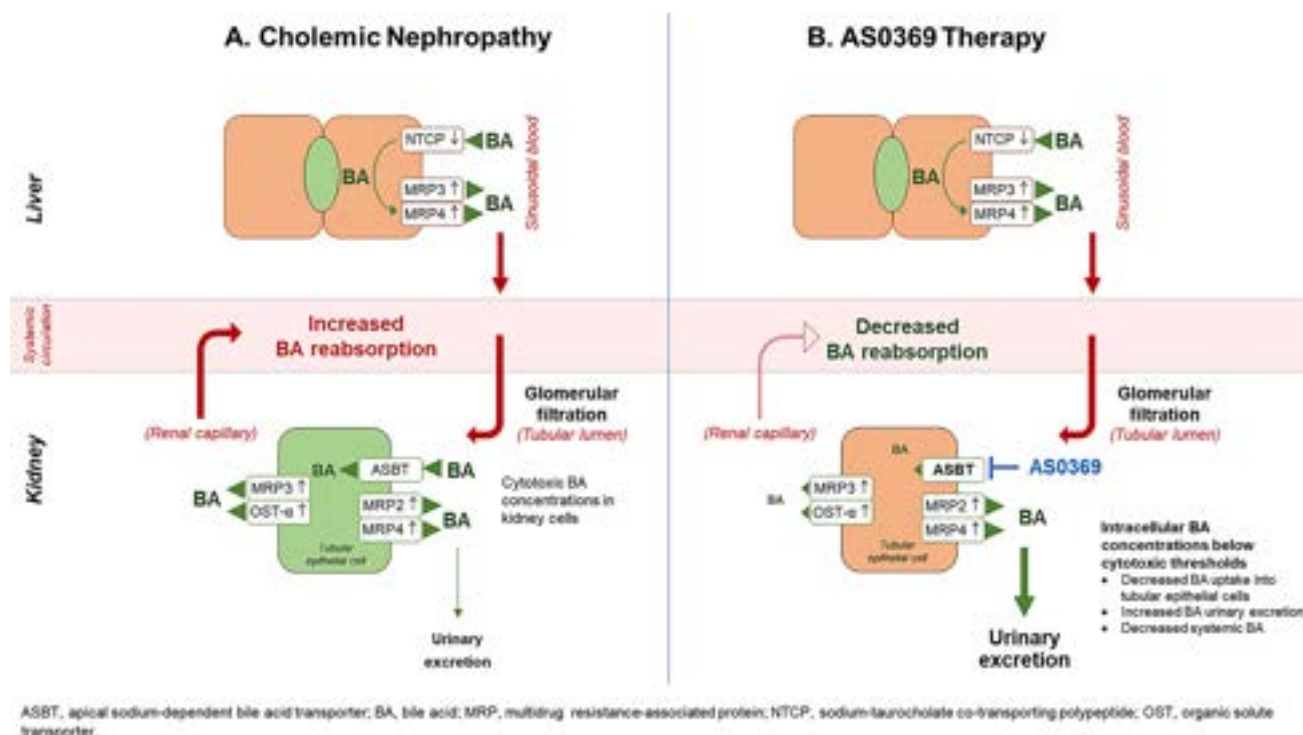


Figure: (abstract: THU-249).

analyses. Translational relevance was evaluated by ASBT immunostaining in renal biopsies from CN patients.

Results: Intravital imaging showed that BAs were reabsorbed from the renal tubular lumen into specific renal tubular epithelial cells (TEC). BA enrichment led to cell death of TEC within the first days after BDL. At week 3 and later, damage of peritubular capillaries and massive leakage of BAs into the renal interstitium were observed, followed by leukocyte infiltration and fibrosis. Renal ASBT expression was maintained in TEC of BDL mice and CN patients, and treatment of BDL mice with AS0369 strongly elevated urinary BA excretion, blocked the uptake of BAs in TEC, and decreased renal tissue BA levels. In addition, AS0369 almost completely prevented kidney injury up to 6 weeks after BDL. All CN hallmarks (ie, cell death events of TEC, tubular casts, immune cell infiltration, and fibrosis) were almost completely absent in AS0369-treated mice. Also, the kidney injury marker neutrophil gelatinase-associated lipocalin (NGAL) in urine was strongly reduced by AS0369 treatment. RNA-Seq analysis demonstrated that ASBT inhibition strongly ameliorated BDL-induced gene expression changes in the kidney, while the corresponding effects in the liver were smaller but still statistically

significant. The efficacy of AS0369 is not sex specific since the results were reproducible in both female and male mice.

Conclusion: BA enrichment in TEC followed by cell death is an early key event in CN. Inhibiting renal ASBT and consequently BA uptake into TEC efficiently prevents CN under conditions where serum and urinary BA concentrations are massively increased (Figure). Moreover, ASBT inhibition reduces endothelial exposure by blocking transepithelial transport. The increased urinary excretion of BAs leads to decreased blood concentrations systemically, which is favourable for all cell types that are compromised by exposure to the circulating high BA concentrations. The present findings may have clinical relevance since TEC ASBT expression is also preserved in CN patients.

THU-250

Common, non-pathogenic variants in genes from monogenic disorders confer additional risk of liver injury later in life

Jake Mann¹, Ye Htun Oo², Girish Gupte¹, Philip N Newsome².

¹Birmingham Children's Hospital, Liver Unit, United Kingdom;

²University of Birmingham, Centre for Liver Research, United Kingdom

Email: jpmann.gsy@gmail.com

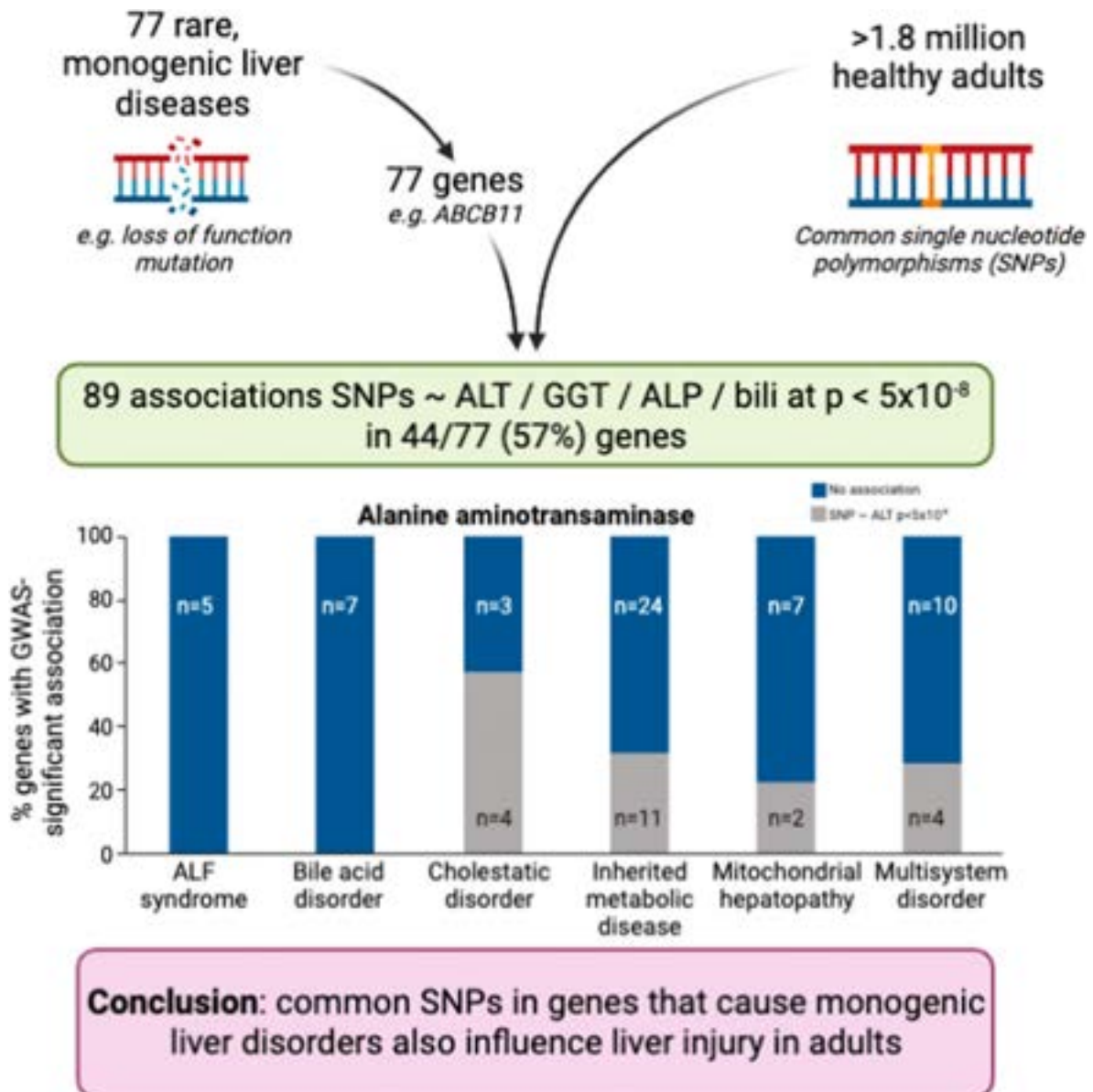


Figure: (abstract: THU-250).

Background and aims: Monogenic liver disease is caused by rare, pathogenic mutations. Exome and genome sequencing frequently identifies variants of unknown significance in these genes. It is not clear whether such non-pathogenic variants confer increased risk of liver injury beyond childhood. Here, we found that these variants increase the severity of liver damage and may act as a 'second hit' in adults.

Method: We identified 77 monogenic paediatric liver diseases. For each gene, we searched for evidence of a liver phenotype in individuals not known to have genetic disease using population-based datasets. We identified genome-wide significant associations ($p < 5 \times 10^{-8}$) between variants (e.g. single nucleotide polymorphisms) and liver biochemistry (ALT, bilirubin, GGT, ALP) in $n = 1,654,950$ participants from the Common Metabolic Disease Portal and $n = 394,841$ from UK BioBank using GeneBass.

Results: We found 89 genome-wide associations for biomarkers of liver injury in otherwise apparently healthy individuals across genes from 44/77 (57%) monogenic disorders (Fig 1). For example, common variants in *ABCB11* (the cause of PFIC type 2) were associated with GGT ($p = 2.0 \times 10^{-33}$) and ALT ($p = 8.4 \times 10^{-39}$). Similarly, common polymorphisms in *JAG1* (that do not cause Alagille's syndrome) were associated with GGT ($p = 2.3 \times 10^{-9}$) and ALT ($p = 5.9 \times 10^{-10}$). Phenotypes were found most frequently in 5/7 (71%) of cholestatic disorders and 5/7 (71%) of bile acid metabolism disorders, compared to 3/8 (38%) of congenital fibrotic disorders. In addition to affecting liver enzymes, serum lipid profile (e.g. total cholesterol) was affected by genes from 23/44 (52%).

Conclusion: Common variants in genes that cause rare monogenic liver disease also confer a risk of liver injury later in life. Understanding the mechanisms of these genes and applying them as predictors for future disease progression in adults may provide an opportunity for treatment of common liver diseases.

THU-251

CD73^{high} biliary tract cancer (BTC): a molecularly-defined subtype with distinct clinical implications

Massimiliano Salati¹, Anna Barbato², Fabiola Piscopo², Lorenzo Evangelista², Gennaro Gambardella², Sergio Sarnataro², Angelica Petrillo³, Bruno Daniele³, Pasquale Pisapia⁴, Maria Salatiello⁴, Umberto Malapelle⁴, Giancarlo Troncone⁴, Andrea Spallanzani¹, Fabio Gelsomino¹, Beatrice Ricco¹, Antonella Iuliano⁵, Luca Reggiani-Bonetti⁶, Colm O'Rourke⁷, Jesper Andersen⁷, Massimo Dominici¹, Brunella Franco^{2,8}, Pietro Carotenuto^{2,8}. ¹University Hospital of Modena, Modena, Italy, ²Department of Oncology and Hematology, Italy; ³Tigem (Telethon Institute of Genetics and Medicine), Pozzuoli, Italy; ⁴Ospedale del Mare, Medical Oncology Unit, Napoli, Italy; ⁵Università degli Studi di Napoli-AOU Federico II, Department of Public Health, Napoli, Italy; ⁶DIMIE, Potenza, Italy; ⁷Section of Pathology, Azienda Ospedaliero-Universitaria Policlinico di Modena, Modena, Italy, Modena, Italy; ⁸Biotech Research and Innovation Centre, Department of Health and Medical Science, Copenhagen, Denmark; ⁸Università degli Studi Federico II di Napoli, DISMET, Napoli, Italy
Email: p.carotenuto@tigem.it

Background and aims: Tumour heterogeneity and the immunotolerant microenvironment are driving forces of biological aggressiveness and treatment refractoriness in BTCs. Recently, CD73, an ecto-5'-nucleotidase, has been increasingly implicated in cancer promotion and treatment resistance, acting through the enzymatic conversion of AMP to immunosuppressive adenosine and the non-catalytic promotion of cancer plasticity, invasion and migration. Interestingly, CD73 has become a clinically validated target with several compounds undergoing advanced-phase development across various cancer types. Here, we aimed at comprehensively characterizing the role of CD73 in a well-annotated cohort of BTC patients.

Method: Medical records and FFPE tissue blocks from 70 radically-resected BTCs were retrospectively retrieved at the University

Hospital of Modena. Immunohistochemistry for CD73, CD4/CD8 and FOXP3 as well as bulk whole-transcriptomic sequencing were performed (Illumina Platform). Silencing of CD73 was achieved by transient transfection of CD73-siRNA, while genetic Knock-out (KO) was performed using CRISPR-Cas system technology in two BTC cell lines (Hucct01; RBE). Tumour growth was assessed in 2D and in 3D cell culture by using MTS assay and spheroid growth analysis before and after treatment with selected drugs. Statistical analyses were performed SPSS software (version 26; SPSS Inc., Chicago, IL, USA).

Results: Overall, 60% of BTC patients showed high CD73 expression (CD73^{high}) and this was associated with older age ($p = 0.01$), gallbladder subsite ($p = 0.03$), and nodal involvement ($p = 0.04$). CD73^{high} tumours were significantly enriched in infiltrating FOXP3+ T lymphocytes ($p < 0.001$) and BTC cells genetically depleted for CD73 were more sensitive to killing by reactive T cells. Transcriptomically, CD73^{high} tumours were characterized by a distinct gene signature over-represented in EMT, TNF-alpha/NFkB, hypoxia and G2/M checkpoint signaling pathways. Clinically, CD73^{high} status was an independent predictor of poorer prognosis in multivariate analysis ($p = 0.03$) with ECOG PS ≥ 2 ($p = 0.001$) and the pathological stage ($p = 0.025$); consistently, the negative prognostic significance of CD73 was externally validated in transcriptome datasets of 436 resected BTC patients from three different cohorts globally (Dong et al., Jasakul et al., Nakamura et al.). Notably, CD73^{high} tumours derived lesser benefit from adjuvant chemotherapy: relapse-free survival was 12.69 vs 6.54 months in chemotreated and non-chemotreated patients, compared to not reached vs 14.37 months in CD73^{low} BTCs. In *in vitro* models, siRNA-mediated depletion and CRISPR-CAS9 gene KO of CD73 sensitized BTC 2D and 3D culture to cisplatin/gemcitabine treatment. Moreover, the pharmacological inhibition of CD73 by AMCP enhanced the sensitivity of BTC cell lines to cisplatin/gemcitabine treatment.

Conclusion: We demonstrated that CD73^{high} disease represent a distinct BTC subtype characterized by an aggressive biological phenotype, resistance to standard chemotherapy and poorer prognosis. Interestingly, we provided proof-of-concept evidence that targeted genetic or pharmacologic inhibition of CD73 enhanced chemotherapy efficacy in both 2D and 3D *in vitro* models of BTC. The clinical targeting of this adenosinergic ectonucleotidase hold promises of improving the efficacy of the recently-established chemo-immunotherapy standard-of-care in BTC.

THU-252

Human cytomegalovirus (HCMV) infection of macrophages induced abnormal development of cholangiocytes in an organoid co-culture model for biliary atresia

Syed Mushfiqur Rahaman¹, Allen KL Cheung², Kenneth KY Wong¹, Paul KH Tam³, Vincent CH Lui¹. ¹The University of Hong Kong, Surgery, Hong Kong, Hong Kong; ²Hong Kong Baptist University, Biology, Hong Kong, Hong Kong; ³Macau University of Science and Technology, Macao, Macao
Email: u3007446@connect.hku.hk

Background and aims: Biliary atresia (BA) is a devastating biliary disease of neonates, but its pathogenesis is unclear. Human cytomegalovirus (HCMV) has been implicated to contribute to BA development from clinical association without mechanistic evidence. Macrophages mediate innate immune responses against HCMV infection. This study addresses how the interactions between HCMV, macrophages and cholangiocytes (bile duct epithelial cells) contribute to BA.

Method: Human induced pluripotent stem cell (iPSC)-derived macrophages infected by HCMV (multiplicity of infection = 1.0) and then cleansed of free viruses were co-cultured with iPSC-derived cholangiocytes in 1:1 ratio. We performed morphological examination; expression analysis of genes relevant for viral propagation/immune responses/cholangiocyte development; single cell RNA-

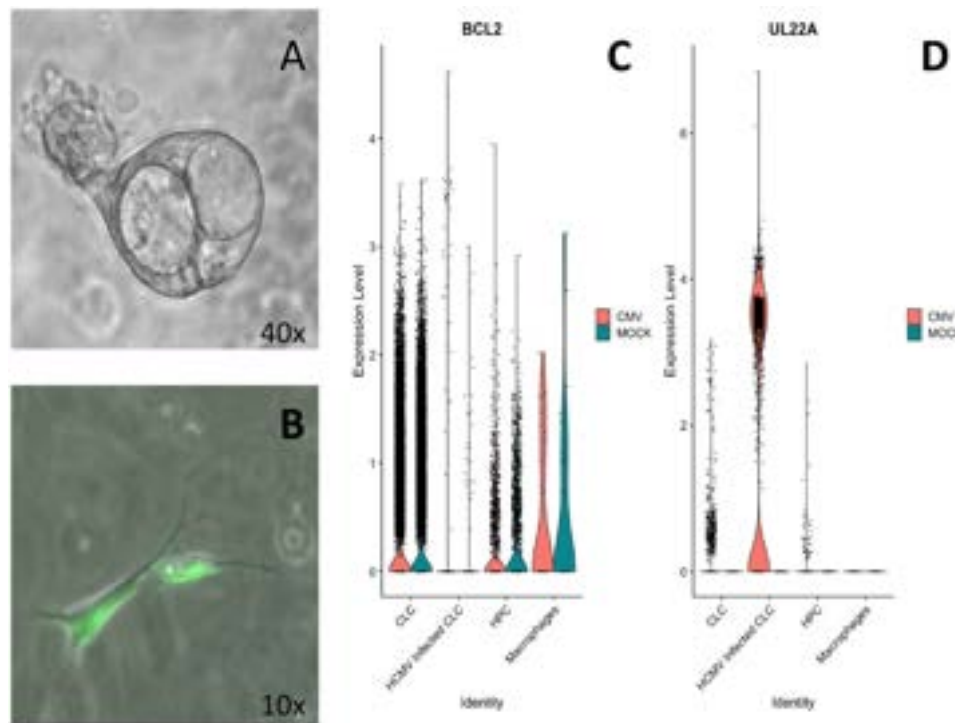


Figure: Microscopic and single cell view of the co-culture system. (A) Poorly expanded organoids with multiple vacuole morphology in the HCMV infected co-culture. (B) HCMV infected macrophages (green fluorescence) in the co-culture system. (C) Small cholangiocytes (BCL2-expressing) but not the large cholangiocytes (BCL2-non-expressing). (D) Viral gene UL22A was highly expressed in the large cholangiocytes. (CLC = Cholangiocyte like cell, HPC = Hepatic progenitor cell)

Figure: (abstract: THU-252).

sequencing (scRNA-seq) of infected and un-infected co-cultures at different post-infection days (PD).

Results: We detected expression of HCMV latent viral genes (UL138 and ULNA), elevated level of pro-inflammatory genes (IL-1 β , TNF- α , CD86) in PD5 infected co-cultures; deformed cholangiocyte organoids in PD7 infected co-cultures. Bioinformatics analysis of the scRNA-seq data on PD5 co-cultures revealed two clusters of cholangiocytes (BCL2-expressing small cholangiocytes and BCL2-non-expressing large cholangiocytes). Viral genes were highly expressed in the large cholangiocytes, suggesting that large cholangiocytes were susceptible to HCMV infection. Moreover, we detected downregulation of cholangiocyte markers (KRT19, KRT18, KRT7, KRT8, EPCAM), pro-apoptotic genes (BAX and CYCS), and pro-apoptotic pathways (MYC-target v1, oxidative phosphorylation and reactive oxygen species pathway) in HCMV-infected cholangiocytes.

Conclusion: Our data showed that (i) HCMV-infected macrophages could transfer the virus to the large cholangiocytes; (ii) HCMV-infected cholangiocytes exhibited dysregulated cholangiocyte development; (iii) HCMV-infection induced upregulation of pro-inflammatory genes. HCMV infection could cause abnormal development of bile duct epithelium, promote inflammatory responses in the liver and contribute to disease initiation/progression of BA.

THU-253

Bacterial vesicles associated virulence factors and epitope mimics in autoimmune hepatitis patients

Swati Thangariyal¹, Chhagan Bihari², Aakriti Jain³, Manish Kumar³, Guresh Kumar¹, Shiv Kumar Sarin⁴, Sukriti Sukriti¹. ¹Institute of Liver and Biliary Sciences, Molecular and Cellular Medicine, New Delhi, India; ²Institute of Liver and Biliary Sciences, Department of Pathology, New Delhi, India; ³University of Delhi, Department of Biophysics, New Delhi, India; ⁴Institute of Liver and Biliary Sciences, Department of Hepatology, New Delhi, India
Email: sukritibiochem@gmail.com

Background and aims: Autoimmune Hepatitis (AIH) is a self-perpetuating, non-resolving hepatic inflammation of unknown cause. Possible mechanism could be epitope mimicry, where antigen shares sequence similarity with self-antigens. We aim to investigate bacterial vesicles BV proteins associated with virulence factors, epitope mimicry, and their role in inducing autoimmune like condition.

Method: Fractionated pre-therapy plasma of AIH patients [n=61, biopsy proven, Hepatic Activity Index (HAI) score >2, ALT (148 \pm 58.4); AST (160.7 \pm 60.2)] and healthy controls (HC) n=30 for BVs using density gradient ultracentrifugation. Confirmed by transmission electron microscopy, western blot of OMP-A and nanoparticle tracking assay. The BV associated proteins were assessed by

POSTER PRESENTATIONS

proteomics, which was further mapped for virulence factors (VF) using VFDB database (mgc.ac.cn/VFs/main.htm) and epitope mimicry using miPrebase (proteininformatics.org/mkumar/mipepbase/) (database of experimentally verified mimicry peptides for both host and pathogen). Further, AIH and Healthy (HC) BV were adoptively transferred intravenously in C57BL/6J female mice. The biochemical, histological and molecular markers of hepatic injury were investigated. The immune cells infiltration was estimated in liver, spleen and whole blood using flow cytometry.

Results: Plasma BV were significantly higher in AIH patients than HC [10.5 vs 3.7; $p=0.003$, 87.7 vs 10.3; $p=0.015$]. Also, the AIH plasma BEVs progressively increase with increasing Histological Activity Index score [$r=0.62$; $p=0.001$], transaminases {ALT, AST [$r=0.59$; $p=0.001$, $r=0.57$; $p=0.001$]} and IgG antibodies [$r=0.37$; $p=0.018$]. Based on BV associated proteins identified by proteomics, upon VF mapping, we found 23% of proteins were associated with virulence factors mainly the elongation factors in AIH plasma, whereas 0% in HC-BV ($p=0.0009$). Depending on the number of residue and homologues sequences, miPrebase mapping identified an experimentally verified peptide sequence IYQIDNHQARKPIAD of methyltransferase family mimicking component of pyruvate dehydrogenase

complex of the host mitochondria. Next, upon AIH-BV administration in WT mice within 12 h, the liver enzymes, Liver weight index were elevated [AST ($p=0.0286$); ALT ($p=0.0452$); LI ($p=0.008$)] than HC-BV. The liver histology showed raised focal acute inflammation in AIH-BV than HC-BV ($p<0.001$) with significantly high infiltration of F4/80⁺ macrophages and Ly6G⁺ neutrophils in the liver ($p<0.001$).

Conclusion: Patients with AIH carry 23% of virulence factors in BV associated proteins and associated Methyltransferase family as the epitope of pyruvate dehydrogenase complex. Also, AIH-BV upon adoptive transfer in WT mice induce AIH-like systemic inflammation, suggesting a role of bacterial products carried through BVs in the pathogenesis of autoimmune hepatitis.

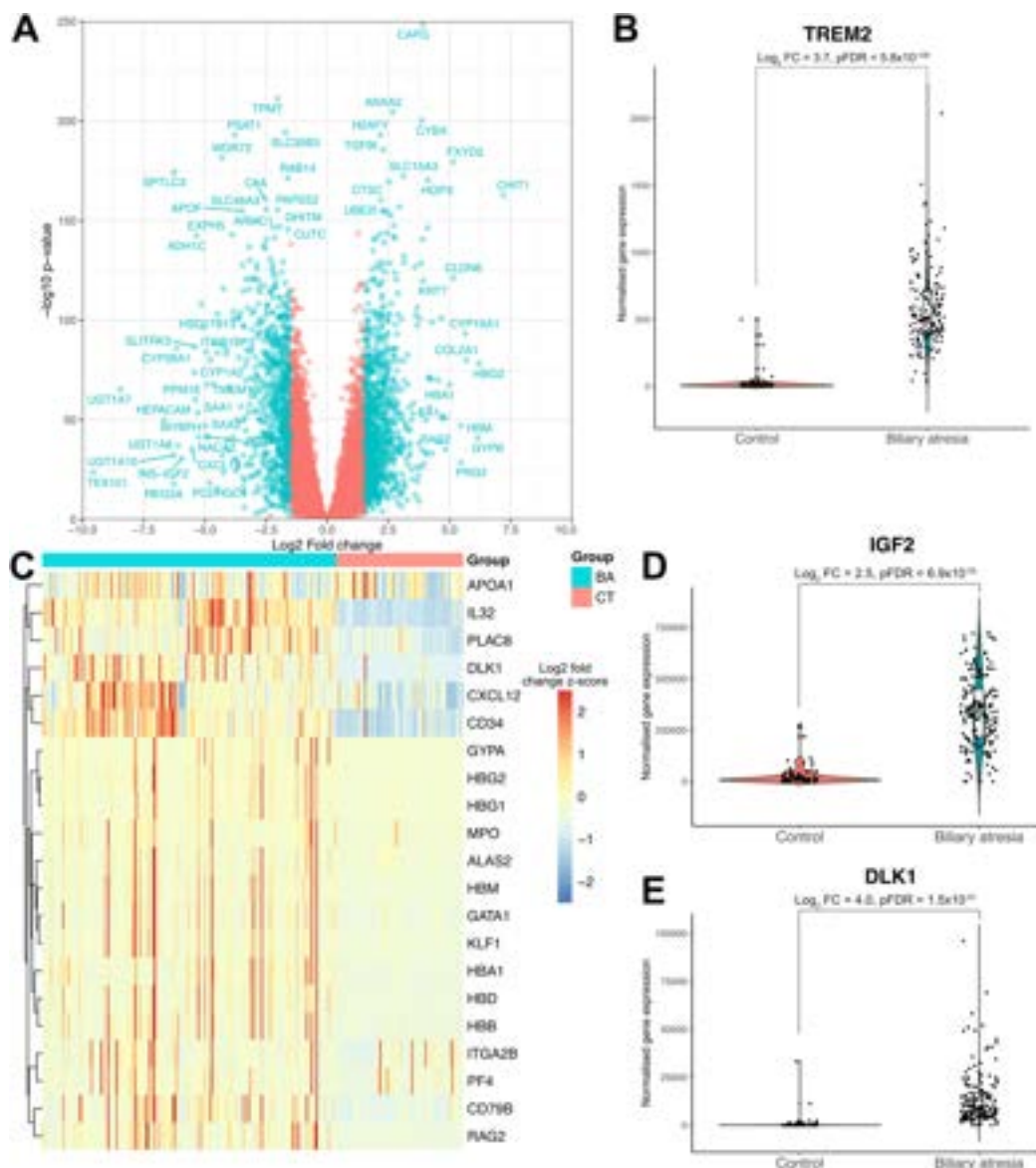
THU-254

Transcriptomic analysis of biliary atresia finds ongoing hepatic hematopoiesis with elevated IGF2

Jake Mann¹, Ye Htun Oo², Girish Gupte¹, Philip N Newsome².

¹Birmingham Children's Hospital, Liver Unit, Birmingham, United Kingdom; ²University of Birmingham, Centre for Liver Research, United Kingdom

Email: jpmann.gsy@gmail.com



Background and aims: Recent single-cell transcriptomic data has implicated foetal immune cells in the pathogenesis of biliary atresia (BA) with the role of immature B-cells in the postnatal liver particularly remaining unclear. To understand the mechanisms behind this, we performed a meta-analysis of RNA sequencing data from infants with BA at the time of Kasai and age-matched controls. Previous analyses had been limited by small numbers of controls; however, here, we have increased power to detect associations.

Method: We obtained transcriptomic data from $n = 177$ children with BA and $n = 78$ controls from Gene Expression Omnibus. After filtering and quality control, we performed differential gene expression analysis comparing BA versus control (using DESeq2), with p value adjustment for multiple testing.

Results: We identified 1,815 significantly differentially expressed genes (Fig. 1A). Many were involved in extracellular matrix remodelling/fibrosis (e.g. *CAPG*, *TGFBI*) and phagocytic activity (e.g. *CHIT1*, *CYBA*). We observed increased expression of *TREM2* (Fig. 1B), which is implicated in profibrogenic scar-associated macrophages in adults and has not previously been described in children. Patients with BA had increased expression of multiple markers of haematopoiesis, including erythroid lineage (e.g. *GYP*, *HBA1*) and early B-cell (e.g. *RAG2*) (Fig. 1C). We identified up-regulation of insulin-like growth factor 2 (*IGF2*, log2 fold change 2.5, $pFDR = 2.8 \times 10^{-40}$, Fig. 1D). *IGF2* is a growth factor for haematopoietic stem cells in the foetal liver. *IGF2* is secreted by hepatocyte progenitors and we observed upregulation of markers of these progenitors (e.g. *DLK1*, Fig. 1E).

Conclusion: Postnatal liver haematopoiesis is active in children with BA but not controls, and we speculate that interactions between haematopoietic and other immune cells may exacerbate intra-hepatic injury in BA. These data suggest that immature B cells production may be driven by *IGF2* secreted by hepatocyte progenitors. Future mechanistic studies exploring interaction of immature immune cells and extracellular matrix remodelling by macrophages will provide pathogenesis mechanism of biliary injury in biliary atresia.

THU-255

Immune cell incompetence and hepatocyte differentiation defects explain mild fibrosis in a model of Alagille syndrome

Jan Mašek^{1,2}, Iva Filipovic³, Simona Hankeova², Jingyan He², Noémi K. M. Van Hul², Lenka Belicova², Anna Maria Frontino¹, Markéta Jiroušková⁴, Daniel Oliveira¹, Fabio Turetti¹, Igor Cervenka², Lenka Sarnová⁴, Elisabeth Verboven², Tomáš Brabec¹, Niklas Björkström³, Martin Gregor⁴, Jan Dobeš¹, Emma Andersson².
¹Charles University, Department of Cell Biology, Prague, Czech Republic; ²Karolinska Institute, Stockholm, Sweden; ³Karolinska Institute, Department of Medicine Huddinge, Stockholm, Sweden; ⁴Institute of Molecular Genetics ASCR, Prague, Czech Republic
Email: jan.masek@natur.cuni.cz

Background and aims: Alagille syndrome (ALGS), caused by mutations in the Notch ligand *JAGGED1*, presents with cholestasis due to bile duct paucity. Remarkably few patients develop severe fibrosis or cancer, while recurring infections are common. Notch regulates liver and immune system development, but how these interact in ALGS is unknown. We aimed to determine whether *Jag1* regulates the immune system in a model of ALGS, and how this affects inflammation and liver disease progression.

Method: In a cancer-prone genetic background, fibrosis and liver cancer prevalence were analysed in *Jag1^{Ndr/Ndr}* mice, an ALGS mouse model. Liver cell populations were analysed using single-cell transcriptomics, and liver, thymus and spleen with flow cytometry. Immune cell function was tested using adoptive immune cell transplantation into *Rag1^{-/-}* mice, challenged with dextran sulphate sodium (DSS, ulcerative colitis model), 3,5-Diethoxycarbonyl-1,4-Dihydrocollidine (DDC, hepatocellular cholestasis) or bile duct ligation (BDL, biliary cholestasis).

Results: Forty-five percent of *Jag1^{+/-}* mice on C3H/57Bl6 background developed liver tumors, but no *Jag1^{Ndr/Ndr}* mice developed tumors. Instead, *Jag1^{Ndr/Ndr}* mice developed mild, ALGS-like, chicken-wire hepatocellular fibrosis, delayed hepatocyte differentiation with blunted cholestasis-induced inflammation, and decreased liver infiltration of CD4⁺ T cells. The splenic CD4⁺/CD8⁺ T cell ratio and Regulatory T-cell numbers were increased. Transplanted *Jag1^{Ndr/Ndr}* lymphocytes were less reactive in a model of ulcerative colitis, with reduced CD4⁺ and CD8⁺ T-cell activation. Finally, *Jag1^{Ndr/Ndr}* lymphocyte-transplanted *Rag1^{-/-}* mice subjected to BDL, but not DDC, displayed three-fold less periportal fibrosis than *Jag1^{+/-}* transplanted *Rag1^{-/-}* mice.

Conclusion: *Jag1* mutation results in delayed hepatocyte differentiation blunting inflammatory signaling. *Jag1* regulates immune cell development and competence, modifying the response to bacterial infection and cholestatic liver insult. The compromised immune response of thymocytes leads to milder-than-expected fibrosis. Our study shows that the immune system interacts with liver disease to modulate fibrosis, in an insult-specific manner, with implications for progression to liver cancer. The compromised immunocompetence further concurs with the reported frequent infections in patients with ALGS. Whether Notch-modulating agents could be utilized to fine-tune fibrosis and prevent liver cancer is thus a key question for future research.

THU-256

SARS-CoV-2 productively infects human hepatocytes and induces cell death

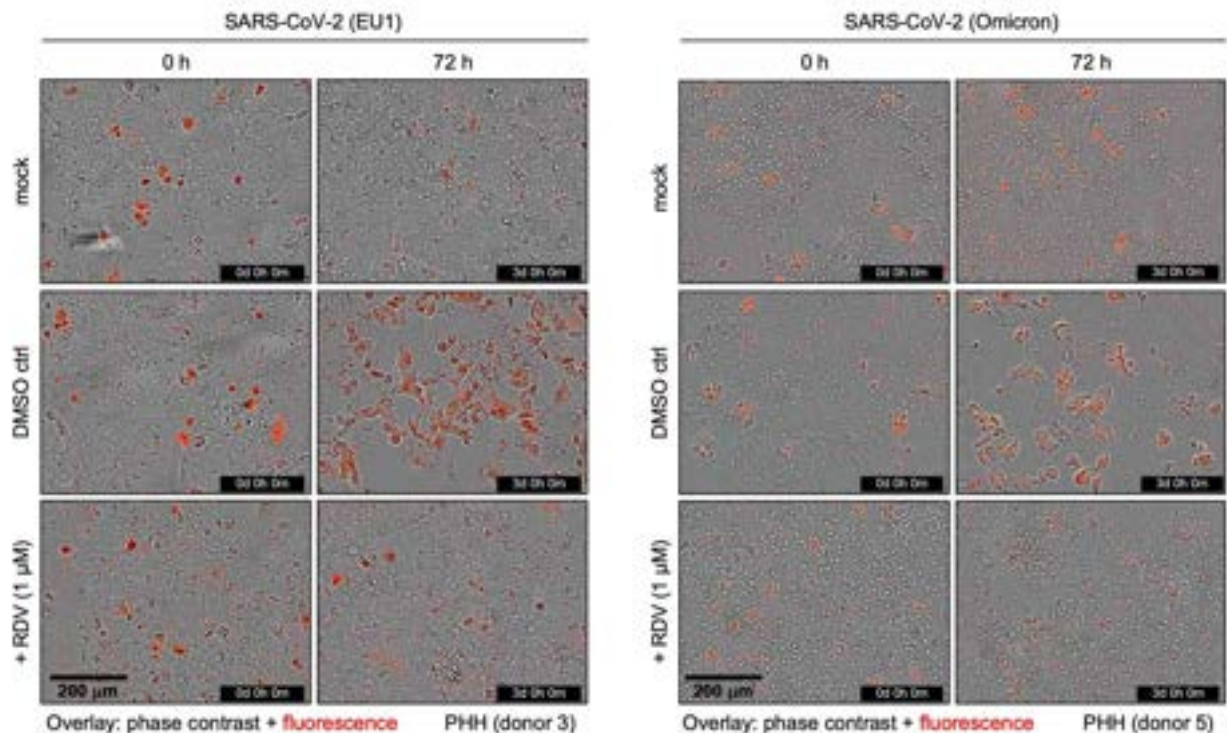
Cho-Chin Cheng¹, Chunkyu Ko^{1,2}, Shubhankar Ambike, Julia Sacherl¹, Stoyan Velkov¹, Bo-Hung Liao¹, Romina Bester¹, Merve Gültan¹, Constanze Jakwerth³, Carsten Schmidt-Weber^{3,4}, Joachim Bugert⁵, Roman Wölfe^{5,6}, Vincent Grass¹, Sandra Essbauer⁵, Oliver Keppler^{4,7}, Carolin Mogler⁸, Florian Vondran^{6,9}, Andreas Pichlmair^{1,6}, Ulrike Protzer^{1,6}.
¹Institute of Virology, Technical University of Munich, Munich, Germany; ²Infectious Diseases Therapeutic Research Center, Korea Research Institute of Chemical Technology, Korea, Rep. of South; ³Center of Allergy and Environment, Technical University of Munich, Germany; ⁴German Center for Lung Research, Germany; ⁵Department of Virology and Intracellular Agents, Bundeswehr Institute of Microbiology, Germany; ⁶German Centre for Infection Research, Germany; ⁷Max von Pettenkofer Institute and Gene Center, University of Munich, Germany; ⁸Institute of Pathology, Technical University of Munich, Germany; ⁹ReMediES, Hannover Medical School, Germany
Email: protzer@tum.de

Background and aims: Growing evidence suggests a liver tropism of SARS-CoV-2. However, it is unknown whether SARS-CoV-2 directly infects primary hepatocytes, how the virus enters the cell, and whether and to which extent the virus replicates and is cytopathic in hepatocytes. We therefore characterized the features of hepatic SARS-CoV-2 infection.

Method: We analyzed mRNA and protein expression of two major cellular entry factors of SARS-CoV-2, ACE2 and TMPRSS2, in primary human hepatocytes (PHH) and hepatoma cell lines and investigated permissiveness to SARS-CoV-2 and the capacity to replicate and spread the virus. Virus-induced cytopathic effect was monitored by real-time live-cell imaging.

Results: PHH and hepatoma cell lines express ACE2 and TMPRSS2, and their expression levels are comparable to those of lung-derived epithelial cells. Upon SARS-CoV-2 infection of hepatocytes with European lineage B.1.177 or Omicron sublineage BA.1, viral markers were readily detectable, whereas remdesivir treatment reduced viral load by 1.8–4.0 log₁₀, indicating productive replication. Knockdown of ACE2 or TMPRSS2 in hepatocytes impaired virus replication, corroborating the use of the canonical entry pathway exploited by SARS-CoV-2 in cells of the respiratory tract. Progeny viruses shed by infected hepatocytes showed the typical coronavirus morphology with “crown-like” appearance and induced plaques after secondary

A



B

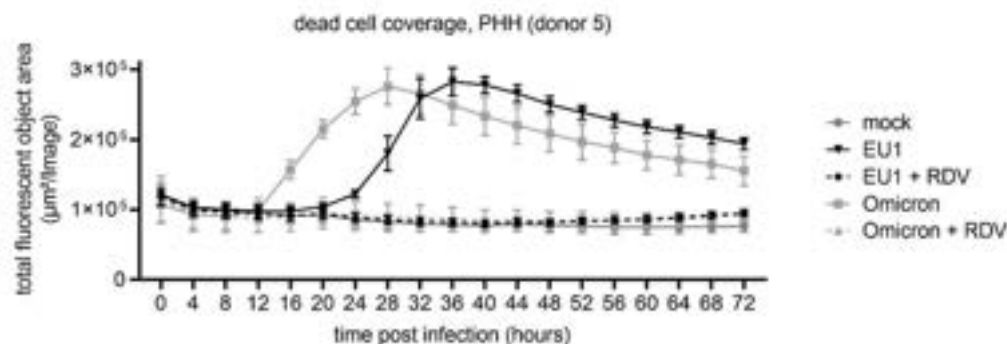


Figure: (abstract: THU-256).

infection, indicating that hepatocytes can support the complete SARS-CoV-2 replication cycle and may thus contribute to virus spread outside of the respiratory tract. Furthermore, SARS-CoV-2 infection of hepatocytes was cytopathic, suggesting that liver damage observed in COVID-19 patients may result from virus-induced cytotoxicity.

Conclusion: SARS-CoV-2 productively infects human hepatocytes via ACE2 and TMPRSS2 and induces hepatocyte death. Our findings help to explain hepatotropism of SARS-CoV-2 and liver damage observed in COVID-19 patients.

THU-257

Characterizing the role of human cytomegalovirus infection associated with biliary atresia

Zuodong Ye¹, Vincent CH Lui², Allen KL Cheung¹, ¹Hong Kong Baptist University, China; ²The University of Hong Kong, China
Email: akcheung@hkbu.edu.hk

Background and aims: Congenital Human cytomegalovirus (HCMV) infection cause a broad spectrum of neonatal diseases including biliary atresia (BA), which is the major cause of infantile obstructive jaundice. Although previous studies have implicated a correlation between HCMV and BA, the pathogenesis of HCMV associated BA remains poorly understood. This study aims to illustrate the intrinsic link between HCMV infection and BA and elucidate the molecular mechanism of HCMV-associated BA.

Method: Liver tissue with BA and non-BA (choledochal cysts [CC] and hepatoblastoma [HB]) were used to perform DNAscope assay to detect HCMV-DNA. Moreover, human induced pluripotent stem cell (iPSC)-derived cholangiocyte-like cells (CLC) organoids were used to establish a direct HCMV infection model to investigate the role of HCMV in the development of BA. Mock and HCMV-infected CLC organoids were used to examine morphological features, mode of virus infection and bulk RNA-seq analysis.

Results: A total of 49 human liver tissues (29 with BA and 20 with non-BA) were investigated for HCMV infection. Among them, 19 of BA (65.5%) and 7 of non-BA (35%) were HCMV-DNA positive. The infection of CLC organoids by HCMV strain TB40/E encoding enhanced green fluorescent protein (TB40/E-eGFP) resulted in reduced organoid growth and induced deformation. DNAScope data showed an overall higher presence of HCMV-DNA than GFP⁺ cells in infected CLC organoids. Very lower virions production in the supernatant of infected CLC organoids was observed. Bioinformatics analysis of the bulk RNA sequencing data showed that the differential expression genes (DEG) between mock and HCMV infected organoids are highly enriched in the epithelial-mesenchymal transition (EMT) pathway. qRT-PCR and immunostaining data verified that HCMV infection decreased the E-cadherin expression and increased N-cadherin expression. Moreover, HCMV infection induced upregulation of pro-inflammatory genes.

Conclusion: Our data showed that: (1) higher percentage of HCMV infection in BA patients than non-BA patients and HCMV infection is closely related to BA pathogenesis; (2) HCMV infection of CLC organoids exhibited low-level productive or persistent infection; (3) HCMV infection promoted the EMT process of CLC organoids. The persistence of HCMV infection likely induce inflammation and EMT that contribute to the development of BA.

THU-258

Rescue of PKU disease phenotype using hepatic progenitor by cytosine base editor and prime editor in vitro

Myounghoi Kim^{1,2}, Sung-Ah Hong³, Hayoon Kim^{1,2}, Elsy Soraya Salas Silva^{1,2}, Michael Adisasmita^{1,2}, Ji hyun Shin^{1,2}, Sangsu Bae⁴, Dongho Choi^{1,2}. ¹Hanyang University College of Medicine, Korea, Rep. of South; ²Hanyang University, Research Institute of Regenerative Medicine and Stem Cells, Korea, Rep. of South; ³Seoul National University College of Medicine, Genomic Medicine, Korea, Rep.

of South; ⁴Seoul National University College of Medicine, Department of Biomedical Sciences, Korea, Rep. of South
Email: crane87@hanyang.ac.kr

Background and aims: Phenylketonuria (PKU) is an autosomal recessive liver disease caused by point mutation. The PKU patient suffers from seizures, skin rashes, and a musty odor in the breath, skin, or urine due to highly accumulated L-phenylalanine (L-Phe) in the blood by the dysfunction of phenylalanine hydroxylase (Pah). Genome editors such as cytosine base editor (CBE) and prime editor (PE) promise great precise and safe editing of DNA. The CBE converts cytosine to thymine (C > T) using deaminase and the prime editor corrects multiple nucleotides (~80 bp) using reverse transcriptase. To overcome genetic-based PKU diseases, genome editors are powerful treatments option.

Method: Mouse primary hepatocytes (mPHs) were isolated from the PKU disease mouse model liver. To generate mouse chemically derived hepatic progenitors (mCdHs), the mPHs were cultured with a reprogramming medium for 7 days by Kim *et al* in 2019. The mCdHs were transfected with CRISPR-Cas9 and guide RNA (gRNA) plasmids by electroporation and performed sequencing of the *Pah* locus to validate the gene correction efficiency.

Results: We generated normal mCdHs (Pah^{+/+}, Wild-mCdHs) and disease mCdHs (Pah^{-/-}, Homo-mCdHs) to demonstrate the similar properties between them. Then, we transfected the editing tools into Homo-mCdHs and expanded them clonally to enhance the correction rate, demonstrating that the cytosine base editor (CBE) group increased the editing rate from 5.5% to 93%. Next, we used prime editor 3, PE3, and its modified version, PE5 to confirm the editing efficiency and showed a 5-fold increase in PE5 than PE3 (PE3, 1.8% to PE5, 10.7%) without clonal expansion. Finally, we analyzed the Tyr level in all hepatic differentiated groups (Wild-mCdH-Heps, Homo-mCdH-Heps, and Homo-edited-mCdH-Heps) and indicated

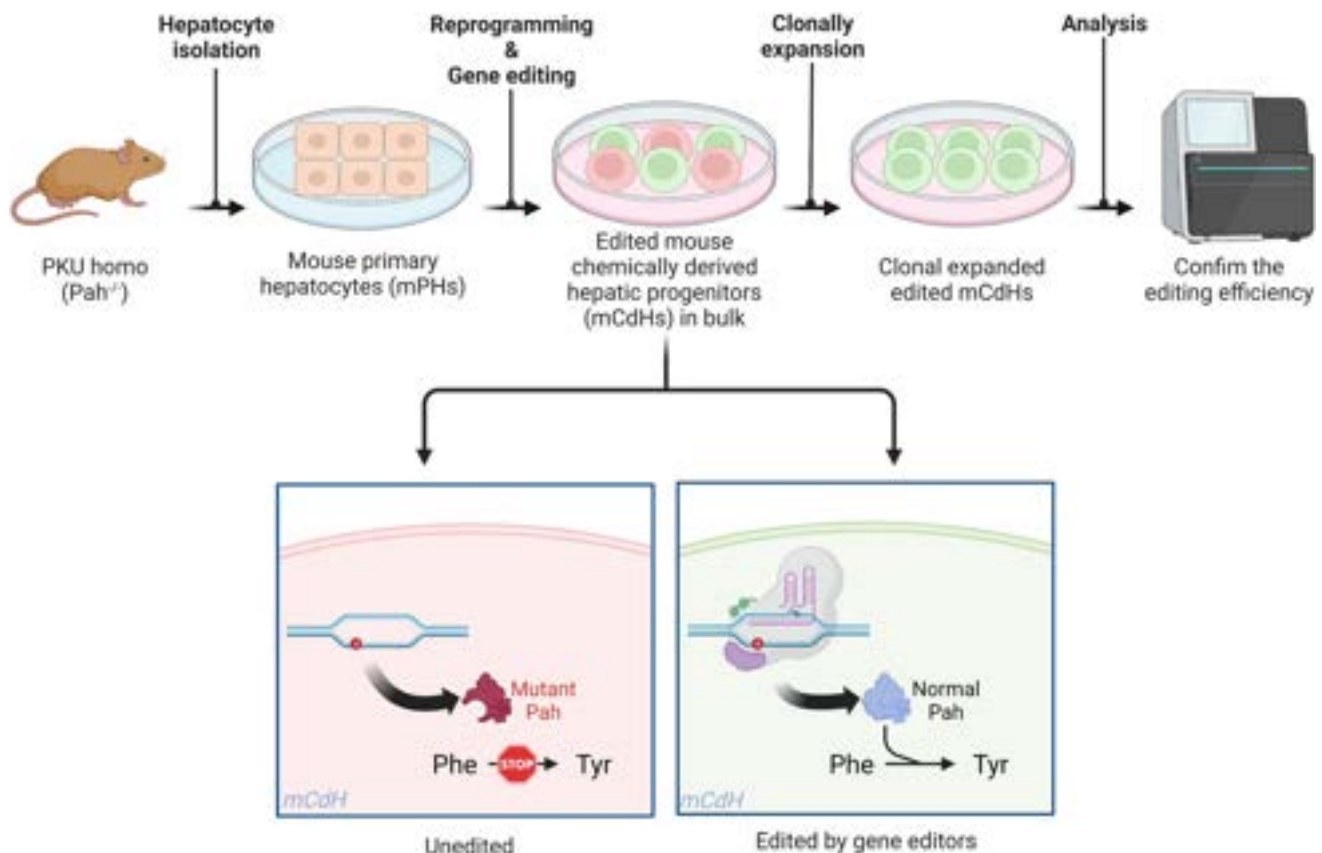


Figure: (abstract: THU-258).

POSTER PRESENTATIONS

increased Tyr level in the edited group indicating restoration of L-Phe metabolism.

Conclusion: These findings demonstrate an effective and safe gene editing system with high efficiency of gene correction and low frequency of insertion/deletion (indel) mutation for the rescue of PKU disease phenotype *in vitro*.

Supported by: This research is funded by grants from National Research Foundation of Korea (2021M3A9H3015390) and National Research Foundation of Korea (2022R1F1A1073058).

THU-259

ARBM-101 as an emerging potent therapeutic option for Wilson disease

Banu Akdogan¹, Eun-Jung Kim², Emilie Munk³, Dasol Kim², Judith Nagel⁴, Eok Park², Byong-Keol Min², Hongjae Lee², Dongsik Park², Chunwon Jung², Weonbin Im², So-Young Eun², Jeremy Semrau⁵, Alan DiSpirito⁶, Simon Hohenester⁷, Thomas Damgaard Sandahl³, Hans Zischka^{1,4}. ¹Helmholtz Munich, Germany; ²ArborMed Co. Ltd, Korea, Rep. of South; ³Aarhus University Hospital, Denmark; ⁴Technical University Munich, Germany; ⁵University of Michigan, United States; ⁶Iowa State University, United States; ⁷LMU Munich, Germany
Email: zischka@helmholtz-muenchen.de

Background and aims: Wilson disease (WD) is a rare genetic disorder manifested by acute or chronic liver dysfunction due to copper overload. WD is caused by failure of copper homeostasis in the liver due to disruptive mutations of a copper transporter, ATP7B. Current copper-chelating drugs in clinical use cannot promptly reduce liver copper levels to a normal physiological range. Besides unwanted drug reactions and non-adherence issues, the progression of liver disease is frequently inevitable due to copper toxicity, representing a highly unmet medical need. As previously introduced, methanobactins are natural, bacteria- originated, high-affinity copper chelators. Here we present our recent data on ARBM-101, also known as Methanobactin-SB2, demonstrating its superior therapeutic efficacy in WD rats, insights into its mode of action and its mobilization paths and studies on its unique safety profile at cellular and molecular levels.

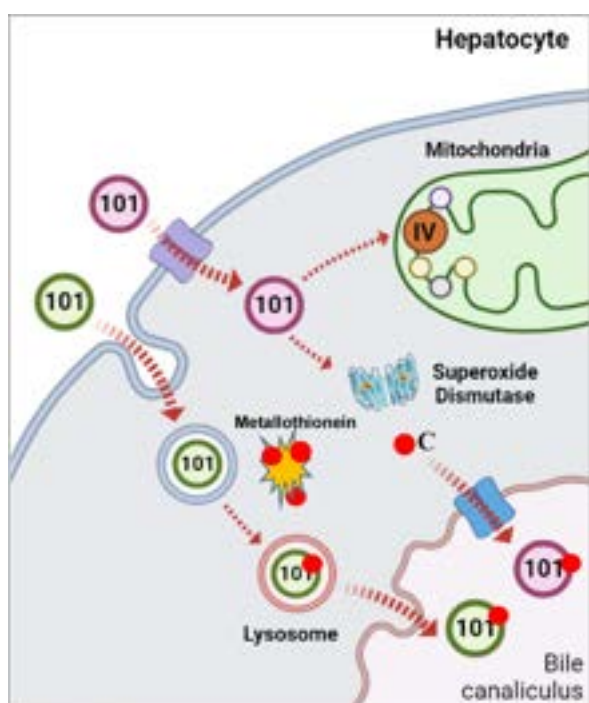


Figure: Potential hepatocyte mechanisms of ADME of ARBM-101.

Method: “LPP” (*Atp7b*^{-/-}) rats, an established WD model, were tested for rescue of severe liver damage by ARBM-101. We assessed animals’ body weight, faecal, urinary, and hepatic copper levels, as well as plasma levels of liver transaminases and bilirubin. Copper distribution, mobilization, and excretion patterns by ARBM101 were studied by PET-scans in live animals using ⁶⁴Cu. HepG2 cell lines with or without intact ATP7B were tested for impacts of ARBM-101 on copper-dependent enzymatic activities (e.g., SOD1). In the same cells, we investigated ADME of ARBM-101 using ARBM-101-specific monoclonal antibodies and quantified copper levels using ICP-MS.

Results: As recently introduced, ARBM-101 demonstrated its superior efficacy of reducing copper overload from WD rat livers. Its uniqueness is in its rapid removal of excess copper via biliary/fecal excretion accompanied by profound ameliorations in liver function. PET-scans further validated these results. *In vitro* cellular assay results, including enzyme activity assays, revealed a strong safety profile of ARBM-101 as well as providing first clues on its ADME.

Conclusion: Our data highlight an unprecedented therapeutic potential with a convincing safety profile of ARBM-101 as an emerging potent therapeutic option for WD.

THU-260

Novel pathogenic ABCC2 variants identified in patients with Dubin-Johnson syndrome and further functional evidence in abnormal bilirubin metabolism

Wenting Tan¹, Yunjie Dan¹, Xing Wan¹, Weiwei He¹, Josiah T. George¹, Yan Zhu¹, Xiaomei Xiang¹, Yi Zhou¹, Guohong Deng¹. ¹Department of Infectious Diseases, Southwest Hospital, Third Military Medical University, China
Email: gh_deng@hotmail.com

Background and aims: Dubin-Johnson syndrome (DJS) is an inherited disorder of bilirubin metabolism, characterized by conjugated hyperbilirubinemia, darkly pigmented liver and presence of brown pigment in hepatocytes due to defective bilirubin excretion into bile. This rare condition is caused by mutation in *ABCC2* gene which encodes the transmembrane protein MRP2 acting as a transporter in bilirubin metabolism. However, only a few pathogenic variants were identified. In this study, we aimed to investigate mutation spectrum and related functional explanation for this condition.

Method: An idiopathic jaundice cohort with 229 patients who visited our hospital between Oct 2017 to Sep 2022 were included in this study. We developed a targeted next-generation sequencing panel in which 43 disease-causing genes known to be associated with inherited metabolic liver disease were involved in, including those resulting in unconjugated (*UGT1A1* for Gilbert syndrome, Crigler-Najjar syndrome) and conjugated hyperbilirubinemia (*ABCC2* for DJS, *SLCO1B1* and *SLCO1B3* for Rotor syndrome). All patients applied this panel to explore relevant causing mutations and identify DJS patients as well as its mutation spectrum. Furthermore, we investigated how the *ABCC2* variants affect the function of MRP2 protein in terms of their production, location, and transport activities in HEK293T cells by construction MRP2 expression plasmids with candidate mutations.

Results: Among all patients, 11 cases were diagnosed as DJS (7 males) by biopsy and genetic test. The median age was 26 years (range 18–51 years). All of them had conjugated hyperbilirubinemia with a median DBIL level of 57.1 $\mu\text{mol/L}$ (32.2–119.0 $\mu\text{mol/L}$) and total serum bilirubin levels of 128.3 $\mu\text{mol/L}$ (64.8–170.2 $\mu\text{mol/L}$), meanwhile with normal liver enzyme, kidney and coagulation function. In accordance with the ACMG guidelines, we identified 12 pathogenic variants on *ABCC2*, as follows, of which 11 are novel including six frameshift variants which finally resulting protein translation termination (Y39fsX40, I452fsX11, A1413fsX49, S1417fsX13, E1462fsX7, I1512fsX11), two nonsense (Y1275X, R911X), three missense (V1419G, R393W, IT1489_1491GPGQ), and one previously reported pathogenic splice donor mutation (c.1815+2T>A). We

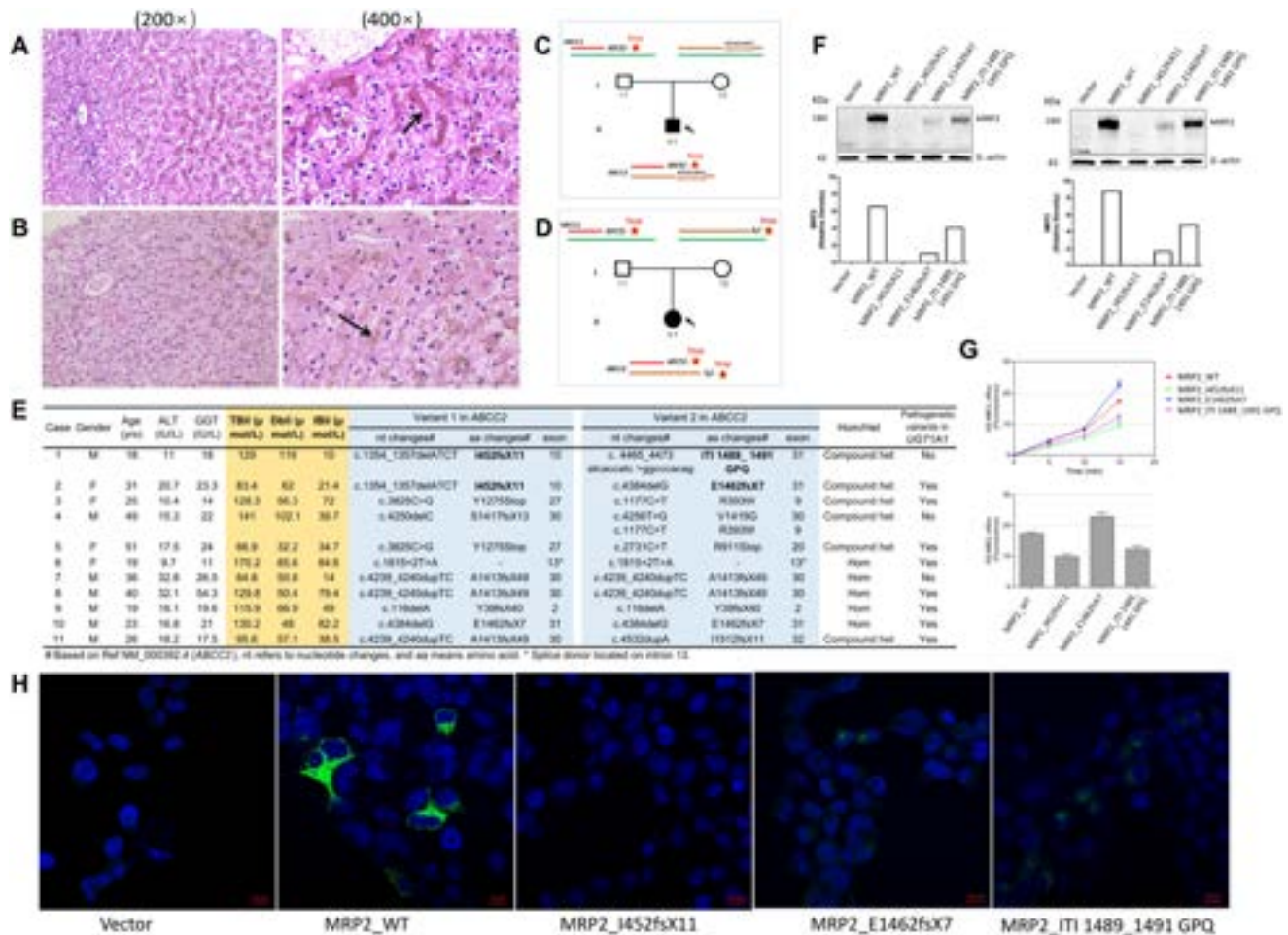


Figure 1. Novel pathogenic ABCG2 variants identified in patients with Dubin-Johnson syndrome and functional analysis. **A-B:** Liver biopsies stain for DJS Case 1 (A) and Case 2 (B), large amounts of pigment deposits found in the hepatocytes, and extensive intrahepatic cholestasis, no evidence of fibrosis was observed. **C-D:** Genogram and mutation patterns for DJS Case 1 (C) and Case 2 (D). Affected individuals are denoted by solid symbols. The mutations were inherited from father and mother respectively for both pedigrees. **E:** Summary of the basic characteristics and pathogenic variants detected in the 11 DJS patients. e.g., I452fsX11 indicates amino acid changed at 452 (Isoleucine, I) due to frameshift mutation and resulting translation termination after 11 amino acids shifting (stop at 453aa). **F:** Western blot analysis of mutant (I452fsX11, E1462fsX7 and ITI 1489_1491 GPQ) MRP2 expressed in HEK293 cells, showing decreased or none protein production. Loading 0.8 µg (left) and 1.6 µg (right) protein. **G:** Export of glutathione-conjugated monochlorobimane (GS-MCLB) by mutant MRP2 from HEK293 cells showing decreased transport activity. **H:** Indirect immunofluorescence for subcellular distribution of mutant MRP2 in HEK293 cells by confocal laser scanning microscopy.

Figure: (abstract: THU-260).

established HEK293 cell lines expressing the first three identified DJS-related variants. Compared to the wild-type, expressed E1462fsX7 and ITI 1489_1491GPQ MRP2 (both in nucleotide-binding domain) were mislocated and mainly retained in the endoplasmic reticulum, meanwhile led to a 50% decreased protein

production and 50% decreased transport activity, suggesting defective bilirubin excretion into bile in this condition. No MRP2 protein was expressed from HEK293 cells transfected with a 452fsX11 mutant (located at membrane-spanning domain), suggesting loss-of-function of transporting substrates like bilirubin. Additionally, 8 of

POSTER PRESENTATIONS

11 cases also presented known pathogenic mutations in *UGT1A1* gene, which suggested an explanation for their accompanying raised serum indirect bilirubin level.

Conclusion: We described here eleven novel pathogenetic *ABCC2* mutations in DJS. The functional analysis indicated that these mutations caused deficient maturation and dysfunction/loss-of-function of MRP2 protein in transport activity. These results expand on the spectrum of *ABCC2* mutations and provide further evidence that these mutations involved in the defective bilirubin excretion in DJS.

THU-261

Albumin levels are associated with portal hypertension in patients with porto sinusoidal vascular disorder

Lucia Lapenna¹, Simone Di Cola¹, Marco Mattana¹, Stefania Gioia¹, Manuela Merli¹. ¹Sapienza University Rome, Department of Translational and Precision Medicine, Italy
Email: lucia.lapenna@uniroma1.it

Background and aims: Porto sinusoidal vascular disorder (PSVD) is a term recently introduced to identify a group of patients with a rare vascular liver disease characterized by hepatic sinusoidal and portal venules lesions, with or without portal hypertension. Little is known about the natural history of these patients and why some patients will develop specific signs of portal hypertension and others will not. The aim of this study was to investigate differences between these two groups: patients with clinically significant portal hypertension (PSVD/PH+) and patients without it (PSVD/PH-).

Method: we retrospectively evaluate data from 32 patients actively followed at our department with diagnosis of PSVD according to VALDIG criteria. T-test and Fisher statistical analysis were performed.

Results: 32 patients were identified. Among them 21 patients were men (66%) and mean age at diagnosis was 43.9 years. Nineteen patients were PSVD/PH+ and showed specific and non-specific signs of portal hypertension at diagnosis (mainly esophageal or gastric varices (75%)). Thirteen patients were PSVD/PH- with no specific signs of portal hypertension. No significant histological differences were observed between the two groups. Albumin levels at diagnosis were normal in all patients as expected, but PSVD/PH+ patients showed significantly lower albumin level compared to those PSVD/PH- (3.65 vs 4.27, $p < 0.05$, respectively) (Table 1). During a median follow-up of 131 ± 64 months, 5 patients in the PSVD/PH- group developed clinically significant portal hypertension. Interestingly, basal albumin level in this sub-group were significantly lower compared to the sub-group of patients that did not develop portal hypertension (3.72 vs 4.43 $p < 0.05$) in the same time frame.

Table:

Characteristics	PSVD/ PH+ (19)	PSVD/ PH- (13)	p value
Sex (M) n (%)	13 (68)	8 (61)	0.72
Age (yrs)	46 ± 17	39 ± 11	0.23
• Histological lesions			
• Obliterative portal venopathy	4	4	0.68
• Incomplete septal fibrosis	6	2	0.41
• Nodular regenerative hyperplasia	5	2	0.67
• Portal tract abnormalities	17	11	0.99
• Perisinusoidal fibrosis	8	7	0.72
• Sinusoidal dilatation	10	10	0.26
Albumin at diagnosis (g/dl)	3.65 ± 0.45	4.27 ± 0.36	0.003

Conclusion: albumin level at diagnosis is associated with the presence of portal hypertension in PSVD patients, despite having the same histological lesions. Furthermore, it may predict which

patients are more likely to develop specific signs of portal hypertension during the natural history of the disease. Further prospective studies are needed in order to confirm this evidence and to be able to implement a prognostic model for this rare disease.

THU-262

Genetic modifiers of liver phenotypes in pediatric Wilson disease: liver biopsy and transient elastography based study

Marcin Krawczyk^{1,2}, Wojciech Janczyk³, Wiktor Smyk⁴, Diana Kamińska³, Piotr Milkiewicz⁵, Susanne N Weber¹, Wiesława Grajkowska⁶, Maciej Pronicki⁶, Piotr Socha³. ¹Department of Medicine II, Saarland University Medical Center, Saarland University, Homburg, Germany; ²Laboratory of Metabolic Liver Diseases, Medical University of Warsaw, Warsaw, Poland; ³Department of Gastroenterology, Hepatology and Nutrition Disorders, The Children's Memorial Health Institute, Warsaw, Poland; ⁴Department of Gastroenterology and Hepatology, Medical University of Gdansk, Gdansk, Poland; ⁵Liver and Internal Medicine Unit, Medical University of Warsaw, Warsaw, Poland; ⁶Department of Pathology, The Children's Memorial Health Institute, Warsaw, Poland
Email: marcin.krawczyk@uks.eu

Background and aims: Wilson disease (WD) is a rare, chronic liver disease caused by mutations in the *ATP7B* gene leading to impaired copper metabolism. The progression of WD varies among patients, but fatty liver is present in most cases. In the current study, we investigate potential genetic modifiers of liver disease progression in children with WD, including fatty liver-associated polymorphisms.

Method: Prospectively, we recruited 84 children (boys 50%, mean age 9 ± 5 years) with WD. There were eight pairs of siblings in this cohort, and one sib from each was randomly picked for further analysis. Liver function tests, including copper metabolism parameters, were measured before the initiation of the treatment. A liver biopsy was conducted in 59 children at diagnosis of WD. During the follow-up (median 3.6 years, range 6 months-10 years), a total of 46 patients underwent non-invasive assessment of liver stiffness measurement (LSM) and controlled attenuation parameter (CAP). Genotyping of the seven variants known to modulate liver injury (i.e., *PNPLA3* p.I148M, *TM6SF2* p.E167 K, *MTARC1* p.A165 T, *HSD17B13* rs72613567, *MBOAT7* p.G17E, *ABCB4* p.T175A and *ABCB4* c.711) was performed using TaqMan assays with fluorescence detection. Genotype frequencies in WD patients were compared to 313 adult controls without liver diseases.

Results: A total of 79% of patients displayed steatosis S1-S2 in liver biopsy; fibrosis F2-F4 was present in 75% of patients, whereas 5% had no fibrosis at baseline. At the follow-up, the median LSM was 5.3 (range 3.1-9.0) kPa and CAP was 248 (range 171-363) dB/m. Patients with steatosis S0, S1, S2 and S3 in liver biopsies presented with increasing median CAP at the follow-up, i.e., 218, 240, 255, and 266 dB/m, respectively. The *TM6SF2* p.E167 K polymorphism was more frequent in children with WD ($p = 0.035$) as compared to controls. Carriers of this variant presented with higher CAP at the follow-up despite receiving WD treatment ($p = 0.04$). The *PNPLA3* polymorphism was linked with a trend of increased risk of developing steatosis $\geq S2$ (OR = 2.40 $p = 0.06$) at baseline. Finally, carriers of the variants associated with protection against fatty liver, namely *HSD17B13* and *MTARC1*, had lower risk of microsteatosis at liver biopsy (OR = 0.34, $p = 0.02$), and presented with a lower CAP at follow-up ($p = 0.01$), respectively.

Conclusion: Common genetic polymorphisms can modulate the course of WD in pediatric patients. Since steatosis is frequent in pediatric WD and persists during follow-up, testing of these genetic variants might help stratify patients risk of disease progression.

THU-263

In vivo adenine base editing reverts C282Y in an HFE- mouse model and improves iron metabolism

Simon Krooss¹, Alice Rovai², Michael Ott¹. ¹Medizinische Hochschule Hannover, Gastroenterology, Hepatology and Endocrinology, Hannover, Germany; ²Medizinische Hochschule Hannover, Transfusion Medicine, Hannover, Germany
Email: krooss.simon@mh-hannover.de

Background and aims: Hereditary Hemochromatosis (HH) is one of the most common genetic diseases in the European population, with a prevalence of 1:200/400. Among the four different types, the most common form is Type 1, a homozygous p.C282Y mutation in the HFE gene, in which a guanosine is replaced by an adenine (c.845 G > A). This mutation results in the misfolding of the HFE protein, thereby losing its ability to work as a sensor for the iron content in the bloodstream. This can cause accumulation of iron in various organs, mostly in the liver, heart and pancreas, thus leading to the development of chronic diseases. Using adenine base editing, we aimed to correct this most common mutation *in vivo* in an HFE-mouse model.

Method: We have developed a precise and sensitive GFP-based reporter system to screen for potent adenine base editor gRNAs targeting the C282Y mutation in the HFE gene. Subsequently 129-Hfetm.1.1Nca mice were treated with an AAV8 split-vector coding for the adenine base editor ABE7.10 and a mutation-specific gRNA. After vector administration, animals were fed with iron-enriched chow and after 4 months, the experiment was terminated. Liver sections and blood parameters were analyzed for changes in iron-specific parameters.

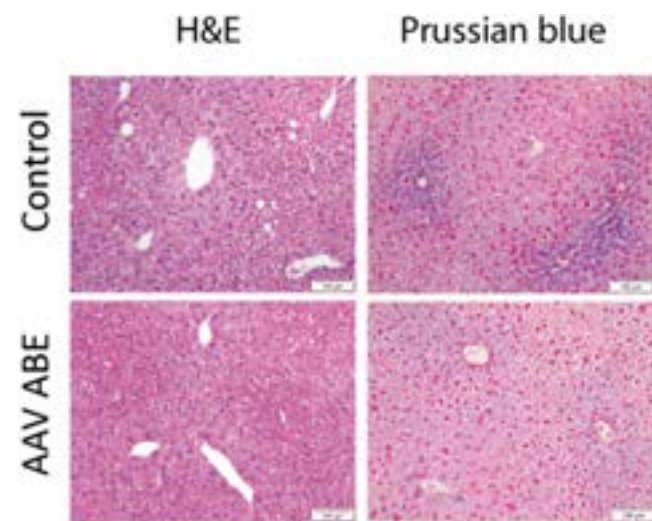


Figure 1: HandE and Prussian blue staining of liver sections obtained from 129-Hfetm.1.1Nca mice either untreated or treated by our AAV8-vector coding for the adenine base editor ABE7.10+gRNA.

Results: Upon a single low-dose (1×10^{11} vector genomes) injection of our therapeutic AAV8 vector, we achieved *in vivo* correction rates of $6.57 \pm 2.31\%$ and significant reduction of iron-specific parameters such as transferrin saturation, UIBC and hepcidin. Hepcidin expression of the treated animals was even comparable to healthy animals. Also on hepatic level, we observed significantly reduced iron accumulation detected via Prussian blue staining (Figure 1). After

administration of a high vector dose (1×10^{12} vector genomes), we achieved an *in vivo* editing efficiency of $10.65 \pm 1.24\%$ and further reduction of hepatic iron accumulation as measured via Prussian blue staining. In addition, using RNAseq analysis of isolated hepatocytes, we could observe the beneficial effect of our therapeutic vector in highly iron-overloaded HFE-mice on transcriptional level.

Conclusion: Both low- and high dose administration of our therapeutic adenine base editing vector led to physiological levels of hepcidin in the blood and significant reduction of hepatic iron overload. Therefore, we consider our therapeutic approach as an important proof-of-principle for future *in vivo* gene correction therapies for monogenic liver diseases.

THU-264

Alpha-1 antitrypsin inclusions sequester 78 kDa glucose-regulated protein in a bile-acid inducible manner

Igor Spivak¹, Nurdan Gueldiken¹, Valentyn Usachov¹, Lei Fu^{1,2}, Fa-Rong Mo¹, Gökce Kobazi Ensari¹, Franziska Hufnagel¹, Malin Fromme¹, Christian Preisinger¹, Pavel Strnad¹. ¹University Hospital RWTH Aachen, Aachen, Germany; ²Ruikang Hospital Affiliated to Guangxi University of Chinese Medicine, Nanning, China
Email: ispivak@ukaachen.de

Background and aims: The homozygous PiZ mutation (PiZZ genotype) is the predominant cause of severe alpha-1 antitrypsin (AAT) deficiency and leads to liver disease via the polymerization and accumulation of AAT in hepatocytes. To better understand this relationship, we systematically analyzed the composition of AAT aggregates in mice and humans. Since a subset of PiZZ subjects develops neonatal cholestasis, we investigated the impact of cholic acid (CA) challenge in PiZ mice, an animal model of PiZZ-associated liver disease.

Method: AAT inclusions were isolated from PiZ mouse and PiZZ human livers via fluorescence-activated and immunomagnetic sorting (FACS/MACS), while Triton X-insoluble proteins were obtained through high salt extraction. Wild-type (WT) mice and individuals without AAT mutation (PiMM genotype) served as controls. Inclusion composition was evaluated by mass spectrometry (MS), immunoblotting, and immunostaining. Mice were administered 2% CA-supplemented chow for seven days.

Results: In insoluble fractions from PiZ mouse livers, MS identified the endoplasmic reticulum chaperone 78 kDa glucose-regulated protein (GRP78) as the most prominent non-AAT protein. This finding was confirmed via immunoblotting of insoluble fractions and reproduced in FACS/MACS isolates (panel A). In PiZ mice, CA-feeding resulted in higher serum liver enzymes than in their WT littermates (AST: 390 ± 680 vs. 180 ± 185 U/l, $p < 0.05$; ALT: 480 ± 241 vs. 213 ± 82 U/l, $p < 0.01$; AP: 170 ± 20 vs. 100 ± 43 U/l, $p < 0.01$; panel B) and higher levels of apoptotic hepatocytes (3.3 ± 0.5 vs. 1.2 ± 0.3 cells/200x-field; $p < 0.01$). This was accompanied by stronger retention of GRP78 in the AAT inclusions of CA treated versus untreated PiZ mice ($32 \pm 12\%$ vs. $4.8 \pm 5.2\%$; $p < 0.05$; panel C) that was seen via immunoblotting and immunostaining, while the total AAT and GRP78 protein levels remained unaltered. The accumulation of GRP78 within AAT inclusions was confirmed in human PiZZ livers (panel D).

Conclusion: Our results demonstrate that GRP78 is a major constituent of AAT inclusions, and its increased retention after CA-feeding may promote cholestatic liver injury.

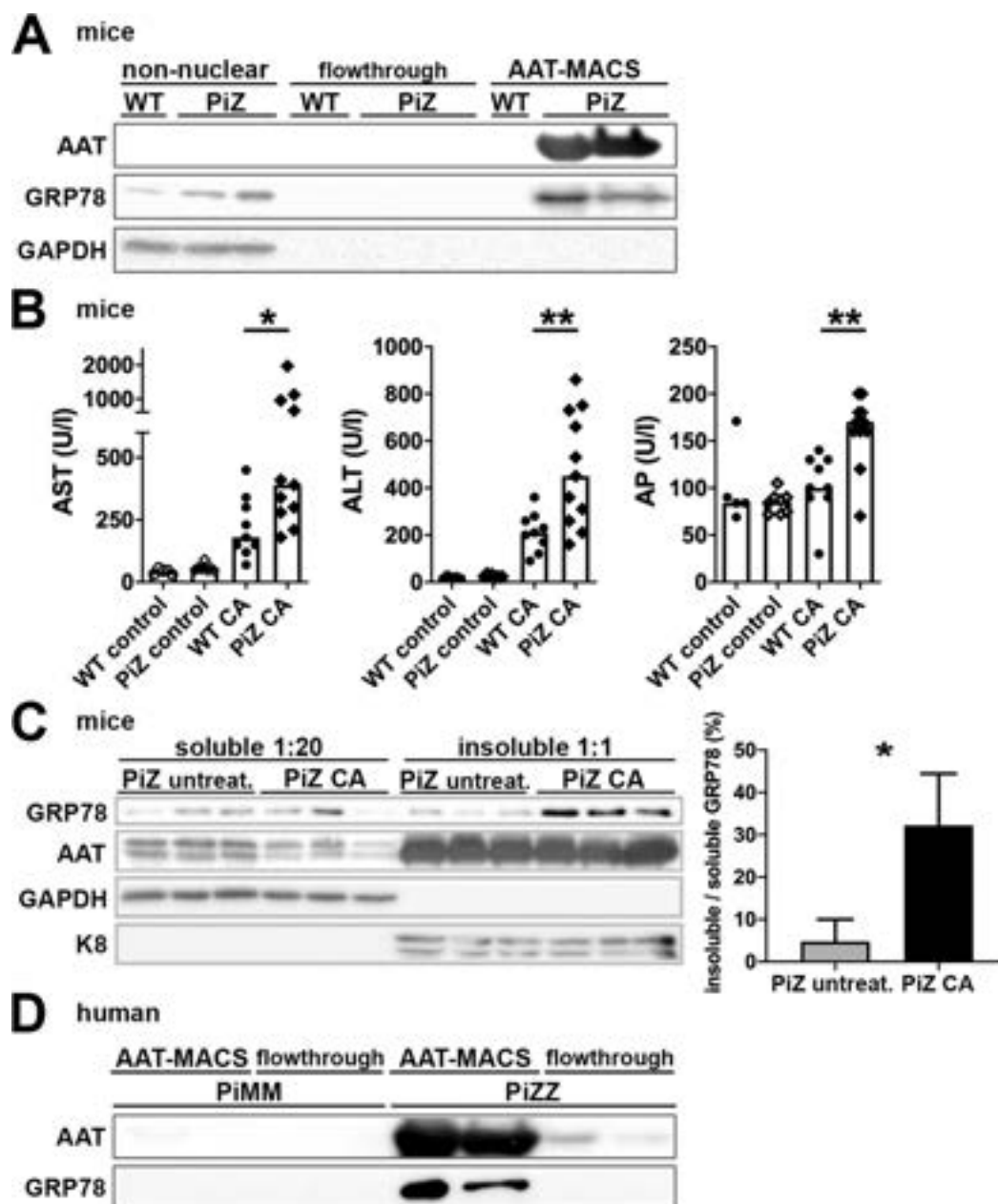


Figure: (abstract: THU-264).

THU-265

Human induced pluripotent stem cells-derived hepatocytes: a very effective tool for functional studies of rare liver diseases

Benedetta Blarasin^{1,2}, Valentina Tiricicco², Sara Maggiore^{1,2}, Eva Dariol^{1,2}, Gabriele Codotto^{1,2}, Claudio Tiribelli², Cristina Bellarosa². ¹University of Trieste, Department of Life Sciences, Italy; ²Fondazione Italiana Fegato-Italian Liver Foundation, Italy
Email: benedetta.blarasin@fegato.it

Background and aims: Among the models for the study of rare liver diseases, established cell lines and primary hepatocytes have numerous limitations, including short survival time, incomplete cell polarization, and invasiveness. Induced Pluripotent Stem Cells (iPSCs) represent an important resource since they can be obtained from the patient in a non-invasive way, expanded indefinitely, and differentiated into hepatocytes, carrying the individual-specific

genetic background. Moreover, iPSCs obtained from healthy donors are an ideal tool since they can be genetically modified using CRISPR-Cas9 technology, introducing specific disease-related mutations before differentiation into hepatocytes. This study aims to obtain human-derived, polarized, and genetically modifiable hepatocytes to study the molecular mechanisms and perform drug screening for rare hepatic diseases.

Method: iPSC-derived human hepatocytes were obtained from urine samples as described by Zhou (Nat Protoc, 2012, doi: 10.1038/nprot.2012.115) and Matakovic (Methods Mol Biol 2022, doi: 10.1007/978-1-0716-2557-6_4.). Urine was collected from healthy donors, children, and adults of both sexes. Exfoliated renal epithelial cells (i.e. urinary cells) were isolated from the specimen and characterized both morphologically and by RT-qPCR. Urinary cells were de-differentiated through lentiviral vector transduction containing the

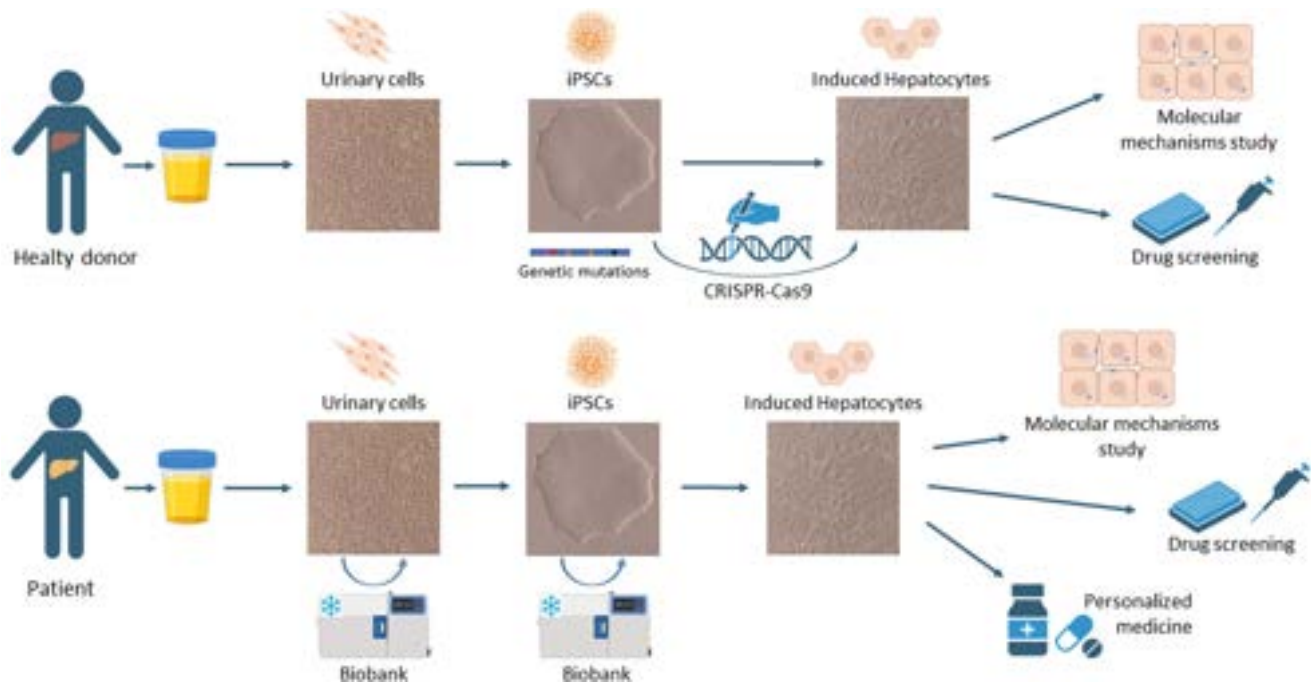


Figure: (abstract: THU-265).

four Yamanaka factors, maintained in culture until iPSC colonies appeared and characterized by RT-qPCR. Differentiation of iPSCs was obtained by sequential changing of culture mediums enriched with specific molecules and growth factors involved in the differentiation process (definitive endoderm, hepatic progenitors, and induced hepatocytes).

Results: Urinary cells m-RNA quantitative PCR analyses confirmed the positive expression of epithelial genes (claudin, E-cadherin) and renal tubular genes (L1CAM, NR3C2) together with the absence of fibroblast gene expression (SLUG). The cells showed to be resistant, enduring without problems with both passaging and thawing. Urinary cells de-differentiated into iPSCs presented the expression of embryonic genes (h-ERT, NANOG and LIN-28). iPSCs showed an unlimited replication potential and sustained repeated freezing and thawing cycles with success. The differentiation of iPSCs to definitive endoderm, hepatic progenitors, and induced hepatocytes was followed morphologically.

Conclusion: We obtained induced hepatocytes from urine-derived iPSC. This model will be used to insert specific disease-related mutations, to study the molecular mechanism of the disease, and to evaluate suitable treatments on iPSC -derived hepatocytes. Urinary cells and iPSCs could be used to establish a biobank. Unfortunately, the entire procedure requires a long time to be performed (2–3 months).

THU-266

Ancillary diagnostic biomarkers in autoimmune hepatitis

Chhagan Bihari¹, S Muralikrishna Shasthry¹, Shabir Hussain¹, Archana Rastogi¹, Shiv Kumar Sarin¹. ¹Institute of Liver and Biliary Sciences, Delhi, India
Email: drcbsharma@gmail.com

Background and aims: There are no specific tests for the diagnosis of autoimmune hepatitis, and it also has overlapping histological features with other conditions like primary biliary cholangitis (PBC), acute hepatitis (AH), drug-induced liver injury (DILI), and

chronic hepatitis (CH). We aimed to identify the circulatory and histological repertoires that can serve as auxiliary tests for autoimmune hepatitis.

Method: Serum samples from age and gender matched treatment naïve histologically confirmed cases of autoimmune hepatitis (PBC, AH, DILI, CH, and healthy control, n=10 each) were subjected to label-free proteomics analysis as a derivation phase. Uniquely expressed proteins in AIH were validated on age and gender matched different subsets of AIH, AH, DILI, CH (N=50 each), and PBC (n=26) by ELISA on serum samples and immunohistochemistry (IHC) on liver biopsies. These proteins were also assessed in seropositive and seronegative cases of AIH, and with the disease activity.

Results: In the initial analysis of autoimmune hepatitis as compared to disease and healthy controls, there were 41 differential proteins compared to CH, 28 compared to PBC, 86 compared to healthy controls, 37 to DILI, and 24 to acute hepatitis. After comparing all the groups, 5 uniquely different protein molecules were identified {afamin, epididymis tissue protein Li-173, gelsolin, vitronectin, and interferon alpha inhibitor Ig delta fc region (IGHD)}. On validation, serum samples of afamin, gelsolin, epididymal tissue protein Li-173, and vitronectin were high in AIH cases, whereas IGHD was lowest in AIH cases as compared to other groups (Fig 1A). Seropositive AIH cases (ANA+, ASMA+) had significant elevation of these proteins than seronegative AIH (Fig 1B) except IGHD, where it was lower in seropositive cases. On tissue IHC the expression of afamin, epididymal tissue protein, gelsolin, and vitronectin was most significant in AIH (Fig. 1C). In autoimmune hepatitis cases, serum levels of epididymis tissue protein and gelsolin correlated with histological activity index (HAI) ($r = 0.721$ and 0.616 , $p < 0.001$), respectively.

Conclusion: Afamin, Epididymis tissue protein Li-173, Gelsolin, Vitronectin and IGHD can be used as non-invasive auxiliary biomarkers for the diagnosis and severity of autoimmune hepatitis.

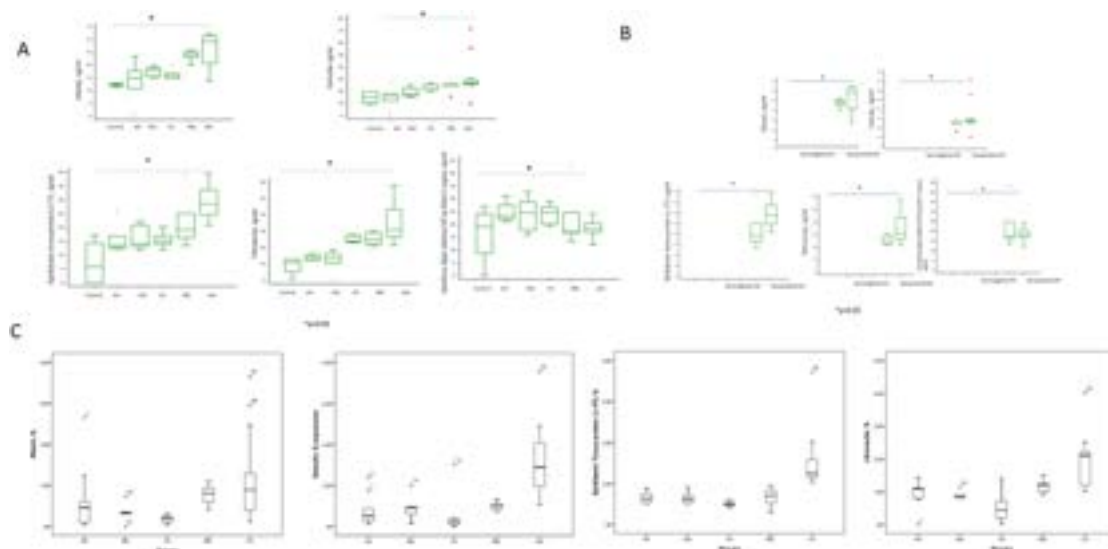


Figure: (abstract: THU-266): A: Serum levels of Afamin, Gelsolin, Epididymis tissue protein Li-173, vitronectin, interferon alpha inhibitor Ig delta fc region (IGHD) among the groups {acute hepatitis (AH), drug induced liver injury (DILI), chronic hepatitis (CH), primary biliary cholangitis (PBC) and autoimmune hepatitis (AIH). B Five protein levels in the serum of AIH based on seronegativity and seropositivity. C. Liver tissue expression of Afamin, Gelsolin, Epididymis tissue protein Li-173, vitronectin in AH, DILI, CH, PBC and AIH.

THU-267

Identification of correctors for traffic-defective ABCB4 variants by a high-throughput screening approach

Mounia Lakli¹, Julie Dumont-Ryckembusch², Veronica Crespi³, Julie Charton², Virginie Vauthier⁴, Amel Ben Saad¹, Elodie Mareux¹, Manon Banet¹, Martine Lapalus¹, Emmanuel Gonzalès¹, Emmanuel Jacquemin¹, Florent Di Meo³, Benoit Deprez², Florence Leroux², Thomas Falguières¹. ¹Université Paris-Saclay, UMR_S 1193 Inserm-Physiopathogenesis and Treatment of Liver Diseases, ORSAY, France; ²Institut Pasteur de Lille, U1177 Inserm, University of Lille-Drugs and Molecules for Living Systems, Lille, France; ³U1248 Pharmacology and Transplantation-Ω-Health Institute, Centre de Biologie et de Recherche en Santé-Université de Limoges, Limoges, France; ⁴Sorbonne Université, Saint-Antoine Research Center, UMR_S 938 Inserm, Paris, France
Email: thomas.falguières@inserm.fr

Background and aims: The ABCB4 (ATP-binding cassette subfamily B member 4) transporter, also known as multidrug resistance protein 3 (MDR3), is a transmembrane protein located at the canalicular membrane of hepatocytes and it ensures the secretion of phosphatidylcholine into bile canaliculi. Phosphatidylcholine is a fundamental component of bile. Through the formation of mixed micelles, it allows the solubilization of cholesterol and the protection of the biliary epithelium from the detergent action of bile salts. Many missense variations in the ABCB4 gene cause several rare cholestatic diseases, the most severe one being progressive familial intrahepatic cholestasis type 3 (PFIC3), which appears during the first years of life and can evolve into cirrhosis and liver failure before adulthood. To date, more than 50% of patients do not respond to conventional treatments, making liver transplantation the ultimate alternative therapy. Thus, this research project is dedicated to characterize and validate new pharmacological correctors first identified by a high-throughput screening approach for traffic-defective ABCB4 variants. **Method:** Six compounds identified by high-throughput screening (CPD-1, 2, 3, 4, 5 and 6) were tested *in vitro* for their capacity to rescue: i) ABCB4 maturation, studied by immunoblot; ii) localization of the transporter at the plasma membrane, analyzed by indirect immunofluorescence; iii) phosphatidylcholine secretion activity, studied by a fluoro-enzymatic assay, of the endoplasmic reticulum-retained ABCB4-I541F, -L556R and -I490T variants. These variants and

ABCB4-WT (wild type) were expressed in HEK293 and HepG2 cell models, treated or not with the drug candidates.

Results: In cell models, only CPD-1, -2, and -3 were able to rescue the maturation and canalicular localization of the I541F and L556R traffic defective ABCB4 variants, while no significant effect was observed on the I490T variant. The functional tests showed a partial but significant rescue of the function of ABCB4-I541F and -L556R variants with only one of these molecules (CPD-3). Moreover, these drug candidates inhibit ABCB4-WT activity at different levels. Dose-response analyses were subsequently performed with the three correctors of interest to find a compromise between correction of ABCB4 traffic and inhibition of the secretory function using lower drugs concentrations. These analyses allowed us to decrease the inhibitory effect of the drugs and partially rescue the function of ABCB4-I541F with CPD-2.

Conclusion: Our results allowed us to validate, on the one hand, three pharmacological correctors of the maturation and canalicular localization of ABCB4-I541F and -L556R variants. On the other hand, these three correctors seem to have a variant-specific effect since they do not significantly rescue ABCB4-I490T traffic. Moreover, these molecules inhibit ABCB4-WT function at different levels. These results might be explained by the direct interaction of these molecules with ABCB4 key functional residues during the protein folding process. However, we were able to compass the inhibitory effect by lowering drug concentration in treated cells, and thus partially rescue the function of ABCB4-I541F and -L556R variants. This study opens the path to chemical optimization of these molecules to increase their benefit/inhibition ratio and further considering their validation in preclinical models.

THU-268

Schistosoma mansoni infection-associated oxidative stress triggers hepatocellular proliferation

Verena von Buelow¹, Nicola Buss², Jakob Lichtenberger², Lukas Härle², Christoph G. Greveling³, Martin Roderfeld², Elke Roeb². ¹Department of Gastroenterology, Justus Liebig University Giessen, Giessen, Germany; ²Department of Gastroenterology, Justus Liebig University Giessen, Giessen, Germany; ³Institute for Parasitology, Justus Liebig University Giessen, Giessen, Germany
Email: verena.von-buelow@innere.med.uni-giessen.de

Background and aims: Schistosomiasis is one of the most common parasitic infections of humans worldwide. The eggs of *Schistosoma mansoni* induce chronic granulomatous liver inflammation. Recent data from animal models and cell culture experiments suggest that this parasite may predispose patients for hepatocellular carcinoma (HCC). Therefore, we analysed whether *S. mansoni* infection-induced oxidative stress provokes hepatocellular replicative stress in a hamster infection model.

Method: Female hamsters (n = 5) were infected either with male and female cercariae of *S. mansoni* (bisex, bs; producing eggs) or cercariae of one gender (monosex sex, ms; no eggs produced) or non-infected (control). Hepatocellular markers for proliferation, DNA repair, oxidative stress, and cell cycle control were analyzed by qRT-PCR, western blotting and immunohistochemistry. The mechanistic interaction of the forementioned cellular processes were analyzed by gain and loss of function experiments in human hepatoma cells (HepG2) and proliferation was determined by a Bromodesoxyuridin (BrdU)-Assay.

Results: The hepatic expression of Minichromosome maintenance 7 (Mcm7)-mRNA was significantly increased in bs-infected hamsters compared to ms- or non-infected hamsters suggesting the involvement of schistosome eggs. Moreover, in vitro treatment of HepG2 cells with soluble egg antigens (SEA) led to an increase of Mcm7-mRNA. We next investigated hepatic Cyclin D1, required for cell cycle G1/S transition and PCNA, which is central to both DNA replication and repair. Both Cyclin D1 and DNA polymerase processivity factor

proliferating cell nuclear antigen (PCNA) were elevated on the protein level in livers of bs-infected hamsters. The addition of GSH diminished SEA-induced Cyclin D1 and PCNA to control levels. p-H2AX, a marker for DNA damage and the proliferation marker Ki67 were colocalized in nuclei of perigranulomatous hepatocytes. SEA-induced proliferation was diminished by the reactive oxygen species (ROS) scavenger GSH.

Conclusion: Recently, *S. mansoni* infection has been discussed as a predisposition for HCC. We demonstrate that *S. mansoni* infection, and in particular schistosome egg antigens, not only disturb the DNA replication but also induce aberrant cell cycle regulation and proliferation by hepatocellular oxidative stress. Our results explain at least partially how *S. mansoni* infection promotes the development of HCC.

THU-269

Biliary atresia human cholangiocyte organoids demonstrate increased oxidative stress response

Yara Hamody¹, Adi Har-Zahav², Keren danan³, Raanan Shamir², Irit Gat-Viks³, Orith Waisbourd-Zinman². ¹Tel aviv universty, Schneider Children's Medical Center of Israel, Petach Tikva, Israel, Israel; ²Schneider Children's Medical Center of Israel, Petach Tikva, Israel, Israel; ³Tel aviv universty, Israel
Email: yarahamody@gmail.com

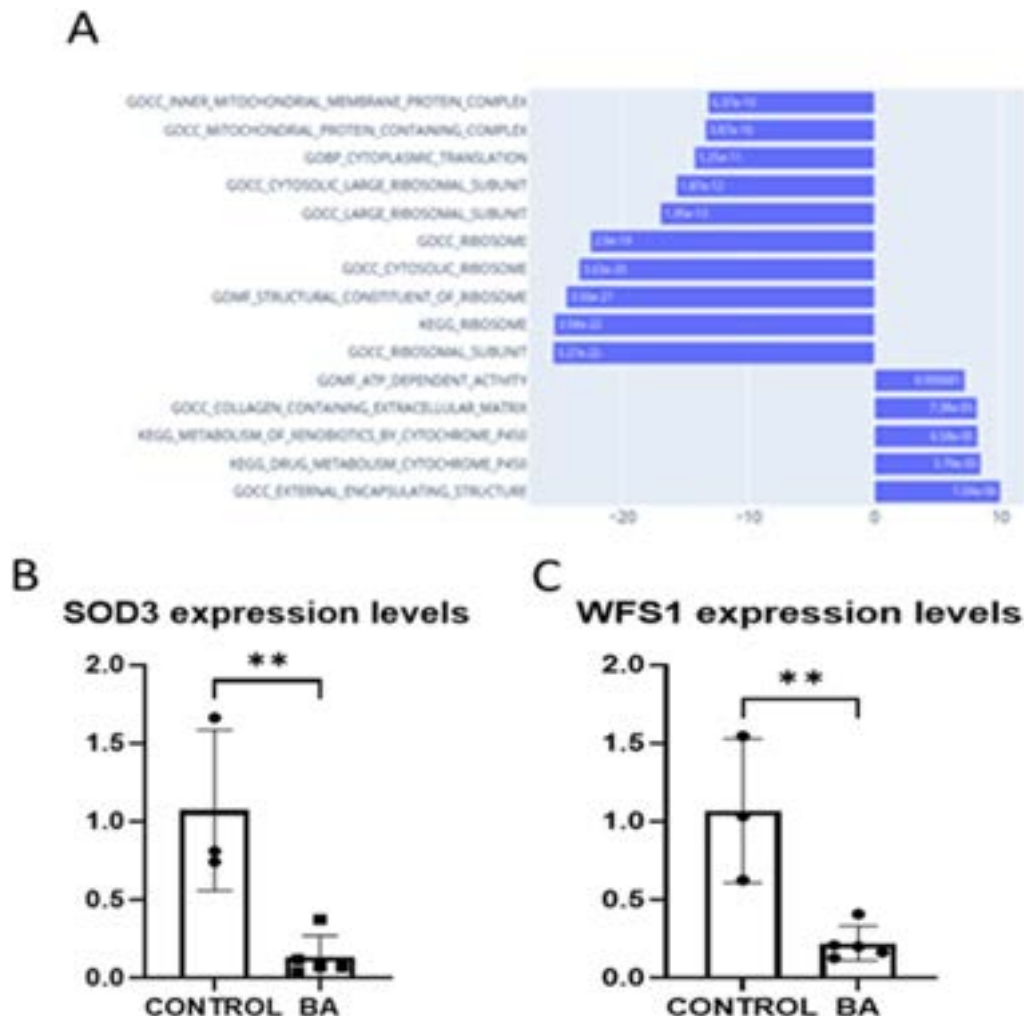


Figure: (abstract: THU-269).

POSTER PRESENTATIONS

Background and aims: Biliary atresia (BA) is a form of biliary fibrosis typically diagnosed in previously healthy newborns before the age of 3 months, with extrahepatic bile duct obstruction and progressive liver fibrosis. The etiology of the disease is unknown. Here we aimed to identify the pathophysiology of the primary cholangiocyte injury in human BA and the potential for recovery, using bulk and single cell gene expression data from different BA patients.

Method: We cultured human cholangiocyte organoids (HCOs) derived from BA patients and non-BA controls, in order to identify pathways involved with BA cholangiocyte injury. Differentially expressed pathways were further studied using qPCR and western blotting in a candidate gene approach.

Results: BA derived HCOs display deformed shape and lumen obstruction. RNA sequencing results identified differentially expressed genes in BA HCOs involved in several biological pathways, including endoplasmic reticulum (ER) stress, unfolded protein response, generation of reactive oxygen species, and drug metabolism (Figure 1A). The results were validated at the RNA and protein levels. We used RT-PCR to compare differences in gene expression-related ER stress between BA patients and non-BA controls. Superoxide dismutase 3 (SOD3) is an extracellular antioxidant defense against oxidative damage, which deficiency induced spontaneous liver injury and fibrosis. SOD3 was downregulated by 7 fold ($p = 0.0067$) in BA patients compared to control (Figure 1B). WFS1 is a component of the IRE1 and PERK signaling pathways which Negatively regulates the ER stress response, was downregulated by 5 fold ($p = 0.0062$) in BA patients compared to control (Figure 1C).

Conclusion: BA derived HCOs are characterized by ER stress and unfolded protein response, which may be result in dysfunctional cell-to-cell adhesion. These findings shed light on mechanisms of injury in BA and may contribute to the discovery of potential therapies.

THU-270

Clinical characteristics and pathogenic mechanism of five new ABCB4 missense mutations in progressive familial intrahepatic cholestasis type 3

Yuhang Weng^{1,2,2}, Yufeng Zheng¹, Dandan Yin¹, Qingfang Xiong¹, Wei Chen¹, Jinlong Li¹, Yongfeng Yang¹. ¹The Second Hospital of Nanjing, Affiliated to Nanjing University of Chinese Medicine, China; ²The Second Hospital of Nanjing, Affiliated to Nanjing University of Chinese Medicine, Department of Hepatology, China
Email: yyf1997@163.com

Background and aims: This study analyzed five new missense variants associated with progressive familial intrahepatic cholestasis type 3 (PFIC-3).

Method: We recruited seven PFIC-3 patients and studied five ABCB4 [adenosine triphosphate (ATP)-binding cassette 4] missense mutations in clinical characteristics and vitro cell model. Especially focus on clinical pathology, ABCB4-mRNA expression, multidrug resistance protein 3 (MDR3) level, cellular sublocalization, stability and phosphatidylcholine functional activity.

Results: We identified five missense mutations in the clinical cohort of this study. Their clinical manifestations are mainly cholestasis. Under HE staining, bile duct injury could be seen, and the immunohistochemical expression could be normal or decreased. In the cell model, the c.1865G>A (p.G622E) mutation resulted in decreased ABCB4-mRNA expression ($p < 0.05$) and endoplasmic reticulum retention in a cell model; c.2777C>T (p.P926L) mutation resulted in MDR3 endoplasmic reticulum retention; The mutations c.1757T>A (p.V586E) ($p < 0.01$), c.2362C>T (p.R788W) and c.3250C>T (p.R1084W) ($p < 0.0001$) reduce MDR3 phosphatidylcholine secretion activity.

Conclusion: The main clinical manifestation of PFIC3 is cholestasis. All five missense mutations were pathogenic in vitro. And the results were also consistent with liver pathology. This further confirms that missense mutations affect clinical outcomes.

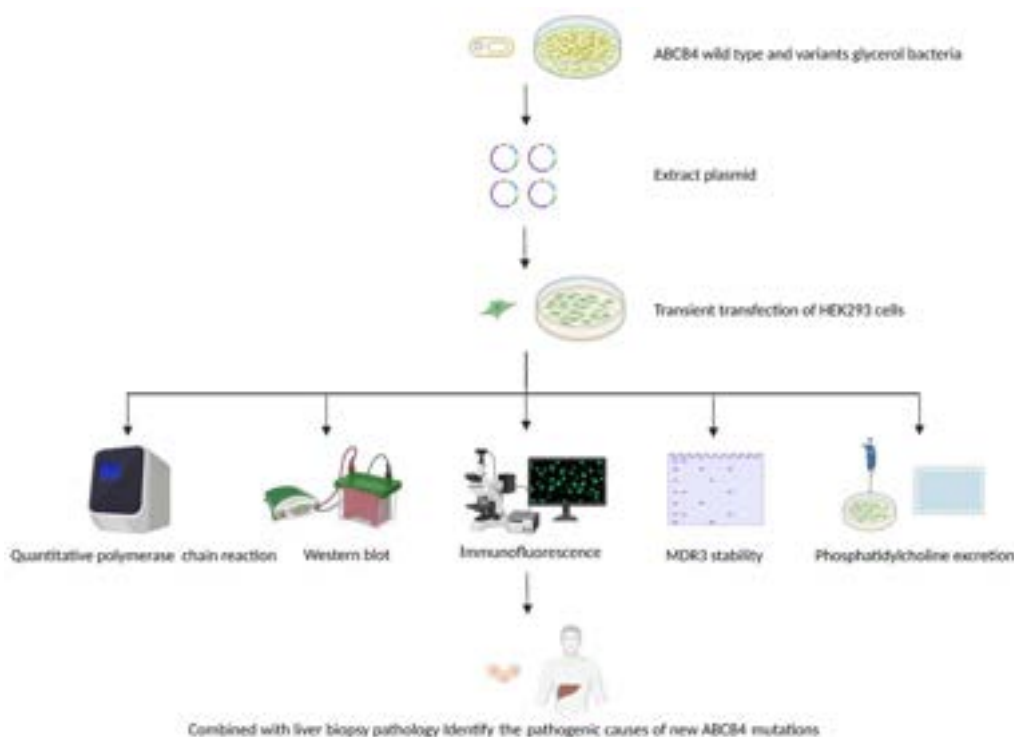


Figure: (abstract: THU-270).

THU-271

Immortalized patient-derived cell models for analysis of liver disease

Matthias Weiland¹, Vanessa Sandfort¹, Oksana Nadzemova¹,

Iyad Kabar², Jonel Trebicka¹, Hartmut Schmidt³, Andree Zibert¹.

¹Münster University Hospital, Medical Clinic B, Münster, Germany;

²Raphaelsklinik Münster, Münster, Germany; ³Essen University Hospital, Essen, Germany

Email: andree.zibert@ukmuenster.de

Background and aims: For many diseases, including rare monogenic liver diseases, patient-derived cells are the gold standard of experimental studies. However, materials derived from biopsies are limited and the proliferation of primary cells is frequently restricted to a few days. Epithelial cells found in the urine (UCs) represent a non-invasive source for establishment of continuously growing cell lines.

The aim of this study was to establish cellular platforms that were used to recapitulate pathomechanisms of liver diseases employing (i) gene transfer of oncogenes and (ii) by reprogramming to induced pluripotent stem cells (iPSCs) followed by differentiation into hepatocyte-like cells (HLCs).

Method: UCs were collected from patients having different liver disease (Wilson disease (WD), hereditary transthyretin amyloidosis (hATTR), HFE-related hemochromatosis, or autosomal dominant polycystic liver disease (ADPLD)). Cells were subjected to immortalization by oncogenes (HPV6E7, cyclinD1/CDK4R24C and hTERT/p53DD) or subjected to reprogramming and differentiation. Cells were analyzed using proliferation assay, flow cytometry, qRT-PCR, and Cyto-ID autophagosome staining.

Results: Gene transfer of several oncogenes led to a stable proliferation of primary cells. Oncogene-immortalized UCs showed similar high expression of epithelial, fibroblast and renal markers. Similarly, primary and immortalized UCs could be efficiently reprogrammed to iPSCs and differentiated to HLCs that showed typical markers of primary hepatocytes. Cells encoding a novel Sec61A1 mutation observed in an ADPLD patient showed a significant

downregulation of autophagy suggesting that a reduced autophagy is related to liver cyst formation. Chloroquine could specifically promote autophagy in ADPLD-derived cells.

Conclusion: In summary, our data suggest that immortalization of primary cells by oncogene transfer or reprogramming/differentiation allow establishment of cellular platforms for molecular studies to explore pathways of pathomechanisms in liver disease and the evaluation of drugs for therapy.

THU-272

CRISPR/Cas9-mediated gene correction of Wilson disease H1069Q mutation in an iPSC cell model

Andree Zibert¹, Matthias Weiland², Oksana Nadzemova¹,

Jonel Trebicka², Vanessa Sandfort¹. ¹Universitätsklinikum Münster,

Medizinische Klinik B, Münster, Germany; ²Universitätsklinikum

Münster, Medizinische Klinik B, Münster, Germany

Email: vanessa.sandfort@ukmuenster.de

Background and aims: Wilson disease (WD) is induced by an autosomal recessive gene defect in the copper transporting protein ATPase7B that leads to cytotoxic copper concentrations in the body, prominently in the liver. The most frequent mutation in the Caucasian population is the point mutation H1069Q. In this study, the H1069Q mutation was targeted by using the clustered regularly interspaced short palindromic repeats (CRISPR) associated nuclease 9 (Cas9) technology in WD specific induced pluripotent stem cells (iPSCs). We asked whether a gene correction is feasible, safe and efficient. Moreover, we studied whether gene-corrected iPSCs maintain the ability to differentiate into hepatocyte-like cells (iHeps) and whether such cells escape from toxic copper.

Method: Epithelial cells from freshly donated urine obtained from a WD patient carrying the compound heterozygous mutation H1069Q/N1270S were collected and reprogrammed into iPSCs. WD iPSCs were transfected with the plasmid PX459.H1069Q plus a set of single-stranded oligo DNA nucleotides (ssODNs) for homology-directed repair (HDR). Single iPSCs clones were analyzed by Sanger sequencing followed by hepatic differentiation and MTT assays.

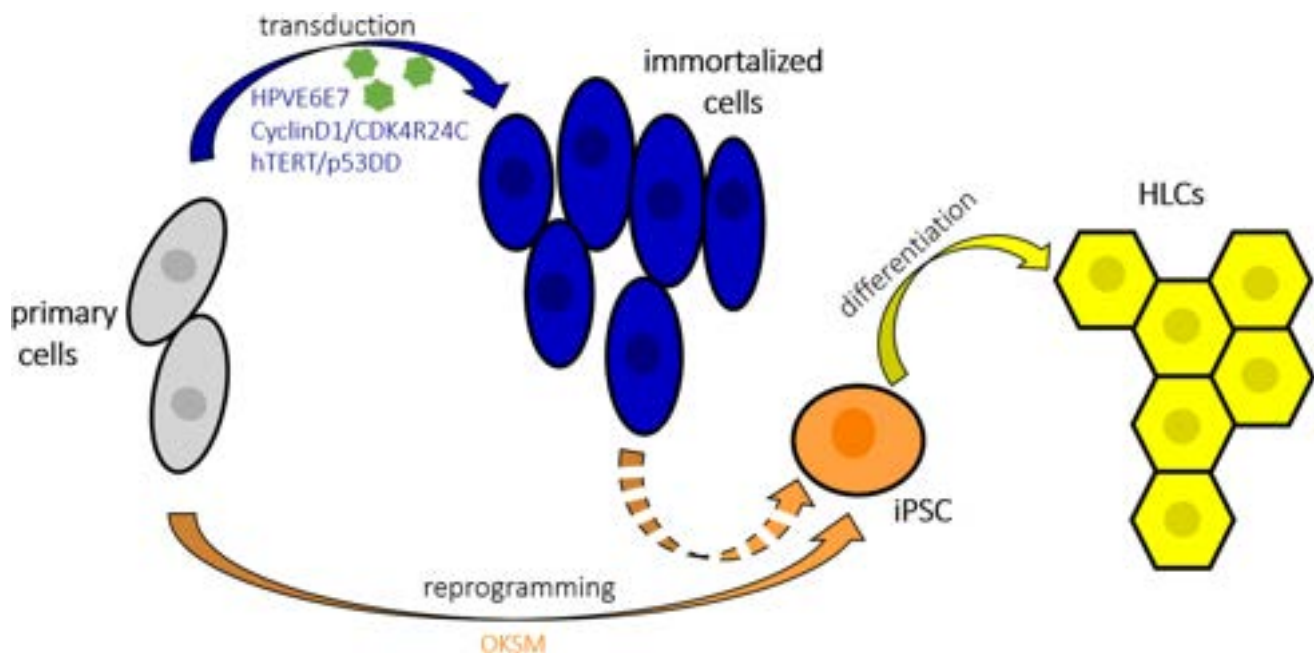


Figure: (abstract: THU-271): Overview of two pathways for immortalization of primary cells. **A** The combined retroviral transfer of oncogenes into primary cells (UCs) was used to gain highly proliferative, immortalized cells (imUCs). **B** Primary cells were reprogrammed to induced pluripotent stem cells (iPSCs) and in vitro differentiation to hepatocyte-like cells (HLCs).

POSTER PRESENTATIONS

Results: After genome engineering, 46% of the cell clones indicated a gene correction of the H1069Q mutation. The second mutation N1270S was not affected indicating the high specificity of the methodology. Corrected iPSCs could be differentiated to iHeps and indicated an improved resistance to a challenge by high copper concentrations.

Conclusion: The current study demonstrates that in vitro genome engineering with CRISPR/Cas9 has a remarkable therapeutic potential to efficiently correct WD, thus further contributing to novel therapeutic approaches for WD specifically and monogenetic rare diseases in general.

THU-273

Liver transplantation for Wilson disease: single center experience

Amnah Alhanaee^{1,2}, Khalid Bzeizi³, Saad Alghamdi¹, Ali Albenmoussa¹, Waleed Alhamoudi¹, Dieter Clemens Broering¹. ¹King Faisal Specialist Hospital and Research Centre, Riyadh, Saudi Arabia; ²Tawam Hospital, أبو ظبي, United Arab Emirates; ³King Faisal Specialist Hospital and Research Centre, liver transplant, Riyadh, Saudi Arabia
Email: amnahalhanaee@gmail.com

Background and aims: Wilson's disease (WD) is a rare genetic disorder with protean manifestations. Even if liver transplantation (LT) could represent an effective therapeutic option for patients with end-stage liver disease. LT however, remains controversial in the presence of neuropsychiatric involvement. We present our experience on transplantation of Saudi patients with WD.

Method: All patients who had LT in King Faisal Specialist hospital during the period January 2004-January 2021 were included in the analysis. The medical records were accessed for all the information, including the demographics of the patients, genetic screen, MELD score and evidence for neuro-psychiatric WD. Graft and patient survival was determined using Kaplan Meier analysis.

Results: A total of 34 patients with WD were transplanted in our center. Females were 18 (53%). The mean age at the onset of symptoms was 24.7 years [range 13–45 years] were included. WD was diagnosed by genetic testing and or Leipzig scoring system using 24-hours urinary collection. The mean MELD score at the time of transplantation was 23.9 and 70% of the patients had Child-C score. Isolated hepatic phenotype was the referral phenotype for LT in 23 patients (67.6%). The combination of neuro-psychiatric and decompensated liver disease was present in 3 patients (8.8%). 5 patients (14.7%) presented with neurological impairment on decompensated liver disease and one patient had isolated neuro-psychiatric WD. Two patients had LT for acute liver failure. One patient had hepatopulmonary syndrome (HPS) and another presented with hepatocellular carcinoma (HCC). Living-related LT was performed on 18 patients (53%). Post-transplant, 5 patients with neuropsychiatric symptoms recovered completely (14.5%). Biopsy proven, acute cellular rejection occurred in 11 and all responded to treatment. Biliary anastomotic strictures developed in 6 patients, managed successfully with ERCP/PTC intervention. PTLT was diagnosed in one patient, 7 years post LT.

Four deaths occurred during the study period (11.7%) and two of them within 30-days post LT. The one, five and ten-years survival rates were 94%, 90% and 80% respectively.

Conclusion: WD remains an uncommon, indication for LT. There was a trend of improvement in the neuro-psychiatric manifestations of WD post transplantation, but more studies are needed. The overall graft and patient survival was excellent and accordingly, LT provides a viable management option for WD with hepatic decompensation.

THU-274

Effects of tetrathiomolybdate, trientine, and penicillamine on intestinal copper uptake: a randomized placebo-controlled ⁶⁴Cu PET/CT study

Frederik Teicher Kirk¹, Ditte Emilie Munk¹, Eugene Scott Swenson², Adam Quicquaro², Mikkel Holm Vendelbo³, Michael Schilsky⁴, Peter Ott¹, Thomas Damgaard Sandahl¹. ¹Aarhus University Hospital, Department of Hepatology and Gastroenterology, Aarhus, Denmark; ²Alexion, AstraZeneca Rare Disease, United States; ³Aarhus University Hospital, Department of Nuclear Medicine and PET-center, Denmark; ⁴Yale School of Medicine, Department of Medicine, Section of Digestive Diseases, and Department of Surgery, Section of Transplant and Immunology, United States
Email: frkirk@rm.dk

Background and aims: In Wilson Disease (WD), ATP7B protein dysfunction leads to copper accumulation with hepatic and neurologic disease. Treatments include D-penicillamine (PEN) and trientine tetrahydrochloride (TRI), which chelate Cu and cause cupriuresis, and the investigational copper binding agent bis-choline-tetrathiomolybdate (TTM). We hypothesized that inhibition of intestinal uptake of copper could be an additional mechanism of action for these drugs. We used PET/CT to investigate the effects of TTM, TRI, PEN and placebo (PLA) on intestinal ⁶⁴Cu uptake. The study was conducted in healthy volunteers as ATP7B is not involved in intestinal copper absorption.

Method: Healthy subjects (n = 32) were included in a partly double blinded placebo-controlled randomized trial. Subjects underwent ⁶⁴Cu PET/CT before treatment and after 7 days of treatment with TTM, TRI, PEN or PLA, each serving as their own controls. Subjects fasted 1 h before and after treatment doses, with final dose 1–2 h prior to ⁶⁴CuCl₂ ingestion. Participants were scanned 1 h and 15 h after an oral dose of ⁶⁴CuCl₂. Radiocopper was quantitated in liver and in blood (aorta). If a drug were to reduce intestinal copper absorption, less copper would be detected in the blood and liver. Subjects followed standardized diets, including a 6 h fast prior to ⁶⁴Cu ingestion.

Results: Compared to pretreatment, hepatic ⁶⁴Cu levels measured 1 h post-⁶⁴Cu dose were reduced by 92% on TTM (p < 0.02), 53% on TRI (p < 0.02), 23% on PEN (p = 0.16), and 3% on PLA (p = 1.00) (Figure 1). At 15 h post-⁶⁴Cu dose, hepatic ⁶⁴Cu levels were reduced by 82% on TTM (p < 0.02), 50% on TRI (p < 0.02), 31% on PEN (p < 0.04) and increased 12% on PLA (p = 0.16). At 15 h, gallbladder ⁶⁴Cu activity demonstrated biliary excretion after TRI, PEN and PLA, but not after TTM.

TRI, PEN and PLA did not significantly change blood ⁶⁴Cu activity at 1 h and 15 h post ⁶⁴Cu administration. Even though TTM reduced hepatic ⁶⁴Cu activity by 80–90%, blood activity was only 40% less at 15 h indicating reduced hepatic clearance. No compensatory increased ⁶⁴Cu activity was detected in other organs. In summary, after TTM, a smaller percent of ingested ⁶⁴Cu dose was present in blood and liver; it was absent in bile and not increased in other organs, indicating significant inhibition of intestinal ⁶⁴Cu absorption. In addition, the reduced ratio of liver/blood ⁶⁴Cu activity indicated reduced hepatic clearance, presumably due to formation of TTM-Cu-albumin complexes in blood.

Conclusion: ⁶⁴Cu PET/CT is useful for evaluating the effect of medical therapy on intestinal copper absorption and copper distribution in the body. The greater inhibition of intestinal copper absorption of TRI compared to PEN may explain recent observations of more urinary copper excretion with PEN but equal efficacy in treating WD patients. TTM markedly reduced hepatic ⁶⁴Cu uptake, reducing both intestinal absorption and hepatic clearance by TTM-Cu-albumin complex formation.

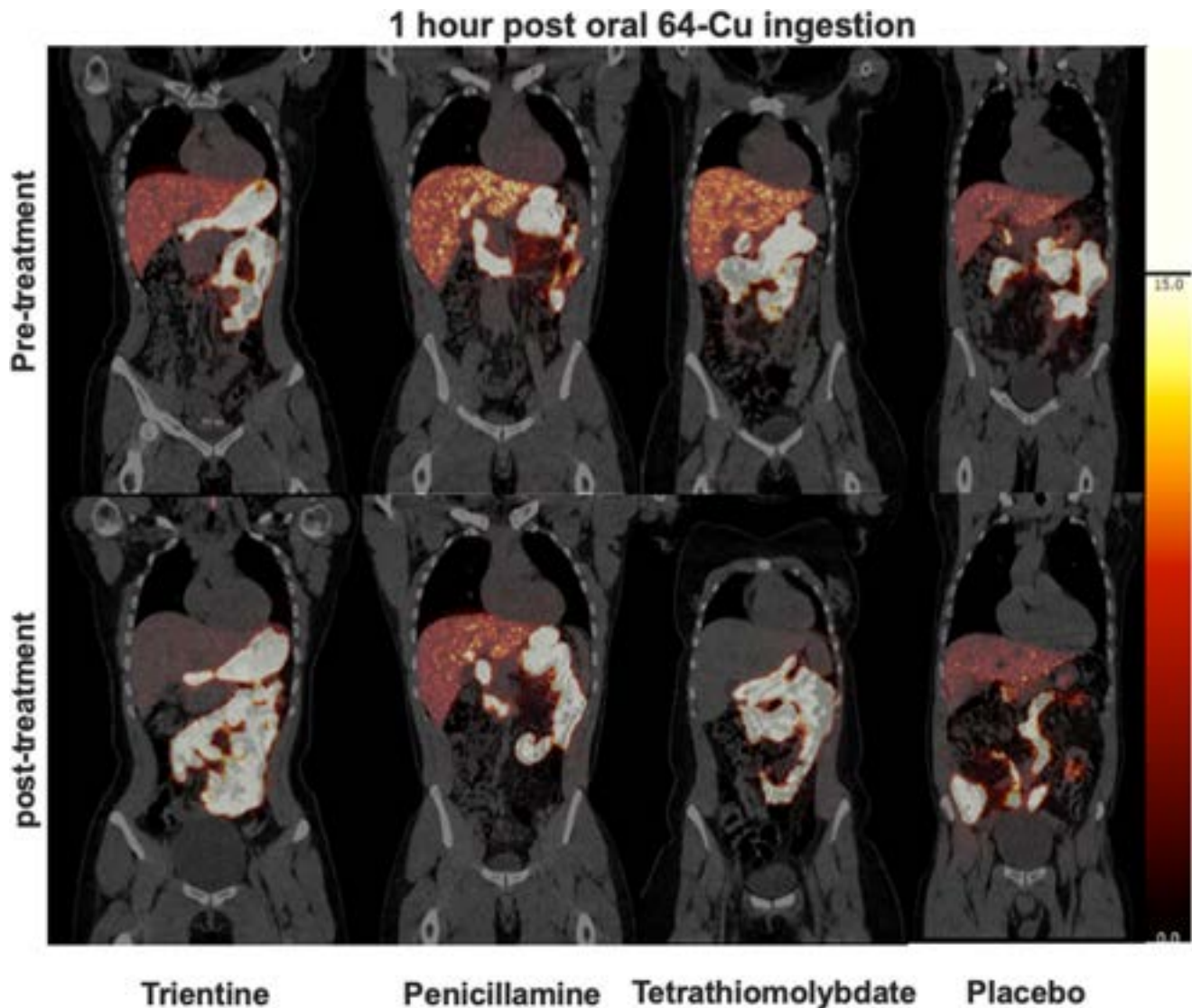


Figure: (abstract: THU-274): Fused coronal paired, representative images from one subject in each group of eight individuals, whole-body PET/CT images showing ^{64}Cu activity in the liver, heart and parts of the small intestine and colon. 1 hour after ^{64}Cu ingestion. Radioactivity scale 0 (black)-15 (white).

THU-275

Four-fold increased mortality rate in patients with Wilson's disease: a population-based cohort study of 151 patients

Fredrik Åberg¹, Ying Shang², Rickard Strandberg², Axel Wester², Linnea Widman², Hannes Hagström². ¹University of Helsinki, Finland; ²Karolinska Institutet, Sweden

Email: hannes.hagstrom@ki.se

Background and aims: Few studies have investigated mortality rates in patients with Wilson's disease and compared these to the general population. Further, there is a lack of information on the risk of other potential outcomes. Here, we examined mortality and other outcomes in a population-based study of patients with Wilson's disease in Sweden.

Method: We did a population-based cohort study, using nation-wide registers to identify all patients with a first diagnosis of Wilson's disease between 2002 and 2020 in Sweden. Each patient was matched by age, sex and municipality with up to 10 reference individuals from the general population. Validated registers were used to investigate outcomes up to 19 years after baseline in patients

and reference individuals. Cox regression was used to examine overall mortality, while Fine and Gray regression models were used for secondary outcomes, considering non-outcome death and liver transplantation as competing events. Validation of the ICD-10 code for Wilson's disease was performed by comparing ICD-codes to medical journals from 26 patients seen at the Karolinska University Hospital.

Results: A total of 151 patients with a first diagnosis of Wilson's disease were identified and matched with 1,441 reference individuals. The positive predictive value for the ICD-10-code for Wilson's disease was 100%. Median age at baseline was 26 years (interquartile range [IQR] 17–42) and 50% were males. At baseline, previous diagnoses of neurologic disease were seen in 17%, and psychiatric diagnoses had been made in 24%, figures considerably higher than in reference individuals (7% and 10%, respectively, both $p < 0.001$). During a mean follow-up of 6.6 years (range 0–19), 10 (6.6%) patients with Wilson's disease died, compared with 31 (2.2%) reference individuals. This translated to a hazard ratio of 3.84 (95%CI = 1.84–8.05). The excess risk of death was confined to patients aged 20 or more at diagnosis. Cumulative mortality at 10 years was estimated to

POSTER PRESENTATIONS

Table: (abstract: THU-275): Incident secondary outcomes in patients with Wilson's disease and matched reference individuals from the general population. Statistically significant estimates are highlighted in bold. Abbreviations: IR = incidence rate, PY = person-years, sHR = subdistribution hazard ratio.

	n/N, Wilson	n/N, controls	IR/1000 PY, Wilson	IR/1000 PY, reference individuals	sHR (95%CI)	p value
Liver-related death	1/151	1/1441	0.85 (0.12–6.06)	0.08 (0.01–0.58)	9.54 (0.60–151.89)	0.11
Liver transplantation	14/141	1/1441	11.94 (7.07–20.17)	0.08 (0.01–0.58)	137.15 (17.94–1048.58)	<0.001
Cardiovascular disease	26/122	92/1111	32.23 (21.95–47.34)	10.26 (8.36–12.59)	2.90 (1.85–4.53)	<0.001
Hepatocellular carcinoma	1/150	1/1432	0.86 (0.12–6.10)	0.08 (0.01–0.58)	9.22 (0.55–154.79)	0.12
Psychiatric diagnoses	24/115	106/988	30.29 (20.30–45.19)	12.79 (10.57–15.47)	2.11 (1.36–3.29)	0.001
Neurologic diagnoses	23/125	102/1120	25.12 (16.70–37.81)	10.91 (8.99–13.25)	2.12 (1.34–3.35)	0.001

12.7% (95%CI = 7.0–22.5) in patients with Wilson's disease, compared to 3.3% (95%CI = 2.2–5.0) in reference individuals. Higher risks of several secondary outcomes in patients with Wilson's disease were identified (Table 1).

Conclusion: In this large, population-based cohort study, patients with Wilson's disease had an almost 4-fold increased rate of death, as well as increased risks for several clinically important outcomes, compared to matched individuals from the general population.

THU-276

Risk of cirrhosis and hepatocellular carcinoma in hemochromatosis: a Swedish nationwide cohort study

Hanne Åström¹, Axel Wester¹, Linnea Widman¹, Per Stal^{1,2}, Hannes Hagström^{1,2}. ¹Karolinska Institutet, Department of Medicine, Huddinge, Sweden; ²Karolinska University Hospital, Division of Hepatology, Department of Upper GI, Sweden
Email: hanne.astrom@ki.se

Background and aims: Hereditary hemochromatosis (HH) is a common genetic disorder of iron metabolism characterized by excessive absorption and accumulation of dietary iron. Patients with HH are thought to be at increased risk of severe liver disease (SLD) and hepatocellular carcinoma (HCC) but current research have produced conflicting results. In this study, we aimed to establish the rates of SLD and HCC in a nationwide cohort study of patients with HH.

Method: Patients with administrative coding for HH (n = 7711) in the Swedish National Patient Register between years 1969–2016 were included. Patients with HH were matched for age, sex and municipality with 74089 controls. Patients were stratified into groups based on age, sex and year of diagnosis. Cox proportional hazards regression was used to determine the rates of SLD and HCC and cumulative incidence was illustrated using Kaplan Meier curves.

Results: In the entire cohort, SLD was diagnosed in 862 persons (HH: 393 [5.1%], vs. Controls: 469 [0.6%]) and HCC was diagnosed in 224 persons (HH: 133 [1.7%], vs. Controls: 91 [0.1%]). During the entire study period, patients with HH had a higher rate of SLD and HCC compared to matched controls (adjusted hazard ratio [aHR] 8.2; 95% CI 7.1–9.5 and aHR 14.1; 95%CI 10.4–19.2 respectively). The rate of SLD development decreased over time with highest rates in 1969–1980 (aHR 19.3; 95%CI 7.4–50.3) and lowest in 2001–2010 (aHR 6.8; 95%CI 5.5–8.4). Men experienced a higher rate of SLD development when compared to women (aHR 8.8; 95%CI 7.4–10.4, vs. aHR 7.1; 95%CI 5.3–9.4) and this was additionally reflected in rate of HCC development (aHR 17.3; 95%CI 12.2–24.7 vs. aHR 6.2; 95%CI 3.0–12.6). Patients older than 66 years of age experienced the highest rate of SLD development (aHR 10.4; 95%CI 8.0–13.6) compared to younger subgroups where rates were observed to be similar (51–65: aHR 7.4; 95%CI 6.0–9.2 and <50: aHR 7.8; 95%CI 5.6–10.9).

Conclusion: In this nationwide cohort study, patients with HH experienced an increased rate of SLD and HCC compared to matched controls from the general population. Over time, the rate of SLD and HCC development in patients with HH seemed to decrease; possibly owing to improved diagnostic techniques and change in management over time. We identified a few subgroups of patients with diverging risk estimates of liver-related outcomes that may require different

clinical follow-up strategies. Thus, further studies are warranted to optimize the management of patients with hemochromatosis.

THU-277

Association of circulating Z-polymer with adverse clinical outcomes and liver fibrosis in adults with the PiZZ alpha-1 antitrypsin deficiency genotype

Malin Fromme¹, Laura Rademacher¹, Samira Amzou¹, John Ripollone², Christi Cook², Isabel Zacharias², Yang Chen², Bing Han², Pavel Strnad¹. ¹University Hospital RWTH Aachen, Aachen, Germany; ²Vertex Pharmaceuticals, Boston, United States
Email: pstrnad@ukaachen.de

Background and aims: The PiZ variant is the most clinically relevant variant in alpha-1 antitrypsin deficiency (AATD), leading to impaired AAT secretion from the liver and Z-polymer formation. To improve the limited knowledge about the biological role of circulating Z-polymers, we studied its association with adverse clinical outcomes, and with liver fibrosis.

Method: PiZZ adults from the European Alpha-1 Liver Cohort, recruited between 2015 and 2020, were included. Serum circulating Z-polymer was measured via an immunoassay method specific for the polymeric form of AAT. Time-to-event analyses were conducted for PiZZ adults followed for adverse clinical outcomes over a median of approximately 4 years. Cox proportional hazards models were used to describe the association between binary circulating Z-polymer (>versus ≤analytic sample median circulating Z-polymer) and adverse clinical outcome (composite of first instance of liver-related hospitalization, listed/realized liver transplant, or all-cause mortality). Cross-sectional associations between circulating Z-polymer and baseline liver fibrosis (FibroScan stiffness) were evaluated using the Spearman correlation (rho). Analyses were stratified by augmentation therapy status because augmentation therapy may infuse polymer, leading to inflated Z-polymer levels.

Results: There were 431 PiZZ adults (baseline: average age of 55 years, 46% female, average body mass index [BMI] of 25.1 kg/m²; 59% reported augmentation therapy use). Baseline mean circulating Z-polymer was higher among PiZZ adults on augmentation therapy (26.0 mg/L, n = 254) than those not on augmentation therapy (19.3 mg/L, n = 173). Of 292 PiZZ adults followed for adverse clinical outcomes, 28 (9.6%) had adverse clinical outcomes (4 liver-related hospitalizations, 4 listed/realized liver transplants, 20 deaths [6 liver-related, 4 lung-related, 10 other/unknown]). Higher circulating Z-polymer (median circulating Z-polymer = 21.5 mg/L) was associated with increased risk of adverse clinical outcome in an age-adjusted model (hazard ratio [HR]: 1.96, 95% confidence interval [CI]: 0.78–4.94, n = 289). Similar associations were observed after stratification by baseline augmentation therapy status (augmented HR: 2.97, 95% CI: 0.95–9.33, n = 182; non-augmented HR: 3.52, 95% CI: 0.73–17.1, n = 106). At baseline, among those not on augmentation therapy, circulating Z-polymer was positively correlated with FibroScan stiffness (rho: 0.29; n = 138).

Conclusion: Higher circulating Z-polymer was associated with shorter time to adverse clinical outcome, and positively correlated with FibroScan stiffness, in PiZZ adults. Circulating Z-polymer may identify patients at risk for rapid liver disease progression in AATD.

THU-278

Blood markers of immune activation help distinguish paediatric activated T-cell hepatitis from other causes

Tamir Diamond^{1,2}, Catherine Chapin^{3,4}, Adriana Perez^{1,2}, Kathleen M. Loomes^{1,2}, Edward Behrens^{1,2}, Estella Alonso^{3,4}.

¹University of Pennsylvania, Pediatrics, Philadelphia, United States;

²Children's Hospital of Philadelphia, Pediatrics, Philadelphia, United States;

³Northwestern University, Feinberg School of Medicine, Pediatrics, Chicago, United States;

⁴Ann and Robert H. Lurie Children's Hospital of Chicago, Chicago, United States

Email: diamondt@chop.edu

Background and aims: Paediatric acute liver failure (PALF) and acute severe hepatitis of unknown cause has recently attracted increased attention due to reports since late 2021 of a possible worldwide increase in cases which may be related to adenovirus infection. To date, a direct viral cause has not been identified in most patients with indeterminate PALF. Instead, recent studies support that many cases of indeterminate acute hepatitis and PALF are driven by an overactive immune response involving effector memory CD8 T-cells, designated activated T-cell hepatitis. Here we describe a multicentre cohort of children with acute hepatitis and PALF presenting between March 2020 and August 2022 and demonstrate how patients can be differentiated by immune phenotype.

Method: Retrospective chart review to identify patients aged 3 months-18 years with acute severe hepatitis and PALF at Ann and Robert H. Lurie Children's Hospital of Chicago and Children's Hospital of Philadelphia. Patients with biochemical evidence of severe liver injury within 8 weeks of onset of illness measured by alanine aminotransferase (ALT) above 500 were included. PALF was defined per the PALF Study Group criteria as previously published. Patients with evidence of chronic liver disease or non-hepatic intrinsic causes for hepatitis were excluded. Demographic, clinical, laboratory, and pathology data were collected by chart review. Patients were classified as activated T-cell hepatitis based on liver biopsy with moderate-dense CD8+ T-cell inflammation (if available) and/or

development of severe aplastic anaemia with negative evaluation for other causes. Patients were labelled unknown (IND-hep) if no aetiology of the liver injury was identified.

Results: 124 patients met inclusion criteria: 83 patients with known diagnoses (23 with PALF) (fig. 1A), 14 with activated T-cell hepatitis (3 PALF), and 27 with IND-hep (11 PALF) (fig 1B). Most patients (97%) had recovery with native liver. Total serum bilirubin and soluble IL-2 receptor at presentation were higher in activated T-cell hepatitis patients compared to IND-hep (fig 1C and 1D). Clinical T- and B-cell flow cytometry studies noted increased percentage of CD8+ T-cells (fig. 1E) and increased HLA-DR+ (activated) T-cells (fig. 1F) in the activated T-cell hepatitis compared to IND-hep group. An increase in CD8 T-cell perforin and granzyme B expression was only seen in patients with activated T-cell hepatitis (figure 1G).

Conclusion: In a multicenter cohort of children with acute liver injury we found that patients with activated T-cell hepatitis have distinctive differences in clinically available peripheral blood immune biomarkers compared to patients with IND-hep which can be used help to identify this diagnostic group. Better characterization of this group will facilitate additional understanding of the underlying pathophysiology, and development of targeted therapies, to improve transplant-free survival.

THU-279

Incidence of hemochromatosis in HFE p.H63D homozygote and p.C282Y/H63D compound heterozygote individuals

Lorenz Michael Pammer¹, Benedikt Schaefer¹, Bernhard Pfeifer^{2,3}, Sabrina Neururer², Claudia Lamina⁴, Florian Kronenberg⁴, Herbert Tilg¹, Heinz Zoller¹. ¹Medizinische Universität Innsbruck, Dept. of Internal Medicine I, Innsbruck, Austria; ²Landesinstitut für Integrierte Versorgung Tirol, Innsbruck, Austria; ³University for Health Sciences, Medical Informatics and Technology, Hall in Tirol, Austria; ⁴Medizinische Universität Innsbruck, Institute of Genetic Epidemiology, Innsbruck, Austria

Email: heinz.zoller@i-med.ac.at

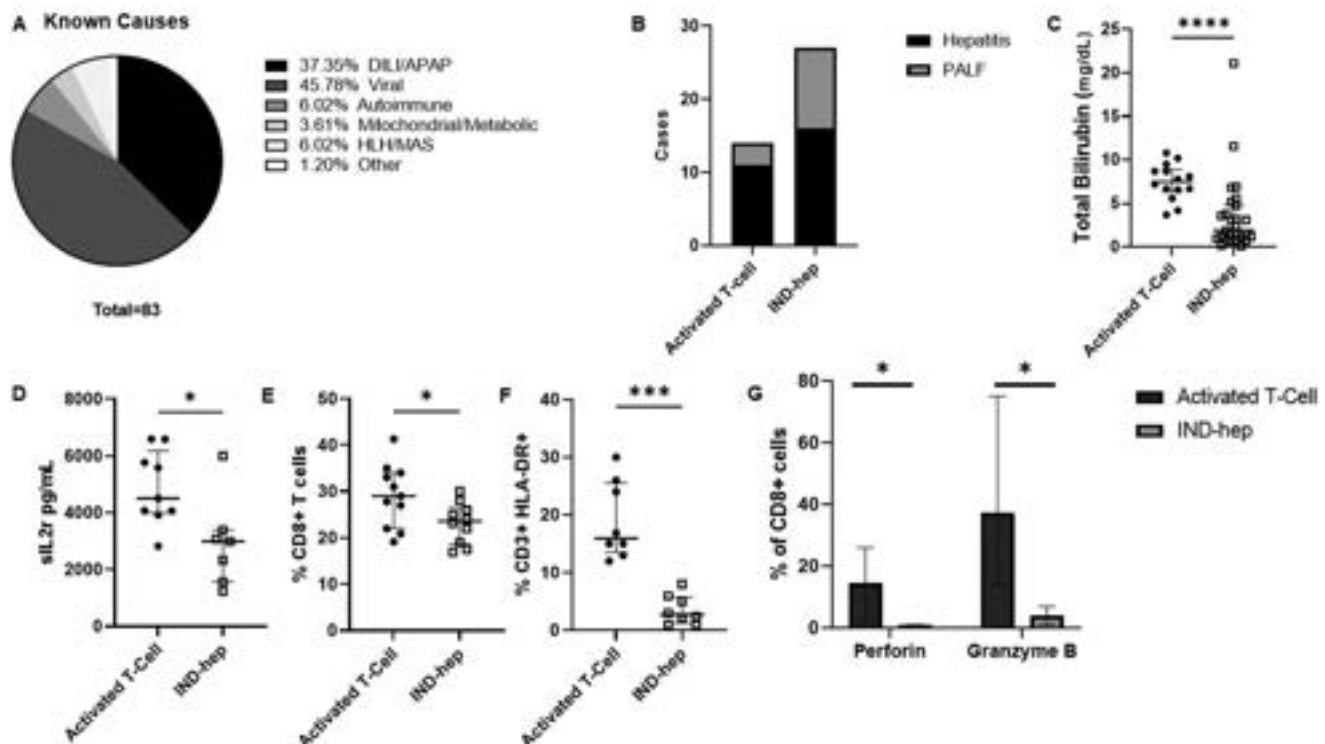


Figure: (abstract: THU-278).

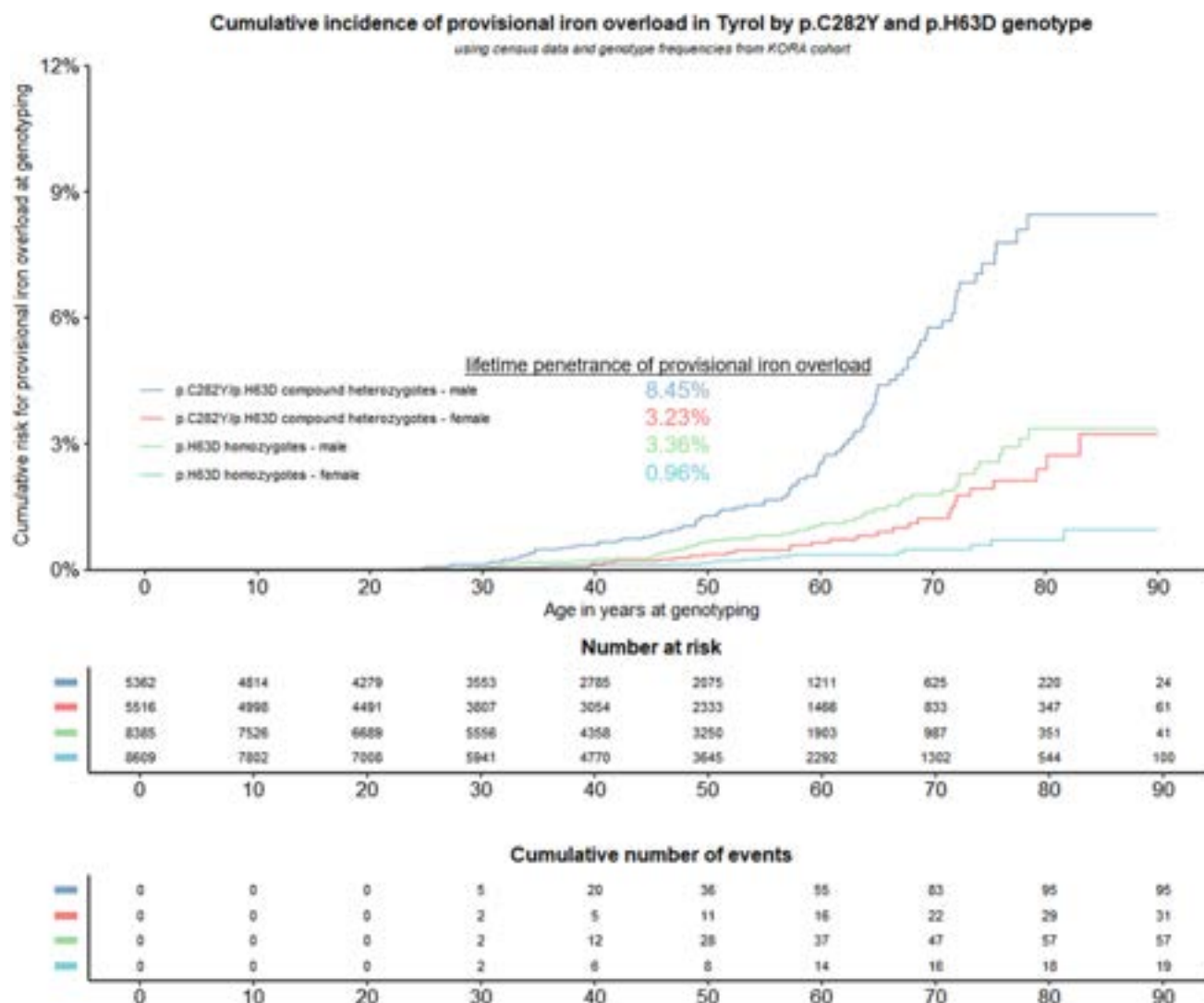


Figure: (abstract: THU-279).

Background and aims: Hemochromatosis is a genetic disease characterized by increased transferrin saturation and liver iron overload. The most common disease-associated genotype is p.C282Y homozygosity in *HFE*. The reported incidence of iron overload in patients who are compound heterozygous for p.C282Y and p.H63D as well as for those patients who are homozygous for p.H63D varies widely between studies. The present study assesses disease penetrance in a large European cohort with a median follow-up of 10.6 years/follow-up of up to 25.1 years

Method: We included 8839 patients, referred for *HFE* genotyping from Tyrol, Austria over a period of 25 years. Penetrant disease was defined as the presence of provisional iron overload (ferritin >300 µg/L for men and postmenopausal women, >200 µg/L for premenopausal women in association with transferrin saturation >55% for men and >45% for women). Using genotype frequencies from a health research database and general population data from Tyrol, expected number for both genotypes were calculated.

Results: In total, we identified 301 p.H63D homozygotes (3.41% of referred patients) and 507 p.C282Y/p.H63D compound heterozygotes (5.73% of referred patients). Lower bounds of lifetime disease penetrance were established at 8.45% for males and 3.23% for females in p.C282Y/p.H63D compound heterozygotes. For p.H63D homozygotes, male lifetime penetrance was 3.36% and female lifetime penetrance was 0.96%. The p.C282Y/p.H63D confers a

higher risk of lifetime provisional iron overload. Compound heterozygous females have comparable lifetime risk to p.H63D homozygous males. Age at diagnosis/genotyping and sex are the strongest modifiers of disease penetrance.

Conclusion: The absolute life-time risk of developing provisional iron overload for p.C282Y/H63D compound heterozygotes and p.H63D homozygotes individuals is low, suggesting that environmental and behavioral risk factors determine disease penetrance.

THU-280

Does earlier introduction of azathioprine result in a reduced cumulative dose of corticosteroid therapy in the treatment of autoimmune hepatitis (AIH) and does this result in the same degree of biochemical response?

Sital Shah¹, Yooyun Chung², Maura Morrison², Catherine McKenzie³, Michael Heneghan². ¹Kings College Hospital NHS Foundation Trust, Institute of Liver Studies, London, United Kingdom; ²King's College Hospital, United Kingdom; ³University Hospital Southampton, Pharmacy and Critical Care, Southampton, United Kingdom
Email: sitalshah@nhs.net

Background and aims: Patients with autoimmune hepatitis (AIH) often receive variable steroid and azathioprine regimens. The purpose of this study was to determine whether earlier introduction

Figure: Table 1: Prednisolone exposure over 5 year follow-up period

Months	Prednisolone dose, mg median (IQR)				Cumulative prednisolone dose, mg, median (IQR)				Cumulative prednisolone dose, mg/kg, median (IQR)			
	Total (n = 226)	Early azathioprine initiation (n = 106)	Late azathioprine initiation (n = 120)	P value	Total (n = 226)	Early azathioprine initiation (n = 106)	Late azathioprine initiation (n = 120)	p value	Total (n = 226)	Early azathioprine initiation (n = 106)	Late azathioprine initiation (n = 120)	p value
3	10 (5)	10 (5)	11.2 (10)	0.71	1626 (840)	1522 (741)	1687 (919)	0.14	23.3 (11.3)	21.7 (9.8)	23.9 (12.0)	0.69
6	10 (7.5)	7.5 (6)	10 (7.5)	0.92	2564 (1288)	2392 (934)	2686 (1369)	0.14	36.4 (19.3)	34.8 (14.2)	37.9 (21.3)	0.35
12	6 (7.5)	5 (7.5)	7.5 (7.5)	0.12	4045 (2104)	3937 (1985)	4060 (2233)	0.69	54.9 (25.8)	51.6 (31.9)	56.6 (36.8)	0.5
24	5 (10)	4.5 (10)	5 (10)	0.7	5815 (4202)	5421 (4036)	5902 (4533)	0.28	73.5 (67.8)	72.84 (70)	74.63 (60.5)	0.99
36	5 (7.5)	2.5 (7.5)	5 (10)	0.11	6870 (7179)	6586 (6977)	6979 (7273)	0.5	95 (103)	90.2 (96)	96.5 (115.7)	0.34
60	0 (6.25)	0 (5)	2.5 (7.5)	0.16	8138 (9158)	7840 (7770)	8802 (9518)	0.19	113 (122)	107 (110)	112 (141)	0.45

Figure: (abstract: WED-280).

of azathioprine for the treatment of AIH allows for reduced cumulative steroid burden in AIH.

Method: We performed a retrospective single centre cohort study. Two hundred and twenty six patients were divided into 2 groups: those who had received azathioprine therapy within 8 weeks of initiation of steroid therapy (early group) and those who had received azathioprine more than 8 weeks after steroid initiation (late group).

Results: The dose and cumulative dose of prednisolone (mg/kg) in the early group was lower compared to the late group at all time-points but this did not reach statistical significance (table 1). The number of patients continuing on steroids was higher in the late group (62%) compared to the early group (52%) at the end of the 5-year follow-up but did not reach statistical significance ($p = 0.33$). The proportion of patients achieving biochemical remission (normal AST and IgG) from induction therapy was 59.1% at 3 months, 71.7% at 6 months and 82% at 12 months. Serum ALT level was normalised in 80% of patients in the early azathioprine group compared to 64.5% in the late group ($p = 0.01$) at 6 months. IgG levels were normalised in 68% of patients in the early group compared to 54% of patients in the late group ($p = 0.05$) at 1-year. Over the 5-year follow-up, more patients in the early group achieved biochemical remission although this was not statistically significant. Within the first 12 months of commencing steroid therapy, 70% of patients experienced steroid related side effects. The odds of experiencing an infection, visual disturbances, fatigue, changes to bone health, weight gain and hyperglycaemia was higher in the late group.

Conclusion: Earlier introduction of azathioprine does not result in a reduced cumulative dose of prednisolone during the first five years of treatment for AIH. However earlier introduction does result in a faster rate of normalisation of AST at 6 months and IgG at 12 months. The odds of experiencing steroid related side effects were higher in late azathioprine group.

THU-281

Impact of alcohol consumption on the liver phenotype in alpha-1 antitrypsin deficiency

Malin Fromme¹, Carolin V. Schneider¹, Nurdan Gueldiken¹, Samira Amzou¹, Yizhao Luo¹, Monica Pons^{2,3}, Joan Genesca^{2,3}, Marc Miravittles⁴, Katrine Thorhauge⁵, Johan Waern⁶, Jan Sperl⁷, Sona Frankova⁷, Marc Bartel⁸, Holger Zimmer⁹, Markus Zorn⁹, Aleksander Krag⁵, Alice Turner¹⁰, Christian Trautwein¹, Pavel Strnad¹.
¹University Hospital RWTH Aachen, Medical Clinic III, Gastroenterology, Metabolic diseases and Intensive Care, Aachen, Germany; ²Vall d'Hebron Institute of Research (VHIR), Vall d'Hebron Barcelona Hospital Campus, Universitat Autònoma de Barcelona, Liver Unit, Hospital Universitari Vall d'Hebron, Barcelona, Spain; ³Instituto de Salud Carlos III, Centro de Investigación Biomédica en Red de Enfermedades Hepáticas y Digestivas

(CIBERehd), Madrid, Spain; ⁴Hospital Universitari Vall d'Hebron, Vall d'Hebron Institut de Recerca (VHIR), Vall d'Hebron Barcelona Hospital Campus, CIBER de Enfermedades Respiratorias (CIBERES), Pneumology Department, Barcelona, Spain; ⁵Odense University Hospital, Department of Gastroenterology and Hepatology, Odense, Denmark; ⁶Sahlgrenska University Hospital, Department of Medicine, Gastroenterology and Hepatology Unit, Gothenburg, Sweden; ⁷Institute for Clinical and Experimental Medicine, Department of Hepatogastroenterology, Prague, Czech Republic; ⁸University Hospital Heidelberg, Institute of Forensic and Traffic Medicine, Heidelberg, Germany; ⁹University Hospital Heidelberg, Central Laboratory, Heidelberg, Germany; ¹⁰University of Birmingham, Institute of Applied Health Research, Birmingham, United Kingdom

Email: mfromme@ukaachen.de

Background and aims: Alpha-1 antitrypsin deficiency (AATD) arises from mutations in the alpha1-antitrypsin (AAT) gene and predisposes to liver cirrhosis. However, the liver phenotype is variable and modifying factors are poorly understood. We studied the impact of alcohol intake on liver-related parameters in individuals with the characteristic heterozygous/homozygous Pi*Z variant (Pi*MZ/Pi*ZZ genotype) found in the community-based United Kingdom Biobank (UKB) and the European Alpha1 liver consortium.

Method: Anamnestic data on alcohol consumption were evaluated in 17 145 Pi*MZ and 141 Pi*ZZ subjects as well as 425 002 non-carriers (Pi*MM) from the UKB. 561 Pi*ZZ individuals from the European Alpha1 liver consortium without concomitant liver disease were assessed and a measurement of carboxydehydrogenase (CDT) was performed. Non-transgenic and Pi*Z mice were subjected to Lieber-DeCarli (LDC) diet containing 3–4% alcohol for 8 weeks.

Results: >80% of individuals reported no/low alcohol intake, while harmful consumption (women ≥ 40 g/d, men ≥ 60 g/d) was rare (~1% in most groups). In UKB participants with Pi*MM/Pi*MZ genotype, significant alcohol consumption (women 12–39 g/d, men 24–59 g/d) resulted only in a <30% increase in transaminases above the upper limit of normal (ULN), while the effect on GGT was more pronounced (Pi*MM: 15.0% vs. 23.0%; Pi*MZ: 15.7% vs. 22.5%), but comparable in both groups. In both genotypes, harmful alcohol intake led to an at least twofold increase in the proportion of Pi*MM and Pi*MZ subject with elevated transaminases, GGT serum levels as well as elevated AST-to-platelet ratio indices (APRI) that were used as a surrogate of liver fibrosis. While liver-related death was >3times more common in Pi*MM/Pi*MZ subjects with harmful alcohol consumption, the difference was not statistically significant in Pi*MZ subjects. In Pi*ZZ individuals from both cohorts, moderate alcohol consumption had no obvious impact on transaminase serum levels, although GGT levels were numerically more frequently elevated. In the European

cohort, Pi*ZZ subjects with moderate alcohol consumption tended to have higher continuous attenuation parameters (CAP) suggestive of liver steatosis, while liver stiffness measurement (LSM) as a surrogate of liver fibrosis did not differ. In addition, 14% of individuals had elevated CDT serum levels ($\geq 1.7\%$). In univariable analysis, Pi*ZZ subjects with elevated CDT levels displayed higher GGT serum levels (72.5 vs. 60.0% ULN, $p = 0.011$) as well as higher APRI scores (0.36 vs. 0.30 units, $p = 0.006$). No differences in LSM, but a trend towards higher CAP results was noted. LDC diet did not increase AAT accumulation in Pi*Z mice, while its impact on collagen mRNA was similar in both genotypes.

Conclusion: Moderate alcohol consumption seems to be tolerated in the majority of Pi*MZ and Pi*ZZ subjects.

THU-282

First nationwide genetic study on Wilson disease (Spanish Wilson registry): high diversity in mutations and in use of genetic evaluation, association with clinical data and influence on diagnosis and health costs

Pablo Alonso Castellano¹, Zoe Mariño², Antonio Oliveira Martin³, Javier Ampuero⁴, Marina Berenguer⁵, Diego Burgos Santamaria⁶, José Ramón Fernández⁷, Jose María Moreno Planas⁸, María Lázaro Ríos⁹, Helena Masnou¹⁰, Maria Luisa Gonzalez Dieguez¹¹, Jose Pinazo Bandera¹², Esther Molina¹³, Manuel Hernández Guerra¹⁴, Concepción gonzalez de frutos¹⁵, Patricia Cordero Ruiz¹⁶, Carolina Muñoz Codoceo¹⁷, Sara Lorente¹⁸, Alba Cachero¹⁹, Manuel Delgado²⁰, Víctor Manuel Vargas Blasco²¹, Judith Gómez-Camarero²², Julia Morillas²³, Francisca Cuenca Alarcon²⁴, Luis Ibañez Samaniego²⁵, Miguel Fernandez-Bermejo²⁶, Beatriz Álvarez-Suárez²⁷, Paula Iruzubieta²⁸, Ana Arencibia Almeida²⁹, Anna Miralpeix², Pilar Castillo³, Luis García-Villarreal³⁰. ¹Servicio Digestivo, Complejo Hospitalario Universitario Insular Materno Infantil (CHUIMI), Las Palmas de Gran Canaria, Spain; ²Liver Unit, Hospital Clínic, CIBERhd, IDIBAPS, ERN-RARE Liver, Universitat de Barcelona, Barcelona, Spain; ³Hospital Universitario La Paz, Madrid, Spain; ⁴Hospital Universitario Virgen del Rocío, Sevilla, Spain; ⁵Hospital Universitari i Politècnic La Fe, València, Spain; ⁶Hospital Ramón y Cajal, Madrid, Spain; ⁷Hospital Universitario de Cruces, Barakaldo, Spain; ⁸Servicio de Aparato Digestivo, Complejo Hospitalario Universitario de Albacete, Facultad de Medicina Universidad de Castilla La Mancha, Spain; ⁹Hospital Universitario Miguel Servet, Zaragoza, Spain; ¹⁰Hospital Universitari Germans Trias i Pujol, Badalona, Spain; ¹¹Hospital Universitario Central de Asturias, Oviedo, Spain; ¹²Unidad de Hepatología, Unidad de Gestión Clínica de Aparato Digestivo, Hospital Universitario Virgen de la Victoria, Instituto de Investigación Biomédica de Málaga-Plataforma Bionand, Málaga, Spain; ¹³Hospital Clínico de Santiago, Santiago de Compostela, Spain; ¹⁴Hospital Universitario de Canarias, Santa Cruz Tenerife, Spain; ¹⁵Hospital Universitario de Toledo, Toledo, Spain; ¹⁶Hospital Universitario Virgen Macarena, Sevilla, Spain; ¹⁷Hospital Universitario 12 de Octubre, Madrid, Spain; ¹⁸Unidad de Hepatología y Trasplante Hepático, Hospital Clínico Lozano Blesa de Zaragoza, IISS Aragón, Spain; ¹⁹Hospital Universitari de Bellvitge, Hospitalet de Llobregat, Spain; ²⁰Hospital Universitario A Coruña, A Coruña, Spain; ²¹Servicio de Hepatología, Hospital Vall d'Hebron, Universitat Autònoma Barcelona, CIBERhd, Barcelona, Spain; ²²Hospital Universitario de Burgos, Burgos, Spain; ²³Hospital Universitario Virgen de la Luz, Cuenca, Spain; ²⁴Unidad de Hígado, Servicio de Aparato Digestivo, Hospital Clínico San Carlos, Madrid, Spain; ²⁵Hospital General Universitario Gregorio Marañón, Madrid, Spain; ²⁶Hospital Universitario de Cáceres, Cáceres, Spain; ²⁷Hospital Universitario Lucus Augusti (CHUL), Lugo, Spain; ²⁸Hospital Universitario Marqués de Valdecilla, Santander, Spain; ²⁹Hospital Universitario Nuestra Señora de La Candelaria, Santa Cruz de Tenerife, Spain; ³⁰Servicio Digestivo, Complejo Hospitalario Universitario Insular Materno Infantil (CHUIMI), Las Palmas de Gran Canaria, Spain
Email: lgarciaavillarreal@gmail.com

Background and aims: We had no wide study about mutations (MUT) and clinical data on Wilson Disease (WD) in Spain. Recently, a National Registry for WD (SWR) was started by the AEEH (Spanish Association for the Study of the Liver). We aimed to study WD mutations and its association with clinical phenotypes and the different use of genetic evaluation among regions.

Method: Multicentre study including genetic and clinical data from patients (pt) from the SWR during the first year. Ethical approval and informed consent was obtained for all cases.

Results: The SWR includes data from 29 hospitals (from 1 to 71 pt) of 13/17 regions (85% nation population). Genetics were available in 233/320 pt with a Leipzig score >2 ; with data of 2 alleles in 206/233 pt (homozygous 27%). More than 130 MUT were registered, the majority in less than 4 alleles, being the most prevalent: M645R (17.3% alleles, mainland and Canaries), L708P (12.6%, only Canaries) and H1069Q (6.5%, only mainland). Only 15 MUT were in homozygosity and 3 in more than 3 pt: L708P (24 pt), c.1708-1G>A (5 pt, restricted to gipsy ethnicity), M645AR (4 pt). Among regions, genetic data ranged from 0% to 100% pt (in 3 regions under 40% and in 4 regions above 85% of their pt). In regions with several centers, the difference among them was higher than 50%. Among the most prevalent MUT, we found differences in the proportion of cirrhosis at diagnosis (higher for L708P $p = 0.002$), asymptomatic pt (higher in H1069Q, $p = 0.027$), clinical presentation (chronic hepatic higher for M645R, recent neurological higher in c.1708-1G>A, chronic neurological higher in L708P, $p < 0.001$). In homozygous pt, we only found differences in recent neurological cases (higher in c.1708-1G>A; $p < 0.05$) and age at diagnosis after 40 yo (low in L708P and high for M645R; $p < 0.001$). In the absence of genetic data up to 45% of pt would not have reached Leipzig score >3 . In screening cases, genetics were used in 49/58 (85%); without genetics, two thirds would not have reached Leipzig >3 (33/49).

Conclusion: We got the first genetic map for WD in Spain, with a great variability of MUT (except in Gran Canaria and the gipsy community, probably with higher inbreeding). The use of genetic testing in WD is very heterogeneous among regions and even within them. Its use is high for screening cases, saving time and costs to both patients and the health care system. The most frequent MUT (M645R) seems to associate with a milder phenotype (lower penetrance), while the Gran Canaria mut (L708P) seems to present earlier and with more severe cases. The MUT of the gipsy ethnicity is associated with recent neurological cases. These data will be confirmed and expanded with further data in the Spanish Wilson Registry.

THU-283

Myeloproliferative neoplasms and splanchnic vein thrombosis: results of a long-term UK prospective cohort study

Rupen Hargreaves¹, Anicee Danaee¹, David Patch², Salil Karkhanis³, Israa Kaddam⁴, Jin Un Kim¹, Hayder Hussein⁴, Frederick Chen⁴, Dominic Yu¹, Mallika Sekhar¹, Dhiraj Tripathi³. ¹Royal Free Hospital NHS Foundation Trust, Department of Haematology, United Kingdom; ²Royal Free Hospital NHS Foundation Trust, Sheila Sherlock Liver Centre, United Kingdom; ³University Hospitals Birmingham NHS Foundation Trust, Liver Unit, United Kingdom; ⁴University Hospitals Birmingham NHS Foundation Trust, Department of Haematology, United Kingdom
Email: rupen.hargreaves@nhs.net

Background and aims: Myeloproliferative neoplasms (MPN) confer an increased risk of thrombosis, including splanchnic vein thrombosis (SVT). SVT comprises porto-mesenteric-splenic axis thrombosis (PMVT) and hepatic vein thrombosis (HVT, Budd-Chiari syndrome). MPN-SVT carries a significant morbidity and clinical management is challenging, requiring surgical and radiological intervention in addition to aggressive anticoagulation. Long term prospective studies of this patient population are lacking. We report the results of a 5-year prospective cohort study assessing outcomes in MPN-SVT patients.

Method: The primary end point was a composite comprised of change in morbidity or portal circulation over 18 months. Secondary end points included 5 year outcome data and antithrombotic and cytoreductive usage, amongst others. Splanchnic thrombotic burden was assessed using cross sectional imaging in line with international standards.

34 patients with MPN-SVT were recruited from two UK specialist centres to an observational study that lasted between 2014 and 2021. **Results:** 34 patients with MPN-SVT were recruited from two UK specialist centres to an observational study that lasted between 2014 and 2021. Median age at diagnosis was 45 (range 22–72) and 59% were female. Median time from SVT to registration was 34 months (range 1–167). There were 3 deaths, two were disease-related. 94% had a JAK2 V617F mutation. The underlying MPN was Polycythaemia vera in 44% and Essential thrombocythaemia in 35%. At 5 years, 39% of patients were taking hydroxycarbamide, 17% interferon, 28% ruxolitinib and 17% no cytoreduction. 28/34 (82%) were on anticoagulation at study recruitment, of whom 89% were on warfarin. 9/34 (26%) were taking an antiplatelet at registration. At 5 years, 28/29 (97%) were on anticoagulation, 68% were on warfarin and 21% on DOACs. HVT accounted for 21% of thrombosis and PMVT for 79%. Cavernoma formation was seen in 19/34 (56%). Imaging outcome data were obtained at 18 months and 60 months. At 18 months, 17/34 (50%) had unchanged abdominal thrombotic appearances, 13/34 (38%) had recanalization, 1 patient (3%) had extension and there were no recurrences. A reduction in thrombotic load was seen in 3 patients (8.8%). At 5 years, 25/29 (86%) had unchanged abdominal thrombotic appearances, 3/29 (10%) had further recanalization and 1/29 (3.4%) had recurrence despite therapeutic anticoagulation. Spleen size increased in 6/29 (21%), reduced in 14/29 (48%) and remained unchanged in 9/29 (31%).

Conclusion: To our knowledge, this is the first prospective study of MPN-SVT. The data show sustained recanalization and low recurrence rates over 5 years, which is a novel finding. Our data provide a contemporary perspective on the natural course of this rare disease entity treated at specialist centres and pave the way for future studies in MPN-SVT.

THU-284

Efficacy and safety outcomes with odevixibat treatment: Pooled data from the phase 3 ASSERT and ASSERT-EXT studies in patients with Alagille syndrome

Nadia Ovchinsky¹, Madeleine Aumar², Alastair Baker³, Ulrich Baumann⁴, Philip Buefler⁵, Mara Cananzi⁶, Ozlem Durmaz⁷, Ryan Fischer⁸, Giuseppe Indolfi⁹, Wikrom Karnsakul¹⁰, Florence Lacaille¹¹, Way Seah Lee¹², Giuseppe Maggione¹³, Philip Rosenthal¹⁴, Mathias Ruiz¹⁵, Etienne Sokal¹⁶, Ekkehard Sturm¹⁷, Wendy L. van der Woerd¹⁸, Henkjan J. Verkade¹⁹, Andrew Wehrman²⁰, Christine Clemson²¹, Qifeng Yu²¹, Quanhong Ni²¹, Jessica Ruvido²¹, Susan Manganaro²¹, Jan Mattsson²¹, Piotr Czubkowski²². ¹Division of Paediatric Gastroenterology, Hepatology, and Nutrition, Children's Hospital at Montefiore, Albert Einstein College of Medicine, United States; ²Univ Lille, CHU Lille, Paediatric Gastroenterology, Hepatology, and Nutrition, Inserm U1286 Infinite, CHU Lille Pôle Enfant, France; ³Paediatric Liver Centre, King's College Hospital, United Kingdom; ⁴Paediatric Gastroenterology and Hepatology, Hannover Medical School, Germany; ⁵Department of Paediatric Gastroenterology, Nephrology, and Metabolic Diseases, Charité Universitätsmedizin Berlin, Germany; ⁶Paediatric Gastroenterology, Digestive Endoscopy, Hepatology, and Care of the Child With Liver Transplantation, Department of Children's and Women's Health, University Hospital of Padova, Italy; ⁷Istanbul University, Istanbul Faculty of Medicine, Turkey; ⁸Division of Paediatric Gastroenterology, Hepatology, and Nutrition, Children's Mercy Hospital,

United States; ⁹Paediatric and Liver Unit, Meyer Children's University Hospital of Florence, Italy; ¹⁰Division of Paediatric Gastroenterology, Nutrition, and Hepatology, Department of Paediatrics, Johns Hopkins University School of Medicine, United States; ¹¹Paediatric Gastroenterology-Hepatology-Nutrition Unit, Hôpital Universitaire Necker-Enfants Malades, France; ¹²Department of Paediatrics, Faculty of Medicine, University of Malaya, Malaysia; ¹³Hepatology, Gastroenterology, Nutrition, Digestive Endoscopy, and Liver Transplantation Unit, Bambino Gesù Children's Hospital IRCCS, Italy; ¹⁴Department of Paediatrics, Division of Gastroenterology, Hepatology, and Nutrition, University of California San Francisco, United States; ¹⁵Department of Paediatric Gastroenterology, Hepatology, and Nutrition, Hospices Civils de Lyon, Hôpital Femme-Mère-Enfant, France; ¹⁶Université Catholique de Louvain, Cliniques St Luc, Belgium; ¹⁷Paediatric Gastroenterology and Hepatology, University Children's Hospital Tübingen, Germany; ¹⁸Department of Paediatric Gastroenterology, Wilhelmina Children's Hospital, University Medical Centre Utrecht, Netherlands; ¹⁹Department of Paediatrics, University of Groningen, Beatrix Children's Hospital/University Medical Centre Groningen, Netherlands; ²⁰Division of Gastroenterology, Hepatology, and Nutrition, Boston Children's Hospital, United States; ²¹Albireo Pharma, Inc., Boston, United States; ²²Department of Gastroenterology, Hepatology, Nutritional Disorders, and Paediatrics, The Children's Memorial Health Institute, Poland
Email: novchins@montefiore.org

Background and aims: Cholestasis in Alagille syndrome (ALGS) is associated with accumulation of bile acids (BAs) and other biliary components in the liver with spill-over into the systemic circulation, as well as severe pruritus that can impair sleep. In the phase 3 ASSERT and ASSERT-EXT trials, odevixibat, an ileal BA transporter inhibitor, improved pruritus and sleep parameters and reduced BAs in patients with ALGS. Using pooled data from these studies, we describe efficacy and safety outcomes with odevixibat in patients with ALGS.

Method: In the completed 24-week ASSERT study, patients with ALGS with history of significant pruritus and elevated serum BAs were randomised 2:1 to odevixibat 120 µg/kg/day or placebo, respectively. Patients who completed ASSERT could enter ASSERT-EXT, an ongoing, 72-week open-label extension study in which all patients receive odevixibat 120 µg/kg/day. This pooled analysis included all odevixibat-treated patients from ASSERT and/or ASSERT-EXT and spans from patients' first dose of odevixibat to a data cut-off of 9 September 2022. Assessments through 36 weeks of treatment included change in observer-reported scratching scores and sleep parameters as well as levels of serum BAs, autotaxin (a proposed mediator of pruritus), and plasma 7- α -hydroxy-4-cholesten-3-one (p-C4; a marker of reduced BA reabsorption). Safety evaluations included monitoring liver function parameters and treatment-emergent adverse events (TEAEs).

Results: At the data cut-off, 52 odevixibat-treated patients (mean age, 6.5 years; 48% female) comprised the pooled population. Compared with baseline, odevixibat treatment resulted in rapid (by week 4) and significant mean improvements in pruritus and reductions in BA levels, as well as significant mean decreases in autotaxin and increases in p-C4 levels (Figure). There were significant decreases from baseline to weeks 33–36 (n = 21) in multiple sleep parameters, including mean percentage of days seeing blood due to scratching, needing help falling asleep, needing soothing, and sleeping with caregiver (–30%, –60%, –59%, and –44%, respectively; all p < 0.001). No patients had concurrent elevations in alanine aminotransferase or total bilirubin that were indicative of drug-induced liver injury. TEAEs were reported in 43 of 52 (83%) odevixibat-treated patients. The most common drug-related TEAE

Mean Change From Baseline in Scratching Scores (A), Bile Acids (B), Autotaxin (C), and p-C4 (D) in a Pooled Population of Patients With ALGS Treated With Odevixibat

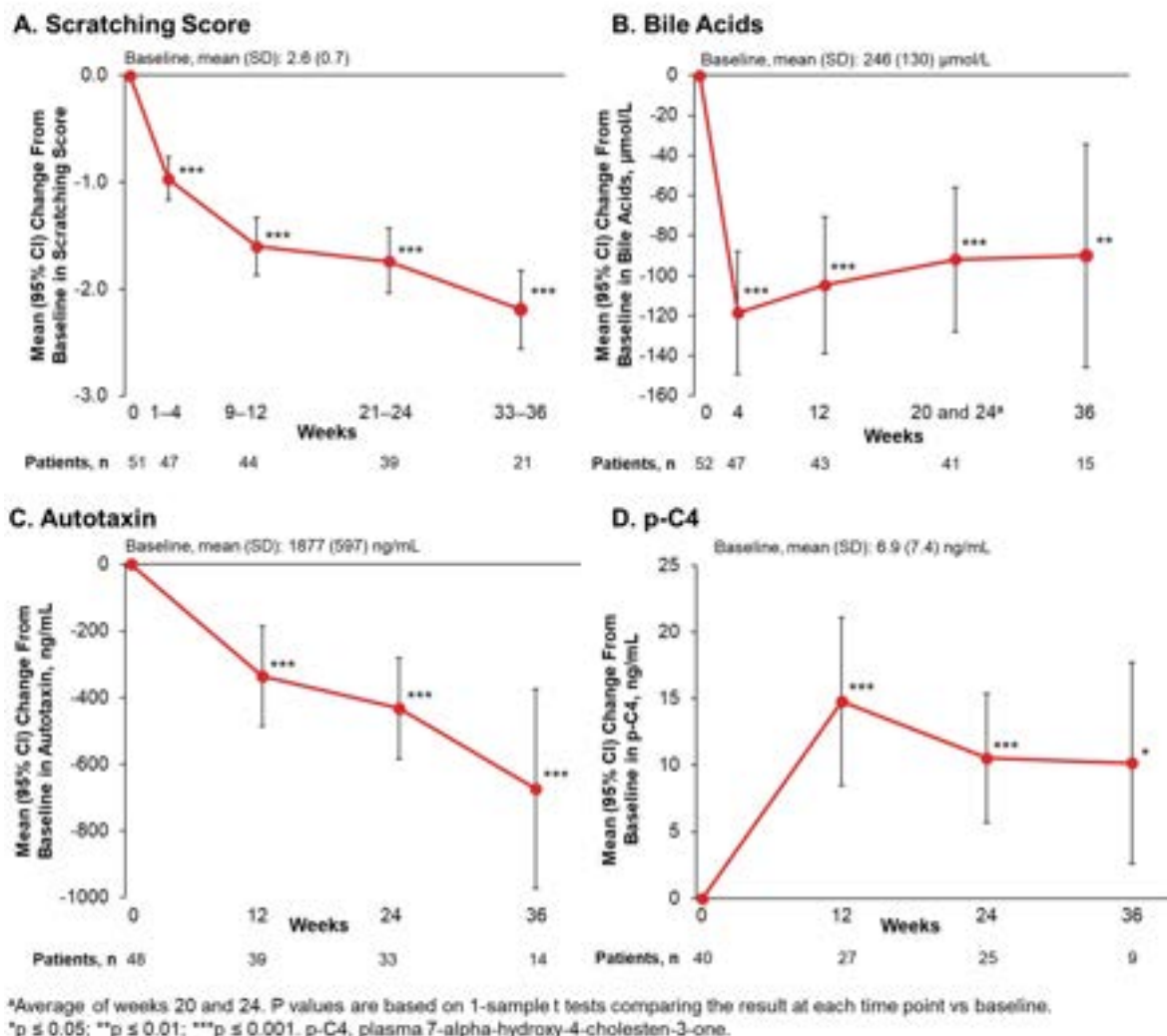


Figure: (abstract: THU-284).

was diarrhoea (n = 6/52 [12%]). At the data cut-off, no patient had TEAEs that led to study discontinuation.

Conclusion: In patients with ALGS, odevixibat treatment for up to 36 weeks led to significant and sustained improvements in pruritus and sleep and significant reductions in BA levels. Consistent with effects on pruritus and BA levels, there were significant changes in autotaxin and p-C4 levels with odevixibat. Odevixibat treatment was generally well tolerated in patients with ALGS.

THU-285

Clinical features, histology and outcome of pediatric porto-sinusoidal vascular disease

Angelo Di Giorgio¹, Lorenza Matarazzo¹, Aurelio Sonzogni², Emanuele Nicastro¹, Andrea Pietrobattista³, Mara Cananzi⁴, Paola Gaio⁴, Marco Sciveres⁵, Grazia Di Leo⁶, Raffaele Iorio⁷, Antonio Marseglia⁸, Giuseppe Maggiore³, Maria Guido⁹, Lorenzo D'Antiga¹. ¹Paediatric Hepatology, Gastroenterology and Transplantation, Hospital Papa Giovanni XXIII, Bergamo, Italy; ²USC Anatomia Patologica ASST Bergamo Est, Italy, Italy; ³Hepatology, Gastroenterology, Digestive Endoscopy, Nutrition, and Liver Transplantation Unit, IRCCS Bambino Gesù, Pediatric Hospital Rome, Italy; ⁴Unit of Gastroenterology, Digestive Endoscopy, Hepatology and

Care of the Child with Liver Transplantation, University Hospital of Padova, Italy; ⁵Paediatric Department and Transplantation, Ismett, Palermo, Italy; ⁶IRCCS Burlo Garofolo, Trieste, Italy; ⁷Department of Translational Medical Science, School of Medicine and Surgery, University of Naples Federico II, Naples, Italy; ⁸Fondazione IRCCS Casa Sollievo della Sofferenza, Division of Pediatrics, San Giovanni Rotondo, Italy; ⁹Department of Medicine-DIMED, University of Padova, Italy
Email: adigiorgio@asst-pg23.it

Background and aims: in paediatrics, porto-sinusoidal vascular disease (PSVD) is likely an underdiagnosed and misdiagnosed condition. We report data of a large cohort of children diagnosed with PSVD.

Method: retrospective, multicentre study of children with PSVD diagnosed by histological criteria in the last 15 years.

Results: 62 children with PSVD (M/F = 36/26, median age 6.6 years, range 3.3–10.6), from 7 centres, were included. Two expert liver pathologists reviewed histological features blindly. Thirty-six patients presented with non-cirrhotic portal hypertension, PH, (PH-PSVD Group = 58%) while 26 had a liver biopsy because of chronic elevation of transaminases without PH (noPH-PSVD Group = 42%). On histology review, the two groups differed for the prevalence of

obliterative portal venopathy (more prevalent in PH-PSVD, $p = 0.005$), and hypervascularised portal tract (more common in noPH-PSVD, $p = 0.039$). At multivariate analysis, platelet count $\leq 185.000/\text{mm}^3$ was the only independent determinant of PH ($p < 0.001$). Linear regression analysis showed a significant reduction in platelet count with increasing age at time of diagnosis and at last follow-up (Pearson coefficient -0.4876 , $p = 0.02$ at diagnosis; 0.4209 ; p value $= 0.04$ at last follow-up). After a median follow-up of 7 years (range 3.0–11.2), in PH-PSVD group 3/36 (8%) required TIPS placement, 5/36 (14%) developed pulmonary vascular complications of PH, and 7/36 (19%) required liver transplantation. In noPH-PSVD none progressed to PH nor had complications. At last follow-up 60/62 patients (97%) were alive.

Conclusion: PSVD present with two different clinical phenotypes, one characterised by PH and one by chronic elevation of transaminases without PH. PSVD should be included among the conditions causing isolated hypertransaminasemia. There is a clear trend to decreased platelet count by age and follow-up at linear regression. On histology, the differences between the two groups are subtle. Medium-term outcome is favourable in patients without PH; progression of the disease is observed in those with PH.

THU-286

Abstract withdrawn

THU-287

High-dose oral thiamine was not superior to placebo in reducing fatigue in patients with primary biliary cholangitis: a randomised, double-blinded, placebo-controlled crossover trial

Palle Bager¹, Lars Bossen¹, Rasmus Hvidbjerg Gantzel¹, Henning Grønbaek¹. ¹Aarhus University Hospital, Department of Hepatology and Gastroenterology, Aarhus N, Denmark
Email: pallbage@rm.dk

Background and aims: Fatigue in primary biliary cholangitis (PBC) is highly frequent and associated with reduced quality of life. The causes of fatigue are multifactorial and have led to a variety of interventions. Despite the impact of fatigue in PBC, only a few interventions have demonstrated clinical effects. However, in patients with inflammatory bowel disease, high-dose thiamine given for 4 weeks showed significant effects on fatigue. We aimed to investigate the effects of high-dose thiamine on fatigue in patients with PBC and conducted a randomised, double-blinded, placebo-controlled crossover trial.

Method: Patients with PBC and significant fatigue, normal renal function, and no obvious other reasons for fatigue were included. Patients were allocated 1:1 to Group 1 (high dose oral thiamine for 4 weeks, a 4 weeks wash-out period, followed by 4-week oral placebo) or Group 2 (oral placebo for 4 weeks, a 4 weeks wash-out period, followed by 4 weeks high dose oral thiamine). The doses of thiamine ranged between 600 and 1800mg/day, based on gender and body weight. Fatigue was measured using the PBC-40 questionnaire. A subscale including 11 questions measures the severity of fatigue (range 11–55). We defined significant fatigue as a score >32, based on data from the general population. The primary end point was a decrease of ≥5 points on the PBC-40 fatigue-subscale. The study adhered to the principles for Good Clinical Practice.

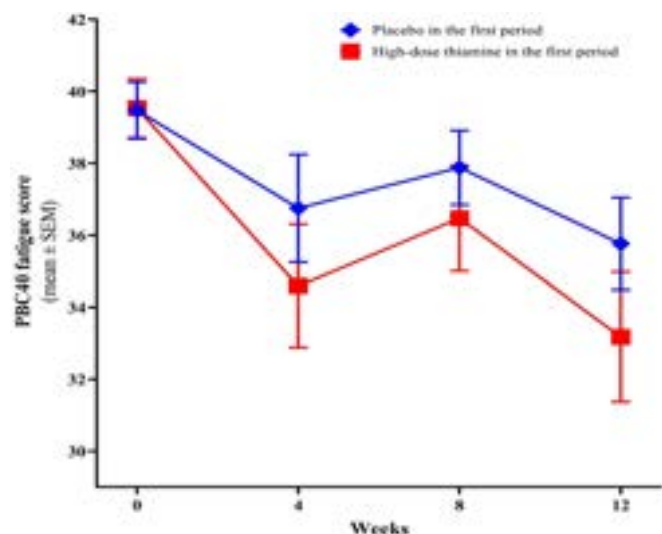


Figure:

Results: Of 36 patients included and randomised, 32 completed the study. Of these, 30 participants (94%) showed >80% adherence to thiamine treatment and were included for further analysis. We observed no statistical differences between the groups at baseline and no carryover effect. At the end of study (week 12), 14 patients (47%) had a reduction ≥5 points in fatigue. The overall mean

reduction of fatigue was 5.4 points (95% CI 2.8–8.0; $p < 0.001$). A delayed treatment model was assessed, showing a 3.7 points (95% CI 1.2–6.2) reduction in fatigue after thiamine treatment, compared to a 3.7 points (95% CI 1.9–5.6) reduction in fatigue after placebo ($p = 0.98$). Furthermore, 44% of Group 1 and 25% of Group 2 showed an improvement of more than 5 points while on thiamine treatment compared with 44% of Group 1 and 31% of Group 2 while on placebo (Figure 1). No serious adverse events were detected. Adverse events were sparse, temporary, and included sore throat and cold symptoms. **Conclusion:** The treatment was well tolerated and safe for the patients. However, the effect of four weeks high-dose oral thiamine was not superior to placebo in PBC patients with significant fatigue. The overall effect could be ascribed to a convincing effect of placebo.

THU-288

Cancer incidence and survival in HFE hemochromatosis-A population-based cohort study

Benedikt Schaefer¹, Lorenz Michael Pammer¹, Bernhard Pfeifer^{2,3}, Sabrina Neururer^{2,3}, Maria Troppmair¹, Marlene Panzer¹, Sonja Wagner¹, Elke Pertler¹, Christian Gieger^{4,5}, Florian Kronenberg⁶, Claudia Lamina⁶, Herbert Tilg¹, Heinz Zoller¹. ¹Medical University of Innsbruck, Department of Medicine I, Gastroenterology, Hepatology and Endocrinology, Austria; ²UMIT Tirol, Division for Digital Medicine and Telehealth, Austria; ³Tirol Kliniken GmbH, Tyrolean Federal Institute for Integrated Care, Austria; ⁴Helmholtz Zentrum München, Institute of Epidemiology, Germany; ⁵Helmholtz Zentrum München, Research Unit of Molecular Epidemiology, Germany; ⁶Medical University of Innsbruck, Institute of Genetic Epidemiology, Austria
Email: heinz.zoller@i-med.ac.at

Background and aims: Hemochromatosis is characterized by progressive iron overload affecting the liver and can cause cirrhosis and hepatocellular carcinoma. Most hemochromatosis patients are homozygous for p.C282Y in *HFE*, but only a minority of individuals with this genotype will develop the disease. The aim was to assess the penetrance of iron overload, liver fibrosis, hepatocellular carcinoma and life expectancy in hemochromatosis patients.

Method: A total of 8839 individuals from the Austrian region of Tyrol were genotyped for the p.C282Y variant between 1997 and 2021. Demographic, laboratory parameters and causes of death were assessed from health records. Survival and cancer incidence were ascertained from the national health insurance and cancer registry. Outcomes were compared to a propensity score matched control population.

Results: Median age at diagnosis in 542 p.C282Y homozygous individuals was 47.8 years (64% male) and the prevalence of biochemical iron overload was 55%. Among all expected Tyrolean residents with p.C282Y homozygosity, biochemical iron overload was confirmed in 15.8% of men as compared to 8.9% of women aged 60 years. The proportion of p.C282Y homozygotes in whom significant fibrosis could be excluded by a FIB-4 score <1.3 decreased with age and was 95.6% in males and 97.3% in females at the age of 60 years. Median life-expectancy was reduced by 6.8 years in individuals homozygous for p.C282Y when compared with population-matched controls ($p = 0.001$). No difference could be found in cancer incidence, including hepatocellular carcinoma.

Conclusion: Penetrance of iron overload in p.C282Y homozygotes is low, but survival is reduced when compared to a matched control population.

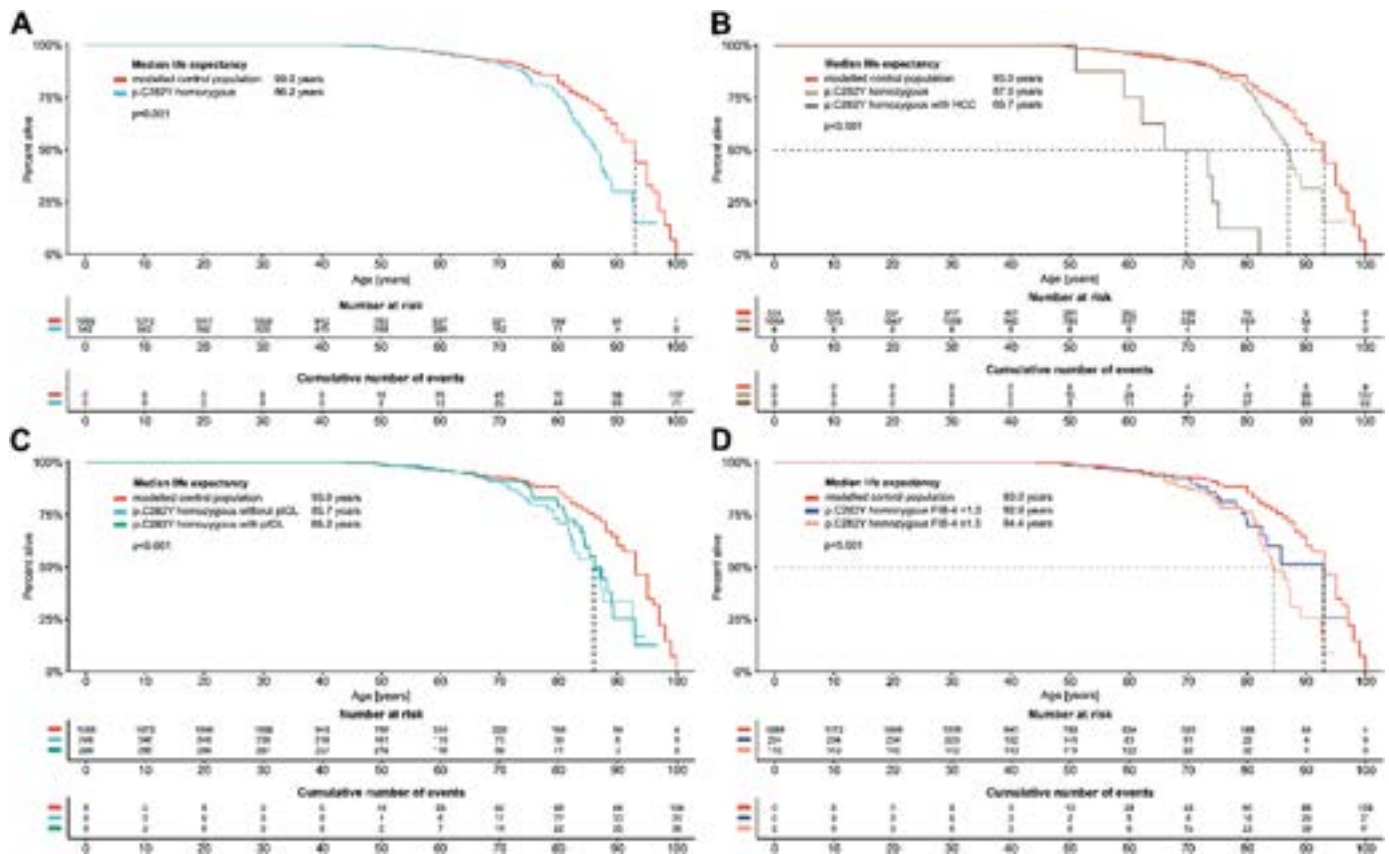


Figure: (abstract: THU-288): (A) Life expectancy of p.C282Y homozygotes (B) with and without hepatocellular carcinoma (C) with and without provisional iron overload (pIOL) and (D) FIB-4 score <1.3 or ≥1.3 compared to a modelled propensity score-matched control population.

THU-289

Analysis of long-term treatment effects of odevixibat on clinical outcomes in children with progressive familial intrahepatic cholestasis in odevixibat clinical studies vs external controls from the NAPPED database

Bettina Hansen¹, Velichka Valcheva², Qifeng Yu², Daan van Wessel³, Richard Thompson⁴, Emmanuel Gonzales⁵, Irena Jankowska⁶, Etienne Sokal⁷, Tassos Grammatikopoulos⁴, Agustina Kadaristiana⁴, Emmanuel Jacquemin⁵, Anne Spraul⁸, Patryk Lipiński⁶, Piotr Czubkowski⁶, Nathalie Rock⁹, Mohammad Shagrani¹⁰, Kishwer Kumar¹⁰, Fowzan Alkuraya¹¹, Meddirevula Sateesh¹², Dieter Clemens Broering¹⁰, Emanuele Nicastro¹³, Deirdre Kelly¹⁴, Gabriella Nebbia¹⁵, Henrik Arnell¹⁶, Björn Fischler¹⁶, Daniele Serranti¹⁷, Cigdem Arkan¹⁸, Esra Polat¹⁹, Dominique Debray²⁰, Florence Lacaille²⁰, Cristina Gonçalves²¹, Loreto Hierro Llanillo²², Gema Muñoz Bartolo²², Yael Mozer-Glassberg²³, Amer Azaz²⁴, Jernej Breclj²⁵, Antal Dezsőfi²⁶, Pier Luigi Calvo²⁷, Enke Grabhorn²⁸, Ekkehard Sturm²⁹, Wendy L. van der Woerd³⁰, Binita M. Kamath³¹, Jian-She Wang³², Li Liting³², Ozlem Durmaz³³, Zerrin Önal³³, Antonia Felzen³, Mark Nomden³, Jaak Sonajalg³⁴, Philip Stein², Quanhong Ni², Christine Clemson², Jan Mattsson², Henkjan J. Verkade³. ¹Department of Epidemiology and Biostatistics, Erasmus MC, Rotterdam, the Netherlands; Toronto Centre for Liver Disease and TGHRI, University Health Network, Canada; IHPME, University of Toronto, Canada; ²Albireo Pharma, Inc., Boston, MA, United States; ³Pediatric Gastroenterology and Hepatology, University Medical Center Groningen, University of Groningen, the Netherlands; European Reference Network on Hepatological Diseases (ERN RARE-LIVER), Netherlands; ⁴Institute of Liver Studies, King's College London, London,

United Kingdom; ⁵Service d'Hépatologie et de Transplantation Hépatique Pédiatriques, Bicêtre Hôpital, AP-HP, Université Paris-Sud, Paris Saclay, Inserm UMR-S 1174, France; European Reference Network on Hepatological Diseases (ERN RARE-LIVER), France; ⁶European Reference Network on Hepatological Diseases (ERN RARE-LIVER); Gastroenterology, Hepatology, Nutritional Disorders and Paediatrics, The Children's Memorial Health Institute, Poland; ⁷European Reference Network on Hepatological Diseases (ERN RARE-LIVER); Université Catholique de Louvain, Cliniques St Luc, Brussels, Belgium; ⁸Service de Biochimie, Bicêtre Hôpital, AP-HP, Université Paris-Sud, Paris Saclay, Inserm UMR-S 1174, France; ⁹Paediatric Gastroenterology, Hepatology and Nutrition Unit, Division of Paediatric Specialties, Department of Paediatrics, Gynaecology and Obstetrics, University Hospitals of Geneva, Switzerland; ¹⁰Liver and SB Transplant and Hepatobiliary-Pancreatic Surgery, King Faisal Specialist Hospital and Research Centre, Riyadh, Saudi Arabia; Alfaisal University, College of Medicine, Riyadh, Saudi Arabia; ¹¹Translation Genomic Department, King Faisal Specialist Hospital and Research Centre, Riyadh, Saudi Arabia; ¹²Clinic Genomics Department, King Faisal Specialist Hospital and Research Centre, Riyadh, Saudi Arabia; ¹³Pediatric Hepatology, Gastroenterology and Transplantation, Ospedale Papa Giovanni XXIII, Bergamo, Italy; ¹⁴European Reference Network on Hepatological Diseases (ERN RARE-LIVER); Liver Unit, Birmingham Women's and Children's Hospital, Birmingham, United Kingdom; ¹⁵Servizio Di Epatologia e Nutrizione Pediatrica, Fondazione Irccs Ca' Granda Ospedale Maggiore Policlinico, Milano, Italy; ¹⁶European Reference Network on Hepatological Diseases (ERN RARE-LIVER); Paediatric Gastroenterology, Hepatology and Nutrition, Astrid Lindgren Children's Hospital and Karolinska University Hospital, Karolinska Institutet, Stockholm, Sweden; ¹⁷Paediatric and Liver Unit, Meyer Children's University Hospital of Florence, Italy; ¹⁸Koc

POSTER PRESENTATIONS

University School of Medicine, Paediatric GI and Hepatology Liver Transplantation Centre, Kuttam System in Liver Medicine, Istanbul, Turkey; ¹⁹Paediatric Gastroenterology, Sancaktepe, Training and Research Hospital, Istanbul, Turkey; ²⁰Unité d'hépatologie Pédiatrique et Transplantation, Hôpital Necker; European Reference Network on Hepatological Diseases (ERN RARE-LIVER), Paris, France; ²¹European Reference Network on Hepatological Diseases (ERN RARE-LIVER); Paediatric Gastroenterology/Hepatology Center Lisbon, Portugal; ²²European Reference Network on Hepatological Diseases (ERN RARE-LIVER); Service of Pediatric Hepatology and Transplantation, Children's Hospital La Paz, La Paz University Hospital, Spain; ²³Institute of Gastroenterology, Nutrition and Liver Diseases, Schneider Children's Medical Centre of Israel, Petah Tikva, Israel; ²⁴Pediatric Gastroenterology, Hepatology and Nutrition, Sheikh Khalifa Medical City, Abu Dhabi, United Arab Emirates; ²⁵Department of Gastroenterology, Hepatology and Nutrition, University Children's Hospital Ljubljana and Department of Paediatrics, Faculty of Medicine, University of Ljubljana, Ljubljana, Slovenia; ²⁶1st Department of Paediatrics, Semmelweis University, Budapest, Hungary; ²⁷Pediatric Gastroenterology Unit, Regina Margherita Children's Hospital, Azienda Ospedaliera Città Della Salute e Della Scienza University Hospital, Torino, Italy; ²⁸Klinik Für Kinder- Und Jugendmedizin, Universitätsklinikum Hamburg Eppendorf, Hamburg, Germany; ²⁹European Reference Network on Hepatological Diseases (ERN RARE-LIVER); University Children's Hospital Tübingen, Tübingen, Germany; ³⁰Wilhelmina Children's Hospital, University Medical Center Utrecht, Paediatric Gastroenterology, Hepatology and Nutrition, Utrecht, Netherlands; ³¹The Hospital for Sick Children and the University of Toronto, Toronto, Canada; ³²Children's Hospital of Fudan University, Shanghai, China; ³³Department of Child Health and Diseases, Gastroenterology, Hepatology and Nutrition, Istanbul Faculty of Medicine, Istanbul University, Istanbul, Turkey; ³⁴Allucent, Cary, NC, United States
Email: bettina.hansen@utoronto.ca

Background and aims: Progressive familial intrahepatic cholestasis (PFIC) is a group of rare cholestatic liver diseases characterized by intractable pruritus, elevated serum bile acids (sBAs), and progressive liver damage. NAPPED (Natural course and Prognosis of PFIC and Effect of biliary Diversion) is a large retrospective database investigating the natural history of PFIC. Odevixibat, an ileal bile acid transporter inhibitor, reduced sBAs and pruritus in patients with PFIC in the phase 3 PEDFIC 1 and PEDFIC 2 studies. We compared clinical outcomes of surgical biliary diversion (SBD), liver transplantation (LT), and death in patients from NAPPED (not treated with odevixibat) with odevixibat-treated patients from the PEDFIC studies.

Method: The analysis population comprised odevixibat-naïve patients from NAPPED and odevixibat-treated patients from PEDFIC 1 and/or PEDFIC 2. BSEP3 patients were excluded in both groups. Eligibility criteria were aligned across cohorts and included genetically proven diagnosis of PFIC1 or PFIC2, sBAs $\geq 100 \mu\text{mol/L}$, alanine aminotransaminase and total bilirubin $\leq 10 \times$ the upper limit of normal, and no prior SBD or LT. Propensity scores, inverse probability of treatment weighting, and matching methods were used to identify and balance baseline covariates, including PFIC type 1, PFIC2-BSEP1 or PFIC2-BSEP2. The primary end point was event-free survival (EFS; time to first event of SBD, LT, or death); secondary end points included native liver survival (NLS), SBD-free survival (DFS), and overall survival (OS). Survival outcomes were measured from study day 1; treatment differences were evaluated by weighted log-rank tests and Cox regression.

Results: A cohort of 80 NAPPED patients (controls) was compared with 69 odevixibat-treated patients. The median study duration in the odevixibat cohort was 22.6 months (range: 1.9–39.2 months). The follow-up duration in the NAPPED cohort was truncated accordingly. Odevixibat-treated patients showed significantly higher EFS and DFS than controls (hazard ratio [HR]: 0.20 and 0.13, respectively); numerical improvements in NLS and OS were also observed (Table).

Results were consistent when different sensitivity analyses were performed. Additional subgroup analyses indicated that EFS was higher in odevixibat-treated patients with PFIC1 (HR [95% CI] = 0.10 [0.02, 0.55]) and PFIC2 (HR [95% CI] = 0.34 [0.12, 1.00]) vs controls.

Conclusion: Odevixibat treatment is associated with higher EFS in patients with PFIC without prior SBD, upon comparison to matched, non-odevixibat-treated patients from the NAPPED registry.

THU-290

Efficacy and safety of vaccination against SARS-CoV-2 in patients with vascular liver disease

Valeria Perez-Campuzano¹, Rautou Pe², Thomas Marjot³, Michael Praktiknjo⁴, Edilmar Alvarado-Tapias⁵, Laura Turco⁶, Luis Ibañez⁷, Carlos González-Alayón⁸, Angela Puente⁹, Elba Llop¹⁰, Macarena Simón-Talero¹¹, Carmen Álvarez-Navascués¹², Thomas Reiberger¹³, Xavier Verhelst¹⁴, Luis Téllez¹⁵, Lara Orts¹, Giuseppe Grassi¹, Anna Baiges¹, Payance Audrey², Jonel Trebicka⁴, Cándid Villanueva⁵, Maria Cristina Morelli⁶, Sam Murray³, Georgina Meacham³, Marc Luetgehetmann¹⁶, Julian Schulze zur Wiesch¹⁷, Juan Carlos Garcia Pagan^{1,18}, Eleanor Barnes³, Aurélie Plessier², Virginia Hernandez-Gea^{1,18}.
¹Hospital Clinic Barcelona, Barcelona, Spain; ²DHU Unity, Pôle des Maladies de l'Appareil Digestif, Service d'Hépatologie, Centre de Référence des Maladies Vasculaires du Foie, Hôpital Beaujon, AP-HP, Clichy, France; ³Nuffield Department of Medicine, University of Oxford, Oxford, United Kingdom; ⁴Department of Medicine B, University Hospital Münster, Germany; ⁵Hospital de la Santa Creu i Sant Pau, Barcelona, Spain; ⁶IRCCS Azienda Ospedaliero-Universitaria di Bologna, Italy; ⁷Hospital General Universitario Gregorio Marañón, Madrid, Spain; ⁸Hospital Universitario de Canarias, Spain; ⁹Hospital Marqués de Valdecilla, Spain; ¹⁰Hospital Puerta del Hierro, Spain; ¹¹Liver Unit, Digestive Diseases, Hospital Universitari Vall d'Hebron, VHIR, Vall d'Hebron Barcelona Hospital Campus, UAB, CIBERehd, Barcelona, Spain; ¹²Hospital Universitario Central de Asturias, Spain; ¹³Division of Gastroenterology and Hepatology, Department of Medicine III, Medical University of Vienna, Austria; ¹⁴Department of Gastroenterology and Hepatology, Ghent University Hospital, Belgium; ¹⁵Hospital Universitario Ramón y Cajal, Madrid, Spain; ¹⁶German Center for Infection Research (DZIF), Partner Site Hamburg-Lübeck-Borstel-Riems, Germany; ¹⁷Department of Internal Medicine, University Medical Center Hamburg-Eppendorf, Germany; ¹⁸University of Barcelona, Barcelona Hepatic Hemodynamic Laboratory, Spain
Email: vihernandez@clinic.cat

Background and aims: Patients with vascular liver diseases (VLD) are at considerable risk for thromboembolic events and are at higher risk of infection by SARS-CoV-2 and a severe course of COVID-19 disease. The immune response to the SARS-CoV-2 vaccination in patients with VLD is unknown. The effectiveness and safety of COVID-19 vaccines, especially the potential risk of thromboembolic events has not been investigated in these individuals. We thus, aimed to determine the efficacy of vaccination against COVID-19, incidence of adverse reactions and outcome post-vaccination in a large cohort of patients with VLD.

Method: International multicentre prospective observational study in patients with VLD. Patients were included at the time of vaccination, with a mean follow-up of 47 weeks (13–71 weeks). We analyzed the incidence of COVID-19 infection after vaccination, severity of side effects, occurrence of thromboembolic events and hepatic decompensation. In a subgroup of patients, the humoral and cellular responses to vaccination were analyzed.

Results: A total of 909 patients from 14 European centers were included, 524 non-cirrhotic-non-malignant-splanchnic vein thrombosis (NCPVT), 234 Portosinusoidal Vascular Disorder (PSVD) and 140 Budd-Chiari Syndrome (BCS). A total of 151 patients were previously infected by COVID-19. A total of 883 patients (97%) received two vaccine doses (fully vaccinated: FV), 681 (75%) also a third dose. In the 755 naïve FV, primary COVID-19 infection occurred in 52 (6.9%), a

Table: (abstract: THU-289): Survival Outcomes

	Odevixibat-Treated Cohort n = 69	NAPPED Control Cohort n = 80
Event-Free Survival (EFS)		
Events, n (%)	6 (9%)	44 (55%)
p value	0.0016	
HR (95% CI)	0.20 (0.09, 0.45)	
Native Liver Survival (NLS)		
Events, n (%)	4 (6%)	21 (26%)
p value	0.0900	
HR (95% CI)	0.33 (0.11, 1.03)	
Diversion-Free Survival (DFS)		
Events, n (%)	2 (3%)	31 (39%)
p value	0.0023	
HR (95% CI)	0.13 (0.04, 0.39)	
Overall Survival (OS)		
Events, n (%)	0 (0%)	4 (5%)
p value	0.0845	
HR (95% CI)	0 (0, NE)	

Sample sizes and events are unweighted. HRs are generated using PS-weighted + covariate-adjusted Cox regression. P values are generated using PS-weighted + covariate-stratified log-rank tests. HR, hazard ratio; NAPPED, NATural course and Prognosis of PFIC and Effect of biliary Diversion; NE, not estimable; PS, propensity score.

rate lower than reported for the un-vaccinated VLD population of 14%. Four FV patients required hospitalization including 2 ICU admissions, and two died from CoVID-19. Incidence of primary CoVID-19 infection after receiving a 3rd dose was 31/600 (5.2%). Prevalence of re-infection was 9/151 (6%), 3 after one dose of vaccination, 4 after two doses, and 2 after a third dose. At least one adverse event was reported in 42.6% patients, 40.6% after the first dose, and 74.9% after the second and third dose. The most frequently reported adverse events were local side effects at the injection site. Systemic side effects were asthenia (15%) and fever (9.4%). No serious adverse events were reported. Thirty-two (3.5%) thromboembolic events were identified, 28 SVT/PVT (23 re-thrombosis and 5 de-novo) and 4 extra-splanchnic. Two after the first dose (23- and 43-days post-vaccination), 23 (71.9%) after the second dose (median 52-days, 12–270), and 7 after a third dose (median 36-days, 19–270). No case of immune-thrombotic-thrombocytopenia (ITP) occurred. Twenty-two (2.4%) patients developed decompensations (median 25-weeks, range 13–42): ascites in n = 11, hepatic encephalopathy in n = 7 and portal hypertensive bleeding in n = 5 in VLD patients. Vaccine immunogenicity was longitudinally assessed in 36 patients receiving an mRNA vaccine. Immune responses were robust in this subgroup, with 36/36 (100%) of patients mounting detectable antibody and T-cell responses after two vaccine doses with comparable levels to those previously reported in healthy populations.

Conclusion: Patients with VLD present an adequate immune response to COVID-19 vaccines, and seem to be effectively protected from serious COVID-19 courses. No cases of vaccine-induced ITP were reported in this large cohort of VLD patients after repeated COVID19 vaccine doses.

THU-291

Serum bile acids are associated with native liver survival in patients with Alagille syndrome: results from the GALA study group

Carla Fiorella Murillo Perez¹, Shannon M. Vandriel¹, Jian-She Wang², Li Liting², Huiyu She², Irena Jankowska³, Piotr Czubkowski³, Dorota Gliwicz³, Emmanuel Gonzalès⁴, Emmanuel Jacquemin⁵, Jérôme Bouligand⁶, Lorenzo D'Antiga⁷, Emanuele Nicastro⁷, Björn Fischler⁸, Henrik Arnell⁹, Susan Siew¹⁰, Michael Stormon¹⁰, Kathleen M. Loomes¹¹, David A. Piccoli¹¹, Elizabeth B. Rand¹¹, James E. Squires¹², Saul J. Karpen¹³, Rene Romero¹³, Mureo Kasahara¹⁴, Zerrin Önal¹⁵, Etienne Sokal¹⁶, Tanguy Demaret¹⁶, Sabina Wiecek¹⁷, Florence Lacaille¹⁸, Dominique Debray¹⁹, Winita Hardikar²⁰, Sahana Shankar²¹, Pamela Valentino²², Shikha Sundaram²³, Alexander Chaidez²³, Noelle Ebel²⁴, Jeffrey Feinstein²⁵, Yael Mozar-Glazberg²⁶, Henry Lin²⁷, Nathalie Rock²⁸, Henkjan J. Verkade²⁹, M.K. Jensen³⁰, Catalina Jaramillo³⁰, Kyungmo Kim³¹, Seak Hee Oh³¹, Jernej Brecelj³², Seema Alam³³, Giuseppe Indolfi³⁴, Niviann Blondet²², Rima Fawaz³⁵, Silvia Nastasio³⁶, Pier Luigi Calvo³⁷, Gabriella Nebbia³⁸, Cigdem Arkan³⁹, Catherine Larson-Nath⁴⁰, Andréanne N. Zizzo⁴¹, Thomas Damgaard Sandahl⁴², Christos Tzivnikos⁴³, Nehal El-Koofy⁴⁴, Mohamed Elmonem⁴⁵, Dev Desai⁴⁶, Wikrom Karnsakul⁴⁷, Palaniswamy Karthikeyan⁴⁸, Pinar Bulut⁴⁹, Nanda Kerkar⁵⁰, Victorien Wolters⁵¹, Amin J Roberts⁵², Helen Evans⁵², Maria Camila Sanchez⁵³, Maria Lorena Cavalieri⁵³, Deirdre Kelly⁵⁴, Way Seah Lee⁵⁵, Christina Hajinicolaou⁵⁶, Chatmanee Lertudomphonwanit⁵⁷, Ryan Fischer⁵⁸, Jesús Quintero Bernabeu^{59,60}, Ruben E. Quiros-Tejeira⁶¹, Melina Melere⁶², Elisa Carvalho⁶³, John Eshun⁶⁴, Aglaia Zellos⁶⁵, Antal Dezsófi⁶⁶, Raquel Borges Pinto⁶⁷, Kathleen Schwarz⁶⁸,

POSTER PRESENTATIONS

- Maria Rogalidou⁶⁹, Jennifer Garcia⁷⁰, María Legarda Tamara⁷¹, Marisa Beretta⁷², Quais Mujawar⁷³, Ermelinda Santos-Silva⁷⁴, Cristina Molera Busoms⁷⁵, Eberhard Lurz⁷⁶, Cristina Gonçalves^{77,78}, Carolina Jimenez-Rivera⁷⁹, Jesús M. Bañales^{80,81,82,83}, Uzma Shah⁸⁴, Richard Thompson⁸⁵, Bettina Hansen^{86,87}, Binita M. Kamath¹, ¹The Hospital for Sick Children and the University of Toronto, Division of Gastroenterology, Hepatology and Nutrition, Toronto, Canada, Canada; ²Children's Hospital of Fudan University, The Center for Pediatric Liver Diseases, Shanghai, China, China; ³The Children's Memorial Health Institute, Department of Gastroenterology, Hepatology, Nutrition Disturbances and Pediatrics, Warsaw, Poland, Poland; ⁴Pediatric Hepatology and Liver Transplantation Unit, National Reference Centre for Rare Pediatric Liver Diseases (Biliary Atresia and Genetic Cholestasis), FILFOIE, ERN RARE LIVER, Bicêtre Hospital, AP-HP, Université Paris-Saclay, Le Kremlin-Bicêtre, France; ⁵Service d'Hépatologie et de Transplantation Hépatique Pédiatriques, Centre de Référence de l'Atresie des Voies Biliaires et des Cholestases Génétiques (AVB-CG), FSMR FILFOIE, ERN RARE LIVER, Hôpital Bicêtre, AP-HP, France; ⁶Service de Génétique Moléculaire, Pharmacogénétique et Hormonologie, Hôpitaux Universitaires Paris-Saclay, Assistance Publique-Hôpitaux de Paris, Centre Hospitalier Universitaire de Bicêtre, Le Kremlin-Bicêtre, France, France; ⁷Ospedale Papa Giovanni XXIII, Pediatric Hepatology, Gastroenterology and Transplantation, Bergamo, Italy, Italy; ⁸Astrid Lindgren Children's Hospital, Department of Paediatric Gastroenterology, Hepatology and Nutrition, Karolinska University Hospital and CLINTEC, Karolinska Institutet, Stockholm, ERN Rare Liver, Sweden; ⁹Astrid Lindgren Children's Hospital, Department of Paediatric Gastroenterology, Hepatology and Nutrition, Karolinska University Hospital and Department of Women's and Children's Health, Karolinska Institutet, Stockholm, Sweden, Sweden; ¹⁰The Children's Hospital at Westmead, Department of Gastroenterology, Sydney, Australia, Australia; ¹¹The Children's Hospital of Philadelphia and the University of Pennsylvania Perelman School of Medicine, Division of Gastroenterology, Hepatology and Nutrition, Philadelphia, Pennsylvania, United States, United States; ¹²University of Pittsburgh School of Medicine, Division of Pediatric Gastroenterology and Hepatology, Department of Pediatrics, Pittsburgh, United States, United States; ¹³Children's Healthcare of Atlanta and Emory University School of Medicine, Division of Pediatric Gastroenterology, Hepatology and Nutrition, Atlanta, United States, United States; ¹⁴Organ Transplantation Center, National Center for Child Health and Development, Tokyo, Japan, Japan; ¹⁵Pediatric Gastroenterology, Hepatology and Nutrition Department, Istanbul University Istanbul Medical Faculty, Istanbul, Turkey, Turkey; ¹⁶Cliniques Universitaires Saint-Luc, Service De Gastroentérologie et Hépatologie Pédiatrique, Brussels, Belgium, Belgium; ¹⁷Medical University of Silesia in Katowice, Department of Pediatrics, Katowice, Poland, Poland; ¹⁸Department of Pediatric Gastroenterology, and Nutrition, Necker-Enfants Malades Hospital, University of Paris, Paris, France, France; ¹⁹Pediatric liver unit, National Reference Centre for Rare Pediatric Liver Diseases (Biliary Atresia and Genetic Cholestasis), FILFOIE, ERN RARE LIVER, Necker-Enfants Malades Hospital, University of Paris, Paris, France, France; ²⁰Royal Children's Hospital, Department of Gastroenterology and Clinical Nutrition, Melbourne, Australia, Australia; ²¹Mazumdar Shaw Medical Center, Narayana Health, Bangalore, India, India; ²²Gastroenterology and Hepatology Division, Department of Pediatrics, University of Washington, Seattle Children's Hospital, Seattle, Washington, United States, United States; ²³Section of Gastroenterology, Hepatology and Nutrition, Department of Pediatrics and the Digestive Health Institute, Children's Hospital of Colorado and University of Colorado School of Medicine, Aurora, United States, United States; ²⁴Division of Gastroenterology, Department of Pediatrics, Stanford University School of Medicine, Palo Alto, California, United States, United States; ²⁵Department of Pediatrics (Cardiology), Stanford University School of Medicine, Lucile Packard Children's Hospital, Palo Alto, California, United States, United States; ²⁶Schneider Children's Medical Center of Israel, Institute of Gastroenterology, Nutrition and Liver Diseases, Petah Tikva, Israel, Israel; ²⁷Oregon Health and Science University, Division of Pediatric Gastroenterology, Department of Pediatrics, Portland, United States, United States; ²⁸Swiss Pediatric Liver Center, Division of Pediatric Specialties, Department of Pediatrics, Gynecology, and Obstetrics, University Hospitals Geneva and University of Geneva, Geneva, Switzerland, Switzerland; ²⁹University Medical Center Groningen, Department of Pediatrics, Center for Liver, Digestive, and Metabolic Diseases, Groningen, Netherlands, Netherlands; ³⁰University of Utah, Division of Pediatric Gastroenterology, Hepatology and Nutrition, Primary Children's Hospital, Salt Lake City, UT, USA, United States; ³¹Department of Pediatrics, University of Ulsan College of Medicine, Asan Medical Center Children's Hospital, Seoul, Korea, Republic of, Korea, Rep. of South; ³²University Medical Center Ljubljana, Pediatric Gastroenterology, Hepatology and Nutrition, and Department of Pediatrics, Faculty of Medicine, Ljubljana, Slovenia, Slovenia; ³³Institute of Liver and Biliary Sciences, Department of Pediatric Hepatology, New Delhi, India, India; ³⁴Department Neurofarba, University of Florence and Meyer Children's University Hospital, Paediatric and Liver Unit, Florence, Italy, Italy; ³⁵Yale University School of Medicine, Department of Pediatrics, New Haven, United States, United States; ³⁶Boston Children's Hospital and Harvard Medical School, Division of Gastroenterology, Hepatology, and Nutrition, Boston, United States, United States; ³⁷Pediatric Gastroenterology Unit, Regina Margherita Children's Hospital, Azienda Ospedaliera-Universitaria Città della Salute e della Scienza, Turin, Italy, Italy; ³⁸Fondazione IRCCS Ca' Granda Ospedale Maggiore Policlinico, Servizio di Epatologia Pediatrica, Milan, Italy, Italy; ³⁹Koc University School of Medicine, Department of Pediatric Gastroenterology and Organ Transplant, Istanbul, Turkey, Turkey; ⁴⁰University of Minnesota, Division of Pediatric Gastroenterology, Hepatology, and Nutrition, Minneapolis, United States, United States; ⁴¹Children's Hospital, London Health Sciences Centre, Division of Paediatric Gastroenterology and Hepatology, Western University, London, Ontario, Canada, Canada; ⁴²Department of Hepatology and Gastroenterology, Aarhus University Hospital, Aarhus, Denmark, Denmark; ⁴³Department of Paediatric Gastroenterology, Al Jalila Children's Specialty Hospital, Mohammed Bin Rashid University of Medicine and Health Sciences, Dubai, United Arab Emirates, United Arab Emirates; ⁴⁴Department of Pediatrics, Faculty of Medicine, Cairo University, Cairo, Egypt, Egypt; ⁴⁵Department of Clinical and Chemical Pathology, Faculty of Medicine, Cairo University, Cairo, Egypt, Egypt; ⁴⁶Solid Organ Transplant Department, Children's Health-Children's Medical Center, Dallas, United States, United States; ⁴⁷Johns Hopkins University School of Medicine, Department of Pediatrics, Baltimore, United States, United States; ⁴⁸Leeds Teaching Hospitals NHS Trust, Leeds Children's Hospital, Leeds, United Kingdom, United Kingdom; ⁴⁹Phoenix Children's Hospital, Division of Pediatric Gastroenterology and Hepatology, Phoenix, United States, United States; ⁵⁰University of Rochester Medical Center, Department of Pediatrics, Div of Pediatric Gastroenterology, Hepatology and Nutrition, Rochester, New York, United States, United States; ⁵¹Department of Pediatric Gastroenterology, University Medical Center Utrecht, Utrecht, The Netherlands, Netherlands; ⁵²Starship Child Health, Department of Paediatric Gastroenterology, Auckland, New Zealand, New Zealand; ⁵³Hospital Italiano Buenos Aires, Pediatric Gastroenterology and Hepatology Division, Buenos Aires, Argentina, Argentina; ⁵⁴Liver Unit, Birmingham Women's and Children's Hospital NHS Trust and University of Birmingham, Birmingham, United Kingdom, United Kingdom; ⁵⁵Faculty of Medicine, Department of Paediatrics, University of Malaya, Kuala Lumpur, Malaysia, Malaysia; ⁵⁶Division of Paediatric Gastroenterology, Chris Hani Baragwanath Academic Hospital, Department of Paediatrics and Child Health, University of the Witwatersrand, Johannesburg, South Africa, South Africa; ⁵⁷Ramathibodi Hospital Mahidol University, Division of Gastroenterology, Department of Pediatrics, Bangkok, Thailand, Thailand; ⁵⁸Children's Mercy Kansas City, Department of Gastroenterology, Section of Hepatology, Kansas City, United States, United States; ⁵⁹Hospital Universitari Vall d'Hebron, Pediatric Hepatology and Liver Transplant Department, Barcelona, Spain, Spain; ⁶⁰Department of Liver and Gastrointestinal Diseases, Biodonostia Health Research Institute-Donostia University Hospital - University of the Basque Country (UPV/EHU), San Sebastian, Spain, 20014, Spain;

⁶¹Children's Hospital and Medical Center and University of Nebraska Medical Center, Department of Pediatrics, Omaha, United States, United States; ⁶²Hospital da Criança Santo Antonio de Porto Alegre, Department of Pediatrics and Gastroenterology Unit, Porto Alegre, Brazil, Brazil; ⁶³Pediatric Gastroenterology Department, Hospital da Criança de Brasília, Centro Universitário de Brasília, Brazil, Brazil; ⁶⁴Department of Pediatric Gastroenterology, Le Bonheur Children's Hospital and The University of Tennessee Health Science Center, Memphis, United States, United States; ⁶⁵Mitera Children's Hospital, Athens, Greece, Greece; ⁶⁶First Department of Paediatrics, Semmelweis University, Budapest, Hungary, Hungary; ⁶⁷Division of Pediatric Gastroenterology of Hospital da Criança Conceição do Grupo Hospitalar Conceição, Porto Alegre, RS, Brazil, Brazil; ⁶⁸University of California San Diego, Rady Children's Hospital San Diego, Division of Pediatric Gastroenterology, San Diego, United States, United States; ⁶⁹Division of Gastroenterology and Hepatology, "Agia Sofia" Children's Hospital, First Department of Pediatrics, University of Athens, Athens, Greece, Greece; ⁷⁰Division of Pediatric Gastroenterology, Hepatology and Nutrition/Miami Transplant Institute, University of Miami, Miami, United States, United States; ⁷¹Paediatric Gastroenterology Unit, Cruces University Hospital, Bilbao, Spain, Spain; ⁷²Faculty of Health Sciences, Wits Donald Gordon Medical Centre, University of the Witwatersrand, Johannesburg, South Africa, South Africa; ⁷³University of Manitoba, Section of Pediatric Gastroenterology, Department of Pediatrics, Winnipeg, Canada, Canada; ⁷⁴Centro Hospitalar Universitário Do Porto, Pediatric Gastroenterology Unit, Porto, Portugal, Portugal; ⁷⁵Pediatric Gastroenterology Hepatology and Nutrition Unit, Hospital Sant Joan de Déu, Esplugues de Llobregat, Spain, Spain; ⁷⁶Department of Pediatrics, Dr. von Hauner Children's Hospital, University Hospital, LMU Munich, Munich, Germany, Germany; ⁷⁷European Reference Network on Hepatological Diseases (ERN RARE-LIVER), Portugal; ⁷⁸Pediatric Gastroenterology/Hepatology Center Lisbon, Portugal, Portugal; ⁷⁹Children's Hospital of Eastern Ontario, Division of Gastroenterology, Hepatology and Nutrition, Ottawa, Canada, Canada; ⁸⁰Department of Liver and Gastrointestinal Diseases, Biodonostia Health Research Institute-Donostia University Hospital, University of the Basque Country (UPV/EHU), San Sebastian, Spain, Spain; ⁸¹National Institute for the Study of Liver and Gastrointestinal Diseases (CIBERehd, "Instituto de Salud Carlos III"), San Sebastian-Donostia, Spain, Spain; ⁸²IKERBASQUE, Basque Foundation for Science, Bilbao, Spain, Spain; ⁸³Department of Biochemistry and Genetics, School of Sciences, University of Navarra, Pamplona, Spain, Spain; ⁸⁴Harvard Medical School, Massachusetts General Hospital for Children, Boston, United States, United States; ⁸⁵Institute of Liver Studies, King's College London, London, United Kingdom, United Kingdom; ⁸⁶Toronto General Hospital University Health Network, Toronto, Canada, Canada; ⁸⁷Institute of Health Policy, Management and Evaluation, Toronto, Canada, Canada
Email: carlafiorella.murilloperez@sickkids.ca

Background and aims: Alagille syndrome (ALGS) is a rare, autosomal dominant multisystem disorder characterized by cholestasis and extrahepatic manifestations. Given the current era of ileal bile acid transporter (IBAT) inhibitor therapies that reduce serum bile acid (SBA) levels, the aim of this study was to determine whether SBA are a predictor of clinical outcomes in ALGS.

Method: Patients were ascertained from the GALA cohort, an international multicentre study including clinically and/or genetically diagnosed children with ALGS. Those with neonatal cholestasis and at least one SBA measurement during follow-up were eligible for inclusion and those with biliary diversion were excluded. An established SBA threshold in progressive familial intrahepatic cholestasis (PFIC) (102 mmol/L) was assessed as a time-dependent covariate in Cox regression analyses for native liver survival (NLS); liver transplantation and death as end points), overall and while adjusting for total bilirubin (TB) levels and stratified by geographical region. Patients who did not meet one of these end points were truncated at the time of Kasai procedure, or their last follow-up, up to a maximum of 18 years of age.

Results: 565 patients from GALA were included, of whom 349 (61.8%) were male with a median year of birth of 2012 (IQR 2007–2016). Rates of NLS at 1, 5 and 18 years were 93.5%, 63.5%, and 50.3%, respectively. The SBA threshold of 102 mmol/L was a significant predictor of outcome (HR = 3.40, 95% CI 2.28–5.06, $p < 0.001$) and there was no significant difference in the impact of SBA between the first year of life and thereafter ($p = 0.90$). SBA remained a significant factor for NLS while adjusting for TB clearance at 1 year (HR = 1.87, 95% CI 1.04–3.33, $p = 0.03$), where clearance is defined as TB < 2 mg/dL. There was no significant interaction between the SBA threshold and clearance of TB.

Conclusion: SBA is an independent predictive factor for NLS in children with ALGS and neonatal cholestasis. Of note, SBA is associated with NLS in children with ALGS who clear their bilirubin i.e. those with anicteric cholestasis. This is relevant in the context of IBAT inhibitors that promote a reduction in SBA and are currently indicated for pruritus but may also impact additional important clinical outcomes.

THU-292

Deep tissue exposure of antibiotics at the target site of infection in patients with cystic liver disease: a randomized pharmacokinetic trial

Lucas H.P. Berns^{1,2}, Roger Brüggemann³, Anouk M.E. Jansen³, Nynke Jager³, Heiman Wertheim², Joost P.H. Drenth¹, Marten A. Lantinga^{1,4}. ¹Radboud University Medical Center, Department of Gastroenterology and Hepatology, Netherlands; ²Radboud University Medical Center, Department of Medical Microbiology, Netherlands; ³Radboud University Medical Center, Department of Pharmacy, Netherlands; ⁴University Medical Centers Amsterdam, Department of Gastroenterology and Hepatology, Amsterdam Gastroenterology and Metabolism, Netherlands
Email: martenlantinga@gmail.com

Background and aims: Successful antibiotic therapy for liver (cyst) infection depends on adequate exposure of the drug at the site of infection. Available pharmacokinetic (PK) data of antibiotics in liver cyst fluid is limited, but such knowledge is critical to manage patients with cyst infections. This study aims to analyse deep tissue exposure of antibiotics using an in vivo human liver cyst model and explore influencing factors.

Method: We performed an explorative, randomized, single-dose, PK study. Patients (≥ 18 years, intact liver and renal function) eligible for percutaneous drainage of liver cysts were, after providing written informed consent, randomized between receiving intravenous (iv) ciprofloxacin and piperacillin/tazobactam (group 1), or trimethoprim/sulfamethoxazole (group 2). Antibiotics were administered as a single iv dose prior to the cyst drainage procedure. Blood samples were drawn at three time-points within 12 hours following administration of antibiotics. The cyst fluid sample was collected during liver cyst drainage. Antibiotic concentrations were measured with liquid chromatography-tandem mass spectrometry using a validated assay for plasma and liver cyst fluid. Primary outcome was deep tissue exposure, expressed as liver cyst to plasma concentration ratio (%). Individual plasma exposure was described by area under the concentration-time curve (AUC). AUC and maximum plasma concentration (C_{max}) were calculated by post hoc estimation based on existing population PK models using non-linear mixed effect modelling. Deep tissue exposure estimates were calculated as cyst concentration to AUC or C_{max} ratio. For exploratory analyses, we used linear regression to assess whether the time interval between antibiotic administration and cyst drainage (minutes), cyst location (left or right liver lobe) or cyst volume (ml) were correlated with deep tissue exposure.

Results: We included 20 patients (90% female, median age 61 years, median eGFR 88 ml/min/1.73 m², median BMI 23.7 kg/m²). Twenty-one liver cysts were drained (group 1: n = 11 cysts, left lobe: n = 5, right lobe: n = 6 and group 2: n = 10 cysts, left lobe: n = 3, right lobe:

POSTER PRESENTATIONS

n = 7). Median drained volume was 700 ml [IQR 375–1200 ml]. Deep tissue exposure for ciprofloxacin was 4.2% [IQR 1.6–8.9%], piperacillin 0.3% [IQR 0.1–1.3%], tazobactam 0.2% [IQR 0.0–1.3%], trimethoprim 12.2% [IQR 6.3–16.1%] and sulfamethoxazole 0.4% [IQR 0.2–3.8%], respectively (Figure 1). Cyst concentration to AUC and Cmax ratios showed comparable distributions. Time between iv administration and cyst drainage increased deep tissue exposure for trimethoprim (R-square 0.63, $p < 0.01$). Deep tissue exposure was numerically higher in left lobe located cysts, except for sulfamethoxazole (Figure 1). Individual cyst volume did not correlate with deep tissue exposure.

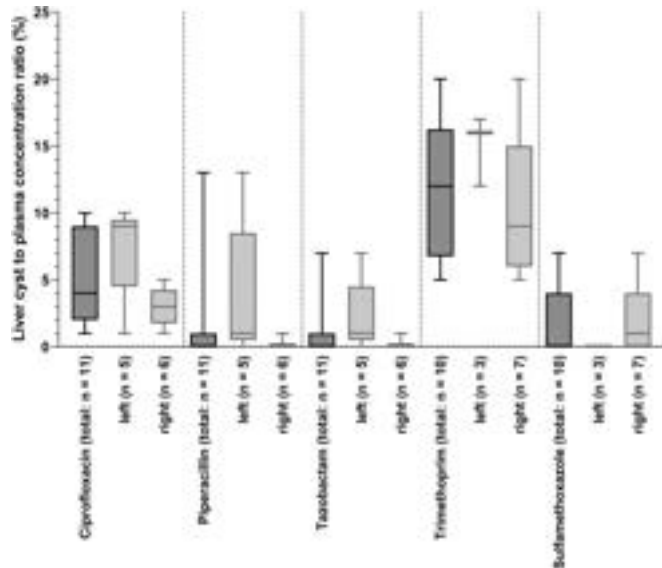


Figure:

Conclusion: Deep tissue exposure of antibiotics in liver cysts was overall low after a single iv dose. Highest exposure in both liver lobes was seen for trimethoprim. Due to low sulfamethoxazole penetration, the synergistic combination with trimethoprim (co-trimoxazole) might be less effective. Exploratory analyses show that complex time-dependent pharmacokinetics and hepatic lobar differences could influence antibiotic exposure at the target site of infection.

THU-293

The non-invasive evaluation of vascular liver disease in patients with cystic fibrosis: a prospective cross-sectional study

Elton Dajti^{1,2,3}, Federico Ravaoli^{1,3}, Giulia Paiola², Sonia Volpi², Luigi Colechia¹, Alberto Ferrarese², Luigina Vanessa Alemanni¹, Caterina Cusumano², Annarita Di Biase⁴, Giovanni Marasco¹, Amanda Vestito⁵, Davide Festi¹, Pierre-Emmanuel Rautou⁶, Marco Cipolli², Antonio Colechia^{2,3}. ¹University of Bologna, Italy; ²Borgo Trento University Hospital of Verona, Italy; ³University of Modena and Reggio Emilia, Dipartimento Chirurgico, Medico, Odontoiatrico e di Scienze Morfologiche con interesse Trapiantologico, Oncologico e di Medicina Rigenerativa, Italy; ⁴University of Modena and Reggio Emilia, Department of Pediatrics, Italy; ⁵IRCCS S. Orsola Hospital, Bologna, Italy; ⁶Université de Paris, AP-HP, Hôpital Beaujon, Service D'Hépatologie, France

Email: e_dajti17@hotmail.com

Background and aims: Porto-sinusoidal vascular disease (PSVD) has recently been described as the prominent pathology in liver explants of patients with cystic fibrosis (CF), but data outside the transplant setting are lacking. We aimed to investigate the prevalence of portal hypertension in cystic fibrosis-associated liver disease (CFLD) and develop a non-invasive algorithm to classify liver involvement in CF patients.

Method: This is a cross-sectional study of consecutive CF patients followed at our tertiary center between 2018 and 2019, who underwent ultrasound examination, liver (LSM), and spleen stiffness (SSM) measurement by transient elastography (TE). CFLD was defined according to abnormal physical examination, liver tests, and ultrasound findings. PSVD was likely if there were portal hypertension (PH) signs in the absence of advanced chronic liver disease (CF-ACLD, LSM <10 kPa).

Results: CFLD was found in 50 (27.5%) of the 182 included patients. At least one sign of PH was found in 47 (26%) patients, but the majority (38/47, 81%) had low LSM (<10 kPa) and were likely to have PSVD, whereas only 9 (5%) had CF-ACLD. PSVD and “mild” CFLD (LSM <10 kPa) co-existed in most (23/36) cases. SSM/LSM ratio could accurately distinguish between likely PSVD and CF-ACLD patients (AUROC = 0.863). In a historical cohort of 599 patients (pre-TE era), survival progressively decreased among patients with no PH, patients with likely PSVD, and patients with CFLD + PH signs (log-rank <0.0001).

Conclusion: PSVD seems to be the prevailing cause of portal hypertension in patients with CF. We developed a new diagnostic

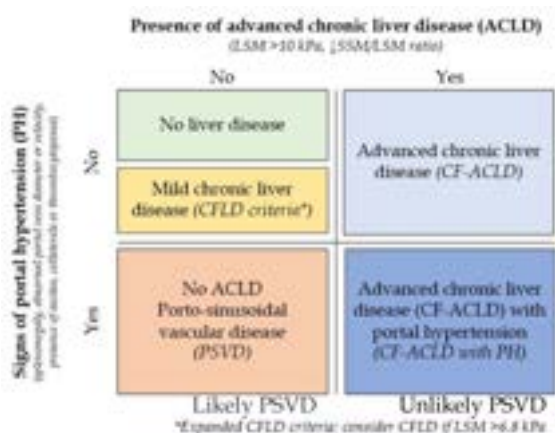
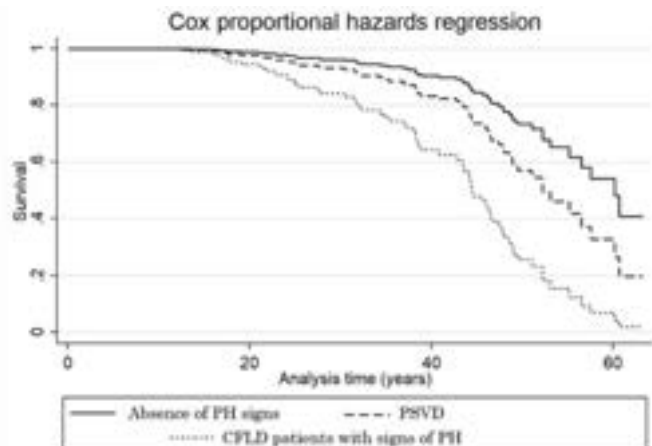


Figure: (abstract: THU-293).



algorithm based on ultrasound, clinical criteria, and TE to classify liver involvement in patients with CF.

THU-294

Monitoring, dosing and clinical outcomes of CFTR modulator triple combination therapy in children with CF post liver transplantation

Dana Cerminara¹, Daniel Leung². ¹Texas Children's Hospital, Pharmacy, United States; ²Baylor College of Medicine, Pediatrics, Houston, United States

Email: dhleung@texaschildrens.org

Background and aims: Triple combination therapy with elexacaftor/tezacaftor/ivacaftor (E/T/I) has revolutionized the lives of people with CF by restoring CF transmembrane regulator (CFTR) function in pulmonary, pancreatic and intestinal tissue, leading to drastically improved lung and nutritional health. There is a known risk of hepatotoxicity and drug interactions with transplant immunosuppressive agents.

Method: This was a retrospective review of 8 patients with CF who were candidates for E/T/I. We describe the protocolized dosing, monitoring, and clinical outcomes of E/T/I use in 8 children with CF post liver transplantation (LT) transplanted between 2014 and 2022. Data was analyzed using descriptive statistics.

Results: From January 2014-December 2022, a total of 14 children with CF received LT at Texas Children's Hospital (TCH) for the indication of portal hypertension. Of these, 8 (25% female) were alive and initiated E/T/I 17.5 months (median) post LT with a mean follow-up of 26 months. Tacrolimus trough (TAC) and liver labs were collected at baseline, 7 days, 14 days, and 28 days post-initiation. Five out of 8 (63%) patients required a TAC dose decrease within the first 2 months; 0 patients required a TAC dose increase. 1–2 TAC dose adjustments were needed in 63% to achieve goal levels and a 20–30% reduction in TAC while on E/T/I was most common. Adverse effects while on E/T/I included mild elevations ($>1.5\times$ baseline) in AST (43%), ALT (43%), GGT (29%), and subjective abdominal pain (29%). No elevations in bilirubin or INR. Only 14% discontinued E/T/I due to intolerance (abdominal pain and diarrhea) and was not liver related. Lung function measured by median FEV₁ improved from 85% to 93% over 13 months (expected 3% decline/year) while on E/T/I. Median BMI pre-E/T/I was 16.6 and increased to 19 post-E/T/I over 12 months but no change in BMI z-score (-0.99 , -1.02 , $p > 0.05$).

Conclusion: While our single center experience appears small, it represents 20% of the US CF pediatric population that received LT during this time period. Treatment with E/T/I post-LT in children with CF appears safe and requires protocolized lab monitoring. 1–2 dose adjustments of tacrolimus (primarily reductions) was most common. E/T/I associated hepatitis was mild with no cholestasis or liver dysfunction. E/T/I was associated with clinically meaningful improvement in lung function and BMI post-LT.

THU-295

Recent splanchnic vein thrombosis occurring during Sars-Cov-2 infection-The VALDIG study

Pierre Deltenre¹, Payance Audrey², Laure Elkrief³, Vincenzo La Mura⁴, Artru Florent⁵, Anna Baiges⁶, Jean Paul Cervoni⁷, Louise China⁸, Isabelle Colle⁹, Elise Lemaitre¹⁰, Bogdan Procopet¹¹, Dietmar Schiller¹², Christophe Bureau¹³, Odile Gorla¹⁴, Isabelle Ollivier-Hourmand¹⁵, Alexandre Nuzzo¹⁶, Pierre-Emmanuel Rautou², Aurélie Plessier^{2,17}. ¹CUB Hôpital Erasme, Belgium; ²Université de Paris, AP-HP, Hôpital Beaujon, Clichy, France; ³CHU Tours, France; ⁴Ospedale Maggiore Policlinico, Italy; ⁵CHUV, Switzerland; ⁶Hospital Clinic, Barcelona; ⁷CHU, Besançon, France; ⁸Royal Free Hospital, United Kingdom; ⁹ASZ Aalst, Belgium; ¹⁰CHU Lille, France; ¹¹Cluj-Napoca, Romania; ¹²Ordensklinikum Linz Barmherzige Schwestern, Linz, Austria; ¹³Hôpital Universitaire Rangueil, Toulouse, France; ¹⁴Hôpital Universitaire Charles Nicolle, Rouen, France; ¹⁵Hôpital Universitaire Côte de la Nacre, Caen, France; ¹⁶Gastroenterology intensive care unit hospital beaujon, Clichy, France; ¹⁷DHU Unity, Pôle des Maladies de l'Appareil Digestif, Service d'Hépatologie, Centre de Référence des Maladies Vasculaires du Foie, Hôpital Beaujon, AP-HP, Clichy, France

Email: pierre.deltenre01@gmail.com

Background and aims: While Sars-Cov-2 infection is a well-known prothrombotic disorder, whether it is a risk factor for splanchnic vein thrombosis (SVT) is unknown. We aimed to assess the impact of Sars-Cov-2 infection on the presentation and prognosis of recent SVT and to assess if the disease profile of these patients differs from patients with recent SVT without Sars-Cov-2 infection.

Method: Retrospective study collecting health-related data of 27 patients presenting with recent SVT in the context of Sars-Cov-2 infection in 12 hospital centers belonging to VALDIG network and comparison to 494 patients with recent SVT prospectively included in a database before the Sars-Cov-2 pandemics.



Figure: (abstract: THU-294): (placeholder)

POSTER PRESENTATIONS

Results: Among the 27 patients with recent SVT and Sars-Cov-2 infection (18 males, median age 51 years), 21 had portal vein thrombosis with or without thrombosis of another splanchnic vein, 2 had isolated superior mesenteric vein thrombosis, 1 isolated splenic

vein thrombosis and 3 isolated hepatic veins thrombosis. Diagnosis of SVT was made 10 days (95% CI: 0–24) after the diagnosis of Sars-Cov-2 infection. Extension of SVT did not differ between patients with and without Sars-Cov-2 infection. No difference was observed in terms of

Table: (abstract: THU-295).

Table. Characteristics of patients with recent SVT with and without Sars-Cov-2 infection

Characteristics	Patients with Sars-Cov-2 infection (n = 27)	Patients without Sars-Cov-2 infection (n = 494)	p-value
Age, years	51 (36-53)	47 (45-49)	0.9
Male sex, n (%)	18 (67%)	298 (61%)	0.7
BMI	26.7 (24.3-29.3)	NA	NA
Fever, n (%)	14 (52%)	74 (15%)	<0.001
Respiratory symptoms, n (%)	12 (44%)	0 (0%)	<0.001
Dyspnea, n (%)	8 (30%)	0 (0%)	<0.001
Anosmia, n (%)	6 (25%)	0 (0%)	<0.001
Ageusia, n (%)	6 (25)	0 (0%)	<0.001
Abdominal pain, n (%)	24 (89%)	404 (82%)	0.6
Ascites, n (%)	7 (26%)	105 (22%)	0.4
CRP, mg/dL	42 (14-106)	35 (21-45)	0.5
D-dimers, ng/mL	3298 (850-10000)	NA	NA
White blood cells (10 ³ /mm ³)	6.1 (4.0-10.0)	7.0 (6.6-7.2)	0.5
Polymorphonuclear neutrophils (10 ³ /mm ³)	3.8 (2.7-6.2)	4.1 (3.9-4.4)	0.8
Lymphocytes (10 ³ /mm ³)	1.1 (0.9-1.5)	1.6 (1.5-1.7)	0.04
Eosinophils (10 ³ /mm ³)	0.03 (0-0.10)	0.10 (0.10-0.10)	0.002
Platelets (10 ³ /mm ³)	220 (178-301)	257 (240-273)	0.6
ASAT, IU/mL	38 (24-43)	32 (30-34)	0.3
ALAT, IU/mL	41 (25-52)	40 (37-43)	0.7
Alkaline Phosphatase, IU/mL	90 (75-134)	83 (79-88)	0.4
Bilirubin, mg/dL	0.9 (0.6-1.1)	0.6 (0.6-0.7)	0.03
INR	1.2 (1.1-1.3)	1.1 (1.0-1.1)	0.01
Creatinine (mg/dL)	0.9 (0.7-1.0)	0.8 (0.8-0.8)	0.3

Abbreviations: ALAT, alanine amino-transferase; ASAT, aspartate amino-transferase; BMI, body mass index; CRP, C-reactive protein; INR: international normalized ratio; NA, not available; SVT, splanchnic vein thrombosis

Continuous variables are presented as median (interquartile range)

age, sex ratio and liver blood tests between patients with and without Sars-Cov-2 infection. Seventeen of Sars-Cov-2 patients (59%) had fever and/or respiratory symptoms (dyspnea, ageusia and/or anosmia). Fever (52% vs. 15%, $p < 0.001$) and respiratory symptoms (44% vs. 0%, $p < 0.001$) were more frequent, and the median count of lymphocytes was lower ($1.1 \times 10^3/\text{mm}^3$ [95% CI: 0.9–1.5] vs. $1.6 \times 10^3/\text{mm}^3$ [95% CI: 1.5–1.7], $p = 0.043$) in patients with than in those without Sars-Cov-2 infection. A prothrombotic condition was identified in 44% patients of Sars-Cov-2 patients and in 52% of non-Sars-Cov-2 patients ($p = 0.5$). No difference was observed regarding associated prothrombotic conditions. Four Sars-Cov-2 patients required ventilation support. All Sars-Cov-2 patients were treated with anticoagulation, including 25 in whom anticoagulation was initiated on the day of SVT diagnosis. During a median follow-up of 250 days (95% CI: 83–394 days), no patient suffered from gastrointestinal bleeding or from another liver-related event and no patient died. Three patients (11%) required intestinal resection for infarction 1 to 3 months after the diagnosis of SVT, which was significantly more frequent than in the control group ($n = 13$ [2.6%], $p = 0.044$). At the end of the follow-up period, partial or complete recanalization of the thrombosed splanchnic vein was observed in 33% of Sars-Cov-2 patients.

Conclusion: Sars-Cov-2 infection can be associated with recent SVT. SVT occurring during Sars-Cov-2 infection is characterized by a higher frequency of respiratory symptoms and a lower lymphocytes count. Intestinal ischemia leading to delayed intestinal resection seems more frequent in Sars-Cov-2 patients. In this cohort study in which all Sars-Cov-2 patients received anticoagulation therapy early on after the diagnosis of SVT, partial or complete recanalization was observed in one third of patients.

THU-296

Liver-related clinical events among adult patients with alpha-1 antitrypsin deficiency-associated liver disease: a longitudinal retrospective study using linked insurance claims data and electronic medical records in the United States

May Hagiwara¹, Victoria Divino², Swapna Munnangi², Mark Delegge², Suna Park¹, Ed G. Marins¹, Kaili Ren¹, Charlton Strange³. ¹Takeda Development Center Americas, Inc., Cambridge, MA, USA, United States; ²IQVIA Inc., Falls Church, VA, USA, United States; ³Medical University of South Carolina, Charleston, SC, USA, United States
Email: ed.marins@takeda.com

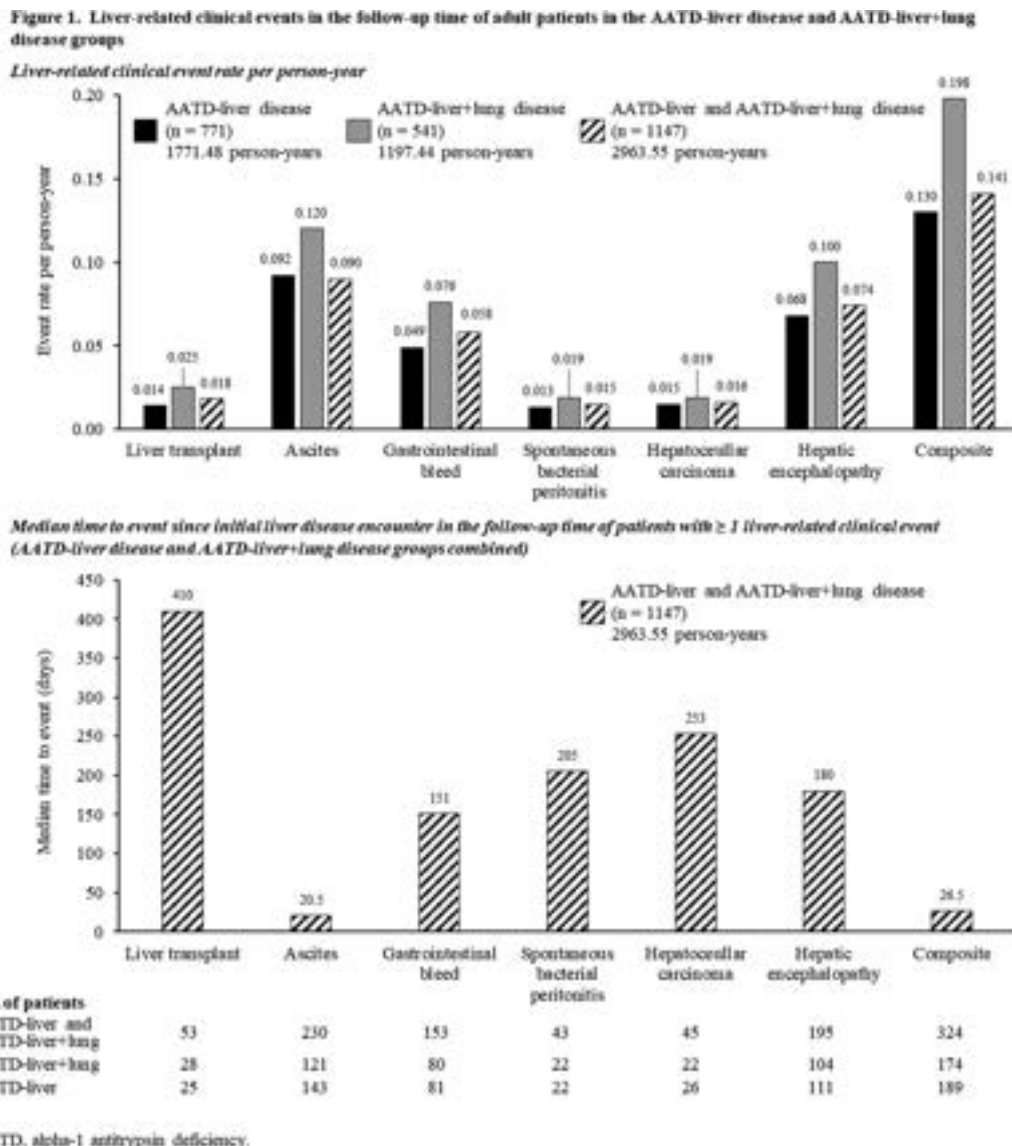


Figure: (abstract: THU-296).

Background and aims: Alpha-1 antitrypsin deficiency (AATD) is a rare genetic disorder occurring in ~1 per 3000–5000 people in the USA. It is characterized by low levels of serum alpha-1 antitrypsin (AAT) and accumulation of misfolded AAT in hepatocytes, which can lead to liver and/or lung disease. Patients with AATD and the protease inhibitor (Pi) ZZ genotype are at increased risk of both diseases. The burden of liver-related clinical events among adult patients with AATD was investigated using large US claims and Ambulatory Electronic Medical Records (AEMR) databases.

Method: This was a retrospective analysis of administrative claims data from the IQVIA PharMetrics® Plus database linked to the IQVIA AEMR database (selection period: January 2012 to October 2021). PharMetrics Plus comprised 142 million enrollees with medical and pharmacy benefits and ≥1-month enrolment during the selection period. Inclusion criteria were: (1) at least one inpatient or at least two outpatient medical claims ≥90 days apart with a diagnosis of AATD in PharMetrics Plus, or (2) with a PiZZ/PiMZ genotype in AEMR and with linkage to PharMetrics Plus; (3) a liver disease diagnosis. A person-time approach was used to maximize the use of data. Follow-up time was assigned to the AATD-liver disease group (for time with liver disease only) and the AATD-liver+lung disease group (for time with both liver and lung disease). Liver-related clinical events of interest (identified by International Classification of Diseases-Ninth/Tenth Revision codes) included liver transplantation, ascites, gastrointestinal bleeds, spontaneous bacterial peritonitis, hepatocellular carcinoma, and hepatic encephalopathy. These were evaluated separately and as a composite (defined as the occurrence of ≥1 of the six clinical events).

Results: In total, 771 and 541 adults aged ≥18 years contributed their time to the AATD-liver disease and AATD-liver+lung disease groups, respectively (combined 1147 patients). The median age was 49 and 55 years, 58% and 51% were male, and the median duration of observation was 22 and 21 months, respectively. Liver-related clinical event rates per person-year among all patients and median time to event for those with liver-related clinical events are shown in Figure 1.

Conclusion: Among adult patients with AATD and liver disease, ascites was the most frequently observed and earliest encountered of the liver-related clinical events studied, followed by gastrointestinal bleeds and hepatic encephalopathy. These rates were higher when patients had both liver and lung disease involvement than liver disease only, possibly related to the higher median age of patients with both diseases. The number of patients with a confirmed PiZZ/PiMZ genotype was very low (AATD-liver disease: n = 11; AATD-liver+lung disease: n = 5), restricting further analysis.

Acknowledgments: Writing assistance was provided by Elena Sugrue, PhD, of Oxford PharmaGenesis, Oxford, UK and funded by Takeda Development Center Americas, Inc.

Funding: This study was funded by Takeda Development Center Americas, Inc.

THU-297

Hepatobiliary malignancies in Wilson Disease: data from an Italian national reference centre

Lorenzo Canova¹, Pier Maria Battezzati¹, Greta Trevisi¹, Elisabetta Boga¹, Emanuela Bertolini¹, Paola Zermiani¹, Sara Monico¹, Massimo Giovanni Zuin¹. ¹ASST Santi Paolo e Carlo, S.C. Gastroenterologia ed Epatologia, Milano, Italy
Email: lorenzo.canova@unimi.it

Background and aims: Wilson disease (WD) is a rare genetic disorder of copper transport leading to its accumulation mainly in the liver and the brain. Clinical course is frequently complicated by development of liver cirrhosis, a recognized risk factor for liver cancer (LC). Data on the risk of LC in WD is limited and controversial. Hepatocellular carcinoma (HCC) and cholangiocarcinoma (CC) have been regarded as a rare complication of WD. In the largest available study (130 patients), a 1.2% prevalence (incidence rate, 0.28 cases per

1,000 person years) has been estimated (van Meer S., 2015). Conversely, HCC estimates in Saudi Arabia (71 patients) were 7.0% and 9.1 cases per 1,000 person years, respectively (Al Fadda M., 2012). We investigated LC risk in a cohort of WD from a single tertiary referral center for liver diseases.

Method: We enrolled all the patients who were consecutively diagnosed WD (Leipzig score >3) between 1975 and 2022. First line therapy was Penicillamine, while intolerant patients received trientine or zinc salts. Patients underwent liver US examinations yearly. Cirrhosis was diagnosed on the basis of histology (if available), clinical, laboratory and US criteria. At time of first evidence of cirrhosis, LC surveillance was started (6-month US scan, alpha-fetoprotein testing). End of follow-up was date of LC diagnosis, liver transplantation (OLT), death, or last visit. 24 h urinary copper excretion was used to monitor treatment adequacy. Cox modeling was used to analyze survival.

Results: Overall, 189 WD patients (52% males) were included. Median age was 17 yr (2–74) on diagnosis and 40 yr (11–74) at time of enrollment. Median follow-up was 11.1 yr (0–47). 158 patients (83%) had hepatic or neurologic symptoms at presentation and 32 (17%) were diagnosed by family screening. On diagnosis, cirrhosis was present in 85 (45%) patients, of whom 11 (13%) had decompensated cirrhosis. At the end of follow-up, 95/189 patients had cirrhosis (3 decompensated, 1 waiting OLT for end-stage liver disease). LC was detected in 8 patients (75% M; age at LC diagnosis, 49–60 yr): 5 had HCC (4 transplanted and alive, 1 died), 2 CC (1 transplanted and alive, 1 died); 1 patient with HCC underwent tumor resection and subsequently developed CC (transplanted and alive). Of the 8 patients diagnosed WD when aged 30+ yr, 6 developed LC (4 HCC, 1 CC, 1 HCC + CC). In 2 patients HCC was diagnosed at time of WD recognition (57, 58 yr). In the remaining 6 patients, 24 h urinary copper excretion was in the therapeutic target. No relationship with mode of presentation or treatment emerged during the treatment period. The incidence of LC was 2.8 cases per 1,000 person years since birth (3 cases per 1,000 person years since time of WD diagnosis) with a prevalence of 4.2%. **Conclusion:** The incidence of LC in WD is higher than formerly estimated, but still lower than other chronic liver diseases. CC represents a substantial part of LC.

THU-298

Beneficial effect of cystic fibrosis transmembrane conductance regulator modulators on adults with cystic fibrosis liver disease

Sofia Manioudaki¹, Larisa Vasilieva², Ilianna Mani³, Filia Diamantea⁴, Theodoros Alexopoulos⁵, Sophia Pouriki⁶, Zoe Athanassa⁷, Aikaterini Sakagianni⁷, Eleni Geladari⁸, Ioannis Elefsiniotis⁹, Emilia Hadziyannis¹⁰, Alexandra Alexopoulou¹⁰. ¹Intensive Care Unit, Sismanogleio General Hospital of Athens, Greece; ²Alexandra General Hospital, Gastroenterology, Athens, Greece; ³2nd Department of Internal Medicine and Research Laboratory, National and Kapodistrian University of Athens, Medical School, Hippokration General Hospital, Athens, Greece; ⁴Adult Cystic Fibrosis Unit, Sismanogleio General Hospital of Athens, Greece; ⁵Laiko General Hospital, Gastroenterology Department, Athens, Greece; ⁶Intensive Care Unit, Sotiria General Hospital of Athens, Greece; ⁷Intensive Care Unit, Sismanogleio General Hospital, Athens, Greece; ⁸Evangelismos General Hospital; ⁹3rd Department of Internal Medicine and Liver Outpatient Clinic, Athens, Greece; ¹⁰Academic Department of Internal Medicine, General Oncology Hospital of Kifisia "Agioi Anargyroi", National and Kapodistrian University of Athens, Greece; ¹⁰2nd Department of Internal Medicine and Research Laboratory, Medical School, National and Kapodistrian University of Athens, Hippokration Hospital, Athens, Greece
Email: alexandra61@med.uoa.gr

Background and aims: In cystic fibrosis (CF), liver disease (CFLD) is the third leading cause of mortality. A combination of modalities including physical examination, biochemical and imaging were utilized in the conventional Debray criteria. New drugs have been approved for the treatment of CF patients who have at least one copy

of the F508del mutation in the CF transmembrane conductance regulator (CFTR) gene. These modulators were reported to improve lung function and symptoms as well as decrease CF exacerbations. However, the drug efficacy and tolerability on CFLD need further investigation.

Method: Longitudinal data were collected from a cohort of genetically confirmed CF adult patients. CFLD was diagnosed by Debray criteria.

Results: Thirty patients with CF [66.7% male, median age at diagnosis 6 (interquartile range 1.83–36) months, median age 27.5 (23–33) years] were included. Nine (30%) met the Debray criteria at first assessment. Seventeen patients (treatment group) treated for ≥ 12 months were compared with 13 treated for < 12 months or untreated (non-treatment group). The median period of drug administration was 45 (21–69) months. Seven patients were receiving from the beginning elxacaftor/tezacaftor/ivacaftor (ELX/TEZ/IVA) while 10 initiated TEZ/IVA or lumacaftor/IVA and continued with ELX/TEZ/IVA. Mild fluctuations in LFTs occurred in 58.8% but did not lead to therapy discontinuation. Only one patient with CFLD received the drug in reduced dose. At the reassessment, 60.5 (57–65.25) months following first assessment, 11 (36.7%) of total patients met the Debray criteria. Two (15.4%) of the non-treatment group were classified as CFLD at first assessment and 6 (46.2%) in the reassessment. Seven (41.2%) in treatment group were classified as CFLD at first assessment and were reduced in 5 (29.4%) at the reassessment. Liver stiffness decreased in the treatment group from 6.8 kPa (5.05–11.95) to 5 kPa (4.15–6.35), ($p = 0.001$). The median time elapsing between two liver stiffness determinations were 87 (57–95) months. Liver stiffness values did not demonstrate a significant alteration in the non-treatment group between the two assessment points ($p = 0.972$).

Conclusion: In a case series of adult patients with CF, some patients from non-treatment group developed CFLD during investigation period while others treated with CFTR modulators were de-classified from CFLD and re-classified in non-CFLD group. Liver stiffness was also improved in treated patients. However, more patients and longer follow-up are needed for solid conclusions to be drawn.

THU-299

Genetic findings and magnetic resonance imaging of multiple biliary hamartomas

Juliana Goediker¹, Philipp Schindler², Judit Horvath³, Julius Heidenreich⁴, Jonel Trebicka¹, Carsten Bergmann⁵, Bernhard Schlevogt¹. ¹University Hospital Muenster, Internal Medicine B, Germany; ²University Hospital Muenster, Department of Radiology, Germany; ³University Hospital Muenster, Department of Human Genetics, Germany; ⁴University Hospital of Würzburg, Department of Diagnostic and Interventional Radiology, Germany; ⁵Medical Center-University of Freiburg, Department of Medicine IV, Germany
Email: juliana.goediker@ukmuenster.de

Background and aims: Biliary hamartomas (BH), which are also known as “von Meyenburg complexes,” are benign and asymptomatic malformations of dilated bile ducts embedded in fibrous stroma, usually smaller than 10 mm. BH are usually incidental findings in liver imaging and there is a risk of misdiagnosis as malignomas. BH are part of a wider spectrum of ductal plate malformations, which are generally presumed to have a genetic basis. However, the specific genetic cause of BH is unknown. This study aims to provide a structured genetic and magnetic resonance imaging (MRI) analysis of BH.

Method: 6 patients with multiple biliary hamartomas (MBH) were identified in a large cohort of a tertiary center. Customized next-generation sequencing was used to identify the underlying genetic cause of MBH. This panel contained more than 650 genes with a known association with ciliopathies. High-resolution contrast-enhanced hepatobiliary MRI was performed in all subjects to provide a structured report of the imaging features of MBH. Quantitative analysis of cystic liver volume was performed with an

artificial-intelligence augmented approach at baseline and follow-up MRI.

Results: In all patients, a heterozygous missense change, truncating or frameshift mutation was found in PKHD1, which encodes for multidomain integral membrane protein fibrocystin. Biallelic mutations are causative for autosomal recessive polycystic kidney disease (ARPKD). Laboratory and clinical abnormalities were missing and acoustic radiation force elastography (ARFI) displayed no signs of liver fibrosis in these patients. MRI showed innumerable small liver cysts without communication with the biliary tree, which allowed diagnosis of MBH. Longitudinal MRI studies revealed that total hepatic cystic volume remained stable over time (mean volume: 104.8 ml; mean proportion of total liver volume: 8.1%, mean follow-up: 3.8 years).

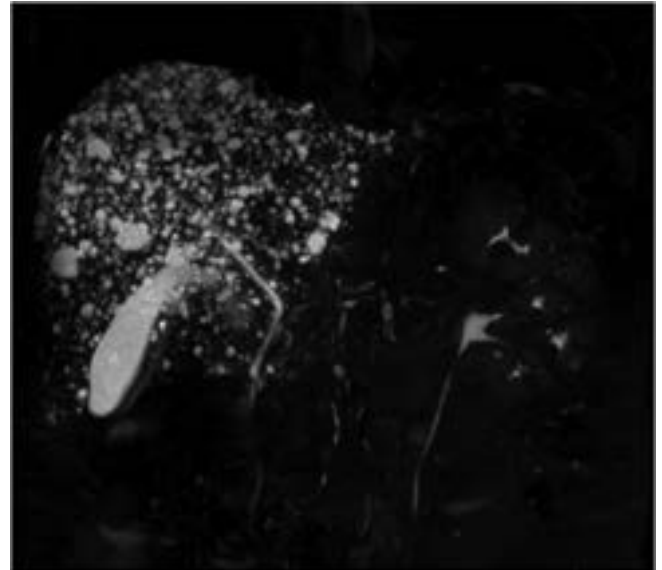


Figure: 3D magnetic resonance cholangiopancreatography (MRCP) showing multiple cystic lesions within the liver, but without communication of the lesions with the biliary ducts.

Conclusion: This case series delivers evidence that MBH and PKHD1-associated polycystic liver disease may belong to the same disease entity, caused by monoallelic mutations in PKHD1. Clinically they share a similar phenotype with innumerable liver cysts within the range of a few millimeters, which remain stable over time.

THU-300

Performance of blood based non-invasive tests for liver fibrosis prediction by transient elastography in Alpha-1 antitrypsin deficiency

Hassaan Yousuf^{1,2}, Tobias Maharaj^{1,2}, Daniel Fraughen^{1,2}, Tomas Carroll^{1,2}, Noel G. McElvaney^{1,2}, John Ryan^{1,2}. ¹Beaumont Hospital, Dublin, Ireland; ²Royal College of Surgeons in Ireland, Ireland
Email: Hassaanmyousuf@hotmail.com

Background and aims: Alpha-1 Antitrypsin Deficiency (AATD) is an inherited disorder characterised by lung and/or liver injury. The most severe form is seen in individuals with the homozygous PiZZ variant, while heterozygous (PiMZ; PiSZ) variants are associated with milder disease. Progressive liver fibrosis may lead to cirrhosis in some cases. In chronic liver disease, liver biopsy is used less often as a staging tool; instead blood-based fibrosis scores such as the NAFLD fibrosis score (NFS), AST to platelet ratio index (APRI) or the Fibrosis-4 (Fib-4) score, or Transient Elastography (TE) by liver stiffness measurement (LSM) may be used to determine fibrosis stage.

Method: Clinical data, blood tests and TE measurements were taken on adult patients presenting to a dedicated AATD clinic over a 18-month period. LSM cutoffs used were > 7.1 kPa for significant

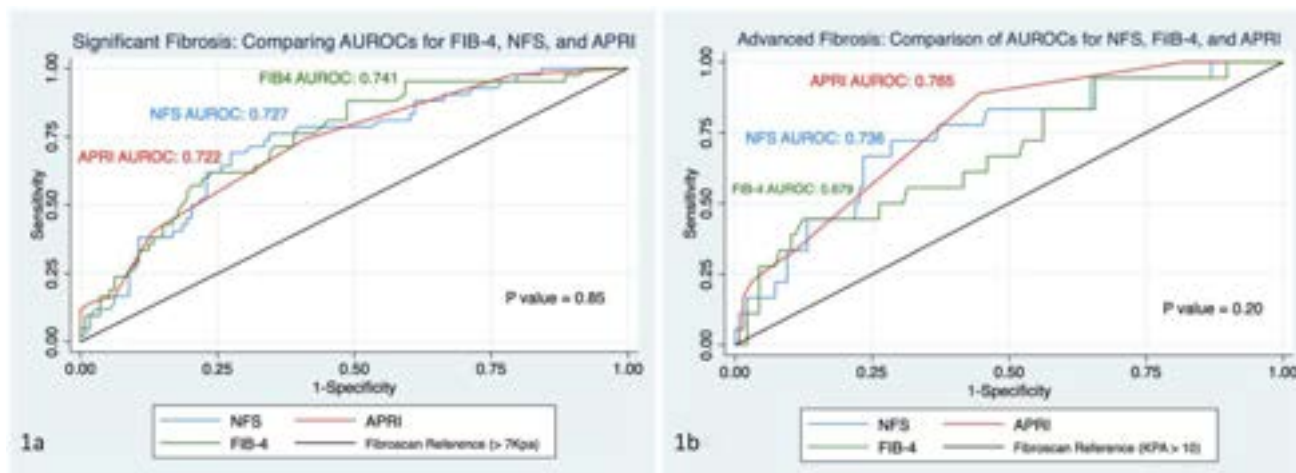


Figure: (abstract: THU-300).

fibrosis, and >10kPa for advanced fibrosis/cirrhosis. Statistics were performed using Stata software.

Results: 155 patients were assessed. Of them, 55% were female, mean age was 52.6 (\pm 16). Regarding AATD phenotype, 69 (44.5%) were PiZZ, and 62 PiMZ and 15 PiSZ. Of the overall cohort, 40 (25.8%) had significant fibrosis based on TE measurement, while 17 (11%) had advanced fibrosis. Of patients with the PiZZ phenotype, 20 (28.9% of PiZZ) had significant fibrosis, while 10 (14.4%) had advanced fibrosis. Of patients with the PiMZ phenotype, 12 (19% of PiMZ) had significant fibrosis, while 4 (6.4%) had advanced fibrosis. NAFLD fibrosis score (NFS), AST to platelet ratio index (APRI) and the Fibrosis-4 (Fib-4) score were compared with liver fibrosis stage as determined by TE. The AUROC curves from significant and advanced fibrosis are outlined in Fig 1. For both stages of fibrosis, these scores showed a modest ability to predict fibrosis stage without significant differences between scores; NFS ($r=0.72$), APRI ($r=0.72$) and Fib-4 ($r=0.74$) for significant fibrosis (Fig1a), and NFS ($r=0.73$), APRI ($r=0.76$) and Fib-4 ($r=0.67$) for advanced fibrosis (Fig1b).

Conclusion: In patients with AATD, existing blood-based, non-invasive markers of liver fibrosis have a modest ability to predict fibrosis. Reliable disease-specific tools are needed to accurately stage liver disease in AATD.

THU-301

Main clinical characteristics and evolutionary events among patients suffering Wilson disease in Spain: first results from the Spanish Wilson registry

Zoe Mariño¹, Luis García-Villarreal², Antonio Oliveira Martin³, Javier Ampuero⁴, Marina Berenguer⁵, Diego Burgos Santamaria⁶, José Ramón Fernández⁷, Jose María Moreno Planas⁸, María Lázaro Ríos⁹, Helena Masnou¹⁰, María Luisa Gonzalez Dieguez¹¹, Jose Pinazo Bandera¹², Esther Molina¹³, Manuel Hernández Guerra¹⁴, Concepción gonzalez de frutos¹⁵, Patricia Cordero Ruiz¹⁶, Carolina Muñoz Codoceo¹⁷, Sara Lorente¹⁸, Alba Cachero¹⁹, Manuel Delgado²⁰, Víctor Manuel Vargas Blasco²¹, Judith Gómez- Camarero²², Julia Morillas²³, Francisca Cuenca Alarcon²⁴, Luis Ibañez Samaniego²⁵, Miguel Fernandez-Bermejo²⁶, Beatriz Álvarez-Suárez²⁷, Paula Iruzubieta²⁸, Ana Arencibia Almeida²⁹, Anna Miralpeix³⁰, Pablo Alonso Castellano³¹, Pilar Castillo³. ¹Liver Unit, Hospital Clínic, CIBERehd, IDIBAPS, ERN-RARE Liver, Universitat de Barcelona, Barcelona., Spain; ²Servicio Digestivo, Complejo Hospitalario Universitario Insular Materno Infantil (CHUIMI), Las Palmas de Gran Canaria., Spain; ³Hospital Universitario La Paz, Madrid., Spain; ⁴Hospital Universitario Virgen del Rocío, Sevilla., Spain; ⁵Hospital Universitari i

Politécnico La Fe, CIBERehd, IIS La Fe, València., Spain; ⁶Hospital Ramón y Cajal, Madrid., Spain; ⁷Hospital Universitario de Cruces, Barakaldo., Spain; ⁸Servicio de Aparato Digestivo, Complejo Hospitalario Universitario de Albacete, Facultad de Medicina Universidad de Castilla La Mancha., Spain; ⁹Hospital Universitario Miguel Servet, Zaragoza., Spain; ¹⁰Hospital Universitari Germans Trias i Pujol, Badalona, Spain; ¹¹Hospital Universitario Central de Asturias, Oviedo., Spain; ¹²Unidad de Hepatología, Unidad de Gestión Clínica de Aparato Digestivo, Hospital Universitario Virgen de la Victoria, Instituto de Investigación Biomédica de Málaga-Plataforma Bionand, Málaga., Spain; ¹³Hospital Clínico de Santiago, Santiago de Compostela., Spain; ¹⁴Hospital Universitario de Canarias, Santa Cruz Tenerife., Spain; ¹⁵Hospital Universitario de Toledo, Toledo., Spain; ¹⁶Hospital Universitario Virgen Macarena, Sevilla., Spain; ¹⁷Hospital Universitario 12 de Octubre, Madrid., Spain; ¹⁸Unidad de Hepatología y Trasplante Hepático, Hospital Clínico Lozano Blesa de Zaragoza, IIS Aragón., Spain; ¹⁹Hospital Universitari de Bellvitge, Hospitalet de Llobregat., Spain; ²⁰Hospital Universitario A Coruña, A Coruña, Spain; ²¹Servicio de Hepatología, Hospital Vall d'Hebron, Universitat Autònoma Barcelona, CIBERehd, Barcelona., Spain; ²²Hospital Universitario de Burgos, Burgos, Spain; ²³Hospital Universitario Virgen de la Luz, Cuenca., Spain; ²⁴Unidad de Hígado, Servicio de Aparato Digestivo, Hospital Clínico San Carlos, Madrid, Spain; ²⁵Hospital General Universitario Gregorio Marañón, Madrid., Spain; ²⁶Hospital Universitario de Cáceres, Cáceres., Spain; ²⁷Hospital Universitario Lucus Augusti (CHUL), Lugo., Spain; ²⁸Hospital Universitario Marqués de Valdecilla, Santander., Spain; ²⁹Hospital Universitario Nuestra Señora de La Candelaria, Santa Cruz de Tenerife, Spain; ³⁰Liver Unit, Hospital Clínic, CIBERehd, IDIBAPS, ERN-RARE Liver, Universitat de Barcelona, Barcelona, Spain; ³¹Servicio Digestivo, Complejo Hospitalario Universitario Insular Materno Infantil (CHUIMI), Las Palmas de Gran Canaria, Spain
Email: zmarino@clinic.cat

Background and aims: Wilson disease (WD) is characterized by a high clinical heterogeneity. In Spain, a National Wilson Registry (supported by the Spanish Association for the Study of the Liver, AEEH) was created in Nov/2021, with the aim of updating clinical information and promote consciousness and interest on the disease. In this first analysis of the global database, we aimed at describing the main baseline characteristics, therapy and long-term clinical events of WD patients.

Method: Multicentric national study including patients from the Wilson AEEH-Registry up to November 2022. Ethical approval from the participant centers and a signed informed consent was required for all cases.

Results: During the first year, 352 patients were registered and 320 had enough data to be analyzed (final cohort): 315 (95.3%) were

adults at inclusion (mean age 42, IQR₂₅₋₇₅ 29–53), 228 (71.3%) were index cases, 167 were male (52.2%), age at WD diagnosis: 16 years (10–27.8), Leipzig score at diagnosis: 7 (5–9) points (93.4% had score ≥ 3), baseline ceruloplasmin <0.2 g/L in 265 (83%), urinary copper >100 $\mu\text{g}/24$ hours in 148 (46.3%), intrahepatic copper >250 $\mu\text{g}/\text{g}$ in 152 (47.5%). Genetics were performed in 242 patients (75%); among them, 85% were compound heterozygote. One third (32.2%) reported a positive family history. Most of the patients (78%) were diagnosed after being studied from a liver disease. Predominant phenotype at diagnosis was chronic liver disease ($n = 158$, 49%), followed by presymptomatic cases ($n = 66$, 20.6%), neurological presentations ($n = 32$, 10.1%), mixed phenotypes ($n = 29$, 9.1%) and acute liver disease ($n = 29$, 9.1%). This last group included 7 cases who required an early liver transplantation (in the first month after diagnosis). Cirrhosis was present in 62 patients (19.4%) at diagnosis. The main initial therapy was based on chelators ($n = 213$, 67%), mainly with D-penicillamine (91.3%). Up to 30% suffered early adverse events (AE). In patients with AE, the therapeutic decision (available in 222) was to remain unchanged in 62%, changed in 32.4% and dose-adjusted in 5.9%. WD treatment is currently different to the initial one in 56% of the cohort. Mean follow-up from diagnosis is 18 years (9–26). Elastography was performed at least once in 203 (64%) cases [mean 6.1KPa (5–8.7)]. Evolutionary events were available from 170 patients (53%): 42 (24.7%) developed *de novo* cirrhosis, 7 (16%) presented hepatic decompensation (mainly ascites), 1 (0.6%) had liver cancer, 5 (2.9%) required liver transplantation within time and 16 (9.4%) patients died (15 deaths were WD-related).

Conclusion: During the first year of the Wilson AEEH-Registry we have recorded data from 320 patients. The hepatic phenotype was predominant in this cohort, as it has been promoted from the Hepatology scientific community. Up to 25% of the patients in Spain still lack from a confirmatory genetic analysis.

THU-302

Endoscopic ultrasound direct portal pressure measurement in patients with porto-sinusoidal vascular disorder and clinically significant portal hypertension: a comparison with hepatic venous pressure gradient measurement

Lucia Giuli¹, Francesco Santopaolo¹, Francesca Ponziani¹, Maria Pallozzi¹, Alberto Larghi¹, Gianenrico Rizzatti¹, Giulia Venturini¹, Andrea Contegiacomo¹, Brigida Eleonora Annicchiarico¹, Antonio Gasbarrini¹. ¹Fondazione Policlinico Universitario Agostino Gemelli IRCCS, Rome, Italy
Email: lucia.giuli92@gmail.com

Background and aims: Hepatic venous pressure gradient (HVPG) represents the gold standard for the evaluation of portal hypertension (PH). HVPG >10 mmHg defines clinically significant portal hypertension (CSPH), a condition that is independently associated with the occurrence of decompensation events. Portal pressure measurement is of fundamental importance for prognostic stratification and assessment of response to therapies. Indeed, a decrement of HVPG by 20% and/or <10 mmHg reduces the decompensation risk. HVPG, however, indirectly measures PH and it may underestimate portal pressure gradient (PPG) in patients with pre-sinusoidal forms of PH, as in porto-sinusoidal vascular disorder (PSVD). Endoscopic ultrasound (EUS)-guided PPG measurement has recently become available. This technique allows measurement of portal pressure directly in the portal vein system and theoretically overcomes HVPG limitations. We investigated the safety and accuracy of EUS measurements as compared to HVPG in evaluating PPG in a cohort of patients with PSVD and CSPH. In patients naïve to non-selective beta-blockers (NSBBs) hemodynamic response to therapy was also evaluated.

Method: Consecutive outpatients with PSVD diagnosed according to Valdig criteria and who presented specific sign (s) of CSPH (gastro-oesophageal varices and/or portosystemic collaterals) underwent HVPG and EUS-guided PPG measurements. In patients naïve to NSBBs, treatment was started and after its titration EUS-PPG

measurement was repeated. Definition and severity of adverse events (AEs) were based on classification of Cotton et al.

Results: Between March 2022 and December 2022, ten patients (mean age 59 ± 16 ; 67% males) were enrolled. Mean platelet count was 64,000 U/microliter with 30% of patients having platelet count $<50,000$ U/microliter. A total of 13 EUS-guided PPG and 10 HVPG measurements were performed. EUS-PPG was technically successful in all cases, without any AEs and requirement for platelet transfusion. EUS-PPG mean value was 19.3 ± 3.2 mmHg versus 8.3 ± 1.3 mmHg of HVPG ($p < 0.0001$) (figure 1). In three patients naïve to NSBBs we repeated a new EUS-PPG measurement after drug titration. The average PPG value in these patients before and after NSBBs titration was respectively $19.3 (\pm 3.8)$ and $16.3 (\pm 2.9)$ mmHg, with one patient out of three who achieved a decrement of PPG $>20\%$.

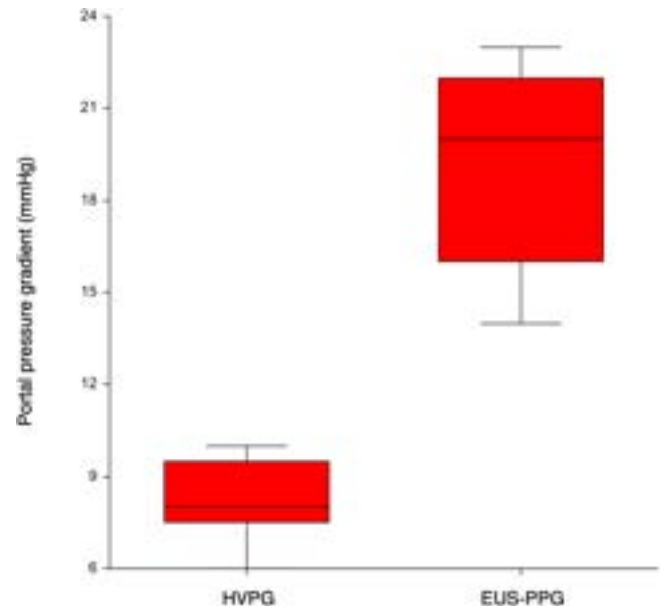


Figure 1:

Conclusion: Direct EUS-guided PPG measurement is safe and significantly more reliable than HVPG in the evaluation of PH in patients with PSVD and CSPH. This technique could be also used to assess hemodynamic response to therapy in pre-sinusoidal forms of PH.

THU-303

Alpha-1 antitrypsin deficiency is underdiagnosed in cirrhotic liver transplant patients: a retrospective multicenter study

Manon Evain¹, Ilias Kounis¹, Isaac Ruiz², Guillaume Lassailly³, Olivier Roux⁴, Alessandro Mazzola⁵, Pauline Houssel-Debry⁶, Laure Elkrief⁷, Rodolphe Anty⁸, Mylène Sebah¹, Teresa Antonini⁹, Didier Samuel¹, Audrey Coilly¹. ¹Hôpital Paul-Brousse Ap-Hp, Villejuif, France; ²CHUM, Montréal, Canada; ³Hôpital Claude Huriez, Lille, France; ⁴Hospital Beaujon AP-HP, Clichy, France; ⁵University Hospitals Pitié Salpêtrière-Charles Foix, Paris, France; ⁶CHU Rennes-Pontchaillou Hospital, Rennes, France; ⁷Chru Hospitals Of Tours, Tours, France; ⁸Hôpital L'archet, Nice, France; ⁹Hôpital de la Croix-Rousse-HCL, Lyon, France
Email: manon.evain@hotmail.fr

Background and aims: Alpha-1 antitrypsin deficiency (AATD) is one of the most common genetic diseases in Europe. It mainly causes pulmonary emphysema. Although it is also responsible for liver fibrosis, AATD is not always diagnosed, even in the most severe patients who are candidates for liver transplantation (LT). The aims of this study was to determine when the diagnosis was made for patients transplanted for AATD, to describe their clinical characteristics and the outcome on the transplant waiting list.

POSTER PRESENTATIONS

Method: We performed a multicenter retrospective study between May 2019 and June 2021 in 9 French and Canadian centers by including all liver transplant patients for AATD. The selection of patients was made or confirmed on the explant analysis with PAS+, diastase-resistant inclusions within hepatocytes. A control group (n = 305) to study the evolution on the transplant waiting list was selected from an existing monocentric cohort of liver transplant patients for decompensated cirrhosis.

Results: We included 58 liver transplant patients with AATD between 1996 and 2020, with a mean age of 55.6 ± 9.9 years at LT, mostly men (78%). Indication of LT was AATD in only 31% of cases whereas excessive alcohol consumption, NASH, cryptogenic cirrhosis represented 43%, 14% and 12% of patients respectively. The diagnosis of AATD was made before LT in only 40% of cases, after LT in 15% of cases. For 45% of patients, the diagnosis was never confirmed before the retrospective analysis. Among them, 62% was diagnosed with cirrhosis due to excessive alcohol consumption. Only 46% of patients in the cohort had confirmation of AATD by phenotyping or genotyping before or after LT. Only 60% of patients had a pre-LT serum AAT assay, which was significantly lower in homozygous versus heterozygous patients (0.36 vs. 0.82 mg/ml, $p < 0.01$). Moreover, 25% of the patients had non-specific pulmonary symptoms, 8% had pulmonary emphysema and 7% had an obstructive syndrome. Compared to the control group, patients transplanted for AATD had a higher MELD score at listing for transplant (21.9 vs 14.2, $p < 0.001$) and a shorter waiting time on the transplant waiting list (4.7 months vs 8.3 months, $p < 0.001$). They were also significantly more often hospitalized in intensive care before transplantation (22 vs. 4.3%, $p < 0.001$), and had more pre-LT sepsis (29 vs. 5.1%, $p < 0.001$).

Conclusion: Our study demonstrates that although patients with AATD are more severe, AATD is largely under-diagnosed in the context of LT. AAT dosage is not sufficient to screen the disease on the waiting list patient. Regarding recent advances and development of curative treatments, systematic phenotype/genotype screening of patients on waiting list could be suggested as well as raising awareness of transplant physician to achieve better management of the patients and their relatives.

THU-304

The impact of a complete biochemical response on health-related quality of life in patients with autoimmune hepatitis: a multicentre prospective cross-sectional study

Romée Snijders^{1,2}, Maciej K. Janik^{2,3}, Meike Mund^{2,4}, Alessio Gerussi^{2,5}, Francesca Bolis^{2,5}, Laura Cristofari^{2,5}, Pietro Invernizzi^{2,5}, Patricia Kovats^{2,6,7}, Maria Papp^{2,6}, Lisbet Grønbaek^{2,8}, Henning Grønbaek^{2,8}, E.T.T.L. Tjwa¹, Luise Aamann^{2,9}, Henriette Ytting^{2,9}, Vincenzo Ronca^{2,10,11}, Katheryn Olsen^{2,10,11}, Ye Htun Oo^{2,10,11}, Adriaan Van der Meer¹², Joao Madaleno^{2,13,14}, Bernardo Canhão^{2,13,14}, Bastian Engel^{2,15}, Alejandro Campos-Murguía^{2,15}, Richard Taubert^{2,15}, Ozgur Koc^{2,16}, Matthijs Kramer¹⁶, José Willemse^{2,17}, Bernd Löwe^{2,18}, Ansgar W. Lohse^{2,19}, Joost P.H. Drenth^{1,2}, Christoph Schramm^{2,4,19}, Piotr Milkiewicz^{2,3,20}, Tom Gevers^{2,16,21}. ¹Department of Gastroenterology and Hepatology, Radboud University Medical Center, Nijmegen, The Netherlands, Netherlands; ²European Reference Network on Hepatological Diseases (ERN RARE-LIVER), Germany; ³Department of Hepatology, Transplantology and Internal Medicine, Medical University of Warsaw, Warsaw, Poland, Poland; ⁴Martin Zeitz Centre for Rare Diseases, University Medical Centre Hamburg-Eppendorf, Hamburg, Germany, Germany; ⁵Division of Gastroenterology and Center for Autoimmune Liver Diseases, Department of Medicine and Surgery, University of Milano-Bicocca, Monza, Italy, Italy; ⁶Division of Gastroenterology, Department of Internal Medicine, Faculty of Medicine, University of Debrecen, Hungary; ⁷Kálmán Laki Doctoral School, Faculty of Medicine, University of Debrecen, Hungary, Hungary; ⁸Department of

Gastroenterology and Hepatology, Aarhus University Hospital, Aarhus, Denmark, Denmark; ⁹Departments of Medical Gastroenterology and Hepatology, Hvidovre University Hospital and Rigshospitalet, Copenhagen, Denmark, Denmark; ¹⁰Liver Transplant and Hepatobiliary Unit, Queen Elizabeth Hospital, University Hospital of Birmingham NHS Foundation Trust, United Kingdom; ¹¹Centre for Liver and Gastro Research, NIHR Biomedical Research Centre, Institute of Immunology and Immunotherapy, University of Birmingham, Birmingham, United Kingdom, United Kingdom; ¹²Department of Gastroenterology and Hepatology, Erasmus University Medical Center, Rotterdam, The Netherlands, Netherlands; ¹³Liver Disease Unit, Internal Medicine Department, Centro Hospitalar e Universitário de Coimbra, Coimbra, Portugal, Portugal; ¹⁴Liver Transplant Unit, Centro Hospitalar e Universitário de Coimbra, Coimbra, Portugal, Portugal; ¹⁵Department of Gastroenterology, Hepatology and Endocrinology, Hannover Medical School, Hannover, Germany, Germany; ¹⁶Department of Gastroenterology and Hepatology, MUMC+, Maastricht, The Netherlands, Netherlands; ¹⁷Dutch Liver Patients Association, Hoogland, The Netherlands, Netherlands; ¹⁸Department of Psychosomatic Medicine and Psychotherapy, University Medical Center Hamburg-Eppendorf, Hamburg, Germany, Germany; ¹⁹I. Department of Medicine, University Medical Center Hamburg-Eppendorf, Hamburg, Germany, Germany; ²⁰Translational Medicine Group, Pomeranian Medical University, Szczecin, Poland, Poland; ²¹Nutrim School for Nutrition and Translational Research in Metabolism, Maastricht University, Maastricht, The Netherlands, Netherlands
Email: Romee.Snijders@radboudumc.nl

Background and aims: Autoimmune hepatitis (AIH) is a rare, chronic liver disease. A complete biochemical response (CBR) is a desired end point in the treatment of AIH. Data suggest that CBR improves the prognosis, but the impact on health-related quality of life (HRQoL) in AIH patients is unclear. The aim of this study is to characterize the relationship between CBR and HRQoL in an international multicentre cohort.

Method: A cross-sectional cohort study was performed in adult patients with AIH who were recruited between July 2020 and December 2022 from 12 European tertiary centres. Patients with a history of liver transplantation or hepatocellular carcinoma were excluded. HRQoL was evaluated using the EQ-5D visual analogue scale (VAS), ranging from 0 (worst imaginable health) to 100 (best imaginable health). The cohort was divided into two groups according to their CBR, which was defined as normal alanine aminotransferase, aspartate aminotransferase, and immunoglobulin G levels. Clinical data were obtained from patient records at the time of HRQoL evaluation. A linear mixed regression analysis was used to explore the relationship between CBR and EQ-5D VAS score.

Results: A total of 748 patients with AIH (mean age: 49.7 years (standard deviation (SD) 17.2); 73.8% female) were evaluated. A total of 25.6% had compensated cirrhosis. The median disease duration was six years (interquartile range (IQR) 2–11). In this cohort, 44.8% had a CBR at the time of HRQoL evaluation. The median EQ-5D VAS score was 80 (IQR 65–90) in the patients with a CBR and 70 (IQR 50–85) in the patients without a CBR. Patients with a CBR used fewer corticosteroids (48.0% vs. 65.4%, $p < 0.001$) and were older (mean (SD) 51.9 (17.1) vs. 48.0 (17.1), $p = 0.002$), while sex and the prevalence of cirrhosis were similar. After controlling for age, sex and corticosteroid use, patients with a CBR reported significantly higher mean EQ-5D VAS scores than those without a CBR ($\beta = 6.71$; 95% CI 2.23, 11.20). We did not observe any association between corticosteroid use and EQ-5D VAS score.

Conclusion: Achieving a CBR in patients with AIH is an important factor associated with improved HRQoL, independent of corticosteroid use, age and sex.

THU-305

Impact of extrahepatic portal vein obstruction on fertility and pregnancy outcomes- a tertiary center experience

Ankita Singh¹, Sidharth Harindranath², Karan Muzumdar², Aditya Kale², Akash Shukla¹. ¹King Edward Memorial Hospital, Gastroenterology, Mumbai, India; ²King Edward Memorial Hospital, Mumbai, India
Email: drakashshukla@yahoo.com

Background and aims: Pregnancy in patients with portal hypertension (PHT) presents a major challenge in terms of management due to plasma volume expansion and increased cardiac output which increases portal pressure and risk of variceal bleeding. PHT is associated with poor pregnancy outcomes in mother and foetus. We aim to study the outcomes of pregnancy (maternal and neonatal) in patients with EHPVO.

Method: This was a single center retrospective analysis of pregnancy outcomes in patients with EHPVO who were registered in the department of Gastroenterology at KEM Hospital between January 2006 to December 2022. All patients underwent endoscopy with prophylactic EVL (for high-risk varices) during second trimester and beta blockers were continued during pregnancy. Second stage of labour was shortened as per obstetric indications. Control group consisted of healthy females without comorbidities and with low-risk pregnancies.

Results: Complete data was available for 100 pregnancies in 45 patients, of which 98 were spontaneous and 2 assisted. There was no maternal mortality. 82 (82%) pregnancies had successful fetal outcomes. Of the 18 unsuccessful pregnancies, 13 (72.2%) were spontaneous abortions, 2 (11.1%) were intra uterine fetal deaths, and 3 (16.7%) were neonatal deaths. 3 (6.7%) patients presented with acute variceal bleed (AVB) for the first-time during pregnancy. Only one of the 17 patients with history of UGIB prior to pregnancy, had repeat hematemesis during pregnancy. During pregnancy, 24 (53.3%) patients were treated with combination (endoscopic with non-selective beta blockers) therapy, 10 (22.3%) with NSBB alone and 11 (24.4%) did not receive any treatment. Anemia was observed in 37 (82.2%) patients; 73% patients had mild, 21.6% moderate and 5.4% severe anemia. 10 (22.2%) patients had thrombocytopenia (platelet count <1L). Infertility was diagnosed in 10 (13.3%) patients, 3 (50%) of them underwent treatment for same and 1 patient had conceived. Of the pregnancies with successful outcomes, 4 (4.9%) were delivered preterm and 19 (23.1%) required Caesarean section; Low birth weight was seen in 23 (28%) and small for gestational age in 9 (10.9%) pregnancies. 105 pregnancies in 45 healthy females formed the control group. 86 (81.9%) successful pregnancies were recorded with 15 (14.28%) low birth weight and 7 (6.66%) small for gestational age births. Neonatal outcomes in patients with EHPVO did not differ significantly from healthy controls ($p > 0.05$). Pregnancy outcomes were also similar between the two groups, with around 82% successful pregnancies. None of the patients were on anticoagulants before or during pregnancy.

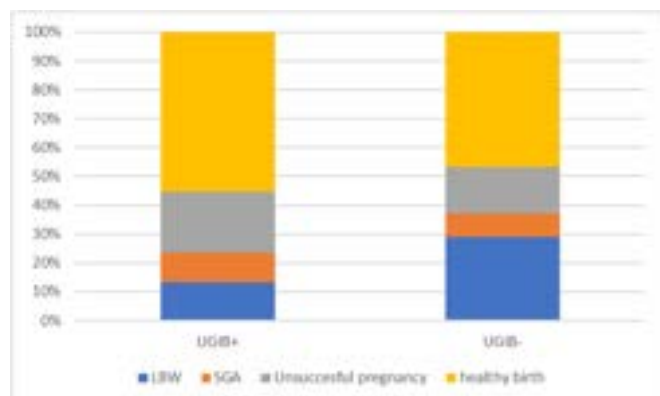


Figure:

Conclusion: Pregnancy in patients with EHPVO has good maternal and neonatal outcomes irrespective of history of variceal bleed before or during pregnancy.

THU-306

Extrahepatic iron loading and disease complications in HFE haemochromatosis

John Olynyk^{1,2}, Tim St Pierre³, Louise Ramm⁴, Grant Ramm⁴. ¹Fiona Stanley Hospital, Murdoch, Australia; ²Edith Cowan University Joondalup Campus, Joondalup, Australia; ³The University of Western Australia, Physics, Crawley, Australia; ⁴QIMR Berghofer Medical Research Institute, Herston, Australia
Email: john.olynyk@health.wa.gov.au

Background and aims: Arthritis and advanced hepatic fibrosis (AHF) are complications of HFE haemochromatosis (HH), more likely at higher degrees of iron overload especially in men. Iron overload is quantified by calculation of mobilizable iron (Fe) stores or the hepatic iron concentration (HIC). Whilst there is a linear relationship between HIC and Fe stores, there is substantial variance, the cause of which is unclear. We aimed to determine if the variance in relationship between HIC and Fe stores may be due to extrahepatic iron load occurring in the presence of arthritis or AHF.

Method: We recorded data on arthritis, liver-biopsy fibrosis, HIC, and Fe stores in 77 male HH subjects. We calculated the hepatic iron index (HII, HIC/age), Fe stores (number of phlebotomies \times 250 mg to reduce ferritin to 50ug/L), and Fe/HIC ratio (a marker of body iron relative to liver iron). To determine if liver volume could confound the relationship between HIC and Fe, we measured liver volume by MRI in an independent group of 17 HH subjects. We conducted linear regression analysis for groups dichotomized for arthritis or AHF and compared HII, HIC, Fe and Fe/HIC relationships.

Results: AHF and arthritis were associated with increased HIC and Fe stores (Table 1). HII was similar across the groups, indicating the rate of hepatic iron loading is independent of arthritis or AHF. Linear regression analysis showed distinctly different relationships between Fe stores and HIC for subjects with arthritis or AHF compared with those without, with less than a 0.01% (for arthritis) or 4% (for AHF) probability of a single relationship being present. Median Fe/HIC values were 50% higher in subjects with arthritis and AHF (0.062 g/(umol/g)) compared with those without (0.040 g/(umol/g), $p = 0.027$). The upper and lower 95% limits of liver volumes varied by a factor of 2.3 (CI 2.1–2.7) which is significantly lower than the factor of 6.7 (CI 5.1–8.7) observed between the 95% limits of Fe for a given HIC, indicating that variability in liver volume does not explain the variability of Fe at a given HIC.

(n)	No AHF No arthritis (36)	No AHF Arthritis (21)	AHF No arthritis (3)	AHF Arthritis (17)
HIC (umol/g)	110 (34–399)	188 (41–361)	384 (295–510)*	228 (57–675) *
HII (HIC/age)	3.7 (1.0–17.4)	4.4 (1.3–10.8)	6.1 (6.0–12.4)	4.9 (1.3–19.3)
Fe (g)	4.8 (1.2–20.0)	7.5 (2.5–19.5)	11.0 (10.0–11.25)	14.0 (4.8–50.0)***
Fe/HIC (g/[umol/g])	0.041 (0.016–0.088)	0.042 (0.023–0.133)	0.029 (0.022–0.034)	0.062 (0.026–0.171)**

All values-Median (range); * $p < 0.05$, *** $p < 0.001$ vs no AHF/no arthritis group, ** $p < 0.05$ vs AHF/no arthritis group.

Conclusion: HH subjects with AHF and arthritis exhibit substantially greater Fe/HIC not explained by variations in hepatic iron deposition or liver volume, raising the possibility of greater extrahepatic iron loading.

THU-307

Longitudinal assessment of plasma immune and bacterial translocation markers in biliary atresia

Vandana Jain¹, Emma Alexander¹, Charlotte Burford¹, Mark Davenport¹, Jessica Nulty¹, Muhammed Yukse¹, Anil Dhawan¹.
¹King's College Hospital, United Kingdom
 Email: vjain@nhs.net

Background and aims: Bacterial translocation (BT), and Pathogen Associated Molecular Patterns (PAMPS), propagate a pro-inflammatory response in chronic liver diseases. However, the role of BT, the immune system, and their interaction, is as-yet incompletely characterised in Biliary Atresia (BA). We aimed to characterise the association of immune markers in BA, before and after Kasai portoenterostomy (KPE), with fibrosis and BT, and clinical outcomes. **Method:** Plasma samples were prospectively collected from BA infants (n = 55) pre-KPE, 6weeks-, 3months-, and 6months-post-KPE. Th1- (IL-2, IFN γ), Th2- (IL-4, IL-10), TH17- (IL-17, IL-23), macrophage-associated (IL-6, IL-8, TNF α , IL-1 β) cytokines, and cellular adhesion molecules (ICAM-1, VCAM-1), BT biomarkers (LBP and D-lactate) were measured. Clinical outcomes: 6month-JC (jaundice clearance), 1year-LT (liver transplantation), cholangitis by 6month-post-KPE, fibrosis biomarkers [Aspartate Aminotransferase-to-platelet ratio index (APRI); Liver Stiffness Measurement (LSM)]. Additionally, we investigated the course of the assessed immune markers via longitudinal analysis, using generalised estimating equations.

Results: Pre-KPE, immune markers were similar between clinical outcome groups. By 6weeks-post-KPE, increased IL-4, IL-8, IL-1 β and ICAM-1 were associated with 1-year-LT. ICAM-1 was associated with poor 6month-JC and with fibrosis biomarkers [APRI;rs=0.6, p<0.001;LSM;rs=0.6, p<0.001]. By 3months-post-KPE, further increases in macrophage-associated cytokines in non-favourable outcome groups (1year-LT and poor 6month-JC), were evident. VCAM-1/ICAM-1, IL-8 and IL-1 β positively correlated with APRI and LSM. We found an increased rise of IL-17 [1.14 ng/L/month], IFN- γ [4.04 ng/L/month] ICAM-1 [76 ug/L/month] and VCAM-1 [142 ug/L/month] over the 6month-period, in 1yr-LT group. IL-17, 6weeks-post-KPE, associated with cholangitis [p=0.03]. At early-post-KPE time-points, macrophage markers (IL-6, IL-8, TNF α) and ICAM-1/VCAM-1

positively correlated with LBP levels; macrophage markers/TH2/Th17 and adhesion molecules, positively correlated with D-lactate.

Conclusion: Divergence of innate (macrophage) and adaptive (Th1/Th2/Th17) immune pathways early post-KPE, strongly discriminates BA infants with non-favourable clinical outcomes. This novel data provides convincing evidence for BT in macrophage activation, upregulation of adhesion molecules, and fibrosis. Consequently, targeted microbiota-modulatory therapy, early-post-KPE, could dampen PAMP-associated damage in BA.

THU-308

Chronic hepatitis B infection and porto-sinusoidal vascular disorder, a non-negligible coexistence

Pol Olivas Alberch^{1,2,3}, Sabela Lens^{3,4}, Genís Campreciós^{3,5}, Carla Montirioni⁶, Marta Magaz^{2,3,4}, Valeria Perez^{2,3,7}, Lara Orts^{3,8}, Anna Baiges^{2,3,4}, Fanny Turon^{2,3,4}, Juan Carlos, Garcia Pagan^{2,3,9}, Virginia Hernandez-Gea^{2,3,10}. ¹Liver Unit, Hospital Clínic de Barcelona, Universitat de Barcelona, IDIBAPS, Spain; ²Hemodynamic Lab, Hospital Clínic de Barcelona, ERN-rare-Liver, Spain; ³Centro de investigación biomédica en red enfermedades hepáticas y digestivas (CIBEREHD), Spain; ⁴Liver Unit, Hospital Clínic de Barcelona, Universitat de Barcelona, IDIBAPS, Spain; ⁵Hemodinamic Lab, Hospital Clínic Barcelona, IDIBAPS, Spain; ⁶Department of Pathology, Hospital Clínic de Barcelona, Universitat de Barcelona, IDIBAPS, Spain; ⁷Liver Unit, Hospital Clínic de Barcelona, Universitat de Barcelona, IDIBAPS, Spain; ⁸Hemodynamic Lab, Hospital Clínic de Barcelona, IDIBAPS, Spain; ⁹Liver Unit, Hospital Clínic de Barcelona, Universitat de Barcelona, IDIBAPS, Spain; ¹⁰Liver Unit, Hospital de Barcelona, Universitat de Barcelona, IDIBAPS, Spain
 Email: olivas.alberch@gmail.com

Background and aims: Porto-sinusoidal vascular disorder (PSVD) diagnostic criteria have recently been redefined (Baveno VII). An important novelty is that the presence of other liver disease etiology does not exclude PSVD diagnosis in absence of cirrhosis. Coexistence of HBV chronic infection (HBVci) and PSVD-like vascular alterations have anecdotally been reported. Our aim is to evaluate the prevalence of this coexistence and its clinical impact.

Method: Retrospective unicentric study. Inclusion of patients meeting Baveno VII PSVD criteria. Detailed characterization of HBV biology. Collection of clinical data at diagnosis and follow-up (11 \pm 9

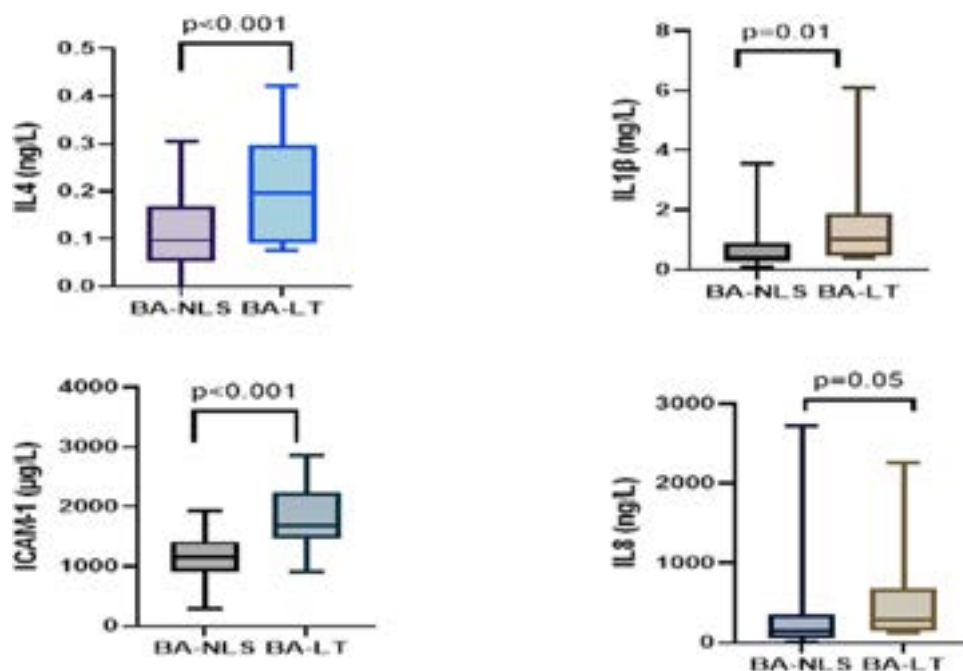


Figure: (abstract: THU-307).

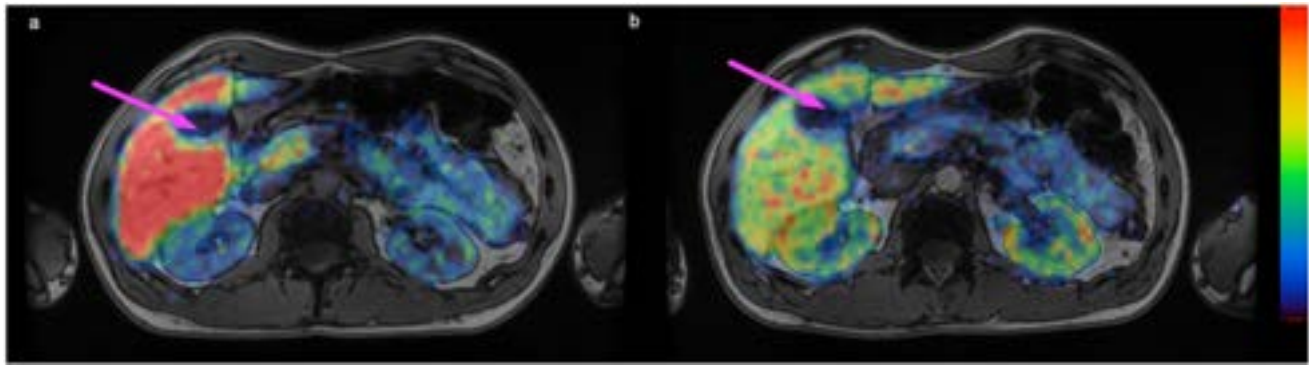


Figure: (abstract: THU-300): Fused axial abdominal PET/MRI showing the liver, kidneys and gallbladder (magenta arrow), 6 hours after i.v. ^{64}Cu injection. a) Pre-treatment after a 3 day pause of treatment with penicillamine. b) After 7 days of treatment with TTM. ^{64}Cu concentration is expressed as Standard uptake Value (SUV). Scale 2.5 (black)-20 (red).

years). Definitions: HBVci (AgHBs + more than 6months), HBV past infection (HBsAg- and anti-HBc+), Non-exposed (HBsAg- and anti-HBc-).

Results: We included 173 patients with PSVD: 151 had a complete HBV biology characterization (HBsAg, anti-HBs, anti-HBc), the other 22 only had HBsAg- information and so, they were only used to calculate prevalence. Prevalence of HBVci was higher in the PSVD cohort than in the general Spanish population (4,49% vs 0,8% $p < 0,001$), as well as the prevalence of past HBV infection (16,85% vs 12,3% $p 0,064$). As HBV and HIV infection may coexist, we analyzed our cohort and did not find differences in HIV infection prevalence in patients with PSVD and HBVci compared to the whole PSVD cohort. The presence of underlying associated conditions (50%) and the biopsy findings were similar in all the HBV serology groups. According to HBV status, patients with HBVci had a significant delay in the diagnosis of PSVD (14 vs 1 year) compared to non-infected ones (Past HBV infection and non-exposed), and the most common misdiagnosis was cirrhosis. At time of PSVD diagnosis HBVci patients had more advanced liver disease with worse hepatic function (MELD 12 (9–16) vs 9 (7–11) $p 0,062$) and slightly higher rate of decompensation (50% vs 38,5% $p 0,712$) and further decompensation (37,5% vs 14,7% $p 0,115$) conditioning higher need of liver transplantation than non-infected patients (25% vs 2, 1% $p 0,023$) and worse liver transplant free survival at one year of diagnosis (75% vs 95, 8%; log-rank 0,002).

Conclusion: HBV chronic infection and PSVD can coexist. Patients with PSVD and HBVci had a more advanced disease at diagnosis and higher need of liver transplantation than non-infected patients. Increased awareness is needed to reduce misdiagnosis and delay in diagnosis reinforcing the idea of managing patients at centers of expertise.

THU-309

Effects of tetrathiomolybdate on copper distribution and biliary excretion: a controlled $^{64}\text{CuCl}_2$ PET/MRI

Frederik Teicher Kirk¹, Ditte Emilie Munk¹, Eugene Scott Swenson², Adam Quicquaro², Mikkel Holm Vendelbo³, Michael Schilsky⁴, Peter Ott¹, Thomas Damgaard Sandahl¹. ¹Aarhus University Hospital, Department of Hepatology and Gastroenterology, Aarhus, Denmark; ²Alexion, AstraZeneca Rare Disease, United States; ³Aarhus University Hospital, Department of Nuclear Medicine and PET-center, Denmark; ⁴Yale School of Medicine, Department of Medicine, Section of Digestive Diseases, and Department of Surgery, Section of Transplant and Immunology, United States
Email: frkirk@rm.dk

Background and aims: Patients with Wilson Disease (WD) experience pathologic hepatic copper accumulation due to reduced biliary copper excretion. Bis-choline tetrathiomolybdate (TTM) is a high affinity copper chelator with therapeutic potential in WD. Reports in

rodents that TTM stimulates hepatic copper excretion into the bile have not been confirmed in humans. In this study, to better understand its mechanism of action, we used ^{64}Cu PET imaging to examine the effects of TTM on copper distribution and hepatic excretion in patients with WD.

Method: Copper distribution and biliary excretion after an intravenous ^{64}Cu dose was investigated in four WD patients on stable chelation therapy using ^{64}Cu PET/MRI. Samples of venous blood were also taken for radiocopper measurement. Patients were scanned 20 minutes post ^{64}Cu dose and 7 more times until 68 h post dose. We compared PET/MRI recordings without treatment (baseline) and after TTM treatment, with each patient serving as their own control.

Results: TTM significantly increased ^{64}Cu levels by 5–700% in venous blood samples and in aorta (measured by PET) during the first 6h after the ^{64}Cu administration. Hepatic levels of ^{64}Cu were significantly decreased from baseline by TTM by 59%–27% (20 min–68 h post dose, respectively). These observations suggested immediate strong binding of ^{64}Cu in blood by TTM with retention of ^{64}Cu in plasma, leading to reduced uptake in organs.

Gallbladder ^{64}Cu levels were below or near detection limit at all time points and did not increase on TTM treatment during the 68 h timeframe, suggesting no induction of biliary radiocopper excretion (Figure). Radiocopper in the kidneys followed a different pattern. Initially, TTM inhibited renal ^{64}Cu accumulation, but from 20 h onwards renal ^{64}Cu was higher after TTM ($p < 0.03$). However, this was not followed by increased ^{64}Cu levels in the bladder.

Conclusion: PET/MRI is a useful tool for examining copper metabolism and mechanism of action of copper chelation therapy. TTM did not enhance biliary excretion of ^{64}Cu after TTM administration to patients with WD, in contrast to earlier reports in rodents, suggesting an alternative mechanism of action for this drug. TTM initially acted to reduce exposure of the liver and other organs to Cu by retaining ^{64}Cu in the plasma, but with time the copper may be redistributed. Further study is needed to delineate the multimodal effect of TTM on copper metabolism.

THU-310

Targeting CCL24 in primary sclerosing cholangitis with CM101: rationale and study design

Douglas Thorburn¹, Massimo Pinzani², Palak Trivedi³, Christopher Bowlus⁴, Rifaat Safadi⁵, Christina Crater⁶, John Lawler^{6,7}, Adi Mor⁶, Chris Cirillo⁶, Matthew Frankel⁶. ¹The Royal Free Hospital, United Kingdom; ²University College London, United Kingdom; ³University of Birmingham, United Kingdom; ⁴University of California, Davis, United States; ⁵Hadassah Hebrew University Hospital, Israel; ⁶Chemomab Therapeutics, Ltd, United States; ⁷Chemomab Therapeutics, INC, Clinical, Israel
Email: douglas.thorburn@nhs.net

POSTER PRESENTATIONS

Background and aims: Primary sclerosing cholangitis (PSC) is a rare, chronic cholestatic liver disease characterized by progressive inflammation, fibrosis, and destruction of the intrahepatic and extra-hepatic bile ducts. Animal models of PSC have shown that cytokines and chemokines may be important pathogenetic mediators of liver inflammation and fibrosis. CCL24 (eotaxin-2) is a chemokine that promotes cell trafficking and regulates inflammatory and fibrotic activities through the CCR3 receptor. Blockade of CCL24 with CM101, a humanized anti-CCL24 monoclonal antibody, has been shown in pre-clinical models to significantly reduce migration and activation of immune cells and fibroblasts, including hepatic stellate cells. In four PSC relevant mouse models (MDR2 knockout, chronic ANIT-induced cholestasis, bile duct ligation, and thioacetamide-induced liver fibrosis), CM101 consistently demonstrated both anti-inflammatory and antifibrotic effects. CM101 was found to reduce alkaline phosphatase (ALP), bile acid and liver fibrosis in the MDR2 knock out mouse model. CM101 was also observed to be safe and well tolerated in healthy subjects and in subjects with non-alcoholic fatty liver disease and patients with non-alcoholic steatohepatitis. Based on the pre-clinical evidence, the safety and tolerability profile of CM101 in phase 1 studies, and the high unmet medical need for patients with PSC, further evaluation of CM101 safety and efficacy is warranted.

Method: A phase 2a biomarker and clinical study was designed to understand the role of CCL24 in the pathogenesis of PSC and the effects of blockade of CCL24 with CM101 in patients with PSC.

Results: This is a Phase 2a, randomized, double-blind, placebo-controlled, multiple-dose, international study evaluating the safety and efficacy of CM101 in patients with PSC (NCT04595825). The overall study design is shown in Figure 1. Up to 93 patients with large duct PSC disease of >24 weeks duration, ALP >1.5 upper limit of normal, and any patients with concurrent stable inflammatory bowel disease will be randomized. The primary end point of the study is safety and tolerability. The pharmacodynamic effects of CM101 will be assessed by changes in CCL24 serum levels, serum inflammatory markers, and immune cell sub-populations. The clinical activity of CM101 will be assessed by changes in ALP, enhanced liver fibrosis (ELF) score, liver enzymes, liver elastography and liver fibrosis markers (e.g. PRO-C3, and PRO-C5). Patient reported outcomes will also be assessed. An independent Data Monitoring Committee has recently reviewed all safety data and had no safety concerns. They endorsed the plan for the next dose escalation per protocol.

Conclusion: Results from this study will provide early evidence of the role of CCL24 in inflammatory and fibrotic disease pathology and the clinical impact of neutralizing CCL24 with CM101, which will guide future development of CM101 in PSC.

THU-311

Intrahepatic cholestasis of pregnancy: genetic testing and genotype-phenotype relations in a cohort from a Danish tertiary liver center

Henning Grønbaek¹, Ida Paulsen¹, Jens Fuglsang², Ida Vogel³, Naja Becher⁴. ¹Aarhus University Hospital, Department of Hepatology and Gastroenterology, Aarhus University Hospital, Aarhus, Denmark, Aarhus N, Denmark; ²Aarhus University Hospital, Department of Obstetrics and Gynaecology, Aarhus N, Denmark; ³Aarhus University Hospital, Department of Obstetrics and Gynaecology, Aarhus N, Denmark; ⁴Aarhus University Hospital, Department of Clinical Genetics, Aarhus N, Denmark
Email: henning.gronbaek@dadlnet.dk

Background and aims: Intrahepatic cholestasis of pregnancy (ICP) affects 0.5–1% of all pregnancies in Denmark. In pregnancy, women present with symptoms of pruritus, elevated liver enzymes and bile acids, and hepatic dysfunction. In severe cases, ICP increases the risk of preterm birth and stillbirth. We aimed to investigate genetic variants related to the development of ICP and describe the genotype-phenotype associations.

Method: We included 34 women (median age 28 years) with ICP and genetic testing of disease causing variants. Thirteen (38%) had a history of cholestatic disease prior to their pregnancy. Patients were screened for disease-causing variants in *ABCB11*, *ABCB4*, *ABCG5*, *ABCC2*, *ATP8B1*, *JAG1*, *NOTCH2*, *TJP2* and *UGT1A1* using a gene panel approach.

Results: Symptoms of cholestatic pruritus occurred in 5 (15%) patients in the 1st trimester, 13 (38%) in the 2nd trimester and in 16 (47%) patients in the 3rd trimester. At first visit the majority presented with elevated ALT (94%), bilirubin (91%), GGT (44%), and bile acids (53%). Thirty-three patients (97%) received treatment; 21 (62%) received monotherapy with Ursodeoxycholic acid, while 12 (35%) patients also received Rifampicin and/or Cholestyramine. In 20 of 34 (59%) patients we identified disease-causing variants, with highest prevalence in *ABCB11* and *ABCB4*. A genotype/phenotype correlation was detected in 21 (62%) women. A total of 13 (38%) women gave birth prematurely (<37 weeks); 7 patients with planned induced labor, and 6 gave birth spontaneously. Four women had an intrauterine foetal demise. Fourteen (41%) had recurrence of ICP in their subsequent pregnancy with one foetal demise.

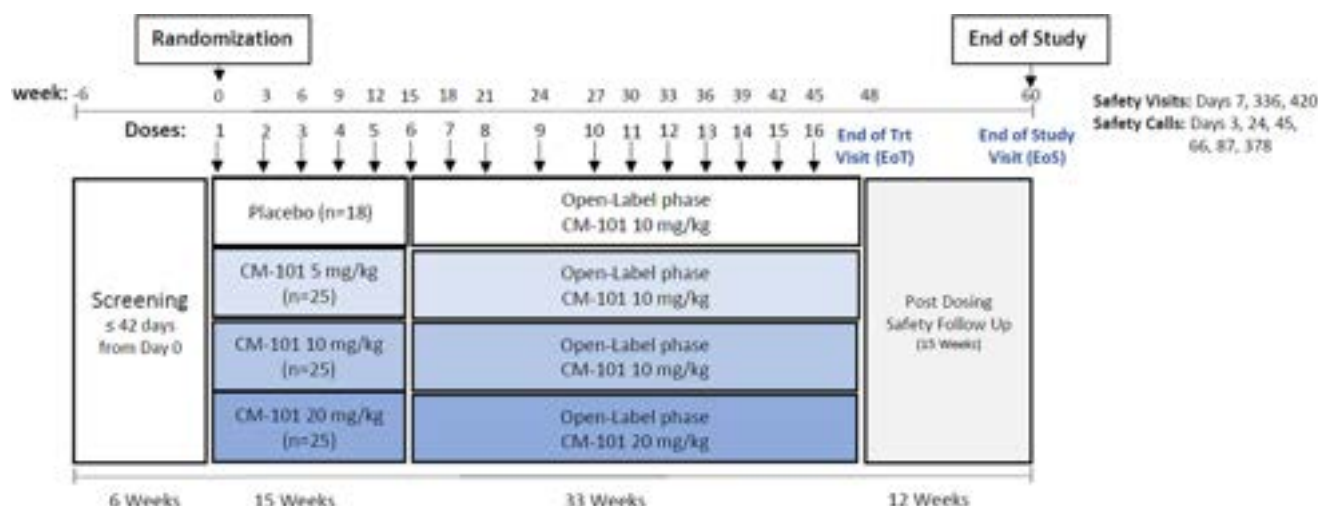


Figure: (abstract: THU-310).

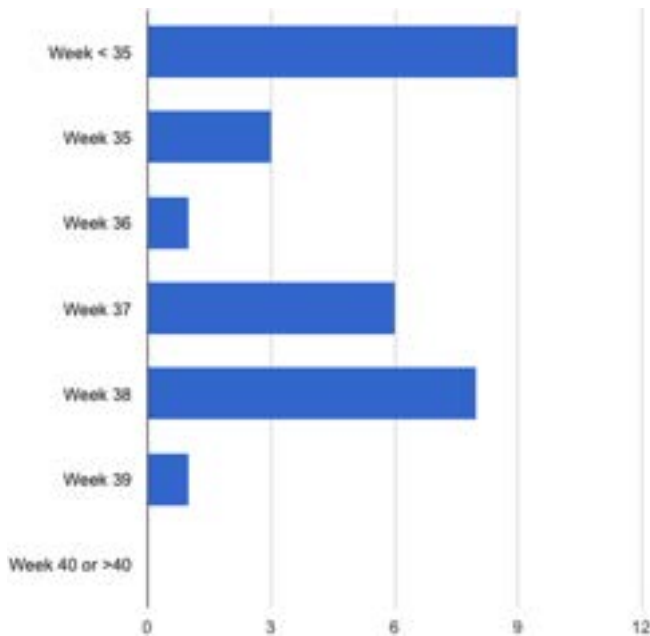


Figure: Overview of gestational week at delivery for patients with ICP.

Conclusion: We detected a genotype/phenotype correlation in 21 (62%) women with ICP. This illustrates the importance of the combination of genetic testing and clinical work-up among women with ICP and may guide handling and treatment of future pregnancies in these women.

THU-312

Longitudinal assessment of gut microbiota, metabolome and intestinal barrier dysfunction in biliary atresia

Vandana Jain¹, Charlotte Burford¹, Emma Alexander¹, Konstantinos Gerasimidis², Anita Verma¹, Mark Davenport¹, Matthew Dalby³, Lindsay Hall³, Anil Dhawan¹. ¹King's College Hospital, United Kingdom; ²University of Glasgow, United Kingdom; ³Quadram Institute, United Kingdom
Email: vjain@nhs.net

Background and aims: Adjuvant therapy post-Kasai Portoenterostomy (KPE), has not reduced liver transplantation (LT) in Biliary Atresia (BA). Increasingly, a gut microbiota (GM)-host interplay, in chronic liver disease, is being described. We aimed to characterise GM, stool short chain fatty acids (SCFAs) and intestinal barrier (IB) markers, in BA, and association with clinical outcomes.

Method: Stool, plasma, were prospectively collected, in BA infants (n = 55) pre-KPE, and 6weeks-, 3months-, 6months-post-KPE. Age-matched healthy (HC; n = 19) and cholestatic control (CC; n = 21) stool was collected. Stool 16S rRNA sequencing (GM) and gas chromatography (SCFAs), were performed. IB markers included plasma Claudin-3 and stool calprotectin (SC). Clinical outcomes: 6month-JC (jaundice clearance), 1year-LT, cholangitis by 6month-post-KPE, fibrosis biomarkers [Aspartate Aminotransferase-to-platelet ratio index (APRI); Liver Stiffness Measurement (LSM)]

Results: Pre-KPE, beta-diversity revealed differences in genus-level-clustering, between BA vs HC [p < 0.03], not CC [p = 0.5] (Fig1). BA incorporated ↓*Bifidobacterium* [p = 0.01], ↑*Enterococcus* [p = 0.01], ↑*Clostridium* [p = 0.04], compared to HC. 6weeks-post-KPE, increased alpha-diversity [p < 0.001], increased genus-level-clustering variation [BA: ↓*Bifidobacterium*, p < 0.001; ↑*Enterococcus*, p = 0.02], and reduced acetate [p < 0.001], was shown in BA vs HC. Pre-KPE, increased alpha-diversity [p = 0.04], and reduced acetate [p = 0.004], was associated with 1year-LT. Increased propionate was associated with poor 6month-JC [p = 0.02]; *Clostridium* positively correlated with propionate [rs = 0.5; p = 0.01]. Early-post-KPE, increased alpha-diversity [p = 0.01], ↑*Streptococcus* [p < 0.001],

↓*Blautia* [p = 0.03], were associated with poor 6month-JC. APRI positively and negatively correlated with *Streptococcus* [rs = 0.4; p = 0.03] and *Bifidobacterium* [rs = -0.5; p = 0.01]. ↓*Bifidobacterium*, 6weeks-post-KPE, was associated with cholangitis development [p = 0.03]. Butyrate, 6weeks-post-KPE, inversely correlated with total bilirubin [rs = -0.3; p = 0.02]. Increased Claudin-3, early-post-KPE, was associated with poor 6month-JC [p = 0.01] and 1year-LT [p = 0.001]. 6months-post-KPE, ↓*Blautia* [p = 0.01], ↓SCFAs [p = 0.04], ↑SC [p = 0.05], were associated with 1year-LT; *Bifidobacterium* inversely correlated with LSM [rs = -0.5; p = 0.02].

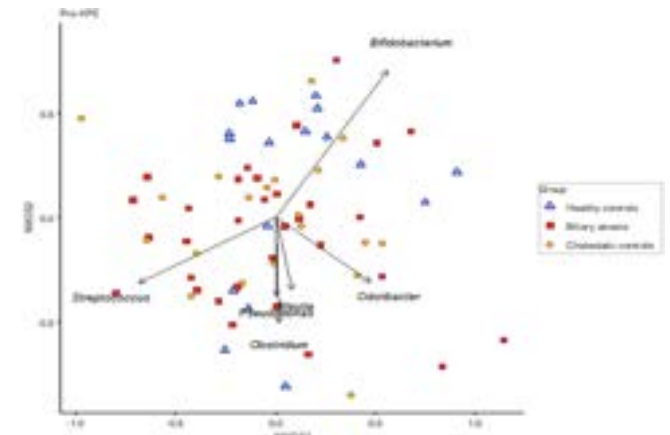


Figure:

Conclusion: Dysbiosis, characterised by pathobiont enrichment and 'probiotic' (*Blautia*, *Bifidobacterium*) deficiency, and subsequent SCFA dysregulation, in pre- and early-post-KPE BA, are associated with non-favourable clinical outcomes. Increased intestinal permeability early-post-KPE, is a likely a key factor in GM-BA-pathogenesis. Early microbiota-modulatory therapy may reduce LT in BA.

THU-313

Odevixibat therapy following liver transplantation in patients with FIC1-deficient progressive familial intrahepatic cholestasis: a retrospective case series

Georg-Friedrich Vogel^{1,2}, Simone Kathemann³, Andrea Pietrobattista⁴, Giuseppe Maggiore⁴, Denise Aldrian¹, Marco Sciveres⁵, Henkjan J. Verkade⁶, Peter Rauschkolb⁷, Christof Maucksch⁷, Velichka Valcheva⁷, Christine Clemson⁷, Elke Lainka³. ¹Department of Paediatrics I, Medical University of Innsbruck, Austria; ²Institute of Cell Biology, Medical University of Innsbruck, Austria; ³Department of Paediatric Gastroenterology, Hepatology, and Liver Transplantation, University Children's Hospital, Germany; ⁴Hepatology, Gastroenterology, Nutrition, Digestive Endoscopy, and Liver Transplantation Unit, Bambino Gesù Children's Hospital IRCCS, Italy; ⁵Paediatric Hepatology and Liver Transplantation, IRCCS ISMETT, Italy; ⁶Department of Paediatrics, University of Groningen, Beatrix Children's Hospital/University Medical Centre Groningen, Netherlands; ⁷Albireo Pharma, Inc., Boston, United States
Email: georg.vogel@i-med.ac.at

Background and aims: *ATP8B1*, encoding FIC1, is expressed in multiple organs such as the liver and small intestine. Mutations in this gene can result in progressive familial intrahepatic cholestasis type 1 (PFIC1), which is characterized by hepatic and extrahepatic manifestations that can ultimately necessitate liver transplantation (LT). Following LT, patients with PFIC1 may develop complications that include graft injury (hepatic steatosis), liver fibrosis, and/or exacerbated diarrhoea, which may impair patients' ability to perform daily activities and reduce their quality of life (QoL). These complications are thought to result from the interplay between physiologic bile acid secretion from the transplanted liver and the native, FIC1-deficient bowel. In this case series, we present clinical

Table: (abstract: THU-313).

Clinical Features, Quality of Life, and Liver Pathology Before and Following Odevixibat Initiation in Patients With PFIC1 And Liver Transplantation

	Patient 1	Patient 2	Patient 3	Patient 4	Patient 5	Patient 6
Before LT						
Symptoms leading to LT	<ul style="list-style-type: none"> Refractory pruritus Cholestasis Dystrophy Feeding disorder 	<ul style="list-style-type: none"> Electrolyte imbalance Dystrophy Pruritus Infections with hospitalization 	<ul style="list-style-type: none"> Intractable pruritus Decreasing liver function 	<ul style="list-style-type: none"> 1st LT: <ul style="list-style-type: none"> Cholestasis Jaundice Failure to thrive Severe pruritus 2nd LT: <ul style="list-style-type: none"> Hepatic artery thrombosis 	<ul style="list-style-type: none"> 1st LT: <ul style="list-style-type: none"> Cholestasis Failure to thrive Severe pruritus 2nd LT*: <ul style="list-style-type: none"> Acidosis Failure to thrive Progressive liver damage 	<ul style="list-style-type: none"> Refractory pruritus and cholestasis Jaundice Fatigue
After LT But Before Odevixibat Initiation						
Description of impact on QoL	Diapers needed during day and/or night	Diapers needed during day and/or night	Wearing diapers unacceptable to patient, so diarrhoea impacted school and family's ability to travel	Diarrhoea frequency negatively impacted the patient's QoL	Diarrhoea frequency negatively impacted the patient's QoL	N/A
Biopsy findings ^a	<ul style="list-style-type: none"> 10% macrovesicular and 5% microvesicular fatty degeneration Liver fibrosis, stage 1 	<ul style="list-style-type: none"> 25% macrovesicular and 50% microvesicular fatty degeneration Liver fibrosis, stage 3 Steatohepatitis and ductular proliferation 	N/A ^b	<ul style="list-style-type: none"> 15% micro-macrovesicular steatosis Expanded portal spaces due to mild fibrosis 	<ul style="list-style-type: none"> 40% steatosis Moderate portal and mild central fibrosis 	N/A
Current daily odevixibat dose (treatment duration)	~ 30 µg/kg (11 months)	~ 100 µg/kg (17 months)	~ 80 µg/kg (13 months)	40 µg/kg (5 months)	40 µg/kg (8 months)	120 µg/kg (16 months ^c)
With Odevixibat						
Description of impact on QoL	<ul style="list-style-type: none"> No diarrhoea Diapers not needed as frequently 	<ul style="list-style-type: none"> No diarrhoea and no nocturnal stools Daytime diapers no longer necessary Reduced fatigue and better concentration at school 	Better able to participate in school and leisure activities	<ul style="list-style-type: none"> No diarrhoea First time in patient's life with normal stool consistency; improved QoL 	Reduced frequency of diarrhoea	N/A
Biopsy findings ^a	<ul style="list-style-type: none"> Liver fibrosis, stage 1–2 Portal inflammation Slight ductular proliferation 	<ul style="list-style-type: none"> < 5% microvesicular fatty degeneration Liver fibrosis, stage 1–2 	N/A	<ul style="list-style-type: none"> 25% to 30% micro-macrovesicular steatosis Expanded portal spaces due to mild fibrosis 	<ul style="list-style-type: none"> 40% steatosis Fibrosis, stage 3–6 	N/A

^aPatient underwent a complete bilocolonic diversion at the same time as the second LT; ^bLast available data before initiating odevixibat; ^cPatient developed steatosis and hepatic inflammation shortly after LT. The patient received surgical biliary diversion approximately 4 years after LT, which resolved the steatosis and liver inflammation; ^dPatient was previously treated with odevixibat for approximately 15 months before undergoing LT on 18 November 2022. Odevixibat was restarted approximately 4 days after LT. Available data are limited due to recent surgery; ^eData from last available assessment. LT, liver transplantation; N/A, not available; PFIC, progressive familial intrahepatic cholestasis; QoL, quality of life.

details of patients with PFIC1 who received odevixibat, an ileal bile acid transporter inhibitor (IBATi), after LT.

Method: Patient demographic, clinical, and treatment data were collected retrospectively using standardised case report forms.

Results: This case series comprises 6 male patients. Common indications for LT included intractable pruritus, cholestasis, and/or growth issues or dystrophy; a second LT was performed in patients 4 and 5 (Table). After LT, 5 patients had fatty degeneration, steatohepatitis, or hepatic steatosis, and patients 1, 2, 4, and 5 had hepatic fibrosis (stage 1–3; Table). Following LT, all patients had diarrhoea (up to 7 stools/day). As a result, QoL and/or school functioning were negatively impacted for these patients and/or their families (Table). Five of 6 physicians cited steatosis and/or unresolved diarrhoea as a reason for initiating odevixibat; in patient 6, who had prolonged episodic cholestasis prior to LT, the drug was prophylactically re-initiated. In patient 5, odevixibat was withdrawn after 8 months due to unchanged steatosis and progression of liver disease despite mild improvement in stool frequency (4–7 to 2–4 stools/day). In other patients with available data who received odevixibat post LT, diarrhoea resolved and/or patients had less frequent bowel movements (approximately 2 stools/day) or improved stool consistency (eg, Bristol Stool Chart type 7 to type 4–5). These patients had improvements in QoL (Table). Changes in liver pathology before and following odevixibat initiation are shown in the Table.

Conclusion: In patients with PFIC1, diarrhoea and hepatic steatosis after LT are frequent and severe, impacting QoL. The real-world data presented here indicate that odevixibat can improve diarrhoea and QoL after LT in patients with PFIC1. In addition, 2 of 4 patients where biopsy was performed following odevixibat initiation had improved steatosis (odevixibat duration: 11 and 17 months, respectively, at last data collection). More studies are needed to determine the role of IBATi treatment in long-term graft survival.

THU-314

A longitudinal study of epidemiology and treatment management of Wilson disease in France based on the French national claims database SNDS

Bernard Benichou¹, Thomas Daniel Robin¹, Jean Philippe Combal¹, Claire Leboucher². ¹Vivet Therapeutics, France; ²Putnam Inizio Advisory, France

Email: bbenichou@vivet-therapeutics.com

Background and aims: The aim of this study was to evaluate longitudinal trends in the epidemiology and management of patients with WD (Wilson disease) identified in the French national health insurance database (SNDS).

Method: The study included all patients with at least one medical claim for hospitalisation with the ICD-10 diagnostic code for WD (E83.0*: copper metabolism disorder) or eligible for ALD status for WD between 1st January 2009 to 31st December 2019. For each patient, data were extracted on age, gender, hospitalisations, liver transplantation, mortality, WD-specific treatments (D-penicillamine, trientine and zinc), disability status and sick leave.

Results: 1,928 patients with WD were identified, of whom 1,520 (78.8%) were analysed. Prevalence of WD in 2019 was estimated as 2.2 cases per 100,000. The median age of the total cohort at inclusion was 39 years and 48% of patients were women. At inclusion, 67% of patients were symptomatic, with a spectrum of hepatic, neurological or psychiatric symptoms. In the first year, 995 patients (65.6%) were hospitalised at least once for a mean duration of 4.4 ± 10.9 days. In the following year, the proportion declined to 41.7% and remained around 40% for the remainder of the follow-up period. 152 patients (10.0%) underwent liver transplantation and 205 died (13.5%). The mean age at death was 57.9 ± 23.1 years. 665 patients (43.8%) received a WD-specific treatment at least once. 167 patients (17.1%) received a government disability pension and 624 (41.1%) benefited from long-term illness status due to WD.

Conclusion: Unexpectedly, less than half of French patients with WD ICD-10 diagnostic code received continuous treatment as recommended in practice guidelines, which with reduce compliance may contribute to a high disease burden in terms of hospitalizations, disability and reduced life expectancy. Interestingly similar results from other countries have been observed (Choe et al. Nature Scientific Reports 2020; Czlonkowska et al. Eur J Neurol 2022) either from national healthcare databases or from large cohort of WD patients followed in reference center. Raising awareness around the limitations of current disease management, patients awareness and improving treatment rates with new transformative treatment alternatives could help reduce the burden of patients living with WD.

THU-315

Impact of suffering Wilson disease in Spain: an observational cross-sectional multicenter study

Zoe Mariño^{1,2}, Marina Berenguer^{3,4}, Luis Peña⁵, Antonio Oliveira Martin⁶, Anna Miralpeix¹, Clara Pérez⁷, Anna Anguera⁸. ¹Hospital Clínic de Barcelona, Liver Unit, Barcelona, Spain; ²CIBERehd, IDIBAPS, ERN-RARE Liver, University of Barcelona, Barcelona, Spain; ³Hospital Universitari i polític La Fe, Department of Gastroenterology and Hepatology, Valencia, Spain; ⁴CIBERehd and IISLaFe, Valencia, Spain; ⁵Complejo Hospitalario Universitario Insular Materno Infantil, Pediatric Gastroenterology, Hepatology and Nutrition Unit, Las Palmas de Gran Canaria, Spain; ⁶Hospital La Paz, Department of Gastroenterology, Madrid, Spain; ⁷Outcomes10, Castellón de la plana, Spain; ⁸Alexion AstraZeneca, Rare Disease Unit, Medical Department, Spain

Email: zmarino@clinic.cat

Background and aims: Wilson disease (WD) can negatively impact health-related quality of life (HRQoL) as well as emotional/social health, two aspects, which have been little explored to date. We aimed to assess the impact of WD on HRQoL, treatment adherence, use of healthcare resources utilization (HRU), and its associated costs.

Method: An observational cross-sectional multicenter study was conducted. Patients with WD aged ≥ 12 years; at least 1 year of previous follow-up and signed informed consent were included. Sociodemographic, clinical and treatment data were collected. The following questionnaires were administered: 1) EQ-5D-5L: HRQoL questionnaire, 2) ad-hoc questionnaire on social/emotional impact of WD, and 3) SMAQ: medication adherence questionnaire. Also, HRU in the last year and productivity were collected, and the costs per patient/month (€) were estimated. A descriptive analysis was performed on 2 subgroups of patients: 1) isolated liver involvement (group H, n = 83, 81.4%) and 2) hepatic and extrahepatic involvement (group EH, n = 19, 18.6%). Data analysis was performed with STATA v.14. Variables were expressed as % or median (IQR_{25–75}).

Results: We included 102 patients: median age of 35 (22–47) years, 57.8% were male, median time since diagnosis 16.2 (10.6–29.4) years, 14.7% with cirrhosis (93.3% Child-Pugh A; 33.3% with esophageal varices), mainly treated with zinc salts (48%) or D-Penicillamine (32.4%). 46.1% received concomitant treatment, especially neuropsychiatric drugs (46.8%). Group H showed better median EQVAS score (88 [75–92]) than EH group (76 [50–85]), with higher scores in mobility, self-care, activities of daily living or pain items. However, up to 42% of patients had some degree of anxiety/depression in both groups. Group EH reported greater impairment in daily activities and executive function. EH group had more difficulty in making friends (42.2% EH vs 16.9% H) or dating (57.9% EH vs 13.2% H). Although emotional affectation was greater in the EH group (47%), up to 30% of the H group reported sadness, anxiety, frustration, or anger related to WD. According to the SMAQ, only 18.1% of the H group showed total treatment adherence vs 42.1% of the EH group. In the last year, patients had a median of 4 outpatient visits to specialists (3 to hepatology). EH group used more extra NHS health resources than the H group (31.6% physiotherapist, 21.1% speech therapist). Overall,

POSTER PRESENTATIONS

the median cost/patient per month was 59.6 (32.4–96.1) € in H group vs 114.9 (76.4–1752) € in EH group.

Conclusion: Patients with extrahepatic involvement showed worse HRQoL, and higher HRU and costs than the hepatic group. Despite the fact that H patients had less general impairment, they showed significant percentages of anxiety/depression and reported difficulties in emotional/social aspects. Treatment adherence was poor, highlighting that there is room for improvement in this area in WD.

THU-316

Role of transient elastography to identify Fontan-associated liver disease (FALD) and novel risk-score to predict failing Fontan

Luisa Cavalletto¹, Roberta Biffanti², Giovanni Di Salvo², Massimo Padalino³, Chiara Giraudo¹, Liliana Chemello¹. ¹University of Padova, Department of Medicine-DIMED, Padova, Italy; ²University of Padova, Department of woman and child's health, Padova, Italy; ³University of Padova, Department of cardiac, thoracic and vascular sciences and public health, Padova, Italy
Email: liliana.chemello@unipd.it

Background and aims: The single ventricle (SV) heart is a rare congenital heart disease (CHD) (7/1000 cases, born alive, with major heart defects) corrected with the palliative Fontan's intervention (cavo-pulmonary shunt) that restores the survival of most child and young patients up to adulthood. Unlikely, these patients develop a series of complications, among all, the Fontan associated liver disease (FALD), which is particularly due to chronic systemic venous hypertension, that causes the occurrence of liver cirrhosis and other severe complications, that negatively impacts the life expectancy in the majority of cases. Our primary aim was to characterize these patients by liver fibrosis and portal hypertension scores (FORNS, LSPS and SSPS) and by liver (LS) and spleen (SS) stiffness measurement in relation to time since Fontan, secondarily to define the risk profile of major complications tailored to the individual patient by selective criteria.

Method: One-hundred and twenty outpatients (68 m/52 f, mean age 24.8 ± 11.6 years) born with SV corrected with Fontan circuit have been recruited prospectively from 2019 to 2022 (mean FU 18.5 ± 13.1 months). Each patient underwent a complete anamnesis, physical examination and specific lab-test profile, and an instrumental evaluation with abdominal US-Doppler or CT/MRI and the LS and SS by transient elastography (VCTE, Fibroscan, Echosens, Paris).

Results: Based on the time elapsed since Fontan's surgery 3 groups, each of 40 cases (group: A <15; B 15–25 and C >25 yrs), were formed to compare the clinical, biochemical and imaging features. ROC curves were built to select the scores cut-off proved to be the most accurate to diagnose FALD (Fig.1). The worsening of the hepatic, renal and cardiac function in relation to time since Fontan surgery appeared in 58/120 cases (group A, B and, C in 17.5%, 47.5% and 80% of cases, respectively; $p < 0.01$). Ten patients (8.3%) died, need OHT or had HCC occurrence. Moreover by identification of advanced liver disease and of portal hypertension selective criteria, we applied a novel risk-score of failing-Fontan, that has predicted a low-moderate risk profile (HR 0.30; CI 0.18–0.52) in 66 patients (55%) and a high risk profile (HR 3, 29, CI 1.93–5.60) in 54 (45%).

Score	Cut-off	Sens. Spec. (%)	AUC ± SE	CI 95%	p-value
FORNS	≥ 4.0	91.2/86.0	0.931±0.024	0.866-0.971	< 0.0001
LSPS	≥ 1.4	91.2/86.2	0.938±0.021	0.877-0.971	< 0.0001
SSPS	≥ 2.3	91.2/91.1	0.960±0.016	0.906-0.988	< 0.0001
LS	≥ 20.2	84.5/79.0	0.907±0.025	0.840-0.952	< 0.0001
SS	≥ 30.7	81.2/85.7	0.915±0.025	0.847-0.950	< 0.0001

Figure 1:

Conclusion: All the scores (Fig.1) showed the capability to improve the FALD diagnosis and the hepatologic management of these young and adult subjects with SV and Fontan circuit. This novel risk score proposed may help to predict the development of major complication and targeting individual surveillance in Fontan patients, to better guide some decision-making process (i.e., the need of surgical interventions or OHT).

LSPS or SSPS, liver or spleen-platelet-score.

THU-317

Real-world experience of Odevixibat in adults with genetic disorders of cholestasis

Palak Trivedi^{1,2}, Alberto Borghi³, Cornelius Engelmann⁴, Vinod Hegade⁵, Simon Hohenester⁶, Deepak Joshi⁷, Jan F. Monkelbaan⁸, Anna Morgando⁹, Praneeta Nagraj¹⁰, Velichka Valcheva¹⁰. ¹National Institute for Health Research Birmingham Biomedical Research Centre, University of Birmingham, Birmingham, United Kingdom; ²Liver Unit, University Hospitals Birmingham, Birmingham, United Kingdom; ³Internal Medicine Unit, Faenza Hospital, Italy; ⁴Medizinische Klinik m. S. Hepatologie und Gastroenterologie, Charité Universitätsmedizin Berlin, Berlin, Germany; ⁵Leeds Liver Unit, Leeds, United Kingdom; ⁶Department of Medicine II, University Hospital, LMU Munich, Munich, Germany; ⁷Institute of Liver Studies, King's College Hospital, London, United Kingdom; ⁸Department of Gastroenterology and Hepatology, University Medical Center, Utrecht, Netherlands; ⁹SC Gastroenterologia U, Città della Salute e della Scienza di Torino, Turin, Italy; ¹⁰Albireo Pharma, Inc, Boston, MA, United States
Email: p.j.trivedi@bham.ac.uk

Background and aims: Genetic disorders of cholestasis, including progressive familial intrahepatic cholestasis (PFIC), typically present in infancy or early childhood. The ileal bile acid transporter inhibitor odevixibat is approved for the treatment of PFIC in patients aged 6 months or older in the European Union and for treatment of pruritus in patients aged 3 months and older with PFIC in the United States. The overarching goal of this study was to seek experience with odevixibat in adult patients with genetic disorders of cholestasis with regard to safety, tolerability, and efficacy.

Method: Data were collected from adults harbouring suspected or confirmed genetic variants associated with cholestasis who initiated odevixibat therapy at age >16 years. Details regarding symptoms and on-treatment biochemical changes are presented.

Results: We accrued data from 10 patients across 8 treatment centres (50% men; age range at diagnosis: 6 months–35 years; current age range, 22–48 years); 6 patients were diagnosed in adulthood (Table). Prior to odevixibat initiation, median serum bile acid (sBA), total bilirubin, and alanine aminotransferase (ALT) values were 138 µmol/L, 18 µmol/L, and 56 U/L, respectively. In most patients, presenting features included pruritus and jaundice, alongside impaired sleep and attention and overall diminished quality of life. Nine patients experienced improvement in pruritus with odevixibat over a median of 3.4 months follow-up (range: 0.9–25.5 months), with 8 patients reporting complete absence of pruritus at the last available assessment. Median (quartile 1, quartile 3) reduction in sBA values was –73 (–174, –38) µmol/L ($p = 0.012$ [Wilcoxon signed-rank test]). Median changes in total bilirubin and ALT values were minimal ($p \geq 0.16$). Two patients experienced gastrointestinal adverse events (increased defecation frequency that resolved with dosage adjustment in 1 patient; mild diarrhoea modifiable with dietary changes in another patient) during treatment with odevixibat; no new safety signals were reported.

Conclusion: In adults with genetic disorders of cholestasis, odevixibat treatment appears to be safe, well tolerated, and associated with a reduction in pruritus intensity.

Table: (abstract: THU-317).

Table. Outcomes in Adult Patients With Genetic Disorders of Cholestasis Treated With Odevixibat

	Age at Diagnosis	Current Age	Sex	Affected Gene(s)	Presenting Features	Dosage (Treatment Duration)	Outcomes With Odevixibat
Patients 1–6: Diagnosed in Adulthood							
Patient 1	35 years	38 years	F	ABCB4 ^a	<ul style="list-style-type: none"> Cholangitis and fibrosis Impaired QoL No pruritus sBAs: 10 µmol/L 	2400 µg/day (1.7 months)	<ul style="list-style-type: none"> No change in pruritus, sleep, ALT or TB Mild diarrhoea modifiable with dietary changes sBAs: 5 µmol/L at month 1
Patient 2	34 years ^b	48 years	M	ABCB11 ^c	<ul style="list-style-type: none"> Pruritus and recurrent jaundice Elevated GGT sBAs: 69 µmol/L 	2400 µg/day (1.3 months)	<ul style="list-style-type: none"> Improved pruritus (no itch within 1 month) Decreased TB sBAs: 76 µmol/L at month 1
Patient 3	32 years	32 years	M	ND ^d	<ul style="list-style-type: none"> Pruritus Jaundice Abdominal pain sBAs: 96 µmol/L 	3600 µg/day (4.6 months)	<ul style="list-style-type: none"> Improved pruritus (VAS=0 by month 2) Decreased ALT, TB Improved sleep, increased energy sBAs: 4 µmol/L at month 2
Patient 4	26 years	41 years	F	ABCB11 ^c	<ul style="list-style-type: none"> Pruritus and recurrent jaundice Elevated GGT sBAs: 84 µmol/L 	2400 µg/day (0.9 months)	<ul style="list-style-type: none"> Improved pruritus (no itch within 1 month) sBAs: 22 µmol/L at month 1
Patient 5	18 years	29 years	F	ABCB11 ^a	<ul style="list-style-type: none"> Pruritus sBAs: 48 µmol/L 	2400 µg/day (4.8 months)	<ul style="list-style-type: none"> Improved pruritus (no itch by month 2) sBAs: 10 µmol/L at month 3 Able to care for child
Patient 6	18 years	23 years	M	ABCB11 ^f	<ul style="list-style-type: none"> Pruritus Jaundice sBAs: 214 µmol/L 	2400 µg/day (3.5 months)	<ul style="list-style-type: none"> Improved pruritus (absent within 3 months) No waking up at night sBAs: 141 µmol/L at month 3
Patients 7–10: Diagnosed in Childhood							
Patient 7	11 years	33 years	M	ATP8B1, ABCB11, ABCB4 ^g	<ul style="list-style-type: none"> Recurrent pruritus, jaundice, liver dysfunction Impaired QoL, psychological distress sBAs: 260 µmol/L 	2400 µg/day (1.8 months ^h)	<ul style="list-style-type: none"> Improved pruritus (absent by month 2) and jaundice Decreased ALT, TB Positive psychological impact sBAs: 6 µmol/L at month 2
Patient 8	9 years	32 years	F	ABCB11 ^f	<ul style="list-style-type: none"> Pruritus sBAs: 284 µmol/L 	2400 µg/day (4.3 months)	<ul style="list-style-type: none"> Improved pruritus (no itch by month 3) Decreased ALT, TB sBAs: 110 µmol/L at month 3 Better mood
Patient 9	4 years	22 years	F	ND ⁱ	<ul style="list-style-type: none"> Pruritus, dry skin Fatigue Short stature Poor QoL and attention sBAs: >180 µmol/L 	1600 µg/day (3.4 months)	<ul style="list-style-type: none"> Pruritus ~20% reduced Decreased TB Eyes are less yellow More engaged in activities of daily living sBAs: ND
Patient 10	6 months	25 years	M	ND ^k	<ul style="list-style-type: none"> Persistent pruritus Intermittent cholestasis Sleep and attention disorders sBAs: 386 µmol/L 	2400 µg/day and 1200 µg/day alternating (25.5 months)	<ul style="list-style-type: none"> Improved pruritus (no itch by month 3) Continued sleep for first time in life sBAs: 27 µmol/L at month 6 Increased defecation frequency

^aHeterozygous c.1445T>C variant; ^bPatient was symptomatic for many years prior to diagnosis; ^cCommon variant in ABCB11 (c.1331T>C); ^dClinical presentation compatible with PFIC; ^eHomozygous c.1331T>C, heterozygous c.149T>C, and heterozygous c.1568C>G variants; ^fHomozygous c.1546T>C, heterozygous c.3148C>T, and heterozygous c.2599C>T variant s; ^gHomozygous ATP8B1 variant (p.R952Q), heterozygous ABCB11 variants (p.A444V and c.3084A>G), and heterozygous ABCB4 variant (c.787A>T); ^hTreatment was stopped due to significant improvement of symptoms, as well as normalized blood values and liver function; ⁱHeterozygous c.1723>T and heterozygous c.1139delT variants; ^jDiagnosis of PFIC type 1; ^kDemonstrated similar haplotype to known patients with recurrent episodic cholestasis.
ALT, alanine aminotransferase; F, female; GGT, gamma-glutamyl transferase; M, male; ND, not determined; PFIC, progressive familial intrahepatic cholestasis; QoL, quality of life; sBAs, serum bile acids; TB, total bilirubin; VAS, visual analogue scale.

POSTER PRESENTATIONS

THU-318

High diagnostic uptake of a targeted panel sequencing in adult patients with chronic hereditary liver disorders

Luisa Ronzoni¹, Ilaria Marini¹, Serena Pelusi¹, Federica Golfetto¹, Angela Lombardi¹, Jessica Rondena¹, Giulia Periti¹, Cristiana Bianco¹, Giulia Passignani¹, Roberta D'Ambrosio², Daniele Prati³, Luca Valenti^{1,4}. ¹Fondazione IRCCS Ca' Granda Ospedale Maggiore Policlinico Milano, 1 Precision Medicine-Biological Resource Centre-Department of Transfusion Medicine, Italy; ²Fondazione IRCCS Ca' Granda Ospedale Maggiore Policlinico Milano, Division of Gastroenterology and Hepatology, Italy; ³Fondazione IRCCS Ca' Granda Ospedale Maggiore Policlinico Milano, Department of Transfusion Medicine, Italy; ⁴Università degli Studi di Milano, Department of Pathophysiology and Transplantation, Italy
Email: luisa.ronzoni@policlinico.mi.it

Background and aims: The pathogenesis of chronic liver diseases (CLD) remains often unexplained despite extended clinical and instrumental evaluations. Next-generation sequencing (Whole Exome [WES] or Targeted Panel Sequencing [TS]) and polygenic risk scores (PRS) determination may improve the diagnostic rate of rare genetic disorders also in adults, but they are not yet widely clinically available. The aim was to evaluate the clinical utility of a TS approach, combined with PRS stratification, in diagnosis CLD in adult patients.

Method: A customized TS including 82 selected liver-diseases genes was performed in 57 unrelated adult patients with CLD of suspected hereditary etiology. For each patient, the genetic predisposition to progressive fatty liver disease was evaluated (PRS based on *PNPLA3* rs738409, *TM6SF2* rs58542926, *MBOAT7* rs641738, *GCKR* rs1260326 and *HSD17B13* rs72613567 variants combination).

Results: Patients' phenotypes were divided into four categories: iron overload, dyslipidemia, cholestatic diseases and fatty liver diseases.

Overall, TS allowed to reach a definitive genetic diagnosis in 16 patients (diagnostic yield: 28%). Heterozygous likely pathogenic variants or rare variants of unknown significance (VUS), but with a high likelihood of altering protein function, were identified in 26 patients, providing a diagnostic rate of 46% for genetic contribution to the phenotype. A total of 15 cases (26%) remained undiagnosed. Stratifying according to the clinical phenotypes, the higher diagnostic yield was obtained in patients with dyslipidemia (36%) and iron overload (35%). Overall, PRS values were over the positive threshold (fixed at 0.495) in 13 patients, 7 of whom (54%) had fatty liver diseases (Figure 1).

Conclusion: TS proved to be a useful first-tier genetic test for the diagnosis of selected adult patients with CLD, mainly if the clinical phenotype is well defined, as in dyslipidemia or iron overload cases. Moreover, TS allowed to identify genetic variants possibly contributing to disease phenotype in a high number of patients, expanding disease pathogenesis understanding. PRS stratification was a useful analysis, mainly in patients with fatty liver diseases, contributing to the diagnosis and allowing to set up a personalized follow-up.

THU-319

Phytoestrogens as a possible hidden driver of cysts proliferation in polycystic liver disease in men and women after menopause

Miki Scaravaglio¹, Antonio Ciacchio^{2,3}, Martina Manna², Giacomo Mulinacci¹, Pietro Invernizzi^{1,2,3}. ¹University of Milano-Bicocca, Department of Medicine and Surgery, Italy; ²Fondazione IRCCS San Gerardo dei Tintori, Gastroenterology Unit, Italy; ³European Reference Network on Hepatological Diseases (ERN RARE-LIVER), Italy
Email: antonio.ciacchio@unimib.it

Background and aims: Polycystic liver disease (PLD) is characterized by the presence of multiple liver cysts with a potential for progressive liver enlargement and cysts growth that may result in visceral compression and poor quality of life, requiring surgery or liver

Figure 1. Diagnostic rate of a customized targeted panel for the analysis of 57 unrelated adult patients with CLD, divided in four disease categories

Clinical Phenotype (number of cases)	Genetic diagnosis		Likely genetic diagnosis		Undiagnosed cases	High PRS (>0.495)
	n. cases (%)	Pathogenic variants	n. cases (%)	Heterozygous likely pathogenic variants or VUS	n. cases (%)	n. cases (%)
Iron Overload (20)	7/20 (35%)	<i>HFE</i> rs1800562 <i>HFE</i> rs179945 <i>FTL</i> rs886037622 <i>HAMP</i> rs104894696 <i>SLC40A1</i> rs770389099 <i>TF</i> rs1799899	9/20 (45%)	<i>PCSK7</i> rs471009 <i>PCSK7</i> rs202038275 <i>NMOR</i> rs142626832 <i>BMPE</i> rs771616962 <i>DGLUK</i> rs372855715	4/20 (20%)	2/20 (10%)
Dyslipidemia (14)	5/14 (36%)	<i>APOB</i> p.S2429* <i>APOB</i> c.3696+2T>G <i>LDLR</i> rs289411776 <i>LDLR</i> rs745343524 <i>LPA</i> rs11269028232	7/14 (50%)	<i>APOE</i> rs1440786605 <i>APOE</i> rs7412 <i>APOE</i> rs429358 <i>GBE1</i> rs80338671 <i>APOB</i> rs53361 <i>APOB</i> rs72653095 <i>LPA</i> rs138408240 <i>PCSK9</i> p.A3155 <i>NPC1</i> rs752453963	2/14 (14%)	4/14 (29%)
Cholestatic disease (4)	0 (0)		2/4 (50%)	<i>ABCB11</i> rs2287622 <i>NRLN4</i> rs370621536	2/4 (50%)	0 (0)
Fatty Liver Disease (19)	4/19 (22%)	<i>TERT</i> rs34094720 <i>JAG1</i> rs761187116 <i>ALDOB</i> rs1800546 <i>PHKB</i> rs117218785 <i>PHKB</i> rs56257827	8/19 (42%)	<i>RTEL1</i> rs748756306 <i>SERPINA1</i> rs28931570 <i>SERPINA1</i> rs2892947 <i>APOB</i> rs12691202 <i>APOB</i> rs186292244 <i>MAN2B1</i> rs45576136 <i>PNPLA2</i> rs749056560 <i>DGLUK</i> rs754623273 <i>GBE1</i> rs759518868	7/19 (37%)	7/19 (37%)
Total cases (57)	16/57 (28%)		26/57 (46%)		15/57 (26%)	13/57 (23%)

Abbreviations: VUS, variant of unknown significance; CLD, Chronic liver disease.

Figure: (abstract: THU-318).

transplantation in some cases. Female sex hormones have been identified as major drivers of liver cysts growth and among them estrogens have been recently pointed as a promising target for new treatment strategies. Phytoestrogens (PEs) are plant-derived non-steroidal compounds mimicking the effects of estrogens by binding estrogen receptors. They are found in plant foods, mainly soy and red clover, and in many dietary supplements prescribed for postmenopausal symptoms and prostate conditions. Nonetheless, possible concerns related to PEs exposure in patients with PLD have been overlooked so far. We aimed to investigate whether PEs-containing supplements might have a role in the progression of liver cysts growth in PLD patients.

Method: We retrospectively assessed the exposure to PEs in all consecutive men and postmenopausal women with a diagnosis of PLD evaluated at the Gastroenterology Unit of Fondazione IRCCS San Gerardo, Monza. Patients with a follow-up less than 12 months were excluded from the analysis.

Results: Of 68 patients diagnosed with PLD, 45 satisfied the study criteria and were included in the analysis, with a median follow-up of 64 months (interquartile range [IQR], 39 to 101 months). Most patients were female after menopause (73.3%) and had a diagnosis of autosomal dominant polycystic kidney disease (51.1%). During the study period, a growth of liver cysts of any grade was reported in 10 out of 45 patients (23.8%), while 7 patients (16.7%) had a significant growth of liver cysts, as defined by an increase of at least 25% per year of the diameter of any cyst and/or the development of signs or symptoms of liver enlargement. Cyst complications, including cyst hemorrhage, cyst infection and cyst rupture, occurred in 8 patients (17.8%). Nobody required liver transplantation. Only one patient died during the study period, for causes unrelated to liver disease. A documented exposure to over-the-counter PEs supplements was identified in 6 out of 41 patients (14.6%). PEs exposure was associated with a higher risk of significant growth of liver cysts (OR 8.3, CI 2.1–42.8, $p = 0.005$). No associations were found when assessing sex, type

of PLD, exposure to estrogen-containing drugs before menopause, metabolic comorbidities.

Conclusion: PEs exposure is associated with a significant risk of liver cysts growth in PLD resulting in a higher burden of symptoms. Pending confirmatory results in larger prospective studies, this pilot study supports the key role of estrogens signaling in the progression of PLD and highlights the need to establish a proper dietary counselling to minimize the risk of exposure to PEs and improve PLD patients care.

THU-320

Patient experience with acute hepatic porphyria before and after long-term givosiran treatment: a qualitative interview study

Stephen Lombardelli¹, Michelle Brown², Stephen Meninger³, Hetanshi Naik⁴. ¹Alnylam Pharmaceuticals, Maidenhead, United Kingdom; ²RTI Health Solutions, Research Triangle, United States; ³Alnylam Pharmaceuticals, United States; ⁴Icahn School of Medicine at Mount Sinai, United States
Email: slombardelli@alnylam.com

Background and aims: Acute hepatic porphyria (AHP) is a family of genetic disorders associated with disruption of heme biosynthesis, accumulation of neurotoxic heme intermediates, and acute neuro-visceral attacks; chronic manifestations may be present. In Phase 1/2 (NCT02949830) and Phase 3 (ENVISION; NCT03338816) studies, givosiran treatment led to sustained improvement in annualized attack rate and other measures. To explore long-term treatment outcomes, qualitative interviews were conducted with study participants.

Method: Patients with AHP (US, Spain, UK) continuing givosiran treatment after completing open-label extension periods of the Phase 1/2 or ENVISION studies participated in 1-hour semistructured telephone interviews. Thematic analysis was conducted.

Results: There were 21 interviewees (86% female; mean [range] age at interview, 39.3 [25–61] years; mean [standard deviation] duration

Table: (abstract: THU-320).

Table. AHP Symptoms, Prestudy and Posttreatment

Symptom	Participant Description of Symptom	
	Prestudy ^a	Posttreatment ^b
Abdominal pain	<i>It would usually start with severe stomach pain, intractable vomiting, it would expand to a full body, horrible, searing, and indescribable level of pain.</i>	<i>The stabbing pain that I used to get in the upper right quadrant is completely gone. Now if it hurts, it's more of an ache. I never have that searing knife-like, sharp pain anymore.</i>
Other pain		
Neuropathic pain/paresthesia ^c	<i>I had this spine pain, which was at the base of my neck; it would hurt so bad; I would be at work like laying on tennis balls to relieve the pressure and I just knew that I'd be hospitalized.</i>	<i>My pain is completely gone. I don't have it on a day-to-day basis anymore. I don't get attacks of pain or nausea at all. On the very odd occasion I do have some discomfort, [but] it's not anywhere near going towards an attack.</i>
Limb pain		
Back pain		
Headache		
Body pain		
Gastrointestinal		
Nausea	<i>[O]nce I started throwing up, I couldn't stop throwing up. Then having thrown up for 3 days and then I'd have to go to the hospital.</i>	<i>I don't really vomit anymore though, that has been a big change.</i>
Vomiting		
Constipation		
Diarrhea		
Mood and emotions		
Anxiety, fear, and worry	<i>To be honest ... I didn't do anything. I didn't want to go outside, I didn't want to speak to anybody, I was angry at life, at the world.</i>	<i>The depression has significantly improved. I kind of feel like I'm getting back to my old self.</i>
Depression and sadness		
Anger, agitation, and aggression		
Other		
Fatigue	<i>I could barely go up the stairs anymore ... when I would get home from work, I felt like I couldn't get up the stairs in my house so I would just stay on the couch the whole night and just keep stuff downstairs.</i>	<i>The fatigue is definitely better, and I actually started trying to get my [work] license back. I've started the process to get that back, so it's definitely improved, and it doesn't affect me on a daily basis.</i>
Sleep (excessive or limited)	<i>I couldn't sleep at all; I would be up sitting there just staring at the ceiling.</i>	<i>I get a better quality of sleep.</i>
Cognition (eg. concentration, confusion)	<i>You can tell me something so simple, and I'll forget.</i>	<i>I was able to think much clearer.</i>
Muscle weakness and paralysis	<i>[I]t feels like you're wearing a lead suit so it's just this heaviness ... I couldn't stand up from a seated position.</i>	<i>Yeah, so just physically able to do more. Slightly stronger muscle tone, able to walk slightly further. I don't fall over anymore. I just have the residual paralysis that I have, but physically I'm definitely stronger than I was.</i>

AHP, acute hepatic porphyria.

^aPrior to Phase 1/2 study or ENVISION.

^bPrestudy and posttreatment symptom descriptions are not necessarily from the same interviewees.

^cNeuropathic pain/paresthesia was coded for any mention of neuropathy, burning, or tingling.

POSTER PRESENTATIONS

of givosiran treatment, 51.8 [7.9] months). When describing their prestudy (ie, prior to Phase 1/2 or ENVISION studies) experience (Table), interviewees reported AHP symptoms in multiple domains, particularly abdominal pain and fatigue (95% for both). The impacts of AHP symptoms were wide-ranging, affecting work/school (100%), family and intimate relationships (95%), and other domains. Most interviewees (19/21; 90%) had used opioids prestudy; relief of acute and/or chronic pain was described as somewhat effective (84%), not effective or mildly effective (26%), and/or effective only in the hospital (intravenous; 21%). Posttreatment, interviewees reported improvement in both symptoms (including abdominal and other types of pain [100%]) and impacts (particularly family and intimate relationships [95%] and work/school [91%]). Most described their attacks as gone (62%) or less frequent/severe (33%). Among 17 interviewees who took opioids, 10 (59%) stopped opioids and 4 (24%) used a lower dose. Pain alleviation was mentioned most frequently as the most important posttreatment improvement (43%). Symptoms that were still present (but less severe) included muscle weakness and paralysis (4/5 interviewees; 80%), fatigue (14/18; 78%), and neuropathic pain and paresthesia (6/9; 67%). All interviewees (100%) were "very satisfied" with givosiran treatment.

Conclusion: Results of these qualitative interviews improve the understanding of the burden of AHP. Interviewees reported meaningful improvements with continuing givosiran treatment.

THU-322

Surveillance of cystic echinococcosis in France: report of the first 103 cases from the French observatory OFREKYS

Solange Bresson-Hadni^{1,2}, Coralie Barrera^{1,2}, Louis Bohard^{1,3}, Noémie Tissot^{1,3}, Paul Calame^{1,4}, Alexandre Doussot^{1,5}, Celia Turco^{1,5}, Eleonore Brumpt^{1,4}, Demonmerot Florent¹, Jenny Knapp^{1,2}, Catherine Chirouze^{1,3}, Laurence Millon^{1,2}. ¹CNR-Echinococcoses, laboratoire de Parasitologie-Mycologie, CHRU Besançon, Besançon, France; ²UMR6249 CNRS Chrono-Environnement, Université de Franche-Comté, Besançon, France; ³Service des Maladies Infectieuses, CHRU Besançon, Besançon, France; ⁴Service de radiologie viscérale CHRU Besançon, Besançon, France; ⁵Service de chirurgie viscérale et carcinologique, transplantation hépatique, CHRU Besançon, Besançon, France

Email: dr.bresson.hadni@wanadoo.fr

Background and aims: Cystic echinococcosis (CE) is a zoonosis due to the larval stage development of *Echinococcus granulosus*. The liver is the organ most often concerned. In France, the available data on CE is limited. In 2016, the French Observatory of CE was launched by the National Reference Center for Echinococcosis (NRC-E) at the request of the Agence Santé Publique France. It aims to study the population diagnosed with CE in France, and to provide an overview of current practices in CE patients care.

Method: Patient's enrolment has been mainly performed through clinical advice requests to the multidisciplinary concilium organized monthly by the NRC-E. After obtaining the patient's consent, demographic, epidemiological and clinical data were recorded through a computerized reporting system (Clean WEB®).

Results: From January 2016 to January 2023, 103 patients were included, (53H/50F), median age 42 yrs (range : 5–89). Most of the reports came from infectious diseases specialists (40% of the cases) and hepato-gastroenterologists (25% of the cases). Eighty five patients (83%) were from foreign countries, Maghreb in 52 cases (50%), Turkey in 10 cases (10%), Eastern Europe in 10 cases (10%). This was a primary diagnosis in 60 patients (59%). A past-history of CE was reported in 42 patients, 16 of them having had an incomplete surgery for CE in their native country. Ten patients seem to have been infected in France. CE discovery was incidental in 41% of the cases. Abdominal

pain was the most common revealing symptom (56% of the cases). An acute inaugural complication (cyst fissuration or rupture, abscess, compression) involved 24% of the cases and resulted in death in 2 patients. There was a single cyst in 45 patients (44%). The liver was the organ most often affected in 84 patients (82%), either alone (n = 61) or in combination with other sites (n = 23). In 18 cases (17%), it was a primary extra-hepatic CE. Cyst characterization according to the WHO classification had only been assessed in 61 cases (59%). Therapeutic data (available on 90 patients) indicated that surgical treatment concerned 72% of the cases and was associated to albendazole (ABZ) in 79%. Instrumental treatments (per-cutaneous and/or biliary interventional endoscopy) concerned 6 cases. Long-term ABZ alone involved 10 patients (11%). In 13% of the cases, CE was considered as inactive and the « Watch and Wait » option was proposed.

Conclusion: This first report of CE case collection in France indicates that most cases are imported and concerns migrant population. The level of knowledge of French practitioners on CE appears insufficient, both at the diagnostic and therapeutic stages. Percutaneous treatments are not developed in this country. Concerning autochthonous cases, prevention actions and animal investigations in the field will be soon set up in the concerned areas. The continuation of this surveillance should help to optimize the management of CE in France.

THU-323

Role of gut-derived endotoxins in porto-sinusoidal vascular disease

Stefania Gioia¹, Roberto Carnevale², Daniele Tavano¹, Diletta Overi³, Lorenzo Ridola¹, Silvia Nardelli¹, Manuela Merli¹, Giulia d'Amati⁴, Adriano Pellicelli⁵, Vincenzo Cardinale¹, Valerio Giannelli⁵, Andrea Baiocchi⁶, Guido Carpino⁷, Oliviero Riggio¹, Eugenio Gaudio³. ¹Sapienza, University of Rome, Department of Translational and Precision Medicine, Italy; ²Sapienza, University of Rome, Department of Medico-Surgical Sciences and Biotechnologies, Latina, Italy; ³Sapienza, University of Rome, Department of Anatomical, Histological, Forensic Medicine and Orthopedics Sciences, Italy; ⁴Sapienza, University of Rome, Department of Radiological, Oncological, and Pathological Sciences, Italy; ⁵Azienda Ospedaliera San Camillo, Department of Transplantation and General Surgery, Italy; ⁶Azienda Ospedaliera San Camillo, Department of Pathology, Italy; ⁷University of Rome "Foro Italico", Department of Movement, Human and Health Sciences, Division of Health Sciences, Italy

Email: stensgioia@hotmail.com

Background and aims: Porto-sinusoidal vascular disease (PSVD) is characterized by histological lesions involving portal veins and sinusoids in absence of cirrhosis. The pathophysiology of PSVD is unclear. However, its association with immunodeficiency, celiac disease, intestinal bowel disorders and abdominal bacterial infections supports the role of altered intestinal permeability and of gut-derived endotoxins. The study aimed at assessing the association between serological markers of increased intestinal permeability, pro-aggregating/pro-coagulant state and liver injury in patients with PSVD.

Method: 33 patients with biopsy-proven PSVD and clinical signs of portal hypertension and 33 healthy subjects, similar for age and sex, were submitted to a peripheral venous blood sampling for the measurement of zonulin and lipopolysaccharides (LPS) as markers of intestinal permeability, of s-Glycoprotein VI, sP-selectin, ADAMTS13 and von Willebrand factor as markers of platelet aggregation, thrombogenesis and microvascular inflammation, factor VIII and F1 +2 as markers of hypercoagulability. Liver biopsy specimens from a subgroup of PSVD patients (n = 18) were available for histomorphological and immunohistochemical study.

Results: Compared to controls, PSVD patients had higher serum levels of LPS (55.4 ± 15.4 vs 19.1 ± 5.3 pg/ml, $p < 0.0001$), zonulin (4.3 ± 1.4 vs 1.9 ± 0.8 ng/ml, $p < 0.0001$), von Willebrand Factor (vWf) (303 ± 88 vs 158 ± 65 U/dl, $p < 0.0001$), factor VIII (185 ± 77 vs 103 ± 33 U/dl, $p < 0.0001$), sP-selectin (37.9 ± 11.9 vs 17.7 ± 5.5 ng/ml, $p < 0.0001$), and F1+2 (158 ± 40 vs 136 ± 27 pmol/l, $p = 0.01$). ADAMTS13 (259 ± 95 vs 497 ± 110 ng/ml, $p < 0.0001$) was reduced. Serum LPS correlated with zonulin ($r = 0.80$, $p < 0.0001$), sP-selectin ($r = 0.85$, $p < 0.0001$), FVIII ($r = 0.42$, $p = 0.02$), and vWF ($r = 0.53$, $p = 0.02$). Histological analysis showed specific signs of PSVD in all patients; particularly, obliterative portal venopathy (OPV) was associated with clinical features, portal inflammation and fibrosis. Compared to samples from healthy subjects (liver donors), PSVD specimens were characterized by increased Toll-like Receptor-4 (TLR4)-positive macrophages and platelet number, located both in portal and perisinusoidal position. TLR4+ macrophage number was correlated with portal inflammation and fibrosis. Sinusoid dilation, perisinusoidal fibrosis, and sinusoidal capillarization were observed. Bile duct alterations and ductular reaction were also observed in PSVD, and their extent correlated with liver fibrosis.

Conclusion: PSVD patients display an altered intestinal permeability with a concomitant endotoxemia correlated to a pro-aggregating and pro-coagulant state; at histologic level, PSVD was associated with increased TLR4+ cell involvement and platelet aggregation within sinusoids. Our study suggests that LPS-TLR4 pathway could play a role in the pathophysiological basis of OPV (figure).

THU-324

Evaluating pruritus and fatigue in patients with treatment-refractory primary biliary cholangitis

Jörn Schattenberg¹, Betsy Williams², France Sowell², Peter Serafini³, Asad Khan⁴, Marwan Sleiman⁵, Julie Dietrich⁶, Carol Addy⁶, Dawn Vargas⁶, Gail Wright⁷, Kris Kowdley⁸. ¹University Medical Centre of the Johannes Gutenberg-University, Mainz, Germany; ²IQVIA, New York, United States; ³Ipsen, Cambridge, United States; ⁴Ipsen, Slough, United Kingdom; ⁵Ipsen, Boulogne, France; ⁶GENFIT Corp, Cambridge, United States; ⁷Canadian PBC Society, Toronto, Canada; ⁸Liver Institute Northwest, Seattle, United States
Email: marwan.sleiman@ipsen.com

Background and aims: Pruritus and fatigue are common symptoms that negatively impact patients with primary biliary cholangitis (PBC). The PBC Worst Itch Numeric Rating Scale (PBC WI NRS) and PROMIS Fatigue Short Form 7a (PFSF 7a) are being used to assess symptoms in a phase III clinical trial of an investigational therapy for PBC.

Method: Semi-structured qualitative interviews were conducted with adult patients diagnosed with PBC using Institutional Review Board-approved materials. PBC WI NRS asks patients to rate their worst itch over the past 24 hours on a scale ranging from 0 (No itch) to 10 (Worst itch imaginable). The PFSF 7a consists of 7 items that measure both the experience of fatigue and interference of fatigue on daily activities over the past 7 days using a Likert response scale. Patients were asked to evaluate the PBC WI NRS and PFSF 7a on ease of understanding of instructions and items, ease of use of scale/response options, and appropriateness of recall period to capture the patient experience. Interviews were conducted by experienced qualitative researchers, and audio recordings were transcribed and analyzed with coding software.

Results: 20 patients (aged 28–68 years; 19 females) diagnosed with PBC, (mean 10.7 years since diagnosis) experiencing pruritus (mild [30%], moderate [45%] or severe [25%]) were interviewed. For the PBC WI NRS, patients reported that instructions (20/20), item wording (20/20), and response options (19/20) were clear (Figure). Most patients (10/18) reported that a 3-point change on the PBC WI NRS scale would constitute a meaningful improvement, which would be pruritus that is “manageable,” and would occur occasionally, for shorter periods of time. This change would lead to less scratching, providing periods of “peace of mind” and less interference with sleep. For the PFSF 7a, all patients asked stated that instructions (18/18), items (18/18), and response options (19/19) were easy to understand. Most patients (12/18) stated a 1-point change on the PFSF 7a would represent a meaningful change in fatigue; this improvement corresponded to changes in alertness and well-being that would be easily noticeable compared to the consistency in their day-to-day experience with fatigue. The energy remaining would also be less fleeting allowing them to accomplish more throughout the day.

Instrument	Instructions were clear	Response options easy to use	Recall period appropriate
PBC WI NRS	20/20	19/20	15/19*
PFSF 7a	18/18**	19/19*	16/20

*One patient was not asked the question

**Two patients were not asked the question

Conclusion: Most patients found the PBC WI NRS and PFSF 7a instruments easy to understand and use for reporting their experience with pruritus and fatigue. These interview results support the content validity of the PBC WI NRS and PFSF 7a instruments in the context of PBC clinical trials; these instruments were selected to measure treatment benefit.

THU-325

Ultrasonographic liver characteristics among patients with Wilson disease

Zoe Mariño¹, Clàudia García², Cristina Collazos², Anna Miralpeix², Xavier Forn¹, Ernest Belmonte³. ¹Liver Unit, Hospital Clínic Barcelona, IDIBAPS, CIBERehd, ERN-RARE Liver, Universitat de Barcelona, Barcelona, Spain; ²Liver Unit, Hospital Clínic Barcelona, Barcelona, Spain; ³Abdominal section, Radiology Department, Hospital Clínic Barcelona, Barcelona, Spain
Email: zmarino@clinic.cat

Background and aims: Wilson disease (WD) may mimic other prevalent liver diseases. A previous work by Akhan O *et al* (Eur J Radiol 2009) suggested that WD may exert some differential ultrasonographic characteristics, such as the presence of hypoechoic nodules or increased periportal thickness (pPT) (more than 2 mm), that could be used for arising WD suspicion. The aim of this work was to analyze the main characteristics of abdominal ultrasounds (aUS) in a cohort of WD patients and correlate them with clinical and elastographic data. **Method:** WD patients followed in our institution with aUS performed between 2018 and 2022 were included. An experienced radiologist blinded to clinical data performed the aUS retrospective analysis. We recorded the closest clinical, elastographic and analytical data for each patient. Statistical analysis was performed with SPSS v.27; variables were expressed as n (%) or mean (IQR_{25–75}).

Results: We included 55 WD patients with aUS: 28 (51%) male, current age 38 (27–47), WD diagnosis done 17 years (11–27) ago, 30 (55%) hepatic phenotype, 14 (25.5%) with cirrhosis (10 at diagnosis, 4 at follow-up), 28 (52.8%) with abnormal ASAT and/or ALAT at US evaluation, elastographic value 5.2 Kpa (4.6–7.4) and CAP 255 dB/m (209–295), available in 47 cases. Transient elastography (TE) was higher in cirrhosis vs non-cirrhosis (9.1Kpa vs. 4.9Kpa, $p < 0.001$). At the aUS, most of the WD patients showed normal hepatic size and morphology (87.3% and 100% respectively). Hepatic contours were normal in 37 (67%). Hepatic parenchyma was heterogeneous in 18 (32.7%), and echogenicity was increased in 31 (56.3%) patients: mild 24 (77.4%), moderate 5 (16.2%), severe 2 (6.4%). The presence of moderate/severe steatosis in aUS ($n = 7$) was significantly associated with a CAP value > 261 dB/m, corresponding to S2-S3 at TE ($p = 0.02$). Eleven patients (20%) presented any solid hepatic lesion (SHL): the majority were hypoechoic nodules (isolated in 2, multiple in 4) or hemangiomas ($n = 3$). Five out of the 6 cases with hypoechoic nodules had cirrhosis; 1 case was hepatocellular carcinoma. pPT was explored in 40 patients (72.7%) and was increased in 14 cases (40%); abnormal pPT was not associated with the presence of cirrhosis, increased transaminases, or SHL. Up to 19 patients (34.5%) had splenomegaly [spleen diameter: 13 cm (12.7–15.5)]: 52.6% of them had cirrhosis ($n = 10$) whereas 47.4% ($n = 9$) had no signs of advanced liver disease ($p < 0.001$). Splenomegaly could only be associated with a reduced platelet count (136 vs 224, $p < 0.001$).

Conclusion: Steatosis showed to be very prevalent in US and correlated with the TE-CAP value among patients with WD. Splenomegaly was observed in one third of the cohort, even in the absence of cirrhosis. The presence of an increased periportal thickness and/or hypoechogenic nodules at the aUS could be helpful for WD diagnosis and should be explored prospectively.

THU-326

Exploring pregnancy, breastfeeding and contraception among women with Wilson disease in Spain: results from the Spanish Wilson registry

Marta Romero-Gutiérrez¹, Pablo Alonso Castellano², Marina Berenguer³, Antonio Oliveira Martin⁴, Maria Luisa Gonzalez Dieguez⁵, Paula Iruzubieta⁶, Helena Masnou⁷, Manuel Delgado⁸, Manuel Hernández Guerra⁹, Sara Lorente¹⁰, María Lázaro Ríos¹¹, Jose María Moreno Planas¹², Concepción gonzalez de frutos¹, Paula Fernandez Alvarez¹³, Francisca Cuenca Alarcon, Julia Morillas¹⁵, Judith Gómez- Camarero¹⁶, Luis García-Villarreal¹⁷, Zoe Mariño¹⁸. ¹Hospital Universitario de Toledo, Spain; ²Complejo Hospitalario Universitario Insular Materno Infantil (CHUIMI), Las Palmas de Gran Canaria, Spain; ³Hospital Universitari i Politècnic La Fe, IISLaFe, Ciberehd, Valencia, Spain; ⁴Hospital Universitario La Paz, Madrid, Spain; ⁵Hospital Universitario Central de Asturias, Oviedo, Spain; ⁶Hospital Universitario Marqués de Valdecilla, Santander, Spain; ⁷Hospital Universitari Germans Trias i Pujol, Badalona, Spain; ⁸Hospital Universitario A Coruña, Spain; ⁹Hospital Universitario de Canarias, Santa Cruz Tenerife, Spain; ¹⁰Hospital Clínico Lozano Blesa de Zaragoza, IISS Aragón, Spain; ¹¹Hospital Universitario Miguel Servet, Zaragoza, Spain; ¹²Complejo Hospitalario Universitario de Albacete, Facultad de Medicina Universidad de Castilla La Mancha, Spain; ¹³Hospital Universitario Virgen Macarena, Sevilla, Spain; ¹⁴Hospital Clínico San Carlos, Madrid, Spain; ¹⁵Hospital Virgen de la Luz, Cuenca, Spain; ¹⁶Hospital Universitario de Burgos, Spain; ¹⁷Complejo Hospitalario Universitario Insular Materno Infantil (CHUIMI), Las Palmas de Gran Canaria, Spain; ¹⁸Hospital Clínic, CIBERehd, IDIBAPS, ERN-RARE Liver, Universitat de Barcelona, Liver Unit, Spain
Email: m.romero.gutierrez@gmail.com

Background and aims: Recommendations about gestation and breastfeeding in patients with Wilson disease (WD) are heterogeneous. Our aim was to collect data on gestational history, lactation,

therapeutic modifications, and contraception in patients with WD in Spain.

Method: Multicenter ambispective study including adult women within the Spanish Wilson Registry. Informed consent was obtained and specific interviews were performed in all cases.

Results: We included 92 women with WD: median age was 43.7 (range: 18–81) years, age at WD diagnosis was 15.7 (3–67) years. Thirty-four women (37%) reported no history of gestation, whereas 58 (63%) referred previous pregnancies [total gestations: 143, median/woman: 2]. WD diagnosis was done during pregnancy in 2 patients (3.4%), before in 41 (70.7%) and after in 15 (25.9%). Up to 35 (33.6%) received no anti-copper therapy while on pregnancy, mostly due to post-gestation diagnosis (91.4%). In those pregnant women with treatment ($n = 69$), the drugs used were: 52.2% D-Penicillamine (D-P), 5.8% trientine and 42% zinc. The therapeutic attitude during pregnancy was: 62.3% unchanged, 10.1% dose reduction, 7.3% changed D-P to zinc; 7.3% women decided to voluntarily abandon therapy; in 13% it was unknown. Up to 49% of women were followed in high-risk gynecological programs. The age at first delivery was 26.1 (18–40) years. Twenty-three WD patients (39.6%) reported previous history of miscarriage, mainly spontaneous (74%) and most occurring during the first trimester. Data regarding 106 newborns was available: 98 term neonates, 6 pre-term, 2 post-term; pathology was reported in 4 children (3.8%). Breastfeeding data was obtained from 78 pregnancies: 26.9% did natural breastfeeding, 60.3% artificial lactation, mixed in 12.8%. Type of lactation was based on patient's choice in 37.2%, hepatology recommendation in 17.9%, gynecology recommendation in 30.8%, others in 7.7%, not available in 6.4%. The use of artificial lactation was mainly (68%) based on physician's recommendations (hepatology/gynecology). After WD diagnosis, 26.1% did not use any contraception, 29.4% used hormonal contraceptives, 21.7% barrier contraceptives, 5.4% IUDs, 10.9% other/combined, and 6.5% unknown. When we asked specifically, WD women were concerned about pregnancy (48.1%), mostly because of the risk of WD and treatment on the fetus (64.5%). However, information received from physicians was considered to be sufficient in more than a half (53.2%).

Conclusion: Gestational history among women with WD in Spain was shown to be heterogeneous. Almost 50% of the patients reported concerns about being pregnant. Artificial breastfeeding was the most frequent method, mainly due to medical recommendations. A clear guide for physicians and WD patients would be desirable.

THU-327

Hepatic alterations in COVID-19: a comparative autopsy study

Sigurd Lax^{1,2}, Kristijan Skok³, Peter Zechner⁴, Stephan Aberle⁵, Ute Bargfrieder¹, Claudia Grosse⁶, Helmut Salzer⁷, Thomas Zlamal⁸, Lisa Setaffy¹, Harald Kessler⁹, Hans-Peter Dienes¹⁰, Michael Trauner¹¹. ¹Hospital Graz II, Pathology, Graz, Austria; ²Johannes Kepler University, Pathology and Molecular Pathology, Linz, Austria; ³Hospital Graz II, Pathology, Graz, Austria; ⁴Hospital Graz II, Cardiology and Intensive Medicine, Graz, Austria; ⁵Medical University Vienna, Virology, Wien, Austria; ⁶Kepleruniklinikum, Pathology and Molecular Pathology, Linz, Austria; ⁷Kepleruniklinikum Linz, Pulmonary Medicine, Linz, Austria; ⁸Hospital Graz II, Cardiology and Intensive Medicine, Graz, Austria; ⁹Medical University Graz, Hygiene, Microbiology and Environmental Medicine, Graz, Austria; ¹⁰Medical University Vienna, Gastroenterology and Hepatology, Wien, Austria; ¹¹Medical University Vienna, Gastroenterology and Hepatology, Vienna, Austria
Email: sigurd.lax@kages.at

Background and aims: COVID-19 is a systemic disease involving particularly the lungs and, in addition, multiple other organs. Whereas the pulmonary changes have been extensively studied, our knowledge on the impact of SARS-CoV-2 on the liver is limited. The aim of this study was to investigate liver changes of COVID-19 deceased in correlation with the hepatic viral status and to compare

the findings with a control group of non-COVID-19 patients matched for age and underlying medical conditions.

Method: Formalin-fixed, paraffin-embedded liver tissue of 50 COVID-19 and 20 non-COVID deceased was studied histologically, by immunohistochemistry and by PCR for SARS-CoV-2 RNA and correlated with clinical and laboratory information.

Results: Viral RNA was detected in liver tissue of 15/50 (30%) COVID-19 deceased but in none of the controls. Livers of COVID-19 deceased showed significantly more frequently moderate to severe (mostly macrovesicular) steatosis, Kupffer cell proliferation and ductular metaplasia of hepatocytes compared to the control group ($p < 0.01$). Portal T-cell infiltrates were significantly less frequent in the PCR-positive COVID-19 subgroup compared to PCR-negative COVID-19 patients and controls ($p < 0.01$). Other findings such as active cholangitis, ductular proliferation, periductular sclerosis, fibrosis, and congestion were present in both COVID-19 patients and controls, without statistically significant differences. Cholestasis and hepatic thrombosis were only found in COVID-19 deceased.

Conclusion: Severe hepatic steatosis, increased Kupffer cell proliferation, ductular proliferation and ductular metaplasia of hepatocytes in COVID-19 may reflect a reaction to the viral infection and/or associated systemic inflammation. However, other histological findings in the liver of elderly COVID-19 deceased, particularly, periductular sclerosis seem to be potentially age-related.

THU-328

The adequacy and safety of liver biopsy performed during cardiac catheterization in patients with Fontan and non-Fontan heart disease

Edward Cytryn¹, Peizi Li², Sara Lewis³, Maria Isabel Fiel², Barry Love⁴, Ali Zaidi⁵, Thomas Schiano⁶, Lauren Grinspan⁶. ¹Icahn School of Medicine at Mount Sinai, Department of Medicine, New York, United States; ²Icahn School of Medicine at Mount Sinai, Department of Pathology, New York, United States; ³Icahn School of Medicine at Mount Sinai, Department of Radiology, New York, United States; ⁴Icahn School of Medicine at Mount Sinai, Department of Pediatrics, Division of Cardiology, New York, United States; ⁵Icahn School of Medicine at Mount Sinai, Department of Medicine (Cardiology), Department of Pediatrics, New York, United States; ⁶Icahn School of Medicine at Mount Sinai, Division of Liver Diseases, Recanati/Miller Transplantation Institute, New York, United States
Email: edward.cytryn@mountsinai.org

Background and aims: Liver biopsy is the gold standard for diagnosis of hepatic fibrosis and cirrhosis. However, it is an invasive procedure and carries risk of bleeding. The surveillance of Fontan-associated liver disease (FALD), an increasingly recognized complication in the growing number of patients post-Fontan procedure, with biopsy during right heart catheterization (RHC) is a unique approach performed at few centers, in part due to questions of risk of biopsy and sampling error. The role and efficacy of transcaval liver biopsy during RHC warrants further investigation. The aim of this study was to review the indications, outcomes, and adequacy of liver biopsy during RHC, with special attention to patients having FALD.

Method: A multidisciplinary, retrospective review of patients at a single institution who underwent liver biopsy during RHC was performed. 94 liver biopsies taken between December 2011 and October 2022 were analyzed. Patient characteristics, RHC and biopsy indications, hemodynamics, complications, and tissue adequacy were evaluated. Specimens were classified as "adequate" if total biopsy linear length was greater than or equal to 20 mm or the total number of portal tracts was greater than or equal to 10, "limited" if the total length was 10 to 20 mm or total number of tracts was 5 to 10, or "inadequate" if the total length was less than 10 mm and total number of tracts was less than 5.

Results: There were 55 biopsies in non-Fontan patients and 39 in Fontan patients with a median age at RHC of 55.5 years and 30 years, respectively. Indications for RHC were routine hemodynamic

assessment (49%), new or progressive heart failure symptoms (47.2%), and arrhythmia (3.6%) in the non-Fontan group and assessment of Fontan circulation (84.6%), heart failure symptoms (10.3%), and arrhythmia (2.6%) in the Fontan group. Indication for liver biopsy in non-Fontan patients was to rule out fibrosis in 92.7% and abnormal LFTs in 7.3%. In Fontan patients, biopsy was indicated to assess FALD in 25.6% with known disease and to rule out fibrosis in 74.4%. Hepatic pressure measurements were obtained in 95.7% of cases (98% non-Fontan, 92.3% Fontan). Average fluoroscopy time was longer in Fontan compared to non-Fontan cases, 12.5 vs 6.4 minutes, with fewer average number of biopsy passes, 2.8 vs 3.6. There were no complications from pain, bleeding, perforation, or infection, and no noted technical difficulties in either group. Average total linear length and number of portal tracts were similar between Fontan and non-Fontan biopsies, 24.3 vs 24.4 mm and 12.7 vs 13.7 portal tracts, respectively. In total, 82/94 (87.2%) were "adequate" and 10/94 (10.6%) were "limited." 4/94 (4.3%) were inadequate by linear length, while 3/94 (3.2%) were inadequate by number of portal tracts, however, only 2/94 (2.1%) met both criteria and were classified as "inadequate." Similar adequacy was noted in sub-analysis of Fontan patients with 34/39 (89.7%) "adequate," 4/39 (10.3%) "limited," and 1/39 (2.6%) "inadequate." A definitive diagnosis was reached on pathology review of 92/94 (97.9%) biopsies.

Conclusion: Liver biopsy performed during a clinically warranted RHC can be safely performed with adequate yield and minimal complication risk. It is especially useful and effective in Fontan patients undergoing RHC to assess FALD development and progression. Liver histology is important to analyze during cardiac decompensation and obtaining a liver biopsy concurrently during a RHC should be considered.

THU-329

Deep learning quantification reveals fundamental prognostic role for ductular reaction in biliary atresia

Iiris Nyholm¹, Nelli Sjöblom², Maria Hukkinen¹, Marjut Pihlajoki³, Jouko Lohi², Aino Mutka², Päivi Heikkilä², Mark Davenport⁴, Markku Heikinheimo³, Johanna Arola², Mikko Pakarinen¹. ¹University of Helsinki and Helsinki University Hospital, Section of Pediatric Surgery, Pediatric Liver and Gut Research Group, Finland; ²University of Helsinki and Helsinki University Hospital, Department of Pathology, Finland; ³University of Helsinki and Helsinki University Hospital, Pediatric Research Center, Finland; ⁴King's College Hospital, Department of Pediatric Surgery, United Kingdom
Email: iiris.nyholm@helsinki.fi

Background and aims: Ductular reaction (DR) is a prominent pathological feature of biliary atresia (BA) associating with unsuccessful Kasai portoenterostomy (KPE) and liver fibrosis in previous small studies using conventional histopathology.

Method: Deep learning model was developed and applied to cytokeratin 7 (CK7) stained native liver biopsies ($n = 257$) in BA patients ($n = 136$). The CharBADR model quantified total proportional DR (DR%) composed of CK7 positive portal biliary epithelium (BEL%) and parenchymal intermediate hepatocytes (PIH%). Results were related to clinical data, Sirius Red quantified liver fibrosis, and serum bile acids.

Results: In total, 116 biopsies were obtained at KPE and 141 during postoperative follow-up. 58% of patients cleared their jaundice (COJ, post-KPE serum bilirubin $< 20 \mu\text{mol/l}$) and overall native liver survival (NLS) was 38%. DR% (8.3 vs 5.9%, $p = 0.045$) and PIH% (13.4 vs 6.3%, $p = 0.004$), but not BEL% (6.8 vs 5.1, $p = 0.09$), were increased at KPE in patients without COJ. During follow-up, increased DR% (13.6 vs 2.9%, $p < 0.001$), PIH% (6.4 vs 0.3%, $p < 0.001$) and BEL% (4.4 vs 2.5%, $p < 0.001$) persisted in patients subsequently transplanted. In Cox regression, high DR% predicted inferior NLS both at KPE (HR = 134, $p = 0.02$) and during post-KPE follow-up (HR = 22, $p < 0.001$). DR% correlated with liver fibrosis at KPE ($R = 0.47$, $p < 0.0001$) and follow-up ($R = 0.27$, $p = 0.004$). A close association between DR% and serum

POSTER PRESENTATIONS

bile acids was observed at follow-up ($R = 0.61$, $p < 0.001$). Fibrosis was not prognostic for NLS at KPE ($HR = 1.00$, $p = 0.96$) or follow-up ($HR = 1.01$, $p = 0.29$).

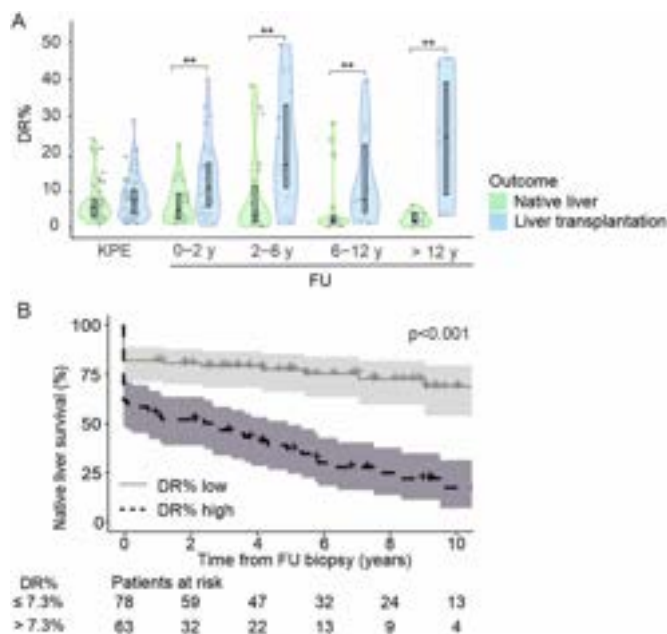


Figure:

Conclusion: DR associated with COJ and, unlike liver fibrosis, predicted need for liver transplantation.

THU-330

Long-term outcomes of patients with Wilson disease: a single center analysis of 361 Korean patients

Hyo Jin Nam¹, Jonggi Choi¹, Won-Mook Choi¹, Danbi Lee¹, Ju Hyun Shim¹, Kang Mo Kim¹, Young-Suk Lim¹, Han Chu Lee¹. ¹Asan Medical Center, Korea, Rep. of South
Email: jkchoi0803@gmail.com

Background and aims: There are few data regarding long-term outcomes and survival of patients with Wilson disease (WD) from large Asian cohorts. We aimed to analyze the clinical long-term data in a large Korean cohort of WD.

Method: Between 2000 and 2022, 361 patients with WD were retrospectively analyzed at Asan Medical Center, Seoul, Republic of Korea. Diagnosis of WD were made on typical symptoms, clinical, biochemical and genetic findings. Primary outcome was liver transplant-free survival. Development of hepatocellular carcinoma (HCC) in the entire patients and progression to liver cirrhosis (LC) in patients without LC at diagnosis were also analyzed. Patients who met the following criteria were excluded: 1) received liver transplantation within 6 months of diagnosis; 2) follow-up period less than 6 months; 3) co-infection with hepatitis B virus; 4) combined alcoholic liver disease. Median follow-up period was 13.0 years.

Results: The mean age was 17.2 years, and 206 (57.1%) of the patients were male. At diagnosis, 146 (40.4%) patients had LC, of which 48 (13.3%) patients showed decompensation. Transplant-free survival rates at 5-, 10-, 15-, and 20-years were 100.0%, 98.4%, 97.9%, and 97.9%, respectively. Cumulative probabilities of HCC development at 5-, 10-, 15-, and 20-years were 0.0%, 0.4%, 1.9%, and 6.1%, respectively. Of the 215 patients without LC at diagnosis, 15 (7.0%) patients showed progression to LC with cumulative risks of 0.0%, 3.0%, 6.1% and 14.1% at 5, 10, 15, and 20 years, respectively. No patients without LC at diagnosis died or developed HCC during the follow-up period. Older age and LC at diagnosis were significantly associated with a worse survival rate ($p < 0.05$ for all).

Conclusion: Korean patients with WD had a favorable long-term prognosis. However, older age and LC at the time of diagnosis increase the risk of death and HCC development.

THU-331

Lessons from population genomics for Wilson disease: Prevalence, penetrance of mutations, clinical implications and design of regional screening programmes

Pablo Alonso Castellano¹, Zoe Mariño², Antonio Oliveira Martin³, Javier Ampuero⁴, Marina Berenguer⁵, Maria Pilar Huarte Muniesa⁶, Diego Burgos Santamaria⁷, José Ramón Fernández⁸, Jose María Moreno Planas⁹, María Lázaro Ríos¹⁰, Helena Masnou¹¹, Maria Luisa Gonzalez Dieguez¹², Jose Pinazo Bandera¹³, Esther Molina¹⁴, Manuel Hernández Guerra^{15,16}, Marta Romero-Gutiérrez¹⁶, Patricia Cordero Ruiz¹⁷, Carolina Muñoz Codoceo¹⁸, Sara Lorente¹⁹, Alba Cachero²⁰, Manuel Delgado²¹, Víctor Manuel Vargas Blasco²², Judith Gómez-Camarero²³, Julia Morillas²⁴, Francisca Cuenca Alarcon²⁵, Luis Ibañez Samaniego²⁶, Miguel Fernandez-Bermejo²⁷, Beatriz Álvarez-Suárez²⁸, Paula Iruzubieta²⁹, Ana Arencibia Almeida³⁰, Anna Miralpeix³¹, Pilar Castillo³, Luis García-Villarreal¹. ¹Servicio Digestivo, Complejo Hospitalario Universitario Insular Materno Infantil (CHUMI), Las Palmas de Gran Canaria, Spain; ²Liver Unit, Hospital Clínic, CIBERehd, IDIBAPS, ERN-RARE Liver, Universitat de Barcelona, Barcelona, Spain; ³Hospital Universitario La Paz, Madrid, Spain; ⁴Hospital Universitario Virgen del Rocío, Sevilla, Spain; ⁵Hospital Universitari i Politècnic La Fe, València, Spain; ⁶Complejo hospitalario Navarra, Pamplona, Spain; ⁷Hospital Ramón y Cajal, Madrid, Spain; ⁸Hospital Universitario de Cruces, Barakaldo, Spain; ⁹Servicio de Aparato Digestivo, Complejo Hospitalario Universitario de Albacete, Facultad de Medicina Universidad de Castilla La Mancha, Spain; ¹⁰Hospital Universitario Miguel Servet, Zaragoza, Spain; ¹¹Hospital Universitari Germans Trias i Pujol, Badalona, Spain; ¹²Hospital Universitario Central de Asturias, Oviedo, Spain; ¹³Unidad de Hepatología, Unidad de Gestión Clínica de Aparato Digestivo, Hospital Universitario Virgen de la Victoria, Instituto de Investigación Biomédica de Málaga-Plataforma Bionand, Málaga, Spain; ¹⁴Hospital Clínico de Santiago, Santiago de Compostela, Spain; ¹⁵Hospital Universitario de Canarias, Santa Cruz Tenerife, Spain; ¹⁶Hospital Universitario de Toledo, Toledo, Spain; ¹⁷Hospital Universitario Virgen Macarena, Sevilla, Spain; ¹⁸Hospital Universitario 12 de Octubre, Madrid, Spain; ¹⁹Unidad de Hepatología y Trasplante Hepático, Hospital Clínico Lozano Blesa de Zaragoza, IIS Aragón, Spain; ²⁰Hospital Universitari de Bellvitge, Hospitalet de Llobregat, Spain; ²¹Hospital Universitario A Coruña, A Coruña, Spain; ²²Servicio de Hepatología, Hospital Vall d'Hebron, Universitat Autònoma de Barcelona, CIBERehd, Barcelona, Spain; ²³Hospital Universitario de Burgos, Burgos, Spain; ²⁴Hospital Universitario Virgen de la Luz, Cuenca, Spain; ²⁵Unidad de Hígado, Servicio de Aparato Digestivo, Hospital Clínico San Carlos, Madrid, Spain; ²⁶Hospital General Universitario Gregorio Marañón, Madrid, Spain; ²⁷Hospital Universitario de Cáceres, Cáceres, Spain; ²⁸Hospital Universitario Lucus Augusti (CHUL), Lugo, Spain; ²⁹Hospital Universitario Marqués de Valdecilla, Santander, Spain; ³⁰Hospital Universitario Nuestra Señora de La Candelaria, Santa Cruz de Tenerife, Spain; ³¹Liver Unit, Hospital Clínic, CIBERehd, IDIBAPS, ERN-RARE Liver, Universitat de Barcelona, Barcelona, Spain
Email: lgarciavillarreal@gmail.com

Background and aims: During the last years several studies have discussed about the prevalence and penetrance of Wilson Disease (WD) mutations with conflicting conclusions. So we decided to compare the estimated data for WD in Spain from genome databases-Lorente et al J Pediatr Gastroenterol Nutr. 2022 Feb 1;74 (2):192-199-with clinical and genetic data obtained from the Spanish Wilson Registry (SWR) by AEEH

Method: We calculated the number of homozygotes of the most frequent mutations in Spain as predicted from the number of carriers found at the Collaborative Spanish Variant Server (assuming that the

	1 (n = 62)	2 (n = 16)	3 (n = 22)	4 (n = 5)	
	Met645Arg	Leu708Pro	His1069Gln	Gly869Arg	
Neurological manifestations	6, 00%	19, 00%	27, 00%	0, 00%	p = 0.05
Hepatic manifestations	72, 00%	81, 00%	31, 00%	60, 00%	p = 0.003
Screening cases	23, 00%	0, 00%	18, 00%	50, 00%	p = 0.023
K-F ring	6, 00%	25, 00%	39, 00%	0, 00%	p = 0.009
Cirrhosis at diagnosis	14, 00%	25, 00%	37, 00%	0, 00%	P < 0.05 1 vs 3

Figure: (abstract: THU-331).

Hardy-Weinberg equilibrium is met), and compared those estimated values with records from the Spanish Wilson Registry (adding late communication from a center not included yet) covering approximately 85% of the Spanish population, and represented mainly by adult cases recruited at digestive services.

Results: The estimated vs real number of homozygotes were as follows: p.Met645Arg (1949 vs 6), p.His1069Gln (20 vs 8), p. Leu708Pro (63 vs 24; only Gran Canaria) and p.Gly869Arg (147 vs 0). Studying homozygous cases from the SWR, the p.Met645Arg homozygous cases compared with those for p.Leu708Pro and p. His1069Gln presented 0% with cirrhosis at diagnosis (vs 40% and 20%, respectively), 20% with extrahepatic disease (vs 46% and 50%, respectively), 20% asymptomatic cases (vs 8% and 0%, respectively), 0% with Kayser-Fleischer (KF) ring (vs 40%, 75% p < 0.05 with p. His1069Gln), and 60% diagnosed after 40 y.o. (vs 0% and 0%, p < 0.001). When comparing p.Met645Arg homozygotes vs p.Met645Arg compound heterozygotes, we found that 60% vs 17%, respectively, were diagnosed after 40 yo (p < 0.05). Finally we studied these 4 mutations in compound heterozygotes with any other mutation, excluding compounds between the frequent mutations (Table):

Conclusion: Considering the limited recruitment time (only one year) of the registry, not covering all patients and only ¼ of cases with a genetic test, it seems that Met645Arg and Gly869Arg are less penetrant mutations, as homozygote patients presented with less cirrhosis at diagnosis, no KF ring, no neurological manifestations and are diagnosed later. From the estimated values, WD in Spain seems to be underdiagnosed possibly, among other reasons, due to the low penetrance of the most frequent mutations (p.Met645Arg and p. Gly869Arg), low suspicion in some cases and atypical presentation in others. Data like these from population genomic studies and clinical records may help to design better screening strategies that could accelerate and improve WD diagnosis.

THU-332

Endogenous ethanol production in biliary atresia and its association with clinical outcomes, liver disease severity, fibrosis, bacterial translocation and intestinal permeability

Emma Alexander¹, Charlotte Burford¹, Mark Davenport¹, Erica Makin¹, Anita Verma¹, Anil Dhawan¹, Vandana Jain¹. ¹King's College Hospital, United Kingdom
Email: vjain@nhs.net

Background and aims: Altered gut microbiota (GM; dysbiosis), have been implicated in the pathogenesis of chronic liver diseases, including Biliary Atresia (BA), and are a major source of endogenous ethanol production. Plasma ethanol concentration was increased in NASH vs obese/healthy controls, and we have previously described an increase in potential ethanol-producing GM in BA. Aim: To characterise ethanol production in BA, and its association with clinical outcomes, liver disease severity, fibrosis, bacterial translocation (BT) and intestinal permeability (IP).

Method: Stool and plasma samples, were prospectively collected, in BA infants (n = 55) pre-Kasai Portoenterostomy (KPE), 6weeks-, 3months-, and 6months-post-KPE. Plasma ethanol, BT [Lipopolysaccharide-Binding Protein (LBP), D-lactate] and IP [Claudin-3] biomarkers, were measured. Stool 16S-rRNA sequencing was performed for GM genus abundance. Outcomes: 6month

jaundice clearance vs 6month jaundice [BA-JC vs BA-J], 1year-liver transplant (LT) status [BA-native liver survivor (NLS) vs BA-LT], Paediatric End Stage Liver Disease (PELD) score, fibrosis [Liver Stiffness Measurement (LSM)].

Results: Plasma ethanol concentration pre-KPE, 6weeks-post-KPE, were not associated with 6month-JC or 1year-LT outcome groups. At 3months-post-KPE, increased ethanol was associated with 1year-LT [BA-NLS, 2.4 mg/L (0, 12.3) vs BA-LT 7 mg/L (1, 140, p = 0.02) and predicted the need for LT at 1year-post-KPE, with AUROC of 0.74. At 6months-post-KPE, ethanol was not associated with clinical outcomes. At 3months-post-KPE, ethanol positively correlated with disease severity [PELD, rs = 0.4, p = 0.02] and fibrosis [LSM, rs = 0.5, p = 0.01]. Regarding BT, ethanol positively correlated with D-lactate at 6weeks-post-KPE [rs = 0.4, p = 0.02] and 3months-post-KPE [rs = 0.5, p = 0.01], but inversely with LBP [3months-post-KPE; rs = -0.3, p = 0.05; 6months-post-KPE, rs = -0.5, p = 0.01]. No correlation between ethanol and individual genus abundance or IP (Claudin-3), was identified.

Conclusion: Ethanol, at 3months-post-KPE, is associated with LT in BA. Ethanol and D-lactate production are linked, suggesting a role for GM-ethanol-BA pathogenesis. The inverse correlation between LBP and ethanol may reflect a protective role for LBP in early endotoxemia. Mechanistic pathways for ethanol-BA pathogenesis, warrant further investigation.

THU-333

Digital pathology using stain-free imaging indices as a tool for fibrosis quantification in patients with congestive hepatopathy

Matthew Yeh¹, Hong-Wen Tsai², Che-Wei Hsu², Cheng-Yi Chen², Yayun Ren³, Kutbuddin Akbary³, Elaine Chng³, Dean Tai³. ¹University of Washington, Department of Pathology, United States; ²National Cheng Kung University Hospital, Taiwan; ³HistoIndex Pte Ltd, Singapore
Email: yehmliver@gmail.com

Background and aims: Congestive hepatopathy (CH) is the result of right heart failure from myriads of heart diseases. It causes centrilobular fibrosis and can progress to portal and bridging fibrosis and even cirrhosis. While histological scoring system for fibrosis in congestive hepatopathy exists, the scores are categorical but not continuous. There are also intra- and inter-observer variation among pathologists. Second harmonic generation/two-photon excitation fluorescence (SHG/TPEF) microscopy has been demonstrated to provide accurate and reproducible fibrosis quantification in preclinical and clinical liver specimens, including biopsies from patients with viral hepatitis and NAFLD. We aim to test the feasibility using SHG/TPEF microscopy in assessing liver fibrosis in congestive hepatopathy. **Method:** Unstained sections from 10 congestive hepatopathy cases with Dai scheme stages 0, 1, 2 and 3 were imaged using SHG/TPEF microscopy. Changes in overall liver fibrosis and in five zonal regions of liver lobules were quantitatively assessed by qFibrosis-a cumulative index based on measuring 184 collagen features on a continuous scale. Using sequential feature selection, 3 parameters were chosen out of 184 fibrosis parameters and a linear regression method was used to construct a congestive hepatopathy index.

Results: 3 parameters chosen for CH fibrosis are all from central vein regions, whereas in NASH, 15 parameters chosen were from total tissue area and portal tract regions. This finding indicates the fibrosis

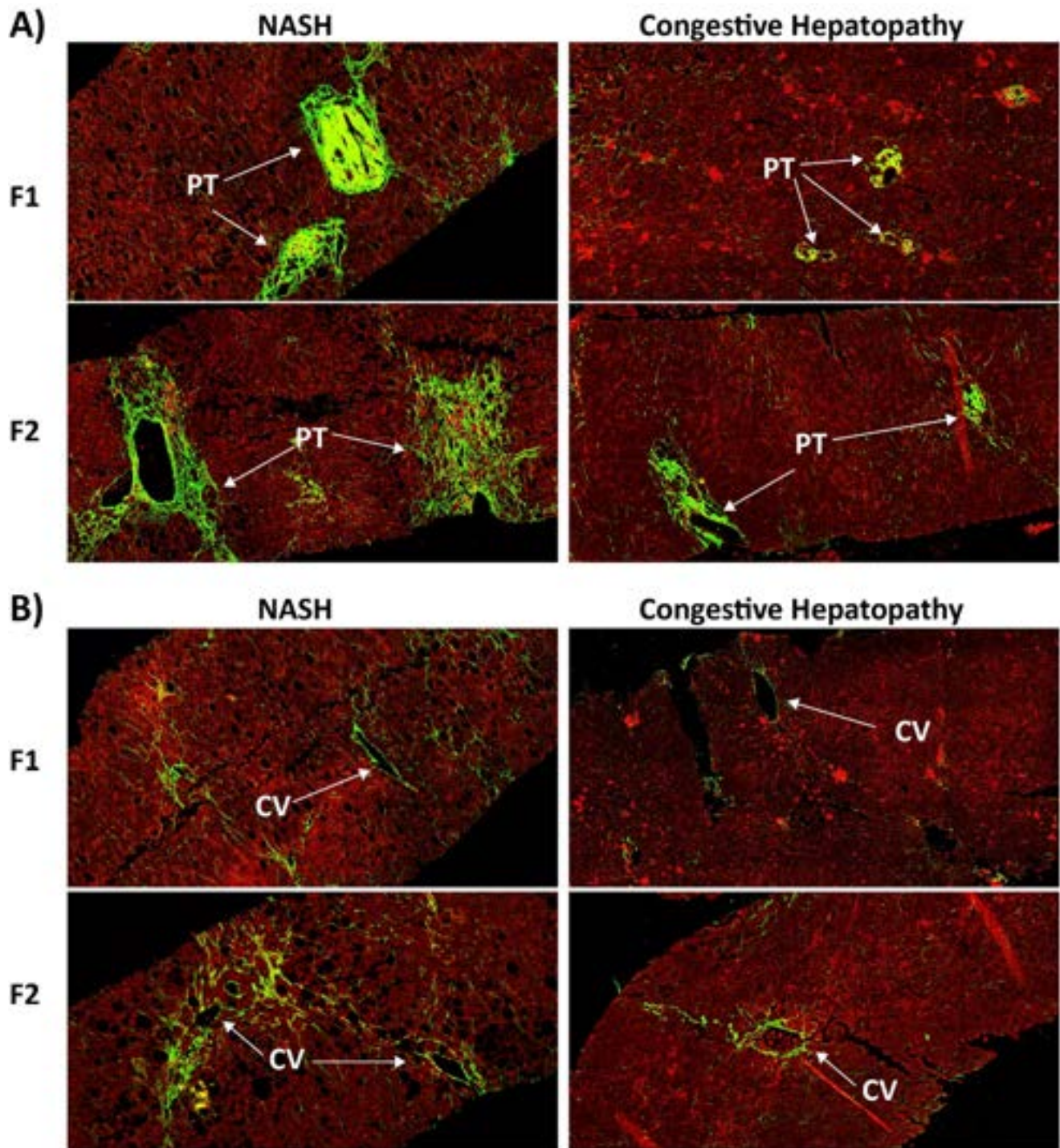


Figure: (abstract: THU-333): Image examples of (A) portal fibrosis and (B) central fibrosis for NASH and CH patients.

progression patterns is quantitatively different in portal tract and central vein regions. This difference can be better visualized in the figures, where SHG/TPEF images shows more fibrosis in NASH comparing to CH. Note that the staging systems used are NASH-CRN and Dai for NASH and CH patients respectively.

Conclusion: This is the first series liver fibrosis in congestive hepatopathy is shown to be assessed using SHG/TPEF microscopy. These data will be expanded and validated in an additional larger number of congestive hepatopathy cohort correlating with clinical and outcome data, and compared with other liver diseases (e.g., NASH and viral hepatitis), which may provide insight evaluating

disease severity that aid clinical management plan algorithm and decision-making.

THU-334

Current transition management of adolescents and young adults with liver diseases: an European reference network rare liver survey

Joao Madaleno^{1,2,3}, Marianne Samyn^{3,4}, Isabel Gonçalves^{3,5}, Zoe Mariño^{3,6}, Ruth de Bruyne^{3,7}, Deirdre Kelly^{3,8}. ¹Liver Disease Unit,

Internal Medicine Department, Centro Hospitalar e Universitário de Coimbra, Coimbra, Portugal; ²Faculty of Medicine, University of Coimbra, Portugal; ³European Reference Network on Hepatological Diseases (ERN RARE-LIVER), Germany; ⁴Paediatric Liver, GI and Nutrition Centre, King's College Hospital NHS Foundation Trust, London, United Kingdom; ⁵Paediatric Liver Transplant Unit, Centro Hospitalar e Universitário de Coimbra, Coimbra, Portugal; ⁶Liver Unit, Hospital Clinic de Barcelona, IDIBAPS, University of Barcelona, CIBEREHD, Barcelona, Spain; ⁷Dept. Pediatric Gastroenterology and Hepatology, Princess Elisabeth Children's Hospital, Ghent University Hospital, Ghent, Belgium; ⁸Liver Unit, Birmingham Women's and Children's NHS Trust and University of Birmingham, Birmingham, United Kingdom
Email: joaocarvalhomadaleno@gmail.com

Background and aims: There is an increased risk for medical complications and morbidity surrounding transfer from pediatric to adult hepatology and transplant services. Health care transition (HCT) is the process of moving from a child/family-centered model of care to an adult or patient-centered model of health care. On behalf of the European Reference Network (ERN) RARE-Liver, the Transition Working group conducted a survey within Europe exploring current practice.

Method: A questionnaire was developed and circulated electronically via ERN members and other national/international professional bodies using the EU Survey platform.

Results: A total of 90 responses (44% adult) from 67 centers in 27 countries were collected. A liver HCT programme was available in 61% (n = 41) centres, organized by paediatrics in 29%, adults 11% and jointly in 57%. Lack of resources was the main reason (56%) for not having a liver HCT programme. Transfer to adult services is mainly

driven by age, with 71% occurring by their 18th/19th birthday but exceptions are allowed in 57%. Transition readiness assessments were only used by 19%, and 70% of health care providers had not received specific training in the care of adolescents and young adults (AYA). The main barriers to adequate HCT were patient/family's dependence on the pediatric provider and inadequate communication between teams with 76.7% and 68.9% responding strongly agree/agree. No feedback system between pediatric and adult services occurs in 45.5% and no evaluation system is in place in 60%.

Conclusion: HCT is important for AYA with chronic liver diseases, but there are crucial limitations and variations in the current provision of transition services across Europe. Standardization of AYA management and specific training are required. This should improve management and continuity of care during adolescence and into adulthood to achieve the best healthcare outcomes.

THU-335

Quality of life in patients with Wilson disease treated with Trientine dihydrochloride: a prospective study

Karl Heinz Weiss¹, Isabelle Mohr², Larissa Wijnberg³, Carlot Kruse³.

¹Salem Medical Centre, Internal Medicine, Germany; ²Heidelberg University Hospital, Gastroenterology, Germany; ³Univar Solutions, Netherlands

Email: larissa.wijnberg@univarsolutions.com

Background and aims: Wilson disease (WD) is a rare genetic disorder, causing copper accumulation in organs, particularly the liver and brain. Life-long chelation therapy is required to remove excess copper and avoid development or worsening of hepatic and neurological symptoms. Chronic illness is known to impact quality of

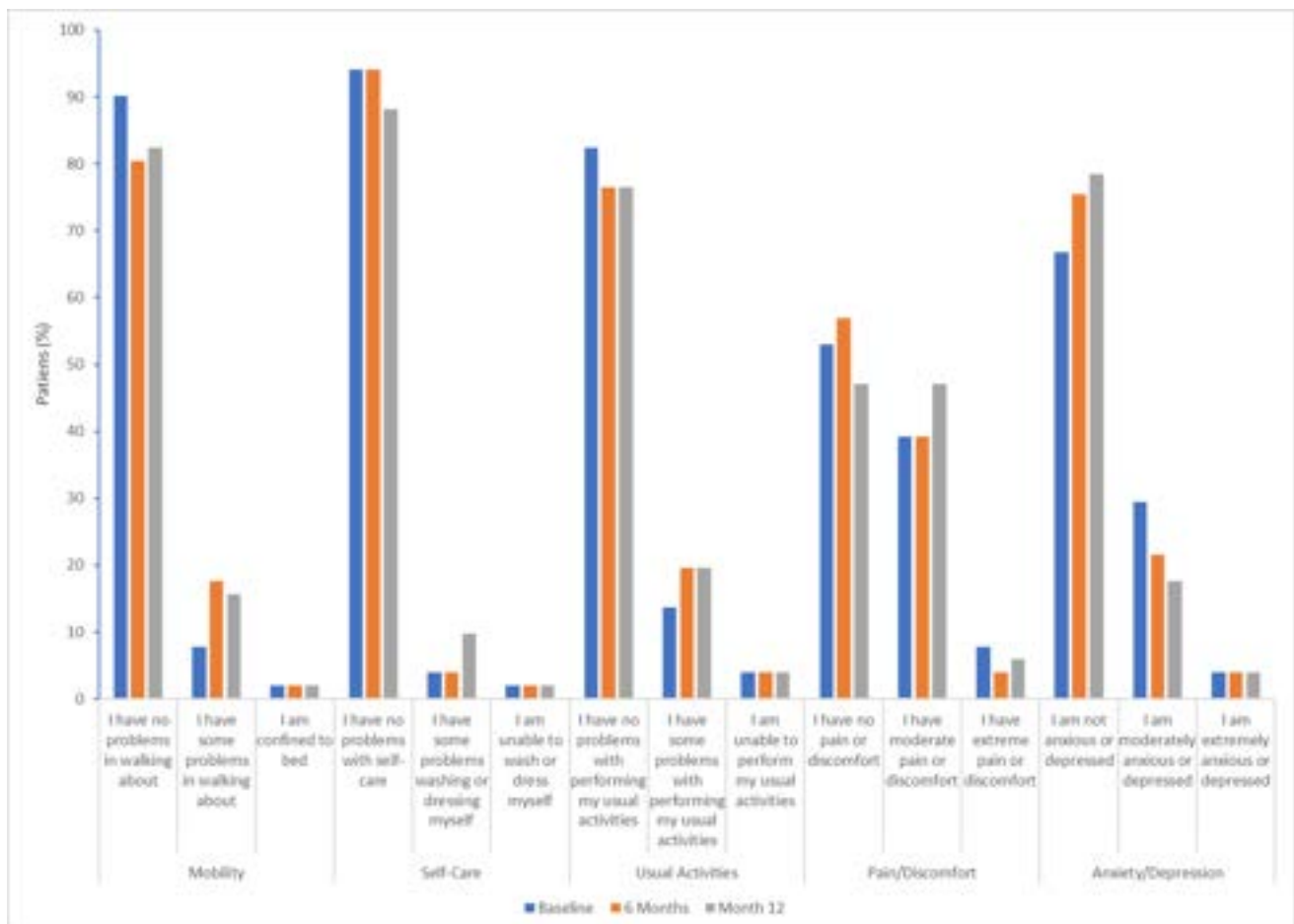


Figure: (abstract: THU-335): Quality of Life (EQ-5D-3L) dimensions at Baseline, Month 6, and Month 12.

POSTER PRESENTATIONS

life (QoL), with lower QoL and increased risk of depression reported in WD. We report QoL outcomes in a prospective study to assess long-term outcomes in patients with WD treated with Trientine dihydrochloride (TETA-2HCl).

Method: Patients with WD who were withdrawn from therapy with D-penicillamine and treated for at least 6 months with 300 mg capsules of TETA-2HCl (equivalent to 200 mg of trientine base) were eligible for this prospective, observational study. Patients were administered their routine dose of TETA-2HCl and completed the EQ-5D-3L questionnaire at Baseline, Month 6, and Month 12.

Results: EQ-5D-3L questionnaires were completed by all patients (N = 51). The five dimensions of the EQ-5D-3L (mobility, self-care, usual activities, pain/discomfort, anxiety/depression) were stable and generally similar at Months 6 and 12. Most patients had no difficulty in mobility or performing self-care activities while on treatment with TETA-2HCl, however one (2%) patient was confined to bed and not able to perform self-care (unable to wash or self-dress) throughout the study. Some problems in performing usual activities were reported by 7 (13.7%) patients, 10 (19.6%) patients and 10 (19.6%) patients at Baseline, Month 6, and Month 12, respectively, while two (3.9%) patients were completely unable to perform any usual activities during the study. Overall, 20 (39.2%) patients, 20 (39.2%) patients and 24 (47.1%) patients experienced moderate pain or discomfort at Baseline, Month 6, and Month 12, respectively. Extreme pain or discomfort was experienced by 4 (7.8%) patients, 2 (3.9%) patients and 3 (5.9%) patients at Baseline, Month 6 and at Month 12 respectively. Moderate anxiety or depression was noted in 15 (29.4%) patients, 11 (21.6%) patients and 9 (17.6%) patients at Baseline, Month 6, and at Month 12, respectively. Extreme anxiety or depression were experienced by 2 (3.9%) patients at Baseline, Month 6 and at Month 12, respectively.

Conclusion: Patients with WD receiving long-term TETA-2HCl therapy generally reported good mobility, self-care and ability to carry out their usual activities. However, pain or discomfort were reported by almost half of patients. Anxiety or depression also

affected up to half of patients at Baseline, although the proportion reporting moderate anxiety or depression decreased substantially during the 12 months of treatment. As a clinical consequence, assessment of anxiety and depression in patients with WD is warranted, even during maintenance therapy.

THU-336

Odevixibat therapy in patients with MYO5B mutations: a retrospective case series

Bertrand Roquelaure¹, Marco Sciveres², Tassos Grammatikopoulos³, Eberhard Lurz⁴, Folke Freudenberg⁵, Lionel Thevathasan⁶, Fatine Elaraki⁶, Velichka Valcheva⁶, Emmanuel Gonzalès⁷. ¹CHU, Hospital de la Timone, France; ²Paediatric Hepatology and Paediatric Liver Transplantation, ISMETT, University of Pittsburgh Medical Center Italy, Palermo, Italy; ³Institute of Liver Studies, King's College London, London, United Kingdom; ⁴Division of Paediatric Gastroenterology and Hepatology, Dr. von Hauner Children's Hospital, University Hospital Munich, LMU, Munich, Germany; ⁵Klinikum Dritter Orden, Division of Pediatric Gastroenterology and Hepatology, Munich, Germany; ⁶Albireo Pharma Inc., Boston, MA, United States; ⁷Hépatologie et Transplantation Hépatique Pédiatriques, Centre de Référence de l'Atrésie des Voies Biliaires et des Cholestases Génétiques, F5MR FILFOIE, ERN RARE LIVER, Hôpital Bicêtre, AP-HP, Université Paris-Saclay, HépatoNov, Inserm U 1193, Paris, France

Email: bertrand.roquelaure@ap-hm.fr

Background and aims: Progressive familial intrahepatic cholestasis type 6 (PFIC6, recently renamed PFIC10 according to Online Mendelian Inheritance in Man [OMIM; <https://www.omim.org/entry/619868>]) is a rare liver disease caused by mutations in the MYO5B gene and characterised by elevated serum bile acids (sBAs) and severe pruritus. This case series reports the effects of treatment with the ileal bile acid transporter inhibitor odevixibat in children with PFIC10.

Serum Bile Acid Levels Before and After Odevixibat Initiation in 5 Patients With MYO5B Deficiency

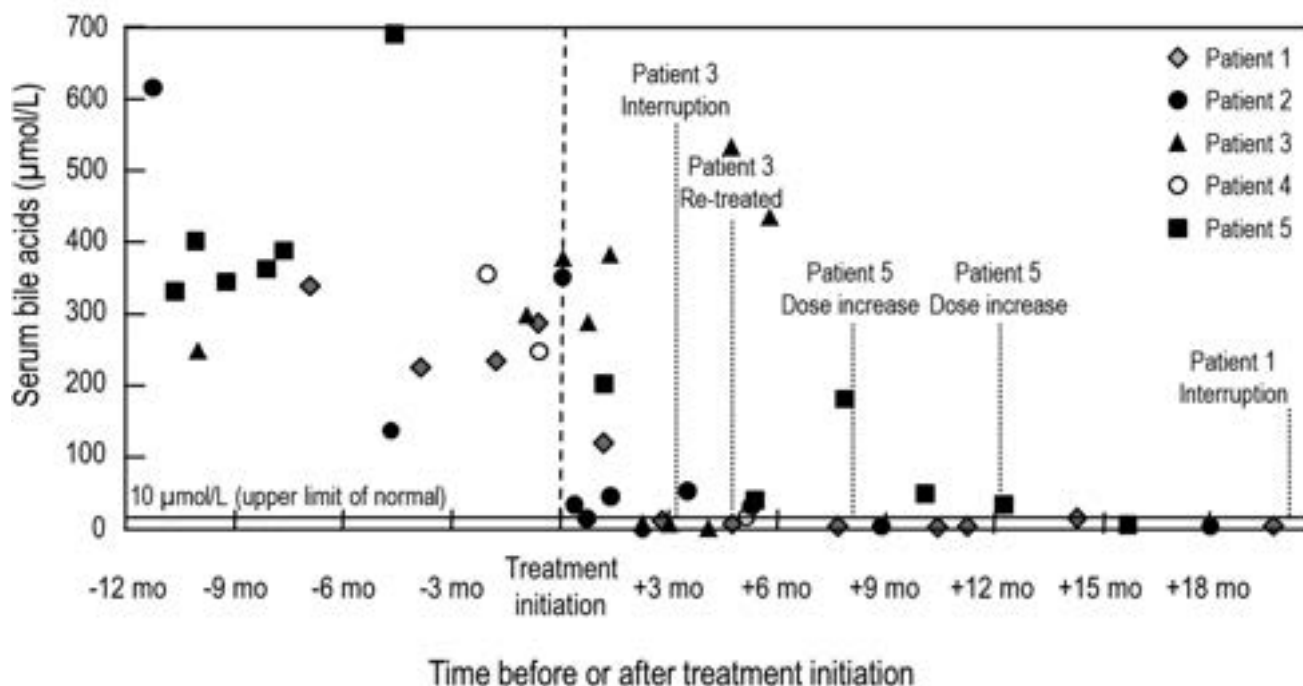


Figure: (abstract: THU-336).

Method: This was a retrospective analysis of 5 children with a diagnosis of MYO5B-related PFIC and pruritus refractory to standard treatment who were treated with odevixibat. Anonymised clinical and laboratory data collected at least quarterly were analysed, including anthropometrics, liver function tests, and treatment history. Pruritus and sleep disorders were rated on a 4-point Likert scale (absent, mild, moderate, or severe).

Results: Odevixibat treatment (40–120 µg/kg/day) was started between 2 and 10 years of age. In the year before starting odevixibat, all patients presented with moderate to severe pruritus despite treatment with rifampicin and ursodeoxycholic acid. Four patients had sleep disturbances. Patient 4 had a history of microvillus inclusion disease and was enterally fed. In the year prior to initiating odevixibat, sBA levels were >150 µmol/L in all patients; total bilirubin levels were >25 µmol/L in 4 patients and <5 µmol/L in Patient 5. In the 3 months after starting odevixibat, sBA levels decreased dramatically (Figure). By 6 months, all patients achieved sBA levels <10 µmol/L and total bilirubin fell to <15 µmol/L. sBA levels remained mostly <10 µmol/L throughout the treatment period (up to 20 months) in 4 patients (Figure). In Patients 3 and 5, compliance and access to treatment were limited, which may explain the fluctuations in sBA levels observed. Pruritus and sleep disturbances improved in the first 3 months and disappeared completely on treatment in all patients (dose increases to 45 µg/kg/day and 65 µg/kg/day were required in Patient 5). In Patients 1 and 3, odevixibat treatment was discontinued following an episode of gastroenteritis associated with a positive test for adenovirus or enteropathogenic *Escherichia coli*. Patient 3 subsequently resumed full-dose odevixibat after 6 weeks of suspension or reduced dosing. Digestive tolerability of odevixibat was good; no new or worsening gastrointestinal symptoms were observed in any child.

Conclusion: Odevixibat treatment in patients with PFIC10 led to a rapid and sustained resolution of pruritus and a significant decrease in or normalisation of sBA levels, supporting the effectiveness of odevixibat. Treatment with odevixibat should be further evaluated in patients with PFIC associated with MYO5B gene mutations.

THU-377

Alkaline phosphatase on admission to the intensive care unit as a new early prognostic biomarker for the development of COVID-19-associated secondary sclerosing cholangitis

Lea Aratari¹, Lea Krauß¹, Vlad Pavel¹, Alexander Mehr¹, Arne Kandulski¹, Karsten Guelow¹, Martina Mueller-Schilling¹, Stephan Schmid¹. ¹University Hospital Regensburg, Department of Internal Medicine I, Gastroenterology, Hepatology, Endocrinology, Infectious Diseases and Rheumatology, Regensburg, Germany
Email: stephan.schmid@ukr.de

Background and aims: In COVID-19, hepatic involvement occurs in up to 53% of patients. Secondary sclerosing cholangitis in critically ill patients (SSC-CIP) is of great importance in the management of critically diseased patients with COVID-19 in the intensive care unit (ICU). In COVID-19 disease cases with SSC-COVID-19-associated SSC-occur. Early detection of this disease and endoscopic treatment is crucial. Therefore, the aim of our study was to identify new and early prognostic biomarkers for developing COVID-19-associated SSC.

Method: 258 patients hospitalized in the ICUs of the University Hospital of Regensburg were analyzed retrospectively. Various clinical, laboratory and intensive care parameters were recorded from the electronic documentation systems. For statistical analyses, IBM SPSS Statistics was used. Receiver operating characteristic (ROC) analysis was conducted, and the area under the curve (AUC) was calculated.

Results: 14 of the 258 patients (5.4%) developed COVID-19-associated SSC during hospitalization in the ICU. 9 of the 14 patients had a high positive end-expiratory pressure (PEEP >10) and were in prone position. In the 9 patients with COVID-19-associated SSC who received Extracorporeal membrane oxygenation (ECMO) therapy, the average duration of ECMO treatment was 55 days. 3 of the 14 patients had a medical history of preexisting liver disease. 8 of the 14 patients survived the hospitalization at the ICU. In the ROC analysis, there was a significant ($p = 0.037$) association between a longer duration of ECMO therapy and the development of SSC. Of note, elevated values of the alkaline phosphatase on admission to the ICU correlated significantly ($p = 0.004$) with the development of COVID-19-associated SSC in the ROC analysis. The area under the curve (AUC) was 0.731.

Conclusion: Elevated alkaline phosphatase on admission was identified as a novel and early prognostic biomarker for the development of COVID-19-associated SSC. Our findings allow optimization of intensive care therapy to reduce the risk of developing COVID-19-associated SSC and early initiation of endoscopic treatment.

THU-378

Outcomes in adult patients with progressive familial intrahepatic cholestasis treated with odevixibat: subgroup analysis from the PEDFIC 2 study

Bertrand Roquelaure¹, Henkjan J. Verkade², Kathleen M. Loomes³, Janis M. Stoll⁴, Christine Clemson⁵, Tao Gu⁵, Jan Mattsson⁵, Philip Stein⁷. ¹CHU, Hospital de la Timone, Marseille, France; ²Department of Paediatrics, University of Groningen, Beatrix Children's Hospital/University Medical Centre Groningen, Groningen, Netherlands; ³Children's Hospital of Philadelphia, Philadelphia, PA, United States; ⁴Department of Paediatrics, Washington University School of Medicine, St. Louis, MO, United States; ⁵Albireo Pharma, Inc., Boston, MA, United States
Email: bertrand.roquelaure@ap-hm.fr

Background and aims: Progressive familial intrahepatic cholestasis (PFIC) is a group of rare genetic liver diseases characterized by cholestasis, pruritus, and progressive liver damage. Symptoms of PFIC typically present in infancy and often progress to end-stage liver disease by early adolescence; however, in some patients, symptom onset may not occur until adulthood. The safety and efficacy of odevixibat, an ileal bile acid transporter inhibitor, was evaluated in patients with PFIC in the phase 3 PEDFIC 1 and PEDFIC 2 studies. To improve our understanding of the effects of odevixibat treatment in adult patients with PFIC, we examined the efficacy and safety of odevixibat in adult patients from PEDFIC 2.

Method: PEDFIC 2 is an ongoing, 72 week, open-label extension study in patients of any age with any type of PFIC; all patients receive odevixibat 120 µg/kg once daily. This analysis includes all adult patients enrolled in PEDFIC 2 and spans from patients' first dose of odevixibat to a data cut-off of 31 January 2022. The following parameters were evaluated: patient-reported pruritus scores (range, 0–4; higher scores indicate worse symptoms), serum bile acid (sBA) levels, hepatic parameters (total bilirubin and alanine aminotransferase [ALT] levels), and treatment-emergent adverse events (TEAEs).

Results: Overall, 5 adult patients with PFIC (mean [range] age, 23.3 [19.5–26] years; 40% female) had enrolled in PEDFIC 2. At baseline, all patients had elevated sBAs and moderate-to-severe pruritus. Of these 5 adult patients, 3 had PFIC1 and 2 had PFIC2. Mean (range) exposure to odevixibat was 36 (24–65) weeks. At the data cut-off, 4 patients were ongoing in the study and 1 patient discontinued the study due to patient withdrawal of consent. From baseline to last assessment, sBA levels varied over time in some patients, but several patients had

Serum Bile Acids, Pruritus, and Hepatic Parameters in Adult Patients With PFIC Treated With Odevixibat

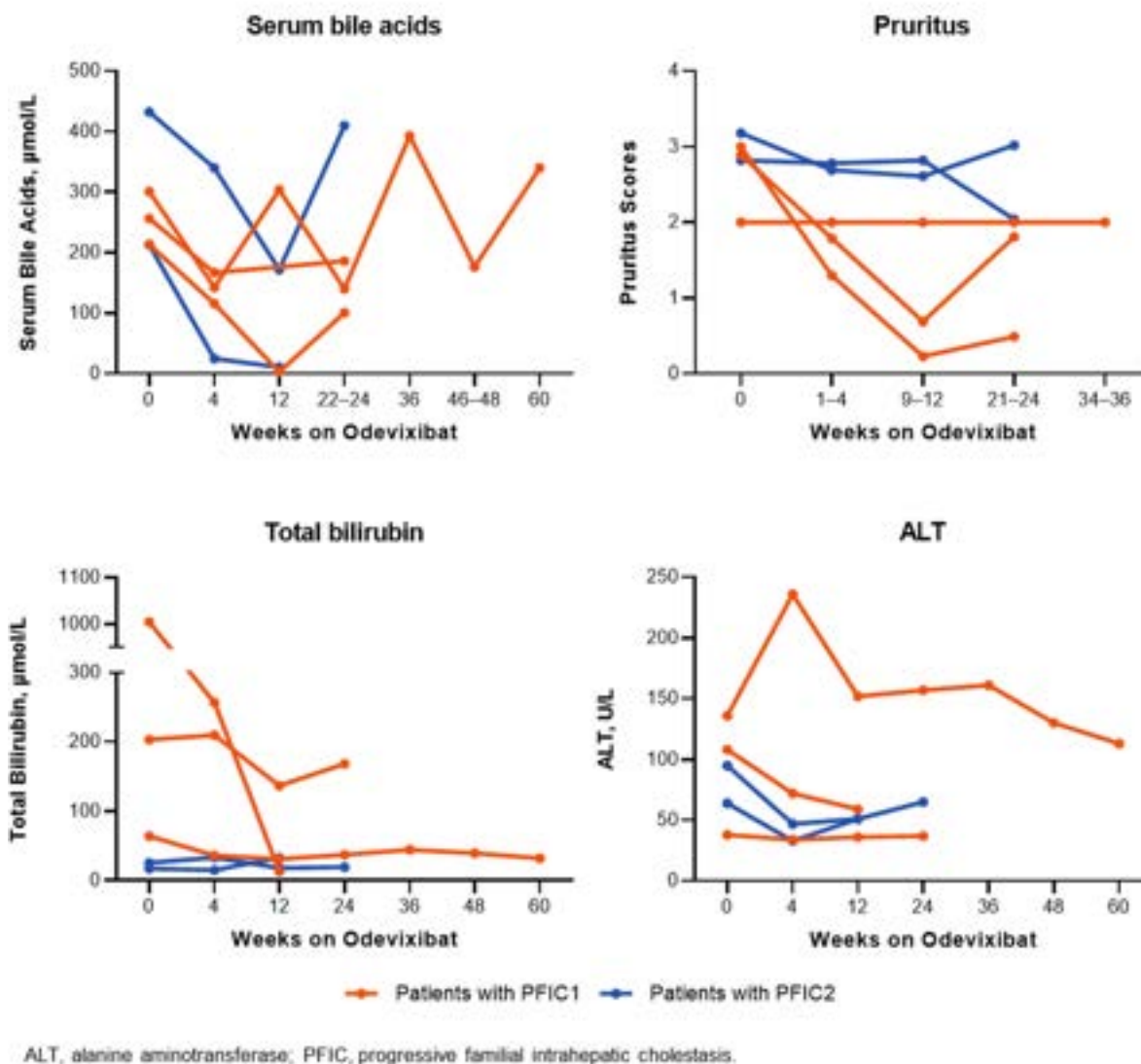


Figure: (abstract: THU-378).

reductions in sBA levels, pruritus scores, total bilirubin levels, and/or ALT (Figure). Three of the 5 patients (60%) had at least 1 TEAE; most were mild to moderate in severity. Two patients experienced a serious TEAE; 1 patient had streptococcal septic arthritis and another patient with a history of pancreatitis experienced acute pancreatitis. None of the TEAEs were considered drug related, and no patient discontinued due to TEAEs.

Conclusion: Several adult patients with PFIC enrolled in the ongoing PEDFIC 2 study have experienced clinical benefits with odevixibat, including reductions in sBAs, pruritus, and/or improvements in hepatic parameters. Odevixibat was generally well tolerated in this adult population.

THU-379

Association of liver injury and prognosis in patients with severe fever with thrombocytopenia syndrome

Rui Huang^{1,2,3}, Jian Wang^{1,2}, Huali Wang⁴, Qun Zhang⁵, Zhiyi Zhang³, Shaoqiu Zhang¹, Yifan Pan⁶, Bei Jia¹, Xiaomin Yan¹, Jie Li^{1,2,3}, Chao Wu^{1,2,3}. ¹Department of Infectious Diseases, Nanjing Drum Tower

Hospital, The Affiliated Hospital of Nanjing University Medical School, China; ²Institute of Viruses and Infectious Diseases, Nanjing University, China; ³Department of Infectious Diseases, Nanjing Drum Tower Hospital Clinical College of Traditional Chinese and Western Medicine, China; ⁴Department of General Practice, Nanjing Second Hospital, Nanjing University of Chinese Medicine, China; ⁵Department of Infectious Diseases, Affiliated Zhongda Hospital of Southeast University, China; ⁶Department of Infectious Diseases, Nanjing Drum Tower Hospital Clinical College of Nanjing Medical University, China
Email: dr.wu@nju.edu.cn

Background and aims: Severe fever with thrombocytopenia syndrome (SFTS) is an epidemic emerging infectious disease caused by a novel bunyavirus with high mortality rate (up to 50%). Liver injury have been reported as a common complication of SFTS patients. However, the prevalence of liver injury related to this disease and its clinical significance is not well characterized.

Method: Two hundred and ninety-one hospitalized SFTS patients were retrospectively included from three hospitals in China between October 2010 and August 2022. Presence of at least one of the

following conditions would be diagnosed as liver injury: alanine transaminase (ALT) or aspartate aminotransferase (AST) more than 3 upper limit of normal (ULN), or alkaline phosphatase (ALP) or total bilirubin (Tbil) more than 2 ULN.

Results: The median age of patients was 63.0 years and male accounted for 51.9%. A total of 65 (22.3%) patients were deceased. 60.1% of patients had liver injury, and the median levels of ALT, AST, ALP, and Tbil at admission were 76.4 U/L, 152.3 U/L, 69.8 U/L, and 9.9 μ mol/L, respectively. Compared to survivors, non-survivors had higher levels of AST (253.0 U/L vs. 131.1 U/L, $p < 0.001$) and ALP (86.2 U/L vs. 67.9 U/L, $p = 0.006$), higher proportion of the elevated ALP (20.0% vs. 4.4%, $p < 0.001$) and liver injury (78.5% vs. 54.9%, $p = 0.001$) at admission. There were increasing trend of ALT, AST, and ALP in non-survivors, while survivors had stable or decrease trend of these parameters during hospitalization. The presence of liver injury (HR 2.015, 95% CI 1.055–3.848, $p = 0.034$) at admission was an independent risk factor of fatal outcome. Patients with liver injury had significant lower cumulative survival probability than patients without liver injury ($p = 0.003$).

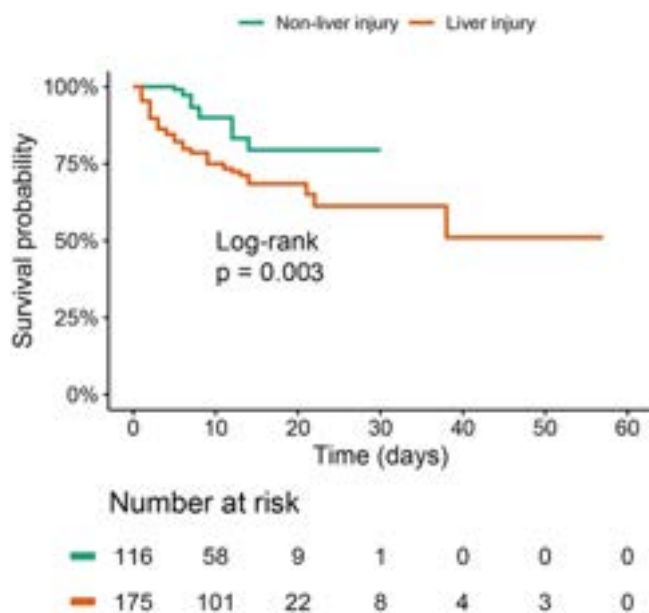


Figure: Cumulative survival probability of SFTS patients with and without liver injury at admission.

Conclusion: Liver injury was common in patients with SFTS. The presence of liver injury is strongly associated with poor prognosis in patients with SFTS, indicating that liver injury indicators should be monitored during hospitalization.

THU-380

State of knowledge of alpha 1 anti-trypsin deficiency among practitioners specialized in liver transplantation in France : a national survey

Manon Evain¹, Ilias Kounis¹, Jérôme Dumortier², Sébastien Dharancy³, Faouzi Saliba¹, Audrey Coilly¹. ¹Hôpital Paul-Brousse Ap-Hp, Villejuif, France; ²Edouard Herriot Hospital, Lyon, France; ³Hospital Claude Huriez, Lille, France
Email: manon.evain@hotmail.fr

Background and aims: Alpha-1 antitrypsin deficiency (AATD) is one of the most common genetic diseases in Europe with a prevalence of heterozygosity of 1.6%. Although it is also responsible for liver damage leading to end stage liver diseases, AATD is not always diagnosed, even in the most severe patients who are candidates for liver transplantation (LT). Considering the recent advances in potential treatment and the understanding of AATD involvement in progression of liver diseases, we aimed to investigate the level of

knowledge on AATD and the current practices of liver transplant physicians in France.

Method: A practice survey of 22 multiple-choice questions in the form of a questionnaire created and distributed via GoogleForm was sent by e-mail to the members of the French think tank in LT, GREF2.

Results: Adherence to the survey was 54%, including 89% hepatologists, 7.5% liver surgeons and 3.5% anesthesiologists. 81% of practitioners rated their level of knowledge as very low, low, or average, and only 22% answered the question of disease prevalence correctly. Half of the responders had >15 years of experience in high-volume LT centers. Only 57% of practitioners routinely performed AATD screening before LT. AAT dosage was used in 97% of cases for the screening but 47% knew that it is decreased by hepatocellular insufficiency and 20% by pregnancy. Only 47% knew that heterozygosity status could be a cofactor of liver disease progression. Furthermore, 62% of practitioners with <5 years of experience considered their level of knowledge to be low but systematically screened before LT in 75% of cases compared to 44% for practitioners with between 5 and 15 years of experience and 61% for practitioners with >15 years.

Conclusion: AATD is a poorly known disease among LT practitioners in France. A better knowledge of screening methods, diagnosis and treatment of the disease would allow a better management of the patients and their relatives.

THU-381

Symptom severity measured by polycystic liver disease-specific questionnaire score partly correlates with both total number of liver cysts and the presence of dominant cysts

Avisnata Das¹, Benjamin Giles¹, Aqeel Jamil¹, Joanna Dowman¹, Andrew Fowell¹, Richard Aspinall¹. ¹Portsmouth Liver Centre, Portsmouth, United Kingdom
Email: avisnata@gmail.com

Background and aims: The polycystic liver disease-specific questionnaire (PLD-Q) has been found to be useful in assessing severity of Polycystic Liver Disease (PLD) related symptoms. The PLD-Q score (from 0 to 100) is based on this questionnaire with higher scores indicating more severe symptoms. PLD-Q score has shown some correlation with PLD disease-severity stage (using Gigot's classification) but not liver volume. Scarce literature exists correlating PLD-Q scores with Qian's Grade of PLD and number of dominant cysts. Here we report variations in PLD-Q scores across Qian's grades 2 to 4 and in patients with varying numbers of dominant cysts.

Method: We evaluated PLD-Q scores in a cohort of 39 fully phenotyped PLD patients in a single centre. Patients had 11 or more liver cysts either as isolated PLD or in conjunction with Polycystic Kidney Disease. We studied PLD-Q scores in three different PLD patient groups classified as per Qian's classification-Grade 2 (11–20 cysts), Grade 3 (>20 cysts) and Grade 4 (>20 cysts with symptomatic hepatomegaly). We also looked at PLD-Q scores in three different patient groups according to number of dominant cysts (size >8 cm) with either zero dominant cyst, 1–2 dominant cysts and 3 or more dominant cysts. Cysts were radiologically evaluated using either CT/MRI/ultrasound scan within 1-year prior to submission of PLD-questionnaire by the patient.

Results: In 7 patients with Qian's Grade 2 disease, the PLD-Q score ranged from 17 to 68 with a mean of 34.7 and median of 33. In 22 Grade 3 patients, PLD-Q score ranged from 6 to 76 with a mean of 32.5 and median of 35. In 10 patients with Grade 4 disease, PLD-Q scores ranged from 31 to 83 with a median of 47 and median of 42.5. However, there was no statistically significant difference between the distributed means of PLD-Q scores within these three groups. (Independent sample t-test, 95% CI). Out of 38 PLD patients with radiologically calculated dominant cyst numbers, 26 had zero dominant cysts (Group A), 10 had 1–2 dominant cysts (Group B) while the remaining two had 3 dominant cysts each (Group C). The mean PLD-Q scores in Groups A, B and C were 36, 44.6 and 33.5

POSTER PRESENTATIONS

respectively while the median scores were 35, 42.5 and 33.5 respectively. No statistically significant difference exists between the distributed means of PLD-Q scores within these groups.

Conclusion: Qian's Grade 4 patients had the highest median PLD-Q score and highest-recorded score of 83 among all grades. Median PLD-score of Grade 3 exceeded that of Grade 2. Patients with 1–2 dominant cysts had the highest mean and median PLD-Q score, suggesting a greater impact on quality of life and supporting targeted intervention. However, there was no statistically significant difference in distributed means of PLD-Q scores between any two groups within the three different Qian's Grade groups or between any two groups within the three dominant cyst numbers-based groups.

THU-382

Online education yields significant gains in gastroenterologists' knowledge of clinical manifestations of Wilson disease

Sukhbir Bahra¹, Adriana Stan¹, Marinella Calle¹, Maya Khalaf¹, Gill Adair¹, Karl Heinz Weiss². ¹Medscape, Education, Netherlands; ²Krankenhaus Salem der Evang. Stadtmission Heidelberg, Germany
Email: astan@medscape.net

Background and aims: WD is a rare disorder in which excessive amounts of copper accumulate in the body, particularly in the liver, brain, and eyes.

We developed an online continuing medical education (CME) activity titled: "Wilson Disease: The Great Masquerader." We hypothesized that participation in this online CME education would lead to improved recognition of the different clinical manifestations of WD.

Method: An online 45 minute video CME activity (www.medscape.org/viewarticle/976141) consisting of a series of 6 expert commentaries was developed. Educational effect was assessed using a

repeated-pair design with pre-/post-assessment (3 knowledge questions and 1 confidence question). A paired samples t-test was conducted for significance testing on overall average number of correct responses and for confidence rating, and a McNemar's test was conducted at the question level (5% significance level). Cohen's d with correction for paired samples estimated the effect size of the education (<0.20 modest, 0.20–0.49 small, 0.59–0.79 moderate, ≥.80 large). Data were collected from 6/30/2022 to 9/30/2022.

Results: A total of 465 gastroenterologists outside US participated, of whom 55 completed all the pre-/post-activity questions. Overall 64% improved their knowledge related to the copper metabolism, clinical manifestations of WD and diagnostic strategies for WD ($p < 0.001$) indicating a considerable effect of the education (Cohen's $d = 0.85$). 4 times more physicians answered all questions correctly after education (9% pre, 47% post). 62% of gastroenterologists had a measurable increase in their confidence in their ability to recognize manifestations of WD in clinical practice.

Conclusion: This online CME activity significantly improved gastroenterologists' knowledge of the clinical manifestations of WD and strategies for timely diagnosis of WD in clinical practice.

THU-383

Progressive familial intrahepatic cholestasis: KFSH and RC

Faisal Abaalkhail¹, Fahad Alsohaibani¹, Musthafa Peedikayil¹, Muath Najmi¹. ¹King Faisal Specialist Hospital and research center, Saudi Arabia
Email: faisal.abaalkhail@gmail.com

Background and aims: Progressive Familial intrahepatic cholestasis (PFIC) is a rare genetic disorder that results from defective mechanisms of bile secretion. There have been no studies describing

Parameter	PFIC 2 (N = 31)	PFIC 3 (N = 49)
Male gender %	51.62	55.10
Age (Mean)	10.2	13.5
Months from birth to diagnosis (Mean)	24.7	82.1
Region%		
Central	33.33	22.45
Eastern	10.00	16.33
Northern	6.67	2.04
Southern	16.67	40.82
Western	33.33	18.37
Positive consanguinity %	89.47	85.71
Family members affected %	52.17	69.57
Jaundice%	61.29	40.82
Pruritus%	41.94	51.02
Failure to thrive%	12.90	8.16
Diarrhea%	6.45	4.08
Splenomegaly%	67.74	61.22
Hepatomegaly%	61.29	59.18

Figure: (abstract: THU-383).

PFIC in Saudi Arabia, Aim: to describe the different types of PFIC and their clinical features, treatment modalities and the outcome in Saudi Arabia.

Method: This is a retrospective study of all patients diagnosed with PFIC at the King Faisal Specialist Hospital and Research Centre in Riyadh from January 1, 2002 to December 31, 2020. All relevant information was

Results: 83 patients were identified with PFIC and type 3 was the commonest (59%), followed by type 2 (37.4%), type 1 (2.4%) and type 4 (1.2%). Males and females were affected equally. Mutation in ATP8B1, ABCB11 and ABCB4 genes were observed in 50% of PFIC type 1, 96% of type 2 and 93% of type 3, respectively. A total of 52 (63.4%) patients underwent liver transplantation; two patients with type 1 (100%), 22/30 (73.3%) with type 2, and 28/49 (57.1%) with type 3. Mean duration of disease before transplantation was 57 ± 71.3 months with a median of 30 months. Following liver transplantation, transplantation, symptomatic control was achieved in 49 patients (94.2%). Recurrence after transplant occurred in 5 (9.61%) patients within average of 41.5 months and a median of 17 months.

Conclusion: PFIC is considered a rare disorder in Saudi Arabia, however early recognition of this disease is important for appropriate management and early referral for liver transplantation evaluation. The overall rate of liver transplantation in our cohort was 63.4% with excellent five-year survival rate.

THU-384

Clinical picture of acute hepatitis in children-single center observations

Anna Mania¹, Paweł Małeck¹, Katarzyna Mazur-Melewska¹, Magdalena Figlerowicz¹. ¹Poznan University of Medical Sciences, Department of Infectious Diseases and Child Neurology, Poznań, Poland
Email: maniaanna@hotmail.com

Background and aims: The aim of the study was to analyze the clinical course and outcome of acute hepatitis in children considering new emerging viral agents.

Method: The study included all children with acute hepatitis admitted to tertiary care centers between 1.10.2021 and 30.11.2022. Clinical data were analysed including potential etiology, clinical and laboratory and imaging tests.

Results: The study included 36 children admitted to the tertiary care center due to acute hepatitis in analysed period. Median (M) age was 13 years (range 3 months-18 years). The most common causing factor was Epstein-Barr virus (EBV) (13/36 cases-13%), autoimmune hepatitis was detected 5/36 children (14%), hemophagocytic lymphohistiocytosis in 3/36 children (8%). SARS-CoV2 infection 2/36 children. Children with EBV-related-hepatitis were older (Median age M = 16 years vs 10 years; $p = 0.0001$) had significantly lower aspartate aminotransferase activity (Median AST M = 121 IU/l) when compared to non-EBV induced hepatitis (Median AST M = 290 IU/l); $p = 0.01$. The majority of children recovered from the infection. One fatal case of unknown etiology was detected.

Conclusion: The most common cause of acute hepatitis was EBV infection of self-limiting course. Certain proportion of patients suffered from life-threatening conditions.

THU-385

Differences in the rates of liver-related clinical events in paediatric patients with alpha-1 antitrypsin deficiency-associated liver disease in the United States

May Hagiwara¹, Victoria Divino², Swapna Munnangi², Mark Delegge², Suna Park¹, Ed G. Marins¹, Kaili Ren¹, Charlton Strange³. ¹Takeda Development Center Americas, Inc., Cambridge, MA, USA, United States; ²IQVIA Inc., Falls Church, VA, USA, United States; ³Medical University of South Carolina, Charleston, SC, USA, United States
Email: ed.marins@takeda.com

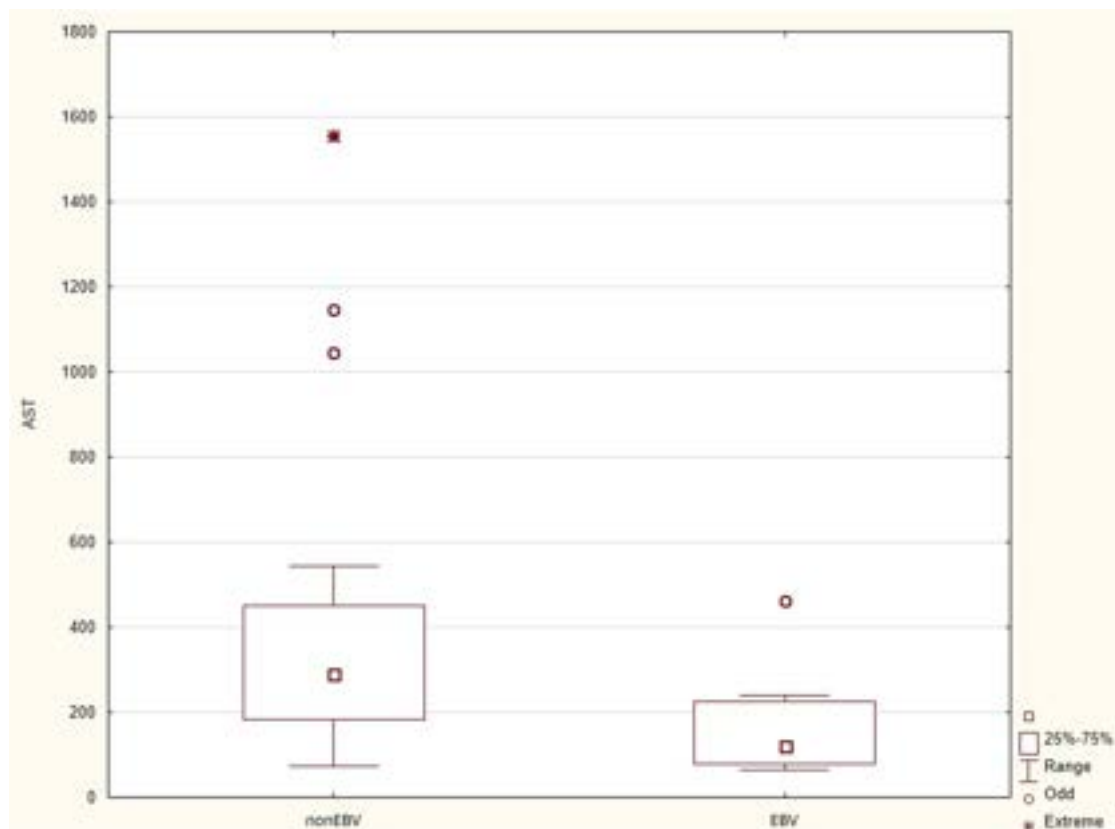


Figure: (abstract: THU-384): Aspartate aminotransferase activity in EBV and non-EBV-related hepatitis.

Figure 1. Liver-related clinical events in the follow-up time of paediatric patients with alpha-1 antitrypsin deficiency-associated liver disease, by age group (event rate per person-year)

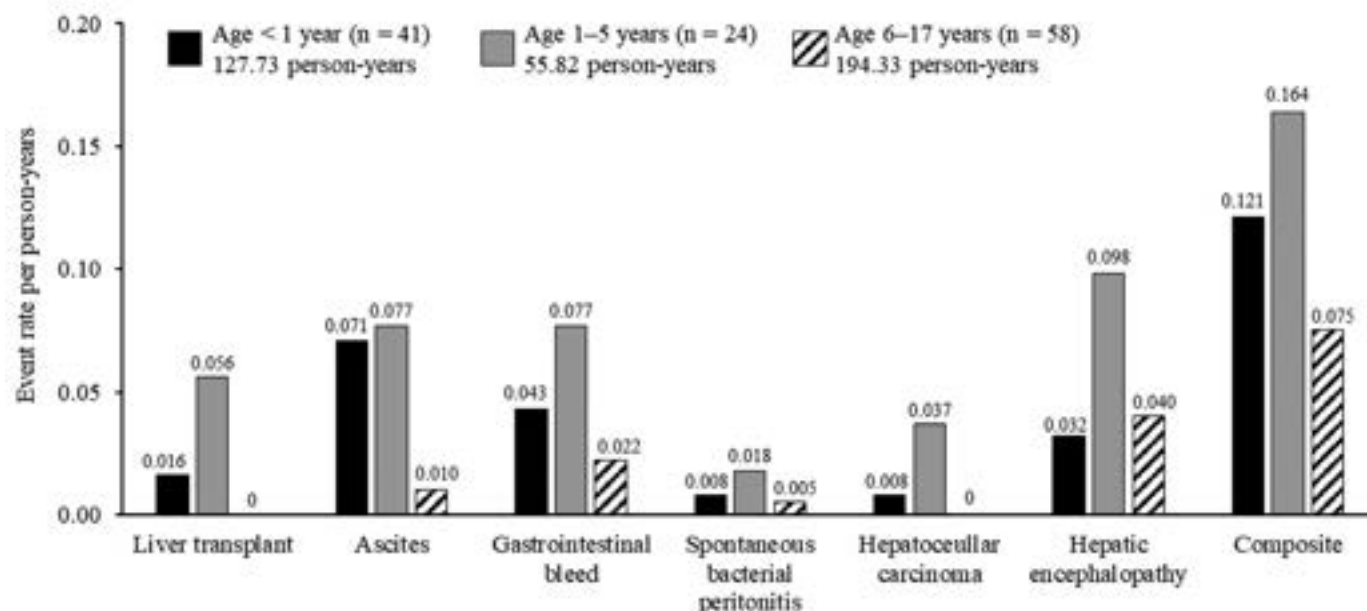


Figure: (abstract: THU-385).

Background and aims: Protease inhibitor (Pi) ZZ genotypes are associated with alpha-1 antitrypsin deficiency (AATD), which affects ~1 per 3000–5000 people in the USA. AATD is characterized by low levels of serum alpha-1 antitrypsin (AAT) and accumulation of misfolded AAT in hepatocytes, which can lead to liver disease in paediatric patients. The burden of liver-related clinical events among paediatric patients with AATD-associated liver disease was investigated by age group using large US claims and Ambulatory Electronic Medical Records (AEMR) databases.

Method: This was a retrospective analysis of administrative claims data from the IQVIA PharMetrics® Plus database linked to the IQVIA AEMR database (selection period: January 2012 to October 2021). PharMetrics Plus comprised 142 million enrollees with medical and pharmacy benefits and ≥1-month enrolment during the selection period. Inclusion criteria were: (1) at least one inpatient or at least two outpatient medical claims ≥90 days apart with a diagnosis of AATD in PharMetrics Plus, or (2) with a PiZZ/PiMZ genotype in AEMR and with linkage to PharMetrics Plus; (3) a liver disease diagnosis. A person-time approach was used to maximize the use of data. Liver-related clinical events of interest (identified by International Classification of Diseases-Ninth/Tenth Revision codes) included liver transplantation, ascites, gastrointestinal bleeds, spontaneous bacterial peritonitis, hepatocellular carcinoma and hepatic encephalopathy. These were evaluated separately and as a composite (defined as the occurrence of ≥1 of the six clinical events), and reported for the overall paediatric population and by age group (<1, 1–5, and 6–17 years).

Results: In total, 123 patients met the eligibility criteria, of whom 41, 24, and 58 were aged <1, 1–5, and 6–17 years, respectively. Median age was 5 years, 60% were male, and the median duration of observation was 31.5 months. Clinical event rates per person-year (PPY) by age group for the liver-related events are shown in Figure 1. Among patients aged <1, 1–5, and 6–17 years, event rates were 0.07, 0.08, and 0.01 PPY for ascites, 0.03, 0.10, and 0.04 PPY for hepatic

encephalopathy, 0.04, 0.08, and 0.02 PPY for gastrointestinal bleeds and 0.02, 0.06, and 0 PPY for liver transplant.

Conclusion: Liver-related clinical event rates were generally similar between paediatric patients with AATD-associated liver disease aged <1 year and 1–5 years. In all age groups, ascites, gastrointestinal bleeds, and hepatic encephalopathy were more common than spontaneous bacterial peritonitis and hepatocellular carcinoma. Liver transplantation was more common in paediatric patients aged 1–5 years than in patients aged <1 year and did not occur in patients aged 6–17 years. Among the study patients, no confirmed PiZZ/PiMZ genotype was identified.

Acknowledgments Writing assistance was provided by Elena Sugrue, PhD, of Oxford PharmaGenesis, Oxford, UK and funded by Takeda Development Center Americas, Inc.

Funding: This study was funded by Takeda Development Center Americas, Inc.

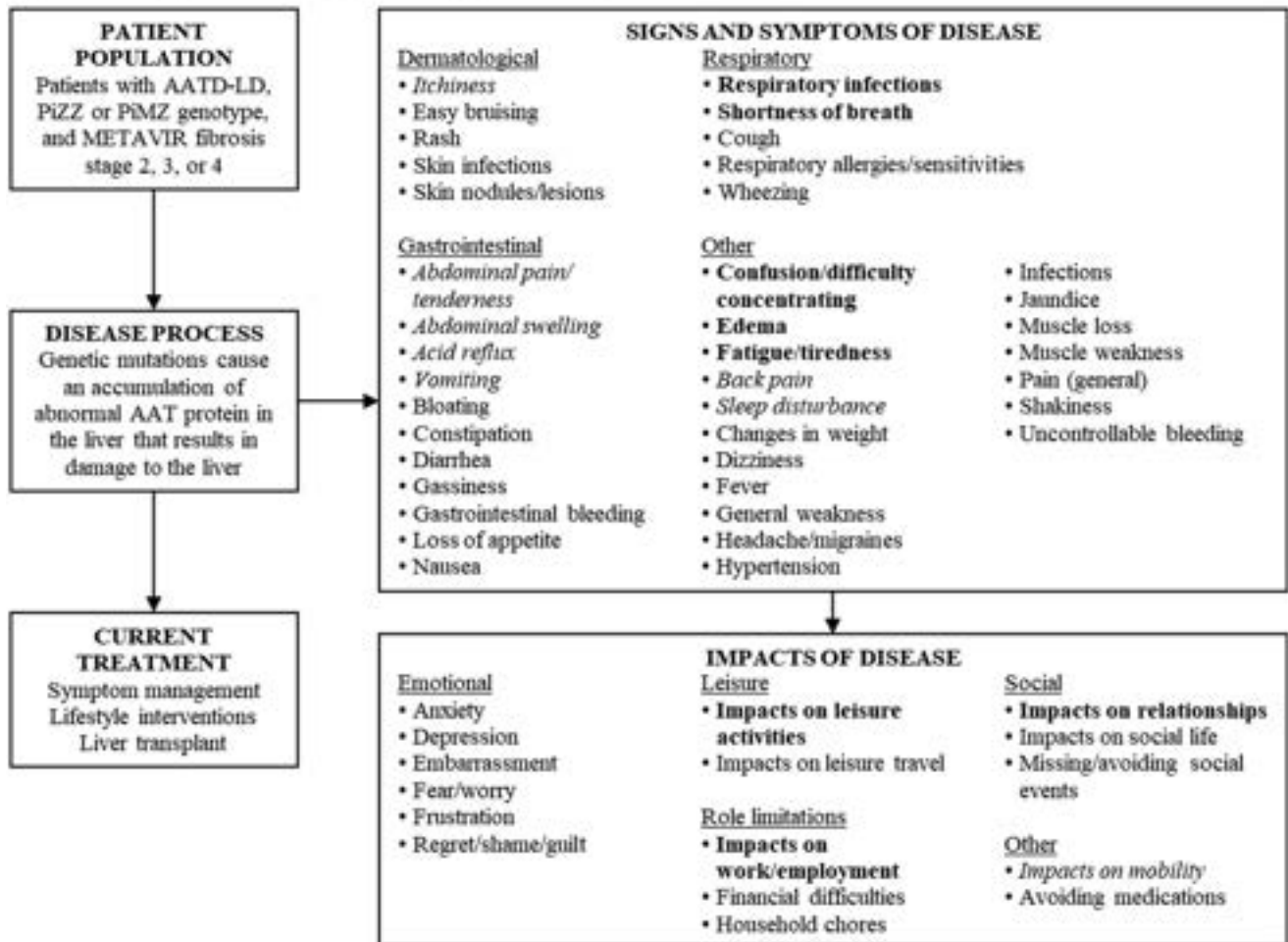
THU-386

Understanding the experience of patients with alpha-1 antitrypsin deficiency (AATD)-associated liver disease

Virginia Clark^{1,2}, Suna Park³, Robert Krupnick⁴, Nicole Sparling⁴, Jason Ritchie⁵, Chitra Karki³, Justin Reynolds⁶. ¹University of Florida, Gainesville, FL, United States; ²University of Florida, Gainesville, United States; ³Takeda Pharmaceuticals USA, Inc, Cambridge, MA, United States; ⁴IQVIA Patient Centered Solutions, Boston, MA, United States; ⁵IQVIA Patient Centered Solutions, New York, NY, United States; ⁶St. Joseph Hospital Medical Center, Phoenix, AZ; Creighton University School of Medicine, Phoenix, AZ, United States
Email: virginia.clark@medicine.ufl.edu

Background and aims: Alpha-1 antitrypsin deficiency (AATD) is a genetic disease that affects ~3.4 million people worldwide and manifests clinically as lung and/or liver disease. This study aimed to elicit characteristics of disease signs, symptoms, and impacts from patient interviews, and inform appropriate selection of clinical outcome assessments.

Figure 1. Conceptual model of alpha-1 antitrypsin deficiency-associated liver disease



Concepts in **bold** were 'most salient', defined as being reported by $\geq 50\%$ of patients and with a mean bothersomeness/disturbance rating of ≥ 5 . Concepts in *italics* were 'highly salient', defined as being reported by $\geq 40\%$ of patients and with a mean bothersomeness/disturbance rating of ≥ 5 .

AATD, alpha-1 antitrypsin deficiency; AATD-LD, alpha-1 antitrypsin deficiency-associated liver disease; METAVIR, Meta-analysis of Histological Data in Viral Hepatitis; Pi, protease inhibitor.

Figure: (abstract: THU-386).

Method: One-to-one telephone interviews involving English-speaking, US adults with AATD-associated liver disease (AATD-LD), with a protease inhibitor (Pi) ZZ or MZ genotype, and without liver cancer were conducted by trained interviewers following a central Institutional Review Board-approved discussion guide. Confirmation of diagnosis was collected for all patients. A preliminary 'concept list' of disease signs, symptoms, and impacts was used to guide the patient interviews and was developed from a targeted literature review, patient blog searches, and clinician interviews with two gastroenterologists, two pulmonologists, and one hepatologist. A conceptual model of AATD-LD was developed based on the findings. Symptoms and impacts of AATD-LD were considered most salient/highly salient if reported by $\geq 50\%/ \geq 40\%$ of patients with a mean bothersomeness/disturbance rating of ≥ 5 on a 0–10 scale (0, not at all bothersome/disturbing; 10, extremely bothersome/disturbing).

Results: Interviews were conducted with 15 patients (male: $n = 8$) with a median (range) age of 57 (28–78) years. Twelve patients had PiZZ and three patients had PiMZ genotypes. METAVIR stages were F2

($n = 6$), F3 ($n = 1$), and F4 ($n = 8$). Eight patients had liver and lung disease; seven had liver disease only. Median time since AATD diagnosis was 12 years. Four patients had received a transplant (liver, $n = 3$; lung, $n = 1$). Of the 41 symptoms reported, the most salient were fatigue/tiredness ($n = 14$), respiratory infections ($n = 10$), shortness of breath ($n = 10$), confusion/difficulty concentrating ($n = 8$), and edema ($n = 8$; Figure 1). Highly salient symptoms were abdominal swelling ($n = 7$), acid reflux ($n = 7$), sleep disturbance ($n = 7$), vomiting ($n = 7$), abdominal pain/tenderness ($n = 6$), itchiness ($n = 6$), and back pain ($n = 6$). The most salient impacts were on work and employment, leisure activities, and relationships. Impacts on mobility ($n = 6$) were highly salient. Overall, emotional impacts were relatively disturbing (mean disturbance rating: 6.3), but each individual impact was reported by few patients.

Conclusion: To our knowledge, this is the first qualitative study of the experience of patients with AATD-LD. Although experiences varied, several concepts were frequently reported and characterized as moderately/highly bothersome/disturbing, even in patients with

POSTER PRESENTATIONS

earlier fibrosis stages which are presumed to be asymptomatic. Clinical outcome assessments that can capture salient concepts are needed to assess the nuances of each patient's experience.

Acknowledgments: Writing assistance was provided by Matthew Reynolds of Oxford PharmaGenesis, Oxford, UK and funded by Takeda Development Center Americas, Inc.

Funding: This study was funded by Takeda Development Center Americas, Inc.

THU-387

Acute liver failure due neonatal hemochromatosis: case with fatal outcome despite early diagnosis and treatment

Liudmyla Shostakovych-Koretska¹, Viktor Mavrutenkov¹, Tetyana Mavropulo². ¹Dnipro State Medical University, Infectious Diseases, Dnipro, Ukraine; ²Dnipro State Medical University, Neonatological, Dnipro, Ukraine
Email: vvmavr@gmail.com

Background and aims: Neonatal hemochromatosis is a very rare, often fatal, iron metabolism disorder in newborns, which is characterized by iron overload of the liver and the development of antenatal acute liver failure. Neonatal hemochromatosis differs from hereditary, although both diseases have similar disorders of iron metabolism. Hereditary hemochromatosis is an autosomal recessive disease while Neonatal hemochromatosis is gestational alloimmune liver disease. The purpose of this study was to show the need to consider the possibility of hemochromatosis diagnosis in all cases of neonatal liver injury.

Method: A descriptive analysis of the features of the presentation and differential diagnosis of neonatal hemochromatosis that developed within the first day after the birth of a child using a wide range of diagnostics and modern approaches to treatment.

Results: The patient (girl) was born from the 2nd pregnancy, 38 weeks of gestation, weight 3500 g, length 55 cm, Apgar score 8 points. The first pregnancy ended in a spontaneous abortion. The girl was on a joint stay with her mother for 13 hours. Then the newborn suddenly had respiratory arrest, cardiac depression, convulsions. In the intensive care unit, the child had signs of acute liver failure with

severe jaundice, hepatosplenomegaly, hemorrhagic, hepatorenal syndrome. Laboratory investigation revealed anemia, leukocytosis, thrombocytopenia, hypoglycemia, hypoalbuminemia, moderate increase transaminases, hyperbilirubinemia 343 mg/dl with the predominance of the direct fraction, severe coagulopathy. There were no data on the incompatibility of maternal and fetal blood types. Differential diagnostics was carried out with viral hepatitis, neonatal hepatitis, herpesvirus, congenital pathology of the biliary system, neonatal sepsis. Plasma Ferritin level 6713 ng/ml was very high compare with the normal level. A high level of ferritin was also confirmed during a second study which, after excluding other causes, made it possible to suspect neonatal hemochromatosis. An liver biopsy revealed giant cell transformation of hepatocytes without specific inclusions. The therapy included antibiotics, fresh frozen plasma, albumin, exchange transfusion session followed by intravenous immunoglobulin. After the therapeutic measures the child's condition showed a short-term improvement, but Ferritin level remained high and the subsequent deterioration was accompanied by the progression of multiple organ disorders, which led to the child death at the age of 40 days. Autopsy revealed hepatosplenomegaly, severe jaundice and hemorrhagic syndrome. Histopathology revealed pathognomonic inclusions of hemosiderin in the liver, kidneys and lungs.

Conclusion: Due to the non-specificity of the first symptoms, neonatal hemochromatosis seems to be one of the most difficult for the differential diagnosis of diseases of the neonatal period. According to reports in one third of cases, mothers have a history of miscarriages with an unknown cause of death. In the presented case, a previous pregnancy ended with spontaneous abortion, which may also be related to these mechanisms. In the reported case, the disease manifested itself in the first hours after birth with rapid progression to fatal liver failure. In real practice, it is necessary to include neonatal hemochromatosis in the differential diagnosis in all cases of severe liver damage, any cases of spontaneous abortion, stillbirth or early postnatal death.

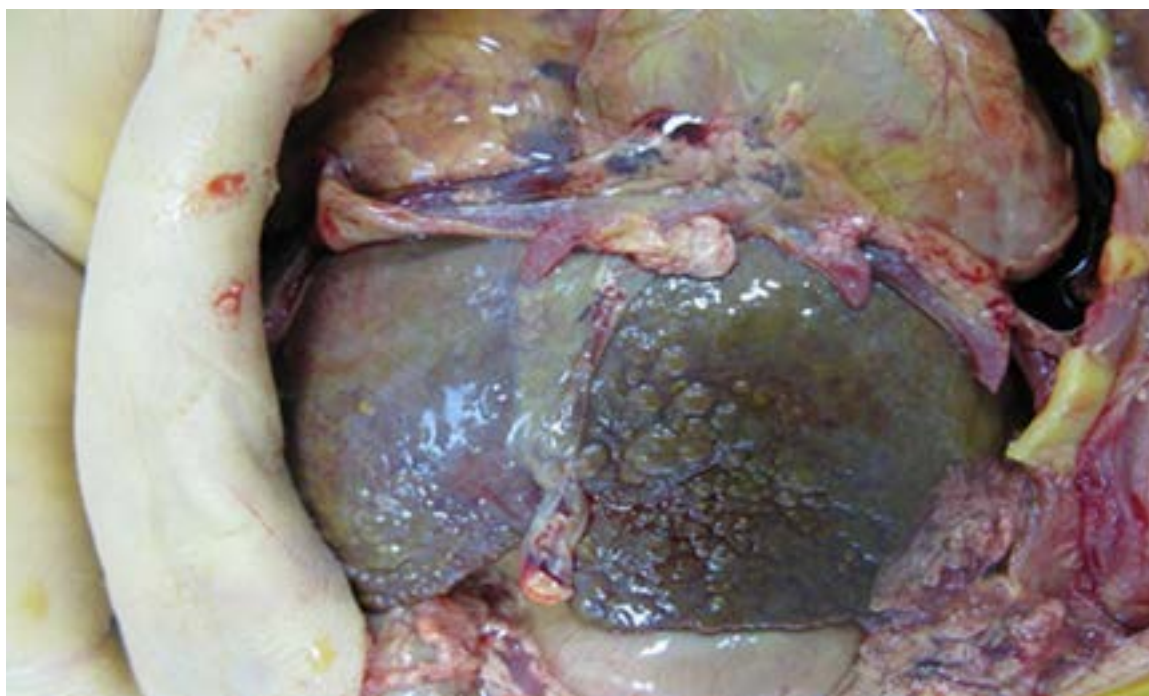


Figure: (abstract: THU-387).

THU-388

Trans-jugular intrahepatic Porto-systemic shunt for Budd Chiari syndrome: single center experience

Amnah Alhanaee^{1,2}, Hamad Alsuhailani¹, Faisal Joueidi³, Ali Albenmoussa¹, Ahmad Elhassan⁴, Abdullah asir⁴, Ahmed Joueidi³, Saad Alghamdi¹, Waleed Alhamoudi¹, Saad Abualghannam¹, Dieter Clemens Broering¹, Khalid Bzeizi¹. ¹King Faisal Specialist Hospital and Research Centre, Riyadh, Saudi Arabia; ²Tawam Hospital, أبو ظبي, United Arab Emirates; ³AlFaisal University, Riyadh, Saudi Arabia, Saudi Arabia; ⁴Alfaisal University, Riyadh, Saudi Arabia
Email: amnahalhanaee@gmail.com

Background and aims: Budd-Chiari syndrome (BCS) is a rare and life-threatening disorder secondary to hepatic venous outflow obstruction. It has a significant mortality rate if untreated. The management differs depending on the clinic presentation and usually follows a step-wise approach. Anticoagulation medication may be the only option, however interventional radiology procedures such as the trans-jugular intrahepatic portosystemic shunt (TIPS) and, if necessary, liver transplantation are lately widely applied. TIPS is regarded a relatively safe and effective treatment. We aimed to evaluate the feasibility and safety of TIPS in the management of BCS in Saudi Arabia

Method: All BCS patients presented to King Faisal Specialist hospital and Research Center and had TIPS during the period January 2010 and November 2022 were included in the analysis. The Aetiology, clinical presentation, laboratory and radiological parameters were all included. All patients underwent surveillance for hepatocellular carcinoma.

Results: A total of 71 patients, mostly females (63.3%) were included in the analysis. The mean age at the onset of symptoms was 38 years (range 19–69 years). Abdominal pain and jaundice were the most common presentations (87.3%). Proteins C and S deficiencies were identified in 31 patients (46.6%), JAK2 mutation in 25 patients (35.2%) and Anti Phospholipid Syndrome in 13 patients (18.2%). The mean MELD score was 19 (range: 8–36) and most patients had Child-Pugh score \geq B (56.3%). BCS confirmation was made by doppler ultrasonography and cross-sectional abdominal imaging in all patients. All patients received anticoagulants pre and post TIPSS. None of the patient died post TIPSS. TIPSS revision was performed on 47 patients (52.8%) and 6 patients (12.7) had more than 10 revisions.

Conclusion: TIPS is an effective modality of treatment for this uncommon condition. Morbidity due to TIPSS failure was relatively low in our cohort. TIPSS occlusion and the need for repeat revisions was the main limitation.

THU-389

The ancestral haplotype HLA-A3 does not influence the likelihood of advanced hepatic fibrosis or cirrhosis in C282Y homozygous hemochromatosis

John Olynyk^{1,2,3,4}, Louise Ramm⁵, Richard Grainger², Helen Currie², Grant Ramm⁵. ¹Edith Cowan University, Medical and Health Sciences, Joondalup, Australia; ²Fiona Stanley Hospital, Murdoch, Australia; ³Curtin University, Bentley, Australia; ⁴Curtin University, Medicine, Bentley, Australia; ⁵QIMR Berghofer Medical Research Institute, Herston, Australia
Email: john.olynyk@health.wa.gov.au

Background and aims: Advanced hepatic fibrosis occurs in up to 25% of individuals with C282Y homozygous hemochromatosis as a result

of progressive iron overload. The aim of the current study was to determine whether human leukocyte antigen (HLA)-A3 haplotypes act as genetic modifiers of the likelihood of advanced hepatic fibrosis. **Method:** Between 1972 and 2013 291 HFE C282Y homozygous individuals underwent clinical and biochemical evaluation, liver biopsy for fibrosis staging and phlebotomy treatment. Of these 133 also underwent HLA typing. Hepatic fibrosis was graded using the system of Scheuer as F0-2 (low grade fibrosis), F3-4 (advanced hepatic fibrosis), and F4 cirrhosis. We analysed the association between the severity of fibrosis and HLA-A3 homozygosity, HLA-A3 heterozygosity or absent HLA-A3 haplotype using categorical analysis.

Results: The mean age of HLA-A3 homozygotes (15 male, 9 female), heterozygotes (43 male, 22 female) and HLA-A3 null individuals (34 male, 10 female) was 40 years. There were no significant differences between the groups for mean (\pm SEM) serum ferritin levels (1320 ± 296 , 1217 ± 124 , 1348 ± 188 ug/L), hepatic iron concentration (178 ± 26 , 213 ± 22 , 199 ± 29 umol/g), mobilizable iron stores (9.9 ± 1.5 , 9.5 ± 1.5 , 11.5 ± 1.7 g iron removed via phlebotomy), frequency of advanced hepatic fibrosis (5/24[12%], 13/63[19%], 10/42[19%], $p = 0.751$) or cirrhosis (3/24[12%], 12/63[21%], 4/42[24%], $p = 0.922$), respectively.

Conclusion: HLA-A3 is not associated with the risk of liver biopsy-proven advanced hepatic fibrosis or cirrhosis in HFE C282Y homozygous haemochromatosis.

THU-390

Demographics, outcomes, and costs of Wilson's disease hospitalizations: a nationwide cohort study

Ankoor Patel¹, Matthew Pelton¹, Carlos Minacapelli², Carolyn Catalano², Vinod Rustgi². ¹Rutgers-Robert Wood Johnson Medical School, Medicine, United States; ²Rutgers-Robert Wood Johnson Medical School, Gastroenterology and Hepatology, United States
Email: ahp60@rwjms.rutgers.edu

Background and aims: Wilson's disease (WD) is a rare, autosomal recessive disorder. Current treatment is focused on chelators and copper antagonists. Data on hospitalization, outcomes, and costs in patients with WD are scarce. Using the National Inpatient Sample (NIS), our study evaluated mortality, length of stay (LOS), and costs among patients with Wilson's Disease in the USA.

Method: We performed a retrospective cohort study using the National Inpatient Sample (NIS) from 2007 to 2017. Wilson's Disease patients were identified using ICD-9/10 codes. Mortality, LOS and costs were primary outcomes. A Charlson Comorbidity Index (CCI) score was calculated for each participant using admission records.

Results: Of the 16,950 WD hospitalizations included, a majority were female (57.01%). Liver failure was diagnosed in 4.93%. The prevalence of depression was 2.01%. The mortality rate and mean LOS were 2.49% and 4.81 days, respectively. The average cost of hospitalization was \$33,483; however, total charges ranged from \$696 to \$1,673,546. The number of hospitalizations with a primary diagnosis of WD peaked in 2010 followed by a gradual decrease in number of hospitalizations between 2011 and 2016.

Conclusion: Our study shows clinical characteristics and outcomes of patients with Wilson's Disease in the USA from an inpatient healthcare database. The risk of liver failure was low. Patients with WD are responsible for significant healthcare cost burden with a wide variation likely due to orthotopic liver transplant.

POSTER PRESENTATIONS

Weighted Summary Statistics for Wilson's Disease Patients in NIS 2007-2017	
Study Measure	Total Weighted Sample (n =16950)
DEMOGRAPHICS	
Age	
Range	18 - 90
Mean (SD)	60.31 (45.42)
Median [IQR]	63 [45, 77]
Age Category, n (%)	
18-34	2655 (15.66)
35-44	1465 (8.64)
45-54	1995 (11.77)
55+	10835 (63.92)
Sex, n (%)	
Male	7285 (42.99)
Female	9660 (57.01)
COMORBIDITIES	
Acute hepatitis, n (%)	180 (1.06)
Cirrhosis, n (%)	2315 (13.66)
Liver Failure, n (%)	835 (4.93)
Jaundice, n (%)	315 (1.86)
Portal Hypertension, n (%)	1535 (9.06)
Depression, n (%)	340 (2.01)
Kayser-Fleischer Rings, n (%)	180 (1.06)
Mild Liver Disease, n (%)	1140 (6.73)
Moderate to Severe Liver Disease, n (%)	1770 (10.44)
PRIMARY OUTCOMES	
Mortality/Patient Death, n (%)	420 (2.49)
Length of Stay (days)	
Range	0 - 96
Mean (SD)	4.81 (0.10)
Median [IQR]	3 [2, 5]
Total Charges (dollars)	
Range	\$696 - \$1,673,546
Mean (SD)	\$33,483 (\$1,073.86)
Median [IQR]	\$18,578 [\$10, 832, \$35, 664]

Figure: (abstract: THU-390): Outcomes of CDI in Patients with NASH, NAFLD, and without NAFLD/NASH.

THU-391

Proteomics for the study of biomarkers in Wilson's disease

Li Li¹, Jie Su^{1,1}, Amina Abudzi^{1,1,1}, Rui Hua^{1,1}. ¹The First Hospital of Jilin University, China

Email: huar@jlu.edu.cn

Background and aims: Wilson's disease (WD), also known as hepatolenticular degeneration, is an autosomal recessive genetic disease caused by ATP7B gene mutation resulting in abnormal copper metabolism and corresponding organ damage. The clinical manifestations are complex and diverse, and genetic, gender, age and other factors make the diagnosis of the disease more difficult. The current

diagnostic methods for WD still have some shortcomings: the determination of ceruloplasmin level, 24-hour urinary copper and hepatic copper is easily affected by other factors; Genetic testing is expensive. Therefore, it is particularly important to explore more sensitive and specific markers for the diagnosis of this disease. This study aims to use proteomics tools to search for potential markers of WD and provide diagnostic basis for WD.

Method: We used quantitative proteomics studies to reveal differentially expressed proteins (DEPs) between 20 WD subjects and 10 healthy controls. Then, we used gene ontology (GO), KEGG and other methods to enrich and cluster the differential proteins, so as to obtain

the signal pathway of significant changes in the differential proteins. Aiming at the differential proteins in the signaling pathway, relevant literature was searched to further clarify the relationship between their biological effects and WD, and explore the potential markers of WD.

Results: Angiotensin, lysosome and TNF signaling pathways. A search of relevant literature found that cathepsin A (CTSA), intercellular adhesion molecule 1 (ICAM1), vascular cell adhesion molecule 1 (VCAM1) and matrix metalloproteinase 9 (MMP9) were significantly correlated with the onset of WD, which may be potential markers of WD.

Conclusion: We preliminarily found that CTSA, ICAM-1, VCAM1 and MMP9 could be used as potential markers of WD by proteomics, which still needs further study.

THU-392

Emphysematous pancreatitis: a sporadic sequela of necrotizing pancreatic infections

Audrey Fonkam¹, George Garriss¹. ¹Wellstar Kennestone Hospital, United States

Email: fonkamaudrey@gmail.com

Background and aims: Emphysematous pancreatitis (EP) is a rare, life-threatening complication of acute necrotizing pancreatitis. EP is associated with various forms of bacteria including gas-forming organisms such as *Escherichia coli* and *Clostridium perfringens*. An abdominal CT is the imaging of choice given its high sensitivity and specificity when gas is seen within or around the pancreatic parenchyma. We present a case of this rare condition that was successfully treated.

Method: A 64 year old male with a history of CAD, HFrEF, type 2 diabetes mellitus, peripheral vascular disease, hyperlipidemia, essential hypertension, and alcohol and tobacco use presented with one-day history of sudden onset, 5/10 sharp, epigastric abdominal pain that radiated to his back and which began after eating an omelet. The pain was worsened by inspiration. Associated symptoms included nausea and vomiting. He denied any fever, chills, constipation, diarrhea or any other symptoms. On exam, his temperature = 99.8o F, pulse = 119 bpm, Bp = 123/78 mm Hg, RR = 18 bpm, and SpO2 = 94% on room air. Abdominal exam was notable for a non-distended abdomen with normoactive bowel sounds. The abdomen was soft with epigastric tenderness to palpation; there was no guarding or rebound tenderness. Pertinent laboratory studies included: WBC = 7.43×10^9 , lipase = 793 U/L, aspartate transaminase = 60 IU/L, alanine transaminase = 102 IU/L, and total bilirubin = 2.4 mg/dL. CT of the abdomen and pelvis with IV contrast showed interstitial edema with hypoenhancement throughout the pancreas and peripancreatic free fluid with gas surrounding the pancreas extending into the retroperitoneum. These findings were suggestive of either an acute gastric ulcer perforation, a fistula, or EP. The patient was admitted, kept N.P.O., and started on intravenous fluids and broad-spectrum antibiotics.

Because of the concerns about a possible fistula, the patient underwent a CT of the abdomen with oral contrast and an EGD; neither study supported the diagnosis of fistula or perforation.

Results: Blood cultures grew *Proteus Mirabilis* and *Escherichia Coli*. Subsequent imaging demonstrated the progression of extraluminal gas and fluid extending between the pancreas and stomach, which developed into a partially-loculated fluid and gas collections in the lesser sac and greater curve of the stomach. These findings were consistent with the diagnosis of EP with possible pseudocyst. The patient completed a course of IV meropenem and had a drain placed by Interventional Radiology which continued to have high volume output throughout his admission. He ultimately required surgical drainage of his abscess, but eventually made a full recovery.

Conclusion: Due to the rarity of this condition, EP is infrequently described in literature, making its diagnosis and management challenging. An interdisciplinary approach between internal medicine, radiology, gastroenterology, and surgery teams is key for successful treatment of these patients.

Viral Hepatitis Experimental and pathophysiology

WEDNESDAY 21 TO SATURDAY 24 JUNE

TOP-102

Proteomics analysis of HBV cccDNA-bound proteins for therapeutic targeting in liver biopsies from hepatitis B patients

Purnima Tyagi¹, Jitendra Kumar¹, Shiv Kumar Sarin², Vijay Kumar¹.

¹Institute of Liver and Biliary Sciences, Molecular and cellular medicine, New Delhi, India; ²Institute of Liver and Biliary Sciences, Department of Hepatology, New Delhi, India

Email: vijaykumar98@gmail.com

Background and aims: There is a growing need to investigate new therapeutics that could target the hepatitis B virus (HBV) reservoir, the cccDNA, since its silencing may facilitate a functional cure for chronic hepatitis B. (CHB). Present study aims to examine the potential roles of cccDNA-bound proteins in HBV reactivation, silencing and contribution to viral replication in the progression of the infection. Identification of cccDNA-bound proteins in both HBeAg-positive (high replicating group) and HBeAg-negative patients (Low replicating group) may aid in better management of HBV patients.

Method: A total of (n = 14) liver biopsies from chronic hepatitis B patients were collected and were sub-grouped on basis of HBeAg

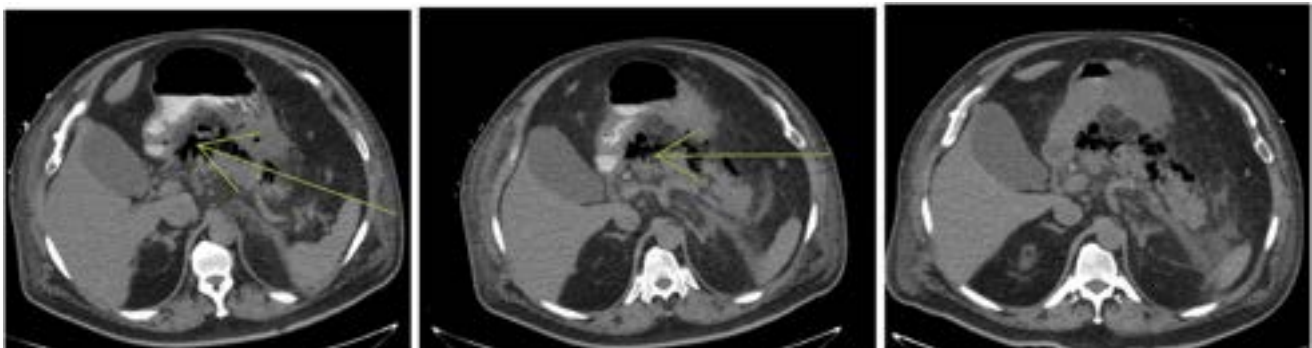


Figure: (abstract: THU-392).

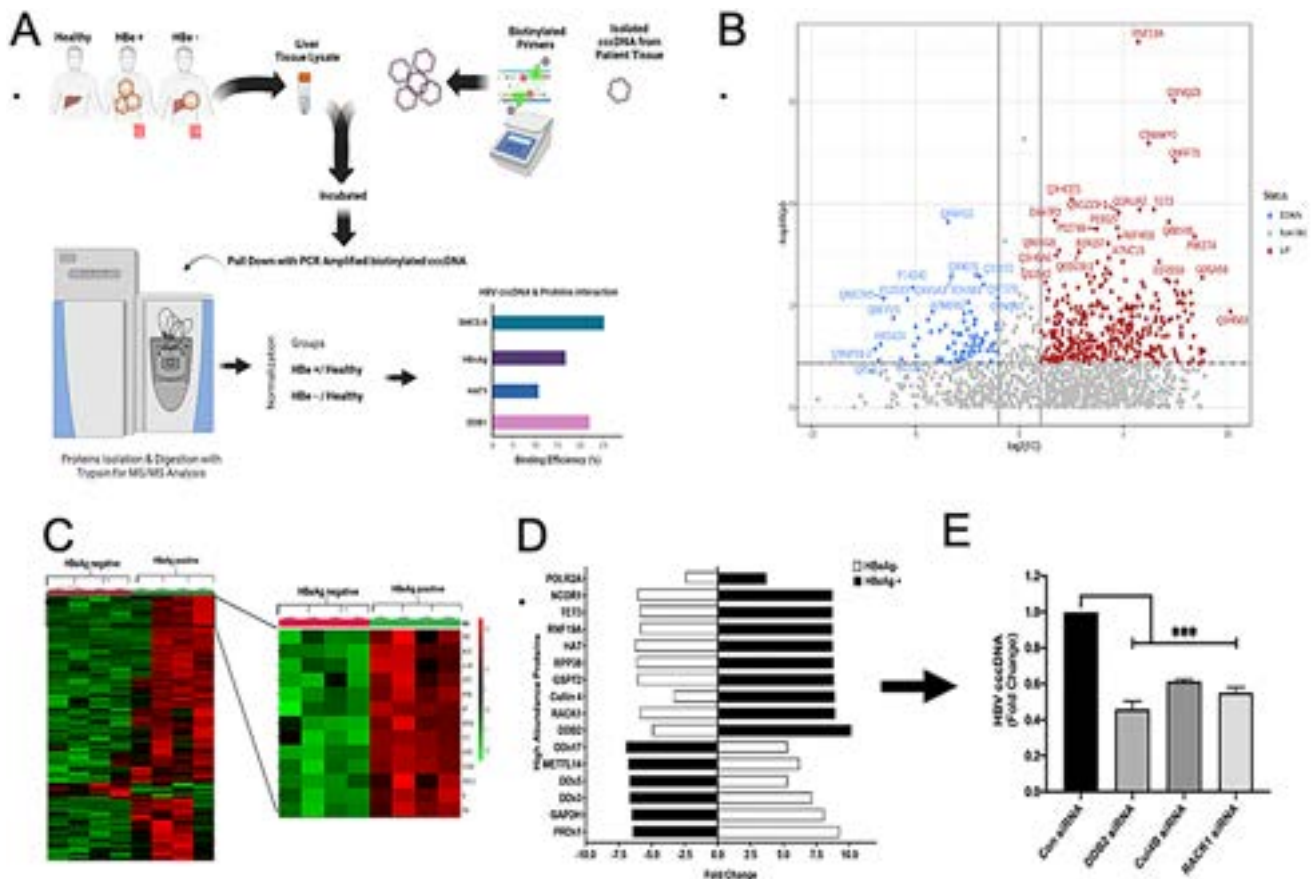


Figure: (abstract: TOP-102): Characterization and identification of HBV cccDNA bound proteins. Illustration of the details study design (A). Volcano plot of the 1350 proteins identified by LC-MS/MS. It shows the fold-change (x-axis) versus the significance (y-axis) of the identified 1350 proteins. The significance (non-adjusted p value) and the fold-change are converted to $-\text{Log}_{10}$ (p value) and Log_2 (fold-change) (B). Heat map of HBeAg positive and HBeAg negative liver biopsies identified proteins in hepatitis B (C). HBV cccDNA bound proteins shown in fold change (D). HBV cccDNA levels after knockdown of selected proteins by using siRNAs in HepG2.2.15 cell lines (E).

negative ($n = 7$) and HBeAg positive ($n = 7$) serum HBsAg positive [\log_{10} IU/ml 3.21 ± 1.09 >6 months] and serum HBV DNA [\log_{10} IU/ml 4 ± 1.09]. Biotinylated DNA oligo complementary to the single stranded region of HBV cccDNA was synthesized. The pull down assay was used to extract cccDNA together along with the binding proteins from both the HBeAg+ and HBeAg- patient's liver tissues, further analysed by nano liquid chromatography coupled with mass spectrometry (nano LC/MS). HepG2.2.15 (with stably integrated HBV genome) was used for the in vitro knockdown studies. After 72 hours of knockdown, the cccDNA levels and the expression pgRNA and HBe and HBsAg proteins were measured by RT-qPCR and ELISA respectively.

Results: cccDNA and the bound proteins were subjected for proteomics analysis. Interestingly, in the HBeAg+, we found total 300 bound proteins significantly upregulated (≥ 2 -fold) and 900 down-regulated (≤ 0.5 -fold). [Culin 4B, RACK1 (Receptor of activated protein C kinase 1), DDB2 (DNA damaging binding protein 2)] significantly upregulated (≥ 2 -fold) and [repressor bound proteins DDx17, DDx5, METTL4 and PRDX1] (≤ 0.5 -fold) were downregulated. We selected top three proteins for knockdown of DDB2, RACK1 and Cul4B using siRNA in vitro (HepG2.2.15) and found the above proteins directly correlated with the expression of HBV parameters like HBsAg ($p < 0.001$), HBeAg ($p < 0.001$), pgRNA ($p < 0.005$), HBV Dna ($p < 0.005$) and cccDNA ($p < 0.005$)

Conclusion: We found cccDNA-bound proteomes correlated with viral load in different patient groups. DDB2, Cul4B and RACK1 were identified as novel nuclear cccDNA-bound proteins in high viral replicating group followed their validation by reduction of cccDNA levels by knockdown. This study provides new insights into the molecular status of cccDNA and potential antiviral targets and for the treatment prognosis of hepatitis B.

TOP-104

The TLR8 agonist Selgantolimod modulates Kupffer cell differentiation status and indirectly impairs HBV entry into hepatocytes via an IL-6-dependent mechanism

Armando Andres Roca Suarez^{1,2}, Marie-Laure Plissonnier^{1,2}, Xavier Grand^{1,2}, Maud Michelet^{1,2}, Guillaume Giraud^{1,2}, Simon Fletcher³, Michel Rivoire⁴, Barbara Testoni^{1,2}, Massimo Levrero^{1,2,5}, Fabien Zoulim^{1,2,5}. ¹INSERM U1052, CNRS Umr-5286, Cancer Research Center of Lyon (CRCL), Lyon, France; ²University of Lyon, Université Claude-Bernard (UCBL), Lyon, France; ³Gilead Sciences Inc., 324 Lakeside Dr., Foster City, CA, 94404, United States; ⁴INSERM U1032, Centre Léon Bérard (CLB), Lyon, France; ⁵Hospices Civils de Lyon (HCL), Lyon, France
Email: fabien.zoulim@inserm.fr

Background and aims: Chronic HBV infection affects close to 300 million people worldwide and is one of the major etiologies for the development of cirrhosis and hepatocellular carcinoma. In spite of universal vaccination programs, HBV is still a global burden due to the limited therapeutic options available. Thus, achieving the goal of HBV cure will require a continuous effort in the development of new molecules and combination therapies. In this regard, the TLR8 agonist Selgantolimod (SLGN) has shown promising results during its clinical evaluation as an immunomodulatory agent against HBV. Although the effect of SLGN has been explored in the peripheral immune compartment, little is known regarding its intrahepatic response. Therefore, we aimed to characterize the transcriptomic changes and intercellular communication events associated with the action of SLGN in the liver microenvironment.

Method: We analyzed publicly available single-cell RNA-seq (scRNA-seq) data in order to identify *TLR8*-expressing cell types in the human liver and established a method for their isolation. We characterized the transcriptomic and cytokine profiles of this population in response to SLGN. The indirect effect of SLGN was evaluated by RNA-seq in primary human hepatocytes (PHH) treated with SLGN-conditioned media (CM) and the quantification of viral parameters following HBV infection. Identified signaling pathways mediating this effect were validated by the analysis of liver transcriptomic data from HBV-infected patients.

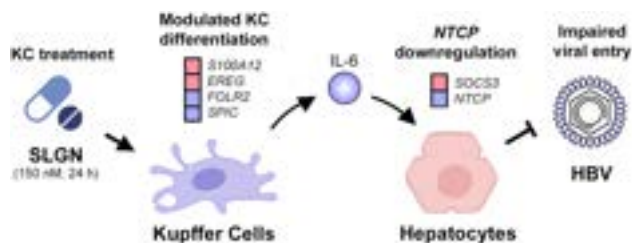


Figure:

Results: Our analysis determined that *TLR8* is primarily expressed in the myeloid compartment of the liver. Therefore, we optimized a method for the isolation of Kupffer cells (KCs) from human liver resections. Using this model, we found that *in vitro* treatment of KCs with SLGN leads to the upregulation of markers that characterize monocyte populations (e.g., *EREG*, *S100A12*) and the downregulation of genes associated with the KC identity (e.g., *SPIC*, *FOLR2*). Interestingly, a similar profile was observed in response to LPS, suggesting this to be part of the general changes associated with an inflammatory response. Moreover, treatment of PHH with SLGN-CM produced in KCs led to the downregulation of NTCP and an impaired HBV entry into hepatocytes. Finally, co-treatment with SLGN-CM and an IL-6-inhibitory antibody identified IL-6 as the cytokine mediating this reduced HBV entry.

Conclusion: Our results suggest that in addition to its previously described therapeutic antiviral activity in HBV-infected hepatocytes, SLGN also has a prophylactic effect via an IL-6-dependent mechanism. Moreover, our characterization of SLGN sheds light into the general transcriptional programs regulating KC activation and underscores the importance of considering cell states when annotating hepatic cell populations based on scRNA-seq data.

TOP-107

Intrahepatic CD8+ T cells correlate with significant declines in HBV viral load and S antigen following a single vaccination with VRON-0200 in an AAV mouse model

Mohadeseh Hasanpourghadi¹, Andrew Luber², Sue Currie², Xiang Zhou¹, Hildegund Ertl¹. ¹The Wistar Institute, United States;

²Virion Therapeutics, United States

Email: scurrie@viriontx.com

Background and aims: VRON-0200 is a therapeutic vaccine developed to achieve functional cure of chronic HBV. The vaccine contains a genetically encoded checkpoint modifier, glycoprotein D (gD), to enhance, broaden and prolong CD8+ T cell responses to HBV core and polymerase with the goal to eliminate HBV-infected hepatocytes and prevent further viral spread. We hypothesized that, by removing virus-infected hepatocytes, S antigen would decline without being targeted by the vaccine. Here we report on correlations between intrahepatic CD8+ T cell responses and HBV viral load and S antigen declines in an AAV mouse model following a single i.m. injection of VRON-0200 (AdC6-gDHBV2).

Method: C57Bl/6 mice were tested for frequency and epitope specificities of IFN-gamma producing vaccine-insert-specific CD8+ T cells in blood, spleens, and livers, following a single i.m. dose of 1×10^{10} vp of a chimpanzee adenovirus vector (AdC6) expressing sequences of polymerase and core within gD (AdC6-gDHBV2), polymerase and core without gD (AdC6-HBV2) or nothing (controls). Efficacy was assessed in C57Bl/6 mice injected i.v. with an AAV8-1.3HBV vector at doses of 10^9 or 10^{10} genome copies. At week 4, mice with high levels of circulating HBV genome copy numbers were vaccinated (n = 5–10/group) with a single i.m. dose of 1×10^{10} vp of AdC6-gDHBV2, AdC6-HBV2, or nothing (control). HBV DNA viral loads and HBsAg titers in sera were assessed before and after vaccination and relationships between viral parameters and frequencies of IFN-gamma producing CD8+ T cells were assessed by Spearman's rank correlations.

Results: gD significantly enhances and broadens CD8+ T cells response in blood, spleens, and livers. In spleens, gD more than doubles the frequencies and breadth of CD8+ T cells. In AAV8-1.3HBV mice, at week 12, a single injection of AdC6-gDHBV2 achieves an HBV viral load decline of $\geq 3 \log_{10}$, the same vaccine without gD reduced viral loads $\leq 1 \log_{10}$. Viral loads increase or remain stable in control mice. HBV DNA copies/ml strongly inversely correlate with the frequency of IFN-gamma CD8+ T cells in livers and spleens (figure); S antigen levels correlate with HBV viral load and inversely correlate with CD8+ T cell frequencies.

Conclusion: VRON-0200 is the first therapeutic vaccine to show significant correlations between intrahepatic CD8+ T cells and HBV viral loads declines. S antigen declines were also observed and directly related to HBV clearance. These data further support the key role of HBV viral load and CD8+ T cells as end points for HBV functional cure and highlight VRON-0200's clinical potential alone or in combination. A VRON-0200 Phase 1b multi-national study is scheduled to begin in 2023.

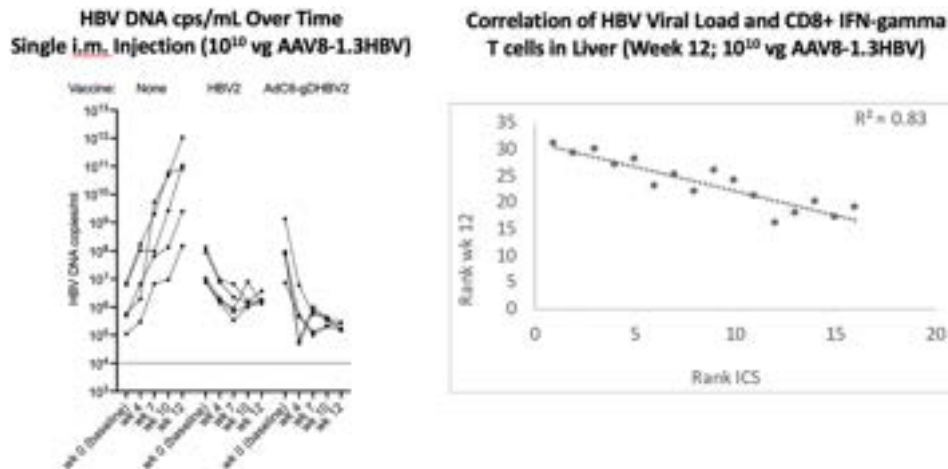


Figure: (abstract: TOP-107).

TOP-108

HBsAg induces mild activation, but not suppression, of intrahepatic immune cells as shown by single-cell RNA sequencing of fine-needle aspirates in chronic HBV patients

Zgjim Osmani¹, Boris Beudeker¹, Gertine Oord¹, Anthony Grooshuismink¹, Robert De Knecht¹, Eric Bindels², Harmen van de Werken³, Andre Boonstra¹. ¹Erasmus Mc, Gastroenterology and hepatology, Rotterdam, Netherlands; ²Erasmus Mc, Hematology, Rotterdam, Netherlands; ³Erasmus Mc, Immunology, Rotterdam, Netherlands
Email: z.osmani@erasmusmc.nl

Background and aims: There is no curative treatment for chronic hepatitis B virus (HBV) infection. Circulating hepatitis B surface antigen (HBsAg) is hypothesized to be responsible for the lack of an effective immune response to HBV. So far, previous attempts have failed to provide us with a complete understanding of the effects of HBsAg. To determine the impact of HBsAg on immune subsets, we optimized a workflow to examine circulating and intrahepatic cells from fine-needle aspirates (FNAs) of the liver.

Method: We included 18 HBeAg-negative patients on tenofovir and entecavir treatment with normal transaminases. Isolated cells from blood and paired liver FNAs were sequenced by 10X Genomics single-cell RNA sequencing. Patients were divided into an HBsAg high (920–12447 IU/ml) and HBsAg low group (1–100 IU/ml). Bioinformatic and differential gene expression analyses were performed comparing the two groups.

Results: Clustering identified 36 clusters in blood (166,351 cells; n = 18) and 29 clusters in liver FNAs (35,513 cells; n = 8). Cluster frequencies were comparable between both groups, except for the *KLRC2+ TIGIT+* NK cell cluster which was significantly decreased in the blood of patients with high HBsAg (avgFC 2.9). When comparing the HBsAg high vs. low group, the highest number of differential expressed genes (DEGs) in blood were observed in the *KLRC2+ TIGIT+* NK cell cluster (78 DEGs). Among others, interferon-related genes and inhibitory KIRs were downregulated in the HBsAg high group. This cluster presumably acquires memory-like properties and is often referred to as “adaptive” NK cells. Similar to blood, cluster frequencies in liver FNAs were comparable between groups except for the *TIGIT+* liver-resident NK cell cluster which was significantly increased in

patients with high HBsAg (avgFC 1.8). In general, gene expression differences were relatively low in FNAs when comparing the HBsAg high vs. low group. The highest number of DEGs were observed in the *CXCR6+ CD69+* liver-resident CD8 T cell cluster (15 DEGs). The inhibitory receptors *KLRB1*, *KLRC1*, and more importantly *IFNG* were upregulated by this cluster in the HBsAg high group, pointing towards a more activated cell state. Interestingly, the memory B cell clusters (10–14 DEGs) upregulated activation markers in the HBsAg high group (e.g., *CD69*, *CD83*), whereas the *TIGIT+* liver-resident NK cell cluster (8 DEGs) significantly upregulated *IL32*. *IL-32* is known to induce pro-inflammatory cytokines and chemokines, yet, its role in the antiviral immune response against HBV remains unknown.

Conclusion: Our workflow provided us with unique insights into the effects of HBsAg at single-cell resolution. Unbiased analyses show us for the first time, to our knowledge, that relatively high HBsAg levels trigger gene expression changes of immune subsets in blood and liver, collectively pointing towards a more activated cell state; primarily in NK-, B- and intrahepatic CD8 T cells.

TOP-111

Dating the origin and evolution dynamics of hepatitis D virus

Yibo Ding¹, Hongbo Guo¹, Qiudi Li¹, Dan Liu¹, Zhijiang Miao², Renxian Tang¹, Kuiyang Zheng¹, Qiuwei Pan³, Wenshi Wang¹. ¹Xuzhou Medical University, Jiangsu Key Laboratory of Immunity and Metabolism, Pathogenic Biology and Immunology, Xuzhou, China; ²Kunming University of Science and Technology, Kunming, China; ³Erasmus Medical Center, Department of Gastroenterology and Hepatology, Netherlands
Email: wenshi.wang@xzhmu.edu.cn

Background and aims: Chronic infection of hepatitis D virus (HDV) causes the most severe form of viral hepatitis. Although discovered more than 40 years ago, the origin and evolutionary landscape of HDV remain elusive. As a satellite virus of hepatitis B virus (HBV), it is poorly understood whether a co-evolution and co-migration relationship exists between HDV and HBV. We aim to map the evolutionary dynamics of HDV geographically and chronologically.

Method: Bayesian coalescent analysis was performed to analyze the phylogenetic relationships, time of origin, the most rapid

dissemination period, area of origin and transmission roadmap of HDV and HBV.

Results: We found the origin time of HDV and HBV and their rapid dissemination period are distantly separated in the timeline. Specifically, HDV jumped into human around 220 years ago and disseminated rapidly since 1990, whereas HBV jumped into human around 37,700 years ago with the most pronounced dissemination period started 4500 years ago. In addition, HDV originated from South America, while HBV originated from Africa. And their propagation roadmaps were also distinct. Moreover, a striking geographic separation of HDV was observed. Both the fitness to HBV genotypes and the adaptation to human lineages contribute to the formation of HDV cladogenesis.

Conclusion: This study has delineated the origin and evolution landscape of HDV. The origin and dispersal of HDV and HBV are distinct both geographically and chronologically. This implies that instead of a co-evolution and co-migration relationship, HDV and HBV evolve in parallel. Nevertheless, the genetic diversity of HDV was driven by multiple factors, including HBV genotypes and human lineages.

FRIDAY 23 JUNE

FRI-215

PD-1 does not suppress effector CD8 T cell differentiation during acute HBV infection and is not required for the induction of HBV-specific CD8 T cell exhaustion in HBV persistent mice

Jia Liu¹. ¹Union Hospital, Tongji Medical College, Huazhong University of Science and Technology, Department of Infectious Diseases, Wuhan, China

Email: jialiu77@hust.edu.cn

Background and aims: PD-1 is one of the key inhibitory receptors regulating CD8 T cell exhaustion during chronic viral infection. However, the role of PD-1 in modulating effector T cell differentiation and function during acute HBV infection is not well defined. Moreover, it is unclear whether PD-1 directly causes HBV-specific CD8 T cell exhaustion during chronic HBV infection.

Method: To address these questions, we examined the impact of genetic depletion of PD-1 from HBV-specific CD8 T cells on their differentiation and function in acute self-resolving and persistent HBV replication mouse models.

Results: We observed a sustained increase of PD-1 expression on CD8 T cells in both the spleen and liver in mice with acute self-resolving HBV replication. PD-1⁺ CD8 T cells demonstrated significantly increased effector T cell differentiation, proliferation, effector cytokine production, and granzyme B expression in compared to PD-1⁻ CD8 T cells. Interestingly, transcriptome sequencing analysis revealed that PD-1⁺ CD8 T cells also expressed significantly higher inhibitory molecules such as TIGIT, LAG-3, CTLA-4 and CD244 compared to PD-1⁻ CD8 T cells. Next, we generated PD-1 knockout (KO) HBcAg-specific TCR transgenic (C93-TCRtg) mouse strain to further analyze the role of PD-1 in regulating HBV-specific CD8 T differentiation and function. Wild type (WT) and PD-1 KO C93-TCRtg CD8 T cells were transfer to naïve mice, and the mice were then challenged with HBV leading to either self-resolving or persistent replication. In the acute self-resolving HBV replication model, both transferred WT and PD-1 KO C93-TCRtg CD8 T cells proliferated efficiently in a comparable level post HBV exposure. The PD-1 KO C93-TCRtg CD8 T cells also showed similar effector differentiation

phenotype, effector cytokine production and cytotoxicity molecule expression compared to the WT C93-TCRtg CD8 T cells. However, the absence of PD-1 led to significant decreases of Tox and Eomes expression in C93-TCRtg CD8 T cells. In HBV persistent mice, the genetic deletion of PD-1 on C93-TCRtg CD8 T cells was insufficient to prevent the development of cell exhaustion. Interestingly, the absence of PD-1 led to significant increases of Tox and Eomes expression and decrease of T-bet expression in C93-TCRtg CD8 T cells in HBV persistent mice.

Conclusion: Our results demonstrate that PD-1 does not suppress effector CD8 T cell differentiation during acute HBV infection and HBV-specific CD8 T cell exhaustion can occur in the absence of PD-1.

FRI-216

Detection and functional analysis of HBV-specific stem cell memory T cells (Tscm)

Hiroshi Abe-Chayama¹, Kazuaki Chayama¹. ¹Hiroshima University, Graduate School of Biomedical and Health Sciences, Hiroshima-shi, Japan

Email: habe@hiroshima-u.ac.jp

Background and aims: CD8⁺ CTLs (Cytotoxic T lymphocytes) play a pivotal role to eliminate HBV. CTLs of chronic HBV patients fail to eliminate infected cells because of exhaustion. Stem cell memory T cells (Tscm) are a rare subset of memory lymphocytes with stem cell-like self-renewal capabilities. Tscm are expected to be useful in cancer therapy. In this study, we detected HBV-specific Tscm in patients with chronic hepatitis and investigated their functions by transferring the Tscm into HBV-infected human hepatocytes transplanted TK-NOG mice.

Method: We isolated CD8⁺ T cells by MACS technology using PBMCs of HBV patients with HLA-A24. HBV core or pol tetramer⁺ HBV-specific Tscm were detected using FACSCanto2. Isolated Tscm from 8 HBV patients were labeled with CFSE and injected into 8 HBV-infected HLA-A24 human hepatocyte transplanted TK-NOG mice. Serum HBV DNA and human albumin levels were monitored until the mice were sacrificed three or four weeks after the Tscm transfer. Hepatic mononuclear cells and splenocytes were isolated to study cell proliferation and intracellular IL-2 and IFN- γ production.

Results: Detection of Tscm from patients with hepatitis B. HLA-A24 core and polymerase tetramer-positive Tscm were detected in 15 and 10 of 18 patients with chronic hepatitis B, respectively. The frequency of Tscm in these patients ranged from 0.6 to 38%. Transfer of Tscm to human hepatocyte transplanted TK-NOG mice. To explore a possibility of Tscm administration therapy to treat HBV infection with Tscm, we transferred 10^5 Tscm from 8 chronic HBV patients to 8 TK-NOG mice with HLA-A24 hepatocytes after HBV infection. Four mice were sacrificed three weeks after human cell injection and remaining four were sacrificed four weeks after the Tscm transfer. Apparent HBV DNA reduction was seen in 5 of the 8 mice. Human albumin levels also declined in these 5 mice suggesting the elimination of HBV-infected hepatocytes. Histological analysis of mouse liver tissue three and four weeks after human cell transfer revealed mild and severe mononuclear cell infiltration. These infiltrating cells were positive for human CD8-alpha staining, suggesting that the transferred TSCMs had differentiated into CTLs and caused hepatitis. No mice showed signs of GVHD. High levels of human blood cells were recovered from the liver and spleen of the mice three weeks after injection but dramatically decreased one week later. IL-2 and IFN- γ producing cells were more abundantly detected in mice sacrificed four weeks after T-cell transfer than three weeks. Most of these

POSTER PRESENTATIONS

cytokine-producing cells were tetramer-positive, suggesting that these cytokines were produced from CTLs reactive to HBV peptides.

Conclusion: We detected Tscm specific to HBV and showed a possibility of Tscm therapy for chronic HBV infection.

FRI-217

RBD1016-a novel anti-HBV GalNAc-siRNA drug resulted in sustained HBsAg reduction and seroconversion in mice models

Li Ming Gan¹, Shuquan Zheng², Feng Li², Zhaoxu Guo², Hong Yu², Hongyan Zhang², Zicai Liang², Shan Gao², ¹Ribocure Pharmaceuticals Ab, Sweden; ²Ribo Life Science Co., Ltd, China
Email: ganlm@ribolia.com

Background and aims: RBD1016 is a siRNA drug intended for treatment of chronic HBV infection, by targeting HBV X gene with pan-genotypic coverage. RBD1016 is in Phase 1 clinical stage for the treatment of CHB patients. Here we report the preclinical data from *in vivo* proof of concept studies using RBD1016 in two relevant mouse models of human HBV.

Method: To evaluate the efficacy of RBD1016, C57B/6N-Tg (1.28HBV)/Vst mice (or HBV transgenic mice) and rAAV8-1.3HBV (or AAV-HBV) animal models were used to investigate the anti-HBV effect of RBD1016 administered at different doses and different treatment regimens.

Results: 1. Single dose of RBD1016 resulted in dose-dependent knockdown of HBV viral markers in transgenic mice. An effective reduction of HBsAg by RBD1016 (max reduction 3.33 log₁₀ IU/ml) was observed in HBV transgenic mice, which lasted for at least three months (Figure 1A). RBD1016 could also achieve substantial and durable reduction of HBeAg and HBV DNA (Figure 1B) in a dose-dependent manner. 2. RBD1016 resulted in HBsAg seroconversion and synergistic effect on HBV DNA reduction combined with ETV (spell out ETV). Rather distinct from other assets in this class, RBD1016 caused *de novo* production of HBsAb in the AAV-HBV mouse model, which was detected in up to 62.5% of the experimental animals after repeated RBD1016 (3 mg/kg, qw*3) treatment

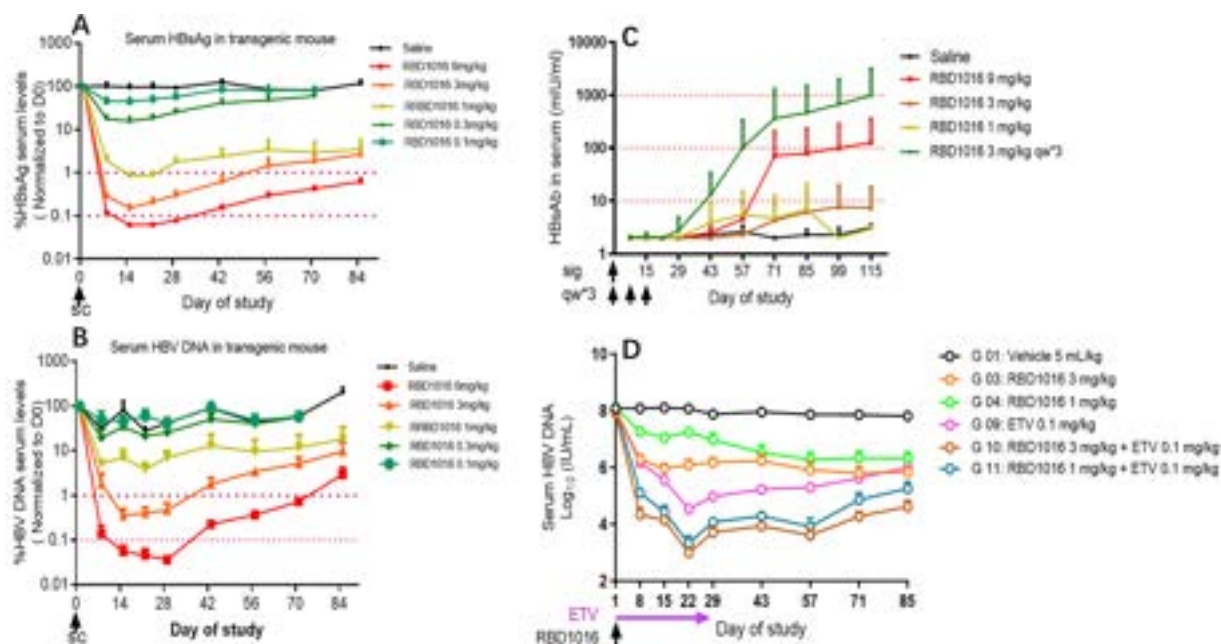
(Figure 1C). The combination of RBD1016 and ETV demonstrated a synergistic effect on serum HBV DNA inhibition, with serum HBV DNA reduced up to 4.91 log₁₀ IU/ml, and the profound inhibition was maintained even after discontinuation of ETV on Day 29 until the end of the study (Figure 1D). 3. A good PKPD correlation between liver RBD1016 concentration and serum HbsAg. There was a good correlation between RBD1016 liver concentration and HBsAg level in the plasma, supporting the use of HBsAg reduction in estimating drug concentration in the liver in human studies. 4. Pre-clinical safety profile. Based on 13 weeks' GLP toxicity studies, no observed adverse effect levels (NOAEL) were defined at 600 and 400 mg/kg in mice and monkeys, respectively, which supports large safety windows for ongoing and future studies in man.

Conclusion: The non-clinical studies of RBD1016 showed a significant and dose-dependent reduction of HBsAg on transgenic mouse model and AAV-HBV mouse model, which was further accompanied with HBsAg seroconversion. RBD1016 alone and in combination with drugs of other mode of action have the potential to contribute to functional cure of HBV in patients with chronic HBV.

FRI-218

HBV infection reshapes host chromatin accessibility and affects choline and iron metabolism

Vincenzo Alfano¹, Giuseppe Rubens Pascucci², Giacomo Corleone³, Francesca De Nicola⁴, Alexia Paturel⁵, Francesca Casascelli di Tocco⁵, Massimiliano Cocca⁵, Claude Caron de Fromental⁵, Oceane Floriot⁵, Rivoire Michel⁶, Massimo Levrero⁷, Francesca Guerrieri⁵. ¹Cancer Research Center of Lyon (CRCL), UMR Inserm 1052 CNRS 5286 Mixte Clb, Université Lyon 1 (UCBL1), Lyon, France; ²IIT Sapienza, Italy; ³UOSD Safu, Italy; ⁴Regina Elena National Cancer Institute, Oncogenomic and Epigenetic Unit, Italy; ⁵Inserm U1052-Crcl, Lyon, France; ⁶Inserm U1032-Clb, France; ⁷Dept of Hépatology, Hospices Civils de Lyon (HCL)-University Claude Bernard Lyon 1, France
Email: vincenzo.alfano@inserm.fr



Effects of RBD1016 on HBV viral markers in transgenic mice. HBsAg was measured by ELISA, HBV DNA was quantified by qPCR, respectively (A, B); Serum HBsAb can be detected after a single or repeated dose of RBD1016 in 62.5% AAV mice, HBsAb level was much higher in repeated dose (C); Additive inhibition of serum HBV DNA was observed for RBD1016 in combination with ETV in HBV transgenic mice (D).

Figure: (abstract: FRI-217).

Background and aims: HBV remains a major health problem worldwide with 250 million people chronically infected and at risk to develop liver cirrhosis and HepatoCellular Carcinoma (HCC). A complex host-virus interaction is responsible for both HBV-specific T and B cells dysfunction and the persistence of the viral cccDNA minichromosome, the two key challenges for HBV cure. The extent of HBV impact on the liver transcriptome remains controversial. Transcriptional activation in eukaryotic cells has been tightly linked with disruption of nucleosome organization at accessible genomic sites of remodeled chromatin. We used ATAC-seq (Assay for Transposase Accessible Chromatin followed by high throughput sequencing) to probe open chromatin and detect early changes in chromatin accessibility in HBV-infected Primary Human Hepatocytes (PHHs).

Method: HBV-infected PHHs (2 h/72 h) from 2 donors were used for ATAC-seq and analysis. The libraries were sequenced (75 × 2 cycles) on a NextSeq 500 Illumina.

Results: ATAC-seq analysis revealed an average of 2000 and 3500 cellular Differentially Accessible Regions (DARs) at 2 h and 72 h post infection (p.i.) respectively, indicating that after HBV infection an increasing number of genomic sites (including promoters, intragenic and distal intergenic regions) change their chromatin accessibility over time. Overall, the regions with different chromatin accessibility were enriched in genes involved in metabolism (KEGG) and GSEA analysis revealed an important role of the chromatin regulating complex PRC2 complex at 72 h p.i. Interestingly, the 1804 DARs, that are equally impacted by HBV infection in both the donors, enriched the pathway of choline metabolism in cancer, which affects PRC2 function. The integration of the ATAC-seq and RNA-seq data allowed us to identify 614 genes that had significant changes in both the analysis at 72 h p.i. These targets confirmed the impact of HBV infection on liver metabolism, and revealed a strong involvement of the iron metabolism in the cellular response to HBV infection. We validated the expression of iron-related genes and we found that HBV infection significantly upregulated the iron uptake in the cells. Finally, using the iron chelator Ferrostain-1, we showed that lowering the available iron levels results in a drastic inhibition of viral replication.

Conclusion: Altogether these results challenge the commonly accepted concept of HBV as a “stealth” virus and show that HBV infection impacts on host cell chromatin landscape and specific transcriptional programs. In particular, HBV imposes a reshaping of key cell metabolic pathways (e.g., choline and iron metabolism). Finally, we showed that available iron levels impact on HBV replication.

FRI-219

Identification of unique liver NK cells in HBV and a new perspective on exhaustion-related NK cell phenotypes by single-cell RNA sequencing

Boris Beudeker¹, Arda Karaoglu¹, Gertine Oord¹, Anthony Grooshuismink¹, Noé Axel Montanari¹, Remco Hoogenboezem², Eric Bindels², Harmen van de Werken³, Robert De Knecht¹, Andre Boonstra¹. ¹Erasmus Mc, Gastroenterology and hepatology, Rotterdam, Netherlands; ²Erasmus Mc, Hematology, Rotterdam, Netherlands; ³Erasmus Mc, Immunology, Rotterdam, Netherlands
Email: p.a.boonstra@erasmusmc.nl

Background and aims: NK cells play an important role in the body's response to chronic hepatitis B virus (HBV) infection. Understanding the impact of stably suppressed HBV on NK cell activation or inhibition is crucial for improving protective immunity and developing effective HBV cure therapies.

Method: Blood NK cells of HBeAg-negative HBV patients with low viral load were phenotyped and functionally tested. To provide a comprehensive and unbiased profile of the composition and transcriptional states of NK cells, paired blood and fine needle liver

aspirates of treated HBV patients were single-cell RNA-sequenced (ScRNAseq) and compared to healthy control datasets.

Results: ScRNAseq analysis revealed distinct NK cell subsets in patients with chronic HBV. We observed a reconfiguration of peripheral NK cells in HBV patients, including a heterogeneous activation-related gene signature and increased TIGIT expression. Contrary to previous hypotheses, we found limited expression of T-cell exhaustion related genes in peripheral NK cells. Our analysis of paired blood and liver NK cells is to date the largest, revealing a unique population of intrahepatic NK cells that clusters with blood NK cells in multidimensional analysis. These intrahepatic cells expressed immediate early genes (*FOS/JUN*), and genes encoding proinflammatory cytokines (*IFNG*). ScRNAseq of unprocessed ex vivo HBV liver aspirates profiled the tissue-resident phenotype of NK cells and revealed pronounced proinflammatory features, accompanied by high expression of the inhibitory factor *TIGIT*, as compared to blood. Our analysis of inhibitory genes in liver-resident NK cells showed a link between TIGIT expression and cytotoxicity and proinflammatory transcriptional profiles in both HBV and healthy liver. Our extensive analysis of NK cell phenotype and function in 101 cases of stably suppressed HBV or healthy patients with spontaneous HBsAg loss showed a link between TIGIT frequency on CD56dim NK cells and the clinical phase of HBeAg-negative HBV, as well as the duration of antiviral therapy. No other well-known activation or inhibitory proteins, such as PD1, TIM-3, KLRG1, HLA-DR or CD38 were found to be associated with these factors.

Conclusion: Blood and liver NK cells of treated HBV patients expressed limited T-cell exhaustion associated features, and expression of TIGIT was linked with favorable clinical outcomes and highly active NK cell subsets. Besides liver-resident NK cells, also activated liver-infiltrating NK cells were observed. In conclusion, our findings demonstrate the potential of targeting blood and liver NK cells as a strategy to cure HBV, especially as novel anti-HBV compounds are being developed in combination with NUC therapy.

FRI-220

Impact of pegylated interferon-alpha in combination with Bulevirtide in HBV/HDV infected humanized mice

Tassilo Volz^{1,2}, Jonathan Kolbe¹, Annika Volmari^{1,2}, Lena Allweiss^{2,3}, Marc Luetgelmann^{2,3}, Simon Fletcher⁴, Meghan Holdorf⁴, Robert Muench⁴, Maura Dandri^{1,2}. ¹University Medical Center Hamburg-Eppendorf, Internal Medicine, Hamburg, Germany; ²German Center for Infection Research, DZIF, Hamburg-Lübeck-Borstel-Riems Site, Germany; ³University Medical Center Hamburg-Eppendorf, Medical Microbiology, Virology and Hygiene, Hamburg, Germany; ⁴Gilead Sciences, Foster City, United States
Email: m.dandri@uke.de

Background and aims: Chronic hepatitis D (CHD) is a complex viral disease for which treatment remains challenging. The entry inhibitor bulevirtide induces a significant decline in HDV RNA and ALT reduction/normalization in CHD patients after 24 weeks, but longer treatment durations and/or combination therapies are needed to accelerate HDV decline and increase cure rates (*Wedemeyer, Lancet Inf Dis* 2022). Pegylated interferon-alpha (pegIFNα) is also used to treat CHD but has high rates of viral relapse. In a small phase II study, the combination of BLV with pegIFNα had superior antiviral efficacy relative to either agent alone (*Wedemeyer, J Hep* 2020). However, the underlying mechanism(s) by which PEG-IFN-α improves the antiviral response to BLV remains unclear. The aim of this in vivo study was to evaluate the antiviral efficacy of BLV and pegIFNα administered alone or in combination using HBV/HDV infected immunodeficient humanized mice.

Method: uPA/SCID/IL2Rγ^{-/-} (USG) mice reconstituted with adult primary human hepatocytes (PHH), were stably infected with HBV and superinfected with a recently cloned patient-derived HDV viral isolate (GT-1p) (*Giersch, JHEP Rep* 2023). Animals (n = 5–6 per group) received BLV (2 μg/g once per day) and pegIFNα (25 ng/g, twice per

POSTER PRESENTATIONS

week) either alone or in combination for a total of 8 weeks. Virological markers and IFN responsiveness in serum and liver were analyzed by qRT-PCR, ELISA, and immunofluorescence.

Results: At baseline of treatment, mice had a median of $9.7 \log_{10}$ HBV DNA copies/ml and a $6.5 \log_{10}$ HDV RNA copies/ml in the serum. Compared to untreated controls, the combination of BLV + pegIFN α resulted in the greatest decrease of serum HDV RNA levels (median $-2.4 \log_{10}$), intrahepatic reduction of HDVAg-positive cells, and intracellular HDV RNA (median $-2.4 \log_{10}$). Monotherapies decreased intrahepatic HDV RNA to a lesser extent (BLV: median $-0.6 \log_{10}$; pegIFN α : median $-0.8 \log_{10}$). As expected, pegIFN α strongly enhanced the expression of human interferon-stimulated genes (ISGs) in liver of humanized mice. In contrast, HDV-mediated intrahepatic ISG induction (e.g., h-ISG15 and h-Mx1) was lower in mice receiving BLV monotherapy compared to untreated HBV/HDV infected controls.

Conclusion: The combination of BLV + peg-IFN- α reduced intrahepatic HDV levels in humanized immunodeficient mice with high levels of HBV and HDV infection to a greater extent than either agent alone. Despite the lack of adaptive immune responses, the block of new infection events mediated by BLV, together with the activation of innate immune responses in hepatocytes by pegIFN α , provide a rationale for the combination effect of these agents observed in CHD patients.

FRI-221

Automated high-throughput image-based screen discovers members of the Akt serine/threonine kinase family as potential targets for treatment of hepatitis E virus infection

Mara Klöhn¹, Yannick Brüggemann¹, Marc Windisch², Daniel Todt¹, Eike Steinmann¹. ¹Ruhr Universität Bochum, Molecular and Medical Virology, Bochum, Germany; ²한국과학기술연구원, Seongnam-si, Korea, Rep. of South

Email: eike.steinmann@rub.de

Background and aims: Nearly four-and-a half decades after the discovery of Hepatitis E virus (HEV) as the etiological agent of viral hepatitis in human, treatment options remain limited to the off-label use of the nucleoside-analog ribavirin (RBV) and pegylated interferon-alpha. Although these drugs have made HEV infections manageable for the majority of patients, a considerable number of patients are either not eligible for or do not respond to currently available treatment options. To find substitute antiviral medications against HEV infections, we developed a simple and effective image-based high-throughput screening assay.

Method: We screened up to 9,500 compounds derived from FDA-approved drug-libraries and carried out dose-response assays of up to 170 of the most promising compounds by utilizing subgenomic HEV reporter replicons of genotype 3 expressing a GFP gene as a marker for viral replication in hepatoma cells. Furthermore, we tested the top hits in infection experiments with the human-derived HEV-3 p6 and the wild-boar HEV-3 83-2 virus.

Results: We discovered at least 5 compounds that markedly inhibit viral infection at low micromolar concentrations in hepatoma cells. Finally, infection experiments with HEV-3 p6-FL and HEV-3 83-2 virus identified Capivasertib and Ipatasertib, two pan-inhibitors of the serine/threonine kinase Akt to inhibit virus infection *in vitro*.

Conclusion: In conclusion, screening drug-repurposing libraries proved to be a versatile tool for identifying novel drugs against HEV infections, but most importantly, our results suggest that pan-Akt inhibitors may be promising therapeutic candidates for the treatment of HEV infections.

FRI-222

The hepatitis E virus ORF2 protein forms amyloid-like protein aggregates which may be pathogenic in human neurons

Jungen Hu¹, Giulia Mizzon², Chiara Olmeo³, Ann-Kathrin Mehnert¹, Rebecca Fu¹, Jan Birkel¹, Andrew Freistaedter¹, Claudio Acuna³, Ralf Bartenschlager^{2,4}, Viet Loan Dao Thi^{1,4}. ¹Chica and Heinz Schaller Research Group, Department of Infectious Diseases, Virology, Heidelberg University Hospital, Germany; ²Molecular Virology, Center for Integrative Infectious Disease Research, Heidelberg University Hospital, Germany; ³Chica and Heinz Schaller Research Group, Institute for Anatomy and Cell Biology, Medical Faculty Heidelberg, Germany; ⁴German Centre for Infection Research (DZIF), Partner Site Heidelberg, Germany

Email: vietloan.daothi@med.uni-heidelberg.de

Background and aims: Hepatitis E virus (HEV) is an important human pathogen. Immunocompromised patients can become chronically HEV-infected and suffer from extrahepatic manifestations, especially neurological disorders. HEV genomic RNA was detected in the cerebrospinal fluid of chronic HEV patients and in the brains of HEV-infected animals. In HEV-infected cells, three different forms of the capsid protein ORF2 have been described: a glycosylated, a cleaved, and an infectious form. How the expression of the different ORF2 forms is regulated, where progeny particles assemble, and how they traffic through the cell is poorly understood. We want to investigate HEV assembly by studying ORF2 in host cells. We also

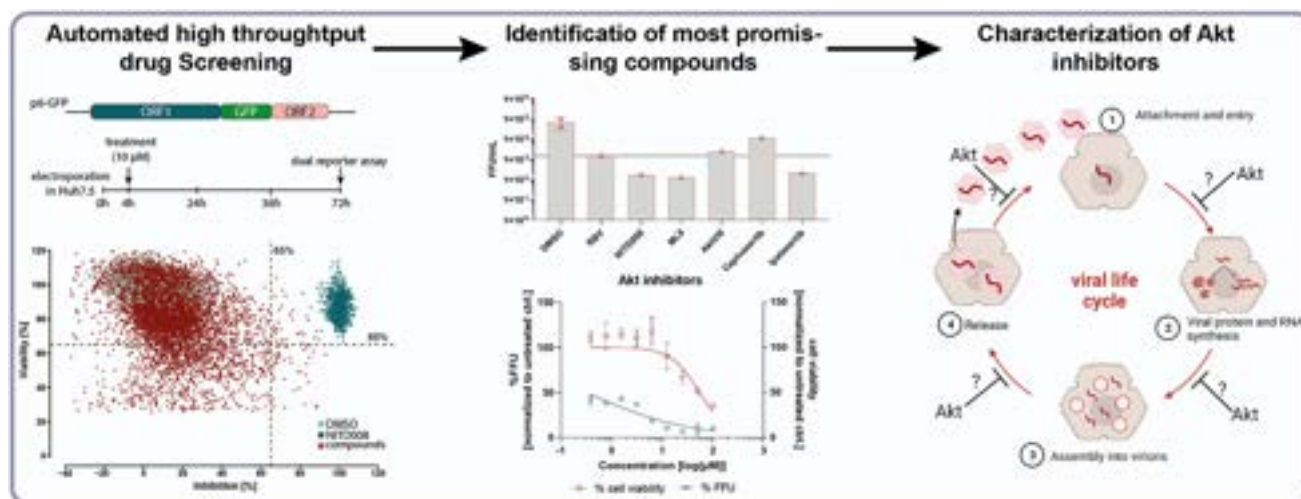


Figure: (abstract: FRI-221).

want to analyze if ORF2 is involved in HEV-induced neuro-pathogenesis.

Method: We engineered a new full-length fluorescence HEV reporter and derivatives by tagging ORF2 using the split GFP system (ORF2-GFP11), which allowed us to perform correlative light-electron microscopy (CLEM) and live-cell imaging studies. We used human induced pluripotent stem cell (iPSC)-derived neurons to study potential HEV-induced neurological disorders.

Results: The ORF2-GFP11 reporter virus replicated to similar levels as WT HEV and made infectious progeny particles. HEV ORF2-GFP11 infection of cells expressing GFP1–10 led to the formation of ~2 µm long rod-shaped GFP-positive ORF2 structures in the cytoplasm. By staining with ORF2 antibodies, we confirmed the formation of these structures in a range of WT HEV-infected cell types, including iPSC-derived hepatocytes and neurons. In HEV WT-infected neurons, calcium concentrations appeared to be lower compared to non-infected neurons. To our surprise, both the supposedly secreted and the infectious ORF2 forms formed large structures in the cytoplasm. Further, ectopically expressed WT ORF2 formed the same structures, suggesting it to be the sole viral determinant. By CLEM and electron tomography analysis, we found that the ORF2 protein formed aggregates composed of orderly stacked tubular filaments with a periodicity of ~35 nm, reminiscent of amyloid fibrils.

Conclusion: We have generated a full-length fluorescence HEV reporter for the first time. The ORF2 protein can form large, cytoplasmic, amyloid-like protein structures which may be involved in the pathogenesis in HEV-infected neurons. We are currently investigating how the structures are formed and if they play a role in progeny HEV assembly processes.

FRI-223.

Hepatitis B virus infected hepatocytes are resistant to cell death induction by virus-specific T cells.

Emely Springer¹, Annika Schneider¹, Joseph Trapani², Daniel Hartmann³, Norbert Hueser³, Melanie Laschinger³, Percy A. Knolle¹, Dirk Wohlleber¹. ¹Technical University of Munich, Institute of molecular Immunology, Munich, Germany; ²Peter MacCallum Cancer Centre, Melbourne, Australia; ³University Hospital München rechts der Isar, Department of Surgery, Munich, Germany
Email: emely.springer@tum.de

Background and aims: Hepatitis B virus (HBV) infection is considered as global health problem with more than 290 million cases of chronic hepatitis B. Although infection of hepatocytes with HBV induces anti-viral CD8 T cell response, viral clearance by CD8 T cells takes weeks or may develop into persistent infection. The reasons for failure of the immune system are manifold and not entirely understood. We recently identified that viral infections renders hepatocytes more susceptible for immune-mediated cell death induction by reducing the mitochondrial stress resilience. Here we aim to analyze if HBV infection renders HBV infected hepatocytes susceptible for enhanced cell death induction or if HBV infected hepatocytes may escape cell death.

Method: Primary human and murine hepatocytes were infected with hepatotropic HBV or transduced with recombinant adenoviruses delivering HBV genomes. T cell effector function against virus-infected hepatocytes were analyzed by co-culture with antigen-specific CD8 T cells or by T cell-derived effector molecules like Fas-ligand, tumor necrosis factor (TNF) or perforin. Cell death induction was monitored by real-time killing assay and caspase activation assay. In addition, we analyzed the mitochondrial stress resilience by challenging with calcium ions. Proof-of-concept experiments were performed in mice to verify the in vitro results.

Results: We found that viral infection with adenoviruses and lymphocytic choriomeningitis virus (LCMV) sensitized infected hepatocytes towards induction of cell death resulting in higher killing efficiency of virus-specific CD8 T cells though reduced mitochondrial resilience. Strikingly, HBV infected hepatocytes did not display such increased susceptibility for cell death induction by CD8 T cell effector molecules. Consequently, mitochondria from HBV infected hepatocytes showed normal stress resilience. Most importantly, co-infection with HBV reversed the adenovirus-induced sensitivity towards immune-mediated cell death induction leading to reduced killing efficiency of HBV-infected hepatocytes.

Conclusion: Here, we demonstrate that HBV infected hepatocytes do not only escape the non-canonical CTL effector function but are also more resistant towards CD8 T cell mediated killing. This identifies a so far not appreciated immune escape of HBV at the level of immune cell effector function against virus-infected hepatocytes. Overcoming this immune escape bears the promise to help in immune-mediated clearance of HBV-infected hepatocytes.

FRI-224

A novel imaging approach to investigate hepatitis E virus entry

Rebecca Fu¹, Zoe Engels¹, Jasmin Weihs¹, Jungen Hu¹, Viet Loan Dao Thi^{1,2}. ¹Schaller Research Group, Department of Infectious Diseases, Virology, University Hospital Heidelberg, Heidelberg, Germany ²German Centre for Infection Research (DZIF), Partner Site Heidelberg, Heidelberg, Germany
Email: vietloan.daothi@med.uni-heidelberg.de

Background and aims: Hepatitis E virus (HEV) is a major causative agent of acute hepatitis and mainly transmitted faecal-orally. HEV particles in faeces are non-enveloped (nHEV) and responsible for host-to-host transmission, while those in the blood possess a cell-derived lipid envelope (eHEV) allowing HEV to disseminate within the host. Studies on nHEV entry pathways have been controversial and no entry receptor has been identified for either form yet. A previous study proposed integrin alpha 3 (ITGA3) as a potential host factor of nHEV entry, but no follow-up studies have been made. In this study, we aimed to develop a new imaging approach, combined with the use of entry inhibitors, to study single HEV particles upon cell entry.

Method: We used fluorescent *in situ* hybridization and immunofluorescence staining to detect the HEV genome and the capsid, respectively. We knocked out (KO) the partner of ITGA3, namely integrin beta 1 (ITGB1), in hepatoma cells. We used chemical inhibitors, siRNAs, GFP-tagged Rab proteins together with their dominant-negative counterparts to study the cell entry pathways used by the two HEV forms.

Results: We successfully established the detection of single incoming HEV particles during early hours of infection (Figure 1A). We found that the binding and infection of nHEV but not eHEV particles was less efficient in ITGB1 KO cells as compared to WT cells. We observed that the genome dissociated from the capsid approximately 7 h post-infection (p.i.), suggesting a rather slow entry process. Endosomal acidification inhibitors led to intracellular capsid accumulation and thus unsuccessful genome release. Affirmingly, these inhibitors decreased both eHEV and nHEV infection in a dose-dependent manner. However, eHEV exhibited higher sensitivity to these inhibitors than nHEV (Figure 1B). For nHEV, knocking down the early endosome marker Rab5 had only a minor effect, while the knockdown of the recycling and late endosome markers Rab11 and Rab7 resulted in strong capsid accumulation and thus unsuccessful cell entry and infection. In contrast, we found eHEV entry to rather depend on the classic endocytic pathway based on Rab5 but not Rab11.

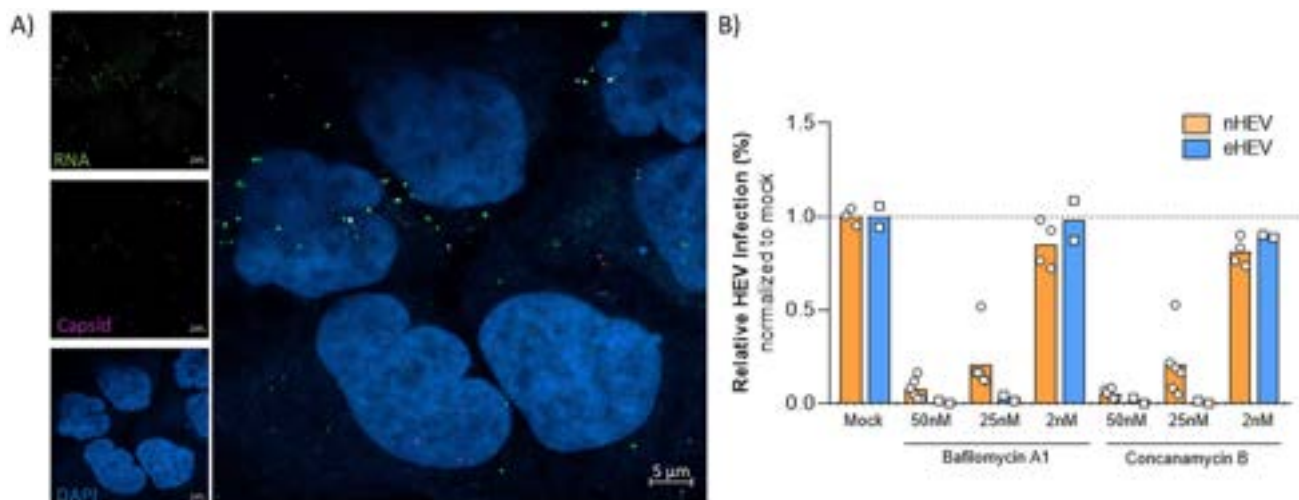


Figure: (abstract: FRI-224): (A) Co-detection of nHEV RNA and capsid 5 hours post-internalization. White arrows indicate co-localized particles. (B) Different sensitivity of nHEV and eHEV to endocytic inhibitors.

Conclusion: Using our novel entry assay, we found that the two HEV forms differentially depend on integrins and that they use likewise differential pathways to enter the cell. Our efforts shall lead to a better understanding of the HEV cell entry mechanism and may ultimately contribute to the development of specific anti-HEV therapies.

FRI-225

CTLA4 inhibits anti-HBs secretion by blocking BCR signaling pathway in chronic hepatitis B infection

Minxin Mao¹, Shengxia Yin², Yawen Wan³, Ming Li¹, Yu Geng¹, Xin Tong², Jie Li², Chao Wu^{1,2}. ¹Department of Infectious Diseases,

Nanjing Drum Tower Hospital Clinical College of Traditional Chinese and Western Medicine, Nanjing University of Chinese Medicine, Nanjing, China; ²Department of Infectious Diseases, Nanjing Drum Tower Hospital, The Affiliated Hospital of Nanjing University Medical School, Nanjing, China; ³Department of Infectious Diseases, Nanjing Drum Tower Hospital Clinical College of Xuzhou Medical University, Xuzhou Medical University, Xuzhou, China
Email: dr.wu@nju.edu.cn

Background and aims: It has been reported that there is no significant change in the number of HBsAg specific B cells in chronic hepatitis B (CHB) patients. However, the vast majority of

Gene sequencing of peripheral blood B cells in CHB patients showed that CTLA4 expression was increased

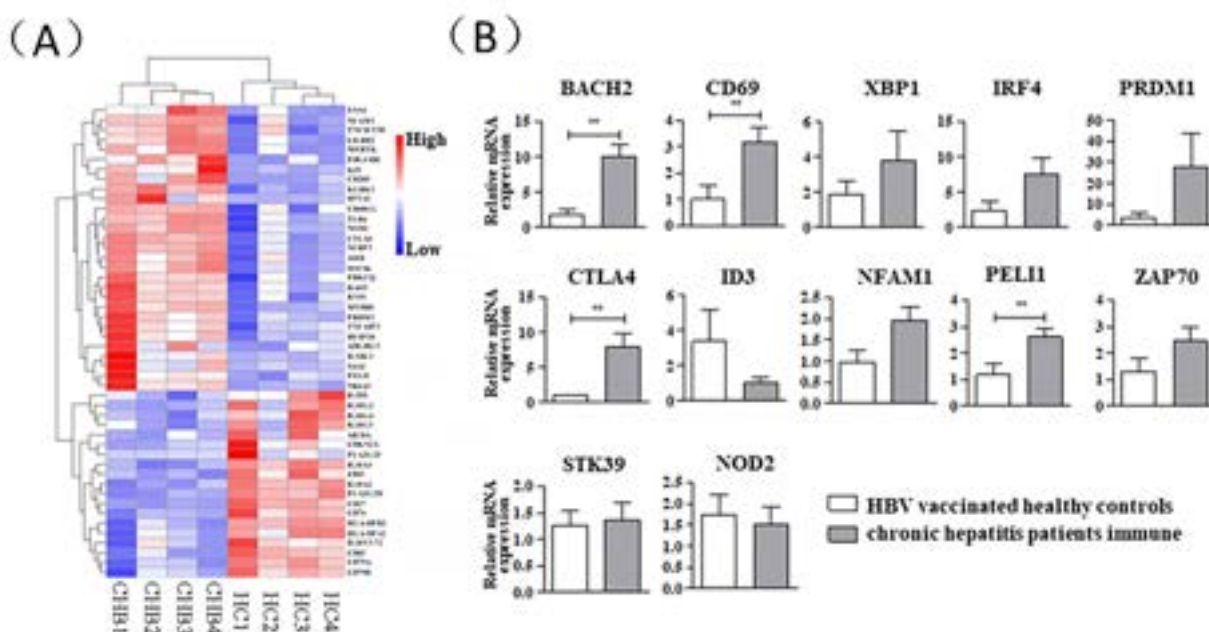


Figure: (abstract: FRI-225).

CHB patients are anti-HBs negative. B cells are the main source of antibodies in humoral immunity against HBV infection. It is believed that the deficiency of anti-HBs is caused by the dysfunction of anti-HBs secretion by HBsAg specific B cells. Therefore, more attention should be paid to the activation of HBsAg specific B cells and the cause of the inhibition of anti-HBs secretion.

Method: Peripheral blood B cells from 4 healthy controls (HC) and 4 CHB patients were collected by flow sorting technology for single cell sequencing, and the sequencing results were analyzed by GO analysis. Blood samples were collected from CHB patients and HC, and the changes in the proportion of peripheral blood B cells were detected by flow cytometry. HBsAg specific B cells were identified by fluorescent dye labeling. Peripheral blood B cells from CHB and HC were sorted by flow cytometry, and B cell cytokines, signaling pathways and antibody secretion by blocking CTLA4 signaling pathway were detected. Using immunoprecipitation (CO-IP), anti-CTLA4 antibody was used to precipitate CTLA4 protein complex, and the protein complex was analyzed by protein general spectrum to identify the differences in phosphorylation levels of downstream proteins and related proteins bound to the complex.

Results: GO analysis showed that the expression levels of multiple proteins in the BCR signaling pathway of B cells were decreased, suggesting that the BCR signaling pathway was blocked. Flow cytometry analysis of peripheral blood B cells from CHB patients and HC showed that CTLA4 protein was highly expressed in B cells from CHB patients, and the increase of CTLA4 expression was more significant in HBsAg specific B cells. We further phenotyped infiltrating B cells in liver biopsy tissues from 5 CHB patients and found that the expression level of CTLA4 in liver B cells was positively correlated with peripheral blood B cells. ELISPOT assay showed that after blocking CTLA4, B cells in some CHB patients recovered the ability to secrete anti-HBs. Calcium flow experiments showed that BCR dependent calcium flow was significantly reduced in HBsAg specific atMBC cells infected with chronic HBV infection, and the conduction of calcium flow was partially restored after the addition of anti-CTLA4. Western Blot test found that HBsAg specific atMBC BCR signaling pathways in cell signal more abnormal protein phosphorylation levels, after adding anti-CTLA4 p-Src, p-BLNK rise obviously, BCR intracellular signal transduction recovered to a certain extent. CO-IP results showed that the phosphorylation level of CTLA4 signaling pathway downstream was inhibited.

Conclusion: High expression of CTLA4 protein in circulating B cells and liver-infiltrating B cells blocks BCR signaling, thereby inhibiting anti-HBs secretion. Therefore, the abnormal expression of CTLA4 protein on B cells may be one of the reasons for the loss of virus specific humoral response during CHB infection.

FRI-226

Transcriptional analysis of HBV infected liver after treatment with selgantolimod reveals longitudinal changes in both inflammation-related pathways and B cell receptor repertoire

Nikita Kolhatkar¹, Circe McDonald¹, Sam Kim¹, Leonard Sowah¹, Jeffrey Wallin¹, Wan-Long Chuang², Yao-Chun (Holden) Hsu³. ¹Gilead Sciences, Inc., Foster City, United States; ²Kaohsiung Medical University Chung-Ho Memorial Hospital, Taiwan; ³E-DA Hospital, Center for Liver Diseases, Taiwan
Email: holdenhhsu@gmail.com

Background and aims: GS-US-389-5458 is an open label phase1b study of selgantolimod, an oral selective small molecule agonist of Toll-like receptor 8 (TLR8) in special populations of subjects with chronic hepatitis B (CHB). Here we investigate the effect of selgantolimod on the periphery and liver microenvironment in the inactive carrier (IC) population of CHB.

Method: IC CHB subjects (HBV DNA <2000 IU/ml, qHBsAg ≤1000 IU/ml and ALT ≤ULN by AASLD 2018 guidelines) received weekly dosing of 3 mg selgantolimod for 24 doses. Paired core needle liver biopsies were collected from 4 IC participants during screening as well at week

23 2-6 hours post selgantolimod dosing. Matching PBMCs and fixed whole blood samples were collected at the same timepoints. RNA was isolated from the peripheral and liver tissue samples and bulk RNAseq, T-cell receptor (TCR), and B-cell receptor (BCR) sequencing was performed using Illumina TruSeq and Takara SMARTer TCR/BCR Profiling Kits. RNAseq alignment was performed using TopHat and Cufflinks. Differentially expressed genes were identified using a linear mixed effect model (DESeq2). Changes in immune pathways of interest were characterized using single-sample Gene Set Enrichment Analysis (ssGSEA). Immune cell composition was estimated using quanTIseq. Clonotype assembly for BCR and TCR sequencing utilized an MiXCR pipeline. Repertoire diversity was quantified using Inverse Simpson Index.

Results: Transcriptional profiles of paired liver biopsies and matched peripheral blood were compared to evaluate modifications in these compartments after treatment with selgantolimod. While we did not observe consistent alterations to the peripheral transcriptional landscape, there were some notable changes in all subjects within the liver. Specifically, a number of genes had increased expression, including regulation of macrophage chemotaxis (*CSF1*), inflammatory cytokines (*STAT1*, *IL6*, *TNFAIP3*, *MYD88*, *TLR7*), activation and proliferation of cytotoxic T cells (*CD69*, *CD44*, *TAP1*), and mature B cell differentiation (*LYN*). Cell deconvolution analyses showed an increase in the averages of M1 Macrophages (1.7-fold), regulatory T cells (4.6-fold), and B cells (1.9-fold) within the liver. TCR analysis of the liver did not indicate consistent expansion or shifts within the liver microenvironment despite increases in T cell activation-related genes. Analysis of B cell receptor repertoires in liver revealed an increase in clonotypic diversity after treatment (mean 1.8-fold). Additionally, we identified a specific heavy chain V gene family, 3-74 that had expanded in the liver but not the periphery upon treatment in two of the four subjects (ranging from ~1.5-5-fold increase within the liver).

Conclusion: Our data indicate that selgantolimod treatment in CHB patients could drive upregulation of inflammation-associated genes within the liver microenvironment, promoting activation of pro-inflammatory myeloid, B and T lymphocytes. Additionally, subsequent weekly treatment with selgantolimod may drive changes to the B cell compartment to both increase diversity of the immunoglobulin repertoire and enrich specific antibody families that may be specific to HBV.

FRI-227

HBs-directed T cell engager antibodies foster efficient recruitment of T cells and lead to strong reduction of hepatitis B virus infection in livers of human liver chimeric mice

Annika Volmari^{1,2}, Oliver Quitt³, Pin Xie⁴, Tassilo Volz^{1,2}, Lena Allweiss^{1,2}, Ke Zhang⁴, Ulrike Protzer^{2,3}, Maura Dandri^{1,2}. ¹University Medical Center Hamburg-Eppendorf, I. Medical Department, Hamburg, Germany; ²German Center for Infection Research (DZIF), Hamburg-Luebeck-Borstel-Riems and Munich sites, Germany; ³Technical University Munich/Helmholtz Munich, Institute of Virology, School of Medicine, Germany; ⁴SCG Cell Therapy, Shanghai, China
Email: a.volmari@uke.de

Background and aims: Current treatment options for chronic Hepatitis B (CHB) efficiently suppress viral replication but rarely achieve a functional cure. Virus-specific adaptive immunity is lacking or dysfunctional in CHB patients and restoration of a functional antiviral T cell response has the potential to promote cure. Recent studies have shown that bispecific antibodies binding HBV envelope proteins (HBVenv) on infected hepatocytes and CD3 and CD28 on T cells target and kill HBV infected cells (Quitt et al. *J Hepatol.* 2021). The aim of this study was to assess liver targeting and antiviral efficacy of these T cell (Tc)-engager antibodies *in vivo* in HBV infected human liver chimeric mice in the presence of high circulating HBsAg levels. **Method:** Humanized mice that were stably (12w) or partially (4w) infected with HBV received PBMCs isolated from healthy human

blood at day 0 and 4 of treatment and four i.p. injections of a combination of bispecific Tc-engager antibodies recognizing HBVenv and either CD3 or CD28 (1 mg/kg body weight, every 3 days). Control mice received PBMCs and PBS. Virological markers and cell infiltration were determined by qPCR, ELISA, immunofluorescence, RNA *in situ* hybridization (RNAscope) and flow cytometry.

Results: *In vitro* assays showed high specificity of the Tc-engager antibodies and determined an optimal treatment ratio of 1:1 to induce efficient activation of T cells, elimination of target cells and antiviral effects. Treatment of stably HBV-infected mice (median viremia of 7×10^5 HBV DNA copies/ml; median HBsAg 3×10^3 IU/ml) with Tc-engager antibodies and human PBMCs induced strong intrahepatic recruitment of human CD4⁺ and CD8⁺ T cells. Antibody treatment resulted in reduction of viremia (1.4log), circulating HBsAg (0.69log) and HBeAg (0.55log) in only 11 days. Intrahepatic levels of HBV pregenomic (pg)RNA (0.7log), HBV DNA (1.4log) and cccDNA (0.9log) were efficiently reduced. Histology and RNAscope revealed reduced numbers of HBcAg⁺ cells and substantially lower HBV-RNA in infected hepatocytes. These changes were accompanied by a transient increase of ALT, increased expression of granzyme B, IFN- γ and TNF- α , and reduction of human serum albumin, indicating human hepatocyte killing. Treatment of partially infected mice efficiently reduced intrahepatic levels of HBV RNA (0.7log), HBV DNA (1log) and cccDNA (0.8log), demonstrating specific recognition of infected cells also in livers harboring lower numbers of HBV⁺ cells.

Conclusion: Treatment of HBV-infected humanized mice with bispecific Tc-engager antibodies after transfer of human PBMCs efficiently reduced HBV viral load *in vivo*, demonstrating their recruitment to the liver and potent recognition of infected hepatocytes despite the presence of high circulating HBsAg levels, as well as induction of both cytolytic and cytokine-mediated HBV-specific T cell immunity.

FRI-228

HBV and HDV interaction and variability in a superinfection mouse model: role of type I interferon

Beatriz Pacín Ruiz^{1,2,3}, Gracián Camps Ramón⁴, María Francesca Cortese^{1,2,3}, Josep Gregori⁵, Selene García-García^{1,2,3}, David Tabernero^{1,3}, África Vales Aranguren⁴, Adrian Najarro¹, Cristina Olague Micheltorena⁴, Ariadna Rando-Segura¹, Josep Quer⁵, Rafael Esteban^{3,6}, Mar Riveiro Barciela^{3,6}, Maria Buti^{3,6}, Gloria González-Aseguinolaza⁴, Francisco Rodríguez-Frías^{1,3,5}. ¹Vall d'Hebron Barcelona Hospital Campus, Microbiology/Liver Unit, Barcelona, Spain; ²Universitat Autònoma de Barcelona, Biochemistry and Molecular Biology Department, Bellaterra, Spain; ³Carlos III Health Institute, Network Center For Biomedical Research in Hepatic and Digestive Diseases (CIBERehd), Madrid, Spain; ⁴University of Navarra, Center for Applied Medical Research (CIMA), Pamplona, Spain; ⁵Vall d'Hebron Barcelona Hospital Campus, Liver Unit, Liver Disease, Laboratory-Viral Hepatitis, Barcelona, Spain; ⁶Vall d'Hebron University Hospital, Liver Unit, Department of Internal Medicine, Barcelona, Spain Email: beatriz.pacin@vhir.org

Background and aims: The hepatitis delta virus (HDV) inhibits the hepatitis B virus (HBV) replication and, differently from its helper, it activates the interferon pathway, inducing the expression of mutagenic enzymes such as ADAR1. This study aimed to inspect the relation between HDV and HBV variability and the role of type I interferon (IFN-I) by studying both viruses' variability upon HDV superinfection in an HBV-expressing transgenic (HBVtg) mouse model knock-out for the IFN α /beta-receptor (HBVtgXIFNAR-KO). **Method:** HBVtgXIFNAR-WT and HBVtgXIFNAR-KO mice were infected with 5×10^{10} viral genomes of an adeno-associated vector expressing luciferase or HDV. HBV expression was weekly monitored by quantifying the HBV DNA and RNA in plasma. Intrahepatic viral RNA was extracted at 7- and 21-days post injection (dpi) to quantify the pregenomic RNA (pgRNA) and to study HBV and HDV

quasispecies (QS) in respectively HBX (5'-HBX between nucleotide [nt] 1255 to 1611 and 3'-HBX between 1596 and 1936) and HDAG (nt 912-1298 in genome) by next-generation sequencing (NGS). QS variability between the groups was evaluated by identifying the single nucleotide variations (SNVs), whereas HDV editing was quantified by evaluating the percentage of haplotypes with the A281G variation (editing site).

Results: A strong reduction of circulating HBV DNA and RNA was observed in presence of HDV especially at 21 dpi. This effect reverted when the IFN-I pathway was inhibited. This trend was not confirmed in liver tissue, where similar concentrations of pgRNA were observed between groups. Several SNVs, especially C to T transition, were detected in the HBX gene over time (CT transition/total mutated positions = 7/15 vs 20/44 at 7 vs 21 dpi, respectively). Some of them were specifically identified in HDV HBVtgXIFNAR-WT mice and involved trans-activation domain of the HBX gene at intrahepatic level. HDV genome editing was low at 7 dpi, and increased at 21 dpi, especially in HDV HBVtgXIFNAR-WT mice ($p = 0.002$). Several SNVs, remarkably A to G transitions, were also spotted in HDAG (75 vs 28 for 7 vs 21 dpi, respectively). Notably, most of the SNVs observed at 7 dpi were also identified at 21 dpi for both HBV and HDV QS.

Conclusion: In our model, the presence of HDV mainly interfered with HBV particle release rather than intrahepatic expression. Of note this effect seems IFN-I dependent. Several transitions, typical of the intracellular mutagenic enzymes, were observed in both HBV and HDV, and some of them were identified at both timepoints, suggesting that these enzymes might contribute to the viral variability by acting on viral mutational hotspot. In HBV, some of these variations specifically interested the trans-activation domain of the HBX gene and could probably contribute to HBV inhibition.

FRI-229

Rapid functional secretome analysis of HBV-specific T cells to guide clinical management of CHB patients

Nina Le Bert¹, Apostolos Koffas², Anthony Tan¹, Lung-Yi Mak², Sophie Stretch², Shou Kit Hang¹, Haiyan Ma³, Ariel Lee³, Yun Ji⁴, Upkar Gill², Qi Chen¹, Qing Zhu⁴, Antonio Bertoletti¹, Patrick Kennedy². ¹Duke-NUS Medical School, Singapore; ²Queen Mary University of London, United Kingdom; ³T Cell Diagnostics/Hyris, Singapore; ⁴Brii Biosciences Limited, United States Email: antonio@duke-nus.edu.sg

Background and aims: Control of Hepatitis B virus (HBV) infection requires functional virus-specific T cells, yet clinical management of patients with chronic HBV infection (CHB) relies exclusively on the assessment of virological and biochemical biomarkers. We aimed to develop a robust rapid assay to measure cytokines secreted or induced by HBV-specific T cells (secretome) with efficient throughput and minimal invasiveness to allow the integration of immunological biomarkers in CHB clinical management.

Method: We designed a rapid HBV-specific T cell test method based on the stimulation of whole blood with customized peptide mixtures covering the envelope, nucleoprotein, polymerase and X protein of different HBV genotypes followed by the quantification of plasma cytokines (IFN- γ , IL-2, IL-10, granzyme B, TNF- α , IL-4). The assay performance was tested in healthy HBs vaccinees ($n = 32$) and in treated ($n = 31$) and treatment naïve ($n = 42$) CHB patients. In selected patients, the sensitivity of the assay was compared with ex vivo and in vitro expansion ELISpot assays and by spiking known numbers of engineered HBV-specific CD8 T cells into whole blood.

Results: Cytokines produced by peptide mixtures covering the different HBV proteins can be individually measured utilizing only 2 ml of whole blood from HBs vaccinees and CHB patients. Sensitivity of the assays was comparable and at times even superior to traditional T cell assays. Spiking known numbers of HBV-specific CD8 T cells into whole blood demonstrated that this assay can detect as little as 50-100 HBV-specific T cells in 400 μ l/whole blood, a sensitivity corresponding to an HBV-specific T cell frequency in total T

cells of 0.02–0.04%. The quantity and ratio of cytokines detected in different CHB patients revealed a vast heterogeneity of secretome profiles. Through multiple logistic regression, the measured immunological parameters were capable of accurately (ROC AUC = 0.9363) segregating untreated CHB patients with high or low viral load.

Conclusion: We demonstrated that we can accurately assess quantity and multi-functionality of HBV-specific T cells in patients without complex in-vitro manipulation in a small volume of whole blood. The assay sensitivity is comparable with known frequencies of circulating HBV-specific T cells in CHB. Global measurement of cytokines secreted or induced by HBV-specific T cells provides a novel biomarker for the interpretation of host-viral interactions in different categories of CHB patients and can signpost the selection of novel immunotherapies.

FRI-230

Identification and functional analysis of miR-4461 associated with hepatitis B-derived hepatocellular carcinomas

Aiko Sakai¹, Masaya Sugiyama¹. ¹National Center for Global Health and Medicine, Japan
Email: msugiyama@hosp.ncgm.go.jp

Background and aims: The development of hepatocellular carcinoma (HCC) due to hepatitis B is difficult to predict. One reason is that its pathogenesis is not due to a persistent accumulation of inflammation. The molecular changes that occur in cells persistently infected with hepatitis B virus (HBV) are not clear on a cell-by-cell basis. The impact of those HBV-infected cells on the pathogenesis of the disease is also unknown. In this study, single-cell RNA-seq (scRNA-seq) analysis of HBV-infected cells was performed to investigate changes in gene expression on a single-cell basis. The molecules relating to HCC were identified and their functions were analysed.

Method: After the infection of primary hepatocytes with HBV, their scRNA-seq analysis was performed. scRNA-seq data were compared between HBV RNA-positive and negative hepatocytes (cell populations in the same environment) in one dish. The miR-4461 levels of HuH7 and HepG2 cells with and without HBV were identified and analyzed for cell proliferation, invasion and migratory capacity. Target genes to which miR-4461 bound were explored by in vitro assay. miR-4461 was quantified in HCC and non-HCC areas using resected liver tissue of hepatitis B and non-B/non-C.

Results: Primary hepatocytes were infected with HBV and then scRNA-seq was performed. miR-4461 was significantly reduced in HBV-infected hepatocytes. miR-4461 expression was reduced when HBV replication plasmids were transfected into HuH7 and HepG2 cells. siRNA knockdown of miR-4461 enhanced the proliferation, invasive and migratory capacity of HuH7 and HepG2 cells. miR-4461 expression levels were confirmed in liver tissues from hepatitis B and non-B/non-C HCC patients. In non-B/non-C specimens, no difference of the miR-4461 expression was observed in both HCC and non-HCC areas compared to normal liver tissue. On the other hand, in hepatitis B specimens, the expression of miR-4461 was lower than that of normal liver ($p < 0.05$). In addition, the expression in HCC areas was lower than non-HCC areas ($p < 0.05$). Target genes of miR-4461 were explored using database and in vitro assay. Then, the FGA gene was one of the targets of miR-4461.

Conclusion: The miR-4461 pathway was suggested to be associated with the establishment and pathogenesis of HBV infection. miR-4461 levels were reduced in liver tissue derived from hepatitis B, and a more significant reduction was observed in HCC area, suggesting that this pathway could be a useful biomarker for HBV-derived HCC.

FRI-231

Reduced hepatic bile acid uptake and blocked hepatitis B viral infection after oral administration of novel small molecule inhibitors of the sodium taurocholate co-transporting polypeptide (NTCP)

Kalliopi Pervolaraki¹, Jean-Christophe Vanherck¹, Charlene Marcadet¹, Lieven Verhoye², Amse De Meyer², Madina Rasulova³, Heyrhyoung Lyoo³, Jasmine Paulissen³, Hendrik Jan Thibaut³, Kristof De Vos³, Patrick Chaltin⁴, Johan Neyts³, Pieter Annaert³, Philip Meuleman², Arnaud Marchand¹, Matthias Versele¹, Stan van de Graaf⁵. ¹CISTIM Leuven vzw, Leuven, Belgium; ²Ghent University, Ghent, Belgium; ³Katholieke Universiteit Leuven, Leuven, Belgium; ⁴Centre for Drug Design and Discovery, Leuven, Belgium; ⁵Amsterdam Umc, locatie AMC, Amsterdam, Netherlands
Email: k.f.vandegraaf@amsterdamumc.nl

Background and aims: The sodium taurocholate co-transporting polypeptide (NTCP, *SLC10A1*) is selectively expressed on the basolateral membrane of hepatocytes and is the main transporter of conjugated bile acids. NTCP also serves as the entry receptor for the hepatitis B virus (HBV) and hepatitis delta virus (HDV). Daily injection with bulevirtide, previously known as Myrcludex-B, a synthetic peptide mimicking the NTCP-binding domain of HBV, is approved in the EU for treatment of patients co-infected with HBV and HDV. Pre-clinical studies suggest that pharmacological inhibition of hepatic bile salt uptake using bulevirtide ameliorates cholestatic liver injury. Both treatment of viral hepatitis and cholestatic liver diseases require chronic treatment, thus indicating the necessity of orally available small molecule inhibitors for this liver-specific transporter/receptor.

Method: A comprehensive drug discovery effort was conducted to identify and optimize potent and selective small-molecule inhibitors of NTCP-mediated bile acid uptake and HBV/HDV entry with adequate *in vitro* ADME characteristics. Several examples were evaluated for impact on bile acid disposition in sandwich-cultured human hepatocytes. Oatp1a/1b deficient mice were used to determine *in vivo* impact on bile acid kinetics. Finally, effects of a lead compound on HBV infection were determined in a urokinase-type plasminogen activator-severe combined immunodeficiency (uPA-SCID) humanized liver mouse model.

Results: Several new compounds were synthesized with single-digit nM potency for NTCP and high selectivity ($>100\times$) against ASBT and BSEP mediated bile acid uptake. Consistently, derivatives of this series dose-dependently reduced intracellular bile acid levels in sandwich-cultured human hepatocytes. PK/PD experiments in Oatp1a/1b deficient mice and in uPA/SCID humanized liver mice illustrated prolonged target engagement (elevation of serum bile acid levels) allowing for once daily oral dosing schedules. *In vitro* infection studies demonstrated low nM HBV and HDV entry inhibition, similar to bulevirtide. Finally, a lead compound completely blocked HBV infection *in vivo* using once daily oral administration in a humanized liver mouse model.

Conclusion: Here we developed orally bioavailable small molecule inhibitors of NTCP with similar anti-HBV efficacy as bulevirtide. This strategy can also be applied to lower hepatocellular bile acid accumulation in cholestatic disease.

FRI-232

The divergent C-terminus of L-HDAg regulates the dynamic life cycle of HDV and the responses to Ionafarnib treatment

Hongbo Guo^{1,1}, Qiudi Li¹, Yi Ni², Kuiyang Zheng¹, Stephan Urban², Wenshi Wang¹. ¹Jiangsu Key Laboratory of Immunity and Metabolism, Department of Pathogenic Biology and Immunology, Xuzhou Medical University, Xuzhou, China; ²Department of Infectious Diseases, Molecular Virology, University Hospital Heidelberg, Germany
Email: wenshi.wang@xzhmu.edu.cn

POSTER PRESENTATIONS

Background and aims: Different life-cycle kinetics of Hepatitis D virus (HDV) genotypes 1–8 were reported previously. C-terminal extension, the only difference between L- and S-HDAg, enables L-HDAg to inhibit HDV replication, but also mediate HDV assembly, thus being the natural drug target of lonafarnib. Strikingly, these residues are highly divergent among genotypes. Therefore, their roles in the life-cycle of HDV and the treatment responses of lonafarnib on HDV were investigated.

Method: Constructs to express chimeric or mutant L-HDAg were created. Their roles in HDV replication and production were investigated using northern blot, reverse-transcription quantitative PCR, and an HDV trans-complementary system established.

Results: C-terminus of L-HDAg of HDV 1–8, although highly divergent, inhibits HDV replication and supports virus production with similar efficacy. The prolines and hydrophobic residues of C-terminus, together with the isoprenylated site, support HBV envelopment HDV, while not needed for non-HBV envelopment. In contrast, the isoprenylated site, but not the prolines and hydrophobic residues, contributes to the trans-inhibitory function of L-HDAg, explaining the double mode-of-actions of lonafarnib on HDV. Besides blocking HDV assembly, lonafarnib promotes intracellular HDV replication solely via inhibiting L-HDAg isoprenylation, while not through an off-target effect on host prenylated proteins.

Conclusion: The divergent C-terminus of L-HDAg *per se* is not the underlying cause to explain the different kinetics of HDV 1–8. During HDV envelopment, the isoprenylated site and the hydrophobic residues of L-HDAg might conduct hydrophobic interactions with the hydrophobic C-terminus of S-HBsAg, while the prolines may extend the C-terminus out of L-HDAg to facilitate this interaction. These findings provide insights into HDV envelopment, and also the usage of lonafarnib against HDV in clinic.

FRI-233

A novel recombinant HBV based selection system allows for a systematic genomic knock-out screening and the identification of host factors involved in HBV infection

Bo-Hung Liao¹, Rupert Öllinger², Wen-Min Chou¹, Andreas Puschnik³, Cho-Chin Cheng¹, Jochen Wettengel¹, Roland Rad², Ulrike Protzer¹.

¹Institute of Virology, Munich, Germany; ²Institute of Molecular Oncology and Functional Genomics, Germany; ³The Chan Zuckerberg Biohub, United States

Email: protzer@tum.de

Background and aims: HBV infection is a global health issues with >285 million of humans living with chronic HBV infection. Unfortunately, our knowledge about the early steps of the virus replication cycle up to the establishment of the nuclear HBV

persistence form, the covalently closed circular DNA (cccDNA), are limited. HBV infection relies on host factors rendering these prospective therapeutic targets. Wild type HBV infection is widely used to screen for these host factors which, however, precludes an analysis on a single cell level. We therefore designed a recombinant HBV (rHBV) expressing part of Cre recombinase complementing a cellular counterpart to perform a systematic genome wide CRISPR-Cas9 knock-out screening at a single cell level.

Method: Fluorescent microscopy and flow-cytometry were conducted to optimize the infection rate of rHBV. The Cre-loxP system consists of a rHBV that encodes the N-terminal Cre and HepG2 cells that stably express the HBV-receptor NTCP and the C-terminal part of Cre recombinase as well as a reporter cassette flanked by loxP sites (HepG2-K7-NTCP-CreC Induced Red (CCIR)). Lentivirus transduction system was applied to introduce Cas9 and a genome-wide human sgRNA knock/out library into the cells. Next generation sequencing (NGS) was performed to deeply sequence the sgRNAs in the cells and followed by the calculation of sgRNA enrichment scores by MAGeCK module analysis.

Results: The split Cre-loxP rHBV infection system allowed for both, positive and negative selection of infected cells. Positive selection uses a reporter gene that is expressed upon rHBV infection and recombination. Negative selection is achieved by antibiotics as antibiotic resistance is lost due to Cre-loxP recombination. Using numerous rounds of infection and subsequent antibiotic selection, we optimized the infection and selection protocol. This allowed us to get around the main drawback of cell-culture HBV infection, its low infection rate. The Cas9 and genome-wide gRNA library introduced into the CCIR cells now allowed to carry out first genome-wide host factors knock-out screenings at the single-cell level. Using NGS, we were able to confirm ZCCHC14 as a top-ranked candidate and identify new host factors involved in HBV infection. We are now validating the discovered candidates and inhibitors that may serve as potential antivirals.

Conclusion: We introduced a novel rHBV infection system that establishes a permanent infection mark via Cre-loxP recombination and enables positive and negative selection of infected cells. After optimization of infection and selection, genome-wide host factor knock-out screenings at the single-cell level identified ZCCHC14 and other host factors participating in the HBV infection. This now allows to dive into the mechanism behind these and explore possible inhibitors targeting these as candidate therapeutics.

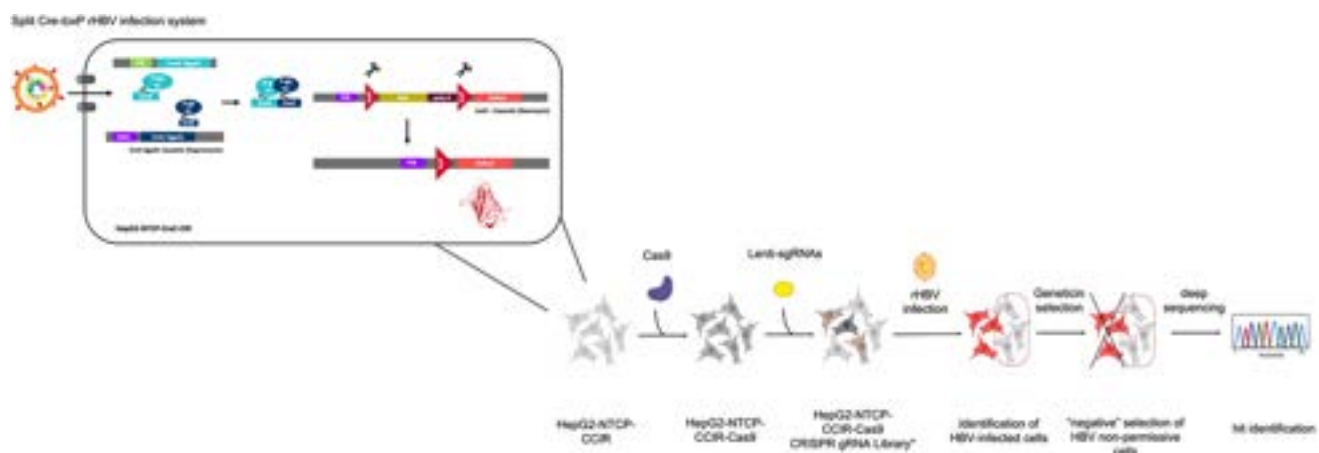


Figure: (abstract: FRI-233).

FRI-234

miR-26a targets USP15 to robustly suppress hepatitis E virus replication via the enhancement of RIG-I-mediated type I interferon response

Jikai Zhang¹, Dan Liu¹, Zijie Wang¹, Renxian Tang¹, Hongbo Guo¹, Wenshi Wang¹. ¹Xuzhou Medical University, China
Email: wenshi.wang@xzhmu.edu.cn

Background and aims: Hepatitis E virus (HEV) infection is the leading cause of acute viral hepatitis globally. However, no specific antivirals are available. Being one of the key host natural antiviral responses, small noncoding RNAs (miRNAs) represent a novel antiviral strategy. Nevertheless, the key miRNAs that regulate HEV life cycle remain largely elusive.

Method: IFN- β promoter activities were determined by dual luciferase reporter (DLR) assay. The mRNA levels of IFN- β , interferon stimulated genes (ISGs) and USP15 or the relative level of HEV RNA were determined by real-time quantitative PCR (qRT-PCR), respectively. The protein levels of USP15, RIG-I, IRF3 and HEV ORF2 were verified by immunoblotting or immunofluorescence assay (IFA). The interaction between USP15 and key elements of IFN pathway or the ubiquitination levels were determined by co-immunoprecipitation (co-IP) and immunoblot analyses.

Results: Herein, we found that miR-26a robustly suppressed HEV replication via the specific inhibition of USP15 expression. Mechanistic investigation revealed that USP15 interacts directly with the retinoic acid-inducible gene I (RIG-I) to deubiquitinate K63-linked RIG-I, thus negatively regulating type I interferon (IFN) signalling. Conversely, miR-26a, by downregulating USP15, promotes RIG-I K63-ubiquitination to enhance type I IFN antiviral responses, resulting in an active antiviral state against HEV. Intriguingly, the activation of type I IFN responses could suppress miR-26a expression,

serving as an intrinsic negative feedback loop to maintain balanced activating signals.

Conclusion: This research identified a new anti-HEV miRNA and elucidated the antiviral mode-of-action. miR-26a may serve as a potential antiviral candidate for combating HEV infection.

FRI-235

Altered metabolic program initiates immune activation leading to hepatitis B surface antigen seroconversion in mild and severe hepatitis B reactivation patients

Jayesh Kumar Sevak¹, Mojahidul Islam¹, Anoushka Saxena¹, Gayantika Verma¹, Manoj Kumar², Ankur Jindal², Gayatri Ramakrishna¹, Shiv Kumar Sarin², Nirupma Trehanpati¹. ¹Institute of Liver and Biliary Sciences, Molecular and Cellular Medicine, New Delhi, India; ²Institute of Liver and Biliary Sciences, Department of Hepatology, New Delhi, India
Email: trehanpati@gmail.com

Background and aims: Rate of seroconversion in hepatitis B reactivation (rHBV) patients is based on the clinical syndrome. Along with elevated bilirubin, coagulopathy, ascites, hepatic encephalopathy, organ failure, systemic immune and metabolic responses play vital role in morbidity and mortality. Therefore, our **aim** was to understand the immune and metabolic responses in mild, severe and ACLF leading to seroconversion.

Method: Total sixty-seven rHBV patients (age 42 ± 13) with raised ALT ($>5\text{XULN}$) and HBV DNAlog 10^{4-8} categorized as mild ($n = 42$, INR < 1.5), severe ($n = 10$, INR > 1.5 , bilirubin $> 2.5\text{XULN}$) and ACLF ($n = 15$) were studied at baseline, week (wk) 12 and 24. Soluble inhibitory molecules and plasma metabolomics was assessed using multiplex bead array and mass spectrometry respectively. High dimensional immune cell profiling was done by flow cytometry.

Results: Of 67 patients, 12 were seroconverted, 7 from mild and five from severe group, but none was seroconverted from ACLF group. At

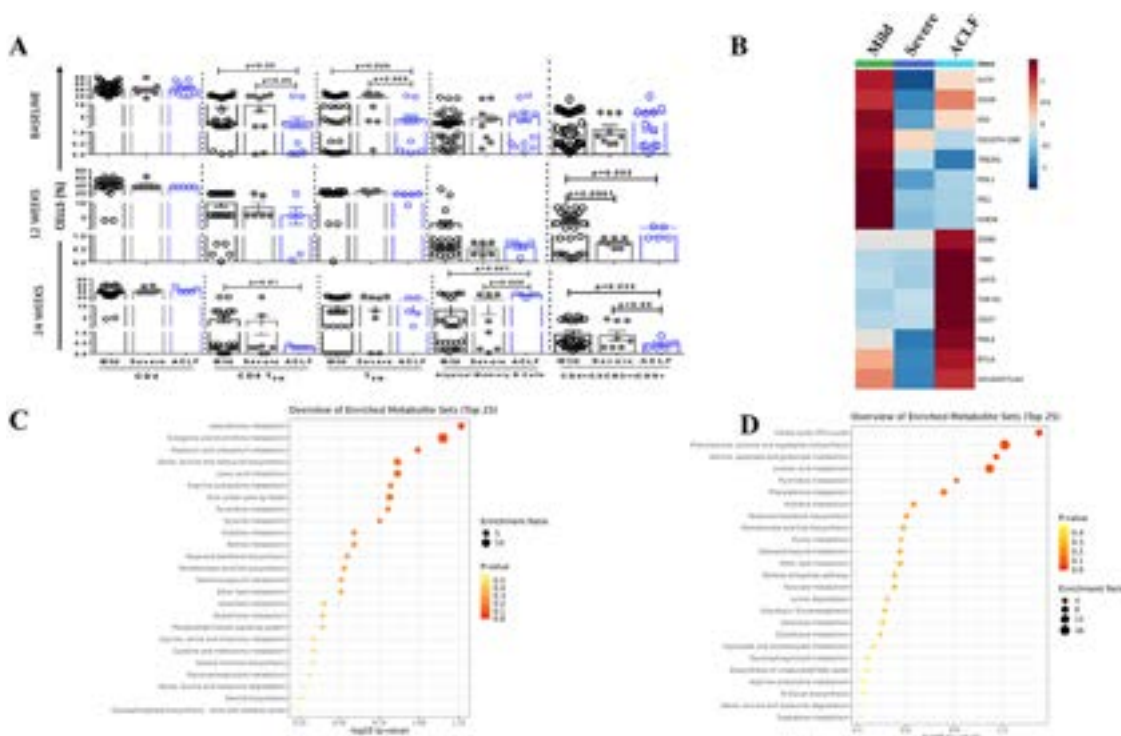


Fig: (A). Kinetic immune changes in mild, severe and ACLF of HBV reactivation. **(B).** Increased soluble inhibitory molecules in mild, severe and ACLF patients. **(C).** Pathway enrichment of mild patients at Baseline. **(D).** Pathway enrichment of ACLF at 24 week.

Figure: (abstract: FRI-235).

POSTER PRESENTATIONS

baseline, no significant difference was observed in the proportions of total CD4/CD8, central memory (CM), TEMRA, B cells, TFH cells and soluble inhibitory receptors except effector memory (EM) which was significantly compromised in ACLF patients compared to mild and severe. At baseline, metabolomics analysis revealed, 32 commonly expressed metabolites associated with beta alanine, arginine, ornithine, porphyrin, urobilinogen metabolism and valine, leucine and isoleucine biosynthesis in mild and severe groups. Which play critical role in exiting T cells from quiescence and leading to T cell activation and cytokine secretion. At wk 12, all B cell subsets including naïve, mature, activated, classical memory, plasma B cells were significantly increased in mild patients compared to severe and ACLF. In severe and ACLF patients, soluble TIM3, LAG3, PDL2, CD27 and CD80 and atypical memory B cells were significantly appeared more with decline in Tfh cells indicating exhausted B cells and formation of short lived plasma B cells. Further, in severe and ACLF patients, unique metabolites pertaining to purine, taurine, hypotaurine, phenylalanine metabolism were expressed with critical role in immune inhibition and anti-inflammatory response. At wk 24, B cells and TFH were significantly increased in mild and severe but declined in ACLF. In ACLF, 75 unique metabolites associated with TCA cycle, Phenylalanine, tyrosine, tryptophan biosynthesis, alanine, aspartate and glutamate metabolism leading to insulin resistance and metabolic alterations.

Conclusion: Our results show that metabolism of beta alanine, arginine, ornithine, porphyrin and urobilinogen contribute immensely to immune activation. Increase levels of soluble inhibitory molecules in ACLF leads to immune and metabolic dysfunction and multiorgan failure.

FRI-236

HBsAg level defines different clinical phenotypes of chronic HBV infection eAg (-) related to the quality of the HBV-specific CD8 cell response

Jeniffer Martínez^{1,2}, Henar Calvo Sánchez^{2,3}, Julia Peña Asensio², Alberto Delgado², Joaquín Miquel², Eduardo Sanz de Villalobos², Alejandro González Praetorius², Miguel Torralba^{2,3}, Juan Ramón Larrubia^{2,3}. ¹University of Alcalá, Department of Biology of Systems, Spain; ²University Hospital of Guadalajara, Translational Hepatology Unit., Spain; ³University of Alcalá, Department of Medicine and Medical Specialties, Spain
Email: juan.larrubia@uah.es

Background and aims: Chronic eAg-negative HBV infection (CIbe (-)) is characterized by little progression of liver fibrosis and a vigorous HBV-multispecific CD8+ cell response. The level of HBV surface antigen (HBsAg) could differentiate different subtypes of CIbe (-). Aims: To evaluate whether HBsAg level correlates with different clinical phenotypes of CIbe (-) and with the quality of the HBV-specific CD8+ cell response.

Method: An analytical cross-sectional study was performed in a cohort of 56 patients with CIbe (-) followed-up for at least one year (95% CI: 5.5–7.5) with ALT<50 IU/ml, HBV viral load (VL) <20,000 IU/ml, APRI<0.5 and Fibroscan <7 KPa. HBsAg level (<300 IU/ml, 300–1000 IU/ml, >1000 IU/ml) was correlated with ALT, AST, APRI, liver stiffness by elastography, platelets, HBV VL, percentage of HBV VL measurements >2000 IU/ml, APRI/years of evolution ratio, Fibroscan (KPa)/years of evolution. In HLA-A2 positive patients we also analyzed the proliferation capacity of HBV-specific CD8+ cells against core18–27, polymerase456–63 and envelope183–91 epitopes after antigenic encounter, using pentameric technology by flow cytometry.

Results: A positive linear trend was observed between HBsAg level and APRI level ($p = 0.002$), Fibroscan ($p = 0.004$), ALT ($p = 0.018$), AST ($p = 0.009$), HBV VL ($p = 0.037$), frequency of HBV VL > 2000 IU/ml ($p = 0.046$) and a negative correlation with platelet level ($p = 0.024$), although all these values were always within the normal range. The frequency of cases with HBV-specific CD8+ cell response against at

least two HBV epitopes was significantly higher in cases with HBsAg < 1000 IU/ml ($p = 0.037$) and this was due to a different response against polymerase456–63 ($p = 0.022$). This response was decreased in cases with HBsAg > 1000 IU/ml, while the response against HBVcore18–27 was preserved and the response against envelope183–91 was abolished, regardless of HBsAg level. Cases with preserved CD8+ cellular response against HBV polymerase456–63 had lower KPa/duration of infection ($p = 0.036$) and APRI/duration of infection ($p = 0.004$). The intensity of specific CD8+ HBV-polymerase456–63 CD8+ response was negatively correlated with Fibroscan (KPa)/years of infection evolution ratio ($p = 0.027$).

Conclusion: Some CIbe (-) patients with HBsAg > 1000 IU/ml present indirect data of higher degree of inflammation, liver stiffness and speed of fibrosis progression which are related to an altered anti-HBV-polymerase456–63 CD8+ cell response. In cases of CIbe (-) with HBsAg > 1000 IU/ml, the cytotoxic T cell response against polymerase should be evaluated and if absent, a liver biopsy should be performed to evaluate the need for treatment.

FRI-237

Chimeric bio-nanoparticles induce targeted HBeAg seroclearance in a HBV hydrodynamic injection mouse model

Yianni Droungas^{1,2}, Hugh Mason¹, Chee Leng Lee¹, Rachel Hammond¹, Stephen Locarnini¹, Renae Walsh¹, Hans Netter¹, Peter Revill^{1,2}. ¹Victorian Infectious Diseases Reference Laboratory, Royal Melbourne Hospital at the Peter Doherty Institute for Infection and Immunity, Australia; ²Department of Microbiology and Immunology, The University of Melbourne, Victoria, Australia
Email: peter.revill@mh.org.au

Background and aims: The hepatitis B e antigen (HBeAg) is a secreted viral protein important for establishing chronic HBV infection. HBeAg seroconversion is a current treatment end point and a preceding step to functional cure. This project utilised HBeAg-epitope expressing bio-nanoparticles (HBeAg-BNP) as immunogens in a hydrodynamic injection (HDI) mouse model of HBV persistent replication. HBeAg clearance was investigated as a novel therapeutic strategy.

Method: HBeAg-BNP candidates were bioengineered using a panel of HBeAg-specific epitopes. Immunogenicity studies were performed in BALB/c mice to identify the most immunogenic HBeAg-BNP candidates, which were then tested using the HDI mouse model. HBV markers of replication, protein expression and antibody production were assessed.

Results: Immunisations of naïve BALB/c mice with HBeAg-BNPs induced HBeAg-specific immune responses against the inserted HBeAg epitopes. Sera from HBeAg-BNP treated BALB/c mice detected HBeAg peptides and native HBeAg by ELISA. Two candidate HBeAg-BNPs (BNP1 and BNP2) were further tested using the HDI mouse model of persistent HBV replication, resulting in 40% (BNP1, 3/7 mice) and 66% (BNP2, 8/12 mice) HBeAg seroclearance. In addition, HBsAg loss was observed almost 20% of the HBeAg-BNP2 group (2/12 mice), with modest (up to 0.9 log) reductions in HBV DNA also observed in some BNP2-treated mice. HBeAg seroclearance, HBsAg loss, or reductions in HBV DNA were not observed in any wild-type BNP control mice (0/7). No difference was observed in the abundance of anti-core positive hepatocytes in BNP treated, or wild-type BNP control mice.

Conclusion: This is the first study to show that HBeAg-BNPs trigger HBeAg-specific immune responses against the native HBeAg and induce its seroclearance. In turn, treatment with HBeAg-BNP2 led to HBsAg loss and HBV DNA reductions in some mice, although did not lead to antibody-mediated clearance of HBV infected hepatocytes. These findings suggest that targeting HBeAg and the induction of anti-HBe antibodies should be further investigated as a novel therapeutic approach.

FRI-238

Pharmacodynamic durability of ALG-125755, a GalNAc-conjugated siRNA, correlated with total and RNA induced complex (RISC) bound siRNA in mouse liver

Kusum Gupta¹, Megan Fitzgerald¹, Jin Hong¹, Cheng Kao¹, Cheng Liu¹, Kha Le¹, Sucheta Mukherjee¹, Dinah Misner¹, Meenakshi Venkatraman¹, Matt McClure¹, Sushmita Chanda², John Fry¹, David Smith¹, Julian Symons¹, Lawrence Blatt¹, Leonid Beigelman¹, Tse-I Lin². ¹Aligos Therapeutics, Inc., United States; ²Aligos Belgium Bv, Leuven, Belgium
Email: kgupta@aligos.com

Background and aims: For the functional cure of chronic hepatitis B, a sustained loss of hepatitis B surface antigen (HBsAg) is required. Targeted small interfering RNAs (siRNAs) have recently demonstrated significant clinical reduction of HBsAg. ALG-125755 is a novel N-acetylgalactosamine (GalNAc)-conjugated siRNA currently in clinical development. Here we demonstrate its mechanism of action, and correlate the durable pharmacodynamics to total and RNA induced silencing complex (RISC) bound siRNA in mouse liver in the adeno-associated virus (AAV)-HBV mouse efficacy model.

Method: To confirm the mechanism of action of ALG-125755, argonaute-2 (AGO-2) degradation of the target S-region HBV RNA sequence induced by the antisense strand (AS), ALG-125736, was qualitatively measured using denaturing polyacrylamide gel electrophoresis. Total and RISC-bound siRNA quantification was performed in the harvested livers from a previously reported adeno-associated virus (AAV)-HBV mouse efficacy study, where a 10 mg/kg single dose or repeat doses up to 70 days at 5 mg/kg every other week (Q2W) or every four weeks (Q4W) demonstrated significant and durable decline in serum HBsAg. Liver samples (Days 14, 28, 70, each prior to the dose, and postdose timepoints at Days 98 and 168) from the single dose and repeat (Q2W) dose groups were analyzed by liquid chromatography-high resolution accurate mass method for total siRNA and immunoprecipitation/reverse transcription-quantitative polymerase chain reaction method for RISC-bound siRNA.

Results: The AS, ALG-125736, complementary to the highly conserved S-region of the HBV RNA sequence, induced cleavage of the target RNA sequence from the S-region of HBV by AGO-2. The engagement of ALG-125755 with AGO-2 protein was confirmed in vitro and also in vivo in the AAV-HBV mouse. Following a single dose in AAV-HBV mice, the half-life of RISC-bound siRNA (23.5 days) was two times longer than that of the total liver siRNA (11.7 days). Upon repeat Q2W dosing, kinetics of RISC-bound siRNA was similar to the total siRNA. Sustained RISC-bound siRNA concentrations were achieved upon repeat dosing. RISC-bound siRNA was quantifiable through the last study day 168 with the repeat dose (Q2W regimen) and at up to 98 days following a single dose. The durability of HBsAg reduction corresponded with both the total and the RISC-bound siRNA.

Conclusion: Binding of ALG-125755 to AGO-2 was demonstrated in vitro and in vivo, confirming that the mechanism of action for ALG-125755 is consistent with that of an siRNA. Pharmacodynamic response of HBsAg reduction and durability correlated with total siRNA and RISC-bound siRNA in mouse liver. The long half-life of the RISC-bound siRNA indicates that dosing in human could be less frequent than monthly dosing.

FRI-239

A potent human PD-L1 siRNA leads to significant reduction of AAV-HBV infected hepatocytes via immune activation in human PD-1/PD-L1 double knock in mice

Jin Hong¹, Dawei Cai¹, Saul Montero¹, Hua Tan¹, Vivek Rajwanshi¹, Aneerban Bhattacharya¹, Kang Hyunsoon¹, Min Luo¹, Megan Fitzgerald¹, David Smith¹, Lawrence Blatt¹, Julian Symons¹, Leonid Beigelman¹. ¹Aligos Therapeutics, South San Francisco, United States
Email: jhong@aligos.com

Background and aims: T cell exhaustion is characteristic of chronic hepatitis B (CHB) and contributes to the persistence of hepatitis B virus (HBV) infection. PD-1/PD-L1 is the dominant co-inhibitory axis mediating T cell exhaustion in CHB patients. Monoclonal antibodies against PD-1 or PD-L1 have been tested in CHB patients and have shown promising results. However, the dose of antibodies administered were significantly lower in CHB patients than in cancer patients to minimize immune related adverse events. Compared with antibodies, subcutaneously (SC) delivered siRNA have a short half-life in plasma and exposure is mainly concentrated in the liver, thereby reducing the potential for systemic toxicities. We have developed a GalNAc conjugated human PD-L1 (hPD-L1) siRNA lead molecule, ALG-072571, that demonstrated significant reduction of AAV-HBV infected hepatocytes through immune activation in human PD-1/PD-L1 double knock in (KI) mice.

Method: siRNAs were synthesized on a MerMade synthesizer. In vitro human PD-L1 knockdown was evaluated in the SNU-387 cell line by RT-qPCR. GalNAc PD-L1 siRNA pharmacodynamics (PD) were studied by assessing Poly IC induced human PD-L1 levels in double KI mice. In double KI mice chronically infected with AAV-HBV, ALG-072571 and HBV siRNA ALG-125819 were dosed SC as single agents (8 × 7.5 mg/kg QW and 4 × 5 mg/kg QOW respectively) or in combination. Serial serum collections were tested for HBsAg, HBeAg, HBV DNA and ALT. Terminal serum samples were assayed for anti-HBsAg antibody. Mouse livers were stained for HBeAg, HBsAg and CD3 using IHC and scored for positive cells.

Results: Unconjugated ALG-072571 containing novel siRNA stabilization chemistries showed an EC₅₀ of 90 pM in reducing hPD-L1 RNA in SNU387 cells. In a PD study, a single SC 7.5 mg/kg dose of ALG-072571 reduced liver hPD-L1 RNA by 71% and protein by 45%. In parallel FACS analysis, the cell surface hPD-L1 level in liver CD45+ immune cells were reduced by 19% and in Kupffer cells by 37%. In an AAV-HBV study using double KI mice, ALG-072571 repeat dosing reduced HBsAg, HBeAg and HBV DNA by 3.3 log₁₀ IU/ml, 1.73 log₁₀ PEIU/ml and 4.5 log₁₀ IU/ml respectively. In the combination group, ALG-072571 and ALG-125819 showed additivity, reducing HBsAg, HBeAg and HBV DNA 4.3 log₁₀ IU/ml, 2.0 log₁₀ PEIU/ml and 6.9 log₁₀ IU/ml respectively. ALT elevation was observed preceding the viral marker reductions. In liver IHC HBeAg staining, the core positive hepatocyte percentages were approximately 60% for the vehicle control and ALG-125819 alone groups, but not detectable in ALG-072571 alone and combination groups. ALG-072571 alone and in combination also showed CD3+ T cell infiltration in the liver and anti HBsAg antibody in the serum of mice with the lowest HBsAg levels.

Conclusion: Liver targeted PD-L1 siRNA therapy may lead to restoration of immune responses against HBV and consequent clearance of HBV infection.

FRI-240

Impact of cirrhosis and long-term follow-up on the inflammatory milieu after hepatitis C virus (HCV) elimination by direct-acting antiviral (DAA) therapy

Moana Witte^{1,2,3,4}, Carlos Oltmanns^{1,2,3,4}, Jan Tauwaldt^{1,2,3,4}, Gordon Grabert^{5,6}, Leon Kalix^{5,6}, Daniel Dehncke^{5,6}, Hagen Schmaus^{3,4}, Heiner Wedemeyer¹, Benjamin Maasoumy¹, Tim Kacprowski^{5,6}, Anke Kraft^{1,2,3,4}, Markus Cornberg^{1,2,3,4}. ¹Hannover Medical School, Department of Gastroenterology, Hepatology and Endocrinology, Germany; ²German Center for Infection Research (DZIF), Hannover, Germany; ³Center for Individualized Infection Medicine (CiiM), Hannover, Germany; ⁴Twincore, Center of Experimental and Clinical Infection Research, Hannover, Germany; ⁵Peter L. Reichertz Institute for Medical Informatics of Technische Universität Braunschweig and Hannover Medical School, Division Data Science, Braunschweig, Germany; ⁶Braunschweig Integrated Centre for Systems Biology (BRICS), Technische Universität Braunschweig, Braunschweig, Germany
Email: witte.moana@mh-hannover.de

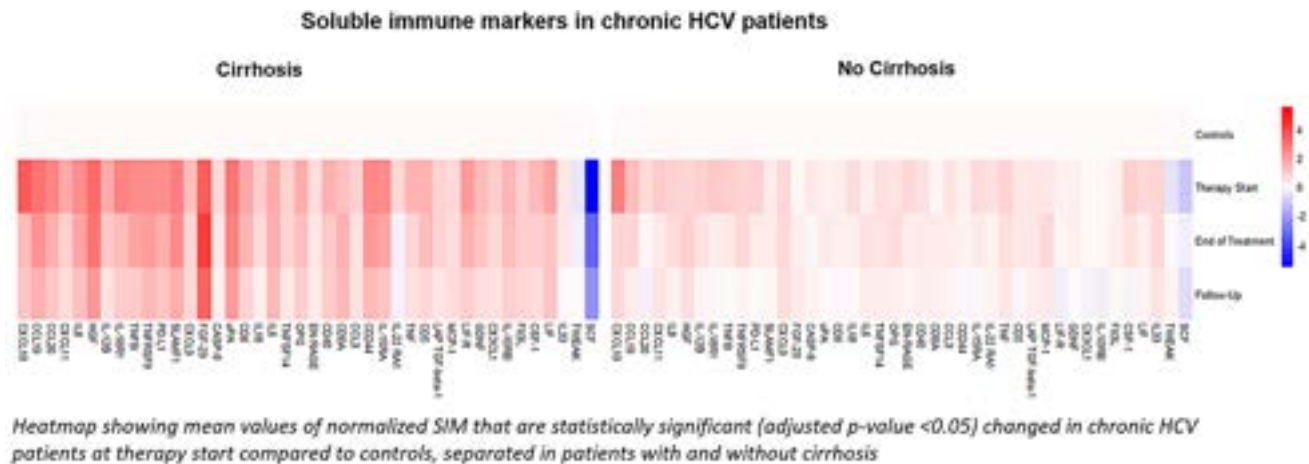


Figure: (abstract: FRI-240): Soluble immune markers (SIM) in chronic HCV patients before and after HCV elimination by DAA and in controls.

Background and aims: DAA therapy results in sustained virologic response in over 99% of patients with chronic HCV. However, a proportion of patients remain at risk for long-term sequelae, such as fatigue or development of hepatocellular carcinoma (HCC), suggesting persistent biological alterations. Following our previous results showing the impact of chronic HCV on the inflammatory milieu in the context of short-term follow-up of 12–24 weeks after DAA therapy, we now aim to further investigate the effect of viral elimination in cirrhotic and non-cirrhotic patients at long-term follow-up.

Method: 104 chronic HCV patients, 47 with cirrhosis (age 57.31 ± 9.37 , elastography 34.17 ± 17.49), of whom 8 developed HCC, and 57 without cirrhosis (age 57.90 ± 11.70 , elastography 7.65 ± 2.50), were treated with DAA. Plasma samples were available at baseline, at the end of treatment, and at long-term follow-up (median: 96 weeks). 40 inactive HBsAg carriers (HBsAg negative, ALT normal) and 16 healthy individuals served as controls. Plasma levels of 92 soluble immune markers (SIM) were measured by Olink Proteomics using a proximity extension assay.

Results: Compared with controls, 43 SIM were statistically significantly altered at baseline in all chronic HCV patients (Welch Two Sample t -test, adjusted p value <0.05). However, an independent comparison between cirrhotic and non-cirrhotic HCV patients revealed very distinct SIM profiles (49 altered SIM in cirrhotics, 24 altered SIM in non-cirrhotics compared to controls). Moreover, SIM dynamics after DAA treatment differed significantly between cirrhotic and non-cirrhotic patients. Compared to controls, no SIM was significantly changed anymore in non-cirrhotics at long-term follow-up, while 39 SIM were still significantly (adjusted p value <0.05) modified in cirrhotics. Of the SIM that were elevated at baseline in both HCV patients with and without cirrhosis, 16 of these "HCV-specific SIM" (including CXCL10, CXCL11, IL-8, PD-L1, IL-15RA, HGF) were still significantly elevated in cirrhotic patients at long-term follow-up in addition to "cirrhosis-specific" SIM (e.g., IL-6, FGF-23, CXCL6, CCL25, MMP-10, MCP-1). Interestingly, some of these "HCV-specific SIM" (e.g., HGF) showed different dynamics in patients who developed HCC compared to matched cirrhotic controls without HCC.

Conclusion: After successful HCV elimination, the HCV specific inflammatory milieu remains altered in cirrhotic patients. Our data suggest that "HCV-specific" and "cirrhosis-specific" changes in the inflammatory milieu can be distinguished. Some of the SIM, known to be associated with carcinogenesis, show different dynamics over time in HCC patients, suggesting a possible link between an altered inflammatory milieu and HCC development.

FRI-241

Preclinical pharmacokinetic, pharmacodynamic and efficacy relationships of ALG-093702, a liver targeted PD-L1 small molecule inhibitor, in different in vivo models

Heleen Roose¹, Qingling Zhang², Kha Le², Andreas Jekle², Kristina Rekstyte-Matiene¹, Sarah Stevens², Ruchika Jaishankhani², Cheng Liu², Sandra Chang², Antitsa Stoycheva², Lawrence Blatt², Leonid Beigelman², Julian Symons², Sushmita Chanda², Francois Gonzalvez¹, Tongfei Wu¹. ¹Aligos Belgium Bv, Belgium; ²Aligos Therapeutics, Inc., United States
Email: twu@aligos.com

Background and aims: The PD-1/PD-L1 immune checkpoint pathway is an attractive target to reverse immune tolerance in chronic hepatitis B (CHB). However, due to the systemic immune adverse effects associated with antibodies, a lower dose of PD-1/PD-L1 antibodies has been used in CHB vs. the dose used for cancer. ALG-093702 is a liver-targeted PD-L1 small molecule inhibitor that preferentially partitions into the liver and thereby may potentially mitigate extra-hepatic on-target related toxicity. Characterizing the relationship between pharmacokinetics (PK), pharmacodynamics (PD) and the efficacy of ALG-093702 is critical for selecting the dosing strategy of new liver targeted PD-L1 inhibitor drugs.

Method: Biochemical PD-1/PD-L1 interaction was assessed by AlphaLISA[®]. Cellular activity was measured using a co-culture reporter assay in which NFAT activity of Jurkat T cells was constitutively inhibited by the engagement of PD-1 by PD-L1-expressing CHO cells. HBV-specific T cell activation assays were performed in PBMCs from an HBV-infected patient and assessed by measuring IFN gamma release. Oral dosing of ALG-093701, a prodrug of ALG-093702, was used for in vivo PK/PD/efficacy studies. In vivo PK/PD/efficacy were assessed in humanized-PD-L1 MC38 subcutaneous xenografts and/or a liver metastasis mouse model.

Results: ALG-093702 inhibited PD-1/PD-L1 interaction with picomolar IC_{50} values ($IC_{50} = 0.048$ nM) and increased TCR signaling in Jurkat cells with an EC_{50} of 5.9 nM. In an ex vivo study, ALG-093702 activated HBV-specific T cells from an HBV-infected patient to a similar extent as durvalumab. In mouse pharmacokinetic studies, ALG-093702 exhibited significantly higher liver concentrations vs. other tested tissues (liver/lung ratio of 10). In a humanized-PD-L1 MC38 subcutaneous mouse model, oral dosing 50 mg/kg of ALG-093701 achieved a similar extent of PD-L1 target occupancy and tumor growth inhibition as durvalumab. This study also demonstrated that the PD-L1 target occupancy was correlated with ALG-093702 tumor concentration.

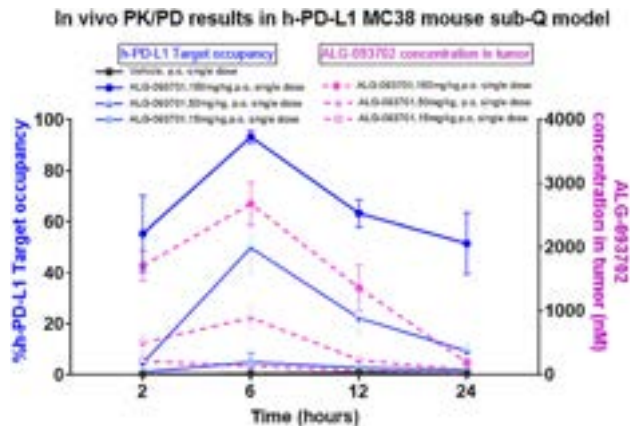


Figure:

Conclusion: We discovered a liver-targeted PD-L1 small molecule inhibitor, ALG-093702, with similar in vitro potency and in vivo PD-L1 target occupancy and tumor growth inhibition as the PD-L1 antibody drug, durvalumab. The preclinical PK/PD/efficacy correlation provides guidance for the efficacious human dose prediction and dosing strategy for clinical studies of oral liver targeted PD-L1 small molecule inhibitor.

FRI-242

The role of gamma delta T cells in chronic hepatitis B virus infection

Katja Steppich^{1,2,3}, Roni Souleiman^{1,2}, Elena Bruni^{3,4,5}, Ximena Leon Lara⁴, Katja Deterding¹, Benjamin Maasoumy¹, Heiner Wedemeyer¹, Immo Prinz^{3,4,5}, Anke Kraft^{1,2,3,6,7}, Markus Cornberg^{1,2,3,6,7}, ¹Hannover Medical School, Department of Gastroenterology, Hepatology and Endocrinology, Germany; ²TWINCORE Centre for Experimental and Clinical Infection Research GmbH, Germany; ³Cluster of Excellence RESIST (EXC 2155), Germany; ⁴Hannover Medical School, Institute of Immunology, Germany; ⁵University Medical Center Hamburg-Eppendorf, Institute of Systems Immunology, Hamburg Center for Translational Immunology (HCTI), Germany; ⁶German Centre for Infection Research, Partner-site Hannover-Braunschweig, Germany; ⁷Centre for Individualized Infection Medicine (CIIM), Germany
Email: steppich.katja@mh-hannover.de

Background and aims: Current treatment options for chronic HBV infection can slow disease progression, but "cure" of HBV infection is a rare event. Therefore, several new therapeutic strategies aimed at "functional cure" (HBsAg loss) are currently being developed. Immune responses are thought to be important for HBV disease progression and HBV cure. Human gamma-delta ($\gamma\delta$) T cells have been shown to play a role in various infectious diseases and are enriched in solid tissues such as the liver, suggesting a role in liver-associated diseases. However, their role in chronic HBV infection remains largely unknown. The aim of this study is to investigate the phenotype, function, and T-cell receptor (TCR) repertoire of $\gamma\delta$ T cells in patients with chronic HBV infection with different viral and clinical characteristics, including patients discontinuing long-term NA therapy.

Method: We performed in-depth ex vivo phenotyping of 87 chronic HBV patients with different HBsAg and HBcrAg levels and controls using a 28-color full-spectrum flow cytometry panel. In addition, PBMC from selected patients were stimulated with phosphoantigens. In addition, TCR sequencing of TCR gamma and TCR delta from mass-sorted V γ 9+ and V γ 9- $\gamma\delta$ T cells was performed using an NGS approach with Illumina MiSeq. In addition, the transcriptome of $\gamma\delta$ T cell subsets was analyzed by single-cell sequencing. Intrahepatic $\gamma\delta$ T cells from some subjects were examined.

Results: We detected and further characterized two distinct $\gamma\delta$ T cell populations (CXCR6+ $\gamma\delta$ T cells and CD16+ $\gamma\delta$ T cells) that were differentially abundant in patients with high (>3.87 log) and low (<3.87 log) HBcrAg levels, whereas HBsAg levels made no difference. Thus, patients with higher HBcrAg levels had a higher frequency of CXCR6+ $\gamma\delta$ T cells (similar phenotype to the recently described CXCR6+CD8+ "autoaggressive" T cells). Analysis of liver tissue samples revealed a higher frequency of CXCR6+ $\gamma\delta$ T cells in the liver compared with blood. A pilot study showed that patients with marked ALT flares after discontinuation of NA treatment had an increase in CXCR6+ $\gamma\delta$ T cells. Interestingly, two patients with similar CXCR6+ $\gamma\delta$ T cell kinetics had similar $\gamma\delta$ TCR diversity and showed subsequent HBsAg loss. In contrast, CD16+ $\gamma\delta$ T cells were significantly increased in patients with low HBcrAg levels, and after stimulation, CD16+ $\gamma\delta$ T cells showed more cytotoxicity (granzyme B) than CD16- $\gamma\delta$ T cells. Transcriptome analyses are ongoing.

Conclusion: Our data suggest that $\gamma\delta$ T cells may be involved in the immunopathogenesis in chronic HBV infection. We describe two distinct $\gamma\delta$ T cell populations that may support viral control in distinct situations but also contribute to hepatitis.

FRI-243

Recombinant hepatitis E viruses harboring a split luciferase tag in the ORF2 capsid protein

Maliki Ankavay¹, Nathalie Da Silva¹, Noémie Oechslin¹, Katja Dinkelborg², Patrick Behrendt², Darius Moradpour¹, Jérôme Gouttenoire¹, ¹Lausanne University Hospital (CHUV) and University of Lausanne, Lausanne, Switzerland, Service of Gastroenterology and Hepatology, Lausanne, Switzerland; ²TWINCORE Centre for Experimental and Clinical Infection Research, Experimental Virology, Germany
Email: maliki.ankavay@chuv.ch

Background and aims: Hepatitis E virus (HEV) infection is the most common cause of acute viral hepatitis worldwide. The viral genome harbors three open reading frames (ORF). The ORF2 protein corresponds to the viral capsid. Molecular studies of the HEV life cycle have been hampered by the lack of robust and sensitive cell culture systems. Hence, the main receptor for HEV cell entry is still elusive and there are no specific antiviral drugs against HEV so far. Here, we aimed to develop a convenient, quantitative and potentially scalable reporter system for HEV infection and replication.

Method: Transposon-mediated random insertion was exploited to identify functional insertion sites within the HEV ORF2 protein. Full-length viral genomes with in-frame insertions of a split luciferase (HiBiT) tag in the capsid protein were characterized by immunofluorescence and immunoblot analyses as well as functional assays. Luciferase activity was quantified by luminometry.

Results: Transposon-mediated random insertion and sequencing of viable genomes identified functional insertion sites in the HEV capsid protein. HEV harboring a HiBiT tag in C-terminal sites remained infectious and functional in terms of RNA replication and capsid secretion, allowing for antibody-free detection and quantitation of capsid protein by luciferase assay. As a proof-of-concept, the antiviral effect of ribavirin and sofosbuvir could be assessed in a quantitative manner. Moreover, neutralization of purified quasi-enveloped and naked HEV by convalescent sera and specific monoclonal antibodies could be measured conveniently. Finally, a broad-scale kinase inhibitor screen identified several compounds with potent antiviral activity that are currently being validated and further characterized in terms of mode of action.

Conclusion: Identification of functional insertion sites enabled tagging of the HEV capsid protein with a highly sensitive and quantitative miniaturized luciferase reporter. Tagged HEV allowed for convenient read-out of infection and replication, with a potential to develop large-scale screening assays for entry inhibitors and other

POSTER PRESENTATIONS

antiviral agents. In addition, the tagged viruses represent a valuable tool for studies aimed at understanding the molecular mechanisms of infection, including the identification of the receptor (s) for HEV cell entry.

FRI-244

Identification of resistance-associated variants after sofosbuvir treatment in chronic hepatitis E patients

Andre Gömer¹, Mara Klöhn¹, Michelle Jagst¹, Maximilian Nocke¹, Thomas Horvatits², Julian Schulze zur Wiesch², Sven Pischke², Svenja Hardtke², Tobias Müller³, Heiner Wedemeyer⁴, Markus Cornberg⁴, Patrick Behrendt⁴, Eike Steinmann¹, Daniel Todt¹.
¹Molecular and Medical Virology, Germany; ²University Medical Center Hamburg-Eppendorf, Germany; ³Charité-Universitätsmedizin Berlin, Berlin, Germany; ⁴Medizinische Hochschule Hannover, Hannover, Germany
Email: andre.goemer@rub.de

Background and aims: Hepatitis E virus (HEV) infections remain a serious problem in immunocompromised patients, leading to chronic infections in about 50% of cases. As of now, off-label use of Ribavirin is the only treatment option, since no HEV-specific antivirals are available. Recently, the hepatitis C virus polymerase inhibitor sofosbuvir was however evaluated as a potential antiviral against HEV in vitro and in vivo. The most comprehensive investigation was a 24-week multicenter phase II pilot trial, where nine chronically HEV-infected patients were treated with sofosbuvir. HEV RNA transiently decreased by 2 log, but increased back to pre-treatment levels within 24 weeks of treatment onset. We aim to identify the reason for viral recurrence by characterizing changes in the viral population during treatment.

Method: For this, we performed amplicon deep sequencing to characterize viral population dynamics in the nine patients treated with sofosbuvir. In addition, we used an HEV-based reporter cell culture system to characterize high-frequency variants that might affect sensitivity to sofosbuvir.

Results: Most patients had highly divergent HEV populations, which suggest a high adaptability to treatment-related selection pressures, possibly associated with the emergence of treatment-resistant variants. We identified amino acid substitution from different time points and singled out substitutions that had become dominant in multiple patients (A1343V, K1383N, D1384N, V1479I, G1634R). These were then cloned into an HEV-3 replicon system to assess their effect on replication fitness and sensitivity to sofosbuvir. The half maximal effective concentration (EC₅₀) was up to 20-fold higher than control, suggesting that variants associated with lower susceptibility were selected during sofosbuvir treatment. In particular, substitution A1343V, which occurred in eight of nine patients during treatment but was not present at baseline, showed a strong increase both in combination with V1479I (20-fold) and as a single substitution (10-fold).

Conclusion: In conclusion, viral population dynamics play a critical role during antiviral treatment. High population diversity during sofosbuvir treatment led to the selection of variants with higher fitness. In particular, the A1343V substitution selected in most patients showed an increased sofosbuvir resistance in vitro, which may have led to treatment failure in vivo.

FRI-245

HBsAg kinetics at month 9 after analogue treatment discontinuation in chronic hepatitis B eAg (-) predicts long-term HBV control

Henar Calvo Sánchez^{1,2}, Julia Peña Asensio¹, Jeniffer Martínez^{1,3}, Alberto Delgado¹, Joaquín Miquel¹, Eduardo Sanz de Villalobos¹, Alejandro González Praetorius¹, Miguel Torralba^{1,2}, Juan Ramón Larrubia^{1,2}.
¹University Hospital of Guadalajara, Translational Hepatology Unit, Spain; ²University of Alcalá, Department of Medicine and Medical Specialties, Spain; ³University of Alcalá, Department of Biology, Spain
Email: juan.larrubia@uah.es

Background and aims: Withdrawal of nucleos(t)ide analogue (NUC) treatment in eAg (-) chronic hepatitis B (CHBeAg (-)) may lead to HBV control. However, there are no markers that predict who benefits from this strategy. Objective: To assess whether HBsAg kinetics after NUC suspension is associated with long-term HBV control.

Method: A longitudinal study of 22 CHBeAg (-) patients previously treated with NUCs for more than 3.5 years and with liver fibrosis <F3 was performed. After discontinuation of treatment, patients were followed monthly in the first quarter and quarterly thereafter, with a follow-up of three years. HBV viral load, HBsAg level and serum alanine aminotransferase (ALT) level were quantified at each follow-up visit. At the end of follow-up (month 36), a patient was considered to be HBV infection controller if the viral load (HBV36) was <2000 IU/ml and the ALT level (ALT36) was normal. We analyzed whether the decrease in HBsAg at month 9 after treatment discontinuation correlated with HBV control at month 36 post-suspension and with the probability of having a multi-specific HBV-functional CD8⁺ cell response, according to the predictive logistic regression model previously described by our group (Peña-Asensio et al. Aliment Pharm Ther 2022).

Results: After discontinuation of treatment with NUCs, an overall decrease in HBsAg level was observed after 36 months of follow-up ($p < 0.001$), which was greater in the group with HBV36 < 2000 IU/ml ($p = 0.004$). The percentage of HBsAg level decrease after 9 months of NUC treatment discontinuation correlated with the presence of HBV36 < 2000 IU/ml and normal ALT36 (Area under ROC curve - 95% CI: 0.58–0.92, $p = 0.037$). The absence of HBsAg decline at month 9 after NUC suspension presented a 100% negative predictive value of viral control at month 36, while a decline $\geq 40\%$ was associated with a 100% predictive positive value of HBV36 < 2000 IU/ml. The level of HBsAg decline at month 9 correlated positively with the probability of having a functional HBV-multispecific CD8⁺ cell response at the end of treatment ($r = 0.566$, $p = 0.009$). Percentage of HBsAg variation after 6-month NUC stop correlated with the clinical status at end of follow-up (HBsAg loss, inactive carrier, grey zone, re-treatment), ($p = 0.002$).

Conclusion: A decrease in HBsAg level $\geq 40\%$ at month 9 after NUC discontinuation in CHBeAg (-) is associated with long-term HBV control, while the absence of decrease implies reactivation of infection during follow-up. The level of HBsAg decline at month 9 correlates positively with the likelihood of having recovered a functional HBV-multispecific CD8⁺ cell response.

FRI-246

Nucleotide analogue therapy does not reverse the hyperexpression of innate-like markers on activated T cells consistent with immunopathology in chronic hepatitis B

Lung Yi Loey Mak^{1,2}, Apostolos Koffas², Sabina Wellington², Sophie Stretch², Anna Riddell³, Man-Fung Yuen¹, Patrick Kennedy², Upkar Gill². ¹The University of Hong Kong, School of Clinical Medicine, Hong Kong; ²Blizard Institute, Barts and The London, School of Medicine and Dentistry, QMUL, Centre for Immunobiology, London, United Kingdom; ³Barts Health NHS Trust, Virology, United Kingdom
Email: u.gill@qmul.ac.uk

Background and aims: There is renewed focus on the importance of non-specific bystander T cells as major contributors to hepatic immunopathology in chronic hepatitis B (CHB). It is key to ascertain details on this understudied immune cell population to provide further insights into the reasons for immunological failure of novel therapies for CHB cure. We studied the phenotypic innate-like properties of global CD4 and CD8 T cells in treatment naïve and experienced patients with CHB compared to healthy controls (HC) to determine any differences and correlated these with clinical parameters.

Method: Forty-six subjects (47.8% male, median age 39.5 years) were studied [CHB; 20, HC; 26]. The proportion of activated (HLA-DR+) T cells was determined along with the expression of NK cell receptors (NKR), markers of T cell differentiation and residency by multi-parameter flow cytometry. The impact of antiviral therapy in a cohort of CHB subjects was also analysed [median tenofovir treatment duration 7.6 years; median ALT: 43 (range: 31–72) U/L; median HBV DNA: 7.1 log IU/ml at treatment initiation].

Results: The overall proportion of HLA-DR+ T cells was higher in CHB patients compared to HCs, and significantly higher on CD4T cells (3.1% vs 1.3%, $p = 0.041$). T cell expression of CXCR6 (0.7% vs 0.3%, $p = 0.010$) and the NKRs, NKG2A (4.4% vs 1.7%, $p = 0.015$) and Nkp30 (2.0% vs 0.9%, $p = 0.023$) was increased in CHB, consistent with immunopathology. We noted augmented expression of NKG2A and CD56 (both $p < 0.0001$) on the activated (HLA-DR+) proportion of CD8 T cells compared to their HLA-DR- counterparts. On analysing CHB subjects undergoing antiviral therapy, the expression of NKRs [NKG2A: CD4; 35.4% vs 2.2% and CD8; 28.4% vs 3.6% (both $p < 0.001$); NKG2D: CD4; 79.6% vs. 2.4% and CD8; 20% vs 5.9% (both $p < 0.01$); Nkp30: CD4; 2.9% vs 0.7% and CD8; 3.3% vs 0.5% (both $p < 0.01$)] and the residency marker CXCR6 (CD4; 10.6% vs 0.4%, $p < 0.0001$, CD8; 2.4% vs 0.3%, $p = 0.011$) remained significantly higher in those on antiviral therapy, despite undetectable HBV DNA and ALT normalisation, compared to those with CHB treatment naïve patients with bona-fide immune control, indicating that the bystander innate like immune defects are not recovered by current antiviral therapy.

Conclusion: CHB is associated with increased non-specific innate like activated T-cells, potentially causing immunopathology. Antiviral therapy is unable to reverse these immune cell defects suggesting the need for earlier treatment or add on therapies to achieve CHB cure.

FRI-247

Baseline plasma lipidome correlates with direct-acting antiviral therapy non-response for HCV in HIV-HCV coinfecting patients

Jaswinder Maras¹, Vasundhra Bindal¹, Gaurav Tripathi¹, Manisha Yadav¹, Nupur Sharma¹, Babu Mathew¹, Sadam H Bhat¹, Abhishak Gupta¹, Neha Sharma¹, Sushmita Pandey¹, Ekta Gupta². ¹Institute of Liver and Biliary Sciences, Department of molecular and cellular medicines, New Delhi, India; ²Institute of Liver and Biliary Sciences, Department of Clinical Virology, New Delhi, India
Email: jassi2param@gmail.com

Background and aims: Direct-acting antivirals have increased the SVR attainment rate to 95%; however, still, there is an HIV-HCV coinfecting population that is non-responders to DAA therapy. As both HIV and HCV co-infection is tightly associated with dyslipidemia characterizing specific alterations in the lipidome of HIV-HCV coinfecting patients will give important pathophysiological insights. The primary aim of the present study is to identify baseline lipid species that could be used for the early stratification of HIV-HCV coinfecting non-responders of the DAA therapy at baseline.

Method: This study identified N=43 of N=2064 HCV patients as HIV-HCV coinfecting. These patients received Sofosbuvir and Daclatasvir as standard HCV therapy. Based on the post-therapy HCV RNA status, these patients were further segregated as responders (n=10) and non-responders (n=10) to standard DAA therapy. Amongst them, 20 paired patient samples were identified, and their baseline and post-therapy (3 months) plasma samples were subjected to untargeted lipidomics analysis using LC-MS/MS.

Results: HCV-HIC coinfecting patients had dyslipidemia; comparative lipid analysis at baseline of DAA non-responders with responders identified 198 differentially expressed lipids ((DEL-90 Up; 108 Down; FC > 1.5, $p < 0.05$). The class with the maximum number of (DELs) was PE (Phosphatidylethanolamine-45 Up; 41 Down), PC (Phosphatidylcholine 20 Up; 21 Down), and others. Comparative analysis of the post-therapy lipidome profile of non-responders with responders revealed 261 DEL (96 UP and 165 Down; FC > 1.5, $p < 0.05$). Among 198 DEL, the class with the maximum number of DEL were PE (30 Up and 66 Down), PC (22 Up; 27 Down), and others. We found that post-therapy downregulation of 27 lipids (Major classes altered PC and PE) and upregulation of 41 lipid species (Major classes altered PC and PE and DG) is linked with DAA therapy response. Surprisingly, non-responders at baseline have very high levels of PE and PC, which decreases post-therapy, suggesting their role in negating the DAA response. DAA therapy induces a net 60X reduction of PE in non-responders and a 12 × reduction in PC. Finally, non-responders at baseline have a very high abundance of lipid species like ((PC (20:1/18.3); FC > 122; $p < 0.05$; AUC > 0.99), ((PE (18:0) p); FC > 589; $p < 0.05$; AUC > 0.99) and, all the selected clinical indicators positively correlated with HCV viral load AST, ALT and APRI score suggesting their role in Viral replication.

Conclusion: The lipidome profile of DAA non-responders and responders is distinct and crucial in determining DAA response. Increase in plasma PE [PE (18:0) p] and PC [PC (20:1/18.3)] are the two major classes that negate DAA response and are key lipid indicator for non-response.

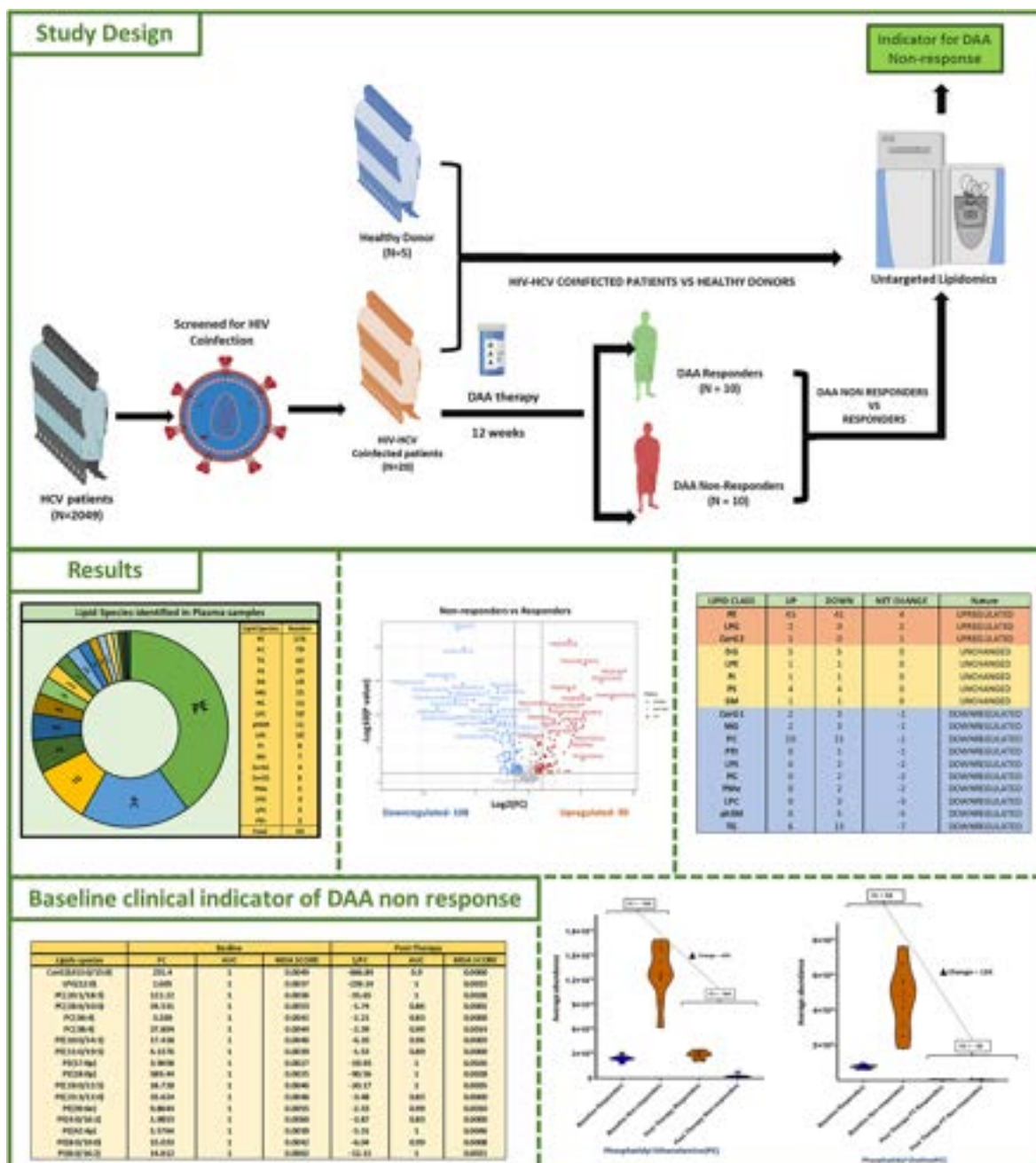


Figure: (abstract: FRI-247).

FRI-248

Intrahepatic characterization of virological and immunological markers in two distinct populations of chronic hepatitis B: baseline assessment of core liver and fine needle aspiration biopsies from the investigational INSIGHT study

Pietro Lampertico^{1,2}, Tarik Asselah³, Edward J. Gane⁴, Scott K. Fung⁵, Patrick Kennedy⁶, Thomas Vanwolleghem⁷, Ewa Janczewska⁸, Julian Schulze zur Wiesch⁹, Mark S. Sulkowski¹⁰, Hans Wils¹¹, Daniele Filippo Colombo¹¹, Nadia Neto¹¹, Ewoud de Troyer¹¹, Koen Van den Berge¹¹, Hinrich Göhlmann¹¹, Jeroen Aerssens¹¹, John Jerzowski¹², Zacharias Anastasiou¹³, Oliver Lenz¹¹, Thierry Verbinen¹¹, Thomas Kakuda¹⁴, Carine Guinard-Azadian¹¹, Marianne Tuefferd¹¹, Michael Biermer¹¹. ¹Foundation IRCCS Ca' Granda

Ospedale Maggiore Policlinico, Division of Gastroenterology and Hepatology, Milan, Italy; ²CRC "A. M. and A. Migliaiavacca" Center for Liver Disease, Department of Pathophysiology and Transplantation, University of Milan, Milan, Italy; ³Université de Paris-Cité, INSERM Umr1149, Department of Hepatology, AP-HP Hôpital Beaujon, Clichy, France; ⁴University of Auckland, New Zealand Liver Transplant Unit, Auckland, New Zealand; ⁵University Health Network, Toronto, Canada; ⁶Barts and The London School of Medicine and Dentistry, London, United Kingdom; ⁷University of Antwerp, Faculty of Medicine and Health Sciences, Laboratory of Experimental Medicine and Pediatrics, Viral Hepatitis Research Group, Antwerp, Belgium; ⁸Medical University of Silesia in Katowice, Faculty of Public Health in Bytom, Bytom, Poland; ⁹University Medical Center Hamburg, Eppendorf, Hamburg, Germany; ¹⁰Johns Hopkins University, Baltimore, United States; ¹¹Janssen Pharmaceutica

Nv, Beerse, Belgium; ¹²Janssen Research and Development, LLC, Titusville, United States; ¹³Janssen-Cilag Pharmaceutical, Pefki, Greece; ¹⁴Janssen Research and Development, LLC, Brisbane, United States
Email: pietro.lampertico@unimi.it

Background and aims: Treatment of chronic hepatitis B (CHB) patients with the siRNA JNJ-73763989 (JNJ-3989) and nucleos (t)ide analogs (NAs) ± the CAM-E JNJ-56136379 (JNJ-6379), has shown profound reductions in hepatitis B viral serum markers. The INSIGHT study (NCT04585789) aims to assess intrahepatic and peripheral changes in immunologic and virologic markers in response to JNJ-3989 based combination regimens in participants with CHB.

Method: INSIGHT is a phase 2, open-label, parallel-group, multicenter study across 9 countries in Europe, North America, and Oceania, in CHB participants who are hepatitis B e-antigen (HBeAg)-positive and not currently treated (NCT; Group 1) or HBeAg-negative and virologically suppressed (VS) by NA (Group 2). Patients are receiving JNJ-3989 + NA ± JNJ-6379 for 48 weeks. Paired percutaneous core liver biopsies as well as fine needle aspiration biopsies (FNABs; uniform protocol across sites) are being collected to investigate potential differences and changes in hepatitis B viral markers and intrahepatic immune status. Viral markers are assessed by immunofluorescent (IF) staining combined with single cell digital droplet PCR from fresh frozen tissue sections; immune cells are characterized by single cell RNA sequencing from FNABs. This analysis focuses on baseline biopsies and the comparison of the two distinct subgroups of CHB participants.

Figure. Baseline serum viral marker levels and frequency of HBV-positive liver cells* by viral marker for Groups 1 and 2.

Range per group (min - max)	Group 1 NCT	Group 2 VS
	HBeAg-positive (n = 4)	HBeAg-negative (n = 4)
Serum viral markers		
HBsAg, log ₁₀ IU/mL	3.5 – 4.9	2.4 – 4.3
HBeAg, log ₁₀ U/mL	6.7 – 9.9	2.7 – 5.7
HBV RNA, log ₁₀ copies/mL	5.3 – 8.6	1.1 – 2.1
HBeAg, log ₁₀ IU/mL	1.5 – 3.0	–
Liver viral markers, %		
HBsAg-positive cells [†]	50.8 – 98.4	17.4 – 49.5
HBeAg-positive cells [†]	40.4 – 92.7	0.02 – 28.3
cccDNA-positive cells [‡]	16.9 – 87.5	35.7 – 58.3
HBV RNA-positive cells [‡]	88.8 – 100.0	8.0 – 30.2
cccDNA positive/HBV RNA negative	0 – 7.4	33.3 – 48.2

Limit of detection = 1.6 copies/cells for both the cccDNA and HBV RNA assay.

*Minimum and maximum fraction of positive cells per sample.

[†]Based on entire section.

[‡]Targeting 90 individual cells/sample.

Results: Baseline liver samples were collected from 20 out of 24 enrolled participants, 10 per group. Currently, analysis of four core liver biopsies from each group has been completed. Ranges of serum viral marker levels were numerically higher for participants in Group 1 vs Group 2, consistent with the higher proportion of HBsAg- and HBeAg-positive hepatocytes in Group 1 vs Group 2 (Figure). Out of individually isolated hepatocytes, a numerically higher frequency of cccDNA positive/HBV RNA positive cells and a lower frequency of cccDNA positive/HBV RNA negative hepatocytes was observed in Group 1 vs Group 2, in line with the difference in liver IF and serum viral markers between the two groups. 19/20 FNAB samples collected at baseline were successfully profiled with approximately 2000 genes/cell quantified (Group 1: n=9; 15,828 liver resident cells; Group 2: n=10; 21,925 liver resident cells). On average, 1988 cells per

sample were profiled, varying from 282 to 5200 cells. Differential expression of interferon stimulated genes between Groups 1 and 2 was observed in liver CD8+ T-cells, mucosal-associated invariant T-cells (MAIT), and natural killer (NK) cells. A few markers in intrahepatic immune cells were associated with peripheral HBsAg levels, including overexpression of TNF in MAIT cells in participants with HBsAg <1000 IU/ml across both groups.

Conclusion: The INSIGHT study successfully employed a harmonized approach of multicenter biopsy collection with central sample analysis of liver resident cells at the single cell level. At baseline, NCT HBeAg-positive participants had numerically higher serum viral biomarker levels reflected by greater proportions of HBsAg-, HBeAg-, and HBV RNA-positive hepatocytes than VS HBeAg-negative participants. Interestingly, differences in immune cell RNA expression were modest between groups, with 14 genes significantly differentially expressed in MAIT/CD8+ T-cells or NK cells (associated with False Discovery Rate <10%).

FRI-249

Epigenetic modulation by DNA methyltransferase inhibition may enhance the effect of immune checkpoint inhibitors to restore HBV-specific T cell responses

Melanie Urbanek-Quaing^{1,2,3,4}, Carlos Oltmanns^{1,2,3,4}, Jasmin Mischke^{1,2,3}, Heiner Wedemeyer^{3,5}, Cheng-Jian Xu^{1,2,4}, Anke Kraft^{1,2,3,4}, Markus Cornberg^{1,2,3,4}. ¹Hannover Medical School, Gastroenterology, Hepatology and Endocrinology, Germany; ²TWINCORE, Hannover, Germany; ³German Center for Infection Research (DZIF), Hannover, Germany; ⁴Center for Individualized Infection Medicine (CiIM), Hannover, Germany; ⁵Hannover Medical School, Gastroenterology, Hepatology and Endocrinology, Hannover, Germany
Email: urbanek-quaing.melanie@mh-hannover.de

Background and aims: Functional cure of chronic hepatitis B virus (HBV) infection (defined by loss of HBsAg) is rarely achieved, emphasizing the need for novel therapeutic approaches. A hallmark of chronic infection is a dysfunctional immune system and the presence of exhausted T cells with a distinct epigenetic signature. There are several approaches to improve their function, such as checkpoint inhibition with anti-PDL1. However, anti-PDL1 alone is unable to remodel the epigenetic patterns associated with exhaustion and thus may prevent durable improvement of the immune response. Our goal is to target these epigenetic imprints of exhaustion in chronic HBV infection to improve the effect of anti-PDL1 on HBV-specific immune responses.

Method: We performed a 10-day stimulation culture with peripheral blood mononuclear cells (PBMC) from 44 individual chronic HBV patients with varying levels of HBsAg and HBeAg. PBMCs were stimulated with HBV core or polymerase overlapping peptide pools (42 patients) or HLA-restricted peptides HBV core₁₈ or pol₄₅₅ (13 patients). In addition, cells were treated with the checkpoint inhibitor anti-PDL1 alone or in combination with the DNA methyltransferase inhibitor (DNMTi) decitabine. HBV-specific immune responses were analyzed by multicolor flow cytometry. In addition, DNA methylation was analyzed using the Illumina Human MethylationEpic Beadchip Array.

Results: After pretreatment with DNMTi followed by anti-PDL1 treatment on day 3 post-stimulation, we observed a markedly improved IFNγ response of HBV-specific CD4⁺ T cells and CD8⁺ T cells in some patients. This effect was heterogeneous, with some patients showing a 2- to 100-fold increase compared with anti-PDL1 treatment alone. For example, the combination of anti-PDL1 and DNMTi increased total HBV core-specific CD4⁺ and CD8⁺ T cell responses in 42% and 39% of cases, respectively, compared with anti-PDL1 alone. HLA-restricted HBV peptide-specific CD8⁺ T cell responses were improved in 46% of cases, with a more pronounced effect on pol₄₅₅-specific responses. Correlation with methylation data and HBV antigen levels is ongoing.

POSTER PRESENTATIONS

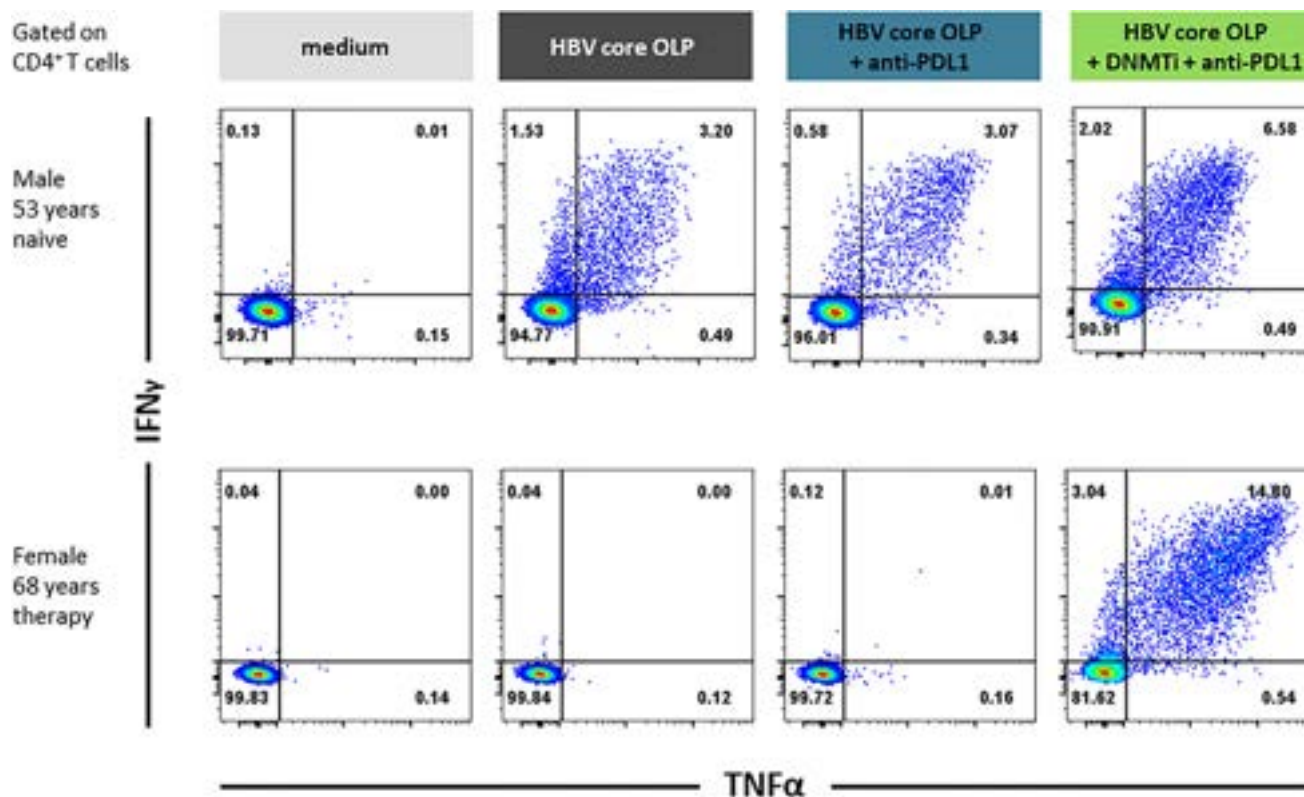


Figure: (abstract: FRI-249): Heterogeneous effect of checkpoint inhibitor anti-PDL1 and DNA methyltransferase inhibitor on HBV core-specific CD4⁺ T cell responses.

Conclusion: The results confirm that epigenetic signatures of T cells may play an important role in the immune response to HBV. Targeting epigenetic modifications by combining DNMTi and checkpoint inhibitors has not been tested in chronic HBV, but seems to be a promising concept to improve HBV-specific immune responses.

FRI-250

Reduction in quantity and function of HBcAg-specific B cells indicates the response to anti-viral therapy in chronic HBV-infected patients receiving ETV or TDF treatment

Li Wang¹, Ning Ling¹, Wenhui Peng¹, Gaoli Zhang¹, Min Chen¹. ¹Key Laboratory of Molecular Biology for Infectious Diseases (Ministry of Education), Institute for Viral Hepatitis, The Second Affiliated Hospital, Chongqing Medical University, China
Email: mchen@hospital.cqmu.edu.cn

Background and aims: Recently, hepatitis B virus core antigen (HBcAg)-specific B cells have been reported to be associated with the disease phase of chronic hepatitis B virus (HBV) infection, but their changes and roles in anti-viral therapy remains unknown yet. Here, features of HBcAg-specific B cells were investigated in chronic HBV-infected (CHB) patients during entecavir (ETV) or tenofovir disoproxil fumarate (TDF) treatment.

Method: Fifty-six treatment-naïve, fifty-one ETV-treated, and twenty-nine TDF-treated CHB patients were enrolled in this study.

The frequency and phenotype of circulating HBcAg-specific B cells were examined by flow cytometry using fluorescently labeled HBcAg and surface markers. The function of antibody-secretion of HBcAg-specific B cells was assessed by HBcAg-specific enzyme-linked immunospot (ELISpot) assays.

Results: Compared to treatment-naïve patients, ETV/TDF-treated CHB patients displayed lower frequencies of total HBcAg-specific B cells, and their memory and class-switched subsets, especially in HBeAg- negative patients. Meanwhile, the proportion and antibody-producing ability of HBcAg-specific B cells progressively declined with the prolonged duration of antiviral therapy. The number of antibody-producing HBcAg-specific B cells positively correlated with the serum level of HBV DNA, HBsAg, or HBeAg. Notably, HBcAg-specific B cells from CHB patients with maintained virological response (MVR) showed significantly lower percentages of total and classic memory population, lower expression of CXCR5 and CD38, while higher expression of CXCR3 than those with low-level viremia (LLV).

Conclusion: Long-term ETV/TDF treatment led to a gradual reduction in the quantity and function of HBcAg-specific B cells. A lower proportion of HBcAg-specific B cells was potential to predict a better response to antiviral therapy.

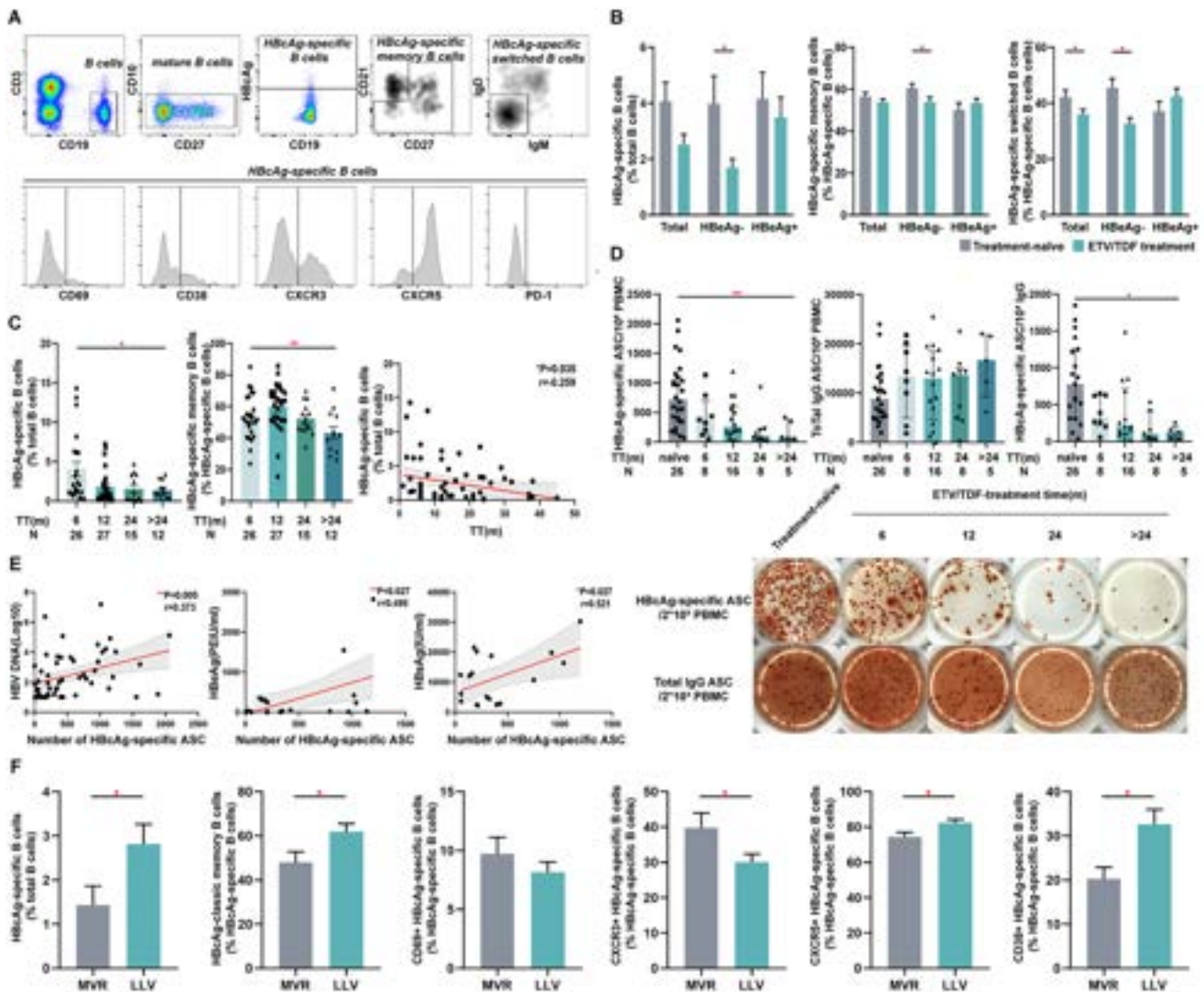


Figure 1. Reduction in quantity and function of HBcAg-specific B cells in chronic HBV infected patients on ETV or TDF treatment. (A) representative FACS plots of HBcAg-specific B cells in CHB patients. (B) decreased percentages of total and memory HBcAg-specific B cells in CHB patients after ETV/TDF treatment. (C) dynamic changes in total and memory HBcAg-specific B cells in ETV/TDF-treated CHB patients at different time-points. (D) gradually decreased antibody-secreting memory HBcAg-specific B cells with the prolongation of ETV/TDF treatment time. (E) a positive correlation of antibody-producing memory HBcAg-specific B cells with serum HBV DNA load, or level of HBsAg or HBeAg. (F) lower HBcAg-specific B cells in CHB patients with better respond to ETV/TDF therapy. TT, treatment time. ASC, antibody-secreting cells. m, month. N, number of cases analyzed. MVR, maintained virological response (defined by persistently undetectable HBV DNA). LLV, low-level viremia (defined by either persistent or intermittent episodes of <2,000 IU/mL detectable HBV DNA). * $p < 0.05$, ** $p < 0.01$.

Figure: (abstract: FRI-250).

FRI-251

Extracellular vesicle-derived microRNA signature in chronic hepatitis C patients with different stages of liver fibrosis

Victoria Cairoli¹, Daniel Valle Millares², Pablo Ryan³, Luz Martin Carbonero⁴, Ignacio De Los Santos⁵, Elena De Matteo¹, Marcela De Sousa⁶, Veronica Briz², María Victoria Preciado¹, Pamela Valva¹, Amanda Fernández Rodríguez². ¹IMIPP-CONICET, Buenos Aires, Argentina; ²ISCIII, Majadahonda, Spain; ³Hospital Universitario Infanta Leonor, Madrid, Spain; ⁴La Paz University Hospital, Madrid, Spain; ⁵Hospital de La Princesa, Madrid, Spain; ⁶Hospital General de Agudos J. M. Ramos Mejía, Buenos Aires, Argentina
Email: amandafr@isciii.es

Background and aims: In the context of chronic hepatitis C (CHC), co-infection with HIV has a negative impact on liver damage progression. Recently, extracellular vesicles (EVs) have gained relevance in liver diseases as intercellular communicators thus

mediating pathological processes. HCV and HIV have been described to modify the microRNA (miRNA) content of EVs, but little is known about their impact on pathogenesis or their possible role as liver damage biomarkers. We aimed to characterize the plasma derived-EVs miRNA signature of HCV+ and HCV+/HIV+ patients and to explore their expression regarding the severity of liver fibrosis, to assess its impact on pathogenesis.

Method: EVs were purified and characterized from 50 CHC plasma samples [36% significant fibrosis ($F \geq 2$)] [21 HCV+ (52.4% $F \geq 2$) and 29 HCV+/HIV+ (22.6% $F \geq 2$)]. EVs-derived total RNA was extracted and massively sequenced. Then, miRNA identification, significant differential expression (SDE) analysis [fold change (FC) ≥ 1.5 ; adjusted p value (p.adj) ≤ 0.2], target gene prediction and pathway enrichment analysis (p.adj ≤ 0.5) were performed. The diagnostic value of SDE miRNAs was assessed by ROC curves analysis.

Results: Differential expression analysis of plasma EVs-miRNAs according to severity of liver fibrosis demonstrated 2 SDE miRNAs

POSTER PRESENTATIONS

(miR-122-5p and miR-92a-3p, up- and down-regulated in the $F \geq 2$ group, respectively) which *in silico* regulate genes involved in cytoskeleton organization. Within HCV+ subgroup, 4 up- (miR-122-5p, miR-320c, miR-3615, miR-320a-3p), and 4 down-regulated miRNAs (miR-374b-5p, let-7a-3p, miR-199a-5p, miR-142-5p) were found in $F \geq 2$ patients. Together, they regulate genes involved in macrophage activity and cell growth/death regulation. In turn, the HCV+/HIV+ subgroup displayed 11 up- (miR-4508, miR-122-5p, miR-451a, miR-1290, miR-1246, miR-107, miR-15b-5p, miR-194-5p, miR-22-5p, miR-20b-5p, miR-142-5p) and 7 down-regulated miRNAs (miR-328-3p, miR-335-3p, miR-125a-5p, miR-423-3p, let-7d-3p, miR-128-3p, miR-10a-5p). These miRNAs regulate the expression of genes involved in the RNA silencing machinery. Regarding diagnostic performance of SDE miRNAs to discriminate $F \geq 2$ cases (AUROC ≥ 0.800) in each group different miRNAs were identified: HCV+: miR-3615 miR-374b-5p, let-7a-3p, miR-142-5p, miR-320a-3p and miR-320c and HCV+/HIV+: miR-423-3p, miR-128-3p, miR-194-5p, miR-10a-5p, miR-328-3p, miR-22-5p, miR-125a-5p, let-7d-3p, miR-335-3p, miR-451a, miR-122-5p and miR-1246.

Conclusion: chronic HCV+ and HCV+/HIV+ patients with different stages of liver fibrosis present a differential profile of EVs-derived miRNAs. This specific miRNA signature would allow elucidation of possible mechanisms involved in clinical evolution and identification of biomarkers of unfavorable progression specific for each group, plausible to be used in a diagnostic panel.

FRI-252

Prophylactic vaccine against hepatitis D virus (HDV) superinfection

Matti Sällberg¹, Lars Frelin¹, Gustaf Ahlén¹, Jingyi Yan¹, Panagiota Maravelia¹, Philip Cunnah², Ana-Rita Ricardo², Nico Mertens³, Richard Bethell⁴. ¹Karolinska Institutet, Laboratory Medicine, Stockholm, Sweden; ²Rodon Biologics, Portugal; ³Bionmer, Netherlands; ⁴SVF Vaccin, Sweden
Email: matti.sallberg@ki.se

Background and aims: Chronic infection with HDV caused by a superinfection of a chronic HBV infection is a major cause for severe liver disease. There is currently no vaccine that can protect patients with chronic HBV infection against a superinfection with HDV. We are therefore developing such a vaccine.

Method: A fusion protein containing multiple PreS1 genotypes and hepatitis D virus antigen (HDAg) of genotypes 1 and 2 was previously generated and to protect against HDV superinfection *in vitro* and *in vivo*. To generate a protein suitable for large scale production according to good manufacturing practice, protein variants were generated that were optimized for protein expression and stability and were tested for immunogenicity.

Results: The original protein described in Burm et al (Gut 2022; 10.1136/gutjnl-2022-327216) was found to be unstable when produced in large scale. Modified versions yielded proteins that were more stable and that were able to be produced at much higher expression levels in E.coli. Importantly, the modified proteins were equal, or even more immunogenic in mice with respect to both PreS1-specific antibodies and PreS1 and HDAg specific T cells.

Conclusion: We have now developed a potential protein-based prophylactic vaccine candidate against HDV superinfection that can be produced at high expression levels and with a good stability for large scale production according to GMP for phase 1, 2, and 3 clinical trials. This may be the first prophylactic vaccine against HDV superinfection.

FRI-253

Rat hepatitis E virus infection in a rat model has multiphasic viral replication kinetics

Zhenzhen Shi¹, Xin Zhang², Niels Cremers², Johan Neyts², Harel Dahari¹, Suzanne Kaptein². ¹Loyola University Chicago, Program for Experimental and Theoretical Modeling, Division of Hepatology, Department of Medicine, Stritch School of Medicine, United States; ²KU Leuven Department of Microbiology and Immunology and Transplantation, Rega Institute, Laboratory of Virology and Chemotherapy, Belgium
Email: suzanne.kaptein@kuleuven.be

Background and aims: Hepatitis E virus (HEV) is the causative agent of hepatitis E in humans and a leading cause of acute viral hepatitis. It is also responsible for chronic hepatitis in immunosuppressed patients worldwide. The virus is mainly transmitted fecal-orally, through the consumption of contaminated drinking water or infected undercooked meat of pigs. Additionally, HEV can also be transmitted via blood transfusions. Previously, we reported that athymic nude rats support the productive replication of rat HEV when injected

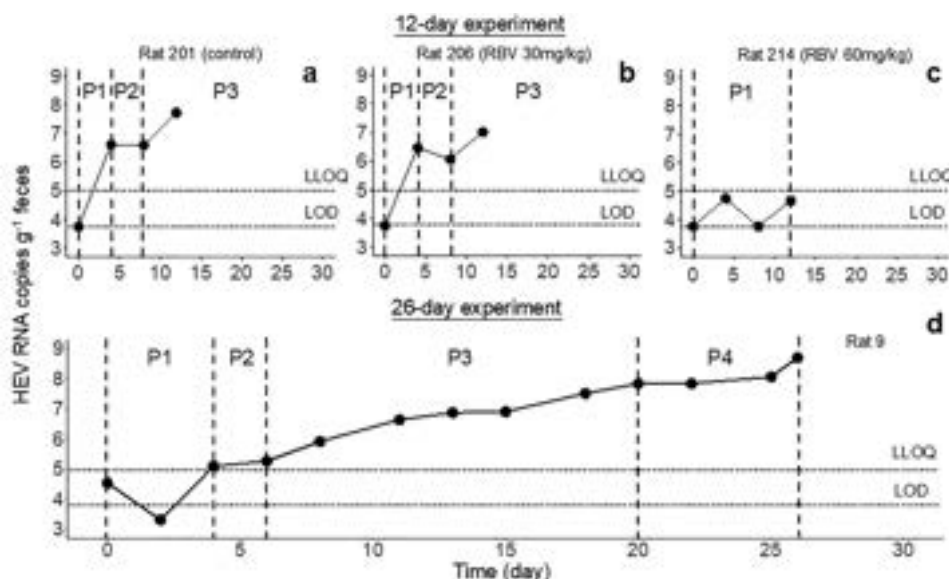


Figure 1. Representative HEV kinetic patterns in the 12-day and 26-day experiments. Solid lines between each experimental data are shown to highlight the trajectory. P1, P2, P3, P4 represent phase 1, phase 2, phase 3, and phase 4, respectively. LLOQ and LOD represent lower limit of quantification and limit of detection, respectively. RBV: ribavirin.

Figure: (abstract: FRI-253).

intravenously with diluted liver homogenate from HEV-infected rats, causing a chronic infection, which resembles the situation in immunocompromised individuals with chronic HEV (PMID: 27483350). Here, we aim to characterize HEV kinetics from infection to steady state in the rat model.

Method: Rat HEV LA-B350 (containing approximately 2×10^7 viral RNA copies) was injected in the tail vein of athymic nude rats in both the 12-day and 26-day experiments ($n = 25$). In the 12-day experiment, rats were treated once daily by oral gavage with either vehicle ($n = 5$) or ribavirin at a dose of 30 mg/kg ($n = 5$) or 60 mg/kg ($n = 5$) for 12 days. In the 26-day experiment, rats were left untreated ($n = 10$) for 26 days. Feces were collected at various time points after infection and analyzed for the presence of viral RNA by quantitative PCR.

Results: In the 12-day experiment, there is no difference in HEV replication kinetics between the control group and the group treated with ribavirin (30 mg/kg, once daily oral administration) (Fig. 1a and b). Three main viral phases were identified in these rats: a LLOQ phase that lasts ~4 days (4.8 ± 1.7 days) (phase 1: P1), a plateau phase that lasts ~4 days (phase 2: P2), and the beginning of a rapid ascension phase (phase 3: P3). In the rats treated with ribavirin 60 mg/kg, the viral load remained in the LLOQ (P1) phase (Fig. 1c). In the 26-day experiment, similar P1 and P2 phases were seen (Fig. 1d) as in the 12-day experiment (Fig. 1a and b). The 26-day experiment helped to fully characterize phase 3 (P3) that lasted until ~day 18 post infection (with viral doubling time of ~5 days) that was followed by a high viral plateau ($7.9 \pm 0.5 \log_{10}$ copies g^{-1} feces) (phase 4: P4) (Fig. 1d).

Conclusion: The rat HEV infection kinetics presented here is an important step in characterizing this experimental model system so that it can be effectively used to elucidate the dynamics of the HEV life cycle and possibly to predict the efficacy of (novel) antiviral therapeutics or vaccine candidates. Future studies need to reveal whether the viral kinetics in the feces reflect that in the liver and/or blood.

FRI-254

(N)one size fits all: Genotype-matched analysis of different disease phases of chronic hepatitis B virus infection

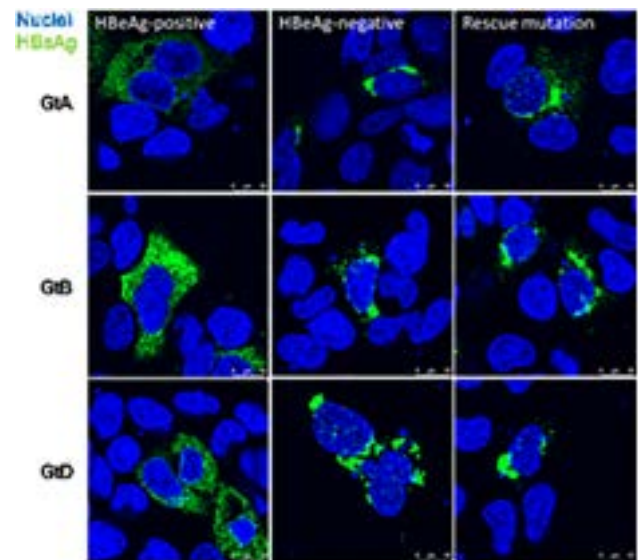
Michael Basic^{1,2}, Keerthihan Keerthihan Thiyagarajah^{1,2}, Mirco Glitscher¹, Anja Schollmeier¹, Qingyan Wu¹, Esra Görgülü^{1,2}, Julia Dietz², Fabian Finkelmeier², Jonel Trebicka³, Stefan Zeuzem², Christoph Sarrazin^{2,4}, Eberhard Hildt¹, Kai-Henrik Peiffer^{1,2,3}. ¹Paul Ehrlich-Institute, Virology, Langen, Germany; ²University Hospital Frankfurt, Department of Gastroenterology and Hepatology, Frankfurt, Germany; ³University Hospital Münster, Medical Clinic B, Münster, Germany; ⁴St. Josefs-Hospital, Department of Internal Medicine and Liver Center, Wiesbaden, Germany
Email: kai-henrik.peiffer@kgu.de

Background and aims: Based on the current EASL guideline chronic HBV infections are divided in five phases. Among others, quantitative (q)HBsAg levels and composition of HBsAg are used for phase-assignment, but depend also on the viral genotype. We aimed to analyse the impact of the disease phase on the clinical and molecular phenotype in a genotype-stratified approach.

Method: Sera of 503 patients, infected with HBV genotype A and D from disease phases 1–4 were analysed for HBV-DNA and qHBsAg levels, HBsAg composition and density of HBsAg-particles. Molecular characteristics of genotype A, B and D HBeAg-negative patient isolates with Precore (PC) mutation G1896A from phase 3 were investigated in comparison to respective HBeAg-positive genomes via WB, RT-PCR, oxyblot, immunofluorescence microscopy, density-, reporter-gen-, infectivity- and kinase-assay. HBeAg-impact was determined by site-directed mutagenesis of PC G1896A.

Results: When stratified by the genotype, no major impact on particle density and HBsAg composition was observed among disease phases 1–4 in the analysed sera of patients infected with genotype A or D. However, in vitro significant differences between HBeAg negative genomes (genotypes A, B and D) from disease phase 3 were observed

in comparison to HBeAg positive wildtype genomes. In HBeAg-negative genomes a strong decrease of intracellular and especially extracellular HBsAg amounts in combination with a HBsAg-retention in the endoplasmic reticulum (Figure) was detected. Interestingly, rescue of HBeAg increased HBsAg amount but not release. However, infectivity of secreted viral particles was unaffected. In addition, the HBV-induced expression of the Nrf2/ARE-dependently regulated gene NQO1 was more pronounced and strikingly ROS/Ras-related signaling was homogeneously deregulated leading to less active MAPK8 and MAPK10 in HBeAg-negative genomes. Sequence analysis revealed no conserved mutations between the HBeAg-negative genomes, which could explain these observations.



Conclusion: Our study indicates limited specificity of HBsAg composition for phase-discrimination when stratified by the viral genotype. In contrast, our in vivo data revealed evidence for a diminished HBsAg synthesis and release in HBeAg-negative genomes isolated from patients of the chronic infection phase. While presence of HBeAg increases HBsAg expression, it does not affect HBsAg release. Through regulation of ARE regulated genes and interference with ROS- and Ras-related pathways including MAPK8 and MAPK10, as key kinases of TNF alpha induced apoptosis, cytoprotective and possible immune escape mechanisms were found to be enhanced in the HBeAg-negative genomes. These changes are caused by an interplay of multiple polymorphisms, which occur naturally over the different phases of the disease, suggesting an evolutionary process.

FRI-255

A primary human hepatocyte system to evaluate antisense oligonucleotide activity against clinically identified hepatitis B virus variants that contain mismatches in the bepirovirsin binding site

Alexander Koenig¹, Jerome Bouquet², Elise Angelini¹, Michael Savarese¹, Hardeep van Gijzel³, Robert Elston⁴, Dickens Theodore⁵, Melanie Paff⁶, Shihyun You¹, Christine Livingston¹. ¹GSK, Infectious Diseases Research Unit, Collegeville, United States; ²GSK, Clinical Biomarkers, United States; ³GSK, Computational Science, United Kingdom; ⁴GSK, Clinical Development, United Kingdom; ⁵GSK, Clinical Development, United States; ⁶GSK, Medicine Development Leaders, United States
Email: christine.m.livingston@gsk.com

Background and aims: Bepirovirsen (BPV; GSK3228836) and GSK3389404, a GalNAc conjugated BPV, are anti-sense oligonucleotides (ASO) that target a conserved 20 nucleotide sequence present

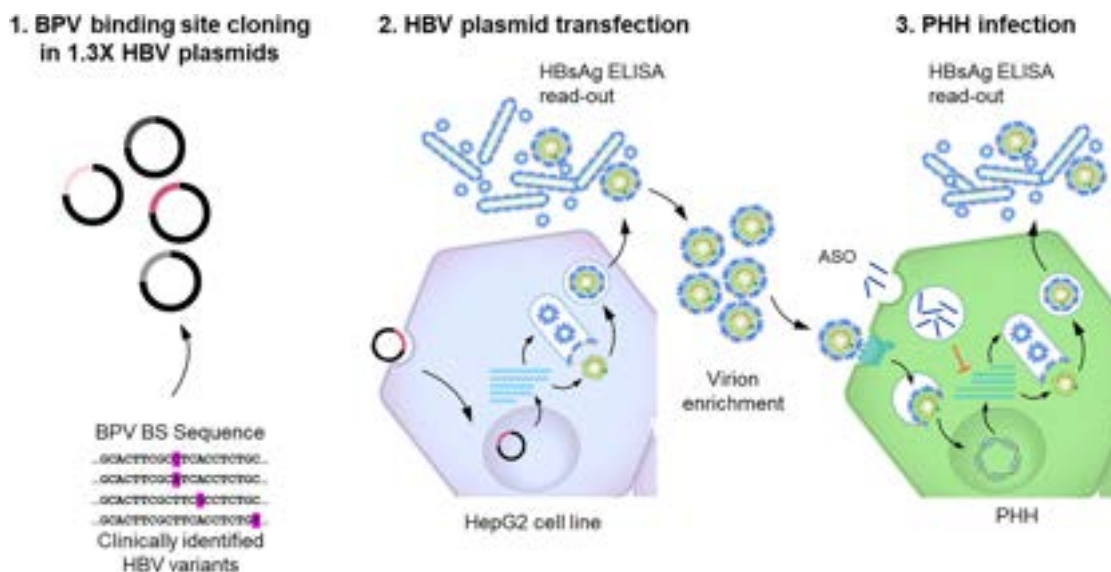


Figure: (abstract: FRI-255).

within all hepatitis B virus (HBV) mRNAs, including pgRNA. Despite the conserved nature of the binding site, single nucleotide polymorphisms (SNPs) within the binding site were identified in a limited number of pre-treatment clinical isolates from BPV B-Clear Phase 2b trial (NCT04449029) or within a publicly available database of sequences derived from clinical isolates. The goal of this study was to develop an *in vitro* system to evaluate the replicative fitness of HBV variants containing SNPs in the BPV/GSK3389404 binding site and to test the susceptibility of progeny virus to ASO treatment.

Method: Clinically identified BPV binding site SNPs, including C7A, C9A, C9T, T10G, A13C, were introduced into genotype D 1.3X HBV genome plasmids that enabled production of infectious viral stocks upon transient transfection in HepG2 cells. Primary human hepatocytes (PHH) were infected with wildtype (WT) HBV or HBV variants for 7 days followed by treatment with ASO GSK3389404 every 3–4 days. Secreted HBsAg levels were measured by ELISA on day 21 post infection. HBsAg levels secreted from mock-treated PHH served as a marker for transcriptional activity of the variants relative to HBV WT. The susceptibility of HBV variants to tool ASO GSK3389404 was evaluated by dose response analysis.

Results: Transfection of each of the 1.3X HBV variant genome plasmids resulted in comparable HBsAg production relative to HBV WT showing successful transfection and that the tested SNPs in the BPV binding site did not appreciably impact plasmid-driven HBsAg levels from HepG2 cells. In PHH, HBV WT and variants C9A, C9T, and T10G collected from HepG2 cells showed comparable infectivity as detected HBsAg levels were similar. In contrast, A13C and C7A variants displayed a several fold reduction of HBsAg, indicating reduced replicative fitness which impedes the interpretation of ASO susceptibility assessments. Among the variants with proportionate fitness to infect PHH and produce HBsAg, dose-response assessment provided evidence that the C9A variant exhibited reduced susceptibility to GSK3389404 compared to HBV WT.

Conclusion: We have developed a two-step *in vitro* model to provide an estimate of replicative fitness and evaluate ASO susceptibility of HBV variants with a SNP in the BPV binding site. Using this system, a few HBV variants identified from B-Clear baseline samples were evaluated. Clinical relevance of HBV variants with reduced susceptibility is under investigation.

FRI-256

Application of magnetic nanoparticle on boosting HBV infection system effectiveness

Bo-Hung Liao¹, Olga Mykhailik², Cho-Chin Cheng¹, Christian Plank^{2,3}, Ulrike Protzer^{1,4}. ¹Institute of Virology, Munich, Germany; ²Ethris GmbH, Planegg, Germany; ³Institute of Molecular Immunology, Germany; ⁴Helmholtz Zentrum München, Germany
Email: protzer@tum.de

Background and aims: Infections with HBV in cell culture is a routine procedure to understand the virus life cycle and to evaluate antiviral strategies. The general drawback in HBV research, however, is its ineffective infection rate, which produces considerable noise effects in downstream analyses and limits its applicability. In contrast to other viruses, HBV infection requires a very high multiplicity of infection (MOI) and still infection rates are limited. To overcome this problem, we used SO-Mag6–11 magnetic nanoparticle (MNP), which have been proven to enhance the potency of lentivirus transduction, to increase the infection rate of HBV and broaden the applicability of the infection system.

Method: We used purified recombinant HBV (rHBV) expressing a red fluorescent protein (rHBV-RFP) to determine infection rates by fluorescence microscopy and flow-cytometry. Incucyte[®] live-cell imaging was applied to observe the dynamics of HBV infection. Quantitative analysis was conducted according to the expression level of fluorescent protein upon rHBV infection.

Results: We first used rHBV-RFP to titrate the optimal ratio of MNP to viral particles using MOI 1, 2, 5, 10, 20 and Incucyte[®] analysis from day 1 to 14. The comparison of RFP expression level indicates that 2 fg iron of MNP per virus particle is optimal. Transgene expression levels positively correlated to the applied MOI. Subsequently, rHBV infection was observed via fluorescent microscopy, and followed by flow-cytometry analysis to determine the infection rate. The infection rates indicated that MNP enabled us to use 1/10 the virus amount to obtain infection rates comparable to that using extremely high MOIs. Furthermore, an additional 10–15% increase in infection rates was achieved by complexing high MOI with MNP. Physical and biochemical validation of MNP and HBV complex are in progress. On one hand, high resolution microscopy is utilized to visualize the complex, and profile conversion upon complex formation will be determined. On the other hand, a spatial-temporal study will be performed to examine if the MNPs alter the kinetics of HBV infection, which step of

virus uptake is enhanced by MNP and how MNP revive less infectious HBV particles.

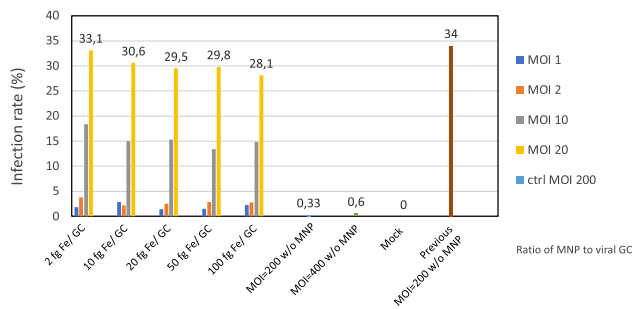


Figure:

Conclusion: The study is the first one reporting the enhancing effect of suitable MNPs on a HBV virus infection system, which is characterized by very low infection rates. We took advantage of the properties of the rHBV infection system that allows visualization of infection and determined the optimal ratio of MNP to viral particles. This increased infection efficacy will allow to extend screening activities in HBV cell culture infection models and provide insights into the limiting steps in these systems.

FRI-257

A new glyco-biomarker for measuring infectious hepatitis B virus targeting surface antigen glycan isomer (HBsAgGi)

Kiyohiko Angata¹, Maki Sogabe¹, Hisashi Narimatsu¹, Ayato Murata², Takuya Genda². ¹RCMG Inc., Japan, ²Juntendo University Shizuoka Hospital, Department of Gastroenterology and Hepatology, Japan
Email: angata@medglyco.com

Background and aims: Hepatitis B virus surface antigen (HBsAg) is a central marker to point-out HBV infection. However, HBsAg test does not always distinguish infectious and non-infectious subviral particles, as it uses antibodies to S-HBs. We aimed to develop a new marker to measure infectious particles more effective than conventional HBsAg. We previously found that DNA-containing particle was enriched by a lectin recognizing O-glycans and then generated a new monoclonal antibody against O-glycosylated PreS2 domain of M-HBs [HBsAg glycan isomer (HBsAgGi)]. Here we show the biochemical characteristics and pilot clinical results of HBsAgGi.

Method: To characterize the HBsAgGi antibody, Western blotting, immunoprecipitation (IP) and immunostaining assays were performed. To investigate clinical utility of the HBsAgGi antibody, we established a new ELISA system and measured sera of chronic hepatitis B (CHB) patients before and after nucleos (t)ide analog (NA) treatment. Reverse-transcription PCR was also performed to detect HBV RNA in HBV particles immunoprecipitated by HBsAgGi antibody.

Results: Biochemical analysis demonstrated that the HBsAgGi antibody recognizes M-HBs but not L-HBs, which is not modified with O-glycan on the PreS2. Mutations in antigenic loop in S-HBs did not affect the binding of HBsAgGi antibody so far tested. HBsAgGi localized in ER to Golgi in M-HBs-expressing cells, suggesting generation of HBsAgGi through glycosylation pathway. ELISA assay showed HBsAgGi antibody specifically bound to M-HBs of genotype C. In treatment naïve CHB patients, serum HBsAgGi level was higher in HBe-positive patients compared to HBe-negative patients at baseline. HBsAgGi levels were significantly correlated with the HBV

DNA level ($p=0.002$, $n=32$). After 48 weeks, HBV DNA was significantly decreased. In contrast, HBsAg level did not show a significant reduction while HBsAgGi level was significantly decreased. Immunoprecipitation experiments confirmed that both HBV DNA- and HBV RNA-containing particles were collected by HBsAgGi antibody.

Conclusion: HBsAgGi specifically presents in minor fraction of HBV particles containing M-HBs of genotype C, and less so in subviral particles, indicating that HBsAgGi antibody can properly detect infectious particles. Since both HBV DNA and HBV RNA were detected in HBsAgGi-bound fraction, HBsAgGi would be a new glyco-biomarker to monitor viral kinetics in CHB patients during NA therapy.

FRI-258

Pregnancy zone protein as a promising biomarker for HEV-related acute liver failure

Jian Wu^{1,2}, Ze Xiang³. ¹Department of Clinical Laboratory, The Affiliated Suzhou Hospital of Nanjing Medical University, Suzhou Municipal Hospital, Gusu School, Nanjing Medical University, 242 Guangji Road, Suzhou 215008, Jiangsu, China; ²The Chinese Consortium for the Study of Hepatitis E (CCSHE), China; ³Zhejiang University School of Medicine, Hangzhou 310009, Zhejiang, China
Email: wujianglinxing@163.com

Background and aims: Timely and effective prognostic biomarkers for hepatitis E virus (HEV)-related acute liver failure (ALF) are urgently needed.

Method: We performed four tandem mass tag (TMT)-labeled quantitative proteomic and targeted proteomics parallel reaction monitoring (PRM) studies on cross-sectional cohort 1 and 2 including 20 acute hepatitis E and 20 HEV-ALF patients respectively.

Results: Pregnancy zone protein (PZP) is a potential prognostic biomarker for HEV-ALF. PZP was identified by TMT and PRM quantitative proteomics. In the derivation cohort, PZP levels of the HEV-ALF patients in survival group were significantly higher than those of the dead group. According to the median level of PZP, HEV-ALF patients in the retrospective cohort 1 were divided into the high PZP (>1316.18 ng/L) and low PZP (≤ 1316.18 ng/L) groups. The survival time of the high PZP group was significantly longer than that of the low PZP group. Decreasing PZP levels were also correlated with the increasing number of failed organs. Compared with PZP levels at admission, levels at discharge increased significantly in the improvement group, and decreased significantly in both the fluctuation and deterioration groups. PZP levels were significantly negatively correlated with alanine aminotransferase, total bilirubin, and international normalized ratio levels. It was revealed that PZP level was highly correlated with survival time, clinical course and organ failure in HEV-ALF patients. Besides, multivariate logistic regression showed that laminin, hepatic encephalopathy, TBil, and PZP were independent factors affecting the prognosis of HEV-ALF patients, which were used to establish a novel prognostic model (ePLT). The assessment in the derivation and validation cohorts showed that the ePLT score was significantly superior to the MELD, KCH and Child-Pugh scores.

Conclusion: PZP is a promising prognostic biomarker, and ePLT is a high-performance prognostic score for HEV-ALF patients, which contribute to clinical decision-making in the management of HEV-ALF.

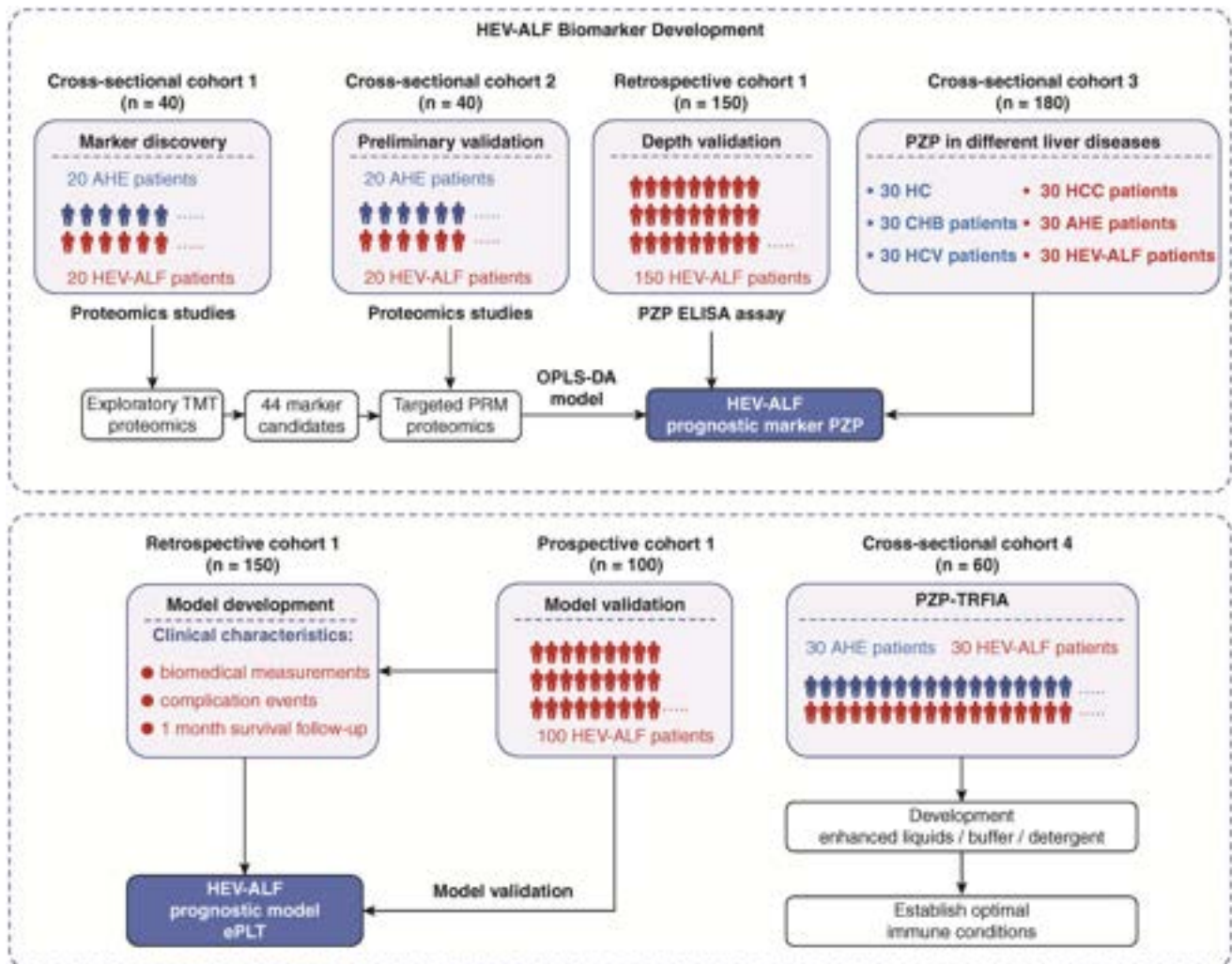


Figure: (abstract: FRI-258).

FRI-259

Quadruple mutation GCAC1809-1812TTCT leads to a better prognosis by decreasing HBV-mediated fibrogenic activity

Esra Görgülü^{1,2}, Michael Basic², Mirco Glitscher², Keerthiyan Keerthiyan Thiyagarajah², Anja Schollmeier², Alica Kubesch³, Julia Dietz³, Stefan Zeuzem¹, Christoph Sarrazin⁴, Kai-Henrik Peiffer^{1,2,5}, Eberhard Hildt^{2,6}. ¹University Hospital Frankfurt, Department of Gastroenterology and Hepatology, Germany; ²Paul Ehrlich-Institute, Virology, Germany; ³University Hospital Frankfurt, Germany; ⁴St. Josefs Hospital, Germany; ⁵University Hospital Muenster, Department of Internal Medicine B, Germany; ⁶German Center for Infection Research (DZIF), Germany
 Email: esra.goerguelue@kgu.de

Background and aims: The quadruple mutation GCAC1809-1812TTCT (TTCT), which coexists with the basal core promoter double mutation A1762T-G1764A (BCP) and is localized in the basal core promoter and/or HBx, is prevalent in inactive carriers and is associated with significantly lower HBV DNA levels and inactive carrier status and thus a better prognosis. In vitro, GCAC1809-1812TTCT leads to decreased replication activity and significantly reduced HBeAg levels. This study aimed to further investigate the

underlying mechanism by which the TTCT mutation impacts HBV pathogenesis, leading to a favorable course of the disease.

Method: Supergenomic constructs harboring BCP and TTCT mutation in different positions localized in the core promoter gene, the HBx gene or both were used to analyze their regulatory activity via reporter gene assays, western blots and qPCR analysis. Reactive oxygen species (ROS) levels were analyzed by oxyblot analyses and flow cytometry. Kinome profiling was performed to investigate the influence of the presence or absence of TTCT on kinase activity.

Results: In our analyses, the TTCT mutation in HBx and basal core promoter leads to a slightly higher induction of the Nrf2/ARE-dependent regulated gene NQO1 as well as lower ROS levels compared to the BCP mutation without TTCT or the wild-type. Strikingly, the presence of the TTCT mutation in HBx and basal core promoter shows downregulation of the serine/threonine kinases PKA, PKG2, and PRKX that contribute to liver fibrosis and upregulation of ERK5 and p38-gamma, which play important roles in hepatic inflammation, whereas the BCP mutation without TTCT enhances the adverse effects in comparison to wild-type HBV.

Conclusion: One potential explanatory approach to the better prognosis in the presence of TTCT mutation is the induction of

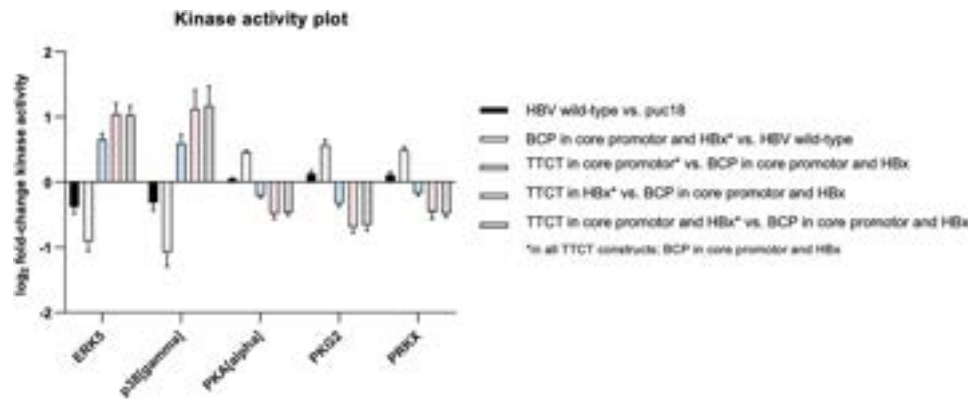


Figure: (abstract: FRI-259).

cytoprotective gene expression and downregulation of major kinases contributing to liver fibrosis.

FRI-260

Growth factor stimulation enhances NTCP expression and improves *in vitro* HBV infection in hepatoma cells

Rodrigue Kanga Wouambo¹, Maria Pfefferkorn¹, Janett Fischer¹, Jonathan Seltsmann¹, Madlen Matz-Soja^{1,2}, Thomas Berg¹, Florian van Bömmel¹. ¹Leipzig University Medical Center, Division of Hepatology, Department of Medicine II, Leipzig, Germany; ²Rudolf-Schönheimer-Institute for Biochemistry, University of Leipzig, Leipzig, Germany

Email: Maria.pfefferkorn@medizin.uni-leipzig.de

Background and aims: Cell culture systems supporting sustained and stable hepatitis B virus (HBV) infection represent an important tool for studying HBV replication and drug efficacy. However, many cell culture models lack stable HBV replication with sufficient expression of replication markers due to an increasing loss of the HBV entry receptor NTCP on the hepatocyte surface. Our study aimed at improving NTCP expression and HBV replication in a cell culture system by using a growth factor stimulation medium.

Method: HepG2-hNTCP-sec+ cells (kindly provided by M. Windisch) were seeded separately and in equal amounts in either Cellartis[®] hepatocytes maintenance medium (HMM; TaKaRa Bio, Ann Arbor, USA) (n=6) or seeding medium (SM; DMEM with 10%FBS, 1%L-Glutamine, 1%Pen/Strep, 2.7%DMSO) (n=6) for 24 h prior HBV inoculation. Consecutively, cells were infected with cell culture derived HBV (ccHBV, genotype D, MOI 10.000) for 18 h.

Supernatant was collected every 2 days during 21 days post infection (dpi). HBV biomarkers HBeAg, HBV DNA, HBV RNA, HBsAg, large (LHBs), and middle (MHBs) antigen were quantified from supernatants. NTCP expression of HBV infected cells in HMM and SM media was quantified by qPCR relative to a stable housekeeping gene (TATABox binding protein-TBP).

Results: The cell growth of HepG2-hNTCP-sec+ cells cultivated with either SM or HMM showed no difference at 6 dpi (p = ns). However, at 14 dpi, cells cultivated in HMM revealed a 2-fold higher NTCP expression compared to cells cultivated in SM. *De novo* secretion of HBV DNA and RNA began 2 dpi in cells cultivated in HMM vs. 2–4 dpi in SM and remained stable over the course of infection. Moreover, levels of HBsAg (ng/ml) increased from day 0 (24.5 ± 6.5 for HMM and 5.6 ± 0.5 for SM, p < 0.0001) to day 2 (157.0 ± 24.6 for HMM and 26.9 ± 4.8 for SM, p < 0.0001) with highest expression after 4 dpi (171.8 ± 31.9 for HMM and 40.8 ± 6.9 for SM, p < 0.0001). Similar to HBsAg levels, HBeAg levels (PEIU/ml) increased in HMM and SM cultivated cells from day 0 (2.6 ± 2.5 vs. 0.6 ± 0.5, p = n.s.) to day 3 (22.9 ± 4.4 vs. 5.8 ± 2.2, p = 0.004), and were highest at 5 dpi (26.1 ± 4 vs. 6.1 ± 0.8, p = 0.001), respectively. Interestingly, in HMM or SM cultivated cells, ratios of MHBs (12.0 ± 4.2% vs. 12.9 ± 3.3%, p = n.s.) and LHBs (11.0 ± 6.2% vs. 11.8 ± 6.5%, p = n.s.) were similar and stable over the course of infection.

Conclusion: Using HMM increases NTCP expression and improves *in vitro* HBV infection and biomarker secretion in HepG2-hNTCP-sec+ cell culture models.

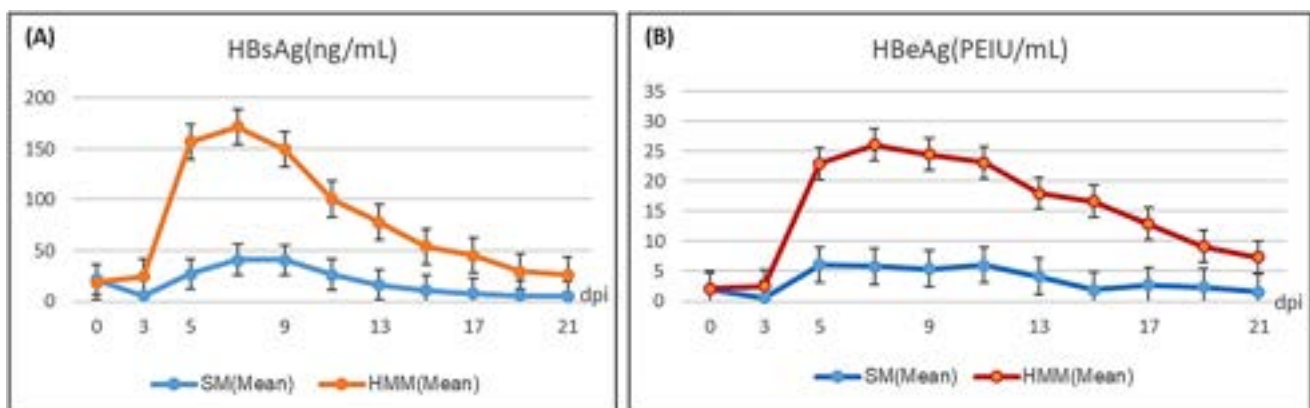


Figure: (abstract: FRI-260).

FRI-261

Hepatitis B virus antigens induce a dramatic LPS-like activation of inflammasome dependent on viral variability

Théophile Cocherie¹, Elisa Teyssou^{1,1}, Adélie Gothland¹, Sophie Sayon¹, Alessandro Mazzola², Anne-Genevieve Marcelin¹, Vincent Calvez¹, Eve Todesco¹. ¹Sorbonne Université, INSERM, Institut Pierre Louis d'Epidémiologie et de Santé Publique, AP-HP, Hôpitaux Universitaires Pitié Salpêtrière-Charles Foix, laboratoire de virologie, F-75013, Paris, France; ²Sorbonne Université, Unité médicale de transplantation hépatique, AP-HP, Hôpital Pitié-Salpêtrière, 75013, Paris, France
Email: eve.todesco@aphp.fr

Background and aims: Inflammation mediated by inflammasome activation leads to pyroptosis, an important innate programmed cell death to control pathogens that could also be associated with multi-organ disturbances. Pyroptosis occurs in two steps. The first, called priming, increases the expression of gene of interests and the second signal leads to activation of caspases and pore formation on the membrane surface, followed by the release of pro-inflammatory cytokines such as IL-1- β and IL-18. Hepatitis B virus (HBV) role regarding pyroptosis is highly disputed and may depend on HBV disease stage, antigens, strains and even on the immune cells studied and their localization.

The aim of this study was to assess the role of HBV antigens on priming step in monocyte-derived cells and to assess the impact of the different serotypes.

Method: The effect of 3 purified proteins {HBsAg (adr, adw and ayw serotypes), HBeAg and HBcAg antigens; Prospect protein specialists, Ness Ziona, Israel} on priming step was assessed on macrophage-like cells. THP-1 circulating monocytes were cultured with RPMI-heses 10% FBS-0.05 mM 2-mercaptoethanol, plated in 96-wells plates and differentiated to macrophages with 10nM of PMA for 24 h. HBV proteins were added at 10ug/ml on the differentiated-THP-1. IL-1 β was measured by luminescence in the supernatant after 18 h of incubation and the addition of the signal 2-activator Nigericin at 10 μ g/ml for 1 h. Controls included mock, cells primed by LPS at 1 μ g/ml for 3 h only and cells primed by LPS at 1 μ g/ml for 3 h and then activated by Nigericin. Comparison of IL-1 β secretions were performed by Turkey's multiple comparisons test after validation by Shapiro test of normality.

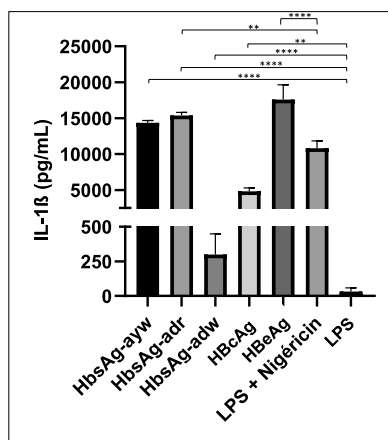


Figure: IL-1 β secretion induced by HBV antigens

The graph represents measure of IL-1 β secretion in supernatants of differentiated-THP-1 cells after incubation with different HBV proteins or LPS only (priming activator) or LPS following by the addition of Nigericin (activator of Signal 2). **p < 0.001; ****p < 0.0001.

Results: We observed that THP-1 cells incubated with HBeAg, HBsAg-adr and ayw serotypes and HBcAg induced a significantly higher IL-1 β secretion than the negative controls. Notably, HBeAg and HBsAg-adr incubation led to huge IL-1 β concentrations in the supernatant (median 17.6 ng/ml IQR [15.0–19.6] and median 15.4 ng/ml IQR [15.1–15.8], respectively), significantly higher than the positive control (cf. Figure 1). Moreover, among HBsAg, a dramatic difference was observed between the adr/ayw and adw serotypes, the latter inducing a much lower secretion than HBsAg derived from adr/ayw serotypes (median 0.3 ng/ml [1.5–4.5], not significantly different from the negative controls).

Conclusion: We observed a very high priming activation for some HBV antigens on monocyte-derived cells, evoking a large and diffuse pyroptosis involvement during HBV infection. Interestingly, HBsAg-adw serotype poorly induced priming. These results suggest that the innate immunity response and, precisely, IL-1 β secretion pathways are influenced by HBV variability. The impact on clinical outcomes should be further studied, particularly regarding the rate of infection chronicity, already reported as high for adw-serotype/genotype A HBV, and the putative impact on systemic inflammation.

FRI-262

Host Sequence snatching identified in-vivo enhances hepatitis E viral replication

Maximilian Nocke¹, Michael Wissing¹, Paula Biedermann², Patrick Behrendt³, C.-Thomas Bock², Heiner Wedemeyer³, Eike Steinmann¹, Daniel Todt^{1,4}. ¹Ruhr University Bochum, Molecular and Medical Virology, Germany; ²Robert Koch Institute, Germany; ³Hannover Medical School, Germany; ⁴European Virus Bioinformatics Center (EVBC), Germany
Email: daniel.todt@rub.de

Background and aims: Hepatitis E virus (HEV) infections are usually asymptomatic and self-limiting, while in immunocompromised or other risk group patients may develop chronic courses. Recent data suggest that HEV has a very heterogeneous hypervariable region (HVR), tolerating major genomic rearrangements, which are mainly observed in chronic patients. Those insertions are correlated with replication fitness *in vitro* and chronicity *in vivo*. We provide a time efficient bioinformatics pipeline tool that automates identification and validation of insertions in high-throughput sequencing (HTS) data, while offering an easy to use graphical user interface (GUI) to simplify accessibility.

Method: Cutadapt and Trimmomatic were used to trim reads in an automated manner. Blastn was integrated in diverse variations to reduce runtime, while assigning reads to genes deposited at NCBI nucleotide database. To receive full insertion sequences, the *de novo* assembler Trinity was introduced into the pipeline. Identified insertions in longitudinal samples of a treatment resistant patient, as well as in public databases were analysed for their influence on viral replication kinetics, virus production capacity and treatment resistance using state-of-the-art HEV cell-culture methods.

Results: During development, runtime was drastically reduced and the need for extended command line usage was bypassed by implementing a GUI. We validated the pipeline by monitoring dynamic rearrangements in the HVR of a chronically HEV infected patient over time. Here, we identify insertions of critical impact for viral fitness while not affecting the sensitivity towards Ribavirin in a sub genomic replicon system and gain further insight into content and distribution of insertions and duplications.

Conclusion: Our pipeline has been designed as a user-friendly tool for detecting insertions of human or viral origin in the HVR of HEV from HTS data using computers with limited RAM and processing power, and includes a graphical user interface to help users interpret and validate the output. This study linked insertions in the HVR to an

increased replication capacity and identified determinants of viral replication *in vitro* and *in vivo*.

FRI-263

Thiourea derivatives exhibit antiviral property by inhibiting hepatitis B virus DNA replication and HBx-induced gene transcription

Jitendra Kumar¹, Purnima Tyagi¹, Shiv Kumar Sarin², Vijay Kumar¹.

¹Institute of Liver and Biliary Sciences, Molecular and Cellular Medicine, India; ²Institute of Liver and Biliary Sciences, Department of Hepatology, India

Email: vijaykumar98@gmail.com

Background and aims: The transactivator HBx protein plays an important role in HBV replication and viral gene expression and has also been implicated in the development of hepatocellular carcinoma (HCC). The current antiviral therapies based on nucleos(t)ide analogs are effective at reducing viral replication but have no impact on the oncogenic functions of HBx. Therefore, HBx is considered as an important therapeutic target to control HBV and HCC. Earlier, we have shown that thiourea derivatives can suppress the expression of HBV DNA and viral antigens. Now we show that the antiviral property of thiourea derivatives is mediated at the Core promoter level resulting in the inhibition of HBx-dependent HBV replication as well as viral gene transcription.

Method: For viral replication studies, HepG2.2.15 cells were transiently transfected with the eukaryotic expression vector for viral HBx (X0) and treated with 10 μ M of thiourea derivatives (DSA-00, DSA-02, and DSA-09) for 48 h. Total RNA was isolated and

quantitated for pre-genomic (pgRNA) expression by RT-qPCR. To HBx-dependent viral gene transcription, HepG2 cells were transiently transfected with either X0 or its three deletion mutants (X5, X12, and X15) along with a luciferase reporter construct for HBV core promoter (nucleotides 1636 to 1851) (Fig. A). Transfected cells were treated with thiourea derivatives (DSA-00, DSA-02, and DSA-09) (10 μ M each) and luciferase activity was measured in cell extracts.

Results: The enhancement in the expression of HBV pre-genomic RNA in the presence of HBx was inhibited to a significant level following treatment with DSA-00, DSA-02, and DSA-09 (Fig. 1B). Further, the HBV core promoter activity induced by HBx was also suppressed by all three thiourea derivatives (Fig. 1C). Interestingly, the three thiourea derivatives also inhibited the core promoter activity induced by two HBx deletion mutants X5 (Δ A) and X12 (partial Δ E) but not X15 (Δ A, B, F) (Fig. 1D).

Conclusion: The thiourea derivatives DSA-00, DSA-02, and DSA-09 were effective at suppressing the HBV pgRNA to significant levels. Further, these compounds also inhibited the HBx-induced HBV core promoter activity. The presence of A and B regions at N-terminus and C-terminal C region appeared to be crucial for the antiviral activity as the transactivation function of X15 mutant could not be suppressed in the presence of these molecules. Alternatively, thiourea derivatives which dock onto HBx *in silico*, are unable to bind to X15 mutant due to the absence of one or more interacting sites. This study suggests that thiourea derivatives specifically target HBx to exhibit its antiviral activity and thus, has the potential to be developed as a new class of HBV therapeutic.

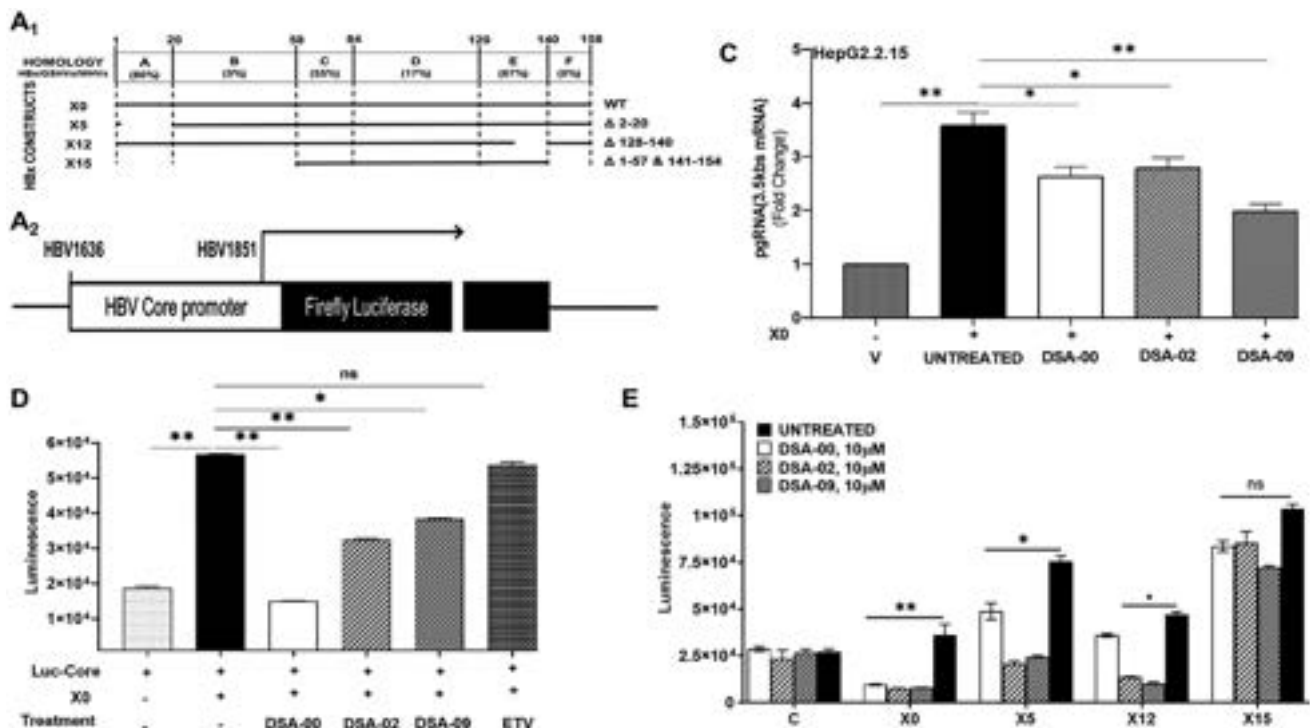


Figure: (abstract: FRI-263): Inhibition of HBV replication and viral gene transcription by Thiourea derivatives. Illustration of HBx wild-type and deletion mutant constructs (A₁). Transient transfection with X-0 and luc-core (A₂) (1 μ g each), the pre-genomic RNAs levels measured by RT-qPCR and calculated by Fold changes in HepG2.2.15 cells treated with thiourea derivatives for 24 hours (B). HBV Core promoter activity with ectopic expression of HBx in HepG2, followed by treatment with thiourea derivatives for 24 hours measured by luciferase assay (C). HBV core promoter activity measured by luciferase assay with HBx wild-type and deletion mutants followed by thiourea derivatives treatment for 24 hours (D). (*p < 0.05; **p < 0.001).

FRI-264

Fas/Fas-ligand induced apoptosis of CD8 (+) lymphocytes in the placenta of women with chronic hepatitis B plays a twofold role in the protection of fetus

Dionysia Mandilara¹, Spyridon Pantzios¹, Georgia Barla¹, Antonia Syriha¹, Ioannis Elefsiniotis¹. ¹General Oncological Hospital of Kifisia Oi Agioi Anargyroi, Kifisia, Greece
Email: deniaa96mand@gmail.com

Background and aims: During pregnancy immunological changes, including the reduction of CD8 (+) T-cells, occur, creating an immunotolerant placental environment. Fas/Fas ligand pathway is responsible for maintaining placental homeostasis. Our study examined the role of Fas/Fas ligand induced apoptosis of CD8 (+) lymphocytes in the protection of fetus, from both HBV infection and CD8 (+) T-cell's cytotoxic effect.

Method: Our study included 50 HBsAg (+)/HBV DNA (+) pregnant women that gave birth with vaginal delivery. Peripheral and umbilical cord blood was collected and placental tissue was examined using hematoxylin-eosin staining, immunohistochemistry and double immunofluorescence in order to identify the T-cell's subpopulations in the decidua and the chorionic villi and detect apoptotic activity.

Results: Umbilical cord HBV-DNA positivity was correlated with high levels of maternal viremia ($p < 0.0001$). Decidua's CD8 (+) lymphocyte count was higher in women with low viral load (LVL) versus women with high viral load (HVL) (11.25 ± 7.23 versus 6.46 ± 3.84 per High Power Field (HPF), $p = 0.043$) and in women with absence of HBV-DNA in contrast with women with positive HBV-DNA in umbilical cord blood (11.00 ± 6.45 versus 4.86 ± 3.02 per HPF, $p = 0.011$). Decidua's CD8 (+)/CD28 (+) and CD8 (+)/Fas-Ligand (+) T-cells' percentage was higher in the LVL group ($13 \pm 1\%$ vs $9 \pm 1\%$, $p = 0.026$ / $51 \pm 1\%$ vs $45 \pm 1\%$, $p = 0.006$), while the percentage of CD8 (+)/Fas (+) was higher in the HVL group ($68 \pm 1\%$ vs $73 \pm 1\%$, $p = 0.035$). The percentage of CD8 (+)/CD28 (+) lymphocytes was statistically lower than the percentage of CD8 (+)/Fas (+) and CD8 (+)/Fas-ligand (+) T-cells in both groups ($p < 0.05$).

Conclusion: High levels of maternal viremia relate to lower levels of CD8 (+) lymphocytes in the decidua probably due to activation of Fas/Fas-ligand apoptotic pathway resulting in the fetus protection both from CD8 (+) lymphocytes cytotoxic effect and HBV transmission.

FRI-265

Intrahepatic hepatitis B virus cccDNA amount and transcriptional activity in a well-characterized cohort of Gambian chronically infected patients: correlation with emerging serum viral markers

Anaëlle Dubois¹, Sarah Heintz¹, Damien Cohen¹, Marie-Laure Plissonnier¹, Françoise Berby¹, Marantha Heil², Massimo Levvero^{1,3,4}, Fabien Zoulim^{1,3,5}, Yusuke Shimakawa⁶, Maud Lemoine⁷, Dalessandro Umberto⁸, Isabelle Chemin¹, Barbara Testoni¹. ¹Inserm U1052, Cancer Research Center of Lyon (CRCL),

France; ²Roche Molecular Diagnostics, United States; ³Croix Rousse hospital, Hospices Civils de Lyon, Department of Hepatology, France; ⁴DMISM and the IIT Center for Life Nanoscience (CLNS), Sapienza University, Rome, Department of Internal Medicine, Italy; ⁵University of Lyon, UMR_S1052, France; ⁶Institut Pasteur, Unité d'Epidémiologie des Maladies Emergentes, France; ⁷Imperial College, Department of Metabolism, Digestion and Reproduction, Division of Digestive Diseases, Hepatology section, United Kingdom; ⁸Medical Research Council Unit The Gambia at the London, School of Hygiene and Tropical Medicine, Banjul, Gambia
Email: barbara.testoni@inserm.fr

Background and aims: Hepatitis B virus (HBV) is highly prevalent in Sub-Saharan Africa, where 80 million people are chronically infected with the virus. One of the most common cancers in the region, hepatocellular carcinoma, is mainly attributable to HBV infection. Natural history of HBV infection has mostly been studied in European and Asian cohorts, thus leaving completely unmet the need of data for the Sub-Saharan Africa, where mode of transmission, age of infection, and various genetic and environmental factors differ completely. Therefore, data relating to the natural history of HBV infection in these patients are much needed.

Method: 96 untreated chronically HBV infected (CHB) patients were retrospectively selected from samples collected in The Gambia in the frame of the PROLIFICA program. Paired liver biopsy and serum samples were analyzed for serum HBV DNA, quantitative (q)HBsAg, HBcrAg (Lumipulse CLEIA Assay) and alanine aminotransferase (ALT) levels. Liver total HBV DNA (tHBV DNA), cccDNA and 3.5Kb RNA were assessed by droplet digital PCR (ddPCR) and cccDNA transcriptional activity was calculated as 3.5Kb RNA/cccDNA ratio. Liver histology scores were also available. Serum HBV RNA (cirB-RNA) was quantified by the Roche HBV RNA investigational assay for use on the cobas® 6800 System (LLOQ 10 cp/ml; linearity range 10 to 10^7 cp/ml; LLOD ~3 cp/ml-Scholtès, J Clin Virol 2022).

Results: The large majority of patients were HBeAg (-), HBV genotype E and only 10% of them had ALT levels above twice the upper limit of normal. Median levels of serum HBV DNA were 2.9 (2.1–4.2) Log IU/ml and qHBsAg were 3.7 (2.5–4.9) Log IU/ml. All patients had quantifiable tHBV DNA in their liver 0.4 (0.1–0.7) copies/cell, 90% had quantifiable cccDNA 0.02 (0.006–0.6) cp/cell and 85% quantifiable 3.5Kb RNA 0.09 (0.02–0.9). cccDNA amount was positively correlated with intrahepatic tHBV DNA, 3.5Kb RNA and serum HBV DNA, but not serum qHBsAg. Moreover, the results clearly indicated the presence of two groups of patients with comparable cccDNA levels, but different transcriptional activity, which was not reflected in differences in the serum HBV DNA or qHBsAg levels. Eighty-five serum samples were available for HBcrAg and cirB-RNA quantification, which were detectable in 35 and 33 samples, respectively. Both markers were highly correlated with intrahepatic HBV markers and in particular with cccDNA levels ($R = 0.7$, $p = 0.0006$ for HBcrAg and $R = 0.6$, $p = 0.02$ for cirB-RNA), which was confirmed also in the group of patients with low cccDNA transcriptional activity.

Table: T-cell's subpopulations in the decidua and chorionic villi in the LVL vs the HVL group

T-CELL SUBTYPE/PLACENTA'S HISTOLOGICAL AREA	LVL (HPF)	HVL (HPF)	P VALUE
CD3 (+) CHORIONIC VILLI	4.80 ± 8.61	2.38 ± 1.50	0.598
CD3 (+) DECIDUA	11.1 ± 6.58	10.00 ± 6.45	0.548
CD4 (+) CHORIONIC VILLI	4.85 ± 4.80	1.00 ± 1.00	0.762
CD4 (+) DECIDUA	6.05 ± 6.31	5.00 ± 1.00	1.00
CD8 (+) CHORIONIC VILLI	6.25 ± 1.07	3.54 ± 5.14	0.265
CD8 (+) DECIDUA	11.25 ± 7.23	6.46 ± 3.84	0.043

Figure: (abstract: FRI-264).

Conclusion: To the best of our knowledge, this is the most comprehensive study evaluating the correlations between intrahepatic and serum HBV activity in people living with CHB in Sub-Saharan Africa. These data will contribute to a better understanding of the natural history of CHB and thus improve the management of African CHB patients.

This work is supported by the French National Research Agency Investissements d'Avenir program (CirB-RNA project-ANR-17-RHUS-0003)

FRI-266

Hepatitis B pre-genomic RNA level has a prospective supporting role for predicting the outcomes of the hepatitis B virus inactive carrier phase

Prooksa Ananchuensook¹, Pakkapon Rattanachaisit¹, Sirinporn Suksawatamnuay¹, Panarat Thaimai¹, Supachaya Sriphoosanaphan¹, Kessarin Thanapirom¹, Piyawat Komolmit¹. ¹Chulalongkorn University, Division of Gastroenterology, Department of Internal Medicine, Bangkok, Thailand
Email: pkomolmit@yahoo.co.uk

Background and aims: Hepatitis B viral (HBV) DNA and quantitative hepatitis B surface antigen (qHBsAg) have been used as biomarkers to classify and predict complications in patients with chronic hepatitis B (CHB) infection. Pregenomic-RNA (pgRNA), the biomarker representing covalently closed circular DNA (cccDNA) activity in hepatocytes, has been associated with viral rebound after cessation of nucleotide analog (NA) treatment. However, the role of pgRNA in the inactive carrier (IC) phase is unclear. Therefore, our study aims to evaluate the utility of pgRNA in IC.

Method: Patients with CHB infection were included in this study and classified into IC and chronic hepatitis (CH) groups according to the European Association for the Study of the Liver (EASL) guidelines. The serum HBV pgRNA, qHBsAg, and HBV viral loads (VL) were quantified using digital polymerase chain reaction (PCR), immunoassay methods, and real-time PCR, respectively. The HBV pgRNA levels and percentage of patients with undetectable HBV pgRNA in each phase were analyzed using the Mann-Whitney U test and chi-square test. The outcomes, including spontaneous HBsAg loss defined as

qHBsAg < 0.05 IU/ml and initiation of antiviral therapy in compliance with the indications outlined in the EASL guidelines, were reviewed. The factors associated with the outcomes were assessed using the Cox regression model.

Results: A total of 309 patients with CHB infection were enrolled. Of these, 154 (49.8%) were in the IC phase and 42 (27.1%) were HBeAg-positive. PgRNA quantity was detectable in 120 patients (38.83%). The log pgRNA showed a moderate correlation with log HBV DNA ($r = 0.376$, $p < 0.001$) and qHBsAg (0.416 , $p < 0.001$). The proportion of patients with detectable pgRNA was significantly lower in the IC group (24.0%) than that in the CH group (53.5%). In the IC group, 126 (81.82%) patients were prospectively observed with a median follow-up time of 26 months (IQR 22.75–29.00). Six (3.9%) patients had spontaneous HBsAg loss, and all of them had qHBsAg < 1,000 IU/ml and undetectable pgRNA. On the other hand, three (1.9%) patients required treatment. Of these, pgRNA was detected in all three (100%), while one (33.3%) had qHBsAg $\geq 1,000$ IU/ml. On univariate analysis, log pgRNA was the only significant factor predicting the need for antiviral therapy, with an odds ratio of 2.85 (95% CI 1.04–7.76).

Conclusion: IC had a lower proportion of detectable pgRNA than the CH group. Furthermore, all patients with spontaneous HBsAg loss had undetectable pgRNA, while all subsequently required treatments had detectable pgRNA. Therefore, pgRNA may be a supporting biomarker that can be added to qHBsAg to improve the accuracy of predicted prognoses for patients in the IC phase of patients in IC.

FRI-267

Droplet digital PCR can quantify cccDNA in plasma of naive chronic HBV infected patients with low HBsAg levels

Ravinder Singh¹, Gayatri Ramakrishna¹, Ekta Gupta², Manoj Kumar³, Shiv Kumar Sarin³, Nirupma Trehanpati⁴. ¹Institute of liver and biliary sciences, Molecular and cellular medicine, Delhi, India; ²Institute of liver and biliary sciences, Virology, India; ³Institute of liver and biliary sciences, Hepatology, India; ⁴Institute of liver and biliary sciences, Molecular and cellular medicine, Delhi, India
Email: trehanpati@gmail.com

Table 1 Factors associated with spontaneous HBsAg loss and future need for antiviral therapy in HBV IC phase.

	Spontaneous HBsAg loss					Future need for antiviral therapy				
	Yes (N = 6)	No (N = 120)	p-value	OR	(95%CI), p-value	Yes (N = 3)	No (N = 123)	p-value	OR	(95%CI), p-value
	N (%) / median (IQR)					N (%) / median (IQR)				
Age (years)	52.50 (39.75–59.00)	49.5 (41.0–54.0)	0.477	1.03	(0.92–1.15), 0.638	46.0 (40.0–53.0)	50.0 (41.0–54.0)	0.605	0.97	(0.84–1.12), 0.674
Male sex	4 (66.7%)	47 (39.2%)	0.143	0.32	(0.06–1.63), 0.201	1 (33.3%)	50 (40.7%)	0.799	1.37	(0.12–15.52), 0.799
AST (U/L)	22.5 (19.0–32.75)	21.5 (19.0–26.0)	0.425	1.05	(0.96–1.14), 0.308	22.0 (18.0–23.0)	22.0 (19.0–26.0)	0.928	0.96	(0.78–1.17), 0.682
ALT (U/L)	22.00 (19.50–47.25)	21.0 (17.0–30.0)	0.442	1.04	(0.99–1.08), 0.104	20.0 (14.0–25.0)	21.0 (17.0–30.0)	0.511	0.94	(0.80–1.10), 0.457
qHBsAg (IU/ml)	10.67 (5.00–69.66)	661.95 (78.79–3,206.00)	0.002*	0.99	(0.97–1.01), 0.206	496.70 (288.40–2,634.00)	621.20 (54.57–3,007.00)	0.845	1.00	(1.00–1.00), 0.611
qHBsAg <1,000 IU/mL	6 (100%)	65 (54.2%)	0.027*			2 (66.7%)	66 (56.1%)	0.715	0.64	(0.06–7.23), 0.717
qHBsAg $\geq 1,000$ IU/mL	0	55 (45.8%)				1 (33.3%)	54 (43.9%)			
pgRNA - Detectable	0	32 (26.7%)	0.143			3 (100%)	29 (23.6%)	0.003*		
pgRNA - Undetectable	6 (100%)	88 (73.3%)				0	94 (76.4%)			
Log pgRNA				0.002	$p < 0.008$				2.85	(1.04–7.76), 0.041*

*Significant p-value ≤ 0.05 .

ALT, alanine aminotransferase; AST, aspartate aminotransferase; CI, confident interval; N, number; NA, nucleotide analog; pgRNA, pregenomic-RNA; qHBsAg, quantitative hepatitis B surface antigen; IU/mL, international unit/ milliliter; OR, odd ratio; U/L, units per liter

Figure: (abstract: FRI-266).

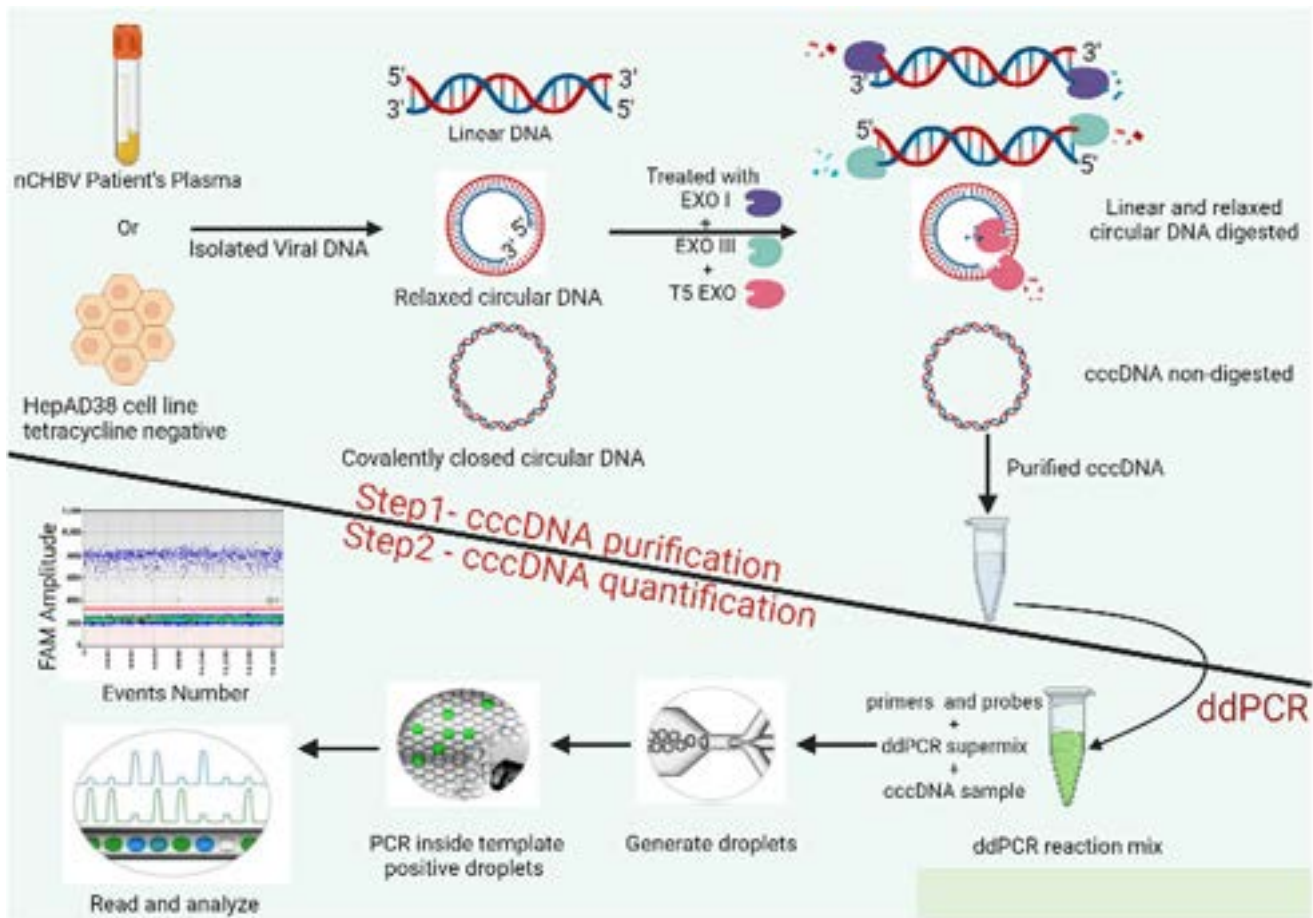


Figure: (abstract: FRI-267): Graphical abstract.

Background and aims: The intranuclear episomal form of HBV DNA i.e., covalently closed circular DNA (cccDNA) is the main replicative and transcriptional unit of HBV. The cccDNA quantification can reflect the transcriptome, active replicon, and persistence of HBV and is done in liver biopsy tissue. There is no sensitive assay for the precise detection of cccDNA in circulation. We aimed to quantify cccDNA in the plasma of chronic HBV (CHBV) patients using three exonucleases followed by droplet digital PCR (ddPCR).

Method: Thirty-six treatment naïve CHBV (nCHBV) patients with low HBsAg (<2,000 IU/ml, HBsAg^{lo}, Gr. I, n=9) and high HBsAg (>2,000 IU/ml, HBsAg^{hi}, Gr. II, n=27) with HBV DNA (<2,000 IU/ml or >2,000 IU/ml) with ALT level >1.2 × ULN (ULN=40 IU/L). To standardize the assay, an HBV genome integrated, tetracycline (tet) regulated HepAD 38 cell line was used as a positive control. Total viral DNA was isolated from tet-off HepAD38 cells and the patient's plasma using Qiagen viral DNA isolation kit. Isolated viral DNA was treated with EXOI and EXO III enzymes to remove linear DNA and T5 exonuclease to remove relaxed circular HBV DNA and got purified cccDNA by phenol:chloroform: isoamyl alcohol (P:C:I) method. Further, to quantitate cccDNA, specific primers with FAM-tagged probe were used in a highly accurate and sensitive droplet digital PCR machine that can detect a single copy of cccDNA. Analysis was done by QuantaSoft Software using the Poisson correction method.

Results: Without enzyme treatment, the tet-off HepAD 38 cell line showed 2210 copies/μl including all three, linear, relaxed circular, and cccDNA forms of HBV DNA. After enzyme treatment, linear and relaxed circular forms were digested and 15 copies/μl cccDNA was evident. Similarly treated viral DNA from chronic HBV patients, showed a median of 9 cccDNA copies (range 1–255)/μl from Gr. I

(HBsAg^{lo}) patients and 11 cccDNA copies (range 2 to 555)/μl from Gr. II (HBsAg^{hi}) patients.

Conclusion: This is the first sensitive and efficient protocol for cccDNA quantification in plasma. Using three exonucleases (EXO I, EXO III, and T5 exonuclease), this assay accurately and specifically quantifies cccDNA by droplet digital PCR even in patients with low HBsAg.

FRI-268

COVID-19 vaccination alters NK cell dynamics and transiently reduces HBsAg titers among patients with chronic hepatitis B

Hyunjae Shin¹, Ha Seok Lee², Ji Yun Noh³, June-Young Koh², So-Young Kim², Jeayeon Park⁴, Sungwon Chung⁴, Moon Haeng Hur⁴, Min Kyung Park⁴, Yun Bin Lee⁴, Yoon Jun Kim⁴, Jung-Hwan Yoon⁴, Jae-Hoon Ko⁵, Kyong Ran Peck⁵, Joon Young Song³, Eui-Cheol Shin², Jeong-Hoon Lee⁴. ¹Seoul National University College of Medicine, Department of Internal Medicine and Liver Research Institute, Seoul, Korea, Rep. of South; ²Korea Advanced Institute of Science and Technology, Korea, Rep. of South; ³Korea University Guro Hospital, Korea, Rep. of South; ⁴Seoul National University College of Medicine, Korea, Rep. of South; ⁵Sungkyunkwan University School of Medicine, Korea, Rep. of South

Email: pindra@empas.com

Background and aims: COVID-19 vaccination may non-specifically alter the host immune system. This study aimed to evaluate the effect of COVID-19 vaccination on HBsAg titer and host immunity in chronic hepatitis B (CHB) patients.

Method: Consecutive CHB patients who had serial HBsAg measurements during antiviral treatment were included in this study.

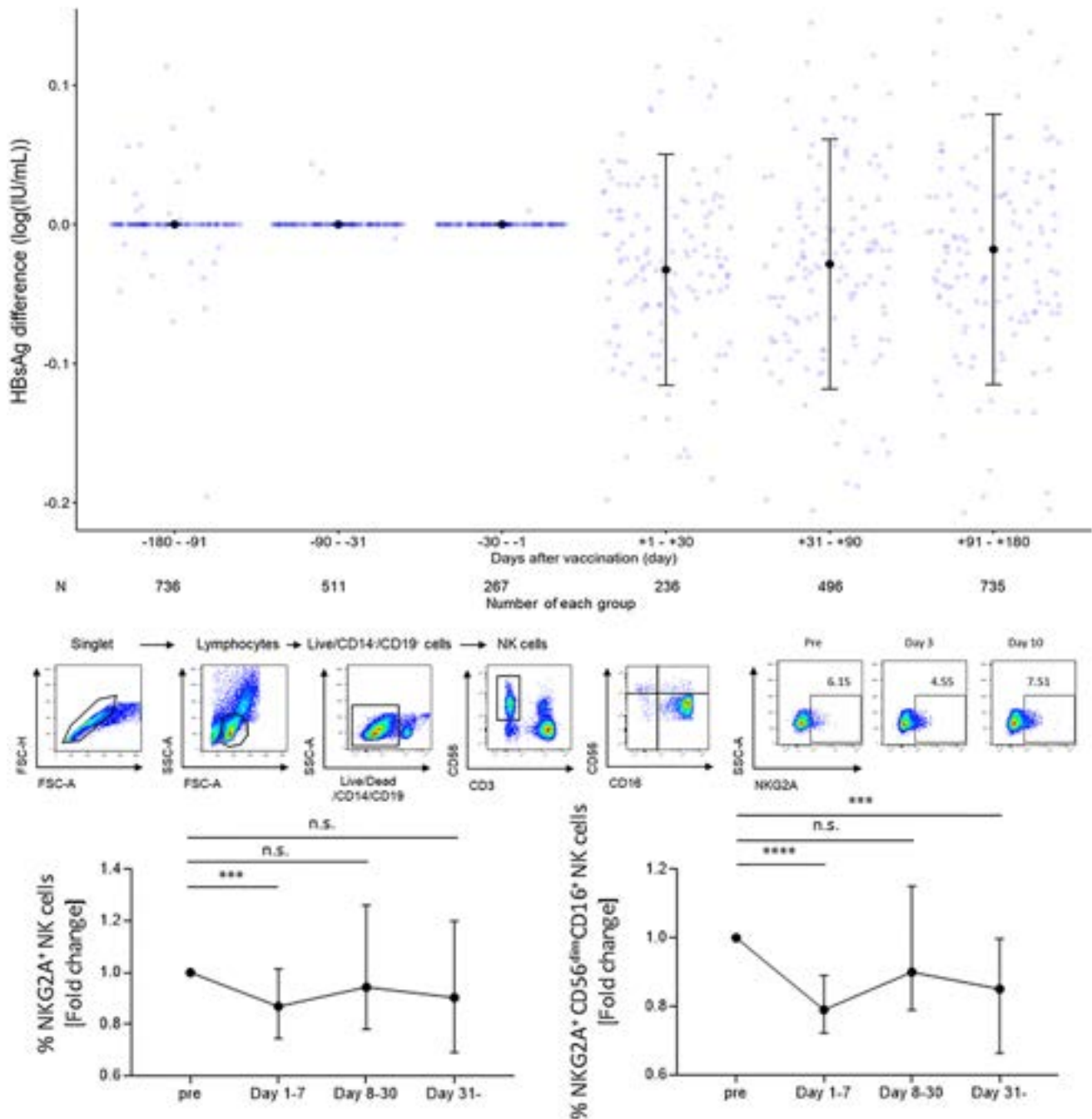


Figure: (abstract: FRI-268).

Changes in the HBsAg levels after COVID-19 vaccination were analyzed. The dynamics of natural killer (NK) cells following COVID-19 vaccination were also examined using serial blood samples collected prospectively from 25 healthy volunteers.

Results: Vaccinated CHB patients (n = 2,329) had significantly lower HBsAg levels 1–30 days post-vaccination compared to baseline (median, –21.4 IU/ml from baseline), but the levels reverted to baseline by 91–180 days (median, –3.8 IU/ml). The velocity of the HBsAg decline was transiently accelerated within 30 days after vaccination (median velocity: –0.06, –0.39, and –0.04 log₁₀ IU/ml/year in pre-vaccination period, days 1–30, and days 31–90,

respectively). In contrast, unvaccinated patients (n = 468) had no change in HBsAg levels. Flow cytometric analysis showed that the frequency of NK cells expressing NKG2A, an NK inhibitory receptor, significantly decreased within 7 days after the first dose of COVID-19 vaccine (median, –13.1% from baseline; p < 0.001). The decrease in the frequency of NKG2A⁺ NK cells was observed in the CD56^{dim}CD16⁺ NK cell population regardless of type of COVID-19 vaccine.

Conclusion: COVID-19 vaccination leads to a rapid, transient decline in HBsAg titer, which may be attributed to a decrease in the frequency of NKG2A⁺ NK cells.

FRI-269

Serum metabolite reveal mitochondrial dysfunction and energy metabolism disruption in chronic hepatitis C virus infection

Amar Deep¹, Sumit Rungta¹, Durgesh Dubey², Ajay Kumar³, Amit Goel², Dhananjay Kumar⁴. ¹King George's Medical University Lucknow, Chowk, Medical Gastroenterology, Lucknow, India; ²SGPGIMS, Gastroenterology, Lucknow, India; ³King George's Medical University Lucknow, Chowk, Internal Medicine, Lucknow, India; ⁴ILBS, Hepatology, New Delhi, India

Email: jsa.amardeep@gmail.com

Background and aims: Hepatitis C virus (HCV) infection is a major public health problem worldwide, with an estimated 170 million people chronically infected. This study aimed to identify patients with HCV infection through an analysis of the 1H NMR spectra of serum samples using multivariate statistical data reduction tools.

Method: The study was a retrospective analysis of 83 chronic hepatitis C patients consecutively treated. To generate an overview of the variations between serological HCV samples and normal controls, an exploratory principal component analysis (PCA) model was created to compare the 800 MHz 1H NMR profiled metabolite concentrations.

Results: The PC1 vs. PC2 scores scatter plot indicated an unsupervised separation trend between HCV and normal controls. A partial least squares discriminant analysis (PLS-DA) model was subsequently constructed, and the corresponding score plot confirmed a conclusive separation between the serum values between the HCV patient and the normal controls. The metabolites were ranked by their contribution to distinguish the HCV from the controls. 10-fold cross-validation was used to assess the statistical robustness of the analysis, and Q2 and R2 values were calculated. Based on the VIP values and p values, 16 serum metabolites were selected for further study as potential biomarkers related to HCV. Compared with the normal control group, the serum contents of several metabolites such as 3-hydroxybutyrate, betaine, carnitine, fucose, glycerol, isopropanol, lysine, mannose, methanol, methionine, and ornithine significantly increased in HCV group, whereas the contents of creatinine, glutamine, proline, serine, and valine decreased significantly. Based on the area under the curve ROC, metabolites were found to have an area under the curve (AUC) greater than 0.8. carnitine can play a role in the transport of fatty acids into the mitochondria for energy production. Proline, serine, and valine are non-essential amino acids that play a role in energy production. They can be converted into intermediates in the TCA cycle and glycolysis. Proline is converted into glutamate, an intermediate in the TCA cycle. Serine can be converted into pyruvate, an intermediate in both the TCA cycle and glycolysis, and also into glucose via gluconeogenesis. Valine can be converted into pyruvate or acetyl-CoA, which can then enter the TCA cycle for energy production. Additionally, Acetyl-CoA is also used in fatty acid biosynthesis. However, none of these amino acids are involved in the PPE (Pentose Phosphate Pathway). These amino acids play an important role in maintaining energy balance in the cells. based on the metabolic signature, mitochondrial damage occurs in CLD-HCV, and the resultant further compromised cellular function, and disease progression occurs.

Conclusion: The study's results indicate a correlation between HCV and mitochondrial damage, as well as potential biomarkers for the disease. it's important to note that the study sample is relatively small, and the findings need to be validated in larger studies to confirm the correlation and biomarkers found in this study.

FRI-270

Characterization of biomarker kinetics in a novel in vitro HBV infection model with the cell line HepG2-hNTCP-sec+ revealed stable HBsAg composition during short- and long-term infection up to four weeks

Lukas Rotter¹, Maria Pfefferkorn¹, Jonathan Selmann¹, Thomas Berg¹, Florian van Bömmel¹. ¹Division of Hepatology, Department of Medicine

li, Leipzig University Medical Center, Leipzig, Germany

Email: Maria.pfefferkorn@medizin.uni-leipzig.de

Background and aims: New reliable HBV infection models are needed, since in existing models a low biomarker secretion *in vitro* often impedes biomarker analysis. The previously reported clone HepG2-hNTCP-sec+ promises to support the viral life cycle of HBV fully and stably for prolonged periods of time. The aim of the study was an extensive characterization of the biomarker pattern *in vitro* during an infection of up to 28 days.

Method: HepG2-hNTCP-sec+ cells (kindly provided by M. Windisch) were seeded and infected with cell culture derived HBV (ccHBV), obtained from HepAD38 cells, at different multiplicities of infection (MOI, copies per cell) ranging from 50 to 10 000. Supernatant was collected after varying intervals of time from every day, every 2 days, every 3 days to every 7 days for a period of 7–28 days. To increase the volume of supernatant for extensive biomarker analysis the infection model was upscaled from an initial 384-well format to a 24-well format. HBV biomarkers (HBV DNA, HBV RNA, HBsAg composition) were measured using our published and validated in-house assays.

Results: After upscaling of the infection model cells were seeded and successfully infected with ccHBV in 96-, 48- and 24-well at MOIs >500. Maximum levels of HBsAg were measured in 24-well (MOI 10 000) at supernatant collection every 3 days with a peak concentration of 404.73 ng/ml at 6 dpi. HBsAg levels were significantly lower (136.46 ng/ml), when intensively washed after infection, compared to the standard protocol. However, the composition of HBsAg was not affected by changed washing or collection protocols. In 24-well (MOI 10000, medium change every 2 days) levels of MHBs and LHBs were 0.79 ng/ml (16.99% of total HBsAg) and 0.31 ng/ml (6.49%) at day 0 and increased to 20.23 ng/ml (13.15%) and 17.74 ng/ml (11.52%) after 6 dpi. In comparison, changing medium every 3 days showed concentrations of MHBs at 3.06 ng/ml (11.72%) and LHBs at 3.28 ng/ml (12.6%) at day 0 and 34, 9 ng/ml (8.57%) and 53, 42 ng/ml (13.08%) after 6 dpi, respectively. Long-term infection revealed a stable HBsAg composition despite a gradual decline of HBsAg to 2.61 ng/ml after 28 dpi. Depending on the protocol, HBV DNA and RNA showed an increase after 2–4 dpi and remained stable during the course of infection.

Conclusion: The new infection model with the cell line HepG2-hNTCP-sec+ was reproducible in several scale-sizes and protocol settings without influencing the HBV biomarker kinetics and might be basis for further studies e.g. regarding new surrogate markers for cccDNA.

FRI-271

Low intraindividual viral evolution is linked to disease progression and need of antiviral treatment initiation in chronic hepatitis B

Magnus Illum Dalegaard^{1,2}, Ulrik Fahnøe^{1,2}, Anni Winckelmann^{1,2}, Signe Bollerup¹, Jens Bukh^{1,2,3}, Nina Weis^{1,2,3}. ¹Copenhagen university hospital, Hvidovre, Department of infectious diseases, Denmark;

²University of Copenhagen, Copenhagen hepatitis C program (COHEP), department of infectious diseases, Copenhagen university hospital, Hvidovre, and department of immunology and microbiology, faculty of health and medical sciences, Denmark; ³University of Copenhagen, Department of clinical medicine, faculty of health and medical sciences, Denmark

Email: magnus.illum.dalegaard.01@regionh.dk

Background and aims: Treatment of chronic hepatitis B (CHB), that is initiated based on factors associated with disease progression, such as viremia, HBeAg status, fibrosis/cirrhosis status and/or family history of hepatocellular carcinoma, is with a nucleoside analogue (NA), and often lifelong. The hepatitis B virus (HBV) genome is relatively short, however quite diverse and can accumulate mutations over time. The impact of viral diversity and evolution on disease progression is not well-established. The objective of this study was to compare intraindividual viral evolution between two groups of CHB

patients over time, using treatment initiation as a measure of disease progression and lack of immunological control.

Method: We included 25 CHB patients; 14 who did (treated group)- and 11 who did not (non-treated group)-initiate NA treatment during the study period, dating back to the establishment of the Danish Database for Hepatitis B and C (DANHEP) biobank in 2004 until 2019. For each patient we obtained three longitudinal plasma/serum samples taken before potential NA treatment initiation, from the DANHEP biobank. HBV DNA was extracted and amplified by PCR before full-length HBV genomes were obtained by deep sequencing. We analyzed the number of mutations that evolved during the study period and calculated the mutation rates using linear regression.

Results: There was no difference between the two groups regarding age, sex, country of origin, genotype and follow-up time (median 60 versus (vs) 57 months) but there was a significant difference in HBV DNA value (median 40, 237, 179 vs 19, 028 IU/ml), HBeAg+ at baseline (n = 9 vs n = 0) and level of alanine aminotransferase (ALT) (median 43 vs 28 IU/ml). Four patients from the non-treated group were excluded from further analysis after quality control of the sequencing data. We found significantly lower mutation rates in the treated group compared to the non-treated (figure 1A). Regrouping the participants by HBeAg status showed a significantly lower mutation rate in the HBeAg+ group (figure 1B). Furthermore, log (HBV DNA) was significantly negatively correlated with mutation rates (Figure 1C).

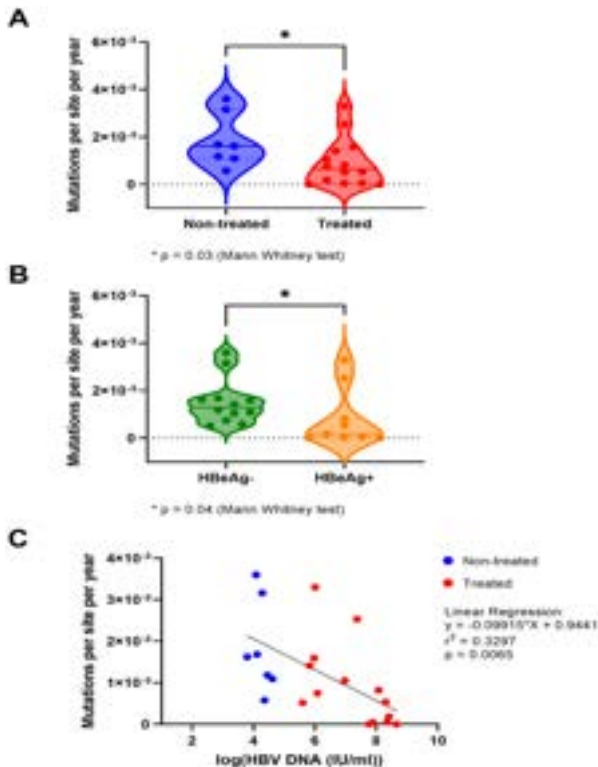


Figure 1. Comparisons of mutation rates of the HBV genome between (A) the treated and non-treated group (B) HBeAg negative and positive individuals and (C) linear regression of log(HBV DNA) and mutation rates.

Conclusion: CHB patients who initiate antiviral treatment have a significantly lower mutation rate prior to treatment initiation compared to patients without treatment indication. This suggests that HBV in individuals with poor immunological control mutates less frequently, which could be due to a lower immune selective pressure. High HBV DNA and HBeAg positivity are good correlates of lower mutation rates.

FRI-272

An in vivo duck hepatitis B virus model recapitulates key aspects of nucleic acid polymer treatment outcomes in chronic hepatitis B patients

Yannick Debing¹, Hannah Vanrusselt¹, Lars Degrauwe^{1,2}, Daniel Apolônio Silva de Oliveira², Christopher Kariuki², Ebanja Joseph Ebwanga², Shahbaz Bashir², Wouter Merckx³, Santhosh Thatikonda⁴, Vikrant Gohil⁴, David Smith⁴, Pierre Raboisson¹, Saul Montero⁴, Jin Hong⁴, Abel Acosta Sanchez⁵, Lawrence Blatt⁴, Julian Symons⁴, Tse-I Lin¹, Leonid Beigelman⁴, Jan Paeshuyse². ¹Aligos Belgium BV, Belgium; ²KU Leuven, Host-Pathogen Interaction Lab, Belgium; ³KU Leuven, TransFARM, Belgium; ⁴Aligos Therapeutics, Inc., United States; ⁵Novalix, Belgium
Email: ydebing@aligos.com

Background and aims: Nucleic acid polymers (NAPs) are an attractive treatment modality for chronic hepatitis B (CHB), with REP2139 and REP2165 having shown efficacy in CHB patients. A significant proportion of patients achieve functional cure, whereas the others exhibit a moderate response or are non-responders. NAP efficacy has been difficult to recapitulate in animal models, with the duck hepatitis B virus (DHBV) model showing some promise but remaining underexplored for NAP efficacy testing. Here we report on an optimized in vivo DHBV duck model and explore several characteristics of NAP treatment in this model.

Method: Pekin ducks (*Anas platyrhynchos domesticus*) were intravenously injected with DHBV-containing serum shortly after hatching. After establishment of infection, animals were treated with entecavir, REP2139 and/or REP2165 and serum DHBV DNA and DHBV surface antigen (DHBsAg) levels were determined weekly. Animals were followed up for several weeks after end of treatment. NAP liver concentrations were determined by mass spectrometry.

Results: REP2139 was efficacious in reducing DHBV DNA and DHBsAg levels in approximately 50% of ducks, both when administered intraperitoneally or subcutaneously. Efficacy was only observed in experimentally infected ducks, not in endogenously infected ducks (vertical transmission). REP2165 showed a different activity profile with a more homogenous antiviral response followed by a faster rebound. Intrahepatic NAP concentrations did not correlate with efficacy. Entecavir pretreatment prior to REP2139 treatment add-on further improved response rates.

Conclusion: Subcutaneous administration of NAPs in the DHBV duck model provides a useful tool for in vivo evaluation of NAPs, recapitulating many aspects of this class of compound's efficacy in CHB patients.

SATURDAY 24 JUNE

Viral hepatitis AE Clinical aspects

SAT-141

Hepatitis A hospitalisations in the United States and risk factors for inpatient mortality: a nationwide population study, 1998–2020

Paul Wasuwanich¹, Joshua So¹, Megan Hofmeister², Saleem Kamili², Songyos Rajborirug³, Wikrom Karnsakul⁴. ¹University of Florida College of Medicine, Department of Medicine, Gainesville, United States; ²Centers for Disease Control and Prevention, Division of Viral Hepatitis, National Center for HIV, Viral Hepatitis, STD and TB Prevention, Atlanta, United States; ³Johns Hopkins Bloomberg School of Public Health, Baltimore, United States; ⁴The Johns Hopkins University School of Medicine, Division of Pediatric Gastroenterology, Hepatology, and Nutrition, Department of Pediatrics, Baltimore, United States
Email: p.wasuwanich@ufl.edu

Background and aims: Hepatitis A virus infections in the United States have been declining due to improvements in sanitation and the introduction of hepatitis A vaccines. However, recent widespread outbreaks associated with person-to-person transmission brought the disease back into the spotlight. We aim to describe the epidemiology of hepatitis A hospitalizations from 1998 to 2020 in the United States and investigate risk factors that increase inpatient mortality.

Method: We utilized the National Inpatient Sample database from the Healthcare Cost and Utilization Project which collects nationwide US hospitalization data. We identified hepatitis A-related hospitalizations using ICD-9 and ICD-10 diagnosis codes. Demographic and geographic data were extracted, as well as clinical data including death, coinfections, comorbidities, pregnancy status, and substance

use. Data were analyzed by logistic and Poisson regression. Significance was defined as $p < 0.01$.

Results: We identified a total of 160,661 hepatitis A-related hospitalizations between 1998 and 2020, with the lowest hospitalization rate in 2015 (21.8 per 1,000,000 people), and the highest in 2019 (62.9 per 1,000,000 people). Hospitalization rates decreased overall during 1998–2015 (Incidence Rate Ratio [IRR] = 0.98; 95% CI = 0.98–0.98; $p < 0.001$) and increased during 2015–2020 (IRR = 1.25; 95% CI = 1.24–1.27; $p < 0.001$). The inpatient mortality rate ranged from 1.7% in 2005 to 3.8% in 2020. Most hospitalizations occurred among males (56.9%), non-Hispanic White persons (72.0%), and in the Southern region (51.2%). Age > 55 years (OR = 2.81; 95% CI = 2.27–3.49; $p < 0.001$), alcoholic cirrhosis (OR = 4.00; 95% CI = 3.00–5.32; $p < 0.001$), autoimmune hepatitis (OR = 3.44; 95% CI = 1.48–8.00; $p = 0.004$), chronic kidney disease (OR = 2.56; 95% CI = 2.02–3.25; $p < 0.001$), heart failure (OR = 2.68; 95% CI = 2.11–3.40; $p < 0.001$), hepatorenal syndrome (OR = 18.32; 95% CI = 13.31–25.22; $p < 0.001$), and portal hypertension (OR = 3.95; 95% CI = 2.97–5.26; $p < 0.001$) increased the odds of inpatient mortality. Hepatitis C virus coinfection (OR = 0.67; 95% CI = 0.51–0.88; $p = 0.004$), tobacco use disorder (OR = 0.38; 95% CI = 0.30–0.49; $p < 0.001$), and intravenous drug use (OR = 0.38; 95% CI = 0.28–0.53; $p < 0.001$) were associated with decreased odds of inpatient mortality. Diabetes, obesity, hepatitis B virus coinfection, fatty liver disease, and solid organ transplantation were not associated with mortality ($p > 0.01$). None of the pregnant women hospitalized with hepatitis A died.

Conclusion: Hepatitis A hospitalizations declined from 1998 to 2015 and then increased rapidly from 2015 to 2020, coinciding with widespread outbreaks associated with person-to-person transmission. Concerningly, inpatient mortality rates also increased. Certain risk factors can be used to predict prognosis of patients hospitalized with hepatitis A.

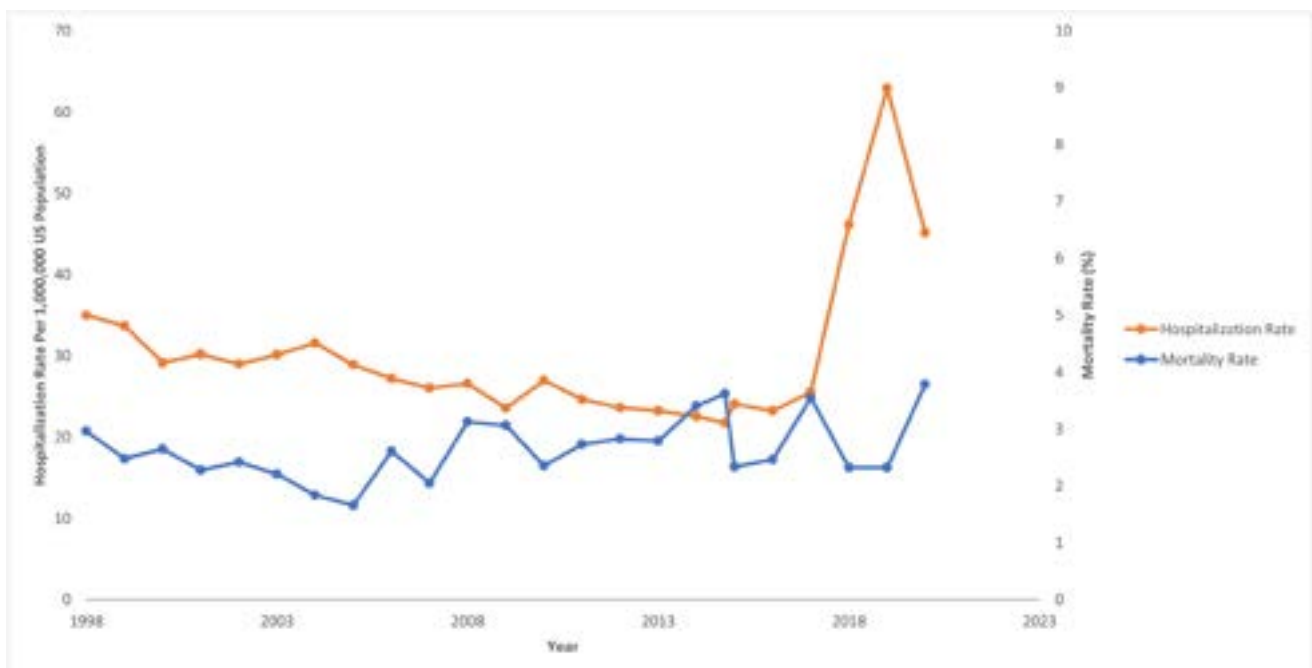


Figure: (abstract: SAT-141): Hospitalization rate and mortality rate of hepatitis A in the United States, 1998–2020.

SAT-142

High prevalence of HEV related to the progression and prognosis of patients with acute pancreatitis: a multicentre cross-sectional and cohort study in China

Jian Wu^{1,2}, Ze Xiang^{2,3}, Lan Huang⁴, Ce Gao⁴, Ling Tong⁵. ¹The Affiliated Suzhou Hospital of Nanjing Medical University, Suzhou Municipal Hospital, Gusu School, Nanjing Medical University, Department of Clinical Laboratory, Suzhou, China; ²The Chinese Consortium for the Study of Hepatitis E (CCSHE), China; ³Zhejiang University School of Medicine, China; ⁴The Affiliated Suzhou Hospital of Nanjing Medical University, Suzhou Municipal Hospital, Gusu School, Nanjing Medical University, China; ⁵The First Affiliated Hospital, Zhejiang University School of Medicine, China
Email: wujianglinxing@163.com

Background and aims: The role of HEV infection in acute pancreatitis (AP) patients remains unclear.

Method: 1000 eligible patients with AP, 1000 healthy controls (HCs) and 300 patients with AHE were recruited from 8 hospitals in China from January 1, 2016 to May 31, 2021.

Results: The positive rates of anti-HEV IgG, anti-HEV IgM and HEV RNA in the AP group were all significantly higher than HCs group. With the increase of the severity of AP, the percentage of HEV infection also increased significantly. According to whether infected with HEV, 1000 AP patients were divided into patients without HEV infection (AP- group, n = 977) and those with HEV infection (AP+AHE

group, n = 23). The percentage of patients with severe AP in the AP +AHE group was significantly higher than the AP- group, and the percentage of patients with mild AP in the AP+AHE group was significantly lower than that in the AP- group. In the AP+AHE group, 12 AP cases were potentially associated with HEV infection, the severity of whom were associated with high level of HEV titre. Moreover, HEV infection was one of the main independent risk factors and owned the high predictive power for the outcome of AP, suggesting that HEV infection was related to poorer outcome of AP. High level of HEV titre would prolong the hospital stay of AP patients, and HEV infection was associated with the higher risk of recurrent AP. In addition, AP+AHE patients receiving conservative treatment showed better prognosis. Among 300 AHE patients, 5 patients were diagnosed with AP. After excluding common AP causes, 2 patients with AP were considered to be potentially associated with HEV infection.

Conclusion: HEV infection plays an important role in the occurrence, development and prognosis of AP, which would have implications for management of AP patients complicated with AHE.

SAT-143

Hepatitis E virus infection before and after liver transplantation

Petra Dinjar Kujundžić¹, Tatjana Vilibic-Cavlek², Tomislav Kelava³, Adriana Vince^{3,4}, Jelena Prpic⁵, Lorena Jemersic⁵, Ana Ostojic⁶, Anna Mrzljak^{3,6}. ¹Merkur Clinical Hospital, Croatia; ²Croatian Institute

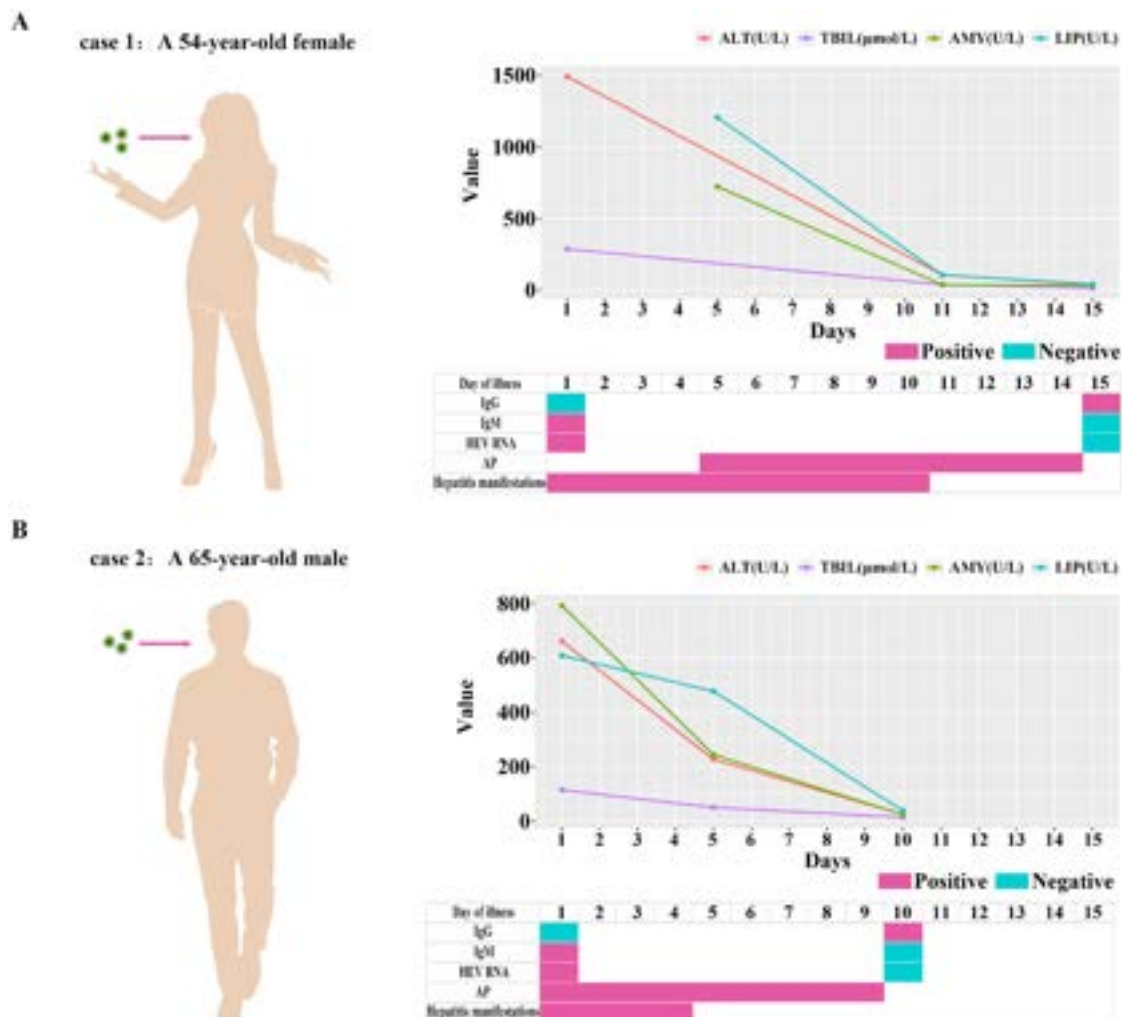


Figure: (abstract: SAT-142).

POSTER PRESENTATIONS

of Public Health, Croatia; ³School of Medicine, University of Zagreb, Croatia; ⁴University Hospital for Infectious Diseases Dr. Fran Mihaljevic, Zagreb, Croatia; ⁵Croatian Veterinary Institute Zagreb, Croatia; ⁶University Hospital Centre Zagreb, Croatia
Email: petra.dinjar@gmail.com

Background and aims: Liver transplant (LT) recipients have an increased risk of developing chronic hepatitis E virus (HEV) infection, which may rapidly progress to graft failure if not treated. The prevalence of HEV infection after LT is unclear and varies geographically. This study aimed to investigate the HEV seroprevalence, acquired risk factors, and the incidence of acute HEV infection in the early post-LT period.

Method: From 2017 to 2019, 766 LT recipients (cohort 1) enrolled in a cross-sectional study during routine post-transplant outpatient visits, and 152 newly transplanted (cohort 2) were prospectively screened at the time of LT assessment and 6- and 12-months post-LT. Cohort 2 was subclassified into three groups according to established HEV IgG status during follow-up: anti-HEV IgG negative (SN), anti-HEV IgG positive (SP), and de novo anti-HEV IgG positive (SP+). Blood samples were tested for anti-HEV IgG and HEV RNA. Medical records and a risk factor assessment questionnaire were reviewed.

Results: The overall anti-HEV IgG seroprevalence in LT recipients was 19.9%, and no HEV RNA was detected. The IgG prevalence was significantly associated with increasing age ($p = 0.033$), however no significant HEV seroprevalence differences were observed regarding gender, the etiology of liver disease listed for LT, place of residence, specific factors within a household (a farm, number of household members, type of drinking water, type of sewage system), production or consumption of cured meat, occupational exposure, blood transfusions in the post-LT period or any of laboratory parameters including level or type of immunosuppressive therapy. A lower risk of infection was observed among recipients with a higher level of education (OR = 0.33; 95%CI = 0.15–0.74), whilst older age was identified as a risk factor for HEV seropositivity (OR = 1.03; 95%CI = 1.01–1.05). In cohort 2, no patient tested HEV RNA positive. Six patients (3.9%) developed seroconversion in the follow-up period. According to anti-HEV IgG status, there were 115 patients in the SN group, 31 in the SP group, and 6 in the SP+ group. No difference between the groups was observed regarding liver tests at 0, 6, and 12 months, respectively.

Conclusion: In Croatia, a substantial proportion of LT recipients are at risk of acquiring HEV infection. The results highlight high HEV seroprevalence among LT recipients (19.9%) but a low risk of developing an acute or chronic HEV infection with the adverse effect of liver graft in the posttransplant period. The source and routes of HEV infection remain unclear in LT recipients.

Viral hepatitis B and D Clinical aspects

WEDNESDAY 21 TO SATURDAY 24 JUNE

TOP-100

Long-term outcome of hepatitis delta in different regions world-wide: results of the hepatitis delta international network (HDIN)

Anika Wranke¹, Emanoil Ceausu², George Dalekos³, Mario Rizzetto⁴, Adela Turcanu⁵, Grazia Niro⁶, Onur Keskin⁷, George Sebastian Gherlan², Minaam Abbas⁸, Patrick Ingiliz⁹, Marion Muche¹⁰, Maria Buti¹¹, Peter Ferenci¹², Thomas Vanwolleghem¹³, Markus Cornberg¹, Zaigham Abbas⁸,

Cihan Yurdaydin¹⁴, Petra Dörge¹, Heiner Wedemeyer¹. ¹Hannover Medical School, Gastroenterology, Hepatology and Endocrinology, Germany; ²Victor Babes Clinical Hospital for Infectious and Tropical Diseases, Romania; ³University of Thessaly, Greece; ⁴University of Torino, Italy; ⁵State University of Medicine "Nicolae Testemitanu," Moldova; ⁶Divisione di Gastroenterologia, Ospedale Generale Regionale "Casa Sollievo della Sofferenza, Italy; ⁷Ankara University, Turkey; ⁸Ziauddin University Hospital Karachi, Pakistan; ⁹Centre for Infectology Berlin (CIB), Germany; ¹⁰Charité, Berlin, Germany; ¹¹Liver Unit, Valle d'Hebron University Hospital and Ciberdel Instituto Carlos III, Spain; ¹²Medical University of Vienna, Austria; ¹³Antwerp University Hospital, Belgium; ¹⁴Koc University Medical School, Turkey
Email: wedemeyer.heiner@mh-hannover.de

Background and aims: Chronic delta hepatitis represents a major global health burden. Clinical features of HDV infection vary largely between different regions world-wide. Moreover, treatment approaches may differ and depend on drugs approved and financial resources. However, factors determining disease progression are poorly defined. The Hepatitis Delta International Network (HDIN) was established in 2011 to compile a comprehensive database to facilitate clinical research on chronic hepatitis delta.

Method: The HDIN registry was developed by the HepNet Study-House of the German Liver Foundation in collaboration with researchers from Europe, Asia, North- and South America. A structured questionnaire specifically developed for hepatitis delta long-term follow-up was implemented. We here report data of 547 patients from 13 centers in 10 countries with ongoing or past HDV infection included until December 2022.

Results: The majority of patients were male ($n = 335$, 61%) and the mean age was 41 years (range 1–79). Most patients were HBeAg-negative (87%). Patients were divided according to the country of birth into Eastern Mediterranean (EM; 26%), Eastern Europe and Central Asia (EE; 38%), Central and Southern Europe (CE; 15%), South Asian (SAS (mainly Pakistan); 16%) and Africa (2%). The median follow-up varied from 9.1 (range 0.6–28) years (EM) to 3.2 (0.6–18) years (SAS) ($p = 0.01$). Liver cirrhosis at baseline was reported in 42% of cases, varying from 41% in EE to 49% in SAS. During follow-up 31% developed a liver-related end point ($n = 168$) after 3.2–4.5 years. Ascites was the most frequent decompensation (22%), followed by encephalopathy (8.8%) and variceal bleeding (7.1%). Hepatocellular carcinoma developed in 47 patients (8.6%) and 68 patients (12%) underwent liver transplantation. Sixty-four patients died (12%), 47% were HDV-related. Clinical liver-related end points developed more frequently in EM patients (42%), compared to 28% in EE patients, 26% in EM patients and 27% in SAS patients ($p < 0.01$). However SAS patients developed end points earlier ($p < 0.01$) and had the highest mortality (Kaplan Meier $p < 0.01$). Additionally, they had lowest Albumin levels and were younger ($p < 0.01$). Antiviral therapy during follow-up was administered to 350 patients (highest treatment uptake in EM and SAS patients, lowest in CE), including 225 patients being treated with IFNa (SAS 59%, EM 49%, EE 35%, CE 23%). Patients who received IFNa-based therapies developed clinical end points less frequently, which was significant in both chi-square and Kaplan-Meier analysis. End points occurred more frequently in patients with positive HDV RNA (at baseline or at end of follow-up) ($p = 0.01$).

Conclusion: The HDIN registry confirmed the particular severity of hepatitis delta. There is an urgent need to generate global data to determine the incidence, the differences in access to care and treatment and consecutively the liver related outcomes.

TOP-101

Identification of liver-associated gene signatures from serum exosomes in patients with chronic hepatitis B

Mario Cortese¹, Liao Zhang², David Pan², Jeffrey Wallin¹, Bryan Downie². ¹Gilead Sciences, Biomarkers, Foster City, United States; ²Gilead Sciences, CBEA, Foster City, United States
Email: mario.cortese@gilead.com

Background and aims: The invasive nature and high costs of liver biopsies pose significant challenges in HBV clinical studies. Serum-based exosome profiling may be an alternative method to profile liver gene expression differences associated with HBV treatment or cure. Here, we generated RNA sequencing data derived from isolated exosomes (Exosome-seq) and peripheral blood to investigate the gene expression characteristics associated with response to pegylated interferon alpha-2a (PEG-IFN) treatment in patients with chronic hepatitis B (CHB).

Method: Clinical study GS-US-174-0149 evaluated PEG-IFN alone or in combination with tenofovir disoproxil fumarate (ClinicalTrials.gov Identifier: NCT01277601). Exosome-seq data was generated from baseline and on-treatment (week 4) samples for study subjects with (n = 14) and without (n = 26) hepatitis B surface antigen (HBsAg) loss at week 48. Additionally, RNA-seq data was obtained from whole blood samples collected at baseline and week 48 from a total of n = 22 CHB patients (n = 13 with and n = 9 without HBsAg loss) in the study. Biological pathway scores were generated using the ssGSEA methodology. Treatment-induced transcriptional signatures were determined using voom-limma or mixed effects models between the two response groups (HBsAg loss vs. no HBsAg loss). Liver specific genes were determined by comparing count-per-million (CPM) expression profiles of liver tissues compared to non-liver tissues using a Wilcoxon-ranked sum test in the Genotype-Tissue Expression (GTEx) dataset.

Results: Exosome profiling revealed broad transcriptional changes 4 weeks following the start of treatment with PEG-IFN. These changes included immune signatures associated with IFN signaling and T cell activation, similarly to those observed in whole blood. Additionally, an increase in liver-specific genes was observed in exosome-seq following PEG-IFN treatment, suggesting that exosome profiling may provide insight into the cellular response of hepatocytes and liver-resident cells elicited by PEG-IFN. Genes encoding markers of liver inflammation (ALB, complement activation (CFHR2, CFHR5), enzymes involved in metabolic pathways (UGT1A3, UGT1A4, HAO1), and coagulation factors (F9, F13B) were among the most enriched liver-specific genes during treatment with PEG-IFN. Despite a large transcriptional overlap, 570 genes demonstrated trending differences after 4 weeks in transcriptional profile (nominal p < 0.05) between Week 48 clinical responders (HBsAg loss) and non-responders. Finally, associations were observed between exosome-derived liver-specific genes and clinical characteristics of HBV disease status, such as HBsAg loss.

Conclusion: Serum-based Exosome-seq revealed liver-associated signatures of response to PEG-IFN treatment in CHB patients. These findings suggest that transcriptional profiling of exosomes has potential as a non-invasive method to profile liver-derived immune responses in HBV clinical studies.

TOP-103

HDV full genome sequencing and sensitive HBV genotyping from a large cohort of HBV/HDV co-infected patients

Savrina Manhas¹, Simin Xu¹, Silvia Chang¹, Thomas Aeschbacher¹, Roberto Mateo¹, Ross Martin¹, Yang Liu¹, Stephanie Narguet², Dzhamal Abdurakhmanov³, Pietro Lampertico⁴, Dmitry Manuilov¹, John F. Flaherty¹, Hongmei Mo¹, Evguenia S Svarovskaia¹, Tarik Asselah². ¹Gilead Sciences, Inc., United States; ²Université de Paris-

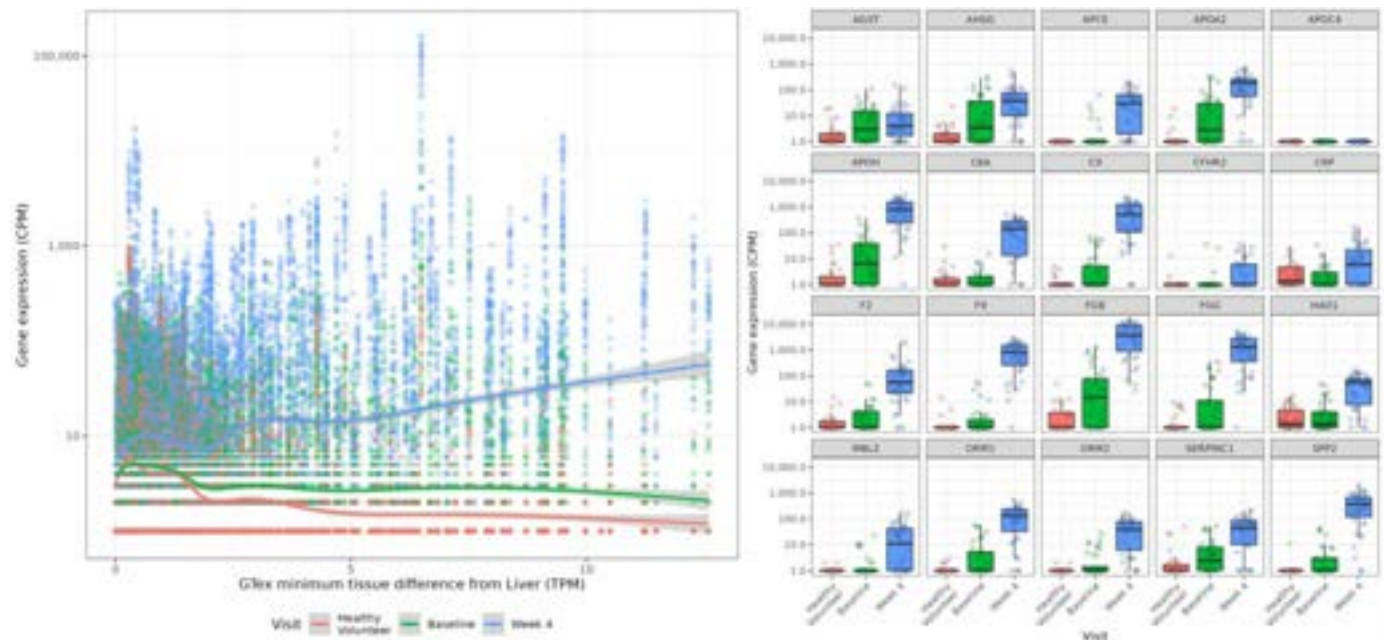


Figure: (abstract: TOP-101): Left panel: Exosome-based gene expression as a function of liver specificity in healthy volunteers (red), and in chronic HBV patients at baseline (green), and 4 weeks post PEG-IFN treatment (blue). Right panel: Exosome-based gene expression in top 20 most liver specific genes based on GTex in healthy volunteers (red), and in chronic HBV patients at baseline (green), and 4 weeks post PEG-IFN treatment (blue).

POSTER PRESENTATIONS

Cité, Department of Hepatology, France; ³Sechenov University, Russian Federation; ⁴Foundation IRCCS Ca' Granda Ospedale Maggiore Policlinico, Italy
Email: savrina.manhas1@gilead.com

Background and aims: Hepatitis Delta virus (HDV) is a 1.7 kb RNA virus that requires Hepatitis B virus (HBV) envelope proteins for hepatocyte entry and virion release. HDV causes the most severe form of viral hepatitis. Evolutionary analysis of nucleotide sequence diversity groups HDV into eight major genotypes (HDV-1 to HDV-8) and HBV into eight major genotypes (GTA to GTH). Most HDV and HBV genotypes have distinct geographical distributions; however, to date, limited HDV and HBV sequencing data is available from HDV/HBV co-infected patients.

Method: HDV and HBV sequencing were attempted for 391 HDV/HBV co-infected patients from 15 countries of birth. For HDV sequencing, full genome (FG) amplification followed by next generation sequencing (NGS) or total RNA sequencing of plasma was used. HDV consensus sequences from NGS were used to determine genotype based on BLAST analyses against a diverse set of HDV sequences representing all HDV genotypes. For HBV sequencing, FG amplification or an ultrasensitive assay using both HBV RNA and DNA amplification of five small fragments across large hepatitis B surface antigen followed by NGS was performed. HBV consensus sequences from NGS were used to determine HBV genotypes based on BLAST analyses against an HBV reference sequence library. If amplification was unsuccessful, HBV genotype was determined using an enzyme immunoassay.

	HBV/HDV Genotype, N											
	A/1	A/2	A/5	A/6	B/1	C/1	D/1	D/2	D/5	E/1	E/5	Failed
Eastern Europe												
Russia	13	4					231	2				2
Romania	1						3					1
Moldova							1					3
Sweden	1											
Western Europe												
Germany	4						29			1	1	
France	1			1		1	6		2	1	2	2
Italy	2				1		19					1
West Africa												
Benin	1									1		
Cameroon			1				1					8
Côte d'Ivoire	1						1		2		1	3
Guinea									1			2
Senegal											1	2
Tunisia							1					
Other												
Afghanistan							1					1
Turkey							1					2
Total	24	4	1	1	1	1	294	2	5	3	5	27

Table. HBV/HDV Genotypes from Co-infected Patients

Results: The majority of patients were from Eastern Europe (n = 264), Western Europe (n = 71) and West Africa (n = 43). HDV and HBV

sequencing were successful for 331 (85%) and 277 (71%) of 391 patients, respectively, while paired HBV/HDV genotypes were determined for 341 (87%) patients. Regarding individual genotypes, HBV GTD and HDV-1 were the most prevalent with 320 (82%) and 327 (84%) of 391 patients, respectively. Paired HBV/HDV genotypes were as follows: D/1 86%, 24 (7%) A/1, 5 (1%) D/5, 5 (1%) E/5, 4 (1%) A/2, 3 (1%) E/1, 2 (1%) D/2, and 1 (<1%) patient each had A/5, A/6, B/1, and C/1 combinations. HBV GTD and HDV-1 were observed in patients from 12/15 and 13/15 countries, respectively while most HBV GTE (11/16) and HDV-5 (9/14) patients were from West Africa. Phylogenetic analyses revealed distinct clusters of sequences within HDV-1 from the same country supported by high bootstrap proportions. Therefore, potential new HDV-1 subtypes can be assigned with the addition of these data to the public domain.

Conclusion: Sequencing and genotyping of HDV and HBV from 391 patients across 15 countries were determined here with HBV/HDV genotypes D/1 being most prevalent. Phylogenetic analyses showed new HDV-1 subtypes that have not been previously reported. To date, this is the largest published dataset of paired HBV/HDV clinical sequences and genotype determinations.

TOP-106

The intrahepatic activity of Hepatitis Delta virus is sustained by an abundant production of HBs transcripts, mainly derived from integrated HBV-DNA, and is not strictly related to the extent of HBV reservoir

Romina Salpini¹, Stefano D'Anna¹, Lorenzo Piermatteo^{1,2}, Elisabetta Teti³, Andrea Di Lorenzo³, Giulia Torre¹, Vincenzo Malagnino³, Marco Iannetta³, Francesca Ceccherini Silberstein¹, Caterina Pasquazzi⁴, Giuseppina Brancaccio⁵, Leonardo Baiocchi⁶, Simona Francioso⁶, Ilaria Lenzi⁶, Umberto Cillo⁵, Alessandro Vitale⁵, Enrico Gringeri⁵, Angelica Magrofuoco⁵, Maria Lorena Abate⁷, Anna Maria Geretti³, Antonella Olivero⁷, Loredana Sarmati³, Mario Rizzetto⁷, Gian Paolo Cavaglia⁷, Valentina Svicher^{1,2}. ¹University of Rome Tor Vergata, Experimental Medicine, Italy; ²University of Rome Tor Vergata, Department of Biology, Italy; ³Tor Vergata University Hospital, Infectious Diseases Unit, Italy; ⁴Sant'Andrea Hospital, Italy; ⁵University of Padua, Italy; ⁶Tor Vergata University Hospital, Hepatology Unit, Italy; ⁷University of Turin, Department of Medical Sciences, Italy
Email: rsalpini@yahoo.it

Background and aims: HDV exploits HBV surface glycoproteins (HBsAg) for viral morphogenesis and de novo entry into hepatocytes. The interplay between the two viruses is poorly understood and has been mainly evaluated in peripheral blood. We investigated HBV and HDV replicative activity and interplay by analysing a well-defined set of liver biopsies from patients with chronic HBV/HDV co-infection.

Method: Liver tissue was analysed from 22 patients (63.6% NUC-treated; 95% HBeAg negative). Intrahepatic levels of covalently closed circular DNA (cccDNA), pregenomic HBV-RNA (pgRNA), total HBV-DNA (itHBV-DNA) and HDV-RNA were quantified by highly sensitive droplet digital PCR (ddPCR). ddPCR assays were also set up to quantify total HBs transcripts and to distinguish HBs transcripts deriving from cccDNA and from integrated HBV-DNA (idDNA-derived HBs) according to Grudva, 2022.

Results: Patients had median (IQR) serum HBsAg, HBV-DNA and HDV-RNA levels of 14,460 (8,868–20,551) IU/ml, 34 (23–65) IU/ml, and 7.3 (3.7–7.7) log₁₀ IU/ml, respectively. Median (IQR) ALT was 75

(64–245) U/L; half of patients has a fibrosis score \geq F5. Intrahepatic HDV-RNA load was median (IQR) 813 (0.3–4266) copies/1000 cells and positively correlated with serum HDV-RNA ($Rho = 0.68$, $P = 0.03$). Regarding HBV intrahepatic reservoir, median (IQR) cccDNA load was 4 (0.04–16) copies/1000 cells, pgRNA load was 10 (2–139) copies/1000 cells and itHBV-DNA load was 185 (61–417) copies/1000 cells. Total HBs transcripts showed a load of median (IQR) 6,257 (591–16,636) copies/1000 cells. Notably, iDNA-derived HBs transcripts exceed by >2 log cccDNA-derived HBs transcripts ($p = 0.01$), supporting an intensive HBs production from integrated HBV-DNA in the setting of HBV/HDV chronic infection. cccDNA load tightly correlated with pgRNA and itHBV-DNA load ($Rho = 0.79$ and 0.74 respectively; $P < 0.01$). Notably, a positive correlation was observed between cccDNA load and total HBs transcripts ($Rho = 0.63$; $P = 0.007$), which was even stronger for cccDNA-derived HBs transcripts ($Rho = 0.9$). Conversely, no correlation was observed between intrahepatic HDV-RNA load and intrahepatic HBV markers ($Rho < 0.36$; $p > 0.15$ for all), supporting independent replicative pathways for the two viruses.

Conclusion: Pathways underlying the persistence of intrahepatic HDV-RNA act independently from the intrahepatic HBV reservoir and are fueled by an abundant production of HBs transcripts, particularly from integrated HBV-DNA. These issues are crucial for understanding mechanisms underlying HDV persistence and for the identification of therapeutic approaches aiming to achieve HDV cure.

TOP-112

Programmed cell death protein 1/ligand 1 inhibitor versus tyrosine kinase inhibitor in the efficacy of HBsAg reduction in chronic hepatitis B patients with hepatocellular carcinoma

Te-Wei Tseng¹, Wei Teng^{1,2}, Po-Ting Lin^{1,2}, Rachel Wen-Juei Jeng^{1,2}, Chun-yen Lin^{1,2}. ¹Linkou Chang Gung Memorial Hospital, Department of Hepatogastroenterology, Taoyuan City, Taiwan; ²Chang Gung University, College of Medicine, Taiwan
Email: rachel.jeng@gmail.com

Background and aims: Recent phase I clinical trial revealed chronic hepatitis B (CHB) patients receiving 0.3 mg/kg/dose Nivolumab, a PD1 inhibitor, had mean HBV surface antigen (HBsAg) decline of 0.30 log₁₀ IU/ml on week 12 and 4.5% HBsAg loss by 6 months follow-up. Whether HBsAg reduction magnitude and HBsAg loss rate will be increased in CHB patients receiving higher dose of PD1 inhibitor remained unknown. We aim to investigate this issue by comparing the HBsAg kinetics between CHB patients with hepatocellular carcinoma (HCC) receiving anti-cancer treatment with either PD1 inhibitor (ICI) or tyrosine kinase inhibitor (TKI).

Method: CHB patients with HCC receiving either [Nivolumab (2–3 mg/kg/dose) or Atezolizumab (1200 mg/dose) plus Bevacizumab (5–10 mg/kg/dose), as ICI group] or [Sorafenib (400–800 mg/day), as TKI group] at least 4 weeks during 2012 to 2023 were retrospectively recruited. All patients were followed for at least 3 months after receiving anti-cancer therapy. Propensity score matching (PSM) was done to adjust baseline characteristics differences (including age, gender, ALT, BCLC stage, HBV DNA level, and nucleotide analogues (NUC) coadministration status) between two groups at a 1:1 ratio. Serial HBsAg levels at 3 months before study entry, at the start of ICI or TKI treatment, and 3 months after treatment were assayed. HBsAg decline and HBsAg loss rate were compared between both groups.

Results: After PSM, there were 36 patients in each group. The median duration of ICI or TKI treatment was 3.32 months and 4.93 months, respectively. Characteristics at study entry were comparable between both groups. The HBsAg reduction magnitude [median: 0.10 vs –0.03 log₁₀ (IU/ml/year), $p = 0.514$], proportion of rapid HBsAg decline (>0.5 log₁₀ IU/ml/year) 8/34 vs 11/34, $p = 0.418$) and HBsAg loss rate (2/36 vs 0/36, $p = 0.493$) after ICI or TKI treatment were all comparable.

Conclusion: CHB patients with HCC receiving anti-cancer dosage of immunotherapy failed to achieve greater HBsAg reduction magnitude nor higher HBsAg loss probability than those receiving TKI. Immunotherapy alone, even with higher dose, may not be potent enough to achieve functional cure.

Table (abstract: TOP-112).

	TKI	ICI	p
N	34	34	
Age	60 (46~81)	61 (26~80)	0.629
Sex (male)	31	24	0.062
ALT (U/L)	42 (16~124)	37 (15~245)	0.594
BCLC stage			0.829
A/B	8	10	
C	26	24	
Anti-cancer therapy			
Atezolizumab/Bevacizumab		18	
Nivolumab		16	
Sorafenib	34		
Anti-cancer treatment duration (m)	4.9 (1.6~37.0)	3.3 (1.0~51.0)	0.052
Baseline HBV DNA level, log ₁₀ IU/ml [#]	1.62 (0~7.35)	0 (0~5.83)	0.027
NUC	33	36	0.239
NUC duration (m)	10.43 (0~1430.18)	19.25 (1.38~141.11)	0.267
HBeAg	4	6	0.509
Baseline HBsAg, IU/ml [#]	675.65 (0.36~16735)	479.5 (0.11~3173)	0.336
Post-treatment HBsAg decline ^{\$}	0.10 (–1.58~5.97)	–0.03 (–3.86~2.09)	0.514
HBsAg decline >0.5 ^{\$}	11	8	0.418
HBsAg decline >1 ^{\$}	5	5	1
HBsAg clearance (<0.05 [#])	0	2	0.493

*median (range);
\$log₁₀ (IU/ml/year);
#IU; m: month

WEDNESDAY 21 JUNE

WED-113

The performance of the cobas® HBV RNA assay for use on the cobas® 5800/6800/8800 Systems (RUO) against genomic variants and transcript heterogeneity

Thomas Meister¹, Victoria Innocent¹, Debra Liggett¹, Dax Javier¹, Alan Blair¹, Zih-Hua Chen¹, Abdellali Kelil¹, Sneha Nishtala¹, Caroline Scholtes², Barbara Testoni², Marie-Laure Plissonnier², Massimo Levrero³, Fabien Zoulim², Marantha Heil¹, Aaron Hamilton¹.
¹Roche Molecular Systems, United States; ²INSERM, France; ³Italy
 Email: aaron.hamilton@roche.com

Background and aims: Circulating HBV RNA has emerged as a novel biomarker reflecting cccDNA presence and transcriptional activity, and is being explored for use as a PCR diagnostic target in monitoring viral clearance and informing treatment decisions. The cobas® HBV RNA assay for use on the cobas® 5800/6800/8800 Systems (RUO) is a quantitative test targeting the 3' poly-A junction of HBV RNA. This allows differentiation from other nucleic acids including products of integrated viral DNA. In this study, HBV genomic polymorphisms and transcript variants were characterized, and the impact on assay performance was assessed.

Method: HBV sequence and transcript diversity were assessed with an *in silico* analysis and an HBV RNA sequencing workflow. For genomic analysis, NCBI and in-house databases were analyzed with a custom algorithm. For assessing HBV RNA sequences, a panel of HBeAg ± samples from genotypes A-E were collected at the Hospices Civils de Lyon. The cobas HBV RNA RUO assay performance was assessed with varying concentrations of *in vitro* transcribed (IVT) RNAs.

Results: Inspection of the polyadenylation cleavage site revealed the most common polymorphism was an A/T at the penultimate nucleotide. Rare genomic variants were present in 4% of the public database. The next six most reported variants had 0.1–1% frequency. A panel of HBeAg ± samples were sequenced. The penultimate A/T variations were observed but none of the rare variants. Analysis of viral RNA revealed that heterogeneity at the HBV poly-A start site varied in a genotype dependent manner. The major variant found alongside the standard poly-A junction is a –2 poly-A start site, which occurs at higher frequencies (30–50%) in genotypes A, D, and E, likely related to the T>A polymorphism at the penultimate nucleotide commonly observed in these genotypes. In contrast, total poly-A alternative start sites in genotypes B and C ranged from 2 to 25%. When the cobas HBV RNA RUO assay was tested with IVT mixtures, the assay performance against the –2 transcript variant was equivalent to the canonical transcript. The next six most reported genomic variants (0.1–1% frequency) were experimentally tested with *in vitro* transcript templates. Additional primers were assessed to mitigate rare mismatches that may affect quantitation of the assay.

Conclusion: The HBV polyadenylation cleavage site was assessed for genomic and transcriptional variation. The major genomic variation was an A/T polymorphism at the penultimate nucleotide of the cleavage site. Alternative poly-A start sites were identified within patient samples, with the major variant being a –2 poly-A start. The detected levels of poly-A heterogeneity had minimal impact on the cobas HBV RNA RUO assay. The assay design was improved with additional primers matching rare genomic mismatches. This diagnostic assay will fulfill a critical unmet need for monitoring chronic HBV infection.

WED-114

Next generation core inhibitors ABI-H3733 and ABI-4334 have significantly improved potency and target coverage for both antiviral and cccDNA formation activities compared to first-generation core inhibitors

Nuruddin Unchwaniwala¹, Katie Zomorodi¹, Michael Shen¹, Ran Yan¹, Xuman Tang¹, Xiang Xu¹, Michel Perron¹, William E. Delaney¹, Kathryn M. Kitrinis¹. ¹Assembly Biosciences, United States
 Email: kkitrinis@assemblybio.com

Background and aims: Core inhibitors (CIs) are a novel class of HBV antivirals with the potential to improve cure rates. CIs have multiple mechanisms of action (MOA), including (1) inhibition of pgRNA encapsidation which prevents formation of new viral particles (antiviral activity), and (2) disruption of incoming capsids which prevents de novo formation of cccDNA (cccDNA activity). CIs typically have greater potency against MOA1 (antiviral) than MOA2 (cccDNA). However, we believe that sufficient target coverage for both MOAs is needed for optimal clinical activity. Assembly Bio has two next generation CI candidates in Phase 1 clinical studies: ABI-H3733 (3733) and ABI-4334 (4334), which have improved potency against both MOAs compared to first-generation CIs including vebicorvir (VBR). Here, we compare human plasma and liver concentrations for VBR, 3733, and 4334 relative to protein adjusted EC₅₀s (paEC₅₀s) for each MOA.

Method: Plasma concentrations of VBR, 3733, and 4334 were measured in ongoing Phase 1a/b studies. Trough concentration (C_{min}) values for 3733 and 4334 at 300 mg once daily (QD) were projected assuming dose proportional exposure using 3733 50 mg (Phase 1b) and 4334 30 mg (Phase 1a) cohort data, respectively. In vitro EC₅₀s for antiviral activity (HBV DNA end point) and cccDNA activity (HBeAg end point) were measured in primary human hepatocytes (PHH) by branched DNA and ELISA, respectively. paEC₅₀s were determined in HepAD38 cells cultured in medium containing physiologic concentrations of human serum albumin and alpha acidic glycoprotein. Liver concentrations relative to plasma were estimated from nonclinical pharmacokinetic (PK) studies.

Results: The PK and antiviral properties of VBR, 3733, and 4334 are summarized in the Table. VBR achieved C_{min} values 1.4- and 0.1-fold above antiviral and cccDNA paEC₅₀s, respectively, at the 300 mg QD clinical dose. Based on the projected C_{min} values at 300 mg QD, 3733 and 4334 are predicted to have C_{min} values >100-fold over paEC₅₀ for antiviral activity and >10-fold over paEC₅₀ for cccDNA activity, with 4334 having an additional 3 to 4 times greater target coverage compared to 3733. VBR, 3733, and 4334 are predicted to have enriched exposure in the liver by 18, 6, and 7-fold, respectively.

Parameter	VBR 300 mg QD	3733 300 mg QD	4334 300 mg QD
Antiviral EC ₅₀ (nM)	281	8.8	0.5
cccDNA EC ₅₀ (nM)	3032	61	2.6
Protein adjustment (fold)	8	9.6	5.5
Plasma C _{min} /paEC ₅₀ (antiviral)	1.4	127	360
Plasma C _{min} /paEC ₅₀ (cccDNA)	0.1	18	69
Liver:plasma ratio	18	6	7

Figure: Summary of Key PK and Antiviral Properties for VBR, 3733, and 4334

Conclusion: Next generation CIs 3733 and 4334 have significantly improved coverage for both antiviral and cccDNA formation activities compared to first generation CIs. 3733 and 4334 are currently completing Phase 1b and Phase 1a studies, respectively.

WED-116

A retrospective observational cohort study of liver-related events among individuals with hepatitis B virus infection with and without hepatitis delta virus infection

Laura Telep¹, Amanda Singer¹, Ben Da¹, Ankita Kaushik¹, Chong Kim¹, Fang Xia¹, Anand Chokkalingam¹, Tatyana Kushner². ¹Gilead Sciences, Inc., Foster City, United States; ²Icahn School of Medicine at Mount Sinai, Division of Liver Diseases, New York, United States
Email: laura.telep@gilead.com

Background and aims: Hepatitis delta virus (HDV) is considered the most severe form of viral hepatitis infection. Among commercially insured patients, there are limited mixed data regarding rates of liver-related events in individuals infected with HDV vs. individuals with HBV mono-infection. The goal of this study is to characterize patients with HDV infection in United States (US) administrative claims data and assess the incidence of liver-related events in this population compared to individuals with HBV mono-infection.

Method: This was a retrospective observational cohort study using data from the IQVIA PharMetrics PlusTM database which contains adjudicated medical and pharmacy claims from commercially insured individuals in the US. All included individuals were age 18+ years at cohort entry with no pauses in enrollment >1 month prior to index or during follow-up. Index date for each cohort (HDV and HBV mono-infected) occurred between January 2007 and September 2021 at either first inpatient, or the first of two outpatient diagnosis codes at least 30 days apart with a 365-day baseline period and follow-up for ≥1 day. Four liver-related events were investigated (cirrhosis/fibrosis, hepatocellular carcinoma (HCC), liver decompensation, or liver transplant) using previously validated definitions. In

each analysis, patients with baseline evidence of the outcome or coinfection with hepatitis C virus (HCV) or human immunodeficiency virus (HIV), were excluded. A unique propensity score (PS) model was constructed using baseline demographic and clinical characteristics including the other three outcomes, nucleot (s)ide analogue (NA) and interferon (IFN) treatment history. Variables with standardized mean differences (SMD) between the exposure groups that were within 0.1 after weighting were considered balanced. Hazard ratios (HR) comparing risk of liver-related events in those with HBV mono-infection vs. HDV infection were estimated using Cox proportional hazards methods after PS weighting.

Results: During the study period, 46,474 individuals with HBV mono-infection and 1,805 with HDV infection were identified. Individuals with HDV were more likely to be older at cohort entry, male, and take NA or IFN treatment than those with HBV mono-infection (Table 1). In addition, baseline prevalence of diabetes, hypertension, hyperlipidemia, and liver-related conditions including HCV coinfection and end stage liver disease (ESLD) was higher in those infected with HDV. After PS weighting, there were no variables with |SMD| >0.1, and individuals infected with HDV had a higher risk for each clinical outcome than those mono-infected with HBV (cirrhosis [HR: 1.44, CI: 1.22–1.70]; liver decompensation [HR: 1.58, CI: 1.34–1.88]; HCC [HR: 1.41, CI: 1.06–1.88]; liver transplant [HR: 2.08, CI: 1.35–3.21]).

Conclusion: In this real-world study of commercially insured individuals with HBV infection in the US, those diagnosed with HDV infection had a higher prevalence of metabolic comorbidities, HCV coinfection, and ESLD at baseline, and an increased risk of liver-related outcomes before and after PS weighting compared to those with HBV mono-infection.

	HBV Mono-infected (n = 46,474)	HBV/HDV Coinfected (n = 1,805)	p-value
Age, years, mean (SD)	48.4 (12.4)	50.1 (11.6)	
	n (%)	n (%)	
Years of age,			
18-34	7,337 (15.8)	174 (9.6)	< 0.01
35-44	10,152 (21.8)	361 (20.0)	
45-54	12,631 (27.2)	730 (29.1)	
55-64	12,618 (27.2)	660 (26.3)	
65-74	3,336 (7.2)	135 (7.5)	
≥75	400 (0.9)	23 (1.3)	
Sex			
Male	25,553 (55.0)	1,125 (62.3)	< 0.01
Baseline liver status			
Cirrhosis/Fibrosis	2,486 (5.4)	267 (14.8)	< 0.01
Liver decompensation	2,369 (5.2)	199 (11.0)	< 0.01
Hepatocellular carcinoma	667 (1.4)	80 (4.4)	< 0.01
Liver transplant	441 (1.0)	54 (3.0)	< 0.01
Baseline comorbidities			
Hepatitis C virus	3,955 (8.5)	285 (15.8)	< 0.01
Human immunodeficiency virus	2,195 (4.7)	92 (5.1)	0.46
Diabetes	6,884 (14.8)	337 (18.7)	< 0.01
Hypertension	14,496 (31.2)	665 (36.8)	< 0.01
Hyperlipidemia	13,386 (28.8)	589 (32.6)	< 0.01
End stage liver disease	976 (2.1)	91 (5.0)	< 0.01
Prescriptions (anytime during study period)			
Nucleot(s)ide analogue	11,429 (24.6)	823 (45.6)	< 0.01
Interferon	568 (1.2)	78 (4.3)	< 0.01
Follow-up, days of person time			
Median (Q1, Q3)	778 (340, 1,509)	820 (367, 1,671)	
PS Weighted HR (95% CI) during follow up period			
Cirrhosis/Fibrosis	1.00 (ref)	1.44 (1.22 – 1.70)	
Liver Decompensation	1.00 (ref)	1.58 (1.34 – 1.88)	
Hepatocellular carcinoma	1.00 (ref)	1.41 (1.06 – 1.88)	
Liver transplant	1.00 (ref)	2.08 (1.35 – 3.21)	

Figure: (abstract: WED-116).

POSTER PRESENTATIONS

WED-117

Novel serum biomarkers for risk stratification in chronic hepatitis B-what do they bring to the table?

Louise Downs^{1,2}, Marion Delphin³, Tingyan Wang^{4,5}, Cori Campbell⁴, Sheila Lumley^{2,4}, Elizabeth Waddilove³, Catherine De Lara⁴, Sue Wareing², Polly Fengou², Kosh Agarwal⁶, Geoffrey Dusheiko^{6,7}, Jacqueline Martin⁸, Azim Ansari⁴, Ivana Carey⁶, Monique Andersson^{2,4}, Eleanor Barnes⁴, Philippa Matthews^{3,7}.

¹University of Oxford, Nuffield Department of Medicine, Oxford, United Kingdom; ²Oxford University Hospitals, Department of Infectious Diseases and Microbiology, Oxford, United Kingdom; ³The Francis Crick Institute, London, United Kingdom; ⁴University of Oxford, Nuffield Department of Medicine, Oxford, United Kingdom; ⁵University of Oxford, NIHR Oxford Biomedical Research Centre, Oxford, United Kingdom; ⁶Kings College London, Institute of Liver Studies, London, United Kingdom; ⁷University College London, London, United Kingdom; ⁸Oxford University Hospitals, Department of Gastroenterology, Oxford, United Kingdom

Email: louise.downs@exeter.ox.ac.uk

Background and aims: Chronic hepatitis B infection (CHB) has diverse clinical phenotypes. Hepatitis B core related antigen (HBcrAg) and pre-genomic RNA (pgRNA) are novel serum biomarkers that provide a proxy signal for cccDNA transcription. We aimed to (i) explore the role of HBcrAg and pgRNA as markers of treatment eligibility in treatment naive patients, and (ii) determine any associations with tissue or immunological phenotypes in patients on nucleoside analogue (NA) treatment.

Method: Serum samples (n = 137) were obtained from adults with CHB at Oxford University Hospitals, UK, including those on and off NA therapy (n = 95 and n = 42 respectively), and HBeAg positive and negative (n = 17 and n = 120 respectively) (Oxford Research Ethics Committee A, reference 09/H0604/20). HBV DNA, Quantitative HBcrAg and HBV pgRNA were measured along with a panel of immune biomarkers. Patient metadata were recorded from the Electronic Health Record (EHR). In untreated patients, we calculated the sensitivity and specificity of previously defined HBcrAg thresholds (>5.3, >4.8 and >3.6 log₁₀ IU/ml) to predict HBV DNA levels relevant to treatment decisions (>200,000, >20,000 and >2000 IU/ml). We compared this with the predictive value of HBeAg status. For those on treatment, we examined the relationship between HBcrAg, pgRNA, ALT, and a panel of ten host immunological markers to reflect liver inflammation and immune phenotype.

Results: (i) In the untreated population, HBcrAg ≥ 5.3 log₁₀ IU/ml was a highly sensitive and specific predictor of HBV DNA >200,000 IU/ml (both 100%). However HBcrAg performed poorly at lower thresholds (e.g. HBcrAg ≥ 4.8 log₁₀ IU/ml had a sensitivity and specificity of 67% and 98% for predicting HBV VL >20,000 IU/ml). HBcrAg was marginally better at predicting both HBV DNA of >200,000 IU/ml and >20,000 IU/ml than HBeAg (HBeAg sens/spec = 100% and 97% for HBV DNA >200,000 IU/ml and 62% and 96% for VL >20,000 IU/ml). In the untreated population with HBV DNA <200,000, the correlation between HBV DNA and HBcrAg is lost, demonstrating a poor correlation between peripheral DNA levels and hepatic reservoir. (ii) In the treated population, mean treatment duration was 24 months at the time of sample collection (range 0–84 months, IQR = 31.5). Median serum HBV DNA levels were below the limit of quantification but HBcrAg and pgRNA were persistent (median 3.6

log₁₀ IU/ml, and 1.7 log₁₀ IU/ml respectively). Neither of these biomarkers correlated with ALT (p = 0.4 and 0.8 respectively), or with any of a panel of host immunological biomarkers (p > 0.2 in all cases).

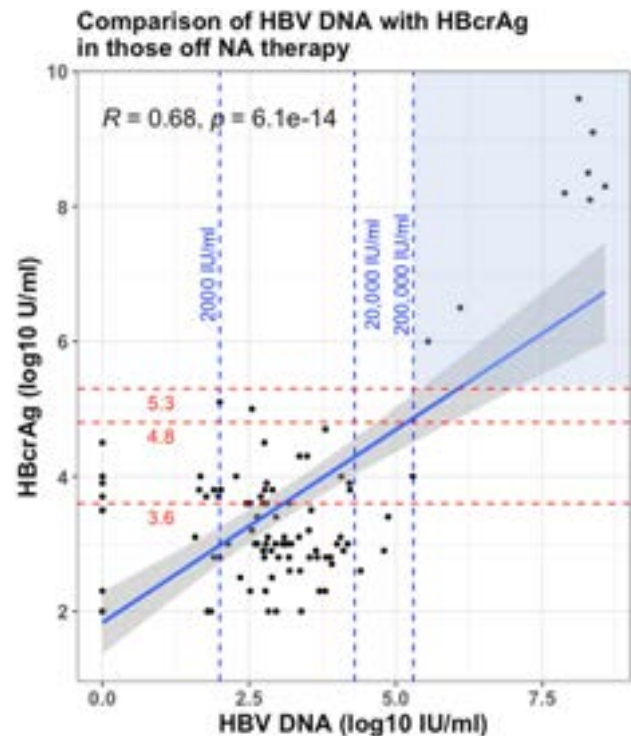


Figure: HBV DNA and HBcrAg levels with HBcrAg thresholds (red dashed lines) and HBV DNA levels used for treatment eligibility (blue dashed lines). Blue shading represents those with HBcrAg >5.3 log₁₀ IU/ml and HBV DNA >200,000 IU/ml.

Conclusion: In settings where HBV DNA quantification is not available, HBcrAg could support treatment decisions, particularly in pregnancy to prevent MTCT (based on WHO thresholds). However, HBcrAg tests are not yet widely available, have cost implications, and may be only marginally better than existing HBeAg testing. In patients on NA therapy, HBcrAg or pgRNA represent quantifiable serum markers of the HBV cccDNA pool and transcriptional activity years after HBV DNA is undetectable in serum. This offers new opportunities for disease stratification. Further longitudinal work in larger cohorts will help determine the use of HBcrAg and pgRNA in prediction of long-term disease outcomes.

WED-118

Long-term outcomes of untreated chronic hepatitis B patients with persistent HBsAg <100 IU/ml

Rachel Wen-Juei Jeng^{1,2}, Mei-Hung Pan³, Chien-Jen Chen³, Hwai-I Yang³. ¹Linkou Chang Gung Memorial Hospital, Gastroenterology and Hepatology, Taoyuan, Taiwan; ²Chang Gung University, College of Medicine, Taoyuan, Taiwan; ³Academia Sinica, Genomic Research Center, Taipei, Taiwan
Email: hiyang@gate.sinica.edu.tw

Background and aims: Chronic hepatitis B patients (CHB) with HBsAg seroclearance had the most favorable outcomes. However, long-term outcomes of CHB patients who had persistent HBsAg <100 IU/ml in natural history remained unknown. This study aimed to investigate HCC incidence and liver-related mortality of CHB patients with persistent HBsAg <100 IU/ml, and to compare with the other population without HBV nor HCV infection (non-HBV).

Method: From the REVEAL cohort, non-cirrhotic CHB subjects with at least two HBsAg assessments were enrolled into the analysis (N = 2708). Subjects with anti-HCV seropositivity, unavailable baseline HBsAg levels or lack of follow-up data, and cirrhosis at study entry were excluded. CHB subjects were categorized into 3 groups by at least two consecutive assessments of HBsAg with a median (Q1-Q3) interval of 1.49 (1.13–3.95) years: persistent HBsAg <100 IU/ml, drop from >100 to persistent <100 IU/ml, and persistent >100 IU/ml. Non-HBV subjects (N = 18960) without cirrhosis at study entry were used for comparison. Propensity score matching (PSM) was performed in a 1:3 ratio between CHB and non-HBV subjects to adjust for characteristics differences including age, gender, levels of ALT, TG, cholesterol, uric acid, smoking, alcohol drinking and DM history. Outcomes including incident HCC and liver-related death were ascertained by data linkage to the national cancer registry and national death database by the end of 2018.

Results: There were 2441 CHB subjects and 7323 non-HBV subjects in the PSM matched cohort, the characteristics were comparable except that the CHB subjects have higher baseline ALT (11 vs. 10 U/L, $P < 0.0001$) and BMI (median: 23.7 vs. 23.6, $P = 0.0349$). During a median follow-up of 26.7 years, the annual incidence of HCC and liver-related death were lowest in non-HBV subjects (0.05% and 0.04%), followed by persistent HBsAg <100 IU/ml (0.09% and 0.09%), HBsAg drop from >100 to persistent <100 IU/ml (0.2% and 0.1%) and highest in persistent HBsAg >100 IU/ml (0.4% and 0.3%). Multivariate Cox regression analysis revealed CHB patients with persistent HBsAg <100 IU/ml did not have a significantly higher risk of HCC or liver-related death than non-HBV (adjusted hazard ratio (aHR): 1.486, $P = 0.1426$ and aHR: 1.675, $P = 0.0699$, respectively). However, a significantly increased relative risk of HCC and liver-related death could be observed for patients with HBsAg drop from >100 to persistent <100 (aHR: 3.775, $P < 0.0001$ and 2.097, $P = 0.0365$, respectively) and persistent >100 IU/ml (aHR: 9.619, $P < 0.0001$ and 9.819, $P < 0.0001$, respectively), when compared with non-HBV.

Conclusion: CHB subjects with persistent HBsAg <100 IU/ml have comparable HCC and liver-related death risk as non-HBV subjects, which may be a good end point for clinical use.

WED-119

HBcrAg-based risk score predicts HCC better than HBV DNA-based risk scores in HBeAg-negative grey zone patients

Tai-Chung Tseng¹, Tetsuya Hosaka², Chun-Jen Liu¹, Fumitaka Suzuki², Chun-Ming Hong³, Hiromitsu Kumada², Tung-Hung Su³, Hung-Chih Yang³, Chen-Hua Liu¹, Pei-Jer Chen³, Jia-Horng Kao³.

¹National Taiwan University Hospital, Internal Medicine, Taipei, Taiwan;

²Toranomon Hospital, Tokyo, Japan; ³National Taiwan University Hospital, Internal Medicine, Taipei, Taiwan

Email: kaojh@ntu.edu.tw

Background and aims: Risk scores have been designed to predict the risk of hepatocellular carcinoma (HCC) in treatment-naïve chronic hepatitis B (CHB) patients. Little is known about their prediction accuracy in hepatitis B e antigen (HBeAg)-negative patients in grey zone (GZ). We aimed to develop a hepatitis B core-related antigen (HBcrAg)-based HCC risk score and explore whether it outperforms other risk scores in GZ patients.

Method: Two retrospective cohorts of HBeAg-negative patients with AASLD-defined GZ were established for derivation and validation (Taiwanese N = 911, Japanese N = 806). All of them were non-cirrhotic at baseline and remained treatment-free during the follow-up. The primary end point was HCC development.

Results: In a median follow-up period of 15.5 years, 85 patients developed HCC in the derivation cohort. We found that age, sex, ALT, platelet count, and HBcrAg, but not HBV DNA levels, were independent predictors and a 20-point GZ-HCC score was developed accordingly. The predicted risk was well calibrated with Kaplan-Meier observed HCC risk. The 10-year and 15-year AUROC was 0.86 (95% CI: 0.80–0.90) and 0.83 (95% CI: 0.78–0.89), respectively, which outperformed other HBV DNA-based HCC risk scores, including REACH-B and GAG-HCC scores (AUROC ranging from 0.63–0.74). There was a consistent finding in the validation cohort that the AUROC of GZ-HCC score was 0.92 (95% CI: 0.88–0.97) and 0.90 (95% CI: 0.83–0.97) at 10-year and 15-year of follow-up, respectively, while the AUROC ranged from 0.66–0.80 in HBV DNA-based risk scores. The better performance was also validated in EASL- and APASL-defined GZ patients. Finally, the low-risk and high-risk GZ patients (stratified by score of 8) had HCC risk close to inactive CHB and immune-active CHB patients, respectively, in both cohorts.

Conclusion: The HBcrAg-based GZ-HCC score predicts HCC better than other HBV DNA-based risk scores in HBeAg-negative GZ patients, which helps optimize their clinical management.

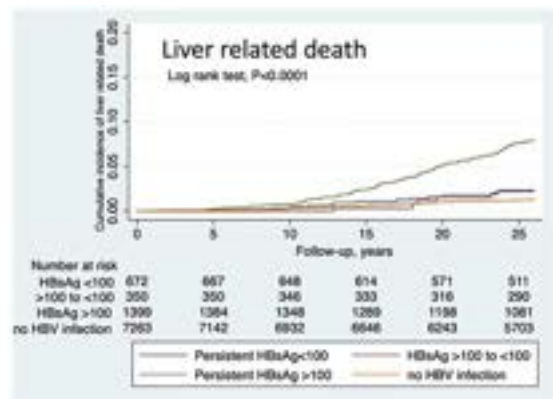
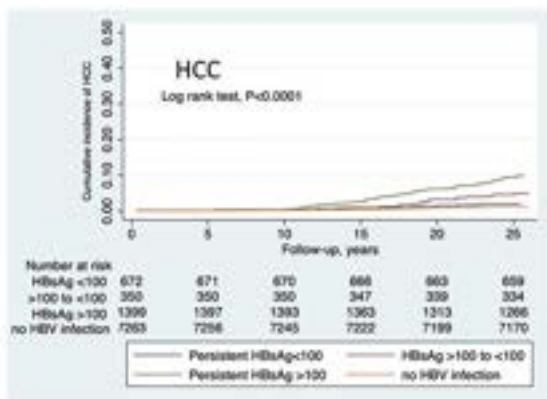


Figure: (abstract: WED-118).

POSTER PRESENTATIONS

WED-120

Extrahepatic malignancies and antiviral drugs for chronic hepatitis B: a nationwide cohort study

Moon Haeng Hur¹, Donghyeon Lee^{1,2}, Jeonghoon Lee¹, Misook Kim³, Jeayeon Park¹, Hyunjae Shin¹, Sungwon Chung¹, Heejin Cho¹, Min Kyung Park¹, Heejoon Jang², Yun Bin Lee¹, Su Jong Yu¹, Won Kim², Yong Jin Jung², Yoon Jun Kim¹, Jung-Hwan Yoon¹. ¹Seoul National University College of Medicine, Department of Internal Medicine and Liver Research Institute, Seoul, Korea, Rep. of South; ²Seoul Metropolitan Government Seoul National University Boramae Medical Center, Department of Internal Medicine, Seoul, Korea, Rep. of South; ³Seoul National University Hospital, Medical Research Collaborating Center, Seoul, Korea, Rep. of South
Email: pindra@empal.com

Background and aims: Many previous studies comparing tenofovir disoproxil fumarate (TDF) and entecavir (ETV) reported that TDF is superior, or at least comparable, to ETV in terms of hepatocellular carcinoma prevention in patients with chronic hepatitis B (CHB). In addition, our recent study suggested that CHB is associated with an increased risk of extrahepatic malignancy (EHM), which normalized with antiviral treatment. We aimed to compare the risk of EHM as well as intrahepatic malignancy (IHM) associated with ETV versus TDF.

Method: Based on claims data of the National Health Insurance Service of Korea, this nationwide cohort study included treatment-naïve CHB patients who initiated antiviral therapy either with ETV (ETV group: n = 24,287) or with TDF (TDF group: n = 29,199) between 2012 and 2014. The primary outcome was the development of any primary EHM. Secondary outcomes were the development of the 10 most prevalent EHMs in Korea and overall IHM.

Results: During median follow-up of 5.9 years, 822 (3.4%) and 706 (2.9%) patients in the ETV and TDF groups, respectively, developed EHM. EHM incidence rate differed significantly between within 3

years and beyond 3 years in both groups (both $P < 0.01$, Davies test). During the first 3 years, there was no difference in EHM risk between groups in the propensity score-matched cohort (subdistribution hazard ratio [SHR] = 1.01, 95% confidence interval [CI] = 0.88–1.17, $P = 0.84$). After year 3, however, TDF was associated with a significantly lower EHM incidence, compared to ETV (SHR = 0.70, 95% CI = 0.60–0.81, $P < 0.01$; Figure). Various sensitivity and subgroup analyses reproduced these results. The TDF group showed a significantly lower incidence of stomach cancer (SHR = 0.57), breast cancer (SHR = 0.53), and non-Hodgkin lymphoma (SHR = 0.34) than the ETV group after 3 years. Regarding the incidence of IHM, the superiority of TDF over ETV was maintained both before year 3 (SHR = 0.88, 95% CI = 0.81–0.95, $P < 0.01$) and after year 3 (SHR = 0.68, 95% CI = 0.62–0.75, $P < 0.01$), with the latter being more prominent.

Conclusion: TDF was associated with about 30% lower risk of EHM as well as IHM than ETV in CHB patients after 3 years of antiviral therapy.

WED-121

Prediction of hepatocellular carcinoma in chronic hepatitis B patients following HBsAg seroclearance: Lage score

Jonggi Choi¹, Eunju Kim², Won-Mook Choi¹, Danbi Lee¹, Kang Mo Kim¹, Ju Hyun Shim¹, Young-Suk Lim¹, Han Chu Lee¹. ¹Asan Medical Center, Department of Gastroenterology, Korea, Rep. of South; ²Chung-Ang University Gwangmyeong Hospital, Korea, Rep. of South
Email: jkchoi0803@gmail.com

Background and aims: Risk of hepatocellular carcinoma (HCC) decreases but remains after HBsAg seroclearance in patients with chronic hepatitis B (CHB). Previous studies focused on predicting the development of HCC in CHB patients without HBsAg seroclearance. The aim of this study was to determine the risk factors for HCC development and develop a prediction model to stratify the risk of HCC after HBsAg seroclearance.

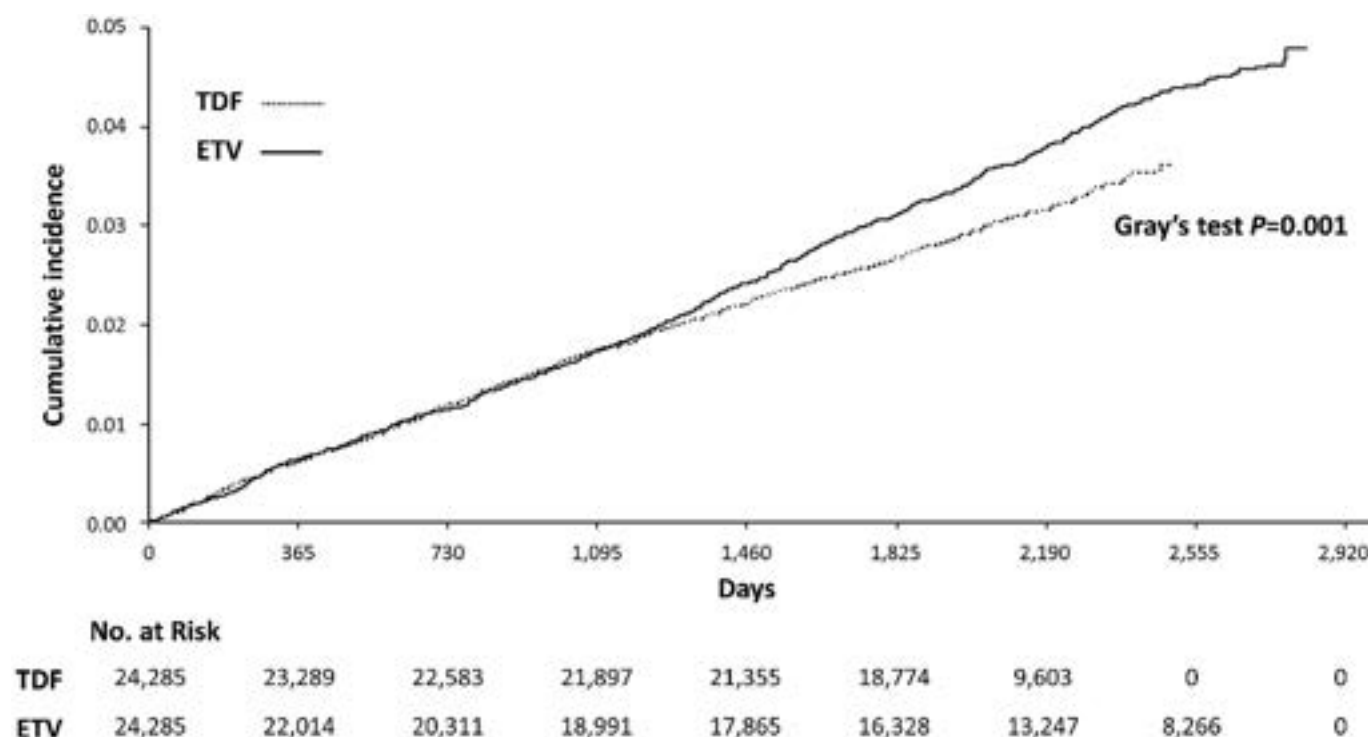


Figure: (abstract: WED-120).

Prediction model (LAGE score) for HCC development after HBsAg seroclearance in 2,421 patients with chronic hepatitis B

Factors			Assigned score
L	Liver cirrhosis	Present	2
A	Age	50≤age <60 Age ≥60	1 2
GE	Gender	Male	3
Risk group	Number of patients	Observation period	Annual incidence of HCC
Low	753	5,667	0.035
Intermediate	986	7,471	0.281
High	682	3,901	1.180

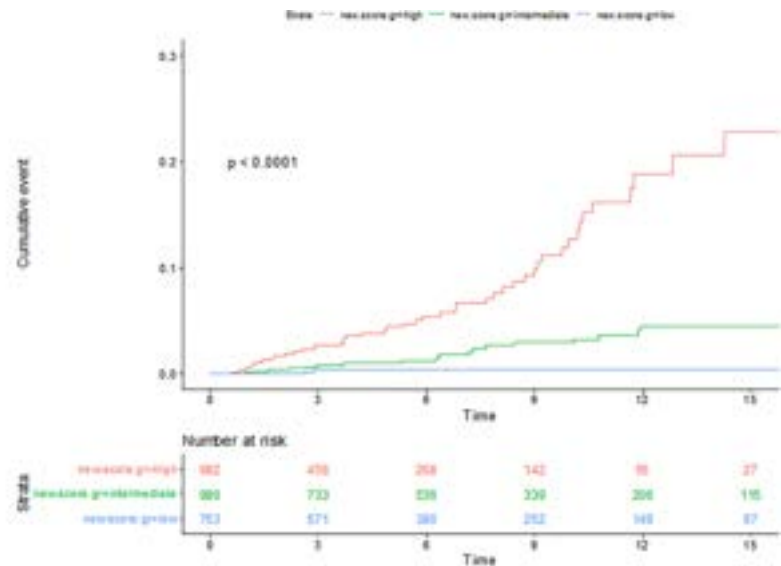


Figure: (abstract: WED-121).

Method: We analyzed 2,421 CHB patients with HBsAg seroclearance at Asan Medical Center in Seoul, Republic of Korea, between 1997 and 2022. HBsAg seroclearance was defined as the HBsAg negativity at least two consecutive tests, 6 months apart, regardless of anti-HBs positivity. The primary outcome was HCC development following HBsAg seroclearance. Cox model was used to determine the factors associated with HCC development. Points were assigned to each risk factor based on the Cox model. Median follow-up period was 5.8 years.

Results: The mean age was 54.6 years, and 64.5% of the patients were male. At the time of HBsAg seroclearance, 414 (17.1%) of patients had liver cirrhosis (LC). During the 17,039 person-years (PYs), 69 of 2421 patients developed HCC, with an annual incidence of 0.41%/100 PYs. At 5, 10, and 15 years, the cumulative incidence of HCC was 1.7%, 4.3%, and 6.8%, respectively. LC [L] (adjusted hazard ratio [AHR]: 6.2), age [A] over 60 years (AHR: 3.9), and male gender [GE] (9.2) were independently associated with an increased risk of HCC in multivariable analysis. Risk scores were assigned to age ≥60 years (2 points), 50≤age <60 (1 point), LC (2 points), male sex (3 points). Low risk (0–2), intermediate risk (3–4), and high risk (5–7) were categorized based on the sum of each point. In the low (n = 753), intermediate (n = 986), and high risk groups (n = 682), the incidence of HCC was 0.04, 0.28, and 1.18/100PYs, respectively. Time-dependent AUROCs of the LAGE score for predicting HCC development at 5-, 10-, and 15-years were 0.808, 0.856, and 0.879, respectively.

Conclusion: LC (L), older age (A), and male gender (GE) at the time of HBsAg seroclearance were highly associated factors with HCC development after HBsAg seroclearance. LAGE score may easily be applicable in real world and aid in stratifying the risk of HCC after HBsAg seroclearance in CHB patients.

WED-122

Eight weeks or less of tenofovir alafenamide to prevent the perinatal hepatitis B transmission: a multicenter, prospective, randomized study

Qing-Lei Zeng¹, Xiao-Ping Dong², Hongxu Zhang³, Wei Li⁴, Ji-Yuan Zhang⁵, Zu-Jiang Yu⁶. ¹The First Affiliated Hospital of Zhengzhou University, Department of Infectious Diseases and Hepatology, Zhengzhou, China; ²Sanmenxia Central Hospital, Department of Infectious Diseases, China; ³Luohe Central Hospital, Department of

Infectious Diseases, China; ⁴Henan Provincial People's Hospital, Department of Infectious Diseases, China; ⁵The Fifth Medical Center of Chinese PLA General Hospital, National Clinical Research Center for Infectious Diseases, Treatment and Research Center for Infectious Diseases, China; ⁶The First Affiliated Hospital of Zhengzhou University, Department of Infectious Diseases and Hepatology, China
Email: zengqinglei2009@163.com

Background and aims: Four weeks of tenofovir alafenamide fumarate (TAF) therapy can lead to 3–4 logs IU/ml of hepatitis B virus (HBV) DNA decrease in clinical practice; meanwhile, young immune tolerant pregnant women commonly have 7–8 logs IU/ml of HBV DNA levels, there was no infant's breakthrough infection reported when the maternal HBV DNA level was below 5.3 logs IU/ml (200 000 IU/ml) after timely standard immunoprophylaxis for the newborns; additionally, the very (gestational weeks [GW] 28–31), moderate (GW 32–33), and late (GW 34–36) preterm rates of singleton pregnancies are 0.6%, 0.7%, 4.3% in China. This study aimed to investigate the feasibility as well as the safety and efficacy of 8 weeks or less of TAF therapy (from GW 33 to delivery date) to prevent mother-to-child transmission of HBV (HBV-MTCT).

Method: In this multicenter, prospective, randomized study, pregnant women with HBV DNA levels ranged from >5.3 logs to <9 logs IU/ml who received TAF from GW 33 to delivery date (group 1) or postpartum month 1 (group 2) were 1:1 enrolled randomly and followed until postpartum month 6, respectively. All infants received standard immunoprophylaxis. The primary end point was the safety of mothers and infants. The secondary end point was the rate of HBV DNA level less than 5.3 logs IU/ml at delivery for mothers, and the hepatitis B surface antigen (HBsAg)-positive rate at 7 months for infants.

Results: In total, 96 and 93 mothers were enrolled, and 96 and 93 infants were born, in groups 1 and 2, respectively (Figure). TAF was well tolerated during a mean treatment duration of 6.5 and 10.3 weeks in groups 1 and 2, respectively. The most common maternal adverse event was nausea (12.5% vs 14.0%), followed by anorexia (7.3% vs 8.6%) and fatigue (6.3% vs 6.5%) in groups 1 and 2, respectively. Only few mothers had abnormal alanine aminotransferase levels at delivery (1[1.0%] vs 0[0%]) and at postpartum months 3 (3[3.1%] vs 3[3.2%]) and 6 (8[8.3%] vs 7[7.5%]), respectively, and no one had alanine aminotransferase levels higher than 100 U/ml. No infants had birth defects in either group. The infants' physical and neurological development at birth and at 7 months were comparable and

POSTER PRESENTATIONS

normal in the two groups. The HBsAg positive rate was 0% at 7 months in all 189 infants.

Characteristics of the mothers at baseline	Group 1 (n=96)	Group 2 (n=93)
Age, years	28.7 ± 5.3	29.1 ± 4.9
Gestational age, weeks	33.2 ± 0.3	33.3 ± 0.3
Hepatitis B e antigen positivity	96 (100)	93 (100)
HBV DNA, log ₁₀ IU/mL	7.7 ± 0.4	7.8 ± 0.3
Alanine aminotransferase, U/L	20.2 ± 11.0	22.5 ± 10.5
Treatment duration, weeks	6.5 ± 1.0	10.3 ± 0.9
Most common maternal adverse events		
Nausea	12 (12.5)	13 (14.0)
Anorexia	7 (7.3)	8 (8.6)
Fatigue	6 (6.3)	6 (6.5)
Most common maternal complications		
Premature rupture of membranes	8 (8.3)	9 (9.7)
Preeclampsia	1 (1.0)	1 (1.1)
Gestational hypertension	1 (1.0)	1 (1.1)
Maternal HBV DNA at delivery, log ₁₀ IU/mL	4.2 ± 0.6	4.1 ± 0.6
< 5.3 log ₁₀ IU/mL	94 (97.9)	91 (97.8)
Characteristics of the infants at birth		
Gestational age, weeks	39.2 ± 1.2	39.3 ± 1.2
Apgar score at 1 minute	9.6 ± 0.5	9.6 ± 0.5
Congenital defects or malformations	0 (0)	0 (0)
Anthropometric indexes	Normal	Normal
At postpartum month 6 for the mothers		
HBV DNA, log ₁₀ IU/mL	7.6 ± 0.3	7.5 ± 0.3
Alanine aminotransferase ≥ 40 U/L	8 (8.3)	7 (7.5)
At 7 months of age for the infants		
Anthropometric indexes	Normal	Normal
HBsAg positive infants	0 (0)	0 (0)

Data are presented as the mean ± standard deviation or n (%).

Figure:

Conclusion: Eight weeks or less of TAF regimen during late pregnancy (from GW 33 to delivery date) to prevent HBV-MTCT are

generally safe for both mothers and infants and obtained 0% of HBV-MTCT rate. Future large-scale validation studies are warranted.

WED-123

HBsAg seroclearance decreases risk of hepatocellular carcinoma but not hepatic decompensation in nucleos (t)ide analogue-treated cirrhotic patients with complete hepatitis B virus suppression: a territory-wide cohort study

Terry Cheuk-Fung Yip¹, Vicki Wing-Ki Hui¹, Vincent Wai-Sun Wong¹, Tsz Fai Yam¹, Che To Lai¹, Yan Liang¹, Yee-Kit Tse¹, Henry LY Chan², Grace Lai-Hung Wong¹. ¹The Chinese University of Hong Kong (CUHK), Department of Medicine and Therapeutics, Hong Kong; ²Union Hospital, Department of Internal Medicine, Hong Kong
Email: wonglaihung@cuhk.edu.hk

Background and aims: We compared the incidence of hepatocellular carcinoma (HCC) and first and further hepatic decompensation in nucleos (t)ide analogue (NA)-treated chronic hepatitis B (CHB) patients with cirrhosis who achieved complete viral suppression alone or hepatitis B surface antigen (HBsAg) seroclearance.

Method: A retrospective cohort study was performed using data from the Clinical Data Analysis and Reporting System, an electronic healthcare database managed by the Hospital Authority, Hong Kong. All adult monoinfected CHB patients with cirrhosis who received entecavir or tenofovir between 1 January 2005 and 30 September 2020 were identified. Baseline date was the start of entecavir or tenofovir treatment. Patients with HCC before or within the first 6 months of baseline, other cancers or liver transplantation before baseline, liver transplantation before HBsAg loss, without hepatitis B virus DNA measurement, and without complete viral suppression were excluded. 1-year landmark analyses were performed; patients with clinical outcome or follow-up ended within 1 year were excluded. The primary outcome was HCC. The secondary outcome was first and further hepatic decompensation, defined as any new occurrence of ascites, spontaneous bacterial peritonitis, variceal bleeding, hepatic encephalopathy, hepatorenal syndrome, liver transplantation, and/or liver-related death.

Results: Of 5,149 patients (mean age 60.1 ± 12.6 years, 66.3% male, 8.0% decompensated cirrhosis) included in the 1-year landmark analysis, 161 (3.1%) achieved HBsAg seroclearance. At a median (25th-75th percentile) follow-up of 4.1 (2.5-5.0) years, 456 (9.1%) and 5

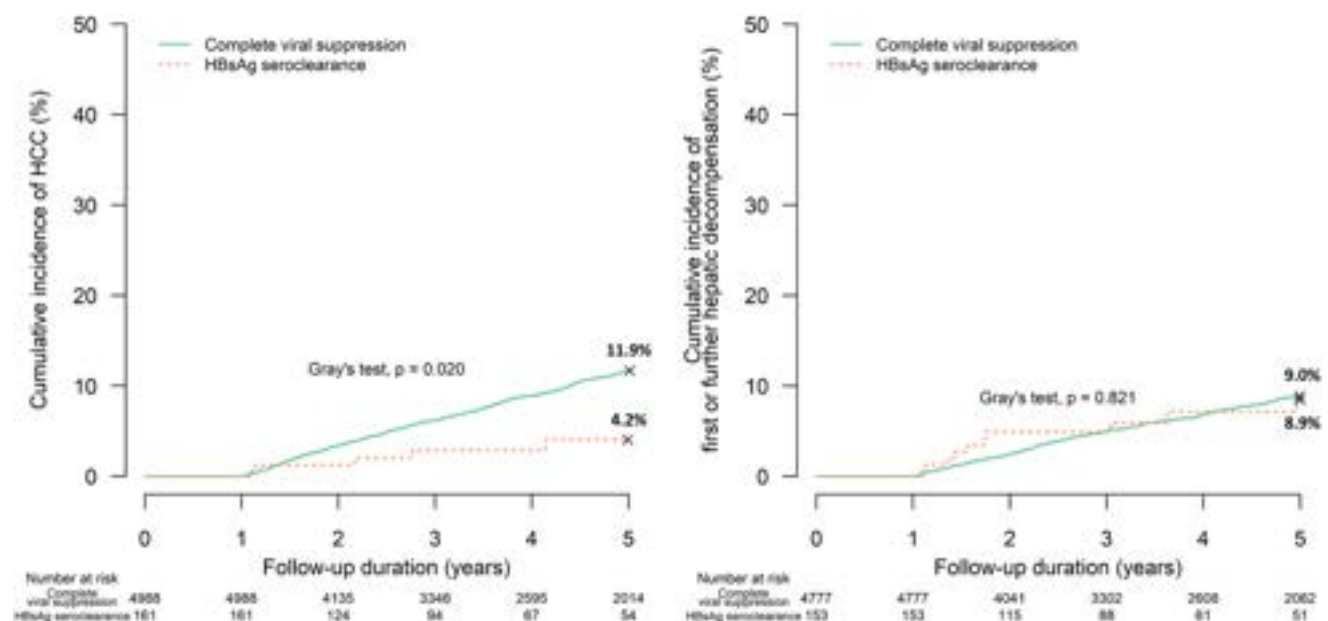


Figure: (abstract: WED-123).

(3.1%) patients with complete viral suppression and HBsAg loss developed HCC respectively; 334/4777 (7.0%) and 10/153 (6.5%) patients with complete viral suppression and HBsAg loss developed first and further hepatic decompensation (Figure). In multivariable analysis, HBsAg seroclearance was associated with a lower risk of HCC (adjusted subdistribution hazard ratio [aSHR] 0.37, 95% confidence interval [CI] 0.15–0.91, $p=0.030$) but not first and further hepatic decompensation (aSHR 1.01, 95% CI 0.52–1.95, $p=0.988$) than complete viral suppression, after adjusting for age, gender, decompensated cirrhosis, diabetes, platelets, albumin, total bilirubin, alanine aminotransferase, international normalised ratio, hepatitis B e antigen status, and use of other NAs. Similar results on HCC were observed in using cause-specific (CS) hazard model (adjusted CSHR [95% CI] 0.40 [0.16–0.96]), patients with compensated cirrhosis (aSHR 0.36 [0.13–0.98]), and 2-year landmark analysis (aSHR 0.37 [0.14–1.04]).

Conclusion: HBsAg seroclearance is associated with a lower risk of HCC but not first and further hepatic decompensation in a territory-wide cohort of NA-treated CHB cirrhotic patients with complete viral suppression.

WED-124

Influence of viral load and fibrotic burden on hepatocellular carcinoma risk at phase change to immune-active phase in chronic hepatitis B

Ho Soo Chun¹, Minjong Lee¹, Hye Ah Lee², Jihye Kim³, Han Ah Lee¹, Hwi Young Kim¹, Tae Hun Kim¹, Eileen Yoon⁴, Dae Won Jun⁴, Sang Hoon Ahn⁵, Seung Up Kim⁵, Yoon Jun Kim³. ¹Department of Internal Medicine, Ewha Womans University College of Medicine, Korea,

Rep. of South; ²Clinical Trial Center, Ewha Womans University Seoul Hospital, Korea, Rep. of South; ³Department of Internal Medicine and Liver Research Institute, Seoul National University College of Medicine, Korea, Rep. of South; ⁴Department of Internal Medicine, Hanyang University College of Medicine, Korea, Rep. of South; ⁵Department of Internal Medicine, Yonsei University College of Medicine, Korea, Rep. of South

Email: ksukorea@yuhs.ac

Background and aims: Recent studies reported that moderate hepatitis B virus (HBV) DNA levels are significantly associated with hepatocellular carcinoma (HCC) risk in hepatitis B e antigen (HBeAg)-positive, non-cirrhotic patients with chronic hepatitis B (CHB). We assessed the association of baseline viral load and fibrotic burden with the risk of HCC development in CHB patients entering the immune-active (IA) phase.

Method: This multicenter cohort study recruited 3,589 HBeAg-positive, non-cirrhotic CHB patients who started antiviral treatment with entecavir or tenofovir disoproxil fumarate at IA phase transitioned from immune-tolerant (IT) phase in twenty-three tertiary university-affiliated hospitals of South Korea (2012–2020). Significant liver fibrosis was defined as fibrosis-4 index (FIB-4) >3.25. Multivariable analysis using the Cox proportional hazards model was performed.

Results: Sixty (1.7%) patients developed HCC (median follow-up, 5.4 years). Patients who developed HCC were significantly older and showed a significantly higher proportion of diabetes, lower platelet counts, and higher FIB-4 levels than those who did not ($n=3,525$, 98.3%) (all $p<0.05$). The HCC risk was highest at moderate HBV DNA levels (5.00–7.99 \log_{10} IU/ml) and significant liver fibrosis. In

Table. (abstract: WED-124): Predictors of HCC development

	Multivariable		P value	Multivariable using FIB-4		
	aHR	95% CI		aHR	95% CI	P value
Demographic variables						
Age, years	1.04	1.02–1.07	<0.001	-	-	-
Male gender	3.58	1.79–7.17	<0.001	3.65	1.84–7.25	<0.001
Diabetes	2.63	1.45–4.77	0.001	3.05	1.72–5.41	<0.001
Antiviral agents						
ETV	-	-	-	-	-	-
TDF	-	-	-	-	-	-
Laboratory variables						
Platelet count, $10^9/L$	0.99	0.98–0.99	<0.001	-	-	-
Aspartate aminotransferase, IU/L	-	-	-	-	-	-
Alanine aminotransferase, IU/L	-	-	-	-	-	-
Total bilirubin, mg/dL	-	-	-	-	-	-
Serum albumin, g/dL	0.92	0.57–1.48	0.725	0.88	0.53–1.47	0.625
Serum creatinine, mg/dL	-	-	-	-	-	-
FIB-4 index						
<1.45	-	-	-	1 (reference)		
1.45–3.25	-	-	-	5.36	2.33–12.33	<0.001
>3.25	-	-	-	7.63	3.05–19.09	<0.001
HBV DNA levels, \log_{10} IU/ml						
≥8.00	-	-	-	-	-	-
7.00–7.99	-	-	-	-	-	-
6.00–6.99	-	-	-	-	-	-
5.00–5.99	-	-	-	-	-	-
<5.00	-	-	-	-	-	-
HBV DNA levels, \log_{10} IU/ml						
≥8.00	1 (reference)			1 (reference)		
5.00–7.99	2.55	1.32–4.91	0.005	2.68	1.40–5.13	0.003
<5.00	1.25	0.50–3.13	0.629	1.77	0.71–4.40	0.221

POSTER PRESENTATIONS

multivariable analysis, moderate HBV DNA levels was independently associated with the increased risk of HCC development (adjusted hazard ratio [aHR]=2.55, 95% confidence interval [CI]=1.32–4.91, $p=0.005$). After adjustment for FIB-4 levels, similar result was maintained (moderate HBV DNA levels: aHR=2.68, 95% CI=1.40–5.13; FIB-4 >3.25: aHR=7.63, 95% CI=3.05–19.09; all $p<0.05$).

Conclusion: Moderate HBV DNA levels and significant liver fibrosis at the time of phase change from IT to IA phase was significantly associated with the risk of HCC development during potent antiviral therapy in patients with CHB.

WED-125

IP10 and anti-HBc can predict virological relapse and HBsAg loss for chronic hepatitis B patients after nucleos (t)ide analogue discontinuation

Yandi Xie¹, Minghui Li², Xiaojuan Ou³, Sujun Zheng⁴, Yinjie Gao⁵, Xiaoyuan Xu⁶, Ying Yang⁷, Anlin Ma⁸, JIA Li⁹, Yuemin Nan¹⁰, Huanwei Zheng^{11,11}, Juan Liu¹², Lai Wei¹³, Bo Feng¹. ¹Peking University People's Hospital, Peking University Hepatology Institute, China; ²Department of Hepatology Division Beijing Ditan Hospital, Capital Medical University, China; ³Liver Research Center, Beijing Friendship

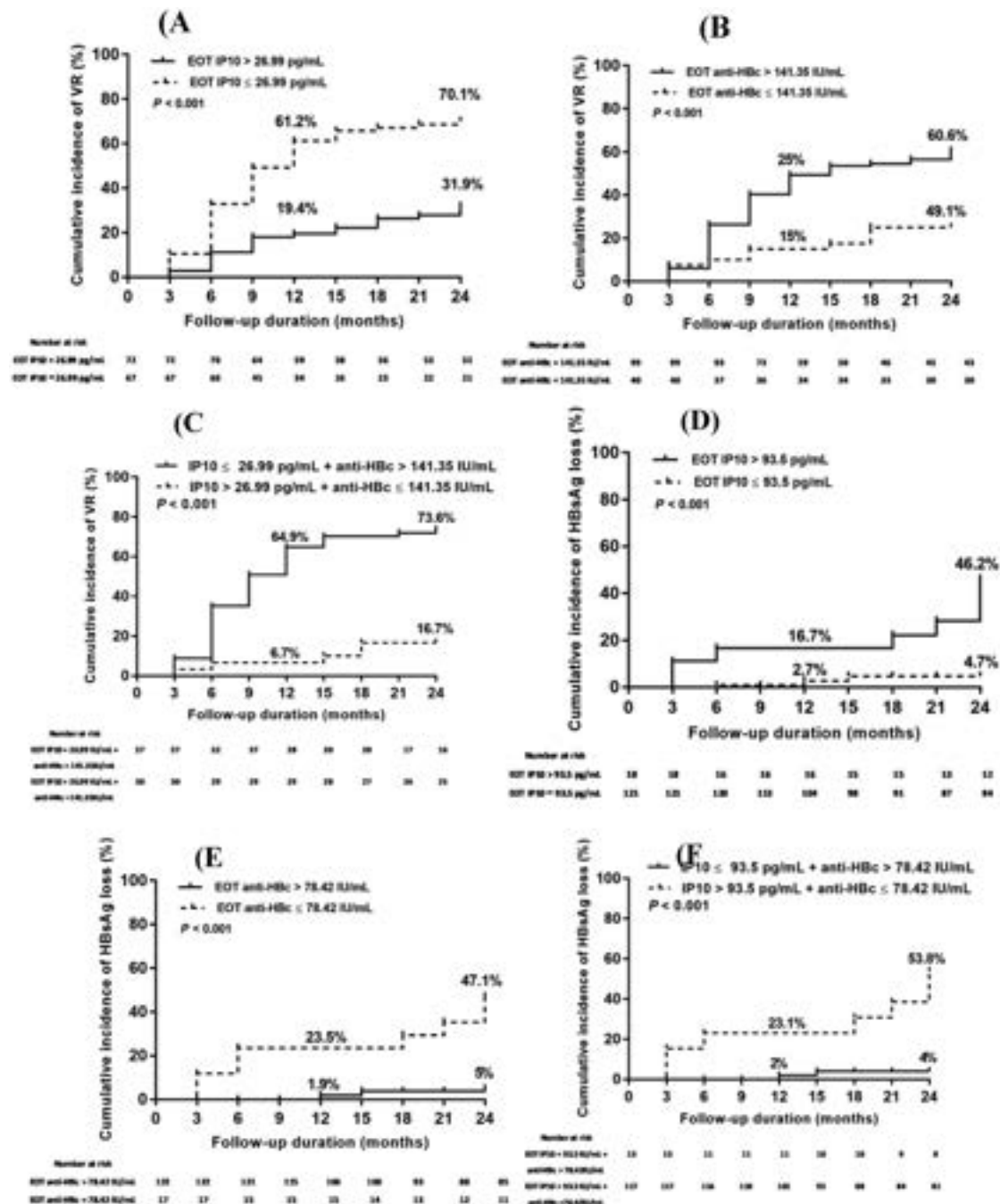


Figure: (abstract: WED-125): Cumulative incidences of virological relapse (VR) and HBsAg loss stratified by end of treatment (EOT) IP10 and anti-HBc. (A)-(C), Cumulative incidences of VR in patients by EOT IP10, anti-HBc or combined two parameters. (D)-(F), Cumulative incidences of HBsAg loss in patients by EOT IP10, anti-HBc or combined two parameters.

Hospital, Capital Medical University, China; ⁴Complicated Liver Diseases and Artificial Liver Treatment and Training Center, Beijing Municipal Key Laboratory of Liver Failure and Artificial Liver Treatment and Research, Beijing Youan Hospital, Capital Medical University, China; ⁵Department of Infectious Diseases, The Fifth Medical Center, General Hospital of PLA, China; ⁶Department of Infectious Diseases, Peking University First Hospital, China; ⁷Department of Infectious Diseases, The Second Hospital of Xingtai, China; ⁸Department of Infectious Disease, China Japan Friendship Hospital; ⁹Department of Liver Disease, Tianjin Second People's Hospital, China; ¹⁰Department of Traditional and Western Medical Hepatology, The Third Hospital of Hebei Medical University, China; ¹¹Department of Liver Disease, Shijiazhuang Fifth Hospital, China; ¹²Research Center for Technologies in Nucleic Acid-Based Diagnostics, China; ¹³Department of Hepatopancreatobiliary Disease, Beijing Tsinghua Changgung Hospital, School of Clinical Medicine, Tsinghua University, China
Email: xyfyfb_1@sina.com

Background and aims: To assess predictive ability of serum interferon-inducible protein 10 (IP10) and hepatitis B core antibody (anti-HBc) levels for virological relapse (VR) and hepatitis B surface antigen (HBsAg) loss after nucleos (t)ide analogue (NA) discontinuation.

Method: In this multicenter prospective study, overall 139 initially hepatitis virus B e antigen-positive patients were followed up for 24 months after NA discontinuation or until clinical relapse.

Results: End of treatment (EOT) IP10 and anti-HBc were 29.2 (5.1–66.4) pg/ml and 193.6 (136.9–221.4) IU/ml. By Cox regression analysis, EOT IP10 (hazard ratio [HR] 0.976, $p < 0.001$) and anti-HBc (HR 1.011, $p < 0.001$) were independent predictors for VR. EOT IP10 (HR, 1.026, $p < 0.001$) and anti-HBc (HR, 0.981, $p < 0.001$) also were independent predictors for HBsAg loss. Until 24 months after NA discontinuation, cumulative rates of VR in patients with EOT IP10 > 26.99 pg/ml and ≤ 26.99 pg/ml were 31.9% and 70.1%, respectively (HR 2.998, $p < 0.001$). Cumulative incidences of VR in patients with EOT anti-HBc ≤ 141.35 IU/ml and > 141.35 IU/ml were 49.1% and 60.6%, respectively (HR 2.99, $p < 0.001$). Cumulative probability of VR was 16.7% in patients with EOT IP10 > 26.99 pg/ml plus anti-HBc ≤ 141.35 IU/ml, which was significant lower than 73.6% (HR 6.464, $p < 0.001$). Cumulative probabilities of HBsAg loss in patients with EOT IP10 > 93.5 pg/ml and ≤ 93.5 pg/ml were 46.2% and 4.7%, respectively (HR 10.94, $p < 0.001$). Cumulative probabilities of HBsAg loss in patients with EOT anti-HBc ≤ 78.42 IU/ml and > 78.42 IU/ml were 47.1% and 5%, respectively (HR 12.27, $p < 0.001$). Patients with EOT IP10 > 93.5 pg/ml plus anti-HBc ≤ 78.42 IU/ml, had the highest 24-month cumulative HBsAg loss rate (53.8% vs 4%, HR 16.83, $p < 0.001$).

Conclusion: High EOT IP10 and low EOT anti-HBc levels were related to both lower risk of VR and higher probability of HBsAg loss.

WED-126

Off-therapy events in hepatitis B e antigen-negative patients with sustained HBV surface antigen < 100 and < 50 IU/ml

Yen-Chun Liu^{1,2}, Rachel Wen-Juei Jeng^{1,2}, Rong-Nan Chien^{1,2}. ¹Chang Gung Memorial Hospital, Linkou branch, Taiwan, Taiwan; ²College of Medicine, Chang Gung University, Taiwan
Email: rachel.jeng@gmail.com

Background and aims: Partial cure is defined as sustained low or undetectable HBV DNA level with low HBsAg level. It has not been well studied that if the long-term durability be different between HBeAg negative chronic hepatitis B (CHB) patients who stop nucleos (t)ide analogue (Nuc) with sustained HBsAg level < 100 versus < 50 IU/ml for 24 weeks from end-of-treatment (EOT). The study aimed to investigate the off-Nuc events incidence in HBeAg negative CHB patients who had achieved sustained qHBsAg < 100 and < 50 IU/ml.

Method: HBeAg-negative CHB patients who stopped Entecavir (ETV) or Tenofovir (TDF) after consecutive undetectable HBV DNA ≥ 1 year were enrolled. Virological relapse (VR) was defined as HBV DNA ≥ 2000 IU/ml. Clinical relapse (CR) and hepatitis flare were defined as alanine aminotransferase (ALT) levels $\geq 2 \times$ ULN and $\geq 5 \times$ ULN with VR. Sustained remission (SR) defined as ALT $< 2 \times$ ULN and HBV DNA less than 2000 IU/ml. Sustained qHBsAg < 100 or < 50 IU/ml was defined as qHBsAg levels persist below 100 or 50 IU/ml for 24 weeks after Nuc discontinuation. Patients who had encountered off-Nuc events within 6 months from EOT were censored from the analysis.

Results: Among 1320 patients, 238 patients (18%) achieved qHBsAg at EOT < 100 IU/ml with mean age of 57 year-old, 87% were male and 37% had liver cirrhosis. Of 238 EOT < 100 IU/ml patients, 144 achieved EOT HBsAg < 50 IU/ml. After excluding 25 patients whose qHBsAg at EOT 6 months being unavailable, 183 patients and 114 patients had achieved SR and sustained EOT < 100 and < 50 IU/ml by EOT week 24, respectively. The 2-year cumulative incidence of VR, CR, hepatitis flare and retreatment showed comparably low in patients with sustained qHBsAg < 100 IU/ml and those with sustained qHBsAg < 50 IU/ml [VR: 46% vs. 37%, CR: 22% (annual incidence, IR: 6%) vs. 19% (IR: 5%), figure A, flare: 11% vs. 10%, retreatment: 19% vs. 19%, all $p > 0.1$]. Patients who achieved sustained EOT HBsAg < 100 or < 50 IU/ml had comparably high 5-year cumulative HBsAg loss incidences [35% (IR: 8%) vs. 44% (IR: 10%), figure B].

Conclusion: HBeAg negative CHB patients who achieved SR and qHBsAg < 100 IU/ml longer than 6 months from EOT showed similarly good off-Nuc durability and high probability for subsequent functional cure compared to those with sustained qHBsAg < 50 IU/ml.

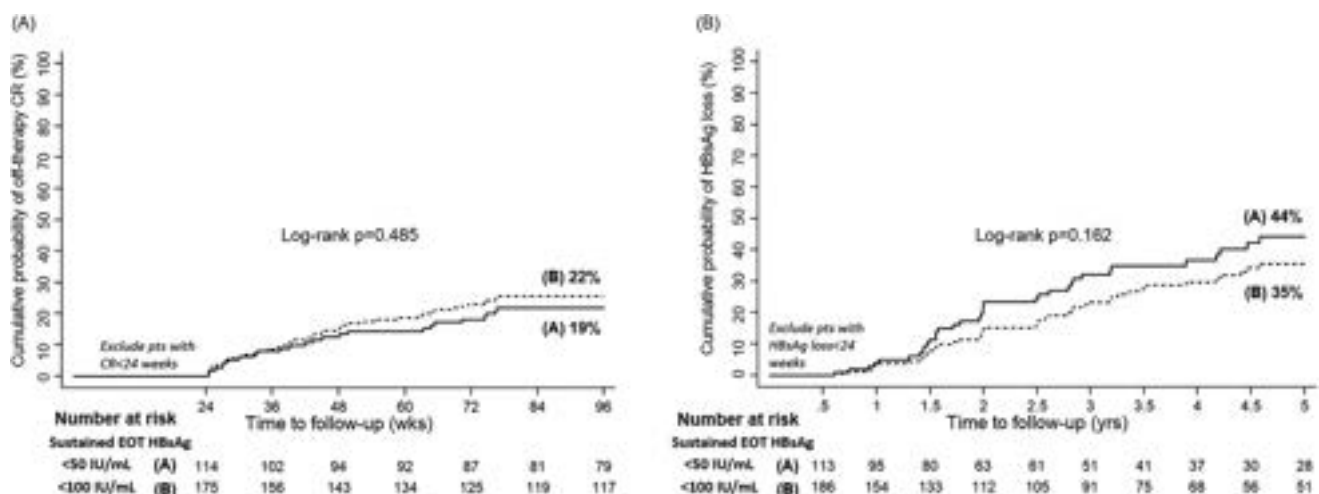


Figure: (abstract: WED-126).

POSTER PRESENTATIONS

WED-127

Improved prediction for liver fibrosis of Fibrosis-4 using machine learning in patients with chronic hepatitis B

Zhiyi Zhang¹, Jian Wang^{2,3}, Shaoqiu Zhang², Yifan Pan⁴, Li Zhu⁵, Yiguang Li⁶, Weimao Ding⁷, Jie Li^{1,2,3,4}, Yuanwang Qiu⁶, Rui Huang^{1,2,3,4}, Chao Wu^{1,2,3,4}, Chuanwu Zhu⁵. ¹Department of Infectious Diseases, Nanjing Drum Tower Hospital Clinical College of Traditional Chinese and Western Medicine, Nanjing University of Chinese Medicine, Nanjing, Jiangsu, China; ²Department of Infectious Diseases, Nanjing Drum Tower Hospital, The Affiliated Hospital of Nanjing University Medical School, Nanjing, Jiangsu, China; ³Institute of

Viruses and Infectious Diseases, Nanjing University, Nanjing, Jiangsu, China; ⁴Department of Infectious Diseases, Nanjing Drum Tower Hospital, Clinical College of Nanjing Medical University, Nanjing, China; ⁵Department of Infectious Diseases, The Affiliated Infectious Diseases Hospital of Soochow University, Suzhou, Jiangsu, China; ⁶Department of Infectious Diseases, The Fifth People's Hospital of Wuxi, Wuxi, Jiangsu, China; ⁷Department of Hepatology, Huai'an No. 4 People's Hospital, Huai'an, Jiangsu, China
Email: zhuchw@126.com

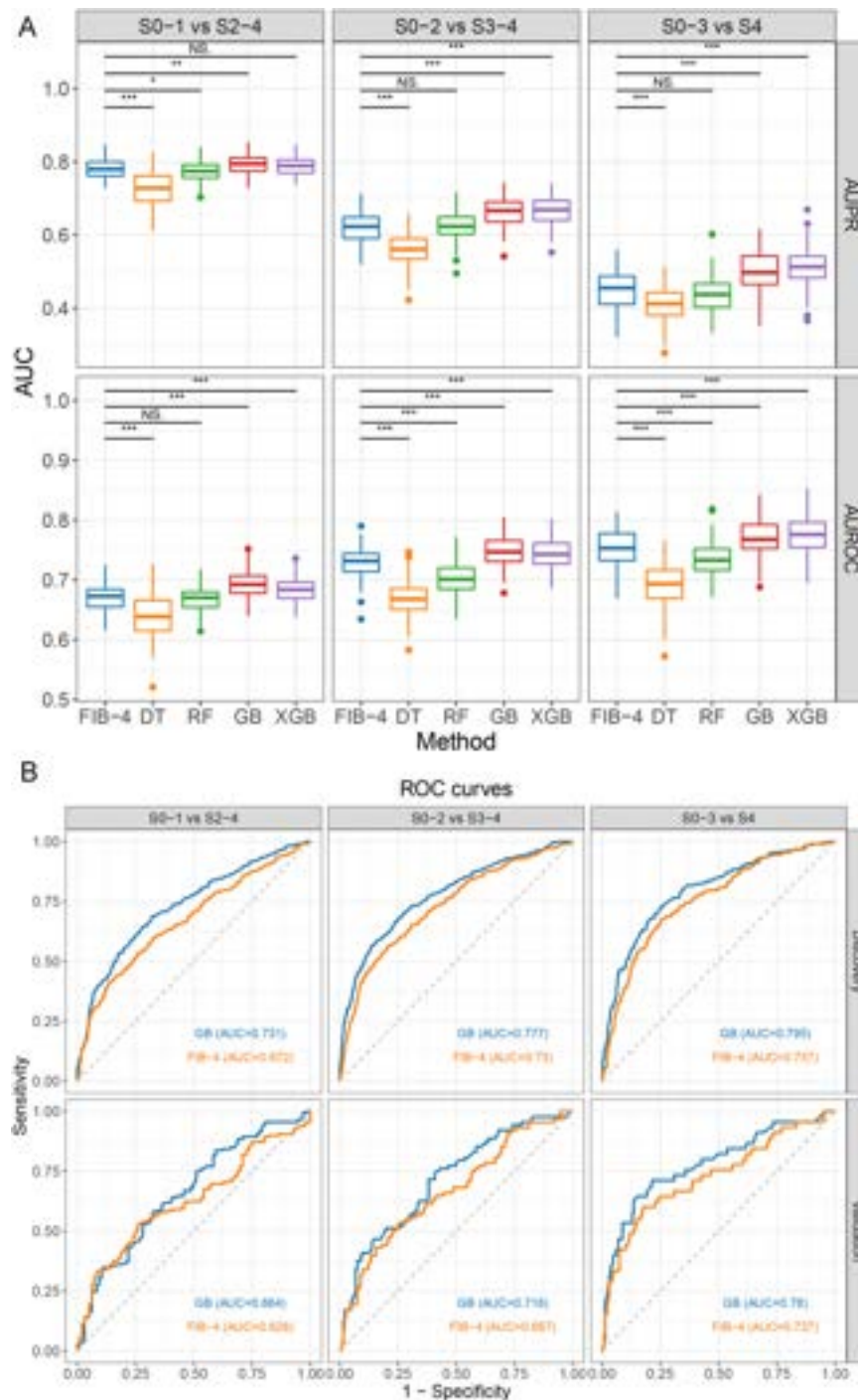


Figure: (abstract: WED-127): Boxplots of AUPR and AUROC on testing sets for five different methods (A) and ROC curves of GB and FIB-4 in fibrosis detection (B).

Background and aims: Fibrosis-4 (FIB-4) index is widely used for predicting liver fibrosis and cirrhosis in patients with chronic hepatitis B (CHB). However, the predictive value of FIB-4 for liver fibrosis and cirrhosis is moderate in CHB. Using cutting-edge machine learning approaches, we aimed to reconstruct FIB-4 for improved prediction of liver fibrosis and cirrhosis.

Method: We included 1231 CHB patients who underwent liver biopsies from four hospitals in this study. To compare the performance of machine learning methods with the FIB-4 index, a discovery set of 957 patients from three hospitals was used. We randomly divided the set into training (70%) and testing (30%) sets 100 times to determine the final model and was externally validated in an independent cohort ($n = 274$), with comparisons to FIB-4 in terms of the area under the receiver-operating-characteristic curve (AUROC).

Results: In predicting significant fibrosis, advanced fibrosis, and cirrhosis, the AUROC of gradient boosting (GB) outperformed other methods and the FIB-4 index ($p < 0.001$). In the validation set, GB performed better than the FIB-4 index for the classification between significant and non-significant fibrosis (AUROC of 0.664 vs. 0.626, $p = 0.09$), significantly greater than the FIB-4 index for the classification between non-advanced and advanced fibrosis (AUROC of 0.716 vs. 0.667, $P = 0.04$) and non-cirrhosis and cirrhosis (AUROC of 0.780 vs. 0.727, $p = 0.01$).

Conclusion: By using the same parameters as FIB-4, the novel GB-based model showed consistent improvements in predicting liver fibrosis and cirrhosis compared to FIB-4 in CHB patients.

WED-128

Passive transfer of hepatitis B core antibody after intravenous immunoglobulin administration in adult patients: a retrospective review

Sital Shah¹, Sophie Mungai¹, Shelley Jones¹. ¹King's College Hospital, London, United Kingdom
Email: sitalshah@nhs.net

Background and aims: After intravenous administration of human normal immunoglobulin (HNlg), patients often test positive for the presence of hepatitis B core antibody (HBcAb). As baseline testing is not common, it is unclear if this is genuine hepatitis B (HBV) exposure or passive transfer during the IV administration of HNlg. Consequently, when patients test positive for HBcAb during screening prior to commencing immunosuppressive therapy, an antiviral to prevent HBV reactivation is commonly prescribed irrespective of true exposure or not. The objective of this study is to highlight the importance of HBcAb testing prior to commencing HNlg infusion, to prevent wrong diagnosis of HBV exposure and incorrect therapeutic decisions.

Method: A retrospective, single center study was carried out at Kings College Hospital, London. Electronic prescription records, dispensing systems and a national HNlg database was used to obtain demographic, clinical information and HNlg specific data of patients receiving long term (>3 months) HNlg treatment during 2011–2021.

Results: Of 493 patients identified, only 71 (14%) received HBcAb testing prior to immunoglobulin administration. 2 were seropositive before infusion, 38 (55%) remained core antibody negative post-infusion, and 31 (45%) became core antibody positive. Those positive for HBcAb, were all hepatitis B surface antigen negative. Because of

uncertainly and poor knowledge around baseline testing, all received antiviral treatment consisting of either tenofovir (10%), entecavir (13%) or lamivudine (77%), prior to being initiated on immunosuppressive therapy. After the initial positive test, only 5 (16%) were re-tested either twice or three times afterwards, where all remained positive. The average number of days between their positive HBcAb test and last infusion was 21 days. The average number of doses between baseline and seropositivity was 5 doses. The most common HNlg used was Privigen/Hizentra with 30 patients (38%) for both seronegative and seropositive patients. Many patients changed to subcutaneous immunoglobulin (SClg) administration of HNlg during the Covid-19 pandemic, which included Hizentra and Cuvitru. Only 2 (6%) patients on SClg became seropositive.

Conclusion: Passive transfer of hepatitis B core antibody is common after HNlg infusions. Hepatitis B core antibody screening should be considered standard practice for each human normal immunoglobulin administration, effectively improving therapeutic decisions by preventing wrong diagnosis of hepatitis B exposure and therefore preventing unnecessary anti-viral use.

WED-129

Secular trends of newly diagnosed chronic hepatitis B in 2000–2022—a territory-wide study

Grace Lai-Hung Wong¹, Vicki Wing-Ki Hui¹, Terry Cheuk-Fung Yip¹, Yee-Kit Tse¹, Che To Lai¹, Vincent Wai-Sun Wong¹. ¹The Chinese University of Hong Kong, Medical Data Analytic Centre (MDAC) and Department of Medicine and Therapeutics, Hong Kong
Email: wonglaihung@cuhk.edu.hk

Background and aims: The World Health Organization (WHO) proposed targets for the reduction of chronic viral hepatitis incidence and mortality of 90% and 65% respectively by 2030. A comprehensive review of the disease burden of chronic viral hepatitis would provide pivotal data to guide strategies to achieve the goals set by WHO. We aimed to estimate the disease burden of newly diagnosed chronic hepatitis B in 2000 to 2022.

Method: This was a territory-wide retrospective cohort study of all patients with chronic hepatitis B who have been under the care at primary, secondary and tertiary medical centres in Hong Kong. Comprehensive virologic parameters related to chronic hepatitis B from the Hospital Authority were analysed. The number of patients with chronic hepatitis B first diagnosed were evaluated according to calendar year.

Results: Between 1 January 2000 and 31 December 2022, 2,120,008 people patients were tested for chronic hepatitis B, of whom 251,987 (11.88%) tested positive. Annually 6623 to 15,075 people were first diagnosed with chronic hepatitis B; the number of new diagnosis peaked in 2009 then gradually dropped similarly in both genders (Figure A). The drop was more prominent in young adults aged below 30 years old and 50 years old or above, whereas the number of new diagnoses remained high in adults aged 30–49 (Figure B).

Conclusion: Newly diagnosed chronic hepatitis B dropped over the last two decades in young adults but remained high in adults aged 30–49. More resources should be allocated to assess the need of antiviral treatment and complication surveillance for patients with chronic hepatitis B in order to meet the WHO targets of 65% reduction in mortality.

POSTER PRESENTATIONS

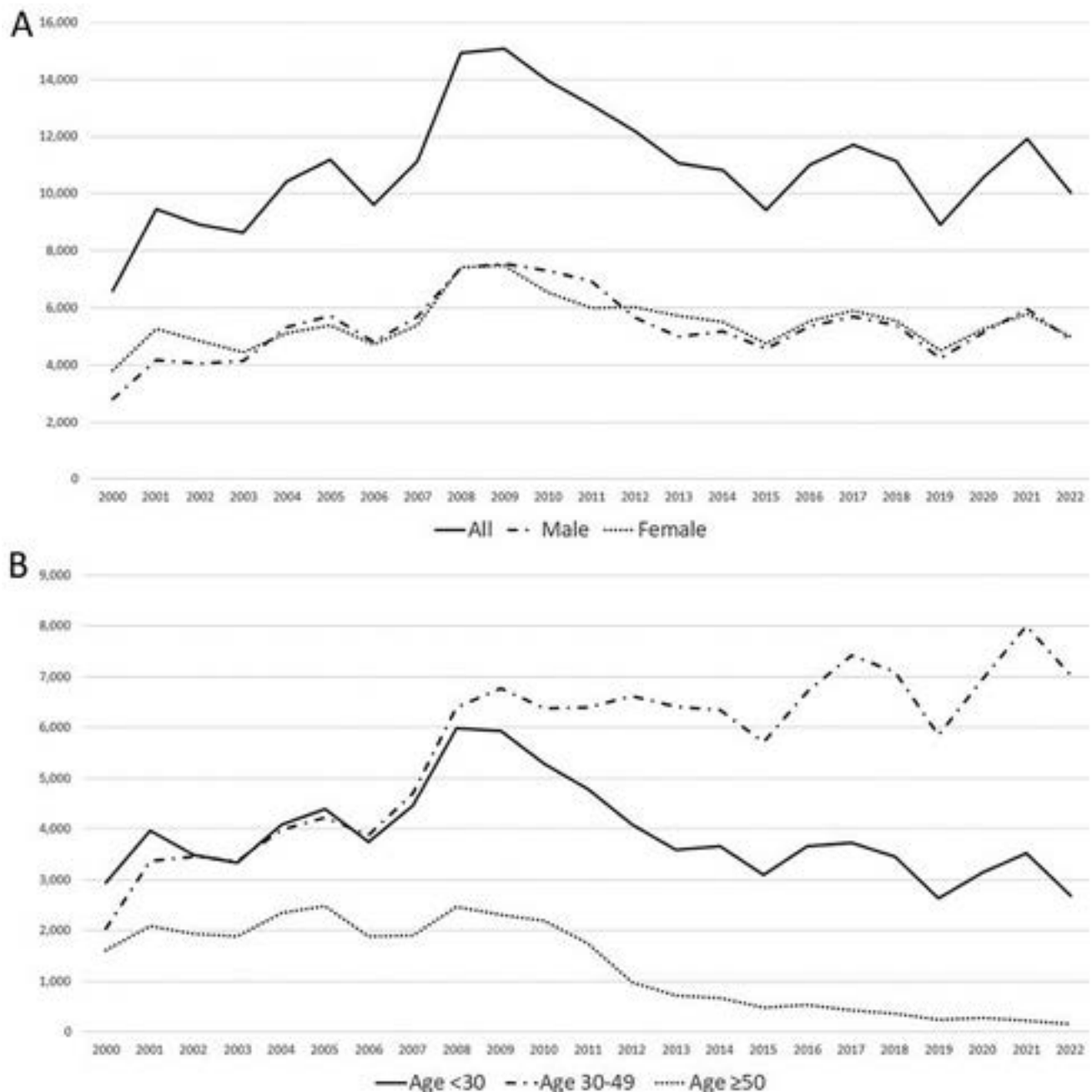


Figure: (abstract: WED-129): Age and gender distribution of patients who were first diagnosed for chronic hepatitis B in 2000 to 2022.

WED-130

Patients with chronic hepatitis delta virus coinfections have higher risk of disease progression than chronic hepatitis B virus monoinfection—results from a Spanish national hospital database

Maria Buti¹, Ankita Kaushik², Mertixell Ascanio³, Josep Darba⁴, Chong Kim². ¹Hospital Universitario Valle Hebrón, Liver Unit, Barcelona, Spain; ²Gilead Sciences, Inc., HEOR-Global Value and Access, Foster City, United States; ³BCN Health Economics and Outcomes Research SL, Barcelona, Spain; ⁴University of Barcelona, Department of Economics, Barcelona, Spain

Email: ankita.kaushik@gilead.com

Background and aims: Patients with chronic hepatitis delta (CHD) infection are at greater risk of developing liver complications than

those with chronic hepatitis B (CHB) monoinfection. This retrospective study compares the rate of disease progression among adult patients with CHD infection vs CHB monoinfection in a national hospital database in Spain.

Method: The study population included patients aged ≥18 years having ≥1 ICD-9/10-CM diagnosis code for HDV or HBV in the Spanish National Health System's Hospital Discharge Records Database (Conjunto Mínimo Básico de Datos) from 1 Jan 2000 to 31 Dec 2019 (study period). HDV-infected and HBV-monoinfected patients were identified from 1 Jan 2001 to 31 Dec 2018 (identification period) with their first diagnosis defined as the diagnosis date, having ≥12 months of continuous enrollment before and after the diagnosis date. Baseline (BL) characteristics including demographics, comorbidities, region, and payer channel were assessed over the entire duration

prior to diagnosis date. HDV-infected and HBV monoinfected patients were propensity score matched (1:5) on BL demographic and clinical characteristics. Multivariable cox proportional hazard regression was performed to assess the differences in risk of compensated cirrhosis (CC), decompensated cirrhosis (DCC), hepatocellular carcinoma (HCC), liver transplantation (LT), and death between the HDV-infected and HBV-monoinfected patients, adjusting for demographics, comorbidities, region, and payer channel.

Results: The study reported 12,317 patients diagnosed with HDV or HBV, of whom 756 matched patients met the inclusion criteria—126 HDV infected and 630 HBV monoinfected. Among HDV-infected vs HBV-monoinfected patients, mean (SD) age was 41.7 (11.8) vs 41.2 (9.9), $p = .581$, and the male to female ratio (roughly 9:1) was similar between cohorts. HDV-infected patients were more likely to transition from noncirrhotic disease (NCD) to CC (HR = 1.89; 95% CI, 1.56, 2.29), CC to DCC (HR = 2.44; 95% CI, 1.74, 4.33), DCC to HCC (HR = 2.80; 95% CI, 1.11, 4.66), HCC to LT (HR = 1.83; 95% CI, 1.18, 3.91), and DCC to death (HR = 5.04; 95% CI, 2.40, 32.44) compared to HBV-monoinfected patients.

Conclusion: In a Spanish national hospital database, HDV-infected patients had significantly greater risk of progressing to greater liver disease severity than HBV-monoinfected patients. These findings underscore the need for early screening, diagnosis, and eventual treatment of HDV to mitigate future disease progression.

WED-131

Dynamic monitoring of HBsAg-specific B cells in CHB patients and its clinical significance in predicting interferon therapy efficacy

Yu Geng¹, Yawen Wan¹, Shengxia Yin¹, Jie Li¹, Chao Wu¹. ¹Nanjing Drum Tower Hospital, Department of Infectious Diseases, Nan Jing Shi, China

Email: dr.wu@nju.edu.cn

Background and aims: The guidelines for the treatment of chronic hepatitis B virus (CHB) patients currently recommend two categories of antiviral drugs: nucleoside analogs and interferons. In comparison to nucleoside analogs, interferons have a higher rate of HBsAg and HBeAg clearance, but their medical compliance, cost, and side effects may hinder clinical application. As a result, the identification of reliable predictive biomarkers to maximize benefits is essential. In HBV infection, the damage and recovery of surface antigen (HBsAg) specific B cells is linked to HBsAg serological conversion. However, current understanding of HBsAg specific B cell immunity is limited, and there are no specific and sensitive methods to detect HBsAg specific B cells. This study presents a method for single-cell level detection of HBsAg specific B cells using an optimized ELISPOT (Enzyme-Linked ImmunoSpot) method. This approach can explore the HBsAg specific B cell responses during different stages of chronic HBV infection and the effect of these responses on the efficacy of interferon treatment in CHB patients.

Method: This study included 142 CHB patients at various stages of immunity, 90 of whom were untreated (21 HBeAg positive patients in the chronic hepatitis stage, 5 HBeAg negative patients in the chronic hepatitis stage, 9 HBeAg positive patients in the chronic infection stage, and 55 HBeAg negative patients in the chronic infection stage). 52 patients received antiviral therapy. Peripheral blood lymphocytes were stimulated over a 5-day period, and the frequency of peripheral blood HBsAg-specific B cells was monitored using ELISPOT. The correlation between serum HBsAb levels and peripheral blood HBsAg-specific B cells was analyzed, and preliminary observations of the dynamic changes of HBsAg-specific B cells before and after interferon treatment were made.

Results: In the chronic hepatitis phase, 6 patients (28.6%) who were HBeAg positive showed positive results in ELISPOT, indicating the presence of peripheral blood HBsAg-specific B cells, while no (0%) HBeAg negative patients in the chronic hepatitis phase showed positive results. Among patients in the chronic infection phase, 3 (30%) who were HBeAg positive and 14 (25.5%) who were HBeAg

negative showed positive results in ELISPOT. The number of peripheral blood-secreting HBsAb-specific B cells was significantly higher in the HBeAg-positive chronic hepatitis group than in the HBeAg-negative chronic infection group ($p < 0.05$). The proportion of "functional cure" in the ELISPOT-positive group was higher after interferon treatment compared to the baseline state (50% in positive group vs. 17.2% in negative group, $P < 0.05$). After interferon treatment, 10 (52.6%) patients showed an increase in HBsAg-specific B cells, with 4 (21.1%) patients achieving "functional cure." Meanwhile, 4 (21.1%) patients with decreased HBsAg-specific B cells and 5 (26.3%) patients with no change in HBsAg-specific B cells did not achieve "functional cure."

Conclusion: In CHB patients in varying immune states, peripheral blood contains HBsAb-secreting B cells that exhibit differing proportions. The peripheral blood's presence of HBsAb-secreting B cells before interferon treatment may be a significant immunological indicator for forecasting interferon therapy efficacy.

WED-132

Association of TLR7 polymorphisms in Caucasians with disease stages and HBsAg loss in hepatitis virus B infections

Janett Fischer¹, Kai-Uwe Krapf¹, Tobias Müller², Heyne Renate³, Thomas Berg¹, Florian van Bömmel¹. ¹Division of Hepatology, Department of Medicine II, Leipzig University Medical Center, Germany;

²Department of Gastroenterology and Hepatology, Charité-Universitätsmedizin Berlin, Berlin, Germany; ³Liver and Study Center Checkpoint, Berlin, Germany

Email: janett.fischer@medizin.uni-leipzig.de

Background and aims: Toll-like receptor 7 (TLR7) activation is major step during innate immune responses against hepatitis B virus (HBV) infections. TLR7 detects single stranded RNA and induces both type 1 interferon and inflammatory responses. Recently, TLR7-directed therapies are under investigation for the treatment of chronic hepatitis B (CHB). Nonetheless, polymorphisms within the *TLR7* gene might affect immune responses and treatment efficacy. Thus, we aimed to evaluate the impact of common *TLR7* polymorphisms (SNPs) on the course of HBV infection and liver disease progression in a Caucasian population.

Method: The study cohort included 519 Caucasian individuals with CHB (60% male, mean age 58 ± 15 years) and 193 with spontaneous HBV surface antigen (HBsAg) seroclearance (SC) with available full blood samples stored at -20°C who had given informed consent for participation in the study. In the CHB group, 206 patients had HBeAg-negative HBV infection and 90 HBeAg-positive and 223 HBeAg-negative CHB. Host genomic DNA extraction and genotyping of the *TLR7* SNPs rs179008, rs864058 and rs2302267 were performed from full blood samples. Serum levels of pro- and anti-inflammatory cytokines were measured in corresponding serum samples from 193 patients.

Results: Genotype distribution of the *TLR7* rs179008 was different between patients with CHB and spontaneous HBsAg SC ($p = 0.0003$). After sex stratification, this difference in genotype distribution only remained significant in female patients ($p = 0.007$). Here, the AT/TT genotypes were associated with an increased likelihood of spontaneous HBsAg SC in adjusted analysis (OR = 1.78 [95% CI: 1.02–3.10], $p = 0.041$). In the HBsAg SC group, female patients carrying the rs179008 AT/TT genotypes showed lower serum levels of interferon (IFN) alpha ($p = 0.028$), IFN beta ($p = 0.016$), IFN gamma ($p = 0.032$) and interleukin (IL)-10 ($p = 0.017$) than carriers of the AA genotype. Furthermore, we found a significant association of *TLR7* rs2302267 TG/GG genotypes with HBeAg-negative infection (OR = 1.51, $p = 0.039$), and an association of *TLR7* rs864058 GG genotype with an increased frequency of liver cirrhosis (OR = 3.48, $p = 0.019$).

Conclusion: In this retrospective study, we confirmed the association of the *TLR7* rs178009 polymorphism with disease stages and functional cure in HBV infected Caucasian patients, and we identified new effects of additional *TLR7* variants on disease progression. Our

POSTER PRESENTATIONS

findings further emphasise the relevance of the genetic and sex predisposition in personalized management of HBV infections and potentially for new TLR7-directed treatment strategies.

WED-133

Higher levels of three HBsAg forms (Large, Middle and Small HBsAg) are associated with HDV replication and with the degree of disease and liver damage

Leonardo Duca¹, Antonella Olivero², Lorenzo Piermatteo^{1,3}, Stefano D'Anna¹, Giulia Torre¹, Elisabetta Teti⁴, Andrea Di Lorenzo⁴, Vincenzo Malagnino⁴, Marco Iannetta⁴, Leonardo Baiocchi⁵, Simona Francioso⁵, Ilaria Lenci⁵, Francesca Ceccherini Silberstein¹, Michele Milella⁶, Annalisa Saracino⁶, Alessia Ciancio², Loredana Sarmati⁴, Mario Rizzetto², Gian Paolo Caviglia², Valentina Svicher^{1,3}, Romina Salpini¹. ¹University of Rome "Tor Vergata", Experimental Medicine, Rome, Italy; ²University of Turin, Department of Medical Sciences, Italy; ³University of Rome "Tor Vergata", Biology, Rome, Italy; ⁴University of Rome "Tor Vergata", Department of Systems Medicine, Infectious Disease Clinic, Italy; ⁵Policlinico Tor Vergata, Hepatology Unit, Italy; ⁶University of Bari "Aldo Moro", Italy
Email: duca.leonardo@hotmail.it

Background and aims: HBV surface proteins (HBsAg) enable the morphogenesis of HDV progeny and entry into hepatocytes. Total HBsAg is composed by 3 different forms: Large-HBs (L-HBs), Middle-HBs (M-HBs), and Small-HBs (S-HBs). Here, we investigate the still unexplored levels of the different HBs forms in the setting of HDV coinfection and their correlation with ALT and the status of cirrhosis.

Method: This study includes 160 plasma samples from patients with HDV-HBV chronic infection classified as high-replicating HDV (HDV-RNA >3 log IU/ml, N = 130) and low-replicating HDV (HDV-RNA <3 log IU/ml, N = 30). Total HBsAg is measured by COBAS HBsAgII assays (Roche Diagnostics) while ad-hoc designed ELISAs are used to quantify L-HBs, M-HBs, S-HBs (Beacle Inc).

Results: Patients have a median (IQR) serum HDV-RNA and total HBsAg of 5.1 (3.4–6.1) log IU/ml and 5716 (1372–10 887) IU/ml, respectively. ALT >40 U/L is observed in 76.9% (median [IQR]: 87 [67–136] U/L) and 63.8% is cirrhotic. The median (IQR) levels of HBs-S, HBs-M and HBs-L are 3,984 (637–6993), 1,147 (141–2299) and 2.3 (0.2–6.5) ng/ml, respectively.

Notably, significantly higher levels of all the 3 HBs forms are observed in patients with high-replicating HDV compared to low-replicating HDV (median [IQR] levels: 4638 [1560–7467] vs 272 [61–3523] ng/ml for S-HBs; 1,409 [228–2647] vs 103 [7.2–615] ng/ml for M-HBs; 3.5 [0.3–9.1] vs 0.3 [0.04–1.2] ng/ml for L-HBs, P < 0.001 for all). A positive correlation is also revealed for the 3 HBs forms with HDV-RNA levels (Rho = 0.42, 0.46 and 0.39 for S-, M- and L-HBs, respectively; P < 0.001 for all).

In low-replicating HDV patients, 51.9% has altered transaminases (median [IQR]: 78 [61–117] U/L). Notably, in this set of patients, M-HBs >200 ng/ml is the best cut-off predicting altered ALT >40 U/L (75% of patients with M-HBs >200 ng/ml vs 37.5% of those with M-HBs <200 ng/ml, PPV = 75%, NPV = 62.5%; P = 0.049), supporting the role of M-HBs in reflecting cytolytic activity even in the setting of a low HDV replication.

Serum HDV-RNA levels were comparable between cirrhotic and non-cirrhotic patients (median [IQR]: 5.1 [4.1–5.9] vs 4.2 [1.2–5.7] log IU/ml; P = 0.11). Nevertheless, a higher ratio of L-HBs/M-HBs (reflecting unbalanced release towards L-HBs) is observed in cirrhotic vs non-cirrhotic patients (median [IQR] % ratio of L-HBs/M-HBs: 0.41 [0.16–1.45] vs 0.18 [0.06–0.45]; P = 0.05). In particular, a % ratio of L-HBs/M-HBs >0.5 correlates with the status of cirrhosis (83.3% with vs 37.3% without L-HBs/M-HBs >0.5 is cirrhotic; P = 0.037).

Conclusion: In chronic HDV coinfection, higher levels of the 3 HBs forms support an enhanced burden of HDV replication and their composition correlates with the degree of cytolytic activity and liver damage. Thus, the quantification of 3 HBs forms can provide an added value in identifying patients with a more advanced disease, in which treatment should be prioritized.

WED-134

Hepatitis delta treatment utilization in the United States: an analysis of commercially insured adults with hepatitis delta virus infection

Robert Wong^{1,2}, Robert G. Gish³, Joseph Lim⁴, Ankita Kaushik⁵, Chong Kim⁵, Gary Leung⁶, Ira M Jacobson⁷. ¹Stanford University School of Medicine, Stanford, United States; ²VA Palo Alto Healthcare System, Palo Alto, United States; ³Hepatitis B Foundation, Doylestown, United States; ⁴Yale University School of Medicine, New Haven, United States; ⁵Gilead Sciences, Inc., HEOR-Global Value and Access, Foster City, United States; ⁶Gilead Sciences, Inc., RWE-Epidemiology, Foster City, United States; ⁷NYU Grossman School of Medicine, New York, United States
Email: rwong123@stanford.edu

Background and aims: Hepatitis delta virus (HDV) infection is associated with more rapid liver disease progression than hepatitis B (HBV) infection alone. Compared with HBV monoinfection, if left untreated, HDV is associated with earlier onset of liver-related complications, such as cirrhosis, liver failure, and liver cancer. While pegylated-interferon (Peg-IFN) is used off-label as a treatment option for HDV, treatment utilization for HDV coinfecting patients in the US are not well understood. This study aims to describe HDV treatment utilization among a large population-based cohort of commercially insured adults with HDV in the US.

Method: Adult patients with ≥1 HDV or HBV diagnosis (ICD-9/10-CM) were identified retrospectively from 1 Jan 2013 to 31 Dec 2021 (study period) using the IQVIA PharMetrics Plus database covering ~210 million patients from primarily commercial payers. HDV patients were identified from 1 Jan 2014 to 31 Dec 2020 (identification period) and defined as those who had ≥1 inpatient or ≥2 outpatient claims ≥30 days apart with an ICD-9/10-CM diagnosis code (070.21, 070.23, 070.31, 070.33, 070.42, 070.52, B160, B170, B161, B180) for HDV during the identification period (earliest date of diagnosis considered index date), ≥1 claim of HBV diagnosis during BL (12-month period prior to index date), and no claims with HDV diagnosis during BL. Continuous enrollment for ≥12 months before and after the index date was required, and patients aged ≥18 years at index with commercial health plans were included. Utilization of antiviral therapies including pegylated interferon, interferon alfa, interferon alfa N3, interferon gamma, tenofovir disoproxil fumarate, tenofovir alafenamide, entecavir, adefovir, telbivudine, and lamivudine were assessed over the entire post-index period (follow-up).

Results: Among 6,002 patients with HDV identified during the identification period, 440 met inclusion criteria. Only five patients (1.1%) received treatment with pegylated interferon (Peg-IFN) within the follow-up period. Fewer than 40% of patients with concurrent HDV infection (n = 175; 39.8%) were receiving HBV-specific antiviral therapy, including tenofovir disoproxil fumarate (91; 20.7%), entecavir (65; 14.8%), tenofovir alafenamide (46; 10.5%), adefovir (7; 1.6%), and lamivudine (2; <0.5%). The majority of patients with HDV were not on any interferon or HBV-related treatments (263; 59.8%).

Conclusion: In a large US national, primarily commercial, healthcare claims database, fewer than 40% of patients with HDV were treated with HBV-specific antiviral therapies, and very few patients (1.1%) were treated with Peg-IFN, the current off label standard of care for HDV infection. Greater awareness of the importance of timely

initiation of antiviral therapy for patients with combined HBV/HDV infection is urgently needed.

WED-135

Comparison of HCC incidence between entecavir and tenofovir in a chronic hepatitis B cohort with balanced censoring

Jang Han Jung¹, Eileen Yoon², Dae Won Jun², Hyunwoo Oh³, Hyo Young Lee³, Sung Eun Kim⁴, Sung-Eun Kim^{5,6}, Soung Won Jeong⁷, Gi-Ae Kim⁸, Jihyun An², Joo Hyun Sohn², Won Sohn⁹, Yong Kyun Cho⁹, Sang Bong Ahn¹⁰. ¹Dongtan Sacred Heart Hospital of Hallym University Medical Center, Korea, Rep. of South; ²Hanyang University, College of Medicine, Department of Internal Medicine, Korea, Rep. of South; ³UiJeongbu Eulji Medical Center, Eulji University College of Medicine, Korea, Rep. of South; ⁴Hallym University Sacred Heart Hospital, Hallym University College of Medicine, Korea, Rep. of South; ⁵Kangdong Sacred Heart Hospital, Hallym University College of Medicine, Korea, Rep. of South; ⁶Hallym University College of Medicine, Internal Medicine, Korea, Rep. of South; ⁷Soonchunhyang University College of Medicine, Soonchunhyang University Seoul Hospital, Korea, Rep. of South; ⁸Kyung Hee University School of Medicine, Korea, Rep. of South; ⁹Kangbuk Samsung Hospital, Sungkyunkwan University School of Medicine, Korea, Rep. of South; ¹⁰Eulji university college of medicine, Korea, Rep. of South Email: noshin@hanyang.ac.kr

Background and aims: The risk of hepatocellular carcinoma (HCC) in patients treated with either entecavir or tenofovir disoproxil fumarate (tenofovir DF) for chronic hepatitis B (CHB) has not been elucidated. Distinct characteristics of patients tend to be treated with tenofovir DF, shorter observation periods for tenofovir DF, and imbalanced rate of censoring between the two drugs have led to contradictory results. Minimizing and balancing the censored data, we aimed to compare the risk of HCC in treatment-naïve patients who were treated with either entecavir or tenofovir DF over the same follow-up duration.

Method: The de-identified data of 9-centered cohort were linked to the record of HCC development in the National Health Insurance Service. To prove the robustness of this analysis, variable subgroup analyses were done on the propensity-score matched with inverse probability of treatment weighting.

Results: We treated 1698 patients (male, 65.3%; mean age, 47.2 ± 11.5 years) with either entecavir (n = 845) or tenofovir DF (n = 853). The mean follow-up duration was 8.7 (IQR 7.9–10.3) years for entecavir and 7.4 years (IQR 6.7–8.4) for tenofovir DF. Sixty-nine and sixty-five patients developed HCC in entecavir group (8.2%) and tenofovir DF group (7.6%), respectively (p = 0.562). Similarly, the incidence of HCC did not differ between the groups (p = 0.268) in 751-pair propensity score-matched patients.

Conclusion: In a retrospective review of 1,698 treatment-naïve patients with CHB, there was no difference in the HCC incidence between the two groups treated with either entecavir or tenofovir DF, over 7-years for both the medications.

WED-136

Serum CXCL16 serves as the predictor for liver inflammation functioning through a NKT cell-depend way in chronic hepatitis B patients

Yawen Wan¹, Shengxia Yin², Ming Li³, Minxin Mao³, Jiacheng Liu², Xin Tong², Jian Wang², Jie Li², Chao Wu^{1,2}. ¹Department of Infectious Diseases, Nanjing Drum Tower Hospital Clinical College of Xuzhou Medical University, Xuzhou Medical University, Xuzhou, China; ²Department of Infectious Diseases, Nanjing Drum Tower Hospital, The Affiliated Hospital of Nanjing University Medical School, Nanjing, China; ³Department of Infectious Diseases, Nanjing Drum Tower Hospital Clinical College of Traditional Chinese and Western Medicine, Nanjing University of Chinese Medicine, Nanjing, China Email: dr.wu@nju.edu.cn

Background and aims: Significant liver inflammation is an important indication for initiating antiviral therapy in chronic hepatitis B (CHB) patients. Liver biopsy has always been regarded as the golden standard for assessing the liver inflammation, while its invasive nature limited the application. The level of alanine aminotransferase (ALT) is currently the most commonly used serum indicator. However, the severity of liver inflammation is not always consistent with ALT levels. Therefore, We aimed to find more effective and non-invasive markers for predicting liver inflammation.

Method: We conducted a cross-sectional study that retrospectively included 120 CHB patients who had underwent liver biopsy and 31 volunteers as health control. Liver inflammation were staged by Scheuer's classification. The expression level of CXC motif chemokine ligand 16 (CXCL16) in peripheral blood of patients with CHB was determined by ELISA and the relationship between CXCL16 and liver inflammation was further analyzed. In addition, the mechanism of CXCL16 affecting liver inflammation was explored by using a mouse model infected with hepatitis B virus (HBV).

Results: We found that the serum level of CXCL16 in CHB patients was much higher than that in healthy subjects. Furthermore, serum CXCL16 was severe significantly higher in severe inflammation group (G ≥ 3, n = 26) than in non-severe inflammation group (G < 3, n = 96) [(median, IQR), 0.42 (0.24–0.71) ng/ml VS 1.01 (0.25–2.09) ng/ml, P < 0.001]. We combined CXCL16 with platelet, ALT and albumin to build a model, which is more effective in predicting severe inflammation than ALT (ROC, 0.92 VS 0.81, P = 0.015). Additionally, by using HBV infected mice model, we found a decreased level of liver inflammation after CXCL16 blockage. A failure of liver infiltration and decreased inflammatory function of natural killer T (NKT) and natural killer (NK) cells were discovered.

Conclusion: CXCL16 could be developed as a promising non-invasive liver inflammation marker for patients with chronic HBV infection. And it could accelerate the hepatic inflammation by a NKT and NK cell depend way.

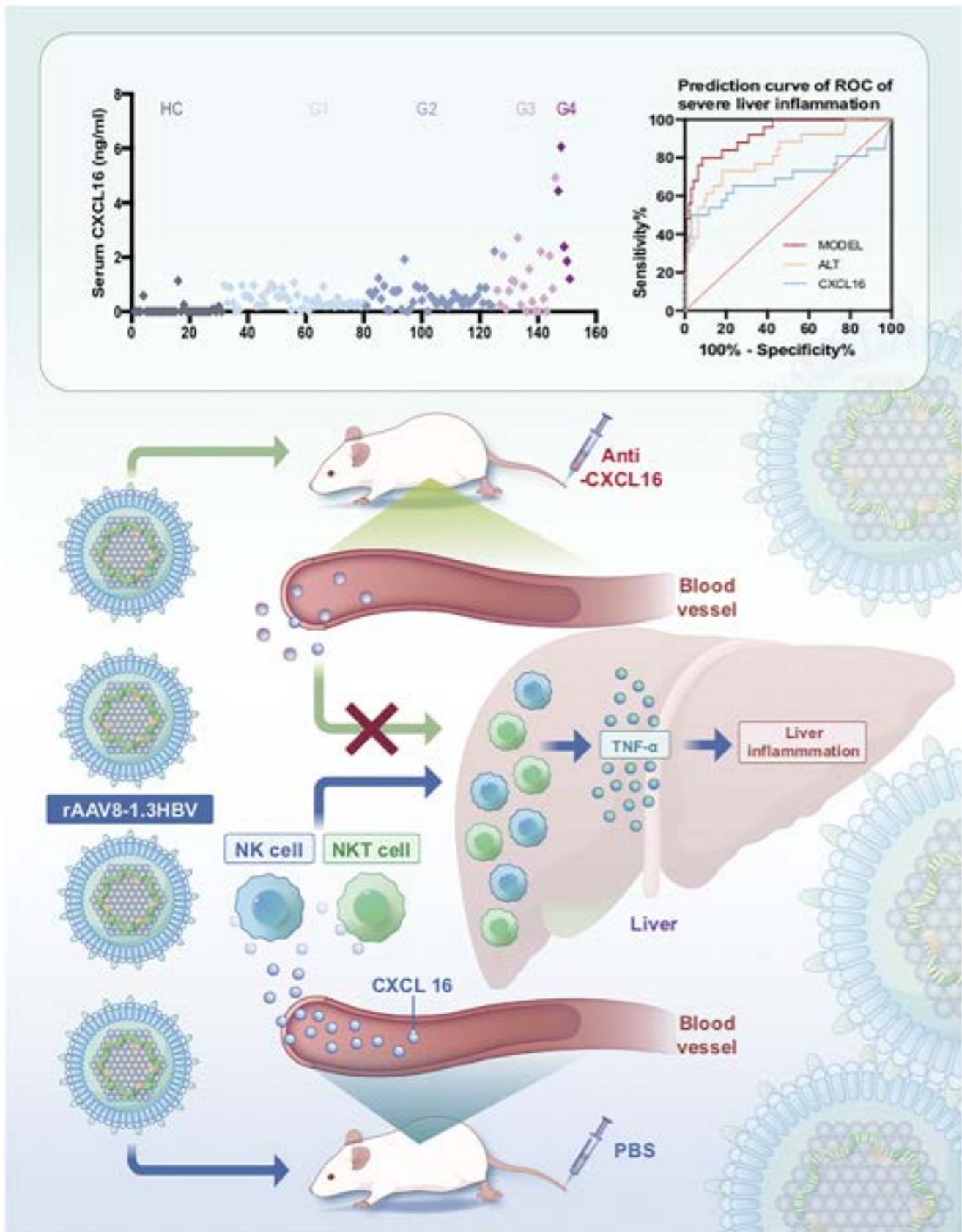


Figure: (abstract: WED-136).

WED-137

Distinct virologic trajectories in chronic hepatitis B patients identify heterogeneity in response to nucleotide analogue therapy

Tingyan Wang^{1,2}, Cori Campbell^{1,2}, Gail Roadknight^{1,3}, Stephanie Little^{1,3}, Alexander Stockdale^{4,5}, Stacy Todd⁵, Karl McIntyre⁶, Andrew Frankland⁶, Jakub Jaworski⁷, Afzal Chaudhry⁷, Ben Glampson^{8,9}, Luca Mercuri^{8,9}, Dimitri Papadimitriou^{8,9}, Christopher R. Jones^{9,10}, Kinga Varnai^{1,3}, Theresa Noble^{1,3}, Hizni Salih^{1,11}, Cai Davis^{12,13}, Ashley Heinson^{12,13}, Michael George^{12,13}, Florina Borca^{12,13}, Josune Olza¹², Louise English¹⁴, Luis Romão¹⁴, David Ramlakhan¹⁴, Eleni Nastouli^{15,16}, Salim Khakoo¹⁷, Will Gelson¹⁸, Graham Cooke^{8,9,19}, Kerrie Woods^{1,3}, Jim Davies^{1,11,20},

Philippa Matthews^{2,3,21,22,23}, Eleanor Barnes^{2,3}. ¹NIHR Oxford Biomedical Research Centre, United Kingdom; ²University of Oxford, Nuffield Department of Medicine, United Kingdom; ³Oxford University Hospitals NHS Foundation Trust, NIHR Health Informatics Collaborative, United Kingdom; ⁴Institute of Infection, Veterinary and Ecological Sciences, University of Liverpool, United Kingdom; ⁵Liverpool University Hospitals NHS Foundation Trust, Tropical Infectious Diseases Unit, Royal Liverpool Hospital, United Kingdom; ⁶Liverpool University Hospitals NHS Foundation Trust, Liverpool Clinical Laboratories, United Kingdom; ⁷Cambridge University Hospitals NHS Foundation Trust, United Kingdom; ⁸Imperial College Healthcare NHS Trust, NIHR Health Informatics Collaborative, United Kingdom; ⁹NIHR Imperial Biomedical

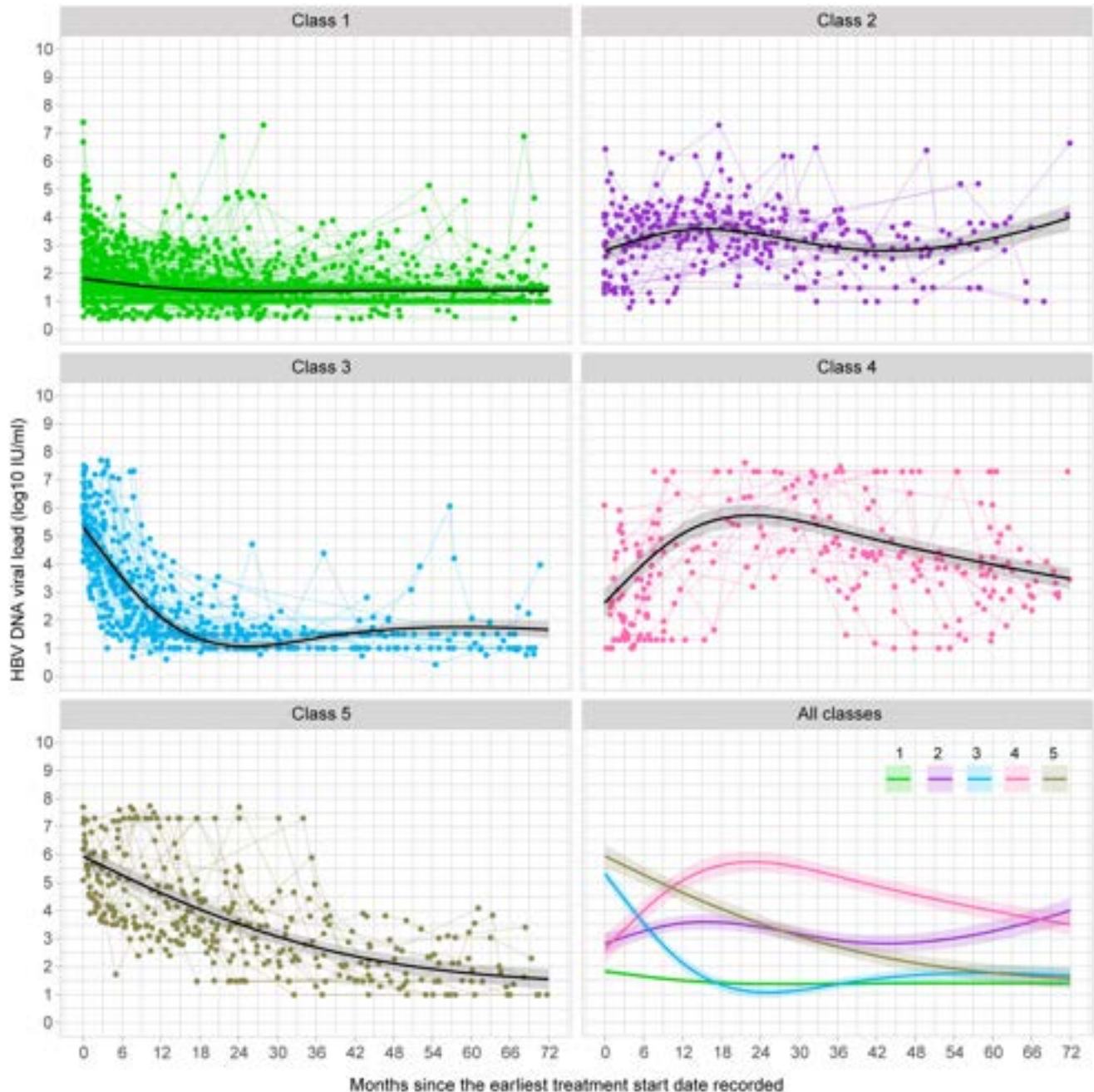


Figure: (abstract: WED-137): Individual trajectories of HBV DNA viral load (VL) and their patterns ('classes 1-5') for chronic hepatitis B patients on treatment. The five VL patterns were identified using latent class mixed model. Dots represent the real values of VL, and solid lines with shading area represent the predicted VL trajectory patterns with 95% confidence intervals.

POSTER PRESENTATIONS

Research Centre, United Kingdom; ¹⁰Imperial College London, Department of Infectious Disease, United Kingdom; ¹¹University of Oxford, Nuffield Department of Population Health, United Kingdom; ¹²University Hospital Southampton NHS Foundation Trust, NIHR Southampton Biomedical Research Centre, United Kingdom; ¹³University of Southampton, Clinical Informatics Research Unit, Faculty of Medicine, United Kingdom; ¹⁴NIHR University College London Hospitals Biomedical Research Centre, United Kingdom; ¹⁵UCLH, Department of Clinical Virology, United Kingdom; ¹⁶UCL Great Ormond Street Institute of Child Health, Department of Infection, Immunity and Inflammation, United Kingdom; ¹⁷University of Southampton, School of Clinical and Experimental Sciences, Faculty of Medicine, United Kingdom; ¹⁸Cambridge University Hospitals NHS Foundation Trust, Cambridge Liver Unit, United Kingdom; ¹⁹Imperial College London, Faculty of Medicine, Department of Infectious Disease, United Kingdom; ²⁰University of Oxford, Department of Computer Science, United Kingdom; ²¹The Francis Crick Institute, London, UK, United Kingdom; ²²University College London, Division of Infection and Immunity, United Kingdom; ²³University College London Hospital, Department of Infectious Diseases, United Kingdom
Email: tingyan.wang@ndm.ox.ac.uk

Background and aims: The longitudinal patterns of HBV DNA viral load (VL) of chronic hepatitis B (CHB) patients on treatment are not well characterised in the UK population. However, understanding the phenotypes of treatment responses is crucial for patient stratification for better care.

Method: We studied a cohort of 8,028 CHB patients from 6 large teaching hospitals in England with longitudinal follow-up, established by the National Institute for Health Research (NIHR) Health Informatics Collaborative (HIC) from electronic patient record systems. We included adults who had two or more VL measurements with >6 months of follow-up on VL for analysis. We applied latent class mixed models to investigate the patterns of VL trajectories since the earliest treatment date recorded (defined as baseline). Repeated and various number of measurements at different time points for patients were considered in the approach, by including fixed effects, and random effects and slope for individuals. The number of VL classes was determined by the Bayesian information criteria, the Akaike information criteria, the discrimination, the odds of correct classification, the relative entropy, and the interpretability of the model. We performed multinomial logistic regressions to assess the determinants of VL trajectories at baseline.

Results: We identified 740 patients on nucleos(t)ide analogue (NA) treatment with longitudinal VL data, with a median follow-up duration of 3.3 years (interquartile range [IQR], 1.6–5.2 years). The total number of VL measurements was 4,642 (median [IQR], 5 [3–8] measurements per patient). Five mutually exclusive patterns of VL trajectories were identified (Figure), i.e., class 1 (N = 557, 75.3%)–‘VL long term suppressed’, class 2 (N = 53, 7.2%)–‘persistent viraemia with moderate VL’, class 3 (N = 74, 10.0%)–‘VL suppressed as expected’, class 4 (N = 24, 3.2%)–‘VL non-suppressing with high VL’, and class 5 (N = 32, 4.3%)–‘VL slowly suppressed’. Univariable analysis showed that baseline age, sex, ethnicity, HBeAg status, ALT, albumin, urea, and treatment regimens, were associated with the VL classes identified. After multivariable analysis, the following independent determinants (all $p < 0.05$) measured at baseline were identified (the reference was class 1): i) age, sex, Mixed or Other ethnicity, albumin, ALT for class 2, ii) sex, HBeAg status, ALT, urea for class 3, iii) age, HBeAg status for class 4, and iv) age, HBeAg status, ALT, combination treatment drugs of entecavir and tenofovir disoproxil for class 5.

Conclusion: There is heterogeneity in virologic response to antiviral treatment with NA agents, and complete virologic suppression for CHB patients on current standard antiviral treatment can be slow. Some of this variability is statistically associated with demographics

and laboratory parameters. Enhanced understanding of treatment response can be used to inform better risk-stratification, improved patient-centric clinical care, and as a foundation to understand the impact of novel therapies as these become available.

WED-138

Utilizing machine learning-based predictive models to identify early virological recurrence in Chinese chronic hepatitis B patients following entecavir withdrawal

Xiaoke Li^{1,2}, Mei Qiu³, Yi Huang⁴, Huanming Xiao⁵, Hening Chen¹, Bingjiu Lu⁶, Yuyong Jiang⁷, Fuli Long⁸, Hui Lin⁹, Jinyu He¹⁰, Mingxiang Zhang¹¹, Qikai Wu¹², Li Wang¹³, Xiaoning Zhu¹⁴, Man Gong¹⁵, Jianguang Sun¹⁶, Xuehua Sun¹⁷, Fengxia Sun¹⁸, Wei Lu¹⁹, Weihua Xu²⁰, Hongbo Du^{1,2}, Yong'an Ye^{1,2}. ¹Dongzhimen Hospital, Beijing University of Chinese Medicine, Hepatology, Beijing, China; ²Beijing University of Chinese Medicine, Liver Diseases Academy of Traditional Chinese Medicine, Beijing, China; ³Shenzhen Traditional Chinese Medicine Hospital, Hepatology, China; ⁴Chongqing Traditional Chinese Medicine Hospital, China; ⁵The Second Affiliated Hospital of Guangzhou University of Chinese Medicine, China; ⁶Liaoning Hospital of Traditional Chinese Medicine, China; ⁷Beijing Ditan Hospital, China; ⁸The First Affiliated Hospital of Guangxi University of Chinese Medicine, China; ⁹Mengchao Hepatobiliary Hospital of Fujian Medical University, China; ¹⁰Shaanxi Hospital of Traditional Chinese Medicine, China; ¹¹The Sixth People's Hospital of Shenyang, China; ¹²The Third People's Hospital of Shenzhen, China; ¹³Public Health Clinical Center of Chengdu, China; ¹⁴Affiliated Traditional Chinese Medicine hospital of Southwest Medical University, China; ¹⁵The Fifth Medical Center of People's Liberation Army of China, China; ¹⁶Shandong Hospital of Traditional Chinese Medicine, China; ¹⁷Shuguang Hospital Affiliated to Shanghai University of Traditional Chinese Medicine, China; ¹⁸Beijing Chinese Medicine Hospital, China; ¹⁹The Second People's Hospital of Tianjin, China; ²⁰The Second Hospital of Shandong University, China
Email: yeyongan@vip.163.com

Background and aims: Although guidelines recommend that chronic hepatitis B (CHB) patients may discontinue nucleos(t)ide analogues (NAs) after consolidation therapy, virological relapses are common. Early virological recurrence (EVR) generally signaling disease flare. However, biomarkers assessing risks of off-treatment virological recurrence are limited. With machine learning techniques, this study aimed to investigate the role of novel biomarkers including hepatitis B virus pregenome RNA (HBV RNA), hepatitis B core-related antigens (HBcrAg), and large surface antigens of HBV (L-HBsAg) in combination with traditional serum assessments such as tests of HBV serological markers, liver enzymes at the end of treatment (EOT) in predicting the risk of EVR in CHB patients within 24 weeks after entecavir (ETV) withdrawal. The study was conducted as part of National Science and Technology Major Project of China, No.2018ZX10725505.

Method: This study was based on data from a prospective multicenter trial in China. In the trial, CHB patients were given a consolidation treatment with ETV for 96 weeks followed by an off-treatment observation for 24 weeks, during which numbers of EVR (defined as serum HBV DNA >10 IU/ml) were counted. With the serological markers collected at the EOT, we developed predictive models to assess the risk of EVR. Multivariable analyses were performed using penalized logistic regression by the LASSO method. Random forest (RF), artificial neural networks (ANNs), and support vector machine (SVM) were used to construct prediction models based on traditional indicators (TI) and novel serum biomarkers, respectively. Area under the curve (AUC) and calibration plots were used to assess the discrimination and calibration.

Results: A total of 420 patients were enrolled in the current study and 172 (40.95%) patients experienced EVR within 24 weeks after ETV withdrawal. LASSO regression revealed that eight variables (levels of

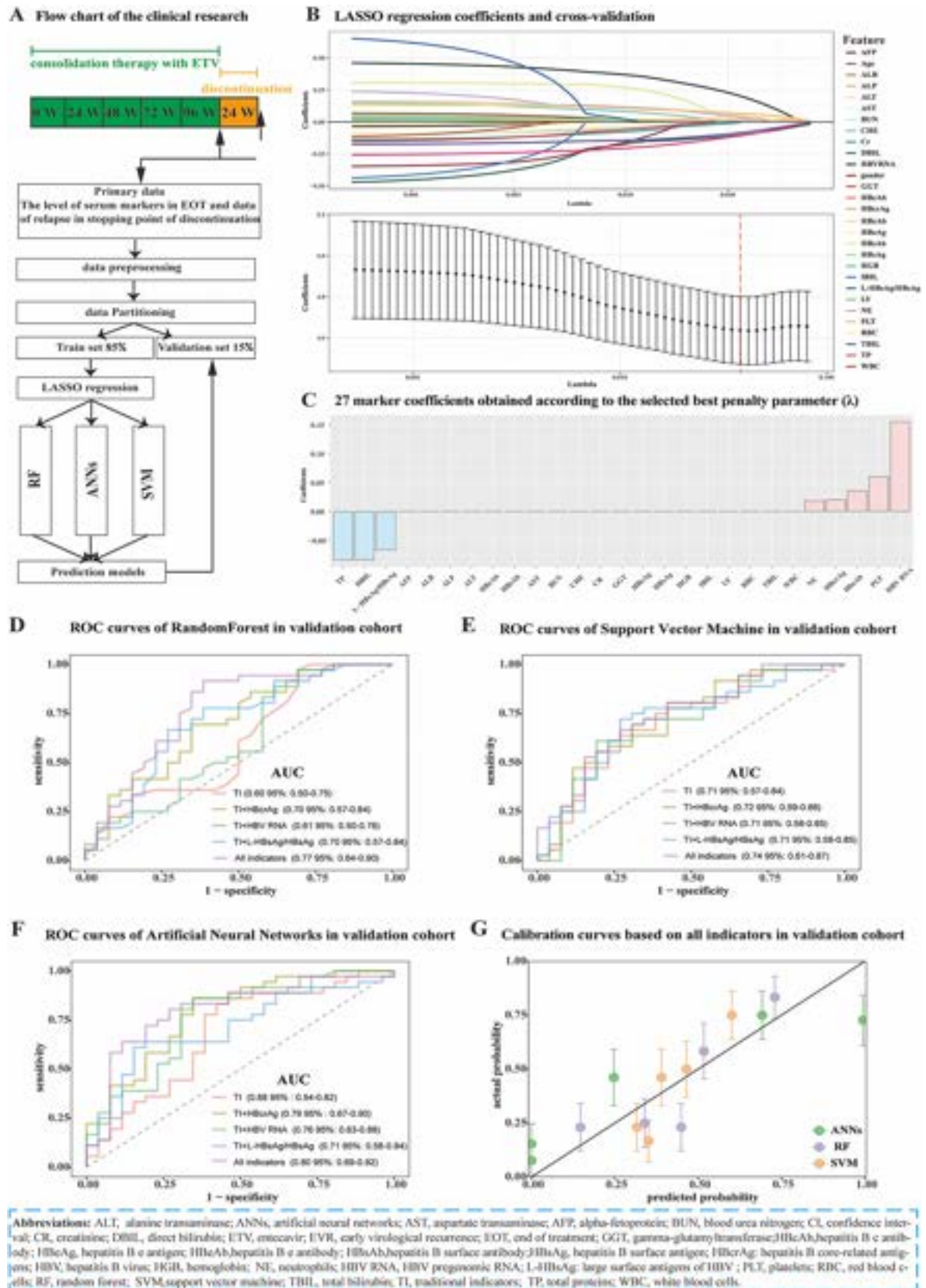


Figure: (abstract: WED-138).

POSTER PRESENTATIONS

HBcAg, HBV RNA, L-HBsAg/HBsAg [hepatitis B surface antigen], platelets [PLT], hepatitis B e antibody [HBeAb], count of neutrophils [NE], direct bilirubin [DBIL] and serum total proteins [TP]) were particularly important features of recurrence. The performance of the SVM model (AUC: 0.71, 95% confidence interval [CI]: 0.57–0.84) based on TI (PLT, HBeAb, NE, DBIL and TP) was superior to RF (AUC: 0.60, 95% CI: 0.50–0.75) and ANNs (AUC: 0.68, 95% CI: 0.54–0.82) models, and the performance of the ANNs (AUC: 0.80, 95% CI: 0.69–0.92) model by integrating TI with all novel serum biomarkers was superior to RF (AUC: 0.77, 95% CI: 0.64–0.90) and SVM (AUC: 0.74, 95% CI: 0.61–0.87) models. Furthermore, the diagnostic efficiency of the combination of TI and all novel serum biomarkers indicators to diagnose EVR was higher than that of a single combined indicator.

Conclusion: Machine learning techniques can be used to create models for predicting EVR following ETV withdrawal in patients with CHB. Patients with certain EOT characteristics, such as high levels of HBcAg, low L-HBsAg/HBsAg ratio, and detectable serum HBV RNA, are at a higher risk for EVR. These models can assist in identifying patients who are suitable for ETV withdrawal with minimal risk in clinical practice.

WED-139

Extrahepatic mortality in patients with chronic hepatitis B infection: a large population-based cohort study

Young Eun Chon¹, Man Young Park², Kwan Sik Lee¹, Dae Won Jun³.

¹CHA Bundang Medical Center, CHA University, Korea, Rep. of South;

²Korea Institute of Oriental Medicine, Korea, Rep. of South; ³Hanyang

University, Korea, Rep. of South

Email: nachivysoo@chamc.co.kr

Background and aims: Accurate statistics on the change in cause of death and mortality in patients with chronic hepatitis B (CHB) are lacking. We investigated the extrahepatic disease-related mortality and its change.

Method: Data of patients who had been newly diagnosed as CHB between 2007 and 2010 (cohort 1, n = 223,424) and between 2012

and 2015 (cohort 2, n = 177,966) from the Korea National Health Insurance Service was used. Mortality and cause of death were obtained from the Statistics Korea. Cause of death were classified as liver-related (hepatic decompensation or HCC) or extrahepatic disease-related (cardiovascular-related, cerebrovascular related, or cancers except HCC).

Results: In cohort 1, death rate was 13.9% yielding overall mortality of 1541/100 000 person-years during 10 years of follow-up. Ten-year overall mortality was 9,234/100 000 person-years in patients with cirrhosis, and 861/100 000 person-years in patients without cirrhosis. Liver-related death in patients with cirrhosis and those without comprised 75.4% and 30.0% of total cause of death, respectively. Most common causes of death in patients with cirrhosis were HCC (62.4%) and liver decompensation (13.0%), whereas those in patients without cirrhosis were cancers except HCC (27.2%) and HCC (22.7%). When 5-year mortality was compared (cohort 1 vs. cohort 2), overall and other mortalities decreased in cohort 2, however, mortality related to cancers except HCC increased (361/100 000 person-years→398/100 000 person-years). Proportion of cancers except HCC as a cause of death has increased (16.7% in cohort→22.4% in cohort 2).

Conclusion: In CHB patients without cirrhosis, extrahepatic disease-related mortality overwhelms liver-related mortality. Compared with the past, the mortality rate and proportion due to cancers except HCC are increasing in the recent cohort.

WED-140

Association of liver fibrosis and hypophosphatemia in treatment-naïve patients with chronic hepatitis B

Suling Jiang¹, Jian Wang^{2,3}, Li Zhu⁴, Zhiyi Zhang⁵, Jie Zhan¹, Weimao Ding⁶, Jie Li^{1,2,3}, Chuanwu Zhu⁴, Rui Huang^{1,2,3}, Chao Wu^{1,2,3}.

¹Department of Infectious Diseases, Nanjing Drum Tower Hospital Clinical College of Nanjing Medical University, Nanjing, Jiangsu, China;

²Department of Infectious Diseases, Nanjing Drum Tower Hospital, The Affiliated Hospital of Nanjing University Medical School, Nanjing, Jiangsu, China; ³Institute of Viruses and Infectious Diseases, Nanjing

Table 3. (abstract: WED-139): All cause and specific mortality rates during 10 years of follow-up in cohort 1

Causes of mortality		Total patient, n	Death, n	Person-years	Death rate, %	Mortality, rate/100 person-years	Mortality, rate/100, 000 person-years	Cause of death, %
All cause mortality	All	223 424	31 157	2 022 180	13.95	1.54	1541	100.0
	Male	125 025	22 197	1 095 217	17.75	2.03	2027	100.0
	Female	98 399	8960	926 963	9.11	0.97	967	100.0
Other cancer related mortality	All	223 424	5348	2 022 180	2.39	0.26	264	17.2
	Male	125 025	3345	1 095 217	2.68	0.31	305	15.1
	Female	98 399	2003	926 963	2.04	0.22	216	22.4
Cardiovascular disease related mortality	All	223 424	2223	2 022 180	0.99	0.11	110	7.1
	Male	125 025	1239	1 095 217	0.99	0.11	113	5.6
	Female	98 399	984	926 963	1.00	0.11	106	11.0
Cerebrovascular disease related mortality	All	223 424	1400	2 022 180	0.63	0.07	69	4.5
	Male	125 025	715	1 095 217	0.57	0.07	65	3.2
	Female	98 399	685	926 963	0.70	0.07	74	7.6
Decompensation related mortality	All	223 424	3139	2 022 180	1.40	0.16	155	10.1
	Male	125 025	2203	1 095 217	1.76	0.20	201	9.9
	Female	98 399	936	926 963	0.95	0.10	101	10.4
HCC related mortality	All	223 424	13 088	2 022 180	5.86	0.65	647	42.0
	Male	125 025	10 803	1 095 217	8.64	0.99	986	48.7
	Female	98 399	2285	926 963	2.32	0.25	247	25.5
Mortality data missing	All	223 424	481	2 022 180	0.22	0.02	24	1.5
	Male	125 025	298	1 095 217	0.24	0.03	27	1.3
	Female	98 399	183	926 963	0.19	0.02	20	2.0
Other mortality	All	223 424	5478	2 022 180	2.45	0.27	271	17.6
	Male	125 025	3594	1 095 217	2.87	0.33	328	16.2
	Female	98 399	1884	926 963	1.91	0.20	203	21.0

University, Nanjing, Jiangsu, China; ⁴Department of Infectious Diseases, The Affiliated Infectious Diseases Hospital of Soochow University, Suzhou, Jiangsu, China; ⁵Department of Infectious Diseases, Nanjing Drum Tower Hospital Clinical College of Nanjing University of Chinese Medicine, Nanjing, Jiangsu, China; ⁶Department of Hepatology, Huai'an No. 4 People's Hospital, Huai'an, Jiangsu, China
Email: dr.wu@nju.edu.cn

Background and aims: The metabolism disorder of serum phosphate is not uncommon in chronic liver diseases. This study investigated the prevalence of hypophosphatemia and the association between hypophosphatemia and liver fibrosis in treatment-naïve patients with chronic hepatitis B (CHB).

Method: Consecutive treatment-naïve CHB patients were included from three medical institutions between January 2015 and April 2022. Significant liver fibrosis and cirrhosis were identified by the aspartate transaminase (AST) to platelet ratio index (APRI), the fibrosis index based on 4 factors (FIB-4), or ultrasonography. Propensity score matching (PSM) and inverse probability weighting (IPW) measures were conducted to balance variables between patients with and without significant fibrosis or cirrhosis.

Results: Of 6,956 patients with CHB, the median age was 41.0 years and male gender accounted for 58.6%. The overall prevalence of hypophosphatemia was 2.7% in treatment-naïve patients with CHB. Patients with significant liver fibrosis and cirrhosis had higher proportions of hypophosphatemia than patients without significant liver fibrosis (4.4% vs. 1.9%, $P < 0.001$) and cirrhosis (4.3% vs. 2.2%, $P < 0.001$). Age ≥ 50 , male sex, and the presence of significant liver fibrosis (OR 1.817, 95% CI 1.291–2.558, $P = 0.001$) and cirrhosis (OR 1.595, 95% CI 1.116–2.279, $P = 0.010$) were independent risk factors of hypophosphatemia. After adjusting for age and sex by PSM and IPW, the prevalence of hypophosphatemia remained higher in patients with significant liver fibrosis and cirrhosis.

Conclusion: The proportion of hypophosphatemia was low in treatment-naïve patients with CHB. Hypophosphatemia was related to more severe liver disease, including significant liver fibrosis and cirrhosis. Close monitoring for hypophosphatemia is warranted in patients with CHB who have significant liver fibrosis or cirrhosis.

WED-141

Treatment eligibility and initiation among chronic hepatitis B patients in a real-world setting in the United States

Mark A Schmidt¹, Yihe G Daida², Sacha Satram³, Teresa M Kimes¹, A Gabriela Rosales¹, Sixiang Nie², Richard Meenan¹, Judy L Donald¹, Michael Chattergoon³, Norah Terrault⁴. ¹Kaiser Permanente Center for Health Research, Portland, OR, United States; ²Kaiser Permanente Center for Integrated Health Care Research, Honolulu, HI, United States; ³Vir Biotechnology, San Francisco, CA, United States; ⁴University of Southern California, Los Angeles, CA, United States
Email: mark.a.schmidt@kpchr.org

Background and aims: Current guidelines for chronic hepatitis B (CHB) management recommend using ALT and HBV DNA levels to guide treatment decisions and monitor individuals who are not in a well-defined immunological disease state ("grey area"), but this remains understudied in the real-world setting. We sought to describe the proportion of untreated CHB patients for whom either treatment or continued monitoring ("grey area") would be indicated and the proportion of those patients subsequently receiving treatment within one, two, and five years of cohort entry.

Method: We identified persons with untreated CHB from two integrated healthcare delivery systems in the United States from 1 January 2000 through 31 December 2015. We abstracted demographic, clinical, laboratory, and pharmacy data from the electronic health records. We first classified all individuals with a Fibrosis-4 score—a non-invasive, biomarker-based index of liver fibrosis—of ≥ 3.25 as *treatment indicated* and then applied the AASLD 2018 Hepatitis B Guidance to classify remaining persons into treatment categories (*grey area*, *treatment indicated*, *treatment not indicated*, and *unknown* [i.e. lacked sufficient laboratory and clinical elements required to assign individuals to another category]).

Results: We observed 2,434 individuals with untreated CHB, of whom 1,237 (50.8%) were female and 1,197 (49.2%), male; 1,565 (64.3%) were Asian, 315 (12.9%) White, 279 (11.5%) Native Hawaiian or Other Pacific Islander, and 275 (11.3%) of other or unknown race; and with a mean (median) age of 42.9 (42) years. At the time of cohort entry, we classified 138 (5.6%) as *treatment indicated*, 364 (15.0%) as *treatment not indicated*, 450 (18.5%) as *grey area*; and 1,482 (60.9%) as *unknown*. The proportion of those with an unknown treatment eligibility decreased from 82.0% in 2000 to 43.5% in 2015 (Figure), with increasing proportions of treatment not indicated and grey area

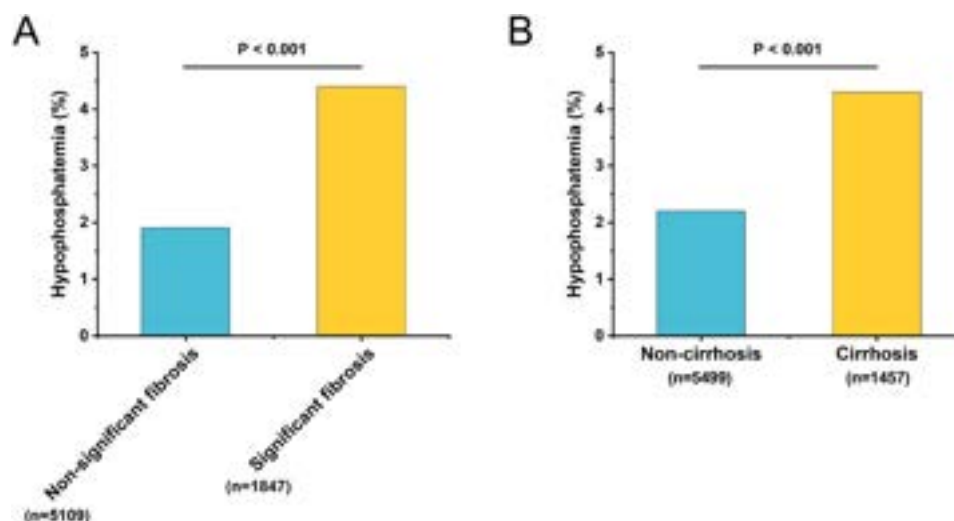


Figure: (abstract: WED-140): The prevalence of hypophosphatemia between patients with and without significant fibrosis/cirrhosis.

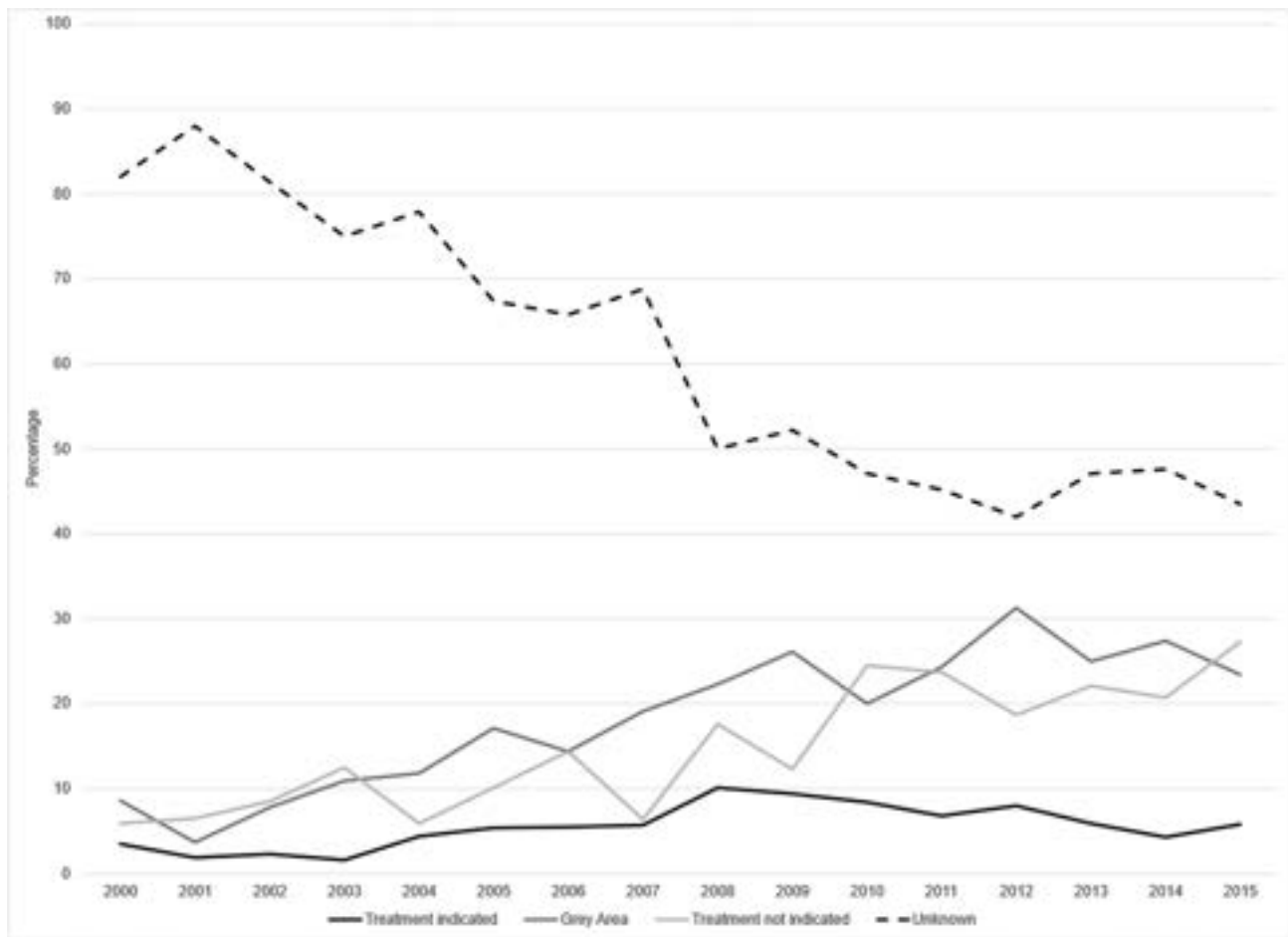


Figure: (abstract: WED-141): Treatment eligibility for individuals with CHB, by year of entry into cohort patients.

patients observed during this time ($p < 0.001$). The proportion of individuals classified as treatment indicated was largely stable. At 1-, 2-, and 5-years of study follow-up, 64 (46.4%), 69 (50.0%), and 75 (54.3%) of treatment indicated had initiated CHB treatment, respectively, as had 46 (10.2%), 59 (13.1%), and 85 (18.9%) of grey area individuals.

Conclusion: The lack of sufficient data to fully characterize treatment eligibility among individuals with CHB is worrisome, especially given that about half of those with treatment eligible CHB are untreated. Although it improved over the course of our study, this proportion has remained over 40%, even in more recent years. The results from this real-world study argue for continued improvement in CHB-related laboratory testing to help clinicians make appropriate treatment decisions for individuals with CHB, especially among those in the grey area who may transition into having active disease.

WED-142

Effects of tenofovir alafenamide fumarate on serum lipids in patients with chronic hepatitis B

Yilin Liu¹, Jian Wang^{2,3}, Zhiyi Zhang¹, Yao Zhang¹, Weimao Ding⁴, Chuanwu Zhu⁵, Rui Huang^{1,2,3}, Chao Wu^{1,2,3}, Jie Li^{1,2,3}. ¹Department of Infectious Diseases, Nanjing Drum Tower Hospital Clinical College of Traditional Chinese and Western Medicine, Nanjing University of Chinese Medicine, Nanjing, Jiangsu, China; ²Department of Infectious Diseases, Nanjing Drum Tower Hospital, The Affiliated Hospital of Nanjing University Medical School, Nanjing, Jiangsu, China; ³Institute of

Viruses and Infectious Diseases, Nanjing University, Nanjing, Jiangsu, China; ⁴Department of Hepatology, Huai'an No. 4 People's Hospital, Huai'an, Jiangsu, China; ⁵Department of Infectious Diseases, The Affiliated Infectious Diseases Hospital of Soochow University, Suzhou, Jiangsu, China

Email: lijier@sina.com

Background and aims: To evaluate the effect of tenofovir alafenamide fumarate (TAF) on lipid metabolism in patients with chronic hepatitis B (CHB).

Method: A total of 298 patients with CHB received antiviral treatment were included between January 2016 to December 2021, including 143 patients treated with TAF and 155 patients treated with tenofovir disoproxil fumarate (TDF). Logistic regression was used to analyze the risk factors for lipid elevation after 24 weeks of antiviral therapy.

Results: Compared to baseline, patients in TAF group had significantly increased total cholesterol (TC) levels (4.22 mmol/l vs. 4.48 mmol/l, $p = 0.009$) after 24 weeks of antiviral treatment, while triglyceride (TG) levels did not change significantly (1.01 mmol/l vs. 0.98 mmol/l, $p = 0.710$). Both TG and TC levels decreased significantly from baseline to 24 weeks in TDF group ($p < 0.001$). After propensity score matching on gender, age, BMI, the presence of fatty liver, alanine transaminase (ALT), TG, TC, and HBeAg status at baseline, there was a significant difference in the change of TG and TC levels at 24 weeks of treatment between the TAF and TDF groups ($p < 0.001$). The levels of TG (1.00 mmol/L vs. 0.76 mmol/L, $p = 0.001$) and TC (4.36 mmol/L vs. 3.67 mmol/L, $p < 0.001$) in TAF group were

significantly higher than in TDF group. Multivariate logistic regression analysis indicated that TAF treatment (OR = 3.646, 95% CI: 2.011–6.642, $p < 0.001$) and ALT level (OR = 1.002, 95% CI: 1.002–1.003, $p = 0.014$) were independent factors for over 10% increased of TC levels after 24 weeks of antiviral treatment.

Conclusion: TAF treatment was associated with increased TC levels in patients with CHB, while had no significant effect on TG levels.

WED-143

Novel serum markers of cccDNA transcriptional activity-HBcrAg and pre-genomic RNA and CXCL10 pro-inflammatory chemokine levels can reduce uncertainty of HBeAg-negative chronic hepatitis B phases

Ivana Carey¹, Mark Anderson², James Lok¹, Christiana Moigboi¹, Bo Wang¹, Gavin Cloherty², Geoffrey Dusheiko¹, Kosh Agarwal¹.

¹King's College Hospital, Institute of Liver Studies, London, United Kingdom; ²Abbott Diagnostics, Department of Infectious Diseases, Chicago, United States

Email: ivana.kraslova@kcl.ac.uk

Background and aims: Two phases of HBeAg-negative chronic hepatitis B are typically determined by HBV DNA and serum ALT concentrations. 'Infection' phase patients have HBV DNA levels <2000 IU/ml and normal ALT (monitoring is recommended), whereas patients in the 'hepatitis' phase have HBV DNA >20000 IU/ml, elevated ALT and moderate-severe liver inflammation on histology, requiring treatment. However up to one third of HBeAg-negative patients fall within a 'grey zone' (HBV DNA 2000–20000 IU/ml and normal ALT) between relatively inactive infection and active disease. Further categorisation of this "grey zone" cohort is required to improve prognostication and treatment indications. Unlike HBsAg, serum levels of hepatitis B core-related antigens (HBcrAg) and pre-genomic HBV RNA (pgRNA) are obligatorily derived from cccDNA, and hence reflect cccDNA transcriptional activity. Thus, these newer markers might be helpful in separating patients with HBeAg-negative infection from patients with more active disease and reduce the number of indeterminate 'grey zone' patients. As HBV disease activity is driven by the interaction of the virus with the host immune system response, serum levels of the pro-inflammatory chemokine CXCL10 could also help in refining 'grey zone' patients. We aimed to compare serum levels of serological, virological and immunological markers in HBeAg negative patients and to determine whether these markers could help in refining HBeAg-negative phases of disease based on HBV DNA and ALT levels (infection, versus grey zone and hepatitis).

Methods: Serum samples from a cross-sectional cohort of 447 HBeAg-negative patients (median age 38 yrs, 170 males) were tested for routine diagnostic markers: HBV DNA (Roche TaqMan, IU/ml), quantitative HBsAg (Abbott ARCHITECT, IU/ml), biochemical (ALT and AST, IU/L) and haematological (INR and platelets counts) and further tests were performed for novel biomarkers-HBcrAg (CLEIA Fujirebio, log₁₀U/ml), pgRNA (Abbott Diagnostics dual-target real-time-PCR assay, LLoQ = 0.48 log₁₀U/ml) and CXCL10 serum levels by ELISA [pg/ml]. FIB-4 and APRI scores were calculated and compared with fibroscan results. The patients were divided into 3 groups based on HBV DNA levels: 'infection' (<2000 IU/ml), 'grey zone' (2000–20 000 IU/ml) and 'hepatitis' (>20 000 IU/ml) phases. The results were compared by AUC-ROC, univariate and multivariate regression analysis.

Results: The levels of all the tested biomarkers were lower in 'infection' phase patients (n = 293) than in 'grey zone' (n = 121) and 'hepatitis' (n = 31) phase patients (Table) by univariate analysis. However, only levels of HBcrAg, pg RNA and CXCL10 differed significantly between groups by multivariate and AUC-ROC analysis (Figure). The proportion of patients with undetectable HBcrAg (<3 log₁₀U/ml) and pgRNA (<0.4 log₁₀U/ml) was highest in 'infection' phase patients than 'grey zone' and 'hepatitis' phase patients (HBcrAg: 64% vs. 25% vs. 6%; pgRNA: 75% vs. 24% vs. 8%, all <0.01).

	Infection phase (n=293)	Grey zone (n=121)	Hepatitis phase (n=31)	p
Median HBV DNA	183 IU/ml	4900 IU/ml	82500 IU/ml	<0.01
Median HBsAg	238.7 IU/ml	4830 IU/ml	5931 IU/ml	<0.01
Median HBcrAg	2.6 log ₁₀ U/ml	3.5 log ₁₀ U/ml	4.5 log ₁₀ U/ml	<0.01
Median pg RNA	1.22 log ₁₀ U/ml	2.13 log ₁₀ U/ml	2.43 log ₁₀ U/ml	<0.01
Median CXCL10	125 pg/ml	218 pg/ml	285 pg/ml	<0.01
Median FIB-4	0.85	0.97	1.08	0.02
Median APRI	0.22	0.26	3.79	<0.01
Median fibroscan	4.3	5.1	7.0	0.01

Figure:

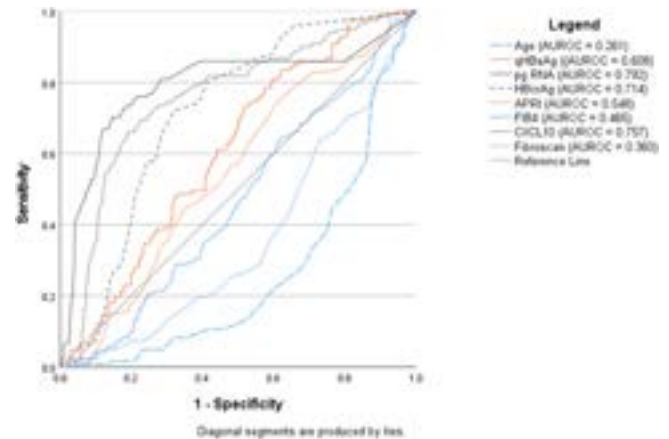


Figure:

Conclusion: Novel serum biomarkers of cccDNA transcriptional activity-HBcrAg and pre-genomic HBV RNA as well as serum CXCL10 levels (<150 pg/ml) can refine active versus inactive HBeAg-negative phases. If larger studies validating these markers confirm their prognostic significance, the finding of undetectable HBcrAg and HBV RNA (by current assay sensitivities) and low CXCL10 levels may qualify a prime group for whom monitoring is appropriate and reduce the uncertainty of 'grey zone' patients.

WED-144

HDV genotypes have an impact on pegylated interferon therapy response and long-term liver disease related outcomes

Ivana Carey¹, Natalie Bolton¹, Mark Anderson², James Lok¹, Christiana Moigboi¹, Gavin Cloherty², Geoffrey Dusheiko¹, Kosh Agarwal¹. ¹King's College Hospital, Institute of Liver Studies, London, United Kingdom; ²Abbott Diagnostics, Department of Infectious Diseases, Chicago, United States

Email: ivana.kraslova@kcl.ac.uk

Background and aims: Although chronic hepatitis delta (HDV) represents the most severe form of chronic viral hepatitis with accelerated rates of advanced liver fibrosis and hepatocellular carcinoma, it is a diverse disease due to differences between HDV genotypes and their impact on the disease outcome. The long-term follow-up (>5 years) data comparing differences of the outcomes between HDV genotypes are lacking. HDV requires HBsAg for propagation. HBsAg originates from both cccDNA and integrated HBV DNA encoded transcripts. Pre-genomic HBV RNA (pg RNA) and HBcrAg are markers of cccDNA transcriptional activity and there are no data comparing these markers according to HDV genotypes. We aimed to investigate whether different virological (HBV DNA, HDV RNA, HDV genotypes and pg RNA) and serological (HBeAg, HBsAg and HBcrAg) markers at diagnosis are able to predict long-term (>5 years) outcomes (morbidity, mortality, response to pegylated interferon (Peg-IFN) and HBsAg loss) in single centre cohort of HDV RNA positive patients.

Methods: Serum samples of 83 HDV RNA positive patients (median age 38 years, 55 males) at diagnosis were tested for the following markers: HBV DNA (Roche TaqMan, IU/ml), HBeAg status and

POSTER PRESENTATIONS

quantitative HBsAg (Abbott ARCHITECT, IU/ml), HBcrAg (CLEIA Fujirebio, log₁₀U/ml), pg RNA (Abbott Diagnostics dual-target real-time-PCR assay, LLoD=0.48 log₁₀U/ml), HDV RNA (in-house real-time PCR, LLoQ=640 copies/ml) and HDV genotypes by the direct sequencing. All patients had clinical follow-up for at least 5 years (median 6.8 years, range 5.3–17.5). Fifty-three (64%) patients underwent at least 24 weeks of therapy with Peg-IFN (>3 years follow-up results after completing therapy). The liver related complications (cirrhosis, decompensation, variceal bleeding, HCC), liver transplantation, mortality and peg-IFN response including HBsAg loss were recorded and compared between patients according to HDV genotypes.

Results: In our cohort-52 (63%) patients had genotype 1 infection vs. 31 (37%) patients infected with genotype 5. There was no difference in patients' age (38.4 vs 38.2 years, $p=0.89$) between genotypes. At diagnosis-cirrhosis was more frequent in genotype 1 than genotype 5 patients (60% vs. 23%, $p<0.01$) and genotype 1 patients ($n=30$) had poorer response to peg-IFN therapy than genotype 5 ($n=23$) patients (7% vs. 61%, $p<0.01$) and less likely achieved HBsAg loss (2% vs. 16%, $p<0.01$). Only virological markers (HDV RNA and pg RNA) were higher in genotype 1 vs. genotype 5 patients and other markers (HBV DNA, HBeAg status, HBsAg, HBcrAg and ALT levels) were similar at diagnosis between genotypes (Table). While there was no difference between numbers of patients who developed HCC between genotypes (4% vs. 6%, $p=0.621$), genotype 1 patients were more likely to have liver related complications-decompensation (32% vs. 10%, $p=0.02$), variceal bleeding (6% vs. 3%, $p=0.04$) or required liver transplantation (23% vs. 3%, $p=0.003$) than genotype 5 patients. The mortality was similar between genotypes (8% vs. 6%, $p=0.646$).

	Genotype 1 (n=52)	Genotype 5 (n=31)	p
Median HBV DNA	0 IU/ml	0 IU/ml	0.877
Median HBsAg	9672 IU/ml	10294 IU/ml	0.261
Median HBcrAg	4 log ₁₀ U/ml	3.5 log ₁₀ U/ml	0.279
Median pg RNA	2.77 log ₁₀ U/ml	1.99 log ₁₀ U/ml	0.03
Median HDV RNA	1.29E5 cp/ml	3.24E4 cp/ml	0.002
Median ALT	67 IU/L	67 IU/L	0.202
Median fibroscan	13.5 kPa	8.5 kPa	<0.01
HBeAg positive [%]	23%	23%	0.958

Figure:

Conclusion: Differences between Peg-IFN responses, liver damage (cirrhosis) and long-term risk of liver disease decompensation were attributed to HDV genotypes in HDV RNA positive patients. Genotype 5 patients were more likely respond to Peg-IFN and had slower progression of liver disease. Lower levels of HDV RNA and pg RNA were more frequent in genotype 5 patients and were linked with better Peg-IFN response and slower disease progression.

WED-145

Systematic screening for hepatitis B at emergency department and linkage to care in Barcelona, Spain

Juan Carlos Ruiz-Cobo¹, Jordi Llaneras², Ariadna Rando-Segura³, Ana Barreira¹, Francisco Rodríguez-Frías³, Adriana Palom¹, Anna Feliu-Prius¹, Mar Riveiro Barciela^{1,4}, Rafael Esteban^{1,4}, Maria Buti^{1,4}. ¹Vall d'Hebron University Hospital, Hepatology, Barcelona, Spain; ²Vall d'Hebron University Hospital, Spain; ³Vall d'Hebron University Hospital, Microbiology, Spain; ⁴CIBERhd, Spain
Email: mbuti@vhebron.net

Background and aims: Spain is considered a low endemicity country for hepatitis B virus (HBV) infection. This is based on a prevalence of HBsAg of 0.22% in the general population attended in primary care centers. Our aim is to perform a screening program for HBV at emergency department where population not attending primary care

centers are represented and analyze the barriers to linkage to care of patients with HBV infection.

Method: We implemented FOCUS program for HBV screening at the emergency department of an academic hospital of an area of 450.000 inhabitants. Adults of >16 years old without HBsAg testing in the previous three months who required a phlebotomy for any purpose were screened. Linkage to care was offered to all patients with a positive result.

Results: We screened 20,941 patients between February 2020 and December 2022, detecting 128 (0.61%) HBsAg positive individuals. The majority were men (67.2%), median age of 61.4 years (IQR 28.8), 98.4% were HBeAg negative and 14% patients had cirrhosis. Anti-HDV was positive in 5 (3.9%) patients and 2 of them had detectable HDV-RNA. Only 12.5% had a risk factor for HBV infection screening following Spanish recommendations. At the time of screening 80 (62.5%) patients were not linked to care or lost to follow-up including 51 (63.8%) who were unaware of HBV and 5 patients with cirrhosis. Of them 63 patients were selected for linkage to care, the reason to not be suitable for linkage were low life expectancy or lack of contact information. Among these patients, 54 (85.7%) were successfully linked to care and 43 had HBeAg-negative chronic infection, 8 HBeAg-negative chronic hepatitis and 3 HBeAg-positive chronic hepatitis. Treatment with nucleos (t)ides analogues was initiated in 9 patients without prior HBV care.

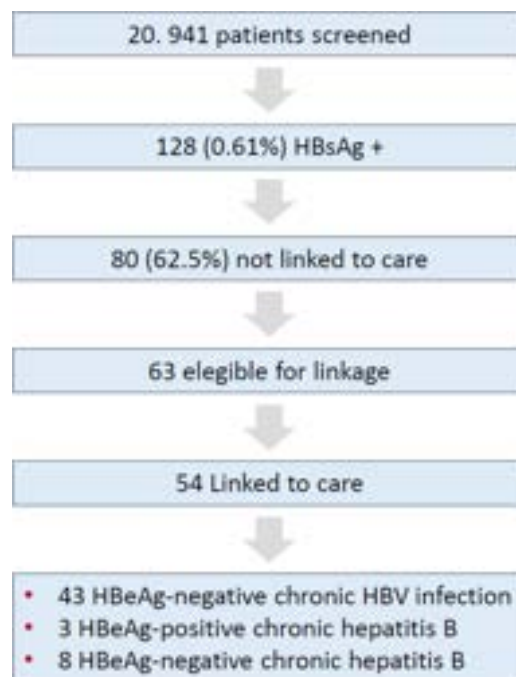


Figure:

Conclusion: The prevalence of HBV in the emergency department is almost three times higher than observed in general population, showing that this strategy allows to identify and link to care a high number of patients without risk factors. In addition, coinfection with HDV is reported in 3.9% of HBsAg positive cases.

WED-146

Epidemiological and clinical profile of HDV infected people in care in Italy: interim analysis from the ongoing PITER cohort

Loreta Kondili¹, Maria Elena Tosti¹, Maria Giovanna Quaranta¹, Alessia Ciancio², Vincenzo Messina³, Giuseppina Brancaccio⁴, Maurizio Brunetto⁵, Mario Capasso⁶, Valerio Rosato⁷, Irene Cacciola⁸, Luisa Pasulo⁹, Teresa Santantonio¹⁰, Carmine Coppola¹¹, Elisa Biliotti¹², Francesco Barbaro⁴, Marco Massari¹³, Nicola Coppola¹⁴, Alberto Ferrarese¹⁵, Francesco Paolo Russo⁴, Vito Di Marco¹⁶, Aldo Marrone¹⁴, Simona Schivazappa¹⁷,

Alessandro Federico¹⁴, Pierluigi Blanc¹⁸, Alba Rocco⁶, Giulia Morsica¹⁹, Donatella Ieluzzi²⁰, Fabio Conti²¹, Martina De Siena²², Maria Grazia Bavetta¹⁶, Michele Milella²³, Ivan Gentile⁶, Carmen Porcu²⁴, Liliana Chemello⁴, Monia Maracci²⁵, Anna Linda Zignego²⁶, Leonardo Baiocchi²⁷, Ivana Rita Maida²⁸, Barbara Coco⁵. ¹Italian National Institute of Health, Roma, Italy; ²Azienda Ospedaliero-Universitaria Città della Salute e della Scienza di Torino, Torino, Italy; ³Sant'Anna Hospital, Caserta, Italy; ⁴University of Padua, Padova, Italy; ⁵University of Pisa, Pisa, Italy; ⁶University of Naples Federico II, Napoli, Italy; ⁷Villa Betania Evangelical Hospital, Napoli, Italy; ⁸The University of Messina, Messina, Italy; ⁹ASST Papa Giovanni XXIII Hospital, Bergamo, Italy; ¹⁰Università degli studi di Foggia, Foggia, Italy; ¹¹Gragnano Hospital, Gragnano (NA), Italy; ¹²National Institute of Infectious Diseases Lazzaro Spallanzani, Roma, Italy; ¹³Azienda Unità Sanitaria Locale, IRCCS di Reggio Emilia, Italy; ¹⁴University of Campania "Luigi Vanvitelli", Caserta, Italy; ¹⁵University Hospital Borgo Trento, Italy; ¹⁶Università degli Studi di Palermo, Palermo, Italy; ¹⁷University of Parma Hospital, Parma, Italy; ¹⁸Santa Maria Annunziata Hospital, Grassano, Italy; ¹⁹San Raffaele Hospital, Milano, Italy; ²⁰University of Verona, Verona, Italy; ²¹Hospital of Faenza, A.U.S.L. of Romagna, Italy; ²²Agostino Gemelli University Policlinic, Rome, Italy; ²³University of Bari, Bari, Italy; ²⁴Università degli Studi di Cagliari, Monserrato, Italy; ²⁵Azienda Osp. Riuniti Marche Nord, Italy; ²⁶University of Florence, Firenze, Italy; ²⁷University of Rome "Tor Vergata", Italy; ²⁸University of Sassari, Sassari, Italy

Email: loreta.kondili@iss.it

Background and aims: With the new therapeutic options available for hepatitis delta infection, epidemiological and clinical profile of patients in care are useful to determine better treatment appropriateness. We aimed to describe the updated epidemiological and clinical profile of HDV infected patients in the PITER HBV cohort.

Method: Data from consecutive HBsAg positive patients enrolled from 2019 up to October 2022 by 50 Clinical centers were evaluated.

Results: Of 4729 patients of whom 1010 (21%) were non-Italian natives, the anti-HDV prevalence was 9.3% (343 of 3679 anti-HDV tested patients): 8.3% (median age 57.5; IQR 53–64) Italian, 13.0% (median age 43 years IQR 43–53 years) non-Italian natives ($p < 0.001$); 22% (1050) have never been tested for HDV infection (23% in Italian and 19% in non-Italian; $p < 0.001$), of whom 21% with liver cirrhosis. Of anti-HDV positive patients, 212 (62%) were tested for HDV RNA, of whom 140 (66%) were HDV RNA positive. Of anti-HDV positive patients, transaminase levels were altered in 63%, cirrhosis was present in 70% (57.5% in Italian and 75.5% in non-Italians; $p = 0.001$), of whom portal hypertension signs in 55%, cirrhosis complications and/or HCC development in 37.5%. Liver disease progression cofactors were present as follows: alcohol use 35.6% (similar in Italians and non-Italians), HCV infection in 11.1% (15.5% in Italian and 1.8% in non-Italian, $p < 0.001$), diabetes in 6.1% (7.5% in Italians and 1.9 in non-Italian $p < 0.001$), other features of potential metabolic syndrome in 23.9%. Overall, 52.8% of patients have no comorbidities, 40.8% has 1–2, 6.4% more than 2 comorbidities.

Conclusion: The updated picture of patients in care in Italy confirms the older Italian cohort and significantly younger non-Italian cohort of patients in care with HDV infection, both with significant proportion of liver cirrhosis. The dysmetabolic comorbidities are more represented in Italians, but the overall comorbidity profile is similar between two cohorts.

WED-147

Effect of Tenofovir and Entecavir on occurrence of hepatocellular carcinoma depends on duration of antiviral treatment and hierarchical PAGE-B risk score

Yi-Hsiang Huang^{1,2,3}, Tsung-Hui Hu⁴, Ming-Lung Yu^{5,6,7}, Chao-Hung Hung^{8,9}, Pin-Nan Cheng^{10,11}, Cheng-Yuan Peng^{12,13}, Chun-Jen Liu^{14,15}, Jyh-Jou Chen¹⁶, Chieh-Ju Lee¹⁷, Rong-Nan Chien^{18,19}. ¹Institute of Clinical Medicine, National Yang Ming Chiao Tung University School of Medicine, Taiwan; ²Taipei Veterans General Hospital, Taipei, Division of Gastroenterology and Hepatology, Department of Medicine, Taiwan; ³Taipei Veterans General Hospital, Therapeutic and Research Center of Liver Cancer, Taipei, Taiwan; ⁴Kaohsiung Chang Gung Memorial Hospital, Division of Hepatogastroenterology, Department of Internal Medicine, Kaohsiung, Taiwan; ⁵Kaohsiung Medical University Hospital, Hepatobiliary Division, Department of Internal Medicine and Hepatitis Center, Taiwan; ⁶Kaohsiung Medical University, Taiwan; ⁷National Sun Yat-sen University, School of Medicine, College of Medicine and Center of Excellence for Metabolic Associated Fatty Liver Disease, Taiwan; ⁸Kaohsiung Chang Gung Memorial Hospital, Division of Hepatogastroenterology, Department of Internal Medicine, Taiwan; ⁹ChiaYi Chang Gung Memorial Hospital, Division of Hepatogastroenterology, Department of Internal Medicine, Taiwan; ¹⁰National Cheng Kung University Hospital, Division of Gastroenterology and Hepatology, Department of Internal Medicine, Taiwan; ¹¹National Cheng Kung University, College of Medicine, Taiwan; ¹²China Medical University Hospital, Center for Digestive Medicine, Department of Internal Medicine, Taiwan; ¹³China Medical University, Taiwan; ¹⁴National Taiwan University College of Medicine, Graduate Institute of Clinical Medicine, Taiwan; ¹⁵National Taiwan University Hospital, Division of Gastroenterology and Hepatology, Taiwan; ¹⁶Chi-Mei Medical Center, Liouying, Taiwan; ¹⁷Taipei Veterans General Hospital, Division of Gastroenterology and Hepatology, Department of Medicine, Taiwan; ¹⁸Linkou Medical Center, Chang Gung Memorial Hospital, Division of Hepatology, Department of Gastroenterology and Hepatology, Taiwan; ¹⁹Keelung Medical Center, Chang Gung Memorial Hospital, Division of Hepatology, Department of Gastroenterology and Hepatology, Taiwan
Email: yhhuang@vghtpe.gov.tw

Background and aims: The nucleos (t)ide analogues (NUCs) entecavir (ETV) and tenofovir disoproxil fumarate (TDF) have been extensively used for the prevention of hepatocellular carcinoma (HCC) in chronic hepatitis B (CHB) patients. However, their comparative efficacy in this regard remains controversial and requires further investigation.

Method: This retrospective, multicenter, study included CHB patients that have been diagnosed with cirrhosis and received ETV or TDF treatment between January 2008 to December 2018, and 2011 to 2018. Risk factor analysis, 1:1 propensity score matching (PSM), and PAGE-B scores were employed in this investigation. Primary outcome included the evaluation of HCC incidence after treatment with either ETV or TDF.

Results: TDF demonstrated a consistently lower risk of HCC occurrence compared to ETV (HR = 0.65; $p = 0.001$), which was maintained after 1:1 PSM (HR = 0.69, $p = 0.030$). But the 2011–2018 time-adjusted analysis revealed that this positive effect was not significantly observed after 1:1 PSM. A higher proportion of ETV patients with PAGE-B scores ≥ 18 before PSM might be the confounder that could be eliminated after PSM in both 2008–2018, and time-adjusted cohort. Interestingly, in subgroup patients with

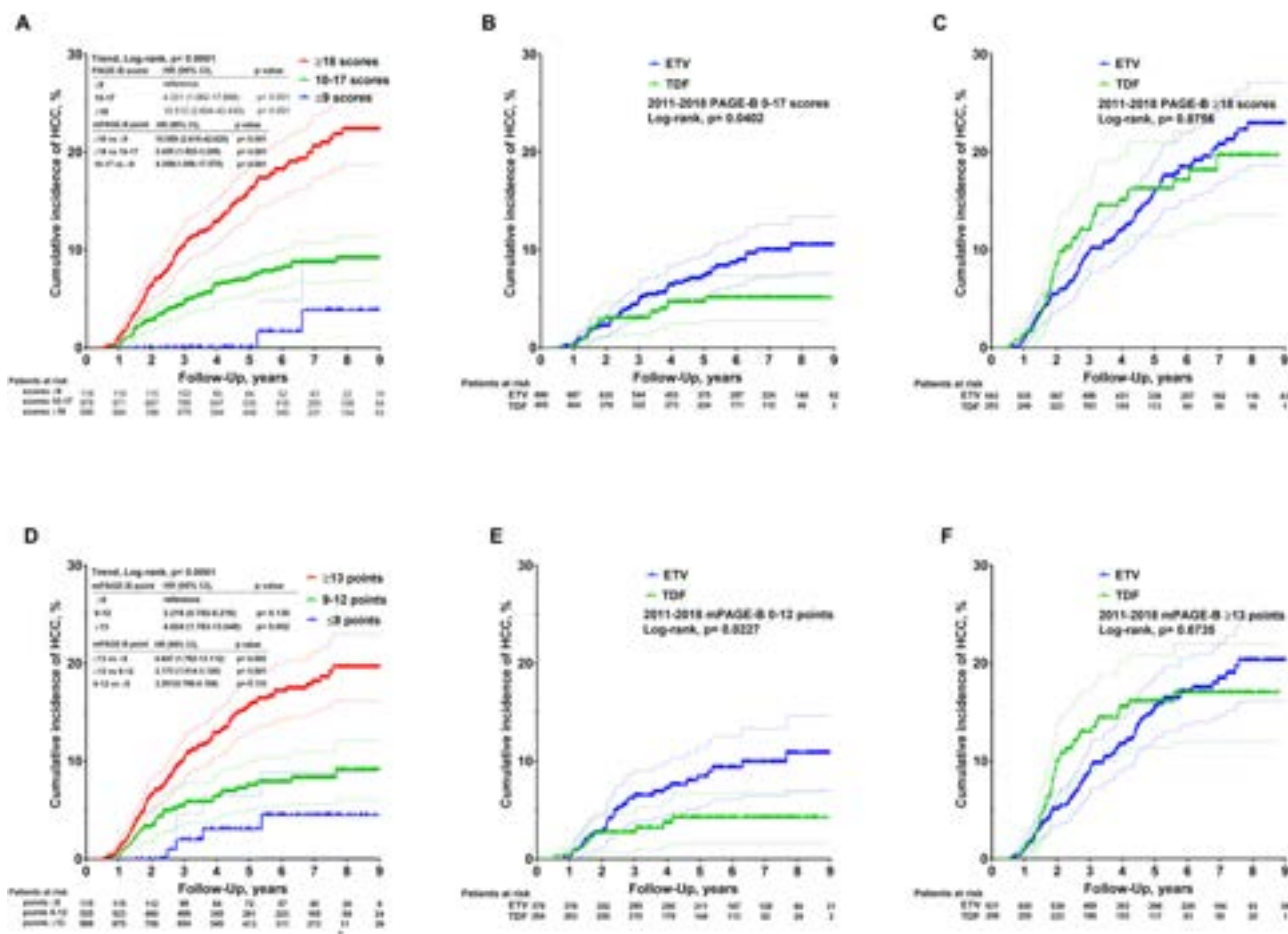


Figure: (abstract: WED-147).

lower PAGE-B scores (0–17), TDF displayed a significantly reduced risk of HCC occurrence than ETV (HR = 0.58, $p = 0.043$), which was maintained even after the 1:1 PSM adjustment (HR = 0.56, $p = 0.048$). **Conclusion:** Duration of antiviral treatment and hierarchical risk scores have impact on outcome analysis to compare ETV vs TDF. TDF intervention, when compared to ETV, elicits favorable outcomes by reducing the occurrence of HCC in patients with lower PAGE-B scores.

WED-148

Significant disparities in risk of cirrhosis and hepatocellular carcinoma among non-cirrhotic, treatment naïve, e-antigen negative hepatitis B patients with low levels of serum alanine aminotransferase

Zeyuan Yang¹, Ramsey C. Cheung², Robert Wong². ¹VA Palo Alto Health Care System, Palo Alto, United States; ²Stanford University School of Medicine, VA Palo Alto Healthcare System, Palo Alto, United States
 Email: rwong123@stanford.edu

Background and aims: The benefit of antiviral therapy in patients with e-antigen (eAg) negative chronic hepatitis B (CHB) with low levels of alanine aminotransferase (ALT) remains unclear given the reported low risk of cirrhosis or hepatocellular carcinoma (HCC). However, it is not clear whether significant heterogeneity in cirrhosis or HCC risk exists, such that certain subsets of this population may benefit from early initiation of antiviral therapy. We evaluated long-term risks of cirrhosis or HCC among non-cirrhotic, treatment-naïve eAg-negative CHB patients with ALT <70 U/L.

Method: Using data from the U.S. National Veterans Affairs database from 2010 to 2022, Veterans with treatment-naïve, e-antigen (eAg)

negative CHB with baseline ALT <70 U/L and minimum 12 months of follow-up were identified. Patients with concurrent HIV, hepatitis C, or hepatitis delta infections were excluded. Patients with cirrhosis or HCC at baseline or within 6 months of study entry were excluded. Incidence of cirrhosis or HCC (per 100 person-years) was stratified by patient demographics, clinical characteristics, and baseline HBV DNA (<2000 IU/ml (Low-DNA), 2000–10⁵ IU/ml (Intermediate-DNA), and >10⁵ IU/ml (High-DNA)). Patients were censored at development of cirrhosis or HCC, death, initiation of antiviral therapy, or end of follow-up period. Comparisons of cirrhosis or HCC incidence between groups utilized the z-statistic using standard equations.

Results: Among 1,531 Veterans with treatment-naïve, eAg negative CHB and ALT <70 U/L (91.4% men, 45% African American, 33% non-Hispanic white, 19% Asian, 4% Hispanic, mean age 55 ± 12, 26.6% with diabetes), 77% had Low-DNA, 15% had Intermediate-DNA, and 7% had High-DNA. Overall incidence of cirrhosis was 0.84 per 100 person-years (95% CI 0.67–1.00) and incidence of HCC was 0.21 per 100 person-years (95% CI 0.12–0.29). No significant difference in long-term risk of cirrhosis or HCC was observed by baseline HBV DNA. When stratified by race/ethnicity, the highest risk of cirrhosis was observed in non-Hispanic whites (1.11 per 100 person-years) and the lowest risk was observed in Hispanics (0.23 per 100 person-years), whereas the highest risk of HCC was observed in non-Hispanic whites (0.25 per 100 person-years) and the lowest risk of HCC was observed in Asians (0.05 per 100 person-years). Older age, presence of concurrent diabetes, and higher FIB-4 score at baseline were associated with higher risk of cirrhosis and HCC (Figure).

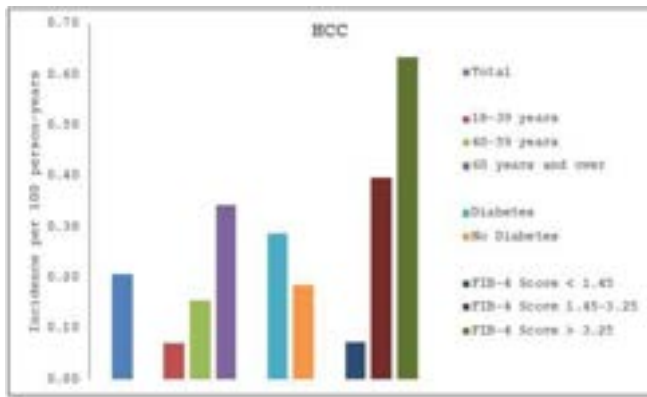


Figure:

Conclusion: Among a large national cohort of treatment-naïve eAg negative patients with non-cirrhotic CHB and baseline ALT <70 U/L, we observed significant heterogeneity in risks of cirrhosis or HCC. Better understanding which sub-populations are at highest risk of disease progression can help guide clinical decisions regarding earlier initiation of antiviral therapy in this group to improve long-term patient outcomes.

WED-149

aMAP score and its combination with liver stiffness measurement accurately assess liver fibrosis in virologically suppressed CHB patients

Rong Fan¹, Guanlin Li^{2,3}, Ning Yu¹, Xiu-Juan Chang⁴, Tamoore Arshad⁵, Wen-Yue Liu⁶, Yan Chen⁴, Grace Lai-Hung Wong^{2,3}, Yiyue Jiang¹,

Xieer Liang¹, Yongpeng Chen¹, Xiao-Zhi Jin⁷, Zheng Dong⁴, Howard Ho-Wai Leung⁸, Xiaodong Wang⁹, Zhen Zeng⁴, Terry Cheuk-Fung Yip^{2,3}, Qing Xie¹⁰, Deming Tan¹¹, Shaoli You⁴, Dong Ji⁴, Jun Zhao⁴, Arun Sanyal¹², Jian Sun¹, Ming-Hua Zheng^{7,9}, Vincent Wai-Sun Wong^{2,3}, Yongping Yang⁴, Jinlin Hou¹. ¹Guangdong Provincial Key Laboratory of Viral Hepatitis Research, Guangdong Provincial Clinical Research Center For Viral Hepatitis, Department of Infectious Diseases, Nanfang Hospital, Southern Medical University, Guangzhou, China; ²Medical Data Analytics Center, Department of Medicine and Therapeutics, The Chinese University of Hong Kong, Hong Kong; ³State Key Laboratory of Digestive Disease, Institute of Digestive Disease, The Chinese University of Hong Kong, Hong Kong; ⁴Senior Department of Hepatology, Fifth Medical Center of Chinese PLA General Hospital, Beijing, China; ⁵Department of Internal Medicine, Virginia Commonwealth University, Richmond, VA, United States; ⁶Department of Endocrinology, the First Affiliated Hospital of Wenzhou Medical University, Wenzhou, China; ⁷NAFLD Research Center, Department of Hepatology, the First Affiliated Hospital of Wenzhou Medical University, Wenzhou, China; ⁸Department of Anatomical and Cellular Pathology, The Chinese University of Hong Kong, Hong Kong; ⁹Key Laboratory of Diagnosis and Treatment for the Development of Chronic Liver Disease in Zhejiang Province, Wenzhou, China; ¹⁰Department of Infectious Diseases, Ruijin Hospital, Shanghai Jiao Tong University School of Medicine, Shanghai, China; ¹¹Department of Infectious Diseases, Xiangya Hospital, Central South University, Changsha, China; ¹²Division of Gastroenterology, Virginia Commonwealth University, Richmond, VA, United States
Email: jlhoumu@163.com

Background and aims: The changes in liver stiffness measurement (LSM) are unreliable to estimate regression of fibrosis during antiviral

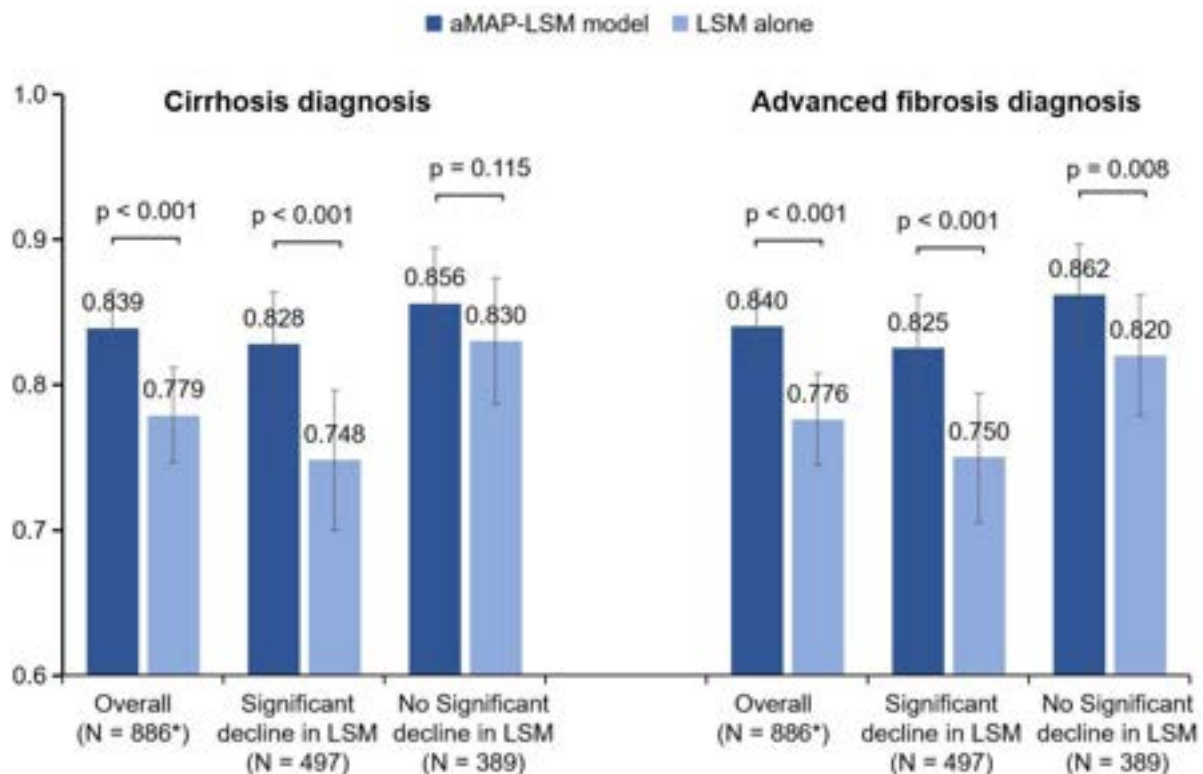


Figure. Comparison between the AUROCs of aMAP-LSM model and LSM alone in diagnosing cirrhosis and advanced fibrosis after treatment among the overall patients and the subgroups of patients stratified by LSM changes during antiviral treatment. *3 patients without available LSM were excluded from the analysis.

Figure: (abstract: WED-149).

POSTER PRESENTATIONS

treatment for chronic hepatitis B (CHB) patients. aMAP score [J Hepatol, 2020], as an accurate hepatocellular carcinoma risk score, may reflect the liver fibrosis stage. Here, we aimed to evaluate the performance of aMAP for diagnosing liver fibrosis in CHB patients with or without treatment.

Method: 2053 patients with liver biopsy from 2 real-world cohorts and 2 multi-centric randomized controlled trials in China were enrolled, among which 2053 CHB were included in the cross-sectional analysis, and 889 CHB patients with paired liver biopsies before and after 72- or 104-week treatment were included in the longitudinal analysis.

Results: In the cross-sectional analysis, the AUROCs of aMAP in diagnosing cirrhosis and advanced fibrosis were 0.788 and 0.757, which were significantly higher or comparable with those of fibrosis index based on four factors (FIB-4, 0.763, $p = 0.010$; 0.753, $p = 0.694$) and aspartate aminotransferase-platelet ratio (APRI, 0.607, $p < 0.001$; 0.613, $p < 0.001$), respectively. Lower and higher cut-off values for each non-invasive test were selected to obtain sensitivity and specificity of 90% or 95%, respectively. When applying these dual cut-off values, aMAP had a trend toward better performance than FIB-4 and APRI with a numerically smaller uncertainty area (UA) and a higher diagnostic accuracy (DA) in diagnosing cirrhosis. The UA was 68.3% for aMAP with DA of 85.2% in cirrhosis detection (74.2%, 84.5% for FIB-4, and 79.0%, 78.0% for APRI, respectively). Moreover, compared with stepwise approaches using FIB-4 (or APRI) and LSM, the stepwise approach using aMAP and LSM also had the smallest UA and satisfactory DA in both cirrhosis (UA: 29.7%; DA: 82.3%) and advanced fibrosis (UA: 46.2%; DA: 79.8%) detection. In the longitudinal analysis, among patients with significant decline in LSM after anti-HBV treatment (defined as LSM at week 72 or 104 decreased $\geq 30\%$ from baseline), the performance of LSM at week 72 (or 104) in diagnosing cirrhosis or advanced fibrosis was unsatisfactory, the AUROCs of which were significantly lower than those without significantly decline (cirrhosis: 0.748 vs. 0.830, $p = 0.012$; advanced fibrosis: 0.750 vs. 0.820, $p = 0.024$). We further established a novel model (aMAP-LSM model) comprising aMAP at baseline, LSM at week 72 (or 104) with or without aMAP at week 72 (or 104) by using logistic regression, which had satisfactory performance in diagnosing cirrhosis and advanced fibrosis after treatment (AUROC: 0.839 and 0.840, respectively), especially for those with significant decline in LSM after treatment (vs. LSM alone: 0.828 vs. 0.748, $p < 0.001$ [cirrhosis]; 0.825 vs. 0.750, $p < 0.001$ [advanced fibrosis]) (Figure).

Conclusion: aMAP score is a promising non-invasive tool for diagnosing fibrosis in CHB patients. The aMAP-LSM model could accurately estimate fibrosis stage for treated CHB patients.

WED-150

Systematic review and meta-analysis: the proportion of chronic hepatitis B patients with different alanine transaminase upper limits and significant hepatic histology

Yuhao Yao¹, Jiaxin Zhang^{1,2}, Xu Cao¹, Xiaoke Li^{1,2}, Xiaobin Zao^{1,2}, Yong'an Ye^{1,2}. ¹Dongzhimen Hospital, Beijing University of Chinese Medicine, China; ²Beijing University of Chinese Medicine, Liver Diseases Academy of Traditional Chinese Medicine, China
Email: yeyong'an@vip.163.com

Background and aims: The proportion of chronic hepatitis B patients (CHB) patients without a history of oral anti-viral medications or interferon use with normal alanine transaminase (ALT) and hepatic histology has been the focus of current research. ALT is one of the most important indicators for initiating antiviral therapy, however, ALT levels alone may not accurately reflect hepatic histology. Furthermore, the current ALT upper limit of normal (ULN) recommended by global guidelines for initiating antiviral therapy varies, leading to controversy on the most appropriate ALT ULN. Thus, this review aims to systematically evaluate the proportion of CHB patients with different ALT upper limits and significant hepatic histology, to provide a reference for the clinical management of this population.

Method: The Medline and EMBASE databases were searched from inception up to November 2022 with the following terms: "Hepatitis B OR "Hepatitis B virus" OR "Hepatitis B, Chronic" OR "chronic hepatitis B" OR "CHB" OR hepatitis B" AND "Alanine Trans-aminase OR "alanine aminotransferase" OR ALT". 'Significant histology' included 'significant fibrosis' and 'significant inflammation'. 'Significant fibrosis' was defined as stage ≥ 2 (Metavir, Batts-Ludwig, HAI, Scheuer or Ishak staging systems) and 'significant inflammation' was defined as stage ≥ 2 (Metavir, Batts-Ludwig or Scheuer staging systems) or score ≥ 4 (Ishak or HAI scoring systems) in the meta-analysis, which was consistent across all studies. Studies with just one of the two outcomes were included in the meta-analysis. Estimation of pooled proportions was calculated using transformed proportions using Freedman-Tukey double arcsine transformation. The protocol was registered at PROSPERO (CRD42021265642, <http://www.crd.york.ac.uk/PROSPERO>).

Results: Twenty studies with 3,624 CHB patients with ALT \leq ULN were included. All patients had no history of prior antiviral or interferon therapy. Most of the patients had HBV DNA levels > 2000 – $20\,000$ IU/ml. The pooled rates of significant fibrosis and significant inflammation in CHB patients with ALT ≤ 40 IU/L were 34.49% (95% CI: 24.31–45.44) and 21.57% (95% CI: 9.20–37.38), respectively. In studies in which ALT upper limits were set below 40 IU/L, significant fibrosis and significant inflammation were observed in 25.61% (95% CI: 16.43–36.03) and 16.68% (95% CI: 6.05–31.21) CHB patients, respectively, without limiting the upper limits. Among studies evaluating CHB patients with ALT ≤ 30 IU/L (males) and 19 IU/L (females), significant fibrosis and significant inflammation were detected in 17% (95% CI: 9.47–26.19) and 14.76% (95% CI: 2.07–36.09), respectively. The comparison of the proportions of CHB patients with significant fibrosis and significant inflammation for different ALT ULN levels was shown in Figure H.

Conclusion: Among untreated CHB patients with normal ALT, a certain percentage of patients still have significant hepatic histology. Approximately one-third of CHB patients with ALT ≤ 40 IU/L may have significant hepatic fibrosis and one-fifth have significant hepatic inflammation. However, the lower the ALT ULN levels set, the lower the proportion of patients with significant histology. Those CHB patients with normal ALT but significant hepatic histology are of concern to clinicians, and further evaluation and treatment may be warranted. Moreover, our study may be helpful for further negotiation of ALT ULN for initiating antiviral therapy.

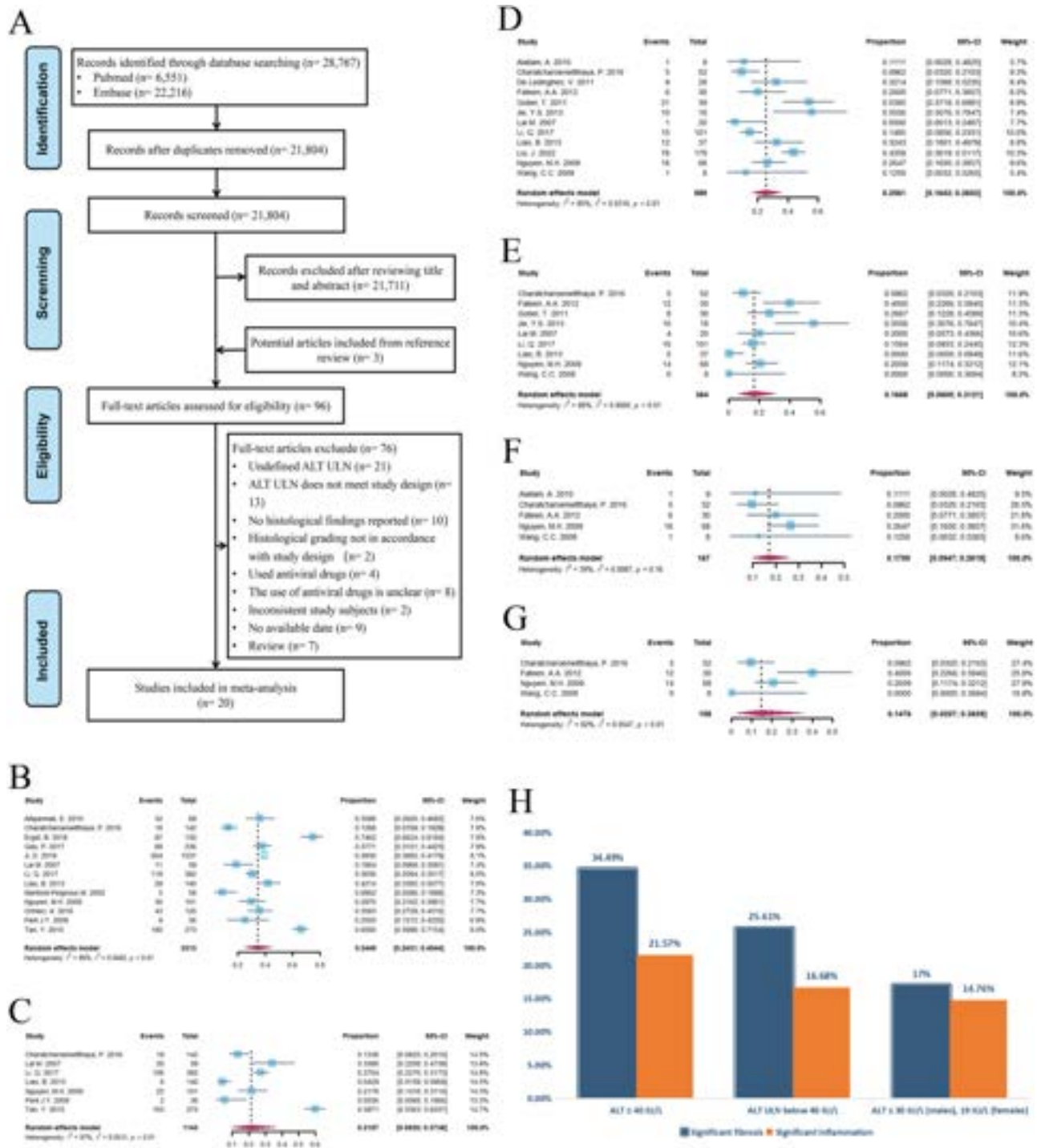


Figure: (abstract: WED-150).

WED-151

Self-stigma in chronic hepatitis B: content and psychometric validation of a new patient-reported outcome instrument

Robert G. Gish¹, Mondher Toumi², Jack Wallace³, Chari Cohen¹, Su Wang^{4,5}, Chris Marshall⁶, Helen Kitchen⁶, Jake Macey⁶, Hannah Pegram⁶, Carrie Houts⁷, Rikki Mangrum⁷, Ashley F. Slagle⁸, Jeffrey Lazarus^{9,10}, Patrick Kennedy¹¹, Florian van Bömmel¹², Maurizia Brunetto¹³, Qin Ning¹⁴, Hiroshi Yatsuhashi^{15,16}, Markus Cornberg¹⁷, Qing Xie¹⁸, Dee Lee¹⁹, Angelina Villasis Keever²⁰, Urbano Sbarigia²¹, Yasushi Takahashi²², John Jerzowski²³, Willem Talloen²¹, Michael Biermer²¹, Eric Chan²⁰. ¹Hepatitis B

Foundation, Doylestown, United States; ²Aix-Marseille University, Jardin du Pharo, Marseille, France; ³Burnet Institute, Melbourne, Australia; ⁴Cooperman Barnabas Medical Center, Florham Park, United States; ⁵World Hepatitis Alliance, London, United Kingdom; ⁶Clarivate (formerly DRG Abacus), London, United Kingdom; ⁷Vector Psychometric Group, Chapel Hill, United States; ⁸Aspen Consulting, LLC, Steamboat Springs, United States; ⁹Barcelona Institute for Global Health (ISGlobal), Barcelona, Spain; ¹⁰CUNY Graduate School of Public Health and Health Policy (CUNY SPH), New York, United States; ¹¹Barts and The London School of Medicine and Dentistry, London, United Kingdom; ¹²Division of

POSTER PRESENTATIONS

Hepatology, Department of Medicine II, Leipzig University Medical Center, Leipzig, Germany; ¹³University Hospital of Pisa, Pisa, Italy; ¹⁴Tongji Hospital, Tongji Medical College, Huazhong University of Science and Technology, Hankou, Wuhan, China; ¹⁵National Hospital Organization (NHO) Nagasaki Medical Center, Kubara, Omura, Nagasaki, Japan; ¹⁶Nagasaki University Graduate School of Biomedical Sciences, Nagasaki City, Japan; ¹⁷Hannover Medical School, Hannover, Germany; ¹⁸Shanghai Jiao Tong University School of Medicine, Ruijin Hospital, Shanghai, China; ¹⁹Inno Community Development Organisation, Guangzhou, Guangdong, China; ²⁰Janssen Global Services, LLC, Raritan, United States; ²¹Janssen Pharmaceutica NV, Beerse, Belgium; ²²Janssen Pharmaceutical K.K., Tokyo, Japan; ²³Janssen Research and Development, LLC, Titusville, United States
Email: rgish@robertgish.com

Background and aims: An estimated 296 million people globally live with chronic hepatitis B (CHB). Stigma against people with CHB is common. Self-stigma (a type of stigma defined as self-induced, internalized negative belief, which affects feelings and function) may negatively impact diagnostics, treatment, and health-related quality of life of people with CHB. We conducted studies to demonstrate the content and psychometric validity of a new patient-reported outcome (PRO) instrument to assess self-stigma in people with CHB, as none currently exists.

Method: Qualitative cognitive debriefing interviews with people living with CHB were conducted to assess the content validity and conceptual coverage of the draft PRO instrument's comprehensiveness and participants' understanding and interpretation of the instructions, items, response scale, and recall period. Quantitative analyses included psychometric evaluation of the PRO instrument using data from the global phase 2b REEF-1 and REEF-2 trials in adults with CHB. The following analyses were conducted: internal consistency and test-retest reliability, known-group validity, exploratory and confirmatory factor analysis, item response theory (IRT), and differential item functioning (DIF).

Results: In the qualitative study, participants in China, Germany, Italy, Japan, and United States (N = 75) informed rephrasing and combining of items for clarity and conceptual overlap, and the addition of a self-stigma definition. Interviews confirmed understanding of the PRO items, instructions, and response scale as intended and confirmed them as relevant and comprehensive. Participants self-reported the frequency with which they experienced each aspect of self-stigma over the past 4 weeks (recall period) and found the response scale appropriate. Quantitative (psychometric) evaluation of responses from participants of REEF-1 (N = 470) and REEF-2 (N = 130) demonstrated that the items possessed good internal consistency (alpha = 0.92) and test-retest reliability (intraclass correlation coefficient [ICC]: summed scores = 0.81; ICC: IRT-based scores = 0.77). Exploratory factor analysis indicated a subset of 9 items that covered important content areas (felt inferior to others, expected others to think less of me, felt people were avoiding me, expected rejection when others found out, worried that people would find out, felt guilty, felt ashamed, avoided social situations, and avoided intimacy) provided a good measurement model fit. Confirmatory factor analysis supported a 1-factor model when fit to these 9 items in the PRO instrument (root mean square error of approximation = 0.04; Tucker-Lewis index = 0.96). The summed scores of the final 9-item scale were supported by results from convergent and discriminant correlations and means of known groups analyses. The 9-item summed scores also detected change over time. DIF analyses indicated no group differences in item performance based on age (≤ 45 vs >45 years), sex, or race/ethnicity (Asian vs non-Asian). The test reliability function of the final 9-item scale indicated that average to high levels of self-stigma had good reliability (>0.70 at -0.8 and higher) supporting the suitability of the instrument for future use in clinical trials.

Conclusion: These results support the content and psychometric validity of this new 9-item PRO instrument for use in clinical studies to assess self-stigma in people with CHB.

WED-152

Hepatitis flare appeared to be more severe with poorer outcome in chronic hepatitis B patients with recent COVID vaccination during the COVID pandemic

Jennifer Tai¹, Yen-Chun Liu^{1,2}, Rachel Wen-Juei Jeng^{1,2}, Rong-Nan Chien^{1,2,3}, Yun-Fan Liaw^{2,3}. ¹Chang Gung Memorial Hospital, Linkou Medical Center, Department of Gastroenterology and Hepatology, Taiwan; ²College of Medicine, Chang Gung University, Taiwan; ³Chang Gung Memorial Hospital, Linkou Medical Center, Liver research unit, Taiwan
Email: liveryfl@gmail.com

Background and aims: Immune-mediated hepatitis following COVID vaccination were reported recently. Further, COVID-19 infection has been reported as one of the possible trigger factors for HBV reactivation. This study aims to investigate the characteristics and severity between chronic hepatitis B (CHB) patients who developed severe flare with and without recent COVID vaccination during Nov 2020-Nov 2021.

Method: From the nucleos (t)ide analogues reimbursement application registry system during Nov 2020-Nov 2021 in Chang Gung Memorial Hospital, Linkou medical center, CHB patients with severe flare, defined as ALT ≥ 1000 U/L or ALT <1000 plus bilirubin ≥ 3.5 mg/dL and/or international normalized ratio (INR) ≥ 1.5 , and/or hepatic decompensation, defined as ALT $\geq 5 \times$ ULN, bilirubin ≥ 2 mg/dL and INR ≥ 1.5 , were recruited. Patients with sepsis, biliary tract infection, advanced liver tumor, alcoholism, acute hepatitis B infection and drug-induced liver injury were excluded. Patients' characteristics along with liver biochemistry, viral markers at onset of hepatitis flare event, and the incidence of mortality or liver transplantation were compared between patients with and without history of recent (<6 months) COVID-19 vaccination.

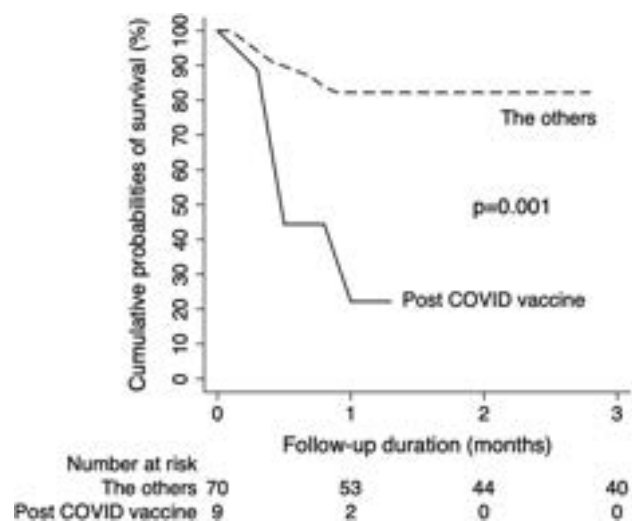


Figure: Kaplan-Meier survival estimates (30-day mortality or liver transplantation).

Results: Among 241 patients registered, 79 patients met the inclusion criteria. Nine patients (11.4%) had history of recent COVID vaccine exposure within 6 months prior to the event (vaccine group), with mean time-to-event of 8 weeks (IQR: 2.9~12.9). The median age, proportion of gender, cirrhosis, and HBeAg positivity were comparable between the vaccine group and non-vaccine group. The median level of HBV DNA at flare was lower in the vaccine group (6.3 vs. 7.0 log₁₀ IU/ml, P = 0.59) and more frequent <5 log₁₀ IU/ml (22.2% vs. 10%, P = 0.29). In addition, the vaccine group had significantly higher

peak INR (median: 3.2 vs 1.7, $p = 0.015$), AST (median: 1789 vs 808 U/L, $p = 0.011$), ALT levels (median: 2079 vs 1500 U/L, $p = 0.018$), more frequent peak ALT >3000 U/L (44.4% vs. 7.1%, $P = 0.008$) and significantly higher rates of 30-day mortality or liver transplant (66.7% vs 21.4%, log rank test, $P < 0.05$).

Conclusion: Recent COVID-19 vaccination may exacerbate severe hepatitis flare, probably due to more vigorous immune response or immune mediated hepatitis following COVID-19 vaccination.

WED-153

Increased baseline comorbidity burden among commercially insured patients with hepatitis delta virus infection vs hepatitis B virus mono-infection in the United States

Robert G. Gish¹, Robert Wong^{2,3}, Chong Kim⁴, Gary Leung⁵, Ira M Jacobson⁶, Joseph Lim⁷, Ankita Kaushik⁴. ¹Hepatitis B Foundation, Doylestown, United States; ²Stanford University School of Medicine, Stanford, United States; ³VA Palo Alto Healthcare System, Palo Alto, United States; ⁴Gilead Sciences, Inc., HEOR-Global Value and Access, Foster City, United States; ⁵Gilead Sciences, Inc., RWE-Epidemiology, Foster City, United States; ⁶NYU Grossman School of Medicine, New York, United States; ⁷Yale University School of Medicine, New Haven, United States

Email: rgish@robertgish.com

Background and aims: Compared to hepatitis B virus (HBV) mono-infection, hepatitis D virus (HDV) is associated with more rapid progression to cirrhosis and liver-related complications. Baseline (BL) characteristics of adults with HBV with concurrent HDV infection were compared to those with HBV mono-infection among commercially insured US patients.

Method: Adults with ≥ 1 HDV or HBV diagnosis (ICD-9/10-CM) were identified retrospectively from 1 Jan 2013 to 31 Dec 2021 (study period) using the IQVIA PharMetrics Plus database covering ~210 million patients from primarily commercial payers. HDV and HBV-mono-infected patients were identified from 1 Jan 2014 to 31 Dec 2020 (identification period). Patients with HDV had ≥ 1 inpatient or ≥ 2 outpatient claims ≥ 30 days apart with an ICD-9/10-CM diagnosis code for HDV during the identification period (earliest date of diagnosis considered index date), ≥ 1 claim of HBV diagnosis during BL, and no claims with HDV diagnosis during BL (12-month period prior to index date). Patients with HBV mono-infection had ≥ 1 inpatient or ≥ 2 outpatient claims ≥ 30 days apart with a claim for HBV only, no claims with HBV diagnosis during BL, and no ICD codes for HDV diagnosis during study period. At least 12 months of continuous enrollment before and after the index date was required, and patients aged ≥ 18 years at index with commercial health plans were included. Patient characteristics were assessed over the 12-month BL period, and comparisons between HDV-infected vs HBV-mono-infected cohorts were made.

Results: Of the 186,376 patients diagnosed with HDV or HBV during the study period, 440 HDV and 22,136 HBV-mono-infected patients

were included. The HDV cohort was significantly older, mean (SD) age 50.3 (10.50) vs 49.1 (11.72) years, $p = .03$; had a significantly greater proportion of males, 65.2% vs 55.2%, $p < .0001$; and had significantly higher mean (SD) Charlson Comorbidity Index scores, 1.97 (2.35) vs 0.91 (1.94), $p < .0001$ than the HBV-mono-infected cohort. Compared to HBV-mono-infected patients, at BL, HDV patients were more likely to have compensated cirrhosis (13% vs 2%), decompensated cirrhosis (12% vs 3%), hepatocellular carcinoma (5% vs 1%), and liver transplant (4% vs 1%); $p < .0001$ for all comparisons. Compared to HBV-mono-infected patients, at BL, HDV patients had significantly higher proportions of hypertension (33% vs 25%; $p = .0001$), obesity (8% vs 5%; $p = .002$), non-alcoholic steatohepatitis (7% vs 2%; $p < .0001$), HCV (6% vs 4%; $p = .003$), and HIV (5% vs 3%; $p = .04$).

Conclusion: Among a nationally representative cohort of commercially insured US patients, patients with HDV had a greater burden of advanced liver disease and complications and other comorbidities at BL compared to HBV-mono-infected patients. This study underscores the importance of early identification and linkage to treatment of patients with HDV to mitigate disease progression and improve patient outcomes.

WED-154

Can we better characterize HBeAg-negative chronically infected hepatitis B patients using novel biomarkers?

Thais Leonel Couto¹, Sergio Rodriguez-Tajes¹, Ariadna Rando-Segura², Ester García-Pras¹, Mireia García-López¹, Sabela Lens¹, Zoe Mariño¹, David Tabernero², Maria Francesca Cortese², Francisco Rodríguez-Frías², Maria Saez-Palma¹, Sofía Pérez-del-Pulgar¹, Xavier Forns¹. ¹Liver Unit, Hospital Clínic Barcelona. University of Barcelona. FCRB-IDIBAPS. CIBEREHD, ISCIII, Spain; ²Unitat de Patologia Hepàtica, Departament de Bioquímica i Microbiologia, Hospital Universitari Vall d'Hebron, CIBEREHD, ISCIII, Barcelona, Spain

Email: xforns@clinic.cat

Background and aims: The natural history of Hepatitis B virus (HBV) infection has different phases that are characterized according to the hepatitis B e antigen (HBeAg) status, HBV-DNA levels and transaminases. Patients with HBeAg-negative chronic infection can be quite heterogeneous, particularly in terms of hepatitis B surface antigen (HBsAg) levels with no apparent association with HBV-DNA levels. In recent years, new biomarkers such as the core-related antigen (HBcrAg) and circulating HBV-RNA (cirB-RNA) have been used as surrogate markers of covalently closed circular DNA (cccDNA) transcriptional activity. Unfortunately, most of these studies focus on patients on nucleos(t)ide analogue (NA) treatment and in the chronic hepatitis phase. The aim of this study was to investigate whether HBcrAg and cirB-RNA could help to better characterize the HBeAg-negative chronic infection phase.

Method: We retrospectively included 184 naive patients with normal ALT divided into 4 groups: HBsAg $>10,000$ IU/ml and HBV-DNA

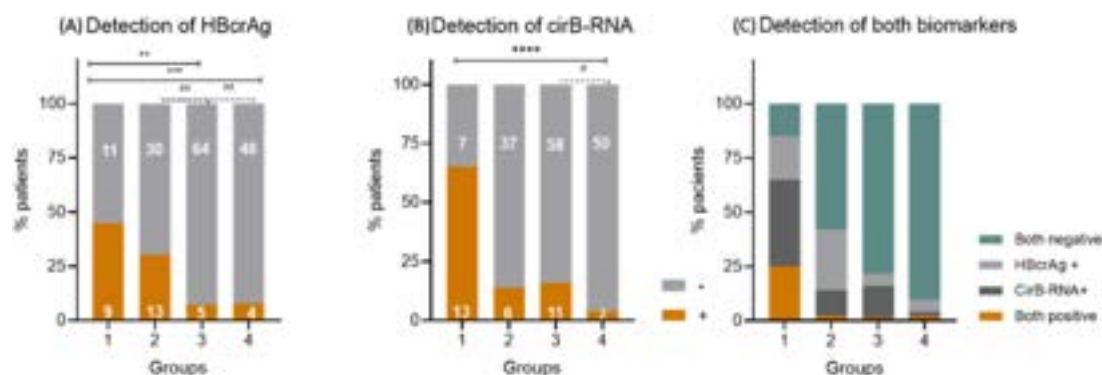


Figure: (abstract: WED-154).

POSTER PRESENTATIONS

2,000–20,000 IU/ml (Group 1, n = 20); HBsAg >10,000 IU/ml and DNA <2,000 IU/ml (Group 2, n = 43); HBsAg 10,000–100 IU/ml and DNA <2,000 IU/ml (Group 3, n = 69); HBsAg <100 IU/ml and DNA <2,000 IU/ml (Group 4, n = 52). HBV-DNA (LLQ <10 IU/ml), HBsAg (LLQ <0.13 IU/ml), HBcrAg (LLQ <3 LogU/ml) and HBV-RNA (LLQ <10 cp/ml) were quantified in all of them at baseline and in 91 patients during follow-up.

Results: Groups were comparable in sex (55% female) and ethnicity (67% Caucasian); age (median 47 years) was greater in group 4 (54 years). The follow-up period after baseline assessment was similar between groups (2.6 years (1.6–3.9)). The presence of HBcrAg and cirB-RNA at baseline varied significantly between groups, ranging from 45% and 65%, respectively, in group 1, to less than 10% in group 4 (Figure). Most of the patients with follow-up remained in the same group (82%) and only 2 patients went from group 2 to group 1 (gray zone). Seventeen patients (18%) achieved functional cure (HBsAg loss) during follow-up (13 from group 4 and 4 from group 3). Neither baseline cirB-RNA detection nor HBcrAg levels predicted change of group or functional cure. Indeed, 2 of the 17 (12%) patients who achieved functional cure had detectable cirB-RNA or HBcrAg at baseline.

Conclusion: In the HBe-negative chronic infection phase, detection of serum HBcrAg and cirB-RNA is not influenced by HBsAg levels, suggesting that it originates from integrated HBV genome. In contrast, HBcrAg and cirB-RNA are frequently detected when HBV-DNA >2000 IU/ml (gray zone), demonstrating increased transcriptional activity of cccDNA. The absence of HBcrAg and cirB-RNA do not predict loss of HBsAg (functional cure). Finally, most patients remain stable overtime and this may indicate that multiple serological marker determination to determine the phase of HBV infection are not required.

WED-155

An online web-based calculator accurately diagnoses immune tolerant phase in chronic HBV-infected patients

Chi Zhang¹, Yiqi Liu¹, Hui Liu², Chen Shao², Hong Zhao¹, Gui-Qiang Wang¹. ¹Peking University First Hospital, Department of Infectious Disease, Center for Liver Disease, China; ²Beijing Youan Hospital, Capital Medical University, Department of Pathology, China
Email: john131212@126.com

Background and aims: There were different antiviral treatment strategies and prognoses between immune tolerant (IT) and non-IT in chronic hepatitis B (CHB) patients. However, existing non-invasive diagnostics were not precision. We aimed to explore new non-invasive models for diagnosing IT and assessed the risk of hepatocellular carcinoma (HCC) in IT patients.

Method: We included treatment-naïve CHB patients with liver biopsy who serological met the diagnostic criteria of IT (HBeAg-positive, HBV DNA >5lgIU/ml, normal ALT). This study included four parts: in step 1, we described the clinical characteristics of IT patients. In step 2, we evaluated the value of non-invasive markers recommended by the guidelines for the diagnosis of IT. In step 3, a

new model for the diagnosis of IT with non-invasive markers were developed and validated. In step 4, to assess the risk of developing HCC using 15 HCC prediction models for IT and non-IT.

Results: According to the criteria for the diagnosis of IT by WHO 2015 guidelines, 196 patients were finally included in this study, of which 83 were liver biopsy-proven IT. In the IT group age, qAnti-HBc, ALT, AST and LSM were lower. While, HBV DNA and HBsAg were higher. The risk of non-IT increased 1.2-fold and 3.92-fold in patients aged 30–40 (95%CI 1.00–4.81, P = 0.049) and >40 years (95%CI 2.28–10.60, P < 0.001), respectively, compared to those aged <30 years. Compared to HBV DNA >8 lg IU/ml, the risk of non-IT was increased 4.33-fold and 9.96-fold in patients 7–8 lg IU/ml (p = 0.001) and <8 lg IU/ml (p < 0.001), respectively. The accuracy of non-invasive marker combinations for the diagnosis of IT did not exceed 0.800, whether in accordance with EASL2017/APASL2015, AASLD2018 or CHINA2019 criteria (0.709, 0.658 and 0.765, respectively). Using univariate analysis, LASSO regression and multivariate analysis, we created a CALA model (qAnti-HBc, LSM, AST, ALP) to diagnosing IT. The AUROC of CALA model reached 0.890 and 0.892 in training and validation sets, respectively, which were significantly higher than APRI, FIB-4 and LSM. For clinical convenience, we have made CALA model in an online web-based calculator and QR code. We included 15 hepatitis B related HCC prediction models (REACH-B, mREACH-BI, mREACH-BII, GAG-HCC, CU-HCC, LSM-HCC, PAGE-B, mPAGE-B, NGM1-HCC, NGM2-HCC, CAMD, RWS-HCC, AASL-HCC, REAL-B, aMAP) by searching the PubMed database. The risk of HCC was significantly lower in biopsy-proven IT than in biopsy-proven non-IT population (all P < 0.01). Subsequently, the CALA model was used to differentiate IT and the same results were obtained as those confirmed by liver biopsy (all P < 0.01, except CU-HCC model P = 0.066).

Conclusion: Online web-based calculator of CALA model can accurately and conveniently diagnose IT. Patients with liver biopsy or CALA model-proven IT were at a lower risk of developing HCC.

WED-156

Hepatitis D screening in HBsAg positive individuals in Germany: insufficient implementation results in a large number of undiagnosed cases

Toni Herta¹, Anna Joachim-Richter², David Petroff³, Ingmar Wolfram⁴, Thomas Berg¹, Jan Kramer², Johannes Wiegand¹, Olaf Bätz². ¹Division of Hepatology, Department of Medicine II, Leipzig University Medical Center, Leipzig, Germany; ²LADR Laboratory Group Dr. Kramer and Colleagues, Geesthacht, Germany; ³Clinical Trial Centre, University of Leipzig, Leipzig, Germany; ⁴General Practitioner, Paderborn, Germany
Email: johannes.wiegand@medizin.uni-leipzig.de

Background and aims: Chronic hepatitis delta (CHD) is the most severe form of viral hepatitis and is caused by hepatitis delta virus (HDV) infection, which can only occur in hepatitis B antigen (HBsAg) positive individuals. Thus, current guidelines recommend an anti-HDV screening in all newly detected HBsAg positive cases. These recommendations received increasing attention after approval of the



Figure: (abstract: WED-155): Online Web-based calculator of CALA model for predicting HBeAg positive chronic hepatitis.

HBV/HDV hepatocyte entry inhibitor bulevirtide as first licensed HDV treatment option in July 2020. We analyzed the implementation of HDV testing in the German health care system during the last 9 years. **Method:** We retrospectively searched the database of 11 LADR laboratory sites throughout Germany for HBsAg positive patients detected between the years 2012 and 2021. Request of anti-HDV and HDV RNA testing, origin of laboratory request (primary care, hospital care, occupational medicine, and asylum center), and basic patient characteristics were recorded.

Results: 13,905 HBsAg positive cases were identified (median age 42 ± 15 years, 47% female). They originated from the primary care level, hospitals, occupational medicine, or an asylum center in 84%, 8%, 2%, 5% of cases, respectively. 2,792/13,905 (20%) of HBsAg positive individuals were tested for anti-HDV antibodies with 142/2,792 (5.1%) positive test results. 32% of these anti-HDV positive patients were female with a mean age of 42 ± 13 years. Anti-HDV testing was requested in 2,544/11,679 (22%) of HBsAg-positive individuals at the primary care level, in 218/1,134 (19%) of cases at hospitals, in 18/304 (6%) of cases at occupational medicine, and in 5/711 (1%) of asylum seekers. This observation likely results from differences in reimbursement policy. Testing of HDV RNA was requested in 57/142 (40%) of anti-HDV positive individuals with 26/57 (45%) positive test results. As 80% of HBsAg positive patients were not tested for anti-HDV, a rough estimate suggests that a factor four more patients could benefit from bulevirtide treatment compared to the current situation. **Conclusion:** Anti-HDV screening in HBsAg positive individuals and subsequent HDV RNA testing in anti-HDV positive patients is poorly implemented in Germany. One possible solution would be anti-HDV and HDV RNA reflex testing at the laboratory level.

WED-157

HDV RNA levels <1000 IU/ml and total anti-HDV titers <1:1000 identify chronic hepatitis D subjects without active liver disease

Gabriele Ricco¹, Daniela Cavallone¹, Piero Colombatto¹, Filippo Oliveri¹, Barbara Coco¹, Veronica Romagnoli¹, Lidia Surace¹, Antonio Salvati¹, Ferruccio Bonino², Maurizia Brunetto^{1,2}. ¹University Hospital of Pisa, Hepatology Unit, Italy; ²Institute of Biostructure and Bioimaging, National Research Council, Italy
Email: maurizia.brunetto@unipi.it

Background and aims: To optimize the management and treatment of chronic hepatitis delta (CHD) urges a better clinical/virologic characterization of the patients (pts). We quantified HDV/HBV markers to investigate their correlation with disease activity/stage and response to Interferon (IFN) treatment in a cohort of 146 pts.

Method: One hundred forty-six consecutive untreated anti HDV+ pts admitted at the University Hospital of Pisa were classified according to their baseline clinical, biochemical, histological and imaging data

in: 1) Pts without liver disease (no-CHD) [ALT<40U/L; LS<6kPa]; 2) CHD without cirrhosis; 3) CHD with cirrhosis; 4) CHD with advanced cirrhosis [previous or ongoing decompensation/HCC/varices]. HDV and HBV makers (HBV DNA/HBsAg/HBcrAg/IgG anti HBc) were tested at baseline (BL) in the overall cohort and at end of therapy (EOT), 24 weeks after EOT (PT-FU) and end of follow-up (EOF) in 31 (21.2%) IFN-treated pts [median 12.4 (6.0–91.7) mos]. Undetectable HDV RNA at EOT, PT-FU and EOF by in house qualitative PCR defined the virologic response. HDV RNA was quantified by RoboGene 2.0 (Roboscreen Diagnostics, LOD 6 IU/ml). Total anti HDV titer was evaluated by 10-fold end point dilution of serum samples (LiaisonXLmurex Anti HDV, DiaSorin).

Results: Eleven (7.6%) subjects were classified as no-CHD: all were viremic, 10 (90.9%) had quantitative (qt) HDV RNA<1000 IU/ml [2.88 Log (0.82–4.14)] and all had anti HDV titer<1:1000. Among 135 CHD pts, qtHDV RNA was higher in pts with cirrhosis [5.55 Log (0.70–7.73)] compared to those without [4.39 Log (0.70–6.75), p=0.002], and among cirrhotics was lower in pts with advanced disease [4.81 Log (0.70–6.48), p=0.008]. Anti HDV≥1:1000 were present in 132 (97.8%) CHD pts. At multivariate analyses HDV RNA [OR=1.816/p=0.007], anti HDV [OR=4.429/p=0.012] and anti HBc IgG [OR=3.260/p=0.041] associated with higher disease activity (ALT>100 U/L); Age [OR=1.059/p=0.032] and HDV RNA [OR=1.643/p=0.006] with cirrhosis. Among 31 IFN-treated pts, 16 (51.6%) were responders at EOT; 13 (41.9%) maintained a virologic response at PT-FU, 15 (48.4%) were non-responders. Data at EOF [median 4.6 (1.3–18) yrs] were available in 28: 14 (50%) pts maintained undetectable HDV RNA and normal ALT, all had HDV RNA <1000 IU/ml by qtPCR [1.69 Log (0.70–2.34); <LOD in 2 (14%)] and 13/14 (92.8%) had anti HDV <1:1000. Among the remaining 14 PCR positive pts, 12 (85.7%) had ALT>40 U/L, 12 (85.7%) had qtHDV RNA >1000 IU/ml [4.66 Log (1.64–6.65)] and all had anti HDV≥1:1000.

Conclusion: HDV RNA<1000 IU/ml and anti HDV titers <1:1000 identify with high diagnostic accuracy (Table) CHD patients without evidence of active liver disease. In CHD pts HDV viremia independently correlates with biochemical activity and stage of liver disease. Quantification of HDV markers qualifies as a useful tool for clinic-virological classification and treatment monitoring of CHD pts.

WED-158

Relationship of hepatitis D viral load, ALT levels, and liver stiffness in untreated patients with chronic hepatitis D

Soo Aleman¹, Pietro Lampertico^{2,3}, Maurizia Brunetto^{4,5}, Pavel Bogomolov⁶, Vladimir Chulanov⁷, Nina Mamonova⁷, Tatyana Stepanova⁸, Dmitry Manuilov⁹, Qi An⁹, Ben Da⁹, John F. Flaherty⁹, Renee-Claude Mercier⁹, Audrey Lau⁹, Stefan Zeuzem¹⁰, Markus Cornberg¹¹, Heiner Wedemeyer¹².

	Untreated n=146 (11 no-CHD/135 CHD)		IFN-treated n=28 (14 EOF Responders/ 14 EOF non-Responders)		Cumulative analysis n=174 (25 no-CHD/ 149 CHD)	
	HDV RNA 1000 IU/mL	anti HDV 1:1000	HDV RNA 1000 IU/mL	anti HDV 1:1000	HDV RNA 1000 IU/mL	anti HDV 1:1000
Sensitivity	90.9%	100.0%	100.0%	92.9%	96.0%	96.0%
Specificity	88.9%	97.8%	85.7%	100.0%	88.6%	98.0%
PPV	40.0%	78.6%	87.5%	100.0%	58.5%	88.9%
NPV	99.2%	100.0%	100.0%	93.3%	99.2%	99.3%
DA	89.0%	97.9%	92.9%	96.4%	89.7%	97.7%

Figure: (abstract: WED-157).

POSTER PRESENTATIONS

¹Karolinska University Hospital/Karolinska Institute, Department of Infectious Diseases, Stockholm, Sweden; ²Foundation IRCCS Ca' Granda Ospedale Maggiore Policlinico, Division of Gastroenterology and Hepatology, Milan, Italy; ³University of Milan CRC "A. M. and A. Migliavacca" Center for Liver Disease, Milan, Italy; ⁴Azienda Ospedaliero-Universitaria Pisana, Italy; ⁵University of Pisa, Department of Clinical and Experimental Medicine, Pisa, Italy; ⁶Moscow Regional Research Clinical Institute after M.F. Vladimirov, Moscow, Russian Federation; ⁷FSBI National Research Medical Center for Phthisiopulmonology and Infectious Diseases of the Ministry of Health of the Russian Federation, Russian Federation; ⁸Limited liability company "Clinic of Modern Medicine," Moscow, Russian Federation; ⁹Gilead

Sciences, Inc., United States; ¹⁰University Hospital Frankfurt, Germany; ¹¹Medizinische Hochschule Hannover, Klinik für Gastroenterologie, Hepatologie und Endokrinologie, Germany; ¹²Medizinische Hochschule Hannover, Klinik für Gastroenterologie, Hepatologie und Endokrinologie, Germany
Email: soo.aleman@ki.se

Background and aims: The clinical significance of hepatitis D virus (HDV) viral load level in chronic hepatitis D (CHD) is unclear. Unlike infection with hepatitis B virus (HBV), HDV may cause both immune-mediated liver injury as well as direct cytopathic damage to hepatocytes. This study aimed therefore to investigate whether HDV viral load is associated with alanine aminotransferase (ALT)

Figure 3a. Scatter Plot of Baseline HDV RNA (log₁₀) and Baseline ALT in the Total Cohort. Full Analysis Set; Studies MYR203, MYR204 and MYR301

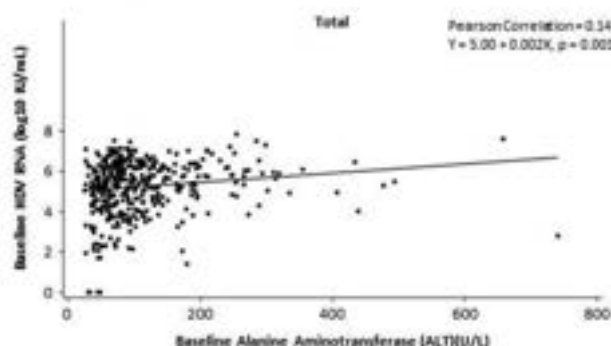


Figure 3b. Scatter Plot of Baseline HDV RNA (log₁₀) and Baseline ALT in Those Without Cirrhosis. Full Analysis Set; Studies MYR203, MYR204 and MYR301

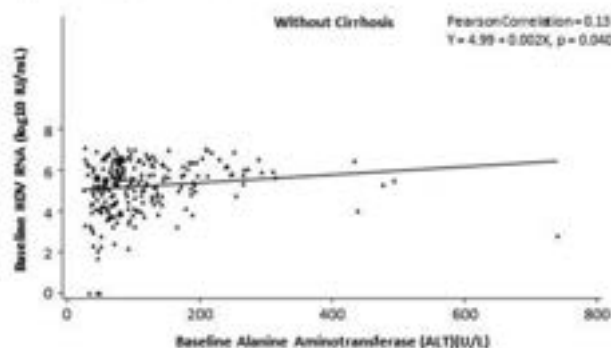
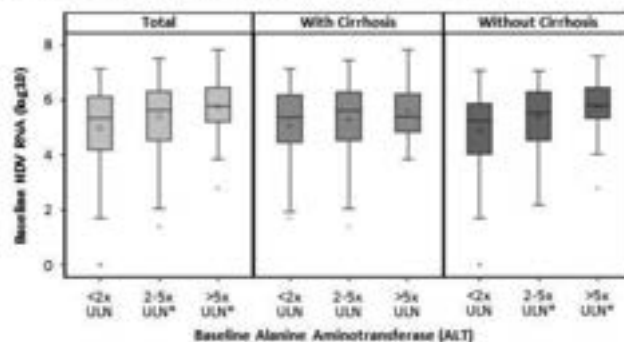


Figure 3c. Baseline HDV RNA (log₁₀) Levels by Baseline ALT (< 2 x ULN, 2-5 x ULN, > 5 x ULN) in the Total Cohort, and Those With/Without Cirrhosis. Full Analysis Set; Studies MYR203, MYR204 and MYR301



Mean HDV RNA increased with higher ALT subgroup category among the total cohort: ALT < 2 x ULN - HDV RNA 5.0 (1.5) log IU/mL; ALT 2-5 x ULN - HDV RNA 5.4 (1.2) log IU/mL; and ALT > 5 x ULN - HDV RNA 5.8 (1.1) log IU/mL.
* Mean HDV RNA of ALT 2-5 x ULN or > 5 x ULN group is significantly different from < 2 x ULN ALT group.

Figure: (abstract: WED-158).

levels and liver stiffness (LS) by transient elastography, which are surrogate markers for hepatic inflammation and liver fibrosis.

Method: A cross-sectional analysis was conducted using pooled baseline data from 3 CHD trials: the phase 2 MYR203 (NCT02888106), phase 2 MYR204 (NCT03852433), and phase 3 MYR301 (NCT03852719) studies. Exclusion criteria included a Child-Pugh-Turcotte score B or C and ALT $<0.5 \times$ upper limit of normal (ULN). Correlation between baseline HDV RNA and ALT levels was performed with Pearson's correlation and linear regression analysis. Subjects were further subclassified by ALT levels: $<2 \times$ ULN, $2-5 \times$ ULN, $>5 \times$ ULN and LS value: <14 vs ≥ 14 kPa. Additional subgroup analyses were performed by baseline cirrhosis status. T-test was used to compare difference of HDV RNA between ALT subgroups. HDV RNA was quantified by Robogene 2.0 (LLOQ 50 IU/ml).

Results: 414 untreated CHD patients were included; the mean (SD) age was 40 (8.6) years, 64% male, 88% white, 35% with cirrhosis and 33% were on nucleoside analogues. Median (Q1, Q3) LS was 11.2 (8.1, 15.4) kPa, mean (SD) ALT-114 (118.6), and mean (SD) HDV RNA-5.3 (1.34) log IU/ml which was similar between those with LS <14 vs ≥ 14 kPa.

Patient distribution across ALT category was: $<2 \times$ ULN (N = 180, 43%), $2-5 \times$ ULN (N = 188, 45%), and $>5 \times$ ULN (N = 46, 11%). Mean HDV RNA in the total cohort increased with higher ALT subgroup category: ALT $<2 \times$ ULN-HDV RNA mean (SD) 5.0 (1.5) log IU/ml, ALT $2-5 \times$ ULN-HDV RNA 5.4 (1.2) log IU/ml, and ALT $>5 \times$ ULN-HDV RNA 5.8 (1.1) log IU/ml. Mean HDV RNA was higher among those with ALT $2-5 \times$ ULN ($p = 0.003$) and $>5 \times$ ULN ($p < 0.001$) compared to those with ALT $<2 \times$ ULN. Mean HDV RNA among those without cirrhosis also increased with higher ALT category. A relationship was seen between the baseline HDV RNA level and ALT in the total cohort ($p = 0.003$, Figure 1a) and non-cirrhotic cohort ($p = 0.040$, Figure 1b). On further analysis by cirrhosis classification, the significant difference in HDV viral load between ALT subgroups remained only among those without cirrhosis (Figure 1c). Similar results were found using AST and HDV viral load. No correlation was seen with baseline HDV RNA level and baseline LS value, regardless of cirrhosis status.

Conclusion: In a large cohort of untreated HDV patients, higher baseline HDV viral load was significantly associated with increased ALT levels among those without cirrhosis. Whether this is associated with a higher rate of progression to cirrhosis and subsequent liver-related events requires further exploration.

WED-159

B cell phenotype, Toll-Like receptor 9 expression and inflammatory cytokines profile in patients with chronic hepatitis B with HBsAg loss or persistent

Nour Nasser^{1,2}, Issam Tout¹, Stephanie Narguet², Nathalie Giuly², Boyer Nathalie², Corinne Castelnau², Valérie Paradis², Pierre Tonnerre³, Vassili Soumelis³, Maria Chartouni¹, Abdel Mansouri^{1,2}, Tarik Asselah^{1,2}. ¹Université Paris Cité, Centre de Recherche sur l'Inflammation, Inserm U1149, CNRS ERL8252, F-75018 Paris, France; ²Assistance Publique-Hôpitaux de Paris (AP-HP), Department of Hepatology, Hôpital Beaujon, F-92110 Clichy, France; ³Université Paris Cité, Human Immunology, Pathophysiology and Immunotherapy (HIPI), team ATIP-Avenir, Inserm UMR 976, F-75010 Paris, France
Email: nour.nasser@inserm.fr

Background and aims: B cells, especially CD38hi plasma cells play a major role in mediating humoral immune responses to clear HBV infection. Hepatitis B s antigen (HBsAg) loss is associated with a better outcome in patients with chronic hepatitis B (CHB). Toll-like receptor 9 (TLR9) is a sensor of viral DNA motifs and activates B cells to generate effective immune responses against infection. We aimed to characterize the B cells phenotype, TLR9 expression and associated-inflammatory cytokines profile in peripheral blood mononuclear cells (PBMCs) and plasma from patients with CHB

who lost HBsAg (HBsAg-) as compared to patients with persistent HBsAg (HBsAg+) and to healthy controls.

Method: HBsAg- patients and HBsAg+ patients (untreated and nucleoside analogues-treated) and healthy controls were included. PBMC and plasma were isolated from the whole patient's blood. B cells phenotype and TLR9 expression were analysed using flow cytometry. Plasma levels of TNF α , IL-10 and IFN γ were analysed using ELISA.

Results: 14 HBsAg-, 40 untreated CHB, and 11 treated CHB with nucleoside analogues patients were recruited and compared to 15 healthy controls. The percent of CD19+, CD27+, CD38hi Plasma B cells was significantly higher in HBsAg+ patients compared to healthy controls (0.76 ± 0.11 , $n = 49$ and 0.50 ± 0.12 , $n = 14$, $p < 0.001$). However, the proportion of CD19+, CD27+, CD38hi Plasma B cells in HBsAg- patients was like that in healthy controls, whereas it significantly increases in HBsAg+ patients as compared to healthy controls (0.83 ± 0.107 , $n = 12$ and 0.502 ± 0.12 , $p < .0001$), indicating a restoration in the percentages of plasma B cells in HBsAg-patients. On the other hand, HBsAg+ patients have shown a significant increase in the percentage of atypical CD19+ CD10+ CD27- CD21- MBC cells when compared to healthy controls (5.68 ± 2.18 , $n = 38$ and 3.13 ± 0.92 , $n = 14$, $p < 0.001$) or to HBsAg- patients (5.68 ± 2.18 and 2.8 ± 0.91 , $n = 12$, $p < .0001$). The relative TLR9 expression was significantly increased in HBsAg+ patients as compared to healthy controls (0.65 ± 0.15 , $n = 39$ and 0.35 ± 0.11 , $n = 14$, $p < 0.0001$) or to HBsAg- patients (0.35 ± 0.11 and 0.63 ± 0.19 , $p < .001$, $n = 14$). Also, plasma TNF α levels significantly increased in HBsAg+ patients compared to healthy controls (15.99 ± 2.83 pg/ml and 11.42 ± 1.67 pg/ml, $p < 0.0001$) but unchanged in HBsAg- group as compared to controls. However, a significant decrease in the levels of TNF α was observed in HBsAg- patients compared to HBsAg+ patients (15.99 ± 2.83 pg/ml and 12.07 ± 1.46 pg/ml, $p < 0.05$). Similarly, IL-10 levels increased in HBsAg+ patients in comparison to healthy controls (8.05 ± 1.67 pg/ml and 10.8 ± 2.9 pg/ml, $p < 0.05$), whereas significantly decreased (10.8 ± 2.9 pg/ml and 8.05 ± 1.67 pg/ml, $p < 0.05$) in HBsAg-patients compared to HBsAg+.

Conclusion: The normal redistribution of B cell subsets was disrupted in patients with persistent HBsAg while restored in patients who lost HBsAg. A restored cytokine environment in HBsAg- patients characterized by a decrease in TNF α and IL-10 plasma levels was observed in comparison HBsAg+ patients. Finally, TLR9 expression was restored upon HBsAg loss. A study of B cell functionality in all groups of patients will be subsequently conducted to better correlate the B cell response to the HBsAg loss.

WED-160

Healthcare resource use and costs associated with hepatitis delta virus infection compared to hepatitis B virus mono-infection among commercially insured patients in the US

Robert Wong^{1,2}, Robert G. Gish³, Chong Kim⁴, Gary Leung⁵, Ira M Jacobson⁶, Joseph Lim⁷, Ankita Kaushik⁴. ¹Stanford University School of Medicine, Stanford, United States; ²VA Palo Alto Healthcare System, Palo Alto, United States; ³Hepatitis B Foundation, Doylestown, United States; ⁴Gilead Sciences, Inc., HEOR-Global Value and Access, Foster City, United States; ⁵Gilead Sciences, Inc., RWE-Epidemiology, Foster City, United States; ⁶NYU Grossman School of Medicine, New York, United States; ⁷Yale University School of Medicine, New Haven, United States
Email: ankita.kaushik@gilead.com

Background and aims: Hepatitis delta virus (HDV) infection occurs in patients with underlying hepatitis B virus (HBV) infection and is associated with more rapid liver disease progression. This retrospective study compared baseline (BL) characteristics, healthcare resource use (HCRU), and costs among commercially insured adults in the US with HBV mono-infection and HDV infection.

Method: The study population included commercially insured adults with ≥ 1 inpatient or ≥ 2 outpatient claims ≥ 30 days apart with an

POSTER PRESENTATIONS

ICD-9/10-CM diagnosis code for HBV in the IQVIA PharMetrics Plus database between 1 Jan 2014 and 31 Dec 2020 (identification period). The HBV index date was the first claim for HBV during the identification period. Patients were required to have ≥ 12 months of continuous enrollment before and after the HBV index date. Patients with HBV had no HDV diagnosis during the study period. Patients with HDV had ≥ 1 inpatient or ≥ 2 outpatient claims ≥ 30 days apart with an HDV diagnosis on or after the HBV index date and ≥ 12 months of continuous enrollment before and after HDV diagnosis. Patients with HBV and HDV were matched for geographic region, BL comorbidities, age, sex, and follow-up time. BL characteristics were assessed over the 12-month pre-HBV index period. Mean per patient per year (PPPY) HCRU and costs were assessed over the entire pre- and post-HDV index periods. Descriptive statistics were summarized, and comparisons were made using Mann-Whitney U and chi-square tests.

Results: Of 152,576 commercial patients diagnosed with HBV and/or HDV during the study period, the matched cohorts for analysis included 325 with HBV mono-infection and 325 with HDV infection. There were no significant differences in BL characteristics or comorbidities between the matched cohorts. The mean PPPY numbers of inpatient visits (1.6 vs 0.7; $p < .0001$), outpatient visits (13.9 vs 7.8; $p < .0001$), and physician office visits (11.6 vs 9.3; $p < .0001$) were greater among patients with HDV infection than HBV mono-infection. Mean PPPY length of stay for inpatient visits was higher among patients with HDV infection than HBV mono-infection (4.6 days vs 1.9 days; $p < .0001$). Patients with HDV infection also had significantly greater total medical costs (\$12,319 vs \$7619; $p < .0001$). The greatest differences in HCRU and cost between patients with HDV infection and HBV mono-infection were from outpatient visits, for which patients with HDV had approximately 6 more visits and spent \$3,094 more per year vs patients with HBV mono-infection.

Conclusion: Among a large national US commercial healthcare claims database, patients with HDV infection cost \$4,700 more in terms of total medical costs annually compared to matched patients with HBV mono-infection. These findings highlight the need for effective screening, diagnosis, and treatment of HDV, which may reduce the clinical and economic burden faced by patients with HDV.

WED-161

Clinical characteristics and phase transition of chronic hepatitis B patients with HBeAg and anti-HBe coexistence

Ruifei Xue¹, Jian Wang^{2,3}, Jie Zhan¹, Zhiyi Zhang⁴, Suling Jiang¹, Juan Xia², Weimao Ding⁵, Jie Li^{1,2,3,4}, Rui Huang^{1,2,3,4}, Chao Wu^{1,2,3,4}.

¹Department of Infectious Diseases, Nanjing Drum Tower Hospital Clinical College of Nanjing Medical University, Nanjing, Jiangsu, China;

²Department of Infectious Diseases, Nanjing Drum Tower Hospital, The

Affiliated Hospital of Nanjing University Medical School, Nanjing, Jiangsu, China; ³Institute of Viruses and Infectious Diseases, Nanjing University, Nanjing, Jiangsu, China; ⁴Department of Infectious Diseases, Nanjing Drum Tower Hospital Clinical College of Traditional Chinese and Western Medicine, Nanjing University of Chinese Medicine, Nanjing, Jiangsu, China; ⁵Department of Hepatology, Huai'an No. 4 People's Hospital, Huai'an, Jiangsu, China
Email: dr.wu@nju.edu.cn

Background and aims: The clinical significance of coexistence of hepatitis B e antigen (HBeAg) and antibody against HBeAg (anti-HBe) remains unclear in patients with chronic hepatitis B (CHB). We aimed to explore the clinical characteristics and phase transition of patients with HBeAg/anti-HBe coexistence.

Method: Eight hundred and forty treatment-naïve HBeAg-positive CHB patients from two medical centers were respectively included. Using cox regression to analyze the associated factors of HBeAg clearance and seroconversion.

Results: Eighty-six (10.2%) patients were HBeAg/anti-HBe coexistence. Patients with anti-HBe had older age (39.0 vs. 34.0 years, $P = 0.016$) and higher FIB-4 value (1.5 vs. 1.0, $P < 0.001$) than patients without anti-HBe. During a median follow-up of 86.5 weeks, 158 (18.8%) and 118 (14.0%) patients achieved HBeAg clearance and HBeAg seroconversion, respectively. Surprisingly, as high as 39.5% of patients with HBeAg and anti-HBe coexistence transitioned to HBeAg positive and anti-HBe negative status. 4.7% of patients with HBeAg and anti-HBe coexistence transitioned to HBeAg negative and anti-HBe negative status. Patients with anti-HBe had higher cumulative HBeAg clearance and HBeAg seroconversion rate than those without anti-HBe ($p < 0.001$). HBeAg/anti-HBe coexistence was associated with higher HBeAg clearance (HR 2.960, 95%CI 1.828, 4.791, $P < 0.001$) and HBeAg seroconversion (HR 4.018, 95%CI 2.372, 6.805, $P < 0.001$).

Conclusion: HBeAg-positive CHB patients with anti-HBe had higher possibility of HBeAg clearance and seroconversion than those of patients without anti-HBe. The presence of coexistent HBeAg and anti-HBe is a predictor of HBeAg clearance and seroconversion. Close follow-up of patients with HBeAg and anti-HBe coexistence are needed to monitor phase transitions of patients.

WED-162

Lower HBV DNA levels is associated more severe liver fibrosis in chronic hepatitis B with serological immune-tolerant phase

Jian Wang^{1,2}, Zhiyi Zhang³, Shaoqiu Zhang¹, Yifan Pan⁴, Xiaomin Yan¹, Weihua Wu¹, Weimao Ding⁵, Chuanwu Zhu⁶, Jie Li^{1,2,3,4}, Rui Huang^{1,2,3,4}, Chao Wu^{1,2,3,4}. ¹Department of Infectious Diseases,

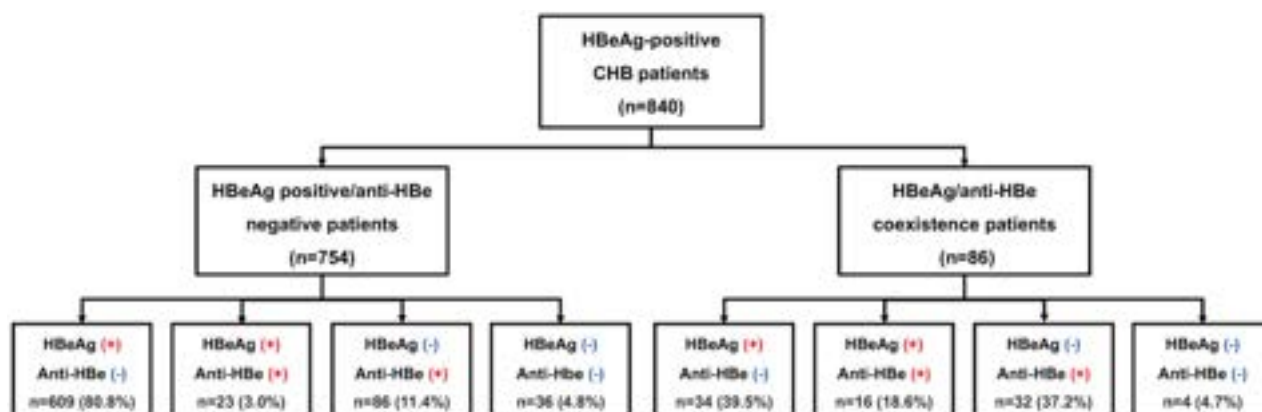


Figure: (abstract: WED-161): Transition of immune status for HBeAg-positive CHB patients with and without anti-HBe.

Nanjing Drum Tower Hospital, The Affiliated Hospital of Nanjing University Medical School, China; ²Institute of Viruses and Infectious Diseases, Nanjing University, China; ³Department of Infectious Diseases, Nanjing Drum Tower Hospital Clinical College of Traditional Chinese and Western Medicine, China; ⁴Department of Infectious Diseases, Nanjing Drum Tower Hospital, Clinical College of Nanjing Medical University, China; ⁵Department of Hepatology, Huai'an No. 4 People's Hospital, China; ⁶Department of Infectious Diseases, The Affiliated Infectious Diseases Hospital of Soochow University, China
Email: doctor_hr@126.com

Background and aims: Patients with chronic hepatitis B (CHB) in serological immune-tolerant (IT) phase might have significant liver fibrosis. However, the association of hepatitis B virus (HBV) DNA levels and liver fibrosis in patients with serological IT phase of CHB remains unclear. This study aimed to compare the severity of liver fibrosis in serological IT patients with different HBV DNA levels.

Method: Six hundred and twenty-two consecutive treatment-naïve serological IT patients with CHB, defined by criteria of positive serum hepatitis B e antigen, HBV-DNA $\geq 10^6$ IU/ml and normal alanine aminotransferase (≤ 35 IU/L for male or ≤ 25 IU/L for female), at three different medical centers were included between January 2015 and August 2022. Patients were divided into three groups according to the serum HBV DNA levels: low ($6 \log_{10}$ IU/ml \leq HBV DNA $< 7 \log_{10}$ IU/ml), moderate ($7 \log_{10}$ IU/ml \leq HBV DNA $< 8 \log_{10}$ IU/ml), and high (HBV DNA $\geq 8 \log_{10}$ IU/ml). Significant liver fibrosis and cirrhosis were identified by aspartate transaminase (AST)-to-platelet ratio index (APRI), fibrosis-4 score (FIB-4), transient elastography, or liver biopsy.

Results: The median age of patients was 33.0 years and 57.9% patients were male. The proportion of patients with lower, moderate, and high HBV DNA levels were 18.8%, 52.1%, and 29.1%, respectively. Patients with low HBV DNA were older and had higher AST levels, while lower platelet, albumin, HBsAg levels, compared to patients with moderate, and high HBV DNA levels. The APRI (0.33 vs. 0.26 vs. 0.26, $p < 0.001$), FIB-4 (1.03 vs. 0.71 vs. 0.68, $p < 0.001$), and liver stiffness values (7.6 kPa vs. 5.6 kPa vs. 5.5 kPa, $p = 0.086$) were higher in patients with low HBV DNA levels than other two groups. Patients with low HBV DNA levels had higher proportions of significant fibrosis (24.8% vs. 9.9% vs. 3.3%, $p < 0.001$) and cirrhosis (7.7% vs. 2.5% vs. 1.1%, $p = 0.004$) compared to patients with moderate and high HBV DNA levels. Compared to patients with high HBV DNA levels, moderate HBV DNA levels (OR 3.095, 95%CI 1.165–8.222, $p = 0.023$) and low HBV DNA levels (OR 4.968, 95%CI 1.706–14.473, $p = 0.003$) were independent risk factors of significant fibrosis, especially for patients aged 30 or older with moderate HBV DNA levels (OR 6.487, 95%CI 1.489–28.255,

$p = 0.013$) and low HBV DNA levels (OR 8.618, 95%CI 1.836–40.458, $p = 0.006$).

Conclusion: Lower HBV DNA level was associated with more severe liver fibrosis in serological IT patients with CHB. Determination of liver fibrosis by liver biopsy or non-invasive methods should be considered without delay for these patients.

WED-163

Clinical evaluation of highly sensitive iTACT hepatitis B core-related antigen and hepatitis B surface antigen assays in the management of HBV reactivation

Takako Inoue¹, Takanori Suzuki², Kentaro Matsuura², Etsuko Iio³, Katsuya Nagaoka³, Masakuni Tateyama³, Hiroko Setoyama³, Yoko Yoshimaru³, Takehisa Watanabe³, Yasuhito Tanaka³. ¹Nagoya City University Hospital, Department of Clinical Laboratory Medicine, Japan; ²Nagoya City University Graduate School of Medical Sciences, Department of Gastroenterology and Metabolism, Japan; ³Kumamoto University, Department of Gastroenterology and Hepatology, Faculty of Life Sciences, Japan
Email: tinoue@fg8.so-net.ne.jp

Background and aims: We developed a highly sensitive hepatitis B core-related antigen assay (iTACT-HBcrAg) and reported its usefulness for the diagnosis of HBV reactivation (J Hepatol, 2021). In Japan, iTACT-HBcrAg has gained pharmaceutical approval and is now available for clinical use. Meanwhile, hepatitis B surface antigen (HBsAg) assays with a higher sensitivity, such as iTACT-HBsAg, have also been developed as an alternative marker to HBV DNA. In this study, we examined the clinical significance of iTACT-HBcrAg and iTACT-HBsAg in the diagnosis of HBV reactivation.

Method: Between 2012 and 2022, patients who had been assessed for HBV markers prior to the introduction of systemic chemotherapy or immunosuppressive therapy, who were diagnosed with HBV-resolved infection, based on positivity for hepatitis B surface antibody or (and) hepatitis B core antibody, were observed. Among them, 33 patients diagnosed with HBV reactivation and whose serial sera were stored were enrolled in this study. Serial sera were measured with iTACT-HBcrAg (cut-off value: 2.1 log U/ml) and iTACT-HBsAg (cut-off value: 0.0005 IU/ml) and compared to the results of HBV DNA monitoring performed as a part of the medical practice. The diagnostic criterion for HBV reactivation was detection of serum HBV DNA. This study was approved by the ethical review committee of our institute.

Results: Thirty-three patients diagnosed with HBV reactivation during or after systemic chemotherapy or immunosuppressive therapy, and with quantitative detection of HBV DNA during the observation period, were selected. Their underlying diseases were

Variables	Entire patients (n=622)	6 <HBV DNA $\leq 7 \log_{10}$ IU/ml (n=117)	7 <HBV DNA $\leq 8 \log_{10}$ IU/ml (n=324)	HBV DNA $\geq 8 \log_{10}$ IU/ml (n=181)	P value
APRI	0.27 (0.22, 0.34)	0.33 (0.24, 0.55)	0.26 (0.22, 0.33)	0.26 (0.21, 0.31)	<0.001
Significant liver fibrosis (≥ 1.5)	9 (1.4)	5 (4.3)	4 (1.2)	0	0.009
Cirrhosis (≥ 2.0)	4 (0.6)	1 (0.9)	3 (0.9)	0	0.436
Missing, No.	0	0	0	0	
FIB-4	0.72 (0.56, 1.03)	1.03 (0.68, 1.99)	0.71 (0.54, 0.98)	0.68 (0.54, 0.87)	<0.001
Significant liver fibrosis (≥ 3.25)	25 (4.0)	16 (13.7)	9 (2.8)	0	<0.001
Cirrhosis (≥ 6.5)	7 (1.2)	5 (4.3)	2 (0.6)	0	0.001
Missing, No.	0	0	0	0	
Liver stiffness (kPa)	5.7 (4.6, 6.8)	7.1 (5.1, 10.1)	5.6 (4.8, 6.8)	5.5 (4.4, 6.4)	0.086
Significant liver fibrosis (≥ 6.0)	19 (3.1)	5 (3.8)	10 (3.1)	4 (2.2)	0.004
Cirrhosis (≥ 11.0)	8 (1.3)	2 (1.6)	4 (1.2)	2 (1.1)	0.180
Missing, No.	470	104	253	113	
Liver biopsy					
Significant liver fibrosis (≥ 2)	24 (3.9)	8 (7.2)	14 (4.3)	2 (1.1)	0.009
Cirrhosis (≥ 4)	3 (0.5)	2 (1.6)	1 (0.3)	0	0.055
Missing, No.	556	106	283	167	

Figure: (abstract: WED-162): Comparison of liver fibrosis among CHB patients with low, moderate, and high HBV DNA levels.

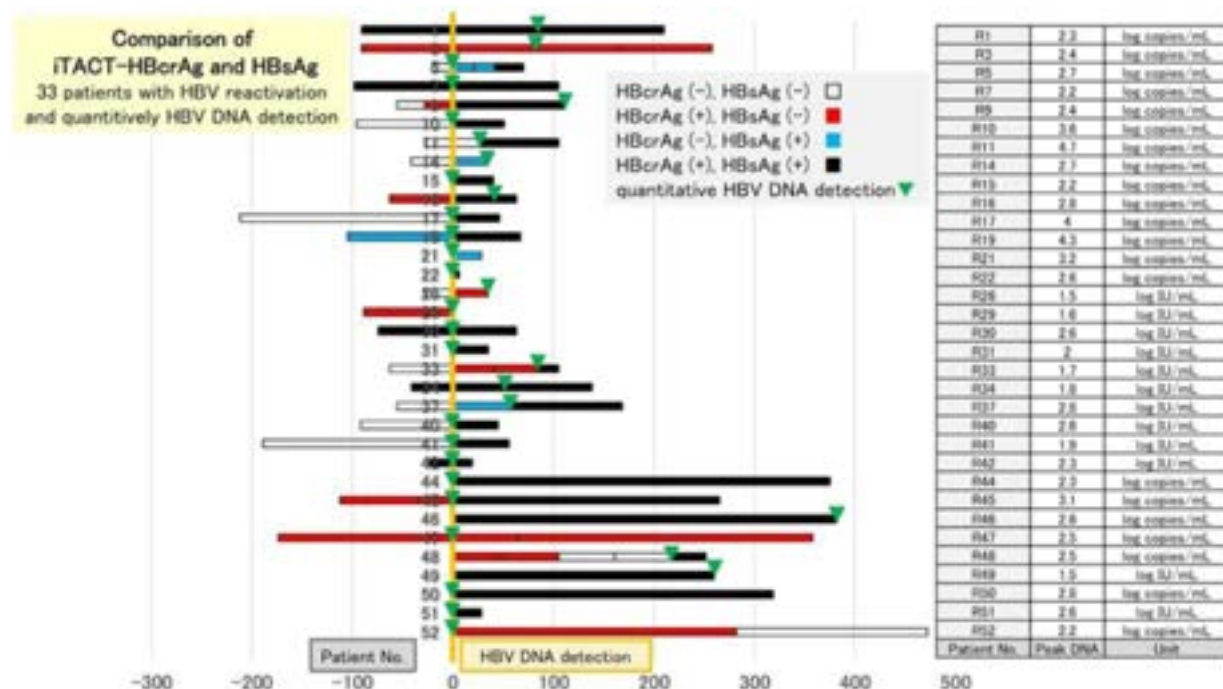


Figure: (abstract: WED-163).

hematopoietic malignancies in 22 patients, non-hematopoietic malignancies in 4 patients, autoimmune diseases in 5 patients, and others in 2 patients. Of the 33 cases in which serum HBV DNA was detected quantitatively, iTACT-HBcrAg was detected early or simultaneously with the diagnosis of HBV reactivation in 85% (28/33), and was detected simultaneously or within 1 month of serum HBV DNA detection quantitatively in 94% (31/33). When iTACT-HBcrAg and iTACT-HBsAg were measured simultaneously, at least one of them was detected earlier or simultaneously with HBV DNA in 100% (33/33).

Conclusion: In the diagnosis of HBV reactivation, a rapid test with comparable sensitivity to quantitative HBV DNA detection, which serves as a guide for administration of nucleos (t)ide analogues, is useful for monitoring outpatients. In this study, the usefulness of iTACT-HBcrAg for the diagnosis of HBV reactivation was reproduced, and the addition of iTACT-HBsAg provided a higher diagnostic performance. iTACT-HBcrAg and iTACT-HBsAg are useful tests for monitoring HBV reactivation because they have the same detection sensitivity as quantitative HBV DNA detection and yield rapid results (within 30 min).

WED-164

Serum thrombospondin-2 for predicting liver fibrosis in patients with chronic hepatitis B virus infection

Yun Chen¹, Yilin Liu², Jian Wang^{3,4}, Zhiyi Zhang², Xin Tong³, Rui Huang^{1,2,3,4}, Chao Wu^{1,2,3,4}. ¹Department of Infectious Diseases, Nanjing Drum Tower Hospital Clinical College of Nanjing Medical University, Nanjing, Jiangsu, China; ²Department of Infectious Diseases, Nanjing Drum Tower Hospital Clinical College of Traditional Chinese and Western Medicine, Nanjing University of Chinese Medicine, Nanjing, Jiangsu, China; ³Department of Infectious Diseases, Nanjing Drum Tower Hospital, The Affiliated Hospital of Nanjing University Medical School, Nanjing, Jiangsu, China; ⁴Institute of Viruses and Infectious Diseases, Nanjing University, Nanjing, Jiangsu, China
Email: dr.wu@nju.edu.cn

Background and aims: Thrombospondin 2 (TSP-2) is a secreted glycoprotein belonging to the thrombospondin family, and is involved in collagen/fibrin formation. Serum TSP-2 level has been

reported to be associated with liver fibrosis in patients with non-alcoholic fatty liver disease and hepatitis C virus infection. We explored the association between TSP-2 and severity of liver fibrosis in patients with chronic hepatitis B virus (HBV) infection.

Method: Serum samples were collected from 228 patients with chronic HBV infection who underwent liver biopsy. Serum TSP-2 was detected by enzyme-linked immunosorbent assays. The Scheuer scoring system was used to evaluate the liver fibrosis stages. Logistic regression analysis was used to analyze the risk factors for fibrosis. The receiver operating characteristic curve (ROC) was used to evaluate the diagnostic accuracy of significant fibrosis ($\geq S2$) and advanced fibrosis ($\geq S3$).

Results: The median age of patients was 40 years, and 146 patients (64.0%) were men. 69 patients (30.3%) had significant fibrosis ($\geq S2$) and 16 patients (7.0%) had advanced fibrosis ($\geq S3$). The median serum TSP-2 level of patients was 16.7 ng/ml (Interquartile range: 13.1–22.1 ng/ml). The serum TSP-2 level increased with fibrosis stages. The areas under the ROC (AUROCs) of serum TSP-2 for predicting significant fibrosis ($\geq S2$) and advanced fibrosis ($\geq S3$) were 0.643 (95% CI: 0.565–0.721, $P = 0.001$) and 0.855 (95% CI: 0.764–0.946, $P < 0.001$), which was comparable with APRI (0.677 and 0.836) and FIB4 (0.646 and 0.823). Serum TSP-2 level was an independent predictor of advanced fibrosis (Odds ratio: 1.042, 95% CI: 1.016–1.069, $P = 0.002$).

Conclusion: Serum TSP-2 correlated with fibrosis stages and could be as a promising predictor of advanced fibrosis in patients with chronic HBV infection.

WED-165

Impact of fatty liver on long-term outcomes in chronic hepatitis B: a systematic review and matched analysis of individual patient data meta-analysis

Yu Jun Wong^{1,2}, Vy H Nguyen^{3,4}, Hwai-I Yang^{5,6,7,8}, Jie Li⁹, Michael Huan Le^{3,10}, Wan-Jung Wu¹¹, Nicole Han¹², Khi Yung Fong¹², Elizabeth Chen¹³, Connie Wong¹⁴, Fajuan Rui¹⁵, Xiaoming Xu¹⁶, Qi Xue¹⁷, Xin Yu Hu¹⁸, Wei Qiang Leow¹⁹, Boon Bee George Goh²⁰, Ramsey C. Cheung^{21,22}, Grace Wong²³, Vincent Wai-Sun Wong²³, Ming-Whei Yu¹¹, Mindie Nguyen²⁴. ¹Changi General Hospital,

Singapore, Gastroenterology and Hepatology, Singapore; ²Duke-NUS Medical School, Singapore, Singapore; ³Stanford University Medical Centre, Palo Alto, California, USA, United States; ⁴Harvard Medical School, Boston, MA, United States; ⁵Genomics Research Centre, Academia Sinica, Taipei, Taiwan; ⁶National Yang Ming Chiao Tung University Yangming Campus, Taiwan; ⁷Kaohsiung Medical University, Taiwan; ⁸Academia Sinica, Taiwan; ⁹Nanjing Drum Tower Hospital, Nan Jing Shi, China; ¹⁰The Robert Larner, M.D. College of Medicine at The University of Vermont, Burlington, United States; ¹¹National Taiwan University College of Public Health, Taiwan; ¹²Yong Loo Lin School of Medicine, Singapore, Singapore; ¹³Department of Gastroenterology and Hepatology, Changi General Hospital, SingHealth, Singapore, Singapore; ¹⁴Stanford University School Medicine, Stanford, United States; ¹⁵Department of Infectious Diseases, Nanjing Drum Tower Hospital Clinical College of Traditional Chinese and Western Medicine, Nanjing University of Chinese Medicine, China; ¹⁶Department of Infectious Diseases, Nanjing Drum Tower Hospital Clinical College of Traditional Chinese and Western Medicine, Nanjing University of Chinese Medicine, China; ¹⁷Department of Infectious Disease, Shandong Provincial Hospital Affiliated to Shandong First Medical University, China; ¹⁸Department of Infectious Disease, Shandong Provincial Hospital, Cheeloo College of Medicine, Shandong University, China; ¹⁹Division of Pathology, Singapore General Hospital, Singapore, Singapore; ²⁰Department of Gastroenterology and Hepatology, Singapore General Hospital, Singapore, Singapore; ²¹Division of Gastroenterology and Hepatology, Department of Medicine, Stanford University Medical Centre, Palo Alto, CA, United States; ²²Division of Gastroenterology and Hepatology, Veterans Affairs Palo Alto Health Care System, Palo Alto, CA, United States; ²³The Chinese University of Hong Kong (CUHK), Hong Kong; ²⁴Department of Epidemiology and Population Health, Stanford University, Stanford, CA, United States
Email: wongyujun1985@gmail.com

Background and aims: Chronic hepatitis B (CHB) and fatty liver (FL) often co-exist, but natural history data of this dual condition (CHB-FL) are sparse. Via a systematic review, conventional meta-analysis (MA) and individual patient-level data MA (IPDMA), we compared liver-related outcomes and mortality between CHB-FL and CHB-no FL patients.

Method: We searched 4 databases from inception to December 2021 and pooled study-level estimates using a random-effects model for conventional MA. For IPDMA, we evaluated outcomes after balancing the two study groups with inverse probability treatment weighting (IPTW) on age, sex, cirrhosis, diabetes, ALT, HBeAg, HBV DNA, and antiviral treatment.

Results: We screened 2157 articles and included 19 eligible studies (17 955 patients: 11 908 CHB-no FL; 6047 CHB-FL) in conventional MA, which found severe heterogeneity ($I^2=88\%-95\%$) and no significant differences in HCC, cirrhosis, mortality, or HBsAg seroclearance incidence ($p=0.27-0.93$). IPDMA included 13 262 patients: 8625 CHB-no FL and 4637 CHB-FL patients who differed in several characteristics. The IPTW cohort included 6955 CHB-no FL and 3346 CHB-FL well-matched patients. CHB-FL patients (vs. CHB-no FL) had significantly lower HCC, cirrhosis, mortality and higher HBsAg seroclearance incidence (all $P\leq 0.002$), with consistent results in subgroups. CHB-FL diagnosed by liver biopsy had a higher 10-year cumulative HCC incidence than CHB-FL diagnosed with non-invasive methods (63.6% vs. 4.3%, $P<0.0001$). On Cox regression, CHB-FL was associated with lower HCC, cirrhosis, mortality and higher HBsAg seroclearance incidence (hazard ratio = 0.68, 0.61, 0.38, 1.35, respectively, all $P\leq 0.004$).

Conclusion: IPDMA data with well-matched CHB patient groups showed that FL (vs. no FL) was associated with significantly lower HCC, cirrhosis, and mortality risk and higher HBsAg seroclearance probability.

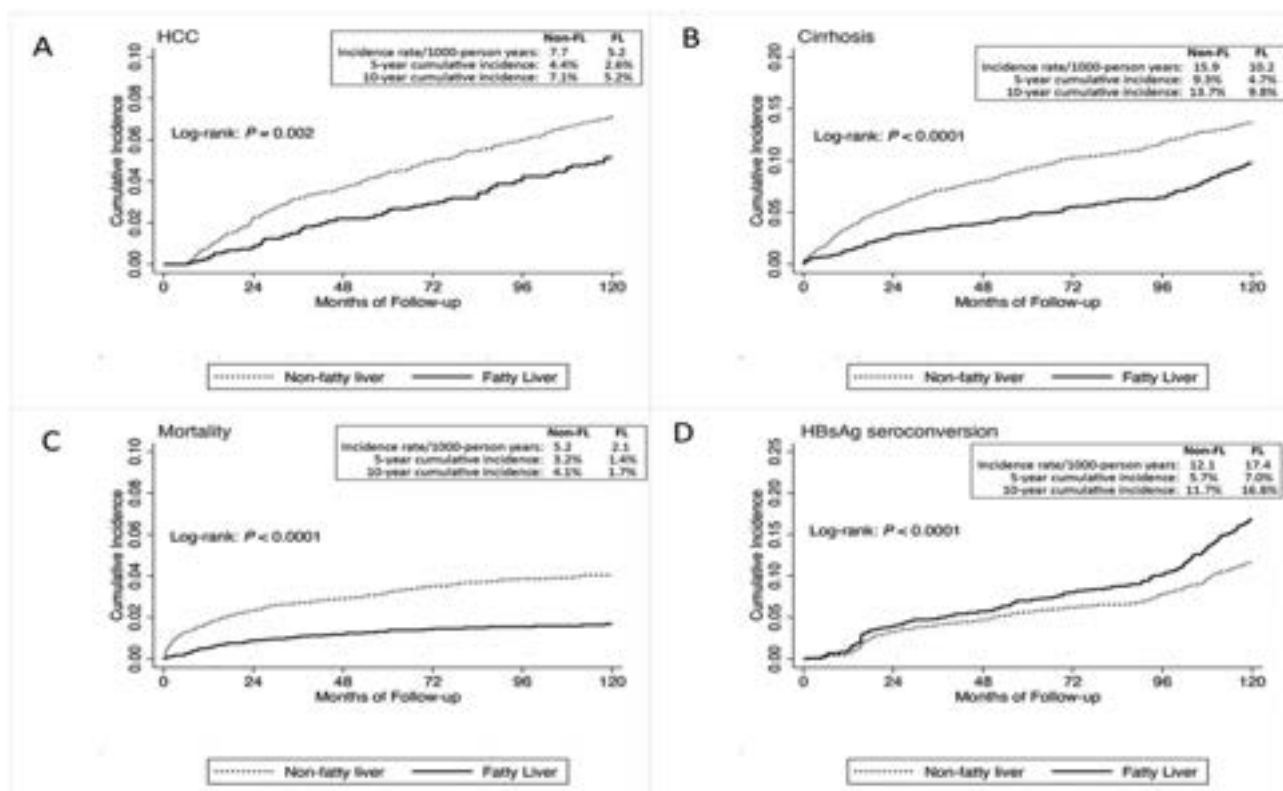


Figure: (abstract: WED-165).

WED-166

Characterizing chronic hepatitis delta in Spain and the gaps in its management

Sergio Rodríguez-Tajes^{1,2}, Adriana Palom^{2,3},
 Alvaro Giraldez-Gallego⁴, Antonio Moreno⁴, Juan José Urquijo⁵,
 Miriam Celada-Sendino⁶, Moises Diago⁵, María García Eliz⁷,
 Javier Fuentes Olmo⁸, Pilar Castillo⁹, Marta Casado¹⁰,
 Ana María Martínez-Sapiña⁸, Elena Pérez Campos¹¹,
 Raquel Muñoz Gómez¹², Marta Hernández Conde¹³,
 Rosa María Morillas^{2,14}, Rafael Granados¹⁵, Mireia Miquel^{2,16},
 Julia Morillas¹⁷, Montserrat García-Retortillo¹⁸, Jose A. Carrión¹⁸,
 Jose María Moreno Planas¹⁹, Mar Riveiro Barciela^{2,3},
 Cristina Montón²⁰, Jesús González Santiago^{2,21}, Sara Lorente²²,
 Susana Llerena²³, Joaquín Cabezas²³, Beatriz Mateos Muñoz²⁴,
 Sergio Vaquez Rodríguez²⁵, Fernando Díaz²⁶, Jose Pinazo Bandera²⁷,
 Merce Delgado Gerra²⁸, Domingo Pérez-Palacios²⁹, Diana Horta³⁰,
 Cristina Fernández Marcos³¹, Carmen López Núñez³²,
 José Luis Calleja Panero¹³, Inmaculada Fernández Vázquez¹²,
 Manuel Rodríguez⁶, Francisco Javier García-Samaniego Rey⁹,
 Xavier Forns^{1,2}, Maria Buti^{2,3}, Sabela Lens^{1,2}. ¹Hospital Clínic,
 Universitat de Barcelona, IDIBAPS, Barcelona, Spain; ²CIBEREHD, Spain;
³Hospital Universitari Vall d'Hebron, Barcelona, Spain; ⁴Hospital Virgen
 del Rocío, IBIS, Sevilla, Spain; ⁵Hospital Universitario General de
 Valencia, Spain; ⁶Hospital Universitario Central de Asturias, Spain;
⁷Hospital Universitario La Fe de Valencia, Spain; ⁸Hospital Miguel Servet,
 Zaragoza, Spain; ⁹Hospital Universitario La Paz, Madrid, Spain;
¹⁰Hospital General Torrecárdenas, Almería, Spain; ¹¹Hospital
 Universitario Torrecárdenas, Almería, Spain; ¹²Hospital Universitario 12
 de Octubre, Madrid, Spain; ¹³Hospital Universitario Puerta de Hierro.
 Majadahonda, Spain; ¹⁴Hospital Germans Trias i Pujol, IGTP, Badalona,
 Spain; ¹⁵Hospital Universitario Dr. Negrín, Gran Canaria, Spain;
¹⁶Hospital Parc Taulí, Institut d'Investigació i innovació I3PT, Sabadell.
 ISCIII, UVic-UCC, Vic, Spain; ¹⁷Hospital Virgen de la Luz, Cuenca, Spain;
¹⁸Hospital del Mar, Parc de Salut Mar, Barcelona, Spain; ¹⁹Centro
 Hospitalario Universitario de Albacete, Spain; ²⁰Hospital Clínico
 Universitario de Valencia, Incliva, Spain; ²¹Hospital Universitario de
 Salamanca, IBSAL, Salamanca, Spain; ²²Hospital Clínico Universitario
 Lozano Blesa, Zaragoza, Spain; ²³Hospital Universitario Marqués de
 Valdecilla, IDIVAL, Santander, Spain; ²⁴Hospital Universitario Ramón y
 Cajal, Madrid, Spain; ²⁵Centro Hospitalario Álvaro Cunqueiro, Vigo,
 Spain; ²⁶Hospital Universitario Gregorio Marañón, Madrid, Spain;
²⁷Hospital Universitario Virgen de la Victoria, Málaga, Spain; ²⁸Hospital
 de Mataró Consorci Sanitari del Maresme, Spain; ²⁹Hospital Infanta
 Elena, Huelva, Spain; ³⁰Hospital Mútua de Terrassa, Spain; ³¹Hospital
 Universitario de Burgos, Spain; ³²Hospital Universitari de Girona Dr.
 Josep Trueta, Spain
 Email: slens@clinic.cat

Background and aims: Chronic hepatitis delta (CHD) is the most severe form of chronic viral hepatitis resulting in high morbidity and mortality due to advanced liver disease. The estimated HDV prevalence in Spain is around 5–10% of patients with hepatitis B. However, true prevalence is probably underestimated due to migration and current limitations in screening and diagnosis. The recent approval of bulevetide and the development of other drugs will change the management of the infection. We aimed to characterize the clinical profile of patients with HDV/HBV infection in Spain and current barriers in their management.

Method: Multicenter registry including patients with positive anti-HDV serology actively monitored in 30 Spanish centers. Epidemiological, clinical and virological variables were recorded at the start of follow-up and at the last visit.

Results: A total of 329 patients were included: 59% were male with median age 51 (IQR: 42–56) years (only 5% were >65 years old), the most common geographical origin was Spain (53%) and East Europe (24%). The median follow-up time since diagnosis was 6 (3–12) years. Importantly, patients from Spain were older and had a longer follow-up with higher presence of cirrhosis and HCV and HIV coinfection

($p < 0.01$). HDV-RNA determination was available in 56% of centers (performed externally in the rest) and its quantification only in 16%. During follow-up, HDV-RNA was assessed in 278 (84%) patients, HDV-RNA was undetectable from baseline in 101 (36%). 133 (48%) had active infection throughout follow-up, while 44 (16%) resolved infection (18 spontaneously and 26 after Peg-INF treatment). At diagnosis 33% had liver cirrhosis (LC), 13% portal hypertension (PH) while only 1% had hepatocellular carcinoma (HCC). During follow-up an additional 10% and 6% developed LC and PH, respectively and 2% HCC. The presence of LC and PH was significantly more frequent in HDV-RNA-positive than in HDV-RNA-negative patients (55% and 27%, $p < 0.01$; 30% and 11% $p < 0.01$).

When performing a gender-based analysis we observed higher rate of active infection among women than men (53% vs. 44%, $p < 0.05$). During follow-up, HDV clearance occurred more among men (19% vs. 11%, $p < 0.05$) despite similar Peg-INF treatment. Despite the high rate of active infection, women had a lower prevalence of LC (36% vs 47%, $p < 0.05$) and HCC (0.7% vs 5%, $p < 0.05$).

Conclusion: The burden of HDV-related disease in Spain is high affecting mostly median age people. One-third of the patients already has cirrhosis at diagnosis and this increases up to 43% after less of a decade of follow-up. Despite a greater rate of active viremia, female sex is associated with less advanced liver disease. Importantly we have identified critical barriers for the management of CHD as it is not possible to locally determine or quantify HDV-RNA in most of the centres. The latter is relevant for prognosis and to assess response to new antiviral therapies.

WED-167

Molecular epidemiology of hepatitis B virus and hepatitis delta virus coinfection in Sudan

Osama Mohamed¹, Birgit Bremer², Sabah Ibrahim³, Sofia Mohamed³,
 Petra Dörge², Yassir Hamadani^{4,5}, Mohamed Hassan⁶, Yasser Mofty⁴,
 Shamsoun Kafi⁷, Heiner Wedemeyer^{2,8}. ¹National University
 Biomedical Research Institute, National University-Sudan, Khartoum,
 Sudan, Department of Molecular Biology, Sudan; ²Hannover Medical
 School, Department for Gastroenterology, Hepatology and
 Endocrinology, Hannover, Germany; ³National University Biomedical
 Research Institute, National University-Sudan, Khartoum, Sudan,
 Department of Bioinformatics and biostatistics, Sudan; ⁴faculty of
 veterinary University of Bahri, Khartoum, Sudan, Department of
 Molecular Biology and bioinformatics, Sudan; ⁵Ibra Hospital, Oman;
⁶faculty of medical laboratory science-National University-Sudan,
 Khartoum, Sudan, Department of hematology, Sudan; ⁷Ribat scientific
 research center, the National Ribat University, Khartoum, Sudan;
⁸German Center for Infection Research, Site Hannover-Braunschweig,
 Germany
 Email: wedemeyer.heiner@mh-hannover.de

Background and aims: Hepatitis D virus (HDV) is dependent on Hepatitis B virus (HBV), and can lead to significant morbidity and mortality. Conflicting data on the impact of hepatitis D have been published for distinct regions in Africa. The aim of this study was to study the molecular epidemiology of HBV/HDV coinfection among a group Sudanese patient.

Method: A total of 324 patient samples (100 patients with hepatocellular carcinoma, 100 with liver cirrhosis and 124 with chronic HBV infection) were collected in Sudan during the year 2019. The CHB group received therapy Pegylated interferon for 48 weeks and Lamivudine for some of patients HBV markers and HDV total antibody were identified by immunoassays. Extracted HBV-DNA and HDV-RNA was quantified by real-time PCR. HBV genotype was determined by multiplex nested PCR and consecutive PCR gel, 11 samples for HBV and 26 samples for HDV were additionally sequenced (Sanger sequencing). Statistical analysis was done using statistical package of social science (IBM SPSS version 20.0) considering a p value ≤ 0.05 as a level of significance.



Figure: (abstract: WED-167).

Results: A total of 319 patients out of 324 were HBsAg positive, were HBV genotyped. the most dominant HBV Genotype was Genotype E in all three groups (52.00%, 44.30%, and 40.30% in HCC, LC and CHB respectively), followed by Genotype D (24.50%, 26.80%, and 31.50% in HCC, LC and CHB respectively). There was a mixed D/E genotypes with 21.40% in HCC group, 24.70% in LC group and 15.30% in CHB group. In addition, some patients possessed genotype A (2.00%, 4.10%, and 7.30% in HCC, LC and CHB respectively). A few Subjects in the CHB group showed a mixed A/E genotype (5.60%) in CHB Individuals with genotype E showed the highest HBV viral load (Median 1550.00, copies/ml, p value=0.008) with 51.9% of them being HDV RNA positive. Anti-HDV was identified in 54 (16.9%) of HBsAg positive patients. HBV genotypes in HDV coinfectd patients were 51.9% E, 27.8% D 20% E/D, while genotype A was not detected. HDV coinfection was more frequent in patients with HCC (27.3%) versus 12.4% of LC, and 17.2% of CHB.

Conclusion: Incidence and existence of HBV and HDV infections in Sudan was documented through the detection of HBV and HDV indicating high prevalence among HCC, LC and chronic HBV patients. Generally, these findings are useful for future studies since there is no information available about HBV and HDV infection in Sudan. HDV coinfectd patients in Sudan show a distinct HBV backbone distribution which may contribute to pathogenesis. These findings establish a baseline for future studies of HBV and HDV coinfection in Sudan.

WED-168

In patients with chronic hepatitis D, the decline of ≥ 2 log HDV-RNA levels that remain detectable is associated with better clinical outcomes

Adriana Palom^{1,2}, Sergio Rodriguez-Tajes^{2,3}, Ariadna Bono⁴, Antonio Madejón^{2,5}, Mar Riveiro Barciela^{1,2}, Ângela Carvalho-Gomes^{2,4}, Sabela Lens^{2,3}, Marina Berenguer^{2,4}, Francisco Javier García-Samaniego Rey^{2,5}, Maria Buti^{1,2}. ¹Liver Unit, Hospital Universitari Vall d'Hebron, Barcelona, Spain; ²Centro de investigación biomédica en red de enfermedades hepáticas y digestivas, Instituto de Salud Carlos III, Madrid, Spain; ³Liver Unit, Hospital Clínic de Barcelona, IDIBAPS, Barcelona, Spain; ⁴Hepatology and Liver

Transplantation Unit, Hospital Universitario y Politécnico La Fe, Valencia, Spain; ⁵Liver Unit, Hospital Universitario La Paz, IdiPAZ, Madrid, Spain Email: mariabutiferret@gmail.com

Background and aims: The end point of treatment for chronic hepatitis D (CHD) is HBsAg loss and/or HDV-RNA undetectability, but these end points are difficult to achieve. An intermediate virological end point of ≥ 2 log decline in HDV-RNA has been considered in clinical trials. However, the impact of this response on the progression of the disease remains unknown. The aim of this study was to evaluate the impact of ≥ 2 log declines in HDV-RNA remaining detectable on the development of clinical events in patients with CHD.

Method: Multicenter study including 80 patients with CHD (all with baseline detectable HDV-RNA) who during the follow-up had consecutive HDV-RNA determinations, which allowed to categorize them into three groups according to HDV-RNA kinetics: Group A) persistently stable levels of HDV-RNA, Group B) ≥ 2 log HDV-RNA decline but remaining detectable (intermediate end point), Group C) achievement of undetectable HDV-RNA. The clinical outcomes (liver decompensation, hepatocellular carcinoma (HCC), transplantation or liver-related death) were analysed. Biochemical (ALT) and virological (HBV-DNA, HDV-RNA) parameters were also compared.

Results: Most patients were male (53.8%), Caucasian (83.8%), median age 46 years and 74% on nucleos(t)ide analogues. Thirty (37.5%) had cirrhosis, and 5 (6%) history of a prior liver decompensation. During a median follow-up of 5.3 (3.1–7.2) years, 42 (52%) subjects had stable HDV-RNA levels, 15 (19%) had a ≥ 2 log decline with detectable HDV-RNA, and 23 (29%) became undetectable. Overall, 19 patients developed clinical events during follow-up. All events occurred while presenting persistently detectable HDV-RNA levels: 13/42 (31%) in HDV-RNA stable subjects (Group A), 3/15 (20%) before reaching ≥ 2 log decline (Group B) and 3/23 (13%) before reaching undetectable HDV-RNA (Group C). After these virological end points, none of the patients with ≥ 2 log decline remaining detectable or undetectable HDV-RNA developed liver-related complications (Figure). Five (13.2%) subjects with undetectable HDV-RNA lost HBsAg during follow-up (p = 0.001). When only the 30 subjects with cirrhosis were analysed, those with a posterior ≥ 2 log decline tended

HDV-RNA end points	N total	Number of patients with a liver-related outcome during follow-up	
		Before end point	After end point
<u>Group A)</u> Persistently detectable	42	13 (31%)* ^Δ Follow-up: 6.7 ± 5.4 years	
<u>Group B)</u> ≥2log decline but detectable	15	3 (20%) Follow-up: 10.2 ± 7.2 years	0 (0%)* Follow-up: 2.1 ± 3.0 years
<u>Group C)</u> Undetectable	23	3 (13%) Follow-up: 4.1 ± 4.3 years	0 (0%) ^Δ Follow-up: 0.7 ± 0.8 years

Follow-up: mean (SD), *p = 0.01, ^Δp = 0.002

Figure: (abstract: WED-168).

to a lower decompensation rate than those with HDV-RNA permanently detectable (1/7 vs 8/17, p=0.149), although the risk of developing HCC (1/7 vs 2/17, p=0.664) was similar. Globally, the risk of clinical events in cirrhotic subjects (decompensation, HCC, mortality/transplantation) also tended to be lower in those with a ≥2log decline in HDV-RNA than in stable subjects (2/7 vs 10/17, p = 0.185).

Conclusion: In this cohort, only patients with stable and persistent HDV-RNA levels present clinical events. No clinical events were observed after patients reached a virological end point. More studies with a larger number of patients and a longer follow-up are needed. This project has been financed by Instituto de Salud Carlos III (PI20/01692).

WED-169

Negligible 10-year risk of liver-related events in chronic hepatitis B patients with low liver stiffness

Lesley Patmore¹, Kirs van Eekhout², Ozgur Koc³, Robert De Knecht¹, Bettina Hansen⁴, Harry LA Janssen^{1,5}, Matthijs Kramer³, Honkoop Pieter⁶, Robert De Man¹, Bart Takkenberg², Milan Sonneveld¹. ¹Erasmus MC, Gastroenterology and hepatology, Rotterdam, Netherlands; ²Amsterdam UMC, locatie AMC, Gastroenterology and Hepatology, Amsterdam, Netherlands; ³Maastricht UMC+, Gastroenterology and Hepatology, Maastricht, Netherlands; ⁴Erasmus MC, Epidemiology and Biostatistics, Rotterdam, Netherlands; ⁵Toronto General hospital, Toronto Centre for Liver Disease, Canada; ⁶Albert Schweitzer Hospital, Gastroenterology and hepatology, Dordrecht, Netherlands
Email: l.patmore@erasmusmc.nl

Background and aims: Patients with chronic hepatitis B (CHB) are at increased risk of hepatocellular carcinoma (HCC) and liver-related mortality. We aimed to study the long-term risk of HCC development and liver-related mortality in relation to the first liver stiffness measurement (LSM).

Method: We conducted a multicentre retrospective cohort study of all consecutive mono-infected CHB patients who underwent at least one LSM by transient elastography with FibroScan (Echosens, France) whilst off antiviral therapy. We analysed the association between liver stiffness as a continuous variable, and after categorization (<or

>9 kPa), with liver-related events, defined as the first of a composite end point of HCC, liver transplantation or liver-related mortality.

Results: We analysed 1102 patients with a median age of 38 years (inter quartile range [IQR] 30–48), predominantly male (53%) and non-Asian (67.5%). The median LSM was 5.3 kPa (IQR 4.3–7.2); 164 patients had an LSM >9 kPa. During a median follow-up of 5.6 years (IQR 2.7–9.3), 12 patients developed an HCC and 10 liver-related deaths were recorded, for a cumulative incidence of 2.3% at 10 years. Higher LSM at study enrolment was associated with an increased risk of liver-related events (hazard ratio [HR] 1.10 per kPa, 95% CI 1.07–1.13, p < 0.001). The cumulative 10-year incidence of liver-related events was 0.7% in patients with a LSM <9 kPa, compared to 9.9% in patients with a LSM >9 kPa (HR 14.62, 95% CI 4.71–45.41, p < 0.001). These results were consistent for patients who subsequently received antiviral therapy (n = 504, p < 0.001) and in patients with an initial HBV DNA >20 000 IU/ml (p = 0.016). LSM >9 kPa was independently associated with an increased risk of liver-related events when adjusting for age, sex, ethnicity, ALT and use of antiviral therapy (adjusted HR 8.9, 95% CI 2.70–29.63, p < 0.001).

Conclusion: An LSM <9 kPa at baseline is associated with negligible 10-year risk of liver-related events in CHB patients. An LSM >9 kPa identifies patients at increased risk of liver-related events who could potentially benefit from treatment with novel antivirals.

WED-170

Steadily decline of HBV DNA load under NAs in lymphoma patients and higher level of qAnti-HBc predict HBV reactivation

Yi-Qi Liu¹, Reyizha Nuersulitan², Chi Zhang¹, Wei Ping Liu², Hong Zhao¹, Gui-Qiang Wang¹. ¹Peking University First Hospital, China; ²Peking University Cancer Hospital, China
Email: zhaohong_pufh@bjmu.edu.cn

Background and aims: Patients with lymphoma and hepatitis B virus infection need to be treated with both chemotherapy and nucleotide analogues therapy. However, the dynamic change of HBV DNA level with the increase of chemotherapy cycles is lacking. Quantitative hepatitis B core antibody (qAnti-HBc), HBV RNA, and hepatitis B virus core-related antigen (HBcrAg) are more sensitive markers to evaluate HBV replication in recent years. It is unknown whether these markers are more sensitive to predict HBV reactivation.

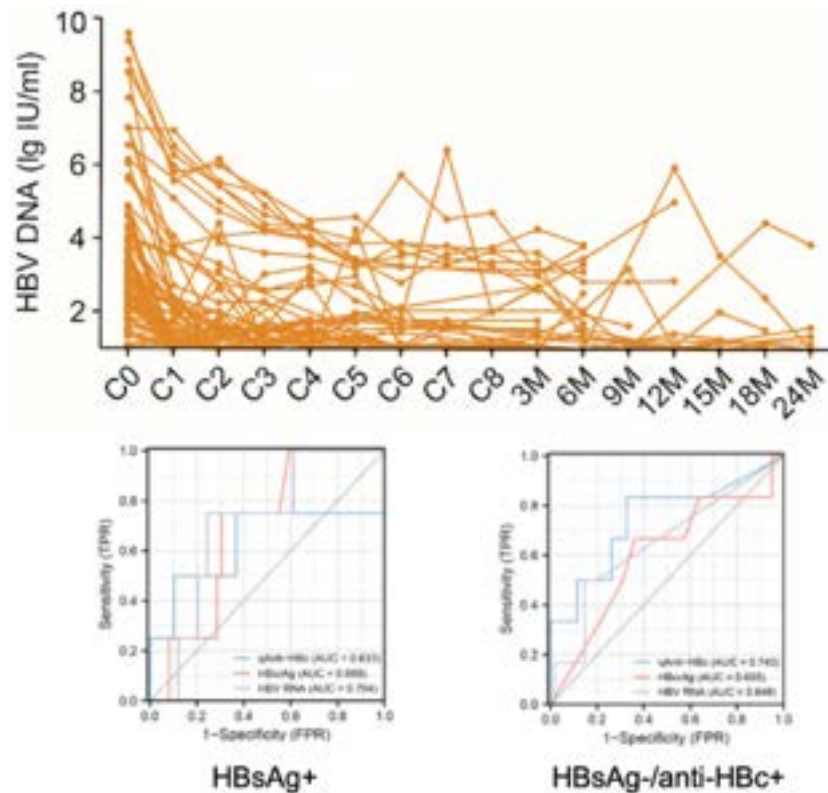


Figure: (abstract: WED-170).

Method: From 29th June 2010 to 6th December 2021, clinical data and serial serum sample were collected from patients with diffuse large B lymphoma and HBV infection. Serum HBV DNA load (real time fluorescent quantitative PCR), qAnti-HBc (developed chemiluminescent particle immunoassay), HBV RNA (simultaneous amplification testing method (HBV-SAT) based on real-time fluorescence detection), and HBcrAg (Lumipulse G HBcrAg assay) were tested before and during chemotherapy. Factors related to HBV DNA reactivation were analyzed by Logistic regression analysis.

Results: Under the NAs, HBV DNA load of 69 with baseline DNA positive HBsAg+ patients declined from 3.15 (2.13–4.73) lg IU/ml at baseline to 1.00 (1.00–1.75) lg IU/ml at the end of chemotherapy, and further declined to 1.00 (1.00–1.04) lg IU/ml at the end of 24-month follow-up. Serum qAnti-HBc level decreased gradually during chemotherapy in HBsAg positive lymphoma patients ($F = 7.090$, $p = 0.009$). The levels of serum HBV RNA and HBcrAg stabled under the chemotherapy. Multivariate analysis revealed that a higher level of qAnti-HBc (1.97 ± 1.20 vs. 1.12 ± 0.84 lg IU/ml, OR = 8.367, [95% CI: 1.439–48.645], $p = 0.018$) and a higher level of HBV RNA (0.86 (0.00–1.94) vs. 0.00 (0.00–0.00) lg copies/ml, OR = 3.654, [95% CI: 1.208–11.048], $p = 0.022$) were related to HBV reactivation in HBsAg-/anti-HBc+ lymphoma patients.

Conclusion: The load of HBV DNA declined steadily by NAs under the chemotherapy in all lymphoma patients. In HBsAg-/anti-HBc+ lymphoma patients, higher level of baseline serum qAnti-HBc and HBV RNA predict the HBV reactivation during chemotherapy.

WED-171

Liver stiffness measurement as a non-invasive method for the diagnosis of liver cirrhosis in patients with chronic hepatitis D virus infection

Lisa Sandmann^{1,2,3}, Kerstin Port¹, Pietro Lampertico^{2,4,5}, Soo Aleman^{2,6,7}, Markus Cornberg^{1,2,3,8,9}, Benjamin Maasoumy^{1,8}, Heiner Wedemeyer^{1,2,3,8}, Katja Deterding¹. ¹Department of

Gastroenterology, Hepatology and Endocrinology, Hannover Medical School, Germany; ²D-SOLVE Consortium, Germany; ³Excellence Cluster RESIST, Excellence Initiative Hannover Medical School, Germany; ⁴Foundation IRCCS Ca' Granda Ospedale Maggiore Policlinico, Division of Gastroenterology and Hepatology, Milan, Italy; ⁵CRC "A. M. and A. Migliavacca" Center for Liver Disease, Department of Pathophysiology and Transplantation, Milan, Italy; ⁶Karolinska University Hospital, Department of Infectious Diseases, Stockholm, Sweden; ⁷Karolinska Institute, Department of Medicine Huddinge, Infectious Diseases, Stockholm, Sweden; ⁸German Center for Infection Research (DZIF), Hannover/Braunschweig, Germany; ⁹Center for Individualised Infection Medicine, Helmholtz Center for Infection Research, Germany
Email: sandmann.lisa@mh-hannover.de

Background and aims: Liver biopsy is the gold standard for the diagnosis of liver cirrhosis. Recently, non-invasive tests (NIT) for determining liver cirrhosis have been proposed as an alternative. Chronic hepatitis D virus infection (CHD) is a rare disease, but associated with high risk of liver cirrhosis. The evidence of NIT for diagnosing liver cirrhosis in this etiology has not been adequately studied due to lack of correlation with histologic findings.

Method: We retrospectively evaluated the diagnostic performance of liver stiffness measurement (LSM) by transient elastography (Fibroscan) for the detection of liver cirrhosis in a cohort of 144 patients with CHD and available liver biopsies. Data was collected from two different German sites and one multicenter clinical trial. LSM was performed within 6 months of liver biopsy, laboratory data was assessed on the day (± 30 days) of LSM. Results were compared to the serological tests AST to ALT ratio (AAR), AST to platelet ratio (APRI), and fibrosis 4 index (FIB-4). Area under the receiver operating characteristic (AUROC) curves was used to assess the performance of NIT, Youden-Index was used to select optimal cut-offs.

Results: Based on histological findings, three groups were defined: Cirrhosis (Metavir 4/Ishak ≥ 5 , $n = 22$), no cirrhosis (Metavir ≤ 1 /Ishak ≤ 2 , $n = 58$) or intermediate fibrosis (Metavir 2–3/Ishak 3–4, $n = 64$).

POSTER PRESENTATIONS

Mean LSM was significantly higher in patients with liver cirrhosis compared to those without it (23.4 vs 10.2 kPa, $p < 0.0001$) or intermediate fibrosis (23.4 vs 13.5 kPa, $p < 0.0001$). For the detection of liver cirrhosis LSM was superior to other NIT with an AUROC of 0.89 as compared to 0.74 (APRI), 0.73 (FIB-4) and 0.69 (AAR), respectively. The optimal cut-off value of LSM for identifying patients with liver cirrhosis was >15.2 kPa (sensitivity 0.91, specificity 0.84, NPV 0.98, PPV 0.50). With this cut-off, liver cirrhosis was correctly diagnosed in 20 of 22 patients and correctly excluded in 102 of 104 patients. When excluding patients with ALT $>5 \times \text{ULN}$, the PPV improved slightly to 55.6%. However, the false positive rate remained high as 15.5% of patients without cirrhosis had an LSM of >15.2 kPa. These patients were more likely to have advanced liver disease with histological staging of Metavir 3 (30% vs 14.7%), lower platelet levels (185 vs $137 \times 1000/\mu\text{l}$, $p < 0.001$) and higher levels of gammaGT (109 vs 44 U/L, $p = 0.015$). The ideal cut-off to exclude advanced fibrosis (Metavir ≥ 3 /Ishak ≥ 4) was <10.2 kPa (sensitivity 0.55, specificity 0.86, NPV 0.45, PPV 0.90). 56 of 62 patients were correctly identified as having no advanced fibrosis. The six misclassified patients were all Metavir 3.

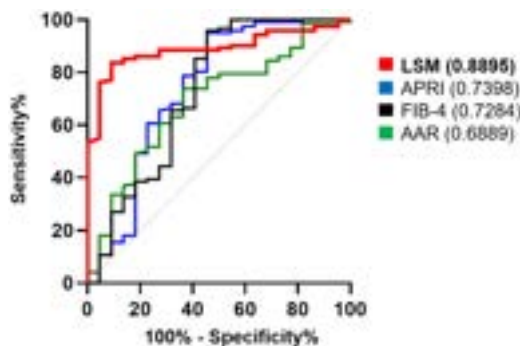


Figure: ROC curves of LSM compared to serological markers for the differentiation of liver cirrhosis defined by histology staging (METAVIR 4/ISHAK 5-6) from absence of liver cirrhosis ($n = 144$).

Conclusion: LSM is a useful NIT to identify patients at risk for liver cirrhosis and is superior to APRI, FIB-4 and AAR. The cut-off of <10.2 kPa correctly excluded liver cirrhosis in all patients while the cut-off of >15.2 kPa correctly identified liver cirrhosis in 91% of patients.

WED-172

Distribution of the natural history stages of pregnant women with chronic hepatitis B virus infection and its association with pregnancy complications and adverse pregnancy outcomes

Xuelian Zhang¹, Yunfei Gao², Jinna Li³, Xueru Yin¹, Yaohua Hao¹, Shimin Yin¹, Jingran Wu⁴, Xiaohuan Jiang¹, Jialin Li¹, Jing Hu⁵,

Zhihua Liu¹. ¹Nanfeng Hospital, Southern Medical University, Department of Infectious Diseases, Guangzhou, China; ²Zengcheng Branch of Nanfeng Hospital, Southern Medical University, Department of Obstetrics and Gynaecology, Guangzhou, China; ³Jiangmen Central Hospital, Department of Infectious Diseases, Jiangmen, China; ⁴Nanfeng Hospital, Southern Medical University, Department of Obstetrics and Gynaecology, Guangzhou, China; ⁵Zhujiang Hospital, Southern Medical University, Department of Nosocomial Infection Administration, Guangzhou, China
Email: zhihualiu@126.com

Background and aims: A large number of pregnant women are living with Hepatitis B virus (HBV). However, there is limited data on the natural history stages of pregnant women with chronic HBV infection. In this study, we aimed to describe the distribution of natural history stages of HBV infection and explore its relationship to pregnancy complications and adverse pregnancy outcomes.

Method: From Jan. 2015 to Aug. 2022, a total of 1276 pregnant women with chronic HBV infection were enrolled in this study. The natural course stages were defined based on AASLD 2018 Hepatitis B Guidance. Patients who cannot be classified into any of the stages are defined as 'grey zone' (GZ), which was classified into three groups: HBeAg positive, regardless of Alanine aminotransferase (ALT) and HBV DNA levels (GZ-A); HBeAg negative, with normal ALT levels and serum HBV DNA $\geq 2 \times 10^3$ IU/ml (GZ-B); HBeAg negative, with elevated ALT levels and serum HBV DNA $\leq 2 \times 10^3$ IU/ml (GZ-C). Logistic regression analysis was used to examine the relationship between natural course stages and pregnancy complications and adverse pregnancy outcomes.

Results: (1) A total of 1276 pregnant women with CHB were enrolled, with 19.04%, 14.73%, 42%, 4.39%, and 19.44% of them in immune-tolerant CHB, HBeAg-positive immune active CHB, inactive CHB and HBeAg-negative immune active CHB, and grey zone CHB, respectively. Among pregnant women in the grey zone, GZ-A, GZ-B and GZ-C accounted for 19.76%, 49.6% and 30.65%, respectively. (2) There were significant differences ($p < 0.05$) in the incidence of thyroid disease in pregnancy, ICP (intrahepatic cholestasis of pregnancy), caesarean section and LGA (greater than gestational age babies) among pregnant women with different natural history stages. The highest incidence of thyroid disease occurred in HBeAg-negative immune active CHB (7.1%); ICP in HBeAg-positive immune active CHB (7.8%); caesarean section in inactive CHB (40.5%); and LGA in the grey zone (12.9%). (3) Analysis of the three groups of "GZ" showed that the incidence of caesarean section was significantly increased in GZ-B compared to GZ-A (43.1% vs 22.4%, $p = 0.014$); the incidence of neonatal weight abnormalities was significantly higher in GZ-C compared to GZ-A (23.7% vs 8.2%, $p = 0.026$); the incidence of GDM (25.0% vs 13.8%), neonatal weight abnormalities (23.7% vs 7.3%) and LGA (21.1% vs 8.9%) were considerably higher in GZ-C compared to GZ-B ($p < 0.05$).

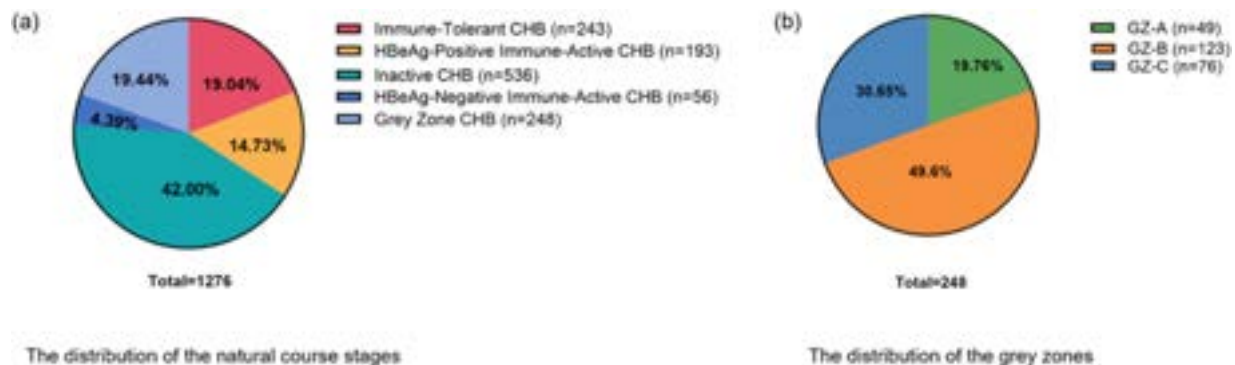


Figure: (abstract: WED-172): Distribution of natural course stages of pregnant women with CHB (a) and distribution of CHB pregnant women of grey zones (b)

Conclusion: Our study showed that inactive CHB was the most common natural course stage among pregnant women, but nearly one-fifth of CHB patients were classified as GZ. The risk of pregnancy complications and adverse pregnancy outcomes varied by natural history stage. Pregnant women with CHB should be closely monitored and managed to further prevent adverse pregnancy outcomes.

WED-173

Comparison of hepatitis B reactivation in patients with resolved hepatitis B infection receiving rituximab or non-rituximab based immunosuppressive therapy: does presence of hepatitis B surface antibody reduce the risk of reactivation?

Wei-Lun Liou¹, Gayathry Morvil¹, Rajneesh Kumar¹. ¹Singapore General Hospital, Gastroenterology and Hepatology, Singapore
Email: liouweilun@gmail.com

Background and aims: Hepatitis B virus (HBV) reactivation and flare may happen in patients with resolved HBV infection (Hepatitis B surface antigen negative, anti-HBc antibody positive) who receive immunosuppressants or chemotherapy. In comparison to Rituximab, most drugs only confer low to medium risk of HBV reactivation to this group of patients. The presence of hepatitis B surface antibody may reduce the risk of HBV reactivation. We compared the outcome of patients with resolved HBV infection who received rituximab or non-Rituximab immunosuppressive therapy and explored the utility of hepatitis B surface antibody in these patients.

Method: We retrospectively collected data of patients who were followed up at HBV immunosuppression clinic at Singapore General Hospital from 2016 to 2022. The lower limit of quantification of HBV DNA was 10 IU/ml. HBV reactivation (HBVr) is defined as a new detectable HBV DNA from previously undetectable DNA. HBV flare is defined as raised alanine aminotransferase of >3 times of upper limit normal in the presence of detectable DNA.

Results: Total 153 patients who did not receive prophylactic nucleoside analogue (NA) were included in the study. There were 70 male patients. The median age of patients was 64 years (IQR 15). The median duration of follow-up following initiation of immunosuppression was 21.4 months (IQR 25.5). 112 patients received non-rituximab therapy, and 41 patients received rituximab therapy. 11

patients in each group developed HBVr. Patients who received rituximab therapy had higher risk of HBVr when compared with non-rituximab group (26.8% vs 9.8%, $p=0.011$). HBVr resolved without needing NA in 8 patients in the rituximab group, and 7 patients in the non-rituximab group. No patient developed HBV flare during the follow-up. A baseline hepatitis B surface antibody level of more than 100 IU/L was associated with lower risk of HBVr in patients who received rituximab therapy (6.7% vs 41.7%, $p=0.019$), but no statistically significant difference in non-rituximab therapy patients (8.8% vs 9.8%, $p=0.573$).

Conclusion: Although the risk of HBVr was higher in patients receiving rituximab therapy, none of the patients developed HBV flare and HBVr resolved spontaneously in the majority. A hepatitis B surface antibody level of more than 100 IU/L may confer additional protection against HBVr in patients receiving rituximab therapy. Regular monitoring instead of prophylactic NA should be considered in this specific group of patients, as well as patients receiving non-rituximab therapy.

WED-174

Hepatitis delta virus (HDV) infection : frequency and outcome in persons living with HIV (PLWH). Data from the ICONA (Italian cohort of naïve for antiretrovirals) cohort

Massimo Puoti^{1,2}, Romina Salpini³, Alessandro Tavelli⁴, Lorenzo Piermatteo⁵, Stefano D'Anna³, Stefania Carrara⁶, Vincenzo Malagnino⁷, Valentina Mazzotta⁸, Giuseppina Brancaccio⁹, Giovanni Battista Gaeta¹⁰, Giulia Marchetti^{11,12}, Pierluigi Viale^{13,14}, Carlo Federico Perno¹⁵, Valentina Svicher³, Antonella d'Arminio Monforte⁴. ¹University of Milano Bicocca, School of Medicine, Milan, Italy; ²ASST GOM Niguarda, Infectious Diseases, Italy; ³University of Rome Tor Vergata, Department of Experimental Medicine, Italy; ⁴Icona Foundation, Milano, Italy; ⁵University of Rome Tor Vergata, Dept of Experimental Medicine, Italy; ⁶INMI, Unity of Microbiology and Biobank, Roma, Italy; ⁷University of Rome Tor Vergata, Department of Medicine of Systems, Clinical Infectious Diseases, Rome, Italy; ⁸INMI, Clinical and Research Infectious Diseases Department, Rome, Italy; ⁹University of Padua, Department of Molecular Medicine, Padua, Italy; ¹⁰University L. Vanvitelli, Infectious Diseases Unit, Naples,

	Rituximab (n = 41)	Non-Rituximab (n = 112)	p value
Gender: Male (%)	23 (56%)	47 (42%)	-
Age, median (IQR)	65.5 (13.8)	63 (13.0)	-
Underlying condition: Haematological condition Chronic condition on immunosuppressants* Breast malignancy	36 (87.8%) 5 (12.2%) -	16 (14.3%) 28 (25%) 28 (25%)	-
Duration of follow-up (months), median (IQR)	24.3 (25.8)	18.6 (25.8)	0.436
Baseline hepatitis B surface antibody >10 >50 >100	28 (68.3%) 20 (48.8%) 15 (36.6%)	83 (74.1%) 57 (50.9%) 45 (40.2%)	0.507 0.852 0.707
Overall hepatitis B reactivation	11 (26.8%)	11 (9.8%)	0.011

*Chronic conditions: autoimmune diseases, rheumatological diseases, renal transplant.

Figure: (abstract: WED-173): Comparison of baseline demographics and hepatitis b reactivation in patients receiving rituximab or non-rituximab therapy.

POSTER PRESENTATIONS

Italy; ¹¹ASST Santi Paolo e Carlo, Clinic of Infectious Diseases, Milano, Italy; ¹²University of Milano, Department of Health Sciences, Milano, Italy; ¹³Alma Mater Studiorum Bologna University, Department of Medical and Surgical Sciences, Bologna, Italy; ¹⁴IRCCS Azienda Ospedaliero Universitaria S. Orsola- Malpighi, Infectious Diseases Unit, Bologna, Italy; ¹⁵Bambino Gesù Pediatric Hospital, Rome, Italy
Email: massimo.puoti@ospedaleniguarda.it

Background and aims: HDV causes the most severe liver disease and suppressive antiviral treatment was recently available for this infection. PLWH are at risk of HDV infection. The factors related to HDV infection and its natural history in PLWH have poorly investigated. In order to assess the need for suppressive anti HDV treatment in PLWH, this retrospective case control study investigates the prevalence, risk factors, clinical correlates and the long-term outcome of people with HDV infection in a large prospective cohort of Italian PLWH naïve for antiretroviral therapy the multicenter prospective ICONA cohort (Italian Cohort of Naïve for Antiretrovirals). **Method:** We retrieved from the database or measured anti HDV reactivity in all HBsAg pos PLWH with an available serum sample: HDVRNA reactivity was tested by Robogene 2.0 (LOD: 6 IU/ml) in all anti HDV pos with an available serum sample. We compared demographic and clinical data between different groups and calculated Hazard Ratio (HR and Adjusted HR AHR) for Liver Related Hard Outcomes (LRHO: Liver decompensation, HCC, liver transplant or Liver Related Death whatever occurred first) from fitting a Cox regression model.

Results: 152/809 HBsAg pos PLWH (18.8%) showed anti HDV reactivity. They were significantly ($p < 0.01$) less frequently female (7.9% vs 18.1%), more frequently IDU (67.1 vs 15.8%), more frequently anti HCV pos (66 vs 16%), less frequently HCVRNA pos (11 vs 15%) and more frequently showed FIB-4 > 3.25 (25 vs 11%). A significantly lower proportion of anti HDV pos pts was still on follow-up in 2022 (23 vs 42%). HDV viremia was detected in 63/95 (68%) anti HDV pos patients. PLWH with HDVRNA reactivity showed more frequently a FIB4 > 3.25 (34 vs 9.7%) without significant differences in other characteristics. 25/95 were still on follow-up in 2022 (25 HDVRNA+ vs 28 HDVRNA-). HR and aHR for LRHO are reported in the table.

Table: Hazard Ratio (HR) and Adjusted HR (AHR) of developing liver failure (ESLD, HCC or Liver related death) after first HDV screening from fitting a Cox Regression model

HDV Status	HR	95% CI	P	AHR*	95% CI	P
HDVAb neg	1.00			1.00		
HDVAb pos/HDV-RNA miss	4.68	1.81 12.09	0.001	2.05	0.68 6.15	0.200
HDVAb pos/HDV-RNA neg	3.87	1.28 11.75	0.017	1.53	0.42 5.60	0.523
HDVAb pos/HDV-RNA pos	6.60	3.08 14.14	<0.001	4.08	1.69 9.86	0.002

Conclusion: One out of five HBV/HIV coinfecting individuals had been infected with HDV; they were more frequently male IDU with HCVAb pos/HCV RNA neg, suggesting a suppressive effect of HDV on HCV replication. Globally, 12% showed coinfection with 4 viruses (HIV, HBV, HDV, HCV). Both previous and active HDV infection are related to advanced liver disease. Only active HDV infection is related to a higher incidence of LRHO on follow-up. Pharmacological suppression

of HDV replication may improve the prognosis in PLWH with active HDV replication.

WED-175

Detection of hepatitis delta virus in seminal fluid and female genital tract

Oyungerel Lkhagva-Ochir¹, Saruul Enkhjargal², Anir Enkhbat³, Nyamtsengel Vangan⁴, Naranjargal Dashdorj³, Odgerel Oidovsambuu⁵. ¹Liver center, Ulaanbaatar, Mongolia; ²National university of mongolia, Ulaanbaatar, Mongolia; ³Liver center, Ulaanbaatar, Mongolia; ⁴Mongolian national university of medical sciences, Ulaanbaatar, Mongolia; ⁵National University of Mongolia, Department of Chemical and Biological Engineering, Ulaanbaatar, Mongolia
Email: l.oyungerel@onomfoundation.org

Background and aims: Mongolia has the highest prevalence of the hepatitis D virus (HDV), leading to high morbidity and mortality from liver diseases and HCC. HDV causes the most severe form of chronic viral hepatitis. In a recent study, it was estimated that anti-HDV prevalence is 67.5% among HBsAg positive population in Mongolia. The prevalence of HDV infection is relatively high among sexually active and young people, thus, the virus might be transmitted during sexual intercourse. Therefore, it is important to confirm the possibility of sexual transmission of HDV by detecting HDV-RNA in the semen and vaginal secretions of patients with chronic hepatitis Delta.

Method: From October 2022 to December 2022, patients from Liver Center, Ulaanbaatar, Mongolia were asked to enroll in this study. A total of 26 patient, (male 18, female 8, aged 23–48 years old) participated in the study. The average age of all participants is 36.5 years and 94% of them are married. The males and females were to refrain from sexual activity for at least 48 hours prior to test. Females also were recommended to do not use any intravaginal products for at least 48 hours prior to the collection of vaginal/cervical swab specimens. The seminal fluids were collected in a sterile container by masturbation. Vaginal/cervical specimens were collected by rubbing with nasopharyngeal swab dedicated for a molecular biology test. Viral RNA was extracted by ... and presence of HDV-RNA was detected subsequently by real time RT-PCR analysis.

Results: In male group, 38.8% (7/18) of seminal fluid samples were positive and in female group, 87.5% (7/8) of vaginal/cervical swab samples were positive. This result indicates that HDV is more likely present in genital cavity of female patients than in seminal fluid of male patients. For male group, correlation between HDV RNA existence in seminal fluid and serum RNA level was not observed. In contrast, female group has a correlation between HDV RNA existence in genital tract and serum RNA level. HDV-RNA was not detected in the sample from only one woman, who had low number of HDV RNA in her serum sample (197IU/ml).

Conclusion: HDV RNA can be detected in seminal fluid of male patient and in genital tract of female patient. This result is solid evidence to indicate the possible risk of sexual transmission of HDV. In the future, we need to study in more detail.

HDV RNA in the blood serum, seminal fluid and genital tract of male and female patients

	Participants	Sex	Age	RT-PCR in blood serum		RT-PCR in seminal fluid and genital tract	
				Ct value	IU/ml	Ct value	IU/ml
1	M1A	Male	38	27	63900	No Ct	0
2	M2A	Male	32	No Ct	0	No Ct	0
3	M3A	Male	34	25.77	78730	No Ct	0
4	M4A	Male	48	21.98	875600	36.03	93
5	M5A	Male	36	20.63	2230000	No Ct	0
6	M6A	Male	35	19.89	6934000	32.28	1010
7	M7A	Male	32	29.27	29500	No Ct	0
8	M8A	Male	32	22.08	4761000	27.33	23700
9	M9A	Male	38	29.29	63510	No Ct	0
10	M10A	Male	34	23.1	902000	No Ct	0
11	M11A	Male	34	21	4320000	33.23	551
12	M12A	Male	35	20.94	5350000	No Ct	0
13	M13A	Male	34	22.52	3052000	No Ct	0
14	M14A	Male	23	24.54	360600	No Ct	0
15	M15A	Male	34	21.79	5904000	33.76	393
16	M17A	Male	32	21.96	2830000	No Ct	0
17	M18A	Male	45	22.39	1303000	35	179
18	M19A	Male	34	19.76	6298000	34.5	246
19	F1B	Female	38	22.74	518400	29.16	7380
20	F2C	Female	41	25.36	7407000	30.48	3190
21	F3B	Female	46	20.79	1865000	31.54	1670
22	F4B	Female	37	23.71	545000	33.58	441
23	F5B	Female	46	19.94	3410000	30.65	2870
24	F6B	Female	33	22.86	3052000	28.43	11800
25	F7C	Female	32	23.99	800000	29.83	4830
26	F8B	Female	35	36.31	197	No Ct	0

Percentage of HDV RNA detected in seminal and genital tract of male and female patients

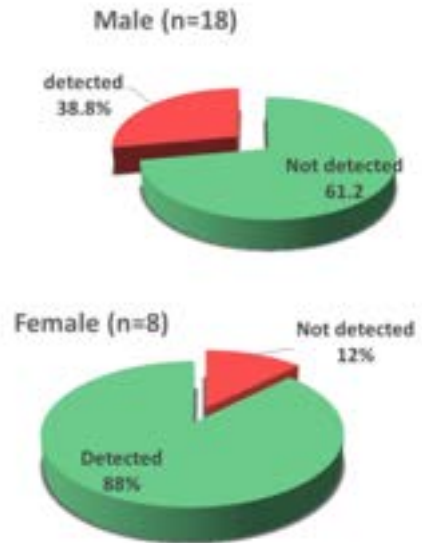


Figure: (abstract: WED-175).

WED-176

Ultrasensitive HBV-RNA quantification by droplet digital PCR is a promising biomarker to optimize the staging of chronic HBV infection and to identify minimal viral activity under prolonged virological suppression

Romina Salpini¹, Lorenzo Piermatteo^{1,2}, Stefano D'Anna¹, Leonardo Duca¹, Giulia Torre¹, Anna Francesca Guerra³, Chiara Boarini³, Alessandro Tavelli⁴, Paolo Ventura³, Francesca Ceccherini Silberstein¹, Antonello Pietrangelo³, Massimo Puoti⁵, Antonella d'Arminio Monforte⁴, Gianluca Abbati³, Upkar Gill⁶, Patrick Kennedy⁶, Valentina Svicher^{1,2}. ¹University of Rome Tor Vergata, Experimental Medicine, Italy; ²University of Rome Tor Vergata, Department of Biology, Italy; ³University of Modena and Reggio Emilia, Italy; ⁴Icona Foundation, Italy; ⁵Niguarda Hospital, Milan, Italy; ⁶Blizard Institute, Barts and The London SMD, QMUL, London, United Kingdom, United Kingdom
Email: rsalpini@yahoo.it

Background and aims: Serum HBV-RNA quantification reflects the burden of virions containing pre-genomic RNA (pgRNA) and is used as surrogate marker of cccDNA transcriptional activity. Here, we define HBV-RNA levels across the natural history of HBV infection, including the under studied phase of occult HBV infection (OBI) and the levels after long-term NUC exposure.

Method: This study includes 106 treatment-naïve patients (pts) categorized in 17 eAg+ with chronic infection (CI), 7 with eAg+ chronic hepatitis (CH), 50 with eAg- CI and 32 with eAg- CH according to EASL guidelines. 38 eAg- virologically suppressed pts under long-term NUC treatment and 28 Anti-HBc+/HBsAg- pts (HIV-coinfected with a serological status compatible with OBI) are also included. Serum HBV-RNA is quantified by droplet digital PCR (ddPCR) targeting pgRNA (LOQ: 5 copies (cps)/ml).

Results: eAg+ CI and CH have elevated HBV-RNA levels (median [IQR]: 7.5 (4.3–8.3) and 7.1 (6.5–7.5) log cps/ml) in line with high HBV-DNA and HBsAg production (median [IQR] HBV-DNA: 9.2 [6.4–9.9] and 8.9 [8.7–9.2] log IU/ml; HBsAg: 20,895 [6,778–72,608] and 52,518 [30,059–80,056] IU/ml).

HBV-RNA undergoes a significant decrease in eAg- phases, achieving the lowest levels in eAg- CI (median [IQR]: 0.6 [0.2–1.4] in eAg- CI vs

2.0 [1.2–2.3] log cps/ml in eAg- CH, $P < 0.001$), paralleling the declining trend of HBV-DNA and HBsAg. In both eAg- phases, HBV-RNA correlates with HBV-DNA ($Rho = 0.49$, $P < 0.001$ for eAg- CI and $Rho = 0.33$, $P = 0.06$ for eAg- CH) while no correlation with HBsAg is revealed ($Rho = 0.2$ and 0.12 , $p > 0.2$), consistent with HBsAg production from integrated HBV-DNA. Notably, by AUROC, HBV-RNA <50 cps/ml shows the best accuracy in predicting the status of eAg- CI (sensitivity: 87.5%, specificity: 71%). In virologically suppressed pts (median [IQR] NUC duration: 6.0 [4.1–9.1] years), HBV-RNA is positive in 78.9% of pts with a median of 1.7 (1.4–2.0) log cps/ml. Notably, the rate of HBV-RNA positivity and HBV-RNA levels remain stable independently from NUC duration, suggesting no decline in intrahepatic HBV activity over prolonged therapy (73.3%, 75% and 90% for NUC duration of <5, 5–9 and ≥9 years, with median [IQR] HBV-RNA of 1.7 [1.5–1.9], 1.4 [1.2–1.4] and 1.8 [1.6–2.3] log cps/ml). Finally, HBV-RNA is also positive in 32.1% of Anti-HBc+/HBsAg- pts (median [IQR]: 1.1 (0.9–1.3) log cps/ml), supporting occult viral activity despite HBsAg negativity.

Conclusion: The production of pgRNA-containing viral particles predominates during the initial phases of chronic infection and decreases after HBeAg-seroconversion. In this context, HBV-RNA can enhance the categorization of chronic HBV infection including the eAg- infection status. The ultra-sensitive HBV-RNA quantification can detect minimal viral activity in the setting of long-term NUC treatment or OBI, providing added value in the identification of patients achieving functional cure.

WED-177

Study of hepatitis delta virus replication markers in anti-HBc positive patients with chronic hepatitis C

Antonio Madejón^{1,2}, Miriam Romero^{1,2}, Araceli García-Sánchez¹, Antonio Oliveira Martin^{1,2}, Pilar Castillo¹, José Carlos Erdozain¹, Francisco Javier Garcia-Samaniego Rey^{1,2}. ¹Hepatology Unit, Hospital Universitario La Paz, Madrid, Spain; ²Centro de Investigación Biomédica en Red (CIBER), Spain
Email: javiersamaniego@telefonica.net

Background and aims: Recent works have identified antibodies and genome sequences from the hepatitis delta virus (HDV) in patients

POSTER PRESENTATIONS

with chronic hepatitis C (CHC) in absence of any marker of infection with hepatitis B virus (HBV). The objective of this work was to analyze the prevalence of active HDV infection (positive for HDV genome) in patients with chronic hepatitis C with evidence of past exposure to HBV.

Method: A cohort of 129 anti-HBc positive patients was retrospectively analyzed, 20 of whom (15%) were positive for anti-HBs antibodies. Seventy-seven patients (60%) were Caucasian and 52 (40%) Sub-Saharan. Regarding co-infection markers, 65 (50%) were HIV positive, with HIV-RNA positivity in 20/65 (31%), and 92 (71%) were anti-HCV positive with detectable HCV-RNA in 23/92 (25%) patients. Fibrosis stage (TE) was: F0-F1 in 42/129 (33%), F2 in 16 (12%), F3 in 5 (4%), F4 in 15 (12%) and indeterminate in 51 (39%) patients. All patients were analysed for the presence of anti-HDV antibodies and delta antigen (HDAg) using commercial kits. The presence of HDV-RNA was also analyzed by in-house RT-PCR. A longitudinal follow-up was performed in those HDV-RNA positive patients, in order to analyze the evolution of HDV viremia. The complete coding region of HDAg was amplified in at least one sample. The presence of HBsAg and HBV-DNA was also confirmed.

Results: Anti-HDV antibodies were detected in 8 (6%) patients. The prevalence of anti-HDV was higher in anti-HCV positive than in negative patients [7/92 (8%) vs 1/37 (3%), respectively; $p=0.03$]; in HIV-negative patients compared to positives [6/64 (9%) vs 2/65 (3%), respectively; $p=0.1$]; and in Caucasian vs Sub-Saharan patients [7/77 (9%) vs 1/52 (2%), respectively; $p=0.09$]. HDAg and HDV-RNA were detected in only 1 patient, who was HCV-RNA positive, HIV negative, and from sub-Saharan origin. The entire coding region of HDAg was amplified. HDV-RNA positivity was confirmed in three sequential samples of this patient taken every 6 months, showing slight fluctuations in viral load (2,540, 1,250, and 6,450 copies/ml, respectively). HBV-DNA and HBsAg were not detected.

Conclusion: These results suggest that active HDV viral replication can be detected in patients with detectable HCV-RNA in the absence of any marker of active HBV infection. Whether HDV replication process is sustained by low levels of HBsAg expression or by interaction with HCV must be further investigated.

WED-178

Long-term outcomes of a population-based cohort of chronic hepatitis B (CHB) patients in West Africa

Gibril Ndow¹, Yusuke Shimakawa², Damien Leith³, Sulayman Bah¹, Rohey Bangura¹, Lamin Bojang¹, Amie Ceesay¹, Queen Bola-Lawal¹, Alhagie Touray¹, Abdoulie Jatta¹, Jainaba Barry¹, Fatou Bintou Nyassi¹, Gabriel Lambert⁴, Amelia Cook⁵, Patrick Ingiliz⁶, Sheikh Omar Bittaye⁷, Yazan Haddadin⁸, Erwan Vo Quang¹, Stéphane Chevaliez⁹, Gavin Cloherty¹⁰, Gora Lo¹¹, Coumba Toure-Kane¹¹, Isabelle Chemin¹², Ramou Njie⁷, Dalessandro Umberto¹, Mark Thursz⁴, Maud Lemoine⁴. ¹MRC Unit The Gambia at LSHTM, Gambia; ²Institut Pasteur, France; ³Glasgow Royal Infirmary, United Kingdom; ⁴Imperial College London, United Kingdom; ⁵Cicely Saunders Institute, United Kingdom; ⁶APHP Henri-Mondor University Hospital, France; ⁷School of Medicine, University of The Gambia, Gambia; ⁸University of Sussex, United Kingdom; ⁹Hopital Henri Mondor, France; ¹⁰Abbott Labs, United States; ¹¹IRESEF, Senegal; ¹²U1052 INSERM, France
Email: gndow@mrc.gm

Background and aims: Longitudinal data in untreated chronic hepatitis B (CHB) infected patients in Africa who are ineligible for antiviral therapy is scarce and urgently needed to inform treatment and monitoring guidelines adapted to this population. We assessed the long-term clinical outcomes of a population-based cohort of CHB subjects in West Africa.

Method: Between 2019 and 2021, all CHB patients enrolled in the PROLIFICA cohort between 2011 and 2014 in The Gambia and Senegal were invited for reassessment of liver disease using fasting liver stiffness measurement (LSM) (Fibroscan), abdominal ultrasound,

HBV DNA measurement (Abbott, USA), HBsAg and HBeAg serologies, liver enzymes, and full blood count.

This analysis focused on untreated participants in The Gambia who were ineligible for antiviral therapy at baseline according to the 2012 EASL criteria. Number of deaths was collected using death certificates and verbal autopsy to assess mortality rate. Liver disease progression was defined as the proportion of patients who: (i) became eligible for antiviral therapy according to the 2017 EASL treatment criteria; and/or (ii) developed clinically significant fibrosis (LSM ≥ 7.8 kPa) or cirrhosis (LSM ≥ 9.5 kPa); and/or (iii) developed hepatocellular carcinoma (HCC).

Results: At baseline, 93 of 943 participants fulfilled EASL treatment criteria or received antiviral therapy, leaving 850 patients who were ineligible and untreated. After a median follow-up of 6.0 years (IQR: 5.5–6.8), 279 (32.8%) participants were lost to follow-up (LTFU) and 27/850 (3.2%) died, including 10 liver-related deaths, giving an overall mortality rate at 584/100,000 person-years (IQR: 400–852). After adjusting for sex and age, baseline APRI ≥ 2 was a strong predictor of overall mortality (OR: 7.2 (1.7–31.3), $p=0.008$). 544/850 (64.0%) had a full liver reassessment: 321/544 (59.0%) were males, median age: 41 (37–48) years, median BMI: 22.8 (20.1–26.1) kg/m², and none reported excessive alcohol intake. Most participants (348/544 (64.0%)) were considered as inactive chronic carriers. 131/544 (24.0%) had viral load ≥ 2000 IU/ml, 49/541 (9.1%) had an ALT level ≥ 40 IU/L and 36/540 (6.7%) had significant liver fibrosis including 13 (2.4%) with cirrhosis and 1 with decompensated cirrhosis. Incidence of HBsAg loss was 0.69 (23/544, CI 0.46–1.04) and higher among females (OR: 2.56 (1.03–6.34) $p=0.042$). Amongst 544 patients reassessed, no HCC was detected but 39 (7.2%) had liver disease progression: 3.3% newly eligible for treatment and 3.9% had liver fibrosis progression, including 15/540 (2.8%) new cirrhotic patients. Amongst patients with no significant liver fibrosis at baseline, 32/492 (6.5%) had liver disease progression including 13 (2.6%) cases of cirrhosis. In multivariate analysis after adjusting for sex and age, baseline HBV DNA viral load ≥ 2000 IU/ml was associated liver disease progression (OR 2.8, 95%CI: 0.9–8.5, $p=0.027$).

Conclusion: This longitudinal study, the first of its kind in Africa, indicates that the number of liver events is not negligible in ineligible and untreated CHB patients, suggesting that monitoring should be maintained with a special focus on patients with viral load ≥ 2000 IU/ml.

WED-179

Incidence of hepatitis D virus super-infection in HBsAg positive patients (The Inci-D cohort study)

Patrick Ingiliz^{1,2,3}, Erwan Vo Quang^{1,4}, Maud Lemoine^{4,5}, Amie Ceesay^{4,6}, Gibril Ndow⁴, Marie-Noëlle Hilleret⁷, Anne Laure Mazialivoua¹, Yusuke Shimakawa⁸, Alhagie Touray⁴, Jean-Michel Pawlotsky^{2,9}, Isabelle Chemin⁶, Stéphane Chevaliez^{2,9}, Vincent Leroy^{1,2}. ¹APHP Henri-Mondor University Hospital, Hepatology, Créteil, France; ²Inserm U955, Créteil, France; ³Maison Médicale Chemin Vert, Paris, France; ⁴MRC The Gambia Unit @ LSHTM, Gambia; ⁵Imperial College London, London, United Kingdom; ⁶Cancer Research Center of Lyon (CRCL), INSERM U1052, CNRS UMR-5286, Lyon, France; ⁷University Grenoble-Alpes, Grenoble, France; ⁸Institut Pasteur, Paris, France; ⁹APHP Henri-Mondor University Hospital, Virology, Créteil, France
Email: patrick.ingiliz@aphp.fr

Background and aims: Super-infection with the hepatitis D virus (HDV) leads to a more aggressive form of chronic hepatitis in patients infected with the hepatitis B virus (HBV). While around 5% of HBsAg-positive individuals are estimated to be HBV-HDV dually infected globally, the timepoint of super-infection is unknown and longitudinal repeated HDV testing is not yet supported by international guidelines. HDV infection occurs most likely parenterally or sexually and depends on the individual's particular risk. In most cases, it remains unclear when super-infection has occurred. Inci-D is a collaborative multicenter and longitudinal cohort study that aims

to evaluate the incidence of HDV super-infection in HBsAg chronic carriers from West Africa and Europe.

Method: The Inci-D cohort consists of two distinct HBV cohorts of clinical meta-data and stored clinical specimens including plasma or dried-blood spots (DBS). Cohort A is a West African cohort derived from the PROLIFICA population-based study in The Gambia. Cohort B is a French cohort including out-patients seen in two university hospitals (Grenoble Alpes and Henri Mondor AHPH). The HBsAg positive patients' first available stored blood sample was used to calculate the baseline prevalence. HDV-antibody (HDVAb) levels were detected using the Diasorin serology kit (Italy). The incidence rate was calculated using the most recent available blood sample. Here, we present preliminary results from cohort A.

Results: For cohort A, 942 blood samples (915 plasma, 27 DBS) of HBsAg-positive individuals were available at baseline. The median age was 35 years (interquartile range (IQR): 31–43), 592/942 (63%) were male, the median ALT levels were 24 U/L (IQR: 19–31), and the median HBV DNA level was 1.90 Log IU/ml (IQR:1–2.6). At baseline, 14/942 individuals (1.5%) were HDVAb-positive: median age 37 years (IQR: 34–57), 7/14 (50%) male, median ALT levels 21 U/L (IQR: 18–33), and median HBV DNA level 1.2 Log IU/ml (IQR:1–2.2). Among HDVAb-negative patients at baseline, 566 individuals had a follow-up sample available (520 plasma, 46 DBS) with an overall follow-up time of 3363 patient-years. After a median follow-up time of 6.0 years (IQR: 5.5–6.8), 8 individuals were detected to be newly HDVAb-positive, representing an incidence rate of 2.37/1000 patient-years. The HDV prevalence at follow-up was 2.1%, indicating a 40% increase from baseline. Median age at of HDV super-infected patients was 35 years (IQR: 34–57), 88% were male. Analyses on cohort B are ongoing and will be presented.

Conclusion: Hepatitis delta superinfection increases considerably in HBsAg-positive carriers in an intermediate HDV prevalence setting, putting patients at risk for advanced liver disease and death. In order to identify individuals with need for treatment or surveillance, repeated HDV serology testing should be implemented by international guidelines.

WED-180

Significant heterogeneity in long-term risks of cirrhosis or hepatocellular carcinoma among a national cohort of U.S. veterans with non-cirrhotic, treatment naïve chronic hepatitis B in the immune tolerant phase

Zeyuan Yang¹, Ramsey C. Cheung², Robert Wong², ¹VA Palo Alto Health Care System, United States; ²Stanford University School of Medicine, VA Palo Alto Healthcare System, Palo Alto, United States
Email: rwong123@stanford.edu

Background and aims: Patients with chronic hepatitis B (CHB) in the “immune-tolerant” phase are not typically recommended for routine antiviral therapy. However, risk of progression to cirrhosis or HCC persists, and debate remains as to whether antiviral therapy is beneficial in certain subsets of this population. We aim to evaluate long-term risks of cirrhosis or HCC among non-cirrhotic, treatment-naïve CHB patients with alanine aminotransferase (ALT) <70 U/L and whether disparities in cirrhosis or HCC risk exist.

Method: Using data from the U.S. National Veterans Affairs database from 2010 to 2022, Veterans with treatment-naïve, e-antigen (eAg) positive CHB with baseline ALT <70 U/L and minimum 12 months of follow-up were identified. Patients with concurrent HIV, hepatitis C, or hepatitis delta infections were excluded. Patients with cirrhosis or HCC at baseline or within 6 months of study entry were excluded. Incidence of cirrhosis or HCC (per 100 person-years) was stratified by patient demographics, clinical characteristics, and baseline HBV DNA (<20 000 IU/ml (Low-DNA), 20 000–10⁷ IU/ml (Intermediate-DNA), and >10⁷ IU/ml (High-DNA)). Patients were censored at development of cirrhosis or HCC, death, initiation of antiviral therapy, or end of follow-up period. Comparisons of cirrhosis or HCC incidence between groups utilized the z-statistic using standard equations.

Results: Among 3,526 Veterans with treatment-naïve CHB and ALT <70 U/L, 19.2% (n = 678) were eAg positive, among whom 91.0% were men, 39.2% African American, 36.6% non-Hispanic white, 20.0% Asian, 4.2% Hispanic, mean age 53 ± 14, 69% had Low-DNA, 13% had Intermediate-DNA, and 18% had High-DNA. Overall incidence of cirrhosis was 1.22 per 100 person-years (95% CI 0.89–1.56) and incidence of HCC was 0.21 per 100 person-years (95% CI 0.07–0.35). Compared to patients with Low-DNA, there was a trend towards higher risk of cirrhosis in patients with Intermediate DNA (2.21 vs. 1.02 per 100 person-years, p = 0.07), but no difference in risk of HCC was observed by baseline HBV DNA. Older age was associated with higher risk of cirrhosis and HCC. Patients with diabetes had significantly higher incidence of cirrhosis (2.49 vs. 0.96 in patients without diabetes, per 100 person-years, p < 0.01). Compared to patients with baseline FIB-4 score <1.45, patients with FIB-4 >3.25 had higher incidence of cirrhosis (5.94 vs. 0.67 per 100 person-years, p < 0.01) and HCC (0.73 vs. 0.27 per 100 person-years, p < 0.05).

Conclusion: Among a national cohort of treatment-naïve, eAg positive patients with non-cirrhotic CHB and baseline ALT <70 U/L, overall long-term risk of cirrhosis or HCC remains low. However, older age, presence of diabetes, and baseline FIB-4 > 3.25 was associated with significantly higher risks of disease progression. Identifying “high risk” features among “immune tolerant” CHB patients may identify individuals that would benefit from earlier treatment initiation.

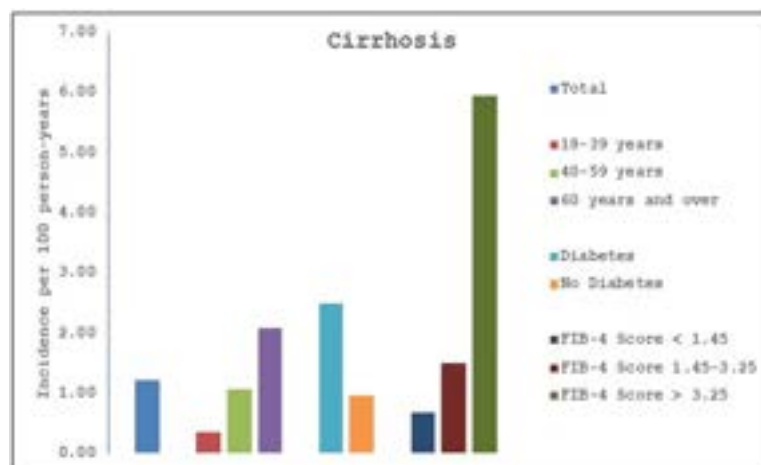


Figure: (abstract: WED-180).

WED-181

Contrasting immune fingerprints of chronic hepatitis B Virus infection in adults from South Africa and the United Kingdom

Marion Delphin¹, Louise Downs^{2,3}, Emily Martyn^{1,4}, Gavin Kelly¹, Marije Van Schalkwyk^{5,6}, Susan Hugo^{5,7}, Elizabeth Waddilove¹, Cori Campbell², Tingyan Wang^{2,8}, Sheila Lumley^{2,3}, Catherine De Lara², Dominique Goedhals^{9,10}, Christo van Rensburg^{5,6}, Sue Wareing³, Polly Fengou³, Jacqueline Martin³, Monique Andersson^{2,6}, Ivana Carey¹¹, Azim Ansari², Wolfgang Preiser^{5,7}, Shiraaz Gabriel^{5,7}, Jantjie Taljaard^{5,6}, Eleanor Barnes^{2,3}, Tongai Gibson Maponga¹², Philippa Matthews^{1,2,13,14}. ¹The Francis Crick Institute, LONDON, United Kingdom; ²Nuffield Department of Medicine, Medawar Building for Pathogen Research, University of Oxford, Oxford, United Kingdom; ³John Radcliffe Hospital, Department of Infectious Diseases and Microbiology, oxford, United Kingdom; ⁴London School of Hygiene and Tropical Medicine, United Kingdom; ⁵Tygerberg Academic Hospital, South Africa; ⁶Stellenbosch University, Faculty of Medicine and Health Sciences, Cape Town, South Africa; ⁷Stellenbosch University, South Africa; ⁸NIHR Oxford Biomedical Research Centre, University of Oxford, Oxford, United Kingdom; ⁹PathCare Vermaak, South Africa; ¹⁰University of the Free State, South Africa; ¹¹Institute of Liver Studies, King's college Hospital, United Kingdom; ¹²Division of Medical Virology, Faculty of Medicine and Health Sciences, Stellenbosch University, South Africa; ¹³University

College London, Division of Infection and Immunity, United Kingdom; ¹⁴University College London Hospital, Department of Infectious Diseases, United Kingdom
Email: marion.delphin@crick.ac.uk

Background and aims: Hepatitis B Virus (HBV) interaction with the immune system is a key determinant of infection outcome. As the HBV field advances towards novel therapies (amongst which immunoregulatory drugs), enhanced risk stratification, and cancer prevention, there is a pressing need to better understand the immunological profiles that underlie diverse disease outcomes. Unfortunately, while accounting for almost 70% of all HBV infections worldwide, African populations have been neglected in clinical studies. We set out to compare circulating levels of ten cytokines, alongside host demographics and viral biomarkers, in cohorts based in the United Kingdom (UK) and South Africa (SA).

Method: Serum samples were obtained from adult patients enrolled at Oxford University Hospitals, UK (n=60), and the Tygerberg Hospital in Cape Town, SA (n=32) with chronic HBV mono-infection (ethics ref.N17/01/013). HBsAg, HBeAg and HBV VL were estimated using standard clinical laboratory protocols, and HBcrAg were quantified using a chemiluminescent assay (Lumipulse G HBcrAg assay, Fujirebio). GM-CSF, IFN α 2 α , IL-2, IL-6, IL-8, IL-10, IL-21, IP-10, PD-1 and TNF- α were quantified using multiplex ELISA (K151AEL-1, MesoScaleDelivery). Patient meta-data were recorded at the time of

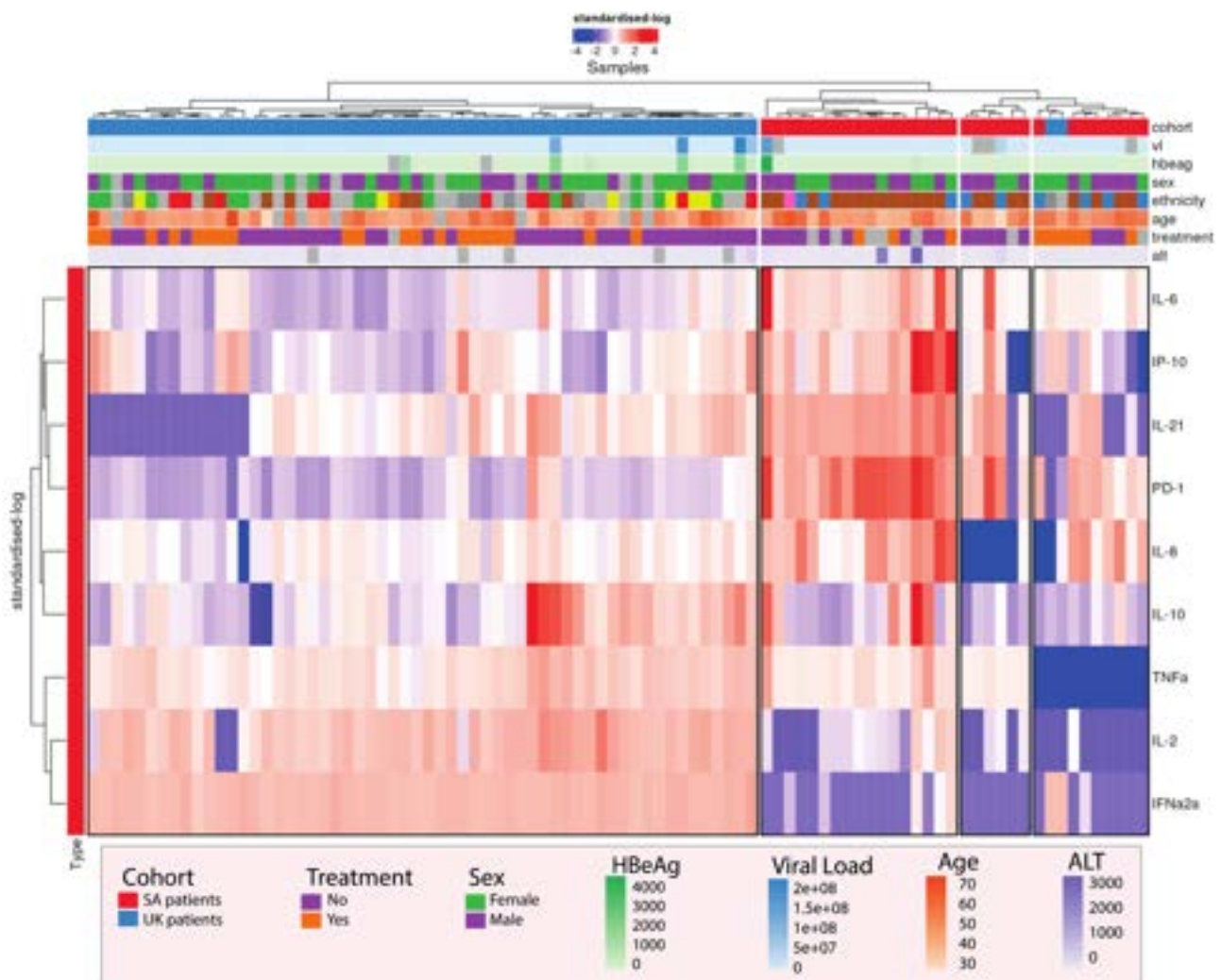


Figure: (abstract: WED-181): Log-standardised heatmap representation of data representing adults with chronic HBV mono- infection (SA cohort in red and UK in blue).

recruitment, supported by Electronic Patient Records where available. For the analysis, using a euclidean distance, samples were hierarchically clustered based purely on standardised log-transformed cytokine measurements using Ward's method for linkage. P values were calculated using Mann Whitney test in Prism v. 8.0.

Results: There were no significant differences between the two cohorts in terms of age ($p = 0.09$), sex ($p = 0.07$) or treatment ($p = 0.61$). HBV related biomarkers were comparable between the two cohorts, including HBcrAg ($p = 0.06$), viral load ($p > 0.99$), HBeAg status ($p = 0.74$) and ALT ($p = 0.81$). However, the two cohorts presented distinct immune profiles. The SA cohort is dominated by a decreased level of IL-2, IL-10 and IFN α 2a, while IP-10, PD-1 and IL-6 are increased ($p < 0.0001$ for all except IFN α 2a, $p = 0.09$) compared to the UK cohort. These clusters did not co-vary with other attributes of the patient, markers of infection or treatment (Figure 1). Of note, the SA cohort could be subdivided into three immune profiles, but without any significant differences.

Conclusion: In this study, CHB patients from SA and the UK have distinct immune profiles, which are not clearly related to other host features or laboratory characteristics of infection. At present, it is unclear if these differences are attributable to host characteristics, viral genetics, exposure to treatment, or other environmental influences. Our data highlight the need for further population-based studies to unravel the diversity in immune profiles. Enhanced understanding of the mechanisms that determine disease outcomes and treatment response are needed to support interventions that reduce the burden of liver disease associated with HBV.

WED-182

Dried blood spot (DBS): a new tool for screening, diagnosis and monitoring of hepatitis D virus (HDV) infection

Rola Matar¹, Alexandre Soulier¹, Valérie Ortonne¹, Olivia Garrigou¹, Pierre Cappy¹, Vincent Leroy², Jean-Michel Pawlotsky¹, Stéphane Chevaliez¹. ¹French National Reference Center for Viral Hepatitis B, C and delta Department of Virology and INSERM U955, Hôpital Henri Mondor, Université Paris-Est Créteil, France; ²Department of Hepatology and Inserm U955, Hôpital Henri Mondor, Université Paris-Est Créteil, France
Email: rola.matar@aphp.fr

Background and aims: Hepatitis D virus (HDV) infection is one of the major public health concerns worldwide. Globally, it is estimated that 5 to 10% of chronic HBsAg carriers are co-infected with HDV. Hepatitis Delta infection can lead to a rapid disease progression towards cirrhosis and hepatocellular carcinoma. The diagnosis of HDV infection is crucial for the management of the disease. Dried blood spot (DBS) sampling is a useful tool for the collection, storage, and shipment of whole blood specimens. The current study was designed to evaluate the performance of standardized HDV diagnostic and monitoring tools in analyzing samples from DBS.

Methods: Paired plasma and whole blood specimens collected using the DBS technique from 110 individuals including 74 patients followed in a tertiary care center and 36 blood donors were tested for virological markers (anti-HD and HDV RNA detection as well as HDV genotype determination) used to diagnose and monitor HDV infection.

Results: Immunological assay detection of anti-HD antibodies in specimens from DBS was reliable after the establishment of a new signal-to-cut-off ratio (0.2545 and 0.2340 using LIAISON XL murex Anti-HDV from DiaSorin and HDV Ab from DIA.PRO assays, respectively). These optimal cutoffs were associated with specificities of 97.5% and 87.5% and sensitivities of 93.1% and 94.2% for the respective

assays. HDV RNA viral load was detected from DBS in the vast majority of patients with active replication using the EurobioPlex HDV qRT-PCR assay, but HDV RNA levels were substantially lower than those detected in the corresponding plasma specimens. The mean HDV RNA detected in whole blood was 1.2 Log IU/disk lower compared to plasma. HDV genotype determination using phylogenetic analysis of a part of R0 region of the delta antigen was achieved in DBS samples with 100% concordance with results obtained from plasma specimens.

Conclusion: This study has shown that whole blood specimens collected on DBS can be used to diagnose and to monitor HDV infection. DBS specimen collection is a clinically relevant tool for improving the access to hepatitis D diagnosis around the world.

WED-183

The role of PAGE-B score in predicting the development of hepatocellular cancer in patients with chronic delta hepatitis

Onur Keskin¹, Cagdas Kalkan², Bengi Ozturk³, Aysun Caliskan², Hasan Sahin⁴, Mesut Gumussoy², Esra Yurdcu⁵, Mithat Bozdayi⁵, Murat Akyildiz⁶, Mujdat Zeybel⁶, Ramazan Idilman⁵, Cihan Yurdaydin⁶. ¹Hacettepe University School of Medicine, Gastroenterology, Ankara, Turkey; ²Ankara University School of Medicine, Gastroenterology, Ankara, Turkey; ³Hacettepe University School of Medicine, Gastroenterology, Turkey; ⁴Hacettepe University School of Medicine, Internal Medicine, Turkey; ⁵Ankara University Hepatology Institute, Ankara, Turkey; ⁶Koc University School of Medicine, Gastroenterology, Turkey
Email: onurkeskin81@gmail.com

Background and aims: The aim of this study is to determine the effectiveness of the PAGE-B score in predicting the development of hepatocellular cancer (HCC) in chronic delta hepatitis (CDH) patients.

Method: 124 CDH patients (88 males/36 females; mean age: 40.3 ± 10 ; 28 cirrhotic-96 noncirrhotic) who received interferon therapy for at least 6 months and had a median follow-up of 115 (12-144) months were included in the study. Patients received median 2 (1-8) episodes of interferon (IFN) therapy. Patients who were found to be HDV RNA negative at the end of 2 years following the end of treatment were considered interferon responsive (n:40). PAGE-B scores of all patients were recorded using previously recorded baseline clinical and laboratory parameters. The clinical and laboratory parameters and PAGE-B scores of the patients who developed and did not develop HCC during the follow-up period were compared and the role of the PAGE-B score in the prediction of HCC in patients with CDH was evaluated.

Results: HCC developed in 21 (18M/3F) patients during the follow-up period. When the patients who developed and did not develop HCC were compared, it was found that the patients who developed HCC were older (47.4 ± 7.5 vs 38.8 ± 10.2 ; $p < 0.01$) and had higher GGT values (121 ± 68 vs 71 ± 74 ; $p < 0.01$). It was observed that HCC developed more frequently in patients with cirrhosis and those who did not respond to IFN (55% cirrhotics vs 11% in noncirrhotics; $p < 0.01$ and 7.5% in IFN-responders vs 21% in IFN-non-responders; $p = 0.04$). By multivariate analysis, age, presence of cirrhosis and GGT level were independent predictors of HCC development. Patients who developed HCC had higher PAGE-B scores than patients who did not develop HCC (15.9 ± 3.4 vs 11.3 ± 4.6 ; $p < 0.01$). Using receiver operating characteristic (ROC) analysis with Youden index, a PAGE-B cut-off score of 13 predicted HCC development with 81% sensitivity, 60% specificity and area under ROC curve of 0.79. Only one patient with a PAGE-B score of < 10 developed HCC on a median follow-up of close to 10 years.

POSTER PRESENTATIONS

Conclusion: PAGE-B score predicts HCC in CDH with a similar strength to that reported for chronic hepatitis B

WED-184

Identification and external validation of the optimal ALT thresholds for ruling in significant histologic disease in chronic hepatitis B

Zhiyi Zhang¹, Jian Wang^{2,3}, Li Zhu⁴, Yilin Liu¹, Xiaomin Yan², Yuanwang Qiu⁵, Chuanwu Zhu⁴, Jie Li^{1,2,3}, Chao Wu^{1,2,3}, Rui Huang^{1,2,3}. ¹Department of Infectious Diseases, Nanjing Drum Tower Hospital Clinical College of Traditional Chinese and Western Medicine, Nanjing University of Chinese Medicine, Nanjing, Jiangsu, China;

²Department of Infectious Diseases, Nanjing Drum Tower Hospital, The Affiliated Hospital of Nanjing University Medical School, Nanjing, Jiangsu, China; ³Institute of Viruses and Infectious Diseases, Nanjing University, Nanjing, Jiangsu, China; ⁴Department of Infectious Diseases, The Affiliated Infectious Diseases Hospital of Soochow University, Suzhou, Jiangsu, China; ⁵Department of Infectious Diseases, The Fifth People's Hospital of Wuxi, Wuxi, Jiangsu, China
Email: doctor_hr@126.com

Background and aims: Identifying the optimal alanine aminotransferase (ALT) threshold for rule-in and rule-out significant liver inflammation and fibrosis is critically important for the management

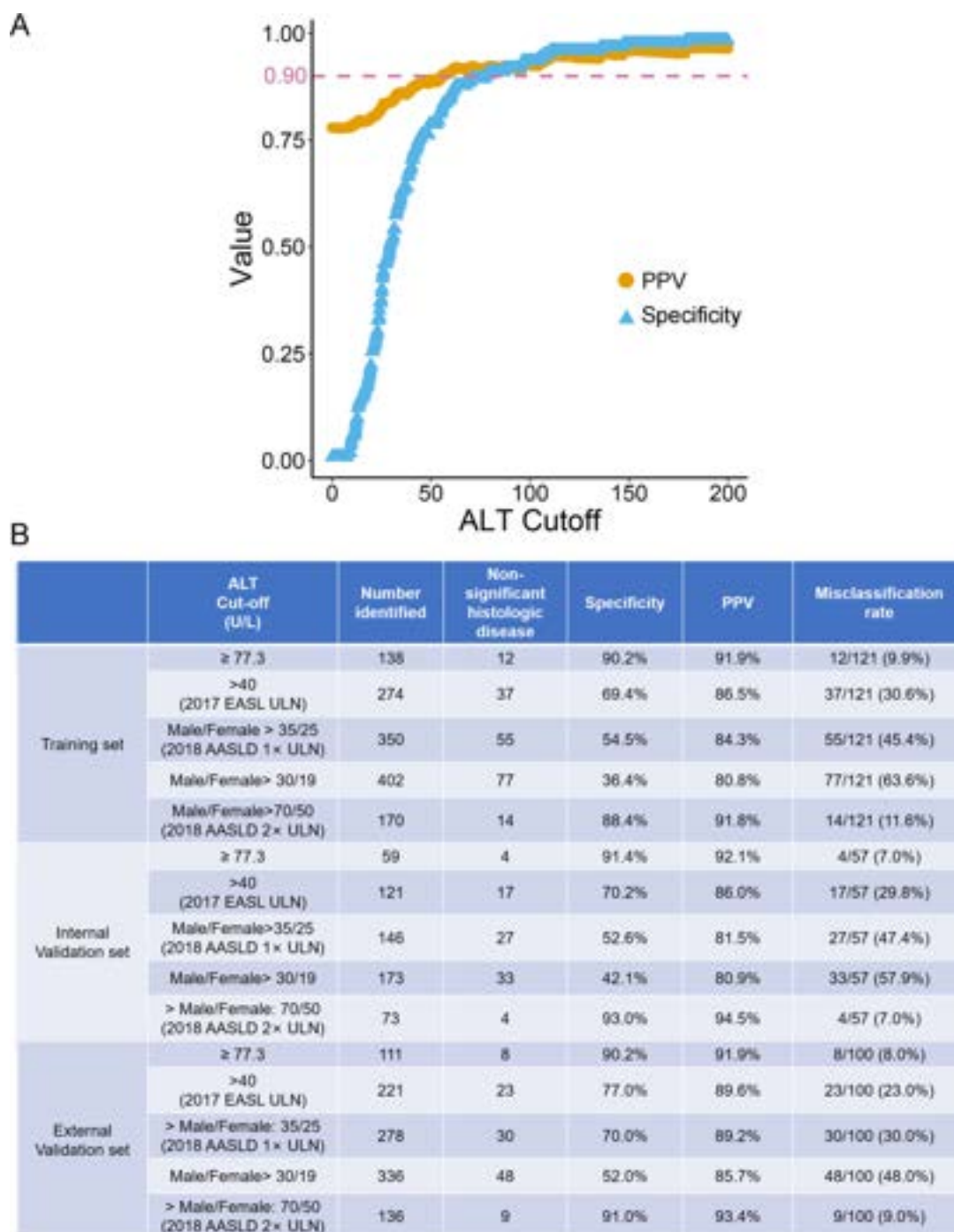


Figure: (abstract: WED-184): Scatterplots showing PPVs, specificities (A) and misdiagnosis rates (B) of ALT cut-offs for ruling in significant histologic disease.

of treat-naïve patients with chronic hepatitis B (CHB). We aimed to explore the optimal ALT threshold for ruling in and ruling out significant liver inflammation and fibrosis in CHB patients.

Method: CHB patients underwent liver biopsy were retrospectively included from four hospitals. Patients from two centers were randomly divided into a training and internal validation set, and patients from two other hospitals comprised the external validation set. The grid-search method was used to determine the cut-offs in the training set with the aim of achieving a specificity and positive predictive value (PPV) of at least 90% for ruling in significant histologic disease. Additionally, the cut-off values were aimed to have a sensitivity of 90% and a negative predictive value exceeding 95% for the exclusion of significant histologic disease. Optimal cut-off values were subsequently validated in both the internal and external validation sets for accuracy. Significant histologic disease was defined as liver inflammation $\geq G2$ or liver fibrosis $\geq S2$ according to Scheuer scoring system.

Results: In proportions of significant histologic disease in the training set ($n = 548$), internal validation set ($n = 235$) and external validation set ($n = 483$) were 77.9%, 75.7% and 79.3%, respectively. The optimal ALT value of 77.3 U/L had a specificity and PPV of 90.22% and 91.9%, respectively, and misclassified only 12 of 121 (9.9%) patients with non-significant histologic disease in the training set. The performance of the newly optimal cut-off of ALT was significantly better than several previous cut-offs of >40 U/L (2017 EASL ULN), male >35 U/L or female >25 U/L (2018 AASLD $1 \times$ ULN), male >30 U/L or female >19 U/L, slightly better than the cut-off of male >70 U/L or female >50 U/L (2018 AASLD $2 \times$ ULN). The specificity and PPV of the newly optimal cut-off of ALT were all above 90% in two validation sets with a misclassification rate of 7% in the internal validation set, and 8% in the external validation set. Regrettably, the cut-offs of ALT to rule out significant histologic disease could not be found.

Conclusion: The newly identified threshold (≥ 77.3 U/L) of ALT had high specificity, PPV and low misclassification rate in ruling in CHB patients with significant histologic disease. The well-validated threshold of ALT could help the antiviral treatment decisions for treat-naïve CHB patients by accurately ruling in significant histologic disease.

WED-185

Predominance of genotype 5 hepatitis delta virus infection in a Portuguese centre

Mariana Cardoso¹, Joana Branco¹, Henrique Coelho¹, Sofia Bragança¹, Gonçalo Alexandrino¹, Mariana Costa¹, Rita Carvalho¹, Elizabeth Padua², Alexandra Martins¹. ¹Hospital Prof. Doutor Fernando Fonseca, Gastroenterology, Portugal; ²National Health Institute Doutor Ricardo Jorge, Portugal
Email: marianafcardoso@gmail.com

Background and aims: Hepatitis delta virus (HDV) infection is the most severe form of viral hepatitis. Genotype (GT) 1 is by far the most prevalent in Europe and globally, while GT5 predominates in Western Africa. Data about HDV seroprevalence in Portugal are scarce and no genotyping studies have been performed to date. We aimed to analyse the seroprevalence of HDV in our centre and to characterize seropositive patients, including HDV genotyping.

Method: Patients followed in our Hepatology clinic between 2012 and 2022 for hepatitis B virus (HBV) infection, defined as positive HBsAg (HBV surface antigen), were retrospectively included. Patients seropositive for HDV and actively followed were subjected to cross-sectional analysis, including blood sample collection. RNA was extracted from the patients' plasma and complementary DNA (cDNA) was synthesized before being submitted to PCR amplification of the 3'-terminal part of the HD (hepatitis delta) gene of HDV. The fragments obtained were analysed by electrophoresis, purified, sequenced and genotyped using an international public database. Clinical, laboratory and imaging data from this subgroup were collected.

Results: From a total of 835 HBsAg positive patients (age 48.3 ± 15.2 years; 56.6% male), 665 (79.6%) had been tested for total anti-HDV antibody. Portuguese patients represented 35.9% of total ($n = 300$), while the majority originated from African countries (57.5%, $n = 480$). The overall HDV seroprevalence was 43/665 (6.5%). Seroprevalence per country/area of origin was 3.0% in Portugal, 12.0% in Central and Eastern Europe and 8.3% in Africa, being as high as 20.3% in Guinea-Bissau. Seropositive patients were younger than the seronegative (41.3 vs 48.9 years, $p < 0.001$).

From the 43 seropositive patients, 21 were included in further studies (age 41.2 ± 9.9 years; 57.1% male). Most patients were HBeAg-negative (85.7% at baseline and currently 95.2%). Advanced chronic liver disease was present in 7 patients (33.3%), including 5 with liver stiffness (LS) ≥ 14 kPa, one with Ishak score of 5/6 and one with imaging findings of cirrhosis and cholangiocarcinoma. Median LS was 7.8 kPa. Most patients (71.4%) were treated with nucleos(t)ide analogs for HBV. One third of patients (7/21) had been treated with peginterferon (HDV clearance: 2; non-response: 4; intolerance: 1). In the current cross-sectional study, HDV RNA was positive in 8/21 (38.0%) patients, 3 of which had previously been classified as RNA negative using a commercial assay. HDV was classified as GT5 in 7 patients (6 from Guinea-Bissau and 1 from Cape Verde), and GT1 in one patient (from Ukraine). Five patients recently started therapy with bulevirtide through the national early access program.

Conclusion: In the largest national cohort to date, seroprevalence and genotype distribution of HDV (with predominance of GT5) were strongly influenced by immigration, notably from African countries.

WED-186

Long-term outcomes of patients with chronic HBsAg positive/HBe-negative infection: differences and transition between inactive carriers and low viremic carriers

Giuseppe Emanuele Maria Rizzo¹, Gabriele Rancatore¹, Pietro Graceffa¹, Giuseppe Falco¹, Fabrizio Bronte², Donatella Ferraro³, Vincenza Calvaruso¹, Vito Di Marco¹. ¹University of Palermo, Section of Gastroenterology and Hepatology, Department of Health Promotion, Mother and Child Care, Internal Medicine and Medical Specialties, PROMISE, Palermo, Italy; ²Ospedali Riuniti Villa Sofia-Cervello, Gastroenterology Unit, Palermo, Italy; ³University of Palermo, Section of Virology, Department of Health Promotion, Mother and Child Care, Internal Medicine and Medical Specialties, PROMISE, Palermo, Italy
Email: gabriele.rancatore@gmail.com

Background and aims: HBsAg-positive/HBeAg-negative Inactive Carrier (IC) with low viral load levels (<2000 IU/ml) has no indication for antiviral treatment, but HBsAg -/HBeAg-negative Low Viremic Carriers (LVC) with viral load between 2000–20 000 IU/ml, belong to a "grey area" of the HBV natural history. IC have a survival comparable to that of the non-infected general population, but it is not clear whether the status of LVC represents a transient phase of low replication in a patient with chronic hepatitis B or whether it is a transition phase to an inactive infection. In this prospective study we evaluated the natural history of a cohort of HBeAg negative patients with viral load $<20\ 000$ IU/ml followed from 2007 to 2022.

Method: At baseline all patients were naïve to antiviral treatment and were evaluated for virus status by quantitative HBsAg (qHBsAg) and serum levels of HBV-DNA, and for disease stage by liver stiffness with FibroScan® and serum transaminase values. Every year patients checked HBV-DNA and transaminase values, performed HBsAg and HBsAb tests, and measured liver stiffness by fibroscan. Change of virological status was defined as an increase or decrease in the value of HBV-DNA levels compared to the cut-off of 2000 IU/ml in at least two consecutive evaluations. A negative test for HBsAg and a positive test for HBsAb was considered a cure for HBV infection.

Results: After the screening, we identified 130 patients (21.6% of the entire cohort of 602 HBsAg positive patients) with HBsAg positive, HBeAg negative, anti-HDV negative, anti-HCV negative, normal transaminase levels and HBV-DNA levels less than 20 000 IU/ml.

POSTER PRESENTATIONS

We identified 91 IC and 39 LCV and two group showed no significant differences regarding age (49 vs 44 years), sex (63% vs 51% males), liver stiffness (mean 5.7 vs 5.3 kPa), and ALT values (28 vs 32 IU/ml) at baseline. At the end of follow-up (median 84 months, range 24–180) the mean of liver stiffness was of 5.5 kPa. Only 10% CI transitioned to LVC status and conversely 51% of LVC transitioned to CI status ($p < 0.001$). During the follow-up 14 patients (10.7%) lost HBsAg and 9 (7%) showed positive HBs-Ab. Furthermore, the identification of IC status had relevant prognostic implications since 15.4% in these patients lost HBsAg compared to no patients in LCV status ($p = 0.01$). Finally, 14 (25%) of 56 IC with baseline levels of qHBsAg < 1000 IU/ml lost HBsAg compared with none of 31 IC with qHBsAg values > 1000 IU/ml.

Conclusion: Our data confirm that both IC and LVC had a good prognosis and no risk of progression to advanced liver disease. HBsAg loss is more frequent in the group of patients with HBV-DNA stably lower than 2000 IU/ml and with quantitative HBsAg values lower than 1000 IU/ml. These evidences can serve as a support in the therapeutic decisions of patients with HBV infection.

WED-187

HBV infected pregnant woman received antiviral treatment and discontinued it postpartum can benefit from retreatment

Qiao Tang¹, Chunrui Wang¹, Peng Hu¹. ¹The Second Affiliated Hospital of Chongqing Medical University, China

Email: hp_cq@163.com

Background and aims: There are limited data on effects of antiviral treatment (AVT) pregnant woman with chronic HBV infection. Previous studies focused on ALT flare but not focused on virological changes. Therefore, we aimed to explore the effects of different antiviral treatments during pregnancy on the mother.

Method: This is a retrospective real-world study on chronic HBV infected pregnant women. We compared the incidences of outcome events (Half decrease in HBsAg, HBV-DNA undetectable and HBeAg clearance) around 1 year postpartum in three groups (Group A: Subjects who started AVT before pregnant and continued it postpartum; Group B: Subjects who who received AVT at 24–28 weeks and continued it postpartum; Group C: Subjects who started AVT at 24–28 weeks and discontinued it postpartum, but retreatment because of abnormal ALT (> 40 U/L)).

Results: A total of 169 chronic HBV infection pregnant women were enrolled in this study, median follow-up time was 18 months. 131 subjects were HBeAg positive and 8 were HBeAg negative, of whom 109 and 7 subjects started antiviral treatment (AVT) at 24–28 weeks, respectively. For those who started AVT but discontinued it postpartum, ALT flare (ALT > 80 U/L) was occurred in 20% (1/5) and 29.8% (28/94) in HBeAg negative and positive, respectively ($p > 0.05$), which was numerically higher than subjects who continued therapy

in HBeAg negative (0%, $p > 0.05$) and positive (9.1%, $p > 0.05$). ALT flare occurred in 61.5% in group C, significantly higher than 9.1% in group B and 0% in group A. The proportion of half decrease in HBsAg occurred in 77.8% in Group C, significantly higher than 20% in group A and comparable with 71.4% in group B. It seems that the proportion was higher in group B than group A ($p = 0.058$). The proportion of HBV-DNA undetectable was comparable between three groups. However, the proportion of HBeAg clearance occurred in group C (25%) was significantly lower than group A (66.7%). And the proportion was comparable between groups A and B (28.6%), between groups B and C.

Conclusion: Although higher ALT flare occurred in pregnant woman who received AVT at 24–28 weeks and discontinued it postpartum, they can benefit from retreatment because of more significantly HBsAg decrease.

WED-188

Higher risk of disease progression in the gray zone relative to hepatitis B e antigen negative chronic hepatitis B infection

YunLing Xue¹, Peng Hu¹, Xiaoqing Liu¹, Qiao Tang¹, GuoRui Wang¹, JinSong Wang¹. ¹The Second Affiliated Hospital of Chongqing Medical University, Department of Infectious Diseases, Institute for Viral Hepatitis, The Key Laboratory of Molecular Biology for Infectious Diseases, Chinese Ministry of Education, China

Email: hp_cq@163.com

Background and aims: Chronic hepatitis B (CHB) remains a global healthcare burden. Hepatitis B e antigen (HBeAg)negative CHB infection is the commonest CHB phase. However, there are some patients with normal alanine aminotransferase (ALT) and negative e antigen that cannot be clearly defined by the guidelines, which we call the gray zone (GZ). There is still confusion about the evolution of disease progression in the GZ and controversy about the need for antiviral therapy. So we aimed to study the natural history and antiviral treatment of HBe negative CHB infection and GZ.

Method: The study retrospectively enrolled 321 patients who were HBeAg negative and had normal ALT (< 40 U/L) without antiviral therapy and without a diagnosis of cirrhosis and hepatocellular carcinoma at baseline. Patients with normal ALT, negative HBe antigen, DNA < 2000 IU/ml and without significant liver fibrosis were diagnosed with HBeAg-negative CHB infection according to the European Liver Association guidelines. Patients who did not meet the above diagnosis were defined as gray zone (GZ). Compared the cumulative incidence of outcome events in GZ and HBeAg-negative CHB infection.

Results: At baseline, 211 (65.73%) of 321 patients were defined as HBeAg negative CHB infection and 110 (34.27%) were defined as GZ. By follow-up, 7 (3.32%) of the total 211 HBeAg negative CHB infection

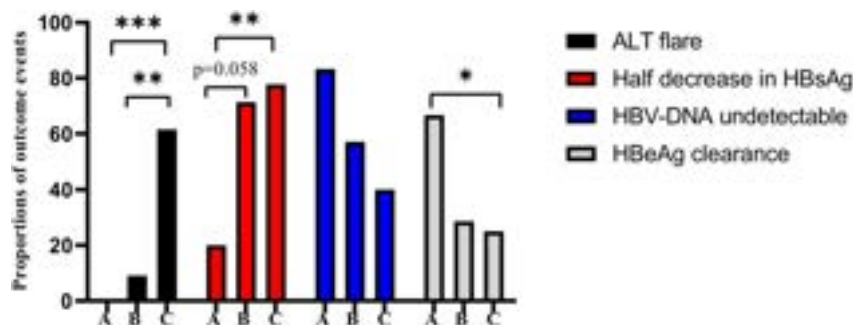


Figure (abstract: WED-187): X axis represents different groups. Group A: Subjects who started AVT before pregnant and continued it postpartum; Group B: Subjects who who received AVT at 24–28 weeks and continued it postpartum; Group C: Subjects who started AVT at 24–28 weeks and discontinued it postpartum, but retreatment because of abnormal ALT (> 40 U/L). Y axis represents proportions of different outcome events.

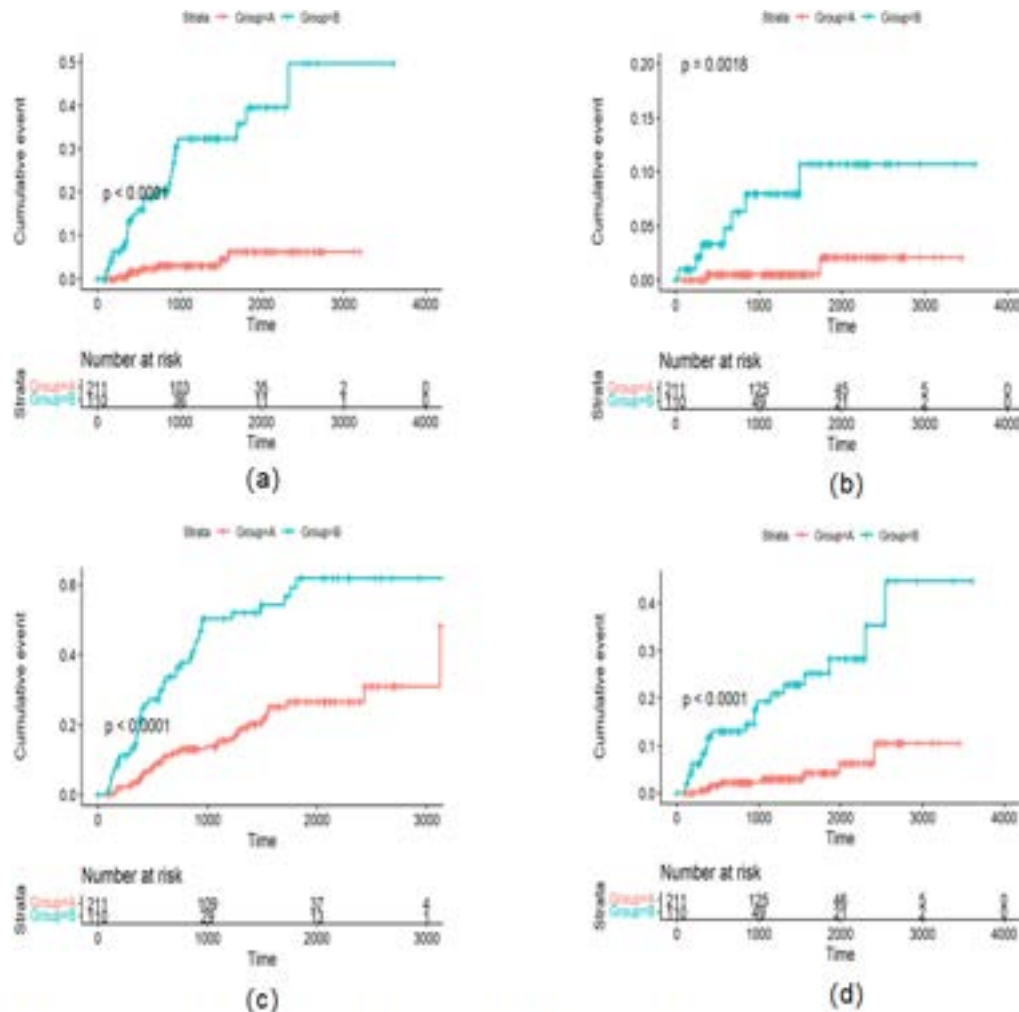


Figure 1: The cumulative incidence between Group A (HBeAg-negative CHB infection) and Group B (GZ) (a) transition to HBeAg-negative chronic hepatitis B and its corresponding gray zone (b) end-stage liver disease (c) elevated ALT (d) antiviral therapy

Figure: (abstract: WED-188).

and 27 (24.5%) of the total 110 patients in GZ at baseline transitioned to HBeAg negative chronic hepatitis B and its corresponding gray zone. The cumulative incidence of transitioning was significantly higher in GZ than HBeAg-negative CHB infection ($p < 0.0001$) (Figure 1a). Meanwhile we defined the occurrence of cirrhosis and/or hepatocellular carcinoma suggested by ultrasound as end-stage liver disease. 9 (2.8%) of in our study population (321) had end-stage liver disease events. 7 (77.78%) patients were in GZ and 2 (22.22%) in HBeAg-negative CHB infection. The cumulative incidence of End-stage liver disease was significantly higher in GZ patients than HBeAg negative CHB infection ($p = 0.0018$) (Figure 1b). We also followed up on the occurrence of ALT elevation and antiviral treatment in patients. ALT elevation occurred in 46 (54.8%) patients in GZ and 38 (45.2%) in HBeAg negative CHB infection. Antiviral therapy occurred in 22 (77.3%) patients in GZ and 8 (22.7%) in HBeAg negative CHB infection. The cumulative incidence of ALT elevation and antiviral therapy was significantly higher in GZ than in HBeAg negative CHB infection ($p < 0.001$, $p < 0.0001$) (Figure 1c, Figure 1d).

Conclusion: In summary, we showed that more than 1/3 of of patients were in GZ at baseline. The cumulative incidence of transition to HBeAg negative chronic hepatitis B and its corresponding gray zone, end-stage liver disease, elevated ALT, and initiation of antiviral therapy were all significantly higher in patients with GZ than in HBeAg-negative CHB infection.

WED-189

Analysis of disease progression in patients with chronic hepatitis B using a large nationwide database

Nobuharu Tamaki¹, Masayuki Kurosaki¹, Yutaka Yasui¹, Kaoru Tsuchiya¹, Hiroyuki Nakanishi¹, Namiki Izumi¹. ¹Musashino Red Cross Hospital, Japan
Email: nobuharu.tamaki@gmail.com

Background and aims: Disease progression in patients with chronic hepatitis B remains unclear. In this study, we aimed to investigate disease progression (hepatocellular carcinoma [HCC] development and decompensation) in patients with chronic hepatitis B using a large claims database.

Method: We used a large claims database established by the Japan Medical Data Center (JMDC Co., Ltd. Tokyo, Japan). The database contains monthly claims from medical institutions and pharmacies, thus it includes all ICD code, prescription history, medical practice, etc.. The database contains records of approximately 14 million insured persons. Among these patients, 3 million patients with health examination data from 2016 to 2021 were examined. Of these, 16,676 persons with chronic hepatitis B disease (based on ICD code) were included. The occurrence of new decompensation (encephalopathy, ascites, varices) and HCC during the observation period was examined.

POSTER PRESENTATIONS

Results: The mean age of the 16676 patients was 51.4 years and 69.2% were male. 3575 (21.4%) were taking nucleic acid analogues (NA). New decompensation occurred in 503 patients (3.0%) and new HCC in 116 patients (0.7%) during the observation period. The 3- and 5-year HCC incidence rates were 0.9% and 1.1%, and the 3- and 5-year decompensation rates were 2.1% and 2.9%. The 5-year HCC incidence was 3.1% and 0.6% in patients with and without NA, respectively. Although patients with NA had a significantly higher incidence of HCC, HCC was also observed in patients without NA. Age, male gender (hazard ratio [HR]:1.7), NA administration (HR:5.3), and alanine aminotransferase (ALT) >20 IU/L (HR:1.5) were significant factors associated with the development of HCC. The 3- and 5-year decompensation rates were 4.1% and 5.2% in patients with NA and 1.5% and 2.1% in patients without NA, respectively. The significant factors associated with decompensation were age, male gender (HR: 1.4), NA administration (HR: 2.4), and ALT >20 IU/L (HR: 1.7). When patients without NA were stratified by ALT level, the 3- and 5-year decompensation rates were 1.3% and 1.8% in patients with ALT \leq 20 IU/L and 1.8% and 2.4% in patients with ALT >20 IU/L. The incidence of decompensation was higher in patients with ALT >20 IU/L ($p = 0.01$).

Conclusion: NA was introduced in high-risk cases for the development of HCC and decompensation. On the other hand, a small number of cases without NA also developed HCC and decompensation, suggesting the need for further verification of the identification of high-risk groups and the criteria for NA administration.

WED-190

The prognosis of hepatitis delta infections in Belgium is poor and determined by the hepatitis delta viremia

Arno Furquim d'Almeida^{1,2}, Erwin Ho², Liesbeth Govaerts², Peter Michiels², Thomas Sersté³, Jean Delwaide⁴, Stefan Bourgeois⁵, Christophe Moreno⁶, Hans Van Vlierberghe⁷, Chantal De Galocsy⁸, Hans Orlent⁹, Michael Peeters¹⁰, Elizaveta Padalko¹¹, Steven Van Gucht¹⁰, Thomas Vanwolleghem^{1,2}.
¹University of Antwerp, Viral Hepatitis Research Group, Laboratory of Experimental Medicine and Pediatrics, Antwerp, Belgium; ²Antwerp University Hospital, Department of Gastroenterology and Hepatology, Antwerp, Belgium; ³CHU Saint-Pierre, Department of Hepato-Gastroenterology, Brussels, Belgium; ⁴CHU de Liège, Department of Hepato-Gastroenterology, Liège, Belgium; ⁵ZNA Antwerp, Department of Gastroenterology, Antwerp, Belgium; ⁶CUB Hôpital Erasme, Department

of Gastroenterology, Hepatopancreatology and Digestive Oncology, Brussels, Belgium; ⁷Ghent University Hospital, Department of Gastroenterology, Ghent, Belgium; ⁸Hôpitaux Iris Sud Bracops, Department of Gastroenterology and Hepatology, Brussels, Belgium; ⁹AZ Sint-Jan, Department of Gastroenterology and Hepatology, Bruges, Belgium; ¹⁰Sciensano, Infectious Diseases in Humans, Viral Diseases, National Reference Centre of Hepatitis Viruses, Brussels, Belgium; ¹¹Ghent University Hospital, Laboratory of Medical Microbiology, Ghent, Belgium

Email: thomas.vanwolleghem@uza.be

Background and aims: Hepatitis B virus (HBV)-hepatitis delta virus (HDV) co-infection is considered the most severe form of chronic viral hepatitis and remains a major global health problem worldwide. Long-term studies that investigate the disease severity are of crucial importance to identify the factors that define the prognosis of this population.

Method: In the present study we retrospectively performed a medical chart review of hepatitis delta patients seen at 8 Belgian hospitals. All relevant data was uniformly collected from July 2001 until January 2023. The inclusion criteria were a) HBsAg or HBV DNA positive at admission; b) anti-HDV or HDV RNA positive; c) at least 1 follow-up visit.

Results: A total of 138 patients were included. The patients were predominantly male (64.5%), had a median age of 36.6 years and had a median follow-up of 5.4 (max 20.4) years. 35.6%, 47.8% and 16.7% of patients respectively were from African, Caucasian and Asian descent. The median AST, ALT and MELD score at admission were 55 (range 9–1735) U/L, 62 (range 13–5463) U/L and 7.9 (range 6–37) respectively. Cirrhosis was diagnosed in 40.6% (52/128) of the patients using liver biopsy ($n = 27$), liver stiffness measurement ($n = 19$) or the combination of clinical and radiological findings ($n = 6$) and did not differ between ethnicity groups ($p = 0.06$). A total of 33 patients (23.9%) had at least one severe adverse outcome during follow-up: 27 liver decompensations (19.6%), 12 HCC's (8.7%), 10 liver transplantations (7.2%) and 9 deaths (6.5%). Patients of Caucasian ethnicity had more frequently an adverse outcome than the other ethnicities ($p = 0.04$). The mean age at time of outcome was 48.6 years. The 1-, 5- and 10-year cumulative outcome probability is 8%, 15% and 49% respectively. The last available HDV RNA was positive in 80/120 (66.7%) patients. These patients had a higher AST (89 vs 49 U/L, $p < 0.001$), ALT (121 vs 61 U/L, $p < 0.001$) at admission and had more frequently cirrhosis (46.7% vs 24.3%, $p = 0.02$) than the patients with a negative last HDV

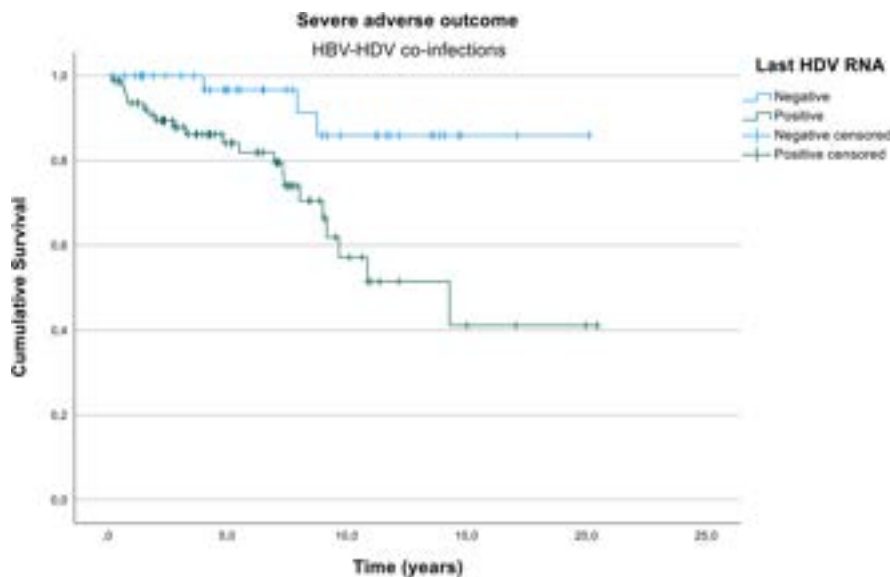


Figure: (abstract: WED-190).

RNA. There was no significant difference in gender ($p = 0.11$), age ($p = 0.74$) and MELD score at admission ($p = 0.08$) between these groups. A detectable HDV viremia at last evaluation was associated with a higher frequency of severe adverse outcomes compared to patients without HDV viremia (1-, 5- and 10-year cumulative outcome probabilities of 10% vs 0%, 18% vs 4% and 59% vs 14% respectively; Kaplan Meier $p = 0.005$). In addition, having a negative HDV RNA at any point during follow-up was associated with not having an outcome ($p = 0.009$).

Conclusion: In this real-world national cohort study, approximately half of HBV-HDV co-infected patients develop a severe liver-related outcome within 10 years of diagnosis. Caucasian patients and those with a positive HDV RNA have a worse prognosis during long-term follow-up.

WED-191

Assessment of clinical and patient reported outcome measures in individuals with chronic hepatitis B who clear HBsAg, followed by the Canadian hepatitis B network

Carla Coffin^{1,2,3}, Magdy Elkhachab⁴, Karen Doucette⁵, Scott K Fung⁶, Alnoor Ramji⁷, Hin Hln Ko⁷, Carla Osioy⁸, Pamela Crotty¹, Anna Manko¹, Chad Saunders⁹, Eric Chan¹⁰, Angelina Villasis Kever¹⁰, TianYan Chen¹¹, Sebastien Poulin¹², Julie Zhu¹³, Mang M⁵, Curtis Cooper¹⁴. ¹University of Calgary, Department of Medicine, Canada; ²University of Calgary, Cumming School of Medicine, Calgary, Canada; ³Cumming School of Medicine, Medicine, Calgary, Canada; ⁴Toronto Liver Centre, Canada; ⁵University of Alberta, Department of Medicine, Canada; ⁶University of Toronto, Department of Medicine, Canada; ⁷University of British Columbia, Division of Gastroenterology, Canada; ⁸Public Health Agency of Canada, National Microbiology Laboratory, Canada; ⁹University of Calgary, Haskayne School of Business, Canada; ¹⁰Janssen Global Services, United States; ¹¹McGill University Health Centre, Canada; ¹²CISSS des Laurentides, Saint-Jérôme, Canada; ¹³Dalhousie University, Division of Gastroenterology, Canada; ¹⁴University of Ottawa, Department of Medicine, Canada
Email: ccoffin@ucalgary.ca

Background and aims: Patient reported outcome measures (PROMs) assessing health-related quality of life (HRQoL) in CHB patients who achieve HBsAg loss compared to untreated HBsAg (+) individuals are not included in most clinical outcome studies.

Method: In this ongoing multi-centre 3-year prospective cohort study we enrolled known CHB patients who achieved HBsAg loss or remained HBsAg (+) but did not require antiviral therapy based on expert guidelines. Subjects consented to serial peripheral blood mononuclear cells and plasma collection for assessment of standard (HBV DNA, qHBsAg, anti-HBs titres) and novel biomarkers, clinical tests (including FibroScan[®]) and completed a Hepatitis B Quality of Life Questionnaire (HBQOL) and a self-stigma questionnaire at each visit. Data were analyzed using SPSS.

Results: In 77 participants enrolled to date, 42 completed 1 year follow-up (median age 55.3, 95% CI 52.6, 57.9), 41.6% Female, 61% Asian, 17% Black, 17% White. NAFLD and diabetes occurred in 22% (17/77) and 10.4%, (8/77) respectively. 57% had prior antiviral therapy (mean 5 years, 3.3, 6.7). 68% were born endemic area, 29% infant/childhood acquisition, and ~3% adult acquired (sexual, drug use, work related exposure). At enrolment, 65 (84%) were HBsAg (-) (8/65, 12.3% HBV DNA+, median HBV DNA 0.15 log), 12 (16%) were HBsAg+ (qHBsAg 200 IU/ml; 109.4, 292) (median HBV DNA 2.1 log IU/ml), ($p = 0.0001$). All tested anti-HBs (+), with higher titres after HBsAg loss (i.e., median 0.7 IU/ml (0.3, 2.0) in HBsAg (+) vs. 18.5 IU/ml (3.9, 46.9) in HBsAg (-) group ($p < 0.05$). All had low risk of liver disease, mean ALT 23 U/L (20.5, 25.6) and mean FibroScan[®] 5.1 kPa (4.7, 5.4). Participants with recent HBsAg loss reported 28% improvement in range of HRQoL indicators. The largest improvements were in reducing fear of bad outcomes, and smallest improvement was in productivity gains (Figure 1).

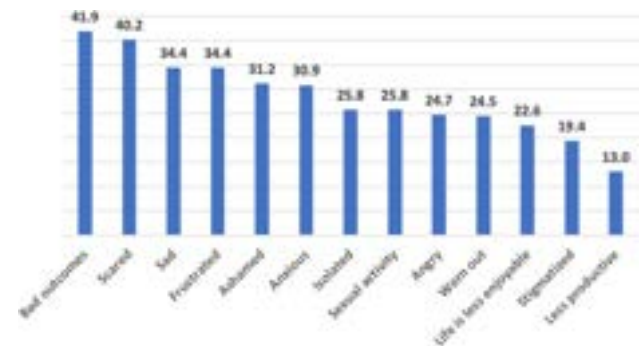


Figure: Participants were asked to report on each of the factors presented on a scale ranging from never to all the time based upon their past experience (prior to HBsAg loss) and current (after HBsAg clearance) (Wilcoxon signed-rank test).

Conclusion: In this prospective cohort study of ethnically diverse CHB patients, participants who achieve HBsAg loss reported improved HRQoL. Patient perspectives are important to consider in assessing benefits of a functional cure.

WED-193

Stability of Hepatitis B virus RNA in plasma and serum under various storage conditions

Valerie Ohlendorf¹, Birgit Bremer¹, Carola Mix¹, Lisa Sandmann¹, Tammo Lambert Tergast¹, Katja Deterding¹, Markus Cornberg¹, Heiner Wedemeyer¹, Benjamin Maasoumy¹. ¹Hannover Medical School, Gastroenterology, Hepatology and Endocrinology, Germany
Email: ohlendorf.valerie@mh-hannover.de

Background and aims: Pregenomic hepatitis B virus (HBV) RNA (pgRNA) is intensively investigated as a biomarker in the management of HBV infected patients. However, prior to the use in routine clinical practice potential confounders of test results need to be identified. This study investigates the stability of HBV RNA under various storage conditions.

Method: HBV RNA levels in 26 hepatitis B patients, of whom 15 received NUC treatment, were determined using the Roche cobas[®] 6800/8800 investigational HBV RNA assay. The lower limit for the quantification of HBV RNA was 10 copies/ml (c/ml). Detectable but not quantifiable HBV RNA level (titer min) were set to 10 c/ml for statistical analyses. Before measurement of HBV RNA, blood samples were stored under the following conditions: baseline (BL) samples were immediately prepared, the supernatant (Su) of plasma (P) and serum (S) samples as well as whole blood (WB) S and P samples of each patient were stored for 6, 48, 169 hours (h) at 4°C, 25°C and 42°C, respectively. HBV RNA level were expressed as median. The unpaired t-test and fishers exact test were performed for statistical analyses.

Results: HBV RNA was detected in 61.5% (N = 16; 122.65 c/ml) of S and 69% (N = 18; 21.9 c/ml) of P samples, respectively. Baseline HBV RNA levels did not differ significantly between P and S samples ($p = 0.45$). Over all samples, a decrease in HBV RNA was detected over time, with higher declines of mean HBV RNA concentrations with increasing storage temperature (BL 4.87×10^6 c/ml; 169 h: 4°C, 4.61×10^6 c/ml; 25°C, 3.56×10^6 c/ml; 42°C, 4.79×10^5 c/ml). The same trend was observed in further subanalysis: In the subgroup of samples with HBV RNA <titer min (P: 33.3%, N=6; S: 25.0%, N=4) the number of all samples with detectable HBV RNA decreased over time. After 48 h of storage at 42°C HBV RNA became undetectable in WB samples and in Su S samples ($p = 0.0022$ to 0.0286). HBV RNA level of 10–100 c/ml were detected in 22.2% (N=4; 15.5 c/ml) of P samples and 25.0% (N=4, 19.45 c/ml) of S samples. Fluctuations in median HBV RNA concentrations ranged from -11.5 to +2.5 c/ml 169 h after BL at 4°C, while at 42°C in WB samples HBV RNA became undetectable after 48–169 h of storage. In samples with HBV RNA level >100 c/ml (P: 44.4%, N=8, 1.55×10^5 c/ml; S: 50%, N=8, 1.78×10^5 c/ml) the number of samples with detectable HBV RNA remained stable at all

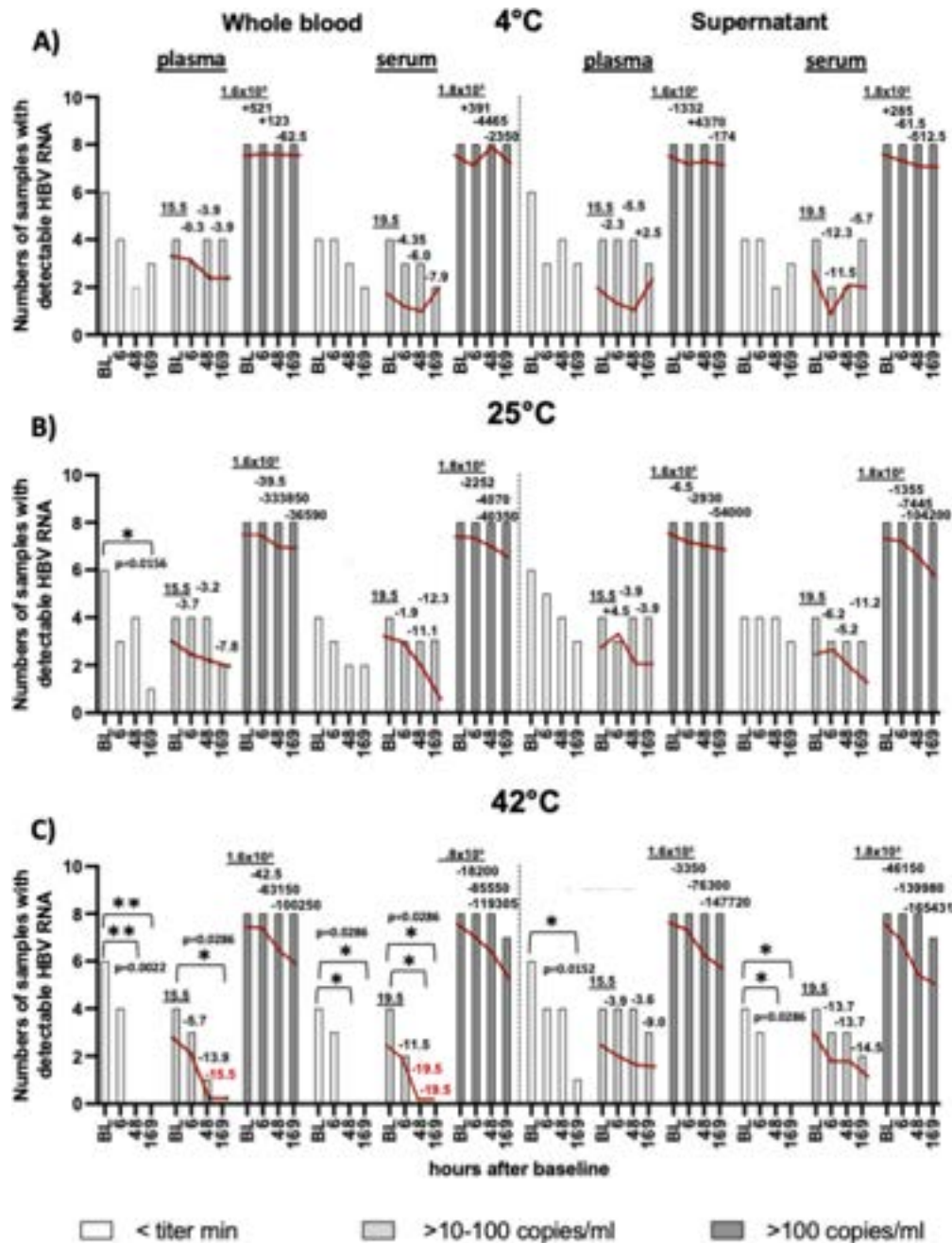


Figure: (abstract: WED-193): Number of samples with detectable HBV RNA (copies/ml) sorted by subgroups of HBV RNA (<titer min, HBV RNA levels ≥ 10 –100 copies/ml and >100 copies/ml, respectively at A) 4°C, B) 25°C and C) 42°C storage condition. Red lines represent median level of HBV RNA, underlined numbers represent median BL level of HBV RNA in copies/ml, not underlined numbers represent the median change in HBV RNA levels compared to BL. Statistically significant changes of RNA level is expressed in red. Brackets indicate a statistically significant decrease in number of samples with detectable HBV RNA.

storage temperatures, except of S samples stored at 42°C. At 4°C, the most stable HBV RNA concentrations over time occurred in WB P samples (median decrease -62.5 c/ml). The maximum median decrease was -4465 c/ml (169 hours after BL in S samples). In contrast, 169 h after BL the maximum decrease in median HBV RNA level was $-104\,200$ c/ml at 25°C and $-165\,431$ c/ml at 42°C, respectively.

Number of samples with detectable HBV RNA (copies/ml) sorted by subgroups of HBV RNA (<titer min, HBV RNA levels ≥ 10 –100 copies/ml and >100 copies/ml, respectively at A) 4°C, B) 25°C and C) 42°C storage condition. Red lines represent median level of HBV RNA,

underlined numbers represent median BL level of HBV RNA in copies/ml, not underlined numbers represent the median change in HBV RNA levels compared to BL. Statistically significant changes of RNA level is expressed in red. Brackets indicate a statistically significant decrease in number of samples with detectable HBV RNA.

Conclusion: A qualitative detection of HBV RNA is feasible in samples with >100 c/ml up to 48 h under storage temperatures of 4–42°C. For most stable quantitative HBV RNA values storage at 4°C should be preferred.

WED-194

Barriers to hepatitis B treatment from the patient's perspectives: survey study by the Canadian hepatitis B network

Hin Hin Ko¹, Curtis Cooper², Anna Manko³, Alnoor Ramji¹, Chad Saunders⁴, Abdel Aziz Shaheen³, Carla Coffin³. ¹University of British Columbia, Division of Gastroenterology, Canada; ²University of Ottawa, Department of Medicine, Canada; ³University of Calgary, Department of Medicine, Canada; ⁴University of Calgary, Haskayne School of Business, Canada
Email: hinnih@gmail.com

Background and aims: Although Canada has a universal health care system, this does not include prescription drug benefits, which vary according to provincial health jurisdiction. There are systemic factors impacting access to treatment leading to poor outcomes. Our previous study has shown undertreatment in patients with chronic hepatitis B who meet treatment guideline criteria. The goal of this survey study is to determine barriers to Hep B treatment from the patient's perspectives.

Method: In this study, an in-person survey was conducted in three specialist hepatology infectious disease clinics for Hep B patients involved in the Canadian HBV Network. Patients' clinical and demographic variables, their knowledge and perception of Hep B and treatment were collected in the survey. Data analyses were performed using SPSS statistics.

Results: Of 83 patient respondents to date from one jurisdiction, 58% (n = 48) were in the 40–59 age group, 50.6% (n = 42) were male. 79.5% (n = 66) were employed and 66.3% (n = 55) worked full time. 25.3% (n = 21) did not have any extended health coverage. 48.2% (n = 40) were currently on treatment and 16.9% (n = 14) sometimes/always had difficulties paying for the anti-viral medication. 44.5% (n = 37) felt 'very knowledgeable/have good knowledge' about Hep B. 30.1% (n = 25) were 'very to extremely worried about developing liver complications' from Hep B. 31.3% (n = 26), 4.8% (4) and 2.4% (2) sometimes, often and always felt stigmatized and isolated because of Hep B, respectively. The percentage of survey respondents who reported challenges in various health related and quality of life factors were summarized in Figure 1. Among those not on treatment (n = 43), 53% (n = 23) 'definitely or probably would accept treatment' if recommended while 18% (n = 8) 'definitely or probably would not accept treatment' despite recommendations. High medication costs, potential medication side effects and needing to take the medication

long term were of concern to 30.3% (n = 13), 65.1% (n = 28) and 60.5% (n = 26) of patients, respectively. Before considering treatment, 39.5% (n = 17) would like to try diet and natural remedies, 32.6% (n = 14) would want to be monitored longer and 27.9% (n = 12) would want to know when the treatment can be stopped.

Conclusion: In this ongoing survey study of CHB population in Canada, about one fifth of the patients would not accept treatment despite physician's recommendations. Lower drug costs, treatment with limited side effects and shorter duration might potentially reduce barriers in people willing to accept treatment.

WED-195

Driving improvements in hepatitis B care in Africa: profile of the hepatitis B in Africa collaborative network (HEPSANET)

Nicholas Riches^{1,2}, Michael Vinikoor³, Alice N. Guingané⁴, Asgeir Johannessen⁵, Maud Lemoine⁶, Philippa Matthews⁷, Edith Okeke⁸, Yusuke Shimakawa⁹, Roger Sombie¹⁰, Alexander Stockdale¹¹, Gilles Wandeler¹², Monique Andersson¹³, Davwar Pantong Mark¹⁴, Hailemichael Desalegn¹⁵, Mary John Duguru¹⁴, Fatou Fall¹⁶, Tongai Gibson Maponga¹⁷, David Nyam P¹⁴, Moussa Seydi¹⁸, Edford Sinkala³, Jantjie Taljaard¹⁹, Mark Sonderup²⁰, Wendy Spearman²⁰. ¹Malawi Epidemiology and Intervention Research Unit, Malawi; ²Liverpool School of Tropical Medicine, Department of Clinical Sciences, Liverpool, United Kingdom; ³University of Zambia, Department of Internal Medicine, Lusaka, Zambia; ⁴Bogodogo University Hospital Center, Hepato-Gastroenterology Department, Ouagadougou, Burkina Faso; ⁵University of Oslo, Institute of Clinical Medicine, Oslo, Norway; ⁶Imperial College London, Department of Metabolism, Digestion and Reproduction, London, United Kingdom; ⁷University of Oxford, Nuffield Department of Medicine, Oxford, United Kingdom; ⁸University of Jos, Faculty of Medical Sciences, Jos, United Kingdom; ⁹Institut Pasteur, Unité d'Epidémiologie des Maladies Emergentes, Paris, France; ¹⁰Yalgado Ouédraogo University Hospital Center, Ouagadougou, Burkina Faso; ¹¹University of Liverpool, Department of Clinical Infection, Microbiology and Immunology, Liverpool, United Kingdom; ¹²University of Bern, Institute of Social and Preventive Medicine, Bern, Switzerland; ¹³Stellenbosch University, Division of Medical Virology, Cape Town, South Africa; ¹⁴University of Jos, Faculty of Medical Sciences, Jos, Nigeria; ¹⁵St Paul's Hospital Millennium Medical College, Medical Department, Addis Ababa, Ethiopia; ¹⁶Hopital

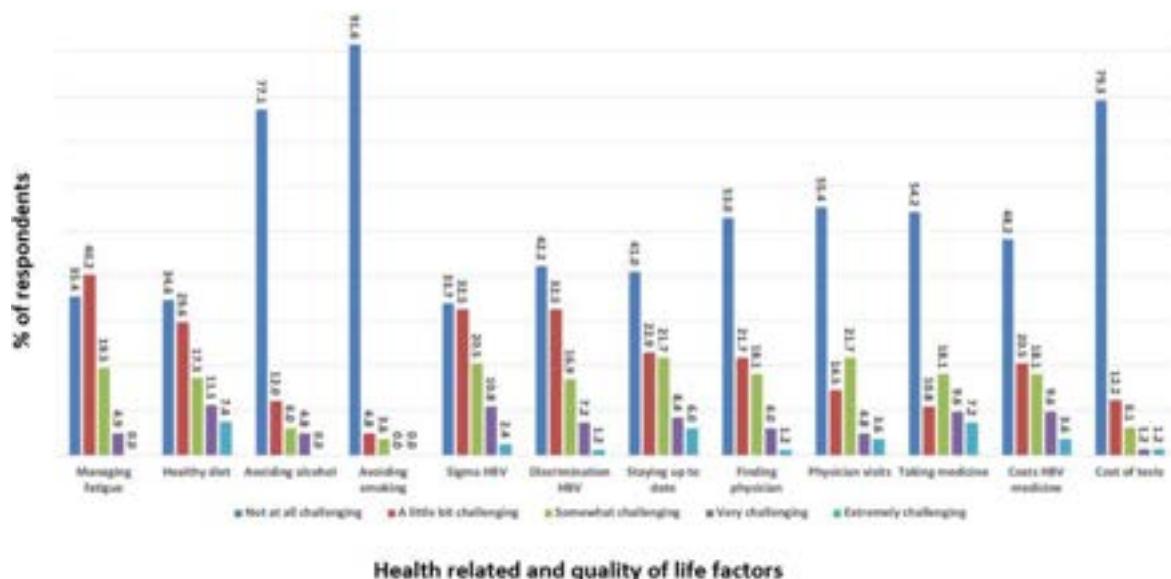


Figure: (abstract: WED-194).

POSTER PRESENTATIONS

Principal de Dakar, Department of Hepatology and Gastroenterology, Dakar, Senegal; ¹⁷Stellenbosch University, Faculty of Medicine and Health Sciences, Cape Town, South Africa; ¹⁸Centre Hospitalier National Universitaire de Fann, Centre Hospitalier National Universitaire de Fann, Dakar, Senegal; ¹⁹Tygerberg Hospital and Stellenbosch University, Division of Infectious Diseases, Cape Town, South Africa; ²⁰University of Cape Town, Division of Hepatology, Department of Medicine, Faculty of Health Sciences, Cape Town, South Africa
Email: nicholas.riches@lstmed.ac.uk

Background and aims: There are approximately one million new cases of chronic hepatitis B virus (HBV) infection each year in the WHO African region, corresponding to two-thirds of all new infections globally. To achieve global elimination of HBV, Africa must be designated a priority region for future research and interventions. Improved understanding of the natural history of HBV in Africa is needed, since disease patterns may be determined by differences in natural history, circulating genotypes, environmental exposures and coinfections. With seed funding from EASL, the Hepatitis B in Africa collaborative network (HEPSANET) was founded to close gaps in knowledge around HBV in Africa.

Method: A systematic review was conducted to identify established and high-quality HBV cohorts in Africa, and those identified were invited to participate. A modified Delphi exercise was conducted with HBV experts across the region to identify research priorities for the initial period of HEPSANET. Ten research priorities were agreed by consensus, with the leading priority being to establish a longitudinal research cohort of people living with chronic HBV in Africa. Working groups for hepatocellular carcinoma, prevention of mother to child transmission, diagnostics, and data harmonization were formed. Baseline data from participating sites were shared. We described HEPSANET research priorities, site characteristics, patient-level demographics and HBV clinical features.

Results: As of October 2022, 13 cohorts representing sites from eight African countries and three regions (East, West, and Southern) had joined HEPSANET and shared their data. An initial cohort of 4,173 participants was analyzed. Median age of the cohort is 34 years (IQR 28–42), 38.8% are women, with 81.3% of cases identified through asymptomatic testing. 9.6% of the cohort are HBeAg-positive, 33.1% have HBV DNA >2000 IU/ml, and 14.3% are cirrhotic based on

transient elastography. Among the 692 with chronic hepatitis (i.e. elevation of both ALT and HBV DNA), the majority (72.8%) were HBeAg-negative.

Conclusion: To address the dearth of longitudinal HBV data in Africa, HEPSANET is combining data from HBV cohorts throughout Africa for the first time. Improved understanding of HBV epidemiology in Africa will lead to better approaches to HBV case finding, care models, and treatment strategies, including with emerging curative therapies. Procedures are now being established to expand this cohort and to allow for collection of longitudinal follow-up data.

WED-196

Risk factors for viral reactivation in patients with overt or occult Hepatitis B virus infection receiving immunosuppressive treatments: a systematic review and meta-analysis

Ciro Celsa¹, Giacomo Emanuele Maria Rizzo¹, Gabriele Rancatore¹, Pietro Graceffa¹, Giuseppe Falco¹, Gabriele Di Maria¹, Marco Vaccaro¹, Marco Enea¹, Vincenza Calvaruso¹, Calogero Camma¹, Vito Di Marco¹.
¹Section of Gastroenterology and Hepatology, PROMISE Department, University of Palermo, Italy
Email: celsaciro@gmail.com

Background and aims: Patients with Hepatitis B virus (HBV) infection receiving immunosuppressive treatments are at risk of HBV reactivation (rHBV). We performed a systematic review with meta-analysis to estimate the risk of rHBV among patients naïve to antiviral prophylaxis and to identify factors associated with rHBV.

Method: Studies of immunosuppressive treatments in HBV patients were identified through literature search using PubMed, MEDLINE, and EMBASE until October 2022. Pooled estimates were obtained using random-effects model. Subgroup analyses were performed according to viral status, drug class and underlying disease. Decision curve analysis (DCA) was used to identify the threshold probability associated with the best net benefit of administering prophylaxis with nucleos (t)ide analogues (NAs) in HBsAg negative anti-HBc positive patients.

Results: Seventy-nine studies (48 retrospective and 31 prospective) were selected, including 9946 patients (1108 HBsAg positive, 8203 anti-HBc positive and 635 isolated anti-HBs positive). Pooled rHBV rate was 6% (95% CI 5–8%; I² 79%; p < 0.001) with a rate of 23% (95% CI

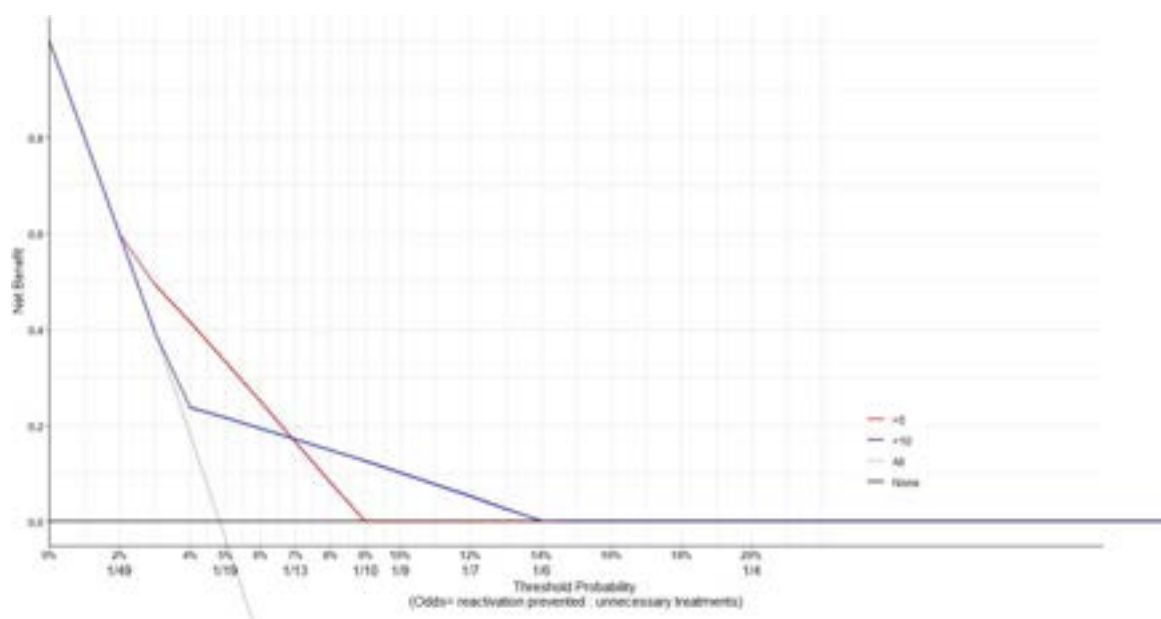


Figure: (abstract: WED-196): Decision curve analysis comparing the net benefit of strategies of administering NAs prophylaxis when HBV reactivation is higher than 5% or 10% with the strategies of treating all or none patients at different threshold probabilities in HBsAg negative anti-HBc positive patients.

16–31%), 4.6% (95% CI, 3.4–6.1%) and 2.9% (95% CI 1.5–10%) in HBsAg positive, anti-HBc positive and isolated anti-HBs positive patients, respectively. In HBsAg positive patients, the risk for rHBV ranged from 22% (95%CI 11–39%) in patients with autoimmune disease receiving immunosuppressants to 30% (95%CI 5–79%) in patients with cancer receiving chemotherapy. In anti-HBc positive patients with cancer, chemotherapy, targeted-therapy and monoclonal antibodies were associated with risk of rHBV of 9% (95%CI 5–15%), 7% (95% CI 1–43%) and 5% (95%CI 2–10%), respectively; in anti-HBc positive with autoimmune diseases, the risk of rHBV was 3% (95% CI 2–4%), 4% (95% CI 2–8%) and 3% (95%CI 1–13%) for anti-TNF α , other monoclonal antibodies and immunosuppressants, respectively. DCA showed that a more aggressive strategy (treating patients with HBV \geq 5%) was associated with higher net benefit when physicians are willing to successfully prevent one rHBV at the cost of unnecessary treatments ranging from 49 to 13, while a less aggressive strategy (treating patients with HBV \geq 10%) was better at the cost of unnecessary treatments ranging from 13 to 6.

Conclusion: This meta-analysis provided consistent results that all HBsAg positive patients should receive NAs prophylaxis. Our decision curve analysis in anti-HBc positive patients provided evidence that in patients with cancer treated with chemotherapy, NAs prophylaxis should be recommended, while in patients with cancer treated with targeted therapies either monitoring or NAs prophylaxis could be appropriate. In patients with cancer treated with monoclonal antibodies and in patients with autoimmune diseases, monitoring and on-demand NAs should be recommended.

WED-197

T-cell responses to PreS1 and PreS2 are correlated to anti-HBs antibody titres, which are higher and persist longer in volunteers vaccinated with 3-antigen than with 1-antigen hepatitis B vaccine in the PROTECT Study: 3.5 year follow-up

Francisco Diaz-Mitoma¹, Timo Vesikari², Tamara Berthoud³, Daniel Plaksin³, David Anderson³, Vlad Popovic³. ¹VBI Vaccines, Inc, Ottawa, Canada; ²Tampereen Rautatieasema, Tampere, Finland; ³VBI Vaccines Inc., Cambridge, United States
Email: fdiazmitoma@vbivaccines.com

Background and aims: PreHevri is a 3-antigen hepatitis B vaccine containing S, PreS1 and PreS2 HBV envelope antigens and Engerix is a 1-antigen HBV vaccine containing the S Ag. PreS antigens have CD4+ T-cell epitopes which may mediate the improved antibody response against HBsAg after vaccination with PreHevri. This study aimed to find the relationship between T-cell activation and induction and persistence of antibody responses after HBV immunization in a Phase 3 study (PROTECT) that compared the immunogenicity of these vaccines and followed volunteers for 3.5 years post vaccination.

Method: Statistical comparisons and correlation analysis between anti-HBs titer and Cultured interferon (IFN)-gamma elispots or stimulation index were measured after the 2nd and 3rd vaccination with PreHevri or with Engerix in a subset of participants (n = 80) in the PROTECT study (N = 1,607). An additional subset of volunteers (N = 347) was followed with antibody titers 3.5 years postvaccination.
Results: Following the third vaccination, there was a statistically significant correlation between anti-HBs titers and T-cell gamma IFN elispot responses to pre-S1 (Pearson's Coefficient = 0.39, p = 0.0137) and pre-S2 (Pearson's Coefficient = 0.33, p = 0.0363), and a trend toward significance between anti-HBs titers and the elispot response to HBsAg (Pearson's Coefficient = 0.31, p = 0.0534) in the PreHevri arm. In contrast, in Engerix-B-vaccinated subjects, a statistically significant correlation was seen only between anti-HBs titers and elispot responses to HBsAg (Pearson's Coefficient = 0.46, p = 0.0026) and no correlation with ELISPOT responses to pre-S1 or pre-S2. The difference in adjusted mean frequency of IFN- γ -secreting SFU/million PBMCs was statistically significant (p < 0.05) and greater in PreHevri arm. These responses to pre-S1 and pre-S2 at Day 35 (7 days post second vaccination) in the Sci-B-Vac group correlated with anti-HBs

titer at Day 56 (4 weeks post second vaccination), 168 (20 weeks post second vaccination) and 196. (4 weeks post 3rd Vaccination) No such correlations to pre-S1 and pre-S2 were seen in the Engerix-B group. Post third vaccination, the adjusted mean stimulation index was 0.8 (95% CI 0.7, 1.0) in the Engerix-B arm and 1.2 (95% CI 1.0, 1.5) in the PreHevri arm. In contrast to the Engerix arm, there was a statistically significant correlation of mean stimulation index of pre-S2 with anti-HBs GMT (Pearson's Coefficient = 0.48, p = 0.0149) in the PreHevri group. 40% (95%CI = 31.9, 48.4) of Engerix and 78% (95%CI = 71.8, 83.7) of PreHevri recipients had anti-HBs \geq 100 mIU/ml at 3.5 years of follow-up post 3rd vaccination.

Conclusion: The 3-antigen Hepatitis B vaccine induces T-cell responses to the PreS domains that are correlated to high and persistent anti-HBs titers observed in the follow-up extension of PROTECT Phase 3 study. Anti-HBs \geq 100 mIU/ml at 3.5 years of follow-up post 3rd vaccination were almost double with 3-antigen than the 1-antigen hepatitis B vaccine.

WED-198

Baseline hepatocyte ballooning is a risk factor for adverse events in patients with chronic hepatitis B complicated with non-alcoholic fatty liver disease

Youwen Tan¹, Wang Jiaming¹. ¹The Third Hospital of Zhenjiang Affiliated Jiangsu University, China
Email: tyw915@sina.com

Background and aims: To study the effect of non-alcoholic fatty liver disease (NAFLD) confirmed by liver pathology on the outcome of long-term serious adverse events (cirrhosis, hepatocellular carcinoma (HCC), and death) in patients with chronic hepatitis B (CHB) virus infection.

Method: Patients with chronic hepatitis B virus (HBV) infection who underwent liver biopsy at the Third People's Hospital of Zhenjiang Affiliated Jiangsu University between January 2005 and September 2020 were enrolled. Baseline clinical and pathological data on liver pathology and clinical data at the end of follow-up were collected. Propensity score matching (PSM) was used to balance the baseline parameters, Kaplan-Meier (K-M) survival analysis was used to evaluate the risk of clinical events, and Cox regression was used to analyze the risk factors of events.

Results: Overall, 456 patients with chronic HBV infection were included in the study, of whom 152 (33.3%) had histologically confirmed NAFLD. The median follow-up time of the entire cohort was 70.5 months. Excluding 67 patients with cirrhosis at baseline, 34 developed cirrhosis, which was diagnosed using ultrasound during the follow-up period. K-M survival analysis showed that NAFLD was not significantly associated with the risk of cirrhosis (log-rank test, p > 0.05). Patients with CHB with fibrosis at baseline were more prone to cirrhosis (log-rank test, p = 0.046). After PSM, multivariate analysis showed that diabetes mellitus, ballooning deformation (BD), and platelet (PLT) were independent risk factors for cirrhosis diagnosed using ultrasound (p < 0.05). A total of 10 patients (2.2%) developed HCC and six patients were in the combined NAFLD group. The median interval between liver biopsy and HCC diagnosis was 100.5 months. K-M survival analysis showed that the cumulative risk of HCC in the NAFLD group was significantly higher (log-rank test, p < 0.05). Lobular inflammation, hepatocyte ballooning, and severe liver fibrosis were also associated with an increased risk of HCC (log-rank test, all p < 0.05). Cox multivariate analysis revealed that hepatocyte ballooning, liver fibrosis, and diabetes mellitus were independent risk factors for HCC.

Conclusion: There was no significant correlation between chronic HBV infection and risk of cirrhosis in patients with NAFLD. Diabetes mellitus, BD, and PLT were independent risk factors for liver cirrhosis. Patients with chronic HBV infection and non-alcoholic steatohepatitis (NASH) have an increased risk of HCC. BD, liver fibrosis, and diabetes mellitus are independent risk factors for HCC.

POSTER PRESENTATIONS

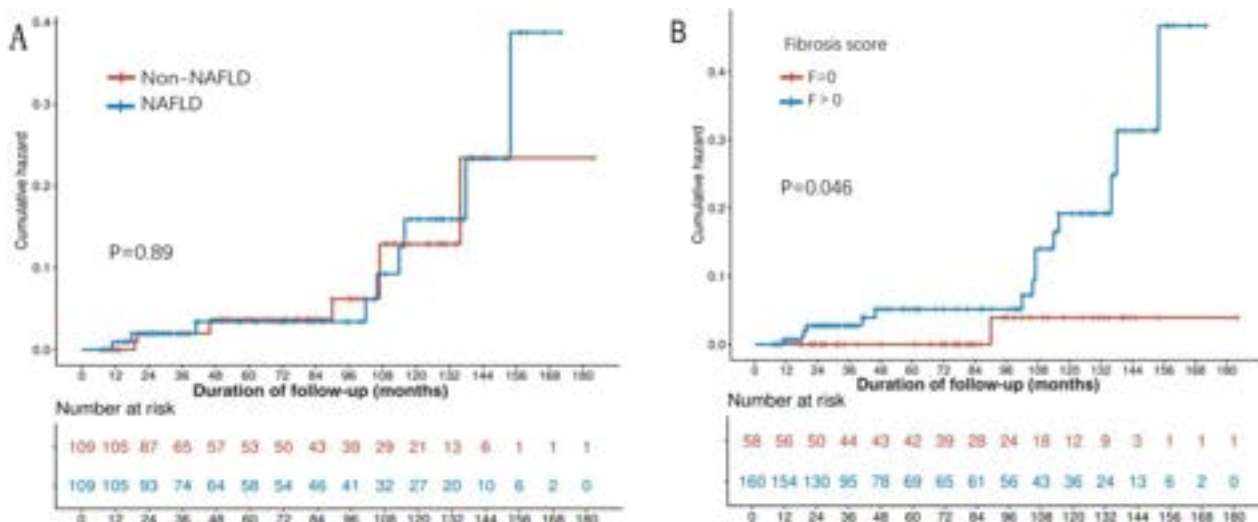


Figure: (abstract: WED-198).

WED-199

Epidemiological landscape and clinical spectrum of chronic hepatitis B in East Africa

Abate Shewaye^{1,2}, Amir Sultan^{1,2}, Zebeaman Tibebe Gorfu², Rabia Redi². ¹Addis Ababa University, College of Health Sciences, Department of Internal Medicine, Addis Ababa, Ethiopia; ²Adera Medical and Surgical Center, Department of Internal Medicine, Addis Ababa, Ethiopia

Email: gzebeaman@gmail.com

Background and aims: According to WHO global report, 296 million people were living with chronic hepatitis B (CHB) infection in 2019, with 1.5 million new infections each year. Nearly 45% of the world's population lives in regions of chronic hepatitis B virus (HBV) endemicity, of which highest percentage is in sub-Saharan Africa including Ethiopia. Fortunately, vaccine and antiviral therapy for CHB has been shown to be effective in preventing the infection and its complications. Thus, this study aims to assess the sociodemographic, clinical and epidemiological pattern of patients with chronic hepatitis B seen at Adera Medical Center, in Addis Ababa, Ethiopia.

Method: Four hundred-three patients were enrolled in this cross-sectional study. Sociodemographic, clinical, and laboratory and imaging parameters were collected and analyzed using SPSS (SPSS, Version 23)

Results: CHB was twice more prevalent amongst males with mean age of 37.96 ± 10.94 . Seventeen patients developed HCC, while five patients died; four of whom were HCC patients and one developed Hepatic Encephalopathy. HCV and HIV coinfecting patients accounted for 2.2% and 1.7% of the study population. HBeAg seropositivity was only 6.5%. Majority (60%) were from Addis Ababa followed by Jijiga, Zeway, and Harar regions. Poor outcomes were noted among older patients (<65 years) with chronic hepatitis B infection ($p < 0.01$)

Conclusion: Majority of our patients (93.5%) were HBeAg negative indicating childhood chronic HBV infection. Male predominance and clustering of CHB in south east Ethiopia was witnessed in our study. Chronic HBV complications like cirrhosis and HCC are more common among elderly patients (>65 yrs) resulting in poorer outcome ($p < 0.01$).

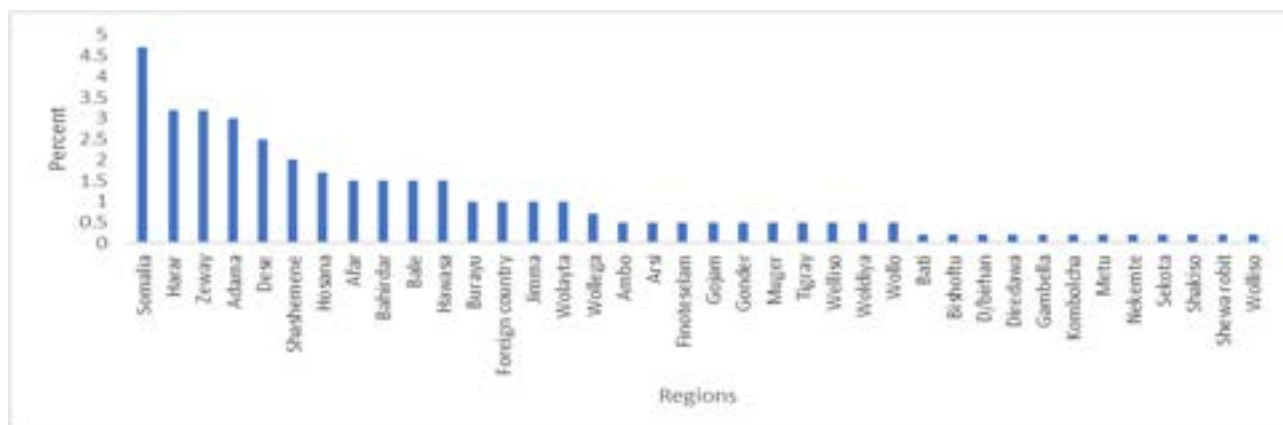


Figure: (abstract: WED-199): Clustering of CHB patients followed at Adera Medical and Surgical Center, Addis Ababa, Ethiopia, 2022.

WED-200

Significantly higher clinical and economic burden following diagnosis of hepatitis delta virus infection among commercially insured adults with chronic hepatitis B in the United States

Robert Wong^{1,2}, Robert G. Gish³, Chong Kim⁴, Gary Leung⁵, Ira M Jacobson⁶, Joseph Lim⁷, Ankita Kaushik⁴. ¹Stanford University School of Medicine, Stanford, United States; ²VA Palo Alto Healthcare System, Palo Alto, United States; ³Hepatitis B Foundation, Doylestown, United States; ⁴Gilead Sciences, Inc., HEOR-Global Value and Access, Foster City, United States; ⁵Gilead Sciences, Inc., RWE-Epidemiology, Foster City, United States; ⁶NYU Grossman School of Medicine, New York, United States; ⁷Yale University School of Medicine, New Haven, United States
Email: ankita.kaushik@gilead.com

Background and aims: Hepatitis delta virus (HDV) is associated with more rapid progression to cirrhosis and liver-related complications compared with other hepatitis virus infections. Baseline (BL) characteristics, healthcare resource use (HCRU), and costs among commercially insured adults with HDV infection in the US were examined.

Method: Adult patients with ≥ 1 HDV or HBV diagnosis (ICD-9/10-CM) were identified retrospectively from 1 Jan 2013 to 31 Dec 2021 (study period) using the IQVIA PharMetrics Plus database covering ~210 million patients from primarily commercial payers. HDV patients were identified from 1 Jan 2014 to 31 Dec 2020 (identification period) and defined as those who had ≥ 1 inpatient or ≥ 2 outpatient claims ≥ 30 days apart with an ICD-9/10-CM diagnosis code for HDV during the identification period (earliest date of diagnosis considered index date), ≥ 1 claim of HBV diagnosis during BL (12-month period prior to index date), and no claims with HDV diagnosis during BL. Continuous enrollment for ≥ 12 months before and after the index date was required, and patients aged ≥ 18 years at index with commercial health plans were included. Patient characteristics were assessed over the BL period and mean per patient per year (PPPY) all-cause HCRU and costs were compared in the 12 months pre- and post-HDV diagnosis.

Results: Among 6,002 patients diagnosed with HDV during the identification period, 440 met inclusion criteria. Baseline characteristics: mean (SD) age, 50.3 (10.50); 65% males; mean (SD) Charlson Comorbidity Index score, 1.97 (2.35). At HDV diagnosis, 13% had compensated cirrhosis, 12% had decompensated cirrhosis, 5% had hepatocellular carcinoma, and 4% had history of liver transplant. Other comorbidities included hypertension (33%), obesity (8%), non-alcoholic steatohepatitis (7%), and hepatitis C (6%). Mean PPPY all-cause total HCRU was significantly greater post-HDV diagnosis vs pre-HDV diagnosis (29.8 vs 24.1, $p < .0001$), driven primarily by significantly increased outpatient visits (8.6 vs 5.5, $p < .0001$), physician office visits (10.8 vs 9.2, $p < .0001$), and pharmacy claims (13.5 vs 11.6, $p < .001$). Mean PPPY all-cause total healthcare costs were significantly greater post-HDV diagnosis vs pre-HDV diagnosis (\$11 197 vs \$9281, $p < .005$), due to increases in total medical costs, including outpatient (\$2471 vs \$1650, $p < .0005$) and physician office (\$1784 vs \$1697, $p < .01$) costs.

Conclusion: Over 20% of commercially insured HDV patients had already developed cirrhosis or liver-related complications at time of diagnosis. Following HDV diagnosis, approximately 6 more visits and claims amounting to \$1916 were observed. These findings underscore

the need for more effective strategies for screening, diagnosis, linkage to care, and treatment of HDV-infected patients, to decrease the burden of disease for patients and the healthcare system.

WED-201

Aspirin use and risk of hepatocellular carcinoma and gastrointestinal bleeding in patients with HBV-related cirrhosis: a landmark analysis

Mi Na Kim¹, Geun U Park², Jae Seung Lee³, Hye Won Lee³, Beom Kyung Kim³, Seung Up Kim³, Jun Yong Park³, Do Young Kim³, Sang Hoon Ahn³. ¹Yonsei University College of Medicine, Department of Internal Medicine, Seoul, Korea, Rep. of South; ²Clinical and Translational Hepatology Laboratory, Korea, Rep. of South; ³Yonsei University College of Medicine, Korea, Rep. of South
Email: ahnsh@yuhs.ac

Background and aims: The use of aspirin in hepatocellular carcinoma (HCC) prevention is still uncertain in patients with hepatitis B virus (HBV)-related cirrhosis. In addition, results regarding whether the risk of gastrointestinal (GI) bleeding is associated with aspirin use in patients with HBV related cirrhosis are controversial. Accordingly, we investigated the association between aspirin use and the risks of HCC and GI bleeding in HBV-related cirrhosis patients using a nationwide cohort.

Method: We conducted a 3-year landmark analysis using nationwide cohort data from the National Health Insurance Service of South Korea. Patients with diagnosed with compensated HBV-related cirrhosis in 2005–2017 were included. Patients who were prescribed aspirin for at least 90 days consecutively during the 3-year exposure period were classified as the aspirin-treated group. A propensity-score matching analysis was applied to balance the aspirin-treated and untreated groups. Using Cox proportional hazard regression analysis, we estimated the risks of HCC and GI bleeding, accounting for competing events.

Results: A total of 12,687 patients (608 aspirin-treated and 12,079 untreated) were included in the analysis. During a median of 7.6 years of follow-up, HCC developed in 219 (36.0%) patients of the aspirin-treated group and 4,265 (35.3%) patients of the untreated group. After multivariate adjustment, the aspirin-treated group showed a significantly lower risk of HCC than the untreated group (adjusted hazard ratio [aHR] = 0.84, 95% confidence interval [CI] = 0.73–0.96; $P = 0.013$). GI bleeding developed in 157 (25.8%) of the aspirin-treated group and 2072 (17.2%) of the untreated group. The aspirin-treated group showed a significantly higher risk of GI bleeding than the untreated group (aHR = 1.21, 95% CI = 1.03–1.43; $P = 0.021$). After propensity-score matching, the cumulative incidence rate of HCC was significantly lower in the aspirin-treated group than the untreated group ($p = 0.013$, log-rank test). Whereas, the cumulative incidence rate of GI bleeding was significantly higher in the aspirin-treated group than the untreated group ($p = 0.025$, log-rank test).

Conclusion: In patients with HBV-related cirrhosis, the aspirin-treated group showed a significantly lower risk of HCC than the untreated group, whereas the risk of GI bleeding was significantly higher in the aspirin-treated group.

WED-202

High prevalence of hepatic steatosis in adults living with hepatitis B, with and without HIV co-infection, in London, UK

Claire Mullender^{1,2}, Angieszka Kemper², Stephen Ogunnaike², Sarah Pett^{1,3}, Irfaan Maan¹, Manik Kohli^{1,2}, Dimitra Peppas^{2,4}, Alejandro Arenas-Pinto^{1,3}, Stuart Flanagan², Indrajit Ghosh², Richard Gilson^{1,2}, Philippa Matthews^{4,5,6}. ¹Institute for Global Health, University College London, United Kingdom; ²Central and North West London NHS Foundation Trust, Department of HIV and Sexual Health, United Kingdom; ³MRC Clinical Trials Unit at University College London, Institute of Clinical Trials and Methodology, United Kingdom; ⁴University College London, Division of Infection and Immunity, United Kingdom; ⁵Francis Crick Institute, United Kingdom; ⁶University College London, Department of Infectious Diseases, United Kingdom
Email: claire-marie.mullender1@nhs.net

Background and aims: Hepatic steatosis is likely to become a leading cause of liver related mortality, and can have a significant impact on the progression of liver disease in the setting of chronic hepatitis B (HBV) and HIV/HBV co-infection. It can be measured using controlled attenuation parameter (CAP), a simple non-invasive test, at the same time as fibrosis assessment by transient elastography. We aimed to describe the prevalence of steatosis in a cohort of adults living with HBV and HIV/HBV co-infection, undergoing routine assessment in a central London clinic.

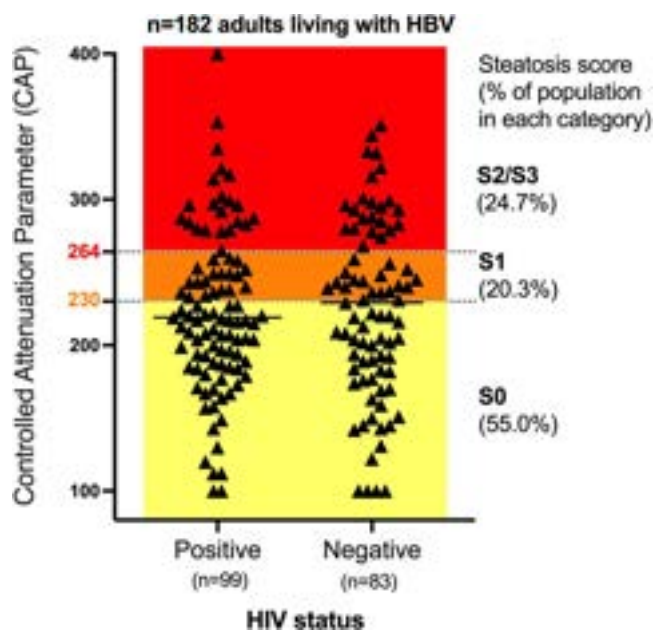


Figure: Distribution of CAP scores in adults living with HBV mono-infection and HBV/HIV co-infection in London. Steatosis graded as S0, S1, S2/3 based on standardised thresholds for HBV. (No difference in distribution between groups, $p = 0.82$)

Method: We performed a retrospective analysis of adults with HBV (including mono-infected and HIV co-infected) who had had CAP measured by Fibroscan® (Echosens) between 1/2017–10/2022. We used CAP scores to categorise steatosis as: S0 <230 dB/m; S1 230–264 dB/m; S2/3 >264 dB/m; and as a continuous scale in a univariate analysis. We investigated for relationships between CAP scores and liver outcomes (based on alanine transaminase [ALT] and fibrosis

score on transient elastography), and age, sex, body mass index (BMI), HIV status and ethnicity.

Results: We reviewed data for 182 patients (80% male; median age 48 years [IQR 39–56]). Ethnicities categorised as 43% White, 30% Black, 10% Asian, remainder mixed/not stated. 99 (54%) had HBV/HIV co-infection. 56% had a BMI ≥ 25 kg/m². Evidence of steatosis was present in 45%, with 20% classified as S1, and 25% stage S2/S3. Median ALT was 23 (IQR 23–41) IU/L. CAP scores were not significantly associated with HIV status (figure 1), sex, or ethnicity, but increased with age ($p = 0.009$) and increased BMI ($p < 0.0001$). Increasing CAP scores were significantly associated with higher ALT ($p = 0.02$) and elevated fibrosis scores ($p = 0.0003$).

Conclusion: We identified a high prevalence of steatosis in our diverse cohort of adults living with HBV, however HIV co-infection was not associated with an increased risk of steatosis in our cohort, which warrants further investigation. We demonstrate that steatosis may contribute to adverse liver outcomes, and as steatosis is a modifiable cause of fibrotic/inflammatory liver disease, further efforts are required to determine its impact and deliver interventions to lower risk in people living with HBV. This is particularly important as people living with HBV and HIV/HBV co-infection are often excluded from therapeutic trials for steatosis.

WED-203

Stable temporal trend of HDV seroprevalence in central Italy across the last two decades with the circulation of HDV sub-genotypes 1 inducing different inflammatory stimuli

Lorenzo Piermatteo^{1,2}, Romina Salpini², Giulia Torre², Stefano D'Anna², Sohaib Khan², Leonardo Duca², Ada Bertoli^{2,3}, Vincenzo Malagnino⁴, Loide Di Traglia³, Pierpaolo Paba³, Marco Ciotti³, Ilaria Lenci⁵, Simona Francioso⁵, Caterina Pasquazzi⁶, Miriam Lichtner⁷, Claudio M. Mastroianni⁷, Francesco Santopaulo⁸, Giuseppe Maria De Sanctis⁹, Massimo Marignani⁶, Adriano Pellicelli¹⁰, Giovanni Galati¹¹, Alessandra Moretti¹², Katia Casinelli¹³, Luciano Caterini¹⁴, Nerio Iapadre¹⁵, Giustino Parruti¹⁶, Jacopo Vecchiet¹⁷, Paoloni Maurizio¹⁸, Sandro Grelli^{2,3}, Francesca Ceccherini Silberstein², Loredana Sarmati⁴, Valentina Svicher^{1,2}. ¹University of Rome "Tor Vergata", Biology, Rome, Italy; ²University of Rome "Tor Vergata", Experimental medicine, Rome, Italy; ³Tor Vergata University Hospital, Virology Unit, Rome, Italy; ⁴Tor Vergata University Hospital, Infectious Diseases Unit, Rome, Italy; ⁵Tor Vergata University Hospital, Hepatology Unit, Rome, Italy; ⁶S. Andrea Hospital, Digestive and Liver Diseases Unit, Rome, Italy; ⁷Sapienza University of Rome, Infectious Diseases Unit, Rome, Italy; ⁸Fondazione Policlinico Universitario Agostino Gemelli IRCCS, Internal Medicine and Gastroenterology, Rome, Italy; ⁹Umberto I University Hospital, Rome, Italy; ¹⁰San Camillo Forlanini Hospital, Liver and Transplant Unit, Rome, Italy; ¹¹University Campus Bio-Medico, Internal Medicine and Hepatology Unit, Roma, Italy; ¹²San Filippo Neri Hospital, Rome, Italy; ¹³Fabrizio Spaziani Hospital, Infectious Disease Unit, Italy; ¹⁴Belcolle Hospital, Viterbo, Italy; ¹⁵San Salvatore Hospital, Italy; ¹⁶Pescara General Hospital, Pescara, Italy; ¹⁷University "G. d'Annunzio" Chieti-Pescara, Italy; ¹⁸Avezzano General Hospital, Italy
Email: lorenzo.piermatteo@uniroma2.it

Background and aims: In Italy, HDV-prevalence and its fluctuations over time are controversial while an extensive characterization of HDV-infected patients (pts) is missing. Here, we assess HDV-seroprevalence in a large cohort of HBsAg-positive pts, followed in Central Italy over time, and the epidemiological/virological characteristics of HDV-infected pts.

Method: This study included 1579 consecutive and well-characterized HBsAg-positive pts, followed in different clinical centers of Central Italy from 2005 to 2022. Factors (demographics, transaminases, HBeAg status) correlated with the lack of HDV screening were defined by multivariable model. HDV sub-genotypes were defined by phylogenetic-analysis.

Results: Most HBsAg-positive pts were male (67%) and Italian (59.4%) with a median (IQR) age of 47 (35–60) years. 75% of pts were HBeAg-negative, median (IQR) serum HBV-DNA and HBsAg were 3.1 (2.8–4.1) IU/ml and 3499 (618–11662) IU/ml, while median ALT was 42 (26–78) U/L. Overall, 45.3% (715/1579) received HDV-screening with an increasing temporal-trend: 17.1% (2005–2010), 43.2% (2011–2015), 56.5% (2016–2019), 75.8% (2020–2022), suggesting a higher awareness towards HDV-screening in recent years. By multivariable model, normal ALT was the only independent factor significantly correlated with the lack of HDV-screening (OR [95%CI]: 1.71 [1.29–2.30], $P < 0.001$). Notably, 13.4% (96/715) of HDV-screened pts resulted anti-HDV+ with a stable temporal trend: 10.7% (2005–2010), 15.6% (2011–2015), 10.8% (2016–2019), 10% (2020–2022). Among them, 80.5% had detectable HDV-RNA (median [IQR] log: 4.6 [3.6–5.6] copies/ml) with altered ALT in 89.3% (median [IQR]: 92 [62–177] U/L). Anti-HDV positivity was higher in pts from Eastern Europe than from Italy (23.6% vs 12.9%, $P = 0.002$) and remained stable over time in both groups. Notably, anti-HDV+ pts from Eastern Europe were younger (44 [37–54] vs 53 [47–62] years, $P < 0.001$) with higher HDV-RNA (4.8 [3.6–5.8] vs 3.9 [1.4–4.9] copies/ml, $P = 0.016$) and HBsAg (9,461 [4,159–24,532] vs 4,447 [737–13,336] IU/ml), $P = 0.032$), indicating more pronounced HDV replicative activity. Phylogenetic analysis revealed the circulation of HDV sub-genotype 1a (25.9%), 1b (33.4%), 1c (25.9%) and 1d (14.8%). Notably, sub-genotype 1a and 1c correlated with 3xULN ALT compared to 1b and 1d (75% versus 27.3%, $P = 0.039$).

Conclusion: The awareness to request HDV-screening is increasing over time even if some gaps persist to achieve HDV-screening in all HBsAg-positive pts. The prevalence of HDV infection remains stable in both foreign and Italian pts over time. Notably, immigration from

Eastern Europe contributes to fuel the circulation of HDV-strains with enhanced replication. The detection of different sub-genotypes, triggering variable inflammatory stimuli, supports the need to expand HDV molecular characterization.

WED-204

Ten years follow-up of patients with chronic hepatitis B and hepatitis D infection

Andreea Dobroaia¹, Simu Razvan-Ioan¹, Letitia Toma¹, Ioana Tanasie¹, Elena Laura Iliescu¹, ¹Fundeni Clinical Institute, Romania
Email: andreea.dobroaia@gmail.com

Background and aims: Hepatitis B virus (HBV) and hepatitis delta virus (HDV) infection is considered the most severe chronic viral hepatitis, due to the rapid onset of complications, such as cirrhosis and hepatocellular carcinoma. The prevalence of HDV and HBV infection is higher among patients from the Mediterranean basin, especially among those with a history of intravenous drug use. The aim of this study is to observe the evolution of the disease, the survival rate of the patients and to determine the key elements that may aid in rising the life expectancy and quality of life of the patients.

Method: We conducted a retrospective observational study on 110 patients diagnosed in our clinic with chronic HBV and HDV infection between January 2012 and December 2012. We monitored the patients for progression to cirrhosis, hepatocellular carcinoma (HCC), as well as APRI, MELD and FIB-4 scores at diagnosis. The survival rate of those patients was expressed as number of months. We only included patients in which interferon therapy was not tolerated or not indicated due to decompensated liver disease. Patients with hepatitis C or HIV co-infection, as well as patients with malignancies or other significant medical conditions with poor prognosis were excluded from the study.

Results: The mean age at diagnosis was 43.82 ± 22.91 years (range between 21 and 65 years). At the time of diagnosis, 52 patients (47.27%) were already diagnosed with cirrhosis (13 patients Child A, 26 patients Child B and 13 patients Child C), while the rest (52.72%) were classified as chronic hepatitis. 15 patients presented HCC at the

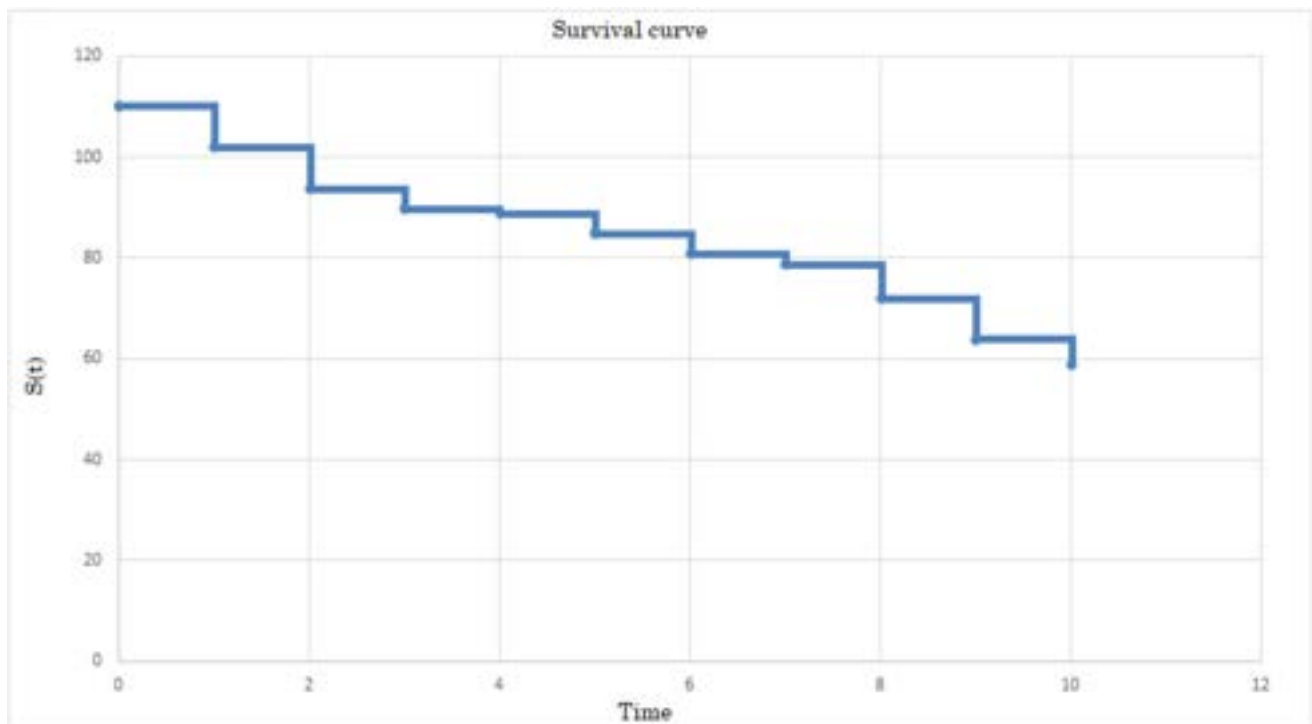


Figure: (abstract: WED-204).

POSTER PRESENTATIONS

time of diagnosis (10 cirrhotic patients and 5 patients with chronic hepatitis). In cirrhotic patients, mean value of MELD was 16.34 ± 8.16 , mean value of APRI was 5.28 ± 1.56 , mean value of Fib-4 was 7.27 ± 4.75 . During the 10 years follow-up, 70.68% of chronic hepatitis patients developed cirrhosis (41 out of 58 patients). New HCC was diagnosed in 18 patients (11 cirrhotic patients and 7 non-cirrhotic patients). Overall survival was 52.72% at 10 years (25% in the cirrhosis group and 34% in the chronic hepatitis group). Notably, only 9 patients underwent liver transplantation. Carcinogenesis rate was 26.19% in cirrhotic patients and 13.2% in non-cirrhotic patients. Increased APRI score as well as Fib-4 score and MELD at diagnosis were associated with mortality ($p = 0.04$, $p = 0.02$, $p = 0.01$ respectively, CI 95%).

Conclusion: While the survival rate for patients with chronic HBV and HDV infection is low, close monitoring for the development of cirrhosis and frequent HCC screening may increase overall survival and may offer bridging possibilities until liver transplantation.

WED-205

Overcoming barriers to care for Delta infected patients

Ariadna Bono¹, Ângela Carvalho-Gomes^{1,2}, Maria Dolores Gómez Ruiz^{1,3}, Susana Sabater Vidal⁴, Juan Carlos, Rodríguez Díaz⁵, Helena Hernández-Èvole⁶, Antonio David Palau Canos⁴, Ana Forés⁴, Maria Rodriguez⁵, Maria L. Molina⁴, Sonia Pascual⁵, Martin Prieto¹, Marina Berenguer^{1,2,3,7}. ¹La Fe Health Research Institute, Spain; ²CIBEREHD, ISCIII, Spain; ³La Fe Polytechnic and University Hospital, Spain; ⁴University General Hospital of Castellon, Spain; ⁵University General Hospital of Alicante, Spain; ⁶Clinical Hospital of Barcelona, Spain; ⁷University of Valencia, Spain
Email: marina.berenguer@uv.es

Background and aims: Delta hepatitis is a rare infectious disease that affects roughly 15 million people worldwide, unevenly distributed, with endemic such as the Mediterranean basin. Due to increasing worldwide migrations, changes in epidemiology have been highlighted recently. In the current setting of advanced therapies and changing epidemiology, a search and phenotyping of HDV cases are warranted. We aim to better understand the local epidemiology of HDV infection, establishing a registry of delta-infected patients in our region as well as linking to care prior undiagnosed or lost to follow-up (FU) cases.

Method: After a search of all possible HDV cases in a Spanish Region, attempts were made to relink to care those lost to follow-up. Approaches were undertaken to detect all HDV infected patients in a Spanish region: (i) database search of the microbiology units for HBsAg positive results plus anti-HDV in 3 Public Healthcare Departments (those without HDV serology in the last 10 years to be further contacted for anti-HDV determination \pm HDV RNA quantitation); (ii) electronic medical records software (ORION program) search from adult patients attending any of the 3 participant Hospitals (Jan 2011–Jun 2021) and codified in the system as HBV HDV.

Results: Two hundred forty-four anti-HDV cases were detected (11% of the chronic HBV patients in our Region), with similar distribution in the three hospital districts. In Hospital 1,133 anti-HDV cases were detected; of these, only 43 were patients that belonged to the Hospital Reference Area. After excluding two possible false positives (only one positive result followed by >5 negative), 41 cases (24 men, 27 European, 12 African, 1 Asian, 1 other) were revised to determine

their phenotype and current linkage to care. Four had previously died (2 liver-related), 19 were adequately being followed up in the liver clinic (5 of these had undergone liver transplantation), 11 were no longer followed up in the hospital (2 Africans had left the country, 1 had moved to another city, and 8 were lost to FU; Of the latter 8, 2 out of 3 European and 1 of 5 African were re-linked to care); The reminder 7 anti-HDV + cases had never been studied and linked to care. Of these, 1 of 3 Europeans, 1 of 3 Africans and 0 of 1 Asians were eventually contacted and re-linked to care. Overall, 28% of patients without adequate local FU were relinked to care. Data on Hospital 2 and 3 will be presented at the meeting.

Conclusion: In a reference center hospital, only half of delta-infected patients are being adequately followed up. After an active search, about a third, particularly non-migrant patients can be relinked to care.

WED-206

Clinical phenotypes of hepatocellular carcinoma in patients with chronic hepatitis D compared to patients with chronic hepatitis B

Matthias Jeschke¹, Leonie Steinhoff¹, Leonie Jochheim¹, Benedikt Hild¹, Moritz Passenberg¹, Hartmut Schmidt¹, Christoph Schramm¹. ¹University of Duisburg-Essen, Department of gastroenterology, hepatology and transplant medicine, Essen, Germany
Email: christoph.schramm@uk-essen.de

Background and aims: Patients with chronic hepatitis D (CHD) are at increased risk for developing hepatocellular carcinoma (HCC) compared to patients with chronic hepatitis B (CHB). CHD-associated HCC may feature a distinct molecular profile compared to CHB-associated HCC. We, therefore, aimed to compare the clinical phenotypes of patients with CHD-associated and CHB-associated HCC.

Method: We conducted a retrospective analysis of all patients with CHD-associated HCC from a single tertiary center in Germany between 2012 and 2022. Patients with first diagnosis of CHD-associated HCC were compared to consecutive patients with CHB-associated HCC between October 2017 and November 2021. Patients with previously treated HCC were excluded.

Results: We identified 15 patients with CHD-associated HCC and compared them to 33 patients with CHB-associated HCC. Patients with CHD-associated HCC were significantly younger (median age 56 years, IQR 52–59, vs. 63 years, IQR 53–67.5; $p = 0.022$), had liver cirrhosis in all cases (100% vs. 62%, $p = 0.025$) and tended to have worse liver function according to Child-Pugh (CP) stage (CP C 31% vs. 6%, $p = 0.080$). There were no differences in gender distribution (male gender 80% vs. 88%, $p = 0.662$), body mass index (median 25.3 vs. 25.3, $p = 0.956$) and ECOG performance status (median 0 vs. 0, $p = 0.577$). Method of HCC diagnosis was comparable between both groups (radiologically in 33% vs. 58%, histologically in 67% vs. 42%, $p = 0.119$). Characteristics of CHD- and CHB-associated HCC are displayed in table 1. HCC in patients with CHD was significantly more likely to be diagnosed in very early (stage 0) and early stages (stage A) according Barcelona Clinic Liver Cancer staging system compared to patients with CHB (67% vs. 21%, $p = 0.004$).

Conclusion: Patients with CHD-associated HCC are younger and present with more advance liver disease compared to patients with CHB-associated HCC. However, tumor burden is lower and HCC is more likely to be diagnosed in early stages and within Milan criteria, whereas a higher ALBI grade would suggest impaired prognosis.

		CHB-associated HCC n = 33	CHD-associated HCC n = 15	p
Tumor grading, n (%)	Good (G1)	3 (21)	4 (40)	0.246
	Moderate (G2)	11 (79)	5 (50)	
	Poor (G3)	0 (0)	1 (10)	
Tumor nodules, n (%)	1 nodule	13 (39)	9 (60)	0.186
	2 nodules	6 (18)	1 (7)	
	3 nodules	1 (3)	2 (13)	
	multifocal	13 (40)	3 (20)	
Tumor extension, n (%)	Unilobular	15 (45.5)	9 (64)	0.341
	Bilobular	18 (54.5)	5 (36)	
Tumor burden, n (%)	>25%	15 (45.5)	2 (14)	0.042
Vascular invasion, n (%)		12 (36)	3 (21)	0.496
Extrahepatic spread, n (%)		7 (21)	0 (0)	0.086
BCLC stage, n (%)	0	1 (3)	1 (7)	0.046
	A	6 (18)	9 (60)	
	B	13 (39)	2 (13)	
	C	12 (36)	3 (20)	
	D	1 (3)	0 (0)	
Milan Criteria, n (%)	Inside	6 (40)	5 (15)	0.074
ALBI score, median (IQR)		-2.700 (-3.054, -2.159)	-2.024 (-2.650, -1.215)	0.513
ALBI grade, n (%)	1	18 (55)	3 (23)	0.036
	2	12 (36)	5 (38.5)	
	3	3 (9)	5 (38.5)	

CHB = chronic hepatitis B; CHD = chronic hepatitis D; HCC = hepatocellular carcinoma; BCLC = Barcelona clinic liver cancer; ALBI = Albumin-Bilirubin-score; IQR = interquartile range

Figure: (abstract: WED-206).

WED-207

Risk stratification for hepatocellular carcinoma in patients with chronic hepatitis D

Leonie Steinhoff¹, Matthias Jeschke¹, Leonie Jochheim¹, Benedikt Hild¹, Moritz Passenberg¹, Hartmut Schmidt¹, Christoph Schramm¹. ¹University of Duisburg-Essen, Department of gastroenterology, hepatology and transplant medicine, Essen, Germany
Email: christoph.schramm@uk-essen.de

Background and aims: Surveillance for hepatocellular carcinoma (HCC) is recommended in patients with increased risk. In recent years, scoring systems have been developed and validated in different populations but not in patients with chronic hepatitis D (CHD) to facilitate risk stratification and to identify subgroups in which surveillance can be safely omitted. We aimed to analyze performance of established scoring systems in CHD-patients.

Method: We retrospectively analyzed all patients with CHD presenting to a single tertiary center from Germany between 2012 and 2022. PAGE B, FIB-4, HCC-Rescue, CAMD, and THRI were calculated at baseline, with was defined as time of first presentation, irrespective of treatment with nucleos (t)id analogs. Patients were followed up until diagnosis of HCC, liver transplantation, or last available data,

whichever came first. Patients with concomitant chronic liver disease, HCC at first presentation and with follow-up (FU) <12 months were excluded.

Results: Sixty-nine patients were identified (64% male gender, median age 41 years, IQR 36–48). Of these, 42 patients had cirrhosis (61%) and 16 patients had history of decompensation (38% of patients with cirrhosis). In the majority of patients (72.5%), FU was <5 years, whereas only 13% were followed up >10 years. During a median FU of 44 months (IQR 21–64.5), four patients developed HCC (6%) and 14 patients underwent liver transplantation (20%), accounting for an incidence of 1.2 per 100 patient years. Results for risk scores are displayed in table 1. One patient (female, age 56 years at HCC diagnosis, FU 49 months), which was categorized as low risk by all risk scores but THRI, did not have signs of cirrhosis at baseline, but histology revealed cirrhosis at time of HCC diagnosis. She had a long-standing CHD, moderate overweight, and history of kidney transplantation and ulcerative colitis, which may contributed to progression to cirrhosis.

Conclusion: FIB-4 and THRI seem most suitable for risk stratification in CHD. However, short FU and low number of patients limit results.

Risk score	Risk category	n (%)	HCC, n	FU (months), (IQR)	Median Incidence per 100 py	Incidence per 100 py
PAGE B	Low	11 (16)	1	47.0 (24.0; 78.0)	2.05	2.05
	Medium	44 (64)	2	44.5 (20.5; 61.0)	0.93	1.06
	High	14 (20)	1	44.5 (22.5; 80.8)	1.49	-
FIB-4	Low	40 (58)	1	46.0 (32.3; 77.0)	0.49	
	High	29 (42)	3	33.0 (19.0; 57.5)	2.37	
HCC-Rescue	Low	33 (48)	2	45.0 (32.0; 67.5)	1.37	1.37
	Medium	26 (38)	1	48.0 (19.3; 80.8)	0.73	1.07
	High	10 (15)	1	34.0 (19.5; 84.8)	2.01	-
CAMD	Low	22 (32)	1	45.5 (37.0; 80.3)	0.93	0.93
	Medium	38 (55)	2	39.5 (19.5; 65.3)	1.15	1.34
	High	9 (13)	1	45.0 (22.0; 98.0)	2.00	-
THRI	Low	6 (9)	0	40.5 (32.0; 57.8)	0	0
	Medium	31 (45)	2	49.0 (31.0; 78.0)	1.10	1.29
	High	32 (46)	2	36.5 (18.5; 51.3)	1.56	-

HCC = hepatocellular carcinoma; IQR = interquartile range; py = patient year

Figure: (abstract: WED-207).

WED-208

Current status of hepatitis delta in Andalusia: multicenter study

Marta Casado¹, Anny Camelo Castillo¹, Pilar Barrera Baena², Ana Belen Perez Jimenez², Jose Pinazo Bandera³, Isabel Viciana³, Juan Cristobal Aguilar⁴, Juan Carlos, Alados Arboledas⁴, German Jose SantaMaria Rodriguez⁵, Carolina Freyre⁵, Carmen Molina Villalba⁶, Joaquin Salas Coronas⁶, M. Pilar Luzón-García⁶, Elena Ruiz⁷, Teresa Cabezas Fernandez¹, Pilar del Pino⁸, Francisco Franco Álvarez De La Luna⁸, Patricia Cordero⁹, Encarnación Ramirez Arellano⁹, Alvaro Giráldez-Gallego¹⁰, María Carmen Lozano Domínguez¹⁰, María Angeles Lopez Garrido¹¹, Antonio Sampedro¹¹, Rocio González-Grande¹², Begoña Palop¹², Manuel Macías¹³, Natalia Montiel¹³, Laura Castillo Molina¹⁴, Carolina Roldan¹⁴, Carmen Sendra Fernández¹⁵, Alberto De La Iglesia Salgado¹⁵, Carlota Jimeno Mate¹⁶, Maria del Carmen Domínguez¹⁶, Fernando Fernández-Sánchez¹⁷, Jose Miguel Rosales Zabal¹⁷, Federico Garcia Garcia⁷. ¹Complejo Hospitalario de Especialidades Torrecárdenas, Almería, Spain; ²Complejo Hospitalario Regional Reina Sofía, Córdoba, Spain; ³Complejo Hospitalario de Especialidades Virgen de la Victoria, Málaga, Spain; ⁴Hospital de Especialidades de Jerez de la Frontera, Jerez de la Frontera, Spain; ⁵Hospital de Especialidades de Puerto Real, Puerto Real, Spain; ⁶Complejo Hospitalario de Poniente, El Ejido, Spain; ⁷Hospital San Cecilio, Granada, Spain; ⁸Complejo Hospitalario de Especialidades Juan Ramón Jiménez, Spain; ⁹Complejo Hospitalario Regional Virgen Macarena, Sevilla, Spain; ¹⁰Complejo Hospitalario Regional Virgen del Rocío, Sevilla, Spain; ¹¹Complejo Hospitalario Regional Virgen de Las Nieves, Granada, Spain; ¹²Complejo Hospitalario Regional de Málaga, Málaga, Spain; ¹³Hospital Puerta del Mar, Cádiz, Spain; ¹⁴Complejo Hospitalario de Jaén, Jaén, Spain; ¹⁵Hospital Comarcal Infanta Elena, Huelva, Spain; ¹⁶Complejo Hospitalario de Especialidades Virgen de Valme, Sevilla, Spain; ¹⁷Complejo Hospital Costa del Sol, Marbella, Spain
Email: mm.casado.m@gmail.com

Background and aims: Chronic hepatitis delta (CHD) is the most severe form of chronic hepatitis, associated with high morbidity and mortality due to its high risk of developing cirrhosis and hepatocellular carcinoma. Its prevalence is unknown, but it is believed to affect around 5% of patients with hepatitis B in Spain. However, this percentage may vary, possibly influenced by migration from countries with higher prevalence. The development of new therapeutic alternatives could modify the management of this infection.

Our aim was to analyze the current state of diagnosis of CHD in hospitals in the autonomous community of Andalusia and describe the profile of patients with chronic infection by active hepatitis delta virus (HDV).

Method: Multicenter, retrospective study, in which the diagnostic workflow of hepatitis delta in the laboratory information systems (SIL) of the 17 participating centers has been analyzed. HBsAg-positive patients, with anti-delta antibodies and detection of HDV RNA, have been included. In patients with active HDV infection, demographic and clinical variables have been analyzed.

Results: The period between January 2018 to October 2022 has been analyzed. 17,899 HBsAg positive patients have been detected; of these, HDV serology (Ig G anti-HDV) was performed in 3314 patients (18%); 205 patients (6.2%) of those tested were anti-HDV positive; of these, HDV RNA was performed in 158 (77%) and finally, 63 patients (39.9%) were RNA-HDV positive, 1.9% of VHD determinations. Regarding the profile of our 63 viremic patients, 69% were men, with an average age of 50 years, 47% were immigrants, half of them coming from Eastern European countries. 37% had HIV or HCV coinfection and 21% history of drug use. 39% of patients had cirrhosis and of them, 6 patients had developed hepatocellular carcinoma, 21% of all viremic patients had presented some episode of decompensation, most of them ascites. 27% had portal hypertension. 40% of patients had been treated with interferon and 6 patients had been transplanted.

Conclusion: The prevalence of anti-HDV positive patients in Andalusia in HBsAg positive patients is 6% and 40% are viremic patients. However, HDV serology has only been performed in 18% of HBsAg-positive patients. The epidemiological profile of patients with active HDV infection has changed as almost half of the patients are immigrants, however, their morbidity remains high. With the new treatment options for HDV, and considering the benefits that the diagnosis of HDV can currently bring, its implementation in the autonomous community of Andalusia seems necessary.

WED-209

Treatment experience and acceptability in a UK HBV cohort- why personalised regimens may be necessary in chronic hepatitis B

Jane Abbott^{1,2}, Patrick Kennedy^{1,2}, Rageshri Dhairyan^{1,2}. ¹Barts Health NHS Trust, United Kingdom; ²Queen Mary University of London, United Kingdom

Email: janeabbott85@gmail.com

Background and aims: Nucleos (t)ide analogues (NA) are the mainstay of treatment for Chronic Hepatitis B (CHB) and whilst they offer potent viral suppression, ultimately they are non-curative. In the context of the functional cure program, and expanding access to anti-viral therapy, it is vital to understand patient acceptability and perspective. We present preliminary results of a patient survey from a multi-ethnic CHB patient cohort.

Method: Patients were recruited from the Barts Health viral hepatitis service, London, UK and consented to a self-guided electronic survey. Patient experience and views on treatment were ascertained, and branch logic was used to tailor subsequent questions dependent on treatment status.

Results: Data are presented on the results of 55 individual patient responses. Respondents had a mean age of 42 years; 59% Male. Ethnicity was predominantly from Asian and African backgrounds: 28.3% Chinese, 20.8% Black African, 18.9% Bangladeshi. 44% of respondents had never taken antiviral therapy. Of the treatment experienced patients, n=2 reported stopping medication due to concerns about side effects. Of patients currently on treatment (n=34); 44% reported being careless or sometimes forgetting to take their medication. Patients not currently on treatment were asked about the factors that would influence their decision to start NA. 83% stated the 'benefit in terms of risk reduction', but 83% were also concerned about treatment side effects. 66.7% stipulated the potential to stop treatment in the future, whilst 44% were worried about the cost. We asked about willingness to take different forms of treatment; 81.5% were willing to take NA daily, 60.4% were willing to take NA indefinitely. 75.9% were willing to take an approved injectable treatment. We asked "How acceptable is it for you to take a daily NA (tablet) that will control viral replication and reduce the risk of harm but not cure your disease?" 31.5% responded extremely acceptable, 42.6% somewhat acceptable. 16.7% stated neutral stance, 3.7% responded somewhat unacceptable and 5.6% extremely

unacceptable. We asked if patients would be open to starting NA therapy if HBV DNA >2000 IU/ml (regardless of ALT level or fibrosis): 20% said yes, 30% said no and 50% were unsure. 66.7% were willing to take part in clinical trials, 61% willing to take an injection as part of a trial, and 74.1% were willing to take a combination of tablets and injections to achieve functional cure. Patients were then asked what duration of this treatment would be acceptable; 3–6 months (27.5%) 6–12 months (37.5%), 12 m–2 yrs (12%) >2 years (25%).

Conclusion: Our results demonstrate a willingness to participate in clinical trials, and an understanding of potential benefits of treatment, which is paralleled with significant concern about side effects. Cost is also a concern. Most patients are willing to take a combination regimen to achieve functional cure but acceptability of treatment duration varies. Clear information about the rationale for treatment and patient education about drug safety may improve treatment uptake. Consultation with patients in drug development should be a vital component of the functional cure program and may usher in an era of personalised treatment regimens.

WED-210

Eliminating viral hepatitis one island at a time-the Hainan experience

Min Liao¹, Jiao Wang¹, Juan Fu¹, Hui Gao¹, Tao Wu¹, Xuexia Zeng², Zhijia Zhao³, Xingyang Zhou⁴, Feng Lin¹, Biao Wu¹. ¹Hainan General Hospital, Haikou, China; ²Hainan Provincial Center for Disease Control and Prevention, Haikou, China; ³People's Hospital of Baoting City, Baoting, China; ⁴Qionghai City Center for Disease Control and Prevention, Qionghai, China

Email: wubiao@hainmc.edu.cn

Background and aims: Hainan Island has the highest incidence of Hepatocellular carcinoma (HCC) in China. In 2021, HCC was the second most common cancer and the first leading cause of death from cancer in Hainan. Most of them are related to Hepatitis B and Hepatitis C in Hainan. However, low disease awareness among Hainanese and lack of disease knowledge among community Health Care Professionals (HCPs) make achieving the WHO targets a great challenge.

Method: Collaborating with Hainan Medical Association, Preventive Medicine Association and Hainan National Health Commission of the Hainan (NHCH), a series of activities were implemented. Education

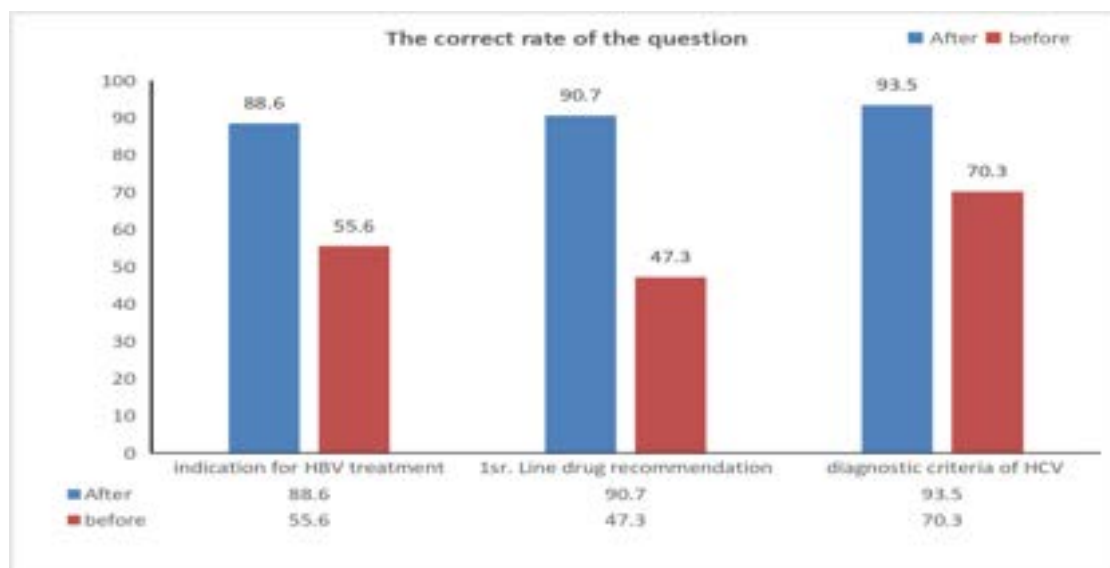


Figure: (abstract: WED-210): The correct rate of the question.

forums to increase awareness of viral hepatitis, screening for HBV in people older than 18 years and HCV in people with high-risk factors were carried out in some cities (Qionghai city, Dongfang city, Baoting city and Haikou city etc) as pilots to create a model of viral hepatitis elimination. It can then be extended to other cities in Hainan to achieve viral hepatitis elimination in Hainan by 2025.

Results: In the past 2 years (2021 Jan–2022 Dec), we have conducted 13 viral hepatitis elimination education conferences in 5 cities for HCPs and a couple of HBV/HCV screening activities in 3 cities. 1683 HCPs were educated and 5,1973 inhabitants were screened for HBV/HCV, respectively. The prevalence of HBV/HCV was 7.3% and 2.3%, respectively, in Dongfang. After education, awareness of viral hepatitis among HCPs has increased significantly. A total of 918 participants were surveyed, including 73% physicians, 19% nurses, 8% medical technicians. 61%, 21% and 18% of the subjects were from primary, secondary and tertiary hospitals respectively. After the education, awareness of HBV/HCV was increased significantly.

Conclusion: This is an efficient way to achieve viral hepatitis elimination in one island through disease education among HCPs and the public to increase awareness of HBV/HCV and screening for HBV in people older than 18 years and HCV in high-risk individuals.

WED-211

Prevalence and predictors of HDV viremia in anti-HDV positive patients of the Hellenic multicenter ReAl-life CLInical Study (HERACLIS-HDV)

George Papatheodoridis¹, Spiliou Manolakopoulos², Stylianos Karapatanis³, Ioannis Elefsiniotis⁴, Dimitrios Christodoulou⁵, Demetrios N. Samonakis⁶, Melanie Deutsch², Christos Oeretanos⁷, Christos Triantos⁸, Konstantinos Mimidis⁹, Emmanouil Manesis¹⁰, Ioannis Vlachogiannakos¹, Ioannis Goulis¹¹, Evangelos Cholongitis¹, Vasilis Sevastianos⁷, Andreas Kapatais¹², Nikolaos Papadopoulos², Panagiota Ioannidou¹, Georgios Germanidis¹³, George Giannoulis¹⁴, Dimitra Lakiotaki¹, Dionisios Kogias⁹, Hariklia Kranidioti², Konstantinos Zisimopoulos⁸, Maria Mela⁷, Georgios Kontos², Paraskevi Fytili¹, Chrysanthi Manolaka³, Polyxeni Agorastou¹¹, Spyridon Pantzios⁴, Margarita Papatheodoridi¹, Eleni Geladari⁷, Nikolaos Psychos⁴, Kalliopi Zachou¹⁴, Anna Chalkidou⁹, Anastasia Spanoudaki², Konstantinos Thomopoulos⁸, George Dalekos¹⁴. ¹General Hospital of Athens "Laiko", Medical School of National and Kapodistrian University of Athens, Greece; ²General Hospital of Athens "Hippokratio", Medical School of National and Kapodistrian University of Athens, Greece; ³General Hospital of Rhodes, Greece; ⁴General and Oncology Hospital of Kifisia "Agiou Anargyroi", Greece; ⁵University General Hospital of Ioannina, Greece; ⁶University General Hospital of Heraklion Crete, Greece; ⁷General Hospital of Athens "Evangelismos", Greece; ⁸University General Hospital of Patras, Greece; ⁹University General Hospital of Alexandroupolis, Greece; ¹⁰Euroclinic SA, Athens, Greece; ¹¹General Hospital of Thessaloniki "Hippokratio", Aristotle University of Thessaloniki, Greece; ¹²General Hospital Nikia-Piraeus "Agios Panteleimon" and General Hospital of Western Attica "Agia Varvara", Greece; ¹³University General Hospital of Thessaloniki "AHEPA", Greece; ¹⁴General University Hospital of Larissa, Greece
Email: gepapath@med.uoa.gr

Background and aims: HDV underdiagnosis remains common varying widely even among different areas of the same country. HDV diagnosis is based on anti-HDV detectability, but not all anti-HDV+ patients (pts) are diagnosed to have HDV viremia. We assessed the rate and predictors of HDV viremia among anti-HDV+ pts of HERACLIS-HDV cohort.

Method: We included 157 (5.8%) anti-HDV+ pts diagnosed among 2696 HBsAg+ adult pts with anti-HDV screening until 03/2022; all had ≥1 visit within 5 years before 10/2021 at one of the 14 participating clinics of HERACLIS-HDV retrospective-prospective cohort study. Epidemiological, clinical and laboratory patients' characteristics were collected using a specifically designed case

report form. Serum HDV RNA was detected by a quantitative real-time polymerase chain reaction assay (Primerdesign Ltd; LLD 400 IU/ml). **Results:** Of the 157 anti-HDV+ pts, 135 (86%) could be tested for HDV RNA at screening, while 6 had died and another 16 had been lost to follow-up. At screening, HDV RNA was detected in 85/135 (63%) pts with median levels of 32,000 (range: 10–22 × 10⁶) IU/ml. All 6 pts who had died and 7/16 pts lost to follow-up had detectable HDV RNA in the past, whereas 8/50 pts with undetectable HDV RNA at screening also had detectable HDV RNA in the past (HDV therapy: 4, liver transplantation: 2, low fluctuating levels: 2). Thus, the overall HDV RNA detectability rate at any time point was 71.6% (106/148 pts tested). HDV RNA at any time point was more frequently detected in anti-HDV+ pts with chronic hepatitis (elevated ALT) than infection (normal ALT) (90/111 or 81.1% vs 16/37 or 43.2%, P < 0.001), advanced (cirrhosis or liver transplantation) than non-advanced liver disease (51/60 or 85.0% vs 55/88 or 62.5%, P = 0.005) and current/past use than no use of HBV therapy (88/108 or 81.5% vs 18/40 or 45.0%, P < 0.001). There was no association between HDV RNA detectability and age, gender, risk group, birth place, center location or size and period of 1st pts visit.

Conclusion: Among anti-HDV+ pts, the probability of serum HDV RNA detectability is significantly higher in those with active and/or advanced liver disease. However, HDV RNA can be frequently detected in all anti-HDV+ subgroups, such as those with normal ALT (>40%), without cirrhosis (>60%) and without a history of HBV therapy (45%).

WED-212

A novel nomogram for predicting HBeAg clearance in HBeAg-positive chronic hepatitis B patients after nucleos (t)ide analogues treatment

Yan Gu¹, Jian Wang^{2,3}, Zhiyi Zhang¹, Shaoqiu Zhang², Yao Zhang¹, Weimao Ding⁴, Jie Li^{1,2,3}, Rui Huang^{1,2,3}, Chao Wu^{1,2,3}. ¹Department of Infectious Diseases, Nanjing Drum Tower Hospital Clinical College of Traditional Chinese and Western Medicine, Nanjing University of Chinese Medicine, Nanjing, Jiangsu, China; ²Department of Infectious Diseases, Nanjing Drum Tower Hospital, The Affiliated Hospital of Nanjing University Medical School, Nanjing, Jiangsu, China; ³Institute of Viruses and Infectious Diseases, Nanjing University, Nanjing, Jiangsu, China; ⁴Department of Hepatology, Huai'an No. 4 People's Hospital, Huai'an, Jiangsu, China
Email: dr.wu@nju.edu.cn

Background and aims: Serum biomarkers for the prediction of HBeAg clearance are important for the management of HBeAg-positive chronic hepatitis B (CHB). This study developed and validated a simple nomogram for predicting HBeAg clearance in hepatitis B e antigen (HBeAg)-positive chronic hepatitis B (CHB) patients treated with nucleos (t)ide analogues (NAs).

Method: Five hundred and sixty-nine CHB patients treated with NAs from two medical institutions between July 2016 to November 2021 were included. Patients were randomly assigned to a derivation cohort (n = 374) and a validation cohort (n = 195) in a 2:1 ratio. A predictive nomogram was established based on cox proportional hazards regression analysis. The predictive value of nomogram was evaluated using the area under the receiver operating characteristic curve (AUC), and the calibration curve.

Results: The 3-year cumulative rates of HBeAg clearance were 27.27% and 21.54% in the derivation cohort and validation cohort, respectively. In the derivation cohort, baseline aspartate aminotransferase, gamma-glutamyl transpeptidase, HBeAg levels and hepatitis B core antibody levels were independently associated with HBeAg clearance and were used to establish the nomogram. The calibration curve revealed that the nomogram had a good agreement with actual observation in both two cohorts. The nomogram showed relatively high accuracy for predicting 48 weeks, 96 weeks, and 144 weeks of HBeAg clearance in the derivation cohort (AUCs: 0.782, 0.734 and 0.671) and validation cohort (AUCs: 0.699, 0.718 and 0.689). The

prediction scores of nomogram ranged from 0 to 100, patients with high scores (79.51–100) had significant higher cumulative incidence of HBeAg clearance than patients with low scores (0–79.51) in both cohorts ($p < 0.05$).

Conclusion: The novel nomogram provided an excellent prediction of antiviral efficacy in HBeAg-positive CHB patients after NAS treatment.

WED-213

The benefit of a local hepatitis B reactivation guideline to improve screening and prophylaxis for patients initiated on rituximab

Helen Boothman¹, Kieran Reynolds¹, Zainab Jadawdji¹, Hannah Hesketh¹, Sarah Clark¹. ¹St George's Hospital, Hepatology, London, United Kingdom

Email: helen.boothman@stgeorges.nhs.uk

Background and aims: Immunosuppressant agents, especially rituximab, have the potential to cause flares and reactivation of hepatitis B virus (HBV) in patients who are currently infected or previously exposed to the virus. The European Association for the Study of the Liver (EASL) Hepatitis B guideline 2017¹ and a Drug Safety Update in England 2014² advise, prior to initiation of rituximab, HBV surface antigen (HBsAg) and HBV core antibody (HBcAb) should be checked and prophylaxis with tenofovir or entecavir should be initiated for any positive results. Despite national guidance, in 2016 there was a fatal HBV reactivation following rituximab at St George's Hospital (SGH). A local guideline was developed in 2018 to highlight the risk and ensure adequate monitoring and prophylaxis. Prior to its implementation, an audit showed 67% of patients receiving rituximab had adequate HBV serology checked.

Method: Newly initiated rituximab prescriptions over a one year period in 2021/22 were identified. Serology results were reviewed to check if pre-screening and initiation of prophylaxis was completed as per the local policy.

Results: 96% of patients started on rituximab had HBV screening. However, only 82% were checked within 3 months of receiving rituximab. 14% of patients had appropriate serology results performed prior to or on the same day as receiving their first dose of rituximab. 10 patients were found to have positive HBsAg or HBcAb, 9 were initiated on prophylaxis (see Table 1).

Conclusion: The introduction of a local guideline and education sessions for specialties responsible for prescribing rituximab resulted in an improvement in HBV screening from 67% to 96%. This has also empowered clinicians to initiate prophylaxis prior to referral to the hepatology team. Despite this, further work is required to ensure the guideline is adhered to in all cases. All 4 patients with no HBV screening were paediatrics, education sessions were offered and the policy is now implemented by the paediatric teams.

References

1. Rituximab: screen for hepatitis B virus before treatment. MHRA. Published 11 December 2014.

2. EASL 2017 Management of hepatitis B virus infection. *Journal of Hepatology* 2017 vol. 67 j 370–398.

WED-214

The comparisons of clinical relapse timing and severity after cessation of prophylactic nucleos(t)ide analogue between chronic hepatitis B patients with lymphoma receiving chemotherapy with and without Rituximab

Yen-Chun Liu^{1,2}, Yu-Jia Shih^{1,2}, Chao-Wei Hsu^{1,2}, Rachel Wen-Juei Jeng^{1,2}. ¹Chang Gung Memorial Hospital, Linkou branch, Taiwan, Taiwan; ²College of Medicine, Chang Gung University, Taiwan, Taiwan

Email: rachel.jeng@gmail.com

Background and aims: Rituximab-based chemotherapy for hematologic malignancies has been well known for high reactivation comparing to other solid tumor chemotherapy regimen. Prophylactic nucleos(t)ide analogues (NUC) treatment is effective to prevent HBV reactivation during chemotherapy. Whether CHB with lymphoma patients will encounter different onset timing or severity of off-Nuc clinical relapse after completion of chemotherapy with and without Rituximab remained unknown. The study aimed to investigate these issues.

Method: HBsAg-positive CHB patients who were diagnosed as lymphoma and had stopped prophylactic Nuc treatment for systemic chemotherapy after at least 12 weeks extended treatment duration were enrolled. In patients with detectable HBV DNA at end-of Nuc treatment (EOT), HBV reactivation was defined at least 2 log₁₀ increase in serum HBV DNA level greater than that at EOT while in patients with undetectable HBV DNA at EOT, reactivation is defined by reappearance of HBV DNA or HBV DNA level ≥ 2000 IU/ml. Clinical relapse (CR) was defined as HBV reactivation with ALT elevation to 2 times upper limit of normal. Hepatic decompensation (HD) was defined as bilirubin ≥ 2 mg/dL and INR ≥ 1.5 with or without clinical syndrome of ascites or hepatic encephalopathy. Cox regressions were analyzed for predictors of off-therapy CR. The cumulative incidence was evaluated by Kaplan-Meier method.

Results: A total of 156 CHB patients with lymphoma were enrolled, mean age of 55-year-old, 51% male, 83% Rituximab-based regimens, and received prophylactic Nuc treatment of a median duration of 48 (range: 29–198) weeks, which the extended Nuc duration of 28 (range: 13–174) weeks. During a median of 56 months follow-up, there were 49 (31%) patients encountered CR with a median time to CR of 24 weeks, and 10 (6%) patients suffering from HD. Compared to patients without Rituximab-based regimens, those receiving Rituximab-based chemotherapy showed numerically higher 2-year cumulative CR incidence (32% vs. 23%, log-rank $p = 0.314$, Figure), three-fold higher peak ALT level at CR (864 vs. 282 U/L, $p = 0.204$), two times greater proportion of ALT ≥ 1000 U/L (47% vs. 20%, $p = 0.362$), but comparable HD rate (6% vs. 8%, $p = 0.673$) and comparable timing to CR (23 vs. 24 weeks, $p = 0.574$). Multivariate cox regression showed male (adjusted hazard ratio (aHR): 1.855, $p = 0.049$), use of less potent Nuc rather than ETV or TDF (versus ETV; aHR:2.516, $p =$

Table 1: (abstract: WED-213): Adherence to local HBV reactivation guideline)

		Receiving rituximab	Adequate screening	Inadequate screening	HBsAg or HBcAb +ve	Prophylaxis initiated
Prior to local guideline	No.	228	152	76	13	8
	pts					
After local guideline	%	100	67	33	6	62
	pts					
After local guideline	No.	106	102	4	10	9
	pts					
	%	100	96	4	9	90
	pts					

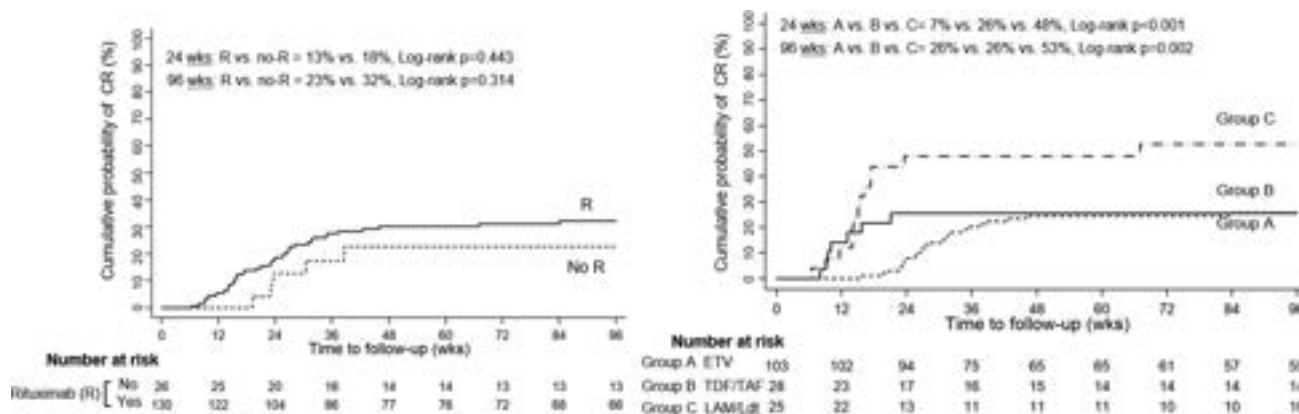


Figure: (abstract: WED-214).

0.007] and pre-treatment HBV DNA $\geq 4 \log_{10}$ IU/ml (aHR:1.953, $p=0.030$) were predictors for CR. Duration of Nuc extension therapy is not an independent factor for CR.

Conclusion: CHB patients who received Rituximab-based regimens for lymphoma had numerically higher off-NUC CR rates and higher ALT level at CR than those without rituximab-based chemotherapy while the timing of CR and hepatic decompensation rate were comparable. Stringent off-therapy monitoring is necessary, especially in patients receiving Rituximab-based regimens.

Viral Hepatitis B and D Current therapies

WEDNESDAY 21 TO SATURDAY 24 JUNE

TOP-105

Tenofovir is associated with a better prognosis of hepatocellular carcinoma compared with entecavir in patients with chronic hepatitis B

Hyun Jun Um¹, Jonggi Choi¹, Young-Suk Lim¹, Won-Mook Choi¹.

¹University of Ulsan College of Medicine, Department of Gastroenterology, Liver Center, Asan Medical Center, Korea, Rep. of South
 Email: dr.choi85@gmail.com

Background and aims: Whether tenofovir or entecavir has different effects on the prevention of hepatitis B virus (HBV)-related hepatocellular carcinoma (HCC) in secondary and tertiary preventive settings remains controversial. This study was aimed to compare the long-term prognosis of HCC between tenofovir and entecavir in patients with chronic hepatitis B (CHB).

Method: CHB patients who were diagnosed with HCC between November 2008 and December 2018 and were treated with either entecavir ($n=3,469$) or tenofovir ($n=3,056$) at a tertiary center in Korea were included. The effect of tenofovir vs. entecavir on the prognosis of HBV-related HCC was evaluated in a propensity score (PS)-matched cohort. Various predefined subgroup analyses were performed.

Results: The mean (SD) age was 54.6 (9.1) years, and 4,351 patients (81.1%) of the PS-matched cohort of 5366 patients were male. During a median follow-up period of 3.0 years, entecavir-treated patients had a mortality rate of 43.0%, whereas tenofovir-treated patients had a mortality rate of 33.5%. Overall survival (OS) was better in tenofovir-treated patients compared with entecavir-treated patients (hazard ratio [HR], 0.80; 95% confidence interval [CI], 0.73–0.88). The difference in OS probability between the two groups became more pronounced over time. The magnitude of the risk difference in OS after 3 years of HCC diagnosis (HR, 0.40; 95% CI, 0.30–0.53) was more prominent than that within 3 years (HR, 0.87; 95% CI, 0.79–0.95). In all subgroup analyses, tenofovir was associated with a better OS than entecavir, except for those with advanced or terminal stage HCC. For those who received curative-intent treatment, recurrence-free survival (HR, 0.83; 95% CI 0.73–0.95) and OS (HR, 0.63; 95% CI 0.50–0.79) were better with tenofovir compared with entecavir.

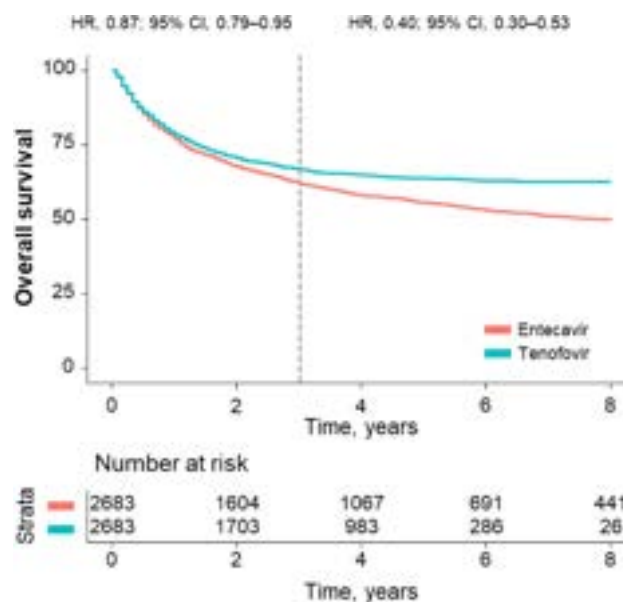


Figure: Survival probability between tenofovir and entecavir in patients with hepatitis B virus-related hepatocellular carcinoma of the propensity score-matched cohort.

Conclusion: In patients with HBV-related HCC, tenofovir showed a better prognosis than ETV, especially in those who survived longer.

SATURDAY 24 JUNE

SAT-144

Predictors of Baveno VII criteria for recompensation in patients with hepatitis B-related decompensated cirrhosis

Vicki Wing-Ki Hui¹, Terry Cheuk-Fung Yip¹, Vincent Wai-Sun Wong¹, Henry LY Chan¹, Grace Lai-Hung Wong¹. ¹Department of Medicine and Therapeutics, Hong Kong

Email: wonglaihung@mect.cuhk.edu.hk

Background and aims: The latest Baveno VII consensus established the foundation of a new concept of hepatic recompensation. The present study sought to investigate potential predictors for recompensation in individuals diagnosed with hepatitis B-related decompensated cirrhosis.

Method: Individuals diagnosed with both chronic hepatitis B and decompensated liver cirrhosis who were treated with first-line oral nucleos (t)ide analogues from March 2006 to December 2022 were identified from a territory-wide database in Hong Kong. A Fine-Gray

subdistribution hazard model, which accounts for competing risks, was employed to identify potential predictors for recompensation.

Results: This study included 2,913 eligible patients, with a mean age of 63.0 ± 11.6 years, of whom 2,184 (75.0%) were male. The baseline Child-Pugh score and MELD score were $7[6, 8]$ and 8.5 ± 6.4 , respectively. During a mean follow-up of 2.1 ± 1.9 years, 435 (14.9%) patients recompensated. High serum albumin correlated with recompensation in cirrhosis (adjusted subdistribution hazard ratio (sHR) 1.03; 95% CI 1.016–1.041; $p < 0.001$), while older age, high alpha-fetoprotein, positive hepatitis B e antigen (HBeAg), and high total bilirubin were associated with a decreased likelihood of recompensation (Age: sHR 0.983; 95% CI 0.975–0.992; $p = 0.001$; Alpha-fetoprotein: sHR 0.697; 95% CI 0.617–0.787; $p < 0.001$; Positive HBeAg: sHR 0.694; 95% CI 0.524–0.919; $p = 0.033$; Total bilirubin: sHR 0.992; 95% CI 0.988–0.996; $p < 0.001$). Patients with recompensation had higher mean serum albumin but lower median AFP, and median total bilirubin compared to those without recompensation over the 5-year follow-up period.

Conclusion: Albumin was an independent protective factor for recompensation, while age, alpha-fetoprotein, positive hepatitis B e antigen, and total bilirubin were identified as risk factors.

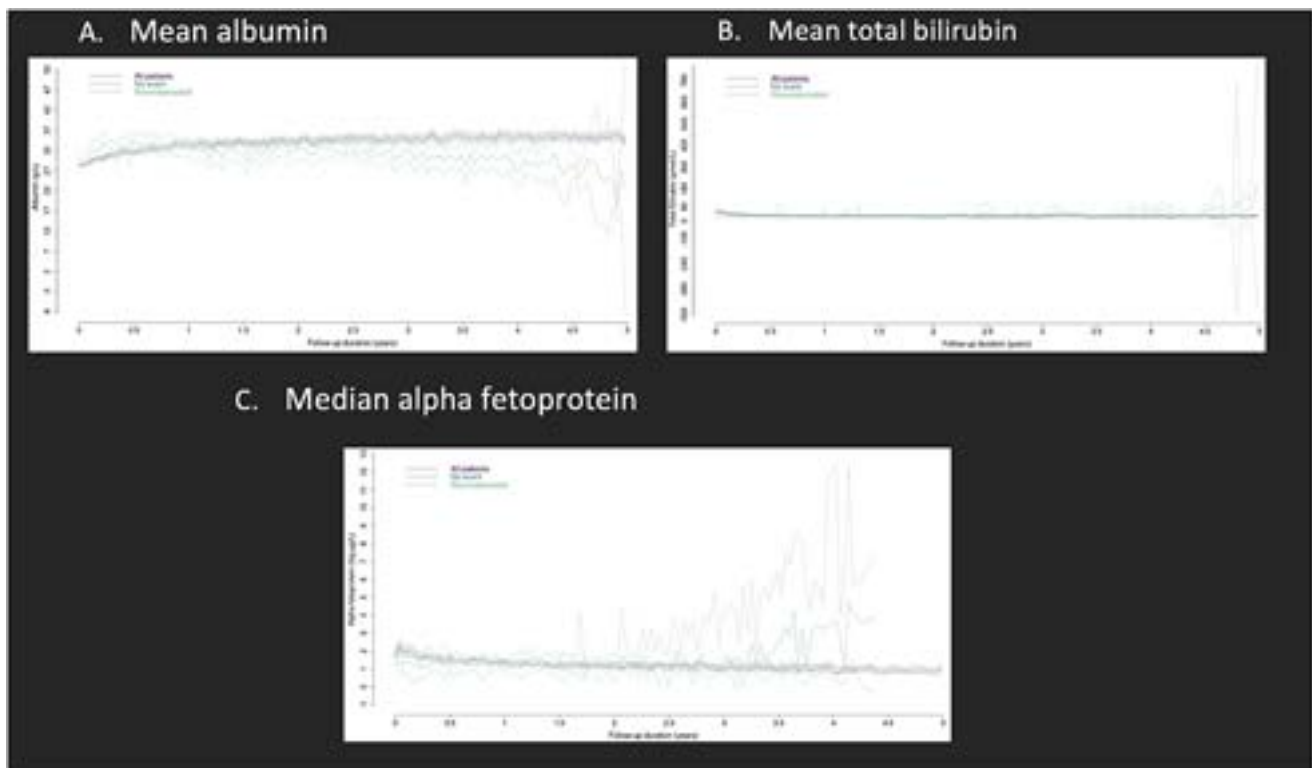


Figure: (abstract: SAT-144).

SAT-145

Utility of partial cure as an end point after nucleos (t)ide analogue withdrawal among chronic hepatitis B patients (RETRACT-B study)

Grishma Hirode^{1,2,3}, Bettina Hansen^{1,4,5}, Chien-Hung Chen⁶, Tung-Hung Su⁷, Grace Wong⁸, Wai-Kay Seto⁹, Arno Furquim d'Almeida¹⁰, Margarita Papatheodoridis¹¹, Sylvia Brakenhoff¹², Sabela Lens¹³, Hannah S.J. Choi¹, Stijn Van Hees¹⁰, Rong-Nan Chien¹⁴, Jordan J. Feld^{1,2,3}, Xavier Forns¹³, Milan Sonneveld¹², George Papatheodoridis¹¹, Thomas Vanwolleghem¹⁰, Man-Fung Yuen⁹, Henry LY Chan⁸, Jia-Horng Kao⁷, Yao-Chun (Holden) Hsu¹⁵, Markus Cornberg¹⁶, Rachel Wen-Juei Jeng¹⁴, Harry LA Janssen^{1,12}. ¹Toronto Centre for Liver Disease, Toronto General Hospital, University Health Network, Toronto, Canada; ²The Toronto Viral Hepatitis Care Network (VIRCAN), Toronto, Canada; ³Institute of Medical Science, University of Toronto, Toronto, Canada; ⁴Institute of Health Policy, Management and Evaluation, University of Toronto, Toronto, Canada; ⁵Department of Epidemiology, Biostatistics, Erasmus University Medical Center, Rotterdam, Netherlands; ⁶Department of Gastroenterology and Hepatology, Kaohsiung Chang Gung Memorial Hospital, Kaohsiung, Taiwan; ⁷Department of Internal Medicine, National Taiwan University Hospital, Taipei, Taiwan; ⁸Medical Data Analytics Centre (MDAC), The Chinese University of Hong Kong, Hong Kong, Hong Kong; ⁹Department of Medicine and State Key Laboratory of Liver Research, The University of Hong Kong, Hong Kong, Hong Kong; ¹⁰Department of Gastroenterology and Hepatology, Antwerp University Hospital, Antwerp, Belgium; ¹¹Department of Gastroenterology, Medical School of National and Kapodistrian University of Athens, Athens, Greece; ¹²Department of Gastroenterology and Hepatology, Erasmus University Medical Center, Rotterdam, Netherlands; ¹³Liver Unit, Hospital Clinic Barcelona, IDIBAPS and CIBEREHD, University of Barcelona, Barcelona, Spain; ¹⁴Department of Gastroenterology and Hepatology, Chang Gung Memorial Hospital Linkou Medical Center, Chang Gung University, Linkou, Taiwan; ¹⁵E-Da Hospital/I-Shou University, Kaohsiung, Taiwan; ¹⁶Department of Gastroenterology, Hepatology and Endocrinology, Hannover Medical School, Germany; Centre for Individualized Infection Medicine (CiIM), Hannover, Germany
Email: grishma.hirode@gmail.com

Background and aims: While functional cure or hepatitis B surface antigen (HBsAg) loss remains the optimal end point for chronic hepatitis B (CHB), recent discussions have suggested the use of "partial cure" as a new primary end point, defined as sustained suppression of HBsAg and HBV DNA undetectability for six months off-therapy. We aim to examine the durability of partial cure after nucleos (t)ide (NA) withdrawal.

Method: Retrospective cohort study of CHB patients who stopped NA therapy and were hepatitis B e antigen (HBeAg) negative with undetectable HBV DNA at cessation. We analyzed differences in

patient characteristics and outcomes between those who achieved HBsAg loss within six months after NA cessation and those with partial cure defined as sustained HBsAg positivity with levels below 100 IU/ml and HBV DNA ≤ 20 IU/ml for at least six months after NA cessation. Survival analysis methods were used to analyze off-therapy outcomes that occurred after six months post-cessation.

Results: Among 1,187 included patients (mean age at end of therapy 54 ± 11 years, 74% male, 88% Asian, 20% HBsAg < 100 IU/ml at end of therapy, median off-therapy follow-up time 18 months [IQR: 6.6–35]), 1.3% had HBsAg loss ($n = 15$) and 4.1% achieved partial cure ($n = 49$) at six months after NA cessation. The partial cure group (vs HBsAg loss group) had a higher proportion of Asian patients (94% vs 60%, $p = .001$) with a shorter median NA duration (3.0 months [IQR: 3.0–3.1] vs 4.5 months [IQR: 3.0–10], $p = .04$). At NA cessation, the partial cure group (vs HBsAg loss group) had higher mean HBsAg levels ($1.0 \pm 0.9 \log_{10}$ IU/ml vs $0.2 \pm 1.8 \log_{10}$ IU/ml, $p = .03$), and median ALT levels ($0.8 \times \text{ULN}$ [IQR: 0.5–1.2] vs $0.5 \times \text{ULN}$ [IQR: 0.4–0.5], $p = .04$) but within the normal range. At 36 months after NA cessation, among the partial cure group, the cumulative probability of HBsAg loss was 48%, sustained response (HBV DNA < 2000 IU/ml and ALT $< 2 \times \text{ULN}$) was 60%, virological relapse (HBV DNA ≥ 2000 IU/ml) was 18%, ALT flare ($\geq 5 \times \text{ULN}$) was 7.7%, and retreatment was 8.4%. Among this group, 1 patient developed hepatic decompensation, 1 patient was diagnosed with HCC, and no patients died during off-therapy follow-up. No patients in the HBsAg loss group experienced relapses or flares and thus none required retreatment. Compared to the group of patients who remained off-therapy without HBsAg loss or partial cure at six months post-cessation, the partial cure group had significantly higher rates of sustained response ($p < .001$), and lower rates of virological relapse ($p < .001$) and ALT flare ($p = .08$) (Figure).

Conclusion: Most patients who achieved partial cure at six months after NA withdrawal, as defined in this study, remained off-therapy thereafter and had favorable outcomes with a high probability of subsequent HBsAg loss. Thus, it may be a viable end point among CHB patients who are well-suppressed and HBeAg negative with low levels of HBsAg at end of therapy.

SAT-146

Effects of tenofovir disoproxil fumarate versus tenofovir alafenamide on risk of osteoporotic fracture in patients with chronic hepatitis B : a nationwide claims study

Eunju Kim¹, Hyun Woong Lee², Kwan Sik Lee³. ¹Chung-Ang University Gwangmyeong Hospital, Department of Gastroenterology, Gwangmyeong-si, Korea, Rep. of South; ²Gangnam Severance Hospital, Yonsei University College of Medicine, Department of Internal Medicine, Seoul, Korea, Rep. of South; ³CHA Bundang Medical Center, CHA University, Department of Gastroenterology, Seongnam, Korea, Rep. of South
Email: leeks519@yuhs.ac

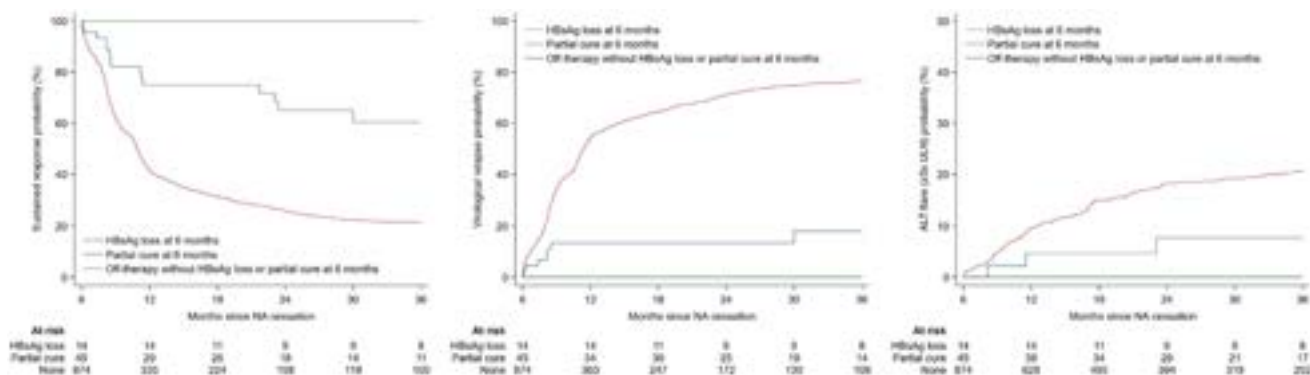


Figure: (abstract: SAT-145).

Background and aims: Since tenofovir disoproxil fumarate (TDF) require long-term use, reduction in bone density should be considered when treating chronic hepatitis B (CHB) patients with aging and systemic diseases. Several studies have shown that patients treated with tenofovir alafenamide (TAF) had less or improved bone mineral density loss compared to patients treated with TDF. However, although improvement in bone density by taking TAF has been reported in previous studies, studies on the actual reduction of fractures are insufficient.

Method: A retrospective cohort study was conducted on 32 582 CHB patients who were initially treated with TDF or TAF from November 2017 to December 2020 using the national claims data of the Health Insurance Review and Assessment Service. The number of patients treated with TDF and TAF was 11 705 and 20 877, respectively. The annual rate of fracture per 100 patients in each group was calculated, and the cox proportional hazard ratio (HR) was analyzed after applying inverse probability treatment weights (IPTW) for both groups.

Results: Among a total of 32 582 patients, the average age was 47.8 ± 11.2 years, males were 64.5%, and the follow-up period was 24.4 ± 11.6 months. The incidence of osteoporotic fractures was 0.78 and 0.49 per 100 person-years in the TDF and TAF groups, respectively. After application of IPTW, HR was 0.68 (95% confidence interval 0.55–0.85, p value = 0.001).

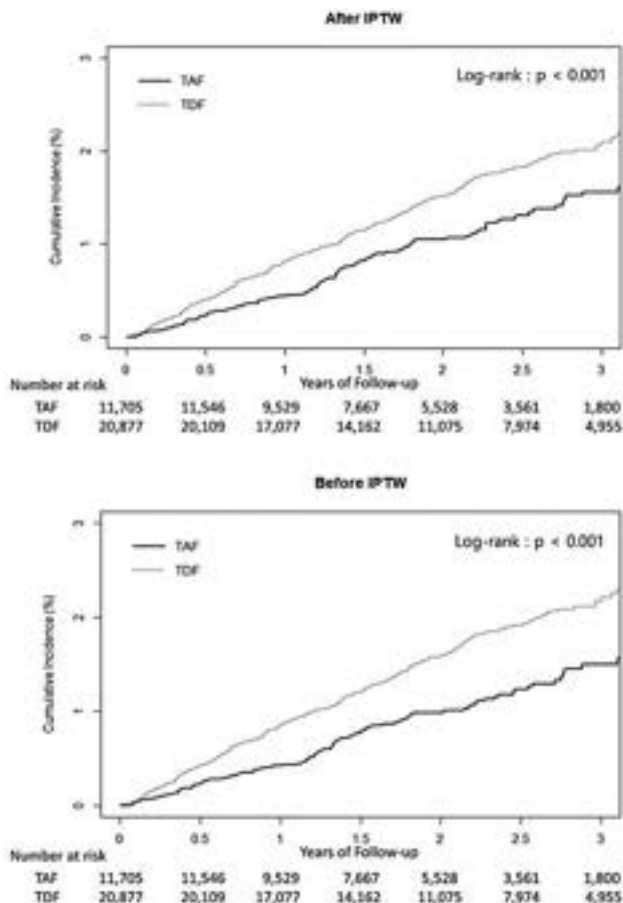


Figure:

Conclusion: In CHB patients, the risk for osteoporotic fracture was significantly lower in the TAF treatment group than the TDF treatment group.

SAT-147

Effects of interferon-based therapies in functional cure and hepatocellular carcinoma risk reduction in patients with chronic hepatitis B: real-world evidence from 2-year data of OASIS project

Qiran Zhang¹, Feng Sun¹, Yiqi Yu¹, Tingting Zhao¹, Shulan Sui¹, Jiming Zhang¹, Jia Shang², Jiawei Geng³, Yiguli He⁴, Ying Guo⁵, Caiyan Zhao⁶, Yueyong Zhu⁷, Xuebing Yan⁸, Wenhong Zhang¹.

¹Huashan Hospital, Fudan University, Department of Infectious Diseases, National Medical Center for Infectious Diseases, Shanghai, China;

²Henan Provincial People's Hospital, Department of Infectious Diseases, Zhengzhou, China; ³The First People's Hospital of Yunnan Province, Department of Infectious Diseases, Kunming, China; ⁴The First Affiliated Hospital of Xian Jiaotong University, Department of Infectious Diseases, Xian, China; ⁵The Third People's Hospital of Taiyuan, Department of Infectious Diseases, Taiyuan, China; ⁶The Third Affiliated Hospital of Hebei Medical University, Department of Infectious Diseases, Shijiazhuang, China; ⁷The First Affiliated Hospital of Fujian Medical University, Department of Infectious Diseases, Fuzhou, China; ⁸Xuzhou Medical University Affiliated Hospital, Department of Infectious Diseases, Xuzhou, China

Email: zhangwenhong@fudan.edu.cn

Background and aims: Interferon (IFN)-based therapy (IFN alone or combined with nucleoside analog [Nuc]) is considered as an effective strategy to improve functional cure rate and reduce hepatocellular carcinoma (HCC) risk in patients with chronic hepatitis B (CHB). We aimed to evaluate the effects of interferon-based therapy in CHB patients with different anti-viral treatment history and baseline HBsAg levels in terms of functional cure and HCC risk reduction, based on large scale real-world data from China.

Method: The analysis was conducted in the data from a multi-center, prospective real-world study (OASIS Project) from China. This project recruited treatment-naïve, IFN-treated and Nuc-treated patients from 32 provinces in China. Participants in OASIS Project received either IFN-based therapy (IFN alone or combined with Nuc) or Nuc monotherapy, and would be followed up for five years. We made this analysis at the time-point of 2 years from project initiation. Data on those who have completed 48 weeks of treatment were analyzed for HBsAg-related events, and all subjects included in this project with complete information were analyzed for cumulative HCC incidence.

Results: A total of 24 946 patients with complete baseline information was included in this analysis, of which 17 210 received IFN-based therapy and 7736 received Nuc therapy. A total of 6978 participants reached 48-week follow-up visit at the timepoint of analysis, of which 4590 were with baseline HBsAg <1500 IU/ml and 2388 with baseline HBsAg ≥1500 IU/ml. In patients with HBsAg <1500 IU/ml, the HBsAg loss rates at 48 weeks of IFN-based therapy were high, regardless of treatment history, either in IFN monotherapy (28.0%–33.3%) or in IFN-Nuc combination therapy (18.1%–28.6%) (Figure 1A). In patients with HBsAg ≥1500 IU/ml, neither IFN monotherapy (2.6%–4.3%) nor IFN-Nuc therapy (1.8%–5.2%) could improve HBsAg loss rates significantly from Nuc monotherapy (0.0%–2.0%) (Figure 1B). The rates of significant HBsAg reduction at 48 weeks (HBsAg decline >1 log₁₀ IU/ml from baseline) were high in patients with IFN-based therapy (26.3%–36.9% in IFN monotherapy and 24.0%–27.8% in IFN-Nuc therapy) (Figure 1C and D). There was significant difference between IFN-based and Nuc treatment, but no significant difference between IFN monotherapy and IFN-Nuc therapy. There were 28 cases developed HCC within 18 months. The cumulative HCC incidence was significantly lower in IFN-based group than Nuc group (0.0301% vs 0.1245%, $P < 0.0001$). After adjusting covariates including age, cirrhosis status and baseline HBsAg levels by COX regression, the difference between two groups was still significant ($p < 0.0001$), and the HR of IFN-based therapy for HCC was 0.153 compared with Nuc therapy (Figure 1E).

Conclusion: IFN-based therapy can significantly improve 48-week HBsAg loss rate from Nuc treatment in patients with low baseline

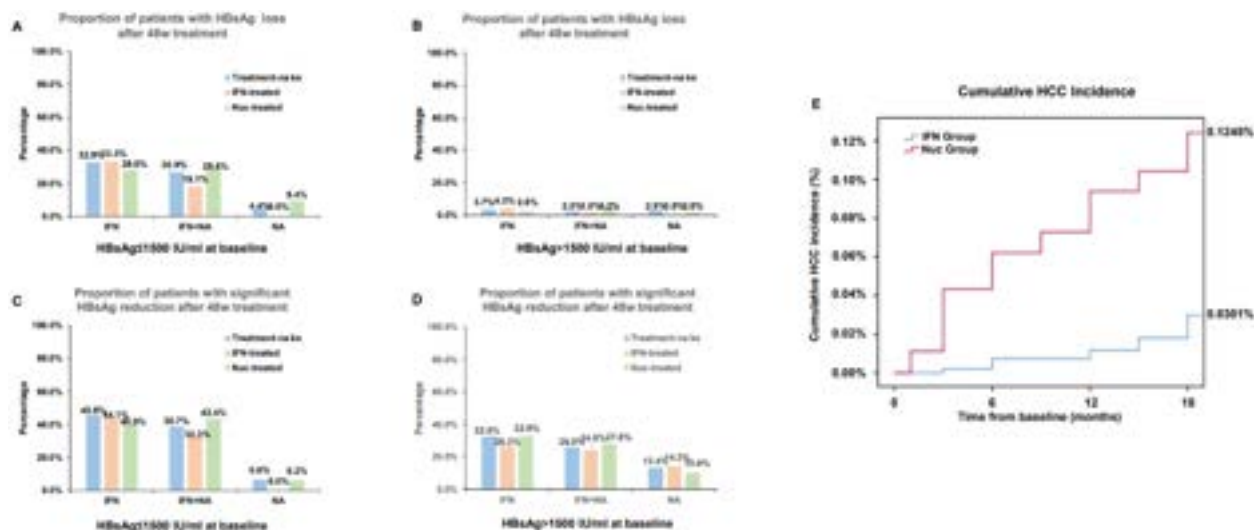


Figure: (abstract: SAT-147).

HBsAg levels, but in patients with high baseline HBsAg levels, HBsAg loss rate is similarly low in either IFN-based or Nuc treatment. However, a high proportion of patients with high baseline HBsAg levels can achieve significant HBsAg reduction after IFN-based therapy, and IFN-treated patients with low HBsAg levels still have relatively high HBsAg loss rates after 48-week IFN based therapy. This suggest that prolonged IFN therapy might be effective for patients with high HBsAg levels to achieve functional cure. Moreover, IFN-based therapy is superior in reducing HCC risks in patients with CHB.

SAT-148

Low HBV DNA and HBsAg levels at 24 weeks off-treatment predict sustained response and HBsAg loss in patients who discontinued antiviral therapy

Milan Sonneveld¹, SM Chiu², Jun Yong Park³, Sylvia Brakenhoff¹, A Kaewdech⁴, Wai-Kay Seto⁵, Yasuhito Tanaka⁶, Ivana Carey⁷, Margarita Papatheodoridis⁸, Piero Colombaro⁹, Florian van Bömmel¹⁰, Thomas Berg¹⁰, Fabien Zoulim¹¹, Sang Hoon Ahn³, George Dalekos¹², Nicole Erler¹, Maurizia Brunetto⁹, Heiner Wedemeyer¹³, Markus Cornberg¹³, Man-Fung Yuen⁵, Kosh Agarwal⁷, Andre Boonstra¹, Maria Buti¹⁴, Teerha Piratvisuth⁴, George Papatheodoridis⁸, Chien-Hung Chen², Benjamin Maasoumy¹³.
¹Erasmus MC, Netherlands; ²Koahsiung Chang Gung Memorial Hospital, Taiwan; ³Yonsei University College of Medicine, Korea, Rep. of South; ⁴Prince of Songkla University, Thailand; ⁵The University of Hong Kong, Hong Kong, Hong Kong; ⁶Kumamoto University, Japan; ⁷Kings College, United Kingdom; ⁸National and Kapodistrian University of Athens, Greece; ⁹University Hospital of Pisa, Italy; ¹⁰Department of Medicine II, Leipzig University Medical Center, Germany; ¹¹INSERM Unit 1052, France; ¹²General University Hospital of Larissa, Greece; ¹³Hannover Medical School, Germany; ¹⁴Hospital Universitari Vall d'Hebron and Ciberehd del Instituto Carlos III de Barcelona, Spain
 Email: m.j.sonneveld@erasmusmc.nl.

Background and aims: Patients who discontinue nucleo (s) tide analogue (NUC) therapy are at risk of severe viral rebound and hepatitis flares, necessitating intensive off-treatment follow-up. We

studied the association between HBsAg and HBV DNA levels at 6 months after therapy cessation (FU W24) with subsequent outcomes.

Method: Chronic hepatitis B patients who discontinued NUC therapy and who were still HBsAg positive and without clinical relapse or retreatment at FU W24 were identified in an existing multicenter database. The association between HBsAg and HBV DNA levels at off-treatment FU W24 with subsequent clinical relapse (defined as HBV DNA >2000 IU/ml + ALT >2× ULN or retreatment) and HBsAg loss was studied through univariable analyses using the Kaplan-Meier method, as well as multivariable Cox regression analysis adjusting for other potential predictors.

Results: We enrolled 641 patients, 86% Asian, 26% pretreatment HBeAg positive, and 59% treated with entecavir. At FU W24, we observed a weak correlation between HBV DNA and HBsAg levels (Pearson's $r = 0.254$, $p < 0.001$). Patients with higher HBV DNA levels at FU W24 had a higher risk of clinical relapse (hazard ratio [HR] 1.617, $p < 0.001$) and a lower chance of HBsAg loss (HR 0.496, $p < 0.001$). Similarly, patients with higher HBsAg levels at FU W24 had a higher risk of clinical relapse (HR 1.616, $p < 0.001$) and a lower chance of HBsAg loss (HR 0.247, $p < 0.001$). A combination of both HBsAg <100 IU/ml and HBV DNA <100 IU/ml at FU W24 identified patients with excellent outcomes (8.5% clinical relapse and 56% HBsAg loss at 192 weeks of subsequent follow-up). Conversely, patients with both HBV DNA >100 IU/ml and HBsAg >100 IU/ml had a very high risk of clinical relapse (68% at 192 weeks), and virtually no chance of HBsAg loss (<1% at 192 weeks). Findings were consistent in multivariable analysis.

Conclusion: Serum levels of HBV DNA and HBsAg at FU W24 can be used to predict subsequent clinical relapse and HBsAg clearance in patients who discontinued NUC therapy. A combination of HBsAg <100 IU/ml with HBV DNA <100 IU/ml identifies patients with very low risk of relapse and excellent chances of HBsAg loss, and could potentially be used as an early surrogate end point for studies aiming at finite therapy in HBV. Patients with both high HBsAg and HBV DNA levels have a very high risk of relapse and virtually no chance of HBsAg loss, and should be closely monitored and/or retreated.

SAT-149

NTCP genetic variants may influence early virological response to bulevirtide monotherapy in patients with HDV related cirrhosis

Pierluigi Toniutto¹, Edmondo Falletti¹, Sara Cmet², Annarosa Cussigh², Elisabetta Degasperis³, Maria Paola Anolli³, Dana Sambarino³, Floriana Facchetti³, Marta Borghi³, Riccardo Perbellini³, Sara Monico³, Pietro Lampertico^{3,4}. ¹University of Udine, Hepatology and liver transplantation unit, Udine, Italy; ²Azienda Sanitaria Universitaria Integrata, Clinical Pathology, Udine, Italy; ³Foundation IRCCS Ca' Granda Ospedale Maggiore Policlinico, Division of Gastroenterology and Hepatology, Milano, Italy; ⁴CRC "A. M. and A. Migliavacca" Center for Liver Disease, Department of Pathophysiology and Transplantation, Milano, Italy

Email: pierluigi.toniutto@uniud.it

Background and aims: Bulevirtide (BLV) is an entry inhibitor conditionally approved by EMA for the treatment of patients with compensated Chronic Hepatitis Delta (CHD). Since it mimics the Na⁺-taurocholate co-transporting polypeptide (NTCP) receptor binding domain, NTCP genetic mutants may potentially contribute to the susceptibility of HDV infection and response to treatment. This study aimed to assess whether NTCP genetic polymorphisms may influence virological and biochemical responses in BLV treated CHD.

Method: Fifty-two patients with CHD (age 49, 26 males, 46 with cirrhosis, pretreatment HDV RNA 5.2 log IU/ml) receiving 2 mg/daily of BLV up to 48 weeks (n = 37) were enrolled. Responses to BLV were categorized as: biochemical (BR), i.e. alanine aminotransferase (ALT) normalization; virological (VR), HDV RNA undetectable or ≥ 2 log IU/ml decline from baseline, and combined (CR), BR+VR. Virological non-response (VNR) was defined as <1 log IU/L decline in HDV RNA from baseline. HDV RNA was quantified by Robogene 2.0 (LOD 6 IU/ml). Six different NTCP single nucleotide polymorphisms (SNPs) (rs943277 C > T, rs943276 C > T, rs76385306 A > C, rs17556915 C > T, rs9323529 A > C, and rs4646296 C > G) were genotyped by Sanger sequencing.

Results: Among all the 6 SNPs investigated, only the carriage of rs17556915 CC (n = 27) vs. CT/TT (n = 25) genotypes was associated with higher HDV RNA levels, both at baseline (5.6 vs. 4.6 log IU/ml, p = 0.016) and at week 24 (3.3 vs. 2.0, p = 0.044), but not at week 48 (2.9 vs. 2.3, p = 0.26). In contrast, no significant correlations were found between these two genotypes and BR, VR, and CR, both at 24 (59.3% vs. 80.0%, p = 0.105; 63.0% vs. 64.0%, p = 0.938; 44.4% vs. 56.0%, p = 0.405) and at week 48 (68.2% vs. 73.3%, p = 0.736; 68.2% vs. 73.3%, p = 0.736; 63.6% vs. 60% p = 0.823). Interestingly, carriers of rs17556915 CC vs. CT/TT genotypes presented more frequently VNR at week 24 (25.9% vs. 4.0%, p = 0.029) but not at week 48 (22.7% vs. 13.3%, p = 0.474). HBsAg serum levels remained unchanged in VR at 48 weeks (3.56 vs. 3.61 Log IU/ml, p = 0.081) but significantly increased in VNR (3.69 vs. 3.83, p = 0.005), independently from the rs17556915 genotypes. Bile acids serum levels increased significantly

from baseline to week 48 (21 vs. 42 mmol/L, p < 0.001) during BLV treatment. Carriers of rs17556915 CC genotype had similar bile acids levels compared to CT/TT both at baseline (21 vs. 30 mmol/L, p = 0.260), at week 24 (32 vs. 38 mmol/L, p = 0.203) and at week 48 (48 vs. 36 mmol/L, p = 0.608).

Conclusion: NTCP genetic variants may influence early virologic response of 2 mg BLV monotherapy in cirrhotic patients with CHD.

SAT-150

Stopping bulevirtide in long-term HDV-RNA suppressed patients seems safe and may enable long treatment-free intervals

Mathias Jachs¹, Marlene Panzer², Lukas Hartl¹, Michael Schwarz¹, Lorenz Balcar¹, Jeremy Camp¹, Petra Munda¹, Mattias Mandorfer¹, Michael Trauner¹, Stephan Aberle¹, Heinz Zoller², Thomas Reiberger¹, Peter Ferenci¹. ¹Medical University of Vienna, Austria; ²Medical University of Innsbruck, Austria

Email: peter.ferenci@meduniwien.ac.at

Background and aims: Bulevirtide (BLV) has been licensed for the treatment of chronic hepatitis D based on on-treatment data overlooking 24–48 weeks, without label recommendations on treatment duration or stopping rules.

Method: Patients included in the ongoing prospective Austrian BLV registry study were offered BLV treatment discontinuation upon the achievement of long-term HDV-RNA suppression to undetectable levels. Off-treatment safety and efficacy were closely monitored.

Results: Seven patients (aged 31–68 years, four with cirrhosis, BLV treatment duration: 46–141 weeks, negative HDV-RNA levels: 12–69 weeks) were included in the study and discontinued treatment. Five had undergone BLV monotherapy, while pegylated interferon-alpha2a (PEG-IFN) was used in combination with BLV in two patients. Until December 2022, patients were followed 10 to 98 weeks (≥ 24 weeks of BLV-free follow-up reached by n = 6). Only one patient showed significant ALT increases within 24 weeks of follow-up. Three patients showed a virological relapse, i.e., detectable HDV-RNA levels, within 24 weeks of BLV-free follow-up, while another relapse occurred after almost one year. So far, relapses occurred exclusively in patients who had undergone BLV monotherapy, while HDV-RNA remained undetectable in the two patients who had undergone combined treatment with PEG-IFN. Overall, treatment with BLV was reintroduced in three patients after 13 to 62 treatment-free weeks. All patients showed antiviral response during their second cycle of BLV treatment. Updated data will be presented at the meeting.

Conclusion: BLV discontinuation upon long-term HDV-RNA suppression appears to be safe, even in patients with cirrhosis, and enable long treatment-free intervals and off-treatment HDV-RNA suppression in some patients, particularly after combined treatment with BLV and PEG-IFN. In case of HDV-RNA relapse, BLV can be safely reintroduced.

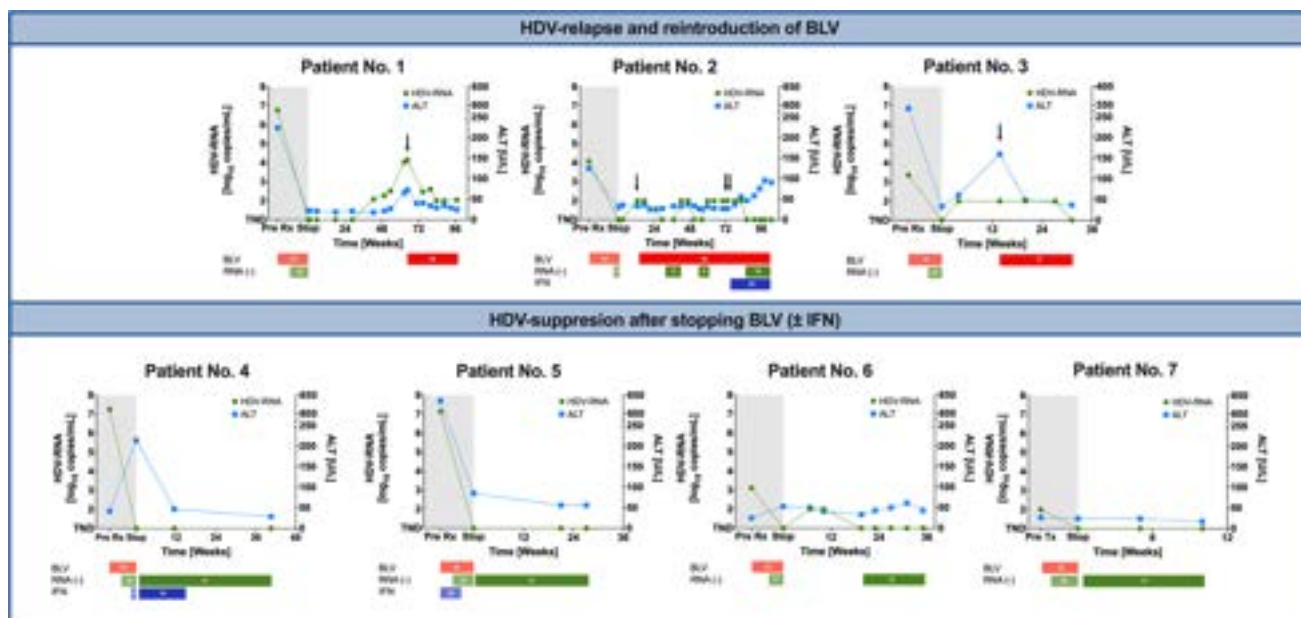


Figure: (abstract: SAT-150).

SAT-151

Switching to Besifovir in chronic hepatitis B patients receiving Tenofovir Disoproxil Fumarate: 96 weeks results of phase 4 trial

Hyung Joon Yim¹, Yeon Seok Seo², Ji Hoon Kim³, Won Kim⁴, Young Kul Jung⁵, Jae Young Jang⁶, Sae Hwan Lee⁷, Yun Soo Kim⁸, Chang Wook Kim⁹, Hyoung Su Kim⁹, Jae-Jun Shim¹⁰, Eun Young Cho¹¹, In Hee Kim¹², Byung Seok Lee¹³, Jeong-Hoon Lee¹⁴. ¹Korea University Ansan Hospital, Internal Medicine, Ansan, Korea, Rep. of South; ²Korea University Anam Hospital, Internal Medicine, Korea, Rep. of South; ³Korea University Guro Hospital, Internal Medicine, Korea, Rep. of South; ⁴Seoul Metropolitan Government Seoul National University Boramae Medical Center, Internal Medicine, Korea, Rep. of South; ⁵Soonchunhyang University Seoul Hospital, Internal Medicine, Korea, Rep. of South; ⁶Soonchunhyang University Cheonan Hospital, Internal Medicine, Korea, Rep. of South; ⁷Gachon University Gil Medical Center, Internal Medicine, Korea, Rep. of South; ⁸Uijeongbu St.Mary's Hospital, the Catholic University of Korea, Internal Medicine, Korea, Rep. of South; ⁹Kangdong Sacred Heart Hospital of Hallym University Medical Center, Internal Medicine, Korea, Rep. of South; ¹⁰Kyunghee University Hospital, Internal Medicine, Korea, Rep. of South; ¹¹Wonkwang University College of Medicine, Internal Medicine, Korea, Rep. of South; ¹²Jeonbuk National University Hospital, Internal Medicine, Korea, Rep. of South; ¹³Chungnam National University Hospital, Internal Medicine, Korea, Rep. of South; ¹⁴Seoul National University Hospital, Internal Medicine, Korea, Rep. of South

Email: gudwns21@korea.ac.kr

Background and aims: In the previous 48-week phase 4 study, switching from TDF to BSV therapy contributed to the maintenance of antiviral effects and improved bone and renal safety in patients with

virologically-suppressed CHB. We evaluated longer-term outcomes in CHB patients in the extended follow-up of the study.

Method: After 48 weeks of comparison of BSV with TDF, eligible patients who had agreed with participating in the extended study continued or switched to either of the drugs, and were followed-up to 96 weeks. We analyzed antiviral efficacy as well as bone and renal safety for the 4 groups.

Results: Among 130 patients who received randomized treatments, 101 patients were included for this observational study (BSV-BSV group, 5; BSV-TDF group, 46; TDF-BSV group, 4; TDF-TDF group, 46). At 96 weeks, 100.0% of patients in the BSV-BSV and TDF-BSV group, and 97.8% in the BSV-TDF and TDF-TDF group maintained virologic response (HBV DNA <20 IU/ml) ($p = 1.00$). Biochemical and serologic responses were comparable between the groups. Of note, bone turnover biomarkers were significantly improved in the BSV-BSV and TDF-BSV groups, and were worsened in the BSV-TDF and TDF-TDF group; accordingly, spine BMD increased in the BSV-BSV and TDF-BSV group, and decreased in the BSV-TDF and TDF-TDF group (% changes; 1.67 ± 1.68 , 3.17 ± 4.31 , -1.35 ± 3.98 , -0.20 ± 3.91 , respectively). The mean %changes of estimated glomerular filtration rates improved in the TDF-BSV group ($2.29 \pm 9.93\%$) while those decreased in the BSV-TDF group ($-2.97 \pm 10.40\%$). There were no adverse events in the BSV-BSV and TDF-BSV groups from 48 to 96 weeks while there were three in the TDF-TDF and BSV-TDF groups.

Conclusion: In this extensional study, antiviral efficacies were comparable between the groups at 96 weeks. Patients receiving BSV for up to 96 weeks showed improved bone and renal safety after the completion of 48 weeks of BSV or TDF therapy in virologically-suppressed CHB patients.

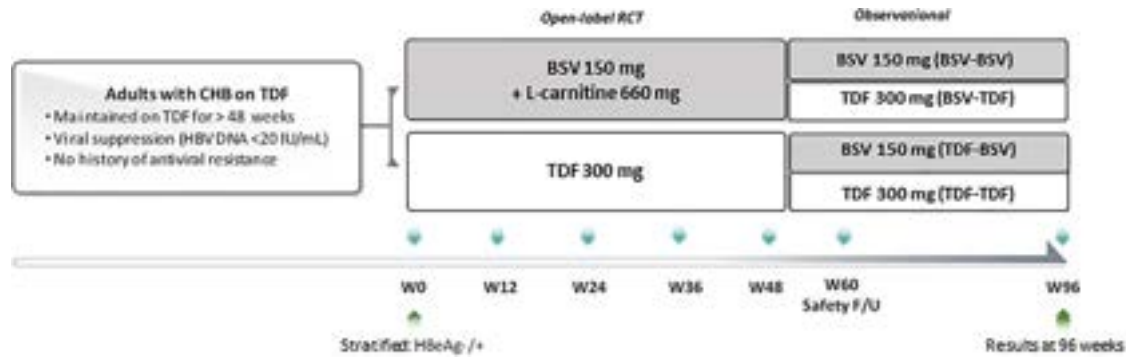


Figure: (abstract: SAT-151): Study scheme.

SAT-152

Five years follow-up of 96 weeks peginterferon plus tenofovir disoproxil fumarate in hepatitis D

Olympia Aevdoxia Anastasiou¹, Florin Alexandru Caruntu², Manuela Gabriela Curescu³, Kendal Yalcin⁴, Ulus S Akarca⁵, Selim Gurel⁶, Stefan Zeuzem⁷, Andreas Erhardt⁸, Stefan Lüth⁹, George Papatheodoridis¹⁰, Onur Keskin¹¹, Kerstin Port¹², Monica Radu², Mustafa Celen⁴, Ramazan Idilman¹¹, Benjamin Heidrich¹², Ingmar Mederacke¹², Heiko von der Leyen¹², Julia Kahlhöfer^{12,13}, Maria von Karpowitz¹², Svenja Hardtke^{9,13}, Markus Cornberg^{12,13}, Cihan Yurdaydin¹¹, Heiner Wedemeyer^{12,13}.

¹Medical Faculty of the University of Duisburg-Essen, Essen, Germany;

²Institutul de Boli Infectioase, Bucharest, Romania; ³Spitalul Clinic de

Boli Infectioase si, Timisoara, Romania; ⁴Dicle University Medical

Faculty, Diyarbakir, Turkey; ⁵Ege University Medical Faculty, Izmir,

Turkey; ⁶Uludağ University Medical Faculty, Bursa, Turkey; ⁷Johann

Wolfgang Goethe University Medical Center, Frankfurt am Main,

Germany; ⁸Heinrich Heine University, Düsseldorf, Germany; ⁹University

Medical Centre Hamburg-Eppendorf, Hamburg, Germany; ¹⁰Medical

School, National and Kapodistrian University of Athens, Athens, Greece;

¹¹Ankara University Medical School, Ankara, Turkey; ¹²Hannover

Medical School, Hanover, Germany; ¹³German Centre for Infection

Research (DZIF), HepNet Study-House/German Liver Foundation,

Hannover, Germany

Email: olympiaevdoxia.anastasiou@uk-essen.de

Background and aims: Until recently pegylated interferon-alfa-2a (PEG-IFNa) therapy was the only treatment option for patients infected with the hepatitis D virus (HDV). Prolonged treatment of hepatitis D with PEG-IFNa with or without tenofovir disoproxil fumarate (TDF) for 96 weeks resulted in HDV RNA suppression in 44% of patients at the end of therapy but did not prevent short-term relapses within 24 weeks after therapy. The virological and clinical long-term effects after prolonged PEG-IFNa-based treatment of hepatitis D are unknown.

Method: The HIDIT-II study comprises of two parallel trials running in Germany, Romania and Greece as an investigator initiated trial and in Turkey as a Roche-sponsored study. Patients (including 41% with liver cirrhosis) received 180 µg PEG-IFNa weekly plus 300 mg TDF once daily (n = 59) or 180 µg PEG-IFNa weekly plus placebo (n = 61) for 96 weeks. Patients were followed until week 356 (5 years after the end of therapy).

Results: Until the end of follow-up 19 (16%) patients developed liver-related complications (n = 6, 32% receiving PEG-IFNa + TDF vs. n = 13, 68% in patients receiving PEG-IFNa plus Placebo, p = 0.113). Achieving HDV suppression at week 96 was associated with decreased long-term risk for the development of hepatocellular carcinoma (p = 0.022) and hepatic decompensation (p = 0.028). The number of patients developing serious complications was similar with (3/18) and without retreatment with PEG-IFNa (16/102, p < 0.999), but was associated with a higher chance of HDV-RNA suppression (p = 0.024, Odds Ratio 3.9 [1.3–12]).

Conclusion: Liver-related clinical events were infrequent and occurred less frequently in patients with virological response to PEG-IFNa treatment. PEG-IFNa treatment should be recommended to HDV-infected patients until alternative therapies become available. Retreatment with PEG-IFNa should be considered for patients with inadequate response to the first cycle of treatment.

SAT-153

Long-term safety profile of tenofovir alafenamide in chronic hepatitis B patients; final 8-year results of 2 Phase 3 studies

Young-Suk Lim¹, Henry LY Chan², Kosh Agarwal³, Patrick Marcellin⁴, Maurizia Brunetto⁵, Wan-Long Chuang⁶, Harry Janssen^{7,8}, Scott Fung⁹, Namiki Izumi¹⁰, Maciej Jablkowski¹¹, Frida Abramov¹², Hongyuan Wang¹², Leland Yee¹², John F. Flaherty¹², Calvin Pan¹³, Shalimar¹⁴, Wai-Kay Seto¹⁵, Edward J. Gane¹⁶, Maria Buti^{17,18}.

¹University of Ulsan College of Medicine, Asan Medical Center, Seoul,

Korea, Rep. of South; ²The Chinese University of Hong Kong (CUHK),

Faculty of Medicine, Tai Wai, Hong Kong; ³King's College Hospital NHS

Foundation Trust, Institute of Liver Studies, London, United Kingdom;

⁴Hôpital Beaujon, APHP, INSERM, University of Paris, Hepatology

department, Clichy, France; ⁵Azienda Ospedaliero-Universitaria Pisana,

Pisa PI, Italy; ⁶Kaohsiung Medical University, Kaohsiung Medical

University Hospital, Kaohsiung City, Taiwan; ⁷University Health

Network, Toronto Centre for Liver Disease, Toronto, Canada; ⁸Erasmus

University Medical Center, Rotterdam, Netherlands; ⁹University of

POSTER PRESENTATIONS

Toronto, Department of Medicine, Toronto, Canada; ¹⁰Japanese Red Cross Musashino Hospital, Department of Gastroenterology and Hepatology, Musashino, Japan; ¹¹Medical University of Lodz, Łódź, Poland; ¹²Gilead Sciences, Inc., Foster City, United States; ¹³New York University Grossman School of Medicine, NYU Langone Health, New York, United States; ¹⁴All India Institute Of Medical Sciences, New Delhi, India; ¹⁵The University of Hong Kong, Department of Medicine and School of Clinical Medicine, Pok Fu Lam, Hong Kong; ¹⁶Auckland Clinical Studies, Auckland, New Zealand; ¹⁷Vall d'Hebron University Hospital Emergency Room, Barcelona, Spain; ¹⁸CIBEREHD del Instituto Carlos III, Madrid, Spain
Email: frida.abramov@gilead.com

Background and aims: In 2 similarly designed double-blind (DB), randomized (2:1), Phase 3 studies (Study 108 in HBeAg-negative [N = 425] and Study 110 in HBeAg-positive [N = 873] patients), tenofovir alafenamide (TAF) demonstrated noninferior efficacy with superior renal and bone safety compared to tenofovir disoproxil fumarate (TDF) at week 96. After completing DB treatment, all patients were eligible to receive open-label (OL) TAF through week 384 (year 8). Here we present the final safety results at year 8.

Method: In a pooled analysis, treatment-emergent adverse events (AEs), serious AEs (SAEs), discontinuations, and laboratory abnormalities were assessed in patients who received OL TAF. Changes from baseline in estimated GFR (by Cockcroft-Gault; eGFR_{CG}) and changes in hip and spine bone mineral density (BMD) by dual x-ray absorptiometry (DXA) scans were assessed.

Results: Of 1298 randomized and treated patients, 1157 (89%; 775 TAF; 382 TDF) entered the OL phase. Overall, 974 (75%) participants completed OL study treatment. The overall incidence of patients experiencing AEs was similar among groups (Table). Rates of Grade 3/4 AEs and AEs leading to discontinuation (D/C) were low and similar among groups. Few Grade 3/4 AEs or SAEs were related to the study drug. Overall, the most common Grade 3/4 lab abnormalities (>2%) were increased amylase (TAF 1.9%, TDF-TAF 2.7%), creatine kinase (TAF 1.4%, TDF-TAF 2.1%), fasting cholesterol (TAF 1.4%, TDF-TAF 2.9%), fasting LDL (TAF 5.9%, TDF-TAF 8.0%), and urine glucose (TAF 5.2%, TDF-TAF 2.7%). After experiencing declines in eGFR_{CG} and hip/spine BMD with TDF treatment in the DB phase, renal and bone outcomes improved following the switch to OL TAF with minimal change through year 8. Overall, low rates of hepatocellular carcinoma (HCC) were observed over 8 years, with 11 cases occurring in the DB and 10 in the OL phases of the study.

Table. OL safety parameters^a

n (%)	TAF n = 775	TDF→TAF total n = 382
Any AE	525 (68)	271 (71)
Grade 3/4 AE	60 (8)	27 (7)
Grade 3/4 AE related to study drug	2 (<1) ^b	0
SAE	97 (13)	49 (13)
SAE related to study drug	4 (1) ^c	0
AE leading to D/C	9 (1)	3 (1)
HCC (DB and OL), n	12	9
Median (Q1, Q3) change in eGFR _{CG} , ml/min	-5.4 (-15.1, 4.9)	-5.0 (-14.6, 6.5)
Mean (SD) %change in hip BMD	-1.64 (4.6180)	-2.05 (5.0434)
Mean (SD) %change in spine BMD	-0.64 (6.4448)	0.04 (6.6041)

^a AEs are treatment-emergent during OL phase; renal/bone changes from original baseline; ^b renal neoplasia [G3] and cerebrovascular accident [G4]; ^c ALT increase [G2], renal neoplasm [G3], osteonecrosis [G2], cerebrovascular accident [G4]; No deaths were treatment-emergent, 6 total deaths (5 DB, 1 OL; TAF 3, TDF 3).

Figure:

Conclusion: Long-term TAF treatment was safe and well tolerated, with minimal changes in eGFR_{CG} and BMD occurring over 8 years.

SAT-154

Association of post-treatment virologic relapse and biochemical flares with HBV serum biomarkers in long-term virologically suppressed HBeAg-negative patients stopping NA treatment: Exploratory analyses from the control arm of the REEF-2 study

Florian van Bömmel¹, Thierry Verbinen², Kosh Agarwal³, Thomas Vanwolleghem⁴, Pietro Lampertico^{5,6}, Maria Buti⁷, Ewa Janczewska⁸, Marc Bourliere⁹, John Jerzowski¹⁰, Thomas Kakuda¹¹, Sandra De Meyer², Adam Bakala², Oliver Lenz², Michael Biermer². ¹Division of Hepatology, Department of Medicine II, Leipzig University Medical Center, Leipzig, Germany; ²Janssen Pharmaceutica NV, Beerse, Belgium; ³Institute of Liver Studies, King's College Hospital, London, United Kingdom; ⁴University of Antwerp, Faculty of Medicine and Health Sciences, Laboratory of Experimental Medicine and Pediatrics, Viral Hepatitis Research Group, Antwerp, Belgium; ⁵Foundation IRCCS Ca' Granda Ospedale Maggiore Policlinico, Division of Gastroenterology and Hepatology, Milan, Italy; ⁶CRC "A. M. and A. Migliavacca" Center for Liver Disease, Department of Pathophysiology and Transplantation, University of Milan, Milan, Italy; ⁷Hospital General Universitari Vall Hebron and CIBER EHD del Instituto Carlos III, Barcelona, Spain; ⁸Medical University of Silesia in Katowice, Faculty of Public Health in Bytom, Bytom, Poland; ⁹Hôpital Saint-Joseph, Department of Hepatology and Gastroenterology, Marseille, France; ¹⁰Janssen Research and Development, LLC, Titusville, United States; ¹¹Janssen Research and Development, LLC, Brisbane, United States
Email: florian.vanboemmel@medizin.uni-leipzig.de

Background and aims: REEF-2 (NCT04129554) assessed efficacy and safety of the combination of siRNA JNJ-73763989, CAM-E JNJ-56136379, and nucleos (t)ide analogues (NA) compared to NA only in virologically suppressed hepatitis B e-antigen (HBeAg)-negative patients with chronic hepatitis B (CHB). All treatments were discontinued in both treatment arms at week 48, followed by 48 weeks of follow-up. In the NA arm, a higher rate of post-treatment virologic relapse and alanine aminotransferase (ALT) flares was observed compared to the JNJ-73763989 arm. We have characterized post-treatment virologic relapses and biochemical flares in the NA arm of the REEF-2 study and assessed their association with end of treatment (EOT) hepatitis B virus (HBV) serum markers.

Method: The association of virologic relapses (confirmed increases in HBV DNA >2000 IU/ml) and biochemical flares (ALT increases ≥3 × upper limit of normal [ULN]) with serum HBV markers was assessed, including HBV RNA (Abbott; lower limit of quantification [LLOQ] = 22 and 11 copies/ml, depending on sample input volume), hepatitis B core related antigen (HBcrAg; Fujirebio; LLOQ/lower limit of detection [LOD] = 3.0/2.6 log₁₀ U/ml), and quantitative anti-hepatitis B core (HBc) IgG (Fujirebio).

Results: 41 of 45 REEF-2 NA-control arm patients (mean NA treatment duration of 8 [range 2–17] years at study entry) who entered follow-up were included. At EOT, all patients had HBV DNA <LLOQ and a mean HBsAg level of 3.41 (range 1.8–4.7) log₁₀ IU/ml. Following NA treatment discontinuation, 27 (66%) and 16 (39%) patients experienced virologic relapses and biochemical flares, respectively. Peak HBV DNA levels during virologic relapse were associated with the magnitude of ALT flares. Ten of 11 (91%) patients with peak HBV DNA >100,000 IU/ml had peak ALT levels ≥10 × ULN versus none of 16 patients with virologic relapse and peak HBV DNA levels >2000–≤100,000 IU/ml. Virologic relapses were generally associated with parallel HBV RNA, HBcrAg, and anti-HBc kinetics, and in few patients with transient HBeAg seroreversion. Six (15%) and 20 (49%) patients had HBV RNA and HBcrAg levels target not

detectable (TND) at EOT, respectively. A similar proportion of patients with HBV RNA detectable and TND at EOT had virologic relapse or ALT flares (Figure). A higher frequency of virologic relapse (peak HBV DNA >100,000 IU/ml) and biochemical flares was observed in patients with detectable HBcrAg and HBsAg <1000 IU/ml at EOT compared to HBcrAg TND and HBsAg ≥1000 IU/ml, respectively (Figure). Patients with quantitative anti-HBc IgG titers <300 IU/ml at EOT had a significantly higher frequency of peak HBV DNA >100 000 IU/ml or biochemical flares than patients with EOT anti-HBc titers ≥300 IU/ml (Figure). None of 11 patients with anti-HBc titers ≥300 IU/ml at EOT had virologic relapse with peak HBV DNA >100,000 IU/ml or peak ALT ≥10× ULN.

Figure. REEF-2 NA-control arm patients with post treatment virologic relapse and ALT flare.

EOT Variables	N	Virological relapse (Confirmed HBV DNA >2000 IU/mL)		Biochemical flare (ALT ≥10× ULN)	
		Any virologic relapse n (%)	Peak HBV DNA >100,000 IU/mL n (%)	Any biochemical flare n (%)	Peak ALT ≥10× ULN n (%)
Patients with EOT data who entered follow-up	41	27 (66%)	11 (27%)	16 (39%)	10 (24%)
HBV RNA					
Detectable*	35	23 (66%)	9 (26%)	13 (37%)	9 (26%)
TND*	6	4 (67%)	2 (33%)	3 (50%)	1 (17%)
p-value*		0.9990	0.5514	0.6624	0.6660
HBcrAg					
Detectable*	21	17 (81%)	9 (43%)	10 (48%)	9 (43%)
TND*	20	10 (50%)	2 (10%)	6 (30%)	1 (5%)
p-value*		0.0116	0.0323	0.3468	0.0689
Anti-HBc IgG					
<300 IU/mL	22	16 (73%)	11 (50%)	12 (55%)	10 (46%)
≥300 IU/mL	19	11 (58%)	0 (0%)	4 (21%)	0 (0%)
p-value*		0.3458	0.0007	0.0129	0.0007
HBsAg					
<1000 IU/mL	13	9 (69%)	4 (46%)	8 (62%)	6 (46%)
≥1000 IU/mL	28	18 (64%)	5 (18%)	8 (29%)	4 (14%)
p-value*		1.000	0.0727	0.0835	0.0485

*<LLQ: detectable or ≥LLQ; †LLQ: target not detected (TND); ‡includes 1 patient with HBsAg <100 IU/mL.
*Two-sided p-value from Fisher's Exact test.
LLQ: HBV RNA assay = 27 and 11 copies/mL, (depending on plasma sample input volume of 0.2 and 0.6 mL, respectively).
LLQ: HBcrAg assay = 3.0 log₁₀ IU/mL. Samples ≥2.6–<3.0 log₁₀ IU/mL are defined as <LLQ: detectable; samples <2.6 log₁₀ IU/mL are defined as <LLQ: TND.

Figure:

Conclusion: In patients discontinuing NA treatment, the level of HBV DNA increases during viral relapse correlated with the peak levels of biochemical flares. EOT anti-HBc IgG levels ≥300 IU/ml were strongly associated with the absence of high peak HBV DNA virologic relapse and high peak ALT flares ≥10× ULN, while this association was weaker for EOT HBcrAg and HBsAg levels and absent for HBV RNA.

SAT-155

Comparable risk of cardiovascular events in chronic hepatitis B patients treated with tenofovir disoproxil fumarate or tenofovir alafenamide

Hyeyeon Hong¹, Jonggi Choi¹, Won-Mook Choi¹, Danbi Lee¹, Ju Hyun Shim¹, Kang Mo Kim¹, Young-Suk Lim¹, Han Chu Lee¹. ¹Asan Medical Center, Department of Gastroenterology, Seoul, Korea, Rep. of South

Email: jkchoi0803@gmail.com

Background and aims: Tenofovir alafenamide (TAF) has been widely used as the first-line antiviral treatment for chronic hepatitis B (CHB) due to its comparable efficacy to tenofovir disoproxil fumarate (TDF) but better safety profile. Previous studies showed that TDF is believed to have lipid-lowering effects, but TAF has exhibited less influence on lipid profiles. Consequently, there were concerns regarding the long-term cardiovascular risk might differ between the two treatments. Thus, we sought to examine the risk of cardiovascular events in a large cohort of patients treated with TAF or TDF.

Method: We retrospectively analyzed 3809 treatment-naïve patients with CHB treated with TDF (n = 2895) or TAF (n = 914) at Asan Medical Center, Seoul, Republic of Korea between 2012 and 2022. The primary

outcome was a composite of major cardiovascular adverse events (MACE), which included myocardial infarction, ischemic stroke, and hospitalization for unstable angina or heart failure. Mean follow-up period was 3.8 years.

Results: The median age was 49.6 years, and 59.1% of the patients were male. At baseline, 365 (9.6%) and 560 (14.7%) of the 3,809 patients had diabetes and hypertension, respectively. Among 2,861 patients for whom smoking history was provided, 633 (22.1%), 514 (18.0%), and 1,714 (59.9%) were current, former, and never smokers, respectively. A total of 41 MACE was occurred with an annual incidence of 0.2%/100 person-years (PYs). At 1, 3, and 5 years, the cumulative risk of MACE was 0.5%, 0.9%, and 1.3% in patients with TDF, and 0.2%, 0.7%, and 0.7% in patients with TAF, respectively. No statistically significant difference in the risk of MACE between the TAF and TDF treatments (p = 0.524). Older age, diabetes, hypertension, coronary artery disease history, and current smoking were associated with an increased risk of MACE in multivariable analysis.

Conclusion: In the present study, patients treated with TAF had a comparable risk of MACE as patients treated with TDF.

SAT-156

Improvements in ALT levels during Bulevirtide treatment for hepatitis D are seen regardless of virologic response

Christopher Dietz-Fricke¹, Frank Tacke², Caroline Zöllner², Münevver Demir², Hartmut Schmidt³, Christoph Schramm³, Katharina Willuweit³, Christian M. Lange⁴, Sabine Weber⁴, Gerald Denk⁴, Christoph Berg⁵, Julia Grottenhaler⁵, Uta Merle⁶, Alexander Olkus⁶, Stefan Zeuzem⁷, Kathrin Sprinzl⁷, Thomas Berg⁸, Florian van Bömmel⁸, Johannes Wiegand⁸, Toni Herta⁸, Thomas Seufferlein⁹, Eugen Zizer⁹, Nektarios Dikopoulos⁹, Robert Thimme¹⁰, Christoph Neumann-Haefelin¹⁰, Peter Galle¹¹, Martin Sprinzl¹¹, Ansgar W. Lohse¹², Jan Kempfski¹², Julian Schulze zur Wiesch¹², Andreas Geier¹³, Florian P. Reiter¹³, Bernhard Schlevogt¹⁴, Juliana Goediker¹⁴, Wolf Peter Hofmann¹⁵, Peter Buggisch¹⁶, Julia Kahlhöfer¹, Kerstin Port¹, Benjamin Maasoumy¹, Markus Cornberg^{1,17,18,19}, Heiner Wedemeyer^{1,17,18}, Katja Deterding¹. ¹Hannover Medical School, Dept. of Gastroenterology, Hepatology, Endocrinology, Germany; ²Dept. of Hepatology and Gastroenterology, Charité Universitätsmedizin Berlin, Campus Virchow-Klinikum (CVK) and Campus Charité Mitte (CCM), Berlin, Germany; ³Dept. of Gastroenterology, Hepatology and Transplantational Medicine, University Hospital Essen, Essen, Germany; ⁴Department of Medicine II, University Hospital, Ludwig Maximilian University Munich, Munich, Germany; ⁵Department of Gastroenterology, Gastrointestinal Oncology, Hepatology, Infectiology, and Geriatrics, University Hospital Tuebingen, Tuebingen, Germany; ⁶Department of Internal Medicine IV, University of Heidelberg, Heidelberg, Germany; ⁷Internal Medicine Department, Goethe University Hospital, Frankfurt, Germany; ⁸Division of Hepatology, Clinic and Polyclinic for Gastroenterology, Hepatology, Infectiology, and Pneumology, University Clinic Leipzig, Leipzig, Germany; ⁹Department of Internal Medicine I, University of Ulm, Ulm, Germany; ¹⁰Department of Medicine II, University Medical Centre Freiburg, Faculty of Medicine, University of Freiburg, Freiburg, Germany; ¹¹Department of Medicine I, University Medical Center of the Johannes-Gutenberg University, Mainz, Germany; ¹²Department of Medicine, University Medical Center Hamburg-Eppendorf, Hamburg, Germany; ¹³University Hospital Würzburg, Division of Hepatology, Dept. of medicine II, Würzburg, Germany; ¹⁴Dept. of Medicine B, University Hospital Münster, Münster, Germany; ¹⁵MVZ for Gastroenterology at Bayerischer Platz, Berlin, Germany; ¹⁶ifl-Institute for interdisciplinary medicine, Hamburg, Germany; ¹⁷German Centre for Infection Research (DZIF), Hannover-Braunschweig, Germany; ¹⁸DSOLVE consortium, a EU Horizon Europe funded project (No 101057917), Germany; ¹⁹Centre for Individualised Infection Medicine (CiIM), a Joint Venture Between the Helmholtz Centre for Infection Research (HZI) and Hannover Medical School (MHH), Hannover, Germany
Email: dietz-fricke.christopher@mh-hannover.de

Background and aims: Hepatitis D is the most form of viral hepatitis leading to liver cirrhosis and hepatocellular carcinoma. The entry inhibitor bulevirtide was approved for the treatment of compensated liver disease in patients with chronic hepatitis D. The FDA and EMA suggest combined end points of virologic and biochemical response for clinical trials. Hence, the conditional approval was based on promising results regarding improvements in biochemical hepatitis activity and reduction of HDV-RNA. We aimed for the characterization of ALT improvements in a real-world setting.

Method: We retrospectively collected anonymized real-world data from 16 German centers treating patients with bulevirtide for chronic hepatitis D. A total of 114 baseline cases was collected. ALT levels were considered normal when <35 IU/l in female and <45 IU/l in male patients. Virologic response was assumed when HDV-RNA was either undetectable, below the lower limit of quantification or had decreased by ≥ 2 log.

Results: Elevated baseline ALT levels were measured in 99/114 patients (mean ALT level 115 IU/l). We covered 4289 patient weeks of bulevirtide treatment with a mean observation time of 38 weeks. Virologic response was observed in 87/114 cases. Mean ALT levels had declined by $68 (\pm 66)$ IU/l at the time point of viral response. Comparable to clinical trials we investigated datapoints at week 12 and week 24 in more detail. A subset of 33 patients had reached treatment week 24. In this group elevated baseline ALT levels were seen in 26/33 patients. At week 12 and 24, ALT had normalized in 9/26 (39%) and 11/26 (42%), respectively. Within the first 12 weeks of treatment a significant decline of ALT was observed (114 IU/l vs. 53 IU/l, $p < 0.001$). This decline was also seen in patients without virologic response (Figure 1). Updated data with additional follow-up weeks will be presented at the meeting.

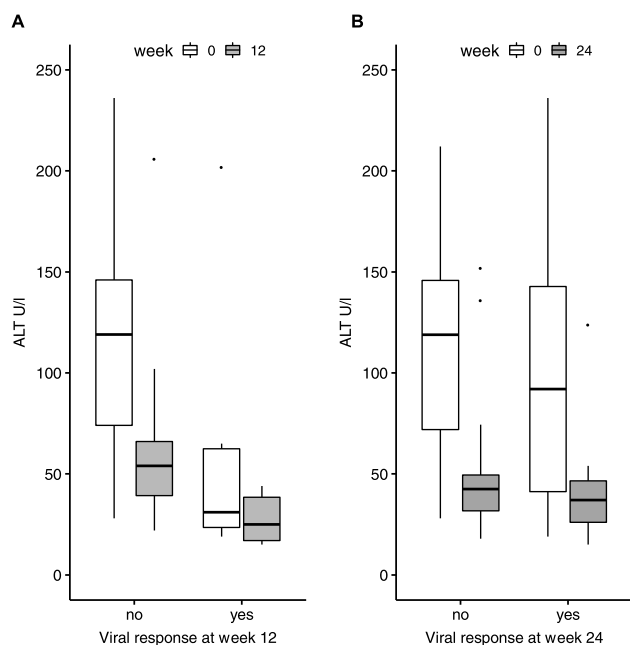


Figure 1: ALT levels at baseline and follow-up weeks grouped by viral response. Boxplots represent ALT levels at week 0 (white), week 12 (grey) and week 24 (dark grey). Outlying data points are visualized by dots. Wilcoxon signed-rank tests were used for comparison of ALT at week 0 and 12 or 24 showing a significant decline of ALT regardless of viral response.

Conclusion: In this real-world cohort ALT levels improved under bulevirtide treatment. This improvement was independent from the virologic response status when investigating distinctive follow-up time points. Different mechanistic explanations for this observation can be considered. The protection of hepatocytes from bile salts through bulevirtide mediated NTCP-blockade may have anti-inflammatory effects. At the same time, the rise in bile salts in the peripheral blood may affect immune cells. The observation of improved ALT values is of clinical relevance as such improvements should theoretically translate into better clinical outcomes.

SAT-157

Comparison of body weight and lipid profiles following tenofovir disoproxil fumarate or entecavir switching to tenofovir alafenamide in chronic hepatitis B patients

Pin-Nan Cheng¹, Chun-Jen Liu², Jyh-Jou Chen³, I-Cher Feng⁴, Hsing-Tao Kuo⁵, Pei-Lun Lee³, Ming-Lung Yu⁵, Yencheng Chiu¹, Chiu Hung-Chih¹, Shih-Chieh Chien¹, Pei-Jer Chen². ¹National Cheng Kung University Hospital, Department of Internal Medicine, Tainan, Taiwan; ²National Taiwan University Hospital, Department of Internal Medicine, Taipei, Taiwan; ³Chi-Mei Medical Center, Liouying, Department of Internal Medicine, Tainan, Taiwan; ⁴Chi-Mei Medical Center, Department of Internal Medicine, Tainan, Taiwan; ⁵Kaohsiung Medical University Hospital, Department of Internal Medicine, Kaohsiung, Taiwan

Email: pncheng@mail.ncku.edu.tw

Background and aims: Body weight (BW) and lipid profiles changes have been reported in HIV infected patients treated with tenofovir alafenamide (TAF) containing regimens. Tenofovir disoproxil fumarate (TDF) treated chronic hepatitis B (CHB) patients exhibited lower lipid profiles in phase III study. The impact of TAF, as a new drug for CHB treatment, on BW and lipid profiles remains unclear and needs to investigate. The aim of this study was to compare the BW changes following switching to a 48-week TAF in prior tenofovir disoproxil fumarate (TDF) or entecavir treated CHB patients.

Method: This was a prospective, multi-center, observational study. CHB patients from seven hospitals in Taiwan treated with TDF or entecavir for at least 1 years and then switched to TAF were enrolled. Treatment indication based on reimbursement criteria. Demography and serial biochemical, hematology, lipid profiles and sugar profiles tests were measured at baseline and then at an interval of 3 or 6 months after switching to TAF. Primary end point was the body weight changes following switching to TAF. Secondary end points included ASCVD score changes, changes of lipid and sugar profiles, and virologic responses following Switching to TAF.

Results: Between June 2020 and May 2021, 159 patients including 100 males and 59 females, were enrolled. The mean age was 56.1 years. Before switching to TAF, 97 patients received TDF and 62 patients received ETV. ETV-switch patients presented with significant older age, lighter BW, lower AST and ALT, higher total bilirubin, lower platelet counts, higher ASCVD risk score, and higher lipid profiles than TDF-switch patients. Significantly lower proportion of TDF-switch patients took lipid lower agents. BW increased shortly after 12 weeks (67.8 ± 12.7 kg, $p < 0.001$) of TAF in TDF-switch patients (Fig. 1). The increased BW maintained following 24 weeks (67.7 ± 12.7 kg, $p = 0.017$), 36 weeks (67.8 ± 12.5 kg, $p = 0.007$), and 48 weeks (67.9 ± 12.9 kg, $p = 0.037$) of TAF treatment. The BW of ETV-switch patients maintained during the first 36 weeks of TAF treatment, but significantly decreased at week 48 (62.6 ± 10.7 kg, $p = 0.033$). In TDF-switch patients, BW of males remained stationary during 48 weeks of TAF, while BW of females at 12 weeks (61.0 ± 8.4 kg, $p < 0.001$), 24 weeks (61.0 ± 9.0 kg, $p = 0.023$), and 36 weeks

Fig. 1 Fig. 2

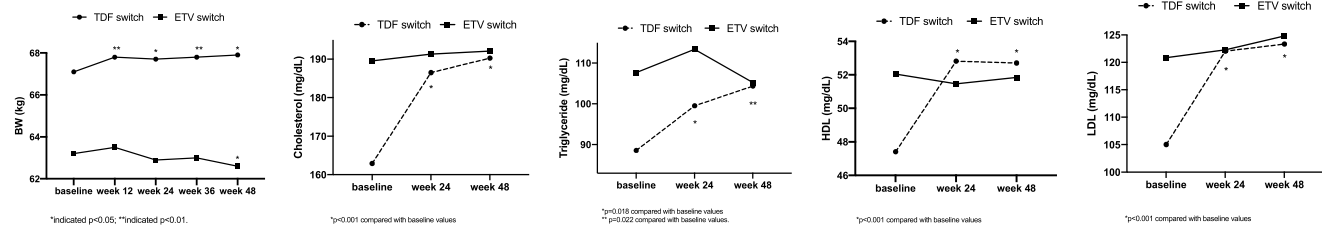


Figure 1: (abstract: SAT-157).

(61.2 ± 9.1 kg, $p = 0.008$) following TAF treatment increased significantly. In TDF-switch patients, cholesterol, triglyceride, HDL, and LDL significantly increased at week 24 and week 48 when compared with baseline (Fig. 2). After 48 weeks of TAF treatment, no significant change of the ASCVD risk score in TDF-switch patients (7.3 ± 9.9 at baseline vs. 7.9 ± 9.9 at week 48, $p = 0.063$) and ETV-switch patients (11.4 ± 13.7 at baseline vs. 12.0 ± 15.4 at week 48, $p = 0.292$).

Conclusion: After 48-week TAF treatment, BW gained significantly in TDF-switched rather than ETV-switched CHB patients. Lipid profiles increase only observed in TDF-switched to TAF CHB patients. ASCVD risk score remained similar following 48-week TAF treatment in either ETV or TDF switched patients.

SAT-158

Model-based meta-analysis of pegylated IFN-alpha induced HBsAg loss at end of treatment and 24 weeks post treatment in chronic hepatitis B virus infection

Nathan Hanan¹, Matthew L Zierhut², Ahmed Nader¹, Anadi Mahajan³, Amandeep Kaur³, Krishna Kumar³, Susan Dixon⁴, Joyeta Das⁴, Mindy Magee¹, Dickens Theodore⁵, Vera Gielen⁴. ¹GSK, Collegeville, United States; ²Certara, San Diego, United States; ³Bridge Medical Consulting, London, United Kingdom; ⁴GSK, Brentford, United Kingdom; ⁵GSK, Durham, United States
Email: vera.x.gielen@gsk.com

Background and aims: Pegylated interferon alpha (Peg-IFNα) is one of two current treatment options for chronic hepatitis B virus (HBV) infection. Peg-IFNα can induce immunological control of HBV with a finite duration treatment, however, response is highly variable. We performed a model-based meta-analysis (MBMA) to establish absolute effect models of hepatitis B surface antigen (HBsAg) loss for peg-IFNα-based regimens at end of treatment (EOT) and 24 weeks post-treatment. This can be leveraged to perform clinical trial simulations that predict outcomes with respect to different populations.

Method: We conducted a systematic review of HBsAg loss rate with peg-IFNα monotherapy or in combination with a nucleos (t)ide analogue (NA) in participants with chronic HBV infection, searching major databases (Embase; MEDLINE; Cochrane) for literature published 2000 to July 2022. HBsAg loss was defined as HBsAg levels reported below the limit of detection (0.05 IU/ml). Models were developed to describe the proportion of participants achieving HBsAg loss at EOT and 24 weeks post treatment as a function of peg-IFNα and peg-IFNα + NA treatment effects. Baseline biological and demographic population characteristics were explored as covariates in both models.

Results: For the peg-IFNα EOT end point of HBsAg loss, a total of 83 study-strata-arms producing HBsAg loss results from 13 235 participants were included. 63 of the study-strata-arms were from randomised controlled trials, the rest are comprised from prospective and retrospective cohorts and single arm trials. For the 24 weeks post-peg-IFNα treatment end point, a total of 58 study-strata-arms producing HBsAg loss results from 4267 participants were included. 43 of the study-strata-arms are from RCTs, 8 from prospective cohorts, 3 retrospective cohorts and 3 single arm trials. In both EOT and post-treatment models, two covariates were identified that describe HBsAg loss in participants treated with peg-IFNα or peg-IFNα + NA: peg-IFNα treatment duration and baseline HBsAg levels. In the EOT model only, HBeAg status was an additional predictor of HBsAg loss. Age, gender, race, and continuation of NA after end of peg-IFNα treatment (24 weeks post-treatment only) were tested but not significant. Degree of missingness for HBV genotype, baseline HBV DNA and baseline alanine aminotransferase (ALT) did not support covariate assessments. The model was then used to simulate 100 000 trials of different populations and treatment arms. Example results of different populations are presented in the table.

Table: Simulated Peg-IFN HBsAg loss rate at EOT and 24 weeks post-treatment following 48 weeks of therapy in HBeAg negative patients (n = 100,000 trials)

Mean baseline HBsAg (log ₁₀ IU/mL)	Peg-IFNα Monotherapy Estimate (95% CI)	Peg-IFNα + NA Estimate (95% CI)
EOT*		
4.5	0.9 (0.2 – 4)	1.2 (0.3 – 5.5)
4.0	1.9 (0.5 – 7.7)	2.7 (0.6 – 10.6)
3.5	4.1 (1 – 15)	5.7 (1.5 – 20.1)
3.0	8.6 (2.2 – 27.7)	11.7 (3.1 – 35.5)
2.5	17 (4.7 – 46.3)	22.5 (6.4 – 55.5)
2.0	31 (9.1 – 66.8)	38.9 (12.2 – 74.5)
1.5	49.6 (16.6 – 82.8)	58.2 (21.4 – 87.6)
1.0	68.3 (27.8 – 92.3)	75.4 (34.4 – 94.6)
0.5	82.6 (42.2 – 96.8)	87 (49.7 – 97.8)
24 weeks post-treatment*		
4.5	1.5 (0.3 – 6.5)	2 (0.4 – 8.5)
4.0	3.1 (0.7 – 12.7)	4.1 (0.9 – 16.3)
3.5	6.4 (1.5 – 23.5)	8.4 (2 – 28.2)
3.0	12.8 (3.2 – 39.7)	16.4 (4.2 – 47.1)
2.5	24 (6.6 – 58.9)	29.5 (8.4 – 66)
2.0	40.4 (12.8 – 75.9)	47.4 (16 – 81.1)
1.5	59.2 (23.1 – 87.6)	65.9 (28.1 – 90.6)
1.0	75.7 (37.9 – 94.1)	80.6 (44.2 – 95.6)
0.5	87 (55.1 – 97.4)	89.9 (61.5 – 98.1)

*Studies informing the EOT and 24 weeks analysis are partially overlapping only, therefore a comparison between these two analyses cannot be made.

Conclusion: The MBMA provides a quantitative description of between-trial variability in peg-IFNα-based regimens and has identified highly influential predictors of HBsAg loss that lend to

POSTER PRESENTATIONS

this variability. These findings provide an evidenced-based approach to predictions of HBsAg in different populations treated with peg-IFN α .

Funding: GSK (217324).

SAT-159

Kinetics of HBsAg forms in chronic hepatitis delta patients treated with bulevirtide for 48 weeks: correlation with virological response

Stefano D'Anna¹, Romina Salpini¹, Elisabetta Degaspero², Leonardo Duca¹, Maria Paola Anolli², Lorenzo Piermatteo^{1,3}, Dana Sambarino², Marta Borghi², Floriana Facchetti², Francesca Ceccherini Silberstein¹, Riccardo Perbellini², Valentina Svicher^{1,3}, Pietro Lampertico^{2,4}. ¹University of Rome "Tor Vergata", Department of Experimental Medicine, Italy; ²Foundation IRCCS Ca' Granda Ospedale Maggiore Policlinico, Division of Gastroenterology and Hepatology, Italy; ³University of Rome "Tor Vergata", Department of Biology, Italy; ⁴CRC "A.M. and A. Migliavacca" Center for Liver Disease, Department of Pathophysiology and Transplantation, Italy
Email: stefanodanna26@gmail.com

Background and aims: HDV exploits the HBV surface protein (HBsAg) for the release of its progeny and entry into hepatocytes. HBsAg consists of three different proteins: Large HBsAg (L-HBs), including preS-1, preS-2 and S regions; Middle HBsAg (M-HBs) including pre-2 and S regions and small HBsAg (S-HBs), containing only the S region. Among them, L-HBs is predominantly present in virions and is crucial for the binding to the NTCp receptor and thus for viral entry into the hepatocytes. Here, we investigate the still unknown kinetics of HBs forms in patients receiving the entry inhibitor bulevirtide (BLV).

Method: Consecutive patients with HDV-related compensated cirrhosis starting BLV monotherapy 2 mg/day were enrolled in this single-center retrospective/longitudinal study. All patients were under effective NUC treatment at entry. L-HBs, M-HBs and S-HBs (Beacle Inc.) were quantified by ad hoc ELISAs assays in baseline and week 48 samples. HDV-RNA was quantified by Robogene 2.0 (LOD: 6 IU/ml). Virological response (VR) was defined as HDV-RNA undetectable (<6 IU/ml) or >2 Log decline compared to baseline, biochemical response as ALT normalization.

Results: Twenty patients with compensated cirrhosis were enrolled: at baseline, median (IQR) age was 50 (40–62) years, 65% males, liver stiffness measurement (LSM) 17.6 (13.1–28.4) kPa, median (IQR) ALT was 110 (83–147) U/L, platelets 72 (59–93) $\times 10^3/\text{mm}^3$, serum HDV-RNA was 4.9 (4.4–5.7) IU/ml and HBsAg levels 3.7 (3.4–3.9) log IU/ml. Pre-treatment, median (IQR) levels of S-HBs, M-HBs and L-HBs were 3421 (1240–6209) ng/ml, 791 (260–1930) ng/ml and 7 (2–15) ng/ml, respectively. Following 48 weeks of BLV, serum HDV-RNA declined by 3.1 (1.8–3.6) log IU/ml and ALT normalized in 14 (70%) patients. VR was observed in 14 (70%) patients while HDV-RNA undetectability in 6 (30%) with 5 of them achieving ALT normalization. During BLV treatment, S-HBs, M-HBs and L-HBs decreased in 60%, 70% and 45% of patients with a median (IQR) decline of 1095 [839–2403] ng/ml, 145

[39–350] ng/ml, 10 [4–15] ng/ml), respectively. HDV-RNA undetectability as well as HDV-RNA undetectability plus ALT normalization at week 48 were significantly greater in patients with low pre-treatment L-HBs levels (54% with vs 11% without L-HBs <9 ng/ml, $P = 0.042$; 50% with vs 0% without L-HBs <9 ng/ml, $P = 0.03$). Notably, the combination of pre-treatment L-HBs levels <9 ng/ml + HDV-RNA levels <5 log IU/ml was the best predictor for achieving combined response (67% with versus 7% without this combination achieved this end point, $P = 0.01$).

Conclusion: Quantification of L-HBs along with serum HDV-RNA may reflect the burden of circulating infectious virions, possibly providing a new tool to identify patients more likely to respond to BLV monotherapy.

SAT-160

Comparison of kidney function decline between chronic hepatitis B patients with versus without antiviral therapy

Jae Seung Lee^{1,2,3}, Chan-Young Jung^{1,4}, Jung Il Lee^{1,2,5}, Sang Hoon Ahn^{1,2,3}, Beom Seok Kim^{1,4}, Seung Up Kim^{1,2,3}. ¹Yonsei University College of Medicine, Department of Internal Medicine, Seoul, Korea, Rep. of South; ²Yonsei University College of Medicine, Institute of Gastroenterology, Seoul, Korea, Rep. of South; ³Severance Hospital, Yonsei Liver Center, Seoul, Korea, Rep. of South; ⁴Yonsei University College of Medicine, Institute of Nephrology, Seoul, Korea, Rep. of South; ⁵Gangnam Severance Hospital, Department of Internal Medicine, Seoul, Korea, Rep. of South
Email: skukorea@yuhs.ac

Background and aims: Kidney function can deteriorate in patients with chronic hepatitis B (CHB). Herein, we compared the risk of kidney function decline between untreated and treated CHB patients receiving antiviral therapy (AVT).

Method: This retrospective study included 1,061 untreated CHB patients, tenofovir alafenamide (TAF) or besifovir dipivoxil maleate (BSV) users ($n = 556$), and entecavir (ETV) users ($n = 2,029$). Primary outcome was kidney function decline, defined as an increase in chronic kidney disease (CKD) stage ≥ 1 for ≥ 3 consecutive months.

Results: The 1:1 propensity score matching yielded 588 pairs in each untreated and treated patient group. The risk of kidney function decline was significantly higher in the treated group (83 patients [2.7 per 1000 person-years (PYs)]) than in the untreated group (39 patients [1.3 per 1000 PYs]) ($p < 0.001$), with an unadjusted hazard ratio of 2.09 (95% confidence interval, 1.43–3.05, $P < 0.001$), which remained the same after adjusting for potential confounders. However, when TAF or BSV users were matched, yielding 259 pairs, no significant difference in the kidney function decline risk was observed between the groups (12 patients in the untreated group [1.6 per 1000 PYs] and 21 in the treated group [2.9 per 1000 PYs], $P = 0.107$). However, when matched, ETV users showed a significantly higher risk of kidney function decline than untreated patients (100 patients [3.6 per 1000 PYs] vs. 31 patients [1.1 per 1000 PYs], $P < 0.001$).

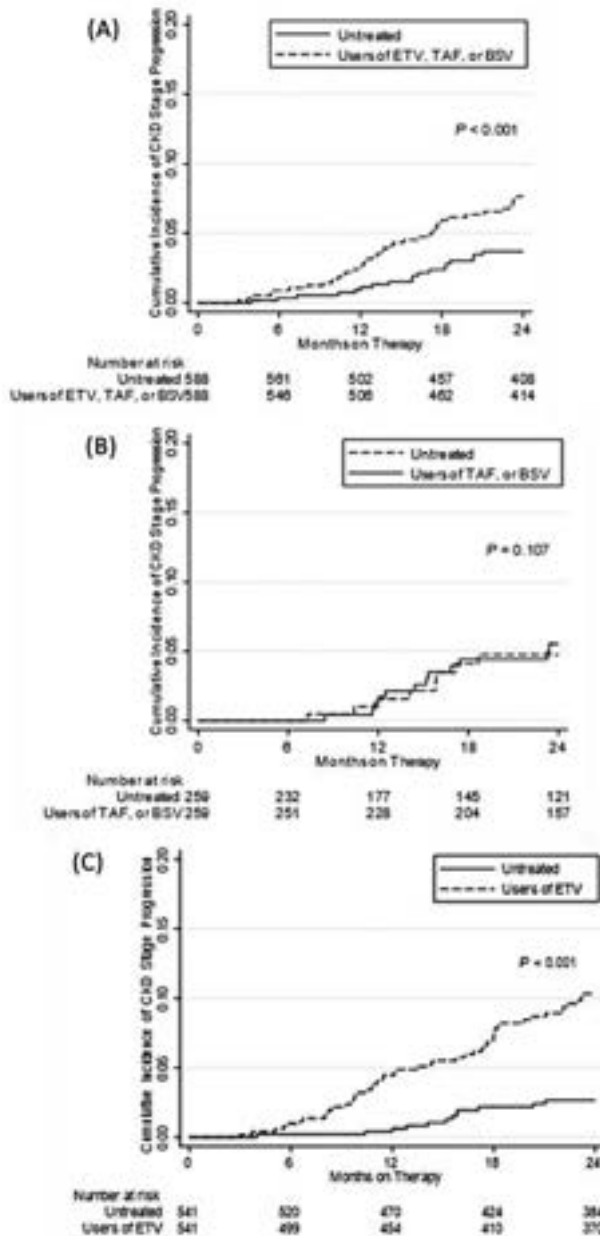


Figure: Cumulative incidence of progression in CKD stage ≥ 1 among (A) untreated patients vs. ETV, TAF, or BSV users, (B) untreated patients vs. TAF or BSV users, and (C) untreated patients vs. ETV users. Abbreviations: CKD, chronic kidney disease; ETV, entecavir; TAF, tenofovir alafenamide; BSV, besifovir disoproxil maleate.

Conclusion: Compared with untreated patients, TAF or BSV users showed a similar risk, whereas ETV users showed a higher risk of kidney function decline.

SAT-161

Effect of first-line nucleot (s)ide analogues on blood lipids in patients with chronic hepatitis B: a network meta-analysis

Kexin Tong¹, Mingjing Chen¹, Danni Wang¹, Jiayi Peng¹, Jia Zhang¹, Jiao Zhou¹, Yujiao Chang¹, Wenxiang Huang¹. ¹The First Affiliated Hospital of Chongqing Medical University, Chongqing, China
Email: wenxiang_huang@163.com

Background and aims: It has been found that blood lipids levels in patients with chronic hepatitis B (CHB) might be changed during antiviral treatment. At present, most studies focused on the comparison of three first-line nucleot (s)ide analogues (NAs), entecavir (ETV), tenofovir disoproxil fumarate (TDF), and tenofovir alafenamide (TAF), but there lacks comprehensive evaluation of their effects on blood lipids under a unified standard. This study aims to evaluate the influence of first-line NAs on blood lipids in CHB patients by using the method of network meta-analysis.

Method: Seven Chinese and English databases were searched from the establishment of the database to November 1, 2022. Studies involving ETV, TDF and TAF on the effects of blood lipids in patients with CHB were included. The changes of serum total cholesterol (TC), triglyceride (TG), low-density lipoprotein cholesterol (LDL-C) and high-density lipoprotein cholesterol (HDL-C) before and after treatment were taken as outcome indicators. We used RevMan5.4 software for direct comparison, and Stata16.0 software for network meta-analysis based on the frequency framework.

Results: Eight articles were included in this study, involving 2614 CHB patients in 10 trials, involving three different antiviral drugs, TAF, TDF and ETV, and the blank control group (inactive CHB patients without antiviral treatment). Direct comparison: Compared with TDF group, blood lipids in TAF group showed an increasing trend (Δ TC SMD = 15.18, 95%CI (11.44, 18.92); Δ TG SMD = 9.24, 95%CI (3.85, 14.63); Δ LDL-C SMD = 6.35, 95%CI (4.41, 8.28); Δ HDL-C SMD = 8.82, 95%CI (2.85, 14.80)); Compared with TDF group, blood lipids in ETV group also increased (Δ TC SMD = 20.39, 95%CI (12.85, 27.93); Δ TG SMD = 18.89, 95%CI (7.28, 30.51); Δ LDL-C SMD = 11.31, 95%CI (4.89, 17.74); Δ HDL-C SMD = 7.65, 95%CI (1.31, 14.00)). Network meta-analysis: TDF can reduce the levels of TC, TG, HDL-C and LDL-C (TDF vs blank control group: Δ TC SMD = -19.43, 95%CI (-27.90, -10.97); Δ TG SMD = -24.11, 95%CI (-44.21, -4.00); Δ LDL-C SMD = -8.91, 95%CI (-16.37, -1.45); Δ HDL-C SMD = -8.6, 95%CI (-14.23, -2.96), while TAF and ETV have no significant difference compared with the blank control group (TAF vs blank control group: Δ TC SMD = 3.39, 95%CI (-4.31, 11.08); Δ TG SMD = 14.2, 95%CI (-5.24, 33.64); Δ LDL-C SMD = 2.37, 95%CI (-4.84, 9.58); Δ HDL-C SMD = -0.37, 95%CI (-4.73, 3.98). ETV vs blank control group: Δ TC SMD = 2.69, 95%CI (-7.04, 12.23); Δ TG SMD = 8.23, 95%CI (-13.07, 29.54); Δ LDL-C SMD = -0.36, 95%CI (-9.02, 8.30); Δ HDL-C SMD = 2.41, 95%CI (-3.81, 8.63)).

Conclusion: TDF had an effect on lowering the levels of TC, TG, HDL-C and LDL-C, and the effect is most obvious within first 24 weeks of treatment initiation. During follow-up for more than 48 weeks, the blood lipids of CHB patients would remain relatively stable. TAF and ETV had neutral effect on lipids change, and no significant difference in blood lipids changes among TAF, ETV and those without antiviral treatment. Switching from TDF to TAF or ETV made the blood lipids of CHB patients increase relatively, but such changes were still within an acceptable range.

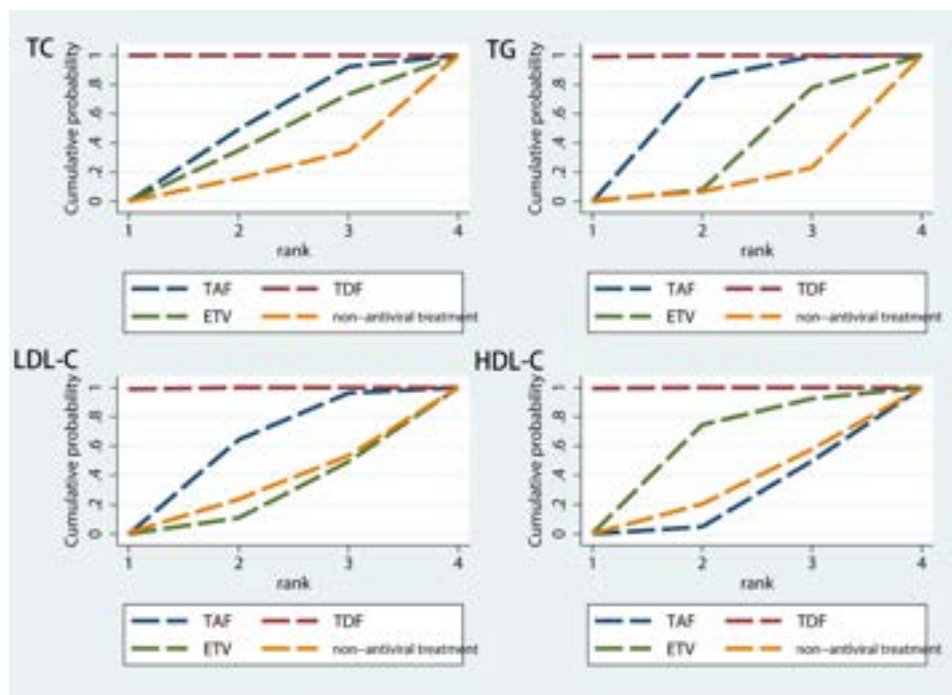


Figure: (abstract: SAT-161): The better the effect of lowering blood lipids, the larger the surface under the cumulative ranking curve (SUCRA).

SAT-162

The different immune response of B cells specific for hepatitis B virus core and envelope antigen in chronic hepatitis B patients with pegylated interferon-alpha treatment

Qi Zheng¹, Ruimin Lai¹, Jiawei Zhang¹. ¹*the First Affiliated Hospital, Fujian Medical University, China*
Email: zhengqi0825@sina.com

Background and aims: The humoral immune response against HBsAg and HBcAg have different functional capabilities during chronic hepatitis B virus (CHB) infection. The phenotype and functional impairment of HBsAg-specific B cells fail to produce detectable anti-HBs and promote the persistence of CHB infection. The seroconversion of the HBsAg provides a promising outcome for pegylated interferon- α (Peg-IFN- α) treated patients with CHB. But a detailed assessment of their impact on HBV-specific B-cell responses is lacking. The study aimed at functional cure including a thorough characterization of hepatitis B-specific B cell responses for Peg-IFN- α treatment.

Method: We included 13 nucleos(t)ide analogue-treated (NUCs) patients with chronic HBV for 48 weeks of Peg-IFN- α treatment. Peripheral blood mononuclear cells (PBMC) were collected before and at 24 weeks, 48 weeks with Peg-IFN- α treatment. Fluorescently labeled HBsAg and HBcAg reagents were synthesized and utilized to characterize ex vivo HBV-specific B cells. The frequency, phenotype and function of HBV-specific B cells and Tfh cells were examined by FACS.

Results: The frequency of HBcAg-specific B cells are similar to HBsAg-specific B cells in NUC-treated patients, and no significant change during Peg-IFN- α treatment. The phenotype and function of B cells specific for HBsAg and HBcAg were different in response to Peg-IFN- α treatment in CHB patients. The expression of CD38 on HBsAg-specific B cells was higher, with the subset of activated memory B cell (actMBC) and IgG+ class-switched memory B cells enriched (PactMBC=0.0065; PIgG=0.0006). And the subset of atypical memory B cells (atMBC) of HBcAg-specific B cells were

increased along with IgG+ class-switched memory B cells reduced and IgM+ class-switched memory B cells increased during Peg-IFN- α treatment. HBsAg-specific B cells showed higher expression of liver-homing marker CXCR3, CD69 and IgG+ class-switched, and lower expression of CXCR5, IgM+ class-switched compared to HBcAg-specific B cells after 48 Weeks Peg-IFN- α treatment. Moreover, the expression of CD40 ligand in Tfh cells was increased ($p=0.0042$) and showed a significant positive correlation with the expression of activation marker CXCR3, CD38 in HBsAg-specific B cells.

Conclusion: The humoral immune response against HBsAg and HBcAg was different in CHB patients with Peg-IFN- α treatment. The exhausted phenotype of HBsAg-specific B cells was recovered whereas HBcAg-specific B cells response was significantly reduced during Peg-IFN- α treatment. Moreover, the frequency of CD40L+Tfh cells was increased and showed a positive correlation with the activation marker of HBsAg-specific B cells indicating the important role of CD40L+Tfh cells in functionally recovering HBsAg-specific B cells with Peg-IFN- α treatment.

SAT-163

Incomplete response with/without genotypic resistance to prior antivirals is not associated with a higher risk of hepatocellular carcinoma during tenofovir treatment for chronic hepatitis B

Ju Yeon Kim¹, Hyunjae Shin¹, Jeayeon Park¹, Moon Haeng Hur¹, Sungwon Chung¹, Min Kyung Park¹, Yun Bin Lee¹, Yoon Jun Kim¹, Jung-Hwan Yoon¹, Jeong-Hoon Lee¹. ¹*Seoul National University College of Medicine, Korea, Rep. of South*
Email: pindra@empas.com

Background and aims: Resistance to antiviral agent is reportedly associated with a higher risk of hepatocellular carcinoma (HCC). However, tenofovir has enabled effective viral suppression even in chronic hepatitis B (CHB) patients who had incomplete response with/without genotypic resistance to previous antivirals. This study aimed to evaluate whether the incomplete response is a risk factor of HCC development in the tenofovir-available era.

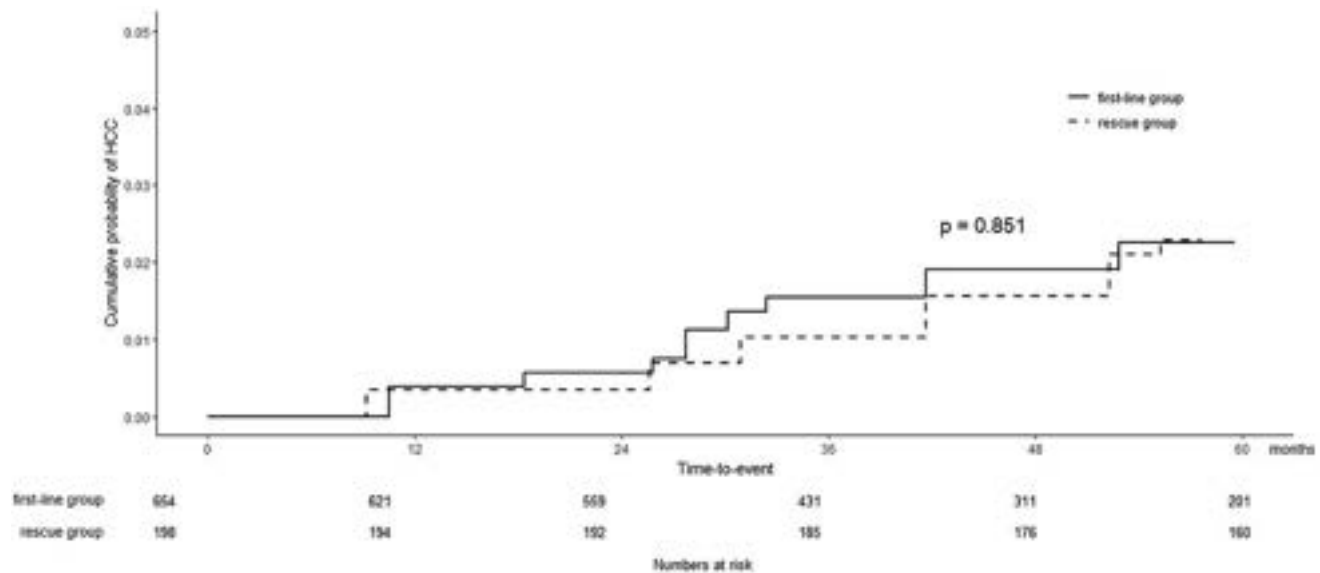


Figure: (abstract: SAT-163).

Method: This retrospective study included 852 consecutive non-cirrhotic CHB patients who started tenofovir between May 2012 and December 2018 at a single tertiary center in Korea: 654 patients started tenofovir as a first-line antiviral treatment (first-line group) and 198 as a rescue therapy for incomplete response to prior antivirals (rescue group). The primary outcome was HCC development. Baseline characteristics were balanced using inverse probability of treatment weighting method.

Results: The rescue group had older age (median, 50 vs. 46 years), included less females (27.3% vs. 47.4%), and lower baseline HBV DNA level (median, 3.1 vs. 6.6 log₁₀ IU/ml) (all $P < 0.05$) compared to the first-line group. 84.3% of the rescue group (167 of 198) had previously documented genotypic resistance. The incidence rates of HCC were comparable between the poor response group (0.63 per 100 person-years [PY]) and the initial therapy group (0.35 per 100 PY) by a univariable Cox proportional hazards model (hazard ratio [HR], 0.91; 95% CI, 0.32–2.54; $P = 0.851$). After adjustment for age, sex, and platelet count, the rescue therapy group was not an independent risk for HCC (adjusted HR, 0.90; 95% CI, 0.33–2.49; $P = 0.840$).

Conclusion: Incomplete response with/without genotypic resistance to prior antiviral therapy was not associated with HCC development in CHB patients with subsequent viral suppression through tenofovir therapy.

SAT-164

Hepatitis B surface antigen loss rate and safety and discontinuations with pegylated interferon alpha in chronic hepatitis B virus infection, a systematic review

Vera Gielen¹, Amandeep Kaur², Krishna Kumar², Saifuddin Kharawala², Joyeta Das¹, Jacob Vincent¹, Anadi Mahajan².
¹GSK, United Kingdom, ²Bridge Medical Consulting, United Kingdom
 Email: vera.x.gielen@gsk.com

Background and aims: Pegylated interferon alpha (Peg-IFNα) is one of two treatment options for chronic hepatitis B virus (HBV) infection. Peg-IFNα can induce immunological control with a finite duration treatment, however, response is highly variable and its safety and tolerable profile impacts eligibility and willingness of patients to take this treatment. The aim was to conduct a systematic review of peg-IFNα treatment in participants with chronic HBV infection, for whom

data on baseline HBsAg levels was available, to understand durability and rates of HBsAg related outcomes, safety and discontinuation.

Method: A systematic review of studies in participants with chronic HBV infection who received PegIFNα, for whom data on baseline hepatitis B surface antigen (HBsAg) was available, was conducted. Outcomes included HBsAg related outcomes for efficacy, safety and treatment discontinuations. Studies included were clinical trials and retrospective and prospective cohorts. Major databases (Embase; MEDLINE; Cochrane) were searched for literature published between 2000 to July 2022.

Results: 126 primary studies were included. 29 studies reported data on durability of HBsAg loss; 10 studies (12 study arms) reported HBsAg loss at end of treatment (EOT), 24 weeks post-treatment and further end points and 19 studies (31 study arms) reported data at EOT and further end points. Range of HBsAg loss in all studies was between 0.0%–84.2% at EOT and in studies assessing durability of response this was 0.0%–44.4%. The majority of studies showed that EOT HBsAg loss with peg-IFNα was durable, 84% or 36 out of 43 study arms showed either no change or increase in HBsAg loss rates over time. Only 7 arms showed a decrease in response rate over time with numerical differences in patients regaining HBsAg being minimal. Data on HBsAg loss at EOT and 24 weeks and factors associated with likelihood of HBsAg loss will be reported in a separate abstract.

Discontinuations were reported in 61 studies and ranged from 0.0% to 62.0%. Discontinuations due to AEs were reported in 52 studies and ranged from 0.0% to 26.8%. AEs were common. Fatigue was reported in 0.0–75.0% (34 studies), asthenia 5–44% (7 studies), headache 2.4–65.1% (30 studies), influenza like illness 8.5–92.9% (9 studies), myalgia 0.0–68.3% (28 studies), depression 0.0–21.5% (10 studies), other neuropsychiatric disorders 0–27% (19 studies, including anxiety, insomnia), and pyrexia 8.2–90% (34 studies).

Conclusion: These results show that some patients can achieve HBsAg loss with peg-IFNα and when achieved HBsAg loss is durable. However, this should be taken in the context of the safety and tolerability profile and therefore patients' willingness to take peg-IFNα with discontinuations ranging between 0 and 62% for a finite regimen.

Funding: GSK (217324).

SAT-165

The efficacy of peginterferon alpha in Chinese inactive hepatitis B carriers and nucleoside analogs-experienced patients: a real world research

Chaojing Wen^{1,2}, Xiaofeng Shi^{1,2}, Yu Lei^{1,2}. ¹The Second Affiliated Hospital, Chong Qing Medical University, Department of Infectious Diseases, Chong Qing, China; ²Key Laboratory of Molecular Biology for Infectious Diseases (Ministry of Education), Institute for Viral Hepatitis, Chong Qing, China

Email: sxf7776@163.com

Background and aims: Due to the different immune states in inactive hepatitis B carriers (IHCs) and nucleoside analogs-experienced patients, whether those two groups of patients show different effectivity to Peginterferon alpha is still unclear. Hence, this study aims to investigate the effectiveness and discrepancy of Peginterferon between inactive hepatitis B carriers and nucleoside analogs-experienced patients.

Method: In this real world, observational study, all subjects were enrolled from June 2010 to September 2021 at the Second Affiliated Hospital of Chong Qing Medical University. A total 58 inactive hepatitis B carriers assigned to receive PEG-IFN α 2b alone for 48 weeks (Peg-IFN group), 84 nucleoside analogs-experienced patients treated with PEG-IFN α 2b plus nucleoside analogs (tenofovir disoproxil fumarate, entecavir or tenofovir alafenamide) for 48 weeks (Peg-IFN plus NAs group), 23 nucleoside analogs-experienced patients receive NAs alone for 48 weeks (NAs group). Patients were followed up 24 weeks after treatment discontinued. Twenty seven untreated IHCs were observed for 72 weeks (control group). The primary end point is the HBsAg clearance and seroconversion at 48 weeks and 72 weeks.

Results: Baseline characteristics are similar in every groups. At week 48, Intention-to-treat analysis showed that the rate of HBsAg clearance were 53.4% (31/58), 45.2% (38/84), 0% (0/27) and 0% (0/23) in Peg-IFN group, Peg-IFN plus NAs group, NAs group and control group respectively (ITT, $P = 0.336$, Peg-IFN VS Peg-IFN plus NAs; $P <$

0.001 Peg-IFN VS controls; $P < 0.001$, Peg-IFN plus NAs VS NAs). HBsAg seroconversion was achieved 36.2% (21/58) of Peg-IFN, 25.8% (23/89) of Peg-IFN plus NAs (ITT, $P = 0.166$). In Peg-IFN group, two patients (2/31, 6.5%) were observed HBsAg reappearance at 12 weeks and 48 weeks after HBsAg loss. Meanwhile, four subjects (4/38, 10.5%) experienced HBsAg relapse at 24 weeks, 32 weeks, 48 weeks and 56 weeks after HBsAg clearance in Peg-IFN plus NAs group ($p = 0.867$). Furthermore, we used the receiver operator curve to analyze HBsAg clearance. A baseline HBsAg level of < 32 IU/ml provide good prediction for HBsAg clearance (sensitivity: 73.7%, specificity: 43.8%). All patients in treatment group exhibited virological response (HBV DNA < 100 IU/ml). Generally, there are no serious adverse events during treatment, and the therapy was well tolerated.

Conclusion: Peg-IFN results in high rates of HBsAg loss and seroconversion in both IHCs and nucleoside analogs-experienced patients, especially, for those patients who HBsAg level below 32 IU/ml. Besides, HBsAg seroclearance achieved after Peg-IFN treatment was durable during 24 weeks' follow-up.

SAT-166

Similarly low risk of chronic kidney disease (CKD) progression in chronic hepatitis B patients with Stage 2 CKD on tenofovir alafenamide versus entecavir

Yan Liang¹, Vicki Wing-Ki Hui¹, Terry Cheuk-Fung Yip¹, Che To Lai¹, Shuk Man Lam¹, Yee-Kit Tse¹, Henry LY Chan¹, Vincent Wai-Sun Wong¹, Grace Lai-Hung Wong¹. ¹the Chinese University of Hong Kong, Hong Kong
Email: wonglaihung@mect.cuhk.edu.hk

Background and aims: Tenofovir alafenamide (TAF) is a novel prodrug of tenofovir. There have been evolving data concerning its positive impact on renal safety as shown in registration trials. We aimed to compare the risk of chronic kidney disease (CKD) progression in chronic hepatitis B (CHB) patients on TAF versus entecavir (ETV).

Method: This is a retrospective cohort study. CKD Epidemiology Collaboration equation was used to determine the estimated

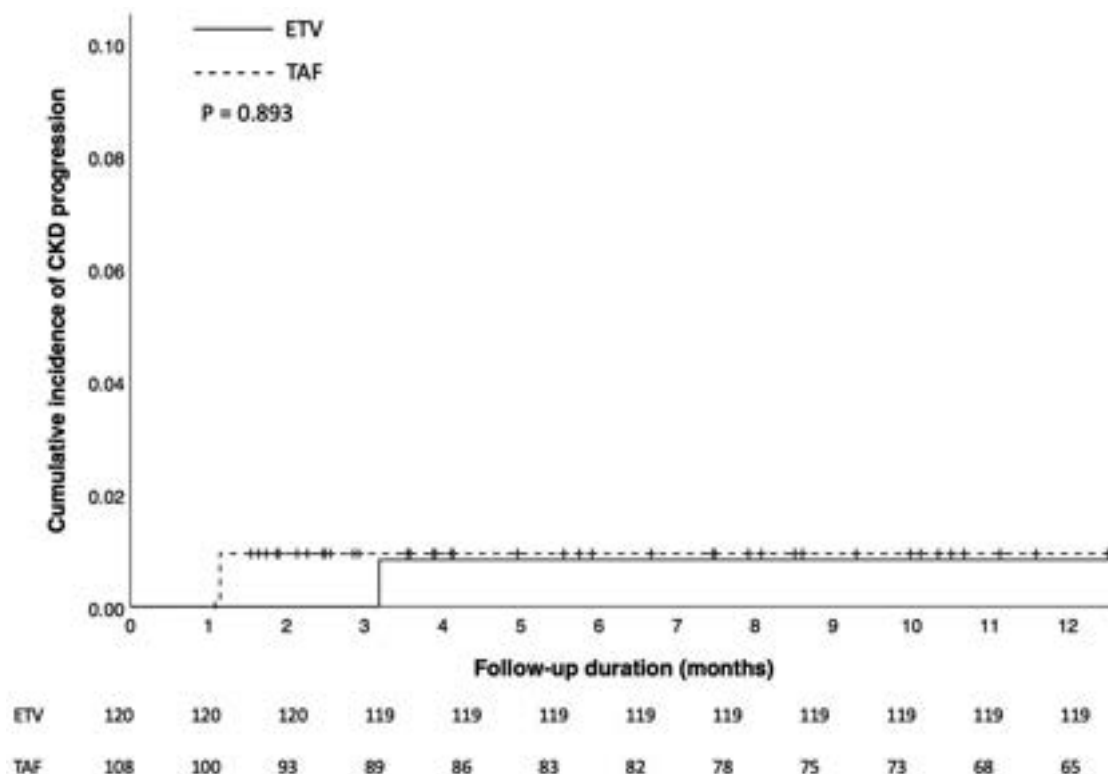


Figure: (abstract: SAT-166).

glomerular filtration rate (eGFR) and classified it into five CKD stages. Those TAF- and ETV-treated CHB patients who had Stage 2 CKD (i.e. eGFR 60–89 ml/min/1.73 m²) and were previously treatment naïve were included. The baseline was defined as the start date of the antiviral treatment. The primary end point was the cumulative incidence of CKD progression at 12 months. Propensity score (PS) with the use of estimated average treatment effect was adopted in the analysis.

Results: 108 TAF-treated and 120 ETV-treated CHB patients were included in the analysis. 306 (58.2%) of them were males and their mean age was 60.0 ± 12.9 years old. Their mean baseline eGFR was 77.1 ± 8.3 and 79.3 ± 7.4 ml/min/1.73 m², respectively. During the first 12 months of follow-up, 1 (0.9%) TAF-treated and 1 (0.8%) ETV-treated patient with baseline Stage 2 CKD had CKD progression of at least one stage for at least three consecutive months, respectively. Kaplan-Meier curves showed that TAF-treated patients had a comparable risk of CKD progression compared with ETV-treated CHB patients (p = 0.893). (Figure).

Conclusion: TAF is associated with a similarly low risk of CKD progression compared with ETV in patients with Stage 2 CKD.

Viral Hepatitis B and D New therapies, unapproved therapies or strategies

WEDNESDAY 21 TO SATURDAY 24 JUNE

TOP-109

VIR-2218 and VIR-3434 therapy is efficacious in preclinical models of hepatitis delta virus infection

Jiayi Zhou¹, Hannah Kaiser¹, Tassilo Volz^{2,3}, Michael A. Schmid⁴, Marc Luetgehmunn^{2,3}, Maura Dandri^{2,3}, Davide Corti⁴, Lisa A. Purcell¹, Andreas Puschnik¹, Florian Lempp¹. ¹Vir Biotechnology, United States; ²University Medical Center Hamburg-Eppendorf, Dept. of Internal Medicine, Germany; ³German Center for Infection Research, Hamburg-Luebeck-Borstel-Riems Site, Germany; ⁴Humabs BioMed SA, a subsidiary of Vir Biotechnology, Switzerland
Email: flempp@vir.bio

Background and aims: Chronic Hepatitis Delta Virus (HDV) infections represent the most severe form of viral hepatitis with limited treatment options. HDV is a satellite virus of Hepatitis B Virus (HBV) that depends on HBV-derived HBsAg for envelopment and viral dissemination in the liver. VIR-2218 is an investigational siRNA therapeutic that targets a highly conserved region within the HBx open reading frame and demonstrates potent knockdown of all HBV transcripts including of HBsAg. VIR-3434 is an investigational neutralizing monoclonal antibody targeting the antigenic loop of HBsAg thereby inhibiting viral entry and reducing circulating HBsAg in preclinical models. VIR-2218 and VIR-3434 are currently being evaluated in clinical trials as monotherapy and in combination. This study aims to determine the antiviral effect of VIR-2218 and VIR-3434 on HDV infection in preclinical models.

Method: *In vitro* antiviral efficacy of VIR-2218 was determined in an HBV/HDV co-infection model of primary human hepatocytes (PHH). After treatment with siRNA, secreted HBsAg was quantified by ELISA and secreted infectious HDV virions were quantified by re-infection of Huh7-NTCP cells. *In vitro* neutralization capacity of VIR-3434 was determined against HDV enveloped with HBsAg of eight different HBV genotypes. *In vivo*, humanized uPA/SCID/beige mice were intraperitoneally injected twice weekly for 4 weeks with VIR-3434 (1 mg/kg) after achieving stable HBV/HDV co-infection. Serological and intrahepatic viral markers were measured by ELISA and (RT-)qPCR.

Results: VIR-2218 reduced HBsAg and secreted infectious HDV with picomolar efficacy in a co-infection model of PHH. VIR-3434 neutralized HDV infection with >10 000-fold higher potency than Hepatitis B Immunoglobulins *in vitro*. Neutralization activity was pan-genotypic as tested with HDV enveloped with HBsAg of HBV genotypes A–H. *In vivo*, HBC34 (the parental molecule of VIR-3434) reduced HBsAg, HBV DNA and HDV RNA serum levels by >2 log₁₀ copies/ml. As expected, intracellular levels of HBV and HDV RNAs were not affected by HBC34 treatment in the chronic infection model.

Conclusion: VIR-2218 and VIR-3434 have previously shown efficacy against HBV infection in multiple *in vitro* and *in vivo* models. Due to the shared usage of HBsAg by HBV and HDV, targeting HBsAg directly also influences concurrent HDV infection. By reducing HBsAg secretion, circulating HBsAg, and HDV virions, as well as blocking entry into hepatocytes, VIR-2218 and VIR-3434 exert antiviral efficacy against HDV through multiple modes of action. These data support the clinical development of VIR-2218 and VIR-3434 for treatment of patients with chronic HDV infection.

TOP-110

Increasing functional cure rate beyond 96 weeks after discontinuation of nucleos (t)ide analogue treatment in HBeAg-negative chronic hepatitis B: follow-up of the stop-NUC trial

Florian van Bömmel¹, Kerstin Stein², Renate Heyne³, Jörg Petersen⁴, Peter Buggisch⁴, Christoph Berg⁵, Stefan Zeuzem⁶, Andreas Stallmach⁷, Martin Sprinzl⁸, Eckart Schott⁹, Anita Pathil-Wartha^{6,10}, Ulrike von Arnim¹¹, Verena Keitel^{12,13}, Jürgen Lohmeyer¹⁴, Simon Karl Georg¹⁵, Christian Trautwein¹⁶, Andreas Trein¹⁷, Dietrich Hüppe¹⁸, Markus Cornberg^{19,20}, Frank Lammert^{21,22}, Patrick Ingiliz^{23,24}, Reinhart Zachoval^{25,26}, Holger Hinrichsen²⁷, Alexander Zipprich^{7,28}, Hartwig Klinker²⁹, Julian Schulze zur Wiesch³⁰, Anett Schmiedeknecht³¹, Oana Brosteanu³¹, Thomas Berg¹. ¹Leipzig University Medical Center, Division of Hepatology, Department of Medicine II, Leipzig, Germany; ²Praxis Hepatologie-Magdeburg, Germany; ³Leberzentrum Checkpoint, Germany; ⁴Leberzentrum Hamburg an der Asklepios Klinik St. Georg, Germany; ⁵Universitätsklinikum Tübingen, Medizinische Klinik I, Germany; ⁶Goethe University, University Hospital Frankfurt, Medizinische Klinik I, Germany; ⁷Universitätsklinikum Jena, Klinik für Innere Medizin IV, Germany; ⁸Johannes Gutenberg Universität, Universitätsmedizin Mainz, I. Medizinische Klinik und Poliklinik, Germany; ⁹Helios Klinikum Emil von Behring, Klinik für Innere Medizin II, Germany; ¹⁰Universitätsklinikum Heidelberg, Innere Medizin IV, Germany; ¹¹Universitätsklinikum Magdeburg AöR, Germany; ¹²Otto-von-Guericke-Universität Magdeburg, Klinik für Gastroenterologie, Hepatologie und Infektiologie, Germany; ¹³Universitätsklinikum Düsseldorf, Klinik für Gastroenterologie, Hepatologie und Infektiologie, Germany; ¹⁴Universitätsklinikum Gießen, Medizinische Klinik II, Germany; ¹⁵MVZ Gastroenterologie Leverkusen GbR, Germany; ¹⁶Uniklinik RWTH Aachen, Medizinische Klinik III, Germany; ¹⁷Gemeinschaftspraxis Schwabstrasse, Germany; ¹⁸Gastroenterologische Gemeinschaftspraxis Herne, Germany; ¹⁹Klinik für Gastroenterologie, Hepatologie und Endokrinologie, Medizinische Hochschule Hannover, Germany; ²⁰Centre for Individualised Infection Medicine (CiIM), Germany; ²¹Medizinische Hochschule Hannover, Klinik für Gastroenterologie, Hepatologie und Endokrinologie, Germany; ²²Universitätsklinikum des Saarlandes, Klinik für Innere Medizin II, Germany; ²³Zentrum für Infektiologie (zibp), Berlin, Germany; ²⁴Henri Mondor University Hospital, Hepatology Department, Germany; ²⁵Leberzentrum München-Sendlinger-Tor-Platz 9, Germany; ²⁶LMU Klinikum Großhadern, Medizinischen Klinik und Poliklinik II, Germany; ²⁷Gastroenterologisch-Hepatologisches Zentrum, Kiel, Germany; ²⁸Martin-Luther-University Halle-Wittenberg, Department of Internal Medicine I, Germany; ²⁹Universitätsklinikum Würzburg, Medizinische Klinik II, Germany; ³⁰Universitätsklinikum Hamburg-Eppendorf, I. Medizinische Klinik und Poliklinik, Germany; ³¹University Leipzig, Clinical Trial Centre, Germany
Email: florian.vanboemmel@medizin.uni-leipzig.de

Background and aims: In the prospective, multicenter, randomized STOP-NUC trial, discontinuation of long-term nucleos (t)ide analogues (NA) treatment resulted in Arm A 8/79 (10%) patients achieving HBsAg loss and 54/79 (68%) patients remaining free of treatment indication within 96 weeks, whereas there were no HBsAg losses in the control Arm B. In the second prospective observation period of the STOP-NUC trial we have assessed effects of NA discontinuation after week 96 up to a maximum follow-up time of 371 weeks (84 months), with a median follow-up time of 200 weeks (46 months).

Method: HBeAg-negative patients without cirrhosis who had achieved suppressed HBV DNA for ≥ 4 years during NA therapy were randomly assigned to either stop (Arm A) or continue (Arm B) treatment. The primary end point was sustained HBsAg loss at week 96. The objectives of the prolonged observation was to investigate the ratios of HBsAg losses, of HBsAg seroconversions, the duration of NUC treatment free follow-up and of response to re-treatment as well as the ratio of HBsAg loss in Arm B.

Results: A total of 99 of 158 originally included patients consented to take part in the prolonged follow-up (46 Arm A, 53 Arm B). At 72 months, the rate of HBsAg loss was 22.3% [95% CI: 7.9%–34.4%] in Arm A and 2.2% [95% CI: 0%–6.4%] in Arm B (Figure 1, $p = 0.0013$). Four further HBsAg losses had occurred after week 96 in Arm A. In Arm B, 13 patients had discontinued NUC treatment according to the discretion of the treating physician of which 1 had lost HBsAg during the follow-up period. Re-treatment with NA during follow-up was introduced at the discretion of the treating physician, and did not necessarily follow-up the stringent rules applied during the first 96 weeks. Re-treatment rate in Arm A was 20.7% [95% CI 9.8%–30.3%] at 72 months after NA stop. No patient in Arm A suffered any serious adverse events possibly related to lack of NA therapy during the prolonged observation period.

Conclusion: The follow-up period of the STOP-NUC trial demonstrates increasing HBsAg loss rates and stable retreatment rates after up to a maximum follow-up time of 84 months of discontinuation of long-term NA treatment in patients with HBeAg negative chronic hepatitis B (EudraCT-Nr.: 2013-004882-15).

SATURDAY 24 JUNE

SAT-167

Switching to peginterferon for chronic hepatitis B patients with hepatitis B e antigen seroconversion on entecavir-a long term follow-up study

Che To Lai¹, Vincent Wai-Sun Wong¹, Angel Mei-Ling Chim¹, Vicki Wing-Ki Hui¹, Yee-Kit Tse¹, Terry Cheuk-Fung Yip¹, Henry LY Chan², Grace Wong¹. ¹The Chinese University of Hong Kong, Department of Medicine and Therapeutics, Hong Kong; ²Union Hospital, Department of Internal Medicine, Hong Kong
Email: wonglaihung@gmail.com

Background and aims: Previous studies looking into switching from entecavir to peginterferon in chronic hepatitis B (CHB) patients showed a high rate of hepatitis B surface antigen (HBsAg) seroclearance; yet long term data are lacking. We aimed to study the long-term virological outcomes of CHB patients with nucleos (t)ide analogue (NA)-induced hepatitis B e antigen (HBeAg) seroconversion switching to peginterferon treatment.

Method: This was a long-term follow-up study of CHB patients recruited from 2013 to 2016 in a prospective, single-arm open-label study receiving 48 weeks of peginterferon alfa-2a monotherapy after achieving HBeAg seroconversion by entecavir. Baseline date was the end of the peginterferon treatment and the patients were followed until the date of latest virological blood tests. Patients were censored upon retreatment with NA. The virological response defined by sustained HBeAg seroconversion and serum hepatitis B virus (HBV) DNA < 2000 IU/ml, as well as the cumulative incidence of HBsAg seroclearance were analysed.

Results: 41 patients from the original study were followed for a mean of 54 months. 30 (73%) were male with a mean age of 44 years. 37 (90%) patients completed the intended 48 weeks course of peginterferon alfa-2a. 11 (27%) patients achieved HBsAg seroclearance, with one patient achieving that at the end of peginterferon

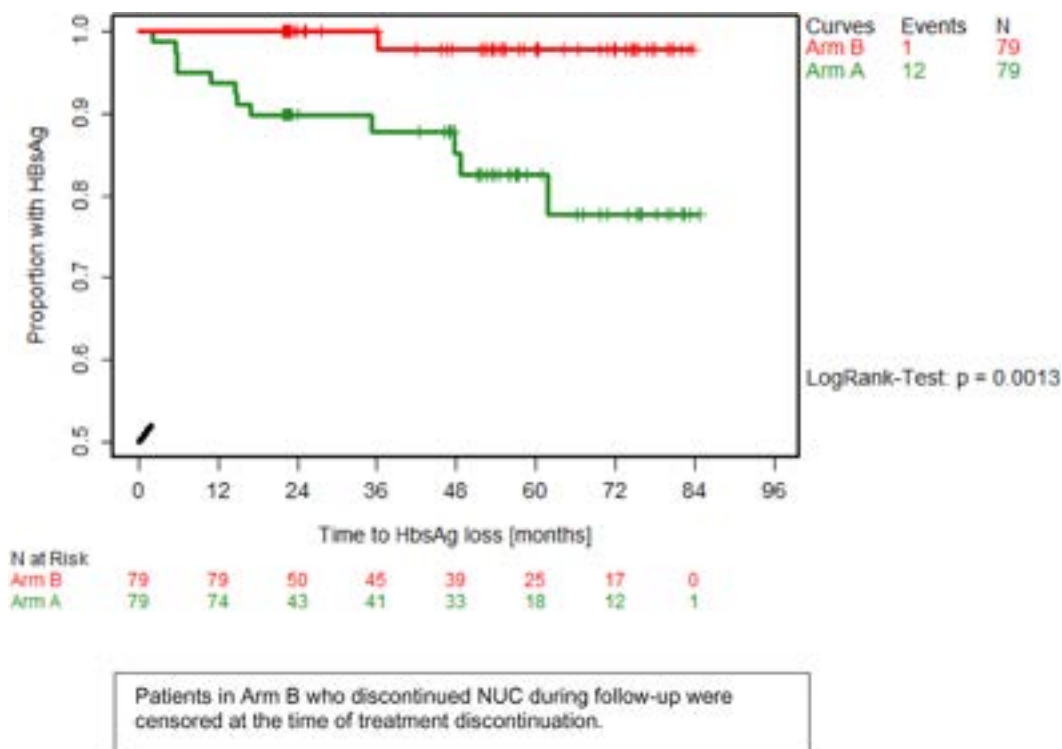


Figure: (abstract: TOP-110).

treatment. The cumulative incidences of HBsAg seroclearance were 16%, 19% and 31% at 12, 24 and 36 months respectively (Figure), and no HBsAg reversion was observed. 26 (63%) patients had sustained virological response with HBeAg seroconversion and serum HBV DNA <2 000 IU/ml throughout, of which 18 of them had undetectable HBV DNA. On the other hand, 15 (37%) patients had virological breakthrough requiring retreatment of NA at a median of 12 months after cessation of peginterferon treatment. End-of-peginterferon treatment HBsAg level <100 IU/ml (odds ratio 6.75, 95% confidence interval 1.24–36.85) was the best predictor for long term HBsAg seroclearance.

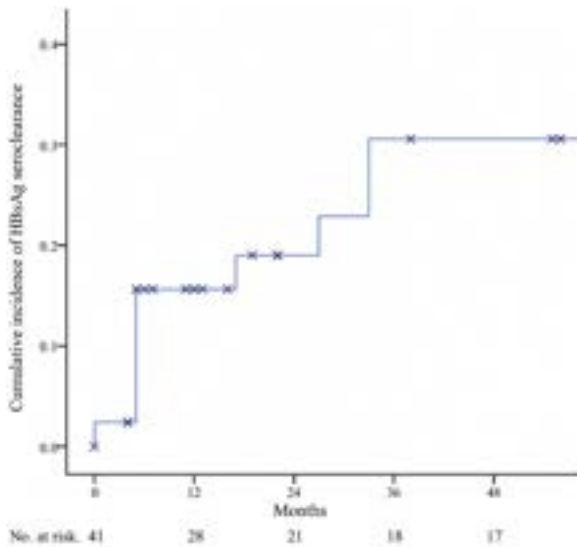


Figure. Cumulative incidence of HBsAg seroclearance in NA-treated CHB patients with HBeAg seroconversion switching to peginterferon alpha-2a

Figure:

Conclusion: In NA-treated patients with HBeAg seroconversion, switching from NA to peginterferon conferred to a high rate of durable HBsAg seroclearance, especially in those with low end-of-peginterferon HBsAg level.

SAT-168

Safety, pharmacokinetics, and antiviral activity of the next-generation hepatitis B core inhibitor ABI-H3733 in patients with hepatitis B e antigen negative chronic hepatitis B infection: preliminary results from a randomized, blinded, Phase 1b study

Edward J. Gane¹, Alina Jucov², Krum Katzarov³, Oana Sandulescu⁴, Ran Yan⁵, Kathryn M. Kitrinis⁵, Jieming Liu⁵, Katie Zomorodi⁵, Luisa M. Stamm⁵, Steven J. Knox⁵, Michele Anderson⁵, Grace Wang⁵, Radoslava Tsrancheva⁶, Anca Streinu-Cercel⁴. ¹University of Auckland,

Auckland, New Zealand; ²ARENSIA Exploratory Medicine GmbH, Düsseldorf, Germany and Department of Gastroenterology, State University of Medicine and Pharmacy, Chisinau, Moldova; ³Department of Gastroenterology, HPB and Transplant Surgery, Military Medical Academy, Sofia, Bulgaria; ⁴Carol Davila University of Medicine and Pharmacy; National Institute for Infectious Diseases "Prof. Dr. Matei Bals", Bucharest, Romania; ⁵Assembly Biosciences, South San Francisco, United States; ⁶Diagnostic Consultative Center Aleksandrovska, Sofia, Bulgaria
Email: edgane@adhb.govt.nz

Background and aims: ABI-H3733-102 (NCT05414981) is an ongoing, randomized, blinded, multiple-dose escalation study assessing the safety, pharmacokinetics (PK), and antiviral activity of the next-generation core inhibitor ABI-H3733 (3733), administered in patients (pts) with chronic hepatitis B virus infection. Here, we report preliminary safety, PK, and antiviral activity in hepatitis B e antigen (eAg) negative pts from completed cohorts.

Method: Each cohort randomized up to 10 pts (8:2 ratio) to 3733 or placebo (PBO) once-daily (QD) for 28 days. The first 2 cohorts evaluated 25 mg and 50 mg 3733. Eligible pts were male or female, aged 18–65 years, eAg positive (HBV DNA $\geq 2 \times 10^4$ IU/ml) or negative (HBV DNA $\geq 2 \times 10^3$ IU/ml), off antiviral therapy, non-cirrhotic with Fibroscan <9 kPa or Metavir F0–F2. Safety was assessed by adverse events (AEs), lab parameters, and electrocardiogram assessments. PK and viral biomarkers (including HBV DNA [Cobas TaqMan, lower limit of quantification = 20 IU/ml]) were assessed throughout.

Results: Baseline (BL) characteristics were similar between the 2 cohorts. As 18/20 pts enrolled were eAg negative, results are described for this subgroup. Most pts were male, White, aged ~40–50 years, with HBV DNA and hepatitis B surface antigen ranging from 3.3–4.5 log₁₀ IU/ml and 3.2–3.9 log₁₀ IU/ml, respectively. Treatment was well tolerated, with no serious AEs, deaths, or AEs leading to study drug discontinuation. AEs were reported in 4 pts and were all Grade 1. Graded lab abnormalities were observed in 53% (8/15) and 100% (3/3) of pts receiving 3733 and PBO, respectively, with most being Grade 1. No alanine aminotransferase (ALT) increases were observed. HBV DNA change from BL at Day 29 was –2.2 and –3.1 log₁₀ IU/ml for 25 mg and 50 mg 3733, respectively. Mean Day 28 C_{max}, AUC_{0–24}, and t_{1/2}, respectively, were 959 ng/ml, 14,820 ng·h/ml, and 24.3 h for 25 mg 3733 and were 2,188 ng/ml, 31,510 ng·h/ml, and 23.9 h for 50 mg 3733.

Conclusion: 3733 was well tolerated at doses up to 50 mg QD for 28 days. All AEs and lab abnormalities were Grade 1 or 2, with no serious AEs, treatment discontinuations, or deaths. No ALT elevations were observed. Increased in vitro potency of 3733 relative to first-generation core inhibitors is reflected in rapid, multi-log declines in HBV DNA at low doses. PK properties of 3733 support daily dosing with C_{min}'s in multiple fold excess of protein-adjusted EC₅₀'s for HBV DNA and covalently closed circular DNA. These findings support further development of 3733.

Table. Summary results for eAg negative pts

Parameter	Cohort 1		Cohort 2	
	3733 50 mg (n = 8)	PBO (n = 1)	3733 25 mg (n = 7)	PBO (n = 2)
BL Characteristics				
Age, years; mean (SD)	40 (5.2)	36 (NA)	42 (5.1)	41 (15.6)
Male; n/N (%)	6/8 (75)	1/1 (100)	4/7 (57)	2/2 (100)
Race, White; n/N (%)	7/8 (88)	1/1 (100)	6/7 (86)	2/2 (100)
HBV DNA (\log_{10} IU/mL); mean (SD)	4.3 (0.83)	3.3 (NA)	4.5 (0.99)	4.3 (0.28)
HBsAg (\log_{10} IU/mL); mean (SD)	3.6 (0.70)	3.9 (NA)	3.8 (0.61)	3.2 (0.24)
Pts with any AE; n/N (%)	1/8 (13)	0	2/7 (29)	1/2 (50)
Pts with any serious AE; n/N (%)	0	0	0	0
Pts with any AE leading to study drug discontinuation; n/N (%)	0	0	0	0
HBV DNA change from BL at Day 29 (\log_{10} IU/mL); mean (SD)	-3.1 (0.71)	-0.60 (NA)	-2.2 (0.85)	-0.7 (0.74)
Day 28 C _{max} , ng/mL; mean (CV%)	2,188 (21)	NA	959 (25)	NA
Day 28 AUC ₀₋₂₄ , ng·h/mL; mean (CV%)	31,510 (25)	NA	14,620 (18)	NA
Day 28 t _{1/2} , hours; mean (CV%)	23.9 (34)	NA	24.3 (43)	NA

^aHBV DNA values <lower limit of quantification (20 IU/mL; 1.30 \log_{10} IU/mL) were imputed as 10 IU/mL (1 \log_{10} IU/mL) for calculation of change from BL.

3733, ASB-H3733; AE, adverse event; AUC₀₋₂₄, area under the plasma concentration-time curve from time zero to 24 hours; BL, baseline; C_{max}, maximum plasma concentration; CV, coefficient of variation; eAg, hepatitis B e antigen; HBV, hepatitis B virus; NA, not available; PBO, placebo; pt, patient; sAg, hepatitis B surface antigen; SD, standard deviation; t_{1/2}, terminal elimination half-life.

Figure: (abstract: SAT-168).

SAT-169

Rescue of cirrhotic HBV/HDV infection from bulevirtide failure by subcutaneous REP 2139-Mg

Marc Bourliere¹, Veronique Loustaud-Ratti², Christiane Stern³, Souad Benali¹, Edouard Bardou-Jacquet⁴, Laurent Alric⁵, Michel Bazinet⁶, Laurence Lecomte¹, Sandrine Francois², Cecilia De-Freitas³, Anita Levacher⁴, Segolene Brichler⁷, Athenais Gerber⁷, Emmanuel Gordien⁷, Stéphane Chevaliez⁸, Andrew Vaillant⁶. ¹Hôpital Saint Joseph, Marseille, France; ²CHU Limoges, Limoges, France; ³Hôpital Beaujon AP-HP, Clichy, France; ⁴CHU Rennes, Rennes, France; ⁵CHU Rangueil, Université Toulouse 3, Toulouse, France; ⁶Replicor Inc., Montreal, Canada; ⁷Centre national de référence des hépatite B, C et Delta-Laboratoire associé, Hôpital Avicenne, Bobigny, France; ⁸Hôpital Henri Mondor, Créteil, France
Email: avillant@replicor.com

Background and aims: REP 2139 blocks HBV subviral particle assembly and hepatitis delta antigen function, driving HBsAg loss in HBV infection and HBsAg/HDV RNA loss in HBV/HDV co-infection. Compassionate access to REP 2139-Mg is being provided under the Replicor Compassionate Access Program (RCAP, NCT05683548). The safety and efficacy of SC injection of REP 2139-Mg in combination therapy is currently being assessed in cirrhotic patients with chronic HBV/HDV co-infection after failure on bulevirtide (BLV).

Method: Compassionate access to REP 2139-Mg has been approved by the ANSM in 11 patients with compensated cirrhosis having no response or viral escape in HDV RNA during 2 or 10 mg BLV. Existing TDF was supplemented with 48 weeks of QW SC 250 mg REP 2139-Mg and 90 µg pegIFN. Weekly safety evaluations were accompanied by virologic assessment every 4 weeks.

Results: As this abstract is submitted, seven patients have at least 4 weeks of REP 2139-Mg exposure. Four patients (#1, 2, 3 and 4) have greater than 24 weeks exposure with three (#1, 2 and 4) having no detectable HDV RNA and >3 \log_{10} IU/ml decline in HBsAg and two (1 and 2) with HBsAg loss and anti-HBs seroconversion. One patient (#1) has completed 48 weeks of therapy and 8 months of TDF monotherapy and still maintains undetectable HDV RNA and HBsAg and anti-HBs seroconversion. TDF therapy has now been stopped in this patient. In patient 3, central obesity likely prevents optimal liver accumulation of REP 2139 with antiviral responses (declines in HDV RNA and HBsAg of 2.2 and 0.63 \log_{10} IU/ml) proceeding with transition from SC injection to IV infusion and from 250 mg qW to 500 mg qW. Three patients (#6, 7 and 10) have completed 4–12 weeks exposure with mild declines in HDV RNA (0.5–1 \log_{10} IU/ml) already present. The administration of SC 250 mg REP 2139-Mg with oral TDF and pegIFN has been well tolerated to date.

Conclusion: Subcutaneous REP 2139-Mg is safe, well tolerated, and effective against HBV and HDV infection in combination with TDF and low dose pegIFN in patients with compensated cirrhosis. REP 2139-Mg is also an effective salvage therapy in bulevirtide failure patients.

SAT-170

The Nuc-Stop study: an open-label, randomized trial of different re-start strategies after treatment withdrawal in HBeAg negative chronic hepatitis B patients

Asgeir Johannessen¹, Dag Henrik Reikvam², Soo Aleman³, Nega Berhe^{4,5}, Nina Weis⁶, Hailemichael Desalegn⁷, Tore Stenstad¹, Lars Heggelund⁸, Ellen Samuelson⁹, Karin Lindahl³, Anni Winkelman⁶, Lars Normann Karlsen¹⁰, Pascal Brugger-Synnes¹¹, Hans Erling Simonsen¹², Jan Svendsen⁸, Marte Holmberg¹, Olav Dalgard⁹. ¹Vestfold Hospital Trust, Tonsberg, Norway; ²Oslo university hospital, Norway; ³Karolinska institutet, Sweden; ⁴Addis Ababa University, Ethiopia; ⁵Oslo University Hospital-Ullevål, Regional Centre for Imported and Tropical Diseases, Oslo, Norway; ⁶Hvidovre Hospital, Denmark; ⁷St. Paul's Hospital Millennium Medical College, Ethiopia; ⁸Vestre Viken Hospital, Norway; ⁹Akershus University Hospital, Norway; ¹⁰Stavanger University Hospital, Norway; ¹¹Ålesund hospital, Norway; ¹²Nordland Hospital Trust, Norway
Email: johannessen.asgeir@gmail.com

Background and aims: Stopping nucleos (t)ide analogue (NA) therapy in patients with chronic hepatitis B (CHB) may trigger a beneficial immune response leading to hepatitis B surface antigen (HBsAg) loss. However, treatment withdrawal may also induce a harmful hepatic necroinflammation that warrants re-start of therapy to prevent progressive liver injury. Whether it might be beneficial to allow patients to undergo a prolonged flare has not been studied in a prospective clinical trial. We therefore carried out the Nuc-Stop Study, an open-label, randomized, multicentre trial of two re-start strategies after stopping NA therapy in hepatitis B e-antigen (HBeAg) negative CHB.

Method: HBeAg negative CHB patients with at least 24 months of full viral suppression on NA therapy were eligible for inclusion. Patients with past or present evidence of cirrhosis were excluded. All study participants stopped antiviral therapy and were randomized to either low-threshold (alanine aminotransferase [ALT] >80 U/L and viral load >2000 IU/ml) or high-threshold (ALT >100 U/L for >4 months, or ALT >400 U/L for >2 month) for re-start of therapy. Patients in both groups re-started NA therapy in case of a severe flare, defined as ALT >800 U/L or any ALT flare with INR ≥1.4 or bilirubin >38 mmol/L. HBsAg loss was the primary end point. Differences between groups were analyzed with Chi-square tests or Fischer's exact tests, and associations with HBsAg loss were analyzed with logistic regression models.

Results: A total of 127 patients were included at 11 centres in Norway, Sweden, Denmark and Ethiopia; 121 patients completed 36 months of follow-up and were included in the final analysis. Median duration of antiviral treatment prior to inclusion was 46 months (interquartile range 32–78). Nine patients (7.4%) experienced a severe flare (maximum ALT 2600 U/L), all of whom quickly normalized after re-start of NA therapy; no other serious adverse events related to treatment withdrawal were observed. There was no statistically significant difference in HBsAg loss between the low-threshold and the high-threshold group (3 of 61; 4.9% vs. 7 of 60; 11.7%; $P=0.205$). After 36 months of follow-up, 26 of 61 (42.6%) patients in the low-threshold group and 8 of 60 (13.3%) patients in the high-threshold group had met the pre-defined re-start criteria (Figure 1). Notably, none of the 34 patients who re-started therapy experienced HBsAg loss, compared to 10 of 87 (11.5%) of those who remained off therapy ($p=0.060$). The only baseline factor independently associated with HBsAg loss was time on antiviral treatment prior to treatment withdrawal (per 1-year, adjusted odds ratio 1.30; 95% confidence interval 1.09–1.54, $P=0.003$).



Figure: Outcome after treatment discontinuation in chronic hepatitis B patients randomized to: A) low-threshold for re-start of treatment, and B) high-threshold for re-start of treatment.

Conclusion: The re-start strategy did not significantly affect the chance of HBsAg loss among non-cirrhotic HBeAg negative CHB patients who stopped antiviral therapy.

SAT-171

Deep learning cluster analysis reveals subtypes in response to antisense oligonucleotide therapy in chronic hepatitis B

Caroline Weis¹, Maria Littmann¹, Aleksei Triastcyn¹, William Jordan², Dickens Theodore³, Melanie Paff², Hannah Tipney⁴, Jenn Singh², Patrick Schwab¹. ¹GSK, Artificial Intelligence and Machine Learning, Zug, Switzerland; ²GSK, Collegeville, PA, United States; ³GSK, Research Triangle Park, NC, United States; ⁴GSK, Stevenage, United Kingdom
Email: patrick.x.schwab@gsk.com

Background and aims: Chronic hepatitis B virus (CHB) infection is characterized by heterogeneity in disease trajectories and response to therapy. A comprehensive mapping of heterogeneity in CHB could potentially aid in supporting future research. In this study, we investigate the use of machine learning for characterizing heterogeneity in CHB from deep phenotypic patient profiles on and off bepirovirsen therapy.

Method: We used data from the B-Clear phase IIb study (NCT04449029) evaluating the efficacy of bepirovirsen in CHB patients (N=408) to identify response groups. We employed machine learning methods to reduce the dimensionality of response data in a manner that conserves information related to patients' response trajectories. The condensed deep phenotypic patient profiles included virologic, immunologic, proteomics and transcriptomics measurements. We performed a cluster analysis on the compressed patient representations to identify subgroups of patients that respond differently in terms of biomarker trajectories following bepirovirsen therapy.

Results: Our results suggest that B-Clear study participants can be stratified into meaningful subpopulations indicative of heterogeneous response to bepirovirsen therapy. The subpopulations recapitulate significant (Benjamini-Yekutieli corrected $p<0.05$) differences in primary efficacy outcomes reflecting CHB virological markers, while identifying new response subtypes and giving a higher resolution on the temporal development of relevant biomarkers. Notably, we observe a high-primary response subtype that is correlated with a considerable decrease in median HBsAg to the lower limit of quantification ($p<0.002$ to closest subtype from day 78 onwards) and a continuous decline of HBV-DNA levels ($p<0.0001$ to the high HBV-DNA non-responder subtype throughout the study). Additionally, the high HBV-DNA non-responder subtype is correlated with higher GFER ($p<0.04$ at baseline, 162, and 324 days) and lower ADGRG1 ($p<0.03$ throughout the study) protein abundances compared to the mixed response subtype.

Conclusion: We present a machine learning-based method to identify meaningful response subgroups within a study cohort. We characterized five subpopulations with heterogeneous clinical trajectories and differences in response to bepirovirsen therapy. The subtypes capture markers associated with patient response trajectories and may guide CHB research. Further validation of the identified markers in additional cohorts is needed.

Funding: GSK (205695).



Figure: (abstract: SAT-171).

SAT-172

Safety and antiviral activity of RBD1016, a RNAi therapeutic, in Chinese subjects with chronic hepatitis B virus (HBV) infection

Wai-Kay Seto^{1,2}, Zicai Liang³, Li Ming Gan³, Jing Fu³, Man-Fung Yuen².

¹The university of Hong Kong-Shenzhen Hospital, Shenzhen, China, China; ²Queen Mary Hospital, The University of Hong Kong, China;

³Suzhou Ribo Life Science Co. Ltd., China

Email: mfyuen@hku.hk

Background and aims: RBD1016, a small interfering RNA (siRNA) drug, is composed of siRNA and the N-acetylgalactosamine delivery system, targeting the conserved region of the X gene of chronic hepatitis B virus (HBV), and can concurrently inhibit 4 gene transcripts of HBV. Here, we report the preliminary data from an ongoing phase I clinical study evaluating the safety and antiviral activity of RBD1016 in subjects with chronic HBV infection.

Method: This randomized, double-blind, placebo-controlled, single and repeated dose escalation, phase I clinical study enrolled treatment naïve or previously treated subjects with chronic HBV infection without hepatic fibrosis or cirrhosis (NCT05017116). Subjects received RBD1016/placebo subcutaneously in combination with nucleos (t)ide analogues (NAs) during the study. In the single dose (SD) group, subjects were recruited in cohorts of six and were randomized 5:1 to receive RBD1016 or placebo. Upon cohort completion, RBD1016's dosage was escalated incrementally from 0.3 mg/kg to 1 mg/kg, 3 mg/kg and 6 mg/kg. For the multiple dose (MD) group, subjects were recruited in cohorts of eight and randomized 6:2 to receive RBD1016 (at 3 mg/kg, followed by 6 mg/kg) or placebo at Day 1 and D 29. Preliminary data for 0.3 mg/kg, 1 mg/kg, 3 mg/kg SD (follow-up to week 24) and 3 mg/kg MD (follow-up to week 16) are presented; dose escalation and follow-up are ongoing.

Results: As of December 28, 2022, twenty-seven subjects (mean age 43.2 years, 44.4% male) (SD = 20, MD = 7) were enrolled, of which 26 (96.3%) were on NAs therapy (entecavir: 17, tenofovir disoproxil fumarate: 6; tenofovir alafenamide: 3) for a median duration of 54.5 (range: 16–150) months. Maximum mean serum HBsAg reductions from baseline in subjects receiving RBD1016 of 0.3 mg/kg, 1 mg/kg, 3 mg/kg SD, 3 mg/kg MD and placebo were 0.48 (at week12), 0.75 (at

week16), 0.97 (at week16), 1.34 (at week16) and 0.01 (at week16) log₁₀ IU/ml, respectively. HBsAg reduction was durable till the end of study at week 24. Serum HBV DNA undetectability (<10 IU/ml) was achieved in three subjects with positive HBV DNA at baseline at weeks 1, 3 and 12, respectively. 9 subjects with RBD1016 therapy had positive serum HBV RNA (lower limit of quantification, 10 copies/ml) at baseline, median HBV RNA among positive subjects was 6240 (range: 11–518 000) copies/ml. By week 24, the median HBV RNA decline was 2450 (range: 1–50 980) copies/ml, with three subjects (one receiving 3 mg/kg SD and two receiving 3 mg/kg MD) achieving HBV RNA undetectability. For subjects with positive HBV RNA, an increased HBV RNA reduction was seen in patients with increased HBsAg decline. The 3 mg/kg MD cohort achieved 0.67 log₁₀ kU/ml HBcrAg reduction at week 6 and 0.5 log₁₀ cp/ml HBV RNA reduction at week 24. RBD1016 was safe, with no serious adverse events or drug-related adverse events reported. No subjects withdrew from the study or discontinued treatment.

Conclusion: A single dose of RBD1016 demonstrated a rapid and durable reduction in serum HBsAg in a dose-dependent manner. Multiple doses of RBD1016 showed increased reduction in HBsAg. Preliminary safety data suggested that RBD1016 was generally safe and well tolerated. The present data supports the further evaluation of RBD1016 for functional cure of patients with chronic HBV infection.

SAT-173

AHB-137, a novel hepatitis B virus antisense oligonucleotide with substantially enhanced in vitro and in vivo antiviral activity

Xiaoli Wu¹, Tingting Lu, Weiguo Zhang¹, Yang Bai¹, Liqun Zhang¹, Shaoyi Ma¹, Ying Chang¹, Jihai Lei¹, Chunxi Li¹, Yuying Liu¹, Zelei Pan¹, Wei Peng¹, Chang Shen¹, Yipeng Wang¹, Qingbo Xing¹, Lisha Zhang¹, Xue Zhou¹, Yang Tian^{1,2}, Chris Yang^{1,2}, Cheng Guofeng^{1,2}. ¹Ausper Biopharma, China; ²AusperBio Therapeutics, United States
Email: guofengcheng1@hotmail.com

Background and aims: Antisense oligonucleotide (ASO) bepirovirsen (BPV) monotherapy has demonstrated activity to achieve sustained HBsAg seroclearance in chronic hepatitis B (CHB) patients, with a promise to be a backbone for HBV cure treatment regimen. However, the current cure rate with BPV remains low, thus a more potent ASO with good safety profile could further improve the

efficacy. Here we report a novel HBV ASO AHB-137 with substantially enhanced in vitro and in vivo antiviral activity.

Method: AHB-137 and BPV were synthesized via solid phase synthesis. In vitro antiviral activity was evaluated in HBV stable cell lines HepG2.2.15 and HepAD38, and in primary human hepatocytes (PHH) infected with HBV. In vivo antiviral activity was evaluated in hydrodynamic injection (HDI) mouse model, AAV-HBV transduced mice, and HBV transgenic mice. Secreted HBsAg was quantified by a clinical HBsAg chemiluminescent immunoassay (AutoBio).

Results: AHB-137 is a novel ASO without conjugation that has a distinct structure from BPV and targets a highly conserved sequence close to the 3' end of HBV mRNA at DR2 region. AHB-137 exhibited potent antiviral activity to inhibit HBsAg production in HepG2.2.15 cells with an EC₅₀ value of 0.13 nM and a selectivity index (SI) >769-fold, compared to BPV with an EC₅₀ of 1.50 nM and SI >67-fold. Similarly, AHB-137 demonstrated 10-fold and 6-fold more potent activity to reduce HBsAg than BPV in HepAD38 and HBV-infected PHH, respectively. More importantly, AHB-137 has shown potent and dose-dependent antiviral activity to reduce serum HBsAg, HBeAg, HBV DNA, and intrahepatic HBV RNA in AAV-HBV mice, HBV transgenic mice, and HDI HBV mice. A single subcutaneous dose of AHB-137 (60 mg/kg) could reduce serum HBsAg 1.3 to 3 log₁₀ (IU/ml) and achieve at least 0.6 log₁₀ additional reduction than BPV in every in vivo model. After 3 doses of AHB-137 (40 mg/kg) in HDI-HBV mice, the serum HBsAg was reduced by >3 log₁₀ (IU/ml) to below LLOQ, compared to a 1.8 log₁₀ (IU/ml) HBsAg reduction by BPV. The broad-spectrum antiviral activity of AHB-137 was also confirmed in HDI-HBV mice with higher potency than BPV across genotypes. As important, there was no significant body weight change and ALT increase in any of the animals treated with AHB-137. Finally, when combined with other classes of anti-HBV agents including Nuc and PEG-IFN in AAV-HBV mice, AHB-137 showed additive/synergistic activity and had no antagonistic activity.

Conclusion: The AHB-137 represents a novel class of HBV ASO that clearly demonstrated strong antiviral activity against HBV mRNA transcribed from both cccDNA and integrated genomes, and had more potent activity in reducing serum HBsAg than BPV across multiple in vitro and in vivo HBV models. Together with its favorable PK and safety profile, AHB-137 is advancing into clinical development.

SAT-174

Vebicorvir, entecavir, and pegylated interferon in patients with hepatitis B e antigen positive chronic hepatitis B virus infection: findings from a phase 2, randomized open-label study in China

Xieer Liang¹, Jinlin Hou¹, Yujuan Guan², Zhanqing Zhang³, Qing Xie⁴, Jidong Jia⁵, Jifang Sheng⁶, Qin Ning⁷, Wang Yang⁸, Afsaneh Mozaffarian⁹, Nuruddin Unchwaniwala¹⁰, Jieming Liu¹⁰, Katie Zomorodi¹⁰, Luisa M. Stamm¹⁰, Steven J Knox¹⁰, Michele Anderson¹⁰, Kathryn M. Kitrinos¹⁰, Grace Wang¹⁰, Yu Chen¹¹, Junqi Niu⁸. ¹Hepatology Unit and Department of Infectious Diseases,

Nanfeng Hospital, Southern Medical University, Guangzhou, China; ²Guangzhou Eighth People's Hospital, Guangzhou, China; ³Fudan University, Shanghai, China; ⁴Ruijin Hospital, Shanghai Jiaotong University School of Medicine, Shanghai, China; ⁵Beijing Friendship Hospital, Capital Medical University, Beijing, China; ⁶The First Affiliated Hospital, College of Medicine, Zhejiang University School of Medicine, Hangzhou, Zhejiang, China; ⁷Tongji Hospital of Tongji Medical College, Huazhong University of Science and Technology, Wuhan, China; ⁸The First Hospital of Jilin University, Jilin, China; ⁹Former employee of Assembly Biosciences during the study; current affiliation Gilead Sciences, Foster City, United States; ¹⁰Assembly Biosciences, South San Francisco, United States; ¹¹Beijing Youan Hospital, Capital Medical University, Beijing, China
Email: freliang@163.com

Background and aims: Vebicorvir (VBR), a first-generation core inhibitor, in combination with entecavir (ETV) previously demonstrated deeper viral suppression compared to ETV alone in untreated patients (pts) with hepatitis B e antigen (eAg) positive chronic hepatitis B virus infection (CHBV). The addition of pegylated interferon alfa (IFN) may further increase the efficacy of VBR + ETV through complementary mechanisms of action. This open-label study (NCT04781647) assessed the relative safety and efficacy of VBR + ETV + IFN.

Method: Fifty-four eAg positive pts with CHBV with F0-F3 fibrosis who were off antiviral therapy were randomized to VBR + ETV (n = 20), VBR + ETV + IFN (n = 17), or IFN + ETV (n = 17) for 24 weeks (wks), after which all pts received VBR + ETV for 24 wks, then a 12-wk follow-up period with ETV alone. HBV DNA was measured by COBAS TaqMan (lower limit of quantification [LLOQ] = 20 IU/ml) and pregenomic (pg)RNA by Assembly Biosciences quantitative polymerase chain reaction assay (LLOQ = 165 U/ml). Quantitative hepatitis B surface antigen (sAg) was measured by Abbott Architect (LLOQ = 0.05 IU/ml). Safety was assessed by adverse events (AEs) and lab parameters.

Results: Baseline (BL) characteristics were similar across treatments; overall, mean (standard deviation [SD]) age was 32 (6.7) years, 39/54 (72%) pts were male, and all were Asian. Twenty-five of 54 (46%) and 29/54 (53%) pts were infected with HBV genotype B and C, respectively. Overall, mean (SD) BL HBV DNA, pgRNA, sAg, and alanine aminotransferase (ALT) were 8.0 (0.96) log₁₀ IU/ml, 6.3 (1.30) log₁₀ U/ml, 4.3 (0.58) log₁₀ IU/ml, and 137 (84.3) U/L, respectively. After 24 wks of randomized treatment, there were no significant differences in change from BL between treatment arms for HBV DNA or HBsAg (Table). VBR + ETV + IFN resulted in a significantly greater reduction in pgRNA than ETV + IFN (p = 0.03). No pts developed anti-sAg antibodies or had evidence of functional cure. The safety profile was consistent with previous reports for VBR and IFN. The proportion of pts reporting treatment emergent AEs was higher in IFN containing arms; 13/20 (65%), 17/17 (100%), and 17/17 (100%) for VBR + ETV, VBR + ETV + IFN, and ETV + IFN, respectively. A single serious AE of Grade 4

Table: LS mean (SE) change from BL at wk 12 and 24 for HBV DNA, pgRNA, and sAg

	VBR + ETV (n = 20)		VBR + ETV + IFN (n = 17)		ETV + IFN (n = 17)	
	Change from BL at Wk 12	Change from BL at Wk 24	Change from BL at Wk 12	Change from BL at Wk 24	Change from BL at Wk 12	Change from BL at Wk 24
n	19	16	12	14	16	15
HBV DNA (log ₁₀ IU/mL); LS mean (SE)	-5.0 (0.26)	-8.0 (0.20) ^a	-4.7 (0.31)	-6.2 (0.22) ^{a,b}	-5.2 (0.29)	-8.3 (0.21) ^a
pgRNA (log ₁₀ U/mL); LS mean (SE)	-2.9 (0.31)	-2.8 (0.36) ^a	-3.4 (0.36)	-3.7 (0.38) ^{a,c}	-2.6 (0.34)	-2.6 (0.39) ^a
sAg (log ₁₀ IU/mL); LS mean (SE)	-0.6 (0.12)	-0.6 (0.14) ^a	-0.4 (0.14)	-0.7 (0.15) ^{a,d}	-0.7 (0.13)	-0.7 (0.15) ^a

^aWk 24: HBV DNA LS means (SE) difference: VBR + ETV + IFN vs VBR + ETV = -0.2 (0.26), p = 0.5018. ^bVBR + ETV + IFN vs ETV + IFN = 0.2 (0.27), p = 0.5065.

^cWk 24: pgRNA LS Means (SE) difference: VBR + ETV + IFN vs VBR + ETV = -0.9 (0.46), p = 0.0535. ^dVBR + ETV + IFN vs ETV + IFN = -1.1 (0.48), p = 0.0300.

^eWk 24: sAg LS Means (SE) difference: VBR + ETV + IFN vs VBR + ETV = -0.1 (0.19), p = 0.6336. ^fVBR + ETV + IFN vs ETV + IFN = 0.1 (0.19), p = 0.7871.

BL, baseline; ETV, entecavir; HBV, hepatitis B virus; IFN, pegylated interferon alfa; LS, least squares; pgRNA, pregenomic RNA; sAg, hepatitis B surface antigen; SE, standard error; VBR, vebicorvir; Wk, week.

Figure: (abstract: SAT-174).

POSTER PRESENTATIONS

ALT elevation was reported in a VBR + IFN + ETV pt that led to study discontinuation. No deaths were reported.

Conclusion: Overall, the addition of IFN to VBR + ETV did not result in significantly greater declines in HBV parameters compared to the dual agent control arms and is unlikely to result in significant rates of functional cure following 24 wks of treatment.

SAT-175

Significant improvement of non-invasive fibrosis tests in HDV compensated cirrhotic patients with clinically significant portal hypertension treated with BLV monotherapy up to 96 weeks

Elisabetta Degasperi¹, Maria Paola Anolli¹, Sara Colonia Uceda Renteria², Dana Sambarino¹, Marta Borghi¹, Riccardo Perbellini¹, Floriana Facchetti¹, Roberta Soffredini¹, Sara Monico¹, Mirella Fraquelli³, Andrea Costantino³, Ferruccio Ceriotti², Pietro Lampertico^{1,4}. ¹Foundation IRCCS Ca' Granda Ospedale Maggiore Policlinico, Department of Gastroenterology and Hepatology, Milan, Italy; ²Foundation IRCCS Ca' Granda Ospedale Maggiore Policlinico, Virology Unit, Milan, Italy; ³Foundation IRCCS Ca' Granda Ospedale Maggiore Policlinico, Division of Gastroenterology and Endoscopy Digestive, Milan, Italy; ⁴CRC "A.M. and A. Migliavacca" Center for Liver Disease, Department of Pathophysiology and transplantation, University of Milan, Milan, Italy
Email: elisabetta.degasperi@policlinico.mi.it

Background and aims: Antiviral treatment of HBV- and HCV-related hepatitis has been shown to significantly improve non-invasive fibrosis tests (NITs), however their course in patients with chronic hepatitis Delta with a virological response during a long-term treatment with Bulevirtide (BLV) monotherapy is currently unknown. **Method:** Consecutive HDV patients with compensated cirrhosis and clinically significant portal hypertension (CSPH) according to Baveno VII criteria with a virological response (≥ 2 Log HDV RNA decline vs. baseline) to BLV monotherapy 2 mg/day up to 96 weeks were enrolled in this single-center study. HDV RNA was quantified by Robogene 2.0 (LOD 6 IU/ml). Clinical variables, AST to Platelet Ratio Index (APRI) and Fibrosis-4 (FIB-4) Index were assessed at baseline and every 8 weeks. Liver (LSM), spleen (SSM) stiffness measurement assessed both by transient elastography (Fibroscan®) and point

shear-wave elastography (ElastPQ) were performed every 24 weeks, as well as liver stiffness-spleen size-to-platelet ratio score (LSPS).

Results: 26 HDV cirrhotic patients were included: pre-treatment, median age was 49 (30–77) years, 54% males, ALT 102 (32–310) U/L, platelets $69 (17–217) \times 10^3/\text{mm}^3$, 73% with varices, spleen 16 (9–25) cm, CPT-A 100%, HDV RNA 5.1 (2.4–6.9) Log IU/ml. During BLV monotherapy, serological NIT significantly improved at all time-points, APRI decreasing from baseline 3.6 (1.2–16.5) to 1.1 (0.3–3.6) at week 96 ($p < 0.001$), and FIB-4 from 7.1 (1.3–28.1) to 4.1 (0.9–7.2) ($p = 0.02$). LSM decreased from baseline 17.3 (7.8–68.1) to 15.7 (5.0–51.9) kPa at week 24 ($p = 0.03$) and LSPS from baseline 5.9 (0.5–23.7) to 3.9 (0.3–9.7) at week 48 ($p = 0.01$), whereas no other significant changes were observed throughout weeks 48 and 72. Conversely, other NITs did not significantly modify during the whole course of BLV treatment: liver ElastPQ 14.3 (4.2–35.2) vs. 16.5 (6.6–25.9) kPa ($p = 0.14$); SSM 51.7 (20–100) vs. 54.7 (18.2–100) kPa ($p = 0.66$), Spleen ElastPQ 42.2 (13.1–102) vs. 43.7 (31.9–94.8) kPa ($p = 0.68$). Four patients underwent liver transplantation (HCC $n = 2$; liver decompensation $n = 2$) and one patient died of liver unrelated causes.

Conclusion: In HDV compensated cirrhotic patients with CSPH, long-term treatment with BLV monotherapy led to a statistically significant improvement of serological fibrosis NITs, liver stiffness and LSPS.

SAT-176

Analysis of HBV genotype association to bepirovirsen treatment response in patients with chronic HBV infection (Phase 2b B-Clear study)

Jerome Bouquet¹, Robert Elston², Phil Yates², Shihyun You³, Amir Youssef³, Ahmed Nader³, Jennifer Cremer⁴, Geoff Quinn², Fiona Campbell², Melanie Paff³, Dickens Theodore⁴. ¹GSK, South San Francisco, United States; ²GSK, Stevenage, United Kingdom; ³GSK, Collegeville, United States; ⁴GSK, Durham, United States
Email: jerome.x.bouquet@gsk.com

Background and aims: Bepirovirsen (BPV; GSK3228836) is an antisense oligonucleotide that targets a conserved 20 nucleotide sequence within HBV pregenomic RNA and mRNAs. B-Clear is a phase 2b trial (NCT04449029) assessing the efficacy and safety of 12 or 24 weeks (wks) of BPV treatment in patients (pts) with chronic hepatitis B (CHB) in which hepatitis B surface antigen (HBsAg) reductions and

Table 1. B-Clear treatment response by genotype

Not-on-NA therapy (pooled treatment arms) N=229					
Genotype	A	B	C	D	Undetermined
N	41 (18%)	49 (21%)	70 (31%)	45 (20%)	9 (4%)
Mean HBsAg (log IU/mL) at baseline	3.982	3.155	3.809	3.765	3.284
Mean reduction HBsAg (log IU/mL) at EOT	-1.872	-2.903	-2.086	-2.617	-1.498
Mean reduction HBsAg (log IU/mL) at OT-WK24	-0.476	-1.601	-0.570	-1.065	-0.634
Number (%) of subjects with HBsAg and HBV DNA <LLOQ at EOT*	2/38 (5%)	18/45 (36%)	5/63 (8%)	5/38 (13%)	1/6 (17%)
Number (%) of subjects with HBsAg and HBV DNA <LLOQ at OT-WK24*	1/39 (3%)	6/44 (14%)	2/62 (3%)	4/35 (11%)	0/5 (0%)
On-NA therapy (pooled treatment arms) N=226					
Genotype	A	B	C	D	Undetermined
N	18 (8%)	20 (9%)	70 (31%)	19 (8%)	93 (41%)
Mean HBsAg (log IU/mL) at baseline	3.724	3.090	3.246	3.406	3.269
Mean reduction HBsAg (log IU/mL) at EOT	-1.380	-2.921	-2.212	-1.641	-2.084
Mean reduction HBsAg (log IU/mL) at OT-WK24	-0.870	-1.670	-0.823	-0.536	-1.155
Number (%) of subjects with HBsAg and HBV DNA <LLOQ at EOT*	2/17 (12%)	7/19 (37%)	12/61 (20%)	0/19 (0%)	17/82 (21%)
Number (%) of subjects with HBsAg and HBV DNA <LLOQ at OT-WK24*	2/18 (11%)	3/18 (17%)	4/68 (6%)	0/17 (0%)	8/85 (9%)

*Denominator indicates number of subjects with data available at EOT or OT-WK24. DNA, deoxyribonucleic acid; EOT, end of treatment; HBsAg, hepatitis B surface antigen; HBV, hepatitis B virus; LLOQ, lower limit of quantification; NA, nucleos(t)ide analogue; OT, off-treatment; WK, week.

Figure: (abstract: SAT-176).

HBsAg seroclearance have been observed. We present the HBsAg response for pts by viral genotype.

Methods: Multicentre, randomised, partial-blind study in pts with CHB who were either receiving concomitant stable nucleos (t)ide analogue therapy (on-NA) or were not receiving NA (not-on-NA). Pts were randomised (3:3:3:1) to receive BPV 300 mg weekly either for 24 wks (Arm 1); for 12 wks then 150 mg for 12 wks (Arm 2); for 12 wks then placebo (PBO) for 12 wks (Arm 3); or PBO for 12 wks then BPV 300 mg for 12 wks (Arm 4). A loading dose of BPV (Arms 1–3) or PBO (Arm 4) was given on days 4 and 11. Pts were followed for 24 weeks (off-treatment [OT]-WK24) after end of treatment (EOT). B-Clear recruited patients in 22 countries encompassing Asia, Europe, the Americas and South Africa. Genotype was determined by HBV DNA or RNA sequencing and/or was investigator reported.

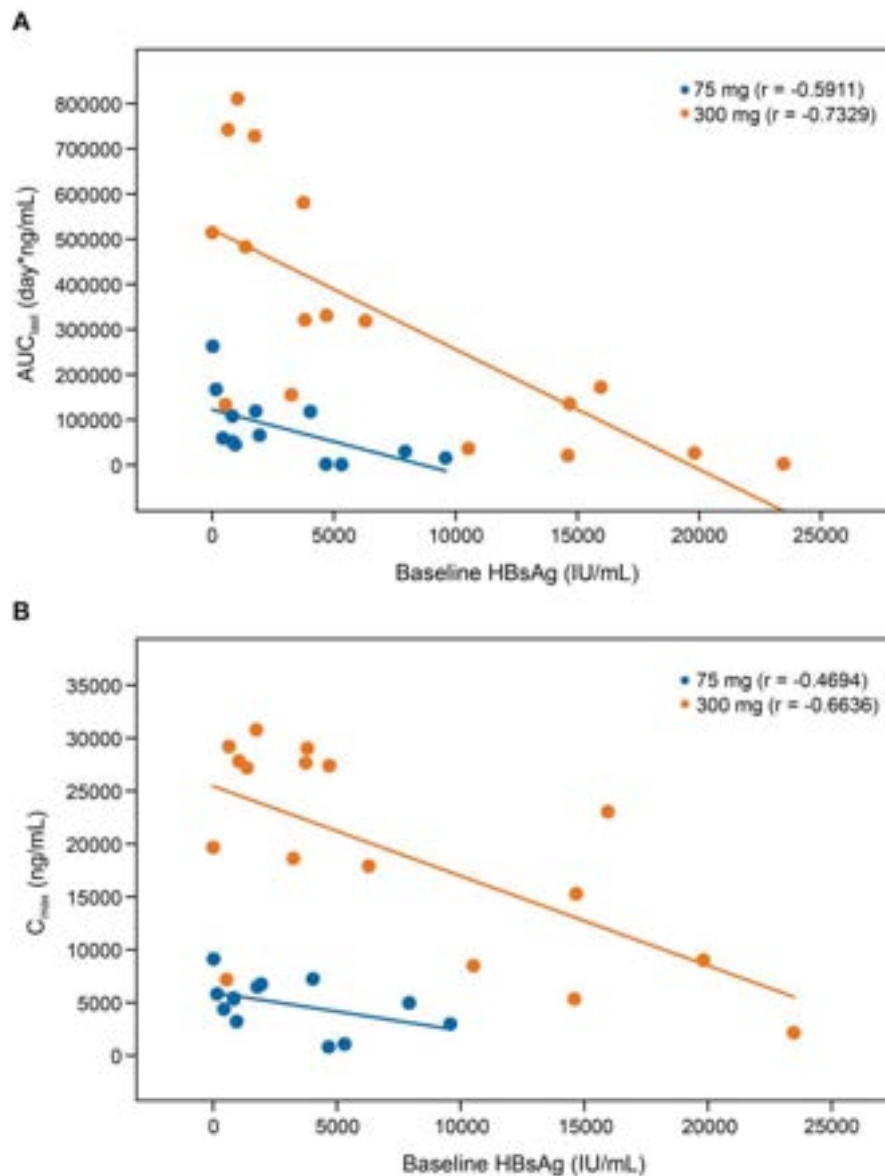
Results: Seven different genotypes were observed: A, B, C, D, E, F and H. Genotypes were in majority B and C in Asia, A and D in Europe, A, B, C and D in the Americas. Not-on-NA: Genotype (GT) C (31%, 70/229 pts) was most frequently observed, followed by GT-B (21%), GT-D (20%), GT-A (18%), other (6%) and undetermined (4%). Pts with GT-B

virus had the lowest mean HBsAg level at baseline (3.155 log IU/ml) and GT-A the highest (3.982 log IU/ml). On-NA: GT-C (31%, 70/226 pts) was most frequently observed, followed by GT-B (9%), GT-D, GT-A (8% each) and others (3%). On-NA pts had low/undetectable RNA/DNA resulting in a high proportion of undetermined genotypes (41%). Pts with GT-B virus had the lowest mean HBsAg level at baseline (3.090 log IU/ml) and GT-A the highest (3.724 log IU/ml). Treatment Response: End of BPV treatment response and 24 wks off BPV treatment response by genotype is shown in Table 1 (treatment arms pooled).

Conclusion: In both not-on-NA and NA cohorts, GT-B had the lowest baseline HBsAg and demonstrated the greatest log reduction in HBsAg, consistent with lower baseline HBsAg predicting the ability to achieve HBsAg seroclearance. HBsAg seroclearance 24 wks off-BPV treatment was achieved in HBV genotypes A, B, C and D.

Funding: GSK (209668).

[on behalf of the B-Clear study group].



Footnote: r refers to Pearson Correlation Coefficient

Figure: (abstract: SAT-177): AUC_{last} vs baseline HBsAg (Figure 1A) and C_{max} vs baseline HBsAg (Figure 1B).

SAT-177

Single dose pharmacokinetics of VIR-3434, a novel neutralizing monoclonal antibody, in participants with chronic hepatitis B virus infection

Sneha V. Gupta¹, Sophia Elie¹, Andre Arizpe¹, George Hristopoulos¹, Pan Wu¹, Daniel Cloutier¹, Maribel Reyes¹. ¹VIR Biotechnology, San Francisco, United States
Email: sgupta@vir.bio

Background and aims: VIR-3434 is an investigational Fc engineered human monoclonal antibody targeting the conserved antigenic loop of hepatitis B surface antigen (HBsAg) in development for the treatment of chronic hepatitis B virus (HBV) and hepatitis D virus (HDV) infection. Here, we report, the free VIR-3434 pharmacokinetics (PK) after single dose administration in participants with chronic HBV infection, including those with HBV viremia and high HBsAg levels.

Method: VIR-3434-1002 is a randomized, double-blind, placebo-controlled phase 1 single ascending dose study evaluating safety, tolerability, antiviral activity, and PK of VIR-3434. Part A enrolled healthy participants whose PK and safety has been previously reported. Parts B-D enrolled noncirrhotic adults with chronic HBV infection. Participants were randomized 6:2 to receive a single subcutaneous (SC) dose of VIR-3434 6 mg, 18 mg, 75 mg, or 300 mg, or placebo. In Parts B and C, participants received nucleos (t)ide reverse transcriptase inhibitor (NRTI) therapy for ≥ 2 months prior to study entry. Parts B and C participants had baseline HBsAg < 3000 and ≥ 3000 IU/ml, respectively. Part D participants were not on NRTI therapy and had baseline HBV DNA ≥ 1000 IU/ml. Participants were followed for up to 40 weeks after study drug administration.

Results: 72 participants were enrolled in Parts B-D; 54 received VIR-3434. Among active participants, median T_{max} was 3–5 days. Larger and more durable HBsAg reductions and higher free VIR-3434 PK for 4 weeks postdose were observed at the 300 mg dose level. Participants with a wide range of baseline HBsAg across Parts B-D and with detectable free VIR-3434 PK received 75 or 300 mg and are described further. Free VIR-3434 PK exposures (AUC_{last} and C_{max}) negatively correlated with HBsAg levels at baseline (Figure 1). Following 300 mg VIR-3434 dose, mean (CV) AUC_{last} and C_{max} was higher in Part B at 967 (21%) ug/ml*day and 32.6 (18%) ug/ml than Part C with 365 (64%) ug/ml*day and 22.5 (39%) ug/ml, respectively. Similarly, VIR-3434 was cleared faster in participants with higher baseline HBsAg. At the 300 mg dose level, median CL/F was 600 ml/day in Part B vs 818 ml/day in Part C, suggestive of target-mediated drug disposition (TMDD).

Conclusion: Among participants who received a single dose of 6 mg, 18 mg, 75 mg, or 300 mg VIR-3434, the highest and most durable free VIR-3434 exposure was observed with the 300 mg dose irrespective of baseline HBsAg. Correlation plots with free PK demonstrate a moderate impact of baseline HBsAg in free VIR-3434 exposure, suggestive of TMDD. These PK data support continued evaluation of 300 mg SC VIR-3434 administered every 4 weeks as monotherapy or in combination for functional cure of participants with chronic HBV infection.

Footnote: r refers to Pearson Correlation Coefficient.

SAT-178

AHB-137, a novel and potent hepatitis B virus antisense oligonucleotide with a favorable preclinical pharmacokinetics and safety profile

Xiao Qiu¹, Tingting Lu¹, Hu Zhou¹, Haixia Cao¹, Weiguo Zhang¹, Guowei Chen¹, Bingxia Lu¹, Xiaoli Wu¹, Yilei Wen¹, Rumeng Cui¹, Qianxi Cui¹, Yuhua Pang¹, Liquan Zhang¹, Qingbo Xing¹, Yuying Liu¹, Lisha Zhang¹, Xue Zhou¹, Yang Tian^{1,2}, Chris Yang^{1,2}, Guofeng Cheng^{1,2}. ¹Ausper Biopharma, China; ²AusperBio Therapeutics, United States
Email: guofeng.cheng@ausperbio.com

Background and aims: Antisense oligonucleotide (ASO) bepirovirsen (BPV) monotherapy has demonstrated activity to achieve sustained HBsAg seroclearance in chronic hepatitis B (CHB) patients, with a promise to be a backbone for HBV cure treatment. AHB-137 is a novel HBV ASO with substantially enhanced antiviral activity over BPV both in vitro and in vivo. Here we report that AHB-137 has a favorable preclinical pharmacokinetics (PK) and safety profile.

Method: CD-1 mice, hydrodynamic injection (HDI) HBV mice, and cynomolgus monkeys were dosed subcutaneously (SC), or by intravenously in monkeys, to assess the PK properties of AHB-137 and BPV. For toxicokinetics and toxicity assessment, 4-week repeat ascending dose studies were conducted in CD-1 mice and cynomolgus monkeys, in which AHB-137 or dosing vehicle was given SC once a week with an additional dose on Day 4 in the first week. Serum and multiple organs were collected at various timepoints and analyzed for AHB-137 concentrations by LC-MS. Safety of AHB-137 was evaluated under GLP toxicology study guideline.

Results: AHB-137 and BPV showed comparable concentration-time profiles in serum in both mice and monkeys at the same dose levels. Despite comparable exposure, three doses of AHB-137 (each dose at 40 mg/kg) reduced the serum HBsAg by $> 3 \log_{10}$ (IU/ml) to below LLOQ in HDI HBV mice while the same doses of BPV only reduced HBsAg by 1.8 \log_{10} (IU/ml), confirming the higher potency of AHB-137 observed both in vitro and in vivo. Furthermore, AHB-137 demonstrated similar pharmacokinetic profile to BPV with a good bioavailability following SC injection (84% bioavailable) in monkeys. Like BPV, the half-life of AHB-137 in serum was approximately 3–4 h in the first 24 h post-dose but was much longer (> 50 h) in latter phase in both mice and monkeys. The serum C_{max} and AUC of AHB-137 was dose-proportional and did not accumulate after 6 repeat doses over 29 days compared to the first dose in either mouse or monkey, as was observed for BPV. The liver and kidney were the main organs for AHB-137 distribution and the tissue concentration of AHB-137 were dose-proportional. AHB-137 is metabolically stable in liver S9 fraction, hepatocytes, and plasma across the mouse, rat, monkey, and human, with little or no drug-drug interaction. In acute tox studies in mice, AHB-137 showed a significantly better safety profile than BPV. In the 4-week repeat dosing GLP studies, AHB-137 was well-tolerated in mice and monkeys with no findings of adverse effect at 60 and 15 mg/kg/dose, respectively. AHB-137 also demonstrated low-risk profile in safety pharmacology studies.

Conclusion: In addition to potent antiviral activity, the novel HBV ASO AHB-137 has demonstrated a favorable preclinical pharmacokinetics and safety profile. AHB-137 is advancing into clinical development for the treatment of CHB patients.

SAT-179

Consolidation treatment with Tiaogan-Buxu-Jiedu granule (Traditional Chinese Medicine compound) plus entecavir reduces virological relapse following entecavir withdrawal in Chinese patients with chronic hepatitis B: a randomized, controlled trial

Xiaoke Li^{1,2}, Mei Qiu³, Yi Huang⁴, Huanming Xiao⁵, Bingjiu Lu⁶, Yuyong Jiang⁷, Fuli Long⁸, Hui Lin⁹, Shuo Li¹, Jinyu He¹⁰, Mingxiang Zhang¹¹, Qikai Wu¹², Li Wang¹³, Xiaoning Zhu¹⁴, Man Gong¹⁵, Jianguang Sun¹⁶, Xuehua Sun¹⁷, Fengxia Sun¹⁸, Wei Lu¹⁹, Weihua Xu²⁰, Hongbo Du^{1,2}, Yong'an Ye^{1,2}. ¹Dongzhimen Hospital, Beijing University of Chinese Medicine, Hepatology, Beijing, China; ²Beijing University of Chinese Medicine, Liver Diseases Academy of Traditional Chinese Medicine, Beijing, China; ³Shenzhen Traditional Chinese Medicine Hospital, Hepatology, China; ⁴Chongqing Traditional Chinese Medicine Hospital, Hepatology, China; ⁵The Second Affiliated Hospital of Guangzhou University of Chinese Medicine, Hepatology,

China; ⁶Liaoning Hospital of Traditional Chinese Medicine, Hepatology, China; ⁷Beijing Ditan Hospital, China; ⁸The First Affiliated Hospital of Guangxi University of Chinese Medicine, China; ⁹Mengchao Hepatobiliary Hospital of Fujian Medical University, Hepatology, China; ¹⁰Shaanxi Hospital of Traditional Chinese Medicine, Hepatology, China; ¹¹The Sixth People's Hospital of Shenyang, China; ¹²The Third People's Hospital of Shenzhen, Hepatology, China; ¹³The Public Health Clinical Center of Chengdu, Hepatology, China; ¹⁴Affiliated traditional Chinese medicine hospital of Southwest Medical University, China; ¹⁵The Fifth Medical Center of People's Liberation Army of China, Hepatology, China; ¹⁶Shandong Hospital of Traditional Chinese Medicine, Hepatology, China; ¹⁷Shuguang Hospital Affiliated to Shanghai University of Traditional Chinese Medicine, Hepatology, China; ¹⁸Beijing Chinese Medicine Hospital, Beijing, China; ¹⁹The Second People's Hospital of Tianjin, China; ²⁰The Second Hospital of Shandong University, China Email: yeyongan@vip.163.com

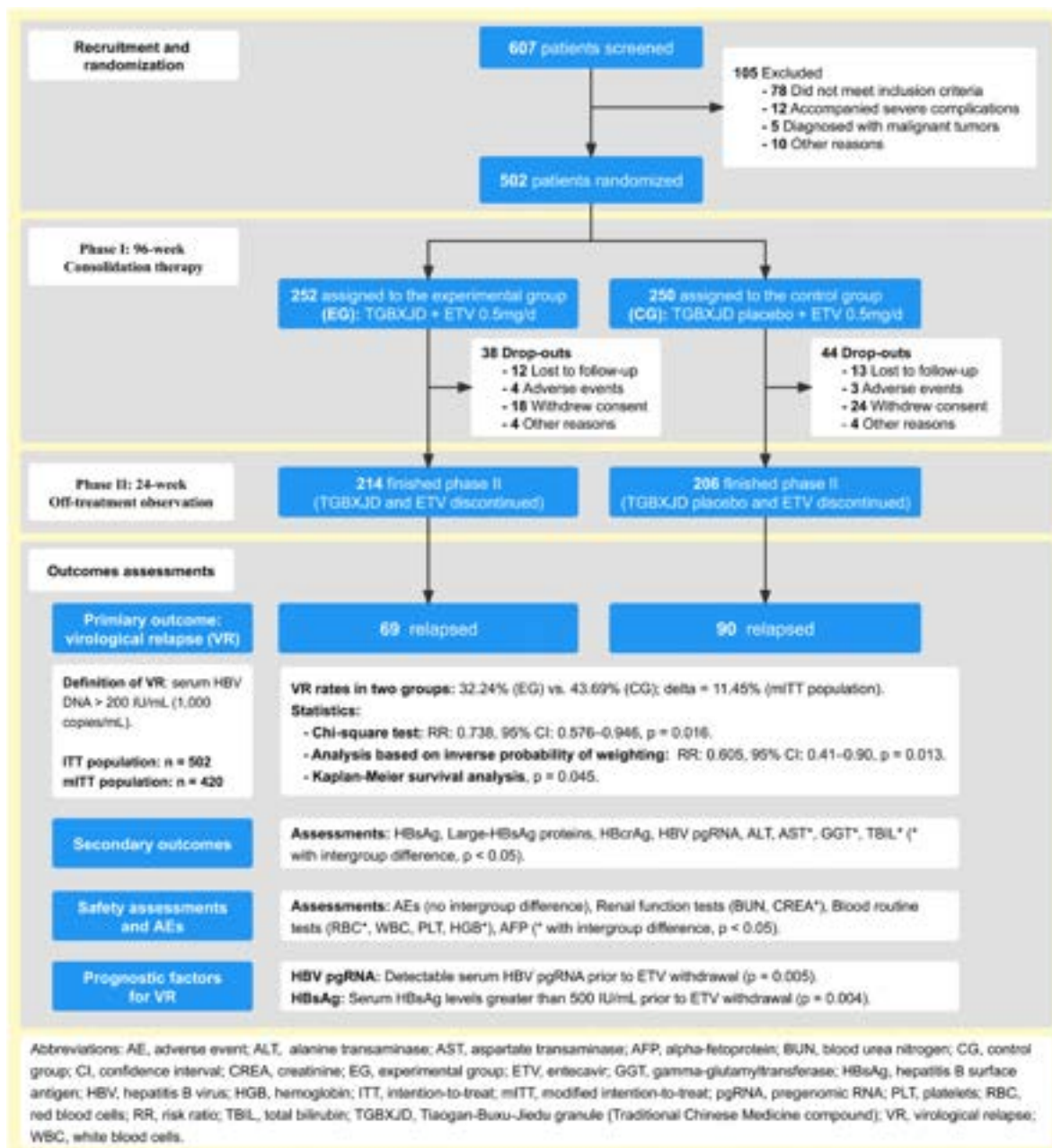


Figure: (abstract: SAT-179).

POSTER PRESENTATIONS

Background and aims: Several guidelines suggest that nucleoside analogues (NAs) may be discontinued in chronic hepatitis B (CHB) patients after hepatitis B e antigen (HBeAg) seroconversion, followed by a certain course of consolidation treatment. However, the withdrawal of NAs often results in virological relapse. In China, Traditional Chinese Medicine (TCM) is widely combined with NAs in treatment. The aim of this double-blind, placebo-controlled, randomized, multicentre trial was to assess whether enhanced consolidation therapy with entecavir (ETV) plus Tiaogan-Buxu-Jiedu granule (TGBXJD), an immune-modulatory TCM compound, can further reduce the risk of virological relapse following ETV withdrawal in CHB patients. The study was conducted as part of National Science and Technology Major Project of China, No.2018ZX10725505. Trial protocol was registered with the Chinese Clinical Trial Registry, ID: ChiCTR-TRC-12002784.

Method: 502 eligible NAs-treated CHB patients were randomly assigned to the experimental group (EG) or the control group (CG) in a 1:1 ratio as the intention-to-treat (ITT) population. During the initial 96-week consolidation phase, the EG received a combination therapy of ETV and TGBXJD, while the CG received ETV and a placebo for TGBXJD. Following the consolidation phase, an off-treatment observation phase of 24 weeks was implemented during which both groups discontinued ETV and TGBXJD (or placebo). The primary outcome measure of the study was the cumulative rate of virological relapse, defined as serum HBV DNA >200 IU/ml. The secondary outcome measures included levels of HBV serological markers, HBV DNA, liver enzymes, HBV pregenome RNA (pgRNA), and HBV large surface proteins.

Results: A total of 420 patients (modified intention-to-treat [mITT] population, 214 in the EG and 206 in the CG) completed consolidation therapy and finished the off-treatment observation. Upon completion of consolidation therapy, the levels of serum HBsAg were comparable between the two groups. During the off-treatment observation phase, 159 patients (69 in the EG and 90 in the CG) experienced virological relapse. In both the ITT population (27.38% vs. 36.00%, delta = 8.62%, relative risk [RR]: 0.761, 95% confidence interval [CI]: 0.586–0.987, $p = 0.037$) and the mITT population (32.24% vs. 43.69%,

delta = 11.45%, RR: 0.738, 95% CI: 0.576–0.946, $p = 0.016$), the relapse rates were statistically lower in the EG than in the CG. According to the Kaplan-Meier survival analysis, the cumulative probability of virological relapse was reduced in the EG ($p = 0.045$). The decreased serum HBsAg levels (under 500 IU/ml, $p = 0.004$) and undetectable serum HBV pgRNA ($p = 0.005$) prior to ETV withdrawal may be related to a reduced risk of virological relapse.

Conclusion: A 96-week consolidation therapy combining the TGBXJD and ETV may improve off-treatment outcomes by reducing virological relapses. Serum HBV pgRNA and HBsAg levels could be evaluated as potential predictors of virological relapse prior to ETV withdrawal.

SAT-180

Positive impact of reflex testing in performing hepatitis delta serology in HBsAg+ patients

Régine Truchi¹, Anne De Monte², Albert Tran¹, Valérie Giordanengo², Laurence Ollier². ¹Archet 2 Hospital, Liver unit, NICE, France; ²Archet 2 Hospital, Virology laboratory, NICE, France

Email: truchi.r@chu-nice.fr

Background and aims: Several studies have shown that screening for the hepatitis Delta virus (HDV) was not optimal: between 30 and 50% of HBs antigen positive (HBsAg+) patients. The virology laboratory of University Hospital Center (CHU) from Nice has been carrying out HDV reflex testing (HDV RT) for several years in HBsAg+ patients.

Method: This work assesses the feasibility and effectiveness of HDV RT within the different departments of our establishment. HDV RT consists of systematically adding HDV serology to HBsAg+ patients if the latter was not requested by the prescriber. In the event of an insufficient quantity of sample, the virology laboratory contacts the clinical department to obtain a second sample in order to carry out HDV screening.

Results: From 01/01/2021 to 12/31/2021, 17 364 HBsAg screenings were carried out at the CHU. 182 HBsAg screenings were positive, corresponding to 138 patients (58 F and 80 M). 80 of these 138 patients (58%) were screened for the first time at the CHU and 58

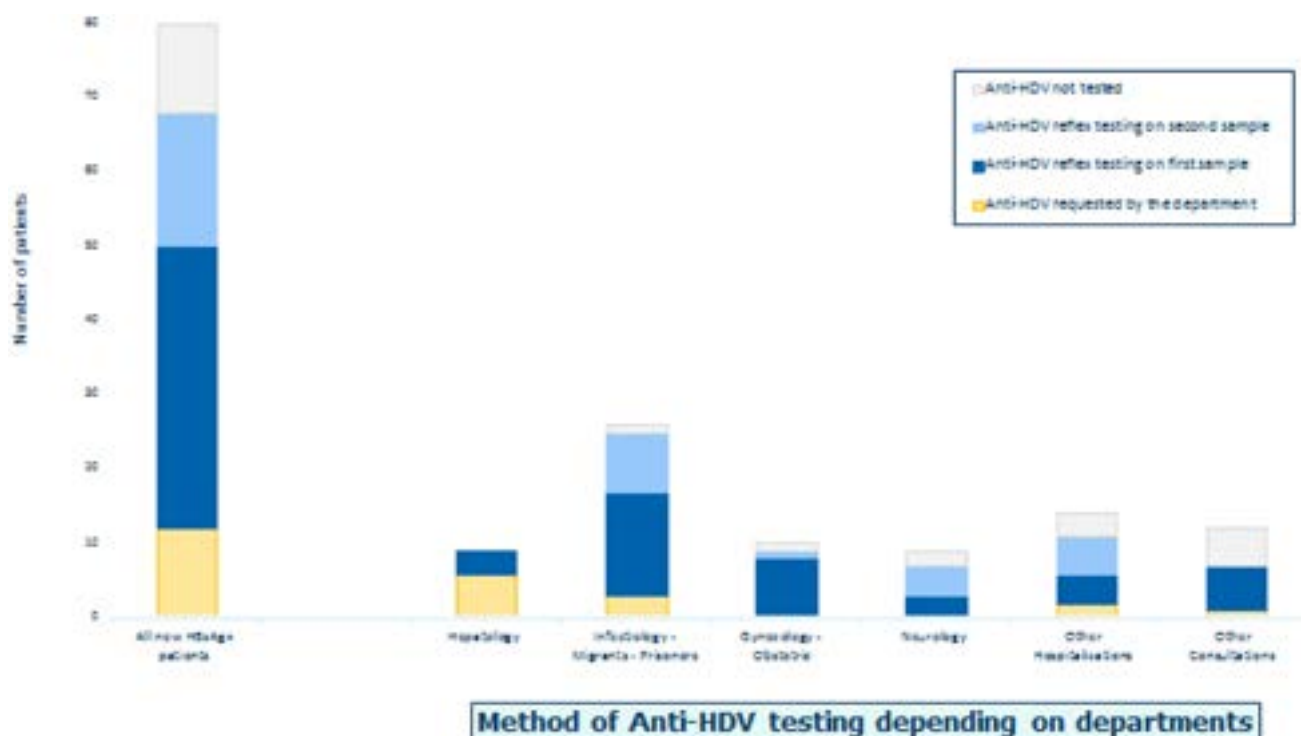


Figure: (abstract: SAT-180).

patients (42%) were already known to be positive for HBsAg. Among the 80 HBsAg+ patients screened for the first time in our center, HDV serology was immediately prescribed by the departments for 12 patients (15%). HDV serology could be added to the first sample for 38 patients (47%) and performed after obtaining a second sample for 18 patients (23%). Thus, 68 of the 80 HBsAg+ patients (85%) had an HDV serology result available, including 56 following reflex testing carried out by the virology laboratory. The operating procedure of the HDV serology is carried out by the different CHU departments is shown in the figure below. Among these 68 HBsAg+ screened for HDV, HDV serology was positive for 4 patients (6%), with HDV replication detected in 3 of them. Concerning the 58 patients already known to be HBsAg+ at the CHU, HDV serology was already available or prescribed from the outset for 49 patients (85%). The reflex testing made it possible to search for co-infection with HDV for 7 additional patients (12%), with a total of 97% of patients screened for HDV.

Conclusion: HDV reflex testing is feasible at the level of an university hospital virology lab and makes it possible to optimize HDV screening in HBV identified patients from different departments, including those not specialized in the management of viral hepatitis.

SAT-181

Pretreatment and on-therapy HDV RNA levels predict response to Bulevirtide monotherapy in HDV compensated cirrhotic patients treated up to 96 weeks

Elisabetta Degasperis¹, Maria Paola Anolli¹, Sara Colonia Uceda Renteria², Dana Sambarino¹, Marta Borghi¹, Riccardo Perbellini¹, Floriana Facchetti¹, Roberta Soffredini¹, Sara Monico¹, Ferruccio Ceriotti², Pietro Lampertico^{1,3}. ¹Foundation IRCCS Ca' Granda Ospedale Maggiore Policlinico, Department of Gastroenterology and Hepatology, Milan, Italy; ²Foundation IRCCS Ca' Granda Ospedale Maggiore Policlinico, Virology Unit, Milan, Italy; ³CRC "A.M. and A. Migliavacca" Center for Liver Disease, Department of Pathophysiology and Transplantation, University of Milan, Milan, Italy
Email: pietro.lampertico@policlinico.mi.it

Background and aims: Bulevirtide (BLV) has been approved for treatment compensated chronic hepatitis Delta (HDV), however baseline and on-therapy predictors of response are still unknown.

Method: Consecutive HDV patients with compensated cirrhosis treated with BLV monotherapy 2 mg/day up to 96 weeks were enrolled in this single-center study. HDV RNA was quantified by Robogene 2.0 (LOD 6 IU/ml). Clinical and virological variables were assessed at baseline and every 8 weeks.

Results: Overall, 49 HDV patients were enrolled: median age 52 (29–77) years, 59% males, platelets $78 (17–217) \times 10^3/\text{mm}^3$, liver stiffness measurement $17.3 (6.4–68.1)$ kPa, ALT $97 (30–1074)$ U/L, HBsAg $3.7 (0.8–4.4)$ LogIU/ml, HDV RNA $5.2 (2.4–6.9)$ LogIU/ml. At baseline, 6% and 24% patients had ALT<ULN (<40 U/L) and <1.5 ULN, respectively. None of the patients had baseline HDV RNA<100 IU/ml, while 8% had HDV RNA<1000 IU/ml, where HDV RNA<1000 IU/ml was associated with ALT<1.5 ULN ($p = 0.02$). Following BLV monotherapy, virological response rates (undetectable or HDV RNA ≥ 2 Log decline vs. baseline) resulted 71% at week 24, 84% at week 48, 75% at week 72 and 80% at week 96, respectively; the corresponding figures for biochemical response rates were 57%, 68%, 81% and 67%, while for combined response 46%, 63%, 63% and 66%, respectively. When considering main treatment timepoints (week 24; week 48; week 72; week 96), HDV RNA <1000 IU/ml at week 48 was associated with ALT <1.5 ULN at the same timepoint ($p = 0.03$). Conversely, no other significant associations were found between HDV RNA with different cut-offs (<6 IU/ml; <100 IU/ml; <1000 IU/ml) and concomitant ALT levels (<ULN; <1.5 ULN) in all remaining treatment timepoints. When analyzing baseline and on-treatment correlations between viremia, ALT and treatment end points, baseline HDV RNA <1000 IU/ml was associated with ALT<1.5 ULN at weeks 48 ($p = 0.0002$), 72 ($p = 0.003$) and 96 ($p = 0.004$) and predicted biochemical response at weeks 72 ($p = 0.01$) and 96 ($p = 0.02$). Baseline HDV RNA <1000 IU/ml was

associated also with virological response at week 48 ($p = 0.007$), 72 ($p = 0.04$) and 96 ($p = 0.04$), while it did not predict combined response at any timepoint. In addition, HDV RNA<1000 IU/ml at week 24 predicted HDV RNA<100 at week 48 ($p = 0.03$), 72 ($p = 0.04$) and 96 ($p = 0.03$) and was also associated with ALT<1.5 ULN at weeks 72 ($p = 0.01$) and 96 ($p = 0.03$). Finally, HDV RNA <1000 IU/ml at week 24 predicted virological response ($p = 0.03$), combined response ($p = 0.02$) and ALT<1.5 ULN ($p = 0.02$) at week 96, but not biochemical response. Conversely, HDV RNA<100 IU/ml at week 24 was not associated with ALT values, virological response and combined response rates at weeks 48, 72 and 96.

Conclusion: In HDV compensated cirrhotic patients treated with BLV monotherapy up to 96 weeks, different baseline and on-treatment HDV RNA cut-offs may predict virological, biochemical and combined response rates.

SAT-182

Preliminary results of a Phase 1b, open-label, multicenter study of selgantolimod (GS-9688) in special populations of patients with chronic hepatitis B

Kosh Agarwal¹, Pin-Nan Cheng², Chun-Jen Liu^{3,4}, Ran Duan⁵, Nikita Kolhatkar⁵, Roberto Mateo⁵, Ben Da⁵, Christopher Richards⁵, Leonard Sowah⁵, Simon Fletcher⁵, Patricia Mendez⁵, Chi-Yi Chen⁶, Wan-Long Chuang⁷, Yao-Chun (Holden) Hsu^{8,9}. ¹King's College Hospital NHS Foundation Trust, Institute of Liver Studies, London, United Kingdom; ²National Cheng Kung University, College of Medicine, National Cheng Kung University Hospital, Tainan, Taiwan; ³National Taiwan University Hospital, Department of Internal Medicine, Division of Gastroenterology, Taipei, Taiwan; ⁴National Taiwan University College of Medicine, Graduate Institute of Clinical Medicine, Taipei, Taiwan; ⁵Gilead Sciences, Inc., Foster City, United States; ⁶Ditmanson Medical Foundation Chiayi Christian Hospital, Division of Gastroenterology and Hepatology, Department of Medicine, Chiayi, Taiwan; ⁷Kaohsiung Medical University Hospital, Kaohsiung Medical University, Department of Internal Medicine, Hepatobiliary Division, Kaohsiung, Taiwan; ⁸E-Da Hospital, Kaohsiung, Taiwan; ⁹I-Shou University, Kaohsiung, Taiwan
Email: kosh.agarwal@nhs.net

Background and aims: Chronic hepatitis B (CHB) is a leading cause of chronic liver disease, cirrhosis, and hepatocellular carcinoma. Selgantolimod (GS-9688), a toll-like receptor 8 agonist (TLR8) in development for CHB treatment, was well tolerated in virally suppressed and viremic patients with CHB. This study evaluated the efficacy and safety of selgantolimod in 3 CHB populations.

Method: This open-label study enrolled 3 unique populations of adults with CHB. Cohort 1 included HBeAg-positive patients with high viral load (HBV DNA $\geq 1 \times 10^7$ IU/ml) and ALT \leq ULN (per AASLD criteria). Cohort 2 included HBeAg-negative patients with HBV DNA ≤ 2000 IU/ml, HBsAg ≤ 1000 IU/ml, and ALT \leq ULN. Cohort 3 included hepatitis D virus (HDV)-coinfected patients on a commercially available oral CHB antiviral. All patients received selgantolimod 3 mg weekly for 24 weeks (w) and were then followed for 24 more. Primary virologic end points at w24 included proportion of patients with $\geq 1 \log_{10}$ IU/ml serum HBsAg decline from baseline (BL), proportion with HBV DNA <LLOQ in Cohorts 1 and 2, and proportion with $\geq 2 \log_{10}$ IU/ml HDV RNA decline from BL in Cohort 3. Safety was evaluated by clinical laboratory tests and documentation of adverse events (AEs). Biomarker analysis for the TLR8 pathway-associated pharmacodynamic readouts was performed.

Results: Patients (N=25) were recruited from sites in the UK and Taiwan; median age was 45 years, 56% were male, 72% were Asian. At w24, no patients in Cohorts 1 and 2 had HBV DNA <LLOQ, and no patients in Cohort 3 had $\geq 2 \log_{10}$ IU/ml decline from BL in HDV RNA. No patients in any cohort had a $\geq 1 \log_{10}$ IU/ml decline from BL in serum HBsAg at w24. In Cohort 3, there was a small decline in the median HDV RNA change from BL at w24 of $-0.25 \log_{10}$ IU/ml (IQR: $-0.25, 0.47$). All patients reported treatment-emergent AEs (TEAEs). In 43% of patients in Cohort 2 and 100% in Cohort 3, TEAEs were

POSTER PRESENTATIONS

judged related to study drug. In Cohort 3, 1 patient had severe nausea and vomiting. All other treatment-related AEs were Grade 2 or lower. No TEAEs led to study drug interruption or discontinuation. ALT elevation was observed in 1 patient in Cohort 1 and 2 patients each in Cohorts 2 and 3; all such increases were Grade 1 or 2. One patient (Cohort 2) met AASLD criteria for an ALT flare. Increases in serum IL-1RA and IL-12p40 levels were observed between 4 and 24 h after selgantolimod treatment in all cohorts.

Conclusion: In these unique populations of CHB, selgantolimod was safe with only 1 severe treatment-related AE. There was a small but consistent HBsAg decline in all cohorts with a trend in HDV RNA decline in the HDV/HBV Cohort. All ALT elevations were <Grade 3, and 1 met AASLD flare criteria.

SAT-183

Safety and efficacy of REP 2139-Mg in association with TDF in chronic hepatitis delta patients with decompensated cirrhosis

Christiane Stern¹, Cecilia De-Freitas¹, Michel Bazinet², Vincent Mackiewicz³, Segolene Brichler⁴, Emmanuel Gordien⁴, Stéphane Chevaliez⁵, Marc Bourliere⁶, Andrew Vaillant². ¹Hôpital Beaujon AP-HP, Clichy, France; ²Replicor Inc., Montreal, Canada; ³Hôpital Bichat, Service de Virologie, Paris, France; ⁴Centre national de référence des hépatite B, C et Delta-Laboratoire associé, Hôpital Avicenne, Bobigny, France; ⁵Hôpital Henri Mondor, Créteil, France; ⁶Hôpital Saint Joseph, Marseille, France

Email: avillant@replicor.com

Background and aims: The only treatment option for chronic hepatitis delta (CHD) patients with decompensated cirrhosis is liver transplantation. REP 2139-Mg blocks the assembly and secretion of HBV subviral particles and hepatitis delta antigen function, providing multiple effects against both HBV and HDV infection. Compassionate access to REP 2139-Mg is being provided under the Replicor Compassionate Access Program (RCAP, NCT05683548). The objective of this study is to describe the safety and efficacy of REP 2139-Mg in CHD patients with decompensated cirrhosis.

Method: Compassionate use in the first three CHD patients with decompensated cirrhosis to receive REP 2139-Mg 250 mg QW SC and TDF 245 mg QD PO for 48 weeks was approved in France by the ANSM. Clinical, biological, virological and imaging data were collected at baseline and every week for the first month, then every month.

Results: Patient 1 is a Caucasian, 56-year-old female, HDV treatment-naïve, with decompensated cirrhosis (Child Pugh B8, portal hypertension and ascites) with HDV RNA 7.04 log₁₀ IU/ml and HBsAg 1177 IU/ml at baseline. Reversal of ascites was confirmed by ultrasound at week 4 HBsAg loss occurred at week 10 with HBsAg seroconversion (27 mIU/ml) at week 14 increasing to 478.5 mIU/ml at week 30. HDV RNA has been undetectable since week 20. Patient 2 is an African, 56-year-old female with CHD and hepatocellular carcinoma (HCC) awaiting liver transplant. She had HDV relapse one year after discontinuing bulevirtide 2 mg and pegIFN 180 µg and progressed to decompensated cirrhosis (Child Pugh C11, portal hypertension, ascites and HCC) with accompanying edema and pronounced fatigue. Baseline HDV RNA was 3.64 log₁₀ IU/ml and HBsAg 4270 IU/ml. A significant reduction of ascites was confirmed at week 4 with marked reduction of peripheral edema and fatigue. Successful liver transplant (due to HCC) was performed in this patient after 10 weeks of therapy. Prior to liver transplant, HDV RNA became undetectable at week 6, HBsAg was 1.75 IU/ml and anti-HBs was 8 mIU/ml. Patient 3 is an African, 47-year-old male, HDV treatment-naïve, with decompensated cirrhosis (Child Pugh C10, portal hypertension, ascites, and hepatic encephalopathy). As observed in the first 2 patients, antiviral response is not yet evident at week 4. A significant reversal of ascites is present at week 6. All three patients experienced no significant adverse events and have presented a good tolerance to subcutaneous injections of REP 2139-Mg to date.

Conclusion: REP 2139-Mg in association with TDF is safe and well tolerated in patients with CHD and decompensated cirrhosis. Liver function improvement with significant ascites reversal was rapid, occurring after only 4 weeks of treatment. HBV-HDV functional cure with HBsAg loss and HBs seroconversion appears achievable for the first time in this special population, which could prevent the need for a future liver transplant.

SAT-184

Is treatment with Bulevirtide 10 mg useful in poor responder patients to 2 mg? Results from the French multicenter early access program

Victor de Lédighen¹, Anne Minello Franza², Nathalie Ganne-Carrié³, Laurent Alric⁴, Sophie Metivier⁴, Martin Siguier³, Bernard Prouvost-Keller⁵, Bruno Roche³, Frederic Heluwaert⁶, Louis d'Alterroche⁷, Leon Muti⁸, Juliette Foucher¹, Fabien Zoulim⁹, Marie-Noëlle Hilleret¹⁰. ¹CHU, Bordeaux, France; ²CHU, Dijon, France; ³APHP, France; ⁴CHU, Toulouse, France; ⁵CHU, Nice, France; ⁶CH, Annecy, France; ⁷CHU, Tours, France; ⁸CHU, Clermont-Ferrand, France; ⁹INSERM, France; ¹⁰CHU, Grenoble, France
Email: victor.deledighen@chu-bordeaux.fr

Background and aims: Significant HDV RNA decline was observed in HBV/HDV patients who received 48 weeks of Bulevirtide (BLV) in monotherapy or in combination with PEG-interferon α 2a (PEG-IFNα) in the French early access program and ANRS Buledelta cohort. However, no data are available of BLV 10 mg in poor responders to 2 mg. The aim of this analysis was to evaluate the efficacy and safety of BLV 10 mg daily with or without PEG-IFNα 2a for at least 6 months in HBV/HDV non-responder patients to BLV 2 mg.

Method: 15 patients (male 66.7%, mean age 43 years, cirrhosis 66.7%, median HDV-RNA at inclusion (BLV 2 mg) 6.52 log₁₀ IU/ml) with chronic HBV/HDV infection, with compensated cirrhosis/severe fibrosis or moderate fibrosis with elevated ALT levels, were included in this study. Patients received BLV 2 mg qd sc alone or in combination with PEG-IFNα once weekly according to physician's choice. All patients received at least 3 months of BLV 2 mg. In case of poor responses according to the physician, BLV was switched from 2 mg to 10 mg. The duration of 10 mg (at least 3 months) was related to the availability of the drug since in January 2022, BLV 10 mg was no longer available.

Results: No specific side-effects were reported. At Day 0 of BLV 10 mg, median HDV RNA was 6.08 log₁₀ IU/ml and median ALT level 63.5 IU/L (2/14 patients had ALT level <40 IU/L). 13 patients received BLV 10 mg monotherapy and 2 patients received BLV 10 mg plus PEG-IFNα. Main results (per protocol analysis) are indicated in Table. At M3, M6 and M9 or M12, median HDV-RNA was 5.29, 3.94, and 5.46 log₁₀ IU/ml. Only one patient (no cirrhosis) had long-term undetectable HDV-RNA. His viral load was 5.15 log₁₀ IU/ml when he started BLV 2 mg and 3.43 log₁₀ IU/ml when he started BLV 10 mg. Two patients switched from 10 to 2 mg when 10 mg was no longer available. No variation of viral load was observed after this switch.

Table: Response to BLV 10 mg after 2 mg.

	Month 3 with BLV 10 mg	Month 6 with BLV 10 mg	Month 9 or 12 with BLV 10 mg
Normal ALT level (<40 IU/L)	30% (3/10)	37.5% (3/8)	33.3% (3/9)
2 log decrease from baseline or undetectable HDV-RNA (%)	18.2% (2/11)	25% (2/8)	9.1% (1/11)
Undetectable HDV-RNA (%)	9.1% (1/11)	25% (2/8)	0% (0/11)

Conclusion: In this first real-world cohort of HDV patients, daily administration of BLV 10 mg in poor responder patients to 2 mg was safe and well tolerated. Unfortunately, no significant virologic effect

was observed after at least 6 months of treatment, even in patients receiving PEG-IFN.

SAT-185

Treatment with Bulevirtide, with or without PEG-interferon, in HIV-HBV/HDV co-infected patients in a real-life setting

Victor de Ledinghen¹, Claire Fougerou-Leurent², Miroslava Subic-Levrero³, Caroline Scholtes³, Emmanuel Gordien⁴, Stanislas Pol⁴, Karine Lacombe⁴, Dulce Alfaia³, Eric Billaud⁵, Vlad Ratziu⁴, Nathalie Ganne-Carrié⁴, Georges-Philippe Pageaux⁶, Vincent Leroy⁴, Isabelle Rosa⁷, Veronique Loustaud-Ratti⁸, Philippe Mathurin⁹, Christelle Tual², Estelle Le Pabic², Fatoumata Coulibaly¹⁰, Dominique Roulot⁴, Fabien Zoulim¹¹. ¹CHU, Bordeaux, France; ²CHU, Rennes, France; ³CHU, Lyon, France; ⁴APHP, France; ⁵CHU, Nantes, France; ⁶CHU, Montpellier, France; ⁷CHI, Créteil, France; ⁸CHU, Limoges, France; ⁹CHU, Lille, France; ¹⁰ANRS, France; ¹¹INSERM, France

Email: victor.deledinghen@chu-bordeaux.fr

Background and aims: Significant HDV RNA decline was observed in HBV/HDV patients who received 48 weeks of Bulevirtide (BLV) in monotherapy or in combination with PEG-interferon α 2a (PEG-IFN α) in the French early access program and ANRS HD EP01 BuleDelta cohort. However, no data are available in HIV co-infected patients. The aim of this analysis was to evaluate the efficacy and safety of BLV 2 mg daily with or without PEG-IFN α 2a for 12 months in HIV/HBV/HDV patients.

Method: 28 HIV patients (male 71.4%, mean age 48.8 years, cirrhosis 53.6%, median HDV-RNA 6.5 log (IU/ml), median HIV RNA 30 copies/ml, median CD4 620 cells/mm³) with chronic HBV/HDV infection were included in the French early access program and ANRS BuleDelta cohort. Patients received BLV 2 mg qd sc alone or in combination with PEG-IFN α once weekly according to physician's choice. HIV drugs regimen were TAF/FTC in 16 (57%) patients, Rilpivirine in 4, Bictegravir in 4, Elvitegravir in 3, Raltegravir in 1, Darunavir in 1, and Dolutegravir in 3.

Results: Twelve (50%) patients had detectable HIV-RNA at day 0 (all <100 cp/ml). At M12/EOT, median CD4 was 602/mm³, and 3 patients had detectable HIV-RNA (all <100 cp/ml). Early discontinuation (before or at M12) was observed in 10 (35.7%) patients (1 (10%) adverse event, 3 (30%) lost to follow-up or patient decision, 6 (60%) other reason). HDV-RNA declined overtime as follow: D0 6.5 log (IU/ml), M3 2.4 log (IU/ml), M6 3.8 log (IU/ml), M9 3.5 log (IU/ml), M12/EOT 3.4 log (IU/ml). At M3, undetectable or HDV-RNA decline >2 log from baseline was observed in 3 (20%) or 8 patients (88.9%) treated with BLV or BLV + PEG-IFN, respectively. Main results at M12 or EOT are presented in Figure 1. Serious adverse events were observed in 7 (5.5%) patients. Mean biliary acid level was 54.9 μ mol/L at M3 and 26.9 μ mol/L at M12.

Conclusion: In this first real-world cohort of HIV/HDV patients, daily administration of BLV 2 mg for 12 months was safe and well tolerated. Strong HDV antiviral responses were observed in real-life whatever the schedule administrated.

	BLV alone (N = 18)	BLV + PEG-IFN (N = 10)
Normal ALT level (<40 IU/L)	10 (55.6 %)	4 (44.4%)
2 log decrease from baseline or undetectable HDV-RNA (%)	11 (61.1%)	6 (60.0%)
Undetectable HDV-RNA (%)	7 (38.9%)	5 (50.0%)

Figure: (abstract: SAT-185).

SAT-186

The safety and pharmacokinetics of ABI-4334, a novel next-generation HBV core inhibitor: interim results from a phase 1 study in healthy volunteers

Edward J. Gane¹, Christian Schwabe², Jieming Liu³, Luisa M. Stamm³, Kathryn M. Kitrinos³, Steven J. Knox³, Michele Anderson³, Grace Wang³, Katie Zomorodi³. ¹University of Auckland, Auckland, New Zealand; ²New Zealand Clinical Research, Auckland, New Zealand; ³Assembly Biosciences, South San Francisco, United States
Email: edgane@adhb.govt.nz

Background and aims: ABI-4334 (4334) is a next-generation hepatitis B virus (HBV) core inhibitor in development for the treatment of chronic HBV infection. 4334 has demonstrated increased in vitro potency against HBV DNA and covalently closed circular (ccc) DNA formation compared with first-generation agents. Here, we report preliminary safety and pharmacokinetic data in healthy volunteers (HVs).

Method: ABI-4334-101 (NCT05569941) is an ongoing, single (SAD) and multiple ascending dose (MAD) study in HVs. During the SAD phase, 8 HVs (6 active, 2 placebo [PBO]) were enrolled in each of 5 dose cohorts, with 6 HVs receiving 4334 in both fasted and fed states to evaluate the effect of a high calorie meal. Following completion of SAD cohort (s), up to 8 HVs (6 active, 2 PBO) were enrolled in two MAD cohorts receiving assigned treatments for 8 days. Safety was assessed by physical exams, adverse events (AEs), and lab parameters. 4334 concentrations were measured by liquid chromatography mass spectrometry.

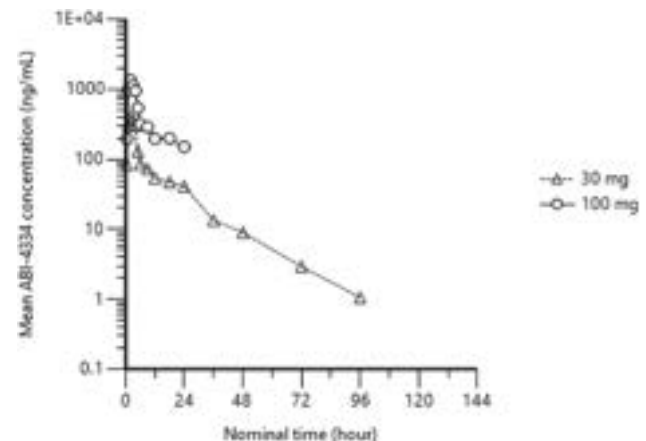


Figure: Mean ABI-4334 plasma concentrations versus time following single ascending doses of ABI-4334 in healthy volunteers (semi-log scale).

Results: At the time of the analysis, two SAD cohorts assessing 30 mg and 100 mg 4334 have been completed. Sixteen HVs enrolled and completed the study. Most were male 11 (69%) and White 11 (69%), with age and body mass index ranging from 20 to 61 years and 19–30 kg/m², respectively. Study drug was well tolerated, with no serious AEs or deaths. Half the HVs each at the 30 mg dose and 100 mg dose

POSTER PRESENTATIONS

(4334 or PBO recipients) reported an AE—7 Grade 1 and 1 Grade 2 (gastroenteritis). The most frequently reported AE was headache, with all cases being Grade 1. None of the AEs were considered related to the study drug. There were no Grade 3 or 4 lab abnormalities. 4334 was rapidly absorbed, with median t_{max} of 2 hrs, and exposure increased proportionally between the 30 mg and 100 mg single doses. Mean C_{max} and AUC_{0-24} values, respectively, were 446 ng/ml and 2503 h-ng/ml after the 30 mg dose, and 1376 ng/ml and 8772 h-ng/ml after the 100 mg dose (Figure). The projected C_{min} values for once daily administration at the 30 mg and 100 mg doses are in multiple-fold excess of protein-adjusted EC_{50} 's for HBV DNA and cccDNA formation.

Conclusion: 4334, a novel next-generation core inhibitor, was well tolerated in SAD cohorts when administered orally up to 100 mg. Plasma concentrations were higher than predicted by non-clinical models and exceeded in vitro EC_{50} values for the inhibition of cccDNA formation. Potent inhibition of HBV with daily dosing is projected.

SAT-187

Frequency of bepirovirsin binding site nucleotide polymorphisms at baseline and impact on end of treatment response to bepirovirsin (Phase 2b B-Clear study)

Jerome Bouquet¹, Robert Elston², Phil Yates², Shihyun You³, Amir Youssef², Ahmed Nader³, Jennifer Cremer⁴, Geoff Quinn², Fiona Campbell², Melanie Paff³, Dickens Theodore⁴. ¹GSK, South San Francisco, United States; ²GSK, Stevenage, United Kingdom; ³GSK, Collegeville, United States; ⁴GSK, Durham, United States
Email: jerome.x.bouquet@gsk.com

Background and aims: Bepirovirsin (BPV; GSK3228836) is an antisense oligonucleotide that targets a conserved 20-nucleotide sequence within HBV pregenomic RNA and mRNAs. B-Clear is a Phase 2b study (NCT04449029) assessing the efficacy and safety of 12 or 24 weeks (wks) of BPV treatment (tmt) in patients (pts) with chronic hepatitis B (CHB). This analysis assessed the frequency of pre-existing BPV binding site single nucleotide polymorphism (SNP) at baseline and the impact on end of tmt (EOT) hepatitis B surface antigen (HBsAg) serum level reduction.

Method: Multicentre, randomised, partial-blind study in pts with CHB who were either receiving concomitant stable nucleos (t)ide analogue therapy (on-NA) or were not receiving NA (not-on-NA). Pts were randomised (3:3:3:1) to receive BPV 300 mg weekly either for 24 wks (Arm 1); for 12 wks then 150 mg for 12 wks (Arm 2); for 12 wks then placebo (PBO) for 12 wks (Arm 3); or PBO for 12 wks then BPV 300 mg for 12 wks (Arm 4). A loading dose of BPV (Arms 1–3) or PBO (Arm 4) was given on days 4 and 11. Next-generation sequencing

was used to sequence HBV DNA or RNA at baseline. A SNP was reported if the frequency was $\geq 5\%$ compared with wild type.

Results: Not-on-NA: Baseline sequence information was available for 219/229 pts. Thirteen pts (13/219, 5.9%) had SNPs detected at a frequency of $\geq 5\%$. The most common BPV binding site SNPs were C9A (n=4/13, 31%) and T10G/C/A (n=6/13, 46%). Pts w/o w/o baseline SNPs had similar mean baseline HBsAg levels (3.605 vs 3.714 log₁₀ IU/ml). On-NA: Baseline sequence information was available for 90/226 pts. Nine pts (9/90, 10%) had a SNP detected at a frequency of $\geq 5\%$. The most common SNP detected was A13G (n=2/9, 22%). Pts w/o w/o a baseline SNP had similar mean baseline HBsAg levels (3.370 vs 3.344 log₁₀ IU/ml). EOT response: The mean log₁₀ reductions in HBsAg levels were lower in pts with a BPV binding site SNP; however, reductions were observed regardless of SNP (Table; tmt arms pooled) and 4 pts with SNP achieved HBsAg <0.05 IU/ml. These 4 pts had SNPs detected at a frequency between 5.417% and 99.943% over wild-type.

Conclusion: SNPs within the BPV binding site were infrequent across tmt arms. Although the HBsAg reduction was lower in the presence of BPV binding site SNPs, reductions were observed, and some pts with SNPs achieved HBsAg <0.05 IU/ml at EOT. Larger studies are needed to confirm these findings.

Funding: GSK (209668)

[on behalf of the B-Clear study group]

SAT-188

Safety, pharmacokinetics, and antiviral activity of single ascending doses of ALG-125755, a GalNAc-conjugated small interfering RNA, in subjects with chronic hepatitis B

Alina Jucov^{1,2}, Edward J. Gane³, Megan Fitzgerald⁴, Kha Le⁴, Stanley Wang⁴, Lynne Ammar⁴, Chris Burnett⁴, Alexei Haceatran¹, Kusum Gupta⁴, Doug Clark⁴, Meenakshi Venkatraman⁴, Leonid Beigelman⁴, Lawrence Blatt⁴, Tse-I Lin⁵, Sushmita Chanda⁴, Matthew McClure⁴, John Fry⁴. ¹ARENSIA Exploratory Medicine, Republican Clinical Hospital, Chisinau, Moldova; ²Nicolae Testemitanu State University of Medicine and Pharmacy, Moldova; ³University of Auckland, New Zealand; ⁴Aligos Therapeutics, Inc., South San Francisco, United States; ⁵Aligos Belgium BV, Belgium
Email: mfitzgerald@aligos.com

Background and aims: To evaluate the safety, pharmacokinetics (PK) and antiviral activity of ALG-125755, a small interfering RNA (siRNA) designed to reduce hepatitis B surface antigen (HBsAg) in subjects with chronic hepatitis B (CHB).

Method: Study ALG-125755-501 (NCT05561530) is a three-part, double-blind, randomized, placebo-controlled phase 1a/1b study. It

Table. Reduction in HBsAg at end of BPV treatment for patients with or without a BPV binding site SNP at Day 1 (pooled treatment arms)

Not-on-NA (n=220)		
	SNP	No SNP
Patients, n (%)	13 (6)	206 (94)
Baseline HBsAg level (log ₁₀ IU/mL)	3.605	3.714
Mean HBsAg reduction (log ₁₀ IU/mL)	-1.734	-2.302
Median HBsAg reduction (log ₁₀ IU/mL)	-1.809	-2.080
Min to Max HBsAg reduction (log ₁₀ IU/mL)	-0.11 to -4.11	0.01 to -5.98
On-NA therapy (n=90)		
	SNP	No SNP
Patients, n (%)	9 (10)	81 (90)
Baseline HBsAg level (log ₁₀ IU/mL)	3.370	3.344
Mean HBsAg reduction (log ₁₀ IU/mL)	-1.629	-2.093
Median HBsAg reduction (log ₁₀ IU/mL)	-2.391	-1.567
Min to Max HBsAg reduction (log ₁₀ IU/mL)	-0.19 to -3.40	0.04 to -5.50

Figure: (abstract: SAT-187).

is evaluating the safety, tolerability, PK and pharmacodynamics of single doses of ALG-125755 in healthy volunteers (HV; Part 1) and single (Part 2) and multiple (Part 3) doses of ALG-125755 in CHB patients. In Part 1, single subcutaneous (SC) doses of ALG-125755 up to 200 mg were well tolerated with linear PK in HVs (Gane et al, APASL 2023). In each cohort in Part 2, which is ongoing, 8 CHB subjects are being randomized 3:1 to receive single SC doses of ALG-125755 or placebo. Safety assessments (adverse events (AEs), vital signs, physical examination, ECG, and laboratories), viral markers (Parts 2 and 3), and plasma and urine PK samples are being collected throughout study conduct. Preliminary blinded results from the first cohort of Part 2 are reported here. Additional available data, including HBsAg, will be presented at the conference.

Results: 8 virologically suppressed hepatitis B e-antigen (HBeAg) negative CHB subjects received a single 50 mg SC dose of ALG-125755 or placebo in Cohort 1. Subjects were mainly female (62.5%), with a mean (SE) age of 58 (2.3) years, mean BMI (SE) of 30.4 (1.3) kg/m², and baseline HBsAg of 2.11 to 4.14 log₁₀ IU/ml. There have been no serious AEs or dose-limiting toxicities. All treatment emergent AEs (TEAEs) were mild (Grade 1) except for one Grade 2 back pain. Other than headache (N = 2), no TEAEs have been reported in more than one subject. No clinically concerning laboratory, physical examinations, vital sign, or ECG abnormalities have been reported. There was low inter-subject variability for ALG-125755 exposures, which were generally similar to those observed in healthy volunteers after dose and body weight adjustment.

Conclusion: Single SC doses of 50 mg ALG-125755 have been well tolerated to date in HBeAg negative CHB subjects with a safety and PK profile supporting further evaluation of higher dose levels.

SAT-189

Efficacy and safety of celecoxib add on nucleos(t)ide analogues on the hepatitis B surface antigen of virally suppressed patients with chronic hepatitis B-interim analysis

Feng Xue^{1,2}, Yingying Li³, Jing Zhang⁴, Qing Ye⁵, Huiying Rao⁶, Zhenhuan Cao⁴, Jun Li⁵, Xiaohe Li⁶, Lai Wei^{1,2}. ¹Beijing Tsinghua Changgung Hospital, Tsinghua University, China; ²School of Clinical Medicine, Tsinghua University, China; ³HolyHaid Artificial Intelligence Drug Development Limited Company, China; ⁴Beijing Youan Hospital, Capital Medical University, China; ⁵Tianjin Third Central Hospital, China; ⁶Peking University People's Hospital, China
Email: weilai@mail.tsinghua.edu.cn

Background and aims: Hepatitis B surface antigen (HBsAg) loss is considered as function cure of chronic hepatitis B (CHB). We found that celecoxib treatment is likely associated with HBsAg loss via artificial intelligence drug screening and has been validated by cytology, in vitro tests and real-world retrospective study. This proof-of-concept study (NCT05256823) is aiming to investigate if celecoxib add on nucleos(t)ide analogues (NUCs) can induce HBsAg loss in virally suppressed patients with CHB.

Method: Virally suppressed patients were defined as patients with CHB taking NUCs for more than 1 year with HBV DNA below the lower limit of quantification. This multi-center, randomized, open-labelled trial was beginning in February, 2022. Patients who were treated with NUCs for more than 1 year with 100 IU/ml < HBsAg < 1500 IU/ml and HBV DNA < 20 IU/ml were recruited. Participants were randomly assigned (in a 3:1 ratio) to receive either celecoxib at a dose of 200 mg twice a day add on NUCs (experimental group) or NUCs continue (control group) for 48 weeks and then followed for another 24 weeks. The primary end points were the ratio of HBsAg loss and the reduction of HBsAg after treatment for 48 weeks and discontinuation for 24 weeks. The safety of celecoxib treatment was evaluated throughout the study. The interim analysis of data for patients by January 11, 2022. All statistical analyses were performed using SAS software (version 9.4), and P < 0.05 were considered significant.

Results: A total of 47 patients participated in this study. 35 participants in the experimental group and 12 participants in the control group. Baseline data were comparable for the two groups. To date, 2 patients withdrew from the study gave no reason. All 45 participants had completed 24 weeks of follow-up and 19 participants completed 36 weeks of follow-up. At week 24, the HBsAg was decreased in 51.5% (17/33) of the patients in the experimental group. The multivariate linear regression analysis suggested the subgroup of patients with HBsAg levels at 200–500 IU/ml was more likely to respond to celecoxib in HBsAg decline. The coefficient is -0.01 compared to reference group. One patient in the experimental group had HBsAg levels of 344.85 IU/ml at baseline, which decreased to 292.29 IU/ml at 12 weeks, to 147.05 IU/ml at 24 weeks and to 79.45 IU/ml at 36 weeks. The incidence of adverse events (AEs) in the experimental group and control group was 91.43% and 91.67%, respectively. The incidence of AEs related to celecoxib treatment was 60%. All AEs were mild or moderate, with no serious adverse events reported.

Figure 1. The change of HBsAg level in 200-500 IU subgroup

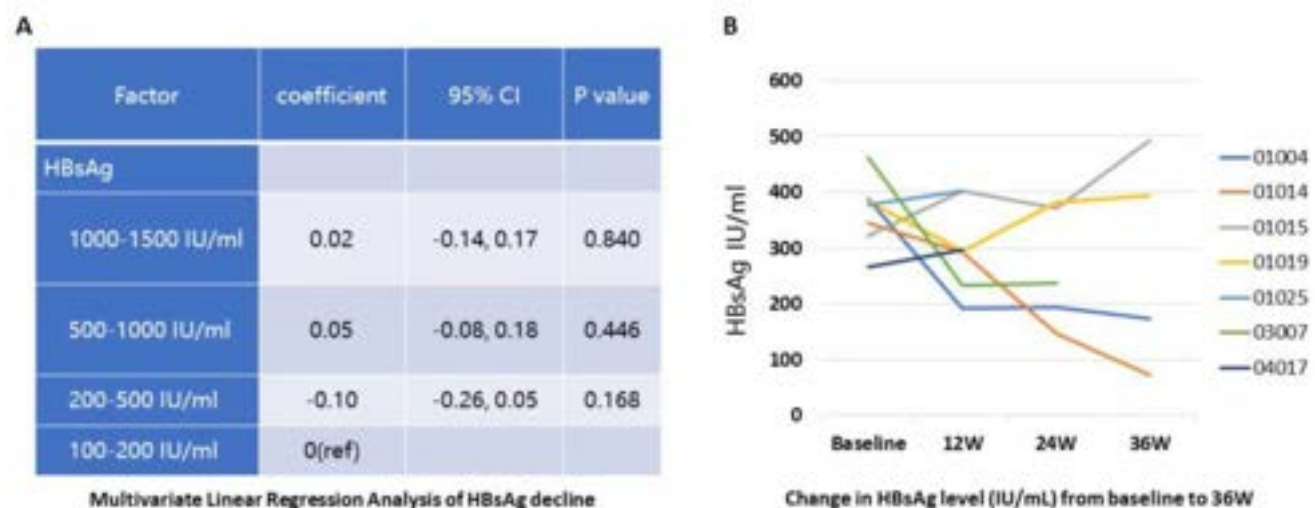


Figure: (abstract: SAT-189).

Conclusion: Celecoxib is safe and well tolerated in virally suppressed patients with CHB within first 24 weeks. Subgroup analysis showed that participants with baseline HBsAg levels between 200 IU/ml and 500 IU/ml had a significant decrease trend in HBsAg. Longer follow-up is needed to assess the long-term efficacy of celecoxib add on NUCs treatment.

SAT-190

Quantification of serum HDV RNA in untreated and Bulevirtide-treated patients with CHD: a comparison between Robogene 2.0 and EurobioPlex

Maria Paola Anolli¹, Sara Colonia Uceda Renteria², Elisabetta Degasperi¹, Dana Sambarino¹, Marta Borghi¹, Floriana Facchetti¹, Riccardo Perbellini¹, Roberta Soffredini¹, Sara Monico¹, Ferruccio Ceriotti², Pietro Lampertico^{1,3}. ¹Foundation IRCCS Ca' Granda Ospedale Maggiore Policlinico, Department of Gastroenterology and Hepatology, Milan, Italy; ²Foundation IRCCS Ca' Granda Ospedale Maggiore Policlinico, Virology unit, Milan, Italy; ³CRC "A.M. and A. Migliavacca" Center for Liver Disease, Department of Pathophysiology and Transplantation, University of Milan, Milan, Italy
Email: maria.anolli@unimi.it

Background and aim: Diagnosis and management of chronic hepatitis Delta (CHD) largely relies on HDV RNA quantification but a significant variability between different assays does exist. Aim of the study was to compare two different methods to quantify serum HDV RNA in untreated and Bulevirtide (BLV)-treated CHD patients.

Method: Frozen plasma from consecutive untreated and BLV treated-CHD patients were tested in a single-center retrospective study for HDV RNA levels by using two different quantification methods: Robogene 2.0 (Roboscreen GmbH, Leipzig, Germany; LOD 6 IU/ml) and EurobioPlex (HDV qRT-PCR, Eurobio, France, LLOQ 100 IU/ml). RNA extraction was performed manually for both assays according to manufacturer indications: INSTANT Virus RNA/DNA kit (Analytik Jena AG, Jena, Germany) for Robogene and NucleoSpin[®] Dx Virus Kit (Macherey-Nagel, Düren, Germany) for EurobioPlex.

Results: A total of 165 plasma samples collected from 123 CHD (88 untreated and 35 BLV-treated) patients were analyzed: median age was 53 (21–78) years, 57% males, 89% of European origin, 61% with cirrhosis, 78% under NUC treatment, 97% HDV genotype 1, ALT were 68 (6–743) U/L, HBsAg 3.8 (0.3–4.6) Log IU/ml, 91% HBeAg negative, 73% HBV DNA undetectable. Overall, median HDV RNA levels were 2.96 (0.30–7.36) vs. 3.03 (1.52–8.19) Log IU/ml by Robogene vs. EurobioPlex ($p < 0.0001$). Compared to the Robogene test, EurobioPlex reported similar HDV RNA levels ($\Delta \pm 0.5$ Log) in 56 (34%) patients, higher in 102 (62%) [Δ between +0.5 and +1 Log in 41; Δ between +1 and +2 Log in 55; $\Delta > 2$ in 6] and lower in 7 (4%) [Δ between – 0.5 and – 1 Log in all 7 cases]. Of the 45 (27%) samples that were target not detected (TND) with Robogene, 73% tested TND with EurobioPlex, 13% <LLOQ, while 13% tested positive (>100 IU/ml). Of the 10 (6%) samples <LOD with Robogene, 80% were TND with EurobioPlex, 10% were <LLOQ and 10% positive. Overall, 55 (33%) of samples tested TND or <LOD with Robogene and 64 (39%) with EurobioPlex ($p < 0.0001$). When setting Robogene as the reference standard, EurobioPlex had a Sensitivity of 86% and a Specificity of 87% in detecting HDV viral load. In BLV treated patients, virological response rates differed according to the assay: the proportion of patients achieving HDV RNA <LOD/LLOQ was 20% with Robogene and 42% with EurobioPlex. 13% of Robogene negative patients tested positive with EurobioPlex while 59% of those negative with EurobioPlex tested positive with Robogene.

Conclusion: Quantification of HDV RNA is significantly influenced by the quantification method, and this could influence clinical management of patients with CHD, being viral load a surrogate treatment end point in CHD

SAT-191

A monoclonal antibody 4G2 exhibits anti-viral activity in mouse models of chronic hepatitis B

Aileen Rubio^{1,2}, Aditi Deshpande³, Renae Walsh⁴, Hans Netter⁴, Chee Leng Lee⁴, Rachel Hammond⁵, Marcela Toro⁴, Stephen Locarnini⁴. ¹ClearB Therapeutics, Inc, Concord, United States; ²ClearB Therapeutics, Inc, United States; ³ClearB Therapeutics, Inc., United States; ⁴Victorian Infectious Diseases Reference Laboratory, Melbourne Health, Australia; ⁵VIDRL, Australia
Email: arubio@clearbtherapeutics.com

Background and aims: We have previously reported that chronic hepatitis B (CHB) patients who achieve functional cure have an antibody clearance profile (CP) associated with the occupation of key loop 1 and 2 epitopes within the Hepatitis B surface antigen (HBsAg) [Walsh, R et al 2019. Liver Int 39 (11) pp2066]. To identify a therapeutic monoclonal antibody (mAb) specifically targeting these epitopes, we immunized a single BALB/c mouse with modified HBsAg to over-represent CP epitopes. The hybridoma pools were screened to select clones producing antibodies with specificity to CP epitopes. The mAb clone 4G2 was selected based on specific recognition to HBsAg loop 1 CP and backbone epitopes. 4G2 mAb was evaluated for anti-viral activity in two murine models of CHB.

Method: Hydrodynamic tail vein injection (HDI) of HBV genotype A2adw2 plasmid into CBA/CaJ mice was performed to establish persistent infection of ~3 log IU/ml HBsAg [Chou H-H et al 2015. PNAS 112 (7) pp2175]. CHB mice were administered 200 or 400 µg 4G2 by intravenous (IV) injection. 4G2 at 400 µg was also assessed in an AAV (serotype 8)/HBV (genotype D ayw) CHB model established in C57BL/6 mice with a stable infection of ~4 log IU/ml HBsAg [Yang D, et al 2014 Cell Mol Immunol 11 (1) pp71–8]. Mice were monitored over time for serological markers of HBsAg, HBV DNA, anti-HBs antibody, as well as liver HBsAg and HBeAg immunohistochemistry at end of study.

Results: Treatment of CHB mice in the HDI model displayed a dose-dependent efficacy with 4G2 at 200 and 400 µg resulting in an average reduction of 2.1 and 2.5 log IU/ml HBsAg respectively, 4 days post-dose antibody administration. A rebound in HBsAg level was observed one week post dose in a subset of animals, but multiple weekly injections of 4G2 at 400 µg maintained the serological HBsAg control. Seroclearance of HBsAg resulted in seroconversion to anti-HBs and clearance of HBsAg and HBeAg positive cells in the liver. 400 µg of 4G2 also displayed efficacy in the AAV/HBV model resulting in an average reduction of 1.5 log IU/ml HBsAg. In both models, placebo and isotype control treatment resulted in no significant change in virological serum markers or seroconversion.

Conclusion: 4G2 mAb therapy was highly efficacious in two CHB murine models with rapid serum HBsAg decline and clearance, anti-HBs seroconversion, and clearance of infected hepatocytes. These findings further support the development of humanized 4G2 mAb for the treatment of CHB.

SAT-192

Treatment for up to 24 weeks with the capsid assembly modulator ALG-000184 results in dose related reductions in HBsAg in subjects with HBeAg positive chronic hepatitis B

Jinlin Hou¹, Yanhua Ding², Junqi Niu², Xieer Liang¹, Man-Fung Yuen³, Edward J. Gane⁴, Kosh Agarwal⁵, Benedetta Massetto⁶, Min Wu⁷, Kha Le⁶, Meenakshi Venkatraman⁶, Qingling Zhang⁶, Christopher Westland⁶, Maida Maderazo⁶, Sushmita Chanda⁶, Leonid Beigelman⁶, Lawrence Blatt⁶, Tse-I Lin⁸, Matt McClure⁶, John Fry⁶. ¹Nanfeng Hospital, Southern Medical University, China; ²Jilin University, the First Hospital, China; ³University of Hong Kong, Hong Kong; ⁴University of Auckland, New Zealand; ⁵Institute of Liver Studies, Kings College Hospital, United Kingdom; ⁶Aligos Therapeutics, Inc., United States; ⁷Aligos Therapeutics (Shanghai) Co., Ltd, China; ⁸Aligos Belgium BV, Belgium
Email: mwu@aligos.com

Table: Mean BL and change from BL in HBV DNA and HBsAg with ALG-000184 plus ETV or ETV alone

	HBV DNA			HBsAg		
	ALG-000184 100 mg + ETV	ALG-000184 300 mg + ETV	ETV	ALG-000184 100 mg + ETV	ALG-000184 300 mg + ETV	ETV
BL, mean (SEM)	8.6 (0.1) N = 8	8.2 (0.3) N = 11	8.1 (0.3) N = 6	4.7 (0.1) N = 8	4.4 (0.2) N = 11	4.3 (0.1) N = 6
CFB, mean (SEM)	- 6.4 (0.2) Week 24 N = 4	- 5.4 (0.3) Week 16 N = 6	- 3.8 (0.3) Week 12 N = 3	- 0.5 (0.1) Week 24 N = 4	- 0.5 (0.2) Week 16 N = 6	+0.05 (0.02) Week 12 N = 3

BL = baseline. ETV = entecavir. CFB = change from baseline. HBV DNA and HBsAg: log₁₀IU/ml

Figure: (abstract: SAT-192).

Background and aims: To evaluate the safety, pharmacokinetics (PK), and antiviral activity of ALG-000184, an oral prodrug of ALG-001075, a novel, pan-genotypic capsid assembly modulator-empty (CAM-E) with picomolar potency.

Method: ALG-000184-201 is a multi-part, multi-center, double-blind, randomized, placebo-controlled study (NCT04536337). Part 4 is evaluating the safety, PK, and antiviral activity of daily doses of ALG-000184 for up to 48 weeks in currently not treated subjects with chronic hepatitis B (CHB). Subjects in Cohorts 1 and 2 were randomized in a 4:1 ratio to ALG-000184 plus entecavir (ETV) or placebo plus ETV for 12 weeks followed by 36 weeks of ALG-000184 plus ETV. Cohorts 1 and 2 evaluated 100 mg and 300 mg of ALG-000184, respectively. A third cohort evaluating open label monotherapy of 300 mg ALG-000184 is also being evaluated. Available data from all three cohorts will be presented at the conference.

Results: To date, 25 subjects have enrolled in Cohorts 1 (100 mg, N = 11) and 2 (300 mg, N = 14) and have dosed for up to 24 and 16 weeks, respectively. All subjects are Asian, most female (52%), mean age 33.2 years, BMI 22.3 kg/m² and HBV genotype B or C. At baseline (BL), most subjects had an ALT less than 1.2 × ULN. Study drug was well tolerated; there were no serious adverse events (AEs) and no discontinuations due to an AE. All treatment emergent AEs were Grade 1 or 2, except for one Grade 4 AE of ALT elevation, which improved despite continuing dosing, and was assessed by the ALT Flare Committee as not due to drug toxicity. No clinically concerning laboratory, ECG, or vital sign findings were reported. The Day 1 PK profile is consistent with earlier findings in healthy volunteers. Mean BL and change from BL in HBV DNA and HBsAg are shown in the table. HBsAg levels were unchanged with ETV, but declined to a maximum of 0.7 log₁₀ IU/ml with 100 mg ALG-000184 plus ETV for at least 22 weeks, and to a maximum of 1.0 log₁₀ IU/ml with 300 mg ALG-000184 plus ETV for at least 14 weeks.

Conclusion: Dosing with ALG-000184 plus ETV for up to 24 weeks was well tolerated, exhibited predictable PK and resulted in substantial reductions in HBV DNA and HBsAg compared to ETV alone. Importantly, dosing with ALG-000184 plus ETV resulted in dose-dependent, clinically relevant declines in HBsAg, suggesting a potential role of ALG-000184 in combination regimens for functional cure.

SAT-193

Efficacy and prediction analysis of pegylated interferon alpha-2b in treatment-naïve HBeAg negative chronic hepatitis B patients with normal ALT: a multicenter real-world study (Ice-breaking Project in China)-Interim analysis

Chong Zhang^{1,1}, Da-Wu Zeng², Da-Chuan Cai³, Xiu-Lan Xue⁴, Ling-Yi Zhang⁵, Bao-Jun Song⁶, Yu-Feng Gao⁷, Yan Huang⁸, Jia Shang⁹, Xiao-Feng Wu¹⁰, Ying Zhang¹¹, Hua Jin¹², Hui Chen¹³, Hong Tang¹⁴, Xiaobo Lu¹⁵, Yujuan Guan¹⁶, Feng Min¹⁷, Liang Xu¹⁸, Gang Li¹⁹, Zhen-Guang Wang²⁰, Xiaoguang Dou¹. ¹Shengjing Hospital of China Medical University, China; ²The First Affiliated Hospital of Fujian Medical University; ³The Second Affiliated Hospital of Chongqing Medical

University, China; ⁴The First Affiliated Hospital of Xiamen University, China; ⁵Lanzhou University Second Hospital, China; ⁶The Sixth People's Hospital of Fushun, China; ⁷The First Affiliated Hospital of Anhui Medical University, China; ⁸Xiangya Hospital Central South University, China; ⁹Henan Provincial People's Hospital, China; ¹⁰The Sixth People's Hospital of Shenyang, China; ¹¹Dalian Public Health Medical Center, China; ¹²The Sixth People's Hospital of Benxi, China; ¹³Hepatobiliary Hospital of Jilin, China; ¹⁴West China Hospital of Sichuan University, China; ¹⁵The First Affiliated Hospital of Xinjiang Medical University, China; ¹⁶Guangzhou Eighth People's Hospital Guangzhou Medical University, China; ¹⁷Army Seventy-three Army Hospital, China; ¹⁸Tianjin Second People's Hospital, China; ¹⁹Liaohu Oilfield General Hospital, China; ²⁰Anshan City Hospital For Infectious Disease, China

Email: douxg@sj-hospital.org

Background and aims: In China, the proportion of HBeAg negative chronic hepatitis B (CHB) patients is gradually increasing, which is related to the pre-C region mutation of long-term HBV infection. The disease progression of Hepatitis B e antigen (HBeAg) negative CHB patients is fast, a large proportion of them have moderate or advanced liver inflammation or fibrosis, even if alanine aminotransferase (ALT) is normal, which requires timely antiviral treatment. The purpose of this study was to analyze the efficacy of pegylated interferon alpha-2b (PegIFN alpha-2b) in HBeAg negative CHB patients with normal ALT, and to explore the predictive factors of virological and serological responses.

Method: This is a multi-center, prospective, non-interventive, real-world clinical study conducted in China, involving 20 hospitals in 12 provinces or municipalities, which enrolled CHB patients with age of 18–60 years, Hepatitis B surface antigen (HBsAg) positive for more than 6 months, HBeAg negative, HBV DNA >20 IU/ml and normal ALT, without antiviral treatment history. PegIFN alpha-2b 180 ug/week was applied on a voluntary basis. The treatment strategy is adjusted according to the virological and serological response every 24 weeks, the total treatment course is not exceed 96 weeks.

Results: A total of 200 patients were planned to be enrolled in the project, which have been completed. Up to now, 75 (37.5%), 95 (47.5%) and 30 (15.0%) patients has completed 48, 72 and 96 weeks of treatment. 53 patients with complete data collection have been summarized for 24 weeks of treatment, and the remaining data are being collected. 35 (66.0%) were male, with an average age of 38.04 ± 8.15 years. The median baseline HBV DNA was 1.01 × 10³ IU/ml (1.46 × 10³~1.94 × 10⁶), of which 56.6% was ≤2000 IU/ml (Figure 1a), the median baseline HBsAg was 657.22 IU/ml (0.92~32828.22), of which 43.4% had HBsAg ≤500 IU/ml (Figure 1b). After 24 weeks of PegIFN alpha-2b treatment, the median HBV DNA was 0 IU/ml, and the rate of HBV DNA negative was 62.3% (Figure 1c), the median HBsAg was decreased to 106.45 IU/ml, and the HBsAg loss rate was 11.3% (Figure 1d). The patients with HBV DNA undetectable at treatment week 24 had much lower baseline HBsAg level than those HBV DNA detectable. (p = 0.032). The rate of HBV DNA negative at 24 weeks was 71.1% in patients with baseline HBsAg ≤1500 IU/ml, significantly higher than those with baseline HBsAg >1500 IU/ml (p = 0.036). There were no adverse events affecting the continued treatment.

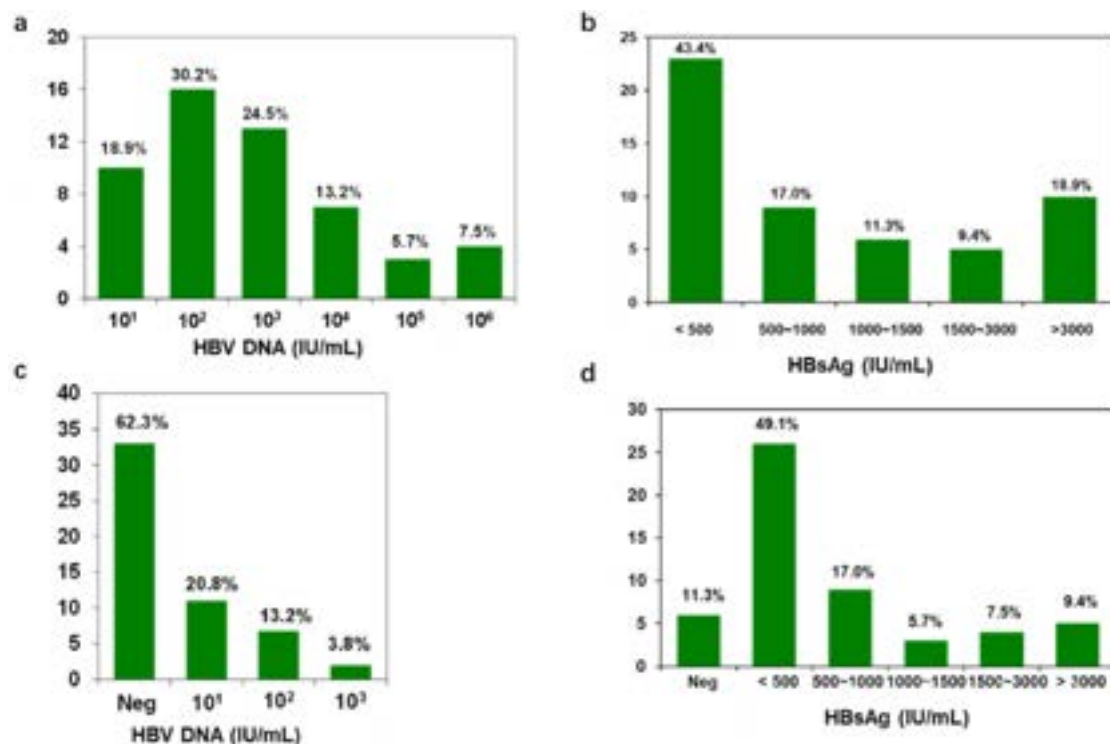


Figure: (abstract: SAT-193): a. Baseline HBV DNA viral load distribution; b. Baseline HBsAg level distribution; c. HBV DNA viral load after 24 weeks of PegIFN alpha-2b treatment; d. HBsAg level after 24 weeks of PegIFN alpha-2b treatment.

Conclusion: For HBeAg negative CHB patients with normal ALT, PegIFN alpha-2b treatment for 24 weeks can achieve a high rate of HBV DNA negative and significant HBsAg decrease, even HBsAg loss. The baseline HBsAg level is related to HBV DNA negative at 24 weeks, and the rate of HBV DNA negative was higher in patients with HBsAg ≤ 1500 IU/ml.

SAT-194

The safety and efficacy of hepalatide (L47) treatment combined with pegylated interferon-alpha 2a in patients with chronic hepatitis B: the preliminary data from a double-blind, RCT phase II trial

Junliang Fu¹, Qing Mao², Qinglong Jin³, Hui Cheng⁴, Yongqian Cheng¹, Xiaolu Tang⁵, Hongli Liu⁵, Fu-Sheng Wang¹. ¹Senior Department of Infectious Diseases, The Fifth Medical Center of Chinese PLA General Hospital, National Clinical Research Center for Infectious Diseases, Beijing, China; ²Department of Infectious Diseases, Southwest Hospital, Army Medical University, Chongqing, China; ³Department of Hepatology, The First Hospital of Jilin University, Jilin University, Changchun, China; ⁴Department of hepatitis, Hepatobiliary hospital of Jilin, Changchun, China; ⁵Shanghai HEP Pharma Co. Ltd., Shanghai, China
Email: fswang302@163.com

Background and aims: Hepalatide (L47), a 47aa synthetic peptide derived from Hepatitis B virus (HBV) Pre-S1, can blocks HBV entry into hepatocytes by competitively binding to HBV entry receptor sodium taurocholate co-transporting polypeptide (NTCP) on the surface of hepatocytes. The aims of this study were to explore the safety and efficacy of hepalatide in the treatment-naïve patients with chronic hepatitis B (CHB).

Method: This randomized, placebo-controlled, double-blind phase 2 clinical trial (NCT 04426968) was planned to enroll 96 treatment-naïve CHB patients with HBV DNA ≥ 20000 IU/ml, $2 \times \text{ULN} \leq \text{ALT} \leq 10 \times \text{ULN}$ from 12 hospitals in China. The CHB patients were randomly

assigned to three groups with different open-label L47 doses (group A 2.10 mg, group B 4.20 mg, and group C 6.30 mg). In each group, patients were double-blindly randomized to receive L47 or placebo treatment in a 3:1 ratio. All patients received subcutaneous injections of L47 or placebo once-daily, combined with subcutaneous injections of pegylated interferon-alpha 2a (PegIFN) (180 μ g/Week) for 24 weeks, then followed up for 24 weeks with PegIFN treatment alone. The primary end point is HBV DNA loss (cut-off value 20 IU/ml at the end of 24 weeks).

Results: As of December 26, 2022, 22 enrolled patients (including 19 patients with HBeAg positive and 3 patients with HBeAg negative) have completed 24-week combination treatment (group A, n=7; group B n=8; group C, n=7). The uncovered preliminary data showed that, in all groups, the adverse events (AEs) were generally grade 1 or 2, and most were identified to be related to PegIFN, such as fever, headache, fatigue, leukocytosis, neutropenia. No treatment-related serious AEs were reported. The baseline HBV DNA levels in the three groups were 8.29 ± 0.61 log IU/ml, 7.34 ± 1.42 log IU/ml and 7.69 ± 0.58 log IU/ml, respectively. At 12 weeks of treatment, the HBV DNA levels were declined by 2.39 ± 1.28 log IU/ml in group A, 2.21 ± 1.53 log IU/ml in group B and 4.23 ± 1.8 log IU/ml in group C, respectively. At the end of 24-week treatment, the HBV DNA levels were further declined by 3.70 ± 2.02 log IU/ml, 2.82 ± 1.71 log IU/ml, 4.54 ± 1.62 log IU/ml in the three groups, respectively. One patient in group A and one patient in group B reached primary end point. The levels of quantitative hepatitis B surface antigen (qHBsAg) were declined from baseline by 1.36 ± 0.99 log IU/ml, 0.89 ± 0.79 log IU/ml, 0.70 ± 0.76 log IU/ml in the three groups at the end of 24-week treatment, respectively. And one patient achieved HBsAg loss (below 0.05 IU/ml) with presence of hepatitis B surface antibody, one patient achieved HBeAg seroconversion. The ALT normalization rate was 28.6%, 37.5% and 57.1% in the three groups at the end of 24-week treatment, respectively.

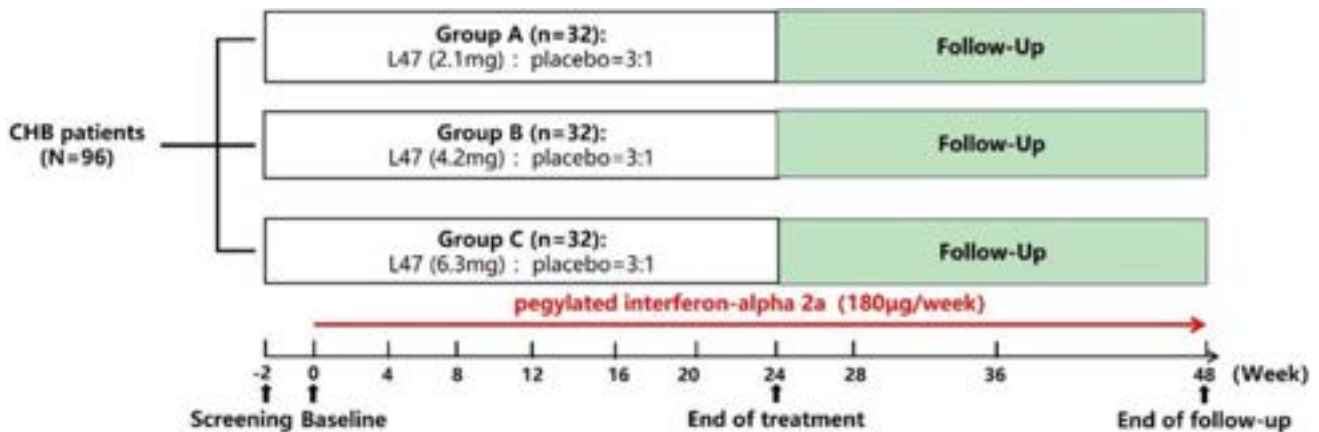


Figure: (abstract: SAT-194): Protocol of clinical trial.

Conclusion: Though the study is not complete, the preliminary data show a good safety and well tolerance of L47 treatment in combination with Peg-IFN. Importantly, the HBV DNA levels were declined rapidly in a L47 dose-dependent manner, highlighting its therapeutic potential in anti-HBV treatment.

SAT-195

A novel class of orally-available small molecules potently inhibiting hepatitis B and D virus entry

Nuruddin Unchwaniwala¹, Heidi Contreras¹, Jinghu Carl Li¹, Dinara Azimova¹, Joseph Tan¹, Lida Guo¹, Francielle Tramontini Gomes de Sousa¹, Kirsten Stray¹, Michael Shen¹, Jiaxin Yu¹, Marc P. Windisch¹, Michel Perron¹, Michael A. Walker¹, William E. Delaney¹, Min Zhong¹. ¹Assembly Biosciences, South San Francisco, United States
Email: mwindisch@assemblybio.com

Background and aims: Approximately 296 and 12 million patients worldwide are chronically infected with hepatitis B virus (HBV) and hepatitis D virus (HDV), respectively. HDV is a small RNA satellite virus that requires HBV envelope proteins to form its own virions. HDV/HBV co-infection is considered the most severe form of chronic viral hepatitis due to faster liver disease progression. Bulevirtide (BLV), a peptide binding to sodium taurocholate co-transporting polypeptide (NTCP), the entry receptor for HBV and HDV, was conditionally approved in Europe for the treatment of chronic HDV. Although clinical trials demonstrated safety and efficacy, BLV requires inconvenient daily injections. Here we describe the preclinical profiling of a novel class of orally-available small molecules that potently inhibit HBV and HDV entry.

Method: EC₅₀s for extracellular hepatitis B e antigen were measured in infected HepG2-NTCP cells and primary human hepatocytes (PHHs) by ELISA. Protein-adjusted HBV EC₅₀s were determined in infected HepG2-NTCP cells cultured with physiologic concentrations of human serum albumin and alpha acidic glycoprotein. EC₅₀s for intracellular hepatitis D antigen were determined by in-cell ELISA in infected HepG2-NTCP cells. The impact on NTCP-dependent bile acid uptake and HBV preS-binding competition were determined in HEK293 cells by measuring fluorescence-labeled bile acid uptake and fluorescence-conjugated preS-binding, respectively. Metabolic stability was evaluated in human, non-human primate (NHP), dog, and rodent liver microsomes (LMs). Pharmacokinetic studies were performed in rodents, dogs, and NHPs.

Results: Three structurally-related compounds potently inhibited HBV in HepG2-NTCP cells (EC₅₀ 4–12 nM) and in PHHs (EC₅₀ 124–233 nM), as well as HDV (EC₅₀ 21–28 nM). A reduction of anti-HBV potency (27- to 36-fold) was observed in a functional serum shift

assay. The compounds inhibited preS-binding (IC₅₀ 22–50 nM) and NTCP-dependent bile acid uptake (NTCP IC₅₀ 8–13 nM). The tested small molecules showed high metabolic stability in rodent LMs (mouse LM CL_{pred} 5–9 ml/min/kg and rat LM CL_{pred} 2–11 ml/min/kg), non-rodent LMs (dog LM 6–8 ml/min/kg and NHP LM 0.6–6 ml/min/kg), and human LMs (CL_{pred} 0.4–1.8 ml/min/kg). Good oral bioavailability was observed in all preclinical species (F = 100% in mice, rats, and NHPs and 76%–100% in dogs) with terminal half-lives of 3.2–3.4 hours in mice, 3.4–5.7 hours in rats, 5–13 hours in dogs, and 7.6–11 hours in NHPs.

Conclusion: We have identified a novel class of highly-potent, orally-bioavailable HBV and HDV entry inhibitors with good drug-like properties, potentially compatible with once-daily dosing in human. Lead optimization of this series of compounds is in progress, with a focus on nominating an investigational clinical development candidate for HDV and HBV therapy in 2023.

SAT-196

Cell-mediated immunity analysis to assess the characteristics of immune response to bepirovirsen: Examples from the B-Clear study

Jenn Singh¹, Bruno Salaun², Shihyun You¹, Stephen Corson³, Melanie Paffl¹, Dickens Theodore⁴. ¹GSK, Collegeville, United States; ²GSK, Rixensart, Belgium; ³Phastar, United Kingdom; ⁴GSK, Research Triangle Park, United States
Email: jennifer.m.singh@gsk.com

Background and aims: B-Clear assessed the efficacy and safety of bepirovirsen (BPV), an antisense oligonucleotide, in participants (pts) with chronic hepatitis B virus (HBV) infection. BPV 300 mg for 24 weeks (wks) resulted in 9–10% of pts achieving the primary end point of HBV DNA and hepatitis B surface antigen (HBsAg) loss maintained for 24 wks post BPV discontinuation. This analysis used T-cell functional characterisation of a subset of pts in B-Clear to understand the immunological response of pts treated with BPV.

Method: B-Clear was a Phase 2b randomised trial in 457 pts either on stable nucleos (t)ide analogue (NA) therapy or not on NA therapy. Methods and results have been published.¹ Briefly, pts were randomized (3:3:3:1) to receive up to 300 mg BPV for 12 or 24 wks with/without loading doses. The primary outcome was the proportion of pts achieving HBsAg <lower limit of detection (LLOD) and HBV DNA <lower limit of quantification (LLOQ) maintained for 24 wks without additional newly initiated antiviral medication after end of BPV treatment. In this analysis, peripheral blood mononuclear cells (collected at baseline, Wk 12 and 24, and off-treatment Wk 1, 12 and 24) from B-Clear study pts were stimulated overnight with overlapping peptide pools to HBV core, surface or polymerase

POSTER PRESENTATIONS

Figure. Example participant profiles.

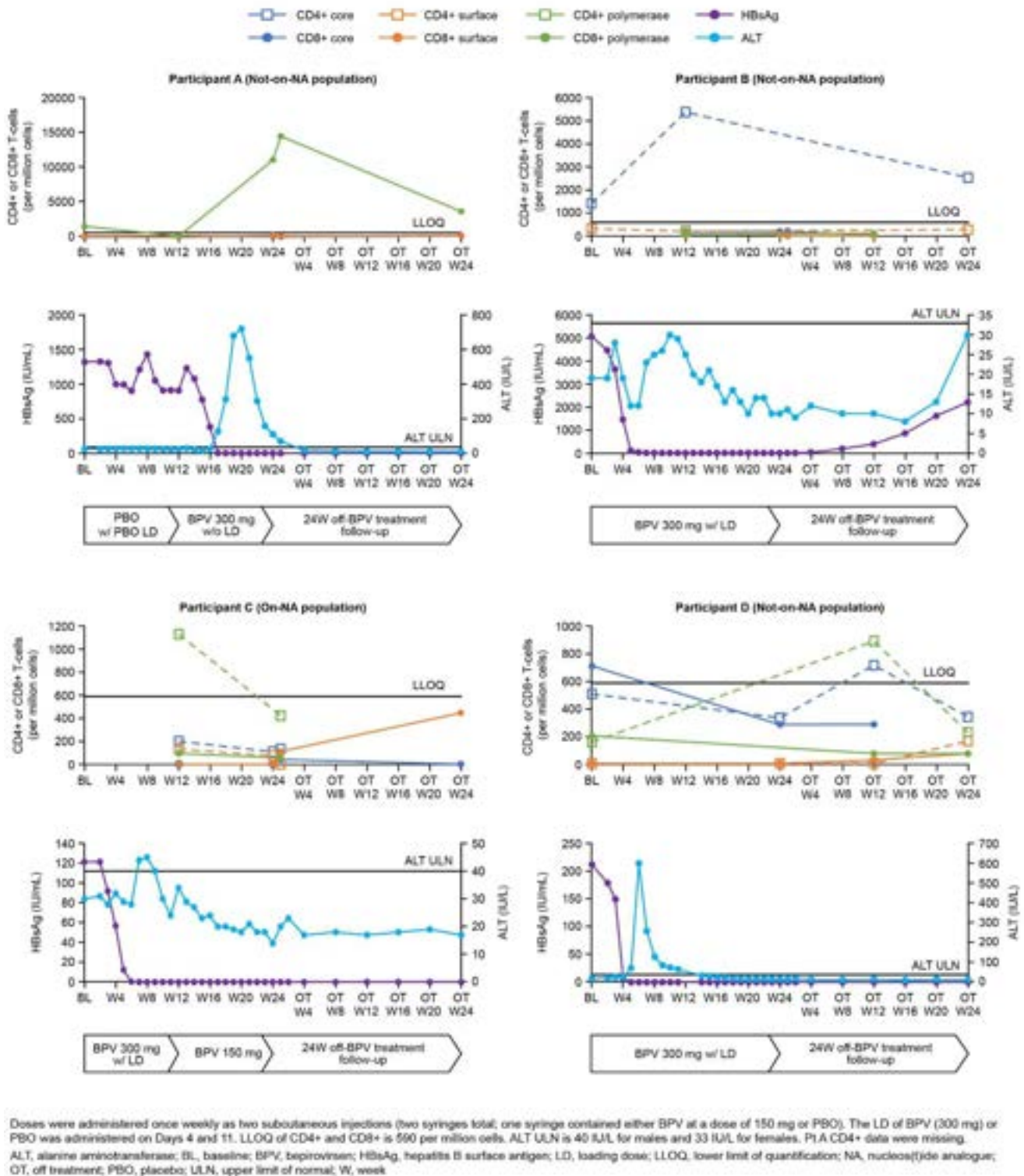


Figure: (abstract: SAT-196).

antigens. Expression of activation markers was analyzed by flow cytometry and used to quantify frequencies of polypositive CD4 and CD8 HBV-specific T-cells (expressing ≥ 2 markers including ≥ 1 cytokine among CD40L, 4-1BB, IFN- γ , TNF- α , IL-2, IL-13 and IL-17).

Results: Here we show individual pt-level example datasets from pts who developed or exhibited core- or polymerase-specific CD4+ or

CD8+ T-cells. None of these example pts exhibited surface-specific CD4+ or CD8+ T-cells. Overall, 159 and 224 pts had CD4+ or CD8+ T-cell data available at any timepoint; 42 pts had at least one CD4+ or CD8+ T-cell value above LLOQ (590 polypositive per million cells) at any timepoint; however, the lack of longitudinal data across the whole dataset due to poor sample quality limited comprehensive

analysis. The pts shown here had variable efficacy responses to BPV. HBsAg level dropped in all 4 pts in this subset (Figure) and at Wk 24 was <LLOD in pts A, C and D and 0.35 IU/ml in pt B. Pt treatment, HBsAg, alanine aminotransferase (ALT), CD4+ and CD8+ T-cell profiles are presented in Figure. Notably, pt A developed polymerase-specific CD8+ T-cells in a similar timeframe as ALT increased; however, the relationship between polymerase-specific CD8+ T-cells and ALT is still unclear.

Conclusion: Some pts have complex and varying HBV-specific T-cell responses during BPV treatment. Available datasets are currently being expanded to clarify the relationships between the multiple factors at play in response to BPV.

Funding: GSK [209668/NCT04449029]

References

1. Yuen MF *et al.* *N Engl J Med* 2022;387 (21):1957–1968.

SAT-197

Therapeutic vaccine candidate CLB-3000 (CLB-405 and CLB-505 adjuvanted with Alhydrogel): a Good Laboratory Practice (GLP)-compliant 15-week intramuscular toxicity study in rabbits with a 4-week recovery

Aileen Rubio¹, Bharat Dixit², Laurie Iciek³. ¹ClearB Therapeutics, Inc, Executive, Concord, United States; ²ClearB Therapeutics, Inc, Concord, United States; ³ClearB Therapeutics, Inc, Concord, United States
Email: arubio@clearbtherapeutics.com

Background and aims: ClearB Therapeutics is developing a therapeutic vaccine candidate, CLB-3000, designed to drive functional cure (FC) in patients with chronic Hepatitis B (CHB). CLB-3000 consists of 2 modified Hepatitis B surface antigens (HBsAg), CLB-405 and CLB-505, expressed in *Pichia pastoris*, purified and adjuvanted with Alhydrogel. CLB-405 and CLB-505 were designed to display clearance profile associated epitopes on HBsAg and were identified from anti-HBs responses of FC patients. The toxicity and immunogenicity of CLB-3000 was evaluated following repeated, intramuscular (IM) injection in New Zealand White (NZW) rabbits for 15 weeks and following a 4-week recovery period.

Method: NZW rabbits (8/sex/group) received 0.9% saline, Alhydrogel only (1000 µg) or CLB-405 and CLB-505 (40 100 and 250 µg each antigen; 80 200, or 500 µg total) with Alhydrogel (1000 µg) via IM injection, Q3W for 15 weeks. Evaluated parameters included: viability, clinical observations, local tolerance, ophthalmology, body weights, food consumption, body temperature, hematology, clinical chemistry, coagulation, organ weights, macroscopic and microscopic pathology, and immunogenicity.

Results: All animals survived to the scheduled necropsy. CLB-3000-related clinical and microscopic pathology findings were limited to effects at the injection sites; no adverse systemic effects were noted. CLB-3000-related clinical pathology changes at ≥80 µg included increases in fibrinogen, CRP, and/or creatine kinase, suggestive of an inflammatory response and muscle damage due to injection site reactions. Microscopic changes including granulomas, macrophage infiltrates, and/or mixed cell inflammation at the injection sites generally occurred at a higher incidence and/or severity in animals administered ≥80 µg CLB-3000. These findings are consistent with expected findings in a vaccine study formulated with adjuvant, did not result in clinical impairment, exhibited some degree of reversibility, and are not considered adverse. CLB-3000 was immunogenic, confirming pharmacologic activity in NZW rabbits.

Conclusion: Repeated IM injection of CLB-3000 was well tolerated at doses up to 500 µg antigen (250 µg CLB-405 and 250 µg CLB-505) with 1000 µg Alhydrogel/animal, the highest dose tested. Findings in this study, which were limited to effects at the injection sites, were consistent with expected findings in a vaccine study formulated with adjuvant and were not considered adverse. The safety profile of CLB-3000 in NZW rabbits supports further investigation for the treatment of CHB patients.

SAT-198

Phase 1b/2a study of heterologous ChAdOx1-HBV/MVA-HBV immunotherapy (VTP-300) combined with low-dose nivolumab (LDN) in virally suppressed patients with CHB on nucleos (t)ide analogues

Tom Evans¹, Eleanor Barnes², Reena Mehta¹, Louise Bussey², Katie Anderson¹, Antonella Vardeu², Anthony Brown¹, Young-Suk Lim³, Wan-Long Chuang⁴, Chiyi Chen⁴, Won Young Tak³, Gin-Ho Lo⁴. ¹Vaccitech Ltd, United Kingdom; ²Oxford University, United Kingdom; ³Asan Medical Center, Korea, Rep. of South; ⁴Kaohsiung Medical University Chung-Ho Memorial Hospital, Taiwan
Email: tom.evans@vaccitech.co.uk

Background and aims: Induction of a functional CD8+ T cell response to HBV is likely a required mechanism to achieve a functional cure of chronic hepatitis B (CHB). The use of a heterologous immunotherapeutic regimen combined with low dose checkpoint inhibition is a promising approach.

Method: Vaccitech's HBV immunotherapeutic (VTP-300) combines an adenoviral vector (ChAdOx1-HBV) and a heterologous Modified Vaccine Ankara boost (MVA-HBV) encoding polymerase, core, and S antigen from a consensus genotype C HBV. A Phase 1b/2a trial to evaluate four different regimens enrolled (n = 55) patients with CHB on prolonged antivirals (VL undetectable and HBsAg <4000 IU/ml) in 4 groups. Group 1 (n = 10), MVA-HBV d0 and d28; Group 2 (n = 18), ChAdOx1-HBV d0 and MVA-HBV d28; Group 3 (n = 18), Group 2 regimen with low dose Nivolumab (LDN) (0.3 mg/kg IV) at d28; Group 4 (n = 9) Group 2 regimen with LDN at d0 and d28.

Results: All 55 patients were enrolled and treated, and there was no concerning safety signal or immunotherapy-related SAE reported. Mild transaminase flares occurred in two patients. Groups 1 and 4 had no appreciable change in mean HBsAg. In Group 3, the mean log10 reduction was -0.76, -0.77 and -0.93 at 3, 6, and 9 months. Two patients in group 3 (genotypes B and C) had non-detectable HBsAg, which persisted until the end of follow-up. In Group 2, three patients with HBsAg <50 IU/ml at screening had HBsAg reductions of -0.94, -0.96 and -1.44 log10 at month 9; reductions >0.5 log10 persisted in most patients for 8 months until study end. Responses were seen in diverse genotypes and were associated in some cases with reductions of pgRNA. HBV T cell responses were assessed in all patients, and responses to all included antigens were observed. Final study results and the relationship between immune response and HBsAg reduction will be presented at the next EASL conference.

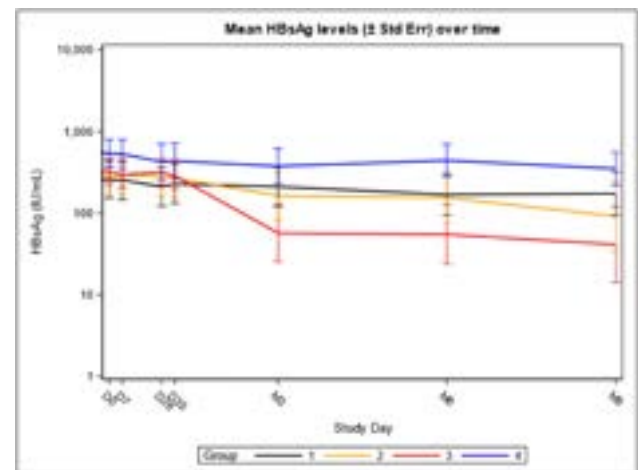


Figure:

Conclusion: VTP-300 immunotherapy, as monotherapy and when combined with low dose nivolumab at the boosting time point, was shown during the Phase 1b/2a trial to be immunogenic and associated with sustained reductions in HBsAg levels in well-

controlled CHB patients, and was administered with no concerning treatment-related SAEs or safety signal observed.

SAT-199

Kinetics of hepatitis B core related antigen in patients with compensated HDV cirrhosis treated with Bulevirtide monotherapy for 72 weeks: a single-center study

Elisabetta Degasper¹, Maria Paola Anolli¹, Dana Sambarino¹, Floriana Facchetti¹, Caroline Scholtes^{2,3,4}, Sara Colonia Uceda Renteria⁵, Alberto Perego⁶, Corinna Orsini⁶, Caroline Charre^{2,3,4}, Marie-Laure Plissonnier², Ferruccio Ceriotti⁵, Sara Monico¹, Barbara Testoni², Massimo Levrero^{2,4,7}, Fabien Zoulim^{2,4,7}, Pietro Lampertico^{1,8}. ¹Foundation IRCCS Ca' Granda Ospedale Maggiore Policlinico, Division of Gastroenterology and Hepatology, Milan, Italy; ²ISERM U1052-Cancer Research Center of Lyon (CRCL), Lyon, France; ³University Claude Bernard Lyon 1 (UCBLI), university of Lyon, Lyon, France; ⁴Hospices Civils de Lyon, Department of Virology, Lyon, France; ⁵Foundation IRCCS Ca' Granda Ospedale Maggiore Policlinico, Virology Unit, Italy; ⁶Fujirebio Italia, Pomezio-Rome, Italy; ⁷Hospices Civils de Lyon, Department of Hepatology, Lyon, France; ⁸CRC "A.M. and A. Migliavacca" Center for Liver disease, Departments of Pathophysiology and Transplantation, university of Milan, Milan, Italy
Email: elisabetta.degasper@policlinico.mi.it

Background and aims: Serum Hepatitis B Core Related Antigen (HBcrAg) has been proposed as a useful biomarker in naïve and treated HBV patients, however its role and kinetics in HDV patients receiving Bulevirtide (BLV) treatment is still unknown.

Method: Consecutive HDV cirrhotic patients treated with BLV 2 mg/day monotherapy for 72 weeks were enrolled in a single-centre study. Clinical/virological characteristics were collected at baseline and every 8 weeks. HDV RNA was quantified by Robogene 2.0 (LOD 6 IU/ml), HBcrAg levels were measured using LUMIPULSE® G HBcrAg assay (Fujirebio Europe, LLOQ 3 log₁₀ U/ml).

Results: Overall, 49 HDV patients were enrolled: median age 52 (29–77) years, 59% males, platelets 78 (17–217) × 10³/mm³, liver stiffness measurement 17.3 (6.4–68.1) kPa, ALT 97 (30–1074) U/L, HBsAg 3.7 (0.8–4.4) LogIU/ml, HDV RNA 5.2 (2.4–6.9) LogIU/ml, HBcrAg 4.1 (3.0–5.2) U/ml. At baseline, HBcrAg was detectable (≥3 U/ml) in 86% of patients and showed a direct correlation with HBsAg levels (r = 0.33, p = 0.03), while no association with HDV RNA or ALT levels was observed. Following 72 weeks of BLV monotherapy, HDV RNA declined by 2.8 (0.2–5.3) LogIU/ml (p < 0.001 vs. baseline), becoming undetectable in 33% of patients. Virological response (undetectable or at least 2 Log HDV RNA decline vs. baseline) was achieved by 78% of patients, a biochemical response (ALT < 40 U/L) was observed in 72% and a combined response (biochemical + virological) in 56%. During BLV treatment, patients testing HBcrAg positive declined from 86% to 70%, however the difference was not significant (p = 0.21). In HBcrAg positive patients, HBcrAg levels significantly declined from 4.1 (3.0–5.2) U/ml at baseline to 3.9 (3.1–4.7) U/ml at week 72 (p = 0.03), while no change in HBsAg levels was observed: from 3.7 (0.8–4.4) to 3.6 (2.5–4.3) LogIU/ml (p = 0.77). In HBcrAg positive patients, HBcrAg levels at week 72 were associated with biochemical response (OR 5.2, p = 0.03), while week 24 (OR 3.9, p = 0.04) and week 48 HBcrAg levels (OR 5.4, p = 0.01) were associated with combined response. Conversely, neither baseline nor on-treatment HBcrAg levels correlated with HDV RNA levels or virological response rates.

Conclusion: In cirrhotic HDV patients treated with BLV monotherapy for 72 weeks, HBcrAg tested positive in most of the patients, being associated with baseline HBsAg levels. During BLV treatment, HBcrAg

levels significantly declined and were associated with biochemical and combined response rates.

SAT-200

Modeling-based response-guided therapy with bulevirtide monotherapy for chronic hepatitis D to identify patients for finite treatment duration

Sarah Duehren¹, Louis Shekhtman^{1,2}, Scott Cotler¹, Stephan Aberle³, Thomas Reiberger^{4,5}, Peter Ferenci⁵, Harel Dahari¹. ¹Loyola University Chicago, Program for Experimental and Theoretical Modeling, Division of Hepatology, Department of Medicine, Stritch School of Medicine, United States; ²Northeastern University, Network Science Institute, United States; ³Medical University Vienna, Center of Virology, Austria; ⁴Medical University of Vienna, Division of Gastroenterology and Hepatology, Department of Medicine III, Austria; ⁵Medical University Vienna, Rare Liver Disease (RALID) Center of the European Reference Network for Rare Hepatological Diseases (ERN RARE-LIVER), Austria
Email: harel.dahari@gmail.com

Background and aims: Bulevirtide (BLV) is a novel antiviral drug against hepatitis D virus (HDV) that was conditionally approved in Europe in 2020. While it recently was suggested that BLV treatment discontinuation may be considered for patients who achieve long-term HDV RNA suppression (PMID:35514008), a computational approach may help to define the required duration of BLV therapy. Here we analyze HDV RNA kinetics in 7 patients undergoing BLV therapy and examine whether mathematical modeling could potentially be used to predict a finite duration of BLV therapy.

Method: Seven chronic HDV-infected patients receiving BLV monotherapy at two clinics in Vienna were included. HDV RNA was quantified by a sensitive PCR assay throughout treatment. ALT and HBsAg data were frequently collected in 7/7 and 3/7 patients, respectively. A recently developed mathematical model (AASLD 2022: late breaking abstract 5031) accounting for HDV RNA, HBsAg and ALT dynamics during BLV treatment was used to predict the time to reach <1 virus copy in the entire extracellular body fluid (BF).

Results: Median pre-treatment HDV RNA, ALT, and HBsAg were 5.0 log IU/ml [interquartile range, IQR 1.7], 44 U/L [IQR 69.5], and 3.1 log IU/ml [IQR 1.0], respectively. Two patients had normal ALT levels at pre-treatment. A delay in HDV RNA decline was seen in 4/7 patients at the beginning of therapy, lasting between 2 and 7 weeks. All 7 patients experienced a rapid phase of HDV decline (median of 0.11 log/week [IQR 0.09]) with a median duration of 14.7 weeks [IQR 13.3] and median magnitude of decline of 2.2 log cp/ml [IQR 0.8]. Thereafter, 2 patients experienced a 2nd slower phase of HDV decline (termed biphasic) of whom only one patient reached HDV undetectable (Fig. 1a). In the remaining 5 patients HDV RNA levels dropped to a subsequent lower viral plateau (termed flat partial response) throughout therapy (Fig. 1b). The two biphasic patients were both young (29 and 30 years old) without cirrhosis, while all flat-partial patients had a median age of 51 [IQR 14] and had cirrhosis. ALT normalized (Female < 35 U/L; Male < 50 U/L) in all but one (biphasic) patient during therapy. Five patients had normal ALT levels by week 24, and one patient by week 36. In 5/6 of these patients, HDV viral load declined ≥ 2 log from pre-treatment levels before ALT normalization. HBsAg remained at pre-treatment levels. In the mathematical model, the predicted values fit well the measured values (Fig. 1). In the biphasic patient who achieved undetectable HDV RNA levels, the model accurately predicted that a duration of ~100 weeks is required to achieve <1 virus copy in the BF (Fig. 1a).

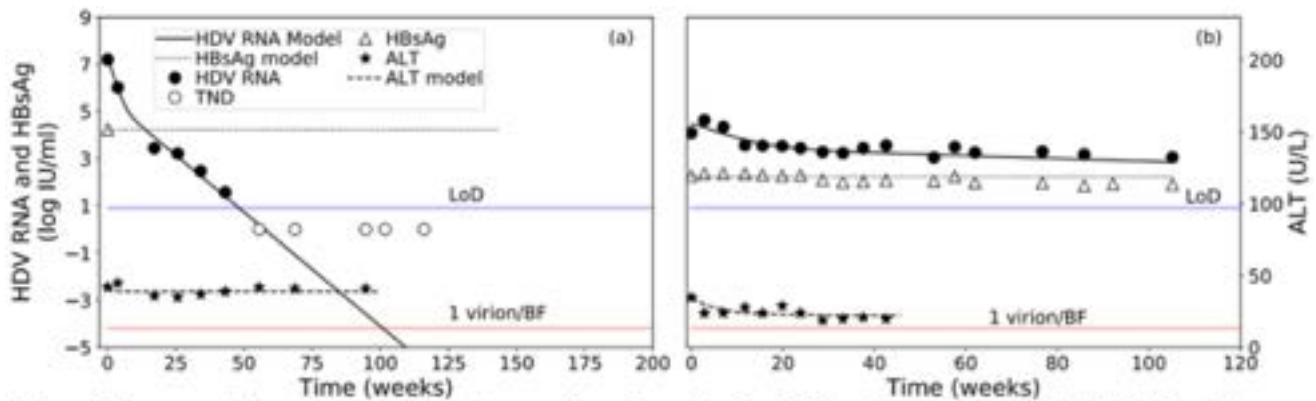


Figure 1. Representative viral kinetic patterns and mathematical modeling: (a) Biphasic (n=2); (b) Flat Partial Response (n=5). LoD, HDV RNA limit of detection (8 IU/ml).

Figure: (abstract: SAT-200).

Conclusion: The developed viral kinetic model provides an initial step toward to guide individualized BLV therapy allowing finite treatment durations in patients with HDV.

SAT-201

A phase 2 study of ASC42, a novel farnesoid X receptor (FXR) agonist, in combination with PEGylated interferon (PEG-IFN) and entecavir(ETV) in chronic hepatitis B patients with 12-week treatment

Jinlin Hou¹, Qianguo Mao², Jing Yuan³, Guoxin Hu⁴, Yao Xie⁵, Handan He⁶, Jinzi Wu⁶. ¹Nanfang Hospital of Southern Medical University, China; ²Xiamen Hospital of Traditional Chinese Medicine, China; ³The third People's Hospital of Shenzhen, China; ⁴Peking university Shenzhen hospital, China; ⁵Beijing Ditan Hospital Capital Medical University, China; ⁶Ascleto BioScience Co., Ltd., China
Email: jlhoumu@163.com

Background and aims: ASC42 is a novel non-steroidal, selective, potent farnesoid X receptor (FXR) agonist. Preclinical studies showed that ASC42 might be a novel anti-viral candidate for hepatitis B virus (HBV) functional cure through inhibiting transcription of HBV covalently closed circular DNA (cccDNA) into HBV RNA and reducing the HBV cccDNA stability. PEGylated interferon (PEG-IFN) and nucleos(t)ide analogs, such as entecavir (ETV), are the major antiviral drugs for chronic hepatitis B (CHB). As ASC42, PEG-IFN and ETV have different mechanisms of action (MoA), a combination of these 3 drugs might enhance the function cure rates in CHB patients. This study aimed to evaluate the safety and efficacy of combined treatment and pharmacokinetic (PK) of ASC42 in CHB patients treated with ASC42 combined with PEGylated interferon- α -2a (PEG-IFN- α -2a) and ETV.

Method: This Phase 2 trial (NCT05107778) was a multi-center, randomized, single-blind, placebo-controlled study conducted in China. Forty-three subjects with CHB were enrolled and randomized into 3 cohorts of 10 mg ASC42 (n = 15), 15 mg ASC42 (n = 14) or matching placebo (n = 14) orally once daily (QD) in combination with ETV (0.5 mg, orally QD) and PEG-IFN- α -2a (180 μ g, subcutaneous injection once a week). Subjects were treated for 12 weeks, and followed for 24 weeks (still on ETV). Serum hepatitis B surface antigen (HBsAg) and hepatitis B virus (HBV) pregenomic RNA (pgRNA) changes from baseline were measured during the 12-week intervention period and 24-week follow-up period.

Results: Two subjects in 15 mg ASC42 cohort withdrew from the study due to grade 2 adverse events (AEs) of dermatitis allergic and pruritus, respectively, while the other subjects completed the study. All subjects in ASC42 and PBO cohorts experienced at least one AE. In total, 153 146, and 127 AEs were reported in 10 mg, 15 mg ASC42 and

PBO cohorts, respectively, and most AEs (94.4%) were mild (grade 1) or moderate (grade 2) in severity. One subject in 15 mg ASC42 cohort experienced a grade 3 serious AE (SAE) of liver function injury with a final outcome of recovered. AEs of pruritus were reported in 2 (2/15, 13.3%), 9 (9/14, 64.3%) and 0 (0%) subjects in 10 mg, 15 mg ASC42 and PBO cohorts, respectively. ASC42 exposure measures (C_{max} and AUC_{0-24}) in 10 mg cohort is 4 times lower than those in 15 mg cohort (C_{max} : 106 versus 441 [ng/ml]; AUC_{0-24} : 733 versus 2920 [h*ng/ml]). There was no accumulation following multiple doses. No significant changes of HBV specific biomarkers from baseline at end of intervention or follow-up were observed among these 3 cohorts.

Conclusion: As a novel FXR agonist, 10 mg ASC42 in combination of PEG-IFN- α -2a and ETV, was safe and well-tolerated and showed minimum and mild pruritus (13.3%) in Chinese CHB patients with a 4-fold safety margin and better efficacy biomarker 7 α -hydroxy-4-cholesten-3-one (C4) inhibition (67%) than obeticholic acid (OCA) at 10–50 mg (40.1–47.3%).

SAT-202

Hepatitis B virus core protein variant profiles observed in chronic hepatitis B patients treated with capsid inhibitor AB-836

Christine L. Espiritu¹, Nagraj Mani², Timothy Eley³, Andrzej Ardzinski², Kim Stever², Joanne Brown⁴, Tilly Varughese⁵, Karen Sims⁵, Gaston Picchio⁶, Angela M Lam², Michael J. Sofia⁶, Emily P. Thi¹. ¹Arbutus Biopharma, Immunology and Biomarkers Research, Warminster, United States; ²Arbutus Biopharma, Biology, United States; ³Arbutus Biopharma, Clinical Pharmacology, United States; ⁴Arbutus Biopharma, Clinical Operations, United States; ⁵Arbutus Biopharma, Clinical Development, United States; ⁶Arbutus Biopharma, United States
Email: ethi@arbutusbio.com

Background and aims: Current treatments for chronic Hepatitis B virus (HBV) infection are limited to nucleos(t)ide analogs (NA) or pegIFN α which have low cure rates and often necessitate life-long treatment. AB-836 is an oral, pan-genotypic, CAM-E (empty) capsid inhibitor that inhibits HBV pre-genomic RNA (pgRNA) encapsidation by binding to HBV core protein and accelerating capsid assembly. In previously described results from the first-in-human clinical study AB-836-001, AB-836 resulted in robust HBV DNA log₁₀ declines of -2.66 (50 mg), -3.04 (100 mg), and -3.55 (200 mg), respectively. Herein we report the prevalence and impact of HBV core protein variants on virologic response to AB-836 treatment. AB-836 is no longer in development.

Method: HBV DNA was extracted from plasma collected from 48 subjects enrolled in AB-836-001 (randomized 10:2 per cohort

POSTER PRESENTATIONS

AB-836:placebo) who were administered AB-836 at either 50 mg, 100 mg, or 200 mg QD for 28 days. Extracted DNA samples underwent HBV-specific PCR amplification followed by Illumina MiSeq next generation sequencing. HBV core protein variant viral fitness and sensitivity to HBV inhibitors was determined using a cell-based *in vitro* system where single point mutations were introduced by site-directed-mutagenesis into an HBV replicating plasmid and then transfected into HepG2 cells.

Results: None of the subjects undergoing AB-836 dosing experienced on-treatment viral rebound. HBV core variants with frequencies of >1% at 31 amino acid sites located in and proximal to the AB-836 binding site were analyzed. No enrichment of core variants was observed between baseline and Day 28 (end of treatment). Higher frequency variants were identified at amino acid sites Y38, I105, T109, T114, I116, and Y118; however, there was no difference in HBV DNA reduction in subjects where core variants were detected at baseline. In cell culture, HBV core variants L30F, T33N, T33Q, L37Q, and I105T resulted in AB-836 EC₅₀ fold changes of 4.7, 64.8, 42.4, 20.8, and 8.3, respectively. Testing of an expanded panel of core variants, including Y38F/H, I105V, T109M/I/S, T114I, Y118F, Y132F, and the Y38F+T109S double variant, showed no effect on AB-836 activity.

Conclusion: No viral breakthrough or enrichment of HBV core protein resistant variants was observed in subjects receiving AB-836 for 28 days. Multiple core protein variants at amino acid positions Y38, I105, T109, T114, and I116 were observed to occur at higher frequencies, suggesting viral plasticity at these sites.

THURSDAY 22 JUNE

Viral Hepatitis C Clinical aspects including follow up after SVR

THU-162

External validation of models to predict hepatocellular carcinoma (HCC) in HCV SVR F3-F4 patients

Iván Sahuco¹, Ângela Carvalho-Gomes^{1,2}, Tsveta Valcheva^{1,3}, Enrique Vidal¹, Laura Martínez-Arenas^{1,2,4}, Carmen Vinaixa^{1,2,5}, Victoria Aguilera Sancho^{1,2,5}, Marina Berenguer^{1,2,3,5}. ¹La Fe Health Research Institute, Spain; ²CIBEREHD, ISCIII, Spain; ³University of Valencia, Spain; ⁴Polytechnic University of Valencia, Spain; ⁵La Fe Polytechnic and University Hospital, Spain
Email: marina.berenguer@uv.es

Background and aims: Several HCC risk-models have been developed to individualize patient surveillance following sustained viral response (SVR) in HCV patients. Validation of these models in different cohorts is an important step to incorporate a more personalized risk assessment in clinical practice. We aimed at applying these models to stratify the risk in our patient population.

Method: Patients with baseline F3-4 fibrosis treated between 2015 and 2018 with interferon-free oral antivirals (DAA) and SVR regularly followed as part of HCC surveillance strategy. The end point of interest was the development of HCC after at least 1 year of FU since end-of-therapy. Five models were applied to our sample population: Pons (<http://doi.org/10.1016/j.jhep.2019.10.005>), aMAP (<https://doi.org/10.1016/j.jhep.2020.07.025>), Ioannou HCC risk (<https://doi.org/10.1016/j.jhep.2018.07.024>), Alonso (<https://doi.org/DOI%2010.1002/hep.31588>) and Semmler (<https://doi.org/10.1016/j.jhep.2021.11.025>). Validation of the models was performed by repeated cross-validation 100 times, choosing randomly in each iteration 75% of the samples to train the model and the remaining 25% to validate it.

Results: Twenty-five (7%) of 357 F3-4 SVR patients regularly followed developed HCC. The number of patients analyzed by each model varied between 82 (Semmler) and 353 (Ioannou) depending on the number of variables available. The sensitivity of the different models varied between 0.17 (Semmler) and 1 (Alonso, aMAP). In our cohort, the model that would allow the most reliable reduction in HCC follow-up visits would be Ioannou HCC risk (see table) with a sensitivity of 96% and a proportion of patients labeled as high risk of 72%. In second place is Semmler model with a sensitivity of 71% and a proportion of patients labeled as high risk of 23%.

Model	N	N high risk	N with HCC	N high risk with HCC	Proportion classified as high risk	Sensitivity
Alonso	133	84	7	7	0.63	1
aMAP	350	313	24	24	0.89	1
Ioannou	352	253	24	23	0.72	0.96
Semmler7	144	33	7	5	0.23	0.71
Semmler7_no OH	144	23	7	4	0.16	0.57
Semmler6	82	10	6	2	0.12	0.33
Semmler6_no OH	82	4	6	1	0.05	0.17
HCCrisk	353	175	24	17	0.5	0.71
Pons	146	31	7	3	0.21	0.43

Figure:

Conclusion: Incorporating the HCC risk model in our center would safely allow for one third reduction in HCC surveillance in HCV SVR F3-4 patients.

THU-163

Impact of direct-acting antiviral therapy on tumor progression and survival in intermediate to advanced hepatocellular carcinoma patient with HCV infection

Chen-Ta Chi¹, I-Cheng Lee¹, Keng-Hsin Lan¹, Chi-Jen Chu¹, Chien-Wei Su¹, Ming-Chih Hou¹, Yi-Hsiang Huang¹. ¹Taipei veterans general hospital, Taiwan
Email: ctchi2@vghtpe.gov.tw

Background and aims: Direct-acting antiviral agents (DAAs) are effective to reduce incidence of hepatocellular carcinoma (HCC) and mortality among hepatitis C virus (HCV) patients. The beneficial impact of DAAs on outcomes in patients with intermediate to advanced HCC remains uncertain. This study aimed to assess the survival of patients with Barcelona Clinic Liver Cancer (BCLC) stage B/C HCC following DAAs treatment.

Method: From April 2015 to May 2022, consecutive 103 HCV-related HCC patients with BCLC stage B or C who had received DAAs therapy were retrospectively reviewed from Taipei Veterans General Hospital. Time to progression (TTP) and overall survival (OS) were assessed and factors associated with TTP and OS were analyzed.

Results: Of the 103 BCLC B/C HCC patients received DAAs, 86 patients were BCLC B and 17 patients were BCLC C. The mean age was 71 years old, and 66% had underlying cirrhosis. Most patients were within Child-Pugh class A (87.4%) and Albumin-bilirubin (ALBI) grade 1/2 (95.1%). Forty-two (40.8%) patients with active HCC during DAAs therapy. Of them, 76 (73.8%) patients received genotype-specific DAAs, and 27 (26.2%) patients received pan-genotypic DAAs. The sustained virological response (SVR) rate was 95.3% (82/86) in BCLC B, and 70.6% (12/17) in BCLC C, respectively. Seral AFP level >200 ng/ml (HR, 2.474; p = 0.010) was the independent predictor of TTP. Presence of cirrhosis, Child-Pugh B/C, seral AFP >200 ng/ml, and fail to achieve SVR were independent risk factors associated with OS. A novel scoring system to predict OS into 3 groups was created based on the multivariate analysis. For the 86 BCLC B HCV-HCC patients, ALBI grade 2/3 (HR, 2.435; p = 0.026) was the only factor associated with unTACEable-progression (TTUP) in multivariate analysis.

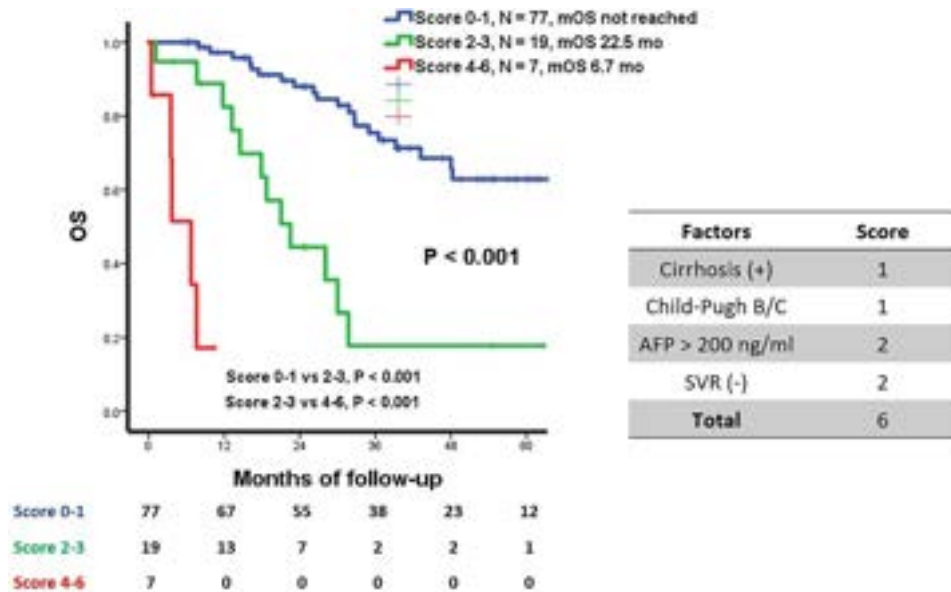


Figure: (abstract: THU-163).

Conclusion: DAAs could achieve a high SVR rate in BCLC B HCC patients even with active HCC. The novel model can be applied to predict survivals after DAAs therapy.

THU-164

The PNPLA3 genotype is the main driver of weight gain after the hepatitis C cure

Veronika Pitova¹, Sona Frankova¹, Mikolas Holinka¹, Magdalena Neroldova¹, Milan Jirsa¹, Jan Sperl¹. ¹Institute for Clinical and Experimental Medicine, Czech Republic
Email: sona.frankova@ikem.cz

Background and aims: The cure of chronic hepatitis C (HCV) is associated with decreased risk of liver-related complications. Body weight gain is currently discussed as a negative consequence of the HCV cure. The aim of the study was to evaluate body weight gain and changes in serum lipid levels, the presence of diabetes mellitus, hypertension and the genotype of PNPLA3, HSD17B13 and IL28B gene in patients treated with direct-acting antiviral (DAA).

Method: We retrospectively evaluated data of 230 patients treated for HCV infection with DAAs who achieved sustained virologic response (127 males, 103 females), with an average age of 52 years. One hundred and seventy-nine (77.8%) were infected with HCV genotype 1, 45 (19.6%) with genotype 3 and 6 with other genotypes (2.6%). Sixty-eight patients (29.6%) had compensated liver cirrhosis. We recorded the body weight, clinical and laboratory data and assessed liver stiffness (LSM) and liver steatosis expressed as the Controlled Attenuation Parameter (CAP) by Fibroscan[®] before treatment and three years after the cure. PNPLA3, HSD17B13 and IL28B genotypes were assessed by the TaqMan predesigned SNP genotyping assays using the Applied Biosystems ABI 7300 Real-Time PCR instrument (Thermo Fischer Scientific).

Results: The mean patients' weight before treatment was 79.9 kg (46-130 kg). Three years after treatment, the mean body weight gain was 3 kg (p < 0.0001). Thirty-five patients (15.2%) gained more than 10% of their initial body weight. The weight gain did not differ between males and females and patients infected with HCV genotypes 1 and 3. The liver stiffness significantly decreased after the treatment, with a mean of 12.1 kPa (range 3.3-73.5 kPa) vs 8.1 kPa (range 1.9-75 kPa), p < 0.0001, but the CAP value did not change significantly (256 dB/m vs 261 dB/m, p = 0.74). There was also an

increased proportion of patients with hypertension (68 vs 93, p < 0.03) and hypercholesterolemia (21 vs 48, p < 0.0006), but not with diabetes (24 vs 31, p = 0.39). The patients with newly diagnosed hypertension or hypercholesterolemia did not have a more pronounced weight gain than patients without the aforementioned (p = 0.14 and 0.14, respectively). The frequency of the genotypes was as follows: PNPLA3 CC 136 (59.1%), CG 85 (37.0%) and GG 9 (3.9%) patients, HSD17B13 TT 136 (59.1%), TTA 75 (32.6%) and TATA 19 (8.3%) patients, and IL28B CC 54 (23.5%), CT 132 (57.4%) and TT 44 (19.1%) patients. The weight gain was associated with the PNPLA3 G allele in the allelic model (CC vs CG+GG, +3 kg vs +0 kg, respectively, p = 0.0035). Dose-dependent effect of the PNPLA3 G allele on weight gain was apparent between different genotypes (CC + 0 kg, CG + 3 kg, GG + 7 kg). There was no association between HSD17B13 and IL28B genotypes and weight gain.

Conclusion: A significant weight gain is common in patients who achieve DAAs-induced HCV cure. PNPLA3 G allele carriage is a risk factor for weight gain after successful HCV therapy.

THU-165

MAFLD (metabolic associated fatty liver disease) outperforms ultrasonographic steatosis to stratify hepatocellular carcinoma risk in patients with advanced hepatitis C cured with direct antiviral agents

Serena Pelusi¹, Cristiana Bianco¹, Massimo Colombo², Giuliana Cologni³, Paolo Del Poggio⁴, Tiziana Re⁵, Nicola Pugliese⁶, Daniele Prati¹, Marie Graciella Pigozzi⁷, Pietro Lampertico¹, Roberta D'Ambrosio¹, Stefano Fagioli⁸, Luca Valenti¹. ¹Fondazione IRCCS Ca' Granda Ospedale Maggiore Policlinico, Milan, Italy; ²San Raffaele Hospital, Milan, Italy; ³Papa Giovanni Hospital, Bergamo, Italy; ⁴Papa Giovanni Hospital, Zingonia, Italy; ⁵Legnano Hospital-ASST Milano Ovest, Milan, Italy; ⁶Humanitas Research Hospital, Milan, Italy; ⁷Spedali Civili Hospital, Brescia, Italy; ⁸Azienda Socio Sanitaria Territoriale Papa Giovanni XXIII, Bergamo, Italy
Email: serenapelusi@libero.it

Background and aims: Metabolic dysfunction associated fatty liver disease (MAFLD) has been proposed to identify individuals at risk of liver events irrespectively of the contemporary presence of other liver disease drivers. Aim of this study was to examine the impact of MAFLD in patients cured of chronic hepatitis C (CHC).

Method: We analyzed data from a real-life cohort of 2611 Italian patients cured of CHC with direct antiviral agents and advanced liver fibrosis, without HBV/HIV, transplantation and negative for hepatocellular carcinoma (HCC) history (age 61.4 ± 11.8 years, 63.9% males, median follow-up 34, i.q.r. 24–40 months). Information about ultrasonographic fatty liver disease (FLD) after sustained virological response was available in 1978.

Results: MAFLD affected 58% of patients, diagnosed due to the presence of diabetes (19%), overweight (37%), or multiple metabolic abnormalities (2%). MAFLD was more frequent than and not coincident with FLD (32% MAFLD-only, 23% MAFLD-FLD, 13% FLD-only). MAFLD was associated with higher liver stiffness ($p < 0.05$), particularly in patients with MAFLD-diabetes and MAFLD-only subgroups, comprising older individuals with more advanced metabolic and liver disease ($p < 0.05$). At Cox proportional hazard multivariable analysis, MAFLD was associated with increased risk of HCC (HR 1.97, 95% c.i. 1.27–3.04; $p = 0.0023$). Further classification according to diagnostic criteria improved risk stratification ($p < 0.0001$), with the highest risk in patients with MAFLD-diabetes. When considering MAFLD together with FLD, patients with MAFLD-only appeared at highest risk since the sustained virological response achievement ($p = 0.008$), with a later catch-up of those with combined MAFLD-FLD, whereas FLD-only was not associated with HCC (figure 1).

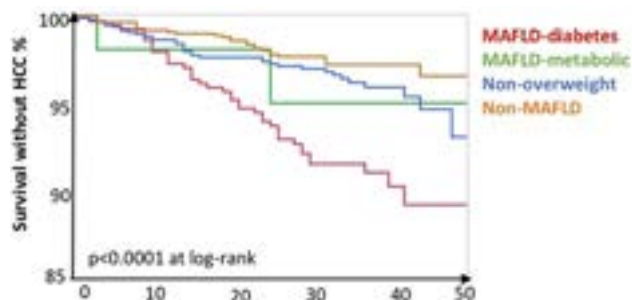


Figure 1:

Conclusion: MAFLD is more prevalent than FLD in patients cured of CHC with advanced fibrosis and identifies more accurately individuals at risk of developing HCC.

THU-166

Most vulnerable HCV patient groups treated with direct acting antivirals achieve high response rates and gain quality of life-data from the German hepatitis C-registry (DHC-R)

Stefan Christensen^{1,2}, Albrecht Stoehr³, Gerlinde Teuber⁴, Jörg Petersen³, Ralph Link⁵, Uwe Naumann⁶, Christine John⁷, Yvonne Serfert⁸, Karl-Georg Simon⁹, Stefan Zeuzem¹⁰, Heiner Wedemeyer^{8,11}. ¹Center for Interdisciplinary Medicine, Muenster, Germany; ²University Hospital Muenster, Department of Gastroenterology and Hepatology, Muenster, Germany; ³ifi-Institute for Interdisciplinary Medicine, Hamburg, Germany; ⁴Practice PD Dr. med. G. Teuber, Frankfurt am Main, Germany; ⁵MVZ-Offenburg GmbH/St. Josefs-Klinik, Offenburg, Germany; ⁶UBN/Praxis, Berlin, Germany; ⁷Center of Gastroenterology, Berlin, Germany; ⁸Leberstiftungs-GmbH Deutschland, Hanover, Germany; ⁹MVZ Dres. Eisenbach, Simon, Schwarz GbR, Leverkusen, Germany; ¹⁰Goethe University Hospital, Department of Internal Medicine I, Frankfurt am Main, Germany; ¹¹Hannover Medical School, Department of Gastroenterology, Hepatology and Endocrinology, Hanover, Germany
Email: christensen@cim-ms.de

Background and aims: DAA therapy cures most HCV-patients. To reach micro-elimination, the focus has to be on most vulnerable patient groups. With the aim to improve patient care we characterize treatment outcomes and quality of life (QoL) of these patients in a large prospective real world cohort.

Method: The DHC-R is a national multicenter real-world registry including about 18,200 patients. The present analysis is based on 6849 patients with available data as of July 15, 2022 and comprises the following subgroups: active drug use (yes N = 478; no N = 6371), alcohol abuse (yes N = 650; no N = 6199), former/current homelessness (yes N = 81, no N = 6768) and prison experience (yes N = 140; no N = 6709). Data on homelessness and prison experience have been obtained since October 2020. One patient can belong to several subgroups. Baseline characteristics, sustained virological response (SVR) rates, QoL (36-Item Short Form Survey, SF-36) at baseline and 12 to 24 weeks after end of treatment (EOT) as well as safety data were analyzed.

Results: The majority of the patients with active drug use, alcohol abuse, former/current homelessness or prison experience were male (79–84%). Patients from these vulnerable subgroups were significantly younger than patients not belonging to these subgroups ($p < 0.05$). With 22 and 23%, respectively, significantly more patients with active drug abuse and alcohol abuse suffered from psychiatric disorders than those without drug or alcohol abuse (12 and 11.8%, respectively; $p < 0.05$). Lost-to-follow-up (LTFU) rates ranged between 31 and 46% in the vulnerable subgroups and were higher after EOT than before EOT. In vulnerable subgroups, Intention-to-treat SVR rates ranged between 61% (active drug abuse) and 67% (alcohol abuse) and was mainly affected by high LTFU rates. In Per-Protocol-Analysis, the SVR rates ranged between 93% (active drug abuse) and 97% (alcohol abuse). According to all SF-36 scales, all vulnerable subgroups benefited significantly from DAA therapy ($p < 0.05$; Figure 1). Of note, the QoL of patients with former/current homelessness improved the most. Adverse events were documented for 19% (prison experience) to 32% (active drug abuse) of the patients. Serious adverse events occurred in a maximum of 5% in each patient group.

Conclusion: Active drug users, people with alcohol abuse, prison experience and former/current homelessness as most vulnerable patient groups respond well to DAA therapy but still need special attention shown by higher rates of LTFU. Although often living in precarious circumstances all these patients gain quality of life from baseline up to 24 weeks after EOT which is a good argument to make efforts to grant access to DAA therapy for the most vulnerable patient groups.

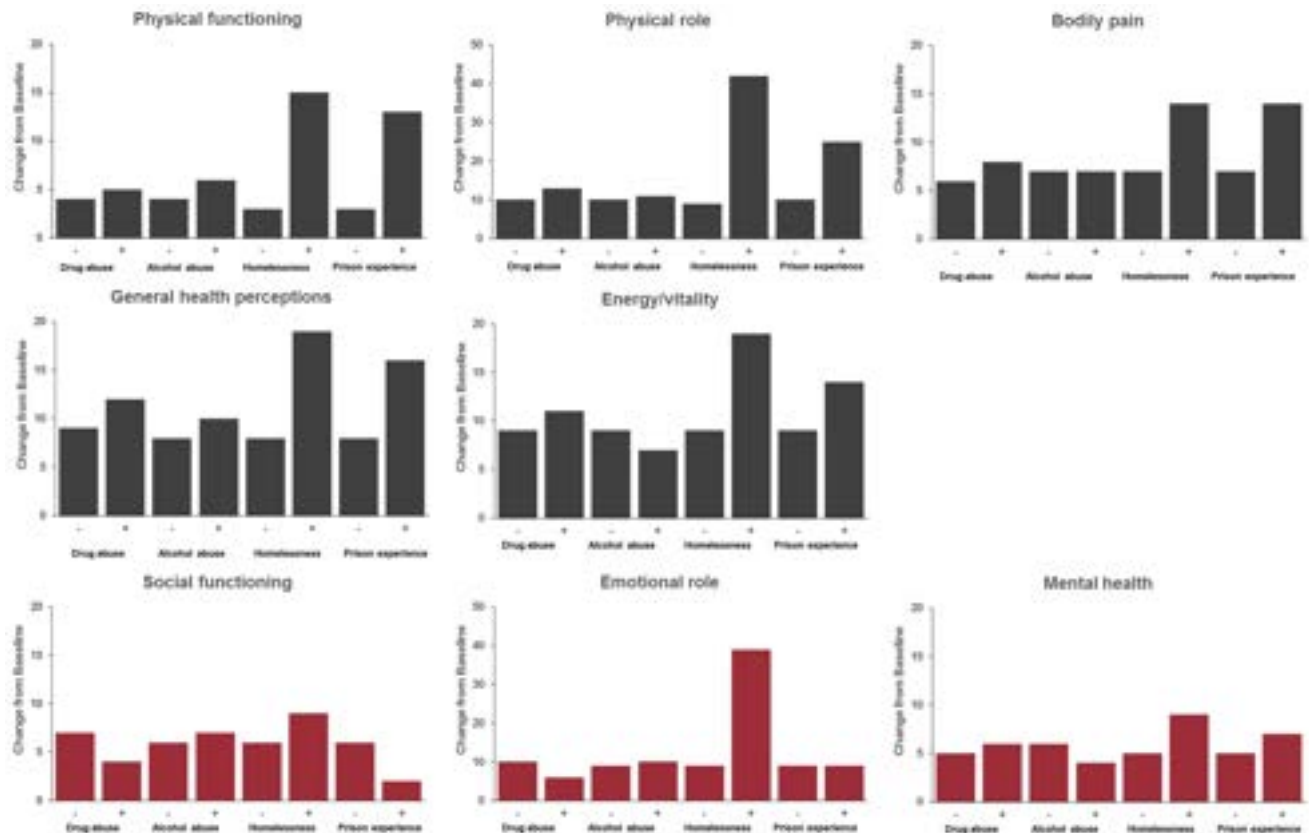


Figure: (abstract: THU-166): Change in SF-36 scales from baseline (BL) to week 12/24 after end of treatment (EOT) according to each subgroup (+yes, -no; changes between BL and week 12/24 after EOT were significant within each subgroup, $p < 0.05$).

THU-167

The impact of 5 years of testing for hepatitis C in prisons in the north east of England

Amy Johnson¹, Jessica Shearer¹, Craig Thompson², Yusri Taha^{1,3}, Stuart Mcpherson^{1,4}. ¹Newcastle upon Tyne Hospitals NHS Foundation Trust, Viral Hepatitis Service, Newcastle upon Tyne, United Kingdom; ²Spectrum Community Health-CIC, Durham, United Kingdom; ³Newcastle upon Tyne Hospitals NHS Foundation Trust, Department of Infection and Tropical Medicine, Newcastle upon Tyne, United Kingdom; ⁴Newcastle upon Tyne, Institute of Cellular Medicine, Newcastle upon Tyne, United Kingdom
Email: amyjohnson12@nhs.net

Background and aims: The prevalence of hepatitis C virus (HCV) in the prison population is high, and diagnosis and treatment of this group is vital to achieving elimination. Universal offering of blood borne virus (BBV) testing was established in all North-East of England (NEE) prisons in March 2016, and data is collected by the prison service. The aim of the study was to review the frequency of HCV among people incarcerated in prison.

Method: Data was collected from three NEE prisons (two male [1 remand, 1 medium sentence], one female). BBV testing offer and screening rates were reviewed for all new inmates between July 2017 and June 2022. HCV antibody (HCV-Ab) and HCV-RNA positivity rates were assessed per quarter. HCV-Ab tests taken within six months of another test were excluded.

Results: There were 39,652 new receptions into prison during the data collection period. 35,906 new receptions (90.6%) were offered BBV testing and 17,068 (47.5%) accepted testing at reception. BBV offer and testing rates over 5 years are shown in Fig. A. Testing rates fell during the COVID-19 pandemic. Despite this reception testing rate, in June 2022, 77.0% of inmates had had BBV testing in 12 months. 3014 tests (17.7%) were HCV-Ab positive and 1249 (7.3%) were HCV-RNA positive (median 238/year). Over time, there was an increase in HCV-Ab frequency from 14% to 17% (Fig. B). There was also an increase in the number of HCV-Ab positive results during the pandemic, suggesting that BBV testing may have been more targeted in the period. Overall, the HCV-RNA positivity rate as a proportion of the total number screened reduced from 7% to 6% during the study period (Fig. C). HCV-RNA prevalence was higher in the female prison than the male prisons (14% vs. 6%). The HCV-RNA positivity rate in HCV-Ab positive individuals fell from 50% to 34% during the study period (Fig. D).

Conclusion: Overall, prevalence of HCV-Ab positivity has increased in NEE prisons over 5 years, but rates of HCV-RNA positivity are falling suggesting that robust testing and treatment programmes are having a meaningful impact. However, the number of individuals with active hepatitis C in prison remains worryingly high. Further work is needed to increase uptake of testing and treatment in this high-prevalence population.

POSTER PRESENTATIONS

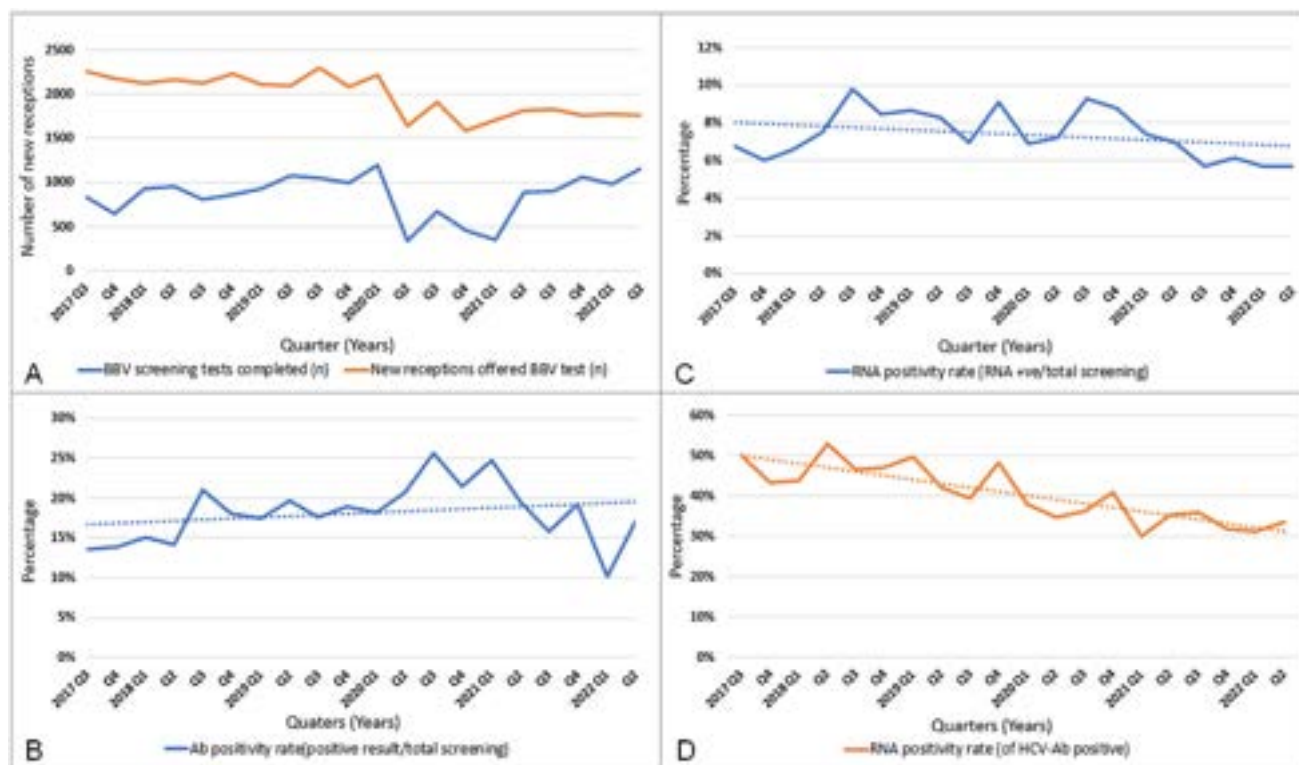


Figure: (abstract: THU-167).

THU-168

Results of the hepatitis B and C screening within the “Check-Up 35+” in the German primary care setting one year after implementation by the federal joint committee

Olaf Bätz¹, David Petroff², Anna Joachim-Richter¹, Katrin Jedrysiak¹, Ingmar Wolfram³, Thomas Berg⁴, Jan Kramer¹, Johannes Wiegand⁴.

¹LADR Laboratory Group Dr Kramer and Colleagues, Germany;

²University of Leipzig, Clinical Trial Center, Germany; ³General Practitioner Paderborn, Germany; ⁴University of Leipzig, Division of Hepatology, Germany

Email: johannes.wiegand@medizin.uni-leipzig.de

Background and aims: The World Health Organization proposed a strategy to eliminate chronic hepatitis C virus (HCV) infection by the year 2030, which was adapted with the BIS2030 program in Germany. One part of this program is adequate screening for hepatitis B virus (HBV) and HCV infection. Therefore, the Federal Joint Committee decided to include a hepatitis B and C screening in the preventive medical examination named “Check-Up 35+,” which is performed in patients of at least 35 years at the primary care level. We investigated the results one year after implementation of the structured screening program.

Method: Analysis of the database of the LADR laboratory group which covers 11 ambulatory health care centers. HBsAg and anti-HCV screenings were identified by the billing categories GOP 01865. The codes GOP 01866 and 01867 were used for HBV-DNA and HCV-RNA (PCR) results in case of positive HBsAg and anti-HCV screening tests.

Results: Between 01 October 2021 and 30 September 2022, 286, 192 laboratory requisitions were analyzed (56% females, median (SD) age 61.2 (14.0) years). HBsAg and anti-HCV prevalence were 0.54% and 0.78%, respectively. 73% of HBsAg positive patients were HBV-DNA positive (prevalence of HBV-DNA: 0.39% (total), 0.48% (male), 0.33% (female)), 16% of anti-HCV positive cases were HCV-RNA positive (HCV-RNA prevalence 0.13% (total), 0.15% (male), 0.11% (female)).

Age and sex specific prevalences of HBsAg, HBV-DNA, anti-HCV, and HCV-RNA are provided in the figure. The highest HCV-RNA prevalence was observed in young men and was 2.4–3 times higher than in young women.

Conclusion: A structured hepatitis screening program at the primary care level could be successfully established and leads to a large number of tests within the first year of implementation.

Age category (years)	HBsAg		HBV DNA		Anti-HCV		HCV-RNA	
	Male (%)	Female (%)	Male (%)	Female (%)	Male (%)	Female (%)	Male (%)	Female (%)
35-44	1.00	0.66	0.86	0.52	1.11	0.58	0.24	0.08
45-54	0.88	0.55	0.66	0.43	1.19	0.70	0.24	0.10
55-64	0.61	0.43	0.45	0.30	1.00	0.76	0.14	0.10
65-74	0.55	0.47	0.36	0.33	0.73	0.67	0.09	0.10
75-84	0.26	0.32	0.16	0.17	0.53	0.64	0.10	0.11
>84	0.17	0.21	0.07	0.11	0.46	0.77	0.04	0.21

Figure: (abstract: THU-168): Prevalence of HBsAg, HBV-DNA, anti-HCV, and HCV-RNA.

THU-169

Clinical outcomes after therapy with direct acting antiviral in patients with HCV-related B-cell Non-Hodgkin lymphomas and/or mixed cryoglobulinemia

Marco Tizzani¹, Roberta Lasco¹, Rosa Claudia Stasio¹, Elisabetta Bretto¹, Yulia Troshina^{1,2}, Giacomo Scaioli³, Fabrizia Pittaluga⁴, Giorgio Maria Saracco^{1,2}, Alessia Ciano^{1,2}. ¹S.C. Gastroenterology U-A.O.U. Città della Salute e della Scienza, Turin, Italy; ²Department of Medical Sciences, University of Turin, Italy; ³Department of public health sciences and pediatrics, University of Turin, Italy; ⁴S.C. Microbiology and virology-AOU Città della Salute e della Scienza, Turin, Italy
Email: marco.tizzani91@gmail.com

Background and aims: Extrahepatic manifestations have always been a difficult-to-manage problem, complicating clinical outcome of Hepatitis C virus (HCV)-infected patients. Direct acting antivirals (DAAs) have significantly changed the history of HCV infection, inducing high rates of sustained virologic response (SVR). The aim of this study is to evaluate the outcomes of patients affected by mixed cryoglobulinemia (MC) and/or B-cell Non-Hodgkin Lymphomas (B-NHL) and HCV after eradication with DAAs.

Method: Virological and haematological end points have been analyzed in 151 patients (62 Male/89 Female, mean age 70.4 (± 13.1)) with MC and/or B-NHL treated with DAAs between February 2015 and March 2022 at 3 months (T1), 6 months (T2) and at their most recent hepatologic/haematologic examination (T3) after SVR12. HCV genotype 1a has been found in 8.2% of patients, 1b in 51.4%, 2 in 27.4%, 3 in 9.6%, 4 in 2.7%, 5 in 0.7%. Ninety-five patients were naive, 34 non-responder and 22 relapser to INF-based therapy. Fifty patients were cirrhotic (33.8%). Symptomatic MC (neuropathy, nephropathy, vasculitis) was present in 57 out of 88 (64.7%) patients and in 13 of them MC was associated with a B-NHL, while asymptomatic MC was present in 31 patients (35.2%). Seventy-three patients had B-NHL: diffuse large B-cell (21), marginal zone (13), follicular (9), mantle (1), others were indolent B cell-NHL not otherwise specified.

Results: SVR12 has been obtained in all 151 patients (100%). Preliminary data showed that, among patients with symptomatic MC, 17 (29.8%) at T1, 16 (28%) at T2 and 26 (45%) at T3 had improvement and/or remission from clinical symptoms, with higher rate among vasculitis symptoms. Cryoglobulines resulted undetectable in 10 (11%), 14 (16%) and 38 (43%) patients at T1, T2 and T3 respectively. Five patients (8.7%), instead, had worsening of symptoms at T3. Among patients with B-NHL, 5 patients had disease progression and 2 of them died during follow-up because of haematological complications, 39 (54.9%) had or stayed in complete remission at T2, while the others had partial haematological regression or disease stability.

Conclusion: HCV eradication with DAAs is safe in patients with MCs and/or B-NHL, and it is associated with clinical improvement and haematological response or stability. Data collection is still ongoing in order to evaluate longer term outcomes.

THU-170

Analysis of mortality rate in the patients after hepatitis C virus elimination using direct acting antivirals and comparison with the general population

Satoshi Miuma¹, Hisamitsu Miyaaki¹, Naota Taura¹, Yasuhiko Nakao¹, Masanori Fukushima¹, Ryu Sasaki¹, Tatsuki Ichikawa², Kazuhiko Nakao¹. ¹Nagasaki university hospital, Department of Gastroenterology and Hepatology, Japan; ²Nagasaki Harbor Medical Center, Department of Gastroenterology, Japan
Email: miuma1002@gmail.com

Background and aims: Direct acting antivirals (DAAs) therapy has enabled the achievement of sustained virologic response (SVR) in many patients with chronic hepatitis C and cirrhosis (post-SVR patients). There have been many studies on the outcomes of post-SVR patients treated with interferon (IFN)-based therapy. However, the outcomes of post-SVR patients treated with DAAs therapy may be different, because patients may be intolerant and refractory to IFN-based therapy, such as older patients and those with liver cirrhosis. In this study, we analyzed the mortality rate and cause of death in post-

Figure 1. Evolution of lymphoma after HCV eradication during the follow up.

T3, three months of follow up; T6, six months of follow up; TL, last follow up; CR, complete disease remission; PR, partial disease remission; S, stable disease; W, disease worsening; DR, disease recurrence; HCV, hepatitis C virus

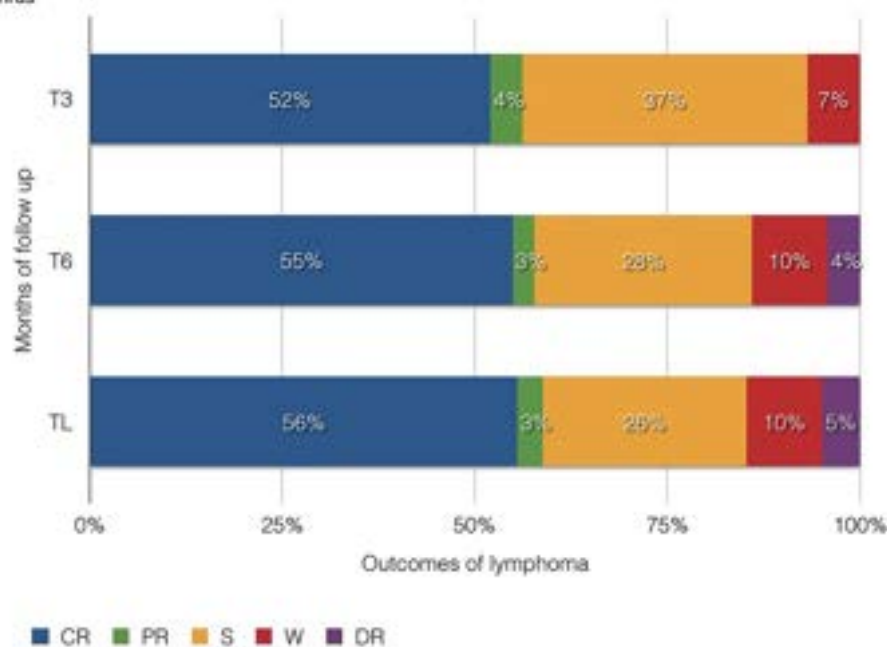


Figure: (abstract: THU-169).

POSTER PRESENTATIONS

SVR patients treated with DAAs therapy. Additionally, the mortality rates were compared with those of the general population.

Method: This was a multicenter retrospective cohort study. A total of 1,682 patients were introduced to DAAs therapy at 15 institutions between September 2014 and December 2020. After excluding those with non-SVR, decompensated liver cirrhosis, previous hepatocellular carcinoma (HCC) treatment history, liver transplantation, and loss to follow-up, 1,298 post-SVR patients were enrolled in this study. The mortality rate after SVR was examined, and the factors contributing to unfavorable outcomes were analyzed using the Cox proportional hazard model. The mortality rates between post-SVR patients and the general population were compared by calculating the standardized mortality ratio (SMR) adjusted for age and sex (referring to the Population Survey Report vital statistics in 2020, reported by the Minister of Health, Labour and Welfare in Japan).

Results: The median age of study participants at DAAs induction was 68 years (555 males and 743 females), and the proportion of patients with cirrhosis was 17.8%. The mortality rate was 12.8 per 1,000 person-years (3-year survival rate, 96.4%; 5-year survival rate, 93.5%). Forty-nine post-SVR patients died during the observation period. Among these, non-liver-related deaths were the most predominant, accounting for 71.4% (35/49), of which malignant neoplasms accounted for the highest proportion of deaths (57.1%, 20/35). The Cox proportional hazards analysis showed that old age was the only factor at DAAs induction contributing to unfavorable outcomes in post-SVR patients (risk ratio = 1.095, $p < 0.001$). Compared with the general population adjusted for sex and age, the SMR for overall mortality in post-SVR patients was 92.8. Additionally, the SMR for malignant neoplasm mortality in post-SVR patients was 118.6; however, the SMR for malignant neoplasm mortality other than HCC was 103.6. These results suggest that the overall mortality rate is lower in post-SVR patients than in the general population and that the malignant neoplasm mortality rate is almost the same between them.

Conclusion: In this study, we found that outcomes of post-SVR patients were favorable, affected only by old age, and were better than those of the general population. Although malignant neoplasms resulted in the highest proportion of non-liver-related deaths, the comparison of mortality rates adjusted for sex and age showed that the malignant neoplasm mortality in post-SVR patients was almost equal to that of the general population.

THU-171

Impact of direct-acting antiviral therapy on survival in patients with liver cirrhosis and ascites. Data from the hepa-C registry

Álvaro Hidalgo Romero¹, Sabela Lens², Beatriz Mateos Muñoz³, María Teresa Ferrer⁴, Marta Hernandez Conde⁵, Manuel Rodríguez⁶, Jose Castellote⁷, Joaquín Cabezas⁸, Jordi Llaneras⁹, Sonia Alonso¹⁰, Jose María Moreno Planas¹¹, José Antonio Carrión¹², Xavier Torras¹³, Esther Badia-Aranda¹⁴, Esther Molina¹⁵, Mercedes Serrano¹⁶, Juan Turnes¹⁷, Paula Fernandez Alvarez¹⁸, Manuel Hernández Guerra¹⁹, Olga Hernandez¹, Pablo Bellot Garcia²⁰, Inmaculada Fernández Vázquez¹. ¹12 de Octubre University Hospital, Hepatology Unit, Digestive System Department, Madrid, Spain; ²Department of Hepatology, Clinic Hospital Barcelona, Spain; ³Department Digestive System, Ramón y Cajal University Hospital, Madrid, Spain; ⁴Clinical Management Unit of the Digestive System, Virgen del Rocío University Hospital, Sevilla, Spain; ⁵Digestive System Department, Puerta de Hierro University Hospital, Madrid, Spain; ⁶Hepatology Unit, Digestive System Department, Asturias Central University Hospital, Spain; ⁷Bellvitge University Hospital, Barcelona, Spain; ⁸Gastroenterology and Hepatology Department, Marqués de

Valdecilla University Hospital, Santander, Spain; ⁹Hepatology Unit, Vall d'Hebron Hospital, Barcelona, Spain; ¹⁰Hepatology Unit, Digestive System Department, Gregorio Marañón University Hospital, Madrid, Spain; ¹¹Digestive System Department, Albacete University Hospital Complex, Spain; ¹²Digestive System Department, Del Mar Hospital, Barcelona, Spain; ¹³Department of Digestive System, Sant Pau University Hospital, Barcelona, Spain; ¹⁴Digestive System Department, Burgos University Hospital, Spain; ¹⁵Digestive System Department, Santiago de Compostela University Hospital, Spain; ¹⁶Department of Digestive System, Hospital of Valme, Sevilla, Spain; ¹⁷Digestive System Department, Pontevedra University Hospital Complex, Spain; ¹⁸Digestive System Department, Virgen de la Macarena University Hospital Complex, Spain; ¹⁹Digestive System Department, Canarias University Hospital, Spain; ²⁰Digestive System Department, Alicante General University Hospital, Spain

Email: alvarohr90@gmail.com

Background and aims: Direct-acting antivirals (DAAs) have changed the natural history of disease in patients with compensated HCV cirrhosis. However, we do not know the long-term impact on liver function and survival in patients with decompensated cirrhosis. Our aim was to evaluate the long-term benefits of DAAs in patients with cirrhosis and ascites.

Method: Observational, multicentre and retrospective study including patients with HCV cirrhosis and ascites, prior or concurrent to treatment with DAAs, who started therapy between 2014–November 2018. We assessed liver function parameters, survival and need for transplantation at 5 years of follow-up. STATA software was used for the analysis, with Cox regression for categorical variables and survival analysis using Kaplan-Meier and log-rank test.

Results: 289 patients were included, 274 (94.8%) with a history of ascites and 132 (45.7%) with ascites at baseline. Mean age was 56 years (50–66), 64% male. Liver function: 144 (49%) Child A and 128 (44%) Child B, mean MELD 11.8 (9–14). Overall survival at 5 years was 77.8%, with negative predictive factors being hypoalbuminaemia ($p: 0.048$) and advanced age ($p: 0.001$). Overall, 43 patients (15%) received a liver transplant. The 5-year transplant-free survival was 84.9%, with hyperbilirubinaemia ($p: 0.000$), MELD ($p: 0.006$) and Child-Pugh classification ($p: 0.000$) being negative predictors. There was a long-term reduction of 2 points in Child ($p < 0.001$), with improvement in bilirubin ($p < 0.001$) and albumin ($p < 0.001$).

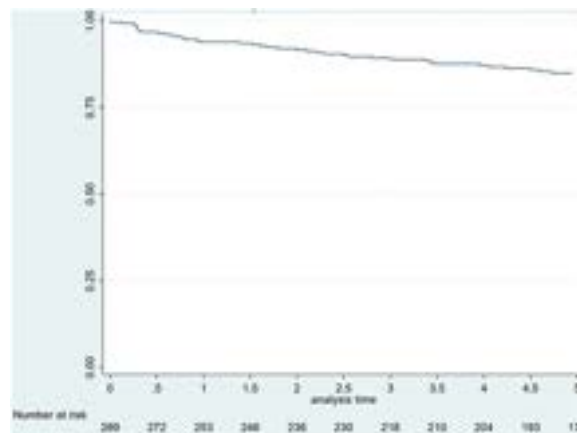


Figure: Transplant-free survival.

Conclusion: Treatment with DAA improves long-term liver function parameters even in patients with ascites, making survival at 5-year follow-up of these patients high compared to that expected based on the natural history of hepatitis C without treatment.

THU-172

HCV elimination: reengagement of previously diagnosed but unlinked patients with chronic hepatitis C to initiate treatment

Maria Guerra Veloz¹, Kate Childs², Teresa Bowyer¹, Kathryn Oakes¹, Esra Derin¹, Claire Mannion¹, Mary D Cannon¹, Geoffrey Dusheiko¹, Kosh Agarwal¹. ¹King's College Hospital, Institute of Liver Studies, London, United Kingdom; ²King's College Hospital, Sexual Health and HIV, United Kingdom

Email: maria.guerraveloz@nhs.net

Background and aims: Hepatitis C elimination requires multiple complex approaches in groups with high-risk factors. Identifying patients with known chronic hepatitis C virus (HCV) infection who have not engaged with the health care system and not been successfully cured has proved to be an effective strategy in many different countries. *The aim of this project was to identify viraemic HCV-infected patients who have been lost in the HCV test and treat care cascade in South-East London, and link them to care.*

Method: All laboratory-positive HCV RNA tests from 2010 to 2020, (but with undocumented SVR status in either the National Hepatitis C registry or the local Kings College Hospital viral hepatitis laboratory data) were included. *In the first phase, each HCV RNA test result was linked with national primary care medical records or with the relevant local London hospital record in order to identify whether or not the HCV care cascade was completed.* In the second phase, subjects who remained without known SVR status were contacted by telephone a maximum of 5 times on different days/months (with voicemails being left) before being sent an appointment reminder by post when contact by telephone was unsuccessful. Subjects were referred to a one-stop clinic at King's, their local viral hepatitis team, or their local outreach service, according to the subject's preference and address.

After treatment, an SVR was confirmed 12 weeks after the end of the treatment.

Results: 1,254 HCV RNA-positive tests (from viraemic patients) with unknown SVR status were included. After reviewing their medical records, 446 subject had not completed the HCV care cascade, and so were eligible for recall. 192/446 individuals were located and 86% (166/192) accepted relevant information and were linked with medical care. 108/166 (65%) initiated direct acting antiviral treatment; 96/108 (89%) completed treatment and 40/96 (42%) attended a post treatment appointment to confirm a SVR. At the end of the project SVR was achieved in 26/40, i.e. 65% of those who attended the SVR appointment or 24% (26/108) of those who initiated treatment (Figure 1).

Conclusion: This simple administrative exercise identified 1,254 HCV viraemic patients and used staff resources already present within the team. Large-scale testing projects are logistically challenging but seldom identify more than a small number of viraemic patients whereas our project proved to be more effective as it identified over 30% of viraemic patients who were previously tested but not linked with treatment. Initiation and treatment completion were high in this project however, there is still a high proportion of non-attendance to confirm HCV cure. This could mean that the treatment initiation rate could be a sensible goal in populations who it is difficult to engage with the system.

Acknowledgements: the authors want to thank the multidisciplinary team involved in this project especially the administrative team, data manager and viral clinical nurse specialists at Kings College Hospital for all of their assistance and efforts to enable the project to be concluded in an efficient manner.

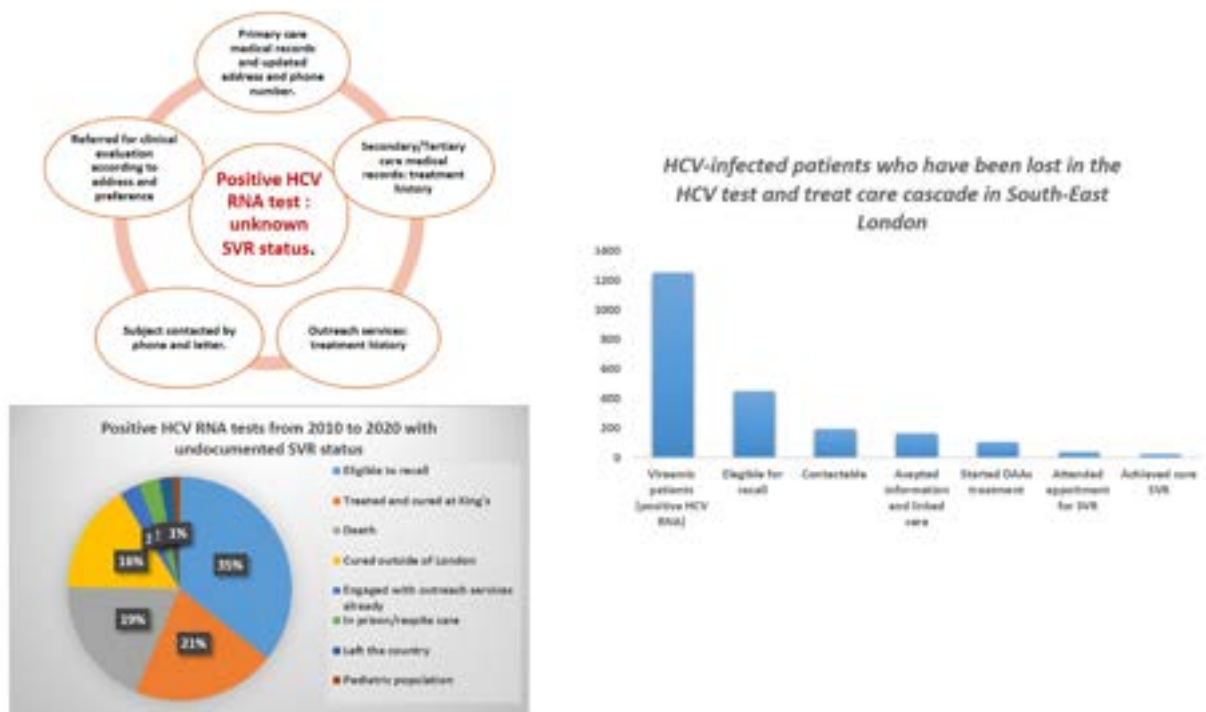


Figure 1: a) Diagram of the project design. b) Positive HCV RNA test and their updated SVR status after the project. c) Hepatitis C care cascade in those who were recall during the project.

Figure 1: (abstract: THU-172).

POSTER PRESENTATIONS

THU-173

HCV screening rates in reproductive age women after universal screening guidelines

Roshni Singh¹, Breanne Biondi², Rachel Epstein^{3,4}, Benjamin Linas⁴.
¹Boston Medical Center, Department of Medicine, United States; ²Boston University School of Public Health, Department of Health Law, Policy and Management, United States; ³Boston University School of Medicine, Department of Pediatrics, Section of Infectious Disease, United States; ⁴Boston University School of Medicine, Department of Medicine, Section of Infectious Disease, United States
 Email: roshni.singh@bmc.org

Background and aims: In 2020, the US Preventative Services Task Force (USPSTF) and the US Centers for Disease Control and Prevention (CDC) recommended screening all asymptomatic adults, including pregnant persons, for hepatitis C virus (HCV) at least once in their lifetime (by CDC guidelines, only if local HCV prevalence is $\geq 0.1\%$ and also during each pregnancy). Yet few studies describe changes in HCV screening since these recommendations, which occurred at the onset of the COVID-19 pandemic. This study aims to compare HCV screening occurring in women with and without a recent pregnancy, before and after the 2020 CDC/USPSTF guidelines.

Method: Using TriNetX, a national electronic medical records database, we calculated HCV screening rates from 2014 to 2022 in 6-month intervals for females of reproductive age (15–44 years old) with and without an encounter for a delivery (ICD10 codes O80–O82) over the study. We counted one HCV antibody test per women, and censored follow-up at the time of the first HCV screening. We compared the change in HCV screening rates between the two groups before and after the universal screening guidelines using a difference-in-differences model with a 6-month washout period (January–June 2020) to account for the onset of the COVID-19 pandemic and publication and dissemination of the revised guidelines. We used year fixed effects and robust standard errors.

Results: Of 17,799,141 females 15–44 years old with a visit at a TriNetX US Collaborative Network health care organization between 2014 and 2022, 704,929 had an encounter for a delivery during that period. The HCV screening rate increased for all women over the study period, but more steeply for those with a recent delivery: from 7.3 screens/1000 person years (PY) in 2014 to 126 screens/1000 PY in 2022 for women without a delivery and from 22.7 to 237 screens/1000 PY for women with a delivery. After the 2020 guidelines, women with a delivery had a 59% increase in HCV screening rate

compared to those without a delivery (95% CI 31–88%, $p < 0.001$; Figure).

Conclusion: Despite interruptions of the COVID-19 pandemic, HCV testing has increased among reproductive age women since the 2020 CDC/USPSTF universal screening recommendations, with a significantly higher increase among women experiencing a recent delivery. These data highlight that pregnancy is a valuable time to capture individuals for healthcare interventions and suggest that perinatal care could be a key venue to test and treat to achieve national HCV elimination goals

THU-174

The impact of HCV cure on glycemic indices in patients using glecaprevir/pibrentasvir from nationwide Taiwan HCV registry

Chung-Feng Huang¹, Hsing-Tao Kuo², Te-Sheng Chang³, Ching-Chu Lo⁴, Chao-Hung Hung³, Chien-Wei Huang⁵, Lee-Won Chong^{6,7}, Pin-Nan Cheng⁸, Ming-Lun Yeh^{1,9}, Cheng-Yuan Peng^{10,11}, Chien-Yu Cheng¹², Jee-Fu Huang^{1,13}, Ming-Jong Bair^{14,15}, Chih-Lang Lin¹⁶, Chi-Chieh Yang¹⁷, Sih-Ren Wang¹⁸, Tsai-Yuan Hsieh¹⁹, Tzong-Hsi Lee²⁰, Pei-Lun Lee²¹, Wen-Chih Wu²², Chih-Lin Lin²³, Wei-Wen Su²⁴, Shengshun Yang²⁵, Chia-Chi Wang²⁶, Jui-Ting Hu²⁷, Lien-Juei Mou²⁸, Chun-Ting Chen^{19,29}, Yi-Hsiang Huang^{30,31}, Chun-Chao Chang^{32,33}, Jia-Sheng Huang³⁴, Guei-Ying Chen³⁵, Jian-Neng Gao³⁶, Chi-Ming Tai^{37,38}, Chun-Jen Liu³⁹, Mei-Hsuan Lee⁴⁰, Pei-Chien Tsai¹, Chia-Yen Dai¹, Jia-Horng Kao³⁹, Han-Chieh Lin^{30,31}, Wan-Long Chuang¹, Chiyi Chen⁴¹, Kuo-Chih Tseng^{42,43}, Ming-Lung Yu¹.
¹Hepatobiliary Division, Department of Internal Medicine and Hepatitis Center, Kaohsiung Medical University Hospital, Kaohsiung Medical University, Kaohsiung, Taiwan; ²Division of Gastroenterology and Hepatology, Department of Internal Medicine, Chi Mei Medical Center, Yongkang District, Tainan, Taiwan; ³Division of Hepatogastroenterology, Department of Internal Medicine, ChiaYi Chang Gung Memorial Hospital and College of Medicine, Chang Gung University, Taoyuan, Taiwan; ⁴Division of Gastroenterology, Department of Internal Medicine, St. Martin De Porres Hospital, Chiayi, Taiwan; ⁵Division of Gastroenterology, Kaohsiung Armed Forces General Hospital, Kaohsiung, Taiwan; ⁶Division of Hepatology and Gastroenterology, Department of Internal Medicine, Shin Kong Wu Ho-Su Memorial Hospital, Taipei, Taiwan; ⁷School of Medicine, Fu-Jen Catholic University, New Taipei City, Taiwan; ⁸Division of Gastroenterology and Hepatology, Department of Internal Medicine, National Cheng Kung University Hospital, College of Medicine, National Cheng Kung University, Tainan, Taiwan; ⁹Department of Internal Medicine, Kaohsiung Municipal

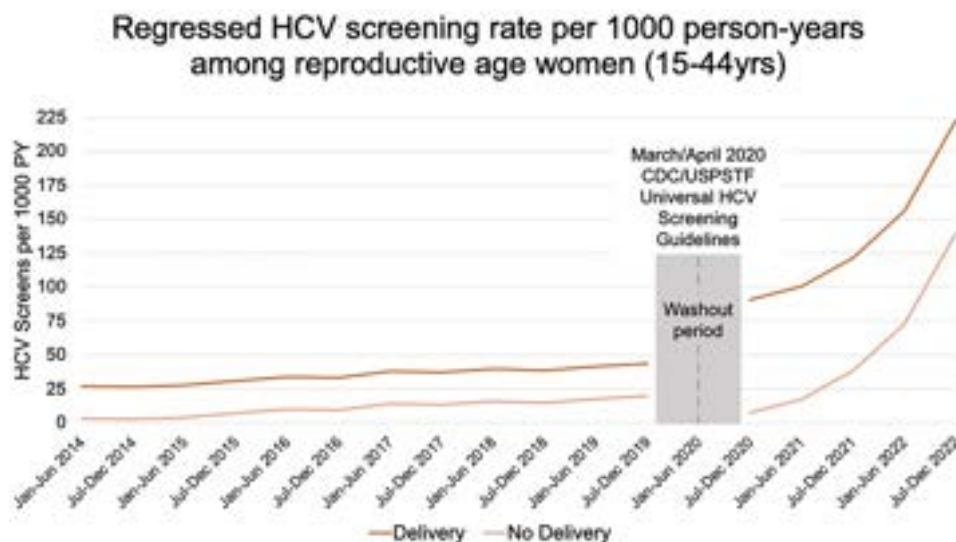


Figure: (abstract: THU-173).

Siaogang Hospital, Kaohsiung Medical University Hospital, Kaohsiung Medical University, Kaohsiung, Taiwan; ¹⁰Center for Digestive Medicine, Department of Internal Medicine, China Medical University Hospital, Taichung, Taiwan; ¹¹School of Medicine, China Medical University, Taichung, Taiwan; ¹²Division of Infectious Diseases, Department of Internal Medicine, Taoyuan General Hospital, Ministry of Health and Welfare, Taoyuan, Taiwan; ¹³Department of Internal Medicine, Kaohsiung Municipal Ta-Tung Hospital, Kaohsiung Medical University Hospital, Kaohsiung Medical University, Kaohsiung, Taiwan; ¹⁴Division of Gastroenterology, Department of Internal Medicine, Taitung Mackay Memorial Hospital, Taitung, Taiwan; ¹⁵Mackay Medical College, New Taipei City, Taiwan; ¹⁶Liver Research Unit, Department of Hepato-Gastroenterology and Community Medicine Research Center, Chang Gung Memorial Hospital at Keelung, College of Medicine, Chang Gung University, Keelung, Taiwan; ¹⁷Department of Gastroenterology, Division of Internal Medicine, Show Chwan Memorial Hospital, Changhua, Taiwan; ¹⁸Division of Gastroenterology, Department of Internal Medicine, Yuan's General Hospital, Kaohsiung, Taiwan; ¹⁹Division of Gastroenterology, Department of Internal Medicine, Tri-Service General Hospital, National Defense Medical Center, Taipei, Taiwan; ²⁰Division of Gastroenterology and Hepatology, Far Eastern Memorial Hospital, New Taipei City, Taiwan; ²¹Division of Gastroenterology and Hepatology, Department of Internal Medicine, Chi Mei Medical Center, Liouying, Tainan, Taiwan; ²²Wen-Chih Wu Clinic, Fengshan, Kaohsiung, Taiwan; ²³Department of Gastroenterology, Renai Branch, Taipei City Hospital, Taipei, Taiwan; ²⁴Department of Gastroenterology and Hepatology, Changhua Christian Hospital, Changhua, Taiwan; ²⁵Division of Gastroenterology and Hepatology, Department of Internal Medicine, Taichung Veterans General Hospital, Taichung, Taiwan; ²⁶Taipei Tzu Chi Hospital, Buddhist Tzu Chi Medical Foundation and School of Medicine, Tzu Chi University, Taipei, Taiwan; ²⁷Liver Center, Cathay General Hospital, Taipei, Taiwan; ²⁸Division of Gastroenterology, Tainan Municipal Hospital (Managed By Show Chwan Medical Care Corporation), Tainan, Taiwan; ²⁹Division of Gastroenterology, Department of Internal Medicine Tri-Service General Hospital Penghu Branch, National Defense Medical Center, Taipei, Taiwan; ³⁰Division of Gastroenterology and Hepatology, Department of Medicine, Taipei Veterans General Hospital, Taipei, Taiwan; ³¹Institute of Clinical Medicine, School of Medicine, National Yang-Ming Chiao Tung University, Taipei, Taiwan; ³²Division of Gastroenterology and Hepatology, Department of Internal Medicine, Taipei Medical University Hospital, Taipei, Taiwan; ³³Division of Gastroenterology and Hepatology, Department of Internal Medicine, School of Medicine, College of Medicine, Taipei Medical University, Taipei, Taiwan; ³⁴Yang Ming Hospital, Chiayi, Taiwan; ³⁵Penghu Hospital, Ministry of Health and Welfare, Penghu, Taiwan; ³⁶National Taiwan University Hospital

Hsin-Chu Branch, Hsinchu, Taiwan; ³⁷Department of Internal Medicine, E-Da Hospital, Kaohsiung, Taiwan; ³⁸School of Medicine, College of Medicine, I-Shou University, Kaohsiung, Taiwan; ³⁹Hepatitis Research Center and Department of Internal Medicine, National Taiwan University Hospital, Taipei, Taiwan; ⁴⁰Institute of Clinical Medicine, National Yang-Ming Chiao Tung University, Taipei, Taiwan; ⁴¹Division of Gastroenterology and Hepatology, Department of Medicine, Dittmanson Medical Foundation Chiayi Christian Hospital, Chiayi, Taiwan; ⁴²Department of Internal Medicine, Dalin Tzu Chi Hospital, Buddhist Tzu Chi Medical Foundation, Chiayi, Taiwan; ⁴³School of Medicine, Tzuchi University, Hualien, Taiwan
Email: fish6069@gmail.com

Background and aims: Hepatitis C virus (HCV) infection impairs insulin signalling and increases the risk of type 2 diabetes mellitus (T2DM). Several studies have shown that the benefits of HCV cure using direct-acting antivirals (DAAs) might improve glycemic indices in chronic hepatitis C (CHC) patients. To further validate the data in the real-world setting, this study aimed to measure the effect of HCV cure by glecaprevir/pibrentasvir (G/P) on glucose parameters in diabetes and non-diabetes patients between baseline and at the time of assessment of sustained virological response at 12 weeks (SVR12) after end of treatment in TASL HCV Registry (TACR).

Method: The TACR is an ongoing nationwide registry program organized and supervised by Taiwan Association for the Study of the Liver (TASL), which aims to setup a database and biobank of patients with CHC in Taiwan. Data was analyzed as of 30 September 2022 for CHC patients treated with G/P. The definition of diabetes are patients documented with diabetes and treated with oral hypoglycemic agents and/or insulin or fulfilled the criteria of fasting plasma glucose (FPG) ≥ 126 (mg/dl) or glycosylated hemoglobin A1C (HbA1c) $> 6.5\%$. In this analysis, the laboratory changes for diabetes and non-diabetes patients, including glycemic and liver-related parameters, which were measured in diabetes and non-diabetes patients between baseline and at SVR12 are presented.

Results: Of the 7,520 patients achieving SVR with G/P, 1,171 were diabetes patients and 6,349 were non-diabetes patients. Overall, the HbA1c (N = 1,473, 6.0 ± 1.3 vs 5.9 ± 1.0 , $p < 0.001$) demonstrated a significant decrease at SVR12 compared to their baseline level. However, the FPG (N = 1,375, 112.0 ± 39.6 vs 112.2 ± 40.3 , $p = 0.461$) did not show the significance. For diabetes patients, the HbA1c (N = 582, $7.4 \pm 1.7\%$ vs $7.0 \pm 1.3\%$, $p < 0.001$) and FPG (N = 513, 148.7 ± 66.7 mg/dL vs 141.0 ± 59.0 mg/dL, $p = 0.017$) at SVR12 decreased significantly compared to their baseline level. For non-diabetes patients, the HbA1c (N = 1,806, $5.6 \pm 0.7\%$ vs $5.5 \pm 0.5\%$, $p = 0.005$) at SVR12 showed a significant improvement compared to their baseline level. However, the FPG did not change significantly (N = 1,713, 100.1

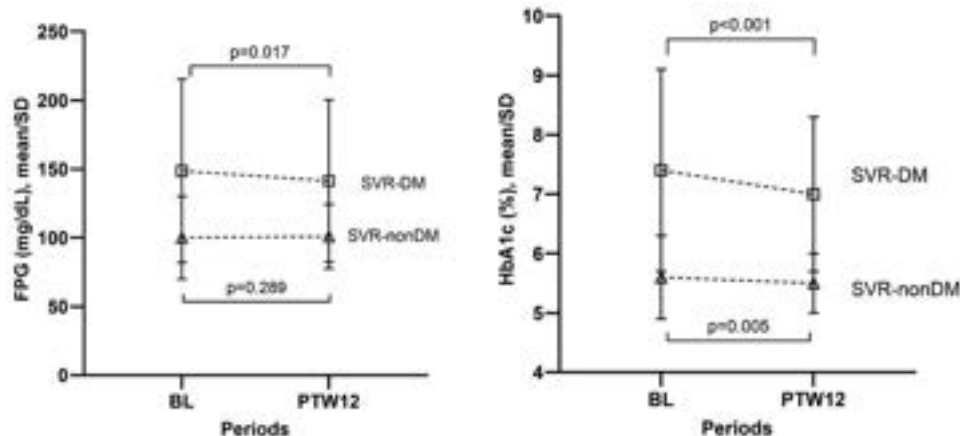


Figure: (abstract: THU-174): Changes in glycemic parameters FPG, HbA1c at baseline (BL) and post-treatment follow-up at week 12 (PTW12) in all SVR, SVR-DM and SVR-nonDM patients using G/P.

POSTER PRESENTATIONS

± 30.1 mg/dL vs 101.0 ± 23.4 mg/dL, $p = 0.289$). The other laboratory data, including AST, ALT, Albumin, Platelet counts, FIB-4, GGT, and creatinine, showed a significant improvement after HCV cure compared to baseline for diabetes and non-diabetes patients.

Conclusion: In this real-world cohort, HCV cure by G/P therapy significantly improved short-term glycemic control in Taiwanese CHC patients.

THU-175

Predicting vertical transmission of hepatitis C in pregnant women using a composite score: a multicenter study

Paul Wasuwanich¹, Joshua So¹, Brett Presnell², Robert Egerman³, Tony Wen³, Wikrom Karnsakul⁴, ¹University of Florida College of Medicine, Gainesville, United States; ²University of Florida, Department of Statistics, Gainesville, United States; ³University of Florida College of Medicine, Division of Maternal-Fetal Medicine, Department of Obstetrics and Gynecology, Gainesville, United States; ⁴The Johns Hopkins University School of Medicine, Division of Pediatric Gastroenterology, Hepatology, and Nutrition, Department of Pediatrics, Baltimore, United States

Email: p.wasuwanich@ufl.edu

Background and aims: Prevention of vertical transmission of hepatitis C virus (HCV) presents an obstetric challenge. We aimed to create a composite score to accurately isolate a population of pregnant women with HCV who will have a high rate of vertical transmission.

Method: In a retrospective, multicenter, cohort study, we identified pregnant women with hepatitis C with linked data to their infants who have had HCV RNA or HCV antibody testing. Demographic data including age and race/ethnicity as well as clinical and laboratory data including tobacco/alcohol history, infection history, liver function tests, HCV RNA titer, HCV antibody, HCV genotype, absolute lymphocyte count, and platelet count were collected. Data were analyzed by logistic regression and receiver operating characteristic (ROC).

Results: We identified 157 pregnant women and 163 corresponding infants. The median maternal delivery age was 29 (IQR: 25–33) years, and the majority (141, or 89.8%) were White. Higher HCV RNA titer (OR = 5.18; 95% CI = 1.95–17.00; $p < 0.001$), higher absolute lymphocyte count (OR = 3.74; 95% CI = 1.24–12.70; $p = 0.020$), and higher platelet count (OR = 2.42; 95% CI = 1.07–5.70; $p = 0.034$) were associated with vertical transmission. Alcohol or tobacco use during pregnancy, diabetes, high BMI, vaginal bleeding, placental previa, history of abnormal pap smear, history of chlamydia/gonorrhea infection, previous cesarean section, ABO blood type, Rh type, white blood cell count, absolute monocyte count, albumin, alanine aminotransferase, aspartate aminotransferase, alkaline phosphatase, total bilirubin, direct bilirubin, HCV genotype, hepatitis B virus infection, HIV infection, and herpes simplex infection were not associated with HCV vertical transmission ($p > 0.05$). A composite score combining the three significant risk factors had an AUROC of 0.902 (95% CI = 0.840–0.964), superior to any of the three risk factors individually. The sensitivity, specificity, and positive predictive value, and negative predictive value were 100.0%, 85.24%, and 40.9%, and 100.0% respectively.

Conclusion: A composite score combining risk factors HCV vertical transmission can isolate a population of pregnant women where the

rate of vertical transmission is high, allowing for potential interventions during antepartum or intrapartum care. The risk-benefit analysis of using antiviral treatment during pregnancy could be determined in selective group of pregnant women with higher probabilities of transmitting HCV to the fetus. Further investigation with larger cohort will be needed to refine the composite score and validate its components.

THU-176

Achieving hepatitis C micro-eliminating in 4 female prisons through a nurse led test and treat approach of pathway optimisation and whole prison testing

Nichola Royal¹, Arran Ludlow-Rhodes¹, Julie Henderson¹, Rob Cheetham¹, Julia Sheehan², Andrew Milner³, Louise Missen³, Andrew Jones³, ¹Practice Plus Group, Health In Justice, Reading, United Kingdom; ²Hepatitis C Trust, London, United Kingdom; ³Gilead Sciences Ltd, Medical, London, United Kingdom

Email: andy.jones@gilead.com

Background and aims: Drug dependence among incarcerated women has been found to be higher than men which correlates to the higher HCV prevalence observed in female prisons. Women only represent approximately 5% of the prison population in England and Wales but research shows they typically enter prison with more acute mental health and substance misuse profiles requiring services to be adapted to their needs. Prisons are an important setting for National Health Service England's plans to eliminate Hepatitis C (HCV) in England by 2025, both in terms of diagnosis and treatment and in understanding prevalence.

Method: In May 2019, a partnership between Gilead Sciences, Practice Plus Group (PPG) and the Hepatitis C Trust (HCT) was formed with the aim of eliminating HCV by 2024 in PPG prisons. This partnership included 4 female prisons where the healthcare was provided by PPG. Regional BBV Lead Nurses, Gilead Medical Scientists and HCT peers worked with prison and HCV stakeholders to optimise test and treat pathways for new prison admissions. HCT peers engaged with staff and residents with the aim of raising awareness and reducing stigma. In the first quarter of 2020, whole prison HCV Intensive Test and Treat events (HITTs) were run in all 4 prisons to ensure testing of residents who were incarcerated before these optimisations were implemented.

Results: In January 2019, 24% of women were screened for HCV within the first 7 days of admission compared to 91% in December 2022, a 279% increase. HITTs were run in February and March of 2020 where 1,096 (98.3%) of the total 1,115 population were tested, with 37 residents being diagnosed as HCV RNA+ and 34 being initiated on DAA therapy. In the final 3 months of 2022, the network of prisons achieved the micro-elimination target of $\geq 95\%$ of residents having been tested in the previous 12 months and $\geq 90\%$ of diagnosed patients having been initiated on treatment with results being 95% and 97% respectively.

RNA prevalence observed in new prison admissions has reduced from 9.1% in quarter 1 of 2019 to 3.5% in quarter 2 of 2022 (figure 1), a 62% reduction despite antibody rates increasing from 12.6% to 14.6 from 2019 to 2022.

Conclusion: Test and treatment optimisation in combination with whole prisons testing has demonstrated that it is feasible to effectively micro-eliminate HCV in this high-risk population. The

Table: (abstract: THU-175): (abstract: THU-175): AUROC with sensitivity and specificity of significant risk factors for hepatitis C vertical transmission and the resulting composite score.

Scoring System	AUROC Curve (95% CI)	Standard Error	Optimized Cutoff	Sensitivity	Specificity
HCV Titer (Log IU/ml)	0.815 (0.730–0.899)	0.043	≥ 6.05	100.0%	59.1%
Lymphocyte Absolute (10^3 /ml)	0.688 (0.530–0.845)	0.080	≥ 1.86	88.9%	46.6%
Platelet (10^3 /ml)	0.709 (0.570–0.849)	0.071	≥ 235	91.7%	49.0%
Composite Score	0.902 (0.840–0.964)	0.032	≥ 12.91	100.0%	85.2%

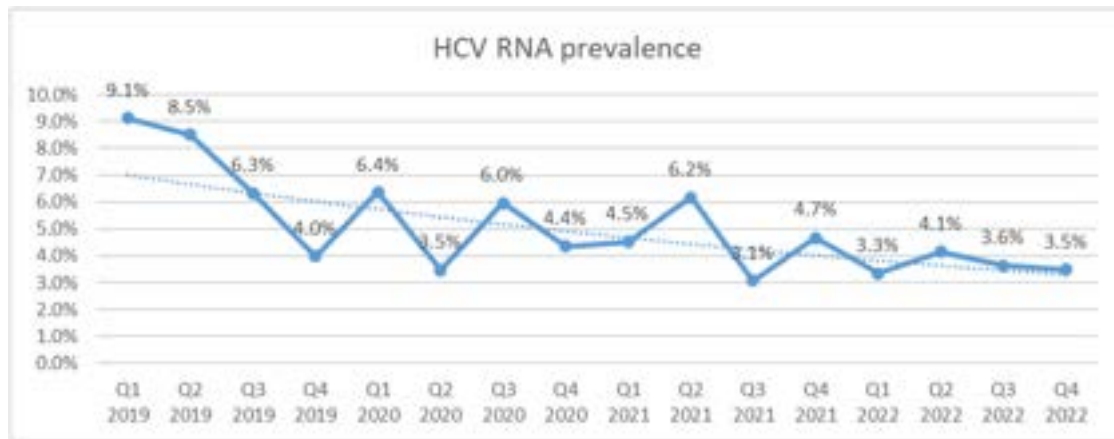


Figure: (abstract: THU-176).

62% reduction in HCV RNA prevalence also demonstrates the effectiveness of England's elimination strategy of optimising HCV services such as those in drug treatment services and prisons.

THU-177

Post-treatment liver function, but not baseline liver function, predicts survival in hepatitis C virus patients with decompensated cirrhosis after direct-acting antiviral treatment

Yuki Tahata¹, Hayato Hikita¹, Satoshi Mochida², Nobuyuki Enomoto³, Akio Ido⁴, Hidekatsu Kuroda⁵, Daiki Miki⁶, Masayuki Kurosaki⁷, Yoichi Hiasa⁸, Ryotaro Sakamori¹, Norifumi Kawada⁹, Taro Yamashita¹⁰, Goki Suda¹¹, Hiroshi Yatsushashi¹², Hitoshi Yoshiji¹³, Naoya Kato¹⁴, Taro Takami¹⁵, Kazuhiko Nakao¹⁶, Kentaro Matsuura¹⁷, Yasuhiro Asahina¹⁸, Yoshito Itoh¹⁹, Ryosuke Tateishi²⁰, Yasunari Nakamoto²¹, Eiji Kakazu²², Shuji Terai²³, Masahito Shimizu²⁴, Yoshiyuki Ueno²⁵, Norio Akuta²⁶, Takahiro Kodama¹, Tomohide Tatsumi¹, Tomomi Yamada²⁷, Tetsuo Takehara¹. ¹Osaka University Graduate School of Medicine, Japan; ²Saitama Medical University, Japan; ³University of Yamanashi, Japan; ⁴Kagoshima University Graduate School, Japan; ⁵Iwate Medical University, Japan; ⁶Hiroshima University, Japan; ⁷Musashino Red Cross Hospital, Japan; ⁸Ehime University Graduate School of Medicine, Japan; ⁹Osaka Metropolitan University, Japan; ¹⁰Kanazawa University, Japan; ¹¹Hokkaido University, Japan; ¹²National Hospital Organization Nagasaki Medical Center, Japan; ¹³Nara Medical University, Japan; ¹⁴Chiba University Graduate School of Medicine, Japan; ¹⁵Yamaguchi University Graduate School of Medicine, Japan; ¹⁶Nagasaki University Hospital, Japan; ¹⁷Nagoya City University Graduate School of Medical Sciences, Japan; ¹⁸Tokyo Medical and Dental University, Japan; ¹⁹Kyoto Prefectural University of Medicine, Japan; ²⁰The University of Tokyo, Japan; ²¹University of Fukui, Japan; ²²National Center for Global Health and Medicine, Japan; ²³Niigata University, Japan; ²⁴Gifu University Graduate School of Medicine, Japan; ²⁵Yamagata University Faculty of Medicine, Japan; ²⁶Toranomon Hospital, Japan; ²⁷Osaka University Hospital, Japan

Email: yuki.tahata@gh.med.osaka-u.ac.jp

Background and aims: Direct-acting antiviral (DAA) treatment has enabled SVR rates of around 90% in patients with hepatitis C virus (HCV)-related decompensated cirrhosis. However, the factors

associated with survival after DAA treatment in patients with decompensated cirrhosis are unclear.

Method: A total of 206 patients with HCV-related decompensated cirrhosis who started DAA treatment between February 2019 and December 2021 at 31 Japanese hospitals was enrolled. Decompensated cirrhosis was defined as Child-Pugh (CP) class B or C or CP class A with previous decompensating events. SVR was defined as undetectable serum HCV-RNA at 12 or 24 weeks after the end of treatment (EOT). We examined the factors associated with liver transplantation (LT)-free survival after DAA treatment in patients with decompensated cirrhosis.

Results: The median age was 68, and 52% of patients were male. The distribution of patients with CP class A, B and C was 10% (20/206), 76% (156/206) and 15% (30/206), respectively. In ITT analysis, the SVR rate was 91.3% (188/206). Six patients had a virological relapse, one had non-response, five died and six were missing. During the median observation period of 28.1 months, 26 patients died (the most common cause of death was liver failure), and two patients underwent LT. LT-free survival rates at 2 and 3 years were 90.0% and 83.2%. Next, we examined the factors associated with LT-free survival by Cox proportional hazard analyses excluding five patients who died by 12 weeks after the EOT to evaluate the impact of post-treatment liver function on LT-free survival. In these analyses, we used 2 models, including either CP class (Model 1) or MELD score (Model 2). In multivariate analysis, serum alanine aminotransferase level ($p = 0.046$), serum creatinine level ($p = 0.003$) and CP class at 12 weeks after the EOT ($p = 0.001$) in Model 1, the presence of hepatic encephalopathy ($p = 0.014$) and MELD score at 12 weeks after the EOT ($p = 0.007$) in Model 2 were identified as significant factors. In these analyses, baseline CP class and MELD score were not significant factors. LT-free survival rates at 3 years were 91.0%, 86.4% and 51.8% in patients with CP class A ($n = 76$), CP class B ($n = 97$) and CP class C ($n = 18$) at 12 weeks after the EOT, respectively. The LT-free survival rates of patients with CP class C at 12 weeks after the EOT were significantly lower than the other two groups. On the other hand, the LT-free survival rate of patients with CP class C at baseline was not significantly lower than the other two groups, whether analyzed with or without the patients who died before 12 weeks after the EOT. **Conclusion:** In patients with decompensated cirrhosis treated with DAA, post-treatment liver function but not baseline liver function were predictors for survival.

THU-178

Network transmission of hepatitis C genotype 2c and 4d in men who have sex with men in Cape Town, South Africa

Mark Sonderup¹, Ziyaad Valley-Omar², Heidi Smuts², Stephen Korsman², Diana Hardie², Wendy Spearman¹. ¹University of Cape Town Faculty of Health Sciences, Division of Hepatology, Cape Town, South Africa; ²University of Cape Town Faculty of Health Sciences and NHLS, Division of Medical Virology, Cape Town, South Africa
Email: msonderup@samedical.co.za

Background and aims: Men who have sex with men (MSM) are at risk for sexual transmission of hepatitis C virus (HCV). Concomitant HIV infection enhances this risk. Network HCV transmission has been reported in Europe, Canada and more recently, Mexico. South Africa is an HCV pan-genotypic region, with genotype (GT) 1 and 5 dominant, followed by GT, 3, 4 and 2, though GT 2c and 4d are infrequent subtypes. We observed a pattern of mostly MSM with HCV 2c or 4d subtype infection presenting for HCV care and investigated for possible HCV network transmission.

Method: All clinical and demographic data of those with the 2 HCV subtypes, and self-identified as MSM, were captured. HCV genotype was determined by sequencing the NS5B gene. Nested NS5B amplification was performed using pan-genotypic primers and sequenced directly with the BigDye terminator cycle. Genotype assignment used the *geno2pheno* algorithm and aligned with reference sequences from the GenBank database using BioEdit version 7.2.5. Phylogenetic trees were constructed in MEGA 6.06 using the maximum-likelihood algorithm with 1000 bootstrap re-samplings to evaluate phylogenetic relatedness within HCV 2c and HCV 4d clusters.

Results: 30 patients, n = 16 GT 2c and n = 14 GT 4d, were evaluated. Median overall age was 50 years [IQR 41–54], with no significant difference in age between GT 2c (52 years) and 4d (47 years) patients, p = 0.08. 73% (n = 22) were HIV infected, with 3% (n = 3) previously or currently having used injecting drugs. All noted casual sex partners and 43% (n = 13) confirmed recreational, non-injecting drug use

during sex. Overall, median baseline HCV viral load was 6.2 [IQR 5.4–6.6] log₁₀ IU/ml; baseline ALT was 71 U/L [IQR 60–153], 50% had F1, 44% F2 and 6% F3 fibrosis. All HIV positive patients were virally suppressed and 90% (n = 27) have completed HCV treatment: 38% (n = 10 with SOF/Daclatasvir), 33% (n = 5 with SOF/Ribavirin); 19% (n = 9 with SOF/Ledipasvir) and 10% (n = 3 with SOF/Velpatasvir), with a 100% SVR rate. Maximum-likelihood trees (fig. 1) support the phylogenetic relatedness within the GT 2c and 4d clusters.

Conclusion: Demonstrated for the first time in South Africa, phylogenetic analysis strongly suggests a network transmission of 2 HCV GT subtypes in MSM in Cape Town. This data emphasizes the need for an important policy focus in the local viral hepatitis strategy for a micro-elimination, targeted education, prevention, and treatment program within this key population. Treatment outcomes to date are excellent.

THU-179

Direct-acting antivirals reduce disease burden in patients with chronic hepatitis C: a Korean nationwide, multicentre, retrospective cohort study

Won Sohn¹, Sang Hoon Ahn², Young Seok Kim³, Seung Up Kim². ¹Kangbuk Samsung Hospital, Sungkyunkwan University School of Medicine, Korea, Rep. of South; ²Severance Hospital, Yonsei University College of Medicine, Korea, Rep. of South; ³Soonchunhyang University, Bucheon Hospital, Korea, Rep. of South
Email: ksukorea@yuhs.ac

Background and aims: Direct-acting antivirals (DAAs) improve the prognosis of patients with chronic hepatitis C (CHC). This study investigated whether DAA treatment improves the disease burden by ameliorating the fibrotic burden in CHC patients.

Method: A nationwide, multicentre, retrospective cohort study was conducted that included patients with CHC recruited from 29 tertiary academic institutes in South Korea. The primary outcome was disease burden, assessed using the measure disability-adjusted life years (DALYs), with age weighting and discounting in untreated and DAA-



Figure 1: (abstract: THU-178).

treated groups. Improvement of fibrotic burden after DAA treatment was assessed using the APRI score and FIB-4 index. The clinical outcomes were hepatocellular carcinoma, liver transplantation, decompensation, or death.

Results: Between January 2007 and December 2022, data from 11,726 patients with CHC, including 8,464 (72%) treated with DAAs, were analysed. During the follow-up period (median 27.5 months), 469 patients died (353 [10.8%] in the untreated group, 116 [1.4%] in the DAA-treated group), 586 developed hepatocellular carcinoma (343 [10.5%] in the untreated group, 243 [2.9%] in the DAA-treated group), 580 developed decompensation (372 [11.4%] in the untreated group, 208 [2.5%] in the DAA-treated group), and 18 underwent liver transplantation (8 [0.2%] in the untreated group, 10 [0.1%] in the DAA-treated group). The multivariable analyses showed that DAA-treated group significantly reduced mortality, HCC risk, and decompensation development compared to the untreated group (hazard ratio [HR] = 0.22, 95% confidence interval [CI] 0.17–0.27; HR = 0.47, 95% CI 0.39–0.58; and HR = 0.31, 95% CI 0.26–0.37, respectively) (all $p < 0.001$). The APRI-based DALY estimate was significantly lower in the DAA-treated group than in the untreated group (mean 5.0 ± 2.9 vs. 5.9 ± 3.8 years, $p < 0.001$), as was the FIB-4-based DAL estimate (mean 5.7 ± 2.7 vs. 6.3 ± 3.5 years, $p < 0.001$). The difference between the two groups with respect to either the APRI- or FIB-4-based DALYs was highest in patients 40–60 years of age.

Conclusion: DAA treatment significantly improved the clinical outcomes of CHC patients and reduced the disease burden, by improving the fibrotic burden after DAA treatment.

THU-180

Hepatitis C micro-elimination program in Zhuhai: a concerted citywide effort to eliminate hepatitis C by 2030

Jinyu Xia¹, Zhongsi Hong¹, Xinchun Zheng¹, Xiaoyan Ye¹, Mengdang Ou¹, Ying Li¹. ¹The Fifth Affiliated Hospital of Sun Yat-Sen University, China
Email: xiajinyu@mail.sysu.edu.cn

Background and aims: To support the World Health Organization's goal of eliminating hepatitis C by 2030, we established a collaborative model called "Lucky Star Program" (LSP) in Zhuhai, Guangdong Province in China and evaluated its effectiveness in screening, treatment and follow-up for HCV infection.

Method: Under the leadership of the Zhuhai Infectious Disease Medical Quality Control Center (ZMQCC), We provide an import platform in bridging the gap between the government, different-level hospitals and communities, a homogeneous mode of Hepatitis C micro-elimination–LSP. ZMQCC is responsible for training and patient network management. Designated hospitals and community hospitals are responsible for HCV antibody (HCV-Ab) screening and activate cascade referral system when necessary. Patients with HCV-Ab positive are referred to a designated hospital for HCV RNA testing, where the positive patients receive standard treatment. We have dedicated staff to supervise and use unique referral QR codes citywide to make the process uniform and minimize patient attrition. Meanwhile, KPI evaluation will be conducted for hepatitis C management in designated hospitals to facilitate the implementation of the program.

Results: LSP kicked off in May 2021. 96,035 in-patients before LSP (from December 2019 to May 2021) and 39,502 in-patients after LSP with dedicated staff (from May 2022 to December 2022) were screened in the Fifth Affiliated Hospital of Sun Yat-Sen University. The seropositive rate of HCV-Ab was 0.43% (410/96,035) before LSP and 0.70% (275/39,502) after LSP, the HCV RNA positive rate were 50% (122/244) before LSP and 86.3% (226/262) after LSP in hospital population. The treatment rate of patients with HCV RNA positive increased from 32.0% (39/122) to 88.1% (199/226) since set up dedicated staff to supervise the whole process. During 2022, 1,175 patients with HIV infection, 36 patients from methadone clinic and 1,571 people from community were screened, the seropositive rate of HCV-Ab were 2.64% (31/1,175), 94.4% (34/36) and 1.02% (16/1,571), the HCV RNA positive rate were 100% (31/31), 52.9% (18/34) and 62.5% (10/16), the DAA treatment rate were 93.5% (29/31), 55.6% (10/18), 80% (8/10) in the HIV-infected, methadone clinic and community population, respectively. SVR12 was greater than 97.0% in all patients with SOF/VEL.

Conclusion: Zhuhai's LSP has already achieved its initial objectives. The successful experience of the pilot hospital should be extended to other designated hospitals citywide. It could improve treatment rates for CHC through focusing on key populations and enhancing follow-up both in the hospitals and in the community.

Figure 1

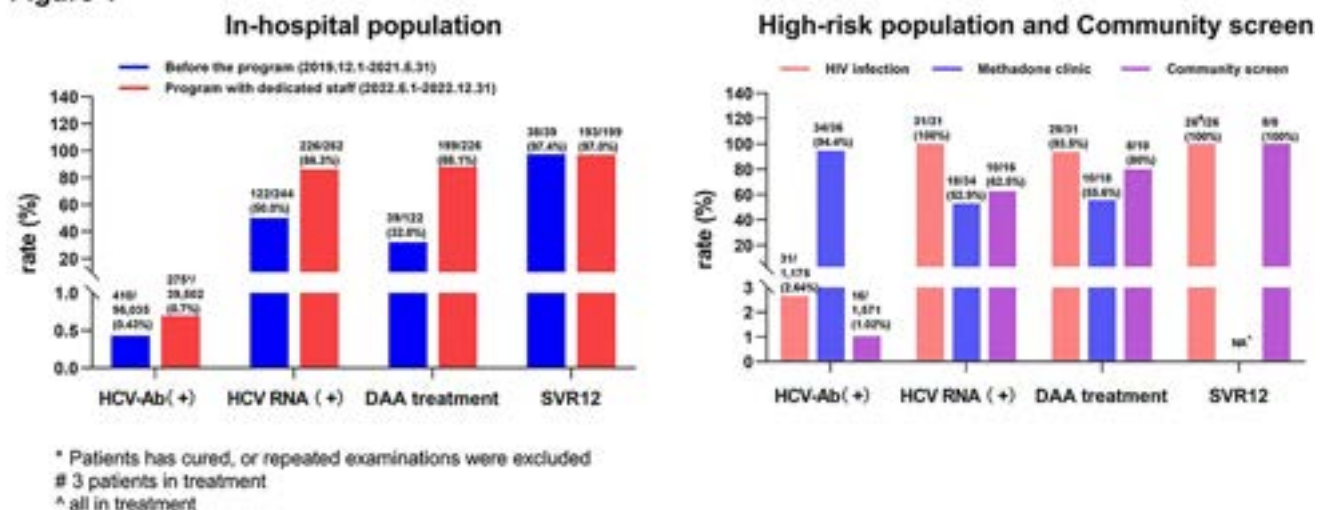


Figure: (abstract: THU-180).

THU-181

Real-world data on long-term quality of life after Glecaprevir/Pibrentasvir therapy: data from the German hepatitis C registry (DHC-R)

Markus Cornberg¹, Albrecht Stoeck², Dennis Hidde³, Gerd Klausen⁴, Willibald Schifflholz⁵, Lutz Thomas⁶, Manfred Nowak⁷, Michelle Collins⁸, Karl-Georg Simon⁹. ¹Hannover Medical School, Department of Gastroenterology, Hepatology and Endocrinology, Hannover, Germany; ²IFI Medizin GmbH, Hamburg, Germany; ³AbbVie Germany GmbH and Co, Wiesbaden, Germany; ⁴Schwerpunktpraxis für Infektionsmedizin am Oranienburger Tor, Berlin, Germany; ⁵Gastroenterologische Schwerpunktpraxis, Augsburg, Germany; ⁶Infektiologikum, Frankfurt am Main, Germany; ⁷f Therapieverbund Ludwigsmühle, Schwerpunktpraxis, Landau in der Pfalz, Germany; ⁸AbbVie Inc, Mettawa, United States; ⁹MVZ Dres Eisenbach/Simon/Schwarz/GbR, Leverkusen, Germany
Email: cornberg.markus@mh-hannover.de

Background and aims: Globally, 58 million people are infected with hepatitis C virus (HCV) many of whom have comorbidities such as injection drug use. Some HCV-infected patients may be motivated by benefits beyond virologic cure; insights into patient-reported outcomes associated with treatment may help efforts to improve linkage to care. This study used data from the German Hepatitis C registry (DHC-R) to evaluate the real-world effect of glecaprevir/pibrentasvir (G/P) on quality of life (QoL) 1-year posttreatment.

Method: The DHC-R is an ongoing, prospective, observational cohort study of patients being treated for chronic HCV infection. Patients were recruited from 159 sites between August 2, 2017, and February 10, 2021, the data cut off for this analysis was November 17, 2021. Patients had HCV genotype (GT) 1–6 and were treated with on-label G/P. Mean short-form 36 health survey questionnaire (SF-36) scores at baseline (BL), posttreatment Week 12 (PTW12) and 1-year posttreatment were reported. Patients achieving sustained virologic

response at PTW12 (SVR12), safety and tolerability were also assessed.

Results: The analysis included 2727 patients. Most were treatment-naïve (91.2%) and noncirrhotic (85.4%). Reported BL comorbidities included opioid substitution therapy (OST; 27.0%), active drug use (6.3%), psychiatric disorders (13.1%), alcohol abuse (8.5%) and HIV coinfection (6.0%). In patients with valid BL, PTW12 and 1-year posttreatment data (n = 119), mean SF-36 physical component score (PCS) and mental component scores (MCS) were improved and maintained in the overall population. Similar improvements were observed for all patient populations, excluding those with alcohol abuse (PCS and MCS scores) and HIV coinfection (MCS score), which showed no improvement. The biggest improvement in MCS scores were seen in patients receiving OST at BL and the biggest different in PCS scores were seen in patients with psychiatric disorders and those receiving OST at BL (Figure 1). The intention to treat (ITT) SVR12 rate was 96.2% (2083/2166) and the modified ITT (mITT) rate was 99.0% (2083/2103). There were no new or unexpected safety signals.

Conclusion: On-label treatment with G/P was highly effective and well-tolerated in routine clinical practice. Improvements in patient QoL were consistent and pronounced across all comorbidities studied, particularly when related to mental components, further supporting the use of G/P in real-world patient populations.

Acknowledgments: Glecaprevir was identified by AbbVie and Enanta. Medical writing support was provided by Laura Whiteley, PhD, and Tom Owen, PhD, of Fishawack Health, funded by AbbVie.

Disclosures: AbbVie sponsored the study; contributed to its design; and participated in the collection, analysis, and interpretation of the data and in the writing, reviewing, and approval of the abstract. All authors had access to relevant data, and participated in the writing, review, and approval of the final abstract.

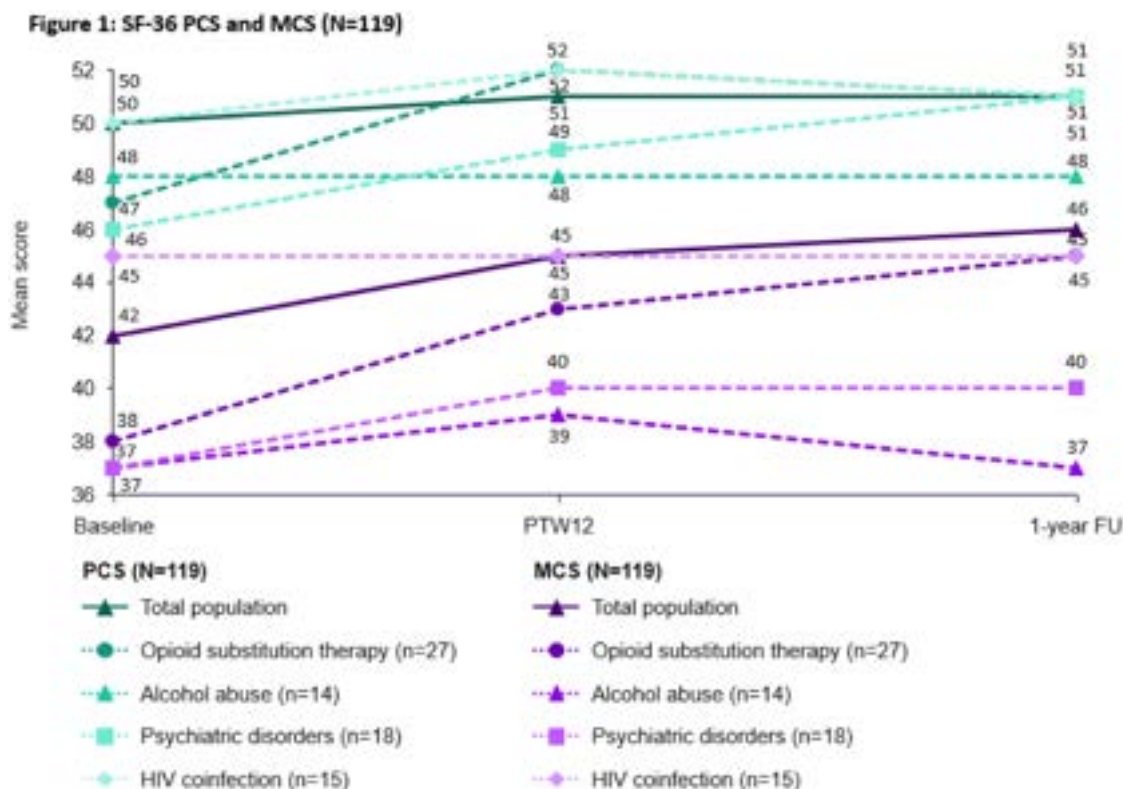


Figure: (abstract: THU-181).

THU-182

What is the impact of a Hepatitis C 'test and trace' pilot using peer workers?

Caroline Allsop¹, Kate McQue¹, Mark Roberts², Suzanne Murphy², Carrie Richardson², Yusri Taha³, Stuart McPherson^{1,4}. ¹The Newcastle upon Tyne Hospitals NHS Foundation Trust, Liver unit, United Kingdom; ²Hepatitis C Trust, United Kingdom; ³The Newcastle upon Tyne Hospitals NHS Foundation Trust, Virology, United Kingdom; ⁴Newcastle University, Translational and Clinical Research Institute, United Kingdom
Email: stuart.mcpherson2@nhs.net

Background and aims: Chronic Hepatitis C virus (HCV) infection is a major cause of morbidity and deaths worldwide. HCV treating teams in England have made steady progress towards the goal of eliminating HCV by 2025. However, HCV reinfection rates are high, particularly in North-East England, suggesting a significant reservoir of untreated infections. Contact tracing, a tool successfully used to identify and treat cases in other infectious diseases, is not routine practice in HCV. Here we present the outcomes of an "HCV Test and Trace" pilot scheme.

Method: Individuals with recently acquired HCV infection or reinfection were invited to participate when they presented to our service for treatment. For those who agreed to participate, a Hepatitis C Trust peer worker approached them to invite potential contacts for HCV test using "dry blood spot." To encourage participation, incentives (vouchers for a food outlet) were given to index individuals and contacts upon HCV testing. We collected data on uptake, HCV test results, treatment rates and reasons for declining.

Results: Between April 2022 and Jan 2023 (9 months), 241 individuals were invited to participate, of whom 118 (49%) agreed. The overall interim outcomes of the pilot are summarised in Fig. 1. To date, 24 (10% of all, 20% of those agreeing) have brought forward contacts for testing. A total of 88 contacts were identified and tested,

averaging 3 or more contacts per participant. Of these, 33 (38%) were HCV RNA positive indicating active HCV. Of these, 16 were new infections and 17 were known cases (7 never seen by HCV services, 10 had treatment prescribed previously, including 5 reinfections). To date, 10 have started antiviral treatment and 14 are awaiting assessment or treatment initiation. The most common reason for individuals declining participation was that they were no longer in contact with at risk individuals (65%).

Conclusion: Overall, about half of individuals with recent HCV infection or reinfection agreed to participate in a test and trace pilot scheme, but to date only 20% actually brought contacts forward. However, the frequency of active HCV among the contacts appears to be high at 38%. Work is ongoing to refine the pathway to increase uptake, and testing and treatment rate.

THU-183

Evaluation of the follow-up in patients with advanced fibrosis after achieve sustained viral response with direct-acting antivirals. Screening and risk of hepatocellular carcinoma

Belén Julian¹, Diego Casas-Deza^{1,2}, Silvia Espina^{1,2}, Luis Javier Lamuela³, Olivia Sierra¹, Carmen Yagüe¹, Sara Lorente Perez^{4,5}, Trinidad Serrano^{4,5}, Jose M Arbones Mainar^{2,6,7}, Vanesa Bernal Monterde^{1,2}. ¹Miguel Servet University Hospital, Zaragoza, Spain; ²IIS Aragon. Unidad de Investigación Clínica HUMS, Zaragoza, Spain; ³Hospital General San Jorge, Huesca, Spain; ⁴Hospital Clínico Universitario Lozano Blesa, Zaragoza, Spain; ⁵IIS Aragon, Spain; ⁶Instituto Aragonés de Ciencias de la Salud, Zaragoza, Spain; ⁷Carlos III Health Institute, Madrid, Spain
Email: vbernal@gmail.com

Background and aims: The risk of developing hepatocellular carcinoma (HCC) persists in patients with hepatitis C virus (HCV) and cirrhosis who achieve sustained viral response (SVR) with direct-

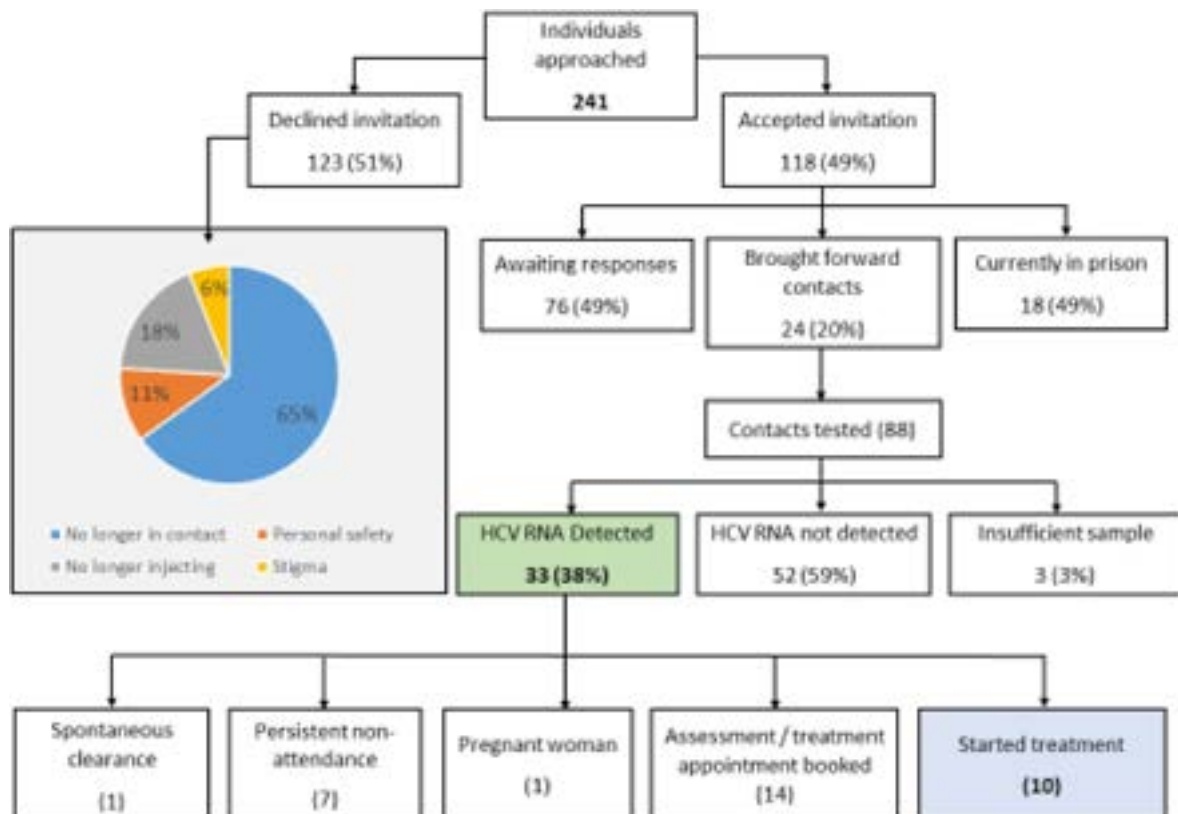


Figure: (abstract: THU-182).

POSTER PRESENTATIONS

acting antiviral agents (DAA). In patients with advanced fibrosis (F3) without cirrhosis the risk is not well established and the different clinical guidelines differ in their recommendations. Our objective was to describe the management and post-SVR evolution of patients with F3 in our community, as well as assessing the incidence of HCC.

Method: Retrospective multicenter study including all patients HCV monoinfected patients with advanced fibrosis without cirrhosis (Fibroscan® [TE] >9, 5 and <14, 5Kpa) who achieved SVR with AAD between November 2015 and April 2021 in the 8 Hospitals of Aragon, an autonomous community of Spain. Follow-up was carried-out until the development of HCC, death, last visit registered or January 2022. A statistical analysis was performed with the R software.

Results: A total of 258 patients (age 58 (11.6) years; 163 (63%) male) were included. Mean [TE] = 10.9 (1.26) Kpa. 39 (15%) were diabetic, 60 (23.3%) hypertensive and 20 (7.8%) affected by harmful use of alcohol. In the pre-SVR ultrasound scan, 42 (17%) presented steatosis and 32 (13.2%) non-specific alterations of the hepatic echostructure. 193 patients (74.8%) have continued HCC screening and 107 (55%) of these underwent a posterior Fibroscan® (F0-1: 27.1%, F2: 5.8%, F3: 7%, F4: 1.6%). Among the factors associated with performing HCC screening after SVR, a higher degree of fibrosis was observed by pre-SVR [TE] (10.6 vs 11.1Kpa; $p = 0.021$), the presence of steatosis (1.5% vs 21.7%, $p < 0.001$) and/or non-specific abnormalities on ultrasound (3.1% vs 38.6%; $p < 0.001$) and the prescribing service (68% Hepatology, 24% General Gastroenterology and 8% Infectious Diseases; $p < 0.001$). During the follow-up (median 53.4 months), 5 of 193 (2.59%) patients developed HCC. Only a post-SVR FIB-4 >3.25 was independently related to its appearance.

Conclusion: HCC screening of patients with F3 and HCV who achieve SVR is heterogeneous in our community, and is determined by the results of pre-SVR [TE] values, pre-SVR ultrasound scan and the prescribing service. HCC incidence is low in these patients. Evaluation of post-SVR fibrosis with the FIB-4 index can help to select for screening the patients with the highest risk.

THU-184

Hepatitis C virus (HCV) infection and neurocognitive impairment in subjects with mild liver disease: the role of neuropsychological and cognitive provoked P300 tests

Marcia Maria Amendola Pires¹, Rafael Espindula², Jefferson Abrantes², Carlos Brandão-Mello¹. ¹Gastrointestinal and Liver Unit, Gaffrée e Güinle University Hospital, Internal Medicine, Rio de Janeiro, Brazil; ²Postgraduate Program in Neurology, Department of Neurology, Neurology, Rio de Janeiro, Brazil
Email: cedubrandao@gmail.com

Background and aims: Hepatitis C virus (HCV) infection is one of the leading causes of liver cirrhosis, hepatocellular carcinoma, and liver-related deaths. It is estimated that 40%-74% of HCV subjects will experience at least one extra-hepatic manifestation within their lifetime, including neurocognitive deficits. Cognitive changes are well documented in patients with chronic liver disease, most often as a result of decompensated liver encephalopathy. However, evidence has shown that cognitive changes can occur before the development of liver cirrhosis. Neuropsychiatric symptoms such as: "brain fog", fatigue and weakness occur in approximately 50% of patients with HCV, regardless of the severity of liver impairment. The long latency auditory evoked potential or cognitive evoked potential (P300) is an endogenous potential dependent on cognitive abilities and it can reflect the individual's functional use of the stimulus, not directly depending on his physical characteristics. The P300 component is evaluated by analysing its amplitude (microvolts (µV) and latency in

milliseconds (ms). The aim of the study was to evaluate the presence of cognitive changes in HCV subjects with the P300 and neuropsychological tests with an emphasis on attention and working memory.

Method: Observational study conducted at the Liver Unit of Gaffrée e Güinle University Hospital (HUGG), from November 2019 through March 2020. All HCV-infected subjects (anti-HCV and HCV-RNA detectable) over 18 years old were considered eligible for investigation. Only HCV subjects with compensated liver disease were included. Liver fibrosis assessment by liver stiffness as well genotyping (sequencing) and HCV-RNA viral load (RT-PCR) were performed. Patients were tested in a single day with cognitive evoked potential and neuropsychological tests (random letter test, form A and B trail test, direct, reverse order digit test and code test). We excluded coinfection with HIV, HBV and syphilis; hypothyroidism or psychiatric illness; neurological diseases that affect the cognition, mainly neurodegenerative diseases; decompensated liver cirrhosis; alcoholism or use of illicit drugs; formal education less than 4 years; complete deafness and subjects over 80 years old. The mean normal value of P300 latency and amplitude was 348.2 milliseconds and 8.9 microvolts, respectively, as described by Torres, Abrantes and Brandão-Mello, 2020

Results: A total of 124 patients were analysed and 91 excluded according to exclusion criteria. Thus 33 HCV subjects (51.5% male) were enrolled. Mild liver fibrosis (F0-F2) was identified in 72.8%. Genotype was predominately 1 (72%). The neuropsychological and P300 results are displayed in table 1. Of the 33 patients with HCV, 57.6% had changes in P300 latency and 60.6% in amplitude, that is, more than 50% globally detectable changes in this complementary method. There was not significant correlation between P300 latency and amplitude and demographic and virological characteristics of HCV subjects, such as gender, education level, age, viral load and liver fibrosis.

RESULTS	HCV SUBJECTS		
	n	%	95% Confidence Interval
Latency P300 (milliseconds)			
< 348.2 (normal)	14	42.4	
≥ 348.2	19	57.6	40.4% - 72.4%
Amplitude P300 (microvolts)			
< 8.9 (normal)	13	39.4	
≥ 8.9	20	60.6	43.4% - 70.0%
Random Letter (number of errors)			
0	21	63.6	
At least 1 mistake	12	36.4	21.4% - 53.6%
Trail Test A (seconds)			
≤ 48.3 (normal)	20	60.6	
> 48.3	13	39.4	23.0% - 56.6%
Trail Test B (seconds)			
≤ 135.7 (normal)	20	60.6	
> 135.7	13	39.4	23.0% - 56.6%
BIA ratio (Executive function)			
≤ 2.91 (normal)	20	60.6	
> 2.91	13	39.4	23.0% - 56.6%
Direct Order Range Scores (DOR)			
> 4 (normal)	32	97.0	
≤ 3	1	3.0	0.15% - 14.1%
Indirect Order Range Scores (IOR)			
> 4 (normal)	15	45.5	
≤ 3	18	54.5	37.5% - 70.8%
Difference in score (DOR-IOR)			
< 3 (normal)	13	39.4	
≥ 4	20	60.6	43.4% - 70.0%
Code testing (points)			
≤ 23 (normal)	31	93.9	
> 22	2	6.1	1.0% - 16.0%

Table 1: HCV Subjects according to P300 and neuropsychological results (n=33)

Figure:

Conclusion: In conclusion, HCV subjects with mild or no fibrosis, presented cognitive deficits in more than 50% in the tests applied to assess working memory and attention. Thus, we suggest that triage for HCV-infection must be included in the list of screening tests in patients who exhibit cognitive decline.

THU-185

A prospective, pragmatic post-authorisation safety study of early recurrence of hepatocellular carcinoma in hepatitis C virus-infected patients after direct-acting antiviral (DAA) therapy: DAA-PASS

Amit Singal¹, Michael Fried², Massimo Colombo³, Roniel Cabrera⁴, Katie Kelley⁵, Neil Mehta⁵, Bruno Sangro⁶. ¹UT Southwestern, United States; ²Target RWE, United States; ³Humanitas Hospital, Italy; ⁴University of Florida, United States; ⁵University of California San Francisco, United States; ⁶Clinica Universidad de Navarra, Spain
Email: bsangro@unav.es

Background and aims: Early reports of DAA therapy for chronic hepatitis C (HCV) after successful treatment of hepatocellular carcinoma (HCC) raised concerns about an increased risk of early and aggressive HCC recurrence. The European Commission recommended that DAA marketing authorisation holders should perform a prospective observational study to assess risk of early recurrence of previously treated HCC after DAA therapy.

Method: A prospective, pragmatic, multinational observational study was designed to estimate the risk of HCC recurrence, after successful treatment of early-stage HCC, associated with DAA therapy exposure during routine clinical care. Patients were eligible if they had HCV mono-infection, no prior DAA therapy, and had radiologically confirmed successful treatment for Barcelona Clinic Liver Cancer (BCLC) stage A HCC. Treatment modalities for HCC and choice/timing of DAA therapy for HCV were at the discretion of investigators. Patients were followed at regular intervals for evidence of HCC recurrence on imaging, beginning from first cross-sectional imaging study (index date) demonstrating complete response to HCC treatment for up to 24 months.

Results: The planned prospective sample size of 600 patients (n = 122 expected HCC recurrences) was not achieved due to the evolving global landscape of DAA therapy resulting in slower than expected enrollment. Of 222 patients screened, 142 were screen failures and 32 did not meet the enrollment criteria. Of the 42 patients enrolled (33 U.S., 9 Italy), median age at HCC diagnosis was 62 (IQR: 8.0) yrs with 79% male and 74% White. Nearly all (95%) had cirrhosis, with 45% with evidence of hepatic decompensation. Treatment for HCC included locoregional therapy (74%) and surgical resection (17%). Eighteen patients never received DAA therapy during follow-up. Twenty-four patients were treated with DAA therapy after index imaging showing complete response (median time from index imaging to DAA initiation = 3.1 months). Median duration of DAA exposure was 2.8 months and median follow-up from DAA initiation was 18.9 months. Ten HCC recurrence events were observed during the study, with 5 each in DAA-treated and DAA-untreated patients (cumulative incidences of 23% and 37%, respectively). The overall crude HCC recurrence rate at 24 months was 17.7 per 100 person-years (PY) with a crude hazard ratio (HR) for HCC recurrence associated with DAA therapy of 0.6 (95% CI, 0.2–2.2). The age-adjusted HR was 0.7 (95% CI, 0.2–2.3). All HCC recurrences occurred intra-hepatic and most (60%) were detected within Milan Criteria, with no differences between the two groups.

Conclusion: Although limited by small sample size, this prospective pragmatic study suggests DAA therapy is not associated with increased HCC recurrence risk among patients with a previous successfully treated HCC.

THU-186

Clinical outcomes after hepatitis C treatment in patients with advanced chronic liver disease

Fabio Correia¹, Gonalo Alexandrino¹, Mariana Cardoso¹, Joana Branco¹, Mariana Costa¹, Rita Carvalho¹, Alexandra Martins¹. ¹Hospital Professor Doutor Fernando Fonseca, Portugal
Email: fabiopcorreia@gmail.com

Background and aims: Patients with advanced chronic liver disease (ACLD) and chronic hepatitis C are at high risk of developing clinically

significant portal hypertension (CSPH) and its complications. Direct-acting antivirals have radically changed the outcomes of hepatitis C treatment. However, data on the impact of cured hepatitis C on the medium-term clinical evolution of patients with ACLD has only recently emerged. We aimed to evaluate the outcomes related to hepatic decompensation, hepatocellular carcinoma (HCC) and mortality in a cohort of patients with ACLD and cured hepatitis C with sustained virological response (SVR).

Method: Prospective, single-centre study, in patients with ACLD and chronic hepatitis C with SVR, treated since February 2015 and with a minimum follow-up (FU) of 2 years. The definition of ACLD was based on liver biopsy or Baveno VII's concepts: liver stiffness measurement (LSM) >10 kPa and/or clinical/imaging elements of CSPH. During FU, hepatic decompensation (ascites, variceal bleeding, and hepatic encephalopathy) unrelated to HCC, development of HCC and mortality were recorded. In decompensated ACLD, the recompensation rate was also evaluated.

Results: We included 147 patients (78.2% male, mean age of 59 years-old). At baseline, 84% (123/147) had compensated ACLD (cACLD), 16% (24/147) had decompensated ACLD (dACLD) and none had suspicious liver nodules. Among patients with cACLD with baseline LSM evaluation (97/123), 65% (63/97) had a LSM >15 kPa. The median follow-up was 52 months. During follow-up, 13% (16/123) of cACLD patients developed complications: first decompensation in 5% (6/123) and HCC in 8% (10/123). All these 16 patients had LSM >15 kPa or clinical/imaging elements of CSPH, and the majority (14/16) had platelet count <150 × 10⁹. The mortality rate was 3% (4/123). In dACLD patients, we observed clinical recompensation in 21% (5/24), HCC in 17% (4/24), with a global mortality rate of 8% (2/24).

Conclusion: In this cohort of patients with ACLD and cured hepatitis C, the medium-term clinical evolution was globally favorable, with emphasis on clinical recompensation in about 25% of dACLD patients. However, HCC remains a major concern, especially in decompensated ACLD, but also in compensated patients. Adverse events occurred only in patients with pre-treatment LSM >15 kPa, the majority with platelets count <150 × 10⁹. These cut-offs, with an established role in ACLD stratification, could perhaps redefine follow-up surveillance in compensated patients. The impact of other cofactors, such as alcohol and obesity, in the development of complications, needs to be further evaluated.

THU-187

Mortality risk following HCV cure among people with HIV coinfection

Naveed Janjua^{1,2}, Stanley Wong¹, Hector Velasquez¹, Dahn Jeong^{1,2}, Sofia Bartlett^{1,2}, Mawuena Binka¹, Jean Damascene Makuza², Prince Adu^{1,2}, Maria Alvarez¹, Jason Wong, Dr.^{1,2}, Mel Krajden^{1,3}. ¹BC Centre for Disease Control, Vancouver, Canada; ²University of British Columbia, School of Population and Public Health, Vancouver, Canada; ³University of British Columbia, Department of Pathology and Laboratory Medicine, Vancouver, Canada
Email: naveed.janjua@bccdc.ca

Background and aims: Hepatitis C (HCV)/human immuno-deficiency virus (HIV) co-infection is associated with higher morbidity and mortality compared to HCV mono-infection. Sustained virologic response (SVR) following HCV treatment is associated with reduced morbidity and mortality. We assessed all-cause, liver-, drug- and non-liver, non-drug- related mortality following SVR among people with HCV/HIV co-infection (PWHI) compared to people with HCV mono-infection (PWHC) in a large population-based cohort in British Columbia (BC), Canada.

Method: We used data from the BC Hepatitis Testers Cohort, which includes ~1.3 million people tested for HCV since 1990, linked with data on medical visits, hospitalizations, prescription drugs and mortality. We followed PWHC and PWHI who achieved SVR following DAA treatment to death or October 31, 2021. We computed mortality rates by HIV co-infection status and performed multivariable

POSTER PRESENTATIONS

proportional hazard modeling to assess the effect of HIV co-infection on all-cause, liver-, drug-, and non-liver, non-drug-related mortality. **Results:** There were 12,150 people who achieved SVR following direct-acting antiviral treatment. PWHI: n = 970, person-years (PY) = 3,188.5, deaths = 171; PWHC: n = 11,180, PY = 36,905.3, deaths = 1,146. Median follow-up time was 3.2 years (interquartile range 1.9–4.5; maximum = 7.4). All-cause, liver-, drug- and non-liver, non-drug-related mortality rate among PWHI and PWHC was 53.6 vs. 31.1/1,000PY, 6.0 vs. 8.2/1,000PY, 24.4 vs. 6.5/1,000PY, 23.2 vs. 16.3/1,000PY, respectively. In the multivariable model, HCV/HIV co-infection was associated with higher all-cause (adjusted hazards ratio (AHR): 1.43, 95%CI: 1.20–1.78), drug-related (AHR: 1.57, 95%CI: 1.17–2.10) and non-liver, non-drug related mortality (AHR: 1.39, 95%CI: 1.07–1.80), while risk of liver-related mortality (AHR: 0.90, 95%CI: 0.54–1.51) was not significantly different compared to HCV mono-infection.

Conclusion: After successful HCV treatment, people with HCV/HIV co-infection have similar liver-related mortality as people with HCV mono-infection, but have higher all-cause, drug- and non-liver, non-drug-related mortality. Higher drug-related and non-liver, non-drug-related mortality indicate tailoring services based on syndemic conditions co-occurring with HIV and HCV infections, such as substance use and mental health support and care for chronic non-communicable conditions.

THU-188

Cholestatic HCV-related cryoglobulinemia, a new clinical and pathological entity: a case-control study

Sara Romeo¹, Andrea Dalbeni¹, Serena Amendola², Filippo Cattazzo¹, Anna Tomezzoli², David Sacerdoti³. ¹University and Azienda Ospedaliera Universitaria Integrata of Verona, Division of General Medicine C, Department of Medicine, Verona, Italy; ²University and Azienda Ospedaliera Universitaria Integrata of Verona, Department of Diagnostics and Public Health, Section of Pathology, Verona, Italy; ³University and Azienda Ospedaliera Universitaria Integrata of Verona, Liver Unit, Department of Medicine, Verona, Italy
Email: sara.romeo26@yahoo.it

Background and aims: Mixed cryoglobulinemia (MC), the most common extrahepatic manifestation in chronic hepatitis C virus (CHC), persisting even after virus eradication with direct-acting antiviral agents, can manifest clinically as a systemic vasculitis with manifestations ranging from purpura, arthralgia, and weakness to more severe neurological and kidney involvement and cirrhosis development. Up today, the relationship between MC and liver intrahepatic cholestasis is unknown. Our study aims to investigate a possible correlation between MC and intrahepatic cholestasis in CHC patients.

Method: 31 hepatitis C virus (HCV) + MC + patients were enrolled, matched for age, sex and genotype with 31 HCV + MC -. Patients with known autoimmune diseases were excluded. For each participant, cholestatic parameters (direct bilirubin, alkaline phosphatase and gamma-glutamyl transferase), HCV-RNA, genotype, plasma MC were measured; liver histology and plasma cells (aggregation and distribution), observed blinded by two different operators, were analyzed. Results were evaluated by the Mann-Whitney U test, Fisher's exact test and by stepwise multivariate analysis ($p \leq 0.05$).

Results: 62 participants (mean age 57.3 ± 11.1 years; males = 50%) with CHC were enrolled. Serum cholestasis (2 or more increased cholestatic parameters) was significantly higher in MC + group ($p = 0.02$) and correlated in univariate analysis with cryoglobulinemia (OR 6.9; $p = 0.02$). Plasma cells on liver histology were found in a significantly higher number in MC + group ($p = 0.01$) and tended to form aggregates more than in the control group ($p = 0.05$). In stepwise multivariate analysis with genotype, HCV-RNA, steatosis, gender and age, cholestasis was only related to MC + (OR 13.57; $p = 0.01$).

Conclusion: Our study identified for the first time a correlation between MC, cholestasis and intrahepatic plasma cells in patients with chronic CHC. Future studies are needed to understand how MC causes cholestasis.

THU-189

Hospitalisation-missing an opportunity to link to hepatitis C care: a retrospective study at a regional Australian health service

Christine Roder^{1,2,3}, Carl Cosgrave⁴, Kathryn Mackie^{1,5}, Bridgette McNamara¹, Joseph Doyle^{3,6}, Amanda Wade^{1,2,3}. ¹Barwon Health, Barwon South West Public Health Unit, Geelong, Australia; ²Deakin University, Centre for Innovation in Infectious Disease and Immunology Research (CIIDIR), Geelong, Australia; ³Burnet Institute, Disease Elimination Program, Melbourne, Australia; ⁴Barwon Health, University Hospital Geelong, Geelong, Australia; ⁵Alfred Health, Pharmacy Department, Melbourne, Australia; ⁶Alfred Health and Monash University, Department of Infectious Disease, Melbourne, Australia
Email: christine.roder@gmail.com

Background and aims: Western Victoria has the highest rate of hepatitis C treatment uptake in Australia. Key to achieving micro-elimination in Western Victoria is developing targeted, data driven strategies to increase testing and linkage to care. This study aimed to assess the proportion of inpatients and emergency department (ED) patients identified at risk of hepatitis C or living with hepatitis C who were tested and linked to care and treatment at University Hospital Geelong (UHG), a regional health service in Victoria, Australia.

Method: A retrospective study was performed of adults admitted as hospital or ED inpatients from November 2018 to November 2021. Data were collected from the following databases: hospital admissions (International Classification of Disease, Tenth revision (ICD-10) coded separations), Australian Clinical Labs (pathology), the hospital pharmacy (direct acting antiviral (DAA) scripts), and Liver Clinic (UHG) outpatient service. Separations were selected if they had a code that indicated intravenous drug use (IDU) or hepatitis C.

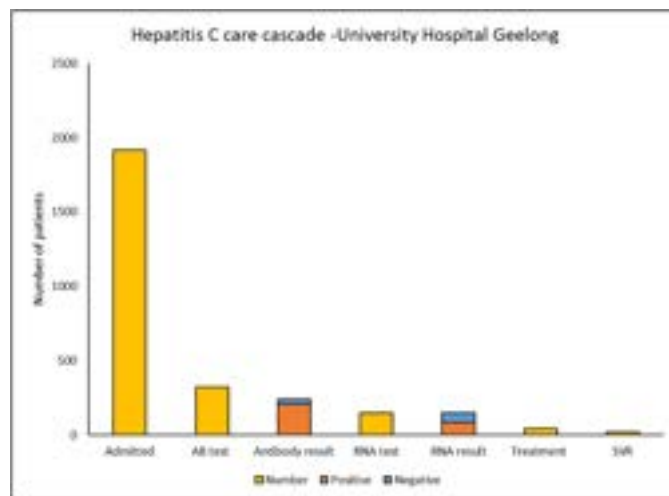


Figure:

Results: There were 1370 patients with IDU coded separations and 628 patients with hepatitis C coded separations (total n = 1917 patients). 16.8% (323/1917) had a documented antibody test and 7.7% (148/1917) had a documented RNA test, 2.2% (43/1917) had a DAA script either dispensed by the hospital pharmacy or prescribed through the Liver Clinic, and 1% (20/1917) had documented cure. Antibody positivity was 65% (210/323) and of those who had an RNA test, RNA was detected in 57.4% (85/148). Of the patients with detectable RNA, 50.6% (43/85) received DAA therapy and 23.5% (20/85) achieved a sustained virologic response (SVR). For hepatitis C coded separations, antibody testing rates were highest in general

medical units (57.1%), and lowest in ED (29.6%). Follow-up RNA testing rates for antibody positivity was similar for all hospital units (67%–73%). For IDU coded separations, antibody testing rates were lower than hepatitis C coded separations, with the highest being hepatitis specialist units (37.5%), and the lowest ED (6.9%). Follow-up RNA testing rates for antibody positivity varied across units (61.5% to 100%).

Conclusion: A targeted intervention that increases hepatitis C antibody testing of people with a history of IDU whilst hospital inpatients is likely to improve linkage to hepatitis C care at our health service, and contribute to micro-elimination.

THU-190

Hepatitis C virus infection follow-up of people who use drugs in the Balearic Islands, Spain

Andrea Herranz¹, Camila Picchio¹, Lucia Bonet², Marita Trelles³, Alicia R Rubi⁴, Leticia Martín⁴, Andreu Sansó⁵, Maria Victoria Moreno⁶, Ana María Sánchez⁶, Jerònima Serra⁷, María Soledad Velasco⁷, Rosa Joy⁸, Marina Lloves⁹, Nora Soria⁹, Maria Buti^{10,11}, Àngels Vilella¹², Jeffrey Lazarus^{1,13}. ¹Barcelona Institute for Global Health (ISGlobal), Hospital Clínic, University of Barcelona, Barcelona, Spain, Spain; ²Department of Gastroenterology, Hospital Universitari Son Espases, Palma, Mallorca, Spain; ³Department of Gastroenterology, Hospital Comarcal d'Inca, Inca, Mallorca, Spain; ⁴Department of Gastroenterology, Hospital Can Misses, Eivissa, Spain; ⁵Department of Gastroenterology, Hospital de Manacor, Manacor, Mallorca, Spain; ⁶Unitat de Conductes Addictives Bons Aires (IBSalut), Palma, Mallorca, Spain; ⁷Unitat de Conductes Addictives Ponent (IBSalut), Palma, Mallorca, Spain; ⁸Centre Inclusió Social (IMAS), Palma, Mallorca, Spain; ⁹Unitat de Conductes Addictives Eivissa, Consell d'Eivissa, Eivissa, Spain; ¹⁰Liver Unit, Hospital Universitari Vall d'Hebron, Barcelona, Spain; ¹¹CIBER Hepatic and Digestive Diseases (CIBERehd), Instituto Carlos III, Madrid, Spain; ¹²Department of Gastroenterology, Hospital Universitari Son Llàtzer, Palma, Mallorca, Spain; ¹³Faculty of Medicine and Health Sciences, University of Barcelona, Barcelona, Spain Email: Jeffrey.Lazarus@isglobal.org

Background and aims: The hepatitis C virus (HCV) infection affects an estimated 56.8 million people and one of the most affected groups are people who use drugs (PWUD). Moreover, PWUD suffer from stigma and discrimination that make it difficult to access healthcare and eliminate HCV infection in this population. In Spain, the *Hepatitis C Free Balears* project was launched to simplify the existing hepatitis C virus (HCV) model of care for people who use drugs (PWUD) in

addiction service centres in the Balearic Islands. This new model of care aims to facilitate treatment completion and monitors for reinfection in this population that, despite being treated, often has difficulties in continued follow-up and has a higher probability of reinfection. The objective of this study is to understand if using simplified and decentralized methods for diagnosis, treatment and follow-up of HCV among PWUD is effective.

Method: This new model of care is being implemented in 21 addiction service centres in the Balearic Islands and includes four phases: 1) recruitment and HCV screening onsite via a point-of-care anti-HCV antibody (Oraquick[®]) and dried blood spot (DBS) testing or blood analysis to confirm viremia (HCV-RNA); 2) linkage to care; 3) treatment prescription via telemedicine; and 4) monitoring onsite of sustained virological response (SVR) at 12 weeks after treatment and monitoring for reinfection after a year, using DBS testing or standard phlebotomy.

Results: Since April 2021, 1251 participants have been recruited of which 409 (33%) were anti-HCV+ and 148 (12%) were HCV-RNA+. Of those, 82 (55%) reported active drug and alcohol use and 25 (17%) had an HIV co-infection.

Of those with active HCV infection, 128 (86%) initiated treatment and 107 (84%) have completed it. SVR12 monitoring was performed in 83 (72%) of those patients who completed treatment, of which 67 (81%) were done by DBS testing. The others (n = 24) did not undergo SVR12 monitoring because the date has not yet arrived (5, 21%) or because they did not show up for the appointment (19, 79%). Of those who were monitored for SVR12, 79 (95%) showed undetectable HCV-RNA. Of the participants screened a year ago or more (612), 70 (11%) have been screened again, using DBS testing in 97% of the cases. Three reinfections were detected in previously treated patients, and no new infections were detected in patients never infected with HCV.

Conclusion: DBS testing is an effective strategy to offer post-treatment and reinfection monitoring in decentralized settings, increasing testing for PWUD participants. With adapted and simplified care models, HCV care can be accessible to those at higher risk of suffering from the infection and facilitates HCV elimination.

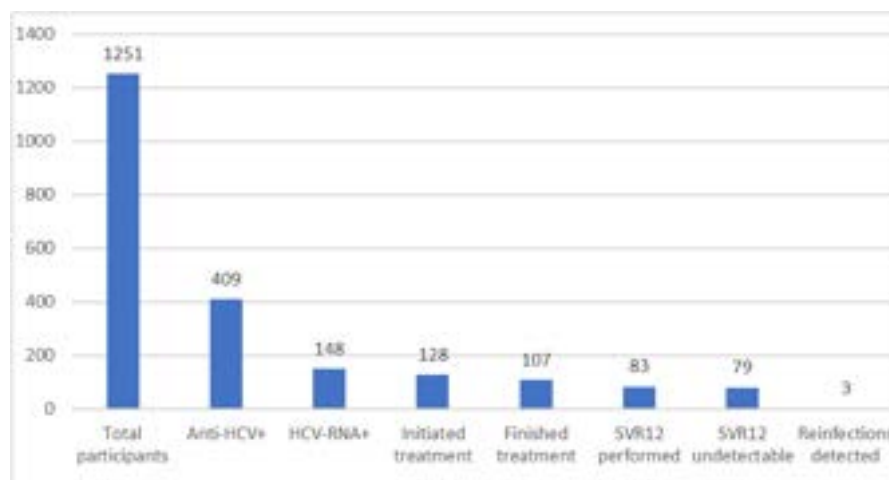


Figure: (abstract: THU-190): *Hepatitis C Free Balears* project treatment cascade (n = 1251).

THU-191

Serum myostatin decreased after direct acting antivirals for cirrhotic patients

Tomoyuki Suehiro¹, Kosuke Matsumoto¹, Yuki Kugiyama¹, Yasuhide Motoyoshi¹, Akira Saeki¹, Shinya Nagaoka¹, Kazumi Yamasaki¹, Atsumasa Komori¹, Hiroshi Yatsushashi¹. ¹Nagasaki Medical Center, Clinical Research Center, Japan
Email: chuntomo0902@gmail.com

Background and aims: Direct-acting antivirals (DAAs) can eradicate HCV even in patients with liver cirrhosis in older age. As cirrhosis itself is also a cause for secondly sarcopenia, optimal and appropriate management of sarcopenia after sustained virological response (SVR) among older patients is of great importance. The purpose of this study is to clarify whether extermination of HCV contributes to the improvement of sarcopenia in patients with type C cirrhosis (LCC), with special attention to chronological changes in sarcopenia-associated molecules including myostatin, which negatively regulate the number and the function of skeletal muscle cells, after secreting from skeletal muscle.

Method: Ninety-nine patients with LCC were treated with DAAs. The median age was 73 (36–92) years. There were 69 patients with Child Pugh (CP)- grade A, and 30 patients with CP-grade B+C. We measured serum myostatin, decorin, follistatin, insulin like growth factor-1 (IGF-1), and skeletal muscle mass index (SMI) at baseline and at SVR 48.

Results: At baseline, patients with CP- B+C group showed significantly higher serum myostatin level than those with CP-A group (CP-B+C, 11409 (3445–26949) pg/dl vs CP-A, 5863 (2292–21795) pg/dl, $p < 0.001$). Multivariate analysis revealed that total bilirubin, prothrombin time, SMI, and M2BPGi were independent factors associated with serum myostatin. Serum myostatin levels were significantly decreased after DAA treatment (baseline 8257 pg/ml vs SVR 48 6394 pg/ml, $p < 0.001$). Though decorin showed similar decrease (baseline 12604 pg/ml vs SVR 48 7953 pg/ml), follistatin and IGF-1 increased significantly (follistatin: baseline 853 pg/ml vs SVR 48 1058 pg/ml, $p < 0.001$; IGF-1: baseline 16.1 ng/ml vs SVR 48 18.2 mg/ml, $p = 0.005$). SMI was restored significantly after DAA treatment (baseline 4.197 vs SVR 48 4.380, $p = 0.009$).

Conclusion: DAA treatment could contribute to improve sarcopenia for LCC patients, possibly by the modulation of sarcopenia-associated molecules.

THU-192

HCV micro-elimination strategy in a tertiary hospital: identification of lost cases and linkage to care

Maria Torner¹, Laura Muñoz Castillo¹, Xavi Grau², Ariadna Clos Parals¹, Aroa Muñoz³, Alba Ardevol Ribalta¹, Gema Fernández-Rivas³, Helena Masnou¹, Águeda Hernández³, Rosa López², Pere Joan Cardona³, Lidia Carabias⁴, Elisa Martró³, Rosa M Morillas¹. ¹Germans Trias i Pujol University Hospital, Hepatology, Badalona, Spain; ²Catalan Institute of Health, North Metropolitan Territorial Management Department, Barcelona province, Spain; ³Germans Trias i Pujol University Hospital, Badalona, Microbiology Department, Spain; ⁴Germans Trias i Pujol University Hospital, Pharmacy Department, Spain
Email: mariatrnsm@gmail.com

Background and aims: Hepatitis C virus (HCV) elimination by 2030 is one of the main goals of the World Health Organization (WHO). The implementation of micro-elimination strategies in each area can help to achieve this goal. Among them, the identification of lost patients (meaning those with active HCV infection not visited and/or treated by a specialist) has been proved to be useful, advisable and cost-effective^{1,2}.

Our aim was to identify patients with active HCV infection lost during the 2010–2022 period in the Northern Metropolitan area of Barcelona, from the Northern Metropolitan Clinical Laboratory (LCMN) registries, describing their characteristics and the success of their linkage to the health system.

Method: As part of an “HCV elimination program” in our area, we designed a strategy based on a computer search of positive HCV-RNA cases with no prior treatment or not cured and retrieval of test results and associated clinical information from clinical records of patients tested at the Microbiology Service of the LCMN, in coordination with the Hospital Information System. The second phase of the intervention focused on the comprehensive review of all clinical records by the Hepatology Unit and selection of candidates for contact, appointment and treatment.

Results: Among the 1461 viremic patients identified, 696 (47.6%) belonged to the area of influence of our tertiary care hospital. Among the latter, 121 (17.4%) were already dead (41.3% due to an hepatic cause). 29 patients (4.2%) had severe comorbidity/frailty and 499 (71.7%) were already under follow-up by an specialist or had already

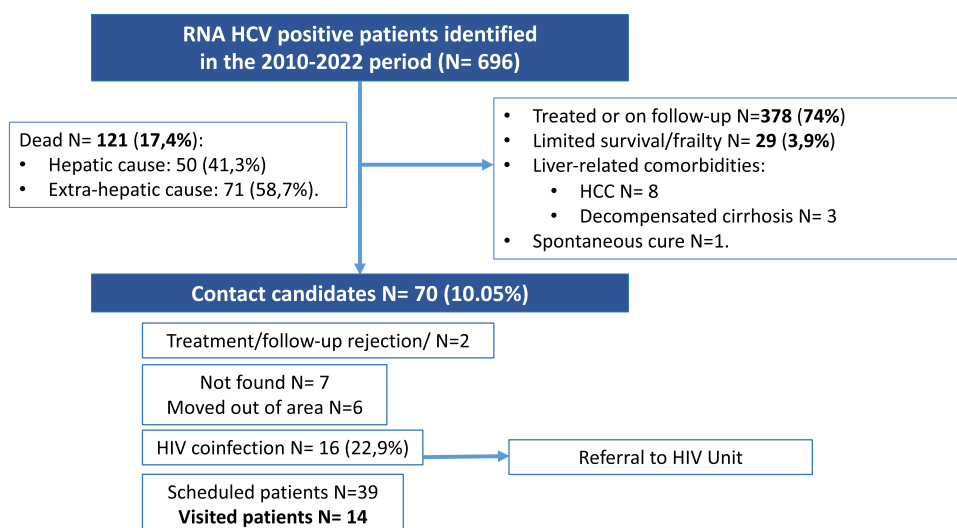


Figure 1. Flowchart of identified patients, selection of candidates for contact and linkage to care. HCC: hepatocellular carcinoma. HIV: human immunodeficiency virus.

Figure: (abstract: THU-192).

been treated. 70 (10.1%) candidates to be contacted were identified, of which 16 (22.9%) had HIV co-infection. Among those not co-infected, 39 patients were referred to the Hepatology Unit and, currently, 10 patients have already started treatment with DAA (3 patients were cured and the rest have a pending evaluation of SVR). Among those patients visited, 3 patients (33%) already had advanced fibrosis/cirrhosis and 1 had an hepatocellular carcinoma.

Conclusion: In our Hospital, up to 10% of RNA-positive patients identified as "lost in the system" were candidates to be contacted. This identification is a demanding task but it has allowed us to identify patients who can benefit from treatment. 33% of patients identified already had advanced liver disease. This strategy can contribute to the elimination of HCV both in our Hospital and others in the Barcelona North Metropolitan region covered by the LCMN.

THU-193

The influence of direct acting antiviral treatment in chronic hepatitis C virus infection on arterial stiffness

Mircea Istrate¹, Letitia Toma¹, Elena Laura Iliescu¹, Razvan Rababoc¹.

¹Fundeni Clinical Institute, Department of Internal Medicine, Bucharest, Romania

Email: mircea.istrate@rez.umfcd.ro

Background and aims: Chronic hepatitis C virus infection represents an important factor of atherosclerosis, related to systemic inflammation and the presence of metabolic syndrome. The aim of this study was to determine the influence of direct acting antiviral treatment in chronic hepatitis C virus infection on arterial stiffness and subsequently on the risk of developing potential cardiovascular pathologies.

Method: We performed a prospective observational study including patients with chronic hepatitis C (all genotypes), without cirrhosis, previously naïve to antiviral therapies. The study was performed during January 2022-January 2023 and included 108 patients receiving Sofosbuvir (400 mg)/Velpatasvir (100 mg), for 12 weeks. Sustained virologic response was defined as undetectable viremia at 12 weeks after the end of therapy. Arterial stiffness was determined both before the initiation of antiviral therapy, as well as after achieving sustained virologic response using oscillometric technique, such as pulse wave velocity (PWV) and pulse wave analysis (PWA) of arterial wave forms. All patients were treated according to current national guidelines and signed informed consent forms regarding the use of their personal data for medical and scientific purposes under the condition of anonymization. Patients with HBV or HIV co-infection were excluded, as well as patients with cirrhosis, solid or hematologic malignancies.

Data analysed were age, sex, Aortic Pulse Wave Velocity (PWVao), Central Systolic Blood Pressure (SBPao) and Aortic Augmentation Index (AIxao). Statistical analysis was performed using IBM SPSS Statistics for Windows, version 26.0 (IBM Corp., Armonk, NY, USA).

Results: The study group included 69 women (69.68%) and 33 men (33.32%), with a mean age and standard deviation of 57.13 ± 8.8 years. Before initiation of antiviral therapy most of the patients had a mean Central Systolic Blood Pressure of 113,13 mmHg (± 10,51 mmHg), a mean Aortic Augmentation Index of 0,29% (± 0,09%) and a mean Aortic Pulse Wave Velocity of 5,27 m/s (± 0,42 m/s). After the 12 weeks of treatment all patients achieved Sustained virologic response and the mean values determined by oscillometric methods varied as follow: the medial Central Systolic Blood Pressure was 108,93 mmHg (± 8,8 mmHg), a mean Aortic Augmentation Index of 0,25% (± 0,1%) and a mean Aortic Pulse Wave Velocity of 5,03 m/s (± 0,35 m/s). While results are not statistically significant, we note a descending trend in arterial stiffness in patients with SVR after DAA.

Conclusion: Obtaining Sustained virologic response in patients with chronic infection with the hepatitis C virus, leads to a decrease in the mean values of Aortic Pulse Wave Velocity, Central Systolic Blood Pressure and Aortic Augmentation Index. The reduction of arterial stiffness merits further longitudinal study in larger cohorts in order

to demonstrate the impact of SVR on the cardiovascular risk of HCV infected patients.

THU-194

One year of HCV/HBV/HIV screening in a psychiatric population consulting in the emergency room (Beaujon Hol/REVHEPAT)

Nathalie Boyer¹, Jamal Abdelkader², Matthieu Gay², Raphael Allali², Prabakar Vaittinada², Cecilia De-Freitas², Murielle Brisson², Béatrice Monnier², Tarik Asselah². ¹Hôpital Beaujon, Service d'hépatologie, France; ²Hôpital Beaujon, France

Email: tarik.asselah@aphp.fr

Background and aims: Hepatitis C virus (HCV) chronic infection is thought to affect 5% of patients with psychiatric pathology. HCV screening in this population is part of the French elimination plan by 2025. In a "patient reach out" approach, seeking medical attention in the emergency room represents an opportunity for contact with care for this precarious population. The treatment of HCV can represent part of the treatment of psychiatric pathology (anxiety, depression). HBV vaccination is also recommended (risk factors, promiscuity). The objective of this pilot work is to evaluate HCV/HBV/HIV screening in the psychiatric population consulting in the emergency room.

Method: Emergency screening (SAU) at Beaujon Hospital (Clichy), of any patient admitted for a psychiatric and/or addiction reason, for whom a Psychiatric expertise is requested. After proposal by the psychiatrist and acceptance by the patient, a screening for the 3 viruses (HCV/HBV/HIV serologies) is carried out at the SAU. The results are collected by the Hepatology department, which makes the diagnosis announcement and ensures, with the REVHEPAT city hospital network, the management of patients tested positive. This collaboration demonstrates the essential role of the hepatologist in a psychiatric setting.

Results: Over 12 months (April 2021–March 2022) (Table) in 665 patients, mean age: 43 years (16–97 years), 64% <50 years, with a F/M ratio of 47%/53%. On the available data, there are consumptions: of alcohol in 32% (189/588) of patients (severe in 54% and moderate in 46%); opiates in 8% (48/565); benzodiazepines = 18% (105/569); cannabis = 23% (131/582); psychostimulants = 10% (56/558). Psychiatric hospitalization was necessary in 50% of cases. Previous viral status was unknown for 90% (357/396) of patients. HCV 3.3% (19/569); HBV 1.6% (9/556); HIV 2.2% (12/558) patients. Among the 19 HCV Antibody positive patients: 10 patients contacted directly: 6 HCV RNA negative patients, 1 refusal of care, 3 appointments not honored; 9 could not be recontacted: 3 psy hospitalizations, 1 remand center, 5 letters to the attending physician. Two patients are co-infected with HIV and 42% patients are to be vaccinated with HBV. All had an unknown prior viral status. Among the 9 HBSAg positive patients: 5 patients have positive HBV DNA (4 F1 patients now followed; 1 PDV), 1 patient already followed by attending physician, 3 letters to the attending physician. Among the 547 HBSAg negative patients: 52% to be HBV vaccinated, 12% immunized and 36% already vaccinated.

Emergency screening	Total : n, (%)	Positive	Positive	Positive
N	665	19	9	12
n/total available		3, 3%	1, 6%	2, 2%
Gender F/H	315/350	5/14	1/8	5/7
Average age (years)	43	52	52	50
Alcohol	32%	60%	38%	20%
Opiates	8%	31%	13%	25%
Benzodiazépines	18%	53%	29%	40%
Cannabis	23%	50%	5%	30%
Psychostimulants	10%	21%	0%	30%

*2 HCV-HIV coinfecting patients; **11 patients already followed with known HIV serology, 1 discovery in a homeless man treated
Figure:

Conclusion: HCV/HBV screening, by going to populations with psychiatric pathology, in particular during emergency contact with care, confirms the high prevalence of viral infection in these

POSTER PRESENTATIONS

populations (HCV ten times higher than in the general population), the opportunity to be able to take care of them, protect them from complications, vaccinate them with HBV and also potentially cure them (HCV) and improve their psychiatric state.

THU-195

Long term normalization of systemic inflammation and endothelial activation after hepatitis C virus (HCV) eradication in HIV/HCV coinfectd, HCV monoinfected patients and HCV-infected liver transplant recipients

Laura Benitez Gutierrez¹, Ana Arias², Ana Duca², Valentin Cuervas-Mons Martínez³, María Jesus Citores⁴. ¹Research Institute and University Puerta de Hierro Majadahonda Hospital, Liver Transplant Unit, Majadahonda, Spain; ²University Puerta de Hierro Majadahonda Hospital, Liver Transplant Unit, Majadahonda, Spain; ³Universidad Autónoma de Madrid, Medicine, Madrid, Spain; ⁴Research Institute Puerta de Hierro- Segovia de Arana, Liver Transplant Unit, Internal Medicine Laboratory, Majadahonda, Spain
Email: lauramariabenitez@gmail.com

Background and aims: Hepatitis C Virus (HCV) infection is associated with a state of chronic inflammation. Patients infected with HCV present increased levels of soluble markers of endothelial dysfunction. We have evaluated the effect of HCV on several soluble markers of systemic inflammation and endothelial activation which favors the development inflammation and result in sustained liver damage in patients infected with HCV, as well as their evolution after long term HCV eradication with DAAs therapy.

Method: A total of 53 patients with chronic HCV infection treated with DAAs were subgroups as: HCV monoinfected (n = 14, group 1), HCV-infected liver transplant recipients (n = 17, group 2) and HIV/HCV coinfectd patients (n = 22, group 3). Blood samples were collected from all subjects at baseline (pre-DAAs treatment), 12 weeks after the end of treatment when sustained virological response (SVR) was evaluated and 4.19 (\pm 0.55) years after the SVR. Liver stiffness (LS) assessed using a FibroScan[®], and the results were expressed in kilopascals (KPa). The next cut-off LS were used: LS < 7.1 KPa F0-F1; 7.1–9.4 KPa F2; 9.5–12.4 KPa F3; and > 12.5 KPa F4, biochemical parameters of liver damage (bilirubin, albumin, ALT, AST, GGT, AP) and ICAM-1 and CXCL10 quantified by Cytometric Bead array (CBA) were recorded at each time point.

Results: Baseline LS was F4 in 45%, F2-F3 in 26% and F1 in 28% patients. F4 stage of LS was present in 80% patients of group 1, while only in 25% and 38% of patients of group 2 and 3 respectively. Levels of ICAM-1, CXCL10, LS (Kpa), bilirubin, ALT, AST, GGT and AP significantly decreased (all p < 0.001) and albumin levels increased (p < 0.01) in SVR and long term post-SVR compared to baseline in all the three study groups. ICAM-1 baseline levels were positively correlated with bilirubin, AST and AP while negatively correlated with albumin levels (all p < 0.05). There was a positive correlation between CXCL10 and ALT/AST basal levels (all p < 0.01) Considering fibrosis stage according the LS ICAM-1 baseline levels were higher in patients with LS \geq F2 (p = 0.008)

Conclusion: The state of chronic inflammation decreases after HCV clearance and it is maintained long term post-SVR in HCV mono-infected patients, HCV-infected liver transplant recipients and HIV/VHC coinfectd patients.

THU-196

Differences in baseline characteristics of direct acting antiviral (DAA)- treated Greek HCV patients according to source of infection

Spyridon (Spyros) Siakavellas¹, Hariklia Kranidioti¹, Anastasia Kourikou¹, Charalampos Karageorgos¹, Anestis Goulas¹, Sofia Vasileiadi¹, Georgios Kontos¹, Nikolaos Papadopoulos¹, Melanie Deutsch¹, Spiliotis Manolopoulos¹. ¹Geniko Nosokomeio Athinon "Ippokrateio", Hepatogastroenterology Unit, 2nd Academic Department of Internal Medicine, Athens, Greece
Email: s.siakavellas@gmail.com

Athinon "Ippokrateio", Hepatogastroenterology Unit, 2nd Academic Department of Internal Medicine, Greece
Email: s.siakavellas@gmail.com

Background and aims: With the introduction of direct-antiviral medication (DAAs), eradication of HCV infection is considered now an achievable goal. While people with history of drug use (PWHU) form the most common population at risk for the infection, in Greece historically there has been a significant proportion of patients arising from the general population with no prior drug use. These two different subgroups exhibit different characteristics, that may be pertinent in the management of HCV infection and long-term follow-up. The aim of this study was to identify potential differences in the makeup of these two HCV patient subgroups.

Method: The HERACLIS cohort, is the largest national HCV registry of patients treated with DAAs in tertiary liver centers from 2015 until 2022. Clinical data and characteristics were obtained from medical records, while transient elastography (TE) measurements and APRI and FIB-4 score calculations were conducted at baseline. Patients were followed up initially for the duration of their treatment.

Results: 680 patients were included in the study, 70.9% (n = 482) of them were men with median age 50.8 years old and 13.6% of these had decompensated liver disease at DAA initiation. 62% (n = 422) of this cohort were PWHU, while the rest had been infected in another manner (non-PWHU). When comparing these two populations, PWHU were younger in age (47.3 ± 9.8 vs 56.3 ± 12.8 years, p < 0.001) and with lower BMI (24.3 ± 4.2 vs 26.1 ± 4.6 kg/m², p < 0.001). Non-PWHU cases had more often diabetes (4.9% vs 1.3%, p < 0.001), hypertension (10.7% vs 8.8%, p < 0.001) as well as decompensated liver disease (8.0% vs 5.6%, p < 0.001). This was also reflected by TE measurements (14.6 ± 11.1 vs 11.3 ± 7.9 kPa, p = 0.001) and FIB-4 score calculations (2.8 ± 2.6 vs 2.2 ± 4.0 vs, p < 0.001) but not by the APRI score. Moreover, PWHU patients tended to have been more often infected with genotype 3 (36.8% vs 8.8%, p < 0.001) while for other genotypes no such stark differences were observed. There was no significant variance observed regarding DAA regimen use but non-PWHU patients tended to suffer more often from adverse events secondary to DAA treatment (1.6% vs 0.3%, p = 0.001).

Conclusion: The Greek PWHU and non-PWHU populations of HCV patients seem to exhibit different baseline characteristics which may be relevant to treatment selection and long-term follow-up regimens. The main differences observed imply the concomitant presence of an element of metabolic syndrome in the non-PWHU cohort with a subsequent potential effect on the degree of underlying liver fibrosis.

THU-197

Incidence and associations of HCV reinfection in the era of direct acting antivirals

Sofia Vasileiadi¹, Kanellos Koustenis¹, Maria Manolakopoulou¹, Charalampos Karageorgos¹, Anestis Goulas¹, Hariklia Kranidioti¹, Spyridon (Spyros) Siakavellas¹, Melanie Deutsch¹, Olga Anagnostou¹, Spiliotis Manolopoulos¹. ¹Geniko Nosokomeio Athinon "Ippokrateio", Hepatogastroenterology Unit, 2nd Academic Department of Internal Medicine, Athens, Greece
Email: s.siakavellas@gmail.com

Background and aims: The introduction of highly effective direct acting antivirals (DAAs) has dramatically changed our practice against HCV infection with high therapy uptake and high response rates; one may argue for higher reinfection rates. The reinfection rates especially in high-risk populations could become a significant barrier in the strategy of HCV elimination. Our aim is to explore the HCV reinfection rate after successful HCV therapy with DAAs in a cohort of people who use drugs (PWUD) and define factors associated with reinfection.

Method: We included patients with chronic compensated hepatitis C who had history of past or current illicit drug use. All had been treated successfully with DAAs in our tertiary center between 2014 and 2021. HCV cure was defined with serum HCV RNA no detectability 3–12

months after the end of treatment (SVR). All patients were contacted at least one year after the end of the treatment via phone call and were invited to a follow-up visit where HCV RNA levels, liver function tests and transient elastography (TE) were performed. Parameters regarding their social-economic status and drug use habits, were also recorded. Serum HCV RNA detectable after SVR was defined as reinfection. This is a preliminary analysis of 174 patients who were called twice; 78 of them did not respond.

Results: 96 patients (82.3% men) were included in the study, with median age 53 (range 34–68) years. 24% (n = 23) had evidence of cirrhosis, 62.5% (n = 60) were unemployed, 66.7% (n = 64) were single and 22.8% (n = 21) had been incarcerated at some point in the past. Almost 60% (n = 57) attended a substitution or therapeutic community program for drug use, with 34.4% (n = 33) reporting drug use in the last 12 months, of which 36.4% (n = 12) shared syringes/other paraphernalia, while 39.4% (n = 13) reported intravenous drug use and 39.4% (n = 13) used drugs via the nasal route. We identified 7 HCV reinfections during 189 PY of follow-up, yielding a reinfection rate of 3.7/100 PY. We found that the reinfection group included younger (44 ± 5 vs 53 ± 8 years, $p = 0.005$) patients, the majority (n = 6, 85.7%) of them under the age of 50, and with a concomitant history of having been imprisoned (85.7% vs 20.2%, $p < 0.001$). Moreover, people in the reinfection group reported longer total history of intravenous drug use (24 ± 8 vs 15 ± 8 years, $p = 0.012$), more often active drug use in the past 12 months (100% vs 29.2%, $p < 0.001$), intravenous drug use (71.4% vs 9%, $p < 0.001$) and shared syringes/paraphernalia (85.7% vs 21.3%, $p < 0.001$). Reinfection was also significantly associated with HIV co-infection (42.9% vs 0%, $p < 0.001$) and cannabis consumption (85.7% vs 37.1%, $p = 0.017$). HCV genotypes in reinfected patients were different compared to baseline pretherapy ones.

Conclusion: HCV reinfection rates after SVR were higher among younger patients who continued high risk behaviors. These data underlined the importance of follow-up assessment for PWUD and the necessity of sustained linkage to health care services.

THU-198

Evaluation of patients treated with direct-acting anti-viral therapy for chronic hepatitis C and their risk of hepatocellular carcinoma in Hong Kong

Victor Yung Sin Chow¹, Veronica Wing I Cheung¹. ¹Our Lady of Maryknoll Hospital, Hong Kong
Email: victor.chow06@gmail.com

Background and aims: To evaluate the risk of early hepatocellular carcinoma (HCC) and its risk factors in chronic hepatitis C patients treated with direct-acting antivirals (DAAs) in Hong Kong.

Method: 333 consecutive chronic hepatitis C patients treated with DAAs from two hospitals over the past 6 years were identified. Kaplan-Meier method was used to calculate cumulative HCC incidence. Cox regression was used to identify factors associated with HCC development. Receiver operating characteristic curve analysis was performed to determine the optimal cut-off levels of AFP for predicting HCC development.

Results: During a median follow-up of 23.4 months after DAA started, 15 (5.4%, 95% Confidence Interval 3.3%–8.7%) out of 279 total included patients developed HCC. The overall sustained virological response (SVR) rate was 98.9%. The 1-year cumulative incidence for de-novo HCC and HCC recurrence were 0.8% and 30.9%, respectively (log-rank test $p < 0.001$). The 1-year cumulative HCC incidence for patients without and with cirrhosis were 0.7% and 5.1%, respectively (log-rank test $p = 0.036$). Univariate analysis showed that significant factors associated with HCC after DAA were: history of previous HCC with curative treatment with subsequent complete radiologic response (Hazard Ratio, HR, 28.88, 95% CI 9.32–89.49, $p < 0.001$), cirrhosis (HR 3.57, 95% CI 1.00–12.77, $p = 0.0499$), evidence of portal hypertension (HR 4.27, 95% CI 1.51–12.07, $p = 0.006$), higher AFP at the start (HR 1.02, 95% CI 1.01–1.03, $p < 0.001$) or end (HR 1.09, 95% CI 1.05–1.14, $p < 0.001$) of DAA therapy, higher bilirubin (HR 1.09, 95% CI 1.04–1.14, $p <$

0.001), lower platelets (HR 0.99, 95% CI 0.98–0.999), lower albumin (HR 0.89, 95% CI 0.81–0.97, $p = 0.007$), and older age (HR 1.07, 95% CI 1.02–1.12, $p = 0.007$). The optimal cut-off level of AFP at the start of DAA therapy for predicting HCC was 10.5 ng/ml (sensitivity 80%, specificity 84.2%, AUROC 0.868). The cumulative incidence of HCC development for the group with AFP level < 10.5 ng/ml at the start of DAA therapy was significantly lower than that for the group with AFP level ≥ 10.5 ng/ml (log-rank test $p < 0.001$). The 1-year cumulative incidence of HCC were 0.5% (95% CI 0%–1.6%) and 12.6% (95% CI 3.1%–22.1%) for the groups with AFP level < 10.5 ng/ml and ≥ 10.5 ng/ml at the start of DAA therapy, respectively. On the other hand, the optimal cut-off level of AFP at the end of DAA therapy for predicting HCC was 5.6 ng/ml (sensitivity 78.6%, specificity 80.5%, AUROC 0.864). The cumulative incidence of HCC development for the group with AFP level < 5.6 ng/ml at the end of DAA therapy was significantly lower than that for the group with AFP level ≥ 5.6 ng/ml (log-rank test $p < 0.001$). The 1-year cumulative incidence of HCC were 0.6% (95% CI 0%–1.7%) and 11.8% (95% CI 2.8%–20.8%) for the groups with AFP level < 5.6 ng/ml and ≥ 5.6 ng/ml at the end of DAA therapy, respectively.

Figure:

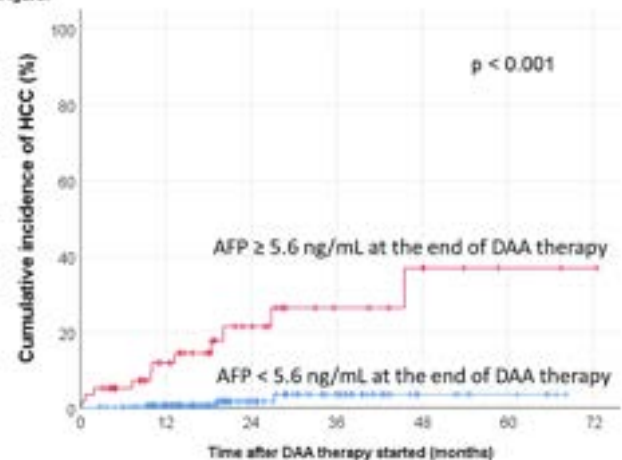


Figure:

Conclusion: Following DAA therapy and achieving SVR in the vast majority of chronic hepatitis C patients, the risk of early de-novo HCC development is low, but the risk of early HCC recurrence remains very high. Higher AFP levels, with cut-off at 10.5 ng/ml and 5.6 ng/ml, at the start and end of DAA therapy respectively, can be useful in stratifying the risk of HCC development.

THU-199

The prevalence of hepatitis C virus infection in high-risk patients with high normal alanine aminotransferase (ALT) in Israel: a bio bank analysis

Amir Shlomai¹, Daniella Beller², Sapir Hadadi³, Galit Rimler⁴, Lilita Schreiber⁴, Gabriel Chodik⁵, Asaf Peretz². ¹Rabin Medical Center, Medicine D, Israel; ²KSM, Maccabi's research and innovation institute, Israel; ³AbbVie Inc, Hod-Hasharon, Israel; ⁴Maccabi MEGA lab, Maccabi Healthcare Services, Israel; ⁵SM, Maccabi's research and innovation institute, Israel
Email: shlomaiaamir@gmail.com

Background and aims: Chronic hepatitis C virus (HCV) infection is a major worldwide problem. Direct antiviral agents (DAAs) are highly effective against HCV and result in nearly 100% cure rate. In Israel, the current prevalence of HCV is estimated at 2% among high-risk adult population, such as former union of soviet socialist republics (USSR) residents. However, the majority of HCV carriers in Israel remain unaware of their disease and are therefore untreated, despite the wide availability of DAAs that are included in the Israeli health-basket. In recent years, it became clear that "healthy" alanine

POSTER PRESENTATIONS

aminotransferase (ALT) values are even lower than previously thought and that a substantial fraction of people with “high normal” ALT might still have an underlying liver disease, including chronic HCV infection. The aim of this study is to determine the prevalence of chronic HCV infection in high-risk population with high-normal ALT.

Method: Adults that opt-in to the Maccabi Healthcare Services biobank and were never tested for HCV before were included. We assessed the prevalence of anti-HCV antibodies in patients who were tested for serum ALT in 2020. Based on inclusion criteria and based on ALT levels, fresh samples from biobank participants were tested for HCV antibodies by CMIA. In case of borderline results, immunoblotting was performed. RT-PCR for HCV RNA was performed on samples with positive HCV antibodies.

Results: The study was conducted in two stages: First, a total of 350 individuals with serum ALT >25 IU/L for women and >33 IU/L for men (mean age = 55 [19, 100]; 36% males; 21% (73/350) former USSR residents, mean ALT = 49.5 [26, 787]) were included in the analysis. Among them, five were positive for HCV antibodies, and only one female patient (0.29%; 95%CI: 0.01% to 1.58%), a former USSR resident with ALT = 30 IU/L, was confirmed positive by PCR. We next focused on former USSR residents with high-normal ALT. Of 202 samples (mean age 57, 39% males) who had high-normal ALT (>25 IU/L <50 IU/L for women, >33 IU/L <50 IU/L for men, mean level 34.3 [25, 50]) tested for anti-HCV antibodies, only 1 patient (0.5%) was found positive by RT-PCR.

Conclusion: The prevalence of HCV positivity in a large Israeli biobank setting is lower than expected. Focusing on high-risk adults with high normal ALT does not improve the yield of screening for HCV carriers in this setting.

THU-200

HCV screening: shortening read time of point-of-care rapid diagnostic test does not effect detection rates of antibodies against hepatitis C virus

Muhammad Nabeel Shafqat¹, Auj Chaudhry², Najam-us-sehar Saeed¹, Asad Choudhry², Muhammad Sohail Khan³, Ghania Shafqat², Fatima Akram¹. ¹District Headquarter Hospital-Gujranwala Medical College, Department of Gastroenterology, Gujranwala, Pakistan; ²PARSA Trust Liver Clinic, Al-Rae Hospital, Gujranwala, Pakistan; ³Univeristy of

the Punjab, Institute of Business and Information Technology, Lahore, Pakistan

Email: nabeelshafqat89@gmail.com

Background and aims: Hepatitis C virus (HCV) infection is a public health threat worldwide and Pakistan has one of the highest HCV prevalence in the world. The WHO has proposed the goal of eliminating viral hepatitis as a public health threat by 2030. This requires a massive scale-up in screening efforts. Simplification of point-of-care (POC) rapid diagnostic test (RDT) which detects anti-HCV antibodies would enhance overall linkage to care, particularly for mass screening and difficult-to-reach populations. Currently, the recommended read time of POC rapid diagnostic detection test to identify antibody positive samples is 20 min. A positive POC RDT result is then followed by a reflex HCV RNA testing to confirm active viremia. This study was conducted to determine whether a shorter read time of 5 minutes could be used to identify all anti-HCV antibody positive samples, and decrease the need for reflex testing by conducting HCV RNA test on the same sample to identify active viremia.

Method: The SD Bioline HCV POC RDT was used for the qualitative detection of antibodies specific to HCV. Any detectable band on RDT was counted as positive, regardless of band intensity. Samples were collected at two sites: a tertiary care hospital and through community screening. HCV screening was done on the mentioned kit at District Headquarter Hospital-Gujranwala Medical College and PARSA Trust Liver Clinic at Gujranwala, Pakistan. Blood samples were tested immediately after collection of whole blood, via finger prick. Two blinded observers, at both collection centres, separately recorded the time-to-positivity by continuous observation during the first 5 minutes, then each minute after, up to 10 minutes and then again at 15 and 20 minutes. The time-to-positivity on RDT was measured by using a stopwatch to note the exact duration of time from the point when sample was placed on RDT kit till the point a positive result appeared. A sample of HCV RNA by PCR was collected in all those who tested positive for anti-HCV antibodies.

Results: Of 1266 patients with a positive test result on anti-HCV antibody POC RDT test, there were 766 (61%) cases with active viremia. In participants with active viremia, 52.7% (404/766) females and 47.3% (362/766) males, the mean age (\pm SD) was 46.37 years (\pm 15.53). In viremic patients, the median time-to-positivity was 1.8

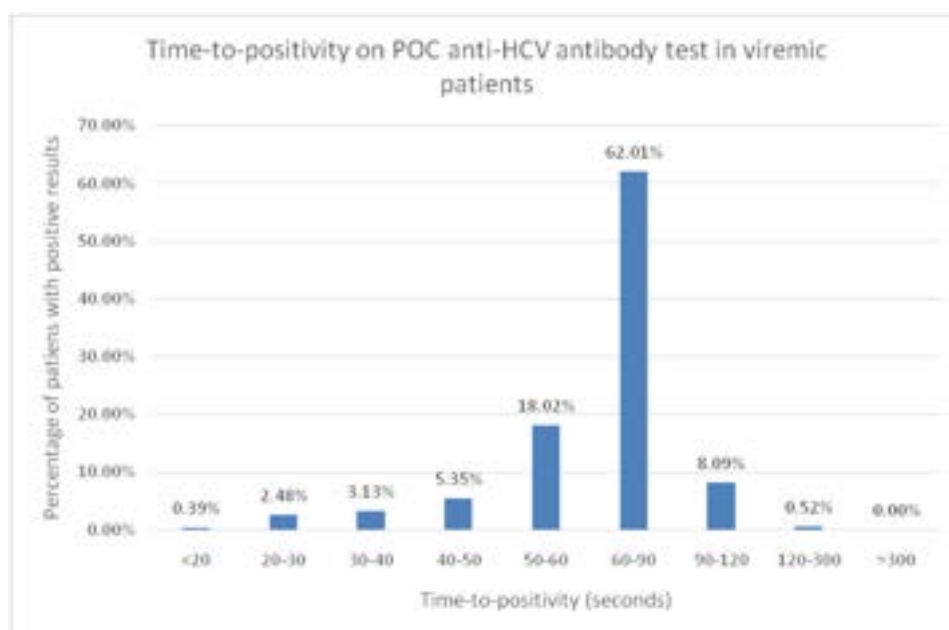


Figure: (abstract: THU-200).

minutes (range, 0.2–2.2 min). Out of all viremic cases, 62.01% of participants had a positive test result in between 60 and 90 seconds whereas 18.02% produced a positive result within 50–60 seconds. Less than 1% of patients with active viremia had a positive screening test within 120–300 seconds. All the patients with active viremia produced a positive result in the antibody RDT test within 5 minutes read time.

Conclusion: Reducing read time of SD bioline rapid antibody POC test from 20 minutes to 5 minutes causes no loss of antibody detection in patients with active viremia. Shortening read time could improve screening efficiency, decrease loss to follow-up rates and can potentially reduce the need for reflex HCV RNA testing. Further studies evaluating POC RDT should be undertaken to explore its utility in replacing HCV RNA by PCR test to detect active viremia in resource poor settings.

THU-201

Digital pathology quantification of cirrhosis severity continuum in human HCV liver biopsies and its correspondence with Laennec and Beijing stages

Louis Petitjean¹, Xiaofei Zhang², Thomas Schiano³, Mathieu Petitjean¹, Maria Isabel Fiel⁴. ¹PharmaNest, Inc, Princeton, United States; ²NYU Long Island School of Medicine, Department of Pathology, Mineola, United States; ³Icahn School of Medicine at Mount Sinai, Intestinal Transplantation, Liver Transplantation, Gastroenterology, New York, United States; ⁴Icahn School of Medicine at Mount Sinai, Department of Pathology, Molecular and Cell-Based Medicine, New York, United States
Email: mathieu.petitjean@pharmanest.com

Background and aims: Cirrhosis severity is defined histologically as a continuous process in which the normal anatomical lobules are replaced by architecturally abnormal nodules separated by fibrous tissue of different morphological phenotypes. The Laennec system, and, more recently the Beijing classification, have been used to subclassify various histological degrees of cirrhosis severity and activity. These methods lack intra-operator reproducibility and have poor detection thresholds. Here, we report on the development of an automated quantitative Digital Pathology and AI method (FibroNest) to quantify cirrhosis severity and activity and assess its correspondence with Laennec and Beijing scores.

Method: 20 consecutive hepatitis C (HCV) patients undergoing liver transplantation consented to participate in an IRB-approved protocol. 5 core biopsies were taken from five segments of the liver immediately after explantation. Formalin-fixed, paraffin embedded sections of the biopsies were stained with Masson trichrome and

scanned at 20X for Digital Pathology. The Laennec system (4A–4C indicating increasing degrees of cirrhosis) and Beijing classification (P–progressive, I–indeterminate, R–regressive,) were assessed by an expert pathologist (MIF). This HCV cohort (n = 100) demonstrated a large variety of severity stages (doi 10.1038/s41379-021-00881-z). Quantitative image analysis was performed to extract single fiber quantitative traits (qFTs, N = 335) to describe the collagen, the fiber morphometric and fibrosis architectural phenotypic dimensions. Principal components of the qFT dataset were automatically identified to account for variability along the Laennec, and the Beijing stages, and then assembled into a normalized Cirrhosis Severity composite Score (CFS) and a Cirrhosis Activity composite Score (CAS).

Results: The AI-enabled CFS and CAS scores classify extreme stages (4A vs 4C, P vs R) with strong statistical significance (p = 0.0011 and p = 0.0004 respectively) in contrast to earlier studies where the Collagen Proportional Area did not correlate with Laennec and Beijing histological scores (doi 10.1038/s41379-021-00881-z). The intermediate stages (4A vs 4B; 4B vs 4C; P vs I; I vs R) are classified with moderate performance (p values = 0.016; 0.082; 0.004; 0.042 respectively) but it is not clear if the uncertainty is driven by the computational method of the pathologist's interpretation. All the three sub-phenotypic layers (for which specific sub-scores are also created) play complementary roles. For instance, the Architecture-CFS classifies 4A vs 4B groups with a p value of 0.001.

Conclusion: The automated quantification of multiple histological phenotypic traits resolves the complexity of the histological assessment of severity and the activity in the cirrhosis continuum with a performance that benchmarks pathologist assessments.

THU-202

Prognostic factors of post-sustained virological response outcome in patients with chronic hepatitis C treated with direct-acting antivirals

Won Sohn¹, Sang Hoon Ahn², Young Seok Kim³, Seung Up Kim⁴. ¹Kangbuk Samsung Hospital, Sungkyunkwan University School of Medicine, Korea, Rep. of South; ²Severance Hospital, Yonsei University College of Medicine, Korea, Rep. of South; ³Soonchunhyang University, Bucheon Hospital, Korea, Rep. of South; ⁴Severance Hospital, Yonsei University College of Medicine, Korea, Rep. of South
Email: ksukorea@yuhs.ac

Background and aims: Direct acting antivirals (DAAs) is the mainstay of antiviral therapy for patients with chronic hepatitis C (CHC). We investigated prognostic factors for the post-sustained virological response (SVR) outcomes in patients with CHC treated DAAs.

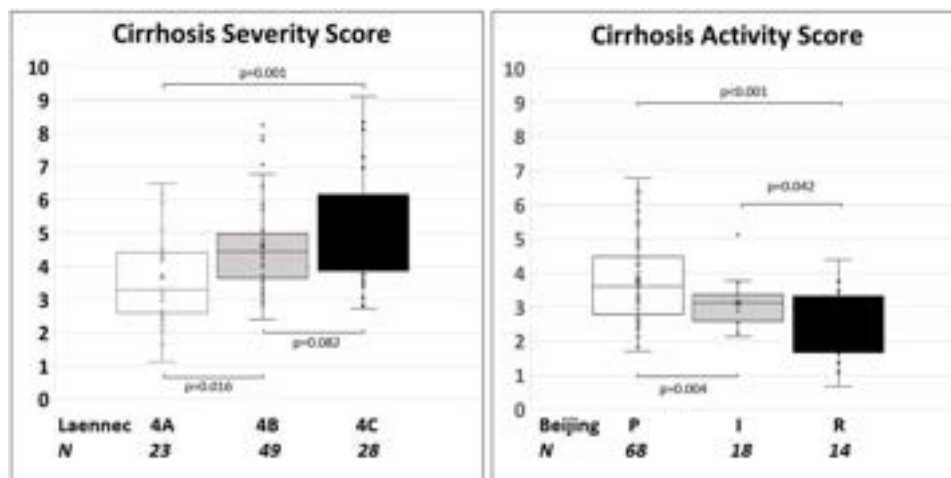


Figure: (abstract: THU-201).

POSTER PRESENTATIONS

Method: This multicentre, retrospective, nationwide cohort study consisted of 1,248 patients with CHC who were seen at 29 expert hepatology centres in Korea from January 2015 to December 2022 and who achieved SVR after DAA therapy. The primary outcome was the development of liver-related events (LREs) after SVR, including all-cause death, hepatocellular carcinoma (HCC), decompensation, or liver transplantation. The fibrotic burden at baseline and at SVR was assessed using transient elastography (TE) and the FIB-4 index.

Results: The mean age of the patients was 59.8 years and 58% (n = 722) were male. The prevalence of genotypes 1 and 2 was 52% and 46%, respectively. The mean liver stiffness value was 11.6 ± 9.8 kPa at baseline and 8.8 ± 7.5 kPa at SVR. LREs developed in 77 (6.2%) patients and consisted of death in 13, HCC in 34, decompensation in 44 and liver transplantation in 2 patients. The multivariable analysis showed that TE-defined cirrhosis at baseline (liver stiffness ≥ 14.4 kPa; hazard ratio [HR] = 2.56; 95% confidence interval [CI] 1.30–5.07) and FIB-4-defined advanced fibrosis stage at SVR (>3.25) (HR = 3.24; 95% CI 1.45–7.22) were independently associated with an increased risk of developing LREs (all $p < 0.05$), together with male sex (HR = 1.99; 95% CI 1.26–3.14) and lower serum albumin level at SVR (<4.0 g/dL) (HR = 1.87; 95% CI 1.12–3.13) (all $p < 0.05$).

Conclusion: The fibrotic burden decreased in patients with CHC after DAA treatment. However, the risk of developing LREs remained even after SVR. Our study showed that an assessment of fibrotic burden before and after DAA treatment is required for predicting outcomes in patients with DAA-treated CHC who achieve SVR.

THU-203

Utilising peer support workers in hepatitis C screening in emergency departments: a pilot study

Alex Caulder^{1,2}, Jane Gitahi¹, Ann Archer^{1,3}, Abigail Sellick^{1,2}, Julie Marshall¹, Kushala Abeysekera^{1,3}, Fiona Gordon¹. ¹University Hospitals Bristol and Weston NHS Foundation Trust, Liver Medicine, Bristol, United Kingdom; ²Hepatitis C Trust, London, United Kingdom; ³University of Bristol, Population Health Sciences, Bristol, United Kingdom

Email: alex.caulder@uhbw.nhs.uk

Background and aims: As widespread availability of directly acting antivirals (DAAs) for hepatitis C (HCV) has improved, engaging with hard-to-reach groups with higher HCV prevalence has become a major focus of public health strategy. People who inject drugs (PWIDs) and the homeless often have difficulty engaging with screening measures and subsequent treatment. Outcomes for patients with liver disease have been repeatedly demonstrated to

be worse in those with greater social deprivation. Baseline HCV testing of PWIDs attending our ED was low (6.3%) with a local HCV RNA positive prevalence of 10% in patients who were current injectors (2022 unpublished NHS England data). Peer support workers (PSW) have been shown to have high acceptability amongst patients with HCV to facilitate community-based screening and treatment. We sought to embed a PSW in the emergency department (ED) to see if this impacted detection of HCV and treatment initiation amongst PWIDs and homeless patients.

Method: 9-month pilot conducted between Feb–Nov 2022. PWIDs and homeless patients attending Bristol Royal Infirmary ED who identified through ED triage nurses and electronic alert systems. Highlighted patients were screened with OraQuick™ antibody and/or capillary blood-borne virus (BBV) testing. HCV positive patients were reviewed by a PSW, supported with Homeless Health team and Drugs and Alcohol nurse specialist. All HCV RNA positive patients were referred for treatment unless declined.

Results: 135 patients (81 males; 60%) were offered HCV testing at 159,126 patient ED episodes during the study period, which was accepted by 113 patients (26 OraQuick™ antibody; 88 BBV testing). In total, 24% of patients offered screening were HCV RNA positive (n = 33/135). 18 of these patients were known HCV RNA positive but had not been treated (54%), whilst 8/53 (15%) HCV RNA negative patients had previously missed their SVR check post-treatment. 5 of the 33 HCV RNA positive patients (15%) had become re-infected post prior successful treatment. 25/33 HCV RNA positive patients were aided by PSW to start treatment, giving a treatment conversion rate of 76% (positive test to treatment initiation). SVR data will be presented.

Conclusion: PSWs embedded within ED encourage high levels of engagement from PWIDs and homeless patients with HCV screening and treatment. This targeted strategy in a hard-to-reach population with high HCV prevalence offers an alternative approach to opt-out BBV testing of ED blood samples.

THU-204

A large-scale, centralized viral hepatitis screening model in Hainan province of China during the COVID-19 pandemic

Tao Wu¹, Biao Wu¹, Feng Lin¹, Jiao Wang¹, Jianzhi Zhao², Lan Chen³, Jinjie Li⁴. ¹Hainan General Hospital, Haikou, China; ²Dongfang Municipal Health Commission, Dongfang, China; ³Dongfang People's Hospital, Dongfang, China; ⁴Dongfang Center for Disease Control and Prevention, Dongfang, China
Email: wutao1_ren@163.com

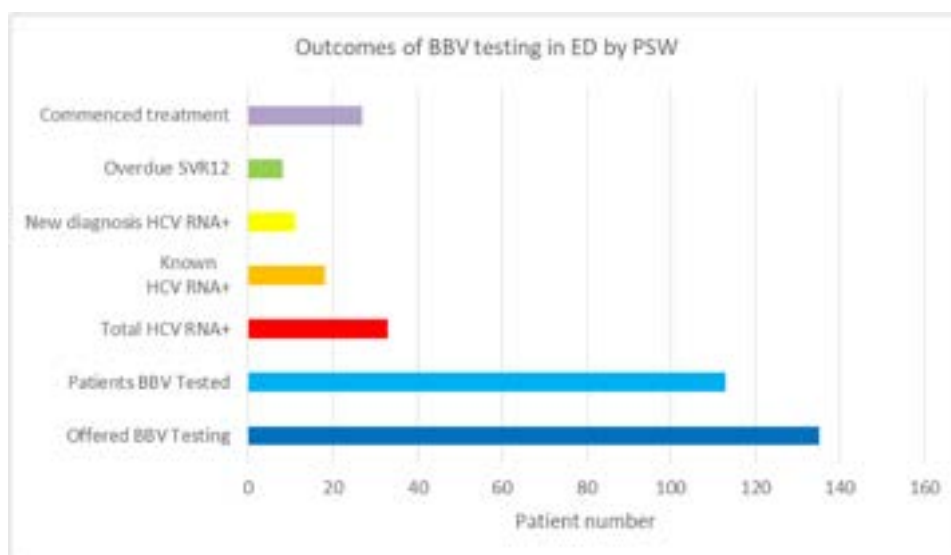


Figure: (abstract: THU-203).

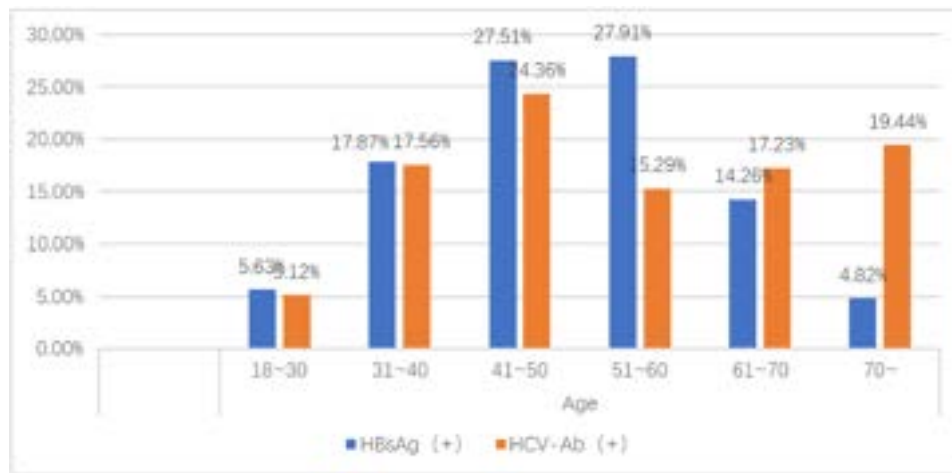


Figure: (abstract: THU-204): The baseline characteristics.

Background and aims: Hainan Province of China is on target to meet the 2030 WHO goal of viral hepatitis elimination by 2025. An increase in screening rates is required to meet this target. The Viral Hepatitis Elimination project kicked off in Jan. 2022. Dongfang city of Hainan Province is listed as a pilot. HBV/HCV screening should be considered a priority in this regard. And over the past year, we have also carried out regular screening for SARS-CoV-2, which means that all people can participate in the screening.

Method: Under the leadership of the Hainan government, the specialists from 3A hospitals in Hainan province worked with the primary doctors in Dongfang city on the training to increase the awareness of viral hepatitis. We have also worked with the staffs of community, who are trained to handle outbreak prevention and control, to conduct screening campaigns. We completed screening for HBV/HCV at one time in pilot areas in Dongfang.

Results: We conducted a daily public screening campaign in the pilot areas from Nov.11th, 2022 to Dec.8th, 2022. Totally, 22,137 people (>18y) were screened in the pilot area, and 38,774 of them were screened HCV at one time, 2.3% of them are HCV-Ab (+), 183,593 of them were screen HBV, 7.3% of them are HBsAg (+). The incidence rate of HBsAg (+) people is higher when they are >30 <70 years old, especially when they are 40-60 years old. There are more cases of HCV-Ab (+) in people over 30 years old, especially in people aged 41-50.

Conclusion: This is a model of government-led and multi-party collaboration to increase awareness about viral hepatitis and successfully conduct screening campaigns. When the resources are limited, it is more beneficial to improve the efficiency of screening by focusing on the screening of HBsAg and HCV-Ab for people over 30 years old. It would be a good model for contributing to viral hepatitis elimination.

THU-205

Usefulness of serum CCL20 as a post sustained viral response biomarker for HCV-associated liver fibrosis

Atsumasa Komori¹, Kosuke Matsumoto², Yuki Kugiyama², Tomoyuki Suehiro², Yasuhide Motoyoshi¹, Akira Saeki², Shinya Nagaoka², Hiroshi Yatsushashi². ¹National Hospital Organization Nagasaki Medical Center, Clinical Research Center, Omura, Japan;

²National Hospital Organization Nagasaki Medical Center, Hepatology, Omura, Japan

Email: atsuriko1027@yahoo.co.jp

Background and aims: CCL20 is one of the advanced fibrosis-associated genes, that were commonly up-regulated among livers in

advanced HCV, HBV, and NASH patients (Komori et al. Hepatology; 68: 909A, 2018). We analysed the chronological changes of serum CCL20 after the treatment with direct acting agents (DAAs) among patients with HCV-associated advanced fibrosis, in order to evaluate its potential as a post sustained viral response (SVR) serum biomarker for liver fibrosis.

Method: A) Serum CCL20 were compared between healthy volunteers (HV, n = 8) and HCV-eradicated patients whose FIB-4 index at SVR24 were larger than 3.25 after DAA treatment (cohort 1, n = 15). B) Serum CCL20 among HCV infected patients whose pre-treatment (Pre) liver stiffness (LS) were larger than 12.5 kPa by transient elastography (FibroScan) (median: 18.1 kPa, range: 13.1-47.2, cohort 2, n = 52) were analysed chronologically at Pre, SVR24, and SVR72. Correlation between serum CCL20 and either LS or serum fibrosis-associated glycosylated marker M2BPGi (Yamasaki et al. Hepatology, 2014) was evaluated (Spearman). Measurement of serum CCL20 was performed with ELISA kit (Quantikine, R&D systems, U.S.A.)

Results: A) Even after SVR, serum CCL20 were higher in cohort 1 than in HV (mean; 33.6 vs. 9.88 pg/ml, p = 0.015) B) Before treatment in cohort 2, serum CCL20 was correlated with serum M2BPGi ($r_s = 0.5806$, p = 0.0002), but not with LS ($r_s = 0.2220$, p = 0.1140). Decrease value from Pre to SVR24 in serum CCL20 (Δ CCL20) was correlated with Δ M2BPGi ($r_s = 0.5129$, p = 0.019), but not with Δ LS ($r_s = 0.2520$, p = 0.1646). Serum CCL20 was significantly decreased from Pre to SVR24, but not from SVR24 to SVR72 (Wilcoxon, p < 0.00001 vs p = 0.12749). Cumulative incidence of hepatocellular carcinoma until the end of observation among patients whose CCL20 were increased from SVR24 to SVR72 (Rebounding, n = 19) was not different to those in decrease (n = 33) (p = 0.12749). 6 out of 19 Rebounding experienced non-HCC liver-related events (de novo AIH, alcohol liver disease, fatty liver: n = 2, ascites, and esophageal varix).

Conclusion: Serum CCL20 may be an alternative biomarker for liver fibrosis that is useful even after SVR, as is M2BPGi. Such integrated character may partly be explained by the literature in which CCL20 was identified as fibrosis and steatosis marker for non-alcoholic steatohepatitis (Govaere et al. Sci Trans Med 2020).

POSTER PRESENTATIONS

THU-206

Hepatitis C and monoclonal gammopathy of undetermined significance: clinical and hematological outcome after eradication with direct acting antivirals

Rosa Claudia Stasio¹, Elisabetta Bretto¹, Marco Tizzani¹, Roberta Lasco¹, Yulia Troshina^{1,2}, Giacomo Scaioli³, Fabrizia Pittaluga⁴, Giorgio Maria Saracco^{1,2}, Alessia Ciano^{1,2}. ¹S.C. Gastroenterology U, AOU città della salute e della scienza, Turin, Italy; ²Departement of medical sciences, University of Turin, Italy; ³Departement of public health sciences and pediatrics, AOU città della salute e della scienza, Turin, Italy; ⁴S.C. Microbiology and virology, AOU città della salute e della scienza, Turin, Italy
Email: stasio.rosa.claudia@gmail.com

Background and aims: Monoclonal gammopathy of undetermined significance (MGUS) has previously been reported among extra-hepatic manifestations of HCV. Currently, limited data are available about the impact of HCV eradication on MGUS progression. Hence, the aim of our study is to investigate the outcome of patients with MGUS and HCV after eradication with Direct acting antivirals (DAAs).

Method: Between February 2015 and March 2022, 2914 patients with HCV were treated with DAAs in our hospital. Among them, 62 patients (29 Male/33 Female, mean age 71.3 (\pm 10.9)) presented MGUS before DAAs therapy. HCV genotype 1a has been found in 9 patients, 1b in 32, 2 in 14, 3 in 4, 4 in 2, 5 in 1 patient. Forty patients were naive, 16 non-responder and 6 relapser to INF-based therapy. Twenty patients were cirrhotic (32.8%). Virological and haematological end points have been retrospectively assessed at 3 months (T1), 6 months (T2) and at the most recent hepatologic/haematologic examination (T3) after sustained viral response (SVR12). MGUS progression was defined as development of symptomatic disease (CRAB criteria) and/or as an increase of monoclonal component (MC) \geq 10%. Disease improvement was defined as reduction of MC \geq 10%.

Results: Prevalence of MGUS in the selected cohort was 2.1%, similar to MGUS prevalence in the general population. SVR12 was obtained in all 62 patients (100%). MGUS improvement was reported in 20.3% of patients at T1, in 21% at T2 and in 19.6% at T3. Six patients (11.7%) showed MC regression at blood testing. Disease progression was reported in 1 patient (1.7%) at T1, in 2 (3.5%) at T2 and in 5 (9.8%) at T3. Only one of them progressed to Multiple myeloma (MM) at T3. All the others remained stable.

Conclusion: HCV eradication with DAAs is efficient and safe in patients with MGUS, and it is associated with very low rates of disease progression. Further studies are required to accurately reinforce their correlation.

THU-207

Ethnic disparity in mortality related to extrahepatic manifestations among people with chronic HCV infection: a large, linked administrative population-based study in British Columbia, Canada

Dahn Jeong¹, Stanley Wong², Mohammad Ehsanul Karim^{1,3}, Ameer Manges^{1,2}, Jean Damascene Makuza¹, Hector Velasquez², Prince Adu², Sofia Bartlett², Eric Yoshida², Maria Alvarez², Amanda Yu², Mawuena Binka², Alnoor Ramji⁴, Mel Krajden⁵, Naveed Janjua^{1,2,3}. ¹The University of British Columbia, School of Population and Public Health, Canada; ²BC Centre for Disease Control, Canada; ³St. Paul's Hospital, Centre for Health Evaluation and Outcome Sciences, Canada; ⁴The University of British Columbia, Division of Gastroenterology, Canada; ⁵The University of British Columbia, Department of Pathology and Laboratory Medicine, Canada
Email: dahn.jeong@bccdc.ca

Background and aims: Previous studies showed ethnic disparities in HCV-related clinical outcomes. Asian Americans living with HCV had higher cirrhosis and hepatocellular carcinoma. As for extrahepatic manifestations (EHM), Asians in US and Canada had a greater risk of diabetes than people of other ethnicities. Currently, there is little research on ethnic disparities in other EHMs. This analysis assessed

the ethnic disparity in EHM-related mortality in a large, population-based cohort.

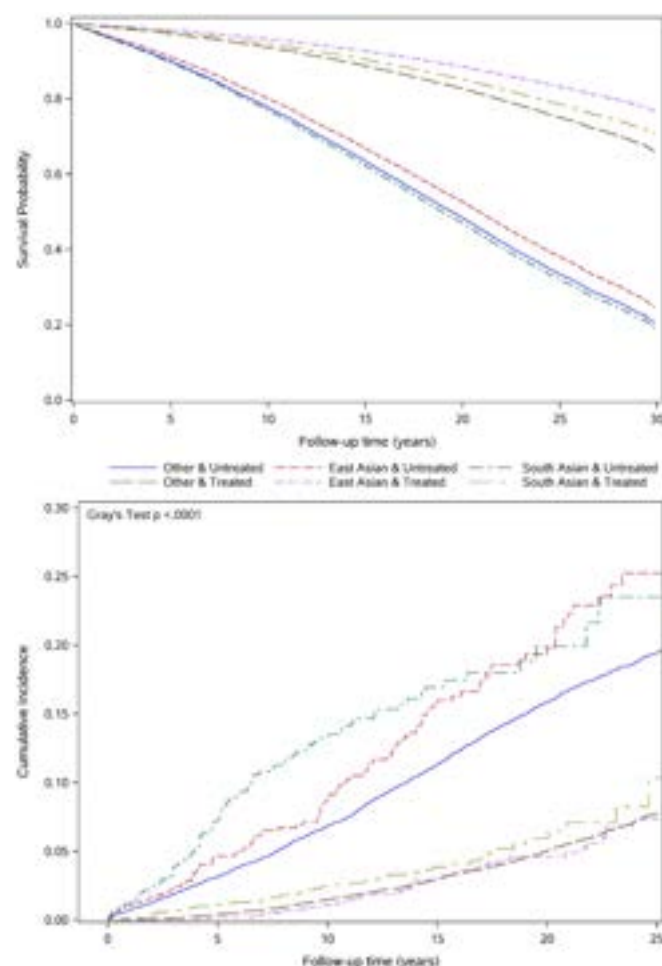


Figure 1: Upper: Overall survival curves for people diagnosed with HCV in BC-HTC, by ethnicity and treatment status. Lower: EHM-related mortality rates for people diagnosed with HCV in BC-HTC, by ethnicity and treatment status.

Method: We used the British Columbia Hepatitis Testers Cohort (BC-HTC) to identify all individuals diagnosed with HCV from 1990 to 2015, linked with administrative health datasets. We defined EHM-related deaths with causes of death from cardiovascular and cerebrovascular diseases, chronic kidney disease (CKD), and diabetes mellitus. Individuals were followed from their first HCV diagnosis until the earliest of: 1) death due to EHM, 2) other death, or 3) end of study (2021/12/31). EHM mortality rates were generated for each ethnic group (East Asian, South Asian, and Other) by HCV treatment (treated, untreated). We used multivariable subdistribution hazards models to account for competing risk and confounders, stratified by HCV treatment.

Results: Study population included 1,399 East Asian, 1,522 South Asian and 37,890 Other people diagnosed with chronic HCV in the BC-HTC. East Asian and South Asian were older compared to Other (45.4% vs 43.0% vs 25.9% \geq 50 years of age, respectively), had a greater prevalence of diabetes (7.4% vs 12.8% vs 4.3%), end-stage renal disease (1.1% vs 2.4% vs 0.6%), and hypertension (15.7% vs 17.5% vs 8.4%), with greater material deprivation (28.6% vs 44.2% vs 23.6%), respectively. However, East and South Asian, compared to Other, had a lower prevalence of alcohol use disorder (2.6% vs 8.3% vs 17.8%) and injection drug use (5.5% vs 7.1% vs 20.9%). The overall EHM-related mortality rate was the highest among untreated South Asian (14.26 per 1,000 PYs) followed by untreated East Asian (13.25 per 1,000 PYs)

and untreated Other (10.44 per 1,000 PYs). The mortality rates were considerably lower for all individuals who were treated (2.52, 3.06, 2.87 per 1,000 PYs, for East Asian, South Asian and Other, respectively). Among untreated people, East Asian had a lower risk of overall EHM-related death (adjusted subdistribution hazard ratio [aHR] 0.79 95%CI 0.63–0.98) compared to Other; South Asian had a higher risk of CKD-related mortality compared to Other (aHR 1.61 95%CI 1.15–2.25). Among those who were treated, the risk of EHM-related death did not statistically differ for East and South Asians compared to Other.

Conclusion: EHM-related mortality was high among East and South Asians diagnosed with HCV, particularly among those who didn't receive treatment. HCV treatment decreased the risk of EHM-related death across all ethnicities and reduced disparities in EHM-related mortality. Continued provider and patient engagement efforts for HCV treatment could reduce HCV-related disease burden.

THU-208

Hepatitis C virus (HCV) infection and neurocognitive impairment in subjects with mild liver disease

Carlos Brandão-Mello¹, Marcia Maria Amendola Pires¹, Max Fakoury¹, Helen Rose Maia Salazar², Sílvia Bastos de Oliveira², Sergio Schmidt².
¹Gastrointestinal and Liver Unit, Gaffrée e Güinle University Hospital, Internal Medicine, Rio de Janeiro, Brazil; ²Postgraduate Program in Neurology, Department of Neurology, Neurology, Rio de Janeiro, Brazil
Email: cedubrandao@gmail.com

Background and aims: Hepatitis C virus (HCV) infection is one of the leading causes of liver cirrhosis, hepatocellular carcinoma, and liver-related deaths. It is estimated that 40%-74% of HCV subjects will experience at least one extra hepatic manifestation within their lifetime, including neurocognitive deficits. The finding of HCV-RNA sequences in post[1]mortem brain tissue raised the possibility that HCV infection may affect the central nervous system and be the source of subtle neuropsychological symptoms, even in non-cirrhotic patients. Our investigation aimed to evaluate whether untreated, asymptomatic, mild HCV-infected subjects showed cognitive disfunctions.

Method: In this case-control observational study conducted at the Liver Unit of Gaffrée e Güinle University Hospital (HUGG), from May 2019 through March 2020. All HCV-infected subjects (anti-HCV and HCV-RNA detectable) over 18 years old were considered eligible for investigation. Only HCV subjects with compensated liver disease were included in the patient group. The comparison group consisted of subjects HCV negative and who were over 18 years old and paired by age and Human Development Index (HDI). HCV[1]subjects and healthy controls were tested at the same moment using three neuropsychological instruments in a random sequence: Symbol Digit Modality Test (SDMT), COWAT and the Continuous Visual Attention test (CVAT). We performed depression screening by DSM-V, liver fibrosis assessment by liver stiffness and blood tests, as well genotyping (sequencing) and HCV-RNA viral load (RT-PCR). A MANCOVA was performed to examine group differences (HCV vs. Healthy) in the six variables: OE (omission-errors), CE (commission-errors), reaction time (RT), variability of RT (VRT), SDMT, COWAT, using age, HDI and sex as covariates. Univariate ANCOVAs assess the effect of HCV on each one of the six neuropsychological variables. A discriminant analysis was performed to identify which variables effectively discriminate HCV-infected subjects and healthy controls.

Results: A sample of 48 subjects was initially evaluated. After applying the exclusion and inclusion criteria, 20 patients were excluded due to the following reasons: a) previous use of α -interferon: n = 8; b) cirrhosis: n = 3 c) type 2 mellitus diabetes: n = 3; d) depression: n = 2; e) patients without assessment of renal function: n = 2; f) hypothyroidism: n = 1 and g) bridging fibrosis (F3 fibrosis) subject with three abnormal liver enzymes: n = 1. Age and HDI did not differ among all groups. Mild fibrosis (F0-F2) was identified in 82.14%. Genotype was predominately 1 (82.14%). There

were no differences in COWAT, (p=0, 614) and SDMT (p=0.608) between the groups. Performance of HCV group was poorer than the controls based on the CVAT. The univariate analysis indicated specific significant differences in RT (p=0.047) and VRT (p=0.046). We found RT to have significant discriminant ability (71.7%).

Table 3: Raw Scores of CVAT, SDMT, Fluency Tests (Animal & Letters) HCV subjects versus Healthy controls

Neuropsychological battery (mean:SD)		HCV - Initial sample (n=48)	Mild Hepatitis HCV (n=20)	Control Group (n=18)
CVAT	OE	2.87 ± 6.37	1.54 ± 4.04	0.67 ± 1.28
	CE	6.14 ± 6.19	6.96 ± 7.23	5.50 ± 2.52
	RT (ms)	453.83 ± 67.31	448.10 ± 58.94	408.33 ± 29.02
	VRT (ms)	93.0 ± 38.43	86.71 ± 18.25	78.94 ± 14.41
COWAT	FL Animal	17.97 ± 5.10	18.67 ± 5.17	18.33 ± 4.21
	FL Flu	14.20 ± 3.59	13.71 ± 3.82	15.61 ± 2.32
	FL F	11.5 ± 5.22	11.42 ± 5.35	12.78 ± 4.95
	FL A	10.91 ± 4.67	11.89 ± 5.13	9.83 ± 4.07
	FL S	11.64 ± 4.30	11.82 ± 3.78	11.39 ± 2.97
	FL (FAS)	34.96 ± 13.13	35.14 ± 13.43	34 ± 9.51
	FL (Animal + Flu) + FAS	66.22 ± 20.89	67.89 ± 19.58	67.94 ± 13.06
SDMT	Number of correct responses	32.35 ± 12.61	35.71 ± 11.57	39.72 ± 10.86

HCV: Hepatitis C virus; CVAT: Continuous Visual attention test; OE: omission error; CE: commission error; RT: reaction time; VRT: variability of reaction time; COWAT: controlled oral word association test; FL: Fluency; SDMT: Symbol digit modality test

Figure:

Conclusion: HCV subjects with mild disease showed deficits in RT and intraindividual VRT as compared to healthy controls in CVAT. The higher VRT and RT exhibited by the HCV group might be explained by lapses in attention which affected the stability of response times and caused an increase in VRT. Our finding suggests that patients with mild HCV exhibit sustained attention problems and it may reflect deficits in the intrinsic alertness subdomain.

THU-209

Chronic hepatitis C and aging: search for cognitive changes

Carlos Brandão-Mello¹, Max Fakoury¹, Marcia Maria Amendola Pires¹, Sergio Schmidt².
¹Gastrointestinal and Liver Unit, Gaffrée e Güinle University Hospital, Internal Medicine, Rio de Janeiro, Brazil; ²Postgraduate Program in Neurology, Department of Neurology, Neurology, Rio de Janeiro, Brazil
Email: cedubrandao@gmail.com

Background and aims: Hepatitis-C virus (HCV) exhibits neurotropism, including brain areas associated with cognitive impairment (CI). Therefore, HCV infection is a risk factor for CI, even without hepatic manifestations. Most infected elderlies acquired HCV when they were young by parenteral route, and the disease remains asymptomatic. However, elderlies chronically infected might be at a greater risk of CI. AIM: To investigate cognitive performance of asymptomatic elderlies with HCV controlling for risk factors commonly associated with cognitive decline.

Method: Cross sectional observational study conducted between May 2018 to February 2020 at the Gastroenterology and Liver outpatient clinic of the Gaffrée e Güinle University Hospital (HUGG). The patients underwent a global health assessment, which provided information on the epidemiological and comorbidity profile, functionality and general well-being, in addition to data on liver function tests, grade of fibrosis (evaluated by liver stiffness), genotype (sequencing) and viral load (RT-PCR). Then, the study participants were subjected to a battery of neurocognitive tests, namely, the Minicog, Mini-Mental State Examination (MMSE), verbal fluency test (VFT) semantic category (animals), and clock drawing test (CDT). Elderlies uninfected (n = 41) and chronically HCV-infected (n = 41) were paired by age, sex, comorbidities, depression, lifestyle, and level of education. HCV-infection was confirmed by anti-HCV reactive and detectable HCV-RNA for more than six months. Participants coinfectd with hepatitis B (HBV) or HIV were excluded. A MANCOVA tested whether HCV infection affected cognitive

POSTER PRESENTATIONS

performance. The possible effect of each covariate and its respective interactions were analysed.

Results: There were not any significant differences between the two groups regarding age, sex, and educational level. However, schooling affected both groups. We found a highly significant main effect of education in relation to cognitive tests ($F=4.42$, 293 df=4/73, $P=0.003$, $\eta^2=0.20$) and a main effect with no difference between groups, that is, nonsignificant effect of Group ($F=1.31$, df=4/73, $P=0.27$, $\eta^2=0.07$). Based on the results of the MANCOVAs, in which education was the only one that had statistical significance in the analyses, we performed the ANCOVAs, where the univariate tests showed that education affected the performance of the MMSE scores ($F=12.3$, 299 df=1/76, $P=0.001$, $\eta^2=0.14$) and VFT ($F=11.1$, df=1/76, $P=0.001$, $\eta^2=0.13$). The difference in education level approached the significance level in the CDT ($F=3.63$, df=1/76, $p=0.06$, $\eta^2=0.05$). In contrast, MINICOG did not differ between the two groups regarding years of formal education (Low and High). All other univariate measures did not reach significant results.

Conclusion: HCV infection did not influence performance of the cognitive screening tests in elderly subjects. Formal years of education (cognitive reserve) may have protected elderlies with HCV-infection. Future studies should be performed using specific tests associated with the brain regions affected by HCV.

THU-210

Coadministration of hepatitis C direct-acting antivirals and enzyme-inducing antiepileptic drugs: real-world experience from a multi-centre case series

Alison Boyle^{1,2}, Fiona Marra^{1,2}, Helen Boothman³, Sonal Patel⁴, Yun Jung Kim⁵, Rachael Kamiri-Ngugi⁶, Aimee Francisco⁷, Rebecca Turley⁸. ¹NHS Greater Glasgow and Clyde, Pharmacy, United Kingdom; ²University of Liverpool, Pharmacology and Therapeutics, United Kingdom; ³St George's University Hospitals NHS Foundation Trust, Pharmacy, United Kingdom; ⁴Guy's and St Thomas' NHS Foundation Trust, Pharmacy, United Kingdom; ⁵University Hospital Southampton NHS Foundation Trust, Pharmacy, United Kingdom; ⁶Royal Surrey NHS foundation trust, Pharmacy, United Kingdom; ⁷King's College Hospital NHS Foundation Trust, Pharmacy, United Kingdom; ⁸Barking, Havering and Redbridge University Hospitals NHS Trust, Pharmacy, United Kingdom
Email: alison.boyle@ggc.scot.nhs.uk

Background and aims: Coadministration of enzyme-inducing antiepileptic drugs (eiAEDs) and hepatitis C (HCV) direct-acting antivirals (DAAs) is not currently recommended due to potential drug-drug interaction (DDI) resulting in significantly reduced DAA levels and risk of treatment failure. This presents a significant barrier to HCV treatment for patients who are unable to stop or switch to alternative antiepileptic agents. There have been a small number of case reports published describing successful outcomes in patients receiving HCV DAA treatment while remaining on eiAEDs^{1,2}. This has led to updated recommendations in the University of Liverpool DDI resource, www.hep-druginteractions.org, to allow consideration of HCV DAA treatment where coadministration is unavoidable. However, the lack of widespread clinical experience may still lead to hesitancy in prescribing in this patient cohort.

Method: A retrospective case series evaluating treatment outcomes of patients prescribed HCV DAAs in combination with eiAEDs in 6 centres across the UK.

Results: A total of 11 patients with chronic, treatment-naïve HCV were treated with HCV DAAs in combination with eiAEDs. Median age was 56 years (range 38–64 years), 8 (73%) patients were non-cirrhotic, 9 (82%) were male and 7 (64%) had GT1A HCV. HCV DAAs were prescribed at standard doses (12 weeks sofosbuvir/velpatasvir (n=6), 8 weeks ledipasvir/sofosbuvir (n=3), 8 weeks glecaprevir/pibrentasvir (n=2)). Coadministered eiAEDs included carbamazepine (n=6), phenytoin (n=3), oxcarbazepine (n=1), phenobarbitone (n=1). High treatment adherence was reported for 10/11 individuals

with 1 patient completing 50% of prescribed treatment course. On-treatment HCV PCR data was available for 7 (64%) patients; of those, 6 had an undetectable HCV PCR and 1 had HCV PCR 156 IU/ml within the first 4–6 weeks of treatment. End of treatment HCV PCR was available for 6 (55%) patients with all achieving undetectable levels. SVR 12 results are available for 3 patients so far with all achieving SVR 12. The remaining 8 patients are awaiting SVR 12 results. Full SVR data will be presented.

Conclusion: This is the largest single case series of coadministered eiAEDs and DAAs. Preliminary data of treatment outcomes are very encouraging and support previously published real-world case reports. These results will help inform HCV treatment decisions in this cohort who continue to face challenges in accessing treatment.

References

1. Natali KM, Jimenez HR, and Slim J. When coadministration cannot be avoided: real world experience of direct acting antivirals for the treatment of hepatitis C virus infection in patients on first generation anticonvulsants. *J Pharm Pract* 2022, 35 (3):495–499.
2. Marcos-Fosch C, Cabezas J, Crespo J *et al.*, Anti-epileptic drugs and hepatitis C therapy: Real-world experience. *J Hepatol*, 2021, 75 (4): 984–5.

THU-211

Impact of hepatitis C treatment on biochemical and metabolic parameters in HIV/HCV coinfecting patient

Lourdes Pedroza¹, Misael Osmar Garcia Martin², Victor Ahumada Topete², Karina Sevilla², Manuel Castillejos Lopez², Gustavo Reyes Teran³, Andrea Carenas Ortega⁴, Akio Murakami Ogasawara⁴, Santiago Ávila Ríos⁴, Arturo Rodea Monroy². ¹Instituto Nacional de Enfermedades Respiratorias, Gastroenterology and Endoscopy, Ciudad de México, Mexico; ²Instituto Nacional de Enfermedades Respiratorias, Hospital Epidemiology and Infectious Disease Unit, Ciudad de México, Mexico; ³CCINSHAE, principal of the coordinating commission of national health institutes and highly specialized hospitals, Ciudad de México, Mexico; ⁴Instituto Nacional de Enfermedades Respiratorias, infectious disease research center, Ciudad de México, Mexico
Email: drapedroza.lourdes@gmail.com

Background and aims: Efficacy and effectiveness of direct-acting antivirals (DAAs) in HIV/HCV coinfecting patients such as mono-infected patients; however, few studies analyze post-treatment improvement in this population. This study aimed to evaluate the changes in renal and hepatic function and fibrosis in coinfecting patients treated with direct-acting antivirals.

Method: In this observational and prospective study, from April 2017 to April 2022, HIV/HCV coinfecting this patient from a specialized care clinic in Mexico; the duration of treatment with DAAs was 12 weeks. Quantitative variables were described using the mean and standard deviation or median and interquartile range. Using the Wilcoxon rank test, the continuous quantitative variables were compared with the 24-week results (sustained viral response).

Results: 86 patients were included, mean age of 40.36 (SD 9.08); 79 (91.9%) men and 7 (8.1%) women, all on ART with virological suppression. The following results were obtained when comparing the baseline data vs. sustained viral response: glomerular filtration 102.0 ml/min/1.73 m² (88.5–114.0) vs. 96. (79.5–109.5) with $p=0.000555$, albumin 4.20 gr/dl (4.01–4.40) vs. 4.32 gr/dl (4.17–4.54) with $p=0.000234$, total bilirubin 0.74 mg/dl (0.50–1.10) vs. 0.65 mg/dl (0.44–0.89) with $p=0.029954$, direct bilirubin 0.16 mg/dl (0.11–0.24) vs. 0.12 mg/dl (0.08–0.15) with $p=0.000714$, GOT 48.50 IU/l (37.0–69.5) vs. 22.0 IU/l (20.0–28.0) with $p=4.3255E-11$, GPT 60.0 IU/l (42.0–86.250) vs. 21.1 IU/l (15.25–26.92) with $p=1.0582E-12$, ALP 105.0 IU/l (79.0–129.85) vs. 92.0 IU/l (74.0–120.0) with $p=0.001719$, GGT 82.35 IU/l (45.5–183.25) vs. 22.0 IU/l (17.0–34.1) with $p=0.000229$, Total cholesterol 149.75 mg/dl (134.55–182.75) vs. 167.95 mg/dl (143.25–187.87) with $p=0.035503$, LDL Cholesterol

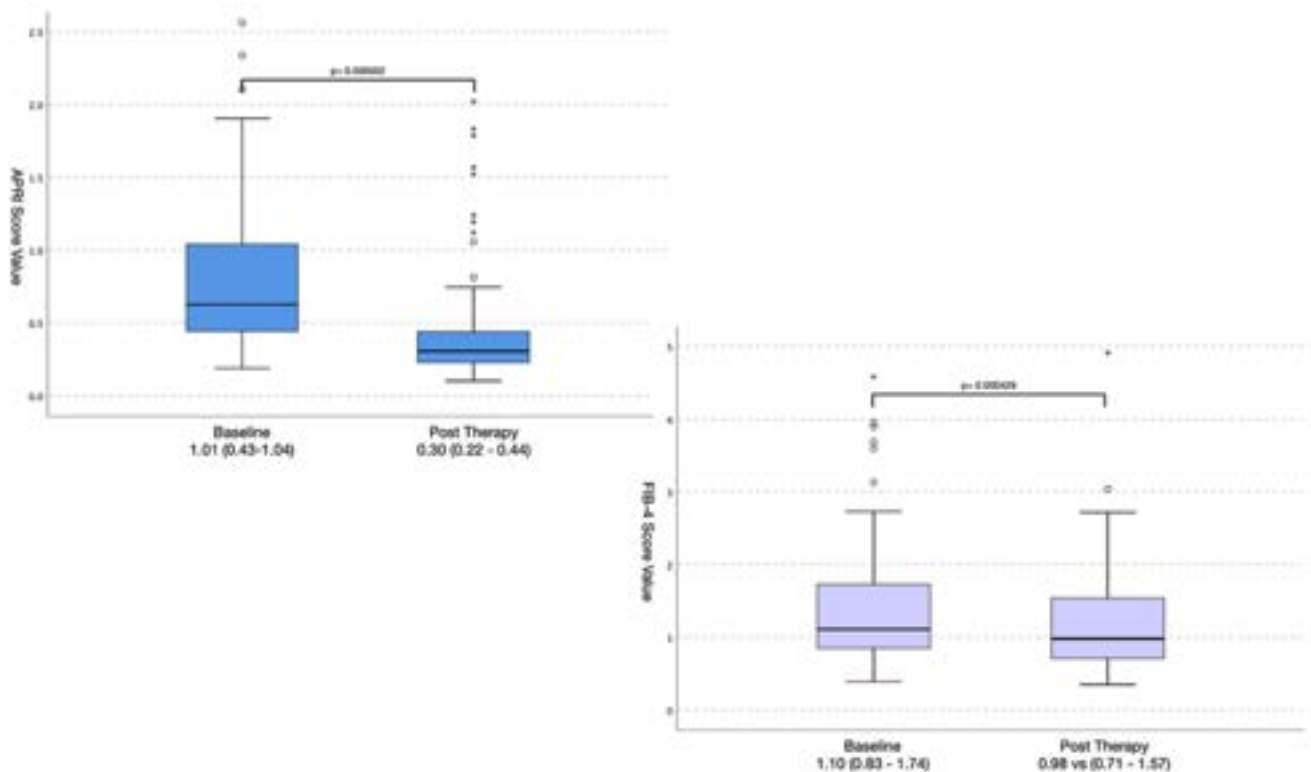


Figure: (abstract: THU-211): Represents the box-and-whisker plots of the Score for hepatic fibrosis.

85.0 mg/dl (63.22–104.05) vs. 102.2 mg/dl (85.65–120.85) with $p = 0.002335$.

Conclusion: HIV/HCV coinfectd patients in virological suppression showed medium-term improvement in most biochemical and metabolic parameters. Simultaneously, a decrease in fibrosis scores was observed after presenting a sustained viral response.

THU-212

Sustained virologic response outcomes in patient with hemodialysis-hepatitis C receiving treatment with direct-acting antivirals agents

Fardhah Akil^{1,2,2}, Rini Bachtiar^{1,2}, Muhammad Luthfi Parewangi^{1,2}, Nu'man AS Daud^{1,2}, Susanto Kusuma^{1,2}, Amelia Rifai^{1,2}, Hasyim Kasim³, Haerani Rasyid³. ¹Centre of Gastroenterology-Hepatology HAM Akil/DR. Wahidin Sudirohusodo General Hospital, Indonesia; ²Hasanuddin University, Division of Gastroenterology-Hepatology, Department of Internal Medicine, Indonesia; ³Hasanuddin University, Division of Nephrology, Department of Internal Medicine, Indonesia
Email: dndakil@gmail.com

Background and aims: Direct-acting antiviral agents (DAAs) have become first-line treatment for hepatitis C virus (HCV) infection and was associated with a survival benefit among persons on hemodialysis. Study of efficacy treatment of DAAs by sustained virologic response (SVR) in dialysis patients are still limited especially in Indonesian population.

Method: This retrospective cohort study was conducted in tertiary care hospital in Makassar, Indonesia between 2017 and 2020. From 90 patients naïve HCV on hemodialysis, 75 of them had received DAAs with regimen Sofosbuvir/Simeprevir, Sofosbuvir/Daclastavir, Sofosbuvir/Ribavirin, and Elbasvir/Grazoprevir. The outcome were sustained virological responses by 12 weeks (SVR12), improvement or deterioration of kidney function by estimated Glomerular Filtration Rate (eGFR)/creatinine, hepatic fibrosis assessed by aspartate aminotransferase-to-platelet ratio index (APRI)/Fibrosis-4 index (FIB-4) scores and the associated factors.

Results: Overall the SVR12 rate was 93.3% and by regimen SOF/SIM, SOF/DAC, SOF/RIB, and ELB/GRV were 95.7%, 90%, 100%, and 80%, while Child-Pugh (CP) class A/B/C had 95.6%/90%/100% respectively. In patients with cirrhosis/no cirrhosis, the SVR rate were similar 93.5%/93.2%. The mean eGFR for SOF/SIM associated with SVR12 were deteriorate from 36.1 to 17.15, while SOF/DAC were improve from 14.54 to 18.79; but no statistically significant for overall eGFR. Both overall mean score APRI and FIB-4 improvement was associated with SVR12 0.16 (95% CI 0.03–0.30) and 0.42 (95% CI 0.13–0.71) respectively; similar to APRI/FIB-4 pre and post treatment regardless of the DAAs regimens ($p < 0.05$).

Conclusion: DAA-mediated SVR12 in HCV dialysis patients resulted in high rate SVR12 >90% and similar rate in all CP class, cirrhosis status with improvement of hepatic fibrosis and kidney function especially on sofosbuvir/daclastavir regimen.

SVR12	(n=75)	(%)	Outcomes, overall	Mean	95% CI	p-value ¹
Overall	70	93.3	HCV-RNA	2.2 x 10 ⁸	1.3 x 10 ⁸ - 3.2 x 10 ⁸	*<0.001
Regimen			eGFR	21.64	19.54 - 24.85	0.06
Sofosbuvir-Simeprevir (SOF/SIM)	44	95.7	APRI	0.16	0.03 - 0.30	*0.01
Sofosbuvir-Daclatasvir (SOF/DAC)	20	90.9	FIB-4	0.42	0.13 - 0.71	*0.002
Sofosbuvir-Ribavirin (SOF/RBV)	2	100	Outcomes	Mean (Std. Deviation)		p-value ²
Elbasvir-Grazoprevir (ELB/GRZ)	4	80		Pre Treatment	Post Treatment	
Child-Pugh Class			eGFR (n=68)			
Class A	42	95.6	SOF/SIM	36.1	17.15	-
Class B	20	90.9	SOF/DAC	14.54	18.79	-
Class C	8	100				
Liver Cirrhosis			Creatinin	7.93 ± 5.87	7.55 ± 4.68	0.06
Yes	29	93.5	APRI	0.48 ± 0.57	0.31 ± 0.12	*0.03
No	41	93.2	FIB-4	1.64 ± 1.09	1.22 ± 0.57	*0.04

¹Paired T-Test ²Wilcoxon Signed Ranks Test *Significant

Figure: (abstract: THU-212).

THURSDAY 22 JUNE

Viral hepatitis C Therapy and resistance

THU-213

Sofosbuvir/Velpatasvir/Voxilaprevir for re-treatment in direct-acting antiviral experienced hepatitis C virus patients: a systematic review and meta-analysis

Devan Pooja¹, Tiong Kai Le Ashley¹, Neo Jean Ee¹, Yu Jun Wong^{2,3}.

¹Yong Loo Lin School of Medicine, National University of Singapore, Singapore; ²Changi General Hospital, Singapore; ³Duke-NUS Medical School, Singapore

Email: wongyujun1985@gmail.com

Background and aims: About 5% of chronic hepatitis virus (HCV) patients treated with direct-acting antiviral did not achieve sustained virological response (SVR12). Data on treatment outcome and predictor of treatment failure on DAA-experienced HCV patients receiving sofosbuvir/velpatasvir/voxilaprevir (SOF/VEL/VOX) is limited. We performed a systematic review and meta-analysis to evaluate the efficacy and safety of SOF/VEL/VOX as salvage treatment in DAA-experienced HCV patients.

Method: A comprehensive search of 5 electronic databases were performed from inception to 1st January 2023. All English literature, irrespective of study design, publication dates were extracted. Pooled estimates were reported in odds ratio (OR) with 95% confidence interval (CI) using random-effect model. Our study outcome was the SVR12, based on modified intention-to-treat; secondary outcome was treatment discontinuation due to treatment-related adverse effect. Subgroup analysis performed based on genotype, status of cirrhosis, HCC, prior SOF/VEL exposure and region.

Results: Over 517 citations identified from 5 databases (PubMed, EMBASE, MEDLINE, Clinical-trial.gov and Web of Science). Data from 24 studies (Asia pacific=5, Africa=3, America=7, Europe=9) involving 2,822 DAA-experienced HCV patients were included. All studies had low to moderate risk of bias. The mean age was 53 years old, 81% were male, 42% had liver cirrhosis. Genotype distributions were diverse (GT1: 74.4%, GT2: 9.9%, GT3: 26.1%, GT4: 8.5%, GT6: 1.4%, indeterminate: 0.9%). 17.2% receive SOF/VEL prior to SOV/VEL/VOX; 25% received ribavirin with SOF/VEL/VOX. 42% had pre-treatment RAS testing performed, where mutation was present in 51%.

Overall pooled SVR12 was 95.0% (95%CI: 94.0–95.8%), with lower SVR12 in Europe compared to region (Europe 84.3% vs Asia Pacific: 96.2%; America 93.0% or Africa 98.9%, $p < 0.0001$ for all). Predictors for treatment failure for retreatment by SOF/VEL/VOX were genotype 3 (OR 0.39, 95%CI: 0.23–0.64, I^2 :7%), active HCC (OR 0.22, 95%CI: 0.08–0.57, I^2 :0%) and baseline cirrhosis (OR 0.25, 95%CI: 0.11–0.60, I^2 :0%), decompensated cirrhosis (OR 0.09, 95%CI: 0.03–0.23, I^2 :3%) and prior SOF/VEL (OR 0.35, 95%CI: 0.13–0.94, I^2 :54%). Baseline RAS mutation and addition of ribavirin to SOF/VEL/VOX was not associated with higher SVR12. Treatment discontinuation due to drug-related was uncommon (10 studies, 0.2%).

Conclusion: SOF/VEL/VOX is efficacious and safe for retreatment in HCV patients with prior DAA failure, even with RAS mutation. Our findings support SOF/VEL/VOX as 1st-line rescue treatment for DAA-experienced HCV patients.

THU-214

Progress towards achieving hepatitis C elimination in the country of Georgia, April 2015-December 2022

Tengiz Tsertsvadze^{1,2}, Amiran Gamkrelidze³, Nikoloz Chkhartishvili¹, Akaki Abutidze^{1,2}, Lali Sharvadze^{2,4}, Maia Butsashvili⁵, Jaba Zarkua⁶, Lia Gvinjilia⁷, Shaun Shadaker⁸, Ekaterine Adamia⁹, Stefan Zeuzem¹⁰, Sanjeev Arora¹¹, Francisco Averhoff¹², Senad Handanagic⁸, Tamar Gabunia⁹. ¹Infectious Diseases, AIDS and Clinical Immunology Research Center, Georgia; ²Ivane Javakhishvili Tbilisi State University, Georgia; ³National Center for Disease Control and Public Health, Georgia; ⁴Hepatology clinic HEPA, Georgia; ⁵Health research union, Georgia; ⁶Medical Center Mrcheveli, Georgia; ⁷Eastern Europe and Central Asia (EECA) Regional Office, Centers for Disease Control and Prevention, Georgia; ⁸Centers for Disease Control and Prevention, Division of Viral Hepatitis National Center for HIV, Hepatitis, STD and TB Prevention, Atlanta, USA, United States; ⁹Ministry of IDPs from the Occupied Territories, Labour, Health and Social Affairs of Georgia, Georgia; ¹⁰Goethe University Hospital, Germany; ¹¹University of New Mexico, United States; ¹²Department of Family and Preventive Medicine, Emory University School of Medicine, United States

Email: tt@aidcenter.ge

Background and aims: The country of Georgia launched the world's first national hepatitis C elimination program in April 2015. Key strategies include nationwide screening, active case finding, linkage to care, decentralized care, and provision of treatment for all persons with hepatitis C virus (HCV) infection, along with effective prevention interventions. The elimination program aims to achieve the following targets: a) diagnose 90% of HCV-infected persons, b) treat

95% of those diagnosed, and c) cure 95% of those treated. We report progress toward elimination targets of the elimination program.

Method: The estimated number of persons with HCV infection was based on a 2015 population-based national seroprevalence survey, which showed that 5.4% of the general adult population had current HCV infection (approximately 150,000 persons). We analyzed data in the national HCV screening and treatment databases during April 2015–December 2022.

Results: As of December 31, 2022, 154,428 adults screened positive for HCV antibodies. Of those, 128,093 (82.9%) received HCV RNA or core antigen testing. A total of 100,576 (78.5%) persons tested had detectable HCV infection, and 80,828 (80.4%) initiated treatment. Of 57,031 adults who were evaluated for sustained virologic response (SVR), 56,447 (99.0%) had no detectable HCV RNA. Based on the 90–95–95 program goals, Georgia has diagnosed 67.1% of the estimated 150,000 adults with current HCV infection, treated 63.0% of the target 128,250 (95% of 150,000), and cured 46.3% of the target 121,837 (95% of 128,250). Treatment effectiveness was comparable among persons with advanced fibrosis (FIB-4 score F3 or F4) with 98.3% achieving SVR, and among patients with mild or no liver fibrosis (FIB-4 score \leq F2), SVR = 99.2%, $p < .0001$.

Conclusion: Georgia has made substantial progress towards eliminating hepatitis C. Over 65% of persons with current HCV infection have been diagnosed, and most have initiated treatment and experienced high cure rates regardless of fibrosis status. Challenges remain in identifying and linking to care persons with current HCV infection in Georgia. The Nationwide integrated, decentralized model of HCV treatment, which is already implemented in many locations, will be critical to improve linkage to care and close gaps in the HCV cascade of care.

THU-215

The most difficult to cure with pangenotypic regimens HCV infected population

Robert Flisiak¹, Hanna Berak², Anna Parfieniuk-Kowder¹, Dorota Dybowska³, Krzysztof Tomasiewicz⁴, Marek Sitko⁵, Dorota Zarębska-Michaluk⁶, Włodzimierz Mazur⁷, Ewa Janczewska⁸, Jakub Klapaczynski⁹, Jerzy Jaroszewicz¹⁰. ¹Medical University of Białystok, Białystok, Poland; ²Hospital for Infectious Diseases in Warsaw, Warsaw, Poland; ³Ludwik Rydygier Collegium Medicum in Bydgoszcz Faculty of Medicine Nicolaus Copernicus University in Toruń, Bydgoszcz, Poland; ⁴Medical University of Lublin, Lublin, Poland; ⁵Jagiellonian University, Kraków, Kraków, Poland; ⁶Jan Kochanowski University Kielce, Kielce, Poland; ⁷Medical University of Silesia, Chorzów, Chorzów, Poland; ⁸ID Clinic, Mysłowice, Poland; ⁹Central Clinical Hospital of the Ministry of Internal Affairs and Administration, Warsaw, Poland; ¹⁰Medical University of Silesia, Katowice, Bytom, Poland
Email: robert.flisiak1@gmail.com

Background and aims: Pangenotypic therapies for HCV infections, although universal and highly effective, leave the risk of treatment failure. The aim of the analysis was to find out the most difficult to cure with pangenotypic regimens population of HCV infected patients.

Method: The analysis included patients selected from the EpiTer-2 database, a large retrospective, multicentre, national real-world study evaluating DAA treatment during period of 2015–2022 in 17, 166 consecutive subjects with hepatitis C virus (HCV) infection. The effectiveness of treatment was assessed in populations known as a worse response to treatment, and then in a population with a combination of all these characteristics.

Results: A total of 5,549 patients were treated with pangenotypic regimens, of which 5,217 achieved SVR, that after excluding 194 lost to follow-up resulted in a response rate of 97.4%. In the group of 1,338 patients infected with genotype 3, the SVR rate was 94.9%, among 1,142 patients with cirrhosis–94.2%, in the population of 2,852 men–96.5%, and among 941 people with BMI > 30 it reached 96.8%. The analysis carried out in a group of 82 men with cirrhosis and obesity,

infected with genotype 3 showed the effectiveness of pangenotypic therapy at the level of only 85.4%, with 89.3% in treatment naive patients and 76.9% in patients with previous therapy failure.

Conclusion: Studying a large population of pangenotypically treated HCV-infected patients, we showed relatively low effectiveness in men with cirrhosis and obesity, infected with genotype 3. Triple therapy should be considered initiating the treatment of HCV infections in this group, which, however, needs to be confirmed in further studies. Previous studies (Polaris-3) were conducted in a less demanding population of patients with cirrhosis infected with genotype 3, so they did not take into account gender and BMI, which significantly worsen the effectiveness.

THU-216

Real-life effectiveness of voxilaprevir/sofosbuvir/velpatasvir in hepatitis C patients previously treated with sofosbuvir/velpatasvir or glecaprevir/pibrentasvir

Juan Carlos Ruiz-Cobo¹, Jordi Llaneras¹, Maria Buti^{1,2}, Xavier Forns^{2,3,4,5}, Isabel Conde^{2,6}, Ana Arencibia Almeida⁷, Moises Diago^{8,9}, Francisco Javier Garcia-Samaniego Rey^{2,10,11}, José Castellote Alonso^{12,13}, Susana Llerena^{14,15}, Elisa Rodriguez^{16,17}, Beatriz Mateos Muñoz^{2,18,19,20}, Manuel Rodríguez^{21,22}, Inmaculada Fernández Vázquez²³, Jose Miguel Rosales Zabal²⁴, José Luis Calleja Panero^{2,25,26}, Rosa M Morillas^{2,27,28,29}, Silvia Montoliu^{30,31}, Adolfo Gallego Moya³², Raul J. Andrade^{2,33,34,35}, Manuel Hernández Guerra³⁶, Esther Badia-Aranda³⁷, Carlota Jimeno Mate³⁸, Jesús González Santiago^{2,39,40}, Beatriz Cuenca⁴¹, Vanesa Bernal Monterde^{42,43}, Manuel Delgado⁴⁴, Juan Turnes^{45,46}, Sabela Lens^{2,3,4,5}. ¹Vall d'Hebron University Hospital, Hepatology, Barcelona, Spain; ²CIBERehd, Spain; ³Hospital Clínic de Barcelona, Liver Unit Hospital Clínic, Barcelona, Spain; ⁴Institut d'Investigacions Biomèdiques August Pi i Sunyer (IDIBAPS), Barcelona, Spain; ⁵Universitat de Barcelona, Barcelona, Spain; ⁶La Fe University and Polytechnic Hospital, Hepatology and Liver Transplantation Unit, Valencia, Spain; ⁷Our Lady of Candelaria University Hospital, Gastroenterology and Hepatology, Santa Cruz de Tenerife, Spain; ⁸Consortium General University Hospital of Valencia, Valencia, Spain; ⁹University of Valencia, Valencia, Spain; ¹⁰IdiPAZ, Madrid, Spain; ¹¹La Paz University Hospital, Madrid, Spain; ¹²Bellvitge University Hospital, L'Hospitalet de Llobregat, Spain; ¹³IDIBELL Institut d'Investigació Biomèdica de Bellvitge, L'Hospitalet de Llobregat, Spain; ¹⁴Marqués de Valdecilla University Hospital, Gastroenterology and Hepatology, Santander, Spain; ¹⁵IDIVAL, Santander, Spain; ¹⁶Virgen del Rocío University Hospital, Digestive Diseases Research Unit, Sevilla, Spain; ¹⁷Facultad de Biología, Cell Biology, Sevilla, Spain; ¹⁸Ramón y Cajal Hospital, Gastroenterology, Madrid, Spain; ¹⁹Instituto Ramón y Cajal de Investigación Sanitaria-IRYCIS, Madrid, Spain; ²⁰Alcalá University, Alcalá de Henares, Spain; ²¹Central University Hospital of Asturias, Gastroenterology and Hepatology, Oviedo, Spain; ²²University of Oviedo, Oviedo, Spain; ²³University Hospital October 12, Gastroenterology and Hepatology, Madrid, Spain; ²⁴Hospital Costa del Sol, Gastroenterology and Hepatology, Marbella, Spain; ²⁵Puerta de Hierro Majadahonda University Hospital, Majadahonda, Spain; ²⁶Instituto de Investigación Sanitaria Puerta del Hierro, Spain; ²⁷Germans Trias i Pujol Hospital, Hepatology, Badalona, Spain; ²⁸IGTP Institut Germans Trias i Pujol, Badalona, Spain; ²⁹Universitat Autònoma de Barcelona, Bellaterra, Spain; ³⁰Hospital Universitari de Tarragona Joan XXIII, Tarragona, Spain; ³¹Institut d'Investigació Sanitària Pere Virgili, Spain; ³²Hospital de la Santa Creu i Sant Pau, Spain; ³³Hospital Universitario Virgen de la Victoria, Málaga, Spain; ³⁴BIONAND, Málaga, Spain; ³⁵University of Malaga, Málaga, Spain; ³⁶Hospital Universitario de Canarias, La Laguna, Spain; ³⁷Burgos University Hospital, Gastroenterology and Hepatology, Burgos, Spain; ³⁸Hospital De Valme, Gastroenterology and Hepatology, Seville, Spain; ³⁹Salamanca University Hospital, Gastroenterology and Hepatology, Salamanca, Spain; ⁴⁰Biomedicine Research Institute (IBSAL) Salamanca, Spain; ⁴¹Getafe University Hospital, Gastroenterology and Hepatology, Getafe, Spain; ⁴²Miguel Servet University Hospital, Gastroenterology and Hepatology, Zaragoza, Spain; ⁴³Instituto de

POSTER PRESENTATIONS

Investigación Sanitaria de Aragón, Spain; ⁴⁴[CHUAC] University Hospital of A Coruña, Gastroenterology and Hepatology, A Coruña, Spain; ⁴⁵Hospital Provincial de Pontevedra, Gastroenterology and Hepatology, Pontevedra, Spain; ⁴⁶Galicia Sur Health Research Institute, Spain
Email: juancarlosrobo@gmail.com

Background and aims: Voxilaprevir/sofosbuvir/velpatasvir (VOX/SOF/VEL) is the recommended therapy for patients with chronic hepatitis C who failed to direct-acting antivirals (DAAs). This is based on studies that mainly included failures to DAAs that are not currently recommended. There is still limited data on retreatment after failure to current first line therapies, sofosbuvir/velpatasvir (SOF/VEL) and glecaprevir/pibrentasvir (GLE/PIB). The aim of the study was to analyze the effectiveness and safety of VOX/SOF/VEL in a real-world setting among only failures to SOF/VEL or GLE/PIB.

Method: Patients with HCV retreated with VOX/SOF/VEL after SOF/VEL or GLE/PIB failure were enrolled in 26 centers in Spain between December of 2017 and December of 2022. All patients received VOX/SOF/VEL ± ribavirin (RBV) for 12 weeks. Sustained virological response (SVR) was defined as undetectable HCV-RNA 12 (SVR12) weeks after the end-of-treatment. Patients with HCV reinfection were excluded.

Results: A total of 135 patients were included, 98 (72.6%) had failed to SOF/VEL and 37 (27.4%) to GLE/PIB. Baseline characteristic were median age 54.1 (IQR 9) years, 84.4% male, 96% Caucasian, 11.9% coinfecting by HIV, 50.9% had history of injected drug use and 44.2% were cirrhotic. GT3 was the predominant in 50.4% of patients followed by GT1 in 36.8%. Median HCV-RNA was 2.9×10^6 (2.4×10^5 – 3.2×10^6). Up to now, 97 (86.6%) of 111 patients who reached follow-up 12 weeks after treatment have achieved SVR. There was a trend to higher rate of SVR in patients previously treated with GLE/PIB than SOF/VEL (88.9% vs 85.5%) ($p = 0.43$). There were no significant differences in SVR between patients with or without cirrhosis (84% vs 90%) ($p = 0.24$), or based on HCV genotype, being 83% for GT3 vs. 89% in other genotypes ($p = 0.29$). Among the 14 patients without SVR to VOX/SOF/VEL despite completing treatment, 9 were GT3, 7 had cirrhosis and 4 (29%) were both GT3, cirrhotic and previously treated with SOF/VEL. RBV was added to VOX/SOF/VEL in 8 (6%) patients and all of them achieved SVR including 5 (63%) GT3 with cirrhosis and prior failure to SOF/VEL. There were no adverse relevant events related to the medication.

Conclusion: VOX/SOF/VEL in the real world is an effective rescue therapy for failures to SOF/VEL or GLE/PIB. There is a trend towards higher SVR in patients previously treated with GLE/PIB. The addition of RBV to VOX/SOF/VEL could rise the rates of SVR and might be considered in patients with GT3, cirrhosis and prior failure to SOF/VEL.

THU-217

An algorithm for simplified hepatitis C virus treatment with non-specialist care based on real-world data from a nationwide registry in Taiwan

Ming-Lung Yu^{1,2,3,4}, Chi-Ming Tai^{5,6}, Lien-Juei Mou⁷, Hsing-Tao Kuo⁸, Chung-Feng Huang^{1,9}, Kuo-Chih Tseng^{10,11}, Chingchu Lo¹², Ming-Jong Bair^{13,14}, Sih-Ren Wang¹⁵, Jee-Fu Huang^{2,3}, Ming-Lun Yeh^{2,3}, Chun-Ting Chen^{16,17}, Ming-Chang Tsai¹⁸, Chien-Wei Huang¹⁹, Pei-Lun Lee²⁰, Tzeng-Hue Yang²¹, Yi-Hsiang Huang^{22,23}, Lee-Won Chong^{24,25}, Chien-Lin Chen²⁶, Chi-Chieh Yang²⁷, Chao-Hung Hung⁴, Sheng-Shun Yang²⁸, Pin-Nan Cheng²⁹, Tsai-Yuan Hsieh¹⁶, Jui-Ting Hu³⁰, Wen-Chih Wu³¹, Chien-Yu Cheng³², Guei-Ying Chen³³, Kwok-Hsiung Chou³⁴, Wei-lun Tsai³⁵, Jian-Neng Gao³⁶, Chih-Lang Lin³⁷, Chia-Chi Wang³⁸, Ta-Ya Lin³⁹, Chih-Lin Lin⁴⁰, Wei-Wen Su⁴¹, Tzong-Hsi Lee⁴², Te-Sheng Chang⁴³, Chun-Jen Liu⁴⁴, Chia-Yen Dai^{2,3}, Chi-Yi Chen⁴⁵, Jia-Horng Kao⁴⁴, Han-Chieh Lin^{22,23}, Wan-Long Chuang^{2,3}, Cheng-Yuan Peng^{46,47}. ¹School of Medicine, College of Medicine and

Center of Excellence for Metabolic Associated Fatty Liver Disease, National Sun Yat-sen University, Kaohsiung, Taiwan; ²Hepatobiliary Division, Department of Internal Medicine and Hepatitis Center, Kaohsiung Medical University Hospital, Kaohsiung Medical University, Kaohsiung, Taiwan; ³Hepatitis Research Center, College of Medicine and Center for Liquid Biopsy and Cohort Research, Kaohsiung Medical University, Kaohsiung, Taiwan; ⁴Division of Hepatogastroenterology, Department of Internal Medicine, Kaohsiung Chang Gung Memorial Hospital, Kaohsiung, Taiwan; ⁵Division of Gastroenterology and Hepatology, Department of Internal Medicine, E-Da Hospital, I-Shou University, Kaohsiung, Taiwan; ⁶School of Medicine for International Students, College of Medicine, I-Shou University, Kaohsiung, Taiwan; ⁷Division of Gastroenterology, Tainan Municipal Hospital (Managed By Show Chwan Medical Care Corporation), Tainan, Taiwan; ⁸Division of Gastroenterology and Hepatology, Department of Internal Medicine, Chi Mei Medical Center, Yongkang District, Tainan, Taiwan; ⁹Ph.D. Program in Translational Medicine, College of Medicine, Kaohsiung Medical University, Kaohsiung, Taiwan; ¹⁰Department of Internal Medicine, Dalin Tzu Chi Hospital, Buddhist Tzu Chi Medical Foundation, Chiayi, Taiwan; ¹¹School of Medicine, Tzuchi University, Hualien, Taiwan; ¹²Division of Gastroenterology, Department of Internal Medicine, St. Martin De Porres Hospital, Chiayi, Taiwan; ¹³Division of Gastroenterology, Department of Internal Medicine, Taitung Mackay Memorial Hospital, Taitung, Taiwan, ¹⁴Mackay Medical College, New Taipei City, Taiwan; ¹⁵Division of Gastroenterology, Department of Internal Medicine, Yuan's General Hospital, Kaohsiung, Taiwan; ¹⁶Division of Gastroenterology, Department of Internal Medicine, Tri Service General Hospital, National Defense Medical Center, Taipei, Taiwan; ¹⁷Division of Gastroenterology, Department of Internal Medicine, Tri Service General Hospital Penghu Branch, National Defense Medical Center, Taipei, Taiwan; ¹⁸School of Medicine, Chung Shan Medical University, Department of Internal Medicine, Chung Shan Medical University Hospital, Taichung, Taiwan; ¹⁹Division of Gastroenterology, Kaohsiung Armed Forces General Hospital, Kaohsiung, Taiwan; ²⁰Division of Gastroenterology and Hepatology, Department of Internal Medicine, Chi Mei Medical Center, Liouying District, Tainan, Taiwan; ²¹Lotung Poh-Ai Hospital, Yilan, Taiwan; ²²Division of Gastroenterology and Hepatology, Department of Medicine, Taipei Veterans General Hospital, Taipei, Taiwan; ²³Institute of Clinical Medicine, School of Medicine, National Yang-Ming Chiao Tung University, Taipei, Taiwan; ²⁴Division of Hepatology and Gastroenterology, Department of Internal Medicine, Shin Kong Wu Ho-Su Memorial Hospital, Taipei, Taiwan; ²⁵School of Medicine, Fu-Jen Catholic University, New Taipei City, Taiwan; ²⁶Department of Medicine, Hualien Tzu Chi Hospital, Buddhist Tzu Chi Medical Foundation and Tzu Chi University, Hualien, Taiwan; ²⁷Department of Gastroenterology, Division of Internal Medicine, Show Chwan Memorial Hospital, Changhua, Taiwan; ²⁸Division of Gastroenterology and Hepatology, Department of Internal Medicine, Taichung Veterans General Hospital, Taichung, Taiwan; ²⁹Division of Gastroenterology and Hepatology, Department of Internal Medicine, National Cheng Kung University Hospital, College of Medicine, National Cheng Kung University, Tainan, Taiwan; ³⁰Liver Center, Cathay General Hospital, Taipei, Taiwan; ³¹Wen-Chih Wu Clinic, Kaohsiung, Taiwan; ³²Division of Infectious Diseases, Department of Internal Medicine, Taoyuan General Hospital, Ministry of Health and Welfare, Taoyuan, Taiwan; ³³Penghu Hospital, Ministry of Health and Welfare, Penghu, Taiwan; ³⁴Zhou Guoxiong Clinic, Penghu, Taiwan; ³⁵Kaohsiung Veterans General Hospital, Kaohsiung, Taiwan; ³⁶National Taiwan University Hospital Hsin-Chu Branch, Hsinchu, Taiwan; ³⁷Liver Research Unit, Department of Hepato-Gastroenterology and Community Medicine Research Center, Chang Gung Memorial Hospital at Keelung, College of Medicine, Chang Gung University, Keelung, Keelung, Taiwan; ³⁸Taipei Tzu Chi Hospital, Buddhist Tzu Chi Medical Foundation and School of Medicine, Tzu Chi University, Taipei, Taiwan; ³⁹Cishan Hospital, Ministry of Health and Welfare, Kaohsiung, Taiwan; ⁴⁰Department of Gastroenterology, Renai Branch, Taipei City Hospital, Taipei, Taiwan; ⁴¹Department of Gastroenterology and Hepatology, Changhua Christian Hospital, Changhua, Taiwan; ⁴²Division of Gastroenterology and Hepatology, Far Eastern Memorial Hospital,

New Taipei City, Taiwan; ⁴³Division of Hepatogastroenterology, Department of Internal Medicine, Chang Gung Memorial Hospital, Chiayi, Taiwan and College of Medicine, Chang Gung University, Taoyuan, Taiwan; ⁴⁴Hepatitis Research Center and Department of Internal Medicine, National Taiwan University Hospital, Taipei, Taiwan; ⁴⁵Division of Gastroenterology and Hepatology, Department of Medicine, Ditmanson Medical Foundation Chiayi Christian Hospital, Chiayi, Taiwan; ⁴⁶Center for Digestive Medicine, Department of Internal Medicine, China Medical University Hospital, Taichung, Taiwan; ⁴⁷School of Medicine, China Medical University, Taichung, Taiwan
Email: waloeh@kmu.edu.tw

Background and aims: Although pan-genotypic direct-acting antivirals (DAA) sofosbuvir/velpatasvir (SOF/VEL) and glecaprevir/pibrentasvir (GLE/PIB) have simplified hepatitis C virus (HCV) treatment, treatment access remains limited due to constraints of specialist resource (e.g., gastroenterologist). Task-sharing by directing non-complicated cases to non-specialists is therefore crucial for upscaling treatment delivery. This study aimed to develop an algorithm to identify patients who can be safely managed by non-specialists.

Method: In this observational study, 10,641 HCV-infected patients registered in the Taiwan HCV Registry (TACR, a nationwide database of HCV-infected patients treated with DAA) between August 2019 and August 2021 were screened, and were included if they received ≥ 1 dose of SOF/VEL or GLE/PIB and fulfilled the eligibility criteria for simplified treatment by either the European Association for the Study of the Liver (EASL) or the American Association for the Study of Liver Diseases (AASLD) guidelines. Multivariate analysis was conducted to

identify patient risk factors associated with Grades 2–4 laboratory abnormalities in liver function parameters (including alanine aminotransferase, aspartate aminotransferase, and total bilirubin) during treatment and the three-month post-treatment follow-up period. An algorithm for simplified treatment with non-specialists (the TACR algorithm) was then developed based on 1) the EASL and AASLD criteria, 2) the risk factors identified, and 3) previous studies regarding additional management needs for special populations.

Results: A total of 7,677 patients were included in this analysis. Multivariate analyses identified the following patient characteristics associated with higher risks of Grades 2–4 abnormalities: age >70 years old, presence of hepatocellular carcinoma, total bilirubin >1.2 mg/dL, estimated glomerular filtration rate (by the Modification of Diet in Renal Disease equation) <60 ml/min/1.73 m², and Fibrosis-4 >3.25 . Incorporating these factors into the algorithm can help better differentiate patient populations with less and more safety management needs. The TACR algorithm for simplified HCV treatment with non-specialists (Figure) was then formulated. Briefly, patients with any ineligibility factors (such as history of hepatic compensation) should seek specialist care due to more complex management needs. Patients with any conditional ineligibility factors (such as age >70 years old) can be managed by specialist care, or by non-specialist care after consultation with a specialist. Patients without any ineligibility factor can be safely managed by non-specialists.

Conclusion: The TACR algorithm can provide important guidance in the effort to promote task sharing to non-specialists, which would be an important step towards HCV elimination.

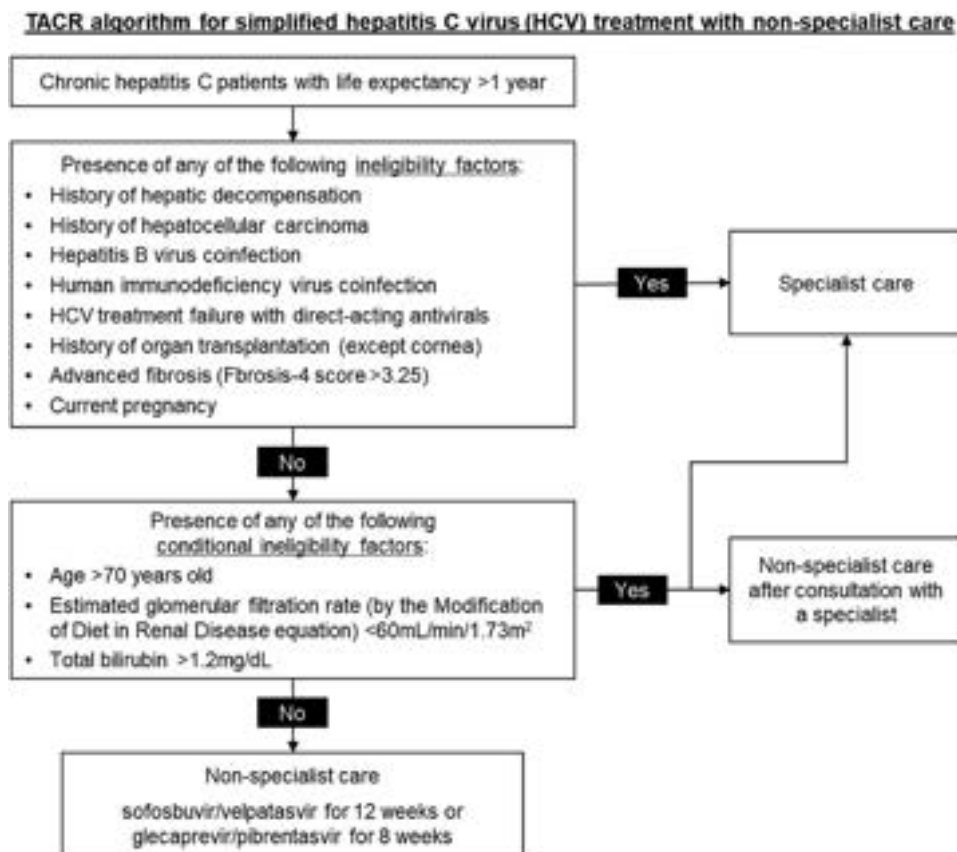


Figure: (abstract: THU-217).

POSTER PRESENTATIONS

THU-218

Evaluating utilization and management of comedications with potential for drug-drug interactions among patients with chronic hepatitis C initiating treatment with sofosbuvir/velpatasvir or glecaprevir/pibrentasvir

Stuart C Gordon¹, Andrea Steffens², Laura Weber², Kimberly McNiff², Alon Yehoshua³. ¹Henry Ford Hospital, United States; ²Optum, United States; ³Gilead Sciences, Inc., United States

Email: andrea.steffens@optum.com

Background and aims: Direct-acting antiviral (DAA) agents for treatment of chronic hepatitis C (HCV) include glecaprevir/pibrentasvir (GLE/PIB), a protease inhibitor with known drug-drug interaction (DDI) effects, and sofosbuvir/velpatasvir (SOF/VEL), a protease inhibitor-free regimen with a more favorable DDI profile. This analysis compared rates and management of comedications with DDI risk (DDI comedications) among patients initiating DAA treatment with SOF/VEL or GLE/PIB.

Method: Adults initiating SOF/VEL or GLE/PIB from July 2016–April 2020 were identified from US administrative claims data in the Optum Research Database. The index date was the first claim for SOF/VEL or GLE/PIB. Continuous enrollment 12 months before (baseline) and 6 months after the index date was required. Patients with baseline liver disease, HCV treatment, or HIV were excluded. Demographics and DDI comedication use were measured. All DDI comedications associated with GLE/PIB and SOF/VEL and DDI comedication severity, defined from more to less severe as red, amber, or yellow, were from the Liverpool HEP Drug Interactions Database. DDI comedication discontinuation, dose decrease, and

change to medication with no DDI risk during DAA treatment were measured in the subset of patients with prevalent DDI comedications 90 days prior to index.

Results: Among 4,528 patients meeting study criteria, 66.6% of GLE/PIB initiators and 43.7% of SOF/VEL initiators had any baseline DDI comedication use ($p < 0.01$). Compared with SOF/VEL initiators, GLE/PIB initiators had higher baseline rates of red (21.4% vs 2.3%), amber (51.9% vs 41.6%), and yellow (31.4% vs 2.8%, all $p < 0.01$) DDI comedications. DDI comedication use decreased during DAA treatment but remained higher in GLE/PIB initiators vs SOF/VEL initiators (41.5% vs 28.9%, $p < 0.01$). Overall, 979 GLE/PIB and 658 SOF/VEL initiators used prevalent DDI comedications in the 90 days pre-index. Of these, GLE/PIB vs SOF/VEL initiators had similar mean age (61.6 vs 61.8 years), proportions of female (42.2% vs 38.8%) and commercially insured (32.0% vs 29.5%) patients; baseline compensated cirrhosis was lower among GLE/PIB vs SOF/VEL initiators (5.8% vs 9.6%, $p < 0.01$). A higher proportion of GLE/PIB vs SOF/VEL initiators discontinued at least 1 DDI comedication before initiating DAA treatment (52.2% vs 38.0%, $p < 0.01$). During DAA treatment, GLE/PIB vs SOF/VEL initiators had higher rates of dose decrease (10.8% vs 6.8%, $p = 0.026$) and change to medication with no DDI risk (3.5% vs 1.1%, $p = 0.014$).

Conclusion: Use of DDI comedications was identified among a substantial proportion of patients, with higher rates of DDI comedication use and actions taken to manage DDI comedication use in GLE/PIB vs SOF/VEL initiators. Additional research is needed to assess real-world consequences of potential DDIs.



Figure: (abstract: THU-218).

THU-219

Concomitant use of proton pump inhibitors and Sofosbuvir/Velpatasvir: evidence from randomized clinical trials and real-world data

Rafael Esteban¹, Steve Flamm², Maria Buti¹, Juan Turnes³, Liyun Ni⁴, Candido Hernández⁵, Alessandra Mangia⁶. ¹Hospital Vall Hebron, Barcelona, Spain; ²Northwestern University Feinberg School of Medicine, Chicago, United States; ³Complejo Hospitalario Universitario de Pontevedra, Gastroenterology and Hepatology Department, Pontevedra, Spain; ⁴Gilead Sciences, Biostatistics Virology, Foster City, United States; ⁵Gilead Sciences, Global Medical Affairs, Madrid, Spain; ⁶IRCCS Casa Sollievo della Sofferenza, UOSD Epatologia, San Giovanni Rotondo, Italy Email: candido.hernandez@gilead.com

Background and aims: Literature and product labels suggest velpatasvir bioavailability may be reduced when administered concomitantly with a proton pump inhibitor (PPI), based mainly on pharmacokinetic studies. We aimed to determine the clinical relationship between PPI use and sustained virologic response rates (SVR) in patients treated with sofosbuvir/velpatasvir (SOF/VEL) for chronic hepatitis C virus (HCV) infection in available data coming from Phase 2/3 clinical trials (RCT) and Real-World Data (RWD).

Method: Retrospective and descriptive analysis of data from patients treated with SOF/VEL for 12 weeks with and without concomitant use of PPIs and participating in Phase 2/3 RCTs and RWD studies. In RCT, PPI use was captured as part of standard concomitant medication reporting, with specific details regarding PPI dosing not collected. Main variables collected for this analysis consisted of SVR12 and relapse rate.

Results: Overall, 546 patients with PPI use were identified, 87 coming from RCT and 459 from RWD. The overall control group of patients without PPI use was 5,201; 2,517 in RCTs and 2,684 in RWD. In RCT, patients receiving PPI and SOF/VEL were mainly male (79%), with a mean age of 57 years (26–78), GT3 in 56% and cirrhotic in 35%. Most patients participating in RCT (66%, 57/87) continuously used PPI during the 12-week course of treatment with SOF/VEL, omeprazole

being the most used PPI (68%). Overall SVR12 in PPI users was 97% (84/87), comparable to the reported by non-PPI users (97%). SVR12 in GT3 patients was 96% (47/49), in F4 was 94% (30/32). In GT3 plus F4 patients, SVR12 was 96% (23/24). Of the 3 patients who did not achieve SVR12 in PPI-users, 2 patients relapsed (relapse rate 2%) and one patient with a history of diabetes discontinued SOF/VEL after 7 days of dosing due to hyperglycemia. In RWD, patients receiving PPI and SOF/VEL were male (54%), with a mean age of 61 years, GT3 in 25% and cirrhotic in 29%. Overall SVR12 in PPI users was 99% (454/459), comparable to the reported by non-PPI users (99%).

Conclusion: In RCTs and RWD, the single-tablet regimen of SOF/VEL for 12 weeks was effective in patients with concomitant PPI use. These data support the use of SOF/VEL according to labeled recommendations with respect to co-administration of PPIs and other acid reducing agents.

THU-220

Sofosbuvir/Velpatasvir plus Ribavirin for chronic hepatitis C virus genotype 3 infected cirrhotic patients with or without HIV or HBV coinfection: real-world experience from southwest China

Ti Wu¹, Ti Wu¹, Kang Huang¹, Xiaofei Li¹, Nihong Lu¹, Zhirong Zhao¹, Lei Wu¹, Jingsong Bai¹, Junyi Li¹, Haiwen Li¹, Yingrong Du¹. ¹The 3rd People's Hospital of Kunming, Yunnan Province, China Email: 2894502062@qq.com

Background and aims: Evidence of direct-acting antiviral (DAA) treatment for refractory chronic hepatitis C (CHC) patients was limited. We aimed to evaluate the effectiveness and safety of Sofosbuvir/Velpatasvir (SOF/VEL) plus Ribavirin (RBV) in cirrhotic patients with hepatitis C virus genotype 3 (GT3) with or without HIV or HBV coinfection.

Method: From June 2018 to December 2021, CHC GT3 patients who received SOF/VEL plus RBV (dosage of RBV depended on weight) for 12 weeks were enrolled. Liver cirrhosis was diagnosed by clinical presentation and radiology examination. The primary end point was

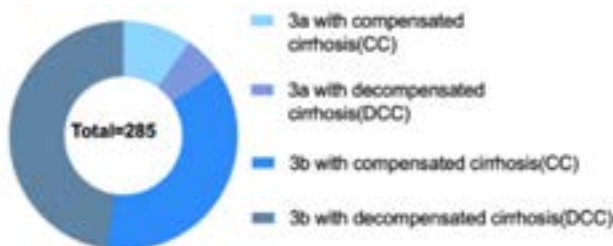


Figure 1. Distribution of HCV GT 3 infected patients with CC or DCC

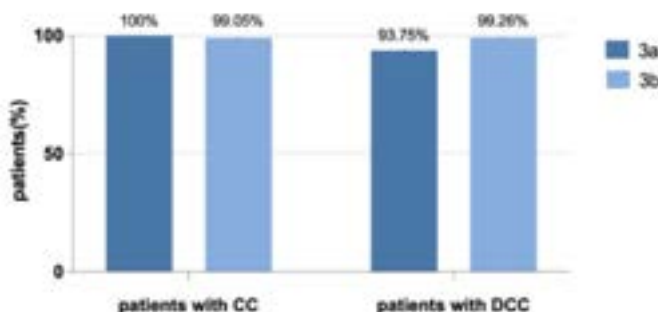


Figure 2. SVR 12 in patients with CC or DCC

Figure: (abstract: THU-220).

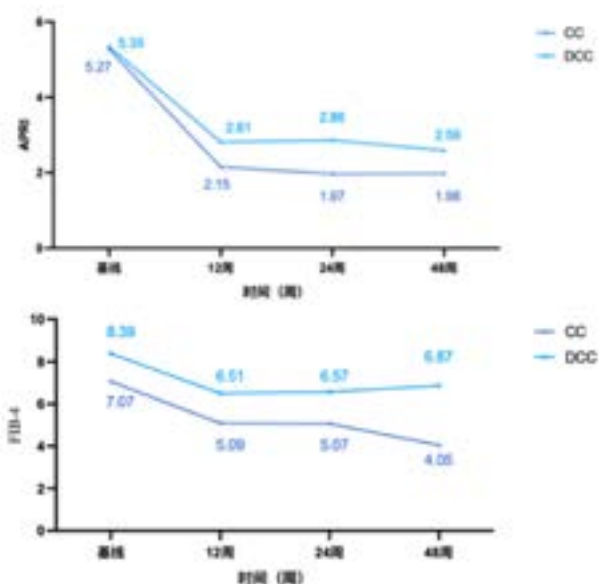


Figure 3. APRI and FIB-4 change in patients with CC or DCC

POSTER PRESENTATIONS

sustained virologic response at 12 weeks off-therapy (SVR12). Adverse events (AE) were assessed during treatment.

Results: In total, 285 treatment-naïve patients were recruited at the Third People's Hospital of Kunming. Mean age was 48.18 ± 8.27 years-old and 74.04% (211/285) were male. All patients had GT3 HCV infection including 44 patients with GT3a and 241 patients with GT3b. All patients had liver cirrhosis, 47% (133/285) had compensated cirrhosis (CC), 53% (152/285) had decompensated cirrhosis (DCC). 98.95% (282/285) patients achieved SVR12 with SOF/VEL plus RBV treatment for 12 weeks, including 97.72% (43/44) in GT3a and 99.17% (239/241) in GT3b. According to coinfection condition, SVR12 rate in CC group were: 99.25% (132/133) in mono-HCV infected patients, and 100% (22/22) in HCV/HIV. In DCC group, 98.68% (150/152) in mono-HCV infected patients, 94.12% (16/17) in HCV/HIV and 100% (7/7) in HBV/HCV coinfecting and 100% (1/1) in HBV/HCV/HIV coinfecting patients achieved SVR12. At the end of treatment, the APRI score and FIB-4 score in CC group and DCC group were improved, and the improvement in the compensated cirrhosis group was better than that in decompensated cirrhosis group (PAPRI = 0.001, PFIB-4 = 0.001). Mean ALT (from 74 ± 27.23 U/L to 39.31 ± 12.22 U/L, $p < 0.05$) and AST (from 73.98 ± 25.54 U/L to 44.17 ± 15.56 U/L, $p < 0.05$) also significantly declined after treatment. 1 patient had serious AE of hemolysis but recovered after 2–3 days of interruption of RBV. Most AEs were consistent with clinical sequelae of advanced liver disease or known toxicities of RBV.

Conclusion: SOF/VEL combined with RBV for cirrhotic GT3 hepatitis C patients all obtained high SVR12 (>95%) and improved liver function during treatment, and SOF/VEL combined with RBV regimen is recommended for cirrhotic GT3 hepatitis C patients.

THU-221

Efficacy of direct-acting antivirals in patients with hepatitis C virus-associated cryoglobulinemia and monoclonal gammopathy

Sofia Gavrisheva¹, Dzhamal Abdurakhmanov², Nikolay Bulanov², Tatiana Krasnova^{1,2}, Elena Tanashchuk², Teona Rozina^{1,2}, Elena Nikulkina², Svetlana Milovanova², Anna Filatova^{1,2}, Sergey Moiseev^{1,2}. ¹Lomonosov Moscow State University, Moscow, Russian Federation; ²Sechenov First Moscow State Medical University, Moscow, Russian Federation
Email: gavrisheva.sofia@gmail.com

Background and aims: Monoclonal gammopathy (MG) is caused by a clonal expansion of plasma cells producing a unique immunoglobulin. MG is common in patients with B-cell lymphoproliferative disorders such as hepatitis C virus (HCV)-associated mixed cryoglobulinemia, and the long-term outcomes of direct-acting antiviral (DAA) therapy in these patients are not fully understood.

Method: We conducted a case series investigation of 10 HCV-positive patients with cryoglobulinemia and MG (diagnosed by serum and urine protein electrophoresis with immunofixation), who received DAA therapy (Table 1). Nine patients met the criteria for HCV-associated cryoglobulinemic vasculitis (HCV-CV) and one patient had asymptomatic cryoglobulinemia (AC). Patients were evaluated at baseline (before starting DAAs) and every 6 months after the end of HCV treatment (EoT). The activity of HCV-CV was assessed by using Birmingham Vasculitis Activity Score version 3 (BVAS.v3).

Results: All patients achieved sustained virological response. Skin purpura was improved in 9/9 (100%) patients, joint involvement – in all 5/5 (100%), sicca syndrome – in 2/2 (100%), and peripheral polyneuropathy – in 2/6 (33.3%) patients. Signs of kidney involvement persisted in 3/5 (60%) patients, including declined glomerular filtration rate in two cases and persistent proteinuria in one patient. In the latter patient a kidney biopsy showed membranoproliferative glomerulonephritis with large subendothelial deposits, there were no typical signs of kidney involvement associated with multiple myeloma. Patient with AC developed Waldenstrom macroglobulinemia 2 years after the EoT and received rituximab-containing chemotherapy. The monoclonal proteins disappeared in 8/10 (80%)

patients with a median time of 13.5 months after EoT, in 2 of them – only after rituximab therapy (including the patient with Waldenstrom macroglobulinemia); 3 other patients received glucocorticosteroids during follow-up (for 3, 6 and 30 months). Immunologic response (defined as absence of circulating cryoglobulins, rheumatoid factor and normal C4 level) was achieved only in 4 (40%) patients, whereas elimination of cryoglobulins occurred in 9 (90%) patients. Complete (defined by a BVAS.v3 score of 0) and partial (defined as BVAS.v3 score <50% of the baseline score) clinical response were achieved by 4 (44.4%) and 5 (55.6%) patients with HCV-CV, respectively. No patient died during follow-up.

Table 1:

Baseline characteristics	n = 10
Age, years	57.5 (49.0–65.8)
Female sex, n (%)	8 (80)
Cirrhosis, n (%)	6 (60)
Clinical manifestations in 9 patients with HCV-CV, n (%)	
Skin purpura	9 (100)
Arthralgia/arthritis	5 (55.6)
Peripheral polyneuropathy	6 (66.7)
Kidney involvement	5 (55.6)
Sicca syndrome	2 (22.2)
Monoclonal immunoglobulin type, n (%)	
IgM kappa	5 (50)
IgA kappa	1 (10)
IgG kappa	1 (10)
IgG lambda and IgM kappa	1 (10)
Not determined	2 (20)
Follow-up period after EoT, months	62.0 (46.5–76.6)

Note: Continuous data are expressed as median (interquartile range)

Conclusion: DAA therapy in patients with HCV-associated cryoglobulinemia and MG was associated with high rates of monoclonal immunoglobulin elimination and clinical improvement, however in some cases additional immunosuppressive therapy is required.

THU-222

Resistance-associated substitutions described after failure of anti-NS5A direct-acting antiviral treatment in 58 hepatitis C virus (HCV) infected patients in Cameroon

Serge Tchamgoue^{1,2,3}, Maurelle Magatsing¹, Tatiana Nganso¹, Marthe Ntep Eboko¹, Mathurin Kowo⁴, Christian Tzeuton⁵.

¹Polyclinique Bordeaux Douala, Infectious Disease, Douala, Cameroon;

²National Network for the fight against viral Hepatitis, deputy chairman, Douala, Cameroon;

³Centre Hospitalier de Libourne, Infectious disease, Libourne, France;

⁴yaounde hospital university, yaounde, Cameroon;

⁵university of douala, douala, Cameroon

Email: stchamgoue@gmail.com

Background and aims: The World Health Organization (WHO) set the goal to eliminate Hepatitis C as a major public health threat by 2030. This goal is challenging in sub-Saharan African countries, where HCV seroprevalence remains too high (i.e. around 3% in Cameroun), due to insufficient funding, lack of screening policies, poor-linkage-to-care strategies, expensive HCV treatments, and more recently, failure of HCV DAA combinations pan-genotypic drugs. Recent European data report suboptimal rates of sustained virological response (SVR) in patients of African origin who were infected with HCV genotype subtypes unusually found in Western Europe (i.e. Genotype (G)1e, G1g, G1l as well as G4c, G4e, G4f, G4r). We aim to describe clinical and virological characteristics of patients escaping from first line HCV treatment including DAA combination in a

national survey data collected in the two biggest Camerounian city: Douala and Yaounde.

Method: Retrospective descriptive study. Data collected from Jan 1st 2020 to Dec 31st 2021. Inclusion criteria: patients escaping from HCV first line treatment including a DAA combination; coming to polyclinic Bordeaux douala's hospital, having a blood test for NS5a genotype virologic test which was sent to Grenoble University hospital (France); giving their consent agreement. This study was agreed by the regional ethical committee.

Results: 58 patients were included; aged 31 to 91 (median 69.5). Women (n = 35; 60%). Weight (BMI>25): (n = 49, 67.2%). HCV was diagnosed since a median of 7.4 years before. All patients received their first line regimen. Fibrosis stage 4 (METAVIR F4) or cirrhosis: (n = 18; 31%). Proven relapsed treatment (n = 32; 55%). HIV co-infected patients (n = 2; 3.4%). Died by dec 31st 2021 (n = 10; 17.2%). Failure associated factors: Anticid or Proton-pump inhibitor IPP (n = 8; 13%). Traditional medicine (n = 5; 8.6%); Poor compliance (n = 3; 5.1%). Treatment regimen on failure: SOFOSBUVIR/LEDIPASVIR (n = 25; 43%); SOFO/LEDI/RIBA/RIBAVIRIN (n = 9; 15.5%); SOFOSBUVIR/DACLATASVIR (n = 9; 15.5%); SOFO/DACLA/RIBA (n = 2; 3.4%), SOFOSBUVIR/VELPATASVIR (n = 11; 18.9%); SOFO/VELPA/RIBA (n = 2; 3.4%). Genotypes distribution : G1 (n = 36; 62%); G4 (n = 15; 25.8%); G2 (n = 4; 6.9%); Non ampli (n = 3; 5.7%). Subtypes Distribution :G11 (n = 19; 32%); G4f (n = 13; 22.4%); G1e (n = 7; 12%); G1 not a not b (n = 3; 5%), Non ampli (n = 3; 5%); G1a (n = 2; 3.4%); G1b (n = 2; 3.4%); one patient for :G1c; G1g; G1h; G2e; G2i; G2k or q; G4t; G4 not a not b. Resistance-associated distribution: L31/M/V (n = 18; 31%); Q30H/KQ/S/R/W (n = 16; 27%); Y93/C/H/M (n = 13; 22%); L31M+Q30R (n = 4;

6%); L28M+Q30R (n = 2; 3%); M28V/M/T (n = 2; 3%); R30/Q (n = 2; 3%); Others (n = 22; 37%)

Conclusion: We described a high proportion of unusual subtypes (G11, G4f, G1e) in HCV patients escaping from their first line treatment including DAA combination, underlining the high interest on accessing to affordable genotypic resistance tests in this context

THU-223

Retreatment of patients experiencing failure with Hepatitis C direct-acting antivirals

Nessa Quinn¹, Colm Bergin², Ciaran Bannan², Susan McKiernan³, Suzanne Norris³, Gillian Farrell², Ciara Houlihan², Catherine Murray², Lewel Alvarado³, Noelle Cullen³, Linda Finnerty³, Suzanne Hunt³, Bernard Carr¹, Gail Melanophy¹, Miriam Coghlan¹. ¹St. James's Hospital, Pharmacy, Ireland; ²St. James's Hospital, Genito Urinary Medicine and Infectious Diseases (GUIDE), Ireland; ³St. James's Hospital, Hepatology, Ireland

Email: nequinn@stjames.ie

Background and aims: The sustained virological response (SVR) rate for first line direct-acting antiviral (DAA) therapy for hepatitis C virus (HCV) infection in Ireland surpasses 95%. Factors associated with the limited number of treatment failures include incomplete adherence, advanced cirrhosis (Child Pugh class B and C) and the presence of resistance associated substitutions (RASs). The aim of this study was to determine the frequency of treatment failure in patients treated in St James Hospital (SJH), Dublin and to review retreatment regimens and outcomes.

Method: Data was extracted from hospital HCV treatment records and the National Hepatitis C Treatment Registry to identify patients

First line treatment	Genotype	RAS conferring reduced susceptibility	Cirrhosis	Re-treatment	Outcome
PrOD/RBV x 8-12/52 (5)	1a (4)	NS5A: Q30R (2)	No (2)	SOF/VEL/VOX/RBV x 12/52 (3)	SVR (3)
		NS5A: Q30R; NS5B: D186V (1)	Yes (1)		
		NS5A: Y93C (1)	No (2)	Pending (1)	N/A
SOF/DAC x 12-24/52 (4)	1b (1)	NS5A: Y93H (1)		SOF/VEL/VOX x 12/52 (1)	SVR (1)
	1a (1)	NS5A: Y93H/N, Q30E, M28V; NS3: Q80K (1)	No (4)	SOF/VEL/VOX/RBV x 12/52 (1)	SVR (4)
		NS5A: A30K (1)		SOF/VEL/VOX x 12/52 (2)	
		NS5A: Y93H (1)		SOF/VEL/VOX/RBV x 12/52 (1)	
SOF/LDV ± RBV x 8-12/52 (11)	1a (7)	NS5A: Q30R, K24N, M208T (1)	No (3)	G/P x 12/52 (1)	Relapse (1)
		NS5A: Q30K (1)		SOF/VEL/VOX x 12/52 (1)	SVR (3)
		NS5A: L31V, H58D, Y93C/W (1)		SOF/G/P x 16/52 (1)	
		NS3: Q80K (1)	Yes (4)	SOF/DAC/RBV x 24/52 (1)	Relapse (1)
		NS5A: Y93C; NS3: Q80K (1)		SOF/VEL x 24/52 (1)	
		Nil resistance (1)		RIP (1)	
		Not tested (1)		Transplant + SOF/VEL/RBV x 24/52 (1)	SVR (5)
	1b (1)	NS5A: Y93H, P58A; NS3: Y56F (1)	No (1)	SOF/VEL/VOX x 12/52 (1)	
	3 (2)	Not tested (2)	Yes (2)	SOF/DAC x 24/52 (1)	
				SOF/DAC/RBV x 24/52 (1)	
SOF/VEL ± RBV x 12/52 (3)	4R (1)	NS5B: S282C/S/T (1)	No (1)	SOF/G/P x 16/52 (1)	
	1a (3)	NS5A: Y93H; NS3: Q80K (1)	Yes (1)	SOF/G/P x 12 weeks (1)	SVR (1)
		NS5A: K24R; NS3: Q80K (1)	No (1)	SOF/VEL/VOX x 12/52 (1)	Relapse (2)
		Nil resistance (1)	Yes (1)	SOF/VEL/VOX/RBV x 12/52 (1)	
G/P x 8/52 (2)	1a (1)	NS3: Q80K (1)	Yes (1)	SOF/G/P x 12/52 (1)	SVR (1)
	3 (1)	NS5A: Y93H (1)	No (1)	SOF/VEL/VOX x 12/52 (1)	Relapse (1)

DAC = daclatasvir; G/p = glecaprevir/pibrentasvir; PrOD = paritaprevir/ritonavir/ombitasvir/dasabuvir; RBV = ribavirin; SOF = sofosbuvir; SVR = sustained virological response; VEL = velpatasvir; VOX = voxilaprevir

Figure: (abstract: THU-223).

who received all-oral DAA treatment for HCV from 2014 to 2021 in SJH.

Results: A total of 2,015 patients received at least one course of all-oral DAA treatment for HCV. A total of 1,589 patients achieved SVR (97.9%) (per protocol analysis). Twenty-five patients failed to achieve SVR, twenty of whom had RASs detected. The most common RASs conferring reduced susceptibility to treatment included NS5A RASs at positions Q30 and Y93 and NS3 RASs at position Q80. Eight patients had >1 NS5A mutation and/or dual class resistance. Of 23 patients who were retreated, 18 achieved SVR (14 of whom received triple therapy with sofosbuvir/velpatasvir/voxilaprevir (SOF/VEL/VOX) or sofosbuvir/glecaprevir/pibrentasvir (SOF/G/P) and 9 of whom received concurrent ribavirin). Five patients failed to achieve SVR with retreatment, two of whom were successfully treated with a third course of DAAs. The remaining three patients are awaiting third line treatment.

Conclusion: Three class DAA regimens are a highly effective retreatment for HCV even in the presence of multiple NS5A and NS3 mutations.

THU-224

Efficacy and safety of Sofosbuvir Plus Daclatasvir bilayer tablet with or without Ribavirin in patients with chronic hepatitis C genotype 4 Infection

Mohamed Hassany¹, Sameh Ramadan², Ehab Moustafa³, Basem Eysa¹, Ahmed Zidan¹, Amany Hassan¹, Heba Abdulaziz¹, Shimaa Afify¹, Mohamed Saeed¹, Hanaa Shalabi¹, Asmaa Gomaa⁴, Naglaa Allam⁴, Eman Abdelsameea⁴, Reda Badr⁴, Aliaa Sabry⁴, Alzhraa Alkhatib⁴, Heba Sameh⁴, Mostafa Elhelbawy⁴, Ahmed Radwan³, Sahar Hassany³, Enas Attia², Mai Abdel Razeq², Fatema Elamrawy⁵, Waseem Medhat⁵, Omar Hamed⁵, Dalia Safwat⁵, Doris Ezzat⁶, Khaled Prince⁵, Imam Waked⁴. ¹National Hepatology and Tropical Medicine Research Institute, Egypt; ²Fayoum General Hospital, Egypt; ³Assuit University, Egypt; ⁴National Liver Institute, Menofia University, Egypt; ⁵ClinMax, Egypt; ⁶Minapharm Pharmaceuticals, Egypt
Email: mohamadhassany@yahoo.com

Background and aims: The evolution of the hepatitis C virus (HCV) therapies, and its very high efficacy, led to a remarkable improvement of the treatment outcome. The combination of sofosbuvir 400 mg and daclatasvir 200 mg is considered one of the best pan-genotypic regimens which was endorsed by many regional and global guidelines, especially after the robust availability of the generic versions of both drugs, which promoted the access to care. Several countries have adopted the concept of developing the bilayer tablets as an innovative drug formula for enhancing the drug delivery and treatment adherence especially in the long-term therapies and multi-medicated diseases. The aim of this study is to evaluate the safety and efficacy of a single bilayer tablet that contains 400 mg of Sofosbuvir (SOF) and 60 mg of Daclatasvir (DAC) administered once daily with or without Ribavirin (RBV) in patients with genotype 4 HCV.

Method: The study is a Phase IV, prospective, open-label, multicenter study. The patients were classified into 2 groups (easy or difficult to treat), patients with no liver cirrhosis, FIB-4 ≤ 3.25 , albumin >3.5 g/dl, total bilirubin ≤ 1.2 mg/dl, INR ≤ 1.2 , platelet count $>150,000$ mm³ and treatment-naïve are considered as the easy to treat group, and

the patients with any opposite parameter were considered as the difficult to treat group. All patients received a single Bilayer tablet that contains 400 mg of SOF and 60 mg of DAC once daily. The difficult-to-treat patients also received RBV divided into two daily doses to reach a total dose of 1200 mg/day if the patient's weight was ≥ 75 kg or 1000 mg/day when the weight was <75 kg. The treatment duration was 12 weeks, and the patients were followed up for an additional 12 weeks after the end of treatment. The safety data and the relation of each of the adverse events to study medications were reported.

Results: A total of 198 patients were screened throughout the study, out of which 142 were enrolled in the study (easy to treat = 120; difficult to treat = 22). The study drug has proven to be effective and safe to be used for patients with HCV disease. The viral load reached the level of low detection and was sustained after 12 weeks of stopping the drug in 88.7% (126/142) of the patients according to the ITT analysis and 100% (99/99) in the per protocol analysis. Only 2 patients (1.4%) showed related AE that were mild or moderate and were resolved by week 24 of the study, additional non-related one death and other adverse events were reported.

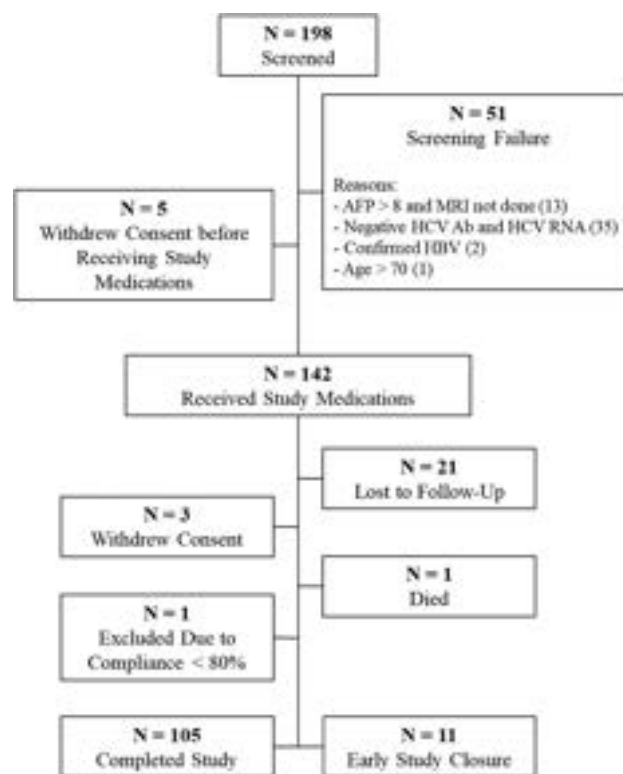


Figure 1: Patient Disposition.

Conclusion: the combination of SOF and DAC in a single bilayer tablet \pm ribavirin is an effective and tolerable treatment regimen for HCV genotype 4 patients.

Author Index

- Aabakken, Lars, S408 (WED-317)
 Aamann, Luise, S982 (THU-304)
 Abaalkhail, Faisal, S859 (SAT-119),
 S1006 (THU-383)
 Abadia, Marta, S697 (SAT-465),
 S705 (SAT-478), S706 (SAT-479)
 Abad, Javier, S291 (SAT-340)
 Abadpour, Shadab, S59 (OS-076)
 Abate, Maria Lorena, S605 (THU-415),
 S1056 (TOP-106)
 Abbasi, Amanullah, S319 (SAT-557)
 Abbas, Minaam, S1054 (TOP-100)
 Abbas, Nadir, S56 (OS-073),
 S398 (WED-299), S466 (THU-497)
 Abbas, Zaigham, S1054 (TOP-100)
 Abbati, Gianluca, S1105 (WED-176)
 Abbott, Jane, S1127 (WED-209)
 Abdallah, Ali, S133 (THU-403)
 Abdalla, Rima, S127 (TOP-093)
 Abdelaal, Hala, S782 (WED-506)
 Abdelhameed, Ahmed, S463 (THU-491)
 Abdelkader, Jamal, S1193 (THU-194)
 Abdelmalek, Manal, S13 (LBO-05),
 S651 (SAT-393), S809 (FRI-467),
 S823 (FRI-517)
 Abdelraouf, Mariam I., S840 (FRI-491)
 Abdelsameea, Eman, S1212 (THU-224)
 Abdrashitov, Ramil, S574 (THU-115),
 S580 (THU-125)
 Abdulaziz, Heba, S1212 (THU-224)
 Abdulle, Amina, S521 (FRI-325),
 S611 (THU-425), S617 (THU-435),
 S626 (THU-452), S637 (THU-470),
 S704 (SAT-474), S713 (SAT-494)
 Abdurakhmanov, Dzhamal,
 S1055 (TOP-103), S1210 (THU-221)
 Abe-Chayama, Hiromi, S72 (OS-098),
 S1017 (FRI-216)
 Abedin, Nada, S276 (WED-385)
 Abe, Hiroshi, S818 (FRI-508)
 Abe, Masanori, S394 (WED-293)
 Abe, Masatoshi, S545 (SAT-246)
 Abenavoli, Ludovico, S40 (OS-045),
 S55 (OS-070)
 Abergel, Armand, S172 (FRI-446),
 S467 (THU-498), S473 (THU-511),
 S498 (FRI-286)
 Åberg, Fredrik, S959 (THU-275)
 Aberle, Stephan, S996 (THU-327),
 S1135 (SAT-150), S1170 (SAT-200)
 Abeysekera, Kushala, S177 (FRI-455),
 S621 (THU-441), S858 (SAT-118),
 S867 (SAT-130), S1198 (THU-203)
 Abiven, Joëlle, S722 (SAT-505),
 S769 (WED-453), S777 (WED-469)
 Ableitner, Elisabeth, S142 (FRI-402)
 Aboagye, Eric, S576 (THU-118)
 Aboelwafa, Reham, S319 (SAT-558)
 Aboona, Majd, S611 (THU-424)
 Abraham, Katie, S918 (FRI-182)
 Abrahams, Tobie, S380 (WED-271)
 Abraldes, Juan, S87 (OS-123-YI)
 Abraldes, Juan G, S10 (LBO-01),
 S865 (SAT-129)
 Abraldes, Juan G., S175 (FRI-451)
 Abramov, Frida, S53 (OS-067),
 S1137 (SAT-153)
 Abrams, Gary, S808 (TOP-091)
 Abrantes, Jefferson, S1188 (THU-184)
 Abril-Fornaguera, Jordi, S48 (OS-059-YI)
 Abualghannam, Saad, S1011 (THU-388)
 Abudzi, Amina, S1012 (THU-391)
 Abugabal, Yehia, S582 (THU-128)
 Abutidze, Akaki, S881 (FRI-123),
 S921 (FRI-187), S1204 (THU-214)
 Accarino, Elena Vargas, S533 (SAT-224),
 S904 (FRI-158)
 Acharya, Subrata, S587 (THU-135)
 Achneck, Hardean, S386 (WED-280)
 Ackermann, Nora, S185 (FRI-341)
 Acosta, Jose Alberto Ferrusquia,
 S86 (OS-121-YI)
 Acosta-López, Silvia, S171 (FRI-445),
 S928 (FRI-198)
 Acquaviva, Antonio, S599 (THU-156)
 Acuna, Claudio, S1020 (FRI-222)
 Adair, Gill, S1006 (THU-382)
 Adali, Gupse, S181 (FRI-463)
 Adames, Enrique, S900 (FRI-151)
 Adam, Gerhard, S285 (SAT-331)
 Adamia, Ekaterine, S931 (FRI-205),
 S1204 (THU-214)
 Adam, René, S46 (OS-053-YI),
 S458 (THU-483)
 Adamson, Colby, S773 (WED-460)
 Adam, Valeria, S251 (WED-344)
 Adanir, Haydar, S195 (FRI-546)
 Adan-Villaescusa, Elena, S526 (TOP-072),
 S537 (SAT-232)
 Addario, Luigi, S105 (LBP-09)
 Addy, Carol, S995 (THU-324)
 Adebayo, Danielle, S195 (FRI-546)
 Adegboye, Oluwatobi, S71 (OS-097)
 Adeniji, Nia, S25 (OS-020-YI)
 Adisasmita, Michael, S437 (SAT-361),
 S563 (SAT-281), S947 (THU-258)
 Adlung, Lorenz, S527 (SAT-213)
 Adori, Csaba, S326 (WED-222),
 S433 (SAT-353)
 Adorini, Luciano, S804 (WED-550)
 Adotti, Valentina, S233 (THU-371),
 S513 (FRI-311)
 Adoukara, Jean-Pierre, S897 (FRI-146)
 Adrien, Lannes, S86 (OS-121-YI),
 S198 (FRI-550), S318 (SAT-556),
 S667 (SAT-419)
 Adu, Prince, S883 (FRI-125), S886 (FRI-130),
 S1189 (THU-187), S1200 (THU-207)
 Aehling, Niklas, S244 (WED-335)
 Aehling, Niklas F, S197 (FRI-549),
 S201 (FRI-555)
 Aerssens, Jeroen, S444 (SAT-374),
 S1034 (FRI-248)
 Aeschbacher, Thomas, S1055 (TOP-103)
 Affronti, Marco, S568 (SAT-288)
 Afify, Shimaa, S1212 (THU-224)
 Afonso, Marta B., S734 (WED-397)
 Afonyushkin, Taras, S224 (THU-358)
 Afroz, Saba, S268 (WED-371),
 S641 (THU-476)
 Agapito, Giuseppe, S568 (SAT-288)
 Agarwal, Ankit, S401 (WED-304),
 S587 (THU-135)
 Agarwal, Banwari, S193 (FRI-543),
 S220 (THU-355)
 Agarwal, Kosh, S31 (OS-030), S53 (OS-067),
 S91 (OS-128), S112 (LBP-18),
 S642 (THU-551), S905 (FRI-161),
 S1060 (WED-117), S1081 (WED-143),
 S1081 (WED-144), S1134 (SAT-148),
 S1137 (SAT-153), S1138 (SAT-154),

*Page numbers for abstracts are followed by the abstract number(s) in parentheses.

Author Index

- S1159 ([SAT-182](#)), S1164 ([SAT-192](#)), S1179 ([THU-172](#))
- Agarwal, Samagra, S6 ([GS-006](#)), S233 ([TOP-041](#))
- Agelopoulos, Konstantin, S377 ([WED-265](#))
- Aggarwal, Arnav, S73 ([OS-101-YI](#)), S297 ([SAT-350](#))
- Aggarwal, Deepankshi, S51 ([OS-064-YI](#))
- Aghemo, Alessio, S54 ([OS-069](#)), S609 ([THU-421](#))
- Agirre Lizaso, Aloña, S57 ([OS-074-YI](#))
- Agirrezabal, Ion, S573 ([THU-114](#))
- Agollah, Germaine D., S13 ([LBO-05](#))
- Agorastou, Polyxeni, S1128 ([WED-211](#))
- Agozino, Marina, S245 ([WED-336](#))
- Agrawal, Prashant, S182 ([TOP-040](#))
- Agrawal, Sudeep, S607 ([THU-419](#))
- Agudo, Rubén Rodríguez, S140 ([FRI-399](#)), S529 ([SAT-216](#))
- Aguilar-Bravo, Beatriz, S78 ([OS-109-YI](#))
- Aguilar-Company, Juan, S375 ([WED-263](#))
- Aguilar, Ferran, S143 ([FRI-404](#)), S206 ([TOP-046](#))
- Aguilar, Juan Cristobal, S1126 ([WED-208](#))
- Aguilar, Laia, S737 ([WED-403](#))
- Aguilar, Raul, S123 ([LBP-35](#))
- Aguilera, Antonio, S921 ([FRI-188](#))
- Aguilera Sancho, Victoria, S87 ([OS-123-YI](#)), S476 ([THU-517](#)), S485 ([THU-535](#))
- Aguilera, Victoria, S2 ([GS-003](#))
- Aguirre, Jose Roberto, S900 ([FRI-151](#))
- Aguyire, Joan, S865 ([SAT-129](#))
- Agyrbay, Aibar, S320 ([SAT-559](#))
- Ahkim, Kyung, S407 ([WED-316](#))
- Ahlén, Gustaf, S1038 ([FRI-252](#))
- Ahmad, Moin, S489 ([TOP-065](#))
- Ahmad, Tariq, S641 ([THU-476](#))
- Ahmed, Aijaz, S894 ([FRI-141](#))
- Ahmed, Anam, S401 ([WED-304](#))
- Ahmed-Belkacem, Hakim, S456 ([THU-478](#))
- Ahmed, Mohamed, S319 ([SAT-558](#)), S678 ([SAT-437](#))
- Ahmed, Osman, S756 ([WED-434](#))
- Ahmed, Rayan, S689 ([SAT-453](#))
- Ahmed, Syed Masroor, S842 ([FRI-497](#))
- Ahmed, Yusuf, S840 ([FRI-492](#))
- Ahn, Keun Soo, S512 ([FRI-309](#)), S594 ([THU-146](#))
- Ahnou, Nazim, S456 ([THU-478](#))
- Ahn, Richard, S322 ([WED-215](#))
- Ahn, Sang Bong, S615 ([THU-431](#)), S662 ([SAT-411](#)), S667 ([SAT-418](#)), S695 ([SAT-462](#)), S704 ([SAT-475](#)), S705 ([SAT-476](#)), S757 ([WED-435](#)), S794 ([WED-531](#)), S821 ([FRI-514](#)), S864 ([SAT-128](#)), S1073 ([WED-135](#))
- Ahn, Sang Hoon, S362 ([FRI-387](#)), S552 ([SAT-259](#)), S595 ([THU-148](#)), S906 ([FRI-162](#)), S1065 ([WED-124](#)), S1121 ([WED-201](#)), S1134 ([SAT-148](#)), S1142 ([SAT-160](#)), S1184 ([THU-179](#)), S1197 ([THU-202](#))
- Ahuja, Vineet, S401 ([WED-304](#))
- Ahumada, Adriana, S90 ([OS-127-YI](#)), S299 ([SAT-521](#))
- Aidoo-Micah, Gloryanne, S558 ([SAT-271](#))
- Aigner, Elmar, S863 ([SAT-126](#))
- Aikata, Hiroshi, S72 ([OS-098](#))
- Ai, Ma, S463 ([THU-490](#))
- Aimaier, Aihetaimu, S543 ([SAT-242](#))
- Aina, Kehinde, S80 ([OS-114-YI](#))
- Aird, Rhona E., S434 ([SAT-355](#))
- Aithal, Guruprasad, S127 ([TOP-092](#)), S157 ([FRI-422](#)), S168 ([FRI-439](#)), S448 ([SAT-381](#)), S708 ([SAT-483](#)), S717 ([SAT-498](#))
- Aizenshtadt, Aleksandra, S59 ([OS-076](#)), S336 ([WED-242](#)), S409 ([TOP-064](#)), S787 ([WED-517](#))
- Ajana, Fatima Zahrae, S842 ([FRI-496](#))
- Ajayi, Omolola, S324 ([WED-218](#))
- Ajaz, Saima, S642 ([THU-551](#))
- Ajee, K L, S846 ([WED-477](#))
- Ajmera, Veeral, S65 ([OS-086](#)), S648 ([TOP-075](#)), S649 ([TOP-083](#))
- Akalu, Tiruwork Fekadu, S865 ([SAT-129](#))
- Akande, Kolawole, S865 ([SAT-129](#))
- Akarca, Ulus, S31 ([OS-030](#)), S181 ([FRI-463](#))
- Akarca, Ulus S, S1137 ([SAT-152](#))
- Akarsu, Mesut, S181 ([FRI-463](#))
- Akbari, Camilla, S605 ([THU-414](#)), S650 ([TOP-085](#)), S653 ([SAT-397](#))
- Akbary, Kutbuddin, S333 ([WED-236](#)), S334 ([WED-237](#)), S334 ([WED-238](#)), S501 ([FRI-290](#)), S999 ([THU-333](#))
- Akbulut, Seval, S408 ([WED-317](#))
- Akdogan, Banu, S948 ([THU-259](#))
- Akerblad, Peter, S57 ([OS-074-YI](#)), S940 ([THU-249](#))
- Akil, Fardhah, S1203 ([THU-212](#))
- Akilli-Oeztuerk, Oezlem, S26 ([OS-022](#))
- Akinobu, Taketomi, S444 ([SAT-373](#))
- Akiyama, Matthew, S100 ([LBP-01](#))
- Akpınar, İhsan Nuri, S645 ([THU-556](#))
- Akram, Fatima, S1196 ([THU-200](#))
- Akushevich, Lucy, S89 ([OS-125](#))
- Akuta, Norio, S1183 ([THU-177](#))
- Akyildiz, Murat, S181 ([FRI-463](#)), S1109 ([WED-183](#))
- Akyuz, Filiz, S709 ([SAT-485](#))
- Alaa, Basma, S779 ([WED-472](#)), S795 ([WED-532](#))
- Ala, Aftab, S967 ([THU-286](#))
- Aladag, Murat, S181 ([FRI-463](#))
- Alagna, Giuliano, S40 ([OS-045](#)), S55 ([OS-070](#))
- Alam, Ejaz, S912 ([FRI-172](#))
- Alam, Imtiaz, S674 ([SAT-431](#))
- Alam, Khurshid, S726 ([SAT-511](#))
- Alam, Seema, S971 ([THU-291](#))
- Alanazi, Alanoud, S724 ([SAT-509](#))
- Alani, Muhsen, S11 ([LBO-03](#))
- Alañón, Paloma, S248 ([WED-341](#))
- Alaparthi, Lakshmi, S782 ([WED-506](#))
- Alarcón, Cristina, S587 ([THU-136](#))
- Alarcon, Francisca Cuenca, S392 ([WED-290](#)), S964 ([THU-282](#)), S980 ([THU-301](#)), S996 ([THU-326](#)), S998 ([THU-331](#))
- Alarcón-Sánchez, Brisa Rodope, S151 ([FRI-414](#)), S160 ([FRI-426](#))
- Alarqan, Reem, S724 ([SAT-509](#))
- Alatrakchi, Nadia, S58 ([OS-075](#))
- Alavi, Maryam, S910 ([FRI-169](#))
- Alazawi, William, S39 ([OS-043](#)), S612 ([THU-426](#)), S621 ([THU-441](#)), S624 ([THU-447](#)), S708 ([SAT-483](#)), S726 ([SAT-512](#)), S740 ([WED-406](#)), S825 ([FRI-520](#))
- Albano, Emanuele, S526 ([SAT-211](#)), S751 ([WED-425](#)), S804 ([WED-551](#))
- Albela, Manuel, S69 ([OS-094](#))
- Albenmoussa, Ali, S958 ([THU-273](#)), S1011 ([THU-388](#))
- Alberch, Pol Olivas, S984 ([THU-308](#))
- Alberio, Lorenzo, S105 ([LBP-08](#))
- Albert Tran, S498 ([FRI-286](#))
- Albhaisi, Somaya, S195 ([FRI-546](#)), S809 ([FRI-466](#))
- Albillos, Agustin, S3 ([GS-003](#)), S8 ([GS-009](#)), S19 ([OS-011-YI](#)), S73 ([OS-102](#)), S87 ([OS-123-YI](#)), S105 ([LBP-09](#)), S220 ([THU-355](#)), S279 ([TOP-043](#)), S475 ([THU-514](#))
- Albir, Marina Garcés, S451 ([SAT-387](#))
- Albrecht, Thomas, S547 ([SAT-248](#))
- Albuquerque, Miguel, S64 ([OS-084-YI](#)), S776 ([WED-467](#))
- Alcaman, Luis Arnaldo Mendez, S840 ([FRI-492](#))
- Alcol, Maria Belen Piqueras, S587 ([THU-136](#))
- Aldana, Andres Gomez, S869 ([SAT-133](#))
- Aldrian, Denise, S987 ([THU-313](#))
- Aldvén, Martina, S857 ([SAT-115](#))
- Alegret, Marta, S356 ([THU-246](#)), S788 ([WED-518](#)), S802 ([WED-546](#))
- Alelyani, Jaber, S724 ([SAT-509](#))
- Alemanni, Luigina Vanessa, S88 ([OS-124-YI](#)), S974 ([THU-293](#))
- Aleman, Soo, S9 ([GS-012](#)), S31 ([OS-030](#)), S53 ([OS-068](#)), S113 ([LBP-20](#)), S1091 ([WED-158](#)), S1101 ([WED-171](#)), S1150 ([SAT-170](#))
- Aleman, Merce Roget, S376 ([WED-264](#))
- Alessandria, Carlo, S10 ([LBO-01](#)), S253 ([WED-348](#))
- Alexander, Emma, S984 ([THU-307](#)), S987 ([THU-312](#)), S999 ([THU-332](#))
- Alexandrino, Gonçalo, S1111 ([WED-185](#)), S1189 ([THU-186](#))
- Alexopoulos, Theodoros, S262 ([WED-362](#)), S978 ([THU-298](#))
- Alexopoulou, Alexandra, S262 ([WED-362](#)), S400 ([WED-302](#)), S978 ([THU-298](#))
- Aleyadeh, Wesam, S89 ([OS-125](#))
- Al-Faddagh, Hind, S724 ([SAT-509](#))
- Alfaiate, Dulce, S876 ([FRI-117](#)), S1161 ([SAT-185](#))
- Alfano, Vincenzo, S1018 ([FRI-218](#))
- Alfaro-Cervello, Clara, S682 ([SAT-442](#))

- Alfaro-Jiménez, Kendall, S529 (SAT-215)
 Alfaro, Omar, S900 (FRI-151)
 Alfonso Martinez-Cruz, Luis, S544 (SAT-244)
 Alghamdi, Saad, S859 (SAT-119), S958 (THU-273), S1011 (THU-388)
 Algibez, Ana Martín, S406 (WED-314), S587 (THU-136)
 Algibez, Ana Martín, S268 (WED-372)
 Alhadhiah, Zahra, S724 (SAT-509)
 Alhamoudil, Walled, S859 (SAT-119)
 Alhamoudi, Waleed, S958 (THU-273), S1011 (THU-388)
 Alhanaee, Amnah, S958 (THU-273), S1011 (THU-388)
 Alibakan, Özlem Kandemir, S279 (WED-391)
 Ali, Basim, S173 (FRI-448)
 Alicia, Delorme, S464 (THU-493)
 Ali, Faiza Sadaqat, S319 (SAT-557)
 Alimenti, Eleonora, S571 (TOP-067), S584 (THU-131)
 Ali, Nida, S935 (FRI-213)
 Ali, Omar, S458 (THU-483)
 Alisi, Anna, S783 (WED-507)
 Ali, Syed Afroz, S225 (THU-360)
 Aliwa, Benard, S346 (THU-230), S354 (THU-242)
 Alizei, Elahe Salimi, S318 (SAT-555)
 Alkhatam, Nazih, S724 (SAT-509)
 Alkhatib, Alzhraa, S1212 (THU-224)
 Alkhatib, Engy, S840 (FRI-491)
 Alkhazashvili, Maia, S891 (FRI-136)
 Alkhouri, Naim, S1 (GS-001), S13 (LBO-05), S29 (OS-026), S30 (OS-027), S118 (LBP-26), S125 (LBP-38), S604 (THU-413), S619 (THU-438), S619 (THU-439), S627 (THU-453), S643 (THU-552), S647 (TOP-074), S655 (SAT-401), S659 (SAT-407), S659 (SAT-408), S684 (SAT-444), S689 (SAT-453), S711 (SAT-488), S812 (FRI-470), S813 (FRI-472), S815 (FRI-476), S822 (FRI-515), S828 (FRI-525)
 Alkuraya, Fowzan, S969 (THU-289)
 Allah, Belimi Hibat, S195 (FRI-546)
 Allaire, Manon, S61 (OS-081), S62 (OS-083-YI), S492 (FRI-274), S494 (FRI-279), S515 (FRI-316), S585 (THU-133), S589 (THU-139), S865 (SAT-129)
 Allali, Raphael, S1193 (THU-194)
 Allalou, Amin, S769 (WED-454)
 Alla, Manasa, S7 (GS-008-YI), S272 (WED-379)
 Allam, Dalia, S195 (FRI-546)
 Allam, Naglaa, S1212 (THU-224)
 Allard, Marc Antoine, S458 (THU-483)
 Allegratti, Andrew S., S10 (LBO-01)
 Allen, Alina, S114 (LBP-21), S627 (THU-453)
 Allen, Christopher, S236 (WED-319), S275 (WED-383)
 Allende, Daniela, S12 (LBO-04)
 Allen, Sophie, S231 (THU-368), S232 (THU-370)
 Aller, Rocío, S700 (SAT-468)
 Alles, Laura García, S936 (FRI-214)
 Alletto, Francesca, S632 (THU-461)
 Allgar, Victoria, S153 (FRI-418)
 Allison, Michael, S46 (OS-053-YI), S157 (FRI-422), S854 (TOP-095)
 Allsop, Caroline, S1187 (THU-182)
 Allsworth, Max, S840 (FRI-492)
 Allweiss, Lena, S1019 (FRI-220), S1023 (FRI-227)
 Almandoz, Edurne, S917 (FRI-181)
 Almeida, Ana Arencibia, S376 (WED-264), S392 (WED-290), S397 (WED-296), S964 (THU-282), S980 (THU-301), S998 (THU-331), S1205 (THU-216)
 Almeida, Bruna, S324 (WED-218), S324 (WED-219)
 Almeida, Isadora, S132 (THU-401)
 Almeida, Nuno, S541 (SAT-237)
 Almishri, Wagdi, S419 (FRI-352)
 Almodovar, Xènia, S250 (WED-343), S737 (WED-403)
 Aloia, Luigi, S75 (OS-105)
 Aloman, Costica, S631 (THU-460)
 Alonso Castellano, Pablo, S980 (THU-301), S996 (THU-326), S998 (THU-331)
 Alonso, Estella, S961 (THU-278)
 Alonso, José Castellote, S2 (GS-003), S1205 (THU-216)
 Alonso, Maria Jesus Medina, S893 (FRI-140)
 Alonso, Maria Luisa Manzano, S90 (OS-127-YI), S299 (SAT-521)
 Alonso, María Luisa Manzano, S268 (WED-372)
 Alonso-Peña, Marta, S390 (WED-288), S868 (SAT-132), S934 (FRI-211)
 Alonso, Rosario González, S73 (OS-102)
 Alonso, Sara, S251 (WED-344), S868 (SAT-132), S911 (FRI-171)
 Alonso, Sonia, S10 (LBO-01), S1178 (THU-171)
 Alqahtani, Saleh, S464 (THU-492), S600 (TOP-081), S627 (THU-453), S859 (SAT-119), S861 (SAT-122), S863 (SAT-125), S905 (FRI-159)
 Alric, Laurent, S52 (OS-066), S498 (FRI-286), S1150 (SAT-169), S1160 (SAT-184)
 Al-Rubaiy, Laith, S864 (SAT-127)
 Al sehemy, Lamiaa, S840 (FRI-491)
 Al Shabeeb, Reem, S464 (THU-492)
 Al-Shabeeb, Reem, S614 (THU-430)
 Al-shari, Aya M., S840 (FRI-491)
 Alsheelkh, Lameya, S724 (SAT-509)
 Alsohaibani, Fahad, S1006 (THU-383)
 Alsua, Nerea Tejado, S921 (FRI-188)
 Alsudaney, Manaf, S489 (TOP-065)
 Alsuhaibani, Hamad, S1011 (THU-388)
 Alswat, Khalid, S627 (THU-453), S863 (SAT-125)
 Altamura, Sandro, S749 (WED-423)
 Altangerel, Enkhjargal, S910 (FRI-168)
 Aluvihare, Varuna, S479 (THU-521)
 Alvarado, Lewel, S1211 (THU-223)
 Alvarado-Tapias, Edilmar, S2 (GS-003), S73 (OS-100-YI), S87 (OS-123-YI), S164 (FRI-433), S279 (TOP-043), S900 (FRI-151), S970 (THU-290)
 Álvares-da-Silva, Mario, S195 (FRI-546), S274 (WED-382), S865 (SAT-129), S900 (FRI-151)
 Alvarez, Alina, S115 (LBP-22)
 Alvarez-Alvarez, Ismael, S18 (OS-007), S126 (TOP-087), S142 (FRI-403)
 Alvarez, Carolina Almohalla, S133 (THU-404), S469 (THU-501), S480 (THU-524), S886 (FRI-129)
 Álvarez, Juan Carlos, S267 (WED-370)
 Alvarez, Laura, S533 (SAT-223)
 Alvarez, Maria, S883 (FRI-125), S1189 (THU-187), S1200 (THU-207)
 Alvarez, Maria del Carmen Plasencia, S894 (FRI-140)
 Alvarez, Marife, S664 (SAT-415)
 Álvarez-Mon, Melchor, S19 (OS-011-YI)
 Álvarez-Navascués, Carmen, S2 (GS-003), S380 (WED-270), S392 (WED-290), S399 (WED-300), S970 (THU-290)
 Alvarez-Navascues, Mari Carmen, S87 (OS-123-YI)
 Alvarez-Ossorio, Angela Rojas, S760 (WED-440), S770 (WED-457)
 Alvarez, Paula Fernandez, S248 (WED-341), S996 (THU-326), S1178 (THU-171)
 Álvarez-Suárez, Beatriz, S964 (THU-282), S980 (THU-301), S998 (THU-331)
 Alvaro, Domenico, S36 (OS-036), S40 (OS-045), S55 (OS-070), S374 (WED-260)
 Alviri, Naz Kanani, S74 (OS-103-YI), S316 (SAT-552)
 Alzola, Carlos, S220 (THU-355)
 Amaddeo, Giuliana, S12 (LBO-04), S61 (OS-081), S577 (THU-119)
 Amado, Luis Enrique Morano, S892 (FRI-139), S898 (FRI-148)
 Amangurbanova, Maral, S65 (OS-086), S649 (TOP-083), S662 (SAT-412), S839 (FRI-490)
 Amaravadi, Lakshmi, S115 (LBP-22)
 Amat, Concepció, S356 (THU-246)
 Ambike, Shubhankar, S945 (THU-256)
 Amendola Pires, Marcia Maria, S1201 (THU-209)
 Amendola, Serena, S1190 (THU-188)
 Ameneni, Gagana, S689 (SAT-453)
 Amengual, J, S560 (SAT-275)
 Amengual, Josep, S331 (WED-231)
 Amer, Johnny, S328 (WED-226), S342 (TOP-039), S484 (THU-532)
 Amin, Amr, S365 (FRI-392)
 Ammann, Markus, S44 (OS-050-YI)
 Ammar, Lynne, S1162 (SAT-188)
 Ammon, Daphni, S44 (OS-050-YI)
 Amo, Maria, S268 (WED-372)

Author Index

- Amor, Carmen, S690 (SAT-454), S697 (SAT-465), S705 (SAT-478), S706 (SAT-479)
- Amorosi, Alessandro, S920 (FRI-185)
- Ampuero, Javier, S2 (GS-003), S35 (OS-035-YI), S248 (WED-341), S366 (TOP-061), S376 (WED-264), S380 (WED-270), S399 (WED-300), S607 (THU-418), S651 (SAT-394), S700 (SAT-468), S703 (SAT-472), S732 (TOP-090), S760 (WED-440), S770 (WED-457), S964 (THU-282), S980 (THU-301), S998 (THU-331)
- Amzou, Samira, S960 (THU-277), S963 (THU-281)
- Anagnostou, Olga, S1194 (THU-197)
- Ananchuensook, Prooksa, S217 (THU-349), S1047 (FRI-266)
- Anand, Abhinav, S73 (OS-101-YI), S297 (SAT-350), S693 (SAT-459)
- Anand, Anil Chandra, S195 (FRI-546)
- Anastasiou, Olympia Aevdoxia, S1137 (SAT-152)
- Anastasiou, Zacharias, S1034 (FRI-248)
- Andara, Maria Teresa, S900 (FRI-151)
- Andersen, Ina, S478 (THU-520)
- Andersen, Jesper, S28 (OS-024-YI), S38 (OS-042-YI), S533 (SAT-223), S534 (SAT-226), S536 (SAT-229), S536 (SAT-230), S541 (SAT-238), S942 (THU-251)
- Andersen, Mette Lehmann, S239 (WED-325)
- Andersen, Peter, S17 (OS-005-YI), S163 (FRI-432), S173 (FRI-449), S175 (FRI-452), S303 (SAT-528), S832 (FRI-479), S845 (TOP-054)
- Anders, Maria Margarita, S253 (WED-348)
- Anderson, Christopher, S445 (SAT-375)
- Anderson, David, S875 (FRI-115), S1119 (WED-197)
- Anderson, Karl, S86 (OS-122)
- Anderson, Katie, S1169 (SAT-198)
- Anderson, Mark, S1081 (WED-143), S1081 (WED-144)
- Anderson, Michele, S1149 (SAT-168), S1153 (SAT-174), S1161 (SAT-186)
- Anderson, Patricia, S852 (WED-488)
- Andersson, Emma, S410 (FRI-330), S433 (SAT-353), S435 (SAT-357), S439 (SAT-365), S945 (THU-255)
- Andersson, Monique, S916 (FRI-178), S1060 (WED-117), S1108 (WED-181), S1117 (WED-195)
- Andrade, Filipe, S61 (OS-080-YI)
- Andrade, Jackie, S153 (FRI-418)
- Andrade, Raul J., S18 (OS-007), S44 (OS-049-YI), S126 (TOP-087), S142 (FRI-403), S144 (FRI-406), S376 (WED-264), S399 (WED-300), S1205 (THU-216)
- András, Budai, S23 (OS-017-YI)
- Andraud, Mickael, S589 (THU-139)
- Andreani, Giulia, S360 (FRI-383)
- Andreata, Francesco, S5 (GS-005)
- Andreis, Alessandro, S713 (SAT-494)
- Andreola, Fausto, S70 (OS-095-YI), S129 (THU-396), S197 (FRI-549), S206 (TOP-046), S220 (THU-355), S767 (WED-450)
- Andreone, Pietro, S53 (OS-068), S374 (WED-260), S729 (SAT-517)
- Andres, Duarte Rojo, S195 (FRI-546)
- Andres-Rozas, Maria, S791 (WED-524)
- Andreu, Jordi Camps, S616 (THU-432)
- Andugulapati, Sai Balaji, S560 (SAT-274)
- Aneja, Jasneet, S58 (OS-075)
- Anfuso, Beatrice, S559 (SAT-273)
- Angata, Kiyohiko, S1041 (FRI-257)
- Ang, Celina, S575 (THU-116), S582 (THU-128), S586 (THU-134)
- Angelakis, Athanasios, S100 (LBP-02)
- Angel, Enrique, S210 (THU-341)
- Angeles Pérez-San-Gregorio, María, S640 (THU-474)
- Angelin, Bo, S57 (OS-074-YI)
- Angelini, Elise, S1039 (FRI-255)
- Angeli, Paolo, S10 (LBO-01), S101 (LBP-03), S185 (FRI-341), S237 (WED-320), S238 (WED-323), S250 (WED-343), S253 (WED-348)
- Angelo, Iacobellis, S105 (LBP-09)
- Angé, Marine, S439 (SAT-364)
- Ang, Tiing Leong, S199 (FRI-552), S257 (WED-353)
- Anguera, Anna, S989 (THU-315)
- Anguita, Juan, S532 (SAT-221)
- An, Jiaxing, S747 (WED-419)
- An, Jihyun, S556 (SAT-266), S558 (SAT-270), S615 (THU-431), S667 (SAT-418), S695 (SAT-462), S701 (SAT-470), S704 (SAT-475), S705 (SAT-476), S757 (WED-435), S794 (WED-531), S864 (SAT-128), S1073 (WED-135)
- Ankarklev, Johan, S410 (FRI-330)
- Ankavay, Maliki, S1031 (FRI-243)
- An, Mahru, S322 (WED-215)
- Annaert, Pieter, S1025 (FRI-231)
- Annicchiarico, Brigida Eleonora, S981 (THU-302)
- Annunziata, Chiara, S797 (WED-535)
- Annunziata, Francesco, S346 (THU-231)
- Anolli, Maria Paola, S107 (LBP-11), S1135 (SAT-149), S1142 (SAT-159), S1154 (SAT-175), S1159 (SAT-181), S1164 (SAT-190), S1170 (SAT-199)
- Anora, Anil, S195 (FRI-546)
- An, Qi, S53 (OS-068), S113 (LBP-20), S1091 (WED-158)
- Ansari, Abu Aasim, S282 (SAT-325)
- Ansari, Azim, S1060 (WED-117), S1108 (WED-181)
- Ansari, Sardar, S308 (SAT-540)
- Anstee, Quentin, S31 (OS-029), S78 (OS-110), S118 (LBP-26), S603 (THU-412), S632 (THU-462), S647 (TOP-074), S651 (SAT-393), S666 (SAT-417), S668 (SAT-421), S685 (SAT-447), S688 (SAT-452), S781 (WED-475), S819 (FRI-509)
- Antal-Szalmás, Péter, S23 (OS-017-YI)
- Antier, Zelig, S69 (OS-094)
- Antinori, Andrea, S907 (FRI-164)
- Antoine, Corinne, S467 (THU-498)
- Antolín, Gloria Sánchez, S480 (THU-524), S886 (FRI-129)
- Anton, Aina, S770 (WED-457)
- Antón, Ángela, S251 (WED-344), S868 (SAT-132), S911 (FRI-171)
- Antonenko, Antonina, S86 (OS-121-YI)
- Antoniades, Charalambos Gustav, S127 (TOP-093)
- Antonietta, Messina, S359 (FRI-382)
- Antonini, Teresa, S62 (OS-083-YI), S981 (THU-303)
- Antonio Diaz, Luis, S145 (TOP-073), S900 (FRI-151)
- Antonoli, Alessandro, S804 (WED-551)
- Antoniou, Katerina, S400 (WED-302)
- Antonucci, Michela, S592 (THU-144)
- Antoran, Belén Ruiz, S8 (GS-009)
- Antoranz-Martinez, Asier, S78 (OS-110)
- Antwi, Milton, S226 (THU-361), S743 (WED-412), S787 (WED-516)
- Anty, Rodolphe, S61 (OS-081), S981 (THU-303)
- Aoto, Yoshimasa, S409 (TOP-060)
- Aouinti, Safia, S170 (FRI-443)
- Apelian, David, S9 (GS-012)
- Apodaka-Biguri, Maider, S137 (FRI-395), S529 (SAT-215), S738 (WED-404), S741 (WED-408)
- Apostolova, Nadezda, S335 (WED-239), S781 (WED-505)
- Aqel, Bashar, S590 (THU-141)
- Aquilanti, Giuliana, S360 (FRI-383)
- Aquino, Marco, S713 (SAT-493), S789 (WED-521)
- Aqul, Amal A., S123 (LBP-35), S387 (WED-282)
- Arab, Juan Pablo, S865 (SAT-129), S900 (FRI-151)
- Aracil, Carlos, S587 (THU-136)
- Aragones, Juan, S220 (THU-355)
- Arai, Kumiko, S744 (WED-415)
- Arai, Masaya, S447 (SAT-380)
- Arai, Taeang, S240 (WED-327), S317 (SAT-554), S584 (THU-131), S818 (FRI-508), S820 (FRI-511)
- Arakawa, Mie, S394 (WED-293)
- Aranguren, África Vales, S1024 (FRI-228)
- Aransay, Ana María, S326 (WED-223), S533 (SAT-224), S560 (SAT-275), S738 (WED-404)
- Araraki, Shingo, S686 (SAT-448)
- Aratari, Lea, S1003 (THU-377)
- Araujo, Roberta, S865 (SAT-129)
- Aravinthan, Aloysius, S195 (FRI-546)
- Arbelaiz, Ander, S541 (SAT-238)
- Arbitrio, Mariamena, S568 (SAT-288)
- Arboledas, Alados, S1126 (WED-208)
- Arbones Mainar, Jose M, S1187 (THU-183)

- Arbune, Manuela, S110 (LBP-15)
 Arce, Angela Novoa, S840 (FRI-492)
 Archambault-Marsan, Alexandre, S937 (TOP-056)
 Archer, Ann, S177 (FRI-455), S621 (THU-441), S858 (SAT-118), S1198 (THU-203)
 Ardevol, Alba, S87 (OS-123-YI)
 Ardiles, Thomas, S188 (FRI-535), S248 (WED-342)
 Ardinski, Andrzej, S1171 (SAT-202)
 Arechederra, Maria, S526 (TOP-072), S537 (SAT-232)
 Arefaine, Mebrihit, S927 (FRI-197)
 Arellanes-Robledo, Jaime, S151 (FRI-414), S160 (FRI-426)
 Arellano, Encarnación Ramirez, S1126 (WED-208)
 Arenas, Juan Ignacio, S366 (TOP-061), S917 (FRI-181)
 Arenas-Pinto, Alejandro, S721 (SAT-504), S1122 (WED-202)
 Arenas, Yaiza, S423 (FRI-359)
 Arena, Umberto, S513 (FRI-311)
 Arevalo, Giselle, S396 (WED-295)
 Argemi, Josep Maria, S12 (LBO-04), S573 (THU-114)
 Argemi, Josepmaria, S164 (FRI-433)
 Argenziano, Maria Eva, S673 (SAT-430)
 Argumáñez Tello, Víctor, S485 (THU-535)
 Arias, Ana, S1194 (THU-195)
 Arias, María de Jesús Loera, S337 (WED-244)
 Arias-Sánchez, Sara, S709 (SAT-484)
 Aricha, Revital, S119 (LBP-28), S415 (FRI-345)
 Ari, Derya, S181 (FRI-463)
 Arif, Ambreen, S912 (FRI-172)
 Arijis, Ingrid, S524 (TOP-066)
 Arikani, Cigdem, S387 (WED-282)
 Ariño, Silvia, S78 (OS-109-YI)
 Aristu, Peio, S791 (WED-524)
 Ariungerel, Nomin, S716 (SAT-497), S718 (SAT-499)
 Ariza, Xavier, S10 (LBO-01)
 Arizpe, Andre, S11 (LBO-02), S32 (OS-031), S1156 (SAT-177)
 Ankan, Cigdem, S123 (LBP-35), S969 (THU-289), S971 (THU-291)
 Armandi, Angelo, S300 (SAT-524), S521 (FRI-325), S605 (THU-415), S611 (THU-425), S617 (THU-435), S618 (THU-437), S626 (THU-452), S637 (THU-470), S652 (SAT-396), S654 (SAT-400), S673 (SAT-430), S704 (SAT-474), S713 (SAT-494)
 Arman, Yücel, S279 (WED-391)
 Armengol, Carolina, S546 (SAT-247), S551 (SAT-256)
 Armisen, Javier, S606 (THU-416)
 Armstrong, Matthew, S231 (THU-368), S232 (THU-370), S827 (FRI-523)
 Armstrong, Paige A., S890 (FRI-135), S891 (FRI-136), S909 (FRI-167), S930 (FRI-203), S933 (FRI-210)
 Armstrong, Paul, S180 (FRI-460)
 Arnal, Pilar Sainz de la Maza, S365 (FRI-391)
 Arnell, Henrik, S969 (THU-289), S971 (THU-291)
 Arnon, Ronen, S128 (THU-394)
 Arola, Johanna, S997 (THU-329)
 Arora, Sanjeev, S1204 (THU-214)
 Arora, Umang, S197 (FRI-548)
 Arora, Vinod, S7 (GS-008-YI), S191 (FRI-539), S272 (WED-379)
 Arpurt, Jean-Pierre, S107 (LBP-11)
 Arraez, Dalia Morales, S2 (GS-003), S164 (FRI-433), S587 (THU-136), S893 (FRI-140)
 Arrese, Marco, S274 (WED-382), S496 (FRI-282), S627 (THU-453), S865 (SAT-129), S900 (FRI-151)
 Arribas, David San Segundo, S251 (WED-344)
 Arroyo, Noelia, S440 (SAT-367)
 Arroyo, Vicente, S220 (THU-355), S452 (SAT-390)
 Arshad, Tamoore, S1085 (WED-149)
 Arslanow, Anita, S15 (OS-001), S250 (WED-343), S845 (TOP-054), S851 (WED-486)
 Arsyad, Nik MA Nik, S274 (WED-382)
 Arteel, Gavin, S145 (TOP-073)
 Artimos, Solange, S112 (LBP-16)
 Arttru, Florent, S74 (OS-104), S127 (TOP-093), S189 (FRI-537), S473 (THU-511)
 Artuch, Rafael, S529 (SAT-216)
 Artzner, Thierry, S459 (THU-484)
 Arufe, Diego, S245 (WED-336)
 Arunima, Ms, S848 (WED-481)
 Arvaniti, Pinelopi, S392 (WED-290), S400 (WED-302), S405 (WED-311), S421 (FRI-354)
 Asahina, Yasuhiro, S1183 (THU-177)
 Ascanio, Mertixell, S1070 (WED-130)
 Ascari, Sara, S493 (FRI-277), S495 (FRI-280)
 Asensio, Julia Peña, S1028 (FRI-236), S1032 (FRI-245)
 Asensio, Maitane, S527 (SAT-212)
 Ashfaq-Khan, Muhammad, S330 (WED-230), S797 (WED-536)
 Ashimkhanova, Aiymkul, S320 (SAT-559)
 Ashley, Tiong Kai Le, S1204 (THU-213)
 Asilaza, Vincent Kinya, S69 (OS-094)
 Asim, Muhammad, S912 (FRI-172)
 asir, Abdullah, S1011 (THU-388)
 Askari, Fred, S967 (THU-286)
 Askgaard, Gro, S4 (GS-004-YI), S160 (FRI-427), S165 (FRI-435)
 Aslan, Rahmi, S274 (WED-382)
 Asokkumar, Ravishankar, S519 (FRI-321)
 Aspas, Jessica, S325 (WED-220)
 Aspichueta, Patricia, S137 (FRI-395), S349 (THU-235), S529 (SAT-215), S533 (SAT-223), S700 (SAT-468), S738 (WED-404), S741 (WED-408)
 Aspinall, Richard, S1005 (THU-381)
 Asrani, Sumeet, S195 (FRI-546), S459 (THU-484)
 Asselah, Tarik, S9 (GS-012), S52 (OS-066), S498 (FRI-286), S1034 (FRI-248), S1055 (TOP-103), S1093 (WED-159), S1193 (THU-194)
 Assenat, Eric, S62 (OS-083-YI), S534 (SAT-225), S577 (THU-119)
 Assinger, Alice, S44 (OS-050-YI), S45 (OS-051-YI), S142 (FRI-402)
 Assis, David N., S388 (WED-283)
 Assumpció Sendra, Maria, S903 (FRI-156)
 Astbury, Stuart, S127 (TOP-092), S448 (SAT-381)
 Åström, Hanne, S960 (THU-276)
 Atallah, Edmond, S127 (TOP-092), S448 (SAT-381)
 Ates-Öz, Edanur, S59 (OS-077)
 Athanassa, Zoe, S978 (THU-298)
 Athavale, Dipti, S80 (OS-113)
 Ather, Bazil, S912 (FRI-172)
 Athira, A, S846 (WED-477)
 Athwal, Varinder, S8 (GS-010), S84 (OS-119-YI)
 Atkinson, Stephen, S145 (TOP-073)
 Atsukawa, Masanori, S110 (LBP-15), S240 (WED-327), S317 (SAT-554), S584 (THU-131), S818 (FRI-508), S820 (FRI-511)
 Attanasio, Maria Rosaria, S903 (FRI-155)
 Attar, Bashar, S900 (FRI-151)
 Attema, Joline, S786 (WED-515)
 Attenberger, Ulrike, S229 (THU-366)
 Atthakitmongkol, Thanapat, S237 (WED-321)
 Attia, Enas, S1212 (THU-224)
 Attia, Yasmeen, S353 (THU-241), S550 (SAT-255), S779 (WED-472), S795 (WED-532)
 Aubé, Christophe, S61 (OS-080-YI), S598 (THU-154)
 Aubin, Adrien, S687 (SAT-450), S701 (SAT-469)
 Audrey, Payance, S970 (THU-290), S975 (THU-295)
 Audureau, Etienne, S46 (OS-055)
 Auer, Timo, S469 (THU-502)
 Augello, Giuseppa, S568 (SAT-288)
 Augusto Martín, Cesar, S544 (SAT-244)
 Aukrust, Pål, S478 (THU-520)
 Au, Kwan Yung, S537 (SAT-231)
 Aumar, Madeleine, S965 (THU-284)
 Auriemma, Alessandra, S510 (FRI-304)
 Aurrekoetxea, Igor, S137 (FRI-395), S529 (SAT-215), S738 (WED-404), S741 (WED-408)
 Authorsen-Grudmann, Roxane, S485 (THU-534)
 Auzinger, Georg, S479 (THU-521)
 Avdicova, Maria, S880 (FRI-121)
 Averhoff, Francisco, S921 (FRI-187), S926 (FRI-195), S1204 (THU-214)
 Avila, Ma, S560 (SAT-275)

Author Index

- Avila, Matías A, S326 (WED-223), S526 (TOP-072), S529 (SAT-216), S532 (SAT-221), S533 (SAT-223), S537 (SAT-232), S544 (SAT-244), S546 (SAT-247), S551 (SAT-256), S732 (TOP-090)
- Avila, Matías A., S349 (THU-235)
- Avitabile, Emma, S163 (FRI-431), S166 (FRI-437)
- Awan, Sana, S336 (WED-241)
- Ayala, Iriscilla, S79 (OS-112)
- Ayares, Gustavo, S865 (SAT-129), S900 (FRI-151)
- Ayonrinde, Oyekoya, S830 (FRI-529)
- Ayoub, Walid S, S489 (TOP-065)
- Ay, Ümran, S350 (THU-236)
- Ayuso, Carmen, S579 (THU-124)
- Azaceta, María Del Barrio, S251 (WED-344), S654 (SAT-400), S700 (SAT-468), S709 (SAT-484), S728 (SAT-515), S868 (SAT-132)
- Azam, Mishal, S912 (FRI-172)
- Azariadi, Kalliopi, S421 (FRI-354)
- Azaz, Amer, S969 (THU-289)
- Azimova, Dinara, S1167 (SAT-195)
- Aziz, Bishoi, S426 (FRI-363)
- Aziz, Fatima, S131 (THU-399)
- Azkargorta, Mikel, S28 (OS-024-YI), S533 (SAT-223), S534 (SAT-226), S541 (SAT-238), S544 (SAT-244)
- Azman, Andrew, S69 (OS-094)
- Azoulay, Daniel, S458 (THU-483), S482 (THU-528)
- Azzaroli, Francesco, S90 (OS-127-YI), S299 (SAT-521)
- Baatarsuren, Uurtsaikh, S475 (THU-516)
- Baba, Hideo, S549 (SAT-253), S562 (SAT-278)
- Babu E, Preedia, S556 (SAT-267)
- Babu, Merin, S848 (WED-481)
- Babu, Rosmy, S228 (THU-362), S357 (THU-248)
- Bachelier, Philippe, S467 (THU-498)
- Bachinger, Fabian, S140 (FRI-400)
- Bachler, Mirjam, S232 (THU-369)
- Bachtar, Rini, S1203 (THU-212)
- Badal, Bryan, S37 (OS-038), S242 (WED-331)
- Badawy, Mohamed, S516 (FRI-317)
- Badell, Martina, S913 (FRI-174)
- Badia-Aranda, Esther, S171 (FRI-445), S1178 (THU-171), S1205 (THU-216)
- Badiali, Sara, S772 (WED-459)
- Badii, Maria, S923 (FRI-190)
- Badri, Prajakta, S49 (OS-062)
- Badr, Reda, S1212 (THU-224)
- Bae, Jae Seok, S512 (FRI-310)
- Baek, Ga Hee, S567 (SAT-287)
- Baek, Marshall, S372 (WED-257)
- Baek, Yang-Hyun, S690 (SAT-455), S698 (SAT-466), S705 (SAT-477), S712 (SAT-491), S785 (WED-513)
- Baena, Pilar Barrera, S1126 (WED-208)
- Baena, Sheila, S325 (WED-220)
- Baerlocher, Gabriela, S105 (LBP-08)
- Bae, Sangsu, S947 (THU-258)
- Bae, Sung Min, S758 (WED-437), S779 (WED-473)
- Bagdadi, Ali, S279 (TOP-043)
- Bager, Palle, S968 (THU-287)
- Baggio, Giovannella, S72 (OS-099)
- Baggus, Elizabeth, S521 (FRI-326)
- Bagiella, Emilia, S461 (THU-488)
- Baguley, Elizabeth, S652 (SAT-395)
- Baheer, Yama, S719 (SAT-501)
- Bahra, Sukhbir, S1006 (THU-382)
- Bah, Sulayman, S67 (OS-090-YI), S1106 (WED-178)
- Baicus, Cristian, S192 (FRI-541)
- Baiges, Anna, S2 (GS-003), S87 (OS-123-YI), S843 (FRI-499), S970 (THU-290), S975 (THU-295), S984 (THU-308)
- Bai, Honglian, S34 (OS-033)
- Bai, Jian, S34 (OS-033)
- Bai, Jingsong, S1209 (THU-220)
- Baik, Soon Koo, S442 (SAT-369)
- Bail, Brigitte Le, S672 (SAT-427)
- Bailly, Sarah, S923 (FRI-190)
- Bailly, Sébastien, S500 (FRI-289), S656 (SAT-403)
- Baiocchi, Leonardo, S40 (OS-045), S55 (OS-070), S1056 (TOP-106), S1072 (WED-133), S1082 (WED-146)
- Baiocchi, Andrea, S994 (THU-323)
- Bair, Ming-Jong, S895 (FRI-143), S1180 (THU-174), S1206 (THU-217)
- Bai, Tao, S581 (THU-126)
- Bai, Yang, S1152 (SAT-173)
- Bajaj, Jasmohan, S101 (LBP-03), S242 (WED-330)
- Bajaj, Jasmohan S, S37 (OS-038), S195 (FRI-546), S236 (WED-319), S242 (WED-331), S256 (WED-352), S258 (WED-355), S274 (WED-382), S275 (WED-383)
- Bajaj, Jasmohan S., S342 (TOP-038), S347 (THU-233), S352 (THU-239), S900 (FRI-151)
- Bajpai, Meenu, S21 (OS-014-YI)
- Bakala, Adam, S1138 (SAT-154)
- Baker, Alastair, S965 (THU-284)
- Baker, Brian, S790 (WED-522)
- Bakewell, Terry, S79 (OS-112)
- Bakieva, Shokhista, S888 (FRI-132)
- Bakker, Sjoerd, S14 (LBO-06)
- Balanesu, Paul, S192 (FRI-541)
- Balcar, Lorenz, S35 (OS-035-YI), S37 (OS-039-YI), S86 (OS-121-YI), S193 (FRI-545), S199 (FRI-551), S224 (THU-358), S244 (WED-334), S282 (SAT-326), S286 (SAT-332), S288 (SAT-335), S292 (SAT-342), S313 (SAT-547), S491 (FRI-273), S498 (FRI-285), S505 (FRI-295), S575 (THU-116), S582 (THU-128), S831 (FRI-477), S939 (TOP-058), S1135 (SAT-150)
- Baldaccini, Valentina, S493 (FRI-277), S495 (FRI-280)
- Baldassarre, Maurizio, S191 (FRI-540), S237 (WED-320)
- Balderramo, Domingo, S496 (FRI-282)
- Baliashvili, Davit, S889 (FRI-133), S890 (FRI-135), S909 (FRI-167), S930 (FRI-203), S931 (FRI-205), S933 (FRI-210)
- Ballerga, Esteban Gonzalez, S105 (LBP-09), S245 (WED-336)
- Ballester, Maria Aguilar, S451 (SAT-387)
- Ballester, María Aguilar, S789 (WED-520)
- Ballester, María Pilar, S35 (OS-035-YI), S220 (THU-355), S682 (SAT-442)
- Ballesteros, Iván, S78 (OS-109-YI)
- Ballestri, Stefano, S729 (SAT-517)
- Balogh, Boglárka, S23 (OS-017-YI)
- Balsano, Clara, S646 (THU-560), S685 (SAT-446)
- Baltayiannis, Gerasimos, S922 (FRI-189)
- Balwani, Manisha, S86 (OS-122)
- Bañales, Jesús, S560 (SAT-275)
- Bañales, Jesús M., S700 (SAT-468), S972 (THU-291)
- Banales, Jesus Maria, S28 (OS-024-YI), S57 (OS-074-YI), S326 (WED-223), S440 (SAT-367), S496 (FRI-282), S527 (SAT-212), S734 (WED-397), S738 (WED-404)
- Bañares, Rafael, S2 (GS-003), S10 (LBO-01), S38 (OS-041-YI), S87 (OS-123-YI), S90 (OS-127-YI), S150 (FRI-412), S279 (TOP-043), S299 (SAT-521), S349 (THU-235), S481 (THU-525), S700 (SAT-468), S732 (TOP-090)
- Banda, Iris, S840 (FRI-492)
- Bandera, Jose Pinazo, S18 (OS-007), S144 (FRI-406), S964 (THU-282), S980 (THU-301), S998 (THU-331), S1098 (WED-166), S1126 (WED-208)
- Bandera, José Pinazo, S171 (FRI-445)
- Bandiera, Lucia, S601 (TOP-082)
- Banet, Manon, S954 (THU-267)
- Bangura, Rohey, S67 (OS-090-YI), S1106 (WED-178)
- Bani, Daniele, S550 (SAT-254)
- Bankwitz, Dorothea, S447 (SAT-379)
- Bannan, Ciaran, S1211 (THU-223)
- Bannas, Peter, S285 (SAT-331)
- Bannon, Lian, S243 (WED-333), S393 (WED-291), S403 (WED-308)
- Bansal, Abhinav, S67 (OS-091)
- Bansal, Meena, S1 (GS-001), S612 (THU-427)
- Bansal, Ruchi, S137 (FRI-394), S553 (SAT-260), S755 (WED-432), S761 (WED-441), S764 (WED-447)
- Bansal, Saurabh, S643 (THU-553)
- Bantel, Heike, S403 (WED-307)
- Banz, Vanessa, S485 (THU-533)
- Bao, Huizhang, S514 (FRI-313)
- Baorda, Francesca, S389 (WED-284), S599 (THU-156)

- Bapaye, Jay, S183 ([FRI-339](#))
 Baptista, Pedro, S365 ([FRI-391](#))
 Barabanchyk, Olena, S637 ([THU-468](#))
 Barange, Karl, S107 ([LBP-11](#))
 Baranova, Elena, S792 ([WED-526](#))
 Bara, Sushma, S235 ([TOP-044](#))
 Baráth, Lukács, S23 ([OS-017-YI](#))
 Barbancho, Sandra Melitón, S365 ([FRI-391](#))
 Barb, Andreea, S151 ([FRI-413](#))
 Barbaro, Francesco, S1082 ([WED-146](#))
 Barbato, Anna, S942 ([THU-251](#))
 Barbato, Francesco, S88 ([OS-124-YI](#))
 Barberá, Aurora, S780 ([WED-474](#))
 Barberi, Laura, S218 ([THU-352](#))
 Barbier, Olivier, S431 ([FRI-368](#))
 Barchuk, William, S11 ([LBO-03](#)), S423 ([FRI-360](#))
 Barciela, Mar Riveiro, S375 ([WED-263](#)), S376 ([WED-264](#)), S392 ([WED-290](#)), S399 ([WED-300](#)), S896 ([FRI-144](#)), S904 ([FRI-158](#)), S917 ([FRI-181](#)), S1024 ([FRI-228](#)), S1082 ([WED-145](#)), S1098 ([WED-166](#)), S1099 ([WED-168](#))
 Barclay, Stephen, S402 ([WED-305](#)), S925 ([FRI-194](#))
 Bardak, Ali Emre, S709 ([SAT-485](#))
 Bardou-Jacquet, Edouard, S52 ([OS-066](#)), S1150 ([SAT-169](#))
 Bargfrieder, Ute, S996 ([THU-327](#))
 Barish, Robert, S13 ([LBO-05](#))
 Barjaktarevic, Igor, S85 ([OS-120](#))
 Barkai, Laszlo, S56 ([OS-073](#))
 Barla, Georgia, S595 ([THU-149](#)), S1046 ([FRI-264](#))
 Barner-Rasmussen, Nina, S370 ([WED-253](#))
 Barnes, Eleanor, S868 ([SAT-131](#)), S970 ([THU-290](#)), S1060 ([WED-117](#)), S1075 ([WED-137](#)), S1108 ([WED-181](#)), S1169 ([SAT-198](#))
 Bar, Nir, S315 ([SAT-550](#))
 Baron, Aurore, S61 ([OS-081](#))
 Barozzi, Iros, S538 ([SAT-233](#))
 Barraud, Hélène, S62 ([OS-083-YI](#))
 Barrault, Camille, S170 ([FRI-442](#))
 Barreira, Ana, S375 ([WED-263](#)), S376 ([WED-264](#)), S399 ([WED-300](#)), S904 ([FRI-158](#)), S1082 ([WED-145](#))
 Barrenechea-Barrenechea, Jon Ander, S546 ([SAT-247](#))
 Barrera, Coralie, S994 ([THU-322](#))
 Barrett, Lisa, S909 ([FRI-166](#))
 Barriales, Diego, S532 ([SAT-221](#))
 Barrio, María Del, S302 ([SAT-526](#))
 Barron, Denis, S762 ([WED-442](#))
 Barron-Millar, Ben, S411 ([FRI-331](#))
 Barry, Jainaba, S67 ([OS-090-YI](#)), S1106 ([WED-178](#))
 Barsukova, Natalia, S9 ([GS-012](#))
 Bartel, Marc, S963 ([THU-281](#))
 Bartenschlager, Ralf, S1020 ([FRI-222](#))
 Barthel, Virginie, S198 ([FRI-550](#)), S807 ([TOP-077](#))
 Barthemon, Justine, S894 ([FRI-142](#))
 Bartlett, Sofia, S883 ([FRI-125](#)), S1189 ([THU-187](#)), S1200 ([THU-207](#))
 Bartneck, Matthias, S416 ([FRI-348](#))
 Bartolo, Gema Muñoz, S969 ([THU-289](#))
 Barutcu, Sezgin, S274 ([WED-382](#))
 Barz, Matthias, S26 ([OS-022](#))
 Baselli, Guido Alessandro, S733 ([WED-393](#))
 Bashir, Mustafa, S813 ([FRI-472](#)), S815 ([FRI-476](#))
 Bashir, Shahbaz, S1051 ([FRI-272](#))
 Basic, Michael, S1039 ([FRI-254](#)), S1042 ([FRI-259](#))
 Basile, Umberto, S723 ([SAT-508](#))
 Basili, Stefania, S217 ([THU-350](#))
 Bassan, Merav, S409 ([TOP-060](#))
 Bassegoda, Octavi, S131 ([THU-399](#)), S737 ([WED-403](#))
 Bassett, Paul, S193 ([FRI-543](#))
 Bassez, Ayse, S524 ([TOP-066](#))
 Basso, Daniela, S183 ([TOP-049](#))
 Basson, Craig, S115 ([LBP-22](#))
 Bastaich, Dustin, S304 ([SAT-532](#)), S832 ([FRI-478](#))
 Basuroy, Ron, S612 ([THU-426](#))
 Bataller, Ramon, S145 ([TOP-073](#)), S158 ([FRI-423](#)), S164 ([FRI-433](#)), S166 ([FRI-437](#)), S865 ([SAT-129](#)), S900 ([FRI-151](#))
 Batchuluun, Battsetseg, S762 ([WED-442](#))
 Bathon, Melanie, S561 ([SAT-277](#))
 Battaglia, Salvatore, S592 ([THU-144](#))
 Battezzati, Pier Maria, S978 ([THU-297](#))
 Battistella, Sara, S54 ([OS-069](#))
 Battisti, Arianna, S118 ([LBP-27](#))
 Battulga, Naranbaatar, S917 ([FRI-181](#))
 Bätz, Olaf, S1090 ([WED-156](#)), S1176 ([THU-168](#))
 Baudin, Martine, S823 ([FRI-517](#))
 Bauer, David JM, S37 ([OS-039-YI](#)), S61 ([OS-080-YI](#)), S193 ([FRI-545](#)), S199 ([FRI-551](#)), S246 ([WED-338](#)), S282 ([SAT-326](#)), S284 ([SAT-330](#)), S286 ([SAT-332](#)), S292 ([SAT-342](#)), S294 ([SAT-345](#)), S313 ([SAT-547](#)), S831 ([FRI-477](#))
 Bauer-Pisani, Tory, S423 ([FRI-358](#))
 Baulande, Sylvain, S12 ([LBO-04](#))
 Baumann, Anja, S154 ([FRI-419](#)), S798 ([WED-539](#))
 Baumann, Anna Katharina, S466 ([THU-496](#))
 Baumann, Ulrich, S123 ([LBP-35](#)), S387 ([WED-282](#)), S965 ([THU-284](#))
 Baumbach, Jan, S527 ([SAT-213](#))
 Baumert, Thomas, S72 ([OS-098](#)), S168 ([FRI-440](#)), S541 ([SAT-237](#))
 Baumgartner, Ruth, S44 ([OS-050-YI](#))
 Bauschen, Alina, S216 ([THU-348](#))
 Bauza, Monica, S682 ([SAT-442](#))
 Baven-Pronk, Martine, S14 ([LBO-06](#))
 Bavetta, Maria Grazia, S1082 ([WED-146](#))
 Bavuso Volpe, Letizia, S774 ([WED-461](#))
 Baxi, Vipul, S31 ([OS-029](#))
 Bayne, David, S274 ([WED-382](#))
 Bazinet, Michel, S1150 ([SAT-169](#)), S1160 ([SAT-183](#))
 Beard, Daniel, S311 ([SAT-544](#))
 Beaufrère, Aurélie, S12 ([LBO-04](#)), S64 ([OS-084-YI](#))
 Beccalli, Benedetta, S920 ([FRI-185](#))
 Becchetti, Chiara, S87 ([OS-123-YI](#))
 Becher, Naja, S986 ([THU-311](#))
 Bech, Katrine, S17 ([OS-005-YI](#)), S173 ([FRI-449](#)), S175 ([FRI-452](#)), S303 ([SAT-528](#)), S845 ([TOP-054](#))
 Bechmann, Lars, S628 ([THU-454](#))
 Bechstein, Wolf, S484 ([THU-531](#))
 Becker, Diana, S536 ([SAT-230](#)), S557 ([SAT-268](#))
 Becker, Lars, S9 ([GS-011](#))
 Becker, Svea, S571 ([SAT-292](#)), S778 ([WED-470](#))
 Beckmann, Sonja, S849 ([WED-482](#))
 Bedewy, Essam, S319 ([SAT-558](#))
 Bedke, Tanja, S525 ([TOP-069](#))
 Bedogni, Giorgio, S191 ([FRI-540](#))
 Bedossa, Pierre, S1 ([GS-001](#)), S13 ([LBO-05](#)), S106 ([LBP-10](#)), S607 ([THU-418](#)), S651 ([SAT-394](#)), S672 ([SAT-427](#)), S753 ([WED-430](#)), S808 ([TOP-091](#)), S820 ([FRI-512](#))
 Bedoya, José Ursic, S74 ([OS-104](#)), S170 ([FRI-443](#)), S467 ([THU-498](#)), S534 ([SAT-225](#)), S577 ([THU-119](#))
 Beeker, Nathanael, S656 ([SAT-402](#))
 Beer, Lucian, S505 ([FRI-295](#))
 Beghdadi, Nassiba, S458 ([THU-483](#))
 Begher-Tibbe, Brigitte, S413 ([FRI-334](#))
 Bégre, Lorin, S101 ([LBP-04](#))
 Béguelin, Charles, S101 ([LBP-04](#))
 Behari, Jaideep, S145 ([TOP-073](#))
 Behling, Cynthia, S715 ([SAT-496](#)), S808 ([TOP-091](#)), S820 ([FRI-512](#))
 Behrendt, Patrick, S1031 ([FRI-243](#)), S1032 ([FRI-244](#)), S1044 ([FRI-262](#))
 Behrens, Edward, S450 ([SAT-386](#)), S961 ([THU-278](#))
 Behrooz, Ali, S671 ([SAT-426](#))
 Beier, Dominik, S596 ([THU-150](#))
 Beigelman, Leonid, S112 ([LBP-18](#)), S548 ([SAT-251](#)), S1029 ([FRI-238](#)), S1029 ([FRI-239](#)), S1030 ([FRI-241](#)), S1051 ([FRI-272](#)), S1162 ([SAT-188](#)), S1164 ([SAT-192](#))
 Bejarano, Ana, S883 ([FRI-126](#))
 Bektaş, Fatih, S709 ([SAT-485](#))
 Bektas, Hicran, S852 ([WED-490](#))
 Beland-Bonenfant, Sarah, S603 ([THU-410](#))
 Belem, Mohamed Aly, S930 ([FRI-202](#))
 Belén Rubio, Ana, S166 ([FRI-437](#))
 Belicova, Lenka, S435 ([SAT-357](#)), S439 ([SAT-365](#)), S945 ([THU-255](#))
 Belilos, Eleanor, S631 ([THU-460](#))
 Belin, Lisa, S607 ([THU-418](#))
 Belkacem, Acidi, S458 ([THU-483](#))
 Bell, Adam, S102 ([LBP-05](#))
 Belladonna, Federica, S713 ([SAT-493](#)), S789 ([WED-521](#))

Author Index

- Bell, Andrew, S792 ([WED-527](#))
- Bellantì, Francesco, S374 ([WED-260](#))
- Bellarosa, Cristina, S952 ([THU-265](#))
- Beller, Daniella, S1195 ([THU-199](#))
- Belletini, Matteo, S713 ([SAT-494](#))
- Bellia, Valentina, S40 ([OS-045](#)), S55 ([OS-070](#))
- Bellido, Sarah Jean, S298 ([SAT-520](#))
- Bellón, José, S474 ([THU-512](#))
- Bellon, Serge, S930 ([FRI-204](#))
- Bell, Sally, S15 ([OS-002](#)), S380 ([WED-271](#)), S852 ([WED-488](#)), S860 ([SAT-121](#))
- Belmonte, Ernest, S843 ([FRI-499](#)), S995 ([THU-325](#))
- Bemeur, Chantal, S233 ([THU-372](#))
- Benali, Souad, S1150 ([SAT-169](#))
- Ben-Ari, Ziv, S719 ([SAT-500](#))
- Bence, Kendra, S786 ([WED-515](#))
- Benderski, Karina, S26 ([OS-022](#))
- Bendtsen, Flemming, S165 ([FRI-434](#)), S239 ([WED-325](#)), S723 ([SAT-507](#)), S748 ([WED-421](#))
- Bendtsen, Kristian, S748 ([WED-421](#))
- Benedé, Raquel, S150 ([FRI-412](#)), S349 ([THU-235](#))
- Benedetti, Andrea, S874 ([FRI-114](#))
- Benedetti, Edoardo, S88 ([OS-124-YI](#))
- Benedetti, Fabio, S88 ([OS-124-YI](#))
- Benedetto, Fabrizio Di, S287 ([SAT-334](#))
- Benedicto, Ana, S335 ([WED-239](#)), S781 ([WED-505](#))
- Benedicto, Ignacio, S732 ([TOP-090](#))
- Benelbarhdadi, Imane, S842 ([FRI-496](#))
- BenGhatnsh, Ahmed, S475 ([THU-515](#))
- Bengsch, Bertram, S582 ([THU-128](#))
- Benhammou, Jihanne, S472 ([THU-508](#))
- Benichou, Bernard, S989 ([THU-314](#))
- Ben-Ishai, Noa, S409 ([TOP-060](#))
- Benitez, Carlos, S195 ([FRI-546](#))
- Benjamin, Jaya, S277 ([WED-388](#)), S293 ([SAT-344](#))
- Benlloch, Salvador, S682 ([SAT-442](#)), S700 ([SAT-468](#))
- Bennett, Ashley, S415 ([FRI-346](#))
- Bennett, Kris, S307 ([SAT-537](#))
- Bennett, Lucy, S84 ([OS-119-YI](#))
- Benninga, Marc, S677 ([SAT-434](#))
- Benoot, Isabelle, S31 ([OS-030](#))
- Bentanachs, Roger, S356 ([THU-246](#)), S788 ([WED-518](#)), S802 ([WED-546](#))
- Benten, Daniel, S285 ([SAT-331](#))
- Bezoubir, Nassima, S359 ([FRI-382](#))
- Beo, Vincent Di, S68 ([OS-092-YI](#))
- Bera, Chinmay, S274 ([WED-382](#))
- Berak, Hanna, S505 ([FRI-296](#)), S1205 ([THU-215](#))
- Berasain, Carmen, S526 ([TOP-072](#)), S537 ([SAT-232](#))
- Beraza, Naiara, S434 ([SAT-356](#))
- Berby, Françoise, S1046 ([FRI-265](#))
- Berdt, Pauline De, S439 ([SAT-364](#))
- Berenguer, Carlota Siljestrom, S690 ([SAT-454](#)), S697 ([SAT-465](#)), S705 ([SAT-478](#)), S706 ([SAT-479](#))
- Berenguer Haym, Marina, S476 ([THU-517](#))
- Berenguer, Marina, S2 ([GS-003](#)), S75 ([OS-105](#)), S133 ([THU-404](#)), S181 ([FRI-462](#)), S366 ([TOP-061](#)), S380 ([WED-270](#)), S469 ([THU-501](#)), S470 ([THU-503](#)), S474 ([THU-512](#)), S481 ([THU-525](#)), S485 ([THU-535](#)), S921 ([FRI-188](#)), S964 ([THU-282](#)), S980 ([THU-301](#)), S989 ([THU-315](#)), S996 ([THU-326](#)), S998 ([THU-331](#)), S1099 ([WED-168](#)), S1124 ([WED-205](#)), S1172 ([THU-162](#))
- Beretta, Laura, S516 ([FRI-317](#))
- Beretta, Marisa, S972 ([THU-291](#))
- Berg, Christoph, S108 ([LBP-12](#)), S403 ([WED-307](#)), S1139 ([SAT-156](#)), S1147 ([TOP-110](#))
- Berg, Christoph P., S90 ([OS-126](#))
- Berger, Annemarie, S113 ([LBP-20](#))
- Berger, Hilmar, S737 ([WED-403](#))
- Berger, Karin, S596 ([THU-150](#))
- Berge, Rolf, S370 ([WED-254](#))
- Berger, Scott, S173 ([FRI-448](#))
- Berges, Jorge Saz, S932 ([FRI-208](#))
- Berggren, Per-Olof, S363 ([FRI-388](#))
- Bergheim, Ina, S154 ([FRI-419](#)), S413 ([FRI-334](#)), S625 ([THU-449](#)), S798 ([WED-539](#))
- Berghe, Tom Vanden, S764 ([WED-446](#))
- Bergin, Colm, S16 ([OS-004](#)), S1211 ([THU-223](#))
- Bergman, David, S82 ([OS-116-YI](#))
- Bergmann, Carsten, S979 ([THU-299](#))
- Bergquist, Annika, S383 ([WED-277](#)), S408 ([WED-317](#)), S857 ([SAT-115](#))
- Bergstrom, Jaclyn, S65 ([OS-086](#)), S839 ([FRI-490](#))
- Bergthaler, Andreas, S739 ([WED-405](#)), S746 ([WED-418](#))
- Berg, Thomas, S90 ([OS-126](#)), S108 ([LBP-12](#)), S197 ([FRI-549](#)), S201 ([FRI-555](#)), S244 ([WED-335](#)), S362 ([FRI-386](#)), S483 ([THU-529](#)), S507 ([FRI-299](#)), S507 ([FRI-300](#)), S576 ([THU-118](#)), S1043 ([FRI-260](#)), S1050 ([FRI-270](#)), S1071 ([WED-132](#)), S1090 ([WED-156](#)), S1134 ([SAT-148](#)), S1139 ([SAT-156](#)), S1147 ([TOP-110](#)), S1176 ([THU-168](#))
- Berhe, Nega, S927 ([FRI-197](#)), S1150 ([SAT-170](#))
- Berlakovich, Gabriela, S465 ([THU-494](#)), S465 ([THU-495](#)), S470 ([THU-505](#)), S489 ([THU-545](#))
- Berliner, Dominik, S240 ([WED-326](#))
- Berman, Mark, S822 ([FRI-515](#))
- Bermúdez, María, S12 ([LBO-04](#)), S533 ([SAT-224](#))
- Bernabeu-Andreu, Francisco A., S683 ([SAT-443](#))
- Bernabeu, Jesús Quintero, S971 ([THU-291](#))
- Bernal, Carmen, S470 ([THU-503](#))
- Bernales, Irantzu, S738 ([WED-404](#))
- Bernal, Sara Borrego, S365 ([FRI-391](#))
- Bernal, William, S479 ([THU-521](#))
- Bernardes, Christina, S846 ([WED-478](#))
- Bernardo-Seisdedos, Ganeko, S736 ([WED-400](#))
- Bernasconi, Davide, S381 ([WED-272](#))
- Bernatik, Sophia, S431 ([FRI-369](#))
- Berndt, Nikolaus, S362 ([FRI-386](#))
- Bernieh, Anas, S417 ([FRI-350](#))
- Bernsmeier, Christine, S77 ([OS-108-YI](#)), S214 ([THU-345](#)), S754 ([WED-431](#))
- Bernts, Lucas H.P., S973 ([THU-292](#))
- Berraondo, Pedro, S537 ([SAT-232](#))
- Berres, Marie-Luise, S571 ([SAT-292](#))
- Bertelli, Cristina, S632 ([THU-461](#)), S645 ([THU-557](#)), S722 ([SAT-506](#))
- Berthoud, Tamara, S1119 ([WED-197](#))
- Bertino, Gaetano, S40 ([OS-045](#)), S55 ([OS-070](#)), S568 ([SAT-288](#))
- Bertolazzi, Giorgio, S803 ([WED-549](#))
- Bertoletti, Antonio, S543 ([SAT-241](#)), S1024 ([FRI-229](#))
- Bertoli, Ada, S1122 ([WED-203](#))
- Bertolini, Emanuela, S978 ([THU-297](#))
- Bertoni, Costanza, S120 ([LBP-29](#)), S837 ([FRI-487](#))
- Bertran, Esther, S331 ([WED-231](#)), S529 ([SAT-216](#))
- Berzigotti, Annalisa, S20 ([OS-012-YI](#)), S61 ([OS-080-YI](#)), S86 ([OS-121-YI](#)), S87 ([OS-123-YI](#)), S279 ([TOP-043](#)), S280 ([TOP-048](#)), S283 ([SAT-327](#)), S481 ([THU-526](#)), S485 ([THU-533](#)), S609 ([THU-421](#)), S664 ([SAT-414](#))
- Besch, Camille, S62 ([OS-083-YI](#))
- Besisik, Fatih, S709 ([SAT-485](#))
- Bes, Marta, S506 ([FRI-298](#))
- Besqueut-Rougerie, Clement, S806 ([WED-555](#))
- Bessa, Isabel, S842 ([FRI-495](#))
- Bessa, Xavier, S267 ([WED-370](#)), S273 ([WED-381](#))
- Besselink, Marc, S836 ([FRI-485](#))
- Bessette, Paul, S5 ([GS-005](#))
- Besson, Adrien, S769 ([WED-453](#)), S777 ([WED-469](#))
- Bessone, Fernando, S132 ([THU-401](#)), S245 ([WED-336](#))
- Bessonova, Leona, S379 ([WED-268](#)), S844 ([FRI-500](#))
- Bester, Romina, S945 ([THU-256](#))
- Best, Jan, S61 ([OS-080-YI](#)), S628 ([THU-454](#))
- Bethell, Richard, S1038 ([FRI-252](#))
- Bettencourt, Ricki, S648 ([TOP-075](#)), S649 ([TOP-083](#)), S662 ([SAT-412](#))
- Bettinger, Dominik, S304 ([SAT-531](#)), S305 ([SAT-534](#)), S318 ([SAT-555](#)), S575 ([THU-116](#)), S586 ([THU-134](#))
- Beudeker, Boris, S496 ([FRI-282](#)), S501 ([FRI-291](#)), S1016 ([TOP-108](#)), S1019 ([FRI-219](#))
- Beuers, Ulrich, S10 ([LBO-01](#)), S14 ([LBO-06](#)), S55 ([OS-071-YI](#)), S403 ([WED-307](#)), S427 ([FRI-364](#))
- Beugger, Anja, S485 ([THU-533](#))
- Bevilacqua, Michele, S203 ([FRI-558](#))

- Beyens, Matthias, S443 (SAT-371)
 Bhadada, Sanjay, S51 (OS-064-YI)
 Bhadoria, Ajeet Singh, S906 (FRI-163)
 Bhakdi, Sebastian Chakrit, S543 (SAT-241)
 Bhamidimarri, Kalyan Ram, S125 (LBP-38)
 Bhandal, Khushpreet, S398 (WED-299)
 Bharadwaj, Sraddha, S542 (SAT-240)
 Bhaskar, Ashima, S17 (OS-006-YI)
 Bhatia, Puja, S277 (WED-388)
 Bhat, Sadam H, S17 (OS-006-YI),
 S21 (OS-014-YI), S76 (OS-107-YI),
 S139 (FRI-398), S326 (WED-222),
 S1033 (FRI-247)
 Bhat, Sadam H., S146 (FRI-407),
 S152 (FRI-416), S414 (FRI-344)
 Bhattacharya, Aneerban, S548 (SAT-251),
 S1029 (FRI-239)
 Bhatt, Deepak, S13 (LBO-05)
 Bhavani, Ruveena, S195 (FRI-546)
 Bhongade, Megha, S517 (FRI-319)
 Bhuiyan, Tasnim, S116 (LBP-23)
 Biancacci, Ilaria, S571 (SAT-292)
 Bianchini, Marcello, S287 (SAT-334)
 Bianchini, Rodolfo, S451 (SAT-388)
 Bianco, Cristiana, S500 (FRI-288),
 S661 (SAT-410), S669 (SAT-422),
 S673 (SAT-430), S803 (WED-549),
 S992 (THU-318), S1173 (THU-165)
 Biancone, Luigi, S460 (THU-485)
 Biase, Annarita Di, S974 (THU-293)
 Biasiolo, Alessandra, S766 (WED-449)
 Biedermann, Paula, S1044 (FRI-262)
 Biermer, Michael, S31 (OS-030),
 S1034 (FRI-248), S1087 (WED-151),
 S1138 (SAT-154)
 Biewenga, Maaike, S14 (LBO-06)
 Biffanti, Roberta, S990 (FRI-316)
 Biggins, Scott, S195 (FRI-546),
 S258 (WED-355)
 Biggins, Scott W, S256 (WED-352)
 Bignamini, Daniela, S814 (FRI-474)
 Bihari, Chhagan, S210 (THU-340),
 S228 (THU-362), S348 (THU-234),
 S357 (THU-248), S943 (THU-253),
 S953 (THU-266)
 Bihary, Dóra, S363 (FRI-389)
 Bijdevaate, Diederik, S306 (SAT-536)
 Bilbao, Jon, S736 (WED-400)
 Bilbao, Jose Ignacio, S573 (THU-114)
 Biliotti, Elisa, S1082 (WED-146)
 Billaud, Eric, S107 (LBP-11), S876 (FRI-117),
 S1161 (SAT-185)
 Billin, Andrew, S64 (OS-085),
 S423 (FRI-360), S678 (SAT-438)
 Billioud, Claire, S318 (SAT-556)
 Bindal, Vasundhara, S17 (OS-006-YI),
 S21 (OS-014-YI), S76 (OS-107-YI),
 S139 (FRI-398), S146 (FRI-407),
 S149 (FRI-410), S152 (FRI-416),
 S326 (WED-222), S414 (FRI-344),
 S1033 (FRI-247)
 Bindels, Eric, S1016 (TOP-108),
 S1019 (FRI-219)
 Bindels, Laure, S772 (WED-458)
 Binder, Christoph, S224 (THU-358)
 Binka, Mawuena, S883 (FRI-125),
 S886 (FRI-130), S919 (FRI-183),
 S1189 (THU-187), S1200 (THU-207)
 Bin Lee, Yun, S630 (THU-457),
 S635 (THU-466)
 Binte Jumat, Nur Halisah, S707 (SAT-482)
 Bin Usman Shah, Syed Hassan,
 S910 (FRI-169)
 Biolato, Marco, S36 (OS-036), S54 (OS-069),
 S660 (SAT-409), S723 (SAT-508)
 Biondi, Breanne, S1180 (THU-173)
 Bird, Thomas, S70 (OS-095-YI)
 Birerdinc, Aybike, S782 (WED-506)
 Birgin, Emrullah, S44 (OS-050-YI)
 Birgit, Kohnke-Ertel, S431 (FRI-369)
 Biriuchenko, Iryna, S637 (THU-468)
 Birkel, Jan, S1020 (FRI-222)
 Birligea, Mihaela, S192 (FRI-541)
 Birrer, Fabienne, S449 (SAT-384)
 Biswas, Sagnik, S73 (OS-101-YI),
 S197 (FRI-548), S297 (SAT-350),
 S587 (THU-135), S693 (SAT-459)
 Bitetto, Davide, S237 (WED-320),
 S402 (WED-306)
 Bittaye, Sheikh Omar, S1106 (WED-178)
 Bittermann, Therese, S398 (WED-298),
 S470 (THU-504)
 Bitto, Niccolò, S87 (OS-123-YI)
 Bi, Yufei, S404 (WED-309)
 Björck, Hanna, S756 (WED-434)
 Björkström, Niklas, S229 (THU-365),
 S945 (THU-255)
 Bjørnholt, Jørgen, S343 (THU-225)
 Björnsson, Einar S., S865 (SAT-129)
 Blach, Sarah, S872 (TOP-096),
 S912 (FRI-173), S934 (FRI-212)
 Black, Georgia, S726 (SAT-512)
 Blair, Alan, S1058 (WED-113)
 Blaise, Lorraine, S492 (FRI-274),
 S585 (THU-133)
 Blaise, Nkegoum, S865 (SAT-129)
 Blake, Connor Henry, S521 (FRI-326)
 Blanc, Jean-Frédéric, S61 (OS-081)
 Blanco, Jesus Miguens, S601 (TOP-088)
 Blanco, Laia, S788 (WED-518),
 S802 (WED-546)
 Blanco, Sonia, S587 (THU-136)
 Blanc, Pierluigi, S1082 (WED-146)
 Blank, Antje, S53 (OS-068)
 Blarasin, Benedetta, S952 (THU-265)
 Blasco, Vargas, S10 (LBO-01)
 Blasco, Víctor Manuel Vargas,
 S253 (WED-348), S964 (THU-282)
 Blas-García, Ana, S335 (WED-239),
 S781 (WED-505)
 Blatt, Lawrence, S112 (LBP-18),
 S548 (SAT-251), S1029 (FRI-238),
 S1029 (FRI-239), S1030 (FRI-241),
 S1051 (FRI-272), S1162 (SAT-188),
 S1164 (SAT-192)
 Blau, Jenny, S606 (THU-416),
 S616 (THU-433)
 Blaya, Delia, S250 (WED-343)
 Blazquez, Alfonso, S444 (SAT-374)
 Blázquez-López, Elena, S732 (TOP-090)
 Blázquez, Víctor, S852 (WED-489)
 Blessing, Kelly, S828 (FRI-525)
 Blissett, Rob, S894 (FRI-141)
 Blizzard, Christopher Leigh, S523 (FRI-329)
 Block, Christophe De, S83 (OS-118)
 Blondet, Niviann, S971 (THU-291)
 Bloom, Patricia, S24 (OS-019),
 S251 (WED-345)
 Blouin, Karine, S874 (FRI-114)
 Bluemel, Benjamin, S880 (FRI-121)
 Boano, Valentina, S40 (OS-045),
 S55 (OS-070)
 Boarini, Chiara, S1105 (WED-176)
 Bobowski-Gerard, Marie, S211 (THU-342)
 Bocca, Claudia, S526 (SAT-211)
 Bock, C.-Thomas, S1044 (FRI-262)
 Bock, Hans, S136 (THU-409)
 Bodakçi, Emin, S477 (THU-518)
 Bode-Boger, Stefanie, S220 (THU-355)
 Bodoque-García, Ana, S142 (FRI-403),
 S144 (FRI-406)
 Boeckmans, Joost, S752 (WED-428),
 S775 (WED-465)
 Boeckx, Bram, S452 (SAT-390),
 S524 (TOP-066)
 Boeckstaens, Guy, S345 (THU-229)
 Boesch, Markus, S363 (FRI-389),
 S452 (SAT-390), S753 (WED-430)
 Boettcher, Jan, S33 (OS-032)
 Bofill, Alex, S486 (THU-536)
 Boga, Elisabetta, S978 (THU-297)
 Bogazliyan, Aycan, S485 (THU-534)
 Bogdanovic, Andriana, S754 (WED-431)
 Bogeski, Ivan, S799 (WED-541)
 Boggio, Elena, S751 (WED-425)
 Bogomolov, Pavel, S53 (OS-068),
 S113 (LBP-20), S1091 (WED-158)
 Bohard, Louis, S994 (THU-322)
 Bohra, Deepika, S414 (FRI-344)
 Boice, Avery, S413 (FRI-335)
 Boichuk, Yuliia, S418 (FRI-351)
 Boillot, Olivier, S62 (OS-083-YI)
 Boiserie, Frederic, S574 (THU-115),
 S580 (THU-125)
 Boix, Paula, S210 (THU-341)
 Bojang, Lamin, S67 (OS-090-YI),
 S1106 (WED-178)
 Bojunga, Jörg, S276 (WED-385)
 Bola-Lawal, Queen, S67 (OS-090-YI),
 S1106 (WED-178)
 Boland, Karen, S255 (WED-350)
 Boldorini, Renzo, S751 (WED-425)
 Boleslawski, Emmanuel, S62 (OS-083-YI),
 S74 (OS-104), S146 (FRI-408)
 Bolis, Francesca, S982 (THU-304)
 Bollerup, Signe, S1050 (FRI-271)
 Bolm, Carsten, S350 (THU-236)
 Bolt, Isabelle, S412 (FRI-333)
 Bolton, Natalie, S1081 (WED-144)
 Bombardieri, Giulia, S920 (FRI-185)
 Bonaiuto, Emanuela, S407 (WED-315)
 Bonazza, Deborah, S768 (WED-452)

Author Index

- Bonder, Alan, S56 ([OS-073](#)), S378 ([WED-267](#)), S844 ([FRI-500](#))
- Bondi, Mario, S729 ([SAT-517](#))
- Bond, Sarah, S49 ([OS-062](#))
- Bonet, Lucia, S1191 ([THU-190](#))
- Bong Ahn, Sang, S633 ([THU-464](#))
- Bonham, C. Andrew, S25 ([OS-020-YI](#))
- Bonifazi, Francesca, S88 ([OS-124-YI](#))
- Bonilla, Eva Fernandez, S392 ([WED-290](#))
- Bonino, Ferruccio, S691 ([SAT-456](#)), S1091 ([WED-157](#))
- Boniquet, Juan Carles Quer, S903 ([FRI-156](#)), S915 ([FRI-177](#))
- Bonn, Stefan, S60 ([OS-079-YI](#))
- Bono, Ariadna, S1099 ([WED-168](#)), S1124 ([WED-205](#))
- Bono, Elisa, S5 ([GS-005](#))
- Bonora, Massimo, S550 ([SAT-254](#))
- Booiijink, Richell, S553 ([SAT-260](#))
- Booij, Tijmen, S532 ([SAT-222](#))
- Boon, Nathalie, S621 ([THU-442](#))
- Boonstra, Andre, S496 ([FRI-282](#)), S501 ([FRI-291](#)), S1016 ([TOP-108](#)), S1019 ([FRI-219](#)), S1134 ([SAT-148](#))
- Boor, Peter, S940 ([THU-249](#))
- Boothman, Helen, S1129 ([WED-213](#)), S1202 ([THU-210](#))
- Boot, James, S740 ([WED-406](#))
- Borahma, Mohamed, S842 ([FRI-496](#))
- Borand, Laurence, S897 ([FRI-146](#))
- Borbath, Ivan, S511 ([FRI-307](#))
- Borca, Florina, S1075 ([WED-137](#))
- Borentain, Patrick, S318 ([SAT-556](#)), S356 ([THU-247](#))
- Borghini, Alberto, S283 ([SAT-327](#)), S990 ([THU-317](#))
- Borghini, Marta, S1135 ([SAT-149](#)), S1142 ([SAT-159](#)), S1154 ([SAT-175](#)), S1159 ([SAT-181](#)), S1164 ([SAT-190](#))
- Borodo, Musa Muhammed, S269 ([WED-373](#))
- Borrego, Sandra, S852 ([WED-489](#))
- Borrello, Maria Teresa, S332 ([WED-232](#))
- Borroto, Danellys, S291 ([SAT-339](#))
- Borssén, Åsa Danielsson, S707 ([SAT-481](#))
- Borzacchiello, Luigi, S326 ([WED-223](#))
- Bosca, Andrea, S133 ([THU-404](#))
- Boscá, Andrea, S469 ([THU-501](#))
- Bosch, Jaime, S20 ([OS-012-YI](#)), S791 ([WED-524](#))
- Bosch, Jaume, S280 ([TOP-048](#))
- Bösch, Johannes, S232 ([THU-369](#))
- Bosch, Miriam, S33 ([OS-032](#)), S59 ([OS-077](#)), S442 ([TOP-053](#))
- Bosco, Oriana, S795 ([WED-533](#))
- Bose, Dipro, S800 ([WED-544](#))
- Bosscher, Karolien De, S743 ([WED-412](#))
- Bosselmann, Emily, S466 ([THU-496](#))
- Bossen, Lars, S390 ([WED-287](#)), S968 ([THU-287](#))
- Bossolasco, Simona, S120 ([LBP-29](#))
- Böttcher, Katrin, S47 ([OS-057](#))
- Botteron, Natalie Vilcinkas Y, S245 ([WED-336](#))
- Bottlander, Jacques, S930 ([FRI-204](#))
- Böttler, Tobias, S403 ([WED-307](#)), S447 ([SAT-379](#))
- Bouam, Samir, S161 ([FRI-429](#))
- Bouattour, Mohamed, S61 ([OS-081](#)), S491 ([FRI-273](#)), S505 ([FRI-295](#)), S577 ([THU-119](#)), S578 ([THU-122](#))
- Boudes, Pol, S333 ([WED-236](#))
- Boudou, Delfina, S924 ([FRI-192](#))
- Boulagnon-Rombi, Camille, S12 ([LBO-04](#))
- Boulanger, Chantal, S435 ([SAT-358](#))
- Boulrier, Dominique, S172 ([FRI-446](#))
- Bouligand, Jérôme, S971 ([THU-291](#))
- Boulter, Luke, S122 ([LBP-33-YI](#))
- Bouma, Gerd, S44 ([OS-049-YI](#))
- Bouquet, Jerome, S1039 ([FRI-255](#)), S1154 ([SAT-176](#)), S1162 ([SAT-187](#))
- Bourdais, Rémi, S589 ([THU-139](#))
- Bourgeois, Alexandre, S233 ([THU-372](#))
- Bourgeois, Stefan, S1114 ([WED-190](#))
- Bourke, Lisa, S861 ([SAT-123](#))
- Bourliere, Marc, S68 ([OS-092-YI](#)), S498 ([FRI-286](#)), S1138 ([SAT-154](#)), S1150 ([SAT-169](#)), S1160 ([SAT-183](#))
- Bourron, Olivier, S487 ([THU-538](#))
- Boursier, Jerome, S12 ([LBO-04](#)), S61 ([OS-080-YI](#)), S105 ([LBP-09](#)), S118 ([LBP-26](#)), S598 ([THU-154](#)), S607 ([THU-418](#)), S651 ([SAT-394](#)), S667 ([SAT-419](#)), S672 ([SAT-427](#))
- Bouvier, Anne-Marie, S82 ([OS-117](#)), S855 ([TOP-098](#))
- Bouvier, Veronique, S82 ([OS-117](#)), S855 ([TOP-098](#))
- Bouzbib, Charlotte, S318 ([SAT-556](#))
- Bowlus, Christopher, S11 ([LBO-03](#)), S367 ([TOP-063](#)), S371 ([WED-256](#)), S388 ([WED-283](#)), S423 ([FRI-360](#)), S431 ([FRI-368](#)), S985 ([THU-310](#))
- Bowyer, Teresa, S1179 ([THU-172](#))
- Boyd, Anders, S101 ([LBP-04](#)), S892 ([FRI-138](#))
- Boyer-Diaz, Zoe, S791 ([WED-524](#))
- Boyer, Nathalie, S1193 ([THU-194](#))
- Boyer, Sylvie, S923 ([FRI-191](#))
- Boyette, Lisa, S64 ([OS-085](#)), S423 ([FRI-360](#)), S678 ([SAT-438](#))
- Boyle, Alison, S1202 ([THU-210](#))
- Boyle, Billy, S840 ([FRI-492](#))
- Bozdayi, Mithat, S1109 ([WED-183](#))
- Bozward, Amber, S443 ([SAT-372](#)), S448 ([SAT-381](#)), S448 ([SAT-382](#))
- Braadland, Peder Rustøen, S370 ([WED-254](#)), S428 ([FRI-365](#))
- Brabec, Tomáš, S945 ([THU-255](#))
- Bracci, Angelica, S685 ([SAT-446](#))
- Bradley, Declan, S850 ([WED-484](#))
- Bradshaw, Jane, S523 ([FRI-329](#))
- Brady, John Michael, S677 ([SAT-436](#))
- Braem, Frédéric, S464 ([THU-493](#))
- Bragança, Sofia, S1111 ([WED-185](#))
- Brahmania, Mayur, S157 ([FRI-422](#)), S175 ([FRI-451](#)), S865 ([SAT-129](#)), S900 ([FRI-151](#))
- Brain, John, S411 ([FRI-331](#))
- Brakenhoff, Sylvia, S52 ([OS-065-YI](#)), S1132 ([SAT-145](#)), S1134 ([SAT-148](#))
- Brañas, Montse, S497 ([FRI-284](#))
- Brancaccio, Giuseppina, S1056 ([TOP-106](#)), S1082 ([WED-146](#)), S1103 ([WED-174](#))
- Branco, Joana, S1111 ([WED-185](#)), S1189 ([THU-186](#))
- Brandão-Mello, Carlos, S1188 ([THU-184](#)), S1201 ([THU-208](#)), S1201 ([THU-209](#))
- Brandt, Annette, S154 ([FRI-419](#)), S798 ([WED-539](#))
- Brandt, Pamela, S464 ([THU-492](#))
- Brantly, Mark, S85 ([OS-120](#))
- Bratos, Gioia, S284 ([SAT-329](#))
- Bratthauer, Gary, S782 ([WED-506](#))
- Braun, Felix, S42 ([OS-047-YI](#))
- Braunwarth, Eva, S44 ([OS-050-YI](#))
- Bravo, Marta Tejedor, S469 ([THU-501](#))
- Bravo, Miren, S532 ([SAT-221](#)), S544 ([SAT-244](#))
- Bray, Fabrice, S146 ([FRI-408](#))
- Brecelj, Jernej, S969 ([THU-289](#)), S971 ([THU-291](#))
- Breen, Leigh, S231 ([THU-368](#)), S232 ([THU-370](#))
- Brees, Dominique, S806 ([TOP-076](#))
- Breitenecker, Kristina, S538 ([SAT-233](#))
- Bremer, Birgit, S1098 ([WED-167](#)), S1115 ([WED-193](#))
- Brenier-Pinchart, Marie-Pierre, S894 ([FRI-142](#))
- Brennan, Todd, S489 ([TOP-065](#))
- Brescia, Paola, S753 ([WED-430](#))
- Bresson-Hadni, Solange, S994 ([THU-322](#))
- Bretto, Elisabetta, S917 ([FRI-180](#)), S1177 ([THU-169](#)), S1200 ([THU-206](#))
- Brew, Bruce, S263 ([WED-364](#))
- Bricard, Orian, S524 ([TOP-066](#))
- Brichler, Segolene, S833 ([FRI-480](#)), S1150 ([SAT-169](#)), S1160 ([SAT-183](#))
- Bridle, Kim, S330 ([WED-229](#))
- Brienza, Giovanni, S646 ([THU-560](#))
- Brigida, Krestina, S888 ([FRI-132](#))
- Brignon, Nicolas, S72 ([OS-098](#))
- Brindley, James Hallimond, S621 ([THU-441](#)), S740 ([WED-406](#))
- Brisac, Cynthia, S58 ([OS-075](#))
- Brisson, Murielle, S1193 ([THU-194](#))
- Briz, Oscar, S527 ([SAT-212](#)), S551 ([SAT-256](#))
- Briz, Veronica, S1037 ([FRI-251](#))
- Brjalin, Vadim, S198 ([FRI-550](#))
- Brochet, Christine, S494 ([FRI-279](#))
- Brockschmidt, Antje, S594 ([THU-147](#))
- Broco, Carolina, S852 ([WED-489](#))
- Brodie, Tess, S449 ([SAT-384](#))
- Brodosi, Lucia, S640 ([THU-475](#)), S673 ([SAT-430](#)), S691 ([SAT-457](#))
- Broering, Dieter Clemens, S958 ([THU-273](#))
- Broering, Ruth, S549 ([SAT-253](#)), S562 ([SAT-278](#))
- Brol, Maximilian Joseph, S185 ([FRI-341](#)), S222 ([THU-356](#)), S313 ([SAT-546](#)), S484 ([THU-531](#)), S712 ([SAT-492](#))

- Bronowicki, Jean-Pierre, S61 (OS-081), S498 (FRI-286)
- Bronte, Fabrizio, S1111 (WED-186)
- Broqua, Pierre, S651 (SAT-393), S823 (FRI-517)
- Broquetas, Teresa, S267 (WED-370), S273 (WED-381)
- Brosch, Mario, S364 (FRI-390)
- Brosi, Phillippe, S162 (FRI-430)
- Bros, Matthias, S26 (OS-022)
- Brosteanu, Oana, S1147 (TOP-110)
- Brotherston, Sophie, S411 (FRI-331)
- Brouard, Cécile, S880 (FRI-121)
- Brousse, Georges, S172 (FRI-446)
- Brouwer, Willem Pieter, S83 (OS-118), S454 (TOP-052)
- Brown, Ambrose, S848 (WED-480)
- Brown, Anthony, S1169 (SAT-198)
- Browne, Sarah, S50 (OS-063)
- Brown, Joanne, S1171 (SAT-202)
- Brown, Joelle, S58 (OS-075)
- Brown, Michelle, S993 (THU-320)
- Brown, Randy, S50 (OS-063)
- Brown, Robert, S35 (OS-034)
- Brown, S. David, S139 (FRI-397)
- Brozat, Jonathan Frederik, S188 (FRI-534)
- Bruccoleri, Mariangela, S571 (TOP-067), S584 (THU-131)
- Brugaletta, Salvatore, S461 (THU-487)
- Bruges, Léa, S12 (LBO-04)
- Brüggemann, Roger, S973 (THU-292)
- Brüggemann, Yannick, S1020 (FRI-221)
- Brugger-Synnes, Pascal, S1150 (SAT-170)
- Bruggmann, Philip, S888 (FRI-131), S933 (FRI-209)
- Bruguera, Pol, S158 (FRI-423), S166 (FRI-437)
- Bruha, Radan, S292 (SAT-341), S727 (SAT-513)
- Bruix, Jordi, S493 (FRI-276), S579 (THU-124)
- Brujats, Ana, S164 (FRI-433)
- Brujats, Anna, S73 (OS-100-YI)
- Brumpt, Eleonore, S994 (THU-322)
- Bruneau, Alix, S351 (THU-238)
- Bruneau, Julie, S874 (FRI-114)
- Brunet, Ludovic, S206 (TOP-046)
- Brunetto, Maurizia, S9 (GS-012), S40 (OS-045), S53 (OS-067), S53 (OS-068), S55 (OS-070), S107 (LBP-11), S113 (LBP-20), S374 (WED-260), S691 (SAT-456), S1082 (WED-146), S1087 (WED-151), S1091 (WED-157), S1091 (WED-158), S1134 (SAT-148), S1137 (SAT-153)
- Bruni, Elena, S1031 (FRI-242)
- Brunner, Nathalie, S933 (FRI-209)
- Brunner, Sarah, S45 (OS-051-YI)
- Brunner, Simon, S481 (THU-526)
- Bruno, Andres, S245 (WED-336)
- Bruno, Benjamin, S260 (WED-358), S809 (FRI-466)
- Bruno, Pierangela, S685 (SAT-446)
- Bruns, Tony, S56 (OS-073), S90 (OS-126), S150 (FRI-412), S188 (FRI-534), S198 (FRI-550), S349 (THU-235)
- Brusa, Stefano, S903 (FRI-155)
- Brusch, Lutz, S364 (FRI-390)
- Brusilovskaya, Ksenia, S246 (WED-338)
- Brussel, Thomas Van, S524 (TOP-066)
- Brusse, Maureen, S553 (SAT-260)
- Brusset, Bleuenn, S62 (OS-083-YI)
- Brutti, Julia, S245 (WED-336)
- Bryce, Kathleen, S872 (TOP-097)
- Bryere, Joséphine, S82 (OS-117)
- Brzezinski, Rafael, S719 (SAT-500)
- Brzustowski, Angélique, S106 (LBP-10), S776 (WED-467)
- Bucci, Laura, S513 (FRI-311)
- Buchard, Benjamin, S172 (FRI-446)
- Büchler, Christa, S521 (FRI-324)
- Buch, Stephan, S548 (SAT-250)
- Bucsics, Theresa, S282 (SAT-326), S313 (SAT-547), S831 (FRI-477)
- Buda, Roxana, S297 (SAT-519)
- Budzyński, Andrzej, S332 (WED-233)
- Bufler, Philip, S965 (THU-284)
- Bugert, Joachim, S945 (THU-256)
- Buggisch, Peter, S90 (OS-126), S108 (LBP-12), S1139 (SAT-156), S1147 (TOP-110)
- Bugianesi, Elisabetta, S500 (FRI-288), S521 (FRI-325), S526 (SAT-211), S605 (THU-415), S609 (THU-421), S611 (THU-425), S617 (THU-435), S620 (THU-440), S626 (THU-452), S637 (THU-470), S646 (THU-559), S652 (SAT-396), S673 (SAT-430), S704 (SAT-474), S713 (SAT-494), S863 (SAT-125)
- Bui, Richard, S173 (FRI-448)
- Bujanda, Luis, S28 (OS-024-YI), S57 (OS-074-YI), S326 (WED-223), S527 (SAT-212), S533 (SAT-223), S534 (SAT-226), S541 (SAT-238), S560 (SAT-275), S741 (WED-408)
- Bukh, Jens, S1050 (FRI-271)
- Bulanov, Nikolay, S1210 (THU-221)
- Bulda, Volodymyr, S637 (THU-468)
- Buliarcă, Alina, S245 (WED-337)
- Bulic, Marko, S229 (THU-366)
- Buller-Taylor, Terri, S919 (FRI-183)
- Bulut, Pinar, S971 (THU-291)
- Bumpass, Brock, S291 (SAT-339)
- Bungay, Rebecca, S291 (SAT-339)
- Bunyan-Woodcraft, Mason, S326 (WED-223)
- Buoro, Sabrina, S920 (FRI-185)
- Buque, Xabier, S137 (FRI-395), S529 (SAT-215), S738 (WED-404), S741 (WED-408)
- Burade, Vinod, S607 (THU-419)
- Burda, Tatiana, S125 (LBP-38)
- Burden, Jemima, S75 (OS-105)
- Bureau, Christophe, S87 (OS-123-YI), S198 (FRI-550), S279 (TOP-043), S318 (SAT-556), S975 (THU-295)
- Buresh, Megan, S913 (FRI-174)
- Burford, Charlotte, S984 (THU-307), S987 (THU-312), S999 (THU-332)
- Burge, Daniel, S139 (FRI-397), S829 (FRI-528)
- Burghart, Lukas, S90 (OS-127-YI), S299 (SAT-521), S936 (TOP-055)
- Burgueño, Beatriz, S480 (THU-524)
- Burke, Emma, S398 (WED-299)
- Burke, Leslie, S330 (WED-229)
- Burlone, Michela, S389 (WED-284), S599 (THU-156)
- Burnett, Chris, S1162 (SAT-188)
- Burra, Patrizia, S54 (OS-069), S183 (TOP-049), S293 (SAT-343), S482 (THU-527), S627 (THU-453)
- Burrel, Marta, S497 (FRI-284)
- Burrer, Renaud, S792 (WED-526)
- Burroughs, Andrew, S105 (LBP-09)
- Burt, Alastair, S671 (SAT-426)
- Buschmann, Tobias, S441 (SAT-368)
- Buschow, Sonja, S561 (SAT-276)
- Busek, Mathias, S59 (OS-076), S409 (TOP-064)
- Bush, Brian, S195 (FRI-546), S274 (WED-382)
- Busoms, Cristina Molera, S972 (THU-291)
- Bussey, Louise, S1169 (SAT-198)
- Buss, Nicola, S954 (THU-268)
- Bustamante, Javier, S481 (THU-525), S541 (SAT-238)
- Butcher, Christian, S649 (TOP-083)
- Buti, Maria, S9 (GS-012), S31 (OS-030), S53 (OS-067), S91 (OS-129-YI), S103 (LBP-06), S113 (LBP-20), S375 (WED-263), S882 (FRI-124), S896 (FRI-144), S901 (FRI-152), S904 (FRI-158), S913 (FRI-175), S917 (FRI-181), S921 (FRI-188), S924 (FRI-192), S1024 (FRI-228), S1054 (TOP-100), S1070 (WED-130), S1082 (WED-145), S1098 (WED-166), S1099 (WED-168), S1134 (SAT-148), S1137 (SAT-153), S1138 (SAT-154), S1191 (THU-190), S1205 (THU-216), S1209 (THU-219)
- Butler, Bryony, S309 (SAT-541)
- Bütow, Laura, S487 (THU-539)
- Butsashvili, Maia, S889 (FRI-133), S930 (FRI-203), S1204 (THU-214)
- Butts, Jordan, S422 (FRI-356)
- Buuren, Nicholas Van, S35 (OS-034)
- Buzzanca, Valerio, S40 (OS-045), S55 (OS-070)
- Buzzee, Benjamin, S838 (FRI-489), S878 (FRI-119)
- Byeon, Jiyeon, S437 (SAT-361)
- Byrne, Mandy, S480 (THU-522)
- Bystrianska, Natalia, S871 (SAT-136)
- Byun, Kwan Soo, S798 (WED-540)
- Bzeizi, Khalid, S958 (THU-273), S1011 (THU-388)
- Caballería, Joan, S171 (FRI-445)
- Caballeria, Llorenç, S664 (SAT-415)

Author Index

- Caballero-Díaz, Daniel, S331 (WED-231)
 Caballero, Federico, S932 (FRI-208)
 Caballero, Francisco J., S57 (OS-074-YI), S527 (SAT-212), S541 (SAT-238)
 Caballol, Berta, S493 (FRI-216)
 Cabello, MR, S18 (OS-007)
 Cabello, Ricardo, S274 (WED-382)
 Cabezas, Joaquín, S911 (FRI-171), S921 (FRI-188), S934 (FRI-211)
 Cabezas, Joaquín, S171 (FRI-445), S1098 (WED-166), S1178 (THU-171)
 Cabibbo, Giuseppe, S592 (THU-144), S593 (THU-145)
 Cable, Edward, S338 (WED-246)
 Cable, Rebecca, S673 (SAT-428)
 Cabral, Loraine Kay, S559 (SAT-273)
 Cabrera, Araceli Bravo, S274 (WED-382)
 Cabrera, Daniel, S145 (TOP-073)
 Cabrera, Roniel, S1189 (THU-185)
 Cabriales, Lucia, S122 (LBP-34)
 Caccamo, Lucio, S457 (THU-481)
 Caccia, Riccardo, S86 (OS-121-YI)
 Cacciatore, Pierluigi, S36 (OS-036)
 Cacciato, Valentina, S233 (THU-371)
 Cacciola, Irene, S457 (THU-481), S1082 (WED-146)
 Cachero, Alba, S964 (THU-282), S980 (THU-301), S998 (THU-331)
 Cadamuro, Luca, S374 (WED-260)
 Cadamuro, Massimiliano, S72 (OS-099), S564 (SAT-283), S804 (WED-550)
 Cadranet, Jean-François, S170 (FRI-442)
 Cagley, Matthew, S516 (FRI-317)
 Cagna, Marta, S795 (WED-533), S804 (WED-550)
 Cai, Da-Chuan, S1165 (SAT-193)
 Cai, Dachuan, S271 (WED-376)
 Cai, Dawei, S1029 (FRI-239)
 Cai, Jianzhong, S557 (SAT-269)
 Caillaud, Ludovic, S170 (FRI-443)
 Caine, Graham, S466 (THU-497)
 Cairns, Helen, S402 (WED-305)
 Cairolí, Victoria, S1037 (FRI-251)
 Cairo, Stefano, S537 (SAT-232), S551 (SAT-256)
 Cai, Xiurong, S745 (WED-416)
 Cai, Yijing, S274 (WED-382)
 Cajka, Tomas, S784 (WED-509)
 Cajochen, Christian, S754 (WED-431)
 Calabrese, Diego, S532 (SAT-222)
 Calabrese, Pietro, S789 (WED-521)
 Calaf, Àngel Rivero, S932 (FRI-208)
 Calame, Paul, S994 (THU-322)
 Calçado, Fernanda, S618 (THU-436)
 Calderaro, Julien, S12 (LBO-04), S577 (THU-119)
 Calderón, Diana Karen Tapia, S683 (SAT-443)
 Caldwell, Stephen H, S258 (WED-356)
 Calero, Silvia, S440 (SAT-367)
 Cales, Paul, S105 (LBP-09), S498 (FRI-286), S667 (SAT-419)
 Caligiuri, Alessandra, S335 (WED-239)
 Caliman-Sturdza, Olga Adriana, S262 (WED-361)
 Calimeri, Francesco, S685 (SAT-446)
 Caliskan, Aysun, S1109 (WED-183)
 Callaghan, Lynne, S153 (FRI-418)
 Calleja Panero, José Luis, S693 (SAT-460), S700 (SAT-468), S934 (FRI-211)
 Callejo-Pérez, Ana, S375 (WED-263)
 Calle, Marinella, S1006 (THU-382)
 Calleri, Alberto, S54 (OS-069), S460 (THU-485)
 Calligaris, Matteo, S457 (THU-480)
 Calmels, Mélanie, S435 (SAT-358)
 Calmy, Alexandra, S101 (LBP-04)
 Calvaruso, Vincenzo, S36 (OS-036), S40 (OS-045), S55 (OS-070), S56 (OS-073), S237 (WED-320), S374 (WED-260), S609 (THU-421), S1111 (WED-186), S1118 (WED-196)
 Calvez, Vincent, S1044 (FRI-261)
 Calvisi, Diego, S529 (SAT-215), S534 (SAT-226), S544 (SAT-244)
 Calvo, Ana Avellon, S902 (FRI-153)
 Calvo, Jorge, S911 (FRI-171)
 Calvo, Mariona, S579 (THU-124)
 Calvo, Pier Luigi, S969 (THU-289)
 Camagni, Stefania, S471 (THU-507)
 Camarinha-Silva, Amélia, S798 (WED-539)
 Cameron, Grace, S177 (FRI-455)
 Cameron, Madeline, S404 (WED-310)
 Cameron, Rainie, S538 (SAT-234), S542 (SAT-239), S565 (SAT-284)
 Camerotto, Riccardo, S564 (SAT-283)
 Camma, Calogero, S374 (WED-260), S586 (THU-134), S592 (THU-144), S609 (THU-421), S803 (WED-549), S1118 (WED-196)
 Cammarota, Antonella, S575 (THU-116), S586 (THU-134)
 Campani, Claudia, S513 (FRI-311), S577 (THU-120), S584 (THU-131), S585 (THU-133), S774 (WED-462)
 Campbell, Cori, S868 (SAT-131), S1060 (WED-117), S1075 (WED-137), S1108 (WED-181)
 Campbell, Fiona, S1154 (SAT-176), S1162 (SAT-187)
 Campello, Elena, S564 (SAT-283)
 Campinoti, Sara, S324 (WED-218), S324 (WED-219)
 Campion, Bertille, S492 (FRI-274), S494 (FRI-279), S515 (FRI-316)
 Campion, Daniela, S10 (LBO-01)
 Camp, Jeremy, S1135 (SAT-150)
 Campo, Rosa del, S19 (OS-011-YI)
 Campos, Elena Pérez, S1098 (WED-166)
 Campos, Maria Carolina, S132 (THU-401)
 Campos-Murguía, Alejandro, S42 (OS-047-YI), S466 (THU-496), S982 (THU-304)
 Campos-Varela, Isabel, S133 (THU-404)
 Campreciós, Genís, S770 (WED-457), S984 (THU-308)
 Camps, Jordi, S670 (SAT-425), S676 (SAT-433)
 Camus, Gregory, S32 (OS-031)
 Cananzi, Mara, S965 (THU-284), S966 (THU-285)
 Cañas, Jorge, S326 (WED-223), S560 (SAT-275)
 Canbay, Ali, S61 (OS-080-YI), S628 (THU-454)
 Cancado, Eduardo, S132 (THU-401)
 Cancelo, Ana Álvarez, S709 (SAT-484)
 Candelaria, Esther Rodríguez, S397 (WED-296), S928 (FRI-198)
 Candels, Lena Susanna, S571 (SAT-292), S778 (WED-470)
 Candia, Valeria, S361 (FRI-384)
 Candusso, Manila, S123 (LBP-35), S387 (WED-282)
 Cañete, Nuria, S171 (FRI-445), S267 (WED-370), S273 (WED-381)
 Canga, Elia, S135 (THU-406)
 Cangelosi, Davide, S446 (SAT-377)
 Cangemi, Roberto, S217 (THU-350)
 Canhão, Bernardo, S982 (THU-304)
 Canhoto, Nuno, S889 (FRI-134)
 Canillas, Lidia, S267 (WED-370), S273 (WED-381)
 Canivet, Clémence M, S667 (SAT-419), S672 (SAT-427)
 Cañizares, Rafael Bañares, S220 (THU-355)
 Cannavò, Maria Rita, S40 (OS-045), S55 (OS-070)
 Cannito, Stefania, S526 (SAT-211), S766 (WED-449)
 Cannon, Mary D, S91 (OS-128), S1179 (THU-172)
 Cano, María Eliece, S911 (FRI-171)
 Canos, Antonio David Palau, S1124 (WED-205)
 Canova, Lorenzo, S978 (THU-297)
 Canto, Carles, S762 (WED-442)
 Canva, Valérie, S52 (OS-066)
 Cao, Dandan, S489 (TOP-065)
 Cao, Haixia, S1156 (SAT-178)
 Cao, Hongcui, S753 (WED-429)
 Cao, Jiacheng, S272 (WED-378)
 Cao, Lu, S330 (WED-229)
 Caon, Elisabetta, S337 (WED-243)
 Cao, Sheng, S145 (TOP-073)
 Cao, Xu, S153 (FRI-417), S224 (THU-359), S569 (SAT-290), S1086 (WED-150)
 Cao, Zhenhuan, S1163 (SAT-189)
 Cao, Zhujun, S195 (FRI-546), S274 (WED-382)
 Caparrós, Esther, S210 (THU-341), S294 (SAT-345)
 Capasso, Mario, S1082 (WED-146)
 Capdevila, Aura, S664 (SAT-415)
 Capel, Jeroen, S242 (WED-330)
 Capelo, Alba, S326 (WED-223), S560 (SAT-275)
 Capeloa, Leon, S26 (OS-022)
 Capinha, Francisco, S86 (OS-121-YI)
 Capodicasa, Luigi, S374 (WED-260)
 Caporali, Cristian, S287 (SAT-334)
 Capozza, Thomas, S118 (LBP-26), S647 (TOP-074), S809 (FRI-467)

- Cappelli, Simone, S691 ([SAT-456](#))
 Cappuyns, Sarah, S48 ([OS-059-YI](#)), S524 ([TOP-066](#))
 Cappy, Pierre, S1109 ([WED-182](#))
 Caputo, Marina, S804 ([WED-551](#))
 Caputo, Sergio Lo, S907 ([FRI-164](#))
 Carabias, Lidia, S1192 ([THU-192](#))
 Caraceni, Paolo, S10 ([LBO-01](#)), S143 ([FRI-404](#)), S191 ([FRI-540](#)), S237 ([WED-320](#)), S238 ([WED-323](#)), S253 ([WED-348](#)), S290 ([SAT-337](#))
 Caravan, Peter, S413 ([FRI-335](#))
 Carazo, Antonio Duarte, S932 ([FRI-207](#))
 Carbonell-Asins, Juan Antonio, S35 ([OS-035-YI](#)), S220 ([THU-355](#))
 Carbonell, Eduardo, S335 ([WED-239](#))
 Carbonell, Nicolas, S318 ([SAT-556](#))
 Carbone, Marco, S40 ([OS-045](#)), S55 ([OS-070](#)), S56 ([OS-073](#)), S374 ([WED-260](#)), S381 ([WED-272](#)), S383 ([WED-277](#))
 Carbonero, Luz Martin, S1037 ([FRI-251](#))
 Carceller-Lopez, Elena, S440 ([SAT-367](#))
 Carcione, Claudia, S457 ([THU-480](#))
 Cardenas, Andres, S486 ([THU-536](#))
 Cárdenas-García, Antonio, S732 ([TOP-090](#))
 Cárdenas, Odila Saucedo, S337 ([WED-244](#))
 Card-Gower, Joshua, S103 ([LBP-06](#))
 Cardinale, Vincenzo, S994 ([THU-323](#))
 Cardona, Katherine Emilia Maldonado, S865 ([SAT-129](#)), S900 ([FRI-151](#))
 Cardona, Pere Joan, S1192 ([THU-192](#))
 Cardoso, Ana Carolina, S618 ([THU-436](#)), S658 ([SAT-405](#))
 Cardoso, Claudia Regina, S626 ([THU-451](#)), S658 ([SAT-405](#))
 Cardoso Delgado, Teresa, S532 ([SAT-221](#)), S544 ([SAT-244](#)), S546 ([SAT-247](#))
 Cardoso, Mariana, S1111 ([WED-185](#)), S1189 ([THU-186](#))
 Cardoso, Miguel, S279 ([WED-390](#))
 Carey, Ivana, S91 ([OS-128](#)), S905 ([FRI-161](#)), S1060 ([WED-117](#)), S1081 ([WED-143](#)), S1081 ([WED-144](#)), S1108 ([WED-181](#)), S1134 ([SAT-148](#))
 Cariou, Bertrand, S603 ([THU-410](#))
 Carleton, Michael, S737 ([WED-401](#))
 Carli, Fabrizia, S605 ([THU-415](#)), S611 ([THU-425](#)), S626 ([THU-452](#))
 Carlomagno, Ilaria, S360 ([FRI-383](#))
 Carlos Álvarez, Juan, S273 ([WED-381](#))
 Carlos, Juan, S984 ([THU-308](#)), S1124 ([WED-205](#)), S1126 ([WED-208](#))
 Carlos Laguna, Juan, S802 ([WED-546](#))
 Carlsson, Björn, S606 ([THU-416](#)), S616 ([THU-433](#))
 Carlton-Smith, Charles, S58 ([OS-075](#))
 Carmona, Isabel, S248 ([WED-341](#))
 Carnero, Amancio, S529 ([SAT-216](#))
 Carnevale, Roberto, S994 ([THU-323](#))
 Caro, Antonia, S267 ([WED-370](#)), S273 ([WED-381](#))
 Carobolante, Francesca, S88 ([OS-124-YI](#))
 Caro, Emilia Rita De, S772 ([WED-459](#))
 Carole, Cagnot, S46 ([OS-055](#))
 Caroline, den Hoed, S184 ([FRI-340](#))
 Carol, Marta, S10 ([LBO-01](#)), S15 ([OS-001](#)), S163 ([FRI-431](#)), S250 ([WED-343](#)), S664 ([SAT-415](#)), S851 ([WED-486](#))
 Caron, Alexandra, S666 ([SAT-417](#))
 Caron de Fromentel, Claude, S1018 ([FRI-218](#))
 Carotenuto, Pietro, S942 ([THU-251](#))
 Carpani, Rossana, S669 ([SAT-422](#))
 Carpino, Guido, S994 ([THU-323](#))
 Carrai, Paola, S482 ([THU-527](#))
 Carrara, Maria, S791 ([WED-525](#))
 Carrara, Stefania, S1103 ([WED-174](#))
 Carrat, Fabrice, S56 ([OS-073](#)), S68 ([OS-092-YI](#)), S498 ([FRI-286](#))
 Carr, Bernard, S850 ([WED-484](#)), S1211 ([THU-223](#))
 Carreño, Fernando, S367 ([TOP-062](#))
 Carrera, Enrique, S496 ([FRI-282](#)), S865 ([SAT-129](#)), S900 ([FRI-151](#))
 Carrieri, Maria Patrizia, S68 ([OS-092-YI](#)), S646 ([THU-559](#)), S923 ([FRI-191](#))
 Carrión, Jose A., S267 ([WED-370](#)), S273 ([WED-381](#)), S1098 ([WED-166](#))
 Carrión, José Antonio, S1178 ([THU-171](#))
 Carrodegua, Alba, S889 ([FRI-134](#)), S902 ([FRI-154](#)), S932 ([FRI-207](#))
 Carroli, Agnese, S54 ([OS-069](#))
 Carroll, Tomas, S979 ([THU-300](#))
 Carucci, Patrizia, S526 ([SAT-211](#))
 Caruntu, Florin Alexandru, S1137 ([SAT-152](#))
 Caruso, Stefano, S12 ([LBO-04](#))
 Carvalhana, Sofia, S279 ([WED-390](#)), S722 ([SAT-506](#))
 Carvalho, Armando, S366 ([TOP-061](#)), S842 ([FRI-495](#))
 Carvalho, Elisa, S971 ([THU-291](#))
 Carvalho-Gomes, Ângela, S1099 ([WED-168](#)), S1124 ([WED-205](#)), S1172 ([THU-162](#))
 Carvalho, Rita, S1111 ([WED-185](#)), S1189 ([THU-186](#))
 Casadei-Gardini, Andrea, S592 ([THU-143](#))
 Casado, Marta, S2 ([GS-003](#)), S248 ([WED-341](#)), S366 ([TOP-061](#)), S380 ([WED-270](#)), S932 ([FRI-207](#)), S1098 ([WED-166](#)), S1126 ([WED-208](#))
 Casado, Miguel Ángel, S896 ([FRI-144](#)), S921 ([FRI-188](#))
 Casal, Giulia, S75 ([OS-105](#))
 Casanovas, Georgina, S2 ([GS-003](#)), S10 ([LBO-01](#))
 Casar, Christian, S42 ([OS-047-YI](#)), S60 ([OS-079-YI](#)), S450 ([SAT-385](#)), S579 ([THU-123](#))
 Casari, Federico, S287 ([SAT-334](#))
 Casas-Deza, Diego, S1187 ([THU-183](#))
 Cascinu, Stefano, S592 ([THU-143](#)), S593 ([THU-145](#))
 Casella, Silvia, S40 ([OS-045](#)), S55 ([OS-070](#))
 Casillas, Linda, S367 ([TOP-062](#)), S398 ([WED-299](#))
 Casinelli, Katia, S1122 ([WED-203](#))
 Casirati, Elia, S733 ([WED-393](#))
 Caskey, Kadon, S173 ([FRI-448](#))
 Caspers, Martien P. M., S763 ([WED-444](#)), S786 ([WED-515](#)), S805 ([WED-553](#))
 Cassani, Barbara, S446 ([SAT-377](#))
 Cassiman, David, S300 ([SAT-524](#)), S452 ([SAT-390](#))
 Cassinotto, Cristophe, S61 ([OS-080-YI](#))
 Casta, Adelaida La, S541 ([SAT-238](#))
 Castagna, Antonella, S120 ([LBP-29](#)), S837 ([FRI-487](#))
 Castagno, Davide, S713 ([SAT-494](#))
 Castaldi, Silvana, S920 ([FRI-185](#))
 Castañeda, Andres, S844 ([FRI-501](#))
 Castañé, Helena, S616 ([THU-432](#)), S670 ([SAT-425](#)), S676 ([SAT-433](#))
 Castano-García, Andrés, S12 ([LBO-04](#)), S579 ([THU-124](#))
 Castaño González, Luis A, S741 ([WED-408](#))
 Castañón, Ylenia Pérez, S541 ([SAT-238](#)), S917 ([FRI-181](#))
 Casteleyn, Christophe, S226 ([THU-361](#))
 Castellana, Fabio, S495 ([FRI-280](#))
 Castellana, Antonino, S40 ([OS-045](#)), S55 ([OS-070](#)), S374 ([WED-260](#))
 Castellano, Pablo Alonso, S964 ([THU-282](#))
 Castellanos-Fernández, Marlen, S900 ([FRI-151](#))
 Castelli, Florence, S206 ([TOP-046](#))
 Castell, Javier, S703 ([SAT-472](#)), S838 ([FRI-488](#))
 Castello, Borja, S526 ([TOP-072](#))
 Castello, Inmaculada, S392 ([WED-290](#)), S399 ([WED-300](#))
 Castellote, Jose, S1178 ([THU-171](#))
 Castelnuovo, Corinne, S1093 ([WED-159](#))
 Castelnuovo, Gabriele, S521 ([FRI-325](#)), S605 ([THU-415](#)), S611 ([THU-425](#)), S617 ([THU-435](#)), S626 ([THU-452](#)), S637 ([THU-470](#)), S704 ([SAT-474](#)), S713 ([SAT-494](#))
 Castelo, Janire, S532 ([SAT-221](#))
 Castera, Laurent, S61 ([OS-080-YI](#)), S612 ([THU-426](#)), S627 ([THU-453](#)), S646 ([THU-559](#)), S838 ([FRI-489](#))
 Castéra, Laurent, S670 ([SAT-424](#)), S681 ([SAT-440](#)), S817 ([FRI-507](#))
 Castiglione, Anna, S917 ([FRI-180](#))
 Castillo, Anny Camelo, S932 ([FRI-207](#)), S1126 ([WED-208](#))
 Castillo, Carmen, S180 ([FRI-462](#))
 Castillo, Elisa, S19 ([OS-011-YI](#))
 Castillo, Joaquin Andrés, S250 ([WED-343](#))
 Castillo, Laura Muñoz, S1192 ([THU-192](#))
 Castillo, Mauricio, S195 ([FRI-546](#))
 Castillo, Pilar, S964 ([THU-282](#)), S980 ([THU-301](#)), S998 ([THU-331](#)), S1098 ([WED-166](#)), S1105 ([WED-177](#))
 Castoldi, Mirco, S562 ([SAT-279](#))
 Castro, María Cristina Reygosa, S893 ([FRI-140](#))
 Castro-Narro, Graciela, S900 ([FRI-151](#))
 Castro, Rui E., S279 ([WED-390](#)), S734 ([WED-397](#)), S738 ([WED-404](#))

Author Index

- Castro, Vanda, S902 (FRI-154)
- Castven, Darko, S277 (WED-387), S527 (SAT-213), S536 (SAT-230), S547 (SAT-248), S557 (SAT-268)
- Castven, Jovana, S536 (SAT-230), S557 (SAT-268)
- Catalano, Carolyn, S273 (WED-380), S312 (SAT-545), S623 (THU-445), S1011 (THU-390)
- Cataluña, Jose Guillain, S599 (THU-157)
- Caterini, Luciano, S1122 (WED-203)
- Caterino, Tina Di, S657 (SAT-404)
- Cathcart, Andrea, S11 (LBO-02)
- Cattan, Stéphane, S61 (OS-081)
- Cattazzo, Filippo, S203 (FRI-558), S668 (SAT-420), S1190 (THU-188)
- Cattin, Anne-Laure, S75 (OS-105)
- Cauduro, Carolina Gomes Da Silveira, S621 (THU-442)
- Caulder, Alex, S1198 (THU-203)
- Causse, Xavier, S52 (OS-066), S107 (LBP-11)
- Caussy, Cyrielle, S603 (THU-410), S687 (SAT-450), S701 (SAT-469)
- Cavaliere, Maria Lorena, S971 (THU-291)
- Cavalletto, Luisa, S990 (THU-316)
- Cavallone, Daniela, S1091 (WED-157)
- Cavallo, Rossana, S917 (FRI-180)
- Cavassini, Matthias, S101 (LBP-04)
- Cavazza, Anna, S127 (TOP-093)
- Cavicchioni, Alessia, S729 (SAT-517)
- Caviglia, Gian Paolo, S521 (FRI-325), S605 (THU-415), S673 (SAT-430), S704 (SAT-474), S713 (SAT-494), S1056 (TOP-106), S1072 (WED-133)
- Cavoli, Tancredi Li, S513 (FRI-311)
- Çavuş, Bilger, S709 (SAT-485)
- Cayon, Lorena, S709 (SAT-484)
- Cazzagon, Nora, S40 (OS-045), S55 (OS-070), S56 (OS-073), S72 (OS-099), S374 (WED-260), S383 (WED-277), S407 (WED-315)
- Ceausu, Emanoil, S1054 (TOP-100)
- Ceccarelli, Daniele, S837 (FRI-487)
- Ceccherini Silberstein, Francesca, S1072 (WED-133), S1122 (WED-203)
- Cederborg, Anna, S276 (WED-384)
- Cedr s, Susana, S375 (WED-263)
- Ceesay, Amie, S1106 (WED-178), S1106 (WED-179)
- Celada-Sendino, Miriam, S171 (FRI-445), S1098 (WED-166)
- Celaj, Stela, S385 (WED-279)
- Celen, Mustafa, S1137 (SAT-152)
- Celik, Ferya, S852 (WED-490)
- Cellner, Linda, S553 (SAT-261)
- Celsa, Ciro, S374 (WED-260), S592 (THU-144), S1118 (WED-196)
- Cendron, Laura, S766 (WED-449)
- Ceni, Elisabetta, S545 (SAT-245), S550 (SAT-254)
- Centelles, Eva, S489 (THU-546)
- Centola, Cielo, S735 (WED-398)
- Cereda, Danilo, S920 (FRI-185)
- Cerezo-Wallis, Daniela, S78 (OS-109-YI)
- Cerini, Federica, S374 (WED-260)
- Cerioti, Ferruccio, S669 (SAT-422), S1154 (SAT-175), S1159 (SAT-181), S1164 (SAT-190), S1170 (SAT-199)
- Cerminara, Dana, S975 (THU-294)
- Cerocchi, Orlando, S503 (FRI-293)
- Cervantes, Vanessa, S648 (TOP-075)
- Cervello, Melchiorre, S568 (SAT-288)
- Cervenka, Igor, S945 (THU-255)
- Cervera, Marta, S15 (OS-001), S163 (FRI-431), S250 (WED-343), S664 (SAT-415), S851 (WED-486)
- Cervoni, Jean Paul, S318 (SAT-556), S975 (THU-295)
- Cesaro, Simone, S88 (OS-124-YI)
- Cescon, Matteo, S519 (FRI-322)
- Cespiati, Annalisa, S500 (FRI-288), S632 (THU-461), S645 (THU-557), S668 (SAT-420), S722 (SAT-506), S814 (FRI-474)
- Ceuleers, Hannah, S776 (WED-466), S790 (WED-523)
- Chabert, Christian, S762 (WED-442)
- Chacon, Carla, S664 (SAT-415)
- Ch fer, Isabel Terol, S476 (THU-517)
- Chaganti, Joga, S263 (WED-364)
- Chaidez, Alexander, S971 (THU-291)
- Chaigneau, Julien, S672 (SAT-427)
- Chai, Jin, S760 (WED-439)
- Chainuvati, Siwaporn, S19 (OS-009), S237 (WED-321), S502 (FRI-292)
- Chairprasert, Amnart, S262 (WED-360)
- Chaiwiriawong, Supakorn, S514 (FRI-314)
- Chalasani, Naga, S171 (FRI-444), S612 (THU-427), S649 (TOP-080)
- Chalkidou, Anna, S1128 (WED-211)
- Challis, Benjamin, S344 (THU-228)
- Chaltin, Patrick, S1025 (FRI-231)
- Chalut, Kevin, S122 (LBP-34)
- Cham, Hawa, S67 (OS-090-YI)
- Chamroonkul, Naichaya, S514 (FRI-314), S721 (SAT-503)
- Chamseddine, Shadi, S582 (THU-128)
- Chan, Connie, S431 (FRI-368)
- Chanda, Sushmita, S112 (LBP-18), S1029 (FRI-238), S1030 (FRI-241), S1162 (SAT-188), S1164 (SAT-192)
- Chandes, Florine, S673 (SAT-429), S694 (SAT-461)
- Chandnani, Sanjay, S405 (WED-312), S643 (THU-553)
- Chan, Doreen, S808 (TOP-091), S820 (FRI-512)
- Chandramouli, Abhishek Shankar, S620 (THU-440)
- Chandra, Nidhi, S790 (WED-522)
- Chandran, Vineesh Indira, S629 (THU-455), S657 (SAT-404)
- Chan, Eric, S1087 (WED-151), S1115 (WED-191)
- Chang, Chun-Chao, S1180 (THU-174)
- Chang, De-Hua, S594 (THU-147)
- Chang, Devon Y., S659 (SAT-408)
- Chang, Eu, S300 (SAT-522)
- Chang, Felicia, S644 (THU-555), S710 (SAT-487)
- Chang, Jason Pik Eu, S283 (SAT-327), S334 (WED-238)
- Chang, Nakho, S817 (FRI-506)
- Chang, Sandra, S1030 (FRI-241)
- Chang, Silvia, S1055 (TOP-103)
- Chang, Te-Sheng, S1180 (THU-174), S1206 (THU-217)
- Chang, Ting, S85 (OS-120)
- Chang, Xiu-Juan, S1085 (WED-149)
- Chang, Ying, S1152 (SAT-173)
- Chang, Young, S916 (FRI-179)
- Chang, Yujiao, S1143 (SAT-161)
- Chan, Henry LY, S29 (OS-025), S506 (FRI-298), S507 (FRI-300), S1064 (WED-123), S1131 (SAT-144), S1132 (SAT-145), S1137 (SAT-153), S1146 (SAT-166), S1148 (SAT-167)
- Chan, Kai En, S629 (THU-456)
- Chan, Kwan Shuen, S537 (SAT-231)
- Chan, Russell, S680 (SAT-439)
- Chan, Stephen, S1 (GS-002-YI), S12 (LBO-04)
- Chanteranne, Brigitte, S172 (FRI-446)
- Chan, Wah-Kheong, S29 (OS-025), S644 (THU-555), S710 (SAT-487), S721 (SAT-503), S863 (SAT-125)
- Chan, Wah Loong, S644 (THU-555), S710 (SAT-487)
- Chao, Hann-Hsiang, S832 (FRI-478)
- Chapin, Catherine, S961 (THU-278)
- Chapman, Brooke, S311 (SAT-543)
- Chapman, Kath, S182 (FRI-464)
- Chappell, Catherine, S913 (FRI-174)
- Chappidi, Sridhar Reddy, S209 (THU-339)
- Charatcharoenwittaya, Phunchai, S19 (OS-009), S237 (WED-321), S721 (SAT-503)
- Charatcharoenwittaya, Punchai, S502 (FRI-292)
- Charlotte, Frederic, S607 (THU-418), S651 (SAT-394)
- Charlton, Michael, S29 (OS-026), S30 (OS-027), S604 (THU-413), S619 (THU-438), S619 (THU-439), S643 (THU-552), S655 (SAT-401)
- Charre, Caroline, S1170 (SAT-199)
- Charri re, Sybil, S603 (THU-410)
- Charton, Julie, S954 (THU-267)
- Chartouni, Maria, S1093 (WED-159)
- Charu, Vivek, S25 (OS-020-YI), S81 (OS-115-YI)
- Cha, Sang-Hoon, S414 (FRI-336), S752 (WED-427)
- Chascsa, David, S590 (THU-141)
- Chattergoon, Michael, S32 (OS-031), S1079 (WED-141)
- Chatterjee, Saurabh, S800 (WED-544)
- Chattopadhyay, Sutirtha, S442 (TOP-053)
- Chaudhan, Neha, S187 (FRI-533)
- Chaudhri, Eirum, S49 (OS-060)
- Chaudhry, Afzal, S1075 (WED-137)
- Chaudhry, Asad, S912 (FRI-172)

- Chaudhry, Auj, S912 (FRI-172),
S1196 (THU-200)
- Chau, Mary, S422 (FRI-356)
- Chavanelle, Vivien, S806 (WED-555)
- Chavey, Carine, S534 (SAT-225)
- Chávez-Tapia, Norberto Carlos,
S865 (SAT-129), S900 (FRI-151)
- Chayama, Kazuaki, S72 (OS-098),
S1017 (FRI-216)
- Chazouillères, Olivier, S408 (WED-317)
- Chazouillères, Olivier, S56 (OS-073),
S498 (FRI-286)
- Chbourk, Sara, S842 (FRI-496)
- Cheesbrough, Jonathan, S123 (LBP-36)
- Cheetham, Rob, S1182 (THU-176)
- Chegary, Malika, S677 (SAT-434)
- Chemello, Liliana, S990 (THU-316),
S1082 (WED-146)
- Chemin, Isabelle, S1046 (FRI-265),
S1106 (WED-178), S1106 (WED-179)
- Chen, Alexander, S623 (THU-445)
- Chen, Chao, S304 (SAT-530)
- Chen, Chengwei, S130 (THU-398)
- Chen, Cheng-Yi, S999 (THU-333)
- Chen, Chien-Hung, S52 (OS-065-YI),
S1132 (SAT-145), S1134 (SAT-148)
- Chen, Chien-Jen, S1060 (WED-118)
- Chen, Chien-Lin, S1206 (THU-217)
- Chen, Chi-Yi, S125 (LBP-38),
S1159 (SAT-182), S1206 (THU-217)
- Chen, Chiyi, S1169 (SAT-198),
S1180 (THU-174)
- Chen, Chun-Ting, S1180 (THU-174),
S1206 (THU-217)
- Chen, Dongbo, S503 (FRI-294),
S540 (SAT-235), S554 (SAT-262)
- Chen, Doris, S564 (SAT-282)
- Chen, Elizabeth, S1096 (WED-165)
- Chen, Frederick, S964 (THU-283)
- Cheng, Alfred Sze-Lok, S1 (GS-002-YI),
S530 (SAT-217)
- Cheng, Andrew, S808 (TOP-091),
S820 (FRI-512)
- Chen, Gang, S488 (THU-540)
- Cheng, Ann-Lii, S9 (GS-011),
S588 (THU-138)
- Cheng, Chien-Yu, S1180 (THU-174),
S1206 (THU-217)
- Cheng, Cho-Chin, S945 (THU-256),
S1026 (FRI-233), S1040 (FRI-256)
- Cheng, Feng, S455 (THU-477)
- Cheng, Guofeng, S1156 (SAT-178)
- Cheng, Ho Ming, S62 (OS-082),
S490 (TOP-068)
- Cheng, Hong Sheng, S79 (OS-111)
- Cheng, Hsu-sheng, S895 (FRI-143)
- Cheng, Hui, S1166 (SAT-194)
- Cheng, Pin-Nan, S1083 (WED-147),
S1140 (SAT-157), S1159 (SAT-182),
S1180 (THU-174), S1206 (THU-217)
- Cheng, Tsung-Yi, S252 (WED-346)
- Chen, Guan-Ju, S825 (FRI-521)
- Chen, Guei-Ying, S1180 (THU-174),
S1206 (THU-217)
- Chen, Guowei, S1156 (SAT-178)
- Cheng, Xuyu, S455 (THU-477)
- Cheng, Yongqian, S1166 (SAT-194)
- Chen, Hening, S153 (FRI-417),
S1076 (WED-138)
- Chen, Hong, S110 (LBP-14)
- Chen, Hongsong, S503 (FRI-294),
S540 (SAT-235), S554 (SAT-262)
- Chen, Hsiu-Hsi, S891 (FRI-137)
- Chen, Hui, S1165 (SAT-193)
- Chen, Jialiang, S193 (FRI-544),
S404 (WED-309)
- Chen, Jie, S581 (THU-126)
- Chen, Jingyi, S291 (SAT-339)
- Chen, Jinjun, S189 (FRI-536),
S195 (FRI-546), S196 (FRI-547),
S202 (FRI-556), S308 (SAT-539)
- Chen, Jinzhang, S525 (TOP-070)
- Chen, Jonathan, S58 (OS-075)
- Chen, Junling, S543 (SAT-242),
S557 (SAT-269)
- Chen, Jyh-Jou, S1083 (WED-147),
S1140 (SAT-157)
- Chen, Kaina, S519 (FRI-321),
S582 (THU-129), S591 (THU-142)
- Chen, Lan, S1198 (THU-204)
- Chen, Lei, S34 (OS-033)
- Chen, Li, S327 (WED-224), S651 (SAT-394),
S715 (SAT-496), S805 (WED-553)
- Chen, Liangxing, S557 (SAT-269)
- Chen, Linda, S67 (OS-091)
- Chen, Li-Tzong, S588 (THU-138)
- Chen, Mei-Tsu, S895 (FRI-143)
- Chen, Min, S1036 (FRI-250)
- Chen, Mingjing, S1143 (SAT-161)
- Chen, Minshan, S9 (GS-011)
- Chen, Pan, S117 (LBP-24)
- Chen, Pei-Jer, S1061 (WED-119),
S1140 (SAT-157)
- Chen, Peng, S543 (SAT-242), S557 (SAT-269)
- Chen, Po-Hsuan Cameron, S671 (SAT-426)
- Chen, Pu, S554 (SAT-262)
- Chen, Qi, S1024 (FRI-229)
- Chen, Sam Li-Sheng, S891 (FRI-137)
- Chen, San-Chi, S588 (THU-138)
- Chen, Shijia, S784 (WED-510)
- Chen, Shin-Wei, S825 (FRI-521)
- Chen, Shiou-Shiang, S891 (FRI-137)
- Chen, Shuai, S745 (WED-416)
- Chen, Sui-Dan, S613 (THU-428)
- Chen, Tianlu, S100 (LBP-02)
- Chen, Tianyan, S426 (FRI-363),
S1115 (WED-191)
- Chen, Vincent, S609 (THU-422),
S611 (THU-424), S658 (SAT-406),
S703 (SAT-473)
- Chen, Wei, S80 (OS-113), S956 (THU-270)
- Chen, Wei-Chia, S361 (FRI-385)
- Chen, Wenyi, S753 (WED-429)
- Chen, Xiaolan, S525 (TOP-070)
- Chen, Xiaoru, S213 (THU-344)
- Chen, Xin, S186 (FRI-342)
- Chen, Yajin, S488 (THU-540)
- Chen, Yan, S1085 (WED-149)
- Chen, Yang, S960 (THU-277)
- Chen, Yanhong, S520 (FRI-323)
- Chen, Yaxi, S574 (THU-115),
S580 (THU-125)
- Chen, Yen-Hao, S588 (THU-138)
- Chen, Yi, S967 (THU-286)
- Chen, Yongpeng, S1085 (WED-149)
- Chen, Yu, S235 (TOP-047), S1153 (SAT-174)
- Chen, Yue, S153 (FRI-417)
- Chen, Yu-Jen, S252 (WED-346)
- Chen, Yujie, S109 (LBP-13)
- Chen, Yun, S395 (WED-294),
S1096 (WED-164)
- Chen, Yunfu, S109 (LBP-13)
- Chen, Yunliang, S696 (SAT-463),
S724 (SAT-510)
- Chen, Zhengming, S69 (OS-093-YI)
- Chen, Zih-Hua, S1058 (WED-113)
- Cheong, Jae Youn, S572 (TOP-071)
- Cheon, Jaekyung, S575 (THU-116),
S582 (THU-128), S586 (THU-134),
S592 (THU-143), S593 (THU-145)
- Cheow, Peng Chung, S591 (THU-142)
- Cher, Gabriel, S300 (SAT-522)
- Chermak, Faiza, S318 (SAT-556),
S467 (THU-498)
- Cherqui, Daniel, S458 (THU-483)
- Cherradi, Sara, S541 (SAT-237)
- Cherubini, Alessandro, S500 (FRI-288),
S733 (WED-393)
- Chessa, Luchino, S40 (OS-045),
S55 (OS-070), S105 (LBP-09)
- Chetcuti, Karen, S522 (FRI-327)
- Cheuk-Fung Yip, Terry, S1069 (WED-129),
S1085 (WED-149)
- Cheung, Allen KL, S942 (THU-252),
S946 (THU-257)
- Cheung, Angela, S426 (FRI-363)
- Cheung, Chin-Cheung, S490 (TOP-068)
- Cheung, Ka Shing, S62 (OS-082)
- Cheung, Pak-To, S680 (SAT-439)
- Cheung, Ramsey C., S1084 (WED-148),
S1096 (WED-165), S1107 (WED-180)
- Cheung, Tan-to, S48 (OS-058)
- Cheung, Veronica Wing I, S1195 (THU-198)
- Chevaliez, Stéphane, S1106 (WED-178),
S1106 (WED-179), S1109 (WED-182),
S1150 (SAT-169), S1160 (SAT-183)
- Chevré, Raphael, S351 (THU-237)
- Chew, Yun, S179 (FRI-459)
- Chia, Nam-Hung, S490 (TOP-068)
- Chiang, CL, S62 (OS-082)
- Chiappori, Federica, S772 (WED-459)
- Chiara, Francesco De, S205 (TOP-042)
- Chiche, Jean-Daniel, S189 (FRI-537)
- Chiche, Laurence, S473 (THU-511)
- Chi, Chen-Ta, S1172 (THU-163)
- Chico, Inmaculada, S587 (THU-136)
- Chidambaram, Nachaippan,
S260 (WED-358), S809 (FRI-466)
- Chien, Elaine, S387 (WED-282)
- Chien, Rong-Nan, S52 (OS-065-YI),
S1067 (WED-126), S1083 (WED-147),
S1088 (WED-152), S1132 (SAT-145)

Author Index

- Chien, Shih-Chieh, S1140 (SAT-157)
 Childs, Kate, S1179 (THU-172)
 Chi, Li-Chi, S361 (FRI-385)
 Chim, Angel Mei-Ling, S1148 (SAT-167)
 Chin, Allison, S304 (SAT-532)
 China, Louise, S74 (OS-103-YI), S975 (THU-295)
 Chinaroonchai, Tanongsak, S237 (WED-321)
 Chinellato, Monica, S766 (WED-449)
 Ching, Carmen, S246 (WED-339)
 Chin, Mike, S5 (GS-005)
 Chiou, Fang Kuan, S123 (LBP-35), S387 (WED-282)
 Chiou, Jen-Jie, S252 (WED-346)
 Chirapongsathorn, Sakkarin, S262 (WED-360)
 Chirouze, Catherine, S994 (THU-322)
 Chi, Susan, S414 (FRI-336), S752 (WED-427)
 Chittajallu, Vibhu, S385 (WED-279)
 Chiu, Chang-Fang, S588 (THU-138)
 Chiu, Keith Wan Hang, S490 (TOP-068)
 Chiu, SM, S1134 (SAT-148)
 Chiu, Yencheng, S1140 (SAT-157)
 Chi, Xiumei, S117 (LBP-24)
 Chkhartishvili, Nikoloz, S881 (FRI-123), S921 (FRI-187), S1204 (THU-214)
 Chng, Elaine, S65 (OS-087), S112 (LBP-17), S333 (WED-236), S334 (WED-237), S334 (WED-238), S501 (FRI-290), S757 (WED-436), S762 (WED-443), S806 (TOP-076), S824 (FRI-518), S999 (THU-333)
 Cho, Dana, S548 (SAT-251)
 Chodik, Gabriel, S1195 (THU-199)
 Cho, Eun Ju, S510 (FRI-306), S610 (THU-423)
 Cho, Eun Young, S438 (SAT-362), S712 (SAT-491), S1136 (SAT-151)
 Chohan, Aishwarya, S901 (FRI-152)
 Cho, Heejin, S494 (FRI-278), S513 (FRI-312), S1062 (WED-120)
 Cho, Hyo Jung, S572 (TOP-071)
 Choi, Dongho, S437 (SAT-361), S456 (THU-479), S563 (SAT-281), S947 (THU-258)
 Choi, Eunho, S798 (WED-540)
 Choi, Gwang Hyeon, S583 (THU-130), S916 (FRI-179)
 Choi, Gyu-Seong, S471 (THU-506), S474 (THU-513)
 Choi, Hannah S.J., S1132 (SAT-145)
 Choi, Hwa Young, S407 (WED-316), S916 (FRI-179)
 Choi, In Young, S758 (WED-437), S779 (WED-473)
 Choi, Jonggi, S393 (WED-292), S573 (THU-113), S589 (THU-140), S998 (THU-330), S1062 (WED-121), S1130 (TOP-105), S1139 (SAT-155)
 Choi, Jong Young, S148 (FRI-409)
 Choi, Joon-Il, S508 (FRI-301)
 Choi, Mi Ran, S156 (FRI-420), S343 (THU-227)
 Choi, Moon Seok, S267 (WED-369), S305 (SAT-533), S631 (THU-459), S821 (FRI-514)
 Choi, Myeung Gi, S141 (FRI-401)
 Choi, Sung Chul, S631 (THU-459)
 Choi, Sung Eun, S25 (OS-021-YI)
 Choi, Tae-Young, S438 (SAT-362)
 Choi, Won-Mook, S573 (THU-113), S589 (THU-140), S998 (THU-330), S1062 (WED-121), S1130 (TOP-105), S1139 (SAT-155)
 Choi, Yun-Jung, S338 (WED-246), S367 (TOP-063), S371 (WED-256)
 Cho, Jai Young, S583 (THU-130)
 Cho, Jang Hwan, S773 (WED-460)
 Cho, Ju-Yeon, S637 (THU-469), S697 (SAT-464)
 Chokkalingam, Anand, S1059 (WED-116)
 Chokshi, Shilpa, S324 (WED-218), S324 (WED-219), S432 (FRI-371)
 Cho, Kyung Joo, S362 (FRI-387), S552 (SAT-259)
 Cholankeril, George, S173 (FRI-448), S472 (THU-508)
 Chollet, Celine, S206 (TOP-046)
 Cholongitas, Evangelos, S400 (WED-302), S1128 (WED-211)
 Chong, Kediende, S69 (OS-094)
 Chong, Lee-Won, S1180 (THU-174), S1206 (THU-217)
 Chong, Shi-En, S644 (THU-555), S710 (SAT-487)
 Chon, Hong Jae, S575 (THU-116), S582 (THU-128), S586 (THU-134), S592 (THU-143)
 Chon, Young Eun, S757 (WED-435), S829 (FRI-527), S916 (FRI-179), S1078 (WED-139)
 Choong, Ingrid, S9 (GS-012)
 Chotiyaputta, Watcharasak, S19 (OS-009), S237 (WED-321), S502 (FRI-292)
 Chotkoe, Shivani, S776 (WED-466), S790 (WED-523)
 Choudhry, Asad, S1196 (THU-200)
 Choudhry, Naheed, S912 (FRI-172)
 Choudhry, Sabina, S179 (FRI-459)
 Choudhury, Ashok, S191 (FRI-539), S195 (FRI-546), S274 (WED-382)
 Choudhury, Tahmid, S803 (WED-548)
 Chouik, Yasmina, S118 (LBP-27), S687 (SAT-450), S701 (SAT-469)
 Chou, Kwok-Hsiung, S1206 (THU-217)
 Chounta, Athina, S400 (WED-302)
 Chou, Wen-Min, S1026 (FRI-233)
 Chowdhury, Swapan, S115 (LBP-22)
 Chowdhury, Tasadduk, S516 (FRI-317)
 Chow, Pierce, S9 (GS-011), S582 (THU-129), S591 (THU-142)
 Chow, Victor Yung Sin, S1195 (THU-198)
 Cho, Yong Kyun, S637 (THU-469), S697 (SAT-464), S1073 (WED-135)
 Cho, Young Seo, S834 (FRI-482)
 Cho, Young Youn, S690 (SAT-455), S698 (SAT-466), S705 (SAT-477), S712 (SAT-491)
 Cho, Yuri, S117 (LBP-25), S510 (FRI-306), S642 (THU-550)
 Christensen-Dalsgaard, Mikkel, S321 (TOP-036)
 Christensen, Lee, S848 (WED-480)
 Christensen, Peer Brehm, S880 (FRI-121)
 Christensen, Stefan, S1174 (THU-166)
 Christinet, Montserrat Fraga, S105 (LBP-08), S481 (THU-526)
 Christodoulou, Dimitrios, S400 (WED-302), S922 (FRI-189), S1128 (WED-211)
 Chua, Damien, S79 (OS-111)
 Chuah, Kee Huat, S644 (THU-555), S710 (SAT-487)
 Chuang, Wan-Long, S53 (OS-067), S125 (LBP-38), S1023 (FRI-226), S1137 (SAT-153), S1159 (SAT-182), S1169 (SAT-198), S1180 (THU-174), S1206 (THU-217)
 Chua, Sin Hui Melissa, S698 (SAT-467), S714 (SAT-495)
 Chua, Siou Sze, S591 (THU-142)
 Chuaypen, Natthaya, S354 (THU-243), S356 (THU-245)
 Chu, Chi-Jen, S1172 (THU-163)
 Chu, Kai-Min, S825 (FRI-521)
 Chulanov, Vladimir, S53 (OS-068), S1091 (WED-158)
 Chung, Alexander, S591 (THU-142)
 Chung, Brian K., S364 (FRI-390), S420 (FRI-353), S421 (FRI-355), S428 (FRI-365)
 Chung, Chuhan, S31 (OS-029), S737 (WED-401)
 Chung, Clive Yik Sham, S537 (SAT-231)
 Chung, Diana, S659 (SAT-407)
 Chung, Goh Eun, S510 (FRI-306), S642 (THU-550)
 Chung, Nakia, S81 (OS-115-YI)
 Chung, Raymond, S58 (OS-075)
 Chung, Sungwon, S610 (THU-423), S630 (THU-457), S635 (THU-466), S1048 (FRI-268), S1062 (WED-120), S1144 (SAT-163)
 Chung, Woo Jin, S588 (THU-137)
 Chung, Yooyun, S432 (FRI-371), S962 (THU-280)
 Chun, Ho Soo, S585 (THU-132), S1065 (WED-124)
 Chu, Niansheng, S450 (SAT-386)
 Chupina, Vilena, S767 (WED-451)
 Chu, Po-sung, S156 (FRI-421), S409 (TOP-060)
 Chu, Xin-Jie, S784 (WED-510)
 Chu, Yin-Lun, S48 (OS-058)
 Ciaccio, Antonio, S992 (THU-319)
 Ciano, Alessia, S107 (LBP-11), S917 (FRI-180), S1072 (WED-133), S1082 (WED-146), S1177 (THU-169), S1200 (THU-206)
 Ciaranello, Andrea, S878 (FRI-119)

- Ciarnelli, Martina, S750 ([WED-424](#))
 Ciccarelli, Olga, S464 ([THU-493](#))
 Ciccia, Roberta, S592 ([THU-144](#))
 Ciccioli, Carlo, S673 ([SAT-430](#))
 Ciceri, Fabio, S88 ([OS-124-YI](#))
 Ciclet, Olivier, S762 ([WED-442](#))
 Cid, Joan, S131 ([THU-399](#))
 Ciesek, Sandra, S113 ([LBP-20](#))
 Ciglemecki, Iza, S69 ([OS-094](#))
 Ciliberto, Domenico, S568 ([SAT-288](#))
 Cillo, Umberto, S293 ([SAT-343](#)),
 S480 ([THU-523](#)), S564 ([SAT-283](#)),
 S1056 ([TOP-106](#))
 Cimermancic, Peter, S671 ([SAT-426](#))
 Cinque, Felice, S632 ([THU-461](#)),
 S645 ([THU-557](#)), S814 ([FRI-474](#))
 Ciordia, Sergio, S537 ([SAT-232](#))
 Ciotti, Marco, S1122 ([WED-203](#))
 Cipolli, Marco, S974 ([THU-293](#))
 Cirella, Antonio, S685 ([SAT-446](#))
 Cirera, Isabel, S105 ([LBP-09](#))
 Cirillo, Chris, S985 ([THU-310](#))
 Ciriminna, Rosaria, S568 ([SAT-288](#))
 Citores, María Jesus, S1194 ([THU-195](#))
 Ciudin, Andreea, S349 ([THU-235](#))
 Ciupkeviciene, Egle, S912 ([FRI-173](#))
 Cives-Losada, Candela, S551 ([SAT-256](#))
 Civitarese, Antonio, S41 ([OS-046](#)),
 S378 ([WED-267](#))
 Claar, Ernesto, S36 ([OS-036](#))
 Claeys, Wouter, S229 ([THU-364](#))
 Clancy, Jennifer-Louise, S660 ([SAT-409](#)),
 S661 ([SAT-410](#)), S812 ([FRI-471](#))
 Clària, Joan, S143 ([FRI-404](#)),
 S206 ([TOP-046](#)), S222 ([THU-356](#)),
 S452 ([SAT-390](#))
 Clark, Doug, S1162 ([SAT-188](#))
 Clark, James, S78 ([OS-110](#))
 Clark, Paul, S176 ([FRI-453](#))
 Clark, Sarah, S284 ([SAT-329](#)),
 S1129 ([WED-213](#))
 Clark, Virginia, S85 ([OS-120](#)),
 S1008 ([THU-386](#))
 Clasen, Frederick, S205 ([TOP-042](#))
 Classen, Arno, S350 ([THU-236](#))
 Classen, Marc, S892 ([FRI-138](#))
 Claudel, Thierry, S739 ([WED-405](#)),
 S746 ([WED-418](#))
 Clauditz, Till, S60 ([OS-079-YI](#))
 Clausen, Susan, S101 ([LBP-03](#))
 Clavel, Thomas, S22 ([OS-015](#))
 Claveria-Cabello, Alex, S537 ([SAT-232](#))
 Clawson, Alicia, S115 ([LBP-22](#))
 Clayton-Chubb, Daniel, S622 ([THU-443](#))
 Cleary, Sean, S44 ([OS-050-YI](#)),
 S465 ([THU-495](#))
 Clemens Broering, Dieter, S969 ([THU-289](#)),
 S1011 ([THU-388](#))
 Clemente, Ana, S145 ([TOP-073](#)),
 S164 ([FRI-433](#)), S171 ([FRI-445](#))
 Clemente, Nausicaa, S751 ([WED-425](#))
 Clément-Leboube, Sophie,
 S751 ([WED-426](#))
 Clement, Thomas, S45 ([OS-052](#))
 Clemson, Christine, S938 ([TOP-057](#)),
 S965 ([THU-284](#)), S969 ([THU-289](#)),
 S987 ([THU-313](#)), S1003 ([THU-378](#))
 Cloherty, Gavin, S67 ([OS-090-YI](#)),
 S1081 ([WED-143](#)), S1081 ([WED-144](#)),
 S1106 ([WED-178](#))
 Cloutier, Daniel, S11 ([LBO-02](#)),
 S32 ([OS-031](#)), S1156 ([SAT-177](#))
 Clusmann, Jan, S492 ([FRI-275](#)),
 S636 ([THU-467](#))
 Cmet, Sara, S402 ([WED-306](#)),
 S1135 ([SAT-149](#))
 Cnop, Miriam, S621 ([THU-442](#))
 Cobbold, Jeremy, S708 ([SAT-483](#))
 Cobham, Ansa, S735 ([WED-398](#))
 Cobreros, Marina, S390 ([WED-288](#))
 Cocca, Massimiliano, S1018 ([FRI-218](#))
 Cocchis, Donatella, S455 ([TOP-059](#))
 Cocherie, Théophile, S1044 ([FRI-261](#))
 Cochran, Blake, S351 ([THU-237](#))
 Coco, Barbara, S40 ([OS-045](#)), S55 ([OS-070](#)),
 S691 ([SAT-456](#)), S1082 ([WED-146](#)),
 S1091 ([WED-157](#))
 Cocolin, Luca Simone, S804 ([WED-551](#))
 Codoceo, Carolina Muñoz, S964 ([THU-282](#)),
 S980 ([THU-301](#)), S998 ([THU-331](#))
 Codotto, Gabriele, S952 ([THU-265](#))
 Coelho, Henrique, S1111 ([WED-185](#))
 Coelho, Henrique Sergio, S618 ([THU-436](#))
 Coelho, Henrique Sérgio, S658 ([SAT-405](#))
 Coelho, Rosa, S835 ([FRI-483](#))
 Coello, Elena, S682 ([SAT-442](#))
 Coenen, Sandra, S306 ([SAT-536](#))
 Coffin, Carla, S875 ([FRI-115](#)),
 S1115 ([WED-191](#)), S1117 ([WED-194](#))
 Coghlan, Miriam, S16 ([OS-004](#)),
 S850 ([WED-484](#)), S1211 ([THU-223](#))
 Cohen-Bacrie, Claude, S722 ([SAT-505](#)),
 S769 ([WED-453](#)), S777 ([WED-469](#))
 Cohen, Chari, S1087 ([WED-151](#))
 Cohen, Damien, S1046 ([FRI-265](#))
 Cohen-ezra, Oranit, S719 ([SAT-500](#))
 Coilly, Audrey, S74 ([OS-104](#)), S189 ([FRI-537](#)),
 S467 ([THU-498](#)), S981 ([THU-303](#)),
 S1005 ([THU-380](#))
 Colapietro, Francesca, S40 ([OS-045](#)),
 S44 ([OS-049-YI](#)), S55 ([OS-070](#))
 Cola, Simone Di, S950 ([THU-261](#))
 Colavolpe, Lucia, S632 ([THU-461](#))
 Colca, Jerry, S826 ([FRI-522](#))
 Colecchia, Antonio, S86 ([OS-121-YI](#)),
 S88 ([OS-124-YI](#)), S283 ([SAT-327](#)),
 S287 ([SAT-334](#)), S519 ([FRI-322](#)),
 S609 ([THU-421](#)), S974 ([THU-293](#))
 Colecchia, Luigi, S88 ([OS-124-YI](#)),
 S974 ([THU-293](#))
 Coletta, Sergio, S493 ([FRI-277](#))
 Collado, Francina, S116 ([LBP-23](#))
 Collazos, Cristina, S135 ([THU-406](#)),
 S885 ([FRI-128](#)), S995 ([THU-325](#))
 Colledan, Michele, S471 ([THU-507](#))
 Colle, Isabelle, S975 ([THU-295](#))
 Colli, Agostino, S283 ([SAT-327](#))
 Collier, Jane, S309 ([SAT-541](#))
 Collier, Mathis, S656 ([SAT-402](#))
 Collins, Amy, S538 ([SAT-234](#)),
 S542 ([SAT-239](#)), S565 ([SAT-284](#))
 Collins, Michelle, S1186 ([THU-181](#))
 Coll, M, S560 ([SAT-275](#))
 Coll, Mar, S38 ([OS-042-YI](#)),
 S250 ([WED-343](#)), S737 ([WED-403](#))
 Coll, Susana, S267 ([WED-370](#)),
 S273 ([WED-381](#))
 Colmenero, Jordi, S461 ([THU-487](#)),
 S481 ([THU-525](#))
 Colnot, Nathalie, S776 ([WED-467](#))
 Colnot, Sabine, S27 ([OS-023-YI](#))
 Colognesi, Martina, S770 ([WED-456](#)),
 S791 ([WED-525](#))
 Cologni, Giuliana, S1173 ([THU-165](#))
 Colombatto, Piero, S691 ([SAT-456](#)),
 S1091 ([WED-157](#)), S1134 ([SAT-148](#))
 Colombo, Massimo, S1173 ([THU-165](#)),
 S1189 ([THU-185](#))
 Colominas, Elena, S267 ([WED-370](#)),
 S273 ([WED-381](#))
 Colom, Joan, S903 ([FRI-156](#)), S913 ([FRI-175](#))
 Colomo, Alan, S105 ([LBP-09](#))
 Colosimo, Santo, S708 ([SAT-483](#))
 Colyn, Leticia, S143 ([FRI-405](#))
 Combail, Jean Philippe, S989 ([THU-314](#))
 Comella, Federica, S797 ([WED-535](#)),
 S800 ([WED-542](#))
 Comoz, Bertille, S82 ([OS-117](#))
 Conaldi, Pier Giulio, S457 ([THU-480](#))
 Conde, Isabel, S133 ([THU-404](#)),
 S180 ([FRI-462](#)), S366 ([TOP-061](#)),
 S392 ([WED-290](#)), S470 ([THU-503](#)),
 S481 ([THU-525](#)), S1205 ([THU-216](#))
 Conde, Marta Hernandez, S1178 ([THU-171](#))
 Conde, Marta Hernández, S272 ([WED-378](#)),
 S291 ([SAT-340](#)), S683 ([SAT-443](#)),
 S693 ([SAT-460](#)), S709 ([SAT-484](#)),
 S1098 ([WED-166](#))
 Congregado, Daniela Mestre,
 S738 ([WED-404](#))
 Connelly, Crystal, S830 ([FRI-529](#))
 Connelly, Margery A., S171 ([FRI-444](#)),
 S666 ([SAT-417](#))
 Connor, Jason, S176 ([FRI-453](#))
 Consortium, The ID LIVER, S84 ([OS-119-YI](#))
 Contegiacomo, Andrea, S981 ([THU-302](#))
 Conti, Fabio, S584 ([THU-131](#)),
 S1082 ([WED-146](#))
 Conti, Filomena, S62 ([OS-083-YI](#)),
 S266 ([WED-368](#)), S467 ([THU-498](#)),
 S473 ([THU-511](#)), S487 ([THU-538](#))
 Contreras, Heidi, S1167 ([SAT-195](#))
 Contreras, Jorge, S840 ([FRI-492](#))
 Conway, Alexander, S815 ([FRI-475](#))
 Conway, Brian, S920 ([FRI-186](#)),
 S929 ([FRI-200](#))
 Conza, Giusy Di, S761 ([WED-441](#))
 Cook, Amelia, S1106 ([WED-178](#))
 Cook, Christi, S960 ([THU-277](#))
 Cooke, Graham, S1075 ([WED-137](#))
 Cooney, Rachel, S123 ([LBP-36](#)),
 S368 ([WED-251](#))

Author Index

- Cooper, Curtis, S1115 ([WED-191](#)), S1117 ([WED-194](#))
- Cooreman, Michael, S651 ([SAT-393](#)), S823 ([FRI-517](#))
- Coppola, Carmine, S1082 ([WED-146](#))
- Coppola, Nicola, S107 ([LBP-11](#)), S1082 ([WED-146](#))
- Corbat, Agustin, S435 ([SAT-357](#))
- Corchado, Cristina, S481 ([THU-525](#))
- Cordero, Patricia, S1126 ([WED-208](#))
- Cordero, Paul, S205 ([TOP-042](#))
- Cordie, Ahmed, S840 ([FRI-491](#))
- Cordingley, Jeremy, S220 ([THU-355](#))
- Cordova, Jacqueline, S195 ([FRI-546](#))
- Corey, Kathleen, S612 ([THU-427](#)), S620 ([THU-440](#))
- Coriat, Romain, S859 ([SAT-120](#))
- Corleone, Giacomo, S1018 ([FRI-218](#))
- Corlianò, Maria, S351 ([THU-237](#))
- Cornberg, Markus, S52 ([OS-065-YI](#)), S53 ([OS-068](#)), S108 ([LBP-12](#)), S113 ([LBP-20](#)), S229 ([THU-365](#)), S283 ([SAT-328](#)), S301 ([SAT-525](#)), S315 ([SAT-551](#)), S1029 ([FRI-240](#)), S1031 ([FRI-242](#)), S1032 ([FRI-244](#)), S1035 ([FRI-249](#)), S1054 ([TOP-100](#)), S1087 ([WED-151](#)), S1091 ([WED-158](#)), S1101 ([WED-171](#)), S1115 ([WED-193](#)), S1132 ([SAT-145](#)), S1134 ([SAT-148](#)), S1137 ([SAT-152](#)), S1139 ([SAT-156](#)), S1147 ([TOP-110](#)), S1186 ([THU-181](#))
- Corneille, Jeremie, S834 ([FRI-481](#))
- Cornejo, Andrea, S728 ([SAT-515](#))
- Coronas, Joaquin Salas, S1126 ([WED-208](#))
- Corpechot, Christophe, S46 ([OS-053-YI](#)), S56 ([OS-073](#)), S408 ([WED-318](#))
- Corradini, Stefano Ginanni, S360 ([FRI-383](#))
- Corradin, Matteo, S920 ([FRI-185](#))
- Corrales, Fernando, S537 ([SAT-232](#))
- Correia, Fabio, S1189 ([THU-186](#))
- Correia, Jorge, S741 ([WED-409](#))
- Correia-Sá, Ana, S842 ([FRI-495](#))
- Corsico, Angelo Guido, S85 ([OS-120](#))
- Corsi, Oscar, S865 ([SAT-129](#))
- Corson, Stephen, S110 ([LBP-15](#)), S1167 ([SAT-196](#))
- Cortellini, Alessio, S575 ([THU-116](#)), S586 ([THU-134](#))
- Cortese, Maria Francesca, S1024 ([FRI-228](#)), S1089 ([WED-154](#))
- Cortese, Mario, S1055 ([TOP-101](#))
- Cortesi, Filippo, S60 ([OS-079-YI](#))
- Cortes, Miren Garcia, S18 ([OS-007](#)), S144 ([FRI-406](#)), S248 ([WED-341](#))
- Cortez, John, S548 ([SAT-251](#))
- Cortez-Pinto, Helena, S103 ([LBP-06](#)), S279 ([WED-390](#)), S722 ([SAT-506](#)), S734 ([WED-397](#)), S865 ([SAT-129](#))
- Corthay, Alexandre, S59 ([OS-076](#))
- Corti, Davide, S1147 ([TOP-109](#))
- Çoruh, Ayşegül Gürsoy, S477 ([THU-518](#))
- Cosgrave, Carl, S1190 ([THU-189](#))
- Cossiga, Valentina, S903 ([FRI-155](#))
- Cossío, Fernando Pedro, S527 ([SAT-212](#))
- Costa, Guido, S446 ([SAT-377](#))
- Costa, Mariana, S1111 ([WED-185](#)), S1189 ([THU-186](#))
- Costa-Moreira, Pedro, S366 ([TOP-061](#))
- Costantino, Andrea, S1154 ([SAT-175](#))
- Costanzo, Giuseppe Di, S593 ([THU-145](#))
- Costanzo, Michele, S38 ([OS-042-YI](#))
- Costa, Roger Flores, S222 ([THU-356](#))
- Costa-Silva, Bruno, S734 ([WED-397](#))
- Coste, Angie, S822 ([FRI-515](#)), S828 ([FRI-525](#))
- Costentin, Charlotte, S61 ([OS-081](#)), S103 ([LBP-07](#)), S500 ([FRI-289](#)), S656 ([SAT-403](#)), S667 ([SAT-419](#)), S672 ([SAT-427](#))
- Cotler, Scott, S1170 ([SAT-200](#))
- Cots, Meritxell Ventura, S164 ([FRI-433](#)), S171 ([FRI-445](#))
- Cotte, Laurent, S876 ([FRI-117](#))
- Cotter, Thomas, S865 ([SAT-129](#)), S900 ([FRI-151](#))
- Cotugno, Rosa, S40 ([OS-045](#)), S55 ([OS-070](#))
- Coughlan, Laura, S909 ([FRI-165](#))
- Coukos, Alexander, S105 ([LBP-08](#))
- Coulibaly, Fatoumata, S1161 ([SAT-185](#))
- Coursier, Severine, S929 ([FRI-201](#))
- Courtois, Anais, S161 ([FRI-429](#))
- Couto, Thais Leonel, S1089 ([WED-154](#))
- Cova, Miguel, S481 ([THU-525](#))
- Cowan, Susan, S880 ([THU-121](#))
- Cox, I. Jane, S205 ([TOP-042](#))
- Cozzolongo, Raffaele, S36 ([OS-036](#)), S40 ([OS-045](#)), S55 ([OS-070](#))
- Crabbe, Marjolein, S444 ([SAT-374](#))
- Craciun, Rares, S245 ([WED-337](#)), S297 ([SAT-519](#))
- Cramer, Thorsten, S542 ([SAT-240](#))
- Cramp, Matthew, S307 ([SAT-537](#))
- Crater, Christina, S985 ([THU-310](#))
- Cravo, Claudia, S618 ([THU-436](#))
- Crawford, Darrell, S330 ([WED-229](#))
- Craxi, Antonio, S609 ([THU-421](#)), S803 ([WED-549](#))
- Creanor, Siobhan, S153 ([FRI-418](#))
- Creasy, Kate Townsend, S636 ([THU-467](#))
- Cremer, Jennifer, S1154 ([SAT-176](#)), S1162 ([SAT-187](#))
- Cremers, Niels, S1038 ([FRI-253](#))
- Crenier, Laurent, S621 ([THU-442](#))
- Crescitelli, Rossella, S740 ([WED-407](#))
- Crespi, Veronica, S954 ([THU-267](#))
- Crespo, Ana, S682 ([SAT-442](#))
- Crespo, Gonzalo, S461 ([THU-487](#))
- Crespo, Javier, S3 ([GS-003](#)), S8 ([GS-009](#)), S38 ([OS-042-YI](#)), S87 ([OS-123-YI](#)), S140 ([FRI-399](#)), S251 ([WED-344](#)), S376 ([WED-264](#)), S390 ([WED-288](#)), S646 ([THU-559](#)), S693 ([SAT-460](#)), S700 ([SAT-468](#)), S709 ([SAT-484](#)), S728 ([SAT-515](#)), S868 ([SAT-132](#)), S911 ([FRI-171](#)), S921 ([FRI-188](#)), S934 ([FRI-211](#))
- Crespo, Maria, S137 ([FRI-395](#))
- Cristofaro, Raimondo De, S252 ([WED-347](#))
- Cristoferi, Laura, S56 ([OS-073](#)), S374 ([WED-260](#)), S381 ([WED-272](#)), S982 ([THU-304](#))
- Critelli, Rosina Maria, S493 ([FRI-277](#))
- Crittenden, Daria B., S371 ([WED-256](#))
- Croagh, Catherine, S306 ([SAT-535](#))
- Croce, Anna Cleta, S795 ([WED-533](#)), S804 ([WED-550](#))
- Croce, Saveria Lory, S40 ([OS-045](#))
- Croce, Saveria Lory, S55 ([OS-070](#)), S711 ([SAT-489](#))
- Crocobbe, Dominic, S812 ([FRI-471](#))
- Crooks, Colin, S4 ([GS-004-YI](#)), S160 ([FRI-427](#))
- Cross, Tim, S521 ([FRI-326](#))
- Crothers, Hannah, S368 ([WED-251](#))
- Crotty, Pamela, S1115 ([WED-191](#))
- Crouch, Emilie, S72 ([OS-098](#)), S541 ([SAT-237](#))
- Cruz-Moreno, Luis, S79 ([OS-112](#))
- Csarmann, Katja, S798 ([WED-539](#))
- Csillag, Aniko, S23 ([OS-017-YI](#))
- Cuadrado, Antonio, S251 ([WED-344](#)), S470 ([THU-503](#)), S777 ([WED-468](#)), S934 ([FRI-211](#))
- Cua, Georgine, S883 ([FRI-125](#)), S919 ([FRI-183](#))
- Cubero, Francisco Javier, S38 ([OS-041-YI](#)), S137 ([FRI-395](#)), S142 ([FRI-403](#)), S150 ([FRI-412](#)), S349 ([THU-235](#)), S544 ([SAT-244](#)), S732 ([TOP-090](#))
- Cubero, Juan Carlos Porres, S844 ([FRI-501](#))
- Cuccorese, Giuseppe, S40 ([OS-045](#)), S55 ([OS-070](#))
- Cuenca, Beatriz, S1205 ([THU-216](#))
- Cuesta, Rubén, S883 ([FRI-126](#))
- Cueto-Sanchez, Alejandro, S144 ([FRI-406](#))
- Cuevas, Cristina Martínez, S480 ([THU-524](#))
- Cuffari, Biagio, S287 ([SAT-334](#))
- Cuffaro, Doretta, S791 ([WED-525](#))
- Cui, Ang, S58 ([OS-075](#))
- Cui, Qianxi, S1156 ([SAT-178](#))
- Cui, Rumeng, S1156 ([SAT-178](#))
- Cullen, Noelle, S1211 ([THU-223](#))
- Cullen, Olivia, S266 ([WED-367](#))
- Cummings, Oscar, S649 ([TOP-080](#))
- Cunha, Antonio Sa, S458 ([THU-483](#))
- Cunnah, Philip, S1038 ([FRI-252](#))
- Cunningham, Morven, S314 ([SAT-548](#))
- Curescu, Manuela Gabriela, S1137 ([SAT-152](#))
- Currà, Jaqueline, S632 ([THU-461](#)), S645 ([THU-557](#))
- Currie, Helen, S1011 ([THU-389](#))
- Currie, Sue, S1015 ([TOP-107](#))
- Curro, Ilaria, S479 ([THU-521](#))
- Curry, Michael, S675 ([SAT-432](#))
- Curtis, Megan, S878 ([FRI-119](#))
- Curto, Anna, S206 ([TOP-046](#))
- Curto, Armando, S774 ([WED-462](#))
- Cusi, Kenneth, S66 ([OS-089](#)), S464 ([THU-492](#)), S627 ([THU-453](#))
- Cussigh, Annarosa, S402 ([WED-306](#)), S1135 ([SAT-149](#))
- Custers, Emma, S763 ([WED-444](#))

- Cusumano, Caterina, S974 (THU-293)
 Cuthbertson, Daniel, S521 (FRI-326),
 S617 (THU-434), S677 (SAT-436)
 Cutolo, Francesco Maria, S903 (FRI-155)
 Cutsem, Eric Van, S48 (OS-059-YI),
 S524 (TOP-066)
 Cuyas, Berta, S10 (LBO-01), S73 (OS-100-YI)
 Cyrille, Stacy, S607 (THU-418)
 Cytryn, Edward, S997 (THU-328)
 Czernuszewicz, Tomasz, S765 (WED-448)
 Czubkowski, Piotr, S123 (LBP-35),
 S387 (WED-282), S965 (THU-284),
 S969 (THU-289), S971 (THU-291)
- Da, Ben, S113 (LBP-20), S1059 (WED-116),
 S1091 (WED-158), S1159 (SAT-182)
 Dąbrowska, Maria, S505 (FRI-296)
 Dachraoui, Mayssa, S72 (OS-098)
 D'Agostino, Daniel, S123 (LBP-35),
 S387 (WED-282)
 Daha, Ioana, S192 (FRI-541)
 Dahari, Harel, S1038 (FRI-253),
 S1170 (SAT-200)
 Dahiya, Monica, S274 (WED-382)
 Dahl, Emilie, S303 (SAT-528)
 Dahlqvist, Géraldine, S464 (THU-493),
 S639 (THU-473), S923 (FRI-190)
 Dahman, Bassam, S304 (SAT-532),
 S832 (FRI-478)
 Dahmen, Uta, S487 (THU-539)
 Dai, Chia-Yen, S895 (FRI-143),
 S1180 (THU-174), S1206 (THU-217)
 Daida, Yihe G, S1079 (WED-141)
 Dai, Wanmin, S756 (WED-434)
 Daix, Valérie, S211 (THU-342)
 Dajti, Elton, S86 (OS-121-YI),
 S88 (OS-124-YI), S90 (OS-127-YI),
 S283 (SAT-327), S299 (SAT-521),
 S519 (FRI-322), S974 (THU-293)
 Dalal, Ashok, S235 (TOP-044)
 Dalbeni, Andrea, S203 (FRI-558),
 S510 (FRI-304), S632 (THU-461),
 S668 (SAT-420), S1190 (THU-188)
 Dalby, Matthew, S987 (THU-312)
 Dalegaard, Magnus Illum,
 S1050 (FRI-271)
 Dalekos, George, S42 (OS-047-YI),
 S44 (OS-049-YI), S56 (OS-073),
 S392 (WED-290), S400 (WED-302),
 S421 (FRI-354), S579 (THU-123),
 S1054 (TOP-100), S1128 (WED-211),
 S1134 (SAT-148)
 D'Alessandro, Umberto, S67 (OS-090-YI)
 D'Alessio, Antonio, S12 (LBO-04),
 S491 (FRI-273), S575 (THU-116),
 S582 (THU-128), S586 (THU-134)
 Dalgard, Olav, S1150 (SAT-170)
 Dalgarno, Kenny, S565 (SAT-284)
 Dallio, Marcello, S105 (LBP-09)
 Dalmau-Bueno, Albet, S932 (FRI-208)
 d'Almeida, Arno Furquim,
 S1114 (WED-190), S1132 (SAT-145)
 d'Alteroche, Louis, S52 (OS-066),
 S318 (SAT-556), S1160 (SAT-184)
- Dalteroche, Louis, S107 (LBP-11),
 S498 (FRI-286)
 Daly, Ann K, S78 (OS-110)
 Damascene, Makuza Jean, S883 (FRI-125)
 Damasio, Marcos, S58 (OS-075)
 d'Amati, Giulia, S994 (THU-323)
 D'Amato, Daphne, S40 (OS-045),
 S55 (OS-070), S521 (FRI-325),
 S605 (THU-415), S617 (THU-435),
 S626 (THU-452), S637 (THU-470),
 S704 (SAT-474), S713 (SAT-494)
 D'Ambrosio, Francesca, S660 (SAT-409),
 S723 (SAT-508)
 D'Ambrosio, Roberta, S91 (OS-129-YI),
 S500 (FRI-288), S673 (SAT-430),
 S920 (FRI-185), S992 (THU-318),
 S1173 (THU-165)
 Damgaard Sandahl, Thomas,
 S958 (THU-274), S971 (THU-291),
 S985 (THU-309)
 D'Amico, Gennaro, S105 (LBP-09)
 D'Amico, Mario, S105 (LBP-09)
 Damink, Steven Olde, S206 (TOP-046),
 S350 (THU-236)
 Danaee, Anicee, S964 (THU-283)
 danan, Keren, S955 (THU-269)
 Dancy, Lucy, S483 (THU-530)
 Dandri, Maura, S1019 (FRI-220),
 S1023 (FRI-227), S1147 (TOP-109)
 Daniele, Bruno, S942 (THU-251)
 Danis, Nilay, S181 (FRI-463)
 D'Anna, Stefano, S1056 (TOP-106),
 S1072 (WED-133), S1103 (WED-174),
 S1105 (WED-176), S1122 (WED-203),
 S1142 (SAT-159)
 Danneberg, Sven, S251 (WED-345)
 Danta, Mark, S11 (LBO-03),
 S263 (WED-364)
 D'Antiga, Lorenzo, S56 (OS-072),
 S123 (LBP-35), S387 (WED-282),
 S966 (THU-285), S971 (THU-291)
 Dan, Yock Young, S698 (SAT-467),
 S707 (SAT-482), S714 (SAT-495)
 Dan, Yock-Young, S721 (SAT-503)
 Dan, Yunjie, S948 (THU-260)
 Dao Thi, Viet Loan, S1020 (FRI-222),
 S1021 (FRI-224)
 Darba, Josep, S1070 (WED-130)
 Darias, Ruth Suarez, S932 (FRI-206)
 Dariol, Eva, S952 (THU-265)
 Darling, Jama, S89 (OS-125)
 d'Arminio Monforte, Antonella,
 S1103 (WED-174), S1105 (WED-176)
 Darnell, Anna, S843 (FRI-499)
 Darvishian, Maryam, S883 (FRI-125)
 Das, Avisnata, S1005 (THU-381)
 D'Ascenzo, Fabrizio, S486 (THU-537)
 Dashdorj, Naranbaatar, S718 (SAT-499)
 Dashdorj, Naranjargal, S716 (SAT-497),
 S718 (SAT-499), S1104 (WED-175)
 Dashputre, Ankur, S291 (SAT-339)
 Da Silva, Nathalie, S1031 (FRI-243)
 Das, Joyeta, S1141 (SAT-158),
 S1145 (SAT-164)
- Das, Prasenjit, S401 (WED-304)
 Das, Srustidhar, S60 (OS-079-YI)
 Das, Sugato, S397 (WED-297)
 Das, Sukanta, S80 (OS-113)
 Datta, Shouren, S402 (WED-305)
 Datusalia, Ashok Kumar, S225 (THU-360)
 Datz, Christian, S19 (OS-010-YI),
 S863 (SAT-126)
 Dauda Dixon, Emmanuel, S746 (WED-418)
 Daud, Nu'man AS, S1203 (THU-212)
 Dauer, Marc, S563 (SAT-280)
 Davenport, Andrew, S220 (THU-355)
 Davenport, Mark, S984 (THU-307),
 S987 (THU-312), S997 (THU-329),
 S999 (THU-332)
 David-Feliciano, Susan, S387 (WED-282)
 Davidov, Yana, S719 (SAT-500)
 Davies, Charlotte E., S177 (FRI-455)
 Davies, Jim, S1075 (WED-137)
 Davies, Kyle, S122 (LBP-33-YI)
 Davies, Melanie, S811 (FRI-469)
 Davies, Nathan, S205 (TOP-042),
 S220 (THU-355)
 Davies, Peter, S925 (FRI-194)
 Davies, Scott, S416 (FRI-347),
 S447 (SAT-380), S448 (SAT-382)
 Davis, Brian, S37 (OS-038)
 Davis, Cai, S1075 (WED-137)
 Davis, Pamela, S809 (FRI-467)
 Dawson, Paul, S415 (FRI-346),
 S940 (THU-249)
 Day, Chris, S603 (THU-412)
 Day, Emily, S762 (WED-442)
 Dayyani, Farshid, S506 (FRI-298)
 Dazzi, Francesco, S127 (TOP-093)
 Dean, Richard, S388 (WED-283),
 S431 (FRI-368)
 de Araujo, Anne-Laure, S722 (SAT-505),
 S769 (WED-453), S777 (WED-469)
 De, Arka, S51 (OS-064-YI)
 Dearlove, David, S731 (TOP-089)
 Deavila, Leyla, S600 (TOP-081),
 S673 (SAT-428), S861 (SAT-122)
 De Azevedo, David, S464 (THU-493)
 de Azevedo, Rita Furtado Feio,
 S452 (SAT-390)
 de Beijer, Monique, S561 (SAT-276)
 De Benedittis, Carla, S389 (WED-284),
 S599 (THU-156)
 Debes, Jose, S496 (FRI-282), S865 (SAT-129)
 Debets, Reno, S561 (SAT-276)
 Debing, Yannick, S1051 (FRI-272)
 de Boer, Ynto, S14 (LBO-06),
 S44 (OS-049-YI)
 Debray, Dominique, S969 (THU-289),
 S971 (THU-291)
 Debroff, Jake, S926 (FRI-196)
 de Bruyne, Ruth, S1000 (THU-334)
 Debzi, Nabil, S274 (WED-382)
 Decaens, Thomas, S61 (OS-081),
 S62 (OS-083-YI), S467 (THU-498),
 S498 (FRI-286), S500 (FRI-289)
 Decaris, Martin, S322 (WED-215)
 Deckmyn, Olivier, S106 (LBP-10)

Author Index

- De Conte, Annachiara, S903 ([FRI-155](#))
 Deep, Amar, S1050 ([FRI-269](#))
 Deepika, S210 ([THU-340](#))
 De-Freitas, Cecilia, S1150 ([SAT-169](#)),
 S1160 ([SAT-183](#)), S1193 ([THU-194](#))
 Degasperri, Elisabetta, S40 ([OS-045](#)),
 S55 ([OS-070](#)), S91 ([OS-129-YI](#)),
 S107 ([LBP-11](#)), S108 ([LBP-12](#)),
 S1135 ([SAT-149](#)), S1142 ([SAT-159](#)),
 S1154 ([SAT-175](#)), S1159 ([SAT-181](#)),
 S1164 ([SAT-190](#)), S1170 ([SAT-199](#))
 de Gauna, Mikel Ruiz, S137 ([FRI-395](#))
 de Gottardi, Andrea, S87 ([OS-123-YI](#))
 de Graaff, Barbara, S523 ([FRI-329](#))
 Degrauwe, Lars, S1051 ([FRI-272](#))
 Degré, Delphine, S621 ([THU-442](#))
 Degroote, Helena, S87 ([OS-123-YI](#)),
 S103 ([LBP-07](#)), S307 ([SAT-538](#))
 de Haan, Jubi, S184 ([FRI-340](#))
 Dehncke, Daniel, S1029 ([FRI-240](#))
 de Hollanda, Ana, S737 ([WED-403](#))
 Deibel, Ansgar, S56 ([OS-073](#))
 Deirós, Roger Paredes, S933 ([FRI-208](#))
 Dejardin, Olivier, S855 ([TOP-098](#))
 De Jonge, Henk-Marijn, S14 ([LBO-06](#))
 de Jonge, Jeroen, S454 ([TOP-052](#))
 de Keizer, Nicolette, S184 ([FRI-340](#))
 Deken, Marcel, S761 ([WED-441](#))
 Dekervel, Jeroen, S48 ([OS-059-YI](#)),
 S524 ([TOP-066](#))
 De Knecht, Robert, S1016 ([TOP-108](#)),
 S1019 ([FRI-219](#))
 De La Luna, Francisco Franco Álvarez,
 S1126 ([WED-208](#))
 Delamarre, Adele, S56 ([OS-073](#)),
 S674 ([SAT-431](#))
 del Amo, Julia, S880 ([FRI-121](#))
 Delaney, William E., S35 ([OS-034](#)),
 S1058 ([WED-114](#)), S1167 ([SAT-195](#))
 de Langlard, Mathieu, S359 ([FRI-382](#))
 Delangre, Etienne, S751 ([WED-426](#))
 de la Peña-Ramirez, Carlos, S197 ([FRI-549](#))
 De Lara, Catherine, S1108 ([WED-181](#))
 de la Rosa, Gloria, S469 ([THU-501](#))
 De las Heras, Berta, S268 ([WED-372](#))
 Delataille, Philippe, S211 ([THU-342](#))
 de la Torre, Manuel, S573 ([THU-114](#))
 De La Torre Sanchez, Mercedes,
 S700 ([SAT-468](#))
 Delaunay, Dominique, S603 ([THU-410](#))
 Delaune, Vaihere, S24 ([OS-018-YI](#))
 Del Barrio Azaceta, María, S693 ([SAT-460](#))
 del Campo Herrera, Enrique, S144 ([FRI-406](#))
 del Campo, Nuria Pérez Diaz,
 S521 ([FRI-325](#)), S704 ([SAT-474](#)),
 S713 ([SAT-494](#))
 Del Carmen Asenjo Lobos, Claudia,
 S840 ([FRI-492](#))
 del Carmen Domínguez, Maria,
 S1126 ([WED-208](#))
 del Carmen Rico, Maria, S728 ([SAT-515](#))
 Delcea, Caterina, S192 ([FRI-541](#))
 DelConte, Anthony, S260 ([WED-358](#)),
 S809 ([FRI-466](#))
 de Lédinghen, Victor, S52 ([OS-066](#)),
 S56 ([OS-073](#)), S61 ([OS-080-YI](#)),
 S107 ([LBP-11](#)), S498 ([FRI-286](#)),
 S609 ([THU-421](#)), S667 ([SAT-419](#)),
 S672 ([SAT-427](#)), S674 ([SAT-431](#)),
 S722 ([SAT-505](#)), S769 ([WED-453](#)),
 S777 ([WED-469](#)), S833 ([FRI-480](#)),
 S1160 ([SAT-184](#)), S1161 ([SAT-185](#))
 Delegge, Mark, S977 ([THU-296](#)),
 S1007 ([THU-385](#))
 Delerive, Philippe, S762 ([WED-442](#)),
 S776 ([WED-467](#))
 Deleuran Hansen, Emil, S175 ([FRI-452](#))
 Deleus, Ellen, S753 ([WED-430](#))
 Delgado, Alberto, S1028 ([FRI-236](#)),
 S1032 ([FRI-245](#))
 Delgado, Igotz, S137 ([FRI-395](#)),
 S529 ([SAT-215](#)), S738 ([WED-404](#)),
 S741 ([WED-408](#))
 Delgado, Manuel, S964 ([THU-282](#)),
 S980 ([THU-301](#)), S996 ([THU-326](#)),
 S998 ([THU-331](#)), S1205 ([THU-216](#))
 Delgado, Teresa Cardoso, S140 ([FRI-399](#)),
 S529 ([SAT-216](#))
 del Hoyo, Javier, S180 ([FRI-462](#))
 Delire, Bénédicte, S134 ([THU-405](#)),
 S511 ([FRI-307](#))
 Delo, Joseph, S452 ([SAT-389](#))
 de los Reyes Luque Urbano, María,
 S736 ([WED-400](#))
 de los Ríos-Arellano, Ericka, S547 ([SAT-249](#))
 De los Santos Fernández, Romina,
 S126 ([TOP-087](#))
 De Los Santos, Ignacio, S1037 ([FRI-251](#))
 Delphin, Marion, S1060 ([WED-117](#)),
 S1108 ([WED-181](#))
 Del Piano, Filomena, S800 ([WED-542](#))
 Delpierre, Julien, S364 ([FRI-390](#))
 del Pino, Pilar, S1126 ([WED-208](#))
 del Rio, Alvaro, S546 ([SAT-247](#))
 del Rio-Cubilledo, Cristina, S892 ([FRI-139](#))
 Deltenre, Pierre, S621 ([THU-442](#)),
 S975 ([THU-295](#))
 Delugré, Fabian, S431 ([FRI-369](#))
 Delvallez, Gauthier, S897 ([FRI-146](#))
 Delwaide, Jean, S1114 ([WED-190](#))
 de Maeyer, Dries, S443 ([SAT-371](#))
 De Man, Joris, S776 ([WED-466](#)),
 S790 ([WED-523](#))
 De Man, Robert, S501 ([FRI-291](#))
 Demard, Nathalie Fabre, S929 ([FRI-201](#))
 Demaret, Tanguy, S971 ([THU-291](#))
 De Maria, Nicola, S54 ([OS-069](#))
 De Martin, Sara, S791 ([WED-525](#))
 De Matteo, Elena, S1037 ([FRI-251](#))
 Demediuk, Barbara, S306 ([SAT-535](#))
 de Meijer, Vincent, S740 ([WED-407](#)),
 S798 ([WED-538](#))
 Demeulenaere, Laurissa, S172 ([FRI-447](#))
 De Meyer, Amse, S1025 ([FRI-231](#))
 Demir, Kadir, S709 ([SAT-485](#))
 Demir, Münevver, S197 ([FRI-549](#)),
 S351 ([THU-238](#)), S1139 ([SAT-156](#))
 Demma, Shirin, S247 ([WED-340](#))
 Denecke, Timm, S483 ([THU-529](#)),
 S507 ([FRI-299](#))
 Deng, Guohong, S196 ([FRI-547](#)),
 S948 ([THU-260](#))
 Deng, Huan, S274 ([WED-382](#))
 Deng, Hui, S549 ([SAT-253](#))
 Deng, Rui, S22 ([OS-016](#))
 Deng, Yangyang, S832 ([FRI-478](#))
 Deng, You, S243 ([WED-332](#))
 den Hoed, Caroline, S46 ([OS-053-YI](#)),
 S454 ([TOP-052](#))
 den Hoed, Marcel, S769 ([WED-454](#))
 De Nicola, Francesca, S1018 ([FRI-218](#))
 Denis, Jérôme, S494 ([FRI-279](#))
 Denk, Gerald, S216 ([THU-348](#)),
 S329 ([WED-228](#)), S403 ([WED-307](#)),
 S417 ([FRI-349](#)), S1139 ([SAT-156](#))
 de Oca Luna, Roberto Montes,
 S337 ([WED-244](#))
 de Oliveira, Silvia Bastos, S1201 ([THU-208](#))
 Depaoli, Alessandro, S486 ([THU-537](#))
 de Pedro, María Sanz, S690 ([SAT-454](#))
 Deprez, Benoit, S954 ([THU-267](#))
 Derben, Finn C., S425 ([FRI-362](#))
 der Borgh, Koen Van, S443 ([SAT-371](#))
 Derdeyn, Jolien, S622 ([THU-444](#))
 der Eijk, Annemiek Van, S892 ([FRI-138](#))
 Derenne, Thomas, S444 ([SAT-374](#))
 Derer, Stefanie, S536 ([SAT-230](#))
 Derin, Esra, S1179 ([THU-172](#))
 Derler, Martina, S142 ([FRI-402](#))
 der Meer, Adriaan Van, S46 ([OS-053-YI](#)),
 S306 ([SAT-536](#)), S454 ([TOP-052](#)),
 S982 ([THU-304](#))
 De Roza, Marianne, S300 ([SAT-522](#))
 D'Errico, Maria Antonietta, S519 ([FRI-322](#))
 De Rudder, Maxime, S438 ([SAT-363](#))
 de Ruiter, Christa, S786 ([WED-515](#))
 Desai, Dev, S971 ([THU-291](#))
 Desai, Monica, S909 ([FRI-165](#))
 Desalegn, Hailemichael, S195 ([FRI-546](#)),
 S274 ([WED-382](#)), S865 ([SAT-129](#)),
 S916 ([FRI-178](#)), S1117 ([WED-195](#)),
 S1150 ([SAT-170](#))
 Desandré, Guillaume, S534 ([SAT-225](#))
 Descamps, Benedicte, S226 ([THU-361](#))
 Descat, Amandine, S355 ([THU-244](#))
 de Schaetzen, Arthur, S76 ([OS-106-YI](#))
 Deschenes, Marc, S645 ([THU-557](#))
 de Sena, Elena, S819 ([FRI-509](#))
 Desert, Romain, S80 ([OS-113](#))
 Deshpande, Aditi, S1164 ([SAT-191](#))
 Deshpande, Kedar, S830 ([FRI-529](#))
 De, Shreemoyee, S436 ([SAT-360](#))
 De Siervi, Silvia, S552 ([SAT-258](#))
 Desjardins, Eris, S762 ([WED-442](#))
 Desmarests, Maxime, S318 ([SAT-556](#))
 Desmond, Paul, S306 ([SAT-535](#))
 de Sousa Damião, Filipe, S87 ([OS-123-YI](#))
 de Sousa, Francielle Tramontini Gomes,
 S1167 ([SAT-195](#))
 De Sousa, Marcela, S1037 ([FRI-251](#))
 Desterke, Christophe, S460 ([THU-486](#)),
 S482 ([THU-528](#))

- de Tarso Aparecida Pinto, Paulo, S112 ([LBP-16](#))
- de Temple, Brittany, S808 ([TOP-091](#)), S820 ([FRI-512](#))
- Deterding, Katja, S90 ([OS-126](#)), S108 ([LBP-12](#)), S1031 ([FRI-242](#)), S1101 ([WED-171](#)), S1115 ([WED-193](#)), S1139 ([SAT-156](#))
- Detlefsen, Sönke, S17 ([OS-005-YI](#)), S163 ([FRI-432](#)), S175 ([FRI-452](#)), S657 ([SAT-404](#)), S845 ([TOP-054](#))
- de Toni, Enrico, S47 ([OS-057](#)), S507 ([FRI-300](#)), S596 ([THU-150](#))
- de Troyer, Ewoud, S1034 ([FRI-248](#))
- Deutsch, Melanie, S400 ([WED-302](#)), S1128 ([WED-211](#)), S1194 ([THU-196](#)), S1194 ([THU-197](#))
- Devalia, Kalpana, S708 ([SAT-483](#)), S740 ([WED-406](#))
- Dev, Anouk, S380 ([WED-271](#))
- Devaux, Carole, S880 ([FRI-121](#))
- de Veer, Rozanne, S46 ([OS-053-YI](#)), S56 ([OS-073](#))
- Deverell, Harriet, S848 ([WED-480](#))
- Devriere, Jacques, S621 ([THU-442](#))
- Devika, S, S846 ([WED-477](#))
- de Villar, Noemi González Pérez, S690 ([SAT-454](#))
- De Vincentis, Antonio, S40 ([OS-045](#)), S55 ([OS-070](#))
- Devisscher, Lindsey, S226 ([THU-361](#)), S743 ([WED-412](#)), S787 ([WED-516](#))
- Devlin, Shannon, S402 ([WED-305](#))
- De Vos, Kristof, S1025 ([FRI-231](#))
- Devresse, Arnaud, S923 ([FRI-190](#))
- de Vries-Sluijs, Theodora, S892 ([FRI-138](#))
- de Waart, Rudi, S427 ([FRI-364](#))
- De Winter, Benedicte, S776 ([WED-466](#)), S790 ([WED-523](#))
- de Wit, Koos, S10 ([LBO-01](#))
- Dezsöfi, Antal, S969 ([THU-289](#)), S971 ([THU-291](#))
- Dhairyawar, Rageshri, S1127 ([WED-209](#))
- Dhaliwal, Amritpal, S231 ([THU-368](#)), S232 ([THU-370](#))
- Dhanasekaran, Renumathy, S25 ([OS-020-YI](#))
- Dhanda, Ashwin, S153 ([FRI-418](#))
- Dharancy, Sebastien, S62 ([OS-083-YI](#)), S467 ([THU-498](#)), S473 ([THU-511](#)), S1005 ([THU-380](#))
- Dharancy, Sébastien, S74 ([OS-104](#))
- Dhawan, Anil, S984 ([THU-307](#)), S987 ([THU-312](#)), S999 ([THU-332](#))
- Dhijimatsu, Ryota, S439 ([SAT-366](#))
- Dhiman, Radha Krishan, S195 ([FRI-546](#))
- Diago, Moises, S376 ([WED-264](#)), S627 ([THU-453](#)), S682 ([SAT-442](#)), S1098 ([WED-166](#)), S1205 ([THU-216](#))
- Diamantea, Filia, S978 ([THU-298](#))
- Diamond, Tamir, S450 ([SAT-386](#)), S961 ([THU-278](#))
- Dianzani, Umberto, S751 ([WED-425](#))
- Díaz, Alba, S12 ([LBO-04](#)), S87 ([OS-123-YI](#)), S493 ([FRI-276](#)), S497 ([FRI-284](#))
- Díaz, Asuncion, S880 ([FRI-121](#)), S902 ([FRI-153](#))
- Díaz del Campo, Nuria Pérez, S605 ([THU-415](#))
- Díaz, Fernando, S481 ([THU-525](#)), S1098 ([WED-166](#))
- Díaz-Ferrer, Javier, S496 ([FRI-282](#)), S865 ([SAT-129](#)), S900 ([FRI-151](#))
- Díaz-Flores, Felicitas, S893 ([FRI-140](#))
- Díaz-González, Álvaro, S380 ([WED-270](#)), S392 ([WED-290](#)), S399 ([WED-300](#))
- Díaz, Irene Gonzalez, S690 ([SAT-454](#)), S697 ([SAT-465](#)), S705 ([SAT-478](#)), S706 ([SAT-479](#))
- Díaz, Luis Antonio, S865 ([SAT-129](#))
- Díaz-Mejía, Nely, S375 ([WED-263](#))
- Díaz-Mitoma, Francisco, S1119 ([WED-197](#))
- Díaz-Muñoz, Mauricio, S547 ([SAT-249](#))
- Díaz, Paula Haridian Quintana, S893 ([FRI-140](#))
- Díaz, Raquel, S87 ([OS-123-YI](#))
- Díaz, Rodríguez, S1124 ([WED-205](#))
- DiBenedetto, Clara, S54 ([OS-069](#))
- Di Benedetto, Davide, S389 ([WED-284](#)), S599 ([THU-156](#))
- di Cesare, Ernesto, S685 ([SAT-446](#))
- Di, Chun, S514 ([FRI-313](#))
- Di Cola, Simone, S217 ([THU-350](#)), S218 ([THU-352](#))
- Diego, Rosa Ortiz De, S936 ([FRI-214](#))
- Dieguez, Maria Luisa Gonzalez, S133 ([THU-404](#)), S481 ([THU-525](#)), S964 ([THU-282](#))
- Diehl, Anna Mae, S800 ([WED-544](#))
- Dienes, Hans-Peter, S996 ([THU-327](#))
- Dieterich, Douglas T, S116 ([LBP-23](#))
- Dieterich, Douglas T., S894 ([FRI-141](#))
- Dietrich, Julie, S995 ([THU-324](#))
- Dietrich, Peter, S377 ([WED-265](#))
- Dietz-Fricke, Christopher, S107 ([LBP-11](#)), S108 ([LBP-12](#)), S1139 ([SAT-156](#))
- Dietz, Julia, S90 ([OS-126](#)), S91 ([OS-129-YI](#)), S1039 ([FRI-254](#)), S1042 ([FRI-259](#))
- Diez, Jose Manuel Olivares, S892 ([FRI-139](#)), S898 ([FRI-148](#))
- Diez, Ruben, S852 ([WED-489](#))
- Diez, Sandra, S852 ([WED-489](#))
- Digiaco, Maria, S791 ([WED-525](#))
- Di Gioia, Cira, S360 ([FRI-383](#))
- Di Giorgio, Angelo, S966 ([THU-285](#))
- Digkilia, Antonia, S12 ([LBO-04](#))
- Dijkstra, Willemijn, S306 ([SAT-536](#))
- Diken, Mustafa, S26 ([OS-022](#))
- Dikopoulos, Nektarios, S1139 ([SAT-156](#))
- Dileo, Eleonora, S626 ([THU-452](#)), S637 ([THU-470](#))
- Dili, Alexandra, S438 ([SAT-363](#))
- Dili, Daer, S261 ([WED-359](#))
- Dill, Michael, S403 ([WED-307](#)), S541 ([SAT-238](#)), S594 ([THU-147](#))
- Dillon, John, S867 ([SAT-130](#))
- Di Lorenzo, Andrea, S1072 ([WED-133](#))
- Dima, Francesco, S203 ([FRI-558](#))
- Di Marco, Vito, S1111 ([WED-186](#)), S1118 ([WED-196](#))
- Dinani, Amreen, S729 ([SAT-516](#))
- Dincer, Dinc, S274 ([WED-382](#))
- Ding, Dora, S64 ([OS-085](#))
- Dingfelder, Jule, S465 ([THU-494](#)), S465 ([THU-495](#)), S470 ([THU-505](#)), S489 ([THU-545](#))
- Ding, Huiguo, S358 ([FRI-381](#))
- Ding, John Nik, S380 ([WED-271](#))
- Ding, Weimao, S638 ([THU-471](#)), S696 ([SAT-463](#)), S724 ([SAT-510](#)), S1068 ([WED-127](#)), S1078 ([WED-140](#)), S1080 ([WED-142](#)), S1094 ([WED-161](#)), S1094 ([WED-162](#)), S1128 ([WED-212](#))
- Ding, Yanhua, S109 ([LBP-13](#)), S110 ([LBP-14](#)), S112 ([LBP-18](#)), S1164 ([SAT-192](#))
- Ding, Yibo, S1016 ([TOP-111](#))
- Dinkelborg, Katja, S1031 ([FRI-243](#))
- Diotalle, Sara, S120 ([LBP-29](#))
- Di Pasqua, Laura Giuseppina, S552 ([SAT-258](#)), S804 ([WED-550](#))
- Dirchwolf, Melisa, S245 ([WED-336](#)), S253 ([WED-348](#)), S865 ([SAT-129](#)), S900 ([FRI-151](#))
- Disayabutr, Suppareark, S19 ([OS-009](#))
- Discher, Thomas, S90 ([OS-126](#))
- DiSpirito, Alan, S948 ([THU-259](#))
- Disse, Emmanuel, S603 ([THU-410](#)), S687 ([SAT-450](#)), S701 ([SAT-469](#))
- Distefano, Marco, S36 ([OS-036](#)), S40 ([OS-045](#)), S55 ([OS-070](#))
- di Tocco, Francesca Casuscelli, S1018 ([FRI-218](#))
- Di Tommaso, Luca, S12 ([LBO-04](#))
- DiTuri, Francesco, S495 ([FRI-280](#))
- Divino, Victoria, S977 ([THU-296](#)), S1007 ([THU-385](#))
- Dixit, Bharat, S1169 ([SAT-197](#))
- Dixon, Emmanuel Dauda, S739 ([WED-405](#))
- Dixon, Susan, S1141 ([SAT-158](#))
- Dixon, Thomas, S193 ([FRI-543](#))
- Di Zeo-Sánchez, Daniel E., S44 ([OS-049-YI](#)), S142 ([FRI-403](#)), S144 ([FRI-406](#))
- Djebbar, Meriem, S498 ([FRI-286](#))
- Djernes, Lars, S257 ([WED-354](#))
- Djokić, Mihajlo, S553 ([SAT-261](#))
- Djuretic, Ivana, S5 ([GS-005](#))
- Dobbermann, Henrike, S277 ([WED-387](#)), S687 ([SAT-449](#))
- Dobeš, Jan, S945 ([THU-255](#))
- Dobracka, Beata, S505 ([FRI-296](#))
- Dobroaia, Andreea, S1123 ([WED-204](#))
- Dobryanksa, Marta, S32 ([OS-031](#))
- Dodd, Maja, S605 ([THU-414](#)), S650 ([TOP-085](#)), S653 ([SAT-397](#))
- Dodge, Jennifer, S161 ([FRI-428](#)), S169 ([FRI-441](#))
- D'Odorico, Anna, S407 ([WED-315](#))
- Dodot, Mihai, S277 ([WED-386](#))
- D'Offizi, Giampiero, S107 ([LBP-11](#))
- Dohan, Anthony, S859 ([SAT-120](#))

Author Index

- Doki, Yuichiro, S439 ([SAT-366](#)), S509 ([FRI-302](#))
- Dold, Leona, S422 ([FRI-357](#)), S429 ([FRI-366](#))
- Dollinger, Matthias, S105 ([LBP-09](#))
- Doll, Michelle, S618 ([THU-437](#))
- Dombrowicz, David, S355 ([THU-244](#))
- Domenech, Gema, S220 ([THU-355](#))
- Domenech, Gemma, S10 ([LBO-01](#)), S579 ([THU-124](#))
- Domenicali, Marco, S191 ([FRI-540](#))
- Domingo-Sàbat, Montserrat, S537 ([SAT-232](#)), S546 ([SAT-247](#))
- Domínguez, Elena Gómez, S268 ([WED-372](#)), S376 ([WED-264](#)), S380 ([WED-270](#)), S392 ([WED-290](#)), S406 ([WED-314](#))
- Domínguez-Hernández, Raquel, S883 ([FRI-126](#)), S896 ([FRI-144](#)), S921 ([FRI-188](#))
- Domínguez, María Carmen Lozano, S1126 ([WED-208](#))
- Dominguez, Nuria, S376 ([WED-264](#))
- Dominici, Massimo, S942 ([THU-251](#))
- Donadon, Matteo, S446 ([SAT-377](#))
- Donald, Judy L, S1079 ([WED-141](#))
- Donate, Jesus, S73 ([OS-102](#))
- Donato, Maria Francesca, S54 ([OS-069](#)), S457 ([THU-481](#))
- Dongelmans, Edo, S52 ([OS-065-YI](#))
- dong, fuchen, S274 ([WED-382](#))
- Donghia, Rossella, S493 ([FRI-277](#))
- Dongiovanni, Paola, S632 ([THU-461](#)), S733 ([WED-393](#)), S739 ([WED-405](#)), S744 ([WED-413](#)), S746 ([WED-418](#)), S772 ([WED-459](#)), S783 ([WED-507](#)), S802 ([WED-547](#)), S803 ([WED-549](#))
- Dong, Jie, S110 ([LBP-15](#)), S520 ([FRI-323](#))
- Dong, Xiao-Ping, S1063 ([WED-122](#))
- Dong, Yawen, S44 ([OS-050-YI](#))
- Dong, Zheng, S1085 ([WED-149](#))
- Dong, Zheyu, S543 ([SAT-242](#)), S557 ([SAT-269](#))
- Donnadieu, Hélène, S170 ([FRI-443](#))
- Donnadieu-Rigole, Hélène, S929 ([FRI-201](#))
- Dooley, Steven, S358 ([FRI-381](#))
- Dopazo, Cristina, S470 ([THU-503](#))
- Dorcaratto, Dimitri, S335 ([WED-239](#)), S451 ([SAT-387](#)), S781 ([WED-505](#))
- Dore, Gregory, S910 ([FRI-169](#))
- Dörge, Petra, S1054 ([TOP-100](#)), S1098 ([WED-167](#))
- Dorival, Celine, S68 ([OS-092-YI](#))
- Dosso, Sara De, S491 ([FRI-273](#))
- Dottor, Francesca, S711 ([SAT-489](#))
- Doucette, Karen, S1115 ([WED-191](#))
- Doukas, Michael, S561 ([SAT-276](#))
- Doussot, Alexandre, S994 ([THU-322](#))
- Dou, Xiaoguang, S34 ([OS-033](#)), S1165 ([SAT-193](#))
- Doverskog, Magnus, S423 ([FRI-359](#))
- D'Ovidio, Erica, S407 ([WED-315](#))
- Dovrat, Sara, S128 ([THU-394](#))
- Dovzhyk, Vira, S845 ([FRI-502](#))
- Dowman, Joanna, S1005 ([THU-381](#))
- Downie, Bryan, S1055 ([TOP-101](#))
- Downs, Louise, S1060 ([WED-117](#)), S1108 ([WED-181](#))
- Downs, Michael, S662 ([SAT-412](#))
- Doyle, Adam, S195 ([FRI-546](#))
- Doyle, Joseph, S1190 ([THU-189](#))
- Draganov, Ventseslav, S198 ([FRI-550](#))
- Dragan, Victor, S192 ([FRI-541](#))
- Drage, Michael, S790 ([WED-522](#))
- Dragomir, Irina, S151 ([FRI-413](#))
- Dragonì, Gabriele, S545 ([SAT-245](#))
- Draijer, Laura, S677 ([SAT-434](#))
- Drammeh, Sainabou, S67 ([OS-090-YI](#))
- Drasdo, Dirk, S359 ([FRI-382](#))
- Dražilová, Sylvia, S871 ([SAT-136](#))
- Drebber, Uta, S712 ([SAT-492](#))
- Dreher, Emely, S547 ([SAT-248](#))
- Dreizler, Dorothee, S339 ([WED-248](#))
- Drenth, Joost P.H., S14 ([LBO-06](#)), S973 ([THU-292](#)), S982 ([THU-304](#))
- Drenth, J.P.H., S579 ([THU-123](#))
- Triessen, Ann, S764 ([WED-446](#))
- Droungas, Yianni, S1028 ([FRI-237](#))
- Duan, Qihua, S338 ([WED-245](#))
- Duan, Ran, S1159 ([SAT-182](#))
- Duan, Zhongping, S235 ([TOP-047](#))
- Dua, Pallavi, S277 ([WED-388](#))
- Duarte, Ivonne Giselle, S245 ([WED-336](#))
- Dubart-Kupperschmitt, Anne, S359 ([FRI-382](#))
- Dube, Asha, S382 ([WED-273](#)), S391 ([WED-289](#))
- Dubey, Durgesh, S1050 ([FRI-269](#))
- Dubey, Vikash, S191 ([FRI-539](#))
- Dubois, Anaëlle, S1046 ([FRI-265](#))
- Dubois, Karine, S233 ([THU-372](#))
- Dubourg, Julie, S29 ([OS-026](#)), S30 ([OS-027](#)), S604 ([THU-413](#)), S619 ([THU-438](#)), S619 ([THU-439](#)), S643 ([THU-552](#)), S655 ([SAT-401](#))
- Dubuquoy, Laurent, S146 ([FRI-408](#))
- Duca, Ana, S1194 ([THU-195](#))
- Duca, Leonardo, S1072 ([WED-133](#)), S1105 ([WED-176](#)), S1122 ([WED-203](#)), S1142 ([SAT-159](#))
- Du, Chengyou, S488 ([THU-540](#))
- Duckely, Myriam, S418 ([FRI-351](#))
- Duckworth, Paul, S677 ([SAT-436](#))
- Duclos-Vallée, Jean-Charles, S359 ([FRI-382](#)), S408 ([WED-318](#)), S498 ([FRI-286](#))
- Ducournau, Gerard, S61 ([OS-081](#))
- Duda, Julia, S778 ([WED-470](#))
- Dudareva, Sandra, S880 ([FRI-121](#))
- Dudek, Michael, S442 ([TOP-050](#))
- Duehren, Sarah, S1170 ([SAT-200](#))
- Dueñas, Maria Emilia, S781 ([WED-475](#))
- Duering, Marco, S763 ([WED-444](#))
- Duffell, Erika, S880 ([FRI-121](#))
- Duffour, Jean-François, S12 ([LBO-04](#)), S491 ([FRI-273](#)), S664 ([SAT-414](#))
- Dufton, Neil, S39 ([OS-043](#))
- Duguru, Mary John, S1117 ([WED-195](#))
- Du, Hongbo, S1076 ([WED-138](#)), S1157 ([SAT-179](#))
- Du, Lixue, S488 ([THU-540](#))
- Düll, Miriam, S377 ([WED-265](#))
- Dultz, Georg, S90 ([OS-126](#)), S91 ([OS-129-YI](#)), S276 ([WED-385](#))
- Duman, Serkan, S477 ([THU-518](#))
- Dumas, Marc-Emmanuel, S344 ([THU-228](#))
- Dumitrascu, Dan, S646 ([THU-559](#))
- Dumitru, Radu, S819 ([FRI-510](#))
- Dumont, Colin, S464 ([THU-493](#))
- Dumont, Etienne, S115 ([LBP-22](#))
- Dumont-Ryckembusch, Julie, S954 ([THU-267](#))
- Dumortier, Jérôme, S52 ([OS-066](#)), S56 ([OS-073](#)), S61 ([OS-080-YI](#)), S62 ([OS-083-YI](#)), S107 ([LBP-11](#)), S170 ([FRI-443](#)), S467 ([THU-498](#)), S473 ([THU-511](#)), S1005 ([THU-380](#))
- Duncker, Jetske, S69 ([OS-094](#))
- Dunn, Winston, S865 ([SAT-129](#))
- Duong, François H.T., S541 ([SAT-237](#))
- Dupont, Daniel Miotto, S510 ([FRI-305](#))
- Dupuy, Julie, S722 ([SAT-505](#)), S769 ([WED-453](#)), S777 ([WED-469](#))
- Duque, Juan Carlos Rodriguez, S709 ([SAT-484](#))
- Durand, Francois, S577 ([THU-120](#))
- Durand, François, S253 ([WED-348](#))
- Durand, Sarah, S72 ([OS-098](#)), S541 ([SAT-237](#))
- Durkalski-Mauldin, Valerie, S136 ([FRI-393](#))
- Durkin, Russell, S879 ([FRI-120](#))
- Durmazer, Esra, S181 ([FRI-463](#))
- Durmaz, Ozlem, S938 ([TOP-057](#)), S965 ([THU-284](#)), S969 ([THU-289](#))
- Duseja, Ajay Kumar, S51 ([OS-064-YI](#)), S195 ([FRI-546](#)), S627 ([THU-453](#)), S863 ([SAT-125](#))
- Dusheiko, Geoffrey, S905 ([FRI-161](#)), S1060 ([WED-117](#)), S1081 ([WED-143](#)), S1081 ([WED-144](#)), S1179 ([THU-172](#))
- Dusky, Heidi, S822 ([FRI-515](#))
- Dutartre, Dan, S722 ([SAT-505](#)), S769 ([WED-453](#)), S777 ([WED-469](#))
- Dutta, Rimlee, S401 ([WED-304](#))
- Duvauchelle, Thierry, S607 ([THU-419](#))
- Duvoux, Christophe, S103 ([LBP-07](#)), S467 ([THU-498](#)), S473 ([THU-511](#))
- Du, Yingrong, S1209 ([THU-220](#))
- Dvorak, Karel, S292 ([SAT-341](#)), S727 ([SAT-513](#))
- Dwarkanathan, Vignesh, S401 ([WED-304](#))
- Dwinnells, Kristen, S45 ([OS-052](#))
- Dwivedi, Ved, S17 ([OS-006-YI](#))
- Dybowska, Dorota, S505 ([FRI-296](#)), S1205 ([THU-215](#))
- Dyson, Jessica, S56 ([OS-073](#)), S411 ([FRI-331](#))
- Dywicki, Janine, S797 ([WED-537](#))
- Dzen, Lucile, S651 ([SAT-393](#)), S823 ([FRI-517](#))
- Dzhagiashvili, Olga, S845 ([FRI-502](#))
- Eapen, CE, S195 ([FRI-546](#))
- Easom, Nicholas, S848 ([WED-480](#))

- Eaton, John, S56 ([OS-073](#))
 Ebadi, Maryam, S377 ([WED-266](#))
 Ebel, Noelle, S971 ([THU-291](#))
 Ebel, Sebastian, S483 ([THU-529](#)),
 S507 ([FRI-299](#))
 Eberly, Katherine, S464 ([THU-492](#)),
 S614 ([THU-430](#)), S905 ([FRI-159](#))
 Ebert, Matthias, S358 ([FRI-381](#)),
 S491 ([FRI-273](#)), S646 ([THU-559](#))
 Eboko, Marthe Ntep, S1210 ([THU-222](#))
 Ebrahimi, Fahim, S82 ([OS-116-YI](#)),
 S600 ([TOP-079](#))
 Ebwanga, Ebanja Joseph, S1051 ([FRI-272](#))
 Echavarria, Victor, S171 ([FRI-445](#)),
 S251 ([WED-344](#)), S911 ([FRI-171](#))
 Echevarria, Juan Emilio, S902 ([FRI-153](#))
 Ecker, Dominik, S90 ([OS-127-YI](#)),
 S299 ([SAT-521](#))
 Edelman, Elazer, S325 ([WED-220](#)),
 S333 ([WED-235](#))
 Edlund, Karolina, S413 ([FRI-334](#)),
 S778 ([WED-470](#)), S940 ([THU-249](#))
 Edwards, Katherine, S822 ([FRI-515](#))
 Edwards, Lindsey A, S7 ([GS-007](#))
 Ee, Neo Jean, S1204 ([THU-213](#))
 Efe, Cumali, S392 ([WED-290](#))
 Efferth, Thomas, S551 ([SAT-256](#))
 Efole, Jean Rene Ngele, S170 ([FRI-442](#))
 Egerman, Robert, S914 ([FRI-176](#)),
 S1182 ([THU-175](#))
 Egger, Robert, S31 ([OS-029](#)),
 S790 ([WED-522](#))
 Egia-Mendikute, Leire, S532 ([SAT-221](#))
 Eguchi, Hidetoshi, S439 ([SAT-366](#)),
 S509 ([FRI-302](#))
 Eguchi, Yuichiro, S627 ([THU-453](#)),
 S863 ([SAT-125](#))
 Ehmer, Ursula, S47 ([OS-057](#)),
 S431 ([FRI-369](#))
 Ehrenbauer, Alena Friederike,
 S251 ([WED-345](#))
 Eiblmaier, Anja, S507 ([FRI-300](#))
 Eichelberger, Beate, S246 ([WED-338](#))
 Eiteneuer, Eva, S547 ([SAT-248](#))
 Ekong, Udeme, S123 ([LBP-35](#)),
 S387 ([WED-282](#))
 Ekstedt, Mattias, S605 ([THU-414](#)),
 S650 ([TOP-085](#)), S653 ([SAT-397](#)),
 S707 ([SAT-481](#))
 Elamin, Yasir, S724 ([SAT-509](#))
 Elamrawy, Fatema, S1212 ([THU-224](#))
 Elaraki, Fatine, S1002 ([THU-336](#))
 Elbaz, Tamer, S570 ([SAT-291](#))
 Elbeshbeshy, Hany, S89 ([OS-125](#))
 Elefsiniotis, Ioannis, S595 ([THU-149](#)),
 S978 ([THU-298](#)), S1046 ([FRI-264](#)),
 S1128 ([WED-211](#))
 Eley, Timothy, S125 ([LBP-38](#)),
 S1171 ([SAT-202](#))
 Elfaituri, Ahmed, S475 ([THU-515](#))
 Elfaituri, Muhammed, S475 ([THU-515](#))
 Elfishawi, Sally, S570 ([SAT-291](#))
 El Garhy, Naeema, S840 ([FRI-491](#))
 Elgretli, Wesal, S645 ([THU-557](#))
 Elguezabal, Natalia, S532 ([SAT-221](#))
 Elhassan, Ahmad, S1011 ([THU-388](#))
 Elhassan, Moawia, S865 ([SAT-129](#))
 Elhelbawy, Mostafa, S1212 ([THU-224](#))
 Elias, Kathleen, S139 ([FRI-397](#)),
 S829 ([FRI-528](#))
 Eliece Cano, María, S921 ([FRI-188](#)),
 S934 ([FRI-211](#))
 Elie, Sophia, S1156 ([SAT-177](#))
 Eliz, María García, S180 ([FRI-462](#)),
 S1098 ([WED-166](#))
 Elizondo, Martín, S245 ([WED-336](#)),
 S253 ([WED-348](#))
 Elkady, Aly, S319 ([SAT-558](#))
 El-Karim, Lima Awad, S503 ([FRI-293](#))
 El Kassas, Mohamed, S865 ([SAT-129](#))
 Elkhatab, Magdy, S1115 ([WED-191](#))
 El-Khatib, Aiman, S353 ([THU-241](#)),
 S550 ([SAT-255](#)), S779 ([WED-472](#)),
 S795 ([WED-532](#))
 El-Koofy, Nehal, S971 ([THU-291](#))
 Elkrief, Laure, S62 ([OS-083-YI](#)),
 S86 ([OS-121-YI](#)), S87 ([OS-123-YI](#)),
 S253 ([WED-348](#)), S283 ([SAT-327](#)),
 S318 ([SAT-556](#)), S975 ([THU-295](#)),
 S981 ([THU-303](#))
 Ellenrieder, Volker, S799 ([WED-541](#))
 Ellik, Zeynep Melekoglu, S477 ([THU-518](#))
 Ellis, Ewa, S433 ([SAT-353](#))
 Ellis, Hilary, S882 ([FRI-124](#))
 Ellmeier, Wilfried, S739 ([WED-405](#)),
 S746 ([WED-418](#))
 Elmonem, Mohamed, S971 ([THU-291](#))
 Elortza, Felix, S28 ([OS-024-YI](#)),
 S533 ([SAT-223](#)), S534 ([SAT-226](#)),
 S541 ([SAT-238](#)), S544 ([SAT-244](#))
 El-Sayed, Manal Hamdy, S875 ([FRI-115](#))
 Elsayes, Khaled, S516 ([FRI-317](#))
 El-Serag, Hashem, S472 ([THU-508](#))
 Elshabrawi, Ahmed, S203 ([FRI-557](#))
 Elsharkawy, Ahmed, S231 ([THU-368](#)),
 S232 ([THU-370](#))
 Elsis, Zizi, S873 ([FRI-113](#))
 Elston, Robert, S110 ([LBP-15](#)),
 S1039 ([FRI-255](#)), S1154 ([SAT-176](#)),
 S1162 ([SAT-187](#))
 Eltepu, Laxman, S548 ([SAT-251](#))
 Elwick, Hannah, S901 ([FRI-152](#))
 Elwing, Jill, S815 ([FRI-475](#))
 Emilie Kann, Anna, S165 ([FRI-435](#))
 Emmanouilidou, Anastasia,
 S769 ([WED-454](#))
 Encinar, José Antonio, S777 ([WED-468](#))
 Encinosa, Mario de Bonis, S397 ([WED-296](#))
 Enea, Marco, S592 ([THU-144](#)),
 S609 ([THU-421](#)), S803 ([WED-549](#)),
 S1118 ([WED-196](#))
 Engblom, Camilla, S60 ([OS-079-YI](#))
 Engel, Bastian, S42 ([OS-047-YI](#)),
 S425 ([FRI-362](#)), S982 ([THU-304](#))
 Engelmann, Cornelius, S70 ([OS-095-YI](#)),
 S71 ([OS-096-YI](#)), S197 ([FRI-549](#)),
 S201 ([FRI-555](#)), S206 ([TOP-046](#)),
 S767 ([WED-450](#)), S990 ([THU-317](#))
 Engel, Samuel, S49 ([OS-060](#)),
 S610 ([THU-423](#)), S650 ([TOP-085](#)),
 S653 ([SAT-397](#))
 Engels, Zoe, S1021 ([FRI-224](#))
 Englebert, Gael, S621 ([THU-442](#))
 English, Louise, S1075 ([WED-137](#))
 Enkhbat, Anir, S1104 ([WED-175](#))
 Enkhjargal, Saruul, S716 ([SAT-497](#)),
 S718 ([SAT-499](#)), S1104 ([WED-175](#))
 Ennequin, Gael, S806 ([WED-555](#))
 Enomoto, Masaru, S566 ([SAT-286](#))
 Enomoto, Nobuyuki, S1183 ([THU-177](#))
 Enrique, Lisandro Moises, S932 ([FRI-208](#))
 Enríquez-Rodríguez, César Jessé,
 S267 ([WED-370](#)), S273 ([WED-381](#))
 Ensari, Gökce Kobazi, S951 ([THU-264](#))
 Entrialgo, Rodrigo, S560 ([SAT-275](#))
 Epstein, Eliana, S58 ([OS-075](#))
 Epstein, Rachel, S838 ([FRI-489](#)),
 S878 ([FRI-119](#)), S1180 ([THU-173](#))
 Erard, Domitille, S62 ([OS-083-YI](#))
 Ercan, Caner, S214 ([THU-345](#))
 Erdemir, Gizem, S477 ([THU-518](#))
 Erdem, Merve, S542 ([SAT-240](#))
 Erden, Ayse, S65 ([OS-086](#))
 Erdmann, Joris, S836 ([FRI-485](#))
 Erdozaín, José Carlos, S1105 ([WED-177](#))
 Ergenc, Ilkay, S389 ([WED-286](#))
 Erhardt, Andreas, S1137 ([SAT-152](#))
 Erice, Oihane, S534 ([SAT-226](#))
 Erickson, Mary, S378 ([WED-267](#)),
 S426 ([FRI-363](#))
 Eriksen, Peter Lykke, S159 ([FRI-424](#)),
 S257 ([WED-354](#))
 Eriksson, Per, S756 ([WED-434](#))
 Erler, Nicole, S1134 ([SAT-148](#))
 Ertle, Judith, S723 ([SAT-507](#))
 Ertl, Hildegund, S1015 ([TOP-107](#))
 Eruzun, Hasan, S279 ([WED-391](#))
 Escandon, Rafael, S822 ([FRI-515](#))
 Escarrabill, Joan, S497 ([FRI-284](#)),
 S849 ([WED-483](#))
 Escorsell, Àngels, S73 ([OS-100-YI](#)),
 S164 ([FRI-433](#))
 Escudero-García, Desamparados,
 S35 ([OS-035-YI](#)), S682 ([SAT-442](#)),
 S693 ([SAT-460](#))
 Escudero-López, Blanca, S732 ([TOP-090](#))
 Escudero, Raquel, S902 ([FRI-153](#))
 Eshun, John, S971 ([THU-291](#))
 Eskridge, Wayne, S627 ([THU-453](#))
 Eslick, Guy, S132 ([THU-402](#))
 Esli, Medina-Morales, S56 ([OS-073](#))
 Esmat, Gamal, S840 ([FRI-491](#))
 Espérance, Claire, S170 ([FRI-443](#))
 Espina, Silvia, S1187 ([THU-183](#))
 Espindula, Rafael, S1188 ([THU-184](#))
 Espinosa, Jorge Simón, S140 ([FRI-399](#))
 Espiritu, Christine L., S1171 ([SAT-202](#))
 Esplugues, Juan V., S335 ([WED-239](#)),
 S781 ([WED-505](#))
 Esquer, Joshua Covarrubias, S123 ([LBP-35](#)),
 S387 ([WED-282](#))
 Essbauer, Sandra, S945 ([THU-256](#))

Author Index

- Esser, Pia, S422 (FRI-357), S429 (FRI-366)
 Eßing, Tobias, S136 (THU-409)
 Esteban-Fabro, Roger, S48 (OS-059-YI)
 Esteban, Rafael, S896 (FRI-144),
 S904 (FRI-158), S913 (FRI-175),
 S1024 (FRI-228), S1082 (WED-145),
 S1209 (THU-219)
 Estep, James M, S673 (SAT-428),
 S782 (WED-506)
 Estes, Chris, S934 (FRI-212)
 Estevez, Matias, S248 (WED-341)
 Estévez, Olga, S150 (FRI-412),
 S349 (THU-235)
 Estulin, Dmitrii, S612 (THU-426)
 Ettich, Julia, S441 (SAT-368)
 Etzion, Ohad, S9 (GS-012)
 Eun, So-Young, S948 (THU-259)
 Eun Yeon, Jong, S798 (WED-540)
 Evain, Manon, S494 (FRI-279),
 S515 (FRI-316), S585 (THU-133),
 S981 (THU-303), S1005 (THU-380)
 Evangelista, Laura, S685 (SAT-446)
 Evangelista, Lorenzo, S942 (THU-251)
 Evans, Hannah, S337 (WED-243)
 Evans, Helen, S971 (THU-291)
 Evans, Ronald, S662 (SAT-412)
 Evans, Tom, S1169 (SAT-198)
 Everson, Greg, S684 (SAT-444),
 S843 (FRI-498)
 Evert, Katja, S521 (FRI-324)
 Evole, Helena Hernández, S131 (THU-399),
 S135 (THU-406), S158 (FRI-423),
 S405 (WED-311)
 Eyal, Yehezkel, S56 (OS-073)
 Eyck, Annelies Van, S764 (WED-446)
 Eysa, Basem, S1212 (THU-224)
 Ezenkwa, Uchenna Simon, S865 (SAT-129)
 Ezhili, Mullai, S473 (THU-510)
 Ezzat, Doris, S1212 (THU-224)
- Fabiani, Françoise Lunel, S897 (FRI-146)
 Fabrega, Emilio, S481 (THU-525)
 Fabregat, Isabel, S331 (WED-231),
 S529 (SAT-216), S560 (SAT-275)
 Fabre, Jeanne, S150 (FRI-412)
 Fabrellas, Núria, S10 (LBO-01),
 S15 (OS-001), S163 (FRI-431),
 S250 (WED-343), S664 (SAT-415),
 S845 (TOP-054), S851 (WED-486)
 Fabre, Odile, S656 (SAT-403)
 Fabris, Luca, S72 (OS-099), S564 (SAT-283),
 S804 (WED-550)
 Fabritius, Matthias, S576 (THU-118)
 Facchetti, Floriana, S1135 (SAT-149),
 S1142 (SAT-159), S1154 (SAT-175),
 S1159 (SAT-181), S1164 (SAT-190),
 S1170 (SAT-199)
 Factor, Valentina M., S456 (THU-479)
 Fagan, Andrew, S37 (OS-038),
 S242 (WED-331), S342 (TOP-038)
 Fagioli, Franca, S88 (OS-124-YI)
 Fagioli, Stefano, S54 (OS-069),
 S381 (WED-272), S471 (THU-507),
 S920 (FRI-185), S1173 (THU-165)
- Fahnøe, Ulrik, S1050 (FRI-271)
 Fahrer, Jörg, S536 (SAT-230)
 Fainboim, Hugo, S245 (WED-336)
 Faisal, Nabiha, S195 (FRI-546)
 Faisaluddin, Mohammed, S183 (FRI-339)
 Faitot, François, S62 (OS-083-YI),
 S473 (THU-511)
 Fajardo, Jemimah Andrea,
 S298 (SAT-520)
 Fakoury, Max, S1201 (THU-208),
 S1201 (THU-209)
 Falari, Sanyam, S414 (FRI-344)
 Falcato, Luis, S888 (FRI-131)
 Falco, Giuseppe, S1111 (WED-186),
 S1118 (WED-196)
 Falcon-Perez, Juan, S541 (SAT-238)
 Falgà, M Àngels, S843 (FRI-499)
 Falguières, Thomas, S954 (THU-267)
 Fallahzadeh, Mohammad Amin,
 S274 (WED-382)
 Fallen-bailey, Roisin, S16 (OS-003)
 Falletti, Edmondo, S1135 (SAT-149)
 Fall, Fatou, S875 (FRI-115), S916 (FRI-178),
 S1117 (WED-195)
 Fallon, Michael, S458 (THU-482),
 S463 (THU-490)
 Fallowfield, Jonathan, S65 (OS-087),
 S601 (TOP-082)
 Falls, Greg, S35 (OS-034)
 Fan, Chunhong, S514 (FRI-313)
 Fanella, Silvia, S40 (OS-045), S55 (OS-070)
 Fanelli, Fabrizio, S233 (THU-371)
 Fang, Jilian, S243 (WED-332)
 Fang, Wen-Hui, S825 (FRI-521)
 Fang, Zheping, S488 (THU-540)
 Fan, Jian-Gao, S627 (THU-453),
 S863 (SAT-125)
 Fan, Jiangao, S744 (WED-414),
 S756 (WED-433)
 Fan, Junqing, S696 (SAT-463),
 S724 (SAT-510)
 Fan, Rong, S22 (OS-016), S34 (OS-033),
 S1085 (WED-149)
 Fantognon, Gildas, S170 (FRI-442)
 Fan, Xiaotang, S34 (OS-033)
 Faraj, Hazem, S475 (THU-515)
 Farges, Olivier, S500 (FRI-289)
 Fargion, Silvia, S632 (THU-461),
 S814 (FRI-474)
 Farhan, Muhammad, S641 (THU-476)
 Faria, Nancy, S889 (FRI-134)
 Farias, Alberto, S489 (THU-546)
 Farias, Alberto Q., S143 (FRI-404),
 S290 (SAT-337)
 Farias, Alberto Queiroz, S195 (FRI-546)
 Farina, Claudio, S920 (FRI-185)
 Farinati, Fabio, S183 (TOP-049),
 S480 (THU-523), S511 (FRI-308)
 Färkkilä, Martti, S370 (WED-253),
 S403 (WED-307)
 Farmer, Douglas, S453 (SAT-391),
 S730 (TOP-086)
 Farre, Jessica, S497 (FRI-284),
 S849 (WED-483)
- Farrell, Gillian, S16 (OS-004),
 S1211 (THU-223)
 Fatih, Noyan, S797 (WED-537)
 Fatima, Ifrah, S678 (SAT-437)
 Fatta, Erika, S632 (THU-461),
 S645 (THU-557)
 Fauler, Günter, S346 (THU-230),
 S354 (THU-242)
 Faulkes, Rosemary, S274 (WED-382)
 Faulkner, Claire, S611 (THU-424)
 Faure, Frédéric, S172 (FRI-446)
 Faure, Stéphanie, S170 (FRI-443),
 S318 (SAT-556)
 Fawaz, Rima, S971 (THU-291)
 Fayazi, Russta, S762 (WED-442)
 Federico, Alessandro, S105 (LBP-09),
 S107 (LBP-11), S500 (FRI-288),
 S1082 (WED-146)
 Fedorov, Dmitri, S715 (SAT-496)
 Feierbach, Becket, S35 (OS-034)
 Feigh, Michael, S530 (SAT-218),
 S742 (WED-410), S746 (WED-417),
 S763 (WED-445), S788 (WED-519),
 S800 (WED-543)
 Feinman, Leighland, S823 (FRI-516)
 Feinstein, Jeffrey, S971 (THU-291)
 Feio de Azevedo, Rita Furtado,
 S753 (WED-430)
 Felaco, Davide, S287 (SAT-334)
 Felber, Marco, S220 (THU-353)
 Feldbacher, Nicole, S346 (THU-230),
 S354 (THU-242)
 Feld, Jordan J., S9 (GS-012),
 S52 (OS-065-YI), S89 (OS-125),
 S314 (SAT-548), S503 (FRI-293),
 S838 (FRI-489), S900 (FRI-151),
 S967 (THU-286), S1132 (SAT-145)
 Feletti, Valentina, S40 (OS-045),
 S55 (OS-070)
 Felicani, Cristina, S729 (SAT-517)
 Felip, Enriqueta, S375 (WED-263)
 Felipe, Vicente, S423 (FRI-359)
 Feliu-Prius, Anna, S904 (FRI-158),
 S1082 (WED-145)
 Felix, Patricia Peña-San,
 S544 (SAT-244)
 Felix, Sean, S673 (SAT-428)
 Felli, Emanuele, S541 (SAT-237)
 Felli, Eric, S20 (OS-012-YI)
 Feltracco, Paolo, S293 (SAT-343)
 Felzen, Antonia, S969 (THU-289)
 Fenaille, Francois, S206 (TOP-046)
 Feng, Bing, S753 (WED-429)
 Feng, Bo, S425 (FRI-361), S692 (SAT-458),
 S1066 (WED-125)
 Feng, Hao, S454 (TOP-051)
 Feng, I-Cher, S1140 (SAT-157)
 Feng, Lili, S235 (TOP-047)
 Fengou, Polly, S1060 (WED-117),
 S1108 (WED-181)
 Feng, Rilu, S358 (FRI-381)
 Feng, Shibao, S13 (LBO-05)
 Feng, Xudong, S753 (WED-429)
 Feng, Yaoting, S557 (SAT-269)

- Feray, Cyrille, S460 (THU-486), S482 (THU-528)
- Ferenc, Anna, S332 (WED-233)
- Ferenci, Peter, S936 (TOP-055), S1054 (TOP-100), S1135 (SAT-150), S1170 (SAT-200)
- Ferguson, James, S123 (LBP-36), S368 (WED-251), S398 (WED-299), S466 (THU-497)
- Ferguson Theodoro, Carmem, S112 (LBP-16)
- Fernandes, Diogo, S279 (WED-390), S734 (WED-397)
- Fernandes, Gail, S610 (THU-423), S650 (TOP-085), S653 (SAT-397)
- Fernandez, Ainhoa, S133 (THU-404), S481 (THU-525)
- Fernandez-Barrena, Maite G, S526 (TOP-072), S533 (SAT-223), S534 (SAT-226), S537 (SAT-232), S546 (SAT-247), S732 (TOP-090), S770 (WED-457)
- Fernandez-Bermejo, Miguel, S964 (THU-282), S980 (THU-301), S998 (THU-331)
- Fernández, Carmen Sendra, S1126 (WED-208)
- Fernández-Carrillo, Carlos, S164 (FRI-433), S171 (FRI-445), S272 (WED-378), S291 (SAT-340), S683 (SAT-443), S934 (FRI-211)
- Fernandez-Checa, José, S38 (OS-042-YI), S142 (FRI-403), S339 (WED-247)
- Fernandez de Ara, Marta, S533 (SAT-223)
- Fernández-de la Varga, Margarita, S474 (THU-512)
- Fernández, Eduardo López, S936 (FRI-214)
- Fernandez-Fernandez, Maria, S38 (OS-042-YI), S339 (WED-247)
- Fernandez, Javier, S131 (THU-399), S220 (THU-355), S253 (WED-348), S489 (THU-546)
- Fernandez, Jorge Alberto Costa, S269 (WED-374)
- Fernández, José Ramón, S964 (THU-282), S980 (THU-301), S998 (THU-331)
- Fernández, Laura Rey, S269 (WED-374)
- Fernández-Lizaranzu, Isabel, S335 (WED-240), S703 (SAT-472)
- Fernandez, Maria Dolores, S902 (FRI-153)
- Fernández, Mario, S529 (SAT-216)
- Fernández, Marlen Ivon Castellanos, S627 (THU-453), S863 (SAT-125)
- Fernandez, Monique, S625 (THU-450)
- Fernández-Palanca, Paula, S554 (SAT-263)
- Fernandez-Paton, Matias, S682 (SAT-442)
- Fernández-Puertas, Idoia, S137 (FRI-395), S529 (SAT-215), S738 (WED-404), S741 (WED-408)
- Fernández-Rivas, Gema, S1192 (THU-192)
- Fernández Rodríguez, Amanda, S1037 (FRI-251)
- Fernández-Rodríguez, Andrea, S709 (SAT-484)
- Fernandez-Rodriguez, Conrado, S366 (TOP-061)
- Fernández-Rodríguez, Conrado, S171 (FRI-445), S380 (WED-270)
- Fernández-Sánchez, Fernando, S1126 (WED-208)
- Fernandez, Teresa Cabezas, S932 (FRI-207), S1126 (WED-208)
- Fernández, Vanessa García, S760 (WED-440), S770 (WED-457)
- Fernando, Nellie, S606 (THU-416)
- Ferrandino, Giuseppe, S840 (FRI-492)
- Ferrarese, Alberto, S54 (OS-069), S183 (TOP-049), S482 (THU-527), S974 (THU-293), S1082 (WED-146)
- Ferrari, Gaetano De, S713 (SAT-494)
- Ferraro, Donatella, S1111 (WED-186)
- Ferreccio, Catterina, S865 (SAT-129), S900 (FRI-151)
- Ferreira, Carlos Noronha, S86 (OS-121-YI)
- Ferreira, Frederico Campos, S618 (THU-436)
- Ferreira-Gonzalez, Sofia, S434 (SAT-355)
- Ferrer, Cristina Suárez, S690 (SAT-454)
- Ferrer, Joana, S493 (FRI-276), S497 (FRI-284)
- Ferrer, Maria Teresa, S1178 (THU-171)
- Ferretti, Sebastian Eduardo, S245 (WED-336)
- Ferri, Flaminia, S54 (OS-069), S360 (FRI-383)
- Ferrigno, Andrea, S795 (WED-533), S804 (WED-550)
- Ferrocino, Ilario, S804 (WED-551)
- Ferronato, Marco, S384 (WED-278)
- Ferstl, Philip, S185 (FRI-341)
- Festi, Davide, S88 (OS-124-YI), S283 (SAT-327), S974 (THU-293)
- Fettiplace, James, S367 (TOP-062)
- Feuerhake, Friedrich, S561 (SAT-277)
- Fevang, Børre, S478 (THU-520)
- Fialla, Annette, S303 (SAT-528)
- Fiancette, Rémi, S448 (SAT-382)
- Fichera, Anna, S56 (OS-073)
- Fickert, Peter, S403 (WED-307)
- Fiel, Maria Isabel, S997 (THU-328), S1197 (THU-201)
- Figge, Anja, S628 (THU-454)
- Figlerowicz, Magdalena, S1007 (THU-384)
- Figredo, Anita, S852 (WED-488)
- Filatova, Anna, S1210 (THU-221)
- Filho, Raymundo Parana, S132 (THU-401)
- Filigheddu, Nicoletta, S804 (WED-551)
- Filipek, Natalia, S274 (WED-382)
- Filipovic, Iva, S945 (THU-255)
- Filippo Colombo, Daniele, S1034 (FRI-248)
- Filippo, Leonardi, S471 (THU-507)
- Filliol, Aveline, S38 (OS-041-YI)
- Filozof, Claudia, S334 (WED-238), S669 (SAT-423)
- Finan, Amanda, S792 (WED-526)
- Finch, Peter, S522 (FRI-327)
- Finkelmeier, Fabian, S491 (FRI-273), S579 (THU-123), S592 (THU-143), S593 (THU-145), S1039 (FRI-254)
- Fink, Michael, S480 (THU-522)
- Finnegan, Peter, S431 (FRI-368)
- Finnerty, Linda, S1211 (THU-223)
- Finn, Heather, S822 (FRI-515)
- Finnigan, Simon, S846 (WED-478)
- Finn, Richard S., S574 (THU-115), S580 (THU-125)
- Fiorillo, Alessandra, S35 (OS-035-YI)
- Fiorini, Cecilia, S40 (OS-045), S55 (OS-070)
- Fiorotto, Romina, S423 (FRI-358)
- Firestein, Nave, S315 (SAT-550)
- Fischer, Janett, S197 (FRI-549), S201 (FRI-555), S244 (WED-335), S483 (THU-529), S507 (FRI-299), S1043 (FRI-260), S1071 (WED-132)
- Fischer, Julian, S330 (WED-230)
- Fischer, Laurent, S671 (SAT-426)
- Fischer, Lutz, S60 (OS-079-YI)
- Fischer, Ryan, S965 (THU-284), S971 (THU-291)
- Fischler, Björn, S433 (SAT-353), S969 (THU-289), S971 (THU-291)
- Fisseha, Henok, S195 (FRI-546)
- Fitzell, Clare, S850 (WED-484)
- Fitzgerald, Megan, S1029 (FRI-238), S1029 (FRI-239), S1162 (SAT-188)
- Fjellstrom, Ola, S606 (THU-416), S616 (THU-433)
- Fjelstrup, Søren, S510 (FRI-305)
- Flack, Steven, S411 (FRI-331)
- Flaherty, John F., S53 (OS-067), S53 (OS-068), S113 (LBP-20), S1055 (TOP-103), S1091 (WED-158), S1137 (SAT-153)
- Flamm, Steve, S1209 (THU-219)
- Flanagan, Eliza, S15 (OS-002), S860 (SAT-121)
- Flanagan, Stuart, S721 (SAT-504), S1122 (WED-202)
- Flatley, Sarah, S382 (WED-273), S391 (WED-289)
- Flemming, Jennifer, S371 (WED-255), S373 (WED-259), S426 (FRI-363)
- Fletcher, Simon, S1014 (TOP-104), S1019 (FRI-220), S1159 (SAT-182)
- Flint, Emilio, S77 (OS-108-YI), S214 (THU-345), S754 (WED-431)
- Flisiak, Robert, S505 (FRI-296), S646 (THU-559), S1205 (THU-215)
- Floreani, Annarosa, S40 (OS-045), S55 (OS-070), S72 (OS-099), S407 (WED-315)
- Florent, Artru, S975 (THU-295)
- Florent, Demonmerot, S994 (THU-322)
- Flores, Rocio Romero, S18 (OS-007)
- Floriot, Oceane, S1018 (FRI-218)
- Flyer, Abbey, S653 (SAT-398)
- Fodor, Andreea, S86 (OS-121-YI), S151 (FRI-413), S295 (SAT-347), S297 (SAT-519)
- Foerster, Friedrich, S47 (OS-057)
- Foglia, Beatrice, S526 (SAT-211)
- Föh, Bandik, S687 (SAT-449)

Author Index

- Folseraas, Trine, S370 ([WED-254](#)), S541 ([SAT-238](#))
- Fondevila, Constantino, S325 ([WED-220](#))
- Fondevila, Marcos Fernandez, S38 ([OS-041-YI](#)), S326 ([WED-223](#)), S560 ([SAT-275](#))
- Fong, Erica, S808 ([TOP-091](#)), S820 ([FRI-512](#))
- Fong, Khi Yung, S1096 ([WED-165](#))
- Fonkam, Audrey, S1013 ([THU-392](#))
- Fonović, Marko, S553 ([SAT-261](#))
- Fontana, Julien, S598 ([THU-154](#))
- Fontana, Robert, S136 ([FRI-393](#))
- Fontanges, Thierry, S118 ([LBP-27](#))
- Fonte, Stefano, S217 ([THU-350](#)), S218 ([THU-352](#))
- Forastiere, Domenico, S54 ([OS-069](#))
- Forbes, Sharon, S266 ([WED-367](#))
- Forbes, Stuart J., S434 ([SAT-355](#))
- Forcelledo, Jose Luis Fernández, S936 ([FRI-214](#))
- Forés, Ana, S1124 ([WED-205](#))
- Forlano, Roberta, S344 ([THU-228](#)), S601 ([TOP-088](#)), S624 ([THU-446](#)), S719 ([SAT-501](#))
- Forman, Lisa, S388 ([WED-283](#))
- Fornaresio, Lisa, S627 ([THU-453](#))
- Fornari, Francesca, S571 ([TOP-067](#))
- Fornasiere, Ezio, S54 ([OS-069](#)), S402 ([WED-306](#))
- Forner, Alejandro, S493 ([FRI-276](#))
- Forns, Xavier, S31 ([OS-030](#)), S52 ([OS-065-YI](#)), S90 ([OS-127-YI](#)), S135 ([THU-406](#)), S299 ([SAT-521](#)), S405 ([WED-311](#)), S885 ([FRI-128](#)), S921 ([FRI-188](#)), S924 ([FRI-192](#)), S995 ([THU-325](#)), S1089 ([WED-154](#)), S1098 ([WED-166](#)), S1132 ([SAT-145](#)), S1205 ([THU-216](#))
- Forrest, Ewan, S157 ([FRI-422](#)), S274 ([WED-382](#)), S402 ([WED-305](#))
- Fortea, Jose Ignacio, S2 ([GS-003](#)), S87 ([OS-123-YI](#)), S251 ([WED-344](#)), S279 ([TOP-043](#))
- Forton, Daniel, S284 ([SAT-329](#)), S452 ([SAT-389](#))
- Foschi, Francesco, S584 ([THU-131](#)), S593 ([THU-145](#))
- Fossdal, Guri, S370 ([WED-254](#))
- Fosse, Pacome, S598 ([THU-154](#))
- Foster, Graham, S909 ([FRI-165](#)), S912 ([FRI-172](#))
- Foster, Robert, S748 ([WED-420](#)), S770 ([WED-455](#))
- Foti, Michelangelo, S751 ([WED-426](#))
- Fouchard, Isabelle, S667 ([SAT-419](#))
- Foucher, Juliette, S52 ([OS-066](#)), S722 ([SAT-505](#)), S769 ([WED-453](#)), S777 ([WED-469](#)), S1160 ([SAT-184](#))
- Fouquier, Julie, S817 ([FRI-507](#))
- Fougerou-Leurent, Claire, S1161 ([SAT-185](#))
- Fourcaudot, Marcel, S79 ([OS-112](#))
- Fournier-Poizat, Céline, S672 ([SAT-427](#)), S817 ([FRI-507](#))
- Fousekis, Fotios, S922 ([FRI-189](#))
- Fowell, Andrew, S1005 ([THU-381](#))
- Fracanzani, Anna Ludovica, S500 ([FRI-288](#)), S609 ([THU-421](#)), S668 ([SAT-420](#)), S722 ([SAT-506](#)), S744 ([WED-413](#)), S814 ([FRI-474](#))
- Fracassi, Giovanna, S646 ([THU-560](#))
- Fraessdorf, Mandy, S66 ([OS-089](#))
- Fraga, Enrique, S272 ([WED-378](#)), S291 ([SAT-340](#)), S683 ([SAT-443](#))
- França, Paulo Henrique, S626 ([THU-451](#))
- Francesca Donato, Maria, S482 ([THU-527](#))
- Francesca, Giulia, S40 ([OS-045](#)), S55 ([OS-070](#))
- Franceschini, Barbara, S446 ([SAT-377](#))
- Francescut, Christian, S711 ([SAT-489](#))
- Francés, Rubén, S210 ([THU-341](#)), S294 ([SAT-345](#))
- Francione, Paolo, S814 ([FRI-474](#))
- Francioso, Simona, S1056 ([TOP-106](#)), S1072 ([WED-133](#)), S1122 ([WED-203](#))
- Francisco, Aimee, S1202 ([THU-210](#))
- Franco, Andrea Jiménez, S616 ([THU-432](#)), S670 ([SAT-425](#)), S676 ([SAT-433](#))
- Franco, Brunella, S942 ([THU-251](#))
- Franco-Cereceda, Anders, S756 ([WED-434](#))
- Francois, Sandrine, S1150 ([SAT-169](#))
- Francoz, Claire, S10 ([LBO-01](#)), S467 ([THU-498](#)), S473 ([THU-511](#))
- France, Sven, S61 ([OS-080-YI](#)), S83 ([OS-118](#)), S279 ([TOP-043](#)), S300 ([SAT-524](#)), S622 ([THU-444](#)), S627 ([THU-453](#)), S651 ([SAT-393](#)), S753 ([WED-430](#)), S764 ([WED-446](#)), S776 ([WED-466](#)), S790 ([WED-523](#)), S807 ([TOP-077](#)), S823 ([FRI-517](#)), S828 ([FRI-526](#)), S865 ([SAT-129](#))
- Frank, Anna Katharina, S59 ([OS-076](#)), S409 ([TOP-064](#))
- Frankel, Matthew, S985 ([THU-310](#))
- Frankland, Andrew, S1075 ([WED-137](#))
- Frank, Leonie, S422 ([FRI-357](#))
- Frankova, Sona, S963 ([THU-281](#)), S1173 ([THU-164](#))
- Franks, Hester, S127 ([TOP-092](#))
- Frank-Soltysiak, Marie, S408 ([WED-318](#))
- Franza, Anne Minello, S52 ([OS-066](#)), S107 ([LBP-11](#)), S1160 ([SAT-184](#))
- Fraquelli, Mirella, S1154 ([SAT-175](#))
- Fraser, Hannah, S909 ([FRI-165](#))
- Frassanito, Gabriella, S54 ([OS-069](#))
- Fratini, Michela, S360 ([FRI-383](#))
- Fraughen, Daniel, S979 ([THU-300](#))
- Frazzetto, Evelise, S40 ([OS-045](#)), S55 ([OS-070](#))
- Frederick, Richard, S241 ([WED-328](#)), S296 ([SAT-348](#))
- Frederiksen, Peder, S688 ([SAT-451](#)), S826 ([FRI-522](#))
- Freeman, Elliot, S380 ([WED-271](#))
- Freemann, Tomer, S549 ([SAT-252](#))
- Freiburghaus, Michèle, S412 ([FRI-332](#))
- Freire, Bárbara, S132 ([THU-401](#))
- Freistaedter, Andrew, S1020 ([FRI-222](#))
- Freitas, José Bruno, S889 ([FRI-134](#))
- Frelin, Lars, S1038 ([FRI-252](#))
- Frenguelli, Luca, S337 ([WED-243](#))
- Freudenberg, Folke, S1002 ([THU-336](#))
- Frey, Alexandra, S485 ([THU-534](#))
- Freyre, Carolina, S1126 ([WED-208](#))
- Frey, Vanessa, S863 ([SAT-126](#))
- Frias, Juan P, S13 ([LBO-05](#)), S808 ([TOP-091](#))
- Fricker, Zachary, S241 ([WED-328](#))
- Friebe, Andreas, S330 ([WED-230](#)), S797 ([WED-536](#))
- Friedman, Joshua, S49 ([OS-062](#))
- Friedman, Marc, S489 ([TOP-065](#))
- Friedman, Scott, S38 ([OS-041-YI](#)), S119 ([LBP-28](#))
- Fried, Michael, S66 ([OS-089](#)), S1189 ([THU-185](#))
- Fried, Michael W., S89 ([OS-125](#))
- Friedrich-Rust, Mireen, S61 ([OS-080-YI](#))
- Fries, Dietmar, S232 ([THU-369](#))
- Frings, Carmen Alexandra Ginesta, S840 ([FRI-492](#))
- Frion-Herrera, Yahima, S791 ([WED-525](#))
- Frisancho, Luis, S171 ([FRI-445](#))
- Fritz, Laurenz, S288 ([SAT-335](#)), S831 ([FRI-477](#))
- Fritzsch, Sarah, S547 ([SAT-248](#))
- Fromme, Malin, S639 ([THU-472](#)), S951 ([THU-264](#)), S960 ([THU-277](#)), S963 ([THU-281](#))
- Frontino, Anna Maria, S945 ([THU-255](#))
- Fruendt, Thorben, S527 ([SAT-213](#))
- Frühhaber, Friederike, S285 ([SAT-331](#))
- Fry, John, S112 ([LBP-18](#)), S1029 ([FRI-238](#)), S1162 ([SAT-188](#)), S1164 ([SAT-192](#))
- Fuchs, Claudia, S19 ([OS-010-YI](#)), S739 ([WED-405](#)), S746 ([WED-418](#))
- Fuchs, Michael, S37 ([OS-038](#)), S149 ([FRI-411](#)), S627 ([THU-453](#))
- Fuentes, David, S516 ([FRI-317](#))
- Fuentes, Eduardo, S900 ([FRI-151](#))
- Fuentes, Matilde, S664 ([SAT-415](#))
- Fuglsang, Jens, S986 ([THU-311](#))
- Fujii, Hideki, S394 ([WED-293](#)), S686 ([SAT-448](#))
- Fujimori, Sota, S409 ([TOP-060](#))
- Fu, Jing, S805 ([WED-554](#)), S1152 ([SAT-172](#))
- Fujiyama, Shigetoshi, S110 ([LBP-15](#))
- Fu, Juan, S1127 ([WED-210](#))
- Fu, Junliang, S1166 ([SAT-194](#))
- Fukada, Hiroo, S180 ([FRI-461](#)), S744 ([WED-415](#)), S793 ([WED-528](#))
- Fuks, David, S859 ([SAT-120](#))
- Fukumoto, Takumi, S559 ([SAT-272](#))
- Fukunishi, Shinya, S584 ([THU-131](#))
- Fukushima, Masanori, S178 ([FRI-458](#)), S565 ([SAT-285](#)), S1177 ([THU-170](#))
- Fu, Lei, S951 ([THU-264](#))
- Fulgenzi, Claudia, S491 ([FRI-273](#)), S575 ([THU-116](#)), S582 ([THU-128](#)), S586 ([THU-134](#))
- Fumolo, Elisa, S402 ([WED-306](#))
- Fundora, Yilliam, S325 ([WED-220](#)), S469 ([THU-501](#)), S486 ([THU-536](#)), S737 ([WED-403](#))

- Fung, Jeremy, S58 (OS-075)
 Fung, Scott, S53 (OS-067), S1137 (SAT-153)
 Fung, Scott K, S314 (SAT-548), S1115 (WED-191)
 Fung, Scott K., S1034 (FRI-248)
 Fung, Yan Yue James, S274 (WED-382)
 Funuyet-Salas, Jesús, S632 (THU-462), S640 (THU-474)
 Fu, Rebecca, S1020 (FRI-222), S1021 (FRI-224)
 Furiosi, Valeria, S749 (WED-423), S774 (WED-461)
 Furquim d'Almeida, Arno, S52 (OS-065-YI)
 Fürst, Anna, S33 (OS-032), S442 (TOP-053)
 Fürst, Stefan, S354 (THU-242)
 Furukawa, Nathan, S890 (FRI-135)
 Furumaya, Alicia, S568 (SAT-289), S836 (FRI-485)
 Fu, Siyu, S496 (FRI-282)
 Fuß, Johannes, S450 (SAT-385)
 Fuster, Carla, S493 (FRI-276)
 Fuster, Josep, S493 (FRI-276)
 Fuster-Martínez, Isabel, S335 (WED-239), S781 (WED-505)
 Fytili, Paraskevi, S1128 (WED-211)
- Gabbia, Daniela, S322 (TOP-037), S770 (WED-456), S791 (WED-525)
 Gabellini, Davide, S749 (WED-423)
 Gabeta, Stella, S400 (WED-302)
 Gabriela, Indre Madalina, S151 (FRI-413)
 Gabrielli, Filippo, S729 (SAT-517)
 Gabriel, Maria Magdalena, S251 (WED-345)
 Gabriel, Shiraaz, S1108 (WED-181)
 Gabunia, Tamar, S881 (FRI-123), S891 (FRI-136), S898 (FRI-147), S909 (FRI-167), S925 (FRI-193), S931 (FRI-205), S933 (FRI-210), S1204 (THU-214)
 Gadano, Adrian, S110 (LBP-15), S245 (WED-336), S253 (WED-348), S274 (WED-382)
 Gadd, Victoria, S434 (SAT-355)
 Gadenne, Cloé, S72 (OS-098)
 Gadge, Pournima, S830 (FRI-530)
 Gadipudi, Laila lavanya, S751 (WED-425)
 Gadi, Zouhir, S83 (OS-118), S622 (THU-444)
 Gaeta, Giovanni Battista, S1103 (WED-174)
 Gagliani, Nicola, S60 (OS-079-YI)
 Gagliardini, Roberta, S907 (FRI-164)
 gagliardi, roberta, S237 (WED-320)
 Gagnon-Sanschagrin, Patrick, S291 (SAT-339)
 Gagnon, William, S431 (FRI-368)
 Gaia, Silvia, S526 (SAT-211)
 Gaio, Paola, S966 (THU-285)
 Gairing, Simon J., S271 (WED-377), S277 (WED-387)
 Gairing, Simon Johannes, S47 (OS-057), S251 (WED-345)
 Gaiser, Timo, S536 (SAT-230)
 Gakima, Primitive, S69 (OS-094)
 Galanis, Petros, S595 (THU-149)
 Galati, Giovanni, S1122 (WED-203)
 Galdavadze, Ketevan, S891 (FRI-136), S898 (FRI-147)
 Gallacher, Jenny, S603 (THU-412), S685 (SAT-447), S688 (SAT-452)
 Gallagher, Mary Leslie, S37 (OS-038)
 Gallay, Philippe, S748 (WED-420), S770 (WED-455)
 Gallego, Adolfo, S376 (WED-264)
 Gallego-Durán, Rocío, S335 (WED-240), S732 (TOP-090), S760 (WED-440), S770 (WED-457)
 Gallego, Esther Quintana, S838 (FRI-488)
 Gallego, Javier, S760 (WED-440)
 Galle, Peter, S26 (OS-022), S251 (WED-345), S264 (WED-365), S271 (WED-377), S277 (WED-387), S536 (SAT-230), S557 (SAT-268), S575 (THU-116), S586 (THU-134), S618 (THU-437), S640 (THU-474), S1139 (SAT-156)
 Galli, Andrea, S545 (SAT-245), S550 (SAT-254)
 Galli, Laura, S120 (LBP-29), S837 (FRI-487)
 Gallo, Paolo, S36 (OS-036)
 Galocsy, Chantal De, S1114 (WED-190)
 Galsgaard, Elisabeth, S321 (TOP-036), S742 (WED-411), S748 (WED-421), S784 (WED-511)
 Galun, Eithan, S549 (SAT-252)
 Gamangatti, Shivanand, S587 (THU-135)
 Gambardella, Gennaro, S942 (THU-251)
 Gambaro, Francesco Luigi, S360 (FRI-383)
 Gambato, Martina, S183 (TOP-049), S482 (THU-527)
 Gambino, Roberto, S605 (THU-415), S611 (THU-425)
 Gámez, Emanuel, S547 (SAT-249)
 Gamkrelidze, Amir, S881 (FRI-123), S891 (FRI-136), S1204 (THU-214)
 Gamkrelidze, Ivane, S872 (TOP-096), S910 (FRI-170), S934 (FRI-212)
 Gampa, Anuhya, S586 (THU-134)
 Ganananadan, Kohilan, S10 (LBO-01), S203 (FRI-557)
 Ganatra, Nazila, S100 (LBP-01)
 Gandelman, Olga, S840 (FRI-492)
 Gander, Amir, S220 (THU-355)
 Gandhi, Harsh, S405 (WED-312)
 Gane, Edward J., S11 (LBO-02), S31 (OS-030), S32 (OS-031), S53 (OS-067), S112 (LBP-18), S967 (THU-286), S1034 (FRI-248), S1137 (SAT-153), S1149 (SAT-168), S1161 (SAT-186), S1162 (SAT-188), S1164 (SAT-192)
 Ganesan, Raja, S156 (FRI-420), S177 (FRI-456), S220 (THU-354), S343 (THU-227)
 Gankina, Natalya Urievna Gankina Urievna, S110 (LBP-15)
 Gan, Li Ming, S794 (WED-530), S1018 (FRI-217), S1152 (SAT-172)
 Ganne-Carrié, Nathalie, S46 (OS-055), S52 (OS-066), S61 (OS-081), S107 (LBP-11), S492 (FRI-274), S498 (FRI-286), S577 (THU-119), S833 (FRI-480), S1160 (SAT-184), S1161 (SAT-185)
 Ganne, Nathalie, S577 (THU-120), S585 (THU-133)
 Ganova-Raeva, Lilia, S891 (FRI-136), S905 (FRI-160)
 Ganry, Olivier, S61 (OS-081), S161 (FRI-429)
 Gansner, John, S49 (OS-062)
 Gantzel, Rasmus Hvidbjerg, S239 (WED-325), S390 (WED-287), S841 (FRI-494), S968 (THU-287)
 Gao, Ce, S1053 (SAT-142)
 Gao, Fangyuan, S193 (FRI-544)
 Gao, Feiqiong, S753 (WED-429)
 gao, haibing, S274 (WED-382)
 Gao, Hongbo, S34 (OS-033)
 Gao, Hui, S1127 (WED-210)
 Gao, Jian-Neng, S1180 (THU-174), S1206 (THU-217)
 Gao, Jing, S773 (WED-460)
 Gao, Juan, S551 (SAT-257)
 Gao, Pujun, S34 (OS-033)
 Gao, Qian, S165 (FRI-434)
 Gao, Rong, S786 (WED-514)
 Gao, Shan, S794 (WED-530), S1018 (FRI-217)
 Gao, Yanhang, S128 (THU-393), S189 (FRI-536), S196 (FRI-547), S202 (FRI-556), S327 (WED-225), S406 (WED-313)
 Gao, Yinjie, S1066 (WED-125)
 Gao, Yiyun, S540 (SAT-236)
 Gao, Yuan, S235 (TOP-047)
 Gao, Yu-Feng, S1165 (SAT-193)
 Gao, Yunfei, S1102 (WED-172)
 gao, zhiliang, S195 (FRI-546)
 Garbin, Marta, S668 (SAT-420)
 Garcia, Alberto Garcia, S248 (WED-341)
 Garcia, Ana Belen Rubio, S250 (WED-343), S664 (SAT-415)
 Garcia-Buey, Luisa, S366 (TOP-061), S380 (WED-270)
 García, Clàudia, S995 (THU-325)
 García-Criado, Maria Ángeles, S87 (OS-123-YI), S497 (FRI-284), S579 (THU-124), S843 (FRI-499)
 Garcia-Delgado, Noemi, S791 (WED-524)
 Garcia, Dwayne, S266 (WED-367)
 Garcia, Federico Garcia, S921 (FRI-188), S1126 (WED-208)
 García-Fernandez de Barrena, Maite, S560 (SAT-275)
 Garcia-Garcia, Selene, S1024 (FRI-228)
 García-García, Sonia, S171 (FRI-445), S180 (FRI-462), S476 (THU-517)
 García-Gaytán, Ana Cristina, S547 (SAT-249)
 Garcia-Guix, Maria, S105 (LBP-09)
 García-Heredia, José Manuel, S529 (SAT-216)
 Garcia, Jennifer, S972 (THU-291)
 Garcia-Larsen, Vanessa, S859 (SAT-119)
 Garcia-Lezana, Teresa, S527 (SAT-213)
 García-López, Mirea, S1089 (WED-154)

Author Index

- García-Luna, Pedro Pablo, S838 ([FRI-488](#))
- García, Maria Luisa Gutierrez, S366 ([TOP-061](#)), S587 ([THU-136](#))
- García, Miriam Soriano, S892 ([FRI-139](#)), S898 ([FRI-148](#))
- García-Monzón, Carmelo, S700 ([SAT-468](#))
- García, Osiris German Idelfonso, S151 ([FRI-414](#))
- García, Pablo Bellot, S1178 ([THU-171](#))
- García, Pablo Miles Wolfe, S936 ([FRI-214](#))
- García Pagan, Juan Carlos, S87 ([OS-123-YI](#))
- García-Palomo, Andrés, S554 ([SAT-263](#))
- García-Pras, Ester, S1089 ([WED-154](#))
- García-Retortillo, Montserrat, S105 ([LBP-09](#)), S267 ([WED-370](#)), S273 ([WED-381](#)), S376 ([WED-264](#)), S380 ([WED-270](#)), S399 ([WED-300](#)), S1098 ([WED-166](#))
- García-Ruiz, M. Carmen, S38 ([OS-042-YI](#)), S339 ([WED-247](#))
- García-Sáez, Juan, S331 ([WED-231](#))
- García-Sánchez, Araceli, S697 ([SAT-465](#)), S1105 ([WED-177](#))
- García, Sergio, S865 ([SAT-129](#)), S900 ([FRI-151](#))
- García, Soledad Sañudo, S480 ([THU-524](#))
- García, Sonia, S485 ([THU-535](#))
- García-Tsao, Guadalupe, S105 ([LBP-09](#)), S256 ([WED-352](#)), S258 ([WED-355](#))
- García-Villarreal, Luis, S964 ([THU-282](#)), S980 ([THU-301](#)), S996 ([THU-326](#)), S998 ([THU-331](#))
- Garcovich, Matteo, S105 ([LBP-09](#))
- Gardener, Matthew, S215 ([THU-346](#))
- Gardini, Andrea Casadei, S12 ([LBO-04](#)), S499 ([FRI-287](#)), S584 ([THU-131](#)), S593 ([THU-145](#))
- Gardy, Joséphine, S855 ([TOP-098](#))
- Garg, Love, S290 ([SAT-338](#))
- Garg, Prince, S228 ([THU-362](#)), S357 ([THU-248](#))
- Garioud, Armand, S930 ([FRI-204](#))
- Garlick, Kelsey, S422 ([FRI-356](#))
- Garnaud, Cécile, S894 ([FRI-142](#))
- Garner, Will, S56 ([OS-072](#)), S370 ([WED-252](#)), S387 ([WED-282](#))
- Garrido, Isabel, S835 ([FRI-483](#))
- Garrido, Maria, S245 ([WED-336](#))
- Garrido, Maria Angeles Lopez, S248 ([WED-341](#)), S1126 ([WED-208](#))
- Garrido, Patricia, S740 ([WED-406](#)), S825 ([FRI-520](#))
- Garrigou, Olivia, S1109 ([WED-182](#))
- Garrison, Louis, S873 ([FRI-113](#))
- Garriss, George, S1013 ([THU-392](#))
- Gart, Eveline, S786 ([WED-515](#))
- Gasbarrini, Antonio, S105 ([LBP-09](#)), S252 ([WED-347](#)), S578 ([THU-122](#)), S660 ([SAT-409](#)), S723 ([SAT-508](#)), S981 ([THU-302](#))
- Gasink, Christopher, S118 ([LBP-26](#)), S647 ([TOP-074](#))
- Gaßler, Nikolaus, S413 ([FRI-334](#))
- Gastaldelli, Amalia, S536 ([SAT-229](#)), S605 ([THU-415](#)), S611 ([THU-425](#)), S626 ([THU-452](#))
- Gato Zambrano, Sheila, S770 ([WED-457](#))
- Gatselis, Nikolaos, S42 ([OS-047-YI](#)), S56 ([OS-073](#)), S400 ([WED-302](#)), S421 ([FRI-354](#)), S579 ([THU-123](#))
- Gatto, Chiara, S457 ([THU-480](#))
- Gat-Viks, Irit, S955 ([THU-269](#))
- Gatzios, Alexandra, S752 ([WED-428](#)), S775 ([WED-465](#))
- Gaudio, Eugenio, S994 ([THU-323](#))
- Gaudio, Francesca Di, S568 ([SAT-288](#))
- Gautam, Jaya, S762 ([WED-442](#))
- Gautam, Pramod, S218 ([THU-351](#)), S228 ([THU-362](#))
- Gautam, Shivani, S348 ([THU-234](#))
- Gautier, Jean-François, S106 ([LBP-10](#)), S670 ([SAT-424](#)), S681 ([SAT-440](#))
- Gautier, Philippe, S122 ([LBP-33-YI](#))
- Gavish, Avishai, S669 ([SAT-423](#))
- Gavrisheva, Sofiya, S1210 ([THU-221](#))
- Gawrieh, Samer, S612 ([THU-427](#)), S649 ([TOP-080](#))
- Gawron, Jana, S447 ([SAT-379](#))
- Gay, Joel, S722 ([SAT-505](#)), S769 ([WED-453](#)), S777 ([WED-469](#))
- Gay, Matthieu, S1193 ([THU-194](#))
- Gazelakis, Kathryn, S380 ([WED-271](#))
- Gaziz, Derek, S66 ([OS-089](#))
- Gaztambide, Sonia, S741 ([WED-408](#))
- Gazzin, Silvia, S768 ([WED-452](#))
- Gebhardt, Rolf, S362 ([FRI-386](#))
- Geenes, Victoria, S36 ([OS-037](#))
- Geeraedts, Tychon, S306 ([SAT-536](#))
- Geerts, Anja, S172 ([FRI-447](#)), S226 ([THU-361](#)), S229 ([THU-364](#)), S307 ([SAT-538](#)), S743 ([WED-412](#)), S787 ([WED-516](#)), S807 ([TOP-077](#))
- Geervliet, Eline, S137 ([FRI-394](#)), S764 ([WED-447](#))
- Gefen, Maytal, S549 ([SAT-252](#))
- Geh, Daniel, S538 ([SAT-234](#)), S542 ([SAT-239](#)), S565 ([SAT-284](#))
- Geier, Andreas, S47 ([OS-057](#)), S90 ([OS-126](#)), S108 ([LBP-12](#)), S596 ([THU-150](#)), S625 ([THU-449](#)), S687 ([SAT-449](#)), S733 ([WED-396](#)), S1139 ([SAT-156](#))
- Geisler, Fabian, S431 ([FRI-369](#))
- Geissler, Edward, S103 ([LBP-07](#))
- Geladari, Eleni, S262 ([WED-362](#)), S978 ([THU-298](#)), S1128 ([WED-211](#))
- Gelsomino, Fabio, S942 ([THU-251](#))
- Gelson, Will, S1075 ([WED-137](#))
- Gelu-Simeon, Moana, S61 ([OS-081](#)), S498 ([FRI-286](#))
- Gencdal, Genco, S181 ([FRI-463](#)), S928 ([FRI-199](#))
- Genç, Sezen, S709 ([SAT-485](#))
- Genda, Takuya, S633 ([THU-463](#)), S1041 ([FRI-257](#))
- Genesca, Joan, S3 ([GS-003](#)), S87 ([OS-123-YI](#)), S90 ([OS-127-YI](#)), S279 ([TOP-043](#)), S299 ([SAT-521](#)), S780 ([WED-474](#)), S963 ([THU-281](#))
- Genescà, Joan, S819 ([FRI-509](#))
- Geng, Anne, S754 ([WED-431](#))
- Genger, Jakob-Wendelin, S739 ([WED-405](#)), S746 ([WED-418](#))
- Geng, Jiawei, S1133 ([SAT-147](#))
- Geng, WenQian, S835 ([FRI-484](#))
- Geng, Yana, S740 ([WED-407](#)), S798 ([WED-538](#))
- Geng, Yu, S1022 ([FRI-225](#)), S1071 ([WED-131](#))
- Genovese, Mark, S11 ([LBO-03](#))
- Genovese, Michela, S640 ([THU-475](#)), S691 ([SAT-457](#))
- Genov, Jordan, S807 ([TOP-077](#))
- Gensluckner, Sophie, S863 ([SAT-126](#))
- Gentile, Ivan, S1082 ([WED-146](#))
- Gentilucci, Umberto Vespasiani, S36 ([OS-036](#)), S374 ([WED-260](#)), S500 ([FRI-288](#)), S665 ([SAT-416](#)), S803 ([WED-549](#))
- Gentleman, Eileen, S324 ([WED-218](#))
- Georgaka, Sokratia, S8 ([GS-010](#))
- George, Jacob, S195 ([FRI-546](#)), S274 ([WED-382](#)), S863 ([SAT-125](#)), S865 ([SAT-129](#))
- George, Josiah T., S948 ([THU-260](#))
- George, Michael, S1075 ([WED-137](#))
- Georges, Bertrand, S50 ([OS-063](#))
- Georg, Simon Karl, S1147 ([TOP-110](#))
- Gerasimidis, Konstantinos, S987 ([THU-312](#))
- Gerber, Athenais, S1150 ([SAT-169](#))
- Gerber, Lynn, S627 ([THU-453](#))
- Gerbes, Alexander, S313 ([SAT-546](#))
- Geretti, Anna Maria, S522 ([FRI-327](#)), S1056 ([TOP-106](#))
- Gerevini, Chiara, S599 ([THU-156](#))
- Gericke, Martin, S753 ([WED-430](#))
- Germanidis, Georgios, S1128 ([WED-211](#))
- Germani, Giacomo, S183 ([TOP-049](#))
- Gerolami, René, S356 ([THU-247](#))
- Gerra, Merce Delgado, S1098 ([WED-166](#))
- Gérus-Durand, Marie, S792 ([WED-526](#))
- Gerussi, Alessio, S374 ([WED-260](#)), S381 ([WED-272](#)), S383 ([WED-276](#)), S982 ([THU-304](#))
- Gervais, Anne, S52 ([OS-066](#)), S107 ([LBP-11](#))
- Gessner, Ryan, S765 ([WED-448](#))
- Getia, Vladimer, S890 ([FRI-135](#)), S925 ([FRI-193](#)), S931 ([FRI-205](#)), S933 ([FRI-210](#))
- Gevers, Tom, S14 ([LBO-06](#)), S373 ([WED-258](#)), S982 ([THU-304](#))
- Ge, Xiaodong, S80 ([OS-113](#))
- Gex, Quentin, S24 ([OS-018-YI](#))
- Geyvandova, Natalia, S53 ([OS-068](#))
- Ghabina, Sherif, S193 ([FRI-543](#))
- Ghadban, Tarik, S60 ([OS-079-YI](#))
- Ghaffari-Laleh, Narmin, S12 ([LBO-04](#))
- Ghai, Megan, S458 ([THU-482](#))
- Ghaleh, Bijan, S456 ([THU-478](#))
- Ghallab, Ahmed, S940 ([THU-249](#))
- Ghallab, Mohammed, S458 ([THU-483](#))

- Ghannouchi, Haroun, S585 (THU-133)
 Gheorghe, Cristian, S899 (FRI-150)
 Gheorghe, Liana, S9 (GS-012),
 S899 (FRI-150)
 Gherardi, Gaia, S322 (TOP-037)
 Gherlan, George Sebastian, S9 (GS-012),
 S1054 (TOP-100)
 Ghesquière, Bart, S452 (SAT-390)
 Ghimire, Sabitri, S433 (SAT-354)
 Ghioca, Mihaela, S899 (FRI-150)
 Ghittoni, Giorgia, S586 (THU-134)
 Ghosh, Indrajit, S721 (SAT-504),
 S1122 (WED-202)
 Giacchetto, Marco, S40 (OS-045),
 S55 (OS-070)
 Giacchetto, Marco, S592 (THU-144)
 Giannelli, Gianluigi, S493 (FRI-277),
 S495 (FRI-280)
 Giannelli, Valerio, S54 (OS-069),
 S247 (WED-340), S482 (THU-527),
 S994 (THU-323)
 Giannini, Edoardo, S511 (FRI-308)
 Giannini, Edoardo Giovanni,
 S40 (OS-045), S54 (OS-069),
 S55 (OS-070), S374 (WED-260),
 S586 (THU-134)
 Giannitrapani, Lydia, S568 (SAT-288)
 Giannone, Fabio, S541 (SAT-237)
 Giannou, Anastasios, S525 (TOP-069)
 Giannoulis, George, S1128 (WED-211)
 Gianoncelli, Alessandra, S360 (FRI-383)
 Gibaja, Veronica, S526 (TOP-072)
 Gibbs, Craig, S5 (GS-005)
 Gibson, Andy, S909 (FRI-165)
 Gibson, Robert, S195 (FRI-546)
 Gieger, Christian, S968 (THU-288)
 Gielen, Vera, S1141 (SAT-158),
 S1145 (SAT-164)
 Giera, Martin, S786 (WED-515)
 Gies, Inge, S65 (OS-088)
 Gigante, Elia, S577 (THU-119)
 Gigi, Eleni, S730 (SAT-518)
 Gigliotti, Luca C., S751 (WED-425)
 Gignoux, Etienne, S69 (OS-094)
 Giladi, Hilla, S549 (SAT-252)
 Gilbert, Benoit, S24 (OS-018-YI)
 Gilbert, Jack, S662 (SAT-412)
 Gil, Erik Ramon, S538 (SAT-234)
 Giles, Benjamin, S1005 (THU-381)
 Gilgenkrantz, Hélène, S435 (SAT-358)
 Gil-Gomez, Antonio, S760 (WED-440),
 S770 (WED-457)
 Gilg, Stefan, S44 (OS-050-YI)
 Gillard, Justine, S772 (WED-458)
 Gillberg, Per-Göran, S57 (OS-074-YI)
 Gillevet, Patrick, S342 (TOP-038),
 S347 (THU-233)
 Gill, Madeleine, S230 (THU-367)
 Gill, Upkar, S118 (LBP-27), S558 (SAT-271),
 S1024 (FRI-229), S1033 (FRI-246),
 S1105 (WED-176)
 Gil, Mar, S780 (WED-474)
 Gilmour, Susan, S123 (LBP-35),
 S387 (WED-282)
 Gil-Pitarch, Claudia, S140 (FRI-399),
 S529 (SAT-216), S544 (SAT-244),
 S546 (SAT-247)
 Gilson, Richard, S721 (SAT-504),
 S1122 (WED-202)
 Gimenez-Garzo, Carla, S423 (FRI-359)
 Gimignani, Giancarlo, S40 (OS-045),
 S55 (OS-070)
 Giné, Alvaro Eguilero, S544 (SAT-244)
 Ginès, Pere, S10 (LBO-01), S15 (OS-001),
 S158 (FRI-423), S163 (FRI-431),
 S166 (FRI-437), S250 (WED-343),
 S664 (SAT-415), S737 (WED-403),
 S845 (TOP-054), S851 (WED-486)
 Ginés, Raquel Fernández, S777 (WED-468)
 Ginion, Audrey, S439 (SAT-364)
 Gioia, Stefania, S87 (OS-123-YI),
 S237 (WED-320), S251 (WED-345),
 S950 (THU-261), S994 (THU-323)
 Giordanengo, Valérie, S1158 (SAT-180)
 Giorgio, Angelo Di, S938 (TOP-057)
 Giorgio, Massimo De, S471 (THU-507)
 Giovannini, Catia, S571 (TOP-067)
 Giral, Marcos, S865 (SAT-129),
 S900 (FRI-151)
 Giráldez-Gallego, Alvaro,
 S1098 (WED-166), S1126 (WED-208)
 Giralt, Albert, S762 (WED-442)
 Girardi, Enrico, S907 (FRI-164)
 Girardi, Noemi, S564 (SAT-283)
 Giraud, Guillaume, S1014 (TOP-104)
 Giraudi, Pablo J, S768 (WED-452),
 S793 (WED-529)
 Giraudo, Chiara, S990 (THU-316)
 Girbes, Alexandre Perez, S682 (SAT-442)
 Giri, Dewan, S729 (SAT-516)
 Girija, Sanal Madhusudana,
 S207 (THU-337)
 Gish, Robert G., S882 (FRI-124),
 S900 (FRI-151), S901 (FRI-152),
 S1072 (WED-134), S1087 (WED-151),
 S1089 (WED-153), S1093 (WED-160),
 S1121 (WED-200)
 Gitahi, Jane, S858 (SAT-118),
 S1198 (THU-203)
 Gitahi, Priscillah, S69 (OS-094)
 Giudicelli, Héloïse, S494 (FRI-279),
 S515 (FRI-316)
 Giudicelli-Lett, Heloïse, S87 (OS-123-YI),
 S589 (THU-139)
 Giuffrè, Mauro, S711 (SAT-489)
 Giuffrida, Paolo, S592 (THU-144)
 Giuli, Lucia, S252 (WED-347),
 S981 (THU-302)
 Giuly, Nathalie, S1093 (WED-159)
 Giunta, Diego, S245 (WED-336),
 S253 (WED-348)
 Giustini, Leonardo, S5 (GS-005)
 Gjini, Kamela, S521 (FRI-325),
 S617 (THU-435), S637 (THU-470),
 S704 (SAT-474), S713 (SAT-494)
 Gkantsinikoudi, Christina, S39 (OS-043)
 Glampson, Ben, S1075 (WED-137)
 Glaus, Jesus, S737 (WED-402)
 Gleeson, Dermot, S382 (WED-273),
 S391 (WED-289)
 Glenister, Kristen, S861 (SAT-123)
 Glenn, Jeffrey, S9 (GS-012)
 Glickman, Jonathan, S31 (OS-029),
 S790 (WED-522)
 Gliddon, Louise, S215 (THU-346)
 Glitscher, Mirco, S1039 (FRI-254),
 S1042 (FRI-259)
 Gliwicz, Dorota, S971 (THU-291)
 Gloor, Severin, S44 (OS-050-YI)
 Gluud, Lise Lotte, S65 (OS-088),
 S165 (FRI-434), S321 (TOP-036),
 S614 (THU-429), S702 (SAT-471),
 S742 (WED-411)
 Gnemmi, Viviane, S12 (LBO-04),
 S146 (FRI-408)
 Gobbo, Giulia, S105 (LBP-09)
 Godec, Sergej, S142 (FRI-403)
 Godey, Sameer, S209 (THU-339)
 Godinho-Santos, Ana, S279 (WED-390)
 Goedhals, Dominique, S1108 (WED-181)
 Goediker, Juliana, S979 (THU-299),
 S1139 (SAT-156)
 Goel, Amit, S1050 (FRI-269)
 Goel, Ashish, S87 (OS-123-YI),
 S274 (WED-382)
 Goeman, Els, S764 (WED-446)
 Goepfert, Benjamin, S547 (SAT-248)
 Goffaux, Alexis, S464 (THU-493),
 S639 (THU-473)
 Goff, Cameron, S173 (FRI-448),
 S472 (THU-508)
 Goffic, Charles Le, S74 (OS-104)
 Gogia, Marine, S921 (FRI-187)
 Gogia, Sudhanshu, S808 (TOP-091)
 Gogna, Apoorva, S582 (THU-129),
 S591 (THU-142)
 Goh, Boon Bee George, S967 (THU-286),
 S1096 (WED-165)
 Goh, Brian, S591 (THU-142)
 Gohil, Vikrant, S1051 (FRI-272)
 Goh, Jade Shu Qi, S591 (THU-142)
 Göhlmann, Hinrich, S1034 (FRI-248)
 Goh, Myungji, S267 (WED-369),
 S305 (SAT-533), S513 (FRI-312),
 S631 (THU-459), S821 (FRI-514)
 Goicoechea, Ibai, S534 (SAT-226)
 Goikoetxea, Naroa, S140 (FRI-399),
 S529 (SAT-216), S532 (SAT-221),
 S544 (SAT-244), S546 (SAT-247)
 Gokcan, Hale, S181 (FRI-463),
 S477 (THU-518)
 Gökden, Yasemin, S279 (WED-391)
 Golabi, Pegah, S600 (TOP-081),
 S627 (THU-453), S861 (SAT-122)
 Golamari, Srinivasa Reddy, S293 (SAT-344)
 Goldberg, David, S398 (WED-298),
 S459 (THU-484), S470 (THU-504)
 Goldberg, Lital, S128 (THU-394)
 Goldenberg, Simon, S7 (GS-007)
 Goldin, Robert D., S624 (THU-446),
 S719 (SAT-501)
 Goldklang, Monica, S85 (OS-120)

Author Index

- Golembo, Myriam, S409 ([TOP-060](#))
 Golfetto, Federica, S992 ([THU-318](#))
 Golla, Rithvik, S587 ([THU-135](#))
 Golovin, Alexey, S59 ([OS-076](#))
 Golse, Nicolas, S458 ([THU-483](#))
 Gomma, Asmaa, S1212 ([THU-224](#))
 Gömer, Andre, S1032 ([FRI-244](#))
 Gomez, Angela Carvalho, S476 ([THU-517](#))
 Gómez, Araceli Casado, S921 ([FRI-188](#))
 Gomez-Cabrero, David, S143 ([FRI-404](#)),
 S290 ([SAT-337](#))
 Gómez- Camarero, Judith, S700 ([SAT-468](#)),
 S980 ([THU-301](#)), S996 ([THU-326](#)),
 S998 ([THU-331](#))
 Gómez-Camarero, Judith, S376 ([WED-264](#)),
 S380 ([WED-270](#)), S392 ([WED-290](#)),
 S399 ([WED-300](#)), S964 ([THU-282](#))
 Gómez, Concepción, S164 ([FRI-433](#))
 Gomez, Diana Carolina, S869 ([SAT-133](#))
 Gómez-Domínguez, Elena, S366 ([TOP-061](#))
 Gomez, Eduardo Vilar, S171 ([FRI-444](#)),
 S612 ([THU-427](#)), S649 ([TOP-080](#))
 Gomez-Gonzalez, Emilio, S335 ([WED-240](#))
 Gómez-Hurtado, Isabel, S210 ([THU-341](#))
 Gomez-Jauregui, Paul, S137 ([FRI-395](#)),
 S529 ([SAT-215](#)), S741 ([WED-408](#))
 Gomez, Manuel Romero, S8 ([GS-009](#)),
 S35 ([OS-035-YI](#)), S49 ([OS-060](#)),
 S248 ([WED-341](#)), S302 ([SAT-526](#)),
 S335 ([WED-240](#)), S609 ([THU-421](#)),
 S632 ([THU-462](#)), S654 ([SAT-400](#)),
 S700 ([SAT-468](#)), S703 ([SAT-472](#)),
 S728 ([SAT-515](#)), S732 ([TOP-090](#)),
 S838 ([FRI-488](#)), S863 ([SAT-125](#))
 Gómez, Mariana Serres, S690 ([SAT-454](#))
 Gómez, Mariano, S587 ([THU-136](#))
 Gomez, Marta Campos, S849 ([WED-483](#))
 Gomez-Martin, Carlos, S573 ([THU-114](#))
 Gómez, Mercedes Vergara,
 S376 ([WED-264](#)), S399 ([WED-300](#))
 Gomez, Paul, S463 ([THU-490](#))
 Gómez-Prat, Jordi, S917 ([FRI-181](#))
 Gómez, Raquel Muñoz, S1098 ([WED-166](#))
 Gómez Santos, Beatriz, S741 ([WED-408](#))
 Gommers, Diederik, S184 ([FRI-340](#))
 Gonçalo, Margarida, S842 ([FRI-495](#))
 Gonçalves, Cristina, S969 ([THU-289](#)),
 S972 ([THU-291](#))
 Gonçalves, Isabel, S1000 ([THU-334](#))
 Gonçalves, João, S279 ([WED-390](#))
 Gong, Jun, S489 ([TOP-065](#))
 Gong, Man, S1076 ([WED-138](#)),
 S1157 ([SAT-179](#))
 Gonsalkorala, Enoka, S266 ([WED-367](#))
 Gonye, Anna, S58 ([OS-075](#))
 Gonzalès, Emmanuel, S954 ([THU-267](#)),
 S969 ([THU-289](#)), S971 ([THU-291](#)),
 S1002 ([THU-336](#))
 González-Alayón, Carlos, S3 ([GS-003](#)),
 S87 ([OS-123-YI](#)), S970 ([THU-290](#))
 Gonzalez, Alvaro Diaz, S376 ([WED-264](#)),
 S390 ([WED-288](#))
 González, Andrea, S251 ([WED-344](#)),
 S911 ([FRI-171](#))
 González-Aseguinolaza, Gloria,
 S1024 ([FRI-228](#))
 González, Daniela, S940 ([THU-249](#))
 gonzalez de frutos, Concepción,
 S964 ([THU-282](#)), S980 ([THU-301](#)),
 S996 ([THU-326](#))
 González, Delia Almeida, S397 ([WED-296](#))
 Gonzalez Dieguez, Maria Luisa,
 S980 ([THU-301](#)), S996 ([THU-326](#)),
 S998 ([THU-331](#))
 González, Elena Tenorio, S314 ([SAT-549](#))
 Gonzalez, Esther Arnaiz, S803 ([WED-548](#))
 Gonzalez, Fabiola Perez, S893 ([FRI-140](#))
 González-Gállego, Javier, S554 ([SAT-263](#))
 González-Grande, Rocio, S314 ([SAT-549](#)),
 S1126 ([WED-208](#))
 Gonzalez, Hector Taboada, S932 ([FRI-208](#))
 González-Huezo, Maria Sarai,
 S195 ([FRI-546](#))
 González, Isabel, S852 ([WED-489](#))
 González, Jesús Manuel, S587 ([THU-136](#))
 González-Jiménez, A, S126 ([TOP-087](#))
 González, Lorena Mosteiro,
 S741 ([WED-408](#))
 González, Marta, S936 ([FRI-214](#))
 González, Miguel García, S73 ([OS-102](#))
 Gonzalez, Monica, S902 ([FRI-153](#))
 González-Navarro, Herminia,
 S451 ([SAT-387](#)), S789 ([WED-520](#))
 Gonzalez-Peralta, Regino, S123 ([LBP-35](#)),
 S387 ([WED-282](#))
 González-Recio, Irene, S140 ([FRI-399](#)),
 S529 ([SAT-216](#)), S532 ([SAT-221](#)),
 S544 ([SAT-244](#))
 Gonzalez-Romero, Francisco,
 S137 ([FRI-395](#)), S738 ([WED-404](#))
 González-Romero, Francisco,
 S529 ([SAT-215](#)), S741 ([WED-408](#))
 Gonzalez-Sanchez, Ester, S331 ([WED-231](#)),
 S560 ([SAT-275](#))
 Gonzalez, Stevan, S241 ([WED-328](#))
 González, Tuñón, S554 ([SAT-263](#))
 Gonzalez, Veronica Enith Prado,
 S865 ([SAT-129](#))
 Gonzalez, Francois, S1030 ([FRI-241](#))
 Goodall, Barbara, S909 ([FRI-166](#))
 Good, Jean-Marc, S105 ([LBP-08](#))
 Goodman, Zachary, S11 ([LBO-03](#)),
 S782 ([WED-506](#))
 Goodwin, Bryan, S422 ([FRI-356](#))
 Goodwin, Tyler, S35 ([OS-034](#))
 Goossens, Nicolas, S481 ([THU-526](#)),
 S751 ([WED-426](#))
 Gopal, Purva, S12 ([LBO-04](#))
 Gophna, Uri, S824 ([FRI-519](#))
 Gopi, Srikanth, S6 ([GS-006](#)),
 S233 ([TOP-041](#))
 Gordien, Emmanuel, S1150 ([SAT-169](#)),
 S1160 ([SAT-183](#)), S1161 ([SAT-185](#))
 Gordillo, Noelia, S198 ([FRI-550](#)),
 S807 ([TOP-077](#))
 Gordon, Fiona, S177 ([FRI-455](#)),
 S858 ([SAT-118](#)), S909 ([FRI-165](#)),
 S1198 ([THU-203](#))
 Gordon, Melita, S522 ([FRI-327](#))
 Gordon, Stuart C, S125 ([LBP-38](#)),
 S863 ([SAT-125](#)), S1208 ([THU-218](#))
 Gordon, Stuart C., S388 ([WED-283](#)),
 S627 ([THU-453](#))
 Gordon, Victoria, S382 ([WED-273](#))
 Gore, John, S555 ([SAT-265](#))
 Gores, Gregory, S28 ([OS-024-YI](#))
 Gorfú, Zebeaman Tibebe, S1120 ([WED-199](#))
 Görgülü, Esra, S1039 ([FRI-254](#)),
 S1042 ([FRI-259](#))
 Gorla, Odile, S86 ([OS-121-YI](#)),
 S975 ([THU-295](#))
 Gormley, Sarah, S877 ([FRI-118](#))
 Gormsen, Lars, S159 ([FRI-424](#))
 Gorsuch, Cassandra, S35 ([OS-034](#))
 Gorter, Alan, S740 ([WED-407](#))
 Gosset, Andréa, S923 ([FRI-191](#))
 Goswami, Rohan, S472 ([THU-509](#))
 Gothland, Adélie, S1044 ([FRI-261](#))
 Gottfredsson, Magnús, S880 ([FRI-121](#))
 Gottfriedová, Halima, S61 ([OS-080-YI](#))
 Gottwald, Millie, S13 ([LBO-05](#))
 Götze, Oliver, S628 ([THU-454](#))
 Gougelet, Angélique, S27 ([OS-023-YI](#))
 Goulas, Anestis, S1194 ([THU-196](#)),
 S1194 ([THU-197](#))
 Goulis, Ioannis, S1128 ([WED-211](#))
 Goundan, Pranava, S67 ([OS-091](#))
 Gountas, Ilias, S880 ([FRI-121](#))
 Gountas, Konstantinos, S880 ([FRI-121](#))
 Gournopanos, Kostas, S122 ([LBP-33-YI](#))
 Gouton, Martial, S833 ([FRI-480](#))
 Goutte, Nathalie, S482 ([THU-528](#)),
 S500 ([FRI-289](#))
 Gouttenoire, Jérôme, S1031 ([FRI-243](#))
 Govaere, Olivier, S78 ([OS-110](#)),
 S781 ([WED-475](#))
 Govaerts, Liesbeth, S1114 ([WED-190](#))
 Gow, Paul, S311 ([SAT-543](#)),
 S380 ([WED-271](#))
 Goyale, Atul, S660 ([SAT-409](#)),
 S661 ([SAT-410](#)), S812 ([FRI-471](#))
 Goyal, Tanvi, S658 ([SAT-406](#)),
 S703 ([SAT-473](#))
 Gozdowska, Jolanta, S563 ([SAT-280](#))
 Gozlan, Yael, S128 ([THU-394](#))
 Grabert, Gordon, S1029 ([FRI-240](#))
 Grabhorn, Enke, S969 ([THU-289](#))
 Graceffa, Pietro, S1111 ([WED-186](#)),
 S1118 ([WED-196](#))
 Gracia-Sancho, Jordi, S20 ([OS-012-YI](#)),
 S732 ([TOP-090](#)), S791 ([WED-524](#))
 Grados, Lucien, S61 ([OS-081](#))
 Graf, Christiana, S90 ([OS-126](#)),
 S91 ([OS-129-YI](#)), S185 ([FRI-341](#))
 Graff, Hannah, S103 ([LBP-06](#))
 Graham, Hiba, S659 ([SAT-407](#))
 Graham, Rondell, S12 ([LBO-04](#))
 Grainger, Richard, S1011 ([THU-389](#))
 Grajkowska, Wiesława, S837 ([FRI-486](#)),
 S950 ([THU-262](#))
 Gralton, Kate, S731 ([TOP-089](#))
 Gramantieri, Laura, S571 ([TOP-067](#))

- Grammatikopoulos, Tassos, S938 (TOP-057), S969 (THU-289), S1002 (THU-336)
- Granados, Rafael, S1098 (WED-166)
- Grancini, Valeria, S814 (FRI-474)
- Grandt, Josephine, S748 (WED-421)
- Grand, Xavier, S1014 (TOP-104)
- Granel, Núria, S849 (WED-483)
- Granito, Alessandro, S499 (FRI-287), S597 (THU-153)
- Grant, Julianne, S860 (SAT-121)
- Granzotto, Marnie, S766 (WED-449)
- Grassi, Anna, S88 (OS-124-YI)
- Grassi, Giuseppe, S40 (OS-045), S55 (OS-070), S843 (FRI-499), S970 (THU-290)
- Grassini, Maria Vittoria, S592 (THU-144)
- Graß, Julia-Kristin, S285 (SAT-331)
- Grasso, Marco, S293 (SAT-343)
- Grass, Vincent, S945 (THU-256)
- Grasu, Cristian Mugur, S819 (FRI-510)
- Gratacos, Jordi, S10 (LBO-01), S15 (OS-001), S158 (FRI-423), S163 (FRI-431), S166 (FRI-437), S171 (FRI-445), S250 (WED-343), S664 (SAT-415), S851 (WED-486)
- Gratien, Maryline Debette, S473 (THU-511)
- Graupera, Isabel, S15 (OS-001), S163 (FRI-431), S250 (WED-343), S279 (TOP-043), S664 (SAT-415), S700 (SAT-468), S737 (WED-403), S845 (TOP-054), S851 (WED-486)
- Graus, Javier, S8 (GS-009)
- Grau, Xavi, S1192 (THU-192)
- Graversen, Jonas, S629 (THU-455), S657 (SAT-404)
- Gray, Kevin, S125 (LBP-38)
- Gray, Meagan, S85 (OS-120)
- Grayston, Alexander, S402 (WED-305)
- Grazia Rendina, Maria, S482 (THU-527)
- Grbic, Dusanka, S426 (FRI-363)
- Greco, Carla, S729 (SAT-517)
- Greco, Gianluigi, S685 (SAT-446)
- Greenaway, Christina, S874 (FRI-114)
- Green, Daniel, S220 (THU-355)
- Green, Edward, S558 (SAT-271)
- Greenham, Olivia, S854 (TOP-095)
- Greenman, Raanan, S415 (FRI-345)
- Gregersen, Nikolaj, S614 (THU-429)
- Gregoire, Damien, S534 (SAT-225)
- Gregori, Josep, S1024 (FRI-228)
- Gregor, Martin, S945 (THU-255)
- Grégory, Jules, S64 (OS-084-YI), S577 (THU-120)
- Gregory, Lindsey, S44 (OS-050-YI), S465 (THU-495)
- Greig, Carolyn, S231 (THU-368), S232 (THU-370)
- Grelli, Sandro, S1122 (WED-203)
- Gremmel, Thomas, S246 (WED-338)
- Greuter, Thomas, S105 (LBP-08)
- Grevelding, Christoph G., S339 (WED-248), S954 (THU-268)
- Grey-Wilson, Charlotte, S433 (SAT-354)
- Grgurevic, Ivica, S61 (OS-080-YI), S283 (SAT-327)
- Grgurević, Ivica, S865 (SAT-129)
- Grieco, Antonio, S482 (THU-527), S660 (SAT-409), S723 (SAT-508)
- Griemsmann, Marie, S90 (OS-127-YI), S283 (SAT-328), S299 (SAT-521), S301 (SAT-525)
- Griffiths, Michael, S174 (FRI-450)
- Grigg, Andrew, S625 (THU-450)
- Grimaldi, Lamiae, S408 (WED-318)
- Grimaudo, Stefania, S774 (WED-462), S803 (WED-549)
- Grimmer, Katharine, S49 (OS-061)
- Grimminger, Peter, S557 (SAT-268)
- Grimsrud, Marit M., S541 (SAT-238)
- Gringeri, Enrico, S564 (SAT-283), S1056 (TOP-106)
- Grinspan, Lauren, S461 (THU-488), S997 (THU-328)
- Grip, Emilie Toresson, S654 (SAT-399), S857 (SAT-115)
- Grischott, Thomas, S933 (FRI-209)
- Groenbaek, Henning, S523 (FRI-328)
- Groen, Bert, S351 (THU-237)
- Grønbaek, Henning, S198 (FRI-550), S239 (WED-325), S390 (WED-287), S510 (FRI-305), S614 (THU-429), S811 (FRI-469), S841 (FRI-494), S968 (THU-287), S982 (THU-304), S986 (THU-311)
- Grønbaek, Lisbet, S982 (THU-304)
- Grønborg, Mads, S742 (WED-411)
- Groneberg, Dieter, S330 (WED-230)
- GrønkJær, Lea Ladegaard, S629 (THU-455), S657 (SAT-404), S851 (WED-487)
- Grooshuismink, Anthony, S496 (FRI-282), S1016 (TOP-108), S1019 (FRI-219)
- Grosse, Claudia, S996 (THU-327)
- Große, Karsten, S56 (OS-073)
- Grossi, Paolo Antonio, S54 (OS-069)
- Grottenthaler, Julia, S108 (LBP-12), S1139 (SAT-156)
- Grova, Alessandro, S592 (THU-144)
- Grove, Jane I., S127 (TOP-092), S448 (SAT-381), S717 (SAT-498)
- Grover, Vijay, S850 (WED-485)
- Grube, Julia, S143 (FRI-405)
- Grueger, Jens, S873 (FRI-113)
- Gruevska, Aleksandra, S323 (WED-217), S335 (WED-239), S781 (WED-505)
- Grünberger, Thomas, S44 (OS-050-YI), S45 (OS-051-YI), S465 (THU-495), S538 (SAT-233), S564 (SAT-282)
- Grzelak, Jan, S331 (WED-231)
- Grzyb, Krzysztof, S478 (THU-520)
- Gschwantler, Michael, S90 (OS-127-YI), S299 (SAT-521), S936 (TOP-055)
- Guan, Jin, S274 (WED-382)
- Guan, Qingtian, S327 (WED-225)
- Guan, Yujuan, S1153 (SAT-174), S1165 (SAT-193)
- Guaraná, Thais, S112 (LBP-16)
- Guariglia, Marta, S521 (FRI-325), S605 (THU-415), S611 (THU-425), S617 (THU-435), S626 (THU-452), S637 (THU-470), S704 (SAT-474)
- Guarin, Jose Miguel Cabrera, S932 (FRI-208)
- Guarino, Maria, S903 (FRI-155)
- Guarneri, Valeria, S640 (THU-475)
- Guasconi, Tomas, S287 (SAT-334)
- Guasti, Daniele, S550 (SAT-254)
- Gucht, Steven Van, S1114 (WED-190)
- Guckenbiehl, Sabrina, S216 (THU-348)
- Gudavalli, Koushik, S86 (OS-121-YI)
- Gueddiken, Nurdan, S639 (THU-472), S951 (THU-264), S963 (THU-281)
- Guelow, Karsten, S1003 (THU-377)
- Guérin, Annie, S291 (SAT-339)
- Guerra, Anna Francesca, S1105 (WED-176)
- Guerra, Javier Abad, S8 (GS-009), S272 (WED-378), S683 (SAT-443), S700 (SAT-468)
- Guerra, Manuel Hernández, S366 (TOP-061), S376 (WED-264), S380 (WED-270), S399 (WED-300), S894 (FRI-140), S964 (THU-282), S980 (THU-301), S996 (THU-326), S998 (THU-331), S1178 (THU-171), S1205 (THU-216)
- Guerra, Patricia, S865 (SAT-129), S900 (FRI-151)
- Guerrero, Antonio, S73 (OS-102)
- Guerrero, Maria, S902 (FRI-153)
- Guerrero, María Torres, S73 (OS-102)
- Guerrieri, Francesca, S1018 (FRI-218)
- Guerrini, Gian Piero, S287 (SAT-334)
- Guettier, Catherine, S359 (FRI-382)
- Guetzlaff, Lea, S466 (THU-496)
- Gugenheim, Jean, S467 (THU-498), S473 (THU-511)
- Guglielmi, Alfredo, S510 (FRI-304)
- Guha, Neil, S84 (OS-119-YI)
- Guha, Rael, S501 (FRI-291)
- Guibal, Aymeric, S61 (OS-080-YI)
- Guichelaar, Maureen, S14 (LBO-06)
- Guichou, Jean-François, S456 (THU-478)
- Guida, Alice, S545 (SAT-245), S550 (SAT-254)
- Guido, Maria, S564 (SAT-283), S766 (WED-449), S966 (THU-285)
- Guiliani, Alejandro Mayorca, S657 (SAT-404), S826 (FRI-522)
- Guillamon, Alex, S78 (OS-109-YI), S737 (WED-403)
- Guillaud, Olivier, S61 (OS-080-YI)
- Guillemin, Gilles, S263 (WED-364)
- Guillot, Adrien, S22 (OS-015), S70 (OS-095-YI), S80 (OS-114-YI), S745 (WED-416)
- Guimaraes, Amanda, S527 (SAT-212)
- Guimarães, Mafalda, S902 (FRI-154)
- Guimaraes, Tatiana, S112 (LBP-16)
- Guinard-Azadian, Carine, S1034 (FRI-248)
- Guinart-Cuadra, Albert, S164 (FRI-433)
- Guingané, Alice, S916 (FRI-178)

Author Index

- Guingané, Alice N., S923 (FRI-191), S1117 (WED-195)
- Guitart, Joan Reguant, S932 (FRI-208)
- Guiu, Boris, S170 (FRI-443)
- Gui, Wenfang, S413 (FRI-334)
- Guixé-Muntet, Sergi, S20 (OS-012-YI), S791 (WED-524)
- Guix, Marta García, S73 (OS-100-YI)
- Gulamhusein, Aliya, S56 (OS-073), S314 (SAT-548), S371 (WED-255), S387 (WED-281), S404 (WED-310), S426 (FRI-363)
- Gulbani, Lasha, S930 (FRI-203)
- Gulck, Ellen Van, S443 (SAT-371)
- Gulden, Lukas, S354 (THU-242)
- Güler Şentürk, Begüm, S928 (FRI-199)
- Guller, Anna, S263 (WED-364)
- Gulpinar, Basak, S477 (THU-518)
- Gulsen, Murat Taner, S181 (FRI-463)
- Gültan, Merve, S945 (THU-256)
- Gumussoy, Mesut, S65 (OS-086), S1109 (WED-183)
- Gümüşsoy, Mesut, S477 (THU-518)
- Gundu Rao, Nagashree, S464 (THU-492)
- Gunduz, Feyza, S195 (FRI-546)
- Gungabissoon, Usha, S388 (WED-283), S398 (WED-299)
- Gunjan, Deepak, S6 (GS-006), S233 (TOP-041)
- Gunn, Nadege, S653 (SAT-398)
- Günsar, Fulya, S181 (FRI-463)
- Günthard, Huldrych, S101 (LBP-04)
- Gunther, Ulrich, S687 (SAT-449)
- Guo, Fang, S784 (WED-510)
- Guofeng, Cheng, S1152 (SAT-173)
- Guo, Hongbo, S1016 (TOP-111), S1025 (FRI-232), S1027 (FRI-234)
- Guo, Jason, S489 (TOP-065)
- Guo, Lida, S1167 (SAT-195)
- Guo, Lining, S196 (FRI-547)
- Guo, Qianqian, S765 (WED-448)
- Guo, Shuling, S774 (WED-461)
- Guo, Ying, S1133 (SAT-147)
- Guo, Zhaoxu, S1018 (FRI-217)
- Gupta, Abhishak, S21 (OS-014-YI), S146 (FRI-407), S152 (FRI-416), S1033 (FRI-247)
- Gupta, Anany, S6 (GS-006)
- Gupta, Ekta, S1033 (FRI-247), S1047 (FRI-267)
- Gupta, Haripriya, S156 (FRI-420), S177 (FRI-456), S220 (THU-354), S343 (THU-227)
- Gupta, Kusum, S1029 (FRI-238), S1162 (SAT-188)
- Gupta, Neil, S885 (FRI-127), S913 (FRI-174), S935 (FRI-213)
- Gupta, Rohit, S906 (FRI-163)
- Gupta, Sarita, S207 (THU-337)
- Gupta, Shivam, S263 (WED-363)
- Gupta, Sneha V., S11 (LBO-02), S32 (OS-031), S1156 (SAT-177)
- Gupte, Girish, S941 (THU-250), S944 (THU-254)
- Gurbindo, Unai, S290 (SAT-337)
- Gurel, Selim, S1137 (SAT-152)
- Gustafson, Jenna, S58 (OS-075)
- Gustot, Thierry, S198 (FRI-550), S621 (THU-442)
- Gu, Tao, S1003 (THU-378)
- Guthrie, Heidi, S688 (SAT-451)
- Guthrie, Nicole, S822 (FRI-515)
- Gutiérrez, Ana Piñar, S838 (FRI-488)
- Gutierrez, Carlos, S251 (WED-344), S911 (FRI-171)
- Gutiérrez de Juan, Virginia, S736 (WED-400)
- Gutierrez, Laura Benitez, S481 (THU-525), S1194 (THU-195)
- Gutiérrez, Luz Goretta Santiago, S928 (FRI-198)
- Gutierrez, Michael, S671 (SAT-426)
- Gutiérrez, Oscar Morales, S274 (WED-382)
- Gutierrez, Sagrario, S180 (FRI-462)
- Guttenberg, Georg, S185 (FRI-341)
- Gu, Wenyi, S61 (OS-080-YI), S185 (FRI-341), S222 (THU-356), S279 (TOP-043), S313 (SAT-546), S484 (THU-531), S712 (SAT-492)
- Gu, Yan, S1128 (WED-212)
- Guy, Cynthia, S1 (GS-001)
- Guy, Margaret, S901 (FRI-152)
- Gu, Yuanlong, S488 (THU-540)
- Gu, Yumei, S117 (LBP-24)
- Guzek, John, S103 (LBP-06)
- Guzman, Grace, S80 (OS-113)
- Guzzo, Antonella, S685 (SAT-446)
- Gvinjilia, Lia, S1204 (THU-214)
- Gwak, Geum-Yon, S267 (WED-369), S305 (SAT-533), S631 (THU-459), S821 (FRI-514)
- Gyoeri, Georg, S465 (THU-494), S465 (THU-495), S470 (THU-505), S489 (THU-545)
- Haan, Sandra De, S439 (SAT-365)
- Haas, Joel, S355 (THU-244)
- Habboub, Nadeen, S344 (THU-228)
- Haber, Philipp, S48 (OS-059-YI), S527 (SAT-213)
- Habersetzer, François, S168 (FRI-440)
- Habtesion, Abeba, S206 (TOP-046)
- Haceatrea, Alexei, S1162 (SAT-188)
- Hacışahinoğulları, Hülya, S709 (SAT-485)
- Hackl, Hubert, S44 (OS-050-YI), S45 (OS-051-YI), S465 (THU-495)
- Hackl, Matthias, S45 (OS-051-YI)
- Hacohen, Nir, S58 (OS-075)
- Hadadi, Sapir, S1195 (THU-199)
- Haddadin, Yazan, S1106 (WED-178)
- Haddon, Lacey, S770 (WED-455)
- Hadjadj, Samy, S603 (THU-410)
- Hadziyannis, Emilia, S978 (THU-298)
- Haele, Matthias Van, S549 (SAT-252)
- Haenzelmann, Sonja, S60 (OS-079-YI)
- Hagiwara, May, S977 (THU-296), S1007 (THU-385)
- Hagström, Hannes, S43 (OS-048-YI), S82 (OS-116-YI), S121 (LBP-30-YI), S157 (FRI-422), S159 (FRI-425), S276 (WED-384), S302 (SAT-527), S600 (TOP-079), S605 (THU-414), S607 (THU-418), S650 (TOP-085), S651 (SAT-394), S653 (SAT-397), S654 (SAT-399), S682 (SAT-441), S707 (SAT-481), S710 (SAT-486), S857 (SAT-115), S959 (THU-275), S960 (THU-276)
- Hähnel, Patrizia, S536 (SAT-230)
- Hahn, Magdalena, S483 (THU-529)
- Haider, Asma, S717 (SAT-498)
- Haider, Raphael, S350 (THU-236)
- Haile, Melat, S69 (OS-094)
- Hailu, Dawit, S927 (FRI-197)
- Hajarizadeh, Behzad, S910 (FRI-169)
- Hajer, Ben Khadhra, S61 (OS-081)
- Hajinicolaou, Christina, S971 (THU-291)
- Hajji, Sofia El, S24 (OS-018-YI), S531 (SAT-220)
- Hajji, Yacine, S666 (SAT-417), S668 (SAT-421)
- Hakeem, Andrew, S795 (WED-532)
- Haktaniyan, Busra, S195 (FRI-546), S274 (WED-382)
- Halford, Melanie, S266 (WED-367)
- Halilbasic, Emina, S403 (WED-307)
- Hall, Andrew, S70 (OS-095-YI), S129 (THU-396), S383 (WED-276)
- Haller, Rosa, S354 (THU-242)
- Hallett, Tim, S923 (FRI-191)
- Halliday, Neil, S383 (WED-276), S579 (THU-123)
- Hall, Lindsay, S987 (THU-312)
- Hallswoth, Kate, S16 (OS-003)
- Hall, Zoe, S323 (WED-217)
- Hamadani, Yassir, S1098 (WED-167)
- Hamandi, Ali, S792 (WED-527)
- Hamdy El-Sayed, Manal, S913 (FRI-174)
- Hamed, Omar, S1212 (THU-224)
- Hametner-Schreil, Stephanie, S90 (OS-127-YI), S299 (SAT-521)
- Hamid, Saeed Sadiq, S9 (GS-012), S863 (SAT-125), S865 (SAT-129), S896 (FRI-145)
- Hamilton, Aaron, S1058 (WED-113)
- Hamilton, Elizabeth, S69 (OS-093-YI)
- Hamilton, James, S85 (OS-120)
- Hammam, Olfat, S353 (THU-241), S550 (SAT-255), S779 (WED-472), S795 (WED-532)
- Hammar, Niklas, S121 (LBP-30-YI)
- Hammerich, Linda, S351 (THU-238)
- Hammersley, Richard, S84 (OS-119-YI)
- Hammond, Nigel, S8 (GS-010)
- Hammond, Rachel, S1028 (FRI-237), S1164 (SAT-191)
- Hammoutene, Adel, S435 (SAT-358), S776 (WED-467)
- Hamody, Yara, S955 (THU-269)
- Hampe, Jochen, S364 (FRI-390), S548 (SAT-250)

- Ham, Young Lim, S343 (THU-227)
 Ham, Younglim, S156 (FRI-420)
 Hanan, Nathan, S1141 (SAT-158)
 Han, Bing, S960 (THU-277)
 Handanagic, Senad, S881 (FRI-123),
 S889 (FRI-133), S890 (FRI-135),
 S898 (FRI-147), S909 (FRI-167),
 S930 (FRI-203), S931 (FRI-205),
 S933 (FRI-210), S1204 (THU-214)
 Han, Dong, S35 (OS-034)
 Hanford, Paula, S398 (WED-299)
 Hanf, Remy, S211 (THU-342)
 Hang, Shou Kit, S1024 (FRI-229)
 Han, Gyoonee, S778 (WED-471)
 Han, Ho Seong, S583 (THU-130)
 Han, Hui, S80 (OS-113)
 Han, Jaekyu, S414 (FRI-336),
 S752 (WED-427)
 Han, Ji Eun, S572 (TOP-071)
 Han, Jinsol, S18 (OS-008-YI)
 Han, Ji Won, S148 (FRI-409)
 Hankeova, Simona, S433 (SAT-353),
 S435 (SAT-357), S945 (THU-255)
 Hanks, Debra, S671 (SAT-426)
 Han, Kyungdo, S510 (FRI-306),
 S642 (THU-550)
 Hanley, Karen Piper, S8 (GS-010),
 S333 (WED-234)
 Hanley, Marion, S255 (WED-350)
 Hanley, Neil, S8 (GS-010),
 S84 (OS-119-YI)
 Han, Ma Ai Thanda, S458 (THU-482)
 Hannah, Nicholas, S380 (WED-271)
 Han Ng, Cheng, S629 (THU-456)
 Hannich, J. Thomas, S939 (TOP-058)
 Han, Nicole, S1096 (WED-165)
 Hanno, Abdelfattah, S319 (SAT-558)
 Hannon, Breffni, S254 (WED-349),
 S255 (WED-351), S270 (WED-375)
 Han, Qinglin, S443 (SAT-371)
 Han, Sangyoung, S785 (WED-513)
 Hansen, Bettina, S52 (OS-065-YI),
 S56 (OS-073), S314 (SAT-548),
 S371 (WED-255), S373 (WED-259),
 S387 (WED-281), S404 (WED-310),
 S426 (FRI-363), S503 (FRI-293),
 S969 (THU-289), S972 (THU-291),
 S1100 (WED-169), S1132 (SAT-145)
 Hansen, Camilla Dalby, S17 (OS-005-YI),
 S163 (FRI-432), S173 (FRI-449),
 S175 (FRI-452), S303 (SAT-528),
 S657 (SAT-404), S832 (FRI-479),
 S845 (TOP-054)
 Hansen, Emil Deleuran, S17 (OS-005-YI),
 S173 (FRI-449), S303 (SAT-528)
 Hansen, Henrik B., S57 (OS-074-YI),
 S321 (TOP-036), S530 (SAT-218),
 S742 (WED-410), S746 (WED-417),
 S788 (WED-519), S800 (WED-543)
 Hansen, Johanne Kragh, S17 (OS-005-YI),
 S163 (FRI-432), S173 (FRI-449),
 S175 (FRI-452), S303 (SAT-528),
 S657 (SAT-404), S832 (FRI-479),
 S845 (TOP-054)
 Hansen, Torben, S17 (OS-005-YI),
 S173 (FRI-449)
 Han, Sojung, S916 (FRI-179)
 Han, Thanda, S463 (THU-490)
 Han, Weiqing, S488 (THU-540)
 Han, Yong-Hyun, S414 (FRI-336),
 S752 (WED-427)
 Hao, Jia-Yu, S825 (FRI-521)
 Hao, Yaohua, S1102 (WED-172)
 Haque, Madhuri, S778 (WED-470)
 Haque, Tanzina, S872 (TOP-097),
 S879 (FRI-120)
 Harada, Akima, S439 (SAT-366)
 Harada, Yoshiyuki, S559 (SAT-272)
 Hara, Eiji, S545 (SAT-246),
 S559 (SAT-272)
 Haraldsson, Borje, S276 (WED-384)
 Harberts, Aenne, S285 (SAT-331)
 Harder, Lea Mørch, S742 (WED-411)
 Hardie, Diana, S1184 (THU-178)
 Hardikar, Winita, S971 (THU-291)
 Hardtke, Svenja, S1032 (FRI-244),
 S1137 (SAT-152)
 Hardtke-Wolenski, Matthias,
 S797 (WED-537)
 Hardwigsen, Jean, S467 (THU-498),
 S473 (THU-511)
 Hardy, Kerry, S523 (FRI-329)
 Hargreaves, Rupen, S964 (THU-283)
 Harindranath, Sidharth, S310 (SAT-542),
 S983 (THU-305)
 Harkin, Kieran, S16 (OS-004)
 Härle, Lukas, S954 (THU-268)
 Harman, David, S708 (SAT-483)
 Harnois, Denise, S472 (THU-509)
 Harputluoglu, Murat, S181 (FRI-463)
 Harris, M. Scott, S50 (OS-063)
 Harris, Nicola, S324 (WED-218)
 Harrison, Emily, S35 (OS-034)
 Harrison, Laura, S382 (WED-273),
 S391 (WED-289)
 Harrison, Stephen, S1 (GS-001),
 S13 (LBO-05), S29 (OS-026),
 S30 (OS-027), S31 (OS-029),
 S49 (OS-061), S50 (OS-063),
 S112 (LBP-17), S118 (LBP-26),
 S604 (THU-413), S619 (THU-438),
 S619 (THU-439), S643 (THU-552),
 S647 (TOP-074), S649 (TOP-080),
 S651 (SAT-393), S653 (SAT-398),
 S655 (SAT-401), S659 (SAT-408),
 S666 (SAT-417), S668 (SAT-421),
 S684 (SAT-444), S790 (WED-522),
 S808 (TOP-091), S812 (FRI-470),
 S813 (FRI-472), S815 (FRI-476),
 S820 (FRI-512), S824 (FRI-518)
 Harris, Ross, S909 (FRI-165)
 Hartel, Gunter, S846 (WED-478)
 Hart, Jennifer, S879 (FRI-120)
 Hartleben, Björn, S425 (FRI-362),
 S466 (THU-496), S797 (WED-537)
 Hartley, Jane, S123 (LBP-35),
 S387 (WED-282)
 Hartl, Johannes, S379 (WED-269)
 Hartl, Lukas, S37 (OS-039-YI),
 S90 (OS-127-YI), S193 (FRI-545),
 S199 (FRI-551), S201 (FRI-554),
 S244 (WED-334), S282 (SAT-326),
 S284 (SAT-330), S286 (SAT-332),
 S288 (SAT-335), S292 (SAT-342),
 S299 (SAT-521), S313 (SAT-547),
 S831 (FRI-477), S939 (TOP-058),
 S1135 (SAT-150)
 Hartmann, Daniel, S1021 (FRI-223.)
 Hartsfield, Cynthia (Cindy), S13 (LBO-05)
 Har-Zahav, Adi, S955 (THU-269)
 Hasanpourghadi, Mohadeseh,
 S1015 (TOP-107)
 Haseeb, Muhammad, S268 (WED-371)
 Hasegawa, Yuta, S317 (SAT-554),
 S820 (FRI-511)
 Hashiguchi, Taishi, S544 (SAT-243)
 Hashim, Ahmed, S74 (OS-103-YI)
 Hasnain, Aliya, S896 (FRI-145),
 S912 (FRI-172)
 Hassan, Amany, S1212 (THU-224)
 Hassanein, Tarek, S675 (SAT-432)
 Hassan, Manal, S516 (FRI-317)
 Hassan, Mohamed, S1098 (WED-167)
 Hassan, Mohsin, S70 (OS-095-YI),
 S71 (OS-096-YI), S197 (FRI-549),
 S206 (TOP-046), S767 (WED-450)
 Hassannia, Behrouz, S764 (WED-446)
 Hassan, Reham, S940 (THU-249)
 Hassany, Mohamed, S1212 (THU-224)
 Hassany, Sahar, S1212 (THU-224)
 Hassan, Zahra, S724 (SAT-509)
 Hasson, Hamid, S120 (LBP-29),
 S837 (FRI-487)
 Hatanaka, Takeshi, S584 (THU-131)
 Hatem, Ammar, S840 (FRI-491)
 Ha, Tina, S239 (WED-324)
 Hatlegjerde, Anne-Lotte Vada,
 S449 (SAT-383)
 Hatting, Maximilian, S571 (SAT-292),
 S778 (WED-470)
 Haubitz, Monika, S105 (LBP-08)
 Hausmann, Fabian, S60 (OS-079-YI)
 Haut, Elliott, S475 (THU-516)
 Havaj, Daniel Jan, S871 (SAT-136)
 Haxhijaj, Labjona, S72 (OS-099)
 Hayama, Korenobu, S240 (WED-327),
 S317 (SAT-554), S820 (FRI-511)
 Hayashi, Hideki, S686 (SAT-448)
 Hayashi, Kazuki, S559 (SAT-272)
 Hayashi, Naoki, S409 (TOP-060)
 Hayat, Umar, S268 (WED-371),
 S641 (THU-476)
 Hayden, Tonya, S905 (FRI-160)
 Ha, Yeonjung, S829 (FRI-527)
 Hayes, Peter, S195 (FRI-546),
 S274 (WED-382)
 Hayward, Kelly, S239 (WED-324)
 Hazebroek, Eric J., S763 (WED-444)
 Hazou, Wadi, S484 (THU-532)
 Heath, Sonya, S612 (THU-427)
 Heaton, Nigel, S324 (WED-218),
 S445 (SAT-376)

Author Index

- Hebbale, Skanda, S79 ([OS-112](#))
Hedman, Hanna Persson, S841 ([FRI-493](#))
Hedrich, Viola, S564 ([SAT-282](#))
Heeboll, Sara, S159 ([FRI-424](#))
Hee Kim, Jung, S190 ([FRI-538](#)),
S192 ([FRI-542](#)), S200 ([FRI-553](#))
Hees, Stijn Van, S52 ([OS-065-YI](#)),
S1132 ([SAT-145](#))
Hegade, Vinod, S411 ([FRI-331](#)),
S990 ([THU-317](#))
Hegel, Johannes Kolja, S507 ([FRI-300](#))
Heger, Zbynek, S546 ([SAT-247](#))
Heggelund, Lars, S1150 ([SAT-170](#))
Hegmar, Hannes, S707 ([SAT-481](#))
He, Handan, S1171 ([SAT-201](#))
Heiden, Denise, S538 ([SAT-233](#))
Heidenreich, Julius, S979 ([THU-299](#))
Heidrich, Benjamin, S1137 ([SAT-152](#))
Heikenwalder, Mathias, S549 ([SAT-252](#))
Heikinheimo, Markku, S997 ([THU-329](#))
Heikkilä, Päivi, S997 ([THU-329](#))
Heikkinen, Sami, S79 ([OS-112](#))
Heil, Marantha, S118 ([LBP-27](#)),
S1046 ([FRI-265](#)), S1058 ([WED-113](#))
Heimanson, Zeev, S236 ([WED-319](#)),
S275 ([WED-383](#)), S291 ([SAT-339](#))
Heimbach, Julie, S465 ([THU-495](#))
Heim, Markus, S481 ([THU-526](#)),
S532 ([SAT-222](#)), S754 ([WED-431](#))
Hein, Moritz, S276 ([WED-385](#))
Heinrich, Sophia, S277 ([WED-387](#)),
S557 ([SAT-268](#))
Heinson, Ashley, S1075 ([WED-137](#))
Heintz, Sarah, S1046 ([FRI-265](#))
Heinz Weiss, Karl, S1006 ([THU-382](#))
Hejda, Vaclav, S41 ([OS-046](#))
He, Jingyan, S439 ([SAT-365](#)),
S945 ([THU-255](#))
He, Jinyu, S1076 ([WED-138](#)),
S1157 ([SAT-179](#))
Helal, Israa, S570 ([SAT-291](#))
Heldens, Anneleen, S226 ([THU-361](#)),
S743 ([WED-412](#)), S787 ([WED-516](#))
He, Liang, S50 ([OS-063](#))
Hellani, Mohammad Fadel,
S865 ([SAT-129](#))
Hellard, Margaret, S875 ([FRI-115](#))
Heller, Bianca, S625 ([THU-449](#))
Heller, Theo, S9 ([GS-012](#))
Helmke, Steve, S843 ([FRI-498](#))
He, Lulu, S20 ([OS-013](#))
Heluwaert, Frederic, S52 ([OS-066](#)),
S107 ([LBP-11](#)), S1160 ([SAT-184](#))
Hemati, Hami, S326 ([WED-222](#)),
S414 ([FRI-344](#))
Henderson, Julie, S1182 ([THU-176](#))
Henderson, Neil, S39 ([OS-044-YI](#)),
S329 ([WED-227](#))
Hendifar, Andrew, S489 ([TOP-065](#))
Hendriks, Tim, S152 ([FRI-415](#))
Heneghan, Michael, S36 ([OS-037](#)),
S46 ([OS-053-YI](#)), S432 ([FRI-371](#)),
S962 ([THU-280](#))
Heng, Benjamin, S263 ([WED-364](#))
Hengstler, Jan G., S413 ([FRI-334](#)),
S535 ([SAT-227](#)), S778 ([WED-470](#)),
S940 ([THU-249](#))
Henin, Guillaume, S464 ([THU-493](#)),
S511 ([FRI-307](#)), S639 ([THU-473](#))
Hennan, Jim, S790 ([WED-522](#))
Hennings, Julia, S22 ([OS-015](#)),
S416 ([FRI-348](#))
Henrique, Mariana Moura,
S279 ([WED-390](#)), S734 ([WED-397](#))
Henry, Camille, S62 ([OS-083-YI](#))
Henry, Linda, S600 ([TOP-081](#)),
S627 ([THU-453](#)), S857 ([SAT-116](#)),
S861 ([SAT-122](#)), S863 ([SAT-125](#))
Henze, Lara, S450 ([SAT-385](#))
Heo, Jeong, S11 ([LBO-02](#)), S125 ([LBP-38](#)),
S588 ([THU-137](#))
He, Qinqun, S189 ([FRI-536](#)), S202 ([FRI-556](#))
Herber, Adam, S201 ([FRI-555](#)),
S244 ([WED-335](#)), S483 ([THU-529](#))
Her, Chris, S322 ([WED-215](#))
Hercun, Julian, S426 ([FRI-363](#))
Herebian, Diran, S415 ([FRI-346](#))
Hériard-Dubreuil, Baptiste,
S769 ([WED-453](#)), S777 ([WED-469](#))
Hermabessière, Paul, S674 ([SAT-431](#))
Hermán-Sánchez, Natalia, S529 ([SAT-216](#))
Hernaez, Ruben, S10 ([LBO-01](#)),
S173 ([FRI-448](#))
Hernández-Abrego, Andy, S547 ([SAT-249](#))
Hernández, Águeda, S1192 ([THU-192](#))
Hernández-Arriaga, Angelica,
S798 ([WED-539](#))
Hernández, Candido, S1209 ([THU-219](#))
Hernandez, Christie, S649 ([TOP-083](#)),
S839 ([FRI-490](#))
Hernández Evole, Helena, S166 ([FRI-437](#))
Hernández-Èvole, Helena, S163 ([FRI-431](#)),
S1124 ([WED-205](#))
Hernández, Francisco Andrés Pérez,
S397 ([WED-296](#)), S928 ([FRI-198](#))
Hernandez-Gea, Virginia, S2 ([GS-003](#)),
S87 ([OS-123-YI](#)), S279 ([TOP-043](#)),
S770 ([WED-457](#)), S843 ([FRI-499](#)),
S970 ([THU-290](#)), S984 ([THU-308](#))
Hernandez-Guerra, Manuel, S2 ([GS-003](#)),
S921 ([FRI-188](#))
Hernandez, Jose Luis Perez, S195 ([FRI-546](#))
Hernandez, Nélia, S132 ([THU-401](#)),
S900 ([FRI-151](#))
Hernandez, Norvin, S173 ([FRI-448](#))
Hernandez, Olga, S1178 ([THU-171](#))
Hernandez, Perla, S489 ([TOP-065](#))
Hernandez, Rocio Calvo, S844 ([FRI-501](#))
Hernandez, Rocio Munoz, S760 ([WED-440](#)),
S770 ([WED-457](#))
Hernández, Rosario, S664 ([SAT-415](#))
Hernandez, Sairy, S9 ([GS-011](#))
Hernandez-Tejero, Maria, S145 ([TOP-073](#)),
S900 ([FRI-151](#))
Hernando, Victoria, S902 ([FRI-153](#))
Heroin, Lucile, S168 ([FRI-440](#))
Herola, Antonio Garcia, S883 ([FRI-126](#))
Herraez, Elisa, S527 ([SAT-212](#))
Herrán, Aitor Odriozola, S251 ([WED-344](#))
Herranz, Andrea, S1191 ([THU-190](#))
Herranz, José María, S349 ([THU-235](#)),
S526 ([TOP-072](#)), S537 ([SAT-232](#)),
S732 ([TOP-090](#)), S770 ([WED-457](#))
Herrera, Blanca, S331 ([WED-231](#))
Herrero, Astrid, S62 ([OS-083-YI](#)),
S74 ([OS-104](#))
Herrero-Cervera, Andrea, S789 ([WED-520](#))
Herrero, Irene Peñas, S480 ([THU-524](#)),
S886 ([FRI-129](#))
Herrero, Jose Ignacio, S133 ([THU-404](#)),
S470 ([THU-503](#))
Herrmann, Carl, S33 ([OS-032](#))
Herrmann, Eva, S91 ([OS-129-YI](#))
Herrmann, Yannic, S45 ([OS-051-YI](#))
Herr, Monika, S687 ([SAT-449](#))
Herta, Toni, S108 ([LBP-12](#)),
S1090 ([WED-156](#)), S1139 ([SAT-156](#))
Herting, Emma Celia, S176 ([FRI-454](#))
Hervieu, Valerie, S603 ([THU-410](#)),
S687 ([SAT-450](#)), S701 ([SAT-469](#)),
S806 ([WED-555](#))
Hesketh, Hannah, S1129 ([WED-213](#))
Hetland, Liv, S702 ([SAT-471](#)),
S742 ([WED-411](#)), S748 ([WED-421](#)),
S784 ([WED-511](#))
Hettiarachchige, Nadilka, S841 ([FRI-493](#))
Heumann, Asmus, S60 ([OS-079-YI](#))
Heurgue-berlot, Alexandra,
S12 ([LBO-04](#))
Heuschmann, Peter, S625 ([THU-449](#))
He, Weiwei, S948 ([THU-260](#))
He, Xiao, S514 ([FRI-313](#))
Heydmann, Laura, S72 ([OS-098](#))
Heyens, Leen, S828 ([FRI-526](#))
He, Yignli, S1133 ([SAT-147](#))
Heymann, Felix, S80 ([OS-114-YI](#)),
S767 ([WED-450](#))
Heyne, Renate, S1147 ([TOP-110](#))
He, Yong, S503 ([FRI-294](#))
He, Yonghong, S406 ([WED-313](#))
He, Zebao, S638 ([THU-471](#)), S696 ([SAT-463](#)),
S724 ([SAT-510](#))
Hiasa, Yoichi, S1183 ([THU-177](#))
Hibner, Urszula, S534 ([SAT-225](#))
Hickman, Matthew, S621 ([THU-441](#)),
S858 ([SAT-118](#)), S909 ([FRI-165](#))
Hicks, Amy, S179 ([FRI-459](#))
Hidalgo, Andrés, S78 ([OS-109-YI](#))
Hidalgo, Hélène Fricker, S894 ([FRI-142](#))
Hidalgo, Nuria Cañete, S105 ([LBP-09](#))
Hidam, Ashini, S187 ([FRI-533](#))
Hidde, Dennis, S1186 ([THU-181](#))
Hiebert, Lindsey, S885 ([FRI-127](#)),
S913 ([FRI-174](#)), S935 ([FRI-213](#))
Higuchi, Mayu, S644 ([THU-554](#))
Higuera, Monica, S533 ([SAT-224](#))
Hikita, Hayato, S1183 ([THU-177](#))
Hilaire, Sophie, S87 ([OS-123-YI](#))
Hild, Benedikt, S1124 ([WED-206](#)),
S1125 ([WED-207](#))
Hildebrandt, Franziska, S410 ([FRI-330](#))
Hildebrandt, Talitha, S754 ([WED-431](#))

- Hildt, Eberhard, S1039 (FRI-254), S1042 (FRI-259)
- Hilleret, Marie-Noëlle, S52 (OS-066), S107 (LBP-11), S473 (THU-511), S894 (FRI-142), S1106 (WED-179), S1160 (SAT-184)
- Hill, Megan, S662 (SAT-412)
- Hilpert, Martin, S664 (SAT-414)
- Hilsenbeck, Susan, S517 (FRI-319)
- Himmelsbach, Vera, S491 (FRI-273)
- Hinrichsen, Holger, S11 (LBO-03), S1147 (TOP-110)
- Hinrichs, Jan, S240 (WED-326), S315 (SAT-551)
- Hinson, Jan, S846 (WED-478)
- Hinz, Sebastian, S364 (FRI-390)
- Hiramatsu, Naoki, S871 (SAT-137)
- Hiraoka, Atsushi, S584 (THU-131)
- Hirayama-Shoji, Kayoko, S409 (TOP-064)
- Hirode, Grishma, S52 (OS-065-YI), S503 (FRI-293), S1132 (SAT-145)
- Hirohara, Junko, S401 (WED-303)
- Hirooka, Masashi, S283 (SAT-327)
- Hirschfield, Benjamin, S398 (WED-299)
- Hirschfield, Gideon, S56 (OS-073), S314 (SAT-548), S367 (TOP-063), S371 (WED-255), S371 (WED-256), S372 (WED-257), S373 (WED-259), S379 (WED-268), S386 (WED-280), S387 (WED-281), S404 (WED-310), S411 (FRI-331), S426 (FRI-363)
- Hirsch, Hans, S101 (LBP-04), S449 (SAT-383)
- Hislop, Colin, S9 (GS-012)
- Hoang, Hai, S325 (WED-221), S566 (SAT-286)
- Hoang, Marjorie, S582 (THU-129)
- Hoare, Matthew, S323 (WED-217)
- hobolth, Lise, S239 (WED-325)
- Hock, Charlotte Sophie, S277 (WED-387)
- Ho, Daniel, S48 (OS-058)
- Hodge, Alex, S622 (THU-443)
- Hodson, Leanne, S731 (TOP-089)
- Hoebinger, Constanze, S152 (FRI-415)
- Hoেকে, Lien Van, S229 (THU-364)
- Hoegl, Annabelle, S742 (WED-411)
- Hoek, Bart Van, S85 (OS-120)
- Hoeroldt, Barbara, S382 (WED-273), S391 (WED-289)
- Ho, Erwin, S1114 (WED-190)
- Hoessly, Linard, S481 (THU-526)
- Hofer, Benedikt, S19 (OS-010-YI), S37 (OS-039-YI), S222 (THU-357), S224 (THU-358), S244 (WED-334), S246 (WED-338), S279 (TOP-043), S286 (SAT-332), S288 (SAT-335), S289 (SAT-336), S316 (SAT-553), S831 (FRI-477)
- Hoffer, Oshrit, S719 (SAT-500)
- Hoffmann, Carsten, S350 (THU-236)
- Hoffmann, Charlotte, S561 (SAT-277)
- Hoffmann, Katrin, S44 (OS-050-YI)
- Hoffman, Sara, S31 (OS-029)
- Hoffstedt, Johan, S710 (SAT-486)
- Hofmann, Maike, S33 (OS-032), S318 (SAT-555), S447 (SAT-379)
- Hofmann, Ute, S940 (THU-249)
- Hofmann, Wolf Peter, S1139 (SAT-156)
- Hofmeister, Megan, S1052 (SAT-141)
- Hofstetter, Thomas, S737 (WED-402)
- Ho, Gideon, S65 (OS-087), S763 (WED-445)
- Hohenester, Simon, S329 (WED-228), S417 (FRI-349), S948 (THU-259), S990 (THU-317)
- Hohlstein, Philipp, S188 (FRI-534)
- Ho, Hsin-Tien, S825 (FRI-521)
- Ho, Jing Liang, S300 (SAT-522)
- Hokkoku, Daiki, S509 (FRI-302)
- (Holden) Hsu, Yao-Chun, S1023 (FRI-226)
- Holdorf, Meghan, S35 (OS-034), S1019 (FRI-220)
- Hole, Mikal Jacob, S413 (FRI-334)
- Holinka, Mikolas, S1173 (THU-164)
- Hollande, Clemence, S578 (THU-122)
- Holmberg, Marte, S1150 (SAT-170)
- Holmes, Heather, S765 (WED-448)
- Holmes, Jacinta, S58 (OS-075), S125 (LBP-38), S306 (SAT-535)
- Holm, Kristian, S343 (THU-225), S421 (FRI-355), S428 (FRI-365)
- Hołowko, Waław, S514 (FRI-313)
- Holt, Jason, S35 (OS-034)
- Holtmann, Gerald, S176 (FRI-453)
- Holtug, Taus, S163 (FRI-432)
- Hompesch, Marcus, S688 (SAT-451)
- Homyk, Andrew, S671 (SAT-426)
- Honda, Akira, S394 (WED-293)
- Hong, Changze, S202 (FRI-556)
- Hong, Chun-Ming, S1061 (WED-119)
- Hong, Hyeyeon, S1139 (SAT-155)
- Hong, Jin, S548 (SAT-251), S1029 (FRI-238), S1029 (FRI-239), S1051 (FRI-272)
- Hong, Mei-Zhu, S869 (SAT-134)
- Hong, Sung-Ah, S947 (THU-258)
- Hong, Zhen Howe, S239 (WED-324)
- Hong, Zhongsi, S1185 (THU-180)
- Hood, Gillian, S621 (THU-441), S740 (WED-406), S825 (FRI-520)
- Hoogenboezem, Remco, S1019 (FRI-219)
- Horakova, Olga, S784 (WED-509), S805 (WED-552)
- Hora, Shainan, S786 (WED-514)
- Horhat, Adelina, S151 (FRI-413), S178 (FRI-457)
- Horisaka, Kisara, S559 (SAT-272)
- Horman, Sandrine, S439 (SAT-364)
- Horn, Michael, S412 (FRI-332)
- Horslen, Simon P., S123 (LBP-35), S387 (WED-282)
- Horsmans, Yves, S134 (THU-405)
- Horta, Diana, S171 (FRI-445), S376 (WED-264), S380 (WED-270), S392 (WED-290), S399 (WED-300), S587 (THU-136), S1098 (WED-166)
- Hortlik, Hannah, S313 (SAT-546), S484 (THU-531)
- Horvath, Angela, S346 (THU-230), S354 (THU-242)
- Horvath, Judit, S979 (THU-299)
- Horvatis, Thomas, S1032 (FRI-244)
- Hosaka, Tetsuya, S1061 (WED-119)
- Hosseini, Mojgan, S715 (SAT-496)
- Ho, Steve, S322 (WED-215)
- Hosui, Atsushi, S871 (SAT-137)
- Hou, Hypatia, S31 (OS-029)
- Hou, Jiajie, S543 (SAT-242)
- Hou, Jinlin, S22 (OS-016), S34 (OS-033), S112 (LBP-18), S507 (FRI-300), S525 (TOP-070), S543 (SAT-242), S1085 (WED-149), S1153 (SAT-174), S1164 (SAT-192), S1171 (SAT-201)
- Houlihan, Ciara, S1211 (THU-223)
- Houmadi, Rhizlane, S722 (SAT-505), S769 (WED-453), S777 (WED-469)
- Hou, Ming-Chih, S252 (WED-346), S496 (FRI-283), S1172 (THU-163)
- Hou, Qiaohao, S347 (THU-232)
- Houri, Inbal, S403 (WED-308), S404 (WED-310)
- Houssel-Debry, Pauline, S86 (OS-121-YI), S473 (THU-511), S981 (THU-303)
- Houts, Carrie, S1087 (WED-151)
- Hou, Yixin, S193 (FRI-544)
- Hovelsø, Nanna, S614 (THU-429)
- Hov, Johannes R., S343 (THU-225), S370 (WED-254), S413 (FRI-334), S428 (FRI-365)
- Howell, Jess, S875 (FRI-115)
- Howell, Jessica, S306 (SAT-535)
- Hoyle, Henry, S409 (TOP-064)
- Hoyo, Jordi, S664 (SAT-415)
- Hradicka, Petra, S343 (THU-225)
- Hristopoulos, George, S1156 (SAT-177)
- Hrynuk, Olha, S712 (SAT-490)
- Hsiang, Chih-Weim, S825 (FRI-521)
- Hsiao, Chih-Yang, S501 (FRI-290)
- Hsieh, Tsai-Yuan, S1180 (THU-174), S1206 (THU-217)
- Hsin-Tzu, Wang, S735 (WED-399), S775 (WED-463)
- Hsiong, Cheng-Huei, S825 (FRI-521)
- Hsu, Chao-Wei, S1129 (WED-214)
- Hsu, Chen-Yang, S891 (FRI-137)
- Hsu, Che-Wei, S999 (THU-333)
- Hsu, Chiun, S588 (THU-138)
- Hsu, Heather, S737 (WED-401)
- Hsu, Shih-Jer, S518 (FRI-320)
- Hsu, Wei-Fan, S491 (FRI-273)
- Hsu, Yao-Chun (Holden), S52 (OS-065-YI), S1132 (SAT-145), S1159 (SAT-182)
- Htun Oo, Ye, S944 (THU-254), S982 (THU-304)
- Huadong, Yan, S196 (FRI-547)
- Huang, Chien-Wei, S1180 (THU-174), S1206 (THU-217)
- Huang, Chi-Wei, S252 (WED-346)
- Huang, Chung-Feng, S1180 (THU-174), S1206 (THU-217)
- Huang, Daniel, S65 (OS-086), S468 (THU-500), S629 (THU-456),

Author Index

- S644 (THU-554), S662 (SAT-412),
S698 (SAT-467), S707 (SAT-482),
S714 (SAT-495), S839 (FRI-490)
Huang, Guangjun, S304 (SAT-530)
Huang, Hian Liang, S582 (THU-129),
S591 (THU-142)
Huang, Jee-Fu, S1180 (THU-174),
S1206 (THU-217)
Huang, Jian, S624 (THU-446)
Huang, Jiaofeng, S634 (THU-465)
Huang, Jia-Sheng, S1180 (THU-174)
Huang, Kai-Wen, S501 (FRI-290)
Huang, Kang, S1209 (THU-220)
Huang, Kuo-Wei, S496 (FRI-283)
Huang, Lan, S1053 (SAT-142)
Huang, Linxiang, S425 (FRI-361),
S862 (SAT-124)
Huang, Rui, S395 (WED-294),
S1004 (THU-379), S1068 (WED-127),
S1078 (WED-140), S1080 (WED-142),
S1094 (WED-161), S1094 (WED-162),
S1096 (WED-164), S1110 (WED-184),
S1128 (WED-212)
Huang, Shang-Chin, S518 (FRI-320)
Huang, Shuo, S145 (TOP-078)
Huang, Tien-Yu, S825 (FRI-521)
Huang, Vera, S548 (SAT-251)
Huang, Wenxiang, S1143 (SAT-161)
Huang, Xiaohong, S127 (TOP-093),
S445 (SAT-376)
Huang, Xuan, S525 (TOP-070)
Huang, Yan, S189 (FRI-536), S196 (FRI-547),
S1165 (SAT-193)
Huang, Yi, S1076 (WED-138),
S1157 (SAT-179)
Huang, Yi-Hsiang, S252 (WED-346),
S490 (TOP-068), S496 (FRI-283),
S575 (THU-116), S582 (THU-128),
S586 (THU-134), S1083 (WED-147),
S1172 (THU-163), S1180 (THU-174),
S1206 (THU-217)
Huang, Ying-Che, S895 (FRI-143)
Huang, Yiyan, S557 (SAT-269)
Huang, Zhenlin, S445 (SAT-376)
Huang, Zuxiong, S189 (FRI-536)
Hua, Rui, S1012 (THU-391)
Huber, Felix, S44 (OS-050-YI)
Huber, Patrick, S304 (SAT-531),
S318 (SAT-555)
Huber, Samuel, S60 (OS-079-YI),
S285 (SAT-331), S525 (TOP-069),
S527 (SAT-213), S579 (THU-123),
S582 (THU-128)
Hubert, Isabelle Fouchard, S52 (OS-066)
Huber, Wolf-Dietrich, S123 (LBP-35),
S387 (WED-282)
Huch, Meritxell, S364 (FRI-390)
Hucke, Florian, S491 (FRI-273)
Hudler, Petra, S553 (SAT-261)
Hudson, Benjamin, S153 (FRI-418)
Huebener, Peter, S285 (SAT-331)
Huebschen, Judith, S930 (FRI-202)
Huelin, Patricia, S2 (GS-003)
Huergo, Estefanía, S290 (SAT-337)
Huerta, Anna, S73 (OS-100-YI)
Huerta, Nuria Del Val, S268 (WED-372)
Hueser, Norbert, S1021 (FRI-223.)
Hufnagel, Franziska, S136 (FRI-393),
S951 (THU-264)
Hughes, Sarah, S284 (SAT-329)
Hugo, Susan, S1108 (WED-181)
Hu, Guoxin, S1171 (SAT-201)
Hu, Haoran, S455 (THU-477),
S540 (SAT-236)
Huiling, Xiang, S243 (WED-332)
Hui, Rex Wan-Hin, S62 (OS-082),
S490 (TOP-068)
Hui, Vicki Wing-Ki, S1064 (WED-123),
S1069 (WED-129), S1131 (SAT-144),
S1146 (SAT-166), S1148 (SAT-167)
Hu, Jing, S1102 (WED-172)
Hu, Jinhua, S243 (WED-332)
Hu, Jui-Ting, S1180 (THU-174),
S1206 (THU-217)
Hu, Jungen, S1020 (FRI-222),
S1021 (FRI-224)
Hukkinen, Maria, S997 (THU-329)
Hull, Diana, S398 (WED-299)
Hul, Noémi K. M. Van, S435 (SAT-357),
S439 (SAT-365)
Hum, Dean, S211 (THU-342),
S666 (SAT-417), S668 (SAT-421)
Hundertmark, Jana, S80 (OS-114-YI)
Hung, Chao-Hung, S1083 (WED-147),
S1180 (THU-174), S1206 (THU-217)
Hung-Chih, Chiu, S1140 (SAT-157)
Hung-Yu, Sun, S735 (WED-399),
S775 (WED-463)
Hun, Monika, S606 (THU-416)
Hunter, Jo, S15 (OS-002)
Hunt, Suzanne, S1211 (THU-223)
Hunyor, Imre, S230 (THU-367)
Huot-Marchand, Philippe, S651 (SAT-393),
S823 (FRI-517)
Hupa-Breier, Katharina Luise,
S466 (THU-496), S797 (WED-537)
Hu, Peng, S195 (FRI-546), S340 (WED-250),
S1112 (WED-187), S1112 (WED-188)
Hupertz, Vera, S123 (LBP-35),
S387 (WED-282)
Hüppe, Dietrich, S1147 (TOP-110)
Hur, Bo-Yun, S506 (FRI-297)
Hur, Junho, S563 (SAT-281)
Hur, Moon Haeng, S1048 (FRI-268),
S1062 (WED-120), S1144 (SAT-163)
Hur, Sumin, S778 (WED-471)
Hurtado-Genovés, Gema, S451 (SAT-387),
S789 (WED-520)
Husebye, Eystein, S370 (WED-254)
Hussain, Nasir, S398 (WED-299)
Hussain, Shabir, S953 (THU-266)
Hussein, Hayder, S964 (THU-283)
Huss, Ryan, S323 (WED-216)
Huth, Thorben, S547 (SAT-248)
Hutsch, Tomasz, S332 (WED-233)
Hu, Tsung-Hui, S125 (LBP-38),
S891 (FRI-137), S1083 (WED-147)
Hu, Xiaoxiao, S271 (WED-376)
Hu, Xin Yu, S1096 (WED-165)
Hu, Yanxia, S747 (WED-419)
Hu, Yoa-Pu, S825 (FRI-521)
Hu, Yuanchang, S446 (SAT-378)
Hvid, Henning, S742 (WED-411),
S748 (WED-421)
Hwang, Carey, S11 (LBO-02), S32 (OS-031)
Hwang, Jow-Jyh, S895 (FRI-143)
Hwang, Jung Ho, S778 (WED-471)
Hwang, Sangyoun, S588 (THU-137)
Hwang, Woonchang, S563 (SAT-281)
Hwang, Yoon Jung, S512 (FRI-310)
Hydes, Theresa, S521 (FRI-326),
S617 (THU-434)
Hyogo, Hideyuki, S686 (SAT-448)
Hyun Kim, Tae, S117 (LBP-25)
Hyun Park, Sang, S779 (WED-473)
Hyun Shim, Ju, S558 (SAT-270)
Hyun Sinn, Dong, S117 (LBP-25)
Hyunsoon, Kang, S548 (SAT-251),
S1029 (FRI-239)
Iacob, Razvan, S899 (FRI-150)
Iacob, Speranta, S899 (FRI-150)
Iakovleva, Viktoriia, S786 (WED-514)
Iannacone, Matteo, S5 (GS-005)
Iannetta, Marco, S1056 (TOP-106),
S1072 (WED-133)
Iannone, Giulia, S191 (FRI-540),
S237 (WED-320)
Iapadre, Nerio, S1122 (WED-203)
Iavarone, Massimo, S12 (LBO-04),
S571 (TOP-067), S584 (THU-131),
S593 (THU-145), S865 (SAT-129)
Ibañez, Luis, S279 (TOP-043),
S700 (SAT-468), S807 (TOP-077),
S970 (THU-290)
Ibarra, Cesar, S541 (SAT-238)
Ibarzábal, Ainitze, S737 (WED-403)
Ibberson, David, S547 (SAT-248)
Iborra, Salvador, S349 (THU-235)
Ibrahim, Reham Awad Awad,
S840 (FRI-491)
Ibrahim, Luqman, S29 (OS-025)
Ibrahim, Sabah, S1098 (WED-167)
Ibrahim, Samar, S765 (WED-448)
Ichai, Philippe, S74 (OS-104),
S189 (FRI-537)
Ichikawa, Masataka, S409 (TOP-060)
Ichikawa, Tatsuki, S1177 (THU-170)
Iciek, Laurie, S1169 (SAT-197)
Idalsoaga, Francisco, S145 (TOP-073),
S865 (SAT-129), S900 (FRI-151)
Idelfonso García, Osiris German,
S160 (FRI-426)
Ide, Tatsuya, S899 (FRI-149)
Idilman, Ramazan, S65 (OS-086),
S181 (FRI-463), S195 (FRI-546),
S274 (WED-382), S477 (THU-518),
S1109 (WED-183), S1137 (SAT-152)
Ido, Akio, S1183 (THU-177)
Iegri, Claudia, S471 (THU-507)
Ieluzzi, Donatella, S203 (FRI-558),
S1082 (WED-146)

- Iglesias, Ainhoa, S137 ([FRI-395](#)), S529 ([SAT-215](#)), S738 ([WED-404](#))
- Iglesias, Estefania Huergo, S143 ([FRI-404](#))
- Igloi-Nagy, Adam, S894 ([FRI-141](#))
- Iglseder, Bernhard, S863 ([SAT-126](#))
- Ignasi, Olivas, S56 ([OS-073](#)), S392 ([WED-290](#)), S405 ([WED-311](#))
- Ignat, Mina, S151 ([FRI-413](#)), S178 ([FRI-457](#)), S297 ([SAT-519](#))
- Ignat, Mina Dana, S295 ([SAT-347](#))
- Ihli, Franziska, S431 ([FRI-369](#))
- Iio, Etsuko, S1095 ([WED-163](#))
- Ijaz, Naeem, S641 ([THU-476](#))
- Ijeoma, Ifeorah, S865 ([SAT-129](#))
- Ijzermans, Jan, S501 ([FRI-291](#)), S561 ([SAT-276](#))
- Ikahihifo-Bender, Jade, S258 ([WED-355](#))
- Ikeda, Yuji, S633 ([THU-463](#))
- Ikejima, Kenichi, S180 ([FRI-461](#)), S744 ([WED-415](#)), S793 ([WED-528](#))
- Ilboudo, Abdoul Kader, S930 ([FRI-202](#))
- Iliescu, Elena Laura, S9 ([GS-012](#)), S277 ([WED-386](#)), S807 ([TOP-077](#)), S819 ([FRI-510](#)), S1123 ([WED-204](#)), S1193 ([THU-193](#))
- Illhardt, Toni, S480 ([THU-522](#))
- Ilyas, Sumera I., S28 ([OS-024-YI](#))
- Imai, Michitaka, S584 ([THU-131](#))
- Imam, Ashraf, S484 ([THU-532](#))
- Imamura, Michio, S72 ([OS-098](#))
- Imanov, Ziya, S709 ([SAT-485](#))
- Im, DaeSeong, S817 ([FRI-506](#))
- Immer, Franz, S888 ([FRI-131](#))
- Imnadze, Paata, S891 ([FRI-136](#))
- Imschoot, Griet Van, S229 ([THU-364](#))
- Im, Weonbin, S948 ([THU-259](#))
- Iñarrairaegui, Mercedes, S12 ([LBO-04](#)), S573 ([THU-114](#))
- Inayat, Faisal, S268 ([WED-371](#))
- Inbar, Dana, S409 ([TOP-060](#))
- Incalzi, Raffaele Antonelli, S665 ([SAT-416](#))
- Incicco, Simone, S250 ([WED-343](#))
- Indersie, Emilie, S537 ([SAT-232](#)), S551 ([SAT-256](#))
- Indolfi, Giuseppe, S965 ([THU-284](#)), S971 ([THU-291](#))
- Indulti, Federica, S86 ([OS-121-YI](#)), S87 ([OS-123-YI](#)), S279 ([TOP-043](#)), S287 ([SAT-334](#))
- Infante, Mirtha, S865 ([SAT-129](#))
- Infelise, Patrizia, S605 ([THU-415](#)), S611 ([THU-425](#))
- Ingavle, Ganesh, S205 ([TOP-042](#))
- Ingiliz, Patrick, S1054 ([TOP-100](#)), S1106 ([WED-178](#)), S1106 ([WED-179](#)), S1147 ([TOP-110](#))
- Ingram, Suzanne, S848 ([WED-480](#))
- Ingram, Wendy, S153 ([FRI-418](#))
- Ingrid, Marcq, S161 ([FRI-429](#))
- Inia, José A., S805 ([WED-553](#))
- Innes, Hamish, S548 ([SAT-250](#))
- Innocenti, Francesco, S645 ([THU-556](#))
- Innocent, Victoria, S1058 ([WED-113](#))
- Inoue, Takako, S1095 ([WED-163](#))
- Invernizzi, Pietro, S11 ([LBO-03](#)), S40 ([OS-045](#)), S55 ([OS-070](#)), S56 ([OS-073](#)), S374 ([WED-260](#)), S381 ([WED-272](#)), S447 ([SAT-380](#)), S982 ([THU-304](#)), S992 ([THU-319](#))
- Ioana, Rusu, S295 ([SAT-347](#))
- Ioannidou, Panagiota, S1128 ([WED-211](#))
- Iori, Anna Paola, S88 ([OS-124-YI](#))
- Iorio, Raffaele, S966 ([THU-285](#))
- Iotti, Stefano, S360 ([FRI-383](#))
- Ippili, Ravi, S67 ([OS-091](#))
- Ippolito, Davide, S381 ([WED-272](#))
- Iqbal, Afshan, S435 ([SAT-357](#))
- Iqbal, Shahed, S64 ([OS-085](#))
- Iqbal, Tariq, S123 ([LBP-36](#)), S368 ([WED-251](#))
- Irani, Farah, S591 ([THU-142](#))
- Iranzo, Patricia, S375 ([WED-263](#))
- Irish, Dianne, S879 ([FRI-120](#))
- Ir Macias, Rocio, S551 ([SAT-256](#))
- Irure, Juan, S390 ([WED-288](#))
- Iruretagoyena, Begoña Rodriguez, S532 ([SAT-221](#))
- Iruzubieta, Paula, S8 ([GS-009](#)), S38 ([OS-042-YI](#)), S140 ([FRI-399](#)), S390 ([WED-288](#)), S693 ([SAT-460](#)), S700 ([SAT-468](#)), S709 ([SAT-484](#)), S728 ([SAT-515](#)), S868 ([SAT-132](#)), S934 ([FRI-211](#)), S964 ([THU-282](#)), S980 ([THU-301](#)), S996 ([THU-326](#)), S998 ([THU-331](#))
- Irving, William, S847 ([WED-479](#))
- Isaak, Alexander, S229 ([THU-366](#))
- Isabel Lucena, Maria, S44 ([OS-049-YI](#))
- Isac, Teodora, S277 ([WED-386](#))
- Isakov, Vasily, S863 ([SAT-125](#))
- Isani, Gloria, S360 ([FRI-383](#))
- Isayama, Hiroyuki, S11 ([LBO-03](#))
- Iser, David, S306 ([SAT-535](#))
- Iserte, Gemma, S497 ([FRI-284](#)), S573 ([THU-114](#)), S579 ([THU-124](#)), S849 ([WED-483](#))
- Ishiba, Hiroshi, S686 ([SAT-448](#))
- Ishido, Shun, S644 ([THU-554](#))
- Ishikawa, Toru, S584 ([THU-131](#)), S818 ([FRI-508](#))
- Islam, Mojahidul, S17 ([OS-006-YI](#)), S218 ([THU-351](#)), S1027 ([FRI-235](#))
- Ismail, Mona, S724 ([SAT-509](#)), S865 ([SAT-129](#))
- Israel, Robert, S236 ([WED-319](#)), S275 ([WED-383](#))
- Israelsen, Mads, S17 ([OS-005-YI](#)), S163 ([FRI-432](#)), S173 ([FRI-449](#)), S175 ([FRI-452](#)), S303 ([SAT-528](#)), S832 ([FRI-479](#)), S845 ([TOP-054](#))
- Istrate, Mircea, S277 ([WED-386](#)), S819 ([FRI-510](#)), S1193 ([THU-193](#))
- Ita-Pérez, Dalia De, S547 ([SAT-249](#))
- Itoh, Kiyoaki, S811 ([FRI-468](#))
- Itoh, Yoshito, S616 ([THU-433](#)), S1183 ([THU-177](#))
- Itokawa, Norio, S240 ([WED-327](#)), S317 ([SAT-554](#)), S584 ([THU-131](#)), S818 ([FRI-508](#)), S820 ([FRI-511](#))
- Ito, Seigo, S453 ([SAT-392](#))
- Itzel, Timo, S646 ([THU-559](#))
- Iuliano, Antonella, S942 ([THU-251](#))
- Ivanecz, Arpad, S553 ([SAT-261](#))
- Ivashkin, Vladimir, S260 ([WED-357](#))
- Iversen, Aske Thorn, S65 ([OS-088](#))
- Iwagami, Yoshifumi, S439 ([SAT-366](#)), S509 ([FRI-302](#))
- Iwaki, Michihiro, S30 ([OS-028](#)), S616 ([THU-433](#)), S686 ([SAT-448](#))
- Iwakiri, Katsuhiko, S240 ([WED-327](#)), S317 ([SAT-554](#)), S818 ([FRI-508](#)), S820 ([FRI-511](#))
- Iwamoto, Hideki, S584 ([THU-131](#))
- Iyer, Janani, S31 ([OS-029](#)), S790 ([WED-522](#))
- Izagirre, Maider Huici, S28 ([OS-024-YI](#))
- Izbicki, Jakob R., S285 ([SAT-331](#))
- Izcue, Ana, S542 ([SAT-240](#))
- Izquierdo-Altarejos, Paula, S423 ([FRI-359](#))
- Izquierdo-Sánchez, Laura, S57 ([OS-074-YI](#)), S541 ([SAT-238](#)), S700 ([SAT-468](#)), S734 ([WED-397](#))
- Izumi, Namiki, S53 ([OS-067](#)), S65 ([OS-086](#)), S598 ([THU-155](#)), S644 ([THU-554](#)), S1113 ([WED-189](#)), S1137 ([SAT-153](#))
- Izzi, Antonio, S36 ([OS-036](#)), S40 ([OS-045](#)), S55 ([OS-070](#))
- Izzy, Manhal, S241 ([WED-328](#)), S555 ([SAT-265](#)), S900 ([FRI-151](#))
- Jaan, Ali, S183 ([FRI-339](#))
- Jaberi, Arash, S314 ([SAT-548](#))
- Jaber, Samir, S74 ([OS-104](#))
- Jablkowski, Maciej, S53 ([OS-067](#)), S1137 ([SAT-153](#))
- Jabri, Yamen, S483 ([THU-530](#))
- Jachs, Mathias, S37 ([OS-039-YI](#)), S90 ([OS-127-YI](#)), S107 ([LBP-11](#)), S108 ([LBP-12](#)), S193 ([FRI-545](#)), S199 ([FRI-551](#)), S201 ([FRI-554](#)), S244 ([WED-334](#)), S282 ([SAT-326](#)), S284 ([SAT-330](#)), S286 ([SAT-332](#)), S288 ([SAT-335](#)), S292 ([SAT-342](#)), S299 ([SAT-521](#)), S313 ([SAT-547](#)), S831 ([FRI-477](#)), S939 ([TOP-058](#)), S1135 ([SAT-150](#))
- Jack, Kathryn, S847 ([WED-479](#))
- Jackson, Kathy, S875 ([FRI-115](#))
- Jacob Hole, Mikal, S428 ([FRI-365](#))
- Jacobs, Daniel, S932 ([FRI-208](#))
- Jacobsen, Birgitte, S629 ([THU-455](#)), S657 ([SAT-404](#)), S851 ([WED-487](#))
- Jacobson, Ira M, S1072 ([WED-134](#)), S1089 ([WED-153](#)), S1093 ([WED-160](#)), S1121 ([WED-200](#))
- Jacommet, Christine, S876 ([FRI-117](#))
- Jacquemin, Emmanuel, S954 ([THU-267](#)), S969 ([THU-289](#)), S971 ([THU-291](#))
- Jadawdji, Zainab, S1129 ([WED-213](#))
- Jaeckel, Elmar, S425 ([FRI-362](#)), S466 ([THU-496](#)), S797 ([WED-537](#))
- Jaekers, Joris, S524 ([TOP-066](#)), S753 ([WED-430](#))
- Jäger, Julius, S413 ([FRI-334](#))

Author Index

- Jager, Nynke, S973 (THU-292)
Jagst, Michelle, S1032 (FRI-244)
Jain, Aakriti, S943 (THU-253)
Jain, Gautam, S282 (SAT-325)
Jain, Priti, S182 (TOP-040)
Jain, Shubham, S405 (WED-312), S643 (THU-553)
Jain, Vandana, S984 (THU-307), S987 (THU-312), S999 (THU-332)
Jaisinghani, Ruchika, S1030 (FRI-241)
Jakate, Shiriam, S631 (THU-460)
Jakhar, Deepika, S208 (THU-338), S228 (THU-363)
Jakwerth, Constanze, S945 (THU-256)
Jalal, Prasun, S516 (FRI-317), S517 (FRI-319)
Jalan, Rajiv, S35 (OS-035-YI), S70 (OS-095-YI), S129 (THU-396), S193 (FRI-543), S197 (FRI-549), S203 (FRI-557), S205 (TOP-042), S206 (TOP-046), S220 (THU-355)
Jambulingam, Nila, S719 (SAT-501)
James, S257 (WED-353), S278 (WED-389)
James, Bethany, S215 (THU-346)
James, Michael, S621 (THU-441), S726 (SAT-512)
Jamialahmadi, Oveis, S665 (SAT-416), S733 (WED-393), S803 (WED-549)
Jamil, Aqeel, S1005 (THU-381)
Jamil, Khurram, S241 (WED-328), S280 (TOP-045), S296 (SAT-348)
Jammal, Alaa, S484 (THU-532)
Janardhan, Sujit, S101 (LBP-03)
Jancoriene, Ligita, S880 (FRI-121), S912 (FRI-173)
Janczewska, Ewa, S198 (FRI-550), S505 (FRI-296), S807 (TOP-077), S1034 (FRI-248), S1138 (SAT-154), S1205 (THU-215)
Janczyk, Wojciech, S837 (FRI-486), S950 (THU-262)
Jandrain, Bernard, S607 (THU-419)
Jane, Joana Codina, S843 (FRI-499)
Janekrongtham, Chawisar, S919 (FRI-184)
Jang, Byoung Kuk, S588 (THU-137)
Jang, Eun Chul, S615 (THU-431), S667 (SAT-418), S695 (SAT-462), S701 (SAT-470), S704 (SAT-475), S757 (WED-435), S794 (WED-531), S864 (SAT-128)
Jang, Eun Sun, S407 (WED-316), S916 (FRI-179)
Jang, Heejoon, S610 (THU-423), S814 (FRI-473), S1062 (WED-120)
Jang, Jae Young, S186 (FRI-343), S190 (FRI-538), S192 (FRI-542), S200 (FRI-553), S1136 (SAT-151)
Jang, Jeong Won, S148 (FRI-409)
Jang, Se Young, S690 (SAT-455), S698 (SAT-466), S705 (SAT-477), S712 (SAT-491)
Jang, Young Saeng, S752 (WED-427)
Janičko, Martin, S871 (SAT-136)
Janik, Maciej K., S42 (OS-047-YI), S400 (WED-301), S982 (THU-304)
Janjua, Naveed, S874 (FRI-114), S883 (FRI-125), S886 (FRI-130), S919 (FRI-183), S1189 (THU-187), S1200 (THU-207)
Jankowska, Irena, S969 (THU-289), S971 (THU-291)
Jankowski, Krzysztof, S563 (SAT-280)
Janowski, Kamil, S837 (FRI-486)
Jans, Alexander, S416 (FRI-348)
Janša, Rado, S553 (SAT-261)
Jansen, Anouk M.E., S973 (THU-292)
Jansen, Christian, S61 (OS-080-YI), S279 (TOP-043)
Janssen, Harry, S53 (OS-067), S1137 (SAT-153)
Janssen, Harry LA, S52 (OS-065-YI), S454 (TOP-052), S503 (FRI-293), S1100 (WED-169), S1132 (SAT-145)
Jan Thibaut, Hendrik, S1025 (FRI-231)
Jantz, Derek, S35 (OS-034)
Japaridze, Maia, S930 (FRI-203)
Jara, Maximilian, S65 (OS-088)
Jaramillo, Catalina, S971 (THU-291)
Jarcuska, Peter, S871 (SAT-136)
Jarman, Edward, S122 (LBP-33-YI)
Jaroszewicz, Jerzy, S505 (FRI-296), S1205 (THU-215)
Jarrin, Denise Monserrat Arroyo, S892 (FRI-139), S898 (FRI-148)
Jarvis, Helen, S867 (SAT-130)
Jasmins, Luís, S889 (FRI-134)
Jasper, Jeffrey, S763 (WED-445)
Jassem, Wayel, S445 (SAT-376), S483 (THU-530)
Jatta, Abdoulie, S67 (OS-090-YI), S1106 (WED-178)
Jaubert, Laura, S170 (FRI-443)
Jauch, Anna, S547 (SAT-248)
Javier, Dax, S1058 (WED-113)
Jaworski, Jakub, S1075 (WED-137)
Jayasekera, Channa, S590 (THU-141)
Jazaeri, Farahnaz, S215 (THU-347)
Jean-Baptiste, Hiriart, S318 (SAT-556)
Jean Damascene, Makuza, S886 (FRI-130)
Jeannin Megnien, Sophie, S619 (THU-438), S619 (THU-439), S643 (THU-552)
Jedrysiak, Katrin, S1176 (THU-168)
Jeglinski, Brenda, S115 (LBP-22)
Jegodzinski, Lina, S687 (SAT-449)
Jekle, Andreas, S1030 (FRI-241)
Jemersic, Lorena, S1053 (SAT-143)
Jemielita, Thomas, S610 (THU-423), S650 (TOP-085), S653 (SAT-397)
Jena, Anuraag, S405 (WED-312), S643 (THU-553)
Jeng, Rachel Wen-Juei, S52 (OS-065-YI), S1057 (TOP-112), S1132 (SAT-145)
Jensen, Anne-Sofie Houlberg, S702 (SAT-471), S748 (WED-421)
Jensen, Boye, S303 (SAT-528)
Jensen, Ellen, S163 (FRI-432), S173 (FRI-449), S303 (SAT-528)
Jensen-Jarolim, Erika, S451 (SAT-388)
Jensen, Majken, S614 (THU-429)
Jensen, M.K., S971 (THU-291)
Jensen, Morten Daniel, S166 (FRI-436)
Jeong, Dahn, S883 (FRI-125), S886 (FRI-130), S919 (FRI-183), S1189 (THU-187), S1200 (THU-207)
Jeong, Jae Yoon, S637 (THU-469), S697 (SAT-464)
Jeong, Jin-Ju, S156 (FRI-420), S177 (FRI-456), S220 (THU-354), S343 (THU-227)
Jeong, Jin Sook, S785 (WED-513)
Jeong, Jong-Min, S25 (OS-021-YI)
Jeong, Kwang Won, S778 (WED-471)
Jeong, Sook-Hyang, S407 (WED-316), S583 (THU-130), S916 (FRI-179)
Jeong, Soung Won, S1073 (WED-135)
Jeong, Won-il, S25 (OS-021-YI)
Jeong, Yun Seong, S555 (SAT-264)
Jeon, Sun Kyung, S506 (FRI-297)
Jepsen, Peter, S4 (GS-004-YI), S103 (LBP-06), S160 (FRI-427), S165 (FRI-435), S166 (FRI-436), S176 (FRI-454), S614 (THU-429)
Jeremie, Corneille, S684 (SAT-445)
Jerome, Ellen, S127 (TOP-093), S445 (SAT-376)
Jerovšek, Marjana Turk, S135 (THU-407)
Jerzowski, John, S31 (OS-030), S1034 (FRI-248), S1087 (WED-151), S1138 (SAT-154)
Jerzynski, Julia, S625 (THU-449)
Jeschke, Matthias, S1124 (WED-206), S1125 (WED-207)
Jessa, Fatema, S316 (SAT-552)
Jesudian, Arun, S291 (SAT-339)
Jesús, María, S554 (SAT-263)
Jesús Perugorria, María, S533 (SAT-223), S534 (SAT-226), S541 (SAT-238)
Jezek, Filip, S311 (SAT-544)
Jezequel, Caroline, S318 (SAT-556)
Jhaisha, Samira Abu, S188 (FRI-534)
Jhaveri, Ravi, S913 (FRI-174)
Jia, Bei, S1004 (THU-379)
Jia, Catherine, S64 (OS-085)
Jia, Gang, S86 (OS-122)
Jia, Ji-Dong, S243 (WED-332)
Jia, Jidong, S1153 (SAT-174)
Jiaming, Wang, S1119 (WED-198)
Jiang, Guoqing, S34 (OS-033)
Jiang, Jing, S20 (OS-013), S186 (FRI-342), S204 (FRI-559), S436 (SAT-359)
Jiang, Longfeng, S453 (SAT-391), S730 (TOP-086)
Jiang, Suling, S1078 (WED-140), S1094 (WED-161)
Jiang, Xiaohuan, S1102 (WED-172)
Jiang, Xiaoyu, S555 (SAT-265)
Jiang, Xixian, S352 (THU-239)
Jiang, Yiyue, S1085 (WED-149)
Jiang, Yongfang, S34 (OS-033), S195 (FRI-546)
Jiang, Yuchuan, S543 (SAT-242)
Jiang, Yuyong, S1076 (WED-138), S1157 (SAT-179)

- Jiang, Z. Gordon, S171 ([FRI-444](#))
 Jiao, Boshen, S873 ([FRI-113](#))
 Jiao, Yan-Mei, S145 ([TOP-078](#))
 Jiarui, Zheng, S425 ([FRI-361](#)),
 S692 ([SAT-458](#))
 Jiayi, Pi, S735 ([WED-399](#)), S775 ([WED-463](#))
 Ji, Dong, S1085 ([WED-149](#))
 Jimenez-Aguero, Raul, S541 ([SAT-238](#))
 Jimenez, Ana Belen Perez,
 S1126 ([WED-208](#))
 Jiménez, César, S10 ([LBO-01](#))
 Jimenez-Esquivel, Natalia, S131 ([THU-399](#)),
 S250 ([WED-343](#))
 Jiménez-González, Carolina,
 S700 ([SAT-468](#)), S709 ([SAT-484](#))
 Jiménez, Javier Rodriguez, S397 ([WED-296](#))
 Jiménez-Martí, Elena, S451 ([SAT-387](#)),
 S789 ([WED-520](#))
 Jiménez-Masip, Alba, S693 ([SAT-460](#))
 Jiménez, Miguel, S248 ([WED-341](#))
 Jiménez-Pérez, Miguel, S314 ([SAT-549](#))
 Jimenez-Rivera, Carolina, S972 ([THU-291](#))
 Jiménez, Wladimiro, S325 ([WED-220](#)),
 S333 ([WED-235](#))
 Jinato, Thananya, S342 ([TOP-038](#)),
 S354 ([THU-243](#)), S356 ([THU-245](#))
 Jindal, Ankur, S1027 ([FRI-235](#))
 Jindal, Disha, S129 ([THU-396](#))
 Jing, Zhang, S138 ([FRI-396](#))
 Jin, Hai, S747 ([WED-419](#))
 Jin, Hua, S1165 ([SAT-193](#))
 Jin, Ming Li, S778 ([WED-471](#))
 Jin, Qinglong, S1166 ([SAT-194](#))
 Jin, Rui, S759 ([WED-438](#)), S862 ([SAT-124](#))
 Jin, Xiao-Zhi, S613 ([THU-428](#)),
 S1085 ([WED-149](#))
 Jin, Yi, S205 ([TOP-042](#))
 Jiroušková, Markéta, S945 ([THU-255](#))
 Jirsa, Milan, S1173 ([THU-164](#))
 Ji, Yun, S1024 ([FRI-229](#))
 Jlaiel, Malik, S834 ([FRI-481](#))
 Jm Bauer, David, S201 ([FRI-554](#))
 Joachim-Richter, Anna, S1090 ([WED-156](#)),
 S1176 ([THU-168](#))
 Jo, Aejeong, S690 ([SAT-455](#)),
 S698 ([SAT-466](#)), S705 ([SAT-477](#)),
 S712 ([SAT-491](#))
 Jobson, Timothy, S877 ([FRI-118](#))
 Jochheim, Leonie, S47 ([OS-057](#)),
 S1124 ([WED-206](#)), S1125 ([WED-207](#))
 Joekes, Elizabeth, S522 ([FRI-327](#))
 Jo, Eunji, S517 ([FRI-319](#))
 Johannes, Chang, S61 ([OS-080-YI](#)),
 S229 ([THU-366](#))
 Johannes Gairing, Simon, S264 ([WED-365](#))
 Johannessen, Asgeir, S916 ([FRI-178](#)),
 S927 ([FRI-197](#)), S1117 ([WED-195](#)),
 S1150 ([SAT-170](#))
 Johansen, Stine, S17 ([OS-005-YI](#)),
 S163 ([FRI-432](#)), S173 ([FRI-449](#)),
 S175 ([FRI-452](#)), S303 ([SAT-528](#)),
 S832 ([FRI-479](#)), S845 ([TOP-054](#))
 Johansson, Edvin, S820 ([FRI-513](#))
 Johansson, Lars, S820 ([FRI-513](#))
 Joh, Jae-Won, S471 ([THU-506](#)),
 S474 ([THU-513](#))
 John, Binu, S110 ([LBP-15](#)), S304 ([SAT-532](#)),
 S832 ([FRI-478](#))
 John, Christine, S1174 ([THU-166](#))
 John, Nimy, S296 ([SAT-349](#))
 Johnson, Amy, S1175 ([THU-167](#))
 Johnson, Elspeth, S731 ([TOP-089](#))
 Johnson, Philip, S521 ([FRI-326](#))
 Johnson, Stephanie, S239 ([WED-324](#))
 Johnston, Michael, S402 ([WED-305](#))
 Jo, Hoon Gil, S438 ([SAT-362](#)),
 S690 ([SAT-455](#)), S698 ([SAT-466](#)),
 S705 ([THU-477](#)), S712 ([SAT-491](#))
 Jokelainen, Kalle, S370 ([WED-253](#))
 Jokl, Elliot, S8 ([GS-010](#)), S71 ([OS-097](#)),
 S333 ([WED-234](#))
 Jones, Andrew, S1182 ([THU-176](#))
 Jones, Christopher, S763 ([WED-445](#))
 Jones, Christopher R., S1075 ([WED-137](#))
 Jones, David, S56 ([OS-073](#)), S367 ([TOP-063](#)),
 S397 ([WED-297](#)), S411 ([FRI-331](#))
 Jones, Lauren, S45 ([OS-052](#))
 Jones, Nicola, S389 ([WED-285](#))
 Jones, Rebecca L., S411 ([FRI-331](#))
 Jones, Robert, S480 ([THU-522](#))
 Jones, Rowena, S901 ([FRI-152](#))
 Jones, Shelley, S1069 ([WED-128](#))
 Jones, Simon, S231 ([THU-368](#)),
 S232 ([THU-370](#))
 Jong, Anja Versteeg-de, S740 ([WED-406](#))
 Jongejan, Aldo, S55 ([OS-071-YI](#))
 Jong-Hon, KANG, S394 ([WED-293](#))
 Jong Yu, Su, S630 ([THU-457](#)),
 S635 ([THU-466](#)), S642 ([THU-550](#))
 Jonker, Johan, S805 ([WED-554](#))
 Joo, Sae Kyung, S603 ([THU-411](#)),
 S814 ([FRI-473](#))
 Jopson, Laura, S411 ([FRI-331](#))
 Jordan, William, S1151 ([SAT-171](#))
 Jördens, Markus, S420 ([FRI-353](#)),
 S421 ([FRI-355](#))
 Jørgensen, Kristin K., S413 ([FRI-334](#))
 Jørgensen, Kristin Kaasen,
 S403 ([WED-307](#))
 Jørgensen, Sebastian, S748 ([WED-421](#))
 Jørgensen, Silje, S478 ([THU-520](#))
 Jørgensen, Søren Peter, S390 ([WED-287](#))
 Jörg, Vincent, S582 ([THU-128](#))
 Jorquera, Francisco, S366 ([TOP-061](#)),
 S380 ([WED-270](#)), S852 ([WED-489](#))
 Jörs, Simone, S431 ([FRI-369](#))
 José Crespo, Alicia San, S480 ([THU-524](#))
 José Ortiz de Urbina, Juan, S554 ([SAT-263](#))
 Joseph, George, S291 ([SAT-339](#))
 Joshi, Amod, S35 ([OS-034](#))
 Joshi, Deepak, S11 ([LBO-03](#)),
 S990 ([THU-317](#))
 Joshita, Satoru, S394 ([WED-293](#))
 Joshi, Yogendrakumar, S277 ([WED-388](#))
 Josué, Mármol Aguilar Carlos,
 S883 ([FRI-126](#))
 Jothimani, Dinesh, S274 ([WED-382](#)),
 S473 ([THU-510](#)), S488 ([THU-544](#))
 Joubel, Camille, S27 ([OS-023-YI](#))
 Joubioux, Florian Le, S806 ([WED-555](#))
 Joueidi, Ahmed, S1011 ([THU-388](#))
 Joueidi, Faisal, S1011 ([THU-388](#))
 Jou, Janice, S832 ([FRI-478](#))
 Joven, Jorge, S670 ([SAT-425](#)),
 S676 ([SAT-433](#))
 Joy, Rosa, S1191 ([THU-190](#))
 Juanola, Adria, S10 ([LBO-01](#)), S15 ([OS-001](#)),
 S163 ([FRI-431](#)), S250 ([WED-343](#)),
 S664 ([SAT-415](#)), S851 ([WED-486](#))
 Juarez, Javier Ventura, S337 ([WED-244](#))
 Ju Cho, Eun, S630 ([THU-457](#)),
 S635 ([THU-466](#)), S642 ([THU-550](#))
 Jucov, Alina, S32 ([OS-031](#)), S1149 ([SAT-168](#)),
 S1162 ([SAT-188](#))
 Judd, Ali, S913 ([FRI-174](#))
 Juel, Helene Bæk, S17 ([OS-005-YI](#)),
 S173 ([FRI-449](#))
 Jühling, Frank, S72 ([OS-098](#))
 Ju, Jin-Sung, S556 ([SAT-266](#)),
 S558 ([SAT-270](#))
 Jukema, J. Wouter, S805 ([WED-553](#))
 Julia, Marino Blanes, S476 ([THU-517](#))
 Julian, Belén, S1187 ([THU-183](#))
 Julian, Luetkens, S229 ([THU-366](#))
 Julla, Jean-Baptiste, S670 ([SAT-424](#)),
 S681 ([SAT-440](#))
 Jumat, Nur Halisah Binte, S698 ([SAT-467](#)),
 S714 ([SAT-495](#))
 Jun, Dae Won, S615 ([THU-431](#)),
 S662 ([SAT-411](#)), S667 ([SAT-418](#)),
 S690 ([SAT-455](#)), S695 ([SAT-462](#)),
 S698 ([SAT-466](#)), S701 ([SAT-470](#)),
 S704 ([SAT-475](#)), S705 ([SAT-476](#)),
 S705 ([SAT-477](#)), S712 ([SAT-491](#)),
 S757 ([WED-435](#)), S794 ([WED-531](#)),
 S864 ([SAT-128](#)), S1065 ([WED-124](#)),
 S1073 ([WED-135](#)), S1078 ([WED-139](#))
 Juneja, Pinky, S208 ([THU-338](#)),
 S228 ([THU-363](#)), S352 ([THU-240](#))
 Junejo, Zeeshan, S204 ([FRI-560](#)),
 S842 ([FRI-497](#))
 Jung, Chan-Young, S1142 ([SAT-160](#))
 Jung, Chunwon, S948 ([THU-259](#))
 Junge, Norman, S383 ([WED-277](#))
 Jung, Hyun Jin, S778 ([WED-471](#))
 Jung, Jang Han, S186 ([FRI-343](#)),
 S190 ([FRI-538](#)), S192 ([FRI-542](#)),
 S200 ([FRI-553](#)), S615 ([THU-431](#)),
 S695 ([SAT-462](#)), S701 ([SAT-470](#)),
 S704 ([SAT-475](#)), S757 ([WED-435](#)),
 S794 ([WED-531](#)), S1073 ([WED-135](#))
 Jung, Jeesun, S792 ([WED-527](#))
 Jung, Jui, S606 ([THU-417](#))
 Jung, Yong Jin, S603 ([THU-411](#)),
 S814 ([FRI-473](#)), S1062 ([WED-120](#))
 Jung, Young Kul, S186 ([FRI-343](#)),
 S190 ([FRI-538](#)), S192 ([FRI-542](#)),
 S578 ([THU-121](#)), S781 ([WED-476](#)),
 S798 ([WED-540](#)), S1136 ([SAT-151](#))
 Jung, Youngmi, S18 ([OS-008-YI](#))
 Junhui, S300 ([SAT-522](#))
 Junien, Jean Louis, S776 ([WED-466](#))

Author Index

- Junien, Jean-Louis, S226 (THU-361), S651 (SAT-393), S823 (FRI-517)
- Junker, Anders, S702 (SAT-471), S742 (WED-411), S748 (WED-421), S784 (WED-511)
- Jun Kim, Yoon, S630 (THU-457), S635 (THU-466), S642 (THU-550)
- Jura, Jolanta, S332 (WED-233), S431 (FRI-370)
- Jurkiewicz, Elżbieta, S837 (FRI-486)
- Ju, Shenghong, S286 (SAT-333)
- Justyna, Janocha-Litwin, S505 (FRI-296)
- Juyal, Dinkar, S790 (WED-522)
- Kabaçam, Gökhan, S181 (FRI-463)
- Kabamba, Benoit, S923 (FRI-190)
- Kabar, Iyad, S957 (THU-271)
- Kablawi, Dana, S645 (THU-557)
- Kacar, Sertac, S470 (THU-505)
- Kachru, Nandita, S857 (SAT-115)
- Kacprowski, Tim, S1029 (FRI-240)
- Kadar, Einat, S926 (FRI-196)
- Kadaristiana, Agustina, S969 (THU-289)
- Kaddam, Israa, S964 (THU-283)
- Kadharia, Anushka, S689 (SAT-453)
- Kaewdech, A, S1134 (SAT-148)
- Kaewdech, Apichat, S514 (FRI-314), S721 (SAT-503)
- Kafi, Shamsoun, S1098 (WED-167)
- Kahlhöfer, Julia, S1137 (SAT-152), S1139 (SAT-156)
- Kahn, Judith, S477 (THU-519)
- Kaina, Bernd, S536 (SAT-230)
- Kain, Renate, S316 (SAT-553)
- Kaiser, Hannah, S1147 (TOP-109)
- Kaiser, Lara, S628 (THU-454)
- Kajaia, Maia, S889 (FRI-133)
- Kajbaf, Farshad, S49 (OS-062)
- Kakazu, Eiji, S444 (SAT-373), S1183 (THU-177)
- Kakisaka, Keisuke, S394 (WED-293)
- Kakizaki, Satoru, S584 (THU-131)
- Kakuda, Thomas, S31 (OS-030), S1034 (FRI-248), S1138 (SAT-154)
- Kalaidzidis, Yannis, S364 (FRI-390)
- Kale, Aditya, S282 (SAT-325), S290 (SAT-338), S310 (SAT-542), S983 (THU-305)
- Kalendova, Veronika, S784 (WED-509), S805 (WED-552)
- Kaliamoorthy, Ilankumaran, S488 (THU-544)
- Kaliaskarova, Kulpash, S320 (SAT-559)
- Kalinowski, Piotr, S563 (SAT-280)
- Kalix, Leon, S1029 (FRI-240)
- Kalkan, Cagdas, S1109 (WED-183)
- Kallin, Nina, S33 (OS-032)
- Kalra, Naveen, S51 (OS-064-YI)
- Kalra, Rupinder, S146 (FRI-407)
- Kaltenecker, Christopher, S316 (SAT-553)
- Kalthoff, Sandra, S422 (FRI-357), S429 (FRI-366)
- Kamada, Yoshihiro, S686 (SAT-448)
- Kamal, Faisal, S268 (WED-371), S641 (THU-476)
- Kamal, Monica A., S570 (SAT-291)
- Kamal, Muhammad, S268 (WED-371)
- Kamar, Nassim, S473 (THU-511)
- Kamath, Binita M., S372 (WED-257), S969 (THU-289), S972 (THU-291)
- Kamath, Patrick S., S10 (LBO-01), S195 (FRI-546), S242 (WED-330), S258 (WED-355), S274 (WED-382), S465 (THU-495), S865 (SAT-129), S900 (FRI-151)
- Kamga Wouambo, Rodrigue, S1043 (FRI-260)
- Kamili, Saleem, S891 (FRI-136), S905 (FRI-160), S1052 (SAT-141)
- Kamimura, Keiko, S899 (FRI-149)
- Kamińska, Diana, S837 (FRI-486), S950 (THU-262)
- Kamiri-Ngugi, Rachael, S1202 (THU-210)
- Kamkamidze, George, S889 (FRI-133), S930 (FRI-203)
- Kanaan, Nada, S923 (FRI-190)
- Kanagalingam, Gowthami, S242 (WED-331)
- Kanai, Takanori, S156 (FRI-421), S409 (TOP-060)
- Kandulski, Arne, S1003 (THU-377)
- Kaneko, Akira, S394 (WED-293)
- Kaneko, Keiko, S240 (WED-327)
- Kang, Bo-Kyeong, S615 (THU-431), S667 (SAT-418), S695 (SAT-462), S701 (SAT-470), S704 (SAT-475), S705 (SAT-476), S757 (WED-435)
- Kang, Garrett, S300 (SAT-522)
- Kang, Hye Jin, S516 (FRI-318)
- Kang, Hyo-Jin, S509 (FRI-303)
- Kang, Ji Hun, S834 (FRI-482)
- Kang, Ju-hee, S778 (WED-471)
- Kang, Keon Wook, S567 (SAT-287), S796 (WED-534)
- Kang, Koo Jeong, S512 (FRI-309), S594 (THU-146)
- Kang, MeeYoung, S583 (THU-130)
- Kang, Min Kyu, S645 (THU-558)
- Kang, Minwoo, S148 (FRI-409)
- Kang, Sang Hee, S555 (SAT-264)
- Kang, Sang-Hee, S578 (THU-121)
- Kang, Seung Goo, S414 (FRI-336), S752 (WED-427)
- Kang, Weiwei, S235 (TOP-047)
- Kang, Wonseok, S267 (WED-369), S305 (SAT-533), S631 (THU-459), S821 (FRI-514)
- Kania, Dramane, S897 (FRI-146)
- Kan, Kejia, S358 (FRI-381)
- Kann, Anna Emilie, S4 (GS-004-YI), S160 (FRI-427)
- Kanto, Tatsuya, S444 (SAT-373), S899 (FRI-149)
- Kanwal, Fasiha, S173 (FRI-448), S472 (THU-508)
- Kao, Cheng, S1029 (FRI-238)
- Kao, Jia-Horng, S52 (OS-065-YI), S518 (FRI-320), S1061 (WED-119), S1132 (SAT-145), S1180 (THU-174), S1206 (THU-217)
- Kapatais, Andreas, S1128 (WED-211)
- Kapiyeva, Raima, S320 (SAT-559)
- Kaplan, David, S188 (FRI-535), S248 (WED-342), S265 (WED-366), S304 (SAT-532), S832 (FRI-478)
- Kappe, Naomi, S85 (OS-120)
- Kappert, Kai, S197 (FRI-549)
- Kaps, Leonard, S26 (OS-022), S264 (WED-365), S271 (WED-377), S277 (WED-387)
- Kaptein, Suzanne, S1038 (FRI-253)
- Karageorgos, Charalampos, S1194 (THU-196), S1194 (THU-197)
- Kara, Leila, S607 (THU-418), S651 (SAT-394), S652 (SAT-396)
- Karam-Allah, Haidi, S840 (FRI-491)
- Karam, Vincent, S46 (OS-053-YI)
- Karanth, Subbu, S102 (LBP-05)
- Karaoglu, Arda, S1019 (FRI-219)
- Karapatanis, Stylianos, S1128 (WED-211)
- Karasu, Zeki, S181 (FRI-463), S195 (FRI-546)
- Karatza, Eleni, S367 (TOP-062)
- Karayannis, Peter, S922 (FRI-189)
- Kardashian, Ani, S169 (FRI-441)
- Karim, Gres, S729 (SAT-516), S926 (FRI-196)
- Karim, Mohammad Ehsanul, S1200 (THU-207)
- Kariuki, Christopher, S1051 (FRI-272)
- Kärjä, Vesa, S803 (WED-549)
- Karkhanis, Salil, S964 (THU-283)
- Karki, Chitra, S1008 (THU-386)
- Karkossa, Isabel, S136 (FRI-393)
- Karlsen, Lars Normann, S1150 (SAT-170)
- Karlsen, Tom Hemming, S364 (FRI-390), S370 (WED-254), S409 (TOP-064), S418 (FRI-351), S420 (FRI-353), S421 (FRI-355), S541 (SAT-238)
- Karner, Vincent, S282 (SAT-326)
- Karnik, Satyajit, S49 (OS-062)
- Karnsakul, Wikrom, S914 (FRI-176), S965 (THU-284), S971 (THU-291), S1052 (SAT-141), S1182 (THU-175)
- Karpen, Saul J., S415 (FRI-346), S971 (THU-291)
- Kar, Premashis, S294 (SAT-346)
- Karriker, Forrest, S35 (OS-034)
- Karsdal, Morten, S173 (FRI-449), S175 (FRI-452), S657 (SAT-404), S688 (SAT-451), S707 (SAT-481), S717 (SAT-498), S723 (SAT-507), S826 (FRI-522)
- Karşıdağ, Kubilay, S709 (SAT-485)
- Karthikeyan, Palaniswamy, S971 (THU-291)
- Karvellas, Constantine, S127 (TOP-093), S189 (FRI-537), S459 (THU-484)
- Kasahara, Mureo, S971 (THU-291)
- Kaseb, Ahmed, S9 (GS-011), S582 (THU-128)
- Kasim, Hasyim, S1203 (THU-212)
- Kasimova, Rano, S113 (LBP-19)

- Kasi, Nagraj, S123 ([LBP-35](#)), S387 ([WED-282](#))
- Kassab, Mohamed, S521 ([FRI-326](#))
- Kassas, Mohamed El, S627 ([THU-453](#)), S863 ([SAT-125](#))
- Kasten, Jennifer, S417 ([FRI-350](#))
- Kastrup, Nanna, S163 ([FRI-432](#))
- Kasuga, Ryosuke, S156 ([FRI-421](#)), S409 ([TOP-060](#))
- Katariya, Nitin, S590 ([THU-141](#))
- Katav, Avi, S415 ([FRI-345](#))
- Katchman, Helena, S195 ([FRI-546](#)), S315 ([SAT-550](#))
- Kateb, Angels, S579 ([THU-124](#))
- Katemann, Christoph, S229 ([THU-366](#))
- Katharina Frank, Anna, S418 ([FRI-351](#))
- Kathawate, Ranganath, S398 ([WED-298](#))
- Kathemann, Simone, S987 ([THU-313](#))
- Kather, Jakob Nikolas, S12 ([LBO-04](#))
- Katja, Füssel, S379 ([WED-269](#))
- Kato, Azusa, S453 ([SAT-392](#))
- Kato, Hideaki, S323 ([WED-216](#))
- Kato, Keizo, S818 ([FRI-508](#))
- Kato, Naoya, S1183 ([THU-177](#))
- Katsahian, Sandrine, S859 ([SAT-120](#))
- Katzarov, Krum, S198 ([FRI-550](#)), S807 ([TOP-077](#)), S1149 ([SAT-168](#))
- Kaufman, Keith, S49 ([OS-060](#))
- Kaufmann, Monika, S719 ([SAT-500](#))
- Kaufman, Stephanie, S31 ([OS-029](#))
- Kauppinen, Sakari, S742 ([WED-410](#))
- Kaur, Amandeep, S1141 ([SAT-158](#)), S1145 ([SAT-164](#))
- Kaur, Amanpreet, S786 ([WED-514](#))
- Kaur, Impreet, S208 ([THU-338](#)), S228 ([THU-363](#)), S352 ([THU-240](#))
- Kaur, Navkiran, S218 ([THU-351](#))
- Kaur, Savneet, S208 ([THU-338](#)), S228 ([THU-363](#)), S326 ([WED-222](#)), S352 ([THU-240](#)), S436 ([SAT-360](#)), S560 ([SAT-274](#))
- Kaur, Senamjit, S309 ([SAT-541](#))
- Kauschke, Stefan Günther, S795 ([WED-533](#))
- Kaushik, Ankita, S882 ([FRI-124](#)), S901 ([FRI-152](#)), S1059 ([WED-116](#)), S1070 ([WED-130](#)), S1072 ([WED-134](#)), S1089 ([WED-153](#)), S1093 ([WED-160](#)), S1121 ([WED-200](#))
- Kautiainen, Hannu, S370 ([WED-253](#))
- Kautz, Achim, S627 ([THU-453](#))
- Kawada, Norifumi, S325 ([WED-221](#)), S395 ([WED-293](#)), S566 ([SAT-286](#)), S1183 ([THU-177](#))
- Kawaguchi, Takumi, S584 ([THU-131](#)), S627 ([THU-453](#)), S686 ([SAT-448](#))
- Kawai, Hidehiko, S633 ([THU-463](#))
- Kawanaka, Miwa, S616 ([THU-433](#)), S686 ([SAT-448](#))
- Kawano, Tadamichi, S240 ([WED-327](#)), S317 ([SAT-554](#)), S818 ([FRI-508](#)), S820 ([FRI-511](#))
- Kawata, Kazuhito, S394 ([WED-293](#)), S584 ([THU-131](#)), S686 ([SAT-448](#))
- Kawli, Kashmira, S290 ([SAT-338](#)), S310 ([SAT-542](#))
- Kaya, Ebru, S254 ([WED-349](#)), S255 ([WED-351](#)), S270 ([WED-375](#))
- Kayani, Kayani, S447 ([SAT-380](#))
- Kaye, Philip, S717 ([SAT-498](#))
- Kayhan, Meral Akdogan, S181 ([FRI-463](#))
- Kaymakoglu, Sabahattin, S709 ([SAT-485](#))
- Kazankov, Konstantin, S176 ([FRI-454](#))
- Kazemier, Geert, S568 ([SAT-289](#)), S836 ([FRI-485](#))
- Kearney, Bradley, S453 ([SAT-392](#))
- Keaveny, Andrew, S101 ([LBP-03](#)), S195 ([FRI-546](#))
- Ke, Bibo, S453 ([SAT-391](#)), S730 ([TOP-086](#))
- Kechagias, Stergios, S605 ([THU-414](#)), S607 ([THU-418](#)), S650 ([TOP-085](#)), S651 ([SAT-394](#)), S653 ([SAT-397](#)), S707 ([SAT-481](#))
- Kedarisetty, Chandan, S209 ([THU-339](#))
- Kee, James, S850 ([WED-484](#))
- Keen, Phyllis, S193 ([FRI-543](#))
- Keerthihan Thiyagarajah, Keerthihan, S1039 ([FRI-254](#)), S1042 ([FRI-259](#))
- Keever, Angelina Villasis, S1087 ([WED-151](#)), S1115 ([WED-191](#))
- Keggenhoff, Friederike, S536 ([SAT-230](#))
- Keijer, Jaap, S786 ([WED-515](#))
- Keitel, Verena, S1147 ([TOP-110](#))
- Keitoku, Taisei, S598 ([THU-155](#)), S644 ([THU-554](#))
- Keklikkiran, Caglayan, S389 ([WED-286](#))
- Kelava, Tomislav, S1053 ([SAT-143](#))
- Kelil, Abdellali, S1058 ([WED-113](#))
- Keller, David, S532 ([SAT-222](#))
- Kelley, Katie, S1189 ([THU-185](#))
- Kelly, Deirdre, S969 ([THU-289](#)), S971 ([THU-291](#)), S1000 ([THU-334](#))
- Kelly, Gavin, S1108 ([WED-181](#))
- Kelsch, Lara, S447 ([SAT-379](#))
- Kelsen, Jens, S510 ([FRI-305](#))
- Kemble, George, S49 ([OS-061](#))
- Kemeç, Gamze, S709 ([SAT-485](#))
- Kemgang, Astrid, S408 ([WED-317](#))
- Ke, Michael, S453 ([SAT-391](#)), S730 ([TOP-086](#))
- Kemos, Polychronis, S912 ([FRI-172](#))
- Kemper, Angieszka, S1122 ([WED-202](#))
- Kempski, Jan, S1139 ([SAT-156](#))
- Kemp, Susan, S174 ([FRI-450](#))
- Kemp, William, S380 ([WED-271](#)), S622 ([THU-443](#)), S861 ([SAT-123](#))
- Kendall, Timothy, S65 ([OS-087](#)), S601 ([TOP-082](#))
- Kendrick, Michael, S44 ([OS-050-YI](#)), S465 ([THU-495](#))
- Kendrick, Stuart, S110 ([LBP-15](#))
- Kennedy, James, S274 ([WED-382](#))
- Kennedy, Patrick, S118 ([LBP-27](#)), S1024 ([FRI-229](#)), S1033 ([FRI-246](#)), S1034 ([FRI-248](#)), S1087 ([WED-151](#)), S1105 ([WED-176](#)), S1127 ([WED-209](#))
- Kenny, Fiona, S324 ([WED-218](#)), S324 ([WED-219](#))
- Keppler, Oliver, S945 ([THU-256](#))
- Kepten, Eldad, S669 ([SAT-423](#))
- Kerbert, Annarein, S35 ([OS-035-YI](#)), S206 ([TOP-046](#))
- Kerins, Caoimhe, S324 ([WED-218](#))
- Kerkar, Nanda, S44 ([OS-049-YI](#)), S971 ([THU-291](#))
- Kerlik, Jana, S880 ([FRI-121](#))
- Kern, Anna, S44 ([OS-050-YI](#)), S45 ([OS-051-YI](#)), S465 ([THU-495](#))
- Kersten, Remco, S55 ([OS-071-YI](#))
- Keskin-Erdogan, Zalike, S337 ([WED-243](#))
- Keskin, Onur, S1054 ([TOP-100](#)), S1109 ([WED-183](#)), S1137 ([SAT-152](#))
- Kessler, Harald, S996 ([THU-327](#))
- Kesten, Jo, S858 ([SAT-118](#)), S909 ([FRI-165](#))
- Ketikoglou, Ioannis, S400 ([WED-302](#))
- Kew, Guan Sen, S300 ([SAT-522](#))
- Khabra, Efrat, S409 ([TOP-060](#))
- Khac, Eric Nguyen, S61 ([OS-081](#)), S161 ([FRI-429](#)), S318 ([SAT-556](#))
- Khaderi, Saira, S173 ([FRI-448](#))
- Khader, Majd, S403 ([WED-308](#))
- Khakayla, Abed, S484 ([THU-532](#))
- Khakoo, Salim, S1075 ([WED-137](#))
- Khalaf, Maya, S1006 ([THU-382](#))
- Khalidi, Marion, S74 ([OS-104](#))
- Khaled, Ala, S475 ([THU-515](#))
- Khaled, Najib Ben, S47 ([OS-057](#)), S596 ([THU-150](#))
- Khalenkow, Maxim, S307 ([SAT-538](#))
- Khalili, Korosh, S503 ([FRI-293](#))
- Khan, Asad, S995 ([THU-324](#))
- Khan, Imran, S272 ([WED-379](#))
- Khan, Muhammad Sohail, S1196 ([THU-200](#))
- Khanna, Deepanshu, S294 ([SAT-346](#))
- Khan, Pir Zarak, S912 ([FRI-172](#))
- Khan, Rayan, S900 ([FRI-151](#))
- Khan, Saniya, S277 ([WED-388](#))
- Khan, Shahid, S864 ([SAT-127](#))
- Khan, Sohaib, S1122 ([WED-203](#))
- Khan, Sulhera, S204 ([FRI-560](#))
- Khan, Waleed, S740 ([WED-406](#))
- Khan, Waqas, S877 ([FRI-118](#))
- Khaoprasert, Sanpolpai, S262 ([WED-360](#))
- Kharawala, Saifuddin, S145 ([SAT-164](#))
- Khatri, Robin, S60 ([OS-079-YI](#))
- Khattab, Mahmoud, S353 ([THU-241](#)), S550 ([SAT-255](#)), S795 ([WED-532](#))
- Khetsuriani, Nino, S113 ([LBP-19](#))
- Khayar, Amel, S456 ([THU-478](#))
- Khokhliuk, Olena, S429 ([FRI-367](#))
- Khorsandi, Shirin Elizabeth, S445 ([SAT-376](#))
- Khosla, Archit, S790 ([WED-522](#))
- Khoury, Tania, S670 ([SAT-424](#)), S681 ([SAT-440](#))
- Khudyakov, Yury, S891 ([FRI-136](#))
- Khukhlina, Oksana, S712 ([SAT-490](#))
- Kiani, Narsis, S290 ([SAT-337](#))
- Kido, Masahiro, S545 ([SAT-246](#)), S559 ([SAT-272](#))
- Kiessling, Fabian, S571 ([SAT-292](#))
- Ki, Han Seul, S442 ([SAT-369](#)), S728 ([SAT-514](#))

Author Index

- Kikuchi, Kentaro, S394 ([WED-293](#))
 Kildegaard, Jonas, S748 ([WED-421](#))
 Kiliaan, Amanda, S763 ([WED-444](#))
 Kilpatrick, Alastair, S434 ([SAT-355](#))
 Kim, Arthur, S58 ([OS-075](#))
 Kim, Aryoung, S267 ([WED-369](#)),
 S305 ([SAT-533](#)), S631 ([THU-459](#))
 Kim, Beom Kyung, S362 ([FRI-387](#)),
 S513 ([FRI-312](#)), S552 ([SAT-259](#)),
 S595 ([THU-148](#)), S906 ([FRI-162](#)),
 S1121 ([WED-201](#))
 Kim, Beom Seok, S1142 ([SAT-160](#))
 Kim, Bo Hyun, S117 ([LBP-25](#))
 Kim, Bohyun, S508 ([FRI-301](#))
 Kim, Byung Ik, S637 ([THU-469](#)),
 S697 ([SAT-464](#))
 Kim, Chang Wook, S1136 ([SAT-151](#))
 Kim, Charlie, S671 ([SAT-426](#))
 Kim, Chong, S1059 ([WED-116](#)),
 S1070 ([WED-130](#)), S1072 ([WED-134](#)),
 S1089 ([WED-153](#)), S1093 ([WED-160](#)),
 S1121 ([WED-200](#))
 Kim, Dae Jin, S758 ([WED-437](#))
 Kim, Dasol, S948 ([THU-259](#))
 Kim, Dong-Hyun, S414 ([FRI-336](#))
 Kim, Dong Joon, S186 ([FRI-343](#)),
 S190 ([FRI-538](#)), S192 ([FRI-542](#)),
 S200 ([FRI-553](#)), S220 ([THU-354](#)),
 S253 ([WED-348](#))
 Kim, Doyoon, S785 ([WED-513](#))
 Kim, Do Young, S362 ([FRI-387](#)),
 S552 ([SAT-259](#)), S595 ([THU-148](#)),
 S906 ([FRI-162](#)), S916 ([FRI-179](#)),
 S1121 ([WED-201](#))
 Kimer, Nina, S165 ([FRI-434](#)),
 S239 ([WED-325](#)), S784 ([WED-511](#))
 Kimes, Teresa M, S1079 ([WED-141](#))
 Kim, Euichang, S573 ([THU-113](#))
 Kim, Eunju, S1062 ([WED-121](#)),
 S1132 ([SAT-146](#))
 Kim, Eun-Jung, S948 ([THU-259](#))
 Kim, Gi-Ae, S606 ([THU-417](#)),
 S1073 ([WED-135](#))
 Kim, Tan, Chin, S278 ([WED-389](#))
 Kim, Haeryoung, S512 ([FRI-310](#))
 Kim, Hayoon, S437 ([SAT-361](#)),
 S563 ([SAT-281](#)), S947 ([THU-258](#))
 Kim, Hwan Mook, S778 ([WED-471](#))
 Kim, Hwi Young, S585 ([THU-132](#)),
 S1065 ([WED-124](#))
 Kim, Hye-Lin, S615 ([THU-431](#)),
 S667 ([SAT-418](#)), S695 ([SAT-462](#)),
 S698 ([SAT-466](#)), S701 ([SAT-470](#)),
 S704 ([SAT-475](#)), S705 ([SAT-477](#)),
 S712 ([SAT-491](#)), S916 ([FRI-179](#))
 Kim, Hye Mi, S362 ([FRI-387](#))
 Kim, Hyoung Su, S186 ([FRI-343](#)),
 S190 ([FRI-538](#)), S192 ([FRI-542](#)),
 S200 ([FRI-553](#)), S1136 ([SAT-151](#))
 Kim, Hyung Jun, S588 ([THU-137](#))
 Kim, Hyun Young, S567 ([SAT-287](#))
 Kim, In Hee, S516 ([FRI-318](#)), S916 ([FRI-179](#)),
 S1136 ([SAT-151](#))
 Kim, Irene, S489 ([TOP-065](#))
 Kim, Jae Hyun, S778 ([WED-471](#))
 Kim, Jaeil, S606 ([THU-417](#))
 Kim, Jeong A, S758 ([WED-437](#)),
 S779 ([WED-473](#))
 Kim, Ji Hoon, S578 ([THU-121](#)),
 S781 ([WED-476](#)), S798 ([WED-540](#)),
 S1136 ([SAT-151](#))
 Kim, Jihye, S817 ([FRI-506](#)),
 S1065 ([WED-124](#))
 Kim, Jin Un, S964 ([THU-283](#))
 Kim, Jin-Wook, S583 ([THU-130](#))
 Kim, Jiyeon, S662 ([SAT-411](#))
 Kim, Jong Man, S471 ([THU-506](#))
 Kim, Jong Su, S720 ([SAT-502](#))
 Kim, Jung Hee, S186 ([FRI-343](#)),
 S637 ([THU-469](#)), S697 ([SAT-464](#))
 Kim, Jung Ju, S778 ([WED-471](#))
 Kim, Jung Kuk, S758 ([WED-437](#))
 Kim, JungMo, S785 ([WED-513](#))
 Kim, Jung Oh, S662 ([SAT-411](#))
 Kim, Ju Yeon, S1144 ([SAT-163](#))
 Kim, Kang Mo, S573 ([THU-113](#)),
 S589 ([THU-140](#)), S998 ([THU-330](#)),
 S1062 ([WED-121](#)), S1139 ([SAT-155](#))
 Kim, KyeWhon, S645 ([THU-558](#))
 Kim, Kyung-ah, S916 ([FRI-179](#))
 Kim, Kyungmo, S971 ([THU-291](#))
 Kim, Kyurae, S25 ([OS-021-YI](#))
 Kim-Lee, Grace, S241 ([WED-328](#))
 Kimmann, Markus, S313 ([SAT-546](#))
 Kim, Mimi, S615 ([THU-431](#)),
 S667 ([SAT-418](#)), S695 ([SAT-462](#)),
 S698 ([SAT-466](#)), S701 ([SAT-470](#)),
 S704 ([SAT-475](#)), S705 ([SAT-476](#)),
 S705 ([SAT-477](#)), S712 ([SAT-491](#)),
 S757 ([WED-435](#))
 Kim, Min, S437 ([SAT-361](#))
 Kim, Mi Na, S513 ([FRI-312](#)), S1121 ([WED-201](#))
 Kim, Minsun, S817 ([FRI-506](#))
 Kim, Min Woo, S778 ([WED-471](#))
 Kim, Misook, S1062 ([WED-120](#))
 Kim, Moon Young, S186 ([FRI-343](#)),
 S192 ([FRI-542](#)), S442 ([SAT-369](#)),
 S728 ([SAT-514](#))
 Kim, Myoung Choi, S437 ([SAT-361](#)),
 S456 ([THU-479](#)), S563 ([SAT-281](#)),
 S947 ([THU-258](#))
 Kim, Nam Hee, S834 ([FRI-482](#))
 Kim, Naomy, S489 ([TOP-065](#))
 Kim, Nomita, S115 ([LBP-22](#))
 Kimono, Beatrice, S688 ([SAT-131](#))
 Ki, Moran, S407 ([WED-316](#))
 Kimoto, Satoshi, S811 ([FRI-468](#))
 Kim, Sam, S1023 ([FRI-226](#))
 Kim, sang gyune, S186 ([FRI-343](#))
 Kim, Sang Kyum, S567 ([SAT-287](#))
 Kim, Sang Wook, S516 ([FRI-318](#))
 Kim, Sarang, S44 ([OS-050-YI](#))
 Kim, Seok-Hwan, S515 ([FRI-315](#))
 Kim, Seong-Hun, S516 ([FRI-318](#))
 Kim, Seon-Ok, S393 ([WED-292](#))
 Kim, Seulgi, S173 ([FRI-448](#))
 Kim, Seung Up, S362 ([FRI-387](#)),
 S513 ([FRI-312](#)), S552 ([SAT-259](#)),
 S595 ([THU-148](#)), S906 ([FRI-162](#)),
 S1065 ([WED-124](#)), S1121 ([WED-201](#)),
 S1142 ([SAT-160](#)), S1184 ([THU-179](#)),
 S1197 ([THU-202](#))
 Kim, Se Woo, S506 ([FRI-297](#))
 Kim, Soon Sun, S572 ([TOP-071](#))
 Kim, So-Young, S1048 ([FRI-268](#))
 Kim, Sung Eun, S794 ([WED-531](#)),
 S1073 ([WED-135](#))
 Kim, Sung-Eun, S186 ([FRI-343](#)),
 S190 ([FRI-538](#)), S192 ([FRI-542](#)),
 S200 ([FRI-553](#)), S253 ([WED-348](#)),
 S1073 ([WED-135](#))
 Kim, Sun Kyoung, S778 ([WED-471](#))
 Kim, Tae Hun, S437 ([SAT-361](#)),
 S456 ([THU-479](#)), S585 ([THU-132](#)),
 S1065 ([WED-124](#))
 Kim, Tae Hyung, S186 ([FRI-343](#)),
 S190 ([FRI-538](#)), S578 ([THU-121](#)),
 S798 ([WED-540](#))
 Kim, Tae-Seok, S512 ([FRI-309](#)),
 S594 ([THU-146](#))
 Kim, Won, S186 ([FRI-343](#)), S190 ([FRI-538](#)),
 S192 ([FRI-542](#)), S603 ([THU-411](#)),
 S814 ([FRI-473](#)), S1062 ([WED-120](#)),
 S1136 ([SAT-151](#))
 Kim, W. Ray, S81 ([OS-115-YI](#)),
 S663 ([SAT-413](#)), S721 ([SAT-503](#))
 Kim, Ye-Jee, S393 ([WED-292](#))
 Kim, Yeonjin, S814 ([FRI-473](#))
 Kim, Yohan, S456 ([THU-479](#)),
 S758 ([WED-437](#)), S779 ([WED-473](#))
 Kim, Yong Hoon, S512 ([FRI-309](#)),
 S594 ([THU-146](#))
 Kim, Yongsoo, S834 ([FRI-482](#))
 Kim, Yoon Jun, S186 ([FRI-343](#)),
 S510 ([FRI-306](#)), S610 ([THU-423](#)),
 S1048 ([FRI-268](#)), S1062 ([WED-120](#)),
 S1065 ([WED-124](#)), S1144 ([SAT-163](#))
 Kim, Young Seok, S1184 ([THU-179](#)),
 S1197 ([THU-202](#))
 Kim, Yun Jung, S1202 ([THU-210](#))
 Kim, Yunki, S817 ([FRI-506](#))
 Kim, Yun Soo, S1136 ([SAT-151](#))
 Kinaani, Fadi, S403 ([WED-308](#))
 Kindler, Thomas, S536 ([SAT-230](#))
 King, Angela, S153 ([FRI-418](#))
 King, Betsy, S475 ([THU-516](#))
 King, Holly, S612 ([THU-427](#))
 King, Jonathan, S74 ([OS-103-YI](#))
 Kinoshita, Manabu, S453 ([SAT-392](#))
 Kirby, John, S411 ([FRI-331](#))
 Kirk, Frederik Teicher, S958 ([THU-274](#))
 Kirsas, Sue, S15 ([OS-002](#))
 Kirstein, Martha M, S579 ([THU-123](#))
 Kiss, András, S23 ([OS-017-YI](#))
 Kister, Bastian, S188 ([FRI-534](#))
 Kita, Yuji, S633 ([THU-463](#))
 Kitchen, Helen, S1087 ([WED-151](#))
 Kitrinou, Kathryn M., S1058 ([WED-114](#)),
 S1149 ([SAT-168](#)), S1153 ([SAT-174](#)),
 S1161 ([SAT-186](#))
 Kittinger, Jakob, S282 ([SAT-326](#))
 Kızıltaş, Cansu, S709 ([SAT-485](#))

- Kjærgaard, Kristoffer, S159 ([FRI-424](#))
 Kjærgaard, Maria, S61 ([OS-080-YI](#)),
 S163 ([FRI-432](#)), S832 ([FRI-479](#)),
 S845 ([TOP-054](#))
 Kjaer, Mette, S817 ([FRI-507](#)), S819 ([FRI-509](#))
 Kjær, Mikkel Breinholt, S510 ([FRI-305](#))
 Kjems, Jørgen, S510 ([FRI-305](#))
 Klaene, Joshua, S422 ([FRI-356](#))
 K L, Ajee, S827 ([FRI-524](#))
 Klapaczynski, Jakub, S505 ([FRI-296](#)),
 S1205 ([THU-215](#))
 Klausen, Gerd, S1186 ([THU-181](#))
 Kleemann, Robert, S763 ([WED-444](#)),
 S786 ([WED-515](#))
 Klein, Christophe, S12 ([LBO-04](#))
 Kleiner, David E, S334 ([WED-238](#)),
 S806 ([TOP-076](#))
 Klein, Hanns-Georg, S507 ([FRI-300](#))
 Kleinlein, Hannah, S377 ([WED-265](#))
 Klein, Marina B., S874 ([FRI-114](#))
 Klein, Sabine, S303 ([SAT-528](#)),
 S712 ([SAT-492](#))
 Kliers, Iris, S811 ([FRI-469](#))
 Klindt-Morgan, Caroline, S415 ([FRI-346](#))
 Klinker, Hartwig, S1147 ([TOP-110](#))
 Klöhn, Mara, S1020 ([FRI-221](#)),
 S1032 ([FRI-244](#))
 Klovstad, Hilde, S880 ([FRI-121](#))
 Klümpen, Heinz-Josef, S576 ([THU-118](#))
 Kluwe, Johannes, S285 ([SAT-331](#))
 Klys, Yuliia, S429 ([FRI-367](#))
 Knapp, Jenny, S994 ([THU-322](#))
 Knecht, Matthias, S280 ([TOP-048](#))
 Kneepkens, Adam, S815 ([FRI-475](#))
 Knegt, Robert De, S83 ([OS-118](#)),
 S1100 ([WED-169](#))
 Knight, Marian, S36 ([OS-037](#))
 Knobler, Hilla, S824 ([FRI-519](#))
 Knolle, Percy A., S33 ([OS-032](#)),
 S59 ([OS-077](#)), S442 ([TOP-050](#)),
 S442 ([TOP-053](#)), S1021 ([FRI-223](#))
 Knowles, Jonathan, S337 ([WED-243](#))
 Knox, Steven J, S1149 ([SAT-168](#)),
 S1153 ([SAT-174](#)), S1161 ([SAT-186](#))
 Knutsson, Douglas, S857 ([SAT-115](#))
 Koay, Eugene, S516 ([FRI-317](#))
 Koball, Sebastian, S220 ([THU-355](#))
 Kobayashi, Shogo, S439 ([SAT-366](#)),
 S509 ([FRI-302](#))
 Kobayashi, Takashi, S30 ([OS-028](#))
 Kocar, Eva, S793 ([WED-529](#))
 Koch, Alexander, S188 ([FRI-534](#)),
 S636 ([THU-467](#))
 Koch, David, S101 ([LBP-03](#))
 Kocheise, Lorenz, S582 ([THU-128](#))
 Ko, Chunkyu, S945 ([THU-256](#))
 Köck, Fiona, S831 ([FRI-477](#))
 Kock, Joery De, S752 ([WED-428](#)),
 S775 ([WED-465](#))
 Koc, Ozgur, S645 ([THU-556](#)),
 S982 ([THU-304](#)), S1100 ([WED-169](#))
 Kodama, Takahiro, S1183 ([THU-177](#))
 Kodama, Yuzo, S559 ([SAT-272](#))
 Koeken, Ine, S764 ([WED-446](#))
 Koek, Ger, S645 ([THU-556](#))
 Koenig, Alexander, S1039 ([FRI-255](#))
 Koenig, Franz, S819 ([FRI-509](#))
 Ko, Eunjung, S781 ([WED-476](#))
 Koffas, Apostolos, S1024 ([FRI-229](#)),
 S1033 ([FRI-246](#))
 Kogias, Dionisios, S1128 ([WED-211](#))
 Koh, Benjamin Wei Feng, S629 ([THU-456](#))
 Koh, Chris, S9 ([GS-012](#))
 Ko, Hin Hln, S426 ([FRI-363](#)), S900 ([FRI-151](#)),
 S1115 ([WED-191](#)), S1117 ([WED-194](#))
 Koh, Jia Hong, S300 ([SAT-522](#))
 Koh, June-Young, S1048 ([FRI-268](#))
 Köhler, Bruno, S506 ([FRI-298](#))
 Köhler, Michael, S313 ([SAT-546](#))
 Kohlhepp, Marlene, S80 ([OS-114-YI](#))
 Kohli, Anita, S125 ([LBP-38](#)), S711 ([SAT-488](#)),
 S828 ([FRI-525](#))
 Kohli, Manik, S721 ([SAT-504](#)),
 S1122 ([WED-202](#))
 Koh, Young-Hwan, S117 ([LBP-25](#))
 Ko, Jae-Hoon, S1048 ([FRI-268](#))
 Kojima, Masami, S733 ([WED-395](#))
 Kolbe, Jonathan, S1019 ([FRI-220](#))
 Kolesnikova, Olena, S767 ([WED-451](#))
 Kolev, Mirjam, S412 ([FRI-332](#))
 Kolhatkar, Nikita, S1023 ([FRI-226](#)),
 S1159 ([SAT-182](#))
 Koller, Michael, S481 ([THU-526](#))
 Koller, Tomas, S865 ([SAT-129](#))
 Koller, Tomáš, S871 ([SAT-136](#))
 Kollmann, Dagmar, S465 ([THU-494](#)),
 S470 ([THU-505](#))
 Komakula, Sai, S80 ([OS-113](#))
 Komeylan, Hamed, S246 ([WED-339](#))
 Komolmit, Piyawat, S217 ([THU-349](#)),
 S1047 ([FRI-266](#))
 Komori, Atsumasa, S394 ([WED-293](#)),
 S401 ([WED-303](#)), S1192 ([THU-191](#)),
 S1199 ([THU-205](#))
 Komura, Takuya, S110 ([LBP-15](#))
 Kõmuru, Kristina, S787 ([WED-517](#))
 Konda, Mikiko, S409 ([TOP-060](#))
 Kondili, Loreta, S1082 ([WED-146](#))
 Kondo, Mayuko, S156 ([FRI-421](#))
 Kone, Amariane, S897 ([FRI-146](#))
 Kong, Alice Pik-Shan, S29 ([OS-025](#))
 Kong, Lianbao, S540 ([SAT-236](#))
 Kong, Ming, S235 ([TOP-047](#))
 Konicek, Anna-Lena, S87 ([OS-123-YI](#))
 Königshofer, Philipp, S222 ([THU-357](#)),
 S224 ([THU-358](#)), S289 ([SAT-336](#)),
 S294 ([SAT-345](#)), S316 ([SAT-553](#))
 König, Stéphane, S531 ([SAT-220](#))
 Konikoff, Fred, S824 ([FRI-519](#))
 Kon, Kazuyoshi, S180 ([FRI-461](#)),
 S744 ([WED-415](#)), S793 ([WED-528](#))
 Kontogianni, Meropi, S262 ([WED-362](#))
 Kontos, Georgios, S1128 ([WED-211](#)),
 S1194 ([THU-196](#))
 Koob, Dennis, S329 ([WED-228](#)),
 S417 ([FRI-349](#))
 Koo, Bo Kyung, S814 ([FRI-473](#))
 Koo, Ja Hyun, S141 ([FRI-401](#))
 Koorneef, Lisa, S743 ([WED-412](#))
 Koot, Bart, S677 ([SAT-434](#))
 Korenaga, Masaaki, S899 ([FRI-149](#))
 Korf, Hannelie, S345 ([THU-229](#)),
 S363 ([FRI-389](#)), S452 ([SAT-390](#)),
 S753 ([WED-430](#))
 Korkmaz, Kerim Sebib, S14 ([LBO-06](#))
 Körner, Christiane, S362 ([FRI-386](#))
 Kornerup, Linda Skibsted, S523 ([FRI-328](#))
 Korolewicz, James, S575 ([THU-116](#)),
 S582 ([THU-128](#))
 Korosec, Ana, S28 ([OS-024-YI](#))
 Korsenik, Joshua, S431 ([FRI-368](#))
 Korsman, Stephen, S1184 ([THU-178](#))
 Kortleve, Dian, S561 ([SAT-276](#))
 Koruth, Roy, S873 ([FRI-113](#))
 Kosari, Kambiz, S489 ([TOP-065](#))
 Kosay, Tolga, S274 ([WED-382](#))
 Koshy, Anoop, S827 ([FRI-524](#))
 Kosinska, Anna, S59 ([OS-077](#))
 Koskinas, Ioannis-Georgios,
 S400 ([WED-302](#))
 Kostadinova, Radina, S327 ([WED-224](#)),
 S737 ([WED-402](#))
 Kostrub, Cory, S417 ([FRI-350](#))
 Kostrzewski, Tomasz, S775 ([WED-464](#))
 Kotaria, Nato, S891 ([FRI-136](#))
 Kotlinowski, Jerzy, S332 ([WED-233](#)),
 S431 ([FRI-370](#))
 Kotorashvili, Adam, S891 ([FRI-136](#))
 Kotski, Sylvain, S500 ([FRI-289](#))
 Koukoulis, George, S400 ([WED-302](#))
 Koulentakis, Mairi, S400 ([WED-302](#))
 Koulla, Yiannoula, S612 ([THU-426](#))
 Koul, Roshan, S326 ([WED-222](#))
 Kounis, Ilias, S460 ([THU-486](#)),
 S981 ([THU-303](#)), S1005 ([THU-380](#))
 Kourikou, Anastasia, S1194 ([THU-196](#))
 Koustenis, Kanellos, S1194 ([THU-197](#))
 Koutny, Florian, S863 ([SAT-126](#))
 Kovats, Patricia, S23 ([OS-017-YI](#)),
 S42 ([OS-047-YI](#)), S982 ([THU-304](#))
 Kovic, Bruno, S9 ([GS-011](#))
 Kow, Alfred, S468 ([THU-500](#))
 Kowalsman, Noga, S409 ([TOP-060](#))
 Kowdley, Kris, S13 ([LBO-05](#)), S115 ([LBP-22](#)),
 S118 ([LBP-26](#)), S371 ([WED-256](#)),
 S378 ([WED-267](#)), S379 ([WED-268](#)),
 S386 ([WED-280](#)), S659 ([SAT-407](#)),
 S678 ([SAT-438](#)), S684 ([SAT-444](#)),
 S995 ([THU-324](#))
 Kowo, Mathurin, S1210 ([THU-222](#))
 Koyano, Kaori, S317 ([SAT-554](#)),
 S820 ([FRI-511](#))
 Koziel, Joanna, S431 ([FRI-370](#))
 Kozma, Emese, S880 ([FRI-121](#))
 Kraaier, Lianne, S535 ([SAT-228](#))
 Kraft, Anke, S229 ([THU-365](#)),
 S1029 ([FRI-240](#)), S1031 ([FRI-242](#)),
 S1035 ([FRI-249](#))
 Krag, Aleksander, S17 ([OS-005-YI](#)),
 S61 ([OS-080-YI](#)), S163 ([FRI-432](#)),
 S173 ([FRI-449](#)), S175 ([FRI-452](#)),
 S253 ([WED-348](#)), S303 ([SAT-528](#)),

Author Index

- S629 (THU-455), S657 (SAT-404), S832 (FRI-479), S845 (TOP-054), S963 (THU-281)
- Kraglund, Frederik, S4 (GS-004-YI), S160 (FRI-427)
- Krajden, Mel, S883 (FRI-125), S1189 (THU-187), S1200 (THU-207)
- Krajewska, Natalia, S448 (SAT-381)
- Krall, Anja, S491 (FRI-273), S582 (THU-128)
- Kramer, Jan, S1090 (WED-156), S1176 (THU-168)
- Kramer, Matthijs, S982 (THU-304), S1100 (WED-169)
- Kramvis, Anna, S875 (FRI-115)
- Kranidioti, Hariklia, S1128 (WED-211), S1194 (THU-196), S1194 (THU-197)
- Kraps, Kai-Uwe, S1071 (WED-132)
- Krarup, Niels, S817 (FRI-507)
- Krasnova, Tatiana, S1210 (THU-221)
- Kratochwil, Clemens, S594 (THU-147)
- Krause, Jenny, S60 (OS-079-YI), S450 (SAT-385)
- Krause, Linda, S373 (WED-258)
- Kraus, Marine, S762 (WED-442)
- Kraus, Nico, S222 (THU-356)
- Krauß, Lea, S1003 (THU-377)
- Krauss, Stefan, S59 (OS-076), S336 (WED-242), S409 (TOP-064), S787 (WED-517)
- Krawczyk, Marcin, S514 (FRI-313), S541 (SAT-238), S563 (SAT-280), S646 (THU-559), S687 (SAT-449), S707 (SAT-480), S733 (WED-396), S950 (THU-262)
- Krebs, Christian F., S60 (OS-079-YI)
- Kredo-Russo, Sharon, S409 (TOP-060)
- Kreimeyer, Henriette, S628 (THU-454)
- Kremer, Andreas E., S56 (OS-073), S849 (WED-482)
- Kremer, Andreas E., S90 (OS-126), S367 (TOP-063), S371 (WED-256), S377 (WED-265), S397 (WED-297)
- Kresevic, Simone, S711 (SAT-489)
- Kreter, Bruce, S67 (OS-091), S873 (FRI-113)
- Kreuels, Benno, S522 (FRI-327)
- Krieg, Laura, S136 (FRI-393)
- Krijgsman, Danielle, S535 (SAT-228)
- Krishnamurthy, Shivani, S263 (WED-364)
- Krishnapriya, S., S848 (WED-481)
- Kroeniger, Konstantin, S507 (FRI-300)
- Kroll, Claudia, S379 (WED-269)
- Kromm, Franziska, S154 (FRI-419)
- Kronborg, Thit Mynster, S165 (FRI-434), S239 (WED-325)
- Kronenberg, Florian, S961 (THU-279), S968 (THU-288)
- Kronsten, Victoria, S7 (GS-007)
- Krooss, Simon, S951 (THU-263)
- Krouma, Lucy, S177 (FRI-455)
- Kruk, Beata, S514 (FRI-313), S563 (SAT-280)
- Krupa, Łukasz, S514 (FRI-313), S563 (SAT-280)
- Krupnick, Robert, S1008 (THU-386)
- Kruse, Carlot, S1001 (THU-335)
- Kuang, Jonathan, S300 (SAT-522)
- Kuběna, Aleš, S292 (SAT-341), S727 (SAT-513)
- Kubesch, Alica, S1042 (FRI-259)
- Kubisch, Ilja, S596 (THU-150)
- Kuchuloria, Tinatin, S891 (FRI-136)
- Kücken, Michael, S364 (FRI-390)
- Kucykowicz, Stephanie, S558 (SAT-271)
- Kudira, Ramesh, S417 (FRI-350)
- Kudo, Masatoshi, S9 (GS-011), S507 (FRI-300), S574 (THU-115), S575 (THU-116), S580 (THU-125), S586 (THU-134), S592 (THU-143), S593 (THU-145)
- Kuenzler, Patrizia, S849 (WED-482)
- Kugelmas, Marcelo, S627 (THU-453)
- Kugiyama, Yuki, S401 (WED-303), S1192 (THU-191), S1199 (THU-205)
- Kuhn, Brooks, S85 (OS-120)
- Kujundžić, Petra Dinjar, S1053 (SAT-143)
- Kuk Kim, Jung, S779 (WED-473)
- Kukla, Michał, S865 (SAT-129)
- Kukolj, George, S443 (SAT-371)
- Kulkarni, Anand, S195 (FRI-546), S865 (SAT-129)
- Kullberg, Joel, S820 (FRI-513)
- Kumada, Hiromitsu, S1061 (WED-119)
- Kumada, Takashi, S584 (THU-131)
- Kumar, Ajay, S235 (TOP-044), S1050 (FRI-269)
- Kumar, Ameeta, S464 (THU-492), S614 (THU-430)
- Kumar, Anupam, S182 (TOP-040), S210 (THU-340), S212 (THU-343)
- Kumar, Ashish, S274 (WED-382)
- Kumar, Dhananjay, S1050 (FRI-269)
- Kumar, Guresh, S277 (WED-388), S943 (THU-253)
- Kumar, Harish, S827 (FRI-524)
- Kumari, Alka, S401 (WED-304)
- Kumari, Suja, S848 (WED-481)
- Kumar, Jitendra, S17 (OS-006-YI), S348 (THU-234), S1013 (TOP-102), S1045 (FRI-263)
- Kumar, Karaddi Venkatanarasimha Nanda, S582 (THU-129), S591 (THU-142)
- Kumar, Kishwer, S969 (THU-289)
- Kumar, Krishna, S1141 (SAT-158), S1145 (SAT-164)
- Kumar, Manish, S943 (THU-253)
- Kumar, Manoj, S182 (TOP-040), S326 (WED-222), S1027 (FRI-235), S1047 (FRI-267)
- Kumar, Pavitra, S70 (OS-095-YI), S71 (OS-096-YI), S206 (TOP-046), S767 (WED-450)
- Kumar, Rahul, S199 (FRI-552), S220 (THU-355), S257 (WED-353), S278 (WED-389)
- Kumar, Rajneesh, S1103 (WED-173)
- Kumar, Raju, S825 (FRI-520)
- Kumar, Sambuddha, S401 (WED-304)
- Kumar Sarin, Shiv, S17 (OS-006-YI), S21 (OS-014-YI), S76 (OS-107-YI), S187 (FRI-533), S191 (FRI-539), S195 (FRI-546), S274 (WED-382), S277 (WED-388), S953 (THU-266)
- Kumar, Shiva, S195 (FRI-546), S274 (WED-382)
- Kumar, Sunil, S830 (FRI-530)
- Kumar, Vijay, S1013 (TOP-102), S1045 (FRI-263)
- Kumar, Vinay, S521 (FRI-326)
- Kunst, Gudrun, S483 (THU-530)
- Kunst, Roni, S412 (FRI-333)
- Kuo, Alexander, S489 (TOP-065)
- Kuo, Hsing-Tao, S1140 (SAT-157), S1180 (THU-174), S1206 (THU-217)
- Kuo, Yong-Fang, S468 (THU-499)
- Kupcinskis, Limas, S912 (FRI-173)
- Küpfer, Lars, S188 (FRI-534)
- Kurahashi, Tomohide, S871 (SAT-137)
- Kurmanova, Gaukhar, S320 (SAT-559)
- Kuroda, Hidekatsu, S1183 (THU-177)
- Kurosaki, Masayuki, S110 (LBP-15), S598 (THU-155), S644 (THU-554), S1113 (WED-189), S1183 (THU-177)
- Kushner, Tatyana, S913 (FRI-174), S1059 (WED-116)
- Kusuma, Susanto, S1203 (THU-212)
- Kwanten, Wilhelmus, S83 (OS-118), S279 (TOP-043), S300 (SAT-524), S622 (THU-444), S764 (WED-446), S776 (WED-466), S790 (WED-523)
- Kwek, Andrew, S199 (FRI-552), S257 (WED-353), S278 (WED-389), S300 (SAT-522)
- Kweon, Young Oh, S110 (LBP-15)
- Kwon, Ari, S141 (FRI-401)
- Kwong, Jeff, S874 (FRI-114)
- Kwong, Tsz Tung, S1 (GS-002-YI)
- Kwon, Hyunjoo, S758 (WED-437), S779 (WED-473)
- Kwon, Jung Hyun, S148 (FRI-409), S186 (FRI-343)
- Kwon, Yu-Jin, S633 (THU-464), S662 (SAT-411)
- Kwo, Paul Yien, S85 (OS-120), S468 (THU-499)
- Kylies, Dominik, S60 (OS-079-YI)
- Kyrrestad, Ingelin, S449 (SAT-383)
- Kyung Park, Min, S630 (THU-457), S635 (THU-466)
- Labanca, Sara, S40 (OS-045), S55 (OS-070)
- Labenz, Christian, S251 (WED-345), S264 (WED-365), S271 (WED-377), S277 (WED-387), S618 (THU-437), S654 (SAT-400), S762 (WED-443)
- Labenz, Joachim, S251 (WED-345), S264 (WED-365)
- Labgaa, Ismail, S12 (LBO-04), S527 (SAT-213)
- Laborde, Nolwenn, S123 (LBP-35), S387 (WED-282)
- Labriola, Dominic, S1 (GS-001), S112 (LBP-17), S813 (FRI-472), S815 (FRI-476)

- Lacaille, Florence, S965 (THU-284), S969 (THU-289), S971 (THU-291)
- Lacalle, Lucas, S865 (SAT-129)
- Laceuille, Franck, S598 (THU-154)
- Lachiondo-Ortega, Sofia, S140 (FRI-399), S529 (SAT-216), S532 (SAT-221), S544 (SAT-244), S546 (SAT-247)
- Lackner, Carolin, S784 (WED-509)
- Lacombe, Karine, S52 (OS-066), S1161 (SAT-185)
- Lacotte, Stéphanie, S24 (OS-018-YI), S531 (SAT-220)
- Łącz, Joanna, S400 (WED-301)
- La, Danie, S89 (OS-125)
- Ladeira, Nuno, S889 (FRI-134)
- Ladelund, Steen, S811 (FRI-469)
- Ladero, Iraia, S532 (SAT-221)
- Lænsman, Eirik, S449 (SAT-383)
- Laferl, Valerie, S45 (OS-051-YI)
- Lagani, Vincenzo, S143 (FRI-404), S290 (SAT-337)
- Laguna, Juan Carlos, S356 (THU-246), S788 (WED-518)
- Lahn, Josefine, S523 (FRI-328)
- Lah, Ponan Ponan Claude Regis, S274 (WED-382)
- Lai, Che To, S29 (OS-025), S1064 (WED-123), S1069 (WED-129), S1146 (SAT-166), S1148 (SAT-167)
- Lai, Huaying, S375 (WED-262)
- Lai, Jennifer, S256 (WED-352), S258 (WED-355), S260 (WED-358)
- Lai, Mandy Sze-Man, S575 (THU-117)
- Laimer, Markus, S664 (SAT-414)
- Lainka, Elke, S987 (THU-313)
- Lai, Qintao, S189 (FRI-536), S202 (FRI-556)
- Lai, Quirino, S103 (LBP-07), S360 (FRI-383)
- Lai, Ruimin, S375 (WED-262), S1144 (SAT-162)
- Lai, Yuxiang, S286 (SAT-333)
- La Janssen, Harry, S83 (OS-118)
- Lake, Jordan, S612 (THU-427)
- Lakiotaki, Dimitra, S1128 (WED-211)
- Lakli, Mounia, S954 (THU-267)
- Lakshmanan, Ajee Kurunjipadath, S848 (WED-481)
- Laleman, Wim, S10 (LBO-01), S61 (OS-080-YI), S238 (WED-323), S279 (TOP-043), S300 (SAT-524), S313 (SAT-546), S452 (SAT-390)
- Lally, James, S762 (WED-442)
- Lalor, Patricia, S215 (THU-346)
- Laloux, Clement, S444 (SAT-374)
- Lama, Adriano, S797 (WED-535), S800 (WED-542)
- Lam, Angela M, S1171 (SAT-202)
- Lamarca, Angela, S541 (SAT-238), S544 (SAT-244)
- Lamarque, Catherine, S467 (THU-498)
- Lamatsch, Sven, S197 (FRI-549)
- Lambert, Gabriel, S1106 (WED-178)
- Lamberti, Viviana, S792 (WED-526)
- Lambrechts, Dieter, S452 (SAT-390)
- Lambrechts, Diether, S48 (OS-059-YI), S363 (FRI-389), S524 (TOP-066)
- Lam, Brian, S627 (THU-453), S863 (SAT-125)
- Lam, David, S167 (FRI-438)
- Lameiras, Sonia, S12 (LBO-04)
- Lamina, Claudia, S961 (THU-279), S968 (THU-288)
- Lam, Laurent, S56 (OS-073)
- Lam, Lok-Ka, S490 (TOP-068)
- Lammers, Twan, S26 (OS-022), S571 (SAT-292)
- Lammert, Craig, S388 (WED-283)
- Lammert, Frank, S563 (SAT-280), S707 (SAT-480), S1147 (TOP-110)
- Lampertico, Pietro, S9 (GS-012), S31 (OS-030), S53 (OS-068), S91 (OS-129-YI), S107 (LBP-11), S108 (LBP-12), S113 (LBP-20), S374 (WED-260), S584 (THU-131), S673 (SAT-430), S882 (FRI-124), S901 (FRI-152), S920 (FRI-185), S1034 (FRI-248), S1055 (TOP-103), S1091 (WED-158), S1101 (WED-171), S1135 (SAT-149), S1138 (SAT-154), S1142 (SAT-159), S1154 (SAT-175), S1159 (SAT-181), S1164 (SAT-190), S1170 (SAT-199), S1173 (THU-165)
- Lampichler, Katharina, S282 (SAT-326), S313 (THU-547), S505 (FRI-295), S939 (TOP-058)
- Lampieri, Marco, S646 (THU-560)
- Lamprecht, Georg, S220 (THU-355)
- Lam, Raymond, S49 (OS-060)
- Lam, Shuk Man, S1146 (SAT-166)
- Lamuela, Luis Javier, S1187 (THU-183)
- Lam, Wendy, S830 (FRI-529)
- Landais, Paul, S460 (THU-486), S482 (THU-528)
- Landa-Magdalena, Ana, S534 (SAT-226)
- Lange, Christian M., S216 (THU-348), S562 (SAT-278), S596 (THU-150), S1139 (SAT-156)
- Lange, Magdalena Swiatek-de, S506 (FRI-298)
- Lange, Naomi, S664 (SAT-414)
- Langer, Harald, S536 (SAT-230)
- Langer, Mona-May, S216 (THU-348)
- Langhans, Bettina, S422 (FRI-357), S429 (FRI-366)
- Langhi, Cédric, S806 (WED-555)
- Lang, Philipp, S562 (SAT-279)
- Langthaler, Patrik, S863 (SAT-126)
- Lan, Keng-Hsin, S1172 (THU-163)
- Lannoo, Matthias, S753 (WED-430)
- Lanoria, Maria, S344 (THU-228)
- Lanthier, Nicolas, S464 (THU-493), S639 (THU-473)
- Lantinga, Marten A., S973 (THU-292)
- Lantvit, Daniel, S80 (OS-113)
- Lan, Xiaojin, S202 (FRI-556)
- Lanza, Alfonso Galeota, S54 (OS-069), S482 (THU-527)
- Lan, Zhixian, S22 (OS-016)
- Laouirem, Samira, S776 (WED-467)
- Lapalus, Martine, S954 (THU-267)
- Lape, Janel, S35 (OS-034)
- Lapenna, Lucia, S218 (THU-352), S950 (THU-261)
- Lapitz, Ainhua, S534 (SAT-226), S541 (SAT-238), S734 (WED-397)
- Laquente, Berta, S579 (THU-124)
- Lara, Catherine De, S1060 (WED-117)
- Lara, Magdalena, S928 (FRI-198), S932 (FRI-206)
- Lara-Romero, Carmen, S609 (THU-421)
- Lara, Ximena Leon, S1031 (FRI-242)
- Larghi, Alberto, S981 (THU-302)
- Larrey, Dominique, S134 (THU-405)
- Larrey, Edouard, S492 (FRI-274), S494 (FRI-279), S515 (FRI-316)
- Larrubia, Juan Ramón, S1028 (FRI-236), S1032 (FRI-245)
- Larrue, Hélène, S87 (OS-123-YI), S279 (TOP-043)
- Larsen, Anett Kristin, S449 (SAT-383)
- Larson-Nath, Catherine, S971 (THU-291)
- Lasagni, Alberto, S564 (SAT-283)
- Lasagni, Simone, S493 (FRI-277)
- Lascau, Anamaria, S123 (LBP-35), S387 (WED-282)
- Laschinger, Melanie, S1021 (FRI-223.)
- Lasco, Roberta, S917 (FRI-180), S1177 (THU-169), S1200 (THU-206)
- Lascoux-Combe, Caroline, S52 (OS-066)
- Lassailly, Guillaume, S62 (OS-083-YI), S981 (THU-303)
- Lasser, Luc, S198 (FRI-550)
- Lassueur, Steve, S762 (WED-442)
- Laszczewska, Maja, S538 (SAT-234), S542 (SAT-239), S565 (SAT-284)
- Latasa, Maria U, S537 (SAT-232)
- Latipov, Renat, S113 (LBP-19)
- Latournerie, Marianne, S318 (SAT-556)
- Latras, Irene, S852 (WED-489)
- Lau, Audrey, S53 (OS-068), S113 (LBP-20), S1091 (WED-158)
- Lau, Daryl, S875 (FRI-115)
- Lauer, Georg, S58 (OS-075)
- Lau, Jessie, S322 (WED-215), S413 (FRI-335)
- Lau, Michelle, S450 (SAT-386)
- Launoy, Guy, S82 (OS-117), S855 (TOP-098)
- Laupsa-Borge, Johnny, S784 (WED-511)
- Laurent, Castera, S86 (OS-121-YI), S106 (LBP-10)
- Lauridsen, Emilie Høegholm Ernst, S841 (FRI-494)
- Lauridsen, Mette, S657 (SAT-404), S851 (WED-487)
- Lauridsen, Mette Munk, S251 (WED-345), S629 (THU-455)
- Lauschke, Volker, S363 (FRI-388)
- Lau, Vince, S48 (OS-058)
- lavanya Gadipudi, Laila, S804 (WED-551)
- Laverdure, Noemie, S123 (LBP-35), S387 (WED-282)
- Lavers, Victoria, S153 (FRI-418)
- Laverty, Lynn, S925 (FRI-194)

Author Index

- Lavery, Gareth, S231 (THU-368), S232 (THU-370)
- Lavezzo, Bruna, S460 (THU-485), S486 (THU-537)
- Lavin, Bernardo Alio, S868 (SAT-132)
- Lavin, JL, S560 (SAT-275)
- Lavin, Philip, S220 (THU-355)
- Lavrado, Natália, S626 (THU-451)
- Lawitz, Eric, S49 (OS-060), S659 (SAT-407), S841 (FRI-493)
- Lawler, John, S119 (LBP-28), S415 (FRI-345), S985 (THU-310)
- Lawrie, Charles, S534 (SAT-226)
- Laxane, Tanmay, S282 (SAT-325)
- Lax, Sigurd, S996 (THU-327)
- Lázaro, Iolanda, S788 (WED-518)
- Lazarus, Jeffrey, S103 (LBP-06), S114 (LBP-21), S600 (TOP-081), S612 (THU-426), S627 (THU-453), S646 (THU-559), S861 (SAT-122), S865 (SAT-129), S900 (FRI-151), S921 (FRI-188), S924 (FRI-192), S1087 (WED-151), S1191 (THU-190)
- Lazas, Don, S13 (LBO-05)
- Lazcano, Ana Lopez, S158 (FRI-423)
- Lazo, Mariana, S865 (SAT-129), S900 (FRI-151)
- Lazzati, Andrea, S859 (SAT-120)
- Lazzeri-Barcelo, Francesca, S363 (FRI-388)
- Leal, Cassia Regina Guedes, S112 (LBP-16)
- Leal, Hector, S150 (FRI-412), S349 (THU-235)
- Leatherbury, Neil, S35 (OS-034)
- Leautaud, Maud, S172 (FRI-446)
- Le Bert, Nina, S1024 (FRI-229)
- Leblanc, Christina, S909 (FRI-166)
- Lebouche, Bertrand, S645 (THU-557)
- Leboucher, Claire, S989 (THU-314)
- Lebuffe, Gilles, S74 (OS-104)
- Leburgue, Angela, S383 (WED-277)
- Leclercq, Isabelle, S76 (OS-106-YI), S438 (SAT-363), S772 (WED-458)
- Lecomte, Laurence, S1150 (SAT-169)
- Lee, Alice, S875 (FRI-115)
- Lee, Ariel, S1024 (FRI-229)
- Lee, Boram, S583 (THU-130)
- Lee, Brian, S161 (FRI-428), S169 (FRI-441)
- Lee, Byung Seok, S1136 (SAT-151)
- Lee, Chanbin, S18 (OS-008-YI)
- Lee, Chang Hun, S516 (FRI-318), S916 (FRI-179)
- Lee, Chee Leng, S1028 (FRI-237), S1164 (SAT-191)
- Lee, ChiehJu, S496 (FRI-283), S1083 (WED-147)
- Lee, Chi Ho, S62 (OS-082)
- Lee, Chul-min, S615 (THU-431), S667 (SAT-418), S695 (SAT-462), S701 (SAT-470), S704 (SAT-475), S705 (SAT-476), S757 (WED-435)
- Lee, Dakyung, S450 (SAT-385)
- Lee, Danbi, S573 (THU-113), S589 (THU-140), S998 (THU-330), S1062 (WED-121), S1139 (SAT-155)
- Lee, Dee, S1087 (WED-151)
- Lee, Dong Ho, S494 (FRI-278), S506 (FRI-297), S512 (FRI-310)
- Lee, Donghyeon, S814 (FRI-473), S1062 (WED-120)
- Lee, Elizabeth, S254 (WED-349), S255 (WED-351), S270 (WED-375)
- Lee, Eun Kong, S552 (SAT-259)
- Lee, Hae Lim, S515 (FRI-315)
- Lee, Hae Won, S583 (THU-130)
- Lee, Han Ah, S585 (THU-132), S1065 (WED-124)
- Lee, Han Chu, S9 (GS-011), S573 (THU-113), S589 (THU-140), S606 (THU-417), S998 (THU-330), S1062 (WED-121), S1139 (SAT-155)
- Lee, Ha Seok, S1048 (FRI-268)
- Lee, Hongjae, S948 (THU-259)
- Lee, Hong Jun, S595 (THU-148)
- Lee, Hye Ah, S1065 (WED-124)
- Lee, Hye Won, S362 (FRI-387), S552 (SAT-259), S595 (THU-148), S906 (FRI-162), S1121 (WED-201)
- Lee, Hyomin, S563 (SAT-281)
- Lee, Hyo Young, S615 (THU-431), S667 (SAT-418), S695 (SAT-462), S701 (SAT-470), S704 (SAT-475), S757 (WED-435), S864 (SAT-128), S1073 (WED-135)
- Lee, Hyun Woong, S1132 (SAT-146)
- Lee, I-Cheng, S490 (TOP-068), S496 (FRI-283), S1172 (THU-163)
- Lee, Jaehyun, S817 (FRI-506)
- Lee, Jae Seung, S362 (FRI-387), S552 (SAT-259), S595 (THU-148), S906 (FRI-162), S1121 (WED-201), S1142 (SAT-160)
- Lee, Jeong-Hoon, S630 (THU-457), S635 (THU-466), S1048 (FRI-268), S1136 (SAT-151), S1144 (SAT-163)
- Lee, Jeonghwa, S610 (THU-423), S1062 (WED-120)
- Lee, Jeonghwa, S817 (FRI-506)
- Lee, Jeong Min, S509 (FRI-303)
- Lee, Jin Suk, S442 (SAT-369)
- Lee, John, S674 (SAT-431)
- Lee, Jonathan, S698 (SAT-467), S707 (SAT-482), S714 (SAT-495)
- Lee, Jong Suk, S758 (WED-437), S779 (WED-473)
- Lee, Joo Ho, S829 (FRI-527)
- Lee, Joon Hyeok, S267 (WED-369), S305 (SAT-533), S631 (THU-459), S821 (FRI-514)
- Lee, Joyce, S48 (OS-058)
- Lee, Joycelyn, S543 (SAT-241)
- Lee, Jung Il, S1142 (SAT-160)
- Lee, Jun-Hyuk, S615 (THU-431), S633 (THU-464), S662 (SAT-411), S695 (SAT-462), S701 (SAT-470), S704 (SAT-475), S705 (SAT-476), S864 (SAT-128)
- Lee, Junyeob, S817 (FRI-506)
- Lee, Ju-Seog, S555 (SAT-264), S578 (THU-121)
- Lee, Kuei-Chuan, S252 (WED-346)
- Lee, Kwan Sik, S829 (FRI-527), S1078 (WED-139), S1132 (SAT-146)
- Lee, Kyu-na, S642 (THU-550)
- Lee, Kyungsun, S414 (FRI-336), S752 (WED-427)
- Lee-Law, Pui-Yuen, S533 (SAT-223)
- Lee, Mei-Hsuan, S1180 (THU-174)
- Leeming, Diana, S173 (FRI-449), S175 (FRI-452), S657 (SAT-404), S688 (SAT-451), S707 (SAT-481), S717 (SAT-498), S723 (SAT-507), S826 (FRI-522)
- Lee, Minjong, S585 (THU-132), S1065 (WED-124)
- Lee, Mi Ra, S442 (SAT-369)
- Lee, Na Young, S141 (FRI-401)
- Lee, Pei-Chang, S252 (WED-346), S496 (FRI-283), S582 (THU-128), S586 (THU-134)
- Lee, Pei-Lun, S1140 (SAT-157), S1180 (THU-174), S1206 (THU-217)
- Lee, Sae Hwan, S1136 (SAT-151)
- Lee, Sang Hyun, S758 (WED-437), S779 (WED-473)
- Lee, Seung Ok, S516 (FRI-318)
- Lee, Silvia, S246 (WED-338)
- Lee, Soon Kyu, S148 (FRI-409)
- Lee, Soo Teik, S516 (FRI-318)
- Lee, Sung-Hwan, S555 (SAT-264)
- Lee, Sung Won, S65 (OS-086)
- Lee, Sunjae, S7 (GS-007)
- Lee, Taesic, S728 (SAT-514)
- Lee, Tanya, S380 (WED-271)
- Lee, Teng-Yu, S588 (THU-138)
- Lee, Tzong-Hsi, S1180 (THU-174), S1206 (THU-217)
- Lee, Tzu-hao, S173 (FRI-448)
- Lee, Way Seah, S965 (THU-284)
- Lee, William M., S127 (TOP-093), S136 (FRI-393)
- Lee, Woojoo, S814 (FRI-473)
- Lee, Yeon-Su, S785 (WED-513)
- Lee, Yeri, S834 (FRI-482)
- Lee, Yong-An, S786 (WED-514)
- Lee, Yong Sun, S785 (WED-513)
- Lee, Yoonseok, S578 (THU-121), S781 (WED-476), S798 (WED-540)
- Lee, Young-Sun, S578 (THU-121), S781 (WED-476), S798 (WED-540)
- Lee, Yun Bin, S610 (THU-423), S1048 (FRI-268), S1062 (WED-120), S1144 (SAT-163)
- Lee, Yu Rim, S588 (THU-137)
- Lefebvre, Eric, S386 (WED-280)
- Lefere, Sander, S172 (FRI-447), S226 (THU-361), S307 (SAT-538), S743 (WED-412), S787 (WED-516)
- Leff, Phillip, S689 (SAT-453), S711 (SAT-488)
- Leggett, Barbara, S266 (WED-367)
- Legoix, Patricia, S12 (LBO-04)
- Legrand, Remy, S656 (SAT-403)
- Legros, Ludivine, S318 (SAT-556)
- Legry, Vanessa, S211 (THU-342)

- Lei, Barbara, S495 (FRI-280)
 Leibiger, Barbara, S363 (FRI-388)
 Leibiger, Ingo, S363 (FRI-388)
 Leibl, Victoria, S377 (WED-265)
 Leibovitzh, Haim, S393 (WED-291)
 Leicht, Hans Benno, S47 (OS-057), S625 (THU-449)
 Lei, Cong, S117 (LBP-24)
 Lei, Jihai, S1152 (SAT-173)
 Leite, Letícia Marques, S842 (FRI-495)
 Leite, Nathalie, S618 (THU-436), S626 (THU-451), S658 (SAT-405)
 Leith, Damien, S195 (FRI-546), S1106 (WED-178)
 Lei, Wei-Yi, S895 (FRI-143)
 Lei, Yu, S1146 (SAT-165)
 Lekakis, Vasileios, S400 (WED-302)
 Le, Kha, S112 (LBP-18), S1029 (FRI-238), S1030 (FRI-241), S1162 (SAT-188), S1164 (SAT-192)
 Lek, Serene, S786 (WED-515)
 Lelasi, Luca, S597 (THU-153)
 Lemaitre, Elise, S975 (THU-295)
 Lemaitre, Lea, S25 (OS-020-YI)
 Lemekhova, Anastasia, S44 (OS-050-YI)
 Le, Michael Huan, S1096 (WED-165)
 Lemke, Steffen, S547 (SAT-248)
 Lemoine, Maud, S67 (OS-090-YI), S875 (FRI-115), S916 (FRI-178), S1046 (FRI-265), S1106 (WED-178), S1106 (WED-179), S1117 (WED-195)
 Lemoine, Sara, S56 (OS-073)
 Lemos, Mateus, S431 (FRI-368)
 Lempp, Florian, S1147 (TOP-109)
 Lenci, Ilaria, S54 (OS-069), S482 (THU-527), S1056 (TOP-106), S1072 (WED-133), S1122 (WED-203)
 Lenicek, Martin, S350 (THU-236), S727 (SAT-513)
 Lens, Sabela, S52 (OS-065-YI), S90 (OS-127-YI), S299 (SAT-521), S885 (FRI-128), S921 (FRI-188), S924 (FRI-192), S984 (THU-308), S1089 (WED-154), S1098 (WED-166), S1099 (WED-168), S1132 (SAT-145), S1178 (THU-171), S1205 (THU-216)
 Lenzen, Henrike, S383 (WED-277)
 Lenzi, Marco, S44 (OS-049-YI), S384 (WED-278)
 Lenz, Oliver, S31 (OS-030), S1034 (FRI-248), S1138 (SAT-154)
 Leo, Grazia Di, S966 (THU-285)
 Leong Ang, Tiing, S278 (WED-389)
 Leontari, Maria, S922 (FRI-189)
 Leor, Jonathan, S719 (SAT-500)
 Leo, So Heun, S584 (THU-131)
 Leow, Wei Qiang, S757 (WED-436), S1096 (WED-165)
 Leow, Wei-Xuan, S29 (OS-025)
 Lepida, Antonia, S621 (THU-442)
 Lepoivre, Bastien, S673 (SAT-429), S694 (SAT-461)
 Leporrier, Karine Bouhier, S577 (THU-119)
 Lequoy, Marie, S12 (LBO-04), S61 (OS-081)
 Lernout, Hannah, S229 (THU-364)
 Leroux, Florence, S954 (THU-267)
 Leroy, Vincent, S467 (THU-498), S498 (FRI-286), S1106 (WED-179), S1109 (WED-182), S1161 (SAT-185)
 Lertudomphonwanit, Chatmanee, S971 (THU-291)
 Leshno, Moshe, S403 (WED-308)
 Leslie, Jack, S323 (WED-217), S538 (SAT-234), S542 (SAT-239), S565 (SAT-284), S783 (WED-508)
 Lesmana, Rinaldi, S253 (WED-348)
 Lestavel, Sophie, S355 (THU-244)
 Le, Suong, S15 (OS-002), S852 (WED-488), S860 (SAT-121)
 Leung, Bernice, S537 (SAT-231)
 Leung, Daniel, S975 (THU-294)
 Leung, Gary, S1072 (WED-134), S1089 (WED-153), S1093 (WED-160), S1121 (WED-200)
 Leung, Howard Ho-Wai, S1085 (WED-149)
 Leung, Kristel, S371 (WED-255), S387 (WED-281), S404 (WED-310)
 Leung, Roland, S48 (OS-058)
 Leung, Wai Keung, S62 (OS-082)
 Leusen, Jeanette, S535 (SAT-228)
 Levacher, Anita, S1150 (SAT-169)
 Leven, Emily, S461 (THU-488)
 Levens, Amar, S14 (LBO-06)
 Levesque, Eric, S74 (OS-104)
 Levine, Alina, S379 (WED-268)
 Levi, Omer, S415 (FRI-345)
 Levrero, Massimo, S68 (OS-092-YI), S101 (LBP-04), S118 (LBP-27), S603 (THU-410), S687 (SAT-450), S701 (SAT-469), S875 (FRI-115), S1014 (TOP-104), S1018 (FRI-218), S1046 (FRI-265), S1058 (WED-113), S1170 (SAT-199)
 Levy, Clementine, S74 (OS-104)
 Levy, Cynthia, S11 (LBO-03), S367 (TOP-063), S371 (WED-256), S386 (WED-280), S388 (WED-283), S398 (WED-298)
 Lévy, Vincent, S577 (THU-120)
 Lewin, Maite, S498 (FRI-286)
 Lewinska, Monika, S536 (SAT-229)
 Lewis, Declan, S479 (THU-521)
 Lewis, James, S398 (WED-298), S470 (THU-504)
 Lewis, Sara, S997 (THU-328)
 Leyh, Catherine, S47 (OS-057)
 Leyva, Rina, S823 (FRI-516)
 Lhotte, Romain, S266 (WED-368)
 Liakina, Valentina, S912 (FRI-173)
 Liang, Jia-Xu, S703 (SAT-472)
 Liang, Junshi, S794 (WED-530)
 Liang, Nian, S812 (FRI-470)
 Liang, Po-Cheng, S895 (FRI-143)
 Liangpunsakul, Suthat, S167 (FRI-438)
 Liang, Tiebing, S612 (THU-427)
 Liang, Xi, S20 (OS-013), S186 (FRI-342), S204 (FRI-559)
 Liang, Xiaowen, S330 (WED-229)
 Liang, Xieer, S22 (OS-016), S112 (LBP-18), S1085 (WED-149), S1153 (SAT-174), S1164 (SAT-192)
 Liang, Yan, S29 (OS-025), S663 (SAT-413), S1064 (WED-123), S1146 (SAT-166)
 Liang, Yaojie, S549 (SAT-253), S562 (SAT-278)
 Liang, Yijun, S224 (THU-359)
 Liang, Zhixian, S530 (SAT-217)
 Liang, Zicai, S794 (WED-530), S1018 (FRI-217), S1152 (SAT-172)
 Lian, Min, S406 (WED-313)
 Lian, Qinshu, S9 (GS-011)
 Liao, Bo-Hung, S945 (THU-256), S1026 (FRI-233), S1040 (FRI-256)
 Liao, Lijun, S347 (THU-232), S413 (FRI-334)
 Liao, Min, S1127 (WED-210)
 Liao, Minjun, S503 (FRI-294)
 Liao, Sih-Han, S518 (FRI-320)
 Liao, Weijia, S503 (FRI-294)
 Liao, Xinxin, S543 (SAT-242)
 Liao, Yee-Tam, S895 (FRI-143)
 Liao, Ian, S531 (SAT-219)
 Liaw, Yun-Fan, S1088 (WED-152)
 Li, Beiling, S189 (FRI-536), S202 (FRI-556), S274 (WED-382)
 Liberal, Rodrigo, S44 (OS-049-YI)
 Liberman, Alexander, S653 (SAT-398)
 Li, Bo, S58 (OS-075), S543 (SAT-242)
 Li, Chris, S443 (SAT-371)
 Lichtenberger, Jakob, S954 (THU-268)
 Lichtenberger, Philipp, S232 (THU-369)
 Lichtner, Miriam, S1122 (WED-203)
 Li, Chuanjiang, S543 (SAT-242)
 Li, Chunxi, S1152 (SAT-173)
 Licina, Mirjana Lana Kosanovic, S880 (FRI-121)
 Li, Di, S794 (WED-530)
 Li, Ditian, S461 (THU-488)
 Lie, Anthony, S763 (WED-445)
 Lieb, David, S58 (OS-075)
 Liebe, Roman, S358 (FRI-381)
 Lieb, Sabine, S507 (FRI-299)
 Liedtke, Christian, S22 (OS-015), S349 (THU-235), S416 (FRI-348)
 Liermann, Jakob, S594 (THU-147)
 Lieto, Raffaele, S903 (FRI-155)
 Li, Fang, S609 (THU-422), S611 (THU-424)
 Li, Feng, S1018 (FRI-217)
 Li, Gang, S1165 (SAT-193)
 Liggett, Debra, S1058 (WED-113)
 Ligoeka, Joanna, S563 (SAT-280)
 Li, Guanlin, S29 (OS-025), S663 (SAT-413), S1085 (WED-149)
 Liguori, Antonio, S500 (FRI-288), S654 (SAT-400), S660 (SAT-409), S661 (SAT-410), S723 (SAT-508), S812 (FRI-471)
 Li, Hai, S195 (FRI-546), S196 (FRI-547)
 Li, Haiwen, S1209 (THU-220)
 Li, James H.W., S680 (SAT-439)
 Li, James Weiquan, S199 (FRI-552)
 Li, Jia, S205 (TOP-042), S1066 (WED-125)
 Li, Jialin, S1102 (WED-172)

Author Index

- Li, Jiaqi, S20 (OS-013)
- Li, Jie, S395 (WED-294), S638 (THU-471), S696 (SAT-463), S724 (SAT-510), S1004 (THU-379), S1022 (FRI-225), S1068 (WED-127), S1071 (WED-131), S1073 (WED-136), S1078 (WED-140), S1080 (WED-142), S1094 (WED-161), S1094 (WED-162), S1096 (WED-165), S1110 (WED-184), S1128 (WED-212)
- Li, Jing, S118 (LBP-26), S844 (FRI-500)
- Li, Jingguo, S329 (WED-228), S417 (FRI-349)
- Li, Jinghu Carl, S1167 (SAT-195)
- Li, Jing-Mao, S869 (SAT-134)
- Li, Jinjie, S1198 (THU-204)
- Li, Jinlong, S956 (THU-270)
- Li, Jinna, S1102 (WED-172)
- Li, Jun, S20 (OS-013), S186 (FRI-342), S204 (FRI-559), S436 (SAT-359), S453 (SAT-391), S730 (TOP-086), S1163 (SAT-189)
- Li, Junyi, S1209 (THU-220)
- Likhitsup, Alisa, S157 (FRI-422), S678 (SAT-437)
- Likhter, Mariya, S719 (SAT-500)
- Li, Lequn, S581 (THU-126)
- Li, Li, S1012 (THU-391)
- Li, Linfang, S520 (FRI-323)
- Lim, Aaron G., S912 (FRI-172)
- Li, Mei, S798 (WED-538)
- Li, Mengfan, S489 (TOP-065)
- Li, Mengqi, S130 (THU-397), S131 (THU-400)
- Lim, Ho Yeong, S592 (THU-143)
- Li, Ming, S1022 (FRI-225), S1073 (WED-136)
- Li, Minghui, S1066 (WED-125)
- Lim, Ji-Hwan, S578 (THU-121)
- Lim, Jihye, S393 (WED-292)
- Lim, Joseph, S856 (SAT-114), S1072 (WED-134), S1089 (WED-153), S1093 (WED-160), S1121 (WED-200)
- Lim, Kai, S300 (SAT-522)
- Lim, Lee-Ling, S29 (OS-025)
- Limones, Maria Jesus Lozano, S365 (FRI-391)
- Lim, Seng Gee, S110 (LBP-15)
- Lim, Sharlene, S423 (FRI-360), S678 (SAT-438)
- Lim, Tien Huey, S11 (LBO-02), S32 (OS-031)
- Lim, Wen Hui, S468 (THU-500), S629 (THU-456)
- Lim, Young-Suk, S11 (LBO-02), S32 (OS-031), S53 (OS-067), S125 (LBP-38), S573 (THU-113), S589 (THU-140), S998 (THU-330), S1062 (WED-121), S1130 (TOP-105), S1137 (SAT-153), S1139 (SAT-155), S1169 (SAT-198)
- Linas, Benjamin, S838 (FRI-489), S878 (FRI-119), S1180 (THU-173)
- Lin, Bingliang, S138 (FRI-396)
- Lin, Chien-Hung, S895 (FRI-143)
- Lin, Chih-Lang, S1180 (THU-174), S1206 (THU-217)
- Lin, Chih-Lin, S1180 (THU-174), S1206 (THU-217)
- Lin, Chuan-Hao, S123 (LBP-35), S387 (WED-282)
- Lin, Chun-yen, S1057 (TOP-112)
- Lindahl, Karin, S1150 (SAT-170)
- Lindfors, Andrea, S682 (SAT-441)
- Lindhauer, Cecilia, S639 (THU-472)
- Lindhorst, Andreas, S753 (WED-430)
- Lindkvist, Björn, S276 (WED-384)
- Lindström, Erik, S57 (OS-074-YI), S940 (THU-249)
- Lindvig, Katrine, S173 (FRI-449)
- Lindvig, Katrine Prier, S17 (OS-005-YI), S163 (FRI-432), S303 (SAT-528), S832 (FRI-479), S845 (TOP-054)
- Line, Pål-Dag, S478 (THU-520)
- Lin, Feng, S1127 (WED-210), S1198 (THU-204)
- Lin, Frederic, S198 (FRI-550), S807 (TOP-077)
- Ling, Ning, S1036 (FRI-250)
- Lin, Han-Chieh, S1180 (THU-174), S1206 (THU-217)
- Lin, Henry, S971 (THU-291)
- Lin, Huapeng, S29 (OS-025), S575 (THU-117), S609 (THU-421), S663 (SAT-413)
- Lin, Hui, S1076 (WED-138), S1157 (SAT-179)
- Lin, Jung-Chun, S825 (FRI-521)
- Lin, Kenneth, S199 (FRI-552), S257 (WED-353), S278 (WED-389)
- Link, Ralph, S1174 (THU-166)
- Lin, Li, S543 (SAT-242)
- Lin, Meiying, S543 (SAT-241)
- Lin, minghua, S195 (FRI-546)
- Lin, Paulo, S35 (OS-034)
- Lin, Pin-Hung, S531 (SAT-219)
- Lin, Po-Ting, S1057 (TOP-112)
- Lin, Quxiang, S406 (WED-313)
- Lin, Su, S70 (OS-095-YI), S129 (THU-396), S634 (THU-465)
- Lin, Tao, S358 (FRI-381)
- Lin, Ta-Ya, S1206 (THU-217)
- Lin, Te-Yu, S825 (FRI-521)
- Lin, Tse-I, S112 (LBP-18), S1029 (FRI-238), S1051 (FRI-272), S1162 (SAT-188), S1164 (SAT-192)
- Lin, Xiaoyu, S375 (WED-262)
- Lin, Xiaoyun, S869 (SAT-134)
- Lin, Yen-Huei, S102 (LBP-05)
- Lin, Yi-Hsuan, S825 (FRI-521)
- Lin, Yuan-Yu, S803 (WED-548)
- Liou, Wei-Lun, S519 (FRI-321), S1103 (WED-173)
- Li, Peijie, S304 (SAT-530)
- Li, Peizi, S997 (THU-328)
- Li, Peng, S186 (FRI-342), S204 (FRI-559)
- Lipiński, Patryk, S969 (THU-289)
- Lipshutz, H. Gabriel, S489 (TOP-065)
- Li, Qinglong, S488 (THU-540)
- Li, Qiudi, S1016 (TOP-111), S1025 (FRI-232)
- Li, Shanshan, S235 (TOP-047)
- Li, Shuo, S340 (WED-249), S1157 (SAT-179)
- Lisker-Melman, Mauricio, S815 (FRI-475)
- Li, Songzi, S574 (THU-115), S580 (THU-125)
- Li, Tengfei, S320 (SAT-560)
- Liting, Li, S969 (THU-289), S971 (THU-291)
- Little, Stephanie, S1075 (WED-137)
- Littmann, Maria, S1151 (SAT-171)
- Liu, Baiyi, S862 (SAT-124)
- Liu, Chang-Hsien, S825 (FRI-521)
- Liu, Cheng, S1029 (FRI-238), S1030 (FRI-241)
- Liu, ChengHai, S195 (FRI-546)
- Liu, Chen-Hua, S1061 (WED-119)
- Liu, Chun-Jen, S1061 (WED-119), S1083 (WED-147), S1140 (SAT-157), S1159 (SAT-182), S1180 (THU-174), S1206 (THU-217)
- Liu, Daming, S514 (FRI-313)
- Liu, Dan, S1016 (TOP-111), S1027 (FRI-234)
- Liu, Dorothy, S597 (THU-151)
- Liu, Fangfang, S759 (WED-438)
- Liu, Feng, S196 (FRI-547), S334 (WED-238), S757 (WED-436), S759 (WED-438), S862 (SAT-124)
- Liu, Gang, S816 (FRI-505)
- Liu, Hanyang, S80 (OS-114-YI), S745 (WED-416)
- Liu, Hongli, S1166 (SAT-194)
- Liu, Hui, S358 (FRI-381), S1090 (WED-155)
- Liu, Jia, S1017 (FRI-215)
- Liu, Jiacheng, S1073 (WED-136)
- Liu, Jie, S49 (OS-060)
- Liu, Jieming, S1149 (SAT-168), S1153 (SAT-174), S1161 (SAT-186)
- Liu, Jing, S274 (WED-382)
- Liu, Jingfeng, S34 (OS-033), S488 (THU-540)
- Liu, Jingwen, S816 (FRI-505)
- Liu, Jinxia, S205 (TOP-042)
- Liu, Jinze, S352 (THU-239)
- Liu, Juan, S1066 (WED-125)
- Liu, Jun, S488 (THU-540)
- Liu, Ken, S380 (WED-271), S575 (THU-117)
- Liu, Margaret, S590 (THU-141)
- Liu, Miaoxia, S189 (FRI-536)
- Liu, Poching, S489 (TOP-065)
- Liu, Qiang, S488 (THU-540)
- Liu, Que, S784 (WED-510), S812 (FRI-470)
- Liu, Ren Ping, S230 (THU-367)
- Liu, Ruijia, S153 (FRI-417), S224 (THU-359), S569 (SAT-290)
- Liu, Shi, S562 (SAT-278)
- Liu, Tian-Qi, S488 (THU-540)
- Liu, Tong, S77 (OS-108-YI)
- Liu, Tsang-Wu, S588 (THU-138)
- Liu, Wei Ping, S1100 (WED-170)
- Liu, Wen-Yue, S613 (THU-428), S1085 (WED-149)
- Liu, Xiangyu, S11 (LBO-03)
- Liu, Xiaoqing, S1112 (WED-188)
- Liu, Xiaowei, S406 (WED-313)
- Liu, Xiaoyu, S530 (SAT-217)
- Liu, Xu, S327 (WED-225)
- Liu, Xuemei, S747 (WED-419)

- Liu, Yali, S34 ([OS-033](#))
 Liu, Yang, S1055 ([TOP-103](#))
 Liu, Yao, S404 ([WED-309](#)),
 S776 ([WED-466](#)), S790 ([WED-523](#))
 Liu, Yen-Chun, S1067 ([WED-126](#)),
 S1088 ([WED-152](#)), S1129 ([WED-214](#))
 Liu, Yilin, S395 ([WED-294](#)),
 S1080 ([WED-142](#)), S1096 ([WED-164](#)),
 S1110 ([WED-184](#))
 Liu, Yi-Qi, S1100 ([WED-170](#))
 Liu, Yiqi, S854 ([TOP-094](#)),
 S1090 ([WED-155](#))
 Liu, Yongheng, S784 ([WED-510](#)),
 S812 ([FRI-470](#))
 Liu, Yudong, S514 ([FRI-313](#))
 Liu, Yuhua, S261 ([WED-359](#))
 Liu, Yuying, S1152 ([SAT-173](#)),
 S1156 ([SAT-178](#))
 Liu, Zhaoli, S425 ([FRI-362](#))
 Liu, Zhicheng, S425 ([FRI-361](#))
 Liu, Zhihua, S1102 ([WED-172](#))
 Liu, Zongyi, S340 ([WED-250](#))
 Livia, Bumbu Andreea, S178 ([FRI-457](#))
 Livingston, Christine, S1039 ([FRI-255](#))
 Li, Wanyu, S835 ([FRI-484](#))
 Li, Wei, S1063 ([WED-122](#))
 Li, Weiquan, S257 ([WED-353](#)),
 S278 ([WED-389](#))
 Li, Wei-Zhe, S145 ([TOP-078](#))
 Li, Wenbin, S371 ([WED-255](#))
 Li, Wenhao, S624 ([THU-447](#)),
 S708 ([SAT-483](#)), S740 ([WED-406](#)),
 S825 ([FRI-520](#))
 Li, Wenhui, S117 ([LBP-24](#))
 Li, Xiaofei, S1209 ([THU-220](#))
 Li, Xiaohe, S759 ([WED-438](#)),
 S1163 ([SAT-189](#))
 Li, Xiaojiao, S109 ([LBP-13](#))
 Li, Xiaoke, S340 ([WED-249](#)),
 S1076 ([WED-138](#)), S1086 ([WED-150](#)),
 S1157 ([SAT-179](#))
 Li, Xiaoqing, S543 ([SAT-242](#))
 Li, Xingzhi, S581 ([THU-126](#))
 Li, Xuehua, S488 ([THU-540](#))
 Li, Yangyang, S613 ([THU-428](#))
 Li, Yiguang, S395 ([WED-294](#)),
 S1068 ([WED-127](#))
 Li, Ying, S1185 ([THU-180](#))
 Li, Yingying, S1163 ([SAT-189](#))
 Li, Yong, S520 ([FRI-323](#))
 Li, Yongyin, S525 ([TOP-070](#)),
 S543 ([SAT-242](#)), S557 ([SAT-269](#))
 Li, You, S273 ([WED-380](#)), S312 ([SAT-545](#))
 Li, Yujia, S358 ([FRI-381](#))
 Li, Yuxin, S193 ([FRI-544](#))
 Lizaola-Mayo, Blanca, S590 ([THU-141](#))
 Lizaso, Aloña Agirre, S28 ([OS-024-YI](#))
 Li, Zhengmao, S34 ([OS-033](#))
 Li, Zhiguo, S340 ([WED-249](#))
 Li, Zhihui, S138 ([FRI-396](#))
 Li, Ziqiang, S261 ([WED-359](#))
 Lkhagvajav, Zoljargal, S475 ([THU-516](#))
 Lkhagva-Ochir, Oyungerel,
 S1104 ([WED-175](#))
 Llaneras, Jordi, S91 ([OS-129-YI](#)),
 S904 ([FRI-158](#)), S1082 ([WED-145](#)),
 S1178 ([THU-171](#)), S1205 ([THU-216](#))
 Llanillo, Loreto Hierro, S969 ([THU-289](#))
 Llansola, Marta, S423 ([FRI-359](#))
 Llarch, Neus, S497 ([FRI-284](#)),
 S579 ([THU-124](#)), S849 ([WED-483](#))
 Lledó, José Luis, S573 ([THU-114](#)),
 S579 ([THU-124](#))
 Lleo, Ana, S40 ([OS-045](#)), S44 ([OS-049-YI](#)),
 S55 ([OS-070](#)), S374 ([WED-260](#)),
 S383 ([WED-277](#)), S446 ([SAT-377](#)),
 S579 ([THU-123](#))
 Llerena, Susana, S911 ([FRI-171](#)),
 S934 ([FRI-211](#)), S1098 ([WED-166](#)),
 S1205 ([THU-216](#))
 Llewelyn, Jessica, S71 ([OS-097](#))
 Llagoña, Anna, S166 ([FRI-437](#))
 Llop, Elba, S2 ([GS-003](#)), S8 ([GS-009](#)),
 S87 ([OS-123-YI](#)), S272 ([WED-378](#)),
 S279 ([TOP-043](#)), S283 ([SAT-327](#)),
 S291 ([SAT-340](#)), S683 ([SAT-443](#)),
 S693 ([SAT-460](#)), S970 ([THU-290](#))
 Lloves, Marina, S1191 ([THU-190](#))
 Llovet, Josep, S48 ([OS-059-YI](#))
 Lloyd, Alison, S75 ([OS-105](#))
 Lloyd, Jonathan, S422 ([FRI-356](#))
 Locarnini, Stephen, S1028 ([FRI-237](#)),
 S1164 ([SAT-191](#))
 Locatelli, Franco, S88 ([OS-124-YI](#))
 Lo, Chen-Yu, S895 ([FRI-143](#))
 Lo, Ching-Chu, S895 ([FRI-143](#)),
 S1180 ([THU-174](#))
 Lo, Chingchu, S1206 ([THU-217](#))
 Lo, Chun-Han, S856 ([TOP-099](#))
 Lockart, Ian, S263 ([WED-364](#))
 Loddó, Massimiliano, S711 ([SAT-489](#))
 Lodge, Peter, S46 ([OS-053-YI](#))
 Lodi, Francesca, S524 ([TOP-066](#))
 Loewe, Christian, S576 ([THU-118](#))
 Loey Mak, Lung Yi, S1033 ([FRI-246](#))
 Lo, Gin-Ho, S1169 ([SAT-198](#))
 Loglio, Alessandro, S107 ([LBP-11](#))
 Lo, Gora, S67 ([OS-090-YI](#)),
 S1106 ([WED-178](#))
 Lohi, Jouko, S997 ([THU-329](#))
 Lohmeyer, Jürgen, S1147 ([TOP-110](#))
 Lohoff, Falk, S792 ([WED-527](#))
 Lohoues, Marie Jeanne, S195 ([FRI-546](#))
 Lohse, Ansgar W., S42 ([OS-047-YI](#)),
 S56 ([OS-073](#)), S285 ([SAT-331](#)),
 S373 ([WED-258](#)), S379 ([WED-269](#)),
 S527 ([SAT-213](#)), S579 ([THU-123](#)),
 S582 ([THU-128](#)), S982 ([THU-304](#)),
 S1139 ([SAT-156](#))
 Loi, Pooi Ling, S300 ([SAT-522](#))
 Lokan, Julie, S625 ([THU-450](#))
 Lok, Anna, S24 ([OS-019](#)), S251 ([WED-345](#)),
 S308 ([SAT-540](#)), S609 ([THU-422](#))
 Loke, Kelvin Siu Hoong, S582 ([THU-129](#)),
 S591 ([THU-142](#))
 Lok, James, S91 ([OS-128](#)), S642 ([THU-551](#)),
 S905 ([FRI-161](#)), S1081 ([WED-143](#)),
 S1081 ([WED-144](#))
 Lolatto, Riccardo, S120 ([LBP-29](#)),
 S837 ([FRI-487](#))
 Lolicato, Marco Gaetano, S552 ([SAT-258](#))
 Lomas, Laura Isusi, S886 ([FRI-129](#))
 Lomasney, Kristen Vieira, S937 ([TOP-056](#))
 Lomax, Joe, S153 ([FRI-418](#))
 Lombardelli, Stephen, S993 ([THU-320](#))
 Lombardi, Angela, S992 ([THU-318](#))
 Lombardi, Ludovica, S217 ([THU-350](#))
 Lombardi, Rosa, S632 ([THU-461](#)),
 S645 ([THU-557](#)), S668 ([SAT-420](#)),
 S722 ([SAT-506](#)), S772 ([WED-459](#)),
 S814 ([FRI-474](#))
 Lombardo, Antonino, S237 ([WED-320](#))
 Lombardo, Daniele, S457 ([THU-481](#))
 Lombardo, Julissa, S900 ([FRI-151](#))
 Loménié, Nicolas, S12 ([LBO-04](#))
 Lonardi, Sara, S592 ([THU-143](#)),
 S593 ([THU-145](#))
 Lonardo, Amedeo, S729 ([SAT-517](#))
 Londoño, Maria Carlota, S376 ([WED-264](#)),
 S380 ([WED-270](#)), S392 ([WED-290](#)),
 S399 ([WED-300](#)), S405 ([WED-311](#))
 Longerich, Thomas, S594 ([THU-147](#))
 Long, Fuli, S1076 ([WED-138](#)),
 S1157 ([SAT-179](#))
 Long, Michelle, S608 ([THU-420](#)),
 S811 ([FRI-469](#))
 Longo, Miriam, S744 ([WED-413](#)),
 S772 ([WED-459](#)), S783 ([WED-507](#)),
 S802 ([WED-547](#))
 Longpre, Lara, S123 ([LBP-35](#))
 Lønsmann, Ida, S173 ([FRI-449](#)),
 S717 ([SAT-498](#)), S723 ([SAT-507](#))
 Loo, Jing Hong, S658 ([SAT-406](#)),
 S703 ([SAT-473](#))
 Loomba, Rohit, S1 ([GS-001](#)), S13 ([LBO-05](#)),
 S31 ([OS-029](#)), S49 ([OS-061](#)),
 S65 ([OS-086](#)), S85 ([OS-120](#)),
 S115 ([LBP-22](#)), S118 ([LBP-26](#)),
 S612 ([THU-427](#)), S627 ([THU-453](#)),
 S647 ([TOP-074](#)), S648 ([TOP-075](#)),
 S649 ([TOP-080](#)), S649 ([TOP-083](#)),
 S659 ([SAT-407](#)), S662 ([SAT-412](#)),
 S666 ([SAT-417](#)), S675 ([SAT-432](#)),
 S678 ([SAT-438](#)), S684 ([SAT-444](#)),
 S790 ([WED-522](#)), S839 ([FRI-490](#)),
 S865 ([SAT-129](#))
 Loomes, Kathleen M., S961 ([THU-278](#)),
 S971 ([THU-291](#)), S1003 ([THU-378](#))
 Loosen, Sven H, S136 ([THU-409](#))
 Loosen, Sven H., S630 ([THU-458](#))
 Lopens, Steffi, S514 ([FRI-313](#))
 López-Bermudo, Lucía, S732 ([TOP-090](#))
 López, Estela Soria, S269 ([WED-374](#))
 López-Gómez, Marta, S272 ([WED-378](#)),
 S291 ([SAT-340](#)), S683 ([SAT-443](#))
 López-Hoyos, Marcos, S251 ([WED-344](#)),
 S390 ([WED-288](#))
 Lopez, Hugo, S158 ([FRI-423](#)), S166 ([FRI-437](#))
 López, Joel, S915 ([FRI-177](#))
 López-Larrubia, Pilar, S777 ([WED-468](#))
 Lopez, Manuel Castillejos, S1202 ([THU-211](#))
 López-Pérez, Ana Rosa, S143 ([FRI-404](#))

Author Index

- López, Rosa, S1192 (THU-192)
 Lopez, Scarlett, S648 (TOP-075)
 Lopez, Sonia Alonso, S90 (OS-127-YI), S299 (SAT-521)
 Loqvist, Pia, S853 (WED-492)
 Lord, Janet, S231 (THU-368), S232 (THU-370)
 Lorduy, Benjamin Polo, S844 (FRI-501)
 Lo, Regina Cheuk Lam, S537 (SAT-231)
 Lorena Abate, Maria, S611 (THU-425), S617 (THU-435), S626 (THU-452), S637 (THU-470)
 Lorenc, Beata, S505 (FRI-296)
 Lorente, Sara, S392 (WED-290), S964 (THU-282), S980 (THU-301), S996 (THU-326), S998 (THU-331), S1098 (WED-166)
 Lorenzo, Andrea Di, S1056 (TOP-106)
 Lorenzo, Laura, S489 (THU-546)
 Lorenzo, Marina Eliana Millan, S883 (FRI-126), S936 (FRI-214)
 Lo, Richard Hoau Gong, S582 (THU-129), S591 (THU-142)
 Lori, Giulia, S536 (SAT-229), S774 (WED-462)
 Losito, Francesco, S40 (OS-045), S55 (OS-070)
 Loste, María Teresa Arias, S8 (GS-009), S693 (SAT-460), S700 (SAT-468), S709 (SAT-484), S728 (SAT-515), S868 (SAT-132)
 Lotersztajn, Sophie, S222 (THU-356)
 Lotte Gluud, Lise, S748 (WED-421), S784 (WED-511)
 Lotto, Marta, S68 (OS-092-YI)
 Loughnan, Alice, S483 (THU-530)
 Louise Reeves, Helen, S542 (SAT-239), S565 (SAT-284)
 Louis Junien, Jean, S790 (WED-523)
 Loumaye, Audrey, S639 (THU-473)
 Loustaud-Ratti, Veronique, S52 (OS-066), S61 (OS-081), S498 (FRI-286), S833 (FRI-480), S1150 (SAT-169), S1161 (SAT-185)
 Louvet, Alexandre, S41 (OS-046), S62 (OS-083-YI), S74 (OS-104), S146 (FRI-408), S161 (FRI-429), S318 (SAT-556), S403 (WED-307), S865 (SAT-129)
 Love, Barry, S997 (THU-328)
 Loveridge, Robert, S479 (THU-521)
 Löwe, Bernd, S373 (WED-258), S982 (THU-304)
 Low, En Xian Sarah, S300 (SAT-522)
 Loy, John, S708 (SAT-483), S740 (WED-406)
 Lozano, Anthony, S534 (SAT-225)
 Lozano, Elisa, S551 (SAT-256)
 Lozano, J, S560 (SAT-275)
 Lozano, Juanjo, S20 (OS-012-YI), S78 (OS-109-YI), S163 (FRI-431), S738 (WED-404), S791 (WED-524)
 Lozano, Miquel, S131 (THU-399)
 Ls, Gouripriya, S827 (FRI-524)
 Luangsang, Souphalane, S33 (OS-032)
 Lubel, John, S380 (WED-271), S523 (FRI-329), S622 (THU-443), S861 (SAT-123)
 Lubber, Andrew, S1015 (TOP-107)
 Lu, Bingjiu, S1076 (WED-138), S1157 (SAT-179)
 Lu, Bingxia, S1156 (SAT-178)
 Lucà, Maria Grazia, S471 (THU-507)
 Lucas, Kathryn Jean, S808 (TOP-091), S813 (FRI-472), S815 (FRI-476)
 Lucejko, Mariusz, S932 (FRI-208)
 Lucena, Ana, S380 (WED-270)
 Lucena, Maria Isabel, S18 (OS-007), S126 (TOP-087), S142 (FRI-403), S144 (FRI-406)
 Lucia, Pietro Di, S5 (GS-005)
 Lücke, Jöran, S525 (TOP-069)
 Lüdde, Tom, S136 (THU-409), S420 (FRI-353), S421 (FRI-355), S562 (SAT-279), S630 (THU-458), S940 (THU-249)
 Ludlow-Rhodes, Arran, S918 (FRI-182), S1182 (THU-176)
 Ludovica Fracanzani, Anna, S632 (THU-461), S645 (THU-557), S772 (WED-459), S802 (WED-547), S803 (WED-549)
 Ludvigsson, Jonas, S82 (OS-116-YI), S600 (TOP-079)
 Luetgehetmann, Marc, S522 (FRI-327), S970 (THU-290)
 Luetgehetmann, Marc, S1019 (FRI-220), S1147 (TOP-109)
 Luft, Juliet, S749 (WED-422)
 Lugari, Simonetta, S729 (SAT-517)
 Lugonja, Sofija, S870 (SAT-135)
 Luhmann, Niklas, S898 (FRI-147)
 Lu, Hsiao-Sheng, S252 (WED-346)
 Luigi Calvo, Pier, S971 (THU-291)
 Luijten, Robbie, S561 (SAT-276)
 Lui, Vincent CH, S942 (THU-252), S946 (THU-257)
 Lu, Kang, S489 (TOP-065)
 Lu, Ligong, S520 (FRI-323)
 Lu, Ling, S528 (SAT-214)
 Luli, Saimir, S538 (SAT-234), S542 (SAT-239)
 Lu, Mengji, S549 (SAT-253), S562 (SAT-278)
 Lu, Mingqin, S195 (FRI-546)
 Lumley, Sheila, S1060 (WED-117), S1108 (WED-181)
 Lu, Nihong, S1209 (THU-220)
 Lun, Liou Wei, S274 (WED-382)
 Lun, Zengjun, S488 (THU-540)
 Luo, Jia, S488 (THU-540)
 Luo, Jinjin, S20 (OS-013), S204 (FRI-559)
 Luo, Ke, S740 (WED-407), S798 (WED-538)
 Luo, Lin, S109 (LBP-13)
 Luo, Min, S548 (SAT-251), S1029 (FRI-239)
 Luo, Wenfan, S202 (FRI-556)
 Luo, Xufeng, S549 (SAT-253), S562 (SAT-278)
 Luo, Yizhao, S963 (THU-281)
 Lupberger, Joachim, S72 (OS-098)
 Lupia, Enrico, S917 (FRI-180)
 Lupo, Giulia, S803 (WED-549)
 Lurje, Georg, S469 (THU-502)
 Lurje, Isabella, S469 (THU-502)
 Lurz, Eberhard, S972 (THU-291), S1002 (THU-336)
 Lu, Shaolong, S581 (THU-126)
 Lu, Shelly C., S736 (WED-400)
 Lusivka-Nzinga, Clovis, S498 (FRI-286)
 Lu, Tess, S803 (WED-548)
 Lüth, Stefan, S1137 (SAT-152)
 Lu, Tingting, S1152 (SAT-173), S1156 (SAT-178)
 Lutsenko, Svetlana, S417 (FRI-349)
 Lutz, Philipp, S422 (FRI-357), S429 (FRI-366)
 Lu, Wei, S1076 (WED-138), S1157 (SAT-179)
 Lu, Wei-Yu, S434 (SAT-355)
 Lu, Xiao-bo, S196 (FRI-547)
 Lu, Xiaobo, S1165 (SAT-193)
 Lu, Xiaomin, S11 (LBO-03)
 Lu, Xinyu, S525 (TOP-070)
 Lu, Zheng, S488 (THU-540)
 Luzko, Irina, S279 (TOP-043), S737 (WED-403)
 Luz Martínez-Chantar, María, S544 (SAT-244), S551 (SAT-256)
 Luzón-García, M. Pilar, S1126 (WED-208)
 Lv, Guoyu, S110 (LBP-14)
 Lv, Guoyue, S327 (WED-225)
 LV, Zicheng, S454 (TOP-051)
 Lyberopoulou, Angeliki, S421 (FRI-354)
 Ly Chan, Henry, S52 (OS-065-YI), S53 (OS-067)
 Lykkesfeldt, Jens, S801 (WED-545)
 Lymanets, Tetiana, S136 (THU-408)
 Lynch-Hill, Yvonne, S909 (FRI-166)
 Lynch, Kate, S380 (WED-271)
 Lyoo, Heyrhyoung, S1025 (FRI-231)
 Lytvak, Ellina, S44 (OS-049-YI), S56 (OS-073), S373 (WED-259), S377 (WED-266), S426 (FRI-363)
 Lyu, Shirley, S48 (OS-058)
 Ma, Aileen, S58 (OS-075)
 Maan, Irfaan, S721 (SAT-504), S1122 (WED-202)
 Ma, Anlin, S1066 (WED-125)
 Ma, Ann T, S10 (LBO-01), S314 (SAT-548)
 Maan, Rael, S306 (SAT-536), S454 (TOP-052)
 Maasoumy, Benjamin, S90 (OS-127-YI), S108 (LBP-12), S198 (FRI-550), S229 (THU-365), S240 (WED-326), S283 (SAT-328), S299 (SAT-521), S301 (SAT-525), S315 (SAT-551), S1029 (FRI-240), S1031 (FRI-242), S1101 (WED-171), S1115 (WED-193), S1134 (SAT-148), S1139 (SAT-156)
 Mabile-Archambeau, Isabelle, S318 (SAT-556)
 Mabrut, Jean-Yves, S473 (THU-511)
 Macchia, Marco, S791 (WED-525)
 MacConell, Leigh, S653 (SAT-398)

- Macdonald, Douglas, S174 ([FRI-450](#)), S872 ([TOP-097](#)), S879 ([FRI-120](#))
- Macdonald, Stewart, S389 ([WED-285](#))
- Macedo, Guilherme, S86 ([OS-121-YI](#)), S366 ([TOP-061](#)), S835 ([FRI-483](#))
- Macek-Jílková, Zuzana, S500 ([FRI-289](#))
- MacEwan, Joanna, S379 ([WED-268](#)), S844 ([FRI-500](#))
- Macey, Jake, S1087 ([WED-151](#))
- Macfarlane, Chelsea, S110 ([LBP-15](#))
- Machain, Matias, S245 ([WED-336](#))
- Ma, Chenyu, S489 ([TOP-065](#))
- Macías, Manuel, S1126 ([WED-208](#))
- Macías-Muñoz, Laura, S333 ([WED-235](#))
- Macias, Rocio IR, S541 ([SAT-238](#))
- Mackie, Kathryn, S1190 ([THU-189](#))
- Mackiewicz, Vincent, S1160 ([SAT-183](#))
- Macnaughtan, Jane, S205 ([TOP-042](#))
- Madaleno, Joao, S383 ([WED-277](#)), S982 ([THU-304](#)), S1000 ([THU-334](#))
- Madamba, Egbert, S65 ([OS-086](#)), S648 ([TOP-075](#)), S649 ([TOP-083](#)), S662 ([SAT-412](#)), S839 ([FRI-490](#))
- Madasu, Susan, S31 ([OS-029](#))
- Madden, Richie, S380 ([WED-271](#))
- Madejón, Antonio, S917 ([FRI-181](#)), S1099 ([WED-168](#)), S1105 ([WED-177](#))
- Made, Lilian Torres, S274 ([WED-382](#))
- Maderazo, Maida, S112 ([LBP-18](#)), S1164 ([SAT-192](#))
- Maderuelo, Esther, S272 ([WED-378](#))
- Madin, Kairat, S507 ([FRI-300](#))
- Madl, Tobias, S354 ([THU-242](#))
- Madrid, Teresa Maria Jordan, S932 ([FRI-207](#))
- Madsen, Andreas Nygaard, S530 ([SAT-218](#))
- Madsen, Bjørn Stæhr, S173 ([FRI-449](#)), S303 ([SAT-528](#))
- Madsen, Lone, S165 ([FRI-435](#))
- Madsen, Martin Rønn, S321 ([TOP-036](#))
- Maeshiro, Tatsuji, S686 ([SAT-448](#))
- Maevskaya, Marina, S260 ([WED-357](#))
- Maeyashiki, Chiaki, S644 ([THU-554](#))
- Mafeld, Sebastian, S314 ([SAT-548](#))
- Maffeis, Claudio, S814 ([FRI-474](#))
- Maffi, Gabriele, S814 ([FRI-474](#))
- Magatsing, Maurelle, S1210 ([THU-222](#))
- Magaz, Marta, S2 ([GS-003](#)), S87 ([OS-123-YI](#)), S843 ([FRI-499](#)), S984 ([THU-308](#))
- Magee, Mindy, S1141 ([SAT-158](#))
- Mageras, Anna, S116 ([LBP-23](#)), S926 ([FRI-196](#))
- Maggioni, Marco, S12 ([LBO-04](#)), S744 ([WED-413](#)), S772 ([WED-459](#))
- Maggiara, Marina, S526 ([SAT-211](#))
- Maggiore, Giuseppe, S965 ([THU-284](#)), S966 ([THU-285](#)), S987 ([THU-313](#))
- Maggiore, Sara, S952 ([THU-265](#))
- Magini, Giulia, S597 ([THU-153](#))
- Magliano, Dianna, S861 ([SAT-123](#))
- Magnanensi, Jeremy, S666 ([SAT-417](#)), S668 ([SAT-421](#))
- Magni, Carlo Federico, S920 ([FRI-185](#))
- Magrofuoco, Angelica, S1056 ([TOP-106](#))
- Mahadeva, Sanjiv, S644 ([THU-555](#)), S710 ([SAT-487](#))
- Ma, Haiyan, S1024 ([FRI-229](#))
- Mahajan, Anadi, S1141 ([SAT-158](#)), S1145 ([SAT-164](#))
- Mahajan, Bhawna, S235 ([TOP-044](#))
- Maharaj, Tobias, S979 ([THU-300](#))
- Maharshi, Sudhir, S235 ([TOP-044](#)), S238 ([WED-322](#))
- Ma, Heming, S327 ([WED-225](#))
- Maheshwari, Deepanshu, S212 ([THU-343](#))
- Mahmood, Hassan, S904 ([FRI-157](#)), S926 ([FRI-195](#))
- Mahmood, Khalid, S904 ([FRI-157](#))
- Mahmoud, Abdelmajeed, S865 ([SAT-129](#))
- Mahmoud, Tasnim, S353 ([THU-241](#)), S550 ([SAT-255](#))
- Mahmud, Nadim, S188 ([FRI-535](#)), S248 ([WED-342](#)), S265 ([WED-366](#))
- Ma, Hong, S34 ([OS-033](#))
- Ma, Huirong, S830 ([FRI-529](#))
- Maida, Ivana Rita, S1082 ([WED-146](#))
- Maieron, Andreas, S863 ([SAT-126](#))
- Maille, Pascale, S12 ([LBO-04](#))
- Mailly, Laurent, S72 ([OS-098](#))
- Mainardi, Victoria, S900 ([FRI-151](#))
- Maini, Mala, S558 ([SAT-271](#))
- Maino, Cesare, S381 ([WED-272](#))
- Maiorca, Francesca, S217 ([THU-350](#))
- Maira, Giovanni Di, S774 ([WED-462](#))
- Maisonnette, Patrick, S44 ([OS-049-YI](#))
- Maiwall, Rakhi, S21 ([OS-014-YI](#)), S76 ([OS-107-YI](#)), S139 ([FRI-398](#)), S182 ([TOP-040](#)), S187 ([FRI-533](#)), S210 ([THU-340](#)), S212 ([THU-343](#)), S218 ([THU-351](#)), S253 ([WED-348](#)), S277 ([WED-388](#))
- Majd, Zouher, S666 ([SAT-417](#)), S668 ([SAT-421](#))
- Majeed, Ammar, S380 ([WED-271](#)), S622 ([THU-443](#)), S861 ([SAT-123](#))
- Majewska, Agata, S36 ([OS-037](#))
- Ma, Jiantao, S608 ([THU-420](#))
- Major, Piotr, S332 ([WED-233](#))
- Majumdar, Avik, S230 ([THU-367](#)), S311 ([SAT-543](#))
- Majzoub, Abdul, S65 ([OS-086](#))
- Makanga, Ronald, S868 ([SAT-131](#))
- Makarova, Nune, S49 ([OS-062](#))
- Makharia, Govind, S401 ([WED-304](#))
- Makin, Erica, S999 ([THU-332](#))
- Makinson, Alain, S876 ([FRI-117](#))
- Makki, Murtaga, S724 ([SAT-509](#))
- Mak, Lung-Yi, S62 ([OS-082](#)), S1024 ([FRI-229](#))
- Mak, Lung Yi Loey, S490 ([TOP-068](#)), S680 ([SAT-439](#))
- Makuza, Jean Damascene, S1189 ([THU-187](#)), S1200 ([THU-207](#))
- Malagnino, Vincenzo, S1056 ([TOP-106](#)), S1072 ([WED-133](#)), S1103 ([WED-174](#)), S1122 ([WED-203](#))
- Malagola, Michele, S88 ([OS-124-YI](#))
- Malapelle, Umberto, S942 ([THU-251](#))
- Maldonado, Valentina, S361 ([FRI-384](#))
- Małeck, Paweł, S1007 ([THU-384](#))
- Maleh, Elias, S658 ([SAT-405](#))
- Malenstein, Hannah Van, S452 ([SAT-390](#))
- Ma, Lichun, S536 ([SAT-230](#))
- Maligireddy, Anand, S472 ([THU-509](#))
- Malik, Jlael, S684 ([SAT-445](#))
- Malik, Sabeen, S336 ([WED-241](#))
- Malik, Shamir, S314 ([SAT-548](#))
- Malik, Sheza, S183 ([FRI-339](#))
- Malik, Tehreem, S336 ([WED-241](#))
- Ma, Lily, S64 ([OS-085](#))
- Malin, Stephen, S756 ([WED-434](#))
- Malinverno, Federica, S374 ([WED-260](#))
- Malkov, Vlad, S64 ([OS-085](#)), S423 ([FRI-360](#)), S678 ([SAT-438](#))
- Mallet, Maxime, S266 ([WED-368](#))
- Mallet, Vincent, S86 ([OS-121-YI](#)), S161 ([FRI-429](#)), S656 ([SAT-402](#)), S859 ([SAT-120](#))
- Mallewa, Jane, S522 ([FRI-327](#))
- Malnick, Stephen, S133 ([THU-403](#))
- Malucelli, Emil, S360 ([FRI-383](#))
- Malvestiti, Francesco, S500 ([FRI-288](#)), S669 ([SAT-422](#)), S803 ([WED-549](#))
- Mameli, Laura, S54 ([OS-069](#)), S482 ([THU-527](#))
- Mamonova, Nina, S53 ([OS-068](#)), S1091 ([WED-158](#))
- Mancuso, Fabrizio, S723 ([SAT-508](#))
- Mandal, Sema, S909 ([FRI-165](#))
- Mandelboim, Michal, S128 ([THU-394](#))
- Mandilara, Dionysia, S595 ([THU-149](#)), S1046 ([FRI-264](#))
- Mandorfer, Mattias, S19 ([OS-010-YI](#)), S35 ([OS-035-YI](#)), S37 ([OS-039-YI](#)), S87 ([OS-123-YI](#)), S90 ([OS-127-YI](#)), S193 ([FRI-545](#)), S199 ([FRI-551](#)), S201 ([FRI-554](#)), S222 ([THU-357](#)), S224 ([THU-358](#)), S244 ([WED-334](#)), S246 ([WED-338](#)), S279 ([TOP-043](#)), S282 ([SAT-326](#)), S284 ([SAT-330](#)), S286 ([SAT-332](#)), S288 ([SAT-335](#)), S289 ([SAT-336](#)), S292 ([SAT-342](#)), S294 ([SAT-345](#)), S299 ([SAT-521](#)), S313 ([SAT-547](#)), S316 ([SAT-553](#)), S498 ([FRI-285](#)), S831 ([FRI-477](#)), S936 ([TOP-055](#)), S939 ([TOP-058](#)), S1135 ([SAT-150](#))
- Mandour, Yasmine M., S570 ([SAT-291](#))
- Mandryk, Olha, S712 ([SAT-490](#))
- Manesis, Emmanouil, S400 ([WED-302](#)), S1128 ([WED-211](#))
- Manfredi, Giulia Francesca, S389 ([WED-284](#)), S599 ([THU-156](#))
- Manfredi, Marcello, S804 ([WED-551](#))
- Manfredi, Sylvain, S61 ([OS-081](#))
- Manganaro, Susan, S965 ([THU-284](#))
- Mang, Anika, S506 ([FRI-298](#))
- Manges, Amee, S1200 ([THU-207](#))
- Mangia, Alessandra, S107 ([LBP-11](#)), S1209 ([THU-219](#))
- Mangini, Chiara, S251 ([WED-345](#))

Author Index

- Mangla, Kamal Kant, S620 (THU-440)
Mangrum, Rikki, S1087 (WED-151)
Manhas, Savrina, S1055 (TOP-103)
Manhota, Menisha, S840 (FRI-492)
Mania, Anna, S1007 (THU-384)
Manigat, Laryssa, S31 (OS-029)
Mani, Ilianna, S262 (WED-362), S978 (THU-298)
Mani, Nagraj, S1171 (SAT-202)
Ma, Ning, S9 (GS-011)
Manioudaki, Sofia, S262 (WED-362), S978 (THU-298)
Man, Joris De, S764 (WED-446)
Manka, Paul, S628 (THU-454)
Man Kim, Jong, S474 (THU-513)
Manko, Anna, S1115 (WED-191), S1117 (WED-194)
Mannalithara, Ajitha, S81 (OS-115-YI)
Manna, Martina, S992 (THU-319)
Mann, Derek, S332 (WED-232), S783 (WED-508)
Mann, Derek A, S323 (WED-217), S538 (SAT-234), S542 (SAT-239), S565 (SAT-284)
Mannion, Claire, S1179 (THU-172)
Männistö, Ville, S803 (WED-549)
Mann, Jake, S941 (THU-250), S944 (THU-254)
Mann, Jelena, S332 (WED-232), S783 (WED-508)
Manns, Michael P, S301 (SAT-525), S403 (WED-307)
Manolaka, Chrysanthi, S1128 (WED-211)
Manolakopoulos, Spiliot, S1128 (WED-211), S1194 (THU-196), S1194 (THU-197)
Manolakopoulou, Maria, S1194 (THU-197)
Manon, Françoise, S722 (SAT-505), S769 (WED-453), S777 (WED-469)
Manousou, Pinelopi, S344 (THU-228), S601 (TOP-088), S624 (THU-446), S708 (SAT-483), S719 (SAT-501)
Man, Robert De, S306 (SAT-536), S496 (FRI-282), S1100 (WED-169)
Mansbach, Hank, S13 (LBO-05), S544 (SAT-243)
Mansoor, Emad, S385 (WED-279)
Mansouri, Abdel, S1093 (WED-159)
Man, Stijn De, S561 (SAT-276)
Man, Tak Yung, S434 (SAT-355)
Mantia, Claudia La, S609 (THU-421)
Mantovani, Alessandro, S668 (SAT-420), S814 (FRI-474)
Mantovani, Anna, S660 (SAT-409), S661 (SAT-410), S812 (FRI-471)
Mantovani, Anna Anna, S668 (SAT-420)
Mantovani, Stefania, S552 (SAT-258)
Manuel, Víctor, S10 (LBO-01)
Manuilov, Dmitry, S53 (OS-068), S113 (LBP-20), S1055 (TOP-103), S1091 (WED-158)
Manuli, Chiara, S54 (OS-069), S486 (THU-537)
Manzano, Ramiro, S693 (SAT-460)
Mao, Minxin, S1022 (FRI-225), S1073 (WED-136)
Mao, Qianguo, S1171 (SAT-201)
Mao, Qing, S1166 (SAT-194)
Maor, Yaakov, S133 (THU-403), S824 (FRI-519)
Mao, Shenghua, S11 (LBO-02), S32 (OS-031)
Mao, Xianhua, S62 (OS-082)
Mao, Yimin, S130 (THU-398)
Maponga, Tongai Gibson, S916 (FRI-178), S1108 (WED-181), S1117 (WED-195)
Maracci, Monia, S107 (LBP-11), S1082 (WED-146)
Marasco, Giovanni, S88 (OS-124-YI), S283 (SAT-327), S974 (THU-293)
Maras, Jaswinder, S17 (OS-006-YI), S21 (OS-014-YI), S76 (OS-107-YI), S139 (FRI-398), S146 (FRI-407), S149 (FRI-410), S152 (FRI-416), S210 (THU-340), S326 (WED-222), S414 (FRI-344), S1033 (FRI-247)
Maravelia, Panagiota, S1038 (FRI-252)
Marazzi, Giovanni, S932 (FRI-208)
Marbach-Breittrück, Eugenia, S362 (FRI-386)
Marcadet, Charlene, S1025 (FRI-231)
Marcelin, Anne-Genevieve, S1044 (FRI-261)
Marcelino-Rodriguez, Itahisa, S397 (WED-296)
Marcellin, Fabienne, S68 (OS-092-YI)
Marcellin, Patrick, S53 (OS-067), S1137 (SAT-153)
Marcello de Araujo Neto, Joao, S618 (THU-436)
Marchand, Arnaud, S1025 (FRI-231)
Marchesi, Julian, S7 (GS-007), S601 (TOP-088)
Marchesi, Luca, S645 (THU-557)
Marchetti, Giulia, S1103 (WED-174)
Marchignoli, Francesca, S640 (THU-475), S673 (SAT-430)
Marciano, Sebastián, S195 (FRI-546), S245 (WED-336), S253 (WED-348)
Marco, Leonardo De, S203 (FRI-558)
Marco, Lorenza Di, S495 (FRI-280)
Marco, Maria, S431 (FRI-368)
Marcos, Cristina Fernández, S587 (THU-136), S1098 (WED-166)
Marco, Vito Di, S237 (WED-320), S374 (WED-260), S609 (THU-421), S803 (WED-549), S1082 (WED-146)
Marescu, Rodrig, S19 (OS-010-YI), S193 (FRI-545), S199 (FRI-551), S292 (SAT-342), S294 (SAT-345)
Marella, Nara, S939 (TOP-058)
Marenco, Simona, S54 (OS-069), S482 (THU-527)
Maresca, Manuel Rodriguez, S932 (FRI-207)
Marette, André, S233 (THU-372)
Mareux, Elodie, S954 (THU-267)
Margalit, Maya, S13 (LBO-05), S544 (SAT-243)
Margarita, Sara, S669 (SAT-422)
Marger, Fabrice, S751 (WED-426)
Margini, Cristina, S61 (OS-080-YI)
Maria Argemi, Josep, S145 (TOP-073)
Maria Banales, Jesus, S529 (SAT-215), S533 (SAT-223), S534 (SAT-226), S541 (SAT-238), S544 (SAT-244), S741 (WED-408)
Maria, Gabriele Di, S374 (WED-260), S592 (THU-144), S609 (THU-421), S803 (WED-549), S1118 (WED-196)
Mariani, Bruno, S247 (WED-340)
Maria, Nicola De, S287 (SAT-334), S482 (THU-527), S495 (FRI-280)
Maria Rizzo, Giacomo Emanuele, S1118 (WED-196)
Maria Saracco, Giorgio, S611 (THU-425), S617 (THU-435), S626 (THU-452), S637 (THU-470)
Maria Schleicher, Eva, S277 (WED-387)
Maried, Jorge Joven, S616 (THU-432)
Marie, Pauline, S534 (SAT-225)
Marignani, Massimo, S40 (OS-045), S55 (OS-070), S1122 (WED-203)
Marigorta, Urko M, S736 (WED-400)
Marín, Eva, S697 (SAT-465), S705 (SAT-478), S706 (SAT-479)
Marini, Ilaria, S500 (FRI-288), S992 (THU-318)
Marin, Jose, S390 (WED-288), S527 (SAT-212), S533 (SAT-223), S537 (SAT-232), S544 (SAT-244), S546 (SAT-247), S551 (SAT-256)
Marino, Mónica, S253 (WED-348)
Mariño, Zoe, S885 (FRI-128), S964 (THU-282), S980 (THU-301), S989 (THU-315), S995 (THU-325), S996 (THU-326), S998 (THU-331), S1000 (THU-334), S1089 (WED-154)
Marin-Rubio, Jose Luis, S781 (WED-475)
Marins, Ed G., S977 (THU-296), S1007 (THU-385)
Marjot, Thomas, S731 (TOP-089), S970 (THU-290)
Mark, Davwar Pantong, S1117 (WED-195)
Markham, Penelope, S101 (LBP-03)
Mark, Henry, S114 (LBP-21)
Marko, Hilken, S549 (SAT-252)
Marlowe, Natalie, S167 (FRI-438)
Marot, Astrid, S621 (THU-442)
Marquardt, Jens, S251 (WED-345), S277 (WED-387), S527 (SAT-213), S536 (SAT-230), S547 (SAT-248), S557 (SAT-268), S687 (SAT-449)
Marquez, Laura, S587 (THU-136)
Marquez, Monserrat, S489 (TOP-065)
Marra, Fabio, S40 (OS-045), S55 (OS-070), S233 (THU-371), S335 (WED-239), S513 (FRI-311), S536 (SAT-229), S584 (THU-131), S593 (THU-145), S609 (THU-421), S774 (WED-462)
Marra, Fiona, S1202 (THU-210)
Marra, Paolo, S381 (WED-272), S471 (THU-507)
Marrapodi, Ramona, S217 (THU-350)
Marrone, Aldo, S1082 (WED-146)

- Marrone, Giuseppe, S660 (SAT-409), S723 (SAT-508)
- Marron, Thomas, S575 (THU-116), S586 (THU-134)
- Marshall, Hanns-Ulrich, S276 (WED-384), S408 (WED-317), S413 (FRI-334), S707 (SAT-481), S778 (WED-470), S940 (THU-249)
- Marseglia, Antonio, S966 (THU-285)
- Marseglia, Mariarosaria, S571 (TOP-067)
- Marshall, Aileen, S383 (WED-276)
- Marshall, Chris, S1087 (WED-151)
- Marshall, Julie, S1198 (THU-203)
- Martell, Claudia, S10 (LBO-01)
- Martell, María, S780 (WED-474)
- Martens, Liesbet, S445 (SAT-375)
- Marti-Aguado, David, S164 (FRI-433), S171 (FRI-445), S682 (SAT-442)
- Marti-Bonmati, Luis, S682 (SAT-442)
- Martí-Carretero, Aina, S171 (FRI-445)
- Martin, Alexander, S103 (LBP-06)
- Martín, Alia, S852 (WED-489)
- Martin, Antonio Oliveira, S366 (TOP-061), S380 (WED-270), S697 (SAT-465), S705 (SAT-478), S706 (SAT-479), S964 (THU-282), S980 (THU-301), S989 (THU-315), S996 (THU-326), S998 (THU-331), S1105 (WED-177)
- Martín, Antonio Oliveira, S690 (SAT-454)
- Martin-Arranz, Maria Dolores, S697 (SAT-465), S705 (SAT-478), S706 (SAT-479)
- Martin-Bermudo, Franz, S732 (TOP-090), S770 (WED-457)
- Martin, Carmen Alonso, S480 (THU-524), S886 (FRI-129)
- Martín, Cesar Augusto, S529 (SAT-216), S738 (WED-404)
- Martin, Daniel, S220 (THU-355)
- Martin, Eleonora De, S74 (OS-104), S134 (THU-405)
- Martínez, Ana Sánchez, S470 (THU-503)
- Martínez-Arenas, Laura, S470 (THU-503), S1172 (THU-162)
- Martínez-Camprecios, Joan, S904 (FRI-158)
- Martínez-Chantar, María Luz, S140 (FRI-399), S326 (WED-223), S529 (SAT-216), S532 (SAT-221), S533 (SAT-223), S537 (SAT-232), S546 (SAT-247), S734 (WED-397)
- Martínez-Cruz, Luis Alfonso, S140 (FRI-399), S529 (SAT-216)
- Martínez, Dilan, S361 (FRI-384)
- Martínez, Edmundo, S865 (SAT-129), S900 (FRI-151)
- Martínez-Escudé, Alba, S664 (SAT-415)
- Martínez, Euridice, S856 (TOP-099)
- Martínez-Gallo, Mónica, S375 (WED-263)
- Martínez-García de la Torre, Raquel A, S78 (OS-109-YI)
- Martínez-García, Mar, S423 (FRI-359)
- Martínez-Geijo, Jennifer, S554 (SAT-263)
- Martínez-Gili, Laura, S601 (TOP-088)
- Martínez-Gómez, María, S780 (WED-474)
- Martínez-Hervás, Sergio, S451 (SAT-387), S789 (WED-520)
- Martínez-Ibárricu, Ana, S135 (THU-406)
- Martínez, Ismael El Hajra, S376 (WED-264), S399 (WED-300)
- Martínez, Javier, S2 (GS-003), S73 (OS-102), S105 (LBP-09), S198 (FRI-550), S376 (WED-264), S380 (WED-270), S399 (WED-300)
- Martínez, Jeniffer, S1028 (FRI-236), S1032 (FRI-245)
- Martínez, Mikel, S336 (WED-242)
- Martínez-Naves, Eduardo, S38 (OS-041-YI)
- Martínez-Ocon, Julia, S461 (THU-487)
- Martínez, Raquel Latorre, S587 (THU-136)
- Martínez-Sánchez, Celia, S38 (OS-042-YI), S737 (WED-403)
- Martínez-Sapiña, Ana María, S1098 (WED-166)
- Martínez, Sara, S133 (THU-404), S664 (SAT-415)
- Martínez, Sebastian, S210 (THU-341)
- Martínez, Sergio Muñoz, S579 (THU-124)
- Martínez, Sergio Muñoz, S819 (FRI-509)
- Martínez, Valentín Cuervas-Mons, S1194 (THU-195)
- Martin, Graham, S854 (TOP-095)
- Martini, Andrea, S766 (WED-449)
- Martin, Isabelle Poizat, S876 (FRI-117)
- Martini, Silvia, S54 (OS-069), S455 (TOP-059), S460 (THU-485), S482 (THU-527), S486 (THU-537)
- Martin, Jacqueline, S1060 (WED-117), S1108 (WED-181)
- Martin, Javier San, S85 (OS-120)
- Martín, Jose Ezequiel, S533 (SAT-224)
- Martín, Leticia, S1191 (THU-190)
- Martin- Mateos, Rosa, S73 (OS-102), S700 (SAT-468)
- Martin-Mateos, Rosa, S171 (FRI-445), S481 (THU-525)
- Martin, Misael Osmar Garcia, S1202 (THU-211)
- Martino, Vincent Di, S318 (SAT-556), S467 (THU-498)
- Martin Padilla, P., S865 (SAT-129)
- Martin, Paul, S832 (FRI-478)
- Martin, Paula Moreno, S397 (WED-296), S932 (FRI-206)
- Martín-Rodríguez, Agustín, S632 (THU-462), S640 (THU-474)
- Martin, Romain, S72 (OS-098)
- Martin, Ross, S1055 (TOP-103)
- Martins, Alexandra, S1111 (WED-185), S1189 (THU-186)
- Martin, Sara De, S322 (TOP-037), S770 (WED-456)
- Martin, Scott, S385 (WED-279)
- Martins, Eduardo Bruno, S49 (OS-061), S671 (SAT-426)
- Martró, Elisa, S921 (FRI-188), S1192 (THU-192)
- Martyn, Emily, S1108 (WED-181)
- Marzioni, Marco, S40 (OS-045), S55 (OS-070), S374 (WED-260)
- Masaki, Tsutomu, S394 (WED-293), S686 (SAT-448)
- Masaroni, Mario, S500 (FRI-288), S713 (SAT-493), S789 (WED-521)
- Mašek, Jan, S945 (THU-255)
- Mashal, Fares, S296 (SAT-349)
- Ma, Shaoyi, S1152 (SAT-173)
- Masi, Gianluca, S575 (THU-116), S584 (THU-131), S586 (THU-134), S592 (THU-143), S593 (THU-145)
- Maslova, Ganna, S136 (THU-408)
- Masnou, Helena, S2 (GS-003), S87 (OS-123-YI), S279 (TOP-043), S964 (THU-282), S980 (THU-301), S996 (THU-326), S998 (THU-331), S1192 (THU-192)
- Mason, Andrew L., S373 (WED-259), S377 (WED-266), S426 (FRI-363)
- Mason, Hugh, S1028 (FRI-237)
- Massari, Marco, S1082 (WED-146)
- Massarwa, Muhammad, S484 (THU-532)
- Massetto, Benedetta, S1164 (SAT-192)
- Masson, Steven, S140 (FRI-399), S157 (FRI-422), S865 (SAT-129)
- Massoulier, Sylvie, S172 (FRI-446)
- Masters, Annie, S782 (WED-506)
- Mastroianni, Claudio M., S1122 (WED-203)
- Masutti, Flora, S711 (SAT-489)
- Masyuko, Sarah, S100 (LBP-01)
- Matarazzo, Lorenza, S966 (THU-285)
- Matar, Rola, S1109 (WED-182)
- Mate, Carlota Jimeno, S248 (WED-341), S1126 (WED-208), S1205 (THU-216)
- Mateescu, Bogdan, S192 (FRI-541)
- Matei, Daniela, S245 (WED-337)
- Mateo, Roberto, S53 (OS-067), S1055 (TOP-103), S1159 (SAT-182)
- Mateos, Rosa María Martín, S133 (THU-404)
- Mathew, Babu, S17 (OS-006-YI), S21 (OS-014-YI), S76 (OS-107-YI), S139 (FRI-398), S146 (FRI-407), S149 (FRI-410), S152 (FRI-416), S326 (WED-222), S414 (FRI-344), S1033 (FRI-247)
- Mathew, Christo, S173 (FRI-448)
- Mathe, Zoltan, S465 (THU-494), S470 (THU-505)
- Mathur, Amit, S590 (THU-141)
- Mathurin, Philippe, S62 (OS-083-YI), S74 (OS-104), S146 (FRI-408), S498 (FRI-286), S1161 (SAT-185)
- Maticic, Mojca, S880 (FRI-121)
- Matilla, Ana, S573 (THU-114), S587 (THU-136)
- Matilla, Gonzalo, S126 (TOP-087), S142 (FRI-403), S144 (FRI-406)
- Mato, José M., S326 (WED-223), S736 (WED-400)
- Matsumoto, Hiroaki, S644 (THU-554)
- Matsumoto, Kosuke, S394 (WED-293), S1192 (THU-191), S1199 (THU-205)

Author Index

- Matsumoto, Tomonori, S545 ([SAT-246](#)), S559 ([SAT-272](#))
- Matsuura, Kentaro, S818 ([FRI-508](#)), S1095 ([WED-163](#)), S1183 ([THU-177](#))
- Matsuura, Takanori, S545 ([SAT-246](#)), S559 ([SAT-272](#))
- Mattace Raso, Giuseppina, S800 ([WED-542](#))
- Mattana, Marco, S950 ([THU-261](#))
- Matter, Matthias, S536 ([SAT-230](#))
- Matthaeis, Nicoletta De, S40 ([OS-045](#)), S55 ([OS-070](#))
- Matthews, Charmaine, S521 ([FRI-326](#))
- Matthews, Gail, S875 ([FRI-115](#)), S910 ([FRI-169](#))
- Matthews, Philippa, S868 ([SAT-131](#)), S916 ([FRI-178](#)), S1060 ([WED-117](#)), S1075 ([WED-137](#)), S1108 ([WED-181](#)), S1117 ([WED-195](#)), S1122 ([WED-202](#))
- Matthews-Rensch, Kylie, S266 ([WED-367](#))
- Mattis, Aras, S715 ([SAT-496](#))
- Mattos, Angelo Z., S496 ([FRI-282](#))
- Mattsson, Jan, S57 ([OS-074-YI](#)), S940 ([THU-249](#)), S965 ([THU-284](#)), S969 ([THU-289](#)), S1003 ([THU-378](#))
- Matzhold, Eva, S477 ([THU-519](#))
- Matz-Soja, Madlen, S244 ([WED-335](#)), S362 ([FRI-386](#)), S1043 ([FRI-260](#))
- Maucksch, Christof, S987 ([THU-313](#))
- Maugard, Thierry, S806 ([WED-555](#))
- Maupoey, Javier, S476 ([THU-517](#))
- Maurer, Jurij, S288 ([SAT-335](#))
- Maurizio, Paoloni, S1122 ([WED-203](#))
- Mauriz, José Luís, S554 ([SAT-263](#))
- Mauro, Ezequiel, S493 ([FRI-276](#)), S579 ([THU-124](#))
- Maurotti, Samantha, S803 ([WED-549](#))
- Mauz, Jim Benjamin, S240 ([WED-326](#)), S315 ([SAT-551](#))
- Mavromatis, Lucas, S792 ([WED-527](#))
- Mavropulo, Tetyana, S1010 ([THU-387](#))
- Mavrutenvkov, Viktor, S1010 ([THU-387](#))
- Ma, Xiong, S406 ([WED-313](#))
- Maya, Douglas, S732 ([TOP-090](#)), S770 ([WED-457](#))
- Maya Miles, Douglas, S760 ([WED-440](#))
- Mayan, David Castano, S351 ([THU-237](#))
- Mayatepek, Ertan, S415 ([FRI-346](#))
- Ma, Ye-Nv, S145 ([TOP-078](#))
- Mayer, Carlotta, S364 ([FRI-390](#))
- Mayerle, Julia, S596 ([THU-150](#))
- Mayer, Pierre, S168 ([FRI-440](#))
- May, Gary, S387 ([WED-281](#))
- May, Jan-Niklas, S571 ([SAT-292](#))
- Maynard, Marianne, S603 ([THU-410](#)), S687 ([SAT-450](#)), S701 ([SAT-469](#))
- Mayne, Tracy, S379 ([WED-268](#)), S844 ([FRI-500](#))
- Mayo, Marilyn J., S367 ([TOP-063](#)), S371 ([WED-256](#))
- Mayo, Patrick, S770 ([WED-455](#))
- May, Tom, S858 ([SAT-118](#))
- Ma, Yun, S127 ([TOP-093](#)), S445 ([SAT-376](#))
- Mazariegos, Marina, S150 ([FRI-412](#))
- Mazialivoua, Anne Laure, S1106 ([WED-179](#))
- Mazumder, Nikhilesh, S308 ([SAT-540](#)), S311 ([SAT-544](#))
- Mazur-Melewska, Katarzyna, S1007 ([THU-384](#))
- Mazur, Włodzimierz, S505 ([FRI-296](#))
- Mazur, Włodzimierz, S1205 ([THU-215](#))
- Mazza, Giuseppe, S337 ([WED-243](#))
- Mazzarelli, Chiara, S482 ([THU-527](#))
- Mazzitelli, Fortunato, S903 ([FRI-155](#))
- Mazzola, Alessandra, S266 ([WED-368](#)), S487 ([THU-538](#))
- Mazzola, Alessandro, S981 ([THU-303](#)), S1044 ([FRI-261](#))
- Mazzoni, Gianluca, S742 ([WED-411](#)), S748 ([WED-421](#))
- Mazzotta, Valentina, S1103 ([WED-174](#))
- Mbachi, Chimezie, S258 ([WED-355](#))
- Mbale, Blessings, S522 ([FRI-327](#))
- Mbaye, Babacar, S356 ([THU-247](#))
- Mbendi, Charles, S865 ([SAT-129](#))
- McAinch, Chloe, S15 ([OS-002](#))
- M'Callum, Marie-Agnès, S937 ([TOP-056](#))
- McCain, Misti, S16 ([OS-003](#)), S140 ([FRI-399](#))
- McCallum, Meaghan, S828 ([FRI-525](#))
- McCann, Adrian, S784 ([WED-511](#))
- McCartan, Jennifer, S850 ([WED-484](#))
- McCaughan, Geoff, S230 ([THU-367](#))
- McClure, Matt, S112 ([LBP-18](#)), S1029 ([FRI-238](#)), S1164 ([SAT-192](#))
- McClure, Matthew, S1162 ([SAT-188](#))
- McConville, Lucinda, S840 ([FRI-492](#))
- McCormick, Aiden, S850 ([WED-484](#))
- McCourt, Peter, S449 ([SAT-383](#))
- McCracken, Celeste, S677 ([SAT-436](#))
- McCune, Anne, S153 ([FRI-418](#)), S157 ([FRI-422](#))
- McDonald, Circe, S1023 ([FRI-226](#))
- McDonnell, Neil D., S139 ([FRI-397](#)), S829 ([FRI-528](#))
- McElvaney, Noel G., S979 ([THU-300](#))
- McGettigan, Neasa, S255 ([WED-350](#))
- McGirr, Ashleigh, S388 ([WED-283](#))
- McGrady, Michele, S230 ([THU-367](#))
- McInnes, Neil, S925 ([FRI-194](#))
- McInnes, Ross, S123 ([LBP-36](#))
- McIntyre, Karl, S1075 ([WED-137](#))
- McIvor, Carolyn, S239 ([WED-324](#))
- McKenzie, Catherine, S962 ([THU-280](#))
- McKevitt, Tara, S848 ([WED-480](#))
- McKiernan, Susan, S1211 ([THU-223](#))
- McLaughlin, Megan, S367 ([TOP-062](#)), S388 ([WED-283](#)), S397 ([WED-297](#)), S398 ([WED-299](#))
- McNamara, Bridgette, S1190 ([THU-189](#))
- McNeil, Carson, S671 ([SAT-426](#))
- McNeil, John, S622 ([THU-443](#))
- McNiff, Kimberly, S1208 ([THU-218](#))
- Mcphail, Mark, S479 ([THU-521](#))
- McPhail, Mark J W, S77 ([OS-108-YI](#)), S127 ([TOP-093](#)), S445 ([SAT-376](#))
- Mcpherson, Stuart, S603 ([THU-412](#)), S624 ([THU-447](#)), S685 ([SAT-447](#)), S688 ([SAT-452](#)), S1175 ([THU-167](#)), S1187 ([THU-182](#))
- Mcque, Kate, S1187 ([THU-182](#))
- McRae, Michael, S843 ([FRI-498](#))
- McReynolds, Cindy, S737 ([WED-401](#))
- McWherter, Charles, S338 ([WED-246](#)), S367 ([TOP-063](#)), S371 ([WED-256](#))
- Meacham, Georgina, S970 ([THU-290](#))
- Mechels, Aurelie, S524 ([TOP-066](#))
- Medel, María Paz, S900 ([FRI-151](#))
- Mederacke, Ingmar, S1137 ([SAT-152](#))
- Medhat, Waseem, S1212 ([THU-224](#))
- Medina-Caliz, Inmaculada, S126 ([TOP-087](#))
- Medina-Cáliz, Inmaculada, S18 ([OS-007](#))
- Medina, Diogo, S889 ([FRI-134](#)), S902 ([FRI-154](#)), S932 ([FRI-207](#))
- Medmoun, Mourad, S170 ([FRI-442](#))
- Medrano-Bosch, Mireia, S325 ([WED-220](#)), S333 ([WED-235](#))
- Medrano, Indhira Perez, S380 ([WED-270](#)), S392 ([WED-290](#))
- Medvedeva, Elina, S125 ([LBP-38](#))
- Meenan, Richard, S1079 ([WED-141](#))
- Meersseman, Philippe, S452 ([SAT-390](#))
- Megnien, Sophie Jeannin, S29 ([OS-026](#)), S30 ([OS-027](#)), S604 ([THU-413](#)), S655 ([SAT-401](#))
- Mehan, Aman, S575 ([THU-116](#))
- Méhes, Gábor, S23 ([OS-017-YI](#))
- Mehnert, Ann-Kathrin, S1020 ([FRI-222](#))
- Mehrabi, Arianeb, S594 ([THU-147](#))
- Mehreen, Sania, S215 ([THU-347](#))
- Mehrl, Alexander, S1003 ([THU-377](#))
- Mehta, Anurag, S620 ([THU-440](#))
- Mehta, Gautam, S193 ([FRI-543](#))
- Mehta, Neil, S1189 ([THU-185](#))
- Mehta, Reena, S1169 ([SAT-198](#))
- Mehta, Shraddha, S31 ([OS-029](#))
- Mehta, Shruti, S282 ([SAT-325](#))
- Mehta, Shubham, S401 ([WED-304](#)), S587 ([THU-135](#))
- Mein, Chaz, S740 ([WED-406](#))
- Meischl, Tobias, S498 ([FRI-285](#))
- Meister, Thomas, S1058 ([WED-113](#))
- Mei, Swee Lin Chen Yi, S306 ([SAT-535](#))
- Mela, Maria, S1128 ([WED-211](#))
- Melanophy, Gail, S850 ([WED-484](#)), S1211 ([THU-223](#))
- Melehani, Jason, S64 ([OS-085](#)), S678 ([SAT-438](#))
- Melere, Melina, S971 ([THU-291](#))
- Melgar-Lesmes, Pedro, S325 ([WED-220](#)), S333 ([WED-235](#))
- Melillo, Tanya, S880 ([FRI-121](#))
- Melini, Stefania, S797 ([WED-535](#)), S800 ([WED-542](#))
- Meli, Rosaria, S797 ([WED-535](#)), S800 ([WED-542](#))
- Melissa Chua, Sin Hui, S707 ([SAT-482](#))
- Melkebeke, Lukas Van, S452 ([SAT-390](#)), S753 ([WED-430](#))
- Mellemkjær, Anders, S390 ([WED-287](#)), S523 ([FRI-328](#))
- Mello, Tommaso, S545 ([SAT-245](#)), S550 ([SAT-254](#))
- Mells, George, S411 ([FRI-331](#))

- Melmer, Andreas, S664 (SAT-414)
Melo, Luma, S145 (TOP-073)
Melum, Espen, S59 (OS-076),
S343 (THU-225), S409 (TOP-064),
S418 (FRI-351), S420 (FRI-353),
S421 (FRI-355), S428 (FRI-365),
S478 (THU-520)
Melzer, Ehud, S133 (THU-403)
Memon, Azra, S438 (SAT-362)
Mena, Adri Ramírez, S916 (FRI-178)
Menconi, Alessio, S774 (WED-462)
Menconi, Maria Cristina, S88 (OS-124-YI)
Mendel, Leore Cohen, S133 (THU-403)
Méndez-Blanco, Carolina, S554 (SAT-263)
Méndez, Isabel, S547 (SAT-249)
Mendez, Marinela, S883 (FRI-126)
Mendez, Patricia, S1159 (SAT-182)
Méndez, Patricia, S903 (FRI-156)
Méndez-Sánchez, Nahum, S863 (SAT-125),
S865 (SAT-129), S900 (FRI-151)
Méndez, Yolanda, S852 (WED-489)
Mendizabal, Manuel, S253 (WED-348),
S865 (SAT-129), S900 (FRI-151)
Mendoza, Yuly, S609 (THU-421)
Mengers, Jan, S185 (FRI-341)
Meng, Qinghua, S243 (WED-332)
Meng, Qing-Jun, S71 (OS-097)
Meng, Zhong-ji, S196 (FRI-547)
Meninger, Stephen, S993 (THU-320)
Menke, Aswin L., S786 (WED-515),
S805 (WED-553)
Mennini, Gianluca, S360 (FRI-383)
Menolascina, Filippo, S601 (TOP-082)
Menon, Devika, S846 (WED-477)
Menon, Krishna, S324 (WED-218),
S479 (THU-521)
Mentink, Sven, S553 (SAT-260)
Meo, Florent Di, S954 (THU-267)
Meoli, Lilianeleny, S7 (GS-007)
Merabet, Yasmina Ben, S61 (OS-081)
Mercade, Jaume, S791 (WED-524)
Mercado-Gómez, María, S140 (FRI-399),
S529 (SAT-216), S532 (SAT-221),
S544 (SAT-244), S546 (SAT-247)
Mercan, Sercan, S799 (WED-541)
Mercan-Stanciu, Adriana, S277 (WED-386),
S819 (FRI-510)
Mercier, Renee-Claude, S53 (OS-068),
S113 (LBP-20), S1091 (WED-158)
Merckx, Wouter, S1051 (FRI-272)
Mercuri, Luca, S1075 (WED-137)
Merelli, Ivan, S772 (WED-459)
Merino, Victor, S682 (SAT-442)
Merino, Xavier, S533 (SAT-224)
Merizian, Talal, S300 (SAT-524),
S654 (SAT-400)
Merle, Philippe, S61 (OS-081)
Merle, Uta, S1139 (SAT-156)
Merli, Manuela, S105 (LBP-09),
S217 (THU-350), S218 (THU-352),
S253 (WED-348), S950 (THU-261),
S994 (THU-323)
Merlos Rodrigo, Miguel Angel,
S546 (SAT-247)
Meroni, Marica, S744 (WED-413),
S772 (WED-459), S783 (WED-507),
S802 (WED-547), S803 (WED-549)
Merrimen, Mike, S617 (THU-434)
Mertens, Christian, S413 (FRI-334)
Mertens, Joachim C., S491 (FRI-273)
Mertens, Nico, S1038 (FRI-252)
Mesenbrink, Peter, S819 (FRI-509)
Mesquita, Mariana, S137 (FRI-395)
Messina, Emanuela, S120 (LBP-29)
Messina, Vincenzo, S36 (OS-036),
S1082 (WED-146)
Mestres, Judit, S461 (THU-487)
Meszaros, Magdalena, S74 (OS-104),
S170 (FRI-443), S473 (THU-511),
S929 (FRI-201)
Metivier, Sophie, S52 (OS-066),
S107 (LBP-11), S498 (FRI-286),
S1160 (SAT-184)
Metselaar, Herold, S46 (OS-053-YI)
Meulbroek, Michael, S932 (FRI-208)
Meuleman, Philip, S1025 (FRI-231)
Meunier, Lucy, S134 (THU-405),
S170 (FRI-443)
Meyer, Bernhard, S240 (WED-326),
S315 (SAT-551)
Meyer, Carsten, S313 (SAT-546)
Meyer, Jasper, S450 (SAT-385)
Meyer, Martin, S754 (WED-431)
Meyer, Sandra De, S1138 (SAT-154)
Meyer, Tim, S558 (SAT-271),
S574 (THU-115), S580 (THU-125)
Meyhöfer, Sebastian, S687 (SAT-449)
Meyhöfer, Svenja, S687 (SAT-449)
Mezzano, Gabriel, S250 (WED-343),
S900 (FRI-151)
Mezzelani, Alessandra, S772 (WED-459)
Mialhes, Patrick, S52 (OS-066)
Miao, Zhijiang, S1016 (TOP-111)
Miar, Ana, S803 (WED-548)
Micah, Eileen Akonobe, S865 (SAT-129)
Miceli, Vitale, S457 (THU-480)
Michael Pammer, Lorenz, S968 (THU-288)
Michailidis, Theodoros, S730 (SAT-518)
Michalak, Sophie, S12 (LBO-04),
S672 (SAT-427)
Michalkova, Hana, S546 (SAT-247)
Michelet, Maud, S1014 (TOP-104)
Michel, Maurice, S618 (THU-437),
S640 (THU-474), S654 (SAT-400),
S762 (WED-443)
Michel, Rivoire, S1018 (FRI-218)
Micheltorena, Cristina Olague,
S1024 (FRI-228)
Michielsen, Peter, S1114 (WED-190)
Michl, Patrick, S594 (THU-147)
Michopoulos, Spyridon, S400 (WED-302)
Middelburg, Tim, S408 (WED-317)
Miele, Luca, S500 (FRI-288),
S654 (SAT-400), S660 (SAT-409),
S723 (SAT-508)
Miethke, Alexander, S56 (OS-072),
S123 (LBP-35), S370 (WED-252),
S387 (WED-282), S417 (FRI-350)
Miette, Véronique, S817 (FRI-507)
Miglione, Marzia, S217 (THU-350)
Miguel de Vega, Beatriz San, S554 (SAT-263)
Miguel Rodrigues, Pedro, S529 (SAT-215),
S533 (SAT-223), S534 (SAT-226),
S541 (SAT-238), S544 (SAT-244)
Mihret, Adane, S927 (FRI-197)
Mikami, Norihisa, S447 (SAT-380)
Mikami, Yohei, S409 (TOP-060)
Miki, Daiki, S1183 (THU-177)
Mikkelsen, Anne Catrine Daugaard,
S159 (FRI-424)
Mikulits, Wolfgang, S538 (SAT-233),
S564 (SAT-282)
Milan, Zoka, S483 (THU-530)
Milardi, Giulia, S446 (SAT-377)
Milella, Michele, S510 (FRI-304),
S1072 (WED-133), S1082 (WED-146)
Milgrom, Yael, S484 (THU-532)
Milia, Marta La, S381 (WED-272)
Milisav, Irina, S142 (FRI-403)
Milkiewicz, Małgorzata, S440 (SAT-367),
S541 (SAT-238), S560 (SAT-275)
Milkiewicz, Małgorzata, S326 (WED-223),
S375 (WED-261)
Milkiewicz, Piotr, S42 (OS-047-YI),
S326 (WED-223), S373 (WED-258),
S375 (WED-261), S400 (WED-301),
S440 (SAT-367), S514 (FRI-313),
S541 (SAT-238), S560 (SAT-275),
S579 (THU-123), S950 (THU-262),
S982 (THU-304)
Millard, Louise, S617 (THU-434)
Millares, Daniel Valle, S1037 (FRI-251)
Miller, Hamish, S708 (SAT-483),
S825 (FRI-520)
Miller, Jennifer, S37 (OS-038)
Millet, Oscar, S376 (WED-400)
Millon, Matthieu, S356 (THU-247)
Millon, Laurence, S994 (THU-322)
Mill, Pleasantine, S122 (LBP-33-YI)
Millwood, Iona, S69 (OS-093-YI)
Milner, Andrew, S1182 (THU-176)
Milot, Laurent, S687 (SAT-450),
S701 (SAT-469)
Milovanova, Svetlana, S1210 (THU-221)
Milovanovic, Tamara, S870 (SAT-135)
Miltenev, Svetlana, S870 (SAT-135)
Mimidis, Konstantinos, S1128 (WED-211)
Minacapelli, Carlos, S273 (WED-380),
S312 (SAT-545), S623 (THU-445),
S1011 (THU-390)
Mina, Joanne, S266 (WED-367)
Min, Byong-Keol, S948 (THU-259)
Minchenberg, Scott, S171 (FRI-444)
Mincheva, Gergana, S423 (FRI-359)
Miners, Alec, S909 (FRI-165)
Min, Feng, S1165 (SAT-193)
Minguez, Beatriz, S12 (LBO-04),
S533 (SAT-224)
Minh, Duc Pham, S325 (WED-221)
Minier, Nicolas, S916 (FRI-178)
Minisini, Rosalba, S389 (WED-284)
Minnich, Anne, S31 (OS-029)

Author Index

- Minnier, Jessica, S601 ([TOP-082](#))
Mino, Masaaki, S444 ([SAT-373](#))
Minoves, Mélanie, S500 ([FRI-289](#))
Minten, Jaak, S220 ([THU-355](#))
Mion, Monica, S183 ([TOP-049](#))
Miquel, Joaquin, S1028 ([FRI-236](#)),
S1032 ([FRI-245](#))
Miquel, Mireia, S587 ([THU-136](#)),
S1098 ([WED-166](#))
Miquel, Rosa, S324 ([WED-218](#)),
S324 ([WED-219](#))
Miralles, Henar las Heras, S892 ([FRI-139](#)),
S898 ([FRI-148](#))
Miralpeix, Anna, S885 ([FRI-128](#)),
S964 ([THU-282](#)), S980 ([THU-301](#)),
S989 ([THU-315](#)), S995 ([THU-325](#)),
S998 ([THU-331](#))
Mirams, Laura, S882 ([FRI-124](#))
Miranda, Joana, S142 ([FRI-403](#))
Miravittles, Marc, S963 ([THU-281](#))
Mirella, Fraquelli, S283 ([SAT-327](#))
Mir, Iris Gines, S740 ([WED-406](#)),
S825 ([FRI-520](#))
Miró, Lluïsa, S356 ([THU-246](#))
Mirshahi, Faridoddin, S749 ([WED-422](#))
Mirza, Darius F., S46 ([OS-053-YI](#))
Mischitelli, Monica, S360 ([FRI-383](#))
Mischke, Jasmin, S1035 ([FRI-249](#))
Misner, Dinah, S1029 ([FRI-238](#))
Missale, Gabriele, S374 ([WED-260](#))
Missen, Louise, S918 ([FRI-182](#)),
S1182 ([THU-176](#))
Mistry, Pratik, S790 ([WED-522](#))
Mita, Dorina, S640 ([THU-475](#))
Mitchell, Catherine, S850 ([WED-485](#))
Mitchell, Eoin, S77 ([OS-108-YI](#))
Mitchyn, Markiyana, S103 ([LBP-06](#))
Mittra, Lalita, S462 ([THU-489](#))
Mitry, Ragai, S445 ([SAT-376](#))
Mitsumoto, Yasuhide, S616 ([THU-433](#))
Mittal, Ashmit, S348 ([THU-234](#))
Mittal, Naveen, S123 ([LBP-35](#)),
S387 ([WED-282](#))
Mitzner, Steffen, S220 ([THU-355](#))
Miura, Satoshi, S178 ([FRI-458](#)),
S565 ([SAT-285](#)), S1177 ([THU-170](#))
Mix, Carola, S1115 ([WED-193](#))
Miyaaki, Hisamitsu, S178 ([FRI-458](#)),
S565 ([SAT-285](#)), S1177 ([THU-170](#))
Miyagawa, Shigeru, S439 ([SAT-366](#))
Miyamoto, Haruka, S644 ([THU-554](#))
Miyamoto, Kentaro, S409 ([TOP-060](#))
Miyata, Misaki, S733 ([WED-395](#))
Miyazaki, Hiromi, S453 ([SAT-392](#))
Mizui, Toshiyuki, S733 ([WED-395](#))
Mizzon, Giulia, S1020 ([FRI-222](#))
Mlitz, Veronika, S739 ([WED-405](#)),
S746 ([WED-418](#))
M, Mang, S1115 ([WED-191](#))
Mngqibisa, Rosie, S110 ([LBP-15](#))
Mo, Cheng, S784 ([WED-510](#))
Mochida, Satoshi, S395 ([WED-293](#)),
S1183 ([THU-177](#))
Möckel, Diana, S571 ([SAT-292](#))
Modest, Dominik, S469 ([THU-502](#))
Moeckli, Beat, S24 ([OS-018-YI](#)),
S531 ([SAT-220](#))
Moe, Fiona Ni Ni, S582 ([THU-129](#)),
S591 ([THU-142](#))
Moehlin, Julien, S72 ([OS-098](#))
Moelker, Adriaan, S306 ([SAT-536](#))
Moescheid, Max, S339 ([WED-248](#))
Moeslein, Magnus, S222 ([THU-356](#))
Mo, Fa-Rong, S951 ([THU-264](#))
Mofty, Yasser, S1098 ([WED-167](#))
Moga, Lucile, S86 ([OS-121-YI](#)),
S279 ([TOP-043](#))
Moggio, Maurizio, S744 ([WED-413](#))
Mogler, Carolin, S431 ([FRI-369](#)),
S945 ([THU-256](#))
Mogul, Douglas, S56 ([OS-072](#)),
S123 ([LBP-35](#)), S370 ([WED-252](#)),
S372 ([WED-257](#)), S387 ([WED-282](#))
Mohamed, Almuthana, S91 ([OS-128](#)),
S877 ([FRI-118](#))
Mohamed, Islam, S517 ([FRI-319](#))
Mohamed, Mohamed Ramadan,
S639 ([THU-472](#)), S778 ([WED-470](#))
Mohamed, Osama, S1098 ([WED-167](#))
Mohamed, Rahma, S840 ([FRI-491](#))
Mohamed, Sofia, S1098 ([WED-167](#))
Mohamed, Wael, S678 ([SAT-437](#))
Mohammad, Tabish, S233 ([TOP-041](#))
Mohammed, Mansur, S269 ([WED-373](#))
Mohan, Nimitha K, S827 ([FRI-524](#))
Möhler, Markus, S26 ([OS-022](#))
Mo, Hongmei, S1055 ([TOP-103](#))
Mohr, Isabelle, S1001 ([THU-335](#))
Mohr, Raphael, S197 ([FRI-549](#))
Mohs, Antje, S413 ([FRI-334](#)),
S416 ([FRI-348](#)), S535 ([SAT-227](#))
Moigboi, Christiana, S905 ([FRI-161](#)),
S1081 ([WED-143](#)), S1081 ([WED-144](#))
Moiseev, Sergey, S1210 ([THU-221](#))
Molendi-Coste, Olivier, S355 ([THU-244](#))
Moles, Anna, S38 ([OS-042-YI](#)),
S339 ([WED-247](#))
Molina, Elena, S532 ([SAT-221](#))
Molina, Esther, S366 ([TOP-061](#)),
S380 ([WED-270](#)), S964 ([THU-282](#)),
S980 ([THU-301](#)), S998 ([THU-331](#)),
S1178 ([THU-171](#))
Molina, Laura Castillo, S1126 ([WED-208](#))
Molina, Maria L, S1124 ([WED-205](#))
Molinari, Eduardo, S903 ([FRI-155](#))
Molinari, Nicolas, S170 ([FRI-443](#))
Molinari, Antonio, S413 ([FRI-334](#))
Møller, Emilie Eifer, S159 ([FRI-424](#)),
S390 ([WED-287](#))
Møllerhøj, Mathias, S321 ([TOP-036](#))
Møllerhøj, Mathias Bonde, S530 ([SAT-218](#))
Möller, Marie, S47 ([OS-057](#))
Møller, Søren, S165 ([FRI-434](#)),
S239 ([WED-325](#)), S748 ([WED-421](#))
Møller, Thomas, S688 ([SAT-451](#)),
S707 ([SAT-481](#))
Molnár, Zsuzsanna, S880 ([FRI-121](#))
Molo, Chiara De, S384 ([WED-278](#))
Moly, K T, S846 ([WED-477](#))
Momoh, Jeffrey, S571 ([SAT-292](#))
Monasterio, Javier Uribe, S900 ([FRI-151](#))
Mondelli, Mario, S552 ([SAT-258](#))
Mondet, Kevin, S64 ([OS-084-YI](#))
Monet, Clement, S74 ([OS-104](#))
Monforte, Antonella d'Arminio,
S907 ([FRI-164](#))
Monge, Fanny, S782 ([WED-506](#))
Monico, Sara, S978 ([THU-297](#)),
S1135 ([SAT-149](#)), S1154 ([SAT-175](#)),
S1159 ([SAT-181](#)), S1164 ([SAT-190](#)),
S1170 ([SAT-199](#))
Monkelbaan, Jan F., S990 ([THU-317](#))
Monllor-Nunell, Teresa, S86 ([OS-121-YI](#))
Monnier, Béatrice, S1193 ([THU-194](#))
Monroy, Arturo Rodea, S1202 ([THU-211](#))
Montagnese, Sara, S251 ([WED-345](#)),
S263 ([WED-364](#))
Montalvá, Eva, S474 ([THU-512](#))
Montanari, Noé Axel, S1019 ([FRI-219](#))
Montanaro, Chiara, S72 ([OS-099](#))
Montano-Loza, Aldo, S44 ([OS-049-YI](#))
Montano-Loza, Aldo J, S11 ([LBO-03](#)),
S56 ([OS-073](#))
Montano-Loza, Aldo J., S373 ([WED-259](#)),
S377 ([WED-266](#)), S426 ([FRI-363](#))
Monte, Anne De, S1158 ([SAT-180](#))
Monte, Maria, S390 ([WED-288](#))
Monterde, Vanesa Bernal, S171 ([FRI-445](#)),
S198 ([FRI-550](#)), S392 ([WED-290](#)),
S587 ([THU-136](#)), S700 ([SAT-468](#)),
S1187 ([THU-183](#)), S1205 ([THU-216](#))
Montero, Saul, S548 ([SAT-251](#)),
S1029 ([FRI-239](#)), S1051 ([FRI-272](#))
Montero-Vallejo, Rocío, S335 ([WED-240](#)),
S732 ([TOP-090](#)), S760 ([WED-440](#)),
S770 ([WED-457](#))
Montesdeoca, Cristina Suárez,
S397 ([WED-296](#)), S932 ([FRI-206](#))
Montesinos, Maria, S788 ([WED-518](#)),
S802 ([WED-546](#))
Montiel, Maria Jesus Perugorria,
S326 ([WED-223](#)), S560 ([SAT-275](#))
Montiel, Natalia, S1126 ([WED-208](#))
Montirioni, Carla, S984 ([THU-308](#))
Montirioni, Carla, S486 ([THU-536](#))
Montoliu, Carmina, S35 ([OS-035-YI](#))
Montoliu, Silvia, S903 ([FRI-156](#)),
S915 ([FRI-177](#)), S1205 ([THU-216](#))
Montón, Cristina, S682 ([SAT-442](#)),
S781 ([WED-505](#)), S1098 ([WED-166](#))
Mookerjee, Raj, S10 ([LBO-01](#)),
S197 ([FRI-549](#)), S203 ([FRI-557](#)),
S205 ([TOP-042](#)), S220 ([THU-355](#))
Moon, Andrew, S268 ([WED-371](#))
Moon, Hye-Sung, S630 ([THU-457](#)),
S635 ([THU-466](#))
Moon, Sang Yi, S690 ([SAT-455](#)),
S698 ([SAT-466](#)), S705 ([SAT-477](#)),
S712 ([SAT-491](#))
Moore, Celia, S344 ([THU-228](#))
Moore, John, S621 ([THU-441](#))
Moore, Kenny, S803 ([WED-548](#))

- Moore, Kevin, S280 ([TOP-045](#))
 Mor, Adi, S119 ([LBP-28](#)), S985 ([THU-310](#))
 Moradpour, Darius, S105 ([LBP-08](#)), S481 ([THU-526](#)), S1031 ([FRI-243](#))
 Morago, Lucia, S902 ([FRI-153](#))
 Moragrega, Ángela B., S781 ([WED-505](#))
 Morales, Nataly Clavo, S840 ([FRI-492](#))
 Morales-Navarrete, Hernan, S361 ([FRI-384](#)), S364 ([FRI-390](#))
 Morales, Rafael, S375 ([WED-263](#))
 Morales-Ruiz, Manuel, S10 ([LBO-01](#)), S250 ([WED-343](#)), S486 ([THU-536](#))
 Morana, Giovanni, S564 ([SAT-283](#))
 Morana, Piera, S592 ([THU-144](#))
 Morán, Elias, S900 ([FRI-151](#))
 Mørch Harder, Lea, S748 ([WED-421](#))
 Mordan, Nicola, S337 ([WED-243](#))
 Mordoch, Ron, S409 ([TOP-060](#))
 Moreau, Richard, S206 ([TOP-046](#)), S452 ([SAT-390](#))
 Moreira, Rebeca, S15 ([OS-001](#))
 Morell, Carola Maria, S122 ([LBP-34](#)), S433 ([SAT-354](#))
 Morelli, Maria Cristina, S54 ([OS-069](#)), S482 ([THU-527](#)), S970 ([THU-290](#))
 Morelli, Olivia, S40 ([OS-045](#)), S55 ([OS-070](#))
 Morello, Fulvio, S917 ([FRI-180](#))
 Moreno, Ángeles Pizarro, S838 ([FRI-488](#))
 Moreno, Antonio, S1098 ([WED-166](#))
 Moreno, Christophe, S90 ([OS-126](#)), S621 ([THU-442](#)), S807 ([TOP-077](#)), S1114 ([WED-190](#))
 Moreno-Gonzalez, Mar, S434 ([SAT-356](#))
 Moreno-Lanceta, Alazne, S325 ([WED-220](#)), S333 ([WED-235](#))
 Moreno, Maria Victoria, S1191 ([THU-190](#))
 Moreno, Pilar, S852 ([WED-489](#))
 Moreno Planas, Jose María, S980 ([THU-301](#)), S996 ([THU-326](#)), S998 ([THU-331](#))
 Moreno, Sarai Romero, S180 ([FRI-462](#)), S470 ([THU-503](#))
 Moreno, Victor, S544 ([SAT-244](#))
 Moreta, Maria Jose, S885 ([FRI-128](#))
 Moretti, Alessandra, S36 ([OS-036](#)), S1122 ([WED-203](#))
 Morgan, Aparna, S15 ([OS-002](#))
 Morgan, Caroline, S220 ([THU-355](#))
 Morgando, Anna, S40 ([OS-045](#)), S55 ([OS-070](#)), S990 ([THU-317](#))
 Morgan, Marsha, S548 ([SAT-250](#))
 Morgenstern, David, S506 ([FRI-298](#))
 Moriarty, Aoife, S180 ([FRI-460](#))
 Morikawa, Rei, S156 ([FRI-421](#)), S409 ([TOP-060](#))
 Morillas, Julia, S587 ([THU-136](#)), S964 ([THU-282](#)), S980 ([THU-301](#)), S996 ([THU-326](#)), S998 ([THU-331](#)), S1098 ([WED-166](#))
 Morillas, Rosa M., S87 ([OS-123-YI](#)), S105 ([LBP-09](#)), S700 ([SAT-468](#)), S1192 ([THU-192](#)), S1205 ([THU-216](#))
 Morillas, Rosa M., S366 ([TOP-061](#)), S376 ([WED-264](#)), S380 ([WED-270](#)), S392 ([WED-290](#)), S399 ([WED-300](#))
 Morillas, Rosa Maria, S1098 ([WED-166](#))
 Morinaga, Maki, S180 ([FRI-461](#))
 Morin, Didier, S456 ([THU-478](#))
 Morisco, Filomena, S903 ([FRI-155](#))
 Morishita, Asahiro, S686 ([SAT-448](#)), S818 ([FRI-508](#))
 Morita, Ippei, S323 ([WED-216](#))
 Mori, Taizo, S444 ([SAT-373](#))
 Moritz, Manuela, S527 ([SAT-213](#))
 Moritz, Thomas, S165 ([FRI-434](#))
 Morling, Joanne, S4 ([GS-004-YI](#)), S84 ([OS-119-YI](#)), S160 ([FRI-427](#)), S168 ([FRI-439](#))
 Mor, Orna, S128 ([THU-394](#))
 Morrin, Martina, S255 ([WED-350](#))
 Morris, Heather, S66 ([OS-089](#))
 Morris, Jude, S402 ([WED-305](#))
 Morrison, Martine C., S763 ([WED-444](#)), S786 ([WED-515](#)), S805 ([WED-553](#))
 Morrison, Maura, S962 ([THU-280](#))
 Morrisette, Jeremy, S450 ([SAT-386](#))
 Morrow, Linda, S115 ([LBP-22](#))
 Morrow, Marisa, S762 ([WED-442](#))
 Morsica, Giulia, S120 ([LBP-29](#)), S837 ([FRI-487](#)), S1082 ([WED-146](#))
 Mortensen, Kim Erlend, S449 ([SAT-383](#))
 Mörtl, Bernhard, S596 ([THU-150](#))
 Moruzzi, Noah, S363 ([FRI-388](#))
 Morvil, Gayathry, S1103 ([WED-173](#))
 Mosca, Ettore, S772 ([WED-459](#))
 Mosig, Alexander, S80 ([OS-114-YI](#))
 Mosina, Liudmila, S113 ([LBP-19](#))
 Mosko, Jeff, S387 ([WED-281](#))
 Mospan, Andrea, S66 ([OS-089](#))
 Moss, Stuart, S230 ([THU-367](#))
 Mostafa, Mohamed, S84 ([OS-119-YI](#))
 Mostafavi, Nahid, S408 ([WED-317](#))
 Motofelea, Ionel-Andrei, S297 ([SAT-519](#))
 Motoyoshi, Yasuhide, S1192 ([THU-191](#)), S1199 ([THU-205](#))
 Motta, Benedetta Maria, S713 ([SAT-493](#)), S789 ([WED-521](#))
 Motta, Rodrigo, S309 ([SAT-541](#))
 Motte, Manon, S792 ([WED-526](#))
 Moukarzel, Adib, S123 ([LBP-35](#)), S387 ([WED-282](#))
 Mou, Lien-Juei, S1180 ([THU-174](#)), S1206 ([THU-217](#))
 Moulin, Philippe, S603 ([THU-410](#))
 Moulis, Lionel, S929 ([FRI-201](#))
 Moura, Miguel, S279 ([WED-390](#))
 Mourya, Akash Kumar, S228 ([THU-363](#)), S352 ([THU-240](#)), S560 ([SAT-274](#))
 Mousel, Travis, S37 ([OS-038](#))
 Moussa, Sam, S1 ([GS-001](#)), S813 ([FRI-472](#)), S815 ([FRI-476](#))
 Moustafa, Ehab, S1212 ([THU-224](#))
 Moya, Adolfo Gallego, S1205 ([THU-216](#))
 Moynihan, Kelly, S5 ([GS-005](#))
 Mozaffarian, Afsaneh, S1153 ([SAT-174](#))
 Mozalevskis, Antons, S898 ([FRI-147](#))
 Mozar-Glazberg, Yael, S128 ([THU-394](#)), S971 ([THU-291](#))
 Mozayani, Behrang, S316 ([SAT-553](#)), S939 ([TOP-058](#))
 Mozer-Glassberg, Yael, S969 ([THU-289](#))
 Mozgovoi, Sergei, S865 ([SAT-129](#))
 Mp, Narmadha, S827 ([FRI-524](#))
 Mrekva, Arpad, S498 ([FRI-285](#))
 Mrzljak, Anna, S383 ([WED-277](#)), S880 ([FRI-122](#)), S1053 ([SAT-143](#))
 Msherghi, Ahmed, S475 ([THU-515](#))
 Muccioli, Giulio G., S772 ([WED-458](#))
 Muche, Marion, S1054 ([TOP-100](#))
 Mucumbi, Sheila Constância Mabote, S865 ([SAT-129](#))
 Mueller, Heike, S339 ([WED-248](#))
 Mueller, Johannes, S162 ([FRI-430](#))
 Mueller-Schilling, Martina, S1003 ([THU-377](#))
 Mueller, Sebastian, S162 ([FRI-430](#)), S283 ([SAT-327](#))
 Muench, Robert, S35 ([OS-034](#)), S1019 ([FRI-220](#))
 Mugisha, Joseph, S868 ([SAT-131](#))
 Muhammad, Taj, S896 ([FRI-145](#))
 Muir, Andrew, S89 ([OS-125](#))
 Mujawar, Quais, S972 ([THU-291](#))
 Mujib, Salma, S127 ([TOP-093](#)), S445 ([SAT-376](#))
 Mujica, Endrina, S769 ([WED-454](#))
 Mukherjee, Sucheta, S1029 ([FRI-238](#))
 Mukherjee, Sujit, S77 ([OS-108-YI](#))
 Mukherjee, Sumanta, S367 ([TOP-062](#)), S388 ([WED-283](#)), S398 ([WED-299](#))
 Mukherji, Atish, S72 ([OS-098](#))
 Mulinacci, Giacomo, S992 ([THU-319](#))
 Mullan, Aidan, S465 ([THU-495](#))
 Mullan, Aoiheann, S8 ([GS-010](#))
 Mullender, Claire, S721 ([SAT-504](#)), S1122 ([WED-202](#))
 Müller, Sascha, S162 ([FRI-430](#))
 Müller, Tobias, S403 ([WED-307](#)), S1032 ([FRI-244](#)), S1071 ([WED-132](#))
 Müllhaupt, Beat, S90 ([OS-126](#)), S403 ([WED-307](#)), S481 ([THU-526](#)), S849 ([WED-482](#))
 Mullish, Benjamin H., S7 ([GS-007](#)), S344 ([THU-228](#)), S601 ([TOP-088](#)), S624 ([THU-446](#)), S719 ([SAT-501](#))
 Müllner-Bucsics, Theresa, S244 ([WED-334](#))
 Mulu, Andargachew, S927 ([FRI-197](#))
 Munda, Petra, S1135 ([SAT-150](#))
 Mund, Meike, S928 ([THU-304](#))
 Munekage, Kensuke, S686 ([SAT-448](#))
 Mungai, Sophie, S1069 ([WED-128](#))
 Muniesa, Maria Pilar Huarte, S998 ([THU-331](#))
 Munk, Ditte Emilie, S958 ([THU-274](#)), S985 ([THU-309](#))
 Munk, Emilie, S948 ([THU-259](#))
 Munker, Stefan, S358 ([FRI-381](#)), S596 ([THU-150](#))
 Munnangi, Swapna, S977 ([THU-296](#)), S1007 ([THU-385](#))

Author Index

- Muños, Beatriz Mateos, S73 ([OS-102](#))
 Muñoz, Aroa, S1192 ([THU-192](#))
 Muñoz, Beatriz Mateos, S90 ([OS-127-YI](#)), S299 ([SAT-521](#)), S392 ([WED-290](#)), S399 ([WED-300](#)), S1098 ([WED-166](#)), S1178 ([THU-171](#)), S1205 ([THU-216](#))
 Munoz-Chimeno, Milagros, S902 ([FRI-153](#))
 Muñoz-Couselo, Eva, S375 ([WED-263](#))
 Muñoz, Elena, S335 ([WED-239](#)), S781 ([WED-505](#))
 Munoz, Leticia, S19 ([OS-011-YI](#))
 Muñoz-Llanes, Nerea, S137 ([FRI-395](#)), S529 ([SAT-215](#)), S741 ([WED-408](#))
 Munteanu, Mona, S674 ([SAT-431](#)), S711 ([SAT-488](#))
 Murad, Sarwa Darwish, S46 ([OS-053-YI](#)), S306 ([SAT-536](#)), S454 ([TOP-052](#))
 Murakami, Eisuke, S323 ([WED-216](#))
 Murata, Ayato, S633 ([THU-463](#)), S1041 ([FRI-257](#))
 Muratori, Luigi, S40 ([OS-045](#)), S55 ([OS-070](#)), S384 ([WED-278](#))
 Muratori, Paolo, S44 ([OS-049-YI](#))
 Mura, Vincenzo La, S87 ([OS-123-YI](#)), S975 ([THU-295](#))
 Murcia, Antonia, S497 ([FRI-284](#))
 Murga, Maria Dolores, S245 ([WED-336](#))
 Murgia, Antonio, S840 ([FRI-492](#))
 Muriel, Pablo, S151 ([FRI-414](#)), S160 ([FRI-426](#))
 Mur, Juan Ignacio Esteban, S506 ([FRI-298](#))
 Murphy, Donald, S874 ([FRI-114](#))
 Murphy, Niamh, S880 ([FRI-121](#))
 Murphy, Suzanne, S1187 ([THU-182](#))
 Murray, Catherine, S1211 ([THU-223](#))
 Murray, Sam, S970 ([THU-290](#))
 Murtuza-Baker, Syed, S8 ([GS-010](#))
 Musabaev, Erkin, S113 ([LBP-19](#)), S888 ([FRI-132](#))
 Musarò, Antonio, S218 ([THU-352](#))
 Muscari, Fabrice, S467 ([THU-498](#))
 Muscate, Franziska, S60 ([OS-079-YI](#))
 Musicha, Crispin, S153 ([FRI-418](#))
 Mussbacher, Marion, S142 ([FRI-402](#))
 Mussetto, Alessandro, S40 ([OS-045](#)), S55 ([OS-070](#))
 Mussini, Cristina, S907 ([FRI-164](#))
 Mustapha, Nik Raihan Nik, S644 ([THU-555](#)), S710 ([SAT-487](#))
 Mustapha, Shettima Kagu, S269 ([WED-373](#))
 Mustapic, Sanda, S61 ([OS-080-YI](#))
 Muthiah, Mark, S468 ([THU-500](#)), S629 ([THU-456](#)), S698 ([SAT-467](#)), S707 ([SAT-482](#)), S714 ([SAT-495](#)), S721 ([SAT-503](#))
 Muthukumarasamy, Uthayakumar, S413 ([FRI-334](#))
 Muti, Leon, S52 ([OS-066](#)), S172 ([FRI-446](#)), S1160 ([SAT-184](#))
 Mutka, Aino, S997 ([THU-329](#))
 Muungani, Lorraine, S549 ([SAT-253](#))
 Muzaale, Florence Nambaziira, S868 ([SAT-131](#))
 Muzaffar, Mahvish, S582 ([THU-128](#))
 Muzumdar, Karan, S983 ([THU-305](#))
 Myers, Robert, S31 ([OS-029](#)), S323 ([WED-216](#))
 Mykhailik, Olga, S1040 ([FRI-256](#))
 Myllys, Maiju, S940 ([THU-249](#))
 Mylvaganam, Ravi, S58 ([OS-075](#))
 Myneni, Sudha, S652 ([SAT-396](#))
 Nabeel, Mohamed Mahmoud, S570 ([SAT-291](#))
 Nabilou, Puria, S702 ([SAT-471](#)), S784 ([WED-511](#))
 Nabi, Oumarou, S170 ([FRI-442](#))
 Nadal, Ruth, S15 ([OS-001](#)), S250 ([WED-343](#)), S664 ([SAT-415](#)), S851 ([WED-486](#))
 Nadeem, Rida, S689 ([SAT-453](#)), S711 ([SAT-488](#))
 Nader, Ahmed, S1141 ([SAT-158](#)), S1154 ([SAT-176](#)), S1162 ([SAT-187](#))
 Nader, Fatema, S627 ([THU-453](#)), S857 ([SAT-116](#))
 Nadzemova, Oksana, S957 ([THU-271](#)), S957 ([THU-272](#))
 Nagahara, Hajime, S545 ([SAT-246](#))
 Naga, Malleswari, S209 ([THU-339](#))
 Naganuma, Atsushi, S584 ([THU-131](#))
 Nagaoka, Katsuya, S1095 ([WED-163](#))
 Nagaoka, Shinya, S1192 ([THU-191](#)), S1199 ([THU-205](#))
 Nagarajan, Perumal, S207 ([THU-337](#))
 Nagaraja, Ravishankara, S607 ([THU-419](#))
 Nagel, Judith, S417 ([FRI-349](#)), S948 ([THU-259](#))
 Nagelkerke, Anika, S798 ([WED-538](#))
 Naggie, Susanna, S612 ([THU-427](#))
 Nagler, Michael, S412 ([FRI-332](#))
 Nagorney, David M., S44 ([OS-050-YI](#)), S465 ([THU-495](#))
 Nagot, Nicolas, S929 ([FRI-201](#))
 Nagraj, Praneeta, S990 ([THU-317](#))
 Nagral, Abha, S195 ([FRI-546](#))
 Nahass, Ronald G, S125 ([LBP-38](#))
 Nahhas, Omar El, S12 ([LBO-04](#))
 Nahnsen, Sven, S547 ([SAT-248](#))
 Nahon, Pierre, S46 ([OS-055](#)), S61 ([OS-081](#)), S103 ([LBP-06](#)), S498 ([FRI-286](#))
 Nai, Antonella, S749 ([WED-423](#)), S774 ([WED-461](#))
 Naidu, Vegi, S560 ([SAT-274](#))
 Naidu, Vishnu, S558 ([SAT-271](#))
 Naik, Hetanshi, S993 ([THU-320](#))
 Naik, Ramavath Nareesh, S751 ([WED-425](#))
 Nair, Manjima, S827 ([FRI-524](#))
 Nair, Manjima P, S848 ([WED-481](#))
 Nair, Priya, S827 ([FRI-524](#)), S846 ([WED-477](#)), S848 ([WED-481](#))
 Nair, Radhika, S379 ([WED-268](#)), S844 ([FRI-500](#))
 Naito, Masafumi, S686 ([SAT-448](#))
 Najarro, Adrian, S1024 ([FRI-228](#))
 Najera, Isabel, S443 ([SAT-371](#))
 Najimi, Mustapha, S198 ([FRI-550](#)), S439 ([SAT-364](#)), S807 ([TOP-077](#))
 Najmi, Muath, S1006 ([THU-383](#))
 Nakadai, Yukie, S156 ([FRI-421](#))
 Nakade, Yukio, S811 ([FRI-468](#))
 Nakai, Manami, S323 ([WED-216](#))
 Nakajima, Atsushi, S30 ([OS-028](#)), S65 ([OS-086](#)), S616 ([THU-433](#)), S686 ([SAT-448](#))
 Nakamoto, Nobuhiro, S156 ([FRI-421](#)), S409 ([TOP-060](#))
 Nakamoto, Yasunari, S1183 ([THU-177](#))
 Nakamura, Yamami, S447 ([SAT-380](#))
 Nakanishi, Hiroyuki, S598 ([THU-155](#)), S644 ([THU-554](#)), S1113 ([WED-189](#))
 Nakano, Toshiaki, S401 ([WED-303](#))
 Nakao, Kazuhiko, S178 ([FRI-458](#)), S565 ([SAT-285](#)), S1177 ([THU-170](#)), S1183 ([THU-177](#))
 Nakao, Yasuhiko, S178 ([FRI-458](#)), S565 ([SAT-285](#)), S1177 ([THU-170](#))
 Nakashima, Hiroyuki, S453 ([SAT-392](#))
 Nakashima, Masahiro, S453 ([SAT-392](#))
 Namburete, Ana, S677 ([SAT-436](#))
 Namer, Barbara, S377 ([WED-265](#))
 Nam, Hyo Jin, S998 ([THU-330](#))
 Namisaki, Tadashi, S394 ([WED-293](#))
 Nam, Ki Tak, S778 ([WED-471](#))
 Nam, Soon Woo, S148 ([FRI-409](#))
 Nana, Melanie, S36 ([OS-037](#))
 Nandekar, Sanket, S830 ([FRI-530](#))
 Nan, Yumin, S243 ([WED-332](#)), S1066 ([WED-125](#))
 Naoumov, Nikolai, S806 ([TOP-076](#))
 Napodano, Cecilia, S723 ([SAT-508](#))
 Napoleone, Laura, S10 ([LBO-01](#))
 Napoli, Laura, S744 ([WED-413](#))
 Napoli, Salvatore, S445 ([SAT-376](#))
 Napolitano, Andrea, S586 ([THU-134](#))
 Narasimhan, Gomathy, S488 ([THU-544](#))
 Nardelli, Silvia, S237 ([WED-320](#)), S251 ([WED-345](#)), S994 ([THU-323](#))
 Nardini, Patrizia, S550 ([SAT-254](#))
 Nardo, Alexander D, S739 ([WED-405](#)), S746 ([WED-418](#))
 Naresh Naik, Ramavath, S804 ([WED-551](#))
 Narguet, Stephanie, S1055 ([TOP-103](#)), S1093 ([WED-159](#))
 Narimatsu, Hisashi, S1041 ([FRI-257](#))
 Nasa, Mukesh, S726 ([SAT-511](#))
 Nascimbeni, Fabio, S729 ([SAT-517](#))
 Nasr, Patrik, S605 ([THU-414](#)), S650 ([TOP-085](#)), S653 ([SAT-397](#)), S707 ([SAT-481](#))
 Nasrullah, Atif, S641 ([THU-476](#))
 Nassar, Islam, S174 ([FRI-450](#))
 Nassauw, Luc Van, S764 ([WED-446](#))
 Nasser, Abdullah, S514 ([FRI-313](#))
 Nasser, Nour, S1093 ([WED-159](#))
 Nastasio, Silvia, S971 ([THU-291](#))
 Nastouli, Eleni, S1075 ([WED-137](#))
 Natarajan, Muthukumar, S607 ([THU-419](#))
 Natella, Pierre-André, S46 ([OS-055](#))
 Nathalie, Boyer, S1093 ([WED-159](#))
 Nathan, Rohit, S458 ([THU-482](#)), S463 ([THU-490](#))

- Natrus, Larysa, S429 ([FRI-367](#))
 Natsui, Kazuki, S124 ([LBP-37](#))
 Natsui, Yui, S124 ([LBP-37](#))
 Nault, Jean Charles, S12 ([LBO-04](#)),
 S577 ([THU-119](#)), S577 ([THU-120](#)),
 S579 ([THU-123](#)), S585 ([THU-133](#))
 Naumann, Uwe, S1174 ([THU-166](#))
 Nautiyal, Nidhi, S212 ([THU-343](#))
 Navale, Pooja, S12 ([LBO-04](#))
 Navari, Nadia, S233 ([THU-371](#))
 Navarro, Jose Luis Lledo, S73 ([OS-102](#))
 Naveed, Shabnam, S842 ([FRI-497](#))
 Naveira, Marcelo, S912 ([FRI-173](#))
 Navidad, Cristian Martínez,
 S616 ([THU-432](#)), S670 ([SAT-425](#)),
 S676 ([SAT-433](#))
 Nawghare, Pankaj, S643 ([THU-553](#))
 Nawrot, Margaux, S355 ([THU-244](#))
 Nayagam, Shevanthi, S923 ([FRI-191](#))
 Nayer, Jamshed, S6 ([GS-006](#))
 Nayfeh, Tarek, S65 ([OS-086](#))
 Ndow, Gibril, S67 ([OS-090-YI](#)),
 S916 ([FRI-178](#)), S1106 ([WED-178](#)),
 S1106 ([WED-179](#))
 Nebbia, Gabriella, S969 ([THU-289](#)),
 S971 ([THU-291](#))
 Neff, Guy, S1 ([GS-001](#)), S653 ([SAT-398](#)),
 S808 ([TOP-091](#)), S813 ([FRI-472](#)),
 S815 ([FRI-476](#))
 Negi, Preeti, S149 ([FRI-411](#))
 Negro, Francesco, S103 ([LBP-06](#)),
 S751 ([WED-426](#))
 Nehring, Sophie, S364 ([FRI-390](#))
 Nelson, Glyn, S565 ([SAT-284](#))
 Nelson, Leonard J, S142 ([FRI-403](#))
 Nemecek, Paige, S35 ([OS-034](#))
 Nemeth-Blazic, Tatjana, S880 ([FRI-121](#))
 Neria, Fernando, S469 ([THU-501](#))
 Neroldova, Magdalena,
 S1173 ([THU-164](#))
 Nery, Filipe Gaio Castro, S87 ([OS-123-YI](#))
 Nesbitt, Robin, S69 ([OS-094](#))
 Ness, Erik, S378 ([WED-267](#)),
 S379 ([WED-268](#)), S844 ([FRI-500](#))
 Neto, Nadia, S443 ([SAT-371](#)),
 S1034 ([FRI-248](#))
 Netter, Hans, S1028 ([FRI-237](#)),
 S1164 ([SAT-191](#))
 Neumann-Haefelin, Christoph,
 S1139 ([SAT-156](#))
 Neumayer, Daniela, S288 ([SAT-335](#))
 Neurath, Markus F., S377 ([WED-265](#))
 Neururer, Sabrina, S961 ([THU-279](#)),
 S968 ([THU-288](#))
 Neuwirth, Teresa, S294 ([SAT-345](#))
 Nevah Rubin, Moises, S463 ([THU-490](#))
 Nevens, Frederik, S41 ([OS-046](#)),
 S56 ([OS-073](#)), S87 ([OS-123-YI](#)),
 S198 ([FRI-550](#)), S345 ([THU-229](#)),
 S452 ([SAT-390](#)), S579 ([THU-123](#))
 Nevzorova, Yulia, S22 ([OS-015](#)),
 S38 ([OS-041-YI](#)), S150 ([FRI-412](#)),
 S349 ([THU-235](#)), S732 ([TOP-090](#))
 Newhouse, Daniel, S78 ([OS-110](#))
 Newsome, Philip N, S66 ([OS-089](#)),
 S672 ([SAT-427](#)), S708 ([SAT-483](#)),
 S941 ([THU-250](#)), S944 ([THU-254](#))
 Newsome, Philip N., S627 ([THU-453](#))
 Neyts, Johan, S1025 ([FRI-231](#)),
 S1038 ([FRI-253](#))
 Nganso, Tatiana, S1210 ([THU-222](#))
 Ng, Cheng Han, S468 ([THU-500](#)),
 S611 ([THU-424](#)), S721 ([SAT-503](#))
 Ng, David Chee Eng, S582 ([THU-129](#)),
 S591 ([THU-142](#))
 Ng, Irene Oi-Lin, S48 ([OS-058](#))
 Ng, Louis, S199 ([FRI-552](#)), S257 ([WED-353](#)),
 S278 ([WED-389](#))
 Ngu, Natalie, S380 ([WED-271](#))
 Nguyen, Brian, S638 ([THU-471](#))
 Nguyen, Henri, S5 ([GS-005](#))
 Nguyen, Le Tuan Anh, S523 ([FRI-329](#))
 Nguyen, Mindie, S468 ([THU-499](#)),
 S638 ([THU-471](#)), S1096 ([WED-165](#))
 Nguyen, Nga, S82 ([OS-117](#))
 Nguyen-Tat, Marc, S277 ([WED-387](#))
 Nguyen, Thi Thu Nga, S855 ([TOP-098](#))
 Nguyen, Tuan, S125 ([LBP-38](#))
 Nguyen, Vy H, S1096 ([WED-165](#))
 Ng, Weng Yan, S582 ([THU-129](#)),
 S591 ([THU-142](#))
 Niazi, Mina, S900 ([FRI-151](#))
 Niaz, Qamar, S215 ([THU-347](#))
 Niaz, Saad, S912 ([FRI-172](#))
 Nibali, Stefano Conti, S552 ([SAT-258](#))
 Nicastro, Emanuele, S966 ([THU-285](#)),
 S969 ([THU-289](#)), S971 ([THU-291](#))
 Nicenboim, Julian, S409 ([TOP-060](#))
 Nicholson-Scott, Louise, S840 ([FRI-492](#))
 Nicholson, Thomas, S231 ([THU-368](#)),
 S232 ([THU-370](#))
 Nicoara-Farcau, Oana, S86 ([OS-121-YI](#)),
 S87 ([OS-123-YI](#)), S151 ([FRI-413](#)),
 S295 ([SAT-347](#)), S297 ([SAT-519](#)),
 S843 ([FRI-499](#))
 Nicolas, Carine, S172 ([FRI-446](#))
 Nicoll, Amanda, S380 ([WED-271](#))
 Niehaus, Christian, S229 ([THU-365](#))
 Nielsen, Elise Jonasson, S251 ([WED-345](#))
 Nielsen, Malte H., S530 ([SAT-218](#)),
 S763 ([WED-445](#))
 Nielsen, Susanne Dam, S841 ([FRI-494](#))
 Nie, Sixiang, S1079 ([WED-141](#))
 Nieß, Hanno, S358 ([FRI-381](#))
 Nieto, Natalia, S80 ([OS-113](#))
 Nieto, Susana, S489 ([THU-546](#))
 Nieuwenhove, Yves Van, S172 ([FRI-447](#)),
 S787 ([WED-516](#))
 Nieva-Zuluaga, Ane, S137 ([FRI-395](#)),
 S529 ([SAT-215](#)), S738 ([WED-404](#)),
 S741 ([WED-408](#))
 Niewczas, Julia, S31 ([OS-030](#))
 Niewola, Karolina, S761 ([WED-441](#))
 Nie, Yaohui, S422 ([FRI-356](#))
 Nioka, Hirohiko, S545 ([SAT-246](#))
 Ni, Irene, S5 ([GS-005](#))
 Nikolic, Katarina, S332 ([WED-232](#))
 Nikolopoulos, Georgios, S880 ([FRI-121](#))
 Nikolopoulou, Georgia, S880 ([FRI-121](#))
 Nikolov, Ivaylo, S198 ([FRI-550](#))
 Nikulkina, Elena, S1210 ([THU-221](#))
 Nikzad, Newsha, S516 ([FRI-317](#))
 Nilius, Henning, S412 ([FRI-332](#))
 Ni, Liyun, S1209 ([THU-219](#))
 Nilusmas, Samuel, S498 ([FRI-286](#))
 Nimanong, Supot, S19 ([OS-009](#)),
 S237 ([WED-321](#)), S502 ([FRI-292](#))
 Nimma, Induja, S472 ([THU-509](#))
 Ningarhari, Massih, S12 ([LBO-04](#)),
 S62 ([OS-083-YI](#))
 Ning, Qin, S1087 ([WED-151](#)),
 S1153 ([SAT-174](#))
 Ning, Yingying, S413 ([FRI-335](#))
 Ninkovic, Marijana, S44 ([OS-050-YI](#))
 Ninomiya, Masashi, S394 ([WED-293](#))
 Ni, Quanhong, S938 ([TOP-057](#)),
 S965 ([THU-284](#)), S969 ([THU-289](#))
 Niro, Grazia, S40 ([OS-045](#)), S55 ([OS-070](#)),
 S374 ([WED-260](#)),
 S1054 ([TOP-100](#))
 Nishida, Naoshi, S575 ([THU-116](#)),
 S586 ([THU-134](#))
 Nishtala, Sneha, S1058 ([WED-113](#))
 Nisingizwe, Marie Paul, S886 ([FRI-130](#))
 Nissen, Nicholas, S489 ([TOP-065](#))
 Niu, Hao, S18 ([OS-007](#)), S126 ([TOP-087](#)),
 S142 ([FRI-403](#))
 Niu, Junqi, S34 ([OS-033](#)), S109 ([LBP-13](#)),
 S112 ([LBP-18](#)), S117 ([LBP-24](#)),
 S327 ([WED-225](#)), S1153 ([SAT-174](#)),
 S1164 ([SAT-192](#))
 Ni, Yi, S1025 ([FRI-232](#))
 Niyomsri, Siwaporn, S912 ([FRI-172](#))
 Ni, Yong, S488 ([THU-540](#))
 Njei, Basile, S856 ([SAT-114](#))
 Njei, Nelvis, S856 ([SAT-114](#))
 Njie, Ramou, S1106 ([WED-178](#))
 Njimi, Hassane, S621 ([THU-442](#))
 Njuguna, Henry, S885 ([FRI-127](#))
 Nkemenang, Patrick, S69 ([OS-094](#))
 Noble, Lisa, S848 ([WED-480](#))
 Noble, Theresa, S1075 ([WED-137](#))
 Nobusawa, Tsubasa, S598 ([THU-155](#)),
 S644 ([THU-554](#))
 Nocke, Maximilian, S1032 ([FRI-244](#)),
 S1044 ([FRI-262](#))
 Noda, Takehiro, S439 ([SAT-366](#)),
 S509 ([FRI-302](#))
 Nogami, Asako, S30 ([OS-028](#))
 Noguchi, Fumie, S156 ([FRI-421](#))
 Nogueiras, Ruben, S38 ([OS-041-YI](#)),
 S140 ([FRI-399](#)), S326 ([WED-223](#)),
 S560 ([SAT-275](#))
 Noh, Ji Yun, S1048 ([FRI-268](#))
 Nørh-Meldgaard, Jacob, S530 ([SAT-218](#)),
 S746 ([WED-417](#)), S788 ([WED-519](#)),
 S800 ([WED-543](#))
 Nolf, Clint De, S229 ([THU-364](#))
 Nomah, Daniel K., S924 ([FRI-192](#))
 Nomden, Mark, S969 ([THU-289](#))
 Nomikos, George, S260 ([WED-358](#))
 Nomura, Takako, S394 ([WED-293](#))

Author Index

- Nong, Qin, S735 (WED-399), S775 (WED-463)
- Nonkovic, Diana, S880 (FRI-121), S880 (FRI-122)
- Noon, Luke, S75 (OS-105)
- Nordestgaard, Børge, S702 (SAT-471)
- Nordhus, Kathrine Sivertsen, S420 (FRI-353)
- Nordøy, Ingvild, S478 (THU-520)
- Norero, Blanca, S865 (SAT-129)
- Noritake, Hiedenao, S686 (SAT-448)
- Norlin, Andreas, S841 (FRI-493)
- Norman, Gary, S375 (WED-261)
- Noronha Ferreira, Carlos, S87 (OS-123-YI)
- Norris, Suzanne, S1211 (THU-223)
- Norton, Luke, S79 (OS-112)
- Nosaka, Ken, S830 (FRI-529)
- Notley, Caitlin, S854 (TOP-095)
- Noureddin, Mazen, S1 (GS-001), S29 (OS-026), S30 (OS-027), S65 (OS-086), S65 (OS-088), S114 (LBP-21), S118 (LBP-26), S604 (THU-413), S619 (THU-438), S619 (THU-439), S629 (THU-456), S643 (THU-552), S655 (SAT-401), S659 (SAT-407), S659 (SAT-408), S678 (SAT-438), S684 (SAT-444), S822 (FRI-515), S828 (FRI-525)
- Noureddin, Nabil, S65 (OS-086)
- Nousbaum, Jean Baptiste, S61 (OS-081), S82 (OS-117), S855 (TOP-098)
- Nova-Camacho, Luiz Miguel, S533 (SAT-223), S541 (SAT-238)
- Novac, Ovidiu, S775 (WED-464)
- Nováková, Barbora, S292 (SAT-341), S727 (SAT-513)
- Novati, Stefano, S863 (SAT-126)
- Novo, Erica, S766 (WED-449)
- Nowak, Manfred, S1186 (THU-181)
- Nowak, Melissa, S441 (SAT-368)
- Nozzoli, Chiara, S88 (OS-124-YI)
- Nuciforo, Sandro, S532 (SAT-222)
- Nuersulitan, Reyizha, S1100 (WED-170)
- Nulan, Yeldos, S20 (OS-012-YI)
- Nulty, Jessica, S984 (THU-307)
- Nunes, Maria De Brito, S280 (TOP-048)
- Nunes, Tiago, S56 (OS-072), S123 (LBP-35), S370 (WED-252), S387 (WED-282)
- Nunes, Vinicius, S132 (THU-401)
- Núñez, Carmen López, S924 (FRI-192), S1098 (WED-166)
- Núñez, Isabel Ruiz, S480 (THU-524)
- Núñez, Susana, S38 (OS-042-YI), S339 (WED-247)
- Nurcis, Jessica, S526 (SAT-211)
- Nuriyev, Kanan, S709 (SAT-485)
- Nuzzo, Alexandre, S975 (THU-295)
- Nwoko, Chinenye, S865 (SAT-129)
- Nyakowa, Mercy, S100 (LBP-01)
- Nyam P, David, S274 (WED-382), S1117 (WED-195)
- Nyassi, Fatou Bintou, S67 (OS-090-YI), S1106 (WED-178)
- Nygård, Sune Boris, S811 (FRI-469), S817 (FRI-507)
- Nyhlin, Nils, S707 (SAT-481)
- Nyholm, Iiris, S997 (THU-329)
- Oakes, Kathryn, S1179 (THU-172)
- Oakley, Fiona, S323 (WED-217), S332 (WED-232), S538 (SAT-234), S542 (SAT-239), S565 (SAT-284), S783 (WED-508)
- Oben, Jude A., S205 (TOP-042)
- Oberti, Frédéric, S61 (OS-081), S318 (SAT-556), S598 (THU-154), S667 (SAT-419)
- Oberti, Giovanna, S632 (THU-461), S645 (THU-557)
- Obmann, Verena, S485 (THU-533)
- Ocal, Osman, S576 (THU-118)
- Ocanit, Anthony, S865 (SAT-129)
- Ochi, Hironori, S584 (THU-131)
- O'Connell, Malene Barfod, S165 (FRI-434)
- Odeghe, Emuobor, S865 (SAT-129)
- Odenthal, Margarete, S712 (SAT-492)
- Odintsova, Viktoria, S349 (THU-235)
- Odriozola, Aitor, S868 (SAT-132)
- Odriozola, Mikel, S527 (SAT-212)
- Odrlijn, Tatjana, S115 (LBP-22)
- Oechslin, Noémie, S1031 (FRI-243)
- Oeda, Satoshi, S686 (SAT-448)
- Oertel, Laetitia, S168 (FRI-440)
- Oetheimer, Christopher, S58 (OS-075)
- Oettl, Karl, S220 (THU-355)
- O'Farrell, Marie, S49 (OS-061)
- Offensperger, Florian, S318 (SAT-555)
- Ofner-Kopeinig, Petra, S477 (THU-519)
- Øgaard, Jonas, S420 (FRI-353), S421 (FRI-355), S588 (FRI-365)
- Ogasawara, Akio Murakami, S1202 (THU-211)
- Ogle, Jonathan, S260 (WED-358), S809 (FRI-466)
- Ogle, Laura, S411 (FRI-331)
- Ogunnaike, Stephen, S1122 (WED-202)
- Ohama, Hideko, S584 (THU-131)
- Oh, Bora, S556 (SAT-266), S558 (SAT-270)
- Oh, Hyunwoo, S615 (THU-431), S695 (SAT-462), S701 (SAT-470), S704 (SAT-475), S757 (WED-435), S794 (WED-531), S864 (SAT-128), S1073 (WED-135)
- Ohira, Hiromasa, S394 (WED-293)
- Oh, Joo Hyun, S615 (THU-431), S667 (SAT-418), S695 (SAT-462), S701 (SAT-470), S704 (SAT-475), S705 (SAT-476), S757 (WED-435), S794 (WED-531), S821 (FRI-514), S864 (SAT-128)
- Oh, Ki Kwang, S156 (FRI-420), S343 (THU-227)
- Ohkura, Naganari, S447 (SAT-380)
- Ohlendorf, Valerie, S1115 (WED-193)
- Öhlinger, Thomas, S465 (THU-494)
- Oh, Seak Hee, S971 (THU-291)
- Oh, Seung Hyun, S778 (WED-471)
- Oh, Tae Gyu, S662 (SAT-412)
- Ohyaabu, Naoki, S323 (WED-216)
- Oidovsambuu, Odgerel, S716 (SAT-497), S718 (SAT-499), S1104 (WED-175)
- Oikawa, Tsunekazu, S818 (FRI-508)
- Okamoto, Natsumi, S447 (SAT-380)
- Okamoto, Ryuichi, S865 (SAT-129)
- Okano, Shinji, S178 (FRI-458)
- Okanoue, Takeshi, S616 (THU-433), S686 (SAT-448), S827 (FRI-523)
- Okeke, Edith, S195 (FRI-546), S916 (FRI-178), S1117 (WED-195)
- Okoye, Ifeoma Joy, S865 (SAT-129)
- Oktyabri, Azzaya, S910 (FRI-168)
- Okubo, Tomomi, S240 (WED-327), S317 (SAT-554), S584 (THU-131), S818 (FRI-508), S820 (FRI-511)
- Olaizola, Irene, S527 (SAT-212), S533 (SAT-223)
- Olaizola, Paula, S57 (OS-074-YI), S527 (SAT-212), S533 (SAT-223), S534 (SAT-226), S541 (SAT-238), S544 (SAT-244)
- Olartekoetxea, Gaizka Errazti, S741 (WED-408)
- Olbrich, Anne, S507 (FRI-299)
- Oldani, Graziano, S24 (OS-018-YI)
- Old, Hannah, S74 (OS-103-YI)
- Oldroyd, Christopher, S854 (TOP-095)
- O'Leary, Jacqueline, S256 (WED-352), S258 (WED-355)
- Olenchock, Benjamin, S49 (OS-062)
- Olinga, Peter, S740 (WED-407), S798 (WED-538)
- Olivas, Pol, S87 (OS-123-YI), S843 (FRI-499)
- Oliveira, Claudia, S865 (SAT-129), S900 (FRI-151)
- Oliveira, Daniel, S945 (THU-255)
- Oliveira, Hugo, S842 (FRI-495)
- Oliveira, Jeffrey, S496 (FRI-282)
- Oliveira, Mafalda, S375 (WED-263)
- Oliveira, Mariana, S233 (THU-372)
- Oliveira, Mariana M., S213 (THU-344)
- Oliveri, Filippo, S691 (SAT-456), S1091 (WED-157)
- Oliver, Mark, S480 (THU-522)
- Olivero, Antonella, S605 (THU-415), S611 (THU-425), S617 (THU-435), S626 (THU-452), S637 (THU-470), S1056 (TOP-106), S1072 (WED-133)
- Olivet, Berta Vazquez, S752 (WED-428)
- Olivieri, Attilio, S88 (OS-124-YI)
- Oliviero, Barbara, S552 (SAT-258)
- Olkus, Alexander, S1139 (SAT-156)
- Ollier, Laurence, S1158 (SAT-180)
- Öllinger, Rupert, S1026 (FRI-233)
- Ollivier-Hourmand, Isabelle, S52 (OS-066), S61 (OS-081), S82 (OS-117), S107 (LBP-11), S318 (SAT-556), S855 (TOP-098), S975 (THU-295)
- Olmeo, Chiara, S1020 (FRI-222)
- Olmo, Javier Fuentes, S1098 (WED-166)
- Olofsson, Peder, S756 (WED-434)
- Olsen, Jens, S614 (THU-429)

- Olsen, Katheryn, S982 (THU-304)
 Olsson, Karen, S240 (WED-326)
 Oltmanns, Carlos, S1029 (FRI-240), S1035 (FRI-249)
 Olynyk, John, S726 (SAT-511), S830 (FRI-529), S983 (THU-306), S1011 (THU-389)
 Olza, Josune, S1075 (WED-137)
 Omar, Ashraf, S570 (SAT-291)
 Omazzi, Barbara, S40 (OS-045), S55 (OS-070)
 Omella, Judit Domenech, S544 (SAT-244)
 Omu, Rifa, S633 (THU-463)
 Önal, Zerrin, S969 (THU-289), S971 (THU-291)
 Ondřej, Podlaha, S443 (SAT-371)
 Ong, Agnes Bee Leng, S786 (WED-514)
 Ong, Charlotte Chung Hui, S629 (THU-456)
 Ong, Christen En Ya, S629 (THU-456)
 Ong, Elden Yen Hng, S629 (THU-456)
 Onghena, Louis, S172 (FRI-447), S226 (THU-361), S743 (WED-412), S787 (WED-516)
 Ong, Janus, S464 (THU-492), S600 (TOP-081), S627 (THU-453), S861 (SAT-122), S905 (FRI-159)
 Onida, Francesco, S88 (OS-124-YI)
 Oniscu, Gabriel, S46 (OS-053-YI)
 Ono, Hiroki, S240 (WED-327), S317 (SAT-554), S820 (FRI-511)
 Ono, Masafumi, S686 (SAT-448)
 Ooe, Chieko, S899 (FRI-149)
 Ooi, London Lucien, S591 (THU-142)
 Oord, Gertine, S496 (FRI-282), S1016 (TOP-108), S1019 (FRI-219)
 Oosterhui, Dorenda, S740 (WED-407)
 Oostvogels, Astrid, S561 (SAT-276)
 Oo, Ye Htun, S416 (FRI-347), S443 (SAT-372), S447 (SAT-380), S448 (SAT-381), S448 (SAT-382), S941 (THU-250)
 Opallo, Nicola, S797 (WED-535), S800 (WED-542)
 Op de Coul, Eline, S880 (FRI-121), S892 (FRI-138)
 Opyrchal, Paulina, S837 (FRI-486)
 Orange, Sam, S16 (OS-003)
 Orazbayeva, Damesh, S320 (SAT-559)
 Orbach, Shari, S844 (FRI-500)
 Ordonez, Felipe, S123 (LBP-35)
 Ordoñez, Felipe, S387 (WED-282)
 Oreistein, Ines, S598 (THU-154)
 Orient, Hans, S1114 (WED-190)
 Orlikowski, Dorian, S527 (SAT-213)
 Orman, Eric, S101 (LBP-03)
 Örmeci, Aslı Çifcibaşı, S709 (SAT-485)
 Oro, Carlos, S932 (FRI-208)
 Oró, Denise, S530 (SAT-218), S746 (WED-417), S763 (WED-445), S788 (WED-519)
 Orpen-Palmer, Josh, S402 (WED-305)
 Orro, Alessandro, S772 (WED-459)
 Orsi, Emanuela, S814 (FRI-474)
 Orsini, Corinna, S1170 (SAT-199)
 Ortega-Alonso, Aida, S18 (OS-007)
 Ortega, Andrea Carenas, S1202 (THU-211)
 Ortega, Lluisa, S166 (FRI-437)
 Ortega, Martin Muñoz, S337 (WED-244)
 Ortega, Miguel A, S19 (OS-011-YI)
 Orti, Luis Sabater, S451 (SAT-387)
 Ortiz, Manuel Gahete, S529 (SAT-216)
 Ortiz-Velez, Carolina, S375 (WED-263)
 Ortmayr, Gregor, S564 (SAT-282)
 Ortonne, Valérie, S1109 (WED-182)
 Orts, Lara, S87 (OS-123-YI), S843 (FRI-499), S970 (THU-290), S984 (THU-308)
 Or, Yat-Sun, S422 (FRI-356)
 Osadchuk, Yulia, S429 (FRI-367)
 Osinusi, Anu, S53 (OS-068)
 Osiowy, Carla, S1115 (WED-191)
 Osipov, Arsen, S489 (TOP-065)
 Osmani, Zgjim, S1016 (TOP-108)
 Osman, Karim, S56 (OS-073)
 Osman, Mahlet, S927 (FRI-197)
 Osman, Mohamed, S426 (FRI-363)
 Osnato, Anna, S433 (SAT-354)
 Ostadreza, Mahnoosh, S733 (WED-393)
 Osta, Eri, S856 (SAT-114)
 Østberg, Nadja, S851 (WED-487)
 Osti, Valentino, S640 (THU-475), S691 (SAT-457)
 Ostojic, Ana, S1053 (SAT-143)
 O'Sullivan, John, S230 (THU-367)
 Osuna-Gómez, Rubén, S164 (FRI-433)
 Otano, Juan Isidro Uriz, S366 (TOP-061)
 Otero, Alejandra, S133 (THU-404), S481 (THU-525)
 Otero, Yolanda, S806 (WED-555)
 Otgonbayar, Badmaa, S910 (FRI-168)
 Otsoa, Fernando Lopitz, S736 (WED-400)
 Ott, Fritz, S362 (FRI-386)
 Ott, Michael, S951 (THU-263)
 Otto, Tobias, S22 (OS-015)
 Ott, Peter, S257 (WED-354), S958 (THU-274), S985 (THU-309)
 Oubaya, Nadia, S467 (THU-498)
 Oude-Elferink, Ronald, S412 (FRI-333), S427 (FRI-364)
 Oudot, Marine, S72 (OS-098)
 Oufella, Amandine Ait, S515 (FRI-316)
 Ou, Mengdang, S1185 (THU-180)
 Ou, Xiaojuan, S1066 (WED-125)
 Ouzan, Denis, S684 (SAT-445), S834 (FRI-481)
 Ouzir, Nora, S64 (OS-084-YI)
 Ovadia, Caroline, S36 (OS-037)
 Ovchinsky, Nadia, S123 (LBP-35), S387 (WED-282), S965 (THU-284)
 Ovenden, William, S284 (SAT-329)
 Overi, Diletta, S994 (THU-323)
 Oversoe, Stine Karlsen, S510 (FRI-305)
 Owen, Christina, S877 (FRI-118)
 Owen, Rhiannon, S721 (SAT-504)
 Øynebråten, Inger, S59 (OS-076)
 Özcürümez, Mustafa, S628 (THU-454)
 Öz, Digidem Kuru, S65 (OS-086)
 Özdırlık, Burcin, S351 (THU-238)
 Ozga, Ann-Kathrin, S285 (SAT-331)
 Özsezen, Serdar, S763 (WED-444)
 Ozturk, Bengi, S1109 (WED-183)
 Paar, Margret, S220 (THU-355)
 Paba, Pierpaolo, S1122 (WED-203)
 Pabic, Estelle Le, S1161 (SAT-185)
 Pablo Arab, Juan, S114 (LBP-21), S145 (TOP-073)
 Pacchioni, Chiara, S729 (SAT-517)
 Pace Palitti, Valeria, S40 (OS-045), S55 (OS-070)
 Pachisia, Aditya Vikram, S401 (WED-304)
 Pachura, Kimberly, S415 (FRI-346)
 Padalino, Massimo, S990 (THU-316)
 Padalko, Elizaveta, S1114 (WED-190)
 Padilla, Marlene, S392 (WED-290)
 Padilla, P. Martin, S900 (FRI-151)
 Padua, Elizabeth, S1111 (WED-185)
 Paeshuyse, Jan, S1051 (FRI-272)
 Paff, Melanie, S110 (LBP-15), S1039 (FRI-255), S1151 (SAT-171), S1154 (SAT-176), S1162 (SAT-187), S1167 (SAT-196)
 Pagadala, Mangesh, S242 (WED-330)
 Paganelli, Massimiliano, S937 (TOP-056)
 Pagan, Garcia, S984 (THU-308)
 Pagani, Alessia, S749 (WED-423), S774 (WED-461)
 Pagan, Juan Carlos Garcia, S3 (GS-003), S279 (TOP-043), S326 (WED-223), S843 (FRI-499), S970 (THU-290)
 Pagano, Duilio, S457 (THU-480)
 Pagano, Giulia, S461 (THU-487)
 Pageaux, Georges-Philippe, S56 (OS-073), S61 (OS-081), S74 (OS-104), S170 (FRI-443), S198 (FRI-550), S473 (THU-511), S498 (FRI-286), S929 (FRI-201), S1161 (SAT-185)
 Pages, Emma, S929 (FRI-201)
 Pages, Josefina, S245 (WED-336)
 Paik, James, S600 (TOP-081), S614 (THU-430), S857 (SAT-116), S861 (SAT-122)
 Paik, Seung Woon, S305 (SAT-533), S631 (THU-459), S821 (FRI-514)
 Paik, Yong-Han, S267 (WED-369), S305 (SAT-533), S631 (THU-459), S821 (FRI-514)
 Paiola, Giulia, S974 (THU-293)
 Pai, Rish, S671 (SAT-426)
 Paisant, Anita, S598 (THU-154)
 Pais, Raluca, S106 (LBP-10), S652 (SAT-396)
 Paiva, Nuno, S534 (SAT-226)
 Pajares, Félix García, S480 (THU-524), S886 (FRI-129)
 Pajinag, Melissa April, S599 (THU-157)
 Pakarinen, Mikko, S997 (THU-329)
 Palaprat, Oriane, S894 (FRI-142)
 Palasantzias, Victoria, S805 (WED-554)
 Palazón, Asís, S532 (SAT-221)
 Palitti, Valeria Pace, S36 (OS-036), S374 (WED-260)
 Palladini, Giuseppina, S804 (WED-550)
 Palle, Mads Sundby, S827 (FRI-523)

Author Index

- Pallett, Laura J, S558 (SAT-271)
 Pallotta, Jonelle, S404 (WED-310)
 Pallozzi, Maria, S252 (WED-347), S981 (THU-302)
 Pallucci, Davide, S217 (THU-350)
 Palma, Carolina Santos, S279 (WED-390), S734 (WED-397)
 Palma, Elena, S324 (WED-218)
 Palmer, Andrew, S176 (FRI-453), S523 (FRI-329)
 Palmer, Daniel, S521 (FRI-326)
 Palmer, Jeremy, S411 (FRI-331), S781 (WED-475)
 Palmese, Francesco, S191 (FRI-540)
 Palmisano, Silvia, S711 (SAT-489), S768 (WED-452), S793 (WED-529)
 Palom, Adriana, S896 (FRI-144), S904 (FRI-158), S917 (FRI-181), S1082 (WED-145), S1098 (WED-166), S1099 (WED-168)
 Palomino, Sara, S143 (FRI-404), S290 (SAT-337)
 Palomo, Albero Rodriguez, S886 (FRI-129)
 Palomo, Consuelo, S396 (WED-295)
 Palop, Begoña, S1126 (WED-208)
 Palou, Eva, S497 (FRI-284), S849 (WED-483)
 Palumbo, Joseph, S101 (LBP-03)
 Paluschinski, Martha, S562 (SAT-279)
 Pamecha, Viniyendra, S207 (THU-337), S326 (WED-222), S357 (THU-248), S414 (FRI-344)
 Pammer, Lorenz Michael, S961 (THU-279)
 Pa, Muhammed Shafi, S827 (FRI-524)
 Pan, Calvin, S53 (OS-067), S1137 (SAT-153)
 Pan, Calvin Q, S243 (WED-332)
 Panchal, Satish, S607 (THU-419)
 Panda, Sameer, S560 (SAT-274)
 Pan, David, S1055 (TOP-101)
 Pandey, Sushmita, S17 (OS-006-YI), S21 (OS-014-YI), S76 (OS-107-YI), S139 (FRI-398), S146 (FRI-407), S149 (FRI-410), S152 (FRI-416), S326 (WED-222), S414 (FRI-344), S1033 (FRI-247)
 Pandya, Aashish, S74 (OS-103-YI)
 Pandya, Keval, S380 (WED-271)
 Pane, Fabrizio, S88 (OS-124-YI)
 Panella, Riccardo, S742 (WED-410)
 Panera, Nadia, S783 (WED-507)
 Panero, José Luis Calleja, S3 (GS-003), S8 (GS-009), S87 (OS-123-YI), S272 (WED-378), S291 (SAT-340), S390 (WED-288), S683 (SAT-443), S709 (SAT-484), S921 (FRI-188), S1098 (WED-166), S1205 (THU-216)
 Pang, Huajin, S543 (SAT-242)
 Pang, Yuhua, S1156 (SAT-178)
 Pan, Jin-Shui, S869 (SAT-134)
 Pan, Mei-Hung, S1060 (WED-118)
 Pan-ngum, Wirichada, S919 (FRI-184)
 Pan, Qin, S756 (WED-433)
 Pan, Qiuwei, S1016 (TOP-111)
 Pantic, Ivana, S870 (SAT-135)
 Pantzios, Spyridon, S595 (THU-149), S1046 (FRI-264), S1128 (WED-211)
 Pan, Xiao-Yan, S613 (THU-428)
 Pan, Yifan, S1004 (THU-379), S1068 (WED-127), S1094 (WED-162)
 Pan, Zelei, S1152 (SAT-173)
 Panzer, Marlene, S968 (THU-288), S1135 (SAT-150)
 Panzer, Simon, S246 (WED-338)
 Paolini, Erika, S739 (WED-405), S744 (WED-413), S746 (WED-418), S772 (WED-459), S783 (WED-507), S802 (WED-547)
 Paolo Caviglia, Gian, S611 (THU-425), S617 (THU-435), S626 (THU-452), S637 (THU-470)
 Paolo Russo, Francesco, S90 (OS-127-YI)
 Paon, Veronica, S203 (FRI-558)
 Papachristoforou, Eleni, S749 (WED-422)
 Papachritoforou, Eleni, S39 (OS-044-YI)
 Papadimitriou, Dimitri, S1075 (WED-137)
 Papadopoulos, Nikolaos, S400 (WED-302), S1128 (WED-211), S1194 (THU-196)
 Papaluca, Tim, S306 (SAT-535)
 Papankorn, Kongnara, S809 (FRI-466)
 Papatheodoridi, Margarita, S52 (OS-065-YI), S337 (WED-243), S400 (WED-302), S475 (THU-514), S1128 (WED-211), S1132 (SAT-145), S1134 (SAT-148)
 Papatheodoridis, George, S52 (OS-065-YI), S107 (LBP-11), S400 (WED-302), S863 (SAT-125), S1128 (WED-211), S1132 (SAT-145), S1134 (SAT-148), S1137 (SAT-152)
 Pape, Simon, S14 (LBO-06)
 Pakiauri, Ana, S891 (FRI-136)
 Pappas, Chris, S296 (SAT-348)
 Papp, Maria, S23 (OS-017-YI), S42 (OS-047-YI), S579 (THU-123), S982 (THU-304)
 Pappo, Orit, S719 (SAT-500)
 Parada, Nelson Daniel Salazar, S268 (WED-372)
 Paradis, Valérie, S12 (LBO-04), S64 (OS-084-YI), S86 (OS-121-YI), S106 (LBP-10), S435 (SAT-358), S577 (THU-119), S670 (SAT-424), S672 (SAT-427), S681 (SAT-440), S776 (WED-467), S1093 (WED-159)
 Paragas, Nathaniel, S599 (THU-157)
 Parals, Ariadna Clos, S1192 (THU-192)
 Paramashivam, Ramya, S473 (THU-510)
 Parasar, Anupama, S212 (THU-343), S326 (WED-222), S348 (THU-234), S556 (SAT-267)
 Pardo, Albert, S903 (FRI-156), S915 (FRI-177)
 Pardo, Melissa Javiera Jerez, S840 (FRI-492)
 Pares, Albert, S56 (OS-073)
 Parewangi, Muhammad Luthfi, S1203 (THU-212)
 Parfieniuk-Kowerda, Anna, S505 (FRI-296), S1205 (THU-215)
 Pariente Zorrilla, Luis Eduardo, S705 (SAT-478), S706 (SAT-479)
 Parisse, Simona, S360 (FRI-383)
 Park, Boram, S117 (LBP-25)
 Park, Dan, S242 (WED-331)
 Park, Dongsik, S948 (THU-259)
 Park, Eok, S948 (THU-259)
 Parker, Richard, S153 (FRI-418), S157 (FRI-422), S179 (FRI-459), S182 (FRI-464), S708 (SAT-483)
 Park, Eun Jin, S758 (WED-437), S779 (WED-473)
 Park, Gaoul, S785 (WED-513)
 Park, Geun U, S1121 (WED-201)
 Park, Hee Chul, S117 (LBP-25)
 Park, Huiyul, S615 (THU-431), S667 (SAT-418), S695 (SAT-462), S701 (SAT-470), S704 (SAT-475), S757 (WED-435), S794 (WED-531)
 Park, Hye Jung, S362 (FRI-387), S552 (SAT-259)
 Park, Jeayeon, S1048 (FRI-268), S1062 (WED-120), S1144 (SAT-163)
 Park, Jeongwoo, S796 (WED-534)
 Park, Jin Joo, S414 (FRI-336), S752 (WED-427)
 Park, Ji Won, S192 (FRI-542)
 Park, Joong-Won, S117 (LBP-25), S586 (THU-134)
 Park, Juil, S506 (FRI-297)
 Park, Jung Gil, S645 (THU-558)
 Park, Junghoan, S506 (FRI-297)
 Park, Jun Yong, S362 (FRI-387), S552 (SAT-259), S595 (THU-148), S906 (FRI-162), S1121 (WED-201), S1134 (SAT-148)
 Park, Kanghee, S573 (THU-113)
 Park, Lauren, S792 (WED-527)
 Park, Man Young, S1078 (WED-139)
 Park, Mi-Hyun, S414 (FRI-336), S752 (WED-427)
 Park, Min Kyung, S610 (THU-423), S1048 (FRI-268), S1062 (WED-120), S1144 (SAT-163)
 Park, Se Yong, S778 (WED-471)
 Park, So Hyun, S508 (FRI-301)
 Park, Soo Young, S513 (FRI-312), S588 (THU-137)
 Park, Su Jung, S442 (SAT-369)
 Park, Suna, S977 (THU-296), S1007 (THU-385), S1008 (THU-386)
 Park, Sungjin, S817 (FRI-506)
 Park, Yeshong, S583 (THU-130)
 Park, Yewan, S606 (THU-417), S821 (FRI-514)
 Park, Young Joo, S588 (THU-137)
 Park, Young Nyun, S12 (LBO-04)
 Parlatti, Lucia, S68 (OS-092-YI), S161 (FRI-429), S656 (SAT-402)
 Parmar, Deven, S649 (TOP-080)
 Parmentier, Fleur, S445 (SAT-375)
 Parnham, Rosie, S177 (FRI-455)
 Parola, Maurizio, S526 (SAT-211), S766 (WED-449)

- Parouei, Fatemeh, S454 ([TOP-052](#))
 Parra-Robert, Marina, S325 ([WED-220](#))
 Parra, Viviana Barrientos, S840 ([FRI-492](#))
 Parruti, Giustino, S1122 ([WED-203](#))
 Parslow, Dominique, S389 ([WED-285](#))
 Parthasaradhy, Kumaraswamy, S207 ([THU-337](#))
 Pascale, Alina, S498 ([FRI-286](#))
 Pascher, Andreas, S484 ([THU-531](#))
 Pascual, Andrea González, S376 ([WED-264](#))
 Pascual, Manuel, S481 ([THU-526](#))
 Pascual, Sonia, S470 ([THU-503](#)), S481 ([THU-525](#)), S587 ([THU-136](#)), S883 ([FRI-126](#)), S1124 ([WED-205](#))
 Pascucci, Giuseppe Rubens, S1018 ([FRI-218](#))
 Pasculli, Giuseppe, S493 ([FRI-277](#))
 Pashtoun, Hasina, S46 ([OS-053-YI](#))
 Pasqua, Laura Giuseppina Di, S795 ([WED-533](#))
 Pasquazzi, Caterina, S1056 ([TOP-106](#)), S1122 ([WED-203](#))
 Passenberg, Moritz, S485 ([THU-534](#)), S1124 ([WED-206](#)), S1125 ([WED-207](#))
 Passigato, Nicola, S814 ([FRI-474](#))
 Passignani, Giulia, S733 ([WED-393](#)), S992 ([THU-318](#))
 Passos-Castilho, Ana Maria, S874 ([FRI-114](#))
 Pasta, Linda, S105 ([LBP-09](#))
 Pasto, Raul, S791 ([WED-524](#))
 Pastore, Mirella, S233 ([THU-371](#)), S536 ([SAT-229](#))
 Pastore, Nunzia, S346 ([THU-231](#))
 Pastor, Helena, S335 ([WED-240](#))
 Pastor, Oscar, S19 ([OS-011-YI](#))
 Pastor, Tania, S541 ([SAT-238](#))
 Pasula, Srikar, S417 ([FRI-350](#))
 Pasulo, Luisa, S54 ([OS-069](#)), S381 ([WED-272](#)), S471 ([THU-507](#)), S482 ([THU-527](#)), S1082 ([WED-146](#))
 Patch, David, S74 ([OS-103-YI](#)), S316 ([SAT-552](#)), S964 ([THU-283](#))
 Patel, Ahsan Shueb, S620 ([THU-440](#)), S817 ([FRI-507](#))
 Patel, Ankoor, S273 ([WED-380](#)), S312 ([SAT-545](#)), S623 ([THU-445](#)), S1011 ([THU-390](#))
 Patel, Ankur, S173 ([FRI-448](#))
 Patel, Bhaumik, S149 ([FRI-411](#))
 Patel, Hailey, S58 ([OS-075](#))
 Patel, Keyur, S314 ([SAT-548](#))
 Patel, Mahesh, S260 ([WED-358](#)), S809 ([FRI-466](#))
 Patel, Manish, S84 ([OS-119-YI](#))
 Patel, Neel, S31 ([OS-029](#))
 Patel, Poulam, S127 ([TOP-092](#))
 Patel, Roshni, S660 ([SAT-409](#)), S661 ([SAT-410](#)), S812 ([FRI-471](#))
 Patel, Sameer, S479 ([THU-521](#))
 Patel, Shray, S689 ([SAT-453](#))
 Patel, Sonal, S1202 ([THU-210](#))
 Patel, Vishal, S7 ([GS-007](#))
 Paternostro, Rafael, S201 ([FRI-554](#)), S244 ([WED-334](#)), S279 ([TOP-043](#)), S282 ([SAT-326](#)), S284 ([SAT-330](#)), S313 ([SAT-547](#))
 Pathak, Gaurav, S623 ([THU-445](#))
 Pathak, Piyush, S73 ([OS-101-YI](#)), S297 ([SAT-350](#))
 Pathil-Warth, Anita, S1147 ([TOP-110](#))
 Patil, Nilesh, S326 ([WED-222](#))
 Patiño, Verónica, S852 ([WED-489](#))
 Patmore, Lesley, S1100 ([WED-169](#))
 Patriarca, Francesca, S88 ([OS-124-YI](#))
 Patrizia, Carrieri, S114 ([LBP-21](#)), S627 ([THU-453](#)), S865 ([SAT-129](#))
 Patseas, Dimitrios, S77 ([OS-108-YI](#))
 Patterson, Scott, S31 ([OS-029](#))
 Paturel, Alexia, S1018 ([FRI-218](#))
 Patwardhan, Vilas, S56 ([OS-073](#)), S844 ([FRI-500](#))
 Patwa, Yashwi Haresh Kumar, S274 ([WED-382](#))
 Paul, Dirk, S606 ([THU-416](#))
 Paule, Lorena, S19 ([OS-011-YI](#))
 Pauling, Josch, S527 ([SAT-213](#))
 Paulissen, Jasmine, S1025 ([FRI-231](#))
 Paul, Sashi, S587 ([THU-135](#))
 Paulsen, Ida, S986 ([THU-311](#))
 Paulweber, Bernhard, S863 ([SAT-126](#))
 Pauly, Jana, S594 ([THU-147](#))
 Pauly, Matthew, S905 ([FRI-160](#))
 Pauw, Michel De, S307 ([SAT-538](#))
 Pavel, Vlad, S1003 ([THU-377](#))
 Pavenstaedt, Hermann, S185 ([FRI-341](#))
 Pavesi, Andrea, S543 ([SAT-241](#))
 Pavesi, Marco, S220 ([THU-355](#))
 Pavicevic, Sandra, S469 ([THU-502](#))
 Pavic, Magda Pletikosa, S880 ([FRI-122](#))
 Pavithran, K, S848 ([WED-481](#))
 Pavlova, Desislava, S198 ([FRI-550](#))
 Pavone, Luigi, S38 ([OS-042-YI](#))
 Pavone, Vincenzo, S88 ([OS-124-YI](#))
 Pawlischak, Piotr, S837 ([FRI-486](#))
 Pawlotsky, Jean-Michel, S12 ([LBO-04](#)), S456 ([THU-478](#)), S1106 ([WED-179](#)), S1109 ([WED-182](#))
 Pawlowska, Agnieszka Pawlowska, S327 ([WED-224](#))
 Payancé, Audrey, S86 ([OS-121-YI](#))
 Payo-Serafin, Tania, S554 ([SAT-263](#))
 Pazi, Swaleh, S865 ([SAT-129](#))
 Peccatori, Jacopo, S88 ([OS-124-YI](#))
 Pech, Maciej, S576 ([THU-118](#))
 Peck, Kyong Ran, S1048 ([FRI-268](#))
 Peck-Radosavljevic, Markus, S491 ([FRI-273](#))
 Pecoraro, Valentina, S729 ([SAT-517](#))
 Pecorella, Irene, S360 ([FRI-383](#))
 Pedersen, Julie Steen, S723 ([SAT-507](#))
 Pedersen, Kamilla, S801 ([WED-545](#))
 Pedica, Federica, S12 ([LBO-04](#))
 Pedrotti, Simona, S749 ([WED-423](#))
 Pedroza, Lourdes, S1202 ([THU-211](#))
 Peedikayil, Musthafa, S1006 ([THU-383](#))
 Peeters, Michael, S923 ([FRI-190](#)), S1114 ([WED-190](#))
 Pegram, Hannah, S1087 ([WED-151](#))
 Pehlivanov, Nonko, S31 ([OS-030](#))
 Peiffer, Kai-Henrik, S90 ([OS-126](#)), S185 ([FRI-341](#)), S313 ([SAT-546](#)), S1039 ([FRI-254](#)), S1042 ([FRI-259](#))
 Pei, Sun, S735 ([WED-399](#))
 Pelacho, Beatriz, S326 ([WED-223](#)), S560 ([SAT-275](#))
 Pelegrina, Amalia, S267 ([WED-370](#)), S273 ([WED-381](#))
 Peleman, Cédric, S764 ([WED-446](#))
 Pelizzaro, Filippo, S511 ([FRI-308](#))
 Pellicano, Rinaldo, S55 ([OS-070](#))
 Pellicelli, Adriano, S40 ([OS-045](#)), S55 ([OS-070](#)), S107 ([LBP-11](#)), S247 ([WED-340](#)), S994 ([THU-323](#)), S1122 ([WED-203](#))
 Pelloux, Hervé, S894 ([FRI-142](#))
 Peloso, Andrea, S24 ([OS-018-YI](#)), S531 ([SAT-220](#))
 Peltekian, Kevork, S426 ([FRI-363](#))
 Peltier, Sébastien, S806 ([WED-555](#))
 Pelton, Matthew, S1011 ([THU-390](#))
 Peltzer, Mona, S535 ([SAT-227](#))
 Pelusi, Serena, S500 ([FRI-288](#)), S535 ([SAT-227](#)), S661 ([SAT-410](#)), S669 ([SAT-422](#)), S733 ([WED-393](#)), S992 ([THU-318](#)), S1173 ([THU-165](#))
 Peña, Luis, S989 ([THU-315](#))
 Penaranda, Guillaume, S684 ([SAT-445](#))
 Peña-San Felix, Patricia, S546 ([SAT-247](#))
 Pencek, Richard, S386 ([WED-280](#))
 Peneranda, Guillaume, S834 ([FRI-481](#))
 Peng, Cheng-Yuan, S444 ([SAT-374](#)), S1083 ([WED-147](#)), S1180 ([THU-174](#)), S1206 ([THU-217](#))
 Peng, Emily, S675 ([SAT-432](#))
 Peng, Feng, S274 ([WED-382](#))
 Peng, Jiayi, S1143 ([SAT-161](#))
 Peng, Ming-Li, S271 ([WED-376](#)), S340 ([WED-250](#))
 Peng, Wei, S1152 ([SAT-173](#))
 Peng, Weng Chuan, S535 ([SAT-228](#))
 Peng, Wenhui, S1036 ([FRI-250](#))
 Peng, Yihong, S784 ([WED-510](#))
 Penicaud, Capucine, S875 ([FRI-115](#))
 Penners, Christian, S22 ([OS-015](#)), S416 ([FRI-348](#))
 Pennisi, Grazia, S500 ([FRI-288](#)), S609 ([THU-421](#)), S673 ([SAT-430](#)), S803 ([WED-549](#))
 Peñuelas, Marina, S902 ([FRI-153](#))
 Peppas, Danielle, S5 ([GS-005](#))
 Pera, Guillem, S664 ([SAT-415](#))
 Peralta, Peregrina, S474 ([THU-512](#))
 Pe, Rautou, S970 ([THU-290](#))
 perbellini, Riccardo, S12 ([LBO-04](#)), S1135 ([SAT-149](#)), S1142 ([SAT-159](#)), S1154 ([SAT-175](#)), S1159 ([SAT-181](#)), S1164 ([SAT-190](#))
 Perdiguero, Gonzalo Gomez, S245 ([WED-336](#))
 Perego, Alberto, S1170 ([SAT-199](#))
 Pereira, Juliana, S483 ([THU-530](#))
 Pereira, Luciano Beltrão, S483 ([THU-530](#))

Author Index

- Pereira, Sheila, S470 (THU-503)
Pereira, Stephen, S408 (WED-317)
Pereira, Vítor Magno, S85 (OS-120), S889 (FRI-134)
Perelló, Christie, S2 (GS-003), S272 (WED-378), S291 (SAT-340), S390 (WED-288), S579 (THU-124), S683 (SAT-443), S693 (SAT-460), S709 (SAT-484)
Perera, Thamara, S466 (THU-497)
Peretz, Asaf, S1195 (THU-199)
Pereyra, David, S44 (OS-050-YI), S45 (OS-051-YI), S465 (THU-495), S470 (THU-505), S489 (THU-545)
Perez, Adriana, S961 (THU-278)
Pérez, Ana, S683 (SAT-443)
Pérez, Beatriz Pillado, S697 (SAT-465), S706 (SAT-479)
Pérez-Bosque, Anna, S356 (THU-246)
Perez-Campuzano, Valeria, S970 (THU-290)
Perez, Carla Fiorella Murillo, S971 (THU-291)
Pérez-Carreón, Julio Isael, S151 (FRI-414), S160 (FRI-426)
Pérez, Clara, S989 (THU-315)
Perez, Cristian, S361 (FRI-384)
Pérez-del-Pulgar, Sofia, S1089 (WED-154)
Pérez Díaz del Campo, Nuria, S611 (THU-425), S617 (THU-435), S626 (THU-452), S637 (THU-470)
Perez, Elena Santos, S272 (WED-378)
Perez-Fernandez, Elia, S366 (TOP-061)
Pérez, Fernando García, S853 (WED-491)
Pérez Hernández, Francisco Andrés, S932 (FRI-206)
Perez-Hernandez, Francisco Javier, S893 (FRI-140)
Perez, Jaime, S385 (WED-279)
Pérez, Javier Fernandez, S932 (FRI-208)
Perez, Juan Manuel Minoz, S674 (SAT-431)
Pérez, Judith, S75 (OS-105), S682 (SAT-442)
Perez, Laura Marquez, S573 (THU-114)
Perez, Martina, S10 (LBO-01), S15 (OS-001), S158 (FRI-423), S163 (FRI-431), S166 (FRI-437), S250 (WED-343), S664 (SAT-415), S851 (WED-486)
Pérez-Palacios, Domingo, S1098 (WED-166)
Perez, Renata, S112 (LBP-16), S618 (THU-436)
Pérez-San-Gregorio, María Angeles, S632 (THU-462)
Perez, Sara Lorente, S133 (THU-404), S470 (THU-503), S573 (THU-114), S1187 (THU-183)
Perez, Valeria, S843 (FRI-499), S984 (THU-308)
Perez, Victor Perez, S894 (FRI-140)
Pericas, Juan M, S693 (SAT-460)
Pericas, Juan M., S349 (THU-235)
Pericàs, Juan M, S700 (SAT-468), S819 (FRI-509)
Pericàs, Juan Manuel, S279 (TOP-043), S780 (WED-474)
Pericoli, Filippo, S880 (FRI-121)
Perignon, Claire, S473 (THU-511)
Perini, Lisa, S407 (WED-315)
Perino, Alessia, S734 (WED-397)
Perisetti, Abhilash, S296 (SAT-349)
Periti, Giulia, S669 (SAT-422), S992 (THU-318)
Perno, Carlo Federico, S1103 (WED-174)
Peron, Jean Marie, S61 (OS-081)
Perramón, Meritxell, S325 (WED-220)
Perron, Michel, S1058 (WED-114), S1167 (SAT-195)
Persano, Mara, S592 (THU-143), S593 (THU-145)
Persico, Marcello, S713 (SAT-493), S789 (WED-521)
Pertler, Elke, S968 (THU-288)
Perucchini, Chiara, S5 (GS-005)
Perugorria, María Jesús, S28 (OS-024-YI), S57 (OS-074-YI), S527 (SAT-212)
Pervolaraki, Kalliopi, S1025 (FRI-231)
Pesatori, Eugenia Vittoria, S381 (WED-272)
Peschard, Simon, S355 (THU-244)
Peschka, Manuela, S527 (SAT-213)
Pesole, Letizia, S493 (FRI-277)
Pesquet, Jean Christophe, S64 (OS-084-YI)
Pessaux, Patrick, S72 (OS-098), S541 (SAT-237)
Pession, Andrea, S88 (OS-124-YI)
Pessoa, Mário, S900 (FRI-151)
Pestana, Madalena, S889 (FRI-134)
Peta, Valentina, S106 (LBP-10)
Petersen, Jörg, S1147 (TOP-110), S1174 (THU-166)
Peters, Erica, S925 (FRI-194)
Peter, Simon, S12 (LBO-04), S561 (SAT-277)
Petitjean, Louis, S327 (WED-224), S335 (WED-240), S651 (SAT-394), S715 (SAT-496), S805 (WED-553), S1197 (THU-201)
Petitjean, Mathieu, S327 (WED-224), S335 (WED-240), S651 (SAT-394), S715 (SAT-496), S805 (WED-553), S1197 (THU-201)
Petit, Jean-Michel, S603 (THU-410)
Petit, Stéphanie, S668 (SAT-421)
Petkeviciene, Janina, S912 (FRI-173)
Petra, Fischer, S151 (FRI-413), S295 (SAT-347), S297 (SAT-519)
Petralli, Giovanni, S691 (SAT-456)
Petrenko, Oleksander, S936 (TOP-055)
Petrenko, Oleksandr, S19 (OS-010-YI), S939 (TOP-058)
Petrić, Miha, S553 (SAT-261)
Petrillo, Angelica, S942 (THU-251)
Petrivna, Tsarynna, S9 (GS-012)
Petroff, David, S1090 (WED-156), S1176 (THU-168)
Petroni, Maria Letizia, S640 (THU-475), S673 (SAT-430)
Petros, Sirak, S201 (FRI-555)
Petrtyl, Jaromir, S292 (SAT-341)
Petrucci, Lucrezia, S660 (SAT-409)
Petrushev, Bobe, S295 (SAT-347)
Petta, Salvatore, S500 (FRI-288), S607 (THU-418), S609 (THU-421), S651 (SAT-394), S673 (SAT-430), S774 (WED-462), S803 (WED-549)
Pettinato, Mariateresa, S749 (WED-423), S774 (WED-461)
Pett, Sarah, S721 (SAT-504), S1122 (WED-202)
Pezzato, Francesco, S407 (WED-315)
Pezzica, Samantha, S605 (THU-415), S611 (THU-425)
Pfefferkorn, Maria, S1043 (FRI-260), S1050 (FRI-270)
Pfeifer, Bernhard, S961 (THU-279), S968 (THU-288)
Pfeiffenberger, Jan, S594 (THU-147)
Pfuhler, Liva, S417 (FRI-350)
Pham, Huong, S600 (TOP-081), S673 (SAT-428)
Pham, Toan, S937 (TOP-056)
Phan, Minh, S197 (FRI-549), S469 (THU-502)
Phen, Samuel, S575 (THU-116), S582 (THU-128), S586 (THU-134)
Philipp, Alexander, S596 (THU-150)
Philippart, Marie, S464 (THU-493), S923 (FRI-190)
Philips, Gino, S48 (OS-059-YI), S452 (SAT-390), S524 (TOP-066)
Phillips, Alexandra, S203 (FRI-557)
Phillips, Sandra, S324 (WED-218)
Phillips, Sheree, S852 (WED-488)
Philo, Mark, S434 (SAT-356)
Pianko, Stephen, S860 (SAT-121)
Piano, Filomena Del, S797 (WED-535)
Piano, Salvatore, S10 (LBO-01), S185 (FRI-341), S237 (WED-320), S250 (WED-343), S253 (WED-348), S865 (SAT-129)
Picalausa, Corinne, S772 (WED-458)
Picardi, Antonio, S36 (OS-036), S665 (SAT-416)
Picariello, Lucia, S545 (SAT-245)
Picchio, Camila, S875 (FRI-115), S924 (FRI-192), S1191 (THU-190)
Picchio, Gaston, S1171 (SAT-202)
Piccinelli, Sara, S920 (FRI-185)
Piccoli, David A., S971 (THU-291)
Piche, Julia, S730 (TOP-084)
Pich, Judit, S10 (LBO-01)
Pichlmair, Andreas, S945 (THU-256)
Piciotti, Roberto, S783 (WED-507), S802 (WED-547), S803 (WED-549)
Piecha, Felix, S285 (SAT-331)
Piermatteo, Lorenzo, S1056 (TOP-106), S1072 (WED-133), S1103 (WED-174), S1105 (WED-176), S1122 (WED-203), S1142 (SAT-159)
Pierre, Tim St, S983 (THU-306)
Piessevaux, Hubert, S923 (FRI-190)
Pieter, Honkoop, S1100 (WED-169)
Pietrangelo, Antonello, S1105 (WED-176)
Pietrobbattista, Andrea, S966 (THU-285), S987 (THU-313)

- Pietschmann, Thomas, S447 ([SAT-379](#))
Pigozzi, Marie Graciella, S1173 ([THU-165](#))
Pihlajamaki, Jussi, S803 ([WED-549](#))
Pihlajoki, Marjut, S997 ([THU-329](#))
Pik, Jason, S300 ([SAT-522](#))
Pilarczyk-Zurek, Magdalena, S431 ([FRI-370](#))
Pileri, Francesca, S107 ([LBP-11](#))
Pillai, Anjana, S586 ([THU-134](#))
Pilone, Vincenzo, S789 ([WED-521](#))
Pinato, David J., S12 ([LBO-04](#)), S491 ([FRI-273](#)), S505 ([FRI-295](#)), S575 ([THU-116](#)), S582 ([THU-128](#)), S586 ([THU-134](#))
Pineda, Abraham Ramos, S274 ([WED-382](#))
Pineda, Antonio A, S537 ([SAT-232](#))
Pineda, Juan, S921 ([FRI-188](#))
Pinelli, Domenico, S471 ([THU-507](#))
Piñero, Federico, S103 ([LBP-07](#)), S865 ([SAT-129](#))
Pino, Belen, S302 ([SAT-526](#)), S654 ([SAT-400](#))
Pinta, Martine Naranjo, S762 ([WED-442](#))
Pinter, Matthias, S12 ([LBO-04](#)), S37 ([OS-039-YI](#)), S201 ([FRI-554](#)), S286 ([SAT-332](#)), S451 ([SAT-388](#)), S491 ([FRI-273](#)), S498 ([FRI-285](#)), S505 ([FRI-295](#)), S575 ([THU-116](#)), S579 ([THU-123](#)), S582 ([THU-128](#)), S586 ([THU-134](#))
Pinto, Elisa, S511 ([FRI-308](#))
Pinto, Inês Vaz, S902 ([FRI-154](#))
Pinto, Jorge Eduardo, S618 ([THU-436](#))
Pinto, Raquel Borges, S971 ([THU-291](#))
Pinyol, Roser, S48 ([OS-059-YI](#))
Pinzani, Massimo, S337 ([WED-243](#)), S415 ([FRI-345](#)), S985 ([THU-310](#))
Piombanti, Benedetta, S233 ([THU-371](#)), S536 ([SAT-229](#)), S774 ([WED-462](#))
Piou, Daphnee, S58 ([OS-075](#))
Piper Hanley, Karen, S71 ([OS-097](#)), S84 ([OS-119-YI](#))
Pipitone, Rosaria, S774 ([WED-462](#))
Pipitone, Rosaria Maria, S803 ([WED-549](#))
Piqué-Gili, Marta, S48 ([OS-059-YI](#))
Pirani, Tasneem, S479 ([THU-521](#))
Piratvisuth, Teerha, S110 ([LBP-15](#)), S506 ([FRI-298](#)), S507 ([FRI-300](#)), S1134 ([SAT-148](#))
Pires, Ananda Staats, S263 ([WED-364](#))
Pires, Marcia Maria Amendola, S1188 ([THU-184](#))
Pirisi, Mario, S389 ([WED-284](#)), S586 ([THU-134](#)), S599 ([THU-156](#))
Pirola, Carlos, S625 ([THU-448](#))
Pironi, Loris, S640 ([THU-475](#)), S673 ([SAT-430](#))
Pirozzi, Claudio, S797 ([WED-535](#)), S800 ([WED-542](#))
Pisano, Giuseppina, S722 ([SAT-506](#)), S814 ([FRI-474](#))
Pisapia, Pasquale, S942 ([THU-251](#))
Piscaglia, Fabio, S499 ([FRI-287](#)), S571 ([TOP-067](#)), S584 ([THU-131](#)), S592 ([THU-143](#)), S593 ([THU-145](#)), S597 ([THU-153](#))
Pischke, Sven, S1032 ([FRI-244](#))
Piscopo, Fabiola, S942 ([THU-251](#))
Pistorio, Valeria, S38 ([OS-042-YI](#)), S339 ([WED-247](#))
Pitova, Veronika, S1173 ([THU-164](#))
Pittaluga, Fabrizia, S917 ([FRI-180](#)), S1177 ([THU-169](#)), S1200 ([THU-206](#))
Pivert, Adeline, S897 ([FRI-146](#))
Pivetta, Stephanie, S500 ([FRI-288](#))
Pivetti, Alessandra, S495 ([FRI-280](#))
Pizaño, Mariana Yazmin Medina, S337 ([WED-244](#))
Pizzirani, Enrico, S293 ([SAT-343](#))
Pizzolante, Fabrizio, S40 ([OS-045](#)), S55 ([OS-070](#))
Placed, Cristina, S616 ([THU-432](#)), S670 ([SAT-425](#)), S676 ([SAT-433](#))
Plagiannakos, Christina, S373 ([WED-259](#))
Plahuta, Irena, S553 ([SAT-261](#))
Plaksin, Daniel, S1119 ([WED-197](#))
Plamper, Andreas, S712 ([SAT-492](#))
Planas, Jose María Moreno, S964 ([THU-282](#)), S1098 ([WED-166](#)), S1178 ([THU-171](#))
Planell, Nuria, S290 ([SAT-337](#))
Planell, Núria, S143 ([FRI-404](#))
Plank, Christian, S1040 ([FRI-256](#))
Platon, Monica, S295 ([SAT-347](#))
Plaza, Francisco Jorquera, S921 ([FRI-188](#))
Plein, Helene, S110 ([LBP-15](#))
Plešnik, Boštjan, S553 ([SAT-261](#))
Plessier, Aurélie, S86 ([OS-121-YI](#)), S970 ([THU-290](#)), S975 ([THU-295](#))
Plettinckx, Els, S880 ([FRI-121](#))
Plissonnier, Marie-Laure, S101 ([LBP-04](#)), S118 ([LBP-27](#)), S1014 ([TOP-104](#)), S1046 ([FRI-265](#)), S1058 ([WED-113](#)), S1170 ([SAT-199](#))
Plo, Isabel, S915 ([FRI-177](#))
Plonowski, Artur, S139 ([FRI-397](#)), S829 ([FRI-528](#))
Poca, Maria, S73 ([OS-100-YI](#))
Pocha, Christine, S242 ([WED-330](#))
Poche, Marguerite, S173 ([FRI-448](#))
Poch, Tobias, S60 ([OS-079-YI](#)), S450 ([SAT-385](#))
Pocurull, Anna, S90 ([OS-127-YI](#)), S135 ([THU-406](#)), S299 ([SAT-521](#)), S405 ([WED-311](#)), S885 ([FRI-128](#))
Poda, Armel, S930 ([FRI-202](#))
Pofi, Riccardo, S731 ([TOP-089](#))
Pogany, Katalin, S892 ([FRI-138](#))
Poggi, Francesca, S471 ([THU-507](#))
Poggi, Guido, S40 ([OS-045](#)), S55 ([OS-070](#))
Poggiolini, Irene, S521 ([FRI-325](#)), S617 ([THU-435](#)), S626 ([THU-452](#)), S637 ([THU-470](#)), S713 ([SAT-494](#))
Poggio, Paolo Del, S1173 ([THU-165](#))
Poiré, Xavier, S923 ([FRI-190](#))
Poisa, Paolo, S40 ([OS-045](#)), S55 ([OS-070](#))
Polak, Wojciech, S46 ([OS-053-YI](#)), S454 ([TOP-052](#))
Polanco, Prido, S689 ([SAT-453](#))
Polat, Esra, S969 ([THU-289](#))
Pollarsky, Florencia, S865 ([SAT-129](#))
Pollicino, Teresa, S457 ([THU-481](#))
Pollmanns, Maike Rebecca, S188 ([FRI-534](#))
Pollock, Richard, S857 ([SAT-116](#))
Pol, Stanislas, S52 ([OS-066](#)), S61 ([OS-080-YI](#)), S106 ([LBP-10](#)), S107 ([LBP-11](#)), S161 ([FRI-429](#)), S498 ([FRI-286](#)), S656 ([SAT-402](#)), S859 ([SAT-120](#)), S1161 ([SAT-185](#))
Polvani, Simone, S545 ([SAT-245](#)), S550 ([SAT-254](#))
Pomej, Katharina, S244 ([WED-334](#)), S282 ([SAT-326](#)), S313 ([SAT-547](#)), S491 ([FRI-273](#)), S498 ([FRI-285](#)), S505 ([FRI-295](#))
Pompili, Enrico, S10 ([LBO-01](#)), S191 ([FRI-540](#)), S237 ([WED-320](#))
Pompili, Maurizio, S36 ([OS-036](#)), S40 ([OS-045](#)), S55 ([OS-070](#)), S88 ([OS-124-YI](#)), S252 ([WED-347](#)), S578 ([THU-122](#))
Ponce-Alonso, Manuel, S19 ([OS-011-YI](#))
Poniachik, Jaime, S396 ([WED-295](#))
Ponnaiah, Maharajah, S652 ([SAT-396](#))
Ponsioen, Cyriel, S408 ([WED-317](#))
Pons, Monica, S2 ([GS-003](#)), S85 ([OS-120](#)), S90 ([OS-127-YI](#)), S299 ([SAT-521](#)), S533 ([SAT-224](#)), S963 ([THU-281](#))
Ponsolles, Clara, S72 ([OS-098](#))
Pontisso, Patrizia, S766 ([WED-449](#))
Ponziani, Francesca, S40 ([OS-045](#)), S54 ([OS-069](#)), S55 ([OS-070](#)), S578 ([THU-122](#)), S981 ([THU-302](#))
Ponziani, Francesca Romana, S252 ([WED-347](#))
Pooja, Devan, S1204 ([THU-213](#))
Poovorawan, Kittiyod, S919 ([FRI-184](#))
Popescu, Alina, S61 ([OS-080-YI](#))
Popovici, Odette, S880 ([FRI-121](#))
Popovic, Vlad, S1119 ([WED-197](#))
Porayko, Michael, S101 ([LBP-03](#))
Porcu, Carmen, S1082 ([WED-146](#))
Porcu, Cristiana, S218 ([THU-352](#))
Porras, José Luis Martínez, S8 ([GS-009](#)), S272 ([WED-378](#)), S291 ([SAT-340](#)), S683 ([SAT-443](#))
Pors, Susanne, S530 ([SAT-218](#)), S746 ([WED-417](#)), S800 ([WED-543](#))
Porta, Gilda, S123 ([LBP-35](#)), S387 ([WED-282](#))
Porteiro, Begonia, S326 ([WED-223](#)), S560 ([SAT-275](#))
Portella, Giuseppe, S903 ([FRI-155](#))
Porte, Robert, S454 ([TOP-052](#))
Portero, Francisco Javier Pamplona, S924 ([FRI-192](#))
Port, Kerstin, S90 ([OS-126](#)), S1101 ([WED-171](#)), S1137 ([SAT-152](#)), S1139 ([SAT-156](#))
Portlock, Theo, S7 ([GS-007](#))
Portone, Greta, S719 ([SAT-501](#))

Author Index

- Pose, Elisa, S10 ([LBO-01](#)), S15 ([OS-001](#)), S158 ([FRI-423](#)), S163 ([FRI-431](#)), S166 ([FRI-437](#)), S171 ([FRI-445](#)), S250 ([WED-343](#)), S664 ([SAT-415](#)), S851 ([WED-486](#))
- Pospiech, Josef, S628 ([THU-454](#))
- Possamai, Lucia, S77 ([OS-108-YI](#)), S214 ([THU-345](#))
- Posselt, Mathias, S163 ([FRI-432](#))
- Poujol-Robert, Armelle, S86 ([OS-121-YI](#))
- Poulard, Severine, S598 ([THU-154](#))
- Poulin, Sebastien, S1115 ([WED-191](#))
- Poulsen, Peter Bo, S614 ([THU-429](#))
- Poumpouridou, Effimia, S465 ([THU-494](#))
- Poupel, Lucie, S27 ([OS-023-YI](#))
- Pouriki, Sophia, S978 ([THU-298](#))
- Powell, Elizabeth, S239 ([WED-324](#)), S846 ([WED-478](#))
- Poynard, Thierry, S106 ([LBP-10](#))
- Poza, Joaquin, S697 ([SAT-465](#)), S705 ([SAT-478](#)), S706 ([SAT-479](#))
- Pozo, Francisco, S902 ([FRI-153](#))
- Pozo-Morales, Macarena, S735 ([WED-398](#))
- Pozzoni, Pietro, S40 ([OS-045](#)), S55 ([OS-070](#)), S105 ([LBP-09](#))
- Pradat, Pierre, S876 ([FRI-117](#))
- Praestholm, Stine Marie, S741 ([WED-409](#))
- Praetorius, Alejandro González, S1028 ([FRI-236](#)), S1032 ([FRI-245](#))
- Praharaj, Dibya Lochan, S274 ([WED-382](#))
- Praktiknjo, Michael, S61 ([OS-080-YI](#)), S87 ([OS-123-YI](#)), S185 ([FRI-341](#)), S229 ([THU-366](#)), S279 ([TOP-043](#)), S313 ([SAT-546](#)), S484 ([THU-531](#)), S970 ([THU-290](#))
- Prampolini, Francesco, S287 ([SAT-334](#))
- Prasad, Mona, S913 ([FRI-174](#))
- Prasad, Preethy, S612 ([THU-426](#))
- Prasad, Shubham, S401 ([WED-304](#))
- Prati, Daniele, S500 ([FRI-288](#)), S669 ([SAT-422](#)), S733 ([WED-393](#)), S992 ([THU-318](#)), S1173 ([THU-165](#))
- Prat, Laura Iogna, S660 ([SAT-409](#)), S661 ([SAT-410](#)), S812 ([FRI-471](#))
- Pratley, Richard E., S607 ([THU-419](#))
- Pratschke, Johann, S469 ([THU-502](#))
- Pratt, Daniel, S388 ([WED-283](#))
- Pravisani, Riccardo, S435 ([SAT-358](#))
- Preciado, María Victoria, S1037 ([FRI-251](#))
- Preiser, Wolfgang, S1108 ([WED-181](#))
- Preisinger, Christian, S951 ([THU-264](#))
- Presa, José, S366 ([TOP-061](#)), S592 ([THU-143](#)), S593 ([THU-145](#))
- Presnell, Brett, S1182 ([THU-175](#))
- Pressiani, Tiziana, S499 ([FRI-287](#)), S575 ([THU-116](#)), S586 ([THU-134](#)), S597 ([THU-153](#))
- Preston, Benjamin, S719 ([SAT-501](#))
- Prete, Arcangelo, S88 ([OS-124-YI](#))
- Prezioso, Lucia, S88 ([OS-124-YI](#))
- Price, Jennifer, S612 ([THU-427](#)), S913 ([FRI-174](#))
- Price, Jillian, S673 ([SAT-428](#)), S861 ([SAT-122](#))
- Prier Lindvig, Katrine, S175 ([FRI-452](#))
- Prieto, Jhon, S496 ([FRI-282](#))
- Prieto, Martin, S921 ([FRI-188](#)), S1124 ([WED-205](#))
- Prieto-Ortiz, Jhon, S83 ([OS-118](#))
- Prieto-Ortiz, Robin G, S83 ([OS-118](#))
- Primignani, Massimo, S87 ([OS-123-YI](#)), S279 ([TOP-043](#))
- Prince, Khaled, S1212 ([THU-224](#))
- Princen, Hans, S805 ([WED-553](#))
- Prinz, Immo, S1031 ([FRI-242](#))
- Pritchett, James, S71 ([OS-097](#))
- Procaccini, Nicholas, S378 ([WED-267](#)), S379 ([WED-268](#))
- Procopet, Bogdan, S86 ([OS-121-YI](#)), S87 ([OS-123-YI](#)), S151 ([FRI-413](#)), S178 ([FRI-457](#)), S245 ([WED-337](#)), S279 ([TOP-043](#)), S295 ([SAT-347](#)), S297 ([SAT-519](#)), S975 ([THU-295](#))
- Prodram, Flavia, S804 ([WED-551](#))
- P Rodrigues, Cecília M., S734 ([WED-397](#))
- Proels, Markus, S403 ([WED-307](#))
- Pronicki, Maciej, S837 ([FRI-486](#)), S950 ([THU-262](#))
- Prosper, Felipe, S526 ([TOP-072](#))
- Prospero, Nicholas Di, S819 ([FRI-509](#))
- Prost, Adrien Ardavan, S170 ([FRI-443](#))
- Protopapa, Francesca, S766 ([WED-449](#))
- Protopapas, Adonis, S400 ([WED-302](#))
- Protopopescu, Camelia, S68 ([OS-092-YI](#))
- Protzer, Ulrike, S33 ([OS-032](#)), S59 ([OS-077](#)), S945 ([THU-256](#)), S1023 ([FRI-227](#)), S1026 ([FRI-233](#)), S1040 ([FRI-256](#))
- Prouvost-Keller, Bernard, S1160 ([SAT-184](#))
- Provenghi, David, S688 ([SAT-451](#))
- Provera, Alessia, S751 ([WED-425](#)), S804 ([WED-551](#))
- Provost, Nicolas, S776 ([WED-467](#))
- Prpic, Jelena, S1053 ([SAT-143](#))
- Prudence, Alexander, S274 ([WED-382](#))
- Psychos, Nikolaos, S1128 ([WED-211](#))
- Ptohis, Nikolaos, S595 ([THU-149](#))
- Puelles, Victor, S60 ([OS-079-YI](#))
- Puente, Angela, S87 ([OS-123-YI](#)), S279 ([TOP-043](#)), S970 ([THU-290](#))
- Puga, Natalia Fernández, S272 ([WED-378](#)), S291 ([SAT-340](#)), S683 ([SAT-443](#))
- Puglia, Victor, S682 ([SAT-442](#))
- Pugliese, Nicola, S609 ([THU-421](#)), S1173 ([THU-165](#))
- Puigvehí, Marc, S267 ([WED-370](#)), S273 ([WED-381](#))
- Pujalwar, Shashank, S282 ([SAT-325](#)), S290 ([SAT-338](#))
- Pujol, Claudia, S73 ([OS-100-YI](#)), S164 ([FRI-433](#)), S171 ([FRI-445](#))
- Pulaski, Hanna, S31 ([OS-029](#))
- Pulwermacher, Philippe, S170 ([FRI-442](#))
- Pungwe, Prisca, S173 ([FRI-448](#))
- Puoti, Massimo, S107 ([LBP-11](#)), S907 ([FRI-164](#)), S920 ([FRI-185](#)), S1103 ([WED-174](#)), S1105 ([WED-176](#))
- Purcell, Lisa A., S1147 ([TOP-109](#))
- Puri, Puneet, S37 ([OS-038](#)), S149 ([FRI-411](#))
- Purrsell, Huw, S84 ([OS-119-YI](#))
- Puschnik, Andreas, S1026 ([FRI-233](#)), S1147 ([TOP-109](#))
- Pusch, Stefan, S547 ([SAT-248](#))
- Putignano, Antonella, S621 ([THU-442](#))
- Putnina, Renate, S880 ([FRI-121](#))
- Puustinen, Lauri, S370 ([WED-253](#))
- Pydyn, Natalia, S332 ([WED-233](#)), S431 ([FRI-370](#))
- Pyrasopoulos, Nikolaos T., S275 ([WED-383](#)), S280 ([TOP-045](#))
- Qadir, Madiha, S842 ([FRI-497](#))
- Qadri, Sami, S803 ([WED-549](#))
- Qian, Junbin, S524 ([TOP-066](#))
- Qian, Shuwen, S347 ([THU-232](#))
- Qian, Yunsong, S34 ([OS-033](#))
- Qian, Zhiping, S196 ([FRI-547](#))
- Qin, Changjiang, S488 ([THU-540](#))
- Qin, Shukui, S9 ([GS-011](#)), S574 ([THU-115](#)), S580 ([THU-125](#))
- Qi, Tingting, S202 ([FRI-556](#))
- Qiu, Mei, S1076 ([WED-138](#)), S1157 ([SAT-179](#))
- Qiu, Tian Yu, S199 ([FRI-552](#))
- Qiu, Tianyu, S257 ([WED-353](#)), S278 ([WED-389](#)), S658 ([SAT-406](#)), S703 ([SAT-473](#))
- Qiu, Xiao, S1156 ([SAT-178](#))
- Qiu, Yuanwang, S395 ([WED-294](#)), S638 ([THU-471](#)), S696 ([SAT-463](#)), S724 ([SAT-510](#)), S1068 ([WED-127](#)), S1110 ([WED-184](#))
- Qi, Wenying, S153 ([FRI-417](#))
- Qi, Xiaolong, S286 ([SAT-333](#))
- Qi, Yonghe, S117 ([LBP-24](#))
- Quack, Thomas, S339 ([WED-248](#))
- Quaglia, Alberto, S70 ([OS-095-YI](#)), S129 ([THU-396](#)), S383 ([WED-276](#))
- Quang, Erwan Vo, S67 ([OS-090-YI](#)), S1106 ([WED-178](#)), S1106 ([WED-179](#))
- Quaranta, Maria Giovanna, S1082 ([WED-146](#))
- Quarta, Santina, S766 ([WED-449](#))
- Queck, Alexander, S484 ([THU-531](#))
- Quer, Josep, S1024 ([FRI-228](#))
- Quezada, Julissa Lombardo, S865 ([SAT-129](#))
- Quiambao, Ronald, S674 ([SAT-431](#))
- Quicquaro, Adam, S958 ([THU-274](#)), S985 ([THU-309](#))
- Quinlan, Jonathan, S231 ([THU-368](#)), S232 ([THU-370](#))
- Quinn, Geoff, S110 ([LBP-15](#)), S1154 ([SAT-176](#)), S1162 ([SAT-187](#))
- Quinn, Nessa, S16 ([OS-004](#)), S850 ([WED-484](#)), S1211 ([THU-223](#))
- Quiñones, Marta, S171 ([FRI-445](#))
- Quiñones, Raisa, S852 ([WED-489](#))
- Quintans, Nerea, S376 ([WED-264](#)), S380 ([WED-270](#))
- Quintas, Ana, S732 ([TOP-090](#))
- Quirk, Erin, S659 ([SAT-407](#))

- Quiros-Roldan, Eugenia, S907 (FRI-164)
 Quiros-Tejeira, Ruben E., S971 (THU-291)
 Quitt, Oliver, S1023 (FRI-227)
 Qumosani, Karim, S426 (FRI-363)
 Quraishi, Nabil, S123 (LBP-36), S368 (WED-251)
 Qurashi, Maria, S864 (SAT-127)
 Qureshi, Huma, S904 (FRI-157), S912 (FRI-172), S926 (FRI-195)
 Qu, Xiaoye, S453 (SAT-391), S730 (TOP-086)
- Rababoc, Razvan, S277 (WED-386), S819 (FRI-510), S1193 (THU-193)
 Rabinowich, Liane, S243 (WED-333), S274 (WED-382)
 Raboisson, Pierre, S1051 (FRI-272)
 Rachynska, Ivanna, S712 (SAT-490)
 Racila, Andrei, S627 (THU-453), S673 (SAT-428), S863 (SAT-125)
 Rac, Marek, S871 (SAT-136)
 Rada, Patricia, S777 (WED-468)
 Radchenko, Anastasiia, S767 (WED-451)
 Rademacher, Laura, S960 (THU-277)
 Rademacher, Sebastian, S483 (THU-529)
 Radenkovic, Silvia, S452 (SAT-390)
 Radenne, Sylvie, S62 (OS-083-YI), S467 (THU-498)
 Rad, Roland, S1026 (FRI-233)
 Radtke, Christine, S739 (WED-405), S746 (WED-418)
 Radu, Codruta, S277 (WED-386)
 Radu, Corina, S151 (FRI-413), S297 (SAT-519)
 Radu, Iuliana Pompilia, S491 (FRI-273)
 Radu, Monica, S1137 (SAT-152)
 Radu, Pompilia, S12 (LBO-04)
 Radwan, Ahmed, S1212 (THU-224)
 Raeven, Pierre, S465 (THU-494)
 Raevens, Sarah, S307 (SAT-538)
 Raffa, Giuseppina, S457 (THU-481)
 Raggi, Chiara, S536 (SAT-229)
 Ragone, Enrico, S36 (OS-036)
 Rahaman, Syed Mushfiqur, S942 (THU-252)
 Rahematpura, Suditi, S274 (WED-382)
 Rahimi, Robert, S275 (WED-383)
 Rahim, Mussarat, S36 (OS-037)
 Rahman, Naheeda, S726 (SAT-512)
 Rahnenführer, Jörg, S778 (WED-470)
 Raimondo, Giovanni, S457 (THU-481)
 Rajalingam, Rajesh, S488 (THU-544)
 Rajamani, Lakshminarayanan, S208 (THU-338)
 Rajan, Vijayraghavan, S182 (TOP-040)
 Rajborirug, Songyos, S1052 (SAT-141)
 Rajcic, Dragana, S152 (FRI-415)
 rajdev, Bishal, S560 (SAT-274)
 Rajender Reddy, K., S468 (THU-499)
 Rajoriya, Neil, S87 (OS-123-YI), S157 (FRI-422), S195 (FRI-546)
 Rajot, Amélie, S603 (THU-410)
 Rajovic, Nina, S870 (SAT-135)
 Rajwana, Yasir, S183 (FRI-339)
 Rajwanshi, Vivek, S548 (SAT-251), S1029 (FRI-239)
- Rakké, Yannick, S561 (SAT-276)
 Ramachandran, Hemalatha, S473 (THU-510), S488 (THU-544)
 Ramachandran, Prakash, S39 (OS-044-YI), S749 (WED-422)
 Ramachandran, Sumathi, S891 (FRI-136)
 Ramadan, Ahmed, S570 (SAT-291)
 Ramadan, Sameh, S1212 (THU-224)
 Ramakrishna, Gayatri, S218 (THU-351), S556 (SAT-267), S1027 (FRI-235), S1047 (FRI-267)
 Ramakrishnan, Shashank, S129 (THU-396)
 Raman, Aria, S689 (SAT-453)
 Ramier, Clémence, S68 (OS-092-YI)
 Ramirez, Carlos, S33 (OS-032)
 Ramirez, Carolina, S900 (FRI-151)
 Ramirez, Ricardo, S35 (OS-034)
 Ramirez, Wagner, S865 (SAT-129), S900 (FRI-151)
 Ramji, Alnoor, S675 (SAT-432), S883 (FRI-125), S886 (FRI-130), S900 (FRI-151), S1115 (WED-191), S1117 (WED-194), S1200 (THU-207)
 Ramlakhan, David, S1075 (WED-137)
 Ramm, Grant, S983 (THU-306), S1011 (THU-389)
 Ramm, Louise, S983 (THU-306), S1011 (THU-389)
 Ramon Gil, Erik, S542 (SAT-239), S565 (SAT-284)
 Ramón, Gracián Camps, S1024 (FRI-228)
 Ramos, Ana Laserna, S928 (FRI-198)
 Ramos, David Fernández, S326 (WED-223), S736 (WED-400)
 Ramos, Maria Jimenez, S601 (TOP-082)
 Rampally, Sai Prasanth, S86 (OS-121-YI)
 Rana, Abbas, S472 (THU-508)
 Ranagan, Jane, S627 (THU-453)
 Rana, Randeep, S233 (TOP-041)
 Rana, Rashmi, S414 (FRI-344)
 Rancatore, Gabriele, S592 (THU-144), S1111 (WED-186), S1118 (WED-196)
 Randall, Jonathan, S489 (TOP-065)
 Rand, Elizabeth B., S971 (THU-291)
 Randhawa, Amarita, S647 (TOP-074), S809 (FRI-467), S823 (FRI-516)
 Rando-Segura, Ariadna, S896 (FRI-144), S904 (FRI-158), S917 (FRI-181), S924 (FRI-192), S1024 (FRI-228), S1082 (WED-145), S1089 (WED-154)
 Randrianarisoa, Mialy, S168 (FRI-440)
 Rangan, Pooja, S458 (THU-482), S463 (THU-490), S611 (THU-424)
 Ranieri, Luisa, S903 (FRI-155)
 Rao, Ankit, S127 (TOP-092)
 Rao, Huiying, S34 (OS-033), S759 (WED-438), S862 (SAT-124), S1163 (SAT-189)
 Rao, Nagashree Gundu, S614 (THU-430), S673 (SAT-428)
 Rao, Nikita, S517 (FRI-319)
 Rao, Pooja, S228 (THU-362), S357 (THU-248)
 Rao, Sudha, S671 (SAT-426)
- Rao, Vikram, S322 (WED-215)
 Rao, Zhuqing, S455 (THU-477), S540 (SAT-236)
 Rapaccini, Gianludovico, S723 (SAT-508)
 Rasheed, Tazeen, S319 (SAT-557)
 Rashidi-Alavijeh, Jassin, S485 (THU-534)
 Rashu, Elias, S702 (SAT-471), S742 (WED-411), S748 (WED-421), S784 (WED-511)
 Rasines, Laura, S709 (SAT-484)
 Rasmussen, Allan, S841 (FRI-494)
 Rasmussen, Ditlev, S17 (OS-005-YI)
 Rasmussen, Ditlev Nytoft, S61 (OS-080-YI)
 Rasmussen, Henrik, S343 (THU-225)
 Raso, Giuseppina Mattace, S797 (WED-535)
 Rastogi, Archana, S207 (THU-337), S212 (THU-343), S953 (THU-266)
 Rastovic, Una, S324 (WED-218)
 Rasulova, Madina, S1025 (FRI-231)
 Rasyid, Haerani, S1203 (THU-212)
 Raszeja-Wyszomirska, Joanna, S42 (OS-047-YI), S400 (WED-301)
 Rath, Pravin, S405 (WED-312), S643 (THU-553)
 Rattanachaisit, Pakkapon, S1047 (FRI-266)
 Ratz, Michael, S439 (SAT-365)
 Rauber, Conrad, S594 (THU-147)
 Rauch, Andri, S101 (LBP-04)
 Rau, Monika, S47 (OS-057), S625 (THU-449), S687 (SAT-449)
 Raurell, Imma, S780 (WED-474)
 Rauschecker, Mitra, S606 (THU-416)
 Rauschkolb, Peter, S987 (THU-313)
 Rausch, Lilli, S767 (WED-450)
 Rausch, Vanessa, S162 (FRI-430)
 Rauter, Laurin, S465 (THU-494), S470 (THU-505)
 Rautou, Pierre-Emmanuel, S61 (OS-080-YI), S86 (OS-121-YI), S87 (OS-123-YI), S143 (FRI-404), S222 (THU-356), S258 (WED-356), S279 (TOP-043), S283 (SAT-327), S290 (SAT-337), S435 (SAT-358), S974 (THU-293), S975 (THU-295)
 Ravaioli, Federico, S86 (OS-121-YI), S88 (OS-124-YI), S283 (SAT-327), S519 (FRI-322), S609 (THU-421), S974 (THU-293)
 Ravindranayagam, Noel, S625 (THU-450)
 Ravi, Samhita, S145 (TOP-073)
 Ray, David, S731 (TOP-089), S792 (WED-527)
 Raymenants, Karlien, S87 (OS-123-YI)

Author Index

- Razavi, Homie, S872 ([TOP-096](#)), S876 ([FRI-116](#)), S888 ([FRI-132](#)), S910 ([FRI-170](#)), S934 ([FRI-212](#))
- Razavi-Shearer, Devin, S872 ([TOP-096](#)), S876 ([FRI-116](#)), S910 ([FRI-170](#)), S934 ([FRI-212](#))
- Razavi-Shearer, Kathryn, S872 ([TOP-096](#)), S876 ([FRI-116](#)), S888 ([FRI-132](#)), S934 ([FRI-212](#))
- Razek, Mai Abdel, S1212 ([THU-224](#))
- Razpotnik, Rok, S553 ([SAT-261](#))
- Razvan-Ioan, Simu, S1123 ([WED-204](#))
- Reano, Simone, S804 ([WED-551](#))
- Reau, Nancy S, S9 ([GS-012](#)), S631 ([THU-460](#))
- Reau, Nancy S., S882 ([FRI-124](#)), S894 ([FRI-141](#)), S901 ([FRI-152](#))
- Rebiha, Aida, S487 ([THU-538](#))
- Rebuzzi, Lisa, S711 ([SAT-489](#))
- Reddy, K. Rajender, S101 ([LBP-03](#)), S195 ([FRI-546](#)), S241 ([WED-328](#)), S242 ([WED-330](#)), S256 ([WED-352](#)), S258 ([WED-355](#))
- Redi, Rabia, S1120 ([WED-199](#))
- Redondo, Ana, S349 ([THU-235](#))
- Redondo, Carlos, S2 ([GS-003](#))
- Reeh, Matthias, S285 ([SAT-331](#))
- Rees, David, S86 ([OS-122](#))
- Reese, Peter, S45 ([OS-052](#))
- Reeves, Helen Louise, S16 ([OS-003](#)), S140 ([FRI-399](#)), S538 ([SAT-234](#))
- Reeves, Katherine, S368 ([WED-251](#))
- Reggiani-Bonetti, Luca, S942 ([THU-251](#))
- Regnault, Helene, S12 ([LBO-04](#)), S577 ([THU-119](#))
- Rehal, Sonia, S762 ([WED-442](#))
- Reiberger, Thomas, S19 ([OS-010-YI](#)), S35 ([OS-035-YI](#)), S37 ([OS-039-YI](#)), S61 ([OS-080-YI](#)), S86 ([OS-121-YI](#)), S87 ([OS-123-YI](#)), S90 ([OS-127-YI](#)), S107 ([LBP-11](#)), S108 ([LBP-12](#)), S193 ([FRI-545](#)), S198 ([FRI-550](#)), S199 ([FRI-551](#)), S201 ([FRI-554](#)), S222 ([THU-357](#)), S224 ([THU-358](#)), S244 ([WED-334](#)), S246 ([WED-338](#)), S279 ([TOP-043](#)), S282 ([WED-326](#)), S283 ([SAT-327](#)), S284 ([SAT-330](#)), S286 ([SAT-332](#)), S288 ([SAT-335](#)), S289 ([SAT-336](#)), S292 ([SAT-342](#)), S294 ([SAT-345](#)), S299 ([SAT-521](#)), S300 ([SAT-524](#)), S313 ([SAT-547](#)), S316 ([SAT-553](#)), S498 ([FRI-285](#)), S831 ([FRI-477](#)), S832 ([FRI-479](#)), S936 ([TOP-055](#)), S939 ([TOP-058](#)), S970 ([THU-290](#)), S1135 ([SAT-150](#)), S1170 ([SAT-200](#))
- Reic, Tatjana, S880 ([FRI-122](#))
- Reider, Lukas, S282 ([SAT-326](#)), S313 ([SAT-547](#))
- Reid, Leila, S909 ([FRI-165](#))
- Reig, María, S12 ([LBO-04](#)), S493 ([FRI-276](#)), S497 ([FRI-284](#)), S573 ([THU-114](#)), S579 ([THU-124](#)), S849 ([WED-483](#)), S865 ([SAT-129](#))
- Reikvam, Dag Henrik, S1150 ([SAT-170](#))
- Reims, Henrik, S478 ([THU-520](#))
- Reincke, Marlene, S304 ([SAT-531](#)), S318 ([SAT-555](#))
- Reineke-Plaaß, Tanja, S561 ([SAT-277](#))
- Reis, Ana, S889 ([FRI-134](#))
- Reis, Daniela, S865 ([SAT-129](#))
- Reißing, Johanna, S150 ([FRI-412](#)), S349 ([THU-235](#)), S778 ([WED-470](#))
- Reiter, Florian P, S47 ([OS-057](#)), S108 ([LBP-12](#)), S596 ([THU-150](#)), S1139 ([SAT-156](#))
- Reiter, Florian P., S625 ([THU-449](#))
- Rekstyte-Matiene, Kristina, S1030 ([FRI-241](#))
- Rela, Mohamed, S473 ([THU-510](#)), S488 ([THU-544](#))
- Rela, Mohd., S12 ([LBO-04](#)), S195 ([FRI-546](#))
- Remih, Katharina, S136 ([FRI-393](#))
- Remmerie, Anneleen, S445 ([SAT-375](#))
- Remy, André-Jean, S930 ([FRI-204](#))
- Renate, Heyne, S1071 ([WED-132](#))
- Rendina, Maria Grazia, S54 ([OS-069](#))
- Rendon, Paloma, S587 ([THU-136](#))
- Ren, Hong, S271 ([WED-376](#)), S340 ([WED-250](#)), S858 ([SAT-117](#))
- Ren, Hong-Gang, S858 ([SAT-117](#))
- Ren, Kaili, S977 ([THU-296](#)), S1007 ([THU-385](#))
- Ren, Liying, S503 ([FRI-294](#)), S540 ([SAT-235](#))
- Rennebaum, Florian, S61 ([OS-080-YI](#)), S484 ([THU-531](#))
- Renne, Thomas, S450 ([SAT-385](#)), S527 ([SAT-213](#))
- Ren, Qingyun, S109 ([LBP-13](#))
- Renteria, Sara Colonia Uceda, S1154 ([SAT-175](#)), S1164 ([SAT-190](#)), S1170 ([SAT-199](#))
- Renteria, Sara Colonia Uceda, S1159 ([SAT-181](#))
- Ren, Tianyi, S744 ([WED-414](#))
- Ren, Yan, S235 ([TOP-047](#))
- Ren, Yayun, S65 ([OS-087](#)), S112 ([LBP-17](#)), S333 ([WED-236](#)), S334 ([WED-237](#)), S334 ([WED-238](#)), S501 ([FRI-290](#)), S613 ([THU-428](#)), S757 ([WED-436](#)), S762 ([WED-443](#)), S806 ([TOP-076](#)), S824 ([FRI-518](#)), S999 ([THU-333](#))
- Repnik, Urska, S364 ([FRI-390](#))
- Requejo, Isabel, S489 ([THU-546](#))
- Rescigno, Maria, S753 ([WED-430](#))
- Reshef, Naama, S824 ([FRI-519](#))
- Resnick, Murray, S31 ([OS-029](#)), S790 ([WED-522](#))
- Restrepo, Juan Carlos, S865 ([SAT-129](#)), S900 ([FRI-151](#))
- Retat, Lise, S103 ([LBP-06](#))
- Re, Tiziana, S1173 ([THU-165](#))
- Reusswig, Friedrich, S441 ([SAT-368](#))
- Reverter, Enric, S131 ([THU-399](#)), S135 ([THU-406](#))
- Revill, Peter, S875 ([FRI-115](#)), S1028 ([FRI-237](#))
- Rey, David, S876 ([FRI-117](#))
- Reyes, Archie C., S422 ([FRI-356](#))
- Reyes, Maribel, S1156 ([SAT-177](#))
- Rey, Francisco Javier Garcia-Samaniego, S917 ([FRI-181](#)), S921 ([FRI-188](#)), S1098 ([WED-166](#)), S1099 ([WED-168](#)), S1105 ([WED-177](#)), S1205 ([THU-216](#))
- Reynolds, Justin, S1008 ([THU-386](#))
- Reynolds, Kieran, S1129 ([WED-213](#))
- Rey, Silvia García, S838 ([FRI-488](#))
- Rezende, Guilherme, S618 ([THU-436](#))
- Rezen, Tadeja, S553 ([SAT-261](#)), S793 ([WED-529](#))
- Rezvani, Milad, S785 ([WED-512](#))
- Rhee, Hyungjin, S12 ([LBO-04](#))
- Rheinwalt, Karl-Peter, S712 ([SAT-492](#))
- Rhu, Jinsoo, S471 ([THU-506](#)), S474 ([THU-513](#))
- Riachi, Ghassan, S61 ([OS-081](#))
- Riado, Daniel, S90 ([OS-127-YI](#)), S299 ([SAT-521](#))
- Riaño, Ioana, S541 ([SAT-238](#))
- Riback, Lindsey, S100 ([LBP-01](#))
- Ribaldone, Davide, S626 ([THU-452](#)), S713 ([SAT-494](#))
- Ribalta, Alba Ardevol, S279 ([TOP-043](#)), S1192 ([THU-192](#))
- Ribeiro, Andrea, S397 ([WED-297](#)), S398 ([WED-299](#))
- Ribera, Jordi, S250 ([WED-343](#))
- Ribes, Carmen, S251 ([WED-344](#)), S911 ([FRI-171](#))
- Ribnikar, Marija, S135 ([THU-407](#))
- Ricardo, Ana-Rita, S1038 ([FRI-252](#))
- Ricciardi, Federico, S840 ([FRI-492](#))
- Ricci, Chiara, S40 ([OS-045](#)), S55 ([OS-070](#))
- Ricco', Beatrice, S942 ([THU-251](#))
- Ricco, Gabriele, S691 ([SAT-456](#)), S1091 ([WED-157](#))
- Richard, Layese, S46 ([OS-055](#)), S833 ([FRI-480](#))
- Richards, Christopher, S1159 ([SAT-182](#))
- Richards, Lisa, S648 ([TOP-075](#)), S649 ([TOP-083](#))
- Richardson, Carrie, S1187 ([THU-182](#))
- Richardson, Naomi, S416 ([FRI-347](#)), S443 ([SAT-372](#)), S447 ([SAT-380](#))
- Riches, Nicholas, S916 ([FRI-178](#)), S1117 ([WED-195](#))
- Rich, Nicole, S472 ([THU-508](#))
- Richter, Martin, S748 ([WED-421](#))
- Ricke, Jens, S576 ([THU-118](#))
- Rico, María Del Carmen, S302 ([SAT-526](#))
- Rico, María del Carmen, S760 ([WED-440](#)), S770 ([WED-457](#))
- Riddell, Anna, S1033 ([FRI-246](#))
- Rider, Elora, S377 ([WED-266](#))
- Ridola, Lorenzo, S105 ([LBP-09](#)), S218 ([THU-352](#)), S994 ([THU-323](#))
- Riedel, Christoph, S285 ([SAT-331](#))
- Riefolo, Mattia, S519 ([FRI-322](#))
- Riegler, Eva, S532 ([SAT-222](#))
- Riescher-Tuczkiewicz, Alix, S258 ([WED-356](#))
- Rifai, Amelia, S1203 ([THU-212](#))
- Rigamonti, Cristina, S40 ([OS-045](#)), S55 ([OS-070](#)), S56 ([OS-073](#)),

- S374 (WED-260), S389 (WED-284), S599 (THU-156)
- Riggio, Oliviero, S87 (OS-123-YI), S217 (THU-350), S994 (THU-323)
- Rigo, Federica, S455 (TOP-059)
- Rigopoulou, Eirini, S400 (WED-302)
- Rijnders, Bart, S892 (FRI-138)
- Riley, David, S617 (THU-434)
- Rimassa, Lorenza, S12 (LBO-04), S575 (THU-116), S582 (THU-128), S586 (THU-134)
- Rimini, Margherita, S12 (LBO-04), S584 (THU-131), S592 (THU-143), S593 (THU-145)
- Rimler, Galit, S1195 (THU-199)
- Rimmer, Peter, S123 (LBP-36)
- Rimola, Jordi, S579 (THU-124)
- Rinaldo, Christine Hanssen, S449 (SAT-383)
- Rincón, Mercedes, S532 (SAT-221)
- Rinella, Mary, S118 (LBP-26), S627 (THU-453), S647 (TOP-074)
- Rio-Cubilledo, Cristina del, S898 (FRI-148)
- Riordan, Stephen, S195 (FRI-546)
- Ríos, María Lázaro, S964 (THU-282), S980 (THU-301), S996 (THU-326), S998 (THU-331)
- Rios, Maria Teresa Ferrer, S587 (THU-136)
- Rios-Ocampo, Alfredo, S805 (WED-554)
- Ríos, Santiago Ávila, S1202 (THU-211)
- Rio, Thomas Mangana Del, S189 (FRI-537)
- Ripamonti, Ilaria, S381 (WED-272)
- Ripault, Marie Pierre, S170 (FRI-443)
- Ripoche, Doriane, S806 (WED-555)
- Ripoll, Cristina, S251 (WED-345)
- Ripollone, John, S960 (THU-277)
- Ripolone, Michela, S744 (WED-413)
- Ritchie, Jason, S1008 (THU-386)
- Riva, Antonio, S432 (FRI-371)
- Rivas, Coral, S709 (SAT-484)
- Rivas, Pablo Palomares, S936 (FRI-214)
- Riveline, Jean-Pierre, S670 (SAT-424), S681 (SAT-440)
- Rivera, Jesús, S279 (TOP-043), S291 (SAT-340), S693 (SAT-460), S700 (SAT-468)
- Rivera, Paula, S145 (TOP-073)
- Rivera, Victor Gabrielli, S840 (FRI-492)
- Riviere, Benjamin, S534 (SAT-225)
- Rivilla, Ivan, S527 (SAT-212)
- Riviotta, Amy, S840 (FRI-492)
- Rivoire, Michel, S1014 (TOP-104)
- Rizzato, Mario Domenico, S584 (THU-131)
- Rizzatti, Gianenrico, S981 (THU-302)
- Rizzetto, Mario, S1054 (TOP-100), S1056 (TOP-106), S1072 (WED-133)
- Rizzo, Giacomo Emanuele Maria, S592 (THU-144), S1111 (WED-186)
- Rizzuto, Rosario, S322 (TOP-037)
- Roach, Millicent, S516 (FRI-317)
- Roadknight, Gail, S1075 (WED-137)
- Robaey, Geert, S828 (FRI-526)
- Robaey, Wouter, S828 (FRI-526)
- Røberg-Larsen, Hanne, S787 (WED-517)
- Robert, Geffers, S425 (FRI-362)
- Robert, Leon, S900 (FRI-151)
- Robert, Marie Gladys, S894 (FRI-142)
- Roberts, Amin J, S971 (THU-291)
- Roberts, Kela, S58 (OS-075)
- Roberts, Mark, S1187 (THU-182)
- Robertson, Marcus, S597 (THU-151)
- Roberts, Scot, S50 (OS-063)
- Roberts, Stuart, S380 (WED-271), S622 (THU-443), S861 (SAT-123), S863 (SAT-125)
- Robic, Marie-Angèle, S318 (SAT-556)
- Robin, Fabien, S62 (OS-083-YI)
- Robinson, Tomos, S632 (THU-462)
- Robin, Thomas Daniel, S989 (THU-314)
- roblero, Juan Pablo, S865 (SAT-129)
- Robles-Díaz, M, S18 (OS-007), S144 (FRI-406)
- Robles-Díaz, Mercedes, S44 (OS-049-YI)
- Robles, Enrique Pérez-Cuadrado, S314 (SAT-549)
- Robles-Frias, Mª José, S732 (TOP-090)
- Roca, Ferran Pujol, S932 (FRI-208)
- Roca Suarez, Armando Andres, S118 (LBP-27), S1014 (TOP-104)
- Roccarina, Davide, S56 (OS-073), S233 (THU-371), S660 (SAT-409), S661 (SAT-410), S812 (FRI-471)
- Rocco, Alba, S1082 (WED-146)
- Roche, Bruno, S52 (OS-066), S107 (LBP-11), S1160 (SAT-184)
- Roch, María Ángeles, S903 (FRI-156)
- Rockall, Andrea, S576 (THU-118)
- Rockey, Don, S275 (WED-383)
- Rock, Nathalie, S969 (THU-289), S971 (THU-291)
- Rockstroh, Jürgen, S101 (LBP-04)
- Rodda, Sheridan, S15 (OS-002)
- Rode, Agnès, S318 (SAT-556)
- Roden, Michael, S66 (OS-089), S827 (FRI-523)
- Roderburg, Christoph, S136 (THU-409), S630 (THU-458)
- Roder, Christine, S1190 (THU-189)
- Roderfeld, Martin, S339 (WED-248), S417 (FRI-349), S954 (THU-268)
- Rodig, Thea, S402 (WED-305)
- Rodney, Kyle, S238 (WED-323)
- Rodrigo, Miguel Angel Merlos, S544 (SAT-244)
- Rodrigo-Torres, Daniel, S434 (SAT-355)
- Rodrigues, Joana, S238 (WED-323)
- Rodrigues, Pedro Miguel, S28 (OS-024-YI), S57 (OS-074-YI), S440 (SAT-367), S527 (SAT-212), S734 (WED-397), S738 (WED-404)
- Rodrigues, Rita Vale, S902 (FRI-154)
- Rodrigues, Robim M, S752 (WED-428), S775 (WED-465)
- Rodríguez, Adrià, S903 (FRI-156), S915 (FRI-177)
- Rodríguez Agudo, Rubén, S532 (SAT-221), S544 (SAT-244)
- Rodríguez, Alvaro Blanes, S365 (FRI-391)
- Rodríguez, Antonio González, S932 (FRI-206)
- Rodríguez, Carlos, S936 (FRI-214)
- Rodríguez, Elisa, S1205 (THU-216)
- Rodríguez-Fraile, Macarena, S573 (THU-114)
- Rodríguez-Frías, Francisco, S896 (FRI-144), S904 (FRI-158), S921 (FRI-188), S924 (FRI-192), S1024 (FRI-228), S1082 (WED-145), S1089 (WED-154)
- Rodríguez-Gandía, Miguel Ángel, S73 (OS-102)
- Rodríguez, Jaime Romero, S932 (FRI-208)
- Rodríguez, Jorge Ruiz, S480 (THU-524)
- Rodríguez, Jose, S115 (LBP-22)
- Rodríguez, Manuel, S2 (GS-003), S87 (OS-123-YI), S921 (FRI-188), S1098 (WED-166), S1178 (THU-171), S1205 (THU-216)
- Rodríguez, Marcela Peña, S347 (THU-233)
- Rodríguez, Maria, S133 (THU-404), S1124 (WED-205)
- Rodríguez-Perálvarez, Manuel, S470 (THU-503)
- Rodríguez, Rafael Gómez, S587 (THU-136)
- Rodríguez, Sergio Vaquez, S171 (FRI-445), S1098 (WED-166)
- Rodríguez-Tajes, Sergio, S90 (OS-127-YI), S299 (SAT-521), S392 (WED-290), S399 (WED-300), S405 (WED-311), S461 (THU-487), S481 (THU-525), S924 (FRI-192), S1089 (WED-154), S1098 (WED-166), S1099 (WED-168)
- Rodwell-Green, Lakisha, S50 (OS-063)
- Roeb, Elke, S339 (WED-248), S417 (FRI-349), S954 (THU-268)
- Roe, Craig, S179 (FRI-459)
- Roediger, Rebecca, S116 (LBP-23), S926 (FRI-196)
- Roehlen, Natascha, S72 (OS-098)
- Roelstraete, Bjorn, S82 (OS-116-YI)
- Roessler, Stephanie, S536 (SAT-230), S547 (SAT-248)
- Rogalidou, Maria, S972 (THU-291)
- Roger, Clementine, S266 (WED-368)
- Rogers, Penelope, S398 (WED-299)
- Roggenbuck, Dirk, S514 (FRI-313)
- Rogiers, Vera, S752 (WED-428), S775 (WED-465)
- Roglans, Núria, S356 (THU-246), S788 (WED-518), S802 (WED-546)
- Rohner, Nicolas, S735 (WED-398)
- Rohr-Udilova, Nataliya, S451 (SAT-388)
- Roig, Clara Amiama, S690 (SAT-454), S697 (SAT-465), S705 (SAT-478), S706 (SAT-479)
- Roig, Cristina, S87 (OS-123-YI)
- Rojas, Anabel, S440 (SAT-367)
- Rojas, German, S245 (WED-336)
- Rojas, Juan, S765 (WED-448)
- Rojo, Ana Isabel, S777 (WED-468)
- Rolando, Christian, S146 (FRI-408)
- Roldan, Carolina, S1126 (WED-208)
- Rollinson, Christopher, S153 (FRI-418)

Author Index

- Rollo, Paolo, S407 ([WED-315](#))
- Rolph, Tim, S808 ([TOP-091](#)), S820 ([FRI-512](#))
- Romagnoli, Renato, S455 ([TOP-059](#)), S460 ([THU-485](#)), S486 ([THU-537](#))
- Romagnoli, Veronica, S691 ([SAT-456](#)), S1091 ([WED-157](#))
- Romano, Antonino, S750 ([WED-424](#))
- Romano, Caroline, S116 ([LBP-23](#))
- Romano, Fabrizio, S480 ([THU-523](#))
- Romano, Javier Sánchez, S449 ([SAT-383](#))
- Romão, Luis, S1075 ([WED-137](#))
- Rombaut, Matthias, S752 ([WED-428](#)), S775 ([WED-465](#))
- Rombouts, Krista, S337 ([WED-243](#))
- Romeo, Sara, S1190 ([THU-188](#))
- Romeo, Sara Sara, S668 ([SAT-420](#))
- Romeo, Stefano, S665 ([SAT-416](#)), S733 ([WED-393](#)), S803 ([WED-549](#))
- Romero, Álvaro Hidalgo, S1178 ([THU-171](#))
- Romero, Carmen Lara, S302 ([SAT-526](#)), S654 ([SAT-400](#)), S703 ([SAT-472](#)), S728 ([SAT-515](#)), S838 ([FRI-488](#))
- Romero, Daniel Brown, S558 ([SAT-271](#))
- Romero Gomez, Manuel, S612 ([THU-426](#)), S627 ([THU-453](#)), S640 ([THU-474](#)), S646 ([THU-559](#)), S760 ([WED-440](#)), S770 ([WED-457](#))
- Romero-Gutiérrez, Marta, S87 ([OS-123-YI](#)), S587 ([THU-136](#)), S996 ([THU-326](#)), S998 ([THU-331](#))
- Romero, Mario, S481 ([THU-525](#))
- Romero, Marta, S544 ([SAT-244](#))
- Romero, Michael, S765 ([WED-448](#))
- Romero, Miriam, S690 ([SAT-454](#)), S697 ([SAT-465](#)), S706 ([SAT-479](#)), S1105 ([WED-177](#))
- Romero, Rene, S971 ([THU-291](#))
- Romero, Sarah, S306 ([SAT-535](#))
- Ronca, Vincenzo, S447 ([SAT-380](#)), S982 ([THU-304](#))
- Ronchi, Davide, S552 ([SAT-258](#))
- Rondena, Jessica, S669 ([SAT-422](#)), S992 ([THU-318](#))
- Ronot, Maxime, S61 ([OS-080-YI](#)), S491 ([FRI-273](#)), S505 ([FRI-295](#)), S577 ([THU-120](#))
- Ronzoni, Luisa, S500 ([FRI-288](#)), S733 ([WED-393](#)), S992 ([THU-318](#))
- Rooseboom, Jalina, S677 ([SAT-434](#))
- Roose, Heleen, S1030 ([FRI-241](#))
- Roque-Cuellar, María C., S838 ([FRI-488](#))
- Roquelaure, Bertrand, S1002 ([THU-336](#)), S1003 ([THU-378](#))
- Roqueta-Rivera, Manuel, S422 ([FRI-356](#))
- Roquin, Guillaume, S105 ([LBP-09](#))
- Rorsman, Fredrik, S605 ([THU-414](#)), S650 ([TOP-085](#)), S653 ([SAT-397](#))
- Rosa, Isabelle, S52 ([OS-066](#)), S107 ([LBP-11](#)), S1161 ([SAT-185](#))
- Rosa, Laura De, S691 ([SAT-456](#))
- Rosales, A Gabriela, S1079 ([WED-141](#))
- Rosat, Aurélie, S481 ([THU-526](#))
- Rosato, Valerio, S36 ([OS-036](#)), S1082 ([WED-146](#))
- Rose, Caren, S886 ([FRI-130](#))
- Rose, Christopher F, S213 ([THU-344](#)), S233 ([THU-372](#))
- Rosell-Cardona, Cristina, S356 ([THU-246](#))
- Rosenberg, Nofar, S549 ([SAT-252](#))
- Rosenberg, William, S867 ([SAT-130](#))
- Rosenquist, Christian, S666 ([SAT-417](#)), S668 ([SAT-421](#))
- Rosenstock, Moti, S544 ([SAT-243](#))
- Rosenthal, Philip, S965 ([THU-284](#))
- Rose, Tim, S527 ([SAT-213](#))
- Rosi, Martina, S513 ([FRI-311](#))
- Rosina, Floriano, S40 ([OS-045](#)), S55 ([OS-070](#))
- Rosinka, Magda, S880 ([FRI-121](#))
- Roskams, Tania, S78 ([OS-110](#)), S549 ([SAT-252](#)), S753 ([WED-430](#))
- Rosler, Elen, S548 ([SAT-251](#))
- Rosoff, Daniel, S792 ([WED-527](#))
- Rosselli, Matteo, S283 ([SAT-327](#))
- Rossi, Alberto, S381 ([WED-272](#))
- Rossi, Alice, S791 ([WED-525](#))
- Rossi, Massimo, S360 ([FRI-383](#))
- Rossini, Benedetta, S519 ([FRI-322](#))
- Rössle, Martin, S305 ([SAT-534](#)), S313 ([SAT-546](#))
- Rossmeisl, Martin, S784 ([WED-509](#)), S805 ([WED-552](#))
- Rössner, Sophia, S710 ([SAT-486](#))
- Rosso, Chiara, S500 ([FRI-288](#)), S521 ([FRI-325](#)), S526 ([SAT-211](#)), S605 ([THU-415](#)), S611 ([THU-425](#)), S617 ([THU-435](#)), S626 ([THU-452](#)), S637 ([THU-470](#)), S652 ([SAT-396](#)), S704 ([SAT-474](#)), S713 ([SAT-494](#))
- Rosso, Natalia, S768 ([WED-452](#)), S793 ([WED-529](#))
- Rossotti, Roberto, S907 ([FRI-164](#))
- Ross, Paul, S91 ([OS-128](#)), S642 ([THU-551](#))
- Rot, Antal, S39 ([OS-043](#))
- Roth, Sofia, S754 ([WED-431](#))
- Rotile, Nicholas, S413 ([FRI-335](#))
- Rotter, Lukas, S1050 ([FRI-270](#))
- Roudot-Thoraval, Françoise, S833 ([FRI-480](#))
- Roulot, Dominique, S52 ([OS-066](#)), S498 ([FRI-286](#)), S833 ([FRI-480](#)), S1161 ([SAT-185](#))
- Roumain, Martin, S772 ([WED-458](#))
- Rourke, Colm O, S28 ([OS-024-YI](#)), S533 ([SAT-223](#)), S534 ([SAT-226](#)), S536 ([SAT-230](#)), S541 ([SAT-238](#)), S942 ([THU-251](#))
- Rout, Ashok, S687 ([SAT-449](#))
- Roux, Charles, S492 ([FRI-274](#))
- Roux, Marine, S672 ([SAT-427](#))
- Roux, Olivier, S10 ([LBO-01](#)), S87 ([OS-123-YI](#)), S981 ([THU-303](#))
- Rovai, Alice, S951 ([THU-263](#))
- Rovida, Elisabetta, S536 ([SAT-229](#)), S774 ([WED-462](#))
- Rowe, Ian, S157 ([FRI-422](#)), S867 ([SAT-130](#))
- Roy, Akash, S274 ([WED-382](#))
- Royal, Nichola, S918 ([FRI-182](#)), S1182 ([THU-176](#))
- Royo, Laura, S546 ([SAT-247](#))
- Royo, Maite, S915 ([FRI-177](#))
- Royo, Sara Pastor, S268 ([WED-372](#))
- Roy, Saswata, S177 ([FRI-455](#))
- Roy, Subhajit, S800 ([WED-544](#))
- Rozina, Teona, S1210 ([THU-221](#))
- Rozman, Damjana, S553 ([SAT-261](#)), S793 ([WED-529](#))
- Rrapaj, Eniada, S733 ([WED-393](#))
- Ruan, Jian, S543 ([SAT-242](#))
- Ruano, Alberto Tinahones, S326 ([WED-223](#))
- Ruan, Qi, S330 ([WED-229](#))
- Ruas, Jorge, S741 ([WED-409](#))
- Rubbia-Brandt, Laura, S531 ([SAT-220](#))
- Rubí, Alicia R, S1191 ([THU-190](#))
- Rubín, Ángel, S470 ([THU-503](#))
- Rubin, Moises Nevah, S458 ([THU-482](#))
- Rubin, Raymond, S241 ([WED-328](#))
- Rubio, Aileen, S1164 ([SAT-191](#)), S1169 ([SAT-197](#))
- Rubio, Ana Belén, S163 ([FRI-431](#)), S851 ([WED-486](#))
- Rubio Garcia, Ana Belen, S15 ([OS-001](#))
- Rubio-Ponce, Andrea, S78 ([OS-109-YI](#))
- Rubio, Sonia Albertos, S913 ([FRI-175](#))
- Rudder, Maxime De, S76 ([OS-106-YI](#))
- Rudilosso, Antonia, S729 ([SAT-517](#))
- Rudkjær, Lise, S321 ([TOP-036](#))
- Rudler, Marika, S198 ([FRI-550](#)), S318 ([SAT-556](#)), S492 ([FRI-274](#)), S494 ([FRI-279](#))
- Rudolf, Erin, S822 ([FRI-515](#))
- Rudolfson, Jan Håkon, S614 ([THU-429](#))
- Rudolph, Bryan, S66 ([OS-089](#))
- Rui, Fajuan, S638 ([THU-471](#)), S696 ([SAT-463](#)), S724 ([SAT-510](#)), S1096 ([WED-165](#))
- Ruiz, Armando Raúl Guerra, S868 ([SAT-132](#))
- Ruiz, Beatriz Pacín, S1024 ([FRI-228](#))
- Ruiz-Blazquez, Paloma, S38 ([OS-042-YI](#)), S339 ([WED-247](#))
- Ruiz-Canovas, Eugenia, S791 ([WED-524](#))
- Ruiz-Cobo, Juan Carlos, S375 ([WED-263](#)), S392 ([WED-290](#)), S904 ([FRI-158](#)), S1082 ([WED-145](#)), S1205 ([THU-216](#))
- Ruiz de Gauna, Mikel, S529 ([SAT-215](#)), S738 ([WED-404](#)), S741 ([WED-408](#))
- Ruiz, Elena, S1126 ([WED-208](#))
- Ruiz-Fernandez, Gloria, S697 ([SAT-465](#)), S705 ([SAT-478](#)), S706 ([SAT-479](#))
- Ruiz, Francisco Rivas, S269 ([WED-374](#))
- Ruiz, Isaac, S981 ([THU-303](#))
- Ruiz, Joaquín, S915 ([FRI-177](#))
- Ruiz, Maria Dolores Gómez, S1124 ([WED-205](#))
- Ruiz, Mathias, S965 ([THU-284](#))
- Ruiz, Pablo, S461 ([THU-487](#)), S486 ([THU-536](#))
- Ruiz, Patricia Cordero, S964 ([THU-282](#)), S980 ([THU-301](#)), S998 ([THU-331](#))
- Ruiz, Pilar Díaz, S928 ([FRI-198](#))
- Ruiz-Tapiador, Juan Ignacio Arenas, S573 ([THU-114](#))
- Rule, Jody, S136 ([FRI-393](#))

- Rull, Monica, S69 ([OS-094](#))
 Rumunu, John, S69 ([OS-094](#))
 Rungta, Sumit, S1050 ([FRI-269](#))
 Ruoppolo, Margherita, S38 ([OS-042-YI](#))
 Ruscica, Massimiliano, S802 ([WED-547](#))
 Rushbrook, Simon, S411 ([FRI-331](#))
 Rushton, Steve, S411 ([FRI-331](#))
 Russell, Erin, S852 ([WED-488](#))
 Russell, Jennifer, S180 ([FRI-460](#))
 Russello, Maurizio, S36 ([OS-036](#)),
 S40 ([OS-045](#)), S55 ([OS-070](#)),
 S374 ([WED-260](#)), S568 ([SAT-288](#))
 Russo, Francesco Paolo, S54 ([OS-069](#)),
 S56 ([OS-073](#)), S183 ([TOP-049](#)),
 S299 ([SAT-521](#)), S322 ([TOP-037](#)),
 S407 ([WED-315](#)), S500 ([FRI-288](#)),
 S770 ([WED-456](#)), S1082 ([WED-146](#))
 Rüstenzade, Aynure, S709 ([SAT-485](#))
 Rustgi, Vinod, S273 ([WED-380](#)),
 S312 ([SAT-545](#)), S623 ([THU-445](#)),
 S1011 ([THU-390](#))
 Rützel, Kristi, S880 ([FRI-121](#))
 Ruvido, Jessica, S965 ([THU-284](#))
 Ruvoletto, Mariagrazia, S766 ([WED-449](#))
 Ruzic, Dusan, S332 ([WED-232](#))
 Ruz-Zafra, Pilar, S171 ([FRI-445](#))
 ruzzenente, andrea, S510 ([FRI-304](#))
 Ryan, Eleanor, S180 ([FRI-460](#))
 Ryan, John, S255 ([WED-350](#)),
 S979 ([THU-300](#))
 Ryan, Marno, S306 ([SAT-535](#))
 Ryan, Pablo, S1037 ([FRI-251](#))
 Ryder, Rachel, S847 ([WED-479](#))
 Ryder, Stephen, S168 ([FRI-439](#)),
 S411 ([FRI-331](#)), S867 ([SAT-130](#))
 Rye, Kerry Ann, S351 ([THU-237](#))
- Saab, Sammy, S101 ([LBP-03](#))
 Saad, Amel Ben, S954 ([THU-267](#))
 Saba, Francesca, S605 ([THU-415](#)),
 S611 ([THU-425](#))
 Sabagh, Ahmed El, S517 ([FRI-319](#))
 Saba, Noor, S912 ([FRI-172](#))
 Sabetta, Annamaria, S217 ([THU-350](#))
 Sabio, Guadalupe, S137 ([FRI-395](#))
 Saborowski, Anna, S561 ([SAT-277](#))
 Sabry, Aliaa, S1212 ([THU-224](#))
 Sacco, Rodolfo, S36 ([OS-036](#)), S40 ([OS-045](#)),
 S55 ([OS-070](#)), S499 ([FRI-287](#)),
 S597 ([THU-153](#))
 Sacerdoti, David, S203 ([FRI-558](#)),
 S510 ([FRI-304](#)), S632 ([THU-461](#)),
 S668 ([SAT-420](#)), S1190 ([THU-188](#))
 Sachdeva, Sanjeev, S235 ([TOP-044](#))
 Sacherl, Julia, S945 ([THU-256](#))
 Sacleux, Sophie-Caroline, S74 ([OS-104](#)),
 S189 ([FRI-537](#)), S220 ([THU-355](#)),
 S318 ([SAT-556](#))
 Sadasivan, Abhishek, S906 ([FRI-163](#))
 Sadasivan, Shine, S827 ([FRI-524](#)),
 S848 ([WED-481](#))
 Sade-Feldman, Moshe, S58 ([OS-075](#))
 Sadiq Hamid, Saeed, S912 ([FRI-172](#)),
 S913 ([FRI-174](#))
- Sadirova, Shakhlo, S888 ([FRI-132](#))
 Saeed, Anwaar, S575 ([THU-116](#)),
 S582 ([THU-128](#)), S586 ([THU-134](#))
 Saeed, Mohamed, S1212 ([THU-224](#))
 Saeed, Najam-us-sehar, S1196 ([THU-200](#))
 Saeed, Quaid, S926 ([FRI-195](#))
 Saeidinejad, Mahdi, S129 ([THU-396](#))
 Saeidi, Reza, S255 ([WED-350](#))
 Saeki, Akira, S1192 ([THU-191](#)),
 S1199 ([THU-205](#))
 Sáenz de Miera, Inés, S903 ([FRI-156](#)),
 S915 ([FRI-177](#))
 Sáenz, José Luis Vega, S932 ([FRI-207](#))
 Saez-Palma, Maria, S1089 ([WED-154](#))
 Safadi2, Rifaat, S549 ([SAT-252](#))
 Safadi, Rifaat, S119 ([LBP-28](#)),
 S328 ([WED-226](#)), S342 ([TOP-039](#)),
 S484 ([THU-532](#)), S985 ([THU-310](#))
 Safdar, Nawaz, S179 ([FRI-459](#))
 Saffioti, Francesca, S56 ([OS-073](#)),
 S309 ([SAT-541](#))
 Saffouri, Baker, S328 ([WED-226](#))
 Safwat, Dalia, S1212 ([THU-224](#))
 Sagakuchi, Shimon, S447 ([SAT-380](#))
 Sagalova, Olga, S53 ([OS-068](#)), S110 ([LBP-15](#))
 Sagie, Lior Hecht, S128 ([THU-394](#))
 Saglietti, Chiara, S105 ([LBP-08](#))
 Sagripanti, Alessandra, S673 ([SAT-430](#))
 Saha, Punnap, S800 ([WED-544](#))
 Sahashiv, Roshni, S199 ([FRI-552](#)),
 S257 ([WED-353](#)), S278 ([WED-389](#))
 Sahin, Eray, S542 ([SAT-240](#))
 Sahin, Hasan, S1109 ([WED-183](#))
 Sahni, Nancy, S51 ([OS-064-YI](#))
 Sahuco, Iván, S1172 ([THU-162](#))
 Sahu, Pabitra, S294 ([SAT-346](#))
 Saihi, Hajar, S825 ([FRI-520](#))
 Sainitin, Donakonda, S33 ([OS-032](#)),
 S59 ([OS-077](#))
 Sainz-Ramírez, Natalia, S137 ([FRI-395](#)),
 S529 ([SAT-215](#)), S741 ([WED-408](#))
 Saito, Satoru, S30 ([OS-028](#))
 Saitta, Carlo, S40 ([OS-045](#)), S55 ([OS-070](#))
 Sakagianni, Aikaterini, S978 ([THU-298](#))
 Sakai, Aiko, S1025 ([FRI-230](#))
 Sakamori, Ryotaro, S1183 ([THU-177](#))
 Sakamoto, Kazumasa, S811 ([FRI-468](#))
 Sakata, Toshihiro, S444 ([SAT-373](#))
 Sakuma, Satoshi, S793 ([WED-528](#))
 Salahuddin, Sultan, S896 ([FRI-145](#))
 Sala, Margarita, S376 ([WED-264](#))
 Sala, Matteo, S907 ([FRI-164](#))
 Salamé, Ephrem, S62 ([OS-083-YI](#)),
 S467 ([THU-498](#)), S473 ([THU-511](#))
 Salani, Francesca, S575 ([THU-116](#)),
 S586 ([THU-134](#))
 Salarzaei, Morteza, S454 ([TOP-052](#))
 Salat, Andreas, S465 ([THU-494](#)),
 S470 ([THU-505](#))
 Salatiello, Maria, S942 ([THU-251](#))
 Salati, Massimiliano, S942 ([THU-251](#))
 Salaun, Bruno, S1167 ([SAT-196](#))
 Sala-Vila, Aleix, S788 ([WED-518](#))
 Salazar, Helen Rose Maia, S1201 ([THU-208](#))
- Salcedo, Magdalena, S376 ([WED-264](#)),
 S392 ([WED-290](#)), S399 ([WED-300](#)),
 S470 ([THU-503](#)), S481 ([THU-525](#))
 Salcedo, María, S12 ([LBO-04](#))
 Salcedo, María-Teresa, S375 ([WED-263](#))
 Saleh, Mohamed Bou, S146 ([FRI-408](#))
 Salgado, Alberto De La Iglesia,
 S1126 ([WED-208](#))
 Salhab, Ahmad, S328 ([WED-226](#)),
 S342 ([TOP-039](#))
 Saliba, Faouzi, S74 ([OS-104](#)), S189 ([FRI-537](#)),
 S220 ([THU-355](#)), S318 ([SAT-556](#)),
 S473 ([THU-511](#)), S807 ([TOP-077](#)),
 S1005 ([THU-380](#))
 Salic, Kanita, S786 ([WED-515](#))
 Salih, Hizni, S1075 ([WED-137](#))
 Salinas, Casper G, S746 ([WED-417](#))
 Salis, Aina, S267 ([WED-370](#)),
 S273 ([WED-381](#))
 Sallahuddin, Sultan, S912 ([FRI-172](#))
 Sällberg, Matti, S1038 ([FRI-252](#))
 Salles, Gil, S626 ([THU-451](#)), S658 ([SAT-405](#))
 Salloum, Shadi, S58 ([OS-075](#))
 Salmerón, Javier, S376 ([WED-264](#)),
 S399 ([WED-300](#))
 Salminen, Kimmo, S11 ([LBO-03](#))
 Salomone, Federico, S605 ([THU-415](#)),
 S611 ([THU-425](#))
 Salpini, Romina, S1056 ([TOP-106](#)),
 S1072 ([WED-133](#)), S1103 ([WED-174](#)),
 S1105 ([WED-176](#)), S1122 ([WED-203](#)),
 S1142 ([SAT-159](#))
 Saltini, Dario, S279 ([TOP-043](#)),
 S287 ([SAT-334](#)), S609 ([THU-421](#))
 Salvati, Antonio, S691 ([SAT-456](#)),
 S1091 ([WED-157](#))
 Salvato, Mauro, S592 ([THU-144](#))
 Salvo, Giovanni Di, S990 ([THU-316](#))
 Salvoza, Noel, S768 ([WED-452](#))
 Salzer, Helmut, S996 ([THU-327](#))
 Samaithongcharoen, Kittichai,
 S19 ([OS-009](#))
 Samakidou, Anna, S400 ([WED-302](#))
 Samala, Niharika, S649 ([TOP-080](#))
 Samaniego, Luis Ibañez, S220 ([THU-355](#)),
 S964 ([THU-282](#)), S980 ([THU-301](#)),
 S998 ([THU-331](#))
 Sambarino, Dana, S1135 ([SAT-149](#)),
 S1142 ([SAT-159](#)), S1154 ([SAT-175](#)),
 S1159 ([SAT-181](#)), S1164 ([SAT-190](#)),
 S1170 ([SAT-199](#))
 Sameh, Heba, S1212 ([THU-224](#))
 Samonakis, Demetrios N.,
 S400 ([WED-302](#)), S1128 ([WED-211](#))
 Sampaziotis, Fotios, S409 ([TOP-064](#)),
 S418 ([FRI-351](#))
 Sampedro, Antonio, S1126 ([WED-208](#))
 Samson, Adel, S575 ([THU-116](#))
 Samuel, Didier, S74 ([OS-104](#)),
 S460 ([THU-486](#)), S482 ([THU-528](#)),
 S981 ([THU-303](#))
 Samuel, Ronald, S173 ([FRI-448](#)),
 S472 ([THU-508](#))
 Samuelsén, Ellen, S1150 ([SAT-170](#))

Author Index

- Samyn, Marianne, S1000 (THU-334)
 Sanabria-Cabrera, Judith, S18 (OS-007)
 Sanai, Faisal, S859 (SAT-119)
 Sanceau, Julie, S27 (OS-023-YI)
 Sanchez, Abel, S865 (SAT-129), S900 (FRI-151)
 Sanchez, Abel Acosta, S1051 (FRI-272)
 Sánchez-Aldehuelo, Rubén, S73 (OS-102), S475 (THU-514)
 Sánchez, Ana María, S1191 (THU-190)
 Sanchez, Angela Puente, S2 (GS-003), S251 (WED-344)
 Sanchez, Antonio, S85 (OS-120)
 Sanchez, Antonio Diaz, S883 (FRI-126)
 Sanchez, Aranzazu, S331 (WED-231)
 Sánchez-Avila, Juan, S939 (TOP-058)
 Sánchez-Bueno, Francisco, S469 (THU-501)
 Sanchez, Cristina, S290 (SAT-337)
 Sánchez-Delgado, Jordi, S10 (LBO-01), S198 (FRI-550)
 Sánchez, Flor M. Fernandez-Gordón, S406 (WED-314)
 Sánchez, Henar Calvo, S1028 (FRI-236), S1032 (FRI-245)
 Sanchez, Lukas Otero, S621 (THU-442)
 Sanchez Luque, Carlos B, S83 (OS-118)
 Sánchez, Marco, S865 (SAT-129), S900 (FRI-151)
 Sanchez, Maria, S664 (SAT-415)
 Sanchez, Maria Camila, S971 (THU-291)
 Sánchez-Martín, Alba, S682 (SAT-442)
 Sanchez, Mercedes De La Torre, S682 (SAT-442)
 Sanchez, Moises, S220 (THU-355)
 Sanchez, Nazaret, S902 (FRI-153)
 Sanchez-Romero, Natalia, S365 (FRI-391)
 Sánchez, Victor, S154 (FRI-419)
 Sanchez, William, S808 (TOP-091)
 Sánchez, Yolanda, S248 (WED-341)
 Sancho-Bru, Pau, S78 (OS-109-YI), S171 (FRI-445), S560 (SAT-275), S737 (WED-403)
 Sancho, Victoria Aguilera, S133 (THU-404), S171 (FRI-445), S180 (FRI-462), S470 (THU-503), S682 (SAT-442), S1172 (THU-162)
 Sanctis, Giuseppe Maria De, S1122 (WED-203)
 Sandahl, Thomas Damgaard, S948 (THU-259)
 Sandeman, Susan, S205 (TOP-042)
 Sander, Beate, S874 (FRI-114)
 Sanders, Matthew, S762 (WED-442)
 Sandford, Richard, S411 (FRI-331)
 Sandfort, Vanessa, S957 (THU-271), S957 (THU-272)
 Sandmann, Lisa, S1101 (WED-171), S1115 (WED-193)
 Sandrin, Laurent, S817 (FRI-507)
 Sandulescu, Oana, S1149 (SAT-168)
 San, Emily Van, S764 (WED-446)
 Sangineto, Moris, S750 (WED-424)
 Sangro, Bruno, S12 (LBO-04), S326 (WED-223), S526 (TOP-072), S537 (SAT-232), S573 (THU-114), S1189 (THU-185)
 Sankar, Kamy, S489 (TOP-065)
 Sanou, Armel Moumouni, S930 (FRI-202)
 Sansó, Andreu, S1191 (THU-190)
 Santamaria, Diego Burgos, S8 (GS-009), S73 (OS-102), S964 (THU-282), S980 (THU-301), S998 (THU-331)
 Santamaria, Eva, S532 (SAT-221)
 SantaMaria Rodriguez, German Jose, S1126 (WED-208)
 Santantonio, Teresa, S107 (LBP-11), S1082 (WED-146)
 Santarone, Stella, S88 (OS-124-YI)
 Santervás, Sandra Izquierdo, S480 (THU-524)
 Santhosh, Arjun, S827 (FRI-524)
 Santiago, Jesús González, S1098 (WED-166), S1205 (THU-216)
 Santi, Alice, S550 (SAT-254)
 Santi, Daniele, S729 (SAT-517)
 Santini, Silvano Junior, S646 (THU-560), S685 (SAT-446)
 Santol, Jonas, S44 (OS-050-YI), S45 (OS-051-YI)
 Santomenna, Floriana, S632 (THU-461), S645 (THU-557)
 Santopaolo, Francesco, S252 (WED-347), S578 (THU-122), S981 (THU-302), S1122 (WED-203)
 Santori, Charles, S671 (SAT-426)
 Santos, André A., S734 (WED-397)
 Santos, Arsénio, S366 (TOP-061), S842 (FRI-495)
 Santos, Beatriz Gómez, S137 (FRI-395), S349 (THU-235), S529 (SAT-215), S738 (WED-404)
 Santos, Catarina Esteves, S902 (FRI-154)
 Santos, Hildo Rodriguez, S397 (WED-296)
 Santos-Laso, Álvaro, S709 (SAT-484)
 Santos, Lorrane, S658 (SAT-405)
 Santos-Silva, Ermelinda, S972 (THU-291)
 Sanyal, Arun, S1 (GS-001), S13 (LBO-05), S31 (OS-029), S49 (OS-062), S171 (FRI-444), S236 (WED-319), S260 (WED-358), S334 (WED-238), S629 (THU-456), S666 (SAT-417), S668 (SAT-421), S715 (SAT-496), S749 (WED-422), S757 (WED-436), S806 (TOP-076), S809 (FRI-466), S811 (FRI-469), S1085 (WED-149)
 Sanz de Villalobos, Eduardo, S1028 (FRI-236), S1032 (FRI-245)
 Sanz, Mario Fernández, S365 (FRI-391)
 Sanz-Martínez, María-Teresa, S375 (WED-263)
 Sanz, Miquel, S489 (THU-546)
 Saphonn, Vonthanak, S875 (FRI-115)
 Saracco, Giorgio Maria, S521 (FRI-325), S605 (THU-415), S713 (SAT-494), S917 (FRI-180), S1177 (THU-169), S1200 (THU-206)
 Saracco, Margherita, S455 (TOP-059), S486 (THU-537)
 Saracino, Annalisa, S907 (FRI-164), S1072 (WED-133)
 Saravanan, Chandra, S806 (TOP-076)
 Saraya, Anoop, S6 (GS-006), S195 (FRI-546), S233 (TOP-041)
 Sarcognato, Samantha, S564 (SAT-283)
 Sardh, Eliane, S86 (OS-122)
 Sardina, Romina García, S251 (WED-344)
 Sardone, Rodolfo, S495 (FRI-280)
 Sarikaya, Ozan, S181 (FRI-463)
 Sarina, Barbara, S88 (OS-124-YI)
 Sarin, Shiv Kumar, S7 (GS-008-YI), S149 (FRI-411), S152 (FRI-416), S182 (TOP-040), S207 (THU-337), S210 (THU-340), S212 (THU-343), S218 (THU-351), S228 (THU-362), S228 (THU-363), S272 (WED-379), S293 (SAT-344), S326 (WED-222), S348 (THU-234), S352 (THU-240), S357 (THU-248), S436 (SAT-360), S556 (SAT-267), S943 (THU-253), S1013 (TOP-102), S1027 (FRI-235), S1045 (FRI-263), S1047 (FRI-267)
 Sarmati, Loredana, S1056 (TOP-106), S1072 (WED-133), S1122 (WED-203)
 Sarnataro, Sergio, S942 (THU-251)
 Sarnecki, Jędrzej, S837 (FRI-486)
 Sarnová, Lenka, S945 (THU-255)
 Sarrazin, Christoph, S90 (OS-126), S91 (OS-129-YI), S1039 (FRI-254), S1042 (FRI-259)
 Sartini, Claudio, S66 (OS-089)
 Sartori, Marco, S711 (SAT-489)
 Sartoris, Riccardo, S491 (FRI-273), S505 (FRI-295)
 Sarvin, Boris, S669 (SAT-423)
 Sarwar, Syeda Zahida, S904 (FRI-157)
 Sasaki, Kazuki, S439 (SAT-366), S509 (FRI-302)
 Sasaki, Ryu, S178 (FRI-458), S565 (SAT-285), S1177 (THU-170)
 Satai, Mayur, S282 (SAT-325)
 Sateesh, Meddirevula, S969 (THU-289)
 Satlikova, Nataliya, S320 (SAT-559)
 Sato, Ken, S394 (WED-293)
 Sato, Sho, S633 (THU-463)
 Sato, Shunsuke, S633 (THU-463)
 Sato, Toshifumi, S180 (FRI-461), S744 (WED-415), S793 (WED-528)
 Satram, Sacha, S1079 (WED-141)
 Sattonnet, Christophe, S792 (WED-526)
 Saunders, Chad, S1115 (WED-191), S1117 (WED-194)
 Sausy, Aurélie, S930 (FRI-202)
 Savarese, Michael, S1039 (FRI-255)
 Saviano, Antonio, S72 (OS-098), S168 (FRI-440), S541 (SAT-237)
 Savino, Alberto, S381 (WED-272)
 Savoldelli, Roberto, S127 (TOP-093)
 Sawada, Koji, S686 (SAT-448)
 Sawhney, Sangeeta, S809 (FRI-467), S823 (FRI-516)
 Saxby, Edward, S15 (OS-002), S860 (SAT-121)

- Saxena, Anoushka, S1027 (FRI-235)
 Saxena, Gaurika, S906 (FRI-163)
 Sayaf, Katia, S322 (TOP-037),
 S770 (WED-456)
 Sayk, Friedhelm, S687 (SAT-449)
 Sayon, Sophie, S1044 (FRI-261)
 Sayuk, Gregory, S815 (FRI-475)
 Sbarigia, Urbano, S1087 (WED-151)
 Scagliotta, Marcelle, S830 (FRI-529)
 Scaioli, Giacomo, S1177 (THU-169),
 S1200 (THU-206)
 Scandali, Giulia, S54 (OS-069)
 Scaravaglio, Miki, S40 (OS-045),
 S55 (OS-070), S374 (WED-260),
 S381 (WED-272), S992 (THU-319)
 Scartozzi, Mario, S592 (THU-143),
 S593 (THU-145)
 Scatton, Olivier, S487 (THU-538)
 Schaadt, Nadine, S561 (SAT-277)
 Schaaf, Louisa, S313 (SAT-546),
 S484 (THU-531)
 Schaap, Frank, S350 (THU-236),
 S542 (SAT-240)
 Schabbauer, Gernot, S28 (OS-024-YI)
 Schaefer, Benedikt, S961 (THU-279),
 S968 (THU-288)
 Schaer, Tifany, S751 (WED-426)
 Schäfer, Volker, S232 (THU-369)
 Schafmayer, Clemens, S364 (FRI-390)
 Schalkwyk, Marije Van,
 S1108 (WED-181)
 Scharitzer, Martina, S505 (FRI-295)
 Schattenberg, Jörn, S1 (GS-001),
 S29 (OS-026), S30 (OS-027),
 S43 (OS-048-YI), S114 (LBP-21),
 S264 (WED-365), S271 (WED-377),
 S300 (SAT-524), S604 (THU-413),
 S607 (THU-418), S612 (THU-426),
 S618 (THU-437), S619 (THU-438),
 S619 (THU-439), S627 (THU-453),
 S640 (THU-474), S643 (THU-552),
 S651 (SAT-394), S652 (SAT-396),
 S654 (SAT-400), S655 (SAT-401),
 S762 (WED-443), S808 (TOP-091),
 S811 (FRI-469), S817 (FRI-507),
 S824 (FRI-518), S865 (SAT-129),
 S995 (THU-324)
 Schaub, Johanna, S322 (WED-215),
 S413 (FRI-335)
 Schaufert, Wendy, S652 (SAT-395)
 Schedlbauer, Anna, S288 (SAT-335)
 Schefczyk, Stefan, S549 (SAT-253),
 S562 (SAT-278)
 Scheiner, Bernhard, S12 (LBO-04),
 S87 (OS-123-YI), S193 (FRI-545),
 S199 (FRI-551), S201 (FRI-554),
 S244 (WED-334), S284 (SAT-330),
 S288 (SAT-335), S292 (SAT-342),
 S294 (SAT-345), S491 (FRI-273),
 S498 (FRI-285), S505 (FRI-295),
 S575 (THU-116), S579 (THU-123),
 S582 (THU-128), S586 (THU-134),
 S831 (FRI-477), S939 (TOP-058)
 Scheller, Juergen, S441 (SAT-368)
 Schemmer, Peter, S477 (THU-519)
 Schepers, Rogier, S524 (TOP-066)
 Schepis, Filippo, S86 (OS-121-YI),
 S87 (OS-123-YI), S279 (TOP-043),
 S287 (SAT-334), S495 (FRI-280),
 S609 (THU-421)
 Schiano, Thomas, S997 (THU-328),
 S1197 (THU-201)
 Schiavo, Luigi, S713 (SAT-493)
 Schiavone, Silvia, S54 (OS-069)
 Schiefer, Judith, S465 (THU-494)
 Schierack, Peter, S514 (FRI-313)
 Schierwagen, Robert, S222 (THU-356),
 S239 (WED-325), S303 (SAT-528),
 S712 (SAT-492)
 Schiffelholz, Willibold, S1186 (THU-181)
 Schiffels, Stephan, S733 (WED-396)
 Schilcher, Gernot, S220 (THU-355)
 Schiller, Dietmar, S975 (THU-295)
 Schilsky, Michael, S958 (THU-274),
 S985 (THU-309)
 Schindler, Aaron, S507 (FRI-299)
 Schindler, Philipp, S61 (OS-080-YI),
 S979 (THU-299)
 Schinoni, Maria, S132 (THU-401)
 Schirmacher, Peter, S547 (SAT-248)
 Schirripa, Marta, S584 (THU-131)
 Schivazappa, Simona, S1082 (WED-146)
 Schlatter, Juliette, S412 (FRI-332)
 Schlattmann, Peter, S487 (THU-539)
 Schleicher, Eva Maria, S264 (WED-365),
 S271 (WED-377)
 Schlenke, Peter, S477 (THU-519)
 Schlevogt, Bernhard, S979 (THU-299),
 S1139 (SAT-156)
 Schluep, Thomas, S85 (OS-120)
 Schlüter, Helmut, S527 (SAT-213)
 Schlüter, Raffael, S277 (WED-387)
 Schmaus, Hagen, S1029 (FRI-240)
 Schmelter, Franziska, S687 (SAT-449)
 Schmid, Michael A., S1147 (TOP-109)
 Schmid, Roland M., S431 (FRI-369)
 Schmid, Stephan, S1003 (THU-377)
 Schmidt, Constantin, S579 (THU-123)
 Schmidt, Dirk Steffen, S238 (WED-323)
 Schmidt, Hartmut, S220 (THU-355),
 S485 (THU-534), S549 (SAT-253),
 S957 (THU-271), S1124 (WED-206),
 S1125 (WED-207), S1139 (SAT-156)
 Schmidt, Mark A., S1079 (WED-141)
 Schmidt, Nathalie, S558 (SAT-271)
 Schmidt, Sergio, S1201 (THU-208),
 S1201 (THU-209)
 Schmidt, Signe, S65 (OS-088)
 Schmidt-Weber, Carsten,
 S945 (THU-256)
 Schmiedeknecht, Anett, S1147 (TOP-110)
 Schmitt-Dischamp, Anne Audrey,
 S172 (FRI-446)
 Schneditz, Georg, S343 (THU-225)
 Schnefeld, Helle Lindholm, S163 (FRI-432),
 S845 (TOP-054)
 Schneider, Annika, S1021 (FRI-223.)
 Schneider, Caitlin, S675 (SAT-432)
 Schneider, Carolin V., S413 (FRI-334),
 S492 (FRI-275), S535 (SAT-227),
 S963 (THU-281)
 Schneider, Carolin Victoria, S636 (THU-467)
 Schneider, Franziska, S229 (THU-366)
 Schneider, Hannah, S240 (WED-326),
 S315 (SAT-551)
 Schneider, Hans, S622 (THU-443)
 Schneider, Kai Markus, S413 (FRI-334),
 S492 (FRI-275), S535 (SAT-227),
 S636 (THU-467)
 Schneider, Paul, S26 (OS-022)
 Schnitzbauer, Andreas, S103 (LBP-07),
 S484 (THU-531)
 Schoder, Maria, S282 (SAT-326),
 S313 (SAT-547)
 Schoelch, Corinna, S723 (SAT-507)
 Schoenlein, Martin, S575 (THU-116),
 S582 (THU-128), S586 (THU-134)
 Schoers, Barbara, S26 (OS-022)
 Schollmeier, Anja, S1039 (FRI-254),
 S1042 (FRI-259)
 Scholtes, Caroline, S1058 (WED-113),
 S1161 (SAT-185), S1170 (SAT-199)
 Schöna, Johanna, S43 (OS-048-YI)
 Schoonjans, Kristina, S734 (WED-397)
 Schoop, Barbara, S849 (WED-482)
 Schophaus, Simon, S636 (THU-467)
 Schott, Eckart, S1147 (TOP-110)
 Schramm, Christoph, S42 (OS-047-YI),
 S56 (OS-073), S60 (OS-079-YI),
 S373 (WED-258), S379 (WED-269),
 S383 (WED-277), S386 (WED-280),
 S403 (WED-307), S450 (SAT-385),
 S541 (SAT-238), S549 (SAT-252),
 S982 (THU-304), S1124 (WED-206),
 S1125 (WED-207), S1139 (SAT-156)
 Schregel, Ida, S42 (OS-047-YI)
 Schreiber, Licita, S1195 (THU-199)
 Schropp, Jonas, S664 (SAT-414)
 Schröter, Dominik, S487 (THU-539)
 Schubert, Kristin, S136 (FRI-393)
 Schulte-Beerbuehl, Sophia,
 S264 (WED-365)
 Schultheiss, Michael, S304 (SAT-531),
 S305 (SAT-534), S318 (SAT-555)
 Schulze, Kornelius, S491 (FRI-273),
 S527 (SAT-213), S575 (THU-116),
 S579 (THU-123), S582 (THU-128),
 S586 (THU-134)
 Schulze zur Wiesch, Julian, S53 (OS-068),
 S970 (THU-290), S1032 (FRI-244),
 S1034 (FRI-248)
 Schulz, Hannah, S836 (FRI-485)
 Schulz, Martin, S185 (FRI-341),
 S313 (SAT-546), S484 (THU-531)
 Schuppan, Detlef, S652 (SAT-396)
 Schuster, Catherine, S72 (OS-098),
 S541 (SAT-237)
 Schwabe, Christian, S1161 (SAT-186)
 Schwabe, Robert F., S38 (OS-041-YI)
 Schwabl, Philipp, S19 (OS-010-YI),
 S222 (THU-357), S244 (WED-334),
 S246 (WED-338), S282 (SAT-326),

Author Index

- S284 (SAT-330), S289 (SAT-336),
S294 (SAT-345), S313 (SAT-547),
S316 (SAT-553), S337 (WED-243),
S939 (TOP-058)
- Schwab, Patrick, S1151 (SAT-171)
- Schwade, Daniel, S596 (THU-150)
- Schwartz, Fionnuala, S483 (THU-530)
- Schwartz, Myron, S527 (SAT-213)
- Schwarzinger, Michael, S859 (SAT-120)
- Schwarz, Kathleen, S971 (THU-291)
- Schwarzl, Jakob, S354 (THU-242)
- Schwarz, Michael, S37 (OS-039-YI),
S90 (OS-127-YI), S193 (FRI-545),
S199 (FRI-551), S201 (FRI-554),
S244 (WED-334), S286 (SAT-332),
S288 (SAT-335), S292 (SAT-342),
S299 (SAT-521), S1135 (SAT-150)
- Schweiger, Sofia, S238 (WED-323)
- Schwiering, Fabian, S330 (WED-230)
- Schwinge, Dorothee, S60 (OS-079-YI),
S450 (SAT-385)
- Scifo, Gaetano, S40 (OS-045), S55 (OS-070)
- Scilabra, Simone, S457 (THU-480)
- Scionti, Francesca, S568 (SAT-288)
- Sciveres, Marco, S966 (THU-285),
S987 (THU-313), S1002 (THU-336)
- Scivetti, Paolo, S40 (OS-045), S55 (OS-070)
- Scott, Charlotte, S445 (SAT-375)
- Seah Lee, Way, S971 (THU-291)
- Seaman, Sian, S434 (SAT-356)
- Sebagh, Mylène, S981 (THU-303)
- Sebastiani, Giada, S609 (THU-421),
S645 (THU-557), S900 (FRI-151)
- Sebode, Marcial, S56 (OS-073)
- Seco, Luis Manuel Cervera, S736 (WED-400)
- Seed, Paul, S36 (OS-037)
- Seehofer, Daniel, S483 (THU-529)
- Segaux, Lauriane, S467 (THU-498)
- Segeral, Olivier, S897 (FRI-146)
- Segovia-Miranda, Fabián, S361 (FRI-384)
- Segovia-Zafra, Antonio, S142 (FRI-403)
- Ségrestin, Bérénice, S603 (THU-410),
S687 (SAT-450), S701 (SAT-469)
- Sehgal, Rashi, S218 (THU-351)
- Seidel, Florine, S763 (WED-444)
- Seidensticker, Max, S576 (THU-118)
- Seidita, Aurelio, S568 (SAT-288)
- Seifert, Sarah, S364 (FRI-390)
- Sejling, Anne-Sophie, S31 (OS-029),
S827 (FRI-523)
- Sekhar, Mallika, S964 (THU-283)
- Seko, Yuya, S616 (THU-433)
- Selcanova, Svetlana Adamcova,
S871 (SAT-136)
- Selicean, Sonia, S20 (OS-012-YI)
- Selinger, Doug, S338 (WED-246)
- Selleri, Silvia, S937 (TOP-056)
- Sellick, Abigail, S1198 (THU-203)
- Seltmann, Jonathan, S1043 (FRI-260),
S1050 (FRI-270)
- Selzer, Niclas, S244 (WED-335)
- Selzner, Nazia, S474 (THU-512)
- Semela, David, S481 (THU-526),
S849 (WED-482)
- Semellini, Filippo, S493 (FRI-277),
S495 (FRI-280)
- Semmler, Georg, S19 (OS-010-YI),
S37 (OS-039-YI), S61 (OS-080-YI),
S87 (OS-123-YI), S90 (OS-127-YI),
S193 (FRI-545), S199 (FRI-551),
S222 (THU-357), S224 (THU-358),
S244 (WED-334), S279 (TOP-043),
S282 (SAT-326), S284 (SAT-330),
S286 (SAT-332), S288 (SAT-335),
S289 (SAT-336), S292 (SAT-342),
S299 (SAT-521), S300 (SAT-524),
S313 (SAT-547), S316 (SAT-553),
S831 (FRI-477), S832 (FRI-479),
S939 (TOP-058)
- Semmo, Nasser, S412 (FRI-332),
S481 (THU-526)
- Semple, Sean, S35 (OS-034)
- Sempoux, Christine, S12 (LBO-04),
S105 (LBP-08)
- Semrau, Jeremy, S948 (THU-259)
- Sen, Binay, S830 (FRI-530)
- Sendra, Carmen, S248 (WED-341)
- Seneshaw, Mulugeta, S749 (WED-422)
- Senkal, Volkan, S709 (SAT-485)
- Senkerikova, Renata, S61 (OS-080-YI)
- Senosiáin, Maria, S133 (THU-404),
S481 (THU-525)
- Senzolo, Marco, S183 (TOP-049),
S293 (SAT-343)
- Seo, Daekwan, S456 (THU-479)
- Seok, Oh Seung, S796 (WED-534)
- Seo, Sang Hyun, S362 (FRI-387),
S552 (SAT-259)
- Seo, Seung Young, S516 (FRI-318)
- Seo, Yeon Seok, S578 (THU-121),
S585 (THU-132), S720 (SAT-502),
S781 (WED-476), S798 (WED-540),
S1136 (SAT-151)
- Serafini, Peter, S995 (THU-324)
- Serdjebi, Cindy, S673 (SAT-429),
S694 (SAT-461)
- Serenari, Matteo, S519 (FRI-322)
- Sererols-Viñas, Laura, S78 (OS-109-YI)
- Serfaty, Lawrence, S110 (LBP-15),
S168 (FRI-440)
- Serfert, Yvonne, S1174 (THU-166)
- Serizawa, Reza, S742 (WED-411),
S748 (WED-421)
- Serper, Marina, S45 (OS-052),
S188 (FRI-535), S248 (WED-342),
S265 (WED-366)
- Serra, Jerònima, S1191 (THU-190)
- Serra, Miguel, S693 (SAT-460),
S921 (FRI-188)
- Serra, Miquel, S10 (LBO-01)
- Serrano, Héctor, S160 (FRI-426)
- Serrano-Macia, Marina, S140 (FRI-399),
S532 (SAT-221), S544 (SAT-244),
S546 (SAT-247)
- Serrano, Mercedes, S1178 (THU-171)
- Serrano, Sara Román, S853 (WED-491)
- Serrano, Trinidad, S1187 (THU-183)
- Serranti, Daniele, S969 (THU-289)
- Serras, Ana, S142 (FRI-403)
- Sersté, Thomas, S1114 (WED-190)
- Serviddio, Gaetano, S750 (WED-424),
S814 (FRI-474)
- Setaffy, Lisa, S996 (THU-327)
- Seto, Wai-Kay, S52 (OS-065-YI),
S53 (OS-067), S62 (OS-082),
S195 (FRI-546), S490 (TOP-068),
S680 (SAT-439), S1132 (SAT-145),
S1134 (SAT-148), S1137 (SAT-153),
S1152 (SAT-172)
- Setoyama, Hiroko, S1095 (WED-163)
- Settmacher, Utz, S487 (THU-539)
- Seufferlein, Thomas, S1139 (SAT-156)
- Sevak, Jayesh Kumar, S218 (THU-351),
S1027 (FRI-235)
- Sevastianos, Vasilis, S262 (WED-362),
S1128 (WED-211)
- Sevenants, Linde, S410 (FRI-330)
- Sevigny, Emma, S35 (OS-034)
- Sevilla, Karina, S1202 (THU-211)
- Seydi, Moussa, S916 (FRI-178),
S1117 (WED-195)
- Seyedkazemi, Star, S671 (SAT-426)
- Seyler, Thomas, S880 (FRI-121)
- Shabaneh, Suha, S484 (THU-532)
- Shabeeb, Reem Al, S905 (FRI-159)
- Shackel, Nicholas, S523 (FRI-329)
- Shadaker, Shaun, S881 (FRI-123),
S889 (FRI-133), S890 (FRI-135),
S891 (FRI-136), S898 (FRI-147),
S909 (FRI-167), S925 (FRI-193),
S930 (FRI-203), S931 (FRI-205),
S933 (FRI-210), S1204 (THU-214)
- Shafqat, Ghania, S1196 (THU-200)
- Shafqat, Muhammad Nabeel,
S912 (FRI-172), S1196 (THU-200)
- Shafir, Asher, S484 (THU-532)
- Shagrani, Mohammad, S969 (THU-289)
- Shagrani, Mohammad Ali, S859 (SAT-119)
- Shaham-Niv, Shira, S669 (SAT-423)
- Shah, Dipam, S600 (TOP-081)
- Shaheen, Abdel Aziz, S371 (WED-255),
S1117 (WED-194)
- Shaheen, Abdel-Aziz, S175 (FRI-451),
S652 (SAT-395)
- Shah, Hemant A, S254 (WED-349),
S255 (WED-351), S270 (WED-375)
- Shahi, Pradeep, S607 (THU-419)
- Shah, Masaud, S785 (WED-513)
- Shah, Parth, S815 (FRI-475)
- Shah, Rushabh, S558 (SAT-271)
- Shah, Sital, S91 (OS-128), S962 (THU-280),
S1069 (WED-128)
- Shah, Uzma, S972 (THU-291)
- Shah, Vijay, S145 (TOP-073), S171 (FRI-444)
- Shah, Wasiuddin, S896 (FRI-145),
S912 (FRI-172)
- Shaikh, Anjiya, S173 (FRI-448)
- Shaji, Aswin, S846 (WED-477)
- Shalabi, Hanaa, S1212 (THU-224)
- Shalaby, Sarah, S87 (OS-123-YI),
S183 (TOP-049), S293 (SAT-343),
S843 (FRI-499)

- Shalimar, S53 (OS-067), S73 (OS-101-YI), S297 (SAT-350), S587 (THU-135), S693 (SAT-459), S1137 (SAT-153)
- Shalimar, Shalimar, S197 (FRI-548), S401 (WED-304)
- Shamir, Raanan, S955 (THU-269)
- Shang, Jia, S34 (OS-033), S196 (FRI-547), S1133 (SAT-147), S1165 (SAT-193)
- Shang, Ying, S159 (FRI-425), S276 (WED-384), S302 (SAT-527), S600 (TOP-079), S605 (THU-414), S650 (TOP-085), S653 (SAT-397), S654 (SAT-399), S959 (THU-275)
- Shankar, R. Ravi, S49 (OS-060)
- Shankar, Sahana, S971 (THU-291)
- Shannon, Christopher, S79 (OS-112)
- Shantanu, P.A., S560 (SAT-274)
- Shao, Anran Shao, S844 (FRI-500)
- Shao, Chen, S358 (FRI-381), S1090 (WED-155)
- Shao, Lan, S808 (TOP-091), S820 (FRI-512)
- Shao, Xiaorong, S64 (OS-085)
- Shapira, Ortal Yzhaky, S859 (SAT-120)
- Sharapov, Said, S113 (LBP-19)
- Sharif, Omar, S28 (OS-024-YI)
- Sharma, Aarti, S208 (THU-338), S228 (THU-363)
- Sharma, Ashish, S507 (FRI-300)
- Sharma, Ashok, S235 (TOP-044)
- Sharma, Barjesh, S235 (TOP-044)
- Sharma, Chhagan, S149 (FRI-411)
- Sharma, Manoj Kumar, S293 (SAT-344)
- Sharma, Mithun, S274 (WED-382)
- Sharma, Naveen, S123 (LBP-36)
- Sharma, Neha, S17 (OS-006-YI), S21 (OS-014-YI), S76 (OS-107-YI), S139 (FRI-398), S146 (FRI-407), S149 (FRI-410), S152 (FRI-416), S326 (WED-222), S414 (FRI-344), S1033 (FRI-247)
- Sharma, Nupur, S17 (OS-006-YI), S21 (OS-014-YI), S76 (OS-107-YI), S139 (FRI-398), S146 (FRI-407), S149 (FRI-410), S152 (FRI-416), S326 (WED-222), S414 (FRI-344), S1033 (FRI-247)
- Sharma, Riddhi, S556 (SAT-267)
- Sharma, Rohini, S575 (THU-116), S576 (THU-118), S586 (THU-134), S864 (SAT-127)
- Sharma, Sanchit, S6 (GS-006), S233 (TOP-041)
- Sharma, Satya Priya, S156 (FRI-420), S177 (FRI-456), S220 (THU-354), S343 (THU-227)
- Sharma, Shakshi, S296 (SAT-349)
- Sharma, Shawn, S920 (FRI-186), S929 (FRI-200)
- Sharma, Shvetank, S17 (OS-006-YI), S76 (OS-107-YI)
- Sharma, Shyam Sunder, S238 (WED-322)
- Sharma, Sonu, S401 (WED-304)
- Sharp, Cassandra, S782 (WED-506)
- Sharvadze, Lali, S881 (FRI-123), S889 (FRI-133), S1204 (THU-214)
- Shasthry, S Muralikrishna, S7 (GS-008-YI), S953 (THU-266)
- Shasthry, Varsha, S277 (WED-388)
- Shavva, Vladimir S, S756 (WED-434)
- Shawa, Isaac, S522 (FRI-327)
- Shawcross, Debbie L, S7 (GS-007), S35 (OS-035-YI)
- Shaw, Jawaaid, S195 (FRI-546), S258 (WED-355)
- Shaw, Tanya, S324 (WED-218), S324 (WED-219)
- Shearer, Jessica, S1175 (THU-167)
- Sheehan, Julia, S1182 (THU-176)
- She, Huiyu, S971 (THU-291)
- Sheikh, Mohammed, S220 (THU-355)
- Sheikh, Muhammad Y, S808 (TOP-091)
- Shekhtman, Louis, S1170 (SAT-200)
- Shen, Chang, S1152 (SAT-173)
- Shen, Feng, S756 (WED-433)
- Sheng, Jifang, S1153 (SAT-174)
- Shen, Michael, S1058 (WED-114), S1167 (SAT-195)
- Shepherd, Amy, S783 (WED-508)
- Sheridan, David, S624 (THU-447), S708 (SAT-483)
- Shermadini, Ketevan, S921 (FRI-187)
- Sheron, Nick, S103 (LBP-06)
- Sheshadri, Somya, S274 (WED-382)
- She, Shaoping, S540 (SAT-235)
- Sheth, Roosey, S127 (TOP-093)
- Shewaye, Abate, S1120 (WED-199)
- She, Wong, S48 (OS-058)
- Shibolet, Oren, S243 (WED-333), S315 (SAT-550), S403 (WED-308)
- Shibo, Meng, S138 (FRI-396)
- Shi, Dan, S858 (SAT-117)
- Shi, Dongyan, S20 (OS-013), S186 (FRI-342), S204 (FRI-559), S436 (SAT-359)
- Shigeo, Shimose, S584 (THU-131), S592 (THU-143), S593 (THU-145)
- Shi, Haobing, S347 (THU-232)
- Shih, Yu-Jia, S1129 (WED-214)
- Shih, Yu-Lueng, S825 (FRI-521)
- Shi, Junping, S638 (THU-471), S696 (SAT-463), S724 (SAT-510)
- Shi, Ke, S193 (FRI-544)
- Shilton, Sonjelle, S898 (FRI-147), S930 (FRI-203)
- Shimada, Yuji, S633 (THU-463)
- Shimakawa, Yusuke, S67 (OS-090-YI), S897 (FRI-146), S916 (FRI-178), S923 (FRI-191), S1046 (FRI-265), S1106 (WED-178), S1106 (WED-179), S1117 (WED-195)
- Shima, Toshihide, S616 (THU-433)
- Shimazaki, Atsuyuki, S323 (WED-216)
- Shi, Mingxia, S406 (WED-313)
- Shimizu, Masahito, S1183 (THU-177)
- Shimizu, Mayuko, S733 (WED-395)
- Shim, Jae-Jun, S1136 (SAT-151)
- Shim, Ju Hyun, S556 (SAT-266), S573 (THU-113), S589 (THU-140), S998 (THU-330), S1062 (WED-121), S1139 (SAT-155)
- Shim, Wan Seob, S567 (SAT-287)
- Shin, Donghun, S438 (SAT-362)
- Shin, Dong Wook, S510 (FRI-306), S642 (THU-550)
- Shin, Eui-Cheol, S1048 (FRI-268)
- Shin, Hyunjae, S1048 (FRI-268), S1062 (WED-120), S1144 (SAT-163)
- Shin, Jaehee, S102 (LBP-05)
- Shin, Ji Hyun, S437 (SAT-361), S456 (THU-479), S563 (SAT-281), S947 (THU-258)
- Shioda, Kaori, S240 (WED-327)
- Shiota, Atsushi, S409 (TOP-060)
- Shirakata, Yuka, S544 (SAT-243)
- Shiri, Ahmad Mustafa, S525 (TOP-069)
- Shi, Xiaofeng, S271 (WED-376), S1146 (SAT-165)
- Shi, Yu, S196 (FRI-547)
- Shi, Yujing, S858 (SAT-117)
- Shi, Zhenzhen, S1038 (FRI-253)
- Shi, Zongkui, S489 (TOP-065)
- Shlomai, Amir, S1195 (THU-199)
- Shlomi, Tomer, S669 (SAT-423)
- Shmanko, Kateryna, S491 (FRI-273)
- Shoaie, Saeed, S7 (GS-007), S205 (TOP-042)
- Shoop, Wendy, S35 (OS-034)
- Shostakovych-Koretska, Liudmyla, S1010 (THU-387)
- Sho, Takuya, S584 (THU-131)
- Shousha, Hend Ibrahim, S570 (SAT-291)
- Shringarpure, Reshma, S808 (TOP-091), S820 (FRI-512)
- Shteyer, Eyal, S128 (THU-394)
- Shuangdi, Duan, S735 (WED-399), S775 (WED-463)
- Shukla, Akash, S87 (OS-123-YI), S282 (SAT-325), S290 (SAT-338), S310 (SAT-542), S983 (THU-305)
- Shulha, Nataliia, S429 (FRI-367)
- Siakavellas, Spyridon (Spyros), S1194 (THU-196), S1194 (THU-197)
- Sica, Simona, S88 (OS-124-YI)
- Sicilia, Mauricio Garcia Saenz De, S296 (SAT-349), S900 (FRI-151)
- Sicuro, Chiara, S519 (FRI-322)
- Sidali, Sabrina, S491 (FRI-273), S505 (FRI-295), S577 (THU-120), S578 (THU-122), S585 (THU-133)
- Siddiqi, Harris, S65 (OS-086), S662 (SAT-412)
- Siddiqi, Najeeha, S383 (WED-276)
- Siddiqui, Mohammad Shadab, S468 (THU-500), S629 (THU-456)
- Sidorova, Julia, S163 (FRI-431)
- Siebenhüner, Alexander, S491 (FRI-273)
- Sieberhagen, Cyril, S617 (THU-434)
- Siena, Martina De, S1082 (WED-146)
- Sierra, Olivia, S1187 (THU-183)
- Sierra, Patricia, S143 (FRI-404)
- Sievert, Alex, S815 (FRI-475)
- Siew, Susan, S971 (THU-291)
- Sifrim, Alejandro, S753 (WED-430)

Author Index

- Sigal, Michael, S351 (THU-238)
 Sigon, Giordano, S624 (THU-446)
 Sigüenza, Rebeca, S700 (SAT-468)
 Siguier, Martin, S1160 (SAT-184)
 Sijtsma, Marijn, S14 (LBO-06)
 Sikaroodi, Masoumeh, S342 (TOP-038), S347 (THU-233)
 Silberhumer, Gerd, S470 (THU-505)
 Silberstein, Francesca Ceccherini, S1056 (TOP-106), S1105 (WED-176), S1142 (SAT-159)
 Si, Lei, S523 (FRI-329)
 Siletta, Marianna, S593 (THU-145)
 Silungwe, Niza, S522 (FRI-327)
 Silva, Daniela, S734 (WED-397)
 Silva de Oliveira, Daniel Apolônio, S1051 (FRI-272)
 Silva, Elsy Soraya Salas, S437 (SAT-361), S456 (THU-479), S563 (SAT-281), S947 (THU-258)
 Silvain, Christine, S61 (OS-081)
 Silva, Joel, S86 (OS-121-YI)
 Silva, Marcelo, S132 (THU-401)
 Silva, Margarida, S734 (WED-397)
 Silva, Raul, S775 (WED-464)
 Silvestri, Alessandra, S753 (WED-430)
 Silvestri, Laura, S749 (WED-423), S774 (WED-461)
 Sim, Alyssa, S300 (SAT-522)
 Simao, Adelia, S842 (FRI-495)
 Simão, André L., S279 (WED-390), S734 (WED-397), S738 (WED-404)
 Simbrunner, Benedikt, S19 (OS-010-YI), S37 (OS-039-YI), S61 (OS-080-YI), S193 (FRI-545), S199 (FRI-551), S201 (FRI-554), S222 (THU-357), S224 (THU-358), S244 (WED-334), S246 (WED-338), S284 (SAT-330), S286 (SAT-332), S288 (SAT-335), S289 (SAT-336), S292 (SAT-342), S294 (SAT-345), S316 (SAT-553), S831 (FRI-477), S939 (TOP-058)
 Simeone, Irene, S545 (SAT-245), S550 (SAT-254)
 Simian, Daniela, S396 (WED-295)
 Simioni, Paolo, S72 (OS-099), S293 (SAT-343), S564 (SAT-283)
 Simmons, David, S861 (SAT-123)
 Simmons, Ruth, S909 (FRI-165)
 Simón-Codina, Blanca, S333 (WED-235)
 Simone, Loredana, S40 (OS-045), S55 (OS-070)
 Simonetto, Douglas, S101 (LBP-03), S241 (WED-328)
 Simon, Evangeline, S488 (THU-544)
 Simoni, Manuela, S729 (SAT-517)
 Simon, Jean-Marc, S589 (THU-139)
 Simon, Karl-Georg, S1174 (THU-166), S1186 (THU-181)
 Simon, Miguel Angel, S380 (WED-270)
 Simón, Miguel Angel, S366 (TOP-061)
 Simón-Santamaria, Jaione, S449 (SAT-383)
 Simonsen, Hans Erling, S1150 (SAT-170)
 Simón-Talero, Macarena, S86 (OS-121-YI), S87 (OS-123-YI), S970 (THU-290)
 Simon, Tracey, S82 (OS-116-YI)
 Simpson, Kara, S8 (GS-010), S71 (OS-097)
 Sims, Karen, S125 (LBP-38), S1171 (SAT-202)
 Sina, Christian, S536 (SAT-230)
 Sinakos, Emmanouil, S400 (WED-302)
 Sinatti, Gaia, S646 (THU-560), S685 (SAT-446)
 Sinclair, Marie, S311 (SAT-543), S625 (THU-450)
 Singal, Amit, S575 (THU-116), S582 (THU-128), S586 (THU-134), S1189 (THU-185)
 Singal, Ashwani, S179 (FRI-459), S468 (THU-499), S627 (THU-453), S863 (SAT-125), S865 (SAT-129), S900 (FRI-151)
 Singanayagam, Arjuna, S284 (SAT-329), S452 (SAT-389)
 Singaraja, Roshni Rebecca, S351 (THU-237)
 Singer, Amanda, S1059 (WED-116)
 Singh, Ankita, S310 (SAT-542), S983 (THU-305)
 Singh, Jenn, S1151 (SAT-171), S1167 (SAT-196)
 Singh, Manavi, S417 (FRI-350)
 Singh, Neetu, S436 (SAT-360)
 Singh, Ravinder, S17 (OS-006-YI), S1047 (FRI-267)
 Singh, Roshni, S1180 (THU-173)
 Singh, Seema, S649 (TOP-083)
 Singh, Shivaram, S253 (WED-348)
 Singh, Shraddha, S228 (THU-362)
 Singh, Sumeet, S735 (WED-398)
 Singh, Virendra, S253 (WED-348)
 Sinkala, Edford, S916 (FRI-178), S1117 (WED-195)
 Sinn, Dong Hyun, S267 (WED-369), S305 (SAT-533), S513 (FRI-312), S585 (THU-132), S631 (THU-459), S821 (FRI-514)
 Sinner, Friedrich, S47 (OS-057)
 Sipeki, Nóra, S23 (OS-017-YI), S42 (OS-047-YI)
 Siribelli, Alessia, S120 (LBP-29), S837 (FRI-487)
 Siripon, Nipaporn, S217 (THU-349)
 Sirlin, Claude, S839 (FRI-490)
 Sironi, Sandro, S381 (WED-272)
 Sirvent, Pascal, S806 (WED-555)
 Sistilli, Gabriella, S784 (WED-509)
 Sista, Ramakrishna, S560 (SAT-274)
 Si, Tengfei, S445 (SAT-376)
 Sitko, Marek, S505 (FRI-296), S1205 (THU-215)
 Sivanath, Tirukonda Prasanna, S278 (WED-389)
 Sivertsen Nordhus, Kathrine, S421 (FRI-355)
 Sjöblom, Nellii, S997 (THU-329)
 Sjöland, Wilhelm, S778 (WED-470)
 Skalicky, Susanna, S45 (OS-051-YI)
 Skinner, Charlotte, S601 (TOP-088)
 Skladany, Lubomir, S871 (SAT-136)
 Skoien, Richard, S266 (WED-367)
 Skok, Kristijan, S996 (THU-327)
 Skröder, Helena, S654 (SAT-399)
 Skrypnyk, Igor, S136 (THU-408)
 Skrypnyk, Roman, S136 (THU-408)
 Skvarkova, Beata, S871 (SAT-136)
 Skyttthe, Maria Kløjgaard, S657 (SAT-404)
 Slagle, Ashley F., S1087 (WED-151)
 Slaughter, Eugene, S230 (THU-367)
 Sleiman, Marwan, S995 (THU-324)
 Slits, Florence, S24 (OS-018-YI), S531 (SAT-220)
 Sljukic, Aleksandra, S364 (FRI-390)
 Sloomer, Charlotte, S44 (OS-049-YI)
 Smadhi, Ryad, S170 (FRI-442), S930 (FRI-204)
 Smedsrød, Bård, S449 (SAT-383)
 Smets, Lena, S345 (THU-229), S452 (SAT-390), S753 (WED-430)
 Smid, Vaclav, S292 (SAT-341), S727 (SAT-513)
 Smit, Colette, S892 (FRI-138)
 Smith, Amy Rhoden, S35 (OS-034)
 Smith, Coleman I., S89 (OS-125)
 Smith, Daniel, S632 (THU-461), S722 (SAT-506)
 Smith, David, S548 (SAT-251), S1029 (FRI-238), S1029 (FRI-239), S1051 (FRI-272)
 Smith, Graham, S411 (FRI-331)
 Smith, Helen, S397 (WED-297)
 Smith, Ian, S434 (SAT-355)
 Smith, Jeff, S35 (OS-034)
 Smolinska, Agnieszka, S840 (FRI-492)
 Smoot, Rory L., S44 (OS-050-YI), S465 (THU-495)
 Smud, Astrid, S245 (WED-336)
 Smuk, Melanie, S726 (SAT-512)
 Smuts, Heidi, S1184 (THU-178)
 Smyk, Wiktor, S950 (THU-262)
 Snabel, Jessica, S786 (WED-515)
 Snijders, Romée, S14 (LBO-06), S373 (WED-258), S982 (THU-304)
 Snir, Tom, S415 (FRI-345)
 Soardo, Giorgio, S500 (FRI-288)
 Soares, Elza, S253 (WED-348)
 Sobenko, Natalia, S56 (OS-073)
 Sobolewski, Cyril, S146 (FRI-408)
 Sobrino, Carmen Iglesias, S397 (WED-296)
 Sobrino, Nieves Martín, S886 (FRI-129)
 Socha, Łukasz, S505 (FRI-296)
 Socha, Piotr, S837 (FRI-486), S950 (THU-262), S967 (THU-286)
 Soeda, Junpei, S205 (TOP-042)
 Soe, Phymar, S886 (FRI-130)
 Soffredini, Roberta, S1154 (SAT-175), S1159 (SAT-181), S1164 (SAT-190)
 Sofia, Michael J., S1171 (SAT-202)
 Sofias, Alexandros Marios, S26 (OS-022)
 Sogabe, Maki, S1041 (FRI-257)
 Sogni, Philippe, S161 (FRI-429), S859 (SAT-120)

- Sohn, Joo Hyun, S615 (THU-431), S667 (SAT-418), S695 (SAT-462), S701 (SAT-470), S704 (SAT-475), S705 (SAT-476), S757 (WED-435), S794 (WED-531), S864 (SAT-128), S1073 (WED-135)
- Sohn, Won, S637 (THU-469), S697 (SAT-464), S1073 (WED-135), S1184 (THU-179), S1197 (THU-202)
- So, Joshua, S914 (FRI-176), S1052 (SAT-141), S1182 (THU-175)
- Sokal, Etienne, S123 (LBP-35), S198 (FRI-550), S387 (WED-282), S439 (SAT-364), S807 (TOP-077), S965 (THU-284), S969 (THU-289), S971 (THU-291)
- Solà, Elsa, S250 (WED-343)
- Soldà, Caterina, S584 (THU-131)
- Soldani, Cristiana, S446 (SAT-377)
- Solé, Cristina, S10 (LBO-01), S250 (WED-343)
- Soliman, Gian Paulo Alberto, S298 (SAT-520)
- Soliman, Riham, S91 (OS-128), S642 (THU-551)
- Soliman, Thomas, S465 (THU-494), S470 (THU-505), S489 (THU-545)
- Solis-Munoz, Pablo, S18 (OS-007)
- Sölter, Ricarda, S339 (WED-248)
- Somasundar, Ponnadai, S472 (THU-508)
- Somay, Kayra, S928 (FRI-199)
- Sombie, Roger, S916 (FRI-178), S1117 (WED-195)
- Some, Fatuma, S865 (SAT-129)
- Sonajalg, Jaak, S969 (THU-289)
- Son, Da-Hye, S633 (THU-464)
- Sonderup, Mark, S875 (FRI-115), S916 (FRI-178), S1117 (WED-195), S1184 (THU-178)
- Song, Bao-Jun, S1165 (SAT-193)
- Song, Byeong Geun, S267 (WED-369), S305 (SAT-533), S631 (THU-459)
- Song, Do Seon, S186 (FRI-343), S190 (FRI-538)
- Song, Eun-Bi, S752 (WED-427)
- Song, Jiankang, S308 (SAT-539)
- Song, Joon Young, S1048 (FRI-268)
- Song, Jung Eun, S645 (THU-558)
- Song, Michael, S658 (SAT-406), S703 (SAT-473)
- Song, Moo Young, S414 (FRI-336), S752 (WED-427)
- Song, Myeong Jun, S515 (FRI-315)
- Song, Qianqian, S489 (TOP-065)
- Song, Sung-Won, S778 (WED-471)
- Song, Zhuolun, S80 (OS-113)
- Sonika, Ujjwal, S235 (TOP-044)
- Sonneveld, Milan, S52 (OS-065-YI), S83 (OS-118), S306 (SAT-536), S454 (TOP-052), S1100 (WED-169), S1132 (SAT-145), S1134 (SAT-148)
- Sonntag, Roland, S416 (FRI-348)
- Sonzogni, Aurelio, S471 (THU-507), S966 (THU-285)
- Sood, Siddarth, S380 (WED-271)
- Sookoian, Silvia, S625 (THU-448)
- Soon, Gwyneth, S757 (WED-436)
- Sorda, Juan Antonio, S105 (LBP-09)
- Sørensen, Karen Kristine, S449 (SAT-383)
- Soresi, Maurizio, S568 (SAT-288)
- Soret, Pierre-Antoine, S56 (OS-073)
- Soria, Anna, S15 (OS-001), S163 (FRI-431), S250 (WED-343), S664 (SAT-415), S737 (WED-403), S851 (WED-486)
- Soriano, German, S10 (LBO-01), S807 (TOP-077)
- Soria, Nora, S1191 (THU-190)
- Sørrig, Rasmus, S65 (OS-088)
- Sorz, Thomas, S222 (THU-357), S289 (SAT-336), S316 (SAT-553)
- So, Shinichi, S559 (SAT-272)
- Sosnovtseva, Svetlana, S102 (LBP-05)
- Soto, Antonio Buño, S690 (SAT-454)
- Soulayrac, Cathy, S170 (FRI-443)
- Souleiman, Roni, S1031 (FRI-242)
- Soulter, Alexandre, S1109 (WED-182)
- Soumelis, Vassili, S1093 (WED-159)
- Sousa-Martin, Jose Manuel, S366 (TOP-061), S380 (WED-270)
- Sovan, Saren, S897 (FRI-146)
- Sowah, Leonard, S1023 (FRI-226), S1159 (SAT-182)
- Sowa, Jan-Peter, S628 (THU-454)
- Sowell, France, S995 (THU-324)
- Soy, Guillem, S87 (OS-123-YI)
- Soza, Alejandro, S900 (FRI-151)
- Spaan, Michelle, S306 (SAT-536)
- Spaggiari, Giorgia, S729 (SAT-517)
- Spallanzani, Andrea, S942 (THU-251)
- Spanoudaki, Anastasia, S1128 (WED-211)
- Sparchez, Zeno, S245 (WED-337), S297 (SAT-519)
- Sparling, Nicole, S1008 (THU-386)
- Spasic, Marija, S465 (THU-494)
- Spearmen, Wendy, S865 (SAT-129), S875 (FRI-115), S916 (FRI-178), S1117 (WED-195), S1184 (THU-178)
- Specchia, Giorgia, S88 (OS-124-YI)
- Spedtsberg, Ida Ziegler, S17 (OS-005-YI), S173 (FRI-449), S175 (FRI-452), S303 (SAT-528)
- Speiciene, Danute, S912 (FRI-173)
- Speksnijder, Arjen, S786 (WED-515)
- Spengler, Ulrich, S422 (FRI-357), S429 (FRI-366)
- Sperl, Jan, S963 (THU-281), S1173 (THU-164)
- Spinetti, Angiola, S920 (FRI-185)
- Spinnato, Francesca, S568 (SAT-288)
- Spivak, Igor, S951 (THU-264)
- Sporea, Ioan, S61 (OS-080-YI)
- Spraul, Anne, S969 (THU-289)
- Sprengers, Dave, S306 (SAT-536), S501 (FRI-291), S561 (SAT-276)
- Springer, Emily, S1021 (FRI-223)
- Springfeld, Christoph, S594 (THU-147)
- Sprinzl, Kathrin, S108 (LBP-12), S1139 (SAT-156)
- Sprinzl, Martin, S640 (THU-474), S1139 (SAT-156), S1147 (TOP-110)
- Squires, James E., S971 (THU-291)
- Squires, Robert H., S123 (LBP-35), S387 (WED-282)
- Sridharan, Shamira, S671 (SAT-426)
- Sridhar, Niranjan, S671 (SAT-426)
- Srinivasan, Sathish, S473 (THU-510)
- Sripchoosanaphan, Supachaya, S217 (THU-349), S1047 (FRI-266)
- Sripongpun, Pimsiri, S514 (FRI-314), S663 (SAT-413), S721 (SAT-503)
- Sritharan, Nanthara, S577 (THU-120)
- Srivastava, Ankur, S867 (SAT-130)
- Srivastava, Siddharth, S235 (TOP-044)
- Sroda, Natalie, S323 (WED-216)
- S, Sudhindran, S827 (FRI-524)
- S, Suja Kumari, S827 (FRI-524)
- Stacey, Duncan, S307 (SAT-537)
- Stadlbauer, Vanessa, S220 (THU-355), S346 (THU-230), S354 (THU-242)
- Stadlmayr, Sarah, S739 (WED-405), S746 (WED-418)
- Staels, Bart, S211 (THU-342), S355 (THU-244), S666 (SAT-417), S668 (SAT-421), S772 (WED-458)
- Stafford, Nina, S864 (SAT-127)
- Stallmach, Andreas, S1147 (TOP-110)
- Stal, Per, S605 (THU-414), S650 (TOP-085), S653 (SAT-397), S865 (SAT-129), S960 (THU-276)
- Staltner, Raphaela, S798 (WED-539)
- Stam, Janine, S740 (WED-407)
- Stamm, Luisa M., S1149 (SAT-168), S1153 (SAT-174), S1161 (SAT-186)
- Stampa, Grit, S339 (WED-248)
- Stampf, Susanne, S481 (THU-526)
- Stan, Adriana, S1006 (THU-382)
- Standen, Mary, S371 (WED-256)
- Ständer, Sonja, S377 (WED-265)
- Stanford-Moore, Adam, S31 (OS-029), S790 (WED-522)
- Stange, Jan, S220 (THU-355)
- Stankevici, Evelina, S173 (FRI-449)
- Stardelova, Kalina Grivcheva, S198 (FRI-550)
- Starke, Ingemar, S57 (OS-074-YI)
- Starlinger, Johannes, S44 (OS-050-YI)
- Starlinger, Patrick, S44 (OS-050-YI), S45 (OS-051-YI), S142 (FRI-402), S465 (THU-495), S538 (SAT-233), S564 (SAT-282)
- Staropoli, Nicoletta, S568 (SAT-288)
- Stary, Georg, S294 (SAT-345)
- Stasio, Rosa Claudia, S917 (FRI-180), S1177 (THU-169), S1200 (THU-206)
- Stathopoulou, Ioanna, S595 (THU-149)
- Stättermayer, Albert, S37 (OS-039-YI), S201 (FRI-554), S286 (SAT-332), S936 (TOP-055)
- Stauber, Rudolf E., S491 (FRI-273), S582 (THU-128), S865 (SAT-129)
- Stauffer, Winston, S748 (WED-420), S770 (WED-455)

Author Index

- Stecchi, Michele, S640 (THU-475), S691 (SAT-457)
- Steenkiste, Christophe Van, S229 (THU-364), S764 (WED-446)
- Stefanescu, Horia, S151 (FRI-413), S178 (FRI-457), S245 (WED-337), S283 (SAT-327), S295 (SAT-347), S297 (SAT-519)
- Stefanini, Benedetta, S586 (THU-134)
- Stefanini, Bernardo, S499 (FRI-287), S597 (THU-153)
- Stefanini, Lucia, S217 (THU-350)
- Steffens, Andrea, S1208 (THU-218)
- Steggerda, Justin, S489 (TOP-065)
- Steib, Christian, S313 (SAT-546)
- Steinberger, Jonathan, S489 (TOP-065)
- Steinberg, Gregory, S762 (WED-442)
- Steinberg, Idan, S773 (WED-460)
- Steiner, Kristina, S264 (WED-365)
- Steinhauser, Toon, S622 (THU-444)
- Stenhoff, Leonie, S1124 (WED-206), S1125 (WED-207)
- Stein, Kerstin, S1147 (TOP-110)
- Steinmann, Eike, S1020 (FRI-221), S1032 (FRI-244), S1044 (FRI-262)
- Steinmann, Silja, S379 (WED-269)
- Stein, Philip, S938 (TOP-057), S969 (THU-289), S1003 (THU-378)
- Stein, Stephanie, S450 (SAT-385)
- Stella, Leonardo, S578 (THU-122)
- İstemihan, Zülal, S709 (SAT-485)
- Stender, Stefan, S702 (SAT-471)
- Stenstad, Tore, S1150 (SAT-170)
- Stepanova, Maria, S464 (THU-492), S627 (THU-453), S673 (SAT-428), S823 (FRI-516), S857 (SAT-116), S863 (SAT-125), S905 (FRI-159)
- Stepanova, Tatyana, S53 (OS-068), S110 (LBP-15), S113 (LBP-20), S1091 (WED-158)
- Stephens, Camilla, S126 (TOP-087), S144 (FRI-406)
- Stepień, Małgorzata, S880 (FRI-121)
- Stappich, Katja, S1031 (FRI-242)
- Sterling, Richard, S89 (OS-125), S612 (THU-427), S838 (FRI-489)
- Stern, Christiane, S52 (OS-066), S833 (FRI-480), S1150 (SAT-169), S1160 (SAT-183)
- Stern, Louisa, S579 (THU-123)
- Stern, Nick, S521 (FRI-326)
- Stettler, Christoph, S664 (SAT-414)
- Stevens, Sarah, S1030 (FRI-241)
- Stever, Kim, S1171 (SAT-202)
- Stewart, Brock, S113 (LBP-19)
- Stewart, Stephen, S180 (FRI-460)
- Sticht, Carsten, S358 (FRI-381), S547 (SAT-248)
- Stickel, Felix, S162 (FRI-430), S548 (SAT-250)
- Stieger, Bruno, S568 (SAT-289)
- Stiess, Michael, S403 (WED-307)
- Stift, Anton, S142 (FRI-402)
- Stirnimann, Guido, S412 (FRI-332), S485 (THU-533), S940 (THU-249)
- Stockdale, Alexander, S522 (FRI-327), S916 (FRI-178), S1075 (WED-137), S1117 (WED-195)
- Stockhoff, Lena, S240 (WED-326), S315 (SAT-551)
- Stockmans, Gert, S828 (FRI-526)
- Stoehr, Albrecht, S1174 (THU-166), S1186 (THU-181)
- Stoelinga, Anna, S14 (LBO-06), S382 (WED-274)
- Stoieva, Tetiana, S845 (FRI-502)
- Stojkovic, Stojan, S536 (SAT-230)
- Stokman, Geurt, S805 (WED-553)
- Stokowiec, Justyna, S59 (OS-076), S336 (WED-242)
- Stoll, Janis M., S1003 (THU-378)
- Stolz, Laura, S304 (SAT-531)
- Stopfer, Katharina, S288 (SAT-335), S831 (FRI-477)
- Stormon, Michael, S971 (THU-291)
- Storni, Federico, S485 (THU-533)
- Stoyanova, Kalina, S501 (FRI-291)
- Stoycheva, Antitsa, S1030 (FRI-241)
- Strandberg, Rickard, S121 (LBP-30-YI), S682 (SAT-441), S959 (THU-275)
- Strängberg, Ellen, S57 (OS-074-YI), S940 (THU-249)
- Strange, Charlton, S85 (OS-120), S977 (THU-296), S1007 (THU-385)
- Straniero, Sara, S57 (OS-074-YI)
- Strassburg, Christian, S61 (OS-080-YI), S229 (THU-366), S403 (WED-307), S422 (FRI-357), S429 (FRI-366)
- Straub, Beate, S536 (SAT-230), S557 (SAT-268), S654 (SAT-400), S762 (WED-443)
- Straub, Mathias, S707 (SAT-480)
- Stray, Kirsten, S1167 (SAT-195)
- Strazzabosco, Mario, S72 (OS-099), S423 (FRI-358), S564 (SAT-283)
- Street, Oliver, S8 (GS-010), S84 (OS-119-YI)
- Streinu-Cercel, Anca, S1149 (SAT-168)
- Stretch, Sophie, S1024 (FRI-229), S1033 (FRI-246)
- Strnad, Pavel, S85 (OS-120), S136 (FRI-393), S639 (THU-472), S951 (THU-264), S960 (THU-277), S963 (THU-281)
- Ströbel, Simon, S327 (WED-224), S737 (WED-402)
- Strogoff-de-Matos, Jorge, S112 (LBP-16)
- Stroka, Deborah, S449 (SAT-384)
- Ström, Oskar, S654 (SAT-399), S857 (SAT-115)
- Strowig, Till, S413 (FRI-334), S778 (WED-470)
- Strumberger, Michael, S754 (WED-431)
- Strunz, Benedikt, S229 (THU-365)
- Struyve, Mathieu, S828 (FRI-526)
- Strzepka, Jessica, S631 (THU-460)
- Stuart, Katherine, S239 (WED-324), S846 (WED-478)
- Studer, Peter, S162 (FRI-430)
- Stupia, Roberta, S203 (FRI-558)
- Sturm, Ekkehard, S938 (TOP-057), S965 (THU-284), S969 (THU-289)
- Sturm, Julia, S142 (FRI-402)
- Sturm, Lukas, S304 (SAT-531), S318 (SAT-555)
- Sturm, Nathalie, S672 (SAT-427)
- Stvilia, Ketevan, S898 (FRI-147)
- Suárez, Cristina, S706 (SAT-479)
- Subhani, Mohsan, S168 (FRI-439)
- Subic-Levrero, Miroslava, S1161 (SAT-185)
- Subramanian, Mani, S31 (OS-029), S323 (WED-216)
- Subudhi, P. Debishree, S348 (THU-234)
- Su, Chien-Wei, S1172 (THU-163)
- Suda, Goki, S584 (THU-131), S592 (THU-143), S593 (THU-145), S1183 (THU-177)
- Suddle, Abid, S445 (SAT-376), S642 (THU-551)
- Sudhindran, S, S848 (WED-481)
- Suehiro, Tomoyuki, S1192 (THU-191), S1199 (THU-205)
- Sugimoto, Shinya, S409 (TOP-060)
- Sugiyama, Masaya, S1025 (FRI-230)
- Sugiyanto, Raisatun, S547 (SAT-248)
- Su, Huan, S413 (FRI-334), S571 (SAT-292), S639 (THU-472), S778 (WED-470)
- Sui, Jianhua, S117 (LBP-24)
- Sui, Shulan, S1133 (SAT-147)
- Su, Jie, S1012 (THU-391)
- Sukeepaisarnjaroen, Wattana, S506 (FRI-298)
- Su, Kim, S333 (WED-234)
- Suk, Ki Tae, S156 (FRI-420), S186 (FRI-343), S190 (FRI-538), S192 (FRI-542), S220 (THU-354), S343 (THU-227)
- Sukowati, Caecilia, S559 (SAT-273)
- Sukriti, Sukriti, S149 (FRI-411), S348 (THU-234), S943 (THU-253)
- Suksamai, Anuchit, S262 (WED-360)
- Suksawatamnua, Sirinporn, S217 (THU-349), S1047 (FRI-266)
- Sulejova, Karolina, S182 (FRI-465), S871 (SAT-136)
- Sulkowski, Mark S, S89 (OS-125)
- Sulkowski, Mark S., S612 (THU-427), S1034 (FRI-248)
- Sultan, Amir, S1120 (WED-199)
- Sultanik, Philippe, S251 (WED-345), S487 (THU-538), S494 (THU-279), S515 (FRI-316), S585 (THU-133)
- Su, Man, S274 (WED-382)
- Sumida, Yoshio, S686 (SAT-448), S811 (FRI-468)
- Su, Minghua, S195 (FRI-546)
- Sumith, Arunima, S827 (FRI-524)
- Sun, Aimin, S34 (OS-033)
- Sundaram, Shikha, S971 (THU-291)
- Sundaram, Vinay, S242 (WED-330)
- Sundbom, Magnus, S820 (FRI-513)
- Sun, Feng, S1133 (SAT-147)
- Sun, Fengxia, S1076 (WED-138), S1157 (SAT-179)

- Sung, Pil Soo, S148 (FRI-409)
 Sun, Jian, S22 (OS-016), S34 (OS-033), S543 (SAT-242), S1085 (WED-149)
 Sun, Jianguang, S1076 (WED-138), S1157 (SAT-179)
 Sun, Jiangwei, S82 (OS-116-YI)
 Sun, Jixuan, S109 (LBP-13)
 Sun, Kejian, S488 (THU-540)
 Sun, Natalie, S608 (THU-420)
 Sun, Ning, S426 (FRI-363)
 Sun, Peng, S795 (WED-533)
 Sun, Suwan, S436 (SAT-359)
 Sun, Xuehua, S1076 (WED-138), S1157 (SAT-179)
 Sun, Ying, S406 (WED-313)
 Sun, Yu, S540 (SAT-236)
 Sun, Zhiyuan, S835 (FRI-484)
 Sun, Zilin, S340 (WED-250)
 Su, Qiaozhu, S338 (WED-245)
 Surabattula, Rambabu, S652 (SAT-396)
 Surace, Lidia, S691 (SAT-456), S1091 (WED-157)
 Suresh, Akanksha, S25 (OS-020-YI)
 Sureshan, Shruti, S228 (THU-362), S348 (THU-234), S357 (THU-248)
 Surguladze, Sophia, S909 (FRI-167), S925 (FRI-193), S931 (FRI-205), S933 (FRI-210)
 Suroliya, Varun, S228 (THU-362), S348 (THU-234), S357 (THU-248)
 Susana del Prado, S73 (OS-102)
 Suschak, John, S50 (OS-063)
 Sussman, Caroline, S765 (WED-448)
 Suter-Riniker, Franziska, S101 (LBP-04)
 Suthanathan, Arul, S466 (THU-497)
 Sutherland, Elena, S39 (OS-044-YI)
 Sutter, Olivier, S585 (THU-133)
 Sutti, Salvatore, S526 (SAT-211), S751 (WED-425), S804 (WED-551)
 Su, Tung-Hung, S12 (LBO-04), S52 (OS-065-YI), S518 (FRI-320), S1061 (WED-119), S1132 (SAT-145)
 Su, Wantong, S528 (SAT-214)
 Su, Wei-Wen, S891 (FRI-137), S1180 (THU-174), S1206 (THU-217)
 Su, Yung-Yeh, S588 (THU-138)
 Su, Zehua, S347 (THU-232)
 Su, Zemin, S136 (FRI-393)
 Suzuki, Fumitaka, S1061 (WED-119)
 Suzuki, Keito, S644 (THU-554)
 Suzuki, Shingo, S733 (WED-395)
 Suzuki, Takahiro, S409 (TOP-060)
 Suzuki, Takanori, S1095 (WED-163)
 Suzzi, Fabrizia, S571 (TOP-067)
 Svängård, Nils, S606 (THU-416)
 Svarovskaia, Evguenia S, S1055 (TOP-103)
 Svegliati-Baroni, Gianluca, S54 (OS-069), S105 (LBP-09), S482 (THU-527), S609 (THU-421), S673 (SAT-430)
 Svendsen, Jan, S1150 (SAT-170)
 Svensson, Eric, S115 (LBP-22)
 Svicher, Valentina, S1056 (TOP-106), S1072 (WED-133), S1103 (WED-174), S1105 (WED-176), S1122 (WED-203), S1142 (SAT-159)
 Swain, Mark G, S652 (SAT-395)
 Swain, Mark G., S175 (FRI-451), S373 (WED-259), S419 (FRI-352), S426 (FRI-363)
 Swaroop, Shekhar, S73 (OS-101-YI), S197 (FRI-548), S297 (SAT-350), S587 (THU-135)
 Sweeney, Kelly, S840 (FRI-492)
 Sweetser, Marianne T, S86 (OS-122)
 Swenson, Eugene Scott, S958 (THU-274), S967 (THU-286), S985 (THU-309)
 Swift, Brandon, S367 (TOP-062)
 Syamprasad, N.P, S560 (SAT-274)
 Sydor, Svenja, S628 (THU-454)
 Syeda, Zehra, S423 (FRI-358)
 Syed, Hussain, S426 (FRI-363)
 Symons, Julian, S548 (SAT-251), S1029 (FRI-238), S1029 (FRI-239), S1030 (FRI-241), S1051 (FRI-272)
 syriha, antonia, S595 (THU-149), S1046 (FRI-264)
 Szalay, Ferenc, S967 (THU-286)
 Szczech, Lynda, S41 (OS-046)
 Sze, Karen, S48 (OS-058)
 Sze, Kenny, S300 (SAT-522)
 Szymanski, Robin, S288 (SAT-335)
 Tabak, Fehmi, S31 (OS-030)
 Taberner-Cortés, Alida, S789 (WED-520)
 Tabernero, David, S1024 (FRI-228), S1089 (WED-154)
 Tabuchi, Takaya, S156 (FRI-421), S409 (TOP-060)
 Tachi, Kenneth, S865 (SAT-129)
 Tacke, Frank, S70 (OS-095-YI), S71 (OS-096-YI), S80 (OS-114-YI), S197 (FRI-549), S351 (THU-238), S469 (THU-502), S646 (THU-559), S737 (WED-403), S745 (WED-416), S767 (WED-450), S819 (FRI-509), S1139 (SAT-156)
 Tada, Faujimas, S584 (THU-131)
 Tada, Toshifumi, S584 (THU-131), S592 (THU-143), S593 (THU-145), S818 (FRI-508)
 Taddei, Maria Letizia, S774 (WED-462)
 Taddei, Tamar, S188 (FRI-535), S248 (WED-342), S304 (SAT-532), S832 (FRI-478)
 Taddei, Tamar H, S265 (WED-366)
 Tadesse, Sewale Anagaw, S865 (SAT-129)
 Tadj, Thierry Fosind, S645 (THU-557)
 Tae Suk, Ki, S177 (FRI-456)
 Tae yoon, Ki, S11 (LBO-02), S32 (OS-031), S712 (SAT-491)
 Tagle, Martin, S865 (SAT-129), S900 (FRI-151)
 Tagliaferri, Pierosandro, S568 (SAT-288)
 Tahata, Yuki, S1183 (THU-177)
 Taha, Yusri, S1175 (THU-167), S1187 (THU-182)
 Taheri, Roya, S936 (FRI-214)
 Tai, Chi-Ming, S1180 (THU-174), S1206 (THU-217)
 Tai, David, S543 (SAT-241)
 Tai, Dean, S65 (OS-087), S112 (LBP-17), S333 (WED-236), S334 (WED-237), S334 (WED-238), S501 (FRI-290), S757 (WED-436), S762 (WED-443), S806 (TOP-076), S824 (FRI-518), S999 (THU-333)
 Tai, Jennifer, S1088 (WED-152)
 Tailleux, Anne, S355 (THU-244), S772 (WED-458)
 Tait, Christopher, S273 (WED-380)
 Tajiri, Kazuto, S584 (THU-131)
 Tajudin, Muna, S710 (SAT-486)
 Takahashi, Atsushi, S394 (WED-293)
 Takahashi, Hidenori, S439 (SAT-366), S509 (FRI-302)
 Takahashi, Hirokazu, S616 (THU-433), S627 (THU-453), S686 (SAT-448)
 Takahashi, Yasushi, S1087 (WED-151)
 Takahashi, Yuka, S644 (THU-554)
 Takami, Taro, S1183 (THU-177)
 Takamura, Masaaki, S394 (WED-293)
 Takaura, Kenta, S644 (THU-554)
 Takeda, Nobutaka, S124 (LBP-37)
 Takehara, Tetsuo, S1183 (THU-177)
 Takeuchi, Akihito, S394 (WED-293)
 Takkenberg, Bart, S836 (FRI-485), S1100 (WED-169)
 Tak, Won Young, S11 (LBO-02), S588 (THU-137), S1169 (SAT-198)
 Talbäck, Mats, S121 (LBP-30-YI)
 Taleb, Shakila, S423 (FRI-358)
 Taljaard, Jantjie, S916 (FRI-178), S1108 (WED-181), S1117 (WED-195)
 Talloen, Willem, S1087 (WED-151)
 Tamaki, Nobuharu, S65 (OS-086), S598 (THU-155), S644 (THU-554), S1113 (WED-189)
 Tamandl, Dietmar, S498 (FRI-285), S505 (FRI-295)
 Tamara, María Legarda, S972 (THU-291)
 Tamargo, Isabel, S805 (WED-554)
 Tamazirt, Sonia, S498 (FRI-286)
 Tamim, Hani, S859 (SAT-119)
 Tamnanloo, Farzaneh, S213 (THU-344)
 Tamori, Akihiro, S566 (SAT-286)
 Tam, Paul KH, S942 (THU-252)
 Tam, Ying, S35 (OS-034)
 Tanabe, Tomohide, S317 (SAT-554), S820 (FRI-511)
 Tanaka, Atsushi, S11 (LBO-03), S395 (WED-293), S401 (WED-303)
 Tanaka, Saiyu, S616 (THU-433)
 Tanaka, Shohei, S644 (THU-554)
 Tanaka, Yasuhito, S897 (FRI-146), S1095 (WED-163), S1134 (SAT-148)
 Tanaka, Yuki, S644 (THU-554)
 Tan, Anthony, S543 (SAT-241), S1024 (FRI-229)
 Tanashchuk, Elena, S1210 (THU-221)
 Tanasie, Ioana, S1123 (WED-204)
 Tan, Chee-Kiat, S519 (FRI-321)

Author Index

- Tan, Chin Kimg, S199 ([FRI-552](#)), S257 ([WED-353](#))
- Tan, Daisong, S782 ([WED-506](#))
- Tan, Damien, S543 ([SAT-241](#))
- Tan, Darren Jun Hao, S468 ([THU-500](#)), S629 ([THU-456](#))
- Tan, Deming, S1085 ([WED-149](#))
- Tandoi, Francesco, S455 ([TOP-059](#))
- Tandon, Nikhil, S693 ([SAT-459](#))
- Tandon, Puneeta, S195 ([FRI-546](#)), S256 ([WED-352](#)), S258 ([WED-355](#))
- Tan, En Ying, S698 ([SAT-467](#)), S707 ([SAT-482](#)), S714 ([SAT-495](#))
- Tan, Eunice, S468 ([THU-500](#)), S698 ([SAT-467](#)), S707 ([SAT-482](#)), S714 ([SAT-495](#))
- Tang, Ansel, S629 ([THU-456](#))
- Tang, Chengwei, S304 ([SAT-530](#))
- Tang, Hong, S195 ([FRI-546](#)), S1165 ([SAT-193](#))
- Tangkijvanich, Pisit, S11 ([LBO-02](#)), S354 ([THU-243](#)), S356 ([THU-245](#)), S919 ([FRI-184](#))
- Tang, Libo, S543 ([SAT-242](#)), S557 ([SAT-269](#))
- Tang, Liming, S745 ([WED-416](#))
- Tang, Qiao, S1112 ([WED-187](#)), S1112 ([WED-188](#))
- Tang, Renxian, S1016 ([TOP-111](#)), S1027 ([FRI-234](#))
- Tanguy, Marion, S435 ([SAT-358](#))
- Tang, Wenshu, S530 ([SAT-217](#))
- Tang, Xiaolu, S1166 ([SAT-194](#))
- Tang, Xuman, S1058 ([WED-114](#))
- Tang, Yingmei, S406 ([WED-313](#))
- Tang, Zhihong, S581 ([THU-126](#))
- Tan, Hiang Keat, S195 ([FRI-546](#))
- Tan, Hong Chang, S351 ([THU-237](#))
- Tan, Hua, S548 ([SAT-251](#)), S1029 ([FRI-239](#))
- Tani, Joji, S818 ([FRI-508](#))
- Taniki, Nobuhito, S156 ([FRI-421](#)), S409 ([TOP-060](#))
- Tan, Jennifer, S597 ([THU-151](#))
- Tan, Jing Tong, S62 ([OS-082](#))
- Tan, Joseph, S1167 ([SAT-195](#))
- Tan, Natassia, S380 ([WED-271](#))
- Tanne, Florence, S318 ([SAT-556](#))
- Tan, Nguan Soon, S79 ([OS-111](#))
- Tannich, Egbert, S522 ([FRI-327](#))
- Tanwandee, Tawesak, S19 ([OS-009](#)), S237 ([WED-321](#)), S502 ([FRI-292](#)), S506 ([FRI-298](#)), S507 ([FRI-300](#))
- Tan, Wenting, S948 ([THU-260](#))
- Tan, Yongfa, S543 ([SAT-242](#))
- Tan, Youwen, S1119 ([WED-198](#))
- Tao, Cui, S463 ([THU-491](#))
- Taourel, Patrice, S929 ([FRI-201](#))
- Tapias, Laura, S885 ([FRI-128](#))
- Tapper, Elliot, S302 ([SAT-527](#)), S308 ([SAT-540](#)), S311 ([SAT-544](#)), S900 ([FRI-151](#))
- Taqi, Soreen, S224 ([THU-358](#))
- Targher, Giovanni, S814 ([FRI-474](#))
- Tarnagda, Zékiba, S930 ([FRI-202](#))
- Tarnawski, Laura, S756 ([WED-434](#))
- Tarrago, David, S902 ([FRI-153](#))
- Taru, Madalina Gabriela, S279 ([TOP-043](#)), S295 ([SAT-347](#))
- Taru, Vlad, S151 ([FRI-413](#)), S222 ([THU-357](#)), S279 ([TOP-043](#)), S289 ([SAT-336](#)), S295 ([SAT-347](#)), S316 ([SAT-553](#))
- Tassone, Pierfrancesco, S568 ([SAT-288](#))
- Tateishi, Ryosuke, S1183 ([THU-177](#))
- Tate, Victoria, S37 ([OS-038](#))
- Tateyama, Masakuni, S1095 ([WED-163](#))
- Tatsumi, Tomohide, S1183 ([THU-177](#))
- Täubel, Jörg, S49 ([OS-062](#))
- Taubert, Richard, S42 ([OS-047-YI](#)), S425 ([FRI-362](#)), S466 ([THU-496](#)), S982 ([THU-304](#))
- Taub, Rebecca, S1 ([GS-001](#)), S112 ([LBP-17](#)), S684 ([SAT-444](#)), S790 ([WED-522](#)), S813 ([FRI-472](#)), S815 ([FRI-476](#))
- Taupin, Jean Luc, S266 ([WED-368](#))
- Taura, Naota, S1177 ([THU-170](#))
- Tautenhahn, Hans-Michael, S487 ([THU-539](#))
- Tauwaldt, Jan, S1029 ([FRI-240](#))
- Tavaglione, Federica, S500 ([FRI-288](#)), S665 ([SAT-416](#)), S803 ([WED-549](#))
- Tavano, Daniele, S994 ([THU-323](#))
- Tavelli, Alessandro, S907 ([FRI-164](#)), S1103 ([WED-174](#)), S1105 ([WED-176](#))
- Tawfik, Mohamed, S827 ([FRI-523](#))
- Tayebi, Hend El, S570 ([SAT-291](#))
- Taylor, Cristin, S31 ([OS-029](#))
- Taylor, Lynn, S838 ([FRI-489](#))
- Taylor-Whiteley, Teresa, S882 ([FRI-124](#))
- Tchamgoue, Serge, S1210 ([THU-222](#))
- Tchorz, Jan, S418 ([FRI-351](#))
- Teague, Amy, S872 ([TOP-097](#))
- Tedesco, Calogero Claudio, S493 ([FRI-277](#))
- Teicher Kirk, Frederik, S985 ([THU-309](#))
- Teisner, Ane Soegaard, S239 ([WED-325](#))
- Teixeira-Clerc, Fatima, S456 ([THU-478](#))
- Teixeira, Rosângela, S112 ([LBP-16](#))
- Tejedor Bravo, Marta, S474 ([THU-512](#))
- Tejedor-Tejada, Javier, S171 ([FRI-445](#))
- Tejera, Felix Pérez, S932 ([FRI-208](#))
- Tekiela, Kamilla, S671 ([SAT-426](#))
- Teklehaymanot, Tilahun, S927 ([FRI-197](#))
- Telep, Laura, S1059 ([WED-116](#))
- Telesca, Claudia, S247 ([WED-340](#))
- Teles, Sara, S122 ([LBP-33-YI](#))
- Tellez, Francisco Félix, S274 ([WED-382](#))
- Téllez, Luis, S2 ([GS-003](#)), S73 ([OS-102](#)), S87 ([OS-123-YI](#)), S279 ([TOP-043](#)), S970 ([THU-290](#))
- Tello, Víctor Argumáñez, S476 ([THU-517](#))
- Tempe, Deepak, S182 ([TOP-040](#))
- Temperli, Simone, S888 ([FRI-131](#))
- Tenca, Andrea, S370 ([WED-253](#))
- Tenes, Andrés, S73 ([OS-102](#))
- Ten-Estève, Amadeo, S682 ([SAT-442](#))
- Teng, Margaret, S300 ([SAT-522](#)), S468 ([THU-500](#)), S629 ([THU-456](#)), S698 ([SAT-467](#)), S707 ([SAT-482](#)), S714 ([SAT-495](#))
- Teng, Wei, S1057 ([TOP-112](#))
- Teng, Xiao, S759 ([WED-438](#)), S763 ([WED-445](#))
- ten Hove, Marit, S755 ([WED-432](#)), S761 ([WED-441](#))
- Ten, Irina, S320 ([SAT-559](#))
- Tenreiro, Ariane Eceiza, S442 ([TOP-050](#))
- Tenta, Roxani, S262 ([WED-362](#))
- Teoh, Xuhui, S300 ([SAT-522](#))
- Terai, Shuji, S124 ([LBP-37](#)), S1183 ([THU-177](#))
- Teran, Gustavo Reyes, S1202 ([THU-211](#))
- Teraoka, Yuji, S72 ([OS-098](#))
- Teratani, Toshiaki, S409 ([TOP-060](#))
- Terbah, Ryma, S311 ([SAT-543](#))
- Tergast, Tammo Lambert, S240 ([WED-326](#)), S283 ([SAT-328](#)), S301 ([SAT-525](#)), S315 ([SAT-551](#)), S1115 ([WED-193](#))
- Termorshuizen, Fabian, S184 ([FRI-340](#))
- Terol Cháfer, Isabel, S485 ([THU-535](#))
- Terracciani, Francesca, S36 ([OS-036](#)), S40 ([OS-045](#)), S55 ([OS-070](#))
- Terrault, Norah, S161 ([FRI-428](#)), S169 ([FRI-441](#)), S1079 ([WED-141](#))
- Terreni, Natalia, S40 ([OS-045](#)), S55 ([OS-070](#))
- Terziroli, Benedetta, S481 ([THU-526](#))
- Tesfai, Kaleb, S648 ([TOP-075](#))
- Tesfaye, Yonas Gedamu, S865 ([SAT-129](#))
- Teshay, Dareskedar, S927 ([FRI-197](#))
- Testillano, Milagros, S573 ([THU-114](#)), S587 ([THU-136](#))
- Testoni, Barbara, S101 ([LBP-04](#)), S118 ([LBP-27](#)), S1014 ([TOP-104](#)), S1046 ([FRI-265](#)), S1058 ([WED-113](#)), S1170 ([SAT-199](#))
- Testro, Adam, S311 ([SAT-543](#))
- Tesz, Gregory, S786 ([WED-515](#))
- Teti, Elisabetta, S1056 ([TOP-106](#)), S1072 ([WED-133](#))
- Tetri, Brent, S66 ([OS-089](#))
- Teuber, Gerlinde, S1174 ([THU-166](#))
- Teufel, Andreas, S491 ([FRI-273](#)), S596 ([THU-150](#)), S646 ([THU-559](#))
- Teyssou, Elisa, S1044 ([FRI-261](#))
- Thabet, Ashraf, S58 ([OS-075](#))
- Thabut, Dominique, S86 ([OS-121-YI](#)), S106 ([LBP-10](#)), S198 ([FRI-550](#)), S251 ([WED-345](#)), S266 ([WED-368](#)), S318 ([SAT-556](#)), S487 ([THU-538](#)), S492 ([FRI-274](#)), S494 ([FRI-279](#)), S498 ([FRI-286](#)), S515 ([FRI-316](#)), S585 ([THU-133](#)), S589 ([THU-139](#))
- Thacker, Leroy, S195 ([FRI-546](#)), S242 ([WED-331](#)), S256 ([WED-352](#)), S258 ([WED-355](#)), S274 ([WED-382](#))
- Thaimai, Panarat, S217 ([THU-349](#)), S1047 ([FRI-266](#))
- Thakar, Shubhankar, S67 ([OS-091](#))
- Thanapirom, Kessarín, S217 ([THU-349](#)), S1047 ([FRI-266](#))
- Thanawala, Vaidehi, S11 ([LBO-02](#))
- Thandassery, Ragesh Babu, S296 ([SAT-349](#))
- Thangariyal, Swati, S943 ([THU-253](#))
- Thang, Sue Ping, S582 ([THU-129](#)), S591 ([THU-142](#))
- Thapar, Shalini, S182 ([TOP-040](#))

- Thatcher, Amy, S850 ([WED-485](#))
 Thatikonda, Santhosh, S1051 ([FRI-272](#))
 Thelwall, Iona, S122 ([LBP-34](#))
 Thennati, Rajamannar, S607 ([THU-419](#))
 Theodore, Dickens, S110 ([LBP-15](#)),
 S1039 ([FRI-255](#)), S1141 ([SAT-158](#)),
 S1151 ([SAT-171](#)), S1154 ([SAT-176](#)),
 S1162 ([SAT-187](#)), S1167 ([SAT-196](#))
 Theodoreson, Mark, S157 ([FRI-422](#))
 Theophanous, Fani, S880 ([FRI-121](#))
 Théophile, Gerster, S318 ([SAT-556](#))
 Therkelsen, Marie Louise, S742 ([WED-411](#))
 Thet, Htay Myat, S300 ([SAT-522](#))
 Thevathasan, Lionel, S1002 ([THU-336](#))
 Thibaut, Morgane, S772 ([WED-458](#))
 Thiele, Maja, S17 ([OS-005-YI](#)),
 S61 ([OS-080-YI](#)), S163 ([FRI-432](#)),
 S173 ([FRI-449](#)), S175 ([FRI-452](#)),
 S303 ([SAT-528](#)), S657 ([SAT-404](#)),
 S832 ([FRI-479](#)), S845 ([TOP-054](#))
 Thiels, Cornelius, S44 ([OS-050-YI](#)),
 S465 ([THU-495](#))
 Thi, Emily P., S125 ([LBP-38](#)),
 S1171 ([SAT-202](#))
 Thierry, Alex Guillaumon, S163 ([FRI-431](#))
 Thimme, Robert, S33 ([OS-032](#)),
 S304 ([SAT-531](#)), S305 ([SAT-534](#)),
 S318 ([SAT-555](#)), S447 ([SAT-379](#)),
 S586 ([THU-134](#)), S1139 ([SAT-156](#))
 Thing, Mira, S165 ([FRI-434](#)), S702 ([SAT-471](#)),
 S742 ([WED-411](#)), S748 ([WED-421](#)),
 S784 ([WED-511](#))
 Thomadakis, Christos, S880 ([FRI-121](#))
 Thomas, Lutz, S1186 ([THU-181](#))
 Thomopoulos, Konstantinos,
 S400 ([WED-302](#)), S1128 ([WED-211](#))
 Thompson, Alexander, S306 ([SAT-535](#)),
 S380 ([WED-271](#))
 Thompson, Craig, S1175 ([THU-167](#))
 Thompson, Marcos Andres, S843 ([FRI-499](#))
 Thompson, Richard, S56 ([OS-072](#)),
 S123 ([LBP-35](#)), S370 ([WED-252](#)),
 S387 ([WED-282](#)), S938 ([TOP-057](#)),
 S969 ([THU-289](#)), S972 ([THU-291](#))
 Thomsen, Anne Bloch, S614 ([THU-429](#))
 Thomsen, Karen Louise, S35 ([OS-035-YI](#)),
 S159 ([FRI-424](#))
 Thomson, Emma, S522 ([FRI-327](#))
 Thoné, Tinne, S445 ([SAT-375](#))
 Thorbek, Ditte Denker, S788 ([WED-519](#))
 Thorburn, Douglas, S11 ([LBO-03](#)),
 S46 ([OS-053-YI](#)), S56 ([OS-073](#)),
 S383 ([WED-276](#)), S411 ([FRI-331](#)),
 S415 ([FRI-345](#)), S579 ([THU-123](#)),
 S985 ([THU-310](#))
 Thorens, Bernard, S607 ([THU-419](#))
 Thorhauge, Katrine, S17 ([OS-005-YI](#)),
 S163 ([FRI-432](#)), S173 ([FRI-449](#)),
 S175 ([FRI-452](#)), S303 ([SAT-528](#)),
 S832 ([FRI-479](#)), S845 ([TOP-054](#)),
 S963 ([THU-281](#))
 Thorne, James, S787 ([WED-517](#))
 Thornton, Michael, S773 ([WED-460](#))
 Thorpe, Molly, S177 ([FRI-455](#))
 Thuluvath, Paul, S101 ([LBP-03](#))
 Thuluvath, Paul J., S195 ([FRI-546](#))
 Thureau, Jérémy, S603 ([THU-410](#))
 Thursz, Mark, S344 ([THU-228](#)),
 S601 ([TOP-088](#)), S624 ([THU-446](#)),
 S719 ([SAT-501](#)), S1106 ([WED-178](#))
 Thuy, Le Thi Thanh, S325 ([WED-221](#)),
 S566 ([SAT-286](#))
 Thylin, Mathias, S370 ([WED-253](#))
 Thys, Kim, S444 ([SAT-374](#))
 Tian, Xiaorong, S696 ([SAT-463](#)),
 S724 ([SAT-510](#))
 Tian, Yang, S1152 ([SAT-173](#)),
 S1156 ([SAT-178](#))
 Tian, Yu, S320 ([SAT-560](#))
 Tiede, Anja, S240 ([WED-326](#)),
 S315 ([SAT-551](#))
 Tie, Jun, S304 ([SAT-530](#))
 Tiendrebego, Abdoul, S897 ([FRI-146](#)),
 S923 ([FRI-191](#))
 Tihi, Matthiew, S531 ([SAT-220](#))
 Tilden, Sally, S858 ([SAT-118](#))
 Tilg, Herbert, S961 ([THU-279](#)),
 S968 ([THU-288](#))
 Tillman, Erik, S808 ([TOP-091](#)),
 S820 ([FRI-512](#))
 Tinahones, Alberto, S560 ([SAT-275](#))
 Tincopa, Monica, S65 ([OS-086](#)),
 S649 ([TOP-083](#))
 Tiniakos, Dina, S78 ([OS-110](#)),
 S400 ([WED-302](#)), S671 ([SAT-426](#))
 Tipney, Hannah, S1151 ([SAT-171](#))
 Tiribelli, Claudio, S559 ([SAT-273](#)),
 S768 ([WED-452](#)), S793 ([WED-529](#)),
 S952 ([THU-265](#))
 Tiriticco, Valentina, S952 ([THU-265](#))
 Tirukonda, Prasanna, S199 ([FRI-552](#)),
 S257 ([WED-353](#))
 Tischendorf, Michael, S185 ([FRI-341](#)),
 S313 ([SAT-546](#)), S484 ([THU-531](#))
 Tissot, Noémie, S994 ([THU-322](#))
 Tiwari, Rajnish, S352 ([THU-240](#))
 Tizzani, Marco, S917 ([FRI-180](#)),
 S1177 ([THU-169](#)), S1200 ([THU-206](#))
 Tješić-Drinković, Ida, S61 ([OS-080-YI](#))
 Tjwa, E.T.T.L., S982 ([THU-304](#))
 Tliba, Maroua, S792 ([WED-526](#))
 Toapanta, David, S131 ([THU-399](#)),
 S135 ([THU-406](#))
 Tobiasch, Anna, S232 ([THU-369](#))
 Tobiasch, Moritz, S232 ([THU-369](#))
 Tobin, William, S241 ([WED-328](#))
 Tobita, Hiroshi, S686 ([SAT-448](#))
 Todd, Stacy, S1075 ([WED-137](#))
 To, Dennis, S102 ([LBP-05](#))
 Todesco, Eve, S1044 ([FRI-261](#))
 Todo, Tsuyoshi, S489 ([TOP-065](#))
 Todt, Daniel, S1020 ([FRI-221](#)),
 S1032 ([FRI-244](#)), S1044 ([FRI-262](#))
 Tokushige, Akihiro, S686 ([SAT-448](#))
 Toledo, Claudio, S253 ([WED-348](#))
 Tolenaars, Dagmar, S55 ([OS-071-YI](#)),
 S427 ([FRI-364](#))
 Tomah, Shaheen, S50 ([OS-063](#))
 Toma, Letitia, S277 ([WED-386](#)),
 S819 ([FRI-510](#)), S1123 ([WED-204](#)),
 S1193 ([THU-193](#))
 Tomasello, Lidia, S723 ([SAT-508](#))
 Tomasiewicz, Krzysztof, S1205 ([THU-215](#))
 Tomasi, Melissa, S669 ([SAT-422](#))
 Tomasini, Simone, S742 ([WED-410](#))
 Tomczak, Aurelie, S594 ([THU-147](#))
 Tomé, Santiago, S171 ([FRI-445](#))
 Tomescu, Dana, S220 ([THU-355](#))
 Tomezzoli, Anna, S1190 ([THU-188](#))
 Tomimaru, Yoshito, S439 ([SAT-366](#)),
 S509 ([FRI-302](#))
 Tomita, Eiichi, S686 ([SAT-448](#))
 Tomlinson, Jeremy, S708 ([SAT-483](#)),
 S731 ([TOP-089](#))
 Tonascia, James, S612 ([THU-427](#))
 Tong, Aaron Kian Ti, S582 ([THU-129](#)),
 S591 ([THU-142](#))
 Tong, Chenhao, S358 ([FRI-381](#))
 Tong, Kexin, S1143 ([SAT-161](#))
 Tong, Ling, S1053 ([SAT-142](#))
 Tong, Xin, S1022 ([FRI-225](#)),
 S1073 ([WED-136](#)), S1096 ([WED-164](#))
 Tong, Yao, S760 ([WED-439](#))
 Toniato, Giorgia, S920 ([FRI-186](#)),
 S929 ([FRI-200](#))
 Toniutto, Pierluigi, S54 ([OS-069](#)),
 S198 ([FRI-550](#)), S237 ([WED-320](#)),
 S402 ([WED-306](#)), S482 ([THU-527](#)),
 S1135 ([SAT-149](#))
 Tonnerre, Pierre, S58 ([OS-075](#)),
 S1093 ([WED-159](#))
 Tonnini, Matteo, S107 ([LBP-11](#)),
 S584 ([THU-131](#)), S597 ([THU-153](#))
 Tonon, Marta, S10 ([LBO-01](#)),
 S237 ([WED-320](#))
 Too, Chow Wei, S582 ([THU-129](#)),
 S591 ([THU-142](#))
 Topal, Baki, S524 ([TOP-066](#)),
 S753 ([WED-430](#))
 Topal, Halit, S524 ([TOP-066](#)),
 S753 ([WED-430](#))
 Topazian, Mark, S195 ([FRI-546](#)),
 S274 ([WED-382](#))
 Topete, Jesus, S822 ([FRI-515](#)),
 S828 ([FRI-525](#))
 Topete, Victor Ahumada,
 S1202 ([THU-211](#))
 Torán, Pere, S664 ([SAT-415](#))
 Tornai, David, S23 ([OS-017-YI](#)),
 S383 ([WED-277](#))
 Tornai, Istvan, S23 ([OS-017-YI](#))
 Tornai, Tamas, S23 ([OS-017-YI](#))
 Torner, Maria, S392 ([WED-290](#)),
 S1192 ([THU-192](#))
 Toro, Luis, S865 ([SAT-129](#))
 Toro, Marcela, S1164 ([SAT-191](#))
 Torp, Nikolaj, S17 ([OS-005-YI](#)),
 S163 ([FRI-432](#)), S173 ([FRI-449](#)),
 S175 ([FRI-452](#)), S303 ([SAT-528](#)),
 S832 ([FRI-479](#)), S845 ([TOP-054](#))
 Torralba, Miguel, S1028 ([FRI-236](#)),
 S1032 ([FRI-245](#))

Author Index

- Torras, Xavier, S73 ([OS-100-YI](#)), S1178 ([THU-171](#))
- Torre, Aldo, S195 ([FRI-546](#)), S274 ([WED-382](#))
- Torre, Giulia, S1056 ([TOP-106](#)), S1072 ([WED-133](#)), S1105 ([WED-176](#)), S1122 ([WED-203](#))
- Torrens, Maria, S533 ([SAT-224](#))
- Torre, Pietro, S713 ([SAT-493](#)), S789 ([WED-521](#))
- Torres, Ana, S248 ([WED-341](#))
- Torre, Sara Della, S733 ([WED-393](#))
- Torres, Callie, S12 ([LBO-04](#))
- Torres, Ferran, S10 ([LBO-01](#))
- Torres, Jorge Calderon, S932 ([FRI-208](#))
- Torres, Laura Monserrat Lopez, S587 ([THU-136](#))
- Torres, Lucía Barbier, S736 ([WED-400](#))
- Torres, Patricia, S489 ([TOP-065](#))
- Torres, Sabrina, S905 ([FRI-160](#))
- Torres-Sangiao, Eva, S911 ([FRI-171](#))
- Tortora, Annalisa, S40 ([OS-045](#)), S55 ([OS-070](#))
- Tortora, Raffaella, S36 ([OS-036](#)), S597 ([THU-153](#))
- Torzilli, Guido, S446 ([SAT-377](#))
- Tosca, Joan, S781 ([WED-505](#))
- Tosetti, Giulia, S86 ([OS-121-YI](#)), S87 ([OS-123-YI](#)), S279 ([TOP-043](#)), S584 ([THU-131](#))
- Toskal, Cagatay, S628 ([THU-454](#))
- Toso, Christian, S24 ([OS-018-YI](#)), S531 ([SAT-220](#))
- Tosti, Maria Elena, S1082 ([WED-146](#))
- Totman, Jennifer, S526 ([TOP-072](#))
- Touboul, Adrien, S680 ([SAT-439](#))
- Touche, Véronique, S355 ([THU-244](#))
- Toumi, Mondher, S1087 ([WED-151](#))
- Touray, Alhagie, S67 ([OS-090-YI](#)), S1106 ([WED-178](#)), S1106 ([WED-179](#))
- Touray, Fatoumatta, S67 ([OS-090-YI](#))
- Toure-Kane, Coumba, S67 ([OS-090-YI](#)), S1106 ([WED-178](#))
- Tout, Issam, S1093 ([WED-159](#))
- Tovoli, Francesco, S499 ([FRI-287](#)), S571 ([TOP-067](#)), S597 ([THU-153](#))
- Toya, Keisuke, S439 ([SAT-366](#))
- Toy, Mehlika, S928 ([FRI-199](#))
- Toyoda, Hidenori, S584 ([THU-131](#)), S686 ([SAT-448](#)), S811 ([FRI-468](#))
- Traglia, Loide Di, S1122 ([WED-203](#))
- Trampert, David, S55 ([OS-071-YI](#))
- Tranah, Thomas, S7 ([GS-007](#)), S35 ([OS-035-YI](#))
- Tran, Albert, S1158 ([SAT-180](#))
- Tran, Nguyen H., S12 ([LBO-04](#))
- Tran, Vinh, S173 ([FRI-448](#))
- Trapani, Joseph, S1021 ([FRI-223](#))
- Trapani, Silvia, S54 ([OS-069](#))
- Trapero, Maria, S272 ([WED-378](#)), S291 ([SAT-340](#)), S683 ([SAT-443](#))
- Trassard, Olivier, S359 ([FRI-382](#))
- Traub, Julia, S346 ([THU-230](#)), S354 ([THU-242](#))
- Trauner, Michael, S11 ([LBO-03](#)), S19 ([OS-010-YI](#)), S37 ([OS-039-YI](#)), S193 ([FRI-545](#)), S199 ([FRI-551](#)), S201 ([FRI-554](#)), S222 ([THU-357](#)), S224 ([THU-358](#)), S244 ([WED-334](#)), S279 ([TOP-043](#)), S282 ([SAT-326](#)), S284 ([SAT-330](#)), S286 ([SAT-332](#)), S288 ([SAT-335](#)), S289 ([SAT-336](#)), S292 ([SAT-342](#)), S294 ([SAT-345](#)), S313 ([SAT-547](#)), S316 ([SAT-553](#)), S352 ([THU-240](#)), S386 ([WED-280](#)), S403 ([WED-307](#)), S423 ([FRI-360](#)), S451 ([SAT-388](#)), S491 ([FRI-273](#)), S498 ([FRI-285](#)), S505 ([FRI-295](#)), S739 ([WED-405](#)), S746 ([WED-418](#)), S831 ([FRI-477](#)), S936 ([TOP-055](#)), S939 ([TOP-058](#)), S940 ([THU-249](#)), S996 ([THU-327](#)), S1135 ([SAT-150](#))
- Trauth, Janina, S90 ([OS-126](#))
- Trautwein, Christian, S22 ([OS-015](#)), S143 ([FRI-405](#)), S188 ([FRI-534](#)), S349 ([THU-235](#)), S413 ([FRI-334](#)), S416 ([FRI-348](#)), S492 ([FRI-275](#)), S535 ([SAT-227](#)), S571 ([SAT-292](#)), S636 ([THU-467](#)), S639 ([THU-472](#)), S730 ([TOP-084](#)), S778 ([WED-470](#)), S963 ([THU-281](#)), S1147 ([TOP-110](#))
- Trček, Hana, S553 ([SAT-261](#))
- Trebicka, Jonel, S10 ([LBO-01](#)), S23 ([OS-017-YI](#)), S61 ([OS-080-YI](#)), S87 ([OS-123-YI](#)), S143 ([FRI-404](#)), S185 ([FRI-341](#)), S222 ([THU-356](#)), S238 ([WED-323](#)), S239 ([WED-325](#)), S279 ([TOP-043](#)), S290 ([SAT-337](#)), S303 ([SAT-528](#)), S313 ([SAT-546](#)), S484 ([THU-531](#)), S712 ([SAT-492](#)), S832 ([FRI-479](#)), S957 ([THU-271](#)), S957 ([THU-272](#)), S970 ([THU-290](#)), S979 ([THU-299](#)), S1039 ([FRI-254](#))
- Treck, Oliver, S521 ([FRI-324](#))
- Treepasertsuk, Sombat, S195 ([FRI-546](#)), S217 ([THU-349](#)), S627 ([THU-453](#)), S721 ([SAT-503](#))
- Trefois, Pierre, S464 ([THU-493](#))
- Trehanpati, Nirupma, S17 ([OS-006-YI](#)), S212 ([THU-343](#)), S218 ([THU-351](#)), S556 ([SAT-267](#)), S1027 ([FRI-235](#)), S1047 ([FRI-267](#))
- Treichel, Nicole, S22 ([OS-015](#))
- Trein, Andreas, S1147 ([TOP-110](#))
- Treleaven, Elise, S266 ([WED-367](#))
- Trelles, Marita, S1191 ([THU-190](#))
- Tremblay, Mélanie, S213 ([THU-344](#)), S233 ([THU-372](#))
- Trentacapilli, Benedetta, S120 ([LBP-29](#))
- Trentini, Muriel, S929 ([FRI-201](#))
- Trenti, Tommaso, S729 ([SAT-517](#))
- Trépo, Eric, S12 ([LBO-04](#)), S621 ([THU-442](#))
- Trevellin, Elisabetta, S766 ([WED-449](#))
- Trevisani, Franco, S480 ([THU-523](#)), S499 ([FRI-287](#)), S511 ([FRI-308](#)), S513 ([FRI-311](#)), S586 ([THU-134](#)), S597 ([THU-153](#))
- Trevisi, Greta, S978 ([THU-297](#))
- Tria, Giada, S744 ([WED-413](#)), S783 ([WED-507](#)), S802 ([WED-547](#))
- Triantafyllou, Evangelos, S77 ([OS-108-YI](#)), S127 ([TOP-093](#)), S214 ([THU-345](#)), S452 ([SAT-389](#))
- Triantos, Christos, S400 ([WED-302](#)), S1128 ([WED-211](#))
- Triastcyn, Aleksei, S1151 ([SAT-171](#))
- Trickey, Adam, S909 ([FRI-165](#))
- Trinh, Amy, S558 ([SAT-271](#))
- Trinka, Eugen, S863 ([SAT-126](#))
- Triolo, Michela, S471 ([THU-507](#))
- Tripathi, Dhiraj, S87 ([OS-123-YI](#)), S964 ([THU-283](#))
- Tripathi, Dinesh Mani, S208 ([THU-338](#)), S228 ([THU-363](#)), S348 ([THU-234](#)), S352 ([THU-240](#)), S436 ([SAT-360](#)), S560 ([SAT-274](#))
- Tripathi, Gaurav, S17 ([OS-006-YI](#)), S21 ([OS-014-YI](#)), S76 ([OS-107-YI](#)), S139 ([FRI-398](#)), S146 ([FRI-407](#)), S149 ([FRI-410](#)), S152 ([FRI-416](#)), S326 ([WED-222](#)), S414 ([FRI-344](#)), S1033 ([FRI-247](#))
- Tripathi, Harshita, S277 ([WED-388](#))
- Tripodo, Claudio, S803 ([WED-549](#))
- Tripson, Simona, S168 ([FRI-440](#))
- Trivedi, Hirsch, S489 ([TOP-065](#))
- Trivedi, Palak, S56 ([OS-073](#)), S123 ([LBP-36](#)), S368 ([WED-251](#)), S386 ([WED-280](#)), S398 ([WED-299](#)), S403 ([WED-307](#)), S416 ([FRI-347](#)), S466 ([THU-497](#)), S985 ([THU-310](#)), S990 ([THU-317](#))
- Trojan, Jörg, S491 ([FRI-273](#)), S507 ([FRI-300](#))
- Troke, Philip, S397 ([WED-297](#))
- Troncone, Giancarlo, S942 ([THU-251](#))
- Troppmair, Maria, S968 ([THU-288](#))
- Troshina, Yulia, S917 ([FRI-180](#)), S1177 ([THU-169](#)), S1200 ([THU-206](#))
- Trost, Jonas, S733 ([WED-396](#))
- Trost, Kajetan, S165 ([FRI-434](#))
- Trost, Matthias, S781 ([WED-475](#))
- Trotovšek, Blaž, S553 ([SAT-261](#))
- Troutman, Ty, S417 ([FRI-350](#))
- Trouw, Leendert, S382 ([WED-274](#))
- Trovato, Francesca, S127 ([TOP-093](#)), S445 ([SAT-376](#))
- Truchi, Régine, S1158 ([SAT-180](#))
- Truong, David, S920 ([FRI-186](#)), S929 ([FRI-200](#))
- Truong, Emily, S659 ([SAT-408](#))
- Truong, Jennifer, S415 ([FRI-346](#))
- Truty, Mark, S44 ([OS-050-YI](#)), S465 ([THU-495](#))
- Trylesinski, Aldo, S672 ([SAT-427](#))
- Trzos, Katarzyna, S332 ([WED-233](#)), S431 ([FRI-370](#))
- Tsafaridou, Maria, S400 ([WED-302](#))
- Tsai, Catherine, S377 ([WED-266](#))
- Tsai, Hong-Wen, S999 ([THU-333](#))
- Tsai, Ming-Chang, S1206 ([THU-217](#))
- Tsai, Pei-Chien, S1180 ([THU-174](#))
- Tsai, Wei-lun, S1206 ([THU-217](#))
- Tsai, Wen-Wei, S49 ([OS-061](#))

- Tsai, Yi-Hsuan, S361 ([FRI-385](#))
Tsakiridis, Evelyn, S762 ([WED-442](#))
Tsang, Simon, S48 ([OS-058](#))
Tschuschner, Annette, S339 ([WED-248](#))
Tseng, Kuo-Chih, S1180 ([THU-174](#)), S1206 ([THU-217](#))
Tseng, Leo, S544 ([SAT-243](#))
Tseng, Tai-Chung, S531 ([SAT-219](#)), S1061 ([WED-119](#))
Tseng, Te-Wei, S1057 ([TOP-112](#))
Tsereteli, Maia, S890 ([FRI-135](#)), S891 ([FRI-136](#)), S898 ([FRI-147](#)), S909 ([FRI-167](#)), S925 ([FRI-193](#)), S931 ([FRI-205](#))
Tsertsvadze, Tengiz, S881 ([FRI-123](#)), S889 ([FRI-133](#)), S921 ([FRI-187](#)), S1204 ([THU-214](#))
Tse, Yee-Kit, S1064 ([WED-123](#)), S1069 ([WED-129](#)), S1146 ([SAT-166](#)), S1148 ([SAT-167](#))
Tsien, Cynthia, S426 ([FRI-363](#))
Tsigas, Alexandros-Pantelis, S262 ([WED-362](#))
Tskhomelidze, Irina, S881 ([FRI-123](#)), S925 ([FRI-193](#)), S931 ([FRI-205](#)), S933 ([FRI-210](#))
Tskhomelidze, Irinka, S898 ([FRI-147](#))
Tsochatzis, Emmanuel, S105 ([LBP-09](#)), S475 ([THU-514](#)), S656 ([SAT-402](#)), S660 ([SAT-409](#)), S661 ([SAT-410](#)), S668 ([SAT-420](#)), S812 ([FRI-471](#))
Tsou, Hsiao-Hui Sophie, S588 ([THU-138](#))
Tsounis, Efthymios, S400 ([WED-302](#))
Tsou, Phoebe, S432 ([FRI-371](#))
Tsrancheva, Radoslava, S110 ([LBP-15](#)), S1149 ([SAT-168](#))
Tsreteli, Maia, S889 ([FRI-133](#)), S933 ([FRI-210](#))
Tsubota, Akihito, S240 ([WED-327](#)), S818 ([FRI-508](#))
Tsuchiya, Atsunori, S124 ([LBP-37](#))
Tsuchiya, Kaoru, S598 ([THU-155](#)), S644 ([THU-554](#)), S1113 ([WED-189](#))
Tsui, Yu, S48 ([OS-058](#))
Tsuneyama, Koichi, S733 ([WED-395](#))
Tsumumi, Tsubasa, S686 ([SAT-448](#))
Tual, Christelle, S1161 ([SAT-185](#))
Tu, Chaoyong, S488 ([THU-540](#))
Tudehope, Fiona, S195 ([FRI-546](#))
Tudor, Andrada, S220 ([THU-355](#))
Tudrujek, Magdalena, S505 ([FRI-296](#))
Tuefferd, Marianne, S444 ([SAT-374](#)), S1034 ([FRI-248](#))
Tufoni, Manuel, S191 ([FRI-540](#))
Tükek, Tufan, S279 ([WED-391](#))
Tun, Nway, S263 ([WED-364](#))
Tuo, Biguang, S329 ([WED-228](#)), S747 ([WED-419](#))
Turan, Dilara, S181 ([FRI-463](#))
Turan, Ilker, S181 ([FRI-463](#))
Turato, Cristian, S552 ([SAT-258](#)), S766 ([WED-449](#))
Turcanu, Adela, S9 ([GS-012](#)), S1054 ([TOP-100](#))
Turco, Celia, S994 ([THU-322](#))
Turco, Laura, S54 ([OS-069](#)), S86 ([OS-121-YI](#)), S87 ([OS-123-YI](#)), S970 ([THU-290](#))
Turetti, Fabio, S945 ([THU-255](#))
Turkina, Anastasia, S260 ([WED-357](#))
Turley, Rebecca, S1202 ([THU-210](#))
Turner, Alice, S963 ([THU-281](#))
Turner, Lucy, S182 ([FRI-464](#))
Turner, Scott, S322 ([WED-215](#)), S413 ([FRI-335](#))
Turnes, Juan, S326 ([WED-223](#)), S376 ([WED-264](#)), S560 ([SAT-275](#)), S700 ([SAT-468](#)), S921 ([FRI-188](#)), S1178 ([THU-171](#)), S1205 ([THU-216](#)), S1209 ([THU-219](#))
Turon, Fanny, S2 ([GS-003](#)), S86 ([OS-121-YI](#)), S87 ([OS-123-YI](#)), S843 ([FRI-499](#)), S984 ([THU-308](#))
Turrubiate, Isaías, S547 ([SAT-249](#))
Tursunova, Dilorom, S113 ([LBP-19](#))
Tushuizen, Maarten, S14 ([LBO-06](#)), S382 ([WED-274](#))
Tuyishime, Albert, S886 ([FRI-130](#))
Tveden-Nyborg, Pernille, S801 ([WED-545](#))
Tyagi, Purnima, S1013 ([TOP-102](#)), S1045 ([FRI-263](#))
Tyakht, Alexander, S349 ([THU-235](#))
Tyc, Katarzyna, S352 ([THU-239](#))
Tzadok, Roie, S393 ([WED-291](#))
Tzedakis, Stylianos, S859 ([SAT-120](#))
Tzeuton, Christian, S1210 ([THU-222](#))
Tzivinikos, Christos, S971 ([THU-291](#))
Uberti-Foppa, Caterina, S120 ([LBP-29](#)), S837 ([FRI-487](#))
Ucbilek, Enver, S195 ([FRI-546](#))
Uchida-Kobayashi, Sawako, S566 ([SAT-286](#))
Uchihara, Naoki, S644 ([THU-554](#))
Uchiyama, Akira, S180 ([FRI-461](#)), S744 ([WED-415](#)), S793 ([WED-528](#))
Ueda, Shinichiro, S686 ([SAT-448](#))
Ueda, Yoshihide, S545 ([SAT-246](#)), S559 ([SAT-272](#))
Ueno, Yoshiyuki, S1183 ([THU-177](#))
Ugiagbe, Rose Ashinedu, S865 ([SAT-129](#))
Uguen, Thomas, S61 ([OS-081](#)), S62 ([OS-083-YI](#)), S467 ([THU-498](#))
Uhlenbusch, Natalie, S373 ([WED-258](#))
Ul Haq, Shamas, S168 ([FRI-439](#))
Uluk, Deniz, S469 ([THU-502](#))
Ulyanov, Anatoly, S489 ([TOP-065](#))
Umair Latif, Muhammad, S799 ([WED-541](#))
Umar, Narmeen, S373 ([WED-259](#))
Umberto, Dalessandro, S1046 ([FRI-265](#)), S1106 ([WED-178](#))
Umemura, Takeji, S394 ([WED-293](#))
Um, Hyun Jun, S1130 ([TOP-105](#))
Unchwaniwala, Nuruddin, S1058 ([WED-114](#)), S1153 ([SAT-174](#)), S1167 ([SAT-195](#))
Unnithan, Gauri, S827 ([FRI-524](#))
Urbanek-Quaing, Melanie, S1035 ([FRI-249](#))
Urbani, Luca, S324 ([WED-218](#)), S324 ([WED-219](#))
Urban, Matthew, S765 ([WED-448](#))
Urban, Stephan, S1025 ([FRI-232](#))
Urbonas, Gediminas, S912 ([FRI-173](#))
Ure, Daren, S324 ([WED-218](#)), S748 ([WED-420](#)), S770 ([WED-455](#))
Uriarte, Iker, S529 ([SAT-216](#)), S537 ([SAT-232](#))
Urias, Esteban, S658 ([SAT-406](#)), S703 ([SAT-473](#))
Urquijo, Juan José, S1098 ([WED-166](#))
Ursic-Bedoya, Jose, S62 ([OS-083-YI](#))
Urzúa, Alvaro, S396 ([WED-295](#))
Usachov, Valentyn, S951 ([THU-264](#))
Uschner, Frank Erhard, S10 ([LBO-01](#)), S185 ([FRI-341](#)), S222 ([THU-356](#)), S313 ([SAT-546](#)), S484 ([THU-531](#)), S712 ([SAT-492](#))
Us, Gediz Dogay, S645 ([THU-556](#))
Uson, Clara, S90 ([OS-127-YI](#)), S299 ([SAT-521](#))
Uson, Eva, S290 ([SAT-337](#))
Utpatel, Kirsten, S521 ([FRI-324](#))
Uva, Paolo, S446 ([SAT-377](#))
Uysal, Alper, S274 ([WED-382](#))
Vaccaro, Marco, S592 ([THU-144](#)), S1118 ([WED-196](#))
Vaidya, Arun, S282 ([SAT-325](#)), S290 ([SAT-338](#))
Vaidyanathan, Akshaya, S576 ([THU-118](#))
Vaillant, Andrew, S1150 ([SAT-169](#)), S1160 ([SAT-183](#))
Vainilovich, Yelena, S198 ([FRI-550](#)), S807 ([TOP-077](#))
Vairetti, Mariapia, S795 ([WED-533](#)), S804 ([WED-550](#))
Vaishnav, Manas, S73 ([OS-101-YI](#)), S197 ([FRI-548](#)), S297 ([SAT-350](#)), S587 ([THU-135](#)), S693 ([SAT-459](#))
Vaittinada, Prabakar, S1193 ([THU-194](#))
Vaknin, Ilan, S119 ([LBP-28](#)), S415 ([FRI-345](#))
Valaydon, Zina, S380 ([WED-271](#))
Valbuena, Mónica Barreales, S171 ([FRI-445](#))
Valcheva, Tsveta, S1172 ([THU-162](#))
Valcheva, Velichka, S969 ([THU-289](#)), S987 ([THU-313](#)), S990 ([THU-317](#)), S1002 ([THU-336](#))
Valdecantos, Pilar, S331 ([WED-231](#))
Valderrama, Alexa Pamela Benitez, S690 ([SAT-454](#))
Valdez, Ivan, S79 ([OS-112](#))
Valdivieso, Miriam, S131 ([THU-399](#)), S489 ([THU-546](#))
Vale, Luke, S632 ([THU-462](#))
Valenti, Chiara, S729 ([SAT-517](#))
Valenti, Luca, S500 ([FRI-288](#)), S535 ([SAT-227](#)), S609 ([THU-421](#)), S646 ([THU-559](#)), S661 ([SAT-410](#)), S669 ([SAT-422](#)), S673 ([SAT-430](#)), S733 ([WED-393](#)), S772 ([WED-459](#)), S803 ([WED-549](#)), S992 ([THU-318](#)), S1173 ([THU-165](#))
Valentin, Nicolas Stankovic, S211 ([THU-342](#))

Author Index

- Valentino, Pamela, S971 ([THU-291](#))
Valenzuela, Esteban Fuentes, S470 ([THU-503](#)), S480 ([THU-524](#))
Valenzuela, María, S171 ([FRI-445](#))
Valerio, Heather, S910 ([FRI-169](#))
Valerio, Luigi, S729 ([SAT-517](#))
Valery, Patricia, S239 ([WED-324](#)), S846 ([WED-478](#))
Valla, Dominique, S106 ([LBP-10](#)), S670 ([SAT-424](#)), S681 ([SAT-440](#)), S776 ([WED-467](#))
Vallée, Greg, S426 ([FRI-363](#))
Valle, Juan, S541 ([SAT-238](#))
Valles, Foix, S131 ([THU-399](#)), S489 ([THU-546](#))
Valley-Omar, Ziyaad, S1184 ([THU-178](#))
Vallez, Emmanuelle, S355 ([THU-244](#))
Vallier, Ludovic, S122 ([LBP-34](#)), S140 ([FRI-400](#)), S433 ([SAT-354](#))
Vallier, Marie, S806 ([WED-555](#))
Vallot, Ariane, S585 ([THU-133](#))
Valsan, Arun, S86 ([OS-121-YI](#)), S827 ([FRI-524](#)), S846 ([WED-477](#)), S848 ([WED-481](#))
Valva, Pamela, S1037 ([FRI-251](#))
Valverde, Angela Martinez, S331 ([WED-231](#)), S440 ([SAT-367](#)), S777 ([WED-468](#))
Van Beekhoven, Dominique, S880 ([FRI-121](#))
van Bömmel, Florian, S108 ([LBP-12](#)), S201 ([FRI-555](#)), S483 ([THU-529](#)), S507 ([FRI-299](#)), S1043 ([FRI-260](#)), S1050 ([FRI-270](#)), S1071 ([WED-132](#)), S1087 ([WED-151](#)), S1134 ([SAT-148](#)), S1138 ([SAT-154](#)), S1139 ([SAT-156](#)), S1147 ([TOP-110](#))
Vandecaveye, Vincent, S48 ([OS-059-YI](#)), S524 ([TOP-066](#))
van de Graaf, Stan, S55 ([OS-071-YI](#)), S412 ([FRI-333](#)), S427 ([FRI-364](#)), S1025 ([FRI-231](#))
van Delden, Otto, S568 ([SAT-289](#)), S836 ([FRI-485](#))
van den Berg, Aad, S14 ([LBO-06](#))
Van den Berge, Koen, S1034 ([FRI-248](#))
van den Beukel, Michelle, S382 ([WED-274](#))
Van den Branden, Astrid, S764 ([WED-446](#))
van den Brand, Floris, S14 ([LBO-06](#)), S44 ([OS-049-YI](#))
Vandenbroucke, Roosmarijn, S229 ([THU-364](#))
van den Heuvel, Marius, S740 ([WED-407](#))
van den Hoek, Anita M., S805 ([WED-553](#))
Van der Meer, Adriaan, S14 ([LBO-06](#)), S56 ([OS-073](#)), S382 ([WED-274](#))
van der Merwe, Schalk, S345 ([THU-229](#)), S363 ([FRI-389](#)), S452 ([SAT-390](#)), S753 ([WED-430](#))
van der Meulen, Stef, S382 ([WED-274](#))
Vanderschueren, Emma, S300 ([SAT-524](#))
van der Valk, Marc, S880 ([FRI-121](#)), S892 ([FRI-138](#))
van der Veen, Lars, S761 ([WED-441](#))
van der Woerd, Wendy L., S965 ([THU-284](#)), S969 ([THU-289](#))
van de Werken, Harmen, S1016 ([TOP-108](#)), S1019 ([FRI-219](#))
Vandriel, Shannon M., S971 ([THU-291](#))
van Duyvenvoorde, Wim, S763 ([WED-444](#)), S786 ([WED-515](#))
van Eekhout, Kirsí, S1100 ([WED-169](#))
van Eijk, Hans, S350 ([THU-236](#))
Vangan, Nyamtsengel, S1104 ([WED-175](#))
Vangara, Sasanka, S209 ([THU-339](#))
van Gerven, Nicole, S14 ([LBO-06](#))
van Gijzel, Hardeep, S1039 ([FRI-255](#))
van Grunsven, Leo, S410 ([FRI-330](#))
Van Gulik, Thomas, S568 ([SAT-289](#))
Vanhaecke, Tamara, S752 ([WED-428](#)), S775 ([WED-465](#))
Vanherck, Jean-Christophe, S1025 ([FRI-231](#))
van Herwaarden, Manon, S14 ([LBO-06](#))
van Heuven, Bertie Joan, S786 ([WED-515](#))
Van Hoek, Bart, S14 ([LBO-06](#)), S382 ([WED-274](#))
van Hooff, Maria, S46 ([OS-053-YI](#))
Vanhove, Christian, S226 ([THU-361](#))
Van Hul, Noémi K. M., S410 ([FRI-330](#)), S433 ([SAT-353](#)), S945 ([THU-255](#))
van IJzendoorn, Manon, S14 ([LBO-06](#))
van Kleef, Laurens, S83 ([OS-118](#))
Vanlemmens, Claire, S473 ([THU-511](#))
Van Melkebeke, Lukas, S363 ([FRI-389](#))
Vanneste, Bavo, S445 ([SAT-375](#))
Vanni, Ester, S40 ([OS-045](#)), S55 ([OS-070](#)), S88 ([OS-124-YI](#)), S374 ([WED-260](#))
van Rensburg, Christo, S1108 ([WED-181](#))
van Rosmalen, Belle, S568 ([SAT-289](#))
van Rosmalen, Marieke, S454 ([TOP-052](#))
Vanrusselt, Hannah, S1051 ([FRI-272](#))
van Schaik, Willem, S123 ([LBP-36](#))
van Selm, Lena, S924 ([FRI-192](#))
Van, Trieu My, S78 ([OS-110](#))
van Weeghel, Michel, S427 ([FRI-364](#))
van Welzen, Berend, S892 ([FRI-138](#))
van Wessel, Daan, S969 ([THU-289](#))
Vanwolleghe, Thomas, S14 ([LBO-06](#)), S52 ([OS-065-YI](#)), S61 ([OS-080-YI](#)), S279 ([TOP-043](#)), S300 ([SAT-524](#)), S622 ([THU-444](#)), S880 ([FRI-121](#)), S1034 ([FRI-248](#)), S1054 ([TOP-100](#)), S1114 ([WED-190](#)), S1132 ([SAT-145](#)), S1138 ([SAT-154](#))
Vaquero, Javier, S38 ([OS-041-YI](#)), S150 ([FRI-412](#)), S331 ([WED-231](#)), S349 ([THU-235](#)), S560 ([SAT-275](#)), S732 ([TOP-090](#))
Varaldo, Riccardo, S88 ([OS-124-YI](#))
Varasa, Tomás Artaza, S171 ([FRI-445](#))
Vardeu, Antonella, S1169 ([SAT-198](#))
Varela, Carmen, S902 ([FRI-153](#))
Varela, Maria, S12 ([LBO-04](#)), S573 ([THU-114](#)), S579 ([THU-124](#))
Varela-Rey, Marta, S326 ([WED-223](#)), S560 ([SAT-275](#))
Vargas Blasco, Víctor Manuel, S980 ([THU-301](#)), S998 ([THU-331](#))
Vargas, Dawn, S995 ([THU-324](#))
Vargas, Hugo, S85 ([OS-120](#)), S195 ([FRI-546](#)), S242 ([WED-330](#)), S256 ([WED-352](#)), S258 ([WED-355](#)), S296 ([SAT-348](#))
Vargas, Montserrat, S903 ([FRI-156](#))
Vargas, Victor, S198 ([FRI-550](#)), S807 ([TOP-077](#))
Variya, Bhavesh, S770 ([WED-455](#))
Varleva, Tonka, S880 ([FRI-121](#))
Varma, Sharat, S620 ([THU-440](#))
Varnai, Kinga, S1075 ([WED-137](#))
Varona, Sarai, S902 ([FRI-153](#))
Varshney, Mohit, S7 ([GS-008-YI](#))
Varughese, Tilly, S1171 ([SAT-202](#))
Vasileiadi, Sofia, S1194 ([THU-196](#)), S1194 ([THU-197](#))
Vasileiadis, Themistokis, S400 ([WED-302](#))
Vasileiou, Despoina, S730 ([SAT-518](#))
Vasileva, Larisa, S262 ([WED-362](#)), S978 ([THU-298](#))
Vásquez-Garzón, Verónica Rocío, S151 ([FRI-414](#)), S160 ([FRI-426](#))
Vassord, Camille, S61 ([OS-080-YI](#))
Vasudevan, Ashwini, S352 ([THU-240](#)), S436 ([SAT-360](#))
Vasuri, Francesco, S519 ([FRI-322](#))
Vauthier, Virginie, S954 ([THU-267](#))
Vaux, Lucinda, S266 ([WED-366](#))
Vaz, Karl, S625 ([THU-450](#)), S861 ([SAT-123](#))
Vázquez, Aitana Carla Morano, S892 ([FRI-139](#)), S898 ([FRI-148](#))
Vázquez, Inmaculada Fernández, S268 ([WED-372](#)), S406 ([WED-314](#)), S1098 ([WED-166](#)), S1178 ([THU-171](#)), S1205 ([THU-216](#))
Vázquez-Ogando, Elena, S732 ([TOP-090](#))
Vazquez, Rafael Godino, S936 ([FRI-214](#))
Vázquez, Valeria, S865 ([SAT-129](#))
V, Dheepak, S462 ([THU-489](#))
Vecchiet, Jacopo, S1122 ([WED-203](#))
Vecchio, Cristina, S751 ([WED-425](#)), S804 ([WED-551](#))
Veckmans, Geraldine, S764 ([WED-446](#))
Veelen, Rhea, S197 ([FRI-549](#)), S201 ([FRI-555](#)), S507 ([FRI-299](#))
Vega, Javier, S683 ([SAT-443](#))
Veidal, Sanne, S321 ([TOP-036](#))
Veillette, Félix, S233 ([THU-372](#))
Velasco, Jose Antonio Velarde-Ruiz, S195 ([FRI-546](#))
Velasco, María Soledad, S1191 ([THU-190](#))
Velasquez, Hector, S883 ([FRI-125](#)), S886 ([FRI-130](#)), S1189 ([THU-187](#)), S1200 ([THU-207](#))
Velazquez, René Malé, S195 ([FRI-546](#))
Velkov, Stoyan, S945 ([THU-256](#))
Veloz, Maria Guerra, S91 ([OS-128](#)), S642 ([THU-551](#)), S905 ([FRI-161](#)), S1179 ([THU-172](#))
Vendelbo, Mikkel Holm, S958 ([THU-274](#)), S985 ([THU-309](#))
Venere, Rosanna, S40 ([OS-045](#)), S55 ([OS-070](#))
Venerito, Marino, S47 ([OS-057](#))

- Veneziano, Marzia, S36 (OS-036)
 Venishetty, Shantanu, S272 (WED-379)
 Venkatachalapathy, Suresh Vasan, S274 (WED-382)
 Venkatraman, Meenakshi, S112 (LBP-18), S1029 (FRI-238), S1162 (SAT-188), S1164 (SAT-192)
 Ventura, Paolo, S1105 (WED-176)
 Ventura, Stephanie, S599 (THU-157)
 Venturini, Giulia, S981 (THU-302)
 Venu, Arathi, S827 (FRI-524)
 Venugopal, Radhika, S473 (THU-510)
 Venuto, Clara De, S191 (FRI-540), S237 (WED-320)
 Verbeek, Jef, S363 (FRI-389), S452 (SAT-390), S753 (WED-430)
 Verbinnen, Thierry, S1034 (FRI-248), S1138 (SAT-154)
 Verboven, Elisabeth, S433 (SAT-353), S945 (THU-255)
 Vercoulen, Yvonne, S535 (SAT-228)
 Verdeguer, Francisco, S327 (WED-224), S737 (WED-402)
 Verderame, Francesco, S568 (SAT-288)
 Verdonk, Robert, S14 (LBO-06)
 Verdonschot, Meggy, S535 (SAT-228)
 Verdoux, Marie, S408 (WED-318)
 Verd, Pep Coll, S932 (FRI-208)
 Vergès, Bruno, S603 (THU-410)
 Verhaege, Daan, S229 (THU-364)
 Verheij, Joanne, S568 (SAT-289), S836 (FRI-485)
 Verhelst, Xavier, S87 (OS-123-YI), S226 (THU-361), S307 (SAT-538), S787 (WED-516), S970 (THU-290)
 Verhoeven, Arthur, S427 (FRI-364)
 Verhoye, Lieven, S1025 (FRI-231)
 Verhulst, Stefaan, S410 (FRI-330), S439 (SAT-365)
 Verkade, Henkjan J., S965 (THU-284), S969 (THU-289), S971 (THU-291), S987 (THU-313), S1003 (THU-378)
 Verma, Anita, S987 (THU-312), S999 (THU-332)
 Verma, Gayantika, S1027 (FRI-235)
 Verma, Nipun, S827 (FRI-524), S848 (WED-481)
 Vermehren, Johannes, S90 (OS-126), S91 (OS-129-YI)
 Verna, Elizabeth, S89 (OS-125)
 Vero, Vittoria, S54 (OS-069)
 Verrijken, An, S83 (OS-118)
 Verschuren, Lars, S763 (WED-444), S805 (WED-553)
 Versele, Matthias, S1025 (FRI-231)
 Verset, Gontran, S12 (LBO-04)
 Verslype, Chris, S48 (OS-059-YI), S524 (TOP-066)
 Verucchi, Gabriella, S107 (LBP-11)
 Vervueren, Laurent, S598 (THU-154)
 Verwaayen, Anna, S22 (OS-015), S416 (FRI-348)
 Verwer, Bart, S14 (LBO-06)
 Vesikari, Timo, S1119 (WED-197)
 Vespasiani Gentilucci, Umberto, S40 (OS-045), S55 (OS-070)
 Vessby, Johan, S605 (THU-414), S650 (TOP-085), S653 (SAT-397), S707 (SAT-481)
 Vesterhus, Mette, S370 (WED-254), S541 (SAT-238)
 Vestito, Amanda, S88 (OS-124-YI), S974 (THU-293)
 Vetter, Marcel, S403 (WED-307)
 Vettori, Giovanni, S374 (WED-260)
 Vettor, Roberto, S766 (WED-449)
 Vezali, Elena, S400 (WED-302)
 Viacheslav, Morozov, S31 (OS-030), S53 (OS-068)
 Viale, Pierluigi, S1103 (WED-174)
 Viayna, Elisabet, S188 (FRI-535), S248 (WED-342), S307 (SAT-537)
 Vibert, Eric, S74 (OS-104), S458 (THU-483), S460 (THU-486), S482 (THU-528)
 Vicardi, Marco, S510 (FRI-304)
 Viceconti, Nicholas, S660 (SAT-409)
 Vicens, Joan Blázquez, S326 (WED-223), S560 (SAT-275)
 Vicent, Silve, S560 (SAT-275)
 Viciano, Isabel, S1126 (WED-208)
 Vicioso, Horacio, S932 (FRI-208)
 Vickerman, Peter, S909 (FRI-165), S912 (FRI-172)
 Vico-Romero, Judit, S904 (FRI-158), S917 (FRI-181)
 Vidal, Enrique, S1172 (THU-162)
 Vidal-González, Judit, S86 (OS-121-YI)
 Vidali, Matteo, S669 (SAT-422)
 Vidal, Pep, S737 (WED-403)
 Vidal, Susana Sabater, S1124 (WED-205)
 Vidal-Trecan, Tiphaine, S670 (SAT-424), S681 (SAT-440)
 Vidmar, Robert, S553 (SAT-261)
 Vidon, Mathias, S930 (FRI-204)
 Viegas, Nuno, S556 (SAT-267)
 Vierling, John M., S85 (OS-120), S371 (WED-256)
 Vierziger, Konstantin, S282 (SAT-326), S313 (SAT-547)
 Viganò, Mauro, S40 (OS-045), S55 (OS-070), S107 (LBP-11), S471 (THU-507), S609 (THU-421)
 Viganò, Raffaella, S40 (OS-045), S55 (OS-070)
 Vignon-Clementel, Irene, S359 (FRI-382)
 Vignone, Anthony, S36 (OS-036)
 Vig, Pamela, S56 (OS-072), S123 (LBP-35), S370 (WED-252), S372 (WED-257), S387 (WED-282), S417 (FRI-350)
 Vijan, Ancuta Elena, S192 (FRI-541)
 Vijayakumar, Archana, S323 (WED-216)
 Vij, Mukul, S12 (LBO-04)
 Vila, Carmen, S392 (WED-290)
 Viladomiu, Lluís, S375 (WED-263)
 Vilarnau, Nuria, S363 (FRI-388)
 Vilar, Teresa De la Rosa, S928 (FRI-198)
 Vilchez-Gómez, Juan Francisco, S38 (OS-041-YI)
 Vilella, Àngels, S1191 (THU-190)
 Vilgrain, Valérie, S61 (OS-080-YI)
 Vilibic-Cavlek, Tatjana, S1053 (SAT-143)
 Villablanca, Eduardo, S60 (OS-079-YI)
 Villadsen, Gerda, S841 (FRI-494)
 Villadsen, Gerda Elisabeth, S403 (WED-307), S523 (FRI-328)
 Villa, Erica, S72 (OS-099), S258 (WED-356), S287 (SAT-334), S493 (FRI-277), S495 (FRI-280)
 Villalba, Carmen Molina, S1126 (WED-208)
 Villamayor, Laura, S440 (SAT-367)
 Villamil, Maria Alejandra Gracia, S56 (OS-073), S392 (WED-290)
 Villani, Roberto, S247 (WED-340)
 Villani, Rosanna, S36 (OS-036), S750 (WED-424), S814 (FRI-474)
 Villano, Gianmarco, S766 (WED-449)
 Villanueva, Augusto, S48 (OS-059-YI), S527 (SAT-213)
 Villanueva, Càndid, S3 (GS-003), S73 (OS-100-YI), S87 (OS-123-YI), S105 (LBP-09), S164 (FRI-433), S279 (TOP-043), S970 (THU-290)
 Villanueva, Dennis, S599 (THU-157)
 Villanueva, Marina, S126 (TOP-087), S142 (FRI-403), S144 (FRI-406)
 Villar, Carmen, S171 (FRI-445)
 Villarroel, Carolina, S926 (FRI-196)
 Villa-Treviño, Saúl, S151 (FRI-414), S160 (FRI-426)
 Villela-Nogueira, Cristiane, S618 (THU-436), S626 (THU-451), S658 (SAT-405)
 Villeret, Francois, S118 (LBP-27)
 Villesen, Ida, S17 (OS-005-YI), S173 (FRI-449), S175 (FRI-452), S303 (SAT-528), S657 (SAT-404)
 Villota-Rivas, Marcela, S114 (LBP-21)
 Vilsbøll, Tina, S607 (THU-419)
 Vilstrup, Hendrik, S159 (FRI-424), S257 (WED-354), S629 (THU-455)
 Vinaixa, Carmen, S476 (THU-517), S485 (THU-535), S1172 (THU-162)
 Vince, Adriana, S1053 (SAT-143)
 Vincent, Catherine, S373 (WED-259), S426 (FRI-363)
 Vincentis, Antonio De, S36 (OS-036), S665 (SAT-416)
 Vincent, Jacob, S1145 (SAT-164)
 Vincent, Jeanne Perpétue, S897 (FRI-146)
 Vinh, Hanh Ngo, S566 (SAT-286)
 Vinikoor, Michael, S916 (FRI-178), S1117 (WED-195)
 Vinod, Vaishnavy S, S827 (FRI-524), S848 (WED-481)
 Vinué, Ángela, S789 (WED-520)
 Viola, Maria, S345 (THU-229)
 Vionnet, Julien, S189 (FRI-537), S481 (THU-526)
 Visentini, Marcella, S217 (THU-350)
 Visentin, Michele, S568 (SAT-289)
 Visic, Ana, S880 (FRI-122)
 Visintin, Alessia, S711 (SAT-489)

Author Index

- Viso, Luis Menchén, S481 (THU-525)
 Visser, Brendan, S25 (OS-020-YI)
 Vitale, Alessandro, S293 (SAT-343), S480 (THU-523), S511 (FRI-308), S1056 (TOP-106)
 Vitale, Giovanni, S86 (OS-121-YI)
 Vitali, Marlena, S31 (OS-029)
 Vitális, Zsuzsanna, S23 (OS-017-YI)
 Vitek, Libor, S727 (SAT-513)
 Vitellius, Carole, S598 (THU-154)
 Vithayathil, Mathew, S576 (THU-118)
 Vits, Lieve, S764 (WED-446)
 Viuff, Birgitte, S748 (WED-421)
 Vivaldi, Caterina, S575 (THU-116), S584 (THU-131), S586 (THU-134)
 Vivanco, Maria, S529 (SAT-216)
 Vizcarra, Pamela, S843 (FRI-499)
 Vizioli, Luca, S54 (OS-069)
 Vizzutti, Francesco, S233 (THU-371)
 Vlachogiannakos, Ioannis, S262 (WED-362), S1128 (WED-211)
 Vlierberghe, Hans Van, S226 (THU-361), S307 (SAT-538), S787 (WED-516), S1114 (WED-190)
 Vnencakova, Janka, S871 (SAT-136)
 Voeller, Alexis, S872 (TOP-096), S910 (FRI-170), S912 (FRI-173), S934 (FRI-212)
 Voet, Francis, S307 (SAT-538)
 Voet, Thierry, S753 (WED-430)
 Vogelaar, Serge, S454 (TOP-052)
 Vogel, Arndt, S12 (LBO-04), S491 (FRI-273), S496 (FRI-282), S507 (FRI-300), S561 (SAT-277), S574 (THU-115), S575 (THU-116), S579 (THU-123), S580 (THU-125), S586 (THU-134)
 Vogel, Georg-Friedrich, S987 (THU-313)
 Vogel, Ida, S986 (THU-311)
 Vogel, Kristina, S441 (SAT-368)
 Vogels, Esther, S412 (FRI-333)
 Vogl, Thomas, S313 (SAT-546)
 Vohl, Marie-Claude, S431 (FRI-368)
 Voidonikolas, Georgios, S489 (TOP-065)
 Voiosu, Andrei, S192 (FRI-541)
 Voiosu, Theodor, S192 (FRI-541)
 Volkert, Ines, S639 (THU-472), S730 (TOP-084)
 Volk, Valery, S561 (SAT-277)
 Volmari, Annika, S1019 (FRI-220), S1023 (FRI-227)
 Volovets, Anastasia, S480 (THU-522)
 Volpe, Letizia Bavuso, S749 (WED-423)
 Volpi, Sonia, S974 (THU-293)
 Volz, Tassilo, S1019 (FRI-220), S1023 (FRI-227), S1147 (TOP-109)
 von Arnim, Ulrike, S1147 (TOP-110)
 von Bergen, Martin, S136 (FRI-393)
 von Buelow, Verena, S339 (WED-248), S954 (THU-268)
 von der Leyen, Heiko, S1137 (SAT-152)
 Vonderlin, Joscha, S285 (SAT-331)
 Vondran, Florian, S945 (THU-256)
 von Felden, Johann, S491 (FRI-273), S527 (SAT-213), S575 (THU-116), S579 (THU-123), S582 (THU-128), S586 (THU-134)
 Vonghia, Luisa, S61 (OS-080-YI), S83 (OS-118), S300 (SAT-524), S622 (THU-444), S764 (WED-446), S776 (WED-466), S790 (WED-523)
 von Karpowitz, Maria, S1137 (SAT-152)
 Vonschallen, Philipp, S737 (WED-402)
 Vorobioff, Julio, S253 (WED-348)
 Voronkova, Natalia, S9 (GS-012)
 Voß, Hannah, S527 (SAT-213)
 Vreeken, Debby, S763 (WED-444)
 Vrolijk, Jan Maarten, S14 (LBO-06)
 Vucur, Mihael, S562 (SAT-279)
 Vu, Hieu, S566 (SAT-286)
 Vuille-Lessard, Élise, S279 (TOP-043)
 Vuppalachchi, Raj, S85 (OS-120), S649 (TOP-080)
 Vyberg, Mogens, S530 (SAT-218), S614 (THU-429), S742 (WED-411), S748 (WED-421)
 Wabitsch, Martin, S65 (OS-088)
 Wack, Katy, S31 (OS-029), S790 (WED-522)
 Waddell, Scott, S122 (LBP-33-YI)
 Waddell, Tom, S677 (SAT-436)
 Waddilove, Elizabeth, S868 (SAT-131), S1060 (WED-117), S1108 (WED-181)
 Wade, Amanda, S1190 (THU-189)
 Wadland, Elaine, S382 (WED-273), S391 (WED-289)
 Waern, Johan, S963 (THU-281)
 Wafula, Rose, S100 (LBP-01)
 Wagner, Josephin, S792 (WED-527)
 Wagner, Mathilde, S492 (FRI-274), S494 (FRI-279), S515 (FRI-316), S585 (THU-133), S589 (THU-139)
 Wagner, Sonja, S968 (THU-288)
 Waich, Eva, S142 (FRI-402)
 Waidmann, Oliver, S579 (THU-123)
 Waisbourd-Zinman, Orith, S128 (THU-394), S955 (THU-269)
 Wai-Sun Wong, Vincent, S114 (LBP-21), S612 (THU-426), S627 (THU-453)
 Wajbrot, Natalia, S626 (THU-451)
 Waked, Imam, S1212 (THU-224)
 Waldmann, Moritz, S527 (SAT-213)
 Waldschmidt, Dirk-Thomas, S491 (FRI-273)
 Walecka, Agnieszka, S193 (FRI-543)
 Walker, Josephine, S912 (FRI-172)
 Walker, Lucy, S389 (WED-285)
 Walker, Maura, S608 (THU-420)
 Walker, Michael A., S1167 (SAT-195)
 Walker, Ruth, S781 (WED-475)
 Wallace, Jack, S1087 (WED-151)
 Wallace, Michael, S58 (OS-075)
 Wallays, Marie, S452 (SAT-390), S753 (WED-430)
 Wallebäck, Anna, S57 (OS-074-YI)
 Waller, Kathryn, S740 (WED-406)
 Wallin, Jeffrey, S1023 (FRI-226), S1055 (TOP-101)
 Walmsley, Martine, S383 (WED-277), S398 (WED-299)
 Walsh, Caroline, S180 (FRI-460)
 Walsh, Renae, S1028 (FRI-237), S1164 (SAT-191)
 Walter, Aurélie, S579 (THU-123)
 Wamala, Joseph, S69 (OS-094)
 Wandeler, Gilles, S101 (LBP-04), S916 (FRI-178), S1117 (WED-195)
 Wandji, Line Carolle Ntandja, S62 (OS-083-YI), S146 (FRI-408)
 Wan, Gang, S130 (THU-397), S131 (THU-400)
 Wang, Baoju, S549 (SAT-253)
 Wang, Bin, S375 (WED-262)
 Wang, Bo, S1081 (WED-143)
 Wang, Bruce, S86 (OS-122)
 Wang, Chaochao, S143 (FRI-405)
 Wang, Chenlu, S490 (TOP-068)
 Wang, Chia-Chi, S1180 (THU-174), S1206 (THU-217)
 Wang, Chuanxin, S34 (OS-033)
 Wang, Chunrui, S1112 (WED-187)
 Wang, Chunying, S34 (OS-033)
 Wang, Cong, S20 (OS-012-YI)
 Wang, Danni, S1143 (SAT-161)
 Wang, Dongdong, S762 (WED-442)
 Wang, Fu-Sheng, S145 (TOP-078), S1166 (SAT-194)
 Wang, Grace, S1149 (SAT-168), S1153 (SAT-174), S1161 (SAT-186)
 Wang, Guangchuan, S304 (SAT-530)
 Wang, Guangyi, S327 (WED-225)
 Wang, Gui-Qiang, S854 (TOP-094), S1090 (WED-155), S1100 (WED-170)
 Wang, GuoRui, S1112 (WED-188)
 Wang, Haiyu, S308 (SAT-539)
 Wang, Hong-Yang, S34 (OS-033)
 Wang, Hongyuan, S53 (OS-067), S1137 (SAT-153)
 Wang, Hua, S358 (FRI-381)
 Wang, Huali, S395 (WED-294), S1004 (THU-379)
 Wang, Huan, S327 (WED-225)
 Wang, Hui, S747 (WED-419)
 Wang, Hui-Fang, S145 (TOP-078)
 Wang, Hung-Wei, S588 (THU-138)
 Wang, Jian, S395 (WED-294), S696 (SAT-463), S724 (SAT-510), S1004 (THU-379), S1068 (WED-127), S1073 (WED-136), S1078 (WED-140), S1080 (WED-142), S1094 (WED-161), S1094 (WED-162), S1096 (WED-164), S1110 (WED-184), S1128 (WED-212)
 Wang, Jian-She, S969 (THU-289), S971 (THU-291)
 Wang, Jiao, S1127 (WED-210), S1198 (THU-204)
 Wang, JinSong, S1112 (WED-188)
 Wang, Jun, S64 (OS-085)
 Wang, Kaifeng, S22 (OS-016)
 Wang, Ke, S733 (WED-396)
 Wang, Lei, S195 (FRI-546)
 Wang, Li, S235 (TOP-047), S1036 (FRI-250), S1076 (WED-138), S1157 (SAT-179)
 Wang, Lianchen, S488 (THU-540)

- Wang, Louis, S199 (FRI-552), S257 (WED-353), S278 (WED-389)
- Wang, Lu, S271 (WED-376)
- Wang, Pei, S489 (TOP-065)
- Wang, Ping, S455 (THU-477), S540 (SAT-236)
- Wang, Qi, S243 (WED-332), S528 (SAT-214)
- Wang, Qingbi, S571 (SAT-292), S778 (WED-470)
- Wang, Roy, S265 (WED-366)
- Wang, Sarah, S377 (WED-266)
- Wangsell, Fredrik, S57 (OS-074-YI)
- Wang, Sih-Ren, S1180 (THU-174), S1206 (THU-217)
- Wang, Sin-Tian, S361 (FRI-385)
- Wang, Stanley, S1162 (SAT-188)
- Wang, Su, S1087 (WED-151)
- Wang, Tao, S885 (FRI-128)
- Wang, Tingyan, S868 (SAT-131), S1060 (WED-117), S1075 (WED-137), S1108 (WED-181)
- Wang, Tongtog, S610 (THU-423)
- Wang, Tongtong, S650 (TOP-085), S653 (SAT-397)
- Wang, Tseng-En, S588 (THU-138)
- Wang, Wei, S274 (WED-382)
- Wang, Wenping, S61 (OS-080-YI)
- Wang, Wenshi, S1016 (TOP-111), S1025 (FRI-232), S1027 (FRI-234)
- Wang, Xian-bo, S196 (FRI-547)
- Wang, Xianbo, S193 (FRI-544), S404 (WED-309)
- Wang, Xiangrui, S347 (THU-232)
- Wang, Xiao, S453 (SAT-391), S730 (TOP-086)
- Wang, Xiaobo, S581 (THU-126)
- Wang, Xiaodong, S613 (THU-428), S1085 (WED-149)
- Wang, Xiaofeng, S520 (FRI-323)
- wang, xiaojing, S202 (FRI-556), S404 (WED-309)
- Wang, Xiaomei, S347 (THU-232)
- Wang, Xiaoming, S243 (WED-332)
- Wang, XiaoXiao, S759 (WED-438), S862 (SAT-124)
- Wang, Xinlei, S613 (THU-428)
- Wang, Xinrui, S117 (LBP-24), S274 (WED-382)
- Wang, Xin W., S536 (SAT-230)
- Wang, Xun, S528 (SAT-214)
- Wang, Yang, S671 (SAT-426)
- Wang, Yayun, S489 (TOP-065)
- Wang, Yinghong, S582 (THU-128)
- Wang, Yingling, S274 (WED-382)
- Wang, Yipeng, S1152 (SAT-173)
- Wang, Yuhao, S543 (SAT-242)
- Wang, Zhen-Guang, S1165 (SAT-193)
- Wang, Zhenyu, S816 (FRI-505)
- Wang, Zijie, S1027 (FRI-234)
- Wan, Xing, S948 (THU-260)
- Wan, Yawen, S1022 (FRI-225), S1071 (WED-131), S1073 (WED-136)
- Waqar, Mariam Fatima, S204 (FRI-560), S842 (FRI-497)
- Ward, John, S885 (FRI-127), S913 (FRI-174), S935 (FRI-213)
- Ward, Ryan, S173 (FRI-448)
- Ward, Zoe, S909 (FRI-165)
- Wareing, Sue, S1060 (WED-117), S1108 (WED-181)
- Warner, Susanne, S44 (OS-050-YI), S465 (THU-495)
- Washington, Kay, S555 (SAT-265)
- Wasser, Jan-Luca, S797 (WED-536)
- Wasuwanich, Paul, S914 (FRI-176), S1052 (SAT-141), S1182 (THU-175)
- Watanabe, Takehisa, S1095 (WED-163)
- Waters, Laura Jane, S721 (SAT-504)
- Waters, Michael, S149 (FRI-411)
- Waterstradt, Katja, S220 (THU-355)
- Watkins, Jennifer, S383 (WED-276)
- Watkins, Timothy R., S11 (LBO-03), S64 (OS-085), S423 (FRI-360), S678 (SAT-438)
- Watson, Hugh, S10 (LBO-01)
- Wdowinski, Simon, S351 (THU-238)
- Weavil, Josh, S260 (WED-358), S809 (FRI-466)
- Webber, Laura, S103 (LBP-06)
- Weber, Florian, S521 (FRI-324)
- Weber, Gerhard, S538 (SAT-233)
- Weber, Laura, S1208 (THU-218)
- Weber, Oliver, S229 (THU-366)
- Weber, Sabine, S1139 (SAT-156)
- Weber, Susanne N, S563 (SAT-280), S687 (SAT-449), S707 (SAT-480), S950 (THU-262)
- Wedemeyer, Heiner, S31 (OS-030), S53 (OS-068), S108 (LBP-12), S113 (LBP-20), S229 (THU-365), S240 (WED-326), S283 (SAT-328), S301 (SAT-525), S315 (SAT-551), S549 (SAT-253), S562 (SAT-278), S797 (WED-537), S882 (FRI-124), S901 (FRI-152), S1029 (FRI-240), S1031 (FRI-242), S1032 (FRI-244), S1035 (FRI-249), S1044 (FRI-262), S1054 (TOP-100), S1091 (WED-158), S1098 (WED-167), S1101 (WED-171), S1115 (WED-193), S1134 (SAT-148), S1137 (SAT-152), S1139 (SAT-156), S1174 (THU-166)
- Wee, Aileen, S757 (WED-436)
- Wege, Henning, S491 (FRI-273), S527 (SAT-213), S575 (THU-116), S579 (THU-123), S582 (THU-128), S586 (THU-134)
- Weghuber, Daniel, S65 (OS-088)
- Wegmann, Liliana Georgiana, S967 (THU-286)
- Wehling, Cyrill, S594 (THU-147)
- Wehrman, Andrew, S965 (THU-284)
- Weiand, Matthias, S957 (THU-271), S957 (THU-272)
- Wei, Bo, S304 (SAT-530)
- Weidemann, Sören Alexander, S379 (WED-269)
- Weidhase, Lorenz, S201 (FRI-555)
- Wei, Ellie, S680 (SAT-439)
- Weihs, Jasmin, S1021 (FRI-224)
- Weihs, Julian, S785 (WED-512)
- Weijer, Gwen, S805 (WED-554)
- Wei, Lai, S324 (WED-218), S324 (WED-219), S334 (WED-238), S757 (WED-436), S1066 (WED-125), S1163 (SAT-189)
- Weiler-Normann, Christina, S522 (FRI-327)
- Wei, Linlin, S274 (WED-382)
- Weil, Merav, S128 (THU-394)
- Weil-Verhoeven, Delphine, S318 (SAT-556)
- Weinberg, Ethan, S101 (LBP-03), S241 (WED-328)
- Weiner, Iddo Nadav, S409 (TOP-060)
- Weinmann, Arndt, S491 (FRI-273), S527 (SAT-213), S557 (SAT-268), S579 (THU-123), S582 (THU-128)
- Weinmann-Menke, Julia, S277 (WED-387)
- Weinstock, Eyal, S409 (TOP-060)
- Weisberg, Ilan, S729 (SAT-516), S926 (FRI-196)
- Weis, Caroline, S1151 (SAT-171)
- Weiskirchen, Ralf, S137 (FRI-394), S764 (WED-447)
- Weis, Nina, S1050 (FRI-271), S1150 (SAT-170)
- Weissenborn, Karin, S251 (WED-345), S629 (THU-455)
- Weissfeld, Lisa, S9 (GS-012)
- Weiss, Karl Heinz, S1001 (THU-335)
- Wei, Tao, S581 (THU-126)
- Weitz, Hendrik, S441 (SAT-368)
- Wejnaruemarn, Salisa, S217 (THU-349), S274 (WED-382)
- Wellington, Sabina, S1033 (FRI-246)
- Welsch, Christoph, S185 (FRI-341), S276 (WED-385)
- Weltman, Martin, S132 (THU-402)
- wemimo, Rasheed mumini, S865 (SAT-129)
- Wen, Biao, S308 (SAT-539)
- Wen, Chaojing, S1146 (SAT-165)
- Wen, Chunhua, S543 (SAT-242)
- Wendon, Julia, S479 (THU-521)
- Wendum, Dominique, S12 (LBO-04)
- Weng, Honglei, S358 (FRI-381)
- Weng, Shangeng, S869 (SAT-134)
- Wen, Guorong, S747 (WED-419)
- Weng, Yuhang, S956 (THU-270)
- Weninger, Jeremias, S44 (OS-050-YI), S45 (OS-051-YI)
- Wen, Jiaying, S117 (LBP-24)
- Wen-Juei Jeng, Rachel, S1060 (WED-118), S1067 (WED-126), S1088 (WED-152), S1129 (WED-214)
- Wentlandt, Kirsten, S254 (WED-349), S255 (WED-351), S270 (WED-375)
- Wen, Tony, S914 (FRI-176), S1182 (THU-175)
- Wen, Xiaoyu, S320 (SAT-560)
- Wen, Yilei, S1156 (SAT-178)
- Werge, Mikkel, S165 (FRI-434), S321 (TOP-036), S702 (SAT-471), S742 (WED-411), S748 (WED-421), S784 (WED-511)

Author Index

- Wernberg, Charlotte, S173 (FRI-449), S629 (THU-455), S657 (SAT-404)
- Werner, Ellen, S306 (SAT-536)
- Werner, Jill, S447 (SAT-379)
- Werner, Merle Marie, S300 (SAT-524), S654 (SAT-400)
- Wernevik, Linda, S606 (THU-416)
- Wernly, Bernhard, S863 (SAT-126)
- Wertheim, Heiman, S973 (THU-292)
- Wesley, Emma, S877 (FRI-118)
- West, Alison, S848 (WED-480)
- Westcott, Felix, S731 (TOP-089)
- Wester, Axel, S43 (OS-048-YI), S276 (WED-384), S302 (SAT-527), S600 (TOP-079), S959 (THU-275), S960 (THU-276)
- West, Joe, S4 (GS-004-YI), S160 (FRI-427), S165 (FRI-435), S166 (FRI-436)
- Westland, Christopher, S112 (LBP-18), S1164 (SAT-192)
- Weston, Chris J, S215 (THU-346)
- Wetten, Aaron, S56 (OS-073), S411 (FRI-331)
- Wettengel, Jochen, S1026 (FRI-233)
- Wettstein, Guillaume, S226 (THU-361), S776 (WED-466), S790 (WED-523)
- Wetzstein, Nils, S91 (OS-129-YI)
- Wewer Albrechtsen, Nicolai J, S748 (WED-421)
- Wharton, Victoria, S309 (SAT-541)
- Wheeler, Darren, S379 (WED-268), S844 (FRI-500)
- White, Jason, S447 (SAT-380)
- White, Laura, S193 (FRI-543)
- White, Laura F., S838 (FRI-489)
- White, Megan, S815 (FRI-475)
- White, Sarah, S731 (TOP-089)
- Whittaker, Robert Neil, S880 (FRI-121)
- Widman, Linnea, S159 (FRI-425), S276 (WED-384), S302 (SAT-527), S600 (TOP-079), S959 (THU-275), S960 (THU-276)
- Wiecek, Sabina, S971 (THU-291)
- Wiegand, Johannes, S108 (LBP-12), S967 (THU-286), S1090 (WED-156), S1139 (SAT-156), S1176 (THU-168)
- Wiencke, Kristine, S478 (THU-520)
- Wiesmann, Maximilian, S763 (WED-444)
- Wiest, Reiner, S220 (THU-353), S280 (TOP-048)
- Wietharn, Brooke, S575 (THU-116), S586 (THU-134)
- Wietz, Ann-Sophie, S159 (FRI-424)
- Wijarnpreecha, Karn, S458 (THU-482), S463 (THU-490), S609 (THU-422), S611 (THU-424), S703 (SAT-473)
- Wijnberg, Larissa, S1001 (THU-335)
- Wilamowski, Mateusz, S332 (WED-233)
- Wilcox, Ian, S230 (THU-367)
- Wilhelmsen, Ingrid, S336 (WED-242), S787 (WED-517)
- Willars, Christopher, S479 (THU-521)
- Willemse, José, S373 (WED-258), S982 (THU-304)
- Williams, Betsy, S995 (THU-324)
- Williams, Felicity, S231 (THU-368), S232 (THU-370)
- Williams, Jack, S909 (FRI-165)
- Williamson, Catherine, S37 (OS-037)
- Williamson, Nicola, S901 (FRI-152)
- Williams, Thomas, S176 (FRI-453)
- Willis, Linda, S673 (SAT-429), S694 (SAT-461)
- Willows, Robin, S762 (WED-442)
- Wills, Quin, S803 (WED-548)
- Willuweit, Katharina, S485 (THU-534), S1139 (SAT-156)
- Wilmer, Alexander, S452 (SAT-390)
- Wils, Hans, S1034 (FRI-248)
- Wilson, David, S329 (WED-227)
- Wilson, Laura, S612 (THU-427)
- Wilson, Mark, S523 (FRI-329)
- Wilson, Steven, S787 (WED-517)
- Wilson, Thomas, S480 (THU-522)
- Wimmer, Ralf, S329 (WED-228), S417 (FRI-349)
- Winckelmann, Anni, S1050 (FRI-271), S1150 (SAT-170)
- Win, Dinja De, S775 (WED-465)
- Windisch, Marc, S1020 (FRI-221)
- Windisch, Marc P., S1167 (SAT-195)
- Winter, Benedicte De, S764 (WED-446)
- Wintersteller, Hannah, S33 (OS-032), S59 (OS-077), S442 (TOP-053)
- Wirtz, Theresa Hildegard, S188 (FRI-534)
- Wisel, Steven, S489 (TOP-065)
- Wissing, Michael, S1044 (FRI-262)
- Withoff, Sebo, S805 (WED-554)
- Witkiewicz, Sherry, S241 (WED-328)
- Witte, Moana, S1029 (FRI-240)
- Wohlleber, Dirk, S33 (OS-032), S59 (OS-077), S442 (TOP-050), S442 (TOP-053), S1021 (FRI-223.)
- Wölfel, Roman, S945 (THU-256)
- Wolf, Florian, S282 (SAT-326)
- Wolffram, Ingmar, S1090 (WED-156), S1176 (THU-168)
- Wolf, Jessica, S429 (FRI-366)
- Wolf, John, S67 (OS-091)
- Wolf, Peter, S193 (FRI-545), S199 (FRI-551), S292 (SAT-342)
- Wolters, Frank, S427 (FRI-364)
- Wolters, Justina, S740 (WED-407)
- Wolters, Victorien, S971 (THU-291)
- Woltsche, Johannes, S354 (THU-242)
- Wong, Cheuk Yan, S537 (SAT-231)
- Wong, Connie, S1096 (WED-165)
- Wong, Darren, S311 (SAT-543)
- Wong, David, S254 (WED-349), S255 (WED-351), S270 (WED-375), S314 (SAT-548)
- Wong, Eddie, S680 (SAT-439)
- Wong, Eugene, S199 (FRI-552), S257 (WED-353), S278 (WED-389)
- Wong, Florence, S195 (FRI-546), S242 (WED-330), S253 (WED-348), S256 (WED-352), S258 (WED-355), S274 (WED-382), S296 (SAT-348)
- Wong, Grace, S52 (OS-065-YI), S1096 (WED-165), S1132 (SAT-145), S1148 (SAT-167)
- Wong, Grace Lai-Hung, S29 (OS-025), S125 (LBP-38), S575 (THU-117), S663 (SAT-413), S1064 (WED-123), S1069 (WED-129), S1085 (WED-149), S1131 (SAT-144), S1146 (SAT-166)
- Wong, Guan Wee, S300 (SAT-522)
- Wong, JasonDr., S1189 (THU-187)
- Wong, Kenneth KY, S942 (THU-252)
- Wong, Mark, S458 (THU-482), S463 (THU-490)
- Wong, Patrick Pak-Chun, S1 (GS-002-YI)
- Wong, Pok Fai, S671 (SAT-426)
- Wong, Robert, S236 (WED-319), S1072 (WED-134), S1084 (WED-148), S1089 (WED-153), S1093 (WED-160), S1107 (WED-180), S1121 (WED-200)
- Wong, Stanley, S883 (FRI-125), S1189 (THU-187), S1200 (THU-207)
- Wong, Vincent Wai-Sun, S29 (OS-025), S575 (THU-117), S609 (THU-421), S663 (SAT-413), S863 (SAT-125), S865 (SAT-129), S1064 (WED-123), S1069 (WED-129), S1085 (WED-149), S1096 (WED-165), S1131 (SAT-144), S1146 (SAT-166), S1148 (SAT-167)
- Wong, Yu Jun, S86 (OS-121-YI), S300 (SAT-522), S658 (SAT-406), S703 (SAT-473), S1096 (WED-165), S1204 (THU-213)
- Won Jun, Dae, S633 (THU-464)
- Won, Sungho, S630 (THU-457), S635 (THU-466)
- Won, Sung-Min, S156 (FRI-420), S177 (FRI-456), S220 (THU-354), S343 (THU-227)
- Wonterghem, Elien Van, S229 (THU-364)
- Woodhoo, Ashwin, S326 (WED-223), S560 (SAT-275)
- Woodhouse, Charlotte, S7 (GS-007)
- Woodruff, Henry, S576 (THU-118)
- Woods, Eric, S116 (LBP-23)
- Woods, Kerrie, S1075 (WED-137)
- Woods, Robyn, S622 (THU-443)
- Woo, Hyun Goo, S785 (WED-513)
- Woo, Hyun Young, S588 (THU-137)
- Wootton, Grace, S416 (FRI-347), S443 (SAT-372), S448 (SAT-381), S448 (SAT-382)
- Woreta, Tinsay, S612 (THU-427)
- Worland, Thomas, S380 (WED-271), S852 (WED-488)
- Worms, Nicole, S805 (WED-553)
- Worni, Mathias, S162 (FRI-430)
- Wörns, Marcus-Alexander, S264 (WED-365), S271 (WED-377)
- Worobetz, Lawrence, S373 (WED-259), S426 (FRI-363)
- Woźniak, Małgorzata, S837 (FRI-486)
- Wranke, Anika, S1054 (TOP-100)
- Wright, Gail, S404 (WED-310), S995 (THU-324)

- Wright, Gavin, S220 (THU-355)
- Wu, Biao, S1127 (WED-210), S1198 (THU-204)
- Wu, Chao, S395 (WED-294), S638 (THU-471), S696 (SAT-463), S724 (SAT-510), S1004 (THU-379), S1022 (FRI-225), S1068 (WED-127), S1071 (WED-131), S1073 (WED-136), S1078 (WED-140), S1080 (WED-142), S1094 (WED-161), S1094 (WED-162), S1096 (WED-164), S1110 (WED-184), S1128 (WED-212)
- Wu, Cheng Hsun, S671 (SAT-426)
- Wu, Chijung, S496 (FRI-283)
- Wu, Chun, S9 (GS-011)
- Wu, Dongming, S455 (THU-477), S540 (SAT-236)
- Wuestefeld, Torsten, S786 (WED-514)
- Wu, Fa-Ling, S613 (THU-428)
- Wu, Feixiang, S581 (THU-126)
- Wu, Hanghang, S38 (OS-041-YI)
- Wu, Hao, S304 (SAT-530)
- Wu, Jian, S1041 (FRI-258), S1053 (SAT-142)
- Wu, Jincai, S488 (THU-540)
- Wu, Jingran, S1102 (WED-172)
- Wu, Jinzi, S1171 (SAT-201)
- Wu, Lei, S1209 (THU-220)
- Wu, Lin, S34 (OS-033)
- Wu, Linda, S575 (THU-116), S582 (THU-128), S586 (THU-134)
- Wu, Min, S112 (LBP-18), S1164 (SAT-192)
- Wu, Na, S858 (SAT-117)
- Wu, Nan, S759 (WED-438)
- Wunsch, Ewa, S373 (WED-258), S375 (WED-261)
- Wu, Pan, S1156 (SAT-177)
- Wu, Qikai, S1076 (WED-138), S1157 (SAT-179)
- Wu, Qingyan, S1039 (FRI-254)
- Wu, Qun, S443 (SAT-371)
- Wurmser, Christine, S59 (OS-077)
- Wu, Sandra, S812 (FRI-470)
- Wu, Sha, S525 (TOP-070)
- Wu, Tao, S1127 (WED-210), S1198 (THU-204)
- Wu, Ti, S1209 (THU-220)
- Wu, Tongfei, S1030 (FRI-241)
- Wu, Wan-Jung, S1096 (WED-165)
- Wu, Wei, S304 (SAT-530)
- Wu, Weihua, S1094 (WED-162)
- Wu, Wen-Chih, S1180 (THU-174), S1206 (THU-217)
- Wu, Xiao-Feng, S1165 (SAT-193)
- Wu, Xiaoli, S1152 (SAT-173), S1156 (SAT-178)
- Wu, Yung-En, S825 (FRI-521)
- Wyatt, Brooke, S116 (LBP-23), S729 (SAT-516)
- Xanthakis, Vanessa, S608 (THU-420)
- Xavier, Elisa, S889 (FRI-134)
- Xavier e Silva, Fernando, S254 (WED-349), S255 (WED-351), S270 (WED-375)
- Xia, Chang-sheng, S514 (FRI-313)
- Xia, Fang, S1059 (WED-116)
- Xia, Jie, S34 (OS-033)
- Xia, Jinyu, S1185 (THU-180)
- Xia, Juan, S1094 (WED-161)
- Xiang, Dejuan, S271 (WED-376)
- Xiang, Hongyan, S340 (WED-250)
- Xiang, Huanyu, S340 (WED-250)
- Xiang, Xiaomei, S948 (THU-260)
- Xiang, Ze, S1041 (FRI-258), S1053 (SAT-142)
- Xian, Yongchao, S195 (FRI-546)
- Xiaobin, Zao, S153 (FRI-417), S224 (THU-359), S569 (SAT-290)
- Xiao, Huanming, S1076 (WED-138), S1157 (SAT-179)
- Xiao, Jieliang, S468 (THU-500)
- Xiao, Jing, S340 (WED-250)
- Xiao, Long, S117 (LBP-24)
- Xiao, Yasi, S387 (WED-281)
- Xia, Qi, S34 (OS-033)
- Xia, Qiang, S453 (SAT-391), S454 (TOP-051), S730 (TOP-086)
- Xia, Yifu, S304 (SAT-530)
- Xie, Dong-Ying, S34 (OS-033)
- Xie, Jianping, S34 (OS-033)
- Xie, Pin, S1023 (FRI-227)
- Xie, Qing, S34 (OS-033), S110 (LBP-15), S195 (FRI-546), S261 (WED-359), S274 (WED-382), S1085 (WED-149), S1087 (WED-151), S1153 (SAT-174)
- Xie, Wen, S130 (THU-397), S130 (THU-398), S131 (THU-400), S243 (WED-332)
- Xie, Yandi, S1066 (WED-125)
- Xie, Yang, S756 (WED-433)
- Xie, Yao, S1171 (SAT-201)
- Xing, Qingbo, S1152 (SAT-173), S1156 (SAT-178)
- Xing, Qing-Qing, S869 (SAT-134)
- Xing, Yufeng, S340 (WED-249)
- Xin, Jiaojiao, S20 (OS-013), S186 (FRI-342), S204 (FRI-559), S436 (SAT-359)
- Xinyi, Yang, S634 (THU-465)
- Xiong, Qingfang, S956 (THU-270)
- Xiong, Yating, S784 (WED-510)
- Xiong, Zhewen, S1 (GS-002-YI), S530 (SAT-217)
- Xirodimas, Dimitris, S546 (SAT-247)
- Xu, Bin, S195 (FRI-546)
- Xu, Cheng-Jian, S425 (FRI-362), S1035 (FRI-249)
- Xu, Dongwei, S453 (SAT-391), S730 (TOP-086)
- Xue, Feng, S1163 (SAT-189)
- Xue, Hui, S304 (SAT-530)
- Xue, Qi, S696 (SAT-463), S724 (SAT-510), S1096 (WED-165)
- Xue, Ruifei, S1094 (WED-161)
- Xue, Xiu-Lan, S1165 (SAT-193)
- Xue, YunLing, S1112 (WED-188)
- Xu, Jia, S109 (LBP-13)
- Xu, Jian, S455 (THU-477), S540 (SAT-236)
- Xu, Jiao, S304 (SAT-530)
- Xu, Jie, S243 (WED-332)
- Xu, Jun, S64 (OS-085), S423 (FRI-360), S678 (SAT-438)
- Xu, Junzhong, S555 (SAT-265)
- Xu, Liang, S1165 (SAT-193)
- Xu, Michael, S784 (WED-510), S812 (FRI-470)
- Xu, Simin, S35 (OS-034), S1055 (TOP-103)
- Xu, Tingfeng, S503 (FRI-294)
- Xu, Weihua, S1076 (WED-138), S1157 (SAT-179)
- Xu, Weikang, S525 (TOP-070)
- Xu, Xiang, S1058 (WED-114)
- Xu, Xiaoming, S1096 (WED-165)
- Xu, Xiaoyuan, S243 (WED-332), S1066 (WED-125)
- Xu, Yayun, S696 (SAT-463), S724 (SAT-510)
- Xu, Zhen, S274 (WED-382)
- Yadav, Devesh, S830 (FRI-530)
- Yadav, Manisha, S17 (OS-006-YI), S21 (OS-014-YI), S76 (OS-107-YI), S139 (FRI-398), S146 (FRI-407), S149 (FRI-410), S152 (FRI-416), S326 (WED-222), S414 (FRI-344), S1033 (FRI-247)
- Yadav, Pushpa, S17 (OS-006-YI), S556 (SAT-267)
- Yagüe, Alvaro, S844 (FRI-501)
- Yagüe, Carmen, S1187 (THU-183)
- Yalaka, Rami Reddy, S209 (THU-339)
- Yalcin, Kendal, S1137 (SAT-152)
- Yalcin, Metin, S284 (SAT-329)
- Yale, Kitty, S808 (TOP-091), S820 (FRI-512)
- Yamada, Daisaku, S439 (SAT-366), S509 (FRI-302)
- Yamada, Michiko, S644 (THU-554)
- Yamada, Tomomi, S1183 (THU-177)
- Yamaguchi, Kanji, S616 (THU-433)
- Yamasaki, Kazumi, S1192 (THU-191)
- Yamashina, Shunhei, S180 (FRI-461), S744 (WED-415), S793 (WED-528)
- Yamashita, Taro, S1183 (THU-177)
- Yamataka, Karin, S156 (FRI-421)
- Yamazoe, Taiji, S444 (SAT-373)
- Yam, Tsz Fai, S1064 (WED-123)
- Yang, Aruhan, S110 (LBP-14)
- Yang, Chao, S520 (FRI-323)
- Yang, Chi-Chieh, S1180 (THU-174), S1206 (THU-217)
- Yang, Chih-Chao, S891 (FRI-137)
- Yang, Chris, S1152 (SAT-173), S1156 (SAT-178)
- Yang, Hao, S34 (OS-033)
- Yang, Hsiao, S330 (WED-229)
- Yang, Hui, S436 (SAT-359)
- Yang, Hung-Chih, S531 (SAT-219), S1061 (WED-119)
- Yang, Hwai-I, S1060 (WED-118), S1096 (WED-165)
- Yang, Jay, S50 (OS-063)
- Yang, Jee-Seon, S897 (FRI-146)
- Yang, Jiayue, S557 (SAT-269)
- Yang, Jin Mo, S186 (FRI-343)
- Yang, Ji won, S573 (THU-113), S589 (THU-140)

Author Index

- Yang, Ju Dong, S489 (TOP-065), S659 (SAT-408)
- Yang, Ke, S371 (WED-256)
- Yang, Li, S406 (WED-313)
- Yang, Ling, S69 (OS-093-YI)
- Yang, Liu, S463 (THU-491)
- Yang, Qiang, S759 (WED-438)
- Yang, Qing, S520 (FRI-323)
- Yang, Rui-Xu, S756 (WED-433)
- Yang, Sheng-Shun, S1206 (THU-217)
- Yang, Shengshun, S588 (THU-138), S1180 (THU-174)
- Yang, Song, S34 (OS-033)
- Yang, Tao, S453 (SAT-391), S730 (TOP-086)
- Yang, Tsung-Chieh, S252 (WED-346)
- Yang, Tzeng-Hue, S1206 (THU-217)
- Yang, Ueng-Cheng, S252 (WED-346)
- Yang vom Hofe, Annika, S417 (FRI-350)
- Yang, Wang, S1153 (SAT-174)
- Yang, Wei Lyn, S300 (SAT-522)
- Yang, Weiqin, S530 (SAT-217)
- Yang, Xianshan, S235 (TOP-047)
- Yang, Xingyue, S747 (WED-419)
- Yang, Ying, S1066 (WED-125)
- Yang, Yongfeng, S34 (OS-033), S956 (THU-270)
- Yang, Yongping, S1085 (WED-149)
- Yang, Zeyuan, S1084 (WED-148), S1107 (WED-180)
- Yang, Zhenwei, S831 (FRI-477)
- Yan, Hai, S489 (TOP-065)
- Yan, Jingyi, S1038 (FRI-252)
- Yanjinkham, Ulziigerel, S716 (SAT-497)
- Yan, Libo, S274 (WED-382)
- Yano, Yoshihiko, S559 (SAT-272)
- Yan, Ran, S1058 (WED-114), S1149 (SAT-168)
- Yan, Sean Xuexian, S582 (THU-129), S591 (THU-142)
- Yan, Sheng, S488 (THU-540)
- Yan, Xiaomin, S1004 (THU-379), S1094 (WED-162), S1110 (WED-184)
- Yan, Xuebing, S1133 (SAT-147)
- Yan-Ying, You You, S869 (SAT-134)
- Yao, Brianna, S58 (OS-075)
- Yao, Heng, S436 (SAT-359)
- Yao, Qigu, S753 (WED-429)
- Yao, Shun, S747 (WED-419)
- Yao, Yuhao, S1086 (WED-150)
- Yao, Zeng-Tao, S145 (TOP-078)
- Yao, Zhiyuan, S443 (SAT-371)
- Yapici, Hasan, S389 (WED-286)
- Yarahmadov, Tural, S449 (SAT-384)
- Yardley, Lucy, S858 (SAT-118)
- Yarra, Silpa, S926 (FRI-196)
- Yasuda, Satoshi, S584 (THU-131), S686 (SAT-448)
- Yasui, Yutaka, S598 (THU-155), S644 (THU-554), S1113 (WED-189)
- Yates, Phil, S1154 (SAT-176), S1162 (SAT-187)
- Yatsuhashi, Hiroshi, S1087 (WED-151), S1183 (THU-177), S1192 (THU-191), S1199 (THU-205)
- Yau, Thomas, S48 (OS-058)
- Yazdanfar, Maryam, S388 (WED-283), S431 (FRI-368)
- Ye, Bin, S117 (LBP-24)
- Yee, Kwang Chien, S523 (FRI-329)
- Yee, Leland, S53 (OS-067), S1137 (SAT-153)
- Yee, Michael, S624 (THU-446), S719 (SAT-501)
- Yegurla, Jatin, S274 (WED-382)
- Yeh, Matthew, S999 (THU-333)
- Yeh, Ming-Lun, S1180 (THU-174), S1206 (THU-217)
- Yehoshua, Alon, S873 (FRI-113), S882 (FRI-124), S894 (FRI-141), S901 (FRI-152), S1208 (THU-218)
- Ye, Hui, S38 (OS-041-YI)
- Yeh, Yen-Po, S891 (FRI-137)
- Yeoman, Andrew, S867 (SAT-130)
- Yeoman, Jeppe, S159 (FRI-424)
- Yeon, Jong Eun, S578 (THU-121), S781 (WED-476)
- Ye, Qin, S67 (OS-091)
- Ye, Qing, S1163 (SAT-189)
- Ye, Qiuyue, S557 (SAT-269)
- Yeung, Andy, S5 (GS-005)
- Ye, Xiaoyan, S1185 (THU-180)
- Ye, Yong'an, S153 (FRI-417), S224 (THU-359), S340 (WED-249), S569 (SAT-290), S1076 (WED-138), S1086 (WED-150), S1157 (SAT-179)
- Ye, Zuodong, S946 (THU-257)
- Yiadam, Akosua Boakye, S767 (WED-450)
- Yi, Kiyoun, S588 (THU-137)
- Yilmaz, ŞGurdal, S31 (OS-030)
- Yilmaz, Yusuf, S389 (WED-286)
- Yimam, Kidist, S11 (LBO-03)
- Yim, Hyung Joon, S578 (THU-121), S781 (WED-476), S916 (FRI-179), S1136 (SAT-151)
- Yim, Hyung Sun, S720 (SAT-502)
- Yi, Min, S85 (OS-120)
- Yim, Sun Young, S555 (SAT-264), S578 (THU-121), S720 (SAT-502), S781 (WED-476), S798 (WED-540)
- Yin, Dandan, S956 (THU-270)
- Yin, Dedong, S274 (WED-382)
- Yin, Guo, S80 (OS-114-YI)
- Yin, Philip, S115 (LBP-22)
- Yin, Shengxia, S1022 (FRI-225), S1071 (WED-131), S1073 (WED-136)
- Yin, Shimin, S1102 (WED-172)
- Yin, Xueru, S1102 (WED-172)
- Yip, Terry Cheuk-Fung, S29 (OS-025), S575 (THU-117), S663 (SAT-413), S1064 (WED-123), S1131 (SAT-144), S1146 (SAT-166), S1148 (SAT-167)
- Yi, Shana, S920 (FRI-186), S929 (FRI-200)
- Yiu, Dorothy Cheuk-Yan, S575 (THU-117)
- Yi, Weimin, S488 (THU-540)
- Yi, Xuan, S525 (TOP-070)
- Yi, Yiling, S406 (WED-313)
- Yıldırım, Abdullah Emre, S195 (FRI-546)
- Yilmaz, Volkan, S181 (FRI-463)
- Yilmaz, Yusuf, S627 (THU-453), S863 (SAT-125)
- Yki-Järvinen, Hannele, S803 (WED-549)
- Yoneda, Masashi, S811 (FRI-468)
- Yoneda, Masato, S30 (OS-028), S616 (THU-433), S686 (SAT-448)
- Yong Hong, Jung, S117 (LBP-25)
- Yoo, Changhoon, S584 (THU-131), S593 (THU-145)
- Yoo, Jeongin, S509 (FRI-303)
- Yoo, Jeong-Ju, S510 (FRI-306), S585 (THU-132), S642 (THU-550)
- Yoon, Eileen, S186 (FRI-343), S190 (FRI-538), S192 (FRI-542), S200 (FRI-553), S615 (THU-431), S633 (THU-464), S662 (SAT-411), S667 (SAT-418), S695 (SAT-462), S698 (SAT-466), S701 (SAT-470), S704 (SAT-475), S705 (SAT-476), S705 (SAT-477), S712 (SAT-491), S757 (WED-435), S794 (WED-531), S864 (SAT-128), S1065 (WED-124), S1073 (WED-135)
- Yoon, Jeong Hee, S509 (FRI-303)
- Yoon, Jung-Hwan, S510 (FRI-306), S610 (THU-423), S630 (THU-457), S635 (THU-466), S642 (THU-550), S1048 (FRI-268), S1062 (WED-120), S1144 (SAT-163)
- Yoon, Ki Tae, S690 (SAT-455), S698 (SAT-466), S705 (SAT-477)
- Yoon, Sang Joon, S177 (FRI-456)
- Yoon, Seung Kew, S148 (FRI-409)
- Yopp, Adam, S9 (GS-011)
- Yoshida, Eric, S883 (FRI-125), S1200 (THU-207)
- Yoshida, Yuichi, S686 (SAT-448)
- Yoshida, Yuji, S317 (SAT-554), S820 (FRI-511)
- Yoshiji, Hitoshi, S395 (WED-293), S1183 (THU-177)
- Yoshikawa, Shiori, S444 (SAT-373)
- Yoshimaru, Yoko, S1095 (WED-163)
- Yoshio, Sachiyo, S444 (SAT-373)
- Yost, Kelli Kosako, S463 (THU-490)
- You, Hong, S243 (WED-332)
- Young, Kung-Chia, S361 (FRI-385)
- Young Lee, Hyo, S794 (WED-531)
- Young, Vincent B., S24 (OS-019)
- Younossi, Elena, S673 (SAT-428)
- Younossi, Issah, S863 (SAT-125)
- Younossi, Zobair, S114 (LBP-21), S118 (LBP-26), S464 (THU-492), S600 (TOP-081), S614 (THU-430), S627 (THU-453), S673 (SAT-428), S782 (WED-506), S823 (FRI-516), S857 (SAT-116), S861 (SAT-122), S863 (SAT-125), S905 (FRI-159)
- Younossi, Zobair M., S468 (THU-499)
- You, Qiuhong, S22 (OS-016)
- You, Shaoli, S1085 (WED-149)
- You, Shihyun, S1039 (FRI-255), S1154 (SAT-176), S1162 (SAT-187), S1167 (SAT-196)

- Youssef, Amir, S1154 (SAT-176), S1162 (SAT-187)
- Yousuf, Hassaan, S979 (THU-300)
- Ytting, Henriette, S42 (OS-047-YI), S165 (FRI-434), S982 (THU-304)
- Yu, Amanda, S883 (FRI-125), S1200 (THU-207)
- Yuan, Haiyang, S613 (THU-428)
- Yuan, Jing, S1171 (SAT-201)
- Yuan, Jin-Hong, S145 (TOP-078)
- yuan, wei, S189 (FRI-536), S202 (FRI-556)
- Yubao, Zheng, S196 (FRI-547)
- Yu, Dominic, S74 (OS-103-YI), S964 (THU-283)
- Yuen, Man-Fung, S11 (LBO-02), S52 (OS-065-YI), S62 (OS-082), S110 (LBP-15), S112 (LBP-18), S125 (LBP-38), S490 (TOP-068), S680 (SAT-439), S1033 (FRI-246), S1132 (SAT-145), S1134 (SAT-148), S1152 (SAT-172), S1164 (SAT-192)
- Yu, Hong, S1018 (FRI-217)
- Yu, Huihong, S406 (WED-313)
- Yu, Jae-Hyun, S141 (FRI-401)
- Yu, Jiabin, S1167 (SAT-195)
- Yujing, Chi, S634 (THU-465)
- Yu, Jiong, S753 (WED-429)
- Yu, Jun, S488 (THU-540)
- Yu, Junxiong, S503 (FRI-294)
- Yukse, Muhammed, S984 (THU-307)
- Yu, Mei, S35 (OS-034)
- Yu, Ming-Lung, S627 (THU-453), S863 (SAT-125), S895 (FRI-143), S1083 (WED-147), S1140 (SAT-157), S1180 (THU-174), S1206 (THU-217)
- Yu, Ming-Whei, S1096 (WED-165)
- Yung, Diana, S195 (FRI-546)
- Yung, Rossitta, S920 (FRI-186), S929 (FRI-200)
- Yu, Ning, S1085 (WED-149)
- Yu, Philip, S490 (TOP-068)
- Yu, Qian, S286 (SAT-333)
- Yu, Qifeng, S965 (THU-284), S969 (THU-289)
- Yurdaydin, Cihan, S9 (GS-012), S928 (FRI-199), S1054 (TOP-100), S1109 (WED-183), S1137 (SAT-152)
- Yurdcu, Esra, S1109 (WED-183)
- Yu, Su Jong, S494 (FRI-278), S510 (FRI-306), S513 (FRI-312), S610 (THU-423), S1062 (WED-120)
- Yusupaliev, Bakhodir, S113 (LBP-19)
- Yu, Tiffany, S48 (OS-058)
- Yu, Xiaojie, S712 (SAT-492)
- Yu, Xudong, S569 (SAT-290)
- Yu, Yanlong, S34 (OS-033)
- Yu, Yan-Yan, S34 (OS-033)
- Yu, Yiqi, S1133 (SAT-147)
- Yu, Zu-Jiang, S1063 (WED-122)
- Yvon, Julé, S673 (SAT-429), S694 (SAT-461)
- Zaaijer, Hans, S892 (FRI-138)
- Zabal, Jose Miguel Rosales, S248 (WED-341), S269 (WED-374), S1126 (WED-208), S1205 (THU-216)
- Zaccherini, Giacomo, S10 (LBO-01), S191 (FRI-540), S237 (WED-320), S238 (WED-323)
- Zacchia, Enza, S903 (FRI-155)
- Zacharias, Isabel, S960 (THU-277)
- Zachou, Kalliopi, S42 (OS-047-YI), S44 (OS-049-YI), S400 (WED-302), S421 (FRI-354), S579 (THU-123), S1128 (WED-211)
- Zachoval, Reinhart, S1147 (TOP-110)
- Zafar, Paul Emile, S64 (OS-084-YI)
- Zafar, Zunaira, S280 (TOP-045)
- Zafra, Federica Benitez, S893 (FRI-140)
- Zago, Alessandra, S56 (OS-073)
- Zaidi, Ali, S997 (THU-328)
- Zakalashvili, Mamuka, S889 (FRI-133)
- Zak, Naomi, S409 (TOP-060)
- Zaksas, Viaceslav, S912 (FRI-173)
- Zaleski, Derek, S45 (OS-052)
- Zallio, Francesco, S88 (OS-124-YI)
- Zamalloa, Ane, S7 (GS-007), S324 (WED-218)
- Zambrano, Elisaul Suarez, S397 (WED-296)
- Zambrano, Sheila Gato, S760 (WED-440)
- Zamora, Ester, S375 (WED-263)
- Zamora, Javier, S470 (THU-503)
- Zamora, Laia, S489 (THU-546)
- Zamparelli, Marco Sanduzzi, S493 (FRI-276), S579 (THU-124)
- Zanaga, Paola, S90 (OS-127-YI), S299 (SAT-521), S500 (FRI-288)
- Zanetto, Alberto, S54 (OS-069), S90 (OS-127-YI), S183 (TOP-049), S287 (SAT-334), S293 (SAT-343), S299 (SAT-521)
- Zangneh, Hooman Farhang, S503 (FRI-293)
- Zanna, Elena Del, S814 (FRI-474)
- Zannini, Martina, S489 (THU-546)
- Zanotto, Ilaria, S322 (TOP-037), S770 (WED-456), S791 (WED-525)
- Zanus, Giacomo, S564 (SAT-283)
- Zao, Xiaobin, S340 (WED-249), S1086 (WED-150)
- Zapata-Pavas, Leidy Estefanía, S544 (SAT-244), S546 (SAT-247)
- Zapatero, Juliana, S131 (THU-399)
- Zaplotnik, Martin, S553 (SAT-261)
- Zarantonello, Lisa, S251 (WED-345)
- Zarbock, Alexander, S185 (FRI-341)
- Zarebska-Michaluk, Dorota, S505 (FRI-296), S1205 (THU-215)
- Zarkua, Jaba, S1204 (THU-214)
- Zazara, Dimitra E., S525 (TOP-069)
- Zazueta, Godolfino Miranda, S195 (FRI-546)
- Zechner, Peter, S996 (THU-327)
- Zeef, Leo, S71 (OS-097)
- Zehn, Dietmar, S59 (OS-077)
- Zeini, Maryam Shokrian, S215 (THU-347)
- Zeini, Mohadese Shokrian, S215 (THU-347)
- Zelber-Sagi, Shira, S103 (LBP-06), S600 (TOP-081), S627 (THU-453), S861 (SAT-122)
- Zelege, Yasmin, S61 (OS-080-YI), S313 (SAT-546), S484 (THU-531)
- Zellos, Aglaia, S971 (THU-291)
- Zeng, Da-Wu, S1165 (SAT-193)
- Zeng, Georgia, S132 (THU-402), S263 (WED-364)
- Zeng, Jingwei, S872 (TOP-097), S879 (FRI-120)
- Zeng, Qinghe, S12 (LBO-04)
- Zeng, Qing-Lei, S145 (TOP-078), S638 (THU-471), S696 (SAT-463), S724 (SAT-510), S1063 (WED-122)
- Zeng, Rebecca Wenling, S468 (THU-500)
- Zeng, Xuexia, S1127 (WED-210)
- Zeng, Zhen, S1085 (WED-149)
- Zen, Yoh, S324 (WED-218)
- Zepeda, Joseph, S388 (WED-283), S431 (FRI-368)
- Zerega, Alina, S245 (WED-336)
- Zerial, Marino, S364 (FRI-390)
- Zermiani, Paola, S978 (THU-297)
- Zetter, Alithea, S49 (OS-061)
- Zeuzem, Stefan, S53 (OS-068), S61 (OS-080-YI), S90 (OS-126), S91 (OS-129-YI), S108 (LBP-12), S113 (LBP-20), S185 (FRI-341), S276 (WED-385), S1039 (FRI-254), S1042 (FRI-259), S1091 (WED-158), S1137 (SAT-152), S1139 (SAT-156), S1147 (TOP-110), S1174 (THU-166), S1204 (THU-214)
- Zeybel, Mujdat, S1109 (WED-183)
- Zhai, Peibin, S784 (WED-510), S812 (FRI-470)
- Zhai, Xing-Ran, S145 (TOP-078)
- Zhanasbayeva, Marzhan, S320 (SAT-559)
- Zhan, Clara-Yongxiang, S621 (THU-442)
- Zhang, Chengchen, S858 (SAT-117)
- Zhang, Chenshu, S100 (LBP-01)
- Zhang, Chi, S854 (TOP-094), S1090 (WED-155), S1100 (WED-170)
- Zhang, Chong, S1165 (SAT-193)
- Zhang, Chunqing, S304 (SAT-530)
- Zhang, Fang Fang, S856 (TOP-099)
- Zhang, Feiyu, S128 (THU-393)
- Zhang, Feng, S304 (SAT-530)
- Zhang, Gaoli, S1036 (FRI-250)
- Zhang, Hanqing, S769 (WED-454)
- Zhang, Heyang, S26 (OS-022)
- Zhang, Hongxu, S1063 (WED-122)
- Zhang, Hongyan, S794 (WED-530), S1018 (FRI-217)
- Zhang, Jeffrey, S101 (LBP-03)
- Zhang, Jia, S1143 (SAT-161)
- Zhang, Jiawei, S1144 (SAT-162)
- Zhang, Jiabin, S1086 (WED-150)
- Zhang, Jikai, S1027 (FRI-234)
- Zhang, Jiming, S1133 (SAT-147)
- Zhang, Jing, S1163 (SAT-189)
- Zhang, Jitao David, S33 (OS-032)
- Zhang, Ji-Yuan, S145 (TOP-078), S1063 (WED-122)
- Zhang, Josephine, S25 (OS-020-YI)
- Zhang, Junhao, S340 (WED-250)
- Zhang, Ke, S1023 (FRI-227)
- Zhang, Lei, S110 (LBP-14)

Author Index

- Zhang, Li, S747 ([WED-419](#))
Zhang, Liao, S1055 ([TOP-101](#))
Zhang, Ling-Yi, S1165 ([SAT-193](#))
Zhang, Lingyun, S530 ([SAT-217](#))
Zhang, Li-Ping, S145 ([TOP-078](#))
Zhang, Liqun, S1152 ([SAT-173](#)),
S1156 ([SAT-178](#))
Zhang, Lisha, S1152 ([SAT-173](#)),
S1156 ([SAT-178](#))
Zhang, Lu, S382 ([WED-274](#))
Zhang, Mingxiang, S1076 ([WED-138](#)),
S1157 ([SAT-179](#))
Zhang, Mingyan, S304 ([SAT-530](#))
Zhang, Ning-Ping, S195 ([FRI-546](#))
Zhang, Pan, S784 ([WED-510](#))
Zhang, Qianren, S744 ([WED-414](#))
Zhang, Qingling, S1030 ([FRI-241](#)),
S1164 ([SAT-192](#))
Zhang, Qingyang, S48 ([OS-058](#))
Zhang, Qiran, S1133 ([SAT-147](#))
Zhang, Qun, S193 ([FRI-544](#)),
S1004 ([THU-379](#))
Zhang, Rui, S562 ([SAT-278](#))
Zhang, Ruihua, S320 ([SAT-560](#))
Zhang, Shaoqiu, S1004 ([THU-379](#)),
S1068 ([WED-127](#)), S1094 ([WED-162](#)),
S1128 ([WED-212](#))
Zhang, Tao, S525 ([TOP-069](#))
Zhang, Ting, S130 ([THU-397](#)),
S131 ([THU-400](#))
Zhang, Wei, S900 ([FRI-151](#))
Zhang, Weiguo, S1152 ([SAT-173](#)),
S1156 ([SAT-178](#))
Zhang, Weituo, S196 ([FRI-547](#))
Zhang, Wenhong, S1133 ([SAT-147](#))
Zhang, Xiao, S610 ([THU-423](#)),
S650 ([TOP-085](#)), S653 ([SAT-397](#))
Zhang, Xiaofei, S1197 ([THU-201](#))
Zhang, Xiaoxun, S760 ([WED-439](#))
Zhang, Xin, S1038 ([FRI-253](#))
Zhang, Xinrong, S29 ([OS-025](#)),
S663 ([SAT-413](#))
Zhang, Xinyuan, S856 ([TOP-099](#))
Zhang, Xuehong, S856 ([TOP-099](#))
Zhang, Xuelian, S1102 ([WED-172](#))
Zhang, Yan, S196 ([FRI-547](#))
Zhang, Yanyun, S274 ([WED-382](#))
Zhang, Yao, S1080 ([WED-142](#)),
S1128 ([WED-212](#))
Zhang, Yiling, S1 ([GS-002-YI](#)),
S530 ([SAT-217](#))
Zhang, Yin, S117 ([LBP-24](#))
Zhang, Ying, S1165 ([SAT-193](#))
Zhang, Yingjun, S109 ([LBP-13](#))
Zhang, Yingyu, S117 ([LBP-24](#))
Zhang, Yuanjian, S308 ([SAT-539](#))
Zhang, Zhanqing, S1153 ([SAT-174](#))
Zhang, Zhiming, S525 ([TOP-070](#))
Zhang, Zhiyi, S395 ([WED-294](#)),
S1004 ([THU-379](#)), S1068 ([WED-127](#)),
S1078 ([WED-140](#)), S1080 ([WED-142](#)),
S1094 ([WED-161](#)), S1094 ([WED-162](#)),
S1096 ([WED-164](#)), S1110 ([WED-184](#)),
S1128 ([WED-212](#))
Zhan, Jie, S1078 ([WED-140](#)),
S1094 ([WED-161](#))
Zhan, Xinyu, S540 ([SAT-236](#))
Zhan, Zhu, S858 ([SAT-117](#))
Zhao, Bigeng, S503 ([FRI-294](#))
Zhao, Caiyan, S195 ([FRI-546](#)),
S1133 ([SAT-147](#))
Zhao, Dejian, S423 ([FRI-358](#))
Zhao, Hong, S130 ([THU-397](#)),
S130 ([THU-398](#)), S131 ([THU-400](#)),
S243 ([WED-332](#)), S854 ([TOP-094](#)),
S1090 ([WED-155](#)), S1100 ([WED-170](#))
Zhao, Jianzhi, S1198 ([THU-204](#))
Zhao, Jun, S1085 ([WED-149](#))
Zhao, Lianhui, S304 ([SAT-530](#))
Zhao, Longgang, S856 ([TOP-099](#))
Zhao, Nan, S760 ([WED-439](#))
Zhao, Siru, S34 ([OS-033](#))
Zhao, Sixian, S159 ([FRI-425](#))
Zhao, Tingting, S1133 ([SAT-147](#))
Zhao, Weizhi, S49 ([OS-062](#))
Zhao, Xinpeng, S784 ([WED-510](#))
Zhao, Zhijia, S1127 ([WED-210](#))
Zhao, Zhirong, S1209 ([THU-220](#))
Zharkova, Maria, S260 ([WED-357](#))
Zheng, Dan, S34 ([OS-033](#))
Zheng, Dekai, S22 ([OS-016](#))
Zheng, Huanwei, S243 ([WED-332](#)),
S1066 ([WED-125](#))
Zheng, Kuiyang, S1016 ([TOP-111](#)),
S1025 ([FRI-232](#))
Zheng, Liming, S747 ([WED-419](#))
Zheng, Ming-Hua, S613 ([THU-428](#)),
S627 ([THU-453](#)), S865 ([SAT-129](#)),
S1085 ([WED-149](#))
Zheng, Qi, S375 ([WED-262](#)),
S638 ([THU-471](#)), S696 ([SAT-463](#)),
S724 ([SAT-510](#)), S1144 ([SAT-162](#))
Zheng, Qichang, S488 ([THU-540](#))
Zheng, Shuquan, S794 ([WED-530](#)),
S1018 ([FRI-217](#))
Zheng, Sujun, S1066 ([WED-125](#))
Zheng, Xin, S195 ([FRI-546](#)), S196 ([FRI-547](#))
Zheng, Xinchun, S1185 ([THU-180](#))
Zheng, Yufeng, S956 ([THU-270](#))
Zhi-Jian, Chen Chen, S869 ([SAT-134](#))
Zhong, Aileen Shiqi, S351 ([THU-237](#))
Zhong, Manhua, S520 ([FRI-323](#))
Zhong, Min, S1167 ([SAT-195](#))
Zhong, Rui, S235 ([TOP-047](#))
Zhong, Weizhe, S540 ([SAT-236](#))
Zhou, Chun-Bao, S145 ([TOP-078](#))
Zhou, Guiqin, S404 ([WED-309](#))
Zhou, Haoming, S455 ([THU-477](#)),
S528 ([SAT-214](#)), S540 ([SAT-236](#))
Zhou, Hu, S1156 ([SAT-178](#))
Zhou, Huijuan, S261 ([WED-359](#))
Zhou, Huiping, S749 ([WED-422](#))
Zhou, Iris Y., S413 ([FRI-335](#)), S680 ([SAT-439](#))
Zhou, Jiao, S1143 ([SAT-161](#))
Zhou, Jiayi, S1147 ([TOP-109](#))
Zhou, Jingying, S1 ([GS-002-YI](#))
Zhou, Li, S235 ([TOP-047](#))
Zhou, Ling, S189 ([FRI-536](#))
Zhou, Lu, S406 ([WED-313](#))
Zhou, Shun, S446 ([SAT-378](#)),
S540 ([SAT-236](#))
Zhou, Taotao, S422 ([FRI-357](#)),
S429 ([FRI-366](#))
Zhou, Xiang, S1015 ([TOP-107](#))
Zhou, Xiaolei, S520 ([FRI-323](#))
Zhou, Xin, S784 ([WED-510](#)), S812 ([FRI-470](#))
Zhou, Xingang, S130 ([THU-397](#)),
S131 ([THU-400](#))
Zhou, Xingping, S204 ([FRI-559](#))
Zhou, Xinyang, S1127 ([WED-210](#))
Zhou, Xue, S1152 ([SAT-173](#)),
S1156 ([SAT-178](#))
Zhou, Yi, S286 ([SAT-333](#)), S948 ([THU-260](#))
Zhou, Yong-Jian, S406 ([WED-313](#))
Zhou, Yuxin, S543 ([SAT-242](#)),
S557 ([SAT-269](#))
Zhou, Zhipeng, S503 ([FRI-294](#))
Zhu, Andrew X., S574 ([THU-115](#)),
S580 ([THU-125](#))
Zhu, Bingbing, S193 ([FRI-544](#))
Zhu, Chuanwu, S195 ([FRI-546](#)),
S395 ([WED-294](#)), S638 ([THU-471](#)),
S696 ([SAT-463](#)), S724 ([SAT-510](#)),
S1068 ([WED-127](#)), S1078 ([WED-140](#)),
S1080 ([WED-142](#)), S1094 ([WED-162](#)),
S1110 ([WED-184](#))
Zhu, Ci, S739 ([WED-405](#)), S746 ([WED-418](#))
Zhuge, Yuzheng, S304 ([SAT-530](#))
Zhu, Jiaqi, S753 ([WED-429](#))
Zhu, Jiaying, S747 ([WED-419](#))
Zhu, Jing, S109 ([LBP-13](#))
Zhu, Julie, S246 ([WED-339](#)),
S1115 ([WED-191](#))
Zhu, Kaiyi, S423 ([FRI-360](#)), S678 ([SAT-438](#))
Zhu, Li, S395 ([WED-294](#)),
S1068 ([WED-127](#)), S1078 ([WED-140](#)),
S1110 ([WED-184](#))
Zhu, Ling, S488 ([THU-540](#))
Zhu, Qian, S271 ([WED-376](#))
Zhu, Qing, S1024 ([FRI-229](#))
Zhuravleva, Ekaterina, S28 ([OS-024-YI](#)),
S38 ([OS-042-YI](#)), S541 ([SAT-238](#))
Zhu, Ren, S443 ([SAT-371](#))
Zhu, Wei, S525 ([TOP-070](#))
Zhu, Xiaoning, S1076 ([WED-138](#)),
S1157 ([SAT-179](#))
Zhu, Xiaoxue, S110 ([LBP-14](#))
Zhu, Yan, S948 ([THU-260](#))
Zhu, Yueyong, S1133 ([SAT-147](#))
Zibert, Andree, S957 ([THU-271](#)),
S957 ([THU-272](#))
Zidan, Ahmed, S1212 ([THU-224](#))
Zierhut, Matthew L, S1141 ([SAT-158](#))
Zigmond, Ehud, S56 ([OS-073](#)),
S393 ([WED-291](#)), S403 ([WED-308](#))
Zignego, Anna Linda, S1082 ([WED-146](#))
Žilincánová, Daniela, S871 ([SAT-136](#))
Zilong, Wang, S425 ([FRI-361](#)),
S862 ([SAT-124](#))
Zimmer, Holger, S963 ([THU-281](#))
Zimmermann, Anca, S646 ([THU-559](#))
Zimmermann, Ruth, S880 ([FRI-121](#))

- Zimmer, Yair, S719 ([SAT-500](#))
- Zimny, Sebastian, S329 ([WED-228](#)), S417 ([FRI-349](#))
- Zimpel, Carolin, S527 ([SAT-213](#)), S536 ([SAT-230](#)), S557 ([SAT-268](#))
- Zingone, Fabiana, S407 ([WED-315](#))
- Zinober, Kerstin, S19 ([OS-010-YI](#)), S222 ([THU-357](#)), S289 ([SAT-336](#)), S316 ([SAT-553](#)), S939 ([TOP-058](#))
- Ziol, Marianne, S12 ([LBO-04](#)), S498 ([FRI-286](#)), S577 ([THU-119](#))
- Zioutas, Maximiliano, S640 ([THU-475](#))
- Zipprich, Alexander, S105 ([LBP-09](#)), S251 ([WED-345](#)), S279 ([TOP-043](#)), S313 ([SAT-546](#)), S1147 ([TOP-110](#))
- Zischka, Hans, S417 ([FRI-349](#)), S948 ([THU-259](#))
- Zisimopoulos, Konstantinos, S1128 ([WED-211](#))
- Zitelli, Patricia, S274 ([WED-382](#)), S489 ([THU-546](#))
- Zito, Giovanni, S457 ([THU-480](#))
- Zito, Rossella, S803 ([WED-549](#))
- Žížalová, Kateřina, S727 ([SAT-513](#))
- Zizer, Eugen, S1139 ([SAT-156](#))
- Zizzo, Andréanne N., S971 ([THU-291](#))
- Zlamal, Thomas, S996 ([THU-327](#))
- Zmora, Niv, S243 ([WED-333](#)), S315 ([SAT-550](#)), S393 ([WED-291](#))
- Zmrzljak, Uršula Prosenc, S553 ([SAT-261](#))
- Zolfino, Teresa, S40 ([OS-045](#)), S55 ([OS-070](#))
- Zoller, Heinz, S232 ([THU-369](#)), S961 ([THU-279](#)), S967 ([THU-286](#)), S968 ([THU-288](#)), S1135 ([SAT-150](#))
- Zöllner, Caroline, S1139 ([SAT-156](#))
- Zomorodi, Katie, S1058 ([WED-114](#)), S1149 ([SAT-168](#)), S1153 ([SAT-174](#)), S1161 ([SAT-186](#))
- Zompo, Fabio Del, S72 ([OS-098](#))
- Zoncapè, Mirko, S660 ([SAT-409](#)), S661 ([SAT-410](#)), S668 ([SAT-420](#)), S812 ([FRI-471](#))
- Zoratti, Caterina, S711 ([SAT-489](#))
- Zorn, Markus, S963 ([THU-281](#))
- Zorrila, Rafael Ruíz, S936 ([FRI-214](#))
- Zorrilla, Luis Eduardo Pariente, S697 ([SAT-465](#))
- Zouari, Fedi, S680 ([SAT-439](#))
- Zoubek, Miguel, S18 ([OS-007](#))
- Zougmore, Honoré, S170 ([FRI-442](#))
- Zou, Heng, S41 ([OS-046](#))
- Zou, Huaibin, S235 ([TOP-047](#))
- Zou, Liangfeng, S117 ([LBP-24](#))
- Zoulim, Fabien, S52 ([OS-066](#)), S101 ([LBP-04](#)), S107 ([LBP-11](#)), S118 ([LBP-27](#)), S498 ([FRI-286](#)), S687 ([SAT-450](#)), S701 ([SAT-469](#)), S1014 ([TOP-104](#)), S1046 ([FRI-265](#)), S1058 ([WED-113](#)), S1134 ([SAT-148](#)), S1160 ([SAT-184](#)), S1161 ([SAT-185](#)), S1170 ([SAT-199](#))
- Zou, Zhaozhen, S591 ([THU-142](#))
- Zou, Zhengsheng, S145 ([TOP-078](#))
- Zuberi, Bader Faiyaz, S319 ([SAT-557](#))
- Zubiaga, Ana, S137 ([FRI-395](#)), S529 ([SAT-215](#)), S738 ([WED-404](#)), S741 ([WED-408](#))
- Zucman-Rossi, Jessica, S537 ([SAT-232](#))
- Zuin, Massimo Giovanni, S978 ([THU-297](#))
- zur Wiesch, Julian Schulze, S1139 ([SAT-156](#)), S1147 ([TOP-110](#))
- Zwicker, Christian, S445 ([SAT-375](#))
- Zyklus, Romanas, S283 ([SAT-327](#))
- Ωeretanos, Christos, S1128 ([WED-211](#))

Disclosures: no commercial relationships

The following abstract submitters have indicated that they have no relationships with commercial entities that might be perceived as having a connection with their presentation:

Abad Guerra Javier	Aslanikashvili Ana	Calleri Alberto
Abdelhameed Ahmed	Astbury Stuart	Calvo Sánchez Henar
Abdulle Amina	Atthakitmongkol Thanapat	Camelo Castillo Anny
Abe-Chayama Hiromi	Attia Yasmeen	Canillas Lidia
Abedin Nada	Aurélie Beaufrère	Cao Hongcui
Adamcova Selcanova Svetlana	Avellon Calvo Ana	Carotenuto Pietro
Adisasmita Michael	Avitabile Emma	Carvalho Armando
Aggarwal Deepankshi	Ay Ümran	Castañé Helena
Agirre Lizaso Aloña	Babu Rosmy	Castañeda Andres
Aguilar Ballester María	Bachinger Fabian	Castelnuovo Gabriele
Ahn Keun Soo	Baliashvili Davit	Castillo Elisa
Ajaz Saima	Bannon Lian	Castoldi Mirco
Alaa Basma	Barabanchyk Olena	Cavazza Anna
Alarcón-Sánchez Brisa Rodope	Barrett Lisa	Celaj Stela
Alegret Marta	Bassegoda Octavi	Celik Ferya
Alexopoulou Alexandra	Battistella Sara	Cespiati Annalisa
Alfaite Dulce	Belkacem Acidi	Chai Jin
Alfano Vincenzo	Beltrão Pereira Luciano	Chatterjee Saurabh
Alhanaee amnah	Benedé Raquel	Chbourk Sara
Alicia Delorme	Benitez Gutierrez Laura	Chemello Liliana
Aliwa Benard	Benitez Zafra Federica	Chi Chen-Ta
Alla Manasa	Benjamin Jaya	Chirapongsathorn Sakkarin
Allaire Manon	Bentanachs Roger	Cho Jai Young
Allen Sophie	Bergquist Annika	Cholankeril George
Almeida Isadora	Berlakovich Gabriela	Chon Young Eun
Alonso Martin Carmen	Bernal Monterde Vanesa	Choudhury Ashok Kumar
Alvarado-Tapias Edilmar	Bevilacqua Michele	Chow Victor Yung Sin
Amador Alberto	Bhadoria Ajeet Singh	Chua Damien
Amer Johnny	Bianco Cristiana	Chun Ho Soo
Amiama Roig Clara	Bindal Vasundhara	Ciacio Antonio
Amin Amr	Birrer Fabienne	Cirella Antonio
Ampuero Javier	Biswas Sagnik	Claeys Wouter
An Ji Hyun	Bitetto Davide	Clark Sarah
Ananchuensook Prooksa	Blarasin Benedetta	Clayton-Chubb Daniel
Andersen Ina	Blázquez Vicens Joan	Clusmann Jan
Andrade Raul J.	Boesch Markus	Coghlan Miriam
Andreea Livia Bumbu	Booijink Richell	Colognesi Martina
Angel Enrique	Boothman Helen	Colyn Leticia
Angelakis Athanasios	Bourgeois Alexandre	Conde Isabel
Ankavay Maliki	Bozward Amber	Correia Fabio
Annunziata Francesco	Brandão-Mello Carlos	Coukos Alexander
Antwi Milton	Breitenecker Kristina	Crocombe Dominic
Apodaka-Biguri Maider	Bresson-Hadni Solange	Crouché Emilie
Archer Ann	Brindley James Hallimond	Csarmann Katja
Ariño Silvia	Brodosi Lucia	Cytryn Edward
Ariungerel Nomin	Brol Maximilian Joseph	Dalbeni Andrea
Armandi Angelo	Brouwer Willem Pieter	D'Amato Daphne
Arnaiz Gonzalez Esther	Bruneau Alix	D'Ambrosio Francesca
Artru Florent	Bryce Kathleen	D'Amico Gennaro
Artzner Thierry	Buch Stephan	Darwish Murad Sarwa
Arvaniti Pinelopi	Büchler Christa	Das Avisnata
Ashfaq-Khan Muhammad	Cadamuro Massimiliano	Davidov Yana
Ashimkhanova Aiyimkul	Cairolì Victoria	De Boer Ynto
Askgaard Gro	Caliman-Sturdza Olga Adriana	De Bonis Encinoso Mario

De Haan Jubi	Fürst Anna	Harindranath Sidharth
De Rudder Maxime	Furtado Feio de Azevedo Rita	Hartl Lukas
de Schaetzen Arthur	Furumaya Alicia	Hashim Ahmed
Deep Amar	Fuster-Martínez Isabel	Hassan Mohsin
Deepika Deepika	Gabbia Daniela	He Jingyan
Del Barrio Azaceta María	Gabrielli filippo	Henin Guillaume
del Rio-Cubilledo Cristina	Gallego-Durán Rocío	Henze Lara
Delo Joseph	Gallo Paolo	Heo Jeong
Delphin Marion	Gandhi Harsh	Hernández-Èvole Helena
Demma Shirin	Gao Juan	Heyens Leen
Derler Martina	Garcia-Larsen Vanessa	Hidalgo Romero Álvaro
Dhaliwal Amritpal	Garg Love	Hiebert Lindsey
Di Cola Simone	Garrido Isabel	Hoebinger Constanze
Di Zeo-Sánchez Daniel E.	Gart Eveline	Hokkoku Daiki
Diamond Tamir	Gato Zambrano Sheila	Hole Mikal Jacob
Dietz Julia	Gatselis Nikolaos	Hora Shainan
Ding Yibo	Gatzios Alexandra	Horakova Olga
Dingfelder Jule	Gautam Pramod	Hryniuk Olha
Dobroaia Andreea	Gavrisheva Sofiia	Hu Haoran
Dogay Us Gediz	Geervliet Eline	Hwang Jung Ho
Dongiovanni Paola	Geh Daniel	Hydes Theresa
Dooley Steven	Geier Andreas	Iacob Speranta
Downs Louise	Gencdal Genco	Idelfonso García Osiris German
Duan Qihua	Geng WenQian	Ignat Mina
Dufton Neil	Ghai Megan	Iliescu Elena Laura
Düll Miriam	Giannitrapani Lydia	Iqbal Afshan
Dzhagiashvili Olga	Gigi Eleni	Ishiba Hiroshi
Easom Nicholas	Gillard Justine	Ismail Mona
Eceiza Tenreiro Ariane	Gil-Pitarch Claudia	İstemihan Zülal
Ehmer Ursula	Gines Mir Iris	Istrate Mircea
Eifer Møller Emilie	Gioia Stefania	Janczyk Wojciech
El Garhy Naeema	Giudicelli-Lett Heloise	JANG Se Young
El Sabagh Ahmed	Giuli Lucia	Janik Maciej K.
El Tayebi Hend	Gjini Kamela	Jazaeri Farahnaz
Elfaituri Muhammed	Goediker Juliana	Jegodzinski Lina
Enkhjargal Saruul	Gömer Andre	Jeng Rachel Wen-Juei
Erdem Merve	Gomez Aldana Andres	Jensen Morten Daniel
Erdemir Gizem	Gómez Santos Beatriz	Jeon Sun Kyung
Ergenc Ilkay	Gonsalkorala Enoka	jiang xiaoyu
Eriksen Peter Lykke	Gonzalez Diaz Irene	Jiarui Zheng
Eruzun Hasan	Gonzalez-Romero Francisco	Jiménez Franco Andrea
Estévez Olga	Goossens Nicolas	Jiménez-Martí Elena
Ettich Julia	Gorfu Zebeaman Tibebe	Jin Yan
Evain Manon	Görgülü Esra	Johannessen Asgeir
Fabregat Isabel	Goyal Tanvi	Johnson Amy
Fajardo Jemimah Andrea	Graf Christiana	Jokl Elliot
Falguières Thomas	Gratacos Jordi	Jördens Markus
Farrell Gillian	Grey-Wilson Charlotte	Jothimani Dinesh
Felber Marco	Griemsmann Marie	Joubel Camille
Feray Cyrille	Guariglia Marta	Juanola Adria
Fernandez Ainhoa	Guarino Maria	Jun Dae Won
Fernández Ginés Raquel	Guedes Leal Cassia Regina	K L Ajee
Fernandez-Gordón Sánchez Flor M	Gui Wenfang	Kaewdech Apichat
Fernández-Lizaranzu Isabel	Guida Alice	Kahn Judith
Ferronato Marco	Gulbani Lasha	Kamkamidze George
Finan Amanda	H Bhat Sadam	Kanani Alviri Naz
Flanagan Eliza	Haddadin Yazan	Kang Ji Hun
Flatley Sarah	Hahn Magdalena	Kann Anna Emilie
Flint Emilio	Hakeem Andrew	KAPS Leonard
Fodor Andreea	Haller Rosa	Karim Gres
Foglia Beatrice	Halliday Neil	Katchman Helena
Fonkam Audrey	Hallsworth Kate	Kaur Savneet
Forlano Roberta	Hamid Saeed Sadiq	Kawano Tadachimi
Fousekis Fotios	Hamilton Elizabeth	Ke Bibo
Francescut Christian	Hamody Yara	Keitoku Taisei
Fu Rebecca	Han Ji Eun	Keskin Onur
Fukushima Masanori	Hanno Abdelfattah	Khanna Deepanshu
Funuyet-Salas Jesús	Hargreaves Rupen	Khetsuriani Nino

Disclosures

Khokhliuk Olena
Kjærgaard Kristoffer
Klöhn Mara
Kobayashi Takashi
Kocar Eva
Komeylian Hamed
Komori Atsumasa
Kon Kazuyoshi
Koob Dennis
Körner Christiane
Kosako Yost Kelli
Kotlinowski Jerzy
Kotorashvili Adam
Koutny Florian
Krause Jenny
Kreimeyer Henriette
Krooss Simon
Kuenzler Patrizia
Kumar Pavitra
Kumari Suja
Kurahashi Tomohide
Lacotte Stéphanie
Ladegaard Grønkjær Lea
Lamarque Catherine
Lamatsch Sven
Langer Mona-May
Lantinga Marten A.
Lapenna Lucia
Lapitz Ainhoa
Larsen Anett Kristin
Lasco Roberta
Latif Muhammad Umair
Lazzeri-Barcelo Francesca
Leite Nathalie
Lewis Declan
Liang Yan
Liguori Antonio
Liou Wei-Lun
Lkhagvajav Zoljargal
Lkhagva-Ochir Oyungerel
Llop Elba
Lo Ching-Chu
Lombardi Rosa
Loosen Sven H
Loqvist Pia
Lu Tingting
Luque Urbano María de los Reyes
M Rodrigues Robim
Ma Ann T
Macias Rocio IR
Madejón Antonio
Maderuelo Esther
Madhusudana Girija Sanal
Maharshi Sudhir
Maheshwari Deepanshu
Mahmoud Tasnim
Malik Sabeen
Mallet Vincent
Mandilara Dionysia
Manuli Chiara
Mao Minxin
Maor Yaakov
Maras Jaswinder
Marciano Sebastián
Marta Garbín Marta
Martell María
Marti-Aguado David
Martín Alia

Martínez Navidad Cristian
Martínez-Sánchez Celia
Mašek Jan
Matar Rola
Mathew Babu
Mayer Carlotta
Mazzola Alessandra
McInnes Neil
Mcpherson Stuart
Medina Pizaño Mariana Yazmin
Mello Tommaso
Méndez Isabel
Mercado-Gómez Maria
Meroni Marica
Meunier Lucy
Milardi Giulia
Millan Lorenzo Marina Eliana
Miller Hamish
Minier Nicolas
Miura Satoshi
Moeckli Beat
Mohammad Tabish
Moles Anna
Montano-Loza Aldo J
Montero-Vallejo Rocío
Moriarty Aoife
Morsica Giulia
Motta Benedetta Maria
Mourya Akash Kumar
Mujica Endrina
Mukherji Atish
Najmi Muath
Nakao Yasuhiko
Nakashima Hiroyuki
Nana Sede Mbakop Raissa
Nandekar Sanket
Nardelli Silvia
Nassar Islam
Nasser Nour
Nesbitt Robin
Nguyen Thi Thu Nga
Nieto Natalia
Nikzad Newsha
Nimanong Supot
Nimma Induja
Ningarhari Massih
Niu Junqi
Njei Basile
Noon Luke
Ntandja Wandji Line Carolle
Odrizola Herrán Aitor
Oh Joo Hyun
Oldroyd Christopher
Olivas Alberch Pol
Onghena Louis
Ono Hiroki
Orpen-Palmer Josh
Ortmayr Gregor
Osmani Zgjim
Osti Valentino
Otero Sanchez Lukas
Ouzan Denis
Pachisia Aditya Vikram
Pacín Ruiz Beatriz
Pagano Giulia
Palasantzas Victoria
Pallozzi Maria
Pandey Sushmita

Pantic Ivana
Pantziros Spyridon
Papachristoforou Eleni
Parisse Simona
Pascale Alina
Patel Ankoor
Paternostro Rafael
Payo-Serafin Tania
Pedroza Lourdes
Peiffer Kai-Henrik
Peltzer Mona
Peñas Herrero Irene
Penners Christian
Pennisi Grazia
Pereyra David
Perez Martina
Pérez Diaz del Campo Nuria
Perez-Campuzano Valeria
Persano Mara
Peschard Simon
Pezzato Francesco
Pfefferkorn Maria
Philippart Marie
Piecha Felix
Piermatteo Lorenzo
Pillado Pérez Beatriz
Piñar Gutiérrez Ana
Pinto Elisa
Piper Hanley Karen
Pirola Carlos
Pocurull Anna
Pollmanns Maike Rebecca
Pooja Devan
Pors Susanne
Pose Elisa
Protopapa Francesca
Provera Alessia
Puente Sanchez Angela
Pujol Claudia
Puri Puneet
Purssell Huw
Qiu Tian Yu
Quinn Nessa
Qurashi Maria
Radchenko Anastasiia
Raevens Sarah
Rahaman Syed Mushfiqur
Rancatore Gabriele
Rashidi-Alavijeh Jassin
Rau Monika
Rausch Lilli
Rauter Laurin
Ravindranayagam Noel
Reic Tatjana
Remih Katharina
Rezen Tadeja
Rhu Jinsoo
Richardson Naomi
Riches Nicholas
Riescher-Tuczkiewicz Alix
Rimini Margherita
Rivera Jesús
Rivero Calaf Àngel
Robert Marie Gladys
Rodda Sheridan
Roderburg Christoph
Rodrigues Pedro Miguel
Rodríguez-Tajes Sergio

Roger Clementine	Strandberg Rickard	Urzúa Alvaro
Romeo Sara	Sturm Lukas	V Dheapak
Romero Sarah	Stvilia Ketevan	Vaidya Arun
Rooseboom Jalina	Su Kim	Vaishnav Manas
Rosenberg Nofar	Suárez Montesdeoca Cristina	Valery Patricia
Rosoff Daniel	Subhani Mohsan	Valsan Arun
Rossmeisl Martin	Suehiro Tomoyuki	van de Graaf Stan
Rosso Chiara	Sugiyama Masaya	van Hooff Maria
Roth Sofia	Sukowati Caecilia	Van Hul Noémi K. M.
Ruan Qi	Sukriti Sukriti	Van Melkebeke Lukas
Rubio Garcia Ana Belen	Sulejova Karolina	Vangara Sasanka
Ruiz de Gauna Mikel	Sultanik Philippe	Vaz Karl
Rusman Resha Dermawansyah	Sumida Yoshio	Vecchio Cristina
Russell Erin	Surguladze Sophia	Veelken Rhea
Saeidi Reza	Syed Hussain	Verboven Elisabeth
Sáenz de Miera Inés	Tai Jennifer	Verdeguer Francisco
Salas Silva Elsy Soraya	Tait Christopher	Verwaayen Anna
Salazar Parada Nelson Daniel	Tamnanloo Farzaneh	Vilar Gomez Eduardo
Saltini Dario	Tang Xiaolu	Villa Erica
Salvoza Noel	Tangkijvanich Pisit	Villamayor Laura
Samuel Ronald	Taru Vlad	Villanueva Marina
Sánchez Victor	Tavaglione Federica	Villaruel Carolina
Sanchez-Romero Natalia	Tavelli Alessandro	Villela-Nogueira Cristiane
Sandfort Vanessa	Teixeira-Clerc Fatima	Vionnet Julien
Sanginetto Moris	Tejedor Bravo Marta	Vitale Alessandro
Sanou Armel Moumouni	Teles Sara	Volkert Ines
Saracco Margherita	Tenca Andrea	Wan Yawen
Sato Shunsuke	Tenorio González Elena	Waqar Marium Fatima
Saviano Antonio	Tergast Tammo Lambert	Ward Zoe
Sayaf Katia	Terracciani Francesca	Weiand Matthias
Schaefer Benedikt	Teufel Andreas	Weil-Verhoeven Delphine
Schramm Christoph	Thanapirom Kessarinn	Wen Chaojing
Schulz Martin	Thandassery Ragesh Babu	Weng Yuhang
Seaman Sian	Thatcher Amy	Werner Jill
Seidel Florine	Thelwall Iona	Wester Axel
Seo Sang Hyun	Thompson Marcos Andres	Wilhelmsen Ingrid
Seul ki Han	Tiede Anja	Williams Thomas
Shafqat Muhammad Nabeel	Tinahones Alberto	Wilson David
Shalaby Sarah	Tizzani Marco	Wintersteller Hannah
Shalimar .	Tobiasch Moritz	Wolters Frank
Sharma Satya Priya	Todesco Eve	Won Sung-Min
She Shaoping	Todt Daniel	Woo Hyun Goo
Shimizu Mayuko	Toma Letitia	Wunsch Ewa
Shostakovych-Koretska Liudmyla	Tong Kexin	Xia Yifu
Shteyer Eyal	Toresson Grip Emilie	Xiang Huanyu
Shuangdi Duan	Torner Maria	Xie Yandi
Si Tengfei	Torre Pietro	Xing Qing-Qing
Sigon Giordano	Toya Keisuke	Xue Feng
Simão André L.	Trampert David	Yim Sun Young
Sinatti Gaia	Tria Giada	Yiu Dorothy Cheuk-Yan
Singaraja Roshni Rebecca	Triantafyllou Evangelos	Yousuf Hassaan
Siribelli Alessia	Triolo Michela	Yu Jun
Skrypnyk Igor	Tripathi Gaurav	Yuan Haiyang
Smets Lena	Truchi Régine	Zanetto Alberto
Smid Vaclav	Trzos Katarzyna	Zannini Martina
Sohn Won	Tseng Tai-Chung	Zapata-Pavas Leidy Estefanía
Sölter Ricarda	Tsertsvadze Tengiz	Zheng Qi
Sonderup Mark	Tsochatzis Emmanuel	Zhou Haoming
Song Byeong Geun	Tuo Biguang	Zigmond Ehud
Springer Emely	Turan Dilara	Zilong Wang
Sripongpun Pimsiri	Turato Cristian	Zito Giovanni
Stan Adriana	Turk Jerovšek Marjana	Zmora Niv
Stasio Rosa Claudia	Turkina Anastasia	Zoncapè Mirko
Stefanini Bernardo	Tyagi Purnima	Zougmore Honoré
Steinmann Silja	Tzedakis Stylianos	Zuin Massimo Giovanni
Stella Leonardo	Urbani Luca	Zwicker Christian
Stephan Schmid	Urias Esteban	
Stockdale Alexander	Ursic Bedoya José	

Disclosures: commercial relationships

The following abstract submitters have indicated that they have relationships with commercial entities that might be perceived as having a connection with their presentation:

Abbott Jane	Boyle Alison	Costello Agnes
Abeysekera Kushala	Broering Ruth	Costentin Charlotte
Aboona Majd	Bruggmann Philip	Craciun Rares
Abramov Frida	Brunner Nathalie	Cristoferi Laura
Agarwal Kosh	Buccsics Theresa	Cui Ang
Aguilera Sancho Victoria	Buller-Taylor Terri	Currie Sue
Ahmed Osman	Bungay Rebecca	Curtis Megan
Aizenshtadt Aleksandra	Burghart Lukas	Dahari Harel
Ajmera Veeral	Caballero Francisco J.	Dajti Elton
Akbary Kutbuddin	Cabezas Joaquin	Dalegaard Magnus Illum
Ala Aftab	Cable Edward	D'Alessio Antonio
Albertos Rubio Sonia	Cales Paul	Dandri Maura
Ali Syed Afroz	Campani Claudia	D'Anna Stefano
Ali Nida	Campbell Cori	De Berdt Pauline
Alkhouri Naim	Caon Elisabetta	De Brito Nunes Maria
Almishri Wagdi	Capel Jeroen	de Graaff Barbara
Altangerel Enkhjargal	Capozza Thomas	de la Torre Manuel
Anderson Phylea	Cappelli Simone	de Langlard Mathieu
Andreola Fausto	Cappuyns Sarah	de Lédinghen Victor
Angata Kiyohiko	Cardenas Andres	de Sena Elena
Armisen Javier	Cardoso Mariana	De Vincentis Antonio
Asselah Tarik	Carey Ivana	Debing Yannick
Åström Hanne	Castéra Laurent	Deltenre Pierre
Atallah Edmond	Castven Darko	Deng You
Bager Palle	Castven Jovana	Deshpande Kedar
Bajaj Jasmohan S	Caussy Cyrielle	Dhanda Ashwin
Balcar Lorenz	Caviglia Gian Paolo	Di Giorgio Angelo
Baldassarre Maurizio	Cederborg Anna	Di Pasqua Laura Giuseppina
Ballester María Pilar	Celsa Ciro	Diaz Luis Antonio
Barchuk William	Chan Wah Loong	Diaz Gonzalez Alvaro
Bauer David JM	Chang Devon Y.	Diaz-Mitoma Francisco
Becker Svea	Chanteranne Brigitte	Dietz-Fricke Christopher
Begré Lorin	Chavanelle Vivien	Dinjar Kujundžić Petra
Belilos Eleanor	Chen San-Chi	Dixon Emmanuel Dauda
Bell Adam	Chen Kaina	Dixon Thomas
Ben Khaled Najib	Chen Shin-Wei	Dodge Esther
Benedicto Ana	Chen Guoliang	Dold Leona
Benichou Bernard	Chen Yue	Domínguez-Hernández Raquel
Bennett Kris	Cheng Cho-Chin	Dongelmans Edo
Bertoletti Antonio	Cherubini Alessandro	Dubourg Julie
Bhanja Abhinab	Chng Elaine	Duca Leonardo
Bihari Chhagan	Choi Won-Mook	Dushaj Elizabeta
Bittermann Therese	Choi Yun-Jung	Ebrahimi Fahim
Bloom Patricia	Chotkoe Shivani	Edwards Katherine
Bobowski-Gerard Marie	CHUNG Sungwon	Edwards Lindsey A
Bono Ariadna	Cimermancic Peter	Elias Kathleen
Booij Tijmen	Civitaresse Antonio	Elshabrawi Ahmed
Boonstra Andre	Collins Amy	Elston Robert
Bosch Miriam	Comoz Bertille	Engel Bastian
Bouquet Jerome	Conway Brian	Epstein Rachel
Boursier Jerome	Cooreman Michael	Espiritu Christine L.
Bowlus Christopher	Corpechot Christophe	Etzion Ohad
Boyd Anders	Cortese Mario	Fatima Ifrah

Feigh Michael
 Felipe Vicente
 Feng Hao
 Fernández- Rodríguez Conrado
 Fernandez-Barrena Maite G
 Ferrandino Giuseppe
 Finnegan Karen
 Fiorotto Romina
 Fischer Janett
 Fitzgerald Megan
 Flisiak Robert
 Frank Anna Katharina
 Frankova Sona
 Friebe Andreas
 Fromme Malin
 Fulgenzi Claudia
 Furquim d'Almeida Arno
 Gadd Victoria
 Gadi Zouhir
 Gairing Simon Johannes
 Gallacher Jenny
 Galsgaard Elisabeth
 García-Villarreal Luis
 Gay Joel
 Ger Flutter
 Gerolami René
 Gessner Ryan
 Gielen Vera
 Gigante Elia
 Gill Madeleine
 Giovannini Catia
 Giralt Albert
 Goikoetxea Naroa
 Golamari Srinivasa Reddy
 González Pascual Andrea
 Gordillo Noelia
 Gorsuch Cassandra
 Gosset Andréa
 Govaere Olivier
 Gracia-Sancho Jordi
 Greenman Raanan
 Grønbæk Henning
 Grueger Jens
 Gruevska Aleksandra
 Gu Wenyi
 Guerra Veloz Maria
 Guofeng Cheng
 Gupta Kusum
 Gupta Neil
 H. Nielsen Malte
 Habboub Nadeen
 Hagström Hannes
 Hajji Yacine
 Hammoutene Adel
 Hansen Emil Deleuran
 Hartsfield Cynthia (Cindy)
 Hassany Mohamed
 Hayat Umar
 Hegmar Hannes
 Heldens Anneleen
 Henrique Mariana Moura
 Herber Adam
 Hernández Candido
 Hernandez-Tejero Maria
 Herting Emma Celia
 Hettiarachchige Nadilka
 Hirode Grishma
 Høegholm Ernst Lauridsen Emilie

Hofer Benedikt
 Hoffmann Charlotte
 Hong Jin
 Hou Jinlin
 Hourli Inbal
 Hradicka Petra
 Hsin-Tzu Wang
 Hsu Heather
 Huang Michael
 Huang Yi-Hsiang
 Huang Linxiang
 Huang Daniel
 Huergo Iglesias Estefania
 HUI Vicki Wing-Ki
 Hupa-Breier Katharina Luise
 Hur Moon Haeng
 Iannacone Matteo
 Ichikawa Masataka
 Ielasi Luca
 Igloi-Nagy Adam
 Ikahihifo-Bender Jade
 Inia José A.
 Inoue Takako
 Iserte Gemma
 Iyer Janani
 Jachs Mathias
 Jain Vandana
 James Bethany
 Janjua Naveed
 Jaroszewicz Jerzy
 Jean Damascene Makuza
 Jeong Dahn
 Jimenez Ramos Maria
 Johannes Chang
 Johansen Stine
 Johansson Lars
 John Binu
 Jois Bhavna
 Jones Andrew
 Jörg Vincent
 Kachru Nandita
 Kahlhöfer Julia
 Kardashian Ani
 Kasuga Ryosuke
 Kendall Timothy
 Kennedy Shannon
 Kent Abigail
 Kerbert Annarein
 Kern Anna
 Khan Sulhera
 Kim Chong
 Kim Jihye
 Kim Ju Yeon
 Kim Bo Hyun
 Kitrinis Kathryn M.
 Kjær Mikkel Breinholt
 Klindt-Morgan Caroline
 Koenig Alexander
 Kolev Mirjam
 Kolhatkar Nikita
 Korenaga Masaaki
 Kostadinova Radina
 Kowalski Amanda
 Krawczyk Marcin
 Kronborg Thit Mynster
 Kupcinkas Limas
 Kwong Tsz Tung
 Lai Che To

Lampertico Pietro
 Lange Naomi
 Lanthier Nicolas
 Lara Romero Carmen
 Lauridsen Mette Munk
 Lax Sigurd
 Lazarus Jeffrey
 Lee Dong Ho
 Lee Sung Won
 Lee Kyungsun
 Lee Pei-Chang
 Lee Brian
 Leff Phillip
 Lempp Florian
 Leonel Couto Thais
 Leung Kristel
 Leung Daniel
 Leven Emily
 Li Guanlin
 Li Xiaojiao
 Liao Min
 Liao Bo-Hung
 Lim Chun Kiat
 Lin Meiyin
 Lindfors Andrea
 Lindholm Schnefeld Helle
 Liu Hanyang
 Liu Jingwen
 Liu Yongheng
 Liu Yuhan
 Liu Zhihua
 Llarch Neus
 Londoño Maria Carlota
 Lønsmann Ida
 Lord Allison
 Lucas Carol
 Luft Juliet
 Lurje Isabella
 Madaleno Joao
 Magaz Marta
 Mageras Anna
 Magnanensi Jeremy
 Magno Pereira Vítor
 Mahmood Hassan
 Maini Mala
 Maiwall Rakhi
 Mak Lung Yi Loey
 Manfredi Giulia Francesca
 Manhas Savrina
 Mania Anna
 Manko Anna
 Mann Jelena
 Margalit Maya
 Mariño Zoe
 Marjot Thomas
 Marlowe Natalie
 Marra Fabio
 Martínez-Arenas Laura
 Matsumoto Tomonori
 Matsuura Takanori
 Mauro Ezequiel
 Mauz Jim Benjamin
 Mayorca Guiliani Alejandro
 Mazumder Nikhilesh
 McClure Matt
 McGarvey Iona
 McRae Michael
 Medical Costello

Disclosures

Medina Diogo
 Meister Thomas
 Melgar-Lesmes Pedro
 Melini Stefania
 Mellemkjær Anders
 Mercier Renee-Claude
 Messamore Eric
 Meszaros Magdalena
 Michel Maurice
 Middelburg Tim
 Miethke Alexander
 Minchenberg Scott
 Mirams Laura
 Missen Louise
 Moga Lucile
 Mohamed Osama
 Mohamed Almuthana
 Mohammed Mansur
 Møller Thomas
 Morelli Maria Cristina
 Morris Heather
 Mueller Sebastian
 Mullender Claire
 MUNTEANU Mona
 Nahon Pierre
 Nana Melanie
 Nanji Zehrah
 Ndow Gibril
 Ness Erik
 NG Irene Oi-Lin
 Ngo Vinh Hanh
 Nguyen Khac Eric
 Niehaus Christian
 Nikolopoulos Georgios
 Niyomsri Siwaporn
 Nøhr-Meldgaard Jacob
 Norton Luke
 Novac Ovidiu
 Nováková Barbora
 Nyholm Iris
 O'Farrell Marie
 Offensperger Florian
 Ohlendorf Valerie
 Olaizola Paula
 Olaizola Irene
 Olynyk John
 Paganelli Massimiliano
 Pagani Alessia
 Pajinag Melissa April
 Palom Adriana
 Palomino Sara
 Pammer Lorenz Michael
 Pan Qin
 Panella Riccardo
 Papatheodoridis George
 Park Min Kyung
 Parker Richard
 Passos-Castilho Ana Maria
 Patmore Lesley
 Patrick Ingiliz
 Pauly Jana
 Pedersen Kamilla
 Peleman Cédric
 Pellegrino Shannnon
 Pelusi Serena
 Pencek Richard
 Pérez Clara
 Peter Joy

Petitjean Mathieu
 Phillips Bethany
 Picchio Camila
 Piñero Federico
 Pirozzi Claudio
 Plonowski Artur
 Pollicino Teresa
 Poulsen Peter Bo
 Poynard Thierry
 Praestholm Stine Marie
 Prier Lindvig Katrine
 Pulaski Hanna
 Puoti Massimo
 Qian Shuwen
 Quaranta Maria Giovanna
 Ramier Clémence
 Rashu Elias
 Rastovic Una
 Ratziu Vlad
 Ravaioli Federico
 Rawles Jacqui
 Razavi Homie
 Razavi-Shearer Devin
 Reiter Florian P
 Remy André-Jean
 Revill Peter
 Riback Lindsey
 Ricco Gabriele
 Rinella Mary
 Roca Suarez Armando Andres
 Roder Christine
 Rodríguez Candelaria Esther
 Roessler Stephanie
 Rohr-Udilova Nataliya
 Romero Gomez Manuel
 Romero-Gutiérrez Marta
 Ronca Vincenzo
 Rønn Madsen Martin
 Roqueta-Rivera Manuel
 Rosenthal Johan
 Rössle Martin
 Roulot Dominique
 Rubio Aileen
 Ruíz-Cobo Juan Carlos
 Ruiz-Fernandez Gloria
 Ryder Rachel
 Saeidinejad Mahdi
 Sakata Toshihiro
 Sällberg Matti
 Salpini Romina
 Sánchez-Aldehuelo Rubén
 Sandmann Lisa
 Sanduzzi Zamparelli Marco
 Santol Jonas
 Sawhney Sangeeta
 Schaub Johanna
 Scheiner Bernhard
 Schleicher Eva Maria
 Schmidt Mark A
 Schneider Caitlin
 Schregel Ida
 Schröter Dominik
 Schwab Patrick
 Schwarz Michael
 Segovia-Miranda Fabián
 Seko Yuya
 Semmler Georg
 Serdjebi Cindy

Serfert Yvonne
 Serper Marina
 Seto Wai-Kay
 Seung Seok Oh
 Sevak Jayesh Kumar
 Shah Syed Hassan Bin Usman
 Shaham-Niv Shira
 Shaheen Abdel-Aziz
 Shang Ying
 Shenvi Swapna
 Shim Wan Seob
 Shin Hyunjae
 Shlomain Amir
 Shringarpure Reshma
 Siakavellas Spyridon (Spyros)
 SIDALI Sabrina
 Silvestri Laura
 Simbrunner Benedikt
 Sims Karen
 Singal Ashwani
 Singh Jenn
 Singh Roshni
 Smith Helen
 Snijders Romée
 Sonneveld Milan
 Sopko Bibb Rachel
 Sorensen Henrik
 Soria López Estela
 Sorz Thomas
 Spivak Igor
 Standen Mary
 Stapleton Beth
 Stauffer Winston
 Steffens Andrea
 Steppich Katja
 Stern Louisa
 Stiess Michael
 Stirnimann Guido
 Stoelinga Anna
 Suess Gregory
 Sun Natalie
 Swearingen Kjersti
 Swiatek-de Lange Magdalena
 Swift Brandon
 Tahata Yuki
 Tajudin Muna
 Tamaki Nobuharu
 Tan Chin Kim
 Tanaka Atsushi
 Taub Rebecca
 Tchamgoue serge
 Teicher Kirk Frederik
 Telep Laura
 Téllez Luis
 Ten Hove Marit
 Teng Margaret
 Terbah Ryma
 Terol Cháfer Isabel
 Testoni Barbara
 Thakar Shubhankar
 Thennati Rajamannar
 Theodoreson Mark
 Thing Mira
 Thorhauge Katrine
 Thornton Michael
 Thuy Le Thi Thanh
 Tincopa Monica
 Tomah Shaheen

Toniutto Pierluigi
 Tornai David
 Torp Nikolaj
 Trehanpati Nirupma
 Trivedi Palak
 Tsuchiya Kaoru
 Urbanek-Quaing Melanie
 Ure Daren
 Uschner Frank Erhard
 Vaillant Andrew
 van Bömmel Florian
 Vanderschueren Emma
 Vandriel Shannon M.
 Vargas Accarino Elena
 Vercoulen Yvonne
 Vesterhus Mette
 Vijayakumar Archana
 Vinaixa Carmen
 Vincent Jeanne Perpétue
 Vithayathil Mathew
 Voeller Alexis
 Voiosu Andrei
 Volmari Annika
 von Buelow Verena

von Felden Johann
 Waddell Tom
 Walker Lucy
 Walker Ruth
 Wang Jun
 Wang Xiaoxiao
 Wang Tingyan
 Wang Wenshi
 Wasuwanich Paul
 Weavil Josh
 Weihs Julian
 Weiss Manuel
 Weiss Karl Heinz
 Werge Mikkell
 Wernberg Charlotte
 Wetten Aaron
 Wiegand Johannes
 Wijarnpreecha Karn
 Wijnberg Larissa
 Witte Moana
 Wong Vincent Wai-Sun
 Wong Grace Lai-Hung
 Wong Robert
 Wong Yu Jun

Wranke Anika
 Wu Min
 Wu Tao
 Wu Tongfei
 Xavier e Silva Fernando
 Xu Jun
 Yadav Pushpa
 Yang Ju Dong
 Yannick Rakké
 Yao Yuhao
 Ye zuodong
 Yeon Jong Eun
 Yip Terry Cheuk-Fung
 Younossi Zobair
 Zeng Qinghe
 Zhan Zhu
 Zhang Chi
 Zhang Josephine
 Zhu Ren
 Ziegler Spedtsberg Ida
 Zischka Hans
 Zou Zhaozhen

Reviewers list

We express our deepest appreciation to the following people, who have given us generous and invaluable help as abstract reviewers for the EASL Congress 2023.

Abdelmalek Manal	Graupera Isabel	Reeves Helene
Adams Leon	Gual Philippe	Reiberger Thomas
Agarwal Kosh	Hagstrom Hannes	Reid Leila
Alazawi William	Hansen Bettina	Reverter Enric
Alisi Anna	Hernandez-Gea Virginia	Rich Nicole
Andersen Jesper	Huch Meri	Rinella Mary
Andersson Emma	Hydes Theresa	Riveiro-Barciela Mar
Andrade Raul Jesús	Iannacone Matteo	Rodríguez-Peralvarez Manuel L.
Bager Palle	Iavarone Massimo	Romeo Stefano
Bansal Ruchi	Idilman Ramazan	Romero Gomez Manuel
Barfod O'Connell Malene	Jalan Rajiv	Rowe Ian
Battaller Ramon	Kondili Loreta	Russo Francesco Paolo
Baumert Thomas	Krag Aleksander	Saborowski Anna
Ben-Ari Ziv	Lemoine Sara	Schäfer Denise
Bengsch Bertram	Leo Ana	Schattenberg Jörn
Berg Thomas	Long Michelle	Schulze-zur Wiesch Julian
Bernal William	Longhi Maria Serena	Scorletti Eleonora
Beuers Ulrich	Lotersztajn Sophie	Scott Charlotte
Böttler Tobias	Lucifora Julie	Semmler Georg
Braconi Chiara	Luukkonen Panu	Senzolo Marco
Bureau Christophe	Macias Rocio	Serfaty Lawrence
Buti Maria	Magnusson Maria	Shawcross Debbie L.
Cabibbo Giuseppe	Mantovani Alessandro	Shiri Sverdlov Ronit
Caraceni Paolo	Mariño Zoe	Shlomai Amir
Carbone Marco	Marra Fabio	Sonneveld Milan
Castera Laurent	Marschall Hans Ulrich	Spee Bart
Cazzagon Nora	Mas Valeria	Steinmann Eike
Childs Kate	Merle Uta	Strick-Marchand Helene
Conti Filomena	Moreno Christophe	Szabo Gyongyi
Corey Kathleen	Morgan Marsha	Tacke Frank
Culver Emma	Moschetta Antonio	Thabut Dominique
Dalekos George	Nault, Jean Charles	Thiele Maja
Dao Thi Viet Loan	Negro Francesco	Thompson Karen
Darwish Murad Sarwa	Newsome Philip	Towey Jennifer
De knegt Robert	Oude Elferink Ronald	Trebicka Jonel
Degasperi Elisabetta	Pais Raluca	Trépo Eric
Degertekin Bülent	Pallett Laura	Tripathi Dhiraj
Dietz Julia	Papatheodoridis George	Trovato Francesca Maria
Edeline Julien	Papp Maria	Tsochatzis Emmanuel
Elsharkawy Ahmed	Parker Richard	Turco Laura
Fabrellas Nuria	Petta Salvatore	Vacca Michele
Fisicaro Paola	Pinzani Massimo	Valenti Luca
Flisiak Robert	Piscaglia Fabio	van Bommel Florian
Folseraas Trine	Pischke Sven	van Mil Saskia
Frances Ruben	Procopet Bogdan	Verma Sumita
Francque Sven	Pollicino Teresa	Vesterhus Mette
Fraquelli Mirella	Pons Monica	Vinken Mathieu
Ganne Carrie Nathalie	Ponziani Francesca	Vonghia Luisa
Garcia Pagan Juan Carlos	Pose Elisa	Wagner Martin
Gilgenkrantz Helene	Postic Catherine	Webb Glynn
Gill Upkar	Protopopescu Camelia	Westbrook Rachel
Goossens Nicolas	Ramachnadran Prakash	Williams Felicity
Gottwein Judith	Ratzu Vlad	Wong Vincent
Gougelet Angelique	Rautou Pierre-Emmanuel	Yasuko Iwakiri
Govaere Olivier	Reesink Hendrik W	